Principles of Bone Biology

FOURTH EDITION

EDITED BY

John P. Bilezikian

T. John Martin

Thomas L. Clemens

Clifford J. Rosen

AP

Principles of Bone Biology

Fourth Edition

Volume 1

Edited by

John P. Bilezikian
Division of Endocrinology, Department of Medicine
College of Physicians and Surgeons
Columbia University, New York, NY, United States

T. John Martin
St. Vincent's Institute of Medical Research;
Department of Medicine at St. Vincent's Hospital
The University of Melbourne
Melbourne, Australia

Thomas L. Clemens
Department of Orthopaedic Surgery
Johns Hopkins University School of Medicine;
Baltimore Veterans Administration Medical Center
Baltimore, MD, United States

Clifford J. Rosen
Maine Medical Center Research Institute
Scarborough, ME, United States

ACADEMIC PRESS
An imprint of Elsevier

Principles of Bone Biology

Fourth Edition

Volume 2

Edited by

John P. Bilezikian
Division of Endocrinology, Department of Medicine
College of Physicians and Surgeons
Columbia University, New York, NY, United States

T. John Martin
St. Vincent's Institute of Medical Research;
Department of Medicine at St. Vincent's Hospital
The University of Melbourne
Melbourne, Australia

Thomas L. Clemens
Department of Orthopaedic Surgery
Johns Hopkins University School of Medicine;
Baltimore Veterans Administration Medical Center
Baltimore, MD, United States

Clifford J. Rosen
Maine Medical Center Research Institute
Scarborough, ME, United States

ACADEMIC PRESS
An imprint of Elsevier

Academic Press is an imprint of Elsevier
125 London Wall, London EC2Y 5AS, United Kingdom
525 B Street, Suite 1650, San Diego, CA 92101, United States
50 Hampshire Street, 5th Floor, Cambridge, MA 02139, United States
The Boulevard, Langford Lane, Kidlington, Oxford OX5 1GB, United Kingdom

Notices
Knowledge and best practice in this field are constantly changing. As new research and experience broaden our understanding, changes in research methods, professional practices, or medical treatment may become necessary.

Practitioners and researchers must always rely on their own experience and knowledge in evaluating and using any information, methods, compounds, or experiments described herein. In using such information or methods they should be mindful of their own safety and the safety of others, including parties for whom they have a professional responsibility.

To the fullest extent of the law, neither the Publisher nor the authors, contributors, or editors, assume any liability for any injury and/or damage to persons or property as a matter of products liability, negligence or otherwise, or from any use or operation of any methods, products, instructions, or ideas contained in the material herein.

Library of Congress Cataloging-in-Publication Data
A catalog record for this book is available from the Library of Congress

British Library Cataloguing-in-Publication Data
A catalogue record for this book is available from the British Library

SET ISBN: 978-0-12-814841-9
Volume 1 ISBN: 978-0-12-819932-9
Volume 2 ISBN: 978-0-12-819933-6

Publisher: Stacy Masucci
Acquisition Editor: Tari Broderick
Editorial Project Manager: Megan Ashdown
Production Project Manager: Poulouse Joseph
Cover designer: Greg Harris

Typeset by TNQ Technologies

Dedication of Fourth Edition to Lawrence G. Raisz

By the end of the 1970s, when the bone research community felt that it was ready for its own scientific society, Larry Raisz was one of the leaders of the group that founded the American Society for Bone and Mineral Research (ASBMR). The ASBMR had its first annual conference in 1979, with Larry serving as its second president. As the first editor of the *Journal of Bone and Mineral Research*, for a decade, Larry set the highest scientific standards for quality and integrity. That standard remains untarnished today.

Larry's knowledge of the facts in our field was prodigious. His expertise and experience in basic elements of bone biology were exceptional. He had great understanding and wisdom in interpretation of the clinical implications of basic bone biology. But he always wanted to know more. At ASBMR and other annual meetings, it was always Larry who rose to the microphone after a presentation to ask, not only the first question, but typically the best one! Remarkably, Larry could translate basic bone biology to the clinical arena. Few in our field then or now could so smoothly integrate clinical aspects of metabolic bone diseases with the burgeoning knowledge of underlying pathophysiological mechanisms. Adding to these talents was a collegiality and an exuberant enthusiasm that pervaded all venues of Larry Raisz's world. As osteoporosis became more widely recognized to be a medical scourge, then and now, Larry quickly grasped the need to speak about the burden of the disease and contributed to the international dialogue, raising awareness among us all. This awareness was a major factor in the recognition among countries that we are dealing with a disease that needs greater understanding at all levels. And, indeed, at all levels, Larry contributed so much.

These qualities made Larry Raisz a wonderfully effective coeditor of the first three editions of *Principles of Bone Biology*. Much more than that, though, he was a pleasure to work with as a colleague and friend, exceptionally efficient and with unfailing humor and optimism when faced with any adversity. Larry would share the highs and lows with you, but the lows were rare and short lived.

We remember him constantly and dedicate to Lawrence G. Raisz, MD, this fourth edition of what he called "Big Gray."

John P. Bilezikian
T. John Martin
Thomas L. Clemens
Clifford J. Rosen

List of Contributors

David Abraham Centre for Rheumatology and Connective Tissue Diseases, University College London, London, United Kingdom

Maria Almeida Division of Endocrinology and Metabolism, Center for Osteoporosis and Metabolic Bone Diseases, University of Arkansas for Medical Sciences, Little Rock, AR, United States; The Central Arkansas Veterans Healthcare System, Little Rock, AR, United States

Elena Ambrogini Center for Osteoporosis and Metabolic Bone Diseases, University of Arkansas for Medical Sciences Division of Endocrinology and Metabolism, Little Rock, AR, United States; Central Arkansas Veterans Healthcare System, Little Rock, AR, United States

Andrew Arnold Center for Molecular Oncology and Division of Endocrinology and Metabolism, University of Connecticut School of Medicine, Farmington, CT, United States

Bence Bakos 1st Department of Medicine, Semmelweis University Medical School, Budapest, Hungary

Clemens Bergwitz Departments of Pediatrics and Internal Medicine, Yale University School of Medicine, New Haven, CT, United States

Daniel D. Bikle VA Medical Center and University of California San Francisco, San Francisco, California, United States

John P. Bilezikian Division of Endocrinology, Department of Medicine, College of Physicians and Surgeons, Columbia University, New York, NY, United States

Neil Binkley University of Wisconsin School of Medicine and Public Health, Madison, Wisconsin, United States

Alessandro Bisello Department of Pharmacology and Chemical Biology, Laboratory for GPCR Biology, University of Pittsburgh School of Medicine, Pittsburgh, PA, United States

L.F. Bonewald Indiana Center for Musculoskeletal Health, Departments of Anatomy and Cell Biology and Orthopaedic Surgery, Indiana University, Indianapolis, IN, USA

George Bou-Gharios Institute of Ageing and Chronic Disease, University of Liverpool, Liverpool, United Kingdom

Roger Bouillon Laboratory of Clinical and Experimental Endocrinology, Department of Chronic Diseases, Metabolism and Aging, KU Leuven, Belgium

Mary L. Bouxsein Center for Advanced Orthopaedic Studies, Beth Israel Deaconess Medical Center, Boston, MA, United States; Department of Orthopaedic Surgery, Harvard Medical School, Boston, MA, United States; Endocrine Unit, Department of Medicine, Massachusetts General Hospital, Boston, MA, United States

Brendan F. Boyce Department of Pathology and Laboratory Medicine, University of Rochester School of Medicine and Dentistry, Rochester, NY, United States

Steven Boyd McCaig Institute for Bone and Joint Health, The University of Calgary, Calgary, AB, Canada

Maria Luisa Brandi Department of Experimental and Clinical Biomedical Sciences, University of Florence, Florence, Italy

David B. Burr Department of Anatomy and Cell Biology, Indiana Center for Musculoskeletal Health, Indiana University School of Medicine, Indianapolis, IN, United States

Laura M. Calvi Department of Medicine and Wilmot Cancer Center, University of Rochester Medical Center, Rochester, NY, United States

Ernesto Canalis Departments of Orthopaedic Surgery and Medicine, and the UConn Musculoskeletal Institute, UConn Health, Farmington, CT, United States

Xu Cao Department of Orthopedic Surgery, Johns Hopkins University School of Medicine, Baltimore, MD, United States

Geert Carmeliet Laboratory of Clinical and Experimental Endocrinology, Department of Chronic Diseases, Metabolism and Ageing, KU Leuven, Leuven, Belgium; Prometheus, Division of Skeletal Tissue Engineering, KU Leuven, Leuven, Belgium

Thomas O. Carpenter Departments of Pediatrics and Internal Medicine, Yale University School of Medicine, New Haven, CT, United States

Wenhan Chang Endocrine Research Unit, Department of Veterans Affairs Medical Center, Department of Medicine, University of California, San Francisco, CA, United States

Shek Man Chim Regeneron Pharmaceuticals, Inc. Tarrytown, NY, United States

Shilpa Choudhary Department of Medicine and Musculoskeletal Institute, UConn Health, Farmington, CT, United States

Sylvia Christakos Department of Microbiology, Biochemistry and Molecular Genetics, Rutgers, New Jersey Medical School, Newark, NJ, United States

Yong-Hee Patricia Chun Department of Periodontics, University of Texas Health Science Center at San Antonio, San Antonio, TX, United States

Cristiana Cipriani Department of Internal Medicine and Medical Disciplines, Sapienza University of Rome, Italy

Roberto Civitelli Washington University in St. Louis, Department of Medicine, Division of Bone and Mineral Diseases, St. Louis, MO, United States

Thomas L. Clemens Department of Orthopaedic Surgery, Johns Hopkins University School of Medicine, Baltimore, MD, United States; Baltimore Veterans Administration Medical Center, Baltimore, MD, United States

Michael T. Collins Skeletal Disorders and Mineral Homeostasis Section, National Institute of Dental and Craniofacial Research, National Institutes of Health, Bethesda, MD, United States

Caterina Conte Vita-Salute San Raffaele University, Milan, Italy; Division of Immunology, Transplantation and Infectious Diseases, IRCCS San Raffaele Scientific Institute, Milan, Italy

Mark S. Cooper The University of Sydney, ANZAC Research Institute and Department of Endocrinology & Metabolism, Concord Hospital, Sydney, NSW, Australia

Jillian Cornish Department of Medicine, University of Auckland, Auckland, New Zealand

Serge Cremers Department of Pathology & Cell Biology and Department of Medicine, Vagelos College of Physicians and Surgeons, Columbia University Irving Medical Center, United States

Bess Dawson-Hughes Jean Mayer USDA Human Nutrition Research Center on Aging at Tufts University, Boston, Massachusetts, United States

Benoit de Crombrugghe The University of Texas M.D. Anderson Cancer Center, Houston, TX, United States

Hector F. DeLuca Department of Biochemistry, University of Wisconsin—Madison, Madison, Wisconsin, United States

David W. Dempster Regional Bone Center, Helen Hayes Hospital, West Haverstraw, NY, United States; Department of Pathology and Cell Biology, College of Physicians and Surgeons, Columbia University, New York, NY, United States

Matthew T. Drake Department of Endocrinology and Kogod Center of Aging, Mayo Clinic College of Medicine, Rochester, MN, United States

Patricia Ducy Department of Pathology & Cell Biology, Columbia University, College of Physicians & Surgeons, New York, NY, United States

Frank H. Ebetino Department of Chemistry, University of Rochester, Rochester, NY, United States; Mellanby Centre for Bone Research, Medical School, University of Sheffield, United Kingdom

Klaus Engelke Department of Medicine, FAU University Erlangen-Nürnberg and Universitätsklinikum Erlangen, Erlangen, Germany; Bioclinica, Hamburg, Germany

Reinhold G. Erben Department of Biomedical Research, University of Veterinary Medicine Vienna, Vienna, Austria

David R. Eyre Department of Orthopaedics and Sports Medicine, University of Washington, Seattle, WA, United States

Charles R. Farber Center for Public Health Genomics, Departments of Public Health Sciences and Biochemistry and Molecular Genetics, University of Virginia School of Medicine, Charlottesville, VA, United States

Marina Feigenson Department of Developmental Biology, Harvard School of Dental Medicine, Boston, MA, United States

Mathieu Ferron Institut de Recherches Cliniques de Montréal, Montréal, QC, Canada

Pablo Florenzano Endocrine Department, School of Medicine, Pontificia Universidad Católica de Chile, Santiago, Chile

Francesca Fontana Washington University in St. Louis, Department of Medicine, Division of Bone and Mineral Diseases, St. Louis, MO, United States

Brian L. Foster Biosciences Division at College of Dentistry at Ohio State University, Columbus, OH, United States

Peter A. Friedman Department of Pharmacology and Chemical Biology, Laboratory for GPCR Biology, University of Pittsburgh School of Medicine, Pittsburgh, PA, United States

Seiji Fukumoto Fujii Memorial Institute of Medical Sciences, Institute of Advanced Medical Sciences, Tokushima University, Tokushima, Japan

Laura W. Gamer Department of Developmental Biology, Harvard School of Dental Medicine, Boston, MA, United States

Thomas J. Gardella Endocrine Unit, Department of Medicine and Pediatric Nephrology, MassGeneral Hospital for Children, Massachusetts General Hospital and Harvard Medical School, Boston, MA, United States

Patrick Garnero INSERM Research Unit 1033-Lyos, Lyon, France

Harry K. Genant Departments of Radiology and Medicine, University of California, San Francisco, CA, United States

Francesca Giusti Department of Experimental and Clinical Biomedical Sciences, University of Florence, Florence, Italy

Andy Göbel Department of Medicine III, Technische Universität Dresden, Dresden, Germany; German Cancer Consortium (DKTK), Partner site Dresden and German Cancer Research Center (DKFZ), Heidelberg, Germany

David Goltzman Calcium Research Laboratories and Department of Medicine, McGill University and McGill University Health Centre, Montreal, QC, Canada

Jeffrey P. Gorski Department of Oral and Craniofacial Sciences, School of Dentistry, and Center for Excellence in Mineralized and Dental Tissues, University of Missouri—Kansas City, Kansas City, MO, United States

James Griffith Department of Imaging and Interventional Radiology, The Chinese University of Hong Kong, Hong Kong, China

R. Graham G Russell Mellanby Centre for Bone Research, Medical School, University of Sheffield, United Kingdom; Nuffield Department of Orthopaedics, Rheumatology and Musculoskeletal Sciences, The Oxford University Institute of Musculoskeletal Sciences, The Botnar Research Centre, Nuffield Orthopaedic Centre, Oxford, United Kingdom

Kurt D. Hankenson Department of Orthopaedic Surgery, University of Michigan Medical School, Ann Arbor, MI, United States

Fadil M. Hannan Department of Musculoskeletal Biology, Institute of Ageing and Chronic Disease, Faculty of Health & Life Sciences, University of Liverpool, Liverpool, United Kingdom; Academic Endocrine Unit, Radcliffe Department of Medicine, University of Oxford, Oxford Centre for Diabetes, Endocrinology and Metabolism (OCDEM), Churchill Hospital, Oxford, United Kingdom

Stephen E. Harris Department of Periodontics, University of Texas Health Science Center at San Antonio, San Antonio, TX, United States

Iris R. Hartley Interinstitute Endocrine Training Program, Eunice Kennedy Shriver National Institute of Child Health and Human Development, National Institutes of Health, Bethesda, MD, United States

Christine Hartmann Institute of Musculoskeletal Medicine, Department of Bone and Skeletal Research, Medical Faculty of the University of Münster, Münster, Germany

Robert P. Heaney Creighton University, Omaha, NE, United States

Geoffrey N. Hendy Metabolic Disorders and Complications, McGill University Health Center Research Institute, and Departments of Medicine, Physiology and Human Genetics, McGill University, Montreal, QC, Canada

Matthew J. Hilton Department of Orthopaedic Surgery, Department of Cell Biology, Duke University School of Medicine, Durham, NC, United States

Lorenz C. Hofbauer Center for Regenerative Therapies Dresden, Center for Healthy Aging and Division of Endocrinology, Diabetes, and Bone Diseases, Department of Medicine III, Technische Universität Dresden, Dresden, Germany

Gill Holdsworth Bone Therapeutic Area, UCB Pharma, Slough, United Kingdom

Yi-Hsiang Hsu Department of Medicine, Beth Israel Deaconess Medical Center and Harvard Medical School, Harvard School of Public Health, Hinda and Arthur Marcus Institute for Aging Research, Hebrew SeniorLife, Boston, MA, United States

David M. Hudson Department of Orthopaedics and Sports Medicine, University of Washington, Seattle, WA, United States

Marja Hurley Department of Medicine, University of Connecticut School of Medicine, UConn Health, Farmington, CT, United States

Karl L. Insogna Departments of Pediatrics and Internal Medicine, Yale University School of Medicine, New Haven, CT, United States

Robert L. Jilka Center for Osteoporosis and Metabolic Bone Diseases, University of Arkansas for Medical Sciences Division of Endocrinology and Metabolism, Little Rock, AR, United States; Central Arkansas Veterans Healthcare System, Little Rock, AR, United States

Mark L. Johnson Department of Oral and Craniofacial Sciences, UMKC School of Dentistry, Kansas City, MO, United States

Rachelle W. Johnson Vanderbilt Center for Bone Biology, Department of Medicine, Division of Clinical Pharmacology, Nashville, TN, United States

Glenville Jones Department of Biomedical and Molecular Science, Queen's University, Kingston, ON, Canada

Stefan Judex Department of Biomedical Engineering, Bioengineering Building, State University of New York at Stony Brook, Stony Brook, NY, United States

Harald Jüppner Endocrine Unit, Department of Medicine and Pediatric Nephrology, MassGeneral Hospital for Children, Massachusetts General Hospital and Harvard Medical School, Boston, MA, United States

Ivo Kalajzic Department of Reconstructive Sciences, UConn Health, Farmington, CT, United States

Gérard Karsenty Department of Genetics and Development, Columbia University Medical Center, New York, NY, United States

Hua Zhu Ke Angitia Biopharmaceuticals Limited, Guangzhou, China

Sundeep Khosla Department of Medicine, Division of Endocrinology, Mayo Clinic College of Medicine, Rochester, MN, United States; The Robert and Arlene Kogod Center on Aging, Rochester, MN, United States

Douglas P. Kiel Department of Medicine, Beth Israel Deaconess Medical Center and Harvard Medical School, Harvard School of Public Health, Hinda and Arthur Marcus Institute for Aging Research, Hebrew SeniorLife, Boston, MA, United States

J. Klein-Nulend Department of Oral Cell Biology, Academic Centre for Dentistry Amsterdam (ACTA), University of Amsterdam and Vrije Universiteit Amsterdam, Amsterdam Movement Sciences, Amsterdam, The Netherlands

Frank C. Ko Center for Advanced Orthopaedic Studies, Beth Israel Deaconess Medical Center, Boston, MA, United States

Yasuhiro Kobayashi Institute for Oral Science, Matsumoto Dental University, Nagano, Japan

Martin Konrad Department of General Pediatrics, University Children's Hospital Münster, Münster, Germany

Paul J. Kostenuik Phylon Pharma Services, Newbury Park, CA, United States; School of Dentistry, University of Michigan, Ann Arbor, MI, United States

Christopher S. Kovacs Faculty of Medicine, Memorial University of Newfoundland, St. John's, NL, Canada

Richard Kremer Calcium Research Laboratories and Department of Medicine, McGill University and McGill University Health Centre, Montreal, QC, Canada

Venkatesh Krishnan Lilly Research Laboratories, Eli Lilly & Company, Lilly Corporate Center, Indianapolis, United States

Henry M. Kronenberg Endocrine Unit, Massachusetts General Hospital, Harvard Medical School, Boston, MA, United States

Peter A. Lakatos 1st Department of Medicine, Semmelweis University Medical School, Budapest, Hungary

Uri A. Liberman Department of Physiology and Pharmacology, Sackler Faculty of Medicine, Tel Aviv University, Tel-Aviv, Israel

Joseph A. Lorenzo The Departments of Medicine and Orthopaedics, UConn Health, Farmington, CT, United States

Conor C. Lynch Department of Tumor Biology, Moffitt Cancer Center, Tampa, FL, United States

Karen M. Lyons Department of Orthopaedic Surgery/ Orthopaedic Hospital, University of California, Los Angeles, CA, United States; Department of Molecular, Cell, & Developmental Biology, University of California, Los Angeles, CA, United States

Y. Linda Ma Biotechnology and Autoimmunity Research, Eli Lilly and Company, Indianapolis, IN, United States

Christa Maes Laboratory of Skeletal Cell Biology and Physiology (SCEBP), Skeletal Biology and Engineering Research Center (SBE), KU Leuven, Leuven, Belgium

Michael Mannstadt Endocrine Unit, Massachusetts General Hospital, Harvard Medical School, Boston, MA, United States

Stavros Manolagas Division of Endocrinology and Metabolism, Center for Osteoporosis and Metabolic Bone Diseases, University of Arkansas for Medical Sciences, Little Rock, AR, United States; The Central Arkansas Veterans Healthcare System, Little Rock, AR, United States

Robert Marcus Stanford University, Stanford, CA, United States

David E. Maridas Department of Developmental Biology, Harvard School of Dental Medicine, Boston, MA, United States

Pierre J. Marie UMR-1132 Inserm (Institut national de la Santé et de la Recherche Médicale) and University Paris Diderot, Sorbonne Paris Cité, Paris, France

Francesca Marini Department of Experimental and Clinical Biomedical Sciences, University of Florence, Florence, Italy

Jasna Markovac California Institute of Technology, Pasadena, CA, United States

T. John Martin St. Vincent's Institute of Medical Research, Melbourne, Australia; Department of Medicine at St. Vincent's Hospital, The University of Melbourne, Melbourne, Australia

Brya G. Matthews Department of Molecular Medicine and Pathology, University of Auckland, Auckland, New Zealand

Antonio Maurizi Department of Biotechnological and Applied Clinical Sciences, University of L'Aquila, L'Aquila, Italy

Sasan Mirfakhraee The University of Texas Southwestern Medical Center, Department of Internal Medicine, Endocrine Division, Dallas, TX, United Sates

Sharon M. Moe Division of Nephrology, Indiana University School of Medicine, Rodebush Veterans Administration Medical Center, Indianapolis, IN, United States

David G. Monroe Department of Medicine, Division of Endocrinology, Mayo Clinic College of Medicine, Rochester, MN, United States; The Robert and Arlene Kogod Center on Aging, Rochester, MN, United States

Carolina A. Moreira Bone Unit of Endocrine Division of Federal University of Parana, Laboratory PRO, Section of Bone Histomorphometry, Pro Renal Foundation, Curitiba, Parana, Brazil

Ralph Müller Institute for Biomechanics, ETH Zurich, Zurich, Switzerland

David S. Musson Department of Medicine, University of Auckland, Auckland, New Zealand

Teruyo Nakatani Department of Basic Science and Craniofacial Biology, New York University College of Dentistry, New York, NY, United States

Dorit Naot Department of Medicine, University of Auckland, Auckland, New Zealand

Nicola Napoli Unit of Endocrinology and Diabetes, University Campus Bio-Medico, Rome, Italy; Division of Bone and Mineral Diseases, Washington University in St Louis, St Louis, MO, United States

Tally Naveh-Many Minerva Center for Calcium and Bone Metabolism, Nephrology Services, Hadassah University Hospital, Hebrew University School of Medicine, Jerusalem, Israel

Edward F. Nemeth MetisMedica, Toronto, ON, Canada

Thomas L. Nickolas Division of Nephrology, Department of Medicine, Columbia University Medical Center, New York, NY, United States

Michael S. Ominsky Radius Health Inc., Waltham, MA, United States

Noriaki Ono Department of Orthodontics and Pediatric Dentistry, University of Michigan School of Dentistry, Ann Arbor, MI, United States

David M. Ornitz Department of Developmental Biology, Washington University School of Medicine, St. Louis, MO, United States

Nicola C. Partridge Department of Basic Science and Craniofacial Biology, New York University College of Dentistry, New York, NY, United States

Vihitaben S. Patel Department of Biomedical Engineering, Bioengineering Building, State University of New York at Stony Brook, Stony Brook, NY, United States

J. Wesley Pike Department of Biochemistry, University of Wisconsin–Madison, Madison, WI, United States

Carol Pilbeam Department of Medicine and Musculoskeletal Institute, UConn Health, Farmington, CT, United States

Lori Plum Department of Biochemistry, University of Wisconsin–Madison, Madison, Wisconsin, United States

John T. Potts, Jr. Endocrine Unit, Department of Medicine and Pediatric Nephrology, MassGeneral Hospital for Children, Massachusetts General Hospital and Harvard Medical School, Boston, MA, United States

J. Edward Puzas Department of Orthopaedics and Rehabilitation, University of Rochester School of Medicine and Dentistry, Rochester, NY, United States

Tilman D. Rachner Department of Medicine III, Technische Universität Dresden, Dresden, Germany; German Cancer Consortium (DKTK), Partner site Dresden and German Cancer Research Center (DKFZ), Heidelberg, Germany; Center for Healthy Aging and Division of

Endocrinology, Diabetes, and Bone Diseases, Technische Universität Dresden, Dresden, Germany

Audrey Rakian Department of Applied Oral Sciences, The Forsyth Institute, Cambridge, MA, United States; Department of Oral Medicine, Infection, Immunity, Harvard School of Dental Medicine, Boston, MA, United States

Rubie Rakian Department of Applied Oral Sciences, The Forsyth Institute, Cambridge, MA, United States; Department of Oral Medicine, Infection, Immunity, Harvard School of Dental Medicine, Boston, MA, United States

Nora E. Renthal Division of Endocrinology, Children's Hospital Boston, Boston, MA, United States

Julie A. Rhoades (Sterling) Department of Veterans Affairs, Nashville, TN, United States; Vanderbilt Center for Bone Biology, Department of Medicine, Division of Clinical Pharmacology, Nashville, TN, United States; Department of Biomedical Engineering, Nashville, TN, United States

Mara Riminucci Department of Molecular Medicine, Sapienza University of Rome, Rome, Italy

Scott J. Roberts Bone Therapeutic Area, UCB Pharma, Slough, United Kingdom

Pamela Gehron Robey National Institute of Dental and Craniofacial Research, National Institutes of Health, Department of Health and Human Services, Bethesda, MD, United States

Michael J. Rogers Garvan Institute of Medical Research and St Vincent's Clinical School; University of New South Wales, Sydney, Australia

G. David Roodman Department of Medicine, Division of Hematology and Oncology, Indiana University School of Medicine, and Roudebush VA Medical Center, Indianapolis, IN, United States

Clifford J. Rosen Maine Medical Center Research Institute, Scarborugh, ME, United States

Vicki Rosen Department of Developmental Biology, Harvard School of Dental Medicine, Boston, MA, United States

David W. Rowe Center for Regenerative Medicine and Skeletal Development, Department of Reconstructive Sciences, Biomaterials and Skeletal Development, School of Dental Medicine, University of Connecticut Health Center, Farmington, CT, United States

Janet Rubin Endocrine Division, Department of Medicine, University of North Carolina, Chapel Hill, NC, United States

Clinton T. Rubin Department of Biomedical Engineering, Bioengineering Building, State University of New York at Stony Brook, Stony Brook, NY, United States

Karl P. Schlingmann Department of General Pediatrics, University Children's Hospital Münster, Münster, Germany

Ego Seeman Department of Endocrinology and Medicine, Austin Health, University of Melbourne, Melbourne, VIC, Australia; Mary MacKillop Institute for Health Research, Australian Catholic University, Melbourne, VIC, Australia

Markus J. Seibel The University of Sydney, ANZAC Research Institute and Department of Endocrinology & Metabolism, Concord Hospital, Sydney, NSW, Australia

Chris Sempos Vitamin D Standardization Program, Havre de Grace, MD, United States

Dolores M. Shoback Endocrine Research Unit, Department of Veterans Affairs Medical Center, Department of Medicine, University of California, San Francisco, CA, United States

Caroline Silve Hôpital Bicêtre, Paris, France; Centre de Référence des Maladies rares du Calcium et du Phosphore and Filière de Santé Maladies Rares OSCAR, AP-HP, Paris, France; Service de Biochimie et Génétique Moléculaires, Hôpital Cochin, AP-HP, Paris, France

Justin Silver Minerva Center for Calcium and Bone Metabolism, Nephrology Services, Hadassah University Hospital, Hebrew University School of Medicine, Jerusalem, Israel

Natalie A. Sims St. Vincent's Institute of Medical Research, Melbourne, Australia; Department of Medicine at St. Vincent's Hospital, The University of Melbourne, Melbourne, Australia

Frederick R. Singer John Wayne Cancer Institute, Saint John's Health Center, Santa Monica, CA, United States

Joseph P. Stains Department of Orthopaedics, University of Maryland School of Medicine, Baltimore, MD, United States

Steve Stegen Laboratory of Clinical and Experimental Endocrinology, Department of Chronic Diseases, Metabolism and Ageing, KU Leuven, Leuven, Belgium; Prometheus, Division of Skeletal Tissue Engineering, KU Leuven, Leuven, Belgium

Paula H. Stern Department of Pharmacology, Northwestern University Feinberg School of Medicine, Chicago, IL, United States

Gaia Tabacco Division of Endocrinology, Department of Medicine, College of Physicians and Surgeons, Columbia University, New York, NY, United States; Endocrinology and Diabetes Unit, Department of Medicine, Campus Bio-Medico University of Rome, Rome, Italy

Istvan Takacs 1st Department of Medicine, Semmelweis University Medical School, Budapest, Hungary

Naoyuki Takahashi Institute for Oral Science, Matsumoto Dental University, Nagano, Japan

Donovan Tay Division of Endocrinology, Department of Medicine, College of Physicians and Surgeons, Columbia University, New York, NY, United States; Department of Medicine, Sengkang General Hospital, Singhealth, Singapore

Anna Teti Department of Biotechnological and Applied Clinical Sciences, University of L'Aquila, L'Aquila, Italy

Rajesh V. Thakker Academic Endocrine Unit, Radcliffe Department of Medicine, University of Oxford, Oxford Centre for Diabetes, Endocrinology and Metabolism (OCDEM), Churchill Hospital, Oxford, United Kingdom

Ryan E. Tomlinson Department of Orthopaedic Surgery, Thomas Jefferson University, Philadelphia, PA, United States

Francesco Tonelli Department of Experimental and Clinical Biomedical Sciences, University of Florence, Florence, Italy

Dwight A. Towler The University of Texas Southwestern Medical Center, Department of Internal Medicine, Endocrine Division, Dallas, TX, United Sates

Elena Tsourdi Department of Medicine III, Technische Universität Dresden, Dresden, Germany; Center for Healthy Aging, Technische Universität Dresden, Dresden, Germany

Chia-Ling Tu Endocrine Research Unit, Department of Veterans Affairs Medical Center, Department of Medicine, University of California, San Francisco, CA, United States

Nobuyuki Udagawa Department of Biochemistry, Matsumoto Dental University, Nagano, Japan

Connie M. Weaver Purdue University, West Lafayette, IN, United States

Marc N. Wein Endocrine Unit, Massachusetts General Hospital, Harvard Medical School, Boston, MA, United States

Lee S. Weinstein Metabolic Diseases Branch, National Institute of Diabetes, Digestive, and Kidney Diseases, Bethesda, MD, United States

MaryAnn Weis Department of Orthopaedics and Sports Medicine, University of Washington, Seattle, WA, United States

Michael P. Whyte Center for Metabolic Bone Disease and Molecular Research, Shriners Hospitals for Children - St. Louis, St. Louis, MO, United States; Division of Bone and Mineral Diseases, Department of Internal Medicine, Washington University School of Medicine at Barnes-Jewish Hospital, St. Louis, MO, United States

Bart O. Williams Program for Skeletal Disease and Center for Cancer and Cell Biology, Van Andel Research Institute, Grand Rapids, MI, United States

Xin Xu State Key Laboratory of Oral Diseases & National Clinical Research Center for Oral Diseases, Department of Cariology and Endodontics, West China Hospital of Stomatology, Sichuan University, Chengdu, PR China

Shoshana Yakar David B. Kriser Dental Center, Department of Basic Science and Craniofacial Biology, New York University College of Dentistry New York, New York, NY, United States

Yingzi Yang Department of Developmental Biology, Harvard School of Dental Medicine, Boston, MA, United States

Stefano Zanotti Departments of Orthopaedic Surgery and Medicine, and the UConn Musculoskeletal Institute, UConn Health, Farmington, CT, United States

Hong Zhou The University of Sydney, ANZAC Research Institute, Sydney, NSW, Australia

Preface to the Fourth Edition

The first edition of *Principles of Bone Biology* was published about 24 years ago, in 1996. Our field was ready then for a compendium of the latest concepts in bone biology. Now, several decades and two editions later, we are pleased to welcome you to the fourth edition of "Big Gray." Since the third edition was published in 2008, our field has continued to undergo sea changes of knowledge and insights. As a result of these advances since then, all chapters have undergone major revisions. In addition, areas not previously covered in depth are featured, such as vascular and nerve interactions with bone, interorgan communicants of bone, hematopoietic−bone cell interactions, nonskeletal aspects of vitamin D and RANK ligand, newly recognized signaling molecules and systems, and advances in methodological aspects of skeletal research. Illustrative of the vibrancy of our field, over 50% of the authors in this edition are new to it. Our returning and new authors are the very best.

We remember Larry Raisz. He, along with Gideon Rodan, constituted the triumvirate of coeditors for the first and second editions. We dedicated the third edition to the memory of Gideon. We dedicate *Principles of Bone Biology*, fourth edition, to the memory of Larry. In these front pages, we reprint our dedication to Gideon and remember Larry with a separate dedication for this edition. We miss them both very much.

We want to acknowledge Jasna Markovac, who has served as our liaison to our authors and our publisher. Given the nature of the times, this book would not have been completed without her dedication, perseverance, and single-minded purpose not to let anything disrupt our publishing goals. She accomplished this feat with an even handedness and a professionalism that was remarkable and remarkably effective. We are grateful to you, Jasna.

Finally, we are grateful to our authors, who have made this book what it is, namely a repository of knowledge and concepts in bone biology and a resource for us all in the years to come.

John P. Bilezikian
T. John Martin
Thomas L. Clemens
Clifford J. Rosen

Chapter 1

Molecular and cellular regulation of intramembranous and endochondral bone formation during embryogenesis

Christine Hartmann[1] and Yingzi Yang[2]

[1]*Institute of Musculoskeletal Medicine, Department of Bone and Skeletal Research, Medical Faculty of the University of Münster, Münster, Germany;*
[2]*Department of Developmental Biology, Harvard School of Dental Medicine, Boston, MA, United States*

Chapter outline

Introduction

The skeletal system performs vital functions: support, movement, protection, blood cell production, calcium storage, and endocrine regulation. Skeletal formation is also a hallmark that distinguishes vertebrate animals from invertebrates. In higher vertebrates (i.e., birds and mammals), the skeletal system contains mainly bones and cartilage, as well as a network of tendons and ligaments that connects them. During embryonic development, bones and cartilage are formed by osteoblasts and chondrocytes, respectively, both of which are derived from common mesenchymal progenitor cells called osteochondral progenitors. Skeletal development starts from mesenchymal condensation, during which mesenchymal progenitor cells aggregate at future skeletal locations. As mesenchymal cells in different parts of the embryo are derived from different cell lineages, the locations of initial skeletal formation determine which of the three mesenchymal cell lineages contribute to the future skeleton. Neural crest cells from the branchial arches contribute to the craniofacial bone, the sclerotome compartment of the somites gives rise to most of the axial skeleton, and lateral plate mesoderm forms the limb mesenchyme, from which limb skeletons are derived.

Principles of Bone Biology. https://doi.org/10.1016/B978-0-12-814841-9.00001-4

How osteoblast cells are induced during bone development is a central question for understanding the organizational principles underpinning a functional skeletal system. Abnormal osteoblast differentiation leads to a broad range of devastating skeletal diseases. Therefore, it is imperative to understand the cellular and molecular mechanisms underlying temporal and spatial controls of bone formation. Bone formation occurs by two essential processes: intramembranous ossification and endochondral ossification during embryonic development. Osteochondral progenitors differentiate into osteoblasts directly to form the membranous bone during intramembranous ossification, whereas during endochondral ossification, they differentiate into chondrocytes instead to form a cartilage template of the future bone. Both ossification processes are essential during the natural healing of bone fractures. In this chapter, we focus on current understanding of the molecular regulation of endochondral and intramembranous bone formation and its implication in diseases.

Intramembranous ossification

Intramembranous ossification mainly occurs during formation of the flat bones of the skull, mandible, maxilla, and clavicles. The mammalian cranium, or neurocranium, is the upper and back part of the skull. It protects the brain and supports the sensory organs, such as the ear, and the viscerocranium, which supports the face. The neurocranium can be divided into calvarium and chondrocranium, which grow to be the cranial vault that surrounds the brain and the skull base, respectively. The calvarium is composed of flat bones: frontal bones, parietal bones, the interparietal part of the occipital bone, and the squamous parts of the temporal bone (Jin et al., 2016). In mice, the calvarium consists of frontal bones, parietal bones, interparietal bone, and squamous parts of the temporal bone, all going through intramembranous ossification (Ishii et al., 2015). By lineage analysis in mouse models, frontal bones show a major contribution from neural crest and a small contribution from head mesoderm, while parietal bones entirely originate from head mesoderm (Jiang et al., 2002; Yoshida et al., 2008; Deckelbaum et al., 2012). Neural crest–derived and head mesoderm–derived cells coalesce to form calvarial bone primordia (Jiang et al., 2002; Yoshida et al., 2008). The mandible and maxilla are derived from the neural crest cells originating in the mid- and hindbrain regions of the neural folds that migrate ventrally, while the clavicles are formed from mesoderm.

The process starts from mesenchymal condensation and progresses through formation of the ossification center, ossification expansion, trabecula formation, and compact bone formation and the development of the periosteum (Fig. 1.1).

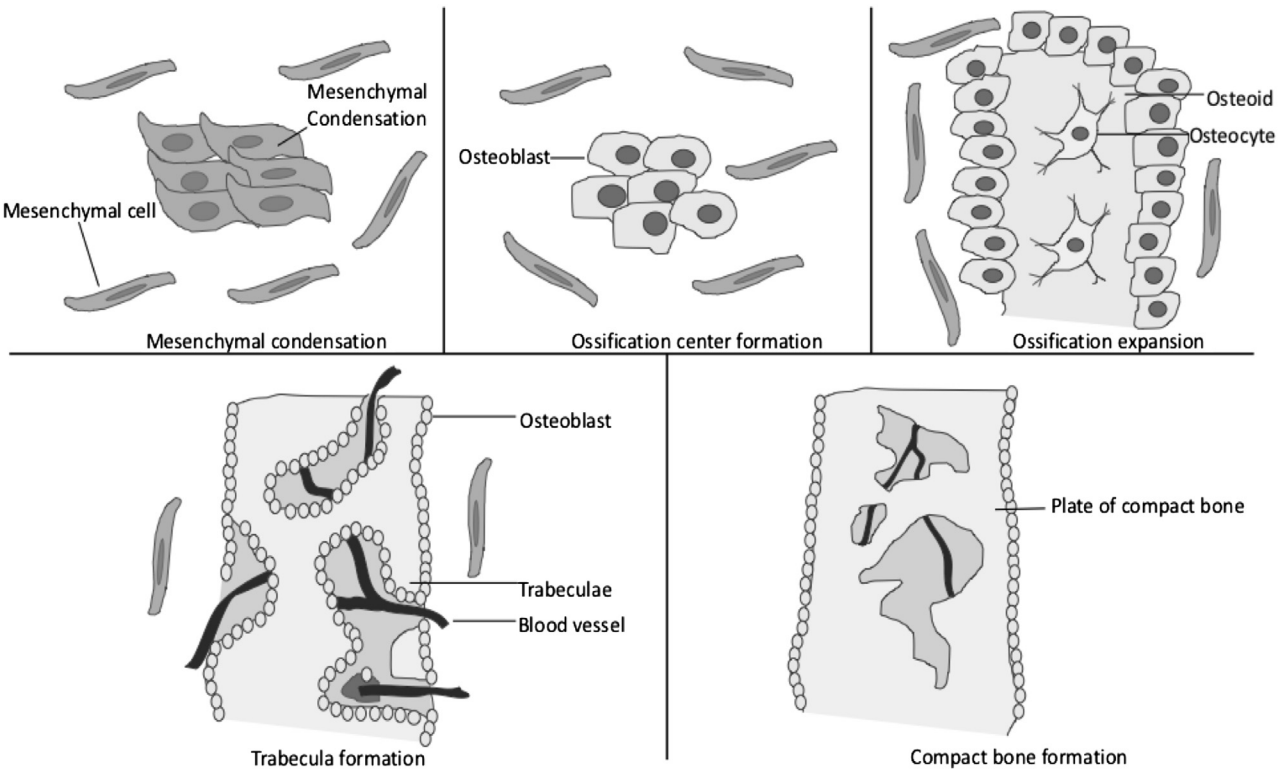

FIGURE 1.1 Schematics of intramembranous cranial bone formation. See text for details.

Condensation of mesenchymal progenitor cells is the first step for both intramembranous and endochondral ossification. During intramembranous ossification, mesenchymal progenitor cells differentiate into osteoblasts instead of chondrocytes as occurs during endochondral ossification. The osteoblasts that appear first in the condensation secrete bone matrix and form the ossification center. The early osteoblasts secrete osteoid, uncalcified matrix, which calcifies soon after, while the osteoblasts mature and terminally differentiate into osteocytes that are entrapped in the osteoid. As osteoblasts differentiate into osteocytes, more mesenchymal progenitors surrounding the osteoid differentiate into new osteoblast cells at the osteoid surface to expand the calcification center. Osteoid expansion around the capillaries results in a trabecular matrix of the spongy bone, while osteoblasts on the superficial layer become the periosteum. The periosteum is a layer that also contains mesenchymal progenitor cells, osteoblast differentiation of which contributes to the formation of a protective layer of compact bone. The blood vessels along with other cells between the trabecular bone eventually form the red marrow. Intramembranous ossification begins in utero during fetal development and continues on into adolescence. At birth, the skull and clavicles are not fully ossified. Sutures and fontanelles are unossified cranial regions that allow the skull to deform during passage through the birth canal. Sutures are joints between craniofacial bones, which are composed of two osteogenic fronts with suture mesenchyme between them (Fig. 1.2). Fontanelles are the space between the skull bones where the sutures intersect and are covered by tough membranes that protect the underlying soft tissues and brain. In humans, cranial sutures normally fuse between 20 and 30 years of age and facial sutures fuse after 50 years of age (Badve et al., 2013; Senarath-Yapa et al., 2012). Most sutures in mice remain patent throughout the animal's lifetime. Sutures and fontanelles allow the craniofacial bones to expand evenly as the brain grows, resulting in a symmetrically shaped head. However, if any of the sutures close too early (fuse prematurely), in the condition called craniosynostosis, there may be no growth in that area. This may force growth to occur in another area or direction, resulting in an abnormal head shape.

Apart from craniofacial bone development, intramembranous ossification also controls bone formation in the perichondral and periosteal regions of the long bone, where osteoblasts directly differentiate from mesenchymal progenitor cells. Yet, this requires a signal from the cartilaginous element. Furthermore, intramembranous ossification is an essential mechanism underlying bone repair and regeneration in the following processes: fracture healing with rigid fixation; distraction osteogenesis, a bone-regenerative process in which osteotomy followed by gradual distraction yields two vascularized bone surfaces from which new bone is formed (Ai-Aql et al., 2008); and blastemic bone creation, which occurs in children with amputations (Fernando et al., 2011).

Intramembranous ossification is tightly regulated at both molecular and cellular levels. Cranial malformations are often progressive and irreversible, and some of them need aggressive surgical management to prevent or mitigate severe impairment such as misshapen head or abnormal brain growth (Bronfin, 2001). For instance, craniosynostosis is a common congenital disorder that affects 1 in 2500 live births. It is characterized by premature cranial suture fusion, which may result in severe conditions such as increased intracranial pressure, craniofacial dysmorphism, disrupted brain development, and mental retardation. Craniosynostosis is generally considered a developmental disorder resulting from a disrupted balance of cellular proliferation, differentiation, and apoptosis within the suture (Senarath-Yapa et al., 2012; Levi et al., 2012; Slater et al., 2008; Lattanzi et al., 2012; Ciurea and Toader, 2009). Surgical correction followed by reshaping of the calvarial bones remains the only treatment available for craniosynostosis patients (Martou and Antonyshyn, 2011; Posnick et al., 2010; Hankinson et al., 2010). In contrast to craniosynostosis, cleidocranial dysplasia (CCD) is caused by reduced intramembranous bone formation, underdeveloped or absent clavicles (collarbones) as well as delayed maturation of the skull, manifested by delayed suture closure and larger than normal fontanelles that are noticeable as "soft spots" on the heads of infants (Farrow et al., 2018). Severe cases of CCD require surgical intervention. Identifying molecular pathways that control intramembranous ossification is critically important in the mechanistic understanding of craniofacial bone diseases and their targeted therapeutic development.

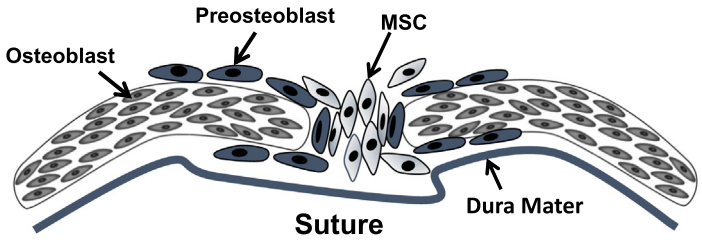

FIGURE 1.2 Schematics of cellular composition of the suture. In the suture, mesenchymal stem cells (MSCs) are located in the middle. They may first become committed preosteoblasts and then finally mature osteoblasts.

Studies of both developmental biology and rare genetic diseases have led to the identification of critical regulators of intramembranous ossification. Transcriptional regulation of the osteoblast lineage is considered in detail in Chapter 7. The runt-related transcription factor 2, RUNX2 (also known as CBFA1), and a zinc finger transcription factor, Osterix (OSX), are osteoblast lineage−determining factors required for both intramembranous and endochondral ossifications. *Runx2* is expressed in osteogenic progenitor cells and required for osteoblast cell fate determination by driving osteoblast-specific gene expression (Ducy et al., 1997; Otto et al., 1997). *Runx2* loss-of-function mutations are found in both mice and humans and cause CCD (Otto et al., 1997; Mundlos et al., 1997; Lee et al., 1997). RUNX2 induces the expression of *Osx*, which is required for osteoblast cell fate commitment, as loss of *Osx* leads to conversion from osteoblasts to chondrocytes (Nakashima et al., 2002). Under the control of RUNX2 and OSX, osteoblast cells produce osteoblast-specific collagen I together with a variety of noncollagenous, extracellular matrix (ECM) proteins that are deposited along with an inorganic mineral phase. The mineral is in the form of hydroxyapatite, a crystalline lattice composed primarily of calcium and phosphate ions.

Cell−cell communication that coordinates cell proliferation and differentiation also plays a critical role in intramembranous ossification. The WNT and Hedgehog (HH) signaling activities are required for cell fate determination of osteoblasts by controlling the expression of *Runx2*. Active WNT/β-catenin signaling is detected in the developing calvarium and perichondrium, where osteoblasts differentiate through intramembranous ossification. Indeed, enhanced WNT/β-catenin signaling enhances bone formation and *Runx2* expression, but inhibits chondrocyte differentiation and *Sox9* expression (Hartmann and Tabin, 2000; Guo et al., 2004; Day et al., 2005). *Sox9* is a master transcription factor that determines chondrocyte cell fate (Bi et al., 1999; Akiyama et al., 2002). Conversely, removal of *β-catenin* in osteochondral progenitor cells resulted in ectopic chondrocyte differentiation at the expense of osteoblasts during both intramembranous and endochondral ossification (Hill et al., 2005; Hu et al., 2005; Day et al., 2005). Therefore, during intramembranous ossification, WNT/β-catenin signaling levels in the mesenchymal condensation are higher, which promotes osteoblast differentiation while inhibiting chondrocyte differentiation. In addition, upregulated WNT/β-catenin signaling in the perichondrium also promoted osteoblast differentiation. In contrast to the WNT/β-catenin signaling, Indian hedgehog (IHH) signaling is not required for osteoblast differentiation of intramembranous bones in the skull (St-Jacques et al., 1999). It is still not clear what controls *Ihh*-independent *Runx2* expression during intramembranous ossification and it is important to understand further the differential regulation of intramembranous versus endochondral ossification by cell signaling. As removing Smoothened, which mediates all HH ligand-dependent signaling, does not abolish intramembranous ossification either (Jeong et al., 2004), HH signaling is likely to be activated in a ligand-independent manner in the developing calvarium. Indeed, it has been found that in the rare human genetic disease progressive osseous heteroplasia, which is caused by null mutations in *Gnas*, which encodes $G\alpha_s$, HH signaling is upregulated. Such activation of HH signaling is independent of HH ligands and is both necessary and sufficient to induce ectopic osteoblast cell differentiation in soft tissues (Regard et al., 2013). Importantly, *Gnas* gain-of-function mutations upregulate WNT/β-catenin signaling in osteoblast progenitor cells, resulting in their defective differentiation and in fibrous dysplasia that also affects intramembranous ossification (Regard et al., 2011). Therefore, $G\alpha_s$ is a key regulator of proper osteoblast differentiation through its maintenance of a balance between the WNT/β-catenin and the HH pathways. The critical role of WNT and HH signaling in intramembranous ossification is also shown in the suture. Mesenchymal stem cells that give rise to the cranial bone and regulate cranial bone repair in adult mice have been identified in the suture. These cells are either $GLI1^+$ or $AXIN2^+$ (Zhao et al., 2015; Maruyama et al., 2016), which marks cells that receive HH or WNT signaling, respectively (Bai et al., 2002; Leung et al., 2002; Jho et al., 2002).

Other signaling pathways, including those mediated by transforming growth factor (TGF) superfamily members, Notch, and fibroblast growth factors (FGFs), are also important in intramembranous ossification. Mutations in the FGF receptors FGFR1, FGFR2, and FGFR3 cause craniosynostosis. The craniosynostosis syndromes involving FGFR1, FGFR2, and FGFR3 mutations include Apert syndrome (OMIM 101200), Beare−Stevenson cutis gyrata (OMIM 123790), Crouzon syndrome (OMIM 123500), Pfeiffer syndrome (OMIM 101600), Jackson−Weiss syndrome (OMIM 123150), Muenke syndrome (OMIM 602849), crouzonodermoskeletal syndrome (OMIM 134934), and osteoglophonic dysplasia (OMIM 166250), a disease characterized by craniosynostosis, prominent supraorbital ridge, and depressed nasal bridge, as well as rhizomelic dwarfism and nonossifying bone lesions. All these mutations are autosomal dominant and many of them are activating mutations of FGF receptors. FGF signaling can promote or inhibit osteoblast proliferation and differentiation depending on the cell context. It does so either directly or through interactions with the WNT and bone morphogenetic protein (BMP) signaling pathways.

Apart from RUNX2 and OSX, other transcription factors are also important, as mutations in them cause human diseases with defects in intramembranous ossification. Mutations in the human *TWIST1* gene cause Saethre−Chotzen syndrome (OMIM 101400), one of the most commonly inherited craniosynostosis conditions. In addition, mutations in the homeobox

genes *MSX1*, *MSX2*, and *DLX* are also associated with human craniofacial disorders (Cohen, 2000; Kraus and Lufkin, 2006). *MSX2* haploinsufficiency decreases proliferation and accelerates the differentiation of calvarial preosteoblasts, resulting in delayed suture closure, whereas its "overexpression" results in enhanced proliferation, favoring early suture closure (Dodig and Raos, 1999). It is likely that *MSX2* normally prevents differentiation and stimulates proliferation of preosteoblastic cells at the osteogenic fronts of the calvariae, facilitating expansion of the skull and closure of the suture. It would be critical to understand further how these transcription factors interact with one another and the signaling pathways to regulate intramembranous bone formation, maintenance, and repair.

The axial skeleton

The axial skeleton consists of the occipital skull bones, the elements of the vertebral column, and the rib cage (ribs and sternum). With the exception of the sternum, the axial skeleton is derived from the paraxial mesoderm, which is segmented into somites during early embryonic development. The occipital skull bones are generated from the fused sclerotomes of the cranial-most 4.5 somites (Goodrich, 1930). The bilateral anlagen of the sternum originate from the lateral plate mesoderm and fuse at the ventral midline in the course of the formation of the rib cage (Chen, 1952).

Somitogenesis

The basic body plan of vertebrates is defined by the metameric segmentation of the musculoskeletal and neuromuscular systems, which originates during embryogenesis from the segmentation of the paraxial mesoderm (for reviews see Winslow et al., 2007; Pourquie, 2000). The paraxial mesoderm is laid down during gastrulation, appearing as bilateral strips of unsegmented tissue (referred to as segmental plate in the avian embryo and presomitic mesoderm in the mouse). It flanks the centrally located neural tube and notochord and gives rise to the axial skeleton (head and trunk skeleton) and all trunk and limb skeletal muscles, as well as the dermis, connective tissue, and vasculature of the trunk. During development, the paraxial mesoderm is segmented through a series of molecular and cellular events in an anterior to posterior (craniocaudal) sequence along the body axis, the anterior-most somites being the more mature ones. The posterior, unsegmented part of the paraxial mesoderm is also referred to as the presomitic mesoderm (PSM), and the sequentially arising, paired tissue blocks are called somites. The PSM is a loose mesenchymal tissue. The cells reaching the anterior border of the PSM progressively undergo a mesenchymal-to-epithelial transition (Christ et al., 2007). Newly formed somites are epithelial balls with a mesenchymal core. As the somites mature, accompanied by the commitment of the cells to the different lineages, this organization changes. In response to signals from the notochord and the ventral floor plate of the neural tube (Sonic Hedgehog [SHH] and the BMP antagonist Noggin), cells on the ventral margin undergo an epithelial−mesenchymal transition, scatter, and move toward the notochord (Christ et al., 2004; Cairns et al., 2008; Yusuf and Brand-Saberi, 2006). These cells will express the transcription factors PAX1, NKX3.1, and NKX3.2 and form the sclerotome, giving rise to the vertebrae and ribs. The dermomyotome is specified by WNT ligands secreted from the dorsal neural tube and the ectoderm covering the dorsal somite. Low levels of SHH signaling are, in combination with WNT signaling, required to maintain the expression of dermomyotomal and myotomal markers (Cairns et al., 2008). The dermomyotome remains epithelial and eventually gives rise to the epaxial muscles of the back and vertebrae, the hypaxial muscles of the body wall and limb, the dermis underneath the skin of the trunk, and the brown adipose tissue (Scaal and Christ, 2004; Atit et al., 2006). Tendons and ligaments of the trunk arise from the fourth somitic compartment, the syndetome, which is induced by the newly formed sclerotome and dermomyotome (Brent et al., 2003; Dubrulle and Pourquie, 2003).

The molecular mechanism driving somitogenesis at the anterior end of the PSM is intrinsic to the PSM, while new cells are continuously added to the PSM from a posteriorly located progenitor pool (Martin, 2016). The so-called segmentation clock, a molecular oscillator coordinating the rhythmic activation of several signaling pathways and the oscillatory expression of a subset of genes in the PSM, is thought to be at the molecular heart of somite formation (Hubaud and Pourquie, 2014). One of the main signaling pathways with oscillatory gene expression is the Notch/Delta/DELTA pathway. This pathway also synchronizes the oscillations between the individual cells (Hubaud and Pourquie, 2014). Also, members of the WNT/β-catenin and the FGF signaling pathway display cyclic gene expression (Aulehla and Pourquie, 2008). The oscillatory expression of these genes appears to go like a wave from the caudal end, sweeping anteriorly through the PSM (Fig. 1.3A). Another molecular system involved in somite formation is the wave front, which is defined by opposing signaling gradients in the PSM (Fig. 1.3B). Here, a posterior−anterior gradient of FGF8 and nuclear β-catenin is opposed by an anterior−posterior gradient of retinoic acid (RA) activity (Mallo, 2016). Despite the fact that the existence of an RA gradient is debated, there is clear genetic evidence that a gradient of WNT signaling activity interacts with the

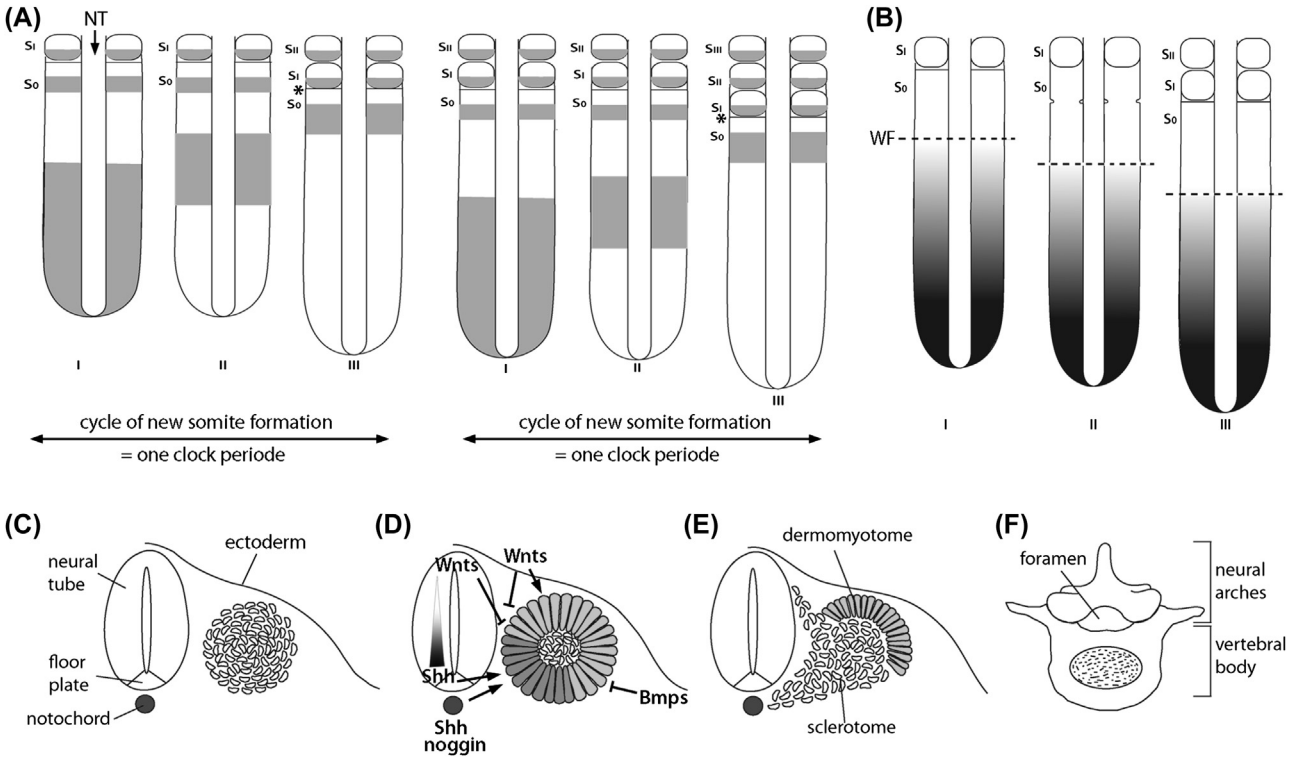

FIGURE 1.3 Somite formation and differentiation. (A) Cyclic gene expression during somite formation. The *asterisk* marks the position of new boundary formation. *NT*, neural tube; S_0, somite stage 0; S_I, somite stage I; S_{II}, somite stage II; S_{III}, somite stage III. (B) Signal gradient within the presomitic mesoderm (PSM), with the *dashed line* marking the position of the wave front (*WF*). (C–E) Schematic representations of the different somite stages. (C) Loose mesenchymal PSM, (D) epithelial ball stage (the ventral darker colored region marks the PAX1-positive sclerotomal region) and factors involved in the somite compartmentalization, (E) sclerotome differentiation. (F) Superior view of a vertebral element derived from the posterior and anterior sclerotomal compartments of two adjacent somites.

segmentation clock to determine the posterior border of a newly forming somite (Mallo, 2016). The morphological changes that eventually lead to the formation of a new somite at the anterior end of the PSM are triggered by Notch activity in combination with the T-box transcription factor, TBX6, and start with the expression of the basic helix–loop–helix transcription factor mesoderm posterior 2 (MESP2) (Saga, 2007; Sasaki et al., 2011). In cells posterior to the determination front, *Mesp2* is repressed by FGF signaling (Sasaki et al., 2011). In addition, *Mesp2* expression becomes restricted to the anterior half of the newly formed somite, as TBX6-mediated transcription of *Mesp2* is suppressed by the RIPPLY1/2 proteins expressed in the posterior part of the somite (Morimoto et al., 2007; Takahashi et al., 2007). MESP2 activity is essential for establishing somite polarity, which is in turn vital for the later formation of the vertebral bodies from the caudal/posterior part of one somite and the rostral/anterior part of the neighboring somite (Christ et al., 2007).

The positional identity of a somite defines the type of vertebral element (occipital, cervical, thoracic, lumbar, or sacral) it will eventually contribute to, and this is controlled, in part, by the regional code of *Hox* genes along the rostral–caudal body axis (for review see Wellik, 2007). Humans and all other bilateral animals have multiple *Hox* genes, encoding transcription factors with a homeobox DNA-binding domain, which are clustered together (Krumlauf, 1992). Through duplication events, the ancestral cluster of originally eight *Hox* genes has been multiplied to four gene clusters (*HoxA*, *HoxB*, *HoxC*, and *HoxD*) of 13 paralogous *Hox* genes in vertebrates. A particular feature of *Hox* gene expression from one cluster is that they are expressed in a temporal and spatial order that reflects their order on the chromosome, with the most 3′ *Hox* gene being expressed first and in the most anterior region. It is thought that the *Hox* genes provide a sort of positional code through their overlapping expression domains, which are characterized by a relatively sharp anterior border. For example, the expression of the *Hox5* paralogs (*HoxA5*, *HoxB5*, and *HoxC5*) correlates in different species such as mouse and chicken, always with the position of the last cervical vertebra, while the anterior domains of the *Hox6* paralogs lie close to the boundary between cervical and thoracic vertebrae (Burke et al., 1995; Burke, 2000). Yet, this correlation is not maintained at the levels of the somites, as mouse and chicken differ in their numbers of cervical elements. Changes in the HOX code can lead to homeotic transformation, which reflects a shift in the regional borders and axial identities.

Members of the polycomb family (*Bmi* and *Eed*) and the TALE class of homeodomain transcription factors are involved in further refining the positional identity provided by the *Hox* code. BMI and EED are transcriptional repressors limiting the rostral (anterior) transcription boundary of individual *Hox* genes (Kim et al., 2006). The TALE proteins, encoded by the *Pbx* and *Meis* genes, further modify the transcriptional activity of the Hox proteins through heterodimerization (Moens and Selleri, 2006).

Sclerotome differentiation

The earliest sclerotomal markers are the transcription factors *Pax1*, *Nkx3.1*, and *Nkx3.2/Bapx1*, which become expressed under the influence of SHH and Noggin signaling in the ventral somite region (Kos et al., 1998; Ebensperger et al., 1995; Murtaugh et al., 2001). *Pax9* expression appears slightly later in the sclerotome and overlaps in part with *Pax1* (Muller et al., 1996). Both genes act redundantly in the ventromedial region of the sclerotome, as in the *Pax1/Pax9* double-mutant mice the development of the ventral vertebra is strongly affected (Peters et al., 1999). NKX3.2 appears to act downstream of *Pax1/Pax9* and can be ectopically induced by PAX1 (Tribioli and Lufkin, 1999; Rodrigo et al., 2003). Although the initial *Pax1* expression is not affected by the loss of *Nkx3.2*, the vertebral differentiation also depends on the function of NKX3.2 (Tribioli and Lufkin, 1999). *Nkx3.1* mutant mice, on the other hand, do not display any skeletal defects (Schneider et al., 2000). As PAX1 is able to activate the expression of early chondroblast markers in vitro, it has been suggested that the activation of PAX1 is the key event that triggers sclerotome formation (Monsoro-Burq, 2005).

After their induction, the sclerotomal cells undergo epithelial−mesenchymal transition and migrate toward the notochord, around the neural tube, and in the thoracic segments also laterally, and then condense to form the vertebral bodies and the intervertebral discs, neural arches, and proximal part of the ribs, respectively (Fig. 1.3C−F). Some notochordal cells surrounded by sclerotomal cells die, while others become part of the intervertebral disc and form the nucleus pulposus (McCann and Seguin, 2016). The neural arches and spinous processes are derived from the mediolateral regions of the sclerotomes and from sclerotomal cells that migrated dorsally. The activity of PAX1/PAX9 is not required for these two compartments (Peters et al., 1999). The dorsally migrating sclerotomal cells contributing to the dorsal part of the neural arches and spinous processes do not express *Pax1* but another set of transcription factors, *Msx1* and Msx2 (reviewed in Monsoro-Burq, 2005; Rawls and Fischer, 2010). Other transcription factors, such as the winged-helix factor, MFH1 (FOXC2), are possibly required for the clonal expansion of cells taking place within the individual sclerotome-derived populations, as they migrate ventrally, laterally, and medially and then condense (Winnier et al., 1997). In addition, the homeodomain transcription factors *Meox1* and *Meox2* have been implicated in vertebral development and may even act upstream of PAX1/PAX9 (Mankoo et al., 2003; Skuntz et al., 2009). Within the individual sclerotomal condensations the chondrogenic and osteogenic programs are then initiated to eventually form the vertebral elements.

The limb skeleton

Overview of limb development

The mesenchymal cells contributing to the skeleton of the appendages (limbs) originate from the bilaterally located lateral plate mesoderm. The lateral plate mesoderm is separated from the somitic mesoderm by the intermediate mesoderm, which gives rise to the kidney and genital ducts. Our knowledge about limb development during embryogenesis is primarily based on two experimental model systems, chick and mouse. In all tetrapods, forelimb development precedes hindlimb development. The axial position of the prospective limb field is in register with the expression of a specific set of *Hox* genes within the somites (Burke et al., 1995). The limb fields are demarcated by the expression of two T-box transcription factors, *Tbx5* in the forelimb and *Tbx4* in the hindlimb field (Petit et al., 2017; Duboc and Logan, 2011). Yet, the identity of the limb is conveyed by the activity of another transcription factor, PITX1, which is expressed specifically in the hindlimb region and specifies hindlimb identity (Logan and Tabin, 1999; Minguillon et al., 2005). In mouse, the forelimb bud starts to develop around embryonic day (E) 9 and the hindlimb around E10. In chick, forelimb development starts on day 2½ (Hamburger Hamilton stage 16) with a thickened bulge (Hamburger and Hamilton, 1992). In humans, the forelimb is visible at day 24 of gestation. Experimental evidence from the chick suggests that WNT signaling induces FGF10 expression and the FGF-dependent initiation of the limb outgrowth (Kawakami et al., 2001). For continuous limb outgrowth the expression of *Fgfs* in the mesenchyme and in an epithelial ridge called the apical ectodermal ridge (AER) is essential (Benazet and Zeller, 2009; Martin, 2001) (Fig. 1.4A). Patterning of the outgrowing limb occurs along all three axes, the proximal−distal, the anterior−posterior, and the dorsal−ventral (Niswander, 2003). For example, in the human arm, the proximal−distal axis runs from the shoulder to the fingertips and can be subdivided into the stylopod (humerus),

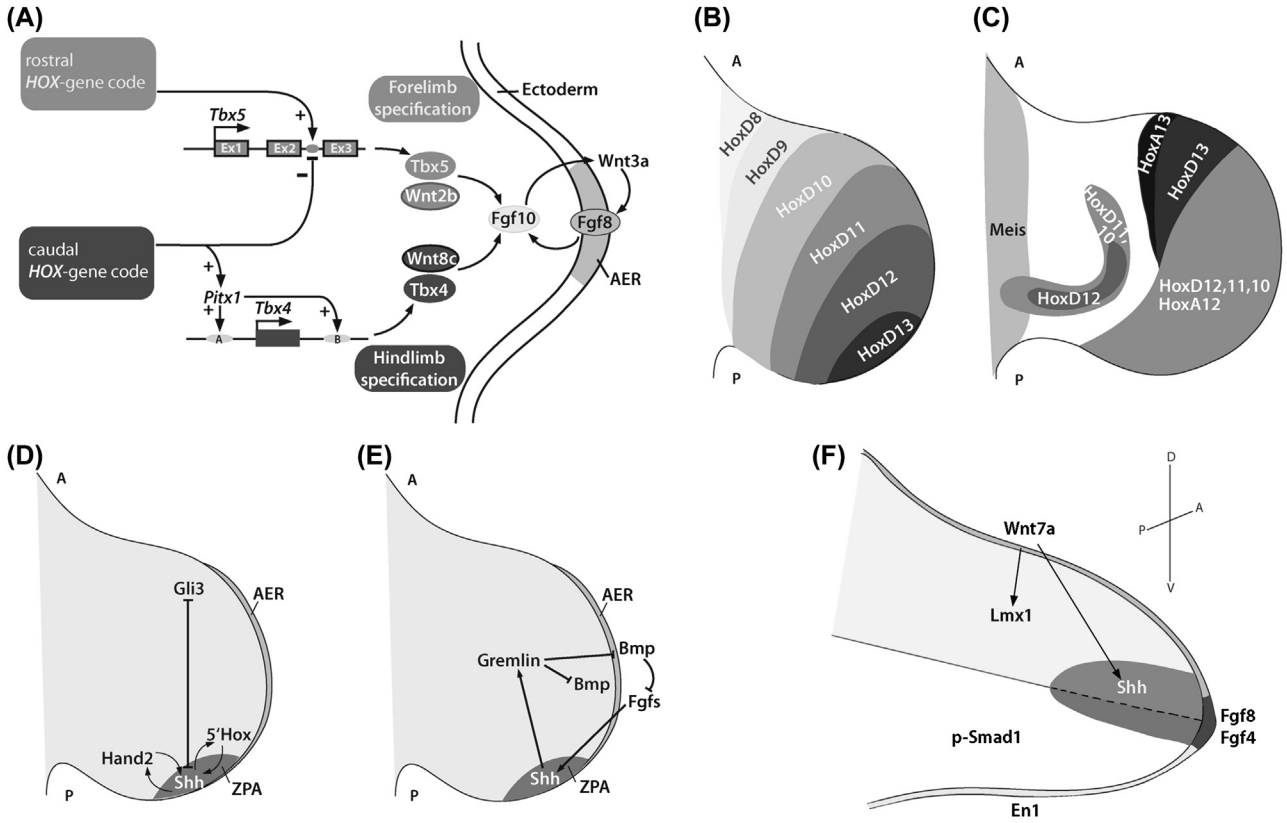

FIGURE 1.4 Limb development overview. (A) Early events in limb bud development: factors involved in the establishment of the limb identity and signals required for the initiation of limb outgrowth. *Hox* genes in the lateral plate mesoderm define the positions where the limbs will develop and activate or repress via specific enhancers the expression of *Pitx1* and the *Tbx4/5* genes. Together with the activity of limb field−specific WNTs an FGF10/WNT3a/FGF8 loop is established, which drives proximal−distal limb outgrowth. *AER*, apical ectodermal ridge. (B) Early nested expression of the HOXD cluster in the limb. *A*, anterior; *P*, posterior. (C) Late expression of the *HoxA* and *HoxD* genes in the autopod stage and expression of the proximal determinant *Meis1*. (D) Factors involved in anterior−posterior patterning of the limb, with *Shh* expressed in the zone of polarizing activity (*ZPA*) under the positive control of the transcription factors HAND2 and the 5′HOX proteins, while its activity in the anterior is opposed by the repressor GLI3. (E) Molecules involved in the interregulation of the anterior−posterior and proximal−distal axes. (F). Molecules involved in the specification of the dorsal−ventral axis: *Wnt7a* expressed in the dorsal ectoderm activates *Lmx1* expression in the dorsal mesenchyme specifying dorsal fate, while EN1 in the ventral ectoderm and phospho-SMAD1 in the ventral mesenchyme specify ventral fate. WNT7a also positively enforces the expression of *Shh*. *(A) Adapted from Fig. 1.2, Petit, F., Sears, K.E., Ahituv, N., 2017. Limb development: a paradigm of gene regulation. Nat. Rev. Genet. 18, 245−258.*

zeugopod (radius and ulna), and autopod regions (wrist and digits of the hand) (Fig. 1.5A). The anterior−posterior axis runs from the thumb to the little finger and the dorsal−ventral axis extends from the back of the arm/hand to the underside of the arm/palm. These three axes are established very early in development, and specific signaling centers, which will be briefly discussed in the following, coordinate the outgrowth and patterning of the limb.

Proximal−distal axis

As already mentioned, during the initiation stage, a positive FGF feedback loop is established between the *Fgfs* expressed in the mesenchyme (*Fgf10*) and the *Fgfs* in the AER (*Fgf8, Fgf4, Fgf9, Fgf17*). Mesenchymal FGF10 activity is essential for the formation of the AER (Sekine et al., 1999). In the positive feedback loop, FGF10 induces *Fgf8* expression in the AER, which is probably mediated by a *Wnt* gene's expression (*Wnt3a* in chick and *Wnt3* in mouse) (Kawakami et al., 2001; Kengaku et al., 1998; Barrow et al., 2003). The AER plays a critical role in the limb outgrowth. Removal of the AER at different time points of development leads to successive truncation of the limb (Saunders, 1948; Summerbell, 1974; Rowe and Fallon, 1982). The *Fgf* genes expressed in the AER confer proliferative and antiapoptotic activity on the distal mesenchyme and maintain the cells in an undifferentiated state (Niswander et al., 1994; Niswander et al., 1993; Fallon et al., 1994; Ten Berge et al., 2008). This is further supported by genetic studies showing that FGF4 and FGF8 are both required for the maintenance of the AER (Boulet et al., 2004; Sun et al., 2002). The most proximal part

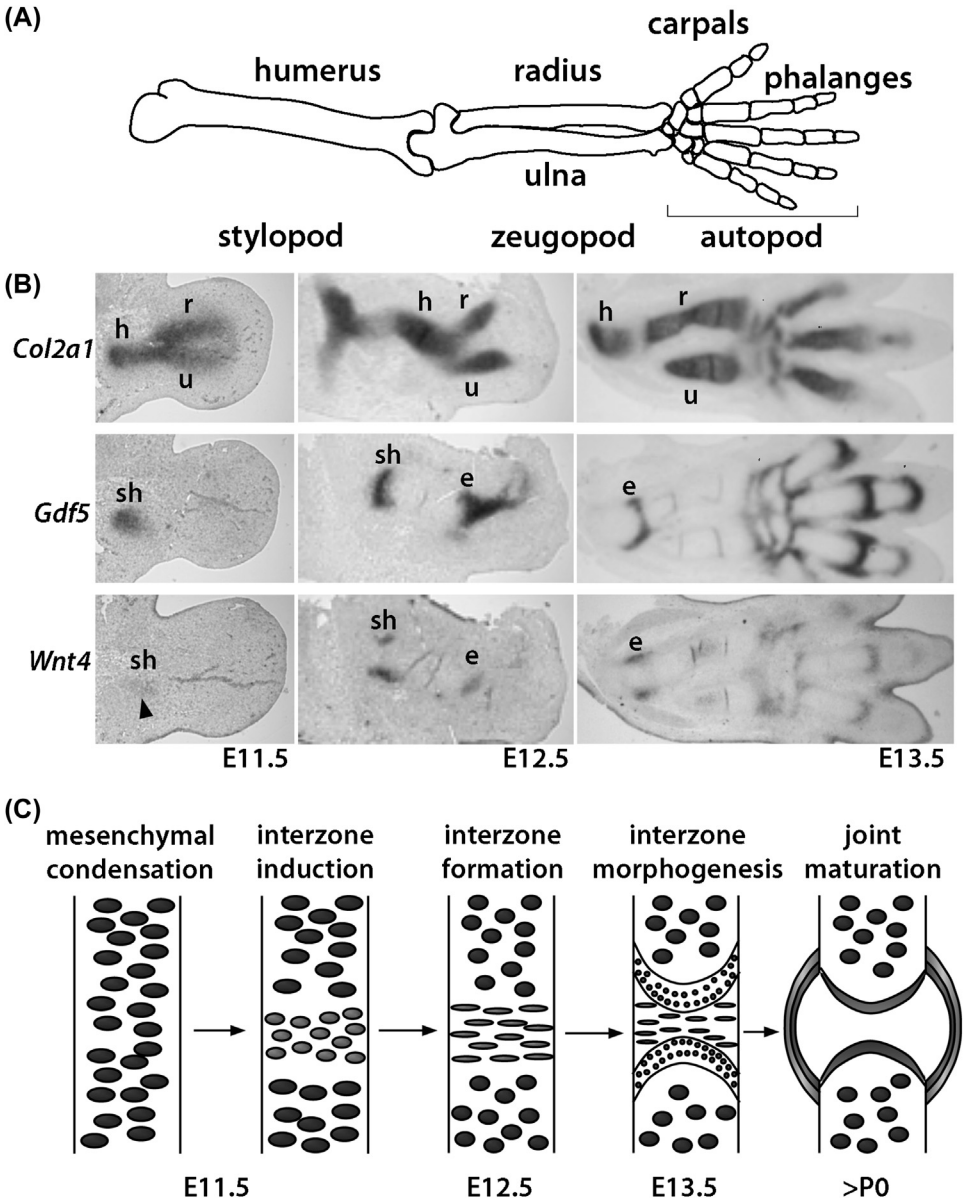

FIGURE 1.5 Patterning of the appendicular skeleton. (A) Schematic overview of the skeletal elements in a human arm. (B) In situ hybridizations on adjacent sections of a mouse forelimb (embryonic stages E11.5, E12.5, and E13.5), showing the branched structure of an early cartilaginous template (*Col2a1* expressing) consisting of the humerus (*h*), radius (*r*), and ulna (*u*). Note that at E11.5 markers of the joint interzone (*Gdf5* and *Wnt4*) are expressed in cells that also express the chondrogenic marker *Col2a1*. At E12.5, during interzone formation, *Col2a1* becomes downregulated in the shoulder (*sh*) and elbow (*e*) region, while the expression patterns of *Gdf5* and *Wnt4* undergo refinement. At E13.5, *Col2a1* is no longer expressed in the joint areas and the expression domains of *Gdf5* and *Wnt4* become distinct. (C) Schematic representation of the major steps during synovial joint formation.

of the limb expresses the TALE homeobox transcription factor MEIS1 under the control of opposing RA and FGF signaling (Mercader et al., 2000). MEIS1 alone is sufficient to proximalize the limb in the chick and mouse systems (Mercader et al., 1999, 2009). Along the proximal–distal axis, the 5′*Hox* genes, which are expressed early in a nested pattern (see Fig. 1.4B), are thought to provide positional cues for growth. As such, members of the group 11 paralogs (HOXA11 and D11 in the forelimb and HOXA11, C11, and D11 in the hindlimb) are required for the growth of the zeugopod, while the autopod establishment depends on the function of group 13 paralogs (Zakany and Duboule, 2007). *Hox* genes are also involved in connective tissue patterning in the limb (Pineault and Wellik, 2014). In addition to their role with regard to the proximal–distal axis, *Hox* genes also play an important role in establishing the signaling center within the limb bud regulating the anterior–posterior axis.

Anterior–posterior axis

Classical embryologic transplantation experiments uncovered the existence of a region present in the posterior limb bud conveying patterning information along the anterior–posterior axis (Saunder and Gasseling, 1968). Transplantation studies also revealed that this region, which was referred to as the zone of polarizing activity (ZPA), must contain some kind of positional information in the form of a secreted morphogen that specifies digit identity along the anterior–posterior axis (Tickle, 1981; Tickle et al., 1975; Wolpert, 1969). The molecular identity of this morphogen was uncovered only in 1993 with the cloning of a vertebrate homolog of the *Drosophila hh* gene, called *Shh*. *Shh* expression overlaps with the ZPA, and Shh-producing cells transplanted into the anterior mesoderm of the limb bud could reproduce mirror-image duplications of ZPA grafts (Riddle et al., 1993). Genetic experiments confirmed that *Shh* is required to establish posterior structures of the limb (Chiang et al., 1996). The *Shh* expression domain is established by the activity of positive and negative regulators. The transcription factor HAND2 (dHAND) is expressed in a posterior domain preceding and encompassing the *Shh* domain and acts as a positive regulator of SHH, which feeds back positively on the expression of HAND2 (Charite et al., 2000; Fernandez-Teran et al., 2000). Early in limb development, *Hand2* is expressed complementary to the transcription factor *Gli3* and GLI3 represses *Hand2* in the anterior (Wang et al., 2000). HAND2, on the other hand, represses *Gli3* in the posterior (Te Welscher et al., 2002). SHH signaling in the posterior prevents the cleavage of the full-length activator GLI3 into the GLI3 repressor (GLI3R) form. Hence, the GLI3R form is restricted to the anterior of the limb bud. The *5′Hox* genes and SHH signaling are also connected by a positive feed-forward regulatory loop (Tarchini et al., 2006; Ros et al., 2003), which may also involve FGF signaling (Rodrigues et al., 2017) (Fig. 1.4D). There is also an interconnection between the anterior–posterior and the proximal–distal axis: SHH signaling upregulates the BMP antagonist Gremlin in the posterior half of the limb. Gremlin antagonism of BMP signaling is required to maintain the expression of *Fgf4*, *Fgf9*, and *Fgf17* in the AER, and FGF signaling feeds positively onto *Shh* (Khokha et al., 2003; Laufer et al., 1994) (Fig. 1.4E).

Dorsal–ventral axis

The third axis that needs to be established is the dorsal–ventral axis. Here, the WNT ligand WNT7a is expressed in the dorsal ectoderm and regulates the expression of the LIM homeobox transcription factor LMX1 (LMX1B in the mouse) in the dorsal mesenchyme (Riddle et al., 1995; Vogel et al., 1995). LMX1B is required to maintain the dorsal identity of structures such as tendons and muscles in the limb (Chen et al., 1998). The ventral counterplayer is the transcription factor Engrailed 1 (EN1), which is expressed in the ventral ectoderm and the ventral half of the AER, and is essential for the formation of ventral structures (Davis et al., 1991; Gardner and Barald, 1992; Cygan et al., 1997; Loomis et al., 1996). BMP signaling appears also to be required for establishment of the dorsal–ventral axis, as the activated downstream component, phospho-SMAD1, is detected throughout the ventral ectoderm and mesenchyme (Ahn et al., 2001) (Fig. 1.4F). Deletion of a BMP receptor gene, *Bmpr1a*, from the limb bud ectoderm results in an expansion of *Wnt7a* and *Lmx1b* into ventral territories, an almost complete loss of *En1*, and severe malformation of the limbs missing the ventral flexor tendons (Ahn et al., 2001).

Mesenchymal condensation and patterning of the skeleton

Patterning of the somitic tissue and the limbs along the different axes is a prerequisite for the mesenchymal condensations to take place. In the craniofacial skeleton, epithelial–mesenchymal interactions occur during the precondensation phase (Hall and Miyake, 1995). Mesenchymal condensations are pivotal for intramembranous and endochondral bone formation. They define the positions and the basic shapes of the future skeletal elements. They can be visualized in the sclerotome, developing skull, and limbs in vivo and in micromass cell cultures in vitro by the presence of cell surface molecules that bind peanut agglutinin (Stringa and Tuan, 1996; Milaire, 1991; Hall and Miyake, 1992). During the prechondrogenic and preosteogenic condensation phase ECM molecules, such as the glycoproteins Fibronectin, Versican, and Tenascin; cell–cell adhesion molecules, such as N-CAM and N-cadherin; the gap-junction molecule Connexin43 (CX43); and Syndecans (type I transmembrane heparan sulfate proteoglycan) become upregulated, but their expression often changes dynamically during the subsequent differentiation process (for review see Hall and Miyake, 2000; DeLise et al., 2000). Cell adhesion and ECM proteins promote the formation of the condensations by establishing cell–cell contacts and cell–matrix interactions. Yet, through genetic studies, their functional requirement for the condensation process has not been demonstrated so far. For the cell–matrix interactions, integrins also play an important role as they act as receptors for Fibronectin (α5β1; αVβ3), types II and VI collagen (α1β1, α2β1, α10β1), Laminin (α6β1), Tenascin (α9β1, αVβ3, α8β1, αVβ6), and Osteopontin (OPN) (αVβ1; αVβ3; αVβ5; α8ßβ1) (Loeser, 2000, 2002; Tucker and Chiquet-Ehrismann, 2015; Docheva et al., 2014).

Various growth factors, such as members of the TGFβ superfamily, regulate the condensation process (reviewed in Moses and Serra, 1996). This has also been elegantly demonstrated in vitro for a subclass of this superfamily of growth factors, the BMP family (Barna and Niswander, 2007). For the proximal elements (femur, tibia, and fibula) in the hindlimb, genetics revealed a dual requirement for the zinc finger transcription factors GLI3 and PLZF to establish the correct temporal and spatial distribution of chondrocyte progenitors (Barna et al., 2005).

Mesenchymal cells within the condensations can differentiate into either osteoblasts (intramembranous ossification) or chondrocytes (endochondral ossification). WNT/β-catenin signaling is essential for the differentiation of osteoblasts, as no osteoblasts develop in conditional mouse mutants in which the β-catenin-encoding gene *Ctnnb1* was deleted in mesenchymal precursor cells of the limb and/or skull (Hu et al., 2005; Hill et al., 2005; Day et al., 2005). Instead, the precursor cells differentiate into chondrocytes (Day et al., 2005; Hill et al., 2005). Hence, β-catenin activity is not essential for chondrogenesis. WNT/β-catenin signaling is most likely acting as a permissive pathway at this early step of differentiation, as too high levels of WNT/β-catenin signaling block osteoblast as well as chondrocyte differentiation (Hill et al., 2005). WNT/β-catenin signaling in perichondrial cells is amplified by SOXC protein family members to further secure the nonchondrogenic fate of these cells (Bhattaram et al., 2014). For osteoblast differentiation to occur, the transcription factor RUNX2 needs to be upregulated within the preosteogenic condensations, while the HMG-box transcription factor SOX9 is required for the further differentiation of cells within the condensations along the chondrocyte lineage and probably also for the condensation process itself (Bi et al., 1999; Akiyama et al., 2002; Karsenty, 2001; Lian and Stein, 2003). The latter aspect has been challenged by the results of in vitro experiments by Barna and Niswander (2007) showing that *Sox9*-deficient mesenchymal cells compact and initially form condensations, yet the cells within the condensations do not differentiate into chondroblasts (Barna and Niswander, 2007).

The skeletal elements in the limbs, which are formed by the process of endochondral ossification, develop in part as continuous, sometimes bifurcated (pre)chondrogenic structures, such as, e.g., the humerus branching into the radius and ulna in the forelimb (Fig. 1.5B), being subsequently segmented by the process of joint formation (Shubin and Alberch, 1986; Hinchliffe and Johnson, 1980; Oster et al., 1988). Furthermore, studies have shown that the cartilage morphogenesis of the developing long bones also occurs in a modular way, with two distinct pools of progenitor cells contributing to the primary structures and the bone eminences (Blitz et al., 2013; Sugimoto et al., 2013). Cells within the bifurcated, $SOX9^{+}$ primary structures express the gene *Col2a1*, characteristic of chondroblasts/chondrocytes. Although they appear during early limb development (E11.5) to be morphologically uninterrupted, the region where a joint (here the shoulder joint) will be formed can be visualized using molecular joint markers, such as *Gdf5* (growth differentiation factor 5) or *Wnt4* (see Fig. 1.5B). Interestingly, the cartilage matrix protein Matrilin-1 is never expressed in the interzone region, nor in the adjacent chondrogenic region, which possibly gives rise to the articular cartilage (Hyde et al., 2007). How the position of joint initiation within the limb is determined is not completely understood as of this writing. A limb molecular clock operating in the distal region may be involved in this process. It has been proposed that two oscillation cycles of the gene *Hairy 2* (*Hes2*) are required to make one skeletal element in the zeugopod and stylopod region of the limb (Sheeba et al., 2016). As the joints develop sequentially along the proximal−distal axis at a certain distance from each other, secreted factors produced by the joint itself may provide some kind of self-organizing mechanism (Hartmann and Tabin, 2001; Hiscock et al., 2017). WNT/β-catenin signaling is also required for joint formation (Hartmann and Tabin, 2001; Guo et al., 2004; Spater et al., 2006a, 2006b). Yet, again, it may act in this process also as a permissive pathway, repressing the chondrogenic potential of the joint interzone cells. However, as WNT/β-catenin signaling also induces the expression of *Gdf5*, it may also play an active role in joint induction by inducing cellular and molecular changes required for joint formation. The AP1-transcription factor family member c-JUN acts upstream of WNT signaling in joint development regulating the expression of *Wnt9a* and *Wnt16*, which are both expressed in the early joint interzone (Kan and Tabin, 2013). Numerous other genes, including *Noggin*, *Hif1α*, *Gdf5*, *Gdf6*, *Gli3*, *Ihh*, *PTH/PTHrPR1*, *Tgfβ*, *Mcp5*, and *Crux1*, have been implicated in a variety of cellular processes during joint formation based on genetic or misexpression experiments (Brunet et al., 1998; Amano et al., 2016; Spagnoli et al., 2007; Longobardi et al., 2012), for review see (Archer et al., 2003; Pacifici et al., 2006).

Endochondral bone formation

Overview

The axial and appendicular skeletal elements are formed by the process of endochondral bone formation starting with a cartilaginous template (Fig. 1.6A−E). This process starts with the condensation of mesenchymal cells at the site of the future skeleton. As mentioned already, this involves alterations in cell−cell adhesion properties and changes in the ECM

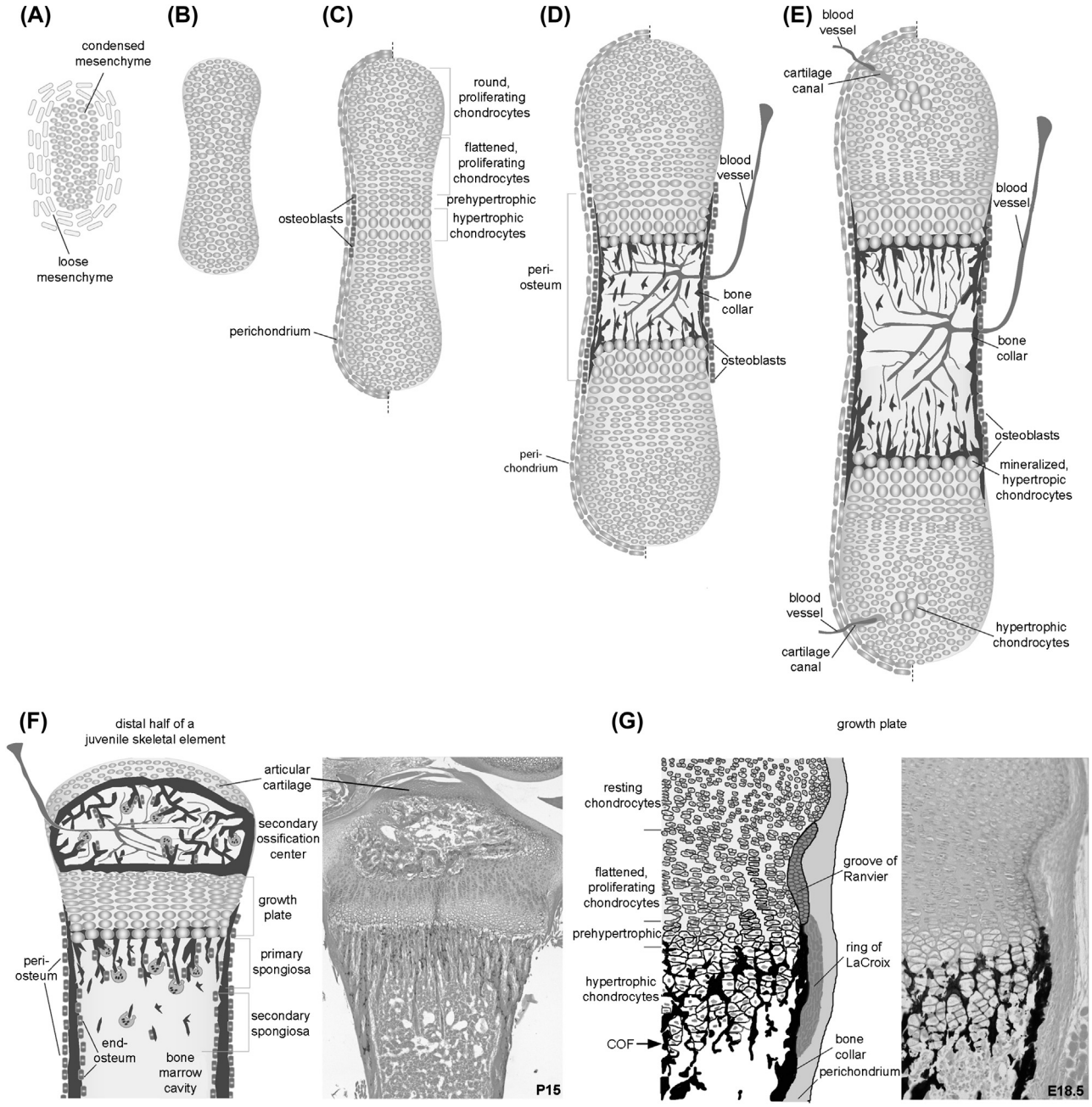

FIGURE 1.6 Schematic representation of the formation and growth of long bones by endochondral ossification. (A) Mesenchymal condensation with surrounding loose mesenchymal cells. (B) Cartilaginous template prefiguring the future skeletal element. (C) Chondrocyte differentiation within the cartilaginous template and differentiation of osteoblasts within a region of the perichondrium, which is then referred to as the periosteum. (D) Blood vessel invasion and onset of bone marrow cavity formation. (E) Onset of the formation of the secondary ossification center with differentiation of hypertrophic chondrocytes in the central region of the epiphysis and blood vessel invasion from the perichondrium through the cartilage canals. (F) Schematic representation on the left and corresponding Alcian blue/eosin−stained image of the proximal end of a postnatal day 15 (P15) mouse tibia on the right. (G) Schematic representation of the different features of a mouse growth plate based on the von Kossa/Alcian blue−stained proximal end of a mouse humerus at embryonic day 18.5 (E18.5). *COF*, chondro-osseous front.

(DeLise and Tuan, 2002a; Delise and Tuan, 2002b; Hall and Miyake, 1995; Bhat et al., 2011). Mesenchymal cells within the condensations start to express chondro-osteogenic markers, such as the transcription factors *Sox9* and *Runx2* (Hill et al., 2005; Akiyama et al., 2005; Wright et al., 1995). Next, the prechondrogenic precursor population of chondroblasts differentiates into chondrocytes, which produce an ECM rich in the proteoglycan aggrecan and fibrillar collagen of type II.

Cartilaginous template formation prefigures the future skeletal element and is surrounded by the so-called perichondrium, a layer of mesenchymal cells. As cartilage is avascular, limb vasculature regression needs to occur where cartilaginous structures form (Hallmann et al., 1987). Yet, interestingly, the chondrogenic condensation does express vascular endothelial growth factor (VEGF) (Eshkar-Oren et al., 2009). The outgrowth of vertebrate limbs occurs progressively along the proximal−distal axis (Newman et al., 2018; Zeller et al., 2009). Concomitantly, the skeletal elements develop in a proximodistal sequence, with the anlagen of the proximal elements (humerus in the forelimb and femur in the hindlimb) forming first, branching into more distal elements, and then being segmented into individual elements as the limb grows (Hinchliffe, 1994). The cartilaginous template increases in size by appositional and interstitial growth (Johnson, 1986). Interstitial growth by dividing chondrocytes allows the cartilage to grow rapidly along the longitudinal axis. The width of the cartilage element is controlled by appositional growth, whereby the perichondrium surrounding the cartilage template serves as the primary source of chondroblasts. Early on, all chondrocytes are still proliferating. As development progresses, the chondrocytes distant to the articulations in the central diaphysis will start to undergo a differentiation program. First, they flatten and rearrange into proliferative stacks of chondrocytes forming the zone of columnar proliferating chondrocytes. The elongation of these columns occurs internally through oriented cell division followed by intercalation movements of the daughters (Ahrens et al., 2009; Li and Dudley, 2009). A 2014 study showed that the daughter cells maintain intimate contact after cell division, preserving cadherin-mediated cell−cell interaction until the end of the rotational movement (Romereim et al., 2014). Interfering with cadherin-mediated cell−cell adhesion stalls the rotation process in vitro (Romereim et al., 2014). A similar rotation defect was observed in mice lacking integrin β1 (Aszodi et al., 2003). Chondrocytes at the lower end of the columns will then exit the cell cycle and become prehypertrophic; a stage that is not morphologically distinct but can be visualized using molecular markers such as the expression of the genes *Ihh* and parathyroid hormone/parathyroid hormone-like peptide receptor 1 (*Pthr1*). Next, the prehypertrophic chondrocytes increase dramatically in volume and become hypertrophic (Cooper et al., 2013; Hunziker et al., 1987). The almost 10-fold increase in volume occurs in parts by true cellular hypertrophy and swelling and significantly contributes to the longitudinal expansion of the skeletal elements as the cells are laterally restricted by matrix channels (Cooper et al., 2013). Hypertrophic chondrocytes (HCCs) are distinct in their ECM producing type X instead of type II collagen. Furthermore, they produce VEGF, which in this context attracts blood vessels to the diaphysis region (Gerber et al., 1999). The ECM of mature HCCs mineralizes and the cells produce matrix metalloproteinase 13 (MMP13) as well as OPN/SSP1. MMP13 (collagenase 3) breaks up the matrix of HCCs for the subsequent removal by osteoclasts (Inada et al., 2004; Stickens et al., 2004), while SSP1 has multiple functions; it regulates mineralization, serves as a chemoattractant for osteoclasts, and is functionally required for their activity (Franzen et al., 2008; Rittling et al., 1998; Boskey et al., 2002; Chellaiah et al., 2003). The final fate of HCCs has long been believed to be apoptotic cell death (Shapiro et al., 2005). Yet, ex vivo and in vitro experiments already hinted at an alternative fate, with HCCs transdifferentiating into osteoblasts (Shapiro et al., 2005). Lineage tracing experiments have confirmed this alternative fate, proposing a model of dual osteoblast origin (Zhou et al., 2014; Yang et al., 2014a, 2014b; Park et al., 2015). At least during embryonic development, about 20% of osteoblasts are chondrocyte derived and about 80% are derived from the perichondrium/periosteum. The latter population migrates into the bone marrow cavity along the invading blood vessels (Maes et al., 2010). This invasion originates from the periosteal collar, the area of the perichondrium in which osteoblasts differentiate and the bone collar is being formed (Colnot et al., 2004). In addition, monocytic osteoclast precursors as well as macrophages, both of which are of hematopoietic origin, enter the remodeling zone via the vascular system, which is attracted by VEGF (Henriksen et al., 2003; Engsig et al., 2000). Blood vessels have additional roles during trabecular bone formation in the primary spongiosa, which will be further discussed in the following. Endothelial cells, chondroclasts, and osteoclasts act together to erode the bone marrow cavity by removing HCC remnants. Interestingly, a bone marrow cavity can form in mouse mutants lacking osteoclasts or even macrophages and osteoclasts (Ortega et al., 2010). In these mutants, MMP9-positive cells are still present at the chondro-osseous junction and may be in part responsible for bone marrow cavity formation (Ortega et al., 2010). With the formation of the marrow cavity in the diaphysis, the two growth plates become separated from each other. The growth plates serve as a continual source of cartilage being converted into bone at the chondro-osseous front during the late stages of development and postnatally. In most species, a second ossification center appears during postnatal development within the epiphyseal cartilage. The onset differs between species for the individual bones and even within one bone for the two epiphyses (Adair and Scammin, 1921; Shapiro, 2001; Zoetis et al., 2003). Here, cartilage canals containing mesenchymal cells and blood vessels enter from the surrounding perichondrium, reaching eventually the hypertrophic center of the epiphysis (Blumer et al., 2008; Alvarez et al., 2005). After the formation of the secondary ossification center, the epiphyseal articular cartilage becomes distinct and the metaphyseal growth plate is sandwiched between the epiphyseal secondary ossification center and the primary ossification center in the diaphysis (Fig. 1.6F).

The growth plate

The cellular organization within the growth plate (schematically depicted in Fig. 1.6F) of a juvenile bone resembles the different zones in embryonic skeletal elements (Fig. 1.6G). There is a zone of small round chondrocytes, some of which are mitotically inert, that is often referred to as the resting zone. Stemlike or progenitor cells are thought to reside in this zone and require the activity of β-catenin for their maintenance (Candela et al., 2014). Concomitant with the growth plate closure that occurs in most vertebrates, with the exception of rodents, these progenitor cells eventually become senescent at the end of puberty and lose their proliferative potential, putting an end to long bone growth (Nilsson and Baron, 2004). The zone next to the resting zone contains flattened, stacked chondrocytes, which are mitotically active and form fairly regular columns. Eventually, the chondrocytes at the lower end of the zone will begin to enlarge, becoming first prehypertrophic and then HCCs (Ballock and O'Keefe, 2003). As already mentioned, some of the HCCs will undergo apoptosis (programmed cell death), while others survive and eventually differentiate into osteoblasts or other cells of the bone marrow cavity (Farnum and Wilsman, 1987; Shapiro et al., 2005; Tsang et al., 2015). The exact cellular and molecular mechanism of the transdifferentiation process of the surviving HCCs is not understood as of this writing. Earlier experiments suggested that this involves asymmetric cell division (Roach et al., 1995). According to the lineage tracing experiments, the transdifferentiating cells express at one point the gene *Col10a1*, encoding the α chain of type X collagen, but were they truly hypertrophic cells? If so, how was their cellular volume adjusted? Or alternatively, is there a pool of "stem cells" residing within the hypertrophic zone? So far, expression of stem cell markers has not been reported in HCCs of a normal growth plate. Yet, cells originating from the hypertrophic zone expressing the lineage tracer also express stem cell markers such as *Sca1* and *Sox2* in vitro (Park et al., 2015). Furthermore, a 2017 publication reported that during fracture healing HCCs express the stem cell markers *Sox2*, *Nanog*, and *Oct4* and that this is triggered by the invading vasculature (Hu et al., 2017). Other experiments such as one in rabbits, in which transdifferentiation was observed after physically preventing vascular invasion at the lower hypertrophic zone, suggest that the vasculature is not required for the transdifferentiation process to occur (Enishi et al., 2014). So far there are only a few molecules known to be required for the chondrocyte-derived differentiation of osteoblasts. One of them is β-catenin (Houben et al., 2016) and the other one SHP2, a protein tyrosine phosphatase (Wang et al., 2017). Mice lacking SHP2 activity in HCCs display a slight reduction in chondrocyte-to-osteoblast differentiation, and the mechanism behind this blockade is the persistence and/or upregulation of SOX9 protein in HCCs (Wang et al., 2017). Mice lacking β-catenin activity in HCCs display an even more severe reduction of chondrocytes differentiating into osteoblasts and its absence also affects in part the transdifferentiation of chondrocytes into other cell types (Houben et al., 2016). The mechanism by which β-catenin affects this transdifferentiation process is unknown as of this writing. Unlike what has been shown in perichondrial osteoblast precursors or in the case of SHP2, persistence of SOX9 protein was not observed (Houben et al., 2016). Furthermore, the loss of β-catenin activity in HCCs affects indirectly the differentiation of perichondrial-derived osteoblast precursors (Houben et al., 2016). HCCs also produce receptor activator of NF-κB ligand (RANKL) and its decoy receptor Osteoprotegerin, which positively and negatively, respectively, influence the differentiation of monocytes into osteoclasts at the chondro-osseous front (Usui et al., 2008; Silvestrini et al., 2005; Kishimoto et al., 2006). The expression of *Rankl* in HCCs is negatively controlled by β-catenin, leading to increased osteoclastogenesis and reduced trabecular bone formation in conditional *Ctnnb1* mice (Houben et al., 2016; Golovchenko et al., 2013; Wang et al., 2014a). As mentioned already, the matrix of the lower rows of HCCs mineralizes. HCCs utilize matrix vesicles to produce large amounts of microcrystalline, Ca^{2+}-deficient, acid-phosphate-rich apatite deposits in the collagen-rich matrix (Wuthier and Lipscomb, 2011). Matrix vesicle release occurs in a polarized fashion from the lateral edges of the growth plate HCCs, resulting in the mineralization of the longitudinal septae, while transverse septae remain unmineralized (Anderson et al., 2005a). The matrix vesicles then release the apatite crystals, which self-nucleate and grow to form spherical mineralized clusters in the calcified zone of the HCCs. Mitochondria may serve as storage containers for Ca^{2+}, with the mitochondria in HCCs reaching the highest Ca^{2+} concentrations and serving as the Ca^{2+} supply for matrix vesicles. The mitochondria loaded with Ca^{2+} can no longer produce sufficient amounts of ATP and the cells undergo a physiological energy crisis. As a consequence, the mitochondria produce increased amounts of reactive oxygen species (ROS) (Wuthier and Lipscomb, 2011). Increased ROS levels feed back on the chondrocytes, inducing them to hypertrophy (Morita et al., 2007).

Through knockout studies in mouse, numerous genes were identified that are involved in the regulation of the mineralization process, such as matrix Gla protein and tissue nonspecific alkaline phosphatase (encoded by the *Akp2* gene), ectonucleotide pyrophosphatase/phosphodiesterase type 1, progressive ankylosis gene, phosphoethanolamine/phosphocholine phosphatase, membrane-anchored metalloproteinase ADAM17, and, as already mentioned, OPN (Anderson et al., 2004, 2005b; Fedde et al., 1999; Hessle et al., 2002; Zaka and Williams, 2006; Harmey et al., 2004; Hall et al., 2013).

After the removal of HCCs, the mineralized longitudinal septae remain and are used by osteoblasts as a scaffold for the deposition of osteoid that calcifies into woven bone.

At the periphery, the growth plate is surrounded by a fibrous structure that consists of the wedge-shaped groove of Ranvier and the perichondrial ring of LaCroix (see Fig. 1.6G) (Brighton, 1978; Langenskiold, 1998). The groove of Ranvier serves as a reservoir for chondro-osteoprogenitor cells and fibroblasts, while the perichondrial ring of LaCroix may serve as a reservoir of precartilaginous cells (Fenichel et al., 2006; Shapiro et al., 1977). Interestingly, the two growth plates within a skeletal element have different activities leading to the differential growth of the distal and proximal parts (Pritchett, 1991, 1992; Farnum, 1994). Curiously, there seems to exist a temporal and local correlation between the appearance of the secondary ossification center and the activity of the nearby growth plate. For instance, in the humerus the secondary ossification center appears first in the proximal epiphysis and here, the proximal growth plate is more active than the distal one.

Mediators of skeleton formation

Accurate skeletogenesis, as well as postnatal growth and repair of the skeleton, depends on the precise orchestration of cellular processes such as coordinated proliferation and differentiation in time and space. Several signaling pathways impinge on the differentiation of the mesenchymal precursors as well as on the subsequent differentiation of chondrocytes and regulate the growth of the skeletal elements. Growth factor signaling is also partly controlled by the ECM and integrins (Munger and Sheppard, 2011; Ivaska and Heino, 2011). Cell-type-specific differentiation is under the control of distinct transcription factors with their activity being modulated by epigenetic factors and microRNAs. In addition to systemic and local factors, oxygen levels and metabolism also influence endochondral bone formation.

Systemic mediators

Longitudinal bone growth after birth is under the influence of various hormones, such as growth hormone (GH), insulin-like growth factors (IGFs), thyroid hormones, estrogen and androgens, glucocorticoids, vitamin D, and leptin. The importance of these hormones in skeletal growth has been demonstrated by genetic studies in animals and by "natural experiments" in humans (for reviews see Nilsson et al., 2005; Wit and Camacho-Hubner, 2011). Many of these systemic mediators interact with one another during linear growth of the juvenile skeleton and are differentially controlled by the nutritional status (Robson et al., 2002; Lui and Baron, 2011; Gat-Yablonski et al., 2008). Yet, only IGF signaling plays a role in endochondral ossification prior to birth.

Mice deficient for either *Igf1* or *Igf2* or the *Igf1r* gene display prenatal as well as postnatal growth defects, suggesting that IGFs act independent of GH on linear growth (Baker et al., 1993; Liu et al., 1993; Powell-Braxton et al., 1993). IGF1 was thought to affect chondrocyte proliferation, yet, a study on longitudinal bone growth in the *Igf1*-null mouse revealed no change in growth plate chondrocyte proliferation or cell numbers, despite the observed 35% reduction in the rate of long bone growth that was attributed to the 30% reduction in the linear dimension of HCCs (Wang et al., 1999). For more detailed information on the activities of GH and IGF signaling see reviews by Giustina et al. (2008), Kawai and Rosen (2012), Svensson et al. (2001), and Lindsey and Mohan (2016).

Local mediators

The various local mediators of endochondral and intramembranous ossification, which will be briefly discussed in the following, interact at multiple levels. Because of space constraints not all of these interactions can be mentioned.

Growth factor signaling pathways

Transforming growth factor β and bone morphogenetic proteins

The TGFβ superfamily is a large family of secreted polypeptides that can be divided into two subfamilies based on the utilization of the downstream signaling mediators, the regulatory SMADs (R-SMADs). The first one, encompassing TGFβ1−β3, activins, inhibins, nodal, and myostatin (GDF8), transduces the canonical signal through the R-SMADs 2 and 3. The second one consists of the BMPs 2 and 4−10 and most GDFs, transducing the canonical signal through R-SMADs 1, 5, and 8. The cofactor SMAD4 is utilized by both groups, forming a complex with the different activated R-SMADs. The receptor complexes are heterodimers consisting of serine/threonine kinase types I (ALKs 1−7) and II (TβRII, ActRII, ActRIIb, BMPRII, and MISRII) receptors. Ligand binding activates the type II receptor, leading to transphosphorylation

of the type I receptor. In addition to the SMAD-dependent canonical signaling, TGFβ/BMPs can signal through numerous SMAD-independent noncanonical signaling pathways (reviewed in Wang et al., 2014c; Wu et al., 2016).

Many of the TGFβ and BMP signaling molecules are involved in endochondral bone formation. In the mouse, all three *Tgfβ* isoforms are expressed in mesenchymal condensations, perichondrium/periosteum, and appendicular growth plates (Pelton et al., 1990, 1991; Schmid et al., 1991). Despite the numerous in vitro reports indicating a role for TGFβ molecules promoting mesenchymal condensation and the onset of chondrocyte differentiation, none of the individual *Tgfβ* knockouts supports such an early role in vivo. It has been proposed that transient activation of TGFβ and/or activin signaling primes mesenchymal cells to become chondroprogenitors (Karamboulas et al., 2010). Of the individual *Tgfβ* knockouts, only the $Tgf\beta2^{-/-}$ mutants displayed defects in intramembranous and endochondral bone formation (Sanford et al., 1997), some of which may be secondary due to defects in tendon formation (Pryce et al., 2009). The conditional ablation of the primary receptor for all three TGFβs and *Alk5*, in mesenchymal cells using the *Dermo1*-Cre line, resulted also in skeletal defects affecting intramembranous and endochondral bones (Matsunobu et al., 2009). The endochondral bone elements in the $Alk5^{-/-}$ animals were smaller and malformed, with ectopic cartilaginous protrusions present in the hindlimb. Conditional deletion of the *Tgfbr2* gene, encoding the TβRII receptor, in the limb mesenchyme with the *Prx1*-Cre line results in the absence of interphalangeal joints, probably due to a defect in downregulation of the chemokine MCP-5 in the joint interzone cells (Spagnoli et al., 2007; Longobardi et al., 2012). The appendicular skeletal elements of the *Tgfbr2*;*Prx1*-Cre embryos are also shorter, associated with altered chondrocyte proliferation and an enlarged HCC zone (Seo and Serra, 2007). This phenotype was also observed upon the expression of a dominant-negative form of the TβRII receptor or by expressing a dominant-negative TβRI (*Alk5*) construct in chondrocytes (Serra et al., 1997; Keller et al., 2011). Surprisingly, deletion of *Tgfbr2* in *Col2a1*-expressing cells resulted in defects only in the axial skeleton and not in the appendicular skeleton (Baffi et al., 2004). Nevertheless, the long bones of the *Tgfbr2;Col2a1*-Cre newborn mice were consistently shorter, but the difference was not significant. Sueyoshi and colleagues reported that deletion of *Tgfbr2* in HCCs results in a minor delay in chondrocyte differentiation around E14.5/15.5. Yet, at birth, no differences regarding the length of the long bones were observed, suggesting that this is a transient effect (Sueyoshi et al., 2012). Deletion of *Tgfbr2* in *Osx*-Cre-positive pre-HCCs and osteoblast precursors in the perichondrium led to postnatal alteration in the growth plate and affected osteoblastogenesis (Peters et al., 2017). This is probably associated with a loss of *TGFβ1* signaling (Tang et al., 2009). Nevertheless, inactivation of *Tgfbr2* may not be sufficient to eliminate all Tgfβ signaling, as TGFβ ligands were still capable of eliciting signals in the $Tgfbr2^{-/-}$ mice (Iwata et al., 2012). Furthermore, TGFβs can activate the canonical BMP/SMAD1/5/8 pathway through engagement of ALK1 (Goumans et al., 2002). TGFβ proproteins are sequestered by the ECM and can then be released and activated through, for instance, the activity of ECM degrading enzymes (Hildebrand et al., 1994; Pedrozo et al., 1998; Annes et al., 2003). For further information, in particular on the involvement of noncanonical TGFβ pathways in chondrogenesis and skeletogenesis and the implications of TGFβ signaling in osteoarthritis, see reviews by van der Kraan et al. (2009), Wang et al. (2014c), and Wu et al. (2016).

The cofactor SMAD4 is thought to mediate canonical signaling downstream of TGFβ and BMP signaling. Yet surprisingly, conditional mutants lacking *Smad4* in *Col2a1*-expressing cells are viable and display only mild phenotypic changes in the growth plate (Zhang et al., 2005; Whitaker et al., 2017). However, the prechondrogenic condensations do not form in mice lacking SMAD4 in the limb mesenchyme, supporting an essential role for TGFβ/BMP signaling in the early steps of chondrocyte differentiation, which appears to be independent of SOX9 (Lim et al., 2015; Benazet et al., 2012). Mice lacking either R-SMAD1/5 in *Col2a1*-expressing cells or all three R-SMADs (SMAD1, 5, and 8) acting downstream of BMP signaling are not viable and display a nearly identical severe chondrodysplasia phenotype (Retting et al., 2009). The axial skeleton is severely compromised, with vertebral bodies replaced by fibroblasts and loose mesenchymal tissue. This suggests that SMAD8 plays only a minor role in chondrogenesis. Furthermore, these results challenge the dogma that SMAD4 is required to mediate SMAD-dependent signaling downstream of BMPs and TGFβs.

Based on the analyses of gene knockout animals, the *Bmp/Gdf* family members *Bmp8*, *Bmp9/Gdf2*, *Bmp10*, and *Gdf10* appear to play no role in embryonic skeletogenesis (Zhao et al., 1996, 1999; Chen et al., 2004; Levet et al., 2013). The *short-ear* mouse is mutant for *Bmp5* and displays defects in skeletal morphogenesis and has weaker bones (Kingsley et al., 1992; Mikic et al., 1995). *Bmp6* mutants have sternal defects (Solloway et al., 1998). Mice mutant for *Bmp7* display skeletal patterning defects restricted to the rib cage, skull, and hindlimbs (Luo et al., 1995; Jena et al., 1997). In addition to *Bmp7*, *Bmp2* and *Bmp4* are expressed in the early limb bud. Conditional deletion of *Bmp2* and *Bmp4* in the limb mesenchyme results in an abnormal patterning of the appendicular skeleton with a loss of posterior elements in the zeugopod and autopod region probably due to a failure of chondrogenic differentiation of the mesenchymal cells caused by insufficient levels of BMP signaling (Bandyopadhyay et al., 2006). In addition, the skeletal elements that form are shorter and thinner. Chondrocyte differentiation within the skeletal elements is delayed but otherwise normal. Concomitantly, the endochondral ossification process is also delayed and bone formation is severely compromised in these

mice (Bandyopadhyay et al., 2006). Yet, of the two BMPs, BMP2 appears to be the crucial regulator of chondrocyte proliferation and maturation (Shu et al., 2011). GDF11/BMP11 is required for axial skeleton patterning and acts upstream of the *Hox* genes (McPherron et al., 1999; Oh et al., 2002). Postnatally, GDF11 acts on bone homeostasis by stimulating osteoclastogenesis and inhibiting osteoblast differentiation (Liu et al., 2016). Mutations in human *GDF5* (*BMP14, CDMP1*) or *BMPR1B* (*ALK6*) cause brachydactyly type C (OMIM 113100) and A2 (OMIM 112600), respectively (Lehmann et al., 2003; Polinkovsky et al., 1997). *Gdf5* and *Bmpr1b* mutant mice also display a brachydactyly phenotype (Storm et al., 1994; Baur et al., 2000; Yi et al., 2000). Closer examination of the *Gdf5* mutant brachypodism mouse revealed that the absence of the joint separating phalangeal elements 1 and 2 is due to the loss of the cartilaginous anlage and subsequent formation of the skeletal element by intramembranous instead of endochondral bone formation (Storm and Kingsley, 1999). The related family members *Gdf5*, *Gdf6*, and *Gdf7* are expressed in the interzone of different subsets of joints. *Gdf6* mutants display fusions of carpal and tarsal joints, and double mutants for *Gdf5/6* show additional skeletal defects (Settle et al., 2003). Interestingly, postnatally, GDF5 and GDF7 modulate the rate of endochondral tibial growth by altering the duration of the hypertrophic phase in the more active growth plate in opposite ways (Mikic et al., 2004, 2008). Bead-implant experiments in chicken and mouse embryos as well as various in vitro experiments revealed a prochondrogenic activity of BMP2, BMP4, or GDF5 protein, which can be antagonized by the secreted molecule Noggin (Zimmerman et al., 1996; Merino et al., 1999; Wijgerde et al., 2005). Consistent with this, Noggin-knockout mice display appendicular skeletal overgrowth and lack synovial joints (Brunet et al., 1998). Yet, surprisingly the caudal axial skeleton does not develop in the *Noggin* mutants. The vertebral phenotype can in part be reverted by the loss of one functional *Bmp4* allele, supporting the notion that too high levels of BMP4 signaling in the axial mesoderm may actually inhibit the differentiation of sclerotomal cells to chondrocytes. Instead, these cells take on a lateral mesodermal fate (Wijgerde et al., 2005; Murtaugh et al., 1999; Hirsinger et al., 1997). Double knockout of the BMP receptors *Bmpr1a* (*Alk3*) and *Bmpr1b* (*Alk6*) revealed a functional redundancy of these two receptors in endochondral ossification. Chondrocyte differentiation in the axial and appendicular skeleton is severely compromised in the mice lacking both receptors (Yoon et al., 2005). Conditional mutants for activin receptor type IA (*Alk2*) display only mild axial phenotypes. Double mutant analysis revealed a functional redundancy with *Bmpr1a* and *Bmpr1b* in endochondral skeletogenesis (Rigueur et al., 2015). Conditional postnatal deletion of *Bmpr1a* revealed a role for BMP signaling in the maintenance of the chondrogenic cell fate in the growth plate (Jing et al., 2013). Constitutively activating mutations in *ALK2* are found in patients with fibrodysplasia ossificans progressiva (OMIM 156400), a rare disorder in which the connective tissue progressively ossifies after traumatic injury (Shore et al., 2006). For further reading see reviews by Rosen (2006), Pogue and Lyons (2006), Wu et al. (2007, 2016), and Wang et al. (2014b).

Parathyroid hormone-related protein and Indian hedgehog

The paracrine hormone parathyroid hormone-related protein (PTHrP) and its receptor PTH1R are part of a crucial regulatory node, also referred to as the IHH/PTHrP feedback loop, coordinating chondrocyte proliferation with maturation in endochondral bone formation (Fig. 1.7). PTHrP is also required for normal intramembranous ossification (Suda et al., 2001). In the appendicular skeletal elements, PTHrP is expressed locally at high levels in the periarticular cells and at lower levels in the proliferating chondrocytes. Its receptor is expressed also at low levels in proliferating and at higher levels in pre-HCCs (Lee et al., 1996; Vortkamp et al., 1996; St-Jacques et al., 1999). *PTHrP* and *Pthr1* mutant mice display similar, but not identical phenotypes, with numerous skeletal abnormalities, including severely shortened long bones (Karaplis et al., 1994; Lanske et al., 1996). In both, the shortening of the long bones is associated with reduced chondrocyte proliferation and accelerated HCC maturation and bone formation (Amizuka et al., 1996; Lee et al., 1996; Lanske et al., 1998). Chimeric mice with $Pth1r^{-/-}$ clones in their growth plates revealed that the effects on chondrocyte maturation were direct but influenced by positional cues, as these clones expressed either *Ihh* or *Col10a1* ectopically dependent on their location within the proliferative zone (Chung et al., 1998). Concomitantly, mice overexpressing either PTHrP or a constitutively active form of PTH1R in chondrocytes show a delay in HCC maturation early and a prolonged persistence of HCCs associated with a delay in blood vessel invasion at later stages of development (Weir et al., 1996; Schipani et al., 1997b). PTH1R is a seven-transmembrane receptor coupled to heterotrimeric G proteins, consisting of α, β, and γ subunits. Its activation by PTHrP results in signaling via either the $G_s(\alpha)$/cAMP or the $G_q(\alpha)$/inositol-3-phosphate-dependent pathway. The two downstream pathways have opposing effects on chondrocyte hypertrophy with $G_q(\alpha)$/inositol-3-phosphate-dependent signaling cell-autonomously accelerating hypertrophic differentiation, while $G_s(\alpha)$/cAMP-signaling delays it (Guo et al., 2002; Bastepe et al., 2004). The intracellular mediator of the canonical WNT signaling pathway, β-catenin, interacts with the PTH1R and may modulate the switch from $G_s(\alpha)$ to the $G_q(\alpha)$ signaling (Yano et al., 2013; Yang and Wang, 2015). The $G_s(\alpha)$/cAMP signaling pathway is also involved in the maintenance of the pool of round proliferating

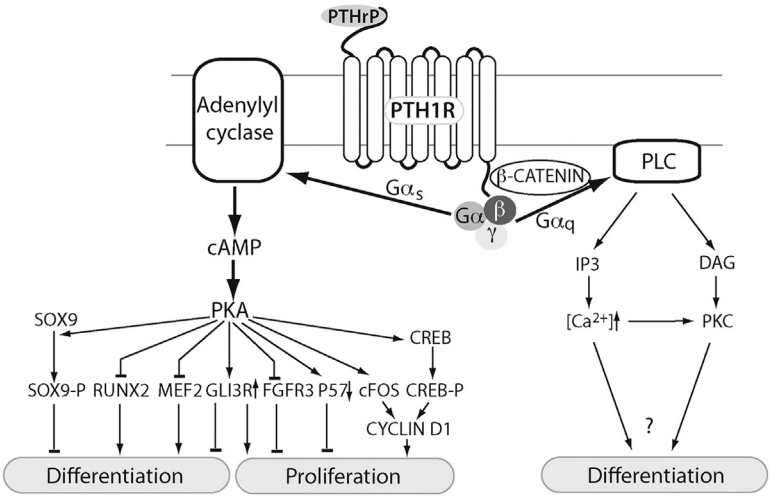

FIGURE 1.7 PTHrP/PTH1R signaling pathways and their functional consequences on chondrocyte differentiation and proliferation. The molecular mechanism underlying the differentiation-promoting effect of the PLC signaling branch is not yet understood. *PKA*, protein kinase A; *PLC*, phospholipase C; *PTHrP*, parathyroid hormone-related protein; *PTH1R*, PTHrP receptor.

chondrocytes (Chagin and Kronenberg, 2014). The inhibitory effect on chondrocyte hypertrophy is mediated through the activation of protein kinase A (PKA) downstream of $G_s(\alpha)$/cAMP signaling. This, in turn, promotes the following response: translocation of histone deacetylase 4 (HDAC4) into the nucleus where it binds to and inhibits the transcriptional activity of MEF2 transcription factors (Kozhemyakina et al., 2009). Furthermore, PTHrP signaling increases the expression of the transcription factor ZFP521, which negatively influences the transcriptional activity of RUNX2, again through recruitment of HDAC4 (Correa et al., 2010). In addition, PTHrP can decrease RUNX2 production and enhance its degradation specifically in chondrocytes (Guo et al., 2006; Zhang et al., 2009, 2010). MEF2 and RUNX2 are both positive regulators of chondrocyte hypertrophy (see later). PKA also phosphorylates SOX9, enhancing its DNA-binding activity, and stimulates GLI3 processing into its repressor fragment, thereby potentially interfering with chondrocyte maturation (Huang et al., 2000; Wang et al., 2000; Mau et al., 2007). PTH1R signal via PKA also inhibits the transcription of FGFR3 (McEwen et al., 1999). Furthermore, it leads to a downregulation of the cell-cycle-dependent inhibitor P57, a negative regulator of chondrocyte proliferation (Yan et al., 1997; MacLean et al., 2004). Last but not least, PTHrP signaling may stimulate proliferation through AP1/CREB dependent activation of cyclin D1 (Ionescu et al., 2001).

The findings in the different *Pthrp*/*Pth1r* mouse models can be correlated with activating mutations in the human PTH1R that lead to ligand-independent cAMP accumulation in patients with Jansen-type metaphyseal dysplasia (OMIM 156400) (Schipani et al., 1995, 1996, 1997a, 1999). On the other hand, the loss-of-function mutants correlate with the Blomstrand chondrodysplasia disorder (OMIM 215045) associated with the absence of a functional PTH1R (Karaplis et al., 1998; Zhang et al., 1998; Jobert et al., 1998). Interestingly, in the recessive Eiken skeletal dysplasia syndrome (OMIM 600002), a mutation leading to a C-terminal truncation of PTH1R has been identified that results in a phenotype opposite to that of Blomstrand chondrodysplasia and resembles a transgenic mouse model in which PTH1R signal transduction via the phospholipase C/inositol-3-phosphate-dependent pathway is compromised (Guo et al., 2002; Duchatelet et al., 2005).

Ihh, encoding a secreted molecule of the HH family, is expressed in pre-HCCs and has been shown to regulate the expression of *PTHrP* (Vortkamp et al., 1996; St-Jacques et al., 1999). This regulation is probably mediated by TGFβ2 signaling (Alvarez et al., 2002). *Ihh*-knockout mice display defects in endochondral and intramembranous bone formation (St-Jacques et al., 1999; Abzhanov et al., 2007; Lenton et al., 2011). In endochondral bone formation, IHH has multiple functions; it regulates proliferation and chondrocyte hypertrophy and is essential for osteoblastogenesis in the perichondrium. The last function of IHH apparently requires additional effectors other than RUNX2 (Tu et al., 2012). Conditional deletion of *Ihh* in *Col2a1*-CRE-expressing cells recapitulates the total knockout phenotype, including the multiple synostosis phenotype, a severe form of synchondrosis (Razzaque et al., 2005). In humans, *IHH* mutations are associated with brachydactyly type A1 (OMIM 112500), while copy number variations including the *IHH* locus are associated with syndactyly and craniosynostosis (Gao et al., 2009; Klopocki et al., 2011). The effects of *Ihh* on chondrocyte hypertrophy are PTHrP dependent as well as independent, while those on proliferation, osteoblastogenesis, and joint formation are PTHrP independent (Karp et al., 2000; Long et al., 2001, 2004; Kobayashi et al., 2005; Amano et al., 2016; Mak et al., 2008).

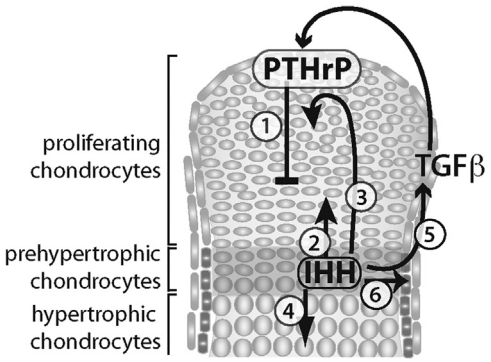

FIGURE 1.8 Parathyroid hormone-related protein (*PTHrP*) and Indian Hedgehog (*IHH*) interactions and functions in the growth plate. IHH and PTHrP participate in a negative feedback loop to regulate chondrocyte proliferation and differentiation. PTHrP is expressed from the perichondrial cells at the articular region and at low levels in round proliferative chondrocytes. It acts on proliferating chondrocytes, keeping them in a proliferative state and preventing their differentiation to prehypertrophic and hypertrophic chondrocytes (**1**). When the PTHrP concentration is sufficiently low enough, chondrocytes drop out of the cell cycle and differentiate into IHH-producing prehypertrophic chondrocytes. IHH, in turn, stimulates the proliferation of the adjacent flattened proliferating chondrocytes (**2**) and accelerates the progression of round to flattened proliferating chondrocytes (**3**) as well as the differentiation of prehypertrophic to hypertrophic chondrocytes (**4**). IHH also stimulates, probably mediated by transforming growth factor β (*TGFβ*) signaling, PTHrP production at the articular ends of the skeletal element (**5**) and acts on perichondrial cells, stimulating their differentiation into osteoblasts (**6**).

As mentioned earlier, the transcription factor GLI3 acts downstream of HH signaling, whereby HH signaling prevents the proteolytic conversion of GLI3 into the repressor form GLI3R. Mutations in *GLI3* are associated with Greig cephalopolysyndactyly (OMIM 175700) and Pallister−Hall syndrome (OMIM 146510) (Demurger et al., 2015). The mouse mutant extra-toes (Xt), a model for Greig cephalopolysyndactyly syndrome, has a deletion in the *Gli3* gene and displays numerous skeletal abnormalities, such as polydactyly, shortened long bones, split sternum, and craniofacial defects (Hui and Joyner, 1993; Vortkamp et al., 1992; Mo et al., 1997). Craniofacial abnormalities and shortened appendicular long bones are also reported in *Gli2* mutants (Mo et al., 1997). Interestingly, in double mutants for *Ihh* and *Gli3* the proliferation defect observed in the *Ihh* mutants is restored and the accelerated HCC differentiation, observed in $Ihh^{-/-}$ specimens, reverted (Hilton et al., 2005; Koziel et al., 2005). In contrast, the defects in osteoblastogenesis and cartilage vascularization are only partially rescued by the loss of *Gli3* (Hilton et al., 2005). Based on the observations in $Ihh^{-/-}$;$Gli3^{-/-}$ double mutants, Koziel and colleagues proposed a model whereby the IHH/GLI3 system regulates two distinct steps in chondrocyte differentiation: first, the transition from distal, round chondrocytes to the columnar chondrocytes, which appears to occur in a PTHrP-independent fashion, and second, the transition from proliferating to HCCs occurring in a PTHrP-dependent fashion (Koziel et al., 2005). Yet, Mak and colleagues proposed that Ihh also promotes chondrocyte hypertrophy in a PTHrP-independent way (Mak et al., 2008) (Fig. 1.8). In addition, Ihh activity is required for the maturation of the perichondrium and, in a cell-autonomous fashion, for the maintenance of endothelial cell fate (Colnot et al., 2005).

WNTs and β-catenin

As mentioned earlier β-catenin-mediated WNT signaling plays an important role as a permissive signal in the early steps of endochondral bone formation, enabling the differentiation of osteoblasts and cells contributing to the joint by repressing the chondrogenic potential within the respective precursor populations. The critical role of WNT/β-catenin signaling in osteoblastogenesis is first shown by the findings that human mutations in the WNT receptor LRP5 cause osteoporosis−pseudoglioma syndrome (OMIM 259770) (Gong et al., 2001; Lara-Castillo and Johnson, 2015). Mutations in the *WNT1* gene are causative for osteogenesis imperfecta, type XV, and an autosomal-dominant form of susceptibility to early onset of osteoporosis (OMIM 615220, 615221) (Keupp et al., 2013; Laine et al., 2013; Pyott et al., 2013). Numerous WNT-pathway molecules have been identified in genome-wide association studies related to skeletal phenotypes (Hsu and Kiel, 2012).

Stabilization of β-catenin in limb mesenchymal cells interferes with the initiation process of endochondral ossification (Hill et al., 2005). In contrast, expression of a constitutively active form of the downstream transcription factor LEF1 in *Col2a1*-expressing cells inhibits further maturation of chondrocytes and interferes with the formation of joints (Tamamura et al., 2005). Later during chondrocyte differentiation, WNT/β-catenin signaling regulates chondrocyte maturation in a positive manner (Hartmann and Tabin, 2001; Enomoto-Iwamoto et al., 2002; Akiyama et al., 2004; Day et al., 2005; Hill et al., 2005; Hu et al., 2005; Spater et al., 2006b; Joeng et al., 2011; Dao et al., 2012). This is mediated in multiple ways,

via direct regulation of *Ihh*, through interference with SOX9, and in a RUNX2-dependent fashion (Akiyama et al., 2004; Yano et al., 2005; Spater et al., 2006b; Dong et al., 2006; Dao et al., 2012; Mak et al., 2008). In HCCs, β-catenin signaling downregulates the expression of *Rankl*, thereby locally regulating the differentiation of osteoclasts at the chondro-osseous border (Golovchenko et al., 2013; Wang et al., 2014a; Houben et al., 2016). Based on overexpression of an intracellular inhibitor of β-catenin, ICAT, it has been proposed that β-catenin positively regulates VEGF and MMP13 (Chen et al., 2008). Yet, this has not been confirmed in conditional β-catenin mutants. Transient activation of β-catenin during early postnatal development leads to abnormal growth plate closure and promotes secondary ossification center formation (Yuasa et al., 2009; Dao et al., 2012). For further information see reviews by Baron and Kneissel (2013), Wang et al. (2014d), and Usami et al. (2016).

In addition to WNT/β-catenin-mediated signaling, a number of additional WNT signaling pathways are important within the growth plate. One that is highly relevant is the planar cell polarity pathway and its components, WNT5a and receptor tyrosine kinase orphan receptor (ROR2). Mutations in WNT5a and ROR2 are associated with Robinow syndrome (OMIM 268310; 164975) and brachydactyly type B1 (OMIM 113000) (Patton and Afzal, 2002; Person et al., 2010; Roifman et al., 2015). In mice, loss-of-function mutations in *Wnt5a*, *Ror2*, *Vangl2*, *Prickle1*, and *Ryk* result in skeletal dysplasias resembling those associated with Robinow syndrome (DeChiara et al., 2000; Takeuchi et al., 2000; Wang et al., 2011; Andre et al., 2012; Macheda et al., 2012; Gao et al., 2011; Yang et al., 2013b; Liu et al., 2014). In mice, *Wnt5a* and its related family member *Wnt5b* are both expressed in pre-HCCs (Yamaguchi et al., 1999; Yang et al., 2003; Witte et al., 2009). WNT5a promotes chondrocyte proliferation, as such mice lacking *Wnt5a* develop shorter skeletal elements due to a reduction in chondrocyte proliferation in zone II of the proliferating chondrocytes, encompassing the flattened proliferating chondrocytes (Yamaguchi et al., 1999; Yang et al., 2003). Furthermore, chondrocyte differentiation of HCCs is severely delayed in $Wnt5a^{-/-}$ mice as it is in *Ror2* mutants (DeChiara et al., 2000; Takeuchi et al., 2000; Oishi et al., 2003). Overexpression of either *Wnt5a* or *Wnt5b* primarily in chondrocytes also delays chondrocyte differentiation, yet, the two WNT ligands act on different chondrocyte subsets (Yang et al., 2003). The intracellular pathways underlying these effects are not known as of this writing. Compromised differentiation of HCCs may be associated with the capacity of WNT5a to induce the proteolytic cleavage of the transcription factor NKX3.2, which inhibits chondrocyte hypertrophy (Provot et al., 2006). In vitro, WNT5a and WNT5b can both activate calcium-dependent signaling leading to nuclear localization of nuclear factor of activated T cells (NFAT), as well as NF-κB signaling, and the kinase JNK (Oishi et al., 2003; Bradley and Drissi, 2010, 2011). The two pathways have differential effects on chondrogenesis (Bradley and Drissi, 2010). WNT5a signaling has also been shown to downregulate WNT/β-catenin signaling (Topol et al., 2003; Mikels and Nusse, 2006). However, experiments suggest that it can also enhance WNT/β-catenin signaling during osteoblastogenesis (Okamoto et al., 2014). Which pathway is preferentially activated may be decided at the level of the coreceptors (Grumolato et al., 2010).

Fibroblast growth factors and their receptors

FGF signaling also plays a critical role in the growth plate. Mutations in all three human *FGFRs* cause skeletal malformations, such as craniosynostosis syndromes (see also intramembranous ossification) and chondrodysplasia. Constitutively activating mutations in *FGFR3* are associated with hypochondrodysplasia (OMIM 146000), achondrodysplasia (OMIM 100800), and thanatophoric dysplasias type I (OMIM 187600) and type II (OMIM 187601). For reviews see Robin et al. (1993) and Ornitz and Marie (2015).

In the murine growth plate, *Fgfr2* is expressed at low levels in the round proliferating zone, also referred to as the resting zone. Proliferating and pre-HCCs express high levels of *Fgfr3*, and HCCs express high levels of *Fgfr1* (Ornitz and Marie, 2015). The growth retardation in conditionally deleted *Fgfr2* mice is attributed to alterations at the chondro-osseous junction (Yu et al., 2003). Yet, chondrocyte proliferation was unaffected in these mice. An increase in the zone of proliferating chondrocytes as well as HCCs was observed upon loss of *Fgfr3* (Colvin et al., 1996; Deng et al., 1996). In contrast, mice carrying an *Fgfr3* gene with human achondroplasia mutations display the opposite phenotype, a decrease in chondrocyte proliferation and a reduced zone of HCCs (Chen et al., 1999; Li et al., 1999). Of the different ligands, FGF9 and FGF18 have been identified based on their mutant phenotypes to be relevant in endochondral bone formation. Both are expressed in the perichondrium and periosteum. FGF9 and FGF18 are both required for chondrocyte maturation, as the onset of hypertrophy is delayed in $Fgf9^{-/-}$ and $Fgf18^{-/-}$ embryos (Hung et al., 2007; Liu et al., 2007). Yet, in the $Fgf9^{-/-}$ mutant only the stylopod elements are affected (Hung et al., 2007). Due to the delay in chondrocyte maturation vascular invasion is also delayed in both mutants. However, there is evidence that FGF18 may directly stimulate the expression of VEGF (Liu et al., 2007). In addition, FGF18 is required for chondrocyte proliferation. A 2016 allelic series study of *Fgf9*/*Fgf18* mutant embryos revealed unique and redundant roles of the two ligands in endochondral ossification (Hung et al., 2016).

C-type natriuretic peptide

In the growth plate, C-type natriuretic peptide (CNP) and its receptor GC-B are primarily expressed in proliferative and pre-HCCs (Chusho et al., 2001). In humans, homozygous loss-of-function mutations in the receptor cause acromesomelic dysplasia Maroteaux type (OMIM 602875), while heterozygous mutations are associated with short stature (Bartels et al., 2004; Olney et al., 2006; Vasques et al., 2013). Yet, the CNP/GC-B system is widely distributed in the body and as such, it was unclear whether it acts systemically or locally on endochondral ossification. Evidence for the latter is based on conditional knockouts of *Cnp* or *Gc-b* in *Col2a1*-Cre-expressing cells that recapitulate the dwarfism phenotypes of the respective full knockouts (Chusho et al., 2001; Tamura et al., 2004; Nakao et al., 2015). Dwarfism is associated with a decrease in the proliferative zone and in the number and size of HCCs. In contrast, loss of the clearance receptor NPR-C results in skeletal overgrowth similar to that in mice overexpressing the related molecule BNP (Suda et al., 1998; Jaubert et al., 1999). Skeletal growth can also be stimulated in a dose-dependent fashion by interfering with the clearance of CNP by overexpressing osteocrin, a natural NPR-C ligand (Kanai et al., 2017). In humans, overexpression of CNP is also associated with skeletal overgrowth (Bocciardi et al., 2007). Craniofacial studies in mice suggest that CNP/GC-B signaling primarily stimulates endochondral ossification (Nakao et al., 2013). Downstream signaling involves cyclic GMP-dependent kinase II but also interferes with the activation of the mitogen-activated protein kinase cascade downstream of FGF signaling (Miyazawa et al., 2002; Ozasa et al., 2005). For further reading see the review by Peake et al. (2014).

Notch signaling

Mutations in the Notch signaling components cause at least two human disorders with vertebral column defects, spondylocostal dysostosis (OMIM 277300, 608681, and 609813) and Alagille syndrome (OMIM 118450 and 610205) (Baldridge et al., 2010). Gain-of-function mutations in *NOTCH2* are found in Hajdu−Cheney syndrome, a rare skeletal disorder characterized by osteoporosis (OMIM 102500) (Majewski et al., 2011; Isidor et al., 2011). These diseases highlight, among others, the critical role of the segmentation clock in human axial skeletal development.

In chick and mouse, the Notch receptors 1−4 and the ligands, Delta1 and Jagged1/2, are expressed in a dynamic way within the developing limb skeleton, and inhibition of Notch signaling disrupts chondrocyte differentiation (Williams et al., 2009; Dong et al., 2010). Misexpression of the ligand Delta1 in chick inhibits the transition from pre-HCC to HCC (Crowe et al., 1999). A similar phenotype is observed upon conditional expression of the active Notch intracellular domain (NICD) in chondrocytes within the long bones, while a loss of skeletal elements due to impaired chondrogenesis is observed in the axial skeleton (Mead and Yutzey, 2009). The latter is associated with a downregulation of *Sox9* and, as shown in additional studies, with an enhanced proliferation of the mesenchymal progenitor cells, which is dependent on the activity of the transcriptional cofactor RBPjκ (recombination signal binding protein for immunoglobulin κ J region), which interacts with the NICD in the nucleus (Dong et al., 2010; Chen et al., 2013). Consistent with the osteoporosis phenotype in humans, the gain of Notch signaling in mice affects osteoblastogenesis of endochondral and membranous bones (Hilton et al., 2008; Mead and Yutzey, 2009; Dong et al., 2010). In contrast, interference with the Notch pathway by conditional deletion of *Presenilin 1/2*, encoding proteins required for the NICD release, or the *Notch1/2* receptors in the limb mesenchyme results initially in a delay of the onset of chondrocyte maturation and later in a delay of terminal differentiation leading to an elongated hypertrophic zone (Hilton et al., 2008). Conditional loss of the Notch effector RBPjκ results in a similar phenotype (Kohn et al., 2012). RBPjκ-independent Notch signaling, in contrast, affects the morphology of all growth plate chondrocytes and enhances osteoblast maturation (Kohn et al., 2012). In the articular chondrocytes, Notch signaling may be required for the maintenance of a chondroprogenitor population (Sassi et al., 2011).

Transcription factors

SOX9 and RUNX2 are master transcription factors that determine chondrocyte and osteoblast cell fates, respectively. It is not surprising that genetic defects in chondrocyte or osteoblast cell fate determination cause severe skeletal defects. Haploinsufficiency of SOX9 protein in humans causes campomelic dysplasia (OMIM 114290) with cartilage hypoplasia and a perinatal lethal osteochondrodysplasia (Meyer et al., 1997). Mutations in human *RUNX2* cause CCD (OMIM 119600), an autosomal-dominant condition characterized by hypoplasia/aplasia of clavicles, patent fontanelles, supernumerary teeth, short stature, and other changes in skeletal patterning and growth (Mundlos et al., 1997). The transcription factor OSX/SP7 acts downstream of RUNX2 within the osteoblast lineage (Nakashima et al., 2002; Nishio et al., 2006). Mutations in the human SP7 gene may be associated with osteogenesis imperfecta type XII (OMIM 613849) (Lapunzina et al., 2010).

Genetic studies in mice revealed that SOX9 plays numerous roles in skeletogenesis, from the initial differentiation of mesenchymal cells to chondrocytes to the maintenance of chondrogenic phenotype, survival, and the control of chondrocyte maturation (reviewed in Lefebvre and Dvir-Ginzberg, 2017). Its necessity for chondrocyte differentiation was first demonstrated by chimeric studies showing that *Sox9*-deficient cells are excluded from the cartilage (Bi et al., 1999). SOX9 activates the expression of two related family members, *Sox5* and *Sox6*, and cooperates with them, establishing and maintaining chondrocyte identity (Smits et al., 2001; Akiyama et al., 2002). SOX9 also interacts directly with and blocks the activity of the transcription factor RUNX2 at target promoters (Zhou et al., 2006). *Runx2* is expressed in pre-HCCs, HCCs, and osteoblast precursors and is important for HCC and osteoblast differentiation (Komori et al., 1997; Otto et al., 1997; Inada et al., 1999; Kim et al., 1999). Thus, this interaction maintains chondrocytes in a proliferative state and blocks their differentiation into HCCs and transdifferentiation into osteoblasts (Dy et al., 2012). RUNX2 acts partially redundantly with the related RUNX-family member RUNX3 on HCC maturation (Yoshida et al., 2004). *Mef2c* and *Mef2d*, members of the myocyte enhancer factor 2 family of transcription factors, are also expressed in pre-HCCs/HCCs. In contrast to *Mef2d*-knockout mice, which have no reported skeletal phenotype, *Mef2c*-deficient mice have shorter long bones associated with a delay in chondrocyte hypertrophy and downregulation of *Runx2* expression (Arnold et al., 2007; Kim et al., 2008). A constitutively active form of MEF2C upregulates *Runx2* and promotes chondrocyte hypertrophy, suggesting that MEF2C acts upstream of RUNX2 (Arnold et al., 2007). The activity of both transcription factors, MEF2C and RUNX2, is modulated by the histone deacetylase HDAC4 (see later). RUNX2 activity in HCCs is probably also modulated by interactions with other transcription factors such as *Dlx5/6*, which both physically interact with RUNX2 (Roca et al., 2005; Chin et al., 2007). Two members of the forkhead family of transcription factors, *Foxa2* and *Foxa3*, also play a role in HCCs. Both are expressed in HCCs and the loss of *Foxa2* results in decreased expression of hypertrophic markers, such as *Col10a1* and *Mmp13*, which is aggravated by the additional loss of *Foxa3* (Ionescu et al., 2012). The *SoxC* genes, *Sox4*, *Sox11*, and *Sox12*, are initially expressed in the mesenchymal progenitors of endochondral and intramembranous bone and become restricted to the perichondrium and joint as the chondrocytes differentiate (reviewed in Lefebvre and Bhattaram, 2016). In the progenitors, SOXC proteins are required for cell survival (Bhattaram et al., 2010). Later, during endochondral ossification, they are required for growth plate formation in part by promoting noncanonical WNT5a signaling (Kato et al., 2015). Other transcription factors, such as *Prrx1/Mhox* in combination with *Prrx2*, *Msx2*, and the *AP1* family member *Fra2*, also play roles in endochondral ossification (Martin et al., 1995; Lu et al., 1999; Karreth et al., 2004; Satokata et al., 2000). These can be acting locally restricted as is the case for *Prrx1/2* (Lu et al., 1999). For further information see reviews by Hartmann (2009), Karsenty (2008), and Nishimura et al. (2018).

The hypoxia-inducible transcription factor HIF consists of an α subunit that is regulated by oxygen and a β subunit that is constitutively expressed (Semenza, 2012; Ratcliffe, 2013). In growth plate chondrocytes, which are hypoxic, the subunit protein HIF-1α is stabilized and, on one hand, induces the expression of VEGF in HCCs and, on the other hand, regulates the oxygen consumption of chondrocytes through stimulation of anaerobic metabolism or glycolysis. Both downstream mechanisms are necessary for chondrocyte survival (Maes et al., 2012; Schipani et al., 2001, 2015; Cramer et al., 2004; Zelzer et al., 2004). The delayed differentiation observed in *Hif1a* mutants is probably a consequence of the initial delay in the initiation of chondrogenesis earlier in development (Provot et al., 2007; Amarilio et al., 2007). In contrast, mutation in the related α-subunit-encoding gene *Hif2a* results in only a transient and modest delay in endochondral ossification (Araldi et al., 2011). Yet, HIF2a appears to play a more prominent role postnatally in articular chondrocyte homeostasis (Pi et al., 2015; Yang et al., 2010).

Epigenetic factors and microRNAs

Since 2009, novel regulators of chondrogenesis and osteoblastogenesis have emerged, including epigenetic factors (reviewed in Furumatsu and Ozaki, 2010; Bradley et al., 2015). Among them is the histone deacetylase HDAC4, which plays a prominent role in HCC differentiation (Vega et al., 2004). HDAC4 binds to and inhibits the activity of two transcription factors that promote HCC differentiation, RUNX2 and MEF2C (Vega et al., 2004; Arnold et al., 2007). Histone-acetyl transferases such as P300 are important cofactors for BMP/SMAD1- and TGFβ/SMAD3-dependent signaling (Furumatsu et al., 2005; Pan et al., 2009; Sun et al., 2009). P300 also acts as a cofactor within the WNT/β-catenin pathway (Levy et al., 2004) and interacts with SOX9 (Furumatsu et al., 2005). SOX9 is also acetylated, which reduces its transcriptional activity, and this can be modulated by the NAD-dependent class III protein deacetylase Sirtuin (SIRT1) (Buhrmann et al., 2014; Bar Oz et al., 2016). SIRT1 and the histone methyltransferases SET7/SET9 also interact with P300 on the type II collagen promoter, promoting transcription (Oppenheimer et al., 2014). Conditional mouse mutants for the histone methyltransferase *Eset* have severely shortened limbs, a split sternum, and a widening of the sagittal suture of the skull (Yang et al., 2013a). The growth plates of *Eset* conditional knockout mice are disorganized, and HCC

differentiation appears to be accelerated. ESET interacts with HDAC4 to repress RUNX2 activity, thereby delaying hypertrophic differentiation (Yang et al., 2013a). Overall changes in the chromatin acetylation status in chondrocytes are induced through the interaction of the transcription factor TRPS1 with HDAC1 and HDAC4 (Wuelling et al., 2013).

Conditional deletion of *Dicer*, an enzyme that is required for the biogenesis of microRNAs, in chondrocytes revealed a functional role for microRNAs in chondrocyte proliferation and differentiation (Kobayashi et al., 2008). The latter is associated with a widened hypertrophic zone. Some of the specific microRNAs involved in these phenotypes are let-7 and miR-140 (Miyaki et al., 2010; Nakamura et al., 2011; Papaioannou et al., 2013). The noncoding RNA Dnm3os, a precursor for the microRNAs miR-199a, miR-199a*, and miR-214, is required for normal growth and skeletal development (Watanabe et al., 2008). In vitro, numerous microRNAs are differentially regulated during chondrogenesis and in osteoarthritis (Swingler et al., 2012; Crowe et al., 2016). For additional information on the role of microRNAs in skeletal development and homeostasis see Hong and Reddi (2012), Mirzamohammadi et al. (2014), and Fang et al. (2015).

Another class of RNA molecules with emerging functions in skeletal development are the long noncoding RNAs (lncRNAs). Mutations in the lncRNA *DA125942*, which interacts with PTHrP, result in brachydactyly type E (OMIM 613382) (Maass et al., 2012). The lncRNA *DANCR* promotes the chondrogenic differentiation of human synovial stem cell−like cells and is involved in osteoblastogenesis (reviewed in Huynh et al., 2017).

The functional roles of the vasculature in endochondral bone formation

Cartilage is an avascular and hypoxic tissue, yet, the ossification process and the remodeling of the cartilage template into cancellous bone require blood vessel invasion. Proliferating chondrocytes express numerous antiangiogenic factors, such as Chondromodulin I, Tenomodulin, Tissue-localized inhibitors of MMPs, and others (Maes, 2013). HCCs, in contrast, express VEGF, which is required to attract blood vessels to the perichondrium flanking the hypertrophic zone, as exemplified by mutant mice in which *Vegf* was deleted in cartilage or which lacked specifically the diffusible splice isoforms VEGF120 and VEGF164 (Zelzer et al., 2004; Maes et al., 2004, 2012). *Vegf* expression in HCCs is controlled by RUNX2 and, as mentioned earlier, by HIF1 (Zelzer et al., 2001). The invasion of blood vessels probably play an important role in the formation of the bone marrow cavity during endochondral ossification. Evidence for this is based on blocking VEGF signaling, which affects cartilage resorption, resulting in the elongation of the zone of HCCs (Gerber et al., 1999). Yet, as the monocytes, which are precursors for chondroclasts and osteoclasts, enter the bone marrow cavity via blood vessels, it is difficult to unambiguously distinguish between the functional requirements of the two components for the formation of the bone marrow cavity. Chondroclasts and osteoclasts produce matrix-degrading enzymes. Yet, the mineral dissolution function of osteoclasts is dispensable for the degradation of HCCs during long bone growth (Touaitahuata et al., 2014). Blood vessel endothelial cells also produce and secrete, among others, MMP9/Gelatinase B under proangiogenic conditions and may, therefore, be actively involved in the degradation of the cartilage matrix (Taraboletti et al., 2002). Blood vessels are, furthermore, important for trabecular bone formation during endochondral ossification. As mentioned previously, osteoblast precursors migrate into the forming bone marrow cavity along the blood vessels (Maes et al., 2010). In addition, it has been shown that the bone marrow cavity contains at least two types of blood vessels. In the embryo, an E and an L type can be distinguished, whereof the E type strongly supports osteoblast lineage cells (Langen et al., 2017). In the adult, the H-type vessels are the ones supporting osteoblast maturation (Kusumbe et al., 2014). Blood vessels also play a role as a structural component in trabecular bone formation. In addition to the mineralized cartilage matrix remnants, the vessels serve as structures for osteoid deposition (Ben Shoham et al., 2016).

References

Abzhanov, A., Rodda, S.J., Mcmahon, A.P., Tabin, C.J., 2007. Regulation of skeletogenic differentiation in cranial dermal bone. Development 134, 3133−3144.

Adair, F.L., Scammin, R.E., 1921. A study of the ossification centers of the wrist, knee and ankle at birth, with particular reference to the physical development and maturity of the newborn. Am. J. Obstet. Gynecol. 2, 35−60.

Ahn, K., Mishina, Y., Hanks, M.C., Behringer, R.R., Crenshaw 3rd, E.B., 2001. BMPR-IA signaling is required for the formation of the apical ectodermal ridge and dorsal-ventral patterning of the limb. Development 128, 4449−4461.

Ahrens, M.J., Li, Y., Jiang, H., Dudley, A.T., 2009. Convergent extension movements in growth plate chondrocytes require gpi-anchored cell surface proteins. Development 136, 3463−3474.

AI-Aql, Z.S., Alagl, A.S., Graves, D.T., Gerstenfeld, L.C., Einhorn, T.A., 2008. Molecular mechanisms controlling bone formation during fracture healing and distraction osteogenesis. J. Dent. Res. 87, 107−118.

Akiyama, H., Chaboissier, M.C., Martin, J.F., Schedl, A., De Crombrugghe, B., 2002. The transcription factor Sox9 has essential roles in successive steps of the chondrocyte differentiation pathway and is required for expression of Sox5 and Sox6. Genes Dev. 16, 2813−2828.

Akiyama, H., Kim, J.E., Nakashima, K., Balmes, G., Iwai, N., Deng, J.M., Zhang, Z., Martin, J.F., Behringer, R.R., Nakamura, T., De Crombrugghe, B., 2005. Osteo-chondroprogenitor cells are derived from Sox9 expressing precursors. Proc. Natl. Acad. Sci. U.S.A. 102, 14665−14670.

Akiyama, H., Lyons, J.P., Mori-Akiyama, Y., Yang, X., Zhang, R., Zhang, Z., Deng, J.M., Taketo, M.M., Nakamura, T., Behringer, R.R., Mccrea, P.D., DE Crombrugghe, B., 2004. Interactions between Sox9 and beta-catenin control chondrocyte differentiation. Genes Dev. 18, 1072−1087.

Alvarez, J., Costales, L., Lopez-Muniz, A., Lopez, J.M., 2005. Chondrocytes are released as viable cells during cartilage resorption associated with the formation of intrachondral canals in the rat tibial epiphysis. Cell Tissue Res. 320, 501−507.

Alvarez, J., Sohn, P., Zeng, X., Doetschman, T., Robbins, D.J., Serra, R., 2002. TGFbeta2 mediates the effects of hedgehog on hypertrophic differentiation and PTHrP expression. Development 129, 1913−1924.

Amano, K., Densmore, M., Fan, Y., Lanske, B., 2016. Ihh and PTH1R signaling in limb mesenchyme is required for proper segmentation and subsequent formation and growth of digit bones. Bone 83, 256−266.

Amarilio, R., Viukov, S.V., Sharir, A., Eshkar-Oren, I., Johnson, R.S., Zelzer, E., 2007. HIF1alpha regulation of Sox9 is necessary to maintain differentiation of hypoxic prechondrogenic cells during early skeletogenesis. Development 134, 3917−3928.

Amizuka, N., Henderson, J.E., Hoshi, K., Warshawsky, H., Ozawa, H., Goltzman, D., Karaplis, A.C., 1996. Programmed cell death of chondrocytes and aberrant chondrogenesis in mice homozygous for parathyroid hormone-related peptide gene deletion. Endocrinology 137, 5055−5067.

Anderson, H.C., Garimella, R., Tague, S.E., 2005a. The role of matrix vesicles in growth plate development and biomineralization. Front. Biosci. 10, 822−837.

Anderson, H.C., Harmey, D., Camacho, N.P., Garimella, R., Sipe, J.B., Tague, S., Bi, X., Johnson, K., Terkeltaub, R., Millan, J.L., 2005b. Sustained osteomalacia of long bones despite major improvement in other hypophosphatasia-related mineral deficits in tissue nonspecific alkaline phosphatase/nucleotide pyrophosphatase phosphodiesterase 1 double-deficient mice. Am. J. Pathol. 166, 1711−1720.

Anderson, H.C., Sipe, J.B., Hessle, L., Dhanyamraju, R., Atti, E., Camacho, N.P., Millan, J.L., Dhamyamraju, R., 2004. Impaired calcification around matrix vesicles of growth plate and bone in alkaline phosphatase-deficient mice. Am. J. Pathol. 164, 841−847.

Andre, P., Wang, Q., Wang, N., Gao, B., Schilit, A., Halford, M.M., Stacker, S.A., Zhang, X., Yang, Y., 2012. The Wnt coreceptor Ryk regulates Wnt/planar cell polarity by modulating the degradation of the core planar cell polarity component Vangl2. J. Biol. Chem. 287, 44518−44525.

Annes, J.P., Munger, J.S., Rifkin, D.B., 2003. Making sense of latent TGFbeta activation. J. Cell Sci. 116, 217−224.

Araldi, E., Khatri, R., Giaccia, A.J., Simon, M.C., Schipani, E., 2011. Lack of HIF-2alpha in limb bud mesenchyme causes a modest and transient delay of endochondral bone development. Nat. Med. 17, 25−26 (author reply 27-9).

Archer, C.W., Dowthwaite, G.P., Francis-West, P., 2003. Development of synovial joints. Birth Defects Res. C Embryo Today 69, 144−155.

Arnold, M.A., Kim, Y., Czubryt, M.P., Phan, D., Mcanally, J., Qi, X., Shelton, J.M., Richardson, J.A., Bassel-Duby, R., Olson, E.N., 2007. MEF2C transcription factor controls chondrocyte hypertrophy and bone development. Dev. Cell 12, 377−389.

Aszodi, A., Hunziker, E.B., Brakebusch, C., Fassler, R., 2003. Beta1 integrins regulate chondrocyte rotation, G1 progression, and cytokinesis. Genes Dev. 17, 2465−2479.

Atit, R., Sgaier, S.K., Mohamed, O.A., Taketo, M.M., Dufort, D., Joyner, A.L., Niswander, L., Conlon, R.A., 2006. Beta-catenin activation is necessary and sufficient to specify the dorsal dermal fate in the mouse. Dev. Biol. 296, 164−176.

Aulehla, A., Pourquie, O., 2008. Oscillating signaling pathways during embryonic development. Curr. Opin. Cell Biol. 20, 632−637.

Badve, C.A., K, M.M., Iyer, R.S., Ishak, G.E., Khanna, P.C., 2013. Craniosynostosis: imaging review and primer on computed tomography. Pediatr. Radiol. 43, 728−742 (quiz 725-7).

Baffi, M.O., Slattery, E., Sohn, P., Moses, H.L., Chytil, A., Serra, R., 2004. Conditional deletion of the TGF-beta type II receptor in Col2a expressing cells results in defects in the axial skeleton without alterations in chondrocyte differentiation or embryonic development of long bones. Dev. Biol. 276, 124−142.

Bai, C.B., Auerbach, W., Lee, J.S., Stephen, D., Joyner, A.L., 2002. Gli2, but not Gli1, is required for initial Shh signaling and ectopic activation of the Shh pathway. Development 129, 4753−4761.

Baker, J., Liu, J.P., Robertson, E.J., Efstratiadis, A., 1993. Role of insulin-like growth factors in embryonic and postnatal growth. Cell 75, 73−82.

Baldridge, D., Shchelochkov, O., Kelley, B., Lee, B., 2010. Signaling pathways in human skeletal dysplasias. Annu. Rev. Genom. Hum. Genet. 11, 189−217.

Ballock, R.T., O'keefe, R.J., 2003. The biology of the growth plate. J. Bone Joint Surg. Am. 85-A, 715−726.

Bandyopadhyay, A., Tsuji, K., Cox, K., Harfe, B.D., Rosen, V., Tabin, C.J., 2006. Genetic analysis of the roles of BMP2, BMP4, and BMP7 in limb patterning and skeletogenesis. PLoS Genet. 2, e216.

Bar oz, M., Kumar, A., Elayyan, J., Reich, E., Binyamin, M., Kandel, L., Liebergall, M., Steinmeyer, J., Lefebvre, V., Dvir-Ginzberg, M., 2016. Acetylation reduces SOX9 nuclear entry and ACAN gene transactivation in human chondrocytes. Aging Cell 15, 499−508.

Barna, M., Niswander, L., 2007. Visualization of cartilage formation: insight into cellular properties of skeletal progenitors and chondrodysplasia syndromes. Dev. Cell 12, 931−941.

Barna, M., Pandolfi, P.P., Niswander, L., 2005. Gli3 and Plzf cooperate in proximal limb patterning at early stages of limb development. Nature 436, 277−281.

Baron, R., Kneissel, M., 2013. WNT signaling in bone homeostasis and disease: from human mutations to treatments. Nat. Med. 19, 179−192.

Barrow, J.R., Thomas, K.R., Boussadia-Zahui, O., Moore, R., Kemler, R., Capecchi, M.R., Mcmahon, A.P., 2003. Ectodermal Wnt3/beta-catenin signaling is required for the establishment and maintenance of the apical ectodermal ridge. Genes Dev. 17, 394−409.

Bartels, C.F., Bukulmez, H., Padayatti, P., Rhee, D.K., Van Ravenswaaij-Arts, C., Pauli, R.M., Mundlos, S., Chitayat, D., Shih, L.Y., Al-Gazali, L.I., Kant, S., Cole, T., Morton, J., Cormier-Daire, V., Faivre, L., Lees, M., Kirk, J., Mortier, G.R., Leroy, J., Zabel, B., Kim, C.A., Crow, Y., Braverman, N.E., Van Den Akker, F., Warman, M.L., 2004. Mutations in the transmembrane natriuretic peptide receptor NPR-B impair skeletal growth and cause acromesomelic dysplasia, type Maroteaux. Am. J. Hum. Genet. 75, 27−34.

Bastepe, M., Weinstein, L.S., Ogata, N., Kawaguchi, H., Juppner, H., Kronenberg, H.M., Chung, U.I., 2004. Stimulatory G protein directly regulates hypertrophic differentiation of growth plate cartilage in vivo. Proc. Natl. Acad. Sci. U.S.A. 101, 14794−14799.

Baur, S.T., Mai, J.J., Dymecki, S.M., 2000. Combinatorial signaling through BMP receptor IB and GDF5: shaping of the distal mouse limb and the genetics of distal limb diversity. Development 127, 605−619.

Ben Shoham, A., Rot, C., Stern, T., Krief, S., Akiva, A., Dadosh, T., Sabany, H., Lu, Y., Kadler, K.E., Zelzer, E., 2016. Deposition of collagen type I onto skeletal endothelium reveals a new role for blood vessels in regulating bone morphology. Development 143, 3933−3943.

Benazet, J.D., Pignatti, E., Nugent, A., Unal, E., Laurent, F., Zeller, R., 2012. Smad4 is required to induce digit ray primordia and to initiate the aggregation and differentiation of chondrogenic progenitors in mouse limb buds. Development 139, 4250−4260.

Benazet, J.D., Zeller, R., 2009. Vertebrate limb development: moving from classical morphogen gradients to an integrated 4-dimensional patterning system. Cold Spring Harb. Perspect. Biol. 1 a001339.

Bhat, R., Lerea, K.M., Peng, H., Kaltner, H., Gabius, H.J., Newman, S.A., 2011. A regulatory network of two galectins mediates the earliest steps of avian limb skeletal morphogenesis. BMC Dev. Biol. 11, 6.

Bhattaram, P., Penzo-Mendez, A., Kato, K., Bandyopadhyay, K., Gadi, A., Taketo, M.M., Lefebvre, V., 2014. SOXC proteins amplify canonical WNT signaling to secure nonchondrocytic fates in skeletogenesis. J. Cell Biol. 207, 657−671.

Bhattaram, P., Penzo-Mendez, A., Sock, E., Colmenares, C., Kaneko, K.J., Vassilev, A., Depamphilis, M.L., Wegner, M., Lefebvre, V., 2010. Organogenesis relies on SoxC transcription factors for the survival of neural and mesenchymal progenitors. Nat. Commun. 1, 9.

Bi, W., Deng, J.M., Zhang, Z., Behringer, R.R., De Crombrugghe, B., 1999. Sox9 is required for cartilage formation. Nat. Genet. 22, 85−89.

Blitz, E., Sharir, A., Akiyama, H., Zelzer, E., 2013. Tendon-bone attachment unit is formed modularly by a distinct pool of Scx- and Sox9-positive progenitors. Development 140, 2680−2690.

Blumer, M.J., Longato, S., Fritsch, H., 2008. Structure, formation and role of cartilage canals in the developing bone. Ann. Anat. 190, 305−315.

Bocciardi, R., Giorda, R., Buttgereit, J., Gimelli, S., Divizia, M.T., Beri, S., Garofalo, S., Tavella, S., Lerone, M., Zuffardi, O., Bader, M., Ravazzolo, R., Gimelli, G., 2007. Overexpression of the C-type natriuretic peptide (CNP) is associated with overgrowth and bone anomalies in an individual with balanced t(2;7) translocation. Hum. Mutat. 28, 724−731.

Boskey, A.L., Spevak, L., Paschalis, E., Doty, S.B., Mckee, M.D., 2002. Osteopontin deficiency increases mineral content and mineral crystallinity in mouse bone. Calcif. Tissue Int. 71, 145−154.

Boulet, A.M., Moon, A.M., Arenkiel, B.R., Capecchi, M.R., 2004. The roles of Fgf4 and Fgf8 in limb bud initiation and outgrowth. Dev. Biol. 273, 361−372.

Bradley, E.W., Carpio, L.R., Van Wijnen, A.J., Mcgee-Lawrence, M.E., Westendorf, J.J., 2015. Histone deacetylases in bone development and skeletal disorders. Physiol. Rev. 95, 1359−1381.

Bradley, E.W., Drissi, M.H., 2010. WNT5A regulates chondrocyte differentiation through differential use of the CaN/NFAT and IKK/NF-kappaB pathways. Mol. Endocrinol. 24, 1581−1593.

Bradley, E.W., Drissi, M.H., 2011. Wnt5b regulates mesenchymal cell aggregation and chondrocyte differentiation through the planar cell polarity pathway. J. Cell. Physiol. 226, 1683−1693.

Brent, A.E., Schweitzer, R., Tabin, C.J., 2003. A somitic compartment of tendon progenitors. Cell 113, 235−248.

Brighton, C.T., 1978. Structure and function of the growth plate. Clin. Orthop. Relat. Res. 22−32.

Bronfin, D.R., 2001. Misshapen heads in babies: position or pathology? Ochsner J. 3, 191−199.

Brunet, L.J., Mcmahon, J.A., Mcmahon, A.P., Harland, R.M., 1998. Noggin, cartilage morphogenesis, and joint formation in the mammalian skeleton. Science 280, 1455−1457.

Buhrmann, C., Busch, F., Shayan, P., Shakibaei, M., 2014. Sirtuin-1 (SIRT1) is required for promoting chondrogenic differentiation of mesenchymal stem cells. J. Biol. Chem. 289, 22048−22062.

Burke, A.C., 2000. Hox genes and the global patterning of the somitic mesoderm. Curr. Top. Dev. Biol. 47, 155−181.

Burke, A.C., Nelson, C.E., Morgan, B.A., Tabin, C., 1995. Hox genes and the evolution of vertebrate axial morphology. Development 121, 333−346.

Cairns, D.M., Sato, M.E., Lee, P.G., Lassar, A.B., Zeng, L., 2008. A gradient of Shh establishes mutually repressing somitic cell fates induced by Nkx3.2 and Pax3. Dev. Biol. 323, 152−165.

Candela, M.E., Cantley, L., Yasuaha, R., Iwamoto, M., Pacifici, M., Enomoto-Iwamoto, M., 2014. Distribution of slow-cycling cells in epiphyseal cartilage and requirement of beta-catenin signaling for their maintenance in growth plate. J. Orthop. Res. 32, 661−668.

Chagin, A.S., Kronenberg, H.M., 2014. Role of G-proteins in the differentiation of epiphyseal chondrocytes. J. Mol. Endocrinol. 53, R39−R45.

Charite, J., Mcfadden, D.G., Olson, E.N., 2000. The bHLH transcription factor dHAND controls Sonic hedgehog expression and establishment of the zone of polarizing activity during limb development. Development 127, 2461−2470.

Chellaiah, M.A., Kizer, N., Biswas, R., Alvarez, U., Strauss-Schoenberger, J., Rifas, L., Rittling, S.R., Denhardt, D.T., Hruska, K.A., 2003. Osteopontin deficiency produces osteoclast dysfunction due to reduced CD44 surface expression. Mol. Biol. Cell 14, 173−189.

Chen, H., Lun, Y., Ovchinnikov, D., Kokubo, H., Oberg, K.C., Pepicelli, C.V., Gan, L., Lee, B., Johnson, R.L., 1998. Limb and kidney defects in Lmx1b mutant mice suggest an involvement of LMX1B in human nail patella syndrome. Nat. Genet. 19, 51−55.

Chen, H., Shi, S., Acosta, L., Li, W., Lu, J., Bao, S., Chen, Z., Yang, Z., Schneider, M.D., Chien, K.R., Conway, S.J., Yoder, M.C., Haneline, L.S., Franco, D., Shou, W., 2004. BMP10 is essential for maintaining cardiac growth during murine cardiogenesis. Development 131, 2219−2231.

Chen, J.M., 1952. Studies on the morphogenesis of the mouse sternum. I. Normal embryonic development. J. Anat. 86, 373−386.

Chen, L., Adar, R., Yang, X., Monsonego, E.O., Li, C., Hauschka, P.V., Yayon, A., Deng, C.X., 1999. Gly369Cys mutation in mouse FGFR3 causes achondroplasia by affecting both chondrogenesis and osteogenesis. J. Clin. Invest. 104, 1517−1525.

Chen, M., Zhu, M., Awad, H., Li, T.F., Sheu, T.J., Boyce, B.F., Chen, D., O'keefe, R.J., 2008. Inhibition of beta-catenin signaling causes defects in postnatal cartilage development. J. Cell Sci. 121, 1455–1465.

Chen, S., Tao, J., Bae, Y., Jiang, M.M., Bertin, T., Chen, Y., Yang, T., Lee, B., 2013. Notch gain of function inhibits chondrocyte differentiation via Rbpj-dependent suppression of Sox9. J. Bone Miner. Res. 28, 649–659.

Chiang, C., Litingtung, Y., Lee, E., Young, K.E., Corden, J.L., Westphal, H., Beachy, P.A., 1996. Cyclopia and defective axial patterning in mice lacking Sonic hedgehog gene function. Nature 383, 407–413.

Chin, H.J., Fisher, M.C., Li, Y., Ferrari, D., Wang, C.K., Lichtler, A.C., Dealy, C.N., Kosher, R.A., 2007. Studies on the role of Dlx5 in regulation of chondrocyte differentiation during endochondral ossification in the developing mouse limb. Dev. Growth Differ. 49, 515–521.

Christ, B., Huang, R., Scaal, M., 2004. Formation and differentiation of the avian sclerotome. Anat. Embryol. 208, 333–350.

Christ, B., Huang, R., Scaal, M., 2007. Amniote somite derivatives. Dev. Dynam. 236, 2382–2396.

Chung, U.I., Lanske, B., Lee, K., Li, E., Kronenberg, H., 1998. The parathyroid hormone/parathyroid hormone-related peptide receptor coordinates endochondral bone development by directly controlling chondrocyte differentiation. Proc. Natl. Acad. Sci. U.S.A. 95, 13030–13035.

Chusho, H., Tamura, N., Ogawa, Y., Yasoda, A., Suda, M., Miyazawa, T., Nakamura, K., Nakao, K., Kurihara, T., Komatsu, Y., Itoh, H., Tanaka, K., Saito, Y., Katsuki, M., Nakao, K., 2001. Dwarfism and early death in mice lacking C-type natriuretic peptide. Proc. Natl. Acad. Sci. U.S.A. 98, 4016–4021.

Ciurea, A.V., Toader, C., 2009. Genetics of craniosynostosis: review of the literature. J. Med. Life 2, 5–17.

Cohen Jr., M.M., 2000. Craniofacial disorders caused by mutations in homeobox genes MSX1 and MSX2. J. Craniofac. Genet. Dev. Biol. 20, 19–25.

Colnot, C., De La Fuente, L., Huang, S., Hu, D., Lu, C., St-Jacques, B., Helms, J.A., 2005. Indian hedgehog synchronizes skeletal angiogenesis and perichondrial maturation with cartilage development. Development 132, 1057–1067.

Colnot, C., Lu, C., Hu, D., Helms, J.A., 2004. Distinguishing the contributions of the perichondrium, cartilage, and vascular endothelium to skeletal development. Dev. Biol. 269, 55–69.

Colvin, J.S., Bohne, B.A., Harding, G.W., Mcewen, D.G., Ornitz, D.M., 1996. Skeletal overgrowth and deafness in mice lacking fibroblast growth factor receptor 3. Nat. Genet. 12, 390–397.

Cooper, K.L., Oh, S., Sung, Y., Dasari, R.R., Kirschner, M.W., Tabin, C.J., 2013. Multiple phases of chondrocyte enlargement underlie differences in skeletal proportions. Nature 495, 375–378.

Correa, D., Hesse, E., Seriwatanachai, D., Kiviranta, R., Saito, H., Yamana, K., Neff, L., Atfi, A., Coillard, L., Sitara, D., Maeda, Y., Warming, S., Jenkins, N.A., Copeland, N.G., Horne, W.C., Lanske, B., Baron, R., 2010. Zfp521 is a target gene and key effector of parathyroid hormone-related peptide signaling in growth plate chondrocytes. Dev. Cell 19, 533–546.

Cramer, T., Schipani, E., Johnson, R.S., Swoboda, B., Pfander, D., 2004. Expression of VEGF isoforms by epiphyseal chondrocytes during low-oxygen tension is HIF-1 alpha dependent. Osteoarthritis Cartilage 12, 433–439.

Crowe, N., Swingler, T.E., Le, L.T., Barter, M.J., Wheeler, G., Pais, H., Donell, S.T., Young, D.A., Dalmay, T., Clark, I.M., 2016. Detecting new microRNAs in human osteoarthritic chondrocytes identifies miR-3085 as a human, chondrocyte-selective, microRNA. Osteoarthritis Cartilage 24, 534–543.

Crowe, R., Zikherman, J., Niswander, L., 1999. Delta-1 negatively regulates the transition from prehypertrophic to hypertrophic chondrocytes during cartilage formation. Development 126, 987–998.

Cygan, J.A., Johnson, R.L., Mcmahon, A.P., 1997. Novel regulatory interactions revealed by studies of murine limb pattern in Wnt-7a and En-1 mutants. Development 124, 5021–5032.

Dao, D.Y., Jonason, J.H., Zhang, Y., Hsu, W., Chen, D., Hilton, M.J., O'keefe, R.J., 2012. Cartilage-specific beta-catenin signaling regulates chondrocyte maturation, generation of ossification centers, and perichondrial bone formation during skeletal development. J. Bone Miner. Res. 27, 1680–1694.

Davis, C.A., Holmyard, D.P., Millen, K.J., Joyner, A.L., 1991. Examining pattern formation in mouse, chicken and frog embryos with an En-specific antiserum. Development 111, 287–298.

Day, T.F., Guo, X., Garrett-Beal, L., Yang, Y., 2005. Wnt/beta-catenin signaling in mesenchymal progenitors controls osteoblast and chondrocyte differentiation during vertebrate skeletogenesis. Dev. Cell 8, 739–750.

Dechiara, T.M., Kimble, R.B., Poueymirou, W.T., Rojas, J., Masiakowski, P., Valenzuela, D.M., Yancopoulos, G.D., 2000. Ror2, encoding a receptor-like tyrosine kinase, is required for cartilage and growth plate development. Nat. Genet. 24, 271–274.

Deckelbaum, R.A., Holmes, G., Zhao, Z., Tong, C., Basilico, C., Loomis, C.A., 2012. Regulation of cranial morphogenesis and cell fate at the neural crest-mesoderm boundary by engrailed 1. Development 139, 1346–1358.

Delise, A.M., Fischer, L., Tuan, R.S., 2000. Cellular interactions and signaling in cartilage development. Osteoarthritis Cartilage 8, 309–334.

Delise, A.M., Tuan, R.S., 2002a. Alterations in the spatiotemporal expression pattern and function of N-cadherin inhibit cellular condensation and chondrogenesis of limb mesenchymal cells in vitro. J. Cell. Biochem. 87, 342–359.

Delise, A.M., Tuan, R.S., 2002b. Analysis of N-cadherin function in limb mesenchymal chondrogenesis in vitro. Dev. Dynam. 225, 195–204.

Demurger, F., Ichkou, A., Mougou-Zerelli, S., Le Merrer, M., Goudefroye, G., Delezoide, A.L., Quelin, C., Manouvrier, S., Baujat, G., Fradin, M., Pasquier, L., Megarbane, A., Faivre, L., Baumann, C., Nampoothiri, S., Roume, J., Isidor, B., Lacombe, D., Delrue, M.A., Mercier, S., Philip, N., Schaefer, E., Holder, M., Krause, A., Laffargue, F., Sinico, M., Amram, D., Andre, G., Liquier, A., Rossi, M., Amiel, J., Giuliano, F., Boute, O., Dieux-Coeslier, A., Jacquemont, M.L., Afenjar, A., Van Maldergem, L., Lackmy-Port-Lis, M., Vincent-Delorme, C., Chauvet, M.L., Cormier-Daire, V., Devisme, L., Genevieve, D., Munnich, A., Viot, G., Raoul, O., Romana, S., Gonzales, M., Encha-Razavi, F., Odent, S., Vekemans, M., Attie-Bitach, T., 2015. New insights into genotype-phenotype correlation for GLI3 mutations. Eur. J. Hum. Genet. 23, 92–102.

Deng, C., Wynshaw-Boris, A., Zhou, F., Kuo, A., Leder, P., 1996. Fibroblast growth factor receptor 3 is a negative regulator of bone growth. Cell 84, 911−921.

Docheva, D., Popov, C., Alberton, P., Aszodi, A., 2014. Integrin signaling in skeletal development and function. Birth Defects Res. C Embryo Today 102, 13−36.

Dodig, S., Raos, M., 1999. [Relation between month of birth and the manifestation of atopic diseases in children and adolescents]. Lijec. Vjesn. 121, 333−338.

Dong, Y., Jesse, A.M., Kohn, A., Gunnell, L.M., Honjo, T., Zuscik, M.J., O'keefe, R.J., Hilton, M.J., 2010. RBPjkappa-dependent Notch signaling regulates mesenchymal progenitor cell proliferation and differentiation during skeletal development. Development 137, 1461−1471.

Dong, Y.F., Soung Do, Y., Schwarz, E.M., O'keefe, R.J., Drissi, H., 2006. Wnt induction of chondrocyte hypertrophy through the Runx2 transcription factor. J. Cell. Physiol. 208, 77−86.

Duboc, V., Logan, M.P., 2011. Regulation of limb bud initiation and limb-type morphology. Dev. Dynam. 240, 1017−1027.

Dubrulle, J., Pourquie, O., 2003. Welcome to syndetome: a new somitic compartment. Dev. Cell 4, 611−612.

Duchatelet, S., Ostergaard, E., Cortes, D., Lemainque, A., Julier, C., 2005. Recessive mutations in PTHR1 cause contrasting skeletal dysplasias in Eiken and Blomstrand syndromes. Hum. Mol. Genet. 14, 1−5.

Ducy, P., Zhang, R., Geoffroy, V., Ridall, A.L., Karsenty, G., 1997. Osf2/Cbfa1: a transcriptional activator of osteoblast differentiation. Cell 89, 747−754.

Dy, P., Wang, W., Bhattaram, P., Wang, Q., Wang, L., Ballock, R.T., Lefebvre, V., 2012. Sox9 directs hypertrophic maturation and blocks osteoblast differentiation of growth plate chondrocytes. Dev. Cell 22, 597−609.

Ebensperger, C., Wilting, J., Brand-Saberi, B., Mizutani, Y., Christ, B., Balling, R., Koseki, H., 1995. Pax-1, a regulator of sclerotome development is induced by notochord and floor plate signals in avian embryos. Anat. Embryol. 191, 297−310.

Engsig, M.T., Chen, Q.J., Vu, T.H., Pedersen, A.C., Therkidsen, B., Lund, L.R., Henriksen, K., Lenhard, T., Foged, N.T., Werb, Z., Delaisse, J.M., 2000. Matrix metalloproteinase 9 and vascular endothelial growth factor are essential for osteoclast recruitment into developing long bones. J. Cell Biol. 151, 879−889.

Enishi, T., Yukata, K., Takahashi, M., Sato, R., Sairyo, K., Yasui, N., 2014. Hypertrophic chondrocytes in the rabbit growth plate can proliferate and differentiate into osteogenic cells when capillary invasion is interposed by a membrane filter. PLoS One 9 e104638.

Enomoto-Iwamoto, M., Kitagaki, J., Koyama, E., Tamamura, Y., Wu, C., Kanatani, N., Koike, T., Okada, H., Komori, T., Yoneda, T., Church, V., Francis-West, P.H., Kurisu, K., Nohno, T., Pacifici, M., Iwamoto, M., 2002. The Wnt antagonist Frzb-1 regulates chondrocyte maturation and long bone development during limb skeletogenesis. Dev. Biol. 251, 142−156.

Eshkar-Oren, I., Viukov, S.V., Salameh, S., Krief, S., Oh, C.D., Akiyama, H., Gerber, H.P., Ferrara, N., Zelzer, E., 2009. The forming limb skeleton serves as a signaling center for limb vasculature patterning via regulation of Vegf. Development 136, 1263−1272.

Fallon, J.F., Lopez, A., Ros, M.A., Savage, M.P., Olwin, B.B., Simandl, B.K., 1994. FGF-2: apical ectodermal ridge growth signal for chick limb development. Science 264, 104−107.

Fang, S., Deng, Y., Gu, P., Fan, X., 2015. MicroRNAs regulate bone development and regeneration. Int. J. Mol. Sci. 16, 8227−8253.

Farnum, C.E., 1994. Differential growth rates of long bones. In: Hall, B.K. (Ed.), Bone: Mechanisms of Bone Development and Growth. CRC Press, Boca Raton.

Farnum, C.E., Wilsman, N.J., 1987. Morphologic stages of the terminal hypertrophic chondrocyte of growth plate cartilage. Anat. Rec. 219, 221−232.

Farrow, E., Nicot, R., Wiss, A., Laborde, A., Ferri, J., 2018. Cleidocranial dysplasia: a review of clinical, radiological, genetic implications and a guidelines proposal. J. Craniofac. Surg. 29, 382−389.

Fedde, K.N., Blair, L., Silverstein, J., Coburn, S.P., Ryan, L.M., Weinstein, R.S., Waymire, K., Narisawa, S., Millan, J.L., Macgregor, G.R., Whyte, M.P., 1999. Alkaline phosphatase knock-out mice recapitulate the metabolic and skeletal defects of infantile hypophosphatasia. J. Bone Miner. Res. 14, 2015−2026.

Fenichel, I., Evron, Z., Nevo, Z., 2006. The perichondrial ring as a reservoir for precartilaginous cells. In vivo model in young chicks' epiphysis. Int. Orthop. 30, 353−356.

Fernandez-Teran, M., Piedra, M.E., Kathiriya, I.S., Srivastava, D., Rodriguez-Rey, J.C., Ros, M.A., 2000. Role of dHAND in the anterior-posterior polarization of the limb bud: implications for the Sonic hedgehog pathway. Development 127, 2133−2142.

Fernando, W.A., Leininger, E., Simkin, J., Li, N., Malcom, C.A., Sathyamoorthi, S., Han, M., Muneoka, K., 2011. Wound healing and blastema formation in regenerating digit tips of adult mice. Dev. Biol. 350, 301−310.

Franzen, A., Hultenby, K., Reinholt, F.P., Onnerfjord, P., Heinegard, D., 2008. Altered osteoclast development and function in osteopontin deficient mice. J. Orthop. Res. 26, 721−728.

Furumatsu, T., Ozaki, T., 2010. Epigenetic regulation in chondrogenesis. Acta. Med. Okayama 64, 155−161.

Furumatsu, T., Tsuda, M., Taniguchi, N., Tajima, Y., Asahara, H., 2005. Smad3 induces chondrogenesis through the activation of SOX9 via CREB-binding protein/p300 recruitment. J. Biol. Chem. 280, 8343−8350.

Gao, B., Hu, J., Stricker, S., Cheung, M., Ma, G., Law, K.F., Witte, F., Briscoe, J., Mundlos, S., He, L., Cheah, K.S., Chan, D., 2009. A mutation in Ihh that causes digit abnormalities alters its signalling capacity and range. Nature 458, 1196−1200.

Gao, B., Song, H., Bishop, K., Elliot, G., Garrett, L., English, M.A., Andre, P., Robinson, J., Sood, R., Minami, Y., Economides, A.N., Yang, Y., 2011. Wnt signaling gradients establish planar cell polarity by inducing Vangl2 phosphorylation through Ror2. Dev. Cell 20, 163−176.

Gardner, C.A., Barald, K.F., 1992. Expression patterns of engrailed-like proteins in the chick embryo. Dev. Dynam. 193, 370−388.

Gat-Yablonski, G., Shtaif, B., Abraham, E., Phillip, M., 2008. Nutrition-induced catch-up growth at the growth plate. J. Pediatr. Endocrinol. Metab. 21, 879–893.

Gerber, H.P., Vu, T.H., Ryan, A.M., Kowalski, J., Werb, Z., Ferrara, N., 1999. VEGF couples hypertrophic cartilage remodeling, ossification and angiogenesis during endochondral bone formation. Nat. Med. 5, 623–628.

Giustina, A., Mazziotti, G., Canalis, E., 2008. Growth hormone, insulin-like growth factors, and the skeleton. Endocr. Rev. 29, 535–559.

Golovchenko, S., Hattori, T., Hartmann, C., Gebhardt, M., Gebhard, S., Hess, A., Pausch, F., Schlund, B., Von Der Mark, K., 2013. Deletion of beta catenin in hypertrophic growth plate chondrocytes impairs trabecular bone formation. Bone 55, 102–112.

Gong, Y., Slee, R.B., Fukai, N., Rawadi, G., Roman-Roman, S., Reginato, A.M., Wang, H., Cundy, T., Glorieux, F.H., Lev, D., Zacharin, M., Oexle, K., Marcelino, J., Suwairi, W., Heeger, S., Sabatakos, G., Apte, S., Adkins, W.N., Allgrove, J., Arslan-Kirchner, M., Batch, J.A., Beighton, P., Black, G.C., Boles, R.G., Boon, L.M., Borrone, C., Brunner, H.G., Carle, G.F., Dallapiccola, B., De Paepe, A., Floege, B., Halfhide, M.L., Hall, B., Hennekam, R.C., Hirose, T., Jans, A., Juppner, H., Kim, C.A., Keppler-Noreuil, K., Kohlschuetter, A., Lacombe, D., Lambert, M., Lemyre, E., Letteboer, T., Peltonen, L., Ramesar, R.S., Romanengo, M., Somer, H., Steichen-Gersdorf, E., Steinmann, B., Sullivan, B., Superti-Furga, A., Swoboda, W., Van Den Boogaard, M.J., Van Hul, W., Vikkula, M., Votruba, M., Zabel, B., Garcia, T., Baron, R., Olsen, B.R., Warman, M.L., Osteoporosis-Pseudoglioma Syndrome Collaborative, G., 2001. LDL receptor-related protein 5 (LRP5) affects bone accrual and eye development. Cell 107, 513–523.

Goodrich, E.S., 1930. Studies on the Structure and Development of Vertebrates. Macmillan, London.

Goumans, M.J., Valdimarsdottir, G., Itoh, S., Rosendahl, A., Sideras, P., TEN Dijke, P., 2002. Balancing the activation state of the endothelium via two distinct TGF-beta type I receptors. EMBO J. 21, 1743–1753.

Grumolato, L., Liu, G., Mong, P., Mudbhary, R., Biswas, R., Arroyave, R., Vijayakumar, S., Economides, A.N., Aaronson, S.A., 2010. Canonical and noncanonical Wnts use a common mechanism to activate completely unrelated coreceptors. Genes Dev. 24, 2517–2530.

Guo, J., Chung, U.I., Kondo, H., Bringhurst, F.R., Kronenberg, H.M., 2002. The PTH/PTHrP receptor can delay chondrocyte hypertrophy in vivo without activating phospholipase C. Dev. Cell 3, 183–194.

Guo, J., Chung, U.I., Yang, D., Karsenty, G., Bringhurst, F.R., Kronenberg, H.M., 2006. PTH/PTHrP receptor delays chondrocyte hypertrophy via both Runx2-dependent and -independent pathways. Dev. Biol. 292, 116–128.

Guo, X., Day, T.F., Jiang, X., Garrett-Beal, L., Topol, L., Yang, Y., 2004. Wnt/beta-catenin signaling is sufficient and necessary for synovial joint formation. Genes Dev. 18, 2404–2417.

Hall, B.K., Miyake, T., 1992. The membranous skeleton: the role of cell condensations in vertebrate skeletogenesis. Anat. Embryol. 186, 107–124.

Hall, B.K., Miyake, T., 1995. Divide, accumulate, differentiate: cell condensation in skeletal development revisited. Int. J. Dev. Biol. 39, 881–893.

Hall, B.K., Miyake, T., 2000. All for one and one for all: condensations and the initiation of skeletal development. Bioessays 22, 138–147.

Hall, K.C., Hill, D., Otero, M., Plumb, D.A., Froemel, D., Dragomir, C.L., Maretzky, T., Boskey, A., Crawford, H.C., Selleri, L., Goldring, M.B., Blobel, C.P., 2013. ADAM17 controls endochondral ossification by regulating terminal differentiation of chondrocytes. Mol. Cell Biol. 33, 3077–3090.

Hallmann, R., Feinberg, R.N., Latker, C.H., Sasse, J., Risau, W., 1987. Regression of blood vessels precedes cartilage differentiation during chick limb development. Differentiation 34, 98–105.

Hamburger, V., Hamilton, H.L., 1992. A series of normal stages in the development of the chick embryo. 1951. Dev. Dynam. 195, 231–272.

Hankinson, T.C., Fontana, E.J., Anderson, R.C., Feldstein, N.A., 2010. Surgical treatment of single-suture craniosynostosis: an argument for quantitative methods to evaluate cosmetic outcomes. J. Neurosurg. Pediatr. 6, 193–197.

Harmey, D., Hessle, L., Narisawa, S., Johnson, K.A., Terkeltaub, R., Millan, J.L., 2004. Concerted regulation of inorganic pyrophosphate and osteopontin by akp2, enpp1, and ank: an integrated model of the pathogenesis of mineralization disorders. Am. J. Pathol. 164, 1199–1209.

Hartmann, C., 2009. Transcriptional networks controlling skeletal development. Curr. Opin. Genet. Dev. 19, 437–443.

Hartmann, C., Tabin, C.J., 2000. Dual roles of Wnt signaling during chondrogenesis in the chicken limb. Development 127, 3141–3159.

Hartmann, C., Tabin, C.J., 2001. Wnt-14 plays a pivotal role in inducing synovial joint formation in the developing appendicular skeleton. Cell 104, 341–351.

Henriksen, K., Karsdal, M., Delaisse, J.M., Engsig, M.T., 2003. RANKL and vascular endothelial growth factor (VEGF) induce osteoclast chemotaxis through an ERK1/2-dependent mechanism. J. Biol. Chem. 278, 48745–48753.

Hessle, L., Johnson, K.A., Anderson, H.C., Narisawa, S., Sali, A., Goding, J.W., Terkeltaub, R., Millan, J.L., 2002. Tissue-nonspecific alkaline phosphatase and plasma cell membrane glycoprotein-1 are central antagonistic regulators of bone mineralization. Proc. Natl. Acad. Sci. U.S.A. 99, 9445–9449.

Hildebrand, A., Romaris, M., Rasmussen, L.M., Heinegard, D., Twardzik, D.R., Border, W.A., Ruoslahti, E., 1994. Interaction of the small interstitial proteoglycans biglycan, decorin and fibromodulin with transforming growth factor beta. Biochem. J. 302 (Pt 2), 527–534.

Hill, T.P., Spater, D., Taketo, M.M., Birchmeier, W., Hartmann, C., 2005. Canonical Wnt/beta-catenin signaling prevents osteoblasts from differentiating into chondrocytes. Dev. Cell 8, 727–738.

Hilton, M.J., Tu, X., Cook, J., Hu, H., Long, F., 2005. Ihh controls cartilage development by antagonizing Gli3, but requires additional effectors to regulate osteoblast and vascular development. Development 132, 4339–4351.

Hilton, M.J., Tu, X., Wu, X., Bai, S., Zhao, H., Kobayashi, T., Kronenberg, H.M., Teitelbaum, S.L., Ross, F.P., Kopan, R., Long, F., 2008. Notch signaling maintains bone marrow mesenchymal progenitors by suppressing osteoblast differentiation. Nat. Med. 14, 306–314.

Hinchliffe, J.R., 1994. Evolutionary developmental biology of the tetrapod limb. Dev. Suppl. 163–168.

Hinchliffe, J.R., Johnson, D.R., 1980. The Development of the Vertebrate Limb. Clarendon Press, Oxford.

Hirsinger, E., Duprez, D., Jouve, C., Malapert, P., Cooke, J., Pourquie, O., 1997. Noggin acts downstream of Wnt and Sonic Hedgehog to antagonize BMP4 in avian somite patterning. Development 124, 4605−4614.

Hiscock, T.W., Tschopp, P., Tabin, C.J., 2017. On the formation of digits and joints during limb development. Dev. Cell 41, 459−465.

Hong, E., Reddi, A.H., 2012. MicroRNAs in chondrogenesis, articular cartilage, and osteoarthritis: implications for tissue engineering. Tissue Eng. B Rev. 18, 445−453.

Houben, A., Kostanova-Poliakova, D., Weissenbock, M., Graf, J., Teufel, S., Von Der Mark, K., Hartmann, C., 2016. beta-catenin activity in late hypertrophic chondrocytes locally orchestrates osteoblastogenesis and osteoclastogenesis. Development 143, 3826−3838.

Hsu, Y.H., Kiel, D.P., 2012. Clinical review: genome-wide association studies of skeletal phenotypes: what we have learned and where we are headed. J. Clin. Endocrinol. Metab. 97, E1958−E1977.

Hu, D.P., Ferro, F., Yang, F., Taylor, A.J., Chang, W., Miclau, T., Marcucio, R.S., Bahney, C.S., 2017. Cartilage to bone transformation during fracture healing is coordinated by the invading vasculature and induction of the core pluripotency genes. Development 144, 221−234.

Hu, H., Hilton, M.J., Tu, X., Yu, K., Ornitz, D.M., Long, F., 2005. Sequential roles of Hedgehog and Wnt signaling in osteoblast development. Development 132, 49−60.

Huang, W., Zhou, X., Lefebvre, V., De Crombrugghe, B., 2000. Phosphorylation of SOX9 by cyclic AMP-dependent protein kinase A enhances SOX9's ability to transactivate a Col2a1 chondrocyte-specific enhancer. Mol. Cell Biol. 20, 4149−4158.

Hubaud, A., Pourquie, O., 2014. Signalling dynamics in vertebrate segmentation. Nat. Rev. Mol. Cell Biol. 15, 709−721.

Hui, C.C., Joyner, A.L., 1993. A mouse model of greig cephalopolysyndactyly syndrome: the extra-toesJ mutation contains an intragenic deletion of the Gli3 gene. Nat. Genet. 3, 241−246.

Hung, I.H., Schoenwolf, G.C., Lewandoski, M., Ornitz, D.M., 2016. A combined series of Fgf9 and Fgf18 mutant alleles identifies unique and redundant roles in skeletal development. Dev. Biol. 411, 72−84.

Hung, I.H., Yu, K., Lavine, K.J., Ornitz, D.M., 2007. FGF9 regulates early hypertrophic chondrocyte differentiation and skeletal vascularization in the developing stylopod. Dev. Biol. 307, 300−313.

Hunziker, E.B., Schenk, R.K., Cruz-Orive, L.M., 1987. Quantitation of chondrocyte performance in growth-plate cartilage during longitudinal bone growth. J. Bone Joint Surg. Am. 69, 162−173.

Huynh, N.P., Anderson, B.A., Guilak, F., Mcalinden, A., 2017. Emerging roles for long noncoding RNAs in skeletal biology and disease. Connect. Tissue Res. 58, 116−141.

Hyde, G., Dover, S., Aszodi, A., Wallis, G.A., Boot-Handford, R.P., 2007. Lineage tracing using matrilin-1 gene expression reveals that articular chondrocytes exist as the joint interzone forms. Dev. Biol. 304, 825−833.

Inada, M., Wang, Y., Byrne, M.H., Rahman, M.U., Miyaura, C., Lopez-Otin, C., Krane, S.M., 2004. Critical roles for collagenase-3 (Mmp13) in development of growth plate cartilage and in endochondral ossification. Proc. Natl. Acad. Sci. U.S.A. 101, 17192−17197.

Inada, M., Yasui, T., Nomura, S., Miyake, S., Deguchi, K., Himeno, M., Sato, M., Yamagiwa, H., Kimura, T., Yasui, N., Ochi, T., Endo, N., Kitamura, Y., Kishimoto, T., Komori, T., 1999. Maturational disturbance of chondrocytes in Cbfa1-deficient mice. Dev. Dynam. 214, 279−290.

Ionescu, A., Kozhemyakina, E., Nicolae, C., Kaestner, K.H., Olsen, B.R., Lassar, A.B., 2012. FoxA family members are crucial regulators of the hypertrophic chondrocyte differentiation program. Dev. Cell 22, 927−939.

Ionescu, A.M., Schwarz, E.M., Vinson, C., Puzas, J.E., Rosier, R., Reynolds, P.R., O'keefe, R.J., 2001. PTHrP modulates chondrocyte differentiation through AP-1 and CREB signaling. J. Biol. Chem. 276, 11639−11647.

Ishii, M., Sun, J., Ting, M.C., Maxson, R.E., 2015. The development of the calvarial bones and sutures and the pathophysiology of craniosynostosis. Curr. Top. Dev. Biol. 115, 131−156.

Isidor, B., Lindenbaum, P., Pichon, O., Bezieau, S., Dina, C., Jacquemont, S., Martin-Coignard, D., Thauvin-Robinet, C., Le Merrer, M., Mandel, J.L., David, A., Faivre, L., Cormier-Daire, V., Redon, R., Le Caignec, C., 2011. Truncating mutations in the last exon of NOTCH2 cause a rare skeletal disorder with osteoporosis. Nat. Genet. 43, 306−308.

Ivaska, J., Heino, J., 2011. Cooperation between integrins and growth factor receptors in signaling and endocytosis. Annu. Rev. Cell Dev. Biol. 27, 291−320.

Iwata, J., Hacia, J.G., Suzuki, A., Sanchez-Lara, P.A., Urata, M., Chai, Y., 2012. Modulation of noncanonical TGF-beta signaling prevents cleft palate in Tgfbr2 mutant mice. J. Clin. Invest. 122, 873−885.

Jaubert, J., Jaubert, F., Martin, N., Washburn, L.L., Lee, B.K., Eicher, E.M., Guenet, J.L., 1999. Three new allelic mouse mutations that cause skeletal overgrowth involve the natriuretic peptide receptor C gene (Npr3). Proc. Natl. Acad. Sci. U.S.A. 96, 10278−10283.

Jena, N., Martin-Seisdedos, C., Mccue, P., Croce, C.M., 1997. BMP7 null mutation in mice: developmental defects in skeleton, kidney, and eye. Exp. Cell Res. 230, 28−37.

Jeong, J., Mao, J., Tenzen, T., Kottmann, A.H., Mcmahon, A.P., 2004. Hedgehog signaling in the neural crest cells regulates the patterning and growth of facial primordia. Genes Dev. 18, 937−951.

Jho, E.H., Zhang, T., Domon, C., Joo, C.K., Freund, J.N., Costantini, F., 2002. Wnt/beta-catenin/Tcf signaling induces the transcription of Axin2, a negative regulator of the signaling pathway. Mol. Cell Biol. 22, 1172−1183.

Jiang, X., Iseki, S., Maxson, R.E., Sucov, H.M., Morriss-Kay, G.M., 2002. Tissue origins and interactions in the mammalian skull vault. Dev. Biol. 241, 106−116.

Jin, S.W., Sim, K.B., Kim, S.D., 2016. Development and growth of the normal cranial vault : an embryologic review. J. Korean Neurosurg. Soc. 59, 192−196.

Jing, J., Ren, Y., Zong, Z., Liu, C., Kamiya, N., Mishina, Y., Liu, Y., Zhou, X., Feng, J.Q., 2013. BMP receptor 1A determines the cell fate of the postnatal growth plate. Int. J. Biol. Sci. 9, 895–906.

Jobert, A.S., Zhang, P., Couvineau, A., Bonaventure, J., Roume, J., LE Merrer, M., Silve, C., 1998. Absence of functional receptors for parathyroid hormone and parathyroid hormone-related peptide in Blomstrand chondrodysplasia. J. Clin. Invest. 102, 34–40.

Joeng, K.S., Schumacher, C.A., Zylstra-Diegel, C.R., Long, F., Williams, B.O., 2011. Lrp5 and Lrp6 redundantly control skeletal development in the mouse embryo. Dev. Biol. 359, 222–229.

Johnson, D.R., 1986. The cartilaginous skeleton. In: The Genetics of the Skeleton. Oxford University Press, New York.

Kan, A., Tabin, C.J., 2013. c-Jun is required for the specification of joint cell fates. Genes Dev. 27, 514–524.

Kanai, Y., Yasoda, A., Mori, K.P., Watanabe-Takano, H., Nagai-Okatani, C., Yamashita, Y., Hirota, K., Ueda, Y., Yamauchi, I., Kondo, E., Yamanaka, S., Sakane, Y., Nakao, K., Fujii, T., Yokoi, H., Minamino, N., Mukoyama, M., Mochizuki, N., Inagaki, N., 2017. Circulating osteocrin stimulates bone growth by limiting C-type natriuretic peptide clearance. J. Clin. Invest. 127, 4136–4147.

Karamboulas, K., Dranse, H.J., Underhill, T.M., 2010. Regulation of BMP-dependent chondrogenesis in early limb mesenchyme by TGFbeta signals. J. Cell Sci. 123, 2068–2076.

Karaplis, A.C., He, B., Nguyen, M.T., Young, I.D., Semeraro, D., Ozawa, H., Amizuka, N., 1998. Inactivating mutation in the human parathyroid hormone receptor type 1 gene in Blomstrand chondrodysplasia. Endocrinology 139, 5255–5258.

Karaplis, A.C., Luz, A., Glowacki, J., Bronson, R.T., Tybulewicz, V.L., Kronenberg, H.M., Mulligan, R.C., 1994. Lethal skeletal dysplasia from targeted disruption of the parathyroid hormone-related peptide gene. Genes Dev. 8, 277–289.

Karp, S.J., Schipani, E., St-Jacques, B., Hunzelman, J., Kronenberg, H., Mcmahon, A.P., 2000. Indian hedgehog coordinates endochondral bone growth and morphogenesis via parathyroid hormone related-protein-dependent and -independent pathways. Development 127, 543–548.

Karreth, F., Hoebertz, A., Scheuch, H., Eferl, R., Wagner, E.F., 2004. The AP1 transcription factor Fra2 is required for efficient cartilage development. Development 131, 5717–5725.

Karsenty, G., 2001. Minireview: transcriptional control of osteoblast differentiation. Endocrinology 142, 2731–2733.

Karsenty, G., 2008. Transcriptional control of skeletogenesis. Annu. Rev. Genom. Hum. Genet. 9, 183–196.

Kato, K., Bhattaram, P., Penzo-Mendez, A., Gadi, A., Lefebvre, V., 2015. SOXC transcription factors induce cartilage growth plate formation in mouse embryos by promoting noncanonical WNT signaling. J. Bone Miner. Res. 30, 1560–1571.

Kawai, M., Rosen, C.J., 2012. The insulin-like growth factor system in bone: basic and clinical implications. Endocrinol Metab. Clin. North Am. 41, 323–333 (vi).

Kawakami, Y., Capdevila, J., Buscher, D., Itoh, T., Rodriguez Esteban, C., Izpisua Belmonte, J.C., 2001. WNT signals control FGF-dependent limb initiation and AER induction in the chick embryo. Cell 104, 891–900.

Keller, B., Yang, T., Chen, Y., Munivez, E., Bertin, T., Zabel, B., Lee, B., 2011. Interaction of TGFbeta and BMP signaling pathways during chondrogenesis. PLoS One 6 e16421.

Kengaku, M., Capdevila, J., Rodriguez-Esteban, C., De La Pena, J., Johnson, R.L., Izpisua Belmonte, J.C., Tabin, C.J., 1998. Distinct WNT pathways regulating AER formation and dorsoventral polarity in the chick limb bud. Science 280, 1274–1277.

Keupp, K., Beleggia, F., Kayserili, H., Barnes, A.M., Steiner, M., Semler, O., Fischer, B., Yigit, G., Janda, C.Y., Becker, J., Breer, S., Altunoglu, U., Grunhagen, J., Krawitz, P., Hecht, J., Schinke, T., Makareeva, E., Lausch, E., Cankaya, T., Caparros-Martin, J.A., Lapunzina, P., Temtamy, S., Aglan, M., Zabel, B., Eysel, P., Koerber, F., Leikin, S., Garcia, K.C., Netzer, C., Schonau, E., Ruiz-Perez, V.L., Mundlos, S., Amling, M., Kornak, U., Marini, J., Wollnik, B., 2013. Mutations in WNT1 cause different forms of bone fragility. Am. J. Hum. Genet. 92, 565–574.

Khokha, M.K., Hsu, D., Brunet, L.J., Dionne, M.S., Harland, R.M., 2003. Gremlin is the BMP antagonist required for maintenance of Shh and Fgf signals during limb patterning. Nat. Genet. 34, 303–307.

Kim, I.S., Otto, F., Zabel, B., Mundlos, S., 1999. Regulation of chondrocyte differentiation by Cbfa1. Mech. Dev. 80, 159–170.

Kim, S.Y., Paylor, S.W., Magnuson, T., Schumacher, A., 2006. Juxtaposed Polycomb complexes co-regulate vertebral identity. Development 133, 4957–4968.

Kim, Y., Phan, D., Van Rooij, E., Wang, D.Z., Mcanally, J., Qi, X., Richardson, J.A., Hill, J.A., Bassel-Duby, R., Olson, E.N., 2008. The MEF2D transcription factor mediates stress-dependent cardiac remodeling in mice. J. Clin. Invest. 118, 124–132.

Kingsley, D.M., Bland, A.E., Grubber, J.M., Marker, P.C., Russell, L.B., Copeland, N.G., Jenkins, N.A., 1992. The mouse short ear skeletal morphogenesis locus is associated with defects in a bone morphogenetic member of the TGF beta superfamily. Cell 71, 399–410.

Kishimoto, K., Kitazawa, R., Kurosaka, M., Maeda, S., Kitazawa, S., 2006. Expression profile of genes related to osteoclastogenesis in mouse growth plate and articular cartilage. Histochem. Cell Biol. 125, 593–602.

Klopocki, E., Lohan, S., Brancati, F., Koll, R., Brehm, A., Seemann, P., Dathe, K., Stricker, S., Hecht, J., Bosse, K., Betz, R.C., Garaci, F.G., Dallapiccola, B., Jain, M., Muenke, M., Ng, V.C., Chan, W., Chan, D., Mundlos, S., 2011. Copy-number variations involving the IHH locus are associated with syndactyly and craniosynostosis. Am. J. Hum. Genet. 88, 70–75.

Kobayashi, T., Lu, J., Cobb, B.S., Rodda, S.J., Mcmahon, A.P., Schipani, E., Merkenschlager, M., Kronenberg, H.M., 2008. Dicer-dependent pathways regulate chondrocyte proliferation and differentiation. Proc. Natl. Acad. Sci. U.S.A. 105, 1949–1954.

Kobayashi, T., Soegiarto, D.W., Yang, Y., Lanske, B., Schipani, E., Mcmahon, A.P., Kronenberg, H.M., 2005. Indian hedgehog stimulates periarticular chondrocyte differentiation to regulate growth plate length independently of PTHrP. J. Clin. Invest. 115, 1734–1742.

Kohn, A., Dong, Y., Mirando, A.J., Jesse, A.M., Honjo, T., Zuscik, M.J., O'keefe, R.J., Hilton, M.J., 2012. Cartilage-specific RBPjkappa-dependent and -independent Notch signals regulate cartilage and bone development. Development 139, 1198–1212.

Komori, T., Yagi, H., Nomura, S., Yamaguchi, A., Sasaki, K., Deguchi, K., Shimizu, Y., Bronson, R.T., Gao, Y.H., Inada, M., Sato, M., Okamoto, R., Kitamura, Y., Yoshiki, S., Kishimoto, T., 1997. Targeted disruption of Cbfa1 results in a complete lack of bone formation owing to maturational arrest of osteoblasts. Cell 89, 755–764.

Kos, L., Chiang, C., Mahon, K.A., 1998. Mediolateral patterning of somites: multiple axial signals, including Sonic hedgehog, regulate Nkx-3.1 expression. Mech. Dev. 70, 25–34.

Kozhemyakina, E., Cohen, T., Yao, T.P., Lassar, A.B., 2009. Parathyroid hormone-related peptide represses chondrocyte hypertrophy through a protein phosphatase 2A/histone deacetylase 4/MEF2 pathway. Mol. Cell Biol. 29, 5751–5762.

Koziel, L., Wuelling, M., Schneider, S., Vortkamp, A., 2005. Gli3 acts as a repressor downstream of Ihh in regulating two distinct steps of chondrocyte differentiation. Development 132, 5249–5260.

Kraus, P., Lufkin, T., 2006. Dlx homeobox gene control of mammalian limb and craniofacial development. Am. J. Med. Genet. 140, 1366–1374.

Krumlauf, R., 1992. Evolution of the vertebrate Hox homeobox genes. Bioessays 14, 245–252.

Kusumbe, A.P., Ramasamy, S.K., Adams, R.H., 2014. Coupling of angiogenesis and osteogenesis by a specific vessel subtype in bone. Nature 507, 323–328.

Laine, C.M., Joeng, K.S., Campeau, P.M., Kiviranta, R., Tarkkonen, K., Grover, M., Lu, J.T., Pekkinen, M., Wessman, M., Heino, T.J., Nieminen-Pihala, V., Aronen, M., Laine, T., Kroger, H., Cole, W.G., Lehesjoki, A.E., Nevarez, L., Krakow, D., Curry, C.J., Cohn, D.H., Gibbs, R.A., Lee, B.H., Makitie, O., 2013. WNT1 mutations in early-onset osteoporosis and osteogenesis imperfecta. N. Engl. J. Med. 368, 1809–1816.

Langen, U.H., Pitulescu, M.E., Kim, J.M., Enriquez-Gasca, R., Sivaraj, K.K., Kusumbe, A.P., Singh, A., DI Russo, J., Bixel, M.G., Zhou, B., Sorokin, L., Vaquerizas, J.M., Adams, R.H., 2017. Cell-matrix signals specify bone endothelial cells during developmental osteogenesis. Nat. Cell Biol. 19, 189–201.

Langenskiold, A., 1998. Role of the ossification groove of Ranvier in normal and pathologic bone growth: a review. J. Pediatr. Orthop. 18, 173–177.

Lanske, B., Divieti, P., Kovacs, C.S., Pirro, A., Landis, W.J., Krane, S.M., Bringhurst, F.R., Kronenberg, H.M., 1998. The parathyroid hormone (PTH)/PTH-related peptide receptor mediates actions of both ligands in murine bone. Endocrinology 139, 5194–5204.

Lanske, B., Karaplis, A.C., Lee, K., Luz, A., Vortkamp, A., Pirro, A., Karperien, M., Defize, L.H., Ho, C., Mulligan, R.C., Abou-Samra, A.B., Juppner, H., Segre, G.V., Kronenberg, H.M., 1996. PTH/PTHrP receptor in early development and Indian hedgehog-regulated bone growth. Science 273, 663–666.

Lapunzina, P., Aglan, M., Temtamy, S., Caparros-Martin, J.A., Valencia, M., Leton, R., Martinez-Glez, V., Elhossini, R., Amr, K., Vilaboa, N., Ruiz-Perez, V.L., 2010. Identification of a frameshift mutation in Osterix in a patient with recessive osteogenesis imperfecta. Am. J. Hum. Genet. 87, 110–114.

Lara-Castillo, N., Johnson, M.L., 2015. LRP receptor family member associated bone disease. Rev. Endocr. Metab. Disord. 16, 141–148.

Lattanzi, W., Bukvic, N., Barba, M., Tamburrini, G., Bernardini, C., Michetti, F., Di Rocco, C., 2012. Genetic basis of single-suture synostoses: genes, chromosomes and clinical implications. Childs Nerv. Syst. 28, 1301–1310.

Laufer, E., Nelson, C.E., Johnson, R.L., Morgan, B.A., Tabin, C., 1994. Sonic hedgehog and Fgf-4 act through a signaling cascade and feedback loop to integrate growth and patterning of the developing limb bud. Cell 79, 993–1003.

Lee, B., Thirunavukkarasu, K., Zhou, L., Pastore, L., Baldini, A., Hecht, J., Geoffroy, V., Ducy, P., Karsenty, G., 1997. Missense mutations abolishing DNA binding of the osteoblast-specific transcription factor OSF2/CBFA1 in cleidocranial dysplasia. Nat. Genet. 16, 307–310.

Lee, K., Lanske, B., Karaplis, A.C., Deeds, J.D., Kohno, H., Nissenson, R.A., Kronenberg, H.M., Segre, G.V., 1996. Parathyroid hormone-related peptide delays terminal differentiation of chondrocytes during endochondral bone development. Endocrinology 137, 5109–5118.

Lefebvre, V., Bhattaram, P., 2016. SOXC genes and the control of skeletogenesis. Curr. Osteoporos. Rep. 14, 32–38.

Lefebvre, V., Dvir-Ginzberg, M., 2017. SOX9 and the many facets of its regulation in the chondrocyte lineage. Connect. Tissue Res. 58, 2–14.

Lehmann, K., Seemann, P., Stricker, S., Sammar, M., Meyer, B., Suring, K., Majewski, F., Tinschert, S., Grzeschik, K.H., Muller, D., Knaus, P., Nurnberg, P., Mundlos, S., 2003. Mutations in bone morphogenetic protein receptor 1B cause brachydactyly type A2. Proc. Natl. Acad. Sci. U.S.A. 100, 12277–12282.

Lenton, K., James, A.W., Manu, A., Brugmann, S.A., Birker, D., Nelson, E.R., Leucht, P., Helms, J.A., Longaker, M.T., 2011. Indian hedgehog positively regulates calvarial ossification and modulates bone morphogenetic protein signaling. Genesis 49, 784–796.

Leung, J.Y., Kolligs, F.T., Wu, R., Zhai, Y., Kuick, R., Hanash, S., Cho, K.R., Fearon, E.R., 2002. Activation of AXIN2 expression by beta-catenin-T cell factor. A feedback repressor pathway regulating Wnt signaling. J. Biol. Chem. 277, 21657–21665.

Levet, S., Ciais, D., Merdzhanova, G., Mallet, C., Zimmers, T.A., Lee, S.J., Navarro, F.P., Texier, I., Feige, J.J., Bailly, S., Vittet, D., 2013. Bone morphogenetic protein 9 (BMP9) controls lymphatic vessel maturation and valve formation. Blood 122, 598–607.

Levi, B., Wan, D.C., Wong, V.W., Nelson, E., Hyun, J., Longaker, M.T., 2012. Cranial suture biology: from pathways to patient care. J. Craniofac. Surg. 23, 13–19.

Levy, L., Wei, Y., Labalette, C., Wu, Y., Renard, C.A., Buendia, M.A., Neuveut, C., 2004. Acetylation of beta-catenin by p300 regulates beta-catenin-Tcf4 interaction. Mol. Cell Biol. 24, 3404–3414.

Li, C., Chen, L., Iwata, T., Kitagawa, M., Fu, X.Y., Deng, C.X., 1999. A Lys644Glu substitution in fibroblast growth factor receptor 3 (FGFR3) causes dwarfism in mice by activation of STATs and ink4 cell cycle inhibitors. Hum. Mol. Genet. 8, 35–44.

Li, Y., Dudley, A.T., 2009. Noncanonical frizzled signaling regulates cell polarity of growth plate chondrocytes. Development 136, 1083–1092.

Lian, J.B., Stein, G.S., 2003. Runx2/Cbfa1: a multifunctional regulator of bone formation. Curr. Pharmaceut. Des. 9, 2677–2685.

Lim, J., Tu, X., Choi, K., Akiyama, H., Mishina, Y., Long, F., 2015. BMP-Smad4 signaling is required for precartilaginous mesenchymal condensation independent of Sox9 in the mouse. Dev. Biol. 400, 132–138.

Lindsey, R.C., Mohan, S., 2016. Skeletal effects of growth hormone and insulin-like growth factor-I therapy. Mol. Cell. Endocrinol. 432, 44–55.
Liu, C., Lin, C., Gao, C., May-Simera, H., Swaroop, A., Li, T., 2014. Null and hypomorph Prickle1 alleles in mice phenocopy human Robinow syndrome and disrupt signaling downstream of Wnt5a. Biol. Open 3, 861–870.
Liu, J.P., Baker, J., Perkins, A.S., Robertson, E.J., Efstratiadis, A., 1993. Mice carrying null mutations of the genes encoding insulin-like growth factor I (Igf-1) and type 1 IGF receptor (Igf1r). Cell 75, 59–72.
Liu, W., Zhou, L., Zhou, C., Zhang, S., Jing, J., Xie, L., Sun, N., Duan, X., Jing, W., Liang, X., Zhao, H., Ye, L., Chen, Q., Yuan, Q., 2016. GDF11 decreases bone mass by stimulating osteoclastogenesis and inhibiting osteoblast differentiation. Nat. Commun. 7, 12794.
Liu, Z., Lavine, K.J., Hung, I.H., Ornitz, D.M., 2007. FGF18 is required for early chondrocyte proliferation, hypertrophy and vascular invasion of the growth plate. Dev. Biol. 302, 80–91.
Loeser, R.F., 2000. Chondrocyte integrin expression and function. Biorheology 37, 109–116.
Loeser, R.F., 2002. Integrins and cell signaling in chondrocytes. Biorheology 39, 119–124.
Logan, M., Tabin, C.J., 1999. Role of Pitx1 upstream of Tbx4 in specification of hindlimb identity. Science 283, 1736–1739.
Long, F., Chung, U.I., Ohba, S., Mcmahon, J., Kronenberg, H.M., Mcmahon, A.P., 2004. Ihh signaling is directly required for the osteoblast lineage in the endochondral skeleton. Development 131, 1309–1318.
Long, F., Zhang, X.M., Karp, S., Yang, Y., Mcmahon, A.P., 2001. Genetic manipulation of hedgehog signaling in the endochondral skeleton reveals a direct role in the regulation of chondrocyte proliferation. Development 128, 5099–5108.
Longobardi, L., Li, T., Myers, T.J., O'rear, L., Ozkan, H., Li, Y., Contaldo, C., Spagnoli, A., 2012. TGF-beta type II receptor/MCP-5 axis: at the crossroad between joint and growth plate development. Dev. Cell 23, 71–81.
Loomis, C.A., Harris, E., Michaud, J., Wurst, W., Hanks, M., Joyner, A.L., 1996. The mouse Engrailed-1 gene and ventral limb patterning. Nature 382, 360–363.
Lu, M.F., Cheng, H.T., Lacy, A.R., Kern, M.J., Argao, E.A., Potter, S.S., Olson, E.N., Martin, J.F., 1999. Paired-related homeobox genes cooperate in handplate and hindlimb zeugopod morphogenesis. Dev. Biol. 205, 145–157.
Lui, J.C., Baron, J., 2011. Effects of glucocorticoids on the growth plate. Endocr. Dev. 20, 187–193.
Luo, G., Hofmann, C., Bronckers, A.L., Sohocki, M., Bradley, A., Karsenty, G., 1995. BMP-7 is an inducer of nephrogenesis, and is also required for eye development and skeletal patterning. Genes Dev. 9, 2808–2820.
Maass, P.G., Rump, A., Schulz, H., Stricker, S., Schulze, L., Platzer, K., Aydin, A., Tinschert, S., Goldring, M.B., Luft, F.C., Bahring, S., 2012. A misplaced lncRNA causes brachydactyly in humans. J. Clin. Invest. 122, 3990–4002.
Macheda, M.L., Sun, W.W., Kugathasan, K., Hogan, B.M., Bower, N.I., Halford, M.M., Zhang, Y.F., Jacques, B.E., Lieschke, G.J., Dabdoub, A., Stacker, S.A., 2012. The Wnt receptor Ryk plays a role in mammalian planar cell polarity signaling. J. Biol. Chem. 287, 29312–29323.
Maclean, H.E., Guo, J., Knight, M.C., Zhang, P., Cobrinik, D., Kronenberg, H.M., 2004. The cyclin-dependent kinase inhibitor p57(Kip2) mediates proliferative actions of PTHrP in chondrocytes. J. Clin. Invest. 113, 1334–1343.
Maes, C., 2013. Role and regulation of vascularization processes in endochondral bones. Calcif. Tissue Int. 92, 307–323.
Maes, C., Araldi, E., Haigh, K., Khatri, R., Van Looveren, R., Giaccia, A.J., Haigh, J.J., Carmeliet, G., Schipani, E., 2012. VEGF-independent cell-autonomous functions of HIF-1alpha regulating oxygen consumption in fetal cartilage are critical for chondrocyte survival. J. Bone Miner. Res. 27, 596–609.
Maes, C., Kobayashi, T., Selig, M.K., Torrekens, S., Roth, S.I., Mackem, S., Carmeliet, G., Kronenberg, H.M., 2010. Osteoblast precursors, but not mature osteoblasts, move into developing and fractured bones along with invading blood vessels. Dev. Cell 19, 329–344.
Maes, C., Stockmans, I., Moermans, K., Van Looveren, R., Smets, N., Carmeliet, P., Bouillon, R., Carmeliet, G., 2004. Soluble VEGF isoforms are essential for establishing epiphyseal vascularization and regulating chondrocyte development and survival. J. Clin. Invest. 113, 188–199.
Majewski, J., Schwartzentruber, J.A., Caqueret, A., Patry, L., Marcadier, J., Fryns, J.P., Boycott, K.M., Ste-Marie, L.G., Mckiernan, F.E., Marik, I., Van Esch, H., Consortium, F.C., Michaud, J.L., Samuels, M.E., 2011. Mutations in NOTCH2 in families with Hajdu-Cheney syndrome. Hum. Mutat. 32, 1114–1117.
Mak, K.K., Kronenberg, H.M., Chuang, P.T., Mackem, S., Yang, Y., 2008. Indian hedgehog signals independently of PTHrP to promote chondrocyte hypertrophy. Development 135, 1947–1956.
Mallo, M., 2016. Revisiting the involvement of signaling gradients in somitogenesis. FEBS J. 283, 1430–1437.
Mankoo, B.S., Skuntz, S., Harrigan, I., Grigorieva, E., Candia, A., Wright, C.V., Arnheiter, H., Pachnis, V., 2003. The concerted action of Meox homeobox genes is required upstream of genetic pathways essential for the formation, patterning and differentiation of somites. Development 130, 4655–4664.
Martin, B.L., 2016. Factors that coordinate mesoderm specification from neuromesodermal progenitors with segmentation during vertebrate axial extension. Semin. Cell Dev. Biol. 49, 59–67.
Martin, G., 2001. Making a vertebrate limb: new players enter from the wings. Bioessays 23, 865–868.
Martin, J.F., Bradley, A., Olson, E.N., 1995. The paired-like homeo box gene MHox is required for early events of skeletogenesis in multiple lineages. Genes Dev. 9, 1237–1249.
Martou, G., Antonyshyn, O.M., 2011. Advances in surgical approaches to the upper facial skeleton. Curr. Opin. Otolaryngol. Head Neck Surg. 19, 242–247.
Maruyama, T., Jeong, J., Sheu, T.J., Hsu, W., 2016. Stem cells of the suture mesenchyme in craniofacial bone development, repair and regeneration. Nat. Commun. 7, 10526.

Matsunobu, T., Torigoe, K., Ishikawa, M., De Vega, S., Kulkarni, A.B., Iwamoto, Y., Yamada, Y., 2009. Critical roles of the TGF-beta type I receptor ALK5 in perichondrial formation and function, cartilage integrity, and osteoblast differentiation during growth plate development. Dev. Biol. 332, 325−338.

Mau, E., Whetstone, H., Yu, C., Hopyan, S., Wunder, J.S., Alman, B.A., 2007. PTHrP regulates growth plate chondrocyte differentiation and proliferation in a Gli3 dependent manner utilizing hedgehog ligand dependent and independent mechanisms. Dev. Biol. 305, 28−39.

Mccann, M.R., Seguin, C.A., 2016. Notochord cells in intervertebral disc development and degeneration. J. Dev. Biol. 4.

Mcewen, D.G., Green, R.P., Naski, M.C., Towler, D.A., Ornitz, D.M., 1999. Fibroblast growth factor receptor 3 gene transcription is suppressed by cyclic adenosine 3',5'-monophosphate. Identification of a chondrocytic regulatory element. J. Biol. Chem. 274, 30934−30942.

Mcpherron, A.C., Lawler, A.M., Lee, S.J., 1999. Regulation of anterior/posterior patterning of the axial skeleton by growth/differentiation factor 11. Nat. Genet. 22, 260−264.

Mead, T.J., Yutzey, K.E., 2009. Notch pathway regulation of chondrocyte differentiation and proliferation during appendicular and axial skeleton development. Proc. Natl. Acad. Sci. U.S.A. 106, 14420−14425.

Mercader, N., Leonardo, E., Azpiazu, N., Serrano, A., Morata, G., Martinez, C., Torres, M., 1999. Conserved regulation of proximodistal limb axis development by Meis1/Hth. Nature 402, 425−429.

Mercader, N., Leonardo, E., Piedra, M.E., Martinez, A.C., Ros, M.A., Torres, M., 2000. Opposing RA and FGF signals control proximodistal vertebrate limb development through regulation of Meis genes. Development 127, 3961−3970.

Mercader, N., Selleri, L., Criado, L.M., Pallares, P., Parras, C., Cleary, M.L., Torres, M., 2009. Ectopic Meis1 expression in the mouse limb bud alters P-D patterning in a Pbx1-independent manner. Int. J. Dev. Biol. 53, 1483−1494.

Merino, R., Macias, D., Ganan, Y., Economides, A.N., Wang, X., Wu, Q., Stahl, N., Sampath, K.T., Varona, P., Hurle, J.M., 1999. Expression and function of Gdf-5 during digit skeletogenesis in the embryonic chick leg bud. Dev. Biol. 206, 33−45.

Meyer, J., Sudbeck, P., Held, M., Wagner, T., Schmitz, M.L., Bricarelli, F.D., Eggermont, E., Friedrich, U., Haas, O.A., Kobelt, A., Leroy, J.G., Van Maldergem, L., Michel, E., Mitulla, B., Pfeiffer, R.A., Schinzel, A., Schmidt, H., Scherer, G., 1997. Mutational analysis of the SOX9 gene in campomelic dysplasia and autosomal sex reversal: lack of genotype/phenotype correlations. Hum. Mol. Genet. 6, 91−98.

Mikels, A.J., Nusse, R., 2006. Purified Wnt5a protein activates or inhibits beta-catenin-TCF signaling depending on receptor context. PLoS Biol. 4, e115.

Mikic, B., Clark, R.T., Battaglia, T.C., Gaschen, V., Hunziker, E.B., 2004. Altered hypertrophic chondrocyte kinetics in GDF-5 deficient murine tibial growth plates. J. Orthop. Res. 22, 552−556.

Mikic, B., Ferreira, M.P., Battaglia, T.C., Hunziker, E.B., 2008. Accelerated hypertrophic chondrocyte kinetics in GDF-7 deficient murine tibial growth plates. J. Orthop. Res. 26, 986−990.

Mikic, B., Van Der Meulen, M.C., Kingsley, D.M., Carter, D.R., 1995. Long bone geometry and strength in adult BMP-5 deficient mice. Bone 16, 445−454.

Milaire, J., 1991. Lectin binding sites in developing mouse limb buds. Anat. Embryol. 184, 479−488.

Minguillon, C., Del Buono, J., Logan, M.P., 2005. Tbx5 and Tbx4 are not sufficient to determine limb-specific morphologies but have common roles in initiating limb outgrowth. Dev. Cell 8, 75−84.

Mirzamohammadi, F., Papaioannou, G., Kobayashi, T., 2014. MicroRNAs in cartilage development, homeostasis, and disease. Curr. Osteoporos. Rep. 12, 410−419.

Miyaki, S., Sato, T., Inoue, A., Otsuki, S., Ito, Y., Yokoyama, S., Kato, Y., Takemoto, F., Nakasa, T., Yamashita, S., Takada, S., Lotz, M.K., Ueno-Kudo, H., Asahara, H., 2010. MicroRNA-140 plays dual roles in both cartilage development and homeostasis. Genes Dev. 24, 1173−1185.

Miyazawa, T., Ogawa, Y., Chusho, H., Yasoda, A., Tamura, N., Komatsu, Y., Pfeifer, A., Hofmann, F., Nakao, K., 2002. Cyclic GMP-dependent protein kinase II plays a critical role in C-type natriuretic peptide-mediated endochondral ossification. Endocrinology 143, 3604−3610.

Mo, R., Freer, A.M., Zinyk, D.L., Crackower, M.A., Michaud, J., Heng, H.H., Chik, K.W., Shi, X.M., Tsui, L.C., Cheng, S.H., Joyner, A.L., Hui, C., 1997. Specific and redundant functions of Gli2 and Gli3 zinc finger genes in skeletal patterning and development. Development 124, 113−123.

Moens, C.B., Selleri, L., 2006. Hox cofactors in vertebrate development. Dev. Biol. 291, 193−206.

Monsoro-Burq, A.H., 2005. Sclerotome development and morphogenesis: when experimental embryology meets genetics. Int. J. Dev. Biol. 49, 301−308.

Morimoto, M., Sasaki, N., Oginuma, M., Kiso, M., Igarashi, K., Aizaki, K., Kanno, J., Saga, Y., 2007. The negative regulation of Mesp2 by mouse Ripply2 is required to establish the rostro-caudal patterning within a somite. Development 134, 1561−1569.

Morita, K., Miyamoto, T., Fujita, N., Kubota, Y., Ito, K., Takubo, K., Miyamoto, K., Ninomiya, K., Suzuki, T., Iwasaki, R., Yagi, M., Takaishi, H., Toyama, Y., Suda, T., 2007. Reactive oxygen species induce chondrocyte hypertrophy in endochondral ossification. J. Exp. Med. 204, 1613−1623.

Moses, H.L., Serra, R., 1996. Regulation of differentiation by TGF-beta. Curr. Opin. Genet. Dev. 6, 581−586.

Muller, T.S., Ebensperger, C., Neubuser, A., Koseki, H., Balling, R., Christ, B., Wilting, J., 1996. Expression of avian Pax1 and Pax9 is intrinsically regulated in the pharyngeal endoderm, but depends on environmental influences in the paraxial mesoderm. Dev. Biol. 178, 403−417.

Mundlos, S., Otto, F., Mundlos, C., Mulliken, J.B., Aylsworth, A.S., Albright, S., Lindhout, D., Cole, W.G., Henn, W., Knoll, J.H., Owen, M.J., Mertelsmann, R., Zabel, B.U., Olsen, B.R., 1997. Mutations involving the transcription factor CBFA1 cause cleidocranial dysplasia. Cell 89, 773−779.

Munger, J.S., Sheppard, D., 2011. Cross talk among TGF-beta signaling pathways, integrins, and the extracellular matrix. Cold Spring Harb. Perspect. Biol. 3 a005017.

Murtaugh, L.C., Chyung, J.H., Lassar, A.B., 1999. Sonic hedgehog promotes somitic chondrogenesis by altering the cellular response to BMP signaling. Genes Dev. 13, 225−237.

Murtaugh, L.C., Zeng, L., Chyung, J.H., Lassar, A.B., 2001. The chick transcriptional repressor Nkx3.2 acts downstream of Shh to promote BMP-dependent axial chondrogenesis. Dev. Cell 1, 411−422.

Nakamura, Y., Inloes, J.B., Katagiri, T., Kobayashi, T., 2011. Chondrocyte-specific microRNA-140 regulates endochondral bone development and targets Dnpep to modulate bone morphogenetic protein signaling. Mol. Cell Biol. 31, 3019−3028.

Nakao, K., Okubo, Y., Yasoda, A., Koyama, N., Osawa, K., Isobe, Y., Kondo, E., Fujii, T., Miura, M., Nakao, K., Bessho, K., 2013. The effects of C-type natriuretic peptide on craniofacial skeletogenesis. J. Dent. Res. 92, 58−64.

Nakao, K., Osawa, K., Yasoda, A., Yamanaka, S., Fujii, T., Kondo, E., Koyama, N., Kanamoto, N., Miura, M., Kuwahara, K., Akiyama, H., Bessho, K., Nakao, K., 2015. The Local CNP/GC-B system in growth plate is responsible for physiological endochondral bone growth. Sci. Rep. 5, 10554.

Nakashima, K., Zhou, X., Kunkel, G., Zhang, Z., Deng, J.M., Behringer, R.R., DE Crombrugghe, B., 2002. The novel zinc finger-containing transcription factor osterix is required for osteoblast differentiation and bone formation. Cell 108, 17−29.

Newman, S.A., Glimm, T., Bhat, R., 2018. The vertebrate limb: an evolving complex of self-organizing systems. Prog. Biophys. Mol. Biol. 137, 12−24.

Nilsson, O., Baron, J., 2004. Fundamental limits on longitudinal bone growth: growth plate senescence and epiphyseal fusion. Trends Endocrinol. Metabol. 15, 370−374.

Nilsson, O., Marino, R., DE Luca, F., Phillip, M., Baron, J., 2005. Endocrine regulation of the growth plate. Horm. Res. 64, 157−165.

Nishimura, R., Hata, K., Nakamura, E., Murakami, T., Takahata, Y., 2018. Transcriptional network systems in cartilage development and disease. Histochem. Cell Biol. 149, 353−363.

Nishio, Y., Dong, Y., Paris, M., O'keefe, R.J., Schwarz, E.M., Drissi, H., 2006. Runx2-mediated regulation of the zinc finger Osterix/Sp7 gene. Gene 372, 62−70.

Niswander, L., 2003. Pattern formation: old models out on a limb. Nat. Rev. Genet. 4, 133−143.

Niswander, L., Jeffrey, S., Martin, G.R., Tickle, C., 1994. A positive feedback loop coordinates growth and patterning in the vertebrate limb. Nature 371, 609−612.

Niswander, L., Tickle, C., Vogel, A., Booth, I., Martin, G.R., 1993. FGF-4 replaces the apical ectodermal ridge and directs outgrowth and patterning of the limb. Cell 75, 579−587.

Oh, S.P., Yeo, C.Y., Lee, Y., Schrewe, H., Whitman, M., Li, E., 2002. Activin type IIA and IIB receptors mediate Gdf11 signaling in axial vertebral patterning. Genes Dev. 16, 2749−2754.

Oishi, I., Suzuki, H., Onishi, N., Takada, R., Kani, S., Ohkawara, B., Koshida, I., Suzuki, K., Yamada, G., Schwabe, G.C., Mundlos, S., Shibuya, H., Takada, S., Minami, Y., 2003. The receptor tyrosine kinase Ror2 is involved in non-canonical Wnt5a/JNK signalling pathway. Genes Cells 8, 645−654.

Okamoto, M., Udagawa, N., Uehara, S., Maeda, K., Yamashita, T., Nakamichi, Y., Kato, H., Saito, N., Minami, Y., Takahashi, N., Kobayashi, Y., 2014. Noncanonical Wnt5a enhances Wnt/beta-catenin signaling during osteoblastogenesis. Sci. Rep. 4, 4493.

Olney, R.C., Bukulmez, H., Bartels, C.F., Prickett, T.C., Espiner, E.A., Potter, L.R., Warman, M.L., 2006. Heterozygous mutations in natriuretic peptide receptor-B (NPR2) are associated with short stature. J. Clin. Endocrinol. Metab. 91, 1229−1232.

Oppenheimer, H., Kumar, A., Meir, H., Schwartz, I., Zini, A., Haze, A., Kandel, L., Mattan, Y., Liebergall, M., Dvir-Ginzberg, M., 2014. Set7/9 impacts COL2A1 expression through binding and repression of SirT1 histone deacetylation. J. Bone Miner. Res. 29, 348−360.

Ornitz, D.M., Marie, P.J., 2015. Fibroblast growth factor signaling in skeletal development and disease. Genes Dev. 29, 1463−1486.

Ortega, N., Wang, K., Ferrara, N., Werb, Z., Vu, T.H., 2010. Complementary interplay between matrix metalloproteinase-9, vascular endothelial growth factor and osteoclast function drives endochondral bone formation. Dis. Model Mech. 3, 224−235.

Oster, G.F., Shubin, N., Murray, J.D., Alberch, P., 1988. Evolution and morphogenetic rules: the shape of the vertebrate limb in ontogeny and phylogeny. Evolution 42, 862−884.

Otto, F., Thornell, A.P., Crompton, T., Denzel, A., Gilmour, K.C., Rosewell, I.R., Stamp, G.W., Beddington, R.S., Mundlos, S., Olsen, B.R., Selby, P.B., Owen, M.J., 1997. Cbfa1, a candidate gene for cleidocranial dysplasia syndrome, is essential for osteoblast differentiation and bone development. Cell 89, 765−771.

Ozasa, A., Komatsu, Y., Yasoda, A., Miura, M., Sakuma, Y., Nakatsuru, Y., Arai, H., Itoh, N., Nakao, K., 2005. Complementary antagonistic actions between C-type natriuretic peptide and the MAPK pathway through FGFR-3 in ATDC5 cells. Bone 36, 1056−1064.

Pacifici, M., Koyama, E., Shibukawa, Y., Wu, C., Tamamura, Y., Enomoto-Iwamoto, M., Iwamoto, M., 2006. Cellular and molecular mechanisms of synovial joint and articular cartilage formation. Ann. N.Y. Acad. Sci. 1068, 74−86.

Pan, Q., Wu, Y., Lin, T., Yao, H., Yang, Z., Gao, G., Song, E., Shen, H., 2009. Bone morphogenetic protein-2 induces chromatin remodeling and modification at the proximal promoter of Sox9 gene. Biochem. Biophys. Res. Commun. 379, 356−361.

Papaioannou, G., Inloes, J.B., Nakamura, Y., Paltrinieri, E., Kobayashi, T., 2013. let-7 and miR-140 microRNAs coordinately regulate skeletal development. Proc. Natl. Acad. Sci. U.S.A. 110, E3291−E3300.

Park, J., Gebhardt, M., Golovchenko, S., Branguli, F., Hattori, T., Hartmann, C., Zhou, X., De Crombrugghe, B., Stock, M., Schneider, H., Von Der Mark, K., 2015. Dual pathways to endochondral osteoblasts: a novel chondrocyte-derived osteoprogenitor cell identified in hypertrophic cartilage. Biol. Open 4, 608−621.

Patton, M.A., Afzal, A.R., 2002. Robinow syndrome. J. Med. Genet. 39, 305−310.

Peake, N.J., Hobbs, A.J., Pingguan-Murphy, B., Salter, D.M., Berenbaum, F., Chowdhury, T.T., 2014. Role of C-type natriuretic peptide signalling in maintaining cartilage and bone function. Osteoarthritis Cartilage 22, 1800−1807.

Pedrozo, H.A., Schwartz, Z., Gomez, R., Ornoy, A., Xin-Sheng, W., Dallas, S.L., Bonewald, L.F., Dean, D.D., Boyan, B.D., 1998. Growth plate chondrocytes store latent transforming growth factor (TGF)-beta 1 in their matrix through latent TGF-beta 1 binding protein-1. J. Cell. Physiol. 177, 343−354.

Pelton, R.W., Dickinson, M.E., Moses, H.L., Hogan, B.L., 1990. In situ hybridization analysis of TGF beta 3 RNA expression during mouse development: comparative studies with TGF beta 1 and beta 2. Development 110, 609−620.

Pelton, R.W., Saxena, B., Jones, M., Moses, H.L., Gold, L.I., 1991. Immunohistochemical localization of TGF beta 1, TGF beta 2, and TGF beta 3 in the mouse embryo: expression patterns suggest multiple roles during embryonic development. J. Cell Biol. 115, 1091−1105.

Person, A.D., Beiraghi, S., Sieben, C.M., Hermanson, S., Neumann, A.N., Robu, M.E., Schleiffarth, J.R., Billington JR., C.J., VAN Bokhoven, H., Hoogeboom, J.M., Mazzeu, J.F., Petryk, A., Schimmenti, L.A., Brunner, H.G., Ekker, S.C., Lohr, J.L., 2010. WNT5A mutations in patients with autosomal dominant Robinow syndrome. Dev. Dynam. 239, 327−337.

Peters, H., Wilm, B., Sakai, N., Imai, K., Maas, R., Balling, R., 1999. Pax1 and Pax9 synergistically regulate vertebral column development. Development 126, 5399−5408.

Peters, S.B., Wang, Y., Serra, R., 2017. Tgfbr2 is required in osterix expressing cells for postnatal skeletal development. Bone 97, 54−64.

Petit, F., Sears, K.E., Ahituv, N., 2017. Limb development: a paradigm of gene regulation. Nat. Rev. Genet. 18, 245−258.

Pi, Y., Zhang, X., Shao, Z., Zhao, F., Hu, X., Ao, Y., 2015. Intra-articular delivery of anti-Hif-2alpha siRNA by chondrocyte-homing nanoparticles to prevent cartilage degeneration in arthritic mice. Gene Ther. 22, 439−448.

Pineault, K.M., Wellik, D.M., 2014. Hox genes and limb musculoskeletal development. Curr. Osteoporos. Rep. 12, 420−427.

Pogue, R., Lyons, K., 2006. BMP signaling in the cartilage growth plate. Curr. Top. Dev. Biol. 76, 1−48.

Polinkovsky, A., Robin, N.H., Thomas, J.T., Irons, M., Lynn, A., Goodman, F.R., Reardon, W., Kant, S.G., Brunner, H.G., Van Der Burgt, I., Chitayat, D., Mcgaughran, J., Donnai, D., Luyten, F.P., Warman, M.L., 1997. Mutations in CDMP1 cause autosomal dominant brachydactyly type C. Nat. Genet. 17, 18−19.

Posnick, J.C., Tiwana, P.S., Ruiz, R.L., 2010. Craniofacial dysostosis syndromes: evaluation and staged reconstructive approach. Atlas Oral Maxillofac. Surg. Clin. North Am. 18, 109−128.

Pourquie, O., 2000. Segmentation of the paraxial mesoderm and vertebrate somitogenesis. Curr. Top. Dev. Biol. 47, 81−105.

Powell-Braxton, L., Hollingshead, P., Warburton, C., Dowd, M., Pitts-Meek, S., Dalton, D., Gillett, N., Stewart, T.A., 1993. IGF-I is required for normal embryonic growth in mice. Genes Dev. 7, 2609−2617.

Pritchett, J.W., 1991. Growth plate activity in the upper extremity. Clin. Orthop. Relat. Res. 235−242.

Pritchett, J.W., 1992. Longitudinal growth and growth-plate activity in the lower extremity. Clin. Orthop. Relat. Res. 274−279.

Provot, S., Kempf, H., Murtaugh, L.C., Chung, U.I., Kim, D.W., Chyung, J., Kronenberg, H.M., Lassar, A.B., 2006. Nkx3.2/Bapx1 acts as a negative regulator of chondrocyte maturation. Development 133, 651−662.

Provot, S., Zinyk, D., Gunes, Y., Kathri, R., Le, Q., Kronenberg, H.M., Johnson, R.S., Longaker, M.T., Giaccia, A.J., Schipani, E., 2007. Hif-1alpha regulates differentiation of limb bud mesenchyme and joint development. J. Cell Biol. 177, 451−464.

Pryce, B.A., Watson, S.S., Murchison, N.D., Staverosky, J.A., Dunker, N., Schweitzer, R., 2009. Recruitment and maintenance of tendon progenitors by TGFbeta signaling are essential for tendon formation. Development 136, 1351−1361.

Pyott, S.M., Tran, T.T., Leistritz, D.F., Pepin, M.G., Mendelsohn, N.J., Temme, R.T., Fernandez, B.A., Elsayed, S.M., Elsobky, E., Verma, I., Nair, S., Turner, E.H., Smith, J.D., Jarvik, G.P., Byers, P.H., 2013. WNT1 mutations in families affected by moderately severe and progressive recessive osteogenesis imperfecta. Am. J. Hum. Genet. 92, 590−597.

Ratcliffe, P.J., 2013. Oxygen sensing and hypoxia signalling pathways in animals: the implications of physiology for cancer. J. Physiol. 591, 2027−2042.

Rawls, A., Fischer, R.E., 2010. Development and functional anatomy of the spine. In: Kusumi, K., Dunwoodie, S.L. (Eds.), The Genetics and Development of Scoliosis. Springer.

Razzaque, M.S., Soegiarto, D.W., Chang, D., Long, F., Lanske, B., 2005. Conditional deletion of Indian hedgehog from collagen type 2alpha1-expressing cells results in abnormal endochondral bone formation. J. Pathol. 207, 453−461.

Regard, J.B., Cherman, N., Palmer, D., Kuznetsov, S.A., Celi, F.S., Guettier, J.M., Chen, M., Bhattacharyya, N., Wess, J., Coughlin, S.R., Weinstein, L.S., Collins, M.T., Robey, P.G., Yang, Y., 2011. Wnt/beta-catenin signaling is differentially regulated by Galpha proteins and contributes to fibrous dysplasia. Proc. Natl. Acad. Sci. U.S.A. 108, 20101−20106.

Regard, J.B., Malhotra, D., Gvozdenovic-Jeremic, J., Josey, M., Chen, M., Weinstein, L.S., Lu, J., Shore, E.M., Kaplan, F.S., Yang, Y., 2013. Activation of Hedgehog signaling by loss of GNAS causes heterotopic ossification. Nat. Med. 19, 1505−1512.

Retting, K.N., Song, B., Yoon, B.S., Lyons, K.M., 2009. BMP canonical Smad signaling through Smad1 and Smad5 is required for endochondral bone formation. Development 136, 1093−1104.

Riddle, R.D., Ensini, M., Nelson, C., Tsuchida, T., Jessell, T.M., Tabin, C., 1995. Induction of the LIM homeobox gene Lmx1 by WNT7a establishes dorsoventral pattern in the vertebrate limb. Cell 83, 631−640.

Riddle, R.D., Johnson, R.L., Laufer, E., Tabin, C., 1993. Sonic hedgehog mediates the polarizing activity of the ZPA. Cell 75, 1401−1416.

Rigueur, D., Brugger, S., Anbarchian, T., Kim, J.K., Lee, Y., Lyons, K.M., 2015. The type I BMP receptor ACVR1/ALK2 is required for chondrogenesis during development. J. Bone Miner. Res. 30, 733−741.

Rittling, S.R., Matsumoto, H.N., Mckee, M.D., Nanci, A., An, X.R., Novick, K.E., Kowalski, A.J., Noda, M., Denhardt, D.T., 1998. Mice lacking osteopontin show normal development and bone structure but display altered osteoclast formation in vitro. J. Bone Miner. Res. 13, 1101−1111.

Roach, H.I., Erenpreisa, J., Aigner, T., 1995. Osteogenic differentiation of hypertrophic chondrocytes involves asymmetric cell divisions and apoptosis. J. Cell Biol. 131, 483−494.

Robin, N.H., Falk, M.J., Haldeman-Englert, C.R., 1993. FGFR-related craniosynostosis syndromes. In: Adam, M.P., Ardinger, H.H., Pagon, R.A., Wallace, S.E., Bean, L.J.H., Stephens, K., Amemiya, A. (Eds.), GeneReviews. Seattle (WA).

Robson, H., Siebler, T., Shalet, S.M., Williams, G.R., 2002. Interactions between Gh, Igf-I, glucocorticoids, and thyroid hormones during skeletal growth. Pediatr. Res. 52, 137−147.

Roca, H., Phimphilai, M., Gopalakrishnan, R., Xiao, G., Franceschi, R.T., 2005. Cooperative interactions between RUNX2 and homeodomain protein-binding sites are critical for the osteoblast-specific expression of the bone sialoprotein gene. J. Biol. Chem. 280, 30845−30855.

Rodrigo, I., Hill, R.E., Balling, R., Munsterberg, A., Imai, K., 2003. Pax1 and Pax9 activate Bapx1 to induce chondrogenic differentiation in the sclerotome. Development 130, 473−482.

Rodrigues, A.R., Yakushiji-Kaminatsui, N., Atsuta, Y., Andrey, G., Schorderet, P., Duboule, D., Tabin, C.J., 2017. Integration of Shh and Fgf signaling in controlling Hox gene expression in cultured limb cells. Proc. Natl. Acad. Sci. U.S.A. 114, 3139−3144.

Roifman, M., Brunner, H.G., Lohr, J.L., Mazzeu, J.F., Chitayat, D., 2015. Autosomal dominant Robinow syndrome. In: Adam, M.P., Ardinger, H.H., Pagon, R.A., Wallace, S.E., Bean, L.J.H., Stephens, K., Amemiya, A. (Eds.), GeneReviews. Seattle (WA).

Romereim, S.M., Conoan, N.H., Chen, B., Dudley, A.T., 2014. A dynamic cell adhesion surface regulates tissue architecture in growth plate cartilage. Development 141, 2085−2095.

Ros, M.A., Dahn, R.D., Fernandez-Teran, M., Rashka, K., Caruccio, N.C., Hasso, S.M., Bitgood, J.J., Lancman, J.J., Fallon, J.F., 2003. The chick oligozeugodactyly (ozd) mutant lacks sonic hedgehog function in the limb. Development 130, 527−537.

Rosen, V., 2006. BMP and BMP inhibitors in bone. Ann. N.Y. Acad. Sci. 1068, 19−25.

Rowe, D.A., Fallon, J.F., 1982. The proximodistal determination of skeletal parts in the developing chick leg. J. Embryol. Exp. Morphol. 68, 1−7.

Saga, Y., 2007. Segmental border is defined by the key transcription factor Mesp2, by means of the suppression of Notch activity. Dev. Dynam. 236, 1450−1455.

Sanford, L.P., Ormsby, I., Gittenberger-DE Groot, A.C., Sariola, H., Friedman, R., Boivin, G.P., Cardell, E.L., Doetschman, T., 1997. TGFbeta2 knockout mice have multiple developmental defects that are non-overlapping with other TGFbeta knockout phenotypes. Development 124, 2659−2670.

Sasaki, N., Kiso, M., Kitagawa, M., Saga, Y., 2011. The repression of Notch signaling occurs via the destabilization of mastermind-like 1 by Mesp2 and is essential for somitogenesis. Development 138, 55−64.

Sassi, N., Laadhar, L., Driss, M., Kallel-Sellami, M., Sellami, S., Makni, S., 2011. The role of the Notch pathway in healthy and osteoarthritic articular cartilage: from experimental models to ex vivo studies. Arthritis Res. Ther. 13, 208.

Satokata, I., Ma, L., Ohshima, H., Bei, M., Woo, I., Nishizawa, K., Maeda, T., Takano, Y., Uchiyama, M., Heaney, S., Peters, H., Tang, Z., Maxson, R., Maas, R., 2000. Msx2 deficiency in mice causes pleiotropic defects in bone growth and ectodermal organ formation. Nat. Genet. 24, 391−395.

Saunder, J.W., Gasseling, M.T. (Eds.), 1968. Ecotdermal and Mesenchymal Interactions in the Origin of Limb Symmetry. Williams and Wilkins, Baltimore.

Saunders JR., J.W., 1948. The proximo-distal sequence of origin of the parts of the chick wing and the role of the ectoderm. J. Exp. Zool. 108, 363−403.

Scaal, M., Christ, B., 2004. Formation and differentiation of the avian dermomyotome. Anat. Embryol. 208, 411−424.

Schipani, E., Jensen, G.S., Pincus, J., Nissenson, R.A., Gardella, T.J., Juppner, H., 1997a. Constitutive activation of the cyclic adenosine 3',5'-monophosphate signaling pathway by parathyroid hormone (PTH)/PTH-related peptide receptors mutated at the two loci for Jansen's metaphyseal chondrodysplasia. Mol. Endocrinol. 11, 851−858.

Schipani, E., Kruse, K., Juppner, H., 1995. A constitutively active mutant PTH-PTHrP receptor in Jansen-type metaphyseal chondrodysplasia. Science 268, 98−100.

Schipani, E., Langman, C., Hunzelman, J., LE Merrer, M., Loke, K.Y., Dillon, M.J., Silve, C., Juppner, H., 1999. A novel parathyroid hormone (PTH)/PTH-related peptide receptor mutation in Jansen's metaphyseal chondrodysplasia. J. Clin. Endocrinol. Metab. 84, 3052−3057.

Schipani, E., Langman, C.B., Parfitt, A.M., Jensen, G.S., Kikuchi, S., Kooh, S.W., Cole, W.G., Juppner, H., 1996. Constitutively activated receptors for parathyroid hormone and parathyroid hormone-related peptide in Jansen's metaphyseal chondrodysplasia. N. Engl. J. Med. 335, 708−714.

Schipani, E., Lanske, B., Hunzelman, J., Luz, A., Kovacs, C.S., Lee, K., Pirro, A., Kronenberg, H.M., Juppner, H., 1997b. Targeted expression of constitutively active receptors for parathyroid hormone and parathyroid hormone-related peptide delays endochondral bone formation and rescues mice that lack parathyroid hormone-related peptide. Proc. Natl. Acad. Sci. U.S.A. 94, 13689−13694.

Schipani, E., Mangiavini, L., Merceron, C., 2015. HIF-1alpha and growth plate development: what we really know. Bonekey Rep. 4, 730.

Schipani, E., Ryan, H.E., Didrickson, S., Kobayashi, T., Knight, M., Johnson, R.S., 2001. Hypoxia in cartilage: HIF-1alpha is essential for chondrocyte growth arrest and survival. Genes Dev. 15, 2865−2876.

Schmid, P., Cox, D., Bilbe, G., Maier, R., Mcmaster, G.K., 1991. Differential expression of TGF beta 1, beta 2 and beta 3 genes during mouse embryogenesis. Development 111, 117−130.

Schneider, A., Brand, T., Zweigerdt, R., Arnold, H., 2000. Targeted disruption of the Nkx3.1 gene in mice results in morphogenetic defects of minor salivary glands: parallels to glandular duct morphogenesis in prostate. Mech. Dev. 95, 163−174.

Sekine, K., Ohuchi, H., Fujiwara, M., Yamasaki, M., Yoshizawa, T., Sato, T., Yagishita, N., Matsui, D., Koga, Y., Itoh, N., Kato, S., 1999. Fgf10 is essential for limb and lung formation. Nat. Genet. 21, 138−141.

Semenza, G.L., 2012. Hypoxia-inducible factors in physiology and medicine. Cell 148, 399−408.

Senarath-Yapa, K., Chung, M.T., Mcardle, A., Wong, V.W., Quarto, N., Longaker, M.T., Wan, D.C., 2012. Craniosynostosis: molecular pathways and future pharmacologic therapy. Organogenesis 8, 103−113.

Seo, H.S., Serra, R., 2007. Deletion of Tgfbr2 in Prx1-cre expressing mesenchyme results in defects in development of the long bones and joints. Dev. Biol. 310, 304−316.

Serra, R., Johnson, M., Filvaroff, E.H., Laborde, J., Sheehan, D.M., Derynck, R., Moses, H.L., 1997. Expression of a truncated, kinase-defective TGF-beta type II receptor in mouse skeletal tissue promotes terminal chondrocyte differentiation and osteoarthritis. J. Cell Biol. 139, 541−552.

Settle JR., S.H., Rountree, R.B., Sinha, A., Thacker, A., Higgins, K., Kingsley, D.M., 2003. Multiple joint and skeletal patterning defects caused by single and double mutations in the mouse Gdf6 and Gdf5 genes. Dev. Biol. 254, 116–130.

Shapiro, F., 2001. Developmental bone biology. In: Pediatric Orthopedic Deformities - Basic Science, Diagnosis, and Treatment. Academic Press, San Diego, San Francisco, New York, Boston, London, Sydney, Tokyo.

Shapiro, F., Holtrop, M.E., Glimcher, M.J., 1977. Organization and cellular biology of the perichondrial ossification groove of ranvier: a morphological study in rabbits. J. Bone Joint Surg. Am. 59, 703–723.

Shapiro, I.M., Adams, C.S., Freeman, T., Srinivas, V., 2005. Fate of the hypertrophic chondrocyte: microenvironmental perspectives on apoptosis and survival in the epiphyseal growth plate. Birth Defects Res. C Embryo Today 75, 330–339.

Sheeba, C.J., Andrade, R.P., Palmeirim, I., 2016. Mechanisms of vertebrate embryo segmentation: common themes in trunk and limb development. Semin. Cell Dev. Biol. 49, 125–134.

Shore, E.M., Xu, M., Feldman, G.J., Fenstermacher, D.A., Cho, T.J., Choi, I.H., Connor, J.M., Delai, P., Glaser, D.L., Lemerrer, M., Morhart, R., Rogers, J.G., Smith, R., Triffitt, J.T., Urtizberea, J.A., Zasloff, M., Brown, M.A., Kaplan, F.S., 2006. A recurrent mutation in the BMP type I receptor ACVR1 causes inherited and sporadic fibrodysplasia ossificans progressiva. Nat. Genet. 38, 525–527.

Shu, B., Zhang, M., Xie, R., Wang, M., Jin, H., Hou, W., Tang, D., Harris, S.E., Mishina, Y., O'keefe, R.J., Hilton, M.J., Wang, Y., Chen, D., 2011. BMP2, but not BMP4, is crucial for chondrocyte proliferation and maturation during endochondral bone development. J. Cell Sci. 124, 3428–3440.

Shubin, N., Alberch, P., 1986. A morphogenic approach to the origin and basic organization of the tetrapod limb. Evol. Biol. 20, 319–387.

Silvestrini, G., Ballanti, P., Patacchioli, F., Leopizzi, M., Gualtieri, N., Monnazzi, P., Tremante, E., Sardella, D., Bonucci, E., 2005. Detection of osteoprotegerin (OPG) and its ligand (RANKL) mRNA and protein in femur and tibia of the rat. J. Mol. Histol. 36, 59–67.

Skuntz, S., Mankoo, B., Nguyen, M.T., Hustert, E., Nakayama, A., Tournier-Lasserve, E., Wright, C.V., Pachnis, V., Bharti, K., Arnheiter, H., 2009. Lack of the mesodermal homeodomain protein MEOX1 disrupts sclerotome polarity and leads to a remodeling of the cranio-cervical joints of the axial skeleton. Dev. Biol. 332, 383–395.

Slater, B.J., Lenton, K.A., Kwan, M.D., Gupta, D.M., Wan, D.C., Longaker, M.T., 2008. Cranial sutures: a brief review. Plast. Reconstr. Surg. 121, 170e-8e.

Smits, P., Li, P., Mandel, J., Zhang, Z., Deng, J.M., Behringer, R.R., De Crombrugghe, B., Lefebvre, V., 2001. The transcription factors L-Sox5 and Sox6 are essential for cartilage formation. Dev. Cell 1, 277–290.

Solloway, M.J., Dudley, A.T., Bikoff, E.K., Lyons, K.M., Hogan, B.L., Robertson, E.J., 1998. Mice lacking Bmp6 function. Dev. Genet. 22, 321–339.

Spagnoli, A., O'rear, L., Chandler, R.L., Granero-Molto, F., Mortlock, D.P., Gorska, A.E., Weis, J.A., Longobardi, L., Chytil, A., Shimer, K., Moses, H.L., 2007. TGF-beta signaling is essential for joint morphogenesis. J. Cell Biol. 177, 1105–1117.

Spater, D., Hill, T.P., Gruber, M., Hartmann, C., 2006a. Role of canonical Wnt-signalling in joint formation. Eur. Cells Mater. 12, 71–80.

Spater, D., Hill, T.P., O'sullivan, R.,J., Gruber, M., Conner, D.A., Hartmann, C., 2006b. Wnt9a signaling is required for joint integrity and regulation of Ihh during chondrogenesis. Development 133, 3039–3049.

St-Jacques, B., Hammerschmidt, M., Mcmahon, A.P., 1999. Indian hedgehog signaling regulates proliferation and differentiation of chondrocytes and is essential for bone formation. Genes Dev. 13, 2072–2086.

Stickens, D., Behonick, D.J., Ortega, N., Heyer, B., Hartenstein, B., Yu, Y., Fosang, A.J., Schorpp-Kistner, M., Angel, P., Werb, Z., 2004. Altered endochondral bone development in matrix metalloproteinase 13-deficient mice. Development 131, 5883–5895.

Storm, E.E., Huynh, T.V., Copeland, N.G., Jenkins, N.A., Kingsley, D.M., Lee, S.J., 1994. Limb alterations in brachypodism mice due to mutations in a new member of the TGF beta-superfamily. Nature 368, 639–643.

Storm, E.E., Kingsley, D.M., 1999. GDF5 coordinates bone and joint formation during digit development. Dev. Biol. 209, 11–27.

Stringa, E., Tuan, R.S., 1996. Chondrogenic cell subpopulation of chick embryonic calvarium: isolation by peanut agglutinin affinity chromatography and in vitro characterization. Anat. Embryol. 194, 427–437.

Suda, M., Ogawa, Y., Tanaka, K., Tamura, N., Yasoda, A., Takigawa, T., Uehira, M., Nishimoto, H., Itoh, H., Saito, Y., Shiota, K., Nakao, K., 1998. Skeletal overgrowth in transgenic mice that overexpress brain natriuretic peptide. Proc. Natl. Acad. Sci. U.S.A. 95, 2337–2342.

Suda, N., Baba, O., Udagawa, N., Terashima, T., Kitahara, Y., Takano, Y., Kuroda, T., Senior, P.V., Beck, F., Hammond, V.E., 2001. Parathyroid hormone-related protein is required for normal intramembranous bone development. J. Bone Miner. Res. 16, 2182–2191.

Sueyoshi, T., Yamamoto, K., Akiyama, H., 2012. Conditional deletion of Tgfbr2 in hypertrophic chondrocytes delays terminal chondrocyte differentiation. Matrix Biol. 31, 352–359.

Sugimoto, Y., Takimoto, A., Akiyama, H., Kist, R., Scherer, G., Nakamura, T., Hiraki, Y., Shukunami, C., 2013. Scx+/Sox9+ progenitors contribute to the establishment of the junction between cartilage and tendon/ligament. Development 140, 2280–2288.

Summerbell, D., 1974. A quantitative analysis of the effect of excision of the AER from the chick limb-bud. J. Embryol. Exp. Morphol. 32, 651–660.

Sun, F., Chen, Q., Yang, S., Pan, Q., Ma, J., Wan, Y., Chang, C.H., Hong, A., 2009. Remodeling of chromatin structure within the promoter is important for bmp-2-induced fgfr3 expression. Nucleic Acids Res. 37, 3897–3911.

Sun, X., Mariani, F.V., Martin, G.R., 2002. Functions of FGF signalling from the apical ectodermal ridge in limb development. Nature 418, 501–508.

Svensson, J., Lall, S., Dickson, S.L., Bengtsson, B.A., Romer, J., Ahnfelt-Ronne, I., Ohlsson, C., Jansson, J.O., 2001. Effects of growth hormone and its secretagogues on bone. Endocrine 14, 63–66.

Swingler, T.E., Wheeler, G., Carmont, V., Elliott, H.R., Barter, M.J., Abu-Elmagd, M., Donell, S.T., Boot-Handford, R.P., Hajihosseini, M.K., Munsterberg, A., Dalmay, T., Young, D.A., Clark, I.M., 2012. The expression and function of microRNAs in chondrogenesis and osteoarthritis. Arthritis Rheum. 64, 1909–1919.

Takahashi, Y., Yasuhiko, Y., Kitajima, S., Kanno, J., Saga, Y., 2007. Appropriate suppression of Notch signaling by Mesp factors is essential for stripe pattern formation leading to segment boundary formation. Dev. Biol. 304, 593–603.

Takeuchi, S., Takeda, K., Oishi, I., Nomi, M., Ikeya, M., Itoh, K., Tamura, S., Ueda, T., Hatta, T., Otani, H., Terashima, T., Takada, S., Yamamura, H., Akira, S., Minami, Y., 2000. Mouse Ror2 receptor tyrosine kinase is required for the heart development and limb formation. Genes Cells 5, 71–78.

Tamamura, Y., Otani, T., Kanatani, N., Koyama, E., Kitagaki, J., Komori, T., Yamada, Y., Costantini, F., Wakisaka, S., Pacifici, M., Iwamoto, M., Enomoto-Iwamoto, M., 2005. Developmental regulation of Wnt/beta-catenin signals is required for growth plate assembly, cartilage integrity, and endochondral ossification. J. Biol. Chem. 280, 19185–19195.

Tamura, N., Doolittle, L.K., Hammer, R.E., Shelton, J.M., Richardson, J.A., Garbers, D.L., 2004. Critical roles of the guanylyl cyclase B receptor in endochondral ossification and development of female reproductive organs. Proc. Natl. Acad. Sci. U.S.A. 101, 17300–17305.

Tang, Y., Wu, X., Lei, W., Pang, L., Wan, C., Shi, Z., Zhao, L., Nagy, T.R., Peng, X., Hu, J., Feng, X., Van Hul, W., Wan, M., Cao, X., 2009. TGF-beta1-induced migration of bone mesenchymal stem cells couples bone resorption with formation. Nat. Med. 15, 757–765.

Taraboletti, G., D'ascenzo, S., Borsotti, P., Giavazzi, R., Pavan, A., Dolo, V., 2002. Shedding of the matrix metalloproteinases MMP-2, MMP-9, and MT1-MMP as membrane vesicle-associated components by endothelial cells. Am. J. Pathol. 160, 673–680.

Tarchini, B., Duboule, D., Kmita, M., 2006. Regulatory constraints in the evolution of the tetrapod limb anterior-posterior polarity. Nature 443, 985–988.

Te Welscher, P., Fernandez-Teran, M., Ros, M.A., Zeller, R., 2002. Mutual genetic antagonism involving GLI3 and dHAND prepatterns the vertebrate limb bud mesenchyme prior to SHH signaling. Genes Dev. 16, 421–426.

Ten Berge, D., Brugmann, S.A., Helms, J.A., Nusse, R., 2008. Wnt and FGF signals interact to coordinate growth with cell fate specification during limb development. Development 135, 3247–3257.

Tickle, C., 1981. The number of polarizing region cells required to specify additional digits in the developing chick wing. Nature 289, 295–298.

Tickle, C., Summerbell, D., Wolpert, L., 1975. Positional signalling and specification of digits in chick limb morphogenesis. Nature 254, 199–202.

Topol, L., Jiang, X., Choi, H., Garrett-Beal, L., Carolan, P.J., Yang, Y., 2003. Wnt-5a inhibits the canonical Wnt pathway by promoting GSK-3-independent beta-catenin degradation. J. Cell Biol. 162, 899–908.

Touaitahuata, H., Cres, G., De Rossi, S., Vives, V., Blangy, A., 2014. The mineral dissolution function of osteoclasts is dispensable for hypertrophic cartilage degradation during long bone development and growth. Dev. Biol. 393, 57–70.

Tribioli, C., Lufkin, T., 1999. The murine Bapx1 homeobox gene plays a critical role in embryonic development of the axial skeleton and spleen. Development 126, 5699–5711.

Tsang, K.Y., Chan, D., Cheah, K.S., 2015. Fate of growth plate hypertrophic chondrocytes: death or lineage extension? Dev. Growth Differ. 57, 179–192.

Tu, X., Joeng, K.S., Long, F., 2012. Indian hedgehog requires additional effectors besides Runx2 to induce osteoblast differentiation. Dev. Biol. 362, 76–82.

Tucker, R.P., Chiquet-Ehrismann, R., 2015. Tenascin-C: its functions as an integrin ligand. Int. J. Biochem. Cell Biol. 65, 165–168.

Usami, Y., Gunawardena, A.T., Iwamoto, M., Enomoto-Iwamoto, M., 2016. Wnt signaling in cartilage development and diseases: lessons from animal studies. Lab. Invest. 96, 186–196.

Usui, M., Xing, L., Drissi, H., Zuscik, M., O'keefe, R., Chen, D., Boyce, B.F., 2008. Murine and chicken chondrocytes regulate osteoclastogenesis by producing RANKL in response to BMP2. J. Bone Miner. Res. 23, 314–325.

Van Der Kraan, P.M., Blaney Davidson, E.N., Blom, A., Van Den Berg, W.B., 2009. TGF-beta signaling in chondrocyte terminal differentiation and osteoarthritis: modulation and integration of signaling pathways through receptor-Smads. Osteoarthritis Cartilage 17, 1539–1545.

Vasques, G.A., Amano, N., Docko, A.J., Funari, M.F., Quedas, E.P., Nishi, M.Y., Arnhold, I.J., Hasegawa, T., Jorge, A.A., 2013. Heterozygous mutations in natriuretic peptide receptor-B (NPR2) gene as a cause of short stature in patients initially classified as idiopathic short stature. J. Clin. Endocrinol. Metab. 98, E1636–E1644.

Vega, R.B., Matsuda, K., Oh, J., Barbosa, A.C., Yang, X., Meadows, E., Mcanally, J., Pomajzl, C., Shelton, J.M., Richardson, J.A., Karsenty, G., Olson, E.N., 2004. Histone deacetylase 4 controls chondrocyte hypertrophy during skeletogenesis. Cell 119, 555–566.

Vogel, A., Rodriguez, C., Warnken, W., Izpisua Belmonte, J.C., 1995. Dorsal cell fate specified by chick Lmx1 during vertebrate limb development. Nature 378, 716–720.

Vortkamp, A., Franz, T., Gessler, M., Grzeschik, K.H., 1992. Deletion of GLI3 supports the homology of the human Greig cephalopolysyndactyly syndrome (GCPS) and the mouse mutant extra toes (Xt). Mamm. Genome 3, 461–463.

Vortkamp, A., Lee, K., Lanske, B., Segre, G.V., Kronenberg, H.M., Tabin, C.J., 1996. Regulation of rate of cartilage differentiation by Indian hedgehog and PTH-related protein. Science 273, 613–622.

Wang, B., Fallon, J.F., Beachy, P.A., 2000. Hedgehog-regulated processing of Gli3 produces an anterior/posterior repressor gradient in the developing vertebrate limb. Cell 100, 423–434.

Wang, B., Jin, H., Zhu, M., Li, J., Zhao, L., Zhang, Y., Tang, D., Xiao, G., Xing, L., Boyce, B.F., Chen, D., 2014a. Chondrocyte beta-catenin signaling regulates postnatal bone remodeling through modulation of osteoclast formation in a murine model. Arthritis Rheum. 66, 107–120.

Wang, B., Sinha, T., Jiao, K., Serra, R., Wang, J., 2011. Disruption of PCP signaling causes limb morphogenesis and skeletal defects and may underlie Robinow syndrome and brachydactyly type B. Hum. Mol. Genet. 20, 271–285.

Wang, J., Zhou, J., Bondy, C.A., 1999. Igf1 promotes longitudinal bone growth by insulin-like actions augmenting chondrocyte hypertrophy. FASEB J. 13, 1985–1990.

Wang, L., Huang, J., Moore, D.C., Zuo, C., Wu, Q., Xie, L., Von Der Mark, K., Yuan, X., Chen, D., Warman, M.L., Ehrlich, M.G., Yang, W., 2017. SHP2 regulates the osteogenic fate of growth plate hypertrophic chondrocytes. Sci. Rep. 7, 12699.

Wang, R.N., Green, J., Wang, Z., Deng, Y., Qiao, M., Peabody, M., Zhang, Q., Ye, J., Yan, Z., Denduluri, S., Idowu, O., Li, M., Shen, C., Hu, A., Haydon, R.C., Kang, R., Mok, J., Lee, M.J., Luu, H.L., Shi, L.L., 2014b. Bone Morphogenetic Protein (BMP) signaling in development and human diseases. Genes Dis. 1, 87–105.

Wang, W., Rigueur, D., Lyons, K.M., 2014c. TGFbeta signaling in cartilage development and maintenance. Birth Defects Res. C Embryo Today 102, 37–51.

Wang, Y., Li, Y.P., Paulson, C., Shao, J.Z., Zhang, X., Wu, M., Chen, W., 2014d. Wnt and the Wnt signaling pathway in bone development and disease. Front. Biosci. 19, 379–407.

Watanabe, T., Sato, T., Amano, T., Kawamura, Y., Kawamura, N., Kawaguchi, H., Yamashita, N., Kurihara, H., Nakaoka, T., 2008. Dnm3os, a non-coding RNA, is required for normal growth and skeletal development in mice. Dev. Dynam. 237, 3738–3748.

Weir, E.C., Philbrick, W.M., Amling, M., Neff, L.A., Baron, R., Broadus, A.E., 1996. Targeted overexpression of parathyroid hormone-related peptide in chondrocytes causes chondrodysplasia and delayed endochondral bone formation. Proc. Natl. Acad. Sci. U.S.A. 93, 10240–10245.

Wellik, D.M., 2007. Hox patterning of the vertebrate axial skeleton. Dev. Dynam. 236, 2454–2463.

Whitaker, A.T., Berthet, E., Cantu, A., Laird, D.J., Alliston, T., 2017. Smad4 regulates growth plate matrix production and chondrocyte polarity. Biol. Open 6, 358–364.

Wijgerde, M., Karp, S., Mcmahon, J., Mcmahon, A.P., 2005. Noggin antagonism of BMP4 signaling controls development of the axial skeleton in the mouse. Dev. Biol. 286, 149–157.

Williams, R., Nelson, L., Dowthwaite, G.P., Evans, D.J., Archer, C.W., 2009. Notch receptor and Notch ligand expression in developing avian cartilage. J. Anat. 215, 159–169.

Winnier, G.E., Hargett, L., Hogan, B.L., 1997. The winged helix transcription factor MFH1 is required for proliferation and patterning of paraxial mesoderm in the mouse embryo. Genes Dev. 11, 926–940.

Winslow, B.B., Takimoto-Kimura, R., Burke, A.C., 2007. Global patterning of the vertebrate mesoderm. Dev. Dynam. 236, 2371–2381.

Wit, J.M., Camacho-Hubner, C., 2011. Endocrine regulation of longitudinal bone growth. Endocr. Dev. 21, 30–41.

Witte, F., Dokas, J., Neuendorf, F., Mundlos, S., Stricker, S., 2009. Comprehensive expression analysis of all Wnt genes and their major secreted antagonists during mouse limb development and cartilage differentiation. Gene Expr. Patterns 9, 215–223.

Wolpert, L., 1969. Positional information and the spatial pattern of cellular differentiation. J. Theor. Biol. 25, 1–47.

Wright, E., Hargrave, M.R., Christiansen, J., Cooper, L., Kun, J., Evans, T., Gangadharan, U., Greenfield, A., Koopman, P., 1995. The Sry-related gene Sox9 is expressed during chondrogenesis in mouse embryos. Nat. Genet. 9, 15–20.

Wu, M., Chen, G., Li, Y.P., 2016. TGF-beta and BMP signaling in osteoblast, skeletal development, and bone formation, homeostasis and disease. Bone Res. 4, 16009.

Wu, X., Shi, W., Cao, X., 2007. Multiplicity of BMP signaling in skeletal development. Ann. N.Y. Acad. Sci. 1116, 29–49.

Wuelling, M., Pasdziernik, M., Moll, C.N., Thiesen, A.M., Schneider, S., Johannes, C., Vortkamp, A., 2013. The multi zinc-finger protein Trps1 acts as a regulator of histone deacetylation during mitosis. Cell Cycle 12, 2219–2232.

Wuthier, R.E., Lipscomb, G.F., 2011. Matrix vesicles: structure, composition, formation and function in calcification. Front. Biosci. 16, 2812–2902.

Yamaguchi, T.P., Bradley, A., Mcmahon, A.P., Jones, S., 1999. A Wnt5a pathway underlies outgrowth of multiple structures in the vertebrate embryo. Development 126, 1211–1223.

Yan, Y., Frisen, J., Lee, M.H., Massague, J., Barbacid, M., 1997. Ablation of the CDK inhibitor p57Kip2 results in increased apoptosis and delayed differentiation during mouse development. Genes Dev. 11, 973–983.

Yang, G., Zhu, L., Hou, N., Lan, Y., Wu, X.M., Zhou, B., Teng, Y., Yang, X., 2014a. Osteogenic fate of hypertrophic chondrocytes. Cell Res. 24, 1266–1269.

Yang, L., Lawson, K.A., Teteak, C.J., Zou, J., Hacquebord, J., Patterson, D., Ghatan, A.C., Mei, Q., Zielinska-Kwiatkowska, A., Bain, S.D., Fernandes, R.J., Chansky, H.A., 2013a. ESET histone methyltransferase is essential to hypertrophic differentiation of growth plate chondrocytes and formation of epiphyseal plates. Dev. Biol. 380, 99–110.

Yang, L., Tsang, K.Y., Tang, H.C., Chan, D., Cheah, K.S., 2014b. Hypertrophic chondrocytes can become osteoblasts and osteocytes in endochondral bone formation. Proc. Natl. Acad. Sci. U.S.A. 111, 12097–12102.

Yang, S., Kim, J., Ryu, J.H., Oh, H., Chun, C.H., Kim, B.J., Min, B.H., Chun, J.S., 2010. Hypoxia-inducible factor-2alpha is a catabolic regulator of osteoarthritic cartilage destruction. Nat. Med. 16, 687–693.

Yang, T., Bassuk, A.G., Fritzsch, B., 2013b. Prickle1 stunts limb growth through alteration of cell polarity and gene expression. Dev. Dynam. 242, 1293–1306.

Yang, Y., Topol, L., Lee, H., Wu, J., 2003. Wnt5a and Wnt5b exhibit distinct activities in coordinating chondrocyte proliferation and differentiation. Development 130, 1003–1015.

Yang, Y., Wang, B., 2015. Disruption of beta-catenin binding to parathyroid hormone (PTH) receptor inhibits PTH-stimulated ERK1/2 activation. Biochem. Biophys. Res. Commun. 464, 27–32.

Yano, F., Kugimiya, F., Ohba, S., Ikeda, T., Chikuda, H., Ogasawara, T., Ogata, N., Takato, T., Nakamura, K., Kawaguchi, H., Chung, U.I., 2005. The canonical Wnt signaling pathway promotes chondrocyte differentiation in a Sox9-dependent manner. Biochem. Biophys. Res. Commun. 333, 1300–1308.

Yano, F., Saito, T., Ogata, N., Yamazawa, T., Iino, M., Chung, U.I., Kawaguchi, H., 2013. beta-catenin regulates parathyroid hormone/parathyroid hormone-related protein receptor signals and chondrocyte hypertrophy through binding to the intracellular C-terminal region of the receptor. Arthritis Rheum. 65, 429–435.

Yi, S.E., Daluiski, A., Pederson, R., Rosen, V., Lyons, K.M., 2000. The type I BMP receptor BMPRIB is required for chondrogenesis in the mouse limb. Development 127, 621–630.

Yoon, B.S., Ovchinnikov, D.A., Yoshii, I., Mishina, Y., Behringer, R.R., Lyons, K.M., 2005. Bmpr1a and Bmpr1b have overlapping functions and are essential for chondrogenesis in vivo. Proc. Natl. Acad. Sci. U.S.A. 102, 5062–5067.

Yoshida, C.A., Yamamoto, H., Fujita, T., Furuichi, T., Ito, K., Inoue, K., Yamana, K., Zanma, A., Takada, K., Ito, Y., Komori, T., 2004. Runx2 and Runx3 are essential for chondrocyte maturation, and Runx2 regulates limb growth through induction of Indian hedgehog. Genes Dev. 18, 952–963.

Yoshida, T., Vivatbutsiri, P., Morriss-Kay, G., Saga, Y., Iseki, S., 2008. Cell lineage in mammalian craniofacial mesenchyme. Mech. Dev. 125, 797–808.

Yu, K., Xu, J., Liu, Z., Sosic, D., Shao, J., Olson, E.N., Towler, D.A., Ornitz, D.M., 2003. Conditional inactivation of FGF receptor 2 reveals an essential role for FGF signaling in the regulation of osteoblast function and bone growth. Development 130, 3063–3074.

Yuasa, T., Kondo, N., Yasuhara, R., Shimono, K., Mackem, S., Pacifici, M., Iwamoto, M., Enomoto-Iwamoto, M., 2009. Transient activation of Wnt/{beta}-catenin signaling induces abnormal growth plate closure and articular cartilage thickening in postnatal mice. Am. J. Pathol. 175, 1993–2003.

Yusuf, F., Brand-Saberi, B., 2006. The eventful somite: patterning, fate determination and cell division in the somite. Anat. Embryol. 211 (Suppl. 1), 21–30.

Zaka, R., Williams, C.J., 2006. Role of the progressive ankylosis gene in cartilage mineralization. Curr. Opin. Rheumatol. 18, 181–186.

Zakany, J., Duboule, D., 2007. The role of Hox genes during vertebrate limb development. Curr. Opin. Genet. Dev. 17, 359–366.

Zeller, R., Lopez-Rios, J., Zuniga, A., 2009. Vertebrate limb bud development: moving towards integrative analysis of organogenesis. Nat. Rev. Genet. 10, 845–858.

Zelzer, E., Glotzer, D.J., Hartmann, C., Thomas, D., Fukai, N., Soker, S., Olsen, B.R., 2001. Tissue specific regulation of VEGF expression during bone development requires Cbfa1/Runx2. Mech. Dev. 106, 97–106.

Zelzer, E., Mamluk, R., Ferrara, N., Johnson, R.S., Schipani, E., Olsen, B.R., 2004. VEGFA is necessary for chondrocyte survival during bone development. Development 131, 2161–2171.

Zhang, J., Tan, X., Li, W., Wang, Y., Wang, J., Cheng, X., Yang, X., 2005. Smad4 is required for the normal organization of the cartilage growth plate. Dev. Biol. 284, 311–322.

Zhang, M., Xie, R., Hou, W., Wang, B., Shen, R., Wang, X., Wang, Q., Zhu, T., Jonason, J.H., Chen, D., 2009. PTHrP prevents chondrocyte premature hypertrophy by inducing cyclin-D1-dependent Runx2 and Runx3 phosphorylation, ubiquitylation and proteasomal degradation. J. Cell Sci. 122, 1382–1389.

Zhang, P., Jobert, A.S., Couvineau, A., Silve, C., 1998. A homozygous inactivating mutation in the parathyroid hormone/parathyroid hormone-related peptide receptor causing Blomstrand chondrodysplasia. J. Clin. Endocrinol. Metab. 83, 3365–3368.

Zhang, Y., Ma, B., Fan, Q., 2010. Mechanisms of breast cancer bone metastasis. Cancer Lett. 292, 1–7.

Zhao, G.Q., Deng, K., Labosky, P.A., Liaw, L., Hogan, B.L., 1996. The gene encoding bone morphogenetic protein 8B is required for the initiation and maintenance of spermatogenesis in the mouse. Genes Dev. 10, 1657–1669.

Zhao, H., Feng, J., Ho, T.V., Grimes, W., Urata, M., Chai, Y., 2015. The suture provides a niche for mesenchymal stem cells of craniofacial bones. Nat. Cell Biol. 17, 386–396.

Zhao, R., Lawler, A.M., Lee, S.J., 1999. Characterization of GDF-10 expression patterns and null mice. Dev. Biol. 212, 68–79.

Zhou, G., Zheng, Q., Engin, F., Munivez, E., Chen, Y., Sebald, E., Krakow, D., Lee, B., 2006. Dominance of SOX9 function over RUNX2 during skeletogenesis. Proc. Natl. Acad. Sci. U.S.A. 103, 19004–19009.

Zhou, X., Von Der Mark, K., Henry, S., Norton, W., Adams, H., De Crombrugghe, B., 2014. Chondrocytes transdifferentiate into osteoblasts in endochondral bone during development, postnatal growth and fracture healing in mice. PLoS Genet. 10 e1004820.

Zimmerman, L.B., De Jesus-Escobar, J.M., Harland, R.M., 1996. The Spemann organizer signal noggin binds and inactivates bone morphogenetic protein 4. Cell 86, 599–606.

Zoetis, T., Tassinari, M.S., Bagi, C., Walthall, K., Hurtt, M.E., 2003. Species comparison of postnatal bone growth and development. Birth Defects Res. B Dev. Reprod. Toxicol. 68, 86–110.

Chapter 2

Skeletal stem cells: tissue-specific stem/progenitor cells of cartilage, bone, stroma, and marrow adipocytes

Pamela Gehron Robey[1] and Mara Riminucci[2]

[1]National Institute of Dental and Craniofacial Research, National Institutes of Health, Department of Health and Human Services, Bethesda, MD, United States; [2]Department of Molecular Medicine, Sapienza University of Rome, Rome, Italy

Chapter outline

Introduction

Stem cells are often thought of as a relatively new discovery, yet the existence of some sort of a stem/progenitor cell in bone from either the periosteum or the marrow was suggested as early as the 1860s in studies on bone regeneration by Ollier and Goujon (Goujon, 1869; Ollier, 1867). The concept of a stem cell was further crystalized in the late 1800s through the early 1900s by a group of astute biologists from diverse fields of interest (e.g., Boveri, Häcker, Regaud, Weidenreich, Dantschakoff, Maximow, and others, reviewed in Ramalho-Santos and Willenbring, 2007; Robey, 2000). They hypothesized that the ability of a tissue to maintain itself throughout the lifetime of an organism is based on the existence of a "stem" cell ("Stammzelle," a term first coined in German by Haeckel; Haeckel, 1868) that would remain primarily quiescent and undifferentiated, but also be able to regenerate the functional parenchyma of its tissue of origin following injury or the need for tissue rejuvenation (tissue turnover). Originally thought to exist only in tissues with high rates of turnover, such as blood, skin, and the gastrointestinal tract, evidence suggested that stem cells do exist in tissues with substantially lower rates of turnover, such as bone, with the ability to repair injury. Even tissues never thought to turn

Principles of Bone Biology. https://doi.org/10.1016/B978-0-12-814841-9.00002-6

over or repair, such as brain, do in fact contain stem cells (reviewed in Robey, 2000; see https://stemcells.nih.gov/info/basics/1.htm for more information). It was subsequently thought that virtually every tissue in the body contains some type of a stem/progenitor cell, although the existence of cardiomyocyte stem cells has been called into question (Kretzschmar et al., 2018). Nonetheless, the very notion of stem cells has had a major impact on both biological and medical sciences since the early 1990s, in terms of understanding the dynamics of tissue homeostasis in health and disease and the thought that they could be useful in tissue regeneration.

Following upon the early work of Ollier and Goujon, the hematologists Tavassoli and Crosby, aiming to better understand the support of hematopoiesis, took bone-free fragments of hematopoietic marrow and transplanted them under the kidney capsule. Remarkably, they found that marrow could be regenerated, but only after the formation of bone (Tavassoli and Crosby, 1968). It was Friedenstein et al., later in collaboration with Owen et al., who determined that the origin of bone in those marrow fragments was in fact a subpopulation of nonhematopoietic cells of the stroma upon which hematopoiesis occurs. When single-cell suspensions of bone marrow were plated into tissue culture plastic dishes at low density, a small proportion of single fibroblastic cells rapidly attached and began to proliferate to form a colony in a density-independent fashion. Friedenstein termed the initial adherent single cells as colony-forming units—fibroblasts (CFU-Fs), being cognizant of the fact that many cells could attach, but could not form a colony in a density-independent fashion. Subsequently, when the progeny of CFU-Fs (bone marrow stromal cells, BMSCs) were transplanted in vivo inside diffusion chambers that prevent vascularization (closed system), cartilage was formed in the relatively anaerobic interior of the chamber, and bone formed at the periphery, which was in close proximity to (but not in direct contact with) blood vessels. When single colonies were transplanted in conjunction with a collagen sponge under the kidney capsule with complete access to the vasculature (an open system), some colonies not only were able to form bone, stroma, and marrow adipocytes of donor origin, but also supported the formation of hematopoietic tissue of recipient origin (an ectopic bone/marrow organ) (Friedenstein et al., 1974). From this clonal analysis (and notice the emphasis on clones; i.e., the progeny of a single cell), Friedenstein and Owen proposed the existence of the first multipotent tissue-specific stem/progenitor cell from a solid connective tissue, which they termed a bone marrow stromal stem cell, able to differentiate into four different phenotypes: chondrogenic, osteoblastic, stromogenic, and adipogenic (Fig. 2.1) (Owen and Friedenstein, 1988). Later, the term "skeletal stem cell" (SSC) was adopted based on this ability to re-create all of the cells found in skeletal tissue proper (reviewed in Bianco and Robey, 2004, 2015; Owen and Friedenstein, 1988). Of note, this groundbreaking work clearly demonstrated that the stroma created by these stem/progenitor cells transfers the hematopoietic microenvironment (Friedenstein et al., 1974), contributing to the concept of a "niche" as later formulated by Schofield (1978).

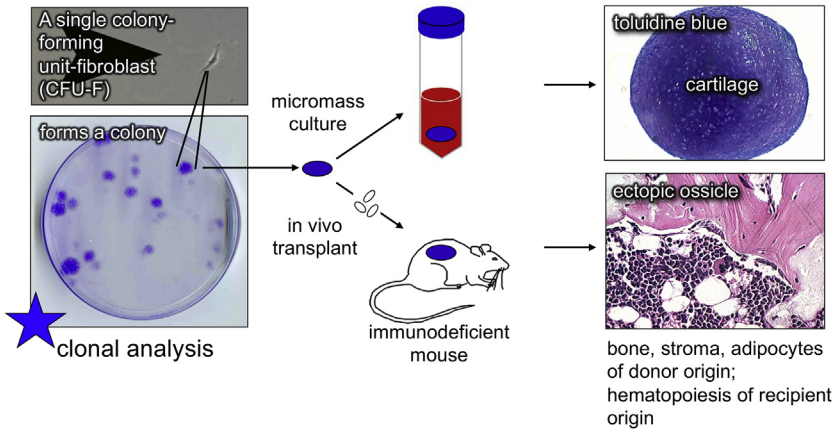

FIGURE 2.1 Proof of the existence of a postnatal multipotent skeletal stem cell. When single-cell suspensions of bone marrow are plated at low density, a single cell (colony-forming unit—fibroblast) rapidly attaches and proliferates to form a colony of bone marrow stromal cells. Clonal analysis is performed by placing clonally derived strains: (1) into micromass cultures (anaerobic) to observe the formation of cartilage or (2) onto appropriate scaffolds followed by subcutaneous transplantation into immunocompromised mice to observe the formation of a bone/marrow organ. This ectopic ossicle is composed of bone, hematopoiesis-supportive stroma, and marrow adipocytes of donor origin and hematopoiesis of recipient origin. *Modified from Bianco, P., Kuznetsov, S., Riminucci, M., Robey, P.G., 2006. Postnatal skeletal stem cells. Meth Enzymol 419, 117—148 and Bianco, P., Robey, P.G., Penessi, G., 2008a. Cell source. In: de Boer, J., van Blitterswijk, C., Thomsen, P., Hubbell, J., Cancedda, R., de Bruijn, J.D., Lindahl, A., Sohler, J., Williams, D.F. (Eds.), Tissue Engineering. Elsevier, Amsterdam, pp. 279—306.*

Developmental origins of bone and skeletal stem cells

Germ-layer specifications

During embryonic development, the body pattern is first laid out by gastrulation of the inner cell mass of the blastocyst (the source of embryonic stem cells) to form germ layers for definitive endoderm, mesoderm, and ectoderm (which includes neural crest). Bone is formed by three different specifications of mesoderm and ectoderm (Olsen et al., 2000). Temporary embryonic cartilages in the cranium are formed from paraxial mesoderm by a process of cartilage regression followed by intramembranous bone formation (Holmbeck et al., 2003). Paraxial mesoderm also forms part of the dorsal cranial vault through primarily intramembranous bone formation, and the axial skeleton through primarily endochondral bone formation. Somatic lateral plate mesoderm forms the appendicular skeleton through intramembranous and endochondral bone formation, and last, neural crest forms the frontal cranium and facial bones through both intramembranous and endochondral pathways (Berendsen and Olsen, 2015; Olsen et al., 2000). It has also been suggested that the dorsal root of the aorta gives rise to skeletal cells through a process whereby specialized angioblasts (mesoangioblasts) bud cells into the extravascular space that go on to form connective tissues, including skeletal tissue (Bianco and Cossu, 1999), analogous to hemangioblasts budding cells into the vessel lumen to form definitive hematopoietic stem cells (HSCs) (Dzierzak and Medvinsky, 2008). Consequently, there are at least three (and possibly four) embryonic sources of skeletal tissue; that is, there is no single common skeletal stem/progenitor cell during embryonic development (Fig. 2.2A and B).

During development of the axial skeleton, the primitive streak (the precursor of mesoderm and endoderm) migrates caudally to form mesendoderm. Cephalic mesendoderm further specifies into paraxial and lateral plate mesoderm. Paraxial mesoderm segments into somites with definitive borders (Pourquie, 2001). Somitomeres with less definitive borders are formed in the head region (Bothe et al., 2011). Somites further differentiate into the dermatome that will form the dermis upon which ectoderm will form skin, the myotome that will form skeletal muscle, the syndetome that will form tendons and ligaments, and the most ventral part of the somite, the sclerotome, which will form the axial skeleton. Lateral plate mesoderm undergoes a splitting process to form the intraembryonic coelom (future peritoneum) and the splanchnic and somatic lateral plate mesoderm, the latter of which goes on to form the appendicular skeleton along with part of the body wall and dermis. Splanchnic mesoderm forms viscera, the heart, and associated blood vessels, including the dorsal root of the aorta (Onimaru et al., 2011). Last, following delamination from the border of the neural plate, neural crest cells migrate into the branchial arches and form cartilage and bone of the head, all epidermal pigment cells, and most of the peripheral nervous system in the trunk (Bronner, 2015) (Fig. 2.2A). It is generally thought that neural crest cells do not contribute to skeletal tissues below the neck; however, based on the expression of the neural crest marker, Wnt1, and expression of Nestin, this concept is currently being questioned (Danielian et al., 1998; Isern et al., 2014).

Patterns of bone formation and development of pericytes/skeletal stem cells

The different patterns of skeletal tissue formation differ from one another based on the involvement (or lack thereof) of cartilage (Fig. 2.2B). During intramembranous bone formation, there is no cartilage template. Embryonic mesenchymal condensations organize into two opposing layers of committed osteoprogenitors that begin to secrete and deposit bone matrix proteins into a sequestered area between the two layers of cells. Due to the activity of alkaline phosphatase on the surface of the committed osteogenic cells, pyrophosphate (a mineralization inhibitor) is cleaved to provide free phosphate for precipitation of a carbonate-rich apatite. In endochondral bone formation, embryonic mesenchyme condenses and differentiates into a cartilage template, the interior portion of which undergoes hypertrophy and calcification, while the outer surface (perichondrium) becomes committed to osteogenesis (periosteum). In this case, bone formation occurs in two ways: (1) between a fully committed osteogenic layer of cells and a layer of hypertrophic chondrocytes, in the bony collar, and (2) through cartilage hypertrophy and subsequent replacement by bone (Hall, 2015). In another pattern of skeletal tissue formation, best exemplified in the cranium, embryonic cartilage templates undergo regression rather than hypertrophy. These cartilages serve as a pathway to guide the formation of new bone by an intramembranous process, and ultimately disappear (Holmbeck et al., 2003) (Fig. 2.2B).

Irrespective of the pattern of formation, newly formed capillaries invade the developing bone, but lack pericytes, a cell type that has numerous cell processes that wrap around developing blood vessels to provide stability (Armulik et al., 2011). As the "naked" blood vessels begin to invade the newly formed woven bone and hypertrophic cartilage (in the case of endochondral bone formation), they form an association with committed osteoprogenitors (and possibly with hypertrophic chondrocytes) based on their expression of fibroblastic cell surface proteins. Because the osteogenic cells are no longer opposing a cell layer that is secreting bone matrix proteins, they undergo a shape change and downregulate expression of bone matrix proteins due to their association with endothelial cells, and become pericytes, cells that wrap around blood

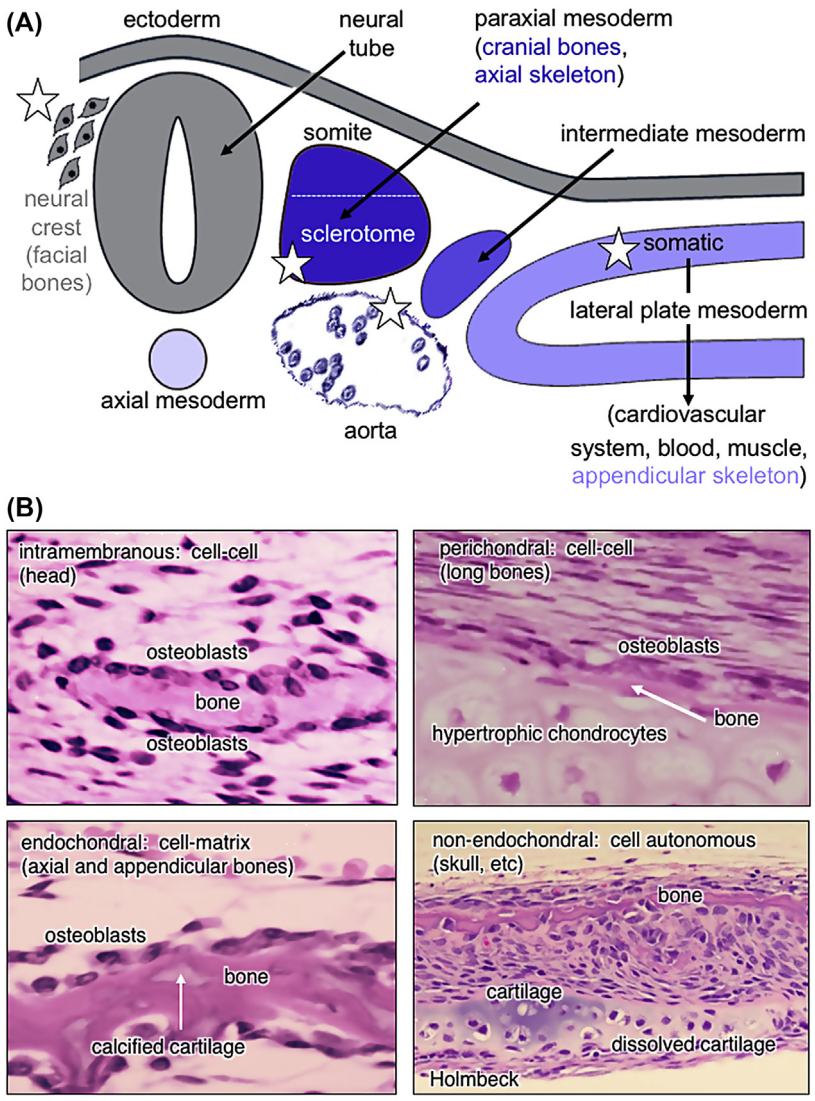

FIGURE 2.2 Development origins and patterns of bone formation. (A) During embryonic development, bone is formed by neural crest cells (ectoderm in origin) and two different specifications of mesoderm (paraxial mesoderm and somatic lateral plate mesoderm). It is also thought that mesangioblasts in the dorsal root of the developing embryo shed cells into the extravascular spaces to give rise to embryonic mesoderm. (B) Bone is formed through several different processes: (1) intramembranous (between two layers of osteoblastic cells), (2) perichondral (between a layer of osteoblastic and hypertrophic cells), (3) endochondral (calcified cartilage is replaced by woven bone), and (4) a nonendochondral replacement process (cartilage regresses, leading the way for intramembranous bone). *(A) Modified from Bianco, P., Robey, P.G., 2015. Skeletal stem cells. Development 142, 1023–1027.*

vessels to provide stability (Fig. 2.3). These pericytic cells proliferate along with the blood vessels into the interior of the bone, with osteoclasts leading the way to carve out the future marrow spaces. The pericytic cells proliferate further into the newly liberated space to form the prehematopoietic bone marrow stroma. Once sufficient bone has formed on the exterior of the rudiment to provide a protected environment, HSCs migrate through the circulation from the thymus, liver, and spleen to the bone, and escape from the circulation to establish definitive hematopoiesis in the bone marrow, the final home of the HSCs under normal conditions (Bianco et al., 1999, 2008b).

The skeletal lineage

As described earlier, embryonic skeletogenic mesenchyme, which contains the most primitive SSC, forms cartilage, bone, bone marrow stroma, and marrow adipocytes in a sequential fashion in time and space. Thus, during fetal development, chondrocytes, osteoblasts, SSCs/BMSCs, and marrow adipocytes can be seen as different stages of maturation rather than

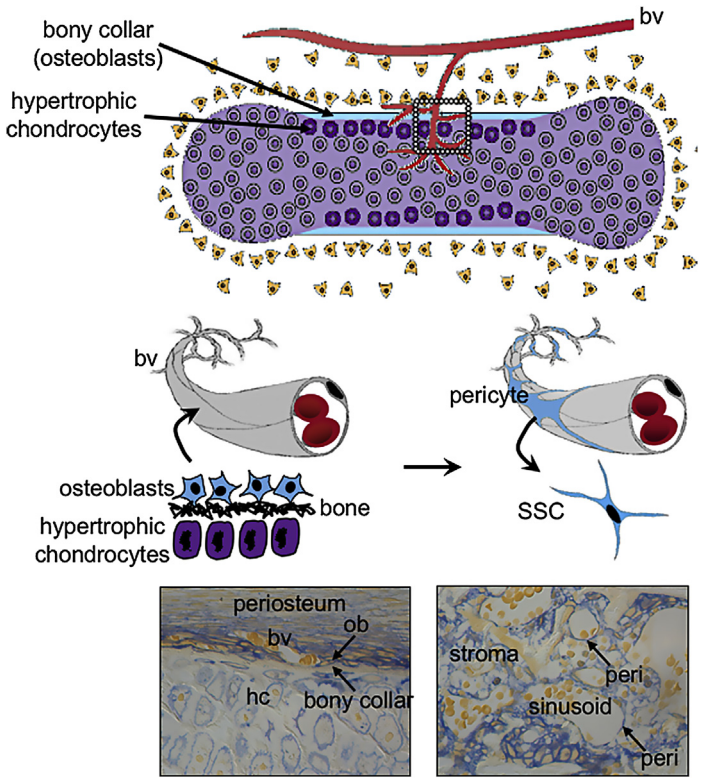

FIGURE 2.3 Development of pericytes/skeletal stem cells. As bone develops (in a long bone, as an example), blood vessels that are devoid of pericytes (cells surrounding blood vessels to give them stability) invade the developing rudiment, passing through the bony collar and hypertrophic cartilage. In doing so, ALP^{+} osteogenic cells (colored blue in the cartoons and photomicrographs) from the perichondrium are relocated into the forming marrow cavity and become primitive stromal cells that coat the forming sinusoids as pericytes, as can be seen in rodents at embryonic day 18. The pericytes (a subset of which are skeletal stem cells) remain quiescent on the blood vessel surfaces until released by injury or the need for bone turnover. *bv*, blood vessel; *hc*, hypertrophic cartilage; *ob*, osteoblast; *peri*, pericyte; *SSC*, skeletal stem cell. *Modified from Bianco, P., Robey, P.G., 2015. Skeletal stem cells. Development 142, 1023–1027.*

as separate lineages (Bianco and Robey, 2015) (Fig. 2.4A). Chondrogenesis, osteogenesis, and adipogenesis are controlled by three master transcription factors: Sox 9 (chondrogenic) (Bi et al., 1999), Runx2 (osteogenic and, to a lesser extent, chondrogenic) (Komori et al., 1997), and peroxisome proliferator-activated receptor γ2 (PPARγ2) (adipogenic) (reviewed in Muruganandan et al., 2009). In the case of cartilage, there are two potential fates: to undergo hypertrophy and be replaced by bone or to remain as hyaline cartilage on the articular surfaces of long bones in joints and in the ears and nose. The factors that maintain cartilage in a hyaline state are not well delineated as of this writing. Knowledge of this key point of regulation is of high interest based on the need to make new cartilage from an appropriate cell type that will not undergo hypertrophy, such as periosteal cells or SSCs/BMSCs.

In the context of embryonic development, a subset of committed osteogenic cells is recruited by blood vessels to form pericytes, which subsequently form stroma that supports hematopoiesis (Bianco et al., 1999, 2008b; Maes et al., 2010). As longitudinal bone growth slows and establishment of hematopoiesis is at a sufficient level to support the organism, stromal cells convert into marrow adipocytes to form yellow marrow, primarily in the distal regions of long bones. During postnatal growth (modeling), homeostasis, and aging (remodeling), cells in bone marrow stroma give rise to bone, hematopoiesis-supportive stroma, and marrow adipocytes (but rarely cartilage under normal conditions), and these tissues are thought to emanate from a single common primordial precursor, the SSC (Fig. 2.4B). Consequently, whether it be during embryonic development, postnatal growth, or adult homeostasis, there is a lineage that gives rise to skeletal tissues (chondrocytes, osteogenic cells, stroma, and marrow adipocytes), not multiple different precursor cells that give rise to different phenotypes. This has implications for the maintenance of skeletal tissues and their adaptations. Cells in the skeletal lineage are flexible; i.e., they can convert from one cell phenotype to another based on changes in the microenvironment. For example, it is well known that with aging, there is an increase in marrow adipocytes (yellow marrow) at the expense of osteogenic differentiation and support of hematopoiesis (red marrow) (Bianco and Riminucci, 1998).

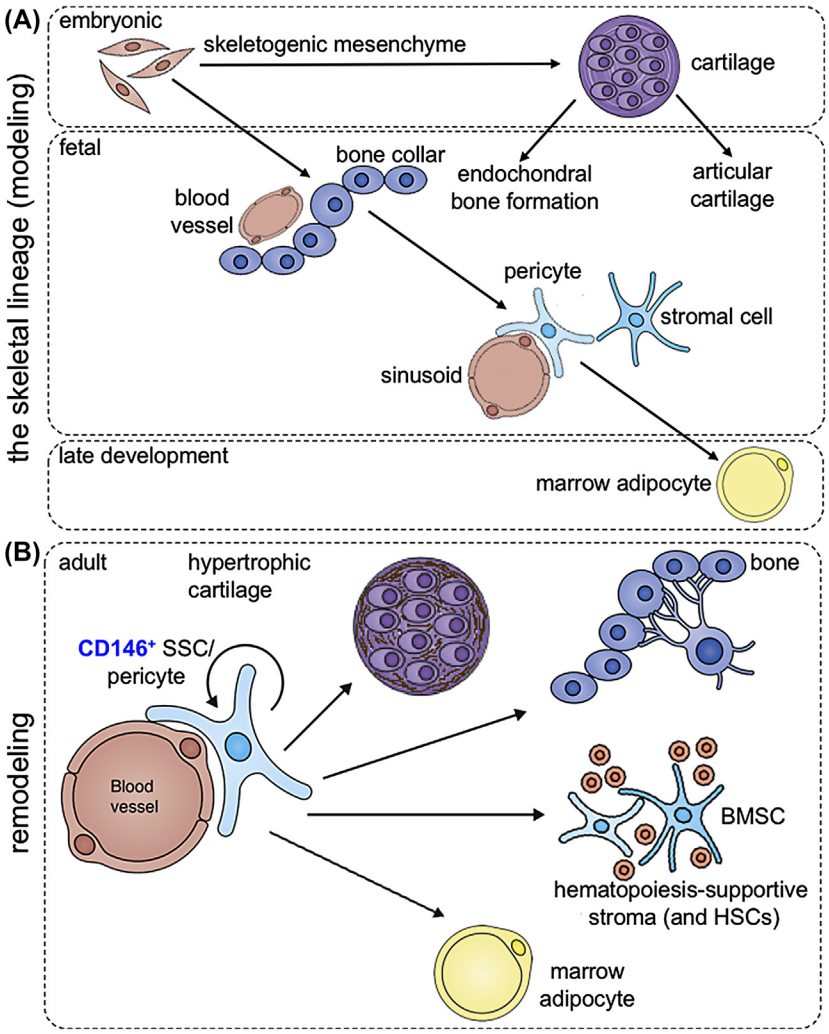

FIGURE 2.4 The skeletal lineage during embryonic development (modeling) and postnatal homeostasis (remodeling). (A) During embryonic development and postnatal maturation (modeling), cells emerging from skeletogenic mesenchyme sequentially form cartilage or bone. Cartilage either undergoes hypertrophy and is replaced by bone or remains as articular cartilage in joints. Osteogenic cells are recruited by blood vessels to form pericytes and stromal cells, which support hematopoiesis. At late stages of postnatal maturation, stromal cells accumulate fat and become marrow adipocytes. (B) In the mature postnatal organism, a subset of pericytes are skeletal stem cells that are capable of forming cartilage (rarely), bone, hematopoiesis-supportive stroma, or marrow adipocytes during skeletal remodeling. *BMSC*, bone marrow stromal cell; *HSC*, hematopoietic stem cell; *SSC*, skeletal stem cell. *Modified from Bianco, P., Robey, P.G., 2015. Skeletal stem cells. Development 142, 1023–1027.*

Cartilage is not normally seen in healthy bone marrow, and during fracture repair, the callus emanates from cells in the periosteum rather than from bone marrow stroma (O'Driscoll and Fitzsimmons, 2001). These periosteal cells are similar to, but not identical with, SSCs from bone marrow (Duchamp de Lageneste et al., 2018; Sacchetti et al., 2016). The role of marrow SSCs/BMSCs is probably to mediate remodeling of the bone in the fracture callus to restore the medullary cavity (reviewed in Einhorn and Gerstenfeld, 2015). This calls into question why SSCs/BMSCs would have the ability to make cartilage at all. The answer may be that during bone development, as blood vessels invade through the bony collar, they capture not only committed osteogenic cells, but hypertrophic chondrocytes as well, and orchestrate their conversion into pericytes. The association with endothelial cells may prevent their demise, but they may also retain a chondrogenic memory, to be recalled when released from the endothelial cell surface. Of note, it is most often reported that cartilage formed by SSCs/BMSCs undergoes hypertrophy and is converted into bone. This notion is supported by reports that not all hypertrophic chondrocytes die, and that some become osteogenic (Holmbeck et al., 2003; Muraglia et al., 2003; Roach et al., 1995; Scotti et al., 2013; Serafini et al., 2014), as has been rediscovered by Yang et al. (2014).

Regulation of SSC/BMSC fate

In postnatal life, SSCs are quiescent due to their association with blood vessels, until liberated by the need for bone turnover or injury. Upon liberation from blood vessel walls during bone turnover or following local injury, SSCs have the possibility of forming osteogenic cells, adipogenic cells, or more hematopoiesis-supportive stroma (Fig. 2.4B). The balance between osteogenic and adipogenic differentiation has received a large amount of attention due to its relevance to bone fragility and osteoporosis (Chen et al., 2016; Devlin and Rosen, 2015; James, 2013; Meyer et al., 2016; Teven et al., 2011). On the other hand, there is little information on how the SSC is directed into becoming a hematopoiesis-supporting stromal cell that is not a stem/progenitor cell. There are clear examples of the expansion of hematopoiesis, which relies on an increase in stroma, such as in hemolytic diseases where bone is lost to accommodate increased blood formation (Bianco and Riminucci, 1998). However, it has not been determined if the increase in hematopoiesis-supportive BMSCs is matched by an increase in SSCs. It has been shown that excess production of erythropoietin by platelet-derived growth factor subunit B-positive ($PDGFB^{+}$) cells (which include SSCs/BMSCs) causes expansion of red marrow (and thus, expansion of stroma) at the expense of bone and marrow adipocytes. However, the colony-forming-efficiency assay, the closest approximation of the number of SSCs available as of this writing, did not show a change in the number of colonies in these mice (Suresh et al., 2019). This suggests that expansion of the stromogenic pool does not necessarily equate with expansion of the SSC population.

Regulation of cell fate is complex, and is controlled by many factors, including hormones, cytokines, growth factors, and their downstream signaling pathways, all of which have an impact on the epigenetic pattern of the genome and subsequent transcriptional activity. Further control arises from posttranscriptional modifications (splice variants and isoforms), translational variation (small noncoding RNAs), and posttranslational modifications (reviewed in Chen et al., 2016). Mechanical forces and cell−matrix and cell−cell interactions are also influential. What follows is a very brief summary of regulatory factors influencing SSC/BMSC fate. However, it must be noted that there is some confusion in adipogenic fate choices based on the fact that it is considered by many that adipocytes from white or brown fat are equivalent to those in marrow, and they are not. Furthermore, in some cases, it is assumed that factors that induce osteogenic differentiation of SSCs/BMSCs will induce osteogenic differentiation of adipose-derived "mesenchymal stem cells" (and other nonskeletal "MSCs"). These nonskeletal "MSCs" are reported to become osteogenic based on an overreliance on artifactual in vitro assays after heavy treatment with chemical modifiers, and/or molecular engineering, but these nonskeletal "MSCs" are not inherently osteogenic.

Hormonal regulation

SSCs/BMSCs express receptors for many of the hormones that control skeletal growth and homeostasis, such as the parathyroid hormone (PTH) receptor, vitamin D receptor, glucocorticoid receptors, sex hormone receptors, thyroid hormone receptor, etc. If and how the corresponding ligands of these receptors control SSC/BMSC fate have not been closely examined in many cases. However, there are a few instances in which hormonal control or changes in their downstream signaling pathways (briefly described in the following) do have an impact on the fate of SSCs/BMSCs. For example, in hyperparathyroidism, it is thought that the ensuing endosteal fibrosis is due to the enhanced proliferation of stromal progenitor cells that accumulate and partially differentiate into osteoblastic cells (Bianco and Bonucci, 1991). Along this same line, excess PTH signaling due to a constitutively activating mutation in the PTH/PTH-related protein receptor (H223R, the causative mutation in Jansen's metaphyseal chondrodysplasia; Schipani et al., 1995), expressed specifically in mature osteoblasts in mice, led to the formation of excessive medullary bone due to the proliferation and maturation of SSCs/BMSCs, at the expense of marrow stromal cells and adipocytes (Kuznetsov et al., 2004). Interestingly, this phenotype resolved with age, with the subsequent removal of excess bone and establishment of a marrow cavity composed of stromal cells that were not multipotent SSCs based on in vivo transplantation assays. On the other side of the coin, it has long been known that estrogen deficiency leads to expansion of adipocytes at the expense of hematopoiesis-supportive stroma and bone, especially in females (e.g., Rosen and Bouxsein, 2006), which is thought to reflect a commitment of SSCs to adipogenesis at the expense of osteogenesis (e.g., Georgiou et al., 2012). However, it is also possible that direct conversion of stromal cells (rather than directing the fate of the SSC) into adipocytes contributes to this phenomenon. Likewise, glucocorticoid treatment in vivo leads to conversion of red marrow to yellow marrow, again thought to be due to a switch in fate of SSCs/BMSCs (e.g., Li et al., 2013). Paradoxically, a glucocorticoid, dexamethasone, is commonly used in medium used to osteogenically differentiate SSCs/BMSCs (Robey et al., 2014), implying that other factors are at play in vivo that drive glucocorticoid-mediated adipogenic differentiation of SSCs/BMSCs.

Signaling pathways and transcription factors

The levels of expression of Runx2, the master regulator of osteogenesis, and PPARγ, the master regulator of adipogenesis, are controlled by a number of signaling pathways activated by Wnts, members of the transforming growth factor β (TGFβ)/bone morphogenetic protein (BMP) superfamily, Notch, Hedgehogs, and fibroblast growth factors (FGFs) (and others), with extensive cross talk between these pathways (reviewed in Chen et al., 2012, 2016; Cook and Genever, 2013; Lin and Hankenson, 2011). Generally speaking, these pathways increase Runx2 expression with a concomitant decrease in PPARγ, or vice versa, during commitment and differentiation of SSCs. Runx2 is the first upregulated gene during osteogenic commitment and, in turn, upregulates Osterix, which along with Runx2 is essential for osteogenesis. Adipogenesis is initiated by upregulation of CCAAT/enhancer binding protein β (C/EBPβ) and C/EBPδ, which in turn induces PPARγ2. PPARγ2 upregulates C/EBPα, which maintains PPARγ2 expression via a positive feedback loop (reviewed in Cook and Genever, 2013).

Perhaps one of the most important signaling pathways that promotes osteogenesis of SSCs at the expense of adipogenesis is the Wnt/β-catenin pathway, which stimulates Runx2 expression and inhibits C/EBPα, thereby inhibiting adipogenesis (Monroe et al., 2012; Taipaleenmaki et al., 2011; reviewed in Cook and Genever, 2013). Members of the TGFβ superfamily also exert major influences mediated by pSmads 2/3, and have multiple effects on differentiation of SSCs/BMSCs. While TGFβs stimulate proliferation, they inhibit osteogenic differentiation (Alliston et al., 2001) and adipogenic differentiation (Kumar et al., 2012). In addition, BMPs play a major role in osteogenic commitment via pSmads 1/5/8 and Msx/Dlx homeoproteins to increase expression of Runx2 (reviewed in Cook and Genever, 2013). However, BMPs also appear to play a role in early adipogenic commitment, although the mechanisms are not clear. Adipogenic differentiation may be related to the type of BMP and its concentration and/or the type of receptors that are present on the cells at different stages of commitment (reviewed in Chen et al., 2012, 2016). It is generally reported that Notch signaling mediated by Delta/Jagged suppresses osteogenic differentiation (Zanotti and Canalis, 2016) and maintains SSCs in a primordial state (Hilton et al., 2008; Tu et al., 2012); however, positive effects on osteoblastogenesis have been reported (reviewed in Chen et al., 2012; Lin and Hankenson, 2011). Notch signaling also appears to have negative and positive effects during adipogenic commitment and differentiation (reviewed in Muruganandan et al., 2009). Indian hedgehog signaling, mediated by the Kinesin family protein Kif7, and the main intracellular Hedgehog pathway regulator, SUFU, is typically thought of in the context of growth plate dynamics, where it promotes osteogenic differentiation (Jemtland et al., 2003). However, in the context of the bone marrow microenvironment, Hedgehog signaling decreases with adipogenic differentiation of SSCs/BMSCs, suggesting that it is a negative regulator of adipogenesis (Fontaine et al., 2008). Hedgehogs may also interact with BMP signaling to promote osteogenic commitment (reviewed in Chen et al., 2016). FGFs can also be osteogenic (FGF2, FGF4, FGF3, FGF9, and FGF19) and adipogenic (FGF1, FGF2, and FGF10) and signal via a number of pathways that include extracellular signal-regulated kinase 1/2 (ERK1/2), p38 mitogen-activated protein kinase, Jun N-terminal kinase (JNK), protein kinase C, and phosphatidylinositol 3-kinase (PI3K) (Ling et al., 2006; Neubauer et al., 2004; reviewed in Chen et al., 2016).

As briefly listed, these are the major players that have been implicated in controlling the fate of SSCs/BMSCs, but there are other pathways initiated by factors such as insulin-like growth factor 1 (IGF-1) and PDGF (liberated from bone matrix during bone resorption), epidermal growth factor, and the transcription factor YAZ (reviewed in Chen et al., 2012, 2016; Cook and Genever, 2013; Lin and Hankenson, 2011). There are likely to be more regulators identified in the future.

Epigenetic controls

It is thought that epigenetic changes induced by signaling pathways operating in SSCs/BMSCs play a major role in fate decisions and stabilization of the osteogenic or adipogenic phenotype (Meyer et al., 2016). Modification of the conformation of chromatin (defined as DNA with bound protein) has an impact on transcription, with open chromatin (euchromatin) being accessible and condensed chromatin (heterochromatin) being inaccessible to transcriptional machinery, transcription factors, and other cofactors. Changes in chromatin architecture are brought about by DNA and histone modification. DNA methylation at CpG dinucleotides and CpG islands by methyltransferases is usually suppressive in nature. In addition to DNA methylation, chromatin structure is also influenced by modifications made to histones bound to DNA, such as methylation and acetylation (and there are others), that occur posttranslationally. Histones 3 and 4 are commonly methylated at specific sites by histone methyltransferases (HMTs). H3K4me3 is usually associated with euchromatin and gene activation, whereas H3K9me3 and H3K27me3 are usually associated with heterochromatin and gene repression. These methyl groups can be removed by histone demethylases (HDMs), and the changes in methylation are very dynamic, promoting flexibility. As an example, it has been demonstrated that formation of H3K27me3 by the

HMT EZH2 promotes adipogenesis of SSCs, whereas its removal by the HDM KDM6A promotes osteogenesis (Hemming et al., 2014). Histone acetylation by histone acetyltransferases and deacetylation by deacetylases (HDACs) is also dynamic. H3K9ac and HRK16ac are generally found in euchromatin and are indicative of transcriptional activation, whereas deacetylation leads to gene inactivation. While use of the HDAC inhibitor trichostatin A was thought to improve osteogenic differentiation of SSCs, it was determined that it profoundly decreased cell proliferation, and did not improve their osteogenic capacity upon in vivo transplantation (de Boer et al., 2006). Further work is needed to demonstrate what role histone acetylation and deacetylation plays in SSC/BMSC cell fate.

MicroRNAs

There are three forms of small noncoding RNAs: short-hairpin RNAs (shRNAs), microRNAs (miRs), and piwi RNAs. shRNAs are generally synthetic, and introduced exogenously (or created by processing of foreign dsRNAs), and piwi RNAs are primarily expressed in germ-line cells (reviewed in Carthew and Sontheimer, 2009; Ha and Kim, 2014); consequently, the role of miRs in controlling cell fate will be briefly summarized. miRs represent a way in which protein expression can be rapidly modified by either blocking translation or inducing the degradation of target mRNAs (reviewed in Jonas and Izaurralde, 2015). Interestingly, regulators of skeletal homeostasis such as BMPs and TGFβs are known to regulate miR expression and processing (reviewed in Lian et al., 2012). Numerous studies have been published indicating that miRs can control cell fate by downregulating the protein level of Runx2 or PPARγ, thereby enhancing adipogenesis or osteogenesis, respectively. Members of the miR-320 family were found to increase during adipogenic differentiation of SSCs/BMSCs by decreasing levels of Runx2 (among other genes) (Hamam et al., 2014). Conversely, miR-20a promotes osteogenesis by targeting PPARγ, as well as inhibitors of the BMP signaling pathway (Zhang et al., 2011). In addition, miR26a was found to decrease in SSCs during rapid bone loss in mice induced by ovariectomy. Overexpression of miR-26a was found to increase osteogenesis by SSCs by reducing levels of Tob1, which is a negative regulator of the BMP/Smad signaling pathway (Li et al., 2015). These are just a few examples, and others can be found in a 2014 review (Clark et al., 2014).

Cell–cell and cell–substrate interactions, cell shape, and mechanical forces

SSCs/BMSCs are not alone in the bone/marrow organ, and their interaction with other cell types undoubtedly influences fate. As already described, interaction with endothelial cells keeps them in a primordial state, and a study has shown that this is due to repression of Osterix (Meury et al., 2006). They also interact with HSCs; however, how HSCs and other hematopoietic cells influence SSC fate is not well known at this time, owing to the rather recent recognition by hematologists that SSCs are members of the HSC niche (reviewed in Ugarte and Forsberg, 2013).

Cell–matrix interactions occur primarily through: (1) integrins (which bind to many of the extracellular matrix components of bone), (2) discoidin domain receptors and urokinase plasminogen activator receptors, which bind to collagens, and (3) other cell surface molecules such as CD44, which binds to osteopontin (a major component of bone matrix) and hyaluronan. Of note, bone marrow is characterized by a preponderance of cell–cell interactions rather than cell–matrix interactions. Marrow contains thin reticular fibers composed primarily of type III collagen, and high levels of hyaluronan, which is gellike in nature (reviewed in Kuter et al., 2007). However, there is no doubt that after isolation from marrow, substrate has a profound influence on cell fate. For example, binding of αVβ1 to osteopontin inhibited adipogenic differentiation and stimulated osteogenic differentiation of murine SSCs, via downregulation of C/EBP expression (Chen et al., 2014). Modulation of cell shape also has an impact on fate. In a study where cell shape was controlled by plating at different densities, it was found that if cells were plated at low density and allowed to spread, the cells were directed toward osteogenesis, whereas plating at high densities, such that the cells remained rounded, induced adipogenesis. These phenomena were found to be mediated by the small GTPase RhoA, which is a regulator of the cytoskeleton (McBeath et al., 2004). There are a number of different methods by which substrates can be patterned, not only in shape, but in their surface character (D'Arcangelo and McGuigan, 2015). Patterns that promoted cytoskeletal contraction via JNK and ERK1/2 activity induced osteogenic differentiation, whereas when cytoskeletal contraction was not supported by a particular pattern, adipogenesis predominated (Kilian et al., 2010). Substrate elasticity and stiffness and the resulting mechanical forces sensed by SSCs/BMSCs control fate as well, with stiffer substrates generally favoring osteogenesis and softer substrates favoring adipogenesis. How substrate interactions control cell fate is extensively reviewed by Guilak et al. (2009). However, again the reader is cautioned that many of these studies purport to show differentiation of SSCs/BMSCs into nonskeletal phenotypes based on morphology and expression of a few markers, without demonstration of functionality. Last, matrix remodeling has a profound effect on the fate of SSCs. A dramatic example is found in the global deletion

of the membrane-type matrix metalloproteinase MT1-MMP (which is a true collagenase), in mice. Although mice appear normal at birth, there is a rapid decrease in growth, and by 40 days, they exhibit severe dwarfism and multiple skeletal defects. Transplantation of SSCs/BMSCs from the mutant mice revealed an almost complete inability to re-form a bone/marrow organ, indicating that MT1-MMP activity is essential for SSC self-renewal (Holmbeck et al., 1999). This mouse model is a direct phenocopy of the human vanishing bone disease Winchester syndrome, now known to be caused by an inactivating mutation in MT1-MMP (Evans et al., 2012).

Isolation of SSCs/BMSCs

While the multipotent stem cell found in marrow is most properly called a bone marrow stromal stem cell or an SSC (reviewed in Bianco and Robey, 2004, 2015; Robey, 2017), it has also gone by the name of "mesenchymal stem cell," based on its ability to re-create bone tissues that originate primarily from embryonic mesenchyme (reviewed in Caplan, 2005). However, not all embryonic mesenchyme forms bone. Furthermore, mesenchyme is an embryonic tissue that forms not only connective tissues, but also blood and blood vessels (MacCord, 2012). No postnatal cell, including any kind of "MSC," has been found to form all three of these tissues. But by applying some of the techniques developed for the isolation and characterization of SSCs/BMSCs, numerous studies purported to identify "MSCs" with the ability to form cartilage, bone, and fat in virtually all connective tissues and beyond. However, the true differentiation capacity and ability to self-renew of non−bone marrow "MSCs" have often not been determined using rigorous assays, leading one to believe that "MSCs" from any tissue are equivalent to SSCs/BMSCs. Furthermore, while some non−bone marrow "MSCs" may form bone, usually after treatment with a BMP, or genetic modification, most, if not all, lack the ability to support the formation of marrow. Few publications on nonmarrow "MSCs" comment on the ability to support hematopoiesis; however, examination of the histological results of in vivo transplantation assays highlight the fact that "MSCs" from adipose tissue (Hicok et al., 2004), dental pulp (Gronthos et al., 2000), periodontal ligament (Miura et al., 2003), and muscle (Sacchetti et al., 2016), as examples, often do not form bone based on rigorous criteria as presented in Phillips et al. (Phillips et al., 2014), and do not support the formation of hematopoietic marrow. In evaluating the results of in vivo transplantation with appropriate scaffolds, it is critical to determine that bone with identifiable osteocytes and osteoblasts of donor origin is formed, rather than dystrophic calcification, which can arise in pathological conditions such as some forms of heterotopic ossification (reviewed in Xu et al., 2018).

SSCs/BMSCs can be isolated from iliac crest aspirates, core biopsies, and surgical waste (Robey, 2011; Robey et al., 2014). While aspirates are less invasive than core biopsies, aspirates are contaminated with large amounts of peripheral blood when large volumes are aspirated, even with frequent repositioning of the aspiration needle, and excess peripheral blood can have a negative impact on the growth of BMSCs (Kharlamova, 1975). When core biopsies and surgical waste are available, repeated washing releases high numbers of cells (reviewed in Bianco et al., 2006). Cells from periosteal tissue, generated via enzymatic treatment or by explant cultures (for examples, see O'Driscoll and Fitzsimmons, 2001; Duchamp de Lageneste et al., 2018), also contain SSCs, but they are not identical to those found in bone marrow.

Characterization of SSCs/BMSCs

The definition of a stem cell is often variable, based on properties that are specific to the tissue from which a stem cell has been isolated. However, the two critical definitions of a stem cell are that the progeny of a single cell are able to re-create the functional parenchyma of a tissue (potency) and that the single cell can self-renew (reviewed in Ramalho-Santos and Willenbring, 2007); i.e., that its divisions are controlled in such a way that the stem cell is maintained within the tissue (Fig. 2.5).

Potency

Rigorous potency assays are critical in defining the differentiation potential of a stem cell and are based on clonal analyses rather than the BMSC population as a whole (Fig. 2.1). Studies by a number of groups (Friedenstein et al., 1974; Gronthos et al., 1994; Kuznetsov et al., 1997; Sacchetti et al., 2007; Sworder et al., 2015) characterized the differentiation capacity of clonal strains by combination of single-colony-derived strains with an appropriate scaffold and transplantation into immunocompromised mice in vivo. From these studies, it was determined that only ∼10% of the CFU-F-derived clonal strains were able to form a complete ossicle composed of bone, stroma, and marrow adipocytes of donor origin and hematopoiesis of recipient origin (multipotent clones), whereas ∼50% of the clones formed only bone and fibrous tissue of donor origin and did not support hematopoiesis (osteogenic clones), and the remainder formed only fibrous tissue

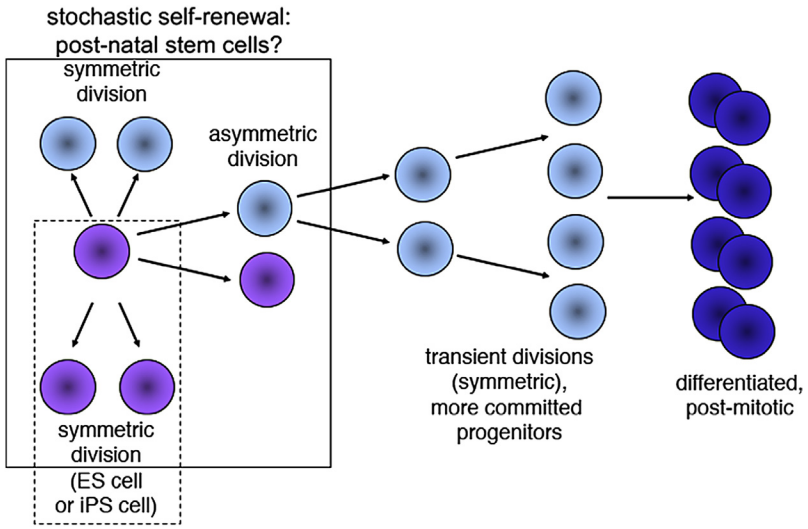

FIGURE 2.5 The kinetics of stem cell self-renewal. A defining feature of stem cells is the ability to self-renew, which is dependent on the type of cell division. Three patterns of stem cell division are possible: (1) asymmetric division in which one daughter cell remains a stem cell and the other is a committed transiently amplifying cell that ultimately differentiates and is postmitotic, (2) symmetric division in which both daughter cells remain as stem cells (as is exemplified by embryonic stem cells and pluripotent stem cells), and (3) symmetric division in which both daughter cells are committed transiently amplifying cells. The exact method by which postnatal stem cells are maintained within a given tissue is not well known, and it has been postulated that postnatal stem cells toggle from one type of division to another, based on the microenvironment and the needs of the tissue (Watt and Hogan, 2000). *ES*, embryonic stem; *iPS*, induced pluripotent stem. *Modified from Bianco, P., Robey, P.G., Penessi, G., 2008a. Cell source. In: de Boer, J., van Blitterswijk, C., Thomsen, P., Hubbell, J., Cancedda, R., de Bruijn, J.D., Lindahl, A., Sohler, J., Williams, D.F. (Eds.), Tissue Engineering. Elsevier, Amsterdam, pp. 279–306.*

(fibroblastic clones). These results indicate that while all of the multipotent clones originated from a single CFU-F, not all CFU-Fs are in fact multipotent. Based on the combination of clonal analysis and in vivo transplantation, one in five of the original CFU-Fs is multipotent, which is the closest approximation to date of the number of SSCs in the total BMSC population.

It must be noted that in vivo transplantation is the gold standard by which to evaluate osteogenic, stromagenic. and adipogenic capacity. Although in vitro assays are often used, they are highly prone to artifact. For the osteogenesis assay, alizarin red S cannot distinguish between dystrophic calcification induced by dead and dying cells versus matrix mineralization. In addition, if the cells make the enzyme alkaline phosphatase, the enzyme cleaves β-glycerophosphate that is in the osteogenic differentiation medium, and when the phosphate concentration in the medium becomes high enough, calcium phosphate precipitates, and it too stains with alizarin red S, but it is not hydroxyapatite. Of interest, there are a number of immortalized cell lines that are used to study the support of hematopoiesis in vitro. However, in vivo transplantation of several of these lines did not result in bone formation, or support hematopoiesis (Chang and Robey, unpublished results). In the adipogenic assay, many cells take up lipid from the serum in the medium and do not synthesize lipids de novo. From these findings, it is clear that in vivo transplantation with an appropriate scaffold is the gold standard by which to assess osteogenic, stromogenic, and adipogenic differentiation.

Conversely, the current gold standard for cartilage formation is the in vivo pellet culture as developed by Johnstone et al. (1998) and Barry et al. (Barron et al., 2015). However, the results of this assay are often misinterpreted. For the chondrogenic pellet culture, one must see bona fide chondrocytes lying in lacunae, surrounded by extracellular matrix that stains purple with toluidine blue (metachromasia). Alcian blue is not specific enough (osteoid stains lightly with Alcian blue), and many reports show pellets of dead cells that stain lightly with Alcian blue. With continued culture of cartilage pellets, the outer surface becomes osteogenic in nature, reminiscent of endochondral bone formation (Muraglia et al., 2003). If cartilage pellets are transplanted in vivo, without any additional scaffold, they remodel into bone either through a hypertrophy pathway (Scotti et al., 2013) or directly into a bone/marrow organ (Serafini et al., 2014). These results harken back to what is seen during development (modeling) and postnatal homeostasis (remodeling): under normal circumstances, SSCs/BMSCs do not form stable cartilage, although they may arise by conversion of a hypertrophic chondrocyte into a pericyte. However, it has been shown that SSCs/BMSCs may be maintained in vivo with an appropriate scaffold, perhaps due to a reawakening of the chondrogenic memory (Kuznetsov et al., 2019).

Markers

Based on their remarkable ability to form cartilage (at least temporarily), and a bone marrow/organ, there have been extensive studies on the characterization of the cell surface markers of human BMSCs, in hopes of identifying a signature that would be useful in isolating SSCs away from more committed BMSCs (reviewed in Bianco et al., 2006; Boxall and Jones, 2012). The consensus is that these cells are uniformly negative for hematopoietic markers such as CD14/LPS receptor, CD34/hematopoietic progenitor cell antigen, and CD45/leukocyte common antigen, and are devoid of many (CD31/PECAM1), but not all, endothelial markers. They are positive for a long list of markers, including (but not limited to) CD13/aminopeptidase N, CD29/ITGB1, CD44/phagocytic glycoprotein 1, CD49a/ITGA1, CD73/ecto-5′-nucleotidase, CD90/Thy-1, CD105/endoglin (also an endothelial marker), CD106/VCAM-2, CD166/ALCAM, Stro1/heat shock protein cognate 70 (a pericyte marker; Fitter et al., 2017; Simmons and Torok-Storb, 1991), and CD146/MCAM (also an endothelial marker) and CD271/LNGFR (Tormin et al., 2011), and there are others. However, these markers are not specific for SSCs/BMSCs and are found on virtually all fibroblastic and/or pericytic cells from many tissues, with some variation depending on the tissue source (Bianco et al., 2008b, 2013). As of this writing, there is no single cell surface marker that can be used to unequivocally identify an SSC, although combinations of markers such as CD146 (Sacchetti et al., 2007) and CD271 (Tormin et al., 2011) may be useful in enriching for SSCs (Robey et al., unpublished results). In addition, cell sorting is best applied to freshly isolated cells, rather than ex vivo-expanded cells. It is known that the expression of many markers changes with time and culture. For example, Stro-1 is known to rapidly decrease with time in culture (Bianco et al., 2008b, 2013).

The aforementioned markers pertain to human cells and in some cases to murine cells. However, there are some significant differences. For example, selection of $CD34^{-}/CD45^{-}/CD146^{+}$ human cells isolates all of the CFU-Fs, whereas murine cells with this phenotype are not CFU-Fs. Selection for CD106/VCAM-1 isolates murine CFU-Fs, but CD146 does not (Chou et al., 2012). With the ability to generate various reporter mice for proper lineage tracing, a number of studies have suggested that Nestin-GFP, Mx1, Lepr, PDGFRα, gremlin (reviewed in Chen et al., 2017, 2018) and CD164/podoplanin (Chan et al., 2018) are potentially relevant markers of murine SSCs.

Determination of skeletal stem cell self-renewal

Friedenstein and Owen, and others that followed, clearly demonstrated that BMSCs fulfilled the first criterion of a stem cell, e.g., they are able to re-create a functional parenchyma (a bone/marrow organ). However, determination of the precise origin and identity came later, along with evidence of self-renewal with the adaptation of a transplantation assay, as has been used by hematologists to determine the presence of HSCs (Sacchetti et al., 2007).

During mitosis, there are three fates for a stem cell: (1) the stem cell divides asymmetrically, and one daughter is maintained as a stem cell, the other as a transiently amplifying cell; (2) the stem cell divides symmetrically, and both daughters remain as stem cells, as in proliferation of embryonic and induced pluripotent stem cells in vitro; or (3) the stem cell divides symmetrically, but both daughters are transiently amplifying cells, with ultimate loss of the stem cell if this type of symmetrical division persists (Fig. 2.5). The allocation of stem cells among these types of divisions during embryonic development, postnatal growth, and homeostasis in adulthood is not well understood. It may be that all three types of divisions are operative under different circumstances, i.e., toggling from one type of division to another (Watt and Hogan, 2000).

Based on these types of cell divisions, it is clear that extensive proliferation is not evidence of self-renewal, as is often claimed in the literature. Using clonal analysis and the transplantation assay (which is key for the demonstration of self-renewal in the hematological system), evidence of self-renewal is linked with: (1) the isolation of a single cell with an identifiable phenotype whose progeny re-create a functional tissue and (2) reisolation of a single cell from the re-created functional tissue with the same identifiable phenotype. By comparing populations of bone-forming cells that were not able to support hematopoiesis to SSCs/BMSCs by fluorescence-activated cell sorting (FACS) for various different markers, it was determined that CD146 (also known as MCAM) was highly expressed by BMSCs, but not by normal human trabecular bone cells. Immunohistochemistry of human marrow identified the $CD146^{+}$ cells as pericytes. Clones established from freshly isolated human marrow were homogeneously positive for CD146, and when clonal strains were transplanted along with scaffolds into mice, again, ~10% were multipotent and able to form a bone/marrow organ. In those transplants, using an antibody specific for human CD146, the only human $CD146^{+}$ cells were pericytes on marrow sinusoids. Human osteocytes and osteoblasts, as identified by staining with antibody specific for human mitochondria, were not, indicating that ex vivo-expanded human $CD146^{+}$ cells were not only able to differentiate into osteogenic cells, but also able to self-renew into pericytes. Furthermore, human cells isolated by collagenase digestion of the transplants by

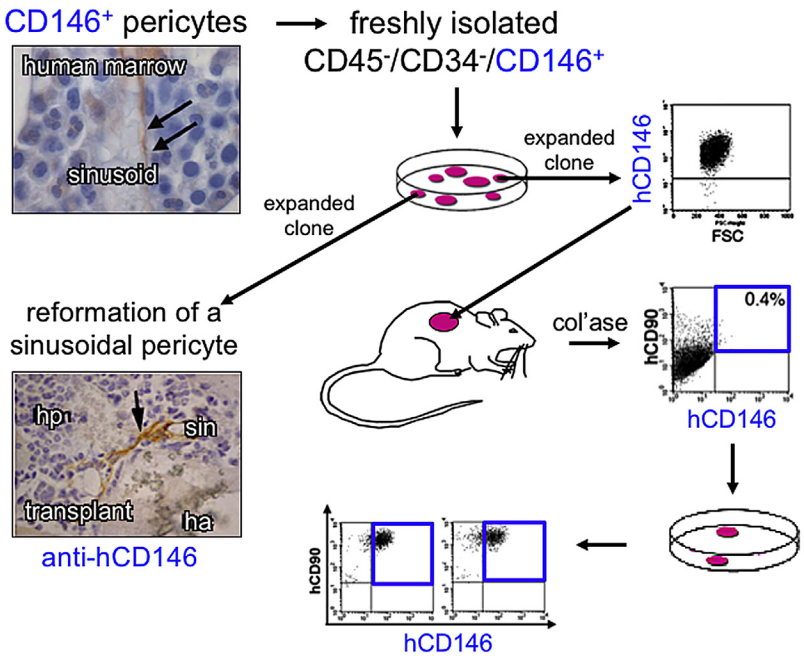

FIGURE 2.6 Skeletal stem cell self-renewal. Based on the use of cloned cells, an antibody specific for human CD146, and in vivo transplantation, it was determined that the multipotent subset of bone marrow stromal cells (BMSCs) does self-renew and contains bona fide skeletal stem cells (SSCs). It was first determined that CD146 is a marker of BMSCs that are able to support hematopoiesis (a defining feature of SSCs) and that these cells are sinusoidal pericytes. Freshly isolated human bone marrow $CD45^{-}/CD34^{-}/CD146^{+}$ cells are clonogenic. When a subset of individual $CD146^{+}$ clones (~1:5) is transplanted, they once again form a bone/marrow organ (ectopic ossicle) and human $CD146^{+}$ pericytes. Human $CD146^{+}$ cells can be reisolated from the ossicle as $CD146^{+}$ CFU-Fs, providing definitive evidence of self-renewal. *ha*, hydroxyapatite/tricalcium phosphate; *hp*, hematopoiesis; *sin*, sinusoid. *Modified from Sacchetti, B., Funari, A., Michienzi, S., Di Cesare, S., Piersanti, S., Saggio, I., Tagliafico, E., Ferrari, S., Robey, P.G., Riminucci, M., Bianco, P., 2007. Self-renewing osteoprogenitors in bone marrow sinusoids can organize a hematopoietic microenvironment. Cell 131, 324–336.*

way of magnetic cell sorting with anti-human-specific CD90 were clonogenic, and $CD146^{+}$, indicative of self-renewal of the CFU-F (Sacchetti et al., 2007) (Fig. 2.6).

The role of SSCs/BMSCs in postnatal bone turnover and remodeling

Bone turnover/remodeling is initiated by many factors, such as PTH, which is released from the parathyroid gland when the calcium-sensing receptor detects a decrease in serum calcium, and when there is a need to replace bone that has become microdamaged through mechanisms that are not yet clear. Formation of receptor activator of NF-κB (RANK)-expressing osteoclast precursors of the monocyte/macrophage series, as well as T cells that influence osteoclast formation (Li et al., 2011), is supported by SSCs/BMSCs by providing a "bed" (στρώμα (Greek)—*stróma*) upon which they are formed. SSCs/BMSCs express a long list of hematopoiesis-associated cytokines and growth factors (Gene Ontology categories "hematological system development and function" and "hematopoiesis" are highly overrepresented in multipotent SSC/BMSC clonal lines; data are in GEO GSE64789; Sworder et al., 2015). SSCs/BMSCs also express high levels of macrophage colony-stimulating factor and RANK ligand (RANKL), both of which are essential for osteoclast formation, and osteoprotegerin (OPG), which serves as a decoy receptor for RANKL, preventing osteoclast formation. Osteoclast formation and bone resorption are dependent on the balance of RANKL and OPG expressed by BMSCs and more mature osteoblastic cells, and BMSCs have long been thought to play a major role in osteoclast formation (reviewed in Boyce and Xing, 2007). Based on mouse models with conditional or cell/tissue-specific deletion of RANKL, it has been proposed that osteocytes also control osteoclast formation based on their expression of RANKL. However, it appears that the $RANKL^{+}$ cell type that controls osteoclastogenesis may be site specific. For example, mice with RANKL deletion in mature osteoblasts and osteocytes using a DMP1-Cre driver maintain tooth eruption, which requires bone resorption to occur, whereas the long bones exhibit an osteopetrotic-like phenotype (reviewed in Sims and Martin, 2014; Xiong and O'Brien, 2012). Further studies are needed to determine the contributions of SSCs/BMSCs, more mature osteoblastic cells, and osteocytes to initiating osteoclast formation throughout the skeleton.

Subsequent to the formation of osteoclasts and dissolution of mineralized matrix, a plethora of growth factors, buried within bone due to their affinity for carbonate-rich apatite, is liberated, including BMPs, PDGF, IGF-1 and IGF-2, and TGFβs. Consequently, PTH, the released factors, as well as those synthesized by local cells (Wnt10b by $CD8^+$ cells, FGF and vascular endothelial growth factor by BMSCs), mediate the reversal stage, which is marked by a cessation in bone resorption and creation of a microenvironment conducive for bone formation, thereby coupling bone resorption with bone formation (reviewed in Crane and Cao, 2014; Sims and Martin, 2014). It is thought that through osteoclastic action, active TGFβ is released and establishes a gradient from the resorption site through the marrow to the pericytes located on a nearby blood vessel. This gradient has two effects. Due to the high concentration of TGFβ at the site of resorption, it inhibits migration of osteoclastic precursors into the area; however, the gradient initiates migration of SSCs/BMSCs into the area in need of restoration, but does not induce differentiation (Tang et al., 2009). Upon arrival in the resorption bay, BMSCs are induced to osteogenic differentiation by the interplay of the TGFβ/BMP, Wnt, and IGF-1 signaling pathways. Interestingly, PTH, in addition to initiating bone resorption, also plays a role in bone formation. PTH bound to its receptor, PTHR1, complexes with Lrp6 (Wnt coreceptor), which leads to stabilization of β-catenin and pSmad1 signaling, along with stimulating cAMP-mediated signaling. The PTH−PTHR1 complex can also bind to the TGFβRII receptor, leading to pSmad2/3 signaling (reviewed in Crane and Cao, 2014). IGF-1 signaling activates mTOR via the PI3K−Akt pathway and induces osteogenic differentiation of BMSCs. Alterations in any of these pathways due to mutation, or alterations in levels of expression due to changes in the microenvironment, can have significant consequences on the balance of bone resorption and formation necessary for skeletal homeostasis (reviewed in Crane and Cao, 2014; Sims and Martin, 2014).

Skeletal stem cells in disease

Based on the fact that SSCs/BMSCs are essential for new bone formation following injury, and the fact that they, in part, control osteoclast formation, these cells are important mediators of skeletal homeostasis. As such, it was hypothesized that any genetic (intrinsic) change or change in their microenvironment (extrinsic) that has an impact on their normal biological activity would result in a skeletal disorder. Furthermore, due to their key role in supporting hematopoiesis and as a component of the HSC's niche (Ugarte and Forsberg, 2013), it was also theorized that there may be some hematological diseases or disorders that are caused, or worsened, by dysfunction of SSCs/BMSCs. Support for these notions came from both genetic (intrinsic) and acquired (extrinsic) diseases that affect bone and hematopoiesis.

Fibrous dysplasia of bone and the McCune−Albright syndrome

The genetic disease, McCune−Albright syndrome (MAS; OMIM: 174800) is characterized by the triad of skin hyperpigmentation (café au lait spots with the "coast of Maine" profile), hyperactive endocrinopathies (renal phosphate wasting, precocious puberty, growth hormone excess, hyperthyroidism, hyperparathyroidism, etc.), and fibrous dysplasia of bone (FD). Patients with FD/MAS are somatic mosaics (the mutation occurs after fertilization) with activating missense mutations of *GNAS*, which codes for Gsα, leading to overproduction of cAMP. FD lesions are characterized by the replacement of normal bone and marrow with woven, poorly organized, and undermineralized bone and replacement of marrow (hematopoiesis and marrow adipocytes) with a fibrotic tissue (reviewed in Boyce et al., 1993) (Fig. 2.7). This fibrotic tissue was found to be composed of a high proportion of mutant BMSCs (Riminucci et al., 1997). The initial effects of the mutation are to dramatically increase their proliferation and to inhibit their ability to form hematopoiesis-supporting stroma and marrow adipocytes. Furthermore, their differentiation into mature osteoblastic cells is severely compromised, as characterized by their retracted morphology and abnormal synthesis and organization of bone matrix, resulting in the formation of Sharpey's fibers (Bianco et al., 2000; Riminucci et al., 1999). The abnormal bone matrix is osteomalacic, due to hypophosphatemia caused by excess production of the phosphate-regulating hormone FGF-23 by the mutated osteogenic cells (Riminucci et al., 2003a). The abnormal composition of the matrix may also play a role in the undermineralization noted in these lesions.

Studies utilizing the fibrotic marrow from FD lesional bone showed that there was a higher colony-forming efficiency compared with normal bone marrow (Fig. 2.7). The presence of transiently amplifying cells present in the FD sample most likely explains the increase in colony-forming efficiency (Kuznetsov et al., 2008).

When FD BMSCs were transplanted along with hydroxyapatite/tricalcium phosphate ceramic particles into immunocompromised mice, they formed a fibrous dysplastic ossicle that completely recapitulated the nature of the FD

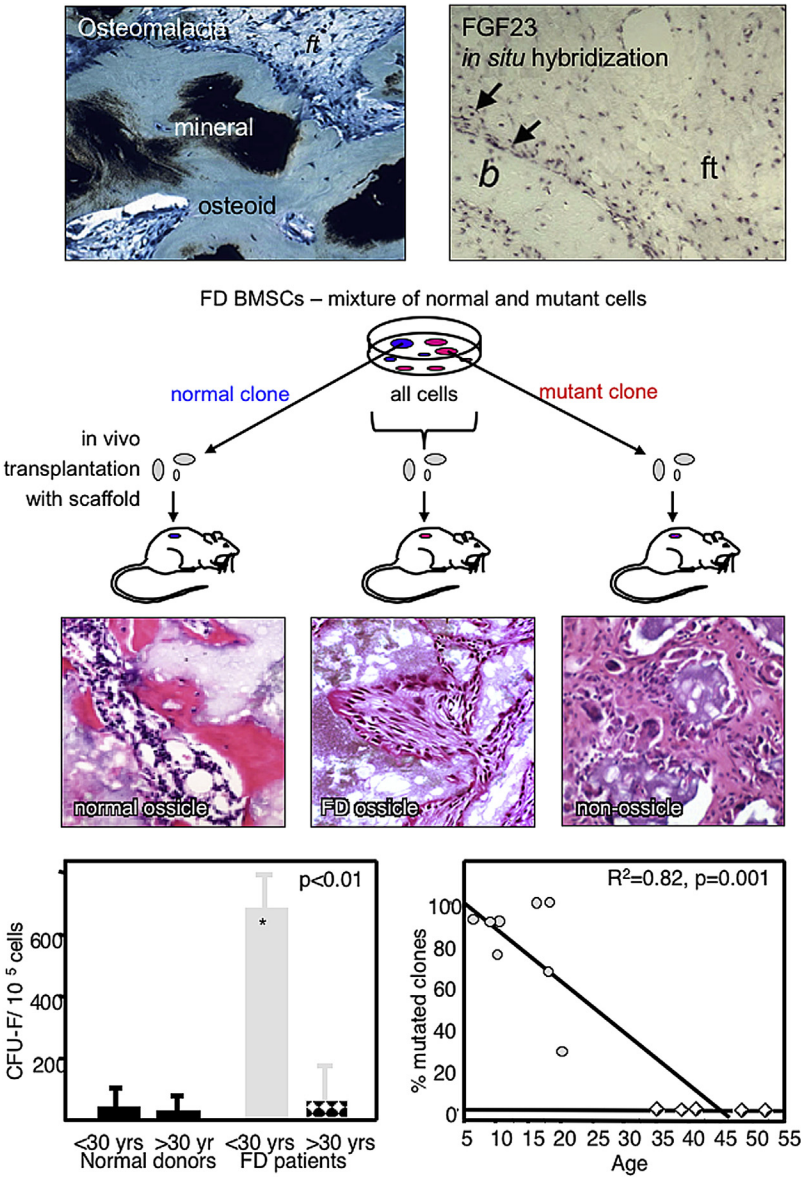

FIGURE 2.7 Fibrous dysplasia of bone/McCune–Albright syndrome (FD/MAS): a disease of skeletal stem cells. FD/MAS is a somatic mosaic disease caused by activating mutations of Gsα. Focal lesions are characterized by replacement of normal bone and marrow by highly disorganized and undermineralized bone and a fibrotic marrow devoid of hematopoiesis and marrow adipocytes. The fibrotic marrow is composed of a mixture of normal stromal cells, which are capable of forming normal bone in in vivo transplants, and mutated stromal cells, which on their own are not capable of surviving. It is only when normal and mutant cells are transplanted together that an FD tissue is formed. Colony-forming efficiency shows that in young patients with FD/MAS, there is a large increase compared with normal donors; however, with age colony-forming efficiency decreases dramatically, suggesting that colony-forming unit–fibroblasts (*CFU-Fs*) from young patients are, in fact, transiently amplifying cells rather than stem cells. Determination of the number of mutant CFU-Fs as a function of age also indicates that there is a dramatic decrease, leading to "normalization" due to the loss of mutated skeletal stem cells/transiently amplifying cells. *b*, bone; *BMSC*, bone marrow stromal cell; *FGF23*, fibroblast growth factor 23; *ft*, fibrous tissue. Arrows point out high levels of FGF23 expression by disfunction osteogenic cells on the bone surface. *Modified from Riminucci, M., Collins, M.T., Fedarko, N.S., Cherman, N., Corsi, A., White, K.E., Waguespack, S., Gupta, A., Hannon, T., Econs, M.J., Bianco, P., Gehron Robey, P., 2003a. FGF-23 in fibrous dysplasia of bone and its relationship to renal phosphate wasting. J. Clin. Invest. 112, 683–692; Riminucci, M., Robey, P.G., Saggio, I., Bianco, P., 2010. Skeletal progenitors and the GNAS gene: fibrous dysplasia of bone read through stem cells. J. Mol. Endocrinol. 45, 355–364; and Robey, P.G., Kuznetsov, S., Riminucci, M., Bianco, P., 2007. The role of stem cells in fibrous dysplasia of bone and the Mccune-Albright syndrome. Pediatr. Endocrinol. Rev. 4 (Suppl. 4), 386–394.*

lesion: abnormal woven and undermineralized bone, Sharpey's fibers, and lack of marrow formation (Bianco et al., 1998) (Fig. 2.7). In addition to transplantation of the total FD BMSC population, individual colonies were also evaluated. Clones were genotyped prior to transplantation, and as expected, clones with a normal genotype made a normal bone/marrow organ. Interestingly, mutant clones failed to survive transplantation; no bone was formed and human cells were not present (Bianco et al., 1998) (Fig. 2.7). This finding supports Happle's hypothesis that the mutation is embryonic lethal (Happle, 1986); that is, mutant cells would survive only when in combination with wild-type cells. Of note, there is no documented case in which FD/MAS was inherited; all cases are examples of de novo mutations after fertilization.

Evidence that FD is a "stem cell" disease (Riminucci et al., 2006) comes from the observation that as FD patients age, they "normalize" (Kuznetsov et al., 2008). Bone biopsies from patients of increasing age showed very high levels of apoptosis, up until approximately 30 years of age. Biopsies of older patients showed decreasing amounts of osteoid and increasing amounts of apparently normal bone and marrow. Marrow samples also showed a decrease in not only colony-forming efficiency, moving toward the normal level with increasing age, but also in the percentage of mutant cells in the total BMSC population, and a near-complete absence of mutant clones (Fig. 2.7). Transplants of BMSCs from older patients also showed increasingly normal ossicles, roughly correlated with age. From these observations, it was hypothesized that mutated SSCs were not able to undergo self-renewing types of division, and with time, transiently amplifying mutant cells differentiated and were ultimately cleared by apoptosis, leaving wild-type SSCs to undergo normal bone formation, albeit on an abnormal preexisting structure. Consequently, it can be reasoned that the impact of the mutation occurs at several levels in the skeletal lineage: (1) the mutation inhibits the self-renewal of mutant SSCs, (2) it causes extensive proliferation of mutant SSCs/BMSCs leading to premature apoptosis, and (3) it causes the derangement of BMSC differentiation into osteogenic, stromogenic, and adipogenic lineages.

Inherited forms of bone marrow failure

Inherited diseases of bone marrow failure are characterized by the inability to make normal numbers of all or specific types of blood cells (pancytopenia, or anemia, leukopenia, and thrombocytopenia) (Khincha and Savage, 2013). There are over 40 genes that have been reported to be mutated in association with these diseases (Ballew and Savage, 2013). Interestingly, many of these genes are not specific for hematopoietic cells based on the fact that patients with these diseases often have multiorgan manifestations. Dyskeratosis congenita (DC) is one such disease that is characterized by the triad of oral leukoplakia, nail dystrophy, and abnormal skin pigmentation, and also severe aplastic anemia, which is the main cause of death. These patients often have pulmonary fibrosis; stenosis of the esophagus, urethra, and/or lacrimal ducts; liver disease; premature graying of hair; and osteopenia (Ballew and Savage, 2013). Mutations have been detected in subunits of telomerase (*DKC1*, *TERT*, *TERC*, *NOP10*, *NHP2*), and in other genes involved in telomere biology (*WRAP53*, *TINF2*, *CTC1*, *RTEL1*). DC can be inherited in an X-linked recessive, autosomal dominant, or autosomal recessive fashion (Ballew and Savage, 2013; Nelson and Bertuch, 2012; Walne et al., 2013). In addition, a small proportion of patients with acquired aplastic anemia but without the other symptoms of DC have been found to have germ-line mutations in genes related to the telomerase complex (Alter et al., 2012; Yamaguchi et al., 2005). Based on these findings, patients with these various diseases and disorders have been grouped together as having telomere biology disorders (TBDs), and present with a very broad clinical spectrum ranging from limited bone marrow aplasia to a severe multiorgan phenotype as in DC.

Bone marrow failure caused by mutations in telomere biology-related genes is almost certainly caused, in part, by an intrinsic dysfunction of HSCs, due to short telomeres and a decrease in their ability to proliferate. However, the HSC's microenvironment (the niche) also controls the normal balance between quiescence and proliferation, self-renewal and differentiation (Schofield, 1978). As shown by Friedenstein et al., BMSCs are able to re-create the hematopoietic microenvironment upon in vivo transplantation into mice (Friedenstein et al., 1974; Owen and Friedenstein, 1988). Mature osteoblastic cells (Calvi et al., 2003), endothelial cells (Kiel et al., 2005), and BMSCs expressing CXCL12 (Omatsu et al., 2010; Sacchetti et al., 2007, 2016; Sugiyama et al., 2006), CD146 (Sacchetti et al., 2007), Nestin-GFP (Mendez-Ferrer et al., 2010), LEPR (Ding and Morrison, 2013), and others (reviewed in Ugarte and Forsberg, 2013) have been suggested to be constituents of the hematopoietic niche. In the quest for an identifiable niche-maintaining cell, current research is directed toward perivascular SSCs/BMSCs (Mendez-Ferrer et al., 2010; Omatsu et al., 2010; Pinho et al., 2013; Raaijmakers et al., 2010; Sacchetti et al., 2007, 2016). Thus, understanding the biological properties of SSCs/BMSCs has important implications not only for skeletal physiology and disease, but also for understanding the regulation of HSC physiology and dysregulation of hematopoiesis in blood disorders.

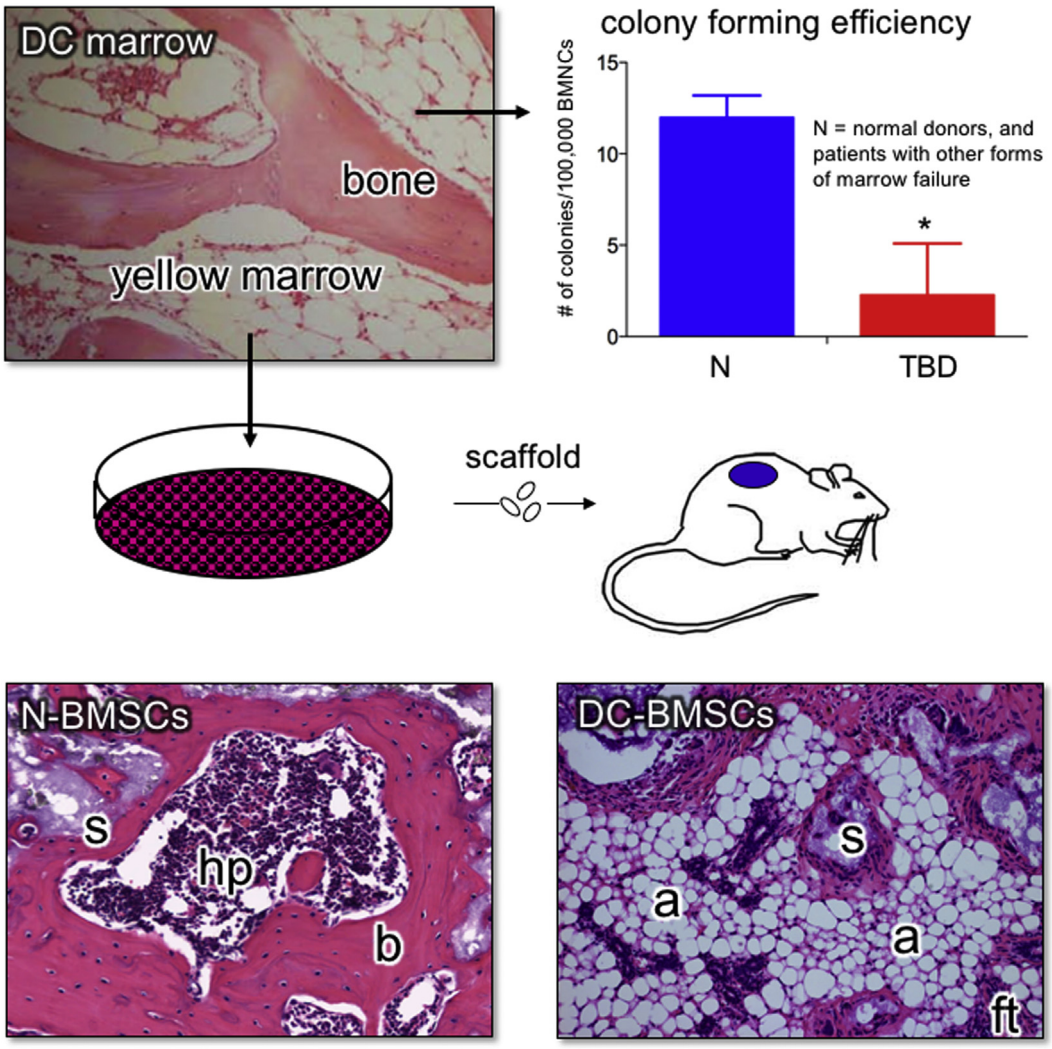

FIGURE 2.8 **Bone marrow failure: the role of skeletal stem cells.** A form of genetically acquired bone marrow failure syndromes is associated with mutations in genes that regulate telomere length, and they have been collectively termed telomere biology disorders (*TBDs*). Dyskeratosis congenita (*DC*) is one such TBD. Iliac crest biopsies from DC patients show predominately yellow marrow and demonstrate a dramatic decrease in colony-forming efficiency compared with normal donors. When DC bone marrow stromal cells (*BMSCs*) are expanded and transplanted, ectopic ossicles show a remarkable similarity to iliac crest biopsies: formation of a yellow marrow, completely devoid of hematopoiesis. *a*, adipocytes; *b,* bone; *BMNCs, bone marrow mono nucleated cells; ft*, fibrous tissue; *hp*, hematopoiesis; *s*, scaffold. *Modified from Balakumaran, A., Mishra, P.J., Pawelczyk, E., Yoshizawa, S., Sworder, B.J., Cherman, N., Kuznetsov, S.A., Bianco, P., Giri, N., Savage, S.A., Merlino, G., Dumitriu, B., Dunbar, C.E., Young, N.S., Alter, B.P., Robey, P.G., 2015. Bone marrow skeletal stem/progenitor cell defects in dyskeratosis congenita and telomere biology disorders. Blood 125, 793–802.*

By using BMSCs isolated from TBD patients to study the biological properties of TBD BMSCs, coupled with in vivo transplantation assay, it was found that SSCs contribute to the hematological phenotype in patients with TBD (Balakumaran et al., 2015) (Fig. 2.8). TBD BMSCs exhibited a drastically reduced colony-forming efficiency, as well as reduced telomerase activity. TBD BMSCs spontaneously differentiated into adipocytes and fibrotic cells even when cultured in osteogenic medium. In addition, they displayed increased senescence in vitro. Unlike normal BMSCs, upon in vivo transplantation into mice, TBD BMSCs failed to form bone or to support hematopoiesis. Knocking down *TERC* (a TBD-associated gene) in normal BMSCs using si*TERC*-RNA recapitulated the TBD BMSC phenotype as exemplified by reduced secondary colony-forming efficiency and growth rate, and accelerated senescence in vitro. Microarray profiles of control and si*TERC* BMSCs showed decreased hematopoietic factors at the mRNA level and decreased secretion of factors at the protein level. These findings are consistent with the notion that defects in SSCs/BMSCs, along with defects in HSCs, contribute to bone marrow failure in TBD patients. SSCs/BMSCs may be a target for drug treatment in some hematological diseases and disorders.

Role of SSCs/BMSCs in acquired inflammation

Changes noted in the ability of SSCs/BMSCs to support hematopoiesis as a function of an intrinsic (genetic) change in TBDs also led to the question whether extrinsic changes would influence the ability of SSCs/BMSCs to support hematopoiesis. Inflammation alters hematopoiesis, often by decreasing erythropoiesis and enhancing myeloid output. The mechanisms behind these changes and how the bone marrow stroma contributes to this process are not well known. These questions were studied in the setting of murine *Toxoplasma gondii* infection (Chou et al., 2012). The data revealed that infection alters early myeloerythroid differentiation, blocking erythroid development beyond the pre-megakaryocyte/erythroblast stage (erythroid crash), while expanding the granulocyte/monocyte precursor population (Fig. 2.9). The effects of infection in animal models deficient in cytokines known to regulate erythropoiesis were examined. The results indicated that in mice deficient in interleukin-6 (IL-6), the decrease in erythropoiesis was partially rescued, and it was also noted that in normal infected mice, serum IL-6 was elevated. From these results, IL-6 was found to be a critical mediator of the erythropoiesis, independent of hepcidin-induced iron restriction. Comparing bone marrow with the spleen showed that the hematopoietic response to infection was driven by the local bone marrow microenvironment. By using bone marrow transplantation to create bone marrow chimeras (IL-6-deficient marrow into normal recipients and vice versa), it was

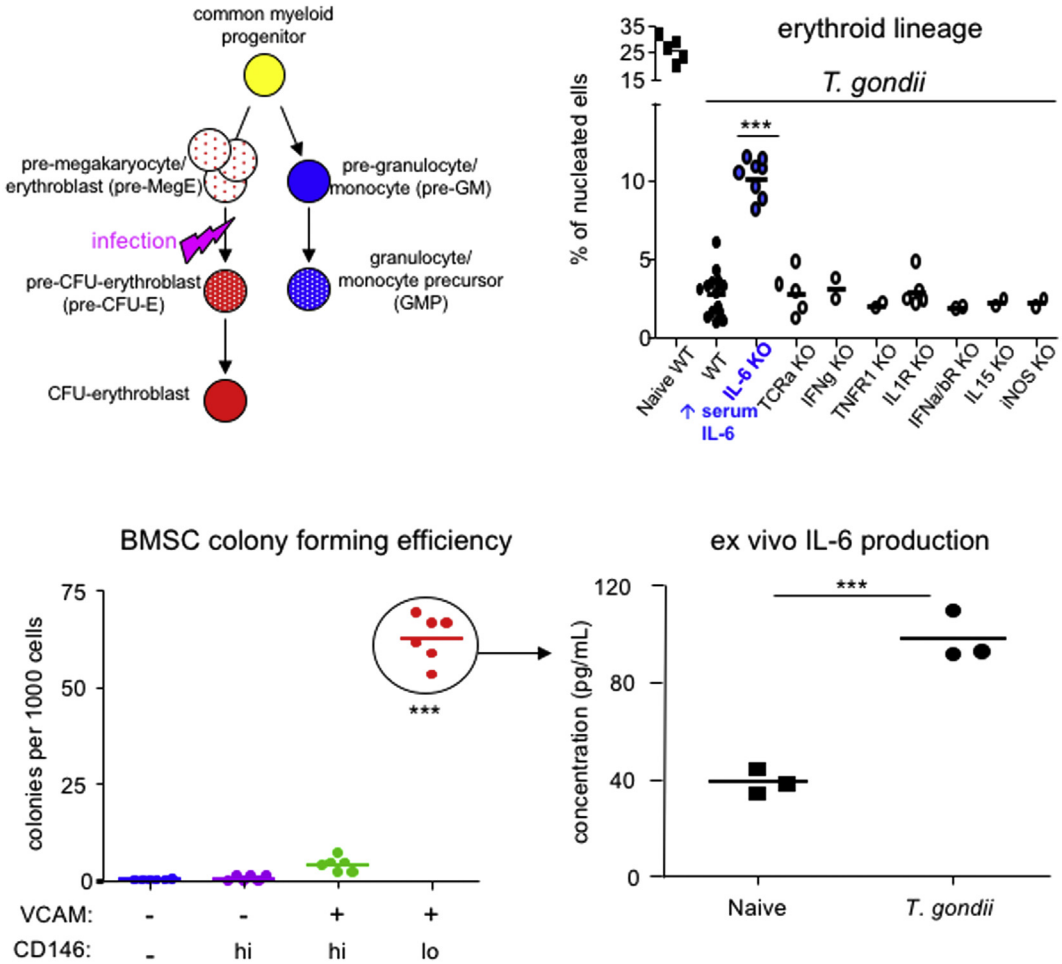

FIGURE 2.9 Skeletal stem cells/bone marrow stromal cells (SSC/BMSCs) in the sculpting of hematopoiesis. *Toxoplasmosis gondii* infection causes a crash in erythropoiesis due the blockade in differentiation of pre-megakaryocytes/erythroblasts into more differentiated cell types and a redirection of the common myeloid progenitor into the lymphoid series. Using mouse models deficient in various cytokines known to modulate erythropoiesis, it was determined that interleukin-6 (*IL-6*) deficiency partially rescued the erythroid crash and that IL-6 was increased in wild-type (*WT*) mice infected with *T. gondii*. Colony-forming unit (*CFU*)—fibroblasts ($CD45^-/Ter119^-/VCAM^+$) were isolated from naïve (uninfected) mice and infected mice, and were found to be the source of IL-6 induced by *T. gondii.* These results suggest that SSCs/BMSCs respond to external stimuli to modulate hematopoietic output and composition. *KO*, knockout. *Modified from Chou, D.B., Sworder, B., Bouladoux, N., Roy, C.N., Uchida, A.M., Grigg, M., Robey, P.G., Belkaid, Y., 2012. Stromal-derived IL-6 alters the balance of myeloerythroid progenitors during Toxoplasma gondii infection. J. Leukoc. Biol. 92, 123–131.*

demonstrated that radioresistant cells (BMSCs) were the relevant source of IL-6 in vivo. Finally, direct ex vivo sorting revealed that CD106/VCAM$^+$ colony-forming BMSCs significantly increased IL-6 secretion after infection (Fig. 2.9). These data suggest that SSCs/BMSCs regulate the hematopoietic changes during inflammation via IL-6 (Chou et al., 2012) and support the notion that extrinsic factors have an impact on stromal cell activity to sculpt hematopoietic output in response to microenvironmental changes.

Skeletal stem cells in tissue engineering

Based on their remarkable ability to form a complete bone/marrow organ, it is no wonder that many have pursued the use of SSCs/BMSCs in tissue engineering. Tissue engineering is typically described as the use of cells, growth factors, and/or cytokines and scaffolds, either alone or in various combinations, to restore tissue function lost due to trauma, tumor removal, and genetic and acquired diseases (Fig. 2.10). For skeletal tissue engineering, there are a number of parameters that affect outcome: the source of cells; the ex vivo expansion conditions, including the use of exogenous growth factors

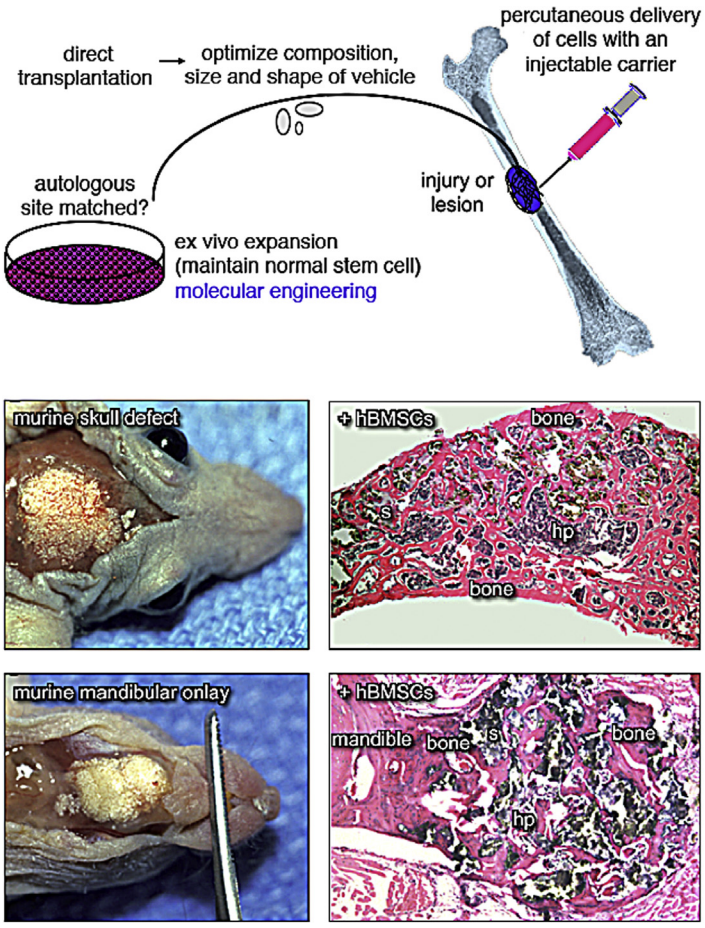

FIGURE 2.10 Skeletal stem cells in bone tissue engineering. In using skeletal stem cells/bone marrow stromal cells (SSCs/BMSCs), appropriate cell sources (e.g., autologous skeletal-derived cells such as bone marrow stromal cells) are needed. Ex vivo expansion conditions must maintain the SSC within the population to ensure that bone turnover can occur as needed. Culture of SSCs/BMSCs also offers the opportunity for molecular engineering to correct genetic defects (Piersanti et al., 2010). Ex vivo-expanded cells must be combined with an appropriate scaffold that will not only be osteoconductive, but also maintain the existence of SSCs. It may be possible to inject lesions directly, but an injectable carrier is needed to prevent their loss to the circulation and to hold them in place. Preclinical studies have been performed in mice to re-create jawbone and cranial bone (and also in dogs; Mankani et al., 2006a). *hp*, hematopoiesis; *s*, scaffold. *Modified from Bianco, P., Robey, P.G., Penessi, G., 2008a. Cell source. In: de Boer, J., van Blitterswijk, C., Thomsen, P., Hubbell, J., Cancedda, R., de Bruijn, J.D., Lindahl, A., Sohler, J., Williams, D.F. (Eds.), Tissue Engineering. Elsevier, Amsterdam, pp. 279–306; Mankani, M.H., Kuznetsov, S.A., Wolfe, R.M., Marshall, G.W., Robey, P.G., 2006b. In vivo bone formation by human bone marrow stromal cells: reconstruction of the mouse calvarium and mandible. Stem Cell. 24, 2140–2149; and Mankani, M.H., Kuznetsov, S.A., Marshall, G.W., Robey, P.G., 2008. Creation of new bone by the percutaneous injection of human bone marrow stromal cell and HA/TCP suspensions. Tissue Eng. Part A 14, 1949–1958.*

and/or cytokines; and the nature of the scaffold. It also must be mentioned that the microenvironment (e.g., gender and age of the recipient, presence or absence of bacterial infection, inflammation, etc.) in which such constructs are placed will have an impact on the outcome of tissue engineering approaches.

Cell sources

By far and away, BMSCs have been the most studied cell population for the use of skeletal tissue regeneration. As shown by clonal analyses, BMSCs, if properly expanded, have a subpopulation of SSCs that are multipotent and able to form a bone/marrow organ. Based on the fact that the SSC is a pericyte on the abluminal side of marrow sinusoids, the presence of marrow in a transplant of BMSCs is indicative of the presence of SSCs. However, that is not to say that more mature populations of osteogenic cells are not useful. There are instances in which building new bone will fit that bill, and mature osteogenic cells isolated from trabecular bone and BMSCs grown in basic FGF make copious amounts of bone, but do not support hematopoiesis (Sacchetti et al., 2007). However, based on the fact that more committed osteogenic cells will eventually disappear and will need to be replaced during bone turnover, it is clear that an SSC is required. Furthermore, based on the fact that differentiated osteogenic cells begin to express histocompatibility antigens, cells used for skeletal tissue regeneration must be autologous and would ultimately be rejected if allogeneic unless immunosuppression is employed, which is not without serious side effects (Robey, 2011).

Finally, it is known that bone arises from three different embryonic specifications during development: paraxial mesoderm, lateral plate mesoderm, and neural crest. It is known that there are subtle histological differences and growth differences of bone from different origins (Akintoye et al., 2006), and studies suggest that there are also differences in the patterns of gene expression (Kidwai et al., unpublished results). Consequently, it is not yet known if SSCs from one embryonic source can substitute for those from another embryonic source. Studies in which iliac crest (appendicular lateral plate mesoderm) was used to build up alveolar bone (neural crest) showed rapid resorption of the iliac crest, suggesting a potential incompatibility (Burnette, 1972). Study of pluripotent stem cells (human embryonic stem cells [ESCs] and human induced pluripotent stem cells [iPSCs]) provides a way to dissect out the regulatory pathways that govern the discrete stages of human bone development operative in the three distinct embryonic sources. Many studies have aimed at differentiating ESCs or iPSCs into SSCs (see Phillips et al., 2014, for examples). However, this and other studies did not attempt to determine from which embryonic specification the cells originated. Studies are under way that are designed to take pluripotent stem cells stepwise through specific stages of bone development (primitive streak, mesendoderm, paraxial and lateral mesoderm, and neural crest) (Kidwai et al., unpublished results).

Scaffolds

There have been a large number of preclinical studies, and a number of small human trials, showing the efficacy of using ex vivo-expanded SSCs/BMSCs in conjunction with an appropriate scaffold for direct orthotopic delivery into large segmental defects (reviewed in Chatterjea et al., 2010; Winkler et al., 2018) (Fig. 2.10). In some approaches, cells are precultured on a scaffold prior to transplantation. However, it is not clear that this is an advantage, especially if osteogenesis is induced, which may preclude the cell population's ability to maintain the SSC. In addition, the nature of the scaffold plays a major role in the performance of the cell population. While many synthetic and natural scaffolds have been fabricated, as of this writing, 3D scaffolds that contain ceramics (usually hydroxyapatite/tricalcium phosphate) as part of their formulation (reviewed in Oh et al., 2006) appear to be the most reliable with respect to the formation of bone and the support of hematopoiesis when seeded with SSCs/BMSCs. However, many of these scaffolds are resorbed very poorly and can persist for long periods of time in vivo. Consequently, scaffolds composed of polymers such as PLGA (poly(lactic-*co*-glycolic acid)) and PCL (poly(ε-caprolactone)), with and without calcium phosphate components or further functionalization, have been developed (reviewed in Kretlow and Mikos, 2007; Rezwan et al., 2006). However, it is not clear that these scaffolds also maintain the SSC/BMSC population's ability to support hematopoiesis. Of note, many studies to identify new scaffolds rely on in vitro assays to evaluate the performance of newly developed scaffolds; however, these assays do not adequately determine osteogenesis or support of hematopoiesis, and in vivo transplantation is required.

In addition to the use of 3D scaffolds, it would also be of benefit to develop techniques for the use of injectable scaffolds that would hold cells in place and support their differentiation, and thereby avoid the need for open surgery (Mankani et al., 2008) (Fig. 2.10). Injection of concentrated bone marrow aspirates has been shown to be beneficial in the treatment of avascular necrosis (Hernigou et al., 2005), but it would be of interest to determine if their efficacy could be enhanced through the use of an injectable carrier. It could also be envisioned that this approach would be useful for the treatment of unicameral bone cysts and nonunions.

Skeletal stem cells and regenerative medicine

It is thought that either systemic infusion of SSCs/BMSCs into the circulation or direct injection into a diseased area has a beneficial effect in treating not only skeletal diseases and disorders, but also a long list of diseases (e.g., graft vs. host disease, cardiovascular disease, osteoarthritis, multiple sclerosis, etc.) (reviewed in Galipeau and Sensebe, 2018). Initially it was thought that SSCs/BMSCs could transdifferentiate into cells outside of the skeletal lineage based on expression of a limited set of markers characteristic of a nonskeletal tissue. However, more rigorous assays have shown that SSCs/BMSCs do not functionally differentiate into nonskeletal tissues without extensive treatment with chemicals or molecular engineering to express tissue-specific transcription factors (reviewed in Bianco et al., 2013). Furthermore, it is known that cells are rapidly cleared from the circulation when injected systemically, and are even rapidly cleared upon direct injection (when they are not attached to a scaffold or carrier) (Bianco and Cossu, 1999; Bianco et al., 2008b). It has been proposed that even though the cells do not seem to home to sites of disease or injury, or to survive long term, they secrete growth factors, cytokines, and/or extracellular vesicles that exert paracrine, immunomodulatory, and/or immunosuppressive effects on recipient cells that initiate an endogenous repair process (reviewed in Galipeau and Sensebe, 2018). While some studies, such as the treatment of certain symptoms of acute graft versus host disease, show that there may be some beneficial effect (Le Blanc and Ringden, 2007), the results of the vast majority of studies have been equivocal (reviewed in Galipeau and Sensebe, 2018). However, it has not been determined that these putative effects are mediated by the subpopulation of SSCs within the BMSC population, and this is unlikely to be the case, based on the fact that SSCs are very rare. Any potential effect is mediated by the BMSC population as a whole, and cannot rightly be called a stem cell therapy at the time of writing. Furthermore, their rapid disappearance in the lungs and the distance of their demise from the site of disease or injury make a mechanism of action obscure.

Stem cell and non–stem cell functions of skeletal stem cells

As described earlier, the regeneration of bone and maintenance of a stem cell on the abluminal side of the marrow sinusoid is of utmost importance in maintaining skeletal homeostasis throughout life (Robey, 2011). However, SSCs/BMSCs also perform other functions that do not rely on their stem/progenitor cell status, that is, not on their potency or their ability to self-renew. For example, based on their pericytic nature, they produce factors that guide the formation of microvessels in conjunction with endothelial cells. In vitro, a mixture of SSCs/BMSCs and endothelial cells plated on Matrigel forms networks with branches, with endothelial cells on the interior, surrounded by SSCs/BMSCs on the exterior. Likewise, when SSCs/BMSCs are cotransplanted in vivo along with human umbilical vein endothelial cells in Matrigel (conditions that are not conducive for bone formation), they again form an extensive capillary-like network after about 3 weeks, and after 8 weeks, a mature thick-walled structure forms with endothelial cells surrounded by pericytes derived from the SSCs/BMSCs. These capillary-like structures are functional based on the presence of recipient blood cells inside their lumens due to anastomosis of the nascent structures with the recipient vasculature (Sacchetti et al., 2016). Furthermore, SSCs/BMSCs support hematopoiesis, one of their defining features, and are thought to be a part of the HSC niche that controls the activities of the HSC (Bianco, 2011). In addition, there is evidence that SSCs/BMSCs play a major role in shaping the composition of hematopoiesis, as presented earlier (Chou et al., 2012). As such, SSCs/BMSCs can be targets for therapeutics designed to control the quantitative and qualitative aspects of hematopoietic cells.

Last, SSCs/BMSCs provide a tool by which to study human skeletal disease. There are many instances in which a mutation associated with a human disease does not re-create the same phenotype when introduced into a mouse. For example, Meunke syndrome is caused by autosomal dominant activating mutations of FGFR3 and is characterized by craniosynostosis, ocular and hearing abnormalities, and fusion or missing bones in the hands and/or feet (Doherty et al., 2007). However, the same mutation in heterozygous mice does not exhibit Meunke syndrome, and only when the mice are homozygous for the mutation do they exhibit some, but not all, of the phenotypic features (Nah et al., 2012). The use of SSCs/BMSCs from human patients with monogenetic disease, or the introduction of mutation with the use of CRISP/Cas9 or other types of genetic engineering, can provide valuable tools with which to elucidate the pathogenetic mechanisms at play by using appropriate in vitro assays and in vivo transplantation assays as described earlier. For example, by studying normal BMSCs transduced with the R201C activating Gsα mutation, it was noted that mutant BMSCs highly overexpress RANKL, an essential factor for osteoclast formation (Piersanti et al., 2010). This finding provided an explanation for the florid increase in osteoclastogenesis during the establishment of expansile lesions (Riminucci et al., 2003b). Furthermore, it suggested the use of denosumab (a humanized anti-RANKL antibody) to treat expansile disease, as has been reported (Boyce et al., 2012). Alternatively, using mutant SSCs/BMSCs to create an ectopic bone/marrow organ provides a model for testing new therapeutics to prevent the formation of diseased bone. The ectopic bone/marrow organ may be useful in

other diseases for which an appropriate animal model does not exist. Finally, the use of SSCs/BMSCs to create cartilage pellets may be helpful in screening small-molecule libraries for factors that prevent hypertrophy.

Summary

It is now clear that the bone/marrow organ contains a multipotent SSC that is able to re-create cartilage, bone, hematopoiesis-supportive stroma, and marrow adipocytes, and is able to self-renew. As such, these cells are central mediators of skeletal homeostasis. In the postnatal organism, fate choices of SSCs into chondrogenic (rarely), osteogenic, stromagenic, and adipogenic progeny are highly influenced by changes in the microenvironment in which they reside, and are mediated by numerous signaling pathways and genomic and epigenetic processes. Mutations (intrinsic changes) that affect their normal biological functions can have a profound effect on the skeleton and even on hematopoiesis based on their presence and activity in the HSC niche. In addition, changes in the microenvironment (extrinsic) that have an impact on SSC/BMSC function can also lead to skeletal and hematological diseases and disorders. Last, SSCs are an essential ingredient for any process aimed at enduring bone regeneration by the cells themselves due to their ability to mediate bone turnover.

Acknowledgments

The authors would like to acknowledge all of the genuinely seminal contributions of Professor Paolo Bianco to the evolution of the field of skeletal stem cell biology. He was truly a pioneer. The authors would also like to acknowledge all of the members, past and present, of the Skeletal Biology Section, NIDCR, and the Stem Cell Lab, Department of Molecular Medicine, Sapienza University of Rome.

The authors declare that they have no conflicts of interest. This work was supported by the DIR, NIDCR, of the IRP, NIH, DHHS, to P.G.R., and by Telethon (grant GGP15198), the EU (PluriMes consortium, FP7-HEALTH-2013-INNOVATION-1−G.A. 602423), and Sapienza University of Rome to M.R.

References

Akintoye, S.O., Lam, T., Shi, S., Brahim, J., Collins, M.T., Robey, P.G., 2006. Skeletal site-specific characterization of orofacial and iliac crest human bone marrow stromal cells in same individuals. Bone 38, 758−768.

Alliston, T., Choy, L., Ducy, P., Karsenty, G., Derynck, R., 2001. TGF-beta-induced repression of CBFA1 by Smad3 decreases cbfa1 and osteocalcin expression and inhibits osteoblast differentiation. EMBO J. 20, 2254−2272.

Alter, B.P., Rosenberg, P.S., Giri, N., Baerlocher, G.M., Lansdorp, P.M., Savage, S.A., 2012. Telomere length is associated with disease severity and declines with age in dyskeratosis congenita. Haematologica 97, 353−359.

Armulik, A., Genove, G., Betsholtz, C., 2011. Pericytes: developmental, physiological, and pathological perspectives, problems, and promises. Dev. Cell 21, 193−215.

Balakumaran, A., Mishra, P.J., Pawelczyk, E., Yoshizawa, S., Sworder, B.J., Cherman, N., Kuznetsov, S.A., Bianco, P., Giri, N., Savage, S.A., Merlino, G., Dumitriu, B., Dunbar, C.E., Young, N.S., Alter, B.P., Robey, P.G., 2015. Bone marrow skeletal stem/progenitor cell defects in dyskeratosis congenita and telomere biology disorders. Blood 125, 793−802.

Ballew, B.J., Savage, S.A., 2013. Updates on the biology and management of dyskeratosis congenita and related telomere biology disorders. Expert Rev. Hematol. 6, 327−337.

Barron, V., Merghani, K., Shaw, G., Coleman, C.M., Hayes, J.S., Ansboro, S., Manian, A., O'Malley, G., Connolly, E., Nandakumar, A., van Blitterswijk, C.A., Habibovic, P., Moroni, L., Shannon, F., Murphy, J.M., Barry, F., 2015. Evaluation of cartilage repair by mesenchymal stem cells seeded on a PEOT/PBT scaffold in an osteochondral defect. Ann. Biomed. Eng. 43, 2069−2082.

Berendsen, A.D., Olsen, B.R., 2015. Bone development. Bone 80, 14−18.

Bi, W., Deng, J.M., Zhang, Z., Behringer, R.R., de Crombrugghe, B., 1999. Sox9 is required for cartilage formation. Nat. Genet. 22, 85−89.

Bianco, P., 2011. Bone and the hematopoietic niche: a tale of two stem cells. Blood 117, 5281−5288.

Bianco, P., Bonucci, E., 1991. Endosteal surfaces in hyperparathyroidism: an enzyme cytochemical study on low-temperature-processed, glycol-methacrylate-embedded bone biopsies. Virchows Arch. A Pathol. Anat. Histopathol. 419, 425−431.

Bianco, P., Cao, X., Frenette, P.S., Mao, J.J., Robey, P.G., Simmons, P.J., Wang, C.Y., 2013. The meaning, the sense and the significance: translating the science of mesenchymal stem cells into medicine. Nat. Med. 19, 35−42.

Bianco, P., Cossu, G., 1999. Uno, nessuno e centomila: searching for the identity of mesodermal progenitors. Exp. Cell Res. 251, 257−263.

Bianco, P., Kuznetsov, S., Riminucci, M., Robey, P.G., 2006. Postnatal skeletal stem cells. Methods Enzymol. 419, 117−148.

Bianco, P., Kuznetsov, S.A., Riminucci, M., Fisher, L.W., Spiegel, A.M., Robey, P.G., 1998. Reproduction of human fibrous dysplasia of bone in immunocompromised mice by transplanted mosaics of normal and Gsalpha-mutated skeletal progenitor cells. J. Clin. Invest. 101, 1737−1744.

Bianco, P., Riminucci, M., 1998. The bone marrow stroma in vivo: ontogeny, structure, cellular composition and changes in disease. In: Beresfore, J., Owen, M.E. (Eds.), Marrow Stromal Cell Culture. Cambridge University Press, Cambridge, UK, pp. 10−25.

Bianco, P., Riminucci, M., Kuznetsov, S., Robey, P.G., 1999. Multipotential cells in the bone marrow stroma: regulation in the context of organ physiology. Crit. Rev. Eukaryot. Gene Expr. 9, 159−173.

Bianco, P., Riminucci, M., Majolagbe, A., Kuznetsov, S.A., Collins, M.T., Mankani, M.H., Corsi, A., Bone, H.G., Wientroub, S., Spiegel, A.M., Fisher, L.W., Robey, P.G., 2000. Mutations of the GNAS1 gene, stromal cell dysfunction, and osteomalacic changes in non-McCune-Albright fibrous dysplasia of bone. J. Bone Miner. Res. 15, 120−128.

Bianco, P., Robey, P.G., 2004. Skeletal stem cells. In: Lanza, R.P. (Ed.), Handbook of Adult and Fetal Stem Cells. Academic Press, San Diego, pp. 415−424.

Bianco, P., Robey, P.G., 2015. Skeletal stem cells. Development 142, 1023−1027.

Bianco, P., Robey, P.G., Penessi, G., 2008a. Cell source. In: de Boer, J., van Blitterswijk, C., Thomsen, P., Hubbell, J., Cancedda, R., de Bruijn, J.D., Lindahl, A., Sohler, J., Williams, D.F. (Eds.), Tissue Engineering. Elsevier, Amsterdam, pp. 279−306.

Bianco, P., Robey, P.G., Simmons, P.J., 2008b. Mesenchymal stem cells: revisiting history, concepts, and assays. Cell Stem Cell 2, 313−319.

Bothe, I., Tenin, G., Oseni, A., Dietrich, S., 2011. Dynamic control of head mesoderm patterning. Development 138, 2807−2821.

Boxall, S.A., Jones, E., 2012. Markers for characterization of bone marrow multipotential stromal cells. Stem Cell. Int. 2012, 975871.

Boyce, A.M., Chong, W.H., Yao, J., Gafni, R.I., Kelly, M.H., Chamberlain, C.E., Bassim, C., Cherman, N., Ellsworth, M., Kasa-Vubu, J.Z., Farley, F.A., Molinolo, A.A., Bhattacharyya, N., Collins, M.T., 2012. Denosumab treatment for fibrous dysplasia. J. Bone Miner. Res. 27, 1462−1470.

Boyce, A.M., Florenzano, P., de Castro, L.F., Collins, M.T., 1993. Fibrous dysplasia/McCune-Albright syndrome. In: Adam, M.P., Ardinger, H.H., Pagon, R.A., Wallace, S.E., Bean, L.J.H., Stephens, K., Amemiya, A. (Eds.), GeneReviews. Seattle, WA.

Boyce, B.F., Xing, L., 2007. The RANKL/RANK/OPG pathway. Curr. Osteoporos. Rep. 5, 98−104.

Bronner, M.E., 2015. Evolution: on the crest of becoming vertebrate. Nature 527, 311−312.

Burnette Jr., E.W., 1972. Fate of an iliac crest graft. J. Periodontol. 43, 88−90.

Calvi, L.M., Adams, G.B., Weibrecht, K.W., Weber, J.M., Olson, D.P., Knight, M.C., Martin, R.P., Schipani, E., Divieti, P., Bringhurst, F.R., Milner, L.A., Kronenberg, H.M., Scadden, D.T., 2003. Osteoblastic cells regulate the haematopoietic stem cell niche. Nature 425, 841−846.

Caplan, A.I., 2005. Review: mesenchymal stem cells: cell-based reconstructive therapy in orthopedics. Tissue Eng. 11, 1198−1211.

Carthew, R.W., Sontheimer, E.J., 2009. Origins and Mechanisms of miRNAs and siRNAs. Cell 136, 642−655.

Chan, C.K.F., Gulati, G.S., Sinha, R., Tompkins, J.V., Lopez, M., Carter, A.C., Ransom, R.C., Reinisch, A., Wearda, T., Murphy, M., Brewer, R.E., Koepke, L.S., Marecic, O., Manjunath, A., Seo, E.Y., Leavitt, T., Lu, W.J., Nguyen, A., Conley, S.D., Salhotra, A., Ambrosi, T.H., Borrelli, M.R., Siebel, T., Chan, K., Schallmoser, K., Seita, J., Sahoo, D., Goodnough, H., Bishop, J., Gardner, M., Majeti, R., Wan, D.C., Goodman, S., Weissman, I.L., Chang, H.Y., Longaker, M.T., 2018. Identification of the human skeletal stem cell. Cell 175, 43−56 e21.

Chatterjea, A., Meijer, G., van Blitterswijk, C., de Boer, J., 2010. Clinical application of human mesenchymal stromal cells for bone tissue engineering. Stem Cell. Int. 2010, 215625.

Chen, G., Deng, C., Li, Y.P., 2012. TGF-beta and BMP signaling in osteoblast differentiation and bone formation. Int. J. Biol. Sci. 8, 272−288.

Chen, K.G., Johnson, K.R., McKay, R.D.G., Robey, P.G., 2018. Concise review: conceptualizing paralogous stem-cell niches and unfolding bone marrow progenitor cell identities. Stem Cell. 36, 11−21.

Chen, K.G., Johnson, K.R., Robey, P.G., 2017. Mouse genetic analysis of bone marrow stem cell niches: technological pitfalls, challenges, and translational considerations. Stem Cell Reports 9, 1343−1358.

Chen, Q., Shou, P., Zhang, L., Xu, C., Zheng, C., Han, Y., Li, W., Huang, Y., Zhang, X., Shao, C., Roberts, A.I., Rabson, A.B., Ren, G., Zhang, Y., Wang, Y., Denhardt, D.T., Shi, Y., 2014. An osteopontin-integrin interaction plays a critical role in directing adipogenesis and osteogenesis by mesenchymal stem cells. Stem Cell. 32, 327−337.

Chen, Q., Shou, P., Zheng, C., Jiang, M., Cao, G., Yang, Q., Cao, J., Xie, N., Velletri, T., Zhang, X., Xu, C., Zhang, L., Yang, H., Hou, J., Wang, Y., Shi, Y., 2016. Fate decision of mesenchymal stem cells: adipocytes or osteoblasts? Cell Death Differ. 23, 1128−1139.

Chou, D.B., Sworder, B., Bouladoux, N., Roy, C.N., Uchida, A.M., Grigg, M., Robey, P.G., Belkaid, Y., 2012. Stromal-derived IL-6 alters the balance of myeloerythroid progenitors during Toxoplasma gondii infection. J. Leukoc. Biol. 92, 123−131.

Clark, E.A., Kalomoiris, S., Nolta, J.A., Fierro, F.A., 2014. Concise review: MicroRNA function in multipotent mesenchymal stromal cells. Stem Cell. 32, 1074−1082.

Cook, D., Genever, P., 2013. Regulation of mesenchymal stem cell differentiation. Adv. Exp. Med. Biol. 786, 213−229.

Crane, J.L., Cao, X., 2014. Bone marrow mesenchymal stem cells and TGF-beta signaling in bone remodeling. J. Clin. Invest. 124, 466−472.

D'Arcangelo, E., McGuigan, A.P., 2015. Micropatterning strategies to engineer controlled cell and tissue architecture in vitro. Biotechniques 58, 13−23.

Danielian, P.S., Muccino, D., Rowitch, D.H., Michael, S.K., McMahon, A.P., 1998. Modification of gene activity in mouse embryos in utero by a tamoxifen-inducible form of Cre recombinase. Curr. Biol. 8, 1323−1326.

de Boer, J., Licht, R., Bongers, M., van der Klundert, T., Arends, R., van Blitterswijk, C., 2006. Inhibition of histone acetylation as a tool in bone tissue engineering. Tissue Eng. 12, 2927−2937.

Devlin, M.J., Rosen, C.J., 2015. The bone-fat interface: basic and clinical implications of marrow adiposity. Lancet Diabetes Endocrinol 3, 141−147.

Ding, L., Morrison, S.J., 2013. Haematopoietic stem cells and early lymphoid progenitors occupy distinct bone marrow niches. Nature 495, 231−235.

Doherty, E.S., Lacbawan, F., Hadley, D.W., Brewer, C., Zalewski, C., Kim, H.J., Solomon, B., Rosenbaum, K., Domingo, D.L., Hart, T.C., Brooks, B.P., Immken, L., Lowry, R.B., Kimonis, V., Shanske, A.L., Jehee, F.S., Bueno, M.R., Knightly, C., McDonald-McGinn, D., Zackai, E.H., Muenke, M., 2007. Muenke syndrome (FGFR3-related craniosynostosis): expansion of the phenotype and review of the literature. Am. J. Med. Genet. 143A, 3204−3215.

Duchamp de Lageneste, O., Julien, A., Abou-Khalil, R., Frangi, G., Carvalho, C., Cagnard, N., Cordier, C., Conway, S.J., Colnot, C., 2018. Periosteum contains skeletal stem cells with high bone regenerative potential controlled by Periostin. Nat. Commun. 9, 773.

Dzierzak, E., Medvinsky, A., 2008. The discovery of a source of adult hematopoietic cells in the embryo. Development 135, 2343−2346.

Einhorn, T.A., Gerstenfeld, L.C., 2015. Fracture healing: mechanisms and interventions. Nat. Rev. Rheumatol. 11, 45–54.

Evans, B.R., Mosig, R.A., Lobl, M., Martignetti, C.R., Camacho, C., Grum-Tokars, V., Glucksman, M.J., Martignetti, J.A., 2012. Mutation of membrane type-1 metalloproteinase, MT1-MMP, causes the multicentric osteolysis and arthritis disease Winchester syndrome. Am. J. Hum. Genet. 91, 572–576.

Fitter, S., Gronthos, S., Ooi, S.S., Zannettino, A.C., 2017. The mesenchymal precursor cell marker antibody STRO-1 binds to cell surface heat shock cognate 70. Stem Cell. 35, 940–951.

Fontaine, C., Cousin, W., Plaisant, M., Dani, C., Peraldi, P., 2008. Hedgehog signaling alters adipocyte maturation of human mesenchymal stem cells. Stem Cell. 26, 1037–1046.

Friedenstein, A.J., Chailakhyan, R.K., Latsinik, N.V., Panasyuk, A.F., Keiliss-Borok, I.V., 1974. Stromal cells responsible for transferring the micro-environment of the hemopoietic tissues. Cloning in vitro and retransplantation in vivo. Transplantation 17, 331–340.

Galipeau, J., Sensebe, L., 2018. Mesenchymal stromal cells: clinical challenges and therapeutic opportunities. Cell Stem Cell 22, 824–833.

Georgiou, K.R., Hui, S.K., Xian, C.J., 2012. Regulatory pathways associated with bone loss and bone marrow adiposity caused by aging, chemotherapy, glucocorticoid therapy and radiotherapy. Am. J. Stem Cells 1, 205–224.

Goujon, E., 1869. Recherches experimentales sur les proprietes physiologiques de la moelle des os. J. de L'Anat et de La Physiol. 6, 399–412.

Gronthos, S., Graves, S.E., Ohta, S., Simmons, P.J., 1994. The STRO-1+ fraction of adult human bone marrow contains the osteogenic precursors. Blood 84, 4164–4173.

Gronthos, S., Mankani, M., Brahim, J., Robey, P.G., Shi, S., 2000. Postnatal human dental pulp stem cells (DPSCs) in vitro and in vivo. Proc. Natl. Acad. Sci. U.S.A. 97, 13625–13630.

Guilak, F., Cohen, D.M., Estes, B.T., Gimble, J.M., Liedtke, W., Chen, C.S., 2009. Control of stem cell fate by physical interactions with the extracellular matrix. Cell Stem Cell 5, 17–26.

Ha, M., Kim, V.N., 2014. Regulation of microRNA biogenesis. Nat. Rev. Mol. Cell Biol. 15, 509–524.

Haeckel, E. (Ed.), Natürliche Schöpfung-Geschichte, 1868, Druck und Verlag von Georg Reimer, Berlin, p. 832.

Hall, B.K., 2015. Bones and Cartilage, second ed. Academic Press, Waltham, MA.

Hamam, D., Ali, D., Vishnubalaji, R., Hamam, R., Al-Nbaheen, M., Chen, L., Kassem, M., Aldahmash, A., Alajez, N.M., 2014. microRNA-320/RUNX2 axis regulates adipocytic differentiation of human mesenchymal (skeletal) stem cells. Cell Death Dis. 5, e1499.

Happle, R., 1986. The McCune-Albright syndrome: a lethal gene surviving by mosaicism. Clin. Genet. 29, 321–324.

Hemming, S., Cakouros, D., Isenmann, S., Cooper, L., Menicanin, D., Zannettino, A., Gronthos, S., 2014. EZH2 and KDM6A act as an epigenetic switch to regulate mesenchymal stem cell lineage specification. Stem Cell. 32, 802–815.

Hernigou, P., Poignard, A., Manicom, O., Mathieu, G., Rouard, H., 2005. The use of percutaneous autologous bone marrow transplantation in nonunion and avascular necrosis of bone. J Bone Joint Surg Br 87, 896–902.

Hicok, K.C., Du Laney, T.V., Zhou, Y.S., Halvorsen, Y.D., Hitt, D.C., Cooper, L.F., Gimble, J.M., 2004. Human adipose-derived adult stem cells produce osteoid in vivo. Tissue Eng. 10, 371–380.

Hilton, M.J., Tu, X., Wu, X., Bai, S., Zhao, H., Kobayashi, T., Kronenberg, H.M., Teitelbaum, S.L., Ross, F.P., Kopan, R., Long, F., 2008. Notch signaling maintains bone marrow mesenchymal progenitors by suppressing osteoblast differentiation. Nat. Med. 14, 306–314.

Holmbeck, K., Bianco, P., Caterina, J., Yamada, S., Kromer, M., Kuznetsov, S.A., Mankani, M., Robey, P.G., Poole, A.R., Pidoux, I., Ward, J.M., Birkedal-Hansen, H., 1999. MT1-MMP-deficient mice develop dwarfism, osteopenia, arthritis, and connective tissue disease due to inadequate collagen turnover. Cell 99, 81–92.

Holmbeck, K., Bianco, P., Chrysovergis, K., Yamada, S., Birkedal-Hansen, H., 2003. MT1-MMP-dependent, apoptotic remodeling of unmineralized cartilage: a critical process in skeletal growth. J. Cell Biol. 163, 661–671.

Isern, J., Garcia-Garcia, A., Martin, A.M., Arranz, L., Martin-Perez, D., Torroja, C., Sanchez-Cabo, F., Mendez-Ferrer, S., 2014. The neural crest is a source of mesenchymal stem cells with specialized hematopoietic stem cell niche function. Elife 3 e03696.

James, A.W., 2013. Review of signaling pathways governing MSC osteogenic and adipogenic differentiation. Scientifica (Cairo) 2013, 684736.

Jemtland, R., Divieti, P., Lee, K., Segre, G.V., 2003. Hedgehog promotes primary osteoblast differentiation and increases PTHrP mRNA expression and iPTHrP secretion. Bone 32, 611–620.

Johnstone, B., Hering, T.M., Caplan, A.I., Goldberg, V.M., Yoo, J.U., 1998. In vitro chondrogenesis of bone marrow-derived mesenchymal progenitor cells. Exp. Cell Res. 238, 265–272.

Jonas, S., Izaurralde, E., 2015. Towards a molecular understanding of microRNA-mediated gene silencing. Nat. Rev. Genet. 16, 421–433.

Kharlamova, L.A., 1975. Colony formation inhibition in human bone marrow stromal cells exposed to a factor formed in vitro by peripheral blood leukocytes. Biull Eksp Biol Med 80, 89–91.

Khincha, P.P., Savage, S.A., 2013. Genomic characterization of the inherited bone marrow failure syndromes. Semin. Hematol. 50, 333–347.

Kiel, M.J., Yilmaz, O.H., Iwashita, T., Yilmaz, O.H., Terhorst, C., Morrison, S.J., 2005. SLAM family receptors distinguish hematopoietic stem and progenitor cells and reveal endothelial niches for stem cells. Cell 121, 1109–1121.

Kilian, K.A., Bugarija, B., Lahn, B.T., Mrksich, M., 2010. Geometric cues for directing the differentiation of mesenchymal stem cells. Proc. Natl. Acad. Sci. U.S.A. 107, 4872–4877.

Komori, T., Yagi, H., Nomura, S., Yamaguchi, A., Sasaki, K., Deguchi, K., Shimizu, Y., Bronson, R.T., Gao, Y.H., Inada, M., Sato, M., Okamoto, R., Kitamura, Y., Yoshiki, S., Kishimoto, T., 1997. Targeted disruption of Cbfa1 results in a complete lack of bone formation owing to maturational arrest of osteoblasts. Cell 89, 755–764.

Kretlow, J.D., Mikos, A.G., 2007. Review: mineralization of synthetic polymer scaffolds for bone tissue engineering. Tissue Eng. 13, 927–938.

Kretzschmar, K., Post, Y., Bannier-Helaouet, M., Mattiotti, A., Drost, J., Basak, O., Li, V.S.W., van den Born, M., Gunst, Q.D., Versteeg, D., Kooijman, L., van der Elst, S., van Es, J.H., van Rooij, E., van den Hoff, M.J.B., Clevers, H., 2018. Profiling proliferative cells and their progeny in damaged murine hearts. Proc. Natl. Acad. Sci. U.S.A. 115, E12245–E12254.

Kumar, A., Ruan, M., Clifton, K., Syed, F., Khosla, S., Oursler, M.J., 2012. TGF-beta mediates suppression of adipogenesis by estradiol through connective tissue growth factor induction. Endocrinology 153, 254–263.

Kuter, D.J., Bain, B., Mufti, G., Bagg, A., Hasserjian, R.P., 2007. Bone marrow fibrosis: pathophysiology and clinical significance of increased bone marrow stromal fibres. Br. J. Haematol. 139, 351–362.

Kuznetsov, S.A., Cherman, N., Riminucci, M., Collins, M.T., Robey, P.G., Bianco, P., 2008. Age-dependent demise of GNAS-mutated skeletal stem cells and "normalization" of fibrous dysplasia of bone. J. Bone Miner. Res. 23, 1731–1740.

Kuznetsov, S.A., Hailu-Lazmi, A., Cherman, N., de Castro, L.F., Robey, P.G., Gorodetsky, R., 2019. In vivo formation of stable hyaline cartilage by naive human bone marrow stromal cells with modified fibrin microbeads. Stem Cells Transl Med.

Kuznetsov, S.A., Krebsbach, P.H., Satomura, K., Kerr, J., Riminucci, M., Benayahu, D., Robey, P.G., 1997. Single-colony derived strains of human marrow stromal fibroblasts form bone after transplantation in vivo. J. Bone Miner. Res. 12, 1335–1347.

Kuznetsov, S.A., Riminucci, M., Ziran, N., Tsutsui, T.W., Corsi, A., Calvi, L., Kronenberg, H.M., Schipani, E., Robey, P.G., Bianco, P., 2004. The interplay of osteogenesis and hematopoiesis: expression of a constitutively active PTH/PTHrP receptor in osteogenic cells perturbs the establishment of hematopoiesis in bone and of skeletal stem cells in the bone marrow. J. Cell Biol. 167, 1113–1122.

Le Blanc, K., Ringden, O., 2007. Immunomodulation by mesenchymal stem cells and clinical experience. J. Intern. Med. 262, 509–525.

Li, J., Zhang, N., Huang, X., Xu, J., Fernandes, J.C., Dai, K., Zhang, X., 2013. Dexamethasone shifts bone marrow stromal cells from osteoblasts to adipocytes by C/EBPalpha promoter methylation. Cell Death Dis. 4, e832.

Li, J.Y., Tawfeek, H., Bedi, B., Yang, X., Adams, J., Gao, K.Y., Zayzafoon, M., Weitzmann, M.N., Pacifici, R., 2011. Ovariectomy disregulates osteoblast and osteoclast formation through the T-cell receptor CD40 ligand. Proc. Natl. Acad. Sci. U.S.A. 108, 768–773.

Li, Y., Fan, L., Hu, J., Zhang, L., Liao, L., Liu, S., Wu, D., Yang, P., Shen, L., Chen, J., Jin, Y., 2015. MiR-26a rescues bone regeneration deficiency of mesenchymal stem cells derived from osteoporotic mice. Mol. Ther. 23, 1349–1357.

Lian, J.B., Stein, G.S., van Wijnen, A.J., Stein, J.L., Hassan, M.Q., Gaur, T., Zhang, Y., 2012. MicroRNA control of bone formation and homeostasis. Nat. Rev. Endocrinol. 8, 212–227.

Lin, G.L., Hankenson, K.D., 2011. Integration of BMP, Wnt, and notch signaling pathways in osteoblast differentiation. J. Cell. Biochem. 112, 3491–3501.

Ling, L., Murali, S., Dombrowski, C., Haupt, L.M., Stein, G.S., van Wijnen, A.J., Nurcombe, V., Cool, S.M., 2006. Sulfated glycosaminoglycans mediate the effects of FGF2 on the osteogenic potential of rat calvarial osteoprogenitor cells. J. Cell. Physiol. 209, 811–825.

MacCord, K., 2012. Mesenchyme. In: Embryo Project Encyclopedia. Arizona State University. https://embryo.asu.edu/pages/mesenchyme.

Maes, C., Kobayashi, T., Selig, M.K., Torrekens, S., Roth, S.I., Mackem, S., Carmeliet, G., Kronenberg, H.M., 2010. Osteoblast precursors, but not mature osteoblasts, move into developing and fractured bones along with invading blood vessels. Dev. Cell 19, 329–344.

Mankani, M.H., Kuznetsov, S.A., Marshall, G.W., Robey, P.G., 2008. Creation of new bone by the percutaneous injection of human bone marrow stromal cell and HA/TCP suspensions. Tissue Eng. Part A 14, 1949–1958.

Mankani, M.H., Kuznetsov, S.A., Shannon, B., Nalla, R.K., Ritchie, R.O., Qin, Y., Robey, P.G., 2006a. Canine cranial reconstruction using autologous bone marrow stromal cells. Am. J. Pathol. 168, 542–550.

Mankani, M.H., Kuznetsov, S.A., Wolfe, R.M., Marshall, G.W., Robey, P.G., 2006b. In vivo bone formation by human bone marrow stromal cells: reconstruction of the mouse calvarium and mandible. Stem Cell. 24, 2140–2149.

McBeath, R., Pirone, D.M., Nelson, C.M., Bhadriraju, K., Chen, C.S., 2004. Cell shape, cytoskeletal tension, and RhoA regulate stem cell lineage commitment. Dev. Cell 6, 483–495.

Mendez-Ferrer, S., Michurina, T.V., Ferraro, F., Mazloom, A.R., Macarthur, B.D., Lira, S.A., Scadden, D.T., Ma'ayan, A., Enikolopov, G.N., Frenette, P.S., 2010. Mesenchymal and haematopoietic stem cells form a unique bone marrow niche. Nature 466, 829–834.

Meury, T., Verrier, S., Alini, M., 2006. Human endothelial cells inhibit BMSC differentiation into mature osteoblasts in vitro by interfering with osterix expression. J. Cell. Biochem. 98, 992–1006.

Meyer, M.B., Benkusky, N.A., Sen, B., Rubin, J., Pike, J.W., 2016. Epigenetic plasticity drives adipogenic and osteogenic differentiation of marrow-derived mesenchymal stem cells. J. Biol. Chem. 291, 17829–17847.

Miura, M., Gronthos, S., Zhao, M., Lu, B., Fisher, L.W., Robey, P.G., Shi, S., 2003. SHED: stem cells from human exfoliated deciduous teeth. Proc. Natl. Acad. Sci. U.S.A. 100, 5807–5812.

Monroe, D.G., McGee-Lawrence, M.E., Oursler, M.J., Westendorf, J.J., 2012. Update on Wnt signaling in bone cell biology and bone disease. Gene 492, 1–18.

Muraglia, A., Corsi, A., Riminucci, M., Mastrogiacomo, M., Cancedda, R., Bianco, P., Quarto, R., 2003. Formation of a chondro-osseous rudiment in micromass cultures of human bone-marrow stromal cells. J. Cell Sci. 116, 2949–2955.

Muruganandan, S., Roman, A.A., Sinal, C.J., 2009. Adipocyte differentiation of bone marrow-derived mesenchymal stem cells: cross talk with the osteoblastogenic program. Cell. Mol. Life Sci. 66, 236–253.

Nah, H.D., Koyama, E., Agochukwu, N.B., Bartlett, S.P., Muenke, M., 2012. Phenotype profile of a genetic mouse model for Muenke syndrome. Childs Nerv. Syst. 28, 1483–1493.

Nelson, N.D., Bertuch, A.A., 2012. Dyskeratosis congenita as a disorder of telomere maintenance. Mutat. Res. 730, 43–51.

Neubauer, M., Fischbach, C., Bauer-Kreisel, P., Lieb, E., Hacker, M., Tessmar, J., Schulz, M.B., Goepferich, A., Blunk, T., 2004. Basic fibroblast growth factor enhances PPARgamma ligand-induced adipogenesis of mesenchymal stem cells. FEBS Lett. 577, 277−283.

O'Driscoll, S.W., Fitzsimmons, J.S., 2001. The role of periosteum in cartilage repair. Clin. Orthop. Relat. Res. S190−S207.

Oh, S., Oh, N., Appleford, M., Ong, J.L., 2006. Bioceramics for tissue engineering applications − a review. Am. J. Biochem. Biotechnol. 2, 49−56.

Ollier, L., 1867. Traite experimentale et clinique de ea regeneration des os et de la production artificielle du tissu osseux. Victor Masson et fils, Paris, France.

Olsen, B.R., Reginato, A.M., Wang, W., 2000. Bone development. Annu. Rev. Cell Dev. Biol. 16, 191−220.

Omatsu, Y., Sugiyama, T., Kohara, H., Kondoh, G., Fujii, N., Kohno, K., Nagasawa, T., 2010. The essential functions of adipo-osteogenic progenitors as the hematopoietic stem and progenitor cell niche. Immunity 33, 387−399.

Onimaru, K., Shoguchi, E., Kuratani, S., Tanaka, M., 2011. Development and evolution of the lateral plate mesoderm: comparative analysis of amphioxus and lamprey with implications for the acquisition of paired fins. Dev. Biol. 359, 124−136.

Owen, M., Friedenstein, A.J., 1988. Stromal stem cells: marrow-derived osteogenic precursors. Ciba Found. Symp. 136, 42−60.

Phillips, M.D., Kuznetsov, S.A., Cherman, N., Park, K., Chen, K.G., McClendon, B.N., Hamilton, R.S., McKay, R.D., Chenoweth, J.G., Mallon, B.S., Robey, P.G., 2014. Directed differentiation of human induced pluripotent stem cells toward bone and cartilage: in vitro versus in vivo assays. Stem Cells Transl. Med. 3, 867−878.

Piersanti, S., Remoli, C., Saggio, I., Funari, A., Michienzi, S., Sacchetti, B., Robey, P.G., Riminucci, M., Bianco, P., 2010. Transfer, analysis, and reversion of the fibrous dysplasia cellular phenotype in human skeletal progenitors. J. Bone Miner. Res. 25, 1103−1116.

Pinho, S., Lacombe, J., Hanoun, M., Mizoguchi, T., Bruns, I., Kunisaki, Y., Frenette, P.S., 2013. PDGFRalpha and CD51 mark human nestin+ sphere-forming mesenchymal stem cells capable of hematopoietic progenitor cell expansion. J. Exp. Med. 210, 1351−1367.

Pourquie, O., 2001. Vertebrate somitogenesis. Annu. Rev. Cell Dev. Biol. 17, 311−350.

Raaijmakers, M.H., Mukherjee, S., Guo, S., Zhang, S., Kobayashi, T., Schoonmaker, J.A., Ebert, B.L., Al-Shahrour, F., Hasserjian, R.P., Scadden, E.O., Aung, Z., Matza, M., Merkenschlager, M., Lin, C., Rommens, J.M., Scadden, D.T., 2010. Bone progenitor dysfunction induces myelodysplasia and secondary leukaemia. Nature 464, 852−857.

Ramalho-Santos, M., Willenbring, H., 2007. On the origin of the term "stem cell". Cell Stem Cell 1, 35−38.

Rezwan, K., Chen, Q.Z., Blaker, J.J., Boccaccini, A.R., 2006. Biodegradable and bioactive porous polymer/inorganic composite scaffolds for bone tissue engineering. Biomaterials 27, 3413−3431.

Riminucci, M., Collins, M.T., Fedarko, N.S., Cherman, N., Corsi, A., White, K.E., Waguespack, S., Gupta, A., Hannon, T., Econs, M.J., Bianco, P., Gehron Robey, P., 2003a. FGF-23 in fibrous dysplasia of bone and its relationship to renal phosphate wasting. J. Clin. Invest. 112, 683−692.

Riminucci, M., Fisher, L.W., Shenker, A., Spiegel, A.M., Bianco, P., Gehron Robey, P., 1997. Fibrous dysplasia of bone in the McCune-Albright syndrome: abnormalities in bone formation. Am. J. Pathol. 151, 1587−1600.

Riminucci, M., Kuznetsov, S.A., Cherman, N., Corsi, A., Bianco, P., Gehron Robey, P., 2003b. Osteoclastogenesis in fibrous dysplasia of bone: in situ and in vitro analysis of IL-6 expression. Bone 33, 434−442.

Riminucci, M., Liu, B., Corsi, A., Shenker, A., Spiegel, A.M., Robey, P.G., Bianco, P., 1999. The histopathology of fibrous dysplasia of bone in patients with activating mutations of the Gs alpha gene: site-specific patterns and recurrent histological hallmarks. J. Pathol. 187, 249−258.

Riminucci, M., Robey, P.G., Saggio, I., Bianco, P., 2010. Skeletal progenitors and the GNAS gene: fibrous dysplasia of bone read through stem cells. J. Mol. Endocrinol. 45, 355−364.

Riminucci, M., Saggio, I., Robey, P.G., Bianco, P., 2006. Fibrous dysplasia as a stem cell disease. J. Bone Miner. Res. 21 (Suppl. 2), P125−P131.

Roach, H.I., Erenpreisa, J., Aigner, T., 1995. Osteogenic differentiation of hypertrophic chondrocytes involves asymmetric cell divisions and apoptosis. J. Cell Biol. 131, 483−494.

Robey, P., 2017. "Mesenchymal stem cells": fact or fiction, and implications in their therapeutic use. F1000Res 6.

Robey, P.G., 2000. Stem cells near the century mark. J. Clin. Invest. 105, 1489−1491.

Robey, P.G., 2011. Cell sources for bone regeneration: the good, the bad, and the ugly (but promising). Tissue Eng. B Rev. 17, 423−430.

Robey, P.G., Kuznetsov, S., Riminucci, M., Bianco, P., 2007. The role of stem cells in fibrous dysplasia of bone and the Mccune-Albright syndrome. Pediatr. Endocrinol. Rev. 4 (Suppl. 4), 386−394.

Robey, P.G., Kuznetsov, S.A., Riminucci, M., Bianco, P., 2014. Bone marrow stromal cell assays: in vitro and in vivo. Methods Mol. Biol. 1130, 279−293.

Rosen, C.J., Bouxsein, M.L., 2006. Mechanisms of disease: is osteoporosis the obesity of bone? Nat. Clin. Pract. Rheumatol. 2, 35−43.

Sacchetti, B., Funari, A., Michienzi, S., Di Cesare, S., Piersanti, S., Saggio, I., Tagliafico, E., Ferrari, S., Robey, P.G., Riminucci, M., Bianco, P., 2007. Self-renewing osteoprogenitors in bone marrow sinusoids can organize a hematopoietic microenvironment. Cell 131, 324−336.

Sacchetti, B., Funari, A., Remoli, C., Giannicola, G., Kogler, G., Liedtke, S., Cossu, G., Serafini, M., Sampaolesi, M., Tagliafico, E., Tenedini, E., Saggio, I., Robey, P.G., Riminucci, M., Bianco, P., 2016. No identical "mesenchymal stem cells" at different times and sites: human committed progenitors of distinct origin and differentiation potential are incorporated as adventitial cells in microvessels. Stem Cell Reports 6, 897−913.

Schipani, E., Kruse, K., Juppner, H., 1995. A constitutively active mutant PTH-PTHrP receptor in Jansen-type metaphyseal chondrodysplasia. Science 268, 98−100.

Schofield, R., 1978. The relationship between the spleen colony-forming cell and the haemopoietic stem cell. Blood Cells 4, 7−25.

Scotti, C., Piccinini, E., Takizawa, H., Todorov, A., Bourgine, P., Papadimitropoulos, A., Barbero, A., Manz, M.G., Martin, I., 2013. Engineering of a functional bone organ through endochondral ossification. Proc. Natl. Acad. Sci. U.S.A. 110, 3997−4002.

Serafini, M., Sacchetti, B., Pievani, A., Redaelli, D., Remoli, C., Biondi, A., Riminucci, M., Bianco, P., 2014. Establishment of bone marrow and hematopoietic niches in vivo by reversion of chondrocyte differentiation of human bone marrow stromal cells. Stem Cell Res. 12, 659–672.

Simmons, P.J., Torok-Storb, B., 1991. Identification of stromal cell precursors in human bone marrow by a novel monoclonal antibody, STRO-1. Blood 78, 55–62.

Sims, N.A., Martin, T.J., 2014. Coupling the activities of bone formation and resorption: a multitude of signals within the basic multicellular unit. Bonekey Rep. 3, 481.

Sugiyama, T., Kohara, H., Noda, M., Nagasawa, T., 2006. Maintenance of the hematopoietic stem cell pool by CXCL12-CXCR4 chemokine signaling in bone marrow stromal cell niches. Immunity 25, 977–988.

Suresh, S., de Castro, L.F., Dey, S., Robey, P.G., Noguchi, C.T., 2019. Erythropoietin modulates bone marrow stromal cell differentiation. Bone Res (in press).

Sworder, B.J., Yoshizawa, S., Mishra, P.J., Cherman, N., Kuznetsov, S.A., Merlino, G., Balakumaran, A., Robey, P.G., 2015. Molecular profile of clonal strains of human skeletal stem/progenitor cells with different potencies. Stem Cell Res. 14, 297–306.

Taipaleenmaki, H., Abdallah, B.M., AlDahmash, A., Saamanen, A.M., Kassem, M., 2011. Wnt signalling mediates the cross-talk between bone marrow derived pre-adipocytic and pre-osteoblastic cell populations. Exp. Cell Res. 317, 745–756.

Tang, Y., Wu, X., Lei, W., Pang, L., Wan, C., Shi, Z., Zhao, L., Nagy, T.R., Peng, X., Hu, J., Feng, X., Van Hul, W., Wan, M., Cao, X., 2009. TGF-beta1-induced migration of bone mesenchymal stem cells couples bone resorption with formation. Nat. Med. 15, 757–765.

Tavassoli, M., Crosby, W.H., 1968. Transplantation of marrow to extramedullary sites. Science 161, 54–56.

Teven, C.M., Liu, X., Hu, N., Tang, N., Kim, S.H., Huang, E., Yang, K., Li, M., Gao, J.L., Liu, H., Natale, R.B., Luther, G., Luo, Q., Wang, L., Rames, R., Bi, Y., Luo, J., Luu, H.H., Haydon, R.C., Reid, R.R., He, T.C., 2011. Epigenetic regulation of mesenchymal stem cells: a focus on osteogenic and adipogenic differentiation. Stem Cell. Int. 2011, 201371.

Tormin, A., Li, O., Brune, J.C., Walsh, S., Schutz, B., Ehinger, M., Ditzel, N., Kassem, M., Scheding, S., 2011. CD146 expression on primary non-hematopoietic bone marrow stem cells is correlated with in situ localization. Blood 117, 5067–5077.

Tu, X., Chen, J., Lim, J., Karner, C.M., Lee, S.Y., Heisig, J., Wiese, C., Surendran, K., Kopan, R., Gessler, M., Long, F., 2012. Physiological notch signaling maintains bone homeostasis via RBPjk and Hey upstream of NFATc1. PLoS Genet. 8 e1002577.

Ugarte, F., Forsberg, E.C., 2013. Haematopoietic stem cell niches: new insights inspire new questions. EMBO J. 32, 2535–2547.

Walne, A.J., Bhagat, T., Kirwan, M., Gitiaux, C., Desguerre, I., Leonard, N., Nogales, E., Vulliamy, T., Dokal, I.S., 2013. Mutations in the telomere capping complex in bone marrow failure and related syndromes. Haematologica 98, 334–338.

Watt, F.M., Hogan, B.L., 2000. Out of Eden: stem cells and their niches. Science 287, 1427–1430.

Winkler, T., Sass, F.A., Duda, G.N., Schmidt-Bleek, K., 2018. A review of biomaterials in bone defect healing, remaining shortcomings and future opportunities for bone tissue engineering: the unsolved challenge. Bone Joint Res 7, 232–243.

Xiong, J., O'Brien, C.A., 2012. Osteocyte RANKL: new insights into the control of bone remodeling. J. Bone Miner. Res. 27, 499–505.

Xu, R., Hu, J., Zhou, X., Yang, Y., 2018. Heterotopic ossification: mechanistic insights and clinical challenges. Bone 109, 134–142.

Yamaguchi, H., Calado, R.T., Ly, H., Kajigaya, S., Baerlocher, G.M., Chanock, S.J., Lansdorp, P.M., Young, N.S., 2005. Mutations in TERT, the gene for telomerase reverse transcriptase, in aplastic anemia. N. Engl. J. Med. 352, 1413–1424.

Yang, L., Tsang, K.Y., Tang, H.C., Chan, D., Cheah, K.S., 2014. Hypertrophic chondrocytes can become osteoblasts and osteocytes in endochondral bone formation. Proc. Natl. Acad. Sci. U.S.A. 111, 12097–12102.

Zanotti, S., Canalis, E., 2016. Notch signaling and the skeleton. Endocr. Rev. 37, 223–253.

Zhang, J.F., Fu, W.M., He, M.L., Xie, W.D., Lv, Q., Wan, G., Li, G., Wang, H., Lu, G., Hu, X., Jiang, S., Li, J.N., Lin, M.C., Zhang, Y.O., Kung, H.F., 2011. MiRNA-20a promotes osteogenic differentiation of human mesenchymal stem cells by co-regulating BMP signaling. RNA Biol. 8, 829–838.

Chapter 3

Bone marrow and the hematopoietic stem cell niche

Laura M. Calvi

Department of Medicine and Wilmot Cancer Center, University of Rochester Medical Center, Rochester, NY, United States

Chapter outline

Introduction

In the adults of land-dwelling vertebrates, the skeleton is the obligate site for normal hematopoiesis during homeostasis. Throughout the life of an organism, hematopoiesis maintains the blood components necessary for oxygenation (erythropoiesis), clotting (megakaryopoiesis/thrombopoiesis), and immunity (myelopoiesis and lymphopoiesis). Since differentiated cells have varying life spans, from hours (in the case of neutrophils) to years (in the case of memory T cells and hematopoietic stem cells [HSCs]), a large component of the hematopoietic system is continually replaced by intermediate committed precursors derived from progenitors that may give rise to more than one differentiated lineage. Progenitors and precursors have limited self-renewal capacity and derive from HSCs, tissue-specific stem cells that persist throughout the life of an organism. While these stem cells are primarily quiescent, they are recruited when there is increased demand for blood products. Given their ability to regenerate the entire hematopoietic system and their relative accessibility, HSCs have been extensively studied as a model system for stem cell behavior. Clinically, HSCs are commonly used in the setting of stem cell transplantation for the treatment of hematologic malignancies and other disorders; therefore, extensive research has focused on understanding their regulation for regenerative purposes. In addition to cell-autonomous programs, a highly complex and dynamic microenvironment in the bone marrow contributes to the support and regulation of HSCs. The components of this system are likely to represent important potential therapeutic targets if their regulation and impact on HSCs are understood. Moreover, since bone and marrow are components of the same organ, dysfunction in bone may contribute to hematopoietic failure and vice versa. Here we present a historical prospective on the concept of the bone marrow microenvironment as a regulatory component for hematopoiesis, and describe the data supporting the role of niche constituents in the regulation of HSCs.

Principles of Bone Biology. https://doi.org/10.1016/B978-0-12-814841-9.00003-8

The niche concept: a historical prospective

In the 1960s and early 1970s the ability to transplant bone marrow cells that could regenerate the hematopoietic system (McCulloch and Till, 1960) and the development of in vivo and cell culture methods that could detect and study hematologic progenitor cells as colony-forming unit cells (Becker et al., 1963; Senn et al., 1967) initiated studies aimed at defining immature cells responsible for sustaining hematopoiesis and their regulation. Based on divergent observations of spleen colony-forming cells compared with in vivo HSCs, the stem cell niche concept was initially proposed in 1978 by Schofield (Schofield, 1978). This investigator single-handedly postulated that the "virtual immortality" of HSCs in the bone marrow may be conferred by association with other cells capable of preventing their maturation, maintaining their reconstitution capacity (Schofield, 1978). At the same time, studies suggested that the distribution of HSCs followed a hierarchical organization, with the most primitive cell populations being found at the endosteal surface of bone (Gong, 1978). Analogous to the niche in ecology, niches conceptually represent the microenvironmental conditions that support specific stem cell populations. Schofield proposed that niche cells would be found in close proximity to supported stem cells, so as to form a relatively "fixed" unit, and that they would provide signals that could modify stem cell fate choices, including bestowing stem cell potential to more differentiated daughter cells (Schofield, 1978). While this innovative idea was stimulated by observations in hematopoiesis, the niche was first demonstrated in the *Drosophila* gonad, where elegant studies showed that niche occupancy could alter cell fate and induce stem cell behavior in progenitor populations (Kiger et al., 2000; Tran et al., 2000; Xie and Spradling, 2000). Since these initial studies, niches have been defined in colonial chordates (Rosental et al., 2018), *Caenorhabditis elegans* (Austin and Kimble, 1987), zebrafish (Tamplin et al., 2015), and murine models for many tissue-based stem cells (Tumbar et al., 2004; Bjerknes and Cheng, 2001), including, most recently, the hematopoietic system. In the bone marrow, many challenges initially delayed identification of niches and critical populations within them. These challenges included the technical difficulties involved in the examination of the boundary between the hard bone tissue and the soft bone marrow, difficulty in direct visualization of the marrow, apparent anatomic disorganization of marrow populations, rarity of HSCs, lack of histologic distinguishing features of these populations, and limited definition of mesenchymal cell populations. However, the regulatory niche, if comprehensively defined, offers the potential for indirect stem cell manipulation and could therefore be a very powerful therapeutic target. In addition, understanding of the critical component of the niche is necessary to design adequate supportive conditions for HSCs ex vivo. For these reasons, definition of the HSC niche has been the focus of intense research efforts since the beginning of the 21st century.

Hematopoietic stem cell microenvironments in the embryo and perinatal period

While in the adult HSCs are found primarily in bone, stem cells with the ability to generate all hematopoietic lineages initially arise in the hemogenic endothelium within the aorta−gonad−mesonephros (AGM) (Ivanovs et al., 2011; Muller et al., 1994; Medvinsky and Dzierzak, 1996; Medvinsky et al., 2011; de Bruijn et al., 2000) as a result of endothelial-to-hematopoietic cell transition (Jaffredo et al., 1998; Bertrand et al., 2010; Boisset et al., 2010; Kissa and Herbomel, 2010; de Bruijn et al., 2002). Additional studies have shown that HSCs may develop not only in the AGM but also in the placenta (Gekas et al., 2005; Ottersbach and Dzierzak, 2005; Rhodes et al., 2008). The role of the placenta as a supportive microenvironment for HSCs has also been demonstrated in humans (Robin et al., 2009). From the AGM and the placenta, HSCs migrate to the fetal liver (murine embryonic day 1, E11), where they are supported by portal vessels (Khan et al., 2016). In the liver, HSCs dramatically expand prior to seeding the bone marrow (Morrison et al., 1995; Bowie et al., 2007; Ema and Nakauchi, 2000). HSC activity is first detected in the bone marrow at E16.5 (Coskun et al., 2014). Contemporary analyses of skeletal and hematopoietic development have shown that, in the mouse, this transition to the bone marrow corresponds to fetal long bone vascularization and incipient osteogenesis (Coskun et al., 2014). Notably, at E16.5, in the long bones osteoblasts are primarily found at the bone collar/periosteum, suggesting that at this developmental stage marrow vascular or mesenchymal populations may drive HSC homing. However, mice with genetic deletion of the transcription factor Osterix ($Sp7^{-/-}$ mice), which lack osteoprogenitors and their progeny, while their marrow vasculature is intact, have bone marrow HSCs that cannot properly home and engraft (Coskun et al., 2014), highlighting the importance of the osteogenic niche in the perinatal time. HSCs continue to migrate to the bone marrow through the first postnatal week, at a time when liver portal vessels are remodeled (Khan et al., 2016), while osteoblastic cell populations are rapidly expanding (Coskun et al., 2014). Once in the bone marrow, during the first 3 weeks of life, HSCs proliferate extensively while bone and marrow grow (Bowie et al., 2006). Subsequently, HSCs become primarily quiescent (Wilson et al., 2008), although the degree of their contribution to daily hematopoiesis remains disputed (Sun et al., 2014; Sawai et al., 2016; Busch et al., 2015).

The adult bone marrow niche

The discovery of cell surface markers that could more easily enrich for and prospectively isolate cells with HSC function using few stains (Kiel et al., 2005; Oguro et al., 2013), combined with advances in tissue imaging, reviewed in Tjin et al. (2018), and the availability of genetic models that could target cellular subsets, reviewed in Kfoury and Scadden (2015), is revolutionizing our understanding of the bone marrow microenvironment. We next summarize bone marrow cell populations that have been shown to contribute to the regulation and support of HSCs.

Mesenchymal stromal/stem cell populations

The definition and identification of mesenchymal stem/stromal cells (MSCs) remain a disputed topic in the bone field; however, niche studies have highlighted specific subsets of these populations that are able to support and modulate HSCs (Mendez-Ferrer et al., 2010). These studies have been performed primarily in the mouse, while the definition of MSCs and their role as HSC niches in the human bone marrow remain poorly understood. By using genetic models in which a key supportive molecule, stromal cell-derived factor 1 (SDF1, also known as C-X-C motif chemokine 12, or CXCL12) or stem cell factor (SCF) (Greenbaum et al., 2013; Ding and Morrison, 2013; Zhou et al., 2017), is genetically deleted in different mesenchymal subsets, and then quantifying HSCs, a number of marrow MSC populations have been reported as participating in HSC support. HSC-supportive cells have also been described, based on their degree of CXCL12 expression, as CXCL12-abundant reticular (or CAR) cells (Sugiyama et al., 2006). A number of populations identified based on either genetic labeling or flow cytometric expression have been shown to support HSCs: nestin−green fluorescent protein (GFP)-positive cells (Mendez-Ferrer et al., 2010), leptin receptor-positive cells (Zhou et al., 2017), paired related homeobox 1 (Prx1)-targeted cells (Greenbaum et al., 2013), and cells identified by their expression of integrin αV (CD51), the platelet-derived growth factor receptor α (Pinho et al., 2013), or CD51 and the cell surface marker Sca1 (Morikawa et al., 2009). Notably, there is evidence that some cell populations, for example, nestin−GFP$^+$ cells, are still heterogeneous (Kunisaki et al., 2013) and that they do not represent multipotent MSCs, since they cannot differentiate to adipocytes (Zhou et al., 2014; Itkin et al., 2016). In addition, there is probably a hierarchy in the organization of these populations. For example, Prx1$^+$ MSCs are able to generate leptin receptor-positive and CAR cells (Zhou et al., 2014; Omatsu et al., 2010), and deletion of the leptin receptor in Prx1$^+$ cells expands osteolineage populations while inhibiting adipocytes (Yue et al., 2016).

More recent data have suggested that the location of supporting cell populations may also have an impact on their ability to functionally influence HSCs. Studies have shown that perivascular cell populations in fact express the highest level of CXCL12 (Ding and Morrison, 2013). Some studies show that nestin−GFP$^+$ cells are distributed along arterioles and sinusoidal structures within the bone marrow (Kunisaki et al., 2013), and at these different locations they provide differential support to HSCs (Asada et al., 2017). Nestin−GFP$^+$ cells at arteriole sites express the pericyte marker neural/glial antigen 2 (NG2), and appear to play a role in the maintenance of HSCs (Pinho et al., 2018). These findings have been debated, as another study has suggested that niches at sinusoidal sites provide a quiescent niche for HSCs (Acar et al., 2015). As we will discuss later, these discrepancies are probably due not only to different experimental models (Joseph et al., 2013), but also to heterogeneity of HSC populations.

Adipocytes

Marrow adipocytes are differentiated from MSC populations (Horowitz et al., 2017). They are rare populations in the juvenile marrow but increase during aging and especially in the setting of myeloablation and anorexia (Calvo et al., 1976; Abella et al., 2002). Studies have suggested that marrow adipocytes have different characteristics compared with adipocytes in other depots and may be heterogeneous (Scheller et al., 2015); however, the lack of a genetic approach to target marrow compared with other adipocyte depots has as of this writing represented a challenge to support these claims. The contribution of marrow adipocytes to the support of HSCs is an area of debate, as is their impact on bone (Doucette et al., 2015; Ambrosi et al., 2017). Initial studies using genetic murine models and pharmacologic tools suggested that adipocytic populations may inhibit HSCs (Naveiras et al., 2009). More recently, Ambrosi et al. presented data that correlate age- and diet-dependent increases in adipocytes with hematopoietic and skeletal stem cell dysfunction (Ambrosi et al., 2017), while Zhou et al. found that adipocytes secrete SCF and promote the regeneration of HSCs (Zhou et al., 2017). While some of these discrepancies have been attributed to differential effects in different bones (Zhou et al., 2017), these data may also tap into the reciprocal relationship of osteolineage and adipocytic cells, long shown in vitro (Ge et al., 2016), and also into the emerging concept that adipocytes may represent a local energy depot to support the

metabolically demanding daily hematopoiesis (Tabe et al., 2017). The ability to target specifically marrow adipocytes genetically will no doubt provide clarity to this important area of investigation, especially as it may modulate skeletal and hematopoietic regeneration, as well as contributing to a supportive microenvironment in the setting of leukemia (Tabe et al., 2017).

Osteoblastic cells

Since bone is the required site for hematopoiesis in adulthood, cells in the osteoblastic lineage were the first candidates as HSC-supportive niche cells. Initial in vitro studies demonstrated that cells of osteoblastic lineage, derived from mice or humans, could provide support to hematopoietic stem and progenitor cells (Taichman and Emerson, 1994; Taichman et al., 1996). Subsequently, data showed that genetic manipulation of osteoblastic populations could expand HSCs, providing the first evidence for the existence of a regulatory hematopoietic microenvironment (Calvi et al., 2003; Zhang et al., 2003). Additional experiments in which osteoblastic populations were ablated in adulthood also demonstrated loss of hematopoietic populations (Visnjic et al., 2004), although lymphocytes were lost prior to HSCs. Moreover, studies using bone marrow samples from patients showed that HSCs are found proximal to endosteal surfaces (Guezguez et al., 2013). In addition, direct imaging of the niche in the calvarial space demonstrated homing of HSCs preferentially to the endosteum (Lo Celso et al., 2009; Xie et al., 2009), even in the absence of myeloablative conditioning (Ellis et al., 2011), with hierarchical organization placing HSCs proximal to the endosteum compared with progenitor cells (Lo Celso et al., 2009). In a genetic model, depletion of osteocalcin-expressing osteolineage cells inhibits mobilization of HSCs (Asada et al., 2013; Ferraro et al., 2011). Finally, when *Sp7*, the gene encoding the transcription factor Osterix, is conditionally deleted, with resulting loss of osteoblastic differentiation, hematopoiesis is almost completely eliminated from the metaphyseal region (Zhou et al., 2010). However, the importance of osteoblastic populations in support of HSCs has been questioned by studies showing that, while the majority of hematopoietic cells reside in the metaphyseal regions, enriched with trabecular bone (Nombela-Arrieta et al., 2013; Guezguez et al., 2013), only a small subset of HSCs are found in direct proximity to osteoblasts (Lo Celso et al., 2009; Kiel et al., 2005, 2009; Sugiyama et al., 2006; Acar et al., 2015), pointing instead to perivascular sites as more frequent niches for HSCs. Later studies clearly demonstrated the close proximity of important endothelial structures to the endosteum, and their interaction with osteoblastic cells, suggesting that these populations collaborate in the support and regulation of HSCs (Kusumbe et al., 2014, 2016; Ramasamy et al., 2014; Xu et al., 2018). Skepticism regarding the role of osteolineage cells in HSC regulation was also supported by studies targeting deletions of two key pro-HSC signals, the chemokine CXCL2 (also known as SDF1) and the growth factor SCF, which demonstrated regulation of HSC numbers and function when removed from mesenchymal stem and progenitor cells but not from osteoblastic populations (Ding and Morrison, 2013; Greenbaum et al., 2013). However, these models reflect primarily the impact of these two factors on HSC numbers and function, and therefore limit the scope of the evaluation of the niche.

Numerous studies provide interesting evidence that osteoblastic cell populations support specifically the common lymphoid progenitor and/or the lymphoid lineage within the bone marrow (Zhu et al., 2007; Ding and Morrison, 2013; Wu et al., 2008), supporting the concept that there may be multiple niches within the bone marrow to support not just HSCs, but also other progenitor populations that are more specialized. For example, data have shown that thymus-seeding progenitors are supported by the Notch ligand Delta-like 4, produced by osteocalcin-expressing osteoblastic cells (Yu et al., 2015).

Within the osteoblastic lineage, there is also evidence that differentiation stage may contribute differentially to HSC support. Data from in vitro studies in which the differentiation stage of osteoblastic populations was controlled showed decreasing support of HSCs with osteoblastic maturation (Cheng et al., 2011; Nakamura et al., 2010). These findings are also supported by proximity-based isolation of endosteal osteoblastic populations found close to HSCs in vivo (Silberstein et al., 2016). Data have shown that genetic disruption of osteoprogenitor cells initiates bone marrow failure and pre-leukemia, while the same defect targeted to osteocalcin-positive populations does not (Raaijmakers et al., 2010). Moreover, while targeting of a constitutively active parathyroid hormone (PTH) receptor to osteoblastic cells expanded HSCs (Calvi et al., 2003), targeting the same construct to osteocytes did not (Calvi et al., 2012), despite similar degrees of osteoblastic expansion. A key PTH-regulated molecule that is produced by osteocytes is sclerostin, the protein encoded by the *Sost* gene, which is known to be downregulated by PTH. Notably, consistent with the data from mice with targeting of the PTH receptor to osteocytes, $Sost^{-/-}$ mice also demonstrate the bone anabolic effect of PTH but not the expansion in HSCs (Cain et al., 2012). Therefore, expansion of osteoblasts alone is not sufficient to expand HSCs, as also shown by treatment with strontium (Lymperi et al., 2008), and osteocyte activation alone does not increase HSCs. However, when osteocytes were depleted in adult mice, lymphopoiesis was disrupted, and mobilization of HSCs induced by granulocyte

colony−stimulating factor (G-CSF) was inhibited (Asada et al., 2013). These data suggest that these populations of terminally differentiated osteoblasts that are embedded in matrix contribute to some aspects of HSC regulation. Interestingly, targeted deletion of $G_s\alpha$ in osteocytes induces a myeloproliferative disorder and splenomegaly through the microenvironment, in a G-CSF-dependent manner (Fulzele et al., 2013). Together these data suggest that cells in the osteoblastic lineage contribute to hematopoietic regulation in a differentiation-dependent manner. One limitation of these data is the unexpected targeting of CAR cells by the DMP-1 promoter (Zhang and Link, 2016). Further data are required to define mechanistically the contributions of these osteolineage populations to the regulation of HSCs and their progeny.

While the importance of osteoblastic cells in normal HSCs remains a hotly debated issue, the role of osteoblastic cells in hematologic malignancies is supported by extensive experimental data. In a murine model of myeloproliferative neoplasia there was an expansion of osteolineage populations that were, however, defective in their ability to support normal HSCs, enhancing clonal hematopoietic populations (Schepers et al., 2013). Numerous models of leukemia have shown its ability to disrupt osteoblastic populations, for example, in a model of blast crisis acute myeloid leukemia (Frisch et al., 2012) and in the MML-AF9 model of acute myeloid leukemia (Silva et al., 2010; Duarte et al., 2018). Loss of osteoblasts accelerated leukemia progression (Silva et al., 2011), and osteoblasts could inhibit leukemia cell engraftment and disease progression (Krevvata et al., 2014). In some cases, activation of the normal niche was able to decrease transformation of preleukemic clones to leukemia (Krause et al., 2013), pointing to the potentially protective role of normal niches.

Osteoblastic cells are also important for the ability of HSCs to recover from radiation injury (Dominici et al., 2009). In this setting, rapid expansion of endosteal osteoblasts required insulin-like growth factor 1 (IGF1) (Caselli et al., 2013). In elegant studies using proximity-based single-cell profiling in the setting of radiation conditioning, Silberstein et al. were able to define characteristics of endosteal osteoblastic populations proximal to HSCs, and identified secreted signals that regulate HSCs, including the secreted RNase angiogenin, interleukin 18, and the adhesion molecule Embigin (Silberstein et al., 2016). Interestingly, these studies were performed in neonatal calvaria, to avoid decalcification, and therefore whether these cell populations contribute to the support and regulation of adult HSCs remains untested. However, the novel signals identified by this approach were found to be important for hematopoietic stem and progenitor cell regulation, strongly implicating osteolineage populations in hematopoietic recovery after myeloablation (Silberstein et al., 2016). Notably, in the case of angiogenin, the same signal had differential effects on stem cell populations and progenitors, indicating a role for osteolineage populations in a coordinated response of the hematopoietic system to acute injury, in which angiogenin maintains HSC quiescence while enhancing progenitor cell proliferation (Goncalves et al., 2016).

Lessons learned from the dissection of mesenchymal osteoblastic components and their matrix were instrumental in attempts at recapitulating a supportive HSC niche ex vivo, as was shown in initial studies describing a biomimetic microenvironment using human cell populations (Bourgine et al., 2018).

Endothelial cells

Initial studies identifying HSCs as lineage$^-$, CD150$^+$, CD48$^-$, and CD41$^-$ cells showed that 60% of these cells were found in proximity to sinusoidal endothelial structures in the adult marrow at homeostasis (Kiel et al., 2005, 2007), suggesting that endothelial cells may contribute to HSC regulation. However, deletion of *CXCL12*, *Jagged1,* or *SCF* in endothelial populations did not have an impact on HSC maintenance although deletion of *Jagged1* in endothelial cells may impact HSF self-renewal (Ding et al., 2012; Greenbaum et al., 2013; Poulos et al., 2013; Ding and Morrison, 2013). However, the endothelium is clearly critical for recovery of HSCs after myeloablation (Hooper et al., 2009; Kobayashi et al., 2010; Butler et al., 2010; Winkler et al., 2012). Just as in the mesenchymal osteoblastic lineage, the heterogeneity of marrow endothelial structures is emerging (Kusumbe et al., 2014; Ramasamy et al., 2014). Vascular heterogeneity clearly imparts differential effects on hematopoiesis (Itkin et al., 2016), to some extent as a result of differential permeability of sinusoids compared with arteriolar structures. Moreover, coupling of vascular with mesenchymal osteolineage populations is being uncovered (Xu et al., 2018; Kusumbe et al., 2016). These data strongly suggest that different niche components are interdependent in their regulation of HSCs.

Hematopoietic cells

The progeny of HSCs are also recognized for their ability to regulate HSCs. In particular, megakaryocytes, marrow macrophages, senescent neutrophils, osteoclasts, and regulatory T cells have been demonstrated to regulate HSCs, either directly or through their ability to modulate the behavior of other niche cells.

Megakaryocytes

Megakaryocytes are the hematologic progenitors that give rise to platelets in the bone marrow when associated with endothelial structures. Several groups have shown that megakaryocytes are direct regulators of HSC quiescence. In the bone marrow, HSCs are often found in close proximity to megakaryocytes (Bruns et al., 2014). Moreover, signals derived from megakaryocytes, including the chemokine CXCL4 (also known as platelet factor 4), Thrombopoietin, and transforming growth factor β1 (TGFβ1), have been shown to mediate the quiescence of HSCs, at least at homeostasis (Bruns et al., 2014; Nakamura-Ishizu et al., 2014, 2015; Zhao et al., 2014). Megakaryocytes also promote murine osteoblastic expansion after radioablation (Olson et al., 2013), and provide a supportive niche preferentially for platelet- and myeloid-biased HSCs (Pinho et al., 2018). The study shows that cells contributing to HSC support can also have an impact on their fate, since deletion of megakaryocytes could induce myeloid- and platelet-biased HSCs to give balanced lineage contribution upon transplantation.

Macrophages

Macrophages are key regulators of both innate and adaptive immunity, and are critical for tissue homeostasis through their capacity to engulf debris, pathogens, and apoptotic cells. Macrophages are highly heterogeneous within different tissues and are derived both from the yolk sac and from the differentiation of monocytes derived from bone marrow (Heideveld and van den Akker, 2017). In the bone marrow, specialized macrophage activities include the engulfment of senescent neutrophils (Casanova-Acebes et al., 2013) and erythropoiesis through their contribution to erythroblastic islands (Bessis, 1958; Chow et al., 2013). Supporting a role for macrophages in the bone marrow niche, HSC dormancy is regulated through the interaction of CD234/Duffy antigen receptor for chemokines expressed on macrophages with CD82/KAI1 expressed on HSCs (Hur et al., 2016). Several lines of evidence demonstrate that marrow macrophages play an important role in trafficking of HSCs to and from the bone marrow. Macrophages regulate the retention of hematopoietic stem and progenitor cells in the bone marrow (Chow et al., 2011; Winkler et al., 2010), and specifically the release of HSCs from the niche, also known as mobilization, induced by G-CSF (Christopher et al., 2011). Interestingly, some of these actions appear to be through their ability to modulate mesenchymal and osteoblastic cell populations. For example, a subset of $CD169^+$ macrophages was found to maintain HSCs in the marrow by regulating MSC production of CXCL12 (Chow et al., 2011). In addition, a population of marrow macrophages marked by smooth muscle actin expresses cyclooxygenase 2 and produces prostaglandin E2 (Ludin et al., 2012). This macrophage population supports HSCs and is expanded by radiation (Ludin et al., 2012) and, on a daily basis, by circadian bursts of darkness-induced norepinephrine that induces melatonin through tumor necrosis factor (Golan et al., 2018). More recently, studies have begun to show that macrophages are also important for homing and engraftment of HSCs. For example, in the zebrafish caudal hematopoietic tissue (equivalent to the mammalian fetal liver), vascular cell adhesion molecule-positive macrophages were found to patrol the venous plexus, interact with HSCs through integrin α4, and regulate HSC retention (Li et al., 2018). In the mammalian bone marrow, a population of $CD169^+$ macrophages located within perivascular and endosteal regions was resistant to conditioning radiation and was found to promote long-term engraftment of HSCs (Kaur et al., 2018). A subset of marrow macrophages found in close proximity to the endosteum, also known as osteomacs, has been shown to regulate osteoblastic function (Chang et al., 2008) and also contribute to support of HSCs through their synergy with osteoblasts and megakaryocytes (Mohamad et al., 2017). Finally, a recent study demonstrated that marrow macrophages from aged mice become defective, with increased inflammatory signals and decreased phagocytic capacity, and that they determine HSC megakaryocytic skewing likely through Interleukin 1 β (Frisch et al 2019 JCI Insight. 2019 Apr 18;5. pii: 124213. doi: 10.1172/jci.insight.124213.PMID: 30998506).

Neutrophils

Neutrophils are hematopoietic cells characterized by segmented nuclei and the presence of granules critical for innate immunity. Neutrophils are very short lived and highly mobile, and represent the "first responder" population in immune and injury responses (Nathan, 2006). They are produced in the bone marrow, where they are preferentially found in close proximity to CAR cells rather than endothelial cells (Evrard et al., 2018). Mature and immature neutrophils exit the bone marrow to the circulation and tissues and senesce rapidly (Evrard et al., 2018). Following a circadian rhythm, a large number of senescent neutrophils expressing the CXCL12 receptor CXCR4 home daily to the bone marrow (Casanova-Acebes et al., 2013). In the bone marrow, senescent neutrophils are phagocytosed by macrophages and indirectly modulate microenvironmental CXCL12 levels (Casanova-Acebes et al., 2013), influencing signals that not only guide senescent neutrophils but also support HSCs.

T cells

High-resolution imaging of the HSC niche after transplantation showed colocalization of hematopoietic stem and progenitor cells with regulatory FoxP3 T cells (T regs) at the endosteum, and demonstrated that depletion of T regs resulted in the loss of HSCs (Fujisaki et al., 2011). These data support the hypothesis that T regs are necessary for the maintenance of allogeneic HSCs after transplantation. Follow-up studies identified a subset of CD150high T regs in the niche that maintain HSC quiescence (Hirata et al., 2018). Transcriptional analysis of these cells found increases in CD39 and CD73, cell surface ectoenzymes that generate extracellular adenosine (Hirata et al., 2018). The authors went on to demonstrate that adenosine is required to mediate the beneficial effects of CD150high T regs, and that adaptive transfer of these cells improves allogeneic engraftment of HSCs (Hirata et al., 2018). In addition to demonstrating the participation of T regs in the regulation of adult HSCs, these data provide strong evidence that definition and targeting of the niche can have a significant impact under clinically relevant conditions.

Osteoclasts

Osteoclasts, key specialized cells that resorb bone, are hematopoietically derived and play a crucial role in the maintenance of skeletal homeostasis. Osteoclasts, as key cells that resorb bone, are necessary for the formation of the bone marrow cavity in the embryo (Mansour et al., 2012). In addition, the ability of osteoclasts to resorb bone may also regulate HSCs through the release of matrix components and minerals. Data using HSCs from mice that lack the calcium sensor have suggested that HSCs preferentially home to regions of high calcium in the marrow (Adams et al., 2006). Similarly, TGFβ is a known matrix factor that can be released by osteoclastic bone resorption that also has been shown to induce quiescence in stem cell populations (Yamazaki et al., 2009).

Neuronal regulation of the hematopoietic stem cell niche

With improvements in the ability to prospectively isolate HSCs, experimentalists observed that the frequency of marrow HSCs is regulated by a circadian rhythm. Studies had uncovered how neuronal innervation of the marrow by the sympathetic nervous system (SNS) plays a role in mobilization of HSCs (Katayama et al., 2006). The same laboratory later discovered that the SNS is responsible for this circadian mobilization of HSCs through β-adrenergic signals (Mendez-Ferrer et al., 2008). Unexpectedly, β-adrenergic receptor agonists induced expression of the vitamin D receptor (VDR) in osteoblasts, and mice lacking the VDR had impairment in G-CSF-mediated osteoblastic inhibition and mobilization of HSCs, suggesting that the VDR is a modulator of HSC trafficking (Kawamori et al., 2010). Neuronal regulation of the hematopoietic stem cell niche is modulated by aging (Maryanovich et al., 2018), chemotherapy (Hanoun et al., 2014), and myeloproliferative syndromes (Arranz et al., 2014), although the mechanisms by which these conditions alter the SNS remain poorly understood. In addition to these direct effects, nonmyelinating marrow Schwann cells have been shown to induce HSC quiescence through their production of TGFβ (Yamazaki et al., 2011). Therefore, neuronal signals are clearly an important target for the manipulation of niches and the HSCs they support.

Hormonal regulation of the hematopoietic stem cell niche

The impact of hormones on the niche indicates that the niche is a dynamic system that is physiologically regulated and therefore represents a homeostatic mechanism to regulate and maintain HSCs. It is likely that these are simply examples of many systemic signals that can regulate HSCs through their niche.

Parathyroid hormone

Studies have demonstrated how constitutive activation of the PTH receptor 1 in osteolineage cells could expand HSCs, and how pharmacologic treatment with anabolic doses of PTH expands HSCs (Calvi et al., 2003; Bromberg et al., 2012; Adams et al., 2007; Itkin et al., 2012). Taking advantage of the use of teriparatide (recombinant PTH1-34) for the treatment of osteoporosis, Yu et al. collected blood from patients with osteoporosis undergoing treatment with teriparatide and quantified circulating HSCs (Yu et al., 2014). This study showed an increase in circulating HSCs in patients receiving anabolic treatment, a first demonstration of the impact of PTH on HSC regulation in humans. Since the bone marrow was

not tested in this patient population, it is not known whether the increase in circulating HSCs was due to increases in their marrow populations or to mobilization to the periphery. Notably, the physiologic role of PTH or PTH-related protein acting through PTH receptor 1 in the niche is poorly understood.

Insulin-like growth factor 1

IGF1 is produced in the liver and by osteoblasts, and its increase in osteoblastic cells after radiation injury appears to have a beneficial impact on the recovery of the hematopoietic systems (Caselli et al., 2013). Since expression of IGF1 is increased with PTH treatment, it is possible that some of the PTH effects on the niche may be mediated by IGF1.

Niche heterogeneity for heterogeneous hematopoietic stem and progenitor cells

From the studies presented thus far, it is clear that, rather than a single niche cell population, the bone marrow microenvironment is heterogeneous and dynamic (Fig. 3.1). Developments in the understanding of hematopoietic stem and progenitor cells now suggest that rather than omnipotent undifferentiated stem cells, there may be functional heterogeneity of HSCs as well. Single-cell transplantation studies have shown that individual HSCs are biased toward myeloid or lymphoid differentiation (Dykstra et al., 2007; Muller-Sieburg et al., 2002; Wilson et al., 2015). This heterogeneity changes with development and with aging (Benz et al., 2012), and appears to be epigenetically imposed (Yu et al., 2017). Evidence of megakaryocytic-biased HSCs has also been shown by numerous laboratories (Sanjuan-Pla et al., 2013; Gekas and Graf, 2013; Shin et al., 2014). This heterogeneity may explain the conflicting data regarding localization of hematopoietic stem and progenitor cells in association with endosteal, periarteriolar, or perisinusoidal sites, or in association with megakaryocytes (as discussed earlier). Initial data to support this contention were provided by the Frenette laboratory, showing that lineage-biased HSCs are regulated by distinct niches, with platelet- and myeloid-biased HSCs

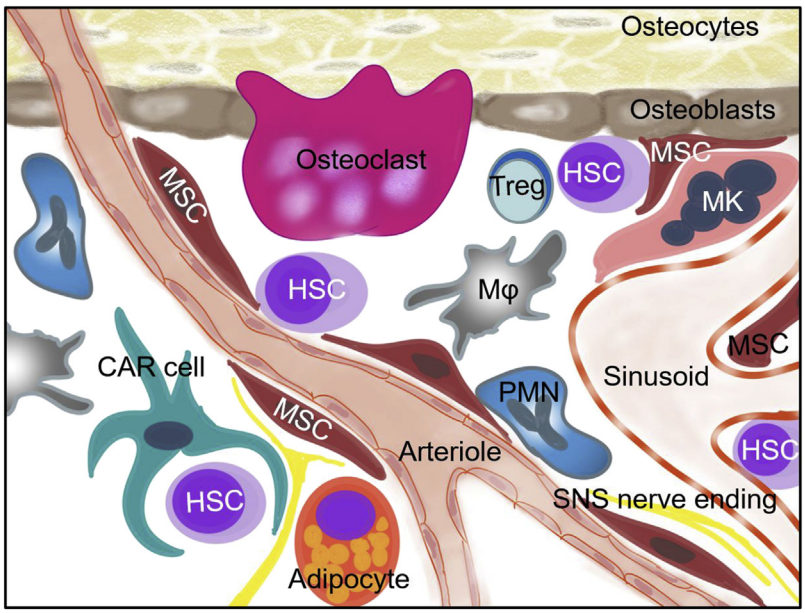

FIGURE 3.1 Heterogeneity of the hematopoietic stem cell niche in the bone marrow. Hematopoietic stem cells (HSCs) are found in close anatomic proximity to multiple regulatory populations in the bone marrow. A diagrammatic representation of the interactions of mesenchymal stroma cells (MSCs), HSCs, and other components of the bone marrow microenvironment is shown. Mesenchymal populations identified as HSC-regulating niche cells through genetic studies include subsets of MSCs (shown in *brown*), found in endosteal and more commonly perivascular locations, with CXCL12-abundant reticular (CAR) cells and leptin receptor-positive cells found primarily in perisinusoidal locations, while nestin−GFP^{+} cells are found primarily in periarteriolar sites. Multiple hematopoietic cells, including macrophages (Mφs), neutrophils (PMNs), megakaryocytes (MKs), osteoclasts, and regulatory T cells (T regs) contribute to HSC regulation. Sympathetic nervous system innervation modulates the circadian mobilization of HSCs in the circulation through its action on the niche.

found in association with and regulated with megakaryocytes, while $NG2^+$ arteriolar niche cells selectively regulate lymphoid-biased HSCs (Pinho et al., 2018).

Conclusions

As the data reviewed here show, our understanding of the HSC and progenitor microenvironment has evolved as our tool kit for their analysis has expanded, and it is likely to continue to increase as our ability to identify rare hematopoietic and mesenchymal populations in both murine models and humans improves. Progress in the definition of the HSC niche has already provided targets that may accelerate hematopoietic recovery and positively influence skeletal disease, especially if there are reciprocal interactions between skeletal stem cells and HSCs and/or their progenies. Moreover, given the potential for microenvironmental contribution to the support of either normal or malignant hematopoiesis, signals regulating interactions between bone microenvironmental populations and cancer cells could provide novel targets for the treatment of metastatic malignancy or primary malignancies in the bone and bone marrow.

Acknowledgments

The author wishes to thank the members of the Calvi, Becker, and Liesveld laboratories for helpful suggestions. This work was supported in part by the National Institutes of Health, National Cancer Institute, and National Institute on Aging awards CA166280 and AG046293; the University of Rochester Core Center for Musculoskeletal Biology and Medicine award AR061307 from the National Institute of Arthritis and Musculoskeletal and Skin Diseases; the Department of Defense (Award W81XWH1810485 to LMC) and the University of Rochester CTSA award UL1 TR002001 from the National Center for Advancing Translational Sciences.

References

Abella, E., Feliu, E., Granada, I., Milla, F., Oriol, A., Ribera, J.M., Sanchez-Planell, L., Berga, L.I., Reverter, J.C., Rozman, C., 2002. Bone marrow changes in anorexia nervosa are correlated with the amount of weight loss and not with other clinical findings. Am. J. Clin. Pathol. 118, 582–588.

Acar, M., Kocherlakota, K.S., Murphy, M.M., Peyer, J.G., Oguro, H., Inra, C.N., Jaiyeola, C., Zhao, Z., Luby-Phelps, K., Morrison, S.J., 2015. Deep imaging of bone marrow shows non-dividing stem cells are mainly perisinusoidal. Nature 526, 126–130.

Adams, G.B., Chabner, K.T., Alley, I.R., Olson, D.P., Szczepiorkowski, Z.M., Poznansky, M.C., Kos, C.H., Pollak, M.R., Brown, E.M., Scadden, D.T., 2006. Stem cell engraftment at the endosteal niche is specified by the calcium-sensing receptor. Nature 439, 599–603.

Adams, G.B., Martin, R.P., Alley, I.R., Chabner, K.T., Cohen, K.S., Calvi, L.M., Kronenberg, H.M., Scadden, D.T., 2007. Therapeutic targeting of a stem cell niche. Nat. Biotechnol. 25, 238–243.

Ambrosi, T.H., Scialdone, A., Graja, A., Gohlke, S., Jank, A.M., Bocian, C., Woelk, L., Fan, H., Logan, D.W., Schurmann, A., Saraiva, L.R., Schulz, T.J., 2017. Adipocyte accumulation in the bone marrow during obesity and aging impairs stem cell-based hematopoietic and bone regeneration. Cell Stem Cell 20, 771–784 e6.

Arranz, L., Sanchez-Aguilera, A., Martin-Perez, D., Isern, J., Langa, X., Tzankov, A., Lundberg, P., Muntion, S., Tzeng, Y.S., Lai, D.M., Schwaller, J., Skoda, R.C., Mendez-Ferrer, S., 2014. Neuropathy of haematopoietic stem cell niche is essential for myeloproliferative neoplasms. Nature 512, 78–81.

Asada, N., Katayama, Y., Sato, M., Minagawa, K., Wakahashi, K., Kawano, H., Kawano, Y., Sada, A., Ikeda, K., Matsui, T., Tanimoto, M., 2013. Matrix-embedded osteocytes regulate mobilization of hematopoietic stem/progenitor cells. Cell Stem Cell 12, 737–747.

Asada, N., Kunisaki, Y., Pierce, H., Wang, Z., Fernandez, N.F., Birbrair, A., MA'ayan, A., Frenette, P.S., 2017. Differential cytokine contributions of perivascular haematopoietic stem cell niches. Nat. Cell Biol. 19, 214–223.

Austin, J., Kimble, J., 1987. glp-1 is required in the germ line for regulation of the decision between mitosis and meiosis in *C. elegans*. Cell 51, 589–599.

Becker, A.J., Mc, C.E., Till, J.E., 1963. Cytological demonstration of the clonal nature of spleen colonies derived from transplanted mouse marrow cells. Nature 197, 452–454.

Benz, C., Copley, M.R., Kent, D.G., Wohrer, S., Cortes, A., Aghaeepour, N., Ma, E., Mader, H., Rowe, K., Day, C., Treloar, D., Brinkman, R.R., Eaves, C.J., 2012. Hematopoietic stem cell subtypes expand differentially during development and display distinct lymphopoietic programs. Cell Stem Cell 10, 273–283.

Bertrand, J.Y., Chi, N.C., Santoso, B., Teng, S., Stainier, D.Y., Traver, D., 2010. Haematopoietic stem cells derive directly from aortic endothelium during development. Nature 464, 108–111.

Bessis, M., 1958. Erythroblastic island, functional unity of bone marrow. Rev. Hematol. 13, 8–11.

Bjerknes, M., Cheng, H., 2001. Modulation of specific intestinal epithelial progenitors by enteric neurons. Proc. Natl. Acad. Sci. U.S.A. 98, 12497–12502.

Boisset, J.C., Van Cappellen, W., Andrieu-Soler, C., Galjart, N., Dzierzak, E., Robin, C., 2010. In vivo imaging of haematopoietic cells emerging from the mouse aortic endothelium. Nature 464, 116–120.

Bourgine, P.E., Klein, T., Paczulla, A.M., Shimizu, T., Kunz, L., Kokkaliaris, K.D., Coutu, D.L., Lengerke, C., Skoda, R., Schroeder, T., Martin, I., 2018. In vitro biomimetic engineering of a human hematopoietic niche with functional properties. Proc. Natl. Acad. Sci. U.S.A. 115, E5688–E5695.

Bowie, M.B., Kent, D.G., Dykstra, B., Mcknight, K.D., Mccaffrey, L., Hoodless, P.A., Eaves, C.J., 2007. Identification of a new intrinsically timed developmental checkpoint that reprograms key hematopoietic stem cell properties. Proc. Natl. Acad. Sci. U.S.A. 104, 5878–5882.

Bowie, M.B., Mcknight, K.D., Kent, D.G., Mccaffrey, L., Hoodless, P.A., Eaves, C.J., 2006. Hematopoietic stem cells proliferate until after birth and show a reversible phase-specific engraftment defect. J. Clin. Invest. 116, 2808–2816.

Bromberg, O., Frisch, B.J., Weber, J.M., Porter, R.L., Civitelli, R., Calvi, L.M., 2012. Osteoblastic N-cadherin is not required for microenvironmental support and regulation of hematopoietic stem and progenitor cells. Blood 120, 303–313.

Bruns, I., Lucas, D., Pinho, S., Ahmed, J., Lambert, M.P., Kunisaki, Y., Scheiermann, C., Schiff, L., Poncz, M., Bergman, A., Frenette, P.S., 2014. Megakaryocytes regulate hematopoietic stem cell quiescence through CXCL4 secretion. Nat. Med. 20, 1315–1320.

Busch, K., Klapproth, K., Barile, M., Flossdorf, M., Holland-Letz, T., Schlenner, S.M., Reth, M., Hofer, T., Rodewald, H.R., 2015. Fundamental properties of unperturbed haematopoiesis from stem cells in vivo. Nature 518, 542–546.

Butler, J.M., Nolan, D.J., Vertes, E.L., Varnum-Finney, B., Kobayashi, H., Hooper, A.T., Seandel, M., Shido, K., White, I.A., Kobayashi, M., Witte, L., May, C., Shawber, C., Kimura, Y., Kitajewski, J., Rosenwaks, Z., Bernstein, I.D., Rafii, S., 2010. Endothelial cells are essential for the self-renewal and repopulation of Notch-dependent hematopoietic stem cells. Cell Stem Cell 6, 251–264.

Cain, C.J., Rueda, R., Mclelland, B., Collette, N.M., Loots, G.G., Manilay, J.O., 2012. Absence of sclerostin adversely affects B-cell survival. J. Bone Miner. Res. 27, 1451–1461.

Calvi, L.M., Adams, G.B., Weibrecht, K.W., Weber, J.M., Olson, D.P., Knight, M.C., Martin, R.P., Schipani, E., Divieti, P., Bringhurst, F.R., Milner, L.A., Kronenberg, H.M., Scadden, D.T., 2003. Osteoblastic cells regulate the haematopoietic stem cell niche. Nature 425, 841–846.

Calvi, L.M., Bromberg, O., Rhee, Y., Weber, J.M., Smith, J.N., Basil, M.J., Frisch, B.J., Bellido, T., 2012. Osteoblastic expansion induced by parathyroid hormone receptor signaling in murine osteocytes is not sufficient to increase hematopoietic stem cells. Blood 119, 2489–2499.

Calvo, W., Fliedner, T.M., Herbst, E., Hugl, E., Bruch, C., 1976. Regeneration of blood-forming organs after autologous leukocyte transfusion in lethally irradiated dogs. II. Distribution and cellularity of the marrow in irradiated and transfused animals. Blood 47, 593–601.

Casanova-Acebes, M., Pitaval, C., Weiss, L.A., Nombela-Arrieta, C., Chevre, R., N, A.G., Kunisaki, Y., Zhang, D., Van Rooijen, N., Silberstein, L.E., Weber, C., Nagasawa, T., Frenette, P.S., Castrillo, A., Hidalgo, A., 2013. Rhythmic modulation of the hematopoietic niche through neutrophil clearance. Cell 153, 1025–1035.

Caselli, A., Olson, T.S., Otsuru, S., Chen, X., Hofmann, T.J., Nah, H.D., Grisendi, G., Paolucci, P., Dominici, M., Horwitz, E.M., 2013. IGF-1-mediated osteoblastic niche expansion enhances long-term hematopoietic stem cell engraftment after murine bone marrow transplantation. Stem Cell 31, 2193–2204.

Chang, M.K., Raggatt, L.J., Alexander, K.A., Kuliwaba, J.S., Fazzalari, N.L., Schroder, K., Maylin, E.R., Ripoll, V.M., Hume, D.A., Pettit, A.R., 2008. Osteal tissue macrophages are intercalated throughout human and mouse bone lining tissues and regulate osteoblast function in vitro and in vivo. J. Immunol. 181, 1232–1244.

Cheng, Y.H., Chitteti, B.R., Streicher, D.A., Morgan, J.A., Rodriguez-Rodriguez, S., Carlesso, N., Srour, E.F., Kacena, M.A., 2011. Impact of maturational status on the ability of osteoblasts to enhance the hematopoietic function of stem and progenitor cells. J. Bone Miner. Res. 26, 1111–1121.

Chow, A., Huggins, M., Ahmed, J., Hashimoto, D., Lucas, D., Kunisaki, Y., Pinho, S., Leboeuf, M., Noizat, C., Van Rooijen, N., Tanaka, M., Zhao, Z.J., Bergman, A., Merad, M., Frenette, P.S., 2013. CD169(+) macrophages provide a niche promoting erythropoiesis under homeostasis and stress. Nat. Med. 19, 429–436.

Chow, A., Lucas, D., Hidalgo, A., Mendez-Ferrer, S., Hashimoto, D., Scheiermann, C., Battista, M., Leboeuf, M., Prophete, C., Van Rooijen, N., Tanaka, M., Merad, M., Frenette, P.S., 2011. Bone marrow CD169+ macrophages promote the retention of hematopoietic stem and progenitor cells in the mesenchymal stem cell niche. J. Exp. Med. 208, 261–271.

Christopher, M.J., Rao, M., Liu, F., Woloszynek, J.R., Link, D.C., 2011. Expression of the G-CSF receptor in monocytic cells is sufficient to mediate hematopoietic progenitor mobilization by G-CSF in mice. J. Exp. Med. 208, 251–260.

Coskun, S., Chao, H., Vasavada, H., Heydari, K., Gonzales, N., Zhou, X., De Crombrugghe, B., Hirschi, K.K., 2014. Development of the fetal bone marrow niche and regulation of HSC quiescence and homing ability by emerging osteolineage cells. Cell Rep. 9, 581–590.

De Bruijn, M.F., Ma, X., Robin, C., Ottersbach, K., Sanchez, M.J., Dzierzak, E., 2002. Hematopoietic stem cells localize to the endothelial cell layer in the midgestation mouse aorta. Immunity 16, 673–683.

De Bruijn, M.F., Speck, N.A., Peeters, M.C., Dzierzak, E., 2000. Definitive hematopoietic stem cells first develop within the major arterial regions of the mouse embryo. EMBO J. 19, 2465–2474.

Ding, L., Morrison, S.J., 2013. Haematopoietic stem cells and early lymphoid progenitors occupy distinct bone marrow niches. Nature 495, 231–235.

Ding, L., Saunders, T.L., Enikolopov, G., Morrison, S.J., 2012. Endothelial and perivascular cells maintain haematopoietic stem cells. Nature 481, 457–462.

Dominici, M., Rasini, V., Bussolari, R., Chen, X., Hofmann, T.J., Spano, C., Bernabei, D., Veronesi, E., Bertoni, F., Paolucci, P., Conte, P., Horwitz, E.M., 2009. Restoration and reversible expansion of the osteoblastic hematopoietic stem cell niche after marrow radioablation. Blood 114, 2333–2343.

Doucette, C.R., Horowitz, M.C., Berry, R., Macdougald, O.A., Anunciado-Koza, R., Koza, R.A., Rosen, C.J., 2015. A high fat diet increases bone marrow adipose tissue (MAT) but does not alter trabecular or cortical bone mass in C57BL/6J mice. J. Cell. Physiol. 230, 2032–2037.

Duarte, D., Hawkins, E.D., Akinduro, O., Ang, H., De Filippo, K., Kong, I.Y., Haltalli, M., Ruivo, N., Straszkowski, L., Vervoort, S.J., Mclean, C., Weber, T.S., Khorshed, R., Pirillo, C., Wei, A., Ramasamy, S.K., Kusumbe, A.P., Duffy, K., Adams, R.H., Purton, L.E., Carlin, L.M., Lo Celso, C., 2018. Inhibition of endosteal vascular niche remodeling rescues hematopoietic stem cell loss in AML. Cell Stem Cell 22, 64−77 e6.

Dykstra, B., Kent, D., Bowie, M., Mccaffrey, L., Hamilton, M., Lyons, K., Lee, S.J., Brinkman, R., Eaves, C., 2007. Long-term propagation of distinct hematopoietic differentiation programs in vivo. Cell Stem Cell 1, 218−229.

Ellis, S.L., Grassinger, J., Jones, A., Borg, J., Camenisch, T., Haylock, D., Bertoncello, I., Nilsson, S.K., 2011. The relationship between bone, hemopoietic stem cells, and vasculature. Blood 118, 1516−1524.

Ema, H., Nakauchi, H., 2000. Expansion of hematopoietic stem cells in the developing liver of a mouse embryo. Blood 95, 2284−2288.

Evrard, M., Kwok, I.W.H., Chong, S.Z., Teng, K.W.W., Becht, E., Chen, J., Sieow, J.L., Penny, H.L., Ching, G.C., Devi, S., Adrover, J.M., Li, J.L.Y., Liong, K.H., Tan, L., Poon, Z., Foo, S., Chua, J.W., Su, I.H., Balabanian, K., Bachelerie, F., Biswas, S.K., Larbi, A., Hwang, W.Y.K., Madan, V., Koeffler, H.P., Wong, S.C., Newell, E.W., Hidalgo, A., Ginhoux, F., Ng, L.G., 2018. Developmental analysis of bone marrow neutrophils reveals populations specialized in expansion, trafficking, and effector functions. Immunity 48, 364−379 e8.

Ferraro, F., Lymperi, S., Mendez-Ferrer, S., Saez, B., Spencer, J.A., Yeap, B.Y., Masselli, E., Graiani, G., Prezioso, L., Rizzini, E.L., Mangoni, M., Rizzoli, V., Sykes, S.M., Lin, C.P., Frenette, P.S., Quaini, F., Scadden, D.T., 2011. Diabetes impairs hematopoietic stem cell mobilization by altering niche function. Sci. Transl. Med. 3, 104ra101.

Frisch, B.J., Ashton, J.M., Xing, L.P., Becker, M.W., Jordan, C.T., Calvi, L.M., 2012. Functional inhibition of osteoblastic cells in an in vivo mouse model of myeloid leukemia. Blood 119, 540−550.

Fujisaki, J., Wu, J., Carlson, A.L., Silberstein, L., Putheti, P., Larocca, R., Gao, W., Saito, T.I., Lo Celso, C., Tsuyuzaki, H., Sato, T., Cote, D., Sykes, M., Strom, T.B., Scadden, D.T., Lin, C.P., 2011. In vivo imaging of Treg cells providing immune privilege to the haematopoietic stem-cell niche. Nature 474, 216−219.

Fulzele, K., Krause, D.S., Panaroni, C., Saini, V., Barry, K.J., Liu, X., Lotinun, S., Baron, R., Bonewald, L., Feng, J.Q., Chen, M., Weinstein, L.S., Wu, J.Y., Kronenberg, H.M., Scadden, D.T., Divieti Pajevic, P., 2013. Myelopoiesis is regulated by osteocytes through Gsalpha-dependent signaling. Blood 121, 930−939.

Ge, C., Cawthorn, W.P., Li, Y., Zhao, G., Macdougald, O.A., Franceschi, R.T., 2016. Reciprocal control of osteogenic and adipogenic differentiation by ERK/MAP kinase phosphorylation of Runx2 and PPARgamma transcription factors. J. Cell. Physiol. 231, 587−596.

Gekas, C., Dieterlen-Lievre, F., Orkin, S.H., Mikkola, H.K., 2005. The placenta is a niche for hematopoietic stem cells. Dev. Cell 8, 365−375.

Gekas, C., Graf, T., 2013. CD41 expression marks myeloid-biased adult hematopoietic stem cells and increases with age. Blood 121, 4463−4472.

Golan, K., Kumari, A., Kollet, O., Khatib-Massalha, E., Subramaniam, M.D., Ferreira, Z.S., Avemaria, F., Rzeszotek, S., Garcia-Garcia, A., Xie, S., Flores-Figueroa, E., Gur-Cohen, S., Itkin, T., Ludin-Tal, A., Massalha, H., Bernshtein, B., Ciechanowicz, A.K., Brandis, A., Mehlman, T., Bhattacharya, S., Bertagna, M., Cheng, H., Petrovich-Kopitman, E., Janus, T., Kaushansky, N., Cheng, T., Sagi, I., Ratajczak, M.Z., Mendez-Ferrer, S., Dick, J.E., Markus, R.P., Lapidot, T., 2018. Daily onset of light and darkness differentially controls hematopoietic stem cell differentiation and maintenance. Cell Stem Cell 23, 572−585 e7.

Goncalves, K.A., Silberstein, L., Li, S., Severe, N., Hu, M.G., Yang, H., Scadden, D.T., Hu, G.F., 2016. Angiogenin promotes hematopoietic regeneration by dichotomously regulating quiescence of stem and progenitor cells. Cell 166, 894−906.

Gong, J.K., 1978. Endosteal marrow: a rich source of hematopoietic stem cells. Science 199, 1443−1445.

Greenbaum, A., Hsu, Y.M., Day, R.B., Schuettpelz, L.G., Christopher, M.J., Borgerding, J.N., Nagasawa, T., Link, D.C., 2013. CXCL12 in early mesenchymal progenitors is required for haematopoietic stem-cell maintenance. Nature 495, 227−230.

Guezguez, B., Campbell, C.J., Boyd, A.L., Karanu, F., Casado, F.L., DI Cresce, C., Collins, T.J., Shapovalova, Z., Xenocostas, A., Bhatia, M., 2013. Regional localization within the bone marrow influences the functional capacity of human HSCs. Cell Stem Cell 13, 175−189.

Hanoun, M., Zhang, D., Mizoguchi, T., Pinho, S., Pierce, H., Kunisaki, Y., Lacombe, J., Armstrong, S.A., Duhrsen, U., Frenette, P.S., 2014. Acute myelogenous leukemia-induced sympathetic neuropathy promotes malignancy in an altered hematopoietic stem cell niche. Cell Stem Cell 15, 365−375.

Heideveld, E., Van Den Akker, E., 2017. Digesting the role of bone marrow macrophages on hematopoiesis. Immunobiology 222, 814−822.

Hirata, Y., Furuhashi, K., Ishii, H., Li, H.W., Pinho, S., Ding, L., Robson, S.C., Frenette, P.S., Fujisaki, J., 2018. CD150(high) bone marrow tregs maintain hematopoietic stem cell quiescence and immune privilege via adenosine. Cell Stem Cell 22, 445−453 e5.

Hooper, A.T., Butler, J.M., Nolan, D.J., Kranz, A., Iida, K., Kobayashi, M., Kopp, H.G., Shido, K., Petit, I., Yanger, K., James, D., Witte, L., Zhu, Z., Wu, Y., Pytowski, B., Rosenwaks, Z., Mittal, V., Sato, T.N., Rafii, S., 2009. Engraftment and reconstitution of hematopoiesis is dependent on VEGFR2-mediated regeneration of sinusoidal endothelial cells. Cell Stem Cell 4, 263−274.

Horowitz, M.C., Berry, R., Holtrup, B., Sebo, Z., Nelson, T., Fretz, J.A., Lindskog, D., Kaplan, J.L., Ables, G., Rodeheffer, M.S., Rosen, C.J., 2017. Bone marrow adipocytes. Adipocyte 6, 193−204.

Hur, J., Choi, J.I., Lee, H., Nham, P., Kim, T.W., Chae, C.W., Yun, J.Y., Kang, J.A., Kang, J., Lee, S.E., Yoon, C.H., Boo, K., Ham, S., Roh, T.Y., Jun, J.K., Lee, H., Baek, S.H., Kim, H.S., 2016. CD82/KAI1 maintains the dormancy of long-term hematopoietic stem cells through interaction with DARC-expressing macrophages. Cell Stem Cell 18, 508−521.

Itkin, T., Gur-Cohen, S., Spencer, J.A., Schajnovitz, A., Ramasamy, S.K., Kusumbe, A.P., Ledergor, G., Jung, Y., Milo, I., Poulos, M.G., Kalinkovich, A., Ludin, A., Kollet, O., Shakhar, G., Butler, J.M., Rafii, S., Adams, R.H., Scadden, D.T., Lin, C.P., Lapidot, T., 2016. Distinct bone marrow blood vessels differentially regulate haematopoiesis. Nature 532 (7599), 323−328.

Itkin, T., Ludin, A., Gradus, B., Gur-Cohen, S., Kalinkovich, A., Schajnovitz, A., Ovadya, Y., Kollet, O., Canaani, J., Shezen, E., Coffin, D.J., Enikolopov, G.N., Berg, T., Piacibello, W., Hornstein, E., Lapidot, T., 2012. FGF-2 expands murine hematopoietic stem and progenitor cells via proliferation of stromal cells, c-Kit activation, and CXCL12 down-regulation. Blood 120, 1843−1855.

Ivanovs, A., Rybtsov, S., Welch, L., Anderson, R.A., Turner, M.L., Medvinsky, A., 2011. Highly potent human hematopoietic stem cells first emerge in the intraembryonic aorta-gonad-mesonephros region. J. Exp. Med. 208, 2417−2427.

Jaffredo, T., Gautier, R., Eichmann, A., Dieterlen-Lievre, F., 1998. Intraaortic hemopoietic cells are derived from endothelial cells during ontogeny. Development 125, 4575−4583.

Joseph, C., Quach, J.M., Walkley, C.R., Lane, S.W., Lo Celso, C., Purton, L.E., 2013. Deciphering hematopoietic stem cells in their niches: a critical appraisal of genetic models, lineage tracing, and imaging strategies. Cell Stem Cell 13, 520−533.

Katayama, Y., Battista, M., Kao, W.M., Hidalgo, A., Peired, A.J., Thomas, S.A., Frenette, P.S., 2006. Signals from the sympathetic nervous system regulate hematopoietic stem cell egress from bone marrow. Cell 124, 407−421.

Kaur, S., Raggatt, L.J., Millard, S.M., Wu, A.C., Batoon, L., Jacobsen, R.N., Winkler, I.G., Macdonald, K.P., Perkins, A.C., Hume, D.A., Levesque, J.P., Pettit, A.R., 2018. Self-repopulating recipient bone marrow resident macrophages promote long-term hematopoietic stem cell engraftment. Blood 132, 735−749.

Kawamori, Y., Katayama, Y., Asada, N., Minagawa, K., Sato, M., Okamura, A., Shimoyama, M., Nakagawa, K., Okano, T., Tanimoto, M., Kato, S., Matsui, T., 2010. Role for vitamin D receptor in the neuronal control of the hematopoietic stem cell niche. Blood 116, 5528−5535.

Kfoury, Y., Scadden, D.T., 2015. Mesenchymal cell contributions to the stem cell niche. Cell Stem Cell 16, 239−253.

Khan, J.A., Mendelson, A., Kunisaki, Y., Birbrair, A., Kou, Y., Arnal-Estape, A., Pinho, S., Ciero, P., Nakahara, F., MA'ayan, A., Bergman, A., Merad, M., Frenette, P.S., 2016. Fetal liver hematopoietic stem cell niches associate with portal vessels. Science 351, 176−180.

Kiel, M.J., Acar, M., Radice, G.L., Morrison, S.J., 2009. Hematopoietic stem cells do not depend on N-cadherin to regulate their maintenance. Cell Stem Cell 4, 170−179.

Kiel, M.J., Radice, G.L., Morrison, S.J., 2007. Lack of evidence that hematopoietic stem cells depend on N-cadherin-mediated adhesion to osteoblasts for their maintenance. Cell Stem Cell 1, 204−217.

Kiel, M.J., Yilmaz, O.H., Iwashita, T., Yilmaz, O.H., Terhorst, C., Morrison, S.J., 2005. SLAM family receptors distinguish hematopoietic stem and progenitor cells and reveal endothelial niches for stem cells. Cell 121, 1109−1121.

Kiger, A.A., White-Cooper, H., Fuller, M.T., 2000. Somatic support cells restrict germline stem cell self-renewal and promote differentiation. Nature 407, 750−754.

Kissa, K., Herbomel, P., 2010. Blood stem cells emerge from aortic endothelium by a novel type of cell transition. Nature 464, 112−115.

Kobayashi, H., Butler, J.M., O'donnell, R., Kobayashi, M., Ding, B.S., Bonner, B., Chiu, V.K., Nolan, D.J., Shido, K., Benjamin, L., Rafii, S., 2010. Angiocrine factors from Akt-activated endothelial cells balance self-renewal and differentiation of haematopoietic stem cells. Nat. Cell Biol. 12, 1046−1056.

Krause, D.S., Fulzele, K., Catic, A., Sun, C.C., Dombkowski, D., Hurley, M.P., Lezeau, S., Attar, E., Wu, J.Y., Lin, H.Y., Divieti-Pajevic, P., Hasserjian, R.P., Schipani, E., Van Etten, R.A., Scadden, D.T., 2013. Differential regulation of myeloid leukemias by the bone marrow microenvironment. Nat. Med. 19, 1513−1517.

Krevvata, M., Silva, B.C., Manavalan, J.S., Galan-Diez, M., Kode, A., Matthews, B.G., Park, D., Zhang, C.A., Galili, N., Nickolas, T.L., Dempster, D.W., Dougall, W., Teruya-Feldstein, J., Economides, A.N., Kalajzic, I., Raza, A., Berman, E., Mukherjee, S., Bhagat, G., Kousteni, S., 2014. Inhibition of leukemia cell engraftment and disease progression in mice by osteoblasts. Blood 124, 2834−2846.

Kunisaki, Y., Bruns, I., Scheiermann, C., Ahmed, J., Pinho, S., Zhang, D., Mizoguchi, T., Wei, Q., Lucas, D., Ito, K., Mar, J.C., Bergman, A., Frenette, P.S., 2013. Arteriolar niches maintain haematopoietic stem cell quiescence. Nature 502, 637−643.

Kusumbe, A.P., Ramasamy, S.K., Adams, R.H., 2014. Coupling of angiogenesis and osteogenesis by a specific vessel subtype in bone. Nature 507, 323−328.

Kusumbe, A.P., Ramasamy, S.K., Itkin, T., Mae, M.A., Langen, U.H., Betsholtz, C., Lapidot, T., Adams, R.H., 2016. Age-dependent modulation of vascular niches for haematopoietic stem cells. Nature 532, 380−384.

Li, D., Xue, W., Li, M., Dong, M., Wang, J., Wang, X., Li, X., Chen, K., Zhang, W., Wu, S., Zhang, Y., Gao, L., Chen, Y., Chen, J., Zhou, B.O., Zhou, Y., Yao, X., Li, L., Wu, D., Pan, W., 2018. VCAM-1(+) macrophages guide the homing of HSPCs to a vascular niche. Nature 564, 119−124.

Lo Celso, C., Fleming, H.E., Wu, J.W., Zhao, C.X., Miake-Lye, S., Fujisaki, J., Cote, D., Rowe, D.W., Lin, C.P., Scadden, D.T., 2009. Live-animal tracking of individual haematopoietic stem/progenitor cells in their niche. Nature 457, 92−96.

Ludin, A., Itkin, T., Gur-Cohen, S., Mildner, A., Shezen, E., Golan, K., Kollet, O., Kalinkovich, A., Porat, Z., D'uva, G., Schajnovitz, A., Voronov, E., Brenner, D.A., Apte, R.N., Jung, S., Lapidot, T., 2012. Monocytes-macrophages that express alpha-smooth muscle actin preserve primitive hematopoietic cells in the bone marrow. Nat. Immunol. 13 (11), 1072−1082.

Lymperi, S., Horwood, N., Marley, S., Gordon, M.Y., Cope, A.P., Dazzi, F., 2008. Strontium can increase some osteoblasts without increasing hematopoietic stem cells. Blood 111, 1173−1181.

Mansour, A., Abou-Ezzi, G., Sitnicka, E., Jacobsen, S.E., Wakkach, A., Blin-Wakkach, C., 2012. Osteoclasts promote the formation of hematopoietic stem cell niches in the bone marrow. J. Exp. Med. 209, 537−549.

Maryanovich, M., Zahalka, A.H., Pierce, H., Pinho, S., Nakahara, F., Asada, N., Wei, Q., Wang, X., Ciero, P., Xu, J., Leftin, A., Frenette, P.S., 2018. Adrenergic nerve degeneration in bone marrow drives aging of the hematopoietic stem cell niche. Nat. Med. 24 (6).

Mcculloch, E.A., Till, J.E., 1960. The radiation sensitivity of normal mouse bone marrow cells, determined by quantitative marrow transplantation into irradiated mice. Radiat. Res. 13, 115−125.

Medvinsky, A., Dzierzak, E., 1996. Definitive hematopoiesis is autonomously initiated by the AGM region. Cell 86, 897–906.

Medvinsky, A., Rybtsov, S., Taoudi, S., 2011. Embryonic origin of the adult hematopoietic system: advances and questions. Development 138, 1017–1031.

Mendez-Ferrer, S., Lucas, D., Battista, M., Frenette, P.S., 2008. Haematopoietic stem cell release is regulated by circadian oscillations. Nature 452, 442–447.

Mendez-Ferrer, S., Michurina, T.V., Ferraro, F., Mazloom, A.R., Macarthur, B.D., Lira, S.A., Scadden, D.T., MA'ayan, A., Enikolopov, G.N., Frenette, P.S., 2010. Mesenchymal and haematopoietic stem cells form a unique bone marrow niche. Nature 466, 829–834.

Mohamad, S.F., Xu, L., Ghosh, J., Childress, P.J., Abeysekera, I., Himes, E.R., Wu, H., Alvarez, M.B., Davis, K.M., Aguilar-Perez, A., Hong, J.M., Bruzzaniti, A., Kacena, M.A., Srour, E.F., 2017. Osteomacs interact with megakaryocytes and osteoblasts to regulate murine hematopoietic stem cell function. Blood Adv. 1, 2520–2528.

Morikawa, S., Mabuchi, Y., Kubota, Y., Nagai, Y., Niibe, K., Hiratsu, E., Suzuki, S., Miyauchi-Hara, C., Nagoshi, N., Sunabori, T., Shimmura, S., Miyawaki, A., Nakagawa, T., Suda, T., Okano, H., Matsuzaki, Y., 2009. Prospective identification, isolation, and systemic transplantation of multipotent mesenchymal stem cells in murine bone marrow. J. Exp. Med. 206, 2483–2496.

Morrison, S.J., Hemmati, H.D., Wandycz, A.M., Weissman, I.L., 1995. The purification and characterization of fetal liver hematopoietic stem cells. Proc. Natl. Acad. Sci. U.S.A. 92, 10302–10306.

Muller-Sieburg, C.E., Cho, R.H., Thoman, M., Adkins, B., Sieburg, H.B., 2002. Deterministic regulation of hematopoietic stem cell self-renewal and differentiation. Blood 100, 1302–1309.

Muller, A.M., Medvinsky, A., Strouboulis, J., Grosveld, F., Dzierzak, E., 1994. Development of hematopoietic stem cell activity in the mouse embryo. Immunity 1, 291–301.

Nakamura-Ishizu, A., Takubo, K., Fujioka, M., Suda, T., 2014. Megakaryocytes are essential for HSC quiescence through the production of thrombopoietin. Biochem. Biophys. Res. Commun. 454, 353–357.

Nakamura-Ishizu, A., Takubo, K., Kobayashi, H., SUZUKI-Inoue, K., Suda, T., 2015. CLEC-2 in megakaryocytes is critical for maintenance of hematopoietic stem cells in the bone marrow. J. Exp. Med. 212, 2133–2146.

Nakamura, Y., Arai, F., Iwasaki, H., Hosokawa, K., Kobayashi, I., Gomei, Y., Matsumoto, Y., Yoshihara, H., Suda, T., 2010. Isolation and characterization of endosteal niche cell populations that regulate hematopoietic stem cells. Blood 116 (9), 1422–1432.

Nathan, C., 2006. Neutrophils and immunity: challenges and opportunities. Nat. Rev. Immunol. 6, 173–182.

Naveiras, O., Nardi, V., Wenzel, P.L., Hauschka, P.V., Fahey, F., Daley, G.Q., 2009. Bone-marrow adipocytes as negative regulators of the haematopoietic microenvironment. Nature 460, 259–263.

Nombela-Arrieta, C., Pivarnik, G., Winkel, B., Canty, K.J., Harley, B., Mahoney, J.E., Park, S.Y., Lu, J., Protopopov, A., Silberstein, L.E., 2013. Quantitative imaging of haematopoietic stem and progenitor cell localization and hypoxic status in the bone marrow microenvironment. Nat. Cell Biol. 15, 533–543.

Oguro, H., Ding, L., Morrison, S.J., 2013. SLAM family markers resolve functionally distinct subpopulations of hematopoietic stem cells and multipotent progenitors. Cell Stem Cell 13, 102–116.

Olson, T.S., Caselli, A., Otsuru, S., Hofmann, T.J., Williams, R., Paolucci, P., Dominici, M., Horwitz, E.M., 2013. Megakaryocytes promote murine osteoblastic HSC niche expansion and stem cell engraftment after radioablative conditioning. Blood 121, 5238–5249.

Omatsu, Y., Sugiyama, T., Kohara, H., Kondoh, G., Fujii, N., Kohno, K., Nagasawa, T., 2010. The essential functions of adipo-osteogenic progenitors as the hematopoietic stem and progenitor cell niche. Immunity 33, 387–399.

Ottersbach, K., Dzierzak, E., 2005. The murine placenta contains hematopoietic stem cells within the vascular labyrinth region. Dev. Cell 8, 377–387.

Pinho, S., Lacombe, J., Hanoun, M., Mizoguchi, T., Bruns, I., Kunisaki, Y., Frenette, P.S., 2013. PDGFRalpha and CD51 mark human Nestin+ sphere-forming mesenchymal stem cells capable of hematopoietic progenitor cell expansion. J. Exp. Med. 210, 1351–1367.

Pinho, S., Marchand, T., Yang, E., Wei, Q., Nerlov, C., Frenette, P.S., 2018. Lineage-biased hematopoietic stem cells are regulated by distinct niches. Dev. Cell 44, 634–641 e4.

Poulos, M.G., Guo, P., Kofler, N.M., Pinho, S., Gutkin, M.C., Tikhonova, A., Aifantis, I., Frenette, P.S., Kitajewski, J., Rafii, S., Butler, J.M., 2013. Endothelial Jagged-1 is necessary for homeostatic and regenerative hematopoiesis. Cell Rep. 4, 1022–1034.

Raaijmakers, M.H., Mukherjee, S., Guo, S., Zhang, S., Kobayashi, T., Schoonmaker, J.A., Ebert, B.L., AL-Shahrour, F., Hasserjian, R.P., Scadden, E.O., Aung, Z., Matza, M., Merkenschlager, M., Lin, C., Rommens, J.M., Scadden, D.T., 2010. Bone progenitor dysfunction induces myelodysplasia and secondary leukaemia. Nature 464, 852–857.

Ramasamy, S.K., Kusumbe, A.P., Wang, L., Adams, R.H., 2014. Endothelial Notch activity promotes angiogenesis and osteogenesis in bone. Nature 507, 376–380.

Rhodes, K.E., Gekas, C., Wang, Y., Lux, C.T., Francis, C.S., Chan, D.N., Conway, S., Orkin, S.H., Yoder, M.C., Mikkola, H.K., 2008. The emergence of hematopoietic stem cells is initiated in the placental vasculature in the absence of circulation. Cell Stem Cell 2, 252–263.

Robin, C., Bollerot, K., Mendes, S., Haak, E., Crisan, M., Cerisoli, F., Lauw, I., Kaimakis, P., Jorna, R., Vermeulen, M., Kayser, M., Van Der Linden, R., Imanirad, P., Verstegen, M., Nawaz-Yousaf, H., Papazian, N., Steegers, E., Cupedo, T., Dzierzak, E., 2009. Human placenta is a potent hematopoietic niche containing hematopoietic stem and progenitor cells throughout development. Cell Stem Cell 5, 385–395.

Rosental, B., Kowarsky, M., Seita, J., Corey, D.M., Ishizuka, K.J., Palmeri, K.J., Chen, S.Y., Sinha, R., Okamoto, J., Mantalas, G., Manni, L., Raveh, T., Clarke, D.N., Tsai, J.M., Newman, A.M., Neff, N.F., Nolan, G.P., Quake, S.R., Weissman, I.L., Voskoboynik, A., 2018. Complex mammalian-like haematopoietic system found in a colonial chordate. Nature 564 (7736), 425–429.

Sanjuan-Pla, A., Macaulay, I.C., Jensen, C.T., Woll, P.S., Luis, T.C., Mead, A., Moore, S., Carella, C., Matsuoka, S., Bouriez Jones, T., Chowdhury, O., Stenson, L., Lutteropp, M., Green, J.C., Facchini, R., Boukarabila, H., Grover, A., Gambardella, A., Thongjuea, S., Carrelha, J., Tarrant, P., Atkinson, D., Clark, S.A., Nerlov, C., Jacobsen, S.E., 2013. Platelet-biased stem cells reside at the apex of the haematopoietic stem-cell hierarchy. Nature 502, 232–236.

Sawai, C.M., Babovic, S., Upadhaya, S., Knapp, D., Lavin, Y., Lau, C.M., Goloborodko, A., Feng, J., Fujisaki, J., Ding, L., Mirny, L.A., Merad, M., Eaves, C.J., Reizis, B., 2016. Hematopoietic stem cells are the major source of multilineage hematopoiesis in adult animals. Immunity 45, 597–609.

Scheller, E.L., Doucette, C.R., Learman, B.S., Cawthorn, W.P., Khandaker, S., Schell, B., Wu, B., Ding, S.Y., Bredella, M.A., Fazeli, P.K., Khoury, B., Jepsen, K.J., Pilch, P.F., Klibanski, A., Rosen, C.J., Macdougald, O.A., 2015. Region-specific variation in the properties of skeletal adipocytes reveals regulated and constitutive marrow adipose tissues. Nat. Commun. 6, 7808.

Schepers, K., Pietras, E.M., Reynaud, D., Flach, J., Binnewies, M., Garg, T., Wagers, A.J., Hsiao, E.C., Passegue, E., 2013. Myeloproliferative neoplasia remodels the endosteal bone marrow niche into a self-reinforcing leukemic niche. Cell Stem Cell 13 (3), 285–299.

Schofield, R., 1978. The relationship between the spleen colony-forming cell and the haemopoietic stem cell. Blood Cells 4, 7–25.

Senn, J.S., Mcculloch, E.A., Till, J.E., 1967. Comparison of colony-forming ability of normal and leukaemic human marrow in cell culture. Lancet 2, 597–598.

Shin, J.Y., Hu, W., Naramura, M., Park, C.Y., 2014. High c-Kit expression identifies hematopoietic stem cells with impaired self-renewal and megakaryocytic bias. J. Exp. Med. 211, 217–231.

Silberstein, L., Goncalves, K.A., Kharchenko, P.V., Turcotte, R., Kfoury, Y., Mercier, F., Baryawno, N., Severe, N., Bachand, J., Spencer, J.A., Papazian, A., Lee, D., Chitteti, B.R., Srour, E.F., Hoggatt, J., Tate, T., LO Celso, C., Ono, N., Nutt, S., Heino, J., Sipila, K., Shioda, T., Osawa, M., Lin, C.P., Hu, G.F., Scadden, D.T., 2016. Proximity-based differential single-cell analysis of the niche to identify stem/progenitor cell regulators. Cell Stem Cell 19, 530–543.

Silva, B., Krevvata, M., Manavalan, J.S., Zhang, C., Brentjens, R., Economides, A., Berman, E., Kousteni, S., 2011. Leukemia Progression Depends on the Presence of Osteoblasts. American Society for Bone and Mineral Research, San Diego, Ca, Usa, p. 1231.

Silva, B., Yoshikawa, Y., Johnson, L., Manavalan, J., Berman, E., Kousteni, S., 2010. Leukemia blasts compromise osteoblast function in a mouse model of acute myelogenous leukemia. In: American Society for Bone and Mineral Research Annual Meeting, October 2010. Toronto, Canada.

Sugiyama, T., Kohara, H., Noda, M., Nagasawa, T., 2006. Maintenance of the hematopoietic stem cell pool by CXCL12-CXCR4 chemokine signaling in bone marrow stromal cell niches. Immunity 25, 977–988.

Sun, J., Ramos, A., Chapman, B., Johnnidis, J.B., Le, L., Ho, Y.J., Klein, A., Hofmann, O., Camargo, F.D., 2014. Clonal dynamics of native haematopoiesis. Nature 514, 322–327.

Tabe, Y., Yamamoto, S., Saitoh, K., Sekihara, K., Monma, N., Ikeo, K., Mogushi, K., Shikami, M., Ruvolo, V., Ishizawa, J., Hail JR., N., Kazuno, S., Igarashi, M., Matsushita, H., Yamanaka, Y., Arai, H., Nagaoka, I., Miida, T., Hayashizaki, Y., Konopleva, M., Andreeff, M., 2017. Bone marrow adipocytes facilitate fatty acid oxidation activating AMPK and a transcriptional network supporting survival of acute monocytic leukemia cells. Cancer Res. 77, 1453–1464.

Taichman, R.S., Emerson, S.G., 1994. Human osteoblasts support hematopoiesis through the production of granulocyte colony-stimulating factor. J. Exp. Med. 179, 1677–1682.

Taichman, R.S., Reilly, M.J., Emerson, S.G., 1996. Human osteoblasts support human hematopoietic progenitor cells in vitro bone marrow cultures. Blood 87, 518–524.

Tamplin, O.J., Durand, E.M., Carr, L.A., Childs, S.J., Hagedorn, E.J., Li, P., Yzaguirre, A.D., Speck, N.A., Zon, L.I., 2015. Hematopoietic stem cell arrival triggers dynamic remodeling of the perivascular niche. Cell 160, 241–252.

Tjin, G., Flores-Figueroa, E., Duarte, D., Straszkowski, L., Scott, M., Khorshed, R.A., Purton, L.E., LO Celso, C., 2019 feb. Imaging methods used to study mouse and human HSC niches: current and emerging technologies. Bone 119, 19–35. https://doi.org/10.1016/j.bone.2018.04.022. Epub 2018 Apr 25. PMID:29704697.

Tran, J., Brenner, T.J., Dinardo, S., 2000. Somatic control over the germline stem cell lineage during Drosophila spermatogenesis. Nature 407, 754–757.

Tumbar, T., Guasch, G., Greco, V., Blanpain, C., Lowry, W.E., Rendl, M., Fuchs, E., 2004. Defining the epithelial stem cell niche in skin. Science 303, 359–363.

Visnjic, D., Kalajzic, Z., Rowe, D.W., Katavic, V., Lorenzo, J., Aguila, H.L., 2004. Hematopoiesis is severely altered in mice with an induced osteoblast deficiency. Blood 103, 3258–3264.

Wilson, A., Laurenti, E., Oser, G., Van Der Wath, R.C., Blanco-Bose, W., Jaworski, M., Offner, S., Dunant, C.F., Eshkind, L., Bockamp, E., Lio, P., Macdonald, H.R., Trumpp, A., 2008. Hematopoietic stem cells reversibly switch from dormancy to self-renewal during homeostasis and repair. Cell 135, 1118–1129.

Wilson, N.K., Kent, D.G., Buettner, F., Shehata, M., Macaulay, I.C., Calero-Nieto, F.J., Sanchez Castillo, M., Oedekoven, C.A., Diamanti, E., Schulte, R., Ponting, C.P., Voet, T., Caldas, C., Stingl, J., Green, A.R., Theis, F.J., Gottgens, B., 2015. Combined single-cell functional and gene expression analysis resolves heterogeneity within stem cell populations. Cell Stem Cell 16, 712–724.

Winkler, I.G., Barbier, V., Nowlan, B., Jacobsen, R.N., Forristal, C.E., Patton, J.T., Magnani, J.L., Levesque, J.P., 2012. Vascular niche E-selectin regulates hematopoietic stem cell dormancy, self renewal and chemoresistance. Nat. Med. 18, 1651–1657.

Winkler, I.G., Sims, N.A., Pettit, A.R., Barbier, V., Nowlan, B., Helwani, F., Poulton, I.J., Van Rooijen, N., Alexander, K.A., Raggatt, L.J., Levesque, J.P., 2010. Bone marrow macrophages maintain hematopoietic stem cell (HSC) niches and their depletion mobilizes HSCs. Blood 116, 4815–4828.

Wu, J.Y., Purton, L.E., Rodda, S.J., Chen, M., Weinstein, L.S., Mcmahon, A.P., Scadden, D.T., Kronenberg, H.M., 2008. Osteoblastic regulation of B lymphopoiesis is mediated by Gs{alpha}-dependent signaling pathways. Proc. Natl. Acad. Sci. U.S.A. 105, 16976−16981.

Xie, T., Spradling, A.C., 2000. A niche maintaining germ line stem cells in the Drosophila ovary. Science 290, 328−330.

Xie, Y., Yin, T., Wiegraebe, W., He, X.C., Miller, D., Stark, D., Perko, K., Alexander, R., Schwartz, J., Grindley, J.C., Park, J., Haug, J.S., Wunderlich, J.P., Li, H., Zhang, S., Johnson, T., Feldman, R.A., Li, L., 2009. Detection of functional haematopoietic stem cell niche using real-time imaging. Nature 457, 97−101.

Xu, R., Yallowitz, A., Qin, A., Wu, Z., Shin, D.Y., Kim, J.M., Debnath, S., Ji, G., Bostrom, M.P., Yang, X., Zhang, C., Dong, H., Kermani, P., Lalani, S., Li, N., Liu, Y., Poulos, M.G., Wach, A., Zhang, Y., Inoue, K., DI Lorenzo, A., Zhao, B., Butler, J.M., Shim, J.H., Glimcher, L.H., Greenblatt, M.B., 2018. Targeting skeletal endothelium to ameliorate bone loss. Nat. Med. 24, 823−833.

Yamazaki, S., Ema, H., Karlsson, G., Yamaguchi, T., Miyoshi, H., Shioda, S., Taketo, M.M., Karlsson, S., Iwama, A., Nakauchi, H., 2011. Nonmyelinating Schwann cells maintain hematopoietic stem cell hibernation in the bone marrow niche. Cell 147, 1146−1158.

Yamazaki, S., Iwama, A., Takayanagi, S., Eto, K., Ema, H., Nakauchi, H., 2009. TGF-beta as a candidate bone marrow niche signal to induce hematopoietic stem cell hibernation. Blood 113, 1250−1256.

Yu, E.W., Kumbhani, R., Siwila-Sackman, E., Delelys, M., Preffer, F.I., Leder, B.Z., Wu, J.Y., 2014. Teriparatide (PTH 1-34) treatment increases peripheral hematopoietic stem cells in postmenopausal women. J. Bone Miner. Res. 29, 1380−1386.

Yu, V.W., Saez, B., Cook, C., Lotinun, S., Pardo-Saganta, A., Wang, Y.H., Lymperi, S., Ferraro, F., Raaijmakers, M.H., Wu, J.Y., Zhou, L., Rajagopal, J., Kronenberg, H.M., Baron, R., Scadden, D.T., 2015. Specific bone cells produce DLL4 to generate thymus-seeding progenitors from bone marrow. J. Exp. Med. 212, 759−774.

Yu, V.W.C., Yusuf, R.Z., Oki, T., Wu, J., Saez, B., Wang, X., Cook, C., Baryawno, N., Ziller, M.J., Lee, E., Gu, H., Meissner, A., Lin, C.P., Kharchenko, P.V., Scadden, D.T., 2017. Epigenetic memory underlies cell-autonomous heterogeneous behavior of hematopoietic stem cells. Cell 168, 944−945.

Yue, R., Zhou, B.O., Shimada, I.S., Zhao, Z., Morrison, S.J., 2016. Leptin receptor promotes adipogenesis and reduces osteogenesis by regulating mesenchymal stromal cells in adult bone marrow. Cell Stem Cell 18, 782−796.

Zhang, J., Link, D.C., 2016. Targeting of mesenchymal stromal cells by cre-recombinase transgenes commonly used to target osteoblast lineage cells. J. Bone Miner. Res. 31, 2001−2007.

Zhang, J., Niu, C., Ye, L., Huang, H., He, X., Tong, W.G., Ross, J., Haug, J., Johnson, T., Feng, J.Q., Harris, S., Wiedemann, L.M., Mishina, Y., Li, L., 2003. Identification of the haematopoietic stem cell niche and control of the niche size. Nature 425, 836−841.

Zhao, M., Perry, J.M., Marshall, H., Venkatraman, A., Qian, P., He, X.C., Ahamed, J., Li, L., 2014. Megakaryocytes maintain homeostatic quiescence and promote post-injury regeneration of hematopoietic stem cells. Nat. Med. 20, 1321−1326.

Zhou, B.O., Yu, H., Yue, R., Zhao, Z., Rios, J.J., Naveiras, O., Morrison, S.J., 2017. Bone marrow adipocytes promote the regeneration of stem cells and haematopoiesis by secreting SCF. Nat. Cell Biol. 19, 891−903.

Zhou, B.O., Yue, R., Murphy, M.M., Peyer, J.G., Morrison, S.J., 2014. Leptin-receptor-expressing mesenchymal stromal cells represent the main source of bone formed by adult bone marrow. Cell Stem Cell 15, 154−168.

Zhou, X., Zhang, Z., Feng, J.Q., Dusevich, V.M., Sinha, K., Zhang, H., Darnay, B.G., DE Crombrugghe, B., 2010. Multiple functions of Osterix are required for bone growth and homeostasis in postnatal mice. Proc. Natl. Acad. Sci. U.S.A. 107, 12919−12924.

Zhu, J., Garrett, R., Jung, Y., Zhang, Y., Kim, N., Wang, J., Joe, G.J., Hexner, E., Choi, Y., Taichman, R.S., Emerson, S.G., 2007. Osteoblasts support B-lymphocyte commitment and differentiation from hematopoietic stem cells. Blood 109, 3706−3712.

Chapter 4

The osteoblast lineage: its actions and communication mechanisms

Natalie A. Sims and T. John Martin

St. Vincent's Institute of Medical Research, Melbourne, Australia; Department of Medicine at St. Vincent's Hospital, The University of Melbourne, Melbourne, Australia

Chapter outline

Introduction

The skeleton is a metabolically active organ in which the organizational pattern of its mineral and organic components determines its successful mechanical function. This is achieved by a combination of dense, compact (cortical) bone and cancellous (trabecular) bone, reinforced at points of stress (Chapter 11). Bone itself is a heterogeneous compound material. The mineral phase of bone, in the form of modified hydroxyapatite crystals, contributes about two-thirds of its weight. The remaining organic matrix consists largely of type I collagen (~90%), with small amounts of lipid (~2%), noncollagenous proteins (~5%), and water. Noncollagenous proteins within the bone matrix include signaling molecules (such as transforming growth factor β and insulin-like growth factor I) and regulators of mineralization (such as osteocalcin and dentin matrix protein 1 [DMP1]).

The word "osteoblast" has been used traditionally to describe those cells in bone responsible for bone collagen matrix production. However, we now know there are multiple stages within the osteoblast lineage, and they perform a much wider range of functions; in fact, these cell types within the lineage, when fully delineated, will merit naming in ways to reflect those functions. In addition to regulating mineralization and osteoclastogenesis directly, the lineage also produces paracrine and autocrine factors (cytokines, growth factors, prostanoids, proteinases), thereby forming communication systems profoundly influencing not only bone formation, but also bone resorption and hematopoiesis (see Chapter 3). To this is added the discoveries revealing bone as an endocrine organ, with cells of the osteoblast lineage being sources of circulating hormones such as fibroblast growth factor 23 (FGF23) and osteocalcin. These two hormones will be discussed in detail in Chapters 64 and 25, respectively.

Principles of Bone Biology. https://doi.org/10.1016/B978-0-12-814841-9.00004-X

Our approach in this chapter is to recognize the mixture of cells comprising the osteoblast lineage. We will consider their range of functions influencing bone structure and strength, without confining the discussion to only those particular cells in the lineage traditionally called osteoblasts because of their ability to produce the bone matrix.

The stages of the osteoblast lineage

The osteoblast lineage consists of a number of stages of differentiation through the mesenchymal lineage. These functions are identifiable by the morphology and location of the cells as well as their gene expression and synthetic capabilities (Fig. 4.1). We will describe each stage of the lineage in turn: mesenchymal precursors, committed preosteoblasts, mature matrix-producing osteoblasts, osteocytes, and bone-lining cells.

Mesenchymal precursors

A detailed discussion of the stem cells of bone will be provided in Chapter 2, but some matters most directly relevant to osteoblasts will be discussed briefly here.

Osteoblasts are derived from stromal mesenchymal cells present in the bone marrow. In vitro, these multipotent precursors are capable of differentiating into osteoblasts, chondrocytes, adipocytes, or myocytes (reviewed in Bianco et al., 2008; Bianco et al., 2010). In vivo their location in the marrow is required for their ability to differentiate into osteoblasts (Sacchetti et al., 2016). Our understanding of these pathways owes much to the work of Alexander Friedenstein and Maureen Owen (Friedenstein, 1976). Their seminal work identified the existence of osteogenic stem cells within the bone marrow stroma. This was achieved when intraperitoneal transplantation of diffusion chambers containing bone marrow cells in rabbits gave rise to a mixture of tissues, including bone and cartilage (Friedenstein, 1976). This diversity of differentiation led Bianco et al. (Bianco et al., 2008) to propose renaming their "osteogenic stem cells" to "skeletal stem cells" (SSCs). The ability of these cells to form bone depended on their location in the marrow: those bone marrow cells taken from close to the endocortical surface of the femora were more osteogenic than cells taken from the central marrow or the intermediate region (Ashton et al., 1984; Bab et al., 1984). Furthermore, when marrow cell distribution was correlated with the colony-forming efficiency of the cells in vitro, stromal fibroblasts from the endocortical surface formed four times as many colonies as the same number of core cells. These observations served to establish Friedenstein's concept of the CFU-F (colony-forming unit—fibroblastic), which he proposed was a self-renewing multipotential stem cell population. An elegant extension of this involved establishing single stromal cell colonies, transplanted under the renal capsule of mice, where they formed plaques containing bone, with the host cells establishing hemopoiesis and excavating a marrow cavity (reviewed in Owen and Friedenstein, 1988). This experiment also provided the first evidence that stromal or osteoblast lineage cells could promote osteoclast recruitment from circulating precursors. Direct evidence for stromal or osteoblast lineage regulation of osteoclast formation was obtained some years later by coculture of osteoblast lineage cells with hemopoietic cells (Takahashi et al., 1988; Udagawa et al., 1989), and is reviewed in Chapter 5.

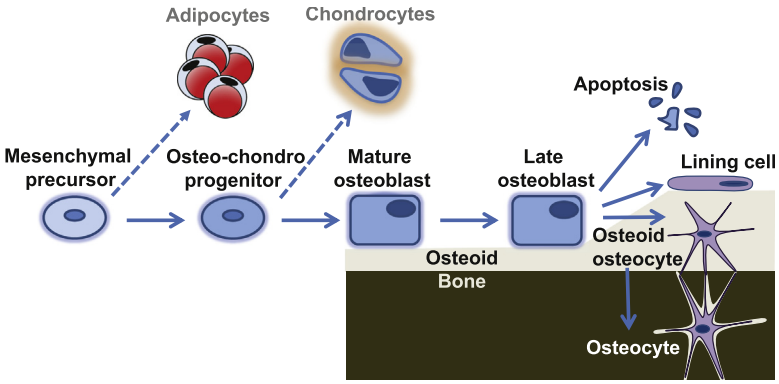

FIGURE 4.1 Stages of differentiation of the osteoblast lineage. Multipotent, replicating mesenchymal precursors, capable also of adipocyte differentiation, become more committed to be replicating osteo-chondro progenitors (osteoblast progenitors). These cells are capable of either chondrocytic or osteoblastic differentiation. When they reach the mature osteoblast stage, they reside on the bone surface above a layer of newly produced collagen-containing osteoid, and continue to differentiate. When they have completed the process of osteoid production, osteoblasts undergo one of three possible fates: (1) cell death through apoptosis; (2) remaining on the bone surface as flattened bone-lining cells, not actively producing osteoid; or (3) becoming embedded in the osteoid as "osteoid osteocytes," gradually becoming encased in mineralized bone, forming a network throughout the bone matrix, and remaining there as osteocytes.

These and subsequent studies using rigorous differentiation assays and CFU-F cells to show multipotency identified an SSC subset capable of forming skeletal tissue within bone marrow stroma. SSCs are rare in the marrow stromal cell population and need to be defined by rigorous clonal and differentiation assays. As an alternative some laboratories turned to the nonhemopoietic adherent cells of the bone marrow, which became known commonly as "mesenchymal stem cells" (MSCs). MSCs could be isolated from many tissues (da Silva Meirelles et al., 2006) and have been claimed to also be capable of forming osteoblasts in vitro. However, such studies have to be viewed with some reservation. The commonly used "osteogenesis assay," often used to confirm osteoblast differentiation, assesses mineral deposition by cells cultured in ascorbic acid and β-glycerophosphate. However, mineral stains rarely distinguish between collagen-containing nodule formation and diffuse mineral deposited by dead or dying cells (Orriss et al., 2014). It should be noted that any cell rich in alkaline phosphatase, including non−osteoblast lineage cells, like chondrocytes, can generate phosphorus by cleaving β-glycerophosphate, resulting in calcium phosphate precipitates, without expressing osteoblast marker genes or producing collagen-rich matrix. The International Society of Cell and Gene Therapy now recommends the term "mesenchymal stromal cells," which reflects only their in vitro properties, without clonal analyses or in vivo studies (Dominici et al., 2006). These caveats were summarized succinctly in a 2017 review (Robey, 2017).

A critical question remains as to whether other stromal cells derived from other sources can generate bone organoids (ossicles) supporting hemopoiesis in vivo. A comparison of stromal cells from bone marrow, white adipose tissue, umbilical cord, and skin led to the conclusion that only bone marrow−derived MSCs have this property (Reinisch et al., 2015). However, a different conclusion was reached when cord blood-borne fibroblasts (CB-BFs) were isolated. These CB-BFs, a rare population of cells, could generate complete ossicles in vivo with a functional hematopoietic stem cell niche, and did so through an endochondral bone formation program (Pievani et al., 2017). This outcome required as a starting point the CB-BF population rather than unselected MSCs from cord blood.

Further advances in understanding the osteoblast progenitor have come through cell lineage tracing methods. These studies localized osteoblast progenitors to vascular structures in the marrow, and suggested the same precursors may also give rise to cells forming the blood vessel and pluripotent perivascular cells (Doherty et al., 1998; Modder and Khosla, 2008; Otsuru et al., 2008). Support for this comes from mice with the smooth muscle α-actin (SMAA) promoter used to direct green fluorescent protein (GFP) to smooth muscle and pericytes; strong osteogenic differentiation was evident in cells positive for SMAA−GFP (Kalajzic et al., 2008). This indicates the capacity of SMAA to mark an osteoblast progenitor population, and reinforced earlier studies proposing the pericyte as an osteoblast progenitor during bone remodeling (Brighton et al., 1992; Doherty et al., 1998). It should be noted that pericytes appear to behave in an organ-specific manner, dictated by their anatomy and position (Bianco et al., 2008). For example, pericytes isolated from muscle generate myocytes in vitro (Dellavalle et al., 2007). Notably, only marrow-residing pericytes appear capable of becoming osteoblasts under normal conditions (Sacchetti et al., 2016). In pathological conditions, there are clearly osteoblast precursor populations resident in other tissues capable of forming bone, including the heterotopic ossifications observed after spinal cord injury (Genet et al., 2015). The generation of osteoblasts from bone marrow−specific pericytes illustrates the importance of the microenvironment in determining differentiation, probably by the generation and influence of local factors. Lineage tracing studies also suggest that bone-lining cells can form a population of osteoblast precursors (see "Bone-lining cells") (Matic et al., 2016).

Commitment of osteoblast progenitors (preosteoblasts)

For many years the "osteoblast phenotype" was studied in rodent cell culture systems, including stable and transformed cell lines, osteogenic sarcoma cell lines, and organ cultures. The limited characterization possible when cells were first grown from rodent bone fragments (Peck et al., 1964) was extended when methods were established to culture cells obtained from newborn rodent calvariae by enzymatic digestion (Luben et al., 1976). At the same time, cells were cultured from osteogenic sarcomata; these, and the clonal cell lines derived from them, were enriched in a number of osteoblastic properties (Majeska et al., 1980; Partridge et al., 1983). The concepts of the osteoblast phenotype developed in these rodent culture systems were extrapolated to adult bone in vivo. Limitations were not always realized, in particular the heterogeneity of primary rodent cultures and the identity of osteosarcoma cells, not as true osteoblasts, but as tumor cells enriched in some osteoblastic features. Nevertheless, these systems have provided useful foundational knowledge, particularly in studying osteoblast lineage intracellular signaling responses to hormones, growth factors, and cytokines (Crawford et al., 1978; Partridge et al. 1981, 1982; Livesey et al., 1982).

Stromal lineage commitment depends on the expression of key transcription factors that, on induction, initiate a cascade of events culminating in differentiation. These are discussed in depth in Chapter 7. Among the transcription factors regulated, osteoblast differentiation requires expression of Runx2 (Komori et al., 1997; Otto et al., 1997) and Osterix

(Nakashima et al., 2002) to commit progenitors to preosteoblasts. Other transcription factors, including ATF4 (Yang et al., 2004), AP-1 (Sabatakos et al., 2000), C/EBPβ, and C/EBPδ (Gutierrez et al., 2002), promote their transition to functional osteoblasts. Alternatively, commitment toward adipocytic differentiation requires expression of other transcription factors, including peroxisome proliferator-activated receptor (PPARγ) (Barak et al., 1999) and C/EBPα (Tanaka et al., 1997).

Because osteoblasts and adipocytes are derived from common progenitors, lineage commitment of precursor cells to osteoblasts results in a proportional decrease in adipogenesis. This inverse relationship is observed in cell culture (Walker et al., 2010; Poulton et al., 2012), and has been described in genetically altered mouse models, both where high osteoblast activity is associated with low marrow adipocyte volume (Sabatakos et al., 2000) and where low osteoblast numbers are associated with high marrow adipocyte volume (Sims et al., 2000; Walker et al., 2010; Poulton et al., 2012). Such reciprocal regulation is also observed clinically: high marrow adiposity is associated with age-related osteoporosis (Justesen et al., 2001) and observed in preclinical models of induced bone loss, such as ovariectomy (Martin et al., 1990) and immobilization (Ahdjoudj et al., 2002). Understanding the relationship between osteoblasts and adipocytes and how its dysregulation contributes to bone loss will provide key information required to improve treatments for skeletal disorders in adult bone metabolism.

The effects of pharmacological parathyroid hormone (PTH) provide another example of the reciprocal regulation of osteoblast/adipocyte commitment. Intermittent administration of amino-terminal preparations of PTH increases bone mass in part by promoting the differentiation of committed osteoblast precursors (Dobnig and Turner, 1995), decreasing osteoblast apoptosis (Manolagas, 2000), and suppressing production of sclerostin by osteocytes (Keller and Kneissel, 2005). Intermittent PTH treatment is also associated with reduced marrow adipocyte numbers in vivo (Sato et al., 2004). Similar observations of reduced osteoprogenitor recruitment and increased marrow adiposity have been noted in mice haploinsufficient for PTH-related protein (PTHrP) (Amizuka et al., 1996; Miao et al., 2005), and increased formation of adipocytes has been noted after cessation of PTH treatment in mice (Balani and Kronenberg, 2018). What is particularly interesting is recent evidence obtained through lineage tracing in mice indicating direct actions of PTH(1−34) through the PTH receptor (PTHR1) on very early osteoblast precursors, favoring osteoblast commitment at the expense of adipocytes (Balani et al., 2017); this is surprising because earlier studies of receptor activation in vitro indicated that responsiveness to PTH required more mature osteoblasts (Allan et al., 2008). The new data suggest that PTHR1 responsiveness is active earlier in the osteoblast lineage. This is consistent with very early work showing suppression of preadipocyte differentiation in vitro by PTHrP (Chan et al., 2001). In support of this, mice with PTHR1 deletion targeted to the osteoblast lineage, including early precursors (using Prx1-Cre), exhibited low bone formation and high marrow fat (Fan et al., 2017). This was associated with altered expression of ZFP467, a transcriptional cofactor, previously described to enhance adipocyte and blunt osteoblast differentiation, which is downregulated in osteoblast lineage cells by PTH or interleukin-6 (IL-6) family cytokine treatment (Quach et al., 2011). Transfection of ZFP467 into mouse calvarial cells substantially increased their transformation into adipocytes when transplanted into marrow (Quach et al., 2011).

A further link between the osteoblast and adipocyte lineages is provided by the finding that knockout of the leptin receptor (LepR) from limb bone marrow stromal cells by crossing *Prrx1.Cre* and *LepR*$^{fl/fl}$ mice revealed that the LepR also mediates local actions on very early SSC precursors to promote adipogenesis and inhibit bone formation (Yue et al., 2016). Such a role for the LepR is opposite to that described above for PTHR1 (Balani et al., 2017; Fan et al., 2017); whether there is any physiological connection between the two is not known.

Osteoblasts and chondrocytes are also derived from a common precursor (sometimes termed an "osteo-chondro progenitor"), and while this does not need to be considered in adult bone remodeling, the commitment of precursors to either of these lineages is important in developmental biology, fracture healing, and approaches being developed for joint cartilage repair. For example, the osteoblast commitment genes *Osterix* and *Runx2* both promote the final stage of chondrocyte differentiation (hypertrophy) preceding vascular invasion in endochondral ossification. This progression through to hypertrophy is blocked in both *Runx2*- (Inada et al., 1999; Kim et al., 1999) and *Osterix*-null mice (Nishimura et al., 2012). These two transcription factors appear to interact directly with each other to promote chondrocyte hypertrophy (Nishimura et al., 2012). In addition, overexpression of *Runx2* promotes chondrocyte hypertrophy, while knockdown reduces it and promotes adipogenesis (Enomoto et al., 2000; Takeda et al., 2001; Ueta et al., 2001). Although reciprocal regulation of chondrogenesis and osteoblastogenesis from the same common precursor has been suggested (Komori, 2018), mechanisms controlling this have not yet been identified. So, too, the question of whether hypertrophic chondrocytes also represent partially committed osteoblast precursors capable of transdifferentiating into osteoblasts continues to be investigated (Yang et al., 2014).

Mature "bone-forming" osteoblasts

Mature osteoblasts synthesize the organic components of bone and contribute to the events resulting in its mineralization. This is discussed in additional detail in Chapter 11.

Mature matrix-producing osteoblasts are recognized as groups of plump, cuboidal mononuclear cells lying on the unmineralized matrix (osteoid) they have synthesized. These cells do not operate in isolation, and in vivo are rarely seen even in small groups of two or three cells. Rather, active bone-forming surfaces are lined by a seam of osteoid, on the surface of which resides a team of osteoblasts with similar morphologic characteristics, including similar nuclear–cytoplasmic alignment, and extensive sites of contact between team members (Fig. 4.2). Formation of mineralized nodules in vitro also depends on a critical mass of differentiated osteoblasts, which form a cobblestone layer before matrix deposition occurs (Ecarot-Charrier et al., 1983; Abe et al., 1993). Matrix-producing osteoblasts communicate with one another, with adjacent bone-lining cells (Doty, 1981), and with osteocytes below the surface through gap junctions and direct cell–cell contact. This requirement of cell–cell contact between matrix-producing osteoblasts emphasizes the importance of juxtacrine and paracrine control mechanisms for osteoblast differentiation and bone formation.

Osteoblasts do not produce "bone" per se, but synthesize a collagen-rich osteoid matrix, which becomes gradually mineralized over time. This process of mineralization is controlled by noncollagenous proteins produced by late-stage osteoblasts and osteocytes. The ability of osteoblasts to produce large quantities of protein is clearly shown by their dense endoplasmic reticulum (Fig. 4.2).

When osteoid is deposited by osteoblasts, it has two potential forms depending on its collagen orientation and speed of production. Within the osteoblast Golgi, procollagen molecules that make up osteoid are biochemically modified to form collagen triple helices, which are released by exocytosis into the extracellular space (Leblond, 1989). During bone

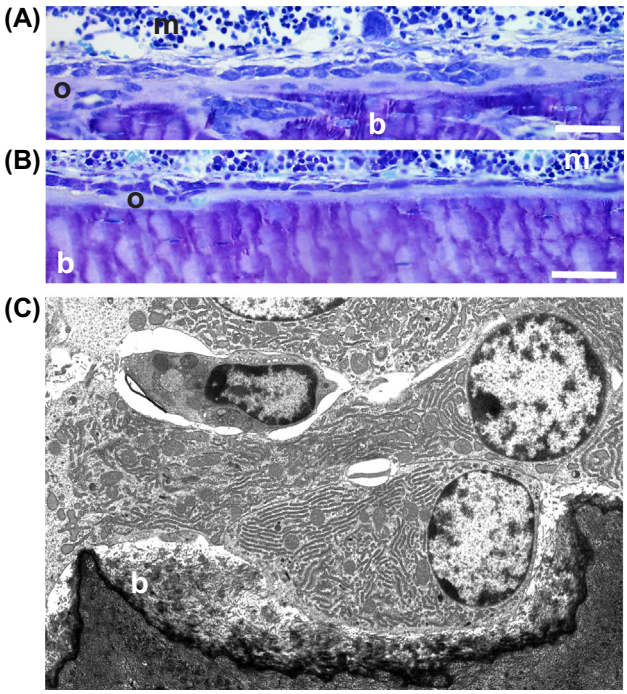

FIGURE 4.2 The appearance of matrix-producing osteoblasts by (A and B) light microscopy and (C) transmission electron microscopy. (A and B) Murine endocortical osteoblasts on newly formed metaphyseal (A) and diaphyseal cortical bone; osteoid (*o*) is the paler substance between the darker mineralized bone (*b*) and the line of cuboidal osteoblasts separating it from the marrow (*m*). Toluidine blue–stained undecalcified tibial sections from 6-week-old female C57BL/6 mice. Scale bar = 50 μm. (C) Osteoblasts on the surface of newly deposited osteoid above calcified cartilage in the primary spongiosa in 6-week-old female mice. Note the extensive contact between the osteoblasts and the extensive endoplasmic reticulum within the cells. *Image (C) courtesy Liliana Tatarczuch and Eleanor Mackie, The University of Melbourne, reproduced from Tonna, S., Takyar, F.M., Vrahnas C., Crimeen-Irwin, B., Ho, P.W., Poulton, I.J., Brennan, H.J., McGregor, N.E., Allan, E.H., Nguyen, H., Forwood, M.R., Tatarczuch, L., Mackie, E.J., Martin, T.J., Sims, N.A., 2014. EphrinB2 signaling in osteoblasts promotes bone mineralization by preventing apoptosis. FASEB J. 28 (10), 4482–4496.*

development and fracture healing, woven bone is deposited rapidly: this contains disordered collagen fibers. During adult bone remodeling, the more slowly deposited, and mechanically stronger, lamellar bone has collagen fibers oriented in perpendicular planes in adjacent lamellae (Giraud-Guille, 1988). How osteoblasts are instructed to form either of these two substances is not known. One clue comes from ultrahigh-voltage electron microscopy studies showing initial sparse and random deposition of collagen fibers, followed, with increasing distance from the surface osteoblasts, by thickening and a shift to being oriented parallel to the direction of growth (Hosaki-Takamiya et al., 2016).

After collagen is deposited it becomes progressively mineralized by the accumulation of hydroxyapatite crystals. This mineralization process has two phases. Within ~5−10 days, osteoid undergoes rapid primary mineralization, and over subsequent weeks, months, and years, secondary mineralization occurs (Glimcher, 1998). Usually, the tissue reaches approximately 50%−70% of its final mineral content during primary mineralization (Boivin and Meunier, 2002; Ruffoni et al., 2007). During secondary mineralization, mineral continues to accumulate at a slower rate (Fuchs et al., 2008), crystals become larger (Glimcher, 1998), and carbonate is substituted for phosphate groups within the matrix (Vrahnas et al. 2016, 2018). As mineral is deposited, the surrounding collagen fibers of bone also change, becoming more cross-linked (Paschalis et al., 2004) and more compact (Vrahnas et al. 2016, 2018).

The processes of mineralization initiation, mineral accrual, and crystal maturation are controlled by a number of noncollagenous proteins expressed by osteoblasts and osteocytes (see Table 4.1). Some proteins promote mineralization, such as the many phosphate-regulating and SIBLING proteins including alkaline phosphatase; phosphate-regulating neutral endopeptidase, X-linked; DMP1; matrix extracellular phosphoglycoprotein; and bone sialoprotein/integrin-binding sialoprotein. The importance of these proteins is clearly illustrated by defective bone mineralization in genetic insufficiencies of these proteins in both humans and mice (Whyte, 1994; Quarles, 2003; Holm et al., 2015). Mineralization inhibitors, such as osteopontin/secreted phosphoprotein-1 (Addison et al., 2010), are also expressed by osteoblasts and osteocytes. The final level of mineralization achieved in the bone substance varies locally within the bone matrix, and depends on the species, sex, age, and anatomical location of the bone (Boskey, 2013).

Bone-lining cells

Bone-lining cells are the abundant flattened cells lining both endocortical and trabecular bone surfaces (Miller and Jee, 1987). These cells have much less synthetic function, little cytoplasm or endoplasmic reticulum, and somewhat less cytoplasmic basophilia and alkaline phosphatase activity. They nevertheless possess gap junctions and may communicate both with one another and, probably through the canaliculi, with osteocytes residing in the bone matrix.

Although long regarded as a "resting" or "quiescent" population, bone-lining cells express receptors for endocrine and paracrine agents in common with mature osteoblasts. Their contraction from the bone surface in response to PTH (Jones and Boyde, 1976) was suggested to be a means of allowing osteoclasts access to the bone surface (Rodan and Martin,

TABLE 4.1 Selected proteins expressed at specific stages of osteoblast differentiation

Committed osteoblast progenitors	Early osteoblasts	Intermediate osteoblasts	Late osteoblasts	Early osteocytes	Late osteocytes
Runx2 (Komori et al., 1997) Osterix (Nakashima et al., 2002)	Pro-a(1)I collagen (Rodan and Noda, 1991) Fibronectin (Stein et al., 1990)	Alkaline phosphatase (Aubin, 1998) Osteonectin (Aubin, 1998) Matrix gla-protein (Stein et al., 1990). Bone sialoprotein Chen et al. (1992) PTH receptor (Allan et al., 2008)	Osteocalcin (Stein et al., 1990) Osteopontin (Stein et al., 1990)	Matrix extracellular phosphoglycoprotein (Igarashi et al., 2002). Dentin matrix protein 1 (Toyosawa et al., 2001) Phosphate-regulating neutral endopeptidase, X-linked (Westbroek et al., 2002)	Sclerostin (van Bezooijen et al., 2004) Fibroblast growth factor 23 (Yoshiko et al., 2007).

Shown is the stage of differentiation at which the marker is most highly expressed. Note: these proteins are expressed at lower levels at other stages of differentiation.

1981). The emergence of bone-lining cells from quiescence has been highlighted much more recently in other ways. This includes reactivation to resume their bone-forming ability by contributing to the anabolic effects of PTH (Kim et al., 2012) and anti-sclerostin treatment (Kim et al., 2017). The ability of bone-lining cells to form active osteoblasts is not restricted to "reactivation." After osteoblast ablation, bone-lining cells have been shown to proliferate and differentiate into mature osteoblasts; marrow-derived precursors were not capable of this (Matic et al., 2016). Bone-lining cells may therefore also provide a source of osteoblast precursors capable of proliferation during adulthood.

Another suggested function for bone-lining cells is their ability to lift from the bone surface to generate a canopy over the basic multicellular unit (BMU) to enclose its activities on the bone surface (Hauge et al., 2001), as discussed in Chapter 10. Bone-lining cells have also been shown to express receptor activator of NF-κB ligand (RANKL) and M-CSF (CSF1), and may therefore also participate in stimulating osteoclastogenesis (Matic et al., 2016). This has been suggested to be particularly important in estrogen deficiency (Streicher et al., 2017).

Osteocytes

Osteocytes, the matrix-embedded cells of the osteoblast lineage, are considered major "controlling cells" or "orchestrators" of bone due to their extensive networks and ability to signal to other cells (Bonewald, 2011; Schaffler et al., 2014). At this stage of the lineage, osteocytes exhibit a distinct pattern of gene expression (Table 4.1), and a distinct phenotype and location. Osteocytes are osteoblasts that became entrapped within the bone matrix during bone formation. As they are trapped, they form extensive dendritic processes through a fluid-filled network of communicating channels, allowing them to sense and respond to mechanical strain and microdamage to bone. They are the most abundant cell in bone by far, forming a highly complex cellular communication network through the bone matrix with a total of ~3.7 trillion connections throughout the adult skeleton (Buenzli and Sims, 2015). The nature and functions of osteocytes are considered in detail in Chapter 6.

One major protein involved in the communication network of osteocytes to osteoblasts is sclerostin, an inhibitor of Wnt-stimulated osteoblast differentiation (Bonewald and Johnson, 2008); the influence of this pathway on bone formation will be considered later. Sclerostin is likely to be important in limiting the amount of bone laid down in modeling, and its production in response to loading (Galea et al., 2011) or to local factors such as prostaglandin E_2 (Genetos et al., 2011), IL-6 family cytokines (Walker et al., 2010), or PTHrP (Ansari et al., 2018) also regulates bone formation.

The process of osteoblast lineage differentiation

Although we have summarized the main subsets of osteoblast lineage cells (precursors, matrix-producing osteoblasts, bone-lining cells, and osteocytes), differentiation is likely to proceed subtly even within each subset, with a range of phenotypic properties likely within any group (i.e., they are probably not homogeneous).

The first approach used to study osteoblast differentiation in vitro was to use primary cultured cells derived from stromal precursors or cell lines such as MC3T3-E1 (Sudo et al., 1983) and Kusa subclones (Allan et al., 2003). These have been used extensively to define pathways of osteoblast differentiation and equate each stage of differentiation and its gene expression profiles with some function in bone. The functions carried out by any member of the lineage depend on its stage of differentiation, its pattern of gene expression, its location in bone, and the influence of local and humoral factors. Thus, it is not appropriate to use the presence or absence of a single gene to define whether a cell is, or is not, an osteoblast. Rather, the expression of multiple genes may be used to define approximately the particular stages of osteoblast lineage differentiation, as illustrated in Table 4.1. While these gene products are often considered osteoblast markers, many are not exclusively expressed by osteoblasts and can be found in other cell types in the body. As single-cell sequencing methods are applied to this question, more will be learned about specific stages of differentiation and potential "subpopulations" of the osteoblast lineage.

When it comes to analyzing mutant mice, or mice treated with agents modifying osteoblast function, attempts to identify changes in the distribution of cells throughout the lineage (i.e., whether there are more cells at the precursor or collagen-producing stage of differentiation) still require morphologic and functional assessment. For example, our work using an antagonist to the EphrinB2/EphB4 interaction in cultured osteoblast lineage cells resulted in low mRNA levels specifically for genes associated with late osteoblasts and osteocytes (Takyar et al., 2013); when cell lineage−specific blockade was assessed in vivo, the midpoint blockade of osteoblast differentiation was reflected in elevated early-stage markers of osteoblast differentiation and reductions in late-stage markers (Tonna et al., 2014), suggesting an EphrinB2/EphB4 checkpoint midway through the differentiation process. Additional histomorphometric data confirmed this: osteoid production was maintained, while the initiation of bone mineralization (which requires expression of late osteoblast and

osteocyte markers) was delayed, leading to a reduction in bone stiffness (Tonna et al., 2014). Thus, stage-specific changes in osteoblast differentiation can lead to changes in the process of bone mineralization, ultimately modifying bone strength.

Defining gene expression patterns at specific stages of osteoblast differentiation has been aided by the use of genetically modified mice with reporter genes under the control of specific promoters. These reporter genes allow sorting of specific populations by fluorescence-activated cell sorting (FACS), a method enabling microarray studies to define specific gene sets expressed by, for example, osteoblasts compared with osteocytes (Kalajzic et al., 2005; Paic et al., 2009). Such studies have led to the identification of gene products associated with bone dissolution expressed by osteocytes (Chia et al., 2015), and allowed purification of cells to confirm gene knockdown in genetically altered mice (Ansari et al., 2018).

Although cell sorting might be helpful for identifying the stages of osteoblasts present in cells isolated from rodents, there remain only very limited cell surface markers available to identify the stages of osteoblast differentiation in non–genetically modified bone. Efforts are being made to develop antibodies specific for SSCs and their progeny, but have to date been unsuccessful. In mice, when cells must be derived from bone by prolonged enzymatic digestion, cell surface markers are inevitably damaged; this hampers FACS analysis. This disadvantage does not apply to the analysis of hemopoietic cells, since they do not require enzymatic digestion; such analyses have been carried out successfully for many years. Despite this limitation, freshly isolated murine bone osteoblast progenitors, which are perhaps less firmly attached to the bone surface, can be separated broadly into early (Sca-1^{+}CD51^{-}) and relatively mature (Sca-1^{-}CD51^{+}) osteoblast progenitors, each of which consist of heterogeneous populations (e.g., Lundberg et al., 2007).

Histology and histomorphometry remain the gold standard for identifying and quantifying mature osteoblasts, osteocytes, and bone-lining cells, and rely on their distinct morphologies and locations; in this way increased osteoblast numbers or changes in the osteocyte network can be identified and compared with changes in osteoid deposition and the rate at which mineralization is initiated. It should be noted that cells very early in the lineage arising from SSCs cannot be recognized morphologically in bone without the use of specific markers. Identifying specific stages of differentiation has been challenging, and requires the use of immunohistochemistry and in situ hybridization. Such methods have been used to identify the presence of Runx2-positive precursors within the marrow space in pathological conditions (for example, Walsh et al., 2009). Needed above all else are markers of osteoblast development and methods of visualization for in situ applications to complement morphologic assessment. The method of laser scanning cytometry, in which image analysis, somewhat like cell sorting, can be carried out on immunostained tissue sections, is a promising approach (Fujisaki et al., 2011).

At their various stages of development, cells of the osteoblast lineage signal to one another

Osteoblast lineage precursors begin their differentiation in the BMU, during which they are likely to be in contact with (or at least in close proximity to) other osteoblast precursors and mature osteoblasts on the bone surface. Bone-lining cells and matrix-producing osteoblasts on the bone surface are also in contact, not only with one another, but also with the highly differentiated osteocytes within the bone matrix. Not surprisingly, therefore, the cells of the lineage exert their influence through communicating signals among its member cells. These may be through direct contact by gap junctions or by paracrine and autocrine signaling. Some influential signaling processes within the osteoblast lineage will be discussed as examples of interactions within the lineage contributing to differentiation and their abilities to form bone, and program the generation of osteoclasts.

An example of contact-dependent communication: EphrinB2/EphB4

We have drawn attention to the role of the contact-dependent interaction between the receptor tyrosine kinase EphB4 and its ligand EphrinB2 as an important checkpoint prior to the late stages of osteoblast differentiation (see earlier) (Takyar et al., 2013; Tonna et al., 2014). EphrinB2 is produced at constant levels throughout osteoblast differentiation in vitro (Allan et al., 2008). In contrast, EphrinB2, but not its receptor, was rapidly increased when cells were exposed in vitro to PTHrP or PTH (Allan et al., 2008). Acute treatment of mice or rats with PTH also results in a rapid increase in EphrinB2 mRNA production in bone (Allan et al., 2008). Osteoblast-specific deletion of EphrinB2 (*OsxCre.Efnb2*$^{f/f}$ mice) caused a mild osteomalacia with compromised bone strength due to impaired late-stage osteoblast differentiation and high levels of osteoblast apoptosis (Tonna et al., 2014). The impairment in osteoblast differentiation was interesting because the osteoblasts expressed all early markers of osteoblast commitment at normal levels, but showed low levels of osteoblast marker expression after the stage of PTHR1 expression. This led to normal osteoid production, but delayed mineralization and diminished bone strength, pinpointing a failure of osteoblasts to pass through the EphrinB2/EphB4 checkpoint to become late-stage osteoblasts and osteocytes. A new insight into such contact-dependent communication

processes came with deletion of EphrinB2 at a later stage of differentiation, in osteocytes. These *Dmp1Cre.Efnb2*$^{f/f}$ mice had brittle bones in which the maturing matrix incorporated mineral and carbonate more rapidly than controls, and strikingly, the osteocytes in the mutant mice exhibited a higher level of cellular autophagy (Vrahnas et al., submitted for publication). Thus EphrinB2-directed actions with differing outcomes can be recognized in these two stages of the osteoblast lineage.

Communication between different stages of differentiation: IL-6 cytokines

The IL-6 family cytokines have many roles in bone physiology mediated by the osteoblast lineage. The first function identified for these cytokines in bone was their ability to promote osteoclast formation in vitro. However, osteoclast formation by IL-6, IL-11, leukemia inhibitory factor (LIF), cardiotrophin 1 (CT-1), and oncostatin M (OSM) in vitro depends on the presence of osteoblast-lineage cells (Tamura et al., 1993), by virtue of their ability to produce RANKL in response to these cytokines (Richards et al., 2000; Palmqvist et al., 2002).

These cytokines also promote bone formation. IL-6, IL-11, CT-1, and OSM all promote osteoblast differentiation in vitro (Bellido et al., 1997; Song et al., 2007; Walker et al., 2008). OSM, CT-1, and LIF, all of which are produced by osteoblasts, stimulate bone formation in vivo (Cornish et al., 1993; Walker et al. 2008, 2010). OSM, CT-1, LIF, and IL-11 also inhibit adipocyte differentiation (Sims et al., 2005; Song et al., 2007; Walker et al. 2008, 2010; Poulton et al., 2012) and stimulate the transcription factors involved in osteoblast commitment described earlier (C/EBPβ and C/EBPδ), while inhibiting the adipogenic transcription factor PPARγ, indicating an influence of these cytokines on early osteoblast/adipocyte commitment; this is confirmed by the low bone formation, high marrow adipose phenotypes of the IL-11 receptor-, CT-1-, LIF-, and OSM receptor-null mice (Sims et al., 2005; Walker et al. 2008, 2010; Poulton et al., 2012). In addition, these cytokines, which are expressed at all stages of osteoblast differentiation, all strongly inhibit expression of sclerostin, confirming a direct action in osteocytes (Walker et al., 2010). Thus, they promote bone formation by direct actions at multiple stages of osteoblast differentiation.

Stage-specific roles of IL-6 family cytokines in the osteoblast lineage were studied further using two mouse models in which the common receptor subunit for these cytokines (gp130) was conditionally deleted either from the entire osteoblast lineage (*Osx1Cre*) or later in osteoblast/osteocyte differentiation (*Dmp1Cre*). Given the role of these cytokines in stimulating osteoclast formation, it was a surprise that no changes in osteoclast formation or RANKL expression were observed. Instead, the mice exhibited a low level of bone formation (Johnson et al., 2014). This indicated that the major physiological effect of these cytokines in the osteoblast lineage is not to support osteoclast formation, but to maintain bone formation (Johnson et al., 2014). Although these cytokines stimulate RANKL expression in the osteoblast lineage, that function is not required for the maintenance of normal bone mass, but may be required to generate osteoclasts specifically in pathological conditions; alternatively, the gp130-dependent support of osteoclast formation within the osteoblast lineage may occur prior to osteoblast commitment. Consistent with differing influences at specific stages of the osteoblast lineage, there was no effect of deletion of gp130 within the osteoblast lineage on marrow adipogenesis (Johnson et al., 2014), suggesting these cytokines also influence osteoblast−adipocyte commitment before the stage of *Osterix* expression. Ultimately, both mice showed the same structural phenotype, indicating that role of gp130 in the osteoblast lineage controlling bone structure is mediated by the osteocyte (Johnson et al., 2014).

Communication at different stages of differentiation: PTHrP/PTHR1

Another communication pathway among the osteoblast lineage is mediated by PTHR1, the G-protein-coupled receptor shared between the hormone PTH and the cytokine PTHrP.

The paracrine action of osteoblast lineage−derived PTHrP to promote bone formation and stimulate osteoclastogenesis has been demonstrated in mice globally deficient in PTHrP and in mice with PTHrP knockdown directed to mature osteoblasts and osteocytes using *ColI(2.3)Cre* (Miao et al., 2005). This revealed a mechanism analogous to the anabolic action of intermittent PTH treatment in osteoporosis (i.e., that local PTHrP retains trabecular bone mass by promoting bone formation). The communication by PTHrP within the lineage has been extended to osteocytes, since osteocyte-specific knockout of PTHrP also results in reduced bone formation and loss of bone mass and strength (Ansari et al., 2018), with the conclusion that osteocyte-derived PTHrP acts in a paracrine/autocrine manner on osteocytes and osteoblasts. Notably, deletion later in the lineage (with *Dmp1Cre*) did not result in reduced osteoclast formation (Ansari et al., 2018), indicating that PTHrP promotes bone formation through actions later in the osteoblast lineage than its actions to stimulate osteoclast formation, analogous to the aforementioned observations in gp130-deficient mice. This topic is considered in detail in Chapter 25.

Physical sensing and signaling by osteoblasts and osteocytes

Another possible signaling mechanism within the osteoblast lineage is their ability to "sense" changes on the bone surface. When rat calvarial cells were provided in vitro to bone slices with crevices made by osteoclasts, or mechanically excavated grooves, the cells made bone in those defects, filling them exactly to a flat surface (Gray et al., 1996). In this way, in bone remodeling, osteoblast filling of a BMU follows the dictates of the size of the resorption cavity made by the osteoclasts, and once the formation process is established, the participating cells themselves sense the spatial limits and fill the space. This may be achieved by the ability of osteoblast precursors to respond to changes in surface topography when the change is either much larger than the cell itself, as in the aforementioned study, or very much smaller than the cell. For example, in response to altered nanotopography, cells adhere to the surface and one another and proceed to differentiate (Dalby et al., 2006). This filling may then occur through chemical communication, possibly involving gap junctions both among matrix-producing osteoblasts and between osteoblasts and osteocytes (Doty, 1981). The changes brought about on the bone surface by cells in the reversal phase may also change the topography and thereby determine osteoblast function. The in vitro study of Gray used bone that did not contain osteocytes, so they are not necessary for osteoblasts to respond to topographic clues, at least in vitro.

Osteocytes also sense the need for new bone formation, in their case, by sensing mechanical strain within the lacuna−canalicular network. Osteocytes respond to these changes by modifying their production of a range of signaling proteins (Mantila Roosa et al., 2011). The most well defined of these modifications is their decreased production of the bone formation inhibitor sclerostin (Robling et al., 2006). This releases a brake on matrix-producing osteoblasts on the bone surface (Robling and Turner, 2009) such that bone formation is increased in response to load in regions under greatest strain, i.e., where new bone is needed. The properties of osteocytes and their actions in mechanotransduction are discussed in detail in Chapter 6; here we use it as an example of how different stages of the osteoblast lineage communicate with one another.

How does the osteoblast lineage promote osteoclast formation?

The first intercellular communication function ascribed to the osteoblast lineage arose when it was proposed that the osteoblast lineage controlled the formation of osteoclasts (Rodan and Martin, 1981). Cell culture methods established this to be the case (Takahashi et al., 1988) by showing that osteoclastogenic cytokines and hormones, such as IL-6, PTH, 1,25-dihydroxyvitamin D_3 ($1,25(OH)_2D$), and OSM, act first on osteoblast lineage cells to promote their production of a membrane-bound regulator of osteoclastogenesis. The essential product from the osteoblast lineage proved to be RANKL, a member of the tumor necrosis factor ligand family that acts upon its receptor RANK in the hematopoietic lineage (Yasuda et al., 1998). The interaction is restricted by a decoy soluble receptor, osteoprotegerin (OPG), also a product of the osteoblast lineage (Simonet et al., 1997). The essential physiological roles of these factors in osteoclastogenesis were established through genetic and pharmacological studies (Boyle et al., 2003).

It continues to be unclear which stage of the osteoblast lineage is most influential in providing RANKL to the osteoclast precursor population. Early studies indicated that RANKL was probably derived from cells relatively early in the osteoblast lineage (Udagawa et al., 1989; Kartsogiannis et al., 1999), which would be more likely to be in contact with the appropriate osteoclast precursor populations. Consistent with a role for pluripotent precursors as a source of RANKL, adipocytes have also been reported to support osteoclastogenesis (Kelly et al., 1998; Hozumi et al., 2009; Quach et al., 2011). It has also been suggested that bone-lining cells may make direct contact with osteoclast precursors (Streicher et al., 2017); this may particularly come into play when they lift from the bone surface to form the canopy prior to bone remodeling. Of all the cells of the osteoblast lineage, probably the least likely to play a part in the regulation of osteoclast formation are mature, bone-synthesizing osteoblasts.

It has also been proposed that osteocytes are a major source of RANKL for osteoclast precursors. This follows the findings that genetic deletion of RANKL causes osteoclast deficiency and osteopetrosis both when the deletion is targeted to the entire osteoblast lineage and (albeit less so) when it is targeted specifically to osteocytes (Nakashima et al., 2011; Xiong et al., 2011). Although genetic deletion of RANKL throughout the osteoblast lineage led to profound osteopetrosis, when genetic deletion of RANKL in that lineage was delayed until adulthood, a reduction of RANKL in the entire osteoblast lineage did not lead to osteopetrosis, leading the authors to suggest that it is only the osteocyte that provides RANKL for osteoclast formation. This finding was not reproduced by Fumoto et al., who achieved a similar level of delayed RANKL knockdown, albeit in younger mice, that resulted in osteopetrosis of the same severity as that in mice lacking RANKL in osteoblast lineage throughout life (Fumoto et al., 2013). Notable in the latter work, in direct contrast to the findings of Nakashima et al. (Nakashima et al., 2011), RANKL mRNA levels were higher in osteoblast-rich cell

preparations compared with osteocyte-rich preparations. In both those studies the cell preparations being compared were impure, and would have contained hematopoietic cells, such as RANKL-expressing T cells, and natural killer cells, which are also capable of promoting osteoclast formation (Horwood et al., 1999; Soderstrom et al., 2010), although the proportion of contamination in each population is unknown. When highly purified populations of osteoblasts and osteocytes were prepared, in which those hematopoietic cells were removed, the level of RANKL expression in non-osteocytic mesenchymal cells (osteoblasts and their precursors) was approximately double that of purified osteocytes (Chia et al., 2015). This is consistent with early in situ hybridization studies, in which few osteocytes were reported to express RANKL (Kartsogiannis et al., 1999). It also parallels two other studies using transgenic expression of marker genes to isolate specific populations of the osteoblast lineage, in which osteoclastogenic support of osteoprogenitors was compared with a mixed population of mature osteoblasts and osteocytes (Li et al., 2010), with purified hematopoietic-cell-free osteocytes (Chia et al., 2015), or with an osteocyte-like cell line (McGregor et al., 2019). In all three works, while osteoblast progenitors supported $1,25(OH)_2D_3$-induced osteoclastogenesis, no osteoclasts were formed when the more mature osteocyte populations were used.

One important concept to consider in the role of osteoblast lineage cells in supporting osteoclastogenesis is that direct contact between the RANKL-expressing osteoblast lineage cells and the RANK-expressing hemopoietic osteoclast precursors was absolutely required for osteoclast formation in vitro (Takahashi et al., 1988; Suda et al., 1992). While recombinant soluble RANKL certainly promotes osteoclast formation from precursors in vitro (Quinn et al., 2001), and in vivo (Tomimori et al., 2009), there remains no evidence for shedding of soluble RANKL in the interaction between osteoblast and hemopoietic lineages, nor any convincing evidence of a physiological role for circulating RANKL. This means it is important to consider the location of the osteoblast lineage cells most likely to support osteoclast formation; cells within or in direct contact with the marrow, such as osteoblast precursors and bone-lining cells, rather than embedded osteocytes, are more likely to come into contact with osteoclast precursors and, therefore, are more likely to support osteoclast formation in normal remodeling. It has been difficult to understand how osteocytes, from within the matrix, could control RANKL availability to osteoclast precursors in the bloodstream through a contact-dependent mechanism, but some mechanisms have been proposed. Early confocal laser scanning microscope images have shown that osteocytic processes extend to the vascular-facing surface of the osteoblast (Kamioka et al., 2001). It has also been suggested that osteocyte-derived exosomes may participate: their release induced by apoptosis can stimulate osteoclastogenesis (Kogianni et al., 2008), and live-cell imaging showed release of microvesicles into the vasculature (Kamel-ElSayed et al., 2015). However, such a mechanism does not overcome the requirement for direct contact between RANKL-producing stromal cells and osteoclast precursors in vitro.

Actions of the osteoblast lineage during the bone remodeling sequence

Osteoblast differentiation is promoted by signals from a range of cell types within the BMU during remodeling. From the perspective of this chapter, it is important to consider the stages of osteoblast differentiation that participate in the remodeling sequence. Of course, their major known function in the bone remodeling sequence is the formation of the appropriate quantity of bone, in response to signals from the bone-resorbing osteoclast, including factors released from the bone matrix or factors produced by the osteoclasts themselves, often termed "coupling factors." Among the many possibilities are CT-1, sphingosine-1-phosphate, Wnt 10b, BMP6, and others (Pederson et al., 2008; Walker et al., 2008; Lotinun et al., 2013; Weske et al., 2018). Osteoclast-derived inhibitors of osteoblast differentiation might also contribute to the outcome. Examples of such inhibitors are Semaphorin 4D (Negishi-Koga et al., 2011), which acts on its receptor Plexin B1 in osteoblastic cells. These factors influence osteoblast precursors, mature matrix-producing osteoblasts, and osteocytes. They are discussed in Chapter 10 and have been described in reviews (Sims and Martin 2014, 2015).

There are additional functions of the osteoblast lineage in remodeling that should also be considered; these are also described in Chapter 10 but are noted briefly here. It has been proposed that the initiation of remodeling may stem from two activities at two different stages of the osteoblast lineage: (1) a signal from osteocytes in response to microdamage within the bone matrix (Schaffler et al., 2014) and (2) the lifting of bone-lining cells to form a canopy over the BMU (Hauge et al., 2001). It has also been proposed that differentiating osteoblast lineage cells on the bone surface are responsible for the duration of the reversal phase (Abdelgawad et al., 2016).

Lessons in osteoblast biology from the Wnt signaling pathway

A major pathway regulating osteoblast differentiation and bone formation identified and defined since 2001 is the Wnt signaling pathway, which modifies bone formation by altering, among other steps, the transcriptional control of

osteoblasts. This new information has had a very great impact on the understanding of control mechanisms within the osteoblast lineage and the development of pharmacological approaches for skeletal fragility. These landmark findings arising out of human genetics are discussed and put into context in detail in Chapters 7 and 8. The implications of these findings for understanding the osteoblast lineage are discussed here.

Wnt signaling is specifically and powerfully inhibited by the action of sclerostin, a protein secreted by osteocytes and encoded by the *SOST* gene. The rare syndromes of skeletal enlargement, sclerosteosis, and van Buchem's disease were discovered to be caused by inactivating mutations in the *SOST* gene (Balemans et al. 2001, 2002). Genetically manipulated mouse models recapitulated the high bone mass observed in the human mutation syndromes (Loots et al., 2005). Within the cell, activation of canonical Wnt signaling leads to stabilization of β-catenin in the cytoplasm through inhibition of glycogen synthase kinase (GSK)-3β-mediated phosphorylation, resulting in accumulation of cytoplasmic β-catenin followed by its translocation to the nucleus and transcription of specific gene targets. Such activation in mesenchymal cells promotes osteoblast activity (Rawadi et al., 2003). Oral delivery of either a small-molecule inhibitor of GSK-3β (Kulkarni et al., 2006) or a less potent inhibitor, lithium chloride (Clement-Lacroix et al., 2005), each enhanced osteoblast differentiation in vitro and increased bone formation, bone mass, and strength in vivo.

It soon became clear that this pathway to control osteoblast differentiation offered appealing therapeutic prospects for the development of anabolic agents. The many possible targets used to increase Wnt/β-catenin signaling included extracellular agonists, inhibition of any of the several extracellular antagonists, and inhibition of GSK-3β. Many of these have been attempted in preclinical experiments, but the chosen approach that is now advanced in clinical development is blockade of sclerostin by treatment with neutralizing antibody.

The effects of the Wnt signaling pathway on bone are not restricted to direct actions on bone matrix production by osteoblasts, however. Mice prepared with a constitutively active β-catenin—and therefore constitutively active Wnt signaling—in the osteoblast lineage surprisingly showed no significant alteration in mature osteoblast numbers; instead the mice had a severe form of osteopetrosis, including failed tooth eruption (Glass et al., 2005). This phenotype appeared to be due to failure of osteoclast formation, caused by increased OPG production by osteoblast lineage cells in which active β-catenin was expressed. A similar osteopetrotic syndrome due to failed osteoclast development and increased OPG was observed in mice lacking the adenomatous polyposis coli protein (APC) in osteoblasts (Holmen et al., 2005). APC acts in a complex of proteins with GSK-3β to maintain the normal degradation of β-catenin. Its absence leads to accumulation of β-catenin, resulting in cell-autonomous activation of Wnt signaling in the osteoblast lineage.

As was predicted, inhibition of production or action of sclerostin resulting in enhanced Wnt canonical signaling led to increased bone mass in preclinical studies (Li et al., 2009; Kramer et al., 2010). In rodents and nonhuman primates, the tissue level mechanism by which anti-sclerostin increases bone is predominantly to promote bone formation on quiescent surfaces—thus a modeling effect. On preresorbed surfaces (remodeling) the amount of new bone formed is greater than that resorbed; this includes bone laid down over quiescent surfaces adjacent to remodeling sites. In the phase II and phase III clinical studies carried out with the humanized monoclonal antibody to sclerostin (romosozumab) (McClung et al., 2014; Cosman et al., 2016), romosozumab recapitulated the rapid increase in bone mineral density that had been seen in preclinical studies. In both clinical studies romosozumab treatment was associated with a transitory increase in the bone formation marker P1NP and a moderate but more sustained decrease in bone resorption markers. The latter effect remains unexplained but could be related to a change in the distribution of cells in the osteoblast lineage population. The profound increase in bone formation may shift the population such that there is a greater proportion of matrix-producing osteoblasts, and the push toward differentiation may lead to a lesser availability of less mature cells that stimulate RANKL production and therefore support osteoclast formation. Alternative explanations could be that Wnt signaling results in sufficient β-catenin activation to promote OPG production (*vide supra*), or that WISP1, induced by Wnt signaling (Holdsworth et al., 2018), inhibits osteoclast formation (Maeda et al., 2015).

The reason for the decrease in bone formation markers after an initial rise poses interesting questions concerning osteocyte/osteoblast interactions. Multiple studies using two different sclerostin antibodies in rats or mice identified a rapid increase in modeling-based bone formation and a transient increase in mineral apposition rate in remodeling sites that was not sustained with continued treatment (Ominsky et al., 2014; Stolina et al., 2014; Nioi et al., 2015; Taylor et al., 2016; Ma et al., 2017). Progressive increases were seen in mRNA levels of Wnt signaling antagonists *Sost* and *Dkk1* in osteoblastic cells, tibiae, and vertebrae. Supporting evidence was recently provided by Holdsworth et al. (Holdsworth et al., 2018), who showed that treatment of mice with anti-sclerostin increased expression in bone of transcripts for antagonists of Wnt signaling, including Sost, Dkk1, Dkk2, WIF1, SFRP2, SFRP4, SFRP5, and FRZB, as well as increased expression of WISP1, which inhibits osteoclast formation (Maeda et al., 2015). Thus, the intriguing possibility has been raised that the transience of anabolic action through sclerostin blockade is the result of self-regulation within the Wnt pathway.

Modulation of the program of osteoblast differentiation can also influence sclerostin expression by the osteoblast lineage. The transcription factor Osterix is absolutely required for osteoblast differentiation and is expressed at early stages of osteoblast commitment (Nakashima et al., 2002). Since sclerostin is expressed by osteoblasts that have reached the osteocytic stage, it was surprising to find that this early osteoblastic transcription factor also binds to the sclerostin promoter, thereby directly stimulating sclerostin expression (Yang et al., 2010). Whether this mechanism plays an important role in continued differentiation of the osteoblast lineage remains to be understood.

These aspects of anti-sclerostin action reveal a complexity of regulation that will undoubtedly be the focus of future attention. Ultimately, activation of Wnt signaling, by whatever means, induces osteoblast differentiation and osteoid formation, but the extent of these effects can be limited by built-in regulation, carried out by later cells of the lineage that produce inhibitors to block further Wnt signaling. They illustrate very well what crucial roles are played in the regulation of bone by cells of the osteoblast lineage; many are new roles revealed in the last 10 years. They draw attention to the fact that the mechanisms involved in sclerostin blockade are new to us, and they illustrate the lack of precision in using the word "osteoblast" as though it is being applied to a group of cells with common properties.

From paracrinology to endocrinology in bone: the secretory osteoblast lineage

The many constituent cells of the osteoblast lineage not only form bone, but also engage in paracrine and juxtacrine signaling among its members, as discussed earlier, as well as with hematopoietic cells in the regulation of osteoclast formation. This makes for a lineage of cells that carry out many functions that extend far beyond the matrix-producing role traditionally ascribed to osteoblasts. These additional functions of osteoblasts include support in physiology of the hematopoietic and immune systems (Calvi et al., 2003). In pathology, the osteoblast lineage also directs how cancer cells are housed, whether having their malignant progression enhanced, as in breast and prostate cancer (Sterling et al., 2011), or inhibited, as in multiple myeloma (Lawson et al., 2015). The osteoblast lineage can also play a central part providing an environment that favors cancer cell dormancy (reviewed in Croucher et al., 2016), in which the large population of lining cells could favor dormancy until changes in local events reawaken malignant cells.

A real surprise came with the realization that the osteoblast lineage also serves as a site of production and secretion of hormones. The first osteoblast lineage endocrine factor identified was FGF23, discovered as responsible for tumor-induced osteomalacia (Yamashita et al., 2000), and with missense mutations causing autosomal dominant hypophosphatemic rickets (Consortium, 2000). Its bone cell of origin was found to be the osteocyte (Liu et al., 2003). Then its hormonal nature was shown: circulating FGF23 acts on the kidney to promote phosphorus excretion and reduce 25(OH)D-1α-hydroxylase expression and hence circulating $1,25(OH)_2D_3$ (Shimada et al., 2004). FGF23 is reviewed in detail in Chapter 64.

Recognition of bone as an endocrine organ (Fukumoto and Martin, 2009) brings with it questions that relate to long-held views of regulatory mechanisms of hormone secretion from endocrine "glands." Usually a specific stimulus, e.g., low calcium for PTH, low glucocorticoid for adrenocorticotropic hormone, results in rapid response secretion of the appropriate hormone. In the case of FGF23, in which the cell source, predominantly osteocytes, is so widely distributed, there must be new endocrine mechanisms by which a need for FGF23 secretion by osteocytes is communicated. A high-phosphate diet increased FGF23 in rats and mice (Perwad et al., 2005), but the mechanism by which this increase occurred is not clear. The substantial increase in FGF23 mRNA and protein production following pharmacological administration of PTH(1−34) was blocked in mice with *Pthr1*-null bones (Fan et al., 2016). Given the evidence for the roles of paracrine PTHrP in osteoblast and osteocyte biology, this would support a view that locally generated PTHrP might regulate FGF23 secretion.

The questions become even more complex in the case of the second bone hormone discovered relatively recently, osteocalcin. Its endocrine role will be considered in detail in Chapter 86. Its direct relevance to this chapter is that it also is a product of the osteoblast lineage, specifically late osteoblasts and early osteocytes, secreted and stored as an abundant component of the bone matrix and with readily assayed circulating levels that can reflect both bone formation and bone resorption.

Osteocalcin is carboxylated at three glutamic acid residues through a vitamin K-dependent process, and is decarboxylated in the acid pH of the bone resorption lacuna to convert GlaOCN (osteocalcin) to GluOCN (undercarboxylated osteocalcin). The latter undercarboxylated and uncarboxylated forms are considered to be the hormonal forms capable of enhancing glucose uptake in muscle, insulin production and cell mass in the pancreatic β-cell, and insulin sensitivity in liver and adipose tissue (Lee et al., 2007; Ferron et al., 2010; Wei et al., 2014; Karsenty and Olson, 2016). These actions are thought to be mediated through the G-protein-coupled receptor family C group 6 member A, GPCR6A (Pi et al., 2011).

Mice with high osteoclast activity levels developed high circulating GluOCN and improved glucose tolerance and insulin sensitivity, while osteoclast suppression was associated with low GluOCN (Lacombe et al., 2013).

The effects of osteocalcin on energy production and utilization were not noted when osteocalcin (*Bglap*)-null mice were first prepared; at that time it was simply surprising to find that there was no striking bone phenotype (Ducy et al. 1996, 1997), although later studies revealed changed bone composition and strength (Boskey et al., 1998). The osteocalcin-null mice were later noted to have larger fat pads and mild hyperglycemia (Lee and Karsenty, 2008). The mice were also noted to breed poorly, and GluOCN was found to enhance male fertility by increasing testosterone production by Leydig cells (Oury et al., 2011). The reproductive role of osteocalcin will also be considered in Chapter 86.

Another feature of the osteocalcin-null mice (Ducy et al., 1997) was a noticeable passivity of behavior that translated into anxiety-like behavior and deficits in memory and learning that could be demonstrated experimentally (Oury et al., 2013). Although GPCR6A was found to be the receptor for osteocalcin in β-cells and myoblasts, the brain actions required a different receptor, since *Gpcr6a*-null mice had none of the behavioral abnormalities of osteocalcin deficiency, and *Gpcr6a* could not be detected at sites of action of osteocalcin in the brain (Khrimian et al., 2017). Rather, genetic experiments indicated that the receptor for osteocalcin in the brain is GPR158. Mice rendered deficient for *Gpr158* exhibited severe cognitive effects that could not be treated by undercarboxylated osteocalcin (Khrimian et al., 2017; Obri et al., 2018).

At the time of writing, these diverse effects of osteocalcin deficiency need confirmation in other species. Complete knockout of osteocalcin in the rat using CRISPR/Cas9 yielded rats with high trabecular thickness and trabecular bone volume, a phenotype not observed in the murine knockout. In addition, although a statistically significant increase in insulin sensitivity was noted in the osteocalcin-null rat, there were no changes in gonadal fat pad weight or body composition (Lambert et al., 2016).

These many effects of uncarboxylated osteocalcin and FGF23 as hormones are fascinating in pointing to an endocrine role for the osteoblast lineage that could never have been predicted. In the case of FGF23 the predominant cell of production is the osteocyte. It is not known whether there are osteocyte subpopulations that preferentially produce FGF23. Whether or not that is the case, FGF23 production is based on a large number of cells that are very widely distributed in the body. To serve as a hormone, mechanisms would be needed to ensure that FGF23 is secreted physiologically in response to signals that come from other organs (endocrine) or from neighboring cells in the same organ (paracrine).

Hormonal osteocalcin presents these same questions and others. Osteocalcin production in the osteoblast lineage is high at later stages of differentiation (e.g., Allan et al., 2003), and is generally regarded as a marker of "late" osteoblasts (Table 4.1). Expression of osteocalcin is also observed in the osteocyte cell line Ocy454 (Spatz et al., 2015), possibly at a lower level than in mature osteoblasts (Ansari et al., 2018). The few studies of osteocalcin localization by in situ hybridization and immunohistochemistry seem to point to either less production in osteocytes than in mature osteoblasts or production restricted to early osteocytes (Weinreb et al., 1990; Ikeda et al., 1992; Zhou et al., 1994). As with FGF23, questions about regulation are raised, such as, what are the immediate signaling mechanisms indicating the need for GluOCN secretion to facilitate energy utilization, reproductive activity, or cognitive activity? If acidification in resorption spaces is an important contributing mechanism, how could the levels be sufficiently tightly regulated for a hormone? Anabolic activity within the osteoblast lineage is associated with increased osteocalcin in the circulation, hence its role as a formation marker as well as a resorption marker, yet how does this modify glucose metabolism and brain function? Answers to these questions could uncover the osteoblast lineage at the center of a new endocrine system and illustrate an even more remarkable diversity in the influence of these cells.

References

Abdelgawad, M.E., Delaisse, J.M., Hinge, M., Jensen, P.R., Alnaimi, R.W., Rolighed, L., Engelholm, L.H., Marcussen, N., Andersen, T.L., 2016. Early reversal cells in adult human bone remodeling: osteoblastic nature, catabolic functions and interactions with osteoclasts. Histochem. Cell Biol. 145 (6), 603−615.

Abe, Y., Akamine, A., Aida, Y., Maeda, K., 1993. Differentiation and mineralization in osteogenic precursor cells derived from fetal rat mandibular bone. Calcif. Tissue Int. 52 (5), 365−371.

Addison, W.N., Masica, D.L., Gray, J.J., McKee, M.D., 2010. Phosphorylation-dependent inhibition of mineralization by osteopontin ASARM peptides is regulated by PHEX cleavage. J. Bone Miner. Res. 25 (4), 695−705.

Ahdjoudj, S., Lasmoles, F., Holy, X., Zerath, E., Marie, P.J., 2002. Transforming growth factor beta2 inhibits adipocyte differentiation induced by skeletal unloading in rat bone marrow stroma. J. Bone Miner. Res. 17 (4), 668−677.

Allan, E.H., Hausler, K.D., Wei, T., Gooi, J.H., Quinn, J.M., Crimeen-Irwin, B., Pompolo, S., Sims, N.A., Gillespie, M.T., Onyia, J.E., Martin, T.J., 2008. EphrinB2 regulation by PTH and PTHrP revealed by molecular profiling in differentiating osteoblasts. J. Bone Miner. Res. 23 (8), 1170−1181.

Allan, E.H., Ho, P.W., Umezawa, A., Hata, J., Makishima, F., Gillespie, M.T., Martin, T.J., 2003. Differentiation potential of a mouse bone marrow stromal cell line. J. Cell. Biochem. 90 (1), 158−169.

Amizuka, N., Karaplis, A.C., Henderson, J.E., Warshawsky, H., Lipman, M.L., Matsuki, Y., Ejiri, S., Tanaka, M., Izumi, N., Ozawa, H., Goltzman, D., 1996. Haploinsufficiency of parathyroid hormone-related peptide (PTHrP) results in abnormal postnatal bone development. Dev. Biol. 175 (1), 166–176.

Ansari, N., Ho, P.W., Crimeen-Irwin, B., Poulton, I.J., Brunt, A.R., Forwood, M.R., Divieti Pajevic, P., Gooi, J.H., Martin, T.J., Sims, N.A., 2018. Autocrine and paracrine regulation of the murine skeleton by osteocyte-derived parathyroid hormone-related protein. J. Bone Miner. Res. 33 (1), 137–153.

Ashton, B.A., Eaglesom, C.C., Bab, I., Owen, M.E., 1984. Distribution of fibroblastic colony-forming cells in rabbit bone marrow and assay of their osteogenic potential by an in vivo diffusion chamber method. Calcif. Tissue Int. 36 (1), 83–86.

Aubin, J.E., 1998. Advances in the osteoblast lineage. Biochem. Cell Biol. 76 (6), 899–910.

Bab, I., Ashton, B.A., Syftestad, G.T., Owen, M.E., 1984. Assessment of an in vivo diffusion chamber method as a quantitative assay for osteogenesis. Calcif. Tissue Int. 36 (1), 77–82.

Balani, D.H., Kronenberg, H.M., 2019. Withdrawal of parathyroid hormone after prolonged administration leads to adipogenic differentiation of mesenchymal precursors in vivo. Bone 118, 16–19.

Balani, D.H., Ono, N., Kronenberg, H.M., 2017. Parathyroid hormone regulates fates of murine osteoblast precursors in vivo. J. Clin. Invest. 127 (9), 3327–3338.

Balemans, W., Ebeling, M., Patel, N., Van Hul, E., Olson, P., Dioszegi, M., Lacza, C., Wuyts, W., Van Den Ende, J., Willems, P., Paes-Alves, A.F., Hill, S., Bueno, M., Ramos, F.J., Tacconi, P., Dikkers, F.G., Stratakis, C., Lindpaintner, K., Vickery, B., Foernzler, D., Van Hul, W., 2001. Increased bone density in sclerosteosis is due to the deficiency of a novel secreted protein (SOST). Hum. Mol. Genet. 10 (5), 537–543.

Balemans, W., Patel, N., Ebeling, M., Van Hul, E., Wuyts, W., Lacza, C., Dioszegi, M., Dikkers, F.G., Hildering, P., Willems, P.J., Verheij, J.B., Lindpaintner, K., Vickery, B., Foernzler, D., Van Hul, W., 2002. Identification of a 52 kb deletion downstream of the SOST gene in patients with van Buchem disease. J. Med. Genet. 39 (2), 91–97.

Barak, Y., Nelson, M.C., Ong, E.S., Jones, Y.Z., Ruiz-Lozano, P., Chien, K.R., Koder, A., Evans, R.M., 1999. PPAR gamma is required for placental, cardiac, and adipose tissue development. Mol. Cell. 4 (4), 585–595.

Bellido, T., Borba, V.Z., Roberson, P., Manolagas, S.C., 1997. Activation of the Janus kinase/STAT (signal transducer and activator of transcription) signal transduction pathway by interleukin-6-type cytokines promotes osteoblast differentiation. Endocrinology 138 (9), 3666–3676.

Bianco, P., Robey, P.G., Saggio, I., Riminucci, M., 2010. Mesenchymal" stem cells in human bone marrow (skeletal stem cells): a critical discussion of their nature, identity, and significance in incurable skeletal disease. Hum. Gene Ther. 21 (9), 1057–1066.

Bianco, P., Robey, P.G., Simmons, P.J., 2008. Mesenchymal stem cells: revisiting history, concepts, and assays. Cell Stem Cell 2 (4), 313–319.

Boivin, G., Meunier, P.J., 2002. The degree of mineralization of bone tissue measured by computerized quantitative contact microradiography. Calcif. Tissue Int. 70 (6), 503–511.

Bonewald, L.F., 2011. The amazing osteocyte. J. Bone Miner. Res. 26 (2), 229–238.

Bonewald, L.F., Johnson, M.L., 2008. Osteocytes, mechanosensing and Wnt signaling. Bone 42 (4), 606–615.

Boskey, A.L., 2013. Bone composition: relationship to bone fragility and antiosteoporotic drug effects. Bonekey Rep. 2, 447.

Boskey, A.L., Gadaleta, S., Gundberg, C., Doty, S.B., Ducy, P., Karsenty, G., 1998. Fourier transform infrared microspectroscopic analysis of bones of osteocalcin-deficient mice provides insight into the function of osteocalcin. Bone 23 (3), 187–196.

Boyle, W.J., Simonet, W.S., Lacey, D.L., 2003. Osteoclast differentiation and activation. Nature 423 (6937), 337–342.

Brighton, C.T., Lorich, D.G., Kupcha, R., Reilly, T.M., Jones, A.R., Woodbury 2nd, R.A., 1992. The pericyte as a possible osteoblast progenitor cell. Clin. Orthop. Relat. Res. 275, 287–299.

Buenzli, P.R., Sims, N.A., 2015. Quantifying the osteocyte network in the human skeleton. Bone 75, 144–150.

Calvi, L.M., Adams, G.B., Weibrecht, K.W., Weber, J.M., Olson, D.P., Knight, M.C., Martin, R.P., Schipani, E., Divieti, P., Bringhurst, F.R., Milner, L.A., Kronenberg, H.M., Scadden, D.T., 2003. Osteoblastic cells regulate the haematopoietic stem cell niche. Nature 425 (6960), 841–846.

Chan, G.K., Deckelbaum, R.A., Bolivar, I., Goltzman, D., Karaplis, A.C., 2001. PTHrP inhibits adipocyte differentiation by down-regulating PPAR gamma activity via a MAPK-dependent pathway. Endocrinology 142 (11), 4900–4909.

Chen, J., Shapiro, H.S., Sodek, J., 1992. Development expression of bone sialoprotein mRNA in rat mineralized connective tissues. J. Bone Miner. Res. 7 (8), 987–997.

Chia, L.Y., Walsh, N.C., Martin, T.J., Sims, N.A., 2015. Isolation and gene expression of haematopoietic-cell-free preparations of highly purified murine osteocytes. Bone 72, 34–42.

Clement-Lacroix, P., Ai, M., Morvan, F., Roman-Roman, S., Vayssiere, B., Belleville, C., Estrera, K., Warman, M.L., Baron, R., Rawadi, G., 2005. Lrp5-independent activation of Wnt signaling by lithium chloride increases bone formation and bone mass in mice. Proc. Natl. Acad. Sci. U. S. A. 102 (48), 17406–17411.

Consortium, A., 2000. Autosomal dominant hypophosphataemic rickets is associated with mutations in FGF23. Nat. Genet. 26 (3), 345–348.

Cornish, J., Callon, K., King, A., Edgar, S., Reid, I.R., 1993. The effect of leukemia inhibitory factor on bone in vivo. Endocrinology 132 (3), 1359–1366.

Cosman, F., Crittenden, D., Adachi, J., Binkley, N., Czerwinski, E., Ferrari, S., Hofbauer, L., Lau, E., Lewiecki, E., Miyauchi, A., Zerbin, C., Milmont, C., Chen, L., Maddox, J., PD, M., Libanati, C., Grauer, A., 2016. Romosozumab treatment in postmenopausal women with osteoporosis. N. Engl. J. Med. https://doi.org/10.1056/NEJMoa1607948.

Crawford, A., Atkins, D., Martin, T.J., 1978. Rat osteogenic sarcoma cells: comparison of the effects of prostaglandins E1, E2, I2 (prostacyclin), 6-keto F1alpha and thromboxane B2 on cyclic AMP production and adenylate cyclase activity. Biochem. Biophys. Res. Commun. 82 (4), 1195–1201.

Croucher, P.I., McDonald, M.M., Martin, T.J., 2016. Bone metastasis: the importance of the neighbourhood. Nat. Rev. Canc. 16 (6), 373–386.

da Silva Meirelles, L., Chagastelles, P.C., Nardi, N.B., 2006. Mesenchymal stem cells reside in virtually all post-natal organs and tissues. J. Cell Sci. 119 (Pt 11), 2204–2213.

Dalby, M.J., McCloy, D., Robertson, M., Wilkinson, C.D., Oreffo, R.O., 2006. Osteoprogenitor response to defined topographies with nanoscale depths. Biomaterials 27 (8), 1306–1315.

Dellavalle, A., Sampaolesi, M., Tonlorenzi, R., Tagliafico, E., Sacchetti, B., Perani, L., Innocenzi, A., Galvez, B.G., Messina, G., Morosetti, R., Li, S., Belicchi, M., Peretti, G., Chamberlain, J.S., Wright, W.E., Torrente, Y., Ferrari, S., Bianco, P., Cossu, G., 2007. Pericytes of human skeletal muscle are myogenic precursors distinct from satellite cells. Nat. Cell Biol. 9 (3), 255–267.

Dobnig, H., Turner, R.T., 1995. Evidence that intermittent treatment with parathyroid hormone increases bone formation in adult rats by activation of bone lining cells. Endocrinology 136 (8), 3632–3638.

Doherty, M.J., Ashton, B.A., Walsh, S., Beresford, J.N., Grant, M.E., Canfield, A.E., 1998. Vascular pericytes express osteogenic potential in vitro and in vivo. J. Bone Miner. Res. 13 (5), 828–838.

Dominici, M., Le Blanc, K., Mueller, I., Slaper-Cortenbach, I., Marini, F., Krause, D., Deans, R., Keating, A., Prockop, D., Horwitz, E., 2006. Minimal criteria for defining multipotent mesenchymal stromal cells. The International Society for Cellular Therapy position statement. Cytotherapy 8 (4), 315–317.

Doty, S.B., 1981. Morphological evidence of gap junctions between bone cells. Calcif. Tissue Int. 33 (5), 509–512.

Ducy, P., Desbois, C., Boyce, B., Pinero, G., Story, B., Dunstan, C., Smith, E., Bonadio, J., Goldstein, S., Gundberg, C., Bradley, A., Karsenty, G., 1996. Increased bone formation in osteocalcin-deficient mice. Nature 382 (6590), 448–452.

Ducy, P., Zhang, R., Geoffroy, V., Ridall, A.L., Karsenty, G., 1997. Osf2/Cbfa1: a transcriptional activator of osteoblast differentiation. Cell 89 (5), 747–754.

Ecarot-Charrier, B., Glorieux, F.H., van der Rest, M., Pereira, G., 1983. Osteoblasts isolated from mouse calvaria initiate matrix mineralization in culture. J. Cell Biol. 96 (3), 639–643.

Enomoto, H., Enomoto-Iwamoto, M., Iwamoto, M., Nomura, S., Himeno, M., Kitamura, Y., Kishimoto, T., Komori, T., 2000. Cbfa1 is a positive regulatory factor in chondrocyte maturation. J. Biol. Chem. 275 (12), 8695–8702.

Fan, Y., Bi, R., Densmore, M.J., Sato, T., Kobayashi, T., Yuan, Q., Zhou, X., Erben, R.G., Lanske, B., 2016. Parathyroid hormone 1 receptor is essential to induce FGF23 production and maintain systemic mineral ion homeostasis. FASEB J. 30 (1), 428–440.

Fan, Y., Hanai, J.-i., Le, P.T., Bi, R., Maridas, D., DeMambro, V., Figueroa, C.A., Kir, S., Zhou, X., Mannstadt, M., Baron, R., Bronson, R.T., Horowitz, M.C., Wu, J.Y., Bilezikian, J.P., Dempster, D.W., Rosen, C.J., Lanske, B., 2017. Parathyroid hormone directs bone marrow mesenchymal cell fate. Cell Metabol. 25 (3), 661–672.

Ferron, M., Wei, J., Yoshizawa, T., Del Fattore, A., DePinho, R.A., Teti, A., Ducy, P., Karsenty, G., 2010. Insulin signaling in osteoblasts integrates bone remodeling and energy metabolism. Cell 142 (2), 296–308.

Friedenstein, A.J., 1976. Precursor cells of mechanocytes. Int. Rev. Cytol. 47, 327–359.

Fuchs, R.K., Allen, M.R., Ruppel, M.E., Diab, T., Phipps, R.J., Miller, L.M., Burr, D.B., 2008. In situ examination of the time-course for secondary mineralization of Haversian bone using synchrotron Fourier transform infrared microspectroscopy. Matrix Biol. 27 (1), 34–41.

Fujisaki, J., Wu, J., Carlson, A.L., Silberstein, L., Putheti, P., Larocca, R., Gao, W., Saito, T.I., Lo Celso, C., Tsuyuzaki, H., Sato, T., Cote, D., Sykes, M., Strom, T.B., Scadden, D.T., Lin, C.P., 2011. In vivo imaging of Treg cells providing immune privilege to the haematopoietic stem-cell niche. Nature 474 (7350), 216–219.

Fukumoto, S., Martin, T.J., 2009. Bone as an endocrine organ. Trends Endocrinol. Metabol. 20 (5), 230–236.

Fumoto, T., Takeshita, S., Ito, M., Ikeda, K., 2013. Physiological functions of osteoblast lineage and T cell-derived RANKL in bone homeostasis. J. Bone Miner. Res.

Galea, G.L., Sunters, A., Meakin, L.B., Zaman, G., Sugiyama, T., Lanyon, L.E., Price, J.S., 2011. Sost down-regulation by mechanical strain in human osteoblastic cells involves PGE2 signaling via EP4. FEBS Lett. 585 (15), 2450–2454.

Genet, F., Kulina, I., Vaquette, C., Torossian, F., Millard, S., Pettit, A.R., Sims, N.A., Anginot, A., Guerton, B., Winkler, I.G., Barbier, V., Lataillade, J.J., Le Bousse-Kerdiles, M.C., Hutmacher, D.W., Levesque, J.P., 2015. Neurological heterotopic ossification following spinal cord injury is triggered by macrophage-mediated inflammation in muscle. J. Pathol. 236 (2), 229–240.

Genetos, D.C., Yellowley, C.E., Loots, G.G., 2011. Prostaglandin E2 signals through PTGER2 to regulate sclerostin expression. PLoS One 6 (3), e17772.

Giraud-Guille, M.M., 1988. Twisted plywood architecture of collagen fibrils in human compact bone osteons. Calcif. Tissue Int. 42 (3), 167–180.

Glass 2nd, D.A., Bialek, P., Ahn, J.D., Starbuck, M., Patel, M.S., Clevers, H., Taketo, M.M., Long, F., McMahon, A.P., Lang, R.A., Karsenty, G., 2005. Canonical Wnt signaling in differentiated osteoblasts controls osteoclast differentiation. Dev. Cell 8 (5), 751–764.

Glimcher, M.G., 1998. The Nature of the Mineral Phase in Bone: Biological and Clinical Implications. Academic Press, San Diego, CA.

Gray, C., Boyde, A., Jones, S.J., 1996. Topographically induced bone formation in vitro: implications for bone implants and bone grafts. Bone 18 (2), 115–123.

Gutierrez, S., Javed, A., Tennant, D.K., van Rees, M., Montecino, M., Stein, G.S., Stein, J.L., Lian, J.B., 2002. CCAAT/enhancer-binding proteins (C/EBP) beta and delta activate osteocalcin gene transcription and synergize with Runx2 at the C/EBP element to regulate bone-specific expression. J. Biol. Chem. 277 (2), 1316–1323.

Hauge, E.M., Qvesel, D., Eriksen, E.F., Mosekilde, L., Melsen, F., 2001. Cancellous bone remodeling occurs in specialized compartments lined by cells expressing osteoblastic markers. J. Bone Miner. Res. 16 (9), 1575–1582.

Holdsworth, G., Greenslade, K., Jose, J., Stencel, Z., Kirby, H., Moore, A., Ke, H.Z., Robinson, M.K., 2018. Dampening of the bone formation response following repeat dosing with sclerostin antibody in mice is associated with up-regulation of Wnt antagonists. Bone 107, 93–103.

Holm, E., Aubin, J.E., Hunter, G.K., Beier, F., Goldberg, H.A., 2015. Loss of bone sialoprotein leads to impaired endochondral bone development and mineralization. Bone 71, 145–154.

Holmen, S.L., Zylstra, C.R., Mukherjee, A., Sigler, R.E., Faugere, M.C., Bouxsein, M.L., Deng, L., Clemens, T.L., Williams, B.O., 2005. Essential role of beta-catenin in postnatal bone acquisition. J. Biol. Chem. 280 (22), 21162–21168.

Horwood, N.J., Kartsogiannis, V., Quinn, J.M., Romas, E., Martin, T.J., Gillespie, M.T., 1999. Activated T lymphocytes support osteoclast formation in vitro. Biochem. Biophys. Res. Commun. 265 (1), 144–150.

Hosaki-Takamiya, R., Hashimoto, M., Imai, Y., Nishida, T., Yamada, N., Mori, H., Tanaka, T., Kawanabe, N., Yamashiro, T., Kamioka, H., 2016. Collagen production of osteoblasts revealed by ultra-high voltage electron microscopy. J. Bone Miner. Metabol. 34 (5), 491–499.

Hozumi, A., Osaki, M., Goto, H., Sakamoto, K., Inokuchi, S., Shindo, H., 2009. Bone marrow adipocytes support dexamethasone-induced osteoclast differentiation. Biochem. Biophys. Res. Commun. 382 (4), 780–784.

Igarashi, M., Kamiya, N., Ito, K., Takagi, M., 2002. In situ localization and in vitro expression of osteoblast/osteocyte factor 45 mRNA during bone cell differentiation. Histochem. J. 34 (5), 255–263.

Ikeda, T., Nomura, S., Yamaguchi, A., Suda, T., Yoshiki, S., 1992. In situ hybridization of bone matrix proteins in undecalcified adult rat bone sections. J. Histochem. Cytochem. 40 (8), 1079–1088.

Inada, M., Yasui, T., Nomura, S., Miyake, S., Deguchi, K., Himeno, M., Sato, M., Yamagiwa, H., Kimura, T., Yasui, N., Ochi, T., Endo, N., Kitamura, Y., Kishimoto, T., Komori, T., 1999. Maturational disturbance of chondrocytes in Cbfa1-deficient mice. Dev. Dynam. 214 (4), 279–290.

Johnson, R.W., Brennan, H.J., Vrahnas, C., Poulton, I.J., McGregor, N.E., Standal, T., Walker, E.C., Koh, T.T., Nguyen, H., Walsh, N.C., Forwood, M.R., Martin, T.J., Sims, N.A., 2014. The primary function of gp130 signaling in osteoblasts is to maintain bone formation and strength, rather than promote osteoclast formation. J. Bone Miner. Res. 29 (6), 1492–1505.

Jones, S.J., Boyde, A., 1976. Experimental study of changes in osteoblastic shape induced by calcitonin and parathyroid extract in an organ culture system. Cell Tissue Res. 169 (4), 499-465.

Justesen, J., Stenderup, K., Ebbesen, E.N., Mosekilde, L., Steiniche, T., Kassem, M., 2001. Adipocyte tissue volume in bone marrow is increased with aging and in patients with osteoporosis. Biogerontology 2 (3), 165–171.

Kalajzic, I., Staal, A., Yang, W.P., Wu, Y., Johnson, S.E., Feyen, J.H., Krueger, W., Maye, P., Yu, F., Zhao, Y., Kuo, L., Gupta, R.R., Achenie, L.E., Wang, H.W., Shin, D.G., Rowe, D.W., 2005. Expression profile of osteoblast lineage at defined stages of differentiation. J. Biol. Chem. 280 (26), 24618–24626.

Kalajzic, Z., Li, H., Wang, L.P., Jiang, X., Lamothe, K., Adams, D.J., Aguila, H.L., Rowe, D.W., Kalajzic, I., 2008. Use of an alpha-smooth muscle actin GFP reporter to identify an osteoprogenitor population. Bone 43 (3), 501–510.

Kamel-ElSayed, S.A., Tiede-Lewis, L.M., Lu, Y., Veno, P.A., Dallas, S.L., 2015. Novel approaches for two and three dimensional multiplexed imaging of osteocytes. Bone 76, 129–140.

Kamioka, H., Honjo, T., Takano-Yamamoto, T., 2001. A three-dimensional distribution of osteocyte processes revealed by the combination of confocal laser scanning microscopy and differential interference contrast microscopy. Bone 28 (2), 145–149.

Karsenty, G., Olson, E.N., 2016. Bone and muscle endocrine functions: unexpected paradigms of inter-organ communication. Cell 164 (6), 1248–1256.

Kartsogiannis, V., Zhou, H., Horwood, N.J., Thomas, R.J., Hards, D.K., Quinn, J.M., Niforas, P., Ng, K.W., Martin, T.J., Gillespie, M.T., 1999. Localization of RANKL (receptor activator of NF kappa B ligand) mRNA and protein in skeletal and extraskeletal tissues. Bone 25 (5), 525–534.

Keller, H., Kneissel, M., 2005. SOST is a target gene for PTH in bone. Bone 37 (2), 148–158.

Kelly, K.A., Tanaka, S., Baron, R., Gimble, J.M., 1998. Murine bone marrow stromally derived BMS2 adipocytes support differentiation and function of osteoclast-like cells in vitro. Endocrinology 139 (4), 2092–2101.

Khrimian, L., Obri, A., Ramos-Brossier, M., Rousseaud, A., Moriceau, S., Nicot, A.S., Mera, P., Kosmidis, S., Karnavas, T., Saudou, F., Gao, X.B., Oury, F., Kandel, E., Karsenty, G., 2017. Gpr158 mediates osteocalcin's regulation of cognition. J. Exp. Med. 214 (10), 2859–2873.

Kim, I.S., Otto, F., Zabel, B., Mundlos, S., 1999. Regulation of chondrocyte differentiation by Cbfa1. Mech. Dev. 80 (2), 159–170.

Kim, S.W., Lu, Y., Williams, E.A., Lai, F., Lee, J.Y., Enishi, T., Balani, D.H., Ominsky, M.S., Ke, H.Z., Kronenberg, H.M., Wein, M.N., 2017. Sclerostin antibody administration converts bone lining cells into active osteoblasts. J. Bone Miner. Res. 32 (5), 892–901.

Kim, S.W., Pajevic, P.D., Selig, M., Barry, K.J., Yang, J.Y., Shin, C.S., Baek, W.Y., Kim, J.E., Kronenberg, H.M., 2012. Intermittent parathyroid hormone administration converts quiescent lining cells to active osteoblasts. J. Bone Miner. Res. 27 (10), 2075–2084.

Kogianni, G., Mann, V., Noble, B.S., 2008. Apoptotic bodies convey activity capable of initiating osteoclastogenesis and localized bone destruction. J. Bone Miner. Res. 23 (6), 915–927.

Komori, T., 2018. Runx2, an inducer of osteoblast and chondrocyte differentiation. Histochem. Cell Biol. 149 (4), 313–323.

Komori, T., Yagi, H., Nomura, S., Yamaguchi, A., Sasaki, K., Deguchi, K., Shimizu, Y., Bronson, R.T., Gao, Y.H., Inada, M., Sato, M., Okamoto, R., Kitamura, Y., Yoshiki, S., Kishimoto, T., 1997. Targeted disruption of Cbfa1 results in a complete lack of bone formation owing to maturational arrest of osteoblasts. Cell 89 (5), 755–764.

Kramer, I., Halleux, C., Keller, H., Pegurri, M., Gooi, J.H., Weber, P.B., Feng, J.Q., Bonewald, L.F., Kneissel, M., 2010. Osteocyte Wnt/beta-catenin signaling is required for normal bone homeostasis. Mol. Cell Biol. 30 (12), 3071–3085.

Kulkarni, N.H., Onyia, J.E., Zeng, Q., Tian, X., Liu, M., Halladay, D.L., Frolik, C.A., Engler, T., Wei, T., Kriauciunas, A., Martin, T.J., Sato, M., Bryant, H.U., Ma, Y.L., 2006. Orally bioavailable GSK-3alpha/beta dual inhibitor increases markers of cellular differentiation in vitro and bone mass in vivo. J. Bone Miner. Res. 21 (6), 910–920.

Lacombe, J., Karsenty, G., Ferron, M., 2013. In vivo analysis of the contribution of bone resorption to the control of glucose metabolism in mice. Mol Metab 2 (4), 498–504.

Lambert, L.J., Challa, A.K., Niu, A., Zhou, L., Tucholski, J., Johnson, M.S., Nagy, T.R., Eberhardt, A.W., Estep, P.N., Kesterson, R.A., Grams, J.M., 2016. Increased trabecular bone and improved biomechanics in an osteocalcin-null rat model created by CRISPR/Cas9 technology. Dis Model Mech 9 (10), 1169−1179.

Lawson, M.A., McDonald, M.M., Kovacic, N., Hua Khoo, W., Terry, R.L., Down, J., Kaplan, W., Paton-Hough, J., Fellows, C., Pettitt, J.A., Neil Dear, T., Van Valckenborgh, E., Baldock, P.A., Rogers, M.J., Eaton, C.L., Vanderkerken, K., Pettit, A.R., Quinn, J.M., Zannettino, A.C., Phan, T.G., Croucher, P.I., 2015. Osteoclasts control reactivation of dormant myeloma cells by remodelling the endosteal niche. Nat. Commun. 6, 8983.

Leblond, C.P., 1989. Synthesis and secretion of collagen by cells of connective tissue, bone, and dentin. Anat. Rec. 224 (2), 123−138.

Lee, N.K., Karsenty, G., 2008. Reciprocal regulation of bone and energy metabolism. Trends Endocrinol. Metabol. 19 (5), 161−166.

Lee, N.K., Sowa, H., Hinoi, E., Ferron, M., Ahn, J.D., Confavreux, C., Dacquin, R., Mee, P.J., McKee, M.D., Jung, D.Y., Zhang, Z., Kim, J.K., Mauvais-Jarvis, F., Ducy, P., Karsenty, G., 2007. Endocrine regulation of energy metabolism by the skeleton. Cell 130 (3), 456−469.

Li, H., Jiang, X., Delaney, J., Franceschetti, T., Bilic-Curcic, I., Kalinovsky, J., Lorenzo, J.A., Grcevic, D., Rowe, D.W., Kalajzic, I., 2010. Immature osteoblast lineage cells increase osteoclastogenesis in osteogenesis imperfecta murine. Am. J. Pathol. 176 (5), 2405−2413.

Li, X., Ominsky, M.S., Warmington, K.S., Morony, S., Gong, J., Cao, J., Gao, Y., Shalhoub, V., Tipton, B., Haldankar, R., Chen, Q., Winters, A., Boone, T., Geng, Z., Niu, Q.T., Ke, H.Z., Kostenuik, P.J., Simonet, W.S., Lacey, D.L., Paszty, C., 2009. Sclerostin antibody treatment increases bone formation, bone mass, and bone strength in a rat model of postmenopausal osteoporosis. J. Bone Miner. Res. 24 (4), 578−588.

Liu, S., Guo, R., Simpson, L.G., Xiao, Z.S., Burnham, C.E., Quarles, L.D., 2003. Regulation of fibroblastic growth factor 23 expression but not degradation by PHEX. J. Biol. Chem. 278 (39), 37419−37426.

Livesey, S.A., Kemp, B.E., Re, C.A., Partridge, N.C., Martin, T.J., 1982. Selective hormonal activation of cyclic AMP-dependent protein kinase isoenzymes in normal and malignant osteoblasts. J. Biol. Chem. 257 (24), 14983−14987.

Loots, G.G., Kneissel, M., Keller, H., Baptist, M., Chang, J., Collette, N.M., Ovcharenko, D., Plajzer-Frick, I., Rubin, E.M., 2005. Genomic deletion of a long-range bone enhancer misregulates sclerostin in Van Buchem disease. Genome Res. 15 (7), 928−935.

Lotinun, S., Kiviranta, R., Matsubara, T., Alzate, J.A., Neff, L., Luth, A., Koskivirta, I., Kleuser, B., Vacher, J., Vuorio, E., Horne, W.C., Baron, R., 2013. Osteoclast-specific cathepsin K deletion stimulates S1P-dependent bone formation. J. Clin. Invest. 123 (2), 666−681.

Luben, R.A., Wong, G.L., Cohn, D.V., 1976. Biochemical characterization with parathormone and calcitonin of isolated bone cells: provisional identification of osteoclasts and osteoblasts. Endocrinology 99 (2), 526−534.

Lundberg, P., Allison, S.J., Lee, N.J., Baldock, P.A., Brouard, N., Rost, S., Enriquez, R.F., Sainsbury, A., Lamghari, M., Simmons, P., Eisman, J.A., Gardiner, E.M., Herzog, H., 2007. Greater bone formation of Y2 knockout mice is associated with increased osteoprogenitor numbers and altered Y1 receptor expression. J. Biol. Chem. 282 (26), 19082−19091.

Ma, Y.L., Hamang, M., Lucchesi, J., Bivi, N., Zeng, Q., Adrian, M.D., Raines, S.E., Li, J., Kuhstoss, S.A., Obungu, V., Bryant, H.U., Krishnan, V., 2017. Time course of disassociation of bone formation signals with bone mass and bone strength in sclerostin antibody treated ovariectomized rats. Bone 97, 20−28.

Maeda, A., Ono, M., Holmbeck, K., Li, L., Kilts, T.M., Kram, V., Noonan, M.L., Yoshioka, Y., McNerny, E.M., Tantillo, M.A., Kohn, D.H., Lyons, K.M., Robey, P.G., Young, M.F., 2015. WNT1-induced secreted protein-1 (WISP1), a novel regulator of bone turnover and Wnt signaling. J. Biol. Chem. 290 (22), 14004−14018.

Majeska, R.J., Rodan, S.B., Rodan, G.A., 1980. Parathyroid hormone-responsive clonal cell lines from rat osteosarcoma. Endocrinology 107 (5), 1494−1503.

Manolagas, S.C., 2000. Birth and death of bone cells: basic regulatory mechanisms and implications for the pathogenesis and treatment of osteoporosis. Endocr. Rev. 21 (2), 115−137.

Mantila Roosa, S.M., Liu, Y., Turner, C.H., 2011. Gene expression patterns in bone following mechanical loading. J. Bone Miner. Res. 26 (1), 100−112.

Martin, R.B., Chow, B.D., Lucas, P.A., 1990. Bone marrow fat content in relation to bone remodeling and serum chemistry in intact and ovariectomized dogs. Calcif. Tissue Int. 46 (3), 189−194.

Matic, I., Matthews, B.G., Wang, X., Dyment, N.A., Worthley, D.L., Rowe, D.W., Grcevic, D., Kalajzic, I., 2016. Quiescent bone lining cells are a major source of osteoblasts during adulthood. Stem Cell. 34 (12), 2930−2942.

McClung, M.R., Grauer, A., Boonen, S., Bolognese, M.A., Brown, J.P., Diez-Perez, A., Langdahl, B.L., Reginster, J.Y., Zanchetta, J.R., Wasserman, S.M., Katz, L., Maddox, J., Yang, Y.C., Libanati, C., Bone, H.G., 2014. Romosozumab in postmenopausal women with low bone mineral density. N. Engl. J. Med. 370 (5), 412−420.

McGregor, N.E., Murat, M., Elango, J., Poulton, I.J., Walker, E.C., Crimeen-Irwin, B., Ho, P.W.M., Gooi, J.H., Martin, T.J., Sims, N.A., 2019. IL-6 exhibits both *cis* and *trans* signaling in osteocytes and osteoblasts, but only *trans* signaling promotes bone formation and osteoclastogenesis. J. Biol. Chem. In Press. 10.1074/jbc.RA119.008074.

Miao, D., He, B., Jiang, Y., Kobayashi, T., Soroceanu, M.A., Zhao, J., Su, H., Tong, X., Amizuka, N., Gupta, A., Genant, H.K., Kronenberg, H.M., Goltzman, D., Karaplis, A.C., 2005. Osteoblast-derived PTHrP is a potent endogenous bone anabolic agent that modifies the therapeutic efficacy of administered PTH 1-34. J. Clin. Invest. 115 (9), 2402−2411.

Miller, S.C., Jee, W.S., 1987. The bone lining cell: a distinct phenotype? Calcif. Tissue Int. 41 (1), 1−5.

Modder, U.I., Khosla, S., 2008. Skeletal stem/osteoprogenitor cells: current concepts, alternate hypotheses, and relationship to the bone remodeling compartment. J. Cell. Biochem. 103 (2), 393−400.

Nakashima, K., Zhou, X., Kunkel, G., Zhang, Z., Deng, J.M., Behringer, R.R., de Crombrugghe, B., 2002. The novel zinc finger-containing transcription factor osterix is required for osteoblast differentiation and bone formation. Cell 108 (1), 17−29.

Nakashima, T., Hayashi, M., Fukunaga, T., Kurata, K., Oh-Hora, M., Feng, J.Q., Bonewald, L.F., Kodama, T., Wutz, A., Wagner, E.F., Penninger, J.M., Takayanagi, H., 2011. Evidence for osteocyte regulation of bone homeostasis through RANKL expression. Nat. Med. 17 (10), 1231−1234.

Negishi-Koga, T., Shinohara, M., Komatsu, N., Bito, H., Kodama, T., Friedel, R.H., Takayanagi, H., 2011. Suppression of bone formation by osteoclastic expression of semaphorin 4D. Nat. Med. 17 (11), 1473−1480.

Nioi, P., Taylor, S., Hu, R., Pacheco, E., He, Y.D., Hamadeh, H., Paszty, C., Pyrah, I., Ominsky, M.S., Boyce, R.W., 2015. Transcriptional profiling of laser capture microdissected subpopulations of the osteoblast lineage provides insight into the early response to sclerostin antibody in rats. J. Bone Miner. Res. 30 (8), 1457−1467.

Nishimura, R., Wakabayashi, M., Hata, K., Matsubara, T., Honma, S., Wakisaka, S., Kiyonari, H., Shioi, G., Yamaguchi, A., Tsumaki, N., Akiyama, H., Yoneda, T., 2012. Osterix regulates calcification and degradation of chondrogenic matrices through matrix metalloproteinase 13 (MMP13) expression in association with transcription factor Runx2 during endochondral ossification. J. Biol. Chem. 287 (40), 33179−33190.

Obri, A., Khrimian, L., Karsenty, G., Oury, F., 2018. Osteocalcin in the brain: from embryonic development to age-related decline in cognition. Nat. Rev. Endocrinol. 14 (3), 174−182.

Ominsky, M.S., Niu, Q.T., Li, C., Li, X., Ke, H.Z., 2014. Tissue-level mechanisms responsible for the increase in bone formation and bone volume by sclerostin antibody. J. Bone Miner. Res. 29 (6), 1424−1430.

Orriss, I.R., Hajjawi, M.O., Huesa, C., MacRae, V.E., Arnett, T.R., 2014. Optimisation of the differing conditions required for bone formation in vitro by primary osteoblasts from mice and rats. Int. J. Mol. Med. 34 (5), 1201−1208.

Otsuru, S., Tamai, K., Yamazaki, T., Yoshikawa, H., Kaneda, Y., 2008. Circulating bone marrow-derived osteoblast progenitor cells are recruited to the bone-forming site by the CXCR4/stromal cell-derived factor-1 pathway. Stem Cell. 26 (1), 223−234.

Otto, F., Thornell, A.P., Crompton, T., Denzel, A., Gilmour, K.C., Rosewell, I.R., Stamp, G.W., Beddington, R.S., Mundlos, S., Olsen, B.R., Selby, P.B., Owen, M.J., 1997. Cbfa1, a candidate gene for cleidocranial dysplasia syndrome, is essential for osteoblast differentiation and bone development. Cell 89 (5), 765−771.

Oury, F., Khrimian, L., Denny, C.A., Gardin, A., Chamouni, A., Goeden, N., Huang, Y.Y., Lee, H., Srinivas, P., Gao, X.B., Suyama, S., Langer, T., Mann, J.J., Horvath, T.L., Bonnin, A., Karsenty, G., 2013. Maternal and offspring pools of osteocalcin influence brain development and functions. Cell 155 (1), 228−241.

Oury, F., Sumara, G., Sumara, O., Ferron, M., Chang, H., Smith, C.E., Hermo, L., Suarez, S., Roth, B.L., Ducy, P., Karsenty, G., 2011. Endocrine regulation of male fertility by the skeleton. Cell 144 (5), 796−809.

Owen, M., Friedenstein, A.J., 1988. Stromal stem cells: marrow-derived osteogenic precursors. Ciba Found. Symp. 136, 42−60.

Paic, F., Igwe, J.C., Nori, R., Kronenberg, M.S., Franceschetti, T., Harrington, P., Kuo, L., Shin, D.G., Rowe, D.W., Harris, S.E., Kalajzic, I., 2009. Identification of differentially expressed genes between osteoblasts and osteocytes. Bone 45 (4), 682−692.

Palmqvist, P., Persson, E., Conaway, H.H., Lerner, U.H., 2002. IL-6, leukemia inhibitory factor, and oncostatin M stimulate bone resorption and regulate the expression of receptor activator of NF-kappa B ligand, osteoprotegerin, and receptor activator of NF-kappa B in mouse calvariae. J. Immunol. 169 (6), 3353−3362.

Partridge, N.C., Alcorn, D., Michelangeli, V.P., Ryan, G., Martin, T.J., 1983. Morphological and biochemical characterization of four clonal osteogenic sarcoma cell lines of rat origin. Cancer Res. 43 (9), 4308−4314.

Partridge, N.C., Kemp, B.E., Livesey, S.A., Martin, T.J., 1982. Activity ratio measurements reflect intracellular activation of adenosine 3',5'-monophosphate-dependent protein kinase in osteoblasts. Endocrinology 111 (1), 178−183.

Partridge, N.C., Kemp, B.E., Veroni, M.C., Martin, T.J., 1981. Activation of adenosine 3',5'-monophosphate-dependent protein kinase in normal and malignant bone cells by parathyroid hormone, prostaglandin E2, and prostacyclin. Endocrinology 108 (1), 220−225.

Paschalis, E.P., Shane, E., Lyritis, G., Skarantavos, G., Mendelsohn, R., Boskey, A.L., 2004. Bone fragility and collagen cross-links. J. Bone Miner. Res. 19 (12), 2000−2004.

Peck, W.A., Birge Jr., S.J., Fedak, S.A., 1964. Bone cells: biochemical and biological studies after enzymatic isolation. Science 146, 1476−1477.

Pederson, L., Ruan, M., Westendorf, J.J., Khosla, S., Oursler, M.J., 2008. Regulation of bone formation by osteoclasts involves Wnt/BMP signaling and the chemokine sphingosine-1-phosphate. Proc. Natl. Acad. Sci. U. S. A. 105 (52), 20764−20769.

Perwad, F., Azam, N., Zhang, M.Y., Yamashita, T., Tenenhouse, H.S., Portale, A.A., 2005. Dietary and serum phosphorus regulate fibroblast growth factor 23 expression and 1,25-dihydroxyvitamin D metabolism in mice. Endocrinology 146 (12), 5358−5364.

Pi, M., Wu, Y., Quarles, L.D., 2011. GPRC6A mediates responses to osteocalcin in beta-cells in vitro and pancreas in vivo. J. Bone Miner. Res. 26 (7), 1680−1683.

Pievani, A., Sacchetti, B., Corsi, A., Rambaldi, B., Donsante, S., Scagliotti, V., Vergani, P., Remoli, C., Biondi, A., Robey, P.G., Riminucci, M., Serafini, M., 2017. Human umbilical cord blood-borne fibroblasts contain marrow niche precursors that form a bone/marrow organoid in vivo. Development 144 (6), 1035−1044.

Poulton, I.J., McGregor, N.E., Pompolo, S., Walker, E.C., Sims, N.A., 2012. Contrasting roles of leukemia inhibitory factor in murine bone development and remodeling involve region-specific changes in vascularization. J. Bone Miner. Res. 27 (3), 586−595.

Quach, J.M., Walker, E.C., Allan, E., Solano, M., Yokoyama, A., Kato, S., Sims, N.A., Gillespie, M.T., Martin, T.J., 2011. Zinc finger protein 467 is a novel regulator of osteoblast and adipocyte commitment. J. Biol. Chem. 286 (6), 4186−4198.

Quarles, L.D., 2003. FGF23, PHEX, and MEPE regulation of phosphate homeostasis and skeletal mineralization. Am. J. Physiol. Endocrinol. Metab. 285 (1), E1−E9.

Quinn, J.M., Itoh, K., Udagawa, N., Hausler, K., Yasuda, H., Shima, N., Mizuno, A., Higashio, K., Takahashi, N., Suda, T., Martin, T.J., Gillespie, M.T., 2001. Transforming growth factor beta affects osteoclast differentiation via direct and indirect actions. J. Bone Miner. Res. 16 (10), 1787−1794.

Rawadi, G., Vayssiere, B., Dunn, F., Baron, R., Roman-Roman, S., 2003. BMP-2 controls alkaline phosphatase expression and osteoblast mineralization by a Wnt autocrine loop. J. Bone Miner. Res. 18 (10), 1842–1853.

Reinisch, A., Etchart, N., Thomas, D., Hofmann, N.A., Fruehwirth, M., Sinha, S., Chan, C.K., Senarath-Yapa, K., Seo, E.Y., Wearda, T., Hartwig, U.F., Beham-Schmid, C., Trajanoski, S., Lin, Q., Wagner, W., Dullin, C., Alves, F., Andreeff, M., Weissman, I.L., Longaker, M.T., Schallmoser, K., Majeti, R., Strunk, D., 2015. Epigenetic and in vivo comparison of diverse MSC sources reveals an endochondral signature for human hematopoietic niche formation. Blood 125 (2), 249–260.

Richards, C.D., Langdon, C., Deschamps, P., Pennica, D., Shaughnessy, S.G., 2000. Stimulation of osteoclast differentiation in vitro by mouse oncostatin M, leukaemia inhibitory factor, cardiotrophin-1 and interleukin 6: synergy with dexamethasone. Cytokine 12 (6), 613–621.

Robey, P., 2017. Mesenchymal stem cells": fact or fiction, and implications in their therapeutic use. F1000Res 6.

Robling, A.G., Bellido, T., Turner, C.H., 2006. Mechanical stimulation in vivo reduces osteocyte expression of sclerostin. J. Musculoskelet. Neuronal Interact. 6 (4), 354.

Robling, A.G., Turner, C.H., 2009. Mechanical signaling for bone modeling and remodeling. Crit. Rev. Eukaryot. Gene Expr. 19 (4), 319–338.

Rodan, G.A., Martin, T.J., 1981. Role of osteoblasts in hormonal control of bone resorption–a hypothesis. Calcif. Tissue Int. 33 (4), 349–351.

Rodan, G.A., Noda, M., 1991. Gene expression in osteoblastic cells. Crit. Rev. Eukaryot. Gene Expr. 1 (2), 85–98.

Ruffoni, D., Fratzl, P., Roschger, P., Klaushofer, K., Weinkamer, R., 2007. The bone mineralization density distribution as a fingerprint of the mineralization process. Bone 40 (5), 1308–1319.

Sabatakos, G., Sims, N.A., Chen, J., Aoki, K., Kelz, M.B., Amling, M., Bouali, Y., Mukhopadhyay, K., Ford, K., Nestler, E.J., Baron, R., 2000. Overexpression of DeltaFosB transcription factor(s) increases bone formation and inhibits adipogenesis. Nat. Med. 6 (9), 985–990.

Sacchetti, B., Funari, A., Remoli, C., Giannicola, G., Kogler, G., Liedtke, S., Cossu, G., Serafini, M., Sampaolesi, M., Tagliafico, E., Tenedini, E., Saggio, I., Robey, P.G., Riminucci, M., Bianco, P., 2016. No identical "mesenchymal stem cells" at different times and sites: human committed progenitors of distinct origin and differentiation potential are incorporated as adventitial cells in microvessels. Stem Cell Reports 6 (6), 897–913.

Sato, M., Westmore, M., Ma, Y.L., Schmidt, A., Zeng, Q.Q., Glass, E.V., Vahle, J., Brommage, R., Jerome, C.P., Turner, C.H., 2004. Teriparatide [PTH(1–34)] strengthens the proximal femur of ovariectomized nonhuman primates despite increasing porosity. J. Bone Miner. Res. 19 (4), 623–629.

Schaffler, M.B., Cheung, W.Y., Majeska, R., Kennedy, O., 2014. Osteocytes: master orchestrators of bone. Calcif. Tissue Int. 94 (1), 5–24.

Shimada, T., Kakitani, M., Yamazaki, Y., Hasegawa, H., Takeuchi, Y., Fujita, T., Fukumoto, S., Tomizuka, K., Yamashita, T., 2004. Targeted ablation of Fgf23 demonstrates an essential physiological role of FGF23 in phosphate and vitamin D metabolism. J. Clin. Invest. 113 (4), 561–568.

Simonet, W.S., Lacey, D.L., Dunstan, C.R., Kelley, M., Chang, M.S., Luthy, R., Nguyen, H.Q., Wooden, S., Bennett, L., Boone, T., Shimamoto, G., DeRose, M., Elliott, R., Colombero, A., Tan, H.L., Trail, G., Sullivan, J., Davy, E., Bucay, N., Renshaw-Gegg, L., Hughes, T.M., Hill, D., Pattison, W., Campbell, P., Sander, S., Van, G., Tarpley, J., Derby, P., Lee, R., Boyle, W.J., 1997. Osteoprotegerin: a novel secreted protein involved in the regulation of bone density. Cell 89 (2), 309–319.

Sims, N.A., Clement-Lacroix, P., Da Ponte, F., Bouali, Y., Binart, N., Moriggl, R., Goffin, V., Coschigano, K., Gaillard-Kelly, M., Kopchick, J., Baron, R., Kelly, P.A., 2000. Bone homeostasis in growth hormone receptor-null mice is restored by IGF-I but independent of Stat5. J. Clin. Invest. 106 (9), 1095–1103.

Sims, N.A., Jenkins, B.J., Nakamura, A., Quinn, J.M., Li, R., Gillespie, M.T., Ernst, M., Robb, L., Martin, T.J., 2005. Interleukin-11 receptor signaling is required for normal bone remodeling. J. Bone Miner. Res. 20 (7), 1093–1102.

Sims, N.A., Martin, T.J., 2014. Coupling the activities of bone formation and resorption: a multitude of signals within the basic multicellular unit. Bonekey Rep. 3. Article number 481.

Sims, N.A., Martin, T.J., 2015. Coupling signals between the osteoclast and osteoblast: how are messages transmitted between these temporary visitors to the bone surface? Front. Endocrinol. 6, 41.

Soderstrom, K., Stein, E., Colmenero, P., Purath, U., Muller-Ladner, U., de Matos, C.T., Tarner, I.H., Robinson, W.H., Engleman, E.G., 2010. Natural killer cells trigger osteoclastogenesis and bone destruction in arthritis. Proc. Natl. Acad. Sci. U. S. A. 107 (29), 13028–13033.

Song, H.Y., Jeon, E.S., Kim, J.I., Jung, J.S., Kim, J.H., 2007. Oncostatin M promotes osteogenesis and suppresses adipogenic differentiation of human adipose tissue-derived mesenchymal stem cells. J. Cell. Biochem. 101 (5), 1238–1251.

Spatz, J.M., Wein, M.N., Gooi, J.H., Qu, Y., Garr, J.L., Liu, S., Barry, K.J., Uda, Y., Lai, F., Dedic, C., Balcells-Camps, M., Kronenberg, H.M., Babij, P., Pajevic, P.D., 2015. The Wnt inhibitor sclerostin is up-regulated by mechanical unloading in osteocytes in vitro. J. Biol. Chem. 290 (27), 16744–16758.

Stein, G.S., Lian, J.B., Owen, T.A., 1990. Relationship of cell growth to the regulation of tissue-specific gene expression during osteoblast differentiation. FASEB J. 4 (13), 3111–3123.

Sterling, J.A., Edwards, J.R., Martin, T.J., Mundy, G.R., 2011. Advances in the biology of bone metastasis: how the skeleton affects tumor behavior. Bone 48 (1), 6–15.

Stolina, M., Dwyer, D., Niu, Q.T., Villasenor, K.S., Kurimoto, P., Grisanti, M., Han, C.Y., Liu, M., Li, X., Ominsky, M.S., Ke, H.Z., Kostenuik, P.J., 2014. Temporal changes in systemic and local expression of bone turnover markers during six months of sclerostin antibody administration to ovariectomized rats. Bone 67C, 305–313.

Streicher, C., Heyny, A., Andrukhova, O., Haigl, B., Slavic, S., Schuler, C., Kollmann, K., Kantner, I., Sexl, V., Kleiter, M., Hofbauer, L.C., Kostenuik, P.J., Erben, R.G., 2017. Estrogen regulates bone turnover by targeting RANKL expression in bone lining cells. Sci. Rep. 7 (1), 6460.

Suda, T., Takahashi, N., Martin, T.J., 1992. Modulation of osteoclast differentiation. Endocr. Rev. 13 (1), 66–80.

Sudo, H., Kodama, H.A., Amagai, Y., Yamamoto, S., Kasai, S., 1983. In vitro differentiation and calcification in a new clonal osteogenic cell line derived from newborn mouse calvaria. J. Cell Biol. 96 (1), 191–198.

Takahashi, N., Akatsu, T., Udagawa, N., Sasaki, T., Yamaguchi, A., Moseley, J.M., Martin, T.J., Suda, T., 1988. Osteoblastic cells are involved in osteoclast formation. Endocrinology 123 (5), 2600–2602.

Takeda, S., Bonnamy, J.P., Owen, M.J., Ducy, P., Karsenty, G., 2001. Continuous expression of Cbfa1 in nonhypertrophic chondrocytes uncovers its ability to induce hypertrophic chondrocyte differentiation and partially rescues Cbfa1-deficient mice. Genes Dev. 15 (4), 467–481.

Takyar, F.M., Tonna, S., Ho, P.W., Crimeen-Irwin, B., Baker, E.K., Martin, T.J., Sims, N.A., 2013. EphrinB2/EphB4 inhibition in the osteoblast lineage modifies the anabolic response to parathyroid hormone. J. Bone Miner. Res. 28 (4), 912–925.

Tamura, T., Udagawa, N., Takahashi, N., Miyaura, C., Tanaka, S., Yamada, Y., Koishihara, Y., Ohsugi, Y., Kumaki, K., Taga, T., et al., 1993. Soluble interleukin-6 receptor triggers osteoclast formation by interleukin 6. Proc. Natl. Acad. Sci. U. S. A. 90 (24), 11924–11928.

Tanaka, T., Yoshida, N., Kishimoto, T., Akira, S., 1997. Defective adipocyte differentiation in mice lacking the C/EBPbeta and/or C/EBPdelta gene. EMBO J. 16 (24), 7432–7443.

Taylor, S., Ominsky, M.S., Hu, R., Pacheco, E., He, Y.D., Brown, D.L., Aguirre, J.I., Wronski, T.J., Buntich, S., Afshari, C.A., Pyrah, I., Nioi, P., Boyce, R.W., 2016. Time-dependent cellular and transcriptional changes in the osteoblast lineage associated with sclerostin antibody treatment in ovariectomized rats. Bone 84, 148–159.

Tomimori, Y., Mori, K., Koide, M., Nakamichi, Y., Ninomiya, T., Udagawa, N., Yasuda, H., 2009. Evaluation of pharmaceuticals with a novel 50-hour animal model of bone loss. J. Bone Miner. Res. 24 (7), 1194–1205.

Tonna, S., Takyar, F.M., Vrahnas, C., Crimeen-Irwin, B., Ho, P.W., Poulton, I.J., Brennan, H.J., McGregor, N.E., Allan, E.H., Nguyen, H., Forwood, M.R., Tatarczuch, L., Mackie, E.J., Martin, T.J., Sims, N.A., 2014. EphrinB2 signaling in osteoblasts promotes bone mineralization by preventing apoptosis. FASEB J. 28 (10), 4482–4496.

Toyosawa, S., Shintani, S., Fujiwara, T., Ooshima, T., Sato, A., Ijuhin, N., Komori, T., 2001. Dentin matrix protein 1 is predominantly expressed in chicken and rat osteocytes but not in osteoblasts. J. Bone Miner. Res. 16 (11), 2017–2026.

Udagawa, N., Takahashi, N., Akatsu, T., Sasaki, T., Yamaguchi, A., Kodama, H., Martin, T.J., Suda, T., 1989. The bone marrow-derived stromal cell lines MC3T3-G2/PA6 and ST2 support osteoclast-like cell differentiation in cocultures with mouse spleen cells. Endocrinology 125 (4), 1805–1813.

Ueta, C., Iwamoto, M., Kanatani, N., Yoshida, C., Liu, Y., Enomoto-Iwamoto, M., Ohmori, T., Enomoto, H., Nakata, K., Takada, K., Kurisu, K., Komori, T., 2001. Skeletal malformations caused by overexpression of Cbfa1 or its dominant negative form in chondrocytes. J. Cell Biol. 153 (1), 87–100.

van Bezooijen, R.L., Roelen, B.A., Visser, A., van der Wee-Pals, L., de Wilt, E., Karperien, M., Hamersma, H., Papapoulos, S.E., ten Dijke, P., Lowik, C.W., 2004. Sclerostin is an osteocyte-expressed negative regulator of bone formation, but not a classical BMP antagonist. J. Exp. Med. 199 (6), 805–814.

Vrahnas, C., Buenzli, P.R., Pearcson, T.A., Pennypacker, B.L., Tobin, M.J., Bambery, K.R., Duong, L.T., Sims, N.A., 2018. Differing effects of parathyroid hormone, alendronate and odanacatib on bone formation and on the mineralisation process in intracortical and endocortical bone of ovariectomized rabbits. Calcif. Tissue Int. 103 (6), 625–637.

Vrahnas, C., Pearson, T.A., Brunt, A.R., Forwood, M.R., Bambery, K.R., Tobin, M.J., Martin, T.J., Sims, N.A., 2016. Anabolic action of parathyroid hormone (PTH) does not compromise bone matrix mineral composition or maturation. Bone 93, 146–154.

Walker, E., McGregor, N., Poulton, I., Pompolo, S., Allan, E., Quinn, J., Gillespie, M., Martin, T., Sims, N.A., 2008. Cardiotrophin-1 is an osteoclast-derived stimulus of bone formation required for normal bone remodeling. J. Bone Miner. Res. 23, 2025–2032.

Walker, E.C., McGregor, N.E., Poulton, I.J., Solano, M., Pompolo, S., Fernandes, T.J., Constable, M.J., Nicholson, G.C., Zhang, J.G., Nicola, N.A., Gillespie, M.T., Martin, T.J., Sims, N.A., 2010. Oncostatin M promotes bone formation independently of resorption when signaling through leukemia inhibitory factor receptor in mice. J. Clin. Invest. 120 (2), 582–592.

Walsh, N.C., Reinwald, S., Manning, C.A., Condon, K.W., Iwata, K., Burr, D.B., Gravallese, E.M., 2009. Osteoblast function is compromised at sites of focal bone erosion in inflammatory arthritis. J. Bone Miner. Res. 24 (9), 1572–1585.

Wei, J., Hanna, T., Suda, N., Karsenty, G., Ducy, P., 2014. Osteocalcin promotes beta-cell proliferation during development and adulthood through Gprc6a. Diabetes 63 (3), 1021–1031.

Weinreb, M., Shinar, D., Rodan, G.A., 1990. Different pattern of alkaline phosphatase, osteopontin, and osteocalcin expression in developing rat bone visualized by in situ hybridization. J. Bone Miner. Res. 5 (8), 831–842.

Weske, S., Vaidya, M., Reese, A., von Wnuck Lipinski, K., Keul, P., Bayer, J.K., Fischer, J.W., Flogel, U., Nelsen, J., Epple, M., Scatena, M., Schwedhelm, E., Dorr, M., Volzke, H., Moritz, E., Hannemann, A., Rauch, B.H., Graler, M.H., Heusch, G., Levkau, B., 2018. Targeting sphingosine-1-phosphate lyase as an anabolic therapy for bone loss. Nat. Med. 24 (5), 667–678.

Westbroek, I., De Rooij, K.E., Nijweide, P.J., 2002. Osteocyte-specific monoclonal antibody MAb OB7.3 is directed against Phex protein. J. Bone Miner. Res. 17 (5), 845–853.

Whyte, M.P., 1994. Hypophosphatasia and the role of alkaline phosphatase in skeletal mineralization. Endocr. Rev. 15 (4), 439–461.

Xiong, J., Onal, M., Jilka, R.L., Weinstein, R.S., Manolagas, S.C., O'Brien, C.A., 2011. Matrix-embedded cells control osteoclast formation. Nat. Med. 17 (10), 1235–1241.

Yamashita, T., Yoshioka, M., Itoh, N., 2000. Identification of a novel fibroblast growth factor, FGF-23, preferentially expressed in the ventrolateral thalamic nucleus of the brain. Biochem. Biophys. Res. Commun. 277 (2), 494–498.

Yang, F., Tang, W., So, S., de Crombrugghe, B., Zhang, C., 2010. Sclerostin is a direct target of osteoblast-specific transcription factor osterix. Biochem. Biophys. Res. Commun. 400 (4), 684–688.

Yang, L., Tsang, K.Y., Tang, H.C., Chan, D., Cheah, K.S., 2014. Hypertrophic chondrocytes can become osteoblasts and osteocytes in endochondral bone formation. Proc. Natl. Acad. Sci. U. S. A. 111 (33), 12097−12102.

Yang, X., Matsuda, K., Bialek, P., Jacquot, S., Masuoka, H.C., Schinke, T., Li, L., Brancorsini, S., Sassone-Corsi, P., Townes, T.M., Hanauer, A., Karsenty, G., 2004. ATF4 is a substrate of RSK2 and an essential regulator of osteoblast biology; implication for Coffin-Lowry Syndrome. Cell 117 (3), 387−398.

Yasuda, H., Shima, N., Nakagawa, N., Yamaguchi, K., Kinosaki, M., Mochizuki, S., Tomoyasu, A., Yano, K., Goto, M., Murakami, A., Tsuda, E., Morinaga, T., Higashio, K., Udagawa, N., Takahashi, N., Suda, T., 1998. Osteoclast differentiation factor is a ligand for osteoprotegerin/osteoclastogenesis-inhibitory factor and is identical to TRANCE/RANKL. Proc. Natl. Acad. Sci. U. S. A. 95 (7), 3597−3602.

Yoshiko, Y., Wang, H., Minamizaki, T., Ijuin, C., Yamamoto, R., Suemune, S., Kozai, K., Tanne, K., Aubin, J.E., Maeda, N., 2007. Mineralized tissue cells are a principal source of FGF23. Bone 40 (6), 1565−1573.

Yue, R., Zhou, B.O., Shimada, I.S., Zhao, Z., Morrison, S.J., 2016. Leptin receptor promotes adipogenesis and reduces osteogenesis by regulating mesenchymal stromal cells in adult bone marrow. Cell Stem Cell 18 (6), 782−796.

Zhou, H., Choong, P., McCarthy, R., Chou, S.T., Martin, T.J., Ng, K.W., 1994. In situ hybridization to show sequential expression of osteoblast gene markers during bone formation in vivo. J. Bone Miner. Res. 9 (9), 1489−1499.

Chapter 5

Osteoclasts

Naoyuki Takahashi[1], Yasuhiro Kobayashi[1] and Nobuyuki Udagawa[2]

[1]*Institute for Oral Science, Matsumoto Dental University, Nagano, Japan;* [2]*Department of Biochemistry, Matsumoto Dental University, Nagano, Japan*

Chapter outline

Introduction

We contributed a chapter with the title "Osteoclast generation" to *Principles of Bone Biology*, third edition, in 2008. Since then, our understanding of osteoclast differentiation and activation has greatly advanced. The previous chapter focused on the regulation of osteoclast differentiation by the receptor activator of NF-κB ligand/receptor activator of NF-κB/osteoprotegerin (RANKL/RANK/OPG) system. In this new chapter, we have added a section called "Function of osteoclasts" in addition to the regulation of osteoclastogenesis. In retrospect, the role of tumor necrosis factor receptor-associated factors (TRAFs) in osteoclast differentiation and activation was not adequately described in the previous chapter. Findings obtained since its publication have clarified the role of TRAFs in osteoclastogenesis. Studies have shown that the removal of endogenous inhibitory molecules from osteoclast precursors is particularly important for inducing osteoclast differentiation and function. We have attempted to summarize the regulatory mechanisms of osteoclastogenesis elucidated in the past decade in this chapter. In a PubMed search, the number of papers hit with the word "osteoclast" was 436 in 1997, when OPG was discovered, and this number increased to 1408 in 2017. Therefore, the identification of important studies has become more challenging. We did not describe the role of osteoclasts in functional coupling between bone resorption and bone formation; this is described in Chapter 10 (Sims and Martin). Since not all important findings on osteoclasts are introduced in this chapter, each reader will obtain a better understanding of osteoclasts by adding the findings that each considers important. We also describe our working hypothesis on osteoclast precursors in vivo in the final section of this chapter. We hope that the contents of this chapter will contribute to the reader's understanding of osteoclasts.

Principles of Bone Biology. https://doi.org/10.1016/B978-0-12-814841-9.00005-1

Function of osteoclasts

Morphological features of osteoclasts

Osteoclasts are multinucleated cells with a size of 20−100 μm, and are formed by the fusion of mononuclear pre-osteoclasts. Osteoclasts have a large number of pleomorphic mitochondria and a well-developed Golgi apparatus with a rough endoplasmic reticulum, indicating that active energy metabolism and protein synthesis are performed in these cells. Many lysosomes are present in osteoclasts, suggesting that the function of osteoclasts is related to protein degradation. The most characteristic feature of bone-resorbing osteoclasts is the presence of ruffled borders and clear zones (also called the sealing zones). Osteoclasts create resorption lacunae (also called Howship's lacunae) under ruffled borders. Resorption lacunae are acidic to promote the dissolution of bone minerals and proteins. The morphological features of a functioning osteoclast and the mechanisms underlying bone resorption are summarized in Fig. 5.1.

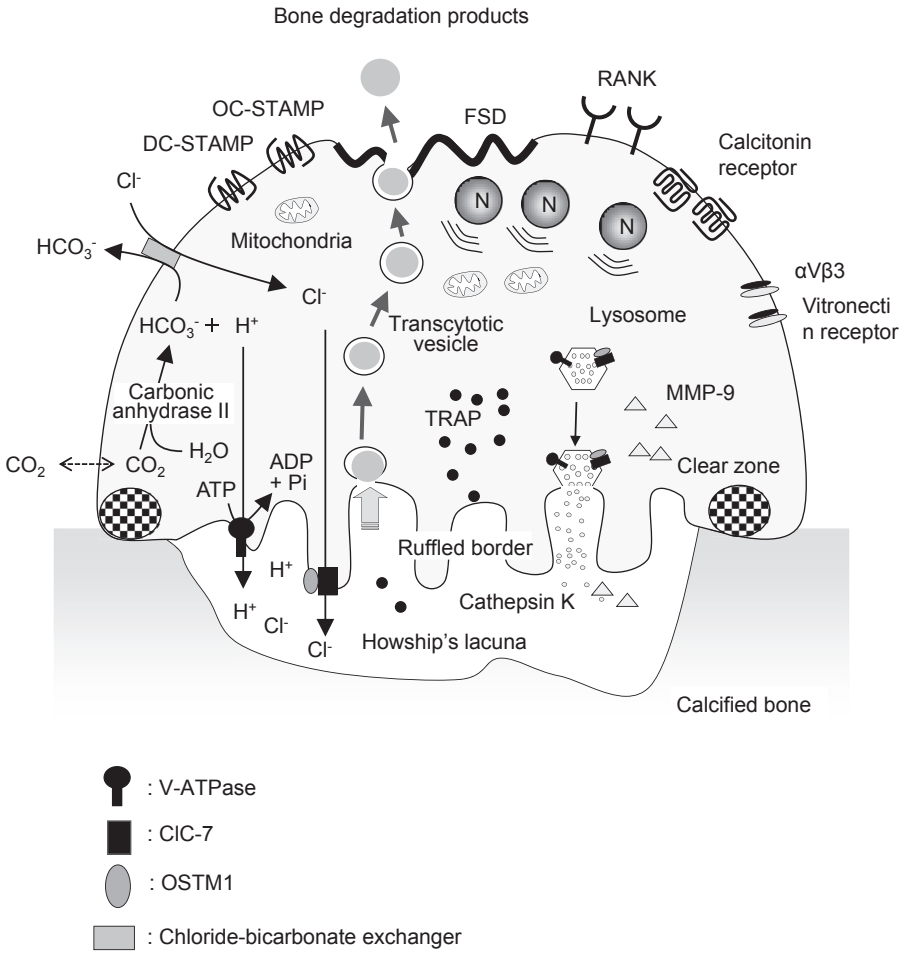

FIGURE 5.1 Schematic representation of a functioning osteoclast. Osteoclasts have several unique ultrastructural characteristics, such as multiple nuclei, abundant mitochondria, and numerous vacuoles and lysosomes. Functioning osteoclasts form ruffled borders and clear zones. The clear zone is recognized as a thick band of actin, isolating resorption lacunae from the surroundings. The resorbing area under the ruffled border is acidic. Vacuolar proton ATPase (*V-ATPase*) exists in the ruffled border and lysosomal membranes. Chloride channel 7 (*ClC-7*) and osteopetrosis-transmembrane protein 1 (*OSTM1*) colocalize in the ruffled border and lysosomal membranes. Matrix metalloproteinase-9 (*MMP-9*) and lysosomal enzymes containing cathepsin K are also secreted into resorption lacunae. Matrix degradation products are endocytosed from a ruffled border region into transcytotic vesicles and then secreted from the functional secretion domain (*FSD*) in the basolateral membrane. Protons are generated by carbonic anhydrase II. Passive chloride−bicarbonate exchangers expressed in the basolateral membrane simultaneously remove HCO_3^- and incorporate Cl^-. Osteoclasts also express large numbers of calcitonin receptors and αVβ3 vitronectin receptors. Dendritic cell-specific transmembrane protein (*DC-STAMP*) and osteoclast-specific transmembrane protein (*OC-STAMP*) are expressed in the osteoclast plasma membrane and play a role in the cell fusion of osteoclasts. Osteoclasts abundantly express calcitonin receptors and receptor activator of NF-κB (*RANK*). *TRAP*, tartrate-resistant acid phosphatase.

The cell membranes of bone-resorbing osteoclasts are divided into four distinct regions: the clear zone, ruffled border, and basolateral and functional secretion domain (FSD) regions (Väänänen and Laitala-Leinonen, 2008). The clear zone is named after its appearance as a bright area under an electron microscope, and this structure is also defined by a thick band of actin called actin rings. Clear zones are involved in the attachment of osteoclasts to bone surfaces and the isolation of resorption lacunae from the surroundings. The ruffled border, which is a foldlike structure formed by the invasion of the cell membrane into the cytoplasm, is the main functional site of bone resorption. Protons and lysosomal enzymes are secreted from ruffled borders into resorption lacunae for the degradation of minerals and matrix proteins. The degradation products of bone are taken up from the specific area of ruffled borders into transcytotic vesicles (Nesbitt and Horton, 1997; Salo et al., 1997; Mulari et al., 2003), are further digested in these vesicles, and are then released from the FSD by vesicular exocytosis.

Mechanism of bone resorption

Osteoclasts possess abundant amounts of carbonic anhydrase II, which is responsible for proton production (Sly et al., 1985). Vacuolar proton ATPase (V-ATPase) localizes to the ruffled border and secretes protons into resorption lacunae in an ATP hydrolysis-dependent manner (Blair et al., 1989; Li et al., 1999; Blair and Athanasou, 2004) (Fig. 5.1). V-ATPase is also detected in lysosomal membranes, and acidifies the inside of lysosomes. Cl^- is transported through chloride channel 7 (ClC-7) to the resorption lacunae to maintain an ionic equilibrium (Kornak et al., 2001). Osteopetrosis-transmembrane protein 1 (OSTM1) is a molecule that is essential for the localization and function of ClC-7 in lysosomes and ruffled borders (Ramírez et al., 2004). OSTM1 acts as the β subunit of ClC-7 (Lange et al., 2006). A mutation in the *OSTM1* gene has been reported in *gl/gl* (gray-lethal) osteopetrotic mice and in patients with hereditary osteopetrosis (Ramírez et al., 2004).

Resorption lacunae are maintained in an acidic environment of approximately pH 4, which favors the dissolution of bone minerals. Proton secretion into resorption lacunae leaves HCO_3^- inside osteoclasts. Passive chloride−bicarbonate exchangers are expressed in the basolateral membrane of osteoclasts and simultaneously remove and incorporate HCO_3^- and Cl^-, respectively (Teti et al., 1989; Wu et al., 2008). The degradation of type I collagen is also promoted under acidic conditions by cathepsin K, a lysosomal enzyme. Cathepsin K has been identified as an enzyme that is specifically expressed in osteoclasts (Tezuka et al., 1994b), and was confirmed to cleave type I collagen at acidic optimum pH (Bossard et al., 1996; Saftig et al., 1998). Matrix metalloproteinase-9 (MMP-9) is highly expressed in osteoclasts (Reponen et al., 1994; Tezuka et al., 1994a). MMP-9 is also secreted into resorption lacunae to digest bone matrix proteins. As described earlier, the degradation products of bone are taken up from the ruffled borders and are ultimately exocytosed to the intercellular space from the FSD. Thus, osteoclasts secrete acids and enzymes and simultaneously absorb degradation products. The flow of vesicles toward the ruffled borders is accompanied by microtubule- and microfilament-mediated vesicle transport (Abu-Amer et al., 1997; Teitelbaum and Ross, 2003; Jurdic et al., 2006). Small GTPases such as RAB7 and RAC are proposed to be involved in vesicle transport in osteoclasts (Zhao et al., 2001; Mulari et al., 2003; Teitelbaum, 2011).

Osteoclasts express a large amount of tartrate-resistant acid phosphatase (TRAP), and release it into blood when they resorb bone (Minkin, 1982). Therefore, TRAP staining is widely used to identify osteoclasts in bone tissues, and serum TRAP activity is measured to evaluate osteoclast number and function in vivo. However, the role of TRAP in bone resorption has not been fully elucidated. Osteoclasts abundantly express the vitronectin receptor, αVβ3 (Horton et al., 1985). This integrin is considered to be involved in the early adhesion of osteoclasts to bone (McHugh et al., 2000). Osteoclasts also abundantly express the calcitonin receptor, a GTP-binding-protein-coupled receptor (Chambers and Magnus, 1982; Nicholson et al., 1986). Calcitonin is secreted from parafollicular cells (C cells) in the thyroids of mammals. Calcitonin activates cAMP/protein kinase A and Ca^{2+}/protein kinase C signaling via a heterotrimeric GTP-binding protein in osteoclasts (Suzuki et al., 1996; Sexton et al., 1999). Calcitonin-induced signals inhibit the bone-resorbing activity of osteoclasts by disrupting the cytoskeletal organization of osteoclasts (Tanaka et al., 2006; Martin and Sims, 2015). RANK is also abundantly expressed on the membrane of osteoclasts (described later).

DC-STAMP/OC-STAMP

Dendritic cell-specific transmembrane protein (DC-STAMP), a seven-transmembrane protein, was discovered as a membrane protein expressed by dendritic cells. Osteoclasts also abundantly express DC-STAMP (Kukita et al., 2004; Yagi et al., 2005). Mononuclear preosteoclasts, but not multinucleated osteoclasts, have been detected in DC-STAMP-deficient mice. Macrophage-derived foreign-body giant cells are also absent in DC-STAMP-deficient mice. Thus, DC-STAMP is a molecule that is needed for the cell fusion of macrophage lineage cells, including osteoclasts and foreign-body giant cells.

Mononuclear preosteoclasts in DC-STAMP-deficient mice express all osteoclast markers and form clear zones and ruffled borders on bone slices. These findings suggest that osteoclastic differentiation is nearly completed by the differentiation of precursor cells into mononuclear preosteoclasts.

Another seven-transmembrane protein, osteoclast-specific transmembrane protein (OC-STAMP), has been identified (Miyamoto et al., 2012b). OC-STAMP-deficient mice showed features very similar to those of DC-STAMP-deficient mice. OC-STAMP-deficient mice express DC-STAMP, whereas no multinucleated osteoclasts are observed in OC-STAMP-deficient mice. Many mononuclear preosteoclasts are also found in OC-STAMP-deficient mice. These findings suggest that DC-STAMP and OC-STAMP both play an important role in the fusion of osteoclasts, but cannot compensate for each other. DC-STAMP-deficient mice and OC-STAMP-deficient mice both develop weak osteopetrosis with age. Thus, DC-STAMP and OC-STAMP are essential factors for the cell fusion of osteoclasts and macrophages, and the multinucleation of osteoclasts appears to be necessary for increasing bone-resorbing capacity. Studies have also shown that the fusion of osteoclasts and macrophages is different from each other in some way. Signal transducer and activator of transcription 6 signals induced by interleukin 4 (IL-4) were required for the cell−cell fusion of macrophages but not osteoclasts (Miyamoto et al., 2012a). DC-STAMP is proposed to play an imperative role in bone homeostasis (Chiu and Ritchlin, 2016). Further studies will unravel the role of this interesting molecule in bone biology.

Ruffled border formation

The fusion of exocytotic vesicles to membranes appears to be mediated by the soluble *N*-ethylmaleimide-sensitive factor attachment protein receptor complex assembly. The synaptotagmin family is also involved in the fusion of exocytotic vesicles. Synaptotagmin I was initially identified as a Ca^{2+} sensor that is abundantly expressed on synaptic vesicles and regulates the fusion step of synaptic vesicle exocytosis. In osteoclasts, synaptotagmin VII plays an essential role in the fusion of lysosomal vesicles to secrete lysosomal enzymes into resorption lacunae (Zao et al., 2008). The degradation of type I collagen by cathepsin K was markedly decreased in synaptotagmin VII-deficient osteoclasts.

Autophagy-related proteins such as autophagy-related protein 5 (ATG5), ATG7, ATG4B, and light-chain protein 3, are also involved in the ruffled border formation of osteoclasts (DeSelm et al., 2011). These findings provide suggestions on how to make ruffled borders in osteoclasts. Osteoclasts possess numerous acidified lysosomes bearing V-ATPase and ClC-7 in the cytoplasm. Bone-resorbing osteoclasts transfer and fuse acidified lysosomes to the side of the plasma membrane facing the bone surface (Mulari et al., 2003; Teitelbaum, 2007). The insertion of vesicles into the plasma membrane markedly increases the surface area of cells and delivers V-ATPase and ClC-7 to the plasma membrane. Osteoclasts form ruffled borders, making extracellular secondary lysosomes and resorbing bone.

Role of osteoblastic cells in osteoclastogenesis

Coculture system

The differentiation and activation of osteoclasts are strictly regulated by the mesenchymal cells of osteoblast lineage cells (referred to as osteoblastic cells), such as osteoblasts, osteocytes, and bone marrow−derived stromal cells. In 1981, Rodan and Martin (1981) proposed a concept that bone-resorbing factors act on osteoblastic cells, but not osteoclasts, to induce osteoclastic bone resorption based on the observation that osteoblastic cells express the receptors for bone-resorbing factors, including parathyroid hormone (PTH) and prostaglandin E_2 (PGE_2). By incorporating this hypothesis, a murine coculture system of osteoblastic cells and hematopoietic cells was established in 1988 (Takahashi et al., 1988). Osteoclasts were formed in a coculture treated with bone-resorbing factors. Osteoblastic cells were shown to strictly regulate osteoclast differentiation and activation in the coculture. Cell-to-cell contact between hematopoietic cells and osteoblastic cells was required to induce osteoclast formation and activation. Experiments using this coculture system established the concept that osteoblastic cells express osteoclast differentiation factor (ODF) as a membrane-associated factor for the induction of osteoclast differentiation (Suda et al., 1992). It was also established that osteoclasts differentiate from various types of monocyte−macrophage lineage precursors in the coculture (Udagawa et al., 1990). The role of osteoblastic cells in the differentiation and function of osteoclasts is summarized in Fig. 5.2.

Macrophage colony-stimulating factor

Macrophage colony-stimulating factor (M-CSF; also called colony-stimulating factor 1) was originally identified as a growth factor that specifically stimulates the development of macrophage colonies. The critical role of M-CSF in osteoclast

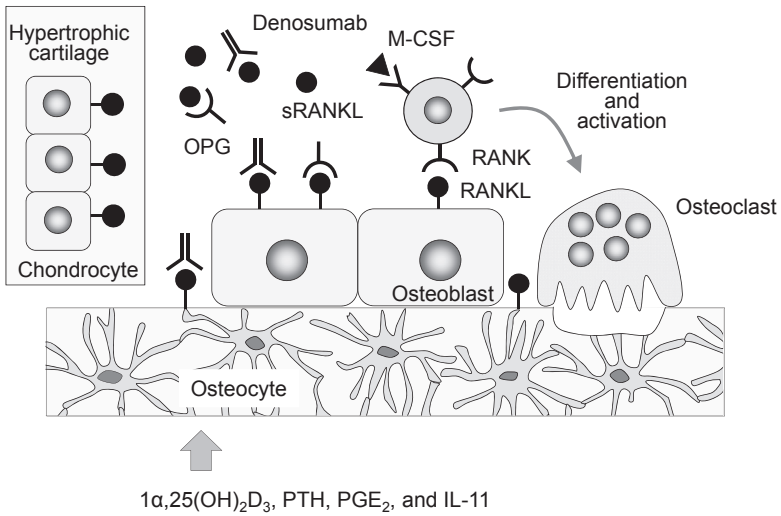

FIGURE 5.2 Schematic representation of osteoclast differentiation and activation. Receptor activator of NF-κB ligand (*RANKL*) expressed by osteoblasts, osteocytes, and hypertrophic chondrocytes supports osteoclast differentiation in the presence of macrophage colony-stimulating factor (*M-CSF*). Osteotropic factors such as 1α,25-dihydroxyvitamin D_3 (*1α,25(OH)$_2$D$_3$*), parathyroid hormone (*PTH*), prostaglandin E_2 (*PGE$_2$*), and interleukin 11 (*IL-11*) stimulate the expression of RANKL in the aforementioned cells. Osteoclast precursors express M-CSF receptor and RANK, and differentiate into osteoclasts in response to both cytokines. The membrane-associated and soluble (s) forms of RANKL support osteoclastogenesis. Osteoprotegerin (*OPG*) secreted by osteoblastic cells and other cells, and denosumab, an anti-RANKL antibody, inhibit osteoclast differentiation and activation by suppressing the RANKL−RANK interaction.

biology was established in a series of experiments on *op/op* (osteopetrosis) mice. Impaired bone resorption in *op/op* mice is associated with a marked reduction in the number of osteoclasts in skeletal tissues (Wiktor-Jedrzejczak et al., 1982). A point mutation in the coding region of the *M-CSF* gene was found in *op/op* mice, leading to the stop codon TGA, 21 bp downstream (Yoshida et al., 1990; Wiktor-Jedrzejczak et al., 1990). The administration of recombinant M-CSF to animals cured their osteopetrotic phenotype, confirming the essential role of this cytokine in the differentiation of osteoclasts (Felix et al., 1990; Kodama et al., 1991b). Hematopoietic cells derived from *op/op* mice differentiated into osteoclasts in a coculture with normal mouse-derived osteoblastic cells. On the other hand, *op/op* mouse-derived osteoblastic cells failed to support osteoclast formation in the coculture with normal hematopoietic cells (Kodama et al., 1991a; Takahashi et al., 1991). These findings further confirmed that M-CSF produced by osteoblastic cells is essentially involved in osteoclastogenesis.

Osteoprotegerin and RANKL

RANKL is a member of the tumor necrosis factor (TNF) superfamily (encoded by TNFSF11) (Anderson et al., 1997), which was originally identified as the T-cell-derived immunomodulatory cytokine, TNF-related activation-induced cytokine (TRANCE), in 1997 (Wong et al., 1997). RANKL is expressed in activated T cells and promotes the survival of dendritic cells by binding to RANK (encoded by *TNFRSF11a*), resulting in enhanced dendritic cell−mediated T cell proliferation. The discovery that RANKL is an essential factor for osteoclastogenesis was made by two independent groups at similar times. In 1997, Simonet et al. cloned a new member of the TNF receptor (TNFR) superfamily (encoded by *TNFRSF11b*) (Simonet et al., 1997). This protein lacked a transmembrane domain, indicating that it is a secreted member of the TNFR family. The hepatic expression of this protein in transgenic mice resulted in severe osteopetrosis. This protein was named "osteoprotegerin," reflecting its protection of bone. Tsuda et al. (1997) independently isolated a novel protein termed "osteoclastogenesis inhibitory factor" (OCIF) from the conditioned medium of a human fibroblast culture. The amino acid sequence of OCIF was identical to that of OPG (Tsuda et al., 1997; Yasuda et al., 1998a). OPG strongly inhibited osteoclast formation induced by 1α,25-dihydroxyvitamin D_3 (1α,25(OH)$_2$D$_3$), PTH, PGE_2, or IL-11 in the coculture. Using OPG as a probe, two groups simultaneously isolated a cDNA with an open reading frame encoding 316 amino acid residues from murine cell lines, and ODF and OPG ligand were found to be identical to RANKL (Yasuda et al., 1998b; Lacey et al., 1998). The expression of RANKL was induced in osteoblastic cells in response to 1α,25(OH)$_2$D$_3$, PTH, PGE_2, and IL-11. The combined treatment of hematopoietic cells with M-CSF and the soluble form of RANKL (sRANKL) induced osteoclast differentiation in vitro in the absence of supporting osteoblastic cells. Moreover, the targeted

disruption of RANKL or RANK induced severe osteopetrosis in mice due to a defect in osteoclast differentiation (Kong et al., 1999; Dougall et al., 1999). RANKL was also shown to activate osteoclast function. Loss-of-function mutations in the genes encoding *RANK*, *OPG*, and *RANKL*, and gain-of-function mutations in the *RANK* gene, were detected in humans (Kobayashi et al., 2009; Crockett et al., 2011). These findings confirmed the essential role of the RANKL–RANK pathway in osteoclast development and function both in vitro and in vivo.

Osteoclastogenesis supported by RANKL

Osteocytes are osteoblast-derived cells embedded in the bone matrix. Osteocytes are connected to one another by gap junctions via cellular processes. Studies have shown that osteocytes also regulate osteoclast formation through the production of RANKL (Nakashima et al., 2011; Xiong et al., 2011). The deletion of RANKL specifically in osteoblastic cells using *osterix*-Cre and *osteocalcin*-Cre resulted in osteopetrosis with impaired tooth eruption, a typical symptom of severe osteopetrosis (Xiong et al., 2011). On the other hand, when *RANKL* was deleted in an osteocyte-specific manner using *dentin matrix protein 1*-Cre, bone resorption was suppressed 6 months after birth and bone mass increased. These findings indicated that RANKL expressed by osteocytes plays an important role in the process of bone remodeling. In addition, hypertrophic chondrocyte-derived RANKL was shown to be important for bone development. An osteopetrotic feature was developed when RANKL was disrupted in hypertrophic chondrocytes using *type X collagen*-Cre mice (Xiong et al., 2011). RANKL was shown to be strongly expressed by T lymphocytes. However, osteopetrosis does not develop with a T-cell-specific *RANKL* deficiency. Based on these findings, it was concluded that RANKL expressed by osteoblasts, osteocytes, and hypertrophic chondrocytes is important for the regulation of bone resorption in mice.

RANKL is produced as an integral membrane protein, and is also cleaved to produce sRANKL (Lacey et al., 1998). Previous studies using the coculture system suggested that the membrane-bound form of RANKL is required for osteoclast formation. However, transgenic mice overexpressing sRANKL or mice injected with sRANKL exhibited increased resorption. To establish the relative importance of membrane-bound versus sRANKL, mice expressing only membrane-bound form of RANKL were produced. The membrane-bound form of RANKL was shown to exert almost all of the functions of RANKL in bone (Xiong et al., 2017).

The anti-RANKL antibody denosumab was developed to suppress excessive bone resorption. Denosumab is a fully humanized monoclonal antibody with affinity and specificity for human RANKL (Lacey et al., 2012). Denosumab blocks the binding of RANKL to RANK expressed on osteoclast precursors and osteoclasts, causing the suppression of osteoclast differentiation and activation. Denosumab is used in the treatment of patients at high risk of bone fractures, including women and men with osteoporosis, men with prostate cancer, and women with breast cancer. Furthermore, denosumab is used to prevent skeletal-related events in patients with bone metastases originating from solid tumors. The roles of RANKL, OPG, and denosumab in osteoclast differentiation and activation are summarized in Fig. 5.2.

RANKL is expressed not only in bone, but also in mammary glands, the lymph nodes, the thymus, and intestinal Peyer's patches (Lacey et al., 1998). Subsequent studies demonstrated that the RANKL–RANK signal is essentially involved in mammary gland development (Fata et al., 2000), lymph node formation (Kong et al., 1999; Yoshida et al., 2002), the elimination of self-reactive T cells in the thymus (Rossi et al., 2007; Akiyama et al., 2008), and microfold cell differentiation in Peyer's patches (Knoop et al., 2009; Kanaya et al., 2012). It was shown in 2017 that the membrane-bound form of RANKL plays an essential role in microfold cell differentiation in intestinal Peyer's patches (Nagashima et al., 2017).

Signal transduction in osteoclastogenesis

The M-CSF receptor FMS

Osteoclasts develop from monocytic precursors from the hematopoietic lineage. PU.1 induces the expression of the M-CSF receptor FMS and is critical for monocyte–macrophage lineage commitment (Tondravi et al., 1997; Zaidi et al., 2003). Signals via FMS are essential for the induction of osteoclast differentiation (Hamilton, 1997; Feng and Teitelbaum, 2013; Stanley and Chitu, 2014). The receptor FMS has a tyrosine kinase domain in the intracellular region. Signals mediated by FMS are required not only for the proliferation of osteoclast progenitors, but also for the differentiation of postmitotic osteoclast precursors (Tanaka et al., 1993). The binding of M-CSF to FMS induces the autophosphorylation of the receptor at several tyrosine residues within the cytoplasmic domain (Feng et al., 2002; Stanley and Chitu, 2014). This phosphorylation of tyrosine residues recruits signaling molecules such as growth factor receptor–bound protein 2 (GRB2) (Insogna et al., 1997) and phosphatidylinositol 3-kinase (PI3K) (Mandal et al., 2009) during osteoclastogenesis. M-CSF mainly activates two signaling pathways: extracellular signal-regulated kinase (ERK) through GRB2 and a serine/

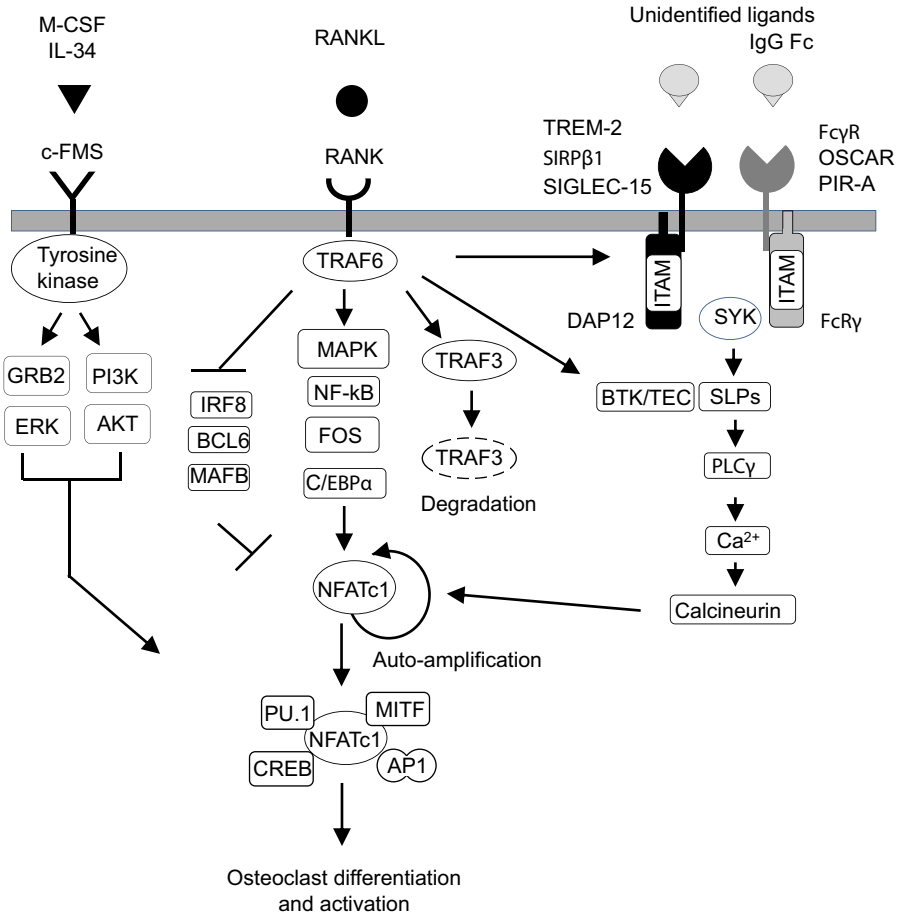

FIGURE 5.3 Signal transduction for osteoclast differentiation and activation. When M-CSF binds to the receptor FMS, the signaling pathways of GRB2−ERK and PI3K−AKT are activated. IL-34 is the second ligand for FMS and induces the same signals as M-CSF. TRAF6 acts as the main adaptor molecule of RANK signaling. TRAF6-mediated signals activate downstream targets such as MAPK, NF-κB, JNK, FOS, and C/EBPα, and ultimately induce the autoamplification of NFATc1. In addition, RANK signals suppress the expression of inhibitory molecules such as IRF8, BCL6, and MAFB. ITAM signaling via immunoglobulin-like receptors is an additional signal that regulates osteoclast differentiation and function. The adaptor proteins DAP12 and FcRγ possess the ITAM sequence and induce ITAM signals. RANK signals also activate ITAM signals. ITAM signals activate SYK, which, in turn, phosphorylates the tyrosine residues of SLPs. RANK signaling activates BTK and TEC. A signaling complex of BTK/TEC and SLPs is formed and activates PLCγ. Activated PLCγ induces the mobilization of intracellular Ca^{2+}, which activates calcineurin to induce the dephosphorylation and autoamplification of NFATc1. Amplified NFATc1 induces the transcription of osteoclast-associated genes in cooperation with PU.1, CREB, and MITF. These signaling cascades induce the differentiation and activation of osteoclasts. *AKT*, serine/threonine kinase; *BCL6*, B cell leukemia/lymphoma 6; *C/EBPα*, CCAAT/enhancer binding protein α; *c-FMS*, M-CSF receptor; *CREB*, cAMP-responsive element binding protein; *DAP12*, DNAX activation protein 12; *ERK*, extracellular signal-regulated kinase; *FcγR*, Fcγ receptor; *FcRγ*, Fc receptor common γ subunit; *GRB2*, growth factor receptor−bound protein 2; *IgG Fc*, immunoglobulin G Fc region; *IL-34*, interleukin-34; *IRF8*, interferon regulatory factor 8; *ITAM*, immunoreceptor tyrosine-based activation motif; *MAPK*, mitogen-activated protein kinase; *M-CSF*, macrophage colony-stimulating factor; *MITF*, microphthalmia-associated transcription factor; *NF-κB*, nuclear factor κB; *NFATc1*, nuclear factor of activated T cells 1; *OSCAR*, osteoclast-associated receptor; *PI3K*, phosphatidylinositol 3-kinase; *PIR-A*, paired immunoglobulin-like receptor A; *PLCγ*, phospholipase Cγ; *RANK*, receptor activator of NF-κB; *RANKL*, receptor activator of NF-κB ligand; *SIGLEC-15*, sialic acid-binding immunoglobulin-like lectin 15; *SIRPβ1*, signal-regulatory protein β1; *SLP*, SRC homology 2 domain-containing leukocyte protein; *SYK*, spleen tyrosine kinase; *TRAF*, tumor necrosis factor receptor-associated factor; *TREM-2,* triggering receptor expressed on myeloid cells 2.

threonine kinase, AKT, through PI3K (Feng and Teitelbaum, 2013; Stanley and Chitu, 2014). Both signaling pathways are considered to be involved in M-CSF-supported osteoclastogenesis. Signals mediated by GRB2 and PI3K are involved in the regulation of cytoskeletal organization in osteoclasts as well as osteoclast differentiation. Signal transduction that induces osteoclast differentiation and activation is summarized in Fig. 5.3.

M-CSF-deficient *op/op* mice exhibit monocytopenia and osteopetrosis (Wiktor-Jedrzejczak et al., 1982). However, several unusual phenomena have been observed in *op/op* mice. Osteoclasts are completely absent in young *op/op* mice, but appear in aged mice (Begg et al., 1993). The osteopetrotic characteristics of FMS-deficient mice are more severe than those

of *op/op* mice (Dai et al., 2002). F4/80-positive macrophages exist in the splenic red pulp in *op/op* mice as well as in wild-type mice, and their number is regulated by a mechanism independent of M-CSF (Cecchini et al., 1994; Yamamoto et al., 2008). These phenomena may be explained by the discovery of IL-34, a second ligand for FMS (Lin et al., 2008; Nakamichi et al., 2013; Stanley and Chitu, 2014). The amino acid sequence of IL-34 is different from that of M-CSF; however, IL-34 binds to FMS and induces the same effects as M-CSF. IL-34 cannot substitute for M-CSF in vivo because its localization differs from that of M-CSF. IL-34 is strongly expressed in the spleen, but not in bone. On the other hand, M-CSF is strongly expressed in bone and the spleen. Osteoclast precursors were previously shown to be present in the spleen, but not in bone in *op/op* mice (Nakamichi et al., 2012). Splenectomy blocked M-CSF-induced osteoclastogenesis in *op/op* mice. Osteoclasts appeared in aged *op/op* mice with the upregulation of IL-34 expression in bone. Splenectomy in *op/op* mice also blocked the age-associated appearance of osteoclasts. These findings suggest that IL-34 plays a pivotal role in maintaining the splenic reservoir of osteoclast precursors, which are transferred from the spleen to bone via the bloodstream in response to diverse stimuli, in *op/op* mice. The administration of FYT720, a sphingosine-1-phosphate agonist, has also been shown to promote the egress of osteoclast precursors from hematopoietic tissues into the bloodstream (Ishii et al., 2009). These findings suggest that some osteoclast precursors are circulating in the bloodstream.

RANK

RANK-mediated signals are also essential for the induction of osteoclast differentiation and function (Fig. 5.3). When RANKL binds to RANK, RANK recruits TRAFs, which are adapter molecules that induce osteoclastogenesis (Wong et al., 1998). TRAFs 1, 2, 3, 5, and 6 are recruited to the cytoplasmic tail of RANK. Among them, the TRAF6-mediated signal is considered to induce osteoclast differentiation and function because TRAF6-deficient mice show severe osteopetrosis with a decreased number of osteoclasts (Lomaga et al., 1999; Naito et al., 1999; Walsh et al., 2015). Osteoclast precursors from TRAF6-deficient mice fail to differentiate into osteoclasts even in the presence of RANKL (Gohda et al., 2005). RANK-mediated signals activate downstream signals such as p38 mitogen-activated protein kinase (MAPK), Jun N-terminal kinase (JNK), and FOS (Wagner and Eferl, 2005; Takayanagi, 2007). These signals ultimately induce the expression of the transcription factor nuclear factor of activated T cells 1 (NFATc1), a master transcription factor that plays a pivotal role in osteoclastogenesis (Ishida et al., 2002; Takayanagi et al., 2002). This robust induction of NFATc1 is based on an autoamplifying mechanism affected through the persistent calcium signal−mediated activation of NFATc1. NFATc1 binds to NFAT-binding sites on its own promoter, constituting a positive feedback loop. In the nucleus, NFATc1 cooperates with other transcription factors, such as PU.1, cAMP-responsive element binding protein, and microphthalmia-associated transcription factor, to induce various osteoclast-specific genes (Sato et al., 2006; Okamoto et al., 2017). *CCAAT/enhancer* binding protein α (C/EBPα) is a key molecular determinant in myeloid lineage commitment. C/EBPα is strongly expressed in osteoclasts and has been identified as a critical *cis*-regulatory element-binding protein in the cathepsin K promoter (Chen et al., 2013). C/EBPα-deficient mice exhibit severely blocked osteoclastogenesis, suggesting that C/EBPα is a key regulator of osteoclast lineage commitment. Peroxisome proliferator-activated receptor γ is also reported to be important for osteoclast differentiation (Okazaki et al., 1999; Wan et al., 2007).

On the other hand, it is important for osteoclastogenesis to exclude factors that inhibit osteoclast differentiation. Interferon regulatory factor 8 (IRF8), a transcription factor expressed in immune cells, is a key inhibitory molecule for osteoclastogenesis (Zhao et al., 2009). IRF8 was found to inhibit osteoclast formation under physiological and pathological conditions, and was downregulated in response to a RANKL stimulation. RANKL also upregulates the expression of the transcription factor B-lymphocyte-induced maturation protein-1 (BLIMP1) (Nishikawa et al., 2010). BLIMP1 then suppresses the expression of other inhibitory transcription factors, such as B cell leukemia/lymphoma 6 and MAFB (Miyauchi et al., 2010). Thus, RANK signaling induces the downregulation of negative regulators together with the upregulation of positive regulators for osteoclastogenesis (Fig. 5.3).

Tumor necrosis factor receptors

TNFα together with M-CSF has been shown to induce osteoclastogenesis in the absence and presence of RANKL (Kobayashi et al., 2000; Zhang et al., 2001). Osteoclast formation induced by TNFα was inhibited by the addition of respective antibodies against TNFR type I (TNFRI, p55) and TNFR type II (TNFRII, p75), but not by OPG. This finding suggests that TNFα stimulates osteoclastogenesis via TNFRs. Osteoclast precursors obtained from RANK- or TRAF6-deficient mice differentiate into osteoclasts when stimulated with TNFα in the presence of cofactors such as transforming growth factor β (Kim et al., 2005). However, the osteoclastogenesis-inducing ability of TNFα is markedly weaker than that of RANKL. Studies have revealed the mechanisms by which TNF induces the differentiation of osteoclasts

(Boyce et al., 2015). When osteoclast precursors prepared from IRF8-deficient mice were used in an osteoclast formation assay, TNFα induced osteoclastogenesis as strongly as RANKL. Recombinant recognition sequence binding protein at the Jκ site (RBP-J) is a DNA-binding protein that functions as a transcriptional repressor or activator depending on the partner proteins. RBP-J strongly suppressed TNFα-induced osteoclastogenesis and inflammatory bone resorption (Zhao et al., 2012). In the absence of RBP-J, TNFα effectively induced osteoclastogenesis and bone resorption in RANK-deficient mice (Yao et al., 2009). In contrast to TRAF6, TRAF3 inhibits osteoclast formation by moderating nuclear factor κB (NF-κB) signaling (Xiu et al., 2014). TRAF3 suppresses the conversion of NF-κB p100 (inhibitory form) into NF-κB p52 (active form) through the degradation of NF-κB-inducing kinase, suggesting that TRAF3 signals induce the accumulation of inhibitory NF-κB p100. RANKL induced the degradation of inhibitory TRAF3 and NF-κB p100 in osteoclast precursors. In contrast, TNFα increased the expression of TRAF3 in osteoclast precursors (Yao et al., 2017). TNFα induced osteoclast formation to the same level as RANKL when NF-κB p100 or TRAF3 was deleted in RANK-deficient osteoclast progenitors. A TNFα injection strongly induced osteoclastogenesis in vivo in mice deficient in RANK together with NF-κB p100 (Yao et al., 2009; Boyce et al., 2015). These findings suggest that TNFα induces osteoclast formation at a similar level compared with RANKL through TNFR under specific conditions, and also that RANKL efficiently eliminates endogenous inhibitory molecules in osteoclast precursors.

ITAM costimulatory signals

Calcium signals

Immunoreceptor tyrosine-based activation motif (ITAM) signaling via immunoglobulin-like receptors is an additional signal regulating osteoclast differentiation and function (Koga et al., 2004; Mocsai et al., 2004; Humphrey and Nakamura, 2016, Okamoto et al., 2017). The adaptor proteins DNAX activation protein 12 (DAP12) and Fc receptor common γ subunit (FcRγ) possess the ITAM sequence (Fig. 5.3). DAP12 is coupled with triggering receptor expressed on myeloid cells 2, signal-regulatory protein β1, and sialic acid-binding immunoglobulin-like lectin 15 (SIGLEC-15), while FcRγ is coupled with osteoclast-associated receptor (Kim et al., 2002; Barrow et al., 2011) and paired immunoglobulin-like receptor A as well as Fcγ receptor (FcγR). DAP12- and FcRγ-mediated ITAM signals activate spleen tyrosine kinase (SYK). RANK-mediated signals also activate ITAM signals as well as MAPK, NF-κB, and FOS signaling. Activated SYK then phosphorylates the tyrosine residues of SRC homology 2 domain-containing leukocyte protein (SLP) adapter molecules such as B cell linker and SLP-76 (Shinohara et al., 2008; Lee et al., 2008). TEC and BTK are tyrosine kinases that belong to the TEC family. RANK signaling activates BTK and TEC by tyrosine phosphorylation. Mice lacking both BTK and TEC showed severe osteopetrosis caused by a defect in bone resorption. ITAM and RANK signaling results in the formation of a signaling complex of BTK/TEC and SLPs. This complex activates phospholipase Cγ (PLCγ), thereby increasing the mobilization of intracellular Ca^{2+}. This increase in intracellular Ca^{2+} activates calcineurin, a Ca^{2+}-dependent serine/threonine phosphatase. Calcineurin induces the dephosphorylation of NFATc1 and promotes its nuclear translocation to enhance the autoamplification of NFATc1. Amplified NFATc1 then induces the transcription of osteoclast-associated genes. Thus, the ITAM signal cooperates with the RANK-mediated signal to induce NFATc1.

Mice lacking both FcRγ and DAP12 exhibit severe osteopetrosis due to impaired osteoclast differentiation, confirming that ITAM signaling is an essential signal promoting osteoclast differentiation. Patients with Nasu−Hakola disease, a rare recessive genetic disease found in Japanese and Finnish people, have cyst formation at the limb epiphysis and exhibit multiple pathological fractures (Humphrey and Nakamura, 2016). Point mutations and defects in the *DAP12* gene have been reported in this disease.

Osteoclast differentiation is also induced from osteoclast precursors deficient in inositol 1,4,5-trisphosphate receptor type 2, which is essential for calcium mobilization. Therefore, there appears to be an osteoclast differentiation pathway that is not dependent on calcium ions (Kuroda et al., 2008; Oikawa et al., 2013). Several common pathways of bone metabolism and the immune system have been elucidated, and the term "osteoimmunology" has been proposed and widely used to obtain a clearer understanding of the regulation of osteoclastogenesis.

SIGLEC-15 and FcγR

Studies have revealed that SIGLEC-15 and FcγR play important roles in osteoclastic bone resorption (Fig. 5.4). SIGLEC family members are sialic acid-binding receptors that are primarily expressed by immune cells. SIGLEC-15 is the only SIGLEC highly conserved throughout vertebrate evolution (Angata et al., 2007). SIGLEC-15 was identified as a gene that is strongly expressed in human osteoclastoma (giant cell tumor of bone) (Hiruma et al., 2011) and also as a gene product

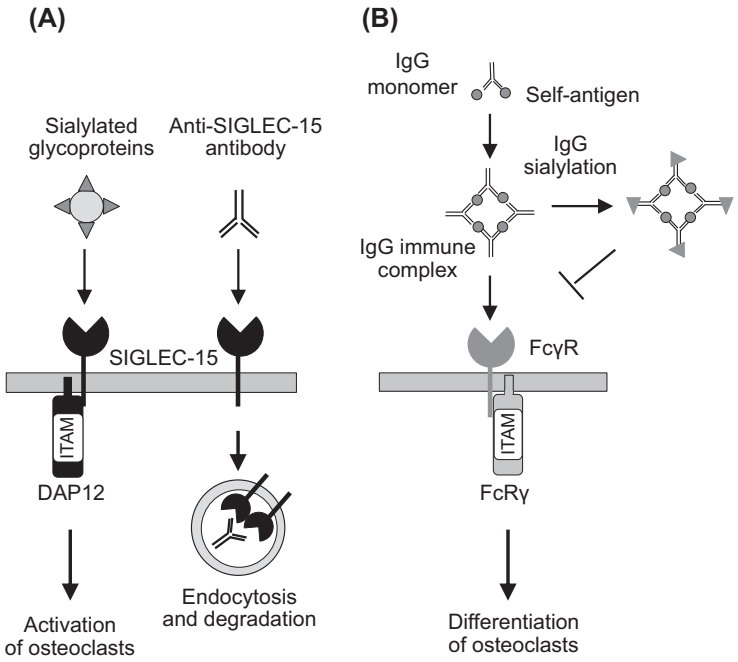

FIGURE 5.4 SIGLEC-15- and FcγR-mediated signaling. (A) Sialic acid-binding immunoglobulin-like lectin 15 (*SIGLEC-15*)-mediated signals. SIGLEC-15 is a sialic acid-binding receptor associated with DNAX activation protein 12 (*DAP12*). It activates spleen tyrosine kinase via DAP12 and promotes the bone resorptive function of osteoclasts. Osteoclasts lacking SIGLEC-15 cannot form actin rings. When an anti-SIGLEC-15 antibody is administered to mice, bone mass increases due to the suppression of bone resorption. Binding of the antibody to SIGLEC-15 induces the dimerization of SIGLEC-15, rapid internalization, and lysosomal degradation. **(B) Fcγ receptor (*FcγR*)-mediated signals.** Although immunoglobulin G (*IgG*) antibodies generally exist as monomers, IgG immune complexes (ICs) are formed in inflammation and autoimmune diseases. IgG ICs promote osteoclast formation via FcγR. The Fc portion of the IgG antibody undergoes sugar chain modifications, and sialic acid is added to a part of its end. Sialylated IgG ICs attenuate its ability to bind to FcγR. *FcRγ*, Fc receptor common γ subunit; *ITAM*, immunoreceptor tyrosine-based activation motif.

induced by NFATc1 (Ishida-Kitagawa et al., 2012). SIGLEC-15 associates with DAP12. SIGLEC-15-deficient mice exhibited osteopetrosis with the suppression of osteoclastic bone resorption. TRAP-positive osteoclasts were detected in SIGLEC-15-deficient mice at levels similar to those in wild-type mice, suggesting that SIGLEC-15 plays a role in osteoclast function (Hiruma et al., 2013; Kameda et al., 2013, 2015). Osteoclasts derived from SIGLEC-15-deficient mice could not form actin rings. In an antigen-induced arthritis model, the degree of periarticular bone loss in the proximal tibia is significantly lower in SIGLEC-15-deficient mice than in wild-type mice (Shimizu et al., 2015). When an anti-SIGLEC-15 neutralizing antibody was administered to mice, bone mass increased due to the suppression of bone resorption (Stuible et al., 2014; Fukuda et al., 2017). The binding of a neutralizing antibody to SIGLEC-15 induces the dimerization of the receptor, rapid internalization, and lysosomal degradation. SIGLEC-15-deficient mice also show resistance to bone loss by ovariectomy. SIGLEC-15-mediated signals activate PI3K and AKT together with PLCγ in osteoclasts. The ligand of SIGLEC-15 is proposed to be a glycoprotein having sialic acid that has not yet been identified. SIGLEC-15 may be a major target for the treatment of bone diseases with excessive bone resorption.

Autoantibody production and IgG immune complex (IC) formation are frequently observed in autoimmune diseases associated with bone loss. Studies have demonstrated that, under pathological conditions such as autoimmune diseases associated with hypergammaglobulinemia, IgG ICs enhance osteoclast formation through FcγR and promote bone resorption (Fig. 5.4) (Negishi-Koga et al., 2015; Harre et al., 2015). The Fc portion of the IgG antibody undergoes various sugar chain modifications. Sialic acid is added to the sugar chain terminal of the Fc portion. This sialylated IgG attenuates its ability to bind to FcγR. The desialylated, but not sialylated, human IgG IC promoted osteoclast formation in vitro. The relationship between the sialylation status of IgG and bone mass was examined in patients with rheumatism. Bone mass was found to decrease as the sialylation rate of IgG in these patients became lower. The administration of the sialic acid precursor *N*-acetyl-D-mannosamine to animals promotes the sialylation of IgG ICs, and suppresses IgG IC-enhanced osteoclast formation. These results demonstrate that ITAM costimulatory signals are important for regulating osteoclast differentiation and function.

WNT signals

Canonical WNT signals

WNT proteins activate β-catenin-dependent canonical and β-catenin-independent noncanonical signaling pathways. In the absence of WNT ligands, β-catenin is phosphorylated by a degradation complex composed of axin, adenomatous polyposis coli, glycogen synthase kinase 3β, and casein kinase 1. Phosphorylated β-catenin is degraded by the ubiquitin proteasome, and cytosolic β-catenin is then maintained at a low level. When the WNT ligand binds to a receptor complex composed of frizzled receptor and low-density lipoprotein receptor-related protein 5/6, the activity of the degradation complex is suppressed, and β-catenin then accumulates in the cytoplasm. Accumulated β-catenin translocates to the nucleus. Nuclear β-catenin together with the transcription factors T cell factor and lymphoid enhancer factor (LEF) induces the transcription of the target gene.

Glass et al. (2005) showed the importance of WNT/β-catenin signals in bone resorption in vivo using genetic approaches. Mice expressing the constitutively active form of β-catenin in mature osteoblasts had an increased bone mass with impaired osteoclast formation. The expression of OPG was increased in the long bones of these mice. The LEF-1 binding sequence is found in the promoter region of the *OPG* gene, and the LEF-1/β-catenin complex induces the expression of OPG. Thus, the activation of WNT/β-catenin signals induces the expression of OPG in mature osteoblasts and markedly inhibits bone resorption. The roles of β-catenin-dependent canonical WNT signaling and β-catenin-independent noncanonical WNT signals that regulate osteoclast differentiation and activation are summarized in Fig. 5.5 (Kobayashi et al., 2016).

WNT3A, a typical canonical WNT ligand, inhibited $1\alpha,25(OH)_2D_3$-induced osteoclast formation in a coculture, but not RANKL-induced osteoclast formation in osteoclast precursor cultures (Yamane et al., 2001). This finding indicates that WNT3A suppresses osteoclastogenesis through the expression of OPG in osteoblasts. The concept that WNT/β-catenin signals inhibit osteoclastogenesis through the expression of OPG was confirmed in a study using OPG-deficient mice (Kobayashi et al., 2015). WNT3A did not inhibit $1\alpha,25(OH)_2D_3$-induced osteoclast formation in a coculture of normal bone marrow cells with OPG-deficient osteoblastic cells.

Moverare-Skrtic et al. (2014) reported important roles for WNT16 in bone mass. WNT16 mRNA was strongly expressed in cortical bone among the various tissues tested, including trabecular bone, suggesting that WNT16 regulates bone formation and resorption in cortical bone. WNT16-deficient mice showed a marked decrease in cortical bone, but not in cancellous bone. WNT16 induced the expression of OPG through the activation of WNT/β-catenin signaling in MC3T3-E1 osteoblastic cells. Furthermore, osteoclast formation was enhanced in cocultures of WNT16-deficient osteoblastic cells with bone marrow cells, suggesting that WNT16 induced OPG through the activation of WNT/β-catenin signals in osteoblastic cells. WNT16 has also been shown to affect osteoclast precursors by activating noncanonical WNT signals. This topic is discussed later.

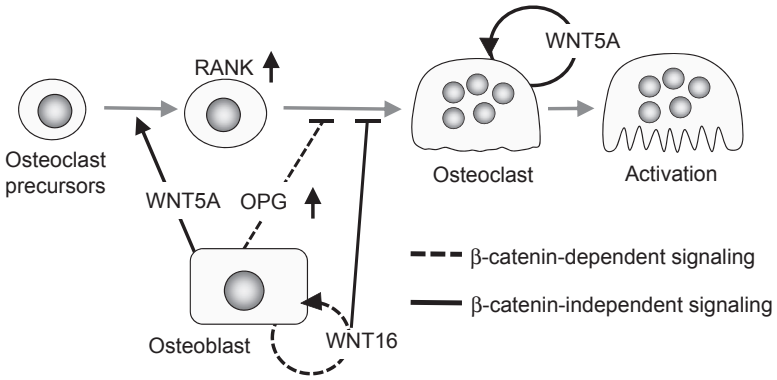

FIGURE 5.5 Regulation of osteoclast differentiation and activation by WNT signals. WNT proteins activate β-catenin-dependent canonical and β-catenin-independent noncanonical signaling pathways. Mice expressing constitutively active β-catenin in mature osteoblasts exhibit an increased bone mass with impaired osteoclast formation. Canonical WNT signals in osteoblastic cells enhance the expression of osteoprotegerin (*OPG*) and inhibit bone resorption. WNT16 is strongly expressed in cortical bone. WNT16 suppresses osteoclast differentiation through the β-catenin-dependent canonical pathway, which enhances OPG production, in osteoblastic cells. WNT16 also acts on osteoclast precursors and inhibits osteoclastic differentiation through noncanonical WNT signaling. WNT5A is a typical ligand for noncanonical WNT signals. WNT5A secreted by osteoblastic cells promotes receptor activator of NF-κB (*RANK*) expression in osteoclast precursors through receptor tyrosine kinase orphan receptor 2 and promotes their osteoclastic differentiation. WNT5A expressed by osteoclasts also induces osteoclast resorptive activity.

The roles of WNT/β-catenin signals in osteoclast precursors have also analyzed. Wei et al. (2011) developed mice expressing a constitutively active form of β-catenin (CA β-cat) or deleted the *β-catenin* gene (Δβ-cat) in osteoclast lineage cells. Both mice with CA β-cat and Δβ-cat osteoclast lineage cells exhibited osteopetrotic phenotypes due to decreased bone resorption. This study showed that β-catenin signals are required for the proliferation of osteoclast precursors, while the sustained activation of β-catenin signals inhibits the differentiation of precursors into osteoclasts. These findings suggest that finely balanced β-catenin signals in osteoclast precursors regulate osteoclastogenesis (Fig. 5.5).

Noncanonical WNT signals

WNT5A is a typical ligand that activates β-catenin-independent noncanonical WNT signals (Mikels et al., 2009) (Fig. 5.5). Receptor tyrosine kinase orphan receptor 1/2 (ROR1/2), coreceptors of WNT proteins, mainly mediate the action of WNT5A. WNT5A secreted by osteoblastic cells promotes osteoclast formation through ROR2, but not ROR1 (Maeda et al., 2012). The conditional deletion of ROR2 in osteoclast precursors and that of WNT5A in osteoblastic cells resulted in impaired osteoclast formation, suggesting that WNT5A−ROR2 signals between osteoblastic cells and osteoclast precursors promote osteoclast differentiation. WNT5A upregulated the expression of RANK in osteoclast precursors through the activation of JNK, thereby enhancing RANKL-induced osteoclast formation.

WNT16 suppressed osteoclast differentiation through the activation of β-catenin-dependent canonical pathways in osteoblastic cells. In contrast, the treatment of osteoclast precursors with WNT16 did not activate WNT/β-catenin signals, but suppressed RANKL-induced NF-κB activation and NFATc1 expression in osteoclast precursors (Moverare-Skrtic et al., 2014; Gori et al., 2015). Furthermore, WNT4 was also reported to inhibit RANKL-induced activation of NF-κB, which in turn suppressed osteoclast formation in a β-catenin-independent manner (Yu et al., 2014). WNT3A activated protein kinase A signals and suppressed the nuclear translocation of NFATc1 in osteoclast precursors, thereby inhibiting osteoclast formation (Weivoda et al., 2016). Thus, WNT16, WNT4, and WNT3A inhibit osteoclast formation through β-catenin-independent noncanonical WNT signals.

The expression of WNT5A and ROR2 was increased in osteoclast precursors during osteoclastic differentiation, suggesting that WNT5A regulates osteoclast function as well as osteoclast differentiation (Uehara et al., 2017). Osteoclast-specific *ROR2* conditional knockout (ROR2 cKO) mice exhibited impaired bone resorption with defects in actin ring formation, but with normal osteoclast formation. The overexpression of the constitutively active form of RHOA, but not that of RAC1, a small GTPase of the RHO family, rescued the impaired bone-resorbing activity of *ROR2* cKO osteoclasts. Osteoclasts strongly expressed protein kinase N3 (PKN3), a RHO effector. *PKN3*-deficient mice exhibited the high bone mass phenotype with the impaired bone-resorbing activity of osteoclasts. SRC activity was weaker in *ROR2* cKO and PKN3-deficient osteoclasts than in wild-type osteoclasts. These findings indicate that WNT5A promotes the bone-resorbing activity of osteoclasts through the ROR2−RHOA−PKN3−SRC signaling axis. The WNT5A−ROR2 signal was also found to promote the invasion of osteosarcoma cells through the activation of SRC and expression of MMP13. These findings suggest that the WNT5A−ROR2 signal plays a role in the degradation of extracellular matrices by activated osteoclasts (Fig. 5.5). Thus, the WNT5A−ROR2 signal in osteosarcomas as well as osteoclasts is critical for degrading extracellular matrices.

Induction of osteoclast function

Adhesion signals

For osteoclasts to become polarized, adhesion signals and cytokine signals need to be simultaneously transmitted into osteoclasts. The induction of osteoclast function begins with the adhesion of osteoclasts to the bone matrix via vitronectin receptors (αVβ3). Adhesion signals transmitted into osteoclasts are summarized in Fig. 5.6. Vitronectin receptors recognize the RGD sequence of extracellular matrix proteins in bone. The targeted disruption of SRC in mice induced osteopetrosis (Soriano et al., 1991). It was also revealed that osteoclasts express high levels of SRC and that SRC-deficient osteoclasts have defects in ruffled border formation (Tanaka et al., 1992; Boyce et al., 1992). Proline-rich tyrosine kinase 2 (PYK2) was identified as a major adhesion-dependent tyrosine kinase in osteoclasts. In osteoclasts derived from SRC-deficient mice, the tyrosine phosphorylation and kinase activity of PYK2 were markedly reduced (Duong et al., 1998). The adaptor molecule, p130 CRK-associated substrate ($p130^{CAS}$), is highly phosphorylated on tyrosine residues and is stably associated with the oncogene products CRK and SRC. Similar to PYK2, $p130^{CAS}$ is highly tyrosine phosphorylated upon osteoclast adhesion to extracellular matrix proteins (Nakamura et al., 1998; Lakkakorpi et al., 1999). $p130^{CAS}$ is not tyrosine

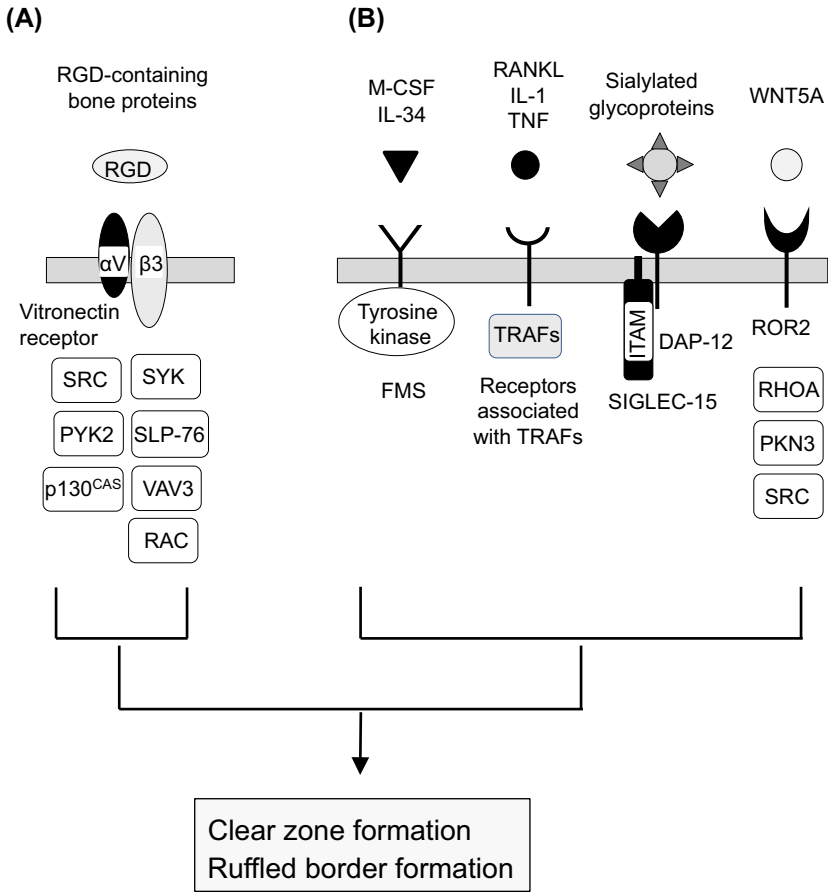

FIGURE 5.6 Signals that induce osteoclast activation. (A) Adhesion signals. The induction of osteoclast function begins with adhesion to the bone matrix via vitronectin receptors (*αVβ3*). Vitronectin receptors recognize the RGD sequence of extracellular matrix proteins in bone. Adhesion signals induce the formation of a signaling complex of SRC, PYK2, and $p130^{CAS}$. This signaling complex induces clear zone formation. Adhesion signals also recruit SLP-76, which functions as an adaptor of VAV3. VAV3 then activates RAC, which participates in αVβ3-mediated cytoskeletal organization in osteoclasts. These adhesion-induced signals are also involved in the induction of the bone-resorbing activity of osteoclasts. **(B) Cytokine signals.** In addition to adhesion signals, cytokine signals need to be transmitted into osteoclasts to induce bone-resorbing activity. M-CSF plays a role in the regulation of bone resorption in collaboration with αVβ3-mediated signals. IL-1 as well as RANKL activates osteoclast function. IL-1 and RANKL use TRAF6 as a signal transducing adaptor. TNFα, which mainly uses TRAF2 as an adaptor, may induce the activation of osteoclasts if each of the endogenous inhibitory molecules is decreased. SIGLEC-15-mediated signals induce the bone-resorbing activity of osteoclasts. WNT5A also promotes the bone-resorbing activity of osteoclasts through the ROR2−RHOA−PKN3−SRC signaling axis. Therefore, adhesion signals and cytokine signals need to be simultaneously transmitted to osteoclasts to induce their bone-resorbing activation. *FMS*, M-CSF receptor; *DAP-12*, DNAX activation protein 12; *IL*, interleukin; *ITAM*, immunoreceptor tyrosine-based activation motif; *M-CSF*, macrophage colony-stimulating factor; *RANKL*, receptor activator of NF-κB ligand; *$p130^{CAS}$*, p130 CRK-associated substrate; *PKN3*, protein kinase N3; *PYK2*, proline-rich tyrosine kinase 2; *ROR2*, receptor tyrosine kinase orphan receptor 2; *SIGLEC-15*, sialic acid-binding immunoglobulin-like lectin 15; *SLP*, SRC homology 2 domain-containing leukocyte protein; *SYK*, spleen tyrosine kinase; *TNF*, tumor necrosis factor; *TRAF*, tumor necrosis factor receptor-associated factor.

phosphorylated in SRC-deficient osteoclasts, indicating that $p130^{CAS}$ is a downstream molecule of SRC. Thus, the three molecules SRC, PYK2, and $p130^{CAS}$ make a complex that plays a role in osteoclast activation (Nakamura et al., 2012).

β3-integrin-null osteoclasts has been shown to be dysfunctional in vivo and in vitro (McHugh et al., 2000; Faccio et al., 2003; Teitelbaum, 2011). VAV3 is a Rho family guanine nucleotide exchange factor. VAV3-deficient osteoclasts showed defective actin cytoskeleton organization and polarization in response to αVβ3 integrin and FMS activation (Faccio et al., 2005). SYK is an upstream regulator of VAV3 in osteoclasts. SYK exerts its effects via intermediaries including SLP adaptor molecules. SLP of 76 kDa (SLP-76) is involved in the SYK-induced activation of VAV3 in osteoclasts (Reeve et al., 2009; Teitelbaum, 2011). Activated VAV3 converts the inactive GDP-bound form of RAC to the active GTP-bound form. RAC then participates in the αVβ3-mediated organization of the osteoclast cytoskeleton. VAV3-deficient mice showed an increased bone mass and were protected from bone loss induced by PTH and RANKL.

Cytokine signals

M-CSF enhances the survival of osteoclasts and also plays a role in the regulation of bone resorption in collaboration with αVβ3-mediated signals (Feng and Teitelbaum, 2013) (Fig. 5.6). The IL-1 receptor (IL-1R) as well as RANK uses TRAF6 as a signal transducing adaptor. IL-1 does not induce osteoclast differentiation, but strongly activates osteoclast function (Thomson et al., 1986; Jimi et al., 1999). Therefore, we considered TRAF6-mediated signals to induce the activation of osteoclasts. However, RANKL stimulation was found to induce the pit-forming activity of TRAF6-deficient osteoclasts when cultured on bone slices (Yao et al., 2017). This finding suggests that a TRAF(s) other than TRAF6 induces the bone-resorbing activity of osteoclasts treated with RANKL. As described previously, TNFα induces the resorptive activity of RANK-deficient osteoclasts in the absence of inhibitory molecules such as NF-κB p100, TRAF3, and RBP-J (Boyce et al., 2015; Zhao et al., 2012). TNFRI and TNFRII mainly use TRAF2 as a signal transducing adaptor. These findings suggest that the TRAF2-mediated signal induces osteoclast activation in the absence of endogenous inhibitory molecules. SIGLEC-15-mediated signals and ROR2-mediated signals in osteoclasts also induce the bone-resorbing activity of osteoclasts. Thus, osteoclast activation is induced through several ligand−receptor systems. These signals appear to cross talk with each other. Importantly, adhesion signals and cytokine signals must be simultaneously transmitted into osteoclasts to induce their resorptive activity (Fig. 5.6).

Characteristics of osteoclast precursors in vivo

RANKL has been considered to influence the site of osteoclast formation because it is expressed by osteoblastic cells. However, when sRANKL is administered to RANKL-deficient mice, osteoclasts are accurately induced in bone (Yamamoto et al., 2006; Takahashi et al., 2010). This is also the case for the administration of M-CSF to *op/op* mice: when M-CSF is administered to M-CSF-deficient *op/op* mice, osteoclasts appear only in bone (Nakamichi et al., 2012). We analyzed the mechanism by which osteoclasts are formed in bone only. Our findings revealed that the lineage-committed precursors that are determined to differentiate into osteoclasts exist in hematopoietic tissues such as bone marrow and the spleen (Mizoguchi et al., 2009; Arai et al., 2012). Lineage-committed precursors are nondividing cells: therefore, we named them "cell cycle-arrested quiescent osteoclast precursors," or qOPs (Muto et al., 2011). As described earlier, qOPs moved from the spleen to bone in *op/op* mice in response to an M-CSF injection. Some qOPs circulate in the bloodstream and settle in bone. qOPs present in bone strongly express RANK. We showed that M-CSF and WNT5A produced by osteoblastic cells induced RANK expression in osteoclast precursors. We named these osteoclast precursors located in bone tissue as "responding osteoclast precursors" (rOPs). rOPs quickly differentiate into osteoclasts without cell cycle progression in response to RANKL. Our hypothesis on osteoclast precursors in vivo is shown in Fig. 5.7.

When TNFα was injected into mice deficient in both RANK and NF-κB p100, osteoclasts formed only in bone. Similarly, a TNFα injection effectively induced osteoclast formation in bone in RBP-J-deficient mice. These findings suggest that if endogenous inhibitory molecules are removed, rOPs differentiate into osteoclasts in response to TNFα. The essential task of RANKL appears to be to effectively eliminate inhibitory molecules in rOPs. We assume that osteoblastic cells play a role in the conversion of qOPs to rOPs. We consider the distribution of rOPs to influence the accurate site of osteoclast formation in vivo.

Conclusion and perspective

Osteoclasts are special cells that secrete hydrochloric acid and proteolytic enzymes from ruffled borders into resorption lacunae and also take up degradation products from ruffled borders into transcytotic vesicles. Degradation products are exocytosed from the FSD. The ruffled border is formed by the fusion of acidified lysosomes to the side of the plasma membrane facing bone. The differentiation of osteoclasts is regulated by M-CSF and RANKL. RANKL expressed by osteoblasts, osteocytes, and hypertrophic chondrocytes, but not by T cells, may support physiological osteoclast formation. In addition to FMS and RANK-mediated signals, ITAM-mediated costimulatory signals are essentially involved in the induction of NFATc1, a master transcription factor for osteoclastogenesis. Canonical and noncanonical WNT signals are important players in the regulation of osteoclast differentiation and function. To induce the resorptive activity of osteoclasts, adhesion signals and cytokine signals must both be simultaneously transmitted into osteoclasts. When RANKL is injected into RANKL-deficient mice, osteoclasts are induced in bone, but not in other tissues. We demonstrate that certain cells such as rOPs are exclusively present in bone. Findings obtained over the past decade have deepened our understanding of osteoclasts. Still, important questions concerning osteoclasts remain as future studies. How do osteoclasts cease bone resorption? Is there a new signaling pathway that controls osteoclast differentiation and function? Is it possible to

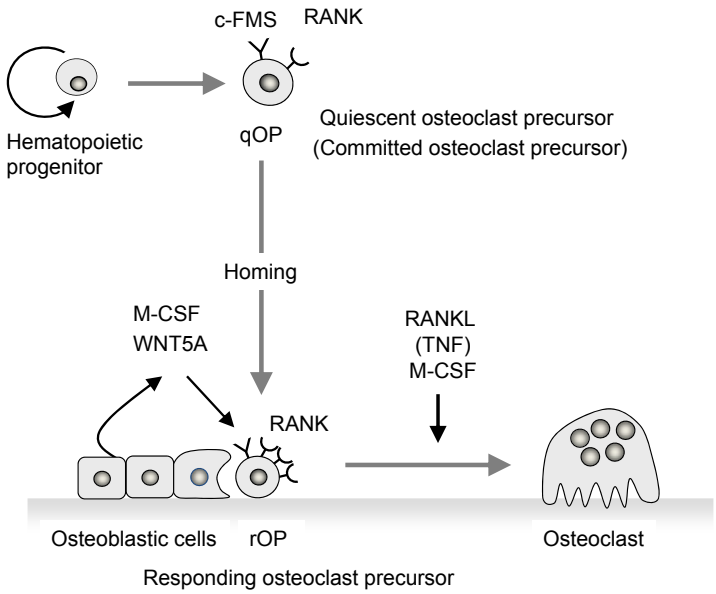

FIGURE 5.7 A hypothetical model of osteoclast differentiation. Osteoclasts are formed from cell cycle−arrested precursors in vivo. These precursor cells are named quiescent osteoclast precursors (*qOPs*). qOPs are the osteoclast lineage−committed precursors derived from hematopoietic tissues. Some qOPs circulate in the bloodstream and settle in bone. qOPs then differentiate into responding osteoclast precursors (*rOPs*). Macrophage colony-stimulating factor (*M-CSF*) and WNT5A produced by osteoblastic cells induce receptor activator of NF-κB (*RANK*) expression in qOPs, suggesting that osteoblastic cells play a role in the appearance of rOPs in bone. rOPs quickly differentiate into osteoclasts in response to receptor activator of NF-κB ligand (*RANKL*). When endogenous inhibitory molecules are removed, rOPs differentiate into osteoclasts in response to tumor necrosis factor α (*TNFα*). When the soluble form of RANKL is administered to RANKL-deficient mice, osteoclasts are induced in bone, but not in other tissues. By assuming rOPs, we may explain why osteoclasts form only in bone. *c-FMS*, M-CSF receptor.

prevent bone loss by adjusting the ITAM and WNT signals? What are the mechanisms integrating adhesion signals and cytokine signals to induce osteoclast activation? How do osteoblastic cells prepare rOPs in bone? These issues are expected to be clarified by future studies.

References

Abu-Amer, Y., Ross, F.P., Schlesinger, P., Tondravi, M.M., Teitelbaum, S.L., 1997. Substrate recognition by osteoclast precursors induces c-src/microtubule association. J. Cell Biol. 137, 247−258.

Akiyama, T., Shimo, Y., Yanai, H., Qin, J., Ohshima, D., Maruyama, Y., Asaumi, Y., Kitazawa, J., Takayanagi, H., Penninger, J.M., Matsumoto, M., Nitta, T., Takahama, Y., Inoue, J., 2008. The tumor necrosis factor family receptors RANK and CD40 cooperatively establish the thymic medullary microenvironment and self-tolerance. Immunity 29, 423−437.

Anderson, D.M., Maraskovsky, E., Billingsley, W.L., Dougall, W.C., Tometsko, M.E., Roux, E.R., Teepe, M.C., DuBose, R.F., Cosman, D., Galibert, L., 1997. A homologue of the TNF receptor and its ligand enhance T-cell growth and dendritic-cell function. Nature 390, 175−179.

Angata, T., Tabuchi, Y., Nakamura, K., Nakamura, M., 2007. Siglec-15: an immune system Siglec conserved throughout vertebrate evolution. Glycobiology 17, 838−846.

Arai, A., Mizoguchi, T., Harada, S., Kobayashi, Y., Nakamichi, Y., Yasuda, H., Penninger, J.M., Yamada, K., Udagawa, N., Takahashi, N., 2012. Fos plays an essential role in the upregulation of RANK expression in osteoclast precursors within the bone microenvironment. J. Cell Sci. 125, 2910−2917.

Barrow, A.D., Raynal, N., Andersen, T.L., Slatter, D.A., Bihan, D., Pugh, N., Cella, M., Kim, T., Rho, J., Negishi-Koga, T., et al., 2011. OSCAR is a collagen receptor that costimulates osteoclastogenesis in DAP12-deficient humans and mice. J. Clin. Invest. 121, 3505−3516.

Begg, S.K., Radley, J.M., Pollard, J.W., Chisholm, O.T., Stanley, E.R., Bertoncello, I., 1993. Delayed hematopoietic development in osteopetrotic (*op/op*) mice. J. Exp. Med. 177, 237−242.

Blair, H.C., Athanasou, N.A., 2004. Recent advances in osteoclast biology and pathological bone resorption. Histol. Histopathol. 19, 189−199.

Blair, H.C., Teitelbaum, S.L., Ghiselli, R., Gluck, S., 1989. Osteoclastic bone resorption by a polarized vacuolar proton pump. Science 245, 855−857.

Bossard, M.J., Tomaszek, T.A., Thompson, S.K., Amegadzie, B.Y., Hanning, C.R., Jones, C., Kurdyla, J.T., McNulty, D.E., Drake, F.H., Gowen, M., Levy, M.A., 1996. Proteolytic activity of human osteoclast cathepsin K. Expression, purification, activation, and substrate identification. J. Biol. Chem. 271, 12517−12524.

Boyce, B.F., Xiu, Y., Li, J., Xing, L., Yao, Z., 2015. NF-kappaB-Mediated regulation of osteoclastogenesis. Endocrinol. Metab. 30, 35−44.

Boyce, B.F., Yoneda, T., Lowe, C., Soriano, P., Mundy, G.R., 1992. Requirement of pp60c-src expression for osteoclasts to form ruffled borders and resorb bone in mice. J. Clin. Invest. 90, 1622–1627.

Cecchini, M.G., Hofstetter, W., Halasy, J., Wetterwald, A., Felix, R., 1994. Role of CSF-1 in bone and bone marrow development. Mol. Reprod. Dev. 46, 75–84.

Chambers, T.J., Magnus, C.J., 1982. Calcitonin alters behaviour of isolated osteoclasts. J. Pathol. 136, 27–39.

Chen, W., Zhu, G., Hao, L., Wu, M., Ci, H., Li, Y.P., 2013. C/EBPalpha regulates osteoclast lineage commitment. Proc. Natl. Acad. Sci. U.S.A. 110, 7294–7299.

Chiu, Y.H., Ritchlin, C.T., 2016. DC-stamp: a key regulator in osteoclast differentiation. J. Cell. Physiol. 231, 2402–2407.

Crockett, J.C., Mellis, D.J., Scott, D.I., Helfrich, M.H., 2011. New knowledge on critical osteoclast formation and activation pathways from study of rare genetic diseases of osteoclasts: focus on the RANK/RANKL axis. Osteoporos. Int. 22, 1–20.

Dai, X.M., Ryan, G.R., Hapel, A.J., Dominguez, M.G., Russell, R.G., Kapp, S., Sylvestre, V., Stanley, E.R., 2002. Targeted disruption of the mouse colony-stimulating factor 1 receptor gene results in osteopetrosis, mononuclear phagocyte deficiency, increased primitive progenitor cell frequencies, and reproductive defects. Blood 99, 111–120.

DeSelm, C.J., Miller, B.C., Zou, W., Beatty, W.L., van Meel, E., Takahata, Y., Klumperman, J., Tooze, S.A., Teitelbaum, S.L., Virgin, H.W., 2011. Autophagy proteins regulate the secretory component of osteoclastic bone resorption. Dev. Cell 21, 966–974.

Dougall, W.C., Glaccum, M., Charrier, K., Rohrbach, K., Brasel, K., De Smedt, T., Daro, E., Smith, J., Tometsko, M.E., Maliszewski, C.R., Armstrong, A., Shen, V., Bain, S., Cosman, D., Anderson, D., Morrissey, P.J., Peschon, J.J., Schuh, J., 1999. RANK is essential for osteoclast and lymph node development. Genes Dev. 13, 2412–2424.

Duong, L.T., Lakkakorpi, P.T., Nakamura, I., Machwate, M., Nagy, R.M., Rodan, G.A., 1998. PYK2 in osteoclasts is an adhesion kinase, localized in the sealing zone, activated by ligation of alpha(v)beta3 integrin, and phosphorylated by src kinase. J. Clin. Invest. 102, 881–892.

Faccio, R., Takeshita, S., Zallone, A., Ross, F.P., Teitelbaum, S.L., 2003. c-Fms and the alphavbeta3 integrin collaborate during osteoclast differentiation. J. Clin. Invest. 111, 749–758.

Faccio, R., Teitelbaum, S.L., Fujikawa, K., Chappel, J., Zallone, A., Tybulewicz, V.L., Ross, F.P., Swat, W., 2005. Vav3 regulates osteoclast function and bone mass. Nat. Med. 11, 284–290.

Fata, J.E., Kong, Y.Y., Li, J., Sasaki, T., Irie-Sasaki, J., Moorehead, R.A., Elliott, R., Scully, S., Voura, E.B., Lacey, D.L., Boyle, W.J., Khokha, R., Penninger, J.M., 2000. The osteoclast differentiation factor osteoprotegerin-ligand is essential for mammary gland development. Cell 103, 41–50.

Felix, R., Cecchini, M.G., Fleisch, H., 1990. Macrophage colony stimulating factor restores *in vivo* bone resorption in the op/op osteopetrotic mouse. Endocrinology 127, 2592–2594.

Feng, X., Takeshita, S., Namba, N., Wei, S., Teitelbaum, S.L., Ross, F.P., 2002. Tyrosines 559 and 807 in the cytoplasmic tail of the macrophage colony-stimulating factor receptor play distinct roles in osteoclast differentiation and function. Endocrinology 143, 4868–4874.

Feng, X., Teitelbaum, S.L., 2013. Osteoclasts: new insights. Bone Res 1, 11–26.

Fukuda, C., Tsuda, E., Okada, A., Amizuka, N., Hasegawa, T., Karibe, T., Hiruma, Y., Takagi, N., Kumakura, S., 2017. Anti-Siglec-15 antibody reduces bone resorption while maintaining bone formation in ovariectomized (OVX) rats and monkeys. In: 2017 ASBMR Annual Meeting, Abstract S112.

Glass 2nd, D.A., Bialek, P., Ahn, J.D., Starbuck, M., Patel, M.S., Clevers, H., Taketo, M.M., Long, F., McMahon, A.P., Lang, R.A., Karsenty, G., 2005. Canonical Wnt signaling in differentiated osteoblasts controls osteoclast differentiation. Dev. Cell 8, 751–764.

Gohda, J., Akiyama, T., Koga, T., Takayanagi, H., Tanaka, S., Inoue, J., 2005. RANK-mediated amplification of TRAF6 signaling leads to NFATc1 induction during osteoclastogenesis. EMBO J. 24, 790–799.

Gori, F., Lerner, U., Ohlsson, C., Baron, R., 2015. A new WNT on the bone: WNT16, cortical bone thickness, porosity and fractures. BoneKEy Rep. 4, 669.

Hamilton, J.A., 1997. CSF-1 signal transduction. J. Leukoc. Biol. 62, 145–155.

Harre, U., Lang, S.C., Pfeifle, R., Rombouts, Y., Fruhbeisser, S., Amara, K., Bang, H., Lux, A., Koeleman, C.A., Baum, W., Dietel, K., Gröhn, F., Malmström, V., Klareskog, L., Krönke, G., Kocijan, R., Nimmerjahn, F., Toes, R.E., Herrmann, M., Scherer, H.U., Schett, G., 2015. Glycosylation of immunoglobulin G determines osteoclast differentiation and bone loss. Nat. Commun. 6, 6651.

Hiruma, Y., Hirai, T., Tsuda, E., 2011. Siglec-15, a member of the sialic acid-binding lectin, is a novel regulator for osteoclast differentiation. Biochem. Biophys. Res. Commun. 409, 424–429.

Hiruma, Y., Tsuda, E., Maeda, N., Okada, A., Kabasawa, N., Miyamoto, M., Hattori, H., Fukuda, C., 2013. Impaired osteoclast differentiation and function and mild osteopetrosis development in Siglec-15-deficient mice. Bone 53, 87–93.

Horton, M.A., Lewis, D., McNulty, K., Pringle, J.A., Chambers, T.J., 1985. Monoclonal antibodies to osteoclastomas (giant cell bone tumors): definition of osteoclast-specific cellular antigens. Cancer Res. 45, 5663–5669.

Humphrey, M.B., Nakamura, M.C., 2016. A comprehensive review of immunoreceptor regulation of osteoclasts. Clin. Rev. Allergy Immunol. 51, 48–58.

Insogna, K.L., Sahni, M., Grey, A.B., Tanaka, S., Horne, W.C., Neff, L., Mitnick, M., Levy, J.B., Baron, R., 1997. Colony-stimulating factor-1 induces cytoskeletal reorganization and c-src-dependent tyrosine phosphorylation of selected cellular proteins in rodent osteoclasts. J. Clin. Investig. 100, 2476–2485.

Ishida-Kitagawa, N., Tanaka, K., Bao, X., Kimura, T., Miura, T., Kitaoka, Y., Hayashi, K., Sato, M., Maruoka, M., Ogawa, T., Miyoshi, J., Takeya, T., 2012. Siglec-15 protein regulates formation of functional osteoclasts in concert with DNAX-activating protein of 12 kDa (DAP12). J. Biol. Chem. 287, 17493–17502.

Ishida, N., Hayashi, K., Hoshijima, M., Ogawa, T., Koga, S., Miyatake, Y., Kumegawa, M., Kimura, T., Takeya, T., 2002. Large scale gene expression analysis of osteoclastogenesis *in vitro* and elucidation of NFAT2 as a key regulator. J. Biol. Chem. 277, 41147–41156.

Ishii, M., Egen, J.G., Klauschen, F., Meier-Schellersheim, M., Saeki, Y., Vacher, J., Proia, R.L., Germain, R.N., 2009. Sphingosine-1-phosphate mobilizes osteoclast precursors and regulates bone homeostasis. Nature 458, 524–528.

Jimi, E., Nakamura, I., Duong, L.T., Ikebe, T., Takahashi, N., Rodan, G.A., Suda, T., 1999. Interleukin 1 induces multinucleation and bone-resorbing activity of osteoclasts in the absence of osteoblasts/stromal cells. Exp. Cell Res. 247, 84–93.

Jurdic, P., Saltel, F., Chabadel, A., Destaing, O., 2006. Podosome and sealing zone: specificity of the osteoclast model. Eur. J. Cell Biol. 85, 195–202.

Kameda, Y., Takahata, M., Komatsu, M., Mikuni, S., Hatakeyama, S., Shimizu, T., Angata, T., Kinjo, M., Minami, A., Iwasaki, N., 2013. Siglec-15 regulates osteoclast differentiation by modulating RANKL-induced phosphatidylinositol 3-kinase/Akt and Erk pathways in association with signaling Adaptor DAP12. J. Bone Miner. Res. 28, 2463–2475.

Kameda, Y., Takahata, M., Mikuni, S., Shimizu, T., Hamano, H., Angata, T., Hatakeyama, S., Kinjo, M., Iwasaki, N., 2015. Siglec-15 is a potential therapeutic target for postmenopausal osteoporosis. Bone 71, 217–226.

Kanaya, T., Hase, K., Takahashi, D., Fukuda, S., Hoshino, K., Sasaki, I., Hemmi, H., Knoop, K.A., Kumar, N., Sato, M., Katsuno, T., Yokosuka, O., Toyooka, K., Nakai, K., Sakamoto, A., Kitahara, Y., Jinnohara, T., McSorley, S.J., Kaisho, T., Williams, I.R., Ohno, H., 2012. The Ets transcription factor Spi-B is essential for the differentiation of intestinal microfold cells. Nat. Immunol. 13, 729–736.

Kim, N., Kadono, Y., Takami, M., Lee, J., Lee, S.H., Okada, F., Kim, J.H., Kobayashi, T., Odgren, P.R., Nakano, H., Yeh, W.C., Lee, S.K., Lorenzo, J.A., Choi, Y., 2005. Osteoclast differentiation independent of the TRANCE-RANK-TRAF6 axis. J. Exp. Med. 202, 589–595.

Kim, N., Takami, M., Rho, J., Josien, R., Choi, Y., 2002. A novel member of the leukocyte receptor complex regulates osteoclast differentiation. J. Exp. Med. 195, 201–209.

Knoop, K.A., Kumar, N., Butler, B.R., Sakthivel, S.K., Taylor, R.T., Nochi, T., Akiba, H., Yagita, H., Kiyono, H., Williams, I.R., 2009. RANKL is necessary and sufficient to initiate development of antigen-sampling M cells in the intestinal epithelium. J. Immunol. 183, 5738–5747.

Kobayashi, K., Takahashi, N., Jimi, E., Udagawa, N., Takami, M., Kotake, S., Nakagawa, N., Kinosaki, M., Yamaguchi, K., Shima, N., Yasuda, H., Morinaga, T., Higashio, K., Martin, T.J., Suda, T., 2000. Tumor necrosis factor alpha stimulates osteoclast differentiation by a mechanism independent of the ODF/RANKL-RANK interaction. J. Exp. Med. 191, 275–286.

Kobayashi, Y., Thirukonda, G.J., Nakamura, Y., Koide, M., Yamashita, T., Uehara, S., Kato, H., Udagawa, N., Takahashi, N., 2015. Wnt16 regulates osteoclast differentiation in conjunction with Wnt5a. Biochem. Biophys. Res. Commun. 463, 1278–1283.

Kobayashi, Y., Udagawa, N., Takahashi, N., 2009. Action of RANKL and OPG for osteoclastogenesis. Crit. Rev. Eukaryot. Gene Expr. 19, 61–72.

Kobayashi, Y., Uehara, S., Udagawa, N., Takahashi, N., 2016. Regulation of bone metabolism by Wnt signals. J. Biochem. 159, 387–392.

Kodama, H., Nose, M., Niida, S., Yamasaki, A., 1991a. Essential role of macrophage colony-stimulating factor in the osteoclast differentiation supported by stromal cells. J. Exp. Med. 173, 1291–1294.

Kodama, H., Yamasaki, A., Nose, M., Niida, S., Ohgame, Y., Abe, M., Kumegawa, M., Suda, T., 1991b. Congenital osteoclast deficiency in osteopetrotic (op/op) mice is cured by injections of macrophage colony-stimulating factor. J. Exp. Med. 173, 269–272.

Koga, T., Inui, M., Inoue, K., Kim, S., Suematsu, A., Kobayashi, E., Iwata, T., Ohnishi, H., Matozaki, T., Kodama, T., Taniguchi, T., Takayanagi, H., Takai, T., 2004. Costimulatory signals mediated by the ITAM motif cooperate with RANKL for bone homeostasis. Nature 428, 758–763.

Kong, Y.Y., Yoshida, H., Sarosi, I., Tan, H.L., Timms, E., Capparelli, C., Morony, S., Oliveira-dos-Santos, A.J., Van, G., Itie, A., Khoo, W., Wakeham, A., Dunstan, C.R., Lacey, D.L., Mak, T.W., Boyle, W.J., Penninger, J.M., 1999. OPGL is a key regulator of osteoclastogenesis, lymphocyte development and lymph-node organogenesis. Nature 397, 315–323.

Kornak, U., Kasper, D., Bosl, M.R., Kaiser, E., Schweizer, M., Schulz, A., Friedrich, W., Delling, G., Jentsch, T.J., 2001. Loss of the ClC-7 chloride channel leads to osteopetrosis in mice and man. Cell 104, 205–215.

Kukita, T., Wada, N., Kukita, A., Kakimoto, T., Sandra, F., Toh, K., Nagata, K., Iijima, T., Horiuchi, M., Matsusaki, H., Hieshima, K., Yoshie, O., Nomiyama, H., 2004. RANKL-induced DC-STAMP is essential for osteoclastogenesis. J. Exp. Med. 200, 941–946.

Kuroda, Y., Hisatsune, C., Nakamura, T., Matsuo, K., Mikoshiba, K., 2008. Osteoblasts induce Ca^{2+} oscillation-independent NFATc1 activation during osteoclastogenesis. Proc. Natl. Acad. Sci. U.S.A. 105, 8643–8648.

Lacey, D.L., Boyle, W.J., Simonet, W.S., Kostenuik, P.J., Dougall, W.C., Sullivan, J.K., San Martin, J., Dansey, R., 2012. Bench to bedside: elucidation of the OPG-RANK-RANKL pathway and the development of denosumab. Nat. Rev. Drug Discov. 11, 401–419.

Lacey, D.L., Timms, E., Tan, H.L., Kelley, M.J., Dunstan, C.R., Burgess, T., Elliott, R., Colombero, A., Elliott, G., Scully, S., Hsu, H., Sullivan, J., Hawkins, N., Davy, E., Capparelli, C., Eli, A., Qian, Y.X., Kaufman, S., Sarosi, I., Shalhoub, V., Senaldi, G., Guo, J., Delaney, J., Boyle, W.J., 1998. Osteoprotegerin ligand is a cytokine that regulates osteoclast differentiation and activation. Cell 93, 165–176.

Lakkakorpi, P.T., Nakamura, I., Nagy, R.M., Parsons, J.T., Rodan, G.A., Duong, L.T., 1999. Stable association of PYK2 and p130(Cas) in osteoclasts and their co-localization in the sealing zone. J. Biol. Chem. 274, 4900–4907.

Lange, P.F., Wartosch, L., Jentsch, T.J., Fuhrmann, J.C., 2006. ClC-7 requires Ostm1 as a beta-subunit to support bone resorption and lysosomal function. Nature 440, 220–223.

Lee, S.H., Kim, T., Jeong, D., Kim, N., Choi, Y., 2008. The tec family tyrosine kinase Btk Regulates RANKL-induced osteoclast maturation. J. Biol. Chem. 283, 11526–11534.

Li, Y.P., Chen, W., Liang, Y., Li, E., Stashenko, P., 1999. Atp6i-deficient mice exhibit severe osteopetrosis due to loss of osteoclast-mediated extracellular acidification. Nat. Genet. 23, 447–451.

Lin, H., Lee, E., Hestir, K., Leo, C., Huang, M., Bosch, E., Halenbeck, R., Wu, G., Zhou, A., Behrens, D., Hollenbaugh, D., Linnemann, T., Qin, M., Wong, J., Chu, K., Doberstein, S.K., Williams, L.T., 2008. Discovery of a cytokine and its receptor by functional screening of the extracellular proteome. Science 320, 807–811.

Lomaga, M.A., Yeh, W.C., Sarosi, I., Duncan, G.S., Furlonger, C., Ho, A., Morony, S., Capparelli, C., Van, G., Kaufman, S., van der Heiden, A., Itie, A., Wakeham, A., Khoo, W., Sasaki, T., Cao, Z., Penninger, J.M., Paige, C.J., Lacey, D.L., Dunstan, C.R., Boyle, W.J., Goeddel, D.V., Mak, T.W., 1999. TRAF6 deficiency results in osteopetrosis and defective interleukin-1, CD40, and LPS signaling. Genes Dev. 13, 1015–1024.

Maeda, K., Kobayashi, Y., Udagawa, N., Uehara, S., Ishihara, A., Mizoguchi, T., Kikuchi, Y., Takada, I., Kato, S., Kani, S., Nishita, M., Marumo, K., Martin, T.J., Minami, Y., Takahashi, N., 2012. Wnt5a-Ror2 signaling between osteoblast-lineage cells and osteoclast precursors enhances osteoclastogenesis. Nat. Med. 18, 405–412.

Mandal, C.C., Ghosh Choudhury, G., Ghosh-Choudhury, N., 2009. Phosphatidylinositol 3 kinase/Akt signal relay cooperates with smad in bone morphogenetic protein-2-induced colony stimulating factor-1 (CSF-1) expression and osteoclast differentiation. Endocrinology 150, 4989–4998.

Martin, T.J., Sims, N.A., 2015. Calcitonin physiology, saved by a lysophospholipid. J. Bone Miner. Res. 30, 212–215.

McHugh, K.P., Hodivala-Dilke, K., Zheng, M.H., Namba, N., Lam, J., Novack, D., Feng, X., Ross, F.P., Hynes, R.O., Teitelbaum, S.L., 2000. Mice lacking beta3 integrins are osteosclerotic because of dysfunctional osteoclasts. J. Clin. Investig. 105, 433–440.

Mikels, A., Minami, Y., Nusse, R., 2009. Ror2 receptor requires tyrosine kinase activity to mediate Wnt5A signaling. J. Biol. Chem. 284, 30167–30176.

Minkin, C., 1982. Bone acid phosphatase: tartrate-resistant acid phosphatase as a marker of osteoclast function. Calcif. Tissue Int. 34, 285–290.

Miyamoto, H., Katsuyama, E., Miyauchi, Y., Hoshi, H., Miyamoto, K., Sato, Y., Kobayashi, T., Iwasaki, R., Yoshida, S., Mori, T., Kanagawa, H., Fujie, A., Hao, W., Morioka, H., Matsumoto, M., Toyama, Y., Miyamoto, T., 2012a. An essential role for STAT6-STAT1 protein signaling in promoting macrophage cell-cell fusion. J. Biol. Chem. 287, 32479–32484.

Miyamoto, H., Suzuki, T., Miyauchi, Y., Iwasaki, R., Kobayashi, T., Sato, Y., Miyamoto, K., Hoshi, H., Hashimoto, K., Yoshida, S., Hao, W., Mori, T., Kanagawa, H., Katsuyama, E., Fujie, A., Morioka, H., Matsumoto, M., Chiba, K., Takeya, M., Toyama, Y., Miyamoto, T., 2012b. Osteoclast stimulatory transmembrane protein and dendritic cell-specific transmembrane protein cooperatively modulate cell-cell fusion to form osteoclasts and foreign body giant cells. J. Bone Miner. Res. 27, 1289–1297.

Miyauchi, Y., Ninomiya, K., Miyamoto, H., Sakamoto, A., Iwasaki, R., Hoshi, H., Miyamoto, K., Hao, W., Yoshida, S., Morioka, H., Chiba, K., Kato, S., Tokuhisa, T., Saitou, M., Toyama, Y., Suda, T., Miyamoto, T., 2010. The Blimp1-Bcl6 axis is critical to regulate osteoclast differentiation and bone homeostasis. J. Exp. Med. 207, 751–762.

Mizoguchi, T., Muto, A., Udagawa, N., Arai, A., Yamashita, T., Hosoya, A., Ninomiya, T., Nakamura, H., Yamamoto, Y., Kinugawa, S., Oda, K., Tanaka, H., Tagaya, M., Penninger, J.M., Ito, M., Takahashi, N., 2009. Identification of cell cycle-arrested quiescent osteoclast precursors *in vivo*. J. Cell Biol. 184, 541–554.

Mocsai, A., Humphrey, M.B., Van Ziffle, J.A., Hu, Y., Burghardt, A., Spusta, S.C., Majumdar, S., Lanier, L.L., Lowell, C.A., Nakamura, M.C., 2004. The immunomodulatory adapter proteins DAP12 and Fc receptor gamma-chain (FcRgamma) regulate development of functional osteoclasts through the Syk tyrosine kinase. Proc. Natl. Acad. Sci. U.S.A. 101, 6158–6163.

Moverare-Skrtic, S., Henning, P., Liu, X., Nagano, K., Saito, H., Borjesson, A.E., Sjogren, K., Windahl, S.H., Farman, H., Kindlund, B., Engdahl, C., Koskela, A., Zhang, F.P., Eriksson, E.E., Zaman, F., Hammarstedt, A., Isaksson, H., Bally, M., Kassem, A., Lindholm, C., Sandberg, O., Aspenberg, P., Sävendahl, L., Feng, J.Q., Tuckermann, J., Tuukkanen, J., Poutanen, M., Baron, R., Lerner, U.H., Gori, F., Ohlsson, C., 2014. Osteoblast-derived WNT16 represses osteoclastogenesis and prevents cortical bone fragility fractures. Nat. Med. 20, 1279–1288.

Mulari, M.T., Zhao, H., Lakkakorpi, P.T., Vaananen, H.K., 2003. Osteoclast ruffled border has distinct subdomains for secretion and degraded matrix uptake. Traffic 4, 113–125.

Muto, A., Mizoguchi, T., Udagawa, N., Ito, S., Kawahara, I., Abiko, Y., Arai, A., Harada, S., Kobayashi, Y., Nakamichi, Y., Penninger, J.M., Noguchi, T., Takahashi, N., 2011. Lineage-committed osteoclast precursors circulate in blood and settle down into bone. J. Bone Miner. Res. 26, 2978–2990.

Nagashima, K., Sawa, S., Nitta, T., Tsutsumi, M., Okamura, T., Penninger, J.M., Nakashima, T., Takayanagi, H., 2017. Identification of subepithelial mesenchymal cells that induce IgA and diversify gut microbiota. Nat. Immunol. 18, 675–682.

Naito, A., Azuma, S., Tanaka, S., Miyazaki, T., Takaki, S., Takatsu, K., Nakao, K., Nakamura, K., Katsuki, M., Yamamoto, T., Inoue, J., 1999. Severe osteopetrosis, defective interleukin-1 signalling and lymph node organogenesis in TRAF6-deficient mice. Genes Cells 4, 353–362.

Nakamichi, Y., Mizoguchi, T., Arai, A., Kobayashi, Y., Sato, M., Penninger, J.M., Yasuda, H., Kato, S., DeLuca, H.F., Suda, T., Udagawa, N., Takahashi, N., 2012. Spleen serves as a reservoir of osteoclast precursors through vitamin D-induced IL-34 expression in osteopetrotic op/op mice. Proc. Natl. Acad. Sci. U.S.A. 109, 10006–10011.

Nakamichi, Y., Udagawa, N., Takahashi, N., 2013. IL-34 and CSF-1: similarities and differences. J. Bone Miner. Metab. 31, 486–495.

Nakamura, I., Jimi, E., Duong, L.T., Sasaki, T., Takahashi, N., Rodan, G.A., Suda, T., 1998. Tyrosine phosphorylation of p130Cas is involved in actin organization in osteoclasts. J. Biol. Chem. 273, 11144–11149.

Nakamura, I., Takahashi, N., Jimi, E., Udagawa, N., Suda, T., 2012. Regulation of osteoclast function. Mod. Rheumatol. 22, 167–177.

Nakashima, T., Hayashi, M., Fukunaga, T., Kurata, K., Oh-Hora, M., Feng, J.Q., Bonewald, L.F., Kodama, T., Wutz, A., Wagner, E.F., Penninger, J.M., Takayanagi, H., 2011. Evidence for osteocyte regulation of bone homeostasis through RANKL expression. Nat. Med. 17, 1231–1234.

Negishi-Koga, T., Gober, H.J., Sumiya, E., Komatsu, N., Okamoto, K., Sawa, S., Suematsu, A., Suda, T., Sato, K., Takai, T., Takayanagi, H., 2015. Immune complexes regulate bone metabolism through FcRgamma signalling. Nat. Commun. 6, 6637.

Nesbitt, S.A., Horton, M.A., 1997. Trafficking of matrix collagens through bone-resorbing osteoclasts. Science 276, 266–269.

Nicholson, G.C., Moseley, J.M., Sexton, P.M., Mendelsohn, F.A., Martin, T.J., 1986. Abundant calcitonin receptors in isolated rat osteoclasts. Biochemical and autoradiographic characterization. J. Clin. Investig. 78, 355–360.

Nishikawa, K., Nakashima, T., Hayashi, M., Fukunaga, T., Kato, S., Kodama, T., Takahashi, S., Calame, K., Takayanagi, H., 2010. Blimp1-mediated repression of negative regulators is required for osteoclast differentiation. Proc. Natl. Acad. Sci. U.S.A. 107, 3117–3122.

Oikawa, T., Kuroda, Y., Matsuo, K., 2013. Regulation of osteoclasts by membrane-derived lipid mediators. Cell. Mol. Life Sci. 70, 3341−3353.

Okamoto, K., Nakashima, T., Shinohara, M., Negishi-Koga, T., Komatsu, N., Terashima, A., Sawa, S., Nitta, T., Takayanagi, H., 2017. Osteoimmunology: the conceptual framework unifying the immune and skeletal systems. Physiol. Rev. 97, 1295−1349.

Okazaki, R., Toriumi, M., Fukumoto, S., Miyamoto, M., Fujita, T., Tanaka, K., Takeuchi, Y., 1999. Thiazolidinediones inhibit osteoclast-like cell formation and bone resorption *in vitro*. Endocrinology 140, 5060−5065.

Ramirez, A., Faupel, J., Goebel, I., Stiller, A., Beyer, S., Stockle, C., Hasan, C., Bode, U., Kornak, U., Kubisch, C., 2004. Identification of a novel mutation in the coding region of the grey-lethal gene OSTM1 in human malignant infantile osteopetrosis. Hum. Mutat. 23, 471−476.

Reeve, J.L., Zou, W., Liu, Y., Maltzman, J.S., Ross, F.P., Teitelbaum, S.L., 2009. SLP-76 couples Syk to the osteoclast cytoskeleton. J. Immunol. 183, 1804−1812.

Reponen, P., Sahlberg, C., Munaut, C., Thesleff, I., Tryggvason, K., 1994. High expression of 92-kD type IV collagenase (gelatinase B) in the osteoclast lineage during mouse development. J. Biol. Chem. 124, 1091−1102.

Rodan, G.A., Martin, T.J., 1981. Role of osteoblasts in hormonal control of bone resorption–a hypothesis. Calcif. Tissue Int. 33, 349−351.

Rossi, S.W., Kim, M.Y., Leibbrandt, A., Parnell, S.M., Jenkinson, W.E., Glanville, S.H., McConnell, F.M., Scott, H.S., Penninger, J.M., Jenkinson, E.J., Lane, P.J., Anderson, G., 2007. RANK signals from CD4(+)3(-) inducer cells regulate development of Aire-expressing epithelial cells in the thymic medulla. J. Exp. Med. 204, 1267−1272.

Saftig, P., Hunziker, E., Wehmeyer, O., Jones, S., Boyde, A., Rommerskirch, W., Moritz, J.D., Schu, P., von Figura, K., 1998. Impaired osteoclastic bone resorption leads to osteopetrosis in cathepsin-K-deficient mice. Proc. Natl. Acad. Sci. U.S.A. 95, 13453−13458.

Salo, J., Lehenkari, P., Mulari, M., Metsikko, K., Vaananen, H.K., 1997. Removal of osteoclast bone resorption products by transcytosis. Science 276, 270−273.

Sato, K., Suematsu, A., Nakashima, T., Takemoto-Kimura, S., Aoki, K., Morishita, Y., Asahara, H., Ohya, K., Yamaguchi, A., Takai, T., Kodama, T., Chatila, T.A., Bito, H., Takayanagi, H., 2006. Regulation of osteoclast differentiation and function by the CaMK-CREB pathway. Nat. Med. 12, 1410−1416.

Sexton, P.M., Findlay, D.M., Martin, T.J., 1999. Curr. Med. Chem. 6, 1067−1093.

Shimizu, T., Takahata, M., Kameda, Y., Endo, T., Hamano, H., Hiratsuka, S., Ota, M., Iwasaki, N., 2015. Sialic acid-binding immunoglobulin-like lectin 15 (Siglec-15) mediates periarticular bone loss, but not joint destruction, in murine antigen-induced arthritis. Bone 79, 65−70.

Shinohara, M., Koga, T., Okamoto, K., Sakaguchi, S., Arai, K., Yasuda, H., Takai, T., Kodama, T., Morio, T., Geha, R.S., Kitamura, D., Kurosaki, T., Ellmeier, W., Takayanagi, H., 2008. Tyrosine kinases Btk and Tec regulate osteoclast differentiation by linking RANK and ITAM signals. Cell 132, 794−806.

Simonet, W.S., Lacey, D.L., Dunstan, C.R., Kelley, M., Chang, M.S., Luthy, R., Nguyen, H.Q., Wooden, S., Bennett, L., Boone, T., Shimamoto, G., DeRose, M., Elliott, R., Colombero, A., Tan, H.L., Trail, G., Sullivan, J., Davy, E., Bucay, N., Renshaw-Gegg, L., Hughes, T.M., Hill, D., Pattison, W., Campbell, P., Sander, S., Van, G., Tarpley, J., Derby, P., Lee, R., Boyle, W.J., 1997. Osteoprotegerin: a novel secreted protein involved in the regulation of bone density. Cell 89, 309−319.

Sly, W.S., Whyte, M.P., Sundaram, V., Tashian, R.E., Hewett-Emmett, D., Guibaud, P., Vainsel, M., Baluarte, H.J., Gruskin, A., Al-Mosawi, M., Sakati, N., Ohlsson, A., 1985. Carbonic anhydrase II deficiency in 12 families with the autosomal recessive syndrome of osteopetrosis with renal tubular acidosis and cerebral calcification. N. Engl. J. Med. 313, 139−145.

Soriano, P., Montgomery, C., Geske, R., Bradley, A., 1991. Targeted disruption of the c-src proto-oncogene leads to osteopetrosis in mice. Cell 64, 693−702.

Stanley, E.R., Chitu, V., 2014. CSF-1 receptor signaling in myeloid cells. Cold Spring Harb. Perspect. Biol 6, a021857.

Stuible, M., Moraitis, A., Fortin, A., Saragosa, S., Kalbakji, A., Filion, M., Tremblay, G.B., 2014. Mechanism and function of monoclonal antibodies targeting siglec-15 for therapeutic inhibition of osteoclastic bone resorption. J. Biol. Chem. 289, 6498−6512.

Suda, T., Takahashi, N., Martin, T.J., 1992. Modulation of osteoclast differentiation. Endocr. Rev. 13, 66−80.

Suzuki, H., Nakamura, I., Takahashi, N., Ikuhara, T., Matsuzaki, K., Isogai, Y., Hori, M., Suda, T., 1996. Calcitonin-induced changes in the cytoskeleton are mediated by a signal pathway associated with protein kinase A in osteoclasts. Endocrinology 137, 4685−4690.

Takahashi, N., Akatsu, T., Udagawa, N., Sasaki, T., Yamaguchi, A., Moseley, J.M., Martin, T.J., Suda, T., 1988. Osteoblastic cells are involved in osteoclast formation. Endocrinology 123, 2600−2602.

Takahashi, N., Muto, A., Arai, A., Mizoguchi, T., 2010. Identification of cell cycle-arrested quiescent osteoclast precursors *in vivo*. Adv. Exp. Med. Biol. 658, 21−30.

Takahashi, N., Udagawa, N., Akatsu, T., Tanaka, H., Isogai, Y., Suda, T., 1991. Deficiency of osteoclasts in osteopetrotic mice is due to a defect in the local microenvironment provided by osteoblastic cells. Endocrinology 128, 1792−1796.

Takayanagi, H., 2007. Osteoimmunology: shared mechanisms and crosstalk between the immune and bone systems. Nat. Rev. Immunol. 7, 292−304.

Takayanagi, H., Kim, S., Koga, T., Nishina, H., Isshiki, M., Yoshida, H., Saiura, A., Isobe, M., Yokochi, T., Inoue, J., Wagner, E.F., Mak, T.W., Kodama, T., Taniguchi, T., 2002. Induction and activation of the transcription factor NFATc1 (NFAT2) integrate RANKL signaling in terminal differentiation of osteoclasts. Dev. Cell 3, 889−901.

Tanaka, S., Suzuki, H., Yamauchi, H., Nakamura, I., Nakamura, K., 2006. Signal transduction pathways of calcitonin/calcitonin receptor regulating cytoskeletal organization and bone-resorbing activity of osteoclasts. Cell. Mol. Biol. 52, 19−23.

Tanaka, S., Takahashi, N., Udagawa, N., Sasaki, T., Fukui, Y., Kurokawa, T., Suda, T., 1992. Osteoclasts express high levels of $p60^{c\text{-}src}$, preferentially on ruffled border membranes. FEBS Lett. 313, 85−89.

Tanaka, S., Takahashi, N., Udagawa, N., Tamura, T., Akatsu, T., Stanley, E.R., Kurokawa, T., Suda, T., 1993. Macrophage colony-stimulating factor is indispensable for both proliferation and differentiation of osteoclast progenitors. J. Clin. Invest. 91, 257–263.

Teitelbaum, S.L., 2007. Osteoclasts: what do they do and how do they do it? Am. J. Pathol. 170, 427–435.

Teitelbaum, S.L., 2011. The osteoclast and its unique cytoskeleton. Ann. N.Y. Acad. Sci. 1240, 14–17.

Teitelbaum, S.L., Ross, F.P., 2003. Genetic regulation of osteoclast development and function. Nat. Rev. Genet. 4, 638–649.

Teti, A., Blair, H.C., Teitelbaum, S.L., Kahn, A.J., Koziol, C., Konsek, J., Zambonin-Zallone, A., Schlesinger, P.H., 1989. Cytoplasmic pH regulation and chloride/bicarbonate exchange in avian osteoclasts. J. Clin. Invest. 83, 227–233.

Tezuka, K., Nemoto, K., Tezuka, Y., Sato, T., Ikeda, Y., Kobori, M., Kawashima, H., Eguchi, H., Hakeda, Y., Kumegawa, M., 1994a. Identification of matrix metalloproteinase 9 in rabbit osteoclasts. J. Biol. Chem. 269, 15006–15009.

Tezuka, K., Tezuka, Y., Maejima, A., Sato, T., Nemoto, K., Kamioka, H., Hakeda, Y., Kumegawa, M., 1994b. Molecular cloning of a possible cysteine proteinase predominantly expressed in osteoclasts. J. Biol. Chem. 269, 1106–1109.

Thomson, B.M., Saklatvala, J., Chambers, T.J., 1986. Osteoblasts mediate interleukin 1 stimulation of bone resorption by rat osteoclasts. J. Exp. Med. 164, 104–112.

Tondravi, M.M., McKercher, S.R., Anderson, K., Erdmann, J.M., Quiroz, M., Maki, R., Teitelbaum, S.L., 1997. Osteopetrosis in mice lacking haematopoietic transcription factor PU.1. Nature 386, 81–84.

Tsuda, E., Goto, M., Mochizuki, S., Yano, K., Kobayashi, F., Morinaga, T., Higashio, K., 1997. Isolation of a novel cytokine from human fibroblasts that specifically inhibits osteoclastogenesis. Biochem. Biophys. Res. Commun. 234, 137–142.

Udagawa, N., Takahashi, N., Akatsu, T., Tanaka, H., Sasaki, T., Nishihara, T., Koga, T., Martin, T.J., Suda, T., 1990. Origin of osteoclasts: mature monocytes and macrophages are capable of differentiating into osteoclasts under a suitable microenvironment prepared by bone marrow-derived stromal cells. Proc. Natl. Acad. Sci. U.S.A. 87, 7260–7264.

Uehara, S., Udagawa, N., Mukai, H., Ishihara, A., Maeda, K., Yamashita, T., Murakami, K., Nishita, M., Nakamura, T., Kato, S., Minami, Y., Takahashi, N., Kobayashi, Y., 2017. Protein kinase N3 promotes bone resorption by osteoclasts in response to Wnt5a-Ror2 signaling. Sci. Signal. 10, 494.

Vaananen, H.K., Laitala-Leinonen, T., 2008. Osteoclast lineage and function. Arch. Biochem. Biophys. 473, 132–138.

Wagner, E.F., Eferl, R., 2005. Fos/AP-1 proteins in bone and the immune system. Immunol. Rev. 208, 126–140.

Walsh, M.C., Lee, J., Choi, Y., 2015. Tumor necrosis factor receptor- associated factor 6 (TRAF6) regulation of development, function, and homeostasis of the immune system. Immunol. Rev. 266, 72–92.

Wan, Y., Chong, L.W., Evans, R.M., 2007. PPAR-gamma regulates osteoclastogenesis in mice. Nat. Med. 13, 1496–1503.

Wei, W., Zeve, D., Suh, J.M., Wang, X., Du, Y., Zerwekh, J.E., Dechow, P.C., Graff, J.M., Wan, Y., 2011. Biphasic and dosage-dependent regulation of osteoclastogenesis by beta-catenin. Mol. Cell Biol. 31, 4706–4719.

Weivoda, M.M., Ruan, M., Hachfeld, C.M., Pederson, L., Howe, A., Davey, R.A., Zajac, J.D., Kobayashi, Y., Williams, B.O., Westendorf, J.J., Khosla, S., Oursler, M.J., 2016. Wnt signaling inhibits osteoclast differentiation by activating canonical and noncanonical cAMP/PKA pathways. J. Bone Miner. Res. 31, 65–75.

Wiktor-Jedrzejczak, W., Bartocci, A., Ferrante Jr., A.W., Ahmed-Ansari, A., Sell, K.W., Pollard, J.W., Stanley, E.R., 1990. Total absence of colony-stimulating factor 1 in the macrophage-deficient osteopetrotic (op/op) mouse. Proc. Natl. Acad. Sci. U.S.A. 87, 4828–4832.

Wiktor-Jedrzejczak, W.W., Ahmed, A., Szczylik, C., Skelly, R.R., 1982. Hematological characterization of congenital osteopetrosis in op/op mouse. Possible mechanism for abnormal macrophage differentiation. J. Exp. Med. 156, 1516–1527.

Wong, B.R., Josien, R., Lee, S.Y., Vologodskaia, M., Steinman, R.M., Choi, Y., 1998. The TRAF family of signal transducers mediates NF-kappaB activation by the TRANCE receptor. J. Biol. Chem. 273, 28355–28359.

Wong, B.R., Rho, J., Arron, J., Robinson, E., Orlinick, J., Chao, M., Kalachikov, S., Cayani, E., Bartlett 3rd, F.S., Frankel, W.N., Lee, S.Y., Choi, Y., 1997. TRANCE is a novel ligand of the tumor necrosis factor receptor family that activates c-Jun N-terminal kinase in T cells. J. Biol. Chem. 272, 25190–25194.

Wu, J., Glimcher, L.H., Aliprantis, A.O., 2008. HCO_3^-/Cl^- anion exchanger SLC4A2 is required for proper osteoclast differentiation and function. Proc. Natl. Acad. Sci. U.S.A. 105, 16934–16939.

Xiong, J., Onal, M., Jilka, R.L., Weinstein, R.S., Manolagas, S.C., O'Brien, C.A., 2011. Matrix-embedded cells control osteoclast formation. Nat. Med. 17, 1235–1241.

Xiong, J., Cawley, K., Piemontese, M., Fujiwara, Y., Macleod, R., Goellner, J., Zhao, H., O'Brien, C., 2017. The soluble form of RANKL contributes to cancellous bone remodeling in adult mice but is dispensable for ovariectomy-induced bone loss. In: 2017 ASBMR Annul Meetinb, Abstract S14.

Xiu, Y., Xu, H., Zhao, C., Li, J., Morita, Y., Yao, Z., Xing, L., Boyce, B.F., 2014. Chloroquine reduces osteoclastogenesis in murine osteoporosis by preventing TRAF3 degradation. J. Clin. Investig. 124, 297–310.

Yagi, M., Miyamoto, T., Sawatani, Y., Iwamoto, K., Hosogane, N., Fujita, N., Morita, K., Ninomiya, K., Suzuki, T., Miyamoto, K., Suzuki, T., Miyamoto, K., Oike, Y., Takeya, M., Toyama, Y., Suda, T., 2005. DC-STAMP is essential for cell-cell fusion in osteoclasts and foreign body giant cells. J. Exp. Med. 202, 345–351.

Yamamoto, T., Kaizu, C., Kawasaki, T., Hasegawa, G., Umezu, H., Ohashi, R., Sakurada, J., Jiang, S., Shultz, L., Naito, M., 2008. Macrophage colony-stimulating factor is indispensable for repopulation and differentiation of Kupffer cells but not for splenic red pulp macrophages in osteopetrotic (op/op) mice after macrophage depletion. Cell Tissue Res. 332, 245–256.

Yamamoto, Y., Udagawa, N., Matsuura, S., Nakamichi, Y., Horiuchi, H., Hosoya, A., Nakamura, M., Ozawa, H., Takaoka, K., Penninger, J.M., Noguchi, T., Takahashi, N., 2006. Osteoblasts provide a suitable microenvironment for the action of receptor activator of nuclear factor-kappaB ligand. Endocrinology 147, 3366−3374.

Yamane, T., Kunisada, T., Tsukamoto, H., Yamazaki, H., Niwa, H., Takada, S., Hayashi, S.I., 2001. Wnt signaling regulates hemopoiesis through stromal cells. J. Immunol. 167, 765−772.

Yao, Z., Lei, W., Duan, R., Li, Y., Luo, L., Boyce, B.F., 2017. RANKL cytokine enhances TNF-induced osteoclastogenesis independently of TNF receptor associated factor (TRAF) 6 by degrading TRAF3 in osteoclast precursors. J. Biol. Chem. 292, 10169−10179.

Yao, Z., Xing, L., Boyce, B.F., 2009. NF-kappaB p100 limits TNF-induced bone resorption in mice by a TRAF3-dependent mechanism. J. Clin. Invest. 119, 3024−3034.

Yasuda, H., Shima, N., Nakagawa, N., Mochizuki, S.I., Yano, K., Fujise, N., Sato, Y., Goto, M., Yamaguchi, K., Kuriyama, M., Kanno, T., Murakami, A., Tsuda, E., Morinaga, T., Higashio, K., 1998a. Identity of osteoclastogenesis inhibitory factor (OCIF) and osteoprotegerin (OPG): a mechanism by which OPG/OCIF inhibits osteoclastogenesis *in vitro*. Endocrinology 139, 1329−1337.

Yasuda, H., Shima, N., Nakagawa, N., Yamaguchi, K., Kinosaki, M., Mochizuki, S., Tomoyasu, A., Yano, K., Goto, M., Murakami, A., Tsuda, E., Morinaga, T., Higashio, K., Udagawa, N., Takahashi, N., Suda, T., 1998b. Osteoclast differentiation factor is a ligand for osteoprotegerin/osteoclastogenesis-inhibitory factor and is identical to TRANCE/RANKL. Proc. Natl. Acad. Sci. U.S.A. 95, 3597−3602.

Yoshida, H., Hayashi, S., Kunisada, T., Ogawa, M., Nishikawa, S., Okamura, H., Sudo, T., Shultz, L.D., Nishikawa, S., 1990. The murine mutation osteopetrosis is in the coding region of the macrophage colony stimulating factor gene. Nature 345, 442−444.

Yoshida, H., Naito, A., Inoue, J., Satoh, M., Santee-Cooper, S.M., Ware, C.F., Togawa, A., Nishikawa, S., Nishikawa, S., 2002. Different cytokines induce surface lymphotoxin-alphabeta on IL-7 receptor-alpha cells that differentially engender lymph nodes and Peyer's patches. Immunity 17, 823−833.

Yu, B., Chang, J., Liu, Y., Li, J., Kevork, K., Al-Hezaimi, K., Graves, D.T., Park, N.H., Wang, C.Y., 2014. Wnt4 signaling prevents skeletal aging and inflammation by inhibiting nuclear factor-kappaB. Nat. Med. 20, 1009−1017.

Zaidi, M., Blair, H.C., Moonga, B.S., Abe, E., Huang, C.L., 2003. Osteoclastogenesis, bone resorption, and osteoclast-based therapeutics. J. Bone Miner. Res. 18, 599−609.

Zhang, Y.H., Heulsmann, A., Tondravi, M.M., Mukherjee, A., Abu-Amer, Y., 2001. Tumor necrosis factor-alpha (TNF) stimulates RANKL-induced osteoclastogenesis via coupling of TNF type 1 receptor and RANK signaling pathways. J. Biol. Chem. 276, 563−568.

Zhao, B., Grimes, S.N., Li, S., Hu, X., Ivashkiv, L.B., 2012. TNF-induced osteoclastogenesis and inflammatory bone resorption are inhibited by transcription factor RBP-J. J. Exp. Med. 209, 319−334.

Zhao, B., Takami, M., Yamada, A., Wang, X., Koga, T., Hu, X., Tamura, T., Ozato, K., Choi, Y., Ivashkiv, L.B., Takayanagi, H., Kamijo, R., 2009. Interferon regulatory factor-8 regulates bone metabolism by suppressing osteoclastogenesis. Nat. Med. 15, 1066−1071.

Zhao, H., Ito, Y., Chappel, J., Andrews, N.W., Teitelbaum, S.L., Ross, F.P., 2008. Synaptotagmin VII regulates bone remodeling by modulating osteoclast and osteoblast secretion. Dev. Cell 14, 914−925.

Zhao, H., Laitala-Leinonen, T., Parikka, V., Vaananen, H.K., 2001. Downregulation of small GTPase Rab7 impairs osteoclast polarization and bone resorption. J. Biol. Chem. 276, 39295−39302.

Chapter 6

The osteocyte

J. Klein-Nulend[1] **and L.F. Bonewald**[2]

[1]Department of Oral Cell Biology, Academic Centre for Dentistry Amsterdam (ACTA), University of Amsterdam and Vrije Universiteit Amsterdam, Amsterdam Movement Sciences, Amsterdam, The Netherlands; [2]Indiana Center for Musculoskeletal Health, Departments of Anatomy and Cell Biology and Orthopaedic Surgery, Indiana University, Indianapolis, IN, USA

Chapter outline

Introduction

The osteocyte is the most abundant cell type in bone. There are approximately 10 times as many osteocytes as osteoblasts in adult human bone (Parfitt, 1977), and the number of osteoclasts is only a fraction of the number of osteoblasts. Our current knowledge of osteocytes lags behind what we know of the properties and functions of both osteoblasts and osteoclasts. However, the striking structural design of bone predicts an important role for osteocytes, and novel techniques have allowed this gap in knowledge to shrink rapidly in the past years.

Considering that osteocytes are located inside the bone, not on the bone surface, and spaced regularly throughout the mineralized matrix, and considering their typical morphology of stellate cells, which are connected to one another via long, slender cell processes, a parallel with the nervous system springs to one's mind. Are the osteocytes the "nerve cells" of the mineralized bone matrix, and if so, what are the stimuli that "excite" these cells? Both theoretical considerations and experimental results have strengthened the notion that osteocytes are the pivotal cells in the biomechanical regulation of bone mass and structure (Cowin et al., 1991; Mullender and Huiskes, 1994, 1995; Klein-Nulend et al., 1995b; Tatsumi et al., 2007; Klein-Nulend et al., 2013 [review]). This idea poses many questions that have to be answered. The development of osteocyte isolation techniques, the use of highly sensitive (immuno)cytochemical and in situ hybridization procedures, and the usefulness of molecular biological methods even when only small numbers of cells are available have rapidly increased our knowledge about this least understood cell type of bone, and will certainly continue to do so in the future. The use of transgenic mouse models to perform targeted deletion of genes has provided considerable information on the function and importance of this bone cell type.

Principles of Bone Biology. https://doi.org/10.1016/B978-0-12-814841-9.00006-3

The osteocytic phenotype

The osteocyte network

Mature osteocytes are stellate-shaped or dendritic cells enclosed within the lacunocanalicular network of bone. The lacunae contain the cell bodies. From these cell bodies, long, slender cytoplasmic processes, dendrites, radiate in all directions, but with the highest density perpendicular to the bone surface (Fig. 6.1). They pass through the bone matrix via small canals, the canaliculi. Processes and their canaliculi may be branched. The more mature osteocytes are connected by these cell processes to neighboring osteocytes, the most recently incorporated osteocytes to neighboring osteocytes and to the cells lining the bone surface. Some of the processes oriented to the bone surface, however, appear not to connect with the lining cells, but pass through this cell layer, thereby establishing a direct contact between the osteocyte network and the extraosseus space. This intriguing observation by Kamioka et al. (2001) suggests the existence of a signaling system between the osteocyte and the bone marrow compartment without intervention of the osteoblasts/lining cells. Osteocytes also appear to be able to retract and extend their dendritic processes, not only between cells in the bone matrix, but also into marrow spaces as shown by dynamic imaging (Veno et al., 2006). This has implications with regard to osteocytes making and breaking communication between cells.

Dramatic changes occur in the distribution of actin-binding proteins during terminal differentiation of osteoblasts to osteocytes (Kamioka et al., 2004). The typical morphology of the osteocyte was originally thought to be enforced on differentiating osteoblasts during their incorporation into the bone matrix. Osteocytes have to remain in contact with other cells and ultimately with the bone surface to ensure the access of oxygen and nutrients. Culture experiments with isolated osteocytes have shown, however, that although the cells lose their stellate shape in suspension, they reexpress this morphology as soon as they settle on a support (Van der Plas and Nijweide, 1992) (Fig. 6.2). Apparently, the typical stellate morphology and the need to establish a cellular network are intrinsic characteristics of terminal osteocyte differentiation.

In bone, gap junctions are present between the tips of the cell processes of connecting osteocytes (Doty, 1981). Within each osteon or hemiosteon (on bone surfaces), therefore, osteocytes form a network of gap junction−coupled cells. As the lacunae are connected via the canaliculi, the osteocyte network represents two network systems: an intracellular one and an extracellular one. Gap junctions are transmembrane channels connecting the cytoplasm of two adjacent cells that regulate the passage of molecules of less than 1 kDa (Goodenough et al., 1966; Bennett and Goodenough, 1978). Gap junction channels are formed by members of a family of proteins known as connexins. One of these members, connexin 43 (Cx43), appears to play an important role in bone cells, as Cx43-null mice have delayed ossification, craniofacial abnormalities, and osteoblast dysfunction (Lecanda et al., 2000). It has been proposed that gap junctions function through the propagation of intracellular signals contributing to mechanotransduction in bone, thereby regulating bone cell differentiation (Donahue, 2000). Fluid-flow-induced shear stress stimulates gap junction−mediated intercellular communication and increases Cx43 expression (Cheng et al., 2001), while oscillating fluid flow has been shown to upregulate gap junction communication by

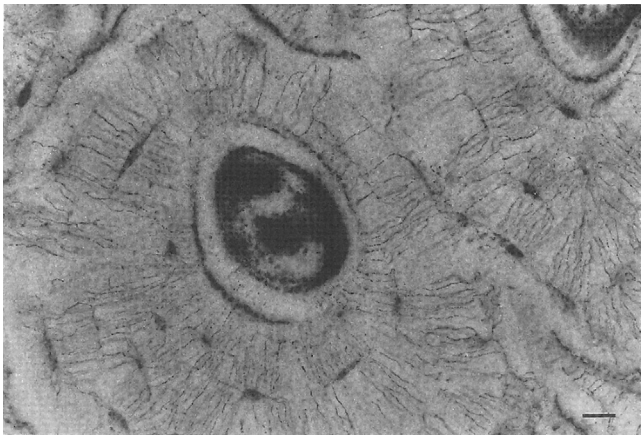

FIGURE 6.1 Osteon in mature human bone. Osteocytes are arranged in concentric circles around the central haversian channel. Note the many cell processes, radiating from the osteocyte cell bodies, in particular in the perpendicular directions. Schmorl staining. (Original magnification, ×390; bar, 25 μm.)

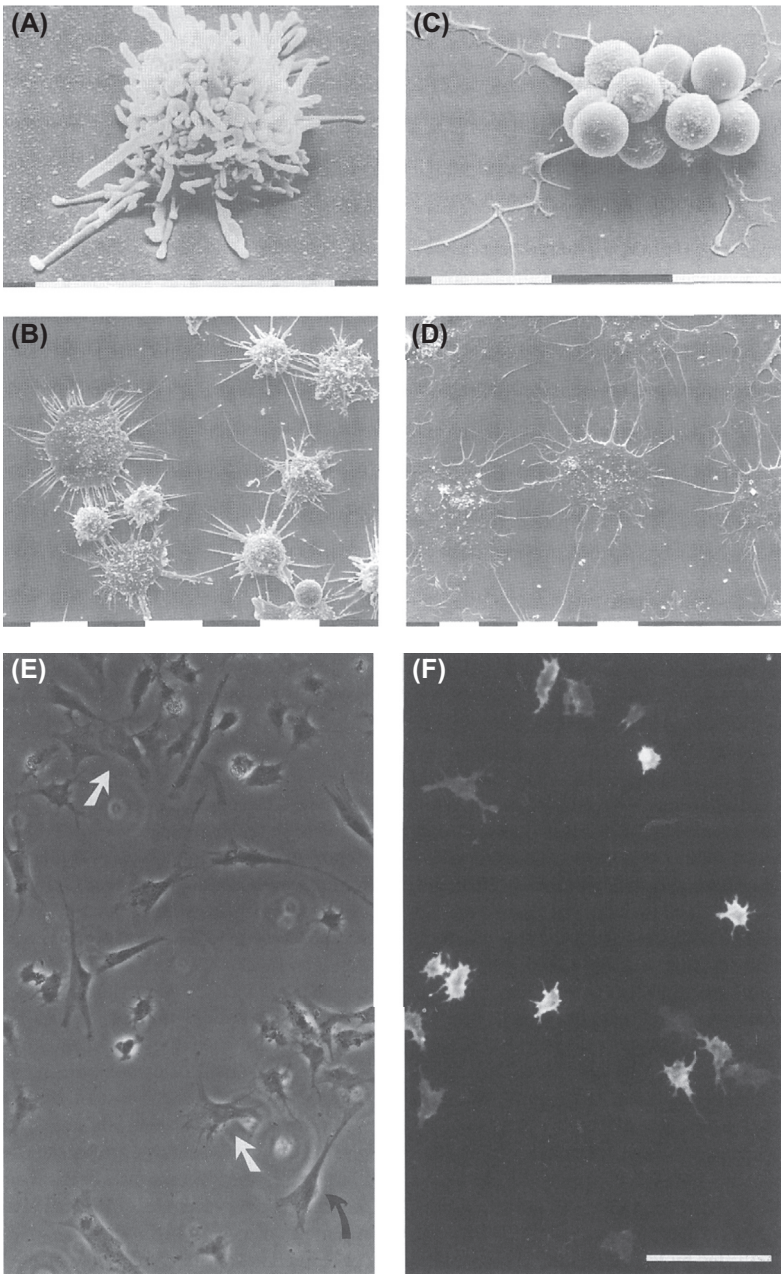

FIGURE 6.2 Isolated osteocytes in culture. Osteocytes were isolated by an immunodissection method using MAb OB7.3-coated magnetic beads. After isolation the cells were seeded on a glass support, cultured for (A) 5 min, (B) 30 min, or (C and D) 24 h and studied with a scanning electron microscope. Immediately after attachment, osteocytes form cytoplasmic extrusions in all directions (A). During subsequent culture the cell processes perpendicular on the support disappear, while the processes in the plane of the support elongate (B) and ultimately form smooth connections between neighboring cells (D). In (A), (B), and (D) the immunobeads were removed from the cells before seeding; in (C) the beads were left on the cells. (Original magnifications, (A) ×7200, (B) ×1400, (C) ×2900, and (D) ×940; bar, 10 μm.) (E and F) Cells were also isolated from periosteum-free 18-day-old chicken calvariae by collagenase digestion, seeded, and cultured for 24 h. Subsequently the osteocytes in the mixed population were specifically stained with MAb OB7.3 in combination with biotinylated horse anti-mouse IgG and streptavidin-Cy3. (E) Phase contrast. (F) Immunofluorescence. *Black arrow*, fibroblast-like cells; *white arrows*, osteoblast-like cells. (Original magnification, ×300; bar, 100 μm.)

an extracellular signal-regulated kinase (ERK) 1/2 mitogen-activated protein kinase-dependent mechanism (Alford et al., 2003) in MLO-Y4 osteocyte-like cells.

Hemichannels, unapposed halves of gap junction channels (Goodenough and Paul, 2003), have been identified in osteocytes localizing at the cell surface, independent of physical contact with adjacent cells. Primary osteocytes and MLO-

Y4 osteocyte-like cells (Kato et al., 1997) express very large amounts of Cx43 compared with other cell types such as osteoblasts, yet these cells are in contact only through the tips of their dendritic processes, raising a question regarding the function of Cx43 on the rest of the cell membrane. The opening of hemichannels results in ATP and NAD^+ release, which in turn raises intracellular Ca^{2+} levels and wave propagation of Ca^{2+}. It has been shown that oscillating fluid flow activates hemichannels in MLO-Y4 osteocyte-like cells, but not in MC3T3-E1 osteoblast-like cells. This activation involved protein kinase C, and resulted in ATP and prostaglandin E_2 (PGE_2) release (Genetos et al., 2007). Hemichannels expressed in bone cells such as MLO-Y4 cells appear to function as essential transducers of the antiapoptotic effects of bisphosphonates (Plotkin et al., 2002) and serve as a portal for the exit of elevated intracellular PGE_2 in osteocytes induced by fluid flow shear stress (Cherian et al., 2005). Integrin $\alpha5\beta1$ interacts with Cx43 to mediate the opening of hemichannels to release prostaglandin in MLO-Y4 cells in response to mechanical stimulation independent of the integrin association with fibronectin and its interaction with the extracellular matrix (Batra et al., 2012). Therefore, gap junctions at the tips of dendrites mediate intracellular communication, while hemichannels along the dendrite and the cell body mediate extracellular communication within the osteocyte network.

In vivo studies have provided additional, sometimes conflicting, information on the functions of Cx43 gap junctions and hemichannels in osteoblasts and osteocytes. Deletion of Cx43 in osteoblasts results in animals with increased osteocyte apoptosis (Bivi et al., 2012). However, mice lacking Cx43 in osteoblasts and/or osteocytes show an increased anabolic response to loading, and decreased catabolic response to unloading (Plotkin et al., 2015). Xu and colleagues generated mice expressing a mutated Cx43 with impaired gap junctions and mice expressing a Cx43 mutant able to form functional hemichannels but unable to form gap junction channels. Mice without both functional gap junctions and functional hemichannels exhibit increased bone mass, whereas mice expressing only hemichannels were not different from wild-type littermate controls (Xu et al., 2015). This study suggests that it is the Cx43 hemichannel and not the gap junction that is responsible for the bone phenotype. It was proposed that hemichannels play a dominant role in osteocyte survival.

Osteocyte formation and death

Osteogenic cells arise from multipotential mesenchymal stem cells (see Chapter 2). These stem cells have the capacity to also differentiate into other lineages, including those of chondroblasts, fibroblasts, adipocytes, and myoblasts (Aubin et al., 1995, Chapter 2). By analogy with hemopoietic differentiation, each of these differentiation lineages is thought to originate from a different committed progenitor, which for the osteogenic lineage is called the osteoprogenitor. Osteodifferentiation progresses via a number of progenitor and precursor stages to the mature osteoblast. Osteoblasts have one of three fates: embedding in their own osteoid, differentiating into an osteocyte; quiescing into a lining cell, or undergoing apoptosis (for review see Manolagas, 2000). The mechanism by which osteoblasts differentiate into osteocytes is, however, still unknown. Imai et al. (1998) found evidence that osteocytes may stimulate osteoblast recruitment and differentiation by expressing osteoblast stimulating factor-1 (OSF-1) (Tezuka et al., 1990). The osteoblasts further differentiate into osteocytes, being surrounded by the osteoid matrix that they produce, and they then may become a new source of OSF-1 for the next round of osteoblast recruitment. The expression of OSF-1 in osteocytes may be activated by local damage to bone or local mechanical stress (Imai et al., 1998). Marotti (1996) has postulated that a newly formed osteocyte starts to produce an osteoblast inhibitory signal when its cytoplasmic processes connecting the cell with the osteoblast layer have reached their maximal length. The osteoid production of the most adjacent, most intimately connected osteoblast will be relatively more inhibited by that signal than that of its neighbors. The inactivated osteoblast then spreads over a larger bone surface area, thereby reducing its linear appositional rate of matrix production even further. A second consequence of the widening and flattening of the cell is that it may intercept more osteocytic processes carrying the inhibitory signal. This positive feedback mechanism results in the embedding of the cell in matrix produced by the neighboring osteoblasts. Ultimately, the cell will acquire the typical osteocyte morphology and the surrounding matrix will become calcified. The theory of Marotti (1996) is based entirely on morphological observations. There is no biochemical evidence on the nature or even the existence of the proposed inhibitory factor. Martin (2000) has, however, used the concept successfully in explaining mathematically the changing rates of matrix formation during bone remodeling.

Osteoid-osteocytes were described by Palumbo (1986) to be cells actively making matrix and calcifying this matrix while the cell body reduces in size in parallel with the formation of cytoplasmic processes. Bordier et al. (1976) and Nijweide et al. (1981) proposed that osteoid-osteocytes play an important role in the initiation and control of mineralization of the bone matrix. During the time in which an osteoblast has become an osteocyte, the cell has manufactured three times its own volume in matrix (Owen, 1995). Franz-Odendaal et al. (2006) propose that once a cell is surrounded by osteoid, the differentiation process has not ended, but continues.

An enzyme that is produced in high amounts by embedding osteoid-osteocytes and not by osteoblasts, casein kinase II, appears to be responsible for the phosphorylation of matrix proteins essential for mineralization (Mikuni-Takagaki et al., 1995). Phosphoproteins appear to be essential for bone mineralization as evidenced in vitro by crystal nucleation assays (Boskey, 1996) and in vivo by osteomalacia in animal models with deletion of (osteocyte-specific) genes such as dentin matrix protein 1 (DMP1) and PHEX (phosphate-regulating gene with homologies to endopeptidases on the X chromosome) (Strom et al., 1997). The roles of these proteins in mineral homeostasis will be discussed later in this chapter. An osteocyte-selective promoter, the 8-kb DMP1, driving green fluorescent protein (GFP) identifies embedding and embedded osteocytes (Kalajzic et al., 2004). With the identification of other markers selective for osteocytes, such as E11/gp38 for early osteocytes (Zhang et al., 2006) and sclerostin for late osteocytes (Poole et al., 2005), new tools have been generated for the study of osteocyte formation.

The life span of osteocytes is probably largely determined by bone turnover, when osteoclasts resorb bone and either "liberate" or destroy osteocytes. Osteocytes may have half-lives of decades if the particular bone they reside in has a slow turnover rate (Parfitt, 1977). The fate of living osteocytes that are liberated by osteoclast action is unknown as of this writing. Some of them, only half released by osteoclastic activity, may be reembedded during new bone formation that follows the resorption process (Suzuki et al., 2000). These osteocytes are then the cells that cross the cement lines between individual osteons, sometimes seen in cross sections of osteonal bone. It has been shown by Kalajzic et al. that isolated osteocytes can partially dedifferentiate into osteoblasts (Torregiani et al., 2013). Most of the osteocytes, however, will probably die by apoptosis and become phagocytosed. Phagocytosis of osteocytes by osteoclasts as part of the bone resorption process has been documented in several reports (Bronckers et al., 1996; Elmardi et al., 1990).

Apoptosis of osteocytes in their lacunae is attracting growing attention because of its expected consequence of decreased bone mechanoregulation, which may lead to osteoclastic bone resorption (Tan et al., 2007, 2008). Osteocyte apoptosis can occur with immobilization, microdamage, estrogen deprivation, elevated cytokines, glucocorticoid treatment, osteoporosis, osteoarthritis, and aging. The resulting fragility is considered to be due to loss of the ability of osteocytes to signal other bone cells for repair due to loss of the capacity to sense microdamage (Manolagas, 2000; Noble et al., 2003). Apoptotic regions around microcracks were found to be surrounded by surviving osteocytes expressing Bcl-2, whereas dying osteocytes appeared to be the target of resorbing osteoclasts (Verborgt et al., 2000, 2002). Apoptotic changes in osteocytes were shown to be associated with high bone turnover (Noble et al., 1997). However, fatigue-related microdamage in bone may cause decreased osteocyte accessibility for nutrients and oxygen, inducing osteocyte apoptosis and subsequent bone remodeling (Burger and Klein-Nulend, 1999; Verborgt et al., 2000). Lack of oxygen elevates hypoxia-inducible factor-1α, a transcription activator, by inactivation of prolyl hydroxylase leading to apoptosis and induction of the osteoclastogenic factor tumor necrosis factor α (TNFα) (Gross et al., 2001), vascular endothelial growth factor, and osteopontin, a mediator of environmental stress and a potential chemoattractant for osteoclasts (Gross et al., 2005).

In contrast to overloading, which induces microdamage, physiological mechanical loads might prevent osteocyte apoptosis in vivo. Mechanical stimulation of osteocytes in vitro, by means of a pulsating fluid flow (PFF), affects TNFα-induced apoptosis. One-hour PFF (0.70 ± 0.30 Pa, 5 Hz) inhibited (25%) TNFα-induced apoptosis in osteocytes, but not in osteoblasts or periosteal fibroblasts (Tan et al., 2006). Although the exact mechanism is not clear, loading-induced nitric oxide production by the osteocytes might be involved in the antiapoptotic effects of mechanical loading. Prostaglandin produced by osteocytes in response to fluid flow shear stress also blocks MLO-Y4 apoptosis (Kitase et al., 2006).

Also, loss of estrogen (Tomkinson et al., 1998) and chronic glucocorticoid treatment (Weinstein et al., 1998) were demonstrated to induce osteocyte apoptosis, which may, at least in part, explain the bone-deleterious effects of these conditions. Several agents, such as bisphosphonates and calcitonin (Plotkin et al., 1999), CD40 ligand (Ahuja et al., 2003), calbindin-D28k (Liu et al., 2004), and estrogen and selective estrogen receptor modulators (Kousteni et al., 2001), have been found to reduce or inhibit osteoblast and osteocyte apoptosis. Bisphosphonates inhibit apoptosis through interaction with Cx43 hemichannels and the ERK pathway (Plotkin and Bellido, 2001). Interestingly, the two antiapoptotic agents parathyroid hormone (PTH) and monocyte chemotactic protein-3 (MCP-3) have been shown to be selective for apoptosis induced by one particular agent, glucocorticoids. Unlike the agents listed earlier, both PTH (Jilka et al., 1999) and MCP-3 will inhibit only glucocorticoid-induced apoptosis, and not TNFα-induced apoptosis, of MLO-Y4 osteocyte-like cells (Kitase et al., 2006).

Osteocyte viability is crucial for the normal functioning of the skeleton and the normal function of other organs such as kidney through fibroblast growth factor 23 (FGF23) production by osteocytes, but also muscle. Osteocyte factors such as PGE_2 and Wnt3a promote myogenesis and enhance muscle function (Mo et al., 2012; Huang et al., 2017). Mice with targeted deletion of Cx43 in osteocytes have a reduced muscle phenotype (Shen et al., 2015). Conversely, secreted muscle factors prevent glucocorticoid-induced osteocyte apoptosis (Jahn et al., 2012), and β-aminoisobutyric acid produced by

contracted muscle with exercise will prevent reactive oxygen−induced osteocyte apoptosis (Kitase et al., 2018). These investigators also found that this muscle metabolite will prevent bone and muscle loss with unloading.

Both mechanical loading and intracellular autophagy play important roles in bone homeostasis. Autophagy is a catabolic process that is regulated by multiple factors and is associated with skeletal diseases. It has been shown that fluid shear stress induces protective autophagy in osteocytes and that mechanically induced autophagy is associated with ATP metabolism and osteocyte survival (Zhang et al., 2018). Moreover, microRNA-199a-3p is involved in the estrogen regulatory networks that mediate MLO-Y4 osteocyte autophagy, potentially by targeting insulin-like growth factor 1 (IGF-1) and mammalian target of rapamycin (Fu et al., 2018).

In summary, osteocyte viability may play a significant role in the maintenance of bone homeostasis and integrity and other organs (Dallas et al., 2013), yet agents that block apoptosis may exacerbate conditions that require repair.

Osteocyte isolation

Analysis of osteocyte properties and functions has long been hampered by the fact that osteocytes are embedded in a mineralized matrix. Although sensitive methods are now available, such as immunocytochemistry and in situ hybridization, by which osteocytes can be studied in the tissue in some detail, osteocyte isolation and culture offer a major step forward. This approach became possible by the development of osteocyte-specific antibodies (Fig. 6.3) directed to antigenic sites on the outside of the cytoplasmic membrane (Bruder and Caplan, 1990; Nijweide and Mulder, 1986). Using an immunodissection method, Van der Plas and Nijweide (1992) subsequently succeeded in the isolation and purification of chicken osteocytes from mixed bone cell populations isolated from fetal bones by enzymatic digestion. A detailed description of the isolation procedure has been published (Semeins et al., 2012). Isolated osteocytes appeared to behave in vitro like they do in vivo in that they reacquired their stellate morphology and, when seeded sparsely, formed a network of cells coupled to one another by long, slender, often branched cell processes (Fig. 6.2). The cells retained this morphology in culture throughout the time studied (5−7 days) and even reexpressed it when passaged for a second time (Van der Plas and Nijweide, 1992).

Mikuni-Takagaki et al. (1995) isolated seven cell fractions from rat calvariae by sequential digestion. They claimed that the last fraction consisted of osteocytic cells. The cells displayed dendritic cell processes, were negative for alkaline phosphatase, had high extracellular activities of casein kinase II and ecto-5′-nucleotidase, and produced large amounts of osteocalcin. After a few days of little change in cell number, the cells of fraction VII, the osteocytic cells, proliferated, but

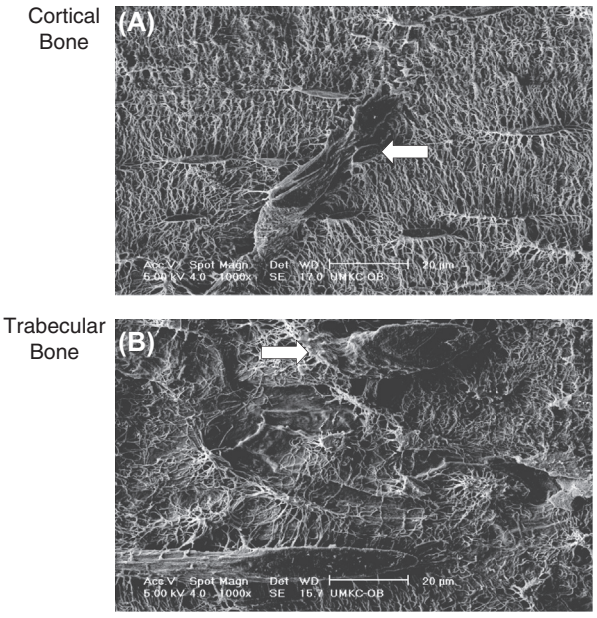

FIGURE 6.3 Images of acid-etched resin-embedded murine (A) cortical and (B) trabecular bone visualized by scanning electron microscopy showing the complexity of the osteocyte lacunocanalicular system and the intimate relationship between the lacunocanalicular system and blood vessels. In the cortical bone, note the linear alignment of the lacunae and the complexity of the canaliculi. In the trabecular bone, the lacunae are not as organized as in the cortical bone. In both sections, note the close relationship of some osteocyte lacunae with blood vessels (*arrows*).

equally fast as those of fraction III, the osteoblastic cells, in culture. With the identification of new osteocyte-selective markers such as Sost, E11/gp38, Dmp1, Phex, and Mepe, it is becoming easier to identify isolated osteocytes (see later).

A methods paper written by Stern and Bonewald (2015) provides a review of the different approaches used to isolate osteocytes from bone. Consistent approaches include collagenase digestions and calcium chelation. In this review, the authors also described isolation of osteocytes from aged bone through the use of bone particle culture. The yield of primary osteocytes decreases with the age of the animal. The isolation is easiest when the bone is hypomineralized as in young animals but becomes more difficult in hypermineralized bone as occurs in aged animals. In summary, whereas primary osteocytes can be isolated from bone, the process is still long compared with soft tissue or bone surface cells.

As of this writing, culture of human osteocytes in vitro remains a challenge. Culture of denuded human bone chips with osteocytes embedded in their native matrix has been shown to overcome this challenge, and provides a three-dimensional model that can be used to study osteocyte function and signaling (Pathak et al., 2016). Pathak and colleagues showed that these osteocytes highly express mRNA of osteocyte-specific signaling molecules (Pathak et al., 2016). The isolation of osteocytes from human trabecular bone samples acquired during surgery has been described (Prideaux et al., 2016). A protocol was used whereby the cells were digested from the bone matrix by sequential collagenase and ethylenediaminetetraacetic acid (EDTA) digestions, and the cells from later digests displayed characteristic dendritic osteocyte morphology when cultured ex vivo. These cells represent an important tool in enhancing current knowledge in human osteocyte biology.

Osteocyte markers

In bone, osteocytes are fully defined by their location within the bone matrix and their stellate morphology. One marker for isolated osteocytes is therefore their typical morphology, which they reacquire in culture (Mikuni-Takagaki et al., 1995; Van der Plas and Nijweide, 1992). Related to this stellate morphology, osteocytes have a typical cytoskeletal organization, which is important for the osteocyte's response to loading (McGarry et al., 2005a,b). It has been shown that the dendrite is the primary mechanosensing part of the osteocyte compared with the cell body (Burra et al., 2010). The prominent actin bundles in the osteocytic processes, together with the abundant presence of the actin-bundling protein fimbrin, are exemplary for osteocytes and are retained after isolation (Tanaka-Kamioka et al., 1998). In addition, osteocytes are generally found to express osteocalcin, osteonectin, and osteopontin, but show little alkaline phosphatase activity, particularly the more mature cells (Aarden et al., 1996b). As stated previously, these metabolic markers have, however, little discriminating value in mixtures of isolated cells. Franz-Odendaal et al. (2006) provide a list of molecular markers for the preosteoblast to the osteocyte.

Initially mainly morphology was used to describe osteocytes until osteocyte-specific antibodies became available. Early examples are the monoclonal antibodies MAb OB7.3 (Nijweide and Mulder, 1986) (Fig. 6.2), MAb OB37.11 (Nijweide et al., 1988), and MAb SB5 (Bruder and Caplan, 1990). All three are specific for avian osteocytes and do not cross-react with mammalian cells. The identities of two of the three antigens involved have not been reported, but that of OB7.3 has been elucidated and found to be the avian homolog of mammalian *Phex* (Westbroek et al., 2002). Using an antibody to Phex allowed purification of avian osteocytes from enzymatically isolated bone cells.

Osteoblast/osteocyte factor 45 (OF45), also known as MEPE (matrix extracellular phosphoglycoprotein), is also highly expressed in osteocytes compared with osteoblasts. Messenger RNA expression of OF45/MEPE begins at embryonic day 20 in more differentiated osteoblasts that have become encapsulated by bone matrix (Igarashi et al., 2002). *Mepe* was isolated and cloned from a TIO tumor cDNA library (Rowe et al., 2000). Cathepsin D or B can cleave MEPE, releasing the highly phosphorylated C-terminal ASARM region that is a potent inhibitor of mineralization in vitro (Bresler et al., 2004; Rowe et al., 2005). OF45/MEPE-null mice have increased bone formation, bone mass, and resistance to age-associated trabecular bone loss (Gowen et al., 2003). The authors speculate that osteocytes act directly on osteoblasts through OF45/MEPE to inhibit their bone-forming activity.

Both Toyosawa et al. (2001) and Feng et al. (2006) found Dmp1 to be highly expressed in osteocytes with very low expression in osteoblasts. DMP1 is specifically expressed along and in the canaliculi of osteocytes within the bone matrix (Feng et al., 2006). Deletion of this gene in mice results in a phenotype similar if not identical to the hyp phenotype, suggesting that Dmp1 and Phex are interactive and essential for phosphate metabolism. Potential roles for DMP1 in osteocytes may be related to the posttranslational processing and modification resulting in a highly phosphorylated protein and regulator of hydroxyapatite formation. Interestingly, Dmp1 and OF45/MEPE belong to the SIBLING (small, integrin-binding ligand, N-linked glycoprotein) family, which also includes bone sialoprotein, osteopontin, and sialophosphoprotein (Fisher and Fedarko, 2003). This family of proteins may function differently in osteocytes compared with other cell

types, especially upon phosphorylation with casein kinase II, a marker of the osteoblast-to-osteocyte transition (Mikuni-Takagaki et al., 1995).

Schulze et al. (1999) and Zhang et al. (2006) have described the expression of E11/gp38 exclusively in osteocytes and not in osteoblasts in vivo. A punctate antibody reaction is observed at the interface between osteoblasts and uncalcified osteoid at the tips and along dendritic processes with less reactivity in osteocytes deeper in the bone matrix. E11/gp38 appears to be responsible for the formation of dendritic processes, as a reduction in protein expression using a short interfering RNA approach led to a decrease in dendrite extension in MLO-Y4 osteocyte-like cells in response to shear stress (Zhang et al., 2006). E11/gp38 colocalizes with ezrin, radixin, and moesin (Scholl et al., 1999), which are concentrated in cell-surface projections where they link the actin cytoskeleton to plasma membrane proteins and are involved in cell motility (Mangeat et al., 1999). CD44 is highly expressed in osteocytes compared with osteoblasts (Hughes et al., 1994), and as E11 is physically associated with CD44 in tumor vascular endothelial cells (Ohizumi et al., 2000), this association most likely occurs in osteocytes to regulate the formation of dendritic processes.

Sclerostin appears to be highly expressed in the mature and not the early osteocyte (Poole et al., 2005). Transgenic mice lacking sclerostin have increased bone mass, and the human condition sclerostosis is due to a premature termination of the SOST gene (Balemans et al., 2001). Sclerostin clearly functions as a Wnt antagonist by binding Lrp5 (Van Bezooijen et al., 2004), a receptor shown to be an important positive regulator of bone mass (Li et al., 2005). Sclerostin protein may be transported through canaliculi to the bone surface to inhibit bone-forming osteoblasts. Sclerostin is downregulated by mechanical loading (Robling et al., 2006). It has also been proposed that the anabolic effects of PTH are through inhibition of SOST expression (Bellido et al., 2005). Neutralizing antibody to sclerostin is being developed as a therapeutic to treat osteoporosis. The antibody blocks or reduces bone loss and supports bone formation, promotes fracture healing, and is a potential therapeutic for a number of conditions of low bone mass, such as osteogenesis imperfecta (Clarke, 2014). In clinical trials, despite very potent effects in increasing bone mass, the FDA rejected approval of the anti-sclerostin antibody romosozumab for osteoporosis treatment due to a higher rate of serious adverse cardiovascular events compared with alendronate (Medscape, 2017). This was a devastating event after following such a potent inducer of bone mass for over a decade. However, as of this writing, the late-phase data from this clinical study are being refiled to show the drug has a positive risk−benefit profile, while other anti-sclerostin monoclonal antibodies are being developed (MacNabb et al., 2016).

FGF23 is a major phosphate-regulating hormone responsible for autosomal dominant hypophosphatemic rickets, for phosphate wasting in tumor-induced osteomalacia, and for X-linked hypophosphatemia. FGF23 is not normally expressed at high levels in osteocytes in the healthy state but is dramatically upregulated in both DMP1- and PHEX-associated hypophosphatemic rickets (Liu et al., 2007). Clinkenbeard and White (2016) performed FGF23 deletion using Col2.3-Cre for osteoblasts and DMP1-Cre for early osteocytes and showed that both osteoblasts and osteocytes are the physiological source of FGF23. More information on the function and regulation of FGF23 is provided later.

It has been shown that receptor activator of NF-κB ligand (RANKL) is a functional marker of osteocytes. Primary osteocytes express RANKL (Kramer et al., 2010), and osteocytes express greater amounts of RANKL than osteoblasts and are better supporters of osteoclast formation (Nakashima et al., 2011; Xiong et al., 2011, 2015). Deletion of RANKL using the 10-kb Dmp1-Cre or Sost-Cre results in mice with increased bone mass. Like sclerostin, RANKL is increased with unloading (Xiong et al., 2011).

In summary, it is becoming easier to define cells as osteocytic. Even though the E11/gp38 molecule is expressed in other tissues (known as podoplanin in kidney and also known as PA2.26, T1a, etc.), it is expressed only in osteocytes, not osteoblasts, in bone (Zhang et al., 2006). While E11/gp38, Phex, and Dmp1 appear to be markers for the early osteocyte, MEPE and Sost/sclerostin are specific markers for the late osteocyte (Poole et al., 2005). Dmp1 and Phex, while expressed in low levels in osteoblasts and other tissues, are highly elevated in early osteocytes. Combining these markers with other properties such as dendricity and low or no alkaline phosphatase can be useful to define not only isolated primary cells, but also cell lines.

Osteocytic cell lines

Since the number of primary osteocytes that can be isolated from chickens each time (Van der Plas and Nijweide, 1992) is limited, several groups have tried to establish osteocytic cell lines. Basically, an osteocytic cell line is a contradiction in terms. Osteocytes are postmitotic. However, a cell line of proliferating precursor cells that would differentiate into osteocytes under specific circumstances could prove to be very valuable in the study of osteocyte properties and functions. HOB-01-C1 (Bodine et al., 1996) is a temperature-sensitive cell line, prepared from immortalized, cloned human adult bone cells. It proliferates at 34°C but stops dividing at 39°C. HOB-01-C1 cells display putative osteocytic markers, such as cellular processes, low alkaline phosphatase activity, high osteocalcin production, and the expression of CD44.

MLO-Y4 (Kato et al., 1997) is an osteocyte-like cell line that expresses high amounts of E11/gp38 (Zhang et al., 2006), CD44, osteocalcin, and osteopontin and has low alkaline phosphatase activity. Numerous investigators have used these cells to examine gap junctions, hemichannels, apoptosis, and other potential functions of osteocytes (Genetos et al., 2007; Plotkin et al., 2005; Vatsa et al., 2006, 2007; Xiao et al., 2006; Zaman et al., 2006; Zhang et al., 2006; Cherian et al., 2005; Liu et al., 2004; Alford et al., 2003; Ahuja et al., 2003; Zhao et al., 2002; Heino et al., 2002, 2004; Cheng et al., 2001; Yellowley et al., 2000) and, as of the updating of this chapter, there are over 250 references using these cells to investigate osteocyte function. Estrogen will reduce support of osteoclast formation by MLO-Y4 cells through an increase in transforming growth factor β3 (Heino et al., 2002) and induce MLO-Y4 cells to support osteoblast mesenchymal stem cell differentiation (Heino et al., 2004), supporting the hypothesis that osteocytes are orchestrators of both bone resorption and bone formation. Observations using these cells have been validated in vivo. For example, MLO-Y4 cells support osteoclast formation through RANKL expression (Zhao et al., 2002) and apoptotic bodies released from MLO-Y4 cells express RANKL (Kogianni et al., 2008). The outcomes using this cell line have been validated using transgenic mouse models generated by two different laboratories showing that RANKL is mainly functional in osteocytes (Nakashima et al., 2011; Xiong et al., 2011).

MLO-A5 cells, a postosteoblast/preosteocyte-like cell line established from the long bones of 14-day-old mice expressing the large T antigen driven by the osteocalcin promoter, differentiate into osteoid-osteocyte-like cells (Kato et al., 2001). MLO-A5 cells express all of the markers of the late osteoblast, such as high alkaline phosphatase, bone sialoprotein, PTH type 1 receptor, and osteocalcin, but begin to express markers of osteocytes such as E11/gp38 as they generate cell processes. MLO-A5 cells generate nanospherites that bud from and mineralize on their developing cellular processes. As the cellular process narrows in diameter, these mineralized structures become associated with and initiate collagen-mediated mineralization (Barragan-Adjemian et al., 2006). PTH has been shown to reduce Sost/sclerostin expression in these cells (Bellido et al., 2005). This is an excellent cell line to study collagen production, regulation, and mineralization, as they are prodigious producers of collagen (Yang et al., 2015; Lu et al., 2018).

Compared with primary osteoblasts and clonal cells, the MLO-Y4 cells show relatively high expression of osteocalcin and Cx43 with low expression of collagen type I and periostin, as well as low alkaline phosphatase activity. However, both MLO-A5 and MLO-Y4 cells have their limitations, such as the lack of sclerostin expression and low DMP1 expression by MLO-Y4 cells. This makes MLO-Y4 cells less suitable for studying signaling molecule production by mature osteocytes. Alternative cell lines that have been used to study sclerostin expression include the SaOS2 osteosarcoma cell line and the osteoblast-like UMR-106 cells. IDG-SW3 (Woo et al., 2011) and Ocy454 (Spatz et al., 2015) are osteocyte cell lines that express relatively high levels of SOST/sclerostin as well as FGF23, both key regulators of bone homeostasis, and could therefore be used to study osteocyte signaling toward other cell types.

The IDG-SW3 osteocyte cell line undergoes a temporally dependent process that replicates the osteoblast-to-osteocyte transition (Woo et al., 2011). This cell line was made from long bones of mice carrying a Dmp1 promoter driving GFP crossed with the Immortomouse. These cells can be expanded at 33°C in the presence of interferon γ (IFN-γ) and then allowed to resume their original phenotype at 37°C in the absence of IFN-γ. Another cell line has been made from the same mice, called Ocy454 (Spatz et al., 2015). Comparisons between the two cell lines suggest that sclerostin expression occurs earlier and is higher in the Ocy454 cells compared with IDG-SW3.

Cementocytes, like osteocytes, are mechanosensory cells, and when the cementocyte cell line IDG-CM6 was compared with IDG-SW3 in their response to shear stress, IDG-CM6 cells significantly increased RANKL, with no change in IDG-SW3 cells, and significantly reduced osteoprotegerin (OPG) in contrast to increased expression by IDG-SW3 cells. The higher OPG/RANKL ratio in IDG-CM6 cementocytes under fluid flow shear stress suggests a potential mechanism for the lack of cementum resorption observed during physiological use and in orthodontic tooth movement (Zhao et al., 2016). Cementocytes in vivo and in vitro express key markers known to be important in osteocyte differentiation, including *Dmp1*/DMP1, *E11/gp38*, and *Sost*/sclerostin. Loss-of-function studies in mice produced cellular cementum phenotypes resembling those in bone, showing that these factors operate in similar fashions in both tissues.

Matrix synthesis

The subcellular morphology of osteocytes and the fact that they are encased in mineralized matrix do not suggest that osteocytes partake to a large extent in matrix production. Osteocytes, especially the more mature cells, have relatively few organelles necessary for matrix production and secretion. Nevertheless, a limited secretion of specific matrix proteins may be essential for osteocyte function and survival. Several arguments are in favor of such limited matrix production. First, as the mineralization front lags behind the osteoid formation front in areas of new bone formation, osteocytes may be involved in the maturation and mineralization of the osteoid matrix by secreting specific matrix molecules. It is, however,

also possible that osteocytes enable the osteoid matrix to be mineralized by phosphorylating certain matrix constituents, as was suggested by Mikuni-Takagaki et al. (1995). Mikuni-Takagaki et al. proposed that casein kinase II, produced in high amounts by embedding osteoid-osteocytes and not by osteoblasts, is responsible for phosphorylation of matrix proteins essential for mineralization. Therefore, the embedding osteoid cell and the osteocyte probably play roles in the mineralization process and potentially in phosphate metabolism (see later). Osteocytes have to inhibit mineralization of the matrix directly surrounding them to ensure the diffusion of oxygen, nutrients, and waste products through the lacunocanalicular system. Osteocalcin, which is expressed to a relatively high extent by osteocytes, may play an important role here (Aarden et al., 1996b; Ducy et al., 1996; Mikuni-Takagaki et al., 1995), as do OF45/MEPE and Sost. Osteocytes have been found positive for osteocalcin and osteonectin (Aarden et al., 1996b), molecules that are probably involved in the regulation of calcification. Osteopontin, fibronectin, and collagen type I (Aarden et al., 1996b) have also been demonstrated in and immediately around (isolated) osteocytes. These proteins may be involved in osteocyte attachment to the bone matrix (see later). Osteocytes also express Notch, which plays a critical role in mineralization (Shao et al., 2018a, 2018b). Finally, if osteocytes are the mechanosensor cells of bone (see later), the attachment of osteocytes to matrix molecules is likely to be of major importance for the transduction of stress signals into cellular signals. Production and secretion of specific matrix molecules offer a possibility for the cells to regulate their own adhesion and, thereby, sensitivity for stress signals.

In addition to collagenous and noncollagenous proteins, the bone matrix contains proteoglycans. These macromolecules consist of a core protein to which one or more glycosaminoglycan side chains are covalently bound. Early electron microscopical studies (Jande, 1971) showed that the osteocyte body, as well as its cell processes, is surrounded by a thin layer of unmineralized matrix containing collagen fibrils and proteoglycans. The proteoglycans were shown to consist of chondroitin 4-sulfate, dermatan sulfate, and keratan sulfate with immunocytochemical methods (Maeno et al., 1992; Smith et al., 1997; Takagi et al., 1997). These observations are supported by the findings of Sauren et al. (1992), who demonstrated an increased presence of proteoglycans in the pericellular matrix by staining with the cationic dye cuprolinic blue. Of special interest is the reported presence of hyaluronan in osteocyte lacunae (Noonan et al., 1996). CD44, which is highly expressed on the osteocyte membrane, is a hyaluronan-binding protein and also binds to collagen, fibronectin, and osteopontin (Nakamura and Ozawa, 1996; Yamazaki et al., 1999). The essential pericellular matrix component perlecan/HSPG2, a large monomeric heparan sulfate proteoglycan, acts as a strong but elastic tether that connects the osteocyte cell body to the bone matrix (Wijeratne et al., 2016). Solute transport in the lacunar–canalicular system plays an important role in osteocyte metabolism and cell–cell signaling. The pericellular matrix-filled lacunar–canalicular system is bone's chromatographic column, where fluid/solute transport to and from the osteocytes is regulated. A better definition of the chemical composition, deposition rate, and turnover rate of the osteocyte pericellular matrix will improve our understanding of osteocyte physiology and bone metabolism (reviewed by Wang, 2018).

The osteocyte cytoskeleton and cell–matrix adhesion

As mentioned earlier, the cell–matrix adhesion of osteocytes is of importance for the translation of biomechanical signals produced by loading of bone into chemical signals. Study of the adhesion of osteocytes to extracellular matrix molecules became feasible with the development of osteocyte isolation and culture methods (Van der Plas and Nijweide, 1992). These studies found little difference between the adhesive properties of osteocytes and osteoblasts, although the patterns of adhesion plaques (osteocytes, many small focal contacts; osteoblasts, larger adhesion plaques) were quite different (Aarden et al., 1996a). Both cell types adhered equally well to collagen type I, osteopontin, vitronectin, fibronectin, and thrombospondin. Integrin receptors are involved, as is shown by the inhibiting effects of small peptides containing an RGD sequence on the adhesion to some of these proteins. Adhesion to all aforementioned matrix molecules was blocked by an antibody reacting with the β_1-integrin subunit (Aarden et al., 1996a). The identity of the α units involved is unknown as of this writing.

Deformation of the bone matrix upon loading may cause a physical "twisting" of integrins at sites where osteocytes adhere to the matrix. Integrins are coupled to the cytoskeleton via molecules such as vinculin, talin, and α-actinin. In osteocytes, especially in the osteocytic cell processes, the actin-bundling protein fimbrin appears to play a prominent role (Tanaka-Kamioka et al., 1998). Mechanical twisting of the cell membrane via integrin-bound beads has been demonstrated to induce cytoskeletal rearrangements in cultured endothelial cells (Wang and Ingber, 1994). The integrin–cytoskeleton complex may therefore play a role as an intracellular signal transducer for stress signals (Litzenberger et al., 2010; Santos et al., 2010). Spectrin, another structural cytoskeletal protein required for the differentiation of osteoblasts to osteocytes (Bonewald, 2011), has been identified as a mechanosensitive element within the osteocyte (Wu et al., 2017). Disruption of the spectrin network promotes Ca^{2+} influx and nitric oxide (NO) secretion as a result of reduced stiffness. In addition to the integrins, the nonintegrin adhesion receptor CD44 may contribute to the attachment of osteocytes to the surrounding

matrix. CD44 is present abundantly on the osteocyte surface (Hughes et al., 1994; Nakamura et al., 1995) and is also linked to the cytoskeleton.

Evidence is accumulating highlighting the crucial role of the cytoskeleton in a multitude of cellular processes. The cytoskeleton, just like our bony skeleton, provides structure and support for the cell, is actively adapted, and is highly responsive to external physical and chemical stimuli. The cytoskeleton is strongly involved in processes such as migration, differentiation, mechanosensing, and even cell death, and largely determines the material properties of the cell (i.e., stiffness).

For bone cells it was shown that the production of signaling molecules in response to an in vitro fluid shear stress (at 5 and 9 Hz) and vibration stress (5−100 Hz) correlated with the applied stress rate (Bacabac et al., 2004, 2006; Bacabac et al., 2006a,b; Mullender et al., 2006). The faster the stress was applied, the stronger the observed response of the cells. Interestingly, high-rate stimuli were found to condition bone cells to be more sensitive to high-frequency, low-amplitude loads (Bacabac et al., 2005). From the field of physics, it is known that the effects of stresses applied at different rates on an object are largely determined by the material properties of that object. This implies that bone cellular metabolic activity (e.g., the production of signaling molecules) and mechanical properties of the cell are related. Bacabac et al. (2006b) developed a novel application of two-particle microrheology, for which he devised a three-dimensional in vitro system using optical traps to quantify the forces induced by cells on attached fibronectin-coated probes (4 μm). The frequency at which the cells generate forces on the beads is related to the metabolic activity of the cell. This system can also be used to apply controlled forces on the cell using the beads, and enables the study of cells under a controlled three-dimensional morphological configuration, with possibilities for a variety of probe coatings for simulating cell−extracellular matrix attachment. Using this setup the generation of forces by different cells was probed to understand the relation between cellular metabolic activities and material properties of the cell. It was shown that at 37°C, CCL-224 fibroblasts exhibited higher force fluctuation magnitude compared with MLO-Y4 osteocytes (Bacabac et al., 2006b). The force fluctuations on the attached probes reflect intracellular movement, which might include actin (and microtubule) polymerization, as well as motor and cross-linker dynamics. Since cell migration involves these dynamic processes, the lower magnitude of force fluctuation might reflect a lower capacity of osteocytes for motility compared with fibroblasts.

Using the optical trap device, the material properties of round suspended MLO-Y4 osteocytes and flat adherent MLO-Y4 osteocytes were characterized. In addition, the cells were loaded with an NO-sensitive fluorescent dye (Vatsa et al., 2006) and the NO response of the cells to forces applied on the cell using the attached probes was studied. Osteocytes under round suspended morphology required lower force stimulation to show an NO response, even though they were an order of magnitude more elastic compared with flat adherent cells (Bacabac et al., 2006b). Apparently, elastic osteocytes require less mechanical force to respond than stiffer cells. On the other hand, flat adherent MLO-Y4 cells, primary chicken osteocytes, MC3T3-E1 osteoblasts, and primary chicken osteoblasts all showed similar elastic moduli of less than 1 kPa (Bacabac et al., 2006b), even though osteocytes are known to be more responsive to mechanical stress than osteoblasts (Klein-Nulend et al., 1995a). This indicates that differences in mechanosensitivity between cells might not be directly related to the elasticity of the cell, but might be more related to other cell-specific properties (i.e., the presence of receptors or ion channels in the membrane). Alternatively, the mechanosensitivity of a cell might be related to how cells change their material properties in relation to deformation.

Simultaneous with the increased NO release in response to mechanical stimulation, MLO-Y4 osteocytes showed increased force traction on the attached beads. In other words, the cells started to "pull harder" on the beads and generated a force up to nearly 30 pN, which interestingly is within the order of forces necessary for activating integrins. Whether there is a causal link between loading-induced NO production by the cells and force generation is under investigation at the time of writing. Since force generation and cell elasticity are (indirectly) related, these results might indicate that osteocytes adapt their elasticity in response to a mechanical stimulus. Indeed, experiments with an atomic force microscope and optical tweezers have shown that osteocytes become "stiffer" after mechanical loading (Bacabac et al., 2006b, and unpublished observations). This stiffening response was related to actual changes in material properties of the cell, suggesting that the cells actively change their cytoskeleton in response to a mechanical load.

Considering the role of the osteocytes as the professional mechanosensors of bone, and the importance of the cytoskeleton for the response of osteocytes to mechanical loading, much is to be expected from research focusing on the cytoskeletal components of the osteocyte (reviewed by Klein-Nulend et al., 2012).

Hormone receptors in osteocytes

PTH receptors have been demonstrated on rat osteocytes in situ (Fermor and Skerry, 1995) and on isolated chicken osteocytes (Van der Plas et al., 1994). Administered in vitro, PTH was reported to increase cAMP levels in isolated chicken

osteocytes (Van der Plas et al., 1994; Miyauchi et al., 2000) and, administered in vivo, to increase fos protein (Takeda et al., 1999) and the mRNAs of c-fos, c-jun, and I1-6 in rat osteocytes (Liang et al., 1999). Matrix metalloproteinase 14 (MMP14) has been shown to be a novel target of PTH signaling in osteocytes that controls resorption by regulating soluble RANKL production (Delgado-Calle et al., 2018). As it is now generally accepted that osteocytes are involved in the transduction of mechanical signals into chemical signals regulating bone (re)modeling, PTH might modulate the osteocytic response to mechanical strain. Injection of PTH into rats was shown to augment the osteogenic response of bone to mechanical stimulation in vivo, whereas thyroparathyroidectomy abrogated the mechanical responsiveness of bone (Chow et al., 1998). However, such an approach cannot separate an effect at the level of osteocyte mechanosensing from one at the level of osteoprogenitor recruitment. One mechanism by which PTH may act on osteocytes was suggested by the reports of Schiller et al. (1992) and Donahue et al. (1995). These authors found that PTH increased Cx43 gene expression and gap-junctional communication in osteoblastic cells. In osteocytes, where cell-to-cell communication is so important, a similar effect might lead to more efficient communication within the osteocyte network. Osteocytes also express the receptor for the carboxy-terminal region of PTH that may play a role in osteocyte viability (Divieti et al., 2001). Activation of receptors for 1,25-dihydroxyvitamin D_3 ($1,25(OH)_2D_3$), which were also shown to be present in osteocytes by immunocytochemistry (Boivin et al., 1987) and by in situ hybridization (Davideau et al., 1996), may have similar effects.

Parfitt concluded in the 1970s that osteocytes control the rapid release of calcium (within minutes) in response to PTH (Parfitt, 1976). More recent in vivo studies have supported Parfitt's hypothesis that osteocytes are the target of PTH. There are profound skeletal effects in transgenic mice with the activation of the PTH receptor in osteocytes (O'Brien et al., 2008; Rhee et al., 2011). Mice lacking the PTH receptor in osteocytes lose less bone with lactation, and an increase in osteocyte lacunar size is absent (Qing et al., 2012). This "perilacunar remodeling" related to "osteocytic osteolysis" (Bélanger, 1969) is achieved by the expression of so-called "osteoclast-specific genes" such as carbonic anhydrases, ATPases, MMP13, cathepsin K, and TRAP (tartrate-resistant acid phosphatase) by the osteocyte. In 2017 it was shown that osteocytes reduce the pH within their lacunocanalicular network during lactation, a process necessary for the release of calcium (Jähn et al., 2017).

Another important hormone involved in bone metabolism is estrogen. Numerous studies have demonstrated that a decrease in blood estrogen levels is accompanied by a loss of bone mass. One explanation for this phenomenon is that estrogen regulates the set point for the mechanical responsiveness of bone (Frost, 1992), i.e., that lowering the ambient estrogen level increases the level of strain in bone necessary for the bone to respond with increased bone formation. If osteocytes are the main mechanosensors of bone, it is reasonable to suppose that osteocytes are the site of set-point regulation by estrogen. Estrogen receptors (ERα) were demonstrated in osteocytes with immunocytochemistry and in situ hybridization (Braidman et al., 1995; Hoyland et al., 1999) in tissue sections. In addition, Westbroek et al. (2000b) found higher levels of ERα in isolated osteocytes than in osteoblasts or osteoblast precursors. It has been shown that the anabolic response of bone to mechanical loading requires ERα (Lee et al., 2003). Studies suggest that osteocytes indeed use ERα to respond to strain, although the ERα content is regulated by estrogen (Zaman et al., 2006). In vivo studies performing targeted deletion of ERα in osteocytes using the Dmp1-Cre model have generally found a reduction in trabecular bone either in females (Kondoh et al., 2014) or in males (Windahl et al., 2013). It is not clear why these studies observed differences in the two sexes.

Receptors for PTH, $1,25(OH)_2D_3$, and estrogen, as well as the androgen receptor (Abu et al., 1997), the glucocorticoid receptor α (Abu et al., 2000; Silvestrini et al., 1999), and various prostaglandin receptors (Lean et al., 1995; Sabbieti et al., 1999), have been described in osteocytes. The prostaglandin receptors, in addition to viability, may be important for communication within the osteocyte network during mechanotransduction (see later). As outlined earlier, glucocorticoids clearly induce osteocyte apoptosis, but may have additional effects. Glucocorticoid treatment causes mature osteocytes to enlarge their lacunae and remove mineral from their microenvironment (Lane et al., 2006). Therefore, osteocytes appear to be able to modify their microenvironment in response to certain factors such as PTH/PTH-related protein and glucocorticoids.

Osteocyte function

Blood–calcium/phosphate homeostasis

The organization of osteocytes as a network of gap junction–coupled cells in each osteon represents such a unique structure that one expects it to have an important function in the metabolism and maintenance of bone. The network offers two advantages that may be exploited by the tissue:

1. a tremendous cell−bone surface contact area, about 2 orders of magnitude larger than the contact area the osteoblasts and lining cells have (Johnson, 1966),
2. an extensive intracellular and an extracellular communication system between sites within the bone and the bone surface.

The first consideration led Bélanger (1969) and others to propose the hypothesis that osteocytes are capable of local bone remodeling or osteocytic osteolysis. According to this hypothesis, osteocytes are coresponsible for blood−calcium homeostasis. Later studies (Boyde, 1980; Marotti et al., 1990) supplied alternative explanations for the observations that appeared to support the osteocytic osteolysis theory. The possibility remains, however, that osteocytes are involved in the facilitation of calcium diffusion in and out of the bone (Bonucci, 1990). Although the bulk of calcium transport in and out of the bone is apparently taken care of by osteoblasts and osteoclasts (Boyde, 1980; Marotti et al., 1990), osteocytes may have a function in the fine regulation of blood−calcium homeostasis. The major emphasis of present-day thinking is, however, on the role of the osteocyte network as a three-dimensional sensor and communication system in bone.

Osteocytes may also play a major role in phosphate homeostasis. PHEX is a metalloendoproteinase found on the plasma membrane of osteoblasts and osteocytes (Ruchon et al., 2000) whose substrate is not known. The precise function of PHEX is unclear but it clearly plays a role in phosphate homeostasis and bone mineralization. *Pex* deletion or loss of function results in X-linked hypophosphatemic rickets (The HYP Consortium, 1995). Nijweide and coworkers (Westbroek et al., 2002) were one of the first groups to propose that the osteocyte network could be considered a gland that regulates bone phosphate metabolism through expression of PHEX.

Other proteins known to regulate mineralization and mineral homeostasis are also highly expressed in osteocytes, such as DMP1, Mepe, and sclerostin. Deletion or mutation of DMP1, a gene that is highly expressed in embedding osteocytes and mature osteocytes, results in hypophosphatemic rickets (Feng et al., 2006), similar to the deletion of Phex. DMP1 is expressed along the canalicular wall, while Phex is expressed on the membrane surface of dendrites and the cell body. Other players in mineral metabolism include MEPE and FGF23, which are also highly expressed in osteocytes (Liu et al., 2006). FGF23 is highly elevated in osteocytes in DMP1-null mice, which results in hypophosphatemia in these animals. The osteocyte network might be viewed as an endocrine gland regulating mineral metabolism. Another fascinating hypothesis is that mineral metabolism is regulated by mechanical loading. DMP1 and Pex gene expression are increased in response to load (Gluhak-Heinrich et al., 2003), Sost expression is inhibited (Robling et al., 2006), while a biphasic response is observed for Mepe expression (Gluhak-Heinrich et al., 2005). Whether FGF23 expression is also regulated by loading is unknown as of this writing. Therefore proteins known to regulate mineralization and mineral homeostasis are also regulated by mechanical loading in osteocytes. These osteocyte regulators of mineral homeostasis can also be responsible for disease. For a review of the physiological and pathological functions of these molecules see Bonewald (2017).

Functional adaptation, Wolff's law

Functional adaptation is the term used to describe the ability of organisms to increase their capacity to accomplish a specific function with increased demand and to decrease this capacity with lesser demand. In the 19th century, the anatomist Julius Wolff proposed that mechanical stress is responsible for determining the architecture of bone and that bone tissue is able to adapt its mass and three-dimensional structure to the prevailing mechanical usage to obtain a higher efficiency of load bearing (Wolff, 1892). For the past century, Wolff's law has become widely accepted. Adaptation will improve an individual animal's survival chance because bone is not only hard but also heavy. Too much of it is probably as bad as too little, leading either to uneconomic energy consumption during movement (for too high a bone mass) or to an enhanced fracture risk (for too low a bone mass). This readily explains the usefulness of mechanical adaptation as an evolutionary driver, even if we do not understand how it is performed.

Osteocytes as mechanosensory cells

In principle, all cells of bone may be involved in mechanosensing, as eukaryotic cells in general are sensitive to mechanical stress (Oster, 1989). However, several features argue in favor of osteocytes as the mechanosensory cells *par excellence* of bone as discussed earlier in this chapter. From a cell biological viewpoint, therefore, bone tissue is a three-dimensional network of cells, most of which are surrounded by a very narrow sheath of unmineralized matrix, followed by a much wider layer of mineralized matrix. The sheath of unmineralized matrix is penetrated easily by macromolecules such as albumin and peroxidase (McKee et al., 1993; Tanaka and Sakano, 1985). However, others have shown that although small

tracers (<6 nm) readily pass through the lacunar–canalicular porosity in the absence of mechanical loading, there appears to be an upper limit of size between 6 and 10 nm for molecular movement from bone capillaries to osteocytic lacunae in rat long bone. It was suggested that this range of pore size represents the fiber spacing that has been proposed for the annular space based on the presence of a proteoglycan fiber matrix surrounding the osteocytes (Wang et al., 2004). Therefore, there is an intracellular as well as an extracellular route for the rapid passage of ions and signal molecules. This allows for several types of cellular signaling from osteocytes lying deep within the bone tissue to surface-lining cells and vice versa (Cowin et al., 1995).

Experimental studies indicate that osteocytes are indeed sensitive to stress applied to intact bone tissue. In vivo experiments using the functionally isolated turkey ulna have shown that immediately following a 6-min period of intermittent (1 Hz) loading, the number of osteocytes expressing glucose-6-phosphate dehydrogenase activity was increased in relation to local strain magnitude (Skerry et al., 1989). The tissue strain magnitude varied between 0.05% and 0.2% (500–2000 microstrain), in line with in vivo peak strains in bone during vigorous exercise. Other models, including strained cores of adult dog cancellous bone, embryonic chicken tibiotarsi, mouse ulnae, rat caudal vertebrae, and rat tibiae, as well as experimental tooth movement in rats, have demonstrated that osteocytes in intact bone change their enzyme activity and RNA synthesis rapidly after mechanical loading (El-Haj et al., 1990; Dallas et al., 1993; Lane et al., 2006; Lean et al., 1995; Forwood et al., 1998; Terai et al., 1999). These studies show that intermittent loading produces rapid changes of metabolic activity in osteocytes and suggest that osteocytes may indeed function as mechanosensors in bone. The mechanical environment of the stress-sensitive osteocyte varies with the geometry of the osteocyte lacuna (McCreadie et al., 2004). Computer simulation studies of bone remodeling, assuming this to be a self-organizational control process, predict a role for osteocytes, rather than lining cells and osteoblasts, as stress sensors of bone (Mullender and Huiskes, 1995, 1997; Huiskes et al., 2000; Ruimerman et al., 2005). A regulating role of strain-sensitive osteocytes in basic multicellular unit (BMU) coupling has been postulated by Smit and Burger (2000). Using finite-element analysis, the subsequent activation of osteoclasts and osteoblasts during coupled bone remodeling was shown to relate to opposite strain distributions in the surrounding bone tissue. In front of the cutting cone of a forming secondary osteon, an area of *decreased* bone strain was demonstrated, whereas a layer of *increased* strain occurs around the closing cone (Smit and Burger, 2000). Osteoclasts therefore attack an area of bone where the osteocytes are underloaded, whereas osteoblasts are recruited in a bone area where the osteocytes are overloaded. Hemiosteonic remodeling of trabecular bone showed a similar strain pattern (Smit and Burger, 2000). Thus, bone remodeling regulated by load-sensitive osteocytes can explain the maintenance of osteonic and trabecular architecture as an optimal mechanical structure, as well as adaptation to alternative external loads (Huiskes et al., 2000; Smit and Burger, 2000; Van Oers et al., 2014 [review]).

Osteocytes are thought to be the major regulator of bone mechanosensation events, but little is known about how osteocytes in vivo acutely respond to tissue-level mechanical loading. A technique has been reported for the direct in vivo observation of osteocyte calcium signaling events with simultaneous whole-bone loading (Lewis et al., 2017). Osteocyte populations were found to integrate mechanical signals by altering the number of responding cells and this effect was dependent on loading frequency (Lewis et al., 2017). Ca^{2+} signaling in the osteocyte network in chick calvariae has been studied using three-dimensional time-lapse imaging (Tanaka et al., 2017). In response to flow, intracellular Ca^{2+} significantly increased in developmentally mature osteocytes in comparison with young osteocytes in the bone matrix, indicating that developmentally mature osteocytes are more responsive to mechanical stress than young osteocytes and have important functions in bone formation and remodeling (Tanaka et al., 2017).

If osteocytes are the mechanosensors of bone, how do they sense mechanical loading? This key question is, unfortunately, still open because it has not yet been established unequivocally how the loading of intact bone is transduced into a signal for the osteocytes. The application of force to bone during movement results in several potential cell stimuli. These include changes in hydrostatic pressure, direct cell strain, fluid flow, and electric fields resulting from electrokinetic effects accompanying fluid flow (Pienkowski and Pollack, 1983). Evidence has been increasing steadily for the flow of canalicular interstitial fluid as the likely stress-derived factor that informs the osteocytes about the level of bone loading (Cowin et al., 1991, 1995; Cowin, 1999; Weinbaum et al., 1994; Klein-Nulend et al., 1995b; Knothe-Tate et al., 2000; Burger and Klein-Nulend, 1999; You et al., 2000; Bakker et al., 2009). Moreover, a realistic high-resolution image-based three-dimensional model has been used to analyze the microscale fluid flow in a human osteocyte canaliculus (Kamioka et al., 2012). In this view, canaliculi are the bone porosity of interest, and the osteocytes the mechanosensor cells.

Canalicular fluid flow and osteocyte mechanosensing

In healthy, adequately adapted bone, strains as a result of physiological loads (e.g., resulting from normal locomotion) are quite small. Quantitative studies of the strain in bones of performing animals (e.g., galloping horses, fast-flying birds, even

a running human volunteer) found a maximal strain not higher than 0.2%−0.3% (Rubin, 1984; Burr et al., 1996). This poses a problem in interpreting the results of in vitro studies of strained bone cells, where much higher deformations, on the order of 1%−10%, were needed to obtain a cellular response (for a review, see Burger and Veldhuijzen, 1993). In these studies, isolated bone cells were usually grown on a flexible substratum, which was then strained by stretching or bending. For instance, unidirectional cell stretching of 0.7% was required to activate PGE_2 production in primary bone cell cultures (Murray and Rushton, 1990). However, in intact bone, a 0.15% bending strain was already sufficient to activate prostaglandin-dependent adaptive bone formation in vivo (Turner et al., 1994; Forwood, 1996). If we assume that bone organ strain is somehow involved in bone cell mechanosensing, then bone tissue seems to possess a lever system whereby small matrix strains are transduced into a larger signal that is detected easily by osteocytes. The canalicular flow hypothesis proposes such a lever system. Indeed, in vitro experiments that relate the effects of fluid flow and substrate straining have shown that fluid-flow-induced shear stress induces higher release of signaling molecules (McGarry et al., 2005a,b). A numerical study showed that the deformation of cells on a two-dimensional substrate caused by fluid flow is fundamentally different from that induced by substrate straining (McGarry et al., 2005a,b). Fluid shear stress had a larger overturning effect on the bone cells, while substrate strain predominantly affected cell−substrate attachments. Whether these observations can be extrapolated toward osteocytes that are embedded in a three-dimensional matrix is a matter of debate, but they clearly indicate that substrate deformation and a flow of interstitial fluid could have differential effects on cells.

The flow of extracellular tissue fluid through the lacunocanalicular network as a result of bone tissue strains was made plausible by the theoretical study of Piekarski and Munro (1977) and has been shown experimentally by Knothe-Tate et al. (1998, 2000). This strain-derived extracellular fluid flow may help keep osteocytes healthy, particularly the deeper ones, by facilitating the exchange of nutrients and waste products between the haversian channel and the osteocyte network of an osteon (Kufahl and Saha, 1990). However, a second function of this strain-derived interstitial fluid flow could be the transmission of "mechanical information" (Fig. 6.4). The magnitude of interstitial fluid flow through the lacunocanalicular network is directly related to the amount of strain of the bone organ (Cowin et al., 1991). Because of the narrow diameter of the canaliculi, bulk bone strains of about 0.1% will produce a fluid shear stress in the canaliculi of roughly 1 Pa (Weinbaum et al., 1994), enough to produce a rapid response in endothelial cells (Frangos et al., 1985; Kamiya and Ando, 1996).

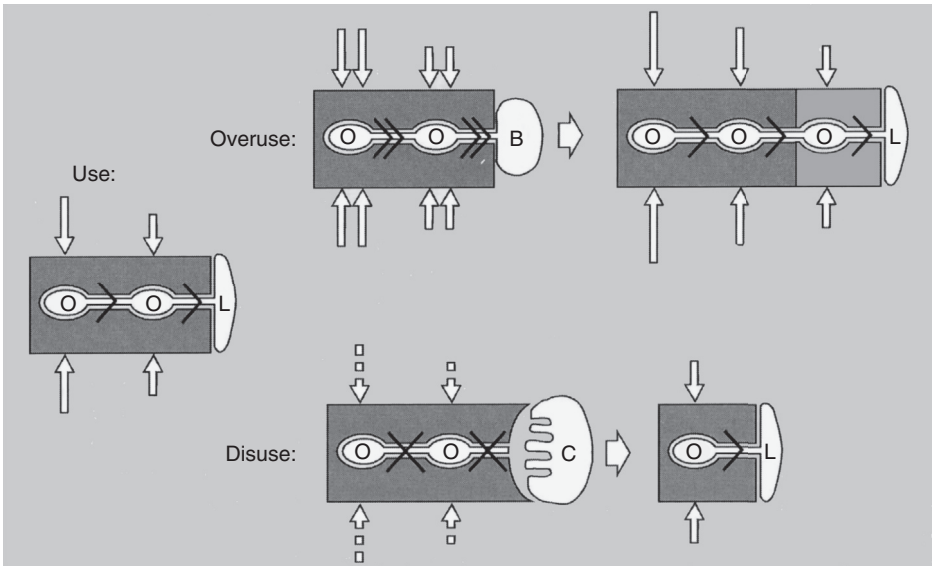

FIGURE 6.4 Schematic representation of how the osteocyte network may regulate bone modeling. In the steady state (*Use*), normal mechanical use ensures a basal level of fluid flow through the lacunocanalicular porosity, indicated by an *arrowhead* through the canaliculi. This basal flow keeps the osteocytes viable and also ensures basal osteocyte activation and signaling, thereby suppressing osteoblastic activity as well as osteoclastic attack. During (local) overuse (*Overuse*), osteocytes are overactivated by enhanced fluid flow (indicated by *double arrowheads*), leading to the release of osteoblast-recruiting signals. Subsequent osteoblastic bone formation reduces the overuse until normal mechanical use is reestablished, thereby reestablishing the steady state of basal fluid flow. During (local) disuse (*Disuse*), osteocytes are inactivated by lack of fluid flow (indicated by *crosses* through canaliculi). Inactivation leads to a release of osteoclast-recruiting signals, to a lack of osteoclast-suppressing signals, or both. Subsequent osteoclastic bone resorption reestablishes normal mechanical use (or loading) and basal fluid flow. *O*, osteocyte; *L*, lining cell; *B*, osteoblast; *C*, osteoclast; *dark gray area*, mineralized bone matrix; *light gray* area, newly formed bone matrix; *white arrows* represent direction and magnitude of loading. *Adapted from Burger, E.H., Klein-Nulend, J., 1999. Mechanotransduction in bone: role of the lacuno-canalicular network. FASEB J. 13, S101−S112.*

Experimental studies in vitro have demonstrated that osteocytes are indeed quite sensitive to the fluid shear stress of such a magnitude compared with osteoblasts and osteoprogenitor cells (Klein-Nulend et al., 1995a,b; Ajubi et al., 1996; Westbroek et al., 2000a,b; Westbroek et al., 2001). These results suggest that the combination of the cellular three-dimensional network of osteocytes and the accompanying porous network of lacunae and canaliculi acts as the mechanosensory organ of bone. Different loading-induced canalicular flow patterns around cutting cone and reversal zone during remodeling could, for instance, explain the typical alignment of haversian canals (Burger et al., 2003). Volumetric strain in the bone around a BMU cutting cone has been related to canalicular fluid flow (Smit et al., 2002), and the predicted area of low canalicular flow around the tip of the cutting cone was proposed to induce local osteocyte apoptosis. Unloading-induced osteocyte apoptosis has been shown in rat bone and was highly associated with osteoclastic bone resorption (Basso and Heersche, 2006). Osteocyte apoptosis at the tip of the cutting cone would attract osteoclasts, leading to further excavation of bone in the direction of loading. Importantly, mechanical loading by fluid shear stress has been shown to promote osteocyte survival (Bakker et al., 2004). The model by Smit et al. (2002) further predicts that at the base of the cutting cone and farther down the reversal zone, osteocytes receive enhanced fluid shear stress during loading. This could prevent osteocyte apoptosis, but may also promote the retraction and detachment of osteoclasts from the bone surface. These two mechanisms, attraction of osteoclasts to the cutting cone tip and induction of osteoclast detachment from the cutting cone base, together explain the mechanically meaningful behavior of osteoclasts during remodeling.

The flow of interstitial fluid through the bone canaliculi will have two effects: a mechanical one derived from the fluid shear stress and an electrokinetic one derived from streaming potentials (Pollack et al., 1984; Salzstein and Pollack, 1987). Either of the two, or both in combination, might activate the osteocyte. For instance, streaming potentials might modulate the movement of ions such as calcium across the cell membrane (Hung et al., 1995, 1996), whereas shear stress will pull at the macromolecular attachments between the cell and its surrounding matrix (Wang and Ingber, 1994). Both ion fluxes and cellular attachment are powerful modulators of cell behavior and therefore good conveyors of physical information (Sachs, 1989; Ingber, 1991). In vitro experiments using bone cells subjected to a flow of fluid of increasing viscosity suggest that fluid shear stress is the major activator of the bone cell response to loading (Bakker et al., 2001). However, care should be taken when extrapolating results obtained with cells seeded on a two-dimensional surface to the three-dimensional in vivo situation.

Mechanosensation and the resulting mechanotransduction of biochemical signals may be a complex event (Bonewald, 2006). Perturbation of dendrites, the cell body, and even primary cilia could be involved in combination or sequentially in this response. The osteocytes' response to different kinds of mechanical loading has predominantly been studied in cell cultures or entire bone, while knowledge of mechanosensing in osteocytes at the single-cell level is essential for understanding the complex process of bone adaptation. For instance, the mechanosensitive part of the osteocytes, the cell body or the cell processes, has not been determined yet. More information is needed on the single osteocyte's response to a localized mechanical stimulation. It has been postulated that the osteocyte processes are an order of magnitude more sensitive to mechanical loading than their cell bodies (Cabahug-Zuckermann et al., 2018). The underlying mechanisms are not clear but may be related to the infrequent $\alpha V\beta 3$ integrin sites where the osteocyte cell processes attach to canalicular walls (Cabahug-Zuckermann et al., 2018). These sites develop dramatically elevated strains during load-induced fluid flow in the lacunar canalicular system and might be primary sites for osteocyte mechanotransduction.

It has been suggested that fluid flow over dendrites in the lacunar–canalicular porosity can induce strains in the actin filament bundles of the cytoskeleton that are more than an order of magnitude larger than tissue level strains. Using the latest ultrastructural data for the cell process cytoskeleton and the tethering elements that attach the process to the canalicular wall, a realistic three-dimensional model was created for the osteocyte process. Using this model, the deformed shape of the tethering elements and the hoop strain on the central actin bundle as a result of loading-induced fluid flow were predicted. It was found that tissue-level strains of >1000 microstrain at 1 Hz resulted in a hoop strain of $>0.5\%$. The tethering elements of the osteocyte process can thus act as a strain amplifier (Han et al., 2004).

It has been published that osteocytes express a single primary cilium (Xiao et al., 2006). These authors also showed that polycystin 1 (PKD1/PC1), a known mechanosensory protein in the kidney, does play a role in normal bone structure. Primary cilia in other cells clearly function as sensors of odors, light, and movement (Singla and Reiter, 2005). It remains to be determined whether the bone defect in animals with defective PKD1 function is due to defective function of PKD1 in cilia, or whether PKD1 has a function in another location in the cell. Early data suggest that loss of cilia results in decreased sensitivity to fluid flow shear stress (Malone et al., 2006). Determining the function of PKD1 and/or cilia should lend insight into mechanotransduction in osteocytes.

The osteocyte has been viewed as either a quiescent cell acting as a "placeholder" in bone or as a mechanosensory cell as outlined in this chapter. Most observations using static two-dimensional imaging suggest that the dendritic processes are somewhat permanently anchored to the lacunar wall. Dallas et al. have shown cell body movement and the extension and retraction of dendritic processes over time using dynamic imaging of living osteocytes within their lacunae (Veno et al., 2006). Calvarial explants from transgenic mice with GFP expression targeted to osteocytes revealed that, far from being a static cell, the osteocyte is highly dynamic. Therefore, dendrites, rather than being permanent connections between osteocytes and with bone surface cells, may have the capacity to connect and disconnect and reconnect. With this new information, theories regarding shear stress within lacunae and osteocyte signaling will require modification.

Osteocyte shape and mechanosensing

The ability of osteocytes to sense and respond to mechanical stimuli depends on many factors, such as the shape of the osteocyte cell bodies, number and length of the cell processes, structure of the cytoskeleton, and presence of primary cilia (Willems et al., 2017). One intriguing factor is osteocyte lacunar shape, which has been hypothesized to affect the transduction of strain on the whole bone to the direct osteocyte microenvironment (Nicolella et al., 2006). It has been shown that considerable variations in the shape of osteocytes and their lacunae exist and that these variations may depend on anatomical location and the age of the bone (Van Hove et al., 2009; Vatsa et al., 2008a,b; Bacabac et al., 2008). Considering that a proper response of osteocytes to mechanical stimuli is highly important to maintain bone strength, the question arises whether changes in lacunar morphology could underlie the alterations in the bone adaptive response seen with aging (reviewed by Hemmatian et al., 2017).

Modifications in the morphology and orientation of osteocytes and their lacunae could result from hormonal changes, as well as from changes in mechanical loading. The alignment and shape of the osteocytes and their lacunae are related to the direction of the mechanical loading (Vatsa et al., 2008a,b; Sugawara et al., 2013). More flattened and elongated osteocytes and lacunae are observed in fibula loaded unidirectionally than in calvarial bone, which is loaded in different directions (Vatsa et al., 2008a,b). Irregularly shaped osteocytes distributed in different directions are found in the femurs of embryonic mice in the absence of mechanical loading, whereas the osteocytes in the femurs of 6-week-old mice subjected to mechanical loading are more flat and spindle shaped, and oriented parallel to the longitudinal axis of the bone (Sugawara et al., 2013). Furthermore, in neurectomized mice under little or no mechanical loading during growth, the osteocytes are round without any preferred orientation (Sugawara et al., 2013). The actin filaments in the osteocyte cytoskeleton distribute in the same direction as the mechanical loading (Vatsa et al., 2008a,b). In addition, the osteocyte morphology might vary in bone pathologies, i.e., the shape of osteocytes and their lacunae are significantly different in the tibia of individuals with osteopetrosis, osteoporosis, and osteoarthritis (Van Hove et al., 2009). Osteocyte lacunae in bone from osteoporotic persons are large and round, lacunae from osteopetrotic persons are small and discoid shaped, whereas lacunae from osteoarthritic persons are large and elongated (Van Hove et al., 2009). Furthermore, in the osteopetrotic bone, the osteocyte lacunae are less oriented to the loading direction in comparison with the orientation of osteocyte lacunae in the osteoarthritic and osteopenic bone (Van Hove et al., 2009). The variations in the shape and alignment of osteocytes and their lacunae in different bone pathologies could reflect an adaptation to the different micromechanical environments with different matrix strain associated with differences in bone mineral density.

Mechanoresponsive osteocytes regulate bone mass, which is important for, among others, dental implant success. Significant differences in osteocyte surface area and orientation seem to exist locally in maxillary bone, which may be related to the tensile strain magnitude and orientation. This might reflect local differences in the osteocyte mechanosensitivity and bone quality, suggesting differences in dental implant success based on the location in the maxilla (Wu et al., 2018).

Response of osteocytes to fluid flow in vitro

The technique of immunodissection, as discussed earlier in this chapter, made it possible to test the canalicular flow hypothesis by comparing the responsiveness of osteocytes, osteoblasts, and osteoprogenitor cells to fluid flow. The strength of the immunodissection technique is that three separate cell populations with a high (90%) degree of homogeneity are prepared, representing (1) osteocytes, with the typical "spider-like" osteocyte morphology and little matrix synthesis, (2) osteoblasts, with a high synthetic activity of bone matrix-specific proteins, and (3) (from the periosteum) osteoprogenitor cells, with a fibroblast-like morphology and very high proliferative capacity (Nijweide and Mulder, 1986). Because the cells are used within 2 days after isolation from the bone tissue, they may well represent the three differentiation steps of osteoprogenitor cell, osteoblast, and osteocyte. In contrast, mixed cell cultures derived from bone that are generally used to

represent "osteoblastic" cells are likely to contain cells in various stages of differentiation. Therefore, changes in mechanosensitivity related to progressive cell differentiation cannot be studied in such cultures. The development of differentiation-stage-specific bone cell lines has facilitated the comparison of cell-type-specific responses to mechanical loading. Ponik et al. (2007) have described significant differences in the response to fluid shear between MC3T3-E1 osteoblasts and MLO-Y4 osteocytes. Stress fibers were formed and aligned within osteoblasts after 1 h of unidirectional fluid flow, but this response was not observed until greater than 5 h of oscillatory fluid flow (Ponik et al., 2007). However, due to their clonal selection, cell lines do not necessarily express the whole range of bone-specific genes characteristic of primary bone cells. Therefore, the use of primary bone cells can be preferred to the use of cell lines when comparing osteoblasts' and osteocytes' behavior.

Using immunoseparated primary cell populations, osteocytes were found to respond far more strongly to fluid flow than osteoblasts, and these stronger than osteoprogenitor cells (Klein-Nulend et al., 1995a,b; Ajubi et al., 1996; Westbroek et al., 2000a). Osteocytes also appeared to be more responsive to fluid flow than osteoblasts or osteoprogenitor cells with respect to the production of soluble signaling molecules affecting osteoblast proliferation and differentiation (Vezeridis et al., 2005). The release of these soluble factors was at least partially dependent on the activation of an NO pathway in osteocytes in response to fluid flow. PFF with a mean shear stress of 0.5 Pa (5 dyn/cm^2) with a cyclic variation of $\pm$0.2 Pa at 5 Hz stimulated the release of NO and PGE_2 and PGI_2 rapidly from osteocytes within minutes (Klein-Nulend et al., 1995a; Ajubi et al., 1996). Osteoblasts showed less response, and osteoprogenitor cells (periosteal fibroblasts) still less. Intermittent hydrostatic compression of 13,000 Pa peak pressure at 0.3 Hz (1 s compression followed by 2 s relaxation) needed more than 1 h application before prostaglandin production was increased, again more in osteocytes than in osteoblasts, suggesting that mechanical stimulation via fluid flow is more effective than hydrostatic compression (Klein-Nulend et al., 1995b). A 1-h treatment with PFF also induced a sustained release of PGE_2 from the osteocytes in the hour following PFF treatment (Klein-Nulend et al., 1995b). This sustained PGE_2 release, continuing after PFF treatment had been stopped, could be ascribed to the induction of prostaglandin G/H synthase-2 (or cyclooxygenase 2, COX-2) expression (Westbroek et al., 2000a). Again, osteocytes were much more responsive than osteoblasts and osteoprogenitor cells, as only a 15-min treatment with PFF increased COX-2 mRNA expression by threefold in osteocytes but not in the other two cell populations (Westbroek et al., 2000a,b). Upregulation of COX-2 but not COX-1 by PFF had been shown earlier in a mixed population of mouse calvarial cells (Klein-Nulend et al., 1997) and was also demonstrated in primary bone cells from elderly women (Joldersma et al., 2000), whereas the expression of COX-1 and COX-2 in osteocytes and osteoblasts in intact rat bone has been documented (Forwood et al., 1998). These in vitro experiments on immunoseparated cells suggest that as bone cells mature, they increase their capacity to produce prostaglandins in response to fluid flow (Burger and Klein-Nulend, 1999). First, their immediate production of PGE_2, PGI_2, and probably $PGF_{2\alpha}$ (Klein-Nulend et al., 1997) in response to flow increases as they develop from osteoprogenitor cell, via the osteoblastic stage, into osteocytes. Second, their capacity to increase expression of COX-2 in response to flow, and thereby to continue to produce PGE_2 even after the shear stress has stopped (Westbroek et al., 2000a), increases as they reach terminal differentiation. Since induction of COX-2 is a crucial step in the induction of bone formation by mechanical loading in vivo (Forwood, 1996), these results provide direct experimental support for the concept that osteocytes, the long-living terminal differentiation stage of osteoblasts, function as the "professional" mechanosensors in bone tissue.

PFF also rapidly induced the release of NO in osteocytes but not osteoprogenitor cells (Klein-Nulend et al., 1995a). Rapid release of NO was also found when whole rat bone rudiments were mechanically strained in organ culture (Pitsillides et al., 1995) and in human bone cells submitted to fluid flow (Sterck et al., 1998). In line with these in vitro observations, inhibition of NO production inhibited mechanically induced bone formation in animal studies (Turner et al., 1996; Fox et al., 1996). NO is a ubiquitous messenger molecule for intercellular communication, involved in many tissue reactions in which cells must collaborate and communicate with one another (Koprowski and Maeda, 1995). The intracellular upregulation of NO after mechanical stimulation has been shown in single bone cells using DAR-4M AM chromophore (Vatsa et al., 2007). It was shown that a single osteocyte can disseminate a mechanical stimulus to its surrounding osteocytes via extracellular soluble signaling factors, which reinforces the putative mechanosensory role of osteocytes and demonstrates a possible mechanism by which a single mechanically stimulated osteocyte can communicate with other cells in a bone multicellular unit, which might help us to better understand the intricacies of intercellular interactions in BMUs and thus bone remodeling (Vatsa et al., 2007). Another interesting example of the involvement of NO in tissue reactions in which cells must collaborate and communicate with one another is the adaptation of blood vessels to changes in blood flow. In blood vessels, enhanced blood flow, e.g., during exercise, leads to widening of the vessel to ensure a constant blood pressure. This response depends on the endothelial cells, which sense the increased blood flow and produce intercellular messengers such as NO and prostaglandins. In response to these messengers, the smooth muscle cells around the vessel relax to allow the vessel to increase in diameter (Kamiya and Ando, 1996). The capacity of endothelial

cells to produce NO in response to fluid flow is related to a specific enzyme, endothelial NO synthase or ecNOS. Interestingly, this enzyme was found in rat bone-lining cells and osteocytes (Helfrich et al., 1997; Zaman et al., 1999) and in cultured bone cells derived from human bone (Klein-Nulend et al., 1998). Both endothelial and neuronal NOS isoforms are present in osteocytes (Caballero-Alias et al., 2004). The rapid release by mechanically stressed bone cells makes NO an interesting candidate for intercellular communication within the three-dimensional network of bone cells. Treatment with pulsatile fluid flow increased the level of ecNOS RNA transcripts in the bone cell cultures (Klein-Nulend et al., 1998), a response also described in endothelial cells (Busse and Fleming, 1998; Uematsu et al., 1995). Enhanced production of prostaglandins is also a well-described response of endothelial cells to fluid flow (Busse and Fleming, 1998; Kamiya and Ando, 1996). It seems, therefore, that endothelial cells and osteocytes possess a similar sensor system for fluid flow and that both cell types are "professional" sensors of fluid flow.

Mechanotransduction starts by the conversion of physical-loading-derived stimuli into cellular signals. Several studies suggest that the attachment complex between intracellular actin cytoskeleton and extracellular matrix macromolecules, via integrins and CD44 receptors in the cell membrane, provides the site of mechanotransduction (Wang et al., 1993; Watson, 1991; Ajubi et al., 1996, 1999; Pavalko et al., 1998). An important early response is the influx of calcium ions through mechanosensitive ion channels in the plasma membrane and the release of calcium from internal stores (Hung et al., 1995, 1996; Ajubi et al., 1999; Chen et al., 2000; You et al., 2000). The rise in intracellular calcium concentration activates many downstream signaling cascades such as protein kinase C and phospholipase A_2 and is necessary for activation of calcium/calmodulin-dependent proteins such as NOS. The activation of phospholipase A_2 results, among others, in the activation of arachidonic acid production and PGE_2 release (Ajubi et al., 1999). Other genes whose expression in osteocytes is modified by mechanical loading include c-fos, MEPE, and IGF-1 (Lean et al., 1995, 1996). MEPE has been shown to be involved in the inhibition of osteoclastogenesis by mechanically loaded osteocytes (Kulkarni et al., 2010).

Many steps in the mechanosignaling cascade are still unknown in osteocytes as well as other mechanosensory cells. One of the most important signaling pathways in response to mechanical loading in the osteocyte is the Wnt/β-catenin pathway. While important for osteoblast differentiation, proliferation, and matrix production, it was hypothesized and then shown that this pathway plays a role in transmitting signals of mechanical loading from osteocytes to cells on the bone surface (Bonewald and Johnson, 2008; Bonewald, 2011). Deletion of various components of the Wnt/β-catenin pathway has effects on bone responses to loading and unloading. For example, deletion of Lrp5 results in impaired osteogenic responses to anabolic loading. It has been shown that the Wnt family of proteins strongly modulates the anabolic response of bone to mechanical loading (Robinson et al., 2006). Mechanical loading by PFF modulates gene expression of proteins involved in Wnt signaling pathways in osteocytes (Santos et al., 2009). Whereas targeted deletion of β-catenin using the Dmp1-Cre driver results in dramatic bone loss (Kramer et al., 2010), deletion of only one allele results in mice with a normal skeleton but a completely abrogated response to anabolic loading (Javaheri et al., 2014). Mechanical loading decreases sclerostin in bone, whereas hindlimb unloading increases expression. Taking all these studies together, it appears that β-catenin signaling plays an important in bone responses to loading. More research will need to be conducted to elucidate the physiological role of Wnts in bone cell mechanotransduction. Undoubtedly, in the meantime, new players in the field of bone cell mechanotransduction will be identified.

Mechanosensitive osteocytes regulate bone mass in adults, while interleukin 6 (IL-6), such as is present during orthodontic tooth movement, also strongly regulates bone mass. Interestingly, IL-6 is produced by shear-loaded osteocytes, suggesting that IL-6 may affect bone mass by modulating osteocyte communication toward osteoblasts (Bakker et al., 2014). Multiple factors contribute to bone loss in inflammatory diseases, but circulating inflammatory factors and immobilization play a crucial role. Systemic inflammation affects human osteocyte-specific protein and cytokine expression (Pathak et al., 2016). Mechanical loading prevents bone loss in the general population, but the effects of mechanical loading in patients with inflammatory disease are less clear. Pathak et al. (2015) found that serum from patients with inflammatory disease upregulated osteocyte-to-osteoclast communication, while mechanical loading nullified this upregulation, suggesting that mechanical stimuli contribute to the prevention of osteoporosis in inflammatory disease. In addition, it has been shown that mechanical loading prevents the stimulating effect of IL-1β, of which plasma and synovial fluid levels are higher in inflammatory diseases, on osteocyte-modulated osteoclastogenesis, suggesting that mechanical loading may abolish IL-1β-induced osteoclastogenesis (Kulkarni et al., 2012).

Summary and conclusion

Tremendous progress has been made in discerning the function of osteocytes since this chapter was first written over 7−8 years ago. One only has to search the term "osteocytes" on PubMed to see the dramatic increase in references to and studies of this elusive bone cell. Markers for osteocytes have been expanded to delineate early to late stages of osteocyte

differentiation and the critical role of mineralization in this process. Genomic profiling of osteocytes is a storehouse of information regarding the potential functions of these cells and their response to strain.

Molecular mechanisms and pathways involved in osteocyte mechanosensation have been identified and expanded significantly. Although some investigators hold to the concept of a single mechanoreceptor initiating a linear cascade of events, new theories suggesting simultaneous triggering events in response to load are being investigated. It remains to be determined what makes these cells more responsive to shear stress than osteoblasts and what role the cell body, dendrites, and even cilia may play in this response.

These cells make up 90%–95% of all bone cells in the adult skeleton. Collectively, any minor modulation of the entire population could have significant local and systemic effects, not only on bone, but also on other organs. Although postulated several decades ago that osteocytes could potentially play a role in calcium metabolism, it appears that this cell may have a more important role in phosphate metabolism. It remains to be determined how factors produced by osteocytes can enter the circulation, suggesting an intimate connection between the lacunocanalicular system and the blood supply.

One reason for the dramatic expansion in knowledge in the field of osteocyte biology is the generation of new tools and advancement of technology. No longer is this cell safe within its mineralized cave from "prying eyes." Transgenic technology has targeted the osteocyte with fluorescent markers and generated conditional deletions. Cell lines and osteocyte-selective and -specific antibodies and probes have been generated. Advanced instrumentation such as Raman spectroscopy and atomic force microscopy can probe and characterize the osteocyte microenvironment. Dynamic imaging has revealed osteocyte movement within their lacuna and canaliculi.

Even with these advances we may still be seeing only "the tip of the iceberg" with regard to osteocyte function. It has been proposed that the osteocyte could be the orchestrator of bone remodeling in the adult skeleton directing both osteoblast and osteoclast function. The future looks exciting and full of new discoveries with regard to the biology of the osteocyte and its role in mechanosensation.

Acknowledgments

The authors would like to acknowledge the pioneering leadership in the field of osteocyte biology of Drs. Els Burger and Peter Nijweide, original authors of this chapter. These two individuals laid the foundation upon which the present authors have founded their research. The authors wish to thank Dr. Astrid Bakker for critically reading the manuscript.

The authors would also like to acknowledge funding support from the National Institutes of Health, NIH NIA PO1AG039355 (L.F.B.) and The Netherlands Foundation for Fundamental Research on Matter (ALW/FOM/NWO project 01FB28/2) (J.K.N.) and The Netherlands Institute for Space Research (SRON grant MG-055) (J.K.N.).

References

Aarden, E.M., Nijweide, P.J., Van der Plas, A., Alblas, M.J., Mackie, E.J., Horton, M.A., Helfrich, M.H., 1996a. Adhesive properties of isolated chick osteocytes in vitro. Bone 18, 305–313.

Aarden, E.M., Wassenaar, A.M., Alblas, M.J., Nijweide, P.J., 1996b. Immunocytochemical demonstration of extracellular matrix proteins in isolated osteocytes. Histochem. Cell Biol. 106, 495–501.

Abu, E.O., Horner, A., Kusec, V., Triffitt, J.T., Compston, J.E., 1997. The localization of androgen receptors in human bone. J. Clin. Endocrinol. Metab. 82, 3493–3497.

Abu, E.O., Horner, A., Kusec, V., Triffitt, J.T., Compston, J.E., 2000. The localization of the functional glucocorticoid receptor alpha in human bone. J. Clin. Endocrinol. Metab. 85, 883–889.

Ahuja, S.S., Zhao, S., Bellido, T., Plotkin, L.I., Jimenez, F., Bonewald, L.F., 2003. CD40 ligand blocks apoptosis induced by tumor necrosis factor alpha, glucocorticoids, and etoposide in osteoblasts and the osteocyte-like cell line murine long bone osteocyte-Y4. Endocrinology 144, 1761–1769.

Ajubi, N.E., Klein-Nulend, J., Nijweide, P.J., Vrijheid-Lammers, T., Alblas, M.J., Burger, E.H., 1996. Pulsating fluid flow increases prostaglandin production by cultured chicken osteocytes—a cytoskeleton-dependent process. Biochem. Biophys. Res. Commun. 225, 62–68.

Ajubi, N.E., Klein-Nulend, J., Alblas, M.J., Burger, E.H., Nijweide, P.J., 1999. Signal transduction pathways involved in fluid flow-induced prostaglandin E_2 production by cultured osteocytes. Am. J. Physiol. 276, E171–E178.

Alford, A.I., Jacobs, C.R., Donahue, H.J., 2003. Oscillating fluid flow regulates gap junction communication in osteocytic MLO-Y4 cells by an ERK1/2 MAP kinase-dependent mechanism small star, filled. Bone 33, 64–70.

Aubin, J.E., Liu, F., Malaval, L., Gupta, A.K., 1995. Osteoblast and chondroblast differentiation. Bone 17 (Suppl. l), 77–83.

Bacabac, R.G., Smit, T.H., Mullender, M.G., Dijcks, S.J., Van Loon, J.J., Klein-Nulend, J., 2004. Nitric oxide production by bone cells is fluid shear stress rate dependent. Biochem. Biophys. Res. Commun. 315, 823–829.

Bacabac, R.G., Smit, T.H., Mullender, M.G., Van Loon, J.J., Klein-Nulend, J., 2005. Initial stress-kick is required for fluid shear stress-induced rate dependent activation of bone cells. Ann. Biomed. Eng. 33, 104–110.

Bacabac, R.G., Mizuno, D., Schmidt, C.F., MacKintosh, F.C., Smit, T.H., Van Loon, J.J.W.A., Klein-Nulend, J., 2006a. Microrheology and force traction of mechanosensitive bone cells. J. Biomech. 39 (Suppl. 1), S231−S232.

Bacabac, R.G., Smit, T.H., Van Loon, J.J., Zandieh Doulabi, B., Helder, M., Klein-Nulend, J., 2006b. Bone cell responses to high-frequency vibration stress: does the nucleus oscillate within the cytoplasm? FASEB J. 20, 858−864.

Bacabac, R.G., Mizuno, D., Schmidt, C.F., MacKintosh, F.C., Van Loon, J.J., Klein-Nulend, J., Smit, T.H., 2008. Round versus flat: bone cell morphology, elasticity, and mechanosensing. J. Biomech. 41, 1590−1598.

Bakker, A.D., Soejima, K., Klein-Nulend, J., Burger, E.H., 2001. The production of nitric oxide and prostaglandin E2 by primary bone cells is shear stress dependent. J. Biomech. 34, 671−677.

Bakker, A.D., Klein-Nulend, J., Burger, E.H., 2004. Shear stress inhibits while disuse promotes osteocyte apoptosis. Biochem. Biophys. Res. Commun. 320, 1163−1168.

Bakker, A.D., Da Silva, V.C., Krishnan, R., Bacabac, R.G., Blaauboer, M.E., Lin, Y.−C., Marcantonio, R.A., Cirelli, J.A., Klein-Nulend, J., 2009. Tumor necrosis factor alpha and interleukin-1beta modulate calcium and nitric oxide signaling in mechanically stimulated osteocytes. Arthritis Rheum. 60, 3336−3345.

Bakker, A.D., Kulkarni, R., Klein-Nulend, J., Lems, W.F., 2014. IL-6 alters osteocyte signaling toward osteoblasts but not osteoclasts. J. Dent. Res. 93, 394−399.

Balemans, W., Ebeling, M., Patel, N., Van Hul, E., Olson, P., Dioszegi, M., Lacza, C., Wuyts, W., Van Den Ende, J., Willems, P., Paes-Alves, A.F., Hill, S., Bueno, M., Ramos, F.J., Tacconi, P., Dikkers, F.G., Stratakis, C., Lindpaintner, K., Vickery, B., Foernzler, D., Van Hul, W., 2001. Increased bone density in sclerosteosis is due to the deficiency of a novel secreted protein (SOST). Hum. Mol. Genet. 10, 537−543.

Barragan-Adjemian, C., Nicolella, D.P., Dusevich, V., Dallas, M., Eick, D., Bonewald, L., 2006. Mechanism by which MLO-A5 late osteoblast/early osteocytes mineralize in culture: similarities with lamellar bone. Calcif. Tissue Int. 79, 340−353.

Basso, N., Heersche, J.N., 2006. Effects of hind limb unloading and reloading on nitric oxide synthase expression and apoptosis of osteocytes and chondrocytes. Bone 39, 807−814.

Batra, N., Burra, S., Siller-Jackson, A.J., Gu, S., Xia, X., Weber, G.F., DeSimone, D., Bonewald, L.F., Lafer, E.M., Sprague, E., Schwartz, M.A., Jiang, J.X., 2012. Mechanical stress-activated integrin α5β1 induces opening of connexin 43 hemichannels. Proc. Natl. Acad. Sci. U.S.A. 109, 3359−3364.

Bélanger, L.F., 1969. Osteocytic osteolysis. Calcif. Tissue Res. 4, 1−12.

Bellido, T., Ali, A.A., Gubrij, I., Plotkin, L.I., Fu, Q., O'Brien, C.A., Manolagas, S.C., Jilka, R.L., 2005. Chronic elevation of parathyroid hormone in mice reduces expression of sclerostin by osteocytes: a novel mechanism for hormonal control of osteoblastogenesis. Endocrinology 146, 4577−4583.

Bennett, M.V., Goodenough, D.A., 1978. Gap junctions, electrotonic coupling, and intercellular communication. Neurosci. Res. Progr. Bull. 16, 1−486.

Bivi, N., Condon, K.W., Allen, M.R., Farlow, N., Passeri, G., Brun, L.R., Rhee, Y., Bellido, T., Plotkin, L.I., 2012. Cell autonomous requirement of connexin 43 for osteocyte survival: consequences for endocortical resorption and periosteal bone formation. J. Bone Miner. Res. 27, 374−389.

Bodine, P.V., Vernon, S.K., Komm, B.S., 1996. Establishment and hormonal regulation of a conditionally transformed preosteocytic cell line from adult human bone. Endocrinology 137, 4592−4604.

Boivin, G., Mesguich, P., Pike, J.W., Bouillon, R., Meunier, P.J., Haussler, M.R., Dubois, P.M., Morel, G., 1987. Ultrastructural immunocytochemical localization of endogenous 1,25-dihydroxyvitamin D and its receptors in osteoblasts and osteocytes from neonatal mouse and rat calvaria. Bone Miner. 3, 125−136.

Bonewald, L.F., 2006. Mechanosensation and transduction in osteocytes. BoneKey-Osteovision 3, 7−15.

Bonewald, L.F., 2011. The amazing osteocyte. J. Bone Miner. Res. 26, 229−238.

Bonewald, L.F., 2017. The role of the osteocyte in bone and non-bone disease. Endocrinol. Metab. Clin. North Am. 46, 1−18.

Bonewald, L.F., Johnson, M.L., 2008. Osteocytes, mechanosensing and Wnt signaling. Bone 42, 606−615.

Bonucci, E., 1990. The ultrastructure of the osteocyte. In: Bonucci, E., Motta, P.M. (Eds.), Ultrastructure of Skeletal Tissues. Kluwer Academic, Dordrecht, The Netherlands, pp. 223−237.

Bordier, P.J., Miravet, L., Ryckerwaert, A., Rasmussen, H., 1976. Morphological and morphometrical characteristics of the mineralization front. A vitamin D regulated sequence of bone remodeling. In: PJ, B. (Ed.), Bone Histomorphometry. Armour Montagu, Paris, France, pp. 335−354.

Boskey, A., 1996. Matrix proteins and mineralization: an overview. Connect. Tissue Res. 35, 357−363.

Boyde, A., 1980. Evidence against "osteocyte osteolysis. Metab. Bone Dis. Relat. Res. 2 (Suppl. l), 239−255.

Braidman, J.P., Davenport, L.K., Carter, D.H., Selby, P.L., Mawer, E.B., Freemont, A.J., 1995. Preliminary *in situ* identification of estrogen target cells in bone. J. Bone Miner. Res. 10, 74−80.

Bresler, D., Bruder, J., Mohnike, K., Fraser, W.D., Rowe, P.S., 2004. Serum MEPE-ASARM-peptides are elevated in X-linked rickets (HYP): implications for phosphaturia and rickets. J. Endocrinol. 183, R1−R9.

Bronckers, A.L., Goei, W., Luo, G., Karsenty, G., D'Souza, R.N., Lyaruu, D.M., Burger, E.H., 1996. DNA fragmentation during bone formation in neonatal rodents assessed by transferase-mediated end labeling. J. Bone Miner. Res. 11, 1281−1291.

Bruder, S.P., Caplan, A.I., 1990. Terminal differentiation of osteogenic cells in the embryonic chick tibia is revealed by a monoclonal antibody against osteocytes. Bone 11, 189−198.

Burger, E.H., Klein-Nulend, J., 1999. Mechanotransduction in bone: role of the lacuno-canalicular network. FASEB J. 13, S101−S112.

Burger, E.H., Veldhuijzen, J.P., 1993. Influence of mechanical factors on bone formation, resorption, and growth in vitro. In: Hall, B.K. (Ed.), Bone, vol. 7. CRC Press, Boca Raton, FL, pp. 37−56.

Burger, E.H., Klein-Nulend, J., Smit, T.H., 2003. Strain-derived canalicular fluid flow regulates osteoclast activity in a remodelling osteon—a proposal. J. Biomech. 3**6**, 1453—1459.

Burr, D.B., Milgran, C., Fyhrie, D., Forwood, M.R., Nyska, M., Finestone, A., Hoshaw, S., Saiag, E., Simkin, A., 1996. In vivo measurement of human tibial strains during vigorous activity. Bone 18, 405—410.

Burra, S., Nicolella, D.P., Francis, W.L., Freitas, C.J., Mueschke, N.J., Poole, K., Jiang, J.X., 2010. Dendritic processes of osteocytes are mechanotransducers that induce the opening of hemichannels. Proc. Natl. Acad. Sci. U.S.A. 107, 13648—13653.

Busse, R., Fleming, I., 1998. Pulsatile stretch and shear stress: physical stimuli determining the production of endothelium derived relaxing factors. J. Vasc. Res. 35, 73—84.

Cabahug-Zuckermann, P., Stout Jr., R.F., Majeska, R.J., Thi, M.M., Spray, D.C., Weinbaum, S., Schaffler, M.B., 2018. Potential role for a specialized β3 integrin-based structure on osteocyte processes in bone mechanosensation. J. Orthop. Res. 36, 642—652.

Caballero-Alias, A.M., Loveridge, N., Lyon, L.E., 2004. NOS isoforms in adult human osteocytes: multiple pathways of NO regulation? Calcif. Tissue Int. 75, 78—84.

Chen, N.X., Ryder, K.D., Pavalko, F.M., Turner, C.H., Burr, D.B., Qiu, J., Duncan, R.L., 2000. Ca(2+) regulates fluid shear-induced cytoskeletal reorganization and gene expression in osteoblasts. Am. J. Physiol. 278, C989—C997.

Cheng, B., Zhao, S., Luo, J., Sprague, E., Bonewald, L.F., Jiang, J.X., 2001. Expression of functional gap junctions and regulation by fluid flow in osteocyte-like MLO-Y4 cells. J. Bone Miner. Res. 16, 249—259.

Cherian, P.P., Siller-Jackson, A.J., Gu, S., Wang, X., Bonewald, L.F., Sprague, E., Jiang, J.X., 2005. Mechanical strain opens connexin 43 hemichannels in osteocytes: a novel mechanism for the release of prostaglandin. Mol. Biol. Cell 16, 3100—3106.

Chow, J.W., Fox, S., Jagger, C.J., Chambers, T.J., 1998. Role for parathyroid hormone in mechanical responsiveness of rat bone. Am. J. Physiol. 274, E146—E154.

Clarke, B.L., 2014. Anti-sclerostin antibodies: utility in treatment of osteoporosis. Maturitas 78, 199—204.

Clinkenbeard, E.L., White, K.E., 2016. Systemic control of bone homeostasis by FGF23 signaling. Curr. Mol. Biol. Rep. 2, 62—71.

Cowin, S.C., 1999. Bone poroelasticity. J. Biomech. 32, 217—238.

Cowin, S.C., Moss-Salentijn, L., Moss, M.L., 1991. Candidates for the mechanosensory system in bone. J. Biomed. Eng. 113, 191—197.

Cowin, S.C., Weinbaum, S., Zeng, Y., 1995. A case for bone canaliculi as the anatomical site of strain generated potentials. J. Biomech. 28, 1281—1297.

Dallas, S.L., Zaman, G., Pead, M.J., Lanyon, L.E., 1993. Early strain-related changes in cultured embryonic chick tibiotarsi parallel those associated with adaptive modeling in vivo. J. Bone Miner. Res. 8, 251—259.

Dallas, S.L., Prideaux, M., Bonewald, L.F., 2013. The osteocyte: an endocrine cell … and more. Endocr. Rev. 34 (5), 658—690.

Davideau, J.L., Papagerakis, P., Hotton, D., Lezot, F., Berdal, A., 1996. In situ investigation of vitamin D receptor, alkaline phosphatase, and osteocalcin gene expression in oro-facial mineralized tissues. Endocrinology 137, 3577—3585.

Delgado-Calle, J., Hancock, B., Likine, E.F., Sato, A.Y., McAndrews, K., Sanudo, C., Bruzzaniti, A., Riancho, J.A., Tonra, J.R., Bellido, T., 2018. MMP14 is a novel target of PTH signaling in osteocytes that controls resorption by regulating soluble RANKL production. FASEB J. https://doi.org/10.1096/fj.201700919RRR [Epub ahead of print].

Divieti, P., Inomata, N., Chapin, K., Singh, R., Juppner, H., Bringhurst, F.R., 2001. Receptors for the carboxyl-terminal region of pth(1-84) are highly expressed in osteocytic cells. Endocrinology 142, 916—925.

Donahue, H.J., 2000. Gap junctions and biophysical regulation of bone cell differentiation. Bone 26, 417—422.

Donahue, H.J., McLeod, K.J., Rubin, C.T., Andersen, J., Grine, E.A., Hertzberg, E.L., Brink, P.R., 1995. Cell-to-cell communication in osteoblastic networks: cell line-dependent hormonal regulation of gap junction function. J. Bone Miner. Res. 10, 881—889.

Doty, S.B., 1981. Morphological evidence of gap junctions between bone cells. Calcif. Tissue Int. 33, 509—512.

Ducy, P., Desbois, C., Boyce, B., Pinero, G., Story, B., Dunstan, C., Smith, E., Bonadio, J., Goldstein, S., Gundberg, C., Bradley, A., Karsenty, G., 1996. Increased bone formation in osteocalcin deficient mice. Nature 382, 448—452.

El-Haj, A.J., Minter, S.L., Rawlinson, S.C., Suswillo, R., Lanyon, L.E., 1990. Cellular responses to mechanical loading in vitro. J. Bone Miner. Res. 5, 923—932.

Elmardi, A.S., Katchburian, M.V., Katchburian, E., 1990. Electron microscopy of developing calvaria reveals images that suggest that osteoclasts engulf and destroy osteocytes during bone resorption. Calcif. Tissue Int. 46, 239—245.

Feng, J.Q., Ward, L.M., Liu, S., Lu, Y., Xie, Y., Yuan, B., Yu, X., Rauch, F., Davis, S.I., Zhang, S., Rios, H., Drezner, M.K., Quarles, L.D., Bonewald, L.F., White, K.E., 2006. Loss of DMP1 causes rickets and osteomalacia and identifies a role for osteocytes in mineral metabolism. Nat. Genet. 38, 1310—1315.

Fermor, B., Skerry, T.M., 1995. PTH/PTHrP receptor expression on osteoblasts and osteocytes but not resorbing bone surfaces in growing rats. J. Bone Miner. Res. 10, 1935—1943.

Fisher, L.W., Fedarko, N.S., 2003. Six genes expressed in bones and teeth encode the current members of the SIBLING family of proteins. Connect. Tissue Res. 44 (Suppl. 1), 33—40.

Forwood, M.R., 1996. Inducible cyclooxygenase (COX-2) mediates the induction of bone formation by mechanical loading in vivo. J. Bone Miner. Res. 11, 1688—1693.

Forwood, M.R., Kelly, W.L., Worth, N.F., 1998. Localization of prostaglandin endoperoxidase H synthase (PGHS)-1 and PGHS-2 in bone following mechanical loading in vivo. Anat. Rec. 252, 580—586.

Fox, S.W., Chambers, T.J., Chow, J.W., 1996. Nitric oxide is an early mediator of the increase in bone formation by mechanical stimulation. Am. J. Physiol. 270, E955—E960.

Frangos, J.A., Eskin, S.G., McIntire, L.V., Ives, C.L., 1985. Flow effects on prostacyclin production by cultured human endothelial cells. Science 227, 1477–1479.

Franz-Odendaal, T.A., Hall, B.K., Witten, P.E., 2006. Buried alive: how osteoblasts become osteocytes. Dev. Dynam. 235, 176–190.

Frost, H.J., 1992. The role of changes in mechanical usage set points in the pathogenesis of osteoporosis. J. Bone Miner. Res. 7, 253–261.

Fu, J., Hao, L., Tian, Y., Liu, Y., Gu, Y., Wu, J., 2018. miR-199a-3p is involved in estrogen-mediated autophagy through the IGF-1/mTOR pathway in osteocyte-like MLO-Y4 cells. J. Cell. Physiol. 233, 2292–2303.

Genetos, D.C., Kephart, C.J., Zhang, Y., Yellowley, C.E., Donahue, H.J., 2007. Oscillating fluid flow activation of gap junction hemichannels induces atp release from MLO-Y4 osteocytes. J. Cell. Physiol. 212, 207–214.

Gluhak-Heinrich, J., Ye, L., Bonewald, L.F., Feng, J.Q., MacDougall, M., Harris, S.E., Pavlin, D., 2003. Mechanical loading stimulates dentin matrix protein 1 (DMP1) expression in osteocytes in vivo. J. Bone Miner. Res. 18, 807–817.

Gluhak-Heinrich, J., Yang, W., Bonewald, L.F., Robling, A.G., Turner, C.H., Harris, S.E., 2005. Mechanically induced DMP1 and MEPE expression in osteocytes: correlation to mechanical strain, osteogenic response and gene expression threshold. J. Bone Miner. Res. 20 (Suppl. 1), S73.

Goodenough, D.A., Goliger, J.A., Paul, D.L., 1996. Connexins, connexons, and intercellular communication. Annu. Rev. Biochem. 65, 475–502.

Goodenough, D.A., Paul, D.L., 2003. Beyond the gap: functions of unpaired connexon channels. Nat. Rev. Mol. Cell Biol. 4, 285–294.

Gowen, L.C., Petersen, D.N., Mansolf, A.L., Qi, H., Stock, J.L., Tkalcevic, G.T., Simmons, H.A., Crawford, D.T., Chidsey-Frink, K.L., Ke, H.Z., McNeish, J.D., Brown, T.A., 2003. Targeted disruption of the osteoblast/osteocyte factor 45 gene (OF45) results in increased bone formation and bone mass. J. Biol. Chem. 278, 1998–2007.

Gross, T.S., Akeno, N., Clemens, T.L., Komarova, S., Srinivasan, S., Weimer, D.A., Mayorov, S., 2001. Selected Contribution: osteocytes upregulate HIF-1alpha in response to acute disuse and oxygen deprivation. J. Appl. Physiol. 90, 2514–2519.

Gross, T.S., King, K.A., Rabaia, N.A., Pathare, P., Srinivasan, S., 2005. Upregulation of osteopontin by osteocytes deprived of mechanical loading or oxygen. J. Bone Miner. Res. 20, 250–256.

Han, Y., Cowin, S.C., Schaffler, M.B., Weinbaum, S., 2004. Mechanotransduction and strain amplification in osteocyte cell processes. Proc. Natl. Acad. Sci. U.S.A. 101, 16689–16694.

Heino, T.J., Hentunen, T.A., Vaananen, H.K., 2002. Osteocytes inhibit osteoclastic bone resorption through transforming growth factor-beta: enhancement by estrogen. J. Cell. Biochem. 85, 185–197.

Heino, T.J., Hentunen, T.A., Vaananen, H.K., 2004. Conditioned medium from osteocytes stimulates the proliferation of bone marrow mesenchymal stem cells and their differentiation into osteoblasts. Exp. Cell Res. 294, 458–468.

Helfrich, M.H., Evans, D.E., Grabowski, P.S., Pollock, J.S., Ohshima, H., Ralston, S.H., 1997. Expression of nitric oxide synthase isoforms in bone and bone cell cultures. J. Bone Miner. Res. 12, 1108–1115.

Hemmatian, H., Bakker, A.D., Klein-Nulend, J., van Lenthe, G.H., 2017. Aging, osteocytes, and mechanotransduction. Curr. Osteoporos. Rep. 15, 401–411.

Hoyland, J.A., Baris, C., Wood, L., Baird, P., Selby, P.L., Freemont, A.J., Braidman, I.P., 1999. Effect of ovarian steroid deficiency on oestrogen receptor alpha expression in bone. J. Pathol. 188, 294–303.

Huang, J., Romero-Suarez, S., Lara, N., Mo, C., Kaja, S., Brotto, L., Dallas, S.L., Johnson, M.L., Jähn, K., Bonewald, L.F., Brotto, M., 2017. Crosstalk between MLO-Y4 osteocytes and C2C12 muscle cells is mediated by the Wnt/β-catenin pathway. J. Bone Miner. Res. 1, 86–100.

Hughes, D.E., Salter, D.M., Simpson, R., 1994. CD44 expression in human bone: a novel marker of osteocytic differentiation. J. Bone Miner. Res. 9, 39–44.

Huiskes, R., Ruimerman, R., van Lenthe, G.H., Janssen, J.D., 2000. Effects of mechanical forces on maintenance and adaptation of form in trabecular bone. Nature 405, 704–706.

Hung, C.T., Pollack, S.R., Reilly, T.M., Brighton, C.T., 1995. Realtime calcium response of cultured bone cells to fluid flow. Clin. Orthop. Relat. Res. 313, 256–269.

Hung, C.T., Allen, F.D., Pollack, S.R., Brighton, C.T., 1996. Intracellular calcium stores and extracellular calcium are required in the real-time calcium response of bone cells experiencing fluid flow. J. Biomech. 29, 1411–1417.

Igarashi, M., Kamiya, N., Ito, K., Takagi, M., 2002. In situ localization and in vitro expression of osteoblast/osteocyte factor 45 mRNA during bone cell differentiation. Histochem. J. 34, 255–263.

Imai, S., Kaksonen, M., Raulo, E., Kinnunen, T., Fages, C., Meng, X., Lakso, M., Rauvala, H., 1998. Osteoblast recruitment and bone formation enhanced by cell matrix-associated heparin-binding growth-associated molecule (HB-GAM). J. Cell Biol. 143, 1113–1128.

Ingber, D.E., 1991. Intergrins as mechanochemical transducers. Curr. Opin. Cell Biol. 3, 841–848.

Jähn, K., Lara-Castillo, N., Brotto, L., Mo, C.L., Johnson, M.L., Brotto, M., Bonewald, L.F., 2012. Skeletal muscle secreted factors prevent glucocorticoid-induced osteocyte apoptosis through activation of beta-catenin. Eur. Cells Mater. 24, 197–210.

Jähn, K., Kelkar, S., Zhao, H., Xie, Y., Tiede-Lewis, L.M., Dusevich, V., Dallas, S.L., Bonewald, L.F., 2017. Osteocytes acidify their microenvironment in response to PTHrP in vitro and in lactating mice in vivo. J. Bone Miner. Res. PMID: 28470757.

Jande, S.S., 1971. Fine structural study of osteocytes and their surrounding bone matrix with respect to their age in young chicks. J. Ultrastruct. Res. 37, 279–300.

Javaheri, B., Stern, A.R., Lara, N., Dallas, M., Zhao, H., Bonewald, L.F., Johnson, M.L., 2014. Deletion of a single β-catenin allele in osteocytes abolishes the bone anabolic response to loading. J. Bone Miner. Res. 29, 705–715.

Jilka, R.L., Weinstein, R.S., Bellido, T., Roberson, P., Parfitt, A.M., Manolagas, S.C., 1999. Increased bone formation by prevention of osteoblast apoptosis with parathyroid hormone. J. Clin. Investig. 104, 439–446.

Johnson, L.C., 1966. The kinetics of skeletal remodeling in structural organization of the skeleton. Birth Defects 11, 66−142.

Joldersma, M., Burger, E.H., Semeins, C.M., Klein-Nulend, J., 2000. Mechanical stress induces COX-2 mRNA expression in bone cells from elderly women. J. Biomech. 33, 53−61.

Kalajzic, I., Braut, A., Guo, D., Jiang, X., Kronenberg, M.S., Mina, M., Harris, M.A., Harris, S.E., Rowe, D.W., 2004. Dentin matrix protein 1 expression during osteoblastic differentiation, generation of an osteocyte GFP-transgene. Bone 35, 74−82.

Kamioka, H., Honjo, T., Takano-Yamamoto, T., 2001. A three-dimensional distribution of osteocyte processes revealed by the combination of confocal laser scanning microscopy and differential interference contrast microscopy. Bone 28, 145−149.

Kamioka, H., Sugawara, Y., Honjo, T., Yamashiro, T., Takano-Yamamoto, T., 2004. Terminal differentiation of osteoblasts to osteocytes is accompanied by dramatic changes in the distribution of actin-binding proteins. J. Bone Miner. Res. 19, 471−478.

Kamioka, H., Kameo, Y., Imai, Y., Bakker, A.D., Bacabac, R.G., Yamada, N., Takaoka, A., Yamashiro, T., Adachi, T., Klein-Nulend, J., 2012. Microscale fluid flow analysis in a human osteocyte canaliculus using a realistic high-resolution image-based three-dimensional model. Integr. Biol. 4, 1198−1206.

Kamiya, A., Ando, J., 1996. Response of vascular endothelial cells to fluid shear stress: Mechanism. In: Hayashi, K., Kamiyn, A., Ono, K. (Eds.), Biomechanics: Functional Adaptation and Remodeling. Springer, Tokyo, pp. 29−56.

Kato, Y., Windle, J.J., Koop, B.A., Mundy, G.R., Bonewald, L.F., 1997. Establishment of an osteocyte-like cell line, MLO-Y4. J. Bone Miner. Res. 12, 2014−2023.

Kato, Y., Boskey, A., Spevak, L., Dallas, M., Hori, M., Bonewald, L.F., 2001. Establishment of an osteoid preosteocyte-like cell MLO-A5 that spontaneously mineralizes in culture. J. Bone Miner. Res. 16, 1622−1633.

Kitase, Y., Jiang, J.X., Bonewald, L.F., 2006. The anti-apoptotic effects of mechanical strain on osteocytes are mediated by PGE_2 and monocyte chemotactic protein, (MCP-3); selective protection by MCP3 against glucocorticoid (GC) and not TNF-a induced apoptosis. J. Bone Miner. Res. 21 (Suppl. 1), S48.

Kitase, Y., Vallejo, J.A., Gutheil, W., Vemula, H., Jahn, K., Yi, J., Zhou, J., Brotto, M., Bonewald, L.F., 2018. Beta-aminoisobutyric acid, I-BAIBA, is a muscle-derived osteocyte survival factor. Cell Rep. 22, 1531−1544.

Klein-Nulend, J., Semeins, C.M., Ajubi, N.E., Nijweide, P.J., Burger, E.H., 1995a. Pulsating fluid flow increases nitric oxide (NO) synthesis by osteocytes but not periosteal fibroblasts-correlation with prostaglandin upregulation. Biochem. Biophys. Res. Commun. 217, 640−648.

Klein-Nulend, J., Van der Plas, A., Semeins, C.M., Ajubi, N.E., Frangos, J.A., Nijweide, P.J., Burger, E.H., 1995b. Sensitivity of osteocytes to biomechanical stress in vitro. FASEB J. 9, 441−445.

Klein-Nulend, J., Burger, E.H., Semeins, C.M., Raisz, L.G., Pilbeam, C.C., 1997. Pulsating fluid flow stimulates prostaglandin release and inducible prostaglandin G/H synthase mRNA expression in primary mouse bone cells. J. Bone Miner. Res. 12, 45−51.

Klein-Nulend, J., Helfrich, M.H., Sterck, J.G.H., MacPherson, H., Joldersma, M., Ralston, S.H., Semeins, C.M., Burger, E.H., 1998. Nitric oxide response to shear stress by human bone cell cultures is endothelial nitric oxide synthase dependent. Biochem. Biophys. Res. Commun. 250, 108−114.

Klein-Nulend, J., Bacabac, R.G., Bakker, A.D., 2012. Mechanical loading and how it affects bone cells: the role of the osteocyte cytoskeleton in maintaining our skeleton. Eur. Cells Mater. 24, 278−291.

Klein-Nulend, J., Bakker, A.D., Bacabac, R.G., Vatsa, A., Weinbaum, S., 2013. Mechanosensation and transduction in osteocytes. Bone 54, 182−190.

Knothe-Tate, M.L., Niederer, P., Knothe, U., 1998. In vivo tracer transport throught the lacunocanalicular system of rat bone in an environment devoid of mechanical loading. Bone 22, 107−117.

Knothe-Tate, M.L., Steck, R., Forwood, M.R., Niederer, P., 2000. In vivo demonstration of load-induced fluid flow in the rat tibia and its potential implications for processes associated with functional adaptation. J. Exp. Biol. 203, 2737−2745.

Kogianni, G., Mann, V., Noble, B.S., 2008. Apoptotic bodies convey activity capable of initiating osteoclastogenesis and localised bone destruction. J. Bone Miner. Res. 23, 915−927.

Kondoh, S., Inoue, K., Igarashi, K., et al., 2014. Estrogen receptor α in osteocytes regulates trabecular bone formation in female mice. Bone 60, 68−77.

Koprowski, H., Maeda, H., 1995. The Role of Nitric Oxide in Physiology and Pathophysiology. Springer-Verlag, Berlin, Germany.

Kousteni, S., Bellido, T., Plotkin, L.I., O'Brien, C.A., Bodenner, D.L., Han, L., Han, K., DiGregorio, G.B., Katzenellenbogen, J.A., Katzenellenbogen, B.S., Roberson, P.K., Weinstein, R.S., Jilka, R.L., Manolagas, S.C., 2001. Nongenotropic, sex-nonspecific signaling through the estrogen or androgen receptors: dissociation from transcriptional activity. Cell 104, 719−730.

Kramer, I., Halleux, C., Keller, H., Pegurri, M., Gooi, J.H., Weber, P.B., Feng, J.Q., Bonewald, L.F., Kneissel, M., 2010. Osteocyte Wnt/beta-catenin signaling is required for normal bone homeostasis. Mol. Cell Biol. 30, 3071−3085.

Kufahl, R.H., Saha, S., 1990. A theoretical model for stress-generated flow in the canaliculi-lacunae network in bone tissue. J. Biomech. 23, 171−180.

Kulkarni, R., Bakker, A.D., Everts, V., Klein-Nulend, J., 2010. Inhibition of osteoclastogenesis by mechanically loaded osteocytes: involvement of MEPE. Calcif. Tissue Int. 87, 461−468.

Kulkarni, R., Bakker, A.D., Everts, V., Klein-Nulend, J., 2012. Mechanical loading prevents the stimulating effect of IL-1β on osteocyte-modulated osteoclastogenesis. Biochem. Biophys. Res. Commun. 420, 11−16.

Lane, N.E., Yao, W., Balooch, M., Nalla, R.K., Balooch, G., Habelitz, S., Kinney, J.H., Bonewald, L.F., 2006. Glucocorticoid-treated mice have localized changes in trabecular bone material properties and osteocyte lacunar size that are not observed in placebo-treated or estrogen-deficient mice. J. Bone Miner. Res. 21, 466−476.

Lean, J.M., Jagger, C.J., Chambers, T.J., Chow, J.W., 1995. Increased insulin-like growth factor I mRNA expression in rat osteocytes in response to mechanical stimulation. Am. J. Physiol. 268, E318−E327.

Lean, J.M., Mackay, A.G., Chow, J.W., Chambers, T.J., 1996. Osteocytic expression of mRNA for c-fos and IGF-I: an immediate early gene response to an osteogenic stimulus. Am. J. Physiol. 270, E937–E945.

Lecanda, F., Warlow, P.M., Sheikh, S., Furlan, F., Steinberg, T.H., Civitelli, R., 2000. Connexin43 deficiency causes delayed ossification, craniofacial abnormalities, and osteoblast dysfunction. J. Cell Biol. 151, 931–944.

Lee, K., Jessop, H., Suswillo, R., Zaman, G., Lanyon, L.E., 2003. Endocrinology: bone adaptation requires oestrogen receptor-alpha. Nature 424, 389.

Lewis, K.J., Frikha-Benayed, D., Louie, J., Stephen, S., Spray, D.C., Thi, M.M., Seref-Ferlengez, Z., Majeska, R.J., Weinbaum, S., Schaffler, M.B., 2017. Osteocyte calcium signals encode strain magnitude and loading frequency in vivo. Proc. Natl. Acad. Sci. U.S.A. 114, 11775–11780.

Li, X., Zhang, Y., Kang, H., Liu, W., Liu, P., Zhang, J., Harris, S.E., Wu, D., 2005. Sclerostin binds to LRP5/6 and antagonizes canonical Wnt signaling. J. Biol. Chem. 280, 19883–19887.

Liang, J.D., Hock, J.M., Sandusky, G.E., Santerre, R.F., Onyia, J.E., 1999. Immunohistochemical localization of selected early response genes expressed in trabecular bone of young rats given hPTH 1–34. Calcif. Tissue Int. 65, 369–373.

Litzenberger, J.B., Kim, J.-B., Tummala, P., Jacobs, C.R., 2010. Beta1 integrins mediate mechanosensitive signaling pathways in osteocytes. Calcif. Tissue Int. 86, 325–332.

Liu, Y., Porta, A., Peng, X., Gengaro, K., Cunningham, E.B., Li, H., Dominguez, L.A., Bellido, T., Christakos, S., 2004. Prevention of glucocorticoid-induced apoptosis in osteocytes and osteoblasts by calbindin-D28k. J. Bone Miner. Res. 19, 479–490.

Liu, S., Zhou, J., Tang, W., Jiang, X., Rowe, D.W., Quarles, L.D., 2006. Pathogenic role of Fgf23 in Hyp mice. Am. J. Physiol. Endocrinol. Metab. 291, E38–E49.

Liu, S., Tang, W., Zhou, J., Vierthaler, L., Quarles, L.D., 2007. Distinct roles for intrinsic osteocyte abnormalities and systemic factors in regulation of FGF23 and bone mineralization in hyp mice. Am. J. Physiol. Endocrinol. Metab. 293, E1636–E1644.

Lu, Y., Kamel-El Sayed, S.A., Grillo, M.A., Veno, P.A., Dusevich, V., Tiede-Lewis, L.M., Phillips, C.L., Bonewald, L.F., Dallas, S.L., February 20, 2018. Live imaging of type I collagen assembly dynamics in cells stably expressing GFP-collagen constructs. J. Bone Miner. Res. https://doi.org/10.1002/jbmr.3409 [Epub ahead of print].

MacNabb, C., Patton, D., Hayes, J.S., 2016. Sclerostin antibody therapy for the treatment of osteoporosis: clinical prospects and challenges. J. Osteoporos. 2016, 6217286.

Maeno, M., Taguchi, M., Kosuge, K., Otsuka, K., Takagi, M., 1992. Nature and distribution of mineral-binding, keratan sulfate-containing glycoconjugates in rat and rabbit bone. J. Histochem. Cytochem. 40, 1779–1788.

Malone, A.M.D., Anderson, C.T., Temiyasathit, S., Tang, J., Tummala, P., Sterns, T., Jacobs, C.R., 2006. Primary cilia: mechanosensory organelles in bone cells. J. Bone Miner. Res. 21 (Suppl. 1), S39.

Mangeat, P., Roy, C., Martin, M., 1999. ERM proteins in cell adhesion and membrane dynamics. Trends Cell Biol. 9, 187–192.

Manolagas, S.C., 2000. Birth and death of bone cells: basic regulatory mechanisms and implications for the pathogenesis and treatment of osteoporosis. Endocr. Rev. 21, 115–137.

Marotti, G., 1996. The structure of bone tissues and the cellular control of their deposition. Ital. J. Anat. Embryol. 101, 25–79.

Marotti, G., Cane, V., Palazzini, S., Palumbo, C., 1990. Structure-function relationships in the osteocyte. Ital. J. Miner. Electrolyte Metab. 4, 93–106.

Martin, R.B., 2000. Does osteocyte formation cause the nonlinear refilling of osteons? Bone 26, 71–78.

McCreadie, B.R., Hollister, S.J., Schaffler, M.B., Goldstein, S.A., 2004. Osteocyte lacuna size and shape in women with and without osteoporotic fracture. J. Biomech. 37, 563–572.

McGarry, J.G., Klein-Nulend, J., Mullender, M.G., Prendergast, P.J., 2005a. A comparison of strain and fluid shear stress in stimulating bone cell responses–a computational and experimental study. FASEB J. 19, 482–484.

McGarry, J.G., Klein-Nulend, J., Prendergast, P.J., 2005b. The effect of cytoskeletal disruption on pulsatile fluid flow-induced nitric oxide and prostaglandin E2 release in osteocytes and osteoblasts. Biochem. Biophys. Res. Commun. 330, 341–348.

McKee, M.D., Farach-Carson, M.C., Butler, W.T., Hauschka, P.V., Nanci, A., 1993. Ultrastructural immunolocalization of noncollagenous (osteopontin and osteocalcin) and plasma (albumin and H_2S-glycoprotein) proteins in rat bone. J. Bone Miner. Res. 8, 485–496.

Medscape FDA Rejects Romosozumab for Osteoporosis, July 17, 2017. Available at: www.medscape.com/viewarticle/882966.

Mikuni-Takagaki, Y., Kakai, Y., Satoyoshi, M., Kawano, E., Suzuki, Y., Kawase, T., Saito, S., 1995. Matrix mineralization and the differentiation of osteocyte-like cells in culture. J. Bone Miner. Res. 10, 231–242.

Miyauchi, A., Notoya, K., Mikuni-Takagaki, Y., Takagi, Y., Goto, M., Miki, Y., Takano-Yamamoto, T., Jinnai, K., Takahashi, K., Kumegawa, M., Chihara, K., Fuijita, T., 2000. Parathyroid hormone-activated volume-sensitive calcium influx pathways in mechanically loaded osteocytes. J. Biol. Chem. 275, 3335–3342.

Mo, C., Romero-Suarez, S., Bonewald, L.F., Johnson, M., Brotto, M., 2012. Prostaglandin E2: from clinical applications to its potential role in bone-muscle crosstalk and myogenic differentiation. Recent Pat. Biotechnol. 6, 223–229.

Mullender, M.G., Huiskes, R., Weinans, H., 1994. A physiological approach to the stimulation of bone remodelling as a self-organisational control process. J. Biomech. 27, 1389–1394.

Mullender, M.G., Huiskes, R., 1995. Proposal for the regulatory mechanism of Wolff's law. J. Orthop. Res. 13, 503–512.

Mullender, M.G., Huiskes, R., 1997. Osteocytes and bone lining cells: which are the best candidates for mechano-sensors in cancellous bone? Bone 20, 527–532.

Mullender, M.G., Dijcks, S.J., Bacabac, R.G., Semeins, C.M., Van Loon, J.J., Klein-Nulend, J., 2006. Release of nitric oxide, but not prostaglandin E_2, by bone cells depends on fluid flow frequency. J. Orthop. Res. 24, 1170–1177.

Murray, D.W., Rushton, N., 1990. The effect of strain on bone cell prostaglandin E2 release: a new experimental method. Calcif. Tissue Int. 47, 35–39.

Nakamura, H., Kenmotsu, S., Sakai, H., Ozawa, H., 1995. Localization of CD44, the hyaluronate receptor, on the plasma membrane of osteocytes and osteoclasts in rat tibiae. Cell Tissue Res. 280, 225–233.

Nakamura, H., Ozawa, H., 1996. Immunolocalization of CD44 and the ERM family in bone cells of mouse tibiae. J. Bone Miner. Res. 11, 1715–1722.

Nakashima, T., Hayashi, M., Fukunaga, T., Kurata, K., Oh-Hora, M., Feng, J.Q., Bonewald, L.F., Kodama, T., Wutz, A., Wagner, E.F., Penninger, J.M., Takayanagi, H., 2011. Evidence for osteocyte regulation of bone homeostasis through RANKL expression. Nat. Med. 17, 1231–1234.

Nicolella, D.P., Moravits, D.E., Galea, A.M., Bonewald, L.F., Lankford, J.L., 2006. Osteocyte lacunae tissue strain in cortical bone. J. Biomech. 39, 1735–1743.

Nijweide, P.J., Mulder, R.J., 1986. Identification of osteocytes in osteoblast-like cultures using a monoclonal antibody specifically directed against osteocytes. Histochemistry 84, 343–350.

Nijweide, P.J., van der Plas, A., Scherft, J.P., 1981. Biochemical and histological studies on various bone cell preparations. Calcif. Tissue Int. 33, 529–540.

Nijweide, P.J., Van der Plas, A., Olthof, A.A., 1988. Osteoblastic differentiation. In: Evered, D., Harnett, S. (Eds.), Cell and Molecular Biology of Vertebrate Hard Tissues, Ciba Foundation Symposium, vol. 136. Wiley, Chichester, UK, pp. 61–77.

Noble, B.S., Stevens, H., Loveridge, N., Reeve, J., 1997. Identification of apoptotic changes in osteocytes in normal and pathological human bone. Bone 20, 273–282.

Noble, B.S., Peet, N., Stevens, H.Y., Brabbs, A., Mosley, J.R., Reilly, G.C., Reeve, J., Skerry, T.M., Lanyon, L.E., 2003. Mechanical loading: biphasic osteocyte survival and targeting of osteoclasts for bone destruction in rat cortical bone. Am. J. Physiol. Cell Physiol. 284, C934–C943.

Noonan, K.J., Stevens, J.W., Tammi, R., Tammi, M., Hernandez, J.A., Midura, R.J., 1996. Spatial distribution of CD44 and hyaluronan in the proximal tibia of the growing rat. J. Orthop. Res. 14, 573–581.

O'Brien, C.A., Plotkin, L.I., Galli, C., Goellner, J.J., Gortazar, A.R., Allen, M.R., Robling, A.G., Bouxsein, M., Schipani, E., Turner, C.H., Jilka, R.L., Weinstein, R.S., Manolagas, S.C., Bellido, T., 2008. Control of bone mass and remodeling by PTH receptor signaling in osteocytes. PLoS One 3, e2942.

Ohizumi, I., Harada, N., Taniguchi, K., Tsutsumi, Y., Nakagawa, S., Kaiho, S., Mayumi, T., 2000. Association of CD44 with OTS-8 in tumor vascular endothelial cells. Biochim. Biophys. Acta 1497, 197–203.

Oster, G., 1989. Cell motility and tissue morphogenesis. In: Stein, W.D., Bronner, F. (Eds.), Cell Shape: Determinants, Regulation and Regulatory Role. Academic Press, San Diego, CA, pp. 33–61.

Owen, M., 1995. Cell population kinetics of an osteogenic tissue. I. (1963). Clin. Orthop. Relat. Res. 313, 3–7.

Palumbo, C., 1986. A three-dimensional ultrastructural study of osteoid-osteocytes in the tibia of chick embryos. Cell Tissue Res. 246, 125–131.

Parfitt, A.M., 1976. The actions of parathyroid hormone on bone: relation to bone remodeling and turnover, calcium homeostasis, and metabolic bone diseases. II. PTH and bone cells: bone turnover and plasma calcium regulation. Metabolism 25, 909–955.

Parfitt, A.M., 1977. The cellular basis of bone turnover and bone loss. Clin. Orthop. Relat. Res. 127, 236–247.

Pathak, J.L., Bravenboer, N., Luyten, F.P., Verschueren, P., Lems, W.F., Klein-Nulend, J., Bakker, A.D., 2015. Mechanical loading reduces inflammation-induced human osteocyte-to-osteoclast communication. Calcif. Tisse Int. 97, 169–178.

Pathak, J.L., Bakker, A.D., Luyten, F.P., Verschueren, P., Lems, W.F., Klein-Nulend, J., Bravenboer, N., 2016. Systemic inflammation affects human osteocyte-specific protein and cytokine expression. Calcif. Tissue Int. 98, 596–608.

Pavalko, F.M., Chen, N.X., Turner, C.H., Burr, D.B., Atkinson, S., Hsieh, Y.F., Qiu, J., Duncan, R.L., 1998. Fluid shear-induced mechanical signaling in MC3T3-E1 osteoblasts requires cytoskeletonintegrin interactions. Am. J. Physiol. 275, C1591–C1601.

Piekarski, K., Munro, M., 1977. Transport mechanism operating between blood supply and osteocytes in long bones. Nature 269, 80–82.

Pienkowski, D., Pollack, S.R., 1983. The origin of stress-generated potentials in fluid-saturated bone. J. Orthop. Res. 1, 30–41.

Pitsillides, A.A., Rawlinson, S.C., Suswillo, R.F., Bourrin, S., Zaman, G., Lanyon, L.E., 1995. Mechanical strain-induced NO production by bone cells: a possible role in adaptive bone (re)modeling? FASEB J. 9, 1614–1622.

Plotkin, L.I., Bellido, T., 2001. Bisphosphonate-induced, hemichannel-mediated, anti-apoptosis through the Src/ERK pathway: a gap junction-independent action of connexin43. Cell Commun. Adhes. 8, 377–382.

Plotkin, L.I., Weinstein, R.S., Parfitt, A.M., Roberson, P.K., Manolagas, S.C., Bellido, T., 1999. Prevention of osteocyte and osteoblast apoptosis by bisphosphonates and calcitonin. J. Clin. Investig. 104, 1363–1374.

Plotkin, L.I., Manolagas, S.C., Bellido, T., 2002. Transduction of cell survival signals by connexin-43 hemichannels. J. Biol. Chem. 277, 8648–8657.

Plotkin, L.I., Mathov, I., Aguirre, J.I., Parfitt, A.M., Manolagas, S.C., Bellido, T., 2005. Mechanical stimulation prevents osteocyte apoptosis: requirement of integrins, Src kinases and ERKs. Am. J. Physiol. Cell Physiol. 289, C633–C643.

Plotkin, L.I., Speacht, T.L., Donahue, H.J., 2015. Cx43 and mechanotransduction in bone. Curr. Osteoporos. Rep. 13, 67–72.

Pollack, S.R., Salzstein, R., Pienkowski, D., 1984. The electric double layer in bone and its influence on stress generated potentials. Calcif. Tissue Int. 36, S77–S81.

Ponik, S.M., Triplett, J.W., Pavalko, F.M., 2007. Osteoblasts and osteocytes respond differently to oscillatory and unidirectional fluid flow profiles. J. Cell. Biochem. 100, 794–807.

Poole, K.E., van Bezooijen, R.L., Loveridge, N., Hamersma, H., Papapoulos, S.E., Lowik, C.W., Reeve, J., 2005. Sclerostin is a delayed secreted product of osteocytes that inhibits bone formation. FASEB J. 19, 1842–1844.

Prideaux, M., Schutz, C., Wijenayaka, A.R., Findlay, D.M., Campbell, D.G., Solomon, L.B., Atkins, G.J., 2016. Isolation of osteocytes from human trabecular bone. Bone 88, 64–72.

Qing, H., Ardeshirpour, L., Pajevic, P.D., Dusevich, V., Jähn, K., Kato, S., Wysolmerski, J., Bonewald, L.G., 2012. Demonstration of osteocytic perilacunar/canalicular remodeling in mice during lactation. J. Bone Miner. Res. 27, 1018−1029.

Rhee, Y., Allen, M.R., Condon, K., Lezcano, V., Ronda, A.C., Galli, C., Olivos, N., Passeri, G., O'Brien, C.A., Bivi, N., Plotkin, L.I., Bellido, T., 2011. PTH receptor signaling in osteocytes governs periosteal bone formation and intra-cortical remodeling. J. Bone Miner. Res. 26, 1035−1046.

Robinson, J.A., Chatterjee-Kishore, M., Yaworsky, P.J., Cullen, D.M., Zhao, W., Li, C., Kharode, Y., Sauter, L., Babij, P., Brown, E.L., Hill, A.A., Akhter, M.P., Johnson, M.L., Recker, R.R., Komm, B.S., Bex, F.J., 2006. Wnt/beta-catenin signaling is a normal physiological response to mechanical loading in bone. J. Biol. Chem. 281, 31720−31728.

Robling, A.G., Bellido, T., Turner, C.H., 2006. Mechanical stimulation in vivo reduces osteocyte expression of sclerostin. J. Musculoskelet. Neuronal Interact. 6, 354.

Rowe, P.S., de Zoysa, P.A., Dong, R., Wang, H.R., White, K.E., Econs, M.J., Oudet, C.L., 2000. MEPE, a new gene expressed in bone marrow and tumors causing osteomalacia. Genomics 67, 54−68.

Rowe, P.S., Garrett, I.R., Schwarz, P.M., Carnes, D.L., Lafer, E.M., Mundy, G.R., Gutierrez, G.E., 2005. Surface plasmon resonance (SPR) confirms that MEPE binds to PHEX via the MEPE-ASARM motif: a model for impaired mineralization in X-linked rickets (HYP). Bone 36, 33−46.

Rubin, C.T., 1984. Skeletal strain and the functional significance of bone architecture. Calcif. Tissue Int. 36, S11−S18.

Ruchon, A.F., Tenenhouse, H.S., Marcinkiewicz, M., Siegfried, G., Aubin, J.E., DesGroseillers, L., Crine, P., Boileau, G., 2000. Developmental expression and tissue distribution of Phex protein: effect of the Hyp mutation and relationship to bone markers. J. Bone Miner. Res. 15, 1440−1450.

Ruimerman, R., Hilbers, P., van Rietbergen, B., Huiskes, R.A., 2005. Theoretical framework for strain-related trabecular bone maintenance and adaptation. J. Biomech. 38, 931−941.

Sabbieti, M.G., Marchetti, L., Abreu, C., Montero, A., Hand, A.R., Raisz, L.G., Hurley, M.M., 1999. Prostaglandins regulate the expression of fibroblast growth factor-2 in bone. Endocrinology 140, 434−444.

Sachs, F., 1989. Ion channels as mechanical transducers. In: Stein, W.D., Bronner, F. (Eds.), Cell Shape: Determinants, Regulation and Regulatory Role. Academic Press, San Diego, CA, pp. 63−94.

Salzstein, R.A., Pollack, S.R., 1987. Electromechanical potentials in cortical bone. II. Experimental analysis. J. Biomech. 20, 271−280.

Santos, A., Bakker, A.D., Zandieh-Doulabi, B., Semeins, C.M., Klein-Nulend, J., 2009. Pulsating fluid flow modulates gene expression of proteins involved in Wnt signaling pathways in osteocytes. J. Orthop. Res. 27, 1280−1287.

Santos, A., Bakker, A.D., Zandieh-Doulabi, B., de Blieck-Hogervorst, J.M.A., Klein-Nulend, J., 2010. Early activation of the ß-catenin pathway in osteocytes is mediated by nitric oxide, phosphatidyl inositol-3 kinase/Akt, and focal adhesion kinase. Biochem. Biophys. Res. Commun. 391, 364−369.

Sauren, Y.M., Mieremet, R.H., Groot, C.G., Scherft, J.P., 1992. An electron microscopic study on the presence of proteoglycans in the mineralized matrix of rat and human compact lamellar bone. Anat. Rec. 232, 36−44.

Schiller, P.C., Mehta, P.P., Roos, B.A., Howard, G.A., 1992. Hormonal regulation of intercellular communication: parathyroid hormone increases connexin 43 gene expression and gap-junctional communication in osteoblastic cells. Mol. Endocrinol. 6, 1433−1440.

Scholl, F.G., Gamallo, C., Vilar, S., Quintanilla, M., 1999. Identification of PA2.26 antigen as a novel cell-surface mucin-type glycoprotein that induces plasma membrane extensions and increased motility in keratinocytes. J. Cell Sci. 112 (Pt 24), 4601−4613.

Schulze, E., Witt, M., Kasper, M., Löwik, C.W., Funk, R.H., 1999. Immunohistochemical investigations on the differentiation marker protein E11 in rat calvaria, calvaria cell culture and the osteoblastic cell line ROS 17/2.8. Histochem. Cell Biol. 111, 61−69.

Semeins, C.M., Bakker, A.D., Klein-Nulend, J., 2012. Isolation of primary avian osteocytes. Methods Mol. Biol. 816, 43−53.

Shao, J., Zhou, Y., Lin, J., Nguyen, T.D., Huang, R., Gu, Y., Friis, T., Crawford, R., Xiao, Y., 2018a. Notch expression by osteocytes plays a critical role in mineralisation. J. Mol. Med. 96, 333−347.

Shao, J., Zhou, Y., Xiao, Y., 2018b. The regulatory roles of Notch in osteocyte differentiation via the crosstalk with canonical Wnt pathways during the transition of osteoblasts to osteocytes. Bone 108, 165−178.

Shen, H., Grimston, S., Civitelli, R., Thomopoulos, S., 2015. Deletion of connexin43 in osteoblasts/osteocytes leads to impaired muscle formation in mice. J. Bone Miner. Res. 30, 596−605.

Silvestrini, G., Mocetti, P., Ballanti, P., Di Grezia, R., Bonucci, E., 1999. Cytochemical demonstration of the glucocorticoid receptor in skeletal cells of the rat. Endocr. Res. 25, 117−128.

Singla, V., Reiter, J.F., 2005. The primary cilium as the cell's antenna: signaling at a sensory organelle. Science 313, 629−633.

Skerry, T.M., Bitensky, L., Chayen, J., Lanyon, L.E., 1989. Early strain-related changes in enzyme activity in osteocytes following bone loading *in vivo*. J. Bone Miner. Res. 4, 783−788.

Smit, T.H., Burger, E.H., 2000. Is BMU-coupling a strain-regulated phenomenon? A finite element analysis. J. Bone Miner. Res. 15, 301−307.

Smit, T.H., Burger, E.H., Huyghe, J.M., 2002. A case for strain-induced fluid flow as a regulator of BMU-coupling and osteonal alignment. J. Bone Miner. Res. 17, 2021−2029.

Smith, A.J., Sinnghrao, S.K., Newman, G.R., Waddington, R.J., Embery, G., 1997. A biochemical and immunoelectron microcopical analysis of chondroitin sulfate-rich proteoglycans in human alveolar bone. Histochem. J. 29, 1−9.

Spatz, J.M., Wein, M.N., Gooi, J.H., Qu, Y., Garr, J.L., Liu, S., Barry, K.J., Uda, Y., Lai, F., Dedic, C., Balcells-Camps, M., Kronenberg, H.M., Babij, P., Pajevic, P.D., 2015. The Wnt inhibitor sclerostin is up-regulated by mechanical unloading in osteocytes in vitro. J. Biol. Chem. 290, 16744−16758.

Sterck, J.G., Klein-Nulend, J., Lips, P., Burger, E.H., 1998. Response of normal and osteoporotic human bone cells to mechanical stress in vitro. Am. J. Physiol. 274, E1113−E1120.

Stern, A.R., Bonewald, L.F., 2015. Isolation of osteocytes from mature and aged murine bone. Methods Mol. Biol. 1226, 3−10.

Strom, T.M., Francis, F., Lorenz, B., Boddrich, A., Econs, M.J., Lehrach, H., Meitinger, T., 1997. Pex gene deletions in Gy and Hyp mice provide mouse models for X-linked hypophosphatemia. Hum. Mol. Genet. 6, 165−171.

Sugawara, Y., Kamioka, H., Ishihara, Y., Fujisawa, N., Kawanabe, N., Yamashiro, T., 2013. The early mouse 3D osteocyte network in the presence and absence of mechanical loading. Bone 52, 189−196.

Suzuki, R., Domon, T., Wakita, M., 2000. Some osteocytes released from thek lacunae are embedded again in the bone and not engulfed by osteoclasts during bone remodeling. Anat. Embryol. 202, 119−128.

Takagi, M., Ono, Y., Maeno, M., Miyashita, K., Omiya, K., 1997. Immunohistochemical and biochemical characterization of sulphated proteoglycans in embryonic chick bone. J. Nihon Univ. Sch. Dent. 39, 156−163.

Takeda, N., Tsuboyama, T., Kasai, R., Takahashi, K., Shimizu, M., Nakamura, T., Higuchi, K., Hosokawa, M., 1999. Expression of the c-fos gene induced by parathyroid hormone in the bones of SAMP6 mice, a murine model for senile osteoporosis. Mech. Ageing Dev. 108, 87−97.

Tan, S.D., Kuijpers-Jagtman, A.M., Semeins, C.M., Bronckers, A.L., Maltha, J.C., Von den Hoff, J.W., Everts, V., Klein-Nulend, J., 2006. Fluid shear stress inhibits TNFalpha-induced osteocyte apoptosis. J. Dent. Res. 85, 905−909.

Tan, S.D., de Vries, T.J., Kuijpers-Jagtman, A.M., Semeins, C.M., Everts, V., Klein-Nulend, J., 2007. Osteocytes subjected to fluid flow inhibit osteoclast formation and bone resorption. Bone 41, 745−751.

Tan, S.D., Bakker, A.D., Semeins, C.M., Kuijpers-Jagtman, A.M., Klein-Nulend, J., 2008. Inhibition of osteocyte apoptosi by fluid flow is mediated by nitric oxide. Biochem. Biophys. Res. Commun. 369, 1150−1154.

Tanaka, T., Sakano, A., 1985. Differences in permeability of microperoxidase and horseradish peroxidase into alveolar bone of developing rats. J. Dent. Res. 64, 870−876.

Tanaka, T., Hoshijima, M., Sunaga, J., Nishida, T., Hashimoto, M., Odagaki, N., Osumi, R., Adachi, T., Kamioka, H., October 12, 2017. Analysis of Ca2+ response of osteocyte network by three-dimensional time-lapse imaging in living bone. J. Bone Miner. Metab. https://doi.org/10.1007/s00774-017-0868-x [Epub ahead of print].

Tanaka-Kamioka, K., Kamioka, H., Ris, H., Lim, S.S., 1998. Osteocyte shape is dependent on actin filaments and osteocyte processes are unique actin-rich projections. J. Bone Miner. Res. 13, 1555−1568.

Tatsumi, S., Ishii, K., Amizuka, N., Li, M., Kobayashi, T., Kohno, K., Ito, M., Takeshita, S., Ikeda, K., 2007. Targeted ablation of osteocytes induces osteoporosis with defective mechanotransduction. Cell Metabol. 5, 464−475.

Terai, K., Takano-Yamamoto, T., Ohba, Y., Hiura, K., Sugimoto, M., Sato, M., Kawahata, H., Inaguma, N., Kitamura, Y., Nomura, S., 1999. Role of osteopontin in bone remodeling caused by mechanical stress. J. Bone Miner. Res. 14, 839−849.

Tezuka, K., Takeshita, S., Hakeda, Y., Kumegawa, M., Kikuno, R., Hashimoto-Gotoh, T., 1990. Isolation of mouse and human cDNA clones encoding a protein expressed specifically in osteoblasts and brain tissue. Biochem. Biophys. Res. Commun. 173, 246−251.

The HYP Consortium, 1995. A gene (PEX) with homologies to endopeptidases is mutated in patients with X-linked hypophosphatemic rickets. Nat. Genet. 11, 130−136.

Tomkinson, A., Gevers, E.F., Wit, J.M., Reeve, J., Noble, B.S., 1998. The role of estrogen in the control of rat osteocyte apoptosis. J. Bone Miner. Res. 13, 1243−1250.

Torreggiani, E., Matthews, B.G., Pejda, S., Matic, I., Horowitz, M.C., Grcevic, D., Kalajzic, I., 2013. Preosteocytes/osteocytes have the potential to dedifferentiate becoming a source of osteoblasts. PLoS One 8, e75204.

Toyosawa, S., Shintani, S., Fujiwara, T., Ooshima, T., Sato, A., Ijuhin, N., Komori, T., 2001. Dentin matrix protein 1 is predominantly expressed in chicken and rat osteocytes but not in osteoblasts. J. Bone Miner. Res. 16, 2017−2026.

Turner, C.H., Forwood, M.R., Otter, M.W., 1994. Mechanotransduction in bone: do bone cells act as sensors of fluid flow? FASEB J. 8, 875−878.

Turner, C.H., Takano, Y., Owan, I., Murrell, G.A., 1996. Nitric oxide inhibitor L-NAME suppresses mechanically induced bone formation in rats. Am. J. Physiol. 270, E639−E643.

Uematsu, M., Ohara, Y., Navas, J.P., Nishida, K., Murphy, T.J., Alexander, R.W., Nerem, R.M., Harrison, D.G., 1995. Regulation of endothelial nitric oxide synthase mRNA expression by shear stress. Am. J. Physiol. 269, C1371−C1378.

Van Bezooijen, R.L., Roelen, B.A., Visser, A., van der Wee-Pals, L., de Wilt, E., Karperien, M., Hamersma, H., Papapoulos, S.E., ten Dijke, P., Lowik, C.W., 2004. Sclerostin is an osteocyte-expressed negative regulator of bone formation, but not a classical BMP antagonist. J. Exp. Med. 199, 805−814.

Van der Plas, A., Nijweide, P.J., 1992. Isolation and purification of osteocytes. J. Bone Miner. Res. 7, 389−396.

Van der Plas, A., Aarden, E.M., Feyen, J.H., de Boer, A.H., Wiltink, A., Alblas, M.J., de Ley, L., Nijweide, P.J., 1994. Characteristics and properties of osteocytes in culture. J. Bone Miner. Res. 9, 1697−1704.

Van Hove, R.P., Nolte, P.A., Vatsa, A., Semeins, C.M., Salmon, P.L., Smit, T.H., Klein-Nulend, J., 2009. Osteocyte morphology in human tibiae of different bone pathologies with different bone mineral density − is there a role for mechanosensing? Bone 45, 321−329.

Van Oers, R.F.M., Klein-Nulend, J., Bacabac, R.G., 2014. The osteocyte as an orchestrator of bone remodeling: an engineers perspective. Clin. Rev. Bone Miner. Metabol. 12, 2−13.

Vatsa, A., Mizuno, D., Smit, T.H., Schmidt, C.F., MacKintosh, F.C., Klein-Nulend, J., 2006. Bio imaging of intracellular NO production in single bone cells after mechanical stimulation. J. Bone Miner. Res. 21, 1722−1728.

Vatsa, A., Smit, T.H., Klein-Nulend, J., 2007. Extracellular NO signalling from a mechanically stimulated osteocyte. J. Biomech. 40 (Suppl. 1), S89−S95.

Vatsa, A., Breuls, R.G., Semeins, C.M., Salmon, P.L., Smit, T.H., Klein-Nulend, J., 2008a. Osteocyte morphology in fibula and calvaria − is there a role for mechanosensing? Bone 43, 452−458.

Vatsa, A., Semeins, C.M., Smit, T.H., Klein-Nulend, J., 2008b. Paxillin localization in osteocytes − is it determined by the direction of loading? Biochem. Biophys. Res. Commun. 377, 1019−1024.

Veno, P., Nicolella, D.P., Sivakumar, P., Kalajzic, I., Rowe, D., Harris, S.E., Bonewald, L., Dallas, S.L., 2006. Live imaging of osteocytes within their lacunae reveals cell body and dendrite motions. J. Bone Miner. Res. 21 (Suppl. 1), S38.

Verborgt, O., Gibson, G.J., Schaffler, M.B., 2000. Loss of osteocyte integrity in association with microdamage and bone remodeling after fatigue in vivo. J. Bone Miner. Res. 15, 60−67.

Verborgt, O., Tatton, N.A., Majeska, R.J., Schaffler, M.B., 2002. Spatial distribution of Bax and Bcl-2 in osteocytes after bone fatigue: complementary roles in bone remodeling regulation? J. Bone Miner. Res. 17, 907−914.

Vezeridis, P.S., Semeins, C.M., Chen, Q., Klein-Nulend, J., 2005. Osteocytes subjected to pulsating fluid flow regulate osteoblast proliferation and differentiation. Biochem. Biophys. Res. Commun. 348, 1082−1088.

Wang, L., 2018. Solute transport in the bone lacunar-canalicular system (LCS). Curr. Osteoporos. Rep. 16, 32−41.

Wang, N., Ingber, D.E., 1994. Control of cytoskeletal mechanisms by extracellular matrix, cell shape and mechanical tension. Biophys. J. 66, 2181−2189.

Wang, N., Butler, J.P., Ingber, D.E., 1993. Mechanotransduction across the cell surface and through the cytoskeleton. Science 260, 1124−1127.

Wang, L., Ciani, C., Doty, S.B., Fritton, S.P., 2004. Delineating bone's interstitial fluid pathway in vivo. Bone 34, 499−509.

Watson, P.A., 1991. Function follows form: generation of intracellular signals by cell deformation. FASEB J. 5, 2013−2019.

Weinbaum, S., Cowin, S.C., Zeng, Y., 1994. A model for the excitation of osteocytes by mechanical loading-induced bone fluid shear stresses. J. Biomech. 27, 339−360.

Weinstein, R.S., Jilka, R.L., Parfitt, A.M., Manolagas, S.C., 1998. Inhibition of osteoblastogenesis and promotion of apoptosis of osteoblasts and osteocytes by glucocorticoids: potential mechanisms of their deleterious effects on bone. J. Clin. Investig. 102, 274−282.

Westbroek, I., Ajubi, N.E., Alblas, M.J., Semeins, C.M., Klein-Nulend, J., Burger, E.H., Nijweide, P.J., 2000a. Differential stimulation of prostaglandin G/H synthase-2 in osteocytes and other osteogenic cells by pulsating fluid flow. Biochem. Biophys. Res. Commun. 268, 414−419.

Westbroek, I., Alblas, M.J., Van der Plas, A., Nijweide, P.J., 2000b. Estrogen receptor α is preferentially expressed in osteocytes. J. Bone Miner. Res. 15 (Suppl. 1), S494.

Westbroek, I., Van der Plas, A., De Rooij, K.E., Klein-Nulend, J., Nijweide, P.J., 2001. Expression of serotonin receptors in bone. J. Biol. Chem. 276, 28961−28968.

Westbroek, I., De Rooij, K.E., Nijweide, P.J., 2002. Osteocyte-specific monoclonal antibody MAb OB7.3 is directed against Phex protein. J. Bone Miner. Res. 17, 845−853.

Wijeratne, S.S., Martinez, J.R., Grindel, B.J., Frey, E.W., Li, J., Wang, L., Farach-Carson, M.C., Kiang, C.H., 2016. Single molecule force measurements of perlecan/HSPG2: a key component of the osteocyte pericellular matrix. Matrix Biol. 50, 27−38.

Willems, H.M.E., van den Heuvel, E.G.H.M., Schoemaker, R.J.W., Klein-Nulend, J., Bakker, A.D., 2017. Diet and exercise: a match made in bone. Curr. Osteoporos. Rep. 15, 555−563.

Windahl, S.H., Borjesson, A.E., Farman, H.H., Engdahl, C., Movérare-Skrtic, S., Sjögren, K., Lagerquist, M.K., Kindblom, J.M., Koskela, A., Tuukkanen, J., Divieti Pajevic, P., Feng, J.Q., Dahlman-Wright, K., Antonson, P., Gustafsson, J.A., Ohlsson, C., 2013. Estrogen receptor-α in osteocytes is important for trabecular bone formation in male mice. Proc. Natl. Acad. Sci. U.S.A. 110, 2294−2299.

Wolff, J.D., 1892. Das Gesetz der Transformation der Knochen. A. Hirschwald, Berlin.

Woo, S.M., Rosser, J., Dusevich, V., Kalajzic, I., Bonewald, L.F., 2011. Cell line IDG-SW3 replicates osteoblast-to-late-osteocyte differentiation in vitro and accelerates bone formation in vivo. J. Bone Miner. Res. 26, 2634−2646.

Wu, X.T., Sun, L.W., Yang, X., Ding, D., Han, D., Fan, Y.B., 2017. The potential role of spectrin network in the mechanotransduction of MLO-Y4 osteocytes. Sci. Rep. 7, 40940.

Wu, V., Van Oers, R.F.M., Schulten, E.A.J.M., Helder, M.N., Bacabac, R.G., Klein-Nulend, J., 2018. Osteocyte morphology and orientation in relation to strain in the jaw bone. Int. J. Oral Sci. 10 (2), 1−8.

Xiao, Z., Zhang, S., Mahlios, J., Zhou, G., Magenheimer, B.S., Guo, D., Dallas, S.L., Maser, R., Calvet, J.P., Bonewald, L., Quarles, L.D., 2006. Cilia-like structures and polycystin-1 in osteoblasts/osteocytes and associated abnormalities in skeletogenesis and Runx2 expression. J. Biol. Chem. 281, 30884−30895.

Xiong, J., Onal, M., Jilka, R.L., Weinstein, R.S., Manolagas, S.C., O'Brien, C.A., 2011. Matrix-embedded cells control osteoclast formation. Nat. Med. 17, 1235−1241.

Xiong, J., Piemontese, M., Onal, M., Campbell, J., Goellner, J.J., Dusevich, V., Bonewald, L.F., Manolagas, S.C., O'Brien, C.A., 2015. Osteocytes, not osteoblasts or lining cells, are the main source of the RANKL required for osteoclast formation in remodeling bone. PLoS One 10, e013818.

Xu, H., Gu, S., Riquelme, M.A., Burra, S., Callaway, D., Cheng, H., Guda, T., Schmitz, J., Fajardo, R.J., Werner, S.L., Zhao, H., Shang, P., Johnson, M.L., Bonewald, L.F., Jiang, J.X., 2015. Connexin 43 channels are essential for normal bone structure and osteocyte viability. J. Bone Miner. Res. 30, 550−562.

Yamazaki, M., Nakajima, F., Ogasawara, A., Moriya, H., Majeska, R.J., Einhorn, T.A., 1999. Spatial and temporal distribution of CD44 and osteopontin in fracture callus. J. Bone Joint Surg. Br. 81, 508−515.

Yang, D., Turner, A.G., Wijenayaka, A.R., Anderson, P.H., Morris, H.A., Atkins, G.J., 2015. 1,25-Dihydroxyvitamin D3 and extracellular calcium promote mineral deposition via NPP1 activity in a mature osteoblast cell line MLO-A5. Mol. Cell. Endocrinol. 412, 140−147.

Yellowley, C.E., Li, Z., Zhou, Z., Jacobs, C.R., Donahue, H.J., 2000. Functional gap junctions between osteocytic and osteoblastic cells. J. Bone Miner. Res. 15, 209−217.

You, J., Yellowley, C.E., Donahue, H.J., Zhang, Y., Chen, Q., Jacobs, C.R., 2000. Substrate deformation levels associated with routine physical activity are less stimulatory to bone cells relative to loading induced oscillating fluid flow. J. Biomech. Eng. 122, 387–393.

Zaman, G., Pitsillides, A.A., Rawlinson, S.C., Suswillo, R.F., Mosley, J.R., Cheng, M.Z., Platts, L.A., Hukkanen, M., Polak, J.M., Lanyon, L.E., 1999. Mechanical strain stimulates nitric oxide production by rapid activation of endothelial nitric oxide synthase in osteocytes. J. Bone Miner. Res. 14, 1123–1131.

Zaman, G., Jessop, H.L., Muzylak, M., De Souza, R.L., Pitsillides, A.A., Price, J.S., Lanyon, L.L., 2006. Osteocytes use estrogen receptor alpha to respond to strain but their ERalpha content is regulated by estrogen. J. Bone Miner. Res. 21, 1297–1306.

Zhang, K., Barragan-Adjemian, C., Ye, L., Kotha, S., Dallas, M., Lu, Y., Zhao, S., Harris, M., Harris, S.E., Feng, J.Q., Bonewald, L.F., 2006. E11/gp38 selective expression in osteocytes: regulation by mechanical strain and role in dendrite elongation. Mol. Cell Biol. 26, 4539–4552.

Zhang, B., Hou, R., Zou, Z., Luo, T., Zhang, Y., Wang, L., Wang, B., 2018. Mechanically induced autophagy is associated with ATP metabolism and cellular viability in osteocytes in vitro. Redox Biol. 14, 492–498.

Zhao, S., Zhang, Y.K., Harris, S., Ahuja, S.S., Bonewald, L.F., 2002. MLO-Y4 osteocyte-like cells support osteoclast formation and activation. J. Bone Miner. Res. 17, 2068–2079.

Zhao, N., Nociti Jr., F.H., Duan, P., Prideaux, M., Zhao, H., Foster, B.L., Somerman, M.J., Bonewald, L.F., 2016. Isolation and functional analysis of an immortalized murine cementocyte cell line, IDG-CM6. J. Bone Miner. Res. 31, 430–442.

Further reading

Aubin, J.E., Turksen, K., 1996. Monoclonal antibodies as tools for studying the osteoblast lineage. Microsc. Res. Tech. 33, 128–140.

Divieti, P., Geller, A.I., Suliman, G., Juppner, H., Bringhurst, F.R., 2005. Receptors specific for the carboxyl-terminal region of parathyroid hormone on bone-derived cells: determinants of ligand binding and bioactivity. Endocrinology 146, 1863–1870.

Ikegame, M., Ishibashi, O., Yoshizawa, T., Shimomura, J., Komori, T., Ozawa, H., Kawashima, H., 2001. Tensile stress induces bone morphogenetic protein 4 in preosteoblastic and fibroblastic cells, which later differentiate into osteoblasts leading to osteogenesis in the mouse calvariae in organ culture. J. Bone Miner. Res. 16, 24–32.

Joldersma, M., Klein-Nulend, J., Oleksik, A.M., Heyligers, I.C., Burger, E.H., 2001. Estrogen enhances mechanical stress-induced prostaglandin production by bone cells from elderly women. Am. J. Physiol. 280, E436–E442.

Kaspar, D., Seidl, W., Neidlinger-Wilke, C., Ignatius, A., Claes, L., 2000. Dynamic cell stretching increases human osteoblast proliferation and CICP synthesis but decreases osteocalcin synthesis and alkaline phosphatase activity. J. Biomech. 33, 45–51.

Kawata, A., Mikuni-Takagaki, Y., 1998. Mechanotransduction in stretched osteocytes, temporal expression of immediate early and other genes. Biochem. Biophys. Res. Commun. 246, 404–408.

Mikuni-Takagaki, Y., Suzuki, Y., Kawase, T., Saito, S., 1996. Distinct responses of different populations of bone cells to mechanical stress. Endocrinology 137, 2028–2035.

Neidlinger-Wilke, C., Stall, I., Claes, L., Brand, R., Hoellen, I., Rubenacker, S., Arand, M., Kinzl, L., 1995. Human osteoblasts from younger normal and osteoporotic donors show differences in proliferation and TGF-beta release in response to cyclic strain. J. Biomech. 28, 1411–1418.

Owan, I., Burr, D.B., Turner, C.H., Qui, J., Tu, Y., Onyia, J.E., Duncan, R.L., 1997. Mechanotransduction in bone: osteoblasts are more responsive to fluid forces than mechanical strain. Am. J. Physiol. 273, C810–C815.

Petersen, D.N., Tkalcevic, G.T., Mansolf, A.L., Rivera-Gonzalez, R., Brown, T.A., 2000. Identification of osteoblast/osteocyte factor 45 (OF45), a bone-specific cDNA encoding an RGD-containing protein that is highly expressed in osteoblasts and osteocytes. J. Biol. Chem. 275, 36172–36180.

Raulo, E., Chernousov, M.A., Carey, D., Nolo, R., Rauvala, H., 1994. Isolation of a neuronal cell surface receptor of heparin-binding growth-associated molecule (HB-GAM): identification as N-syndecan (syndecan-3). J. Biol. Chem. 269, 12999–13004.

Rauvala, H., 1989. An 18-kD heparin-binding protein of developing brain that is distinct from fibroblastic growth factors. EMBO J. 8, 2933–2941.

Wetterwald, A., Hoffstetter, W., Cecchini, M.G., Lanske, B., Wagner, C., Fleisch, H., Atkinson, M., 1996. Characterization and cloning of the E11 antigen, a marker expressed by rat osteoblasts and osteocytes. Bone 18, 125–132.

Chapter 7

Transcriptional control of osteoblast differentiation and function

Gérard Karsenty
Département of Genetics and Development, Columbia University Medical Center, New York, NY, United States

Chapter outline

As is the case for every cell differentiation process, differentiation of a mesenchymal pluripotent cell into any cell type is governed in large part by transcription factors that trigger the entire program of cell differentiation. Our knowledge about the transcriptional control of osteoblast differentiation made its main strides at the end of the 20th century and has been significantly refined since then, with the emergence of novel mechanisms regulating gene expression in addition to transcription factors. Briefly and ideally, a transcription factor that is a differentiation factor for a given cell type should (1) be expressed in progenitors of this cell type, (2) regulate the expression of all cell-specific genes in this cell type, (3) induce expression of the aforementioned genes when ectopically expressed in other cell types (sufficiency criterion), and (4) be necessary for the differentiation of this cell type in vivo, in mice, and at best in humans. As presented in this chapter, the transcription factor currently viewed as the master gene of osteoblast differentiation is one of the very few differentiation factors to fulfill all these criteria.

Runx2, a master control gene of osteoblast differentiation in bony vertebrates

The power of a combined effort between molecular biologists and human geneticists in identifying key genes regulating cell differentiation, which has been so beneficial for our understanding of skeletal biology, is best illustrated by the realization at the end of the 1990s that Runt-related transcription factor 2 (Runx2) is a master gene of osteoblast differentiation. Runx2, previously termed Pebp2a1, AmI3, or Cbfa1, was originally cloned in 1993 as one of three mammalian homologs of the *Drosophila* transcription factor Runt (Kagoshima et al., 1993; Ogawa et al., 1993). Based on the premise that it might be expressed in thymus and T cell lines, but not in B cell lines, Runx2 was thought to be involved in T cell differentiation and was deleted to study T cell differentiation (Ogawa et al., 1993; Satake et al., 1995). However, 4 years after the cloning of Runx2, its crucial role as a transcriptional determinant of osteoblast differentiation was demonstrated by several investigators working independent of one another and using different yet complementary experimental approaches (Ducy et al., 1997; Komori et al., 1997; Lee et al., 1997; Mundlos et al., 1997; Otto et al., 1997).

Principles of Bone Biology. https://doi.org/10.1016/B978-0-12-814841-9.00007-5

One approach, purely molecular, was aimed at the identification of osteoblast-specific transcription factors through the systematic analysis of the promoter of what was then the only osteoblast-specific gene, *Osteocalcin*. The analysis of a proximal promoter fragment of one of the two mouse *Osteocalcin* genes led to the identification of the only two known osteoblast-specific *cis*-acting elements, termed OSE1 and OSE2 (Ducy and Karsenty, 1995). Remarkably, as of this writing, those two *cis*-acting elements remain the only known strictly osteoblast-specific *cis*-acting elements. Sequence inspection of OSE2 revealed homology for the DNA-binding site of Runt family transcription factors, and subsequent analysis demonstrated that the factor binding to OSE2 is related immunologically to transcription factors of the Runt family (Geoffroy et al., 1995; Merriman et al., 1995). Eventually, screening of a mouse osteoblast cDNA library revealed that only one of the three mammalian *Runx* genes, namely *Runx2*, is expressed predominantly in cells of the osteoblast lineage (Ducy et al., 1997). Indeed, in situ hybridization further revealed that during mouse development, *Runx2* expression is first detected in the lateral plate mesoderm at 10.5 days postcoitus (dpc), and later is confined in cells of the mesenchymal condensations. Until 12.5 dpc these cells, which prefigure the future skeleton, represent common precursors of osteoblasts and chondrocytes. At 14.5 dpc osteoblasts first appear and maintain the expression of *Runx2*, whereas in chondrocytes *Runx2* expression decreases significantly and becomes restricted to prehypertrophic and hypertrophic chondrocytes. After birth, *Runx2* expression is strictly restricted to osteoblasts and cells of the perichondrium. This spatial and temporal expression pattern suggested Runx2 might play a critical role as a regulator of osteoblast differentiation (Ducy et al., 1997).

The demonstration that Runx2 was indeed an osteoblast differentiation factor came from several synergistic lines of molecular and genetic evidence. First, in addition to the *Osteocalcin* promoter, functional OSE2-like elements were identified in the promoter regions of most other genes that are expressed at relatively high levels in osteoblasts, such as *α1(II)-collagen*, *Osteopontin*, and *Bone sialoprotein*, and eventually many more (Ducy et al., 1997). Second, and more decisively, forced expression of *Runx2* in nonosteoblastic cell lines or primary skin fibroblasts induced osteoblast-specific gene expression in these cells, demonstrating that Runx2 acts as a transcriptional activator of osteoblast differentiation in vitro (Ducy et al., 1997). This was subsequently verified in vivo, where it was shown that the constitutive expression of Runx2 at low levels in nonhypertrophic chondrocytes triggered the entire cascade of endochondral bone formation, which normally does not occur in the cartilaginous ribs. Remarkably, however, ectopic expression of Runx in chondrocytes cannot cause transdifferentiation of chondrocytes into osteoblasts (Takeda et al., 2001). This suggests that if trans-differentiation of chondrocytes into osteoblasts can exist it remains a rather rare event. Third, the ultimate demonstration that Runx2 is an indispensable transcriptional activator of osteoblast differentiation came from genetic studies in mice and humans. At the same time, two groups deleted the *Runx2* gene from the mouse genome, both expecting an immunological phenotype based on the assumption that *Runx2* was involved in T cell differentiation (Komori et al., 1997; Otto et al., 1997). Instead, all *Runx2*-deficient mice had no skull, because intramembranous bone formation did not occur. In the rest of their skeleton, there are no osteoblasts in *Runx2*-deficient mice, an observation confirmed by the lack of expression of osteoblast marker genes.

The critical importance of Runx2 for osteoblast differentiation was further emphasized by the finding that mice lacking only one allele of *Runx2* display hypoplastic clavicles and delayed closure of the fontanelles, i.e., defects of intra-membranous ossification (Otto et al., 1997). This phenotype is identical to what is seen in a human disease termed cleidocranial dysplasia (CCD), and subsequent genetic analysis of CCD patients revealed disease-causing heterozygous mutations of the *RUNX2* gene, thereby demonstrating the relevance of Runx2 for osteoblast differentiation also in humans (Lee et al., 1997; Mundlos et al., 1997). Taken together, this overwhelming molecular and genetic evidence has led to the generally accepted view that Runx2 is a master control gene of osteoblast differentiation, providing a molecular switch inducing osteoblast-specific gene expression in mesenchymal progenitor cells (Lian and Stein, 2003). Remarkably, many, although not all, of the subsequent advances that have been made in the field are centered around the biology of Runx2.

In addition to its prominent role in osteoblast differentiation and skeletogenesis, Runx2 is also involved in the regulation of bone formation beyond development. This has been demonstrated in several ways. First, transgenic mice expressing a dominant-negative variant of Runx2 specifically in fully differentiated osteoblasts are viable, but develop severe osteopenia caused by a decreased rate of bone formation, in the face of normal osteoblast numbers (Ducy et al., 1999). This phenotype is readily explained by the finding that several Runx2 target genes encoding bone extracellular matrix proteins are expressed at much lower levels. Second, mice lacking *StatI*, a transcription factor attenuating the nuclear translocation of Runx2, as discussed later, display a high-bone-mass phenotype that is explained not only by increased osteoblast differentiation, but also by increased bone matrix deposition (Kim et al., 2003). Third, a similar, but even more severe, phenotype is observed in mice lacking the nuclear adapter protein Shn3. Because Shn3, as discussed later, is involved in the ubiquitination and proteasomal degradation of Runx2, the increased bone formation of the Shn3-deficient mice is readily explained by increased Runx2 levels in osteoblasts that in turn lead to enhanced bone matrix deposition (Jones et al., 2006). Given these results, it came as a surprise that another transgenic mouse model,

overexpressing intact *RU/u2* under the control of an osteoblast-specific 0.1 *(I)-collagen* promoter fragment, did not display the expected high-bone-mass phenotype, but a severe osteopenia accompanied by an increased fracture risk (Liu et al., 2001). Although these mice had increased numbers of osteoblasts, their bone formation rate was strikingly reduced, which likely illustrates the fact that the dosage of Runx2 needs to be tightly regulated to orchestrate proper bone formation in vivo.

Runx2 functions during skeletogenesis beyond osteoblast differentiation

Although most of these results demonstrating a key role for Runx2 in osteoblasts were already discussed in the last edition of this book, there is accumulating novel evidence that the role of Runx2 in skeletogenesis is much more complex than previously anticipated. The starting point for these findings was the observation that Runx2-deficient mice also display defects of chondrocyte hypertrophy in some skeletal elements (Inada et al., 1999; Kim et al., 1999). Moreover, because *Runx2* is transiently expressed in prehypertrophic chondrocytes of mouse embryos, there was a possibility of a function of Runx2 in chondrocyte differentiation. One way to address this possibility was the generation of a transgenic mouse model expressing *Runx2* in nonhypertrophic chondrocytes, using an *α1(II)-collagen* promoter/enhancer construct (Takeda et al., 2001).

In line with the suspected role of Runx2 as a positive regulator of chondrocyte hypertrophy, these transgenic mice displayed accelerated chondrocyte maturation in the growth plates, but also evidence of ectopic cartilage formation in the rib cage or in the trachea, among other locations. Moreover, the presence of this transgene in a Runx2-deficient genetic background prevented the absence of skeletal mineralization that is normally associated with *Runx2* deficiency. However, the skeleton of these mice contained only hypertrophic cartilage, and no bone matrix, thereby demonstrating that Runx2 induces chondrocyte hypertrophy, but not a transdifferentiation into osteoblasts (Takeda et al., 2001).

Because *Runx2* expression in prehypertrophic chondrocytes is transient, the main function of Runx2 here is probably to establish the growth plate. However, through another site of expression, namely in perichondrial cells, Runx2 has an additional function in the regulation of chondrogenesis. In these cells Runx2 positively regulates the expression of Fgfl8, a diffusible molecule that inhibits chondrocyte maturation and osteoblast differentiation (Hinoi et al., 2006; Liu et al., 2002; Ohbayashi et al., 2002). Taken together, these results establish that Runx2 is more than the master gene of osteoblast differentiation; it is, in fact, along with Sox9, the major transcriptional regulator of cell differentiation during skeletogenesis, acting positively and negatively on osteoblast and chondrocyte differentiation.

Regulation of Runx2 accumulation and function

In essence, the accumulation and demonstration that Runx2 exhibits, in vivo in mice and humans, all the characteristics of an osteoblast differentiation factor raised the usual questions: (1) What is upstream of Runx2? (2) How is Runx2 function regulated? (3) What is downstream of Runx2?

The search for mechanisms regulating *Runx2* expression is still ongoing. However, progress in this area of research came when a peculiarity of osteoblast differentiation was confronted in other progress in bone biology. This peculiarity of osteoblast biology is that the synthesis of type I collagen, the overwhelmingly most abundant protein of the bone extracellular matrix, precedes the expression of Runx2 (Wei et al., 2015). The fact that osteoblasts regulate glucose metabolism through the hormone osteocalcin prompted, of course, the study of the regulation of glucose metabolism in osteoblasts (Lee et al., 2007). This 2007 study showed that glucose is the main nutrient of osteoblasts and that, in vivo, glucose is transported in osteoblasts through Glut1, whose expression in cells of the osteoblasts lineage precedes that of Runx2. Glucose uptake favors osteoblast differentiation by preventing the proteasomal degradation of Runx2. Accordingly, Runx2 cannot induce osteoblast differentiation when glucose uptake is compromised, and raising blood glucose levels is sufficient to initiate bone formation in Runx2-deficient embryos. That Runx2 favors Glut1 expression determines the onset of osteoblast differentiation during development (Wei et al., 2015).

In addition to this strong metabolic regulation of osteoblast differentiation, other transcription factors have been shown to act upstream of Runx2. There are several lines of evidence showing that, for instance, certain homeodomain-containing transcription factors are involved in the regulation of *Runx2* expression. One of these proteins is Msx2, whose role in skeletal development was demonstrated through the identification of gain- and loss-of-function mutations in human patients suffering from Boston-type craniosynostosis or enlarged parietal foramina, respectively (Jabs et al., 1993; Wilke et al., 2000). Likewise, *Msx2*-deficient mice display defective ossification of the skull and of bones developing by endochondral ossification (Satokata et al., 2000). Moreover, because the expression of *Osteocalcin* and *Runx2* is strongly reduced in *Msx2*-deficient mice, it appears that Msx2 acts upstream of Runx2 in a transcriptional cascade regulating

osteoblast differentiation. A similar observation has been described for mice lacking the homeodomain-containing transcription factor *Bpx* (Tribioli and Lufkin, 1999). These mice die at birth owing to a severe dysplasia of the axial skeleton, whereas the appendicular skeleton is virtually unaffected. *Runx2* expression in *Bpx*-deficient mice is strongly reduced in osteo-chondrogenic precursor cells of the prospective vertebral column, thereby indicating that *Bpx* is required for *Runx2* expression specifically in these skeletal elements.

There are also negative regulators of *Runx2* expression. One of them is another homeodomain-containing transcription factor, Hoxa2. *Hoxa2*-deficient mice display ectopic bone formation in the second branchial arch, which is readily explained by an induction of *Runx2* expression exactly in this region (Kanzler et al., 1998). Consistent with these observations, transgenic mice expressing *Hoxa2* in craniofacial bones under the control of an *Msx2* promoter fragment lack several bones in the craniofacial area. Beyond development there is at least one factor required to limit *Runx2* expression in osteoblast precursor cells, namely, the high-mobility group−containing transcription factor Sox8. Sox8-deficient mice display an osteopenia that is caused by accelerated osteoblast differentiation accompanied by enhanced expression of *Runx2* (Schmidt et al., 2005). Likewise, transgenic mice expressing *Sox8* under the control of an osteoblast-specific *α1(I)-collagen* promoter fragment virtually lack differentiated osteoblasts because of a decreased expression of *Runx2*. In addition to the existence of transcriptional regulators of *Runx2* expression, there are also factors interacting with the Runx2 protein, thereby activating or repressing its activity. One identified positive regulator of Runx2 action is the nuclear matrix protein Satb2. The importance of this protein in skeletogenesis was first discovered in human patients with cleft palate that carry a heterozygous chromosomal translocation inactivating the *SATB2* gene (Fitzpatrick et al., 2003). The generation of a *Satb2*-deficient mouse model confirmed the importance of this gene in craniofacial development, skeletal patterning, and osteoblast differentiation (Dobreva et al., 2006). The last function was in part attributed to an increased expression of *Hoxa2*, a negative regulator of bone formation discussed earlier, whose expression is repressed by the binding of Satb2 to an enhancer element of the *Hoxa2* gene.

In addition to this type of action, there is also a Hoxa2-independent influence of Satb2 on the transcription of *Bone sialoprotein* and *Osteocalcin*. Whereas in the case of *Bone sialoprotein*, Satb2 directly binds to an osteoblast-specific element in the promoter of this gene, the activation of *Osteocalcin* expression by Satb2 requires a physical interaction with Runx2. This was demonstrated by cotransfection assays using a *Luciferase* reporter gene under the control of an osteoblast-specific *Osteocalcin* promoter fragment, but also by coimmunoprecipitation experiments. Moreover; the synergistic action of Satb2 and Runx2 in osteoblasts was genetically confirmed through the generation and analysis of compound heterozygous mice lacking one allele of each gene (Dobreva et al., 2006). Taken together, these results identified Satb2 as an important regulator of osteoblast differentiation in mice and humans. Moreover, the finding that Satb2 also interacts with Activating transcription factor 4 (ATF4), another transcription factor involved in osteoblast differentiation and function that will be discussed later, illustrates that the transcriptional network regulating bone formation is much more complex than previously anticipated.

This is further highlighted by the discovery of several other proteins that physically interact with Runx2, thereby attenuating its activity. One of these proteins is Stat1, a transcription factor regulated by extracellular signaling molecules, such as interferons. Stat1-deficient mice, as already mentioned, are viable, but develop a high-bone-mass phenotype explained by enhanced bone formation (Kim et al., 2003). The increase in osteoblast differentiation and function in these mice is molecularly explained by the lack of a Stat1-mediated inhibition of the transcriptional activity of Runx2. Interestingly, the physical interaction of both proteins is independent of Stat1 activation by phosphorylation, and it inhibits the translocation of Runx2 into the nucleus. Thus, overexpression of Stat1 in osteoblasts leads to a cytosolic retention of Runx2, and the nuclear translocation of Runx2 is much more prominent in Stat1-deficient osteoblasts (Kim et al., 2003).

Another protein interacting with Runx2, thereby decreasing its availability in the nucleus, is Shn3. Shn3 is a zinc finger adapter protein originally thought to be involved in VDJ recombination of immunoglobulin genes (Wu et al., 1993). Unexpectedly, however, the generation of an Shn3-deficient mouse model revealed that it plays a major function in bone formation. In fact, the *Shn3*-deficient mice display a severe adult-onset osteosclerotic phenotype owing to a cell-autonomous increase in bone matrix deposition (Jones et al., 2006). Interestingly, although several Runx2 target genes are expressed at higher rates in Shn3-deficient osteoblasts, *Runx2* expression itself is not affected by the absence of Shn3. Importantly, however, the Runx2 protein level is strikingly increased in *Shn3*-deficient osteoblasts. This finding is molecularly explained by the function of Shn3 as an adapter molecule linking Runx2 to the E3 ubiquitin ligase WWP1. The Shn3-mediated recruitment of WWP1 in turn leads to an enhanced proteasomal degradation of Runx2, which is best highlighted by the finding that RNA interference−mediated downregulation of WWP1 in osteoblasts leads to increased Runx2 protein levels and enhanced extracellular matrix mineralization, thus virtually mimicking the defects observed in the absence of Shn3 (Jones et al., 2006). Taken together, these data identify Shn3 as a key negative regulator of Runx2 actions in vivo. Accordingly, and as anticipated, *Glut1* expression and glucose uptake are significantly increased in

shn3$^{-/-}$ osteoblasts, as is *Runx2* expression (Wei et al., 2015). Moreover, given the postnatal onset of the bone phenotype of the *Shn3*-deficient mice, it has been speculated that compounds blocking the interaction of Runx2, Shn3, and WWP1 may serve as specific therapeutic agents for the treatment of bone loss diseases, such as osteoporosis. This does not exclude the possibility that *Shn3* may regulate osteoblast differentiation through additional mechanisms (Shim et al., 2013).

While Stat1 and Shn3 exemplify the importance of a negative regulation of Runx2 in postnatal bone remodeling, there is also a need for a negative regulation of Runx2 activity before bone development starts and when *Runx2* is already expressed. This is highlighted by the finding that *Runx2* expression in the lateral plate mesoderm is already detectable as early as embryonic day (E) 10 of mouse development, whereas the expression of molecular markers of differentiated osteoblasts cannot be detected before E13.5 at the earliest (Ducy, 2000). One molecular explanation for this delay between *Runx2* expression and osteoblast differentiation came from the functional analysis of Twist proteins that are transiently coexpressed with *Runx2* early during development and inhibit osteoblast differentiation by interacting with Runx2. In essence, the initiation of osteoblast differentiation occurs only when *Twist* gene expression fades away.

In brief, the fact that Runx2 expression precedes osteoblast differentiation by more than 4 days led to the assumption that Runx2 function must be regulated negatively in Runx2-expressing cells. The identification of such a factor relied on human genetic evidence. Haploinsufficiency at the *RUNX2* locus causes a lack of bone in the skull, whereas haploinsufficiency at the *TWIST1* locus causes essentially too much bone in the skull, a condition called craniosynostosis (EI Ghouzzi et al., 1997; Howard et al., 1997). Because the same phenotypes are observed in the corresponding mouse models lacking one allele of either gene, it was possible to demonstrate a genetic interaction of *Runx2* and *Twist1* through the generation of compound heterozygous mice. In fact, these mice did not display any detectable defects of skull development and suture fusion (Bialek et al., 2004). In contrast, the defects of clavicle development caused by haploinsufficiency of *Runx2* were not rescued by heterozygosity of *Twist1*, but by the deletion of *Twist2*. Thus, both Twist proteins have similar functions but in different skeletal elements. This is totally consistent with their expression pattern in mouse embryos (Bialek et al., 2004).

Both Twist proteins are presumably basic helix−loop−helix (bHLH) transcription factors, yet this function of Twist is not determined by the bHLH domain, but rather by the C-terminal 20 amino acids, the so-called Twist box, whose sequence is fully conserved in both Twist proteins, in mice and humans. Through the Twist box, Twist proteins interact with the Runx2 DNA-binding domain and prevent its DNA binding. The importance of this sequence motif for Twist function in vivo was confirmed by the existence of a Twist-box mutation within the human *TWISTI* gene that causes a severe form of craniosynostosis (Gripp et al., 2000). Moreover, an ethylnitrosourea-mutagenesis approach in mice led to the identification of an amino acid substitution within the Twist box of Twist1 that causes premature osteoblast differentiation in vivo (Bialek et al., 2004).

Unexpectedly, this mouse model, termed Charlie Chaplin, also displayed decreased chondrocyte maturation, thereby suggesting an additional physiological role of Twist1, independent of its antiosteogenic function (Hinoi et al., 2006). Because *Twist1* is not expressed in chondrocytes, but in mesenchymal cells of the perichondrium, it appears that it is required to inhibit the induction of *Fgf18* expression in these cells by the action of Runx2, which was described earlier. Indeed, whereas transgenic mice overexpressing *Twist1* under the control of an osteoblast-specific 0.1 *(I)-collagen* promoter fragment displayed enhanced chondrocyte maturation, the decreased chondrocyte maturation in the *CC/CC* mice was normalized by haploinsufficiency of *Runx2* (Hinoi et al., 2006). Taken together, these data demonstrate that Twist1, through inhibition of Runx2 DNA binding, not only limits osteoblast differentiation and bone formation, but also enhances chondrocyte maturation during skeletal development. Other negative regulators of Runx2 function in vivo have been described based on their abilities to influence the CCD phenotype of *Runx2*$^{+/-}$ mice. One of them, another zinc finger−containing protein termed zinc finger protein 521 (2fp521), antagonizes Runx2 function in a histone deacetylase 3 (HDAC3)-dependent manner.

Osterix, a Runx2-dependent osteoblast-specific transcription factor required for bone formation

In addition to Runx2, there is at least one more transcription factor, termed Osterix (Osx), whose activity is absolutely required in mice for osteoblast differentiation. Osx is a zinc finger−containing transcription factor that is specifically expressed in osteoblasts of all skeletal elements. Inactivation of Osx in mice results in perinatal lethality owing to a complete absence of bone formation (Nakashima et al., 2002). Unlike the *Runx2*-deficient mice whose skeleton is completely unmineralized, the *Osx*-deficient mice lacked a mineralized matrix only in bones formed by intramembranous ossification. In contrast, the bones formed by endochondral ossification contained mineralized matrix, but this resembled

calcified cartilage, not mineralized bone matrix. This finding suggested that Osx, unlike Runx2, is not required for chondrocyte hypertrophy, thereby demonstrating that it specifically induces osteoblast differentiation and bone formation in vivo. The comparative expression analysis by in situ hybridization further revealed that *Osx* is not expressed in *Runx2*-deficient embryos, and that *Runx2* is normally expressed in *Osx*-deficient embryos (Nakashima et al., 2002). These results demonstrated that Osx acts downstream of Runx2 in a transcriptional cascade of osteoblast differentiation, and its expression is apparently directly regulated by the binding of Runx2 to a responsive element in the promoter of the Osx gene (Nishio et al., 2006).

In contrast to the steadily increasing knowledge about the function of Runx2 and its regulation by other molecules, the molecular mechanisms underlying the action of Osx in osteoblasts are less well understood. Moreover, unlike for *RUNX2*, no human mutations of the *OSX* gene have yet been identified that would be associated with decreased bone formation. Nevertheless, one 2005 publication indicates that Osx contributes to the negative effects of nuclear factor of activated T cells (NFAT) inhibitors on bone mass (Koga et al., 2005). NFAT inhibitors, such as *FKS06* or cyclosporin A, are commonly used as immune suppressants, e.g., after organ transplantation. However, this treatment is often accompanied by the development of osteopenia in the patient (Rodino and Shane, 1998). Likewise, treatment of mice with *FKS06* leads to decreased bone mass owing to impaired bone formation, and the same phenotype was observed in mice lacking the transcription factor Nfatc1. The deduced role of Nfatc1 as a physiological activator of osteoblast differentiation and function can be molecularly explained by an interaction with *Osx*. In fact, both proteins synergistically activate transcription of a *Luciferase* reporter gene driven by an osteoblast-specific *α1(I)-collagen* promoter fragment, which is based on the formation of a DNA-binding complex of Nfatc1 and Osx (Koga et al., 2005). It has been shown that Osx might act as a cofactor for Dlx5 for osteoblast specification (Hojo et al., 2016).

ATF4, a transcriptional regulator of osteoblast functions and a mediator of the neural regulation of bone mass

The role of ATF4 in skeletal biology also arose from a combination of molecular biology and human and mouse genetic data. *RSK2*, which encodes a kinase, is the gene mutated in Coffin–Lowry syndrome, an X-linked mental retardation condition associated with skeletal abnormalities (Trivier et al., 1996). Like Rsk2-deficient mice, $Atf4^{-/-}$ mice display a lower bone mass owing to impaired bone formation (Yang et al., 2004). In vitro kinase assays demonstrated that ATF4 is strongly phosphorylated by Rsk2, and that this phosphorylation is undetectable in osteoblasts derived from *Rsk2*-deficient mice. The subsequent analysis of an *Atf4*-deficient mouse model revealed that this transcription factor plays a crucial role in bone formation. In fact, *Atf4*-deficient mice display a delayed skeletal development and thereafter develop a severe low-bone-mass phenotype caused by a decrease in bone formation (Yang et al., 2004).

Molecularly, ATF4 was identified as the factor binding to the osteoblast-specific element OSE1 in the *Osteocalcin* promoter, thereby directly activating the transcription of this gene. Moreover, ATF4 is required for proper synthesis of type I collagen, although this function is not mediated by a transcriptional regulation of *type I collagen* expression. In fact, because type I collagen synthesis in the absence of nonessential amino acids is specifically reduced in primary osteoblast cultures lacking ATF4, it appears that ATF4 is required for efficient amino acid import in osteoblasts, as has been described for other cell types (Harding et al., 2003). Because a reduced type I collagen synthesis was subsequently also observed in mice lacking Rsk2, these data provided evidence that the diminished ATF4 phosphorylation in the absence of Rsk2 may contribute to the skeletal defects associated with Coffin–Lowry syndrome (Yang et al., 2004).

In addition to its role in bone formation, ATF4, through its expression in osteoblasts, regulates bone resorption (Elefteriou et al., 2005). This function is molecularly explained by the fact that ATF4 binds to the promoter of the *Rankl* (receptor activator of NF-κB ligand) gene to promote osteoclast differentiation (Teitelbaum and Ross, 2003). As a result, ATF4-deficient mice have a decreased number of osteoclasts because of their reduced *Rankl* expression. Most importantly, this function of ATF4 is involved in the control of bone resorption by the sympathetic nervous system. In fact, treatment of normal osteoblasts with isoproterenol, a surrogate of sympathetic signaling, enhanced osteoclastogenesis of cocultured bone marrow macrophages through an induction of osteoblastic *Rankl* expression (Elefteriou et al., 2005). As expected, this effect was blunted when the osteoblasts were derived from mice lacking the β2-adrenergic receptor Adrb2. However, the effect of isoproterenol was also blunted by an inhibitor of protein kinase A, or by using osteoblasts derived from ATF4-deficient mice (Elefteriou et al., 2005). Taken together, these results demonstrated that ATF4 is an important mediator of extracellular signals, such as β-adrenergic stimulation, in osteoblasts.

Thus, it is not surprising that the function of ATF4 is mostly regulated posttranslationally. For example, as already mentioned, ATF4 also interacts with other proteins, such as the nuclear matrix protein Satb2 (Dobreva et al., 2006). Also as

described earlier, the proximal *Osteocalcin* promoter contains two osteoblast-specific elements, termed OSE1 and OSE2, that serve as binding sites for ATF4 and Runx2, respectively (Ducy and Karsenty, 1995; Ducy et al., 1997; Schinke and Karsenty, 1999; Yang et al., 2004). Because of the proximity of both elements, there is indeed a physical interaction of the two proteins, which is stabilized by Satb2, which acts as a scaffold enhancing the synergistic activity of Runx2 and ATF4, which is required for optimum *Osteocalcin* expression (Xiao et al., 2005; Dobreva et al., 2006).

Other aspects of ATF4 biology are also regulated posttranslationally. In fact, even the osteoblast specificity of ATF4 function is not determined by osteoblast-specific *ATF4* expression, but by a selective accumulation of the ATF4 protein in osteoblasts, which itself is explained by the lack of proteasomal degradation (Yang and Karsenty, 2004). This is best demonstrated by the finding that the treatment of nonosteoblastic cell types with the proteasome inhibitor MG 115 leads to accumulation of the ATF4 protein, thereby resulting in ectopic *Osteocalcin* expression. Taken together, these data provided the first evidence for the achievement of a cell-specific function of a transcriptional activator by a posttranslational mechanism. They are therefore of general importance for our understanding of the transcriptional networks controlling cellular differentiation and function.

Remarkably, ATF4 biology further illustrates how the molecular understanding of a disease-causing gene can translate into therapeutic interventions. Indeed, an increased Rsk2-dependent phosphorylation of ATF4 may also be involved in the development of the skeletal abnormalities in human patients suffering from neurofibromatosis (Ruggieri et al., 1999; Stevenson et al., 1999). This disease, which is primarily known for tumor development within the nervous system, is caused by inactivating mutations of the *NF1* gene, which encodes a Ras-GTPase-activating protein (Klose et al., 1998). The generation of a mouse model lacking *Nf1* specifically in osteoblasts ($Nf1^{-/-}_{ob}$) led to the demonstration that this gene plays a major physiological role in bone remodeling. In fact, the $Nf1^{-/-}_{ob}$ mice displayed a high-bone-mass phenotype that is caused by increased bone turnover and is accompanied by enrichment of unmineralized osteoid (Elefteriou et al., 2006). The analysis of this phenotype revealed an increased production of type I collagen in the absence of *Nf1*, which is molecularly explained by an Rsk2-dependent activation of ATF4. Likewise, transgenic mice overexpressing *ATF4* in osteoblasts display a phenotype similar to that of the $Nf1^{-/-}_{ob}$ mice, and the increased type I collagen production and osteoid thickness in the latter are significantly reduced by haploinsufficiency of ATF4 (Elefteriou et al., 2006).

These molecular findings may also have therapeutic implications. Given the previously discussed function of ATF4 in amino acid import, it appeared reasonable to analyze whether the skeletal defects of the $Nf1^{-/-}_{ob}$ mice can be affected by dietary manipulation. Indeed, the increased bone formation and osteoid thickness of $Nf1^{-/-}_{ob}$ mice can be normalized by a low-protein diet, and the same was the case in the transgenic mice overexpressing *ATF4* in osteoblasts (Elefteriou et al., 2006). Likewise, the defects of osteoblast differentiation and bone formation observed in both the *ATF4*- and the Rsk2-deficient mice were corrected by feeding a high-protein diet. Taken together, these data not only emphasize the importance of ATF4 in osteoblast biology, but also demonstrate how knowledge about its specific functions in osteoblasts can be useful for the treatment of skeletal diseases.

Additional transcriptional regulators of osteoblast differentiation and function

Activator protein 1 (AP-1) is a heterodimeric transcription factor composed of members of the Jun and Fos families of basic leucine zipper proteins (Karin et al., 1997). These include the Jun proteins c-Jun, JunB, and JunD, as well as the Fos proteins c-Fos, Fra1, Fra2, and Fosb, respectively. Although AP-1 transcription factors have been demonstrated to fulfill various functions in different cell types, it is striking that some of the family members play specific roles in bone remodeling, as demonstrated by several loss- or gain-of-function studies in mice (Wagner and Eferl, 2005). For instance, the deletion of *c-Fos* from the mouse genome results in severe osteopetrosis owing to an arrest of osteoclast differentiation, whereas the transgenic overexpression of *c-Fos* results in osteosarcoma development (Grigoriadis et al., 1993, 1994). Moreover, transgenic mice overexpressing either *Fml* or *i1fosB*, a splice variant of *FosB*, display a severe osteosclerotic phenotype caused by increased osteoblast differentiation and function (Jochum et al., 2000; Sabatakos et al., 2000). Likewise, mice lacking Fra1 in extraplacental tissues display an osteopenia associated with reduced bone formation, indicating a physiological role of Fra1 in osteoblasts (Eferl et al., 2004). When the same approach was used to inactivate JunB in extraplacental tissues, thereby circumventing the embryonic lethality caused by a complete genomic deletion of *JunB*, the resulting mice developed a state of low bone turnover, owing to cell-autonomous defects in osteoblasts, but also in osteoclast differentiation (Kenner et al., 2004).

Taken together, these data provide evidence for a crucial role of AP-1 transcription factors in the regulation of bone formation, although their connection to the other transcriptional regulators described earlier still needs to be further investigated. For instance, it is known from other cell types that Jun proteins can also interact with ATF family members, thus raising the possibility that heterodimerization with ATF4 may be one mechanism by which these proteins can regulate

osteoblast-specific gene expression (Chinenov and Kerppola, 2001). Interestingly, it has been demonstrated that the osteosarcoma development of *c-Fos* transgenic mice is dramatically decreased in an Rsk2-deficient genetic background (David et al., 2005). This observation is molecularly explained by the lack of c-Fos phosphorylation by Rsk2, thereby leading to increased proteasomal degradation. Thus, Rsk2 apparently not only is involved in the physiological regulation of bone formation via phosphorylation of ATF4, but may also have an influence on the development of osteosarcomas via phosphorylation of c-Fos.

Another potential mechanism by which AP-1 family members might be involved in the regulation of bone formation came- from the analysis of mouse models with impaired circadian regulation. These mice, which lack components of the molecular clock, namely the *Per* or *Cry* genes, display a high-bone-mass phenotype caused by increased bone formation (Fu et al., 2005). Moreover, they respond to intracerebroventricular infusion of leptin with a further increase in bone mass, suggesting that the components of the molecular clock are involved in the regulation of bone formation via the sympathetic nervous system. Interestingly, virtually all genes encoding members of the AP-1 transcription factor family were expressed at higher levels in osteoblasts derived from mice lacking either the *Per* genes or the β2-adrenergic receptor Adrb2 (Fu et al., 2005). This increase was especially pronounced in the case of the *c-Fos* gene, whose expression can also be induced by the addition of isoproterenol in wild-type osteoblasts. In turn, c-Fos leads to a direct activation of *c-Myc* transcription, thereby indirectly increasing the intracellular levels of cyclin D1 and promoting osteoblast proliferation. Taken together, these data demonstrated that the expression of AP-1 components is activated via sympathetic signaling, and that this induction is counteracted by the activity of clock gene products.

Finally, another transcription factor that, like AP-1, is not cell specific but plays a great role in osteoblast biology, is the cAMP-responsive element binding protein (CREB), a transcription factor mediating changes in gene expression caused by signaling through various G-protein-coupled receptors. The demonstration that gut-derived serotonin is an inhibitor of bone formation in mice, rats, and humans, the regulation of the synthesis of which is under the control of Lrp5 signaling in the gut, raised the question of how serotonin signals in osteoblasts (Yadav et al., 2008; Frost et al., 2011). Expression analysis and cell-specific gene deletion experiments in the mouse showed that Htr1B is the receptor of serotonin, mediating its function in osteoblasts, namely, an inhibition of proliferation, and that the transcription factor mediating this effect is CREB (Yadav et al., 2008).

Transcription factors acting downstream of Wnt signaling in osteoblasts: what do they actually do in differentiated osteoblasts?

The discovery of the *LRP5* gene as a major determinant of bone mass in humans because of its homology to a Wnt coreceptor in *Drosophila* has generated an enormous interest and hope in what the canonical Wnt signaling could do in cells of the osteoblast lineage and especially in differentiated osteoblasts. An obligatory implication of this belief, an implication that cannot be ignored or dismissed, is that ablating canonical Wnt signaling in differentiated osteoblasts should lead to an osteopetrotic phenotype. Unfortunately, when taken at face value as they should, the experiments performed to test this hypothesis not only did not provide any evidence that it is the case, but in fact clearly showed that it is not the case.

Indeed, the osteoblast-specific inactivation of β-catenin, the molecular node of the canonical Wnt signaling pathway, resulted in the expected low-bone-mass phenotype; however, this was caused by an isolated and massive increase in bone resorption (Glass et al., 2005). The molecular explanation for the regulation of osteoclast differentiation by β-catenin expression in osteoblasts came from the expression analysis of *Osteoprotegerin* (*Opg*), a well-known inhibitor of bone resorption, blocking the activity of Rankl (Simonet et al., 1997; Yasuda et al., 1998). Surprisingly, although *Opg* expression was markedly increased in osteoblasts from mice expressing the stabilized form of β-catenin, its expression was decreased in mice harboring an osteoblast-specific deletion of β-catenin (Glass et al., 2005). That similar results were observed when β-catenin was deleted from osteocytes established that it is a general rule of bone biology. Of note, these results need to be considered together with the experimental evidence gathered by two different laboratories, using for that purpose mutant mouse strains also generated in two different laboratories, that mice lacking Lrp5 signaling in osteoblasts only do not have any bone phenotype to speak of (Yadav et al., 2008; Kode et al., 2014).

One of the transcription factors activated by β-catenin in osteoblasts has already been identified as Tcfl, whose importance for the regulation of gene expression in osteoblasts is highlighted by several lines of evidence. First, in situ hybridization revealed that *Tcfl* is expressed in osteoblasts during bone development and after birth. Second, *Tcfl*-deficient mice display a low-bone-mass phenotype caused by an increase in bone resorption. Third, the compound heterozygosity of *Tcfl* and *β-catenin* in osteoblasts also results in low bone mass, which is not observed when one allele of each gene is

inactivated alone. Fourth, *Opg* expression is decreased in osteoblasts of *Tcfl*-deficient mice, and the molecular analysis of the *Opg* promoter revealed the existence of a Tcf1-binding site, whose functional activity was subsequently proven by chromatin immunoprecipitation and DNA cotransfection assays (Glass et al., 2005). The implication of these results cannot be underestimated, without taking great and yet predictable risks, when proposing to harness the canonical Wnt signaling pathway for therapeutic purposes in the context of osteoporosis.

Regulation of osteoblast differentiation by means other than transcription factors

Chromatin structure, which influences by posttranslational modifications of histone proteins around which the DNA is wrapped, is a major determinant of gene expression (Allis et al., 2007). Histone acetylation promotes gene transcription by relaxing the chromatin structure, whereas deacetylation of histones by HDACs induces chromatin condensation and transcriptional repression (Berger, 2002; Verdin et al., 2003; Allis et al., 2007). Class II HDACs contain a poorly active catalytic domain and a long N-terminal extension to which transcription factors can bind. The existence of this domain has suggested that class II HDACs can link extracellular cues to the genome of a given cell (Verdin et al., 2003; Haberland et al., 2009). Several class I HDACs (Hdac1 and Hdac3) are expressed in osteoblasts, and conditional deletion of Hdac3 within osteo-chondroprogenitor cells decreases osteoblast number, and, as mentioned earlier, one mechanism whereby Zpf521 inhibits Runx2 functions during osteoblast differentiation is by interacting with HDAC3. On the other hand, one class II HDAC, HDAC4, acts as a central integrator of two extracellular cues acting on osteoblasts. One is parathyroid hormone, which targets HDAC4 for degradation and thereby releases MeF2c that can now transactivate *Rankl*, and thus favors osteoclast differentiation. The other is sympathetic tone, which instead favors HDAC4 accumulation in the nucleus, its association with ATF4, and again Rankl expression and osteoclast differentiation (Obri et al., 2014).

Another mode of regulation of osteoblast differentiation that has received much attention since the last edition of this book is the one fulfilled by small noncoding RNAs. MicroRNAs (miRNAs) are small noncoding RNAs that down-regulate expression of their target genes by either mRNA degradation or translational inhibition (Valencia-Sanchez et al., 2006; Bartel, 2009; Djuranovic et al., 2011; Huntzinger and Izaurralde, 2011). Although most miRNAs are broadly expressed, some have a more restricted pattern of expression and influence cell differentiation (Poy et al., 2004). The importance of this mode of gene regulation during skeletogenesis is inferred from the observation that inactivation of

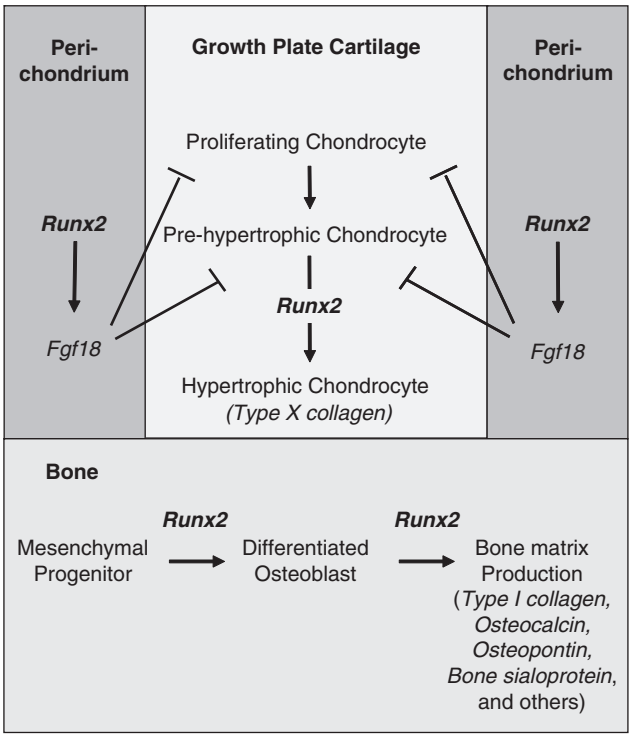

FIGURE 7.1 *Schematic representation of the functions of Runx2 during chondrogenesis and osteoblast differentiation.*

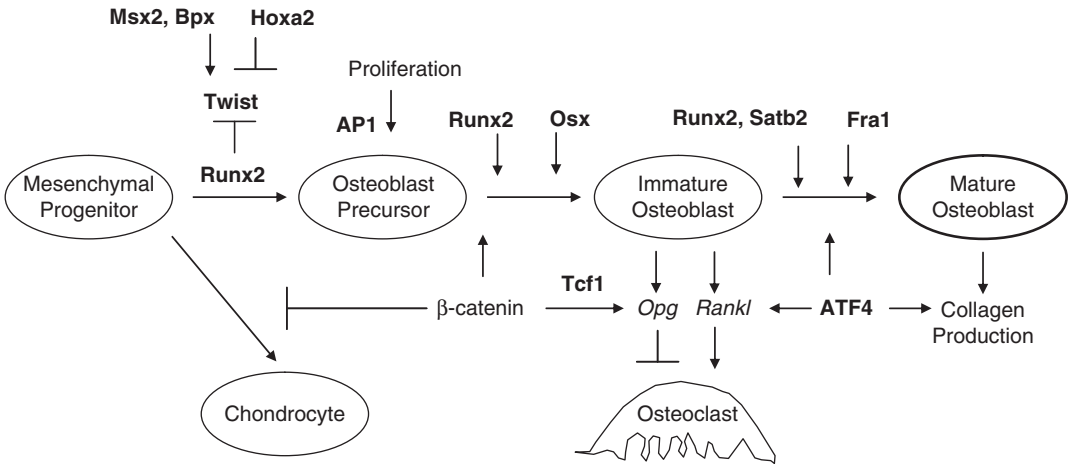

FIGURE 7.2 *Schematic representation of the transcriptional control of osteoblast differentiation and functions.*

DICER, a protein necessary for processing of miRNAs, affects osteoblast differentiation (Gaur et al., 2010). Accordingly, it has been suggested that miRNAs may be involved in osteoblast proliferation and/or differentiation (Hassan et al., 2010). However, these observations were derived from gain-of-function experiments performed in cell culture. Few miRNAs had been shown, through cell-specific loss-of-function experiments performed in the mouse, to regulate osteoblast proliferation and/or differentiation in vivo. A first example of these was miRNA-2561, whose silencing in the mouse reduces Runx2 accumulation without, however, causing a characteristic CCD phenotype (Li et al., 2009). Two other miRNAs, miR-34b and miR-34c, were shown through cell-specific gene deletion to inhibit osteoblast proliferation by suppressing cyclin D1, CDK4, and CDK6 accumulation (Wei et al., 2012). They also hampered osteoblast differentiation by inhibiting the function of SATB2, a protein interacting with Runx2 and ATF4 (Wei et al., 2012). Another miRNA, miR-124, inhibits bone formation by targeting another transcription factor implicated in osteoblast differentiation, ATF4, whereas miR-188 was shown to favor bone formation in an HDAC9-dependent manner (Li et al., 2015) (Fig. 7.1 and 7.2).

References

Allis, C.D., Berger, S.L., Cote, J., Sent, S., Jenuwein, T., Kouzarides, T., Pillus, L., Reinber, D., Shi, Y., Shiekhaltar, R., Shilatifard, A., Workman, J., Zhang, Y., 2007. New nomenclature for chromatin-modifying enzymes. Cell 131 (4), 633–636.

Bartel, D.P., 2009. MicroRNAs:target recognition and regulatory functions. Cell 136 (2), 215–233.

Berger, S.L., 2002. Histone modification in transcriptional regulation. Curr. Opin. Genet. Dev. 12 (2), 142–148.

Bialek, P., Kern, B., Yang, X., Schrock, M., Sosic, D., Hong, N., Wu, H., Yu, K., Ornitz, D.M., Olson, E.N., Justice, M.J., Karsenty, G., 2004. A twist code determines the onset of osteoblast differentiation. Dev. Cell 6, 423–435.

Chinenov, Y., Kerppola, T., 2001. Close encounters of many kinds: fos-Jun interactions that mediate transcription regulatory specificity. Oncogene 20, 2438–2452.

David, J.P., Mehic, D., Bakiri, L., Schilling, A.E., Mandic, V., Priemel, M., Idarraga, M.H., Reschke, M.O., Hoffmann, O., Amling, M., Wagner, E.E., 2005. Essential role of"RSK2 in c-Fos-dependent osteosarcoma development. J. Clin. Invest. 115, 664–672.

Djuranovic, S., Nahvi, A., Green, R., 2011. A parsimonious model of gene regulation by miRNAs. Science 331 (6017), 550–553.

Dobreva, G., Chahrour, M., Dautzenberg, M., Chirivella, L., Kanzler, B., Farinas, 1., Karsenty, G., Grosschedl, R., 2006. SATB2 is a multifunctional determinant of craniofacial patterning and osteoblast differentiation. Cell 125, 971–986.

Ducy, P., Karsenty, G., 1995. Two distinct osteoblast-specific cis-acting elements control expression of a mouse osteocalcin gene. Mol. Cell. Biol. 15, 1858–1869.

Ducy, P., Zhang, R., Geoffroy, v., Ridall, A.L., Karsenty, G., 1997. Osf2/Cbfa1: a transcriptional activator of osteoblast differentiation. Cell 89, 747–754.

Ducy, P., Starbuck, M., Priemel, M., Shen, J., Pinero, G., Geoffroy, V., Amling, M., Karsenty, G., 1999. A Cbfal-dependent genetic pathway controls bone formation beyond embryonic development. Genes Dev. 13, 1025–1036.

Ducy, P., 2000. Cbfal: a molecular switch in osteoblast biology. Dev. Dynam. 219, 461–471.

Eferl, R., Hoebertz, A., Schilling, A.E., Rath, M., Karreth, E., Kenner, L., Amling, M., Wagner, E.E., 2004. The Fos-related antigen Fra-l is an activator of bone matrix formation. EMBO J. 23, 2789–2799.

Elefteriou, E., Ahn, J.D., Takeda, S., Starbuck, M., Yang, X., Liu, X., Kondo, H., Richards, W.G., Bannon, T.W., Noda, M., Clement, K., Vaisse, c., Karsenty, G., 2005. Leptin regulation of bone resorption by the sympathetic nervous system and CART. Nature 434, 514–520.

Elefteriou, E., Benson, M.D., Sowa, H., Starbuck, M., Liu, X., Ron, D., Parada, L.F., Karsenty, G., 2006. ATF4 mediation of NF1 functions in osteoblast reveals a nutritional basis for congenital skeletal dysplasiae. Cell Metabol. 4, 441–451.

Frost, M., Andersen, T., Gossiel, F., hansen, S., Bollerslev, J., Van Hul, W., Eastell, R., Kassem, M., Brixen, K., 2011. Levels of serotonin, sclerostin, bone turnover markers as well as bone density and microachitecture in patients with high bone mass phenoptype due to a mutation in Lrp5. J. Bone Miner. Res. 8, 1721–1728.

El Ghouzzi, v., Le Merrer, M., Perrin-Schmitt, F., Lt0eunie, E., Benit, P., Renier, D., Bourgeois, P., Bolcato-Bellemin, A.L., Munnich, A., Bonaventure, J., 1997. Mutations of the TWIST gene in the SaethreChotzen syndrome. Nat. Gellet. 15, 42–46.

Fitzpatrick, D.R., Carr, L.M., McLaren, L., Leek, 1. P., Wightman, P., Williamson, K., Gautier, P., McGill, N., Hayward, c., Firth, H., Markham, A.E., Fantes, 1. A., Bonthron, D.T., 2003. Identification of SATB2 as the cleft palate gene on 2q32-q33. Hum. Mol. Genet. 12, 2491–2501.

Fu, L., Patel, M.S., Bradley, A., Wagner, E.E., Karsenty, G., 2005. The molecular clock mediates leptin-regulated bone formation. Cell 122, 803–815.

Gaur, T., Hussain, S., Mudhasani, R., Parulkar, I., Colby, J.L., Frederick, D., Kream, B.E., Van Wijnen, A.J., Stein, Jl, Stein, G.S., Jones, S.N., Lian, J.B., 2010. Diver inactivation in osteoprogenitor cells compromises fetal survival and bone formation while excision in differentiated osteoblasts increases bone mass in the adult mouse. Dev. Biol. 340 (1), 1–21.

Geoffroy, v., Ducy, P., Karsenty, G., 1995. A PEBP2/AML-Related factor increases osteocalcin promoter activity through its binding to an osteoblast-specific cis-acting element. J. Biol. Chem. 270, 30973–30979.

Glass, D.A., II, Bialek, P., Ahn, J.D., Starbuck, M., Patel, M.S., Clevers, H., Taketo, M.M., Long, F., McMahon, A.P., Lang, R.A., Karsenty, G., 2005. Canonical Wnt signaling in differentiated osteoblasts controls osteoclast differentiation. Dev. Cell 751–764.

Grigoriadis, A.E., Schellander, K., Wang, Z.Q., Wagner, E.F., 1993. Osteoblasts are target cells for transformation in c-fos transgenic mice. J. Cell Biol. 122, 685–701.

Grigoriadis, A.E., Wang, Z.Q., Cecchini, M.G., Hofstetter, w., Felix, R., Fleisch, H.A., Wagner, E.E., 1994. c-Fos: a key regulator of osteoclast-macrophage lineage determination and bone remodeling. Science 266, 443–448.

Gripp, K. w., Zackai, E.H., Stolle, C.A., 2000. Mutations in the human TWIST gene. Hum. Mutat. 15, 479.

Haberland, M., Mokalled, M.H., Montgomery, R.L., Olson, E.N., 2009. Epigenetic control of skull morphogenesis by histone deacetylase 8Genes. Dev 23 (14), 1625–1630.

Harding, H.P., Zhang, y, Zeng, H., Novoa, J., Lu, P.D., Calfon, M., Sadri, N., Yun, C., Popko, B., Paules, R., Stojdl, D.F., Bell, J.C., Hettmann, T., Leiden, J.M., Ron, D., 2003. An integrated stress response regulates amino acid metabolism and resistance to oxidative stress. Mol. Cell 11, 619–633.

Hassan, M.Q., Gordon, J.A., Beloti, M.M., Croce, C.M., van Wijnen, A.J., Stein, J.L., Stein, G.S., Lian, J.B., 2010. A network connecting Runx2, SATB2 and the miR-23a-27a-24-2 cluster regulates the osteoblast differentiation program. Proc. Natl. Acad. Sci. U.S.A. 107 (46), 19879–19884.

Hinoi, E., Bialek, P., Chen, Y.T., Rached, M.T., Groner, Y., Behringer, R.R., Ornitz, D.M., Karsenty, G., 2006. Runx2 inhibits chondrocyte proliferation and hypertrophy through its expression in the perichondrium. Genes Dev. 20, 2937–2942.

Hojo, H., Ohba, S., He, X., Lai, L.P., McMahon, A.P., 2016. Sp7/Osterix is restricted to bone-forming vertebrates where it acts as a Dlx Co-factor in osteoblast specification. Dev. Cell 37 (3), 238–253.

Howard, T.D., Paznekas, W.A., Green, E.D., Chiang, L. c., Ma, N., Ortiz de Luna, R.I., Garcia Delgado, C., Gonzalez-Ramos, M., Kline, A.D., Jabs, E.W., 1997. Mutations in TWIST, a basic helix-loop-helix transcription factor, in Saethre-Chotzen syndrome. Nat. Genet. 15, 36–41.

Huntzinger E, Izaurralde E. Gene silencing by microRNAs: contributions of translational repression and mRNA decay. Nat. Rev. Genet. 12(2): 99–110

Inada, M., Yasui, T., Nomura, S., Miyake, S., Deguchi, K., Himeno, M., Sato, M., Yamagiwa, H., Kimura, T., Yasui, N., Ochi, T., Endo, N., Kitamura, Y., Kishimoto, T., Komori, T., 1999. Maturational disturbance of chondrocytes in Cbfal-deficient mice. Dev. Dynam. 214, 279–290.

Jabs, E. w., Muller, U., Li, X., Ma, L., Luo, w., Haworth, I.S., Klisak, I., Sparkes, R., Warman, M.L., Mulliken, J.B., 1993. A mutation in the homeodomain of the human MSX2 gene in a family affected with autosomal dominant craniosynostosis. Cell 75, 443–450.

Jochum, W., David, J.P., Elliott, C., Wutz, A., Plenk, H.J., Matsuo, K., Wagner, E.F., 2000. Increased bone formation and osteosclerosis in mice overexpressing the transcription factor Fra-1. Nat. Med. 6, 980–984.

Jones, D. c., Wein, M.N., Oukka, M., Hofstaetter, J.G., Glimcher, M.J., Glimcher, L.H., 2006. Regulation of adult bone mass by the zinc finger adapter protein Schnurri-3. Science 312, 1223–1227.

Kagoshima, H., Shigesada, K., Satake, M., Ito, Y., Miyoshi, H., Ohki, M., Pepling, M., Gergen, P., 1993. The Runt domain identifies a new family of heteromeric transcriptional regulators. Trends Genet. 9, 338–341.

Kanzler, B., Kuschert, S.J., Liu, Y.-H., Mallo, M., 1998. Hoxa-2 restricts the chondrogenic domain and inhibits bone formation during development of the branchial area. Development 125, 2587–2597.

Karin, M., Liu, Z., Zandi, E., 1997. AP-1 function and regulation. Curr. Opin. Cell. Bioi. 9, 240–246.

Kenner, L., Hoebertz, A., Beil, T., Keon, N., Karreth, F., Eferl, R., Scheuch, H., Szremska, A., Amling, M., Schorpp-Kistner, M., Angel, P., Wagner, E.E., 2004. Mice lacking JunB are osteopenic due to cell-autonomous osteoblast and osteoclast defects. J. Cell Biol. 164, 613–623.

Kim, I.S., Otto, F., Abel, B., Mundlos, S., 1999. Regulation of chondrocyte differentiation by Cbfa1. Mech. Dev. 80, 159–170.

Kim, S., Koga, T., Isobe, M., Kern, B.E., Yokochi, T., Chin, Y.E., Karsenty, G., Taniguchi, T., Takayanagi, H., 2003. Stat! functions as a cytoplasmic attenuator of Runx2 in the transcriptional program of osteoblast differentiation. Genes Dev. 17, 1979–1991.

Klose, A., Ahmadian, M.R., Schuelke, M., Scheffzek, K., Hoffmeyer, S., Gewies, A., Schmitz, E., Kaufmann, D., Peters, H., Wittinghofer, A., Nurnberg, P., 1998. Selective disactivation of neurofibromin GAP activity in neurofibromatosis type 1. Hum. Mol. Genet. 7, 1261–1268.

Kode, A., Obri, A., Paone, R., Kousteni, S., Ducy P Karsenty, G., 2014. Lrp5 regulation of bone mass and serotonin synthesis in the gut. Nat. Med. 20, 1228–1229.

Koga, T., Matsui, Y., Asagiri, M., Kodama, T., de Crombrugghe, B., Nakashima, K., Takayanagi, H., 2005. NFAT and Osterix cooperatively regulate bone formation. Nat. Med. 11, 880−885.

Komori, T., Yagi, H., Nomura, S., Yamaguchi, A., Sasaki, K., Deguchi, K., Shimizu, Y., Bronson, R.T., Gao, Y.H., Inada, M., Sato, M., Okamoto, R., Kitamura, Y., Yoshiki, S., Kishimoto, T., 1997. Targeted disruption of Cbfal results in a complete lack of bone formation owing to maturational arrest of osteoblasts. Cell 89, 755−764.

Lee, B., Thirunavukkarasu, K., Zhou, L., Pastore, L., Baldini, A., Hecht, J., Geoffroy, V., Ducy, P., Karsenty, G., 1997. Missense mutations abolishing DNA binding of the osteoblast-specific transcription factor *OSF2/CBFAl* in cleidocranial dysplasia. Nat. Genet. 16, 307−310.

Lee, N.K., Sowa, H., Hinoi, E., Ferron, M., Ahn, J.D., Confavreux, C., Dacquin, R., Mee, P.J., McKee, M., Jung, D.Y., Zhang, Z., Kim, J.K., Mauvais-Jarvis, F., Ducy, P., Karsenty, G., 2007. Endocrine regulation of energy metabolism by the skeleton. Cell 130, 456−469.

Lian, J.B., Stein, G.S., 2003. Runx2/Cbfal: a multifunctional regulator of bone formation. Curr. Pharm. Des. 9, 2677−2685.

Li, H., Xie, H., Liu, W., Hu, R., Huang, B., Tan, Y.F., Xu, K., Sheng, Z.F., Zhou, H.D., Wu, X.P., Luo, X.H., 2009. A novel micorRNA targeting HDAC5 regulates osteoblast differentiation in mice and contributes to primary osteoporosis in humans. J. Clin. Invest. 119 (120), 3666−3677.

Li, C.J., Cheng, P., Liang, M.K., Chen, Y.S., Lu, Q., Wang, J.Y., Xia, Z.Y., Zhou, H.D., Cao, X., Xie, H., Liao, E.Y., Luo, X.H., April 2015. MicroRNA-188 regulates age-related switch between osteoblast and adipocyte differentiation. J. Clin. Investig. 125 (4), 1509−1522.

Liu, w., Toyosawa, S., Furuichi, T., Kanatani, N., YosQida, c., Liu, Y., Himeno, M., Narai, S., Yamaguchi, A., Komori, T., 2001. Overexpression of Cbfal in osteoblasts inhibits osteoblast maturation and causes osteopenia with multiple fractures. J. Cell Biol. 155, 157−166.

Liu, Z., Xu, J., Colvin, J.S., Omitz, D.M., 2002. Coordination of chondrogenesis and osteogenesis by fibroblast growth factor 18. Genes Dev. 16, 859−869.

Merriman, H.L., vanWijnen, A.J., Hiebert, S., Bidwell, J.P., Fey, E., Lian, J., Sein, J., Stein, G.S., 1995. The tissue-specific nuclear matrix protein, NMP-2, is a member of the *MAL/CBFIPEBP21Runt* domain transcription factor family: interactions with the osteocalcin gene promoter. Biochemistry 34, 13125−13132.

Mundlos, S., Otto, E., Mundlqs, c., Mulliken, J.B., Aylsworth, A.S., Albright, S., Lindhout, D., Cole, W.G., Henn, w., Knoll, J.H., Owen, M.J., Mertelsmann, R., Zabel, B.D., Olsen, B.R., 1997. Mutations involving the transcription factor CBFAI cause cleidocranial dysplasia. Cell 89, 773−779.

Nakashima, K., Zhou, X., Kunkel, G., Zhang, Z., Deng, J.M., Behringer, R.R., de Crombrugghe, B., 2002. The novel zinc finger-containing transcription factor osterix is required for osteoblast differentiation and bone formation. Cell 108, 17−29.

Nishio, Y., Dong, Y., Paris, M., O'Keefe, R.J., Schwarz, E.M., Drissi, H., 2006. Runx2-mediated regulation of the zinc finger OsterixlSp7 gene. Gene 372, 62−70.

Obri A., Mkinistoglu MP, Zhang H, Karsenty G., HDAC4 integrates PTH and sympathetic signaling in osteoblasts. J. Cell Biol. 205 (6): 771-780

Ogawa, E., Maruyama, M., Kagoshima, H., Inuzuka, M., Lu, J., Satake, M., Shigesada, K., Ito, Y., 1993. PEBP2IPEA2 represents a family of transcription factors homologous to the products of the Drosophila runt gene and the human AMLl gene. Proc. Natl. Acad. Sci. U.S.A. 90, 6859−6863.

Ohbayashi, N., Shibayama, M., Kurotaki, Y., Imanishi, M., Fujimori, T., Itoh, N., Takada, S., 2002. FGF18 is required for normal cell proliferation and differentiation during osteogenesis and chondrogenesis. Genes Dev. 16, 870−879.

Otto, E., Thronelkl, A.P., Crompton, T., Denzel, A., Gilmour, K. c., Rosewell, 1. R., Stamp, G.W.H., Beddington, R.S.P., Nundlos, S., Olsen, B.R., Selby, P.B., Owen, M.J., 1997. Cbfal, a candidate gene for cleidocranial dysplasia syndrome, is essential for osteoblast differentiation and bone development. Cell 89, 765−771.

Poy, M.N., Eliasson, L., Krutzfeldt, J., Kuwajima, S., Ma, X., Macdonald, P.E., Pfeffer, S., Tuschl, T., Rajewsky, N., Rorsman, P., Stoffel, M., 2004. A pancreatic islet-specific microRNA regulates insulin secretion. Nature 432 (7014), 226−230.

Rodino, M.A., Shane, E., 1998. Osteoporosis after organ transplantation. Am. J. Med. 104, 459−469.

Ruggieri, M., Pavone, v., De Luca, D., Franzo, A., Tine, A., Pavone, L., 1999. Congenital bone malformations in patients with neurofibromatosis type I (Nfl). J. Pediatr. Orthop. 19, 301−305.

Sabatakos, G., Sims, N.A., Chen, J., Aoki, K., Kelz, M.B., Amling, M., Bouali, Y., Mukhopadhyay, K., Ford, K., Nestler, E.J., Baron, R., 2000. Overexpression of 6FosB transcription factor(s) increases bone formation and inhibits adipogenesis. Nat. Med. 6, 985−990.

Satake, M., Nomura, S., Yamaguchi-Iwai, Y., Yousuke, T., Hashimoto, Y., Niki, M., Kitamura, Y., Ito, Y., 1995. Expression of the Runt Domain encoding PEBP2 alpha genes in T cells during thymic development. Mol. Cell. Biol. 15, 1662−1670.

Satokata, 1., Ma, L., Ohshima, H., Bei, M., Woo, I., Nishizawa, K., Maeda, T., Takano, Y., Uchiyama, M., Heaney, S., Peteres, H., Tang, Z., Maxson, R., Maas, R., 2000. Msx2 deficiency in mice causes pleotropic defects in bone growth and ectodermal organ formation. Nat. Genet. 24, 391−395.

Schmidt, K., Schinke, T., Haberland, M., Priemel, M., Schilling, A.E., Mueldner, C., Rueger, J.M., Sock, E., Wegner, M., Amling, M., 2005. The high mobility group transcription factor Sox8 is a negative regulator of osteoblast differentiation. J. Cell Biol. 168, 899−910.

Schinke, T., Karsenty, G., 1999. Characterization of Osfl, an osteoblast-specific transcription factor binding to a critical cis-acting element in the mouse osteocalcin promoter. J. Biol. Chem. 274, 30182−30189.

Shim, Jae-Hyuck, Greenblatt, Matthew B., Zou, Weiguo, Huang, Zhiwei, Wein, Marc N., Brady, Nicholas, Hu, Dorothy, et al., 2013. Schnurri-3 regulates ERK downstream of WNT signaling in osteoblasts. The Journal of clinical investigation 123 (9), 4010−4022.

Simonet, W.S., Lacey, D.L., Dunstan, C.R., Kelley, M., Chang, M.S., Luthy, R., Nguyen, H.Q., Wooden, S., Bennett, L., Boone, T., Shimamoto, G., DeRose, M., Elliott, R., Colombero, A., Tan, H.L., Trail, G., Sullivan, J., Davy, E., Bucay, N., Renshaw-Gegg, L., Hughes, T.M., Hill, D., Pattison, w., Campbell, P., Sander, S., Van, G., Tarpley, 1., Derby, P., Lee, R., Boyle, W.J., 1997. Osteoprotegerin: a novel secreted protein involved in the regulation of bone density. Cell 89, 309−319.

Stevenson, D.A., Birch, P.H., Friedman, J.M., Viskochil, D.H., Balestrazzi, P., Boni, S., Buske, A., Korf, B.R., Niimura, M., Pivnick, E.K., Schorry, E.K., Short, M.P., Tenconi, R., Tonsgard, J.H., Carey, J.C., 1999. Descriptive analysis of tibial pseudarthrosis in patients with neurofibromatosis 1. Am. J. Med. Genet. 84, 413−419.

Takeda, S., Bonnamy, J.P., Owen, M.J., Ducy, P., Karsenty, G., 2001. Continuous expression of Cbfal in nonhypertrophic chondrocytes uncovers its ability to induce hypertrophic chondrocyte differentiation and partially rescues Cbfal-deficient mice. Genes Dev. 15, 467−481.

Teitelbaum, S.L., Ross, E.P., 2003. Genetic regulation of osteoclast development and function. Nat. Rev. Genet. 4, 638−649.

Tribioli, C., Lufkin, T., 1999. The murine *Bapxl* homeobox gene plays a critical role in embryonic development of the axial skeleton and spleen. Development 126, 5699−5711.

Trivier, E., De Cesare, D., Jacquot, S., Pannetier, S., Zackai, E., Young, L., Mandel, J.L., Sassone-Corsi, P., Hanauer, A., 1996. Mutations in the kinase Rsk-2 associated with Coffin-Lowry syndrome. Nature 384, 567−570.

Valencia-Sanchez, M.A., Liu, J., Hannon, G.J., Parker, R., 2006. Control of translation and mRNA degradation by miRNAs and siRNAs. Genes Dev 20 (5), 515−524.

Verdin, E., Ott, M., 2013. Acetylphosphate: a novel link between lysine acetylation and intermediary metabolism in bacteria. Mol Cell 51 (2), 132−134.

Wagner, E.F., Eferi, R., 2005. Fos! AP-I proteins in bone and the immune system. Immunol. Rev. 208, 126−140.

Wei, J., Shi, Y., Zheng, L., Zhou, B., Inose, H., Wang, J., Guo, X.E., Grosschedl, R., Karsenty, G., May 14, 2012. miR-34s inhibit osteoblast proliferation and differentiation in the mouse by targeting SATB2. J. Cell Biol. 197 (4), 509−521.

Wei, J., Shimazu, J., Makinistoglu, M., Maurizi, A., Kajimura, D., Zong, H., Takarada, T., Iezaki, T., Pessin, J.E., Hinoi, E., Karsenty, G., 2015. Glucose uptake and Runx2 synergize to orchestrate osteoblast differentiation and bone formation. Cell 161, 1576−1591.

Wilke, A.O.M., Tang, Z., Eianko, N., Walsh, S., Twigg, S.R.E., Hurst, J.A., Wall, S.A., Chrzanowska, K.H., Maxson, R.E.J., 2000. Functional haploinsufficiency of the human homeobox gene MSX2 causes defects in skull ossification. Nat. Genet. 24, 387−390.

Wu, L.C., Mak, C.H., Dear, N., Boehm, T., Foroni, L., Rabbitts, T.H., 1993. Molecular cloning of a zinc finger protein which binds to the heptamer of the signal sequence for V(D)J recombination. Nucleic Acids Res. 21, 5067−5073.

Xiao, G., Jiang, D., Ge, C., Zhao, Z., Lai, Y., Boules, H., Phimphilai, M., Yang, X., Karsenty, G., Franceschi, R.T., 2005. Cooperative interactions between activating transcription factor 4 and Runx2! Cbfal stimulate osteoblast-specific osteocalcin gene expression. J. Biol. Chem. 280, 30689−30696.

Yadav, V.K., Ryu, J.H., Suda, N., Tanaka, K., Gingrich, J., Schutz, G., Glorieux, F.H., Insogna, K., Mann, J.J., Hen, R., Ducy, P., Karsenty, G., 2008. Lrp5 control bone mass by inhibiting serotonin synthesis in the duodenum. Cell 135, 825−837.

Yang, X., Karsenty, G., 2004. ATF4, the osteoblast accumulation of w∼ich is determined post-translationally, can induce osteoblastspecific gene expression in non-osteoblastic cells. J. Biol. Chem. 279, 47109−47114.

Yang, X., Matsuda, K., Bialek, P., Jacquot, S., Masuoka, H.C., Schinke, T., Li, L., Brancorsini, S., Sassone-Corsi, P., Townes, T.M., Hanauer, A., Karsenty, G., 2004. ATF4 is a substrate of RSK2 and an essential regulator of osteoblast biology; implication for Coffin-Lowry syndrome. Cell 117, 387−398.

Yasuda, H., Shima, N., Nakagawa, N., Mochizuki, S.I., Yano, K., Fujise, N., Sato, Y., Goto, M., Yamaguchi, K., Kuriyama, M., Kanno, T., Murakami, A., Tsuda, E., Morinaga, T., Higashio, K., 1998. Identity of osteociastogenesis inhibitory factor (OCIF) and osteoprotegerin (OPG): a mechanism by which OPG/OCIF inhibits osteoclastogenesis in vitro. Endocrinology 139, 1329−1337.

Further reading

Boyden, L.M., Mao, J., Belsky, J., Mitzner, L., Farhi, A., Mitnick, M.A., Wu, D., Insogna, K., Lifton, R.P., 2002. High bone density due to a mutation in LDL-receptor-related protein 5. N. Engl. J. Med. 346, 1513−1521.

Day, T.E., Guo, X., Garrett-Beal, L., Yang, Y., 2005. Wntlbetacatenin signaling in mesenchymal progenitors controls osteoblast and chondrocyte differentiation during vertebrate skeletogenesis. Dev. Cell 8, 739−750.

Gong, Y., Slee, R.B., Fukai, N., Rawadi, G., Roman-Roman, S., Reginato, A.M., Wang, H., Cundy, T., Glorieux, E.H., Lev, D., Zacharin, M., Oexle, K., Marcelino, J., Suwairi, W., Heeger, S., Sabatakos, G., Apte, S., Adkins, W.N., Allgrove, J., Arslan-Kirchner, M., Batch, J.A., Beighton, P., Black, G.c., Boles, R.G., Boon, L.M., BOlTone, c., Brunner, H.G., Carle, G.E., Dallapiccola, B., De Paepe, A., Floege, B., Halfhide, M.L., Hall, B., Hennekam, R.C., Hirose, T., Jans, A., Juppner, H., Kim, C.A., Keppler-Noreuil, K., Kohlschuetter, A., LaCombe, D., Lambert, M., Lemyre, E., Letteboer, T., Peltonen, L., Ramesar, R.S., Romanengo, M., Somer, H., Steichen-Gersdorf, E., Steinmann, B., Sullivan, B., Superti-Furga, A., Swoboda, W., van den Boogaard, M.J., Van Hul, w., Vikkula, M., Votruba, M., Zabel, B., Garcia, T., Baron, R., Olsen, B.R., Warman, M.L., 2001. LDL receptor-related protein 5 (LRP5) affects bone accrual and eye development. Cell 107, 513−523.

Hecht, J., Seitz, V., Urban, M., Wagner, E., Robinson, P.N., Stiege, A., Dieterich, c., Kornak, U., Wilkening, U., Brieske, N., Zwingman, c., Kidess, A., Stricker, S., Mundlos, S., 2007. Detection of novel skeletogenesis target,genes by comprehensive analysis of a Runx 2(-/-) mouse model. Gene Expr. Patterns 7, 102−112.

Hill, T.P., Spater, D., Taketo, M.M., Birchmeier, W., Hartmann, C., 2005. Canonical Wntlbeta-catenin signaling prevents osteoblasts from differentiating into chondrocytes. Dev. Cell 727−738.

Huelsken, J., Birchmeier, W., 2001. New aspects of Wnt signaling pathways in higher vertebrates. Curr. Opin. Genet. Dev. 11, 547−553.

Kato, M., Patel, M.S., Levasseur, R., Lobov, I., Chang, B.H., Glass II, D.A., Hartmann, C., Li, L., Hwang, T.H., Brayton, C.F., Lang, R.A., Karsenty, G., Chan, L., 2002. Cbfa1-independent decrease in osteoblast proliferation, osteopenia, and persistent embryonic eye vascularization in mice deficient in Lrp5, a Wnt coreceptor. J. Cell Biol. 157, 303−314.

Little, R.D., Carulli, J.P., Del Mastro, R.G., Dupuis, J., Osborne, M., Folz, C., Manning, S.P., Swain, P.M., Zhao, S.C., Eustace, B., Lappe, M.M., Spitzer, L., Zweiei, S., Braunschweiger, K., Benchekroun, Y., Hu, X., Adair, R., Chee, L., FitzGerald, M.G., Tulig, C., Caruso, A., Tzellas, N., Bawa, A., Franklin, B., McGuire, S., Nogues, X., Gong, G., Allen, K.M., Anisowicz, A., Morales, A.J., Lomedico, P.T., Recker, S.M., Van Eerdewegh, P., Recker, R.R., Johnson, M.L., 2002. A mutation in the LDL receptor-related protein 5 gene results in the autosomal dominant high-bone-mass trait. Am. J. Hum. Genet. 70, 11−19.

Mao, J., Wang, J., Liu, B., Pan, W., Farr III, G.H., Flynn, C., Yuan, H., Takada, S., Kimelman, D., Li, L., Wu, D., 2001. Low-density lipoprotein receptor-related protein-5 binds to Axin and regulates the canonical Wnt signaling pathway. Mol. Cell 7, 801−809.

Vaes, B.L., DlIey, P., Sijbers, A.M., Hendriks, J.M., van Someren, E.P., de Jong, N.G., van den Heuvel, E.R., Olijve, W., van Zoelen, E.J., Dechering, K.J., 2006. Microarray analysis on Runx2-deficient mouse embryos reveals novel Runx2 functions and target genes during intrame! llbranous and endochondral bone formation. Bone 39, 724−738.

Zheng, Q., Zhou, G., Morello, R., Chen, Y., Garcia-Rojas, X., Lee, B., 2003. Type X collagen gene regulation by Runx2 contributes directly to its hypertrophic chondrocyte-specific expression in vivo. J. Cell Biol. 162, 833−842.

Chapter 8

Wnt signaling and bone cell activity

Bart O. Williams[1] **and Mark L. Johnson**[2]

[1]*Program for Skeletal Disease and Center for Cancer and Cell Biology, Van Andel Research Institute, Grand Rapids, MI, United States;*
[2]*Department of Oral and Craniofacial Sciences, UMKC School of Dentistry, Kansas City, MO, United States*

Chapter outline

Introduction

The first two decades of the 21st century have witnessed a literal explosion in our understanding of fundamental biological processes, catalyzed in large part by the human genome project and the vast repertoire of technologies that are now available to identify genes and study gene function. The field of bone biology has certainly benefited from these advances as illustrated by many of the chapters in this book. Not surprisingly perhaps, the genetic dissection of single-gene human disorders that present with skeletal abnormalities has led to advances in our understanding of bone biology, oftentimes in directions that could not have been anticipated by the current state of knowledge.

The Wnt/β-catenin pathway and its sister pathways (planar cell polarity, or PCP, and Wnt/Ca^{2+}) are one of five key signaling pathway families critical for normal development. They control a spectrum of cellular functions from differentiation to proliferation and growth and are involved in many aspects of patterning during development. As such it is not surprising that we now recognize that a wide spectrum of diseases have been attributed to mutations in members of the pathway or aberrant regulation of one of the Wnt pathways (Goggolidou and Wilson, 2016; Libro et al., 2016; Wang et al., 2016; Abou Ziki and Mani, 2017; Butler and Wallingford, 2017; Lodish, 2017; Nusse and Clevers, 2017). The field of bone biology was introduced to the Wnt/β-catenin signaling pathway in 2001−2 as a result of the discovery of mutations in the low-density lipoprotein receptor (LDLR)-related protein 5 (*LRP5*) gene that give rise to conditions of decreased (Gong et al., 2001) or increased bone mass (Boyden et al., 2002; Little et al., 2002). This was followed shortly after by the identification of *SOST* gene mutations as causal for sclerosteosis (Balemans et al., 2001; Brunkow et al., 2001) and, in the next year, for Van Buchem disease (Balemans et al., 2002; Staehling-Hampton et al., 2002). However, the recognition that sclerostin, the product of the *SOST* gene, was a key negative regulator of Wnt/β-catenin signaling was not made until 2005 (Li et al., 2005). Targeting sclerostin with humanized anti-sclerostin antibodies has become the focus of major clinical trials for the treatment of osteoporosis and has several other potential applications (see later). Since those initial descriptions of altered bone mass, several key components of the Wnt signaling pathway (see Fig. 8.1) have been shown to underlie a large number of monogenic bone diseases (see for review Maupin et al., 2013; Malhotra and Yang, 2014; Lara-Castillo and Johnson, 2015; Wang et al., 2016; Reppe et al., 2017). In many cases normal polymorphisms in these genes are associated

Principles of Bone Biology. https://doi.org/10.1016/B978-0-12-814841-9.00008-7

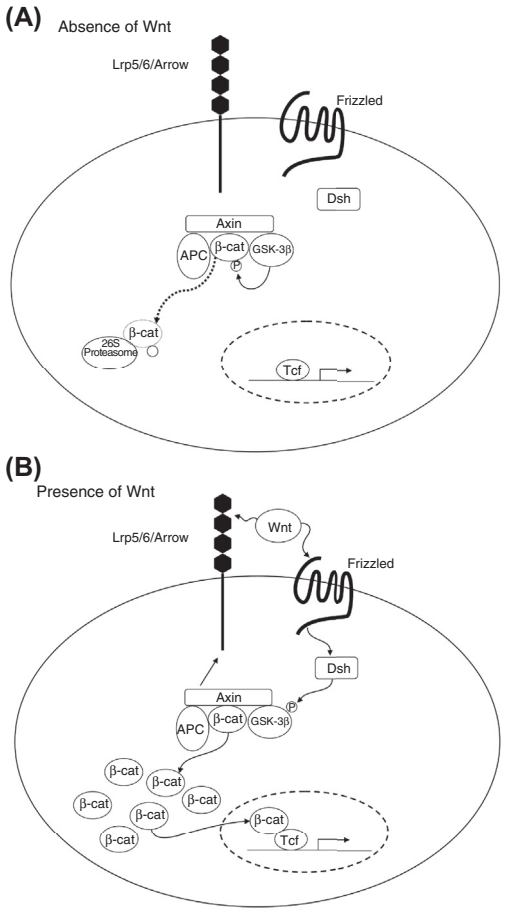

FIGURE 8.1 The Wnt/β-catenin signaling pathway. The Wnt/β-catenin signaling pathway is controlled by two cell surface coreceptors, Frizzled and one of the low-density lipoprotein receptor–related proteins (Lrp5 or Lrp6) in vertebrates or Arrow in *Drosophila*, that cooperatively bind the Wnt protein ligand. (A) In the absence of Wnt, the degradation complex consisting of the scaffolding protein Axin, adenomatous polyposis coli (*APC*), and glycogen synthase kinase-3β (*GSK-3β*), along with several other proteins (not shown), coordinates the phosphorylation (*P*) of β-catenin (*β-cat*), which is then ubiquitinated and degraded by the 26S proteasome complex. This serves to keep the intracellular levels of free β-catenin at a low level. (B) When Wnt ligand is bound by the Lrp5/6/Arrow and Frizzled coreceptors the protein Dishevelled (*Dsh*) is activated, which results in the phosphorylation of GSK-3β, thereby inhibiting its activity. The degradation complex is also induced to bind to the cytoplasmic tail of Lrp5/6/Arrow and the combination of events leads to the intracellular accumulation of high levels of free β-catenin. β-Catenin can then translocate into the nucleus, and upon binding to the T cell factor/lymphoid enhancer-binding factor (*Tcf*/LEF) family of transcription factors, regulate the expression of a number of target genes.

with or contribute to some degree of variance in complex bone traits such as bone density (see for review Urano and Inoue, 2014; Lara-Castillo and Johnson, 2015; Rocha-Braz and Ferraz-de-Souza, 2016; Reppe et al., 2017).

Prior to these human genetic studies the role of Wnt/β-catenin signaling in bone was limited mainly to skeletal development, but because of the explosion of research that occurred as a result of those seminal publications we now appreciate the role of this pathway in bone cell differentiation, proliferation, and apoptosis; bone mass regulation; and the ability of bone to respond to changes in mechanical load. While Wnts can signal through multiple pathways, in this chapter the focus will be on what is known about the Wnt/β-catenin signaling pathway and its regulation as pertains to bone.

Wnt genes and proteins

As of this writing, there are 19 known *Wnt* genes in humans. Wnt proteins are secreted, highly posttranslationally modified proteins that play key roles in development and homeostasis through their involvement in cell differentiation, proliferation, and apoptosis. Nusse and Varmus first described Wnt as the mouse protooncogene integration site/locus (*int-1*) of the murine mammary tumor virus that resulted in breast tumors (Nusse and Varmus, 1982). Because of the challenges in purifying Wnt in a biologically active form, Nusse turned to a genetic system to help characterize the downstream components of the pathway when it was found that the *Drosophila* segment polarity gene *Wingless* (*Wg*) was homologous

to the *int-1* gene (Rijsewijk et al., 1987). In 1991, several of the founding researchers in this field who came from the fields of *Drosophila* genetics, mammary viral oncogenesis, and early embryonic development in *Xenopus* came together to standardize the nomenclature for the growing number of Int-1- and Wg-related genes that were being identified and coined the term "Wnt" as a combination of Wingless and Int-1 (Nusse et al., 1991).

The Wnt proteins are difficult to study because of posttranslational modifications (mainly palmitoylation) that make them extremely hydrophobic and difficult to purify in a biologically active form. In fact, it took 21 years after the initial discovery of Wnt to work out the conditions to purify recombinant Wnt protein in a manner that retained its signaling activity (Willert et al., 2003). Thus, historically, much of what we know about Wnt proteins was based on their DNA sequence analysis and genetic screens in *Drosophila* and, later, *Caenorhabditis elegans* (Sawa and Korswagen, 2013). The various Wnt genes share general homology in the range of 35%, although within subgroups the homology can be as high as 83%. The molecular weight of the various Wnt proteins ranges from 39 to 46 kDa. All Wnts contain 23 or 24 conserved cysteine residues that are spaced similarly between proteins, suggesting an important conservation of function, possibly proper folding of the protein, which is required for Wnt activity.

Nusse and colleagues successfully purified Wnt3a from mouse L cells (Willert et al., 2003). Subsequently Schulte et al. (Schulte et al., 2005) used a similar strategy to purify Wnt5a. Both groups originally thought that the addition of a palmitate to the first, most amino-terminally conserved of the cysteine residues was absolutely required for Wnt3a and Wnt5a activity. In fact, the identification of this cysteine residue as the site of palmitoylation turned out to be incorrect, as subsequent studies showed that, in fact, a serine residue was the target of palmitoylation in Wnt proteins (Takada et al., 2006; Janda et al., 2012). The implications for this are discussed in the following.

In *Drosophila* the gene *porcupine* and in *C. elegans* the gene *mom-1* encode acyltransferase enzymes that are the proteins responsible for the palmitoylation of Wnts (Kadowaki et al., 1996; Nusse, 2003). Interestingly, these proteins are membrane bound and found in the endoplasmic reticulum, indicating that the palmitoylation occurs intracellularly. While palmitoylation of secreted proteins is somewhat unusual (Dunphy and Linder, 1998), the hedgehog family of proteins is also palmitoylated and secreted in this manner (Nusse, 2003). Subsequent work revealed two functional aspects related to palmitoylation of this serine. First, it is essential for transport of Wnt ligands from the endoplasmic reticulum to the cell surface for secretion. Upon palmitoylation, a multipass transmembrane protein, Wntless, binds to the palmitoylated Wnt and acts as a chaperone protein to facilitate its transport through the Golgi to the cell surface (Banziger et al., 2006; Bartscherer et al., 2006). Loss of either Porcupine or Wntless renders a cell functionally null for the ability to secrete any Wnt ligands.

The second functional role of the palmitoylated serine residue is its requirement for facilitating the binding of Wnt to Frizzled on the cell surface. This role was identified as a result of the first successful crystal structure of the Wnt−Frizzled interaction (Janda et al., 2012). This structure revealed that the palmitoleic group attached to the serine fits into a deep, hydrophobic group in the cysteine-rich domain (CRD) of Frizzleds.

Components of the Wnt/β-catenin signaling pathway

A detailed description of the various components of the Wnt/β-catenin signaling pathway can be found at the Wnt homepage website maintained by Dr. Roel Nusse (http://web.stanford.edu/group/nusselab/cgi-bin/wnt/). The major players in the Wnt/β-catenin signaling pathway in bone are (1) the cell surface coreceptors Lrp5/6 and Frizzled; (2) the intracellular proteins Dishevelled (Dsh), glycogen synthase kinase-3β (GSK-3β), Axin, and β-catenin; and (3) the T cell factor/lymphoid enhancer-binding factor (TCF/LEF) nuclear transcription factors that bind β-catenin and regulate gene expression. In addition, there are a number of other extracellular and intracellular proteins involved in regulation of this pathway that serve to modify the functionality of one of these key proteins. Particularly important are a number of proteins that bind Lrp5/6 to modulate its binding of Wnt ligand.

The details of the Wnt/β-catenin pathway are illustrated in Fig. 8.1. Ultimately the Wnt/β-catenin signaling pathway controls the intracellular levels of free β-catenin. In the absence of Wnt ligand the intracellular levels of β-catenin are extremely low due to the activity of a degradation complex comprising Axin, GSK-3β, the adenomatous polyposis coli (APC) protein, and several other proteins. This complex, specifically GSK-3β or -3α, is responsible for the phosphorylation of β-catenin, which leads to its ubiquitination and degradation by the 26S proteasome complex (Fig. 8.1A). Wnt binding to the Lrp5/6-Frizzled coreceptors results in Dsh activation and Axin binding to the cytoplasmic tail of Lrp5/6. Dsh activation leads to GSK-3β phosphorylation and inhibition of its activity. β-Catenin is no longer phosphorylated and this, coupled with the binding of Axin to the cytoplasmic tail of Lrp5/6, releases β-catenin. β-Catenin accumulates in the cytoplasm and then translocates into the nucleus where it binds to the TCF/LEF family of transcription proteins and regulates the expression of specific target genes (Fig. 8.1B).

Lrp5, Lrp6, and frizzled

Lrp5 and Lrp6 (Arrow in *Drosophila*) are highly homologous proteins that until their role in bone biology was described were considered orphan members of the LDLR family, which includes at least 13 members (Strickland et al., 2002). One of the hallmark structural characteristics of this family is the presence of YWTD (tyrosine−tryptophan−threonine−aspartic acid) repeat motifs framed by epidermal growth factor repeats in the extracellular domain of the proteins. These repeat clusters form β-propeller structures that are important for ligand binding. Based on the amino acid sequence of Lrp5 and Lrp6 derived from cDNA cloning (Brown et al., 1998; Dong et al., 1998; Hey et al., 1998; Kim et al., 1998), Lrp5/6 each contain four of these repeat clusters. However, the YWTD motif is degenerate and one of the six repeat sequences comprising each motif in Lrp5 is substituted by LFAN (leucine−phenylalanine−alanine−asparagine) or FFTN sequences (Johnson and Summerfield, 2005). Many of these LDLR family members have a consensus sequence of NPxY (asparagine−proline−x−tyrosine) in their cytoplasmic tail that is required for endocytosis of the receptor (Chen et al., 1990). Lrp5 and Lrp6 lack an NPxY sequence. Also the orientation of their extracellular domain is reversed relative to other members of the LDLR family in that LDL-A type repeats (complement-like repeats) are adjacent to the transmembrane spanning region rather than at the amino-terminal end (or clustered throughout the extracellular domain). There are also only three of these LDL-A type repeats in Lrp5 and Lrp6.

Originally human *LRP5* was proposed as a candidate gene for susceptibility to type 1 diabetes in the insulin-dependent diabetes mellitus 4 locus that was mapped to chromosome 11q13 (Figueroa et al., 2000; Twells et al., 2001). However, subsequent genetic association studies failed to confirm this functional role (Twells et al., 2003). At the same time, Arrow (Wehrli et al., 2000) and Lrp6 (Tamai et al., 2000) were shown to mediate Wnt/β-catenin signaling and $Lrp6^{-/-}$ mutant mouse embryos displayed skeletal abnormalities similar to those found in mice carrying mutations in various Wnt genes (Pinson et al., 2000). Subsequently mutations in human *LRP5* were shown to cause osteoporosis pseudoglioma syndrome (OPPG) (Gong et al., 2001), which is characterized by low bone mass and progressive blindness, and the high bone mass (HBM) mutation G171V was reported in two separate kindreds (Boyden et al., 2002; Little et al., 2002). A large number of additional mutations that give rise to conditions of increased or decreased bone mass have been reported in the literature (Balemans and Van Hul, 2007). Also, allelic variants of *LRP5* have been shown to contribute to variation in bone mass in several studies, although the relative degree varies and sex differences are noted in many of the studies (Karasik et al., 2016).

The role of LRP6 in human bone density variation has been studied to a limited degree. One report indicates that the *LRP6* Ile1062Val allele contributes to a higher risk for fragility and vertebral fracture in men and that this allelic variant in combination with the *LRP5* A1330V allele accounted for 10% of the fractures in males (van Meurs et al., 2006). It has also been shown that $Lrp6^{+/-}$:$Lrp5^{-/-}$ mice have lower adult bone mineral density compared with $Lrp6^{+/+}$:$Lrp5^{-/-}$ mice, suggesting a role for Lrp6 in bone mass accrual (Holmen et al., 2004). A mutation in *LRP6* ($LRP6^{R611C}$) was linked to early-onset coronary artery disease in a family, and the five mutation carriers that were studied also had low bone density, confirming a role for LRP6 in bone mass accrual as suggested by the studies in mice (Mani et al., 2007). Also, a hypomorphic *Lrp6* mutation in the mouse (called *ringelschwanz*) has been identified, and studies in that model confirm a role for Lrp6 in somitogenesis and osteogenesis (Kokubu et al., 2004).

Given that both appear to be coexpressed in most cells/tissues that have been examined, it was of interest to determine whether Lrp5 and Lrp6 served totally redundant roles in skeletal development and homeostasis. Using the Dermo1-Cre strain to drive conditional gene deletion in mesenchymal progenitors, it was demonstrated that Lrp5 and Lrp6 played redundant roles at this stage (Joeng et al., 2011). Interestingly, deletion of the genes in mature osteoblasts (using OCN-Cre) revealed that Lrp6 and Lrp5 played overlapping, but not redundant, roles at that stage (Riddle et al., 2013). The role of Lrp5 and the Wnt/β-catenin signaling pathway in the response of bone to mechanical loading has been firmly established. Based upon analysis of the phenotype of affected members of the HBM trait kindred we had speculated that the *LRP5* G171V mutation gene might somehow have altered the sensitivity of the skeleton to mechanical loading (Johnson et al., 2002). Several lines of evidence now support a central role for Lrp5 and the Wnt/β-catenin signaling pathway in the response of bone/bone cells to mechanical loading. Sawakami et al. (Sawakami et al., 2006) have shown that the bone formation response after loading is reduced by 88% in male and 99% in female $Lrp5^{-/-}$ mice compared with wild-type loaded mice. Mice carrying the LRP5 cDNA containing the G171V mutation have increased sensitivity to mechanical loading (Cullen et al., 2004). Osteocyte β-catenin haploinsufficiency protects against bone loss in male mice subjected to hindlimb unloading (Maurel et al., 2016). Changes in the expression of Wnt/β-catenin signaling pathway target genes have been shown to occur both in vivo in bone (Robinson et al., 2006) and in vitro in bone cells (Lau et al., 2006; Robinson et al., 2006) in response to mechanical loading. Given that Lrp5 is required for the response of bone to mechanical loading, the question that next needs to be answered is, where does Lrp5/Wnt/β-catenin signaling fit into the cellular cascade events

that occur in response to mechanical loading? A partial answer to this question will be discussed further later in this chapter. Another unanswered question is, does Lrp6 play a role in the response to loading? At this writing we have no definitive answer, but given the results of the ulna loading studies performed with the $Lrp5^{-/-}$ mice and that these mice have normal alleles of Lrp6, it would seem that Lrp6 plays little or no role in mechanoresponsiveness in bone.

As of this writing there are 10 known members of the Frizzled family of proteins in humans and a homologous protein called Smoothened that functions in Hedgehog signaling. The Frizzled proteins contain a CRD at the amino terminus and seven transmembrane-spanning domains. The CRD is responsible for binding of Wnt ligands (Bhanot et al., 1996). The Frizzled proteins are generally thought to be coupled to trimeric G proteins (Sheldahl et al., 1999; Katanaev et al., 2005). It also seems evident that different Frizzleds regulate different intracellular signaling cascades. However, the specific combinations are not completely understood. Specific Frizzleds functioning in combination with Lrp5 or Lrp6 in the binding of specific Wnt proteins lead to activation of β-catenin signaling; however, some Frizzleds acting alone appear to be involved in the activation of at least three other Wnt signaling pathways. These other Wnt pathways are the PCP (Mlodzik, 2002), the Wnt/Ca^{2+} involving protein kinase C (Kuhl et al., 2000), and a protein kinase A (PKA) pathway involved in muscle myogenesis (Chen et al., 2005). Dsh also appears to be involved in the first two of these Frizzled-regulated pathways. It is still not clear which of the 10 different Frizzleds are involved in the activation of each of the four Wnt pathways. However, it is known that some of the Wnt proteins preferentially activate the β-catenin signaling pathway (e.g., Wnt1 and Wnt3A), whereas other Wnts activate only one of the other pathways (e.g., Wnt5A activates the Wnt/Ca^{2+} signaling pathway) (Miller, 2001).

Recent work has begun to link specific Frizzled genes to skeletal development and homeostasis. Mouse strains carrying global deletions in most of the 10 Frizzled genes have been created (Wang et al., 2016). However, only two have been evaluated in detail for skeletal phenotypes. $Fzd8^{-/-}$ mice have osteopenia with normal bone formation and increased osteoclast activity (Albers et al., 2013), while $Fzd9^{-/-}$ mice have low bone mass associated with reduced chemokine expression but normal Wnt/β-catenin signaling (Albers et al., 2011; Heilmann et al., 2013). Based on work in human patients, Fzd2 probably plays a central role in early limb development. Specifically, deleterious heterozygous mutations in Fzd2 were associated with autosomal dominant omodysplasia or variations of Robinow syndrome, syndromes in which skeletal dysplasia is characterized by facial dysmorphism and shortening of the limbs (Saal et al., 2015; Turkmen et al., 2017). It is not clear whether the alteration of Fzd2 produces a protein that acts in a dominant negative fashion or if phenotypes are a result of haploinsufficiency for Fzd2. One report showed that an Fzd2 allele associated with autosomal dominant omodysplasia produced a protein truncated shortly after the seventh transmembrane domain of Fzd2 that was unable to activate β-catenin signaling. However, this work did not distinguish whether the underlying mechanistic effect was due to haploinsufficiency or a dominant negative effect of the truncated protein (Saal et al., 2015). Identification of the genetic alterations underlying the development of Robinow syndrome has revealed that mutations causing similar human phenotypes can be found in the following genes: WNT5A, FZD2, ROR2, DVL1, DVL3, and RAC3 (White et al., 2018). One interpretation of this is that a pathway initiated by WNT5A binding to the FZD2 and ROR2 receptors activates DVL proteins, resulting in the activation of RAC3 and its downstream targets.

The discovery that Lrp5/6/Arrow was also required for the activation of the Wnt/β-catenin signaling pathway suggested a model in which Lrp5/6/Arrow and Frizzled function as coreceptors (Tamai et al., 2000; Wehrli et al., 2000). The role of Wnt was proposed to perhaps facilitate the association/interaction of the coreceptors and this was the key event leading to pathway activation. Several lines of evidence obtained from the construction of various fusion proteins suggest that this is most likely the case (Holmen et al. 2002, 2005; Tolwinski et al., 2003). Wnt binding and the formation of this ternary complex leads to a Frizzled-dependent activation of Dsh. However, the exact molecular mechanism mediating Dsh activation is not clear. Dsh phosphorylation appears to be one common feature in all of the signaling pathways through which it is known to act. The kinases casein kinase 1 (CK1) (Peters et al., 1999) and CK2 (Willert et al., 1997) and PAR-1 (Sun et al., 2001) are the leading candidates for carrying out the phosphorylation of Dsh, which can occur through both Lrp5/6-dependent (leading to the β-catenin signaling pathway) and independent mechanisms (Wnt binding to Frizzled in the absence of Lrp5/6) (Gonzalez-Sancho et al., 2004). Three different models of how Frizzled and Dsh may interact have been proposed (He et al., 2004), but it is not clear which one functions in conjunction with Wnt and Lrp5/6/Arrow.

Dishevelled, glycogen synthase kinase-3β, Axin, and β-catenin

Dsh serves an important intermediary function between Frizzled and GSK-3β in the Wnt/β-catenin signaling pathway. Dsh also serves as an intermediary in the Wnt/Ca^{2+} signaling pathway (Kuhl et al., 2000) and the PCP pathway (Mlodzik, 2002). The PCP pathway is responsible for the proper orientation of wing hairs and thoracic bristles in *Drosophila.* Mutants with hairs/bristles that were improperly oriented led to the identification of the *Frizzled* and *Dishevelled* genes

(see for review Adler, 2002). Evidence suggests that Frizzled signals through the $G\alpha_o$ subunit in both the Wnt/β-catenin pathway and the PCP pathway (Katanaev et al., 2005). While it is not fully understood how Dsh becomes activated upon Wnt binding and how it can discriminate between which pathway(s) to activate, a model has been proposed that suggests that differential intracellular localization of Dsh may be involved in determining some aspects of its function. Dsh associated with cytoplasmic vesicles has been proposed to be linked to signaling through the Wnt/β-catenin pathway, while Dsh associated with actin and the plasma membrane is proposed to signal via the PCP pathway (Capelluto et al., 2002; Povelones and Nusse, 2002). It may also be that Frizzled localization and the specific Frizzled present in the cell, along with the distribution of downstream components and the specific Wnt ligand participating in the initial binding events, are critical as well (Bejsovec, 2005; Katoh, 2005).

The mechanism responsible for the activation of Dsh is not fully understood nor is the mechanism whereby Dsh acts known. There are three domains in Dsh that appear to be critical for its function. There is a DIX domain, which is also found in Axin; a PDZ domain; a conserved stretch of basic amino acids; and a DEP domain that is found in other vertebrate proteins that interact with trimeric G proteins (Cadigan and Nusse, 1997; He et al., 2004). Activation of Dsh occurs through phosphorylation and this appears to occur in the other Wnt signaling pathways that involve Dsh. The kinases CK1 (Peters et al., 1999) and CK2 (Willert et al., 1997) and PAR-1 (Sun et al., 2001) are the leading candidates to carry out the phosphorylation of Dsh. Gonzalez-Sancho et al. (Gonzalez-Sancho et al., 2004) have suggested that Frizzled−Dsh−Axin and Lrp5/6/Arrow−Axin associations occur in parallel and both are required for stabilization of β-catenin. However, much remains to be understood about the role of Dsh in Wnt/β-catenin signaling and with regard to its role in the other Wnt signaling pathways.

GSK-3 has two isoforms, α and β. While most of the current evidence implicates GSK-3β in the control of intracellular levels of β-catenin, GSK-3α may also play a role (McManus et al., 2005; Asuni et al., 2006). GSK-3β was first identified as playing a key role in the regulation of glycogen synthesis by phosphorylating (and thereby inhibiting) glycogen synthase (see for review Hermida et al., 2017). GSK-3α and -3β are themselves both inhibited by phosphorylation at an amino-terminal serine residue, serine 21 (α) (Sutherland and Cohen, 1994) or serine-9 (β) (Sutherland et al., 1993; Stambolic and Woodgett, 1994). This phosphorylation is known to be catalyzed by a number of kinases, including mitogen-activated protein (MAP) kinase (Sutherland and Cohen, 1994), protein kinase B (PKB)/Akt (Haq et al., 2000), protein kinase C (Cook et al., 1996), and PKA (Fang et al., 2000). However, this inhibitory phosphorylation may not be linked to GSK-3-mediated regulation of β-catenin signaling (Papadopoulou et al., 2004; McManus et al., 2005). To explain this paradox, Forde and Dale (Forde and Dale, 2007) have suggested that GSK-3β phosphorylation is a redundant form of regulation with respect to β-catenin signaling. Integrin-linked kinase also regulates GSK-3β, but apparently not through phosphorylation at serine 9 (Delcommenne et al., 1998). While there are many other regulators of GSK-3β (Hardt and Sadoshima, 2002), the aforementioned kinases all have described roles in bone and, as will be discussed later, this intersection with the Wnt/β-catenin signaling pathway suggests possible cross talk between pathways.

The kinase activity of GSK-3β appears to be enhanced by a priming phosphorylation at nearby sites. In proteins such as Lrp5/6, where multiple GSK-3β phosphorylation sites are present in the cytoplasmic tail, GSK-3β can self-prime. The initial priming phosphorylation of β-catenin needed for the subsequent GSK-3β phosphorylation is carried out by CK1 (Liu et al., 2002). GSK-3β has also been shown to phosphorylate two sites within Axin (T609 and S614), which is prerequisite for the binding of β-catenin (Jho et al., 1999). It has been proposed that Wnt signaling leads to a dephosphorylation of these sites and this is part of the mechanism leading to the release of β-catenin from the degradation complex. In addition, protein phosphatase 2A (PP2A), which binds to Axin, APC, and Dsh (Hsu et al., 1999; Seeling et al., 1999; Yamamoto et al., 2001), plays an important counterbalancing role opposing GSK-3β. When CK1 phosphorylates its substrates within the degradation complex, PP2A dissociates, which favors further net phosphorylation and the release of β-catenin (Gao et al., 2002). Phosphorylated β-catenin is then ubiquitinated and degraded by the 26S proteasome complex (Aberle et al., 1997).

Axin acts as a scaffolding protein that directly interacts with/binds Dsh, GSK-3β, APC, PP2A, and β-catenin (Behrens et al., 1998; Hart et al., 1998; Ikeda et al., 1998; Itoh et al., 1998; Nakamura et al., 1998; Sakanaka et al., 1998; Yamamoto et al., 1998; Fagotto et al., 1999; Farr et al., 2000). Axin was first identified as the product of the mouse fused locus (Zeng et al., 1997). In vertebrates there are two forms of Axin: Axin 1, which is constitutively expressed and is the main form of the degradation complex, and Axin 2 (also known as Conductin). Axin 2 expression is induced by Wnt signaling and it functions as a negative feedback inhibitor of β-catenin signaling (Jho et al., 2002). Axin has several functional domains required for its interactions with the various other proteins of the degradation complex. It appears that amino acids 581−616 are responsible for binding β-catenin, while the RGS domain interacts with APC, and GSK-3β appears to bind to amino acids 444−543 (Nakamura et al., 1998), although GSK-3β was observed only when β-catenin was present. The Armadillo repeats in β-catenin mediate the interaction with Axin, while a Dix domain similar to the one found in Dsh

probably mediates the interactions between Axin and Dsh. Mutations in the human AXIN2 gene have been linked to familial tooth agenesis and are predisposing for colon cancer (Lammi et al., 2004).

The collapse of the degradation complex and the release of β-catenin is a complex cascade of poorly understood events. Wnt binding to the coreceptors induces Axin to bind to the cytoplasmic tail of Lrp5/6/Arrow (after the coreceptor is phosphorylated and FRAT-1 binds). When Wnt is not present, β-catenin is bound to APC and APC to Axin as a consequence of specific phosphorylations mediated by GSK-3β (and other kinases). In the presence of Wnt and the activation of Dsh, these phosphorylation events are inhibited, and binding of Axin to the cytoplasmic tail of Lrp5/6/Arrow leads to the collapse of the complex and release of β-catenin into the cytoplasm.

β-Catenin is highly homologous to the *Drosophila* segment polarity gene *armadillo* (McCrea et al., 1991). The human β-catenin gene (*CTNNB*) is located on chromosome 3p21 and encodes a protein of 781 amino acids (~85 kDa). Two pools of β-catenin exist within the cell: one associated with E-cadherin and the other in the cytoplasm (Nelson and Nusse, 2004). β-Catenin contains a cassette of 12 Armadillo repeats in the middle of the protein that are the interaction sites with E-cadherin, APC, and the nuclear transcription factors (Cadigan and Nusse, 1997; Willert and Nusse, 1998). A number of mutations in β-catenin have been identified that give rise to human cancers. The amino-terminal end of the protein (mainly between amino acids 29–49) contains key residues whose phosphorylation by GSK-3β plays a critical role in the subsequent degradation of the protein, and when one or more of these residues are mutated the protein is more stable and the increased signaling results in tumor formation/growth (Yost et al., 1996; Polakis, 2000). Exactly how β-catenin is translocated from the cytoplasm into the nucleus is not fully understood, although there is evidence that this may require participation with estrogen receptor α (ERα) (Armstrong et al., 2007).

Transcriptional regulation by β-catenin

Once inside the nucleus, β-catenin binds to the TCF/LEF family of transcription factors and regulates the expression of a large (and ever-increasing) list of target genes. It has been shown that β-catenin can also interact with the FOXO family of transcriptional regulators and that this association is particularly important during oxidative stress (Essers et al., 2005), which may play a role in age-associated bone loss (Almeida et al., 2006). A consensus TCF/LEF core sequence has been identified that is required for binding of the TCF/LEF proteins (CCTTTGATC) (Korinek et al., 1997). The TCF/LEF proteins have DNA-binding ability but require the transactivating domain of β-catenin (at the C-terminal end) to regulate transcription.

A large number of proteins (see http://www.stanford.edu/~rnusse/ for a detailed listing) participate in the transcriptional regulation mediated by β-catenin. As of this writing, the model for how β-catenin regulates target gene transcription involves the formation of a larger complex of proteins that induces a change in chromatin structure (Barker et al., 2001). In *Drosophila*, when Wnt is not present, TCF acts as a repressor of Wnt/Wg target genes by forming a complex with Groucho (Cavallo et al., 1998), whose repressing ability is regulated by the histone deacetylase enzyme, Rpd3 (Chen et al., 1999). Studies in *Xenopus* have shown that β-catenin interacts with the acetyltransferases p300 and CBP to activate the *siamois* gene promoter (Hecht et al., 2000). Other proteins that control β-catenin signaling include the antagonist Chibby, which binds to the C-terminal end (Takemura et al., 2003), and the protein ICAT (Tago et al., 2000), which negatively regulates the interaction between β-catenin and TCF-4. TCF/LEF can also be phosphorylated by the MAP kinase–related protein NLK/Nemo (Ishitani et al., 2003), which reduces the affinity for β-catenin. Considerably less is known about the interaction of β-catenin with the FOXO family of transcription factors, but presumably it also involves cooperative and repressive interactions with a number of proteins. Also, it is not understood how choices are made as to which interactions are favored under any given set of cellular circumstances.

There are a large number of known Wnt/β-catenin target genes. Interestingly, many of these targets are components of the Wnt signaling pathway (see http://www.stanford.edu/~rnusse/ for a more complete listing), which creates a complicated set of feedback loops that can potentially serve to further amplify or inhibit signaling through the pathway. Some of these target genes will be discussed further in the following sections as they play important roles in bone.

Wnt signaling and bone cell function

Osteoblast differentiation and function

Many aspects of osteoblast differentiation have been covered in other chapters in this book (see Chapters 4 and 7). Wnt/β-catenin signaling plays important roles at several levels. A search of the PubMed database using the terms "Wnt and osteoblast and differentiation" yielded over 1000 published articles since 2002. Obviously a comprehensive, detailed

review of what we now understand regarding the role of Wnt/β-catenin signaling in osteoblast differentiation is not possible, but several excellent reviews have been published that cover key aspects (Hartmann, 2006; Baron and Kneissel, 2013; Zhong et al., 2014; Lerner and Ohlsson, 2015; Ahmadzadeh et al., 2016; Kobayashi et al., 2016).

Skeletal stem cells (Robey, 2017) are capable of differentiating into adipocytes, chondrocytes, and osteoblastic lineage cells. In part, the commitment to these different cell lineages is controlled by Wnt ligands that activate either the Wnt/β-catenin or the noncanonical Wnt signaling pathway. MacDougal and colleagues (Ross et al., 2000; Bennett et al., 2005) demonstrated that Wnt10b stimulates osteoblastogenesis and inhibits adipogenesis. Subsequently, Zhou et al. (Zhou et al., 2008) suggested a model involving glucocorticoid-induced *Wnt* gene expression in osteoblasts, and the expressed Wnt proteins then induce Runx2 expression and inhibit peroxisome proliferator-activated receptor γ expression in progenitor cells, thereby leading to increased osteoblastogenesis versus adipogenesis. Control of chondrogenesis is complex, with both canonical Wnt/β-catenin and noncanonical signaling having been demonstrated in the regulation of chondrogenesis at various levels in the differentiation pathway. Wnt1 and Wnt7a have been shown to play inhibitory roles in the early prechondrogenic mesenchyme. Hartmann and Tabin (Hartmann and Tabin, 2000) demonstrated specific patterns of expression of Wnt5a, Wnt5b, and Wnt4 in the chicken limb chondrogenic regions, with Wnt5a and Wnt4 having opposing effects. Wnt5a inhibits chondrogenesis and bone collar formation, while Wnt4 accelerates these processes. Church et al. (Church et al., 2002) have shown that Wnt5a is expressed in the joints and perichondrium, with Wnt5b and Wnt11 localized to the region of prehypertrophic chondrocytes. Akiyama et al. (Akiyama et al., 2004) have shown that Sox9, a transcription factor required for chondrogenesis, directly binds to β-catenin and thereby competes for Tcf/Lef-mediated transcription by β-catenin. Reciprocally, Wnt3a has been shown to inhibit chondrocyte differentiation by upregulating the expression of *c-Jun* leading to activation of activator protein 1, which suppresses Sox-9 (Hwang et al., 2005). Hill et al. (Hill et al., 2005) proposed a model in which β-catenin is necessary, but not sufficient, for suppressing chondrogenic commitment of progenitor cells. Thus, the role of Wnt signaling in the fate decisions for differentiation between adipogenesis, chondrogenesis, and osteogenesis within the skeletal stem population is complex and fine-tuned by various Wnt ligands and is tightly controlled both spatially and temporally.

The commitment toward osteoblastogenesis is driven by the Runt domain−containing transcription factor, Runx2 (Ducy et al., 1997; Komori et al., 1997; Lee et al., 1997; Otto et al., 1997) (AML3/PEB2α/CBFA1), and the transcription factor Osterix (Osx) (Nakashima et al., 2002), which acts downstream of Runx2. The original descriptions of human LRP5 mutations in low- and high-bone-mass traits suggested an important role for Wnt signaling in osteoblast proliferation and differentiation (Gong et al., 2001; Boyden et al., 2002; Little et al., 2002). Subsequent studies with a transgenic mouse expressing the HBM $LRP5^{G171V}$ mutation provided further support for Wnt/β-catenin signaling in the regulation of osteoblast differentiation and function (Babij et al., 2003). There is a complicated relationship between activation of Wnt/β-catenin signaling and Runx2. Gaur et al. (Gaur et al., 2005) demonstrated that β-catenin induced Runx2 expression and Haxaire et al. have shown that Runx2 is a negative regulator of Wnt/β-catenin signaling (Haxaire et al., 2016). Runx2 and Osx activate the expression of SOST (Perez-Campo et al., 2016), a negative regulator of the pathway, which may partially explain the decrease in Wnt/β-catenin signaling.

Studies have also shown an important role for microRNAs (miRNAs) in the regulation of osteoblastogenesis, in part through their regulation of Wnt/β-catenin signaling. DICER, which is a key component of miRNA processing, has been shown to be significantly upregulated by Runx2 (Zheng et al., 2017). The miRNAs miR-335-5p and miR-17-92 decrease Dickkopf-1 (Dkk-1) levels (Zhang et al., 2017; Zheng et al., 2017). miR-142-3p inhibits APC, leading to increased β-catenin nuclear translocation and signaling (Hu et al., 2013). During osteoblast differentiation miR-218 is induced, which leads to activation of Wnt/β-catenin signaling by downregulating the expression of SOST, DKK-2, and sFRP2, but in a feed-forward loop the activation of the pathway subsequently further increases expression of miR-218 (Hassan et al., 2012). Similarly, miR-29 expression has also been shown to be induced by activation of Wnt/β-catenin signaling, and miR-29a and -29c repress the expression of several pathway inhibitors in a positive feedback loop (Kapinas et al. 2009, 2010).

In addition to its role in osteoblast differentiation, Wnt/β-catenin signaling also plays important roles in the proliferation, apoptosis, metabolism, and mineralization of the skeleton driven by osteoblasts. The role of Wnt signaling in regulating these functions is complex and includes both direct effects on the osteoblast itself and indirect effects through the expression of other osteoblast-derived factors that affect other bone cells and involves both canonical and noncanonical Wnt signaling pathways. For example, Wnt3a has been shown to induce matrix extracellular phosphoglycoprotein (Mepe) by stimulating expression of the *Mepe* gene. Wnt3a has also been shown to stimulate bone morphogenetic protein 2 (BMP-2) gene expression (Cho et al., 2012; Zhang et al., 2013), which also regulates *Mepe* gene expression (Cho et al., 2012). Studies have demonstrated differentiation-stage-specific effects of Wnt signaling in osteoblasts (Eijken et al., 2008; Bao et al., 2017).

Kato et al. (Kato et al., 2002) demonstrated in the $Lrp5^{-/-}$ mouse that the low-bone-mass phenotype was due to decreased osteoblast proliferation and reduced matrix deposition. Gong et al. (Gong et al., 2001) demonstrated that Wnt3a, but not Wnt5a, increased alkaline phosphatase activity in C3H10T1/2 and ST2 cell lines. Based on their data, they suggested that LRP5 and the Wnt/β-catenin signaling pathway play important roles in osteoblast differentiation and proliferation. Boyden et al. (Boyden et al., 2002) observed elevated serum osteocalcin levels, a marker of bone formation, but normal collagen type I urinary N-telopeptide levels, a marker of bone resorption. This suggested that the $LRP5^{G171V}$ mutation leads to exuberant osteoblast activity resulting in increased bone density. Babij et al. (Babij et al., 2003) developed a transgenic mouse (over)expressing the human $LRP5^{G171V}$ cDNA and also observed normal osteoclast activity with increased mineralizing surface and enhanced alkaline phosphatase staining in osteoblasts. However, Glass et al. (Glass et al., 2005), using mouse models with targeted deletion or overexpression of β-catenin in osteoblasts, identified another important role in the regulation of osteoclast activity through the production of osteoprotegerin (OPG). Why mutations in the Wnt receptor lead to increased osteoblast activity and alterations in β-catenin levels resulting in altered osteoclast activity is not entirely clear.

Another area of osteoblast function that has garnered attention is the role of Wnt signaling in the regulation of cellular energy metabolism in osteoblasts (Frey et al., 2017; Yao et al., 2017). The Wnt effects appear to be mediated by β-catenin in the case of fatty acid catabolism (Frey et al., 2017), mTORC2 in the case of aerobic glycolysis (Esen et al., 2013), and mTORC1 involving glutamine metabolism (Karner et al., 2015). Interestingly, both of the mTORC1/2-mediated effects appear to involve LRP5/Lrp6/Frizzled binding of a Wnt ligand (Karner and Long, 2017).

Studies have clearly shown an important role for the Wnt/β-catenin signaling pathway in the prevention of both osteoblast and osteocyte apoptosis. Kato et al. (Kato et al., 2002) demonstrated in the $Lrp5^{-/-}$ mouse that the hyaloid vessels failed to undergo apoptosis, resulting in the persistence of this vasculature network into the adult, which could explain the blindness associated with human OPPG patients carrying LRP5-null mutations. Babij et al. (Babij et al., 2003), using the HBM transgenic mouse, showed decreased osteoblast and osteocyte apoptosis attributable to the $LRP5^{G171V}$ mutation. Secreted Frizzled-related protein-1 (sFRP-1) is a Wnt/β-catenin signaling pathway inhibitor (Bodine et al., 2004), and blocking sFRP with a small-molecule inhibitor caused a significant reduction in osteoblast apoptosis in cell culture (Bodine et al., 2009).

Osteoclast function

Osteoclasts are derived from hematopoietic (myeloid lineage) progenitors. Macrophage colony-stimulating factor (M-CSF) (Yoshida et al., 1990) and receptor activator of NF-κB ligand (RANKL) (Kong et al., 1999) are critical for osteoclast replication and differentiation, respectively. The early studies of osteoblast-targeted deletion or constitutive activation of β-catenin in mice surprisingly demonstrated a critical role for the pathway in the regulation of osteoclastogenesis, which was attributed to altered expressed of the RANKL ligand decoy receptor OPG (Glass et al., 2005; Holmen et al., 2005). Studies in MC3T3-E1 cells also demonstrated that activation of Wnt/β-catenin signaling downregulates the expression of RANKL (Spencer et al., 2006). Thus, by regulating the OPG/RANKL ratio, the Wnt/β-catenin signaling pathway in osteoblasts can control osteoclastogenesis. It is now recognized that the osteocyte is an important source of RANKL, and its role in osteoclastogenesis will be discussed further in a subsequent section.

Wnt signaling within osteoclasts is also an important role. The Wnt pathway inhibitor sFRP-1 has been shown to bind to RANKL and inhibit osteoclast formation (Hausler et al., 2001). Wei et al. (Wei et al., 2011) demonstrated that β-catenin-mediated Wnt signaling was induced during the M-CSF quiescence-to-replication/proliferation phase, but downregulated during the RANKL proliferation-to-differentiation phase of osteoclastogenesis. Mechanistically, Wnt/β-catenin signaling promoted proliferation of osteoclast precursors by increasing expression of GATA2 and Evi1 and blocked differentiation by inhibiting c-Jun phosphorylation. Extending this work further, Weivoda et al (Weivoda et al., 2016) have demonstrated that Lrp5/6/Frizzled binding of Wnt3a affects osteoclastogenesis through β-catenin and the noncanonical cAMP/PKA pathway. The latter pathway functions to block early osteoclast progenitors from differentiating by phosphorylation of nuclear factor of activated T cells 1.

Human genome-wide association studies have revealed that Wnt16 contributes to variation in bone density (Medina-Gomez et al., 2012; Zheng et al., 2012). Wnt16 through Wnt/β-catenin signaling has been shown to be involved in intramembranous ossification and to suppress osteoblast differentiation and mineralization (Jiang et al., 2014). Osteoblast-derived Wnt16 has been shown to stimulate OPG production by osteoblasts, which indirectly affects osteoclastogenesis, and to directly inhibit RANKL-mediated action in preosteoclasts through a c-Jun-mediated mechanism, rather than by canonical Wnt/β-catenin signaling (Weivoda et al., 2016). Additional Wnt ligands that have been implicated in osteoclast differentiation include Wnt4 and Wnt5a (Kobayashi et al. 2015a, 2015b).

Osteocyte function

In recent years, the role of the osteocyte in orchestrating the activity of osteoblasts and osteoclasts has been clearly established. Several excellent reviews have been published that detail the myriad of mechanisms through which osteocytes exert their regulation of bone formation and resorption (Bonewald and Johnson, 2008; Baron and Kneissel, 2013; Burgers and Williams, 2013; O'Brien et al., 2013; Schaffler et al., 2014; Johnson and Recker, 2017) (see also Chapter 6).

Based upon the skeletal phenotype of the HBM kindred, Johnson et al. (Johnson et al., 2002) first proposed that one of the main roles of the Wnt/β-catenin signaling pathway in bone was as a key component of the response to mechanical loading. In support of this hypothesis it was subsequently demonstrated that the $LPR5^{G171V}$ mutation resulted in increased bone formation (Bex et al., 2003; Cullen et al., 2004) and that loss of Lrp5 resulted in a lack of bone formation in response to load (Sawakami et al., 2006). Activation of Wnt/β-catenin signaling occurs following in vivo loading (Kamel et al., 2006; Lau et al., 2006; Robinson et al., 2006; Sawakami et al., 2006; Javaheri et al., 2014; Lara-Castillo et al., 2015), and targeted deletion of osteocyte β-catenin results in severe bone loss and compromised load responsiveness (Kramer et al., 2010; Javaheri et al., 2014; Kang et al., 2016). While the exact mechanism by which osteocytes (bone cells) perceive mechanical load is unresolved, a number of downstream events are now known to occur that are central to the biochemical response by the cell. Bonewald and Johnson (Bonewald and Johnson, 2008) suggested a model describing how the Wnt/β-catenin signaling pathway activates in response to mechanical load. In support of this model, Kamel et al. (Kamel et al., 2010) demonstrated that prostaglandin E_2 (PGE_2) was able to stimulate β-catenin nuclear translocation through a phosphatidylinositol 3-kinase (PI3K)/Akt-mediated mechanism. Lara-Castillo et al. (Lara-Castillo et al., 2015) subsequently demonstrated in vivo that loading rapidly activated β-catenin signaling in osteocytes and, in agreement with prior work by Sawakami et al. (Sawakami et al., 2006), found a concordant reduction in sclerostin and Dkk-1 levels in osteocytes. Pretreatment with Carpofen, a cyclooxygenase 2 inhibitor, blocked activation of Wnt/β-catenin signaling (Lara-Castillo et al., 2015), in agreement with their in vitro studies (Kamel et al., 2010).

Several other functions of the osteocyte involve aspects of Wnt/β-catenin pathway regulation, either directly or through the expression of its downstream targets. It is now recognized that the osteocyte is a key regulator of osteoblast and osteoclast function via its production of sclerostin (Poole et al., 2005; van Bezooijen et al., 2005) and RANKL (Nakashima et al., 2011; Xiong et al., 2011) and that sclerostin plays a role in osteocyte RANKL production (Wijenayaka et al., 2011). Glucocorticoids are known to induce osteocyte autophagy or apoptosis depending upon the dose (Jia et al., 2011). Protection against glucocorticoid-induced apoptosis is mitigated, in part, by the induction of PGE_2 upon mechanical loading and subsequent activation of Wnt/β-catenin signaling (Kitase et al., 2010). Parathyroid hormone (PTH) has been implicated in the regulation of sclerostin expression (Bellido et al., 2005; Keller and Kneissel, 2005) through regulation of the *Sost* gene enhancer involving MEF2 family transcription factors (Leupin et al., 2007). However, the bone anabolic effects of PTH cannot be fully explained by its regulation of sclerostin and/or interaction with Wnt/β-catenin signaling (Powell et al., 2011; Kedlaya et al., 2016; Delgado-Calle et al., 2017).

The fact that mutations in another member of the LDLR-related family, LRP4, were linked to phenotypes similar to those seen in human patients carrying loss-of-function mutations in the sclerostin gene was the catalyst for studies that eventually showed that LRP4 serves as a receptor for sclerostin, facilitating its presentation to Lrp5 or Lrp6 at the membrane and allowing it to inhibit Wnt/β-catenin signaling (Leupin et al., 2011). The importance of this interaction and its inhibition of both Lrp5 and Lrp6 signaling have been demonstrated by genetically engineered mouse models and inhibitory antibody studies (Chang et al., 2014).

Interactions between Wnt/β-catenin signaling and other pathways important in bone mass regulation

The Wnt/β-catenin signaling pathway is not the only pathway that is known to be important in the regulation of bone cell activities, and considerable effort is now being focused on understanding how all of these various pathways interact to regulate bone mass. As already discussed, GSK-3β is the critical intracellular enzyme controlling β-catenin levels. Therefore any pathway that can regulate GSK-3β activity has the potential to interact with the Wnt/β-catenin signaling pathway independent of the Lrp5/6/Frizzled coreceptors and any modulators that function at that level.

One set of well-known pathways that have the potential to cross talk with the Wnt/β-catenin signaling pathway comprises those pathways that signal through Akt/PKB. Akt/PKB is activated by PI3K, whose activity is opposed by the phosphatase and tensin homolog deleted on chromosome 10 (PTEN) tumor suppressor (Datta et al., 1999; Kandel and Hay, 1999). Akt/PKB has been shown to be stimulated by Wnt and, in association with Dsh, to phosphorylate GSK-3β (Fukumoto et al., 2001). This raises the potential for several growth factors to potentially cross talk with the Wnt/β-catenin

signaling pathway. It has been shown that the growth of colon cancer cells induced by PGE_2 is partially the result of activation of the Wnt/β-catenin pathway through a dual mechanism involving Akt-mediated phosphorylation of GSK-3β and the $G\alpha_s$ subunit trimeric G proteins associated with the PGE_2 EP2 receptor binding to Axin and thereby promoting dissociation of the degradation complex (Castellone et al., 2005). PGE_2 release/production in bone cells is a well-known early response to mechanical loading. Fluid-flow shear stress has been shown to increase the phosphorylation of both Akt and GSK-3β in osteoblasts (Norvell et al., 2004). Fluid-flow shear stress results in an initial activation of the β-catenin signaling that is Lrp5 independent and probably mediated through cross talk with PGE_2 signaling (Kamel et al. 2006, 2010). As of this writing, we are testing a model in which this initial activation results in a feedback amplification loop that functions at the level of Lrp5 and leads to new bone formation. When Lrp5 is not present, the amplification loop does not occur and no new bone formation can occur, as was observed in the loading studies on the $Lrp5^{-/-}$ mouse (Sawakami et al., 2006). It has also been shown that integrin-linked kinase can regulate Akt/PKB and GSK-3β (Delcommenne et al., 1998), which potentially connects the important role of integrins in the response of bone cells to mechanical loading (Pavalko et al., 1998; Wozniak et al., 2000) with the Wnt/β-catenin signaling pathway through a cross talk mechanism.

In addition, signaling pathways that regulate the expression of activators or inhibitors (discussed previously) of the Wnt/β-catenin pathway thereby interact at this level. For example, results of studies with PTH suggest that PTH acts in part through a complementary pathway and not entirely through the Lrp5 Wnt/β-catenin signaling pathway. Continuous PTH treatment of rats in vivo or UMR 106 cells in culture results in a downregulation of *Lrp5* and *Dkk1* and an upregulation of *Lrp6* and *Fzd1* (Kulkarni et al., 2005) and, based on these studies, it was suggested that the effects of PTH are in part mediated by a cAMP/PKA pathway. In studies with the sFRP-1-knockout mouse, it was concluded that PTH and Wnt signaling may share some common components, but PTH action appears to extend beyond the Wnt pathway (Bodine et al., 2004). However, studies with the $Lrp5^{-/-}$ mouse have shown that Lrp5 is not required for the anabolic effects of PTH on bone (Iwaniec et al., 2004; Sawakami et al., 2006). Evidence has been presented that PTH infusion in mice decreases *Sost* mRNA expression and sclerostin levels in osteocytes (Bellido et al., 2005). This finding implies a negative feedback control mechanism in which sclerostin production by osteocytes opposes the actions of Wnts and/or BMPs on osteoblast precursors, and PTH, by decreasing sclerostin levels, indirectly therefore stimulates osteoblast differentiation and bone formation. Thus the picture of PTH that emerges is complex.

Likewise, several groups have examined potential cross talk between the BMP signaling pathway and Wnt/β-catenin signaling (Rawadi et al., 2003; He et al., 2004; van den Brink, 2004; Nakashima et al., 2005; Tian et al., 2005; Gaur et al., 2006; Liu et al., 2006). One model that has been proposed (Liu et al., 2006) for cross talk between these two pathways in bone marrow stromal cells involves a Dsh−Smad1 interaction in the unstimulated state that becomes disrupted when Wnt is present. When both Wnt and BMP-2 are present the phosphorylation of Smad1 stabilizes the interaction and thereby inhibits Wnt/β-catenin signaling (Liu et al., 2006). In intestinal crypt stem cell self-renewal, BMP inhibitory effects have been proposed to be mediated through the suppression of Wnt/β-catenin signaling through a mechanism involving PTEN, PI3K, and Akt (He et al., 2004). In bone, it has been proposed that BMP-2 increases the expression of Wnt proteins that then activate the Wnt/β-catenin signaling pathway in an autocrine/paracrine feedback loop (Rawadi et al., 2003). It has also been proposed that Wnts induce the expression of BMPs and this induction is necessary for expression of alkaline phosphatase (Winkler et al., 2005). This model also implicated sclerostin as imposing a level of control preferentially at the level of BMP signaling versus Wnt signaling. However, there is now clear evidence for sclerostin being a negative regulator of the Wnt/β-catenin signaling through binding to Lrp5 (Ellies et al., 2006; Semenov and He, 2006). Thus, while it is clear that these two pathways are somehow intertwined, the exact nature of their interaction(s) is complex (Marcellini et al., 2012).

As mentioned previously, there is now compelling evidence for the involvement of Lrp5 and the Wnt/β-catenin signaling pathway in the formation of new bone induced by mechanical loading of bone. Evidence also indicates that the $LRP5^{G171V}$ mutation may also protect against bone loss related to disuse, but that bone loss due to estrogen withdrawal is not affected by this mutation (Bex et al., 2003). However, it has been shown that ERα and β-catenin can/do form a functional interaction and potentially regulate gene expression (Kousmenko et al., 2004). It has also been suggested that in bone there is a convergence of the ER, kinases, BMP, and Wnt signaling pathways that regulates the differentiation of osteoblasts (Kousteni et al., 2007).

What other pathways might also interact with the Wnt/β-catenin signaling pathway? An emerging concept in the Wnt field is that there are numerous β-catenin-independent pathways that are altered upon inhibition of GSK-3. The term "Wnt-dependent stabilization of proteins," or Wnt-STOP, has been proposed for this aspect of Wnt signaling (Acebron et al., 2014; Huang et al., 2015; Koch et al., 2015; Acebron and Niehrs, 2016). One such example of this type of regulation is the GSK-3-dependent (but β-catenin-independent) regulation of the mammalian target of rapamycin (mTOR) pathway (Inoki et al., 2006; Karner and Long, 2017). This example may be particularly relevant for understanding the role of Wnt

signaling in bone biology (Esen et al., 2013; Chen et al., 2014; Karner et al., 2015; Sun et al., 2016). It is likely that more Wnt-dependent pathways will be identified and that only by understanding the complex interplay of these various pathways will the control of the differentiation, proliferation, and function of bone cells be fully appreciated.

The Wnt signaling pathway as a target for anabolic therapy in bone

The $LRP5^{G171V}$ mutation results in an HBM phenotype and a skeleton that is resistant to fracture (Johnson et al., 1997). The affected members of this kindred seem to have no other health consequences related to the presence of this mutation, although in a second kindred with the $LRP5^{G171V}$ mutation affected members all had torus lesions in the oral cavity to varying degrees (Boyden et al., 2002). It has also been reported that some mutations in *LRP5* (Gong et al., 2001; Whyte et al., 2004) may have associated pathology. The finding that Lrp5 and Wnt/β-catenin signaling are critical components of bone responsiveness to mechanical loading (Bonewald and Johnson, 2008; Javaheri et al., 2014; Lara-Castillo et al., 2015) suggests a potentially novel pharmaceutical approach. Perhaps one strategy would be to use a pharmaceutical agent that can alter regulation of the pathway (mimicking the effect of the LRP^{G171V} mutation) in combination with an exercise regimen to produce an optimal bone anabolic effect. It might even be possible to use such a combination therapy approach with a drug dose that by itself has little consequence on bone mass and thus perhaps avoid undesirable side effects.

Given the major role of Wnt/β-catenin signaling in skeletal development and adult bone mass regulation, it is not surprising that soon after the description of the LRP5 mutations that regulate bone mass, considerable attention was focused on using key components of the pathway as targets for new drug development (Janssens et al., 2006; Baron and Rawadi, 2007; Baron and Kneissel, 2013). Caution was raised in these early discussions that misregulation of the pathway could lead to undesirable side effects such as cancer (Polakis, 2000; Moon et al., 2002; Prunier et al., 2004; Nusse, 2005; Johnson and Rajamannan, 2006). The discovery that sclerostin, the product of the *SOST* gene and a key negative regulator of the Wnt/β-catenin signaling pathway, was expressed mainly by osteocytes provided a potential solution to this paradox (Bellido et al., 2005; Li et al., 2005; Poole et al., 2005; van Bezooijen et al., 2005).

Two major pharmaceutical clinical trials using humanized monoclonal antibodies to sclerostin (romosozumab and blosozumab) have been reported in the literature (McClung, 2017). Clinical trials with romosozumab (Cosman et al., 2016; Ishibashi et al., 2017; Langdahl et al., 2017; Saag et al., 2017) consistently showed significant gains in areal bone mineral density at the lumbar spine, total hip, and femoral neck and reduced fracture risk. Studies in rats suggested that there was no significant carcinogenic risk in humans (Chouinard et al., 2016), which had been a concern identified as a result of rat studies on the use PTH(1−34) (Vahle et al., 2002). However, in a 2017 study (Saag et al., 2017) there was a slight, but significant, increase in adverse cardiovascular events that was not observed in previous studies. The basis for this cardiovascular issue is not clear. However, it is known that Wnt/β-catenin signaling plays a role in vascular calcification (Johnson and Rajamannan, 2006; Towler et al., 2006; Bostrom et al., 2011), and the question that needs to be more fully explored is whether these cardiovascular adverse events occurred in individuals with underlying vascular disease that was not excluded in the enrollment of subjects for these studies. Interestingly, the other reports did not report any observable differences in adverse events between treatment groups. Phase II clinical trials with blosozumab have also yielded similar positive gains in bone density (McColm et al., 2014; Recker et al., 2015; Recknor et al., 2015), with no significant differences in adverse events being detected in these initial studies between groups. Blosozumab has been removed from consideration for FDA approval as of this writing, and the impact of the adverse cardiovascular risk observed in the romosozumab phase III trials on FDA approval is unclear.

Are there other possibilities for exploiting this pathway pharmaceutically to treat diseases of low bone mass (Baron and Kneissel, 2013)? The majority of pharmaceutical agents on the market target either receptors or specific enzymes. In the Wnt/β-catenin pathway the obvious targets in this regard are the coreceptors Lrp5 and Frizzled and GSK-3β, which is the key enzyme controlling intracellular β-catenin levels.

Regulation of GSK-3β activity has already been reported to produce a bone anabolic effect. LiCl treatment, which inhibits GSK-3β, restores bone mass in the $Lrp5^{-/-}$ mouse (Clement-Lacroix et al., 2005), and in humans the use of lithium appears to have an associated decreased fracture risk and a trend for decreased risk of osteoporotic fractures of the spine and wrist (Colles fracture) (Vestergaard et al., 2005). GSK-3β inhibitors have also been shown to produce a bone anabolic effect in vivo and to increase expression of bone formation markers and induce osteoblast cell differentiation in vitro (Kulkarni et al., 2006; Robinson et al., 2006). In one of these studies, changes in gene expression profile that were obtained from treatment with these agents were virtually identical to changes observed in HBMtg mouse bones, in bone cells after mechanical loading, and in primary bone cells from affected members of HBM (Robinson et al., 2006). What these studies suggest is that, as we learn more about how the Wnt/β-catenin signaling pathway functions in bone, it will be possible to design better and more specific pharmaceutical agents and approaches.

Given the cross talk between other signaling pathways and the Wnt/β-catenin signaling pathway it may be that as we understand more about the nature of these complex interactions and regulation of the pathway, these studies will reveal targets/approaches for treatment (Johnson and Recker, 2017). PTH has been proposed to decrease levels of sclerostin produced by osteocytes and thus release the inhibition on osteoblast differentiation (Bellido et al., 2005). Could it be possible to regulate *Sost* gene expression through other means and thereby affect a bone anabolic effect? BMPs appear to induce the expression of Wnts (and perhaps vice versa), and so understanding what regulates Wnt gene expression in bone may provide a key to new pharmaceutical approaches. The result of β-catenin nuclear translocation is a change in expression of a number of genes, many of which function in a feedback loop as inhibitors or activators of the pathway. As we understand more about the nature of these genes/proteins and their regulation, it may be possible to design drugs that can alter the activity of these proteins and thereby tip the balance between bone formation and bone resorption in favor of formation and either increase bone mass or prevent bone loss. DKK-1 is another inhibitor of the pathway, and early animal studies have shown promise for this approach, which is similar to the anti-sclerostin antibodies therapies discussed earlier (Glantschnig et al., 2010; Li et al., 2011; Florio et al., 2016). DKK-1 antibodies have also gained considerable interest as a therapy to treat and manage myeloma bone disease (Terpos et al., 2017).

Interestingly, the importance of the Wnt pathway in bone homeostasis has also been emphasized by work in human clinical trials for cancer treatment. Several therapeutic strategies for blocking Wnt signaling to treat cancer are being tested in phase I trials (Rey and Ellies, 2010; Krishnamurthy and Kurzrock, 2018). In some instances, these trials had to be at least temporarily halted because patients displayed evidence of fracture or significant bone loss (Jimeno et al., 2017). This is consistent with several mouse models in which mice that have been genetically engineered to lack the ability to secrete Wnt ligands from osteoblasts have extremely low bone mass (Zhong et al., 2012; Wan et al., 2013; Tan et al., 2014). Strategies designed to mitigate these effects are undoubtedly being evaluated in animal models, and a greater knowledge of the specific Wnt receptors that are necessary for adult bone homeostasis may facilitate more targeted treatments.

While many of these ideas about creating new therapies targeting this pathway in bone may be considered fanciful speculation at this point, if we have learned anything since the discovery in the early years of the 21st century of the mutations in *LRP5* that give rise to low and high bone mass, it may simply be that the discoveries of the next five years may be even more enlightening in terms of our understanding of the role of Wnt/β-catenin signaling in bone.

References

Aberle, H., Bauer, A., Stappert, J., Kispert, A., Kemler, R., 1997. β-Catenin is a target for the ubiquitin-proteasome pathway. EMBO J. 16, 3797−3804.

Abou Ziki, M.D., Mani, A., 2017. Wnt signaling, a novel pathway regulating blood pressure? State of the art review. Atherosclerosis 262, 171−178.

Acebron, S.P., Niehrs, C., 2016. Beta-catenin-independent roles of wnt/LRP6 signaling. Trends Cell Biol. 26 (12), 956−967.

Acebron, S.P., Karaulanov, E., Berger, B.S., Huang, Y.L., Niehrs, C., 2014. Mitotic wnt signaling promotes protein stabilization and regulates cell size. Mol. Cell. 54 (4), 663−674.

Adler, P.N., 2002. Planar signaling and morphogenesis in *Drosophila*. Dev. Cell. 2, 525−535.

Ahmadzadeh, A., Norozi, F., Shahrabi, S., Shahjahani, M., Saki, N., 2016. Wnt/beta-catenin signaling in bone marrow niche. Cell Tissue Res. 363 (2), 321−335.

Akiyama, H., Lyons, J.P., Mori-Akiyama, Y., Yang, X., Zhang, R., Zhang, Z., Deng, J.M., Taketo, M.M., Nakamura, T., Behringer, R.R., McCrea, P.D., de Crombrugghe, B., 2004. Interactions between Sox9 and beta-catenin control chondrocyte differentiation. Genes Dev. 18 (9), 1072−1087.

Albers, J., Schulze, J., Beil, F.T., Gebauer, M., Baranowsky, A., Keller, J., Marshall, R.P., Wintges, K., Friedrich, F.W., Priemel, M., Schilling, A.F., Rueger, J.M., Cornils, K., Fehse, B., Streichert, T., Sauter, G., Jakob, F., Insogna, K.L., Pober, B., Knobeloch, K.P., Francke, U., Amling, M., Schinke, T., 2011. Control of bone formation by the serpentine receptor Frizzled-9. J. Cell Biol. 192 (6), 1057−1072.

Albers, J., Keller, J., Baranowsky, A., Beil, F.T., Catala-Lehnen, P., Schulze, J., Amling, M., Schinke, T., 2013. Canonical Wnt signaling inhibits osteoclastogenesis independent of osteoprotegerin. J. Cell Biol. 200 (4), 537−549.

Almeida, M., Han, L., Lowe, V., Warren, A., Kousteni, S., O'Brien, C.A., Manolagas, S., 2006. Reactive oxygen species antagonize the skeletal effects of wnt/β-catenin in vitro and aging mice by diverting β-catenin from TCF- to FOXO-mediated transcription. J. Bone Miner. Res. 21 (Suppl. 1), S26 (abst 1092).

Armstrong, V.J., Muzylak, M., Sunters, A., Zaman, G., Saxon, L.K., Price, J.S., Lanyon, L.E., 2007. Wnt/beta-catenin signaling is a component of osteoblastic bone cell early responses to load-bearing and requires estrogen receptor alpha. J. Biol. Chem. 282 (28), 20715−20727.

Asuni, A.A., Hooper, C., Reynolds, C.H., Lovestone, S., Anderton, B.H., Killick, R., 2006. GSK3alpha exhibits beta-catenin and tau directed kinase activities that are modulated by wnt. Eur. J. Neurosci. 24, 3387−3392.

Babij, P., Zhao, W., Small, C., Kharode, Y., Yaworsky, P., Bouxsein, M., Reddy, P., Bodine, P., Robinson, J., Bhat, B., Marzolf, J., Moran, R., Bex, F., 2003. High bone mass in mice expressing a mutant LRP5 gene. J. Bone Miner. Res. 18, 960−974.

Balemans, W., Van Hul, W., 2007. The genetics of low-density lipoprotein receptor-related protein 5 in bone: a story of extremes. Endocrinology 148 (6), 2622−2629.

Balemans, W., Ebeling, M., Patel, N., Van Hul, E., Olson, P., Dioszegi, M., Lacza, C., Wuyts, W., Van Den Ende, J., Willems, P., Paes-Alves, A.F., Hill, S., Bueno, M., Ramos, F.J., Tacconi, P., Dikkers, F.G., Stratakis, C., Lindpaintner, K., Vickery, B., Foernzler, D., Van Hul, W., 2001. Increased bone density in sclerosteosis is due to the deficiency of a novel secreted protein (SOST). Hum. Mol. Genet. 10 (5), 537–543.

Balemans, W., Patel, N., Ebeling, M., Van Hul, E., Wuyts, W., Lacza, C., Dioszegi, M., Dikkers, F.G., Hildering, P., Willems, P.J., Verheij, J.B., Lindpaintner, K., Vickery, B., Foernzler, D., Van Hul, W., 2002. Identification of a 52 kb deletion downstream of the SOST gene in patients with van Buchem disease. J. Med. Genet. 39 (2), 91–97.

Banziger, C., Soldini, D., Schutt, C., Zipperlen, P., Hausmann, G., Basler, K., 2006. Wntless, a conserved membrane protein dedicated to the secretion of wnt proteins from signaling cells. Cell 125, 509–522.

Bao, Q., Chen, S., Qin, H., Feng, J., Liu, H., Liu, D., Li, A., Shen, Y., Zhong, X., Li, J., Zong, Z., 2017. Constitutive beta-catenin activation in osteoblasts impairs terminal osteoblast differentiation and bone quality. Exp. Cell Res. 350 (1), 123–131.

Barker, N., Hurlstone, A., Musisi, H., Miles, A., Bienz, M., Clevers, H., 2001. The chromatin remodelling factor Brg-1 interacts with β-catenin to promote target gene activation. EMBO J. 20, 4935–4943.

Baron, R., Kneissel, M., 2013. WNT signaling in bone homeostasis and disease: from human mutations to treatments. Nat. Med. 19 (2), 179–192.

Baron, R., Rawadi, G., 2007. Targeting the wnt/β-catenin pathway to regulate bone formation in the adult skeleton. Endocrinology 148 (6), 2635–2643.

Bartscherer, K., Pelte, N., Ingelfinger, D., Boutros, M., 2006. Secretion of wnt ligands requires Evi, a conserved transmembrane protein. Cell 125, 523–533.

Behrens, J., Jerchow, B.A., Wurtele, M., Grimm, J., Asbrand, C., Wirtz, R., Kuhl, M., Wedlich, D., Birchmeier, W., 1998. Functional interaction of an axin homolog, conductin, with β-catenin, APC and GSK3β. Science 280, 596–599.

Bejsovec, A., 2005. Wnt pathway activation: new relations and locations. Cell 120, 11–14.

Bellido, T., Ali, A.A., Gubrij, I., Plotkin, L.I., Fu, Q., O'Brien, C.A., Manolagas, S.C., Jilka, R.L., 2005. Chronic elevation of parathyroid hormone in mice reduces expression of sclerostin by osteocytes: a novel mechanism for hormonal control of osteoblastogenesis. Endocrinology 146 (11), 4577–4583.

Bennett, C.N., Longo, K.A., Wright, W.S., Suva, L.J., Lane, T.F., Hankenson, K.D., MacDougald, O.A., 2005. Regulation of osteoblastogenesis and bone mass by Wnt10b. Proc. Natl. Acad. Sci. U. S. A. 102 (9), 3324–3329.

Bex, F., Green, p., Marsolf, J., Babij, P., Yaworsky, P., Kharode, Y., 2003. The human LRP5 G171V mutation in mice alters the skeletal response to limb unloading but not to ovariectomy. J. Bone Miner. Res. 18 (Suppl. 2), S60.

Bhanot, P., Brink, M., Harryman Samos, C., Hsieh, J.C., Wang, Y.S., Macke, J.P., Andrew, D., Nathans, J., Nusse, R., 1996. A new member of the frizzled family from *Drosophila* functions as a wingless receptor. Nature 382 (6588), 225–230.

Bodine, P.V.N., Kharode, Y.P., Seestaller-Wehr, L., Green, P., Milligan, C., Bex, F.J., 2004a. The bone anabolic effects of parathyroid hormone (PTH) are Blunted by deletion of the wnt antagonist secreted frizzled-related protein (sFRP)-1. J. Bone Miner. Res. 19 (Suppl. 1), S17 (abstract 1063).

Bodine, P.V.N., Zhao, W., Kharode, Y.P., Bex, F.J., Lambert, A.-J., Goad, M.B., Gaur, T., Stein, G.S., Lian, J.B., Komm, B.S., 2004b. The wnt antagonist secreted frizzled-related protein-1 is a negative regulator of trabecular bone formation in adult mice. Mol. Endocrinol. 18, 1222–1237.

Bodine, P.V., Stauffer, B., Ponce-de-Leon, H., Bhat, R.A., Mangine, A., Seestaller-Wehr, L.M., Moran, R.A., Billiard, J., Fukayama, S., Komm, B.S., Pitts, K., Krishnamurthy, G., Gopalsamy, A., Shi, M., Kern, J.C., Commons, T.J., Woodworth, R.P., Wilson, M.A., Welmaker, G.S., Trybulski, E.J., Moore, W.J., 2009. A small molecule inhibitor of the Wnt antagonist secreted frizzled-related protein-1 stimulates bone formation. Bone 44 (6), 1063–1068.

Bonewald, L.F., Johnson, M.L., 2008. Osteocytes, mechanosensing and Wnt signaling. Bone 42 (4), 606–615.

Bostrom, K.I., Rajamannan, N.M., Towler, D.A., 2011. The regulation of valvular and vascular sclerosis by osteogenic morphogens. Circ. Res. 109 (5), 564–577.

Boyden, L.M., Mao, J., Belsky, J., Mitzner, L., Farhi, A., Mitnick, M.A., Wu, D., Insogna, K., Lifton, R.P., 2002. High bone density due to a mutation in LDL-receptor-related protein 5. N. Engl. J. Med. 346, 1513–1521.

Brown, S.D., Twells, R.C., Hey, P.J., Cox, R.D., Levy, E.R., Soderman, A.R., Metzker, M.L., Caskey, C.T., Todd, J.A., Hess, J.F., 1998. Isolation and characterization of LRP6, a novel member of the low density lipoprotein receptor gene family. Biochem. Biophys. Res. Commun. 248, 879–888.

Brunkow, M.E., Gardner, J.C., Van-Ness, J., Paeper, B.W., Kovacevich, B.R., Proll, S., Skonier, J.E., Zhao, L., Sabo, P.J., Fu, Y., Alisch, R.S., Gillett, L., Colbert, T., Tacconi, P., Galas, D., Hamersma, H., Beighton, P., Mulligan, J., 2001. Bone dysplasia sclerosteosis results from loss of the SOST gene product, a novel cystine knot-containing protein. Am. J. Hum. Genet. 68, 577–589.

Burgers, T.A., Williams, B.O., 2013. Regulation of Wnt/beta-catenin signaling within and from osteocytes. Bone 54 (2), 244–249.

Butler, M.T., Wallingford, J.B., 2017. Planar cell polarity in development and disease. Nat. Rev. Mol. Cell Biol. 18 (6), 375–388.

Cadigan, K.M., Nusse, R., 1997. Wnt signaling: a common theme in animal development. Genes Dev. 11, 3286–3305.

Capelluto, D.G.S., Kutateladze, T.G., Habas, R., Finklestein, C.V., He, X., Overduin, M., 2002. The DIX domain targets dishevelled to actin stress fibres and vesicular membranes. Nature 419, 726–729.

Castellone, M.D., Teramoto, H., Williams, B.O., Druey, K.M., Gutkind, J.S., 2005. Prostaglandin E_2 promotes colon cancer cell growth through a G_s-axin-β-catenin signaling Axis. Science 310, 1504–1510.

Cavallo, R.A., Cox, R.T., Moline, M.M., Roose, J., Polevoy, G.A., Clevers, H., Peifer, M., Bejsovec, A., 1998. *Drosophila* Tcf and Groucho interact to repress wingless signalling activity. Nature 395, 604–608.

Chang, M.K., Kramer, I., Huber, T., Kinzel, B., Guth-Gundel, S., Leupin, O., Kneissel, M., 2014. Disruption of Lrp4 function by genetic deletion or pharmacological blockade increases bone mass and serum sclerostin levels. Proc. Natl. Acad. Sci. U. S. A. 111 (48), E5187–E5195.

Chen, W.J., Goldstein, J.L., Brown, M.S., 1990. NPXY, a sequence often found in cytoplasmic tails, is required for coated pit-mediated internalization of the low density lipoprotein receptor. J. Biol. Chem. 265, 3116–3123.

Chen, G., Fernandez, J., Mische, S., Courey, A.J., 1999. A functional interaction between the histone deacetylase Rpd3 and the corepressor Groucho in Drosophila development. Genes Dev. 13, 2218–2230.

Chen, A.E., Ginty, D.B., Fan, C.-M., 2005. Protein kinase a signalling via CREB controls myogenesis induced by wnt proteins. Nature 433, 317–322.

Chen, J., Tu, X., Esen, E., Joeng, K.S., Lin, C., Arbeit, J.M., Ruegg, M.A., Hall, M.N., Ma, L., Long, F., 2014. WNT7B promotes bone formation in part through mTORC1. PLoS Genet. 10 (1), e1004145.

Cho, Y.D., Kim, W.J., Yoon, W.J., Woo, K.M., Baek, J.H., Lee, G., Kim, G.S., Ryoo, H.M., 2012. Wnt3a stimulates Mepe, matrix extracellular phosphoglycoprotein, expression directly by the activation of the canonical Wnt signaling pathway and indirectly through the stimulation of autocrine Bmp-2 expression. J. Cell. Physiol. 227 (6), 2287–2296.

Chouinard, L., Felx, M., Mellal, N., Varela, A., Mann, P., Jolette, J., Samadfam, R., Smith, S.Y., Locher, K., Buntich, S., Ominsky, M.S., Pyrah, I., Boyce, R.W., 2016. Carcinogenicity risk assessment of romosozumab: a review of scientific weight-of-evidence and findings in a rat lifetime pharmacology study. Regul. Toxicol. Pharmacol. 81, 212–222.

Church, V., Nohno, T., Linker, C., Marcelle, C., Francis-West, P., 2002. Wnt regulation of chondrocyte differentiation. J. Cell Sci. 115 (Pt 24), 4809–4818.

Clement-Lacroix, P., Ai, M., Morvan, F., Roman-Roman, S., Vayssiere, B., Belleville, C., Estrera, K., Warman, M.L., Baron, R., Rawadi, G., 2005. Lrp5-independent activation of wnt signaling by lithium chloride increases bone formation and bone mass in mice. Proc. Natl. Acad. Sci. U.S.A. 102, 17406–17411.

Cook, D., Fry, M.J., Hughes, K., Sumathipala, R., Woodgett, J.R., Dale, T.C., 1996. Wingless inactivates glycogen synthase kinase-3 via an intracellular signalling pathway which involves a protein kinase C. EMBO J. 15, 4526–4536.

Cosman, F., Crittenden, D.B., Adachi, J.D., Binkley, N., Czerwinski, E., Ferrari, S., Hofbauer, L.C., Lau, E., Lewiecki, E.M., Miyauchi, A., Zerbini, C.A., Milmont, C.E., Chen, L., Maddox, J., Meisner, P.D., Libanati, C., Grauer, A., 2016a. Romosozumab treatment in postmenopausal women with osteoporosis. N. Engl. J. Med. 375 (16), 1532–1543.

Cosman, F., Gilchrist, N., McClung, M., Foldes, J., de Villiers, T., Santora, A., Leung, A., Samanta, S., Heyden, N., McGinnis 2nd, J.P., Rosenberg, E., Denker, A.E., 2016b. A phase 2 study of MK-5442, a calcium-sensing receptor antagonist, in postmenopausal women with osteoporosis after long-term use of oral bisphosphonates. Osteoporos. Int. 27 (1), 377–386.

Cullen, D.M., Akhter, M.P., Johnson, M.L., Morgan, S., Recker, R.R., 2004. Ulna loading response altered by the HBM mutation. J. Bone Miner. Res. 19 (Suppl. 1), S396 (abstract M217).

Datta, S.R., Brunet, A., Greenberg, M.E., 1999. Cellular survival: a play in three Akts. Genes Dev. 13, 2905–2927.

Delcommenne, M., Tan, C., Gray, V., Rue, L., Woodgett, J., Dedhar, S., 1998. Phosphoinositide-3-OH kinase-dependent regulation of glycogen synthase kinase 3 and protein kinase B/AKT by the integrin-linked kinase. Proc. Natl. Acad. Sci. U.S.A. 95, 11211–11216.

Delgado-Calle, J., Tu, X., Pacheco-Costa, R., McAndrews, K., Edwards, R., Pellegrini, G.G., Kuhlenschmidt, K., Olivos, N., Robling, A., Peacock, M., Plotkin, L.I., Bellido, T., 2017. Control of bone anabolism in response to mechanical loading and PTH by distinct mechanisms downstream of the PTH receptor. J. Bone Miner. Res. 32 (3), 522–535.

Dong, Y., Lathrop, W., Weaver, D., Qiu, Q., Cini, J., Bertolini, D., Chen, D., 1998. Molecular cloning and characterization of LR3, a novel LDL receptor family protein with mitogenic activity. Biochem. Biophys. Res. Commun. 251, 784–790.

Ducy, P., Zhang, R., Geoffroy, V., Ridall, A.L., Karsenty, G., 1997. Osf2/Cbfa1: a transcriptional activator of osteoblast differentiation. Cell 89 (5), 747–754.

Dunphy, J.T., Linder, M.E., 1998. Signalling functions of protein palmitoylation. Biochim. Biophys. Acta 1436, 245–261.

Eijken, M., Meijer, I.M., Westbroek, I., Koedam, M., Chiba, H., Uitterlinden, A.G., Pols, H.A., van Leeuwen, J.P., 2008. Wnt signaling acts and is regulated in a human osteoblast differentiation dependent manner. J. Cell. Biochem. 104 (2), 568–579.

Ellies, D.L., Viviano, B., McCarthy, J., Rey, J.-P., Itasaki, N., Saunders, S., Krumlauf, R., 2006. Bone density ligand, sclerostin, directly interacts with LRP5 but not LRP5^{G171V} to modulate wnt activity. J. Bone Miner. Res. 21, 1738–1749.

Esen, E., Chen, J., Karner, C.M., Okunade, A.L., Patterson, B.W., Long, F., 2013. WNT-LRP5 signaling induces Warburg effect through mTORC2 activation during osteoblast differentiation. Cell Metabol. 17 (5), 745–755.

Essers, M.A.G., de Vries-Smits, L.M.M., Barker, N., Polderman, P.E., Burgering, B.M.T., Korswagen, H.C., 2005. Functional interactional between β-catenin and FOXO in oxidative stress signaling. Science 308, 1181–1184.

Fagotto, F., Jho, E., Zeng, L., Kurth, T., Joos, T., Kaufmann, C., Costantini, F., 1999. Domains of axin involved in protein-protein interactions, wnt pathway inhibiiton, and intracellular localization. J. Cell Biol. 145, 741–756.

Fang, X., Yu, S.X., Lu, Y., Bast, R.C., Woodgett, J.R., Mills, G.B., 2000. Phosphorylation and inactivation of glycogen synthase kinase 3 by protein kinase A. Proc. Natl. Acad. Sci. U.S.A. 97, 11960–11965.

Farr, G.H., Ferkey, D.M., Yost, C., Pierce, S.B., Weaver, C., Kimelman, D., 2000. Interaction among GSK-3, GBP, axin, and APC in *Xenopus* Axis specification. J. Cell Biol. 148, 691–701.

Figueroa, D.J., Hess, J.F., Ky, B., Brown, S.D., Sandig, V., Hermanowski-Vosatka, A., Twells, R.C., Todd, J.A., Austin, C.P., 2000. Expression of the type I diabetes-associated gene LRP5 in macrophages, vitamin A system cells, and the islets of langerhans suggests multiple potential roles in diabetes. J. Histochem. Cytochem. 48, 1357–1368.

Florio, M., Gunasekaran, K., Stolina, M., Li, X., Liu, L., Tipton, B., Salimi-Moosavi, H., Asuncion, F.J., Li, C., Sun, B., Tan, H.L., Zhang, L., Han, C.Y., Case, R., Duguay, A.N., Grisanti, M., Stevens, J., Pretorius, J.K., Pacheco, E., Jones, H., Chen, Q., Soriano, B.D., Wen, J., Heron, B., Jacobsen, F.W., Brisan, E., Richards, W.G., Ke, H.Z., Ominsky, M.S., 2016. A bispecific antibody targeting sclerostin and DKK-1 promotes bone mass accrual and fracture repair. Nat. Commun. 7, 11505.

Forde, J.E., Dale, T.C., 2007. Glycogen synthase kinase 3: a key regulator of cellular fate. Cell. Mol. Life Sci. 64 (15), 1930−1944.

Frey, J.L., Kim, S.P., Li, Z., Wolfgang, M.J., Riddle, R.C., 2018. beta-catenin directs long-chain fatty acid catabolism in the osteoblasts of male mice. Endocrinology 159 (1), 272−284.

Fukumoto, S., Hsieh, C.-M., Maemura, K., Layne, M.D., Yet, S.-F., Lee, K.-H., Matsui, T., Rosenzweig, A., Taylor, W.G., Rubin, J.S., Perrella, M.A., Lee, M.-E., 2001. Akt participation in the wnt signaling pathway through dishevelled. J. Biol. Chem. 276, 17479−17483.

Gao, Z.-H., Seeling, J.M., Hill, V., Yochum, A., Virshup, D.M., 2002. Casein kinase I phosphorylates and destabilizes the β-catenin degradation complex. Proc. Natl. Acad. Sci. U.S.A. 99, 1182−1187.

Gaur, T., Lengner, C.J., Hovhannisyan, H., Bhat, R.A., Bodine, P.V.N., Komm, B.S., Javed, A., van Wijnen, A.J., Stein, J.L., Stein, G.S., Lian, J.B., 2005. Canonical wnt signaling promotes osteogensis by directly stimulating *Runx2* gene expression. J. Biol. Chem. 280, 33132−33140.

Gaur, T., Rich, L., Lengner, C.J., Hussain, S., Trevant, B., Ayers, D., Stein, J.L., Bodine, P.V.N., Komm, B.S., Stein, G.S., Lian, J.B., 2006. Secreted frizzled related protein 1 regulates wnt signaling for BMP2 induced chondrocyte differentiation. J. Cell. Physiol. 208, 87−96.

Glantschnig, H., Hampton, R.A., Lu, P., Zhao, J.Z., Vitelli, S., Huang, L., Haytko, P., Cusick, T., Ireland, C., Jarantow, S.W., Ernst, R., Wei, N., Nantermet, P., Scott, K.R., Fisher, J.E., Talamo, F., Orsatti, L., Reszka, A.A., Sandhu, P., Kimmel, D., Flores, O., Strohl, W., An, Z., Wang, F., 2010. Generation and selection of novel fully human monoclonal antibodies that neutralize Dickkopf-1 (DKK1) inhibitory function in vitro and increase bone mass in vivo. J. Biol. Chem. 285 (51), 40135−40147.

Glass, D.A., Bialek, P., Ahn, J.D., Starbuck, M., Patel, M.S., Clevers, H., Taketo, M.M., Long, F., McMahon, A.P., Lang, R.A., Karsenty, G., 2005. Canonical wnt signaling in differentiated osteoblasts controls osteoclast differentiation. Dev. Cell 8, 751−764.

Goggolidou, P., Wilson, P.D., 2016. Novel biomarkers in kidney disease: roles for cilia, Wnt signalling and ATMIN in polycystic kidney disease. Biochem. Soc. Trans. 44 (6), 1745−1751.

Gong, Y., Slee, R.B., Fukai, N., Rawadi, G., Roman-Roman, S., Reginato, A.M., Wang, H., Cundy, T., Glorieux, F.H., Lev, D., Zacharin, M., Oexle, K., Marcelino, J., Suwairi, W., Heeger, S., Sabatakos, G., Apte, S., Adkins, W.N., Allgrove, J., Arsian-Kirchner, M., Batch, J.A., Beighton, P., Black, G.C.M., Boles, R.G., Boon, L.M., Borrone, C., Brunner, H.G., Carle, G.F., Dallapiccola, B., De Paepa, A., Floege, B., Halfide, M.L., Hall, B., Hennekam, R.C., Hirose, T., Jans, A., Juppner, H., Kim, C.A., Keppler-Noreuil, K., Kohlschuetter, A., LaCombe, D., Lambert, M., Lemyre, E., Letteboer, T., Peltonen, L., Ramesar, R.S., Romanengo, M., Somer, H., Steichen-Gersdorf, E., Steinmann, B., Sullivan, B., Superta-Furga, A., Swoboda, W., van den Boogaard, M.-J., Van Hul, W., Vikkula, M., Votruba, M., Zabel, B., Garcia, T., Baron, R., Olsen, B.R., Warman, M.L., 2001. LDL receptor-related protein 5 (LRP5) affects bone accrual and eye development. Cell 107, 513−523.

Gonzalez-Sancho, J.M., Brennan, K.R., Castelo-Soccio, L.A., Brown, A.M., 2004. Wnt proteins induce dishevelled phosporylation via an LRP5/6 independent mechanism, irrespective of their ability to stabilize β-catenin. Mol. Cell Biol. 24, 4757−4768.

Haq, S., Choukroun, G., Kang, Z.B., Ranu, H., Matsui, T., Rosenzweig, A., Molkentin, J.D., Alessandrini, A., Woodgett, J., Hajjar, R., Michael, A., Force, T., 2000. Glycogen synthase kinase-3β is a negative rgulator of cardiomyocyte hypertrophy. J. Cell Biol. 151, 117−130.

Hardt, S.E., Sadoshima, J., 2002. Glycogen synthase kinase-3b: a novel regulator of cardiac hypertrophy and development. Circ. Res. 90, 1055−1063.

Hart, M.J., de los Santos, R., Albert, I.N., Rubinfeld, B., Polakis, P., 1998. Downregulation of β-catenin by HUman axin and its association with the APC tumor suppressor, β-catenin. Curr. Biol. 8, 573−581.

Hartmann, C., 2006. A Wnt canon orchestrating osteoblastogenesis. Trends Cell Biol. 16 (3), 151−158.

Hartmann, C., Tabin, C.J., 2000. Dual roles of Wnt signaling during chondrogenesis in the chicken limb. Development 127 (14), 3141−3159.

Hassan, M.Q., Maeda, Y., Taipaleenmaki, H., Zhang, W., Jafferji, M., Gordon, J.A., Li, Z., Croce, C.M., van Wijnen, A.J., Stein, J.L., Stein, G.S., Lian, J.B., 2012. miR-218 directs a Wnt signaling circuit to promote differentiation of osteoblasts and osteomimicry of metastatic cancer cells. J. Biol. Chem. 287 (50), 42084−42092.

Hausler, K.D., Horwood, N.J., Uren, A., Ellis, J., Lengel, C., Martin, T.J., Rubin, J.S., Gillespie, M.T., 2001. Secreted frizzled-related protein (sFRP-1) binds to RANKL to inhibit osteoclast formation. J. Bone Miner. Res. 16, S153.

Haxaire, C., Hay, E., Geoffroy, V., 2016. Runx2 controls bone resorption through the down-regulation of the wnt pathway in osteoblasts. Am. J. Pathol. 186 (6), 1598−1609.

He, X., Semenov, M., Tamai, K., Zeng, X., 2004a. LDL receptor-related proteins 5 and 6 in wnt/β-catenin signaling: arrows points the way. Development 131 (8), 1663−1677.

He, X.C., Zhang, J., Tong, W.-G., Tawfik, O., Ross, J., Scoville, D.H., Tian, Q., Zeng, X., He, X., Wiedemann, L.M., Mishinia, Y., Li, L., 2004b. BMP signaling inhibits intestinal stem cell self-renewal through suppression of wnt-β-catenin signaling. Nat. Genet. 36, 1117−1121.

Hecht, A., Vleminckx, K., Stemmler, M.P., van Roy, F., Kemler, R., 2000. The p300/CBP acetyltransferases function as transcriptional coactivators of β-catenin in vertebrates. EMBO J. 19, 1839−1850.

Heilmann, A., Schinke, T., Bindl, R., Wehner, T., Rapp, A., Haffner-Luntzer, M., Nemitz, C., Liedert, A., Amling, M., Ignatius, A., 2013. The Wnt serpentine receptor Frizzled-9 regulates new bone formation in fracture healing. PLoS One 8 (12), e84232.

Hermida, M.A., Dinesh Kumar, J., Leslie, N.R., 2017. GSK3 and its interactions with the PI3K/AKT/mTOR signalling network. Adv. Biol. Regul. 65, 5−15.

Hey, P.J., Twells, R.C., Phillips, M.S., Yusuke, N., Brown, S.D., Kawaguchi, Y., Cox, R., Guochun, X., Dugan, V., Hammond, H., Metzker, M.L., Todd, J.A., Hess, J.F., 1998. Cloning of a novel member of the low-density lipoprotein receptor family. Gene 216, 103−111.

Hill, T.P., Spater, D., Taketo, M.M., Birchmeier, W., Hartmann, C., 2005. Canonical wnt/β-catenin signaling prevents osteoblasts from differentiating into chondrocytes. Dev. Cell 8, 727−738.

Holmen, S.L., Salic, A., Zylstra, C.R., Kirschner, M.W., Williams, B.O., 2002. A novel set of wnt-frizzled fusion proteins identifies receptor components that activate β-catenin-dependent signaling. J. Biol. Chem. 277, 34727−34735.

Holmen, S.L., Giambernardi, T.A., Zylstra, C.R., Buckner-Berghuis, B.D., Resau, J.H., Hess, J.F., Glatt, V., Bouxsein, M.L., Ai, M., Warman, M.L., Williams, B.O., 2004. Decreased BMD and limb deformities in mice carrying mutations in both Lrp5 and Lrp6. J. Bone Miner. Res. 19, 2033−2040.

Holmen, S.L., Robertson, S.A., Zylstra, C.R., Williams, B.O., 2005a. Wnt-independent activation of b-catenin mediated by a dkk-fz5 fusion protein. Biochem. Biophys. Res. Commun. 328, 533−539.

Holmen, S.L., Zylstra, C.R., Mukherjee, A., Sigler, R.E., Faugere, M.C., Bouxsein, M.L., Deng, L., Clemens, T.L., Williams, B.O., 2005b. Essential role of beta-catenin in postnatal bone acquisition. J. Biol. Chem. 280 (22), 21162−21168.

Hsu, W., Zeng, L., Costantini, F., 1999. Identification of a domain of axin that binds to the serine/threonine protein phosphatase 2A and a self-binding domain. J. Biol. Chem. 274, 3439−3445.

Hu, W., Ye, Y., Zhang, W., Wang, J., Chen, A., Guo, F., 2013. miR1423p promotes osteoblast differentiation by modulating Wnt signaling. Mol. Med. Rep. 7 (2), 689−693.

Huang, Y.L., Anvarian, Z., Doderlein, G., Acebron, S.P., Niehrs, C., 2015. Maternal Wnt/STOP signaling promotes cell division during early Xenopus embryogenesis. Proc. Natl. Acad. Sci. U. S. A. 112 (18), 5732−5737.

Hwang, S.G., Yu, S.S., Lee, S.W., Chun, J.S., 2005. Wnt-3a regulates chondrocyte differentiation via c-Jun/AP-1 pathway. FEBS Lett. 579 (21), 4837−4842.

Ikeda, S., Kishida, S., Yamamoto, H., Murai, H., Koyama, S., Kikuchi, A., 1998. Axin, a negative regulator of the wnt signaling pathway, forms a complex with GSK-3β and β-catenin and promotes GSK-3β-dependent phosphorylation of β-catenin. EMBO J. 17 (5), 1371−1384.

Inoki, K., Ouyang, H., Zhu, T., Lindvall, C., Wang, Y., Zhang, X., Yang, Q., Bennett, C., Harada, Y., Stankunas, K., Wang, C.Y., He, X., MacDougald, O.A., You, M., Williams, B.O., Guan, K.L., 2006. TSC2 integrates Wnt and energy signals via a coordinated phosphorylation by AMPK and GSK3 to regulate cell growth. Cell 126 (5), 955−968.

Ishibashi, H., Crittenden, D.B., Miyauchi, A., Libanati, C., Maddox, J., Fan, M., Chen, L., Grauer, A., 2017. Romosozumab increases bone mineral density in postmenopausal Japanese women with osteoporosis: a phase 2 study. Bone 103, 209−215.

Ishitani, T., Ninomiya-Tsuji, J., Matsumoto, K., 2003. Regulation of lymphoid enhancer factor/T-cell factor by mitogen-activated protein kinase-related nemo-like kinase dependent phosphorylation in wnt/β-catenin signaling. Mol. Cell Biol. 23, 1379−1389.

Itoh, K., Krupnick, V.E., Sokol, S.Y., 1998. Axis determination in Xenopus involves biochemical interactions of axin, glycogen synthase kinase 3 and β-catenin. Curr. Biol. 8, 591−598.

Iwaniec, U.T., Liu, G., Arzaga, R.R., Donovan, L.M., Brommage, R., Wronski, T.J., 2004. Lrp5 is not essential for the stimulatory effect of PTH on bone formation in mice. J. Bone Miner. Res. 19 (Suppl. 1), S18 (abstract 1064).

Janda, C.Y., Waghray, D., Levin, A.M., Thomas, C., Garcia, K.C., 2012. Structural basis of wnt recognition by frizzled. Science 337 (6090), 59−64.

Janssens, N., Janicot, M., Perera, T., 2006. The wnt-dependent signaling pathways as targets in oncology drug discovery. Investig. New Drugs 24 (4), 263−280.

Javaheri, B., Stern, A.R., Lara, N., Dallas, M., Zhao, H., Liu, Y., Bonewald, L.F., Johnson, M.L., 2014. Deletion of a single beta-catenin allele in osteocytes abolishes the bone anabolic response to loading. J. Bone Miner. Res. 29 (3), 705−715.

Jho, E., Lomvardas, S., Costanti, F., 1999. A GSK3beta phosphorylation site in axin modulates interaction with beta-catenin and tcf-mediated gene expression. Biochem. Biophys. Res. Commun. 266, 28−35.

Jho, E.-h., Zhang, T., Domon, C., Joo, C.-K., Freund, J.-N., Costantini, F., 2002. Wnt/β-Catenin/Tcf signaling induces the transcription of Axin2, a negative regulator of the signaling pathway. Mol. Cell Biol. 22, 1172−1183.

Jia, J., Yao, W., Guan, M., Dai, W., Shahnazari, M., Kar, R., Bonewald, L., Jiang, J.X., Lane, N.E., 2011. Glucocorticoid dose determines osteocyte cell fate. FASEB J. 25 (10), 3366−3376.

Jiang, Z., Von den Hoff, J.W., Torensma, R., Meng, L., Bian, Z., 2014. Wnt16 is involved in intramembranous ossification and suppresses osteoblast differentiation through the Wnt/beta-catenin pathway. J. Cell. Physiol. 229 (3), 384−392.

Jimeno, A., Gordon, M., Chugh, R., Messersmith, W., Mendelson, D., Dupont, J., Stagg, R., Kapoun, A.M., Xu, L., Uttamsingh, S., Brachmann, R.K., Smith, D.C., 2017. A first-in-human phase I study of the anticancer stem cell agent ipafricept (OMP-54F28), a decoy receptor for wnt ligands, in patients with advanced solid tumors. Clin. Cancer Res. 23 (24), 7490−7497.

Joeng, K.S., Schumacher, C.A., Zylstra-Diegel, C.R., Long, F., Williams, B.O., 2011. Lrp5 and Lrp6 redundantly control skeletal development in the mouse embryo. Dev. Biol. 359 (2), 222−229.

Johnson, M.L., Rajamannan, N.M., 2006. Diseases of wnt signaling. Rev. Endocr. Metab. Disord. 7, 41−49.

Johnson, M.L., Recker, R.R., 2017. Exploiting the WNT signaling pathway for clinical purposes. Curr. Osteoporos. Rep. 15 (3), 153−161.

Johnson, M.L., Summerfield, D.T., 2005. Parameters of LRP5 from a structural and molecular perspective. Crit. Rev. Eukaryot. Gene Expr. 15, 229−242.

Johnson, M.L., Gong, G., Kimberling, W.J., Recker, S.M., Kimmel, D.K., Recker, R.R., 1997. Linkage of a gene causing high bone mass to human chromosome 11 (11q12-13). Am. J. Hum. Genet. 60, 1326−1332.

Johnson, M.L., Picconi, J.L., Recker, R.R., 2002. The gene for high bone mass. Endocrinololgist 12, 445−453.

Kadowaki, T., Wilder, E., Klingensmith, J., Zachary, K., Perrimon, N., 1996. The segment polarity gene porcupine encodes a putative multitransmembrane protein involved in wingless processing. Genes Dev. 10 (24), 3116−3128.

Kamel, M.A., Holladay, B.R., Johnson, M.L., 2006. Potential interaction of prostaglandin and wnt signaling pathways mediating bone cell responses to fluid flow. J. Bone Miner. Res. 21 (Suppl. 1), S92 (abs F166).

Kamel, M.A., Picconi, J.L., Lara-Castillo, N., Johnson, M.L., 2010. Activation of beta-catenin signaling in MLO-Y4 osteocytic cells versus 2T3 osteoblastic cells by fluid flow shear stress and PGE2: implications for the study of mechanosensation in bone. Bone 47 (5), 872−881.

Kandel, E.S., Hay, N., 1999. The regulation and activities of the multifuncitonal serine/threonin kinase Akt/PKB. Exp. Cell Res. 253, 210−229.

Kang, K.S., Hong, J.M., Robling, A.G., 2016. Postnatal beta-catenin deletion from Dmp1-expressing osteocytes/osteoblasts reduces structural adaptation to loading, but not periosteal load-induced bone formation. Bone 88, 138−145.

Kapinas, K., Kessler, C.B., Delany, A.M., 2009. miR-29 suppression of osteonectin in osteoblasts: regulation during differentiation and by canonical Wnt signaling. J. Cell. Biochem. 108 (1), 216−224.

Kapinas, K., Kessler, C., Ricks, T., Gronowicz, G., Delany, A.M., 2010. miR-29 modulates Wnt signaling in human osteoblasts through a positive feedback loop. J. Biol. Chem. 285 (33), 25221−25231.

Karasik, D., Rivadeneira, F., Johnson, M.L., 2016. The genetics of bone mass and susceptibility to bone diseases. Nat. Rev. Rheumatol. 12 (6), 323−334.

Karner, C.M., Long, F., 2017. Wnt signaling and cellular metabolism in osteoblasts, 74 (9), 1649−1657.

Karner, C.M., Esen, E., Okunade, A.L., Patterson, B.W., Long, F., 2015. Increased glutamine catabolism mediates bone anabolism in response to WNT signaling. J. Clin. Investig. 125 (2), 551−562.

Katanaev, V.L., Ponzielli, R., Semeriva, M., Tomlinson, A., 2005. Trimeric G protein-dependent frizzled signaling in *Drosophila*. Cell 120, 111−122.

Kato, M., Patel, M.S., Levasseur, R., Lobov, I., Chang, B.H.-J., Glass, D.A., Hartmann, C., Li, L., Hwang, T.H., Brayton, C.F., Lang, R.A., Karsenty, G., Chan, L., 2002. Cbfa 1-independent decrease in osteoblast proliferation, osteopenia, and persistent embryonic eye vascularization in mice deficient in Lrp5, a wnt coreceptor. J. Cell Biol. 157, 303−314.

Katoh, M., 2005. Wnt/PCP signaling pathway and human cancer. Oncol. Rep. 14, 1583−1588.

Kedlaya, R., Kang, K.S., Hong, J.M., Bettagere, V., Lim, K.E., Horan, D., Divieti-Pajevic, P., Robling, A.G., 2016. Adult-onset deletion of beta-catenin in (10kb)dmp1-expressing cells prevents intermittent PTH-induced bone gain. Endocrinology 157 (8), 3047−3057.

Keller, H., Kneissel, M., 2005. SOST is a target gene for PTH in bone. Bone 37 (2), 148−158.

Kim, D.H., Inagaki, Y., Suzuki, T., Ioka, R.X., Yoshioka, S.Z., Magoori, K., Kang, M.J., Cho, Y., Nakano, A.Z., Liu, Q., Fujino, T., Suzuki, H., Sasano, H., Yamamoto, T.T., 1998. A new low density lipoprotein receptor related protein, LRP5, is expressed in hepatocytes and adrenal cortex, and recognizes apolipoprotein E. Eur. J. Biochem. 124, 1072−1076.

Kitase, Y., Barragan, L., Qing, H., Kondoh, S., Jiang, J.X., Johnson, M.L., Bonewald, L.F., 2010. Mechanical induction of PGE2 in osteocytes blocks glucocorticoid-induced apoptosis through both the beta-catenin and PKA pathways. J. Bone Miner. Res. 25 (12), 2657−2668.

Kobayashi, Y., Thirukonda, G.J., Nakamura, Y., Koide, M., Yamashita, T., Uehara, S., Kato, H., Udagawa, N., Takahashi, N., 2015a. Wnt16 regulates osteoclast differentiation in conjunction with Wnt5a. Biochem. Biophys. Res. Commun. 463 (4), 1278−1283.

Kobayashi, Y., Uehara, S., Koide, M., Takahashi, N., 2015b. The regulation of osteoclast differentiation by Wnt signals. Bonekey Rep. 4, 713.

Kobayashi, Y., Uehara, S., Udagawa, N., Takahashi, N., 2016. Regulation of bone metabolism by Wnt signals. J. Biochem. 159 (4), 387−392.

Koch, S., Acebron, S.P., Herbst, J., Hatiboglu, G., Niehrs, C., 2015. Post-transcriptional wnt signaling governs epididymal sperm maturation. Cell 163 (5), 1225−1236.

Kokubu, C., Heinzmann, U., Kokubu, T., Sakai, N., Kubota, N., Kawai, M., Wahl, M.B., Galceran, J., Grosschedt, R., Ozono, K., Imai, K., 2004. Skeletal defects in *ringelshwanz* mutant mice reveal that Lrp6 is required for proper somitogenesis and osteogenesis. Development 131, 5469−5480.

Komori, T., Yagi, H., Nomura, S., Yamaguchi, A., Sasaki, K., Deguchi, K., Shimizu, Y., Bronson, R.T., Gao, Y.H., Inada, M., Sato, M., Okamoto, R., Kitamura, Y., Yoshiki, S., Kishimoto, T., 1997. Targeted disruption of Cbfa1 results in a complete lack of bone formation owing to maturational arrest of osteoblasts. Cell 89 (5), 755−764.

Kong, Y.Y., Yoshida, H., Sarosi, I., Tan, H.L., Timms, E., Capparelli, C., Morony, S., Oliveira-dos-Santos, A.J., Van, G., Itie, A., Khoo, W., Wakeham, A., Dunstan, C.R., Lacey, D.L., Mak, T.W., Boyle, W.J., Penninger, J.M., 1999. OPGL is a key regulator of osteoclastogenesis, lymphocyte development and lymph-node organogenesis. Nature 397 (6717), 315−323.

Korinek, V., Barker, N., Morin, P.J., van Wichen, D., de Weger, R., Kinzler, K.W., Vogelstein, B., Clevers, H., 1997. Constitutive transcriptional activation by a β-catenin-tcf complex in $APC^{-/-}$ colon carcinoma. Science 275, 1784−1787.

Kousmenko, A.P., Takeyama, K., Ito, S., Furutani, T., Sawatsubashi, S., Maki, A., Suzuki, E., Kawasaki, Y., Akiyama, T., Tabata, T., Kato, S., 2004. Wnt/β-catenin and estrogen signaling converge *in vivo*. J. Biol. Chem. 279, 40255−40258.

Kousteni, S., Almeida, M., Han, L., Bellido, T., Jilka, R.L., Manolagas, S., 2007. Induction of osteoblast differentiation by selective activation of kinase-mediated actions of the estrogen receptor. Mol. Cell Biol. 27, 1516−1530.

Kramer, I., Halleux, C., Keller, H., Pegurri, M., Gooi, J.H., Weber, P.B., Feng, J.Q., Bonewald, L.F., Kneissel, M., 2010. Osteocyte Wnt/beta-catenin signaling is required for normal bone homeostasis. Mol. Cell Biol. 30 (12), 3071−3085.

Krishnamurthy, N., Kurzrock, R., 2018. Targeting the Wnt/beta-catenin pathway in cancer: update on effectors and inhibitors. Cancer Treat Rev. 62, 50−60.

Kuhl, M., Sheldahl, L.C., Park, M., Miller, J.R., Moon, R.T., 2000. The wnt/Ca+2 pathway: a new vertebrate wnt signaling pathway takes shape. Trends Genet. 16, 279−283.

Kulkarni, N.H., Halladay, D.L., Miles, R.R., Gilbert, L.M., Frolik, C.A., Galvin, R.J.S., Martin, T.J., Gillespie, M.T., Onyia, J.E., 2005. Effects of parathyroid hormone on wnt signaling pathway in bone. J. Cell. Biochem. 95, 1178−1190.

Kulkarni, N.H., Onyia, J.E., Zeng, Q.Q., Tian, X., Liu, M., Halladay, D.L., Frolik, C.A., Engler, T., Wei, T., Kriauciunas, A., Martin, T.J., Sato, M., Bryant, H.U., Ma, Y.L., 2006. Orally Bioavailable GSK-3α/β dual inhibitor increases markers of cellular differentiation *in vitro* and bone mass *in vivo*. J. Bone Miner. Res. 21, 910−920.

Lammi, L., Arte, S., Somer, M., Jarvinen, H., Lahermo, P., Thesleff, I., Pirinen, S., Nieminen, P., 2004. Mutations in AXIN2 cause familil tooth agenesis and predispose to colorectal cancer. Am. J. Hum. Genet. 74, 1043−1050.

Langdahl, B.L., Libanati, C., Crittenden, D.B., Bolognese, M.A., Brown, J.P., Daizadeh, N.S., Dokoupilova, E., Engelke, K., Finkelstein, J.S., Genant, H.K., Goemaere, S., Hyldstrup, L., Jodar-Gimeno, E., Keaveny, T.M., Kendler, D., Lakatos, P., Maddox, J., Malouf, J., Massari, F.E., Molina, J.F., Ulla, M.R., Grauer, A., 2017. Romosozumab (sclerostin monoclonal antibody) versus teriparatide in postmenopausal women with osteoporosis transitioning from oral bisphosphonate therapy: a randomised, open-label, phase 3 trial. Lancet 390 (10102), 1585−1594.

Lara-Castillo, N., Johnson, M.L., 2015. LRP receptor family member associated bone disease. Rev. Endocr. Metab. Disord. 16 (2), 141−148.

Lara-Castillo, N., Kim-Weroha, N.A., Kamel, M.A., Javaheri, B., Ellies, D.L., Krumlauf, R.E., Thiagarajan, G., Johnson, M.L., 2015. In vivo mechanical loading rapidly activates beta-catenin signaling in osteocytes through a prostaglandin mediated mechanism. Bone 76, 58−66.

Lau, K.-H.W., Kapur, S., Kesavan, C., Baylink, D.J., 2006. Up-regulation of the wnt, estrogen receptor, insulin-like growth factor-I, and bone morphogenetic protein pathways in C57BL/6J osteoblasts as opposed to C3H/HeJ osteoblasts in Part Contributes to the differential anabolic response to fluid shear. J. Biol. Chem. 281, 9576−9588.

Lee, B., Thirunavukkarasu, K., Zhou, L., Pastore, L., Baldini, A., Hecht, J., Geoffroy, V., Ducy, P., Karsenty, G., 1997. Missense mutations abolishing DNA binding of the osteoblast-specific transcription factor OSF2/CBFA1 in cleidocranial dysplasia. Nat. Genet. 16 (3), 307−310.

Lerner, U.H., Ohlsson, C., 2015. The WNT system: background and its role in bone. J. Intern. Med. 277 (6), 630−649.

Leupin, O., Kramer, I., Collette, N.M., Loots, G.G., Natt, F., Kneissel, M., Keller, H., 2007. Control of the SOST bone enhancer by PTH using MEF2 transcription factors. J. Bone Miner. Res. 22 (12), 1957−1967.

Leupin, O., Piters, E., Halleux, C., Hu, S., Kramer, I., Morvan, F., Bouwmeester, T., Schirle, M., Bueno-Lozano, M., Fuentes, F.J., Itin, P.H., Boudin, E., de Freitas, F., Jennes, K., Brannetti, B., Charara, N., Ebersbach, H., Geisse, S., Lu, C.X., Bauer, A., Van Hul, W., Kneissel, M., 2011. Bone overgrowth-associated mutations in the LRP4 gene impair sclerostin facilitator function. J. Biol. Chem. 286 (22), 19489−19500.

Li, X., Liu, P., Liu, W., Maye, P., Zhang, J., Zhang, Y., Hurley, M., Guo, C., Boskey, A., Sun, L., Harris, S.E., Rowe, D.W., Ke, H.Z., W. D, 2005a. Dkk2 has a role in terminal osteoblast differentiation and mineralized matrix formation. Nat. Genet. 37, 945−952.

Li, X., Zhang, Y., Kang, H., Liu, W., Liu, P., Zhang, J., Harris, S.E., Wu, D., 2005b. Sclerostin binds to LRP5/6 and antagonizes canonical wnt signaling. J. Biol. Chem. 280, 19883−19887.

Li, X., Grisanti, M., Fan, W., Asuncion, F.J., Tan, H.L., Dwyer, D., Han, C.Y., Yu, L., Lee, J., Lee, E., Barrero, M., Kurimoto, P., Niu, Q.T., Geng, Z., Winters, A., Horan, T., Steavenson, S., Jacobsen, F., Chen, Q., Haldankar, R., Lavallee, J., Tipton, B., Daris, M., Sheng, J., Lu, H.S., Daris, K., Deshpande, R., Valente, E.G., Salimi-Moosavi, H., Kostenuik, P.J., Li, J., Liu, M., Li, C., Lacey, D.L., Simonet, W.S., Ke, H.Z., Babij, P., Stolina, M., Ominsky, M.S., Richards, W.G., 2011. Dickkopf-1 regulates bone formation in young growing rodents and upon traumatic injury. J. Bone Miner. Res. 26 (11), 2610−2621.

Libro, R., Bramanti, P., Mazzon, E., 2016. The role of the Wnt canonical signaling in neurodegenerative diseases. Life Sci. 158, 78−88.

Little, R.D., Carulli, J.P., Del Mastro, R.G., Dupuis, J., Osborne, M., Folz, C., Manning, S.P., Swain, P.M., Zhao, S.C., Eustace, B., Lappe, M.M., Spitzer, L., Zweier, S., Braunschweiger, K., Benchekroun, Y., Hu, X., Adair, R., Chee, L., FitzGerald, M.G., Tulig, C., Caruso, A., Tzellas, N., Bawa, A., Franklin, B., McGuire, S., Nogues, X., Gong, G., Allen, K.M., Anisowicz, A., Morales, A.J., Lomedico, P.T., Recker, S.M., Van Eerdewegh, P., Recker, R.R., Johnson, M.L., 2002. A mutation in the LDL receptor-related protein 5 gene results in the autosomal dominant high-bone-mass trait. Am. J. Hum. Genet. 70, 11−19.

Liu, C., Li, Y., Semenov, M., Han, C., Baeg, G.-H., Tan, Y., Zhang, Z., Lin, X., He, X., 2002. Control of β-catenin phosphorylation/degradation by a dual-kinase mechanism. Cell 108, 837−847.

Liu, Z., Tang, Y., Xu Cao, T.Q., Clemens, T.L., 2006. A dishevelled-1/smad-1 interaction couples WNT and bone morphogenetic protein signaling pathways in uncommitted bone marrow stromal cells. J. Biol. Chem. 281, 17156−17163.

Lodish, M., 2017. Genetics of adrenocortical development and tumors. Endocrinol Metab. Clin. N. Am. 46 (2), 419−433.

Malhotra, D., Yang, Y., 2014. Wnts' fashion statement: from body stature to dysplasia. Bonekey Rep. 3, 541.

Mani, A., Radhakrishman, J., Wang, H., Mani, A., Mani, M.-A., Nelson-Williams, C., Carew, K.S., Mane, S., Najmabadi, H., Wu, D., Lifton, R.P., 2007. LRP6 mutation in a family with early coronary disease and metabolic risk factors. Science 315, 1278−1582.

Marcellini, S., Henriquez, J.P., Bertin, A., 2012. Control of osteogenesis by the canonical Wnt and BMP pathways in vivo: cooperation and antagonism between the canonical Wnt and BMP pathways as cells differentiate from osteochondroprogenitors to osteoblasts and osteocytes. Bioessays 34 (11), 953−962.

Maupin, K.A., Droscha, C.J., Williams, B.O., 2013. A comprehensive overview of skeletal phenotypes associated with alterations in wnt/beta-catenin signaling in humans and mice. Bone Res. 1 (1), 27−71.

Maurel, D.B., Duan, P., Farr, J., Cheng, A.L., Johnson, M.L., Bonewald, L.F., 2016. Beta-catenin haplo insufficient male mice do not lose bone in response to hindlimb unloading. PLoS One 11 (7), e0158381.

McClung, M.R., 2017. Sclerostin antibodies in osteoporosis: latest evidence and therapeutic potential. Ther Adv Musculoskelet Dis 9 (10), 263−270.

McColm, J., Hu, L., Womack, T., Tang, C.C., Chiang, A.Y., 2014. Single- and multiple-dose randomized studies of blosozumab, a monoclonal antibody against sclerostin, in healthy postmenopausal women. J. Bone Miner. Res. 29 (4), 935−943.

McCrea, P.D., Turck, C.W., Gumbiner, B., 1991. A homolog of the armadillo protein in Drosophila (plakoglobin) associated with E-cadherin. Science 254, 1359−1361.

McManus, E.J., Sakamoto, K., Armit, L.J., Ronaldson, L., Shpiro, N., Marquez, R., Alessi, D.R., 2005. Role that phosphorylation of GSK3 plays in insulin and wnt signaling defined by knockin analysis. EMBO J. 24, 1571−1583.

Medina-Gomez, C., Kemp, J.P., Estrada, K., Eriksson, J., Liu, J., Reppe, S., Evans, D.M., Heppe, D.H., Vandenput, L., Herrera, L., Ring, S.M., Kruithof, C.J., Timpson, N.J., Zillikens, M.C., Olstad, O.K., Zheng, H.F., Richards, J.B., St Pourcain, B., Hofman, A., Jaddoe, V.W., Smith, G.D., Lorentzon, M., Gautvik, K.M., Uitterlinden, A.G., Brommage, R., Ohlsson, C., Tobias, J.H., Rivadeneira, F., 2012. Meta-analysis of genome-wide scans for total body BMD in children and adults reveals allelic heterogeneity and age-specific effects at the WNT16 locus. PLoS Genet. 8 (7), e1002718.

Miller, J.R., 2001. The Wnts. Genome Biol. 3 reviews 3001.3001-3001.3015.

Mlodzik, M., 2002. Planar cell polarization: do the same mechanisms regulate Drosophila tissue polarity and vertebrate gastrulation? Trends Genet. 18, 564–571.

Moon, R.T., Bowerman, B., Boutros, M., Perrimon, N., 2002. The promise and perils of wnt signaling through β-catenin. Science 296, 1644–1646.

Nakamura, T., Hamada, F., Ihidate, T., Anai, K., Kawahara, K., Toyoshima, K., Akiyama, T., 1998. Axin, an inhibitor of the wnt signalling pathway, interacts with β-catenin, GSK-3β and APC and reduces the β-catenin level. Genes Cells 3, 395–403.

Nakashima, K., Zhou, X., Kunkel, G., Zhang, Z., Deng, J.M., Behringer, R.R., de Crombrugghe, B., 2002. The novel zinc finger-containing transcription factor osterix is required for osteoblast differentiation and bone formation. Cell 108 (1), 17–29.

Nakashima, A., Katagiri, T., Tamura, M., 2005. Cross-talk between wnt and bone morphogenetic protein 2 (BMP-2) signaling in differentiation pathway of C2C12 myoblasts. J. Biol. Chem. 280, 37660–37668.

Nakashima, T., Hayashi, M., Fukunaga, T., Kurata, K., Oh-Hora, M., Feng, J.Q., Bonewald, L.F., Kodama, T., Wutz, A., Wagner, E.F., Penninger, J.M., Takayanagi, H., 2011. Evidence for osteocyte regulation of bone homeostasis through RANKL expression. Nat. Med. 17 (10), 1231–1234.

Nelson, W.J., Nusse, R., 2004. Convergence of wnt, β-catenin, and cadherin pathways. Science 303, 1483–1487.

Norvell, S.M., Alvarez, M., Bidwell, J.P., Pavalko, F.M., 2004. Fluid shear stress induces β-catenin signaling in osteoblasts. Calcif. Tissue Int. 75, 396–404.

Nusse, R., 2003. Wnts and hedgehogs: lipid-modified proteins and similarities in signaling mechanisms at the cell surface. Development 130, 5297–5305.

Nusse, R., 2005. Wnt signaling in disease and development. Cell Res. 15, 28–32.

Nusse, R., Clevers, H., 2017. Wnt/beta-Catenin signaling, disease, and emerging therapeutic modalities. Cell 169 (6), 985–999.

Nusse, R., Varmus, H.E., 1982. Many tumors induced by the mouse mammary tumor virus contain a provirus integrated in the same region of the host genome. Cell 31, 99–109.

Nusse, R., Brown, A., Papkoff, J., Scambler, P., Shackleford, G., McMahon, A., Moon, R., Varmus, H., 1991. A new nomenclature for int-1 and related genes: the Wnt gene family. Cell 64 (2), 231.

O'Brien, C.A., Nakashima, T., Takayanagi, H., 2013. Osteocyte control of osteoclastogenesis. Bone 54 (2), 258–263.

Otto, F., Thornell, A.P., Crompton, T., Denzel, A., Gilmour, K.C., Rosewell, I.R., Stamp, G.W., Beddington, R.S., Mundlos, S., Olsen, B.R., Selby, P.B., Owen, M.J., 1997. Cbfa1, a candidate gene for cleidocranial dysplasia syndrome, is essential for osteoblast differentiation and bone development. Cell 89 (5), 765–771.

Papadopoulou, D., Bianchi, M.W., Bourouis, M., 2004. Functional studies of shaggy/glycogen synthase kinase 3 phosphorylation sites in *Drosophila melanogaster*. Mol. Cell Biol. 24 (11), 4909–4919.

Pavalko, F.M., Chen, N.X., Turner, C.H., Burr, D.B., Atkinson, S., Hsieh, Y., Qui, J., Duncan, R.L., 1998. Fluid shear-induced mechanical signaling in MC3T3-E1 osteoblasts requires cytoskeleton-integrin interactions. Am. J. Physiol. 275 (C), C1591–C1601.

Perez-Campo, F.M., Santurtun, A., Garcia-Ibarbia, C., Pascual, M.A., Valero, C., Garces, C., Sanudo, C., Zarrabeitia, M.T., Riancho, J.A., 2016. Osterix and RUNX2 are transcriptional regulators of sclerostin in human bone. Calcif. Tissue Int. 99 (3), 302–309.

Peters, J.M., McKay, R.M., McKay, J.P., Graff, J.M., 1999. Casein kinase I transduces wnt signals. Nature 401, 345–350.

Pinson, K.I., Brennan, J., Monkley, S., Avery, B.J., Skarnes, W.C., 2000. An LDL-receptor-related protein mediates wnt signalling in mice. Nature 407, 535–538.

Polakis, P., 2000. Wnt signaling and cancer. Genes Dev. 14, 1837–1851.

Poole, K.E.S., van Bezooijen, R.L., Loveridge, N., Hamersma, H., Papapoulos, S.E., Lowik, C.W., Reeve, J., 2005. Sclerostin is a delayed secreted product of osteocytes that inhibits bone formation. FASEB J. 19, 1842–1844.

Povelones, M., Nusse, R., 2002. Wnt signalling sees spots. Nat. Cell Biol. 4, E249–E250.

Powell Jr., W.F., Barry, K.J., Tulum, I., Kobayashi, T., Harris, S.E., Bringhurst, F.R., Pajevic, P.D., 2011. Targeted ablation of the PTH/PTHrP receptor in osteocytes impairs bone structure and homeostatic calcemic responses. J. Endocrinol. 209 (1), 21–32.

Prunier, C., Hocevar, B.A., Howe, P.H., 2004. Wnt signaling: physiology and pathology. Growth Factors 22, 141–150.

Rawadi, G., Vayssiere, B., Dunn, F., Baron, R., Roman-Roman, S., 2003. BMP-2 controls alkaline phosphatase expression and osteoblast mineralization by a wnt autocrine loop. J. Bone Miner. Res. 18, 1842–1953.

Recker, R.R., Benson, C.T., Matsumoto, T., Bolognese, M.A., Robins, D.A., Alam, J., Chiang, A.Y., Hu, L., Krege, J.H., Sowa, H., Mitlak, B.H., Myers, S.L., 2015. A randomized, double-blind phase 2 clinical trial of blosozumab, a sclerostin antibody, in postmenopausal women with low bone mineral density. J. Bone Miner. Res. 30 (2), 216–224.

Recknor, C.P., Recker, R.R., Benson, C.T., Robins, D.A., Chiang, A.Y., Alam, J., Hu, L., Matsumoto, T., Sowa, H., Sloan, J.H., Konrad, R.J., Mitlak, B.H., Sipos, A.A., 2015. The effect of discontinuing treatment with blosozumab: follow-up results of a phase 2 randomized clinical trial in postmenopausal women with low bone mineral density. J. Bone Miner. Res. 30 (9), 1717–1725.

Reppe, S., Datta, H.K., Gautvik, K.M., 2017. Omics analysis of human bone to identify genes and molecular networks regulating skeletal remodeling in health and disease. Bone 101, 88–95.

Rey, J.P., Ellies, D.L., 2010. Wnt modulators in the biotech pipeline. Dev. Dynam. 239 (1), 102–114.

Riddle, R.C., Diegel, C.R., Leslie, J.M., Van Koevering, K.K., Faugere, M.C., Clemens, T.L., Williams, B.O., 2013. Lrp5 and Lrp6 exert overlapping functions in osteoblasts during postnatal bone acquisition. PLoS One 8 (5), e63323.

Rijsewijk, F., Schuermann, M., Wagenaar, E., Parren, P., Weigel, D., Nusse, R., 1987. The drosphila homology of the mouse mammary oncogen int-1 is identical to the segment polarity gene wingless. Cell 50, 649−657.

Robey, P., 2017. "Mesenchymal stem cells": fact or fiction, and implications in their therapeutic use. F1000Res (6).

Robinson, J.A., Chatterjee-Kishore, M., Yaworsky, P., Cullen, D.M., Zhao, W., Li, C., Kharode, Y.P., Sauter, L., Babij, P., Brown, E.L., Hill, A.A., Akhter, M.P., Johnson, M.L., Recker, R.R., Komm, B.S., Bex, F.J., 2006. Wnt/β-Catenin signaling is a normal physiological response to mechanical loading in bone. J. Biol. Chem. 281, 31720−31728.

Rocha-Braz, M.G., Ferraz-de-Souza, B., 2016. Genetics of osteoporosis: searching for candidate genes for bone fragility. Arch Endocrinol Metab 60 (4), 391−401.

Ross, S.E., Hemati, N., Longo, K.A., Bennett, C.N., Lucas, P.C., Erickson, R.L., MacDougald, O.A., 2000. Inhibition of adipogenesis by Wnt signaling. Science 289 (5481), 950−953.

Saag, K.G., Petersen, J., Brandi, M.L., Karaplis, A.C., Lorentzon, M., Thomas, T., Maddox, J., Fan, M., Meisner, P.D., Grauer, A., 2017. Romosozumab or alendronate for fracture prevention in women with osteoporosis. N. Engl. J. Med. 377 (15), 1417−1427.

Saal, H.M., Prows, C.A., Guerreiro, I., Donlin, M., Knudson, L., Sund, K.L., Chang, C.F., Brugmann, S.A., Stottmann, R.W., 2015. A mutation in FRIZZLED2 impairs Wnt signaling and causes autosomal dominant omodysplasia. Hum. Mol. Genet. 24 (12), 3399−3409.

Sakanaka, C., Weiss, J.B., Williams, L.T., 1998. Bridging of β-catenin and glycogen syhase kinase-3b by axin and inhibiiton of β-Catenin-mediated transcription. Proc. Natl. Acad. Sci. U.S.A. 95, 3020−3030.

Sawa, H., Korswagen, H.C., 2013. Wnt signaling in *C. elegans*. Worm 1−30.

Sawakami, K., Robling, A.G., Ai, M., Pitner, N.D., Liu, D., Warden, S.J., Li, J., Maye, P., Rowe, D.W., Duncan, R.L., Warman, M.L., Turner, C.H., 2006. The wnt Co-receptor Lrp5 is essential for skeletal mechanotransduction, but not for the anabolic bone response to parathyroid hormone treatment. J. Biol. Chem. 281, 23698−23711.

Schaffler, M.B., Cheung, W.Y., Majeska, R., Kennedy, O., 2014. Osteocytes: master orchestrators of bone. Calcif. Tissue Int. 94 (1), 5−24.

Schulte, G., Bryja, V., Rawal, N., Castelo-Branco, G., Sousa, K.M., Arenas, E., 2005. Purified wnt-5a increases differentiation of midbrain dopaminergic cells and dishevelled phosphorylation. J. Neurochem. 92, 1550−1553.

Seeling, J.M., Miller, J.R., Gil, R., Moon, R.T., White, R., Virshup, D.M., 1999. Regulation of β-catenin signaling by the B56 subunit of protein phosphatase 2A. Science 283, 2089−2091.

Semenov, M., He, X., 2006. LRP5 mutations linked to high bone mass diseases cause reduced LRP5 binding and inhibition by SOST. J. Biol. Chem. 281, 38276−38284.

Sheldahl, L.C., Park, M., Malbon, C.C., Moon, R.T., 1999. Protein kinase C is differentially stimulated by wnt and frizzled homologs in a G-protein-dependent manner. Curr. Biol. 9, 695−698.

Spencer, G.J., Utting, J.S., Etheridge, S.L., Arnett, T.R., Genever, P.G., 2006. Wnt signalling in osteoblasts regulates expression of the receptor activator of NFkB ligand and inhibits osteoclastogenesis in vitro. J. Cell Sci. 119, 1283−1296.

Staehling-Hampton, K., Proll, S., Paeper, B.W., Zhao, L., Charmley, P., Brown, A., Gardner, J.C., Galas, D., Schatzman, R.C., Beighton, P., Papapoulos, S., Hamersma, H., Brunkow, M.E., 2002. A 52-kb deletion in the SOST-MEOX1 intergenic region on 17q12-q21 is associated with van Buchem disease in the Dutch population. Am. J. Med. Genet. 110 (2), 144−152.

Stambolic, V., Woodgett, J.R., 1994. Mitogen inactivation of glycogen synthase kinase-3β in intact cells via serine 9 phosphorylation. Biochem. J. 303, 701−704.

Strickland, D.K., Gonias, S.L., Argraves, W.S., 2002. Diverse roles for the LDL receptor family. Trends Endocrinol. Metabol. 13 (2), 66−74.

Sun, T.Q., Lu, B., Feng, J.J., Reinhard, C., Jan, Y.N., Fantl, W.J., Williams, L.T., 2001. PAR-1 is a dishevelled-associated kinase and a positive regulator of wnt signaling. Nat. Cell Biol. 3, 628−636.

Sun, W., Shi, Y., Lee, W.C., Lee, S.Y., Long, F., 2016a. Rictor is required for optimal bone accrual in response to anti-sclerostin therapy in the mouse. Bone 85, 1−8.

Sun, Y., Zhu, D., Chen, F., Qian, M., Wei, H., Chen, W., Xu, J., 2016b. SFRP2 augments WNT16B signaling to promote therapeutic resistance in the damaged tumor microenvironment. Oncogene 35 (33), 4321−4334.

Sutherland, C., Cohen, P., 1994. The α-isoform of glycogen synthase kinase-3 from rabbit skeletal muscle is inactivated by p70 S6 kinase or MAP kinase-activated protein kinase-1 in vitro. FEBS (Fed. Eur. Biochem. Soc.) Lett. 338, 37−42.

Sutherland, C., Leighton, I.A., Cohen, P., 1993. Inactivation of glycogen synthase kinase-3β by phosphorylation: new kinase connections in insulin and growth-factor signaling. Biochem. J. 296, 15−19.

Tago, K., Nakamura, T., Nishita, M., Hyodo, J., Nagai, S., Murata, Y., Adachi, S., Ohwada, S., Morishita, Y., Shibuya, H., Akiyama, T., 2000. Inhibition of wnt signaling by ICAT, a novel β-catenin-interacting protein. Genes Dev. 14, 1741−1749.

Takada, R., Satomi, Y., Kurata, T., Ueno, N., Norioka, S., Kondoh, H., Takao, T., Takada, S., 2006. Monounsaturated fatty acid modification of Wnt protein: its role in Wnt secretion. Dev. Cell 11 (6), 791−801.

Takemura, K., Yamaguchi, S., Lee, Y., Zhang, Y., Carthew, R.W., Moon, R.T., 2003. Chibby, a nuclear β-catenin-associated antagonist of the wnt/wingless pathway. Nature 422, 905−909.

Tamai, K., Semenov, M., Kato, Y., Spokony, R., Liu, C., Katsuyama, Y., Hess, F., Saint-Jeannet, J.P., He, X., 2000. LDL-Receptor-Related proteins in wnt signal transduction. Nature 407, 530−535.

Tan, S.H., Senarath-Yapa, K., Chung, M.T., Longaker, M.T., Wu, J.Y., Nusse, R., 2014. Wnts produced by Osterix-expressing osteolineage cells regulate their proliferation and differentiation. Proc. Natl. Acad. Sci. U. S. A. 111 (49), E5262–E5271.

Terpos, E., Christoulas, D., Gavriatopoulou, M., 2018. Biology and treatment of myeloma related bone disease. Metabolism 80, 80–90.

Tian, Q., He, X.C., Li, L., 2005. Bridging the BMP and wnt pathways by PI3 kinase/Akt and 14-3-3zeta. Cell Cycle 4, 215–216.

Tolwinski, N.S., Wehrli, M., Rives, A., Erdeniz, N., DiNardo, S., Wieschaus, E., 2003. Wg/Wnt signal can Be transmitted through arrow/LRP5,6 and axin independently of Zw3/Gsk3beta activity. Dev. Cell 4 (3), 407–418.

Towler, D.A., Shao, J.S., Cheng, S.L., Pingsterhaus, J.M., Loewy, A.P., 2006. Osteogenic regulation of vascular calcification. Ann. N. Y. Acad. Sci. 1068, 327–333.

Turkmen, S., Spielmann, M., Gunes, N., Knaus, A., Flottmann, R., Mundlos, S., Tuysuz, B., 2017. A Novel de novo FZD2 Mutation in a Patient with Autosomal Dominant Omodysplasia. Mol Syndromol 8 (6), 318–324.

Twells, R.C., Metzker, M.L., Brown, S.D., Cox, R., Garey, C., Hammond, H., Hey, P.J., Levy, E., Nakagawa, Y., Philips, M.S., Todd, J.A., Hess, J.F., 2001. The sequence and gene characterization of a 400-kb candidate region for IDDM4 on chromosome 11q13. Genomics 72, 231–242.

Twells, R.C., Mein, C.A., Payne, F., Veijola, R., Gilbey, M., Bright, M., Timms, A., Nakagawa, Y., Snook, H., Nutland, S., Rance, H.E., Carr, P., Dudridge, F., Cordell, H.J., Cooper, J., Tuomilehto-Wolf, E., Tuomilehto, J., Phillips, M., Metzker, M., Hess, J.F., Todd, J.A., 2003. Linkage and association mapping of the LRP5 locus on chromosome 11q13 in type I diabetes. Hum. Genet. 113, 99–105.

Urano, T., Inoue, S., 2014. Genetics of osteoporosis. Biochem. Biophys. Res. Commun. 452 (2), 287–293.

Vahle, J.L., Sato, M., Long, G.G., Young, J.K., Francis, P.C., Engelhardt, J.A., Westmore, M.S., Linda, Y., Nold, J.B., 2002. Skeletal changes in rats given daily subcutaneous injections of recombinant human parathyroid hormone (1-34) for 2 years and relevance to human safety. Toxicol. Pathol. 30 (3), 312–321.

van Bezooijen, R.L., ten Dijke, P., Papapoulos, S.E., Lowik, C.W., 2005. SOST/sclerostin, an osteocyte-derived negative modulator of bone formation. Cytokine Growth Factor Rev. 16, 319–327.

van den Brink, G.R., 2004. Linking pathways in colorectal cancer. Nat. Genet. 36, 1038–1039.

van Meurs, J.B., Rivadeneira, F., Jhamai, M., Hugens, W., Hofman, a., van Leeuwen, J.P., Pols, H.A., Uitterlinden, A.G., 2006. Common genetic variation of the low-density lipoprotein receptor-related protein 5 and 6 genes determine fracture risk in elderly white men. J. Bone Miner. Res. 21, 141–150.

Vestergaard, P., Rejnmark, L., Mosekilde, L., 2005. Reduced relative risk of fractures among users of lithium. Calcif. Tissue Int. 77, 1–8.

Wan, Y., Lu, C., Cao, J., Zhou, R., Yao, Y., Yu, J., Zhang, L., Zhao, H., Li, H., Zhao, J., Zhu, X., He, L., Liu, Y., Yao, Z., Yang, X., Guo, X., 2013. Osteoblastic Wnts differentially regulate bone remodeling and the maintenance of bone marrow mesenchymal stem cells. Bone 55 (1), 258–267.

Wang, Y., Chang, H., Rattner, A., Nathans, J., 2016. Frizzled receptors in development and disease. Curr. Top. Dev. Biol. 117, 113–139.

Wehrli, M., Dougan, S.T., Caldwell, K., O'Keefe, L., Schwartz, S., Vaizel-Ohayon, D., Schejter, E., Tomlinson, A., DiNardo, S., 2000. Arrow encodes an LDL-receptor-related protein essential for wingless signaling. Nature 407, 527–530.

Wei, W., Zeve, D., Suh, J.M., Wang, X., Du, Y., Zerwekh, J.E., Dechow, P.C., Graff, J.M., Wan, Y., 2011. Biphasic and dosage-dependent regulation of osteoclastogenesis by beta-catenin. Mol. Cell Biol. 31 (23), 4706–4719.

Weivoda, M.M., Ruan, M., Hachfeld, C.M., Pederson, L., Howe, A., Davey, R.A., Zajac, J.D., Kobayashi, Y., Williams, B.O., Westendorf, J.J., Khosla, S., Oursler, M.J., 2016. Wnt signaling inhibits osteoclast differentiation by activating canonical and noncanonical cAMP/PKA pathways. J. Bone Miner. Res. 31 (1), 65–75.

White, J.J., Mazzeu, J.F., Coban-Akdemir, Z., Bayram, Y., Bahrambeigi, V., Hoischen, A., van Bon, B.W.M., Gezdirici, A., Gulec, E.Y., Ramond, F., Touraine, R., Thevenon, J., Shinawi, M., Beaver, E., Heeley, J., Hoover-Fong, J., Durmaz, C.D., Karabulut, H.G., Marzioglu-Ozdemir, E., Cayir, A., Duz, M.B., Seven, M., Price, S., Ferreira, B.M., Vianna-Morgante, A.M., Ellard, S., Parrish, A., Stals, K., Flores-Daboub, J., Jhangiani, S.N., Gibbs, R.A., Brunner, H.G., Sutton, V.R., Lupski, J.R., Carvalho, C.M.B., 2018. WNT signaling perturbations underlie the genetic heterogeneity of Robinow syndrome. Am. J. Hum. Genet. 102 (1), 27–43.

Whyte, M., Reinus, W., Mumm, S., 2004. High-bone-mass disease and LRP5. N. Engl. J. Med. 350 (20), 2096–2098.

Wijenayaka, A.R., Kogawa, M., Lim, H.P., Bonewald, L.F., Findlay, D.M., Atkins, G.J., 2011. Sclerostin stimulates osteocyte support of osteoclast activity by a RANKL-dependent pathway. PLoS One 6 (10), e25900.

Willert, K., Nusse, R., 1998. β-Catenin: a key mediator of wnt signaling. Development 8, 95–102.

Willert, K., Brink, M., Wodarz, a., Varmus, H., Nusse, R., 1997. Casein kinase 2 associates with and phosphorylates dishevelled. EMBO J. 16, 3089–3096.

Willert, K., Brown, J.D., Danenberg, E., Duncan, A.W., WeissmanI, L., Reya, T., Yates, J.R., Nusse, R., 2003. Wnt proteins are lipid-modified and can act as stem cell growth factors. Nature 423 (6938), 448–452.

Winkler, D.G., Sutherland, M.S.K., Ojala, E., Turcott, E., Geoghegan, J.C., Shpektor, D., Skonier, J.E., Yu, C., Latham, J.A., 2005. Sclerostin inhibition of wnt-3a-induced C3H10t1/2 cell differentiation is indirect and mediated by bone morphogenetic proteins. J. Biol. Chem. 280, 2498–2502.

Wozniak, M., Fausto, A., Carron, C.P., Meyer, D.M., Hruska, K.A., 2000. Mechanically strained cells of the osteoblast lineage organize their extracellular matrix through unique sites of avß3-integrin expression. J. Bone Miner. Res. 15, 1731–1745.

Xiong, J., Onal, M., Jilka, R.L., Weinstein, R.S., Manolagas, S.C., O'Brien, C.A., 2011. Matrix-embedded cells control osteoclast formation. Nat. Med. 17 (10), 1235–1241.

Yamamoto, H., Kishida, S., Uochi, T., Ikeda, S., Koyama, S., Asashima, M., Kikuchi, A., 1998. Axil, a member of the axin family, interacts with both glycogen synthase kinase 3β and β-catenin and inhibits Axis formation of *Xenopus* embryos. Mol. Cell Biol. 18, 2867–2875.

Yamamoto, H., Hinoi, T., Michiue, T., Fukui, A., Usui, H., Janssens, V., Van Hoof, C., Goris, J., Asashima, M., Kikuchi, A., 2001. Inhibition of the wnt signaling pathway by the PR61 subunit of protein phosphatase 2A. J. Biol. Chem. 276, 26875−26882.

Yao, Q., Yu, C., Zhang, X., Zhang, K., Guo, J., Song, L., 2017. Wnt/beta-catenin signaling in osteoblasts regulates global energy metabolism. Bone 97, 175−183.

Yoshida, H., Hayashi, S., Kunisada, T., Ogawa, M., Nishikawa, S., Okamura, H., Sudo, T., Shultz, L.D., Nishikawa, S., 1990. The murine mutation osteopetrosis is in the coding region of the macrophage colony stimulating factor gene. Nature 345 (6274), 442−444.

Yost, C., Torres, M., Miller, J.R., Huang, E., Kimelman, D., Moon, R.T., 1996. The axis-inducing activity, stability, and subcellular distribution of b-catenin is regulated in *Xenopus* embryos by glycogen synthase kinase 3. Genes Dev. 10, 1443−1454.

Zeng, L., Fagotto, F., Zhang, t., Hsu, W., Vasicek, T.J., Perry, W.L., Gumbiner, B.M., Constantini, F., 1997. The mouse fused locus encodes axin, an inhibitor of the wnt signaling pathway that regulates embryonic Axis formation. Cell 90, 181−192.

Zhang, R., Oyajobi, B.O., Harris, S.E., Chen, D., Tsao, C., Deng, H.W., Zhao, M., 2013. Wnt/beta-catenin signaling activates bone morphogenetic protein 2 expression in osteoblasts. Bone 52 (1), 145−156.

Zhang, L., Tang, Y., Zhu, X., Tu, T., Sui, L., Han, Q., Yu, L., Meng, S., Zheng, L., Valverde, P., Tang, J., Murray, D., Zhou, X., Drissi, H., Dard, M.M., Tu, Q., Chen, J., 2017. Overexpression of MiR-335-5p promotes bone formation and regeneration in mice. J. Bone Miner. Res. 32 (12), 2466−2475.

Zheng, H.F., Tobias, J.H., Duncan, E., Evans, D.M., Eriksson, J., Paternoster, L., Yerges-Armstrong, L.M., Lehtimaki, T., Bergstrom, U., Kahonen, M., Leo, P.J., Raitakari, O., Laaksonen, M., Nicholson, G.C., Viikari, J., Ladouceur, M., Lyytikainen, L.P., Medina-Gomez, C., Rivadeneira, F., Prince, R.L., Sievanen, H., Leslie, W.D., Mellstrom, D., Eisman, J.A., Moverare-Skrtic, S., Goltzman, D., Hanley, D.A., Jones, G., St Pourcain, B., Xiao, Y., Timpson, N.J., Smith, G.D., Reid, I.R., Ring, S.M., Sambrook, P.N., Karlsson, M., Dennison, E.M., Kemp, J.P., Danoy, P., Sayers, A., Wilson, S.G., Nethander, M., McCloskey, E., Vandenput, L., Eastell, R., Liu, J., Spector, T., Mitchell, B.D., Streeten, E.A., Brommage, R., Pettersson-Kymmer, U., Brown, M.A., Ohlsson, C., Richards, J.B., Lorentzon, M., 2012. WNT16 influences bone mineral density, cortical bone thickness, bone strength, and osteoporotic fracture risk. PLoS Genet. 8 (7), e1002745.

Zheng, L., Tu, Q., Meng, S., Zhang, L., Yu, L., Song, J., Hu, Y., Sui, L., Zhang, J., Dard, M., Cheng, J., Murray, D., Tang, Y., Lian, J.B., Stein, G.S., Chen, J., 2017. Runx2/DICER/miRNA pathway in regulating osteogenesis. J. Cell. Physiol. 232 (1), 182−191.

Zhong, Z., Zylstra-Diegel, C.R., Schumacher, C.A., Baker, J.J., Carpenter, A.C., Rao, S., Yao, W., Guan, M., Helms, J.A., Lane, N.E., Lang, R.A., Williams, B.O., 2012. Wntless functions in mature osteoblasts to regulate bone mass. Proc. Natl. Acad. Sci. U. S. A. 109 (33), E2197−E2204.

Zhong, Z., Ethen, N.J., Williams, B.O., 2014. WNT signaling in bone development and homeostasis. Wiley Interdiscip. Rev. Dev. Biol. 3 (6), 489−500.

Zhou, H., Mak, W., Zheng, Y., Dunstan, C.R., Seibel, M.J., 2008. Osteoblasts directly control lineage commitment of mesenchymal progenitor cells through Wnt signaling. J. Biol. Chem. 283 (4), 1936−1945.

Further Reading

Rudnicki, J.A., Brown, A.M., 1997. Inhibition of chondrogenesis by Wnt gene expression in vivo and in vitro. Dev. Biol. 185 (1), 104−118.

Aghajanova, L., Velarde, M.C., Giudice, L.C., 2009. The progesterone receptor coactivator Hic-5 is involved in the pathophysiology of endometriosis. Endocrinology 150 (8), 3863−3870.

Bao, G.Y., Lu, K.Y., Cui, S.F., Xu, L., 2015a. DKK1 eukaryotic expression plasmid and expression product identification. Genet. Mol. Res. 14 (2), 6312−6318.

Bao, M.W., Cai, Z., Zhang, X.J., Li, L., Liu, X., Wan, N., Hu, G., Wan, F., Zhang, R., Zhu, X., Xia, H., Li, H., 2015b. Dickkopf-3 protects against cardiac dysfunction and ventricular remodelling following myocardial infarction. Basic Res. Cardiol. 110 (3), 25.

Bell, K.L., Garrahan, N., Kneissel, M., Loveridge, N., Grau, E., Stanton, M., Reeve, J., 1996. Cortical and cancellous bone in the human femoral neck: evaluation of an interactive image analysis system. Bone 19 (5), 541−548.

Betts, A.M., Clark, T.H., Yang, J., Treadway, J.L., Li, M., Giovanelli, M.A., Abdiche, Y., Stone, D.M., Paralkar, V.M., 2010. The application of target information and preclinical pharmacokinetic/pharmacodynamic modeling in predicting clinical doses of a Dickkopf-1 antibody for osteoporosis. J. Pharmacol. Exp. Ther. 333 (1), 2−13.

Binnerts, M.E., Tomasevic, N., Bright, J.M., Leung, J., Ahn, V.E., Kim, K.A., Zhan, X., Liu, S., Yonkovich, S., Williams, J., Zhou, M., Gros, D., Dixon, M., Korver, W., Weis, W.I., Abo, A., 2009. The first propeller domain of LRP6 regulates sensitivity to DKK1. Mol. Biol. Cell 20 (15), 3552−3560.

Bjorklund, P., Svedlund, J., Olsson, A.K., Akerstrom, G., Westin, G., 2009. The internally truncated LRP5 receptor presents a therapeutic target in breast cancer. PLoS One 4 (1), e4243.

Bourhis, E., Tam, C., Franke, Y., Bazan, J.F., Ernst, J., Hwang, J., Costa, M., Cochran, A.G., Hannoush, R.N., 2010. Reconstitution of a frizzled8.Wnt3a.LRP6 signaling complex reveals multiple Wnt and Dkk1 binding sites on LRP6. J. Biol. Chem. 285 (12), 9172−9179.

Bourhis, E., Wang, W., Tam, C., Hwang, J., Zhang, Y., Spittler, D., Huang, O.W., Gong, Y., Estevez, A., Zilberleyb, I., Rouge, L., Chiu, C., Wu, Y., Costa, M., Hannoush, R.N., Franke, Y., Cochran, A.G., 2011. Wnt antagonists bind through a short peptide to the first beta-propeller domain of LRP5/6. Structure 19 (10), 1433−1442.

Briot, K., Rouanet, S., Schaeverbeke, T., Etchepare, F., Gaudin, P., Perdriger, A., Vray, M., Steinberg, G., Roux, C., 2015. The effect of tocilizumab on bone mineral density, serum levels of Dickkopf-1 and bone remodeling markers in patients with rheumatoid arthritis. Joint Bone Spine 82 (2), 109−115.

Bu, G., Lu, W., Liu, C.C., Selander, K., Yoneda, T., Hall, C., Keller, E.T., Li, Y., 2008. Breast cancer-derived Dickkopf1 inhibits osteoblast differentiation and osteoprotegerin expression: implication for breast cancer osteolytic bone metastases. Int. J. Cancer 123 (5), 1034−1042.

Burton, D.W., Foster, M., Johnson, K.A., Hiramoto, M., Deftos, L.J., Terkeltaub, R., 2005. Chondrocyte calcium-sensing receptor expression is up-regulated in early Guinea pig knee osteoarthritis and modulates PTHrP, MMP-13, and TIMP-3 expression. Osteoarthr. Cartil. 13 (5), 395–404.

Campos-Obando, N., Castano-Betancourt, M.C., Oei, L., Franco, O.H., Stricker, B.H., Brusselle, G.G., Lahousse, L., Hofman, A., Tiemeier, H., Rivadeneira, F., Uitterlinden, A.G., Zillikens, M.C., 2014. Bone mineral density and chronic lung disease mortality: the rotterdam study. J. Clin. Endocrinol. Metab. 99 (5), 1834–1842.

Caraci, F., Busceti, C., Biagioni, F., Aronica, E., Mastroiacovo, F., Cappuccio, I., Battaglia, G., Bruno, V., Caricasole, A., Copani, A., Nicoletti, F., 2008. The Wnt antagonist, Dickkopf-1, as a target for the treatment of neurodegenerative disorders. Neurochem. Res. 33 (12), 2401–2406.

Clohisy, J.C., Connolly, T.J., Bergman, K.D., Quinn, C.O., Partridge, N.C., 1994. Prostanoid-induced expression of matrix metalloproteinase-1 messenger ribonucleic acid in rat osteosarcoma cells. Endocrinology 135 (4), 1447–1454.

Cook, T.F., Burke, J.S., Bergman, K.D., Quinn, C.O., Jeffrey, J.J., Partridge, N.C., 1994. Cloning and regulation of rat tissue inhibitor of metalloproteinases-2 in osteoblastic cells. Arch. Biochem. Biophys. 311 (2), 313–320.

Costa, A.G., Bilezikian, J.P., Lewiecki, E.M., 2014. Update on romosozumab : a humanized monoclonal antibody to sclerostin. Expert Opin. Biol. Ther. 14 (5), 697–707.

Culley, K.L., Dragomir, C.L., Chang, J., Wondimu, E.B., Coico, J., Plumb, D.A., Otero, M., Goldring, M.B., 2015. Mouse models of osteoarthritis: surgical model of posttraumatic osteoarthritis induced by destabilization of the medial meniscus. Methods Mol. Biol. 1226, 143–173.

Daoussis, D., Liossis, S.N., Solomou, E.E., Tsanaktsi, A., Bounia, K., Karampetsou, M., Yiannopoulos, G., Andonopoulos, A.P., 2010. Evidence that Dkk-1 is dysfunctional in ankylosing spondylitis. Arthritis Rheum. 62 (1), 150–158.

Darlavoix, T., Seelentag, W., Yan, P., Bachmann, A., Bosman, F.T., 2009. Altered expression of CD44 and DKK1 in the progression of Barrett's esophagus to esophageal adenocarcinoma. Virchows Arch. 454 (6), 629–637.

de Andres, M.C., Imagawa, K., Hashimoto, K., Gonzalez, A., Goldring, M.B., Roach, H.I., Oreffo, R.O., 2011. Suppressors of cytokine signalling (SOCS) are reduced in osteoarthritis. Biochem. Biophys. Res. Commun. 407 (1), 54–59.

Deal, C., 2009. Future therapeutic targets in osteoporosis. Curr. Opin. Rheumatol. 21 (4), 380–385.

Favero, M., Ramonda, R., Goldring, M.B., Goldring, S.R., Punzi, L., 2015. Early knee osteoarthritis. RMD Open 1 (Suppl. 1), e000062.

Fillmore, R.A., Mitra, A., Xi, Y., Ju, J., Scammell, J., Shevde, L.A., Samant, R.S., 2009. Nmi (N-Myc interactor) inhibits Wnt/beta-catenin signaling and retards tumor growth. Int. J. Cancer 125 (3), 556–564.

Fleury, D., Gillard, C., Lebhar, H., Vayssiere, B., Touitou, R., Rawadi, G., Mollat, P., 2008. Expression, purification and characterization of murine Dkk1 protein. Protein Expr. Purif. 60 (1), 74–81.

Galasso, O., Panza, S., Santoro, M., Goldring, M.B., Aquila, S., Gasparini, G., 2015. Pten elevation, autophagy and metabolic reprogramming may Be induced in human chondrocytes during steroids or nutrient depletion and osteoarthritis. J. Biol. Regul. Homeost. Agents 29 (4 Suppl. l), 1–14.

Gasser, J.A., Kneissel, M., Thomsen, J.S., Mosekilde, L., 2000. PTH and interactions with bisphosphonates. J. Musculoskelet. Neuronal Interact. 1 (1), 53–56.

Gavriatopoulou, M., Dimopoulos, M.A., Christoulas, D., Migkou, M., Iakovaki, M., Gkotzamanidou, M., Terpos, E., 2009. Dickkopf-1: a suitable target for the management of myeloma bone disease. Expert Opin. Ther. Targets 13 (7), 839–848.

Goldhahn, J., Feron, J.M., Kanis, J., Papapoulos, S., Reginster, J.Y., Rizzoli, R., Dere, W., Mitlak, B., Tsouderos, Y., Boonen, S., 2012. Implications for fracture healing of current and new osteoporosis treatments: an ESCEO consensus paper. Calcif. Tissue Int. 90 (5), 343–353.

Goldring, M.B., 2009a. The link between structural damage and pain in a genetic model of osteoarthritis and intervertebral disc degeneration: a joint misadventure. Arthritis Rheum. 60 (9), 2550–2552.

Goldring, S.R., 2009b. Needs and opportunities in the assessment and treatment of osteoarthritis of the knee and hip: the view of the rheumatologist. J. Bone Joint Surg. Am. 91 (Suppl. 1), 4–6.

Goldring, S.R., 2009c. Periarticular bone changes in rheumatoid arthritis: pathophysiological implications and clinical utility. Ann. Rheum. Dis. 68 (3), 297–299.

Goldring, M.B., 2012a. Articular cartilage degradation in osteoarthritis. HSS J. 8 (1), 7–9.

Goldring, M.B., 2012b. Chondrogenesis, chondrocyte differentiation, and articular cartilage metabolism in health and osteoarthritis. Ther. Adv. Musculoskelet. Dis. 4 (4), 269–285.

Goldring, M.B., 2012c. Do mouse models reflect the diversity of osteoarthritis in humans? Arthritis Rheum. 64 (10), 3072–3075.

Goldring, S.R., 2012d. Alterations in periarticular bone and cross talk between subchondral bone and articular cartilage in osteoarthritis. Ther. Adv. Musculoskelet Dis. 4 (4), 249–258.

Goldring, M.B., Berenbaum, F., 2015. Emerging targets in osteoarthritis therapy. Curr. Opin. Pharmacol. 22, 51–63.

Goldring, S.R., Goldring, M.B., 2006. Clinical aspects, pathology and pathophysiology of osteoarthritis. J. Musculoskelet. Neuronal Interact. 6 (4), 376–378.

Goldring, S.R., Goldring, M.B., 2010. Bone and cartilage in osteoarthritis: is what's best for one good or bad for the other? Arthritis Res. Ther. 12 (5), 143.

Goldring, M.B., Otero, M., 2011. Inflammation in osteoarthritis. Curr. Opin. Rheumatol. 23 (5), 471–478.

Goldring, S.R., Scanzello, C.R., 2012. Plasma proteins take their toll on the joint in osteoarthritis. Arthritis Res. Ther. 14 (2), 111.

Goldring, S., Wright, T., 2012. Frontiers in osteoarthritis: executive summary of the scientific meeting: executive summary of the scientific meeting. HSS J. 8 (1), 2–3.

Goldring, M.B., Otero, M., Plumb, D.A., Dragomir, C., Favero, M., El Hachem, K., Hashimoto, K., Roach, H.I., Olivotto, E., Borzi, R.M., Marcu, K.B., 2011. Roles of inflammatory and anabolic cytokines in cartilage metabolism: signals and multiple effectors converge upon MMP-13 regulation in osteoarthritis. Eur. Cells Mater. 21, 202–220.

Goldring, S., Lane, N., Sandell, L., 2012. Foreword: osteoarthritis. Bone 51 (2), 189.

Gong, Y., Bourhis, E., Chiu, C., Stawicki, S., DeAlmeida, V.I., Liu, B.Y., Phamluong, K., Cao, T.C., Carano, R.A., Ernst, J.A., Solloway, M., Rubinfeld, B., Hannoush, R.N., Wu, Y., Polakis, P., Costa, M., 2010. Wnt isoform-specific interactions with coreceptor specify inhibition or potentiation of signaling by LRP6 antibodies. PLoS One 5 (9), e12682.

Graeff, C., Campbell, G.M., Pena, J., Borggrefe, J., Padhi, D., Kaufman, A., Chang, S., Libanati, C., Gluer, C.C., 2015. Administration of romosozumab improves vertebral trabecular and cortical bone as assessed with quantitative computed tomography and finite element analysis. Bone 81, 364−369.

Granchi, D., Baglio, S.R., Amato, I., Giunti, A., Baldini, N., 2008. Paracrine inhibition of osteoblast differentiation induced by neuroblastoma cells. Int. J. Cancer 123 (7), 1526−1535.

Gregson, C.L., Wheeler, L., Hardcastle, S.A., Appleton, L.H., Addison, K.A., Brugmans, M., Clark, G.R., Ward, K.A., Paggiosi, M., Stone, M., Thomas, J., Agarwal, R., Poole, K.E., McCloskey, E., Fraser, W.D., Williams, E., Bullock, A.N., Davey Smith, G., Brown, M.A., Tobias, J.H., Duncan, E.L., 2016. Mutations in known monogenic high bone mass loci only explain a small proportion of high bone mass cases. J. Bone Miner. Res. 31 (3), 640−649.

Halleux, C., Kramer, I., Allard, C., Kneissel, M., 2012. Isolation of mouse osteocytes using cell fractionation for gene expression analysis. Methods Mol. Biol. 816, 55−66.

Hansson, M., Olesen, D.R., Peterslund, J.M., Engberg, N., Kahn, M., Winzi, M., Klein, T., Maddox-Hyttel, P., Serup, P., 2009. A late requirement for Wnt and FGF signaling during activin-induced formation of foregut endoderm from mouse embryonic stem cells. Dev. Biol. 330 (2), 286−304.

Hay, E., Nouraud, A., Marie, P.J., 2009. N-cadherin negatively regulates osteoblast proliferation and survival by antagonizing Wnt, ERK and PI3K/Akt signalling. PLoS One 4 (12), e8284.

Hernandez, L., Park, K.H., Cai, S.Q., Qin, L., Partridge, N., Sesti, F., 2007. The antiproliferative role of ERG K+ channels in rat osteoblastic cells. Cell Biochem. Biophys. 47 (2), 199−208.

Hey, F., Giblett, S., Forrest, S., Herbert, C., Pritchard, C., 2016. Phosphorylations of serines 21/9 in glycogen synthase kinase 3alpha/beta are not required for cell lineage commitment or WNT signaling in the normal mouse intestine. PLoS One 11 (6), e0156877.

Hoeppner, L.H., Secreto, F.J., Westendorf, J.J., 2009. Wnt signaling as a therapeutic target for bone diseases. Expert Opin. Ther. Targets 13 (4), 485−496.

Imagawa, K., de Andres, M.C., Hashimoto, K., Pitt, D., Itoi, E., Goldring, M.B., Roach, H.I., Oreffo, R.O., 2011. The epigenetic effect of glucosamine and a nuclear factor-kappa B (NF-kB) inhibitor on primary human chondrocytes–implications for osteoarthritis. Biochem. Biophys. Res. Commun. 405 (3), 362−367.

Jin, H., Wang, B., Li, J., Xie, W., Mao, Q., Li, S., Dong, F., Sun, Y., Ke, H.Z., Babij, P., Tong, P., Chen, D., 2015. Anti-DKK1 antibody promotes bone fracture healing through activation of beta-catenin signaling. Bone 71, 63−75.

John, M.R., Widler, L., Gamse, R., Buhl, T., Seuwen, K., Breitenstein, W., Bruin, G.J., Belleli, R., Klickstein, L.B., Kneissel, M., 2011. ATF936, a novel oral calcilytic, increases bone mineral density in rats and transiently releases parathyroid hormone in humans. Bone 49 (2), 233−241.

Johnson, K., Svensson, C.I., Etten, D.V., Ghosh, S.S., Murphy, A.N., Powell, H.C., Terkeltaub, R., 2004. Mediation of spontaneous knee osteoarthritis by progressive chondrocyte ATP depletion in Hartley Guinea pigs. Arthritis Rheum. 50 (4), 1216−1225.

Kneissel, H., 1976. Treatment of lumbar disk herniation with depot cortisone intrathecally and peridurally (author's transl). Med. Klin. 71 (37), 1506−1507.

Kneissel, H., Horcajada, J., 1970. The moment for angiography after subarachnoid hemorrhage. Wien Med. Wochenschr. 120 (47), 863−865.

Kneissel, H., Hofer, R., Horcajada, J., 1972. [Scintigraphic demonstration of the subarachnoid space for the evaluation of disorders in liquor circulation]. Wien Klin. Wochenschr. 84 (27), 457−458.

Kneissel, S., Queitsch, I., Petersen, G., Behrsing, O., Micheel, B., Dubel, S., 1999. Epitope structures recognised by antibodies against the major coat protein (g8p) of filamentous bacteriophage fd (Inoviridae). J. Mol. Biol. 288 (1), 21−28.

Kneissel, M., Boyde, A., Gasser, J.A., 2001. Bone tissue and its mineralization in aged estrogen-depleted rats after long-term intermittent treatment with parathyroid hormone (PTH) analog SDZ PTS 893 or human PTH(1-34). Bone 28 (3), 237−250.

Koh, J.M., Jung, M.H., Hong, J.S., Park, H.J., Chang, J.S., Shin, H.D., Kim, S.Y., Kim, G.S., 2004. Association between bone mineral density and LDL receptor-related protein 5 gene polymorphisms in young Korean men. J. Korean Med. Sci. 19, 407−412.

Komatsu, D.E., Mary, M.N., Schroeder, R.J., Robling, A.G., Turner, C.H., Warden, S.J., 2010. Modulation of Wnt signaling influences fracture repair. J. Orthop. Res. 28 (7), 928−936.

Kuang, H.B., Miao, C.L., Guo, W.X., Peng, S., Cao, Y.J., Duan, E.K., 2009. Dickkopf-1 enhances migration of HEK293 cell by beta-catenin/E-cadherin degradation. Front. Biosci. 14, 2212−2220.

Larsen, B.M., Hrycaj, S.M., Newman, M., Li, Y., Wellik, D.M., 2015. Mesenchymal Hox6 function is required for mouse pancreatic endocrine cell differentiation. Development 142 (22), 3859−3868.

Lee, M., Partridge, N.C., 2010. Parathyroid hormone activation of matrix metalloproteinase-13 transcription requires the histone acetyltransferase activity of p300 and PCAF and p300-dependent acetylation of PCAF. J. Biol. Chem. 285 (49), 38014−38022.

Leong, D.J., Choudhury, M., Hanstein, R., Hirsh, D.M., Kim, S.J., Majeska, R.J., Schaffler, M.B., Hardin, J.A., Spray, D.C., Goldring, M.B., Cobelli, N.J., Sun, H.B., 2014. Green tea polyphenol treatment is chondroprotective, anti-inflammatory and palliative in a mouse post-traumatic osteoarthritis model. Arthritis Res. Ther. 16 (6), 508.

Li, X., Liu, H., Qin, L., Tamasi, J., Bergenstock, M., Shapses, S., Feyen, J.H., Notterman, D.A., Partridge, N.C., 2007. Determination of dual effects of parathyroid hormone on skeletal gene expression in vivo by microarray and network analysis. J. Biol. Chem. 282 (45), 33086−33097.

Li, X., Qin, L., Partridge, N.C., 2008. In vivo parathyroid hormone treatments and RNA isolation and analysis. Methods Mol. Biol. 455, 79−87.

Li, M., Wu, X.H., Yin, G., Xie, Q.B., 2015. Correlation of RANKL/OPG, dickkopf-1 and bone marrow edema in rheumatoid arthritis with the complaint of knee pain. Sichuan Da Xue Xue Bao Yi Xue Ban 46 (2), 276–279.

Liu, J., Ho, S.C., Su, Y.X., Chen, W.Q., Zhang, C.X., Chen, Y.M., 2009. Effect of long-term intervention of soy isoflavones on bone mineral density in women: a meta-analysis of randomized controlled trials. Bone 44 (5), 948–953.

Liu, Y., Kodithuwakku, S.P., Ng, P.Y., Chai, J., Ng, E.H., Yeung, W.S., Ho, P.C., Lee, K.F., 2010. Excessive ovarian stimulation up-regulates the Wnt-signaling molecule DKK1 in human endometrium and may affect implantation: an in vitro co-culture study. Hum. Reprod. 25 (2), 479–490.

Liu, Z., Kennedy, O.D., Cardoso, L., Basta-Pljakic, J., Partridge, N.C., Schaffler, M.B., Rosen, C.J., Yakar, S., 2016. DMP-1-mediated Ghr gene recombination compromises skeletal development and impairs skeletal response to intermittent PTH. FASEB J. 30 (2), 635–652.

Loeser, R.F., Goldring, S.R., Scanzello, C.R., Goldring, M.B., 2012. Osteoarthritis: a disease of the joint as an organ. Arthritis Rheum. 64 (6), 1697–1707.

Martinez, G., Wijesinghe, M., Turner, K., Abud, H.E., Taketo, M.M., Noda, T., Robinson, M.L., de Iongh, R.U., 2009. Conditional mutations of beta-catenin and APC reveal roles for canonical Wnt signaling in lens differentiation. Investig. Ophthalmol. Vis. Sci. 50 (10), 4794–4806.

Martyn-St James, M., Carroll, S., 2009. A meta-analysis of impact exercise on postmenopausal bone loss: the case for mixed loading exercise programmes. Br. J. Sports Med. 43 (12), 898–908.

Mauriello Jr., J.A., Wasserman, B., Kraut, R., 1993. Use of Vicryl (polyglactin-910) mesh implant for repair of orbital floor fracture causing diplopia: a study of 28 patients over 5 years. Ophthalmic Plast. Reconstr. Surg. 9 (3), 191–195.

Meng, S., Zhou, F.L., Zhang, W.G., Cao, X.M., Wang, B.Y., Wang, Y., Bai, G.G., 2012. The research on the expression and localization of multiple myeloma associated antigen MMSA-1. Xi Bao Yu Fen Zi Mian Yi Xue Za Zhi 28 (1), 63–66.

Meyer, T., Kneissel, M., Mariani, J., Fournier, B., 2000. In vitro and in vivo evidence for orphan nuclear receptor RORalpha function in bone metabolism. Proc. Natl. Acad. Sci. U. S. A. 97 (16), 9197–9202.

Minisola, S., 2014. Romosozumab: from basic to clinical aspects. Expert Opin. Biol. Ther. 14 (9), 1225–1228.

Mitsuyama, H., Healey, R.M., Terkeltaub, R.A., Coutts, R.D., Amiel, D., 2007. Calcification of human articular knee cartilage is primarily an effect of aging rather than osteoarthritis. Osteoarthr. Cartil. 15 (5), 559–565.

Moors, M., Bose, R., Johansson-Haque, K., Edoff, K., Okret, S., Ceccatelli, S., 2012. Dickkopf 1 mediates glucocorticoid-induced changes in human neural progenitor cell proliferation and differentiation. Toxicol. Sci. 125 (2), 488–495.

Muka, T., de Jonge, E.A., de Jong, J.C., Uitterlinden, A.G., Hofman, A., Dehghan, A., Zillikens, M.C., Franco, O.H., Rivadeneira, F., 2016. The influence of serum uric acid on bone mineral density, hip geometry, and fracture risk: the rotterdam study. J. Clin. Endocrinol. Metab. 101 (3), 1113–1122.

Neogi, T., Booth, S.L., Zhang, Y.Q., Jacques, P.F., Terkeltaub, R., Aliabadi, P., Felson, D.T., 2006. Low vitamin K status is associated with osteoarthritis in the hand and knee. Arthritis Rheum. 54 (4), 1255–1261.

Ng, K.W., Martin, T.J., 2014. New therapeutics for osteoporosis. Curr. Opin. Pharmacol. 16, 58–63.

Nusse, R., Varmus, H.E., 1992. Wnt genes. Cell 69 (7), 1073–1087.

Olivotto, E., Otero, M., Marcu, K.B., Goldring, M.B., 2015. Pathophysiology of osteoarthritis: canonical NF-kappaB/IKKbeta-dependent and kinase-independent effects of IKKalpha in cartilage degradation and chondrocyte differentiation. RMD Open 1 (Suppl. 1), e000061.

Ootani, A., Li, X., Sangiorgi, E., Ho, Q.T., Ueno, H., Toda, S., Sugihara, H., Fujimoto, K., Weissman, I.L., Capecchi, M.R., Kuo, C.J., 2009. Sustained in vitro intestinal epithelial culture within a Wnt-dependent stem cell niche. Nat. Med. 15 (6), 701–706.

Otero, M., Goldring, M.B., 2007. Cells of the synovium in rheumatoid arthritis. Chondrocytes. Arthritis Res. Ther. 9 (5), 220.

Partridge, N.C., Alcorn, D., Michelangeli, V.P., Kemp, B.E., Ryan, G.B., Martin, T.J., 1981. Functional properties of hormonally responsive cultured normal and malignant rat osteoblastic cells. Endocrinology 108 (1), 213–219.

Partridge, N.C., Hillyard, C.J., Nolan, R.D., Martin, T.J., 1985. Regulation of prostaglandin production by osteoblast-rich calvarial cells. Prostaglandins 30 (3), 527–539.

Pettit, A.R., Walsh, N.C., Manning, C., Goldring, S.R., Gravallese, E.M., 2006. RANKL protein is expressed at the pannus-bone interface at sites of articular bone erosion in rheumatoid arthritis. Rheumatology 45 (9), 1068–1076.

Power, J., Poole, K.E., van Bezooijen, R., Doube, M., Caballero-Alias, A.M., Lowik, C., Papapoulos, S., Reeve, J., Loveridge, N., 2010. Sclerostin and the regulation of bone formation: effects in hip osteoarthritis and femoral neck fracture. J. Bone Miner. Res. 25 (8), 1867–1876.

Purro, S.A., Dickins, E.M., Salinas, P.C., 2012. The secreted Wnt antagonist Dickkopf-1 is required for amyloid beta-mediated synaptic loss. J. Neurosci. 32 (10), 3492–3498.

Qiang, Y.W., Hu, B., Chen, Y., Zhong, Y., Shi, B., Barlogie, B., Shaughnessy Jr., J.D., 2009. Bortezomib induces osteoblast differentiation via Wnt-independent activation of beta-catenin/TCF signaling. Blood 113 (18), 4319–4330.

Qin, L., Tamasi, J., Raggatt, L., Li, X., Feyen, J.H., Lee, D.C., Dicicco-Bloom, E., Partridge, N.C., 2005. Amphiregulin is a novel growth factor involved in normal bone development and in the cellular response to parathyroid hormone stimulation. J. Biol. Chem. 280 (5), 3974–3981.

Raggatt, L.J., Partridge, N.C., 2010. Cellular and molecular mechanisms of bone remodeling. J. Biol. Chem. 285 (33), 25103–25108.

Recchia, I., Rucci, N., Funari, A., Migliaccio, S., Taranta, A., Longo, M., Kneissel, M., Susa, M., Fabbro, D., Teti, A., 2004. Reduction of c-Src activity by substituted 5,7-diphenyl-pyrrolo[2,3-d]-pyrimidines induces osteoclast apoptosis in vivo and in vitro. Involvement of ERK1/2 pathway. Bone 34 (1), 65–79.

Rivadeneira, F., Styrkarsdottir, U., Estrada, K., Halldorsson, B.V., Hsu, Y.H., Richards, J.B., Zillikens, M.C., Kavvoura, F.K., Amin, N., Aulchenko, Y.S., Cupples, L.A., Deloukas, P., Demissie, S., Grundberg, E., Hofman, A., Kong, A., Karasik, D., van Meurs, J.B., Oostra, B., Pastinen, T., Pols, H.A., Sigurdsson, G., Soranzo, N., Thorleifsson, G., Thorsteinsdottir, U., Williams, F.M., Wilson, S.G., Zhou, Y., Ralston, S.H., van Duijn, C.M., Spector, T., Kiel, D.P., Stefansson, K., Ioannidis, J.P., Uitterlinden, A.G., 2009. Twenty bone-mineral-density loci identified by large-scale meta-analysis of genome-wide association studies. Nat. Genet. 41 (11), 1199–1206.

Roschger, P., Grabner, B.M., Rinnerthaler, S., Tesch, W., Kneissel, M., Berzlanovich, A., Klaushofer, K., Fratzl, P., 2001. Structural development of the mineralized tissue in the human L4 vertebral body. J. Struct. Biol. 136 (2), 126–136.

Rosi, M.C., Luccarini, I., Grossi, C., Fiorentini, A., Spillantini, M.G., Prisco, A., Scali, C., Gianfriddo, M., Caricasole, A., Terstappen, G.C., Casamenti, F., 2010. Increased Dickkopf-1 expression in transgenic mouse models of neurodegenerative disease. J. Neurochem. 112 (6), 1539–1551.

Rundle, C.H., Wang, H., Yu, H., Chadwick, R.B., Davis, E.I., Wergedal, J.E., Lau, K.H., Mohan, S., Ryaby, J.T., Baylink, D.J., 2006. Microarray analysis of gene expression during the inflammation and endochondral bone formation stages of rat femur fracture repair. Bone 38 (4), 521–529.

Sahithi, K., Swetha, M., Prabaharan, M., Moorthi, A., Saranya, N., Ramasamy, K., Srinivasan, N., Partridge, N.C., Selvamurugan, N., 2010. Synthesis and characterization of nanoscale-hydroxyapatite-copper for antimicrobial activity towards bone tissue engineering applications. J. Biomed. Nanotechnol. 6 (4), 333–339.

Sato, N., Yamabuki, T., Takano, A., Koinuma, J., Aragaki, M., Masuda, K., Ishikawa, N., Kohno, N., Ito, H., Miyamoto, M., Nakayama, H., Miyagi, Y., Tsuchiya, E., Kondo, S., Nakamura, Y., Daigo, Y., 2010. Wnt inhibitor Dickkopf-1 as a target for passive cancer immunotherapy. Cancer Res. 70 (13), 5326–5336.

Scanzello, C.R., Goldring, S.R., 2012. The role of synovitis in osteoarthritis pathogenesis. Bone 51 (2), 249–257.

Schneider, S.F., 1990. Psychology at a crossroads. Am. Psychol. 45 (4), 521–529.

Schrader, R., Kneissel, G.D., Sievert, H., Bussmann, W.D., Kaltenbach, M., 1992. [Clinical features and therapy of persistent ductus arteriosus in adults]. Dtsch. Med. Wochenschr. 117 (47), 1805–1809.

Selvamurugan, N., Shimizu, E., Lee, M., Liu, T., Li, H., Partridge, N.C., 2009. Identification and characterization of Runx2 phosphorylation sites involved in matrix metalloproteinase-13 promoter activation. FEBS Lett. 583 (7), 1141–1146.

Shalhoub, V., Conlon, D., Tassinari, M., Quinn, C., Partridge, N., Stein, G.S., Lian, J.B., 1992. Glucocorticoids promote development of the osteoblast phenotype by selectively modulating expression of cell growth and differentiation associated genes. J. Cell. Biochem. 50 (4), 425–440.

Sottile, V., Seuwen, K., Kneissel, M., 2004. Enhanced marrow adipogenesis and bone resorption in estrogen-deprived rats treated with the PPARgamma agonist BRL49653 (rosiglitazone). Calcif. Tissue Int. 75 (4), 329–337.

Streeten, E.A., Morton, H., McBride, D.J., 2003. Osteoporosis pseudoglioma syndrome: 3 siblings with a novel LRP5 mutation. J. Bone Miner. Res. 18 (Suppl. 2), S35.

Tella, S.H., Gallagher, J.C., 2014. Biological agents in management of osteoporosis. Eur. J. Clin. Pharmacol. 70 (11), 1291–1301.

Terkeltaub, R., Johnson, K., Murphy, A., Ghosh, S., 2002. Invited review: the mitochondrion in osteoarthritis. Mitochondrion 1 (4), 301–319.

Tripathi, A., Saravanan, S., Pattnaik, S., Moorthi, A., Partridge, N.C., Selvamurugan, N., 2012. Bio-composite scaffolds containing chitosan/nano-hydroxyapatite/nano-copper-zinc for bone tissue engineering. Int. J. Biol. Macromol. 50 (1), 294–299.

Tutak, W., Park, K.H., Vasilov, A., Starovoytov, V., Fanchini, G., Cai, S.Q., Partridge, N.C., Sesti, F., Chhowalla, M., 2009. Toxicity induced enhanced extracellular matrix production in osteoblastic cells cultured on single-walled carbon nanotube networks. Nanotechnology 20 (25), 255101.

Uderhardt, S., Diarra, D., Katzenbeisser, J., David, J.P., Zwerina, J., Richards, W., Kronke, G., Schett, G., 2010. Blockade of Dickkopf (DKK)-1 induces fusion of sacroiliac joints. Ann. Rheum. Dis. 69 (3), 592–597.

Ulm, C.W., Kneissel, M., Hahn, M., Solar, P., Matejka, M., Donath, K., 1997. Characteristics of the cancellous bone of edentulous mandibles. Clin. Oral Implant. Res. 8 (2), 125–130.

Vajda, E.G., Kneissel, M., Muggenburg, B., Miller, S.C., 1999. Increased intracortical bone remodeling during lactation in beagle dogs. Biol. Reprod. 61 (6), 1439–1444.

Wang, Q., Rozelle, A.L., Lepus, C.M., Scanzello, C.R., Song, J.J., Larsen, D.M., Crish, J.F., Bebek, G., Ritter, S.Y., Lindstrom, T.M., Hwang, I., Wong, H.H., Punzi, L., Encarnacion, A., Shamloo, M., Goodman, S.B., Wyss-Coray, T., Goldring, S.R., Banda, N.K., Thurman, J.M., Gobezie, R., Crow, M.K., Holers, V.M., Lee, D.M., Robinson, W.H., 2011. Identification of a central role for complement in osteoarthritis. Nat. Med. 17 (12), 1674–1679.

Weng, L.H., Wang, C.J., Ko, J.Y., Sun, Y.C., Su, Y.S., Wang, F.S., 2009. Inflammation induction of Dickkopf-1 mediates chondrocyte apoptosis in osteoarthritic joint. Osteoarthr. Cartil. 17 (7), 933–943.

Williams, B.O., 2014. Insights into the mechanisms of sclerostin action in regulating bone mass accrual. J. Bone Miner. Res. 29 (1), 24–28.

Wixted, J.J., Fanning, P., Rothkopf, I., Stein, G., Lian, J., 2010. Arachidonic acid, eicosanoids, and fracture repair. J. Orthop. Trauma 24 (9), 539–542.

Wright, T., Goldring, S., 2012. Reaching consensus and highlighting future directions for research: the osteoarthritis summit breakout sessions. HSS J. 8 (1), 80–83.

Wu, C.W., Terkeltaub, R., Kalunian, K.C., 2005. Calcium-containing crystals and osteoarthritis: implications for the clinician. Curr. Rheumatol. Rep. 7 (3), 213–219.

Xu, N., Zhou, W.J., Wang, Y., Huang, S.H., Li, X., Chen, Z.Y., 2015. Hippocampal Wnt3a is necessary and sufficient for contextual fear memory acquisition and consolidation. Cerebr. Cortex 25 (11), 4062–4075.

Yi, Q., 2009. Novel immunotherapies. Cancer J. 15 (6), 502–510.

Yoshikawa, Y., Fujimori, T., McMahon, A.P., Takada, S., 1997. Evidence that absence of wnt-3a signaling promotes neuralization instead of paraxial mesoderm development in the mouse. Dev. Biol. 183, 234–242.

Zechner, W., Kneissel, M., Kim, S., Ulm, C., Watzek, G., Plenk Jr., H., 2004. Histomorphometrical and clinical comparison of submerged and nonsubmerged implants subjected to experimental peri-implantitis in dogs. Clin. Oral Implant. Res. 15 (1), 23–33.

Zhang, S.N., Sun, A.J., Ge, J.B., Yao, K., Huang, Z.Y., Wang, K.Q., Zou, Y.Z., 2009. Intracoronary autologous bone marrow stem cells transfer for patients with acute myocardial infarction: a meta-analysis of randomised controlled trials. Int. J. Cardiol. 136 (2), 178–185.

Zhao, J., Kim, K.A., Abo, A., 2009. Tipping the balance: modulating the Wnt pathway for tissue repair. Trends Biotechnol. 27 (3), 131–136.

Zhu, Y., Sun, Z., Han, Q., Liao, L., Wang, J., Bian, C., Li, J., Yan, X., Liu, Y., Shao, C., Zhao, R.C., 2009. Human mesenchymal stem cells inhibit cancer cell proliferation by secreting DKK-1. Leukemia 23 (5), 925−933.

Zillikens, M.C., Uitterlinden, A.G., van Leeuwen, J.P., Berends, A.L., Henneman, P., van Dijk, K.W., Oostra, B.A., van Duijn, C.M., Pols, H.A., Rivadeneira, F., 2010. The role of body mass index, insulin, and adiponectin in the relation between fat distribution and bone mineral density. Calcif. Tissue Int. 86 (2), 116−125.

Zirwes, R.F., Eilbracht, J., Kneissel, S., Schmidt-Zachmann, M.S., 2000. A novel helicase-type protein in the nucleolus: protein NOH61. Mol. Biol. Cell 11 (4), 1153−1167.

Chapter 9

Vascular and nerve interactions

Ryan E. Tomlinson[1], Thomas L. Clemens[2,3] and Christa Maes[4]

[1]Department of Orthopaedic Surgery, Thomas Jefferson University, Philadelphia, PA, United States; [2]Department of Orthopaedic Surgery, Johns Hopkins University School of Medicine, Baltimore, MD, United States; [3]Baltimore Veterans Administration Medical Center, Baltimore, MD, United States; [4]Laboratory of Skeletal Cell Biology and Physiology (SCEBP), Skeletal Biology and Engineering Research Center (SBE), KU Leuven, Leuven, Belgium

Chapter outline

Introduction

Bone is a highly vascularized and innervated organ. During development, all the long bones of the skeleton form via an avascular and noninnervated cartilage template. The conversion of the cartilaginous model into bone is dependent on its primary invasion by blood vessels, a process that is associated with the development of a bone marrow cavity and its infiltration by various cell types populating the bone, including bone-forming osteolineage cells, bone-resorbing osteoclasts, and hematopoietic cells. The presence of an adequate vascular supply is absolutely required for further bone formation and remodeling, to supply the necessary oxygen, nutrients, and hormones and to remove waste products (Maes, 2013). Furthermore, the close physical relationship and molecular crosstalk between the endothelial cells of the blood vessels and the osteoprogenitors residing in the perivascular space are thought to contribute to angiogenic−osteogenic coupling (Maes, 2013; Dirckx et al., 2013). This term refers to the close spatial−temporal association of angiogenesis and osteogenesis, as observed during fetal skeletal development, during the juvenile growth spurt, in remodeling bone throughout adulthood, and in fracture healing (Schipani et al., 2009; Maes, 2013; Wang et al., 2007). For some time, compromised vascularity and reduced blood flow in bone have been associated with age-related declines in bone mass and osteoporosis as well as poor bone repair, emphasizing the potential therapeutic value of understanding the vasculature of bone and how to modulate it (Maes, 2013; Ramasamy et al., 2016; Tomlinson et al., 2013; Tomlinson and Silva, 2013; Mekraldi et al., 2003; Burkhardt et al., 1987; Saran et al., 2014; Carano and Filvaroff, 2003; Street et al., 2002). Interestingly, nerves accompany the blood vessels that supply bone tissue; in fact, innervation and vascularization of developing bone are tightly coordinated and possibly interdependent processes. The presence of nerves in bone has been appreciated since work of the early microscopists, who utilized routine histological methods such as toluidine blue or silver staining to reveal nerve axons in calcified tissue (Miller and Kasahara, 1963; Milgram and Robinson, 1965; Linder, 1978; Thurston, 1982). These studies helped validate the numerous clinical observations regarding skeletal pain emanating from bone tissue itself, particularly following surgery necessitated by neoplastic bone disease. Immunohistochemical studies, beginning in the mid-1980s (Hohmann et al., 1986), began to dissect the various types and subtypes of neuronal axons in bone. This work gradually revealed that the skeleton is richly innervated by sensory, sympathetic, and parasympathetic axons of the

Principles of Bone Biology. https://doi.org/10.1016/B978-0-12-814841-9.00009-9

peripheral nervous system, with axons found in the periosteum and marrow space as well as calcified tissue (Bjurholm et al., 1988; Wojtys et al., 1990; Hill and Elde, 1991; Hukkanen et al., 1992; Mach et al., 2002; Castañeda-Corral et al., 2011). Furthermore, each of these nerve types appears to serve unique functions within the bone microenvironment, many of which are under active investigation. In this chapter, we will review the current understanding of the origin, location, and function of the blood vessels and different nerve types in bone.

The vasculature of bone

Vascularization of developing bone

The development of the long bones of the skeleton by endochondral ossification is characterized by the initial formation of a cartilage template that prefigures the future bone. Cartilage is inherently avascular, in line with the typical production of angiogenic inhibitors by chondrocytes during their immature and differentiating states. When chondrocytes reach their final maturation stage and become hypertrophic chondrocytes, the balance shifts toward the predominant expression of angiogenic stimulators. At this stage, hypertrophic chondrocytes begin expressing vascular endothelial growth factor (VEGF). As a consequence, hypertrophic cartilage becomes invaded by blood vessels, which triggers the formation of the primary ossification center and the nascent bone marrow cavity. Osteoprogenitors coinvade the middiaphyseal bone region along with blood vessels originating from the perichondrium, and instigate bone formation inside the shaft (Maes et al., 2010a). The excavation of the original cartilaginous template is probably steered by both angiogenesis-related tissue remodeling and osteoclastic resorption of the calcified cartilage matrix. While the fate of the hypertrophic chondrocytes proper was classically considered to be apoptotic cell death, studies using genetic lineage tracing strategies in mice have revived the long-standing hypothesis of transdifferentiation of terminally differentiated growth plate chondrocytes into osteoblasts (Zhou et al., 2014; Yang et al., 2014; Park et al., 2015). Whether the incoming vasculature may have an instructive role in defining the fate of the hypertrophic chondrocyte, which seems highly plausible, needs to be defined.

The concept that hypertrophic chondrocytes direct the cartilage-to-bone transition through VEGF release during endochondral bone growth was established through the use of a variety of mouse models. First, administration of a soluble VEGF receptor chimeric protein (sFlt-1) that acts to inhibit VEGF was shown to impair vascular invasion of the growth plate in juvenile mice, which was associated with reduced longitudinal bone growth and trabecular bone formation (Gerber et al., 1999). Concomitantly, the mice showed a pronounced extension of the layer containing hypertrophic chondrocytes in their growth plates (Gerber et al., 1999), a feature that had also been transiently observed in knockout mice lacking the matrix metalloproteinase 9 (MMP-9) (Vu et al., 1998). In joining these findings, the theory was proposed that capillary invasion of the growth cartilage brings osteoclasts—cells of hematopoietic origin sharing a precursor with macrophages—to the chondro-osseous junction. MMP-9 production and matrix resorption by osteoclasts or postulated related cells called "chondroclasts" would progressively release matrix-bound VEGF from the degrading cartilage matrix, creating a positive-feedback system steering capillary growth, hypertrophic cartilage matrix decay and resorption, and trabecular bone formation (Karsenty and Wagner, 2002). Although the fine details of the cellular sources and situated actions of MMP-9 are as yet to be resolved, the important role of VEGF as coordinator of the progressive turnover of cartilage into bone and driver of longitudinal bone growth has been further substantiated and refined through the use of conditional knockout mice and knock-in models (reviewed in greater detail in Maes, 2013, 2017; Dirckx et al., 2013; Dirckx and Maes, 2016). These studies furthermore annotated specific functions to the major VEGF splice isoforms (VEGF120, VEGF164, and VEGF188 in the mouse), primarily based on their differential solubility versus matrix-binding characteristics. The shorter, soluble VEGF isoforms (VEGF120 and to some extent VEGF164) can diffuse and attract distant blood vessels toward the source of VEGF secretion, thus stimulating angiogenic growth of the capillary bed. The longer isoforms (VEGF164 and especially VEGF188) have strong affinity to bind heparin-containing matrix components, become sequestered in the cartilage matrix, and are released upon proteolytic degradation of the matrix, thereby serving a coordinating role in linking cartilage-to-bone turnover to the progressive vascularization of the growing bone (Maes, 2017; Maes et al., 2002, 2004; Zelzer et al., 2002) (Fig. 9.1).

VEGF plays essential roles in the initial osteo-angiogenic invasion of fetal bones during primary ossification center (POC) formation, as well as in triggering the vascularization processes that mediate the formation of the secondary ossification centers in the epiphyses later in skeletal development (Maes et al., 2004, 2012a; Duan et al., 2015). Mice engineered to express only the VEGF120 isoform or only the VEGF188 isoform showed a delay in the initial vascular invasion and development of the long bones, indicating the importance of the VEGF164 isoform or a combination of soluble and matrix-bound VEGF (Maes et al., 2002, 2004; Zelzer et al., 2002). The levels of VEGF need to be tightly

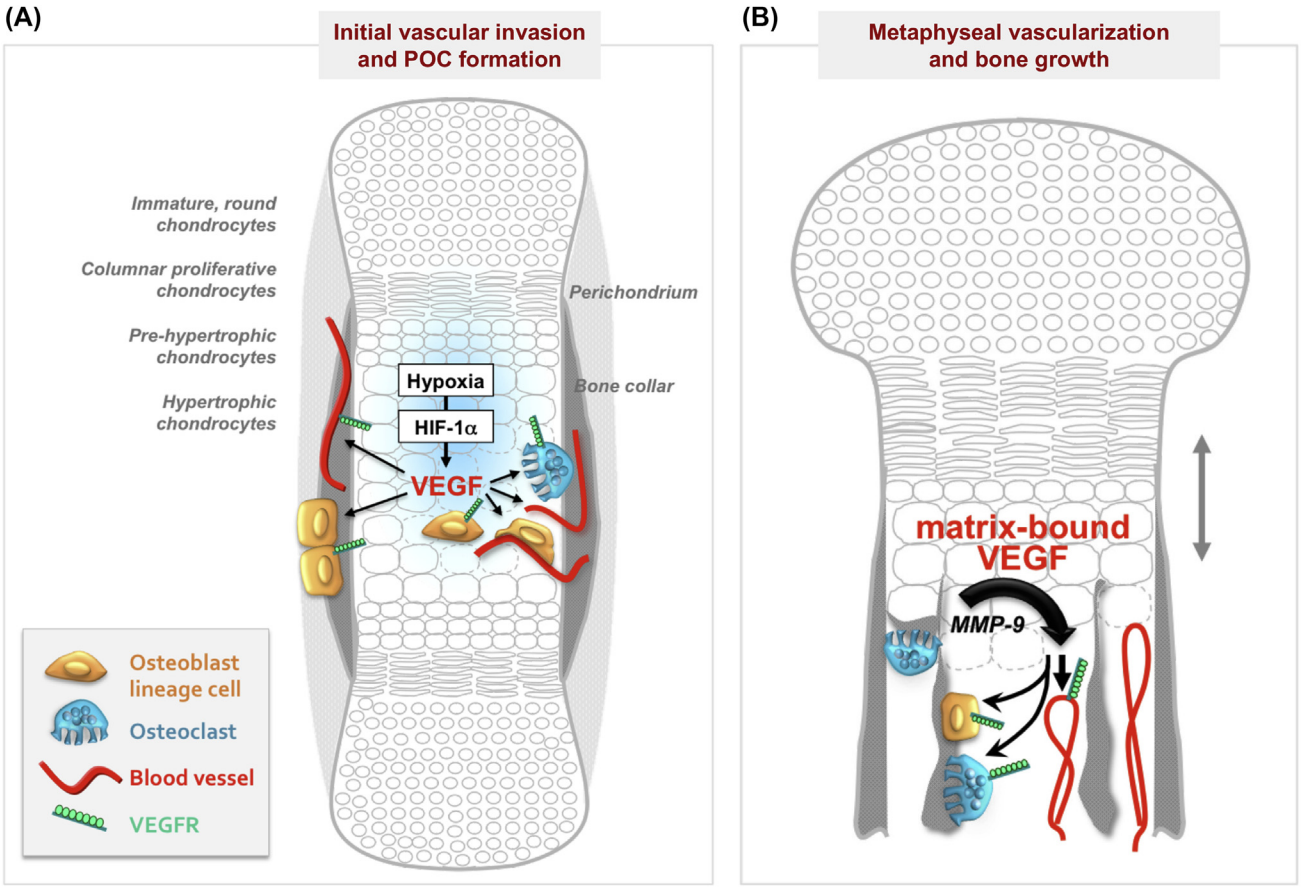

FIGURE 9.1 The roles of hypoxia-inducible factor (HIF) and vascular endothelial growth factor (VEGF) in the neovascularization of cartilage and its conversion to bone. (A) VEGF controls the initial osteo-angiogenic invasion of the endochondral bone template. During long bone development, hypertrophic chondrocytes in the middle diaphyseal region of the avascular cartilage template become hypoxic and express high levels of VEGF. Both HIF-1α and VEGF are required for the timely invasion of the template by blood vessels from the perichondrium. Along with the endothelium, osteoprogenitors move into the tissue, start to deposit bone, and establish the primary ossification center (POC). Osteoclasts, cells of hematopoietic origin, also appear, coinciding with vascular accumulation in the perichondrium, and coinvade the cartilage. All the cell types involved express VEGF receptors (*VEGFR*) and can respond directly to VEGF signaling by enhanced migration, recruitment, proliferation, and/or differentiation. **(B) VEGF actions at the chondro-osseous junction and the metaphysis of growing long bones.** The matrix-binding isoforms of VEGF, VEGF164 and VEGF188, are stored in the cartilage matrix after their secretion by hypertrophic chondrocytes. Upon cartilage resorption, mediated by osteoclasts and matrix metalloproteinase-9 (*MMP-9*), the released VEGF attracts blood vessels toward the growth plate and stimulates angiogenesis. Indirectly (via the vascular growth) and directly (via VEGFR signaling), VEGF stimulates bone formation by osteoblasts and cartilage resorption and bone remodeling by osteoclasts, thereby coordinating the conversion of cartilage into bone at the chondro-osseous junctions and stimulating the growth of the long bones. *Figure reproduced from Maes, C., 2017. Signaling pathways effecting crosstalk between cartilage and adjacent tissues: seminars in cell and developmental biology: the biology and pathology of cartilage. Semin. Cell Dev. Biol. 62, 16–33.*

controlled though, as either partial loss or local increase of VEGF is detrimental to bone development (Maes et al., 2010b; Haigh et al., 2000). In fact, Col2-Cre-driven conditional overexpression of VEGF164 in the fetal skeleton led to premature osteo-angiogenic invasion of developing bones, hypervascularization of the primary ossification center, aberrant bone deposition, and severely misshapen limbs (Maes et al., 2010b). The physiological induction of high levels of VEGF expression in hypertrophic chondrocytes appears to be fundamentally coupled to the differentiation progression of the cells and involves several transcriptional regulators, including Runx2, Osterix (Osx), and hypoxia-inducible factors (HIFs), particularly HIF-1α, the prime driver of the cellular responses to low-oxygen conditions (Chen et al., 2012; Zelzer et al., 2001; Tang et al., 2012; Cramer et al., 2004; Lin et al., 2004). HIF-1α signaling and other hypoxia-driven control mechanisms also contribute to the fine regulation of the more moderate VEGF levels in the hypoxic center of the developing growth plate and the preinvasion cartilaginous template; these signals are important for stimulating perichondrial angiogenesis as well as ensuring survival of the hypoxic chondrocytes (Maes et al., 2004, 2012a; Duan et al., 2015; Schipani et al., 2001; Provot et al., 2007; Amarilio et al., 2007; Eshkar-Oren et al., 2009).

Vascularization of the mature skeleton

Also beyond development, the skeletal vascular system remains an essential player in the regulation of bone formation and remodeling, as characterized most comprehensively in the long bones. These bones are supplied by a dense network of blood vessels comprising epiphyseal, metaphyseal, and periosteal blood vessels. The nutrient arteries provide the main entry of the blood into the bone shaft. Within the shaft, the vessels are organized in a highly branched and organized network of sinusoidal capillaries, arteries, and arterioles in the bone marrow environment, with endosteal vessels near the cortical bone and metaphyseal capillaries arranged in longitudinal orientation among the trabecular bone spicules toward the chondro-osseous junction of the growth plate (Brookes and Revell, 1998; Roche et al., 2012). Recent work has termed the endosteal and metaphyseal capillaries "H-type" blood vessels, because of their strong reactivity to antibodies recognizing the endothelial cell markers CD31/PECAM-1 and endomucin (EMCN) ($CD31^{high}$;$EMCN^{high}$). The sinusoidal blood vessel network in the diaphyseal bone shaft is by these molecular criteria designated as the "L-type" endothelium in bone ($CD31^{low}$;$EMCN^{low}$) (Kusumbe et al., 2014). Processes of adult bone remodeling and bone mass homeostasis, fracture repair, and bone tissue regeneration, as well as proper hematopoiesis, all rely on optimal bone and bone marrow vascularization. Yet, different types of skeletal blood vessels may provide differential support and contributions to these various processes. For instance, particularly H-type capillaries in growing and mature bones are heavily associated with perivascular osteoprogenitor cells, including Runx2-, Osx-, and platelet-derived growth factor (PDGF) receptor β-expressing cells, which are thought to be important for bone formation. The vascular system may thus help deliver these osteoprogenitor populations to bone formation sites, in addition to providing the necessary oxygen, nutrients, and growth factors for their controlled differentiation and activity (Dirckx et al., 2013; Maes et al., 2010a). Loss of these populations is observed with aging in mice and may be related to the well-documented age-related and osteoporosis-linked declines in both vascular density and bone mass (Maes, 2013; Ramasamy et al., 2016; Mekraldi et al., 2003; Burkhardt et al., 1987; Kusumbe et al., 2014). On the other hand, bone marrow arterioles and sinusoidal L-type vessels are surrounded by specific subsets of hematopoietic stem cells (HSCs) and provide critical components of the niche microenvironments that control their quiescence and differentiation balances (Ramasamy et al., 2016; Kusumbe et al., 2016; Itkin et al., 2016). Impaired revascularization has been long known to be detrimental to bone repair, but the specifics of the angiogenic processes and blood vessel types in fracture healing are only starting to be determined (Wang et al., 2017). Clearly, angiogenesis in bone and its coupling with osteogenesis provide promising therapeutic angles for low bone mass—associated diseases and for bone repair and regeneration, highlighting the importance of understanding the underlying crosstalk and regulatory mechanisms operating in osteolineage cells and in endothelial cells, as outlined next in this section (Fig. 9.2).

Bone cells' control of skeletal vascularization and oxygenation

Signaling from hypertrophic chondrocytes, osteoblast lineage cells, and osteoclasts has been found instructive toward the development, growth, and maintenance of the skeletal vascular system (Maes, 2013; Maes et al., 2012b). As the prime angiogenic factor, VEGF produced by these cell types plays a major role in adult bone. Moreover, the hypoxia-induced and HIF-mediated signaling pathways represent major regulators of the tight coupling between angiogenesis and osteogenesis in postnatal bone formation and bone remodeling, at least in part by functioning as key upstream inducers of VEGF expression (Maes et al., 2012b; Schipani et al., 2009). Some of the mouse models that exposed these roles include Cre-loxP-mediated conditional knockouts employing Osx-Cre, type I collagen-Cre, and osteocalcin (OC)-Cre driver strains to target osteoprogenitors, maturing osteoblasts, and differentiated osteoblasts, respectively. The first evidence for the importance of the HIF pathway components in the adult murine skeleton was provided by genetic targeting of HIF-1α and the upstream negative regulator of HIF activity, Von Hippel—Lindau (VHL), in OC-expressing osteoblasts (Wang et al., 2007). Mice lacking HIF-1α in osteoblasts exhibited narrower bones and reduced trabecular bone volume, associated with reduced vascular density and decreased bone formation (Wang et al., 2007; Shomento et al., 2010). Conversely, VHL inactivation, which is associated with constitutive HIF stabilization and boosted hypoxia signaling pathway activity, was associated with increased trabecular bone volume and increased VEGF levels and vascular density in bone (Wang et al., 2007). This study implicated osteoblastic HIF signaling in the regulation of angiogenesis in the bone microenvironment in response to hypoxia and postulated the principle of angiogenic—osteogenic coupling by hypoxia-sensing mechanisms, involving the indirect stimulation of osteogenesis as a consequence of skeletal vascular expansion (Wang et al., 2007). The critical oxygen-sensing prolyl hydroxylase enzymes (PHDs), which regulate HIF degradation in normoxia and control hypoxic HIF activity, have correspondingly been found to play important roles in the control of skeletal vascularization, bone formation, and bone remodeling (Wu et al., 2015). Combined inactivation of PHD1, PHD2, and PHD3 in osteoprogenitors resulted in extreme HIF signaling and excessive bone accumulation associated with overstimulation of angiogenic—osteogenic coupling (Wu et al., 2015).

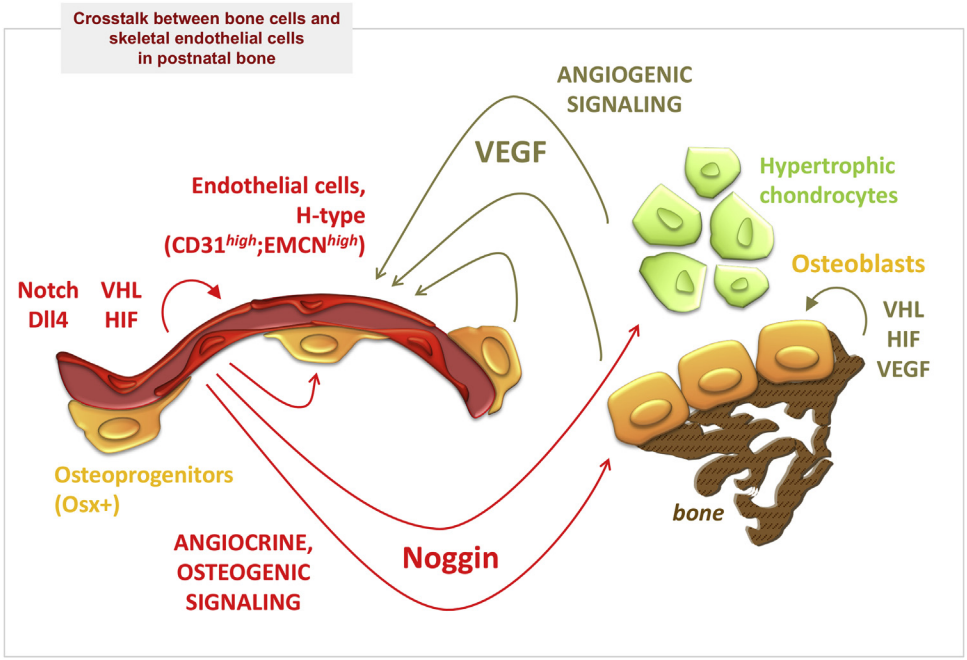

FIGURE 9.2 Bidirectional crosstalk between chondro-osteoblast lineage cells and skeletal endothelial cells, mediating angiogenic–osteogenic coupling in postnatal bone. Schematic view of the dynamic and reciprocal interplay between the different cell types in the bone environment that couples angiogenesis and osteogenesis. (Right and upper part) In the osteogenic compartment of the long bones, the signaling pathway governed by Von Hippel–Lindau (VHL), hypoxia-inducible factor (HIF), and vascular endothelial growth factor (VEGF) has been identified as a key driver of angiogenic–osteogenic coupling, by exerting both (1) cell-autonomous roles in chondrocytes, osteoprogenitors, and osteoblasts and (2) VEGF-mediated paracrine effects on the blood vessels in the bone environment, stimulating angiogenesis. (Left and lower part) In the vasculature of the bone and bone marrow environment, a specialized subtype of endothelial cells (ECs) expressing high levels of the endothelial markers CD31 and endomucin (EMCN) constitute the "type H" vessels in the metaphysis and endosteum. These ECs mediate the growth of the blood vessels in bone, through a tissue-selective mechanism of angiogenesis involving positive regulation by the VHL/HIF and Notch/Dll4 signaling pathways. Coupling of angiogenesis back to osteogenesis is mediated by osteoregulatory signals produced by ECs (i.e., angiocrine, osteogenic signals), such as Noggin. Osx, Osterix. *Figure adapted from Maes, C., Clemens, T.L., 2014. Angiogenic-osteogenic coupling: the endothelial perspective. Bonekey Rep. 3, 578.*

Work has also revealed additional roles of the hypoxia signaling pathways in the complex bone environment, as shown by using the Osx-Cre mouse to inactivate VHL in osteoprogenitors, either constitutively from fetal life onward or induced only later in the postnatal skeleton (by applying doxycycline/reverse tetracycline-controlled transactivator–mediated suppression of the activity of the Osx-Cre driver), and through other related mouse models. These studies revealed that the combined actions of the HIFs (both HIF-1 and HIF-2) increase angiogenesis and osteogenesis, alter hematopoiesis (mainly erythropoiesis), and enhance glycolytic cell metabolism in osteolineage cells (Shomento et al., 2010; Dirckx et al., 2018; Rankin et al., 2012; Regan et al., 2014). The last aspect appeared to be also associated with effects beyond bone on global energy metabolism, as hyperactivated hypoxia signaling through VHL deletion caused excessive glucose uptake and glycolysis in osteoblasts and an overall increased skeletal glucose consumption, along with impaired systemic control of glucose homeostasis (Dirckx et al., 2018). Altogether, the combined functions of the hypoxia pathway in bone are mediated by a large number of proteins encoded by direct HIF target genes (Semenza, 2012), with key roles ascribed to VEGF, erythropoietin, and genes involved in anaerobic cell metabolism, such as glucose transporters (e.g., Glut1) and key glycolytic enzymes including pyruvate dehydrogenase kinase 1, phosphoglycerate kinase 1, and lactate dehydrogenase A. As such, a growing number of effector proteins are being implicated in the responses to low oxygen in osteoblasts and other bone cell types, ensuring both cellular adaptation as well as remediation of the low oxygenation state within the tissue.

For VEGF specifically, the advantageous effects on osteogenesis are mediated partly indirectly by its paracrine proangiogenic actions—thereby stimulating the delivery of oxygen, nutrients, hormones, and angiocrine signaling factors (also see later) to the bone-forming osteoblasts—and partly directly. Indeed, most bone cell types express VEGF receptors, and ample in vitro studies have evidenced that VEGF signaling in osteolineage cells can induce their migration, differentiation, and bone-forming activity (reviewed in Maes, 2013). In vivo, a study overexpressing VEGF in the bone environment of adult mice suggested that cell-autonomous effects mediated by β-catenin signaling in osteoblast lineage

cells contributed to the phenotype, which was overall characterized by high bone mass, expansion of the osteoprogenitor pool, bone marrow fibrosis, and hematopoietic defects (Maes et al., 2010b). Conversely, conditional inactivation of *VEGF* in osteoprogenitors (driven by the Osx-Cre mouse strain) was shown to result in increased bone marrow adipogenesis at the expense of osteogenesis, and implicated intracrine-acting VEGF in cell fate decisions of stromal progenitors in the bone environment (Liu et al., 2012). Proper angiogenic–osteogenic coupling thus requires tight regulation and dynamic fine-tuning of the hypoxia signaling events and VEGF levels within the bone environment.

These hypoxia-related mechanisms have also been implicated in widespread bone pathologies, and pharmacological PHD inhibitors could be of great therapeutic value, for instance, in age-related osteoporosis and compromised fracture healing. Genetic inactivation of VHL or PHDs in mice or treatment with PHD-inhibiting compounds was effective in protecting mice against age- or ovariectomy-induced bone loss (Kusumbe et al., 2014; Wu et al., 2015; Zhao et al., 2012; Weng et al., 2014; Liu et al., 2014). Furthermore, activation of HIFs can be a successful strategy to improve fracture repair and bone regeneration, as supported by experimental animal models (Wan et al., 2008; Shen et al., 2009).

Endothelial and angiocrine signaling in bone

The aforementioned studies amply showed that osteolineage cells are equipped with the molecular tools to sense oxygen tension and direct adjustments in vascularization by signaling to endothelial cells. In addition, the regulation of skeletal vascularization and angiogenic–osteogenic coupling also involves endothelial cell-intrinsic mechanisms and angiocrine signals secreted by the endothelium, including the HIF signaling pathway, Notch, and bone morphogenetic protein (BMP) family signaling. Indeed, the oxygen-regulated program mediated by HIFs is also key in the endothelial cells of the skeletal blood vessels, in line with the hypoxic status of the postnatal bone and bone marrow environment. This has been shown by endothelium-specific, inducible inactivation of VHL in mice (using the vascular endothelial–cadherin [or Cdh5] promotor to drive the expression of CreERt2), which led to a striking increase in H-type blood vessels in the bones of juvenile mice (Kusumbe et al., 2014). Concomitantly, the pool of $Runx2^{+}$ or Osx^{+} cells associated with these vessels was expanded and the bone volume increased. The converse phenotype was seen upon endothelial cell-targeted inactivation of HIF-1α, as this mutation led to severe vascular defects and reduced numbers of osteoprogenitors (Kusumbe et al., 2014). It is thought that endothelial cells of H-type blood vessels secrete pro-osteogenic factors such as fibroblast growth factors, PDGFs, and BMPs, and as such contribute to the coupling of angiogenesis and osteogenesis (Ramasamy et al., 2016; Kusumbe et al., 2014). One signaling system that was found to be very important in the local production of angiocrine signals by vascular endothelial cells in the bone microenvironment is the Notch pathway (Ramasamy et al., 2014). Loss- and gain-of-function mouse models established that Notch/Dll4 signaling in H-type capillary endothelial cells regulated angiogenesis but also osteogenesis, by influencing the endothelial production and secretion of the BMP antagonist Noggin, which surprisingly was found to positively influence osteolineage cells and bone formation in vivo (Ramasamy et al., 2014).

These studies and further work are increasingly revealing that the endothelial cells of the skeletal blood vessels exert important signaling functions contributing to the control of bone development, growth, homeostasis, and regeneration, as well as to hematopoiesis. Indeed, within the skeletal system, blood vessels also constitute critical components of the niche microenvironments for HSCs in the bone marrow; the specific localization, nature, and molecular determinants of the vascular niches for HSCs are topics of intensive ongoing investigations at the interface between bone biology and hematology, with broad therapeutic application (Kusumbe et al., 2016; Itkin et al., 2016).

The nerve system of bone

Innervation of developing bone

The development of the nervous system is a complex process of axonal growth, synapse formation, and cellular signaling, during which the spinal cord forms from the neural tube during neurulation (Ciani and Salinas, 2005). Sensory axons enter the spinal cord through the dorsal roots and then ascend through the emerging white matter to the brain, whereas sympathetic neurons migrate ventrally to coalesce in prevertebral sympathetic ganglia (Glebova and Ginty, 2005). Both sensory and sympathetic axons are guided to their appropriate peripheral target tissues, including bone, by neurotrophic factors (Pezet and McMahon, 2006). In fact, developing tissues dictate the amount and type of innervation they require by secreting the specific neurotrophin that promotes neuronal survival of its corresponding axon type (Reichardt, 2006). At least one such neurotrophin is known to be active in developing long bone: nerve growth factor (NGF). In a 2016 study, this prototypical neurotrophic factor was found to be expressed by osteoprogenitor cells during both primary and secondary ossification (Tomlinson et al., 2016). Moreover, sensory neurons located in the dorsal root ganglion project axons

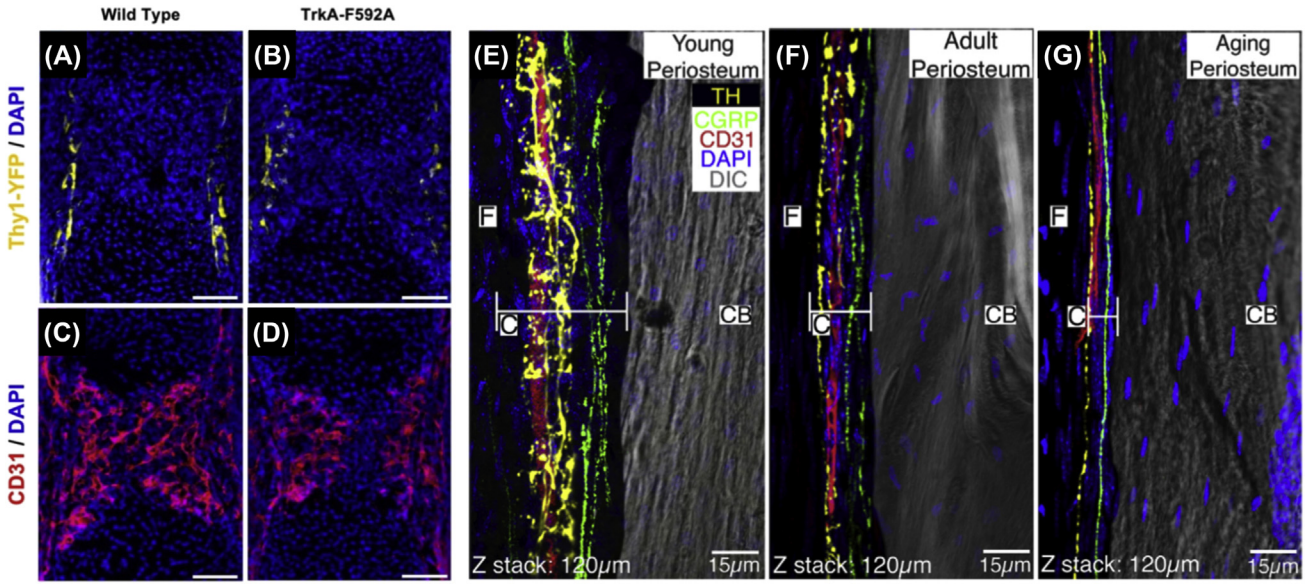

FIGURE 9.3 Skeletal nerves in the periosteum from beginning to end. (A) Thy1-YFP reporter mice were used to visualize nerve axons in the perichondrial region at embryonic day 15.5, just after primary ossification centers have formed. (B) Inhibition of nerve growth factor (NGF)−tyrosine kinase receptor 1 (TrkA) signaling in TrkA-F592A mice diminished nerve axons in the perichondrial region. (C, D) Similarly, inhibition of NGF−TrkA signaling impaired vascular invasion of the ossification center, as visualized by staining against CD31. Scale bars, 100 μm. (E) The periosteum of a young mouse is teeming with $CD31^+$ blood vessels (*red*), calcitonin gene-related peptide $(CGRP)^+$ sensory nerve axons (*green*), and tyrosine hydroxylase (TH)+ sympathetic nerve axons (*yellow*). (F, G) As the mouse ages to adulthood and beyond, the cambium layer shrinks but sensory and sympathetic nerve fibers along with blood vessels remain intact in the periosteum. Cambium (*C*) and fibrous (*F*) layers of the periosteum and cortical bone (*CB*) are labeled. *(C, D) Adapted from Tomlinson R.E., Li, Z., Zhang, Q., Goh B.C., Li, Z., Thorek D.L.J., Rajbhandari, L., Brushart T.M., Minichiello, L., Zhou, F., Venkatesan, A., Clemens T.L., 2016. NGF-TrkA signaling by sensory nerves coordinates the vascularization and ossification of developing endochondral bone. Cell Rep. 16 (10), 2723−2735. (F, G) Adapted from Chartier, S.R., Mitchell, S.A.T., Majuta, L.A., Mantyh, P.W., 2018. The changing sensory and sympathetic innervation of the young, adult and aging mouse femur. Neuroscience 387, 178−190.*

expressing neurotrophic tyrosine kinase receptor 1 (TrkA), the high-affinity receptor for NGF, which reach perichondrial bone surfaces adjacent to primary ossification centers at a time coincident with the initiation of NGF expression in osteochondral progenitor cells. Inactivation of TrkA signaling in mice impaired skeletal innervation, delayed vascular invasion, and decreased the number of osteoprogenitor cells, resulting in decreased femoral bone length and volume. These results were consistent with previous studies on the skeletal action of semaphorin 3A (Sema3A), a well-characterized inhibitor of neuronal outgrowth. Mice lacking Sema3a were observed to have gross defects in nerve, heart, and skeletal patterning (Behar et al., 1996). Subsequent work found that selective loss of Sema3a in neurons, but not osteoblasts, decreased skeletal sensory innervation and postnatal bone mass (Fukuda et al., 2013). To date, no studies have conclusively examined the timing and location of the arrival of sympathetic or parasympathetic nerves in bone. Given that sympathetic innervation of the mesenteric arteries in mouse takes place postnatally, it is unlikely that autonomic nerve fibers play a major role in primary or secondary ossification (Brunet et al., 2014) (Fig. 9.3).

Innervation of the mature skeleton

Somatic nervous system

Sensory nerves of the somatic nervous system are distributed throughout the body, including the skin, bones, joints, tendons, and muscles, and transduce signals involved in spatial orientation (proprioception), pain and noxious stimuli (nociception), temperature changes, and the perception of nonpainful tactile stimuli (Julius and Basbaum, 2001; McKemy et al., 2002; Proske and Gandevia, 2012; Jones and Smith, 2014). To accomplish these functions, nerve endings generally express a wide variety of receptors and channels that will initiate the appropriate signaling cascades in response to perturbations (Pongratz and Straub, 2013). These include Toll-like receptors, cytokine and prostaglandin receptors, transient receptor potential ion channels, and growth factor receptors, among many others (Pongratz and Straub, 2013). Surprisingly, the vast majority (>80%) of nerves in mature bone are thinly myelinated or unmyelinated sensory nerves that express

TrkA, a consequence of the expression of NGF during development (Castañeda-Corral et al., 2011; Tomlinson et al., 2016; Jimenez-Andrade et al., 2010). Furthermore, the density of sensory nerves in the adult mouse femur is highest in the periosteum and marrow space, relatively low in the mineralized bone, and essentially zero in healthy cartilage (Mach et al., 2002; Castañeda-Corral et al., 2011).

In general, the most familiar and best understood function of sensory nerves is pain sensation, which is profoundly apparent following traumatic bone fracture or in patients with bone malignancies. The central mediator of osseous pain sensation is NGF, which transmits nociceptive signals either by directly activating the abundant TrkA+ sensory nerves in bone or through indirect mechanisms that enhance the response of other nociceptive pathways (Mantyh, 2014). This upstream position of the NGF−TrkA signaling pathway in pain sensation has made it an attractive target for developing pharmaceuticals for treating pain associated with cancer and osteoarthritis as well as an active area of research. Several studies have documented upregulated expression of NGF in progenitor cells, osteoblasts, and chondrocytes during fracture repair in rodents (Asaumi et al., 2000; Grills and Schuijers, 1998). Correspondingly, blockade of NGF function has been observed to significantly decrease behavior associated with pain following fracture in mice (Jimenez-Andrade et al., 2007; Koewler et al., 2007), and additional studies demonstrated that this analgesia can be provided without affecting standard fracture healing outcomes (Rapp et al., 2015). However, others have shown that topical application of NGF to rib fractures in rats and the distraction callus in rabbit mandibles significantly decreases healing time and improves subsequent repair strength (Grills et al., 1997; Wang et al., 2006). This effect is thought to be mediated through NGF-induced release of neuropeptides such as calcitonin gene-related peptide (CGRP) and substance P (Malcangio et al., 1997; Quarcoo et al., 2004), which are both known to positively influence bone formation (Baldock et al., 2007; Goto et al., 2001, 2007; Li et al., 2010; Long et al., 2010; Lundberg et al., 2007; Sample et al., 2011). As a result, more work must be done to fully understand the role of NGF−TrkA signaling in bone fracture repair. Nonetheless, widespread therapeutic use of the highly effective anti-NGF antibodies for pain relief may be imminent (Lane et al., 2010; Jayabalan and Schnitzer, 2017; Birbara et al., 2018). Although phase III clinical trials were halted in 2010 due to an increased incidence of adverse events (Hochberg, 2015), the humanized monoclonal anti-NGF antibody tanezumab (Pfizer and Lilly) received FDA fast-track approval in 2017 as the first in a new class of nonopioid pain relievers.

In addition to pain sensation, sensory nerves in bone have also been found to play an important role in responding to mechanical loads placed on the skeleton. This line of inquiry was initiated based on the observation that primary afferent sensory nerves are present in a dense meshlike network on the periosteal and endosteal surfaces (Martin et al., 2007), which are the preferential sites for the perception of skeletal deformation. Mature, OC-expressing osteoblasts on the periosteal and endosteal surfaces of bone were observed to robustly express NGF in response to mechanical loading in mice (Tomlinson et al., 2017). Furthermore, the researchers found that inactivation of NGF−TrkA signaling significantly attenuated bone formation in response to load, via a decrease in osteocytic Wnt/β-catenin signaling. Since sensory nerves remain essentially intact in the periosteum throughout life, even as bone undergoes marked changes associated with aging (Chartier et al., 2018), targeting NGF−TrkA signaling for bone accrual may be a viable strategy in cases in which bone cell−targeted therapies may fail. Importantly, more research is necessary to determine if anti-NGF therapeutic agents for pain will substantially affect strain-adaptive bone remodeling in humans.

Autonomic nervous system

The autonomic nervous system (ANS), part of the peripheral nervous system, is divided into two antagonistic branches: the sympathetic nervous system and the parasympathetic nervous system. Whereas sympathetic nerves primarily signal through the release of norepinephrine to activate α- and β-adrenergic receptors, parasympathetic nerves release acetylcholine that activates muscarinic acetylcholine receptors (mAChRs) and nicotinic acetylcholine receptors (nAChRs). In general, these two nerve types serve to coordinate bodily functions not consciously directed, such as breathing or the regulation of blood pressure. Both nerve types are present in bone tissue, and have been primarily visualized in close contact with the main arteries that provide the blood supply to long bones (Bjurholm et al., 1988; Hill and Elde, 1991; Tabarowski et al., 1996). In particular, nerves expressing tyrosine hydroxylase (TH) (the rate-limiting enzyme in the synthesis of catecholamines) are routinely observed wrapping around blood vessels in bone with a spiral-type morphology (Mach et al., 2002; Castañeda-Corral et al., 2011). Similarly, parasympathetic nerves with immunoreactivity against vesicular acetylcholine transporter and choline acetyltransferase can be observed readily, particularly in the marrow space (Artico et al., 2002; Bajayo et al., 2012). However, the specific locations, densities, and distributions throughout the bone and marrow space are not well described.

Generally, it is held that the ANS exerts its effect on the skeleton via close contact with bone cells. However, given the limited direct interaction of ANS nerve fibers with skeletal cells (Dénes et al., 2005), others have proposed that a diffusion mechanism may have a role (Elefteriou, 2018). Nonetheless, osteoblasts and osteoclasts have both been observed to express a wide variety of adrenergic receptors, most notably the β2-adrenergic receptor (Kajimura et al., 2011), which can respond to the norepinephrine released by sympathetic nerve terminals (Togari, 2002). Work has shown that neither osteoblasts nor osteoclasts express detectable levels of mAChRs, but nAChRs are readily observable, particularly the α2 and β2 subunits, which may respond to the release of acetylcholine from parasympathetic nerve terminals (Bajayo et al., 2012).

Bone remodeling activity is at least partially restrained by signals emanating from the ANS via regulation of bone resorption (Elefteriou et al., 2005). Several studies have shown that sympathetic nervous outflow stimulates bone resorption that, in turn, negatively affects bone formation (Elefteriou et al., 2005; Katayama et al., 2006), whereas parasympathetic signaling appears to favor bone accrual by inhibiting bone resorption (Bajayo et al., 2012). This paradigm is consistent with the circadian rhythm of the ANS. Generally, sympathetic nervous activity is dominant during the day, during peak bone resorption; conversely, parasympathetic nervous activity is dominant during the night, during peak bone formation (Dudek and Meng, 2014; Komoto et al., 2012; Shao et al., 2003). Furthermore, mice lacking β2-adrenergic receptor in the osteoblast lineage have significantly increased bone formation coupled with decreased bone resorption, leading to an eventual increase in total bone mass in adulthood (Kajimura et al., 2011). However, pharmacological studies do not recapitulate this encouraging result: treatment with either a β-adrenergic receptor agonist (salbutamol) or an antagonist (isoprenaline) was associated with bone loss in mice, mainly through increased bone resorption (Bonnet et al., 2007; Kondo and Togari, 2011). Nonetheless, the known safety profile of "β blockers," which block activation of β-adrenergic receptors and have achieved widespread use for the treatment of cardiovascular disease, has resulted in significant interest in modulating ANS signaling to increase bone mass in humans. Encouragingly, a recent meta-analysis of seven cohort and nine case−control studies found that the use of β blockers was associated with a 15% decrease in overall fracture risk, with β1-specific blockers most strongly associated with the risk reduction (Toulis et al., 2014). Nonetheless, a 2015 randomized clinical trial was unable to establish an effect of β2-adrenergic agonists or antagonists on human bone turnover (Veldhuis-Vlug et al., 2015). Furthermore, preclinical studies have concluded that the contribution of sympathetic signaling to load-induced bone formation in bone is minimal (de Souza et al., 2005); no studies have investigated the role of parasympathetic signaling in this process. In total, much work remains to determine the direct and specific effects of the ANS on bone metabolism.

Conclusion

The pre-eminent role of vascularization in bone was originally reported in the 1960s (Trueta and Buhr, 1963; Trueta and Caladias, 1964) and is now well established. Moreover, much has been learned about the regulation of vascular growth in bone and the roles of VEGF and the hypoxia signaling pathways, both in physiology and in bone defect repair. Altogether, studies performed in this field are progressively uncovering the molecular underpinnings of osteo-angiogenic coupling, which obviously involves a vigorous bidirectional crosstalk between endothelial cells and osteolineage cells that is only beginning to be uncovered. Especially little is known, as of this writing, about the nature of angiocrine signaling factors emanating from the endothelium and their roles in developing, growing, remodeling, and healing bones. Many other aspects of the organization, integrity, and functioning of the vasculature in the skeletal system remain to be investigated in further depth, including the molecular specifics of the specialized vascular environments for skeletal stem/progenitor cell harboring and bone formation, and of the niches controlling the maintenance of HSCs and the support of hematopoiesis in the bone marrow environment. Increasing insights into these areas will direct future studies exploring how the bone vasculature can ultimately be modulated to achieve anabolic treatments of osteoporosis and other bone disorders, to support compromised fracture repair and tissue engineering therapies, and to improve treatments of hematological pathologies and stem cell transplantation protocols.

Similarly, the skeleton is densely innervated by a wide variety of somatic and autonomic nerve axons that carry out their unique functions in a complex microenvironment. Despite tremendous advances, much remains to be uncovered regarding the nerves in bone. These lingering questions include the timeline of sympathetic innervation in bone, the role of NGF−TrkA signaling in bone repair, the identification of nerve-derived osteogenic cues, the specific action of the ANS on bone remodeling, and the alterations in nerve signaling that occur with aging.

Finally, the mechanisms by which bone vascular and nerve systems interact during development, homeostatic bone remodeling, and fracture repair still need to be uncovered. Answers to these fundamental questions will inevitably lead to novel approaches for improving overall skeletal health.

References

Amarilio, R., Viukov, S.V., Sharir, A., Eshkar-Oren, I., Johnson, R.S., Zelzer, E., 2007. HIF-1alpha regulation of Sox9 is necessary to maintain differentiation of hypoxic prechondrogenic cells during early skeletogenesis. Development 134 (21), 3917–3928.

Artico, M., Bosco, S., Cavallotti, C., Agostinelli, E., Giuliani-Piccari, G., Sciorio, S., Cocco, L., Vitale, M., 2002. Noradrenergic and cholinergic innervation of the bone marrow. Int. J. Mol. Med. 10 (1), 77–80.

Asaumi, K., Nakanishi, T., Asahara, H., Inoue, H., Takigawa, M., 2000. Expression of neurotrophins and their receptors (TRK) during fracture healing. Bone 26 (6), 625–633.

Bajayo, A., Bar, A., Denes, A., Bachar, M., Kram, V., Attar-Namdar, M., Zallone, A., Kovács, K.J., Yirmiya, R., Bab, I., 2012. Skeletal parasympathetic innervation communicates central IL-1 signals regulating bone mass accrual. Proc. Natl. Acad. Sci. U.S.A. 109 (38), 15455–15460.

Baldock, P.A., Allison, S.J., Lundberg, P., Lee, N.J., Slack, K., Lin, E.J., Enriquez, R.F., McDonald, M.M., Zhang, L., During, M.J., Little, D.G., Eisman, J.A., Gardiner, E.M., Yulyaningsih, E., Lin, S., Sainsbury, A., Herzog, H., 2007. Novel role of Y1 receptors in the coordinated regulation of bone and energy homeostasis. J. Biol. Chem. 282 (26), 19092–19102.

Behar, O., Golden, J.A., Mashimo, H., Schoen, F.J., Fishman, M.C., 1996. Semaphorin III is needed for normal patterning and growth of nerves, bones and heart. Nature 383 (6600), 525–528.

Birbara, C., Dabezies Jr., E.J., Burr, A.M., Fountaine, R.J., Smith, M.D., Brown, M.T., West, C.R., Arends, R.H., Verburg, K.M., 2018. Safety and efficacy of subcutaneous tanezumab in patients with knee or hip osteoarthritis. J. Pain Res. 11, 151–164.

Bjurholm, A., Kreicbergs, A., Brodin, E., Schultzberg, M., 1988. Substance P- and CGRP-immunoreactive nerves in bone. Peptides 9 (1), 165–171.

Bonnet, N., Benhamou, C.L., Beaupied, H., Laroche, N., Vico, L., Dolleans, E., Courteix, D., 2007. Doping dose of salbutamol and exercise: deleterious effect on cancellous and cortical bones in adult rats. J. Appl. Physiol. 102 (4), 1502–1509.

Brookes, M., Revell, W.J., 1998. Blood Supply of Bone: Scientific Aspects. Springer, London; New York xx, 359 p.

Brunet, I., Gordon, E., Han, J., Cristofaro, B., Broqueres-You, D., Liu, C., Bouvrée, K., Zhang, J., del Toro, R., Mathivet, T., Larrivée, B., Jagu, J., Pibouin-Fragner, L., Pardanaud, L., Machado, M.J.C., Kennedy, T.E., Zhuang, Z., Simons, M., Levy, B.I., Tessier-Lavigne, M., Grenz, A., Eltzschig, H., Eichmann, A., 2014. Netrin-1 controls sympathetic arterial innervation. J. Clin. Invest. 124 (7), 3230–3240.

Burkhardt, R., Kettner, G., Bohm, W., Schmidmeier, M., Schlag, R., Frisch, B., Mallmann, B., Eisenmenger, W., Gilg, T., 1987. Changes in trabecular bone, hematopoiesis and bone marrow vessels in aplastic anemia, primary osteoporosis, and old age: a comparative histomorphometric study. Bone 8 (3), 157–164.

Carano, R.A., Filvaroff, E.H., 2003. Angiogenesis and bone repair. Drug Discov. Today 8 (21), 980–989.

Castañeda-Corral, G., Jimenez-Andrade, J.M., Bloom, A.P., Taylor, R.N., Mantyh, W.G., Kaczmarska, M.J., Ghilardi, J.R., Mantyh, P.W., 2011. The majority of myelinated and unmyelinated sensory nerve fibers that innervate bone express the tropomyosin receptor kinase a. Neuroscience 178, 196–207.

Chartier, S.R., Mitchell, S.A.T., Majuta, L.A., Mantyh, P.W., 2018. The changing sensory and sympathetic innervation of the young, adult and aging mouse femur. Neuroscience 387, 178–190.

Chen, D., Tian, W., Li, Y., Tang, W., Zhang, C., 2012. Osteoblast-specific transcription factor osterix (Osx) and HIF-1alpha cooperatively regulate gene expression of vascular endothelial growth factor (VEGF). Biochem. Biophys. Res. Commun. 424 (1), 176–181.

Ciani, L., Salinas, P.C., 2005. Wnts in the vertebrate nervous system: from patterning to neuronal connectivity. Nat. Rev. Neurosci. 6 (5), 351–362.

Cramer, T., Schipani, E., Johnson, R.S., Swoboda, B., Pfander, D., 2004. Expression of VEGF isoforms by epiphyseal chondrocytes during low-oxygen tension is HIF-1 alpha dependent. Osteoarthritis Cartilage 12 (6), 433–439.

de Souza, R.L., Pitsillides, A.A., Lanyon, L.E., Skerry, T.M., Chenu, C., 2005. Sympathetic nervous system does not mediate the load-induced cortical new bone formation. J. Bone Miner. Res. 20 (12), 2159–2168.

Dénes, A., Boldogkoi, Z., Uhereczky, G., Hornyák, A., Rusvai, M., Palkovits, M., Kovács, K.J., 2005. Central autonomic control of the bone marrow: multisynaptic tract tracing by recombinant pseudorabies virus. Neuroscience 134 (3), 947–963.

Dirckx, N., Maes, C., 2016. Hypoxia-driven pathways in endochondral bone development. In: Grässel, S., Aszodi, A. (Eds.), Cartilage, Physiology and Development, vol. 1. Springer International Publishing, Switzerland, pp. 143–168 (Chapter 6).

Dirckx, N., Van Hul, M., Maes, C., 2013. Osteoblast recruitment to sites of bone formation in skeletal development, homeostasis, and regeneration. Birth Defects Res. C Embryo Today 99 (3), 170–191.

Dirckx, N., Tower, R.J., Mercken, E.M., Vangoitsenhoven, R., Moreau-Triby, C., Breugelmans, T., Nefyodova, E., Cardoen, R., Mathieu, C., Van der Schueren, B., Confavreux, C.B., Clemens, T.L., Maes, C., 2018. VHL deletion in osteoblasts boosts cellular glycolysis and improves global glucose metabolism. J. Clin. Invest. 128 (3), 1087–1105.

Duan, X., Murata, Y., Liu, Y., Nicolae, C., Olsen, B.R., Berendsen, A.D., 2015. Vegfa regulates perichondrial vascularity and osteoblast differentiation in bone development. Development 142 (11), 1984–1991.

Dudek, M., Meng, Q.-J., 2014. Running on time: the role of circadian clocks in the musculoskeletal system. Biochem. J. 463 (1), 1–8.

Elefteriou, F., Ahn, J.D., Takeda, S., Starbuck, M., Yang, X., Liu, X., Kondo, H., Richards, W.G., Bannon, T.W., Noda, M., Clement, K., Vaisse, C., Karsenty, G., 2005. Leptin regulation of bone resorption by the sympathetic nervous system and cart. Nature 434 (7032), 514–520.

Elefteriou, F., 2018. Impact of the autonomic nervous system on the skeleton. Physiol. Rev. 98 (3), 1083–1112.

Eshkar-Oren, I., Viukov, S.V., Salameh, S., Krief, S., Oh, C.D., Akiyama, H., Gerber, H.P., Ferrara, N., Zelzer, E., 2009. The forming limb skeleton serves as a signaling center for limb vasculature patterning via regulation of VEGF. Development 136 (8), 1263–1272.

Fukuda, T., Takeda, S., Xu, R., Ochi, H., Sunamura, S., Sato, T., Shibata, S., Yoshida, Y., Gu, Z., Kimura, A., Ma, C., Xu, C., Bando, W., Fujita, K., Shinomiya, K., Hirai, T., Asou, Y., Enomoto, M., Okano, H., Okawa, A., Itoh, H., 2013. Sema3a regulates bone-mass accrual through sensory innervations. Nature 497 (7450), 490–493.

Gerber, H.P., Vu, T.H., Ryan, A.M., Kowalski, J., Werb, Z., Ferrara, N., 1999. VEGF couples hypertrophic cartilage remodeling, ossification and angiogenesis during endochondral bone formation. Nat. Med. 5 (6), 623–628.

Glebova, N.O., Ginty, D.D., 2005. Growth and survival signals controlling sympathetic nervous system development. Annu. Rev. Neurosci. 28, 191–222.

Goto, T., Kido, M.A., Yamaza, T., Tanaka, T., 2001. Substance p and substance p receptors in bone and gingival tissues. Med. Electron. Microsc. 34 (2), 77–85.

Goto, T., Nakao, K., Gunjigake, K.K., Kido, M.A., Kobayashi, S., Tanaka, T., 2007. Substance P stimulates late-stage rat osteoblastic bone formation through neurokinin-1 receptors. Neuropeptides 41 (1), 25–31.

Grills, B.L., Schuijers, J.A., 1998. Immunohistochemical localization of nerve growth factor in fractured and unfractured rat bone. Acta Orthop. Scand. 69 (4), 415–419.

Grills, B.L., Schuijers, J.A., Ward, A.R., 1997. Topical application of nerve growth factor improves fracture healing in rats. J. Orthop. Res. 15 (2), 235–242.

Haigh, J.J., Gerber, H.P., Ferrara, N., Wagner, E.F., 2000. Conditional inactivation of VEGF-A in areas of collagen2a1 expression results in embryonic lethality in the heterozygous state. Development 127 (7), 1445–1453.

Hill, E.L., Elde, R., 1991. Distribution of c CGRP-, VIP-, D beta H-, SP-, and NPY-immunoreactive nerves in the periosteum of the rat. Cell Tissue Res. 264 (3), 469–480.

Hochberg, M.C., 2015. Serious joint-related adverse events in randomized controlled trials of anti-nerve growth factor monoclonal antibodies. Osteoarthritis Cartilage 23 (Suppl. 1), S21.

Hohmann, E.L., Elde, R.P., Rysavy, J.A., Einzig, S., Gebhard, R.L., 1986. Innervation of periosteum and bone by sympathetic vasoactive intestinal peptide-containing nerve fibers. Science 232 (4752), 868–871.

Hukkanen, M., Konttinen, Y.T., Rees, R.G., Gibson, S.J., Santavirta, S., Polak, J.M., 1992. Innervation of bone from healthy and arthritic rats by substance P and calcitonin gene related peptide containing sensory fibers. J. Rheumatol. 19 (8), 1252–1259.

Itkin, T., Gur-Cohen, S., Spencer, J.A., Schajnovitz, A., Ramasamy, S.K., Kusumbe, A.P., Ledergor, G., Jung, Y., Milo, I., Poulos, M.G., Kalinkovich, A., Ludin, A., Kollet, O., Shakhar, G., Butler, J.M., Rafii, S., Adams, R.H., Scadden, D.T., Lin, C.P., Lapidot, T., 2016. Distinct bone marrow blood vessels differentially regulate haematopoiesis. Nature 532 (7599), 323–328.

Jayabalan, P., Schnitzer, T.J., 2017. Tanezumab in the treatment of chronic musculoskeletal conditions. Expert Opin. Biol. Ther. 17 (2), 245–254.

Jimenez-Andrade, J.M., Martin, C.D., Koewler, N.J., Freeman, K.T., Sullivan, L.J., Halvorson, K.G., Barthold, C.M., Peters, C.M., Buus, R.J., Ghilardi, J.R., Lewis, J.L., Kuskowski, M.A., Mantyh, P.W., 2007. Nerve growth factor sequestering therapy attenuates non-malignant skeletal pain following fracture. Pain 133 (1–3), 183–196.

Jimenez-Andrade, J.M., Mantyh, W.G., Bloom, A.P., Xu, H., Ferng, A.S., Dussor, G., Vanderah, T.W., Mantyh, P.W., 2010. A phenotypically restricted set of primary afferent nerve fibers innervate the bone versus skin: therapeutic opportunity for treating skeletal pain. Bone 46 (2), 306–313.

Jones, L.A., Smith, A.M., 2014. Tactile sensory system: encoding from the periphery to the cortex. Wiley Interdiscip. Rev. Syst. Biol. Med. 6 (3), 279–287.

Julius, D., Basbaum, A.I., 2001. Molecular mechanisms of nociception. Nature 413 (6852), 203–210.

Kajimura, D., Hinoi, E., Ferron, M., Kode, A., Riley, K.J., Zhou, B., Guo, X.E., Karsenty, G., 2011. Genetic determination of the cellular basis of the sympathetic regulation of bone mass accrual. J. Exp. Med. 208 (4), 841–851.

Karsenty, G., Wagner, E.F., 2002. Reaching a genetic and molecular understanding of skeletal development. Dev. Cell 2 (4), 389–406.

Katayama, Y., Battista, M., Kao, W.-M., Hidalgo, A., Peired, A.J., Thomas, S.A., Frenette, P.S., 2006. Signals from the sympathetic nervous system regulate hematopoietic stem cell egress from bone marrow. Cell 124 (2), 407–421.

Koewler, N.J., Freeman, K.T., Buus, R.J., Herrera, M.B., Jimenez-Andrade, J.M., Ghilardi, J.R., Peters, C.M., Sullivan, L.J., Kuskowski, M.A., Lewis, J.L., Mantyh, P.W., 2007. Effects of a monoclonal antibody raised against nerve growth factor on skeletal pain and bone healing after fracture of the C57BL/6J mouse femur. J. Bone Miner. Res. 22 (11), 1732–1742.

Komoto, S., Kondo, H., Fukuta, O., Togari, A., 2012. Comparison of β-adrenergic and glucocorticoid signaling on clock gene and osteoblast-related gene expressions in human osteoblast. Chronobiol. Int. 29 (1), 66–74.

Kondo, H., Togari, A., 2011. Continuous treatment with a low-dose β-agonist reduces bone mass by increasing bone resorption without suppressing bone formation. Calcif. Tissue Int. 88 (1), 23–32.

Kusumbe, A.P., Ramasamy, S.K., Adams, R.H., 2014. Coupling of angiogenesis and osteogenesis by a specific vessel subtype in bone. Nature 507 (7492), 323–328.

Kusumbe, A.P., Ramasamy, S.K., Itkin, T., Mae, M.A., Langen, U.H., Betsholtz, C., Lapidot, T., Adams, R.H., 2016. Age-dependent modulation of vascular niches for haematopoietic stem cells. Nature 532 (7599), 380–384.

Lane, N.E., Schnitzer, T.J., Birbara, C.A., Mokhtarani, M., Shelton, D.L., Smith, M.D., Brown, M.T., 2010. Tanezumab for the treatment of pain from osteoarthritis of the knee. N. Engl. J. Med. 363 (16), 1521–1531.

Li, J., Ahmed, M., Bergstrom, J., Ackermann, P., Stark, A., Kreicbergs, A., 2010. Occurrence of substance P in bone repair under different load comparison of straight and angulated fracture in rat tibia. J. Orthop. Res. 28 (12), 1643–1650.

Lin, C., McGough, R., Aswad, B., Block, J.A., Terek, R., 2004. Hypoxia induces HIF-1alpha and VEGF expression in chondrosarcoma cells and chondrocytes. J. Orthop. Res. 22 (6), 1175–1181.

Linder, J.E., 1978. A simple and reliable method for the silver impregnation of nerves in paraffin sections of soft and mineralized tissues. J. Anat. 127 (Pt 3), 543–551.

Liu, Y., Berendsen, A.D., Jia, S., Lotinun, S., Baron, R., Ferrara, N., Olsen, B.R., 2012. Intracellular VEGF regulates the balance between osteoblast and adipocyte differentiation. J. Clin. Invest. 122 (9), 3101–3113.

Liu, X., Tu, Y., Zhang, L., Qi, J., Ma, T., Deng, L., 2014. Prolyl hydroxylase inhibitors protect from the bone loss in ovariectomy rats by increasing bone vascularity. Cell Biochem Biophys 69 (1), 141–149.

Long, H., Ahmed, M., Ackermann, P., Stark, A., Li, J., 2010. Neuropeptide Y innervation during fracture healing and remodeling. A study of angulated tibial fractures in the rat. Acta Orthop. 81 (5), 639–646.

Lundberg, P., Allison, S.J., Lee, N.J., Baldock, P.A., Brouard, N., Rost, S., Enriquez, R.F., Sainsbury, A., Lamghari, M., Simmons, P., Eisman, J.A., Gardiner, E.M., Herzog, H., 2007. Greater bone formation of Y2 knockout mice is associated with increased osteoprogenitor numbers and altered Y1 receptor expression. J. Biol. Chem. 282 (26), 19082–19091.

Mach, D.B., Rogers, S.D., Sabino, M.C., Luger, N.M., Schwei, M.J., Pomonis, J.D., Keyser, C.P., Clohisy, D.R., Adams, D.J., O'Leary, P., Mantyh, P.W., 2002. Origins of skeletal pain: sensory and sympathetic innervation of the mouse femur. Neuroscience 113 (1), 155–166.

Maes, C., Clemens, T.L., 2014. Angiogenic-osteogenic coupling: the endothelial perspective. Bonekey Rep. 3, 578.

Maes, C., Carmeliet, P., Moermans, K., Stockmans, I., Smets, N., Collen, D., Bouillon, R., Carmeliet, G., 2002. Impaired angiogenesis and endochondral bone formation in mice lacking the vascular endothelial growth factor isoforms VEGF164 and VEGF188. Mech. Dev. 111, 61–73.

Maes, C., Stockmans, I., Moermans, K., Van Looveren, R., Smets, N., Carmeliet, P., Bouillon, R., Carmeliet, G., 2004. Soluble VEGF isoforms are essential for establishing epiphyseal vascularization and regulating chondrocyte development and survival. J. Clin. Invest. 113 (2), 188–199.

Maes, C., Kobayashi, T., Selig, M.K., Torrekens, S., Roth, S.I., Mackem, S., Carmeliet, G., Kronenberg, H.M., 2010a. Osteoblast precursors, but not mature osteoblasts, move into developing and fractured bones along with invading blood vessels. Dev. Cell 19 (2), 329–344.

Maes, C., Goossens, S., Bartunkova, S., Drogat, B., Coenegrachts, L., Stockmans, I., Moermans, K., Nyabi, O., Haigh, K., Naessens, M., Haenebalcke, L., Tuckermann, J.P., Tjwa, M., Carmeliet, P., Mandic, V., David, J.P., Behrens, A., Nagy, A., Carmeliet, G., Haigh, J.J., 2010b. Increased skeletal VEGF enhances beta-catenin activity and results in excessively ossified bones. EMBO J. 29 (2), 424–441.

Maes, C., Araldi, E., Haigh, K., Khatri, R., Van Looveren, R., Giaccia, A.J., Haigh, J.J., Carmeliet, G., Schipani, E., 2012a. VEGF-independent cell-autonomous functions of HIF-1alpha regulating oxygen consumption in fetal cartilage are critical for chondrocyte survival. J. Bone Miner. Res. 27 (3), 596–609.

Maes, C., Carmeliet, G., Schipani, E., 2012b. Hypoxia-driven pathways in bone development, regeneration and disease. Nat. Rev. Rheumatol. 8 (6), 358–366.

Maes, C., 2013. Role and regulation of vascularization processes in endochondral bones. Calcif. Tissue Int. 92 (4), 307–323.

Maes, C., 2017. Signaling pathways effecting crosstalk between cartilage and adjacent tissues: seminars in cell and developmental biology: the biology and pathology of cartilage. Semin. Cell Dev. Biol. 62, 16–33.

Malcangio, M., Garrett, N.E., Tomlinson, D.R., 1997. Nerve growth factor treatment increases stimulus-evoked release of sensory neuropeptides in the rat spinal cord. Eur. J. Neurosci. 9 (5), 1101–1104.

Mantyh, P.W., 2014. The neurobiology of skeletal pain. Eur. J. Neurosci. 39 (3), 508–519.

Martin, C.D., Jimenez-Andrade, J.M., Ghilardi, J.R., Mantyh, P.W., 2007. Organization of a unique net-like meshwork of CGRP+ sensory fibers in the mouse periosteum: implications for the generation and maintenance of bone fracture pain. Neurosci. Lett. 427 (3), 148–152.

McKemy, D.D., Neuhausser, W.M., Julius, D., 2002. Identification of a cold receptor reveals a general role for TRP channels in thermosensation. Nature 416 (6876), 52–58.

Mekraldi, S., Lafage-Proust, M.H., Bloomfield, S., Alexandre, C., Vico, L., 2003. Changes in vasoactive factors associated with altered vessel morphology in the tibial metaphysis during ovariectomy-induced bone loss in rats. Bone 32 (6), 630–641.

Milgram, J.W., Robinson, R.A., 1965. An electron microscopic demonstration of unmyelinated nerves in the haversian canals of the adult dog. Bull. Johns Hopkins Hosp. 117, 163–173.

Miller, M.R., Kasahara, M., 1963. Observations on the innervation of human long bones. Anat. Rec. (145), 13–23.

Park, J., Gebhardt, M., Golovchenko, S., Branguli, F.P., Hattori, T., Hartmann, C., Zhou, X., deCrombrugghe, B., Stock, M., Schneider, H., von der Mark, K., 2015. Dual pathways to endochondral osteoblasts: a novel chondrocyte-derived osteoprogenitor cell identified in hypertrophic cartilage. Biol. Open 4 (5), 608–621.

Pezet, S., McMahon, S.B., 2006. Neurotrophins: mediators and modulators of pain. Annu. Rev. Neurosci. 29, 507–538.

Pongratz, G., Straub, R.H., 2013. Role of peripheral nerve fibres in acute and chronic inflammation in arthritis. Nat. Rev. Rheumatol. 9 (2), 117–126.

Proske, U., Gandevia, S.C., 2012. The proprioceptive senses: their roles in signaling body shape, body position and movement, and muscle force. Physiol. Rev. 92 (4), 1651–1697.

Provot, S., Zinyk, D., Gunes, Y., Khatri, R., Le, Q., Kronenberg, H., Johnson, R., Longaker, M., Giaccia, A., Schipani, E., 2007. HIF-1alpha regulates differentiation of limb bud mesenchyme and joint development. J. Cell Biol. 177, 451–464.

Quarcoo, D., Schulte-Herbrüggen, O., Lommatzsch, M., Schierhorn, K., Hoyle, G.W., Renz, H., Braun, A., 2004. Nerve growth factor induces increased airway inflammation via a neuropeptide-dependent mechanism in a transgenic animal model of allergic airway inflammation. Clin. Exp. Allergy 34 (7), 1146–1151.

Ramasamy, S.K., Kusumbe, A.P., Wang, L., Adams, R.H., 2014. Endothelial notch activity promotes angiogenesis and osteogenesis in bone. Nature 507 (7492), 376–380.

Ramasamy, S.K., Kusumbe, A.P., Itkin, T., Gur-Cohen, S., Lapidot, T., Adams, R.H., 2016. Regulation of hematopoiesis and osteogenesis by blood vessel-derived signals. Annu. Rev. Cell Dev. Biol. 32, 649–675.

Rankin, E.B., Wu, C., Khatri, R., Wilson, T.L., Andersen, R., Araldi, E., Rankin, A.L., Yuan, J., Kuo, C.J., Schipani, E., Giaccia, A.J., 2012. The HIF signaling pathway in osteoblasts directly modulates erythropoiesis through the production of EPO. Cell 149 (1), 63–74.

Rapp, A.E., Kroner, J., Baur, S., Schmid, F., Walmsley, A., Mottl, H., Ignatius, A., 2015. Analgesia via blockade of NGF/TrkA signaling does not influence fracture healing in mice. J. Orthop. Res. 33 (8), 1235–1241.

Regan, J.N., Lim, J., Shi, Y., Joeng, K.S., Arbeit, J.M., Shohet, R.V., Long, F., 2014. Up-regulation of glycolytic metabolism is required for HIF-1alpha-driven bone formation. Proc. Natl. Acad. Sci. U.S.A. 111 (23), 8673–8678.

Reichardt, L.F., 2006. Neurotrophin-regulated signalling pathways. Philos. Trans. R. Soc. Lond. B Biol. Sci. 361 (1473), 1545–1564.

Roche, B., David, V., Vanden-Bossche, A., Peyrin, F., Malaval, L., Vico, L., Lafage-Proust, M.H., 2012. Structure and quantification of microvascularisation within mouse long bones: what and how should we measure? Bone 50 (1), 390–399.

Sample, S.J., Hao, Z., Wilson, A.P., Muir, P., 2011. Role of calcitonin gene-related peptide in bone repair after cyclic fatigue loading. PLoS One 6 (6) e20386.

Saran, U., Gemini Piperni, S., Chatterjee, S., 2014. Role of angiogenesis in bone repair. Arch. Biochem. Biophys. 561, 109–117.

Schipani, E., Ryan, H.E., Didrickson, S., Kobayashi, T., Knight, M., Johnson, R.S., 2001. Hypoxia in cartilage: HIF-1alpha is essential for chondrocyte growth arrest and survival. Genes Dev. 15 (21), 2865–2876.

Schipani, E., Maes, C., Carmeliet, G., Semenza, G.L., 2009. Regulation of osteogenesis-angiogenesis coupling by HIFs and VEGF. J. Bone Miner. Res. 24 (8), 1347–1353.

Semenza, G.L., 2012. Hypoxia-inducible factors in physiology and medicine. Cell 148 (3), 399–408.

Shao, P., Ohtsuka-Isoya, M., Shinoda, H., 2003. Circadian rhythms in serum bone markers and their relation to the effect of etidronate in rats. Chronobiol. Int. 20 (2), 325–336.

Shen, X., Wan, C., Ramaswamy, G., Mavalli, M., Wang, Y., Duvall, C.L., Deng, L.F., Guldberg, R.E., Eberhart, A., Clemens, T.L., Gilbert, S.R., 2009. Prolyl hydroxylase inhibitors increase neoangiogenesis and callus formation following femur fracture in mice. J. Orthop. Res. 27 (10), 1298–1305.

Shomento, S.H., Wan, C., Cao, X., Faugere, M.C., Bouxsein, M.L., Clemens, T.L., Riddle, R.C., 2010. Hypoxia-inducible factors 1alpha and 2alpha exert both distinct and overlapping functions in long bone development. J. Cell. Biochem. 109 (1), 196–204.

Street, J., Bao, M., deGuzman, L., Bunting, S., Peale Jr., F.V., Ferrara, N., Steinmetz, H., Hoeffel, J., Cleland, J.L., Daugherty, A., van Bruggen, N., Redmond, H.P., Carano, R.A., Filvaroff, E.H., 2002. Vascular endothelial growth factor stimulates bone repair by promoting angiogenesis and bone turnover. Proc. Natl. Acad. Sci. U.S.A. 99 (15), 9656–9661.

Tabarowski, Z., Gibson-Berry, K., Felten, S.Y., 1996. Noradrenergic and peptidergic innervation of the mouse femur bone marrow. Acta Histochem. 98 (4), 453–457.

Tang, W., Yang, F., Li, Y., de Crombrugghe, B., Jiao, H., Xiao, G., Zhang, C., 2012. Transcriptional regulation of vascular endothelial growth factor (VEGF) by osteoblast-specific transcription factor osterix (Osx) in osteoblasts. J. Biol. Chem. 287 (3), 1671–1678.

Thurston, T.J., 1982. Distribution of nerves in long bones as shown by silver impregnation. J. Anat. 134 (Pt 4), 719–728.

Togari, A., 2002. Adrenergic regulation of bone metabolism: possible involvement of sympathetic innervation of osteoblastic and osteoclastic cells. Microsc. Res. Tech. 58 (2), 77–84.

Tomlinson, R.E., Silva, M.J., 2013. Skeletal blood flow in bone repair and maintenance. Bone Research 1 (4), 311–322.

Tomlinson, R.E., McKenzie, J.A., Schmieder, A.H., Wohl, G.R., Lanza, G.M., Silva, M.J., 2013. Angiogenesis is required for stress fracture healing in rats. Bone 52 (1), 212–219.

Tomlinson, R.E., Li, Z., Li, Z., Minichiello, L., Riddle, R.C., Venkatesan, A., Clemens, T.L., 2017. NGF-TrkA signaling in sensory nerves is required for skeletal adaptation to mechanical loads in mice. Proc. Natl. Acad. Sci. U.S.A. 114 (18), E3641.

Tomlinson, R.E., Li, Z., Zhang, Q., Goh, B.C., Li, Z., Thorek, D.L.J., Rajbhandari, L., Brushart, T.M., Minichiello, L., Zhou, F., Venkatesan, A., Clemens, T.L., 2016. NGF-TrkA signaling by sensory nerves coordinates the vascularization and ossification of developing endochondral bone. Cell Rep. 16 (10), 2723–2735.

Toulis, K.A., Hemming, K., Stergianos, S., Nirantharakumar, K., Bilezikian, J.P., 2014. β-Adrenergic receptor antagonists and fracture risk: a meta-analysis of selectivity, gender, and site-specific effects. Osteoporos. Int. 25 (1), 121–129.

Trueta, J., Buhr, A.J., 1963. The vascular contribution to osteogenesis. V. The vasculature supplying the epiphysial cartilage in rachitic rats. J. Bone Joint Surg. Br. 45, 572–581.

Trueta, J., Caladias, A.X., 1964. A study of the blood supply of the long bones. Surg. Gynecol. Obstet. 118, 485–498.

Veldhuis-Vlug, A.G., Tanck, M.W., Limonard, E.J., Endert, E., Heijboer, A.C., Lips, P., Fliers, E., Bisschop, P.H., 2015. The effects of beta-2 adrenergic agonist and antagonist on human bone metabolism: a randomized controlled trial. Bone 71, 196–200.

Vu, T.H., Shipley, J.M., Bergers, G., Berger, J.E., Helms, J.A., Hanahan, D., Shapiro, S.D., Senior, R.M., Werb, Z., 1998. MMP-9/gelatinase b is a key regulator of growth plate angiogenesis and apoptosis of hypertrophic chondrocytes. Cell 93 (3), 411–422.

Wan, C., Gilbert, S.R., Wang, Y., Cao, X., Shen, X., Ramaswamy, G., Jacobsen, K.A., Alaql, Z.S., Eberhardt, A.W., Gerstenfeld, L.C., Einhorn, T.A., Deng, L., Clemens, T.L., 2008. Activation of the hypoxia-inducible factor-1alpha pathway accelerates bone regeneration. Proc. Natl. Acad. Sci. U.S.A. 105 (2), 686–691.

Wang, L., Zhou, S., Liu, B., Lei, D., Zhao, Y., Lu, C., Tan, A., 2006. Locally applied nerve growth factor enhances bone consolidation in a rabbit model of mandibular distraction osteogenesis. J. Orthop. Res. 24 (12), 2238–2245.

Wang, Y., Wan, C., Deng, L., Liu, X., Cao, X., Gilbert, S.R., Bouxsein, M.L., Faugere, M.C., Guldberg, R.E., Gerstenfeld, L.C., Haase, V.H., Johnson, R.S., Schipani, E., Clemens, T.L., 2007. The hypoxia-inducible factor alpha pathway couples angiogenesis to osteogenesis during skeletal development. J. Clin. Invest. 117 (6), 1616−1626.

Wang, J., Gao, Y., Cheng, P., Li, D., Jiang, H., Ji, C., Zhang, S., Shen, C., Li, J., Song, Y., Cao, T., Wang, C., Yang, L., Pei, G., 2017. CD31hiEmcnhi vessels support new trabecular bone formation at the frontier growth area in the bone defect repair process. Sci. Rep. 7 (1), 4990.

Weng, T., Xie, Y., Huang, J., Luo, F., Yi, L., He, Q., Chen, D., Chen, L., 2014. Inactivation of VHL in osteochondral progenitor cells causes high bone mass phenotype and protects against age-related bone loss in adult mice. J. Bone Miner. Res. 29 (4), 820−829.

Wojtys, E.M., Beaman, D.N., Glover, R.A., Janda, D., 1990. Innervation of the human knee joint by substance-P fibers. Arthroscopy 6 (4), 254−263.

Wu, C., Rankin, E.B., Castellini, L., Alcudia, J.F., LaGory, E.L., Andersen, R., Rhodes, S.D., Wilson, T.L., Mohammad, K.S., Castillo, A.B., Guise, T.A., Schipani, E., Giaccia, A.J., 2015. Oxygen-sensing PHDs regulate bone homeostasis through the modulation of osteoprotegerin. Genes Dev. 29 (8), 817−831.

Yang, L., Tsang, K.Y., Tang, H.C., Chan, D., Cheah, K.S.E., 2014. Hypertrophic chondrocytes can become osteoblasts and osteocytes in endochondral bone formation. Proc. Natl. Acad. Sci. U.S.A. 111 (33), 12097−12102.

Zelzer, E., Glotzer, D.J., Hartmann, C., Thomas, D., Fukai, N., Soker, S., Olsen, B.R., 2001. Tissue specific regulation of VEGF expression during bone development requires Cbfa1/Runx2. Mech. Dev. 106 (1−2), 97−106.

Zelzer, E., McLean, W., Ng, Y.S., Fukai, N., Reginato, A.M., Lovejoy, S., D'Amore, P.A., Olsen, B.R., 2002. Skeletal defects in VEGF (120/120) mice reveal multiple roles for VEGF in skeletogenesis. Development 129, 1893−1904.

Zhao, Q., Shen, X., Zhang, W., Zhu, G., Qi, J., Deng, L., 2012. Mice with increased angiogenesis and osteogenesis due to conditional activation of HIF pathway in osteoblasts are protected from ovariectomy induced bone loss. Bone 50 (3), 763−770.

Zhou, X., von der Mark, K., Henry, S., Norton, W., Adams, H., de Crombrugghe, B., 2014. Chondrocytes transdifferentiate into osteoblasts in endochondral bone during development, postnatal growth and fracture healing in mice. PLoS Genet. 10 (12), e1004820.

Chapter 10

Coupling of bone formation and resorption

Natalie A. Sims and T. John Martin

St. Vincent's Institute of Medical Research, Melbourne, Australia; Department of Medicine at St. Vincent's Hospital, The University of Melbourne, Melbourne, Australia

Chapter outline

Introduction:—bone modeling and bone remodeling

Skeletal structure and function are regulated by hormones, cytokines, and the central and sympathetic nervous systems in response to a range of factors, including changes in mechanical loading and stimuli emanating from the immune and reproductive systems. Not only does the skeleton provide mechanical strength to the body, protection of internal organs, and sites of muscle attachment for locomotion, but bone is also a very significant endocrine organ with major influences on calcium, phosphate, and glucose metabolism.

Skeletal structure is determined by two processes: modeling and remodeling. The key difference between these two processes is the relationship between bone-forming osteoblasts and bone-resorbing osteoclasts. In modeling, actions of osteoblasts and osteoclasts occur in separation (i.e., on different surfaces), while in remodeling, the actions of osteoblasts and osteoclasts occur in sequence on the same bone surface.

Modeling modifies the shape of the skeleton. This includes both the construction of bone, which takes place from the beginning of skeletogenesis during fetal life until the end of the second decade, when the longitudinal growth of the skeleton is completed (Frost, 1964), and changes in bone shape associated with aging (Parfitt et al., 1983; Robling and Turner, 2009) or in response to mechanical load. In modeling bone formation occurs independently (i.e., without prior bone resorption), as does bone resorption (without subsequent bone formation). In this way bone is formed at sites of greatest mechanical load and removed where it is not required. For example, bone formed and deposited on the outer surface of the bone widens a growing bone; at the same time, bone is resorbed at a different location to enlarge the medullary cavity containing the bone marrow.

Principles of Bone Biology. https://doi.org/10.1016/B978-0-12-814841-9.00010-5

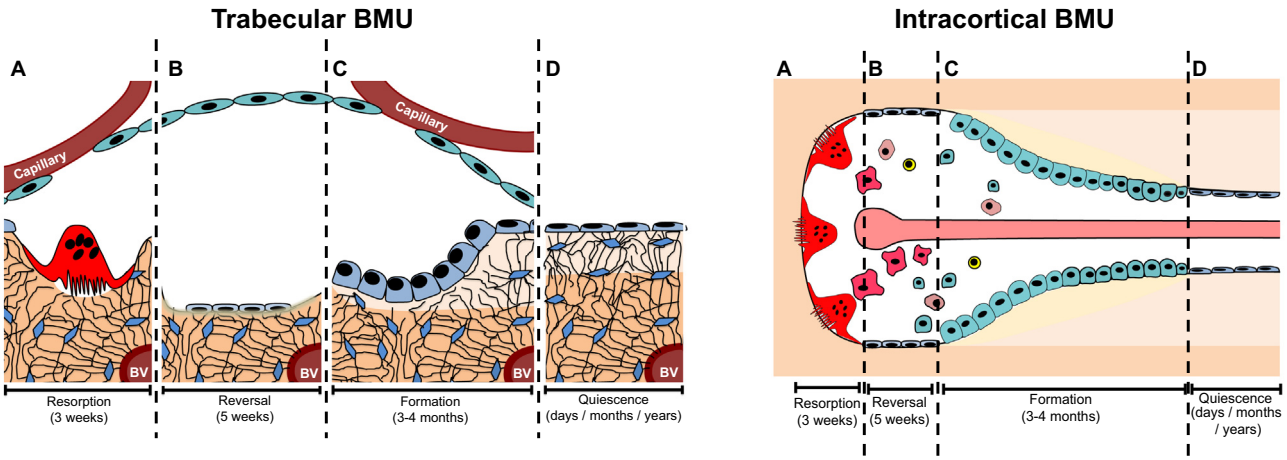

FIGURE 10.1 The basic structure of trabecular (left) and intracortical (right) basic multicellular units (*BMUs*), showing how the cell populations present on the surface change over time. (A) Initiation of remodeling, with lifting of the canopy, and osteoclast-mediated resorption on the bone surface. Osteoclast progenitors may be supplied by the capillaries adjacent to the canopy. (B) After bone resorption, the surface is covered by osteoblast lineage reversal cells. (C) Following the reversal period, osteoblasts fill the pit resorbed by osteoclasts by generating new osteoid, which is gradually mineralized over time; again, osteoblasts may be supplied by the nearby vasculature. (D) The process is complete, the pit filled, the surface is covered with bone-lining cells, and the canopy can no longer be detected. Mineralization of the osteoid continues until it reaches maximal levels, or until the next remodeling cycle occurs. *BV*, blood vessel.

Remodeling was initially described as two linked processes: (1) a destructive process, wrought by bone-resorbing osteoclasts, followed by (2) a productive process ascribed to bone-forming osteoblasts; this was based on Harold Frost's examination of multiple sections through trabecular bone from normal adult skeletons (Hattner et al., 1965). The sequence of resorption followed by formation was likened to the healing of a soft-tissue wound, and analogous progressions were noted to take place in the formation of several epithelia (e.g., Ford and Young, 1963). The tissue wound analogy is apt, since the principal functions of bone remodeling are to provide a means of adapting the skeleton to changes in loading and to remove and replace damaged or old bone. Remodeling occurs asynchronously throughout the skeleton at many anatomically distinct sites termed basic multicellular units (BMUs) (Frost, 1964; Hattner et al., 1965). In BMUs, tiny packets of bone are removed by osteoclasts and subsequently replaced by new bone matrix (osteoid) produced by osteoblasts; that matrix is mineralized to form new bone substance. In trabecular bone the BMU is located on the bone surface. In Haversian cortical bone the BMU comprises cutting zones led by osteoclasts that proceed through bone, followed by differentiating osteoblasts (Fig. 10.1) (Parfitt, 1982; Eriksen, 1986; Eriksen et al., 1993; Hauge et al., 2001). The roles of remodeling and modeling will be discussed in detail elsewhere in this book (Seeman, Chapter 11).

Development of the concept of coupling

When Frost introduced the BMU, he also introduced the concept of "coupling" as the process by which resorption of a certain amount of bone is followed by formation of the amount sufficient to replace it (Hattner et al., 1965). This was a remarkable insight given that little was known of the cells of bone at that time; their origins were not at all understood, and it was more than another decade before they could be studied directly. The events within the BMU progress from quiescence to activation, resorption, and formation, and finally return to quiescence when filling of the resorbed space is complete (Fig. 10.1).

The bone resorption activity in a BMU in adult human bone takes approximately 3 weeks (Eriksen et al., 1984b), the formation response 3−4 months (Eriksen et al., 1984a), and between the two activities there is a "reversal phase" (Tran Van et al., 1982), which takes several weeks (Eriksen et al., 1984b). The process occurs with sufficient frequency, and at sufficient sites, to replace 5%−10% of the skeleton per year, with the entire adult human skeleton replaced in around 10 years (Parfitt, 1980). In rodents the duration of this sequence is compressed, but a time delay between resorption and formation still exists: in rat alveolar bone the reversal phase lasts for approximately 3.5 days (Vignery and Baron, 1980). These numbers vary also with site, skeletal health, and treatment (Jensen et al., 2014), and in some conditions, including osteoporosis, there is an increased duration, or even arrest, of the reversal phase (Parfitt, 1982; Andersen et al., 2013).

Coupled remodeling is asynchronous throughout the skeleton

When we consider the time course over which remodeling occurs it must be noted that BMUs throughout the skeleton are active at different stages of the remodeling cycle. Indeed, it is an essential feature of bone remodeling that it does not occur uniformly throughout the skeleton, but takes place where it is needed to repair damaged or replace old bone. The events are initiated asynchronously, at sites geographically and chronologically separated from one another. Therefore, at any one time, bone is being resorbed in BMUs at some locations, while at others, a BMU is in its formation or reversal phase. Systemically administered drugs that influence bone remodeling will therefore act upon BMUs at all sites and in differing phases of their remodeling cycle. This presents a special challenge to pharmacological interventions aimed at preventing and reversing the structural decay associated with menopause and advancing age. It also needs to be borne in mind when considering ways in which circulating hormones might influence bone remodeling.

The development of a BMU in bone begins with resorption by osteoclasts, leaving scalloped contours in Howship's lacunae, followed by generation of the cement line, upon which bone formation by osteoblasts would take place (Fig. 10.1). Scalloped cement lines are used in histology to indicate that formation has taken place on previously resorbed surfaces, whereas smooth cement lines signify bone being formed on surfaces without previous resorption, i.e., modeling; while these are observed in larger mammals, they are rarely observed in murine bone, because the pits formed by mouse osteoclasts are more shallow. In adult trabecular bone, about 96% of bone formation takes place on resorbed surfaces (i.e., remodeling surfaces), the remainder on intact surfaces (modeling), with some of the latter reflecting overfilling of the resorbed lacunae (Hattner et al., 1965). The remodeling sequence proposed by Frost, of activation, resorption, and formation (ARF) (Frost, 1964), was extended by Baron, who proposed the existence of a reversal phase between resorption and formation, a stage characterized by the presence of mononuclear cells and the formation of a cement line separating new from old bone (Baron, 1977). Although the reversal phase, lasting as long as 5 weeks in human bone remodeling, has been poorly understood, it is now being investigated in some detail and will be discussed later. Frost's view of bone remodeling was readily adopted by others (Frost, 1964; Harris and Heaney, 1969; Parfitt, 1982).

Coupling is unidirectional and sequential: bone formation following bone resorption

The term "coupling" is illustrative, because it calls to mind the coupling of a train carriage to a locomotive: the osteoclast is analogous to the engine commencing the process of remodeling, with osteoblasts being the carriage coupled to it and following behind.

The first essential step in the remodeling cycle was proposed to be the generation of active osteoclasts. This suggestion was made even before it was recognized that osteoclasts develop from hemopoietic precursors. Osteoclasts are probably derived from early and late precursors available in marrow adjacent to activation sites (reviewed by Takahashi et al., Chapter 5); they may be drawn to the site by chemoattractants derived from osteocytes or from the bone matrix itself (Sims and Gooi, 2008). They may also be recruited from blood available at the bone interface through a sinus structure of bone remodeling compartments (Hauge et al., 2001; Kristensen et al., 2013). At each BMU, the resorption of a volume of bone is followed by new bone formation sufficient to fill the space. The BMU resorbs and replaces old bone at the same location so there is no change in bone size or shape. If the volumes of bone removed and replaced are equal, there will be no permanent loss of bone or compromise in bone mass.

Coupling does not include the major mechanism of intercellular communication in bone that was proposed some years later, of osteoblastic lineage cells controlling osteoclast formation (Chambers, 1980; Rodan and Martin, 1981) by their production of receptor activator of NF-κB ligand (RANKL) and osteoprotegerin (OPG) (Lacey et al., 1998; Yasuda et al., 1998; Suda et al., 1999). The Frost coupling concept preceded this by decades. The control of osteoclast formation and function by osteoblasts (or cells in that lineage) is not coupling, although this mistake is commonly made in the literature. Coupling refers strictly to *the process by which products of bone resorption and of osteoclasts and other cells within the BMU influence recruitment and differentiation of the osteoblast lineage to mature osteoblasts that synthesize bone and mineralize it*. Frost provided a great service in identifying the coupling mechanism as one that was likely to be important physiologically and important in devising therapeutic approaches; this simple concept has come to be recognized as a complex process with many participants, as will be discussed.

Coupling as a multicellular process

The balance between bone formation and resorption requires participation of a number of cell types beyond differentiated osteoclasts and osteoblasts. Coupling is therefore not simply an event taking place between osteoclasts and osteoblasts, but

an extensive process of information transfer involving diverse cells and interactions aimed ultimately at regulating osteoblast differentiation/bone formation (Sims and Martin, 2015). Since the several stages of the process are prolonged in duration, any cellular communication mechanisms have to provide for the separation of these events in time.

Coupling occurs locally within a basic multicellular unit

In discussing the mechanisms of coupling, including osteoclast formation, activity, and maintenance, we are considering only local factors. They seem better equipped than circulating hormones to activate asynchronous events throughout the skeleton.

Although very little was known about osteoclasts at the time of Frost's proposal, the key initial event was agreed to be the initiation of resorption by osteoclasts. When the steps in osteoclast formation and activation were eventually revealed as being derived from precursors in the bone marrow, the question of how osteoclasts commenced BMU formation at a site of need was asked.

Much interest has developed in the data showing the development of a canopy extending over the active BMU during its initiation. This was proposed first by Rasmussen and Bordier (Rasmussen and Bordier, 1974) and suggests a mechanism to isolate the BMU and allow local communication between differing cell types. Direct evidence came from Hauge et al. (Hauge et al., 2001), who suggested that lining cells lift from the underlying bone at the start of remodeling activity and form a canopy over the site to be resorbed, whether on the surface in trabecular bone or within the substance of cortical bone undergoing haversian remodeling. The capillary blood supply closely associated with the canopy (Kristensen et al., 2013) was proposed as a source of hematopoietic precursors for osteoclast formation (Fig. 10.1). Osteoclast formation can take place rapidly in vivo; this may be made possible by partially differentiated niches of cells available for the BMU. Such partially differentiated osteoclast precursors, designated as "quiescent osteoclast precursors," have been characterized in mouse and rat (Mizoguchi et al., 2009), having arrived there in the circulation (Muto et al., 2011), but have not yet been identified in human subjects. They are reported in Takahashi et al. (Chapter 5).

Capillaries associated with the canopy also provide a mechanism for ingress of other cells, including mesenchymal precursors (Eghbali-Fatourechi et al., 2007) and immune and endothelial cells. Consistent with such supply from blood was the demonstration that red blood cells could be seen within the active cortical BMU (Andersen et al., 2009). The canopy has also been demonstrated in rabbit bone (Jensen et al., 2014), which undergoes Haversian remodeling in the cortex, although the canopy has not been convincingly shown yet in intracortical "cutting cones." Although a similar canopy has been predicted in the mouse, it has been observed only above bone-forming surfaces (Narimatsu et al., 2010). Tissue-specific macrophages ("osteomacs") have been found to form a canopy over bone-forming sites in the mouse (Chang et al., 2008), but the relationship between the two canopies remains unclear.

Osteocytes are recognized as important in mechanosensing and regulation of bone remodeling (Bonewald and Johnson, 2008). They are the most abundant cell of bone and are situated to communicate both throughout the skeleton and with bone-lining cells on the surface. Recognition of the need to remove or repair a region of bone could be achieved by osteocytes. Indeed, apoptosis of osteocytes as a result of microdamage coincides with bone resorption by osteoclasts (Verborgt et al., 2000; Noble et al., 2003; Heino et al., 2009; Kennedy et al., 2012), implicating this as a mechanism to target the initiation of remodeling for bone repair. A signal emitted by osteocytes to lining cells could lead them to lift and begin to form the canopy overlying and containing the BMU (Eghbali-Fatourechi et al., 2007; Eriksen et al., 2007). The nature of the signal to attract osteoclast precursors to the bone surface is unknown, but a number of chemoattractants have been suggested (Sims and Gooi, 2008). RANKL and macrophage colony-stimulating factor (M-CSF) production by local mesenchymal-derived cells may also play a role in the initial formation of the BMU. Since the canopy mesenchymal cells themselves have been suggested to be a source of osteoblast precursors (Delaisse, 2014), they may, in addition to lining cells, mesenchymal precursors within the BMU, and osteocytes, also be sources of RANKL and M-CSF as the necessary stimuli for osteoclast generation at the site.

Coupling and balance: what is the difference?

The amount and quality of bone is retained in the skeleton during balanced bone remodeling because the processes within BMUs are matched: the amount of bone synthesized replaces the amount removed. The two processes are "balanced" through mechanisms of intercellular communication (see later). This is the key to integrity of the remodeling process and the success of the BMU system in ensuring maintenance of normal bone during young adult life, when bone mass is maintained at a constant level. It is what led Frost to propose the coupling of bone formation and resorption processes within the remodeling BMU. At other times in life, the balance is negative (bone mass is lost) or positive (bone mass is

gained), but this does not mean there a loss of coupling (although the term "uncoupling" is frequently used): formation still follows resorption, but there is an imbalance in the activities between the bone cells. This caution is especially pertinent in studies claiming (for example) that pharmacological agents or genetic alterations uncouple bone formation from resorption on the basis of serum biochemical markers; these markers represent the sum of all formation and resorption activities in the skeleton, including both modeling and remodeling.

Some forms of uncoupling or dissociation may occur at the BMU level, for example, when osteoclasts are nonfunctional or not present (and therefore are unable to initiate remodeling and provide signals to osteoblasts) (Henriksen et al., 2011) or in instances of reversal phase "arrest," when the canopy over the BMU is disrupted as in myeloma bone disease (Andersen et al., 2010) and some cases of osteoporosis (Andersen et al., 2014). This will be discussed later.

The resorption phase of remodeling and its cessation in the basic multicellular unit

Once a BMU site is activated, resorption must be limited in some way. An important unanswered question about osteoclast behavior and the control of resorption in the remodeling cycle is: how does each osteoclast know when to stop resorbing? The process is likely to finish with osteoclast death, which has been studied in vitro to some extent, but its regulation in vivo remains obscure. There are several possible mechanisms. Osteoclasts phagocytose osteocytes, which might provide a mechanism to remove the signal for resorption (Elmardi et al., 1990). The very high (millimolar) concentrations of calcium generated during mineral dissolution, capable of inhibiting osteoclasts (Zaidi et al., 1989), might come into play particularly in the localized and focused conditions of the BMU. Transforming growth factor β (TGFβ) is available either when it is resorbed from the matrix and activated by acid pH or when it is secreted by the osteoblast lineage and can promote osteoclast apoptosis (Hughes and Boyce, 1997). A direct effect of estrogen to enhance osteoclast apoptosis has been identified in mouse genetic experiments (Nakamura et al., 2007). Some insights into the control of apoptosis arise from genetic and pharmacological studies showing that inhibition of acidification of the resorption space by blockade of either chloride channel-7 (ClC-7) or the V-type H^+ ATPase of the osteoclast results in prolonged osteoclast survival (Henriksen et al., 2004; Karsdal et al. 2005, 2007). This might suggest a role for acidification in determining osteoclast life span, perhaps even through TGFβ activation. In determining how resorption ends in the BMU, there is much to be learned of mechanisms regulating osteoclast apoptosis. There might be several events limiting resorption to only a certain amount of bone at each BMU, including the possibility that accumulation of osteoblast progenitors provides a signal, but no dominant governing control has yet been identified.

Coupling mechanisms originate from several cellular sources

The development of the coupling concept led to an extensive search for possible "coupling factors"— messengers from the active osteoclast controlling the differentiation and activity of subsequent osteoblasts on the same surface. Many candidate factors have now been identified and are listed in Table 10.1. We propose, however, that rather than a single coupling factor, or even a team of coupling factors, there are a range of "coupling mechanisms" promoting and limiting bone formation in the BMU (Fig. 10.2). Some coupling mechanisms derive from osteoclasts and their activities: (1) matrix-derived signals released by osteoclasts during bone resorption and (2) factors synthesized by the mature osteoclast (which may include secreted factors, membrane-bound factors, or factors released in cell-derived vesicles). But there are also coupling mechanisms emanating from other cell types within the BMU: (3) topographical changes effected by the osteoclast on the bone surface and sensed by osteoblasts; (4) secreted and membrane-bound products of osteoblast lineage cells, including osteoblast precursors, lining cells, and osteocytes; (5) secreted products of immune and endothelial cells; and (6) neurogenic stimuli arising from the extensive innervation circuitry in bone. The last will not be considered in this chapter since they are speculative and have not been subject to direct experiment. The others will each be discussed in turn.

It is also important to note the many different contexts in which osteoclasts communicate to osteoblasts: not every signal from an osteoclast that changes osteoblast differentiation or function should be considered a coupling factor. There are three pertinent examples of this. First, during endochondral ossification, the process by which the cartilage surrounding hypertrophic chondrocytes is resorbed by osteoclast-like cells and replaced by osteoblasts is analogous to remodeling of bone; it is sequential, and both resorption of matrix and formation of new bone occur on the same surface (Baron and Sims, 2000). However, the control mechanisms existing in that anatomical location are likely to be different, because of contributions from the hypertrophic chondrocytes and adjacent invading blood vessels (Poulton et al., 2012). Second, osteoclasts appear to produce "osteotransmitter" signals transmitted through the cortical osteocyte network (either by lacunocanalicular transport or by a signal relay) to influence the function of osteoblasts on the periosteal surface (Johnson et al., 2015). Third, in murine calvariae, in which there is no remodeling and hence no coupling, osteoblasts and

TABLE 10.1 A summary of osteoclast-derived coupling factors and their other sources and influences near or in the basic multicellular unit. Influences listed are from *in vitro* studies, unless otherwise indicated. RANKL, receptor activator of NF-kappa B ligand.

Factor	Production by osteoclasts	Other potentially relevant sources	Influences on osteoblast differentiation and bone formation	Other potential influences in remodeling
Transforming growth factor β	Released from matrix (Oreffo et al., 1989)	Osteoblasts (Robey et al., 1987) T lymphocytes (Chen et al., 1998) Macrophages (Fadok et al., 1998)	Stimulates progenitor expansion (Robey et al., 1987; Hock et al., 1990) Stimulates progenitor migration and differentiation (Tang et al., 2009) Stimulates bone formation in organ culture (Hock et al., 1990)	Stimulates osteoclastogenesis by direct action on osteoclast precursors (Sells Galvin et al., 1999) Stimulates sclerostin expression (Loots et al., 2012)
Bone morphogenetic protein (BMP) 2	Released from matrix (Oreffo et al., 1989) Secreted (Garimella et al., 2008)	Osteoblasts (Robubi et al., 2014) Macrophages (Champagne et al., 2002)	Stimulates progenitor expansion and migration (Fiedler et al., 2002) Stimulates osteoblast differentiation (Rickard et al., 1994)	Stimulates osteoclast activity (Hanamura et al., 1980; Kanatani et al., 1995)
Insulin-like growth factors	Released from matrix (Centrella and Canalis, 1985a)	Osteoblasts (Canalis and Gabbitas, 1994) Macrophages (Fournier et al., 1995)	Stimulates progenitor expansion (Xian et al., 2012)	Stimulates osteoclastogenesis (Wang et al., 2006)
Platelet-derived growth factor BB	Released from matrix (Centrella and Canalis, 1985a) Secreted (Kreja et al., 2010)	Osteoblasts (Zhang et al., 1991) Endothelial cells (Daniel and Fen, 1988) Osteoclasts (Lees et al., 2001)	Promotes progenitor replication (Hock and Canalis, 1994) Promotes progenitor migration (Sanchez-Fernandez et al., 2008; Kreja et al., 2010) Stimulates bone formation in vivo (Mitlak et al., 1996) Inhibits osteoblast differentiation (Hock and Canalis, 1994; Kubota et al., 2002)	Stimulates osteoclast precursor recruitment (Hock and Canalis, 1994)
Cardiotrophin-1	Secreted (Walker et al., 2008)		Stimulates bone formation in vivo (Walker et al., 2008) Stimulates osteoblast commitment (Walker et al., 2008) Suppresses sclerostin expression (Walker et al., 2008) Bone formation is low in null mice (Walker et al., 2008)	Stimulates osteoclastogenesis (Richards et al., 2000) Bone resorption is low in null mice (Walker et al., 2008)
BMP-6	Secreted (Garimella et al., 2008)	Mesenchymal and hematopoietic stem cells (Martinovic et al., 2004; Friedman et al., 2006)	Stimulates osteoblast differentiation (Friedman et al., 2006)	Stimulates osteoclastogenesis from human marrow cells (Wutzl et al., 2006)

Wnt10b	Secreted (Pederson et al., 2008)	T cells (Terauchi et al., 2009)	Stimulates osteoblast differentiation in vivo (Bennett et al., 2007)	Stimulates osteoclast activity in vivo (Bennett et al., 2007)
Sphingosine-1-phosphate (S1P)	S1P production catalyzed by secreted sphingosine-1-kinase (Pederson et al., 2008)	Vasculature (Scariano et al., 2008) Red blood cells (Pappu et al., 2007)	Induces osteoblast precursor recruitment (Pederson et al., 2008) Promotes osteoblast survival (Ryu et al., 2006; Pederson et al., 2008) Promotes osteoblast migration (Ryu et al., 2006)	Stimulates osteoclast recruitment (Scariano et al., 2008). Stimulates RANKL expression by osteoblasts and T cells (Ryu et al., 2006) Stimulates osteoclast precursor chemotaxis (Ishii et al., 2010) Intracellular S1P inhibits osteoclast differentiation (Ryu et al., 2006)
collagen triple-helix repeat –containing 1	Secreted (Takeshita et al., 2013)	Mesenchymal cells, osteoblasts (Kimura et al., 2008), and osteocytes (Y-R Jin Bone, 2017, p153)	Stimulates osteoblast differentiation (Kimura et al., 2008) Stimulates bone formation in vivo (Kimura et al., 2008; Takeshita et al., 2013) Osteoclast-specific null mice show reduced bone formation (Takeshita et al., 2013) Osteoblast-specific overexpression causes increased bone formation (Kimura et al., 2008)	Inhibits osteoclast formation and activity (Y-R Jin Bone, 2017, p153)
Complement 3a	Secreted (Matsuoka et al., 2014)	Circulating (50 ng/mL in human serum) (Wlazlo et al., 2013)	Stimulates alkaline phosphatase activity and mineralization in calvarial osteoblasts (Matsuoka et al., 2014).	Increases cytokine output from macrophages and T cells (Carroll, 2004) Osteoclast recruitment (Sato et al., 1993)
Oncostatin M	Secreted (Fernandes et al., 2013)	Macrophages (Zarling et al., 1986) Osteoblasts (Walker et al., 2010) Osteocytes (Walker et al., 2010) T lymphocytes (Clegg et al., 1996)	Promotes osteoblast commitment (Walker et al., 2010) Stimulates bone formation in vivo (Walker et al., 2010)	Synergizes with BMP-2 (Fernandes et al., 2013) Stimulates osteoclast formation (Tamura et al., 1993)
Semaphorin 4D	Membrane bound (Negishi-Koga et al., 2011)	T lymphocytes (including soluble forms) (Wang et al., 2001)	Inhibits bone formation (Negishi-Koga et al., 2011) Gene deletion leads to enhanced bone formation (Negishi-Koga et al., 2011)	Stimulates osteoclastogenesis (Dacquin et al., 2011).
EphrinB2	Membrane bound (Zhao et al., 2006)	Osteoblasts (Zhao et al., 2006) Osteocytes (Allan et al., 2008)	Promotes osteoblast differentiation through EphB4 (Zhao et al., 2006) Suppresses osteoblast apoptosis (Tonna et al., 2014) Promotes late-stage osteoblast differentiation in vivo (Takyar et al., 2013)	Inhibits osteoclast differentiation (Zhao et al., 2006) Inhibits RANKL production by osteoblasts (Tonna et al., 2014)

Continued

TABLE 10.1 A summary of osteoclast-derived coupling factors and their other sources and influences near or in the basic multicellular unit. Influences listed are from *in vitro* studies, unless otherwise indicated. RANKL, receptor activator of NF-kappa B ligand.—cont'd

Factor	Production by osteoclasts	Other potentially relevant sources	Influences on osteoblast differentiation and bone formation	Other potential influences in remodeling
Cxcl16	Secreted (Ota et al., 2013)	Vascular smooth muscle cells (Wagsater et al., 2004) Macrophages (Barlic et al., 2009)	May stimulate osteoblast precursor migration (Ota et al., 2013)	
Leukemia inhibitory factor	Secreted (Ota et al., 2013)	Mesenchymal stem cells (Sims and Johnson, 2012)	Stimulates bone formation in vivo (Cornish et al., 1993) Stimulates osteoblast precursor expansion (Cornish et al., 1997) Promotes osteoblast differentiation (Poulton et al., 2012) Suppresses sclerostin expression (Walker et al., 2010) Gene deletion leads to low bone formation in remodeling (Poulton et al., 2012)	Stimulates osteoclastogenesis (Reid et al., 1990) Inhibits marrow adipogenesis (Poulton et al., 2012)
miR-214-3p	Exocytosed (Li et al., 2016)	Monocytes	Circulating miR-214-3p associated with less bone formation in vivo (Li et al., 2016) Suppresses osteoblast differentiation (Li et al., 2016)	
RANKL reverse signal	Membrane bound (Furuya et al., 2018)	Osteoblast precursors, osteocytes (Kartsogiannis et al., 1999; Lacey et al., 1998; Matsuzaki et al., 1998)	Promotes bone formation (Ikebuchi et al., 2018)	

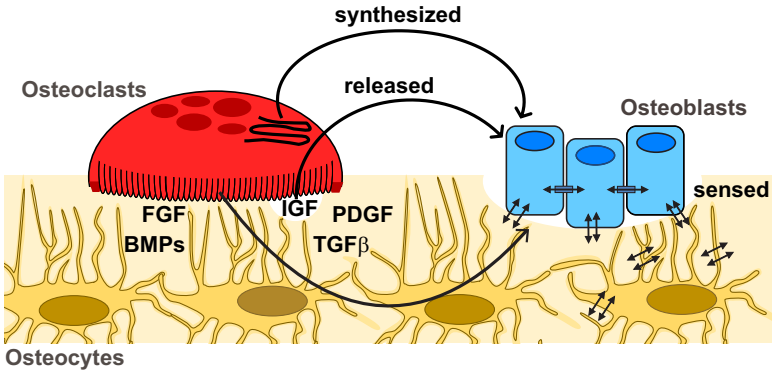

FIGURE 10.2 How do osteoblasts know how much bone to make? Signals, including proteins, are synthesized and secreted by osteoclasts and act directly on cells of the osteoblast lineage (including precursors and osteocytes). Osteoclasts also release matrix-bound growth factors such as insulin-like growth factor (*IGF*), bone morphogenetic proteins (*BMPs*), transforming growth factor β (*TGFβ*), platelet-derived growth factor (*PDGF*), and fibroblast growth factor (*FGF*) during the process of resorption; these also modify the function of osteoblast lineage cells. Osteoblasts also themselves sense the size of the pit left by the osteoclast, and signal to one another either via gap junctions or through secreted and membrane-bound proteins. Osteocytes also sense the changing mechanical strain both during the process of resorption and during bone formation, which changes the nature of the signals they release to influence bone-forming activity.

nonresorbing osteoclasts come into direct contact with each other (Furuya et al., 2018). This implies that osteoblasts may therefore inhibit osteoclast function by a direct contact mechanism in this context; this example of direct contact between the cells may also mediate communication from the osteoclast to the osteoblast, but mechanisms have not yet been identified. The range of coupling factors already identified may have also functions extending beyond coupling to these other examples of communication between these two lineages.

Matrix-derived resorption products as coupling factors

The first suggestion of a molecular mechanism for coupling came from Howard et al. (Howard et al., 1981). The bone matrix had long been known to contain a store of latent growth factors, including TGFβ, bone morphogenetic protein 2 (BMP-2), platelet-derived growth factor (PDGF), and the insulin-like growth factors (IGFs) (Hanamura et al., 1980; Centrella and Canalis, 1985a,b; Oreffo et al., 1989; Hock et al., 1990; Pfeilschifter et al., 1995). All are deposited by osteoblasts during matrix production and then released from the bone surface and activated by acidification during osteoclastic resorption, at which point they become available as agents influencing cells within the BMU, including osteoblasts and their precursors. The amount of bone resorbed by the osteoclast would determine the concentration of factors released, thereby modifying bone formation in a manner proportional to resorption.

Availability of these matrix-derived growth factors does not depend exclusively on resorption. Each is also synthesized by the osteoblasts themselves in latent forms activated by plasmin generated by plasminogen activators (Campbell et al., 1992; Yee et al., 1993) or matrix metalloproteinases (Dallas et al., 2002). In the case of PDGF-BB, its local involvement might be predominantly from a cell source, since it is produced by both osteoblasts and osteoclasts (Canalis and Ornitz, 2000), and its secretion by osteoclast precursors induces vessel formation and bone formation during both modeling and remodeling (Xie et al., 2014).

The hypothesis that coupling could be exerted by resorption-derived growth factors brought the issue before the field. It needed to take into account, though, that growth factor concentrations in matrix are high but variable in locations throughout the skeleton. The quantity and identity of growth factors contained within the matrix are determined by their production and release by osteoblasts and their incorporation into the matrix during bone formation in the previous remodeling cycle(s). Since precise replacement of bone at each site is a key requirement in coupling within the BMU, the active growth factor activities would need to be made available precisely in the quantities needed and in a spatially and temporally controlled manner. That could be difficult to achieve. Furthermore, if resorbed matrix is the main source of the growth factors, their primary availability would be at the earliest stage of the remodeling cycle (during resorption), which is temporally separate from the commencement of bone formation in the BMU (see Fig. 10.1). It seems unlikely that these growth factors would remain within the bone microenvironment for some weeks during the reversal phase until they could influence mature osteoblasts upon their arrival at the bone surface.

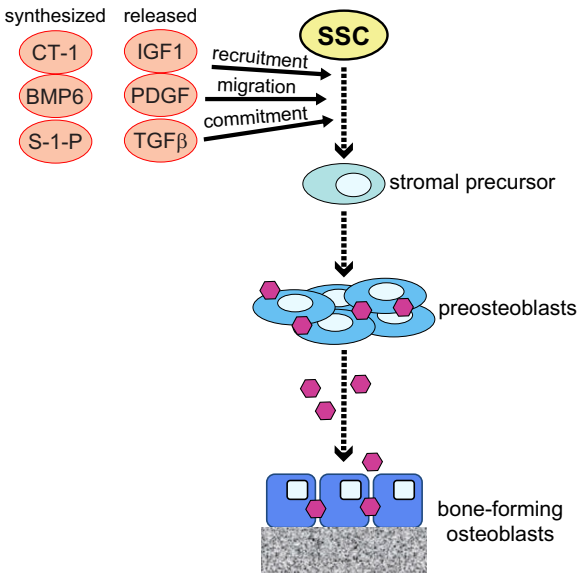

FIGURE 10.3 How do growth factors released by osteoclasts influence bone formation? Factors are synthesized by osteoclasts (such as cardiotrophin-1 [*CT-1*], bone morphogenetic protein 6 [*BMP6*], or sphingosine-1-phosphate [*S-1-P*]; see Table 10.1 for other examples) or released by osteoclast-mediated bone resorption of the matrix (such as insulin-like growth factor 1 [*IGF1*], platelet-derived growth factor [*PDGF*], and transforming growth factor β [*TGFβ*]; see Table 10.1 for other examples). These are likely to act on stromal stem cells (*SSCs*) to stimulate progenitor recruitment, to promote their migration to the bone surface, and to stimulate their early commitment to differentiate into mature, bone-forming osteoblasts. Preosteoblasts and mature osteoblasts throughout their differentiation communicate to each other through the release of factors such as TGFβ and parathyroid hormone–related protein and through the action of membrane-bound molecules such as EphrinB2 (represented by hexagons).

This conceptual difficulty with the growth factor/coupling concept has been helped by the outcome of mouse genetic experiments showing that active TGFβ release during bone resorption acts as a chemoattractant to induce migration of osteoblast precursors to prior sites of resorption (Tang et al., 2009) (Fig. 10.3). This provides osteoblast precursor cells within the BMU where they are available for stimulation by other signals promoting their differentiation and matrix production. The ability of osteoblast- and matrix-derived IGF-1 to promote osteoblast differentiation by favoring recruitment of mesenchymal stem cells (MSCs) (Xian et al., 2012) also links early release of growth factors to later differentiation of osteoblasts. These proposals for the mechanisms of growth factor action make it easier to understand how growth factors released by resorption, or from cell sources, could enhance subsequent bone formation in the BMU. Rather, their main influences would be to stimulate osteoblast progenitors, including their recruitment (Xian et al., 2012), migration (Fiedler et al., 2002; Sanchez-Fernandez et al., 2008; Tang et al., 2009; Kreja et al., 2010), and differentiation (Mitlak et al., 1996). The necessary precise quantitation could be achieved during the next stage through influences on the number and progression of stem cells after they enter the remodeling site.

Coupling factors synthesized and secreted by osteoclasts

Osteoclasts themselves might also be the source of coupling activity. This first arose during consideration of the anabolic action of intermittently injected parathyroid hormone (PTH), which was known to be achieved through activation of new and existing BMUs (Martin and Sims, 2005). This raised the question, what mechanisms determine replacement of the precise amount of bone resorbed in a BMU to preserve bone balance (Fig. 10.2)? Attention began to focus on identifying contributing osteoclast-derived factors, acting either independently or cooperatively with matrix-derived factors.

There were clues from human and mouse genetics. The failure of bone resorption results in the clinical syndrome of osteopetrosis: this may occur due to osteoclast deficiency or impaired activity. In forms of osteopetrosis with failed osteoclast formation—"osteoclast-poor" osteopetrosis—such as in the rare example of individual human subjects with lost RANKL/RANK signaling (Sobacchi et al., 2007), the bone is devoid of osteoclasts. This can be mimicked in a murine model by genetic ablation of *c-fos*, a transcription factor essential for osteoclast formation, and such mice have osteopetrosis noted by their failure to generate osteoclasts, and theirgreatly reduced bone formation (Grigoriadis et al., 1994).

The other form of osteopetrosis is "osteoclast-rich." Individuals with osteopetrosis due to defective osteoclast function, caused by mutations in either ClC-7 or the corresponding osteoclastic V-ATPase subunit A3 (also called TCIRG1), had

high numbers of inactive osteoclasts (Henriksen et al., 2004; Karsdal et al., 2005). Unlike osteoclast-poor osteopetrosis, bone formation was normal or even increased, rather than diminished, as might be expected because of the greatly impaired resorption (Alatalo et al., 2004; Del Fattore et al., 2006). The level of bone formation has been linked directly to the presence of increased numbers of nonresorbing osteoclasts by direct correlation between the number of osteoclasts and the number of bone-forming osteoblasts (Del Fattore et al., 2006). Furthermore, when osteoclasts generated from the peripheral blood of a patient with osteopetrosis due to a mutation in the V-ATPase subunit A3 were cultured in vitro, conditioned medium from those osteoclasts was able to stimulate mineralized nodule formation in vitro despite their inability to resorb bone (Henriksen et al., 2012). This correlated well with earlier work in osteoclasts cultured on plastic (and therefore not resorbing bone), which were found to secrete factors promoting nodule formation (Karsdal et al., 2008; Pederson et al., 2008).

The findings from human genetics were supported by several studies in mice, whether deficient in *c-src* (Marzia et al., 2000), cathepsin K (Pennypacker et al., 2009), or *Pyk2* (Gil-Henn et al., 2007); in each case bone resorption is inhibited without inhibition of formation. In each of these knockout mice, while resorption is greatly reduced, osteoclast numbers are not. This is strikingly different from the case of *c-fos*-deficient mice that lack osteoclasts and have impaired bone formation (Grigoriadis et al., 1994). In support of the idea that the mutant osteoclasts might have impaired resorptive capacity but retain their ability to promote bone formation, transplantation of hematopoietic precursor cells deficient in the osteoclastic V-ATPase subunit a3 required for resorptive function into normal adult mice led to a significant reduction in resorption with increased osteoclast numbers but no reduction in bone formation (Lee et al., 2006). This was observed for up to 18 weeks following induction of osteopetrosis and was associated with improved bone volume and strength (Henriksen et al., 2011). A further instructive study (Thudium et al., 2014) compared osteopetrosis induced by transplanting irradiated normal mice with osteoclast precursors from oc/oc mice (osteoclast-rich osteopetrosis) or with RANK-deficient (osteoclast-poor) cells. The increase in bone volume was larger with the oc/oc cell transplantation, despite a similar reduction in bone resorption, indicating that the nonfunctional osteoclasts retained their ability to support bone formation also in vivo.

Other genetic evidence in mice indicated an intrinsic anabolic activity emanating from osteoclasts. An example is an early in vivo study showing that a signal from the active osteoclast is required for bone formation in mice lacking the osteoclast inhibitor OPG (Nakamura et al., 2003). These mice exhibit very high levels of osteoclastogenesis and resorption, resulting in severe osteopenia. They also show a high level of bone formation. Risedronate treatment reduced osteoclast activity, while osteoclast numbers remained high. The reduction in osteoclast activity was associated with a low level of bone formation, even in the presence of a BMP-2 implant, indicating that active osteoclasts produce bone formation-simulating activity. In a later study these authors (Koide et al., 2017) found that conditioned medium from osteoclasts of OPG-deficient mice included leukemia inhibitory factor as a potential osteoclast-derived coupling factor, as had been suggested by others (Pederson et al., 2008; Poulton et al., 2012). It should be emphasized, though, that it is difficult to prove whether it is a coupling factor in the context of bone remodeling or simply a factor produced by osteoclasts that can also stimulate bone formation.

Based on experiments in mice with inactivating mutations of each of the two alternative signaling pathways of gp130 it was concluded that resorption alone was insufficient to promote coupled bone formation, but that active osteoclasts are the likely source, and that the coupling pathway is interleukin-6 dependent (Sims et al., 2004; Martin and Sims, 2005). Another proposed pathway of gp130 involvement was through the gp130-signaling cytokine cardiotrophin-1 (CT-1). In mice with global deletion of CT-1, although osteoclast numbers are high, their activity is low, and so too is the activity of their osteoblasts, indicating a lack of coupling factor production (Walker et al., 2008). CT-1 was detected in resorbing osteoclasts by immunohistochemistry (IHC) and shown to stimulate osteoblast differentiation in vitro and bone formation in vivo (Walker et al., 2008).

When osteoclast conditioned medium stimulated MSC migration and osteoblastic differentiation, Pedersen et al. (Pederson et al., 2008) undertook a microarray study identifying sphingosine-1-phosphate (S1P), Wnt10b, and BMP-6 as osteoclast products, suggesting they might be coupling factors. Each of these skeletal anabolic agents was known to be secreted by osteoclasts to a greater extent than by macrophages (Baron and Rawadi, 2007; Vukicevic and Grgurevic, 2009). Whether important as an osteoclast product or not, Wnt10b has been invoked as a T cell product mediating the anabolic effect of PTH (Terauchi et al., 2009; Bedi et al., 2012). The roles of S1P in bone are also likely to be quite complex. It can have inhibitory or stimulatory effects on osteoblasts depending on the stage of cell differentiation and on the source of precursors, such as human MSCs, immortalized MSCs, and mouse calvarial osteoblasts (Ryu et al., 2006; Pederson et al., 2008; Quint et al., 2013). S1P is also expressed by cells in the vasculature and acts on its receptor, expressed in osteoclast precursors, to stimulate osteoclastic recruitment in vitro (Ishii et al., 2009). Furthermore, in vivo and in vitro studies indicated that S1P can limit bone resorption by regulating the chemotaxis and migration of osteoclast precursors, essentially resulting in increased recirculation from bone to blood (Ishii et al., 2010). In that same work,

knockout of the S1P receptor S1PR1 yielded mice with excessive bone loss and enhanced osteoclast attachment to bone surfaces, and treatment with FTY720, a drug agonist of four of the five S1P receptors, including S1PR1, was effective in preventing bone loss in ovariectomized mice. Data more likely suggesting a role for osteoclast-derived S1P in the coupling mechanism came from a study in which *cathepsin K* was rendered null in osteoclasts, resulting in impaired resorption, while osteoclast numbers and bone formation were maintained (Lotinun et al., 2013). Ex vivo cultures showed that the mutated osteoclasts had a greater capability to promote aspects of osteoblast differentiation in coculture, an effect inhibited by an S1P receptor antagonist. Suggestive though this is of a role for S1P in the coupling process in the BMU, it needs to be explored further and put into the context of other actions of S1P, which has been invoked as a signaling mechanism in the actions of a number of cytokines, growth factors, and hormones (reviewed in Alvarez et al., 2007).

Other candidate osteoclast-secreted coupling factors have emerged from in vitro and ex vivo studies (listed in Table 10.1). These include afamin, a member of the albumin/vitamin D-binding protein family (Lichenstein et al., 1994); it is produced by osteoclasts and caused the recruitment of a mouse preosteoblastic cell line in vitro, in a manner that was lost by in vitro knockdown of afamin production (Kim et al., 2012). Another is PDGF-BB, produced by nonresorbing osteoclasts, which induces migration of bone marrow−derived human MSCs (Kreja et al., 2010) and mouse preosteoblasts (Sanchez-Fernandez et al., 2008), although an earlier study indicated that PDGF-BB inhibited osteoblastogenesis (Kubota et al., 2002). Perhaps more convincing evidence for a role for PDGF-BB in remodeling is from the mouse genetic studies that show its promotion of angiogenesis when mobilized by resorption and acting early in remodeling (Xie et al., 2014). Two candidate coupling activities, collagen triple-helix repeat−containing 1 and complement factor 3A (C3A), were put forward by one group (Takeshita et al., 2013; Matsuoka et al., 2014), but in each case they were produced by cells other than osteoclasts, and the high circulating level of C3A tended to exclude it from a role as a local regulator of coupling within the BMU. A more recent suggestion has been that microRNAs are released as coupling factors contained within exosomes that reach the circulation (Li et al., 2016). While it is appealing that osteoclast-derived membranous vesicles could provide a way of regulating osteoblast function, it is difficult to see how this could be controlled, either within the confines of the BMU or at the level of the whole individual.

Membrane-bound coupling factors synthesized by osteoclasts

Some of the osteoclast-derived coupling factors proposed are membrane-bound molecules, expressed on the cell surface of osteoclasts. Such molecules therefore require direct cell−cell contact with osteoblast lineage cells to produce effects that might favor osteoblast differentiation. These membrane-bound proteins have been discovered through a combination of genetic and pharmacological approaches. Factors proposed to act in this cell-contact-dependent manner include EphrinB2 (Zhao et al., 2006) and semaphorin D (Negishi-Koga et al., 2011). While plausible in vitro, and observed in the highly active murine calvarial suture that lacks BMUs (Furuya et al., 2018), such cell-contact-dependent mechanisms are problematic in the BMU because osteoclasts and osteoblasts are present on the bone surface at different times during remodeling, and therefore are rarely, if ever, in contact. If such mechanisms occur, they may exist between osteoclasts and osteoblast precursors very early in remodeling, or between osteoclasts and osteoblast lineage cells in the remodeling canopy. The latter possibility will be discussed in light of anatomic structural studies of the reversal phase, later.

The Eph family constitutes the largest family of receptor tyrosine kinases, notable because both receptors (Eph proteins) and ligands (Ephrin proteins) are membrane bound and both forward (through receptor) and reverse (through ligand) signaling takes place upon their interaction. EphrinB2 is expressed at all stages of osteoblast differentiation, as well as in osteoclasts and their precursors (Zhao et al., 2006; Allan et al., 2008). The first study of ephrin/Eph interaction in bone seemed to present an exciting prospect of EphrinB2 from the osteoclast acting as a coupling factor through a cell-contact-dependent mechanism with osteoblasts (Zhao et al., 2006). In vitro data indicated that contact between osteoclasts and osteoblasts initiated signaling in both cells such that EphrinB2 signaling in the osteoclast lineage limited their differentiation, while simultaneous EphB4 signaling in the osteoblast stimulated bone formation. However, osteoclast lineage−specific deletion of EphrinB2 presented no detectable in vivo bone phenotype (Zhao et al., 2006), nor did osteoclast precursors from an osteoclast-specific knockout of EphrinB2 show any alteration in osteoclast differentiation (Tonna et al., 2014). Further, EphrinB2/EphB4 interaction within the osteoblast lineage in vivo played a crucial role in maintaining osteoblast differentiation and attaining normal bone strength (Takyar et al., 2013). Specific blockade of EphrinB2/EphB4 signaling both in vitro and in vivo impaired osteoblast function and the anabolic response to PTH in vivo (Tonna et al., 2014). The latter was dependent on the availability of EphrinB2 for reverse signaling. Indeed, the earlier published evidence (Zhao et al., 2006) for a mild anabolic effect of transgenic EphB4 overexpression in vivo, and treatment of osteoblasts with clustered EphB4-Fc in vitro, might be explained by such an action through EphrinB2 signaling within osteoblasts. Given the extensive contact among osteoblasts that is required for bone formation (Ecarot-Charrier et al., 1983;

Abe et al., 1993; Gerber and ap Gwynn, 2001), it seems logical that such membrane-bound proteins are more likely to regulate bone formation through communication between osteoblast lineage cells than in osteoclast−osteoblast coupling activity that links two cell types without physical contact.

Semaphorins include both secreted and membrane-associated molecules that use plexins and neuropilins as their primary receptors. Plexins are the usual receptors for membrane−associated semaphorins, and neuropilins are obligate coreceptors in the case of most soluble class III receptors (Winberg et al., 1998; Takahashi et al., 1999; Tamagnone et al., 1999). Transcriptional arrays carried out on osteoclasts revealed substantial expression of semaphorin 4D (Sema4D), with none detectable in osteoblasts (Negishi-Koga et al., 2011). Targeted genetic ablation of Sema4D in osteoclasts resulted in increased trabecular bone mass, due to increased number and activity of osteoblasts, whereas osteoclast numbers were normal. Marrow transfer to wild-type mice from Sema4D-null mice resulted in increased bone formation and trabecular bone mass, and treatment of osteoblasts in vitro with recombinant soluble Sema4D-Fc decreased formation of mineralized nodules. The data point to Sema4D as an osteoclast-derived inhibitor of osteoblast differentiation and bone formation; these properties would equip it to be a fine-tuning mediator of remodeling in the BMU, acting as an inhibitor of the process. Just as OPG counters RANKL action by providing a powerful negative influence on osteoclast formation and function, it comes as no surprise that there should exist inhibitors of coupling; this raises the possibility that more such activities might exist.

A further membrane-bound coupling activity that has gained support is “outside-in” or “reverse” signaling within osteoblasts by RANK, the receptor for RANKL that signals action to generate osteoclasts (Suda et al., 1999). In addition to its actions to inhibit osteoclastogenesis, a RANKL-binding agent was found to also increase bone formation in vivo and promote osteoblast differentiation in vitro (Furuya et al., 2013). This was confirmed in an animal model of inflammatory arthritis (Kato et al., 2015), and was discussed in an editorial published in the same issue (Sims and Romas, 2015). These pharmacological studies have been supported by identification of an endogenous and potentially physiological action of RANK. RANK secreted in vesicles from maturing osteoclasts was found to increase bone formation by promoting RANKL reverse signaling to activate *runx2* (Ikebuchi et al., 2018). This is an interesting possibility that would require controlled delivery from osteoclasts early in the life of a BMU to appropriate targets in the osteoblast lineage, just as is the case with TGFβ (Tang et al., 2009) and IGF-1 (Xian et al., 2012) (*vide supra*, discussion under “Matrix-derived resorption products as coupling factors”).

Perspective on candidate osteoclast-derived coupling factors identified to date

Research activity focused on the search for local osteoclast-derived coupling factors (whether by active secretion or resorption of bone matrix) has yielded many candidate molecules, summarized in Table 10.1, indicating the nature of the experiment used and the cells capable of producing those molecules. Since many of these have been identified only since 2009, most require validation by independent groups of researchers working in multiple systems. This is particularly true of those factors identified in conditioned media. These can point to factors that may be important, but they each require validation of their specificity and their in vivo relevance.

A striking feature of these published data is that none of these candidate osteoclast-derived coupling factors can be said confidently to be exclusively derived from the osteoclast. Many are also products of cells in close proximity with, and even within, the BMU, such as macrophages and other immune cells, and many circulate in concentrations high enough to exclude a primary function as local regulators at multiple sites throughout the skeleton. The frequency of contradictory reports, variability of experimental systems that have been used, and limited nature of in vitro studies have made some of these reports difficult to interpret. Observations arising out of activities discovered in conditioned medium of osteoclast cultures need to be interpreted in light of substantial macrophage contamination in such cultures that is variable between donors and laboratories, and cannot be avoided with existing methods. Furthermore, none of the in vitro studies have set out to determine whether osteoclast products influence different stages of osteoblast differentiation, which seems a likely mechanism by which they could act, given the temporal delay between bone resorption and formation at the BMU. It would seem likely that the coupling process within the BMU would require actions at different stages, as osteoblasts progress through differentiation during remodeling (Fig. 10.3).

How other cells contribute to coupling

In addition to factors released by osteoclasts through resorption, secretion, or membrane budding, other cell types may mediate the signals required to ensure that bone formed during remodeling in the BMU matches the prior level of bone

resorption to maintain bone mass. Some possibilities include signaling by osteoblast lineage cells themselves, macrophages and immune cells, and the cell population resident during the reversal phase.

Osteoblast lineage cells—sensing the surface and signaling to one another

Osteoblast lineage precursors begin their differentiation in the BMU, during which they are in contact with (or at least in close proximity to) other precursors and mature osteoblasts on the bone surface. Bone-forming osteoblasts on the bone surface are also in contact, not only with one another, but also with the highly differentiated osteocytes within the bone matrix. This lends itself to communication within the lineage as part of the overall coupling process.

An example of such intralineage information transfer is the production of latent TGFβ, produced by osteoblasts, activated by proteases, and supplementing the resorption-derived TGFβ that contributes to the initial stages of coupling in the BMU (Yee et al., 1993; Pfeilschifter et al., 1995). We have drawn attention to the role of EphrinB2/EphB4 interaction between osteoblast lineage cells as an important checkpoint that must be passed for the lineage to reach late stages of osteoblast differentiation (Takyar et al., 2013; Tonna et al., 2014). EphrinB2 production remains unchanged throughout osteoblast differentiation, but responds with rapidly increased production when exposed to PTH-related protein (PTHrP) (Allan et al., 2008). Through such interactions within the osteoblast lineage, osteoblast precursors are able to respond to the cues initiated by osteoclast-derived factors to enter the BMU and differentiate to osteoblasts capable of bone matrix production (Fig. 10.3).

The osteocyte, the most abundant cell in bone by far, forms a highly complex cellular communication network through the bone matrix, with a total of ∼3.7 trillion connections throughout the adult skeleton (Buenzli and Sims, 2015). This network has crucial regulatory functions by its production of sclerostin, which limits bone formation though its powerful inhibition of Wnt-stimulated osteoblast differentiation (Bonewald and Johnson, 2008). This action is likely to be important in limiting the amount of bone laid down in modeling, but its production in response to loading (Galea et al., 2011), or to local factors such as prostaglandin E_2 (Genetos et al., 2011) or PTHrP (Ansari et al., 2018), is capable of regulating the bone formation within BMUs. Just as osteoblast precursors are available in the BMU at the time when osteoclasts are present, resorbing bone and releasing or producing coupling factors, so too are osteocytes available to respond to coupling factors. Indeed, a number of osteoclast-derived coupling factors promote bone formation and suppress sclerostin production by osteocytes: these include CT-1 and Leukemia Inhibitory Factor (LIF) (Walker et al., 2008, 2010; Poulton et al., 2012).

Another mechanism to which osteoblasts can respond that would allow them to produce sufficient bone matrix to refill the cavity left by osteoclasts, is their ability to "sense" changes on the bone surface. It was shown in vitro that if rat calvarial cells were provided to bone slices with crevices made by osteoclasts or mechanically excavated grooves, the cells made bone in those defects, filling them exactly to a flat surface (Gray et al., 1996). Osteoblast precursors have been shown to respond to changes in surface topography, whether the change is much larger than the cell itself, as in the aforementioned study, or very much smaller than the cell (Dalby et al., 2006). In response to altered nanotopography, osteoblast lineage cells adhere to the surface and one another and proceed to differentiate. In this way, osteoclasts control osteoblast activity from a distance by establishing the size and shape of the resorptive pit to be filled. It is also possible that the changes brought about on the bone surface by cells in the reversal phase change the topography in a way that determines osteoblast function. Both the proposed growth factor actions and the work of Gray et al. imply that once the formation process is established, the participating cells themselves are able to sense the spatial limits and fill the space through chemical communication, possibly involving gap junctions or cell-contact-dependent communication processes both between bone-forming osteoblasts and between osteoblasts and osteocytes (Tonna and Sims, 2014). Since the in vitro study of Gray used bone that did not contain osteocytes, while they may contribute, osteocytes are not necessary for osteoblasts to respond to topographic clues, at least in vitro.

Osteocytes are the major controlling cells of bone (Bonewald, 2011; Schaffler et al., 2014), producing sclerostin as a powerful inhibitor of bone formation, whether in modeling or remodeling (van Bezooijen et al., 2004). Through their fluid-filled network of communicating channels they sense and respond to mechanical strain; this system might provide an additional coupling mechanism. Osteocytes would sense the increased strain resulting from weakening of the bone as resorption progresses (McNamara et al., 2006), and respond by producing a signal to halt resorption. They would also detect when the strain is relieved as the resorbed pit is refilled by osteoblasts. Such a strain-based model for coupling was proposed some years ago (Rodan, 1991), and as our understanding of osteocyte signaling increases, possible mediators are coming to light. As the mechanical properties of the excavated bone improve, the osteocytes may signal to osteoblasts that enough bone has been made in the BMU, a task that could be filled by sclerostin or by other osteocyte-derived regulators of bone formation such as oncostatin M (OSM) (Walker et al., 2010) or PTHrP (Ansari et al., 2018). Clearly many steps are

required to achieve precision in the coupling process: precursor replication, differentiation, limiting the cell mass to exactly what is required, correct shaping, and level of mineralization.

Macrophages, immune cells, and endothelial cells

As discussed earlier, a key problem of studying osteoclastic effects on osteoblasts is the technical difficulty of obtaining sufficiently purified osteoclasts. Furthermore, the extensive overlap in gene expression between osteoclasts and macrophages suggests that factors produced by osteoclasts can be also produced by macrophages in the vicinity of the BMU.

OSM, a cytokine that signals through gp130, stimulates bone formation in mouse calvariae in vivo and in bone remodeling, as indicated by impaired bone formation in OSM-null mice, and promotes osteoblast commitment by calvarial osteoblasts in vitro (Walker et al., 2010). Although not expressed in osteoclasts, OSM was originally identified in macrophages (Zarling et al., 1986) and was present in media from enriched cultures of human osteoclasts. It was found to be the factor responsible for strongly inducing alkaline phosphatase activity and mineralization by human adipose tissue-derived MSCs (pluripotent osteoblast precursors) (Fernandes et al., 2013), where macrophage populations formed from the same source as the osteoclasts were found to be even more efficient at driving MSC maturation, probably due to higher OSM production. A cautionary finding from some of this work was that differing responses can occur with different types of macrophage activation (Guihard et al., 2012; Nicolaidou et al., 2012). These findings serve to make a broader point: factors identified as osteoclast-derived coupling factors are produced not only by osteoclasts but also by macrophages (to which they have a close ontogenic relationship).

Like the contaminating macrophages in osteoclast cultures, macrophages are present in primary osteoblast cultures from calvariae and promote osteoblast differentiation (Chang et al., 2008). This finding led to the identification of bone-resident tissue macrophages (osteal macrophages defined by F4/80 antigen expression) mingled in large numbers with osteoblasts at the endosteal and periosteal bone surfaces and forming a canopy-like layer above osteoblasts and bone-lining cells at endosteal surfaces (Chang et al., 2008). Despite their emerging importance, defining the resident osteal macrophage population remains problematic since they are primarily defined by location, and as of this writing, cell surface markers do not exist that allow the resident cells to be specifically purified. Such regulatory macrophages would be expected to be sensitive to cues from the immune system. In addition, either a change in their activation state or replacement by recruited inflammatory macrophages and availability within the BMU canopy, by modifying their secretion of factors such as OSM, might alter local bone metabolism, perhaps profoundly (Fig. 10.4).

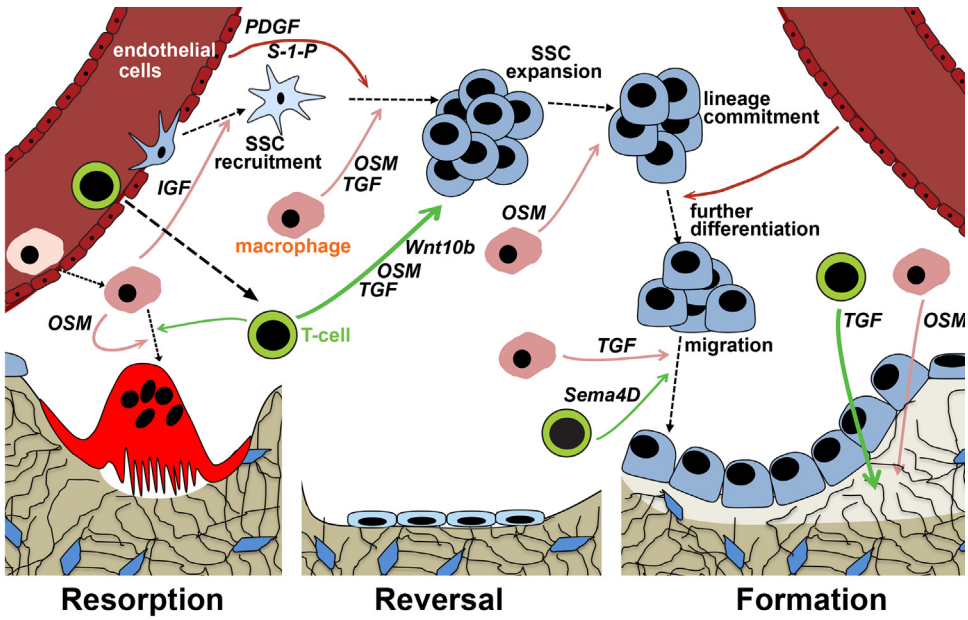

FIGURE 10.4 Signals from "nonresident bone cells" that enter the bone remodeling compartment from the vasculature, such as endothelial cells, T lymphocytes, and macrophages, also contribute to the matching of bone formation to bone resorption during the resorption, reversal, and formation phases of remodeling. Some examples of potential factors from each cell type are illustrated, such as platelet-derived growth factor (*PDGF*), sphingosine-1-phosphate (*S-1-P*), oncostatin M (*OSM*), Wnt10b, and transforming growth factor (*TGF*) are shown. See Table 10.1 for more examples. Factors act on each stage of osteoblast differentiation, including on osteocytes. *IGF*, insulin-like growth factor; *Sema4D*, semaphorin 4D; *SSC*, stromal stem cell.

Immune cells are also able to gain access to remodeling sites through the blood supply at the canopy (Fig. 10.4). Just as OSM may promote bone formation by virtue of its production by macrophages (Zarling et al., 1986), T lymphocytes (Clegg et al., 1996), osteoblasts, and osteocytes (Walker et al., 2010), the same is true of many of the other coupling factors (summarized in Table 10.1). T cells have been invoked as playing a part in normal remodeling by mediating the anabolic effect of intermittent PTH injection in the mouse (Terauchi et al., 2009; Bedi et al., 2012). In that work Wnt10b was reported as the T cell product acting upon the osteoblast lineage to achieve the PTH anabolic effect. The significance of this work might go further, though. Since the PTH anabolic effect is considered to be predominantly through promotion of remodeling, can these findings imply that T cells contribute to normal remodeling events within the BMU? It is relevant to note that Wnt10b was also one of the osteoclast conditioned medium−derived coupling factors identified by Pederson et al. (2008).

The data summarized in Table 10.1 illustrate the redundancy among cell types of secretory products that might promote osteoblast differentiation. They also illustrate the difficulty in identifying any exclusive osteoclast-derived activity. None of these considerations reduces the potential importance of these factors in bone biology. Rather, they illustrate multiple roles for these factors, the likely complexity of the coupling process, the possible involvement of multiple cell types, and the likely cross-regulation of each of these regulatory pathways.

The reversal phase as a coupling mechanism

Publications have suggested a regulatory role for the reversal phase in coupling of osteoblast to osteoclast activity. The existence of a reversal phase between the resorptive and the formative phases of remodeling was proposed originally by Baron, (1977) on the basis of studies in rat bone. Twenty years after Frost's remodeling proposals it was found that toward the end of resorption, mononuclear cells gather at the bottom of resorption pits, where they prepare the pits for the engagement of osteoblasts in bone formation (Villanueva et al., 1986). In this reversal phase of remodeling, macrophages had been long considered responsible for the postresorption digestion of collagen fragments in the BMU. The identification that cells of the osteoblast lineage were able to engulf collagen fragments (Takahashi et al., 1986) was taken further by Everts et al. (Everts et al., 2002), who identified osteoblast lineage bone-lining cells cytologically at sites of resorption, both in calvariae and in long bones, and showed that these cells actually engulf collagen fragments remaining on the bone surface after osteoclasts have resorbed and left it (Everts et al., 2002). This activity appeared to be mediated by membrane matrix metalloproteinases. Thus, although these osteoblast lineage cells are not equipped to lay down an adequate matrix, they nevertheless are able to lay down a thin layer of collagen along Howship's lacuna, closely associated with a cement line. This reversal line (cement line) contains a large abundance of osteopontin (Chen et al., 1994), which is produced by both osteoclasts and osteoblasts. Osteopontin is an RGD-containing extracellular matrix protein that interacts with integrin receptors $\alpha V\beta 3$ in osteoclasts and primarily $\alpha V\beta 5$ in osteoblasts, mediating cell attachment to the bone surface and signaling within the cell. The presence of osteopontin on the reversal line raises the possibility that it may be one of the signals for cessation of osteoclast activity or initiation of osteoblastic bone formation or possibly both.

These findings of Everts et al. were of interest in themselves, in drawing attention to a function of osteoblast lineage cells in remodeling during the period between bone resorption and formation. Further than that, though, the question of whether these lining cells might become "activated" to become matrix-producing osteoblasts after the reversal phase became an active question.

When in situ hybridization (ISH) and IHC were used in human bone biopsy samples, the reversal cells on the surface were confirmed to be of the osteoblastic lineage by virtue of their expression of osteoblast marker genes (Andersen et al., 2013). Furthermore, those next to bone-forming osteoblasts were more mature than those next to osteoclasts (Andersen et al., 2013). This was in contrast to earlier findings in human and other bones, indicating that cells near osteoclasts are tartrate-resistant acid phosphatase (TRAP)-positive mononuclear osteoclasts (Tran Van et al., 1982; Eriksen et al., 1984b; Eriksen, 1986; Bianco et al., 1988). To resolve this, sensitive ISH and IHC methods were used and showed functional and phenotypic changes in the mesenchymal reversal cells as they progressed from near the osteoclasts (TRAP positive by IHC) to near the osteoblasts (TRAP negative) (Abdelgawad et al., 2016). TRAP immunoreactivity was shown to be occurring in cells with no detectable TRAP mRNA, leading to the conclusion that TRAP positivity in the early reversal cells resulted from ingestion from nearby osteoclasts. Runx2 immunoreactivity was uniform throughout the reversal cells, reflecting their osteoblastic lineage.

Removal of the collagen remnants in Howship's lacunae is another potential coupling mechanism, since it is obligatory for bone formation to occur. It is carried out by cells close to osteoclasts, early reversal cells with enhanced collagenolytic activity mediated through production of matrix metalloproteinase-13 (MMP-13) (Abdelgawad et al., 2016) and the

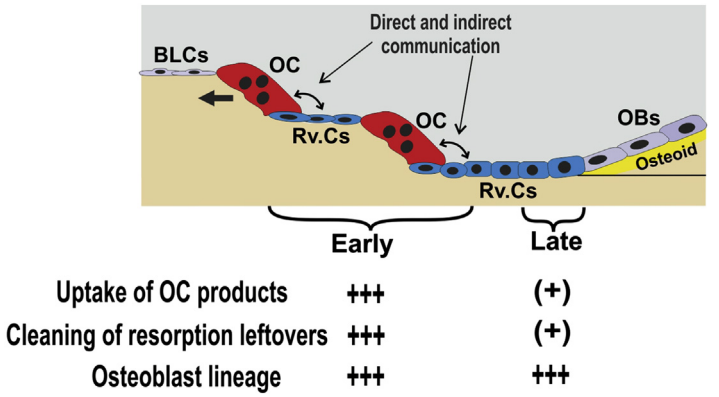

FIGURE 10.5 A new model of the reversal phase of remodeling. During quiescence, bone-lining cells (*BLC*) cover the inactive bone surface. Osteoclasts (*OC*) resorb the bone matrix and are intercalated with osteoblast lineage reversal cells (*Rv.Cs*) in the early reversal phase. In this phase osteoclast products released from the bone matrix or synthesized and secreted by osteoclasts are taken up by reversal cells, and may influence osteoblast progenitors. In the late reversal phase, reversal cells differentiate, on the bone surface, to become bone-forming osteoblasts (*OBs*) capable of synthesizing osteoid. Figure provided by Thomas L Andersen.

endocytic collagen receptor uPARAP/Endo180 (Madsen et al., 2011). With progression to late reversal cells there is much less expression of MMP-13 and uPARAP, constant Runx2, and no TRAP (Abdelgawad et al., 2016).

This evidence indicates a phenotypic change during the reversal phase in the cells on the bone surface. The cells progress from early to late reversal cells, with the latter differentiating directly into osteoid-synthesizing osteoblasts (Delaisse, 2014) (Fig. 10.5). The findings point to potential connections between osteoclasts and early osteoblast lineage cells that could transmit contact-independent or contact-dependent signals. Such contact could influence the function and progress of those osteoblast lineage cells. As an area of cell biology to study it is a fascinating one, if difficult to approach through any other than in vivo experimentation. In contrast to these potential communication points, mature osteoclasts and mature bone-forming osteoblasts are probably almost never in contact in ways that can transfer information.

Evidence consistent with these mechanisms was also obtained from remodeling in cortical bone, which is carried out with different cellular organization. The resorbing osteoclasts generate a cutting cone directed parallel to the diaphysis of long bones, with this resorption followed by the reversal zone and then osteoblasts synthesizing matrix (Eriksen, 1986; Jaworski, 1992) (Fig. 10.1).

Additional work from the same group examined the continuum of the BMU in cutting cones by IHC and ISH to identify osteoblast lineage cells and osteoclasts. In doing so, they described a reversal phase in which osteoblast progenitors differentiate until a critical mass of mature osteoblasts is reached and matrix formation follows (Abdelgawad et al., 2016; Lassen et al., 2017). They also noted the presence of sparsely distributed osteoclasts in the reversal phase in decreasing numbers as time after resorption increased. These osteoclasts are close enough to osteoblast lineage cells to be capable of transmitting signals, and seem to be responsible for a slow "secondary" bone resorption period needed to widen the osteon, as opposed to the longitudinal resorption in the cutting zone (Jaworski and Lok, 1972; Parfitt, 1983). The dynamics of these cells in the reversal phase that are modeled graphically in Fig. 10.5 confer an important role on the reversal phase in the coupling process of bone remodeling. First, it draws attention to the need for the supply of osteoblast precursors at that stage, if they are to progress to form bone. Where do they come from and how? The capillary blood supply identified near the canopy (Kristensen et al., 2013; Delaisse, 2014) is a potential source, as are the very early mesenchymal cells (pericytes) adherent to those nearby capillaries (Bianco et al., 2011). Second, while they are differentiating, these osteoblast lineage cells have osteoclasts distributed among them and are capable of signaling to them with secreted or even membrane-bound coupling activities (Lassen et al., 2017). Where do these "interstitial" osteoclasts come from? Are they newly generated or are they osteoclasts continuing to function from the initial resorption phase? Third, the onset of bone formation, with synthesis of ample osteoid, is an effective signal that dampens osteoclastic resorption, since osteoclasts are not known to attach to osteoid. Fourth, prolongation of the reversal phase for any reason, such as inadequate supply of progenitors with aging, can prolong the process and increase the osteon width, even contributing to porosity (Andreasen et al., 2017). On the other hand, the sooner bone formation starts, the faster secondary/radial bone resorption will stop.

Thus, in considering coupling of bone formation to resorption, the reversal phase is engaged in a remarkable abundance of biological interactions. In attempts to characterize coupling, intercellular communication mechanisms during the

reversal phase might be a more rewarding focus of attention rather than a narrow search for signals from mature osteoclasts to osteoblasts. The many participating signals are likely to have targets and outcomes that are heavily dependent upon the stages of differentiation of cells within the osteoblast lineage.

Conclusion

The coupling of bone formation to bone resorption is the dominant biological feature of bone remodeling. It is useful to consider the relative contributions to its control of circulating hormones and of locally generated factors. The latter might come from osteoclasts, osteoblasts, osteocytes, the matrix, or other cells in the environment, such as immune cells, macrophages, and endothelial cells.

Bone remodeling takes place simultaneously and asynchronously at very many sites throughout the skeleton, with those sites being selected because damaged or old bone needs to be removed and replaced. How those sites are selected we do not know. Once a BMU is initiated, though, it needs to have its activities regulated—its osteoclast formation, activity, and death; its osteoblast differentiation from precursors as primitive as tissue stem cells—and cessation of that process is needed when the filling of the BMU is complete.

All of these are processes and mechanisms that lend themselves readily to local regulation. This makes the process of coupling such an important one to understand. It is less easy to imagine how the progression of the remodeling process could be regulated satisfactorily by circulating hormones. This is especially so when thinking of the initiation of BMUs at specific sites, control of osteoclast activity at those sites, control of the supply of mesenchymal lineage precursors, and then their differentiation.

For these reasons we ask, how could a circulating hormone be a useful contributor to the bone formation process in remodeling? The question arises with PTH, for example, where the available published information tells us that there is a circadian rhythm of circulating PTH levels, but the total change throughout 24 h is on the order of 20% (Jubiz et al., 1972; el-Hajj Fuleihan et al., 1997; Fraser et al., 1998; White et al., 2007; Redmond et al., 2016). Such constancy of circulating PTH seems to equip it poorly for the initiation and/or control of BMUs generated stochastically throughout the skeleton. Locally generated PTHrP, though, could be the way that action through the PTHR1 contributes to remodeling (see Chapter 25).

There might be quite a different view in the case of an inhibitory hormone, such as estrogen. If the function of estrogen is to be available always to maintain a constitutive brake on osteoclast formation and/or activity, complemented by a more effective local inhibitor, e.g., OPG, this could be achieved as a circulating hormone. Lowering of estrogen would be expected to result in escape of control and increased remodeling by initiation of new BMUs, which is indeed what happens. If this line of reasoning is correct, perhaps by analogy we should think of the possibility of there being circulating activity that acts as a constitutive brake on osteoblast differentiation and thence bone formation. Its relationship with the local inhibitor of formation, sclerostin, would be analogous to that between estrogen and OPG.

The process of bone remodeling is a complex one with many participating cells and effectors and many identifiable stages that we are only beginning to understand. What is becoming evident, though, is that it is much easier to inhibit remodeling than it is to stimulate it. That is why therapeutic approaches to inhibit resorption are simple compared with approaches to stimulate formation.

References

Abdelgawad, M.E., Delaisse, J.M., Hinge, M., Jensen, P.R., Alnaimi, R.W., Rolighed, L., Engelholm, L.H., Marcussen, N., Andersen, T.L., 2016. Early reversal cells in adult human bone remodeling: osteoblastic nature, catabolic functions and interactions with osteoclasts. Histochem. Cell Biol. 145 (6), 603–615.

Abe, Y., Akamine, A., Aida, Y., Maeda, K., 1993. Differentiation and mineralization in osteogenic precursor cells derived from fetal rat mandibular bone. Calcif. Tissue Int. 52 (5), 365–371.

Alatalo, S.L., Ivaska, K.K., Waguespack, S.G., Econs, M.J., Vaananen, H.K., Halleen, J.M., 2004. Osteoclast-derived serum tartrate-resistant acid phosphatase 5b in Albers-Schonberg disease (type II autosomal dominant osteopetrosis). Clin. Chem. 50 (5), 883–890.

Allan, E.H., Hausler, K.D., Wei, T., Gooi, J.H., Quinn, J.M., Crimeen-Irwin, B., Pompolo, S., Sims, N.A., Gillespie, M.T., Onyia, J.E., Martin, T.J., 2008. EphrinB2 regulation by PTH and PTHrP revealed by molecular profiling in differentiating osteoblasts. J. Bone Miner. Res. 23 (8), 1170–1181.

Alvarez, S.E., Milstien, S., Spiegel, S., 2007. Autocrine and paracrine roles of sphingosine-1-phosphate. Trends Endocrinol. Metabol. 18 (8), 300–307.

Andersen, T.L., Abdelgawad, M.E., Kristensen, H.B., Hauge, E.M., Rolighed, L., Bollerslev, J., Kjaersgaard-Andersen, P., Delaisse, J.M., 2013. Understanding coupling between bone resorption and formation: are reversal cells the missing link? Am. J. Pathol. 183 (1), 235–246.

Andersen, T.L., Hauge, E.M., Rolighed, L., Bollerslev, J., Kjaersgaard-Andersen, P., Delaisse, J.M., 2014. Correlation between absence of bone remodeling compartment canopies, reversal phase arrest, and deficient bone formation in post-menopausal osteoporosis. Am. J. Pathol. 184 (4), 1142–1151.

Andersen, T.L., Soe, K., Sondergaard, T.E., Plesner, T., Delaisse, J.M., 2010. Myeloma cell-induced disruption of bone remodelling compartments leads to osteolytic lesions and generation of osteoclast-myeloma hybrid cells. Br. J. Haematol. 148 (4), 551–561.

Andersen, T.L., Sondergaard, T.E., Skorzynska, K.E., Dagnaes-Hansen, F., Plesner, T.L., Hauge, E.M., Plesner, T., Delaisse, J.M., 2009. A physical mechanism for coupling bone resorption and formation in adult human bone. Am. J. Pathol. 174 (1), 239–247.

Andreasen, C.M., Delaisse, J.M., Cj van der Eerden, B., van Leeuwen, J.P., Ding, M., Andersen, T.L., 2018. Understanding age-induced cortical porosity in women: the accumulation and coalescence of eroded cavities upon existing intracortical canals is the main contributor. J. Bone Miner. Res. 33 (4), 606–620.

Ansari, N., Ho, P.W., Crimeen-Irwin, B., Poulton, I.J., Brunt, A.R., Forwood, M.R., Divieti Pajevic, P., Gooi, J.H., Martin, T.J., Sims, N.A., 2018. Autocrine and paracrine regulation of the murine skeleton by osteocyte-derived parathyroid hormone-related protein. J. Bone Miner. Res. 33 (1), 137–153.

Barlic, J., Zhu, W., Murphy, P.M., 2009. Atherogenic lipids induce high-density lipoprotein uptake and cholesterol efflux in human macrophages by up-regulating transmembrane chemokine CXCL16 without engaging CXCL16-dependent cell adhesion. J. Immunol. 182 (12), 7928–7936.

Baron, R., 1977. Importance of the intermediate phase between resorption and formation in the measurement and understanding of the bone remodelling sequence. In: Meunier, P. (Ed.), I. Bone Remodelling, 2nd Int Workshop. Lab Armour Montague, Paris, pp. 179–183.

Baron, R., Rawadi, G., 2007. Targeting the Wnt/beta-catenin pathway to regulate bone formation in the adult skeleton. Endocrinology 148 (6), 2635–2643.

Baron, R., Sims, N.A., 2000. Bone Cells and Their Function. Skeletal Growth Factors. E. Canalis. Lippincott Williams and Wilkins, Philadelphia, pp. 1–16.

Bedi, B., Li, J.Y., Tawfeek, H., Baek, K.H., Adams, J., Vangara, S.S., Chang, M.K., Kneissel, M., Weitzmann, M.N., Pacifici, R., 2012. Silencing of parathyroid hormone (PTH) receptor 1 in T cells blunts the bone anabolic activity of PTH. Proc. Natl. Acad. Sci. U.S.A. 109 (12), E725–E733.

Bennett, C.N., Ouyang, H., Ma, Y.L., Zeng, Q., Gerin, I., Sousa, K.M., Lane, T.F., Krishnan, V., Hankenson, K.D., MacDougald, O.A., 2007. Wnt10b increases postnatal bone formation by enhancing osteoblast differentiation. J. Bone Miner. Res. 22 (12), 1924–1932.

Bianco, P., Ballanti, P., Bonucci, E., 1988. Tartrate-resistant acid phosphatase activity in rat osteoblasts and osteocytes. Calcif. Tissue Int. 43 (3), 167–171.

Bianco, P., Sacchetti, B., Riminucci, M., 2011. Osteoprogenitors and the hematopoietic microenvironment. Best Pract. Res. Clin. Haematol. 24 (1), 37–47.

Bonewald, L.F., 2011. The amazing osteocyte. J. Bone Miner. Res. 26 (2), 229–238.

Bonewald, L.F., Johnson, M.L., 2008. Osteocytes, mechanosensing and Wnt signaling. Bone 42 (4), 606–615.

Buenzli, P.R., Sims, N.A., 2015. Quantifying the osteocyte network in the human skeleton. Bone 75, 144–150.

Campbell, P.G., Novak, J.F., Yanosick, T.B., McMaster, J.H., 1992. Involvement of the plasmin system in dissociation of the insulin-like growth factor-binding protein complex. Endocrinology 130 (3), 1401–1412.

Canalis, E., Gabbitas, B., 1994. Bone morphogenetic protein 2 increases insulin-like growth factor I and II transcripts and polypeptide levels in bone cell cultures. J. Bone Miner. Res. 9 (12), 1999–2005.

Canalis, E., Ornitz, D.M., 2000. Biology of Platelet-Derived Growth Factor. Skeletal Growth Factors. E. Canalis. Lippincott Williams and Wilkins, Philadelphia, USA, pp. 153–166.

Carroll, M.C., 2004. The complement system in regulation of adaptive immunity. Nat. Immunol. 5 (10), 981–986.

Centrella, M., Canalis, E., 1985a. Local regulators of skeletal growth: a perspective. Endocr. Rev. 6 (4), 544–551.

Centrella, M., Canalis, E., 1985b. Transforming and nontransforming growth factors are present in medium conditioned by fetal rat calvariae. Proc. Natl. Acad. Sci. U.S.A. 82 (21), 7335–7339.

Chambers, T.J., 1980. The cellular basis of bone resorption. Clin. Orthop. Relat. Res. 151, 283–293.

Champagne, C.M., Takebe, J., Offenbacher, S., Cooper, L.F., 2002. Macrophage cell lines produce osteoinductive signals that include bone morphogenetic protein-2. Bone 30 (1), 26–31.

Chang, M.K., Raggatt, L.J., Alexander, K.A., Kuliwaba, J.S., Fazzalari, N.L., Schroder, K., Maylin, E.R., Ripoll, V.M., Hume, D.A., Pettit, A.R., 2008. Osteal tissue macrophages are intercalated throughout human and mouse bone lining tissues and regulate osteoblast function in vitro and in vivo. J. Immunol. 181 (2), 1232–1244.

Chen, J., McKee, M.D., Nanci, A., Sodek, J., 1994. Bone sialoprotein mRNA expression and ultrastructural localization in fetal porcine calvarial bone: comparisons with osteopontin. Histochem. J. 26 (1), 67–78.

Chen, W., Jin, W., Wahl, S.M., 1998. Engagement of cytotoxic T lymphocyte-associated antigen 4 (CTLA-4) induces transforming growth factor beta (TGF-beta) production by murine CD4(+) T cells. J. Exp. Med. 188 (10), 1849–1857.

Clegg, C.H., Rulffes, J.T., Wallace, P.M., Haugen, H.S., 1996. Regulation of an extrathymic T-cell development pathway by oncostatin M. Nature 384 (6606), 261–263.

Cornish, J., Callon, K., King, A., Edgar, S., Reid, I.R., 1993. The effect of leukemia inhibitory factor on bone in vivo. Endocrinology 132 (3), 1359–1366.

Cornish, J., Callon, K.E., Edgar, S.G., Reid, I.R., 1997. Leukemia inhibitory factor is mitogenic to osteoblasts. Bone 21 (3), 243–247.

Dacquin, R., Domenget, C., Kumanogoh, A., Kikutani, H., Jurdic, P., Machuca-Gayet, I., 2011. Control of bone resorption by semaphorin 4D is dependent on ovarian function. PLoS One 6 (10), e26627.

Dalby, M.J., McCloy, D., Robertson, M., Wilkinson, C.D., Oreffo, R.O., 2006. Osteoprogenitor response to defined topographies with nanoscale depths. Biomaterials 27 (8), 1306–1315.

Dallas, S.L., Rosser, J.L., Mundy, G.R., Bonewald, L.F., 2002. Proteolysis of latent transforming growth factor-beta (TGF-beta)-binding protein-1 by osteoclasts. A cellular mechanism for release of TGF-beta from bone matrix. J. Biol. Chem. 277 (24), 21352−21360.

Daniel, T.O., Fen, Z., 1988. Distinct pathways mediate transcriptional regulation of platelet-derived growth factor B/c-sis expression. J. Biol. Chem. 263 (36), 19815−19820.

Del Fattore, A., Peruzzi, B., Rucci, N., Recchia, I., Cappariello, A., Longo, M., Fortunati, D., Ballanti, P., Iacobini, M., Luciani, M., Devito, R., Pinto, R., Caniglia, M., Lanino, E., Messina, C., Cesaro, S., Letizia, C., Bianchini, G., Fryssira, H., Grabowski, P., Shaw, N., Bishop, N., Hughes, D., Kapur, R.P., Datta, H.K., Taranta, A., Fornari, R., Migliaccio, S., Teti, A., 2006. Clinical, genetic, and cellular analysis of 49 osteopetrotic patients: implications for diagnosis and treatment. J. Med. Genet. 43 (4), 315−325.

Delaisse, J.M., 2014. The reversal phase of the bone-remodeling cycle: cellular prerequisites for coupling resorption and formation. Bonekey Rep. 3, 561.

Ecarot-Charrier, B., Glorieux, F.H., van der Rest, M., Pereira, G., 1983. Osteoblasts isolated from mouse calvaria initiate matrix mineralization in culture. J. Cell Biol. 96 (3), 639−643.

Eghbali-Fatourechi, G.Z., Modder, U.I., Charatcharoenwitthaya, N., Sanyal, A., Undale, A.H., Clowes, J.A., Tarara, J.E., Khosla, S., 2007. Characterization of circulating osteoblast lineage cells in humans. Bone 40 (5), 1370−1377.

el-Hajj Fuleihan, G., Klerman, E.B., Brown, E.N., Choe, Y., Brown, E.M., Czeisler, C.A., 1997. The parathyroid hormone circadian rhythm is truly endogenous–a general clinical research center study. J. Clin. Endocrinol. Metab. 82 (1), 281−286.

Elmardi, A.S., Katchburian, M.V., Katchburian, E., 1990. Electron microscopy of developing calvaria reveals images that suggest that osteoclasts engulf and destroy osteocytes during bone resorption. Calcif. Tissue Int. 46 (4), 239−245.

Eriksen, E.F., 1986. Normal and pathological remodeling of human trabecular bone: three dimensional reconstruction of the remodeling sequence in normals and in metabolic bone disease. Endocr. Rev. 7 (4), 379−408.

Eriksen, E.F., Eghbali-Fatourechi, G.Z., Khosla, S., 2007. Remodeling and vascular spaces in bone. J. Bone Miner. Res. 22 (1), 1−6.

Eriksen, E.F., Gundersen, H.J., Melsen, F., Mosekilde, L., 1984a. Reconstruction of the formative site in iliac trabecular bone in 20 normal individuals employing a kinetic model for matrix and mineral apposition. Metab. Bone Dis. Relat. Res. 5 (5), 243−252.

Eriksen, E.F., Melsen, F., Mosekilde, L., 1984b. Reconstruction of the resorptive site in iliac trabecular bone: a kinetic model for bone resorption in 20 normal individuals. Metab. Bone Dis. Relat. Res. 5 (5), 235−242.

Eriksen, E.F., Vesterby, A., Kassem, M., Melsen, F., Mosekilde, L. (Eds.), 1993. Bone Remodeling and Bone Structure. Handbook of Experimental Pharmacology. Springer Verlag, Berlin.

Everts, V., Delaisse, J.M., Korper, W., Jansen, D.C., Tigchelaar-Gutter, W., Saftig, P., Beertsen, W., 2002. The bone lining cell: its role in cleaning Howship's lacunae and initiating bone formation. J. Bone Miner. Res. 17 (1), 77−90.

Fadok, V.A., Bratton, D.L., Konowal, A., Freed, P.W., Westcott, J.Y., Henson, P.M., 1998. Macrophages that have ingested apoptotic cells in vitro inhibit proinflammatory cytokine production through autocrine/paracrine mechanisms involving TGF-beta, PGE2, and PAF. J. Clin. Investig. 101 (4), 890−898.

Fernandes, T.J., Hodge, J.M., Singh, P.P., Eeles, D.G., Collier, F.M., Holten, I., Ebeling, P.R., Nicholson, G.C., Quinn, J.M., 2013. Cord blood-derived macrophage-lineage cells rapidly stimulate osteoblastic maturation in mesenchymal stem cells in a glycoprotein-130 dependent manner. PLoS One 8 (9), e73266.

Fiedler, J., Roderer, G., Gunther, K.P., Brenner, R.E., 2002. BMP-2, BMP-4, and PDGF-bb stimulate chemotactic migration of primary human mesenchymal progenitor cells. J. Cell. Biochem. 87 (3), 305−312.

Ford, J.K., Young, R.W., 1963. Cell proliferation and displacement in the adrenal cortex of young rats injected with tritiated thymidine. Anat. Rec. 146, 125−137.

Fournier, T., Riches, D.W., Winston, B.W., Rose, D.M., Young, S.K., Noble, P.W., Lake, F.R., Henson, P.M., 1995. Divergence in macrophage insulin-like growth factor-I (IGF-I) synthesis induced by TNF-alpha and prostaglandin E2. J. Immunol. 155 (4), 2123−2133.

Fraser, W.D., Logue, F.C., Christie, J.P., Gallacher, S.J., Cameron, D., O'Reilly, D.S., Beastall, G.H., Boyle, I.T., 1998. Alteration of the circadian rhythm of intact parathyroid hormone and serum phosphate in women with established postmenopausal osteoporosis. Osteoporos. Int. 8 (2), 121−126.

Friedman, M.S., Long, M.W., Hankenson, K.D., 2006. Osteogenic differentiation of human mesenchymal stem cells is regulated by bone morphogenetic protein-6. J. Cell. Biochem. 98 (3), 538−554.

Frost, H.M., 1964. Dynamics of bone remodeling. Bone Biodynamics 315−333.

Furuya, M., Kikuta, J., Fujimori, S., Seno, S., Maeda, H., Shirazaki, M., Uenaka, M., Mizuno, H., Iwamoto, Y., Morimoto, A., Hashimoto, K., Ito, T., Isogai, Y., Kashii, M., Kaito, T., Ohba, S., Chung, U.I., Lichtler, A.C., Kikuchi, K., Matsuda, H., Yoshikawa, H., Ishii, M., 2018. Direct cell-cell contact between mature osteoblasts and osteoclasts dynamically controls their functions in vivo. Nat. Commun. 9 (1), 300.

Furuya, Y., Inagaki, A., Khan, M., Mori, K., Penninger, J.M., Nakamura, M., Udagawa, N., Aoki, K., Ohya, K., Uchida, K., Yasuda, H., 2013. Stimulation of bone formation in cortical bone of mice treated with a receptor activator of nuclear factor-kappaB ligand (RANKL)-binding peptide that possesses osteoclastogenesis inhibitory activity. J. Biol. Chem. 288 (8), 5562−5571.

Galea, G.L., Sunters, A., Meakin, L.B., Zaman, G., Sugiyama, T., Lanyon, L.E., Price, J.S., 2011. Sost down-regulation by mechanical strain in human osteoblastic cells involves PGE2 signaling via EP4. FEBS Lett. 585 (15), 2450−2454.

Garimella, R., Tague, S.E., Zhang, J., Belibi, F., Nahar, N., Sun, B.H., Insogna, K., Wang, J., Anderson, H.C., 2008. Expression and synthesis of bone morphogenetic proteins by osteoclasts: a possible path to anabolic bone remodeling. J. Histochem. Cytochem. 56 (6), 569−577.

Genetos, D.C., Yellowley, C.E., Loots, G.G., 2011. Prostaglandin E2 signals through PTGER2 to regulate sclerostin expression. PLoS One 6 (3), e17772.

Gerber, I., ap Gwynn, I., 2001. Influence of cell isolation, cell culture density, and cell nutrition on differentiation of rat calvarial osteoblast-like cells in vitro. Eur. Cells Mater. 2, 10−20.

Gil-Henn, H., Destaing, O., Sims, N.A., Aoki, K., Alles, N., Neff, L., Sanjay, A., Bruzzaniti, A., De Camilli, P., Baron, R., Schlessinger, J., 2007. Defective microtubule-dependent podosome organization in osteoclasts leads to increased bone density in Pyk2(-/-) mice. J. Cell Biol. 178 (6), 1053−1064.

Gray, C., Boyde, A., Jones, S.J., 1996. Topographically induced bone formation in vitro: implications for bone implants and bone grafts. Bone 18 (2), 115−123.

Grigoriadis, A.E., Wang, Z.Q., Cecchini, M.G., Hofstetter, W., Felix, R., Fleisch, H.A., Wagner, E.F., 1994. c-Fos: a key regulator of osteoclast-macrophage lineage determination and bone remodeling. Science 266 (5184), 443−448.

Guihard, P., Danger, Y., Brounais, B., David, E., Brion, R., Delecrin, J., Richards, C.D., Chevalier, S., Redini, F., Heymann, D., Gascan, H., Blanchard, F., 2012. Induction of osteogenesis in mesenchymal stem cells by activated monocytes/macrophages depends on oncostatin M signaling. Stem Cell. 30 (4), 762−772.

Hanamura, H., Higuchi, Y., Nakagawa, M., Iwata, H., Nogami, H., Urist, M.R., 1980. Solubilized bone morphogenetic protein (BMP) from mouse osteosarcoma and rat demineralized bone matrix. Clin. Orthop. Relat. Res. 148, 281−290.

Harris, W.H., Heaney, R.P., 1969. Skeletal renewal and metabolic bone disease. N. Engl. J. Med. 280 (6), 303−311 concl.

Hattner, R., Epker, B.N., Frost, H.M., 1965. Suggested sequential mode of control of changes in cell behaviour in adult bone remodelling. Nature 206 (983), 489−490.

Hauge, E.M., Qvesel, D., Eriksen, E.F., Mosekilde, L., Melsen, F., 2001. Cancellous bone remodeling occurs in specialized compartments lined by cells expressing osteoblastic markers. J. Bone Miner. Res. 16 (9), 1575−1582.

Heino, T.J., Kurata, K., Higaki, H., Vaananen, H.K., 2009. Evidence for the role of osteocytes in the initiation of targeted remodeling. Technol. Health Care 17 (1), 49−56.

Henriksen, K., Andreassen, K.V., Thudium, C.S., Gudmann, K.N., Moscatelli, I., Cruger-Hansen, C.E., Schulz, A.S., Dziegiel, M.H., Richter, J., Karsdal, M.A., Neutzsky-Wulff, A.V., 2012. A specific subtype of osteoclasts secretes factors inducing nodule formation by osteoblasts. Bone 51 (3), 353−361.

Henriksen, K., Flores, C., Thomsen, J.S., Bruel, A.M., Thudium, C.S., Neutzsky-Wulff, A.V., Langenbach, G.E., Sims, N., Askmyr, M., Martin, T.J., Everts, V., Karsdal, M.A., Richter, J., 2011. Dissociation of bone resorption and bone formation in adult mice with a non-functional V-ATPase in osteoclasts leads to increased bone strength. PLoS One 6 (11), e27482.

Henriksen, K., Gram, J., Schaller, S., Dahl, B.H., Dziegiel, M.H., Bollerslev, J., Karsdal, M.A., 2004. Characterization of osteoclasts from patients harboring a G215R mutation in ClC-7 causing autosomal dominant osteopetrosis type II. Am. J. Pathol. 164 (5), 1537−1545.

Hock, J.M., Canalis, E., 1994. Platelet-derived growth factor enhances bone cell replication, but not differentiated function of osteoblasts. Endocrinology 134 (3), 1423−1428.

Hock, J.M., Canalis, E., Centrella, M., 1990. Transforming growth factor-beta stimulates bone matrix apposition and bone cell replication in cultured fetal rat calvariae. Endocrinology 126 (1), 421−426.

Howard, G.A., Bottemiller, B.L., Turner, R.T., Rader, J.I., Baylink, D.J., 1981. Parathyroid hormone stimulates bone formation and resorption in organ culture: evidence for a coupling mechanism. Proc. Natl. Acad. Sci. U.S.A. 78 (5), 3204−3208.

Hughes, D.E., Boyce, B.F., 1997. Apoptosis in bone physiology and disease. Mol. Pathol. 50 (3), 132−137.

Ikebuchi, Y., Aoki, S., Honma, M., Hayashi, M., Sugamori, Y., Khan, M., Kariya, Y., Kato, G., Tabata, Y., Penninger, J.M., Udagawa, N., Aoki, K., Suzuki, H., 2018. Coupling of bone resorption and formation by RANKL reverse signalling. Nature 561 (7722), 195−200.

Ishii, M., Egen, J.G., Klauschen, F., Meier-Schellersheim, M., Saeki, Y., Vacher, J., Proia, R.L., Germain, R.N., 2009. Sphingosine-1-phosphate mobilizes osteoclast precursors and regulates bone homeostasis. Nature 458 (7237), 524−528.

Ishii, M., Kikuta, J., Shimazu, Y., Meier-Schellersheim, M., Germain, R.N., 2010. Chemorepulsion by blood S1P regulates osteoclast precursor mobilization and bone remodeling in vivo. J. Exp. Med. 207 (13), 2793−2798.

Jaworski, Z.F., 1992. Haversian Systems and Haversian Bone. CRC, London.

Jaworski, Z.F., Lok, E., 1972. The rate of osteoclastic bone erosion in Haversian remodeling sites of adult dog's rib. Calcif. Tissue Res. 10 (2), 103−112.

Jensen, P.R., Andersen, T.L., Pennypacker, B.L., Duong, L.T., Engelholm, L.H., Delaisse, J.M., 2014. A supra-cellular model for coupling of bone resorption to formation during remodeling: lessons from two bone resorption inhibitors affecting bone formation differently. Biochem. Biophys. Res. Commun. 443 (2), 694−699.

Jin YR, Stohn JP, Wang Q, Nagano K, Baron R, Bouxsein ML, Rosen CJ, Adarichev VA, Lindner V. Inhibition of osteoclast differentiation and collagen antibody-induced arthritis by CTHRC1, Bone 97 (4), 153−167.

Johnson, R.W., McGregor, N.E., Brennan, H.J., Crimeen-Irwin, B., Poulton, I.J., Martin, T.J., Sims, N.A., 2015. Glycoprotein130 (Gp130)/interleukin-6 (IL-6) signalling in osteoclasts promotes bone formation in periosteal and trabecular bone. Bone 81, 343−351.

Jubiz, W., Canterbury, J.M., Reiss, E., Tyler, F.H., 1972. Circadian rhythm in serum parathyroid hormone concentration in human subjects: correlation with serum calcium, phosphate, albumin, and growth hormone levels. J. Clin. Investig. 51 (8), 2040−2046.

Kanatani, M., Sugimoto, T., Kaji, H., Kobayashi, T., Nishiyama, K., Fukase, M., Kumegawa, M., Chihara, K., 1995. Stimulatory effect of bone morphogenetic protein-2 on osteoclast-like cell formation and bone-resorbing activity. J. Bone Miner. Res. 10 (11), 1681−1690.

Karsdal, M.A., Henriksen, K., Sorensen, M.G., Gram, J., Schaller, S., Dziegiel, M.H., Heegaard, A.M., Christophersen, P., Martin, T.J., Christiansen, C., Bollerslev, J., 2005. Acidification of the osteoclastic resorption compartment provides insight into the coupling of bone formation to bone resorption. Am. J. Pathol. 166 (2), 467−476.

Karsdal, M.A., Martin, T.J., Bollerslev, J., Christiansen, C., Henriksen, K., 2007. Are nonresorbing osteoclasts sources of bone anabolic activity? J. Bone Miner. Res. 22 (4), 487−494.

Karsdal, M.A., Neutzsky-Wulff, A.V., Dziegiel, M.H., Christiansen, C., Henriksen, K., 2008. Osteoclasts secrete non-bone derived signals that induce bone formation. Biochem. Biophys. Res. Commun. 366 (2), 483–488.

Kartsogiannis, V., Zhou, H., Horwood, N.J., Thomas, R.J., Hards, D.K., Quinn, J.M., Niforas, P., Ng, K.W., Martin, T.J., Gillespie, M.T., 1999. Localization of RANKL (receptor activator of NF kappa B ligand) mRNA and protein in skeletal and extraskeletal tissues. Bone 25, 525–534.

Kato, G., Shimizu, Y., Arai, Y., Suzuki, N., Sugamori, Y., Maeda, M., Takahashi, M., Tamura, Y., Wakabayashi, N., Murali, R., Ono, T., Ohya, K., Mise-Omata, S., Aoki, K., 2015. The inhibitory effects of a RANKL-binding peptide on articular and periarticular bone loss in a murine model of collagen-induced arthritis: a bone histomorphometric study. Arthritis Res. Ther. 17, 251.

Kennedy, O.D., Herman, B.C., Laudier, D.M., Majeska, R.J., Sun, H.B., Schaffler, M.B., 2012. Activation of resorption in fatigue-loaded bone involves both apoptosis and active pro-osteoclastogenic signaling by distinct osteocyte populations. Bone 50 (5), 1115–1122.

Kim, B.J., Lee, Y.S., Lee, S.Y., Park, S.Y., Dieplinger, H., Ryu, S.H., Yea, K., Choi, S., Lee, S.H., Koh, J.M., Kim, G.S., 2012. Afamin secreted from nonresorbing osteoclasts acts as a chemokine for preosteoblasts via the Akt-signaling pathway. Bone 51 (3), 431–440.

Kimura, H., Kwan, K.M., Zhang, Z., Deng, J.M., Darnay, B.G., Behringer, R.R., Nakamura, T., de Crombrugghe, B., Akiyama, H., 2008. Cthrc1 is a positive regulator of osteoblastic bone formation. PLoS One 3 (9), e3174.

Koide, M., Kobayashi, Y., Yamashita, T., Uehara, S., Nakamura, M., Hiraoka, B.Y., Ozaki, Y., Iimura, T., Yasuda, H., Takahashi, N., Udagawa, N., 2017. Bone formation is coupled to resorption via suppression of sclerostin expression by osteoclasts. J. Bone Miner. Res. 32 (10), 2074–2086.

Kreja, L., Brenner, R.E., Tautzenberger, A., Liedert, A., Friemert, B., Ehrnthaller, C., Huber-Lang, M., Ignatius, A., 2010. Non-resorbing osteoclasts induce migration and osteogenic differentiation of mesenchymal stem cells. J. Cell. Biochem. 109 (2), 347–355.

Kristensen, H.B., Andersen, T.L., Marcussen, N., Rolighed, L., Delaisse, J.M., 2013. Increased presence of capillaries next to remodeling sites in adult human cancellous bone. J. Bone Miner. Res. 28 (3), 574–585.

Kubota, K., Sakikawa, C., Katsumata, M., Nakamura, T., Wakabayashi, K., 2002. Platelet-derived growth factor BB secreted from osteoclasts acts as an osteoblastogenesis inhibitory factor. J. Bone Miner. Res. 17 (2), 257–265.

Lacey, D.L., Timms, E., Tan, H.L., Kelley, M.J., Dunstan, C.R., Burgess, T., Elliott, R., Colombero, A., Elliott, G., Scully, S., Hsu, H., Sullivan, J., Hawkins, N., Davy, E., Capparelli, C., Eli, A., Qian, Y.X., Kaufman, S., Sarosi, I., Shalhoub, V., Senaldi, G., Guo, J., Delaney, J., Boyle, W.J., 1998. Osteoprotegerin ligand is a cytokine that regulates osteoclast differentiation and activation. Cell 93 (2), 165–176.

Lassen, N.E., Andersen, T.L., Ploen, G.G., Soe, K., Hauge, E.M., Harving, S., Eschen, G.E.T., Delaisse, J.M., 2017. Coupling of bone resorption and formation in real time: new knowledge gained from human haversian BMUs. J. Bone Miner. Res. 32 (7), 1395–1405.

Lee, S.H., Rho, J., Jeong, D., Sul, J.Y., Kim, T., Kim, N., Kang, J.S., Miyamoto, T., Suda, T., Lee, S.K., Pignolo, R.J., Koczon-Jaremko, B., Lorenzo, J., Choi, Y., 2006. v-ATPase V0 subunit d2-deficient mice exhibit impaired osteoclast fusion and increased bone formation. Nat. Med. 12 (12), 1403–1409.

Lees, R.L., Sabharwal, V.K., Heersche, J.N., 2001. Resorptive state and cell size influence intracellular pH regulation in rabbit osteoclasts cultured on collagen-hydroxyapatite films. Bone 28 (2), 187–194.

Li, D., Liu, J., Guo, B., Liang, C., Dang, L., Lu, C., He, X., Cheung, H.Y., Xu, L., Lu, C., He, B., Liu, B., Shaikh, A.B., Li, F., Wang, L., Yang, Z., Au, D.W., Peng, S., Zhang, Z., Zhang, B.T., Pan, X., Qian, A., Shang, P., Xiao, L., Jiang, B., Wong, C.K., Xu, J., Bian, Z., Liang, Z., Guo, D.A., Zhu, H., Tan, W., Lu, A., Zhang, G., 2016. Osteoclast-derived exosomal miR-214-3p inhibits osteoblastic bone formation. Nat. Commun. 7, 10872.

Lichenstein, H.S., Lyons, D.E., Wurfel, M.M., Johnson, D.A., McGinley, M.D., Leidli, J.C., Trollinger, D.B., Mayer, J.P., Wright, S.D., Zukowski, M.M., 1994. Afamin is a new member of the albumin, alpha-fetoprotein, and vitamin D-binding protein gene family. J. Biol. Chem. 269 (27), 18149–18154.

Loots, G.G., Keller, H., Leupin, O., Murugesh, D., Collette, N.M., Genetos, D.C., 2012. TGF-beta regulates sclerostin expression via the ECR5 enhancer. Bone 50 (3), 663–669.

Lotinun, S., Kiviranta, R., Matsubara, T., Alzate, J.A., Neff, L., Luth, A., Koskivirta, I., Kleuser, B., Vacher, J., Vuorio, E., Horne, W.C., Baron, R., 2013. Osteoclast-specific cathepsin K deletion stimulates S1P-dependent bone formation. J. Clin. Investig. 123 (2), 666–681.

Madsen, D.H., Ingvarsen, S., Jurgensen, H.J., Melander, M.C., Kjoller, L., Moyer, A., Honore, C., Madsen, C.A., Garred, P., Burgdorf, S., Bugge, T.H., Behrendt, N., Engelholm, L.H., 2011. The non-phagocytic route of collagen uptake: a distinct degradation pathway. J. Biol. Chem. 286 (30), 26996–27010.

Martin, T.J., Sims, N.A., 2005. Osteoclast-derived activity in the coupling of bone formation to resorption. Trends Mol. Med. 11 (2), 76–81.

Martinovic, S., Mazic, S., Kisic, V., Basic, N., Jakic-Razumovic, J., Borovecki, F., Batinic, D., Simic, P., Grgurevic, L., Labar, B., Vukicevic, S., 2004. Expression of bone morphogenetic proteins in stromal cells from human bone marrow long-term culture. J. Histochem. Cytochem. 52 (9), 1159–1167.

Marzia, M., Sims, N.A., Voit, S., Migliaccio, S., Taranta, A., Bernardini, S., Faraggiana, T., Yoneda, T., Mundy, G.R., Boyce, B.F., Baron, R., Teti, A., 2000. Decreased c-Src expression enhances osteoblast differentiation and bone formation. J. Cell Biol. 151 (2), 311–320.

Matsuoka, K., Park, K.A., Ito, M., Ikeda, K., Takeshita, S., 2014. Osteoclast-derived complement component 3a stimulates osteoblast differentiation. J. Bone Miner. Res. 29 (7), 1522–1530.

Matsuzaki, K., Udagawa, N., Takahashi, N., Yamaguchi, K., Yasuda, H., Shima, N., Morinaga, T., Toyama, Y., Yabe, Y., Higashio, K., Suda, T., 1998. Osteoclast differentiation factor (ODF) induces osteoclast-like cell formation in human peripheral blood mononuclear cell cultures. Biochem Biophys Res Commun 246, 199–204.

McNamara, L.M., Van der Linden, J.C., Weinans, H., Prendergast, P.J., 2006. Stress-concentrating effect of resorption lacunae in trabecular bone. J. Biomech. 39 (4), 734–741.

Mitlak, B.H., Finkelman, R.D., Hill, E.L., Li, J., Martin, B., Smith, T., D'Andrea, M., Antoniades, H.N., Lynch, S.E., 1996. The effect of systemically administered PDGF-BB on the rodent skeleton. J. Bone Miner. Res. 11 (2), 238–247.

Mizoguchi, T., Muto, A., Udagawa, N., Arai, A., Yamashita, T., Hosoya, A., Ninomiya, T., Nakamura, H., Yamamoto, Y., Kinugawa, S., Nakamura, M., Nakamichi, Y., Kobayashi, Y., Nagasawa, S., Oda, K., Tanaka, H., Tagaya, M., Penninger, J.M., Ito, M., Takahashi, N., 2009. Identification of cell cycle-arrested quiescent osteoclast precursors in vivo. J. Cell Biol. 184 (4), 541–554.

Muto, A., Mizoguchi, T., Udagawa, N., Ito, S., Kawahara, I., Abiko, Y., Arai, A., Harada, S., Kobayashi, Y., Nakamichi, Y., Penninger, J.M., Noguchi, T., Takahashi, N., 2011. Lineage-committed osteoclast precursors circulate in blood and settle down into bone. J. Bone Miner. Res. 26 (12), 2978–2990.

Nakamura, M., Udagawa, N., Matsuura, S., Mogi, M., Nakamura, H., Horiuchi, H., Saito, N., Hiraoka, B.Y., Kobayashi, Y., Takaoka, K., Ozawa, H., Miyazawa, H., Takahashi, N., 2003. Osteoprotegerin regulates bone formation through a coupling mechanism with bone resorption. Endocrinology 144 (12), 5441–5449.

Nakamura, T., Imai, Y., Matsumoto, T., Sato, S., Takeuchi, K., Igarashi, K., Harada, Y., Azuma, Y., Krust, A., Yamamoto, Y., Nishina, H., Takeda, S., Takayanagi, H., Metzger, D., Kanno, J., Takaoka, K., Martin, T.J., Chambon, P., Kato, S., 2007. Estrogen prevents bone loss via estrogen receptor alpha and induction of Fas ligand in osteoclasts. Cell 130 (5), 811–823.

Narimatsu, K., Li, M., de Freitas, P.H., Sultana, S., Ubaidus, S., Kojima, T., Zhucheng, L., Ying, G., Suzuki, R., Yamamoto, T., Oda, K., Amizuka, N., 2010. Ultrastructural observation on cells meeting the histological criteria for preosteoblasts–a study in the mouse tibial metaphysis. J. Electron. Microsc. 59 (5), 427–436.

Negishi-Koga, T., Shinohara, M., Komatsu, N., Bito, H., Kodama, T., Friedel, R.H., Takayanagi, H., 2011. Suppression of bone formation by osteoclastic expression of semaphorin 4D. Nat. Med. 17 (11), 1473–1480.

Nicolaidou, V., Wong, M.M., Redpath, A.N., Ersek, A., Baban, D.F., Williams, L.M., Cope, A.P., Horwood, N.J., 2012. Monocytes induce STAT3 activation in human mesenchymal stem cells to promote osteoblast formation. PLoS One 7 (7), e39871.

Noble, B.S., Peet, N., Stevens, H.Y., Brabbs, A., Mosley, J.R., Reilly, G.C., Reeve, J., Skerry, T.M., Lanyon, L.E., 2003. Mechanical loading: biphasic osteocyte survival and targeting of osteoclasts for bone destruction in rat cortical bone. Am. J. Physiol. Cell Physiol. 284 (4), C934–C943.

Oreffo, R.O., Mundy, G.R., Seyedin, S.M., Bonewald, L.F., 1989. Activation of the bone-derived latent TGF beta complex by isolated osteoclasts. Biochem. Biophys. Res. Commun. 158 (3), 817–823.

Ota, K., Quint, P., Weivoda, M.M., Ruan, M., Pederson, L., Westendorf, J.J., Khosla, S., Oursler, M.J., 2013. Transforming growth factor beta 1 induces CXCL16 and leukemia inhibitory factor expression in osteoclasts to modulate migration of osteoblast progenitors. Bone 57 (1), 68–75.

Pappu, R., Schwab, S.R., Cornelissen, I., Pereira, J.P., Regard, J.B., Xu, Y., Camerer, E., Zheng, Y.W., Huang, Y., Cyster, J.G., Coughlin, S.R., 2007. Promotion of lymphocyte egress into blood and lymph by distinct sources of sphingosine-1-phosphate. Science 316 (5822), 295–298.

Parfitt, A., 1980. Morphological basis of bone mineral measurements: transient and steady state effects of treatment in osteoporosis. Mineral and Elecrolyte Metabolism 4, 273–287.

Parfitt, A., 1983. Bone histomorphometry: techniques and interpretations. In: Recker, R.R. (Ed.), Histomorphometry. CRC Press, Baton Rouge, USA, pp. 142–221.

Parfitt, A.M., 1982. The coupling of bone formation to bone resorption: a critical analysis of the concept and of its relevance to the pathogenesis of osteoporosis. Metab. Bone Dis. Relat. Res. 4 (1), 1–6.

Parfitt, A.M., Mathews, C.H., Villanueva, A.R., Kleerekoper, M., Frame, B., Rao, D.S., 1983. Relationships between surface, volume, and thickness of iliac trabecular bone in aging and in osteoporosis. Implications for the microanatomic and cellular mechanisms of bone loss. J. Clin. Investig. 72 (4), 1396–1409.

Pederson, L., Ruan, M., Westendorf, J.J., Khosla, S., Oursler, M.J., 2008. Regulation of bone formation by osteoclasts involves Wnt/BMP signaling and the chemokine sphingosine-1-phosphate. Proc. Natl. Acad. Sci. U.S.A. 105 (52), 20764–20769.

Pennypacker, B., Shea, M., Liu, Q., Masarachia, P., Saftig, P., Rodan, S., Rodan, G., Kimmel, D., 2009. Bone density, strength, and formation in adult cathepsin K (-/-) mice. Bone 44 (2), 199–207.

Pfeilschifter, J., Laukhuf, F., Muller-Beckmann, B., Blum, W.F., Pfister, T., Ziegler, R., 1995. Parathyroid hormone increases the concentration of insulin-like growth factor-I and transforming growth factor beta 1 in rat bone. J. Clin. Investig. 96 (2), 767–774.

Poulton, I.J., McGregor, N.E., Pompolo, S., Walker, E.C., Sims, N.A., 2012. Contrasting roles of leukemia inhibitory factor in murine bone development and remodeling involve region-specific changes in vascularization. J. Bone Miner. Res. 27 (3), 586–595.

Quint, P., Ruan, M., Pederson, L., Kassem, M., Westendorf, J.J., Khosla, S., Oursler, M.J., 2013. Sphingosine 1-phosphate (S1P) receptors 1 and 2 coordinately induce mesenchymal cell migration through S1P activation of complementary kinase pathways. J. Biol. Chem. 288 (8), 5398–5406.

Rasmussen, H., Bordier, P., 1974. The Physiological Basis of Metabolic Bone Disease. Williams and Wilkins, Waverley Press, Baltimore.

Redmond, J., Fulford, A.J., Jarjou, L., Zhou, B., Prentice, A., Schoenmakers, I., 2016. Diurnal rhythms of bone turnover markers in three ethnic groups. J. Clin. Endocrinol. Metab. 101 (8), 3222–3230.

Reid, L.R., Lowe, C., Cornish, J., Skinner, S.J., Hilton, D.J., Willson, T.A., Gearing, D.P., Martin, T.J., 1990. Leukemia inhibitory factor: a novel bone-active cytokine. Endocrinology 126 (3), 1416–1420.

Richards, C.D., Langdon, C., Deschamps, P., Pennica, D., Shaughnessy, S.G., 2000. Stimulation of osteoclast differentiation in vitro by mouse oncostatin M, leukaemia inhibitory factor, cardiotrophin-1 and interleukin 6: synergy with dexamethasone. Cytokine 12 (6), 613–621.

Rickard, D.J., Sullivan, T.A., Shenker, B.J., Leboy, P.S., Kazhdan, I., 1994. Induction of rapid osteoblast differentiation in rat bone marrow stromal cell cultures by dexamethasone and BMP-2. Dev. Biol. 161 (1), 218–228.

Robey, P.G., Young, M.F., Flanders, K.C., Roche, N.S., Kondaiah, P., Reddi, A.H., Termine, J.D., Sporn, M.B., Roberts, A.B., 1987. Osteoblasts synthesize and respond to transforming growth factor-type beta (TGF-beta) in vitro. J. Cell Biol. 105 (1), 457–463.

Robling, A.G., Turner, C.H., 2009. Mechanical signaling for bone modeling and remodeling. Crit. Rev. Eukaryot. Gene Expr. 19 (4), 319–338.

Robubi, A., Berger, C., Schmid, M., Huber, K.R., Engel, A., Krugluger, W., 2014. Gene expression profiles induced by growth factors in in vitro cultured osteoblasts. Bone Joint Res. 3 (7), 236–240.

Rodan, G.A., 1991. Mechanical loading, estrogen deficiency, and the coupling of bone formation to bone resorption. J. Bone Miner. Res. 6 (6), 527–530.

Rodan, G.A., Martin, T.J., 1981. Role of osteoblasts in hormonal control of bone resorption–a hypothesis. Calcif. Tissue Int. 33 (4), 349–351.

Ryu, J., Kim, H.J., Chang, E.J., Huang, H., Banno, Y., Kim, H.H., 2006. Sphingosine 1-phosphate as a regulator of osteoclast differentiation and osteoclast-osteoblast coupling. EMBO J. 25 (24), 5840–5851.

Sanchez-Fernandez, M.A., Gallois, A., Riedl, T., Jurdic, P., Hoflack, B., 2008. Osteoclasts control osteoblast chemotaxis via PDGF-BB/PDGF receptor beta signaling. PLoS One 3 (10), e3537.

Sato, T., Abe, E., Jin, C.H., Hong, M.H., Katagiri, T., Kinoshita, T., Amizuka, N., Ozawa, H., Suda, T., 1993. The biological roles of the third component of complement in osteoclast formation. Endocrinology 133 (1), 397–404.

Scariano, J.K., Emery-Cohen, A.J., Pickett, G.G., Morgan, M., Simons, P.C., Alba, F., 2008. Estrogen receptors alpha (ESR1) and beta (ESR2) are expressed in circulating human lymphocytes. J. Recept. Signal Transduct. Res. 28 (3), 285–293.

Schaffler, M.B., Cheung, W.Y., Majeska, R., Kennedy, O., 2014. Osteocytes: master orchestrators of bone. Calcif. Tissue Int. 94 (1), 5–24.

Sells Galvin, R.J., Gatlin, C.L., Horn, J.W., Fuson, T.R., 1999. TGF-beta enhances osteoclast differentiation in hematopoietic cell cultures stimulated with RANKL and M-CSF. Biochem. Biophys. Res. Commun. 265 (1), 233–239.

Sims, N.A., Gooi, J.H., 2008. Bone remodeling: multiple cellular interactions required for coupling of bone formation and resorption. Semin. Cell Dev. Biol. 19 (5), 444–451.

Sims, N.A., Jenkins, B.J., Quinn, J.M., Nakamura, A., Glatt, M., Gillespie, M.T., Ernst, M., Martin, T.J., 2004. Glycoprotein 130 regulates bone turnover and bone size by distinct downstream signaling pathways. J. Clin. Investig. 113 (3), 379–389.

Sims, N.A., Johnson, R.W., 2012. Leukemia inhibitory factor: a paracrine mediator of bone metabolism. Growth Factors. 30 (2), 76–87.

Sims, N.A., Martin, T.J., 2015. Coupling signals between the osteoclast and osteoblast: how are messages transmitted between these temporary visitors to the bone surface? Front. Endocrinol. 6, 41.

Sims, N.A., Romas, E., 2015. Is RANKL inhibition both anti-resorptive and anabolic in rheumatoid arthritis? Arthritis Res. Ther. 17, 328.

Sobacchi, C., Frattini, A., Guerrini, M.M., Abinun, M., Pangrazio, A., Susani, L., Bredius, R., Mancini, G., Cant, A., Bishop, N., Grabowski, P., Del Fattore, A., Messina, C., Errigo, G., Coxon, F.P., Scott, D.I., Teti, A., Rogers, M.J., Vezzoni, P., Villa, A., Helfrich, M.H., 2007. Osteoclast-poor human osteopetrosis due to mutations in the gene encoding RANKL. Nat. Genet. 39, 960.

Suda, T., Takahashi, N., Udagawa, N., Jimi, E., Gillespie, M.T., Martin, T.J., 1999. Modulation of osteoclast differentiation and function by the new members of the tumor necrosis factor receptor and ligand families. Endocr. Rev. 20 (3), 345–357.

Takahashi, T., Fournier, A., Nakamura, F., Wang, L.H., Murakami, Y., Kalb, R.G., Fujisawa, H., Strittmatter, S.M., 1999. Plexin-neuropilin-1 complexes form functional semaphorin-3A receptors. Cell 99 (1), 59–69.

Takahashi, T., Kurihara, N., Takahashi, K., Kumegawa, M., 1986. An ultrastructural study of phagocytosis in bone by osteoblastic cells from fetal mouse calvaria in vitro. Arch. Oral Biol. 31 (10), 703–706.

Takeshita, S., Fumoto, T., Matsuoka, K., Park, K.A., Aburatani, H., Kato, S., Ito, M., Ikeda, K., 2013. Osteoclast-secreted CTHRC1 in the coupling of bone resorption to formation. J. Clin. Investig. 123 (9), 3914–3924.

Takyar, F.M., Tonna, S., Ho, P.W., Crimeen-Irwin, B., Baker, E.K., Martin, T.J., Sims, N.A., 2013. EphrinB2/EphB4 inhibition in the osteoblast lineage modifies the anabolic response to parathyroid hormone. J. Bone Miner. Res. 28 (4), 912–925.

Tamagnone, L., Artigiani, S., Chen, H., He, Z., Ming, G.I., Song, H., Chedotal, A., Winberg, M.L., Goodman, C.S., Poo, M., Tessier-Lavigne, M., Comoglio, P.M., 1999. Plexins are a large family of receptors for transmembrane, secreted, and GPI-anchored semaphorins in vertebrates. Cell 99 (1), 71–80.

Tamura, T., Udagawa, N., Takahashi, N., Miyaura, C., Tanaka, S., Yamada, Y., Koishihara, Y., Ohsugi, Y., Kumaki, K., Taga, T., Kishimoto, T., Suda, T., 1993. Soluble interleukin-6 receptor triggers osteoclast formation by interleukin 6. Proc. Natl. Acad. Sci. U. S. A. 90 (24), 11924–11928.

Tang, Y., Wu, X., Lei, W., Pang, L., Wan, C., Shi, Z., Zhao, L., Nagy, T.R., Peng, X., Hu, J., Feng, X., Van Hul, W., Wan, M., Cao, X., 2009. TGF-beta1-induced migration of bone mesenchymal stem cells couples bone resorption with formation. Nat. Med. 15 (7), 757–765.

Terauchi, M., Li, J.Y., Bedi, B., Baek, K.H., Tawfeek, H., Galley, S., Gilbert, L., Nanes, M.S., Zayzafoon, M., Guldberg, R., Lamar, D.L., Singer, M.A., Lane, T.F., Kronenberg, H.M., Weitzmann, M.N., Pacifici, R., 2009. T lymphocytes amplify the anabolic activity of parathyroid hormone through Wnt10b signaling. Cell Metabol. 10 (3), 229–240.

Thudium, C.S., Moscatelli, I., Flores, C., Thomsen, J.S., Bruel, A., Gudmann, N.S., Hauge, E.M., Karsdal, M.A., Richter, J., Henriksen, K., 2014. A comparison of osteoclast-rich and osteoclast-poor osteopetrosis in adult mice sheds light on the role of the osteoclast in coupling bone resorption and bone formation. Calcif. Tissue Int. 95 (1), 83–93.

Tonna, S., Sims, N.A., 2014. Talking among ourselves: paracrine control of bone formation within the osteoblast lineage. Calcif. Tissue Int. 94 (1), 35–45.

Tonna, S., Takyar, F.M., Vrahnas, C., Crimeen-Irwin, B., Ho, P.W., Poulton, I.J., Brennan, H.J., McGregor, N.E., Allan, E.H., Nguyen, H., Forwood, M.R., Tatarczuch, L., Mackie, E.J., Martin, T.J., Sims, N.A., 2014. EphrinB2 signaling in osteoblasts promotes bone mineralization by preventing apoptosis. FASEB J. 28 (10), 4482–4496.

Tran Van, P.T., Vignery, A., Baron, R., 1982. Cellular kinetics of the bone remodeling sequence in the rat. Anat. Rec. 202 (4), 445–451.

van Bezooijen, R.L., Roelen, B.A., Visser, A., van der Wee-Pals, L., de Wilt, E., Karperien, M., Hamersma, H., Papapoulos, S.E., ten Dijke, P., Lowik, C.W., 2004. Sclerostin is an osteocyte-expressed negative regulator of bone formation, but not a classical BMP antagonist. J. Exp. Med. 199 (6), 805–814.

Verborgt, O., Gibson, G.J., Schaffler, M.B., 2000. Loss of osteocyte integrity in association with microdamage and bone remodeling after fatigue in vivo. J. Bone Miner. Res. 15 (1), 60–67.

Vignery, A., Baron, R., 1980. Dynamic histomorphometry of alveolar bone remodeling in the adult rat. Anat. Rec. 196 (2), 191–200.

Villanueva, A.R., Sypitkowski, C., Parfitt, A.M., 1986. A new method for identification of cement lines in undecalcified, plastic embedded sections of bone. Stain Technol. 61 (2), 83–88.

Vukicevic, S., Grgurevic, L., 2009. BMP-6 and mesenchymal stem cell differentiation. Cytokine Growth Factor Rev. 20 (5–6), 441–448.

Wagsater, D., Olofsson, P.S., Norgren, L., Stenberg, B., Sirsjo, A., 2004. The chemokine and scavenger receptor CXCL16/SR-PSOX is expressed in human vascular smooth muscle cells and is induced by interferon gamma. Biochem. Biophys. Res. Commun. 325 (4), 1187–1193.

Walker, E.C., McGregor, N.E., Poulton, I.J., Pompolo, S., Allan, E.H., Quinn, J.M., Gillespie, M.T., Martin, T.J., Sims, N.A., 2008. Cardiotrophin-1 is an osteoclast-derived stimulus of bone formation required for normal bone remodeling. J. Bone Miner. Res. 23 (12), 2025–2032.

Walker, E.C., McGregor, N.E., Poulton, I.J., Solano, M., Pompolo, S., Fernandes, T.J., Constable, M.J., Nicholson, G.C., Zhang, J.G., Nicola, N.A., Gillespie, M.T., Martin, T.J., Sims, N.A., 2010. Oncostatin M promotes bone formation independently of resorption when signaling through leukemia inhibitory factor receptor in mice. J. Clin. Investig. 120 (2), 582–592.

Wang, X., Kumanogoh, A., Watanabe, C., Shi, W., Yoshida, K., Kikutani, H., 2001. Functional soluble CD100/Sema4D released from activated lymphocytes: possible role in normal and pathologic immune responses. Blood 97 (11), 3498–3504.

Wang, Y., Nishida, S., Elalieh, H.Z., Long, R.K., Halloran, B.P., Bikle, D.D., 2006. Role of IGF-I signaling in regulating osteoclastogenesis. J. Bone Miner. Res. 21 (9), 1350–1358.

White, H.D., Ahmad, A.M., Durham, B.H., Peter, R., Prabhakar, V.K., Corlett, P., Vora, J.P., Fraser, W.D., 2007. PTH circadian rhythm and PTH target-organ sensitivity is altered in patients with adult growth hormone deficiency with low BMD. J. Bone Miner. Res. 22 (11), 1798–1807.

Winberg, M.L., Noordermeer, J.N., Tamagnone, L., Comoglio, P.M., Spriggs, M.K., Tessier-Lavigne, M., Goodman, C.S., 1998. Plexin A is a neuronal semaphorin receptor that controls axon guidance. Cell 95 (7), 903–916.

Wlazlo, N., van Greevenbroek, M.M., Ferreira, I., Jansen, E.H., Feskens, E.J., van der Kallen, C.J., Schalkwijk, C.G., Bravenboer, B., Stehouwer, C.D., 2013. Activated complement factor 3 is associated with liver fat and liver enzymes: the CODAM study. Eur. J. Clin. Investig. 43 (7), 679–688.

Wutzl, A., Brozek, W., Lernbass, I., Rauner, M., Hofbauer, G., Schopper, C., Watzinger, F., Peterlik, M., Pietschmann, P., 2006. Bone morphogenetic proteins 5 and 6 stimulate osteoclast generation. J. Biomed. Mater. Res. A 77 (1), 75–83.

Xian, L., Wu, X., Pang, L., Lou, M., Rosen, C.J., Qiu, T., Crane, J., Frassica, F., Zhang, L., Rodriguez, J.P., Xiaofeng, J., Shoshana, Y., Shouhong, X., Argiris, E., Mei, W., Cao, X., 2012. Matrix IGF-1 maintains bone mass by activation of mTOR in mesenchymal stem cells. Nat. Med. 18 (7), 1095–1101.

Xie, H., Cui, Z., Wang, L., Xia, Z., Hu, Y., Xian, L., Li, C., Xie, L., Crane, J., Wan, M., Zhen, G., Bian, Q., Yu, B., Chang, W., Qiu, T., Pickarski, M., Duong, L.T., Windle, J.J., Luo, X., Liao, E., Cao, X., 2014. PDGF-BB secreted by preosteoclasts induces angiogenesis during coupling with osteogenesis. Nat. Med. 20 (11), 1270–1278.

Yasuda, H., Shima, N., Nakagawa, N., Yamaguchi, K., Kinosaki, M., Mochizuki, S., Tomoyasu, A., Yano, K., Goto, M., Murakami, A., Tsuda, E., Morinaga, T., Higashio, K., Udagawa, N., Takahashi, N., Suda, T., 1998. Osteoclast differentiation factor is a ligand for osteoprotegerin/osteoclastogenesis-inhibitory factor and is identical to TRANCE/RANKL. Proc. Natl. Acad. Sci. U.S.A. 95 (7), 3597–3602.

Yee, J.A., Yan, L., Dominguez, J.C., Allan, E.H., Martin, T.J., 1993. Plasminogen-dependent activation of latent transforming growth factor beta (TGF beta) by growing cultures of osteoblast-like cells. J. Cell. Physiol. 157 (3), 528–534.

Zaidi, M., Datta, H.K., Patchell, A., Moonga, B., MacIntyre, I., 1989. Calcium-activated' intracellular calcium elevation: a novel mechanism of osteoclast regulation. Biochem. Biophys. Res. Commun. 163 (3), 1461–1465.

Zarling, J.M., Shoyab, M., Marquardt, H., Hanson, M.B., Lioubin, M.N., Todaro, G.J., 1986. Oncostatin M: a growth regulator produced by differentiated histiocytic lymphoma cells. Proc. Natl. Acad. Sci. U.S.A. 83 (24), 9739–9743.

Zhang, L., Leeman, E., Carnes, D.C., Graves, D.T., 1991. Human osteoblasts synthesize and respond to platelet-derived growth factor. Am. J. Physiol. 261 (2 Pt 1), C348–C354.

Zhao, C., Irie, N., Takada, Y., Shimoda, K., Miyamoto, T., Nishiwaki, T., Suda, T., Matsuo, K., 2006. Bidirectional ephrinB2-EphB4 signaling controls bone homeostasis. Cell Metabol. 4 (2), 111–121.

Chapter 11

Modeling and remodeling: the cellular machinery responsible for bone's material and structural strength during growth, aging, and drug therapy

Ego Seeman

Department of Endocrinology and Medicine, Austin Health, University of Melbourne, Melbourne, VIC, Australia; Mary MacKillop Institute for Health Research, Australian Catholic University, Melbourne, VIC, Australia

Chapter Outline

Summary

During growth, the cellular machinery of bone modeling and remodeling assembles bone's size, shape, and microstructure. Bone matrix is synthesized as a composite of organic and inorganic material configured with varying volumes of extracellular fluid—containing void to form its cortical and trabecular compartments. Endocortical resorptive modeling excavates a medullary cavity void volume, which shifts the cortex radially, increasing resistance to bending exponentially while minimizing cortical thickening and so avoiding bulk; larger bone cross sections are assembled with a relatively thinner cortex.

During young adulthood, balanced remodeling renews the mineralized bone matrix volume without permanently compromising bone microstructure. As modeling and remodeling are surface dependent, the large surface area/matrix volume configuration of interconnected thin trabecular plates facilitates accessibility of the matrix to being renewed; this is

Principles of Bone Biology. https://doi.org/10.1016/B978-0-12-814841-9.00011-7

an advantage provided that remodeling remains balanced. The lower surface area/matrix volume of compact cortical bone makes it less accessible to being renewed and so liable to damage accumulation.

Around midlife, remodeling becomes unbalanced in both sexes and rapid in postmenopausal women. Unbalanced remodeling transactions deposit less bone than was resorbed, producing permanent cortical thinning, porosity, trabecular thinning, perforation, and loss of connectivity, which compromise bone strength disproportionate to the bone loss producing this deterioration.

Antiresorptive agents do not reverse microstructural deterioration or bone fragility present at the time of initiating treatment. Most antiresorptives only slow remodeling, they do not abolish it, so that total bone matrix volume and microstructure continue to deteriorate, albeit more slowly than without treatment. The slowly declining bone matrix volume is less often remodeled and so becomes more fully mineralized and less ductile, predisposing to damage accumulation. Teriparatide, the only available anabolic agent, produces predominantly remodeling-based bone formation and appears to reduce vertebral and nonvertebral fracture risk more efficaciously than antiresorptive therapy. Encouraging observations have been reported using modeling-based anabolic therapy and combined antiresorptive and anabolic therapy, but reducing the population burden of fractures remains a challenging unmet need.

Bone modeling and remodeling during growth and the attainment of bone's peak material and structural strength

Definition of bone modeling and remodeling

Bone *modeling* or construction is usually thought of as bone formation. Bone modeling is both formative and resorptive. Formative modeling is carried out by osteoblasts, cells that synthesize and deposit a volume of osteoid upon a quiescent bone surface that has not undergone prior bone resorption (Parfitt, 1996). Resorptive modeling is carried out by osteoclasts, cells that resorb a volume of bone without a subsequent phase of bone formation.

Formative and resorptive modeling occur mainly during growth and confer the paradoxical properties of strength for loading, yet lightness for mobility, and resistance to deformation, yet flexibility to allow energy absorption. These properties are conferred by the deposition of bone at locations where it is needed and by removal of bone from locations where it is not needed, thereby changing bone's external and internal size and shape.

Bone *remodeling* or reconstruction maintains the composition and properties of the mineralized bone matrix during young adulthood. Remodeling is carried out by teams of osteoclasts and osteoblasts, basic multicellular units (BMUs), which respectively resorb and replace a volume of damaged or older bone with the same volume of newly synthesized osteoid at the same location (see chapters 4 and 10 for further detail).

The osteoid undergoes rapid primary mineralization within days of deposition to become "bone" and then slower secondary mineralization, a physicochemical process of enlargement of crystals of calcium hydroxyapatite deposited during primary mineralization. The crystals enlarge and displace water without change in the dimensions of the collagen fibrils (Akkus, 2003).

Bone's material and structural strength

Bone is a specialized connective tissue. Type I collagen is tough; it is distensible in tension but lacks resistance to bending, i.e., stiffness. Stiffening is achieved by mineralizing the collagen with platelets of calcium hydroxyapatite. The mineral confers material stiffness but sacrifices the ability to absorb and store energy by deforming. For a given increase in the percentage of mineral ash, stiffness increases fivefold, but the amount of work needed to produce a fracture decreases 14-fold, almost three times more (Currey, 2002) (Fig. 11.1, top).

Nature selects a mineralization density that is suited to the function a bone usually performs. Ossicles of the ear are over 80% mineral, a feature conferring stiffness that is selected for so that they can vibrate like tuning forks and transmit sound with high fidelity. The ability to store energy by deforming is sacrificed, but it is unnecessary (Fig. 11.1, bottom). Cracking is unlikely because ossicles are housed safely in the skull. Deer antlers are less densely mineralized to facilitate deformation, so they can absorb energy like springs during head butting in mating season. Greater energy-absorbing ability of antlers, "toughness" or resilience, is selected for over stiffness, but stiffness is unnecessary because antlers are not load bearing (Currey, 1969).

Although mineral stiffens bone, it is also the most brittle component of bone; an increase in mineral density decreases toughness more than it increases stiffness. So to defend against loss of toughness, the platelets of mineral are protected from being excessively loaded by noncollagenous proteins, glue-like material that releases energy imposed during loading

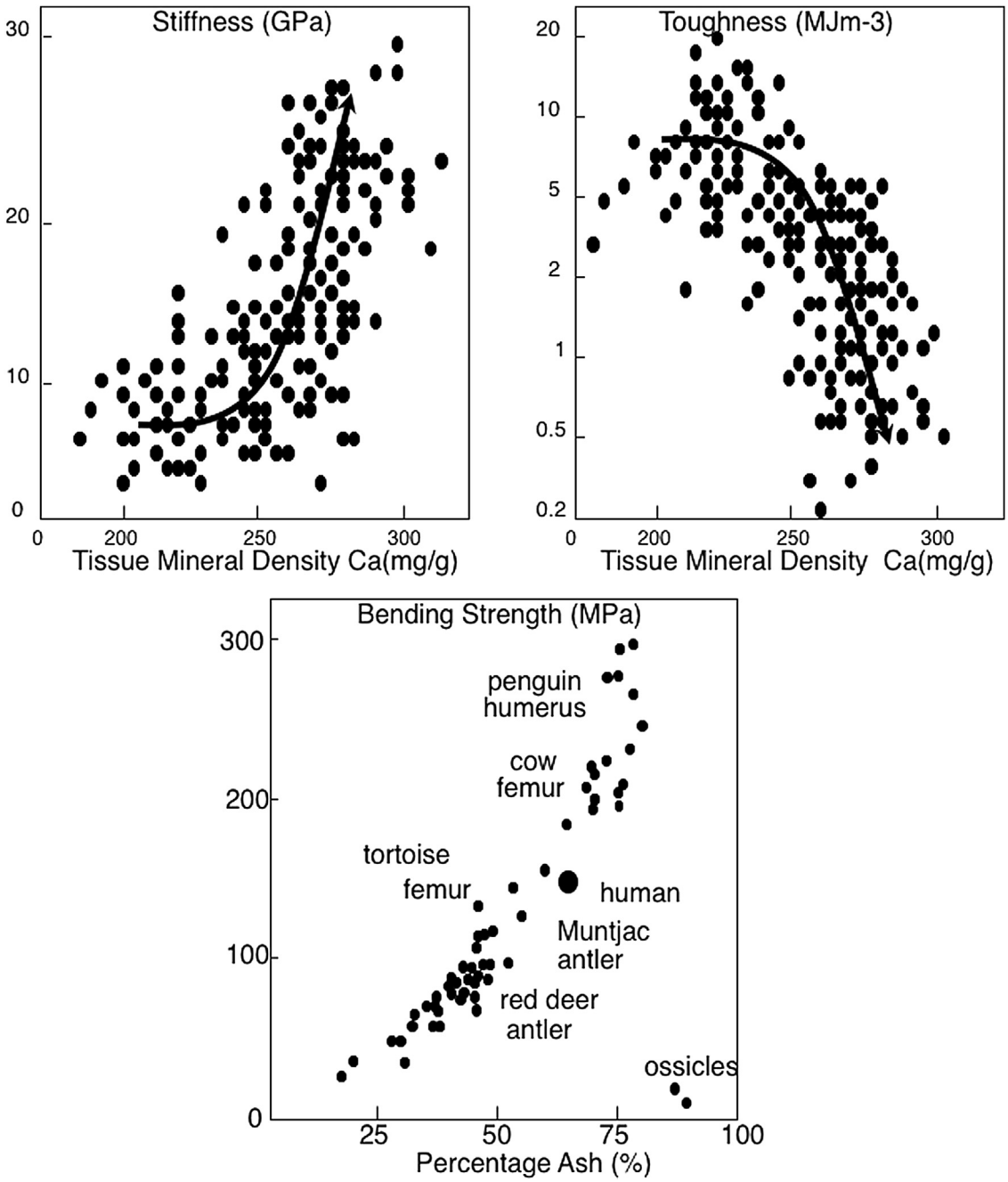

FIGURE 11.1 (Top) As tissue mineral content increases, stiffness increases, but toughness decreases disproportionately. (Bottom) Ossicles of the ear are 90% mineral. They have little resistance to bending. Antlers are about 40% mineral, allowing them to deform without cracking. *(Top) Adapted from Currey, J.D., 2002. Bones. Structure and Mechanics. Princeton UP, New Jersey, pp. 1–380. (Bottom) Adapted from Curry, J.D., 1969. Mechanical consequences of variation in the mineral content of bone. J. Biomechan. 2, 1–11.*

by breaking intrahelical "sacrificial" bonds, which allows uncoiling of the noncollagenous proteins. This provides "hidden" length. Stresses at the tissue, fiber, and mineral levels decrease in proportions of 12:5:2 (Fantner et al., 2005, Gupt et al., 2006) (Fig. 11.2).

Advancing age compromises this mechanism as advanced glycation end products accumulate, reducing the ability of noncollagenous proteins to protect the mineral platelets (Ural and Vashishth, 2014). This predisposes to the development of diffuse damage, which differs from microcracking. Diffuse damage occurs within the osteon. Microcracks occur in the interosteonal (interstitial) matrix. Diffuse damage is reversible and its repair does not involve bone remodeling.

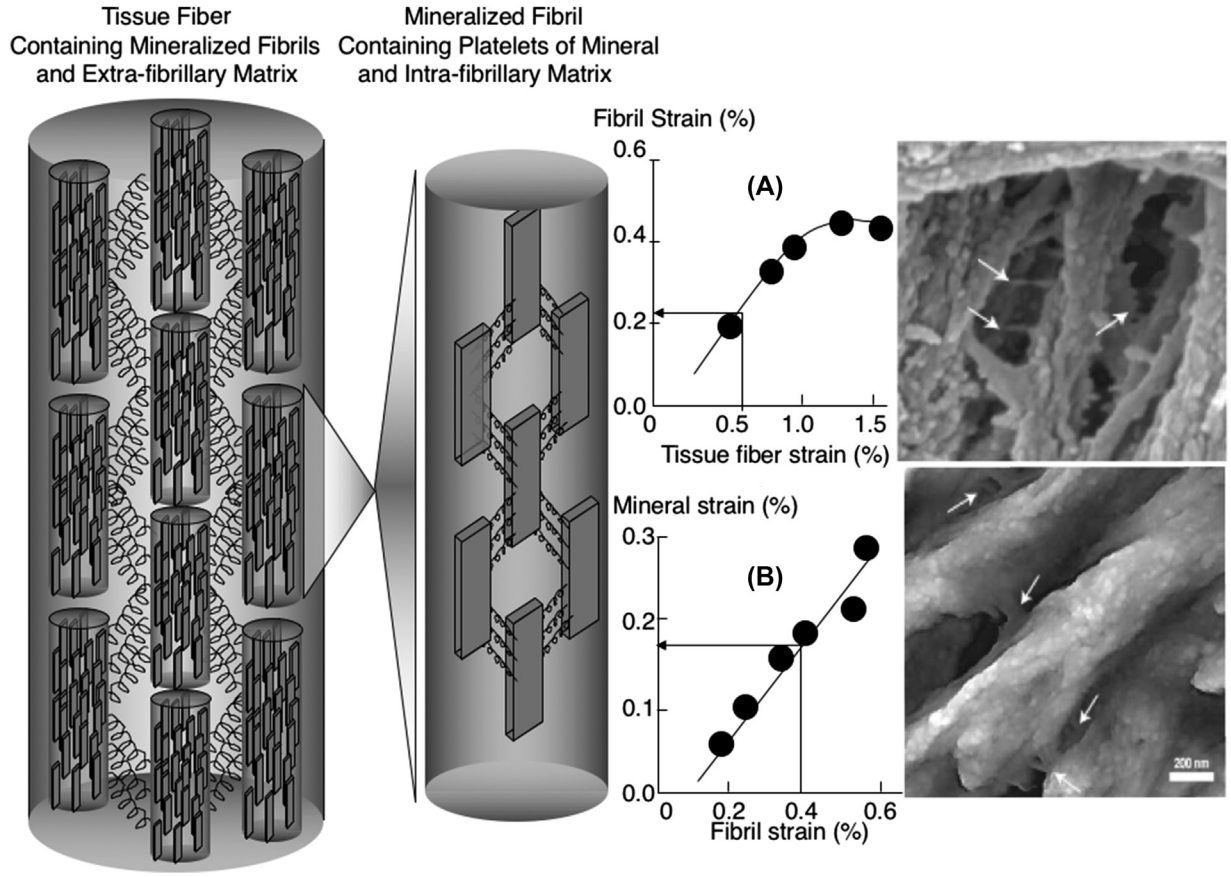

FIGURE 11.2 A collagen tissue fiber contains mineralized fibrils. The fibrils contain mineral platelets bound by noncollagenous proteins, helical structures that can lengthen via the breakage of sacrificial intrahelical bonds to provide "hidden length" and avoid overloading the mineral platelets. (Graph A) Tissue fiber strain distributed to fibrils. (Graph B) Fibrils absorb strain, minimizing mineral strain. *Adapted from Gupta et al. (2005). Images of non-collagenous glue like proteins. From Fantner, G., Hassen kam, T., Kindt, J.H., Weaver, J.C., Birkedal, H., Pechenik, L., Cutroni, J.A., Cidade, G.C., Stucky, G.D., Morse, D.E., Hansma, P.K., 2005. Nat. Mater. 4, 612–616.*

During growth, the mineralized bone matrix volume is fashioned into three-dimensional structures. Although there is variability in the material composition of bone, this composition is similar among land-dwelling mammals (Keaveney et al., 1998). Most of the diversity in bone strength is the result of structural diversity, which is obvious at the macroscopic level from bone to bone and from species to species, but how this diversity in size and shape is achieved is neither obvious nor intuitive.

If bone had only to be strong, this could be achieved by bulk alone—more mass. But mass takes time to grow, is costly to maintain, and limits mobility. Bone also must serve as a lever to facilitate mobility and so it must be light. Longer tubular bones need more mass than shorter bones to construct their length, but in an individual, the diversity in total external and internal cross-sectional areas (CSAs) and varying shapes of a cross section, from cross section to adjacent cross section along the length of a bone is achieved using *similar* amounts of mineralized matrix volume.

In an individual, differences in the total cross section size, shape, and internal architecture of adjacent cross sections of a long bone are achieved by varying the volume of void, not the volume of mineralized bone matrix. For example, at the radius, the large total CSA of the distal metaphysis is assembled using more void volume forming a large medullary canal, not more mineralized matrix volume (Fig. 11.3, left). Most of the mineralized matrix is fashioned as trabecular bone, a porous sponge-like configuration of intersecting thin plates of mineralized matrix. Only a small amount of mineralized matrix is assembled as cortical bone. The cortex is thin and porous with a low matrix mineral density (Ghasem-Zadeh et al., 2017).

More proximally, the *same* mineralized matrix volume is contained within the smaller total CSA of diaphyseal shaft achieved, by assembling it with a smaller medullary void volume, not less material. The constant amount of mineralized bone matrix is fashioned here as a thicker compact cortex with a low porosity and high matrix mineral density. There is little, if any, trabecular bone. This design serves the need for the lever function of a long bone or a cantilever function of a

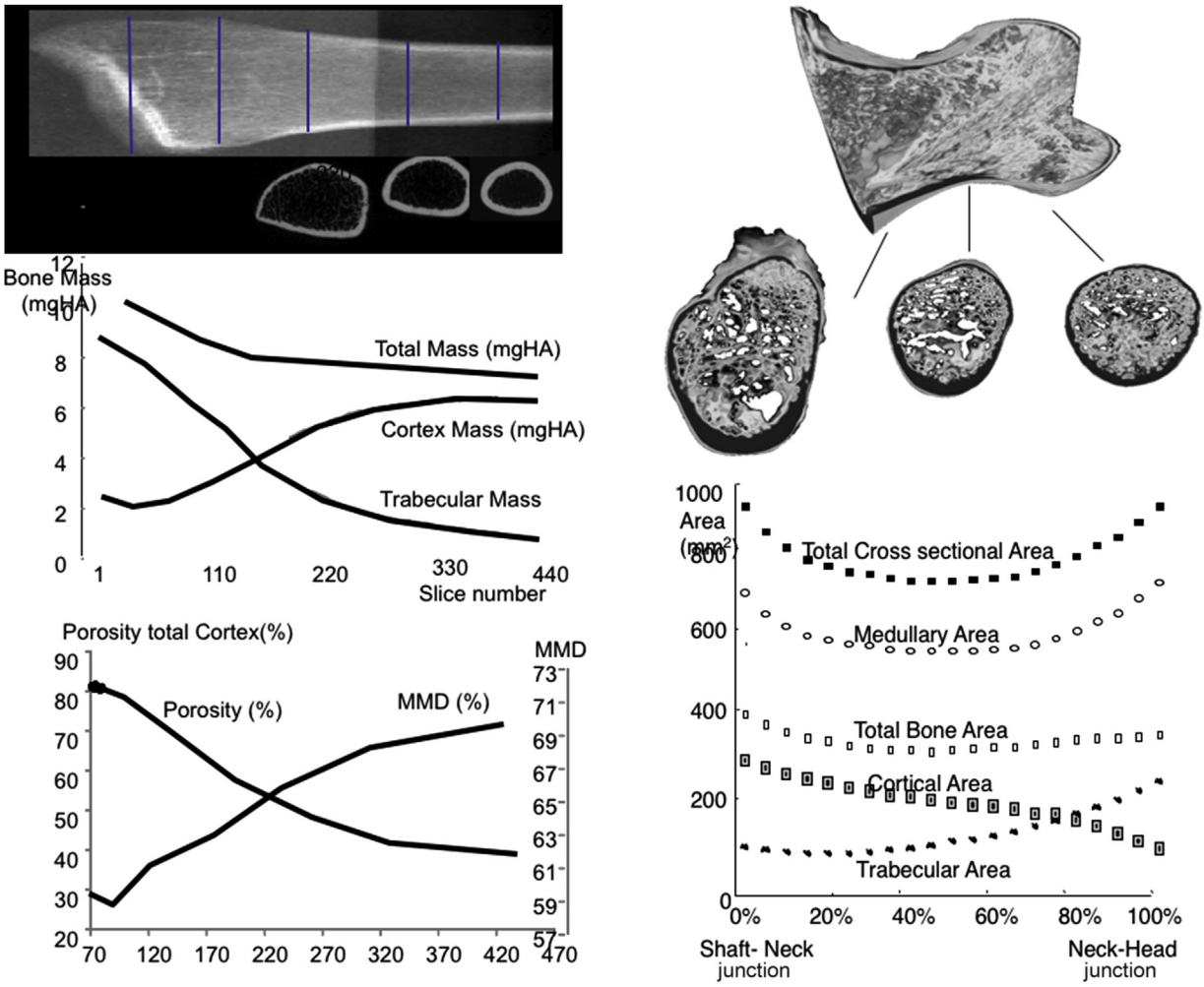

FIGURE 11.3 (Left) Distal radius. The mass is relatively constant along the metaphysis but it is assembled more as trabecular than cortical bone distally, with cortices of higher porosity and lower matrix mineral density. Proximally, the similar amount of material is mainly cortical with low porosity and higher matrix mineral density. (Right) The femoral neck differs in size but each cross section is assembled with a similar amount of material, forming more cortical bone adjacent to the femoral shaft and more trabecular bone nearer the femoral head. *MMD*, Matrix mineral density. *Adapted from Zebaze, R.M., Jones, A., Knackstedt, M., Maalouf, G., Seeman, E., 2007. Construction of the femoral neck during growth determines its strength in old age. J. Bone Miner. Res. 22 (7), 1055–1061.*

shorter bone like the femoral neck. Similar observations have been reported in studies of the femoral neck (Fig. 11.3, right panel).

Thus, the total CSA of a tubular bone and its mineralized matrix mass are inversely associated; larger cross sections are assembled with less material relative to their total CSA, producing a lower apparent volumetric bone mineral density (vBMD); there is less bone within the periosteal envelope of a bigger bone, avoiding bulk. Smaller cross sections are assembled with more material relative to their size, producing a higher apparent vBMD; there is more bone within the periosteal envelope of a smaller bone, minimizing the liability to fracture of slenderness.

Bulk is avoided in larger cross sections by greater modeling-based endocortical resorption during growth. A larger medullary cavity is excavated so that thickening of the cortex by periosteal apposition is offset, thereby minimizing mass, yet radial displacement by this radial modeling drift achieves the same cortical bone area and compressive strength because the thinner "ribbon" of cortex is distributed around a larger perimeter. The radial drift of the cortex increases resistance to bending even though the cortex is thinner relative to the total CSA (Ruff and Hayes, 1988).

Thus, long bones are not drinking straws; they do not have a single cross-sectional diameter, a single cortical thickness, or medullary cavity diameter. Group means are used to express these dimensions but they obscure the diversity in structure and matrix mineral distribution so critical to determining diversity in bone strength. Diameters of a bone cross section

differ at each degree around the periosteal perimeter, creating differences in the external shape. Differences in the medullary diameters at corresponding points around the endocortical perimeter determine the shape of the medullary cavity, and the proximity of the periosteal and endocortical envelopes determines the cortical thicknesses around the perimeter of the cross section and the distances at which the cortical mass at each point around a cross section is placed from the neutral axis (Zebaze et al. 2005, 2007).

This diversity in bone size, shape, and mass distribution is achieved by differing degrees of focal formative and resorptive modeling at each point around the periosteal and endocortical perimeters. Intracortical remodeling assembles osteons, which are bone structural units with a central canal and concentric lamellae of differently oriented mineralized collagen fibers. A cement line delineates each osteon from the interstitial (interosteonal) bone matrix and other osteons.

An example of this regional specificity of remodeling is seen in studies of the femoral neck, the location of fractures associated with high morbidity and mortality. Remodeling upon the periosteal, intracortical, and endocortical surfaces varies according to the location chosen (Fig. 11.4, left). This heterogeneity produces the varying shape of the femoral neck cross sections. Greater periosteal apposition superiorly and inferiorly relative to mediolaterally produces the elliptical shape. Differences in periosteal apposition and endocortical resorption produce a thicker cortex inferiorly and a thinner cortex superiorly (Zebaze et al., 2007). The loss of bone during aging is also heterogeneous and varies depending on the location measured. It is greatest at the superior segment where the cortex is thinnest.

This principle of optimizing strength and minimizing mass is illustrated in a prospective study of the growth of a tibial cross section (Wang et al., 2005a, 2005b). In prepubertal girls, tibial cross-sectional shape was already elliptical at 10 years of age. During 2 years, focal periosteal apposition increased the ellipticity by adding twice the amount of bone anteroposteriorly than mediolaterally. Consequently, estimates of bending strength increased more in the anteroposterior (I_{max})

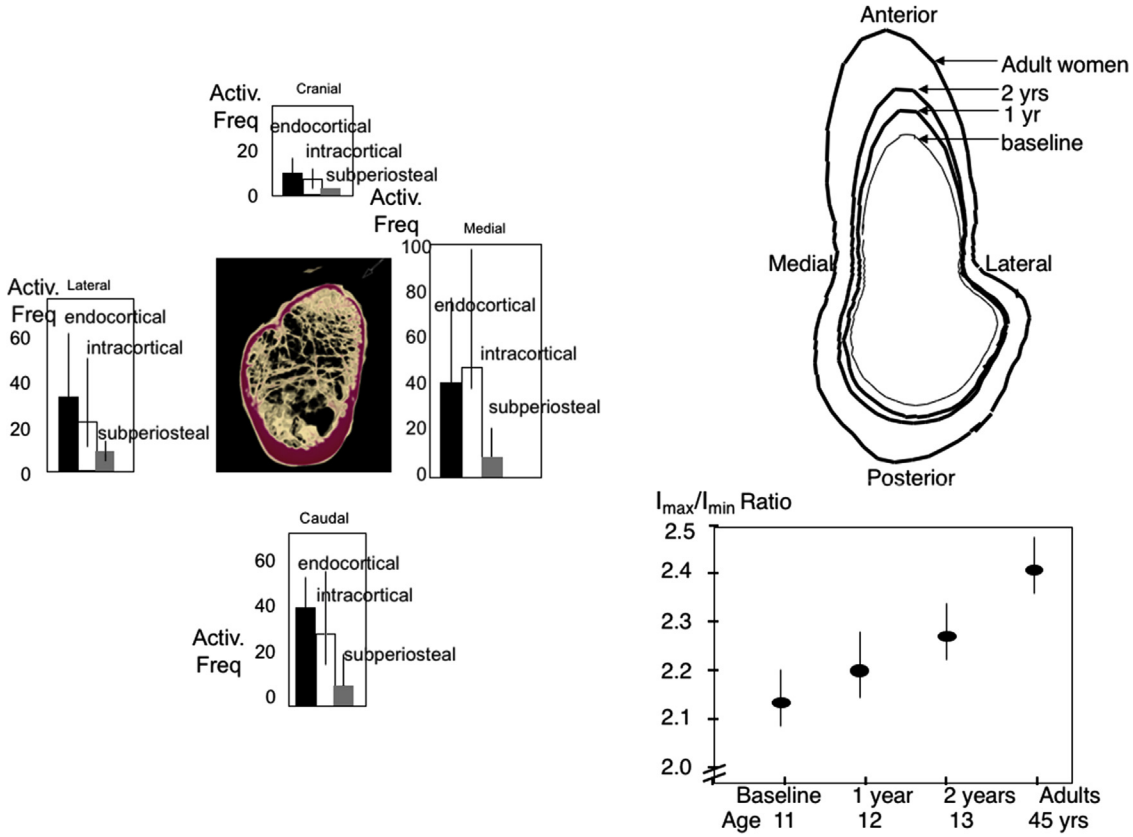

FIGURE 11.4 (Left) The femoral neck cross section. Activation frequency (*Activ. Freq*) of remodeling events differs on the periosteal, intracortical, and endocortical surface depending on the location studied. (Right) Bone mass distribution around the center of the tibial cross section. More bone is deposited anteriorly and posteriorly than medially and laterally during 2 years of growth, increasing the ellipticity of the cross section. Bending resistance increases more along the anteroposterior axis (I_{max}) than the mediolateral axis (I_{min}) as reflected in the increasing ratio. *Adapted from Wang, Q., Alen, M., Nicholson, P., Lyytikainen, A., Suurubuenu, M., Helkala, E., Suominen, H., Cheng, S., 2005a. Growth patterns at distal radius and tibial shaft in pubertal girls: a 2-year longitudinal study. J. Bone Miner. Res. 20 (6), 954–961, Wang, X.F., Duan, Y., Beck, T., Seeman, E.R., 2005b. Varying contributions of growth and ageing to racial and sex differences in femoral neck structure and strength in old age. Bone 36 (6), 978–986.*

than the mediolateral direction (I_{min}) (Fig. 11.4, right). Marrow area changed little, so more mass was distributed as a thicker cortex anteroposteriorly due to periosteal apposition without concurrent endocortical resorption. Resistance to bending increased by 44% along the principal axis (I_{max}) with a 22% increase in mass. If cortical thickness increased by the same amount of periosteal apposition at each point around the tibial perimeter, the amount of bone producing the same increase in bending resistance would be 205 mg, four-fold more than observed.

While it is intuitive that a bone with a larger CSA must be constructed with more periosteal bone than a smaller cross section, the contrary is observed. During 2 years, the absolute amount of bone deposited on the periosteal surface of the tibial cross section was similar in children with baseline tibial total CSA in the upper, middle, and lower tertile at 10 years of age. Thus, larger cross sections were assembled with less mass relative to their starting cross-sectional size, avoiding bulk, and smaller cross sections were assembled with more mass relative to their starting total CSA, offsetting the fragility associated with slenderness.

Deposition of similar amounts of bone on the periosteal surface of larger and smaller cross sections (and so less in relative terms on the former and more on the latter) was possible because the differences in bone size were established early, probably in utero (see later). Consequently, the deposition of an amount of bone on the periosteal surface of a larger cross section confers more bending resistance than the deposition of the same amount of bone on the periosteal surface of a smaller cross section, because resistance to bending is proportional to the fourth power of the distance from the neutral axis (Ruff and Hayes, 1988).

The increase in strength of a bone achieved by modifying its size and shape rather than increasing its mass is convincingly documented in racket sports. During growth, greater loading of the playing arm achieves greater bone strength by modifying its external size, its shape, and its internal architecture. Focal periosteal apposition and endocortical resorption at some locations, but endocortical bone formation at others, change the distribution of bone in space *without* a net change in its mass to accommodate loading patterns; apparent vBMD does not change; bending strength increases without increasing bulk (Haapsalo et al., 2000; Bass et al., 2002).

Trait variances in adulthood originate before puberty

Although adults have larger skeletons than children, differences in bone size and mass in adult life probably begin early in life. In a 3-year prospective study of growth in 40 boys and girls, Loro et al. reported that the variance at Tanner stage 2 (prepuberty) in vertebral CSA and volumetric trabecular BMD, femoral shaft CSA, and cortical area was no less than at Tanner stage 5 (maturity); 60%–90% of the variance at maturity was accounted for by the variance present before puberty. Thus, the magnitude of trait variances (dispersion around the age-specific mean) is largely established before puberty (Loro et al., 2000).

The ranking of individual values at Tanner stage 2 was unchanged during 3 years in girls. These traits tracked, so that an individual with a large vertebral or femoral shaft cross section, or higher vertebral vBMD or femoral cortical area, before puberty retained this position at maturity. The regression lines for each of the quartiles did not cross during 3 years. Similar observations were made in boys.

Similar observations have been reported using peripheral computed tomography of the tibia in 258 girls. The magnitude of variance at 10–13 years of age did not differ from that 2 years later, and did not differ from that of their premenopausal mothers. Likewise, in a study monitoring 744 women and men during 25 years, about 90% of the variance in cortical thickness in adulthood was accounted for by variance at completion of growth 25 years earlier (Garn et al., 1992). Similarly, studies from Tromso suggest that distal and ultradistal radial size and mass tracked during 6.5 years of follow-up of 5366 women and men ages 45–84 years (Emaus et al. 2005, 2006).

Finding that the magnitude of the trait variances at maturity is no different from the magnitude of their variances before puberty suggests that growth in larger and smaller bones occurs the same rate. (If larger bones deposit more bone during growth than smaller bones, variance will increase.) In addition, the constant variance and tracking also suggest that environmental factors are likely to contribute little to total variance of a trait in the population.

In infants and children at ages between 1 and 10 years, variances in diaphyseal diameter and muscle diameter were established at 1–2 years of age (Maresh, 1961). In a cross-sectional study of 146 stillborn fetuses of 20–41 weeks gestation, the percentage of a femur, tibia, and humerus diaphyseal cross section that was cortical area was about 80%–90% at 20 weeks gestation and remained so across the 20 weeks of intrauterine life, suggesting that as bone size increased during advancing intrauterine life, the proportion of bone within the cross section was established prior to 20 weeks gestation (Rodriguez et al., 1992).

The inference from the early establishment and constancy of trait variances is that genetic rather than environmental factors account for this variance. Studies in family members, twins, and birth cohorts followed for many decades and

studies of fetal limb buds grown in vitro support this view (Murray and Huxley, 1925; Pocock et al., 1987; Seeman et al., 1996).

This does not mean that traits *in an individual* are immutably fixed. This flawed notion confuses the proportion of the *population* variance in a trait attributable to genetic or environmental differences in that population with the effect of an environmental factor or disease on a trait in an individual. Muscle paralysis in utero, exercise during growth, or effects of disease in adulthood all have profound effects on bone structure in individuals (Bass et al., 2002; Pitsillides, 2006). Lifestyle changes influence the population mean of a trait as documented many times by secular increases in height, a highly heritable trait (Bakwin, 1964; Meredith, 1978; Cameron et al., 1982; Tanner et al., 1982; Malina and Brown, 1987). However, under stable conditions, lifestyle *differences* within a population make only a small contribution to trait variances compared with genetic *differences* in that population.

Sex and racial differences in bone structure

For the vertebrae, increasing bone size by periosteal apposition builds a wider vertebral body in males than in females and in some races than in others (Seeman, 1998). Trabecular number per unit area is constant during growth (Fig. 11.5, bottom left). Therefore, individuals with a low trabecular number in young adulthood are likely to have lower trabecular numbers in childhood (Parfitt et al., 2000). The age-related increase in trabecular density is the result of increased thickness of existing trabeculae (Fig. 11.5, top left). Before puberty there is no difference in trabecular density in boys and girls of either Caucasian or African American origin (Gilsanz et al 1988, 1991) (Fig. 11.5, right). This suggests that both vertebral body size and the mass within its periosteal envelope increase in proportion until Tanner stage 3.

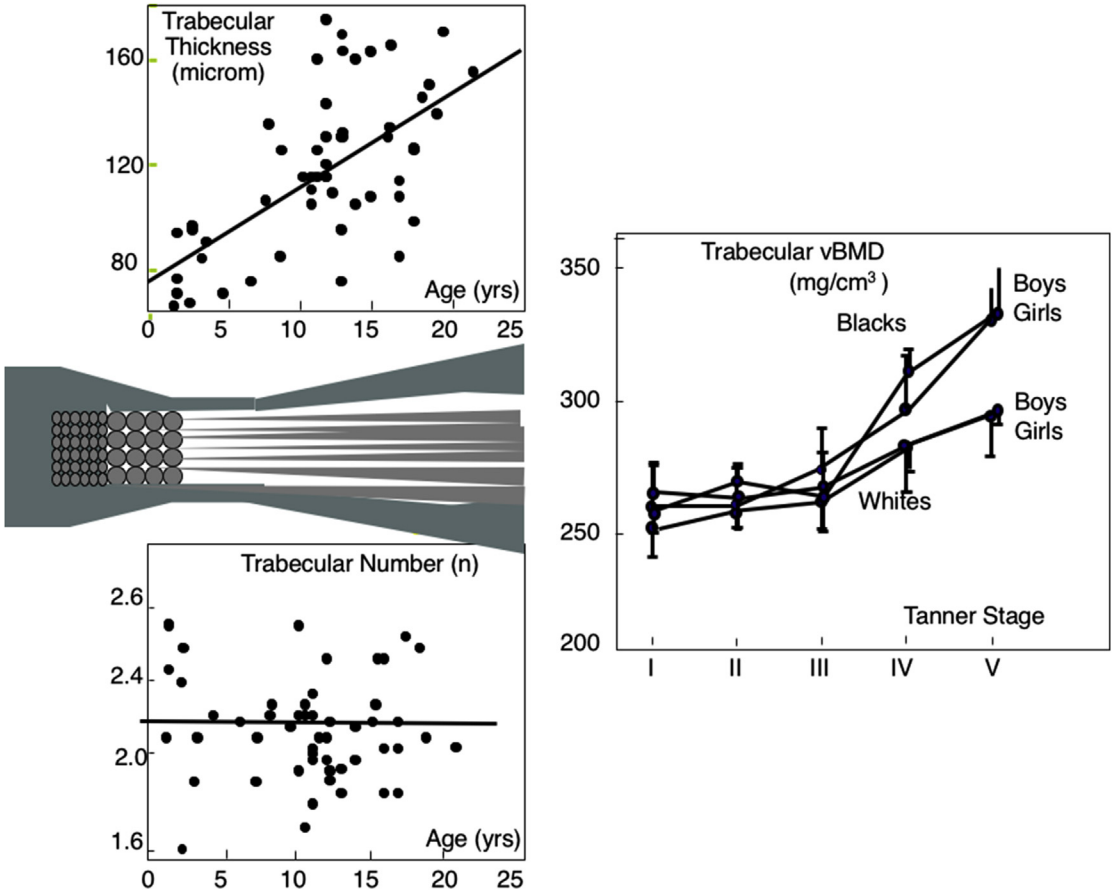

FIGURE 11.5 (Left) Trabecular volumetric bone mineral density (*vBMD*) increases with advancing age owing to an increase in trabecular thickness (top), not number (bottom). (Right) Before puberty, trabecular vBMD is no different by sex or race and increases at Tanner stage 3 similarly by sex within a race, but more greatly in blacks than in whites. *(Left) Adapted from Parfitt, A.M., Travers, R., Rauch, F., Glorieux, F.H., 2000. Structural and cellular changes during bone growth in healthy children. Bone 27, 487–494. (Right) Adapted from Gilsanz, V., Roe, T.F., Stefano, M., Costen, G., Goodman, W.G., 1991. Changes in vertebral bone density in black girls and white girls during childhood and puberty. N. Engl. J. Med. 325, 1597–1600.*

At puberty, trabecular density increases by race and sex, but there is no sex difference in trabecular density within a race. This increase is probably the result of the cessation of external growth in bone size but continued bone formation upon trabecular and endocortical surfaces, resulting in more bone within the periosteal surface of the bone—higher apparent vBMD. Thus, growth does not build a "denser" vertebral body in males than females, it builds a bigger vertebral body in males. Strength of the vertebral body is greater in young males than females because of size differences. Within a sex, African Americans have a higher trabecular density than whites due to a greater increase in trabecular thickness (Han et al., 1996). The mechanisms responsible for the racial dimorphism in trabecular density but lack of sexual dimorphism within a race are not known. The greater trabecular thickness in African Americans partly accounts for the lower remodeling rate in adulthood because there is less surface available upon which remodeling can occur (Han et al., 1996).

Sex differences in appendicular growth are largely the result of differences in timing of puberty (Fig. 11.6, left). Before puberty, there are already sex differences in diaphyseal diameter (Iuliano-Burns et al., 2008). As long bones increase in length by endochondral apposition, periosteal apposition widens the lengthening long bone. Concurrent endocortical resorption excavates the medullary cavity. As periosteal apposition is greater than endocortical resorption, the cortex thickens. In females, earlier completion of longitudinal growth with epiphyseal fusion and earlier inhibition of periosteal apposition produces a smaller bone.

Bone length continues to increase in males and periosteal apposition increases cortical thickness. However, cortical thickness is similar in males and females because endocortical apposition in females contributes to final cortical thickness (Garn, 1970; Bass et al., 1999). Cortical thickness is similar by race and sex (Fig. 11.6, right). What differs is the position of the cortex in relationship to the long axis of the long bone (Wang et al., 2005a, 2005b; Duan et al., 2005). It is not clear

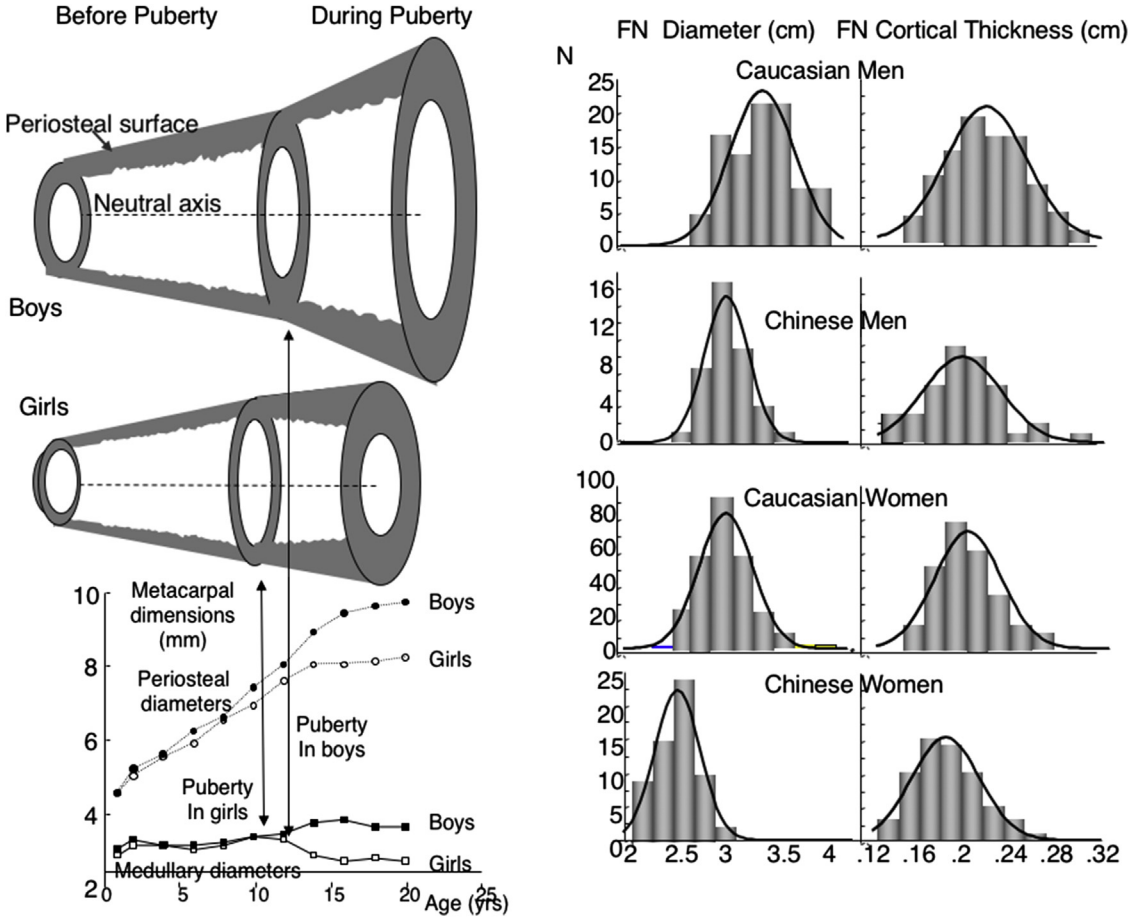

FIGURE 11.6 (Left) Long bone diameter is greater in males than females before puberty. Growth in length and width continues longer in males because puberty occurs later. Endocortical apposition in females contributes to cortical thickness so that final cortical thickness is similar in males and females but displaced further radially in males. (Right) Distribution of femoral neck (*FN*) diameter differs by sex and race but FN cortical thickness is similar by sex and race. *(Left) Adapted from Garn, S., 1970. The Earlier Gain and Later Loss of Cortical Bone. Nutritional Perspectives. Charles C. Thomas, Springfield, IL, pp. 3–120. (Right) E. Seeman with permission.*

whether the wider diaphysis in males than in females is the result of more rapid periosteal apposition in males, as commonly believed, or more protracted longitudinal growth at the same rate, as males enter puberty 1−2 years after females (Garn, 1970).

Bone remodeling by the basic multicellular unit

Osteocyte death in signaling bone remodeling

Bone, like roads, buildings, and bridges, develops fatigue damage during repeated loading, but only bone has a mechanism enabling it to detect the location and magnitude of the damage, remove it, replace it with new bone, and restore the bone's material composition while maintaining its micro- and macroarchitecture (Parfitt 1996, 2002).

Bone resorption is not necessarily bad for bone. On the contrary, the resorptive phase of remodeling removes old or damaged mineralized matrix. The formation phase of the remodeling cycle renews the material composition of bone and restores bone's microstructure provided that the volume of bone formed and deposited is the same as the volume of damaged bone removed. This process depends on the normal production, work, and life span of osteoclasts and osteoblasts. While these are the two executive cells of the BMU, the BMU consists of a range of cells that participate in the renewal of bone matrix composition, as discussed elsewhere (see chapters 4 and 10 for further detail).

It is likely that the osteocyte plays a pivotal role in bone modeling and remodeling. Osteocytes are the most numerous, longest-lived cells of bone. There are about 10,000 cells per cubic millimeter of mineralized bone matrix volume and each cell possesses about 50 neuron-like processes that connect osteocytes with one another and with flattened lining cells on the endosteal surface (Marotti et al., 1990) (Fig. 11.7A, see legend also).

The dense lacelike network of osteocytes with their processes ensures that no part of bone is more than several micrometers from a lacuna containing its osteocyte, suggesting that these cells are part of the machinery guarding the integrity of the composition and structure of bone (Parfitt, 2002). Microcracks sever osteocyte processes in their canaliculi, producing osteocyte apoptosis (Hazenberg et al., 2006) (Fig. 11.7B and C). Prevention of osteocyte death may be an attractive therapeutic target if they are the result of damage, if they become a form of damage themselves when they become apoptotic, or if they produce damage (O'Brien et al., 2004; Keller and Kneissel, 2005; Manolagas, 2006).

Apoptotic osteocytes, for example, may be a form of damage themselves, perhaps reducing the energy-absorbing/dissipating capacity of bone when lacunae mineralize. Estrogen deficiency and corticosteroid therapy result in their apoptosis (Manolagas, 2006). Osteocyte apoptosis may damage surrounding mineralized matrix, producing bone fragility (independent of bone loss). Corticosteroid-treated mice have large osteocyte lacunae surrounded by matrix with a 40% reduction in mineral and reduced elastic modulus (Lane et al., 2006). Genetic ablation of osteocytes produces bone fragility (Tatsumi et al., 2007). Whether the increased rate of remodeling in midlife in women is partly the result of osteocyte death is not known.

The number of dead osteocytes provides the topographical information needed to identify the location and size of damage (Verborgt et al., 2000; Taylor, 1997; Schaffler and Majeska, 2005) (Fig. 11.11C). Osteocyte apoptosis is likely to be one of the first events signaling the need for remodeling. It precedes osteoclastogenesis (Clark et al., 2005). In vivo, osteocyte apoptosis occurs within 3 days of immobilization and is followed within 2 weeks by osteoclastogenesis (Aguirre et al., 2006). In vitro, death of the osteocyte-like MLO-Y4 cells, induced by scratching, results in the formation of TRACP-positive (osteoclast-like) cells along the scratching path (Kurata et al., 2006).

Thus, just as the spider knows the location and size of its wriggling prey by signals sent along its vibrating web, the need for reparative remodeling is likely to be signaled by osteocyte death. This takes place via their processes connected to viable osteocytes and to flattened osteoblasts lining the three intracortical, endocortical, and trabecular components of the inner (endosteal) surface of bone upon which remodeling is initiated.

The bone remodeling compartment

Bone remodeling is initiated at points upon on the endocortical, trabecular, and intracortical components of the endosteal envelope. The endocortical and trabecular surfaces are adjacent to marrow. The intracortical surface is formed by the surface of Haversian and Volkmann's canals. While remodeling is initiated at points upon these surfaces, damage occurs deep to them, within the matrix of osteons or the interstitial (interosteonal) bone in the case of cortical bone or within hemiosteons in the case of trabecular bone. Information concerning the location and size of damage must reach these surfaces, and cells involved in remodeling must reach the site of damage beneath the endosteal surface. This anatomical

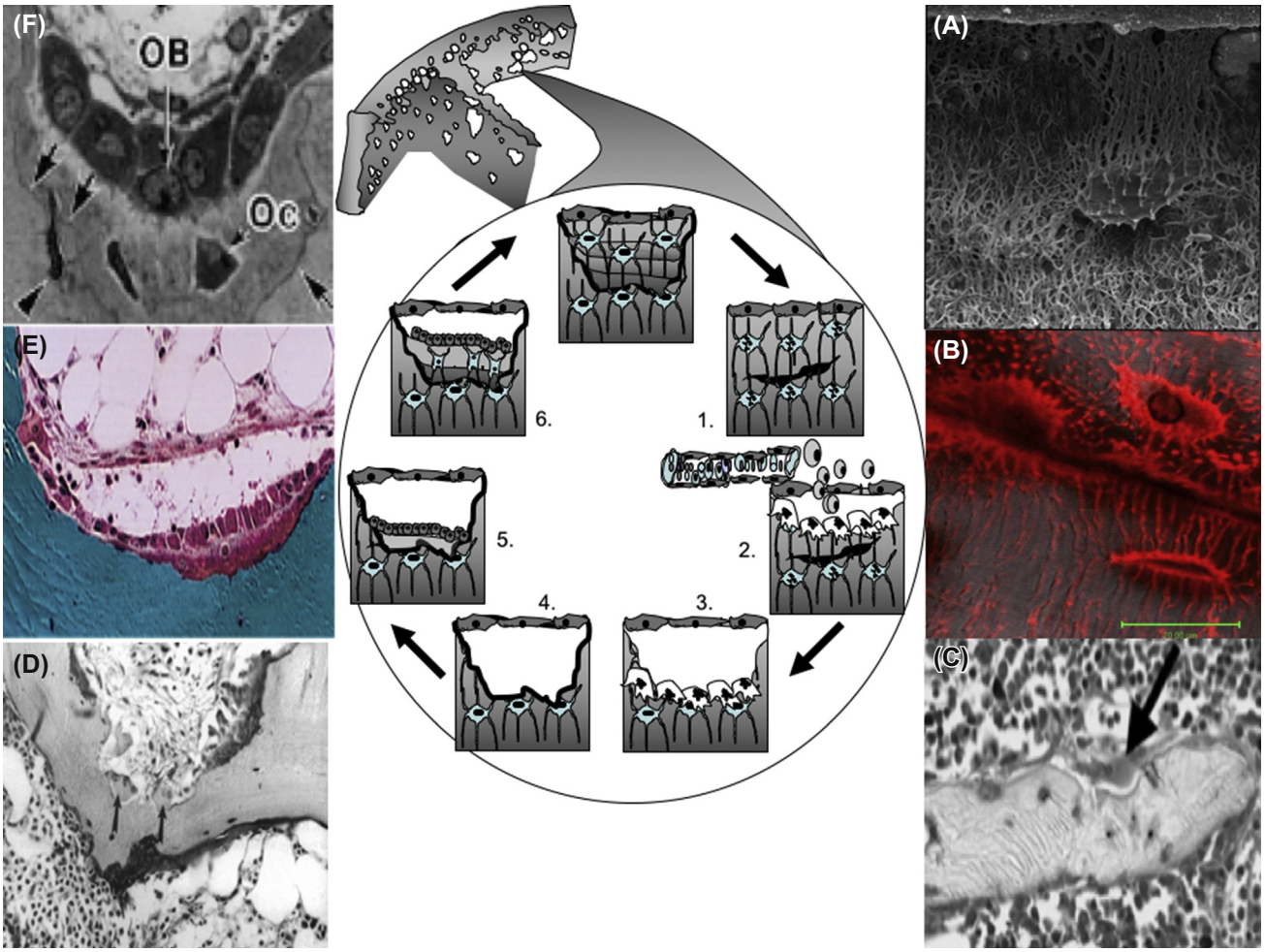

FIGURE 11.7 (A) Osteocytes are connected to one another and to lining cells on the endosteal surface adjacent to the marrow. (B) Damage to osteocytic processes by a microcrack produces osteocyte apoptosis. (C) The distribution of apoptotic osteocytes provides the topographical information needed to target osteoclasts (identified by arrow) to the damage. (D) Osteoclasts (arrows) resorb bone. (E) Osteoblasts deposit osteoid. (F) Some osteoblasts are entombed in the osteoid (arrows) they deposit. Central cartoons depict the remodeling events with (1) damage causing osteocytes to apoptose; (2) formation of a bone remodeling compartment with a vascular supply and osteoclasts resorbing bone; (3 and 4) osteoclasts resorbing damage; (5) a cement line being formed; and (6) bone formation following refilling of the cavity with entombment of osteoblasts that become osteocytes. *OB*, osteoblast; *Oc*, osteocyte. *(B) Courtesy J. Hazenberg. (C) Courtesy M. Schaffler. (F) From Suzuki, R., Domon, T., Wakita, M., 2000. Some osteocytes released from their lacunae are embedded again in the bone and not engulfed by osteoclasts during remodelling. Anat. Embrol. 202, 119–128.*

arrangement makes the flattened lining cells likely conduits transmitting the health status of the bone matrix to the bone marrow environment, which in turn is a source of the cells of the BMU, but not the only source.

Apoptotic osteocytes signal the location and size of the damage burden to the flattened lining cells of the endosteal surface, leading to the formation of a bone remodeling compartment (BRC), which confines and targets remodeling to the damage that is removed by osteoclasts (Hauge et al., 2001) (Fig. 11.7D). The regulatory steps between osteocyte apoptotic death and creation of the BRC are not known. Bone-lining cells express collagenase mRNA (Fuller and Chambers, 1995). An early event creating the BRC may be collagenase digestion of unmineralized osteoid to expose mineralized bone, a requirement for osteoclastic bone resorption.

The flattened bone-lining cells express markers of the osteoblast lineage, particularly lining cells forming the BRC canopy (Hauge et al., 2001; Parfitt, 2001). These canopy cells also express markers for growth factors and regulators of osteoclastogenesis, such as receptor activator of NF-κB ligand (RANKL), suggesting that the canopy has a central role in the differentiation of precursor cells of marrow stromal origin, monocyte–macrophage origin, and vascular origin toward their respective osteoblast, osteoclast, or vascular phenotype.

The multidirectional steps of the remodeling cycle

While the two classical events of remodeling—resorption of a volume of bone by osteoclasts and formation of a similar volume of bone by osteoblasts—occur sequentially (Hattner et al., 1965), the cellular and molecular regulatory events leading to these two fully differentiated functions may not be sequential. Some may be contemporaneous and multidirectional; osteoblastogenesis and its regulators determine osteoclastogenesis, and so the volume of bone to be resorbed, while osteoclastogenesis and the products of the resorbed matrix regulate osteoblastogenesis. Both pathways may be regulated to some extent by osteocytes and their products (e.g., sclerostin). How this cellular and molecular traffic is orchestrated from beginning to end remains unclear (see chapters 4 and 10 for further detail).

Signaling from apoptotic osteocytes to cells in the canopy expressing the osteoblast phenotype may influence further differentiation toward osteoblast precursors expressing RANKL and fully differentiated osteoblasts producing osteoid. Even at this stage, regulation of osteoclastogenesis and osteoblastogenesis occurs simultaneously through osteoblast precursors. In the MLO-Y4 cell line, damaged osteocyte-like cells have been reported to secrete macrophage colony-stimulating factor and RANKL (Kurata et al., 2006). Whether this occurs in human subjects in vivo is not known, but it raises the possibility that osteocytes participate in the differentiation of monocyte−macrophage precursor cells toward the osteoclast lineage. Both osteoblast and osteoclast precursors circulate and so may arrive at the BRC via the circulation and via capillaries penetrating the canopy (Eghbai-Fatourechi et al 2005, 2007; Fujikawa et al., 1996).

The contribution of precursors from the canopy or the marrow via sinusoids or capillaries is not well defined. Angiogenesis is essential to bone remodeling. Osteoprogenitor cells are associated with vascular structures in the marrow and several studies suggest there may be common progenitors giving rise to cells forming the blood vessels and the perivascular cells that can differentiate toward cells of multiple lineages (Doherty et al., 1998; Howson et al., 2005; Sacchetti et al., 2007; Matsumoto et al., 2006; Kholsa, 2007; Otsura et al., 2007; Khosla et al., 2008).

Little is known about the factors determining the volume of bone resorbed or how resorption stops after the damaged region has been resorbed. Osteoclasts phagocytose osteocytes and this may be one way the signal for resorption is removed (Elmardi et al., 1990). Products from the osteoclasts, independent of their resorption activity, and products from the resorbed matrix partly regulate osteoblastogenesis and bone formation (Suda et al., 1999; Martin and Sims, 2005; Lorenzo, 2000). Sclerostin, a negative regulator of bone formation, is an osteocyte product that inhibits bone formation and its inhibition is permissive for bone formation.

After the reversal phase, osteoblasts deposit osteoid, partly or completely filling the cavity (establishing the size of any negative BMU balance) (Fig. 11.7E). Osteoblasts deposit type I collagen, which is configured as the lamellae that undergo primary and secondary mineralization. How the osteoblasts change polarity to produce the differently oriented collagen fibers from lamella to lamella is not known. Most osteoblasts die, others become lining cells, while others are entombed in the osteoid they form, leaving reconstruction and "rewiring" of the osteocytic canalicular communicating system for later mechanotransduction, damage detection, and repair (Fig. 11.7F) (Han et al., 2004).

Perhaps the most fundamental and challenging question remains unanswered. Why is remodeling initiated at a given location and at a given time? While it is commonly stated that remodeling is initiated by "damaged" or "old" bone, the definitions of "damaged" and "old" remain enigmatic. Damage at the nano- or microstructural level has not been categorized in morphological terms, so the causes of damage, the biomechanical effects, and the biochemical and structural means of detecting, signaling, and repairing different types of damage remain uncertain (Akkus et al., 2004; Burr et al., 1998; Danova et al., 2003; Diab et al., 2006; Diab T and Vashisha D 2005; Garnero et al., 2006; Landis 2002; Ruppel et al., 2006; Silva et al., 2006; Taylor et al., 1997).

Bone remodeling and microstructure during young adulthood, menopause, and advanced age

Young adulthood: reversible bone loss and microstructural deterioration

Remodeling is balanced during young adulthood; the same volumes of bone are removed and eventually replaced at specific locations upon the endocortical, intracortical, and trabecular components of bone's endosteal envelope (Hattner et al., 1965). There is no net focal gain or loss of bone so that the external and internal dimensions of the mineralized bone matrix volume remain unchanged. Remodeling also occurs upon the outer (periosteal) surface but to a minimal extent (Orwoll 2003; Blizoites et al., 2006).

The resorption of a volume of bone, its replacement with an identical volume of osteoid, and primary and secondary mineralization of osteoid are not instantaneous events. The resorptive phase of remodeling takes ~3 weeks, the reversal

phase takes ~1 week, the formation phase takes ~3 months, and completion of mineralization takes many months, if not years (Baron et al., 1984; Hattner et al., 1965; Parfitt, 1996).

Remodeling occurs simultaneously at different locations but it is asynchronous. BMUs at different locations are at different phases of their remodeling cycle. While remodeling is balanced, the deficit in matrix and its mineral content is *focally* transient and fully reversible. However, as concurrent events are asynchronous, there is a *globally* ever-present deficit in matrix and its mineral content formed by the BMUs at different stages of their remodeling cycle. The more rapid the remodeling, the greater the number of BMUs, and so the greater size of the reversible deficit in matrix and its mineral content.

In morphological terms, the ever-present reversible global deficit in matrix and its mineral content consists of BMUs in their resorption phase, BMUs with cavities in their reversal phase, cavities containing osteoid that has undergone primary mineralization, and other cavities containing matrix at various stages of secondary mineralization (Parfitt, 1996). More BMUs are at varying stages of their formation or mineralization phase than in their resorption or reversal phase because the matrix formation phase is longer than the resorption phase and the matrix mineralization phase is very much longer than the matrix deposition phase. As secondary mineralization is so much slower than the matrix deposition, the ever-present global deficit in mineralized bone matrix volume is largely the result of a deficit in the mineral content of the matrix, not the matrix. New osteons in cortical bone or hemiosteons in trabecular bone are fully reconstructed by the cellular activity of osteoblastic bone formation many months before they become fully mineralized.

In premenopausal women, the ever-present global deficit is ~10% of the total mineralized bone matrix volume. After menopause, when remodeling rate increases, the deficit is ~20% of the total mineralized bone matrix volume. Of the 20% of the skeleton being remodeled—"turned over"—annually, not all is reversible because of the emergence of the remodeling imbalance and the appearance of the irreversible deficit in bone matrix and its mineral content.

The recognition of the existence of the reversible and irreversible deficits in matrix volume and its mineral content and the differing time course of completion of matrix resorption, matrix deposition, and the much slower secondary mineralization of the matrix is important because each event contributes differently to aspects of the pathogenesis of menopause and age-related loss of bone matrix, its mineral content, and so bone's material and structural strength and whole-bone strength.

This "deconstruction" into the reversible and irreversible deficits of bone matrix and mineral content is also relevant to understanding the morphological changes produced by antiresorptive and anabolic therapy, particularly when these two classes of drugs are combined. These treatments have opposite effects on matrix mineral density and so have effects on material and microstructural strength not captured by the BMD measurement, and indeed obscured by the measurement, which is used as a surrogate of "bone strength." Several examples of the effects of the reversible and irreversible deficits in matrix and mineral follow here and in the section concerning modeling and remodeling during drug therapy.

The reversible deficit in matrix and its mineral content produces no permanent microstructural deterioration before menopause. If remodeling is rapid, the presence of many excavated cavities may increase bone fragility independent of the temporary small deficit in matrix and its mineral content produced by the delay and slowness of the formation phase. These cavities form stress "risers" or stress "concentrators," which are likely to contribute to the pathogenesis of fractures (Hernandez, 2006).

Before menopause, remodeling is balanced and the deficit in matrix and mineral at a given location is transitory, yet several studies suggest that bone loss occurs before menopause. For example, Riggs et al. reported that women lose 37% and men 42% of the total trabecular bone before age 50 years and 6% and 15% of lifetime cortical bone is lost (Riggs et al 1986, 2007; Gilsanz et al., 1987). However, a prospective study of female twins remaining premenopausal or entering peri- or postmenopause did not support the occurrence of bone loss or microstructural deterioration before menopause (Bjørnerem et al., 2018).

The loss of bone (measured as a decrease in BMD) may be an artifact produced by an increase in medullary cavity fat, which attenuates photons less than water or cells, producing a seeming decline in BMD giving the impression of bone "loss" (Bolotin and Sievänen, 2001). Alternatively, a remodeling imbalance may exist before menopause but is below the detection limits of current methods. If bone loss does occur before menopause, the structural and biomechanical consequences are likely to be less than those of bone loss later in life because the remodeling rate is slow, and trabecular bone loss probably proceeds by reduced bone formation and thinning rather than increased bone resorption with perforation and loss of connectivity. Thinning is less deleterious to loss of strength than perforation and loss of connectivity (Van der Linden et al., 2001). Moreover, continued periosteal apposition partly offsets endocortical bone loss, shifting the cortices radially, maintaining cortical area and resistance to bending (Szulc et al., 2006).

Menopause: reversible and irreversible bone loss and microstructural deterioration

At the time of menopause, there is an early accelerated phase of bone loss and an accelerated decrease in BMD. The worsening of the reversible deficit in matrix and mineral is the net result of the concurrent appearance of many more BMUs in their resorptive phase than the BMUs generated before menopause only now entering their refilling phase. The deficit in matrix and mineral produced by perturbation of steady-state surface level remodeling is fully reversible.

If the increase in the rate of bone remodeling was the only effect of menopause, BMD would decrease to a level determined by the higher rate of remodeling at the new steady state with BMUs in varying states of incompleteness of their remodeling cycle. No further bone loss would occur. Bone fragility would increase as a function of numbers of stress concentrators. If estrogen deficiency was reversed and remodeling returned to its premenopausal rate, BMD would be fully restored to its premenopausal level and there would be no permanent microstructural deterioration. This is not the case.

The percentages of the endosteal surface participating in bone resorptive activity and in formative activity at other locations are increased because the birth rate of BMUs increases after menopause. This alone does not determine whether bone is irreversibly lost from the skeleton. Whether bone loss occurs depends on the presence of a remodeling imbalance at the level of each BMU. Menopause is accompanied by the appearance of remodeling imbalance; less bone is deposited than was resorbed during each remodeling transaction. This differs from the reversible deficit and reversible microstructural deterioration produced by the normal delay and slowness of the refilling phase of remodeling.

Remodeling imbalance with less bone deposited than formed may occur in a range of ways. The most common and demonstrated by histomorphometry is a reduction in *both* the volumes of bone resorbed and the volumes deposited by each BMU, but a greater reduction in the volume of bone formed (Lips et al., 1978; Vedi et al., 1984). The decrease in resorption by the BMU is reflected in a smaller resorption cavity and an age-related increase in interstitial thickness (Croucher et al., 1991; Ericksen et al., 1999). (If resorption depth increased, interstitial wall thickness, the distance between cement lines of adjacent hemiosteons in trabecular bone, should decrease.) The reduction in the volume of bone resorbed results in the formation of smaller osteons, as the diameter of the resorption cavity defines the outer diameter of the osteon to be reassembled, while the reduction in the volume of bone deposited in the smaller cavity produces fewer lamellae and a larger central Haversian canal (porosity).

Another mechanism producing remodeling imbalance is an increase (not decrease) in the volume of bone resorbed and a decrease in the volume of bone formed due to an increase in the life span of osteoclasts and decrease in the life span of the osteoblasts, respectively (Manolagas Bonyadi et al., 2003; Nishida et al., 1999; Stenderup et al., 2001; Oreffo et al., 1998). The observation that menopause is accompanied by reduced numbers of trabeculae not thinning is consistent with larger cavities perforating these trabeculae (Aaron et al., 1987; Bjornerem et al., 2018). The observation of reduced cavity depth is consistent with a reduction in bone resorption. The differing observations can be reconciled if the increased life span of osteoclasts produced by estrogen deficiency is transitory (Ericksen et al 1986, 1999; Manolagas, 2000; Compston et al., 1995).

The factor driving the early accelerated bone loss is the perturbation of the surface extents of resorption and formation, not remodeling imbalance. Whether the early accelerated loss of bone at menopause is partly due to a reduction in the volume of bone formed by BMUs generated just *before* menopause is uncertain, because osteoblasts of these BMUs may not yet have a reduced life span. The reduction in osteoblast life span may emerge only during menopause.

Remodeling returns to steady state 6−12 months postmenopause at a higher remodeling rate than the steady-state remodeling before menopause, but at a slower rate than in early menopause. This slowing is not the result of slowing of the rate of remodeling. On the contrary, the rate of remodeling continues to be rapid. Bone loss is driven by the size of the remodeling imbalance and the birth rate of the new BMUs, but no longer by perturbation of the surface extents of resorption and formation. Now, the great many new BMUs generated in early menopause refill incompletely, and concurrently, a similarly large number of BMUs in their resorptive phase are generated**.** The rates of increase in cortical porosity, decrease in trabecular density due to reduced numbers of trabeculae, and reduction in matrix mineral density accelerate in women transitioning from peri- to postmenopause, and then decelerate (Bjørnerem et al., 2018) (Fig. 11.8).

Whatever the mechanisms producing remodeling imbalance, the imbalance in the volumes of bone resorbed and deposited by each BMU is the necessary and sufficient morphological basis for bone loss, microstructural deterioration, and bone fragility. Bone can no longer accommodate its loading circumstance by adaptive modeling and remodeling because each time a remodeling event occurs in an attempt to maintain bone's material composition, there is a loss of bone and microstructural deterioration. Most importantly, the loss of strength is out of proportion to the bone loss producing this deterioration; an increase in porosity of a compact structure like cortical bone reduces resistance to bending to the seventh power of the rise in porosity. A rise in porosity of an already porous structure like cortical bone reduces its resistance to bending to the third power (Schaffler and Burr, 1988).

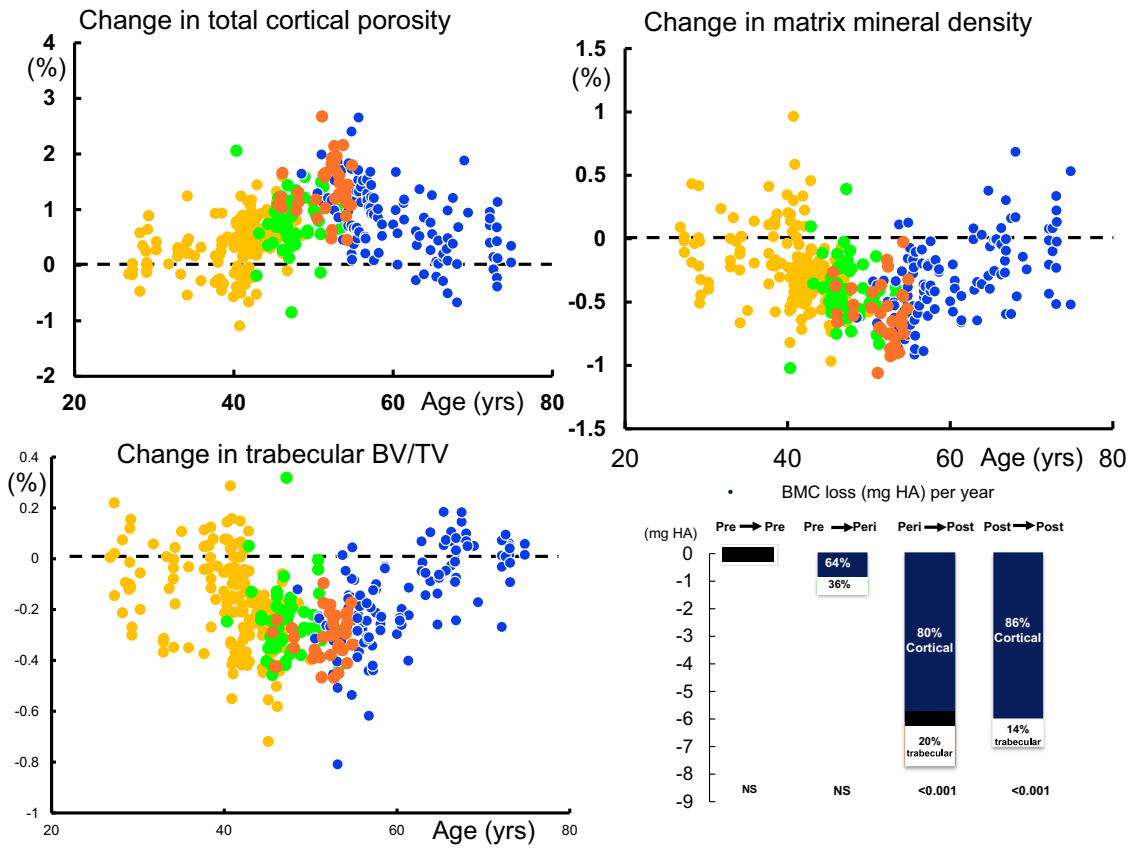

FIGURE 11.8 Annual changes in distal tibia total cortical porosity, trabecular bone volume/total volume (*BV/TV*), and matrix mineral density as a function of baseline age in women remaining premenopausal (*light orange dots* [light gray in print version]), becoming perimenopausal (*green dots* [medium gray in print version]), becoming postmenopausal (*dark orange dots* [dark gray in print version]), and remaining postmenopausal (*blue dots* [black in print version]). The bottom right shows the amount of tibial cortical and trabecular bone loss as a percentage of annual loss of total bone mineral content (*BMC*; mg hydroxyapatite [*HA*]) in women remaining premenopausal (*Pre* → *Pre*), becoming perimenopausal (*Pre* → *Peri*), moving from peri- to postmenopausal (*Peri* → *Post*), and remaining postmenopausal (*Post* → *Post*). *P* values within each group tested whether the total annual loss was different from zero.

Thus, BMD may decrease only into the so-called "low normal" range or osteopenic range, but bone fragility is present and is obscured by these modest reductions in BMD, which misleadingly suggest fracture risk is low. Fracture risk is lower than in women with BMD within the osteoporosis range (T score < -2.5 SD), but osteopenia or normal BMD in a postmenopausal woman is no assurance of absence of fracture risk; on the contrary, most fractures in the community arise among women and men with osteopenia (Siris et al., 2004).

Advanced age: the predominance of cortical bone loss

Modeling and remodeling are surface-dependent cellular events. For remodeling to occur there must be a surface upon which it is initiated. The larger the surface area, the greater the likelihood that remodeling can be initiated by events occurring deep to that surface, whether this event is matrix damage, osteocyte death, or other still undefined factors. Trabecular bone is fashioned as thin plates with a large surface area and a high surface area/matrix volume configuration. This is an advantage for matrix damage repair because damage can be easily signaled to the trabecular surface and the initiated remodeling can then easily be targeted to return to the matrix damage, remove it, and replace it with new bone. Hence, trabecular bone is more readily "turned over," a liability when remodeling becomes unbalanced. Indeed, when this occurs, rapid loss of complete trabeculae removes them and their surface so that trabecular remodeling diminishes as trabeculae disappear. In addition, loss of strength is greater with perforation of trabeculae, as found in women, rather than thinning, as occurs in men (Van der Linden, 2001) (Fig. 11.9).

As trabeculae are lost with their surfaces, bone loss from this compartment slows as less trabecular surface is available for resorption, but remodeling upon the endocortical and intracortical surfaces continues and increases as the endocortical

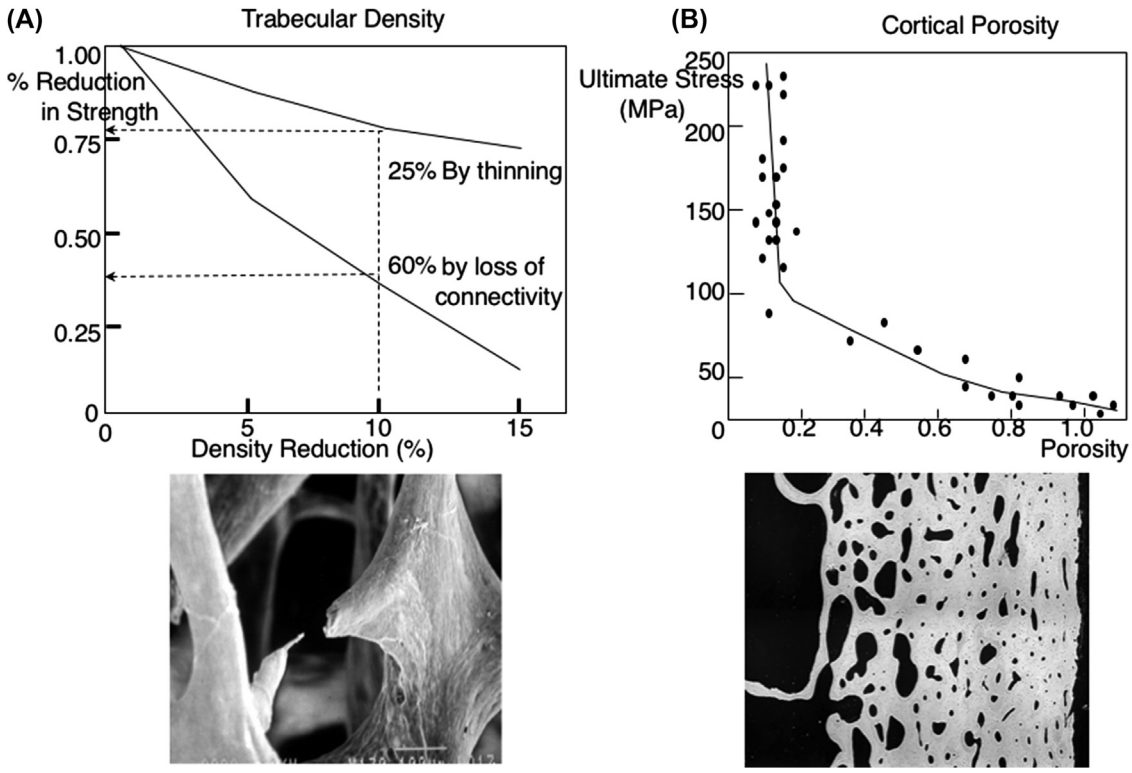

FIGURE 11.9 (A) Reduction in strength produced by a 10% deficit in trabecular density is greater when this deficit is produced by loss of trabecular connectivity than by thinning. Image shows loss of connectivity (Mosekilde et al., 1990). (B) A small increase in cortical porosity by a few percentage points is associated with a decline in ultimate stress and reduction in toughness. Scanning electron microscopic image of irregularly shaped enlarged pores in cortical bone. *(A) Adapted from Van der Linden, J.C., Homminga, J., Verhaar, J.A.N., Weinans, H., 2001. Mechanical consequences of bone loss in cancellous bone. J. Bone Miner. Res. 16, 457–465. (B) Adapted from Martin, R.B., 1984. Porosity and specific surface of bone. CRC Critical Rev. Biomed. Eng. 10, 179–221; and Yeni, Y.N., Brown, C.U., Wang, Z., Norman, T.L., 1997. The Influence of bone morphology on fracture toughness of the human femur and tibia. Bone 21, 453–459.*

surface undergoes bone resorption, so that its surface area increases like the folds of a curtain (Parfitt, 1984; Brown et al., 1987; Arlot et al., 1990; Foldes et al., 1991). The main source of bone loss is intracortical remodeling initiated upon the surface of the myriads of Haversian canals traversing the cortex (Martin, 1984; Brockstedt et al., 1993; Yeni et al., 1997). Increased porosity is mainly due to increased size of existing canals that coalesce, forming irregularly shaped pores (canals seen in cross section). As the canals enlarge, the surface area of the canals also enlarges as does the surface area/matrix volume configuration, making cortical matrix accessible to being turned over and lost by the unbalanced remodeling (Bui et al., 2013). Total bone surface area either does not change (increasing in cortical bone, decreasing in trabecular bone) or increases (in regions of cortical bone only) so that late in life, bone loss is more cortical than trabecular in origin (Zebaze et al., 2010).

Increased intracortical remodeling of cortex adjacent to the medullary canal fragments the cortex, causing it to "trabecularize"; the cortical fragments look like trabecular bone and the porosity is erroneously "seen" as part of an enlarging medullary canal. Apportioning the intracortical porosity to the medullary compartment underestimates the age-related increase in cortical porosity and the trabecularized cortical fragments are regarded as trabecular bone within the seemingly expanded medullary canal, leading to an underestimation of the decrease in trabecular density with age (Zebaze et al., 2010). Both errors underestimate fracture risk in individuals and so fail to signal the imperative to initiate treatment.

Solutions to these problems have been found by segmenting a corticotrabecular outer and inner transitional zone using non-threshold-based image analysis. This approach allocates and confines cortical porosity to this "third" compartment, rather than erroneously expanding the medullary canal void, and cortical fragments to the outer transitional zone and partly to the inner transitional zone, which also contains true trabecular fragments (Zebaze et al., 2013).

As age advances and rapid unbalanced remodeling continues due to permanent estrogen deficiency and perhaps emerging secondary hyperparathyroidism, the extent of coalescence of pores increases, so the number of intracortical pores decreases, but the total area of porosity increases, as reported in patients with hip fractures (Bell et al., 1999). Cortical

porosity reduces the ability of bone to limit crack propagation so that bone cannot absorb the energy imparted by the impact of a fall. This energy is released in the worst possible way, by fracture (Martin, 1984; Yeni et al., 1997). The continued unbalanced remodeling at a similar intensity removes the same volume of bone from an ever-decreasing amount of bone, accelerating the rate of bone loss and microstructural deterioration (Zebaze et al. 2013).

While the unbalanced remodeling produces bone loss and microstructural deterioration, remodeling is a transaction. Older, more completely mineralized bone is replaced with a smaller volume of younger bone that is less completely mineralized. This results in a decrease in mean matrix mineral density and an increase in the heterogeneity in the degree of mineralization of adjacent osteons and the interstitial (interosteonal) bone between osteons (which is more fully mineralized) (Boivin and Meunier, 2002; Boivin et al., 2003). This heterogeneity may limit microcrack propagation because more energy is needed to propagate a microcrack through a heterogeneously than a homogeneously mineralized material (Ural and Vashishth, 2014). However, interstitial (interosteonal) bone is less remodeled and becomes more highly mineralized and cross-linked with advanced glycation end products like pentosidine, both of which reduce the ductility of the matrix, facilitating microcrack propagation (Bailey et al., 1999; Banse et al., 2002; Nalla et al., 2004; Qui et al., 2005; Yeni et al., 1997; Viguet-Carrin et al., 2006).

The net effects of reduced periosteal apposition and endosteal bone loss

Over 80 years ago, Fuller Albright suggested that osteoporosis was a disorder of reduced bone formation (Albright et al., 1941). Research into the pathogenesis of bone fragility has focused on the role of bone resorption. During aging, reduced bone formation plays a central role in producing remodeling imbalance and so net bone loss takes place from the three components of the endosteal surface and reduced periosteal bone formation.

As age advances bone modeling by periosteal apposition continues, but much more slowly than during growth and much more slowly than endosteal bone loss. The net effect is an imperceptibly small increase in bone size but a reduction in total mineralized bone matrix volume and microstructural deterioration, with eventual almost complete loss of trabecular bone, cortical thinning, and a reduction in the number of cortical pores, but an increase in the cortical porosity as enlarging pores coalesce, so that all that is left is an eggshell rim of cortical bone (Balena et al., 1992; Seeman et al., 2003; Szulc et al., 2006).

Periosteal apposition is believed to increase as an adaptive response to compensate for the loss of strength produced by endocortical bone loss, so there will be no *net* loss of bone, no cortical thinning, and no loss of bone strength (Ahlborg et al., 2003). While this is often claimed, there are formidable challenges in identifying the existence of periosteal apposition during adulthood, its site specificity, its magnitude, and sex differences. In cross-sectional studies, secular changes in bone size may obscure or exaggerate periosteal apposition. Secular increases in stature are variously reported in one or both sexes, in some races but not others, and in the skeleton of the upper or lower body or both (Bakwin, 1964; Meredith, 1978; Cameron et al., 1982; Tanner et al., 1982; Malina and Brown, 1987).

These secular trends can produce misleading inferences when increments or lack of increments in bone diameters are used as surrogates of periosteal apposition. For example, in cross-sectional studies, the absence of an increment in periosteal diameter across age may not mean periosteal apposition failed to occur. Earlier born individuals (the elderly in a cross-sectional sample) are likely to have been shorter and to have had more slender bones than later born individuals (young normals in a cross-sectional sample). When periosteal apposition occurs, earlier born persons (forming the older subjects in a cross-sectional sample) with more slender bones have an increase in bone diameter that comes to equal that in later born persons (who have not yet had age-related periosteal apposition), leading to the flawed inference that there was no periosteal apposition.

When comparisons are made between sexes (or races) in cross-sectional studies, if the truth is that periosteal apposition is greater in men than in women but men have a secular increase in bone size and women do not, then the secular increase in men will blunt the increment in bone width across age in men and make it appear that the age-related increase in vertebral and femoral neck diameters (and so periosteal apposition) is similar in women and men.

Longitudinal studies are also problematic because changes in periosteal apposition during aging are small (Balena et al., 1992). The precision of methods to determine bone diameter, usually bone densitometry, and problems with edge detection when BMD is changing, limit the credibility of these measurements. Nevertheless, in one prospective study of over 600 women, Szulc et al. reported that endocortical bone loss occurred in premenopausal women with concurrent periosteal apposition (Szulc et al., 2006) (Fig. 11.10). As periosteal apposition was less than endocortical resorption, the cortices thinned but there was no *net* bone loss because the thinner cortex was now distributed around a larger perimeter, conserving total bone mass. Resistance to bending increased despite bone loss and cortical thinning, because this same amount of bone was now distributed farther from the neutral axis. So bone mass alone is a poor predictor of strength,

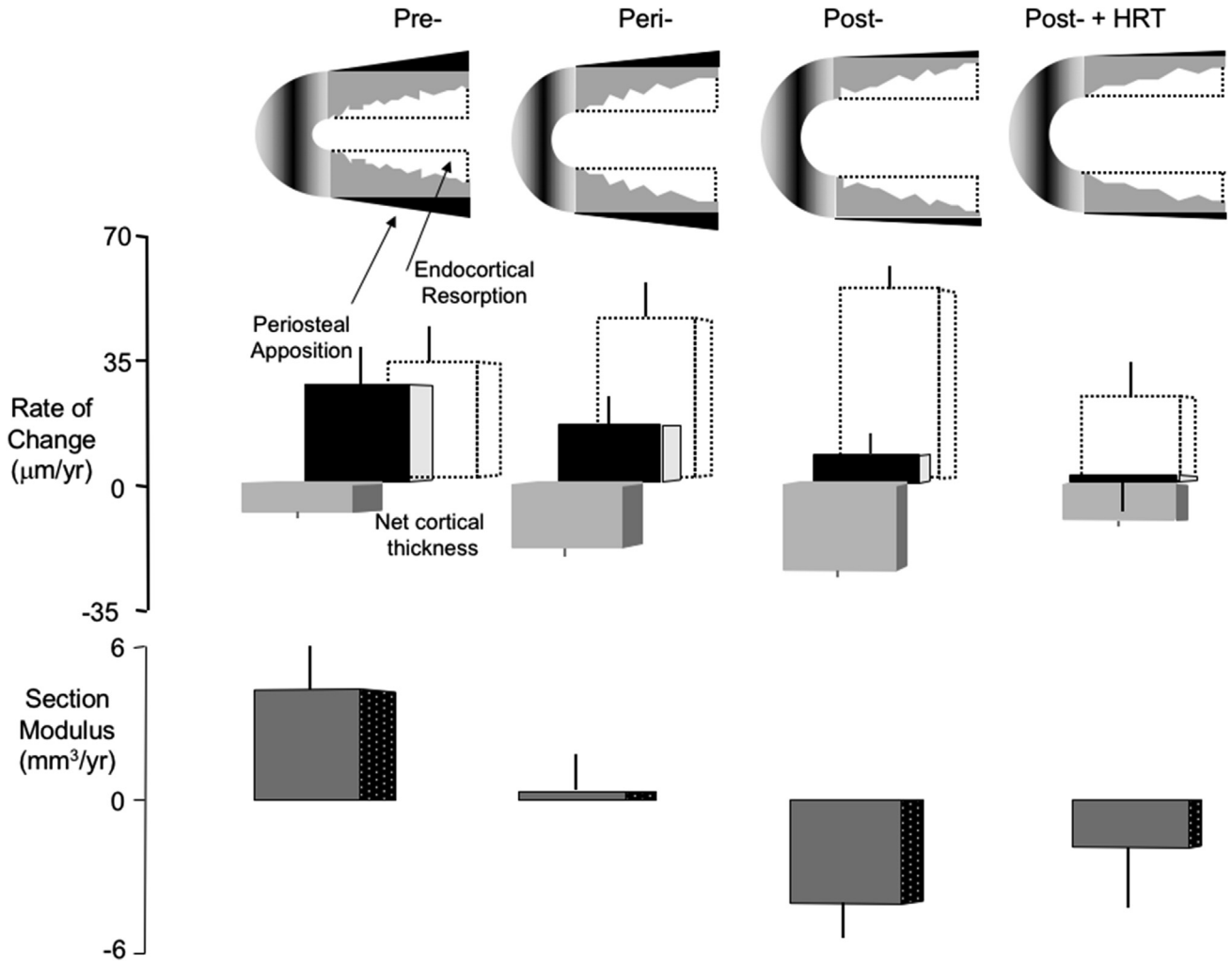

FIGURE 11.10 The amount of bone resorbed by endocortical resorption (*open bar*) increases with age. The amount deposited by periosteal apposition (*black bar*) decreases. The net effect is a decline in cortical thickness (*gray bar*). In premenopausal women, the thinner cortex is displaced radially, increasing section modulus (Z). In perimenopausal women Z does not decrease, despite cortical thinning, because periosteal apposition still produces radial displacement. In postmenopausal women, Z decreases because endocortical resorption continues, periosteal apposition declines, and little radial displacement occurs. In women treated with hormone replacement therapy (*HRT*), resorption is decreased with no effect on periosteal apposition. Z is less reduced than in untreated women. *Adapted from Szulc, P., Seeman, P., Duboeuf, F., Sornay-Rendu, E., Delmas, P.D., 2006. Bone fragility: failure of periosteal apposition to compensate for increased endocortical resorption in postmenopausal women. J. Bone Miner. Res. 21, 1856−1863.*

because resistance to bending is determined by the spatial distribution of the bone and increases as a fourth-power function of the radial distance a volume of bone is positioned from the neutral axis.

Endocortical resorption increased during the perimenopausal period, yet periosteal apposition decreased: it did not increase as expected if periosteal apposition is compensatory. The cortices thinned as periosteal apposition declined further. Nevertheless, bending strength remained unchanged, despite bone loss and cortical thinning, because periosteal apposition was still sufficient to shift the thinning cortex outward (Fig. 11.10).

Bone fragility emerged after menopause when acceleration in endocortical bone resorption and deceleration in periosteal apposition produced further net cortical thinning. As periosteal apposition was now minimal, there was little outward displacement of the thinning cortex, so cortical area now declined as did resistance to bending. Endocortical resorption was reduced but not abolished in women receiving hormone replacement therapy, while periosteal apposition was no different from that of untreated women; cortical thinning was reduced and the resistance to bending occurred, but less than in untreated women.

Periosteal envelope is not an exclusively bone-forming surface. During growth, bone resorption is critical for the in-wasting that produces the fan-shaped metaphyses (Rauch et al., 2001). Bliziotes and colleagues report that bone

resorption occurs in adult nonhuman primates (Blizoites et al., 2006). Femur specimens from 16 intact adult male and female nonhuman primates showed that periosteal remodeling of the femoral neck in intact animals was slower than in cancellous bone but more rapid than at the femoral shaft. Gonadectomized females showed an increase in osteoclast number on the periosteal surface compared with intact controls. If these data are correct, adult skeletal dimensions may decrease in size as age advances.

Sexual dimorphism in trabecular and cortical bone loss

A greater proportion of women than men sustain fragility fractures. Men have a larger skeleton than women so that resistance to bending is greater in men. Bone loss in both sexes is the result of remodeling imbalance but remodeling rate does not increase in midlife in men. If there is a transitory increase in the volume of bone resorbed by each BMU in women, this does not seem to be the case in men. So, trabecular thinning occurs in men, trabecular perforation with greater loss of trabecular strength occurs in women (Aaron et al., 1987; Van der Linden et al., 2001). Net trabecular bone loss across age is reported to be only slightly greater in women than in men (Riggs et al., 2004), or is similar (Aaron et al., 1987; Meunier et al., 1990; Kalender et al., 1989; Mosekilde and Mosekilde, 1990; Seeman, 1997; Seeman et al., 2001). However, measurement error is likely to produce this observation because greater intracortical remodeling with trabecularization of the cortex in women underestimates their loss of trabecular bone. Cortical porosity increases less in men than in women because remodeling rate is lower in men and so crack propagation in cortical bone is probably better resisted in men than in women. Research is needed because cortical porosity is underestimated by imaging methods that use threshold-based image analysis (Zebaze et al., 2013).

Thus, several methodological issues leave the question of the morphological basis of sex differences in bone fragility unanswered (Seeman et al., 2004). The absolute risks for fracture in women and men of the same age and BMD are similar (Kanis et al., 2001, 2005). If this is correct, then the reason fewer men than women suffer fractures in their lifetime is likely to be that fewer men than women have material and structural properties that cause bone fragility, such as high cortical porosity and low trabecular density. Structural failure occurs less often in men because the relationship between load and bone strength is better maintained in men than in women (Riggs et al., 2006; Bouxsein et al., 2006).

The heterogeneous material and structural basis of bone fragility in patients with fractures

Patients with fractures are grouped by having "one or more minimal trauma fractures" or sustaining a fall from "no greater than the standing position." However, the pathogenesis and structural basis of the bone fragility underlying the fractures are heterogeneous. Patients with fractures may have high, normal, or low remodeling rates (Brown et al., 1984; Arlot et al., 1990; Delmas, 2000). Some have a negative BMU balance due to reduced formation, increased resorption, or both, or no negative BMU balance (Ericksen et al., 1990). Some patients with fractures have increased, while others have reduced, matrix mineral density (Ciarelli et al., 2003) (Fig 11.11). Some patients have reduced osteocyte density, others do not (Qui et al 2003, 2005). Contemporary therapeutics gives no consideration to selecting a treatment based on the underlying pathogenesis or structural abnormalities of bone fragility. Consequently, there are no data to support the notion that selecting treatment according to the causes of bone fragility will lead to reducing the number needed to treat to avert one person from having a fracture.

Bone modeling, remodeling, and drug therapy

Antiresorptive therapy reduces the reversible but not the irreversible deficit in mineralized matrix volume

The effects of antiresorptive therapy are the reciprocal of the effects of menopause in several ways. When an antiresorptive agent is administered, the early accelerated increase in BMD is largely due to the rapid reduction in the reversible deficit in matrix and its mineral content. At the time of administration, the number of BMUs in their resorptive phase decreases in proportion to the antiresorptive efficacy of the drug. Bisphosphonates reduce remodeling by 50%–60% (as estimated using remodeling markers). The net effect of fewer new BMUs excavating resorption cavities and the many more resorption cavities excavated shortly before treatment concurrently entering their refilling phase is the rapid early net increase in BMD and reduction in cortical porosity reported during the first 6–12 months of treatment (Seeman, 2010).

The rise in BMD is often mistakenly interpreted as an increase in bone "mass" or "volume" and a restoration of microstructural deterioration. This is not the case; the incomplete refilling of cavities excavated just before treatment is the

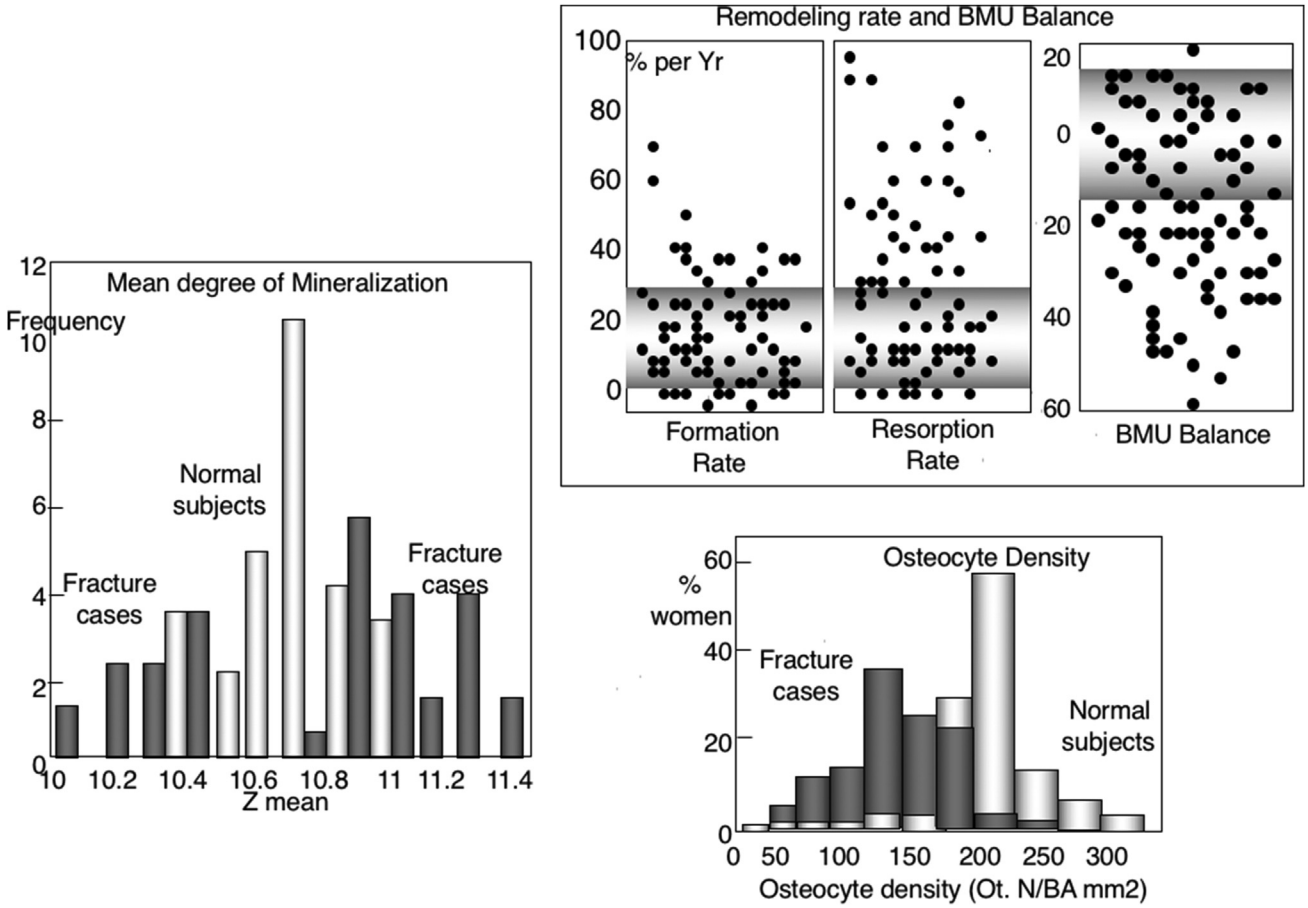

FIGURE 11.11 Bone fragility in patients with fractures has a heterogeneous pathogenesis and structural basis. Patients have tissue mineral density in the upper or lower part of the normal distribution. Some have reduced or normal osteocyte density. Formation and resorption rates may be lower normal or high; bone balance in the basic multicellular level (*BMU*) may be normal or negative. *Adapted from Ciarelli, T.E., Fyhrie, D.P., Parfitt, A.M., 2003. Effects of vertebral bone fragility and bone formation rate on the mineralization levels of cancellous bone from white females. Bone 32, 311–315. Qui, S., Rao, R.D., Saroj, I., Sudhaker, I., Palnitkar, S., Parfitt, A.M., 2003. Reduced iliac cancellous osteocyte density in patients with osteoporotic vertebral fracture. J. Bone Miner. Res. 18, 1657–1663. Eriksen et al. (1990).*

same in a treated and a placebo group. The reason BMD increases in the treated group is that fewer cavities are being excavated than are being incompletely refilled. BMD decreases in the control group because similar numbers of cavities are being excavated and incompletely refilled. In the treated group there is no change in the external or internal dimensions of bone; the periosteal perimeter does not increase, as occurs during growth or anabolic therapy; the endocortical perimeter does not decrease, as occurs during endocortical apposition using anabolic therapy; and trabeculae do not thicken.

There may be focal trabecular thickening at the remodeled location as incomplete refilling of the resorption cavity occurs due to the reversible component of the deficit. The irreversible deficit is not corrected, so that there is no focal restitution of the dimensions of a trabecular plate or cortical thickness to the level before menopause, because the remodeling imbalance is not corrected. Thickening above the premenopausal level would require overfilling of the resorption cavity. As antiresorptives may reduce the size of the resorption cavity, it is plausible that refilling or overfilling might occur (Allen et al., 2010). Even so, antiresorptives cannot reconstruct the skeleton because the remodeling rate is suppressed. Only about 5%–7% of the skeleton is remodeled annually.

The trabecular and cortical "thickening" often reported using imaging methods is an artifact produced by an increase in matrix mineral density (part of the reversible deficit in mineral), which leads to edge detection as photons are attenuated by the same deficit matrix that is now more densely mineralized (Seeman, 2010). Nevertheless, incomplete refilling of cavities may reduce stress risers and this may partly account for the rapid reduction in vertebral fracture risk achieved when remodeling is suppressed by antiresorptive agents.

As steady-state remodeling is restored at the new slower rate determined by the drug's antiresorptive efficacy, bone loss continues because the unsuppressed unbalanced remodeling continues to deteriorate the bone. Total bone matrix volume

decreases despite treatment. Moreover, matrix mineral density of the declining matrix volume increases due to continued secondary mineralization, which is part of the *reversible* deficit in *mineral*. So BMD continues to increase, obscuring the decrease in total bone matrix volume, and this increase may be mistaken as an increase in bone matrix mass or volume and a reversal of microstructural deterioration (Fig. 11.12).

The only antiresorptive that virtually abolishes bone loss is denosumab, because it is widely distributed and reduces osteoclast synthesis from its precursors and reduces the life span of osteoclasts existing at the time of treatment. Denosumab profoundly suppresses serum C-terminal telopeptide of type I collagen (CTX), so there is almost complete separation of the frequency distribution curves of serum CTX in treated and untreated subjects (Zebaze et al., 2014). This is not the case when alendronate is administered. About half of the women receiving alendronate had serum CTX no different from that of untreated controls, probably because of continued cortical bone loss despite alendronate treatment. Bisphosphonates bind avidly to mineral and fail to penetrate deep peri-Haversian cortical matrix (Smith, 2003). The concentrations of bisphosphonates are lower in cortical than in trabecular bone. When an osteoclast imbibes deeper cortical matrix its resorptive activity is not inhibited. In studies of nonhuman primates, ibandronate reduces remodeling upon endocortical and trabecular, but not Haversian canal, surfaces and improves trabecular, not cortical, bone strength (Smith et al., 2003).

As reported in human subjects and nonhuman primates, upon the return of steady state at a slow remodeling rate in the second 6 months of therapy, continued intracortical remodeling with alendronate probably accounts for cortical porosity no longer being lower than in controls by 12 months (Zebaze et al., 2014). With weak antiresorptive agents like calcium supplements or selective estrogen receptor modulators, the rate of remodeling is only modestly reduced relative to pretreatment, perhaps by 20%−30%; so after steady state is restored from its initial perturbed state, bone loss and microstructural deterioration continue, but only slightly more slowly than prior therapy (Reid et al., 2006; Silverman et al., 2012).

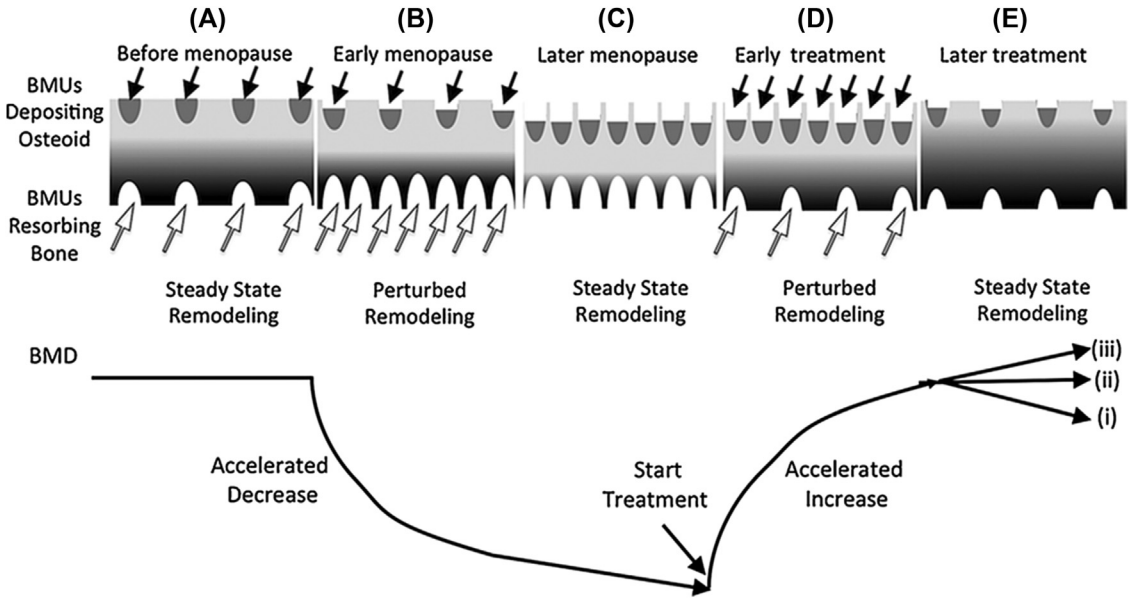

FIGURE 11.12 (A) Before menopause, remodeling is slow and in steady state. Similar numbers of sites are excavated (*white arrows*) and completely refilled (*black arrows*). No net bone loss occurs. (B) During early menopause, surface level remodeling is perturbed as more basic multicellular units (BMUs) resorb bone and each resorbs more bone (*white arrows*), while concurrently, the fewer cavities excavated before menopause now refill but do so incompletely (*black arrows*). Bone mineral density (*BMD*) decreases rapidly (bottom). (C) During later menopause, surface level remodeling returns to steady state but at a higher rate. The number of BMUs excavating bone approximately equals the number excavated in early menopause, only now refilling but doing so incompletely. Bone loss continues but more slowly. (D) During early antiresorptive therapy remodeling now becomes perturbed at the surface level but in a reciprocal fashion to early menopause. Fewer BMUs excavate smaller cavities (*white arrows*), while the many more BMUs excavating in later menopause refill incompletely (*black arrows*). BMD increases rapidly. (E) During later antiresorptive therapy, remodeling returns to steady state at the surface level at a slower rate, much like premenopause, but remodeling is unbalanced. The fewer and smaller cavities excavated during early antiresorptive treatment refill incompletely as similarly few new BMUs excavate smaller cavities. (i) If the negative BMU balance remains, BMD slowly declines from its higher level. (ii) If BMU balance is restored, there is no change in BMD. (iii) If remodeling remains unbalanced, secondary mineralization increases BMD, obscuring continued structural deterioration and the slow decrease in bone matrix volume.

With protracted remodeling suppression beyond the first 3 years, there is continued slow increase in BMD due to slow completion of secondary mineralization, which may take years (Akkus, 2004). Increases in matrix mineral density should become asymptotic with full mineralization of matrix after about 3−5 years of treatment (Dempster et al., 2018). During denosumab therapy there is continued increase in BMD reported after 5 years of treatment. This is not an anabolic effect of this antiresorptive agent. Studies of nonhuman primates suggest that age-related bone modeling upon the endocortical surface remains obscured by rapid remodeling prior to treatment and becomes detectable when remodeling is markedly suppressed by denosumab (Ominsky et al., 2015). Whether this occurs during treatment in human subjects remains uncertain.

Anabolic therapy: restoring the irreversible deficit in mineralized matrix volume and microstructural deterioration by remodeling- and modeling-based bone formation

Thus, the reversible deficit in matrix produced by the slowness of its deposition (∼3 months) and the slowness of matrix mineralization (taking ∼2 years), both respond to antiresorptive therapy. Slowing remodeling allows completion of the deposition of matrix and its complete mineralization. The irreversible deficit is not responsive to antiresorptive therapy. Reconstruction of the skeleton, "curing" bone fragility, requires anabolic therapy. Anabolic agents produce modeling- or remodeling-based bone formation.

Modeling-based bone formation occurs upon quiescent bone surfaces. Remodeling-based bone formation occurs within BMUs present at the time of treatment or by the initiation of new BMUs. Of necessity, the latter is preceded by the initial resorptive phase of remodeling removing mineralized bone by excavating a cavity within cortical bone or upon trabecular surfaces. Refilling of the cavity may correct the remodeling imbalance. If achieved, this will allow continued remodeling without causing microstructural deterioration. This will not reconstruct the skeleton.

Overfilling of existing and newly created cavities is needed to begin reconstruction of the skeleton, but this will result in focal reconstruction only. This approach is limited in scope because, at best, only 10%−20% of the skeleton is remodeled annually. Thus, reconstruction of an already deteriorated microstructure is a formidable challenge and probably requires sustained modeling-based bone formation.

Modeling upon the periosteal surface increases bone's total cross-sectional area, modeling upon the intracortical surface reduces intracortical porosity, modeling upon the endocortical surface thickens the cortex and increases its CSA. Modeling upon trabecular surfaces thickens them and may improve their connectivity, provided some connectivity is preserved at the time of treatment. Modeling upon surfaces of trabeculae abutting the cortex may "corticalize" them, thickening the cortex in a way that is the opposite of cortical trabecularization and cortical thinning from "within" the cortex during aging. Corticalization of trabeculae is similar to the formation of the metaphyseal cortex, which is the result of the coalescence of trabeculae emerging from the periphery of the growth plate (Cadet et al., 2003).

If successful, modeling produces an absolute increase in mineralized bone matrix volume, an increase in periosteal perimeter, a decrease in endocortical perimeter and medullary area, cortical thickening, a reduction in cortical porosity, and an increase in trabecular density. This differs from the increase in mineralized matrix density of a slowly diminishing total bone matrix volume produced by remodeling suppression using antiresorptive agents: both treatments increase BMD, but the morphological basis of the increase in BMD is of course very different and is likely to have different effects on bone strength.

About 80% of the total osteoid formed by parathyroid hormone (PTH) (1−34)- or PTH(1−84)-mediated bone formation is remodeling based. This is likely to be the same using abaloparatide, a peptide acting on the PTHR1 receptor that shares some of its amino acid sequence with PTH(1−34) and PTH-related protein (PTHrP) (Miller et al., 2016; Martin and Seeman, 2017). The proportion of the remodeling-based bone formation derived from anabolic agents acting on existing BMUs and newly generated BMUs resulting from PTH(1−34) treatment is uncertain, but the more rapid the remodeling, the greater the surface extent of remodeling, and the larger the number of existing BMUs at various stages of remodeling available to PTH.

During the resorptive phase of a remodeling cycle, PTH is likely to promote osteocyte and osteoblast precursor production of RANKL, osteoclastogenesis, bone resorption, and an increase in cortical porosity, until production of local factors from osteoclasts and the matrix they resorb influences bone formation. PTH acting on BMUs in their reversal phase may promote differentiation of osteoblast lineage cells into mature osteoid-producing forms. PTH acting on BMUs in their formation phase is likely to increase matrix production by inhibiting osteoblast apoptosis. Of necessity, BMU-based bone formation must follow resorption; the earlier increase in resorption markers is not a signal of the closure of a mythological "anabolic window." Excavated cavities upon endocortical or trabecular surfaces may refill or overfill, the latter thickening cortices and trabeculae focally.

Periosteal apposition is modest during adulthood and is advantageous because of the disproportionate increase in bending strength achieved by a small increment in bone diameter. However, there is no evidence that intermittent PTH produces measurable changes in periosteal circumference, even though there is evidence of increased apposition using quadruple labeling procedures (Lindsay et al., 2006).

Modeling-based bone formation upon intracortical canal surfaces may reduce canal diameter focally. However, many studies suggest that cortical porosity increases during early intermittent PTH therapy. Even though this increase in porosity is likely to be transient, bone fragility may increase transiently. Whether this occurs is not known. Trabecular thickening is likely to increase connectivity, provided some connectivity is present, but thickening may remain undetected by noninvasive imaging methods (that depend on photon attenuation by mineral) because replacement of older mineralized matrix with newly synthesized osteoid transmits rather than attenuates photons.

Abaloparatide, a peptide with partial amino acid homology to PTH(1−34) and PTHrP, has been reported to reduce the incidence of vertebral and nonvertebral fractures (Miller et al., 2016). There is no evidence quantifying the proportions of any anabolic effect due to existing BMUs at the time of treatment, newly generated BMUs in response to treatment, or modeling-based bone formation. A claim is made that the anabolic effect occurs with relatively less resorptive effect than observed using PTH(1−34). This is partly based on finding less of an increase in serum CTX relative to the increase in procollagen type 1 N-terminal propeptide (P1NP) in clinical trials in human subjects. The higher ratio of P1NP to CTX is inferred to be a surrogate of greater net bone formation relative to resorption, which in turn is responsible for the 1%−2% greater gain in BMD with abaloparatide than with PTH(1−34). These inferences are problematic for several reasons that are discussed elsewhere (Seeman, 2016; Martin and Seeman, 2017).

About 80% of the intracortical, endocortical, and trabecular components of the endosteal surface are quiescent and provide a vast surface area upon which osteoid can be deposited. Sclerostin antibodies (Scl-Abs) like romosozumab block the action of sclerostin, an inhibitor of bone formation. The anabolic effect is largely modeling based and is accompanied by a transient reduction in circulating serum CTX, suggesting that there is also a reduction in bone resorption. Ominsky et al. (2017) quantified the bone modeling and remodeling activity on bone surfaces in OVX rats administered vehicle or Scl-Ab (25 mg/kg) twice a week for 5 weeks, and in adolescent cynomolgus monkeys administered vehicle or Scl-Ab (30 mg/kg) subcutaneously every 2 weeks for 10 weeks. In OVX rats, Scl-Ab increased modeling eightfold from 7% to 63% of the bone surface. In cynomolgus monkeys, Scl-Ab increased modeling-based formation on trabeculae from 0.6% to 34% and on the endocortical surface from 7% to 77%. Scl-Ab did not increase remodeling-based bone formation despite decreased resorption surface in both species.

These observations have been confirmed by unpublished data reported by Chavassieux et al. (JBMR, 2019). The effects of 210 mg romosozumab on iliac crest histomorphometry at 2 and 12 months in postmenopausal women with osteoporosis were reported. For histomorphometry, 29 women had quadruple labeling at 2 m and 70 double labeling at 12 m. For microcomputed tomography (microCT), 28 women were evaluable at 2 m, and 71 at 12 m. At 2 months, bone formation rate increased in cancellous bone by 328% and by 233% upon endocortical surfaces. At 2 and 12 months, eroded surface decreased in cancellous and endocortical bone. At 12 months, wall thickness, bone mass, and trabecular and cortical thickness increased with romosozumab. At 2 months, microCT showed a decrease in trabecular separation; at 12 months, trabecular BMD, matrix density, and bone volume increased. There is robust evidence of vertebral and nonvertebral fracture risk reduction that appears to be more effective than that obtained with antiresorptive therapy or PTH(1−34) (Saag et al., 2017; Kendler et al., 2018). Details of the anti-fracture efficacy are presented elsewhere (Reid, 2015; Ramchand and Seeman, 2018).

Combined antiresorptive and anabolic therapy

Combining antiresorptive and anabolic therapy makes sense. The justification for any additional cost and exposure to the side effects of two drugs is evidence of greater fracture risk reduction than achieved by either drug alone. A prospective randomized blinded placebo-controlled trial is a formidable challenge to execute and has never been done. A lower level of evidence comes from animal experiments demonstrating that combined therapy increases the breaking strength of bone ex vivo more greatly than either drug alone. Only one study comparing PTH(1−34)/alendronate and PTH(1−34)/osteoprotegerin (OPG) versus PTH(1−34) alone has been reported. While trabecular bone volume increased more greatly than PTH(1−34) alone, bone strength assessed ex vivo in this study of rodents was not greater than that produced by PTH(1−34) alone (Samadfam et al., 2007).

Short of evidence of improved bone strength is morphological data showing that combined therapy produces a greater net increase in the volumes of bone deposited upon the periosteal surface and the three (intracortical, endocortical, and trabecular) components of the endosteal surface than therapy with either drug alone. Combined therapy has not been

reported to produce a greater periosteal perimeter, a smaller endocortical perimeter, increased cortical thickness and area, lower cortical porosity, or thicker, more connected, or greater numbers of trabeculae than therapy with either drug alone.

Most comparator studies have been done using changes in BMD, bone remodeling markers, or bone microstructure as the outcome. This approach is fraught with challenges because a change in BMD may be the result of a change in bone matrix volume, its mineral content, or both, and often, these traits change in the opposite direction, even with single therapy. For example, antiresorptives slow unbalanced remodeling; matrix volume continues to decrease and microstructure continues to deteriorate, but matrix mineral density increases, producing a net increase in BMD of the deteriorating structure. PTH(1−34) increases bone matrix volume but decreases its matrix mineral density as remodeling-based bone formation replaces older more mineralized bone with younger less mineralized bone. BMD has been reported variously to increase, decrease, or remain unchanged. Thus, the behavior of these traits even during single-drug therapy makes inferences about the effects on bone strength challenging, but more so when these drugs are combined.

Indeed, combined therapy has been reported to blunt the BMD response to PTH in some, but not all, studies. Blunting is held to be due to antiresorptive treatment suppressing remodeling so that remodeling-based bone formation by PTH(1−34) is prevented. Scrutiny of the data does not support this notion. If blunting of the BMD response was due to fewer BMUs, then blunting should be *more* severe with coadministration of PTH(1−34) with zoledronate, denosumab, or OPG than with alendronate. The opposite is reported (Tsai et al., 2015), and many studies report additive effects (Seeman and Martin, 2015). Blunting is not *greater* with denosumab/PTH(1−34) than with alendronate/PTH, even though denosumab suppresses remodeling more greatly than alendronate. Additive effects on BMD are reported with PTH/denosumab relative to PTH(1−34) alone (Tsai et al., 2015; Leder et al., 2014) and comparing PTH/OPG versus PTH (Kostenuik et al., 2001).

The difficulties using bone densitometry are only partly overcome by independently measuring changes in matrix mineral density and microstructure, because image acquisition and analysis using high-resolution peripheral computed tomography also depends on photon attenuation by a region's mineral content. Challenges in the interpretation of the effects of combined therapy are illustrated in the study by (Tsai et al., 2015; Leder et al., 2014).

These investigators report that combined therapy increased cortical vBMD. However, PTH reduced cortical vBMD, while denosumab had no detectable effect, leaving unexplained the increased cortical vBMD using combined therapy. Combined therapy increased cortical matrix mineral density, yet PTH decreased it, and denosumab had no detectable effect, again leaving unexplained the increased cortical matrix density using combined therapy. Combined therapy had no effect on porosity, yet PTH increased it, while denosumab had no detectable effect, leaving the combined effect unexplained. Finally, combined therapy increased cortical thickness, PTH had no detectable effect, but denosumab increased it; the opposite of what was expected.

The findings reasonably to be expected are as follows: for cortical vBMD combined therapy should have no net effect, because PTH increases porosity and reduces matrix mineral density; denosumab does the reverse. Combined therapy therefore should also have no net effect on cortical porosity or matrix mineral density, but should increase cortical thickness. Failure to detect an increase in cortical thickness is probably the result of replacement of mineralized bone with younger bone. Finding an increase in cortical thickness with denosumab is likely to be due to an edge detection error, as antiresorptives increase matrix mineral density, they do not thicken cortices. Most pores are <100 μm. At a resolution of 130 μm, voxels containing a pore or part of a pore also contain matrix and so attenuate photons above the threshold designated as "porosity."

Conclusion

Deterioration of the cellular machinery of modeling and remodeling compromises the many qualities of bone conferred by its material composition and structural design. For the past 60 years, the bone strength conferred by these qualities and the bone fragility resulting from their deterioration have been inferred using BMD. This was a good beginning because it provided a quantitative measure of fracture risk, but BMD is insensitive; most fractures occur in individuals with modest deficits in BMD. These individuals have fragile bones caused by microstructural deterioration. BMD does not capture this fragility because the loss of strength produced by microstructural deterioration is disproportionate to the bone loss producing it and the modest reductions in BMD. There is progress in image acquisition and quantification of microstructure, but whether measurement of microstructural deterioration improves detection of individuals at imminent risk for a first fracture and whether treatment allocation based on the severity of microstructural deterioration reduces the number of persons that need to be treated to avert one event remain unknown. Answers to these questions are needed because longevity and the burden of fractures are increasing. Antiresorptive agents neither reverse existing microstructural deterioration nor abolish its progression. These drugs only slow continued microstructural deterioration and reduce vertebral

and hip fracture risk by ~50%. For nonvertebral fractures, 80% of all fractures, the risk reduction is only 20%–30%. Teriparatide, the only anabolic agent widely available for clinical use, produces predominantly remodeling-based bone formation and transitory cortical porosity but may have better vertebral and nonvertebral anti-fracture efficacy than antiresorptives. The recently marketed abaloparatide reduces vertebral and nonvertebral fractures and is also likely to produce remodeling-based bone formation. Neither drug reduces the risk of hip fracture, the most devastating fracture. Modeling-based bone formation using romosozumab, an Scl-Ab, has antivertebral and nonvertebral fracture efficacy within 12 months. Whether anabolic agents in combination with antiresorptive agents offer better anti-fracture efficacy than either drug alone is not known. The challenge of reducing the burden of fractures remains an unmet need.

References

Aaron, J.E., Makins, N.B., Sagreiy, K., 1987. The microanatomy of trabecular bone loss in normal aging men and women. Clin. Orthop. Relat. Res. 215, 260–271.

Aguirre, J.I., Plotkin, L.I., Stewart, S.A., Weinstein, R.S., Parfitt, A.M., Manolagas, S.C., Bellido, T., 2006. Osteocyte apoptosis is induced by weightlessness in mice and precedes osteoclast recruitment and bone loss. J. Bone Miner. Res. 21, 605–615.

Ahlborg, H.G., Johnell, O., Turner, C.H., Rannevik, G., Karlsson, M.K., 2003. Bone loss and bone size after the menopause. N. Engl. J. Med. 349, 327–334.

Akkus, O., Polyakova-Akkus, A., Adar, F., Schaffler, M.B., 2003. Aging of microstructural compartments in human compact bone. J. Bone Miner. Res. 18, 1012–1019.

Akkus, O., Adar, F., Schaffler, M.B., 2004. Age-related changes in physicochemical properties of mineral crystals are related to impaired mechanical function of cortical bone. Bone 34, 443–453.

Albright, F., Smith, P.H., Richardson, A.M., 1941. Postmenopausal osteoporosis. J. Am. Med. Assoc. 116, 2465–2474.

Allen, M.R., Erickson, A.M., Wang, X., Burr, D.B., Martin, R.B., Hazelwood, S.J., 2010. Morphological assessment of basicmulticellular unit resorption parameters in dogs shows additional mechanisms of bisphosphonate effects on bone. Calcif. Tissue Int. 86 (1), 67–71.

Arlot, M.E., Delmas, P.D., Chappard, D., Meunier, P.J., 1990. Trabecular and endocortical bone remodelling in postmenopausal osteoporosis: comparison with normal postmenopausal women. Osteoporos. Int. 1, 41–49.

Bailey, A.J., Sims, T.J., Ebbesen, E.N., Mansell, J.P., Thomsen, J.S., Mosekilde, L., 1999. Age-related changes in the biochemical properties of human cancellous bone collagen: relationship to bone strength. Calcif. Tissue Int. 65, 203–210.

Bakwin, H., 1964. Secular increase in height: is the end in sight? Lancet 2, 1195–1196.

Balena, R., Shih, M.-S., Parfitt, 1992. Bone resorption and formation on the periosteal envelope of the ilium: a histomorphometric study in healthy women. J. Bone Miner. Res. 7, 1475–1482.

Banse, X., Sims, T.J., Bailey, A.J., 2002. Mechanical properties of adult vertebral cancellous bone: correlation with collagen intermolecular cross-links. J. Bone Miner. Res. 17, 1621–1628.

Baron, R., Tross, R., Vignery, A., 1984. Evidence of sequential remodeling in rat trabecular bone: morphology, dynamic histomorphometry, and changes during skeletal maturation. Anat. Rec. 208 (1), 137–145.

Bass, S., Delmas, P.D., Pearce, G., Hendrich, E., Tabensky, A., Seeman, E., 1999. The differing tempo of growth in bone size, mass and density in girls is region-specific. J. Clin. Investig. 104, 795–804.

Bass, S.L., Saxon, L., Daly, R., Turner, C.H., Robling, A.G., Seeman, E., 2002. The effect of mechanical loading on the size and shape of bone in pre-, peri- and post-pubertal girls: a study in tennis players. J. Bone Miner. Res. 17 (12), 2274–2280.

Bell, K.L., Loveridge, N., Power, J., Garrahan, N., Meggitt, B.F., Reeve, J., 1999. Regional differences in cortical porosity in the fractured femoral neck. Bone 24, 57–64.

Bjørnerem, Å., Wang, X., Bui, M., Ghasem-Zadeh, A., Hopper, J.L., Zebaze, R., Seeman, E., 2018. Menopause-Related Appendicular Bone Loss is Mainly Cortical and Results in Increased Cortical Porosity. J. Bone Miner. Res. 33 (4), 598–605.

Blizoites, M., Sibonga, J.D., Turner, R.T., Orwoll, E., 2006. Periosteal remodeling at the femoral neck in nonhuman primates. J. Bone Miner. Res. 21, 1060–1067.

Boivin, G., Lips, P., Ott, S.M., Harper, K.D., Sarkar, S., Pinette, K.V., Meunier, P.J., 2003. Contribution of raloxifene and calcium and vitamin D supplementation to the increase of the degree of mineralization of bone in postmenopausal women. J. Clin. Endocrinol. Metab. 88, 4199–4205.

Boivin, G., Meunier, P.J., 2002. Changes in bone remodeling rate influence the degree of mineralization of bone. Connect. Tissue Res. 43, 535–537.

Bolotin, H.H., Sievänen, H., 2001. Inaccuracies inherent in dual-energy x-ray absorptiometry in vivo bone mineral density can seriously mislead diagnostic/prognostic interpretations of patient –specific bone fragility. J. Bone Miner. Res. 16, 799–805.

Bouxsein, M.L., Melton 3rd, L.J., Riggs, B.L., Muller, J., Atkinson, E.J., Oberg, A.L., Robb, R.A., Camp, J.J., Rouleau, P.A., McCollough, C.H., Khosla, S., 2006. Age- and sex-specific differences in the factor of risk for vertebral fracture: a population-based study using QCT. J. Bone Miner. Res. 21 (9), 1475–1482.

Brockstedt, H., Kassem, M., Eriksen, E.F., Mosekilde, L., Melsen, F., 1993. Age- and sex-related changes in iliac cortical bone mass and remodeling. Bone 14 (4), 681–691.

Brown, J.P., Delmas, P.D., Arlot, M., Meunier, P.J., 1987. Active bone turnover of the cortico-endosteal envelope in postmenopausal osteoporosis. J. Clin. Endocrinol. Metab. 64, 954–959.

Brown, J.P., Delmas, P.D., Malaval, L., Edouard, C., Chapuy, M.C., Meunier, P.J., 1984. Serum bone gla-protein: a specific marker for bone formation in postmenopausal osteoporosis. Lancet i, 1091–1093.

Bui, M., Bjornerem, A., Ghasem-Zadeh, A., Dite, G.S., Hopper, J.L., Seeman, E., 2013. Architecture of cortical bone determines in part its remodelling and structural decay. Bone 55 (2), 353–358.

Burr, D.B., Turner, C.H., Naick, P., Forwood, M.R., Ambrosius, W., Hasan, S., Pidaparti, R., 1998. Does microdamage accumulation affect the mechanical properties of bone? J. Biomech. 31, 337–345.

Cadet, E.R., Gafni, R.I., McCarthy, E.F., McCray, D.R., Bacher, J.D., Barnes, K.M., et al., 2003. Mechanisms responsible for longitudinal growth of the cortex: coalescence of trabecular bone into cortical bone. J. Bone Joint Surg. Am. 85-A (9), 1739–1748.

Cameron, N., Tanner, J.M., Whitehouse, R.H., 1982. A longitudinal analysis of the growth of limb segments in adolescence. Ann. Hum. Biol. 9, 211–220.

Chavassieux, P., Chapurlat, R., Portero-Muzy, N., Roux, J.P., Garcia, P., Brown, J.P., Libanati, C., Boyce, R.W., Wang, A., Grauer, A., 2019. Bone-forming and antiresorptive effects of romosozumab in postmenopausal women with osteoporosis: bone histomorphometry and microcomputed tomography analysis after 2 and 12 months of treatment. J. Bone Miner. Res. doi: 10.1002/jbmr.3735. [Epub ahead of print]

Ciarelli, T.E., Fyhrie, D.P., Parfitt, A.M., 2003. Effects of vertebral bone fragility and bone formation rate on the mineralization levels of cancellous bone from white females. Bone 32, 311–315.

Clark, W.D., Smith, E.L., Linn, K.A., Paul-Murphy, J.R., Muir, P., Cook, M.E., 2005. Osteocyte apoptosis and osteoclast presence in chicken radii 0–4 days following osteotomy. Calcif. Tissue Int. 77, 327–336.

Compston, J.E., Yamaguchi, K., Croucher, P.I., Garrahan, N.J., Lindsay, P.E., Shaw, R.W., 1995. The effects of gonadotrophin releasing hormone agonists on iliac crest cancellous bone structure in women with endometriosis. Bone 16, 261–267.

Croucher, P.I., Garrahan, N.J., Mellish, R.W.E., Compston, J.E., 1991. Age-related changes in resorption cavity characteristics in human trabecular bone. Osteoporos. Int. 1, 257–261.

Currey, J.D., 2002. Bones. Structure and Mechanics. Princeton UP, New Jersey, pp. 1–380.

Curry, J.D., 1969. Mechanical consequences of variation in the mineral content of bone. J. Biomech. 2, 1–11.

Danova, N.A., Colopy, S.A., Radtke, C.L., Kalscheur, V.L., Markel, M.D., Vanderby Jr., R., McCabe, R.P., Escarcega, A.J., Muir, P., 2003. Degradation of bone structural properties by accumulation and coalescence of microcracks. Bone 33, 197–205.

Delmas, P.D., 2000. The use of biochemical markers in the evaluation of fracture risk and treatment response. Osteoporos. Int. 11 (Suppl. 1), S5–S6.

Dempster, D.W., Brown, J.P., Fahrleitner-Pammer, A., Kendler, D., Rizzo, S., Valter, I., Wagman, R.B., Yin, X., Yue, S.V., Boivin, G., 2018. Effects of long- term denosumab on bone histomorphometry and mineralization in women with postmenopausal osteoporosis. J. Clin. Endocrinol. Metab. 103, 2498–2509.

Diab, T., Condon, K.W., Burr, D.B., Vashishth, D., 2006. Age-related change in the damage morphology of human cortical bone and its role in bone fragility. Bone 38, 427–431.

Diab, T., Vashisha, D., 2005. Effects of damage morphology on cortical bone fragility. Bone 37, 96–102.

Doherty, M.,J., Ashton, B.A., Walsh, S., Beresford, J.N., Grant, M.E., Canfield, A.E., 1998. Vascular pericytes express osteogenic potential in vitro and in vivo. J. Bone Miner. Res. 13, 828–838.

Duan, Y., Wang, X.F., Evans, A., Seeman, E., 2005. Structural and biomechanical basis of racial and sex differences in vertebral fragility in Chinese and Caucasians. Bone 36, 987–998.

Eghbali-Fatourechi, G.Z., Lamsam, J., Fraser, D., Nagel, D.A., Riggs, B.L., Khosla, S., 2005. Circulating osteoblast lineage cells in humans. N. Engl. J. Med. 352, 1959–1966.

Eghbali-Fatourechi, G.Z., Moedder, U.I., Charatcharoenwitthaya, N., Sanyal, A., Undale, A.H., Clowes, J.A., Tarara, J.E., Khosla, S., 2007. Characterization of circulating osteoblast lineage cells in humans. Bone 40, 1370–1377.

Elmardi, A.S., Katchburian, M.V., Katchburian, E., 1990. Electron microscopy of developing calvaria reveal images that suggest that osteoclasts engulf and destroy osteocytes during bone resorption. Calcif. Tissue Int. 46, 239–245.

Emaus, N., Berntsen, G.K., Joakimsen, R., Fonnebo, V., 2005. Longitudinal changes in forearm bone mineral density in women and men aged 25–44 years: the Tromso Study, a population-based study. Am. J. Epidemiol. 162, 633–643.

Emaus, N., Berntsen, G.K., Joakimsen, R., Fonnebo, V., 2006. Longitudinal changes in forearm bone mineral density in women and men aged 45–84 years: the Tromso Study, a population-based study. Am. J. Epidemiol. 163 (5), 441–449.

Ericksen, E.F., 1986. Normal and pathological remodeling of human trabecular bone: three dimensional reconstruction of the remodelling sequence in normals and in metabolic disease. Endocr. Rev. 4, 379–408.

Eriksen, E.F., Hodgson, S.F., Eastell, R., Cedel, S.L., O'Fallon, W.M., Riggs, B.L., 1990. Cancellous bone remodeling in type I (postmenopausal) osteoporosis: quantitative assessment of rates of formation, resorption, and bone loss at tissue and cellular levels. J. Bone Miner. Res. 5, 311–319.

Eriksen, E.F., Langdahl, B., Vesterby, A., Rungby, J., Kassem, M., 1999. Hormone replacement therapy prevents osteoclastic hyperactivity: a histomorphometric study in early postmenopausal women. J. Bone Miner. Res. 14, 1217–1221.

Fantner, G., Hassen kam, T., Kindt, J.H., Weaver, J.C., Birkedal, H., Pechenik, L., Cutroni, J.A., Cidade, G.C., Stucky, G.D., Morse, D.E., Hansma, P.K., 2005. Nat. Mater. 4, 612–616.

Foldes, J., Parfitt, A.M., Shih, M.-S., Rao, D.S., Kleerekoper, M., 1991. Structural and geometric changes in iliac bone: relationship to normal aging and osteoporosis. J. Bone Miner. Res. 6, 759–766.

Fujikawa, Y., Quinn, J.M., Sabokbar, A., McGee, J.O., Athanasou, N.A., 1996. The human osteoclast precursor circulates in the monocyte fraction. Endocrinology 137, 4058–4060.

Fuller, K., Chambers, T.J., 1995. Localisation of mRNA for collagenase in osteocytic, bone surface and chondrocytic cells but not osteoclasts. J. Cell Sci. 106, 2221–2230.

Garn, S., 1970. The Earlier Gain and Later Loss of Cortical Bone. Nutritional Perspectives. Charles C. Thomas, Springfield, IL, pp. 3–120.

Garn, S.M., Sullivan, T.V., Decker, S.A., Larkin, F.A., Hawthorne, V.M., 1992. Continuing bone expansion and increasing bone loss over a two-decade period in men and women from a total community sample. Am. J. Hum. Biol. 4 (1), 57–67.

Garnero, P., Borel, O., Gineyts, E., Duboeuf, F., Solberg, H., Bouxsein, M.L., Christiansen, C., Delmas, P.D., 2006. Extracellular post-translational modifications of collagen are major determinants of biomechanical properties of fetal bovine cortical bone. Bone 38, 300–309.

Ghasem-Zadeh, A., Burghardt, A., Wang, X.F., Iuliano, S., Bonaretti, S., Bui, M., et al., 2017. Quantifying sex, race, and age specific differences in bone microstructure requires measurement of anatomically equivalent regions. Bone 101, 206–213.

Gilsanz, V., Gibbens, D.T., Carlson, M., Boechat, I., Cann, C.E., Schulz, E.S., 1987. Peak trabecular bone density: a comparison of adolescent and adult. Calcif. Tissue Int. 43, 260–262.

Gilsanz, V., Gibbens, D.T., Roe, T.F., Carlson, M., Senac, M.O., 1988. Vertebral bone density in children: effect of puberty. Radiology 166, 847–850.

Gilsanz, V., Roe, T.F., Stefano, M., Costen, G., Goodman, W.G., 1991. Changes in vertebral bone density in black girls and white girls during childhood and puberty. N. Engl. J. Med. 325, 1597–1600.

Gupta, H.S., Seto, J., Wagermier, W., Zaslansky, P., Boesecke, P., Fratzl, P., 2006. Cooperative deformation of mineral and collagen in bone at the nanoscale. Proc. Natl. Acad. Sci. U. S. A. 103 (47), 17741–17746.

Gupta, S.H., Wagermaier, W., Zickler, G.A., Raz-Ben Aroush, D., Funari, S.S., Roschger, P., Wagner, H.D., Fratzl, P., 2005. Nanoscale Deformation Mechanisms in Bone. Nano Lett. 5 (10), 2108–2111.

Haapasalo, H., Kontulainen, S., Sievanen, H., Kannus, P., Jarvinen, M., Vuori, I., 2000. Exercise-induced bone gain is due to enlargement in bone size without a change in volumetric bone density: a peripheral quantitative computed tomography study of the upper arms of male tennis players. Bone 27 (3), 351–357.

Han, Y., Cowin, S.C., Schaffler, M.B., Weinbaum, S., 2004. Mechanotransduction and strain amplification in osteocyte cell processes. Proc. Natl. Acad. Sci. U. S. A. 101 (47), 16689–16694.

Han, Z.-H., Palnitkar, S., Rao, D.S., Nelson, D., Parfitt, A.M., 1996. Effect of ethnicity and age or menopause on the structure and geometry of iliac bone. J. Bone Miner. Res. 11, 1967–1975.

Hattner, R., Epker, B.N., Frost, H.M., 1965. Suggested sequential mode of control of changes in cell behaviour in adult bone remodelling. Nature 963, 489–490.

Hauge, E.M., Qvesel, D., Eriksen, E.F., Mosekilde, I., Melsen, F., 2001. Cancellous bone remodelling occurs in specialized compartments lined by cells expressing osteoblastic markers. J. Bone Miner. Res. 16, 1575–1582.

Hazenberg, J.G., Freeley, M., Foran, E., Lee, T.C., Taylor, D., 2006. Microdamage: a cell transducing mechanism based on ruptured osteocyte processes. J. Biomech. 39, 2096–2103.

Hernandez, C.J., Gupt, A., Keaveny, T.M., 2006. A biomechanical analysis of the effects of resorption cavities on cancellous bone strength. J. Bone Miner. Res. 21, 1248–1255.

Howson, K.M., Aplin, A.C., Gelati, M., Alessandri, E.A., Nicosia, R.F., 2005. The postnatal rat aorta contains pericyte progenitor cells that form spheroidal colonies in suspension culture. Am. J. Cell Physiol. 289, 1396–1407.

Iuliano-Burns, S., Hopper, J., Seeman, E., 2008. Sexual Dimorphism in Bone Structure Is Present before Puberty: A Male:female Co-twin Study (Submitted for publication).

Kalender, W.A., Felsenberg, D., Louis, O., Lopez, O., Lopez, P., Klotz, E., Osteaux, M., Fraga, J., 1989. Reference values for trabecular and cortical vertebral bone density in single and dual-energy quantitative computed tomography. Eur. J. Radiol. 9, 75–80.

Kanis, J.A., Borgstrom, F., Zethraeus, Z., Johmell, O., Oden, A., Jonsson, B., 2005. Intervention thresholds for osteoporosis in men and women. Bone 36, 22–32.

Kanis, J.A., Johnell, O., Oden, A., Dawson, A., De laet, C., Jonsson, B., 2001. Ten year probabilities of osteoporotic fractures according to BMD and diagnostic thresholds. Osteoporos. Int. 12, 989–995.

Keaveney, T.M., 1998. Cancellous bone. In: Black, J., Hastings, G. (Eds.), Handbook of Biomaterials Properties. Chapman and Hall, London.

Keller, H., Kneissel, M., 2005. SOST is a target gene for PTH in bone. Bone 37, 148–158.

Kendler, D.L., Marin, F., Zerbini, C.A.F., Russo, L.A., Greenspan, S.L., Zikan, V., Bagur, A., Malouf-Sierra, J., Lakatos, P., Fahreieitner-Pammer, A., et al., 2018. Effects of teriparatide and risedronate on new fractures in post- menopausal women with severe osteoporosis (VERO): a multicentre, double- blind, double- dummy, randomised controlled trial. Lancet 391, 230–240.

Kholsa, S., Westendorf, J.J., Oursler, M.J., 2008. Building bone to reverse osteoporosis and repair fractures. J. Clin. Investig. 118 (2), 421–428.

Khosla, S., 2008. Building bone to rcverse osteoporosis and repair fractures. J. Clin. Investig. 118 (2), 421–428.

Kostenuik, P.J., Capparelli, C., Morony, S., Adamu, S., Shimamoto, G., Shen, V., Lacey, D.L., Dunstan, C.R., 2001. OPG and PTH(1-34) have additive effects on bone density and mechanical strength in osteopenic ovariectomized rats. Endocrinology 142, 4295–4304.

Kurata, K., Heino, T.J., Higaki, H., Väänänen, H.K., 2006. Bone marrow cell differentiation induced by mechanically damaged osteocytes in 3D gel-embedded culture. J. Bone Miner. Res. 21, 616–625.

Landis, W.J., 2002. The strength of a calcified tissue depends in part on the molecular structure and organization of its constituent mineral crystals in their organic matrix. Bone 30, 492–497.

Lane, N.E., Yao, W., Balooch, M., Nalla, R.K., Balooch, G., Habelitz, S., Kinney, J.H., Bonewald, L.F., 2006. Glucocorticoid-treated mice have localized changes in trabecular bone material properties and osteocyte lacunar size that are not observed in placebo-treated or estrogen-deficient mice. J. Bone Miner. Res. 21, 466–476.

Leder, B.Z., Tsai, J.N., Uihlein, A.V., Burnett-Bowie, S.A., Zhu, Y., Foley, K., Lee, H., Neer, R.M., 2014. Two years of denosumab and teriparatide administration in postmenopausal women with osteoporosis (The DATA Extension Study): a randomized controlled trial. J. Clin. Endocrinol Metab. 99, 1694−1700.

Lindsay, R., Cosman, F., Zhou, H., Bostrom, M.P., Shen, V.W., Cruz, J.D., Nieves, J.W., Dempster, D.W., 2006. A novel tetracycline labeling schedule for longitudinal evaluation of the short- term effects of anabolic therapy with a single iliac crest bone biopsy: early actions of teriparatide. J. Bone Miner. Res. 21, 366−373.

Lips, P., Courpron, P., Meunier, P.J., 1978. Mean wall thickness of trabecular bone packets in the human iliac crest: changes with age. Calcif. Tissue Res. 10, 13−17.

Lorenzo, J., 2000. Interactions between immune and bone cells: new insights with many remaining questions. J. Clin. Investig. 106, 749−752.

Loro, M.L., Sayre, J., Roe, T.F., Goran, M.I., Kaufman, F.R., Gilsanz, V., 2000. Early identification of children predisposed to low peak bone mass and osteoporosis later in life. J. Clin. Endocrinol. Metab. 85 (10), 3908−3918.

Malina, R.M., Brown, K.H., 1987. Relative lower extremity length in Mexican American and in American black and white youth. Am. J. Phys. Anthropol. 72, 89−94.

Manolagas, S.C., 2000. Birth and death of bone cells: basic regulatory mechanisms and implications for the pathogenesis and treatment of osteoporosis. Endocr. Rev. 21, 115−137.

Manolagas, S.C., 2006. Choreography from the tomb: an emerging role of dying osteocytes in the purposeful, and perhaps not so purposeful, targeting of bone remodeling. BoneKEy Osteovision 3 (1), 5−14.

Maresh, M.M., 1961. Bone, muscle and fat measurements. Longitudinal measurements of the bone, muscle and fat widths from roentgenograms of the extremities during the first six years of life. Pediatrics 28, 971−984.

Marotti, G., Cane, V., Palazzini, S., Palumbo, C., 1990. Structure-function relationships in the osteocyte. Ital. J. Miner. Electrolyte Metab. 4, 93−106.

Martin, R.B., 1984. Porosity and specific surface of bone. CRC Crit. Rev. Biomed. Eng. 10, 179−221.

Martin, T.J., Seeman, E., 2017. Abaloparatide is an anabolic, but does it spare resorption? J. Bone Miner. Res. 32, 11−16.

Martin, T.J., Sims, N.A., 2005. Osteoclast-derived activity in the coupling of bone formation to resorption. Trends Mol. Med. 11, 76−81.

Matsumoto, T., Kawamoto, A., Kuroda, R., Ishikawa, M., Mifune, Y., Iwasaki, H., Miwa, M., Horii, M., Hayashi, S., Oyamada, A., Nishimura, H., Murasawa, S., Doita, M., Kurosaka, M., Asahara, T., 2006. Therapeutic potential of vasculogenesis and osteogenesis promoted by peripheral blood CD34 positive cells for functional bone healing. Am. J. Pathol. 169, 1440−1457.

Meredith, H.V., 1978. Secular change in sitting height and lower limb height of children, youths, and young adults of Afro-black, European, and Japanese ancestry. Growth 42, 37−41.

Meunier, P.J., Sellami, S., Briancon, D., Edouard, C., 1990. Histological heterogeneity of apparently idiopathic osteoporosis. In: Deluca, H.F., Frost, H.M., Jee, W.S.S., Johnston, C.C., Parfitt, A.M.U.P.P. (Eds.), *Osteoporosis.* Recent Advances in Pathogenesis and Treatment, pp. 293−301. Baltimore.

Miller, P.D., Hattersley, G., Riis, B.J., Williams, G.C., Lau, E., Russo, L.A., Alexandersen, P., Zerbini, C.A.F., Hu, Ming-yi, Harris, A.G., Fitzpatrick, L.A., Cosman, F., Christiansen, C., 2016. Effect of abaloparatide versus placebo on new vertebral fractures in postmenopausal women with osteoporosis: a randomized clinical trial. JAMA 316, 722−733.

Mödder, U.I., Khosla, S., 2008. Skeletal stem cell/osteoprogenitor cells: current concepts, alternate hypotheses and relationsjip to the bone remodelling compartment. J. Cell. Biochem. 103 (2), 393−400.

Mosekilde, L., Mosekilde, L., 1990. Sex differences in age-related changes in vertebral body size, density and biochemical competence in normal individuals. Bone 11, 67−73.

Murray, P.D.F., Huxley, J.S., 1925. Self-differentiation in the grafted limb bud of the chick. J. Anat. 59, 379−384.

Nalla, R.K., Kruzic, J.J., Kinney, J.H., Ritchie, R.O., 2004. Effect of aging on the toughness of human cortical bone: evaluation by R-curves. Bone 35, 1240−1246.

Nishida, S., Endo, N., Yamagiwa, H., Tanizawa, T., Takahashi, H.E., 1999. Number of osteoprogenitor cells in human bone marrow markedly decreases after skeletal maturation. J. Bone Miner. Metab. 17, 171−177.

O'Brien, C.A., Jia, D., Plotkin, L.I., Bellido, T., Powers, C.C., Steward, S.Q., Manolagas, S.C., Weinstein, R.S., 2004. Glucocorticoids act directly on osteoblasts and osteocytes to induce their apoptosis and reduce bone formation and strength. Endocrinology 145, 1925−1941.

Ominsky, M.S., Boyce, R.W., Li, X., Ke, H.Z., 2017. Effects of sclerostin antibodies in animal models of osteoporosis. Bone 96, 63−75.

Ominsky, M.S., Libanati, C., Niu, Qing-Tian, Boyce, R.W., Kosteniol, P.J., Baron, R., Dempster, D.W., 2015. Sustained modeling-based bone formation during adulthood in cynomolgus monkeys may contribute to continuous BMD gains with denosumab. J. Bone Miner. Res. 30, 1280−1289.

Oreffo, R.O., Bord, S., Triffitt, J.T., 1998. Skeletal progenitor cells and ageing human populations. Clin. Sci. 94, 549−555.

Orwoll, E.S., 2003. Toward an expanded understanding of the role of the periosteum in skeletal health. J. Bone Miner. Res. 18, 949−954.

Otsura, S., Tamai, K., Yamazaki, T., Yoshjkawa, H., Kaneda, Y., 2007. Bone marrow-derived osteoblast progenitor cells in circulating blood contribute to ectopic bone formation in mice. Biochem. Biophys. Res. Commun. 354, 453−458.

Parfitt, A.M., 1984. Age-related structural changes in trabecular and cortical bone: cellular mechanisms and biomechanical consequences. Calcif. Tissue Int. 36, S123−S128.

Parfitt, A.M., 1996. Skeletal heterogeneity and the purposes of bone remodelling: implications for the understanding of osteoporosis. In: Marcus, R., Feldman, D., Kelsey, J. (Eds.), Osteoporosis. Academic, San Diego, CA, pp. 315−339.

Parfitt, A.A., 2001. The bone remodelling compartment: a circulatory function of bone lining cells. J. Bone Miner. Res. 16 (9), 1583−1585.

Parfitt, A.M., 2002. Targeted and non-targeted bone remodeling: relationship to basic multicellular unit origination and progression. Bone 30, 5–7.
Parfitt, A.M., Travers, R., Rauch, F., Glorieux, F.H., 2000. Structural and cellular changes during bone growth in healthy children. Bone 27, 487–494.
Pitsillides, A.A., 2006. Early effects of embryonic movement: 'a shot out of the dark'. J. Anat. 206, 417–431.
Pocock, N.A., Eisman, J.A., Hopper, J.L., Yeates, M.G., Sambrook, P.N., Eberl, S., 1987. Genetic determinants of bone mass in adults. A twin study. J. Clin. Investig. 80 (3), 706–710.
Qiu, S., Rao, D.S., Fyhrie, D.P., Palnitkar, S., Parfitt, A.M., 2005. The morphological association between microcracks and osteocyte lacunae in human cortical bone. Bone 37, 10–15.
Qui, S., Rao, R.D., Saroj, I., Sudhaker, 1., Palnitkar, S., Parfitt, A.M., 2003. Reduced iliac cancellous osteocyte density in patients with osteoporotic vertebral fracture. J. Bone Miner. Res. 18, 1657–1663.
Ramchand, S.K., Seeman, E., 2018. Advances and unmet needs in the therapeutics of bone fragily. Front Endocrinol. https://doi.org/10.3389/fendo.2018.00505.
Rauch, F., Neu, C., Manz, F., Schoenau, E., 2001. The development of metaphyseal cortex – implications for distal radius fractures during growth. J. Bone Miner. Res. 16, 1547–1555.
Reid, I.R., 2015. Short-term and long-term effects of osteoporosis therapies. Nat. Rev. Endocrinol. 11, 418–428.
Reid, I.R., Mason, B., Horne, A., Ames, R., Reid, H.E., Bava, U., Bolland, M.J., Gamble, G.D., 2006. Randomized controlled trial of calcium in healthy older women. Am. J. Med. 119, 777–785.
Riggs, B.L., Melton, L.J., Robb, R., Camp, J.J., Atkinson, E.J., McDaniel, L., Amin, S., Rouleau, P.A., Khosla, S., 2007. A population-based assessment of rates of bone loss at multiple skeletal sites: evidence for substantial trabecular bone loss in young women and men. J. Bone Miner. Res. 23, 205–214.
Riggs, B.L., Melton 3rd, L.J., Robb, R.A., Camp, J.J., Atkinson, E.J., Oberg, A.L., Rouleau, P.A., McCollough, C.H., Khosla, S., Bouxsein, M.L., 2006. Population-based analysis of the relationship of whole bone strength indices and fall-related loads to age- and sex-specific patterns of hip and wrist fractures. J. Bone Miner. Res. 21 (2), 315–323.
Riggs, B.L., Melton III., L.J., Robb, R.A., Camp, J.J., Atkinson, E.J., Peterson, J.M., Rouleau, P.A., McCollough, C.H., Bouxsein, M.L., Khosla, S., 2004. A population-based study of age and sex differences in bone volumetric density, size, geometry and structure at different skeletal sites. J. Bone Miner. Res. 19, 1945–1954.
Riggs, B.L., Wahner, H.W., Melton, L.J., Richelson, L.S., Judd, H.L., Offord, K.P., 1986. Rates of bone loss in the appendicular and axial skeletons of women: evidence of substantial vertebral bone loss before menopause. J. Clin. Investig. 77, 1487–1491.
Rodriguez, I., Palacios, J., Rodriguez, S., 1992. Transverse bone growth and cortical bone mass in the human prenatal period. Biol. Neonate 62–69.
Ruff, C.B., Hayes, W.C., 1988. Sex differences in age-related remodeling of the femur and tibia. J. Orthop. Res. 6, 886–896.
Ruppel, M.E., Burr, D.B., Miller, L.M., 2006. Chemical makeup of micro-damaged bone differs from undamaged bone. Bone 39, 318–324.
Saag, K.G., Petersen, J., Brandi, M.L., Karaplis, A.C., Lorentzon, M., Thomas, T., Maddox, J., Fan, M., Meisner, P.D., Grauer, A., 2017. Romosozumab or alendronate for fracture prevention in women with osteoporosis. N. Engl. J. Med. 377, 1417–1427.
Sacchetti, B., Funari, A., Michienzi, S., Di Cesare, S., Piersanti, S., Saggio, I., Tagliafico, E., Ferrari, S., Robey, P.G., Riminucci, M., Bianco, P., 2007. Marrow sinusoids can organise a hematopoietic microenvironment. Cell 131, 324–336.
Samadfam, R., Xia, Q., Goltzman, D., 2007. Co-treatment of PTH with osteoprotegerin or alendronate increases its anabolic effect on the skeleton of oophorectomized mice. J. Bone Miner. Res. 22, 55–63.
Schaffler, M.B., Burr, D.B., 1988. Stiffness of compact bone: effects of porosity and density. J. Biomech. 21, 13–16.
Schaffler, M.B., Majeska, R.J., 2005. Role of the osteocyte in mechanotransduction and skeletal fragility. Abst 20, p. 12. In: Proceedings of Meeting. Bone Quality: What Is It and Can We Measure It? Besthesda, Maryland May 2–3.
Seeman, E., 1997. From density to structure: growing up and growing old on the surfaces of bone. J. Bone Miner. Res. 12, 1–13.
Seeman, E., 1998. Growth in bone mass and size–are racial and gender differences in bone mineral density more apparent than real? J. Clin. Endocrinol. Metab. 83 (5), 1414–1419.
Seeman, E., 2003. Periosteal bone formation – a neglected determinant of bone strength. N. Engl. J. Med. 349, 320–323.
Seeman, E., 2010. Bone Morphology in Response to Alendronate as Seen by High-Resolution Computed Tomography: Through a Glass Darkly. J. Bone Miner. Res. 25 (12), 2277–2281.
Seeman, E., Bianchi, G., Adami, S., Kanis, J., Khosla, S., Orwoll, E., 2004. Osteoporosis in men-consensus is premature. Calcif. Tissue Int. 75, 120–122.
Seeman, E., Duan, Y., Fong, C., Edmonds, J., 2001. Fracture site-specific deficits in bone size and volumetric density in men with spine or hip fractures. J. Bone Miner. Res. 16 (1), 120–127.
Seeman, E., Hopper, J.L., Young, N.R., Formica, C., Goss, P., Tsalamandris, C., 1996. Do genetic factors explain associations between muscle strength, lean mass, and bone density? A twin study. Am. J. Physiol. 270 (2 Pt 1), E320–E327.
Seeman, E., Martin, T.J., 2015. Combined antiresorptive and anabolic therapy: a missed opportunity. J. Bone Miner. Res. 30, 753–764.
Silva, M.J., Brodt, M.D., Wopenka, B., Thomopoulos, S., Williams, D., Wassen, M.H., Ko, M., Kusano, N., Bank, R.A., 2006. Decreased collagen organization and content are associated with reduced strength of demineralized and intact bone in the SAMP6 mouse. J. Bone Miner. Res. 21, 78–88.
Silverman, S.L., Chines, A.A., Kendler, D.L., Kung, A.W., Teglbjærg, C.S., Felsenberg, D., Mairon, N., Constantine, G.D., Adachi, J.D., 2012. Sustained efficacy and safety of bazedoxifene in preventing fractures in postmenopausal women with osteoporosis: results of a 5-year, randomized, placebo-controlled study. Osteoporos Int. 23, 351–363.

Siris, E.S., Chen, Y.T., Abbott, T.A., Barrett-Connor, E., Miller, P.D., Wehren, L.E., Berger, M.L., 2004. Bone mineral density thresholds for pharmacological intervention to prevent fractures. Arch. Intern. Med. 164, 1108–1112.

Smith, S.Y., Recker, R.R., Hannan, M., Müller, R., Bauss, F., 2003. Intermittent intravenous administration of the bisphosphonate ibandronate prevents bone loss and maintains bone strength and quality in ovariectomized cynomolgus monkeys. Bone 32, 45–55.

Stenderup, K., Justesen, J., Eriksen, E.F., Rattan, S.I., Kassem, M., 2001. Number and proliferative capacity of osteogenic stem cells are maintained during aging and in patients with osteoporosis. J. Bone Miner. Res. 16, 1120–1129.

Suda, T., Takahashi, N., Udagawa, N., Jimi, E., Gillespie, M.T., Martin, T.J., 1999. Modulation of osteoclast differentiation and function by the new members of the tumor necrosis factor receptor and ligand families. Endocr. Rev. 20 (3), 345–357.

Suzuki, R., Domon, T., Wakita, M., 2000. Some osteocytes released from their lacunae are embedded again in the bone and not engulfed by osteoclasts during remodelling. Anat. Embrol. 202, 119–128.

Szulc, P., Seeman, P., Duboeuf, F., Sornay-Rendu, E., Delmas, P.D., 2006. Bone fragility: failure of periosteal apposition to compensate for increased endocortical resorption in postmenopausal women. J. Bone Miner. Res. 21, 1856–1863.

Tanner, J.M., Hayashi, T., Preece, M.A., Cameron, N., 1982. Increase in length of leg relative to trunk in Japanese children and adults from 1957 to 1977: comparison with British and with Japanese Americans. Ann. Hum. Biol. 9, 411–423.

Tatsumi, S., Ishii, K., Amizuka, N., Li, M., Kobayashi, T., Kohno, K., Ito, M., Takeshita, S., Ikeda, K., 2007. Targeted ablation of osteocytes induces osteoporosis with defective mechanotransduction. Cell Metabol. 5, 464–475.

Taylor, D., 1997. Bone maintenance and remodeling: a control system based on fatigue damage. J. Orthop. Res. 15, 601–606.

Tsai, J.N., Uihlein, A.V., Burnett-Bowie, S.A., Neer, R.M., Zhu, Y., Derrico, N., Lee, H., Bouxsein, M.L., Leder, B.Z., 2015. Comparative effects of teriparatide, denosumab, and combination therapy on peripheral compartmental bone density, microarchitecture, and estimated strength: the DATA-HRpQCT study. J. Bone Miner. Res. 30, 39–45.

Ural, A., Vashishth, D., 2014. Hierarchical perspective of bone toughness – from molecules to fracture. Int. Mater. Rev. 59 (5), 245–263.

Van der Linden, J.C., Homminga, J., Verhaar, J.A.N., Weinans, H., 2001. Mechanical consequences of bone loss in cancellous bone. J. Bone Miner. Res. 16, 457–465.

Vedi, S., Compston, J.E., Webb, A., Tighe, J.R., 1984. Histomorphometric analysis of dynamic parameters of trabecular bone formation in the iliac crest of normal British subjects. Metab. Bone Dis. Relat. Res. 5, 69–74.

Verborgt, O., Gibson, G.J., Schaffler, M.B., 2000. Loss of osteocyte integrity in association with microdamage and bone remodeling after fatigue damage in vivo. J. Bone Miner. Res. 15, 60–67.

Viguet-Carrin, S., Garnero, S.P., Delmas, P.D.D., 2006. The role of collagen in bone strength. Osteoporos. Int. 17, 319–336.

Wang, Q., Alen, M., Nicholson, P., Lyytikainen, A., Suurubuenu, M., Helkala, E., Suominen, H., Cheng, S., 2005a. Growth patterns at distal radius and tibial shaft in pubertal girls: a 2-year longitudinal study. J. Bone Miner. Res. 20 (6), 954–961.

Wang, X.F., Duan, Y., Beck, T., Seeman, E.R., 2005b. Varying contributions of growth and ageing to racial and sex differences in femoral neck structure and strength in old age. Bone 36 (6), 978–986.

Yeni, Y.N., Brown, C.U., Wang, Z., Norman, T.L., 1997. The Influence of bone morphology on fracture toughness of the human femur and tibia. Bone 21, 453–459.

Zebaze, R., Ghasem-Zadeh, A., Bohte, A., Iuliano-Burns, S., Mirams, M., Price, R.I., et al., 2010. Intracortical remodelling and porosity in the distal radius and post-mortem femurs of women: a cross-sectional study. Lancet 375 (9727), 1729–1736.

Zebaze, R., Ghasem-Zadeh, A., Mbala, A., Seeman, E., 2013. A new method of segmentation of compact-appearing, transitional and trabecular compartments and quantification of cortical porosity from high resolution peripheral quantitative computed tomographic images. Bone 54 (1), 8–20.

Zebaze, R.M., Jones, A., Knackstedt, M., Maalouf, G., Seeman, E., 2007. Construction of the femoral neck during growth determines its strength in old age. J. Bone Miner. Res. 22 (7), 1055–1061.

Zebaze, R.M., Jones, A., Welsh, F., Knackstedt, M., Seeman, E., 2005. Femoral neck shape and the spatial distribution of its mineral mass varies with its size: clinical and biomechanical implications. Bone 37 (2), 243–252.

Zebaze, R.M., Libanati, C., Austin, M., Ghasem-Zadeh, A., Hanley, D.A., Zanchetta, J.R., Thomas, T., Boutroy, S., Bogado, C.E., Bilezikian, J.P., Seeman, E., 2014. Differing Effects of Denosumab and Alendronate on Cortical and Trabecular Bone. Bone 59, 173–179.

Chapter 12

Aging and bone

Maria Almeida[1,2] and Stavros Manolagas[1,2]

[1]*Division of Endocrinology and Metabolism, Center for Osteoporosis and Metabolic Bone Diseases, University of Arkansas for Medical Sciences, Little Rock, AR, United States;* [2]*The Central Arkansas Veterans Healthcare System, Little Rock, AR, United States*

Chapter outline

Characteristics of the aged skeleton

Human

The proportion of elderly humans among the global population is now higher than at any time in history. Old age is a major risk factor for several chronic diseases, including osteoporosis, and increases exponentially the risk of fractures (Almeida et al., 2017; Niccoli and Partridge, 2012). Soon after the attainment of peak bone mass the balance between bone formation and bone resorption begins to progressively tilt in favor of the latter, in both women and men (Looker et al., 1998). This process is slowed by the presence of sex steroids and accelerates following menopause. The rate of bone loss due to the menopause is followed, within 5−10 years, by a slower phase of bone loss (Black and Rosen, 2016; Seeman, 2013). This later phase occurs also in men and causes structural deterioration of cortical bone, a significant portion of which is due to increased intracortical porosity (Bala et al., 2015). Postmenopausal women have greater cortical porosity than men over the age of 50 (Nirody et al., 2015; Shanbhogue et al., 2016). It is unknown, however, whether this difference is due to decreased estrogen levels. Importantly, about 80% of fractures occur in the appendicular skeleton, at regions containing large amounts of cortical bone.

A histological hallmark of aged human bone is decreased wall width, an index of the reduced amount of work performed by teams of osteoblasts (Lips et al., 1978; Parfitt, 1990). This is due primarily to an insufficient number of osteoblasts relative to the need for the replacement of bone created by increased osteoclastic resorption (Manolagas, 2000). Another common histologic feature of aged human bone is decreased osteocyte density (Manolagas and Parfitt, 2010; Qiu et al., 2002b). The decrease in osteocyte lacunar density in cortical bone with age correlates with microcrack accumulation (Vashishth et al., 2000). In contrast, a dense osteocyte network is associated with better bone material quality (Kerschnitzki et al., 2013). Mineralization of osteocyte lacunae, a process known as micropetrosis, may contribute to the decrease in osteocytes with age (Busse et al., 2010; Frost, 1960). Micropetrosis may be one potential outcome of osteocyte death; however, the conditions that cause it are unclear. Be that as it may, it is now abundantly clear that the integrity or lack thereof of the osteocyte network plays a major role in skeletal health and disease.

Principles of Bone Biology. https://doi.org/10.1016/B978-0-12-814841-9.00012-9

Rodents

Like humans, both female and male mice lose bone mass and strength with age. Aging female mice do not experience menopause, but become acyclic while retaining functional levels of estrogens (Almeida et al., 2017; Ucer et al., 2017). Androgen levels in aged male mice are maintained at a 20-fold higher level than in females (Nilsson et al., 2015). Yet, both female and male mice exhibit all of the major features of skeletal aging, including the decline of cancellous and cortical bone mass and the development of cortical porosity by 18 months of age (Almeida et al., 2007b; Ferguson et al., 2003; Glatt et al., 2007; Halloran et al., 2002; Jilka et al., 2010; Ucer et al., 2017). In C57BL/6J (B6) mice the accrual of bone mass occurs up to 6−7 months of age, and soon after bone mineral density starts to slowly decline at a constant rate until the end of life. Micro-computed tomography (microCT) analysis performed at about 12 months (equivalent to 40 years in humans; Dutta and Sengupta, 2016) shows that the marrow begins to expand and additional bone is slowly added to the periosteum, but the former exceeds the latter, leading to a thinner and more fragile cortex. The number of osteoclasts also decreases in cancellous bone with advancing age.

The structural and cellular features of aged bone in mice have been well characterized. Old age causes a decline in osteoblast number, bone formation rate, and wall width, which is seen in cancellous and endocortical bone surfaces of both female and male mice (Almeida et al., 2007b; Tiede-Lewis et al., 2017; Ucer et al., 2017). Osteoclast number, however, also declines with age in the cancellous compartment (Almeida et al., 2007b). Thus, an insufficient number of osteoblasts must be the key mechanism for the unbalanced remodeling and the age-dependent loss of cancellous bone.

It has been argued earlier that the endosteal surface of adult mice undergoes osteoclastic modeling but not basic multicellular unit (BMU)-based remodeling. Several lines of evidence refute this idea. Specifically, the endosteal surface of both 7- and 21-month-old B6 mice exhibits scalloped cement lines, which are associated with fluorochrome labeling, indicating that BMU-based remodeling of the endosteal surface persists with advancing age. Moreover, administration of osteoprotegerin to adult mice ablates both endosteal bone resorption and formation. The same is true in adult rats, as shown by histologic analysis of 12-month-old female Fischer-344 rats (Erben, 1996) and a strong inhibitory effect of risedronate on endosteal fluorochrome labeling in 15-month-old ovariectomized Sprague−Dawley rats (Baumann, 1995). The loss of bone at the endosteal surface is caused by inadequate filling of resorption cavities due to an increase in osteoclasts and decrease in osteoblasts (Li et al., 2015; Ucer et al., 2017). As is the case in humans (Han et al., 1997; Power et al., 2003), cortical thinning with aging in mice is due to loss of bone from the endosteal surface that exceeds the amount of bone added to the periosteal surface.

Another feature of skeletal aging in both female and male mice is an increase in cortical porosity (Ferguson et al., 2003; Jilka et al., 2014; Tiede-Lewis et al., 2017). Like humans, aged female mice exhibit higher cortical porosity than aged males (Piemontese et al., 2017). In female B6 mice, the number and size of pores are much higher in the femoral cortex of 21-month-old mice than in 7-month-old young adults. Large pores are especially prominent in the metaphyseal cortex. Unbalanced remodeling is most evident near the endosteal surface and leads to the penetration of the endosteal boundary and the trabecularization of the endocortical part of the cortex, similar to the situation in humans. In young adult mice, cortical capillaries formed during development persist in the cortex, and osteons arise only occasionally from these capillaries (Piemontese et al., 2017; Schneider et al., 2009). With advancing age, however, osteons exhibit several histologic hallmarks of remodeling activity, including osteoclasts and fluorochrome-labeled bone matrix adjacent to scalloped cement lines. Histologic and microCT imaging studies in aged mice suggest that new osteons may arise from preexisting cortical capillaries, from redirection of endosteal BMUs from the endosteal surface into the cortex in tandem with vascular invasion from the marrow, or from both mechanisms. However, murine osteons do not exhibit the numerous concentric lamellae that characterize the much larger osteons of human bone. Instead, they resemble rabbit osteons (Pazzaglia et al., 2015). The highly organized networks seen in humans are not present in murine osteons, perhaps due to the lack of a preexisting haversian system. Nevertheless, this is probably a consequence of body size rather than phylogenetic determinants.

Interestingly, genetic background greatly influences the gain or loss of murine cortical bone mass during growth, in old age, or following sex steroid deficiency (Li et al., 2005; Piemontese et al., 2017; Price et al., 2005). In contrast, genetic background does not influence trabecular bone loss (Piemontese et al., 2017). This and the evidence that an increase in bone resorption accounts for the loss of cortical, but not cancellous, bone with age, indicates that distinct molecular mechanisms underlie the age-dependent dysregulation of endosteal and trabecular remodeling in mice.

Bone cell aging

Cellular aging is frequently described as a decline in function due to the accumulation of damage to lipids, proteins, and DNA (Droge, 2002). Damage of long-lived cells, together with the cellular response to damage, is thought to be involved

in the functional deterioration of many tissues with advancing age (55). Mesenchymal progenitors and osteocytes are long-lived cells and, most likely, are more prone to suffer the damaging effects of aging. The declining osteoblast number in the aging skeleton has been attributed to a decrease in the number of mesenchymal stem cells (MSCs), defective proliferation/differentiation of progenitor cells, or diversion of these progenitors toward the adipocyte lineage (Almeida and O'Brien, 2013; Kassem and Marie, 2011).

The loss of functional adult stem/progenitor cells (Rossi et al., 2008; Sharpless and DePinho, 2007) might contribute to the defective regenerative capacity of different tissues with age. Indeed, old mice exhibit a reduction in the number, proliferative capacity, or differentiation potential of distinct stem cells such as germ-line (Ryu et al., 2006; Zhang et al., 2006), neuronal (Kuhn et al., 1996; Molofsky et al., 2006), hematopoietic (Morrison et al., 1996), and muscle progenitor cells (Conboy et al., 2003; Shefer et al., 2006). Genetic mutations, epigenetic changes, and the extrinsic environmental milieu alter stem cell function with aging (Goodell and Rando, 2015).

Osteocytes orchestrate bone resorption and formation via the production of receptor activator of nuclear factor κB (NF-κB) ligand (RANKL), sclerostin (Sost), and other factors. Osteocytes formed during growth are still present in the cortical bone of skeletally mature and of aged mice (Piemontese et al., 2017). Findings indicate that aging of osteocytes can affect their expression profile and, consequently, alter both bone resorption and bone formation (Farr et al., 2016; Piemontese et al., 2017).

Osteoblast progenitors

MSCs are generally defined by their ability to self-replicate and differentiate into chondrocytes, osteoblasts, and adipocytes (Caplan, 1991; Friedenstein et al., 1974). MSCs are found in the bone marrow and in the perivascular niche in multiple human organs (Crisan et al., 2008). Mesenchymal cells in the bone marrow of long bones in mice express smooth muscle α-actin, myxovirus resistance-1, leptin receptor, and/or collagen II, and give rise to osteoblasts on the bone surfaces (Grcevic et al., 2012; Ono et al., 2014; Park et al., 2012; Zhou et al., 2014). Of note, cells expressing leptin receptor are the source of the majority of osteoblasts and osteocytes in adult mice. However, the effects of aging in these or other adult skeletal MSC populations remain unknown.

Because of the very limited number of MSCs, and the laborious procedures required to isolate pure populations, cultures of bone marrow stromal cells from humans and rodents are commonly used as surrogates for progenitor cells. These cultures have been used to elucidate changes in MSCs with aging in both humans and rodents (Coipeau et al., 2009; Kasper et al., 2009; Sethe et al., 2006; Stenderup et al., 2003). Changes in the behavior of bone marrow−derived MSCs with aging, such as loss of potential to proliferate and differentiate, loss of capacity to form bone in vivo, and increased senescence, have been also reported (Coipeau et al., 2009; Kasper et al., 2009; Sethe et al., 2006; Stenderup et al., 2003). Multipotent cells derived from adipose tissue similarly show an age-dependent loss of self-renewal capacity as well as an increased propensity for adipogenesis (Huang et al., 2010). Furthermore, cultures of MSCs from patients with Hutchinson−Gilford progeria syndrome, a disease characterized by accelerated aging, exhibit defective ability to differentiate (Scaffidi and Misteli, 2008). Similar findings have been reported in murine models of progeria (Chen et al., 2013; Diderich et al., 2012).

The transcription factor Osterix1 (Osx1) is required for osteoblast differentiation. Bone marrow mesenchymal progenitor cells expressing Osx1 give rise to all osteoblast and adipocytes in bone (Horowitz et al., 2017; Xiong et al., 2011), suggesting that expression of Osx1 marks a bipotent progenitor. In a mouse model in which Osx1-expressing cells are labeled with a fluorescent protein, the number of these cells in the bone marrow greatly decreases between adulthood and old age (Kim et al., 2017). Moreover, the cells from old mice exhibit decreased proliferation and several markers of cellular senescence, as determined in freshly isolated cells. Notably, the decline in the number of Osx1-expressing cells with age is associated with a decrease in type H capillaries at the distal end of the arterial network, which are critical for the maintenance of perivascular osteoprogenitors (Kusumbe et al., 2014). Aging leads to an increase in the expression of peroxisome proliferator-activated receptor γ—the master transcription factor for adipogenesis—in Osx1-expressing progenitor cells (Kim et al., 2017), in line with their propensity to differentiate toward adipocytes. Indeed, an increase in marrow adipocytes is a well-established consequence of skeletal aging in humans and mice (Horowitz et al., 2017). It remains unclear, however, whether any of the changes noted in osteoblast progenitors contribute to the decrease in bone formation with age and whether they are functionally related to skeletal involution.

Osteocytes

Depending on their anatomical location, osteocyte life span in humans can range from a few months to several decades. Osteocytes are as old as the bone matrix in which they are embedded and this depends on the rate of remodeling at that site.

Within cancellous bone and remodeling cortical bone, a subset of osteoblasts becomes embedded in bone matrix with each remodeling cycle, thereby generating a fresh population of osteocytes within the new packet of bone. Osteocytes near the periosteum are derived from the osteoblasts that continuously expand the periosteum via modeling. As mentioned earlier, osteocyte survival and number decline with age in rodents and humans (Jilka et al., 2013; Noble et al., 1997; Qiu et al., 2002a). In aged mice, there is a concomitant and dramatic decrease in dendrite number per osteocyte. This effect is more severe in females compared with males (Tiede-Lewis et al., 2017). A loss of dendrites with age is also seen in neuronal cells and is associated with impaired nervous system function in a variety of disorders such as Parkinson's and Alzheimer's disease (Koleske, 2013; McNeill et al., 1988). Dendrite loss in neuronal disorders has been linked to defective autophagy (Coleman, 2013; Tang et al., 2014). Interestingly, young mice with defective autophagy in osteocytes show an aging bone phenotype, including reduced trabecular and cortical bone volume, increased cortical porosity, and loss of dendrites (Piemontese et al., 2016). Nevertheless, it remains unknown whether loss of dendrites is causally related to the low bone mass in this model or in wild-type aged mice.

Because of the difficulty in isolating pure populations of osteocytes, there has been little quantitative information on molecular damage in osteocytes from aged mice. Based on the evidence that osteocytes control bone resorption via RANKL and bone formation via sclerostin, reduced osteocyte number might lead to altered production of these factors, leading to changes in bone remodeling. The levels of sclerostin decrease in cortical bone with age (Piemontese et al., 2017). However, the low sclerostin levels should promote Wnt signaling and thereby osteoblast formation; yet osteoblast number is reduced with age. In contrast to sclerostin, RANKL expression levels in cortical bone increase with age, consistent with the increase in endocortical bone resorption. The increase of RANKL along with an increase in other cytokines, chemokines, and metalloproteinases indicates that aging alters the synthetic capacity of osteocytes.

Although the cellular and molecular mechanisms responsible for the increase in cortical porosity with age remain unclear, there is evidence to suggest that osteocytes are the mediators of this effect. Increased osteocyte apoptosis, perhaps in response to age-dependent bone microdamage, is thought to contribute to the development of cortical porosity (Bentolila et al., 1998; Cardoso et al., 2009; Jilka and O'Brien, 2016). This notion is based on evidence that apoptotic osteocytes release factors that stimulate RANKL production by neighboring viable osteocytes. The age-dependent increases in RANKL and cortical porosity are exacerbated in female mice with apoptosis-resistant osteocytes (Jilka et al., 2014), probably due to accumulation of damaged osteocytes that cannot complete the apoptotic death program. Senescent osteocytes might be also involved in the activation of de novo intracortical remodeling via the senescence-associated secretory phenotype (SASP) (see section on "Cellular senescence"). As of this writing, there is no explanation for the lower porosity in male compared with female mice, in the face of a seemingly equivalent increase in osteocyte senescence in both sexes. Similarly, the highly variable magnitude and preferential development of cortical porosity near the metaphyses remain unexplained. In addition, it remains unclear why these mechanisms have different effects on the rate of remodeling in cancellous versus cortical bone.

Molecular mechanisms of aging

The time-dependent accumulation of cellular damage is widely considered the general cause of aging (Gems and Partridge, 2013; Lithgow and Kirkwood, 1996; Vijg and Campisi, 2008). Nevertheless, the sources of aging-caused damage, the compensatory responses that attempt to reestablish homeostasis, the interconnection between the different types of damage and compensatory responses, and the optimal means to intervene exogenously to delay aging remain unknown. Nonetheless, several cellular and molecular hallmarks of aging have been identified (Kennedy et al., 2014; Lopez-Otin et al., 2013). A hallmark should ideally fulfill the following criteria: it should manifest during normal aging, its experimental aggravation should accelerate aging, and its experimental amelioration should delay aging. Below, we review evidence that aging hallmarks such as mitochondrial dysfunction, cell senescence, and loss of proteostasis contribute to skeletal involution with old age.

Mitochondrial dysfunction

The mitochondrial free radical theory of aging proposes that as cells and organisms age, the efficacy of the respiratory chain diminishes, thus reducing ATP generation and increasing electron leakage and production of reactive oxygen species (ROS) (Green et al., 2011; Harman, 1956). The respiration-produced free radicals cause damage to macromolecules, resulting in cellular and tissue loss of function observed during aging (Balaban et al., 2005; Droge, 2002). The majority of cellular ROS are generated by the mitochondria during oxidative phosphorylation. H_2O_2 is the most stable and abundant form of ROS and is produced from the conversion of superoxide by superoxide dismutase enzymes (Balaban et al., 2005;

Chance et al., 1979; D'Autreaux and Toledano, 2007). ROS are also produced in other cellular compartments by NADPH oxidases, lipoxygenases, and other enzymes, in response to growth factors and cytokines (Janssen-Heininger et al., 2008). To prevent excessive ROS production, cells scavenge ROS by multiple mechanisms, including superoxide dismutases and catalase as well as thiol-containing oligopeptides with redox-active sulfhydryl moieties. The most abundant of the last are glutathione and thioredoxin (Dickinson and Forman, 2002).

Several lines of evidence have called into question the idea that an increase in ROS limits life span at the organismal level. Specifically, mouse models of increased mitochondrial ROS and oxidative damage do not exhibit accelerated aging (Van Remmen et al., 2003; Zhang et al., 2009). In addition, increased ROS may prolong life span in lower organisms (Doonan et al., 2008; Mesquita et al., 2010). In line with these observations, ROS can trigger proliferation and survival in response to physiological signals and stress conditions (Sena and Chandel, 2012). Nevertheless, many other studies indicate that oxidative stress is responsible for age-related pathologies, including diabetes, cardiovascular disease, cancer, and neurodegeneration (Dai et al., 2014; Lee et al., 2010; Schriner et al., 2005; Wanagat et al., 2010). A reevaluation of these apparent contradictory lines of evidence posits that the primary effect of ROS is the activation of compensatory homeostatic responses. Above certain threshold levels, ROS betray their original homeostatic purpose and exacerbate, rather than ameliorate, the age-associated damage (Hekimi et al., 2011; Salmon et al., 2010). This new conceptual framework accommodates seemingly conflicting evidence regarding the positive, negative, or neutral effects of ROS on aging.

It has been well established that ROS play a role in osteoclast differentiation and bone resorption (Garrett et al., 1990). RANKL and macrophage colony-stimulating factor—the two critical cytokines for osteoclast generation—promote mitochondrial biogenesis and the accumulation of H_2O_2 in osteoclasts, and H_2O_2 stimulates osteoclastogenesis (Bartell et al., 2014; Garrett et al., 1990; Ha et al., 2004; Ishii et al., 2009; Lee et al., 2005). The increase in H_2O_2 by proosteoclastogenic cytokines is due to an Akt-mediated inhibition of FoxO transcription factors, which causes a decrease in the expression of antioxidant enzymes (Bartell et al., 2014; Liu et al., 2005; Tan et al., 2015). Importantly, lowering H_2O_2 generation in osteoclasts, by overexpressing human catalase targeted to the mitochondria, reduces osteoclast numbers and increases bone mass (Bartell et al., 2014).

As in other tissues, skeletal aging is associated with an increase in ROS levels in bone cells (Almeida et al., 2007b; Jilka et al., 2010; Lean et al., 2003, 2005; Manolagas, 2010). The loss of bone mass caused by sex steroid deficiency in mice is also associated with an increase in ROS (Almeida et al., 2007b; Lean et al., 2003; Manolagas, 2010; Yamasaki et al., 2009). These findings raised the possibility that elevated ROS may be a common mechanism of the adverse effects of sex steroid deficiency and old age on bone; and that sex steroid deficiency may accelerate the effects of aging. Studies involving administration of antioxidants or decreasing mitochondrial levels of H_2O_2 (by expressing a mitochondria-targeted catalase transgene) have revealed that mitochondrial ROS are required for the increase in osteoclast number and the loss of bone caused by ovariectomy or orchidectomy. Surprisingly, however, mitochondrial ROS in osteoclasts do not contribute to the adverse effects of aging on either cortical or cancellous bone. Attenuation of H_2O_2 generation in cells of the mesenchymal lineage, on the other hand, ameliorates the age-dependent decline in mineralizing surfaces and prevents the loss of cortical bone. Together, these studies have indicated a major role of ROS in the bone loss associated with aging and estrogen deficiency. Yet, the evidence that distinct cell types are implicated in the effects of ROS within each condition suggests that the cellular and molecular mechanisms responsible for the loss of bone mass with aging and estrogen deficiency are distinct.

Oxidative stress decreases the life span of an osteoblast, as evidenced by the observation that administration of antioxidants abrogates osteoblast apoptosis in ovariectomized or aged mice (Almeida et al., 2007b; Jilka et al., 2010). ROS also inhibit the Wnt/β-catenin signaling pathway, which is indispensable for osteoblastogenesis during development and adulthood (Baron and Kneissel, 2013). Wnt proteins bind to the Frizzled/low-density lipoprotein (LDL) receptor—related protein 5 (LRP5) or LRP6 receptor complex, thereby preventing the degradation of the transcriptional coactivator β-catenin (Clevers and Nusse, 2012). In the nucleus β-catenin associates with the T cell factor (TCF) lymphoid-enhancer binding factor family of transcription factors and regulates the expression of Wnt target genes. In the setting of oxidative stress or nutrient depletion, FoxOs divert the limited pool of active β-catenin from TCF- to FoxO-mediated transcription in diverse cell types, including osteoblasts, colon cancer cells, and hepatocytes (Almeida et al., 2007a; Hoogeboom et al., 2008; Liu et al., 2011). In murine models of targeted deletion of FoxOs in osteoblast progenitors FoxOs restrain the pro-proliferative effects of Wnt signaling and attenuate bone formation (Iyer et al., 2013). Likewise, FoxOs in enteroendocrine progenitors or in neuronal progenitors suppress β-catenin/TCF-mediated transcription and proliferation (Paik et al., 2009; Talchai et al., 2012). Thus, diversion of β-catenin from TCF- to FoxO-mediated transcription in response to stressful conditions, such as increased ROS and growth factor deficiency, may represent a pathogenetic mechanism for osteoporosis. Support for this idea is provided by the evidence that mice that lack FoxOs in the osteoblast lineage maintain high bone mass throughout life (Iyer et al., 2013).

Cellular senescence

Cellular senescence is a process in which cells stop dividing and initiate a gene expression pattern known as SASP (Campisi, 2013; Kuilman et al., 2010; Lopez-Otin et al., 2013; Newgard and Sharpless, 2013). An increase in senescent cells occurs in most tissues with age; however, its impact on age-related diseases and longevity has remained unknown until recently. Senescent cells can be identified by several features, including cell cycle arrest, DNA damage foci that contain phosphorylated histone H2AX, activated ataxia−telangiectasia mutated (ATM) kinase ATM(Ser^{1981}), p53 binding protein, activated p53 (phospho-Ser^{15}), elevated levels of the cell cycle inhibitor $p21^{CIP1}$ or $p16^{INK4a}$, and high senescence-associated β-galactosidase activity. Although none of these markers is, in and of itself, specific or universal for all senescent types, there is a clear consensus that senescent cells express most of them (Campisi, 2013; Childs et al., 2015; Munoz-Espin and Serrano, 2014). Another characteristic of senescent cells is a resistance to apoptosis. Notably, postmitotic cells also exhibit key characteristics of senescence. For example, neurons in various parts of human and mouse brains are known to accumulate high amounts of DNA damage (Sedelnikova et al., 2004) along with other senescence-associated markers, including heterochromatinization, accumulation of GATA4 and activation of NF-κB, synthesis of proinflammatory interleukins, and senescence-associated β-galactosidase activity (Jurk et al., 2012). Senescence-like features are similarly seen in adipocytes of mice on a high-fat diet (Minamino et al., 2009).

Selective elimination of senescent cells expressing p16 in mice, through an INK-ATTAC or p16-3MR transgene, has revealed that senescent cells reduce organismal life and health span (reviewed in Childs et al., 2017). For example, genetic depletion of senescent cells rejuvenates the hematopoietic stem cells (HSCs), counters frailty and the loss of renal function in aged mice, diminishes cancer relapse, and prevents the development of atherosclerosis and osteoarthritis (Baar et al., 2017; Chang et al., 2016; Childs et al., 2016; Demaria et al., 2017; Jeon et al., 2017). The evidence that genetic ablation of senescent cells counters the effects of aging has prompted a rush to the discovery of small molecules that can selectively kill senescent cells (Baker et al., 2011; Zhu et al., 2015). These drugs, called senolytics, have the potential to be novel antiaging agents. Ablation of senescent cells using senolytics delays age-related pathologies in naturally aged mice, similar to the elimination of senescence with genetic means (Baar et al., 2017; Baker et al., 2011, 2016; Jeon et al., 2017; Ogrodnik et al., 2017; Schafer et al., 2017).

In vitro studies using serially passaged bone marrow−derived stromal cells have suggested that cells from aged humans become senescent at earlier passages compared with cells from young individuals (Stenderup et al., 2003; Zhou et al., 2008). However, because serial passaging by itself causes replicative senescence (Hayflick and Moorhead, 1961), it has remained unclear whether osteoblast progenitors become senescent with old age in vivo. As we discussed earlier, studies using freshly isolated osteoprogenitor cells have elucidated that the age-related decline in number of these cells is associated with several markers of senescence, including DNA damage foci, G1 cell cycle arrest, activated p53, and elevated levels of $p21^{CIP1}$. Markers of senescence, including elevated p16 and expression of the SASP, were also present in osteocyte-enriched bone fractions from old mice. Elimination of p16-expressing cells in 20-month-old mice, using the INK-ATTAC transgene or senolytics, increases bone mass (Farr et al., 2017). This effect is associated with a decrease in osteoclasts and an increase in osteoblasts at the endocortical surfaces.

One of the causes of senescence is DNA damage. Of all DNA lesions, DNA double-strand breaks are the most harmful. DNA double-strand breaks can be induced by radiation, radiomimetic chemicals, or ROS, but also during DNA replication when a polymerase encounters a single-strand lesion at a replication fork (Jackson, 2002). DNA double-strand breaks pose problems for cells because their immediate and efficient repair by ligation is often constrained by their physical separation and/or the need to process damaged DNA termini (Mine-Hattab and Rothstein, 2012; Soutoglou and Misteli, 2008). In the absence of repair, damaged cells can be eliminated by apoptosis. Alternatively, mitotically active cells respond to DNA double-strand breaks by becoming senescent. DNA damage triggers a repair response known as the DNA damage response (DDR). This response is characterized by the activation of ATM and the recruitment of RAD-3-related kinase (or ATR) (Rouse and Jackson, 2002) to the site of damage, leading to phosphorylation of Ser^{139} of histone H2AX molecules adjacent to the site of DNA damage. The phosphorylation of histone H2AX activates the transducer kinases Chk1 and Chk2, which converge on p53/p21 and p16 (Smogorzewska and de, 2002). In addition, the DDR stimulates the SASP by upregulating GATA4 and NF-κB (Kang et al., 2015).

Markers of DNA damage increase with age in both osteoprogenitors and osteocytes and are associated with cell senescence (Kim et al., 2017; Piemontese et al., 2017). While it remains unclear whether DNA damage is indeed the cause of skeletal cell senescence, DNA damage induced by irradiation causes changes in osteoprogenitors that are similar to the ones seen with aging (Kim et al., 2017). In addition, DNA damage due to focal irradiation in long bones causes senescence of osteoblast lineage cells, decreases bone formation, and leads to bone loss in mice (Chandra et al., 2017). Additional support for the deleterious effects of DNA damage on the skeleton is provided from the phenotype of murine models of

progeroid syndromes due to defective DNA damage repair. For example, a mouse model of trichothiodystrophy (Diderich et al., 2012; Nicolaije et al., 2012; Wijnhoven et al., 2005) exhibits features of accelerated aging, including loss of trabecular and cortical bone mass and a reduction in bone strength, from 9 months onward. Similar observations have been made in a murine model of Werner syndrome (Brennan et al., 2014). Bone marrow–derived osteoblastic cell cultures from these models exhibit increased senescence (Chen et al., 2013; Saeed et al., 2011). Nevertheless, caution should be exercised in interpreting results from progeroid mice, as several of these models exhibit impaired growth, poor health, and short life spans (Chen et al., 2013; Niedernhofer et al., 2006; Saeed et al., 2011). Furthermore, not all the cellular features of natural aging are replicated in the progeroid models. Specifically, the loss of trabecular bone mass in several progeroid models is associated with an increase in osteoclast number, which is not seen with natural aging (Almeida et al., 2007b; Brennan et al., 2014; Chen et al., 2013; Saeed et al., 2011).

Together these lines of evidence implicate cellular senescence in the loss of bone mass with age. Future work should elucidate the cell targets and the molecular mechanisms mediating the effects of senescence in skeletal aging. These studies should also clarify the extent to which elimination of cell senescence ameliorates the loss of bone mass with age.

Loss of autophagy

Proteostasis, the process by which cells control the abundance and folding of the proteome, is maintained by proteolytic systems, such as the ubiquitin–proteasome system and the autophagy–lysosomal system, both of which decrease in old age (Cuervo, 2008; Morimoto and Cuervo, 2014). These changes occur in age-related diseases characterized by the accumulation of intracellular or extracellular protein aggregates, including neurodegeneration. These observations have led to the idea that a decline in proteostasis is a common mechanism of aging.

Autophagy is a quality control system that removes defective organelles or protein aggregates to maintain the health and viability of the cell (Yang and Klionsky, 2010). However, under stress conditions, for example, hypoxia or nutrient deprivation, autophagy increases to break down cellular components that can be reused as an energy source. During macroautophagy large components of the cytoplasm, including protein aggregates and mitochondria, are surrounded by a double-membrane structure to form a vacuole known as an autophagosome. This structure then fuses with the lysosome to allow the degradation of its components. Autophagosome formation is controlled by a ubiquitin-like protein known as LC3 (Geng and Klionsky, 2008), which, in turn, is activated by the E1-like enzyme Atg7 and is eventually conjugated to phosphatidylethanolamine in the double-membrane structure. This process is dependent on Atg7, and genetic inactivation of Atg7 effectively abrogates autophagy (Komatsu et al., 2007). Other forms of autophagy include chaperone-mediated autophagy and microautophagy (Levine and Kroemer, 2008). Chaperone-mediated autophagy targets proteins containing a specific five-amino-acid motif directly to the lysosome for degradation. Microautophagy is characterized by invagination of the lysosomal membrane to engulf small portions of the cytoplasm. Because macroautophagy is the most prevalent form of autophagy in many cell types, hereafter, we will use the general term autophagy to refer to this particular process.

Many organisms show signs of decreased autophagic capacity with aging in tandem with the accumulation of damaged cellular components, suggesting that a decline in autophagy may contribute to organismal aging (Cuervo, 2008; Hansen et al., 2018; Lopez-Otin et al., 2013). Specifically, expression of autophagy-related genes declines in muscle tissue from aged humans and in the hypothalamus, muscle, liver, and osteoarthritic bone chondrocytes from aged rodents (Carames et al., 2015; Carnio et al., 2014; Cuervo and Dice, 2000). Furthermore, suppression of autophagy in neurons or myocytes mimics the effects of aging on the nervous or muscle tissue, respectively (Carnio et al., 2014; Komatsu et al., 2007).

Deletion of ATG7 in osteoblasts and osteocytes decreases cancellous and cortical bone mass (Onal et al., 2013). These changes are associated with lower osteoclast and osteoblast numbers in cancellous bone. In addition, ROS levels are increased in the bones of mice lacking autophagy in osteocytes. This is probably due to the accumulation of damaged mitochondria, which in turn produce more ROS. Nevertheless, autophagy exerts positive effects on the skeleton by mechanisms other than suppression of H_2O_2 levels in the mitochondria of osteoblasts and osteocytes (Piemontese et al., 2016). Strikingly, deletion of Atg7 in the entire osteoblast lineage using an Osx1-Cre transgene causes fractures and decreases bone mass. The low-bone-mass phenotype is more pronounced than the one of mice in which ATG7 is deleted from mature osteoblasts and osteocytes (Piemontese et al., 2016). Lack of autophagy in early progenitors of osteoblasts alters osteocyte cell body morphology and reduces the extent of osteocyte cellular projections, suggesting that autophagy contributes to the transition of osteoblasts into osteocytes.

A critical role for autophagy in bone homeostasis is further supported by evidence that mice with deletion of ATG5 or the focal adhesion kinase family–interacting protein of 200 kDa (FIP200) in cells of the osteoblast lineage have compromised autophagy and low bone mass (Liu et al., 2013; Nollet et al., 2014).

Autophagy is important for the long-term health of stem cells as well as fully differentiated long-lived cell types. For example, autophagy is required for the maintenance of the HSC compartment in adult mice (Mortensen et al., 2011; Warr et al., 2013). The FoxO transcription factors are critical for the expression of autophagy genes and the induction of autophagy in response to stress in HSCs and other cell types (Warr et al., 2013; Zhao et al., 2008). It is possible that autophagy plays a similar role in the maintenance of MSCs in bone and this may underlie changes in MSC behavior with age.

In conclusion, suppression of autophagy in the osteoblast lineage is sufficient to replicate in young adult mice the skeletal changes observed in aged wild-type mice. Future studies will be required to identify the molecular mechanisms by which autophagy in cells of the osteoblast lineage controls bone remodeling and bone mass and whether autophagy does indeed decline with age in osteocytes or other cell types of the lineage.

Contribution of bone extrinsic mechanisms to skeletal aging

Loss of sex steroids

A decrease in estrogen levels at menopause, or both estrogens and androgens in elderly men, causes an imbalance between bone resorption and formation, leading to loss of bone mass and strength and increased risk of osteoporotic fractures (Almeida et al., 2017; Khosla, 2010; Manolagas, 2000; Manolagas et al., 2013; Vanderschueren et al., 2014). Within 5−10 years after menopause, the slope of the decline of bone mass in women slows and becomes indistinguishable from the slope of bone loss seen in elderly males. This slower phase of bone loss in both sexes later in life affects primarily the cortical compartment and is characterized by cortical thinning as well as increased cortical porosity (Nicks et al., 2012; Zebaze et al., 2010). Consequently, after the age of 65 most fractures are nonvertebral and predominantly occur at cortical sites (Zebaze et al., 2010).

Estrogens and androgens slow the rate of bone remodeling, and estrogen or androgen deficiency accelerates it. In addition, cell and biochemical studies have revealed that the antiremodeling effects of these two hormones result from their ability to restrain the birth rate of osteoclasts and shorten their life span (Almeida et al., 2017; Hughes et al., 1996; Manolagas, 2000, 2010, 2013). Conditional deletion models of the estrogen receptor α or the androgen receptor have provided critical new insights into the cellular targets of sex steroid action in vivo (Almeida et al., 2013; Chiang et al., 2009; Maatta et al., 2013; Martin-Millan et al., 2010; Nakamura et al., 2007; Notini et al., 2007; Sinnesael et al., 2012; Ucer et al., 2015). This body of work, reviewed elsewhere (Almeida et al., 2017), has produced two seminal but unexpected findings. First, the effects of estrogens and androgens on the cancellous bone compartment are mediated via different cell types. In females, estrogens protect against the loss of cancellous bone via direct actions on cells of the osteoclast lineage. In males, on the other hand, androgens protect against the loss of cancellous bone via actions on mature osteoblasts or osteocytes. Second, in both females and males, estrogens alone protect against the resorption of cortical bone, via actions on osteoprogenitors. In males, the estrogens responsible for this effect derive from the aromatization of androgens. In support of this conclusion, administration of estrogens to orchidectomized B6 mice prevents the loss of cortical thickness, while administration of dihydrotestosterone has no effect (Ucer et al., 2017). Notably, in men, estrogens account for ~70% and testosterone for at most ~30% of the protective effect of sex steroids on bone resorption (Khosla, 2015), remarkably consistent with the fact that the skeleton is ~80% cortical and ~20% cancellous.

Because of the abrupt decline in ovarian function at menopause in women and a slower decline of both androgen and estrogen levels in men with advancing age, the two conditions inexorably overlap, making it impossible to dissect their independent contributions to the cumulative anatomic deficit. Experiments using B6 mice ovariectomized at 4 or 18 months of age have elucidated that at least up to the age of 19.5 months mice remain functionally estrogen sufficient (Ucer et al., 2017). Six weeks following the loss of ovarian function at either age, we observed the expected decrease in uterine weight and increase in body weight in both young and old mice. Nonetheless, femoral cortical thickness and vertebral cancellous bone volume declined and cortical porosity increased in the estrogen-sufficient mice between 5.5 and 19.5 months of age. These findings clearly show that in mice the adverse effects of aging are independent of sex steroid status.

The canonical inhibitor of NF-κB kinase β/NF-κB pathway plays a seminal role in the SASP (Salminen et al., 2012). As discussed earlier under "Cellular senescence," the transcription factors GATA4 and NF-κB are major activators of the SASP (Kang et al., 2015). GATA4 protein levels, NF-κB activity, and the expression of common SASP genes are increased in both bone marrow stromal cells and osteocytes from old B6 mice (Farr et al., 2016; Kim et al., 2017; Piemontese et al., 2017). In line with these findings, the number of osteoclasts formed in cocultures of macrophages with

bone marrow−derived stromal cells is higher when stromal cells originate from old mice compared with cells from young mice (Cao et al., 2005; Kim et al., 2017). Estrogens suppress NF-κB activation via direct interactions of the estrogen receptor α with NF-κB (De Bosscher et al., 2006; Stice and Knowlton, 2008). Moreover, some of the same cytokines of the SASP have been implicated in the loss of cortical bone caused by estrogen deficiency (Almeida et al., 2017). It is, therefore, quite likely that in the aged skeleton, senescence of mesenchymal lineage cells and the SASP, driven by NF-κB activation, are the predominant mechanism of the increased osteoclast number and resorption in the endosteal surface. Because NF-κB is also upregulated by estrogen deficiency, the two pathologies may act in concert. In other words, NF-κB may be a key molecular nexus where the two pathologies intersect, and as a result estrogen deficiency accelerates the adverse effects of aging on cortical bone in both sexes.

Lipid peroxidation and declining innate immunity

ROS-induced oxidative damage causes lipid peroxidation and thereby produces highly reactive degradation products, including oxidized phosphatidylcholine, malondialdehyde (MDA), and 4-hydroxynonenal (Witztum and Lichtman, 2014). These neoepitopes interact with amino groups of proteins and other lipids to create oxidation-specific epitopes (OSEs). The same neoepitopes occur on apoptotic cell bodies. OSEs are part of a larger group of proinflammatory molecules, collectively known as damage-associated molecular patterns (DAMPs), that are produced in response to cellular stressors, including oxidative stress. DAMPs share structural homology with another group of moieties present on microbes and collectively known as pathogen-associated molecular patterns (PAMPs). Because of their shared molecular signatures, PAMPs and DAMPs bind to evolutionarily conserved pattern recognition receptors (PRRs) of the innate immune system.

Natural antibodies (nAbs) of the innate immune system are the first line of defense against microbial pathogens. nAbs are produced by B-1 lymphocytes and are predominantly of the IgM class. The antigen binding sites of nAbs are generated by rearrangement of germ-line-encoded variable-region genes in the complete absence of foreign antigen exposure, hence the term "natural" as opposed to antibodies produced by the "adaptive" immune system. As opposed to the adaptive immune system, nAbs have only a limited repertoire of binding specificities (Ehrenstein and Notley, 2010; Vas et al., 2013). nAbs are soluble PRRs that recognize OSEs and block their adverse effects.

When OSEs are not neutralized and/or their production is excessive, relative to the capacity of the innate immune system, the physiologic response is overwhelmed and becomes instead a disease-causing mechanism (Witztum and Lichtman, 2014). A series of clinical studies has provided compelling evidence that anti-OSE-specific IgM antibodies made by B-1 cells play a role in the development of disease in humans, as they do in mice (Binder et al., 2016; Griffin et al., 2011). Indeed, OSE-specific natural IgM antibodies protect against cardiovascular disease (Tsiantoulas et al., 2014), and titers of IgM antibody against oxidized LDL (OxLDL) and MDA−LDL are inversely correlated with cardiovascular disease (Karvonen et al., 2003; Tsimikas et al., 2007). In particular, anti-PC (phosphocholine) IgM levels are inversely correlated with cardiovascular disease risk in patients with systemic lupus erythematous (Anania et al., 2010; Gronwall et al., 2012), stroke (Fiskesund et al., 2010), and heart attacks (de Faire et al., 2010; Fiskesund et al., 2012; Gronlund et al., 2009; Imhof et al., 2015). Notably, in humans, B-1 cells decline with age (Griffin et al., 2011), raising the possibility that declining levels of nAbs against OSEs contribute to the pathogenesis of age-related diseases.

Hyperlipidemia leads to atherogenesis by promoting the formation of oxidized forms of LDL and phospholipids. These oxidation-modified moieties, in turn, induce potent inflammatory responses in the subendothelial matrix of the arteries, thereby triggering the pathogenetic changes that are ultimately responsible for the generation of the atherosclerotic lesions (Steinberg and Witztum, 2010). Consistent with this mechanism, genetic animal models of hyperlipidemia exhibit disruption of normal lipoprotein regulation and metabolism. Indeed, B6 mice maintained on an atherogenic high-fat diet, or genetically modified B6 mice lacking the LDL receptor or its ligand (ApoE), develop hyperlipidemia and atherosclerosis as a result of reduced clearance of non−high-density lipoproteins (Tintut and Demer, 2014).

Osteoporosis and atherosclerosis are epidemiologically linked (Makovey et al., 2009; Tintut and Demer, 2014). Moreover, bone mineral density and LDL-cholesterol levels are inversely correlated in mice as well as rats (Liu et al., 2016; Tintut and Demer, 2014). Diet-induced hyperlipidemia adversely affects bone growth and bone mineral density in these models. In line with the evidence for an adverse effect of lipids on bone, lipid accumulation has been demonstrated by histochemical staining in the subendothelial spaces of haversian canals from patients with osteoporosis (Tintut et al., 2004). Based on this evidence, it has been hypothesized that, similar to the situation in the subendothelial space of the vasculature, lipids accumulating in the subendothelial spaces of the haversian canals undergo nonenzymatic modifications, such as oxidation by ROS, rendering them capable of inducing inflammatory responses. Oxidized lipids may then induce

bone loss by inhibiting the differentiation of bone-forming osteoblasts and promoting the differentiation of bone-resorbing osteoclasts (Almeida et al., 2009; Liu et al., 2016).

Witztum and colleagues have generated transgenic mice that overexpress a single-chain variable fragment of the IgM nAb E06 (Que et al., 2018). The fragment is secreted from liver and macrophages and achieves sufficient plasma levels to inhibit macrophage uptake of OxLDL. High-fat diet—fed LDL receptor—null mice expressing E06 develop less atherosclerosis compared with controls. Importantly, high-fat diet—induced bone loss is also attenuated in mice expressing the E06 transgene due to an increase in osteoblast number and bone formation (Ambrogini et al., 2018). More strikingly, E06-scFv increases bone mass in mice fed a normal diet. Moreover, the levels of anti-PC IgM decrease in aged mice. These results indicate that OSEs chronically occurring with or without a high-fat diet in mice exert a restraining effect on bone formation. Moreover, the age-related bone loss might be due in part to diminished innate immune system defense against OSEs. Taken together with the evidence that the same nAbs prevent atherosclerosis, these discoveries demonstrate that anti-OSE nAbs may well represent a novel therapeutic approach against atherosclerosis and osteoporosis simultaneously.

Decreased physical activity

Mechanical strains are critical signals for bone mass accrual and strength (Frost, 2003). Mechanical loading tilts the balance between bone formation and resorption in favor of the former, by stimulating bone formation and suppressing bone resorption (Robling et al., 2006; Rubin and Lanyon, 1985; Zhao et al., 2013). For example, exposure to frequent high-impact loading increased bone mass in the dominant arm of tennis players (Ireland et al., 2013; Jones et al., 1977). Conversely, unloading due to lack of ambulation or weightlessness during space flights causes a marked reduction in bone mass, due to decreased bone formation and increased bone resorption (Lang et al., 2004; LeBlanc et al., 1990). A decrease in physical activity with aging, most likely, contributes to skeletal fragility. Exercise that is beneficial to bone in premenopausal women is typically not effective in elderly women (Korpelainen et al., 2006; Vainionpaa et al., 2007). Likewise, in animals the stimulatory effects of loading on bone are greater in growing or young adult animals compared with older ones (Holguin et al., 2014; Meakin et al., 2014; Razi et al., 2015; Rubin et al., 1992; Turner et al., 1995). These findings indicate that with aging, there is reduced responsiveness of the skeleton to mechanical loading (Srinivasan et al., 2012).

Osteocytes are thought of as critical mediators of the effects of mechanical loading by virtue of their location and connectivity with one another and with cells at the bone surface. Because osteocyte dendrites are critical for mechanotransduction (Burra et al., 2010), reduced dendrite connectivity may contribute to the impaired bone response to mechanical loading in aged animals. In addition, altered cell proliferation and decreased Wnt signaling have been implicated in the age-related decline in bone mechanoresponsiveness. The importance of Wnt signaling in loading-induced bone formation is well documented. Mechanical loading in young adult animals downregulates Sost/sclerostin at sites of subsequent bone formation and stimulates canonical Wnt signaling (Lara-Castillo et al., 2015; Moustafa et al., 2012; Robinson et al., 2006; Robling et al., 2008). Moreover, the osteogenic response to loading in mice is disrupted by overexpression of Sost, deletion of Lrp5, or heterozygous deletion of β-catenin in bone cells (Javaheri et al., 2014; Sawakami et al., 2006; Tu et al., 2012; Zhao et al., 2013). Activation of Wnt signaling by mechanical loading is impaired in bone of aged mice (Holguin et al., 2016). Meakin et al. reported that osteoblasts from old mice are less proliferative after in vitro stretching, and that tibial compression in old mice produces a smaller increase in periosteal osteoblast number than in young mice (Meakin et al., 2014). The age-related decline in osteoprogenitor number might contribute to the deficient response of the skeleton to mechanical loading (Kim et al., 2017).

Future directions

Research in animal models has revealed that the rate of physiological aging can be ameliorated by a variety of behavioral, genetic, and pharmacological means. There is great enthusiasm that this can also be accomplished in humans. Most importantly, decreased rate of aging in animal models is often accompanied by a delay (and decreased severity) of a number of age-associated diseases. This evidence strongly suggests that therapeutic interventions that can either delay the onset or decrease the rate of aging could have a beneficial effect on the health of the elderly. As a result, there is a race to develop drugs that may alleviate several degenerative diseases simultaneously. Current antiosteoporotic treatments have limited impact on public health, despite their effectiveness at the individual level. It is, therefore, imperative to elucidate mechanisms of skeletal aging so that osteoporosis is added to the list of degenerative diseases that are amenable to treatment with antiaging drugs.

References

Almeida, M., Ambrogini, E., Han, L., Manolagas, S.C., Jilka, R.L., 2009. Increased lipid oxidation causes oxidative stress, increased PPAR{gamma} expression and diminished pro-osteogenic Wnt signaling in the skeleton. J. Biol. Chem. 284, 27438–27448.

Almeida, M., Han, L., Martin-Millan, M., O'Brien, C.A., Manolagas, S.C., 2007a. Oxidative stress antagonizes Wnt signaling in osteoblast precursors by diverting beta-catenin from T cell factor- to forkhead box O-mediated transcription. J. Biol. Chem. 282, 27298–27305.

Almeida, M., Han, L., Martin-Millan, M., Plotkin, L.I., Stewart, S.A., Roberson, P.K., Kousteni, S., O'Brien, C.A., Bellido, T., Parfitt, A.M., et al., 2007b. Skeletal involution by age-associated oxidative stress and its acceleration by loss of sex steroids. J. Biol. Chem. 282, 27285–27297.

Almeida, M., Iyer, S., Martin-Millan, M., Bartell, S.M., Han, L., Ambrogini, E., Onal, M., Xiong, J., Weinstein, R.S., Jilka, R.L., et al., 2013. Estrogen receptor-alpha signaling in osteoblast progenitors stimulates cortical bone accrual. J. Clin. Investig. 123, 394–404.

Almeida, M., Laurent, M.R., Dubois, V., Claessens, F., O'Brien, C.A., Bouillon, R., Vanderschueren, D., Manolagas, S.C., 2017. Estrogens and androgens in skeletal physiology and pathophysiology. Physiol. Rev. 97, 135–187.

Almeida, M., O'Brien, C.A., 2013. Basic biology of skeletal aging: role of stress response pathways. J. Gerontol. A Biol. Sci. Med. Sci. 68, 1197–1208.

Ambrogini, E., Que, X., Wang, S., Yamaguchi, F., Weinstein, R.S., Tsimikas, S., Manolagas, S.C., Witztum, J.L., Jilka, R.L., 2018. Oxidation-specific epitopes restrain bone formation. Nat. Commun. 9, 2193.

Anania, C., Gustafsson, T., Hua, X., Su, J., Vikstrom, M., de Faire, U., Heimburger, M., Jogestrand, T., Frostegard, J., 2010. Increased prevalence of vulnerable atherosclerotic plaques and low levels of natural IgM antibodies against phosphorylcholine in patients with systemic lupus erythematosus. Arthritis Res. Ther. 12, R214.

Baar, M.P., Brandt, R.M., Putavet, D.A., Klein, J.D., Derks, K.W., Bourgeois, B.R., Stryeck, S., Rijksen, Y., van Willigenburg, H., Feijtel, D.A., et al., 2017. Targeted apoptosis of senescent cells restores tissue homeostasis in response to chemotoxicity and aging. Cell 169, 132–147 e116.

Baker, D.J., Childs, B.G., Durik, M., Wijers, M.E., Sieben, C.J., Zhong, J., Saltness, R.A., Jeganathan, K.B., Verzosa, G.C., Pezeshki, A., et al., 2016. Naturally occurring p16(Ink4a)-positive cells shorten healthy lifespan. Nature 530, 184–189.

Baker, D.J., Wijshake, T., Tchkonia, T., LeBrasseur, N.K., Childs, B.G., van de Sluis, B., Kirkland, J.L., Van Deursen, J.M., 2011. Clearance of p16Ink4a-positive senescent cells delays ageing-associated disorders. Nature 479, 232–236.

Bala, Y., Zebaze, R., Seeman, E., 2015. Role of cortical bone in bone fragility. Curr. Opin. Rheumatol. 27, 406–413.

Balaban, R.S., Nemoto, S., Finkel, T., 2005. Mitochondria, oxidants, and aging. Cell 120, 483–495.

Baron, R., Kneissel, M., 2013. WNT signaling in bone homeostasis and disease: from human mutations to treatments. Nat. Med. 19, 179–192.

Bartell, S.M., Kim, H.N., Ambrogini, E., Han, L., Iyer, S., Serra, U.S., Rabinovitch, P., Jilka, R.L., Weinstein, R.S., Zhao, H., et al., 2014. FoxO proteins restrain osteoclastogenesis and bone resorption by attenuating H_2O_2 accumulation. Nat. Commun. 5, 3773.

Baumann, B.D., Wronski, T.J., 1995. Response of cortical bone to antiresorptive agents and parathyroid hormone in aged ovariectomized rats. Bone 16, 247–253.

Bentolila, V., Boyce, T.M., Fyhrie, D.P., Drumb, R., Skerry, T.M., Schaffler, M.B., 1998. Intracortical remodeling in adult rat long bones after fatigue loading. Bone 23, 275–281.

Binder, C.J., Papac-Milicevic, N., Witztum, J.L., 2016. Innate sensing of oxidation-specific epitopes in health and disease. Nat. Rev. Immunol. 16, 485–497.

Black, D.M., Rosen, C.J., 2016. Clinical practice. Postmenopausal osteoporosis. N. Engl. J. Med. 374, 254–262.

Brennan, T.A., Egan, K.P., Lindborg, C.M., Chen, Q., Sweetwyne, M.T., Hankenson, K.D., Xie, S.X., Johnson, F.B., Pignolo, R.J., 2014. Mouse models of telomere dysfunction phenocopy skeletal changes found in human age-related osteoporosis. Dis. Model. Mech. 7, 583–592.

Burra, S., Nicolella, D.P., Francis, W.L., Freitas, C.J., Mueschke, N.J., Poole, K., Jiang, J.X., 2010. Dendritic processes of osteocytes are mechanotransducers that induce the opening of hemichannels. Proc. Natl. Acad. Sci. U. S. A. 107, 13648–13653.

Busse, B., Djonic, D., Milovanovic, P., Hahn, M., Puschel, K., Ritchie, R.O., Djuric, M., Amling, M., 2010. Decrease in the osteocyte lacunar density accompanied by hypermineralized lacunar occlusion reveals failure and delay of remodeling in aged human bone. Aging Cell 9, 1065–1075.

Campisi, J., 2013. Aging, cellular senescence, and cancer. Annu. Rev. Physiol. 75, 685–705.

Cao, J.J., Wronski, T.J., Iwaniec, U., Phleger, L., Kurimoto, P., Boudignon, B., Halloran, B.P., 2005. Aging increases stromal/osteoblastic cell-induced osteoclastogenesis and alters the osteoclast precursor pool in the mouse. J. Bone Miner. Res. 20, 1659–1668.

Caplan, A.I., 1991. Mesenchymal stem cells. J. Orthop. Res. 9, 641–650.

Carames, B., Olmer, M., Kiosses, W.B., Lotz, M.K., 2015. The relationship of autophagy defects to cartilage damage during joint aging in a mouse model. Arthritis Rheum. 67, 1568–1576.

Cardoso, L., Herman, B.C., Verborgt, O., Laudier, D., Majeska, R.J., Schaffler, M.B., 2009. Osteocyte apoptosis controls activation of intracortical resorption in response to bone fatigue. J. Bone Miner. Res. 24, 597–605.

Carnio, S., LoVerso, F., Baraibar, M.A., Longa, E., Khan, M.M., Maffei, M., Reischl, M., Canepari, M., Loefler, S., Kern, H., et al., 2014. Autophagy impairment in muscle induces neuromuscular junction degeneration and precocious aging. Cell Rep. 8, 1509–1521.

Chance, B., Sies, H., Boveris, A., 1979. Hydroperoxide metabolism in mammalian organs. Physiol. Rev. 59, 527–605.

Chandra, A., Lin, T., Young, T., Tong, W., Ma, X., Tseng, W.J., Kramer, I., Kneissel, M., Levine, M.A., Zhang, Y., et al., 2017. Suppression of sclerostin alleviates radiation-induced bone loss by protecting bone-forming cells and their progenitors through distinct mechanisms. J. Bone Miner. Res. 32, 360–372.

Chang, J., Wang, Y., Shao, L., Laberge, R.M., Demaria, M., Campisi, J., Janakiraman, K., Sharpless, N.E., Ding, S., Feng, W., et al., 2016. Clearance of senescent cells by ABT263 rejuvenates aged hematopoietic stem cells in mice. Nat. Med. 22, 78–83.

Chen, Q., Liu, K., Robinson, A.R., Clauson, C.L., Blair, H.C., Robbins, P.D., Niedernhofer, L.J., Ouyang, H., 2013. DNA damage drives accelerated bone aging via an NF-kappaB-dependent mechanism. J. Bone Miner. Res. 28, 1214–1228.

Chiang, C., Chiu, M., Moore, A.J., Anderson, P.H., Ghasem-Zadeh, A., McManus, J.F., Ma, C., Seeman, E., Clemens, T.L., Morris, H.A., et al., 2009. Mineralization and bone resorption are regulated by the androgen receptor in male mice. J. Bone Miner. Res. 24, 621–631.

Childs, B.G., Baker, D.J., Wijshake, T., Conover, C.A., Campisi, J., van Deursen, J.M., 2016. Senescent intimal foam cells are deleterious at all stages of atherosclerosis. Science 354, 472–477.

Childs, B.G., Durik, M., Baker, D.J., Van Deursen, J.M., 2015. Cellular senescence in aging and age-related disease: from mechanisms to therapy. Nat. Med. 21, 1424–1435.

Childs, B.G., Gluscevic, M., Baker, D.J., Laberge, R.M., Marquess, D., Dananberg, J., van Deursen, J.M., 2017. Senescent cells: an emerging target for diseases of ageing. Nat. Rev. Drug Discov. 16, 718–735.

Clevers, H., Nusse, R., 2012. Wnt/beta-Catenin signaling and disease. Cell 149, 1192–1205.

Coipeau, P., Rosset, P., Langonne, A., Gaillard, J., Delorme, B., Rico, A., Domenech, J., Charbord, P., Sensebe, L., 2009. Impaired differentiation potential of human trabecular bone mesenchymal stromal cells from elderly patients. Cytotherapy 11, 584–594.

Coleman, M.P., 2013. The challenges of axon survival: introduction to the special issue on axonal degeneration. Exp. Neurol. 246, 1–5.

Conboy, I.M., Conboy, M.J., Smythe, G.M., Rando, T.A., 2003. Notch-mediated restoration of regenerative potential to aged muscle. Science 302, 1575–1577.

Crisan, M., Yap, S., Casteilla, L., Chen, C.W., Corselli, M., Park, T.S., Andriolo, G., Sun, B., Zheng, B., Zhang, L., et al., 2008. A perivascular origin for mesenchymal stem cells in multiple human organs. Cell Stem Cell 3, 301–313.

Cuervo, A.M., 2008. Autophagy and aging: keeping that old broom working. Trends Genet. 24, 604–612.

Cuervo, A.M., Dice, J.F., 2000. Age-related decline in chaperone-mediated autophagy. J. Biol. Chem. 275, 31505–31513.

D'Autreaux, B., Toledano, M.B., 2007. ROS as signalling molecules: mechanisms that generate specificity in ROS homeostasis. Nat. Rev. Mol. Cell Biol. 8, 813–824.

Dai, D.F., Chiao, Y.A., Marcinek, D.J., Szeto, H.H., Rabinovitch, P.S., 2014. Mitochondrial oxidative stress in aging and healthspan. Longev. Health. 3, 6.

De Bosscher, K., Vanden Berghe, W., Haegeman, G., 2006. Cross-talk between nuclear receptors and nuclear factor kappaB. Oncogene 25, 6868–6886.

de Faire, U., Su, J., Hua, X., Frostegard, A., Halldin, M., Hellenius, M.L., Wikstrom, M., Dahlbom, I., Gronlund, H., Frostegard, J., 2010. Low levels of IgM antibodies to phosphorylcholine predict cardiovascular disease in 60-year old men: effects on uptake of oxidized LDL in macrophages as a potential mechanism. J. Autoimmun. 34, 73–79.

Demaria, M., O'Leary, M.N., Chang, J., Shao, L., Liu, S., Alimirah, F., Koenig, K., Le, C., Mitin, N., Deal, A.M., et al., 2017. Cellular senescence promotes adverse effects of chemotherapy and cancer relapse. Cancer Discov. 7, 165–176.

Dickinson, D.A., Forman, H.J., 2002. Glutathione in defense and signaling: lessons from a small thiol. Ann. N. Y. Acad. Sci. 973, 488–504.

Diderich, K.E., Nicolaije, C., Priemel, M., Waarsing, J.H., Day, J.S., Brandt, R.M., Schilling, A.F., Botter, S.M., Weinans, H., van der Horst, G.T., et al., 2012. Bone fragility and decline in stem cells in prematurely aging DNA repair deficient trichothiodystrophy mice. Age 34, 845–861.

Doonan, R., McElwee, J.J., Matthijssens, F., Walker, G.A., Houthoofd, K., Back, P., Matscheski, A., Vanfleteren, J.R., Gems, D., 2008. Against the oxidative damage theory of aging: superoxide dismutases protect against oxidative stress but have little or no effect on life span in *Caenorhabditis elegans*. Genes Dev. 22, 3236–3241.

Droge, W., 2002. Free radicals in the physiological control of cell function. Physiol. Rev. 82, 47–95.

Dutta, S., Sengupta, P., 2016. Men and mice: relating their ages. Life Sci. 152, 244–248.

Ehrenstein, M.R., Notley, C.A., 2010. The importance of natural IgM: scavenger, protector and regulator. Nat. Rev. Immunol. 10, 778–786.

Erben, R.G., 1996. Trabecular and endocortical bone surfaces in the rat: modeling or remodeling? Anat. Rec. 246, 39–46.

Farr, J.N., Fraser, D.G., Wang, H., Jaehn, K., Ogrodnik, M.B., Weivoda, M.M., Drake, M.T., Tchkonia, T., LeBrasseur, N.K., Kirkland, J.L., et al., 2016. Identification of senescent cells in the bone microenvironment. J. Bone Miner. Res. 31, 1920–1929.

Farr, J.N., Xu, M., Weivoda, M.M., Monroe, D.G., Fraser, D.G., Onken, J.L., Negley, B.A., Sfeir, J.G., Ogrodnik, M.B., Hachfeld, C.M., et al., 2017. Targeting cellular senescence prevents age-related bone loss in mice. Nat. Med. 23, 1072–1079.

Ferguson, V.L., Ayers, R.A., Bateman, T.A., Simske, S.J., 2003. Bone development and age-related bone loss in male C57BL/6J mice. Bone 33, 387–398.

Fiskesund, R., Stegmayr, B., Hallmans, G., Vikstrom, M., Weinehall, L., de Faire, U., Frostegard, J., 2010. Low levels of antibodies against phosphorylcholine predict development of stroke in a population-based study from northern Sweden. Stroke 41, 607–612.

Fiskesund, R., Su, J., Bulatovic, I., Vikstrom, M., de Faire, U., Frostegard, J., 2012. IgM phosphorylcholine antibodies inhibit cell death and constitute a strong protection marker for atherosclerosis development, particularly in combination with other auto-antibodies against modified LDL. Results Immunol. 2, 13–18.

Friedenstein, A.J., Chailakhjan, R.K., Latsinik, N.V., Panasyuk, A.F., Keiliss-Borok, I.V., 1974. Stromal cells responsible for transferring the microenvironment of the hemopoietic tissues. Cloning in Vitro and Retransplantation in Vivo. Transplantation 17, 331–340.

Frost, H.M., 1960. Micropetrosis. J. Bone Joint. Surg. Am. 42A, 144–150.

Frost, H.M., 2003. Bone's mechanostat: a 2003 update. Anat. Rec. A Discover. Mol. Cel. Evolut. Biol. 275, 1081–1101.

Garrett, I.R., Boyce, B.F., Oreffo, R.O., Bonewald, L., Poser, J., Mundy, G.R., 1990. Oxygen-derived free radicals stimulate osteoclastic bone resorption in rodent bone in vitro and in vivo. J. Clin. Investig. 85, 632–639.

Gems, D., Partridge, L., 2013. Genetics of longevity in model organisms: debates and paradigm shifts. Annu. Rev. Physiol. 75, 621–644.

Geng, J., Klionsky, D.J., 2008. The Atg8 and Atg12 ubiquitin-like conjugation systems in macroautophagy. 'Protein modifications: beyond the usual suspects' review series. EMBO Rep. 9, 859–864.

Glatt, V., Canalis, E., Stadmeyer, L., Bouxsein, M.L., 2007. Age-related changes in trabecular architecture differ in female and male C57BL/6J mice. J. Bone Miner. Res. 22, 1197–1207.

Goodell, M.A., Rando, T.A., 2015. Stem cells and healthy aging. Science 350, 1199–1204.

Grcevic, D., Pejda, S., Matthews, B.G., Repic, D., Wang, L., Li, H., Kronenberg, M.S., Jiang, X., Maye, P., Adams, D.J., et al., 2012. In vivo fate mapping identifies mesenchymal progenitor cells. Stem Cell. 30, 187–196.

Green, D.R., Galluzzi, L., Kroemer, G., 2011. Mitochondria and the autophagy-inflammation-cell death axis in organismal aging. Science 333, 1109–1112.

Griffin, D.O., Holodick, N.E., Rothstein, T.L., 2011. Human B1 cells in umbilical cord and adult peripheral blood express the novel phenotype $CD20^{+}$ $CD27^{+}$ $CD43^{+}$ $CD70^{-}$. J. Exp. Med. 208, 67–80.

Gronlund, H., Hallmans, G., Jansson, J.H., Boman, K., Wikstrom, M., de Faire, U., Frostegard, J., 2009. Low levels of IgM antibodies against phosphorylcholine predict development of acute myocardial infarction in a population-based cohort from northern Sweden. Eur. J. Cardiovasc. Prev. Rehabil. 16, 382–386.

Gronwall, C., Akhter, E., Oh, C., Burlingame, R.W., Petri, M., Silverman, G.J., 2012. IgM autoantibodies to distinct apoptosis-associated antigens correlate with protection from cardiovascular events and renal disease in patients with SLE. Clin. Immunol. 142, 390–398.

Ha, H., Kwak, H.B., Lee, S.W., Jin, H.M., Kim, H.M., Kim, H.H., Lee, Z.H., 2004. Reactive oxygen species mediate RANK signaling in osteoclasts. Exp. Cell Res. 301, 119–127.

Halloran, B.P., Ferguson, V.L., Simske, S.J., Burghardt, A., Venton, L.L., Majumdar, S., 2002. Changes in bone structure and mass with advancing age in the male C57BL/6J mouse. J. Bone Miner. Res. 17, 1044–1050.

Han, Z.H., Palnitkar, S., Rao, D.S., Nelson, D., Parfitt, A.M., 1997. Effects of ethnicity and age or menopause on the remodeling and turnover of iliac bone: implications for mechanisms of bone loss. J. Bone Miner. Res. 12, 498–508.

Hansen, M., Rubinsztein, D.C., Walker, D.W., 2018. Autophagy as a promoter of longevity: insights from model organisms. Nat. Rev. Mol. Cell Biol. 19, 579–593.

Harman, D., 1956. Aging: a theory based on free radical and radiation chemistry. J. Gerontol. 11, 298–300.

Hayflick, L., Moorhead, P.S., 1961. The serial cultivation of human diploid cell strains. Exp. Cell Res. 25, 585–621.

Hekimi, S., Lapointe, J., Wen, Y., 2011. Taking a "good" look at free radicals in the aging process. Trends Cell Biol. 21, 569–576.

Holguin, N., Brodt, M.D., Sanchez, M.E., Silva, M.J., 2014. Aging diminishes lamellar and woven bone formation induced by tibial compression in adult C57BL/6. Bone 65, 83–91.

Holguin, N., Brodt, M.D., Silva, M.J., 2016. Activation of Wnt signaling by mechanical loading is impaired in the bone of old mice. J. Bone Miner. Res. 31, 2215–2226.

Hoogeboom, D., Essers, M.A., Polderman, P.E., Voets, E., Smits, L.M., Burgering, B.M., 2008. Interaction of FOXO with beta-catenin inhibits beta-catenin/T cell factor activity. J. Biol. Chem. 283, 9224–9230.

Horowitz, M.C., Berry, R., Holtrup, B., Sebo, Z., Nelson, T., Fretz, J.A., Lindskog, D., Kaplan, J.L., Ables, G., Rodeheffer, M.S., et al., 2017. Bone marrow adipocytes. Adipocyte 6, 193–204.

Huang, S.C., Wu, T.C., Yu, H.C., Chen, M.R., Liu, C.M., Chiang, W.S., Lin, K.M., 2010. Mechanical strain modulates age-related changes in the proliferation and differentiation of mouse adipose-derived stromal cells. BMC Cell Biol. 11, 18.

Hughes, D.E., Dai, A., Tiffee, J.C., Li, H.H., Mundy, G.R., Boyce, B.F., 1996. Estrogen promotes apoptosis of murine osteoclasts mediated by TGF-b. Nat. Med. 2, 1132–1136.

Imhof, A., Koenig, W., Jaensch, A., Mons, U., Brenner, H., Rothenbacher, D., 2015. Long-term prognostic value of IgM antibodies against phosphorylcholine for adverse cardiovascular events in patients with stable coronary heart disease. Atherosclerosis 243, 414–420.

Ireland, A., Maden-Wilkinson, T., McPhee, J., Cooke, K., Narici, M., Degens, H., Rittweger, J., 2013. Upper limb muscle-bone asymmetries and bone adaptation in elite youth tennis players. Med. Sci. Sports Exerc. 45, 1749–1758.

Ishii, K.A., Fumoto, T., Iwai, K., Takeshita, S., Ito, M., Shimohata, N., Aburatani, H., Taketani, S., Lelliott, C.J., Vidal-Puig, A., et al., 2009. Coordination of PGC-1beta and iron uptake in mitochondrial biogenesis and osteoclast activation. Nat. Med. 15, 259–266.

Iyer, S., Ambrogini, E., Bartell, S.M., Han, L., Roberson, P.K., de Cabo, R., Jilka, R.L., Weinstein, R.S., O'Brien, C.A., Manolagas, S.C., et al., 2013. FOXOs attenuate bone formation by suppressing Wnt signaling. J. Clin. Investig. 123, 3409–3419.

Jackson, S.P., 2002. Sensing and repairing DNA double-strand breaks. Carcinogenesis 23, 687–696.

Janssen-Heininger, Y.M., Mossman, B.T., Heintz, N.H., Forman, H.J., Kalyanaraman, B., Finkel, T., Stamler, J.S., Rhee, S.G., van der Vliet, A., 2008. Redox-based regulation of signal transduction: principles, pitfalls, and promises. Free Radic. Biol. Med. 45, 1–17.

Javaheri, B., Stern, A.R., Lara, N., Dallas, M., Zhao, H., Liu, Y., Bonewald, L.F., Johnson, M.L., 2014. Deletion of a single beta-catenin allele in osteocytes abolishes the bone anabolic response to loading. J. Bone Miner. Res. 29, 705–715.

Jeon, O.H., Kim, C., Laberge, R.M., Demaria, M., Rathod, S., Vasserot, A.P., Chung, J.W., Kim, D.H., Poon, Y., David, N., et al., 2017. Local clearance of senescent cells attenuates the development of post-traumatic osteoarthritis and creates a pro-regenerative environment. Nat. Med. 23, 775–781.

Jilka, R.L., Almeida, M., Ambrogini, E., Han, L., Roberson, P.K., Weinstein, R.S., Manolagas, S.C., 2010. Decreased oxidative stress and greater bone anabolism in the aged, when compared to the young, murine skeleton with parathyroid hormone administration. Aging Cell 9, 851–867.

Jilka, R.L., Noble, B., Weinstein, R.S., 2013. Osteocyte apoptosis. Bone 54, 264–271.

Jilka, R.L., O'Brien, C.A., 2016. The role of osteocytes in age-related bone loss. Curr. Osteoporos. Rep. 14, 16–25.

Jilka, R.L., O'Brien, C.A., Roberson, P.K., Bonewald, L.F., Weinstein, R.S., Manolagas, S.C., 2014. Dysapoptosis of osteoblasts and osteocytes increases cancellous bone formation but exaggerates cortical porosity with age. J. Bone Miner. Res. 29, 103−117.

Jones, H.H., Priest, J.D., Hayes, W.C., Tichenor, C.C., Nagel, D.A., 1977. Humeral hypertrophy in response to exercise. J. Bone Joint Surg. Am. 59, 204−208.

Jurk, D., Wang, C., Miwa, S., Maddick, M., Korolchuk, V., Tsolou, A., Gonos, E.S., Thrasivoulou, C., Saffrey, M.J., Cameron, K., et al., 2012. Postmitotic neurons develop a p21-dependent senescence-like phenotype driven by a DNA damage response. Aging Cell 11, 996−1004.

Kang, C., Xu, Q., Martin, T.D., Li, M.Z., Demaria, M., Aron, L., Lu, T., Yankner, B.A., Campisi, J., Elledge, S.J., 2015. The DNA damage response induces inflammation and senescence by inhibiting autophagy of GATA4. Science 349 aaa5612.

Karvonen, J., Paivansalo, M., Kesaniemi, Y.A., Horkko, S., 2003. Immunoglobulin M type of autoantibodies to oxidized low-density lipoprotein has an inverse relation to carotid artery atherosclerosis. Circulation 108, 2107−2112.

Kasper, G., Mao, L., Geissler, S., Draycheva, A., Trippens, J., Kuhnisch, J., Tschirschmann, M., Kaspar, K., Perka, C., Duda, G.N., et al., 2009. Insights into mesenchymal stem cell aging: involvement of antioxidant defense and actin cytoskeleton. Stem Cell. 27, 1288−1297.

Kassem, M., Marie, P.J., 2011. Senescence-associated intrinsic mechanisms of osteoblast dysfunctions. Aging Cell 10, 191−197.

Kennedy, B.K., Berger, S.L., Brunet, A., Campisi, J., Cuervo, A.M., Epel, E.S., Franceschi, C., Lithgow, G.J., Morimoto, R.I., Pessin, J.E., et al., 2014. Geroscience: linking aging to chronic disease. Cell 159, 709−713.

Kerschnitzki, M., Kollmannsberger, P., Burghammer, M., Duda, G.N., Weinkamer, R., Wagermaier, W., Fratzl, P., 2013. Architecture of the osteocyte network correlates with bone material quality. J. Bone Miner. Res. 28, 1837−1845.

Khosla, S., 2010. Update on estrogens and the skeleton. J. Clin. Endocrinol. Metab. 95, 3569−3577.

Khosla, S., 2015. New insights into androgen and estrogen receptor regulation of the male skeleton. J. Bone Miner. Res. 30, 1134−1137.

Kim, H.N., Chang, J., Shao, L., Han, L., Iyer, S., Manolagas, S.C., O'Brien, C.A., Jilka, R.L., Zhou, D., Almeida, M., 2017. DNA damage and senescence in osteoprogenitors expressing Osx1 may cause their decrease with age. Aging Cell.

Koleske, A.J., 2013. Molecular mechanisms of dendrite stability. Nat. Rev. Neurosci. 14, 536−550.

Komatsu, M., Wang, Q.J., Holstein, G.R., Friedrich Jr., V.L., Iwata, J., Kominami, E., Chait, B.T., Tanaka, K., Yue, Z., 2007. Essential role for autophagy protein Atg7 in the maintenance of axonal homeostasis and the prevention of axonal degeneration. Proc. Natl. Acad. Sci. U. S. A. 104, 14489−14494.

Korpelainen, R., Keinanen-Kiukaanniemi, S., Heikkinen, J., Vaananen, K., Korpelainen, J., 2006. Effect of impact exercise on bone mineral density in elderly women with low BMD: a population-based randomized controlled 30-month intervention. Osteoporos. Int. 17, 109−118.

Kuhn, H.G., Dickinson-Anson, H., Gage, F.H., 1996. Neurogenesis in the dentate gyrus of the adult rat: age-related decrease of neuronal progenitor proliferation. J. Neurosci. 16, 2027−2033.

Kuilman, T., Michaloglou, C., Mooi, W.J., Peeper, D.S., 2010. The essence of senescence. Genes Dev. 24, 2463−2479.

Kusumbe, A.P., Ramasamy, S.K., Adams, R.H., 2014. Coupling of angiogenesis and osteogenesis by a specific vessel subtype in bone. Nature 507, 323−328.

Lang, T., LeBlanc, A., Evans, H., Lu, Y., Genant, H., Yu, A., 2004. Cortical and trabecular bone mineral loss from the spine and hip in long-duration spaceflight. J. Bone Miner. Res. 19, 1006−1012.

Lara-Castillo, N., Kim-Weroha, N.A., Kamel, M.A., Javaheri, B., Ellies, D.L., Krumlauf, R.E., Thiagarajan, G., Johnson, M.L., 2015. In vivo mechanical loading rapidly activates beta-catenin signaling in osteocytes through a prostaglandin mediated mechanism. Bone 76, 58−66.

Lean, J.M., Davies, J.T., Fuller, K., Jagger, C.J., Kirstein, B., Partington, G.A., Urry, Z.L., Chambers, T.J., 2003. A crucial role for thiol antioxidants in estrogen-deficiency bone loss. J. Clin. Investig. 112, 915−923.

Lean, J.M., Jagger, C.J., Kirstein, B., Fuller, K., Chambers, T.J., 2005. Hydrogen peroxide is essential for estrogen-deficiency bone loss and osteoclast formation. Endocrinology 146, 728−735.

LeBlanc, A.D., Schneider, V.S., Evans, H.J., Engelbretson, D.A., Krebs, J.M., 1990. Bone mineral loss and recovery after 17 weeks of bed rest. J. Bone Miner. Res. 5, 843−850.

Lee, H.Y., Choi, C.S., Birkenfeld, A.L., Alves, T.C., Jornayvaz, F.R., Jurczak, M.J., Zhang, D., Woo, D.K., Shadel, G.S., Ladiges, W., et al., 2010. Targeted expression of catalase to mitochondria prevents age-associated reductions in mitochondrial function and insulin resistance. Cell Metabol. 12, 668−674.

Lee, N.K., Choi, Y.G., Baik, J.Y., Han, S.Y., Jeong, D.W., Bae, Y.S., Kim, N., Lee, S.Y., 2005. A crucial role for reactive oxygen species in RANKL-induced osteoclast differentiation. Blood 106, 852−859.

Levine, B., Kroemer, G., 2008. Autophagy in the pathogenesis of disease. Cell 132, 27−42.

Li, C.J., Cheng, P., Liang, M.K., Chen, Y.S., Lu, Q., Wang, J.Y., Xia, Z.Y., Zhou, H.D., Cao, X., Xie, H., et al., 2015. MicroRNA-188 regulates age-related switch between osteoblast and adipocyte differentiation. J. Clin. Investig. 125, 1509−1522.

Li, C.Y., Schaffler, M.B., Wolde-Semait, H.T., Hernandez, C.J., Jepsen, K.J., 2005. Genetic background influences cortical bone response to ovariectomy. J. Bone Miner. Res. 20, 2150−2158.

Lips, P., Courpron, P., Meunier, P.J., 1978. Mean wall thickness of trabecular bone packets in the human iliac crest: changes with age. Calcif. Tissue Res. 26, 13−17.

Lithgow, G.J., Kirkwood, T.B.L., 1996. Mechanisms and evolution of aging. Science 273, 80.

Liu, F., Fang, F., Yuan, H., Yang, D., Chen, Y., Williams, L., Goldstein, S.A., Krebsbach, P.H., Guan, J.L., 2013. Suppression of autophagy by FIP200 deletion leads to osteopenia in mice through the inhibition of osteoblast terminal differentiation. J. Bone Miner. Res. 28, 2414−2430.

Liu, H., Fergusson, M.M., Wu, J.J., Rovira, I.I., Liu, J., Gavrilova, O., Lu, T., Bao, J., Han, D., Sack, M.N., et al., 2011. Wnt signaling regulates hepatic metabolism. Sci. Signal. 4, ra6.

Liu, W., Wang, S., Wei, S., Sun, L., Feng, X., 2005. Receptor activator of NF-kappaB (RANK) cytoplasmic motif, 369PFQEP373, plays a predominant role in osteoclast survival in part by activating Akt/PKB and its downstream effector AFX/FOXO4. J. Biol. Chem. 280, 43064–43072.

Liu, Y., Almeida, M., Weinstein, R.S., O'Brien, C.A., Manolagas, S.C., Jilka, R.L., 2016. Skeletal inflammation and attenuation of Wnt signaling, Wnt ligand expression, and bone formation in atherosclerotic ApoE-null mice. Am. J. Physiol. Endocrinol. Metab. 310, E762–E773.

Looker, A.C., Wahner, H.W., Dunn, W.L., Calvo, M.S., Harris, T.B., Heyse, S.P., Johnston Jr., C.C., Lindsay, R., 1998. Updated data on proximal femur bone mineral levels of US adults. Osteoporos. Int. 8, 468–489.

Lopez-Otin, C., Blasco, M.A., Partridge, L., Serrano, M., Kroemer, G., 2013. The hallmarks of aging. Cell 153, 1194–1217.

Maatta, J.A., Buki, K.G., Ivaska, K.K., Nieminen-Pihala, V., Elo, T.D., Kahkonen, T., Poutanen, M., Harkonen, P., Vaananen, K., 2013. Inactivation of the androgen receptor in bone-forming cells leads to trabecular bone loss in adult female mice. BoneKEy Rep. 2, 440.

Makovey, J., Chen, J.S., Hayward, C., Williams, F.M., Sambrook, P.N., 2009. Association between serum cholesterol and bone mineral density. Bone 44, 208–213.

Manolagas, S.C., 2000. Birth and death of bone cells: basic regulatory mechanisms and implications for the pathogenesis and treatment of osteoporosis. Endocr. Rev. 21, 115–137.

Manolagas, S.C., 2010. From estrogen-centric to aging and oxidative stress: a revised perspective of the pathogenesis of osteoporosis. Endocr. Rev. 31, 266–300.

Manolagas, S.C., 2013. Steroids and osteoporosis: the quest for mechanisms. J. Clin. Investig. 123, 1919–1921.

Manolagas, S.C., O'Brien, C.A., Almeida, M., 2013. The role of estrogen and androgen receptors in bone health and disease. Nat. Rev. Endocrinol. 9, 699–712.

Manolagas, S.C., Parfitt, A.M., 2010. What old means to bone. Trends Endocrinol. Metab. 21, 369–374.

Martin-Millan, M., Almeida, M., Ambrogini, E., Han, L., Zhao, H., Weinstein, R.S., Jilka, R.L., O'Brien, C.A., Manolagas, S.C., 2010. The estrogen receptor-alpha in osteoclasts mediates the protective effects of estrogens on cancellous but not cortical bone. Mol. Endocrinol. 24, 323–334.

McNeill, T.H., Brown, S.A., Rafols, J.A., Shoulson, I., 1988. Atrophy of medium spiny I striatal dendrites in advanced Parkinson's disease. Brain Res. 455, 148–152.

Meakin, L.B., Galea, G.L., Sugiyama, T., Lanyon, L.E., Price, J.S., 2014. Age-related impairment of bones' adaptive response to loading in mice is associated with sex-related deficiencies in osteoblasts but no change in osteocytes. J. Bone Miner. Res. 29, 1859–1871.

Mesquita, A., Weinberger, M., Silva, A., Sampaio-Marques, B., Almeida, B., Leao, C., Costa, V., Rodrigues, F., Burhans, W.C., Ludovico, P., 2010. Caloric restriction or catalase inactivation extends yeast chronological lifespan by inducing H_2O_2 and superoxide dismutase activity. Proc. Natl. Acad. Sci. U. S. A. 107, 15123–15128.

Minamino, T., Orimo, M., Shimizu, I., Kunieda, T., Yokoyama, M., Ito, T., Nojima, A., Nabetani, A., Oike, Y., Matsubara, H., et al., 2009. A crucial role for adipose tissue p53 in the regulation of insulin resistance. Nat. Med. 15, 1082–1087.

Mine-Hattab, J., Rothstein, R., 2012. Increased chromosome mobility facilitates homology search during recombination. Nat. Cell Biol. 14, 510–517.

Molofsky, A.V., Slutsky, S.G., Joseph, N.M., He, S., Pardal, R., Krishnamurthy, J., Sharpless, N.E., Morrison, S.J., 2006. Increasing p16INK4a expression decreases forebrain progenitors and neurogenesis during ageing. Nature 443, 448–452.

Morimoto, R.I., Cuervo, A.M., 2014. Proteostasis and the aging proteome in health and disease. J. Gerontol. A Biol. Sci. Med. Sci. 69 (Suppl. 1), S33–S38.

Morrison, S.J., Wandycz, A.M., Akashi, K., Globerson, A., Weissman, I.L., 1996. The aging of hematopoietic stem cells. Nat. Med. 2, 1011–1016.

Mortensen, M., Soilleux, E.J., Djordjevic, G., Tripp, R., Lutteropp, M., Sadighi-Akha, E., Stranks, A.J., Glanville, J., Knight, S., Jacobsen, S.E., et al., 2011. The autophagy protein Atg7 is essential for hematopoietic stem cell maintenance. J. Exp. Med. 208, 455–467.

Moustafa, A., Sugiyama, T., Prasad, J., Zaman, G., Gross, T.S., Lanyon, L.E., Price, J.S., 2012. Mechanical loading-related changes in osteocyte sclerostin expression in mice are more closely associated with the subsequent osteogenic response than the peak strains engendered. Osteoporos. Int. 23, 1225–1234.

Munoz-Espin, D., Serrano, M., 2014. Cellular senescence: from physiology to pathology. Nat. Rev. Mol. Cell Biol. 15, 482–496.

Nakamura, T., Imai, Y., Matsumoto, T., Sato, S., Takeuchi, K., Igarashi, K., Harada, Y., Azuma, Y., Krust, A., Yamamoto, Y., et al., 2007. Estrogen prevents bone loss via estrogen receptor alpha and induction of Fas ligand in osteoclasts. Cell 130, 811–823.

Newgard, C.B., Sharpless, N.E., 2013. Coming of age: molecular drivers of aging and therapeutic opportunities. J. Clin. Investig. 123, 946–950.

Niccoli, T., Partridge, L., 2012. Ageing as a risk factor for disease. Curr. Biol. 22, R741–R752.

Nicks, K.M., Amin, S., Atkinson, E.J., Riggs, B.L., Melton III, L.J., Khosla, S., 2012. Relationship of age to bone microstructure independent of areal bone mineral density. J. Bone Miner. Res. 27, 637–644.

Nicolaije, C., Diderich, K.E., Botter, S.M., Priemel, M., Waarsing, J.H., Day, J.S., Brandt, R.M., Schilling, A.F., Weinans, H., Van der Eerden, B.C., et al., 2012. Age-related skeletal dynamics and decrease in bone strength in DNA repair deficient male trichothiodystrophy mice. PLoS One 7, e35246.

Niedernhofer, L.J., Garinis, G.A., Raams, A., Lalai, A.S., Robinson, A.R., Appeldoorn, E., Odijk, H., Oostendorp, R., Ahmad, A., van, L.W., et al., 2006. A new progeroid syndrome reveals that genotoxic stress suppresses the somatotroph axis. Nature 444, 1038–1043.

Nilsson, M.E., Vandenput, L., Tivesten, A., Norlen, A.K., Lagerquist, M.K., Windahl, S.H., Borjesson, A.E., Farman, H.H., Poutanen, M., Benrick, A., et al., 2015. Measurement of a comprehensive sex steroid profile in rodent serum by high-sensitive gas chromatography-tandem mass spectrometry. Endocrinology 156, 2492–2502.

Nirody, J.A., Cheng, K.P., Parrish, R.M., Burghardt, A.J., Majumdar, S., Link, T.M., Kazakia, G.J., 2015. Spatial distribution of intracortical porosity varies across age and sex. Bone 75, 88–95.

Noble, B.S., Stevens, H., Loveridge, N., Reeve, J., 1997. Identification of apoptotic changes in osteocytes in normal and pathological human bone. Bone 20, 273–282.

Nollet, M., Santucci-Darmanin, S., Breuil, V., Al-Sahlanee, R., Cros, C., Topi, M., Momier, D., Samson, M., Pagnotta, S., Cailleteau, L., et al., 2014. Autophagy in osteoblasts is involved in mineralization and bone homeostasis. Autophagy 10, 1965–1977.

Notini, A.J., McManus, J.F., Moore, A., Bouxsein, M., Jimenez, M., Chiu, W.S., Glatt, V., Kream, B.E., Handelsman, D.J., Morris, H.A., et al., 2007. Osteoblast deletion of exon 3 of the androgen receptor gene results in trabecular bone loss in adult male mice. J. Bone Miner. Res. 22, 347–356.

Ogrodnik, M., Miwa, S., Tchkonia, T., Tiniakos, D., Wilson, C.L., Lahat, A., Day, C.P., Burt, A., Palmer, A., Anstee, Q.M., et al., 2017. Cellular senescence drives age-dependent hepatic steatosis. Nat. Commun. 8, 15691.

Onal, M., Piemontese, M., Xiong, J., Wang, Y., Han, L., Ye, S., Komatsu, M., Selig, M., Weinstein, R.S., Zhao, H., et al., 2013. Suppression of autophagy in osteocytes mimics skeletal aging. J. Biol. Chem. 288, 17432–17440.

Ono, N., Ono, W., Nagasawa, T., Kronenberg, H.M., 2014. A subset of chondrogenic cells provides early mesenchymal progenitors in growing bones. Nat. Cell Biol. 16, 1157–1167.

Paik, J.H., Ding, Z., Narurkar, R., Ramkissoon, S., Muller, F., Kamoun, W.S., Chae, S.S., Zheng, H., Ying, H., Mahoney, J., et al., 2009. FoxOs cooperatively regulate diverse pathways governing neural stem cell homeostasis. Cell Stem Cell 5, 540–553.

Parfitt, A.M., 1990. Bone-forming cells in clinical conditions. In: Hall, B.K. (Ed.), Bone, The Osteoblast and Osteocyte, vol. 1. Telford Press and CRC Press, Boca Raton, FL, pp. 351–429.

Park, D., Spencer, J.A., Koh, B.I., Kobayashi, T., Fujisaki, J., Clemens, T.L., Lin, C.P., Kronenberg, H.M., Scadden, D.T., 2012. Endogenous bone marrow MSCs are dynamic, fate-restricted participants in bone maintenance and regeneration. Cell Stem Cell 10, 259–272.

Pazzaglia, U.E., Sibilia, V., Congiu, T., Pagani, F., Ravanelli, M., Zarattini, G., 2015. Setup of a bone aging experimental model in the rabbit comparing changes in cortical and trabecular bone: morphological and morphometric study in the femur. J. Morphol. 276, 733–747.

Piemontese, M., Almeida, M., Robling, A.G., Kim, H.N., Xiong, J., Thostenson, J.D., Weinstein, R.S., Manolagas, S.C., O'Brien, C.A., Jilka, R.L., 2017. Old age causes de novo intracortical bone remodeling and porosity in mice. JCI Insight 2.

Piemontese, M., Onal, M., Xiong, J., Han, L., Thostenson, J.D., Almeida, M., O'Brien, C.A., 2016. Low bone mass and changes in the osteocyte network in mice lacking autophagy in the osteoblast lineage. Sci. Rep. 6, 24262.

Power, J., Loveridge, N., Lyon, A., Rushton, N., Parker, M., Reeve, J., 2003. Bone remodeling at the endocortical surface of the human femoral neck: a mechanism for regional cortical thinning in cases of hip fracture. J. Bone Miner. Res. 18, 1775–1780.

Price, C., Herman, B.C., Lufkin, T., Goldman, H.M., Jepsen, K.J., 2005. Genetic variation in bone growth patterns defines adult mouse bone fragility. J. Bone Miner. Res. 20, 1983–1991.

Qiu, S., Rao, D.S., Palnitkar, S., Parfitt, A.M., 2002a. Age and distance from the surface but not menopause reduce osteocyte density in human cancellous bone. Bone 31, 313–318.

Qiu, S., Rao, D.S., Palnitkar, S., Parfitt, A.M., 2002b. Relationships between osteocyte density and bone formation rate in human cancellous bone. Bone 31, 709–711.

Que, X., Hung, M.Y., Yeang, C., Gonen, A., Prohaska, T.A., Sun, X., Diehl, C., Maatta, A., Gaddis, D.E., Bowden, K., et al., 2018. Oxidized phospholipids are proinflammatory and proatherogenic in hypercholesterolaemic mice. Nature 558, 301–306.

Razi, H., Birkhold, A.I., Weinkamer, R., Duda, G.N., Willie, B.M., Checa, S., 2015. Aging leads to a dysregulation in mechanically driven bone formation and resorption. J. Bone Miner. Res. 30, 1864–1873.

Robinson, J.A., Chatterjee-Kishore, M., Yaworsky, P.J., Cullen, D.M., Zhao, W., Li, C., Kharode, Y., Sauter, L., Babij, P., Brown, E.L., et al., 2006. Wnt/beta-catenin signaling is a normal physiological response to mechanical loading in bone. J. Biol. Chem. 281, 31720–31728.

Robling, A.G., Castillo, A.B., Turner, C.H., 2006. Biomechanical and molecular regulation of bone remodeling. Annu. Rev. Biomed. Eng. 8, 455–498.

Robling, A.G., Niziolek, P.J., Baldridge, L.A., Condon, K.W., Allen, M.R., Alam, I., Mantila, S.M., Gluhak-Heinrich, J., Bellido, T.M., Harris, S.E., et al., 2008. Mechanical stimulation of bone in vivo reduces osteocyte expression of Sost/sclerostin. J. Biol. Chem. 283, 5866–5875.

Rossi, D.J., Jamieson, C.H., Weissman, I.L., 2008. Stems cells and the pathways to aging and cancer. Cell 132, 681–696.

Rouse, J., Jackson, S.P., 2002. Interfaces between the detection, signaling, and repair of DNA damage. Science 297, 547–551.

Rubin, C.T., Bain, S.D., McLeod, K.J., 1992. Suppression of the osteogenic response in the aging skeleton. Calcif. Tissue Int. 50, 306–313.

Rubin, C.T., Lanyon, L.E., 1985. Regulation of bone mass by mechanical strain magnitude. Calcif. Tissue Int. 37, 411–417.

Ryu, B.Y., Orwig, K.E., Oatley, J.M., Avarbock, M.R., Brinster, R.L., 2006. Effects of aging and niche microenvironment on spermatogonial stem cell self-renewal. Stem Cell. 24, 1505–1511.

Saeed, H., Abdallah, B.M., Ditzel, N., Catala-Lehnen, P., Qiu, W., Amling, M., Kassem, M., 2011. Telomerase-deficient mice exhibit bone loss owing to defects in osteoblasts and increased osteoclastogenesis by inflammatory microenvironment. J. Bone Miner. Res. 26, 1494–1505.

Salminen, A., Kauppinen, A., Kaarniranta, K., 2012. Emerging role of NF-kappaB signaling in the induction of senescence-associated secretory phenotype (SASP). Cell. Signal. 24, 835–845.

Salmon, A.B., Richardson, A., Perez, V.I., 2010. Update on the oxidative stress theory of aging: does oxidative stress play a role in aging or healthy aging? Free Radic. Biol. Med. 48, 642–655.

Sawakami, K., Robling, A.G., Ai, M., Pitner, N.D., Liu, D., Warden, S.J., Li, J., Maye, P., Rowe, D.W., Duncan, R.L., et al., 2006. The Wnt co-receptor LRP5 is essential for skeletal mechanotransduction but not for the anabolic bone response to parathyroid hormone treatment. J. Biol. Chem. 281, 23698–23711.

Scaffidi, P., Misteli, T., 2008. Lamin A-dependent misregulation of adult stem cells associated with accelerated ageing. Nat. Cell Biol. 10, 452–459.

Schafer, M.J., White, T.A., Iijima, K., Haak, A.J., Ligresti, G., Atkinson, E.J., Oberg, A.L., Birch, J., Salmonowicz, H., Zhu, Y., et al., 2017. Cellular senescence mediates fibrotic pulmonary disease. Nat. Commun. 8, 14532.

Schneider, P., Krucker, T., Meyer, E., Ulmann-Schuler, A., Weber, B., Stampanoni, M., Muller, R., 2009. Simultaneous 3D visualization and quantification of murine bone and bone vasculature using micro-computed tomography and vascular replica. Microsc. Res. Tech. 72, 690–701.

Schriner, S.E., Linford, N.J., Martin, G.M., Treuting, P., Ogburn, C.E., Emond, M., Coskun, P.E., Ladiges, W., Wolf, N., Van, R.H., et al., 2005. Extension of murine life span by overexpression of catalase targeted to mitochondria. Science 308, 1909–1911.

Sedelnikova, O.A., Horikawa, I., Zimonjic, D.B., Popescu, N.C., Bonner, W.M., Barrett, J.C., 2004. Senescing human cells and ageing mice accumulate DNA lesions with unrepairable double-strand breaks. Nat. Cell Biol. 6, 168–170.

Seeman, E., 2013. Age- and menopause-related bone loss compromise cortical and trabecular microstructure. J. Gerontol. A Biol. Sci. Med. Sci. 68, 1218–1225.

Sena, L.A., Chandel, N.S., 2012. Physiological roles of mitochondrial reactive oxygen species. Mol. Cell. 48, 158–167.

Sethe, S., Scutt, A., Stolzing, A., 2006. Aging of mesenchymal stem cells. Ageing Res. Rev. 5, 91–116.

Shanbhogue, V.V., Brixen, K., Hansen, S., 2016. Age- and sex-related changes in bone microarchitecture and estimated strength: a three-year prospective study using HRpQCT. J. Bone Miner. Res. 31, 1541–1549.

Sharpless, N.E., DePinho, R.A., 2007. How stem cells age and why this makes us grow old. Nat. Rev. Mol. Cell Biol. 8, 703–713.

Shefer, G., Van de Mark, D.P., Richardson, J.B., Yablonka-Reuveni, Z., 2006. Satellite-cell pool size does matter: defining the myogenic potency of aging skeletal muscle. Dev. Biol. 294, 50–66.

Sinnesael, M., Claessens, F., Laurent, M., Dubois, V., Boonen, S., Deboel, L., Vanderschueren, D., 2012. Androgen receptor (AR) in osteocytes is important for the maintenance of male skeletal integrity: evidence from targeted AR disruption in mouse osteocytes. J. Bone Miner. Res. 27, 2535–2543.

Smogorzewska, A., de Lange, T., 2002. Different telomere damage signaling pathways in human and mouse cells. EMBO J. 21, 4338–4348.

Soutoglou, E., Misteli, T., 2008. On the contribution of spatial genome organization to cancerous chromosome translocations. J. Natl. Cancer Inst. Monogr. 16–19.

Srinivasan, S., Gross, T.S., Bain, S.D., 2012. Bone mechanotransduction may require augmentation in order to strengthen the senescent skeleton. Ageing Res. Rev. 11, 353–360.

Steinberg, D., Witztum, J.L., 2010. Oxidized low-density lipoprotein and atherosclerosis. Arterioscler. Thromb. Vasc. Biol. 30, 2311–2316.

Stenderup, K., Justesen, J., Clausen, C., Kassem, M., 2003. Aging is associated with decreased maximal life span and accelerated senescence of bone marrow stromal cells. Bone 33, 919–926.

Stice, J.P., Knowlton, A.A., 2008. Estrogen, NFkappaB, and the heat shock response. Mol. Med. 14, 517–527.

Talchai, C., Xuan, S., Kitamura, T., DePinho, R.A., Accili, D., 2012. Generation of functional insulin-producing cells in the gut by Foxo1 ablation. Nat. Genet. 44, 406–412. S401.

Tan, P., Guan, H., Xie, L., Mi, B., Fang, Z., Li, J., Li, F., 2015. FOXO1 inhibits osteoclastogenesis partially by antagonizing MYC. Sci. Rep. 5, 16835.

Tang, G., Gudsnuk, K., Kuo, S.H., Cotrina, M.L., Rosoklija, G., Sosunov, A., Sonders, M.S., Kanter, E., Castagna, C., Yamamoto, A., et al., 2014. Loss of mTOR-dependent macroautophagy causes autistic-like synaptic pruning deficits. Neuron 83, 1131–1143.

Tiede-Lewis, L.M., Xie, Y., Hulbert, M.A., Campos, R., Dallas, M.R., Dusevich, V., Bonewald, L.F., Dallas, S.L., 2017. Degeneration of the osteocyte network in the C57BL/6 mouse model of aging. Aging 9, 2190–2208.

Tintut, Y., Demer, L.L., 2014. Effects of bioactive lipids and lipoproteins on bone. Trends Endocrinol. Metab. 25, 53–59.

Tintut, Y., Morony, S., Demer, L.L., 2004. Hyperlipidemia promotes osteoclastic potential of bone marrow cells ex vivo. Arterioscler. Thromb. Vasc. Biol. 24, e6–10.

Tsiantoulas, D., Diehl, C.J., Witztum, J.L., Binder, C.J., 2014. B cells and humoral immunity in atherosclerosis. Circ. Res. 114, 1743–1756.

Tsimikas, S., Brilakis, E.S., Lennon, R.J., Miller, E.R., Witztum, J.L., McConnell, J.P., Kornman, K.S., Berger, P.B., 2007. Relationship of IgG and IgM autoantibodies to oxidized low density lipoprotein with coronary artery disease and cardiovascular events. J. Lipid Res. 48, 425–433.

Tu, X., Rhee, Y., Condon, K.W., Bivi, N., Allen, M.R., Dwyer, D., Stolina, M., Turner, C.H., Robling, A.G., Plotkin, L.I., et al., 2012. Sost down-regulation and local Wnt signaling are required for the osteogenic response to mechanical loading. Bone 50, 209–217.

Turner, C.H., Takano, Y., Owan, I., 1995. Aging changes mechanical loading thresholds for bone formation in rats. J. Bone Miner. Res. 10, 1544–1549.

Ucer, S., Iyer, S., Bartell, S.M., Martin-Millan, M., Han, L., Kim, H.N., Weinstein, R.S., Jilka, R.L., O'Brien, C.A., Almeida, M., et al., 2015. The effects of androgens on murine cortical bone do not require AR or ERalpha signaling in osteoblasts and osteoclasts. J. Bone Miner. Res. 30, 1138–1149.

Ucer, S., Iyer, S., Kim, H.N., Han, L., Rutlen, C., Allison, K., Thostenson, J.D., de, C.R., Jilka, R.L., O'Brien, C., et al., 2017. The effects of aging and sex steroid deficiency on the murine skeleton are independent and mechanistically distinct. J. Bone Miner. Res. 32, 560–574.

Vainionpaa, A., Korpelainen, R., Sievanen, H., Vihriala, E., Leppaluoto, J., Jamsa, T., 2007. Effect of impact exercise and its intensity on bone geometry at weight-bearing tibia and femur. Bone 40, 604–611.

Van Remmen, H., Ikeno, Y., Hamilton, M., Pahlavani, M., Wolf, N., Thorpe, S.R., Alderson, N.L., Baynes, J.W., Epstein, C.J., Huang, T.T., et al., 2003. Life-long reduction in MnSOD activity results in increased DNA damage and higher incidence of cancer but does not accelerate aging. Physiol. Genom. 16, 29–37.

Vanderschueren, D., Laurent, M.R., Claessens, F., Gielen, E., Lagerquist, M.K., Vandenput, L., Borjesson, A.E., Ohlsson, C., 2014. Sex steroid actions in male bone. Endocr. Rev. 35, 906–960.

Vas, J., Gronwall, C., Silverman, G.J., 2013. Fundamental roles of the innate-like repertoire of natural antibodies in immune homeostasis. Front. Immunol. 4, 4.

Vashishth, D., Verborgt, O., Divine, G., Schaffler, M.B., Fyhrie, D.P., 2000. Decline in osteocyte lacunar density in human cortical bone is associated with accumulation of microcracks with age. Bone 26, 375−380.

Vijg, J., Campisi, J., 2008. Puzzles, promises and a cure for ageing. Nature 454, 1065−1071.

Wanagat, J., Dai, D.F., Rabinovitch, P., 2010. Mitochondrial oxidative stress and mammalian healthspan. Mech. Ageing Dev. 131, 527−535.

Warr, M.R., Binnewies, M., Flach, J., Reynaud, D., Garg, T., Malhotra, R., Debnath, J., Passegue, E., 2013. FOXO3A directs a protective autophagy program in haematopoietic stem cells. Nature 494, 323−327.

Wijnhoven, S.W., Beems, R.B., Roodbergen, M., van den Berg, J., Lohman, P.H., Diderich, K., van der Horst, G.T., Vijg, J., Hoeijmakers, J.H., van Steeg, H., 2005. Accelerated aging pathology in ad libitum fed Xpd(TTD) mice is accompanied by features suggestive of caloric restriction. DNA Repair 4, 1314−1324.

Witztum, J.L., Lichtman, A.H., 2014. The influence of innate and adaptive immune responses on atherosclerosis. Annu. Rev. Pathol. 9, 73−102.

Xiong, J., Onal, M., Jilka, R.L., Weinstein, R.S., Manolagas, S.C., O'Brien, C.A., 2011. Matrix-embedded cells control osteoclast formation. Nat. Med. 17, 1235−1241.

Yamasaki, N., Tsuboi, H., Hirao, M., Nampei, A., Yoshikawa, H., Hashimoto, J., 2009. High oxygen tension prolongs the survival of osteoclast precursors via macrophage colony-stimulating factor. Bone 44, 71−79.

Yang, Z., Klionsky, D.J., 2010. Eaten alive: a history of macroautophagy. Nat. Cell Biol. 12, 814−822.

Zebaze, R.M., Ghasem-Zadeh, A., Bohte, A., Iuliano-Burns, S., Mirams, M., Price, R.I., Mackie, E.J., Seeman, E., 2010. Intracortical remodelling and porosity in the distal radius and post-mortem femurs of women: a cross-sectional study. Lancet 375, 1729−1736.

Zhang, X., Ebata, K.T., Robaire, B., Nagano, M.C., 2006. Aging of male germ line stem cells in mice. Biol. Reprod. 74, 119−124.

Zhang, Y., Ikeno, Y., Qi, W., Chaudhuri, A., Li, Y., Bokov, A., Thorpe, S.R., Baynes, J.W., Epstein, C., Richardson, A., et al., 2009. Mice deficient in both Mn superoxide dismutase and glutathione peroxidase-1 have increased oxidative damage and a greater incidence of pathology but no reduction in longevity. J. Gerontol. A Biol. Sci. Med. Sci. 64, 1212−1220.

Zhao, J., Brault, J.J., Schild, A., Goldberg, A.L., 2008. Coordinate activation of autophagy and the proteasome pathway by FoxO transcription factor. Autophagy 4, 378−380.

Zhao, L., Shim, J.W., Dodge, T.R., Robling, A.G., Yokota, H., 2013. Inactivation of Lrp5 in osteocytes reduces young's modulus and responsiveness to the mechanical loading. Bone 54, 35−43.

Zhou, B.O., Yue, R., Murphy, M.M., Peyer, J.G., Morrison, S.J., 2014. Leptin-receptor-expressing mesenchymal stromal cells represent the main source of bone formed by adult bone marrow. Cell Stem Cell 15, 154−168.

Zhou, S., Greenberger, J.S., Epperly, M.W., Goff, J.P., Adler, C., Leboff, M.S., Glowacki, J., 2008. Age-related intrinsic changes in human bone-marrow-derived mesenchymal stem cells and their differentiation to osteoblasts. Aging Cell 7, 335−343.

Zhu, Y., Tchkonia, T., Pirtskhalava, T., Gower, A.C., Ding, H., Giorgadze, N., Palmer, A.K., Ikeno, Y., Hubbard, G.B., Lenburg, M., et al., 2015. The Achilles' heel of senescent cells: from transcriptome to senolytic drugs. Aging Cell 14, 644−658.

Chapter 13

Type I collagen structure, synthesis, and regulation

George Bou-Gharios[1], David Abraham[2] and Benoit de Crombrugghe[3]

[1]Institute of Ageing and Chronic Disease, University of Liverpool, Liverpool, United Kingdom; [2]Centre for Rheumatology and Connective Tissue Diseases, University College London, London, United Kingdom; [3]The University of Texas M.D. Anderson Cancer Center, Houston, TX, United States

Chapter outline

Introduction

It has been over 150 years since the term "collagen" was first adopted in the English language. This ropelike structure that yields gelatin upon boiling made its early appearance in evolution in primitive animals such as jellyfish, coral, and sea anemones (Bergeon, 1967). Today, the collagen family of proteins has grown to 28 different types and is used as a versatile biomaterial for delivery of drugs as well as for cosmetic purposes.

The work of Nageotte in the early 1920s used acid solubilization to reveal the fibers that histologists had earlier described in sections of connective tissues (Nageotte, 1927); X-ray diffraction and then electron microscopy characterized those fibers that made up the collagen molecule. In addition to collagens involved in fibril formation, several other groups

Principles of Bone Biology. https://doi.org/10.1016/B978-0-12-814841-9.00013-0

of nonfibrillar collagen have been discovered. Among these, some are involved in the formation of membranes that surround tissues, such as basement and Descemet's membranes, the cuticle of worms, and the skeleton of sponges. During those 150 years our understanding of collagen has evolved with advances in techniques and technology. This led to the discovery that collagens mediate adulthood extracellular matrix (ECM) remodeling and are needed for aging to be delayed (Ewald et al., 2015). The importance of collagen production in diverse antiaging interventions implies that ECM remodeling is a generally essential signature of longevity assurance.

In this chapter, we are focusing on fibrillar collagens and, in particular, collagen type I, the most abundant extracellular protein, especially in bone where it is essential for bone strength and in soft connective tissues where it confers compliance, flexibility, and resilience. We will discuss the structure and biosynthesis, regulation, and degradation of type I collagen and associated proteins that maintain its homeostasis and recent insights into the organization of regulatory elements in type I collagen genes, many of which are based on studies in transgenic mice. Then we will address how collagen synthesis is regulated by cytokines and growth factors.

The accepted definition of collagens is "structural proteins of the extracellular matrix which contain one or more domains harboring the conformation of a collagen triple helix" (Myllyharju and Kivirikko, 2004; van der Rest and Garrone, 1991). The triple-helix motif is composed of three polypeptide chains whose amino acid sequence consists of Gly−X−Y repeats. Because of this particular peptide sequence, each chain is coiled in a left-handed helix, and the three chains assemble in a right-handed triple helix, where Gly residues are in the center of the triple helix and the lateral chains of X and Y residues are on the surface of the helix (van der Rest and Garrone, 1991). In about one-third of the cases, X is a proline and Y is a hydroxyproline; the presence of hydroxyproline is essential to stabilize the triple helix and is a unique characteristic of collagen molecules. At the time of this review, 28 different types of collagens have been described, which are grouped in subfamilies depending on their structure and/or their function. The Roman numerals denoting collagen types follow the order in which they were reported. For each collagen type, the α chains are identified with Arabic numerals (Myllyharju and Kivirikko, 2001). Although a standard nomenclature has been agreed on, the representation of the collagen names can be sometimes confusing. Throughout this chapter, we will address the unassembled collagen molecules as procollagens, the mouse genes as Col1a1 or Col1a2 (lower case), and the human genes in capital letters (COL1A1 or COL1A2).

The family of fibrillar collagens

Types I, II, III, V, and XI and the newly described types XXIV and XXVII collagens (Boot-Handford et al., 2003; Koch et al., 2003) form the group of fibrillar collagens. The characteristic feature of fibrillar collagens is that they consist of a long continuous triple helix that self-assembles into highly organized fibrils. These fibrils have a very high tensile strength and play a key role in providing a structural framework for body structures such as skeleton, skin, blood vessels, intestines, or fibrous capsules of organs. Type I collagen, which is the most abundant protein in vertebrates, is present in many organs and is a major constituent of bone, tendons, ligaments, and skin. Type III collagen is less abundant than type I collagen, but its distribution essentially parallels that of type I collagen with the exception of bones and tendons, which contain virtually no type III collagen. Moreover, type III collagen is relatively more abundant in distensible tissues, such as blood vessels, than in nondistensible tissues. Type V collagen is present in tissues that also contain type I collagen. Type II collagen is a major constituent of cartilage and is also present in the vitreous body. Like type II, type XI and type XXVII collagens are present in cartilage. However, unlike other collagens, type XXVII appears to express in epithelial cells of cochlea, lung, gonad, and stomach (Boot-Handford et al., 2003), suggesting that its function in these epithelial layers cannot depend on the copolymerization with other collagens. Collagen type XXIV displays unique structural features of invertebrate fibrillar collagens and is expressed predominantly in bone tissue (Matsuo et al., 2006).

Bone formation is a complex and tightly regulated genetic program that involves two distinct pathways at different anatomical locations (de Crombrugghe et al., 2001; Karsenty and Wagner, 2002; Olsen et al., 2000). In intramembranous ossification, mesenchymal cells condense and differentiate directly into mainly collagen type I−producing osteoblasts, whereas in endochondral bone formation, a cartilage model that is initially rich in type II and type XI collagens, which are secreted by chondrocytes, is replaced by an ostium rich in collagen type I matrix. Cartilage formation in endochondral skeletal elements is initiated by the condensation of chondrogenic mesenchymal cells followed by the overt differentiation of cells in these condensations. After undergoing a unilateral form of proliferation, these cells gradually become hypertrophic. At the same time, cells around the condensations form the perichondrial layer that gives rise to the osteoblast-forming periosteum and ultimately to cortical bone. The process of cartilage replacement by a bone matrix involves invasion by preosteoblasts in the periosteum as well as blood vessels and hematopoietic cells of the zone of hypertrophic chondrocytes. Expression of the genes for collagen type I and those for collagen types II and XI follows distinct

transcriptional codes that control osteoblastogenesis and chondrogenesis (Bridgewater et al., 1998; de Crombrugghe et al., 2001; Karsenty and Wagner, 2002; Lefebvre et al., 2001; Lefebvre and de Crombrugghe, 1998). In addition to fibrillar collagens, collagen type X has been implicated in the morphogenic events of hypertrophic cartilage prior to its replacement by bone. Although knockout mice for collagen X showed no apparent phenotype (Rosati et al., 1994), significant reduction in the amount and quality of bone minerals was evident (Paschalis et al., 1996).

Collagen types XXIV and XXVII display mutually exclusive patterns of expression in the developing and adult mouse skeleton. Gene expression studies have shown that, whereas Col24a1 transcripts accumulate at ossification centers of the craniofacial, axial, and appendicular skeleton, Col27a1 activity is instead confined to the cartilaginous anlagen of skeletal elements (Boot-Handford et al., 2003; Koch et al., 2003; Pace et al., 2003). In addition, structural considerations have suggested that collagens XXIV and XXVII are likely to form distinct homotrimers (Koch et al., 2003). Together these observations have been interpreted to indicate that these newly discovered fibrillar collagens may participate in the control of important physiological processes in bone and cartilage, such as collagen fibrillogenesis and/or matrix calcification and mineralization (Boot-Handford et al., 2003; Koch et al., 2003; Pace et al., 2003).

Structure, biosynthesis, transport, and assembly of type I collagen

Structure

Fibril-forming collagens are synthesized in precursor form, procollagens. Each molecule of type I collagen is typically composed of two α1 chains and one α2 chain (α1(I)2−α2(I)) coiled around one another in a characteristic triple helix. Both the α1 chain and the α2 chain consist of a long helical domain preceded by a short N-terminal peptide and followed by a short C-terminal peptide (for reviews, see Myllyharju and Kivirikko, 2001, 2004, and van der Rest and Garrone, 1991).

The mechanism that controls the 2:1 stoichiometry of the collagen chains in type I collagen is not well understood. It is evident that a number of type I collagen molecules can be formed by three α1 chains (α1(I)3). The homotrimeric type I collagen isotype containing three pro-α1(I) collagen chains (α1(I)3) is a minor isotype, whose role is not well understood. Homotrimers are found embryonically (Jimenez et al., 1977; Rupard et al., 1988), in small amounts in skin (Uitto, 1979), in certain tumors and cultured cancer cell lines (Moro and Smith, 1977; Rupard et al., 1988), and also during wound healing (Haralson et al., 1987). Mesangial cells, which do not synthesize collagen type I in vivo, produce homotrimeric type I collagen in culture, further suggesting that homotrimers play a role in wound healing (Johnson et al., 1992). The collagen I α2-deficient mouse, otherwise known as the oim mouse (osteogenesis imperfecta [OI] model), is homozygous for a spontaneous nucleotide deletion in the Col1a2 gene, resulting in a frameshift altering the carboxy propeptide of the pro-Col1a2 chain. Although the carboxy propeptide is not present in mature type I collagen, it is responsible for association of the Col1a2 chain with the Col1a1 chains during assembly of the triple helix (Chipman et al., 1993; Deak et al., 1983; McBride et al., 1997) (see sections on collagen diseases).

Type I collagen is secreted as a propeptide, but the N telopeptide and the C telopeptide are cleaved rapidly by specific proteases, ADAMTS- 2 and bone morphogenetic protein 1 (BMP-1), respectively, so that shorter molecules assemble to form fibrils (Canty and Kadler, 2005). In fibrils, molecules of collagen are parallel to one another (Fig. 13.1); they overlap one another by multiples of 67 nm (distance D), with each molecule being 4.4 D (300 nm) long; there is a 40-nm (0.6 D) gap between the end of a molecule and the beginning of the next (see Fig. 13.1). This quarter-staggered assembly explains the banded aspect displayed by type I collagen fibrils in electron microscopy. In tissues, type I collagen fibrils can be parallel to one another and form bundles (or fibers), as in tendons, or they can be oriented randomly and form a complex network of interlaced fibrils, as in skin. In bone, hydroxyapatite crystals seem to lie in the gaps between collagen molecules.

Regulation of transcription

In humans the gene coding for the α1 chain of type I collagen is located on the long arm of chromosome 17 (17q21.3−q22; chromosome 11 in mouse), and the gene coding for the α2 chain is located on the long arm of chromosome 7 (7q21.3−q22; chromosome 6 in mouse). Both genes have very similar structures (Chu et al., 1984; D'Alessio et al., 1988), and this structure is also very similar to that of genes coding for other fibrillar collagens (Vuorio and de Crombrugghe, 1990). The difference in size between the two genes (18 kb for the Col1a1 gene and 38 kb for the Col1a2 gene) is explained by differences in the sizes of the introns.

The triple-helical domain of the α1 chain is coded by 41 exons, which code for Gly−X−Y repeats, and by two so-called joining exons. These joining exons code in part for the telopeptides and in part for Gly−X−Y repeats, which

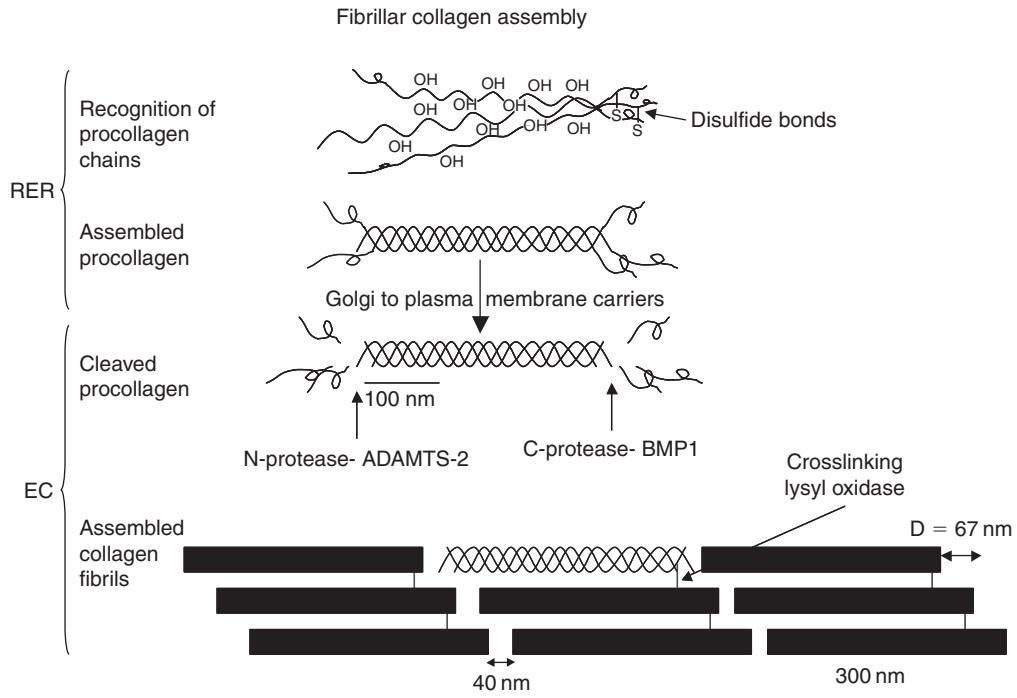

FIGURE 13.1 Schematic diagram of collagen assembly depicting the recognition of the α chains in the rough endoplasmic reticulum (*RER*) and the helix formation strengthened by the hydroxylated proline and lysine residues (*OH*). The collagen is then transported by the Golgi to plasma membrane vesicles to the extracellular space (*EC*) where the propeptides are removed by proteinases and the fibrils are assembled into collagen fibers that are cross-linked by lysyl oxidase. *ADAMTS-2*, a disintegrin and metalloproteinase with thrombospondin motifs-2; *BMP1*, bone morphogenetic protein-1.

are part of the triple-helical domain. The triple-helical domain of the α2 chain is coded by 42 exons, plus two joining exons. The corresponding exons coding for the triple-helical domain of the α1 chain and for the triple-helical domain of the α2 chain have similar lengths (Table 13.1). The only exception is that exons 34 and 35 in Col1a2, which are 54 bp long each, correspond to a single 108-bp 34/35 exon in the a1 gene. Except for the two joining exons, each exon starts exactly with a G codon and ends precisely with a Y codon, and all the exons are 54, 108 (54 3 2), 162 (54 3 3), 45, or 99 bp long (see Table 13.1). This organization suggests that exons coding for triple-helical domains could have originated from the amplification of a DNA unit containing a 54-bp exon embedded in intron sequences. Exons of 108 and 162 bp would result from a loss of intervening introns. Exons of 45 and 99 bp would result from recombinations between two 54-bp exons (Vuorio and de Crombrugghe, 1990).

For both the α1 chain and the α2 chain, the C propeptide plus the C telopeptide are coded by four exons (exons 48−51 of the Col1a1 gene, exons 49−52 of the Col1a2 gene). The first of these exons codes for the end of the triple-helical domain, the C-terminal telopeptide, and the beginning of the C-terminal propeptide. The three other exons code for the rest of the C-terminal propeptide. The C-terminal propeptide has a globular structure that is stabilized by two intrachain disulfide bonds (see Fig. 13.1). It contains three (α2 chain) and four (α1 chain) additional cysteine residues that form interchain disulfide bonds. The formation of disulfide bonds precedes the triple-helix formation and plays an essential role in the intracellular assembly of the three α chains (see sections on translational and posttranslational modifications). Prdm5 is a member of a family of transcriptional regulators that predominantly bind exonic regions of collagen genes and associate with RNA polymerase II to sustain collagen I transcription. Prdm5 targets all mouse collagen genes as well as several small leucine-rich proteoglycan (SLRP) genes. Prdm5 controls both collagen I transcription and fibrillogenesis by binding inside the Col1a1 gene body and maintaining RNA polymerase II occupancy. In vivo, Prdm5 loss results in delayed ossification involving a pronounced impairment in the assembly of fibrillar collagens (Galli et al., 2012).

The signal peptide, the N propeptide, and the N telopeptide of the 1 chain, as well as of the α2 chain, are coded by the first six exons. The N propeptide of the α1 chain contains a cysteine-rich (10-cysteine-residue) globular domain, a short triple-helical domain, and a short globular domain, which harbors the N-terminal peptidase cleavage site (see Fig. 13.1). The N-terminal propeptide of the α2 chain does not contain a cysteine-rich domain but a short globular domain. The 3′-untranslated region (UTR) of both the Col1a1 gene and the Col1a2 gene contains more than one polyadenylation site,

TABLE 13.1 Sizes of exons coding for the triple-helical domain of type I collagen[a].

Exon	Size (bp)	Exon	Size (bp)	Exon	Size (bp)
7	45	21	108	35	54
8	54	22	54	36	54
9	54	23	99	37	108
10	54	24	54	38	54
11	54	25	99	39	54
12	54	26	54	40	162
13	45	27	54	41	108
14	54	28	54	42	108
15	45	29	54	43	54
16	54	30	45	44	108
17	99	31	99	45	54
18	45	32	108	46	108
19	99	33	54	47	54
20	54	34	54	48	108

[a]In the pro-α1(I) collagen gene, exons 33 (54 bp) and 34 (54 bp) are replaced by a single 108-bp 33/34 exon. The two joining exons (exons 6 and 49) are not considered in this table (see text for details).

which indicates that mRNAs with different sizes will be generated. As in many other genes, the functional role of the different polyadenylation sites is still unknown.

Control of translation

After being transcribed, the pre-mRNA undergoes exon splicing, capping, and addition of a poly(A) tail, which gives rise to a mature mRNA. These mature mRNAs are then translated in polysomes, and the resulting proteins undergo extensive posttranslational modifications before being assembled into a triple helix and released in the extracellular space (for reviews, see Lamande and Bateman, 1999; Myllyharju and Kivirikko, 2001).

Signal peptides are cleaved from the chains when their N-terminal end enters the cisternae of the rough endoplasmic reticulum (ER). Both the pro-α1 chain and the pro-α2 chain undergo hydroxylation and glycosylation, and these modifications are essential for the assembly of type I collagen chains in a triple helix. About 100 proline residues in the Y position of the Gly−X−Y repeats, a few proline residues in the X position, and about 10 lysine residues in the Y position undergo hydroxylation, respectively, by a prolyl 4-hydroxylase, a prolyl 3-hydroxylase, and a lysyl hydroxylase. Hydroxylation of proline to hydroxyproline is critical to obtain a stable triple helix, and at 37°C, stable folding in a triple-helical conformation cannot be obtained before at least 90 prolyl residues have been hydroxylated. These hydroxylases have different requirements to be active, and, in particular, they can act only when prolyl or lysyl residues occupy the correct position in the amino acid sequence of the α chain and when peptides are not in a triple-helical configuration. Moreover, these enzymes require ferrous ions, molecular oxygen, α-ketoglutarate, and ascorbic acid to be active. This requirement for ascorbic acid could explain some of the consequences of scurvy on wound healing. When lysyl residues become hydroxylated, they serve as a substrate for a glycosyltransferase and for a galactosyltransferase, which add glucose and galactose, respectively, to the E−OH group. As for hydroxylases, glycosylating enzymes are active only when the collagen chains are not in a triple-helical conformation. Glycosylation interferes with the packaging of mature molecules into fibrils, and increased glycosylation tends to decrease the diameter of fibrils.

While hydroxylations and glycosylations described previously occur, after a mannose-rich oligosaccharide is added to the C propeptide of each pro-α chain, C propeptides from two α1 chains and one α2 chain associate, with the formation of intrachain and interchain disulfide bonds. After prolyl residues have been hydroxylated, and the three C propeptides have associated, a triple helix will form at the C-terminal end of the molecule and then extend toward the N-terminal end (see Fig. 13.1). This propagation of the triple-helical configuration occurs in a "zipper-like" fashion (Prockop, 1990). If prolyl

residues are not hydroxylated or if interchain disulfide bonds are not formed between the C propeptides, the α chain will not fold into a triple helix. Although the functions of the C-terminal sequences, which have been associated with initiation of triple-helix formation, are thought to be well established, those of the N-terminal propeptide are poorly understood (Bornstein, 2002). The N propeptide of type I procollagen, as released physiologically by procollagen N-protease (ADAMTS-2), contains a globular domain largely encoded by exon 2 in the Col1a1 gene and a short triple helix that terminates in a non-triple-helical telopeptide sequence, which separates this helix from the major collagen helix. Bornstein and colleagues generated a mouse with a targeted deletion of exon 2 in the Col1a1 gene, thus replicating the type IIB splice form of type II procollagen in type I procollagen (Bornstein et al., 2002); surprisingly, homozygous mutant mice were essentially normal. In particular, none of the steps in collagen biogenesis thought to be dependent on the N propeptide were defective. However, there was a significant, but background-dependent, fetal mortality, which suggested a role for the type I collagen N propeptide in developmental processes.

Toman and colleagues have gone even further to demonstrate that propeptide may not be necessary for the selection and folding of procollagen. They engineered type I collagen genes that encode the N and C telopeptides with the entire triple-helical domain and showed that these sequences are sufficient for the assembly of a triple helix in *Saccharomyces cerevisiae* (Olsen et al., 2001). Other fibrillar collagens (types II, III, V, and XI) have similar structures and thus would be expected to fold into triple helices without the propeptide regions in an analogous system.

Intracellular transport

The transport of newly synthesized secretory proteins begins at their site of synthesis, the ER, a network of dynamically interconnected membrane tubules and cisternae (Fig. 13.1). All vesicles then detach from the ER through membrane fission and move to the ER−Golgi intermediate compartment. From there, carriers containing secretory cargoes are transported forward to the Golgi complex.

The newly formed triple-helical forms are then stabilized by heat shock protein 47 (Hsp47), a molecular chaperone of type I collagen molecules (Nagai et al., 2000; Tasab et al., 2000). This protein belongs to the serine protease inhibitor (serpin) superfamily containing a serpin signature sequence. Hsp47 resides in the ER, as inferred from the presence of a carboxyl-terminal RDEL sequence similar to the ER retrieval signal, KDEL. After folding, proteins enter the exit sites of the ER, where they are sorted into large pleomorphic budding vesicles that are generated through the membrane-bending properties of coat protein complex II (COPII). Disrupting the Hsp47 gene in mice resulted in embryonic lethality in mice by 11.5 days postcoitus and caused a molecular abnormality in procollagens (Nagai et al., 2000). Type I procollagen chains containing propeptides accumulated in the tissues, but the mature collagen chains normally processed were scarcely observed, suggesting that HSP47 is essential as a collagen-specific molecular chaperone for the proper processing of procollagen molecules, and the Hsp47 gene is needed for the normal development of mouse embryo (Nagai et al., 2000). However, the transfer from ER to the Golgi was unexplained since the mean fibrillar collagen, when formed into a trimer, adopts a rigid, rodlike structure of >300 nm in length and could not fit into a generic COPII vesicle of 60−90 nm diameter.

A genome-wide screen was performed in *Drosophila* tissue culture S2 cells to identify transport components (Bard et al., 2006). This screen revealed a number of previously unidentified genes required for transport and Golgi organization (TANGO genes). TANGO1 was shown to transport carriers without following the cargo into the vesicle itself. Thus, the mechanism of TANGO1-mediated cargo loading of collagen VII into COPII carriers (j.cell. 2008.12.025). A null allele of Mia3 in the mouse. Melanoma inhibitory activity member 3 (MIA3/TANGO1) is an evolutionarily conserved ER resident transmembrane protein.

Mia3 knockouts display a chondrodysplasia that causes dwarfing of the fetus, peripheral edema, and perinatal lethality. Thus far, our understanding of Mia3 (*Drosophila melanogaster* homolog of the vertebrate gene MIA3, also known as TANGO1) in escorting all collagens examined to date, including collagens I, II, III, IV, VII, and IX, but not other ECM components, such as fibronectin or aggrecan, indicates that this protein plays a unique role within the cell to facilitate the nucleation of large ER transport vesicles. However, collagen secretion indeed still occurs in Mia3-null cells. Either an alternate independent pathway of egress remains open to large ECM cargoes, or these proteins can still exit via large COPII vesicles (Wilson et al., 2011). Interestingly, studies in mice focusing on liver fibrogenesis and hepatic stellate cell (HSC) function noted that the loss of MIA3/TANGO1 resulted in retention of procollagen I in the ER and promotion of the unfolded protein response. In vivo this was manifest as a reduction in hepatic fibrosis following liver injury and a dysregulation in HSC homeostasis leading to enhanced apoptosis (Maiers et al., 2017). A critical role for correct intracellular transport of procollagen I has also been highlighted in HSCs deficient in the ER oxidase 1α enzyme (ERO1α), which mediates protein modifications crucial to the transport of secreted proteins. Silencing of ERO1α caused impaired secretion of collagen type I and intracellular accumulation severely inhibiting cell proliferation (Fujii et al., 2017). It is notable that

mutations in the ubiquitous COPII component Sec23a or in the transport protein particle complex subunit TRAPPC2 (which is involved in trafficking between the ER and the Golgi complex) can selectively affect osteocytes and chondrocytes, resulting in craniolenticulosutural dysplasia (Boyadjiev et al., 2006) and spondyloepiphyseal dysplasia tarda (Gedeon et al.,1999), respectively.

After passing through the Golgi complex and reaching the *trans*-Golgi network (TGN), different cargoes are packaged in specialized membranous carriers, within which they are shipped out to the plasma membrane. There they are secreted into the extracellular space, where removal of the N and C propeptides from procollagens I, II, and III is catalyzed by specific Zn^{2+}-dependent metalloendopeptidases, procollagen N- and C-proteinase, respectively (Prockop, 1998). Procollagen C-proteinase, also known as BMP-1, is a member of the astacin family of proteases and triggers spontaneous self-assembly of collagen molecules into fibrils, giving rise to mature collagen molecules (Kadler, 2004; Kadler et al., 1990). Cleavage of the propeptide decreases the solubility of collagen molecules dramatically. Thus a major extracellular function of C propeptides is thought to prevent fibril formation, while N propeptides influence fibril shape and diameter (Hulmes, 2002).

The free propeptides are believed to be involved in feedback regulation of the synthesis of types I and III collagens by fibroblasts in culture (Wiestner et al., 1979). However, the mechanism of this inhibition remained elusive despite attempts by several groups to characterize it.

Fibrillogenesis

In the extracellular space, the molecules of mature collagen assemble spontaneously into quarter-staggered fibrils; this assembly is directed by the presence of clusters of hydrophobic and of charged amino acids on the surface of the molecules. Fibril formation has been compared with crystallization in that it follows the principle of "nucleated growth" (Prockop, 1990). Once a small number of molecules have formed a nucleus, it grows rapidly to form large fibrils. During fibrillogenesis, some lysyl and hydroxylysyl residues are deaminated by a lysine oxidase, which deaminates the «-NH_2 group, giving rise to aldehyde derivatives. These aldehydes will associate spontaneously with «-NH_2 groups from a lysyl or hydroxylysyl residue of adjacent molecules, forming interchain cross-links. These cross-links will increase the tensile strength of the fibrils considerably (see Fig. 13.1). In vitro studies have shown that procollagen molecules and their various structural domains have a remarkable capacity to control all stages of collagen assembly, from intracellular assembly to extracellular suprafibrillar assembly at a micrometer scale. The in vivo process is much more complex, but we are beginning to understand some of this in particular cell types. Kadler and coworkers have shown that GPCs are indeed present in vivo in embryonic tendon fibroblasts and that some GPCs contain 28-nm-diameter collagen fibrils. Moreover, GPCs are targeted to novel plasma membrane protrusions, which they have termed "fibripositors" (fibril depositors). What was intriguing in this study is the fact that procollagen can be converted to collagen within the confines of the cell membrane, which is consistent with the observation of collagen fibrils in some GPCs and the known intracellular activation of BMP-1 in the TGN compartment (Canty-Laird et al., 2012). In addition, fibripositors were shown to be always oriented along the tendon axis, which establishes a link between intracellular transport and the organization of the ECM (Canty et al., 2004). Interestingly, fibripositor formation is not a constitutive process in procollagen-secreting cells. It is absent in postnatal development despite active procollagen synthesis, and occurs only during a narrow window of embryonic development when tissue architecture is being established. It is not known whether this phenomenon occurs in other types of specialized collagen-secreting cells. More recently, the Kadler group has shown that fibripositors are specialized sites of fibril assembly and fibril transport. The fibripositors form an extended mechanical interface between the cytoskeleton and extracellular collagen fibrils. This interface serves to transmit cell-derived tensioning force to the tissue, which is critical in maintaining fibril alignment. The dynamic transport of new collagen fibrils occurs at the plasma membrane and this process is driven by nonmuscle myosin II, since inhibition of dynamin-dependent endocytosis with dynasore blocked fibricarrier formation and caused accumulation of fibrils in fibripositors (Kalson et al., 2013).

Assembly

The final assembly of fibrillar collagen involves the direct interaction of several molecules, which include other collagens, SLRPs, and others. These interactions shape the diameter of the fibrils (Kuc and Scott, 1997; Vogel and Trotter, 1987) and patterning of the final matrix. SLRPs are a group of secreted proteins, including decorin, biglycan, fibromodulin, lumican, and keratocan, among others, that play major roles in tissue development and assembly, especially in collagen fibrillogenesis (Iozzo, 1999). Biglycan and decorin are highly expressed in extracellular bone matrix and there is now substantial evidence to support an increasing role for biglycan and decorin in influencing bone cell differentiation and proliferative

activity (Waddington et al., 2003). The ability of decorin and biglycan to interact with collagen molecules and to facilitate fibril formation has implicated these macromolecules in important roles in the provision of a collagenous framework in bone, which eventually allows for mineral deposition. Initial mineral deposition is proposed to occur within or near the gap zones along the collagen fibers, and the structural architecture of the collagen fibers along with interacting noncollagenous proteins is likely to play a key role in directing placement of the mineral crystals (Dahl and Veis, 2003).

Molecular modeling techniques have led to the proposal that decorin and biglycan adopt an open-horseshoe structure (Weber et al., 1996) where the inner cavity interacts with a single triple-helical molecule. The generation of mutated forms of decorin has demonstrated the importance of leucine-rich sequences 4− to 6 in mediating this interaction (Kresse et al., 1997). In addition, reduction in the disulfide bridges at the C- and N-terminal ends of decorin also abolished interaction with type I collagen (Ramamurthy et al., 1996) and this led to the proposal that the disulfide loop at the C terminus binds to adjacent collagen fibrils, thereby facilitating the lateral assembly and stabilization of the fibrils.

Interestingly, molecular analysis data have put forward the idea that decorin exists as a dimer in solution (Scott et al., 2003), and if this is the case in vivo, then the nature of this interaction will be important when considering the mechanistic role of decorin in fibril assembly. The glycosaminoglycan moieties of decorin and biglycan have also been deemed to play an important role in collagen fibrillogenesis, where the interaction of glycosylated forms of these SLRPs with collagen appeared to be greater than that of nonglycosylated forms (Bittner et al., 1996). Adding to the macro- and microstructural information of collagen type I, three important studies using high-resolution mapping, crystallographic techniques, and modeling have highlighted the spatial arrangement and packaging of the collagen molecules in fibrils and fibril domain architecture. These investigations have helped to evolve our understanding of cell−collagen−matrix interactions via the presentation of organized domains and provide novel solutions and information relevant to the functional interactions of decorin in assembly and matrix metalloproteinases (MMPs) in collagenolysis (Orgel et al., 2006; Sweeney et al., 2008; Varma et al., 2016). Further evidence for the role of decorin and biglycan in bone formation is provided by targeted deletion of the genes. The biglycan-knockout (Bgn 2/2) mouse (Xu et al., 1998), unlike the Dcn 2/2 mouse (Danielson et al., 1997), showed no gross skin abnormalities but rather a reduction in bone density. These mice were seen to develop an osteoporotic phenotype, failing to achieve peak bone mass, owing to decreased bone formation, with significantly shorter femurs (Ameye et al., 2002). Within these animals lower osteoblast numbers and osteoblast activity were observed. In vitro experiments demonstrated that the number and responsiveness of bone marrow stromal cells to transforming growth factor β (TGFβ), and hence osteogenic precursor cells, decreased dramatically with age, but apoptosis rates increased (Chen et al., 2002a,b). The effects were not confined only to the skeletal tissues. Within the teeth the transition of predentin to dentin appeared to be impaired and the thickness of the enamel was dramatically increased (Goldberg et al., 2002). Taken together these results would suggest that biglycan plays an important role in the formation of mineralized tissue. Furthermore, despite high sequence identity and somewhat similar patterns of localization, decorin and biglycan are not interchangeable in function and do not have the ability to rescue each other's knockout phenotypes. Notably, Bgn 2/2 and Dcn 2/2 double-knockout animals revealed that the effects of both gene deficiencies were additive in the dermis and synergistic in bone (Corsi et al., 2002). The lack of both genes caused a phenotype with severe skin fragility and osteopenia, resembling a rare progeroid variant of Ehlers−Danlos syndrome.

Consequences of genetic mutations on type I collagen formation

OI (also known as "brittle bone disease") is a genetic disease characterized by an extreme fragility of bones. Genetic studies have shown that it is due to a mutation in the coding sequence of either the pro-COL1A1 gene or the pro-COL1A2 gene, and more than 150 mutations have been identified (for review, see Byers, 2001). Most severe cases of OI result from mutations that lead to the synthesis of normal amounts of an abnormal chain, which can have three consequences (Marini et al., 2007). First, the structural abnormality can prevent the complete folding of the three chains in a triple helix, e.g., if a glycine is substituted by a bulkier amino acid that will not fit in the center of the triple helix. In this case, the incompletely folded triple-helical molecules will be degraded intracellularly, resulting in a phenomenon known as "procollagen suicide." Second, some mutations appear not to prevent folding of the three chains in a triple helix, but presumably prevent proper fibril assembly. For example, Prockop's group has shown that a mutation of the pro-Col1a1 gene that changed the cysteine at position 748 to a glycine produced a kink in the triple helix (Kadler et al., 1991). Finally, some mutations will not prevent triple-helical formation or fibrillogenesis but might modify the structural characteristics of the fibrils slightly and thus affect their mechanical properties. In all these cases, the consequences on the mechanical properties of bone are probably similar. Mild forms of OI most often result from a functionally null allele, which decreases the production of normal type I collagen. Null mutations are usually the result of the existence of a premature stop codon or of an abnormality in mRNA splicing. In these cases, the abnormal mRNA appears to be retained

in the nucleus (Johnson et al., 2000). A mouse model of OI has been obtained by using a knock-in strategy that introduced a $Gly^{349} \rightarrow Cys$ mutation into the pro-Col1a1 gene (Forlino et al., 1999). This model faithfully reproduced the human disease. Another spontaneous mouse mutation, the oim/oim mouse, analogous to human type III OI, carries a spontaneous deletion of G at nucleotide 3983 in the α2 chain of collagen type I, which alters the reading frame to result in the final 48 amino acids of the COOH-terminal propeptide generating a new stop codon, with addition of an extra amino acid (Chipman et al., 1993). In these mice, collagen type I is made of α(I)3 homotrimers in place of the normal α1(I)2 α2(I)1 heterotrimers (Chipman et al., 1993; Kuznetsova et al., 2004; Miles et al., 2002), which results in marked skeletal fragility, with thinning of the long bones and reduced mechanical strength (Chipman et al., 1993; Pereira et al., 1995). An additional organ pathology has been described by Phillips and coworkers, namely a glomerulopathy characterized by abnormal renal collagen deposition (Brodeur et al., 2007; Phillips et al., 2002). Interestingly, data have also provided an insight into a fourth mechanism potentially resulting in OI. Here, a mutation at the signal peptide cleavage site of collagen type I, a domain not well characterized, caused reduced production and the intracellular retention of collagen I, leading to a severe OI phenotype (Lindert et al., 2018). This study is consistent with the notion that mechanisms influencing intracellular transport of collagen I may exert a profound impact on bone and other connective tissues in which collagen type I plays an important structural role.

Ehlers–Danlos syndrome types VIIA and VIIB are two rare dominant genetic diseases characterized mainly by an extreme joint laxity. They result from mutations in the pro-COL1A1 gene (Ehlers–Danlos syndrome type VIIA) or in the pro-COL1A2 gene (Ehlers–Danlos syndrome type VIIB) that interfere with the normal splicing of exon 6, and a little fewer than 20 mutations have been described. These mutations can affect the splice donor site of intron 7 or the splice acceptor site of intron 5; in the latter case, there is efficient recognition of a cryptic site in exon 6 (Byers et al., 1997). Thus, these mutations induce a partial or complete excision of exon 6. They do not appear to affect the secretion of the abnormal procollagen molecules, but they are responsible for the disappearance of the cleavage site of the N-terminal propeptide and thus for the presence of partially processed collagen molecules in fibrils that fail to provide normal tensile strength to tissues (Byers, 2001). Nevertheless, these mutations seem to affect the rate of cleavage of the N-terminal propeptide rather than completely prevent it, which explains why the phenotype is less severe than for patients who do not have a functional N-proteinase (Ehlers–Danlos syndrome type VIIC).

Collagen type I degradation and catabolism

The absolute requirement to critically regulate collagen type I synthesis and assembly in health is paralleled by the necessity to control the level and deposition of collagen type I once produced at the level of degradation and catabolism (for reviews see Fields 2013; Van Doren 2015; Zigrino et al., 2016). Furthermore, work over the past 5–10 years has begun to unravel the molecular pathways mediating degradation of collagen (Mi et al., 2017; Sprangers et al., 2019). These studies have shown that several key intracellular and extracellular pathways exist, and both mechanisms are important for maintaining collagen homeostasis. Different pathways for extracellular and intracellular degradation are employed by a wide range of tissue and cell types (i.e., bone, cartilage, and skin). There are at least three main types of enzymes that possess collagenolytic activity, including the MMPs (Nagase et al., 2006), cathepsins (Novinec et al., 2013), and neutrophil elastase (Fields, 2013). One of the most typical vertebrate collagenases and the most studied with respect to collagen type I cleavage is MMP-1 (Arakaki et al., 2009; Fields, 2013). MMP-1 cleaves collagen type I into one-quarter- and three-quarter-length fragments (Lauer-Fields, 2002). Once cleaved, a number of factors appear to influence further collagenolysis and sequential degradation. These include conformational dynamics and the mechanism by which the MMPs disrupt the stable collagen triple helix (Adhikari, 2012), cross-linking (Kwansa et al., 2014), cell surface binding that facilitates collagen unwinding (Adhikari et al., 2011), and the presence of membrane-bound proteases such as MT1-MMP (Yañez-Mó et al., 2008). Several other MMPs, such as MMP-2, MMP-8, MMP-9, MMP-12, MMP-13, and MMP-14, are also known to degrade collagen, but in general the precise modes of action of many have not been studied in detail. For MMP-12, the catalytic domain has been studied, and it recognizes, binds, and cleaves at specific sites in the triple helix in regions of relatively less proline, notably between Gly^{775} and Leu/Ile^{776} in the α1 and α2 collagen chains, respectively, in a manner that is characteristic of the unique collagenolytic activity of MMP collagenases (Bigg et al., 2007; Tam et al., 2004; Taddese et al., 2010).

It is clear that correct proteolytic processing and collagenolysis are critical in development and for normal tissue homeostasis, and abnormalities in these processes or their dysregulation in disease and aging can significantly contribute to many severe pathologies (reviewed in 2017 by Amar et al.,). It has also become apparent that many studies aimed at defining the molecular mechanism(s) have taken advantage of animal systems or in vitro analysis. For instance, in models of diabetes in rodents, reduced MMP (MMP-2 and MMP-9) activity was noted to be associated with increased collagen

deposition and stromal growth (Santos et al., 2017), and an imbalance in MMP/tissue inhibitor of metalloproteinases (TIMP) levels (creating reduced MMP-1 and MMP-3) appears to be responsible for the elevated collagen type I production in an in vitro model of chronic liver disease using HSCs (Robert et al., 2016). Enhanced type I collagen levels can directly promote fibroblast differentiation by altering integrin expression in models of cardiac fibrosis (Hong et al., 2017). Abnormally high collagen turnover by enhanced MMP activity can be equally disruptive such as aortic aneurysms, where elevated MMP-3, MMP-9, and MMP-12 are present and associated with collagen degradation (Klaus et al., 2017). Another important aspect of dysregulated collagen catabolism is the direct impact excessive levels of collagen type I can exert on cells via surface receptors. Studies have shown type I collagen promotes differentiation, proliferation, and scar formation by cardiac and ligament fibroblasts and astrocytes via interactions with specific integrins, cadherins, and SPARC (secreted protein acidic and cysteine rich) (Hara et al., 2017; Hong et al., 2017; Rosset et al., 2017), and plays a proinflammatory role by altering the release of cytokines by monocytes (Schultz et al., 2016). These data provide an insight into the distinct and pivotal role of collagen type I in regulating critical cell functions and the deleterious impact resulting from failure of correct collagen type I degradation and homeostasis. A greater understanding of role of MMPs and the molecule mechanisms that underlie their distinct roles in collagenolysis will enable the development of selective, specific, or targeted approaches for the effective treatment of an array of human conditions.

Collagen type I and bone pathologies

Because type I collagen is the most abundant protein in bone and because mutations in the COL1A1 gene are a major cause of OI, this gene has been considered a strong candidate for susceptibility to osteoporosis (Ralston and de Crombrugghe, 2006). Indeed polymorphisms in both the promoter (Garcia-Giralt et al., 2002) and the first intron of COL1A1 (Grant et al., 1996) have been associated with changes in bone mineral density (BMD). The polymorphism of intron 1 is located in a binding site for the transcription factor Sp1 and has been associated with various osteoporosis-related symptoms such as bone density and fractures (Grant et al., 1996; Uitterlinden et al., 1998), postmenopausal bone loss (Harris et al., 2000; MacDonald et al., 2001), bone geometry (Qureshi et al., 2001), bone quality (Mann et al., 2001), and bone mineralization (Stewart et al., 2005). The osteoporosis-associated Sp1 polymorphism causes increased Sp1 binding, enhanced transcription, and abnormally high production of COLIA1 mRNA and protein (Mann et al., 2001), which result in an imbalance between the COLIA1 and the COLIA2 chains. This is thought to lead to impairment of bone strength and reduced bone mass in carriers of the Sp1 polymorphism (Stewart et al., 2005). Retrospective meta-analyses of previous studies have indicated that the Sp1 polymorphic allele is associated with reduced BMD and with vertebral fractures (Efstathiadou et al., 2001; Mann and Ralston, 2003). In a large prospective meta-analysis of more than 20,000 participants from several European countries in the GENOMOS study, homozygotes for the Sp1 polymorphism were found to be associated with lower BMD at the lumbar spine and femoral neck and a predisposition to vertebral fractures (Ralston et al., 2006). In this study, however, the BMD association was observed only for homozygotes of the Sp1 polymorphism, in contrast to previous studies in which heterozygotes also showed a reduction in BMD (Mann and Ralston, 2003). It should be noted that the association between COLIA1 alleles and vertebral fracture reported in GENOMOS and other studies was not fully accounted for by the reduced bone density, suggesting that the Sp1 allele may also be a measure of bone quality. Furthermore, the existence of an extended haplotype defined by the Sp1 polymorphism and other promoter polymorphisms has been proposed to exert stronger effects on BMD than the individual polymorphisms (Garcia-Giralt et al., 2002; Stewart et al., 2006). Evidence has been presented that suggests that the promoter polymorphism at position 21,663 interacts with the transcription factor NMP4, which plays a role in osteoblast differentiation by interacting with Smads (Garcia-Giralt et al., 2005).

Although collagen type I assembly stipulates a heterotrimer assembly, a homotrimer assembly appears to occur in fetal tissues, fibrosis, and cancer (Han et al., 2010). Genetic studies indicate that collagen (I) homotrimers may be detrimental to bone structure, as in the mouse model of OI (oim), in which only $(\alpha 1)3$ homotrimers are present and the bone contains smaller and more tightly packed apatite crystals, but has a lower BMD due to altered collagen organization and bone structure (Vanleene et al., 2012).

However, the homotrimer can reduce the risk of tendon/ligament rupture, possibly because of the laxity in the fibrils. Translational mechanisms may also play a role in collagen (I) homotrimer biosynthesis, as nonmuscle myosin has been reported to coordinate cotranslational translocation of collagen (I) heterotrimers (Cai et al., 2010). However, disassembly of nonmuscle myosin filaments appeared to result in collagen (I) homotrimer production in lung fibroblasts but not in scleroderma skin fibroblasts, indicating that translational control may be specific to particular cell or tissue types. Collagen (I) homotrimer is resistant to proteolytic degradation by MMPs through its resistance to local unwinding at the MMP cleavage site (Han et al., 2010) and may therefore persist in tissues during remodeling and contribute to tissue sclerosis. In

cancer, invasive cancer cells may use homotrimers for building MMP-resistant invasion paths, supporting local proliferation and directed migration of the cells, whereas surrounding normal stromal collagens are cleaved.

Transcriptional regulation of type I collagen genes

Expression of the pro-Col1a1 gene and the pro-Col1a2 gene is coordinately regulated in a variety of physiological and pathological situations. In many of these instances it is likely that the control of expression of these two genes is mainly exerted at the level of transcription, suggesting that similar transcription factors control the transcription of both genes.

This section considers successively the proximal promoter elements of these genes and then the nature of cell-specific enhancers located in other areas of these genes, including intronic sequences. Information about the various DNA elements has come from transient expression experiments in tissue culture cells, in vitro transcription experiments, and experiments in transgenic mice. In vitro transcription experiments and, in large measure, transient expression experiments identify DNA elements that have the potential of activating or inhibiting promoter activity. These DNA elements can be used as probes to detect DNA-binding proteins. However, transient expression and in vitro transcription experiments do not take into account the role of the chromatin structure in the control of gene expression. Transgenic mice are clearly the most physiological system to identify tissue-specific elements; the DNAs that are tested are integrated into the mouse genome and their activities are presumably also influenced by their chromatin environment. In transgenic mice experiments, reporter genes such as green fluorescent protein, luciferase, or the *Escherichia coli* β-galactosidase offer the advantage that their activity is indicative of promoter activation and location of the expression. All three transgenes can be detected in vivo without having to kill the mouse. In addition, X-Gal histochemical stain for β-galactosidase can identify the cell types in which the transgene is active by histology.

Transient transfection experiments using various sequences upstream of the transcription start site of either the pro-α1(I) or the pro-α2(I) promoter, cloned upstream of a reporter gene, and introduced into fibroblasts have delineated positive *cis*-acting regulatory segments in these two sequences that were designated as minimal proximal promoters. Footprint experiments and gel-shift assays performed using these regulatory elements as DNA templates have also characterized sequences that interact with DNA-binding proteins to modulate the expression of the two genes.

Proximal promoters of type I collagen genes

Transcription factors binding to the pro-α1(I) proximal promoter

In the pro-α1(1) collagen gene, a close homology exists between human and mouse promoters. Brenner and colleagues demonstrated by progressively deleting the mouse pro-Col1a1 promoter that sequences downstream of 2181 bp are needed for high-level transient transfection (Brenner et al., 1989). Therefore, the sequence between 2220 and 1110 has been used as the proximal promoter (Fig. 13.2) and contains binding sites for DNA-binding factors that also bind to the proximal pro-Col1a2 promoter (Ghosh, 2002). These DNA elements include an RFX consensus binding site surrounding the transcription start site (−11 to +10) that contains three methylation sites, rather than one in the COL1A2 gene RFX-binding site. RFX1 interacts weakly with the unmethylated COL1A1 site, and binds with higher affinity to the methylated site (Sengupta et al., 2005).

RFX1 represses the unmethylated COL1A1 less efficiently than COL1A2, while RFX5 interacts with both collagen type I genes with similar binding affinity and represses both promoters equally.

The mouse pro-Col1a1 proximal promoter includes a binding site for the CCAAT-binding protein CBF between 290 and 2115 (Karsenty and de Crombrugghe, 1990). A second CCAAT box located slightly more upstream is, however, unable to bind CBF, suggesting that sequences surrounding the CCAAT motif also have a role in CBF binding. Similar results were observed in the human COL1A1 promoter (Saitta et al., 2000). DNA transfection experiments with the pro-Col1a1 promoter showed that point mutations in the CBF-binding site decreased promoter activity (Karsenty and de Crombrugghe, 1990). The CBF-binding site is flanked by two identical 12-bp repeat sequences that are binding sites for Sp1 and probably other GC-rich binding proteins (Nehls et al., 1991). In transient transfection experiments, a mutation in the binding site that prevents the binding of Sp1 surprisingly increased the activity of the promoter, and overexpression of Sp1 decreased the activity of the promoter (Nehls et al., 1991). It is possible that several transcription factors with different activating potentials bind to overlapping binding sites and compete with one another for binding to these sites; the overall activity of the promoter could then depend on the relative occupancy of the different factors on the promoter DNA. Substitution mutations in two apparently redundant sites between 2190 and 2170 and between 2160 and 2130 that abolished DNA binding resulted in an increase in transcription (Karsenty and de Crombrugghe, 1990). Formation of a

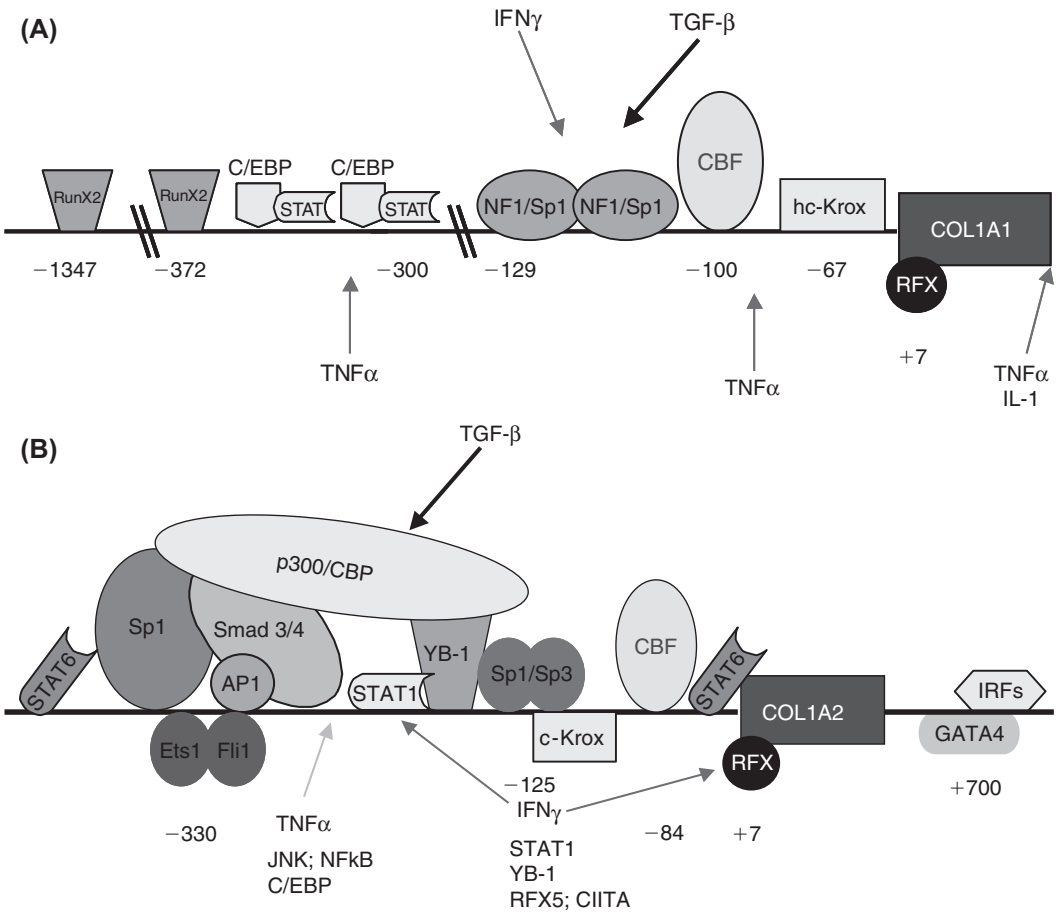

FIGURE 13.2 Schematic diagrams illustrating the known transcription factors that bind to the proximal promoter of the human and murine (A) Col1a1 and (B) Col1a2 promoters. Also shown are the cytokines that modulate the expression of these genes. The data are accumulated from several papers as cited in the text. *AP1*, activator protein 1; *CBF*, CCAAT-binding factor; *CBP*, CREB-binding protein; *C/EBP*, CCAAT/enhancer-binding protein; *CIITA*, class II, major histocompatibility complex, transactivator; *hc-Krox*, human collagen Krox; *IFNγ*, interferon-γ; *IL-1*, interleukin 1; *IRF*, interferon regulatory factor; *JNK*, Jun N-terminal kinase; *NF1*, nuclear factor 1; *NF-κB*, nuclear factor κB; *STAT*, signal transducer and activator of transcription; *TGF-β*, transforming growth factor β; *TNFα*, tumor necrosis factor α; *YB-1*, Y-box binding factor.

DNA−protein complex with these two redundant elements in the pro-Col1a1 promoter was also shown to be completed by the sequence of the pro-Col1a2 promoter between 2173 and 2143, suggesting that both type I promoters contained similar binding sites (Karsenty and de Crombrugghe, 1991). A member of the Krox family, designated c-Krox, binds to these two sites in the pro-Col1a1 promoter (Galera et al., 1994). In addition, c-Krox binds to a site located near the CCAAT box in the pro-Col1a1 promoter and to three GC-rich sequences in the pro-Col1a2 proximal promoter, located between 2277 and 2264 bp, between 2175 and 2143 bp, and near the CCAAT box, respectively (Galera et al., 1996). More recently, c-Krox has been shown to exert its action by synergistic association with SP1 (Kypriotou et al., 2007).

The Col1a1 promoter region spanning bp 29 to 256 bound purified recombinant YY1, and the corresponding binding activity in nuclear extracts was supershifted using a YY1-specific antibody. Mutation of the TATA box to TgTA enhanced YY1 complex formation. YY1 functions as a positive regulator of constitutive activity in fibroblasts. Although YY1 is not sufficient for transcriptional initiation, it is a required component of the transcription machinery in this promoter (Riquet et al., 2001).

A RunX2/Cbfa1-binding element is present in the Col1a1 promoter of mouse, rat, and human at approximately position 2372 (Kern et al., 2001). This site binds RunX2/Cbfa1 only weakly and does not act as a *cis*-acting activator of transcription when tested in DNA transfection experiments. These may interact with the upstream osteoblast-specific element (OSF2) site at 21,347 (Kern et al., 2001), as discussed under "Upstream elements in the pro-*Col1a1* gene" later.

A study exploring the impact of hypoxia on human cartilage identified the role of Sp3 transcription factor in down-regulating collagen type I by binding to a region in the human COL1A1 promoter (between −2300 and −1816) upstream

of the initiation site. This motif contains two GC boxes and the data support the competition between Sp1 and Sp3 for binding, and the accumulation of Sp3 in response to cartilage hypoxia switches from Sp1 binding, a positive regulator toward transcriptional suppression via Sp3 (Duval et al., 2016).

It is likely that the transcriptional function of various transcription factors and eventually their DNA-binding properties offer opportunities for regulation by intracellular signaling pathways. These pathways are triggered by a variety of cytokines such as tumor necrosis factor α (TNFα), which exerts its inhibitory action on Col1a1 expression through nuclear factor κB (NF-κB) (Rippe et al., 1999).

Factors binding to the pro-COL1A2 proximal promoter

Several functional *cis*-acting elements have been identified in the approximately 400-bp proximal promoter of the mouse pro-Col1a2 gene (154−2350 bp) and the human minimal sequence between 152 and 2378 bp. The first transcription factor found to bind to this promoter was the ubiquitous CCAAT-binding protein CBF. This transcription factor is formed by three separate subunits, named A, B, and C, which have all been cloned and sequenced (Maity and de Crombrugghe, 1998). All three subunits are needed for CBF to bind to the sequence containing the CCAAT box located between 284 and 280 and activate transcription in both human and mouse genes (see Fig. 13.2B). In vitro data suggest that the A and C subunits first associate to form an A−C complex and that this complex then forms a heteromeric molecule with the B subunit (Sinha et al., 1995). Mutations in the CCAAT box that prevent the binding of CBF decrease the transcriptional activity of the pro-Col1a2 proximal promoter three to five times in transient transfection experiments of fibroblastic cell lines (Coustry et al., 1995). Purified CBF as well as CBF composed of its three recombinant subunits also activate the pro-Col1a2 promoter in cell-free nuclear extracts previously depleted of CBF (Coustry et al., 1995). Two of the three subunits of CBF contain transcriptional activation domains. More recently, a single substitution of T to an A in vivo in the presence of an upstream enhancer of the human sequence suggested that CBF is involved in patterning of the collagen type I expression in the dorsoventral as well as the rostrocaudal axis of mouse skin fibroblasts (Tanaka et al., 2004).

In addition to the binding site for CBF, footprinting experiments and gel-shift studies identified other binding sites in the first 350 bp of the mouse pro-Col1a2 promoter. Three GC-rich sequences, located at about 2160 bp (between 2176 and 2152 bp) and 2120 bp (between 2131 and 2114 bp) have been shown to interact with DNA-binding proteins by footprint experiments and gel-shift assays (Hasegawa et al., 1996). A deletion in the mouse promoter encompassing these three footprinted sequences completely abolished the transcriptional activity of the pro-Col1a2 proximal promoter in transient transfection experiments using fibroblastic cell lines. The corresponding regions in the human pro-COL1A2 promoter were also protected in in vivo and in vitro footprinting experiments (Ihn et al., 1996) and bound transcriptional activators. However, gel-shift assays performed using the human pro-COL1A2 promoter have suggested that a *cis*-acting element located at 2160 bp represents a repressor element (Ihn et al., 1996), implying that interactions between proteins interacting with the activator elements at 2300, 2125, and 280 bp and proteins binding to a repressor element at 2160 bp regulate this gene. More recently it was shown that CUX1, a CCAAT displacement protein, is associated with reduced expression of type I collagen both in vivo and in vitro and that enhancing the expression of CUX1 results in effective suppression of type I collagen by interfering with CBF binding (Fragiadaki et al., 2011).

Sp1 and Sp3 have been shown to bind the TCCTCC motif located between 2123 and 2128 bp; both transcription factors activate this promoter (Ihn et al., 2001) (see Fig. 13.2B). Furthermore, proteins that bind to the two proximal segments also bind to the most upstream GC-rich segment, at 2300 bp, with the exception of CBF, suggesting a redundancy among functionally active DNA segments of the pro-COL1A2 proximal promoter.

TGFβ mediates its action in the human promoter through the combination of the ubiquitous transcription factor Sp1, the Smad3/4 complex, and the coactivators p300/CREB-binding protein (CBP) in what is termed a TGFβ-responsive element (TβRE) (Zhang et al., 2000). This segment contains three GC-rich motifs between 2330 and 2255, capable of binding Sp1, CCAAT/enhancer-binding protein (C/EBP), activator protein 1 (AP1), and Smad complexes (Chen et al., 1999, 2000a,b; Kanamaru et al., 2003; Tamaki et al., 1995; Zhang et al., 2000). Interaction among these nuclear factors is synergistic and requires binding of Sp1 and Smad3/4 to the GC-rich elements and the downstream CAGAC Smad site, respectively (Ghosh et al., 2000; Poncelet and Schnaper, 2001; Zhang et al., 2000). At the turn of this century, there was a great debate over whether Smads are more important than AP1 in the proximal promoter. This was resolved some 10 years later when it was shown that TGFβ also activates the COL1A2 gene via a noncanonical (Smad-independent) signaling pathway, which requires enhancer/promoter cooperation involving exchange of c-Jun/JunB transcription factor occupancy of a critical enhancer site, resulting in the stabilization of enhancer/promoter coalescence (Ponticos et al., 2009). A report exploring the effects of hypoxia and TGFβ on the COL1A2 gene has added to the potential role of Smads, in particular Smad3, in regulating collagen expression. These studies in human mesangial cells suggest that under hypoxic conditions and in the

presence of TGFβ, hypoxia-inducible factor 1α (HIF-1α) and Smad3 can form transcriptional complexes and preferentially enhance binding to one of the three hypoxia response elements within the human COL1A2 promoter at position −335 bp (Baumann et al., 2016). The authors suggest that this novel interaction provides a mechanism that accounts for the synergy observed between HIF and TGFβ in kidney fibrosis.

TNFα and interferon-γ (IFN-γ) suppress matrix production. In contrast to the single DNA element that mediates TGFβ stimulation of the COL1A2 proximal promoter, both TNFα and IFN-γ have been shown to inhibit COL1A2 transcription by interfering with the formation of the TGFβ-induced complex, and by stimulating the interaction of negative factors with responsive DNA elements located 5′ and 3′ of it. This so-called "cytokine responsive element" plays an important role in maintaining homeostasis. Involvement of AP1 and NF-κB in transducing the inhibitory action of TNFα on COL1A2 gene expression has been shown using immortalized fibroblasts from mice that lack either the AP1 activator Jun N-terminal kinase 1 (JNK1) or the NF-κB essential modulator NEMO. Specifically, the loss of JNK1 prevented the TNFα antagonism of TGFβ, but preserved TNFα inhibition of constitutive COL1A2 expression. TGFβ antagonism by TNFα involves JNK1 phosphorylation of c-jun, leading to off-DNA competition of the latter molecule for Smad3 binding to the cognate DNA site and/or for interaction with the p300/CBP coactivators (Kouba et al., 1999; Verrecchia et al., 2001, 2002).

Binding of IFN-γ to its receptors leads to tyrosine phosphorylation of janus kinase (JAK) tyrosine kinases and this in turn results in signal transducer and activator of transcription (STAT1) phosphorylation. In COL1A2, STAT1 activation results in competition with Smad3 for interaction with p300/CBP (Inagaki et al., 2003). In addition, JAK1 can also activate transcription factor Y-box binding factor (YB-1); this activation results in both inhibition of constitutive promoter activity through YB-1 binding of the 2125TC box and antagonism of TGFβ signals through YB-1 competition with Smad3 and/or p300/CBP (Ghosh et al., 2001; Higashi et al., 2003). For more details, see "Growth factors" and "Cytokines."

Est1/Fli1 have also been shown to bind the same sequence with opposite effects on collagen type I transcription. A functional Ets transcription factor was identified in COL1A2 in close proximity of Sp1 sites. Ets1 stimulated, whereas Fli1 inhibited, promoter activity. Sp1 binding was essential for inhibition of Fli1. Moreover, overexpression of Fli1 in dermal fibroblasts led to a decrease in COL1A2 mRNA and protein levels (Czuwara-Ladykowska et al., 2001). Furthermore, TGFβ treatment of dermal fibroblasts leads to dissociation of Ets1 from the CBP/p300 complexes and alters their response to TGFβ in favor of matrix degradation (Czuwara-Ladykowska et al., 2002).

Furthermore, a CpG motif at 17 bp has been shown to be preferentially methylated and bound by RFX proteins in cells acquiring a collagen I—negative state. Cell transfection experiments in conjunction with DNA-binding assays have assigned positive or negative properties to each of the proteins binding to the proximal promoter of pro-COL1A2 (Sengupta et al., 2002). The degree of methylation at the 17 CpG site, on the other hand, has been shown to modulate the binding affinity of RFX proteins and, consequently, their ability to downregulate promoter activity by recruiting associated proteins that interfere with the assembly of positively acting transcriptional complexes (Xu et al., 2003, 2004).

Structure and functional organization of upstream segments of type I collagen genes

Upstream elements in the pro-*Col1a1* gene

In complete contrast with its high-level activity in transient expression and in vitro transcription experiments, the 220-bp pro-Col1a1 proximal promoter is almost completely inactive in stable transfection experiments and in transgenic mice (Rossert et al., 1996). By increasing the length of this promoter, evidence from different groups showed that the 2.3-kb human promoter linked to different transgenes resulted in a high degree of tissue-specific expression of the reporter gene in bone, tail, and skin. However, this expression of the transgene was not identical to that of the endogenous gene (Slack et al., 1991). Indeed, in later experiments using embryos from the same mice, in situ hybridization assays showed no expression of the transgene in perichondrium and in skeletal muscle, implying that additional sequences might be needed to obtain expression of the gene in all type I collagen—producing cells (Liska et al., 1994). In newborn mice carrying a 3.6-kb rat Col1a1 promoter linked to a chloramphenicol acetyltransferase (CAT) reporter gene, high levels of transgene expression were found in extracts of bone, tooth, and tendon (Bogdanovic et al., 1994; Pavlin et al., 1992). Similarly, the mouse 3.6-kb promoter fused to β-galactosidase transgene resulted in a similar pattern, but localized to three distinct *cis*-acting sequences that directed expression in the skin, bone, and tendon (Rossert et al., 1995). The skin element was between 2220 and 2900 bp. The bone element was further delineated to 117 bp between 21,656 and 21,540 bp, and the tendon to a sequence between 22,300 and 23,600 bp (Rossert et al., 1996) (Fig. 13.3). These experiments suggested a modular arrangement of separate *cis*-acting elements that activate the pro-Col1a1 gene in different type I collagen-

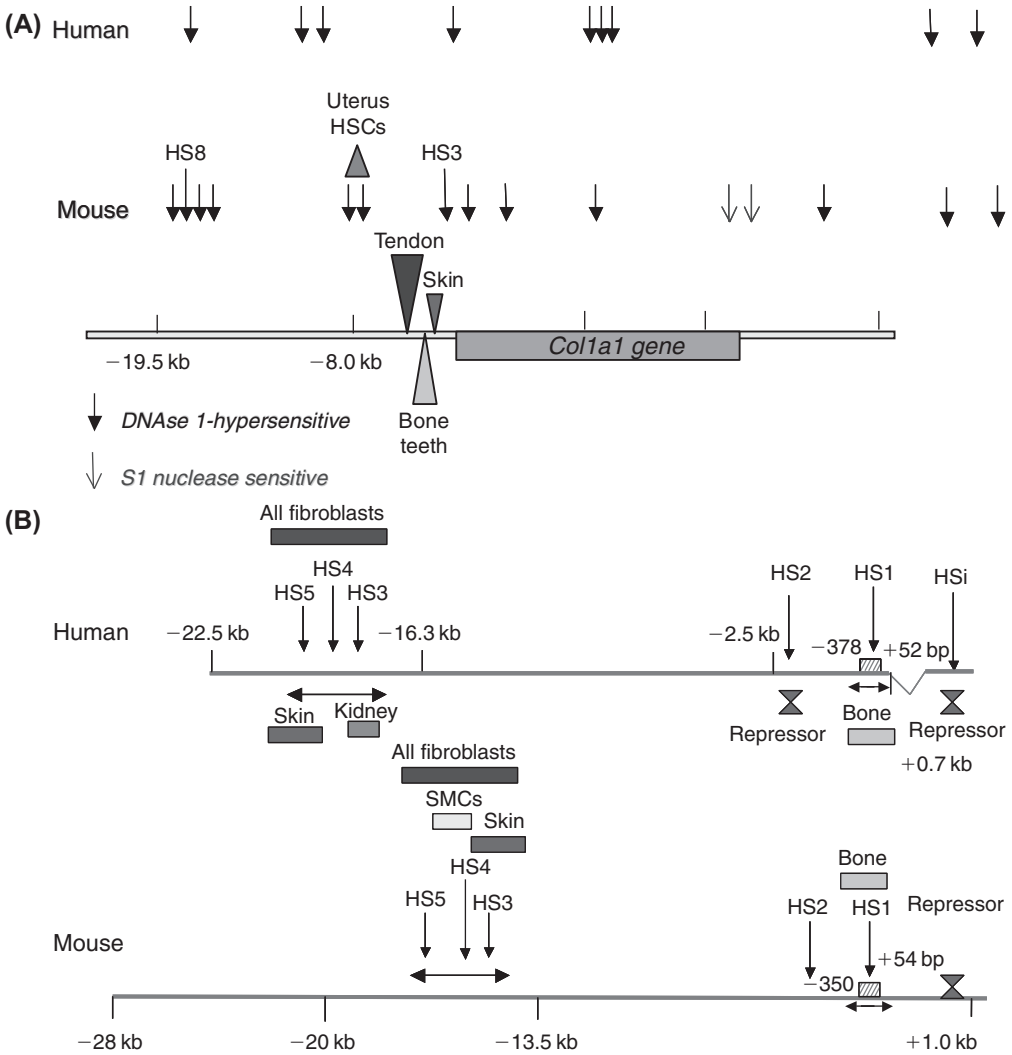

FIGURE 13.3 DNase I hypersensitive sites (*HS*) of the human and murine (A) Col1a1 and (B) Col1a2 genes depicted by *vertical arrows*, which indicate the position within the gene where the sequence may be involved in transcriptional regulation. Areas of high homology in the promoter (0.85%) are indicated by *horizontal arrows*. Also indicated are the regions in which *cis*-acting sequences have been shown to be expressed in transgenic mice, and the tissues or cells in which they are expressed, and which are called "elements" SMCs, smooth muscle cells.

producing cells. The direct consequence of such a modular arrangement is that it should be possible to selectively modulate the activation of type I collagen genes in well-defined subpopulations of type I collagen−producing cells. Perhaps the best illustration of a *cis*-acting element responsible for the activation of the mouse pro-Col1a1 gene is the osteoblast element. This 117-bp segment is very well conserved among species. In the mouse promoter, located between 21,656 and 21,540 bp, is a minimal sequence able to induce high levels of expression of the reporter gene exclusively in osteoblasts. In these mice the transgene becomes active at the same time during embryonic development when osteoblasts first appear in the different ossification centers. This so-called "osteoblast-specific element" can be divided into three subsegments that have different functions. The 29-bp A segment, which is located most 5′ (21,656−21,628 bp), is required to activate the gene in osteoblasts. A deletion of the A element or a 4-bp mutation in the TAAT sequence of this segment completely abolished the expression of the reporter gene in osteoblasts of transgenic mice. The C segment, which is located at the 3′ end of the 117-bp sequence (21,575−21,540 bp), is required to obtain consistent high-level expression of the reporter gene in transgenic mice (Rossert et al., 1996). When this C segment was deleted, the lacZ gene was expressed at very low levels and only in a small proportion of transgenic mice. The function of the intermediary segment (B segment) is still poorly understood, but it could be to prevent a promiscuous expression of the gene and, in particular, expression of the gene in the nervous system.

In addition to the 117-bp region, a consensus Cbfa1-binding site, termed oxidation-specific epitope 2 (OSE2), is present at approximately 21,347 bp of the rat, mouse, and human genes (Kern et al., 2001). RunX2/Cbfa1 can bind to this site, as demonstrated by electrophoretic mobility shift assay and supershift experiments using an anti-Cbfa1 antibody. Mutagenesis of the Col1a1 OSE2 at 21,347 bp reduces the activity of a Col1a1 promoter fragment - to threefold. Moreover, multimers of this OSE2 at 21,347 bp confer osteoblast-specific activity to a minimum Col1a1 collagen promoter fragment in DNA transfection experiments. However, this region did not confer expression in transgenic mice, suggesting that other specific factors contribute to expression of collagen type I in osteoblasts. Indeed, Osterix (Osx), a zinc finger transcription factor, was found to be essential for bone formation and to act downstream of RunX2/Cbfa1. It was shown to bind to segment C of the osteoblast element. The tendon element was found to be a combination of sequences between 23.2 and 23.6 kb termed TSE1 and TSE2 (Terraz et al., 2002). Gel-shift experiments of this region showed that scleraxis, which is a basic helix−loop−helix transcription factor that is expressed selectively in tendon fibroblasts, binds TSE2, whereas TSE1 binds NFATc (nuclear factor of activated T cells) transcription factors (Lejard et al., 2007).

In pursuit of the controlling regions of this gene, a chromatin structure analysis of the human COL1A2 gene has revealed the presence of several proximal and distal 5′ and 3′ DNase I hypersensitive sites (HSs) (Barsh et al., 1984). Breindl's team used the same technique and mapped a 55-kb sequence spanning the mouse gene, including 24 kb of 5′- and 13 kb of 3′-flanking sequences (Salimi-Tari et al., 1997). Nine HSs were found, seven of which were in the promoter sequence (HS3−HS9) up to 220 kb (see Fig. 13.3A). All of these HSs were present in collagen type I−producing cells except for HS8. When these sequences were fused to a reporter gene in transgenic animals, they revealed an additional *cis*-acting sequence in uterine smooth muscle cells between 27 and 28 kb (Krempen et al., 1999) and in liver stellate cells (Yata et al., 2003).

Upstream elements of the mouse pro-*Col1a2* gene

The activity of the mouse 350-bp pro-Col1a2 proximal promoter in transgenic mice is very low compared with that of the corresponding endogenous gene. Although this low-level activity appears to be present selectively in fibroblasts and mesenchymal cells (Niederreither et al., 1992), the precise sequences and the factors responsible for this tissue specificity have not yet been identified. An element located 13.5−17 kb upstream of the start site of transcription, and named "far-upstream enhancer," increased the levels of expression of the lacZ and luciferase reporter genes considerably when it was cloned upstream of the 350-bp mouse pro-Col1a2 proximal promoter. Moreover, this element by itself contributed to the tissue-specific expression of a reporter gene. Indeed, when it was cloned upstream of a minimal promoter that has no tissue-specific expression by itself, i.e., the first 220 bp of the pro-Col1a1 proximal promoter, it conferred a tissue-specific expression to the lacZ reporter gene in transgenic mice (Bou-Gharios et al., 1996). The enhancer was reduced in size to 1.5 kb between −15.5 and −17 kb and was shown to depend on HS4 around 250 bp to drive the expression. Interestingly, in transgenic mice harboring the lacZ reporter gene cloned downstream of a pro-Col1a2 promoter segment containing the far-upstream enhancer, fibroblastic cells expressed the lacZ reporter gene at very high levels, but only a subset of osteoblastic cells expressed this reporter gene, and odontoblasts and fully differentiated tendon fibroblasts did not (Bou-Gharios et al., 1996; Li et al., 2017), suggesting that a *cis*-acting element active in all osteoblasts is missing from this promoter/enhancer sequence. Other than this heterogeneous expression of the lacZ reporter gene in bone, the lack of expression of the lacZ gene in odontoblasts suggests that other elements exist that control expression in these cells and strongly supports a modular organization of different regulatory domains in the mouse pro-Col1a2 promoter, as described for the pro-Col1a1 promoter.

To verify the transgene staining results, both luciferase and β-galactosidase activity in tissue homogenate was measured, because the transgenic line used harbored both β-galactosidase and luciferase transgenes. Although β-galactosidase staining was no longer present in many tissues by the time transgenic mice were weaned, luciferase activity of the same tissues remained significantly higher than in controls. The endogenous mRNA level followed the overall trend of the transgene, and very little transgene mRNA was detected by 3 months of age. The skin showed the highest level of endogenous mRNA during development, which was matched by transgene expression (Ponticos et al., 2004a, b), and although mRNA level dropped by day 10 after birth, the transgene remained significantly high until 3 weeks of age, suggesting perhaps a specific role of this enhancer in the dermis.

The role of the enhancer in the regulation of the collagen type I gene was also revealed by measuring activation of the transgenes after injury to tissues, either by injection of fibrogenic cytokines such as TGFβ1 or by physical injury. Such challenge appears to stimulate a significant increase in transcription of both the endogenous collagen gene and the transgenes. Although mRNA levels of collagen have been shown to diminish in many tissues after birth and throughout adulthood (Goldberg et al., 1992), acute injury reactivates the lacZ transgene to a level that is visually apparent

(Ponticos et al., 2004a, b). This finding makes such transgenic animals an important tool and provides a model to address questions about the nature of cells that are active in fibrosis. For example, in muscular dystrophy, where fibrosis bears the hallmark of the disease (Morrison et al., 2000), this model can be used to identify those cells that are active in producing collagen type I as shown with glomerulosclerosis (Chatziantoniou et al., 1998) and the Tsk mouse model bred with these transgenic mice (Denton et al., 2001). More importantly, this will allow us to test the direct effects of various antifibrotic agents on the cells that are actively synthesizing collagen type I.

In the human COL1A2 gene, six distinct DNase I−HSs were mapped within 22 kb upstream and around the start site of transcription. Their spatial arrangement, cell type specificity, and relative availability to DNase I digestion are comparable to those of the mouse gene (Antoniv et al., 2001). The more striking finding of the chromatin survey was the identification of three strong cell-type-specific HSs (HS3−5), at a location comparable to those of the mouse far-upstream enhancer and residing within nearly identical sequences (see Fig. 13.3B). DNase I footprinting correlated areas of sequence identity with 12 distinct binding sites of nuclear proteins, the majority of which are likely not to be tissue specific. Using transgenic analysis, it was found that the proximal 2378 promoter contains elements that drive tissue-specific transcription in subsets of fibroblastic and osteoblastic cells, and this activity is significantly augmented when the proximal promoter is linked to the far-upstream enhancer. The results of the human transgenes thus indicate that the predominant function of the upstream element is to broaden and intensify tissue-specific transcription from the proximal promoter. Unlike the mouse enhancer that was active only in a subset of osteoblasts, the human sequence was active in all osteoblasts and it is most likely that the osteoblast element resides in the proximal promoter (Antoniv et al., 2001). Focusing on the mouse Col1a2 gene, a study by Marongiu et al. has identified a potentially new long-range autoregulatory mechanism controlling collagen transcription. The group investigated FOXL2, a member of the evolutionarily conserved forkhead box transcription factors, and found, using chromatin immunoprecipitation experiments followed by genomic DNA sequencing (ChIP-seq) and electrophoretic mobility shift assays, that this factor bound to a DNA element ∼65 kb upstream of the collagen gene. This region was found to contain a putative forkhead transcription factor binding site (ACAAACA), thereby providing a mechanism antagonizing transcription from the promoter. These experiments were centered on studies of the mouse reproductive system and therefore whether this represents a general automodulatory process governing Col1a2 transcription or is a tissue-restricted process is unclear as of this writing (Marongiu et al., 2016).

Delineating the mode of action of tissue-specific elements

The mode of action of the different lineage-specific transcription elements and their postulated cognate-binding proteins is still unknown, but studies of HSs (Antoniv et al., 2001; Bou-Gharios et al., 1996) and in vivo footprinting experiments (Chen et al., 1997) strongly suggest that the chromatin structure of discrete areas in the regulatory regions of type I collagen genes is different in cells when these genes are being transcribed actively, compared with cells in which they are silent. These experiments suggest that, in intact cells, transcription factors such as CBF bind to the proximal promoters of type I collagen genes only in cells in which the genes are transcribed actively (Coustry et al., 2001). Although in vivo footprint experiments show a protection of the CCAAT box in different fibroblastic cell lines, such a protection does not exist in cell lines that do not produce type I collagen. Similarly, HSs corresponding to the far-upstream enhancer of the pro-Col1a2 promoter can be detected only in cells that express type I collagen. The importance of chromatin structure is also highlighted by comparison of transient and stable transfection experiments. When a chimeric construct harboring the pro-Col1a1 osteoblast-specific element cloned upstream of a minimal promoter and of the lacZ reporter gene was transfected stably in different cell lines, it was expressed in the ROS17/2 osteoblastic cell line, but not in two fibroblastic cell lines or in a cell line that does not produce type I collagen. In contrast, in transient transfection experiments, the same chimeric construction was expressed at high levels by all cell lines. These results suggest a model in which the binding of a lineage-specific transcription factor to specific enhancer segments of type I collagen genes would result in opening the chromatin around the promoter and allow ubiquitous transcription factors to bind to the proximal promoter and to activate transcription of the genes.

The discovery of the far-upstream enhancer raised the question of whether the enhancer could confer tissue specificity on its own, and if individual elements of the proximal promoter contribute differently to COL1A2 transcription in vivo. A series of mutations introduced into each of the transcription factors' binding sites within the proximal promoter, such as the three Sp1 sites, GC-rich Sp1/Sp3-binding sites, and the CBF-binding site, reduced transgene activity, providing strong evidence that these protein interactions operate in vivo as well, and in concert with the enhancer-bound complex (Tanaka et al., 2004). The unique expression pattern of transgenic mice harboring mutations in the binding site of transcription factor CBF/NFY led to loss of lacZ expression in the ventral and head regions of the dermis, as well as in the muscles of the forelimbs. The patterning of specific cell lineages implies that CBF/NFY may be essential for COL1A2 activity in those

cells that do not express the transgene. These transgenic data therefore raise the intriguing possibility that CBF/NFY may be implicated in patterning COL1A2 expression in some mesenchyme cell lineages through a yet-to-be-defined mechanism. The results suggested cooperativity between the far-upstream enhancer and the proximal promoter in assembling tissue-specific protein complexes. They confirmed in vitro observations indicating that interactions among proximal promoter elements are required for optimal transcription. They also indicated that transcription factors binding to individual promoter elements are responsible for distinct properties of COL1A2 expression in vivo (Ramirez et al., 2006). More importantly, the upstream enhancer was shown to play a part in the fibrotic process of connective tissue disease, such as diffuse cutaneous systemic sclerosis (SSc), where the accumulation of JunB in the COL1A2 enhancer in fibroblast DNA resulted in altered mammalian target of rapamycin (mTOR)/protein kinase B (AKT) signaling and a failure of proteolytic degradation of collagen, which underpins the aberrant overexpression of type I collagen in this disease (Ponticos et al., 2015).

In the enhancer sequence of the mouse Col1a2 gene, the first tissue-specific element to be characterized was a vascular smooth muscle cell (vSMC) element: a 100-bp sequence at about 216.6 kb upstream of the transcription start site regulates collagen expression exclusively in vSMCs (Ponticos et al., 2004a, b). This expression was shown to be activated through the binding of the homeodomain protein Nkx2.5, and further potentiated by the presence of GATA6. In contrast, this element was repressed by the binding of the zinc finger protein δ-EF1/ZEB1. A model of regulation was proposed in which the activating transcription factor, Nkx2.5, and the repressor, δ-EF1/ZEB1, compete for an overlapping DNA-binding site. This element is important in understanding the molecular mechanisms of vessel remodeling and is a potential target for intervention in vascular diseases in which there is excessive deposition of collagen in the vessel wall.

Role of the first intronic elements in regulating collagen type I

First intron of the pro-*COL1A1* gene

Different negative or positive regulatory segments have been identified within the first intron, but most of the transcription factors binding to these regulatory segments are still unknown. A sequence of the first intron of the human COL1A2 gene located about 1600 bp downstream of the transcription start site binds AP1, and a mutation that abolished this binding diminished the expression of a reporter gene in transient transfection experiments (Liska et al., 1990) This AP1 was also found to mediate the repressive effect of ras in fibroblasts (Slack et al., 1995). Another segment of the first intron of the human gene, which extends from 820 to 1093 bp, has been shown to inhibit the activity of a reporter gene in transient transfection experiments (Liska et al., 1992). This sequence contains two binding sites for an Sp1-like transcription factor, and mutations in these two Sp1-binding sites tended to increase the activity of the reporter gene (Liska et al., 1992). An Sp1-binding site is also located at about 1240 bp, in the human gene, and a frequent G-to-T polymorphism in this Sp1-binding site (G1242T) has been linked with low BMD and increased risk of osteoporotic vertebrate fracture (Grant et al., 1996), which suggests that it may be important for normal levels of type I collagen synthesis by osteoblasts.

The phenotype of Mov 13 mice suggested that the first intron of the pro-α1(I) collagen gene could play a role in the expression of this gene. These mice, which harbor a retrovirus in the first intron of the pro-Col1a1 gene (Harbers et al., 1984), express this gene in osteoblasts and odontoblasts, but not in fibroblastic cells (Schwarz et al., 1990). Nevertheless, the presence of tissue-specific regulatory elements in the first intron of the pro-Col1a1 gene has long been controversial. Two groups have reported that, in transgenic mice harboring the proximal promoter of either the human or the rat pro-Col1a1 gene, the pattern of expression of the reporter gene was the same whether or not these mice harbored the first intron of the pro-Col1a1 collagen gene (Sokolov et al., 1993). In contrast, data obtained by in situ hybridization in transgenic mice harboring 2.3 kb of the human pro-Col1a1 proximal promoter suggested that the first intron of this gene was necessary to obtain high-level expression of the transgene in the dermis of skin (Liska et al., 1994). Only mice harboring the first intron, in addition to the 2.3-kb proximal promoter segment, expressed the human growth hormone reporter gene at high levels in skin. To clarify this issue, Bornstein's group generated knock-in mice with a targeted deletion of most of the first intron (Hormuzdi et al., 1998). Mice homozygous for the mutated allele developed normally and showed no apparent abnormalities. Nevertheless, in heterozygous mice, the mutated allele was expressed at normal levels in skin, but at lower levels in lung and muscle, and its levels of expression decreased with age in these two tissues more than in wild-type mice. Thus, the first intron does not play a role in the tissue-specific expression of the pro-Col1a1 gene, but it seems to be important for maintaining normal transcriptional levels of this gene in certain tissues (Hormuzdi et al., 1999).

First intron of the pro-*COL1A2* gene

The first intron of the mouse pro-Col1a2 gene has also been shown to contain a tissue-specific enhancer in transient transfection experiments (Rossi and de Crombrugghe, 1987). In transgenic mice, however, the presence of this tissue-specific enhancer apparently had no effect on the pattern of expression of a CAT reporter gene (Goldberg et al., 1992). However, transgenic analysis of the human gene suggested that, despite the homologies between the two genes, species-specific differences have been reported regarding the function of individual *cis*-acting elements, such as the first intron sequence (Antoniv et al., 2005). In vitro DNase I footprinting of the sequence corresponding to the open chromatin site identified a cluster of three distinct areas of nuclease protection that span from nucleotide 1647 to 1759 of the COL1A2 gene. These areas contain consensus sequences for GATA and interferon regulatory factor (IRF) transcription factors. Gel mobility shift and chromatin immunoprecipitation assays corroborated this finding by documenting binding of GATA4 and IRFs 1and 2 to the first intron sequence (Antoniv et al., 2005). Moreover, a short sequence encompassing the three footprints was found to inhibit expression of transgenic constructs containing the COL1A2 proximal promoter and far-upstream enhancer in a position-independent manner. Mutations inserted into each of the footprints restored transgenic expression to different extents. These results therefore indicated that the intronic sequence corresponds to a repressor element, the activity of which seems to be mediated by the concerted action of GATA and IRF proteins (see Fig. 13.2B). Furthermore, GATA4 was found to bind the promoter sequence of HS2 at 22.3 kb in the COL1A2 gene. Overexpression of this transcription factor inhibited the expression of the transgene as well as the endogenous gene in fibroblasts (Wang et al., 2005). The presence of a common repressor transcription factor in both HS2 and HS intron led to the suggestion that the "switch-off" of collagen in adults may occur via cooperation of the intronic sequence and HS2 to block the enhancer activity from exerting its effect through its cooperation with the proximal promoter in HS1 (Ramirez et al., 2006).

ChIP-seq with chromatin of mouse calvarial cells has been used to identify Osx/Sp7 interaction sites (Hojo et al., 2016). Osx was previously shown to be a transcription factor completely required for osteoblast differentiation and for bone formation (Nakashima *et al.* 2002). In this ChIP-seq study one major peak of Osx/Sp7 interaction in the chromatin of the Col1a1 gene was localized in the segment that was previously identified to be osteoblast specific in transgenic mice (Rossert et al., 1996; Bedalov et al., 1995). Other peaks of Osx/Sp7 interactions were also identified farther upstream of the sequence previously identified as osteoblast specific. The same ChIP-seq study also provided evidence that Osx/Sp7, which belongs to the Sp1 family of transcription factors, was itself not strongly binding to a GC-rich DNA target, unlike the other members of the SP1 family, but interacted as a coactivator with another DNA-binding protein, most likely a member of the Dlx family of transcription factors (Hojo et al., 2016). ChIP-seq is a powerful method to identify interaction sites for specific transcription factors in the genome of specific cell types. These sites can then further be characterized either by reporter assays in vivo in transgenic mice or by transfection of tissue culture cells. In addition, ChIP-seq can be used to characterize epigenomic modifications of histones or other chromatin proteins in the genome of specific cells.

In other ChIP-seq experiments interactions of the Runx2 transcription factor, which is also required for osteoblast differentiation and for bone formation, with the Col1a1 gene were examined (Wu et al., 2014). A major site of interactions was found at a promoter-proximal site of this gene. This study compared the interactions of Runx2 in the genome of a preosteoblastic cell line at three stages of osteoblast differentiation.

Posttranscriptional regulation of type I collagen

Even if the control of expression of type I collagen genes appears to be mainly exerted at the level of transcription, type I collagen production is also regulated at a posttranscriptional level. For example, TGFβ and IFN-γ modulate not only the levels of transcription of type I collagen genes, but also the stability of the corresponding mRNAs. Similarly, activation of HSCs is associated with a dramatic increase in the stability of the pro-Col1a1 mRNA. Run-on experiments have shown that the half-life of this mRNA was increased about 15-fold in activated rat HSCs compared with quiescent ones (Stefanovic et al., 1997). Several lines of evidence indicate that expression of the genes coding for the two collagens I and III is controlled predominantly posttranscriptionally at the mRNA level, as the 3′-UTR of the collagen family mRNA has been shown to be a target for mRNA-binding protein. Heterogeneous nuclear ribonucleoproteins (hnRNPs) A1, E1, and K substantially participate in the coordinative upregulation of collagen I and III synthesis, which is involved in mRNA stabilization (Lindquist et al., 2000). Indeed, all three COL1A1, COL1A2, and COL3A1 3′-UTRs contain hnRNP K-like consensus motifs and do actually bind it. COL1A1 and COL1A2 contain a classical CU-rich hnRNP E1-binding site, and it is also able to bind hnRNP E1, although not in COL3A1, which lacks a more extended CU-rich region. Furthermore, these mRNA-binding proteins have been shown to increase in fibrotic conditions and are suggested to coordinate expression of

type I and III collagens by common posttranscriptional mechanisms targeted at the mRNA 3′-UTR level (Thiele et al., 2004).

The sequence of the mouse pro-Col1a1 mRNA surrounding the start codon could also play a role in regulating mRNA stability. This sequence has been shown to form a stem−loop structure, and mutations that prevent its formation decreased the stability of the mRNA dramatically (Stefanovic et al., 1999). Indeed, the 5′-UTRs of COL1A1, COL1A2, and COL3A1 mRNAs are involved in such translational control. These 5′ stem−loops, together with their cognate binding proteins, should help coordinate translation and couple the translation apparatus to the rest of the collagen biosynthetic pathway (Stefanovic and Brenner, 2003).

MicroRNAs (miRNAs) mediate the posttranscriptional regulation of gene expression by binding to partially complementary sites in the 3′-UTR of target mRNA. The formation of miRNA−mRNA duplexes leads to mRNA degradation or translational repression (Ambros, 2003) The first miRNAs that were shown to be involved in collagen regulation were members of the miR-29 family. TGF is activated and triggers the downregulation of miR-29 in cardiac fibroblasts and consequent upregulation of the expression of collagens and other ECM proteins involved in fibrosis (pnas.0805038105). This was also evident in other fibrotic disease. Moreover, miR-185 and miR-98 have been shown to regulate TGFβ and collagen type I in hypertrophic scar tissue fibroblasts. miR-185 loss of function resulted in elevated TGFβ1 and collagen expression, suggesting miR-185 might serve as a potential therapeutic target for scarring. miR-98 was shown to directly target the Col1A1 3′-UTR, resulting in reduced expression, and therefore likely to have an impact on scar formation. In addition to miRs that directly interact and inhibit collagen and TGFβ, the study of keloid fibroblasts has highlighted the role of miR-21in promoting Col1A1 production via the targeting of Smad7. Negatively regulating the expression of the inhibitory Smad, Smad 7, appears to alter the TGFβ/Smad7 signaling pathway favoring increased collagen production and keloid scarring. Similarly, downregulation of miRNA let-7a or miR-196a was shown to contribute to scarring in SSc by the intrinsic activation of TGFβ (jimmunol.1200822) and the expression of miR-21 or miR-145 and decreased mRNA levels of Smad7 or Smad3, respectively. Similarly, the cytokine decreased the expression of miR-29b and increased α1(I) collagen mRNA. Accordingly, these miRNAs may contribute to the pathogenesis of SSc via the regulation of Smad7, Smad3, and α1(I) collagen (Zhu et al., 2012).

Critical factors involved in type I collagen gene regulation

Various cytokines, hormones, vitamins, and growth factors can modify type I collagen synthesis by osteoblasts and/or fibroblasts. The effects of these molecules have been studied mainly in vitro by using either bone organ cultures or cell cultures. However, in some instances the in vivo effects of these factors on type I collagen synthesis have also been studied. A degree of complexity is due to the fact that some factors can act on type I collagen synthesis but can also act indirectly by modifying the secretion of other factors, which will themselves affect type I collagen synthesis. For example, TNFα will inhibit type I collagen production through the NF-κB pathway, but it will also induce the secretion of prostaglandin E_2 (PGE_2) and of interleukin 1 (IL-1), which themselves affect type I collagen production. Furthermore, PGE_2 will induce the production of insulin-like growth factor 1 (IGF-1), which also modifies the rate of type I collagen synthesis.

Growth factors

Transforming growth factor β

In mammals, the TGFβ family consists of three members (TGFβ1, TGFβ2, and TGFβ3), which have similar biological effects but different spatial and temporal patterns of expression. These three molecules are part of a large family, the TGFβ superfamily, which also contains proteins such as BMPs, activins/inhibins, and growth and differentiation factors, as well as Nodal and its related proteins (Chang et al., 2002; Massague and Chen, 2000). Members of the TGFβ family are multifunctional proteins that regulate cell proliferation and differentiation, ECM modification, angiogenesis, apoptosis, and immunosuppression (Feng and Derynck, 2005; Jones et al., 2006; Schier and Shen, 2000). A TGFβ protein exerts its function by binding to and bringing together on the cell surface type I and II receptors to form a ligand−receptor complex (Leask and Abraham, 2004). Five members of type II and seven members of type I receptors (Activin receptor-like kinase 1−7) have been characterized in mammals (Graham and Peng, 2006). Upon phosphorylation by the type II receptor, the type I receptor phosphorylates and activates Smads, which are intracellular signaling molecules for members of the TGFβ superfamily. Phosphorylated Smads are released from the receptors and form oligomeric complexes with a common-partner Smad, Smad4, and translocate into the nucleus where they bind to specific DNA sequences called Smad-binding elements and act as transcription factors to regulate the transcription of target genes. Smad2 and Smad3

respond to TGFβs, Activins, Nodal, and Lefty, whereas Smad1, Smad5, and Smad8 mediate BMP signaling (Miyazawa et al., 2002). Several transcription factors and transcriptional coactivators have been shown to cooperate with Smad complexes, such as Sp1, AP1, PEBP2/CBF, TFE-3, ATF-2, and CBP/p300 (reviewed in Attisano and Wrana, 2000).

TGFβs are secreted by many cell types, including monocytes/macrophages, lymphocytes, platelets, fibroblasts, osteoblasts, and osteoclasts (Leask and Abraham, 2004). Synthesis by bone cells is quantitatively important because, in vivo, the highest levels of TGFβ are found in platelets and bone (Seyedin et al., 1985). Nearly all cells, including osteoblasts and fibroblasts, have TGFβ receptors (Verrecchia and Mauviel, 2007).

The three mammalian TGFβ isoforms are synthesized as homodimeric proproteins (pro-TGFβ) that have a mass of 75 kDa. The dimeric propeptides are cleaved from the mature TGFβ 24-kDa dimer in the *trans*-Golgi by furin-type enzymes. Mature TGFβ1 then associates noncovalently with a dimer of its N-terminal propeptide (also called LAP, for latency-associated peptide). This complex is referred to as the small latent complex (Annes et al., 2003). Early in the assembly of TGFβ and LAP, disulfide linkages are formed between cysteine residues of LAP and specific cysteine residues in another protein, the latent-TGFβ-binding protein (LTBP), to form the large latent complex (Annes et al., 2003). The LTBP is removed extracellularly by either proteolytic cleavage by various proteases, such as plasmin, thrombin, plasma transglutaminase, or endoglycosylases, or by physical interactions of the LAP with other proteins, such as thrombospondin-1, which is able to transform latent TGFβ1 into active TGFβ1 in vitro. Analysis of mice harboring a targeted disruption of the thrombospondin-1 gene suggests that it probably plays an important role in vivo (Crawford et al., 1998). In particular, the phenotype of thrombospondin-1-null mice was relatively similar to that of TGFβ1-null mice, and fibroblasts isolated from the former mice had a decreased ability to activate TGFβ1. Nevertheless, thrombospondin-1 is probably not the only molecule that activates TGFβ in vivo (Abdelouahed et al., 2000).

The four LTBPs (LTBP1−4) belong to the LTBP/fibrillin family of large extracellular glycoproteins (Todorovic et al., 2005). LTBP1, LTBP3, and LTBP4 form a subgroup within the family, because they covalently interact with latent TGFβ and have an important role as regulators of TGFβ function: LTBPs facilitate the secretion of latent TGFβ, direct its localization in the ECM, and regulate the activation of the cytokine. In mice ablation of the Ltbp3 gene and attenuation of Ltbp4 expression both result in developmental defects associated with reduced TGFβ activity (Dabovic et al., 2002; Sterner-Kock et al., 2002), further demonstrating that Ltbp3 and Ltbp4 modulate extracellular TGFβ levels in a specific and nonredundant manner.

The role of TGFβ on type I collagen synthesis has been demonstrated both in vivo and in vitro. In vivo, subcutaneous injections of platelet-derived TGFβ in newborn mice increased type I collagen synthesis by dermal fibroblasts with formation of granulation tissue (Roberts et al., 1986). Injections of platelet-derived TGFβ onto the periostea of parietal bone of newborn rats stimulated bone formation, and thus accumulation of ECM (Noda and Camilliere, 1989). Transgenic mice that overexpressed mature TGFβ1 developed hepatic fibrosis and renal fibrosis (Sanderson et al., 1995). Increased expression of TGFβ2 in osteoblasts in transgenic mice resulted in an osteoporosis-like phenotype with progressive bone loss. The bone loss was associated with an increase in osteoblastic matrix deposition and osteoclastic bone resorption (Erlebacher and Derynck, 1996). Conversely, expression of a dominant-negative TGFβ receptor mutant in osteoblasts led to decreased bone remodeling and increased trabecular bone mass (Filvaroff et al., 1999). In humans, mutations in the LAP of TGFβ1 cause Camurati−Engelmann disease, a rare sclerosing bone dysplasia inherited in an autosomal-dominant matter. It is unclear whether these mutations impair the ability of the LAP to inhibit TGFβ activity or cause accelerated degradation of TGFβ (Janssens et al., 2000; Kinoshita et al., 2000).

More recently, transgenic mice expressing a kinase-deficient type II TGF receptor (T-RIIΔk) in fibroblasts demonstrated unexpected skin and lung fibrosis (Denton et al., 2003). Moreover, the fibrotic phenotype of explanted dermal fibroblasts from the T-RIIΔk-deficient transgenic mice showed that expression of the mutant receptor leads to multilevel activation of the TGFβ ligand−receptor axis and that activation depends on endogenous T-RI receptor kinase activity (Denton et al., 2005). This paradoxical increased activity of the TGFβ ligand−receptor axis in these transgenic mice occurs despite previous findings that the kinase-deficient TGFβ receptors are dominant-negative inhibitors of signaling in several experimental systems, when expressed at high levels compared with wild-type receptors. Further evidence that TGFβ and its signaling pathways significantly influence collagen gene regulation is manifested in Smad3 2/2 mice exposed to a single dose of 30−50 Gy of γ-irradiation. These mice showed significantly less epidermal acanthosis and dermal influx of mast cells, macrophages, and neutrophils and decreased expression of TGFβ compared with skin from wild-type littermates, suggesting that inhibition of Smad3 could decrease tissue damage and reduce fibrosis after exposure to ionizing radiation (Flanders et al., 2002). Conversely, C57BL/6 mice with bleomycin-induced lung fibrosis receiving an intratracheal injection of a recombinant adenovirus expressing Smad7 demonstrated suppression of type I procollagen mRNA, reduced hydroxyproline content, and no morphological fibrotic responses in the lungs, indicating that gene transfer of Smad7 prevents bleomycin-induced lung fibrosis (Nakao et al., 1999). More recently, using mice with a targeted deletion of

Smad3, Roberts et al. (2006) demonstrated that lack of Smad3 prevents the epithelial-to-mesenchymal transition of lens epithelial cells following injury, and attenuates the development of fibrotic sequelae. Together, these various experimental approaches demonstrate the direct implication of Smad3 and TGFβ and molecular changes in collagen type I in fibrotic diseases.

In vitro, TGFβ stimulates the synthesis of most of the structural components of the ECM by fibroblasts and osteoblasts, including type I collagen (for a review, see Leask and Abraham, 2004). It also decreases ECM degradation by repressing the synthesis of collagenases and stromelysins and by increasing the synthesis of TIMPs. It increases lysyl-oxidase activity, which may favor interchain cross-linking in collagen fibrils (Feres-Filho et al., 1995). Finally, it stimulates the proliferation of both fibroblasts and osteoblasts, in contrast to its inhibitory effect on the proliferation of epithelial cells. Moreover, TGFβ may have a role in controlling the lineage-specific expression of type I collagen genes during embryonic development, because there is an excellent temporal and spatial correlation between the activation of type I collagen genes and the presence of immunoreactive TGFβ in the extracellular environment (Niederreither et al., 1992). As noted earlier, Fli1 is a key transcriptional repressor of the *COL1A2* gene. Interestingly, TGFβ induces a sequential displacement of Fli1 from the COL1A2 promoter by posttranslational modifications. The molecular mechanism underlying this process has been delineated and involves the TGFβ-induced phosphorylation of Fli1 leading to the dissociation of the transcriptional repressor protein complex composed of Fli1, histone deacetylase (HDAC), and p300. Thus by alleviating the chromatin remodeling by histone deacetylation, the repressor complex that occupies the COL1A2 promoter (at −404 to −237) is disassembled, leading to transcriptional activation (Asano et al., 2013).

Another way in which TGFβ exerts its action is at a pretranslational level, by increasing mRNA levels of the pro-Col1a1 and pro-Col1a2 transcripts. This increase in type I collagen mRNA levels can be caused by an increase in the transcription rate of type I collagen genes and/or by an increase in procollagen mRNA stability, with the relative contribution of these two mechanisms depending on cell type and on culture conditions. The second effect is through Smad proteins as indicated later: The effect of TGFβ on transcription of the human pro-COL1A2 gene involves Smad complexes (reviewed by Ramirez et al., 2006). This effect is mediated through a sequence of the promoter located between 2378 and 2183 bp upstream of the start site of transcription and is called the TβRE, as demonstrated by transfection experiments (Inagaki et al., 1994). Footprinting experiments performed with this sequence revealed two distinct segments interacting with DNA-binding proteins (Inagaki et al., 1994). It contains two binding sites for Sp1, as well as a binding site for C/EBP (Greenwel et al., 1997; Inagaki et al., 1994). The DNA sequence between 2271 and 2250 contains a CAGA box that binds Smad 3/Smad4 complexes (Chen et al., 1999; Zhang et al., 2000), as well as a binding site for AP1 (Chung et al., 1996). Data have shown that Smad 3/Smad4 complexes can bind to the CAGA box and mediate TGFβ-induced stimulation of the pro-COL1A2 gene, in cooperation with Sp1 proteins (Zhang et al., 2000). Other studies have suggested a role of AP1 in mediating the effects of TGFβ (Chung et al., 1996). This Smad/AP1 interaction was later found to take place "off DNA" (Verrecchia et al., 2001). The transcriptional coactivator CBP/p300, which can bind to Smad complexes, also plays an important role in mediating the effects of TGFβ on the transcriptional activity of the pro-COL1A2 gene (Ghosh et al., 2000). Thus, TGFβ probably activates the transcription of the pro-COL1A2 gene through the binding of a multimeric complex, which includes Smad3/Smad4, Sp1, CBP/p300, and possibly AP1. More recently, using Affymetrix microarrays to detect cellular genes whose expression is regulated by TGFβ through Smad3, Chen et al. identified the gene for early growth response factor-1 (EGR-1) as a Smad3-inducible gene (Chen et al., 2006a,b). It was also found that TGFβ enhanced endogenous Egr-1 interaction with a consensus Egr-1-binding-site element and with GC-rich DNA sequences of the human COL1A2 promoter in vitro and in vivo. Furthermore, forced expression of Egr-1 by itself caused dose-dependent upregulation of COL1A2 promoter activity and further enhanced the stimulation induced by TGFβ (Chen et al., 2006a,b). Other transcriptional coactivators such as the steroid receptor coactivator-1 may also participate in TGFβ effects (Dennler et al., 2005).

In the rat pro-Col1a1 gene, a TβRE has been described at about 1.6 kb upstream of the start site of transcription (Ritzenthaler et al., 1993) and between 2174 and 284 bp in the human pro-α1 collagen gene (Jimenez et al., 1994). The latter sequence contains an Sp1-like binding site, but neither of these two sequences seems to contain a potential Smad-binding site. In addition to direct action of TGFβ, part of the profibrotic properties may be indirect, mediated by increased production of a cysteine-rich protein called connective tissue growth factor (CTGF) (Leask and Abraham, 2003).

Connective tissue growth factor

CTGF (also called CCN2), a member of the CCN family of matricellular proteins, has long been known to promote differentiation and proliferation of chondrocytes and osteoblasts (for a review, see Takigawa et al., 2003). CCN2 promotes fibroblast proliferation, matrix production, and granulation tissue formation, as well as cell adhesion and migration.

Experiments using recombinant CTGF and neutralizing antibodies targeting CTGF have suggested that CTGF mediates at least some of the effects of TGFβ on fibroblast proliferation, adhesion, and ECM production, including collagen and fibronectin (Crean et al., 2002; Weston et al., 2003). Moreover, an expression vector encoding CTGF transfected into fibroblasts can activate a reporter driven by the type I collagen promoter, suggesting that a CTGF response element exists in the promoter of type I collagen (Shi-wen et al., 2000). Perhaps the most significant recent insights into the specific physiological roles of CCN2 have come from the generation of mutant mice lacking CCN2 (Ivkovic et al., 2003). Ccn2 2/2 mice display severely malformed rib cages and die soon after birth owing to a failure to breathe. These mice exhibit impaired chondrocyte proliferation and proteoglycan production within the hypertrophic zone. Excessive chondrocytic hypertrophy and a concomitant reduction in endochondral ossification are also observed. Further support for the idea that CCN2 regulates bone formation in development comes from studies of transgenic mice that overproduce CCN2 under the control of the mouse type XI collagen promoter. These mice develop normally but show dwarfism within a few months of birth owing to a reduced bone density (Nakanishi et al., 2001). The molecular basis for this deformity has not yet been explored; however, a possible explanation is that CCN2 overexpression results in abnormally premature ossification, before proper chondrocyte maturation.

CCN2 is constitutively expressed in fibrotic and embryonic fibroblasts independent of TGFβ (Chen et al., 2006a,b; Holmes et al., 2001, 2003). Experiments using Ccn2 2/2 mouse embryonic fibroblasts (MEFs) have shown that loss of CCN2 results in an inability of TGFβ to induce expression of approximately one-third of those mRNAs induced in Ccn2 1/1 MEFs (Shi-wen et al., 2006). Consistent with the fact that CCN2 is required for only a subset of TGF responses, Ccn2 2/2 MEFs show no impairment of the generic Smad pathway, emphasizing the relative selectivity of CCN2-dependent action. In contrast to the lack of effect of loss of CCN2 expression on basal type I collagen and α-smooth muscle actin expression, the ability of TGFβ to induce these proteins is impaired in Ccn2 2/2 MEFs (Shi-wen et al., 2006).

Expression of the CTGF gene in fibroblasts is strongly induced by TGFβ but not by other growth factors, and intradermal injections of TGFβ in neonatal mice induced an overexpression of CTGF in skin fibroblasts (Frazier et al., 1996; Igarashi et al., 1993). The ability of TGFβ to induce CCN2 also requires protein kinase C and the Ras/MEK/ERK MAP kinase cascade (Chen et al., 2002a,b; Stratton et al., 2002). As in the case of other TGFβ-responsive promoters that do not require the transcription factor AP1, the induction of CCN2 by TGFβ is antagonized by hyperactive AP1 or JNK (Leask et al., 2003) because of the ability of active Jun to bind to Smads off DNA and inhibit Smads from interacting with the target DNA sequences (Verrecchia et al., 2001). The role of CTGF in scarring and fibrosis regulating collagen type I also appears to be via mediating the activity of other factors such as adenosine or by modulating critical signaling pathways such as the AKT/mTOR pathways. For instance, activation of the adenosine (2A) receptor was shown to suppress the expression of the transcriptional repressor Fli1, yet induce the secretion of CTGF. Together, the release of the inhibitory activity of Fli1 (able to suppress both collagen type I and CTGF) and the elevation in CTGF level resulted in a significant enhancement of collagen type I production (Chan et al., 2013). In addition, the targeting of the CTGF 3′-UTR by an endogenous miRNA (miR-143-3p) reduced CTGF levels and inhibited collagen expression. This observation was further refined to reveal that reducing CTGF concomitantly attenuated AKT/mTOR signaling, and suggested that restraining the AKT/mTOR pathway by targeting CTGF represents a mechanism to effectively block collagen ECM production (Mu et al., 2016). Interestingly, platelet-derived growth factor receptor β also uses the AKT/mTOR signaling pathway to promote collagen (1α2) expression in an in vitro model of tubulointerstitial fibrosis (Das et al., 2017).

Although a specific CTGF receptor has yet to be identified, CTGF appears to perform many of its functions through integrins, heparan sulfate-containing proteoglycans, and the low-density lipoprotein receptor-related protein (Gao and Brigstock, 2003; Segarini et al., 2001; Weston et al., 2003).

Fibroblast growth factor

Fibroblasts growth factors (FGFs) comprise a family of 23 genes encoding structurally related proteins divided into six subfamilies of FGFs (Ornitz and Marie, 2002). The most recent member is FGF23, which is mainly produced by osteocytes in bone and acts as a hormone primarily to inhibit phosphate reabsorption in the proximal tubules of the kidney (Liu et al., 2007; Razzaque and Lanske, 2007). Most members of the FGF family bind to four distinct FGF receptor tyrosine kinase molecules (FGFRs) and activate the receptors. Historically, FGF2 (basic FGF) was the first FGF ligand to be isolated from growth-plate chondrocytes (Sullivan and Klagsbrun, 1985). Subsequently, Fgf2 gene expression has also been observed in periosteal cells and in osteoblasts (Hurley et al., 1999; Sabbieti et al., 1999). FGF signaling affects the expression and activity of several transcription factors that are required for calvarial osteogenesis. In rat or mouse calvarial cells, FGF2 activates osteocalcin transcription. This activity is inhibited by the transcription factor MSX2 and is activated by DLX5

(Newberry et al., 1997, 1999). FGF2 can upregulate Twist expression in mouse calvarial mesenchyme (Rice et al. 2000). Twist-heterozygous mice show altered FGFR protein expression (Rice et al., 2000), suggesting that Twist acts upstream of FGF signaling pathways. In addition, Twist could be a potential transcriptional regulator that mediates the negative effect of FGF2 on type I collagen expression in calvarial cells (Fang et al., 2001). Thus, FGF/FGFR, MSX, and Twist functionally interact to control cranial suture development in a coordinated manner. FGF2 production by calvarial osteoblasts is upregulated by FGF2 itself and by parathyroid hormone (PTH), PGE_2, and TGFβ. Thus, the balance between high and low levels of endogenous FGF2 may constitute a mechanism to control proliferation and ensure normal cranial vault development (Moore et al., 2002).

Bone resorption by osteoclasts is required to maintain the shape of craniofacial bones during development. It is therefore significant that FGF2 can increase the formation of osteoclast-like cells and activate mature osteoclasts through FGFR1 (Chikazu et al., 2000). In addition, FGF2 increases the expression of metalloproteinases, collagenases 1 and 3 (Newberry et al., 1997; Tang et al., 1996; Varghese et al., 2000), TIMPs 1 and 3 (Varghese et al., 1995), and stromelysin-3, which regulates collagenase activity in calvarial cells (Delany and Canalis, 1998). These mechanisms may control bone matrix degradation and remodeling by FGFs during calvarial expansion. Targeted deletion of FGF2 causes a relatively subtle defect in osteoblastogenesis, leading to decreased bone growth and bone density. However, no defects in chondrogenesis were observed (Montero et al., 2000).

Insulin-like growth factor

IGF-1 is synthesized by many cells, including cells of the osteoblastic lineage, as well as chondroblasts and osteoclasts (Rajaram et al., 1997). IGF-1 plays an important role in regulating peak BMD and bone size (Mohan and Baylink, 2005; Mohan et al., 2003). The IGFs interact with specific cell surface receptors, designated type 1 and type 2 IGF receptors (IGF-1R and IGF-2R). Most of the actions of IGF-1 and IGF-2 are mediated by the IGF-1R, which is a transmembrane receptor with tyrosine kinase activity.

The IGFs in serum and other extracellular environments are bound to specific IGF-binding proteins (IGFBPs), which represent a family of six secreted proteins with a common domain organization. Each IGFBP has unique properties and exhibits specific functions. IGFBPs 2− to 5 are present in bone; IGFBPs 4 and 5 are expressed at the highest levels. Unlike IGFBP-4, which has an inhibiting effect on IGF actions, IGFBP-5 has a potentiating effect, both in vivo and in vitro, probably by binding directly to sites that are independent of the IGF receptor (Govoni et al., 2005).

IGF-1 and IGF-2 can stimulate osteoblast and fibroblast proliferation and increase type I collagen production by these cells. Their effect on type I collagen production by osteoblasts has been demonstrated by using both fetal rat calvariae and osteoblastic cells, and it is related to an increase in corresponding mRNA transcripts (McCarthy et al., 1989; Thiebaud et al., 1994; Woitge and Kream, 2000). IGF-1 can also promote osteogenic differentiation and Col1a2 synthesis via induction of the mRNA-binding La ribonucleoprotein 6 gene (LARP6). Here, IGF-1 treatment of primary osteoblasts caused an increase in LARP6, which bound to the Col1a2 mRNA, promoting expression. Although in this study the precise mechanism by which LARP6 binding promoted COL1A2 expression was not delineated, a previous series of experiments by another group had noted that IGF-1 rapidly increased LARP6 expression, which was able to bind to the 5′ stem−loop motif structures of both the COL1a1 and the COL1a2 mRNAs. This suggested that increased synthesis of collagen would result from alterations in mRNA stability/accessibility or the ability of LARP6 to enhance or coordinate its translation into the heterotrimeric collagen type I molecule (Blackstock et al., 2014).

In vivo, administration of IGF-1 to hypophysectomized rats increased mRNA transcripts for pro-Col1a1 and pro-Col1a2 genes in parietal bones (Schmid et al., 1989). Furthermore, in calvariae of mice in which the Igf1 gene was disrupted, there was a reduced rate of collagen synthesis. By using the Cre-LoxP model to disrupt IGF-1 in all Col1a2-expressing cells it was demonstrated that locally produced IGF-1 plays a critical role in embryonic and postnatal growth. Local IGF-1 from Col1a2-producing cells is required for bone matrix mineralization during embryonic development and postnatal growth (Govoni et al., 2007). Moreover, to determine the effects of locally expressed IGF-1 on bone remodeling, a transgene was produced in which murine IGF-1 cDNA was cloned downstream of a gene fragment comprising 3.6 kb of 5′ upstream regulatory sequence and most of the first intron of the rat Col1a1 gene. Transgenic calvariae showed an increase in osteoclast numbers per bone surface, as well as increased collagen synthesis and cell proliferation. Femur length, cortical width, and cross-sectional area were also increased in transgenic femurs, whereas femoral trabecular bone volume displayed little change. Thus, broad overexpression of IGF-1 in cells of the osteoblast lineage increased indices of bone formation and resorption (Jiang et al., 2006). Furthermore, in calvariae of mice in which the IGF-1 gene was disrupted, there was a reduced rate of collagen synthesis (Woitge and Kream, 2000).

Cytokines

Tumor necrosis factor α

TNFα is a cytokine secreted mainly by monocytes/macrophages, but osteoblasts seem to be able to produce TNFα under certain conditions (Gowen et al., 1990). After being cleaved from its propeptide, TNFα undergoes trimerization and binds to type I receptors, which transduce most of the effects of TNFα, or to type II receptors, which activates them and transmits signals to the nucleus via different transcription factors.

TNFα levels are elevated in various bone disorders, such as rheumatoid arthritis and osteoporosis (Beutler and Cerami, 1988; Pacifici, 1996). In bone tissue, TNFα inhibits osteoblast function and increases osteoclastogenesis, thus favoring net matrix destruction (Centrella et al., 1988; Chou et al., 1996; Panagakos et al., 1996). Similarly, TNFα stimulates fibroblast and osteoblast proliferation and inhibits the production of ECM components, including type I collagen and its modifying enzyme, lysyl oxidase (Kouba et al., 1999; Pischon et al., 2004; Verrecchia et al., 2000), as well as the transcription factor Sox9 (Murakami et al., 2000), and increases collagenase production and thus ECM degradation (Iraburu et al., 2000).

In vivo, inoculation of nude mice with TNFα-producing cells decreased type I collagen production in skin and liver, impaired wound healing, and decreased TGFβ1 synthesis in skin (Houglum et al., 1998). TNFα also increases PGE_2 and interleukin 1 production by osteoblasts and fibroblasts, which themselves modulate type I collagen synthesis.

In dermal fibroblasts, inhibition of collagen synthesis in fibroblasts by TNFα is associated with a decrease in mRNA levels for the pro-Col1a1 and pro-Col1a2 transcripts and in the transcription of type I collagen genes (Solis-Herruzo et al., 1988). Inagaki et al. (1995) showed that TNFα increases the binding of a protein complex that recognizes the negative *cis*-acting element located immediately next to the TβRE, and postulated that TNFα counteracts the TGFβ-elicited stimulation of collagen gene expression through overlapping nuclear signaling pathways. Kouba et al. (1999) characterized this specific TNFα-response element between nucleotides 2271 and 2235 relative to the transcription initiation site and termed it TαRE. Electrophoretic mobility supershift assays identified the NF-κB family members NF-κB1 and RelA as transcription factors binding the TαRE and mediating TNFα repression of COL1a2 promoter activity. By using a gene-knockout approach, the same group showed that, in primary fibroblasts from NEMO-knockout mice, lack of NF-κB activation prevented repression of basal COL1a2 gene expression by TNFα. Similar regulatory mechanisms take place in dermal fibroblasts transfected with dominant-negative forms of IKK-α, a critical kinase upstream of NF-κB (Verrecchia et al., 2002). More interestingly, the antagonist activities of TGFβ and TNFα in COL1a2 may be the result of steric interactions between transcription factors binding to TβRE and TαRE, respectively (Greenwel et al., 2000; Verrecchia et al., 2001).

The inhibitory effects of TNFα on the rat pro-Col1a1 proximal promoter were shown to be mediated by a sequence located between 2378 and 2345 bp through the binding of proteins of the C/EBP family, such as C/EBPδ and p20C/EBPβ (Iraburu et al., 2000). Other TNFα response elements have been identified within the pro-Col1a1 gene between 2101 and 238 bp and between 68 and 86 bp, in dermal fibroblasts and HSCs, respectively (Hernandez et al., 2000; Mori et al., 1996). The latter *cis*-acting element binds proteins of the Sp1 family, whereas the proteins binding to the former have not been identified (Hernandez et al., 2000; Mori et al., 1996). Using two lines of transgenic mice harboring a growth hormone reporter gene under the control of either at 2.3 kb, the human pro-COL1A1 proximal promoter plus the first intron, or at 440 bp, this promoter plus the first intron, Chojkier's group reported that different *cis*-acting elements mediate the inhibitory effects of TNFα, depending on the tissue (Houglum et al., 1998). In skin, the inhibitory effect of TNFα on the activity of the reporter gene was mediated through a *cis*-acting element located between 22.3 kb and 2440 bp (Buck et al., 1996). In contrast, this inhibitory effect of TNFα was mediated in liver through an element located between 2440 and 11,607 bp (Houglum et al., 1998).

Interferon γ

IFN-γ is a cytokine produced both by monocytes/macrophages and by type 1 helper T cells. IFN-γ binds to the IFN-γ receptor complex (IFNGR1 and IFNGR2), followed by the activation of receptor-associated JAK, which in turn phosphorylates and activates STAT1. Once phosphorylated, STAT1 molecules dimerize and translocate to the nucleus where they modulate target gene transcription either by direct interaction with specific sequences or through protein−protein interactions (Darnell et al., 1994; Horvai et al., 1997).

In vitro, IFN-γ decreases osteoblast and fibroblast proliferation and type I collagen synthesis by these cells. This effect seems to be caused both by a decrease in type I collagen mRNA stability (Czaja et al., 1987; Kahari et al., 1990) and by a decrease in the transcription rate of the pro-Col1a1 gene (Diaz and Jimenez, 1997; Yuan et al., 1999). Transfection studies

using different segments of the human pro-COL1A1 proximal promoter have shown the existence of an IFN-γ response element between 2129 and 2107 bp that can bind transcription factors NF1 and members of the Sp1 family (Yuan et al., 1999). However, mutations in NF1 and Sp1 sites, which abrogate the binding of these factors, repress the basal COL1A1 promoter activity but are unable to abrogate the IFN-γ-mediated inhibition, suggesting that NF1 and Sp1 are not involved in this inhibitory action of IFN-γ (Yuan et al., 1999). The activation of major histocompatibility complex II by IFN-γ requires activation of a trimeric DNA-binding transcriptional complex, the RFX5 complex, containing RFXB (also called RFXANK or Tvl-1), RFXAP, and RFX5 protein. RFX5 was later shown to bind to the collagen transcription start site and repress collagen gene expression (Sengupta et al., 2002). Moreover, two studies have provided further evidence for the role of the RFX5 repressor complex in suppressing COL1A2 transcription and have noted a prominent role of epigenetics in this mode of regulation of collagen synthesis. Both studies identified components of the HDAC complex (SIRT1 and SIN3B) acting upon RFX5, altering its acetylation status. In smooth muscle cells IFN-γ repressed COL1A2 transcription by downregulating the sirtuin SIRT1, leading to acetylation, preventing nuclear expulsion and degradation and thereby modulating RFX5 repressor activity. IFN-γ also promoted the recruitment of SIN3B to the COL1A2 transcription start site, where it cooperated with G9a, a histone H3K9 methyltransferase, to effect a repressive chromatin structure. Taken together these studies strongly suggest that IFN-γ coordinates the assembly of a potent repressor complex containing RFX5, HDACs, Sirt1, Sin3B, and G9a on the COL1A2 promoter. In the human COL1A2 gene, an IFN-γ response element has been identified between 2161 and 125 bp by using transfection experiments in dermal fibroblasts (Higashi et al., 1998). Similar to the action of TNFα, Ulloa et al. (1999) reported that IFN-γ abrogates the TGFβ stimulation of TβRE-containing reporter constructs in fibrosarcoma cells by inducing the level of Smad7 via the JAK−STAT1 signaling pathway. To account for the antagonistic action of IFN-γ and TGFβ on the expression of the COL1a2 gene, however, evidence suggests another mechanism involving p300/CBP. This evidence indicates that IFN-γ-activated STAT1 sequesters the endogenous p300 and reduces its interaction with Smad3, thus inhibiting the TGFβ/Smad-induced collagen gene transcription (Ghosh et al., 2001). Moreover, Higashi et al. (2003) showed that YB-1 binds to the IFN-γ responsive element at 2165 to 2150 and mediates transcriptional repression of COL1A2. YB-1 was used successfully as a therapeutic target to downregulate collagen type I as a strategy to treat liver fibrosis in vivo. This effect was potentiated by the addition of exogenous IFN-γ (Inagaki et al., 2005).

Other cytokines

Interleukin 1

IL-1 is a cytokine secreted mainly by monocytes/macrophages, but also by other cells, including fibroblasts, osteoblasts, synoviocytes, and chondrocytes. Two forms of IL-1 have been described, IL-1α and IL-1β, which have little primary structure homology but bind to the same receptor and have similar biological activities (Stylianou and Saklatvala, 1998).

IL-1 modulates the type I collagen synthesis at different levels, and the variations may be attributable to cell type, species, and age differences, but, at this writing, the molecular mechanisms by which IL-1 modulates type I collagen gene transcription are not clear. In vitro, IL-1 has an inhibitory effect on type I collagen production by osteoblasts, which is due to an inhibition of type I collagen gene transcription (Harrison et al., 1990). Nevertheless, it can be masked when low doses of IL-1 are used, as this cytokine stimulates the production of PGE_2, which in turn can modulate type I collagen synthesis. Slack et al. (1995) have suggested that the inhibitory effects of IL-1 on the transcription of the human pro-COL1A1 collagen gene by osteoblasts could be mediated through the binding of AP1 to the first intron of the gene (Slack et al., 1995), but this has not been confirmed. In vitro, IL-1β inhibits the expression of the COL1A2 in human lung fibroblasts at the transcriptional level by a PGE_2-independent effect, as well as through the effect of endogenous fibroblast PGE_2 released under the stimulus of the cytokine (Diaz et al., 1993). More recently, in SSc fibroblasts, pre-IL-1α was shown to form a complex with IL-1β-binding proteins that are translocated into the nuclei of fibroblasts via HAX-1 (HS1-associated protein X-1) and IL-1 receptor type II to increase production of collagen and IL-6 (Kawaguchi et al., 2006). In contrast, the biological impact of IL-1β on tendon fibroblasts showed that the presence of IL-1β significantly decreased the level of collagen type I mRNA. These effects were found to be mediated by selective upregulation of the EP(4) receptor, which is a member of the G-protein-coupled receptors that transduces the PGE_2 signal via the p38 MAP kinase pathway (Thampatty et al., 2007).

Interleukin 13

IL-13 is a major inducer of fibrosis. Indeed, IL-13 induces expression of TGF 2 β1 in macrophages. The increase in TGFβ expression requires both TNFα and signaling through the IL-13 receptor α2 (IL-13Ra2) to activate an AP1 variant, which stimulates the TGFβ promoter. Prevention of IL-13Ra2 expression, IL-13Ra2 gene silencing, or blockade of IL-13Ra2

signaling leads to marked downregulation of TGFβ1 production and collagen deposition in bleomycin-induced lung fibrosis (Fichtner-Feigl et al., 2006). Thus, IL-13Ra2 signaling during prolonged inflammation could be an important therapeutic target for the prevention of TGFβ1-mediated fibrosis. Evidence has also suggested that IL-13 can mediate the increased deposition of collagen type I via TGFβ (Firszt et al., 2014) and independent of the action of TGFβ via STAT6. By showing a direct effect of IL-13 on collagen expression using specific STAT6 small interfering RNAs and miR-135b, an endogenous miRNA that targets STAT6, and methylation inhibitors, the authors were able to show a clear role for STAT6 and epigenetic mechanisms regulating IL-13-mediated collagen production (O'Reilly et al., 2016).

Interleukin 4

IL-4 is secreted by type 2 helper T cells and by mastocytes. In vitro, IL-4 increases type I collagen production by human fibroblasts by increasing both transcriptional levels of type I collagen genes and the stability of the corresponding mRNAs (Serpier et al., 1997). In bronchial fibroblasts, IL-4 positively regulates pro-COL1A1 transcription by direct promoter activation and increases the TIMP2/MMP-2 ratio, thereby supporting the profibrotic effect of this cytokine. Furthermore, a combined action of SP1, NF-κB, and STAT6 contributes to the IL-4-mediated COL1A2 gene activation. An AP2 site adjacent to a STAT6 consensus motif, TTC N(3/4) GCT, is located within 205 bases of the transcription start site and seems to support the moderate IL-4 induction of COL1A1 gene expression (Bergeron et al., 2003; Buttner et al., 2004).

Interleukin 6 IL-6 has been shown to induce collagen type I and is elevated in patients with SSc (Kawaguchi et al., 1999) and in cultured HSCs (Nieto, 2006). Two studies have indicated that IL-6 can regulate collagen type I via STAT3 by two distinct mechanisms. First, IL-6 induction of STAT3 (phospho-STAT3/S727) led to noncanonical STAT3 activation and to increased TGFβ and collagen expression (Li et al., 2015). Second, at both the transcriptional level, through the upstream elements of the COL1A2 enhancer and their interaction with the proximal promoter, and the posttranscriptional level, where IL-6 *trans* signaling and high levels of STAT3 activation led to increased COL1A2 protein expression by (Papaioannou et al., 2018).

Other interleukins

IL-10 is secreted mainly by monocytes/macrophages and inhibits type I collagen gene transcription and type I collagen production by skin fibroblasts (Reitamo et al., 1994). In addition, several other cytokines have also been reported to regulated type I collagen production, for instance, IL-17, IL-18, and the IL-12 family of cytokines, such as IL-23. Although the molecular mechanisms responsible for changes in collagen have not been fully explored, they often show alterations in the levels of transcription factors, upstream signaling pathways, and miRNA expression. For example, IL-18 appears to involved in the activation of the ERK signaling cascade leading to the induction of the collagen type I transcriptional repressor Ets1 (Kim et al., 2010). With respect to IL-17, this cytokine exerts a direct impact on the expression of TGFβ type II receptors (TGFβRIIs) via JNK-dependent signaling pathways, with the resultant upregulation and stabilization of TGFβRII leading to enhance Smad2/3 signaling and the induction of collagen gene expression (Fabre et al., 2014). The dysregulation in IL-23 signaling reported in fibrosis and contributing to increased collagen production has been attributed to an IL-23-dependent imbalance between two miRNAs (miR-4458 and miR-18a) that target type I collagen, and in particular the IL-23 downregulation of miR-18a resulting in collagen upregulation (Nakayama et al., 2017).

Oncostatin M is produced mainly by activated T cells and monocytes/macrophages and belongs to the hematopoietic cytokine family. It is mitogenic for fibroblasts and stimulates type I collagen production by fibroblasts by increasing transcriptional levels of type I collagen genes (Ihn et al., 1997). Transfection studies performed using different segments of the human pro-α2(I) collagen gene have shown that a 12-bp segment located between 2131 and 2120 bp, and that contains a TCCTCC motif, mediated the stimulatory effects of oncostatin M (Ihn et al., 1997).

Arachidonic acid derivatives

PGE_2, a product of the cyclooxygenase pathway, is synthesized by various cell types, including endothelial cells, monocytes/macrophages, osteoblasts, and fibroblasts. Its production by fibroblasts is increased by IL-1 and TNFα. PGE_2 has a biphasic effect on type I collagen synthesis by bone organ cultures and by osteoblastic cells (Ono et al., 2005). At low concentrations, it increases type I collagen synthesis, whereas at higher concentrations it decreases type I collagen synthesis. PGE_2 induces the production of IGF-1 by osteoblastic cells, and part of the stimulatory effect of low doses of PGE_2 on type I collagen production seems to be indirect, mediated by a stimulation of IGF-1 production (Raisz et al., 1993a, b). Nevertheless, part of this stimulatory effect is independent of IGF-1 production and persists after blocking the

effects of IGF-1 (Raisz et al., 1993a, b). It is notable that when PGE_2 is added to fibroblasts in culture, it inhibits type I collagen synthesis and decreases the levels of the corresponding mRNAs. Most of the effects of PGE_2 are mediated through an increase in cAMP levels (Sakuma et al., 2004) and the activation of collagen synthesis by low doses of PGE_2 could be caused by such a mechanism, because cAMP analogs can also increase collagen synthesis in bone (Fall et al., 1994). In contrast, the inhibitory effect of PGE_2, which has been shown to be caused by an inhibition of transcription of type I collagen genes, is not mediated through a cAMP-dependent pathway but through a pathway involving the activation of protein kinase C (Sakuma et al., 2004). A study using an osteoblastic cell line transfected stably with various segments of the rat pro-Col1a1 promoter cloned upstream of a CAT reporter gene has shown that PGE_2 acts through an element located more than 2.3 kb upstream of the start site of transcription (Raisz et al., 1993a, b). A more recent study using fibroblasts transfected transiently with a construct containing 220 bp of the mouse pro-Col1a1 proximal promoter has shown that PGE_2 can also act through a *cis*-acting element located within this promoter segment (Riquet et al., 2000).

Hormones and vitamins

Corticosteroids

It has been known for many years that the administration of corticosteroids to patients results in osteoporosis and growth retardation. In mice, corticosteroids have also been shown to decrease collagen production in calvariae (Advani et al., 1997). In vitro, incubation of fetal rat calvariae with high doses of corticosteroids, or with lower doses but for a prolonged period of time, decreased the synthesis of type I collagen (Canalis, 1983; Dietrich et al., 1979); this inhibitory effect could also be observed with osteoblastic cell lines (Hodge and Kream, 1988). Moreover, cortisol increases interstitial collagenase transcript levels by posttranscriptional mechanisms in osteoblastic cells (Delany et al., 1995a, b). Nuclear run-off experiments performed using osteoblasts derived from fetal rat calvariae showed that glucocorticoids downregulate transcriptional levels of the pro-Col1a1 gene, as well as the stability of the corresponding mRNA (Delany et al., 1995a, b). Because corticosteroids inhibit the secretion of IGF-1, part of their inhibitory effect on type I collagen synthesis could be indirect, but calvariae from IGF-1-null mice maintain their responsiveness to glucocorticoids (Woitge and Kream, 2000).

When added to fibroblasts in culture, corticosteroids usually decrease type I collagen synthesis by acting at a pretranslational level, which is in agreement with their in vivo effect on wound healing (Cockayne et al., 1986). Stable transfection experiments using the mouse pro-Col1a2 proximal promoter fused to a CAT reporter gene and transfected into fibroblasts have shown that sequences located between 22,048 and 2981 bp and between 2506 and 2351 bp were important for the corticosteroid-mediated inhibition of transcription (Perez et al., 1992). However, the *cis*-acting element(s) responsible was not sufficient to block the effect alone (Meisler et al., 1995), and further experiments from the same group indicated that glucocorticoids coordinately regulate procollagen gene expression through TGFβ elements. Depression of procollagen gene expression by glucocorticoids through the TGFβ element is mediated by decreased TGFβ secretion, possibly involving a secondary effect on regulatory proteins encoded by noncollagenous protein genes (Cutroneo and Sterling, 2004).

BMD decreases by 2%−4.5% after just 6 months of glucocorticoid administration to healthy men, but subsequently the rate of bone loss declines (LoCascio et al., 1990). Considerable evidence indicates that glucocorticoid-induced bone loss occurs in two phases in both humans and mice: an early, rapid phase in which bone mass is lost because of excessive bone resorption and a slower, later phase in which bone is lost because of inadequate bone formation (LoCascio et al., 1990; Weinstein et al., 1998). Transgenic mice overexpressing 11β-hydroxysteroid dehydrogenase type 2 (11β-HSD2) using the osteoclast-specific murine tartrate-resistant acid phosphatase promoter (Reddy et al., 1995) exhibited decreased cancellous osteoclasts after glucocorticoid administration and were protected from the glucocorticoid-induced early, rapid loss of BMD (Jia et al., 2006), suggesting that direct effects of glucocorticoids on osteoclasts are more important than these mediators in the early, rapid loss of bone mass that follows glucocorticoid administration. Similarly, when an osteoblast-specific 2.3-kb Col1a1 promoter drives 11β-HSD2 expression in mature osteoblasts, 11β-HSD2 should metabolically inactivate endogenous glucocorticoids in the targeted cells, thereby reducing glucocorticoid signaling; collagen synthesis rates were lower in calvarial organ cultures of transgenic mice than in wild-type. Furthermore, the inhibitory effect of 300 nM hydrocortisone on collagen synthesis was blunted in transgenic calvariae. Trabecular bone parameters measured by microcomputed tomography were also reduced in L3 vertebrae, but not femurs, of 7- and 24-week-old transgenic females. This effect was not seen in male mice, suggesting that endogenous glucocorticoid signaling is required for normal vertebral trabecular bone volume and architecture in female mice (Sher et al., 2004).

Thyroid hormones

Thyroid hormones have been shown to inhibit type I collagen production by cardiac fibroblasts, and this effect was associated with a decrease in the levels of pro-Col1a1 mRNA (Chen et al., 2000a,b). Transfection studies have shown that thyroid hormones modulate transcriptional levels of the pro-Col1a1 gene through a *cis*-acting element located between 2224 and 115 bp (Chen et al., 2000a,b). In addition, thyroid hormone (T3) regulates the FGFR1 promoter in osteoblasts through a thyroid receptor-binding site at position 2279/2264 (O'Shea P et al., 2007). With respect to chondrocyte differentiation, a study has indicated that thyroid hormone receptor-associated protein 3 negatively regulates SOX9 transcriptional activity as a cofactor of a SOX9 transcriptional complex during chondrogenesis (Sono et al., 2018).

Parathyroid hormone

PTH binds to specific receptors in osteoblasts and upregulates the expression of receptor activator of NF-κB ligand, a protein essential for osteoclast development and survival. PTH signaling occurs via a PTH receptor 1/cAMP/protein kinase A/CREB cascade. Runx2 may contribute to the osteoblast specificity of PTH signaling (Fu et al., 2006) by downregulating osteoprotegerin expression (Boyle et al., 2003). In vitro, PTH inhibits type I collagen synthesis by osteoblastic cell lines as well as by bone organotypic cultures (Kream et al., 1986). This inhibitory effect is associated with a decrease in the levels of procollagen mRNAs (Kream et al., 1986). When calvariae of transgenic mice harboring a 1.7-, 2.3-, or 3.6-kb segment of the rat pro-Col1a1 proximal promoter were cultured in the presence of PTH, there was a parallel decrease in the incorporation of [^{3}H]proline and in the activity of the reporter gene, suggesting that the pro-Col1a1 promoter contains a *cis*-acting element located downstream of 21.7 kb, which mediates the inhibition of the pro-Col1a1 gene expression induced by PTH (Bogdanovic et al., 2000; Kream et al., 1993). Furthermore, the effect of PTH on the levels of expression of the reporter gene were mimicked by cAMP and potentiated by a phosphodiesterase inhibitor, suggesting that the inhibitory effects of PTH are mediated mainly by a cAMP signaling pathway (Bogdanovic et al., 2000).

Vitamin D

The classic role of the vitamin D endocrine system is to stimulate calcium absorption in the intestine, thus maintaining normocalcemia and indirectly regulating bone mineralization (van Driel et al., 2004). The actions of vitamin D are mediated through the vitamin D receptor (VDR), which acts as a ligand-activated transcription factor to regulate the expression of target genes. The VDR heterodimerizes with retinoid X receptor (RXR) and associates with the transcriptional complex on promoters of target genes. In vitro, the active metabolite of vitamin D3, $1,25(OH)_2D_3$, has been shown to inhibit type I collagen synthesis by bone organ cultures and by osteoblastic cells, and this inhibitory effect is caused by an inhibition of the transcription of type I collagen genes (Bedalov et al., 1998; Harrison et al.,1989). Transfection studies performed with the rat pro-Col1a1 proximal promoter led to the identification of a vitamin D-responsive element between 22.3 and 21.6 kb (Pavlin et al., 1994). Nevertheless, when transgenic mice harboring a 1.7-kb segment of the rat pro-Col1a1 promoter cloned upstream of a CAT reporter gene were treated with $1,25(OH)_2D_3$, the levels of expression of the CAT reporter gene decreased, which suggests that a vitamin D-response element is located downstream of 21.7 kb (Bedalov et al., 1998). Similarly, when calvariae from these transgenic mice were cultured in the presence of $1,25(OH)_2D_3$, it inhibited reporter gene expression (Bedalov et al., 1998). It is of note that part of the effects of vitamin D on type I collagen could be mediated through an inhibition of the production of IGF-1, because vitamin D has been shown to inhibit IGF-1 production and increase the concentrations of inhibitory IGFBP-4 (Scharla et al., 1991). Indeed, the effects of $1,25(OH)_2D_3$ on release of the IGFs were independent of bone resorption and support the conclusion that $1,25(OH)_2D_3$ modulated the production and secretion of IGF-1 and IGF-2 in calvarial cells (Linkhart and Keffer, 1991). The results of these and similar studies on PTH in calvarial cells suggest that PTH, TGFβ, and $1,25(OH)_2D_3$ differentially regulate mouse calvarial cell IGF-1 and IGF-2 production. Furthermore, IGFBP-5 has been shown to reduce the effects of $1,25(OH)_2D_3$ by blocking cell cycle progression at G0/G1 in osteoblasts and by decreasing the expression of cyclin D1. Moreover, IGFBP-5 can interact with VDR to prevent RXR:VDR heterodimerization and IGFBP-5 may attenuate the $1,25(OH)_2D_3$-induced expression of bone differentiation markers (Schedlich et al., 2007).

Many studies have reported an inverse relationship between vitamin D and PTH concentrations, where PTH plateaued at concentrations of 25OHD between 75 and 100 nmol/L (30−40 ng/mL). Biochemical markers of bone metabolism are increasingly used in the management of patients with osteoporosis and other metabolic bone diseases.

Among bone formation markers is procollagen type 1 amino-terminal propeptide (P1NP), which is released into the circulation during bone formation. Bone resorption markers include carboxy-terminal cross-linked telopeptide of type I collagen (CTX). CTX is a degradation product of type I collagen and is released into the circulation during bone resorption

(Vasikaran et al., 2011). The Bone Marker Standards Working Group recommends P1NP and CTX as reference standard markers of bone formation and resorption (Vasikaran et al., 2011; Stokes et al., 2011). In humans, many studies have reported deficiencies or insufficiencies in vitamin D, even in equatorial countries (Tan et al., 2013), and a confusing picture of the markers of bone turnover, P1NP and CTX, and vitamin D levels, which may be influenced by reduced PTH, has emerged.

References

Abdelouahed, M., Ludlow, A., Brunner, G., Lawler, J., 2000. Activation of platelet-transforming growth factor beta-1 in the absence of thrombospondin-1. J. Biol. Chem. 275, 17933−17936.

Adhikari, A.S., Chai, J., Dunn, A.R., 2011. Mechanical load induces a 100-fold increase in the rate of collagen proteolysis by MMP-1. J. Am. Chem. Soc. 133 (6), 1686−1689.

Adhikari, A.S., Glassey, E., Dunn, A.R., 2012. Conformational dynamics accompanying the proteolytic degradation of trimeric collagen I by collagenases. J. Am. Chem. Soc. 134 (32), 13259−13265. https://doi.org/10.1021/ja212170b.

Advani, S., LaFrancis, D., Bogdanovic, E., Taxel, P., Raisz, L.G., Kream, B.E., 1997. Dexamethasone suppresses in vivo levels of bone collagen synthesis in neonatal mice. Bone 20, 41−46.

Amar, S., Smith, L., Fields, G.B., 2017. Matrix metalloproteinase collagenolysis in health and disease. Biochim. Biophys. Acta. Mol. Cell. Res. 1864 (11 Pt A), 1940−1951. https://doi.org/10.1016/j.bbamcr.2017.04.015.

Ambros, 2003. Cell 113, 673−676.

Ameye, L., Aria, D., Jepsen, K., Oldberg, A., Xu, T., Young, M.F., 2002. Abnormal collagen fibrils in tendons of biglycan/fibromodulin-deficient mice lead to gait impairment, ectopic ossification, and osteoarthritis. FASEB J. 16, 673−680.

Annes, J.P., Munger, J.S., Rifkin, D.B., 2003. Making sense of latent TGFbeta activation. J. Cell Sci. 116, 217−224.

Antoniv, T.T., De Val, S., Wells, D., Denton, C.P., Rabe, C., de Crombrugghe, B., Ramirez, F., Bou-Gharios, G., 2001. Characterization of an evolutionarily conserved far-upstream enhancer in the human alpha 2(I) collagen (COL1A2) gene. J. Biol. Chem. 276, 21754−21764.

Antoniv, T.T., Tanaka, S., Sudan, B., De Val, S., Liu, K., Wang, L., Wells, D.J., Bou-Gharios, G., Ramirez, F., 2005. Identification of a repressor in the first intron of the human alpha 2(I) collagen gene (COL1A2). J. Biol. Chem.

Arakaki, P.A., Marques, M.R., Santos, M.C., 2009. MMP-1 polymorphism and its relationship to pathological processes. J. Biosci. 34 (2), 313−320.

Asano, Y., Trojanowska, M., 2013. Fli1 represses transcription of the human α2(I) collagen gene by recruitment of the HDAC1/p300 complex. PLoS One 8 (9), e74930.

Attisano, L., Wrana, J.L., 2000. Smads as transcriptional co-modulators. Curr. Opin. Cell Biol. 12, 235−243.

Barsh, G.S., Roush, C.L., Gelinas, R.E., 1984. DNA and chromatin structure of the human alpha 1 (I) collagen gene. J. Biol. Chem. 259, 14906−14913.

Baumann, B., Hayashida, T., Liang, X., Schnaper, H.W., 2016. Hypoxia-inducible factor-1α promotes glomerulosclerosis and regulates COL1A2 expression through interactions with Smad3. Kidney Int. 90 (4), 797−808.

Bedalov, A., Salvatori, R., Dodig, M., Kapural, B., Pavlin, D., Kream, B.E., Clark, S.H., Woody, C.O., Rowe, D.W., Lichtler, A.C., 1998. 1,25-Dihydroxyvitamin D3 inhibition of col1a1 promoter expression in calvariae from neonatal transgenic mice. Biochim. Biophys. Acta 1398, 285−293.

Bergeon, M.T., 1967. Collagen: a review. J. Okla. State Med. Assoc. 60, 330−332.

Bergeron, C., Page, N., Joubert, P., Barbeau, B., Hamid, Q., Chakir, J., 2003. Regulation of procollagen I (alpha1) by interleukin-4 in human bronchial fibroblasts: a possible role in airway remodelling in asthma. Clin. Exp. Allergy 33, 1389−1397.

Beutler, B., Cerami, A., 1988. Cachectin (tumor necrosis factor): a macrophage hormone governing cellular metabolism and inflammatory response. Endocr. Rev. 9, 57−66.

Bigg, H.F., Rowan, A.D., Barker, M.D., Cawston, T.E., 2007. Activity of matrix metalloproteinase-9 against native collagen types I and III. FEBS J. 274 (5), 1246−1255.

Bittner, K., Liszio, C., Blumberg, P., Schonherr, E., Kresse, H., 1996. Modulation of collagen gel contraction by decorin. Biochem. J. 314 (Pt 1), 159−166.

Blackstock, C.D., Higashi, Y., Sukhanov, S., Shai, S.Y., Stefanovic, B., Tabony, A.M., Yoshida, T., Delafontaine, P., 2014. Insulin-like growth factor-1 increases synthesis of collagen type I via induction of the mRNA-binding protein LARP6 expression and binding to the 5' stem-loop of COL1a1 and COL1a2 mRNA. J. Biol. Chem. 289 (11), 7264−7274.

Bogdanovic, Z., Bedalov, A., Krebsbach, P.H., Pavlin, D., Woody, C.O., Clark, S.H., Thomas, H.F., Rowe, D.W., Kream, B.E., Lichtler, A.C., 1994. Upstream regulatory elements necessary for expression of the rat COL1A1 promoter in transgenic mice. J. Bone Miner. Res. 9, 285−292.

Bogdanovic, Z., Huang, Y.F., Dodig, M., Clark, S.H., Lichtler, A.C., Kream, B.E., 2000. Parathyroid hormone inhibits collagen synthesis and the activity of rat col1a1 transgenes mainly by a cAMP-mediated pathway in mouse calvariae. J. Cell. Biochem. 77, 149−158.

Boot-Handford, R.P., Tuckwell, D.S., Plumb, D.A., Rock, C.F., Poulsom, R., 2003. A novel and highly conserved collagen (pro(alpha)1(XXVII)) with a unique expression pattern and unusual molecular characteristics establishes a new clade within the vertebrate fibrillar collagen family. J. Biol. Chem. 278, 31067−31077.

Bornstein, P., 2002. The NH(2)-terminal propeptides of fibrillar collagens: highly conserved domains with poorly understood functions. Matrix Biol. 21, 217−226.

Bornstein, P., Walsh, V., Tullis, J., Stainbrook, E., Bateman, J.F., Hormuzdi, S.G., 2002. The globular domain of the proalpha 1(I) N-propeptide is not required for secretion, processing by procollagen N-proteinase, or fibrillogenesis of type I collagen in mice. J. Biol. Chem. 277, 2605−2613.

Bou-Gharios, G., Garrett, L.A., Rossert, J., Niederreither, K., Eberspaecher, H., Smith, C., Black, C., Crombrugghe, B., 1996. A potent far-upstream enhancer in the mouse pro alpha 2(I) collagen gene regulates expression of reporter genes in transgenic mice. J. Cell Biol. 134, 1333–1344.

Boyadjiev, S.A., et al., 2006. Cranio-lenticulo-sutural dysplasia is caused by a SEC23A mutation leading to abnormal endoplasmic-reticulum-to-Golgi trafficking. Nat Genet 38, 1192–1197.

Boyle, W.J., Simonet, W.S., Lacey, D.L., 2003. Osteoclast differentiation and activation. Nature 423, 337–342.

Brenner, D.A., Rippe, R.A., Veloz, L., 1989. Analysis of the collagen alpha 1(I) promoter. Nucleic Acids Res. 17, 6055–6064.

Bridgewater, L.C., Lefebvre, V., de Crombrugghe, B., 1998. Chondrocyte-specific enhancer elements in the Col11a2 gene resemble the Col2a1 tissue-specific enhancer. J. Biol. Chem. 273, 14998–15006.

Brodeur, A.C., Wirth, D.A., Franklin, C.L., Reneker, L.W., Miner, J.H., Phillips, C.L., 2007. Type I collagen glomerulopathy: postnatal collagen deposition follows glomerular maturation. Kidney Int. 71, 985–993.

Buck, M., Houglum, K., Chojkier, M., 1996. Tumor necrosis factor-alpha inhibits collagen alpha1(I) gene expression and wound healing in a murine model of cachexia. Am. J. Pathol. 149, 195–204.

Buttner, C., Skupin, A., Rieber, E.P., 2004. Transcriptional activation of the type I collagen genes COL1A1 and COL1A2 in fibroblasts by interleukin-4: analysis of the functional collagen promoter sequences. J. Cell. Physiol. 198, 248–258.

Byers, P.H., 2001. Folding defects in fibrillar collagens. Philos. Trans. R. Soc. Lond. B Biol. Sci. 356, 151–157 discussion 157–158.

Byers, P.H., Duvic, M., Atkinson, M., Robinow, M., Smith, L.T., Krane, S.M., Greally, M.T., Ludman, M., Matalon, R., Pauker, S., Quanbeck, D., Schwarze, U., 1997. Ehlers–Danlos syndrome type VIIA and VIIB result from splice-junction mutations or genomic deletions that involve exon 6 in the COL1A1 and COL1A2 genes of type I collagen. Am. J. Med. Genet. 72, 94–105.

Cai, et al., 2010. J Mol Biol. 401, 564–578.

Canty, E.G., Kadler, K.E., 2005. Procollagen trafficking, processing and fibrillogenesis. J. Cell Sci. 118, 1341–1353.

Canty, E.G., Lu, Y., Meadows, R.S., Shaw, M.K., Holmes, D.F., Kadler, K.E., 2004. Coalignment of plasma membrane channels and protrusions (fibripositors) specifies the parallelism of tendon. J. Cell Biol. 165, 553–563.

Canty-Laird, E.G., Lu, Y., Kadler, K.E., 2012. Stepwise proteolytic activation of type I procollagen to collagen within the secretory pathway of tendon fibroblasts in situ. Biochem. J. 441 (2), 707–717. https://doi.org/10.1042/BJ20111379.

Centrella, M., McCarthy, T.L., Canalis, E., 1988. Tumor necrosis factor-alpha inhibits collagen synthesis and alkaline phosphatase activity independently of its effect on deoxyribonucleic acid synthesis in osteoblast-enriched bone cell cultures. Endocrinology 123, 1442–1448.

Chan, E.S., Liu, H., Fernandez, P., Luna, A., Perez-Aso, M., Bujor, A.M., Trojanowska, M., Cronstein, B.N., 2013. Adenosine A(2A) receptors promote collagen production by a Fli1- and CTGF-mediated mechanism. Arthritis Res. Ther. 15 (3), R58.

Chang, H., Brown, C.W., Matzuk, M.M., 2002. Genetic analysis of the mammalian transforming growth factor-beta superfamily. Endocr. Rev. 23, 787–823.

Chatziantoniou, C., Boffa, J.J., Ardaillou, R., Dussaule, J.C., 1998. Nitric oxide inhibition induces early activation of type I collagen gene in renal resistance vessels and glomeruli in transgenic mice. Role of endothelin. J. Clin. Investig. 101, 2780–2789.

Chen, Y., Blom, I.E., Sa, S., Goldschmeding, R., Abraham, D.J., Leask, A., 2002. CTGF expression in mesangial cells: involvement of SMADs, MAP kinase, and PKC. Kidney Int. 62, 1149–1159.

Chen, W.J., Lin, K.H., Lee, Y.S., 2000. Molecular characterization of myocardial fibrosis during hypothyroidism: evidence for negative regulation of the pro-alpha1(I) collagen gene expression by thyroid hormone receptor. Mol. Cell. Endocrinol. 162, 45–55.

Chen, S.J., Ning, H., Ishida, W., Sodin-Semrl, S., Takagawa, S., Mori, Y., Varga, J., 2006. The early-immediate gene EGR-1 is induced by transforming growth factor-beta and mediates stimulation of collagen gene expression. J. Biol. Chem. 281, 21183–21197.

Chen, S.S., Ruteshouser, E.C., Maity, S.N., de Crombrugghe, B., 1997. Cell-specific in vivo DNA-protein interactions at the proximal promoters of the pro alpha 1(I) and the pro alpha 2(I) collagen genes. Nucleic Acids Res. 25, 3261–3268.

Chen, X.D., Shi, S., Xu, T., Robey, P.G., Young, M.F., 2002. Age-related osteoporosis in biglycan-deficient mice is related to defects in bone marrow stromal cells. J. Bone Miner. Res. 17, 331–340.

Chen, Y., Shi-wen, X., Eastwood, M., Black, C.M., Denton, C.P., Leask, A., Abraham, D.J., 2006. Contribution of activin receptor-like kinase 5 (transforming growth factor beta receptor type I) signaling to the fibrotic phenotype of scleroderma fibroblasts. Arthritis Rheum. 54, 1309–1316.

Chen, S.J., Yuan, W., Lo, S., Trojanowska, M., Varga, J., 2000. Interaction of smad3 with a proximal smad-binding element of the human alpha2(I) procollagen gene promoter required for transcriptional activation by TGF-beta. J. Cell. Physiol. 183, 381–392.

Chen, S.J., Yuan, W., Mori, Y., Levenson, A., Trojanowska, M., Varga, J., 1999. Stimulation of type I collagen transcription in human skin fibroblasts by TGF-beta: involvement of Smad 3. J. Investig. Dermatol. 112, 49–57.

Chikazu, D., Hakeda, Y., Ogata, N., Nemoto, K., Itabashi, A., Takato, T., Kumegawa, M., Nakamura, K., Kawaguchi, H., 2000. Fibroblast growth factor (FGF)-2 directly stimulates mature osteoclast function through activation of FGF receptor 1 and p42/p44 MAP kinase. J. Biol. Chem. 275, 31444–31450.

Chipman, S.D., Sweet, H.O., McBride Jr., D.J., Davisson, M.T., Marks Jr., S.C., Shuldiner, A.R., Wenstrup, R.J., Rowe, D.W., Shapiro, J.R., 1993. Defective pro alpha 2(I) collagen synthesis in a recessive mutation in mice: a model of human osteogenesis imperfecta. Proc. Natl. Acad. Sci. U.S.A. 90, 1701–1705.

Chou, D.H., Lee, W., McCulloch, C.A., 1996. TNF-alpha inactivation of collagen receptors: implications for fibroblast function and fibrosis. J. Immunol. 156, 4354–4362.

Chu, M.L., de Wet, W., Bernard, M., Ding, J.F., Morabito, M., Myers, J., Williams, C., Ramirez, F., 1984. Human pro alpha 1(I) collagen gene structure reveals evolutionary conservation of a pattern of introns and exons. Nature 310, 337–340.

Chung, K.Y., Agarwal, A., Uitto, J., Mauviel, A., 1996. An AP-1 binding sequence is essential for regulation of the human alpha 2(I) collagen (COL1A2) promoter activity by transforming growth factor-beta. J. Biol. Chem. 271, 3272–3278.

Cockayne, D., Sterling Jr., K.M., Shull, S., Mintz, K.P., Illeyne, S., Cutroneo, K.R., 1986. Glucocorticoids decrease the synthesis of type I procollagen mRNAs. Biochemistry 25, 3202–3209.

Corsi, A., Xu, T., Chen, X.D., Boyde, A., Liang, J., Mankani, M., Sommer, B., Iozzo, R.V., Eichstetter, I., Robey, P.G., Bianco, P., Young, M.F., 2002. Phenotypic effects of biglycan deficiency are linked to collagen fibril abnormalities, are synergized by decorin deficiency, and mimic Ehlers–Danlos-like changes in bone and other connective tissues. J. Bone Miner. Res. 17, 1180–1189.

Coustry, F., Hu, Q., de Crombrugghe, B., Maity, S.N., 2001. CBF/NF-Y functions both in nucleosomal disruption and transcription activation of the chromatin-assembled topoisomerase IIalpha promoter. Transcription activation by CBF/NF-Y in chromatin is dependent on the promoter structure. J. Biol. Chem. 276, 40621–40630.

Coustry, F., Maity, S.N., de Crombrugghe, B., 1995. Studies on transcription activation by the multimeric CCAAT-binding factor CBF. J. Biol. Chem. 270, 468–475.

Crean, J.K., Finlay, D., Murphy, M., Moss, C., Godson, C., Martin, F., Brady, H.R., 2002. The role of p42/44 MAPK and protein kinase B in connective tissue growth factor induced extracellular matrix protein production, cell migration, and actin cytoskeletal rearrangement in human mesangial cells. J. Biol. Chem. 277, 44187–44194.

Cutroneo, K.R., Sterling, K.M., 2004. How do glucocorticoids compare to oligo decoys as inhibitors of collagen synthesis and potential toxicity of these therapeutics? J. Cell. Biochem. 92, 6–15.

Czaja, M.J., Weiner, F.R., Eghbali, M., Giambrone, M.A., Eghbali, M., Zern, M.A., 1987. Differential effects of gamma-interferon on collagen and fibronectin gene expression. J. Biol. Chem. 262, 13348–13351.

Czuwara-Ladykowska, J., Sementchenko, V.I., Watson, D.K., Trojanowska, M., 2002. Ets1 is an effector of the transforming growth factor beta (TGF-beta) signaling pathway and an antagonist of the profibrotic effects of TGF-beta. J. Biol. Chem. 277, 20399–20408.

Czuwara-Ladykowska, J., Shirasaki, F., Jackers, P., Watson, D.K., Trojanowska, M., 2001. Fli-1 inhibits collagen type I production in dermal fibroblasts via an Sp1-dependent pathway. J. Biol. Chem. 276, 20839–20848.

D'Alessio, M., Bernard, M., Pretorius, P.J., de Wet, W., Ramirez, F., 1988. Complete nucleotide sequence of the region encompassing the first twenty-five exons of the human pro alpha 1(I) collagen gene (COL1A1). Gene 67, 105–115.

Dabovic, B., Chen, Y., Colarossi, C., Obata, H., Zambuto, L., Perle, M.A., Rifkin, D.B., 2002. Bone abnormalities in latent TGF-[beta] binding protein (Ltbp)-3-null mice indicate a role for Ltbp-3 in modulating TGF-[beta] bioavailability. J. Cell Biol. 156, 227–232.

Dahl, T., Veis, A., 2003. Electrostatic interactions lead to the formation of asymmetric collagen-phosphophoryn aggregates. Connect. Tissue Res. 44 (Suppl. 1), 206–213.

Danielson, K.G., Baribault, H., Holmes, D.F., Graham, H., Kadler, K.E., Iozzo, R.V., 1997. Targeted disruption of decorin leads to abnormal collagen fibril morphology and skin fragility. J. Cell Biol. 136, 729–743.

Darnell Jr., J.E., Kerr, I.M., Stark, G.R., 1994. Jak-STAT pathways and transcriptional activation in response to IFNs and other extracellular signaling proteins. Science 264, 1415–1421.

Das, F., Ghosh-Choudhury, N., Venkatesan, B., Kasinath, B.S., Ghosh Choudhury, G., 2017. PDGF receptor-β uses Akt/mTORC1 signaling node to promote high glucose-induced renal proximal tubular cell collagen I (α2) expression. Am. J. Physiol. Renal. Physiol. 313 (2), F291–F307.

de Crombrugghe, B., Lefebvre, V., Nakashima, K., 2001. Regulatory mechanisms in the pathways of cartilage and bone formation. Curr. Opin. Cell Biol. 13, 721–727.

Deak, S.B., Nicholls, A., Pope, F.M., Prockop, D.J., 1983. The molecular defect in a nonlethal variant of osteogenesis imperfecta. Synthesis of pro-alpha 2(I) chains which are not incorporated into trimers of type I procollagen. J. Biol. Chem. 258, 15192–15197.

Delany, A.M., Canalis, E., 1998. Dual regulation of stromelysin-3 by fibroblast growth factor-2 in murine osteoblasts. J. Biol. Chem. 273, 16595–165600.

Delany, A.M., Gabbitas, B.Y., Canalis, E., 1995. Cortisol downregulates osteoblast alpha 1 (I) procollagen mRNA by transcriptional and post-transcriptional mechanisms. J. Cell. Biochem. 57, 488–494.

Delany, A.M., Jeffrey, J.J., Rydziel, S., Canalis, E., 1995. Cortisol increases interstitial collagenase expression in osteoblasts by post-transcriptional mechanisms. J. Biol. Chem. 270, 26607–26612.

Dennler, S., Pendaries, V., Tacheau, C., Costas, M.A., Mauviel, A., Verrecchia, F., 2005. The steroid receptor co-activator-1 (SRC-1) potentiates TGF-beta/Smad signaling: role of p300/CBP. Oncogene 24, 1936–1945.

Denton, C.P., Lindahl, G.E., Khan, K., Shiwen, X., Ong, V.H., Gaspar, N.J., Lazaridis, K., Edwards, D.R., Leask, A., Eastwood, M., Leoni, P., Renzoni, E.A., Bou Gharios, G., Abraham, D.J., Black, C.M., 2005. Activation of key profibrotic mechanisms in transgenic fibroblasts expressing kinase-deficient type II Transforming growth factor-{beta} receptor (T{beta}RII{delta}k). J. Biol. Chem. 280, 16053–16065.

Denton, C.P., Zheng, B., Evans, L.A., Shi-wen, X., Ong, V.H., Fisher, I., Lazaridis, K., Abraham, D.J., Black, C.M., de Crombrugghe, B., 2003. Fibroblast-specific expression of a kinase-deficient type II transforming growth factor beta (TGFbeta) receptor leads to paradoxical activation of TGFbeta signaling pathways with fibrosis in transgenic mice. J. Biol. Chem. 278, 25109–25119.

Denton, C.P., Zheng, B., Shiwen, X., Zhang, Z., Bou-Gharios, G., Eberspaecher, H., Black, C.M., de Crombrugghe, B., 2001. Activation of a fibroblast-specific enhancer of the proalpha2(I) collagen gene in tight-skin mice. Arthritis Rheum. 44, 712–722.

Diaz, A., Jimenez, S.A., 1997. Interferon-gamma regulates collagen and fibronectin gene expression by transcriptional and post-transcriptional mechanisms. Int. J. Biochem. Cell Biol. 29, 251–260.

Diaz, A., Munoz, E., Johnston, R., Korn, J.H., Jimenez, S.A., 1993. Regulation of human lung fibroblast alpha 1(I) procollagen gene expression by tumor necrosis factor alpha, interleukin-1 beta, and prostaglandin E2. J. Biol. Chem. 268, 10364–10371.

Duval, E., Bouyoucef, M., Leclercq, S., Baugé, C., Boumédiene, K., 2016. Hypoxia inducible factor 1 alpha down-regulates type i collagen through Sp3 transcription factor in human chondrocytes. IUBMB Life 68 (9), 756–763.

Efstathiadou, Z., Tsatsoulis, A., Ioannidis, J.P., 2001. Association of collagen Ialpha 1 Sp1 polymorphism with the risk of prevalent fractures: a meta-analysis. J. Bone Miner. Res. 16, 1586–1592.

Erlebacher, A., Derynck, R., 1996. Increased expression of TGF-beta 2 in osteoblasts results in an osteoporosis-like phenotype. J. Cell Biol. 132, 195–210.

Ewald, C.Y., Landis, J.N., Porter Abate, J., Murphy, C.T., Blackwell, T.K., 2015. Dauer-independent insulin/IGF-1-signalling implicates collagen remodelling in longevity. Nature 519 (7541), 97–101.

Fabre, T., Kared, H., Friedman, S.L., Shoukry, N.H., 2014. IL-17A enhances the expression of profibrotic genes through upregulation of the TGF-β receptor on hepatic stellate cells in a JNK-dependent manner. J. Immunol. 193 (8), 3925–3933. https://doi.org/10.4049/jimmunol.1400861.

Fang, M.A., Glackin, C.A., Sadhu, A., McDougall, S., 2001. Transcriptional regulation of alpha 2(I) collagen gene expression by fibroblast growth factor-2 in MC3T3-E1 osteoblast-like cells. J. Cell. Biochem. 80, 550–559.

Feng, X.H., Derynck, R., 2005. Specificity and versatility in tgf-beta signaling through Smads. Annu. Rev. Cell Dev. Biol. 21, 659–693.

Feres-Filho, E.J., Choi, Y.J., Han, X., Takala, T.E., Trackman, P.C., 1995. Pre- and post-translational regulation of lysyl oxidase by transforming growth factor-beta 1 in osteoblastic MC3T3-E1 cells. J. Biol. Chem. 270, 30797–30803.

Fichtner-Feigl, S., Strober, W., Kawakami, K., Puri, R.K., Kitani, A., 2006. IL-13 signaling through the IL-13alpha2 receptor is involved in induction of TGF-beta1 production and fibrosis. Nat. Med. 12, 99–106.

Fields, G.B., 2013 Mar 29. Interstitial collagen catabolism. J. Biol. Chem. 288 (13), 8785–8793. https://doi.org/10.1074/jbc.R113.451211.

Filvaroff, E., Erlebacher, A., Ye, J., Gitelman, S.E., Lotz, J., Heillman, M., Derynck, R., 1999. Inhibition of TGF-beta receptor signaling in osteoblasts leads to decreased bone remodeling and increased trabecular bone mass. Development 126, 4267–4279.

Firszt, R., Francisco, D., Church, T.D., Thomas, J.M., Ingram, J.L., Kraft, M., 2014. Interleukin-13 induces collagen type-1 expression through matrix metalloproteinase-2 and transforming growth factor-β1 in airway fibroblasts in asthma. Eur. Respir. J. 43 (2), 464–473.

Flanders, K.C., Sullivan, C.D., Fujii, M., Sowers, A., Anzano, M.A., Arabshahi, A., Major, C., Deng, C., Russo, A., Mitchell, J.B., Roberts, A.B., 2002. Mice lacking Smad3 are protected against cutaneous injury induced by ionizing radiation. Am. J. Pathol. 160, 1057–1068.

Forlino, A., Porter, F.D., Lee, E.J., Westphal, H., Marini, J.C., 1999. Use of the Cre/lox recombination system to develop a non-lethal knock-in murine model for osteogenesis imperfecta with an alpha1(I) G349C substitution. Variability in phenotype in BrtlIV mice. J. Biol. Chem. 274, 37923–37931.

Fragiadaki, M., Ikeda, T., Witherden, A., Mason, R.M., Abraham, D., Bou-Gharios, G., 2011. High doses of TGF-β potently suppress type I collagen via the transcription factor CUX1. Mol. Biol. Cell 22 (11), 1836–1844.

Frazier, K., Williams, S., Kothapalli, D., Klapper, H., Grotendorst, G.R., 1996. Stimulation of fibroblast cell growth, matrix production, and granulation tissue formation by connective tissue growth factor. J. Investig. Dermatol. 107, 404–411.

Fu, Q., Manolagas, S.C., O'Brien, C.A., 2006. Parathyroid hormone controls receptor activator of NF-kappaB ligand gene expression via a distant transcriptional enhancer. Mol. Cell Biol. 26, 6453–6468.

Fujii, M., Yoneda, A., Takei, N., Sakai-Sawada, K., Kosaka, M., Minomi, K., Yokoyama, A., Tamura, Y., 2017. Endoplasmic reticulum oxidase 1α is critical for collagen secretion from and membrane type 1-matrix metalloproteinase levels in hepatic stellate cells. J. Biol. Chem. 292 (38), 15649–15660. https://doi.org/10.1074/jbc.M117.783126.

Galera, P., Musso, M., Ducy, P., Karsenty, G., 1994. c-Krox, a transcriptional regulator of type I collagen gene expression, is preferentially expressed in skin. Proc. Natl. Acad. Sci. U.S.A. 91, 9372–9376.

Galera, P., Park, R.W., Ducy, P., Mattei, M.G., Karsenty, G., 1996. c-Krox binds to several sites in the promoter of both mouse type I collagen genes. Structure/function study and developmental expression analysis. J. Biol. Chem. 271, 21331–21339.

Galli, G.G., Honnens de Lichtenberg, K., Carrara, M., Hans, W., Wuelling, M., Mentz, B., Multhaupt, H.A., Fog, C.K., Jensen, K.T., Rappsilber, J., Vortkamp, A., Coulton, L., Fuchs, H., Gailus-Durner, V., Hrabě de Angelis,, M., Calogero, R.A., Couchman, J.R., Lund, A.H., 2012. Prdm5 regulates collagen gene transcription by association with RNA polymerase II in developing bone. PLoS Genet. 8 (5) e1002711. Epub 2012 May 10.

Gao, R., Brigstock, D.R., 2003. Low density lipoprotein receptor-related protein (LRP) is a heparin-dependent adhesion receptor for connective tissue growth factor (CTGF) in rat activated hepatic stellate cells. Hepatol. Res. 27, 214–220.

Garcia-Giralt, N., Enjuanes, A., Bustamante, M., Mellibovsky, L., Nogues, X., Carreras, R., Diez-Perez, A., Grinberg, D., Balcells, S., 2005. In vitro functional assay of alleles and haplotypes of two COL1A1-promoter SNPs. Bone 36, 902–908.

Garcia-Giralt, N., Nogues, X., Enjuanes, A., Puig, J., Mellibovsky, L., Bay-Jensen, A., Carreras, R., Balcells, S., Diez-Perez, A., Grinberg, D., 2002. Two new single-nucleotide polymorphisms in the COL1A1 upstream regulatory region and their relationship to bone mineral density. J. Bone Miner. Res. 17, 384–393.

Gedeon, A.K., et al., 1999. Nat Genet 22, 400–404.

Ghosh, A.K., 2002. Factors involved in the regulation of type I collagen gene expression: implication in fibrosis. Exp. Biol. Med. 227, 301–314.

Ghosh, A.K., Yuan, W., Mori, Y., Chen, S., Varga, J., 2001. Antagonistic regulation of type I collagen gene expression by interferon-gamma and transforming growth factor-beta. Integration at the level of p300/CBP transcriptional coactivators. J. Biol. Chem. 276, 11041–11048.

Ghosh, A.K., Yuan, W., Mori, Y., Varga, J., 2000. Smad-dependent stimulation of type I collagen gene expression in human skin fibroblasts by TGF-beta involves functional cooperation with p300/CBP transcriptional coactivators. Oncogene 19, 3546–3555.

Goldberg, H., Helaakoski, T., Garrett, L.A., Karsenty, G., Pellegrino, A., Lozano, G., Maity, S., de Crombrugghe, B., 1992. Tissue-specific expression of the mouse alpha 2(I) collagen promoter. Studies in transgenic mice and in tissue culture cells. J. Biol. Chem. 267, 19622–19630.

Goldberg, M.D., Septier, O., Rapoport, M., Young, L., Ameye, 2002. Biglycan is a repressor of amelogenin expression and enamel formation: an emerging hypothesis. J. Dent. Res. 81, 520−524.

Govoni, K.E., Baylink, D.J., Mohan, S., 2005. The multi-functional role of insulin-like growth factor binding proteins in bone. Pediatr. Nephrol. 20, 261−268.

Govoni, K.E., Wergedal, J.E., Florin, L., Angel, P., Baylink, D.J., Mohan, S., 2007. Conditional deletion of IGF-I in collagen type 1{alpha}2 (Col1 {alpha}2) expressing cells results in postnatal lethality and a dramatic reduction in bone accretion. Endocrinology.

Gowen, M., Chapman, K., Littlewood, A., Hughes, D., Evans, D., Russell, G., 1990. Production of tumor necrosis factor by human osteoblasts is modulated by other cytokines, but not by osteotropic hormones. Endocrinology 126, 1250−1255.

Graham, H., Peng, C., 2006. Activin receptor-like kinases: structure, function and clinical implications. Endocr. Metab. Immune Disord. - Drug Targets 6, 45−58.

Grant, S.F., Reid, D.M., Blake, G., Herd, R., Fogelman, I., Ralston, S.H., 1996. Reduced bone density and osteoporosis associated with a polymorphic Sp1 binding site in the collagen type I alpha 1 gene. Nat. Genet. 14, 203−205.

Greenwel, P., Inagaki, Y., Hu, W., Walsh, M., Ramirez, F., 1997. Sp1 is required for the early response of alpha2(I) collagen to transforming growth factor-beta1. J. Biol. Chem. 272, 19738−19745.

Greenwel, P., Tanaka, S., Penkov, D., Zhang, W., Olive, M., Moll, J., Vinson, C., Di Liberto, M., Ramirez, F., 2000. Tumor necrosis factor alpha inhibits type I collagen synthesis through repressive CCAAT/enhancer-binding proteins. Mol. Cell Biol. 20, 912−918.

Han, et al., 2010. J Biol Chem. 285, 22276−22281.

Hara, M., Kobayakawa, K., Ohkawa, Y., Kumamaru, H., Yokota, K., Saito, T., Kijima, K., Yoshizaki, S., Harimaya, K., Nakashima, Y., Okada, S., 2017. Interaction of reactive astrocytes with type I collagen induces astrocytic scar formation through the integrin-N-cadherin pathway after spinal cord injury. Nat. Med. 23 (7), 818−828.

Haralson, M.A., Jacobson, H.R., Hoover, R.L., 1987. Collagen polymorphism in cultured rat kidney mesangial cells. Lab. Invest. 57, 513−523.

Harbers, K., Kuehn, M., Delius, H., Jaenisch, R., 1984. Insertion of retrovirus into the first intron of alpha 1(I) collagen gene to embryonic lethal mutation in mice. Proc. Natl. Acad. Sci. U.S.A. 81, 1504−1508.

Harris, S.S., Patel, M.S., Cole, D.E., Dawson-Hughes, B., 2000. Associations of the collagen type Ialpha1 Sp1 polymorphism with five-year rates of bone loss in older adults. Calcif. Tissue Int. 66, 268−271.

Harrison, J.R., Petersen, D.N., Lichtler, A.C., Mador, A.T., Rowe, D.W., Kream, B.E., 1989. 1,25-Dihydroxyvitamin D3 inhibits transcription of type I collagen genes in the rat osteosarcoma cell line ROS 17/2.8. Endocrinology 125, 327−333.

Harrison, J.R., Vargas, S.J., Petersen, D.N., Lorenzo, J.A., Kream, B.E., 1990. Interleukin-1 alpha and phorbol ester inhibit collagen synthesis in osteoblastic MC3T3-E1 cells by a transcriptional mechanism. Mol. Endocrinol. 4, 184−190.

Hasegawa, T., Zhou, X., Garrett, L.A., Ruteshouser, E.C., Maity, S.N., de Crombrugghe, B., 1996. Evidence for three major transcription activation elements in the proximal mouse proalpha2(I) collagen promoter. Nucleic Acids Res. 24, 3253−3560.

Hernandez, I., de la Torre, P., Rey-Campos, J., Garcia, I., Sanchez, J.A., Munoz, R., Rippe, R.A., Munoz-Yague, T., Solis-Herruzo, J.A., 2000. Collagen alpha1(I) gene contains an element responsive to tumor necrosis factor-alpha located in the 5' untranslated region of its first exon. DNA Cell Biol. 19, 341−352.

Higashi, K., Inagaki, Y., Suzuki, N., Mitsui, S., Mauviel, A., Kaneko, H., Nakatsuka, I., 2003. Y-box-binding protein YB-1 mediates transcriptional repression of human alpha 2(I) collagen gene expression by interferon-gamma. J. Biol. Chem. 278, 5156−5162.

Higashi, K., Kouba, D.J., Song, Y.J., Uitto, J., Mauviel, A., 1998. A proximal element within the human alpha 2(I) collagen (COL1A2) promoter, distinct from the tumor necrosis factor-alpha response element, mediates transcriptional repression by interferon-gamma. Matrix Biol. 16, 447−456.

Hojo, et al., 2016. Dev Cell. 37, 238−253.

Holmes, A., Abraham, D.J., Chen, Y., Denton, C., Shi-wen, X., Black, C.M., Leask, A., 2003. Constitutive connective tissue growth factor expression in scleroderma fibroblasts is dependent on Sp1. J. Biol. Chem. 278, 41728−41733.

Holmes, A., Abraham, D.J., Sa, S., Shiwen, X., Black, C.M., Leask, A., 2001. CTGF and SMADs, maintenance of scleroderma phenotype is independent of SMAD signaling. J. Biol. Chem. 276, 10594−10601.

Hong, J., Chu, M., Qian, L., Wang, J., Guo, Y., Xu, D., 2017. Fibrillar type I collagen enhances the differentiation and proliferation of myofibroblasts by lowering α2β1 integrin expression in cardiac fibrosis. Biomed. Res Int. 2017, 1790808. https://doi.org/10.1155/2017/1790808.

Hormuzdi, S.G., Penttinen, R., Jaenisch, R., Bornstein, P., 1998. A gene-targeting approach identifies a function for the first intron in expression of the alpha1(I) collagen gene. Mol. Cell Biol. 18, 3368−3375.

Hormuzdi, S.G., Strandjord, T.P., Madtes, D.K., Bornstein, P., 1999. Mice with a targeted intronic deletion in the Col1a1 gene respond to bleomycin-induced pulmonary fibrosis with increased expression of the mutant allele. Matrix Biol. 18, 287−294.

Horvai, A.E., Xu, L., Korzus, E., Brard, G., Kalafus, D., Mullen, T.M., Rose, D.W., Rosenfeld, M.G., Glass, C.K., 1997. Nuclear integration of JAK/STAT and Ras/AP-1 signaling by CBP and p300. Proc. Natl. Acad. Sci. U.S.A. 94, 1074−1079.

Houglum, K., Buck, M., Kim, D.J., Chojkier, M., 1998. TNF-alpha inhibits liver collagen-alpha 1(I) gene expression through a tissue-specific regulatory region. Am. J. Physiol. 274, G840−G847.

Hulmes, D.J., 2002. Building collagen molecules, fibrils, and suprafibrillar structures. J. Struct. Biol. 137, 2−10.

Hurley, M.M., Tetradis, S., Huang, Y.F., Hock, J., Kream, B.E., Raisz, L.G., Sabbieti, M.G., 1999. Parathyroid hormone regulates the expression of fibroblast growth factor-2 mRNA and fibroblast growth factor receptor mRNA in osteoblastic cells. J. Bone Miner. Res. 14, 776−783.

Igarashi, A., Okochi, H., Bradham, D.M., Grotendorst, G.R., 1993. Regulation of connective tissue growth factor gene expression in human skin fibroblasts and during wound repair. Mol. Biol. Cell 4, 637−645.

Ihn, H., Ihn, Y., Trojanowska, M., 2001. Spl phosphorylation induced by serum stimulates the human alpha2(I) collagen gene expression. J. Investig. Dermatol. 117, 301–308.

Ihn, H., LeRoy, E.C., Trojanowska, M., 1997. Oncostatin M stimulates transcription of the human alpha2(I) collagen gene via the Sp1/Sp3-binding site. J. Biol. Chem. 272, 24666–24672.

Ihn, H., Ohnishi, K., Tamaki, T., LeRoy, E.C., Trojanowska, M., 1996. Transcriptional regulation of the human alpha2(I) collagen gene. Combined action of upstream stimulatory and inhibitory cis-acting elements. J. Biol. Chem. 271, 26717–26723.

Inagaki, Y., Kushida, M., Higashi, K., Itoh, J., Higashiyama, R., Hong, Y.Y., Kawada, N., Namikawa, K., Kiyama, H., Bou-Gharios, G., Watanabe, T., Okazaki, I., Ikeda, K., 2005. Cell type-specific intervention of transforming growth factor beta/Smad signaling suppresses collagen gene expression and hepatic fibrosis in mice. Gastroenterology 129, 259–268.

Inagaki, Y., Nemoto, T., Kushida, M., Sheng, Y., Higashi, K., Ikeda, K., Kawada, N., Shirasaki, F., Takehara, K., Sugiyama, K., Fujii, M., Yamauchi, H., Nakao, A., de Crombrugghe, B., Watanabe, T., Okazaki, I., 2003. Interferon alfa down-regulates collagen gene transcription and suppresses experimental hepatic fibrosis in mice. Hepatology 38, 890–899.

Inagaki, Y., Truter, S., Ramirez, F., 1994. Transforming growth factor-beta stimulates alpha 2(I) collagen gene expression through a cis-acting element that contains an Sp1-binding site. J. Biol. Chem. 269, 14828–14834.

Inagaki, Y., Truter, S., Tanaka, S., Di Liberto, M., Ramirez, F., 1995. Overlapping pathways mediate the opposing actions of tumor necrosis factor-alpha and transforming growth factor-beta on alpha 2(I) collagen gene transcription. J. Biol. Chem. 270, 3353–3358.

Iozzo, R.V., 1999. The biology of the small leucine-rich proteoglycans. Functional network of interactive proteins. J. Biol. Chem. 274, 18843–18846.

Iraburu, M.J., Dominguez-Rosales, J.A., Fontana, L., Auster, A., Garcia-Trevijano, E.R., Covarrubias-Pinedo, A., Rivas-Estilla, A.M., Greenwel, P., Rojkind, M., 2000. Tumor necrosis factor alpha down-regulates expression of the alpha1(I) collagen gene in rat hepatic stellate cells through a p20C/EBPbeta- and C/EBPdelta-dependent mechanism. Hepatology 31, 1086–1093.

Ivkovic, S., Yoon, B.S., Popoff, S.N., Safadi, F.F., Libuda, D.E., Stephenson, R.C., Daluiski, A., Lyons, K.M., 2003. Connective tissue growth factor coordinates chondrogenesis and angiogenesis during skeletal development. Development 130, 2779–2791.

Janssens, K., Gershoni-Baruch, R., Guanabens, N., Migone, N., Ralston, S., Bonduelle, M., Lissens, W., Van Maldergem, L., Vanhoenacker, F., Verbruggen, L., Van Hul, W., 2000. Mutations in the gene encoding the latency-associated peptide of TGF-beta 1 cause Camurati-Engelmann disease. Nat. Genet. 26, 273–275.

Jia, D., O'Brien, C.A., Stewart, S.A., Manolagas, S.C., Weinstein, R.S., 2006. Glucocorticoids act directly on osteoclasts to increase their life span and reduce bone density. Endocrinology 147, 5592–5599.

Jiang, J., Lichtler, A.C., Gronowicz, G.A., Adams, D.J., Clark, S.H., Rosen, C.J., Kream, B.E., 2006. Transgenic mice with osteoblast-targeted insulin-like growth factor-I show increased bone remodeling. Bone 39, 494–504.

Jimenez, S.A., Bashey, R.I., Benditt, M., Yankowski, R., 1977. Identification of collagen alpha1(I) trimer in embryonic chick tendons and calvaria. Biochem. Biophys. Res. Commun. 78, 1354–1361.

Jimenez, S.A., Varga, J., Olsen, A., Li, L., Diaz, A., Herhal, J., Koch, J., 1994. Functional analysis of human alpha 1(I) procollagen gene promoter, Differential activity in collagen-producing and -nonproducing cells and response to transforming growth factor beta 1. J. Biol. Chem. 269, 12684–12691.

Johnson, R.J., Floege, J., Yoshimura, A., Iida, H., Couser, W.G., Alpers, C.E., 1992. The activated mesangial cell: a glomerular "myofibroblast"? J. Am. Soc. Nephrol. 2, S190–S197.

Johnson, C., Primorac, D., McKinstry, M., McNeil, J., Rowe, D., Lawrence, J.B., 2000. Tracking COL1A1 RNA in osteogenesis imperfecta, splice-defective transcripts initiate transport from the gene but are retained within the SC35 domain. J. Cell Biol. 150, 417–432.

Jones, R.L., Stoikos, C., Findlay, J.K., Salamonsen, L.A., 2006. TGF-beta superfamily expression and actions in the endometrium and placenta. Reproduction 132, 217–232.

Kadler, K., 2004. Matrix loading: assembly of extracellular matrix collagen fibrils during embryogenesis. Birth Defects Res. C Embryo Today 72, 1–11.

Kadler, K.E., Hulmes, D.J., Hojima, Y., Prockop, D.J., 1990. Assembly of type I collagen fibrils de novo by the specific enzymic cleavage of pC collagen. The fibrils formed at about 37 degrees C are similar in diameter, roundness, and apparent flexibility to the collagen fibrils seen in connective tissue. Ann. N. Y. Acad. Sci. 580, 214–224.

Kadler, K.E., Torre-Blanco, A., Adachi, E., Vogel, B.E., Hojima, Y., Prockop, D.J., 1991. A type I collagen with substitution of a cysteine for glycine-748 in the alpha 1(I) chain copolymerizes with normal type I collagen and can generate fractallike structures. Biochemistry 30, 5081–5088.

Kahari, V.M., Chen, Y.Q., Su, M.W., Ramirez, F., Uitto, J., 1990. Tumor necrosis factor-alpha and interferon-gamma suppress the activation of human type I collagen gene expression by transforming growth factor-beta 1. Evidence for two distinct mechanisms of inhibition at the transcriptional and posttranscriptional levels. J. Clin. Investig. 86, 1489–1495.

Kalson, N.S., Starborg, T., Lu, Y., Mironov, A., Humphries, S.M., Holmes, D.F., Kadler, K.E., 2013. Nonmuscle myosin II powered transport of newly formed collagen fibrils at the plasma membrane. Proc. Natl. Acad. Sci. U.S.A. 110 (49), E4743–E4752. https://doi.org/10.1073/pnas.1314348110.

Kanamaru, Y., Nakao, A., Tanaka, Y., Inagaki, Y., Ushio, H., Shirato, I., Horikoshi, S., Okumura, K., Ogawa, H., Tomino, Y., 2003. Involvement of p300 in TGF-beta/Smad-pathway-mediated alpha 2(I) collagen expression in mouse mesangial cells. Nephron Exp. Nephrol. 95, e36–e42.

Karsenty, G., de Crombrugghe, B., 1990. Two different negative and one positive regulatory factors interact with a short promoter segment of the alpha 1 (I) collagen gene. J. Biol. Chem. 265, 9934–9942.

Karsenty, G., de Crombrugghe, B., 1991. Conservation of binding sites for regulatory factors in the coordinately expressed alpha 1 (I) and alpha 2 (I) collagen promoters. Biochem. Biophys. Res. Commun. 177, 538–544.

Karsenty, G., Wagner, E.F., 2002. Reaching a genetic and molecular understanding of skeletal development. Dev. Cell 2, 389–406.

Kawaguchi, Y., Hara, M., Wright, T.M., 1999. Endogenous IL-1alpha from systemic sclerosis fibroblasts induces IL-6 and PDGF-A. J. Clin. Investig. 103, 1253–1260.

Kawaguchi, Y., Nishimagi, E., Tochimoto, A., Kawamoto, M., Katsumata, Y., Soejima, M., Kanno, T., Kamatani, N., Hara, M., 2006. Intracellular IL-1alpha-binding proteins contribute to biological functions of endogenous IL-1alpha in systemic sclerosis fibroblasts. Proc. Natl. Acad. Sci. U.S.A. 103, 14501–14506.

Kern, B., Shen, J., Starbuck, M., Karsenty, G., 2001. Cbfa1 contributes to the osteoblast-specific expression of type I collagen genes. J. Biol. Chem. 276, 7101–7107.

Kim, H.J., Song, S.B., Choi, J.M., Kim, K.M., Cho, B.K., Cho, D.H., Park, H.J., 2010. IL-18 downregulates collagen production in human dermal fibroblasts via the ERK pathway. J. Invest. Dermatol. 130 (3), 706–715.

Kinoshita, A., Saito, T., Tomita, H., Makita, Y., Yoshida, K., Ghadami, M., Yamada, K., Kondo, S., Ikegawa, S., Nishimura, G., Fukushima, Y., Nakagomi, T., Saito, H., Sugimoto, T., Kamegaya, M., Hisa, K., Murray, J.C., Taniguchi, N., Niikawa, N., Yoshiura, K., 2000. Domain-specific mutations in TGFB1 result in Camurati-Engelmann disease. Nat. Genet. 26, 19–20.

Klaus, V., Tanios-Schmies, F., Reeps, C., Trenner, M., Matevossian, E., Eckstein, H.H., Pelisek, J., 2017. Association of matrix metalloproteinase levels with collagen degradation in the context of abdominal aortic aneurysm. Eur. J. Vasc. Endovasc. Surg. 53 (4), 549–558.

Koch, M., Laub, F., Zhou, P., Hahn, R.A., Tanaka, S., Burgeson, R.E., Gerecke, D.R., Ramirez, F., Gordon, M.K., 2003. Collagen XXIV, a vertebrate fibrillar collagen with structural features of invertebrate collagens: selective expression in developing cornea and bone. J. Biol. Chem. 278, 43236–43244.

Kouba, D.J., Chung, K.Y., Nishiyama, T., Vindevoghel, L., Kon, A., Klement, J.F., Uitto, J., Mauviel, A., 1999. Nuclear factor-kappa B mediates TNF-alpha inhibitory effect on alpha 2(I) collagen (COL1A2) gene transcription in human dermal fibroblasts. J. Immunol. 162, 4226–4234.

Kream, B.E., LaFrancis, D., Petersen, D.N., Woody, C., Clark, S., Rowe, D.W., Lichtler, A., 1993. Parathyroid hormone represses alpha 1(I) collagen promoter activity in cultured calvariae from neonatal transgenic mice. Mol. Endocrinol. 7, 399–408.

Kream, B.E., Rowe, D., Smith, M.D., Maher, V., Majeska, R., 1986. Hormonal regulation of collagen synthesis in a clonal rat osteosarcoma cell line. Endocrinology 119, 1922–1928.

Krempen, K., Grotkopp, D., Hall, K., Bache, A., Gillan, A., Rippe, R.A., Brenner, D.A., Breindl, M., 1999. Far upstream regulatory elements enhance position-independent and uterus-specific expression of the murine alpha1(I) collagen promoter in transgenic mice. Gene Expr. 8, 151–163.

Kresse, H., Liszio, C., Schonherr, E., Fisher, L.W., 1997. Critical role of glutamate in a central leucine-rich repeat of decorin for interaction with type I collagen. J. Biol. Chem. 272, 18404–18410.

Kuc, I.M., Scott, P.G., 1997. Increased diameters of collagen fibrils precipitated in vitro in the presence of decorin from various connective tissues. Connect. Tissue Res. 36, 287–296.

Kuznetsova, N.V., Forlino, A., Cabral, W.A., Marini, J.C., Leikin, S., 2004. Structure, stability and interactions of type I collagen with GLY349-CYS substitution in alpha 1(I) chain in a murine Osteogenesis Imperfecta model. Matrix Biol. 23, 101–112.

Kwansa, A.L., De Vita, R., Freeman, J.W., 2014. Mechanical recruitment of N- and C-crosslinks in collagen type I. Matrix Biol. 34, 161–169.

Kypriotou, M., Beauchef, G., Chadjichristos, C., Widom, R., Renard, E., Jimenez, S., Korn, J., Maquart, F.X., Oddos, T., Von Stetten, O., Pujol, J.P., Galera, P., 2007. Human collagen-Krox (hc-Krox) up-regulates type I collagen expression in normal and scleroderma fibroblasts through interaction with Sp1 and Sp3 transcription factors. J. Biol. Chem.

Lamande, S.R., Bateman, J.F., 1999. Procollagen folding and assembly: the role of endoplasmic reticulum enzymes and molecular chaperones. Semin. Cell Dev. Biol. 10, 455–464.

Lauer-Fields, J.L., Juska, D., Fields, G.B., 2002. Matrix metalloproteinases and collagen catabolism. Biopolymers 66 (1), 19–32.

Leask, A., Abraham, D.J., 2003. The role of connective tissue growth factor, a multifunctional matricellular protein, in fibroblast biology. Biochem. Cell Biol. 81, 355–363.

Leask, A., Abraham, D.J., 2004. TGF-beta signaling and the fibrotic response. FASEB J. 18, 816–827.

Leask, A., Holmes, A., Black, C.M., Abraham, D.J., 2003. Connective tissue growth factor gene regulation. Requirements for its induction by transforming growth factor-beta 2 in fibroblasts. J. Biol. Chem. 278, 13008–13015.

Lefebvre, V., Behringer, R.R., de Crombrugghe, B., 2001. L-Sox5, Sox6 and Sox9 control essential steps of the chondrocyte differentiation pathway. Osteoarthritis Cartilage 9 (Suppl. A), S69–S75.

Lefebvre, V., de Crombrugghe, B., 1998. Toward understanding SOX9 function in chondrocyte differentiation. Matrix Biol. 16, 529–540.

Lejard, V., Brideau, G., Blais, F., Salingcarnboriboon, R., Wagner, G., Roehrl, M.H., Noda, M., Duprez, D., Houillier, P., Rossert, J., 2007. Scleraxis and NFATc regulate the expression of the pro-alpha1(I) collagen gene in tendon fibroblasts. J. Biol. Chem. 282, 17665–17675.

Li, I.M.H., Horwell, A.L., Chu, G., de Crombrugghe, B., Bou-Gharios, G., 2017. Characterization of mesenchymal-fibroblast cells using the Col1a2 promoter/enhancer. Methods Mol. Biol. 1627, 139–161.

Li, C., Iness, A., Yoon, J., Grider, J.R., Murthy, K.S., Kellum, J.M., Kuemmerle, J.F., 2015. Noncanonical STAT3 activation regulates excess TGF-β1 and collagen I expression in muscle of stricturing Crohn's disease. J. Immunol. 194 (7), 3422–3431.

Lindert, U., Gnoli, M., Maioli, M., Bedeschi, M.F., Sangiorgi, L., Rohrbach, M., Giunta, C., 2018. Insight into the pathology of a COL1A1 signal peptide heterozygous mutation leading to severe osteogenesis imperfecta. Calcif. Tissue Int. 102 (3), 373–379.

Lindquist, J.N., Marzluff, W.F., Stefanovic, B., 2000. Fibrogenesis. III. Posttranscriptional regulation of type I collagen. Am. J. Physiol. 279, G471–G476.

Linkhart, T.A., Keffer, M.J., 1991. Differential regulation of insulin-like growth factor-I (IGF-I) and IGF-II release from cultured neonatal mouse calvaria by parathyroid hormone, transforming growth factor-beta, and 1,25-dihydroxyvitamin D3. Endocrinology 128, 1511–1518.

Liska, D.J., Reed, M.J., Sage, E.H., Bornstein, P., 1994. Cell-specific expression of alpha 1(I) collagen-hGH minigenes in transgenic mice. J. Cell Biol. 125, 695–704.

Liska, D.J., Robinson, V.R., Bornstein, P., 1992. Elements in the first intron of the alpha 1(I) collagen gene interact with Sp1 to regulate gene expression. Gene Expr. 2, 379–389.

Liska, D.J., Slack, J.L., Bornstein, P., 1990. A highly conserved intronic sequence is involved in transcriptional regulation of the alpha 1(I) collagen gene. Cell Regul. 1, 487–498.

Liu, S., Gupta, A., Quarles, L.D., 2007. Emerging role of fibroblast growth factor 23 in a bone-kidney axis regulating systemic phosphate homeostasis and extracellular matrix mineralization. Curr. Opin. Nephrol. Hypertens. 16, 329–335.

LoCascio, V., Bonucci, E., Imbimbo, B., Ballanti, P., Adami, S., Milani, S., Tartarotti, D., DellaRocca, C., 1990. Bone loss in response to long-term glucocorticoid therapy. Bone Miner. 8, 39–51.

MacDonald, H.M., McGuigan, F.A., New, S.A., Campbell, M.K., Golden, M.H., Ralston, S.H., Reid, D.M., 2001. COL1A1 Sp1 polymorphism predicts perimenopausal and early postmenopausal spinal bone loss. J. Bone Miner. Res. 16, 1634–1641.

Maiers, J.L., Kostallari, E., Mushref, M., deAssuncao, T.M., Li, H., Jalan-Sakrikar, N., Huebert, R.C., Cao, S., Malhi, H., Shah, V.H., 2017. The unfolded protein response mediates fibrogenesis and collagen I secretion through regulating TANGO1 in mice. Hepatology 65 (3), 983–998. https://doi.org/10.1002/hep.28921.

Maity, S.N., de Crombrugghe, B., 1998. Role of the CCAAT-binding protein CBF/NF-Y in transcription. Trends Biochem. Sci. 23, 174–178.

Mann, V., Hobson, E.E., Li, B., Stewart, T.L., Grant, S.F., Robins, S.P., Aspden, R.M., Ralston, S.H., 2001. A COL1A1 Sp1 binding site polymorphism predisposes to osteoporotic fracture by affecting bone density and quality. J. Clin. Investig. 107, 899–907.

Mann, V., Ralston, S.H., 2003. Meta-analysis of COL1A1 Sp1 polymorphism in relation to bone mineral density and osteoporotic fracture. Bone 32, 711–717.

Marini, J.C., Forlino, A., Cabral, W.A., Barnes, A.M., San Antonio, J.D., Milgrom, S., Hyland, J.C., Korkko, J., Prockop, D.J., De Paepe, A., Coucke, P., Symoens, S., Glorieux, F.H., Roughley, P.J., Lund, A.M., Kuurila-Svahn, K., Hartikka, H., Cohn, D.H., Krakow, D., Mottes, M., Schwarze, U., Chen, D., Yang, K., Kuslich, C., Troendle, J., Dalgleish, R., Byers, P.H., 2007. Consortium for osteogenesis imperfecta mutations in the helical domain of type I collagen: regions rich in lethal mutations align with collagen binding sites for integrins and proteoglycans. Hum. Mutat. 28, 209–221.

Marongiu, M., Deiana, M., Marcia, L., Sbardellati, A., Asunis, I., Meloni, A., Angius, A., Cusano, R., Loi, A., Crobu, F., Fotia, G., Cucca, F., Schlessinger, D., Crisponi, L., 2016. Novel action of FOXL2 as mediator of Col1a2 gene autoregulation. Dev. Biol. 416 (1), 200–211.

Massague, J., Chen, Y.G., 2000. Controlling TGF-beta signaling. Genes Dev. 14, 627–644.

Matsuo, N., Tanaka, S., Gordon, M.K., Koch, M., Yoshioka, H., Ramirez, F., 2006. CREB-AP1 protein complexes regulate transcription of the collagen XXIV gene (Col24a1) in osteoblasts. J. Biol. Chem. 281, 5445–5452.

McBride Jr., D.J., Choe, V., Shapiro, J.R., Brodsky, B., 1997. Altered collagen structure in mouse tail tendon lacking the alpha 2(I) chain. J. Mol. Biol. 270, 275–284.

McCarthy, T.L., Centrella, M., Canalis, E., 1989. Regulatory effects of insulin-like growth factors I and II on bone collagen synthesis in rat calvarial cultures. Endocrinology 124, 301–309.

Meisler, N., Shull, S., Xie, R., Long, G.L., Absher, M., Connolly, J.P., Cutroneo, K.R., 1995. Glucocorticoids coordinately regulate type I collagen pro alpha 1 promoter activity through both the glucocorticoid and transforming growth factor beta response elements: a novel mechanism of glucocorticoid regulation of eukaryotic genes. J. Cell. Biochem. 59, 376–388.

Mi, Y., Wang, W., Zhang, C., Liu, C., Lu, J., Li, W., Zuo, R., Myatt, L., Sun, K., 2017. Autophagic degradation of collagen 1A1 by cortisol in human amnion fibroblasts. Endocrinology 158 (4), 1005–1014. https://doi.org/10.1210/en.2016-1829.

Miles, C.A., Sims, T.J., Camacho, N.P., Bailey, A.J., 2002. The role of the alpha2 chain in the stabilization of the collagen type I heterotrimer: a study of the type I homotrimer in oim mouse tissues. J. Mol. Biol. 321, 797–805.

Miyazawa, K., Shinozaki, M., Hara, T., Furuya, T., Miyazono, K., 2002. Two major Smad pathways in TGF-beta superfamily signalling. Genes Cells 7, 1191–1204.

Mohan, S., Baylink, D.J., 2005. Impaired skeletal growth in mice with haploinsufficiency of IGF-I: genetic evidence that differences in IGF-I expression could contribute to peak bone mineral density differences. J. Endocrinol. 185, 415–420.

Mohan, S., Richman, C., Guo, R., Amaar, Y., Donahue, L.R., Wergedal, J., Baylink, D.J., 2003. Insulin-like growth factor regulates peak bone mineral density in mice by both growth hormone-dependent and -independent mechanisms. Endocrinology 144, 929–936.

Montero, A., Okada, Y., Tomita, M., Ito, M., Tsurukami, H., Nakamura, T., Doetschman, T., Coffin, J.D., Hurley, M.M., 2000. Disruption of the fibroblast growth factor-2 gene results in decreased bone mass and bone formation. J. Clin. Investig. 105, 1085–1093.

Moore, R., Ferretti, P., Copp, A., Thorogood, P., 2002. Blocking endogenous FGF-2 activity prevents cranial osteogenesis. Dev. Biol. 243, 99–114.

Mori, K., Hatamochi, A., Ueki, H., Olsen, A., Jimenez, S.A., 1996. The transcription of human alpha 1(I) procollagen gene (COL1A1) is suppressed by tumour necrosis factor-alpha through proximal short promoter elements: evidence for suppression mechanisms mediated by two nuclear–factor binding sites. Biochem. J. 319 (Pt 3), 811–816.

Moro, L., Smith, B.D., 1977. Identification of collagen alpha1(I) trimer and normal type I collagen in a polyoma virus-induced mouse tumor. Arch. Biochem. Biophys. 182, 33–41.

Morrison, J., Lu, Q.L., Pastoret, C., Partridge, T., Bou-Gharios, G., 2000. T-cell-dependent fibrosis in the mdx dystrophic mouse. Lab. Invest. 80, 881–891.

Mu, S., Kang, B., Zeng, W., Sun, Y., Yang, F., 2016. MicroRNA-143-3p inhibits hyperplastic scar formation by targeting connective tissue growth factor CTGF/CCN2 via the Akt/mTOR pathway. Mol. Cell Biochem. 416 (1-2), 99−108.

Murakami, S., Lefebvre, V., de Crombrugghe, B., 2000. Potent inhibition of the master chondrogenic factor Sox9 gene by interleukin-1 and tumor necrosis factor-alpha. J. Biol. Chem. 275, 3687−3692.

Myllyharju, J., Kivirikko, K.I., 2001. Collagens and collagen-related diseases. Ann. Med. 33, 7−21.

Myllyharju, J., Kivirikko, K.I., 2004. Collagens, modifying enzymes and their mutations in humans, flies and worms. Trends Genet. 20, 33−43.

Nagai, N., Hosokawa, M., Itohara, S., Adachi, E., Matsushita, T., Hosokawa, N., Nagata, K., 2000. Embryonic lethality of molecular chaperone hsp47 knockout mice is associated with defects in collagen biosynthesis. J. Cell Biol. 150, 1499−1506.

Nagase, H., Visse, R., Murphy, G., 2006. Structure and function of matrix metalloproteinases and TIMPs. Cardiovasc. Res. 69 (3), 562−573.

Nageotte, J., 1927. Action des sels neutres sur la formation du caillot artificiel de collagene. C. R. Soc. Biol. 96, 828−830.

Nakanishi, T., Yamaai, T., Asano, M., Nawachi, K., Suzuki, M., Sugimoto, T., Takigawa, M., 2001. Overexpression of connective tissue growth factor/hypertrophic chondrocyte-specific gene product 24 decreases bone density in adult mice and induces dwarfism. Biochem. Biophys. Res. Commun. 281, 678−681.

Nakao, A., Fujii, M., Matsumura, R., Kumano, K., Saito, Y., Miyazono, K., Iwamoto, I., 1999. Transient gene transfer and expression of Smad7 prevents bleomycin-induced lung fibrosis in mice. J. Clin. Investig. 104, 5−11.

Nakayama, W., Jinnin, M., Tomizawa, Y., Nakamura, K., Kudo, H., Inoue, K., Makino, K., Honda, N., Kajihara, I., Fukushima, S., Ihn, H., 2017. Dysregulated interleukin-23 signalling contributes to the increased collagen production in scleroderma fibroblasts via balancing microRNA expression. Rheumatology (Oxford) 56 (1), 145−155.

Nehls, M.C., Rippe, R.A., Veloz, L., Brenner, D.A., 1991. Transcription factors nuclear factor I and Sp1 interact with the murine collagen alpha 1 (I) promoter. Mol. Cell Biol. 11, 4065−4073.

Newberry, E.P., Latifi, T., Towler, D.A., 1999. The RRM domain of MINT, a novel Msx2 binding protein, recognizes and regulates the rat osteocalcin promoter. Biochemistry 38, 10678−10690.

Newberry, E.P., Willis, D., Latifi, T., Boudreaux, J.M., Towler, D.A., 1997. Fibroblast growth factor receptor signaling activates the human interstitial collagenase promoter via the bipartite Ets-AP1 element. Mol. Endocrinol. 11, 1129−1144.

Niederreither, K., D'Souza, R.N., De Crombrugghe, B., 1992. Minimal DNA sequences that control the cell lineage-specific expression of the pro alpha 2(I) collagen promoter in transgenic mice. J. Cell Biol. 119, 1361−1370.

Nieto, N., 2006. Oxidative-stress and IL-6 mediate the fibrogenic effects of [corrected] Kupffer cells on stellate cells. Hepatology 44, 1487−1501.

Noda, M., Camilliere, J.J., 1989. In vivo stimulation of bone formation by transforming growth factor-beta. Endocrinology 124, 2991−2994.

Novinec, M., Lenarčič, B., 2013. Cathepsin K: a unique collagenolytic cysteine peptidase. Biol. Chem. 394 (9), 1163−1179. https://doi.org/10.1515/hsz-2013-0134.

O'Reilly, S., Ciechomska, M., Fullard, N., Przyborski, S., van Laar, J.M., 2016. IL-13 mediates collagen deposition via STAT6 and microRNA-135b: a role for epigenetics. Sci. Rep. 6, 25066.

O'Shea, P.J., Guigon, C.J., Williams, G.R., Cheng, S.Y., 2007. Regulation of fibroblast growth factor receptor-1 by thyroid hormone: identification of a thyroid hormone response element in the murine Fgfr1 promoter. Endocrinology.

Olsen, D.R., Leigh, S.D., Chang, R., McMullin, H., Ong, W., Tai, E., Chisholm, G., Birk, D.E., Berg, R.A., Hitzeman, R.A., Toman, P.D., 2001. Production of human type I collagen in yeast reveals unexpected new insights into the molecular assembly of collagen trimers. J. Biol. Chem. 276, 24038−24043.

Olsen, B.R., Reginato, A.M., Wang, W., 2000. Bone development. Annu. Rev. Cell Dev. Biol. 16, 191−220.

Ono, K., Kaneko, H., Choudhary, S., Pilbeam, C.C., Lorenzo, J.A., Akatsu, T., Kugai, N., Raisz, L.G., 2005. Biphasic effect of prostaglandin E2 on osteoclast formation in spleen cell cultures: role of the EP2 receptor. J. Bone Miner. Res. 20, 23−29.

Orgel, J.P., Irving, T.C., Miller, A., Wess, T.J., 2006. Microfibrillar structure of type I collagen in situ. Proc. Natl. Acad. Sci. U.S.A. 103 (24), 9001−9005. Epub 2006 Jun 2.

Ornitz, D.M., Marie, P.J., 2002. FGF signaling pathways in endochondral and intramembranous bone development and human genetic disease. Genes Dev. 16, 1446−1465.

Pace, J.M., Corrado, M., Missero, C., Byers, P.H., 2003. Identification, characterization and expression analysis of a new fibrillar collagen gene, COL27A1. Matrix Biol. 22, 3−14.

Pacifici, R., 1996. Estrogen, cytokines, and pathogenesis of postmenopausal osteoporosis. J. Bone Miner. Res. 11, 1043−1051.

Panagakos, F.S., Fernandez, C., Kumar, S., 1996. Ultrastructural analysis of mineralized matrix from human osteoblastic cells: effect of tumor necrosis factor-alpha. Mol. Cell. Biochem. 158, 81−89.

Papaioannou, I., Xu, S., Denton, C.P., Abraham, D.J., Ponticos, M., 2018. STAT3 controls COL1A2 enhancer activation cooperatively with JunB, regulates type I collagen synthesis posttranscriptionally, and is essential for lung myofibroblast differentiation. Mol. Biol. Cell 29 (2), 84−95.

Paschalis, E.P., Jacenko, O., Olsen, B., deCrombrugghe, B., Boskey, A.L., 1996. The role of type X collagen in endochondral ossification as deduced by Fourier transform infrared microscopy analysis. Connect. Tissue Res. 35, 371−377.

Pavlin, D., Bedalov, A., Kronenberg, M.S., Kream, B.E., Rowe, D.W., Smith, C.L., Pike, J.W., Lichtler, A.C., 1994. Analysis of regulatory regions in the COL1A1 gene responsible for 1,25-dihydroxyvitamin D3-mediated transcriptional repression in osteoblastic cells. J. Cell. Biochem. 56, 490−501.

Pavlin, D., Lichter, A., Bedalov, A., Kream, B., Harrison, J., Thomas, H., Gronowicz, G., Clark, S., Woody, C., Rowe, D., 1992. Differential utilization of regulatory domains within the a(1) collagen promoter in osseous and fibroblastic cells. J. Cell Biol. 116, 227−236.

Pereira, R.F., Hume, E.L., Halford, K.W., Prockop, D.J., 1995. Bone fragility in transgenic mice expressing a mutated gene for type I procollagen (COL1A1) parallels the age-dependent phenotype of human osteogenesis imperfecta. J. Bone Miner. Res. 10, 1837−1843.

Perez, J.R., Shull, S., Gendimenico, G.J., Capetola, R.J., Mezick, J.A., Cutroneo, K.R., 1992. Glucocorticoid and retinoid regulation of alpha-2 type I procollagen promoter activity. J. Cell. Biochem. 50, 26−34.

Phillips, C.L., Pfeiffer, B.J., Luger, A.M., Franklin, C.L., 2002. Novel collagen glomerulopathy in a homotrimeric type I collagen mouse (oim). Kidney Int. 62, 383−391.

Pischon, N., Darbois, L.M., Palamakumbura, A.H., Kessler, E., Trackman, P.C., 2004. Regulation of collagen deposition and lysyl oxidase by tumor necrosis factor-alpha in osteoblasts. J. Biol. Chem. 279, 30060−30065.

Poncelet, A.C., Schnaper, H.W., 2001. Sp1 and Smad proteins cooperate to mediate transforming growth factor-beta 1-induced alpha 2(I) collagen expression in human glomerular mesangial cells. J. Biol. Chem. 276, 6983−6992.

Ponticos, M., Abraham, D., Alexakis, C., Lu, Q.L., Black, C., Partridge, T., Bou-Gharios, G., 2004. Col1a2 enhancer regulates collagen activity during development and in adult tissue repair. Matrix Biol. 22, 619−628.

Ponticos, M., Partridge, T., Black, C.M., Abraham, D.J., Bou-Gharios, G., 2004. Regulation of collagen type I in vascular smooth muscle cells by competition between Nkx2.5 and deltaEF1/ZEB1. Mol. Cell Biol. 24, 6151.

Ponticos, M., Harvey, C., Ikeda, T., Abraham, D., Bou-Gharios, G., 2009. JunB mediates enhancer/promoter activity of COL1A2 following TGF-beta induction. Nucleic Acids Res. 37 (16), 5378−5389.

Ponticos, M., Papaioannou, I., Xu, S., Holmes, A.M., Khan, K., Denton, C.P., Bou-Gharios, G., Abraham, D.J., 2015. Failed degradation of JunB contributes to overproduction of type I collagen and development of dermal fibrosis in patients with systemic sclerosis. Arthritis & Rheumato. (Hoboken, N.J) 67 (1), 243−253.

Prockop, D.J., 1990. Mutations that alter the primary structure of type I collagen. The perils of a system for generating large structures by the principle of nucleated growth. J. Biol. Chem. 265, 15349−15352.

Qureshi, A.M., McGuigan, F.E., Seymour, D.G., Hutchison, J.D., Reid, D.M., Ralston, S.H., 2001. Association between COLIA1 Sp1 alleles and femoral neck geometry. Calcif. Tissue Int. 69, 67−72.

Raisz, L.G., Fall, P.M., Gabbitas, B.Y., McCarthy, T.L., Kream, B.E., Canalis, E., 1993. Effects of prostaglandin E2 on bone formation in cultured fetal rat calvariae: role of insulin-like growth factor-I. Endocrinology 133, 1504−1510.

Raisz, L.G., Fall, P.M., Petersen, D.N., Lichtler, A., Kream, B.E., 1993. Prostaglandin E2 inhibits alpha 1(I)procollagen gene transcription and promoter activity in the immortalized rat osteoblastic clonal cell line Py1a. Mol. Endocrinol. 7, 17−22.

Rajaram, S., Baylink, D.J., Mohan, S., 1997. Insulin-like growth factor-binding proteins in serum and other biological fluids: regulation and functions. Endocr. Rev. 18, 801−831.

Ralston, S.H., de Crombrugghe, B., 2006. Genetic regulation of bone mass and susceptibility to osteoporosis. Genes Dev. 20, 2492−2506.

Ralston, S.H., Uitterlinden, A.G., Brandi, M.L., Balcells, S., Langdahl, B.L., Lips, P., Lorenc, R., Obermayer-Pietsch, B., Scollen, S., Bustamante, M., Husted, L.B., Carey, A.H., Diez-Perez, A., Dunning, A.M., Falchetti, A., Karczmarewicz, E., Kruk, M., van Leeuwen, J.P., van Meurs, J.B., Mangion, J., McGuigan, F.E., Mellibovsky, L., del Monte, F., Pols, H.A., Reeve, J., Reid, D.M., Renner, W., Rivadeneira, F., van Schoor, N.M., Sherlock, R.E., Ioannidis, J.P., 2006. Large-scale evidence for the effect of the COLIA1 Sp1 polymorphism on osteoporosis outcomes: the GENOMOS study. PLoS Med. 3, e90.

Ramamurthy, P., Hocking, A.M., McQuillan, D.J., 1996. Recombinant decorin glycoforms. Purification and structure. J. Biol. Chem. 271, 19578−19584.

Ramirez, F., Tanaka, S., Bou-Gharios, G., 2006. Transcriptional regulation of the human alpha 2(I) collagen gene (COL1A2), an informative model system to study fibrotic diseases. Matrix Biol. 25, 365.

Razzaque, M.S., Lanske, B., 2007. The emerging role of the fibroblast growth factor-23-klotho axis in renal regulation of phosphate homeostasis. J. Endocrinol. 194, 1−10.

Reddy, S.V., Hundley, J.E., Windle, J.J., Alcantara, O., Linn, R., Leach, R.J., Boldt, D.H., Roodman, G.D., 1995. Characterization of the mouse tartrate-resistant acid phosphatase (TRAP) gene promoter. J. Bone Miner. Res. 10, 601−606.

Reitamo, S., Remitz, A., Tamai, K., Uitto, J., 1994. Interleukin-10 modulates type I collagen and matrix metalloprotease gene expression in cultured human skin fibroblasts. J. Clin. Investig. 94, 2489−2492.

Rice, D.P., Aberg, T., Chan, Y., Tang, Z., Kettunen, P.J., Pakarinen, L., Maxson, R.E., Thesleff, I., 2000. Integration of FGF and TWIST in calvarial bone and suture development. Development 127, 1845−1855.

Rippe, R.A., Schrum, L.W., Stefanovic, B., Solis-Herruzo, J.A., Brenner, D.A., 1999. NF-kappaB inhibits expression of the alpha1(I) collagen gene. DNA Cell Biol. 18, 751−761.

Riquet, F.B., Lai, W.F., Birkhead, J.R., Suen, L.F., Karsenty, G., Goldring, M.B., 2000. Suppression of type I collagen gene expression by prostaglandins in fibroblasts is mediated at the transcriptional level. Mol. Med. 6, 705−719.

Riquet, F.B., Tan, L., Choy, B.K., Osaki, M., Karsenty, G., Osborne, T.F., Auron, P.E., Goldring, M.B., 2001. YY1 is a positive regulator of transcription of the Col1a1 gene. J. Biol. Chem. 276, 38665−38672.

Ritzenthaler, J.D., Goldstein, R.H., Fine, A., Smith, B.D., 1993. Regulation of the alpha 1(I) collagen promoter via a transforming growth factor-beta activation element. J. Biol. Chem. 268, 13625−13631.

Robert, S., Gicquel, T., Bodin, A., Lagente, V., Boichot, E., 2016. Characterization of the MMP/TIMP imbalance and collagen production induced by IL-1β or TNF-α release from human hepatic stellate cells. PLoS One 11 (4), e0153118.

Roberts, A.B., Sporn, M.B., Assoian, R.K., Smith, J.M., Roche, N.S., Wakefield, L.M., Heine, U.I., Liotta, L.A., Falanga, V., Kehrl, J.H., et al., 1986. Transforming growth factor type beta: rapid induction of fibrosis and angiogenesis in vivo and stimulation of collagen formation in vitro. Proc. Natl. Acad. Sci. U.S.A. 83, 4167–4171.

Roberts, A.B., Tian, F., Byfield, S.D., Stuelten, C., Ooshima, A., Saika, S., Flanders, K.C., 2006. Smad3 is key to TGF-beta-mediated epithelial-to-mesenchymal transition, fibrosis, tumor suppression and metastasis. Cytokine Growth Factor Rev. 17, 19–27.

Rosati, R., Horan, G.S., Pinero, G.J., Garofalo, S., Keene, D.R., Horton, W.A., Vuorio, E., de Crombrugghe, B., Behringer, R.R., 1994. Normal long bone growth and development in type X collagen-null mice. Nat. Genet. 8, 129–135.

Rossert, J.A., Chen, S.S., Eberspaecher, H., Smith, C.N., de Crombrugghe, B., 1996. Identification of a minimal sequence of the mouse pro-alpha 1(I) collagen promoter that confers high-level osteoblast expression in transgenic mice and that binds a protein selectively present in osteoblasts. Proc. Natl. Acad. Sci. U.S.A. 93, 1027–1031.

Rossert, J., Eberspaecher, H., de Crombrugghe, B., 1995. Separate cis-acting DNA elements of the mouse pro-alpha 1(I) collagen promoter direct expression of reporter genes to different type I collagen-producing cells in transgenic mice. J. Cell Biol. 129, 1421–1432.

Rosset, E.M., Trombetta-eSilva, J., Hepfer, G., Yao, H., Bradshaw, A.D., 2017. SPARC and the N-propeptide of collagen I influence fibroblast proliferation and collagen assembly in the periodontal ligament. PLoS One 12 (2), e0173209.

Rossi, P., de Crombrugghe, B., 1987. Identification of a cell-specific transcriptional enhancer in the first intron of the mouse alpha 2 (type I) collagen gene. Proc. Natl. Acad. Sci. U.S.A. 84, 5590–5594.

Rupard, J.H., Dimari, S.J., Damjanov, I., Haralson, M.A., 1988. Synthesis of type I homotrimer collagen molecules by cultured human lung adenocarcinoma cells. Am. J. Pathol. 133, 316–326.

Sabbieti, M.G., Marchetti, L., Abreu, C., Montero, A., Hand, A.R., Raisz, L.G., Hurley, M.M., 1999. Prostaglandins regulate the expression of fibroblast growth factor-2 in bone. Endocrinology 140, 434–444.

Saitta, B., Gaidarova, S., Cicchillitti, L., Jimenez, S.A., 2000. CCAAT binding transcription factor binds and regulates human COL1A1 promoter activity in human dermal fibroblasts: demonstration of increased binding in systemic sclerosis fibroblasts. Arthritis Rheum. 43, 2219–2229.

Sakuma, Y., Li, Z., Pilbeam, C.C., Alander, C.B., Chikazu, D., Kawaguchi, H., Raisz, L.G., 2004. Stimulation of cAMP production and cyclooxygenase-2 by prostaglandin E(2) and selective prostaglandin receptor agonists in murine osteoblastic cells. Bone 34, 827–834.

Salimi-Tari, P., Cheung, M., Safar, C.A., Tracy, J.T., Tran, I., Harbers, K., Breindl, M., 1997. Molecular cloning and chromatin structure analysis of the murine alpha1(I) collagen gene domain. Gene 198, 61–72.

Sanderson, N., Factor, V., Nagy, P., Kopp, J., Kondaiah, P., Wakefield, L., Roberts, A.B., Sporn, M.B., Thorgeirsson, S.S., 1995. Hepatic expression of mature transforming growth factor beta 1 in transgenic mice results in multiple tissue lesions. Proc. Natl. Acad. Sci. U.S.A. 92, 2572–2576.

Santos, S.A.A.D., Porto Amorim, E.M., Ribeiro, L.M., Rinaldi, J.C., Delella, F.K., Justulin, L.A., Felisbino, S.L., 2017. Hyperglycemic condition during puberty increases collagen fibers deposition in the prostatic stroma and reduces MMP-2 activity. Biochem. Biophys. Res. Commun. 493 (4), 1581–1586.

Schedlich, L.J., Muthukaruppan, A., O'Han, M.K., Baxter, R.C., 2007. Insulin-like growth factor binding protein-5 interacts with the vitamin D receptor and modulates the vitamin D response in osteoblasts. Mol. Endocrinol. 21, 2378–2390.

Schier, A.F., Shen, M.M., 2000. Nodal signalling in vertebrate development. Nature 403, 385–389.

Schmid, C., Guler, H.P., Rowe, D., Froesch, E.R., 1989. Insulin-like growth factor I regulates type I procollagen messenger ribonucleic acid steady state levels in bone of rats. Endocrinology 125, 1575–1580.

Schultz, H.S., Guo, L., Keller, P., Fleetwood, A.J., Sun, M., Guo, W., Ma, C., Hamilton, J.A., Bjørkdahl, O., Berchtold, M.W., Panina, S., 2016. OSCAR-collagen signaling in monocytes plays a proinflammatory role and may contribute to the pathogenesis of rheumatoid arthritis. Eur. J. Immunol. 46 (4), 952–963.

Schwarz, M., Harbers, K., Kratochwil, K., 1990. Transcription of a mutant collagen I gene is a cell type and stage-specific marker for odontoblast and osteoblast differentiation. Development 108, 717–726.

Scott, P.G., Grossmann, J.G., Dodd, C.M., Sheehan, J.K., Bishop, P.N., 2003. Light and X-ray scattering show decorin to be a dimer in solution. J. Biol. Chem. 278, 18353–18359.

Segarini, P.R., Nesbitt, J.E., Li, D., Hays, L.G., Yates III, J.R., Carmichael, D.F., 2001. The low density lipoprotein receptor-related protein/alpha2-macroglobulin receptor is a receptor for connective tissue growth factor. J. Biol. Chem. 276, 40659–40667.

Sengupta, P.K., Fargo, J., Smith, B.D., 2002. The RFX family interacts at the collagen (COL1A2) start site and represses transcription. J. Biol. Chem. 277, 24926–24937.

Sengupta, P., Xu, Y., Wang, L., Widom, R., Smith, B.D., 2005. Collagen alpha1(I) gene (COL1A1) is repressed by RFX family. J. Biol. Chem. 280 (22), 21004–21014.

Serpier, H., Gillery, P., Salmon-Ehr, V., Garnotel, R., Georges, N., Kalis, B., Maquart, F.X., 1997. Antagonistic effects of interferon-gamma and interleukin-4 on fibroblast cultures. J. Investig. Dermatol. 109, 158–162.

Seyedin, S.M., Thomas, T.C., Thompson, A.Y., Rosen, D.M., Piez, K.A., 1985. Purification and characterization of two cartilage-inducing factors from bovine demineralized bone. Proc. Natl. Acad. Sci. U.S.A. 82, 2267–2271.

Sher, L.B., Woitge, H.W., Adams, D.J., Gronowicz, G.A., Krozowski, Z., Harrison, J.R., Kream, B., 2004. Transgenic expression of 11beta-hydroxysteroid dehydrogenase type 2 in osteoblasts reveals an anabolic role for endogenous glucocorticoids in bone. Endocrinology 145, 922–929.

Shi-wen, X., Pennington, D., Holmes, A., Leask, A., Bradham, D., Beauchamp, J.R., Fonseca, C., du Bois, R.M., Martin, G.R., Black, C.M., Abraham, D.J., 2000. Autocrine overexpression of CTGF maintains fibrosis: RDA analysis of fibrosis genes in systemic sclerosis. Exp. Cell Res. 259, 213–224.

Shi-wen, X., Stanton, L.A., Kennedy, L., Pala, D., Chen, Y., Howat, S.L., Renzoni, E.A., Carter, D.E., Bou-Gharios, G., Stratton, R.J., Pearson, J.D., Beier, F., Lyons, K.M., Black, C.M., Abraham, D.J., Leask, A., 2006. CCN2 is necessary for adhesive responses to transforming growth factor-beta1 in embryonic fibroblasts. J. Biol. Chem. 281, 10715–10726.

Sinha, S., Maity, S.N., Lu, J., de Crombrugghe, B., 1995. Recombinant rat CBF-C, the third subunit of CBF/NFY, allows formation of a protein-DNA complex with CBF-A and CBF-B and with yeast HAP2 and HAP3. Proc. Natl. Acad. Sci. U.S.A. 92, 1624–1628.

Slack, J.L., Liska, D.J., Bornstein, P., 1991. An upstream regulatory region mediates high-level, tissue-specific expression of the human alpha 1(I) collagen gene in transgenic mice. Mol. Cell Biol. 11, 2066–2074.

Slack, J.L., Parker, M.I., Bornstein, P., 1995. Transcriptional repression of the alpha 1(I) collagen gene by ras is mediated in part by an intronic AP1 site. J. Cell. Biochem. 58, 380–392.

Sokolov, B.P., Mays, P.K., Khillan, J.S., Prockop, D.J., 1993. Tissue- and development-specific expression in transgenic mice of a type I procollagen (COL1A1) minigene construct with 2.3 kb of the promoter region and 2 kb of the 39-flanking region. Specificity is independent of the putative regulatory sequences in the first intron. Biochemistry 32, 9242–9249.

Solis-Herruzo, J.A., Brenner, D.A., Chojkier, M., 1988. Tumor necrosis factor alpha inhibits collagen gene transcription and collagen synthesis in cultured human fibroblasts. J. Biol. Chem. 263, 5841–5845.

Sono, T., Akiyama, H., Miura, S., Deng, J.M., Shukunami, C., Hiraki, Y., Tsushima, Y., Azuma, Y., Behringer, R.R., Matsuda, S., 2018. THRAP3 interacts with and inhibits the transcriptional activity of SOX9 during chondrogenesis. J. Bone Miner. Metab. 36 (4), 410–419.

Sprangers, S., Everts, V., 2019. Molecular pathways of cell-mediated degradation of fibrillar collagen. Matrix Biol. 75-76, 190–200. https://doi.org/10.1016/j.matbio.2017.11.008.

Stefanovic, B., Brenner, D.A., 2003. 5' stem-loop of collagen alpha 1(I) mRNA inhibits translation in vitro but is required for triple helical collagen synthesis in vivo. J. Biol. Chem. 278, 927–933.

Stefanovic, B., Hellerbrand, C., Holcik, M., Briendl, M., Aliebhaber, S., Brenner, D.A., 1997. Posttranscriptional regulation of collagen alpha1(I) mRNA in hepatic stellate cells. Mol. Cell Biol. 17, 5201–5209.

Sterner-Kock, A., Thorey, I.S., Koli, K., Wempe, F., Otte, J., Bangsow, T., Kuhlmeier, K., Kirchner, T., Jin, S., Keski-Oja, J., von Melchner, H., 2002. Disruption of the gene encoding the latent transforming growth factor-beta binding protein 4 (LTBP-4) causes abnormal lung development, cardiomyopathy, and colorectal cancer. Genes Dev. 16, 2264–2273.

Stewart, T.L., Jin, H., McGuigan, F.E., Albagha, O.M., Garcia-Giralt, N., Bassiti, A., Grinberg, D., Balcells, S., Reid, D.M., Ralston, S.H., 2006. Haplotypes defined by promoter and intron 1 polymorphisms of the COLIA1 gene regulate bone mineral density in women. J. Clin. Endocrinol. Metab. 91, 3575–3583.

Stewart, T.L., Roschger, P., Misof, B.M., Mann, V., Fratzl, P., Klaushofer, K., Aspden, R., Ralston, S.H., 2005. Association of COLIA1 Sp1 alleles with defective bone nodule formation in vitro and abnormal bone mineralization in vivo. Calcif. Tissue Int. 77, 113–118.

Stokes, F.J., Ivanov, P., Bailey, L.M., Fraser, W.D., 2011. The effects of sampling procedures and storage conditions on short-term stability of blood-based biochemical markers of bone metabolism. Clin. Chem. 57 (1), 138–140.

Stratton, R., Rajkumar, V., Ponticos, M., Nichols, B., Shiwen, X., Black, C.M., Abraham, D.J., Leask, A., 2002. Prostacyclin derivatives prevent the fibrotic response to TGF-beta by inhibiting the Ras/MEK/ERK pathway. FASEB J. 16, 1949–1951.

Stylianou, E., Saklatvala, J., 1998. Interleukin-1. Int. J. Biochem. Cell Biol. 30, 1075–1079.

Sullivan, R., Klagsbrun, M., 1985. Purification of cartilage-derived growth factor by heparin affinity chromatography. J. Biol. Chem. 260, 2399–2403.

Sweeney, S.M., Orgel, J.P., Fertala, A., McAuliffe, J.D., Turner, K.R., Di Lullo, G.A., Chen, S., Antipova, O., Perumal, S., Ala-Kokko, L., Forlino, A., Cabral, W.A., Barnes, A.M., Marini, J.C., San Antonio, J.D., 2008. Candidate cell and matrix interaction domains on the collagen fibril, the predominant protein of vertebrates. J. Biol. Chem. 283 (30), 21187–21197. https://doi.org/10.1074/jbc.M709319200.

Taddese, S., Jung, M.C., Ihling, C., Heinz, A., Neubert, R.H., Schmelzer, C.E., 2010. MMP-12 catalytic domain recognizes and cleaves at multiple sites in human skin collagen type I and type III. Biochim. Biophys. Acta. 1804 (4), 731–739.

Takigawa, M., Nakanishi, T., Kubota, S., Nishida, T., 2003. Role of CTGF/HCS24/ecogenin in skeletal growth control. J. Cell. Physiol. 194, 256–266.

Tam, E.M., Moore, T.R., Butler, G.S., Overall, C.M., 2004. Characterization of the distinct collagen binding, helicase and cleavage mechanisms of matrix metalloproteinase 2 and 14 (gelatinase A and MT1-MMP): the differential roles of the MMP hemopexin c domains and the MMP-2 fibronectin type II modules in collagen triple helicase activities. J. Biol. Chem. 279 (41), 43336–43344.

Tamaki, T., Ohnishi, K., Hartl, C., LeRoy, E.C., Trojanowska, M., 1995. Characterization of a GC-rich region containing Sp1 binding site(s) as a constitutive responsive element of the alpha 2(I) collagen gene in human fibroblasts. J. Biol. Chem. 270, 4299–4304.

Tan, K.M., Saw, S., Sethi, S.K., 2013. Vitamin D and its relationship with markers of bone metabolism in healthy Asian women. J. Clin. Lab. Anal. 27 (4), 301–304.

Tanaka, S., Antoniv, T.T., Liu, K., Wang, L., Wells, D.J., Ramirez, F., Bou-Gharios, G., 2004. Cooperativity between far upstream enhancer and proximal promoter elements of the human {alpha}2(I) collagen (COL1A2) gene instructs tissue specificity in transgenic mice. J. Biol. Chem. 279, 56024–56031.

Tang, K.T., Capparelli, C., Stein, J.L., Stein, G.S., Lian, J.B., Huber, A.C., Braverman, L.E., DeVito, W.J., 1996. Acidic fibroblast growth factor inhibits osteoblast differentiation in vitro: altered expression of collagenase, cell growth-related, and mineralization-associated genes. J. Cell. Biochem. 61, 152–166.

Tasab, M., Batten, M.R., Bulleid, N.J., 2000. Hsp47: a molecular chaperone that interacts with and stabilizes correctly-folded procollagen. EMBO J. 19, 2204–2211.

Terraz, C., Brideau, G., Ronco, P., Rossert, J., 2002. A combination of cis-acting elements is required to activate the pro-alpha 1(I) collagen promoter in tendon fibroblasts of transgenic mice. J. Biol. Chem. 277, 19019−19026.

Thampatty, B.P., Li, H., Im, H.J., Wang, J.H., 2007. EP4 receptor regulates collagen type-I, MMP-1, and MMP-3 gene expression in human tendon fibroblasts in response to IL-1 beta treatment. Gene 386, 154−161.

Thiebaud, D., Guenther, H.L., Porret, A., Burckhardt, P., Fleisch, H., Hofstetter, W., 1994. Regulation of collagen type I and biglycan mRNA levels by hormones and growth factors in normal and immortalized osteoblastic cell lines. J. Bone Miner. Res. 9, 1347−1354.

Thiele, B.J., Doller, A., Kahne, T., Pregla, R., Hetzer, R., Regitz-Zagrosek, V., 2004. RNA-binding proteins heterogeneous nuclear ribonucleoprotein A1, E1, and K are involved in post-transcriptional control of collagen I and III synthesis. Circ. Res. 95, 1058−1066.

Todorovic, V., Jurukovski, V., Chen, Y., Fontana, L., Dabovic, B., Rifkin, D.B., 2005. Latent TGF-beta binding proteins. Int. J. Biochem. Cell Biol. 37, 38−41.

Uitterlinden, A.G., Burger, H., Huang, Q., Yue, F., McGuigan, F.E., Grant, S.F., Hofman, A., van Leeuwen, J.P., Pols, H.A., Ralston, S.H., 1998. Relation of alleles of the collagen type Ialpha1 gene to bone density and the risk of osteoporotic fractures in postmenopausal women. N. Engl. J. Med. 338, 1016−1021.

Uitto, J., 1979. Collagen polymorphism: isolation and partial characterization of alpha 1(I)-trimer molecules in normal human skin. Arch. Biochem. Biophys. 192, 371−379.

Ulloa, L., Doody, J., Massague, J., 1999. Inhibition of transforming growth factor-beta/SMAD signalling by the interferon-gamma/STAT pathway. Nature 397, 710−713.

van der Rest, M., Garrone, R., 1991. Collagen family of proteins. FASEB J. 5, 2814−2823.

Van Doren, S.R., 2015. Matrix metalloproteinase interactions with collagen and elastin. Matrix Biol. 44-46, 224−231. https://doi.org/10.1016/j.matbio.2015.01.005.

van Driel, M., Pols, H.A., van Leeuwen, J.P., 2004. Osteoblast differentiation and control by vitamin D and vitamin D metabolites. Curr. Pharmaceut. Des. 10, 2535−2555.

Vanleene, et al., 2012. Bone 50, 1317−1323.

Varghese, S., Ramsby, M.L., Jeffrey, J.J., Canalis, E., 1995. Basic fibroblast growth factor stimulates expression of interstitial collagenase and inhibitors of metalloproteinases in rat bone cells. Endocrinology 136, 2156−2162.

Varghese, S., Rydziel, S., Canalis, E., 2000. Basic fibroblast growth factor stimulates collagenase-3 promoter activity in osteoblasts through an activator protein-1-binding site. Endocrinology 141, 2185−2191.

Varma, S., Orgel, J.P., Schieber, J.D., 2016. Nanomechanics of type I collagen. Biophys J. 111 (1), 50−56. https://doi.org/10.1016/j.bpj.2016.05.038.

Vasikaran, S., Eastell, R., Bruyere, O., Foldes, A.J., Garnero, P., Griesmacher, A., et al., 2011. Markers of bone turnover for the prediction of fracture risk and monitoring of osteoporosis treatment: a need for international reference standards. Osteoporos. Int. 22 (2), 391−420.

Verrecchia, F., Mauviel, A., 2007. Transforming growth factor-beta and fibrosis. World J. Gastroenterol. 13, 3056−3062.

Verrecchia, F., Pessah, M., Atfi, A., Mauviel, A., 2000. Tumor necrosis factor-alpha inhibits transforming growth factor-beta/Smad signaling in human dermal fibroblasts via AP-1 activation. J. Biol. Chem. 275, 30226−30231.

Verrecchia, F., Vindevoghel, L., Lechleider, R.J., Uitto, J., Roberts, A.B., Mauviel, A., 2001. Smad3/AP-1 interactions control transcriptional responses to TGF-beta in a promoter-specific manner. Oncogene 20, 3332−3340.

Verrecchia, F., Wagner, E.F., Mauviel, A., 2002. Distinct involvement of the Jun-N-terminal kinase and NF-kappaB pathways in the repression of the human COL1A2 gene by TNF-alpha. EMBO Rep. 3, 1069−1074.

Vogel, K.G., Trotter, J.A., 1987. The effect of proteoglycans on the morphology of collagen fibrils formed in vitro. Collagen Relat. Res. 7, 105−114.

Vuorio, E., de Crombrugghe, B., 1990. The family of collagen genes. Annu. Rev. Biochem. 59, 837−872.

Waddington, R.J., Roberts, H.C., Sugars, R.V., Schonherr, E., 2003. Differential roles for small leucine-rich proteoglycans in bone formation. Eur. Cells Mater. 6, 12−21 discussion 21.

Wang, L., Tanaka, S., Ramirez, F., 2005. GATA-4 binds to an upstream element of the human alpha2(I) collagen gene (COL1A2) and inhibits transcription in fibroblasts. Matrix Biol. 24, 333−340.

Weber, I.T., Harrison, R.W., Iozzo, R.V., 1996. Model structure of decorin and implications for collagen fibrillogenesis. J. Biol. Chem. 271, 31767−31770.

Weinstein, R.S., Jilka, R.L., Parfitt, A.M., Manolagas, S.C., 1998. Inhibition of osteoblastogenesis and promotion of apoptosis of osteoblasts and osteocytes by glucocorticoids. Potential mechanisms of their deleterious effects on bone. J. Clin. Investig. 102, 274−282.

Weston, B.S., Wahab, N.A., Mason, R.M., 2003. CTGF mediates TGF-beta-induced fibronectin matrix deposition by upregulating active alpha5beta1 integrin in human mesangial cells. J. Am. Soc. Nephrol. 14, 601−610.

Wiestner, M., Krieg, T., Horlein, D., Glanville, R.W., Fietzek, P., Muller, P.K., 1979. Inhibiting effect of procollagen peptides on collagen biosynthesis in fibroblast cultures. J. Biol. Chem. 254, 7016−7023.

Wilson, et al., 2011. J Cell Biol. 194 (2), 347.

Woitge, H.W., Kream, B.E., 2000. Calvariae from fetal mice with a disrupted Igf1 gene have reduced rates of collagen synthesis but maintain responsiveness to glucocorticoids. J. Bone Miner. Res. 15, 1956−1964.

Wu, et al., 2014. Genome Biol 15, R52.

Xu, T., Bianco, P., Fisher, L.W., Longenecker, G., Smith, E., Goldstein, S., Bonadio, J., Boskey, A., Heegaard, A.M., Sommer, B., Satomura, K., Dominguez, P., Zhao, C., Kulkarni, A.B., Robey, P.G., Young, M.F., 1998. Targeted disruption of the biglycan gene leads to an osteoporosis-like phenotype in mice. Nat. Genet. 20, 78−82.

Xu, Y., Wang, L., Buttice, G., Sengupta, P.K., Smith, B.D., 2003. Interferon gamma repression of collagen (COL1A2) transcription is mediated by the RFX5 complex. J. Biol. Chem. 278, 49134−49144.

Xu, Y., Wang, L., Buttice, G., Sengupta, P.K., Smith, B.D., 2004. Major histocompatibility class II transactivator (CIITA) mediates repression of collagen (COL1A2) transcription by interferon gamma (IFN-gamma). J. Biol. Chem. 279, 41319−41332.

Yañez-Mó, M., Barreiro, O., Gonzalo, P., Batista, A., Megías, D., Genís, L., Sachs, N., Sala-Valdés, M., Alonso, M.A., Montoya, M.C., Sonnenberg, A., Arroyo, A.G., Sánchez-Madrid, F., 2008. MT1-MMP collagenolytic activity is regulated through association with tetraspanin CD151 in primary endothelial cells. Blood 112 (8), 3217−3226.

Yata, Y., Scanga, A., Gillan, A., Yang, L., Reif, S., Breindl, M., Brenner, D.A., Rippe, R.A., 2003. DNase I-hypersensitive sites enhance alpha1(I) collagen gene expression in hepatic stellate cells. Hepatology 37, 267−276.

Yuan, W., Yufit, T., Li, L., Mori, Y., Chen, S.J., Varga, J., 1999. Negative modulation of alpha1(I) procollagen gene expression in human skin fibroblasts: transcriptional inhibition by interferon-gamma. J. Cell. Physiol. 179, 97−108.

Zhang, W., Ou, J., Inagaki, Y., Greenwel, P., Ramirez, F., 2000. Synergistic cooperation between Sp1 and Smad3/Smad4 mediates transforming growth factor beta1 stimulation of alpha 2(I)-collagen (COL1A2) transcription. J. Biol. Chem. 275, 39237−39245.

Zhu, et al., 2012. J clin Immunol 32, 514−522.

Zigrino, P., Brinckmann, J., Niehoff, A., Lu, Y., Giebeler, N., Eckes, B., Kadler, K.E., Mauch, C., 2016. Fibroblast-derived MMP-14 regulates collagen homeostasis in adult skin. J. Invest. Dermatol. 136 (8), 1575−1583. https://doi.org/10.1016/j.jid.2016.03.036.

Chapter 14

Collagen cross-linking and bone pathobiology

David M. Hudson, MaryAnn Weis and David R. Eyre
Department of Orthopaedics and Sports Medicine, University of Washington, Seattle, WA, United States

Chapter outline

Introduction

Lysyl oxidase (LOX)-mediated covalent cross-links between individual collagen molecules are essential for the strength of collagen fibrils. They appeared at the dawn of metazoan evolution (Rodriguez-Pascual and Slatter, 2016) and can be argued to have been a critical step in allowing larger animals to evolve (Boot-Handford and Tuckwell, 2003). Divergencies in the content, placement, and chemical stability of these intermolecular cross-links have clearly evolved to modulate the properties of collagen fibrils in different tissue types.

Collagen accounts for about a third of all protein in the human body (Verzár, 1964) and is the main organic component of bone (Myllyharju and Kivirikko, 2004; Eyre, 1980). Fibrillar collagen molecules consist of three polypeptide α-chains, each about 1000 residues of a single repeating Gly−Xaa−Yaa primary amino acid sequence, which folds into the defining triple-helical conformation of a collagen molecule. Variations in the extensive posttranslational modifications of the major fibril-forming collagen type I contribute to the structural and functional differences between tissues (Eyre et al., 1984a,b;

Principles of Bone Biology. https://doi.org/10.1016/B978-0-12-814841-9.00014-2

Hudson and Eyre, 2013). Indeed, cross-linking chemistry differs fundamentally between skin, tendon, and bone type I collagen, with distinct changes continuing during tissue growth and maturation (Light and Bailey, 1979).

LOXs initiate fibrillar collagen cross-linking, in the sole enzymatic step, by forming aldehyde side-chains from specific telopeptide lysine and hydroxylysine residues. From then on, further reactions are driven by the local protein environment at the cross-linking sites. All the fibril-forming collagens (types I, II, III, V, and XI) can have up to four cross-linking loci per molecule, one per telopeptide domain and two placed symmetrically at opposite ends of the triple helix. Certain chains (α2(I), α1(V), α2(V), α1(XI) and α2(XI)) lack C-telopeptide cross-linking lysines. Upon collagen fibril assembly, the triple-helical cross-linking lysines align and spontaneously react with telopeptide lysine and hydroxylysine aldehydes in adjacent molecules staggered axially by 4D periods (where D = 67nm, the axial stagger of adjacent collagen molecules packed in a fibril). The mature cross-linking chemistry in bone collagen is distinctive, with products containing both lysine and hydroxylysine aldehyde precursors (Fig. 14.1).

Advances in collagen cross-link analysis

Mature cross-link analysis

The content of pyridinoline cross-links, readily quantified by their natural fluorescence, has been used as a gold standard for assessing collagen cross-linking quality for decades (Eyre et al., 1984a). Specifically, high-performance liquid chromatography-based assays were developed to measure the quantitative distribution of hydroxylysyl pyridinoline (HP) and lysyl pyridinoline (LP) across tissues and collagen genetic types (Eyre et al., 1984b; Wu and Eyre, 1985; Fujimoto, 1977). Variances in the total amount and/or HP/LP ratio of these trifunctional residues have been one of the traditional measures of collagen quality and pathobiology (Eyre et al., 1984a,b). Although informative, the content of pyridinolines is only a fraction of the total LOX-mediated cross-links in most tissues, including bone.

Even mature bone contains more divalent cross-links and more pyrrolic cross-links than total pyridinolines. Trivalent pyrrole cross-links are measured in collagenous tissues using a colorimetric assay. Ehrlich's reagent (*p*-dimethylaminobenzaldehyde) reacts with pyrrole residues to yield a quantifiable pink color (Scott et al., 1981). Pyrrole cross-links appear to be limited mostly to fibrillar collagens of bone and load-bearing tendons (Hanson and Eyre, 1996; Horgan et al., 1990).

Divalent cross-link analysis

Divalent cross-linking amino acids were originally profiled in tissues as tritiated products after sodium borotritide reduction on the amino acid analyzer, with quantitation relative to nonreducible cross-links by ninhydrin detection (Eyre, 1987; Avery et al., 2009). Mass spectrometric approaches have begun to supplement the traditional methods of amino acid analysis and N-terminal sequencing for studying divalent collagen cross-links (Hudson et al., 2017; Eyre et al., 2004; Kalamajski et al., 2014; Terajima et al., 2014; Naffa et al., 2016).

Electrospray mass spectrometry

Early mass spectrometric methods were used to structurally characterize collagen cross-links beginning in the 1960s (Blumenfeld and Gallop, 1966; Schneider et al., 1967). However, using ion-trap mass spectrometry, collagen cross-linked peptides could be identified by their peptide fragmentation patterns (Fig. 14.2) (Eyre et al., 2004). Collagen peptides can be generated for mass spectrometric analysis using several approaches, including sodium dodecyl sulfate–polyacrylamide gel electrophoresis of whole chains and CNBr peptides and in-gel protease digestion (e.g., trypsin, endo-Asp) or bacterial collagenase digestion followed by liquid chromatography, or directly from urine after Sep-Pak enrichment (Eyre et al., 2008). By using sequence-specific antibodies for detection followed by mass spectrometric analysis, heterotypic cross-links between α-chains of different collagen types were identified (Eyre et al., 2008).

Cross-link formation

Bone collagen cross-linking

The distinctive profile of mature cross-links in bone collagen is controlled by the partial hydroxylation of lysine residues at both telopeptide and triple-helical cross-linking sites (Fig. 14.3). Telopeptide lysines at both ends are about 50%

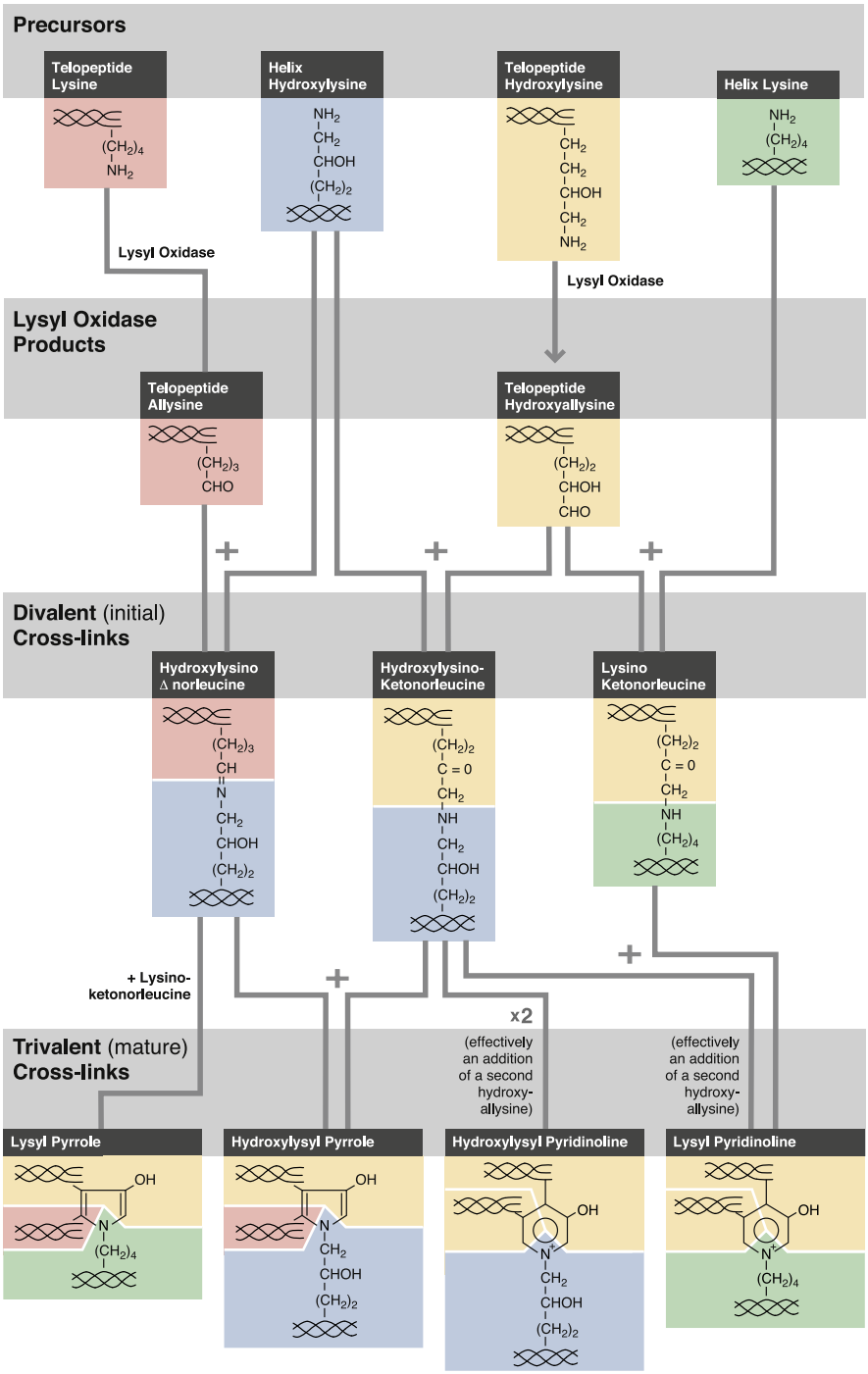

FIGURE 14.1 Lysyl oxidase–derived collagen cross-linking pathway in bone. Type I collagen cross-linking in bone is unique in using both lysine (allysine) and hydroxylysine (hydroxyallysine) aldehyde precursors in the telopeptide domains. In growing fibrils, the aldehydes interact with specific lysine or hydroxylysine residues at helical sites (K87 and K930) in neighboring collagen molecules. The resulting divalent cross-links are the predominant cross-links found in bone. These initial divalent cross-links can add an additional telopeptide aldehyde (from a second divalent cross-link) to form trivalent (mature) cross-links. In adult human bone, the trivalent cross-links are a mixture of about equal amounts of pyridinolines and pyrroles.

hydroxylated (human, bovine) compared with 0% in skin type I collagen and 100% in cartilage type II collagen (Eyre et al., 2008). This results in a unique pattern of both divalent and mature, trivalent cross-linked peptides from bone collagen including a mixture of mature pyrrole and pyridinoline structures (Hanson and Eyre, 1996). The formation of the trifunctional cross-links requires the precise lateral packing of collagen molecules in the native staggered structure that

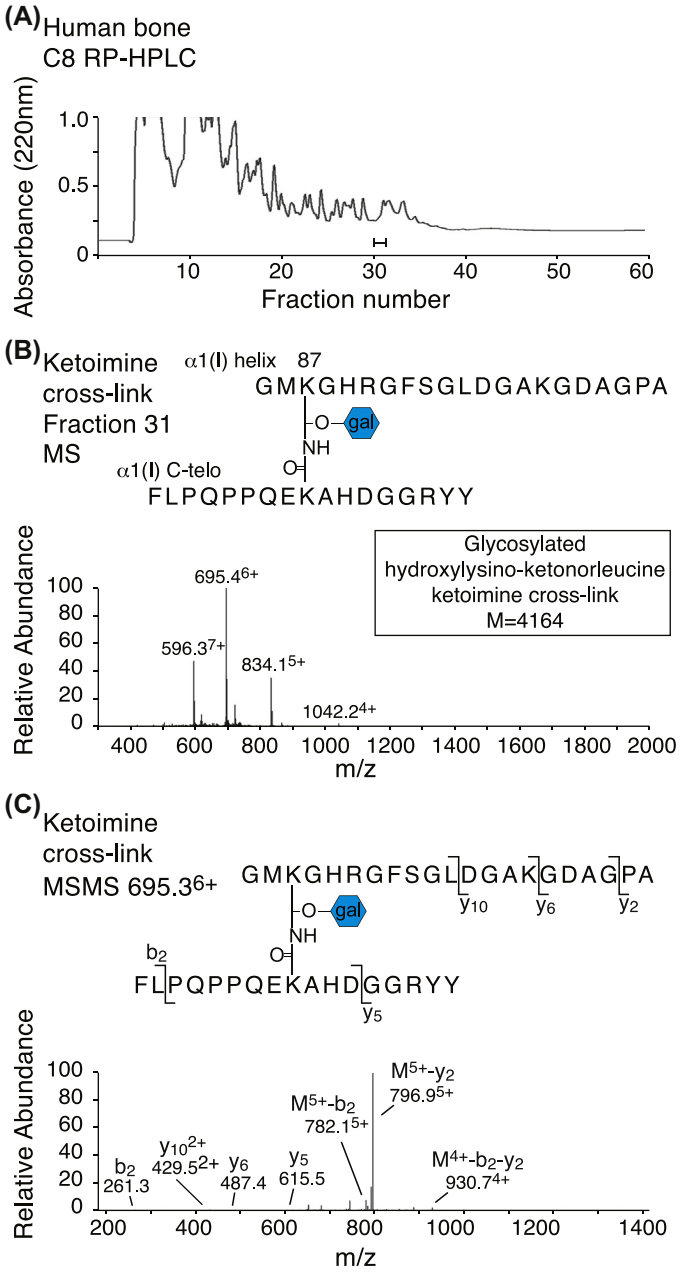

FIGURE 14.2 The identification of a divalent cross-linked peptide from bone collagen (Lys-87 to C-telopeptide) using mass spectrometry. (A) Reverse-phase high-performance liquid chromatography resolution of cross-linked peptides from human bone collagen digested with bacterial collagenase. (B) Mass spectrometry (*MS*) profile of fraction 31 reveals a glycosylated (galactosyl-) ketoimine structure from human bone (596.3^{7+}, 695.4^{6+}, 834.1^{5+}, and 1042.2^{4+}). (C) Tandem MS fragmentation spectrum of the parent ion (695.3^{6+}) confirms the mass of the glycosylated ketoimine cross-link.

provides the appropriate nearest-neighbor intermolecular relationships for reactions to occur. The well-characterized chemical pathway of cross-linking interactions in bone collagen is shown in Fig. 14.1.

Cross-link structures

Divalent cross-links

The predominant cross-links in mature bone collagen are divalent residues (Eyre et al., 1984a; Eyre, 1981, 1987). With increasing age the mean sum of divalent cross-links (dihydroxylysinonorleucine [DHLNL] and hydroxylysinonorleucine

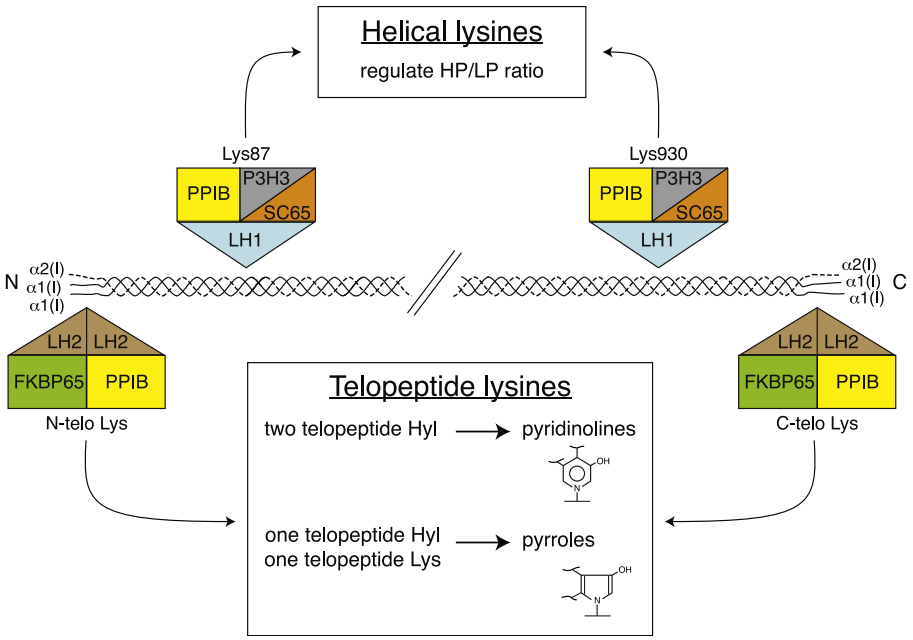

FIGURE 14.3 Regulation of collagen cross-linking in bone by the lysyl hydroxylase (*LH*) complexes. The four lysine sites of cross-linking are symmetrically located in type I collagen (two telopeptide sites and two triple-helical sites). The LH1 complex (LH1, PPIB, SC65, P3H3) catalyzes the hydroxylation of helical lysines 87 and 930. The LH2 complex (LH2 dimer, PPIB, FKBP65) catalyzes the hydroxylation of N- and C-telopeptide lysines. The pattern of lysyl hydroxylation determines the chemical nature of the cross-links, which varies between tissue types. In bone collagen, LH2 partially hydroxylates the telopeptide lysines and LH1 partially hydroxylates the two helical-site lysines of both α-chains. This pattern is a distinguishing post-translational feature of bone type I collagen compared with type I collagen of skin, tendon, and other soft tissues. *FKBP65*, 65-kDa FK506-binding protein; *HP*, hydroxylysyl pyridinoline; *Hyl*, hydroxylysine; *LP*, lysyl pyridinoline; *P3H3*, prolyl 3-hydroxylase 3; *PPIB*, cyclophilin B (peptidyl-prolyl isomerase B); *SC65*, synaptonemal complex 65.

[HLNL]) decreases from 1.9 mol/mol in young bone (13 years) to 0.8 mol/mol in adult bone (41 years) (Eyre, 1987). This decrease coincides with cross-link maturation from bifunctional to trifunctional structures. It is important to note that the physiological bone cross-links, such as dehydro-DHLNL and dehydro-HLNL, and their respective ketoamine forms are reduced to stable secondary amines, DHLNL and HLNL, upon borohydride treatment, allowing their quantitation after acid hydrolysis. Several studies have applied mass spectrometry to further investigate the divalent cross-links in normal tissue (Terajima et al., 2014) and in mouse models that alter tendon (Kalamajski et al., 2014), skin and bone cross-linking chemistry (Hudson et al., 2017).

Pyridinium cross-links

Telopeptide hydroxylysines are a prerequisite for pyridinoline formation (Bank et al., 1999), and the degree of helical cross-linking lysine hydroxylation determines the ratio of HP to LP (Eyre and Wu, 2005). HP and LP each show molecular site and α-chain selectivity in their concentrations (Hanson and Eyre, 1996). Their levels in urine relative to creatinine offer a convenient measure of bone resorption (Beardsworth et al., 1990). Even more specific to osteoclastic bone resorption are the NTx and CTx urine and serum immunoassays directed at short type I collagen telopeptide fragments that were protected by the cross-links through to excretion (Hanson et al., 1992; Singer and Eyre, 2008).

Pyrrole cross-links

Pyrroles are the product of an interaction between a telopeptide lysine aldehyde, a telopeptide hydroxylysine aldehyde, and a triple-helical-domain lysine or hydroxylysine. We believe pyrrole formation involves an interaction between an initial ketoimine and an aldimine divalent cross-link, analogous to that proposed between two divalent cross-links to form HP and LP (Eyre and Oguchi, 1980). This mechanism produces the trivalent structure and releases one triple-helical domain donor sequence. The highest pyrrole cross-link levels will occur when the telopeptide lysines are 50% hydroxylated as they roughly are in normal human bone collagen (Hanson and Eyre, 1996). There is evidence that the content of pyrrole cross-links is positively associated with bone strength (Knott and Bailey, 1998), perhaps by aiding in the assembly of the highly

ordered mineral nanocrystal/protein composite of normal bone. Thus the ratio of pyrrole/pyridinoline cross-links has been shown to be associated with bone quality, with a lower pyrrole content and altered trabecular organization in osteoporotic bone compared with control bone (Banse et al., 2002).

Pyridinoline and pyrrolic cross-linked peptides in urine

The 3-hydroxy pyrrole cross-linking structures, unlike pyridinolines, are labile to acid hydrolysis and so cannot be measured in the same tissue acid hydrolysates as pyridinolines. They can, however, be recovered in cross-linked peptides from mild, proteolytic digests of bone matrix (Hanson and Eyre, 1996) and also in cross-linked peptides excreted in urine as products of osteoclastic bone resorption along with their pyridinoline counterparts.

Fig. 14.4 shows an example of liquid chromatography–mass spectrometry analysis of the urinary pool of cross-linked peptides from osteoclastic resorption that were derived from the N-telopeptide cross-linking site. The results shown reveal a mix of pyridinoline- and pyrrole-linked, otherwise identical trivalent peptides from the main site of pyrrole cross-linking (Hanson and Eyre, 1996). The resulting estimate of pyridinoline-to-pyrrole ratio can provide a potentially useful, noninvasive index of the posttranslational quality of a patient's bone.

Histidine-containing collagen cross-links and other maturation products

It is becoming increasingly evident that the diversity in biomechanical properties between different collagen-rich tissues is very much a function of evolved differences in cross-linking chemistry. Although beyond the scope of this review, collagen cross-linking variations include the apparent involvement of histidine residues in the pathway of lysine aldehyde cross-linking in skin collagen (Yamauchi et al., 1987); an arginine-bound adduct, arginoline, from divalent ketoimine cross-links in cartilages (Eyre et al., 2010); and the sulfilimine cross-links created by the enzyme peroxidasin between specific hydroxylysine and methionine residues in all forms of type IV collagen that are crucial for the biological function of basement membranes (Vanacore et al., 2009; Bhave et al., 2012).

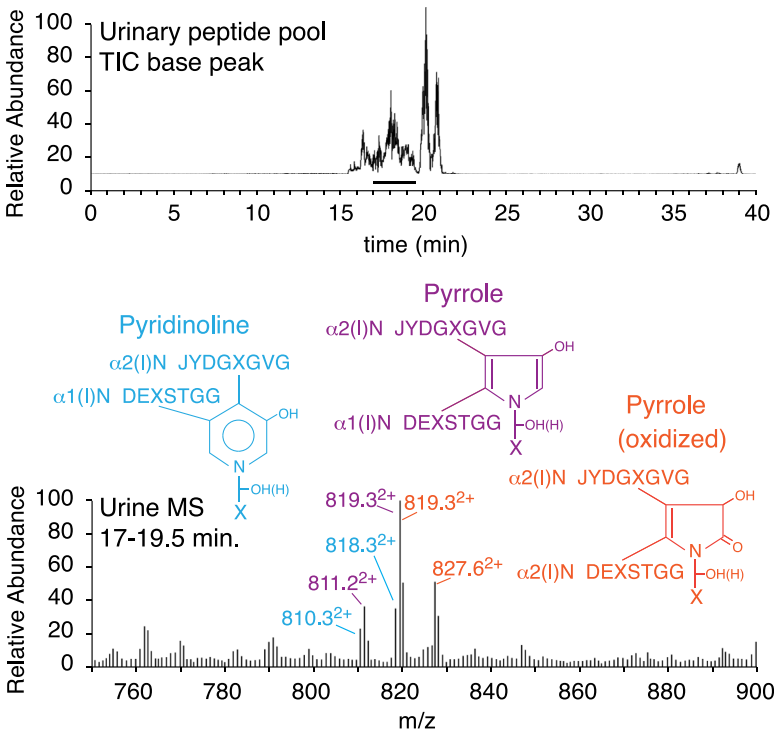

FIGURE 14.4 Liquid chromatography–mass spectrometry (LC–MS) analysis of cross-linked collagen peptides in human urine. The top shows the total ion current (*TIC*) elution profile of peptides on reverse-phase LC and the bottom the ion-trap mass spectral analysis of the *underlined* peptide component peak. The pool of peptides was initially enriched for analysis by ion-exchange and reverse-phase cartridge extraction. The structures shown were identified by their MS/MS fragmentation patterns on tandem mass spectrometry and fitting of the masses of the trivalent cross-linking residues shown. The 3-hydroxy pyrrole ring is readily oxidizable to the +16 Da oxo C2 ring form (819.3^{2+} and 827.6^{2+}), and so gives two pairs of peptides for the lysyl- and hydroxylysyl-derived variants.

In recent work, we have shown that the stable maturation product histidinohydroxylysinonorleucine (HHL), believed to form naturally in the lysine aldehyde pathway of cross-linking that dominates in skin, cornea, and other soft tissue collagens (Yamauchi et al., 1987), is an artifactual product of acid hydrolysis. It is a reaction product formed at sites of C-telopeptide allysine aldol in species with a neighboring C-telopeptide histidine residue (Eyre et al., 2019). This and other evidence is consistent with a role for nearby histidines in catalyzing cross-link formation. Histidine incorporation into mature cross-linking structures is seen only after borohydride reduction (HHMD, histidinohydroxymerodesmosine) or acid hydrolysis (HHL), not on mass spectral analysis of proteolytic digests of tissue collagen (Eyre et al., 2019).

Glycosylations and glycations

Enzymatic glycosylation

Hydroxylysine glycoside content can vary significantly between tissues and collagen types. Bone type I collagen is particularly limited. Only one site, hydroxylysine (Hyl)-87, in each α-chain appears to be fully glycosylated, and Gal-Hyl dominates over Glc-Gal-Hyl. The Gal-Hyl residue participates in cross-link formation with α1(I) C-telopeptide aldehydes (Hanson and Eyre, 1996). Additional partial glycosylation sites include Hyl-174 and Hyl-219 in both α-chains, but only at low occupancy (Terajima et al., 2014; Pokidysheva et al., 2013).

Enzymatic glycosylation is a specific and regulated intracellular modification of nascent collagen α-chains in the endoplasmic reticulum (ER) prior to triple-helix formation (Myllyharju and Kivirikko, 2004; Kivirikko and Myllyla, 1982). The predominant hydroxylysyl galactosyltransferase for bone type I collagen, glycosyltransferase 25 domain 1, is encoded by the GLT25D1 gene (Schegg et al., 2009; Sricholpech et al., 2011). Interestingly, a member of the lysyl hydroxylase (LH) family, the multifunctional LH3, is the principal galactosyl−hydroxylysyl glucosyltransferase in basement membrane collagen (Rautavuoma et al., 2004; Ruotsalainen et al., 2006) and potentially bone type I collagen biosynthesis (Sricholpech et al., 2011).

Tissue-dependent variations in cross-link glycosylation

The ratio of glycosylated to nonglycosylated cross-links can reflect maturational age, tissue type, and even disease state of a collagen sample. Such variation was demonstrated by a 2014 study of adult bovine bone collagen peptides using tandem mass spectrometry (Terajima et al., 2014). Glycosylated pyridinolines and pyrroles were more prevalent than their non-glycosylated forms, and the Gal form dominated. Divalent cross-links were mostly glycosylated too, but with about equal Gal and Glc-Gal forms. The results suggest a steric selectivity for the Gal-Hyl-87 ketoimine cross-link being incorporated into the trivalent structure.

This is consistent with a preference for nonglycosylated pyridinolines being formed during type II collagen maturation in cartilage (Eyre et al., 2008). Divalent ketoimines containing Glc-Gal-Hyl-87 are the primary cross-links in fetal cartilage, whereas nonglycosylated HP is the main pyridinoline in adult articular cartilage (Eyre et al., 2008). An attached disaccharide may therefore sterically hinder a ketoimine cross-link from being the precursor of Glc-Gal HP. A preference for nonglycosylated > Gal > Glc-Gal precursors is indicated.

Potential functions

Potentially, glycosyl groups on bone collagen could either aid or interfere with fibril mineralization. A role for type I collagen overglycosylation in the pathogenesis of osteogenesis imperfecta (OI) has been suggested (Bateman et al., 1984; Tenni et al., 1993; Taga et al., 2013). Altered levels of bone collagen glycosylation have been noted in several musculoskeletal disorders, including postmenopausal osteoporosis (Michalsky et al., 1993), osteosarcoma, and osteofibrous dysplasia (Lehmann et al., 1995). Although in general the functional effects of sugar residues on collagen α-chains are unclear, a broad spectrum of roles have been proposed. They include activities in matrix remodeling (Yang et al., 1993; Jürgensen et al., 2011), collagen fibrillogenesis (Notbohm et al., 1999; Bätge et al., 1997; Torre-Blanco et al., 1992), collagen cross-linking (Rautavuoma et al., 2004; Ruotsalainen et al., 2006; Wang et al., 2002; Moro et al., 2000), and bone mineralization (Sricholpech et al., 2012).

Nonspecific glycations

Among the known and proposed cross-links in collagens, perhaps the least understood but most speculative pathologically are those identified as advanced glycation end products (AGEs). Collagens are frequently cited targets for these adventitious sugar additions since they are typically very long-lived proteins with half-lives ranging for humans from about

5 years in bone (Manolagas, 2000) and 10 years in skin (Avery and Bailey, 2006) to 100 years or more in tendon (Thorpe et al., 2010; Heinemeier et al., 2013) and cartilage (Verzijl et al., 2000). Interestingly, whereas LOX-controlled collagen cross-links appear to plateau in content at a relatively young tissue age (Haut et al., 1992; Eyre et al., 1988), these nonenzymatic cross-links seem to increase steadily over time and cause host tissues to stiffen (Bank et al., 1998; Snedeker and Gautieri, 2014).

Being generally stochastic in nature, AGE cross-linking is proposed to result from randomly accumulated lysine, and perhaps arginine, side-chain glycation adducts that by their placement have potential to go on to form intra- and intermolecular cross-links (Monnier et al., 2005). There is evidence, however, that collagen glycations and AGE formation sites are not random, but will tend to occur at restricted sites (Reiser et al., 1992; Hudson et al., 2018).

Advanced glycation end products

AGEs are formed following the reaction of the carbonyl of a reducing sugar (commonly glucose) with a lysine residue (Fig. 14.5). This nonenzymatic process is the first step in the classical Maillard reaction pathway. The initial product is a relatively unstable Schiff base with the ε-amine of the lysine, which Amadori rearranges to the ketoimine fructosyllysine. This can undergo dehydration, condensation, fragmentation, and cross-linking to form various AGE products. The most prominent is glucosepane, formed by dehydration, carbonyl migration along the sugar carbon chain, and arginine side-chain addition. For this to produce interchain or intrachain protein cross-links, arginine and lysine side-chains need to be 7 Å or less apart (Dai et al., 2008). Several potential sites of glucosepane formation in collagen type I fibrils have been predicted on theoretical grounds (Gautieri et al., 2014; Collier et al., 2015, 2016), but direct analytical proof on connective tissue samples is limited at best. The potential for hydroxylysine as well as lysine residues to be glycated in collagens tends also to have been largely ignored.

Types of advanced glycation end products

From the analysis of complete protease hydrolysates, glucosepane is by far the most prevalent of the potential AGE cross-links in connective tissues (Biemel et al., 2002). Although many more glycation-based structures and potential cross-links have been predicted from experiments in vitro (Snedeker and Gautieri, 2014; Monnier et al., 2005; Sell and Monnier, 2012), their natural tissue levels and significance are less clear. For example, most AGEs arise as monovalent side-chain

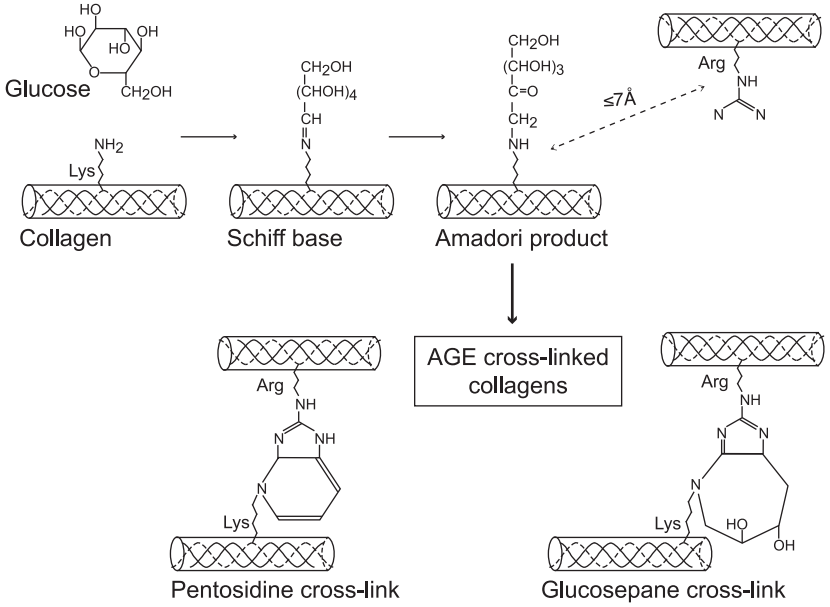

FIGURE 14.5 Glycation products as potential collagen cross-links in bone. The covalent attachment of glucose to collagens and other long-lived proteins leads to advanced glycation end products (*AGEs*) that include candidate cross-links. The Maillard reaction pathway is initiated when the carbonyl of a reducing sugar (commonly glucose) reacts with lysine residues (commonly collagen). The relatively unstable initial Schiff base Amadori rearranges to the ketoimine fructosyllysine. This product can undergo dehydration, condensation, fragmentation, and cross-linking to form various AGE products, which include glucosepane and pentosidine. Such pathological cross-links are thought to contribute to age-related soft tissue stiffening, but the significance for bone is largely unknown.

modifications, which include the arginine product, ornithine; the lysine adduct, fructosyllysine; and the lysine product, carboxymethyllysine. The last has been proposed to cause tissue damage through its ability to chelate transitional metals that can produce reactive oxygenated species (Saxena et al., 1999).

Glucosepane can in theory form intrachain, interchain, and intermolecular collagen cross-links. Based on quantitation in whole-tissue proteolytic digests, glucosepane has been proposed to be the most significant AGE cross-link in older tissues (~0.3 mol/mol of collagen (age 80 skin) (Monnier et al., 2005). Pentosidine, the fluorescent AGE, is quantitatively minor (0.019 mol/mol of collagen (age 80 bone) (Viguet-Carrin et al., 2009). However, to put this in perspective, even if all the measured tissue glucosepane was in collagen as intermolecular cross-links, the levels reached are still an order of magnitude lower than those of the main LOX-based cross-links introduced at synthesis.

Potential consequences

Diabetes mellitus seems to accelerate the age-related decline in bone quality. Increased risk of bone fractures has long been associated with both type 1 and type 2 diabetes (Vestergaard et al., 2009). Bone biopsies from patients with type 1 diabetes revealed a positive association between bone fracture incidence and pentosidine content (Farlay et al., 2016). However, despite decades of research, the pathogenesis of the skeletal effects in diabetes is still poorly understood.

Cross-linking lysine-modifying enzymes

Lysyl hydroxylases

The LH isoenzymes (LH1−3) are encoded by procollagen-lysine, 2-oxoglutarate 5-dioxygenases (*PLOD1−3*). These LH isoenzymes catalyze the hydroxylation of specific collagen lysine residues in a reaction requiring several cofactors (Fe^{2+}, 2-oxoglutarate, O_2, and ascorbate). Unlike prolyl hydroxylation, the extent of lysine hydroxylation varies significantly between tissues and collagen types.

The exact substrate sequence specificity of each isoenzyme has not been fully resolved. It is becoming increasingly clear, however, that LH1 is mainly responsible for catalyzing the hydroxylation of lysine residues within the triple-helical sequence Gly-Xaa-Lys of type I collagen, with particular preference for the cross-linking sites. LH2 is responsible for hydroxylating cross-linking lysine residues in the telopeptide sequences Xaa-Lys-Gly, Xaa-Lys-Ala, and Xaa-Lys-Ser of fibrillar collagens. *PLOD2* encodes two splice variants of LH2, a short form termed LH2a and a long form with an extra exonic 21 amino acids termed LH2b. It has long been thought that LH2b is responsible for collagen telopeptide lysine hydroxylation in bone (Yamauchi and Shiiba, 2008) and hence is the splice variant that controls expression of a hydroxylysine−aldehyde cross-linking tissue phenotype. However, findings in our laboratory are consistent with each splice variant having a unique tissue-specific function. Indeed, although LH2b is ubiquitously expressed in many tissues (Yeowell and Walker, 1999), we suspect that its predominant activity is in bone, tendon, and ligaments, and LH2a is the likely active isoform in connective tissues other than bone.

LH3 is the only multifunctional PLOD isoenzyme, which not only has LH activity, but also hydroxylysyl−galactosyltransferase and galactosylhydroxylysyl−glucosyltransferase activities (Wang et al., 2002). The LH activity of LH3 may be more important functionally for basement membrane collagens, such as type IV collagen, than for fibrillar collagens (Ruotsalainen et al., 2006).

Consequences of lysyl hydroxylase gene mutations

The kyphoscoliotic type of Ehlers−Danlos syndrome (EDS VIA) is caused by homozygous or compound heterozygous mutations in *PLOD1*. *Plod1*-null mice, which exhibit muscle hypotonia and aortic ruptures but not kyphoscoliosis or skin laxity, have a milder phenotype than the human *PLOD1* mutations (Takaluoma et al., 2007; Steinmann et al., 2002). A lack of helical lysine hydroxylation will systemically alter normal collagen cross-linking. In bone, for example, the HP/LP ratio is severely reduced due to the disruption of HP formation. Mutations in *PLOD2* have been identified in Bruck syndrome, an autosomal recessive disorder characterized by bone fragility and congenital joint contractures (Ha-Vinh et al., 2004). Mutations in *PLOD3* have been shown to cause epidermolysis bullosa simplex and other severe connective tissue defects (Salo et al., 2008). The *Plod3*-null mouse is embryonically lethal, which was attributed to an intracellular accumulation of type IV collagen lacking Glc-Gal-Hyl (Rautavuoma et al., 2004). However, if Glc-Gal-Hyl was also lost from some tissue fibrillar collagens, their cross-linking chemistry and supramolecular assembly may also have been affected.

Lysyl oxidases

LOX is responsible for the oxidative deamination of side-chain lysine and hydroxylysine primary amine substrates to produce reactive aldehydes (Siegel et al., 1970). The LOX-driven conversion of telopeptide lysine and hydroxylysine residues to allysines is the sole enzymatic step driving collagen cross-linking chemistry (Siegel and Fu, 1976). This enzyme reaction occurs outside the cell, specifically on the extracellular matrix substrates elastin and collagen (Eyre et al., 1984a). Five additional, LOX-like (LOXL) isoenzymes have been identified in eukaryotes (Grau-Bové et al., 2015; Wordinger and Clark, 2014). Despite all having a similar, highly conserved catalytic domain, two LOXL subfamilies can be classified, LOXL2/L3/L4 and LOX/L1/L5 (Grau-Bové et al., 2015). The former is proposed to influence collagen IV cross-linking in basement membranes and the latter to be involved in chordate/vertebrate-specific matrix remodeling (Grau-Bové et al., 2015).

A range of disease states, from glaucoma to thoracic aortic aneurysm and dissection, have been associated with mutations in the *LOX* and *LOXL* genes (Lee et al., 2016; Thorleifsson et al., 2007). The $Lox^{-/-}$ mice are perinatal lethal and exhibit cardiovascular instability with arterial and diaphragmatic ruptures (Hornstra et al., 2003; Maki, 2002). Desmosine cross-links in elastin were shown to be reduced by approximately 60% in the aorta and lungs of these knockout mice (Maki, 2002).

Heritable disorders and mouse models

Heritable disorders

OI, also known as brittle bone disease, is a generalized connective tissue disorder characterized by low bone mass and bone fragility. An array of systemic features is associated with the disease, but none are as pronounced as the skeletal phenotype. Approximately 90% of OI cases are caused by dominantly inherited mutations in the type I collagen gene *COL1A1* or *COL1A2*. The most common of these mutations substitute glycine residues with bulkier or charged residues. Generally, severity increases the more C-terminal the mutation is located, consistent with triple-helix folding from the C terminus, but with many site-related inconsistencies, suggesting a regional severity model (Marini et al., 2007).

In 2006, the first recessively inherited OI, caused by CRTAP mutation, was characterized (Morello et al., 2006). A long list of additional genes quickly followed (Table 14.1) (Kang et al., 2017; Eyre and Weis, 2013). The new insights into OI pathological mechanisms also revealed previously unappreciated genes that regulate collagen cross-linking chemistry and homeostasis. A decade later, new genes linked to rare musculoskeletal disorders, including OI, Bruck syndrome, and EDS, continued to emerge. Many of the new OI-causing genes (>10) encode proteins with essential roles in collagen post-translational modification, cross-linking, and mineralization, and some function as collagen chaperones and transporters through the ER and Golgi. The expanding list of OI-causing genes includes X-linked, dominant, and recessive variants that affect osteoblast function without any detected effect on collagen cross-linking. Although beyond the present scope, several comprehensive reviews cover them (Cundy, 2012; Forlino and Marini, 2016; Marini et al., 2017).

Collagen posttranslational modifications

CRTAP, LEPRE1, PPIB

An association between a collagen posttranslational modification and OI was discovered from studying the cartilage-associated protein (CRTAP)-null mouse (Morello et al., 2006). This led to the identification of other OI-causing genes encoding subunits of the prolyl 3-hydroxylase enzyme complex, which is composed of CRTAP, cyclophilin B (also called peptidylprolyl isomerase B; PPIB), and prolyl 3-hydroxylase 1 (P3H1) in a 1:1:1 ratio (Vranka et al., 2004). P3H1 (*LEPRE1*) and CRTAP (*LEPREL3*) are both members of the leprecan family of genes; however, only P3H1 has enzyme activity. P3H1 is the enzyme responsible for 3-hydroxylation of specific Pro residues in the X-position of the collagen Gly-Xaa-Yaa triplet repeat, to form 3-hydroxyproline (3*S*,2*S*-L-hydroxyproline; 3Hyp) (Vranka et al., 2004; Ogle et al., 1962; Ogle et al., 1961). The other two proteins in the enzyme complex, PPIB and CRTAP, act as a peptidylprolyl isomerase and an essential "helper" protein, respectively. Disruption of the P3H1 complex results in the loss or reduction of prolyl 3-hydroxylation at two sites in type I collagen, α1(I)Pro986 and α2(I)Pro707 (Morello et al., 2006).

Gene mutations that disrupt expression of any protein in the P3H1 complex (P3H1, CRTAP, and PPIB) have been shown to cause recessive OI (Morello et al., 2006; Barnes et al., 2006, 2010; Cabral et al., 2007; van Dijk et al., 2009). A common consequence of the gene mutations includes altered bone collagen cross-linking (Eyre and Weis, 2013). Bone from the *Crtap*-null mouse and a *LEPRE1*-mutant OI patient had abnormally high HP/LP ratios and overhydroxylated

TABLE 14.1 Noncollagen genes in which mutations cause osteogenesis imperfecta variants or related bone collagen abnormalities.

Gene	Protein	Phenotype	Bone collagen abnormalities
CRTAP *LEPRE1* *PPIB*	CRTAP P3H1, prolyl hydroxylase CYPB, cyclophilin B } P3H1 Complex	Mild to severe OI, reduced mineral density	α1(I)P986 and α2(I)P707 under prolyl-3-hydroxylation, high HP/LP (CRTAP and LEPRE1), low HP/LP (PPIB)
TMEM38B	TRIC-B	Bone fragility, moderate/severe OI	Reduced helical Lys hydroxylation, increased telopeptide hydroxylation
FKPB10 *PLOD2*	FKBP65 LH2, lysyl hydroxylase 2	Bruck syndrome: bone fragility, joint contractures	Lack of telopeptide hydroxylysines produces skin-like cross-links
LEPREL2 *LEPREL4*	P3H3 Sc65	Low bone mass, skin fragility	Low HP/LP, reduced helical Lys hydroxylation, altered divalent cross-links
MBTPS2	SP2, site-2 metalloprotease	Moderate/severe X-linked OI	Reduced helical Lys-87 hydroxylation and glycosylation
BMP1	Procollagen type I C-propeptidase	High mineral density, mild to severe OI	Defective C-propeptide removal, potential cross-linking defects
SERPINH1	HSP47, heat shock protein 47	Moderate/severe OI, bone fragility	High HP/LP and abnormal arrangement of cross-linking bonds
IFITM5	Bril, osteoblast-specific small transmembrane protein	Normal to severe OI, bone fragility	Altered mineralization, no other collagen abnormalities
SERPINF1	PEDF, pigment epithelium-derived factor	Moderate/severe OI, low mineral density, osteoid seams	Failed mineralization, no other collagen abnormalities

HP, hydroxylysyl pyridinoline; *LP*, lysyl pyridinoline; *OI*, osteogenesis imperfecta.

telopeptide lysines (Eyre and Weis, 2013). In contrast, bone and tendon from the *PPIB*-null mouse and bone from a *PPIB*-mutant OI patient had abnormally low HP/LP ratios but overhydroxylated telopeptide lysines in type I collagen (Eyre and Weis, 2013; Terajima et al., 2016). How an absent P3H1 complex can bring about these differential effects on collagen cross-linking is not fully clear. If it delays triple-helix folding, then helix lysine overmodification (higher HP/LP) might be expected. In the case of PPIB, which is a vital component of several ER complexes, including the LH1 complex (Cabral et al., 2014), both the P3H1 complex and LH1 activity are knocked down. The overhydroxylation of telopeptide lysines in the absence of a P3H1 complex is harder to explain, but may involve recently recognized interactions between prolyl 3-hydroxylase and LH complexes in the ER (see "SC65 and P3H3"). The effects on cross-linking are therefore most likely due mainly to an absence of the P3H1 complex and consequences of ER distress, not the absence of 3Hyp residues at α1(I) P986 and α2(I)P707 (Cabral et al., 2014; Pyott et al., 2011).

Solid-phase binding studies do, however, support a role for 3Hyp in collagen intermolecular recognition and binding during assembly (Hudson et al., 2012). Loss of prolyl 3-hydroxylation in CRTAP, P3H1, and PPIB forms of OI could potentially disrupt the fundamental short-range order in the supramolecular assembly within collagen fibrils of bone (Hudson et al., 2012). A compromised polymeric architecture might hinder the ordered hydroxyapatite nanocrystal growth within collagen fibrils (Eyre and Weis, 2013).

TMEM38B

TMEM38B encodes the ER-membrane monovalent cation channel TRIC-B. Mutations in *TMEM38B* have been shown to cause moderately severe recessive OI (Volodarsky et al., 2013; Shaheen et al., 2012). Disruption of TRIC-B-driven intracellular calcium homeostasis was proposed to dysregulate collagen synthesis and cause OI (Cabral et al., 2016). Type I collagen exhibited altered posttranslational modifications as a consequence of altering the function and expression of vital modifying enzymes. For example, cross-linking lysine hydroxylation was reduced in the helix and increased in telopeptides (Cabral et al., 2016). Much like P3H1 complex mutations, TMEM38B defects were proposed to cause intracellular accumulation of collagen, which resulted in ER stress and the unfolded protein response.

PLOD2 and FKBP10

PLOD2 and *FKBP10* mutations have both been linked to Bruck syndrome (Bank et al., 1999; Ha-Vinh et al., 2004). *FKBP10* encodes the 65-kDa FK506-binding protein FKBP65, a collagen chaperone protein with peptidylprolyl isomerase activity (Ishikawa et al., 2008). *FKBP10* mutations were also shown to cause both Bruck syndrome with severe OI (Kelley et al., 2011; Schwarze et al., 2013; Alanay et al., 2010) and Kuskokwim syndrome with minimal skeletal defects (Barnes et al., 2013). Notably, an *FKBP10* homozygous null mutation, which yields bone collagen with only lysine aldehyde-derived cross-links, does not seem to affect cartilage or ligament collagen (Bank et al., 1999). The lack of telopeptide hydroxylysines precludes pyridinoline formation in bone, and results in skin-like cross-links. The reduction of hydroxyallysine-derived cross-links observed in bone collagen is phenocopied in patients with *PLOD2* and *FKBP10* mutations (Bank et al., 1999; Schwarze et al., 2013). Interestingly, the *Fkbp10*-null mouse exhibited severe embryonic growth defects and did not survive birth (Lietman et al., 2014). The *Plod2*-null mouse is also embryonic lethal (Hyry et al., 2009); however, a zebrafish model carrying a biallelic nonsense mutation in *plod2* displayed severe musculoskeletal abnormalities resembling Bruck syndrome (Gistelinck et al., 2016). The bone collagen defects in *PLOD2* and *FKBP10*–derived Bruck syndrome can be detected as abnormal ratios of HP/LP in patients' urine (Schwarze et al., 2013). Indeed, biochemical data revealed that FKBP65 was part of an enzyme complex with LH2, as a deficiency of FKBP65 resulted in reduced telopeptide cross-linking lysine hydroxylation (Schwarze et al., 2013; Barnes et al., 2012). Consequently, FKBP65-deficient bone produced skin-like collagen cross-links with complete absence of pyridinolines (Schwarze et al., 2013).

SC65 and P3H3

Synaptonemal complex 65 (SC65 or P3H4) is another member of the leprecan gene family and a homolog of CRTAP. Like CRTAP, SC65 has no known enzymatic activity and appears to also function as a "helper" protein. SC65 operates in an enzymatic multiprotein complex, comprising LH1, PPIB, and prolyl 3-hydroxylase 3 (P3H3) (Heard et al., 2016). Although no known human mutation has yet been described, two *Sc65*-null mice have been characterized as having low bone mass and skin fragility (Heard et al., 2016; Gruenwald et al., 2014). *P3h3*-null mouse skin was similarly characterized as having a lack of structural integrity and fragile collagen fabric (Hudson et al., 2017). Both the *Sc65*-null and the *P3h3*-null mice were found to have decreased collagen lysine hydroxylation and abnormal cross-linking (Hudson et al., 2017).

The ratio of mature HP/LP cross-links in bone of both *Sc65*-null and *P3h3*-null mice was reversed compared with wild-type, consistent with the level of lysine underhydroxylation seen in individual chains at cross-linking sites. This was the first direct evidence of an ER complex controlling collagen modification that combines both a lysyl- and a prolyl-hydroxylase activity.

Mechanistically, lysine underhydroxylation at the helical-domain cross-linking sites altered the divalent aldimine cross-link chemistry of the mutant collagen. In normal skin, fully glycosylated Hyl-87 preferentially forms an intermolecular aldimine cross-link with a C-telopeptide lysine aldehyde. However, in the *Sc65*-null and *P3h3*-null mice, the type I collagen LH1 substrate sites are underhydroxylated and subsequently underglycosylated. As a result, the C-telopeptide lysine aldehydes preferentially form intramolecular aldol cross-links (as opposed to intermolecular aldols). We predict that under normal conditions the presence of the disaccharide on Hyl-87 favors aldimine formation with a single C-telopeptide aldehyde. This glycosylated aldimine then sterically hinders intramolecular aldol formation with the second α1(I) C-telopeptide aldehyde of the molecule, which favors intermolecular aldol formation. So, the net effect of underhydroxylated Lys-87 is fewer aldol intermolecular cross-links. A very similar underhydroxylation of triple-helical domain lysines occurs in human EDS VIA and *Plod1*-null mouse tissues (Takaluoma et al., 2007; Steinmann et al., 2002; Eyre et al., 2002), suggesting that *P3H3* and *SC65* mutations may cause as yet undefined EDS variants.

MBTPS2

The regulated intramembrane proteolysis of transmembrane proteins is an essential cellular process that releases functional protein domains into signaling pathways (Lal and Caplan, 2011). *MBPTS2* (membrane-bound transcription factor peptidase, site 2) encodes the serine protease S2P (site-2 metalloprotease), which spans the Golgi membrane (Ye et al., 2000). Missense mutations in MBTPS2 have been shown to cause moderately severe X-linked OI (Lindert et al., 2016). S2P was found to have impaired function, which ultimately resulted in reduced secretion of type I collagen in fibroblast cultures. Type I collagen also exhibited altered posttranslational modifications with decreased lysine hydroxylation and glycosylation on the K87 cross-linking lysines of both α-chains (Lindert et al., 2016). The main contributor to the bone phenotype from loss of S2P may be the impaired activation of several transcription factors fundamental to normal bone development (Lindert et al., 2016).

Collagen processing

Bone morphogenetic protein 1

Bone morphogenetic protein 1 is the type I procollagen C-propeptide protease. Homozygous missense mutations in *BMP1* have been shown to cause a recessively inherited form of OI with a severe skeletal phenotype (Martinez-Glez et al., 2012). Missense mutations at the type I collagen propeptide cleavage site result in a phenotypically similar but less severe form of OI characterized by unusually high mineral density bone (Lindahl et al., 2011, Cundy et al., 2018). Although not established, retention of the type I collagen C-propeptide presumably disrupts fibril assembly and could alter collagen cross-linking (Eyre and Weis, 2013). It is tempting to speculate that the retained propeptide could alter collagen fibril three-dimensional packing so that the ratio of bone mineral to collagen and bone density are increased.

Collagen chaperone

SERPINH1

SERPINH1 encodes heat shock protein 47 (HSP47), an ER-resident and collagen-specific chaperone protein. HSP47 functions as a quality control protein that prevents premature aggregation of native procollagen molecules during transport through the ER (Widmer et al., 2012). Mutations in *SERPINH1* cause OI with severe skeletal deformity (Christiansen et al., 2010). Loss of HSP47 chaperone function resulted in protein misfolding and intracellular retention of type I collagen with subsequent ER stress (Drogemuller et al., 2009). The importance of *SERPINH1* was highlighted by the embryonic lethality observed in *Hsp47*-null mice (Nagai et al., 2000). An OI dachshund with a loss-of-function mutation in *SERPINH1* (Drogemuller et al., 2009) revealed bone collagen cross-linking abnormalities consistent with a defective molecular assembly and posttranslational chemistry (Lindert et al., 2015). Mutations in *SERPINH1* yield brittle bones with a high HP/LP ratio, telopeptide lysine overhydroxylation, and resulting overabundance of stable pyridinoline cross-links (Eyre and Weis, 2013).

Bone mineralization

IFITM5

Mutations in *IFITM5* yield an autosomal dominant form of OI with a moderate to severe skeletal phenotype (Glorieux et al., 2000). The *IFITM5* gene encodes interferon-induced transmembrane protein 5 (IFITM5), a 14.8-kDa transmembrane protein thought to function in early bone mineralization (Moffatt et al., 2008). The *IFITM5*-null mouse had stunted growth with smaller long bones (Hanagata et al., 2011). No defects in collagen posttranslational chemistry have been found in the bone of mice expressing the type V OI-causing IFITM5 mutation (Lietman et al., 2015).

SERPINF1

OI caused by homozygous null mutations in *SERPINF1* result in bone mineralization defects without any known effect on collagen structure (Glorieux et al., 2002). *SERPINF1* encodes pigment epithelium-derived factor (PEDF), a member of the serine protease inhibitor serpin superfamily (Rauch et al., 2012). PEDF is a 50-kDa glycoprotein known as a potent inhibitor of angiogenesis (Becker et al., 2011). PEDF has been shown to bind to type I collagen from bone and is thought to help regulate bone angiogenesis and matrix remodeling (Tombran-Tink and Barnstable, 2004). Indeed, the absence of PEDF results in large quantities of unmineralized osteoid and an abnormal lamellar pattern on histology of patient bone (Homan et al., 2011). It is likely that the bone phenotype is the result of a dysregulated step in the mineral deposition machinery.

Implications for bone fragility and mineral deposition

Abnormal collagen cross-linking emerges as a recurring theme in many of these rare musculoskeletal disorders. We end with a hypothesis that the abnormal collagen cross-linking seen in bone from many variants of OI is a responsible contributor to the underlying brittleness. Clearly, collagen strength rests heavily on its cross-linking, but other properties of bone, including ductility and resistance to microdamage and crack propagation, may depend on the unique pattern of LOX-mediated cross-links that characterize normal bone collagen of higher vertebrates. The placement of cross-links and the chemical lability of a significant fraction of them (those formed from lysine aldehydes) may be required to produce a malleable framework in which highly ordered hydroxyapatite nanocrystals can grow optimally within the fibrils (Eyre and Weis, 2013).

Fig. 14.6 illustrates this concept of labile, aldimine cross-links breaking as mineral crystallites grow in the interior of bone collagen fibrils. If, as the data suggest, lysine aldehyde and hydroxylysine aldehyde cross-links are each distributed in an orderly (nonrandom) pattern in the packed collagen lattice, this could channel a parallel, ordered growth of

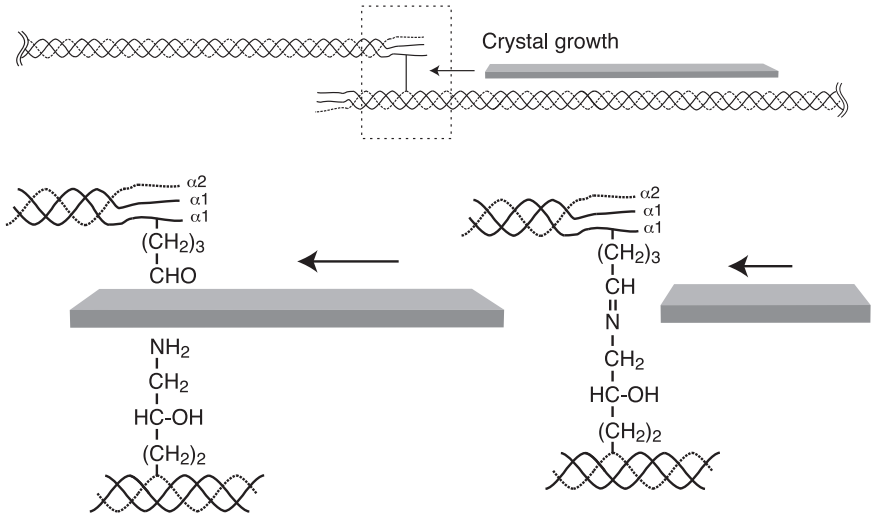

FIGURE 14.6 Illustrated concept that labile (aldimine) cross-links break as part of the orderly growth of hydroxyapatite crystal in mineralizing collagen fibrils.

hydroxyapatite crystals. In theory, for human bone, up to half the initial divalent cross-links (aldimines) would break, reverting back to their aldehyde plus amine precursors. The result is potentially increased intermolecular packing space for growing crystallites in a still stably cross-linked collagen fibril lattice (Eyre and Weis, 2013).

Future challenges

After more than half a century of study, we still do not understand at the molecular level the mechanism that drives the orderly mineralization of bone collagen. To what degree mineralization is driven by bone-specific features of the fibrils themselves, particularly their unique cross-linking chemistry, or is a process driven by extrafibrillar factors is still unclear. Understanding more broadly how differences in cross-linking chemistry between tissues and during development confer functional advantages will also help in understanding how defects in bone collagen cross-linking cause a compromised bone structure. Whether pyrrole cross-links contribute to the unique material properties of normal bone and how their loss might increase bone fragility in OI are also important questions. It should also not escape attention that the mechanisms causing bone collagen cross-linking abnormalities revealed by the study of rare genetic disorders may well be operative in more common brittle bone disorders, including osteoporosis and diabetes.

References

Alanay, Y., Avaygan, H., Camacho, N., Utine, G.E., Boduroglu, K., Aktas, D., et al., April 9, 2010. Mutations in the gene encoding the RER protein FKBP65 cause autosomal-recessive osteogenesis imperfecta. Am. J. Hum. Genet. 86 (4), 551–559.

Avery, N.C., Bailey, A.J., September 2006. The effects of the Maillard reaction on the physical properties and cell interactions of collagen. Pathol. Biol. 54 (7), 387–395.

Avery, N.C., Sims, T.J., Bailey, A.J., 2009. Quantitative determination of collagen cross-links. In: Extracellular Matrix Protocols. Methods in Molecular Biology, vol. 522. Humana Press, Totowa, NJ, pp. 103–121.

Bank, R.A., Bayliss, M.T., Lafeber, F.P., Maroudas, A., Tekoppele, J.M., February 15, 1998. Ageing and zonal variation in post-translational modification of collagen in normal human articular cartilage. The age-related increase in non-enzymatic glycation affects biomechanical properties of cartilage. Portland Press Limited Biochem. J. 330 (Pt 1), 345–351.

Bank, R.A., Robins, S.P., Wijmenga, C., Breslau-Siderius, L.J., Bardoel, A.F., van der Sluijs, H.A., et al., February 2, 1999. Defective collagen crosslinking in bone, but not in ligament or cartilage, in Bruck syndrome: indications for a bone-specific telopeptide lysyl hydroxylase on chromosome 17. National Academy of Sciences Proc. Natl. Acad. Sci. U. S. A. 96 (3), 1054–1058.

Banse, X., Devogelaer, J.P., Lafosse, A., Sims, T.J., Grynpas, M., Bailey, A.J., July 2002. Cross-link profile of bone collagen correlates with structural organization of trabeculae. Bone 31 (1), 70–76.

Barnes, A.M., Chang, W., Morello, R., Cabral, W.A., Weis, M., Eyre, D.R., et al., December 28, 2006. Deficiency of cartilage-associated protein in recessive lethal osteogenesis imperfecta. N. Engl. J. Med. 355 (26), 2757–2764.

Barnes, A.M., Carter, E.M., Cabral, W.A., Weis, M., Chang, W., Makareeva, E., et al., February 11, 2010. Lack of cyclophilin B in osteogenesis imperfecta with normal collagen folding. N. Engl. J. Med. 362 (6), 521–528.

Barnes, A.M., Cabral, W.A., Weis, M., Makareeva, E., Mertz, E.L., Leikin, S., et al., November 2012. Absence of FKBP10 in recessive type XI osteogenesis imperfecta leads to diminished collagen cross-linking and reduced collagen deposition in extracellular matrix. Wiley Subscription Services, Inc., A Wiley Company Hum. Mutat. 33 (11), 1589–1598.

Barnes, A.M., Duncan, G., Weis, M., Paton, W., Cabral, W.A., Mertz, E.L., et al., September 2013. Kuskokwim syndrome, a recessive congenital contracture disorder, extends the phenotype of FKBP10 mutations. Hum. Mutat. 34 (9), 1279–1288.

Bateman, J.F., Mascara, T., Chan, D., Cole, W.G., January 1, 1984. Abnormal type I collagen metabolism by cultured fibroblasts in lethal perinatal osteogenesis imperfecta. Portland Press Ltd Biochem J. 217 (1), 103–115.

Bätge, B., Winter, C., Notbohm, H., Acil, Y., Brinckmann, J., Müller, P.K., July 1997. Glycosylation of human bone collagen I in relation to lysyl-hydroxylation and fibril diameter. J. Biochem. 122 (1), 109–115.

Beardsworth, L.J., Eyre, D.R., Dickson, I.R., July 1990. Changes with age in the urinary excretion of lysyl- and hydroxylysylpyridinoline, two new markers of bone collagen turnover. John Wiley and Sons and The American Society for Bone and Mineral Research (ASBMR). J. Bone Miner. Res. 5 (7), 671–676.

Becker, J., Semler, O., Gilissen, C., Li, Y., Bolz, H.J., Giunta, C., et al., March 11, 2011. Exome sequencing identifies truncating mutations in human SERPINF1 in autosomal-recessive osteogenesis imperfecta. Am. J. Hum. Genet. 88 (3), 362–371.

Bhave, G., Cummings, C.F., Vanacore, R.M., Kumagai-Cresse, C., Ero-Tolliver, I.A., Rafi, M., et al., September 2012. Peroxidasin forms sulfilimine chemical bonds using hypohalous acids in tissue genesis. Nat. Chem. Biol. 8 (9), 784–790.

Biemel, K.M., Friedl, D.A., Lederer, M.O., July 12, 2002. Identification and quantification of major maillard cross-links in human serum albumin and lens protein. Evidence for glucosepane as the dominant compound. American Society for Biochemistry and Molecular Biology J. Biol. Chem. 277 (28), 24907–24915.

Blumenfeld, O.O., Gallop, P.M., October 1966. Amino aldehydes in tropocollagen: the nature of a probable cross-link. National Academy of Sciences Proc. Natl. Acad. Sci. U. S. A. 56 (4), 1260–1267.

Boot-Handford, R.P., Tuckwell, D.S., February 2003. Fibrillar collagen: the key to vertebrate evolution? A tale of molecular incest. Bioessays 25 (2), 142–151.

Cabral, W.A., Chang, W., Barnes, A.M., Weis, M., Scott, M.A., Leikin, S., et al., March 2007. Prolyl 3-hydroxylase 1 deficiency causes a recessive metabolic bone disorder resembling lethal/severe osteogenesis imperfecta. Nat. Genet. 39 (3), 359–365.

Cabral, W.A., Perdivara, I., Weis, M., Terajima, M., Blissett, A.R., Chang, W., et al., June 2014. Abnormal type I collagen post-translational modification and crosslinking in a cyclophilin B KO mouse model of recessive osteogenesis imperfecta. Public Library of Science. In: Cohn, D. (Ed.), PLoS Gen. 10 (6), e1004465.

Cabral, W.A., Ishikawa, M., Garten, M., Makareeva, E.N., Sargent, B.M., Weis, M., et al., July 2016. Absence of the ER cation channel TMEM38B/TRIC-B disrupts intracellular calcium homeostasis and dysregulates collagen synthesis in recessive osteogenesis imperfecta. PLoS Gen. 12 (7), e1006156. Bateman, J.F., editor.

Christiansen, H.E., Schwarze, U., Pyott, S.M., AlSwaid, A., Balwi Al, M., Alrasheed, S., et al., March 12, 2010. Homozygosity for a missense mutation in SERPINH1, which encodes the collagen chaperone protein HSP47, results in severe recessive osteogenesis imperfecta. Am. J. Hum. Genet. 86 (3), 389–398.

Collier, T.A., Nash, A., Birch, H.L., de Leeuw, N.H., October 2015. Preferential sites for intramolecular glucosepane cross-link formation in type I collagen: a thermodynamic study. Matrix Biol. 48, 78–88.

Collier, T.A., Nash, A., Birch, H.L., de Leeuw, N.H., November 2016. Intra-molecular lysine-arginine derived advanced glycation end-product cross-linking in Type I collagen: a molecular dynamics simulation study. Biophys. Chem. 218, 42–46.

Cundy, T., June 2012. Recent advances in osteogenesis imperfecta. Calcif. Tissue Int. 90 (6), 439–449.

Cundy, T., Dray, M., Delahunt, J., Hald, J.D., Langdahl, B., Li, C., et al., July 2018. Mutations that alter the carboxy-terminal-propeptide cleavage site of the chains of type I procollagen are associated with a unique osteogenesis imperfecta phenotype. J. Bone. Miner. Res. 33 (7), 1260–1271. https://doi.org/10.1002/jbmr.3424. Epub 2018 Apr 18. PubMed PMID: 29669177; PubMed Central PMCID: PMC6031457.

Dai, Z., Wang, B., Sun, G., Fan, X., Anderson, V.E., Monnier, V.M., July 2008. Identification of glucose-derived cross-linking sites in ribonuclease A. American Chemical Society J. Proteome Res. 7 (7), 2756–2768.

Drogemuller, C., Becker, D., Brunner, A., Haase, B., Kircher, P., Seeliger, F., et al., July 2009. A missense mutation in the SERPINH1 gene in Dachshunds with osteogenesis imperfecta. PLoS Gen. 5 (7), e1000579.

Eyre, D.R., Oguchi, H., January 29, 1980. The hydroxypyridinium crosslinks of skeletal collagens: their measurement, properties and a proposed pathway of formation. Biochem. Biophys. Res. Commun. 92 (2), 403–410.

Eyre, D.R., Weis, M.A., October 2013. Bone collagen: new clues to its mineralization mechanism from recessive osteogenesis imperfecta. Springer US Calcif. Tissue Int. 93 (4), 338–347.

Eyre, D.R., Wu, J.-J., 2005. Collagen cross-links. In: Collagen. Topics in Current Chemistry, vol. 247. Springer Berlin Heidelberg, Berlin, Heidelberg, pp. 207–229.

Eyre, D.R., Paz, M.A., Gallop, P.M., 1984a. Cross-linking in collagen and elastin. Annu. Rev. Biochem. 53, 717–748.

Eyre, D.R., Koob, T.J., Van Ness, K.P., March 1984. Quantitation of hydroxypyridinium crosslinks in collagen by high-performance liquid chromatography. Anal. Biochem. 137 (2), 380–388.

Eyre, D.R., Dickson, I.R., Van Ness, K., June 1, 1988. Collagen cross-linking in human bone and articular cartilage. Age-related changes in the content of mature hydroxypyridinium residues. Portland Press Ltd Biochem. J. 252 (2), 495–500.

Eyre, D., Shao, P., Weis, M.A., Steinmann, B., July 2002. The kyphoscoliotic type of Ehlers-Danlos syndrome (type VI): differential effects on the hydroxylation of lysine in collagens I and II revealed by analysis of cross-linked telopeptides from urine. Mol. Genet. Metabol. 76 (3), 211–216.

Eyre, D.R., Pietka, T., Weis, M.A., Wu, J.-J., January 23, 2004. Covalent cross-linking of the NC1 domain of collagen type IX to collagen type II in cartilage. J. Biol. Chem. 279 (4), 2568–2574.

Eyre, D.R., Weis, M.A., Wu, J.-J., May 2008. Advances in collagen cross-link analysis. Methods 45 (1), 65–74.

Eyre, D.R., Weis, M.A., Wu, J.J., May 28, 2010. Maturation of collagen Ketoimine cross-links by an alternative mechanism to pyridinoline formation in cartilage. J. Biol. Chem. 285 (22), 16675–16682.

Eyre, D.R., March 21, 1980. Collagen: molecular diversity in the body's protein scaffold. Science 207 (4437), 1315–1322.

Eyre, D.R., Weis, M., Rai, J., February 7, 2019. Analyses of lysine aldehyde cross-linking in collagen reveal that the mature cross-link histidinohydroxylysinonorleucine is an artifact. J. Biol. Chem. pii: jbc.RA118.007202. doi: 10.1074/jbc.RA118.007202. [Epub ahead of print] PubMed PMID: 30733334.

Eyre, D.R., 1981. Crosslink maturation in bone collagen. Dev. Biochem. 22, 51–55.

Eyre, D., 1987. Collagen cross-linking amino acids. Methods Enzymol. 144, 115–139.

Farlay, D., Armas, L.A.G., Gineyts, E., Akhter, M.P., Recker, R.R., Boivin, G., January 2016. Nonenzymatic glycation and degree of mineralization are higher in bone from fractured patients with type 1 diabetes mellitus. J. Bone Miner. Res. 31 (1), 190–195.

Forlino, A., Marini, J.C., April 16, 2016. Osteogenesis imperfecta. Lancet 387 (10028), 1657–1671.

Fujimoto, D., June 20, 1977. Isolation and characterization of a fluorescent material in bovine achilles tendon collagen. Biochem. Biophys. Res. Commun. 76 (4), 1124–1129.

Gautieri, A., Redaelli, A., Buehler, M.J., Vesentini, S., February 2014. Age- and diabetes-related nonenzymatic crosslinks in collagen fibrils: candidate amino acids involved in Advanced Glycation End-products. Matrix Biol. 34, 89–95.

Gistelinck, C., Witten, P.E., Huysseune, A., Symoens, S., Malfait, F., Larionova, D., et al., November 2016. Loss of type I collagen telopeptide lysyl hydroxylation causes musculoskeletal abnormalities in a zebrafish model of Bruck syndrome. J. Bone Miner. Res. 31 (11), 1930–1942.

Glorieux, F.H., Rauch, F., Plotkin, H., Ward, L., Travers, R., Roughley, P., et al., September 2000. Type V osteogenesis imperfecta: a new form of brittle bone disease. John Wiley and Sons and The American Society for Bone and Mineral Research (ASBMR). J. Bone Miner. Res. 15 (9), 1650−1658.

Glorieux, F.H., Ward, L.M., Rauch, F., Lalic, L., Roughley, P.J., Travers, R., January 2002. Osteogenesis imperfecta type VI: a form of brittle bone disease with a mineralization defect. John Wiley and Sons and The American Society for Bone and Mineral Research (ASBMR). J. Bone Miner. Res. 17 (1), 30−38.

Grau-Bové, X., Ruiz-Trillo, I., Rodriguez-Pascual, F., May 29, 2015. Origin and evolution of lysyl oxidases. Nature Publishing Group Sci. Rep. 5 (1), 651.

Gruenwald, K., Castagnola, P., Besio, R., Dimori, M., Chen, Y., Akel, N.S., et al., March 2014. Sc65 is a novel endoplasmic reticulum protein that regulates bone mass homeostasis. J. Bone Miner. Res. 29 (3), 666−675.

Hanagata, N., Li, X., Morita, H., Takemura, T., Li, J., Minowa, T., May 2011. Characterization of the osteoblast-specific transmembrane protein IFITM5 and analysis of IFITM5-deficient mice. J. Bone Miner. Metab. 29 (3), 279−290.

Hanson, D.A., Eyre, D.R., October 25, 1996. Molecular site specificity of pyridinoline and pyrrole cross-links in type I collagen of human bone. J. Biol. Chem. 271 (43), 26508−26516.

Hanson, D.A., Weis, M.A., Bollen, A.M., Maslan, S.L., Singer, F.R., Eyre, D.R., November 1992. A specific immunoassay for monitoring human bone resorption: quantitation of type I collagen cross-linked N-telopeptides in urine. J. Bone Miner. Res. 7 (11), 1251−1258.

Haut, R.C., Lancaster, R.L., DeCamp, C.E., February 1992. Mechanical properties of the canine patellar tendon: some correlations with age and the content of collagen. J. Biomech. 25 (2), 163−173.

Ha-Vinh, R., Alanay, Y., Bank, R.A., Campos-Xavier, A.B., Zankl, A., Superti-Furga, A., et al., December 1, 2004. Phenotypic and molecular characterization of Bruck syndrome (osteogenesis imperfecta with contractures of the large joints) caused by a recessive mutation in PLOD2. Am. J. Med. Genet. 131 (2), 115−120.

Heard, M.E., Besio, R., Weis, M., Rai, J., Hudson, D.M., Dimori, M., et al., April 2016. Sc65-Null mice provide evidence for a novel endoplasmic reticulum complex regulating collagen lysyl hydroxylation. Public Library of Science. In: Bateman, J.F. (Ed.), PLoS Gen. 12 (4), e1006002.

Heinemeier, K.M., Schjerling, P., Heinemeier, J., Magnusson, S.P., Kjaer, M., May 2013. Lack of tissue renewal in human adult Achilles tendon is revealed by nuclear bomb (14)C. FASEB J. 27 (5), 2074−2079.

Homan, E.P., Rauch, F., Grafe, I., Lietman, C., Doll, J.A., Dawson, B., et al., December 2011. Mutations in SERPINF1 cause osteogenesis imperfecta type VI. Wiley Subscription Services, Inc., A Wiley Company J. Bone Miner. Res. 26 (12), 2798−2803.

Horgan, D.J., King, N.L., Kurth, L.B., Kuypers, R., August 1990. Collagen crosslinks and their relationship to the thermal properties of calf tendons. Arch. Biochem. Biophys. 281 (1), 21−26.

Hornstra, I.K., Birge, S., Starcher, B., Bailey, A.J., Mecham, R.P., Shapiro, S.D., April 18, 2003. Lysyl oxidase is required for vascular and diaphragmatic development in mice. American Society for Biochemistry and Molecular Biology J. Biol. Chem. 278 (16), 14387−14393.

Hudson, D.M., Archer, M., King, K.B., Eyre, D.R., October 5, 2018. Glycation of type I collagen selectively targets the same helical domain lysine sites as lysyl oxidase-mediated cross-linking. J. Biol. Chem. 293 (40), 15620−15627.

Hudson, D.M., Eyre, D.R., 2013. Collagen prolyl 3-hydroxylation: a major role for a minor post-translational modification? Connect. Tissue Res. 54 (4−5), 245−251.

Hudson, D.M., Kim, L.S., Weis, M., Cohn, D.H., Eyre, D.R., March 27, 2012. Peptidyl 3-hydroxyproline binding properties of type I collagen suggest a function in fibril supramolecular assembly. Biochemistry (Mosc.) 51 (12), 2417−2424.

Hudson, D.M., Weis, M., Rai, J., Joeng, K.S., Dimori, M., Lee, B.H., et al., March 3, 2017. P3h3-null and Sc65-null mice phenocopy the collagen lysine under-hydroxylation and cross-linking abnormality of Ehlers-danlos syndrome type VIA. J. Biol. Chem. 292 (9), 3877−3887.

Hyry, M., Lantto, J., Myllyharju, J., November 6, 2009. Missense mutations that cause Bruck syndrome affect enzymatic activity, folding, and oligomerization of lysyl hydroxylase 2. J. Biol. Chem. 284 (45), 30917−30924.

Ishikawa, Y., Vranka, J., Wirz, J., Nagata, K., Bachinger, H.P., November 14, 2008. The rough endoplasmic reticulum-resident FK506-binding protein FKBP65 is a molecular chaperone that interacts with collagens. J. Biol. Chem. 283 (46), 31584−31590.

Jürgensen, H.J., Madsen, D.H., Ingvarsen, S., Melander, M.C., Gårdsvoll, H., Patthy, L., et al., September 16, 2011. A novel functional role of collagen glycosylation: interaction with the endocytic collagen receptor uparap/ENDO180. J. Biol. Chem. 286 (37), 32736−32748.

Kalamajski, S., Liu, C., Tillgren, V., Rubin, K., Oldberg, Å., Rai, J., et al., July 4, 2014. Increased C-telopeptide cross-linking of tendon type I collagen in fibromodulin-deficient mice. American Society for Biochemistry and Molecular Biology J. Biol. Chem. 289 (27), 18873−18879.

Kang, H., Aryal, A.C.S., Marini, J.C., March 2017. Osteogenesis imperfecta: new genes reveal novel mechanisms in bone dysplasia. Transl. Res. 181, 27−48.

Kelley, B.P., Malfait, F., Bonafe, L., Baldridge, D., Homan, E., Symoens, S., et al., March 2011. Mutations in FKBP10 cause recessive osteogenesis imperfecta and Bruck syndrome. J. Bone Miner. Res. 26 (3), 666−672.

Kivirikko, K.I., Myllyla, R., 1982. Posttranslational enzymes in the biosynthesis of collagen: intracellular enzymes. Methods Enzymol. 82 (Pt A), 245−304.

Knott, L., Bailey, A.J., March 1998. Collagen cross-links in mineralizing tissues: a review of their chemistry, function, and clinical relevance. Bone 22 (3), 181−187.

Lal, M., Caplan, M., February 2011. Regulated intramembrane proteolysis: signaling pathways and biological functions. Physiology 26 (1), 34−44.

Lee, V.S., Halabi, C.M., Hoffman, E.P., Carmichael, N., Leshchiner, I., Lian, C.G., et al., August 2, 2016. Loss of function mutation in LOX causes thoracic aortic aneurysm and dissection in humans. Proc. Natl. Acad. Sci. U. S. A. 113 (31), 8759−8764.

Lehmann, H.W., Wolf, E., Röser, K., Bodo, M., Delling, G., Müller, P.K., 1995. Composition and posttranslational modification of individual collagen chains from osteosarcomas and osteofibrous dysplasias. J. Cancer Res. Clin. Oncol. 121 (7), 413–418.

Lietman, C.D., Rajagopal, A., Homan, E.P., Munivez, E., Jiang, M.-M., Bertin, T.K., et al., September 15, 2014. Connective tissue alterations in Fkbp10-/- mice. Oxford University Press Hum. Mol. Genet. 23 (18), 4822–4831.

Lietman, C.D., Marom, R., Munivez, E., Bertin, T.K., Jiang, M.-M., Chen, Y., et al., March 2015. A transgenic mouse model of OI type V supports a neomorphic mechanism of the IFITM5 mutation. J. Bone Miner. Res. 30 (3), 489–498.

Light, N.D., Bailey, A.J., January 1, 1979. Changes in crosslinking during aging in bovine tendon collagen. FEBS Lett. 97 (1), 183–188.

Lindahl, K., Barnes, A.M., Fratzl-Zelman, N., Whyte, M.P., Hefferan, T.E., Makareeva, E., et al., June 2011. COL1 C-propeptide cleavage site mutations cause high bone mass osteogenesis imperfecta. Hum. Mutat. 32 (6), 598–609.

Lindert, U., Weis, M.A., Rai, J., Seeliger, F., Hausser, I., Leeb, T., et al., July 17, 2015. Molecular consequences of the SERPINH1/HSP47 mutation in the Dachshund natural model of osteogenesis imperfecta. J. Biol. Chem. 290 (29), 17679–17689.

Lindert, U., Cabral, W.A., Ausavarat, S., Tongkobpetch, S., Ludin, K., Barnes, A.M., et al., July 6, 2016. MBTPS2 mutations cause defective regulated intramembrane proteolysis in X-linked osteogenesis imperfecta. Nature Publishing Group Nat. Commun. 7, 11920.

Maki, J.M., October 14, 2002. Inactivation of the lysyl oxidase gene lox leads to aortic aneurysms, cardiovascular dysfunction, and perinatal death in mice. American Heart Association, Inc Circulation 106 (19), 2503–2509.

Manolagas, S.C., April 2000. Birth and death of bone cells: basic regulatory mechanisms and implications for the pathogenesis and treatment of osteoporosis. Endocr. Rev. 21 (2), 115–137.

Marini, J.C., Forlino, A., Cabral, W.A., Barnes, A.M., San Antonio, J.D., Milgrom, S., et al., March 2007. Consortium for osteogenesis imperfecta mutations in the helical domain of type I collagen: regions rich in lethal mutations align with collagen binding sites for integrins and proteoglycans. Hum. Mutat. 28 (3), 209–221.

Marini, J.C., Forlino, A., Bächinger, H.P., Bishop, N.J., Byers, P.H., Paepe, A.D., et al., August 18, 2017. Osteogenesis imperfecta. Primers Nat. Rev. Dis. 3, 17052.

Martinez-Glez, V., Valencia, M., Caparros-Martin, J.A., Aglan, M., Temtamy, S., Tenorio, J., et al., February 2012. Identification of a mutation causing deficient BMP1/mTLD proteolytic activity in autosomal recessive osteogenesis imperfecta. Hum. Mutat. 33 (2), 343–350.

Michalsky, M., Norris-Suarez, K., Bettica, P., Pecile, A., Moro, L., May 14, 1993. Rat cortical and trabecular bone collagen glycosylation are differently influenced by ovariectomy. Biochem. Biophys. Res. Commun. 192 (3), 1281–1288.

Moffatt, P., Gaumond, M.-H., Salois, P., Sellin, K., Bessette, M.-C., Godin, E., et al., September 2008. Bril: a novel bone-specific modulator of mineralization. John Wiley and Sons and The American Society for Bone and Mineral Research (ASBMR). J. Bone Miner. Res. 23 (9), 1497–1508.

Monnier, V.M., Mustata, G.T., Biemel, K.L., Reihl, O., Lederer, M.O., Zhenyu, D., et al., June 2005. Cross-linking of the extracellular matrix by the maillard reaction in aging and diabetes: an update on "a puzzle nearing resolution". Blackwell Publishing Ltd Ann. N. Y. Acad. Sci. 1043 (1), 533–544.

Morello, R., Bertin, T.K., Chen, Y., Hicks, J., Tonachini, L., Monticone, M., et al., October 20, 2006. CRTAP is required for prolyl 3- hydroxylation and mutations cause recessive osteogenesis imperfecta. Cell 127 (2), 291–304.

Moro, L., Romanello, M., Favia, A., Lamanna, M.P., Lozupone, E., February 2000. Posttranslational modifications of bone collagen type I are related to the function of rat femoral regions. Calcif. Tissue Int. 66 (2), 151–156.

Myllyharju, J., Kivirikko, K.I., January 2004. Collagens, modifying enzymes and their mutations in humans, flies and worms. Trends Genet. 20 (1), 33–43.

Naffa, R., Holmes, G., Ahn, M., Harding, D., Norris, G., December 23, 2016. Liquid chromatography-electrospray ionization mass spectrometry for the simultaneous quantitation of collagen and elastin crosslinks. J. Chromatogr. A 1478, 60–67.

Nagai, N., Hosokawa, M., Itohara, S., Adachi, E., Matsushita, T., Hosokawa, N., et al., September 18, 2000. Embryonic lethality of molecular chaperone hsp47 knockout mice is associated with defects in collagen biosynthesis. The Rockefeller University Press J. Cell Biol. 150 (6), 1499–1506.

Notbohm, H., Nokelainen, M., Myllyharju, J., Fietzek, P.P., Müller, P.K., Kivirikko, K.I., March 26, 1999. Recombinant human type II collagens with low and high levels of hydroxylysine and its glycosylated forms show marked differences in fibrillogenesis in vitro. J. Biol. Chem. 274 (13), 8988–8992.

Ogle, J.D., Arlinghaus, R.B., Logan, M.A., July 1961. Studies on peptides obtained from enzymic digests of collagen with evidence for the presence of an unidentified compound in this protein. Arch. Biochem. Biophys. 94, 85–93.

Ogle, J.D., Arlinghaus, R.B., Logan, M.A., December 1962. 3-Hydroxyproline, a new amino acid of collagen. J. Biol. Chem. 237, 3667–3673.

Pokidysheva, E., Zientek, K.D., Ishikawa, Y., Mizuno, K., Vranka, J.A., Montgomery, N.T., et al., August 23, 2013. Posttranslational modifications in type I collagen from different tissues extracted from wild type and prolyl 3-hydroxylase 1 null mice. American Society for Biochemistry and Molecular Biology J. Biol. Chem. 288 (34), 24742–24752.

Pyott, S.M., Schwarze, U., Christiansen, H.E., Pepin, M.G., Leistritz, D.F., Dineen, R., et al., April 15, 2011. Mutations in PPIB (cyclophilin B) delay type I procollagen chain association and result in perinatal lethal to moderate osteogenesis imperfecta phenotypes. Hum. Mol. Genet. 20 (8), 1595–1609.

Rauch, F., Husseini, A., Roughley, P., Glorieux, F.H., Moffatt, P., August 2012. Lack of circulating pigment epithelium-derived factor is a marker of osteogenesis imperfecta type VI. J. Clin. Endocrinol. Metab. 97 (8), E1550–E1556.

Rautavuoma, K., Takaluoma, K., Sormunen, R., Myllyharju, J., Kivirikko, K.I., Soininen, R., September 28, 2004. Premature aggregation of type IV collagen and early lethality in lysyl hydroxylase 3 null mice. National Acad Sciences Proc. Natl. Acad. Sci. U. S. A. 101 (39), 14120–14125.

Reiser, K.M., Amigable, M.A., Last, J.A., December 5, 1992. Nonenzymatic glycation of type I collagen. The effects of aging on preferential glycation sites. J. Biol. Chem. 267 (34), 24207–24216.

Rodriguez-Pascual, F., Slatter, D.A., November 23, 2016. Collagen cross-linking: insights on the evolution of metazoan extracellular matrix. Nature Publishing Group Sci. Rep. 6 (1), 1955.

Ruotsalainen, H., Sipilä, L., Vapola, M., Sormunen, R., Salo, A.M., Uitto, L., et al., February 15, 2006. Glycosylation catalyzed by lysyl hydroxylase 3 is essential for basement membranes. J. Cell Sci. 119 (Pt 4), 625–635.

Salo, A.M., Cox, H., Farndon, P., Moss, C., Grindulis, H., Risteli, M., et al., October 2008. A connective tissue disorder caused by mutations of the lysyl hydroxylase 3 gene. Am. J. Hum. Genet. 83 (4), 495–503.

Saxena, A.K., Saxena, P., Wu, X., Obrenovich, M., Weiss, M.F., Monnier, V.M., July 5, 1999. Protein aging by carboxymethylation of lysines generates sites for divalent metal and redox active copper binding: relevance to diseases of glycoxidative stress. Biochem. Biophys. Res. Commun. 260 (2), 332–338.

Schegg, B., Hülsmeier, A.J., Rutschmann, C., Maag, C., Hennet, T., February 2009. Core glycosylation of collagen is initiated by two beta(1-O)galactosyltransferases. American Society for Microbiology Mol. Cell. Biol. 29 (4), 943–952.

Schneider, A., Henson, E., Blumenfeld, O.O., Gallop, P.M., June 9, 1967. The presence of lysinal (2,6-diaminohexanal) in tropocollagen. Biochem. Biophys. Res. Commun. 27 (5), 546–551.

Schwarze, U., Cundy, T., Pyott, S.M., Christiansen, H.E., Hegde, M.R., Bank, R.A., et al., January 1, 2013. Mutations in FKBP10, which result in Bruck syndrome and recessive forms of osteogenesis imperfecta, inhibit the hydroxylation of telopeptide lysines in bone collagen. Hum. Mol. Genet. 22 (1), 1–17.

Scott, J.E., Hughes, E.W., Shuttleworth, A., August 1981. A collagen-associated Ehrlich chromogen: a pyrrolic cross-link? Portland Press Limited Biosci. Rep. 1 (8), 611–618.

Sell, D.R., Monnier, V.M., 2012. Molecular basis of arterial stiffening: role of glycation - a mini-review. Karger Publishers Gerontology 58 (3), 227–237.

Shaheen, R., Alazami, A.M., Alshammari, M.J., Faqeih, E., Alhashmi, N., Mousa, N., et al., October 2012. Study of autosomal recessive osteogenesis imperfecta in Arabia reveals a novel locus defined by TMEM38B mutation. J. Med. Genet. 49 (10), 630–635.

Siegel, R.C., Fu, J.C., September 25, 1976. Collagen cross-linking. Purification and substrate specificity of lysyl oxidase. J. Biol. Chem. 251 (18), 5779–5785.

Siegel, R.C., Pinnell, S.R., Martin, G.R., November 10, 1970. Cross-linking of collagen and elastin. Properties of lysyl oxidase. Biochemistry 9 (23), 4486–4492.

Singer, F.R., Eyre, D.R., October 2008. Using biochemical markers of bone turnover in clinical practice. Clevel. Clin. J. Med. 75 (10), 739–750.

Snedeker, J.G., Gautieri, A., July 2014. The role of collagen crosslinks in ageing and diabetes - the good, the bad, and the ugly. CIC Edizioni Internazionali Muscles Ligaments Tendons J. 4 (3), 303–308.

Sricholpech, M., Perdivara, I., Nagaoka, H., Yokoyama, M., Tomer, K.B., Yamauchi, M., March 18, 2011. Lysyl hydroxylase 3 glucosylates galactosylhydroxylysine residues in type I collagen in osteoblast culture. American Society for Biochemistry and Molecular Biology J. Biol. Chem. 286 (11), 8846–8856.

Sricholpech, M., Perdivara, I., Yokoyama, M., Nagaoka, H., Terajima, M., Tomer, K.B., et al., June 29, 2012. Lysyl hydroxylase 3-mediated glucosylation in type I collagen: molecular loci and biological significance. American Society for Biochemistry and Molecular Biology J. Biol. Chem. 287 (27), 22998–23009.

Steinmann, B., Royce, P.M., Superti-Furga, A., 2002. The Ehlers-danlos syndrome. In: Connective Tissue and its Heritable Disorders. John Wiley & Sons, Inc, Hoboken, NJ, USA, pp. 431–523.

Taga, Y., Kusubata, M., Ogawa-Goto, K., Hattori, S., May 3, 2013. Site-specific quantitative analysis of overglycosylation of collagen in osteogenesis imperfecta using hydrazide chemistry and SILAC. American Chemical Society J. Proteome Res. 12 (5), 2225–2232.

Takaluoma, K., Hyry, M., Lantto, J., Sormunen, R., Bank, R.A., Kivirikko, K.I., et al., March 2, 2007. Tissue-specific changes in the hydroxylysine content and cross-links of collagens and alterations in fibril morphology in lysyl hydroxylase 1 knock-out mice. American Society for Biochemistry and Molecular Biology J. Biol. Chem. 282 (9), 6588–6596.

Tenni, R., Valli, M., Rossi, A., Cetta, G., January 15, 1993. Possible role of overglycosylation in the type I collagen triple helical domain in the molecular pathogenesis of osteogenesis imperfecta. Wiley Subscription Services, Inc., A Wiley Company Am. J. Med. Genet. 45 (2), 252–256.

Terajima, M., Perdivara, I., Sricholpech, M., Deguchi, Y., Pleshko, N., Tomer, K.B., et al., August 15, 2014. Glycosylation and cross-linking in bone type I collagen. American Society for Biochemistry and Molecular Biology J. Biol. Chem. 289 (33), 22636–22647.

Terajima, M., Taga, Y., Chen, Y., Cabral, W.A., Hou-Fu, G., Srisawasdi, S., et al., March 2, 2016. Cyclophilin-B modulates collagen cross-linking by differentially affecting lysine hydroxylation in the helical and telopeptidyl domains of tendon type I collagen. American Society for Biochemistry and Molecular Biology J. Biol. Chem. jbc.M115.699470.

Thorleifsson, G., Magnusson, K.P., Sulem, P., Walters, G.B., Gudbjartsson, D.F., Stefansson, H., et al., September 7, 2007. Common sequence variants in the LOXL1 gene confer susceptibility to exfoliation glaucoma. Science 317 (5843), 1397–1400.

Thorpe, C.T., Streeter, I., Pinchbeck, G.L., Goodship, A.E., Clegg, P.D., Birch, H.L., May 21, 2010. Aspartic acid racemization and collagen degradation markers reveal an accumulation of damage in tendon collagen that is enhanced with aging. J. Biol. Chem. 285 (21), 15674–15681.

Tombran-Tink, J., Barnstable, C.J., April 2, 2004. Osteoblasts and osteoclasts express PEDF, VEGF-A isoforms, and VEGF receptors: possible mediators of angiogenesis and matrix remodeling in the bone. Biochem. Biophys. Res. Commun. 316 (2), 573–579.

Torre-Blanco, A., Adachi, E., Hojima, Y., Wootton, J.A., Minor, R.R., Prockop, D.J., February 5, 1992. Temperature-induced post-translational overmodification of type I procollagen. Effects of over-modification of the protein on the rate of cleavage by procollagen N-proteinase and on self-assembly of collagen into fibrils. J. Biol. Chem. 267 (4), 2650–2655.

van Dijk, F.S., Nesbitt, I.M., Zwikstra, E.H., Nikkels, P.G., Piersma, S.R., Fratantoni, S.A., et al., October 2009. PPIB mutations cause severe osteogenesis imperfecta. Am. J. Hum. Genet. 85 (4), 521–527.

Vanacore, R., Ham, A.J., Voehler, M., Sanders, C.R., Conrads, T.P., Veenstra, T.D., et al., September 4, 2009. A sulfilimine bond identified in collagen IV. Science 325 (5945), 1230–1234.

Verzár, F., 1964. Aging of the collagen fiber. Elsevier Int. Rev. Connect. Tissue Res. 2, 243–300.

Verzijl, N., DeGroot, J., Thorpe, S.R., Bank, R.A., Shaw, J.N., Lyons, T.J., et al., December 15, 2000. Effect of collagen turnover on the accumulation of advanced glycation end products. J. Biol. Chem. 275 (50), 39027–39031.

Vestergaard, P., Rejnmark, L., Mosekilde, L., January 2009. Diabetes and its complications and their relationship with risk of fractures in type 1 and 2 diabetes. Calcif. Tissue Int. 84 (1), 45–55.

Viguet-Carrin, S., Gineyts, E., Bertholon, C., Delmas, P.D., January 1, 2009. Simple and sensitive method for quantification of fluorescent enzymatic mature and senescent crosslinks of collagen in bone hydrolysate using single-column high performance liquid chromatography. J. Chromatogr. B, Anal. Technol. Biomed. Life Sci. 877 (1–2), 1–7.

Volodarsky, M., Markus, B., Cohen, I., Staretz-Chacham, O., Flusser, H., Landau, D., et al., January 2013. A deletion mutation in TMEM38B associated with autosomal recessive osteogenesis imperfecta. Hum. Mutat. 34 (4) (n/a–n/a).

Vranka, J.A., Sakai, L.Y., Bächinger, H.P., May 28, 2004. Prolyl 3-hydroxylase 1, enzyme characterization and identification of a novel family of enzymes. American Society for Biochemistry and Molecular Biology J. Biol. Chem. 279 (22), 23615–23621.

Wang, C., Risteli, M., Heikkinen, J., Hussa, A.-K., Uitto, L., Myllyla, R., May 24, 2002. Identification of amino acids important for the catalytic activity of the collagen glucosyltransferase associated with the multifunctional lysyl hydroxylase 3 (LH3). J. Biol. Chem. 277 (21), 18568–18573.

Widmer, C., Gebauer, J.M., Brunstein, E., Rosenbaum, S., Zaucke, F., Drogemuller, C., et al., August 14, 2012. Molecular basis for the action of the collagen-specific chaperone Hsp47/SERPINH1 and its structure-specific client recognition. Proc. Natl. Acad. Sci. U. S. A. 109 (33), 13243–13247.

Wordinger, R.J., Clark, A.F., October 2014. Lysyl oxidases in the trabecular meshwork. J. Glaucoma 23 (8 Suppl. 1), S55–S58.

Wu, J.J., Eyre, D.R., December 30, 1985. Studies on the distribution of hydroxypyridinium cross-links in different collagen types. Ann. N. Y. Acad. Sci. 460, 520–523.

Yamauchi, M., Shiiba, M., 2008. Lysine hydroxylation and cross-linking of collagen. In: Post-translational Modifi Cations of Proteins. Methods in Molecular Biology?, vol. 446. Humana Press, Totowa, NJ, pp. 95–108.

Yamauchi, M., London, R.E., Guenat, C., Hashimoto, F., Mechanic, G.L., August 25, 1987. Structure and formation of a stable histidine-based trifunctional cross-link in skin collagen. J. Biol. Chem. 262 (24), 11428–11434.

Yang, C.L., Rui, H., Mosler, S., Notbohm, H., Sawaryn, A., Müller, P.K., May 1, 1993. Collagen II from articular cartilage and annulus fibrosus. Structural and functional implication of tissue specific posttranslational modifications of collagen molecules. Eur. J. Biochem. 213 (3), 1297–1302.

Ye, J., Rawson, R.B., Komuro, R., Chen, X., Davé, U.P., Prywes, R., et al., December 2000. ER stress induces cleavage of membrane-bound ATF6 by the same proteases that process SREBPs. Mol. Cell. 6 (6), 1355–1364.

Yeowell, H.N., Walker, L.C., April 1999. Tissue specificity of a new splice form of the human lysyl hydroxylase 2 gene. Matrix Biol. 18 (2), 179–187.

Chapter 15

Secreted noncollagenous proteins of bone

Jeffrey P. Gorski[1] **and Kurt D. Hankenson**[2]

[1]Department of Oral and Craniofacial Sciences, School of Dentistry, and Center for Excellence in Mineralized and Dental Tissues, University of Missouri–Kansas City, Kansas City, MO, United States; [2]Department of Orthopaedic Surgery, University of Michigan Medical School, Ann Arbor, MI, United States

Chapter outline

Introduction

Bone differs from soft connective tissues in that it is composed of a mineralized hydroxyapatite phase and an organic phase. Although the organic matrix of bone consists primarily of collagen(s) (as reviewed early in this volume), the existence of other secreted noncollagenous components was first proposed by Herring and coworkers in the 1960s (Herring and Ashton, 1974). Historically, using degradative techniques, a variety of carbohydrate-containing moieties were extracted and partially characterized. A major breakthrough in the isolation and characterization of noncollagenous proteins of bone came with the development of "dissociative" techniques whereby proteins could be extracted in an intact, nonaggregated form (Termine et al., 1980, 1981a,b). Although they are not as abundant as so-called structural components such as collagen, their importance in bone physiology cannot be underestimated. This is emphasized by the identification of mutations in a number of these proteins that result in abnormal bone (Gorski, 2011). This chapter discusses secreted noncollagenous proteins found in bone matrix. Since the publication of the previous edition of this work in 2008, substantial additions have been made to include recently reported functional studies, inclusion of noncollagenous proteins that were not previously considered, and new information regarding the developing area of bone–muscle/fat/pancreas/testis cross-talk signaling and the role that these proteins play in these interactions.

Principles of Bone Biology. https://doi.org/10.1016/B978-0-12-814841-9.00015-4

Proteoglycans

This class of molecules is characterized by the covalent attachment of long-chain polysaccharides (glycosaminoglycans, GAGs) to core protein molecules. GAGs are composed of repeating disaccharide units that are sulfated to varying degrees and include chondroitin sulfate, dermatan sulfate, keratan sulfate, and heparan sulfate (HS). Hyaluronic acid is also a GAG found in bone, but itself is not attached to a core protein. Different subclasses of proteoglycans are generally characterized by the structure of the core protein and by the nature of the GAG (Table 15.1). Although other types of molecules can be sulfated, proteoglycans bear greater than 95% of the sulfate groups within any organic matrix (Lamoureux et al., 2007).

Aggrecan and versican (PG-100)

There are two large chondroitin sulfate proteoglycans associated with skeletal tissue that are characterized by core proteins with globular domains at the amino and carboxy termini and by binding to hyaluronan to form large aggregates. Aggrecan was assumed to be virtually cartilage specific, but its mRNA is detected in developing bone (Wong et al., 1992) and is present in high-throughput gene expression studies of osteoblasts. It should also be noted that aggrecan is an important component of the primary spongiosa that forms during endochondral ossification. In the nanomelic chick, there is a mutation in the aggrecan core protein such that it is not expressed in cartilage (Primorac et al., 1999). However, there is an impact on bones that form via the intramembranous pathway, an unanticipated finding because these bones would not be expected to be affected by abnormal cartilage development. This suggests a role for aggrecan in bone matrix separate from its role in cartilage. Mutation of the aggregan gene results in a form of spondyloepiphyseal dysplasia in humans leading to premature osteoarthritis (Gleghorn et al., 2005), and in mice, a mutation leading to a null allele results in cartilage matrix deficiency with severe skeletogenesis defects and perinatal death (*cdm* mice) (Watanabe et al., 1994). While not specifically examined, there also appear to be defects in bones that form via intramembranous ossification. However, conditional mouse models that disrupt the aggrecan gene in an osteoblast-specific manner have not been described.

Closely related, but not identical, is a soft connective tissue—enriched proteoglycan termed versican, which is mostly localized to loose, interstitial mesenchyme in developing bone. It has been hypothesized that it captures space that will ultimately become bone. It is this proteoglycan that is destroyed as osteogenesis progresses. It is noteworthy that the core protein of versican contains epidermal growth factor (EGF)-like sequences (Wight, 2002), and release of these sequences may influence the metabolism of cells in the osteoblastic lineage. As osteogenesis progresses, versican is replaced by two members of another class of proteoglycans that contain core proteins of a different chemical nature (decorin and biglycan; Fisher et al., 1989). In the *hdf* (heart defect) mouse, the versican gene is disrupted and the protein is not expressed. The mutation is embryonic lethal, and in vitro studies have shown defective chondrogenesis by limb mesenchyme (Williams et al., 2005). A conditional versican allele has been generated and mice with limb bud mesenchymal disruption show altered digit formation and alterations in transforming growth factor β (TGFβ) localization, but an effect on bone has not been described (Choocheep et al., 2010).

Decorin (PG-II) and biglycan (PG-I)

The two small proteoglycans that are heavily enriched in bone matrix are decorin and biglycan, both of which contain chondroitin sulfate chains in bone, but bear dermatan sulfate in soft connective tissues. They are characterized by core proteins that contain a leucine-rich repeat (LRR) sequence, a property shared with proteins that are associated with morphogenesis such as *Drosophila* toll protein and chaoptin, the leucine-rich protein of serum, and adenylyl cyclase (Fisher et al., 1989). As leucine-rich proteoglycans, they are included in a family referred to as small leucine-rich proteoglycans (SLRPs). The crystal structures of decorin (McEwan et al., 2006) and biglycan (Scott et al., 2006) have been determined, and based on this analysis, it appears that the SLRPs are not as curved as ribonuclease and that they may dimerize.

Although decorin and biglycan share many properties owing to the high degree of homology of their core proteins, they are also quite distinct, as best demonstrated by their patterns of expression (Bianco et al., 1990). In cartilage, decorin is found in the interterritorial matrix away from the chondrocytes, whereas biglycan is in the intraterritorial matrix. In keeping with this pattern, during endochondral bone formation, decorin is widely distributed in a pattern that is virtually indistinguishable from that of type I collagen. It first appears in preosteoblasts, is maintained in fully mature osteoblasts, and is subsequently downregulated as cells become buried in the extracellular matrix to become osteocytes. However, biglycan exhibits a much more distinctive pattern of distribution. It is found in a pericellular location in unique areas undergoing morphological delineation. It is upregulated in osteoblasts and, interestingly, its expression is maintained in osteocytes and

TABLE 15.1 Proteoglycans in bone matrix.

Molecule	Structural characteristics	Gene ontology biological processes
Aggrecan	1×10^6 to 3×10^6 MW; 210- to 250-kDa core protein; 100–150 kDa GAG chains (CS and KS); two globular domains (G1 and G2) and a third globular domain (G3)	Skeletal system development; chondrocyte development; proteolysis; cell adhesion; central nervous system development; heart development; keratan sulfate biosynthetic process; extracellular matrix disassembly; proteoglycan biosynthetic process; extracellular matrix organization; collagen fibril organization; keratan sulfate catabolic process
Versican (PG-100)	1×10^6 MW intact protein ; 360-kDa core; 12 CS chains of 45 kDa, G1 and G3 globular domains with hyaluronan-binding sites; EGF- and CRP-like sequences	Skeletal system development; osteoblast differentiation; cell adhesion; multicellular organism development; central nervous system development; cell recognition; extracellular matrix organization; GAG metabolic process; CS metabolic, biosynthetic, and catabolic processes; dermatan sulfate biosynthetic process; posttranslational protein modification; cellular protein metabolic process
Decorin	130-kDa intact protein; 38- to 45-kDa core with 10 leucine-rich repeat sequences, 1 CS chain of 40 kDa	RNA binding; protein kinase inhibitor activity; protein binding; collagen binding; GAG binding; protein N-terminus binding; extracellular matrix binding
Biglycan	270-kDa intact protein, 38- to 45-kDa core protein with 12 leucine-rich repeat sequences, two CS chains of 40 kDa	May bind to collagen; may bind to TGFβ; pericellular environment; a genetic determinant of peak bone mass
Fibromodulin	59-kDa intact protein, 42-kDa core protein with leucine-rich repeat sequences, one N-linked KS chain	TGFβ receptor complex assembly; NOT axonogenesis; KS biosynthetic process; collagen fibril organization; KS catabolic process
Osteoglycin (mimecan)	299-aa precursor, 105-aa mature protein, leucine-rich repeat sequences	Axonogenesis; regulation of receptor activity; KS biosynthetic process; KS catabolic process; negative regulation of smooth muscle cells
Asporin	43-kDa core protein	Negative regulation of protein kinase activity; cytokine-mediated signaling pathway; bone mineralization; negative regulation of TGFβ receptor signaling pathway; biomineral tissue development; negative regulation of JAK–STAT cascade; negative regulation of tooth mineralization
Osteoadherin (osteomodulin)	85-kDa intact protein, 47-kDa core protein, 11 leucine-rich repeat sequences, RGD sequence	Cell adhesion; NOT axonogenesis; KS biosynthetic process; regulation of bone mineralization; KS catabolic process
Syndecan	32-kDa intact protein	Retinoid metabolic process; ureteric bud development; GAG biosynthetic process; GAG catabolic process; inflammatory response; response to toxic substance; response to organic substance; cell migration; GAG metabolic process; wound healing; odontogenesis; response to hydrogen peroxide; myoblast development; leukocyte migration; response to glucocorticoid; response to cAMP; response to calcium ion; striated muscle cell development; Sertoli cell development; canonical Wnt signaling; positive regulation of exosomal secretion; positive regulation of extracellular exosome assembly
Perlecan	660-kDa intact protein, 450-kDa core protein, three 70- to 100-kDa HS GAGs	Interacts with matrix components, regulates cell signaling
Glypican	Lipid-linked HSPG, 66-kDa core, two HS GAGs	Copper ion binding; fibroblast growth factor binding; laminin binding; HS proteoglycan binding
Hyaluronan	Multiple proteins associated outside of the cell, structure unknown	May work with versican-like molecule to capture space destined to become bone

CRP, C-reactive protein; *CS*, chondroitin sulfate; *EGF*, epidermal growth factor; *GAG*, glycosaminoglycan; *HS*, heparan sulfate; *HSPG*, heparan sulfate proteoglycan; *KS*, keratan sulfate; *MW*, molecular weight; *TGFβ*, transforming growth factor β.
Gene ontologies listed are derived in large part from one of two on-line sources: www.informatics.jax.org/vocab/gene_ontology or www.genecards.org/search/keyword.

is localized to lacunae and canaliculi. Osteocytes act as mechanoreceptors within the bone matrix (Bonewald, 2006), and proteoglycans, possibly biglycan or cell surface–associated molecules (such as HS proteoglycans), may play a role as force transducers.

Transgenic mice that are deficient in decorin have primarily thin skin (Danielson et al., 1997), whereas mice deficient in biglycan fail to achieve peak bone mass and develop osteopenia (Xu et al., 1998). Animals that are double deficient for decorin and biglycan exhibit a phenotype reminiscent of the progeroid form of Ehlers–Danlos syndrome, whereby collagen fibrils are highly disrupted in both the dermis and the bone (Corsi et al., 2002). Disruption of biglycan in mice also impairs fracture healing, possibly through regulation of endostatin (Myren et al., 2016).

Both decorin and biglycan have been found to bind to TGFβ and to regulate its availability and activity (Markmann et al., 2000). In view of current interest in bone muscle cross talk, it is interesting that decorin also binds specifically to myostatin, another activin superfamily member, and is able to block its inhibitory actions on myoblasts by sequestration (Miura et al., 2006). Subsequent work has shown that decorin's anti-myostatin action can be largely mimicked by an N-terminal Nos. 48–71 peptide, which is capable of blocking myostatin's binding to the activin type II receptor (El Shafey et al., 2016). Interestingly, anti-myostatin peptides derived from decorin are associated with human atrial fibrillation (Barallobre-Barreiro et al., 2016). Further work is needed to determine if decorin and decorin N-terminal peptides can modulate the receptor-mediated actions of TGFβ on osteoblastic cells in a similar manner.

A novel role for biglycan, and another SLRP, fibromodulin, has also been demonstrated in regulating osteoclastogenesis (Kram et al., 2017). Double-knockout mice for both genes show significant osteopenia because of enhanced osteoclastogenesis. Biglycan and fibromodulin bind to both tumor necrosis factor α and receptor activator of NF-κB ligand (RANKL) and thereby regulate osteoclastogenesis. In the absence of the proteins, osteoblasts are unable to sequester these proosteoclastic factors, and osteoclastogenesis is unregulated.

Decorin also binds to collagen (decorating collagen fibrils), as does biglycan. This interaction has dramatic effects on collagen fibril assembly and on the mechanical properties, including tensile strength, of the resultant matrix (Reese et al., 2013). Another activity has been demonstrated by in vitro cell attachment assays in which decorin and biglycan were both found to inhibit bone cell attachment, presumably by binding to fibronectin and inhibiting its cell–matrix binding capabilities (Grzesik and Robey, 1994).

Other leucine-rich repeat sequence proteins and proteoglycans

Interestingly, there are at least 60 proteins that have been found to contain LRRs, and many of them are also SLRPs (Matsushima et al., 2000). Another SLRP found in bone is osteoglycin, previously termed "osteoinductive factor" and later found to be a protein bound to TGFβ (Ujita et al., 1995). This molecule is similar but not identical to the proteoglycan PG-Lb, which has now been found to be epiphycan, localized primarily in epiphyseal cartilage. More recently, another LRR, asporin, has been localized to developing bone. Unlike other LRRs, it has an aspartic acid–rich amino sequence (Henry et al., 2001). Asporin-knockout mice have been generated and a defect in bone was not reported (Maccarana et al., 2017).

Other members of the SLRP family found in bone include fibromodulin, as previously mentioned, which contains keratan sulfate and binds to collagen fibrils in regions distinctly different from those of decorin (Hedbom and Heinegard, 1993); osteoadherin, also known as osteomodulin, which contains the cell attachment sequence Arg-Gly-Asp (RGD) (Sommarin et al., 1998); and lumican, which may regulate collagen fibril formation. Osteomodulin is highly upregulated during bone morphogenetic protein (BMP)-induced osteoblast differentiation, but it's impacts on bone in knockout mice are minimal.

Although SLRPs appear to be "born to bind," definitive functions are not known. The mouse deficient for both biglycan and fibromodulin exhibits initial joint laxity, followed by development of extra sesamoid bones in many tendons and development of an osteoarthritis-like condition (Ameye and Young, 2002). The lumican/fibromodulin-knockout mouse resembles a variant of Ehlers–Danlos syndrome (OMIM: 130000) and has ectopic calcification (Chakravarti et al., 2003). Other proteoglycans have been isolated from a variety of animal species by using varying techniques, for example, HAPGIII (so named for its ability to bind to hydroxyapatite) and PG-100, which has been shown subsequently to be homologous to versican, as reviewed previously (Zu et al., 2007).

Although not generally found in the extracellular matrix, HS proteoglycans found associated with, or intercalated into, cell membranes may be very influential in regulating bone cell metabolism. Receptors for several growth factors (TGFβ and fibroblast growth factor 2 [FGF2], to name two) have been found to associate with HS (either bound covalently to core proteins or as free GAGs). Deficiency in the *EXT1* or *EXT2* genes in humans, which encode Golgi glycosyltransferases that are responsible for HS synthesis, results in hereditary multiple exostoses (HME) (OMIM: 133700). In HME, patients develop osteochondromas because of dysregulated BMP signaling (Pacifici, 2017).

Intercalated HS proteoglycans (the syndecan family) have been postulated to regulate cell growth, perhaps through modulation of growth factor and receptor activity (Markmann et al., 2000). Work shows that over-expression of syndecan-2 in mouse osteoblasts results in alterations in Wnt signaling and a reduction in the osteoclast regulatory protein RANKL (Mansouri et al., 2017). Perlecan is highly expressed in cartilage and has been found to interact with matrix components and to regulate cell signaling proteins, including FGF. Knockout mice have a phenotype that resembles thanatophoric dysplasia type I (OMIM: 187600) (Arikawa-Hirasawa et al., 1999), and mutations in humans are associated with Schwartz–Jampel syndrome (OMIM: 142461). Glypicans are another class of HS proteoglycans linked to cell membranes by phosphoinositol linkages that are cleavable by phospholipase C. Consequently, their activity may be in the pericellular environment or in the extracellular matrix. Mutations in glypican 3 give rise to Simpson–Golabi–Behmel syndrome (OMIM: 300037), and the knockout mouse has delayed endochondral bone formation and impaired osteoclastic development (Viviano et al., 2005). The complete cast of HS proteoglycans present in the cellular and pericellular environment in bone is not yet complete (see Zu et al., 2007, for a review).

Hyaluronan

This unsulfated GAG is not attached to a protein core and is synthesized by a completely different pathway. Hyaluronan is synthesized in the extracellular environment by a group of three plasma membrane hyaluronic acid synthases, which use cytoplasmic UDP-glucuronic acid and UDP-*N*-acetylglucosamine as substrates (Vigetti et al., 2014). Large amounts of hyaluronan are synthesized during the early stages of bone formation and may associate with versican to form high molecular weight aggregates (Fedarko et al., 1992; Falconi and Aubin, 2007). Interestingly, the long bones of hyaluronic acid synthase 2 (Has2)-deficient mice are severely shortened, implying that hyaluronic acid synthesis is required for normal longitudinal growth of all limbs (Matsumoto et al., 2009). A series of changes in the cartilage of *Has2*-null mice, e.g., reduced number of hypertrophic chondrocytes, disorganized growth plates, and lower expression of hypertrophic differentiation markers, indicate that hyaluronic acid is also needed for normal chondrocyte maturation. In other tissues, hyaluronic acid is believed to participate in cell migration and differentiation (Fedarko et al., 1992).

Glycoproteins

Virtually all noncollagenous bone matrix proteins are modified post-translationally to contain either N- or O-linked oligosaccharides, many of which can be modified further by the addition of phosphate and/or sulfate (Table 15.2). In general, compared with their soft connective tissue counterparts, bone matrix proteins are modified more extensively and in a different pattern. In some cases, differences in posttranslational modifications result from differential splicing of heterogeneous nuclear RNA, but, in general, they result from differences in the activities of enzymes located along the intracellular pathway of secretion. The pattern of post-translational modifications may be cell type specific and consequently may be of use in distinguishing protein metabolism from one tissue type versus another.

The number of secreted glycoproteins that have been identified in bone matrix grows every year. This, in part, is because of the explosion of information from high-throughput expression techniques, including RNA sequencing. What follows next is a brief description of secreted bone proteins that most likely play structural as well as metabolic roles. Other glycoprotein species have been identified primarily as growth factors and will be covered in more detail elsewhere in this volume.

Alkaline phosphatase

Tissue nonspecific alkaline phosphatase (TNAP) is a product of the *ALPL* gene. TNAP is localized to the cell membrane of osteoblasts and plays an essential role in bone mineralization. Human mutations in *ALPL* are responsible for hypophosphatasia (OMIM: 146300, 241510, and 241500), a disease condition characterized by hypomineralized bones, abnormal bone formation and skeleton growth, and dental abnormalities. TNAP is present in abundance on matrix vesicles and thus in developing bone matrix, where it degrades extracellular pyrophosphate, a potent inhibitor of bone mineralization. Mice with deficiency in TNAP have severe bone abnormalities (Millan and Whyte, 2016).

Sclerostin

Sclerostin is a product of the *SOST* gene and is secreted by kidney, vascular cells, and bone osteocytes. Early work suggested that sclerostin may work in combination with noggin to form complexes that antagonize BMP mitogenic activity

TABLE 15.2 Characteristics of glycoproteins in bone matrix.

Molecule	Structural characteristics	Gene ontology biological processes
Alkaline phosphatase	Two identical subunits of 80 kDa, disulfide-bonded, tissue-specific posttranslational modifications	Skeletal system development; osteoblast differentiation; endochondral ossification; developmental process involved in reproduction; C-terminal protein lipidation; metabolic process; dephosphorylation; biomineral tissue development; response to lipopolysaccharide; response to vitamin D; response to antibiotic; response to glucocorticoid; cellular response to organic cyclic compound; cementum mineralization
Sclerostin	24 kDa, C-terminal cysteine knot-like domain similar to BMP antagonists	Ossification; response to mechanical stimulus; Wnt signaling; negative regulation of ossification; negative regulation of BMP signaling pathway; negative regulation of protein complex assembly; positive regulation of transcription, DNA-templated; cellular response to parathyroid hormone stimulus; negative regulation of canonical Wnt signaling pathway; negative regulation of Wnt signaling pathway involved in dorsal/ventral axis specification
Periostin	93 kDa	Skeletal system development; response to hypoxia; negative regulation of cell–matrix adhesion; regulation of systemic arterial blood pressure; cell adhesion; regulation of notch signaling pathway; response to mechanical stimulus; tissue development; response to muscle activity; positive regulation of smooth muscle cell migration; extracellular matrix organization; response to estradiol; wound healing; cellular response to fibroblast growth factor stimulus; cellular response to vitamin K; cellular response to tumor necrosis factor; cellular response to transforming growth factor β stimulus; negative regulation of substrate adhesion-dependent cell spreading; positive regulation of chemokine (C–C motif) ligand 2 secretion; neuron projection extension; bone regeneration
Osteonectin/ SPARC	35–45 kDa, intramolecular disulfide bonds; α-helical amino terminus with multiple low-affinity, Ca^{2+} binding sites; two EF-hand high-affinity, Ca^{2+} sites; ovomucoid homology; glycosylated, phosphorylated, tissue-specific modifications	Ossification; negative regulation of endothelial cell proliferation; platelet degranulation; receptor-mediated endocytosis; signal transduction; heart development; response to gravity; response to lead ion; positive regulation of endothelial cell migration; negative regulation of angiogenesis; regulation of cell morphogenesis; extracellular matrix organization; lung development; response to lipopolysaccharide; response to L-ascorbic acid; response to cytokine; wound healing; regulation of cell proliferation; response to peptide hormone; pigmentation; response to ethanol; response to cadmium ion; inner ear development; response to glucocorticoid; response to cAMP; response to calcium ion; bone development; cellular response to growth factor stimulus
Tetranectin	21-kDa protein composed of four identical subunits of 5.8 kDa, sequence homologies with asialoprotein receptor and G3 domain of aggrecan	Ossification; platelet degranulation; positive regulation of plasminogen activation; bone mineralization; cellular response to organic substance; cellular response to transforming growth factor β stimulus

BMP, bone morphogenetic protein.
Gene ontologies listed are derived in large part from one of two on-line sources: www.informatics.jax.org/vocab/gene_ontology or www.genecards.org/search/keyword.

by physically sequestering the latter (Winkler et al., 2004). However, more recently, sclerostin is most recognized as an inhibitor of Wnt signaling. Sclerostin expression has been shown to be important for skeletal function because deficient individuals homozygous for a nonsense mutation in the N-terminal coding region exhibit characteristics of sclerosteosis (severe bone overgrowth often including syndactyly; Brunkow et al., 2001). Van Buchem's disease represents a milder form of sclerosteosis caused by a regulatory mutation that reduces the expression of sclerostin and results in abnormal bone growth (Vanhoenacker et al., 2003). These sclerosteosis conditions are similar to a high-bone-mass disorder caused by an activating mutation in the Wnt co-receptor, *LRP5* (Gong et al., 2001). Sclerostin is recognized as a key osteocyte-produced feedback mechanism that serves to modulate the development and activity of osteoblasts.

The functional importance of sclerostin as an inhibitor of bone formation has been reinforced through many mouse knockout and transgenic studies, as well through clinical and translational studies (Ominsky et al., 2010; Padhi et al., 2011). For example, multiple myeloma is associated with increased fracture risk and low bone density, due to the production of paracrine factors that stimulate osteoclastic bone resorption (Roodman, 2011). Blocking osteoclast action with bisphosphonates has been shown to reduce bone loss; however, it does not stimulate replacement of bone and treated

patients still experience low bone mass and increased fracture risk. It has now been shown that anti-sclerostin antibodies are able to induce new bone formation in a mouse model of multiple myeloma (McDonald et al., 2017) and, importantly, tumor-bearing mice treated with both bisphosphonate and anti-sclerostin antibodies gained more bone mass and displayed better vertebral fracture resistance than bisphosphonate-treated tumor control mice. These results suggest that antibody therapy against sclerostin may ultimately be beneficial in stimulating new bone formation. However, a number of issues remain to be resolved before therapeutic anti-sclerostin antibodies can be prescribed safely for building bone mass in multiple myeloma or osteoporosis patients (Bhattacharya et al., 2018).

Periostin

The *POSTN* gene encodes a secreted $M_r = 90$ kDa extracellular protein involved in integrin-mediated adhesion of epithelial cells in heart, bone, and teeth. Deletion of *POSTN* leads to cardiac valve disease, as well as skeletal and dental abnormalities including low bone mineral density (BMD) and reduced cortical bone strength (Rios et al., 2005). As it is highly expressed in periosteal bone cells, work by Bonnet et al., 2017) suggests that periostin plays a positive role in the formation of cortical bone. They showed that periostin is a substrate and direct target of cathepsin K both in vivo and in vitro. Importantly, when cathepsin K was inhibited either pharmacologically or through genetic ablation, expression of periostin was increased in vivo, especially in the periosteum. Interestingly, the bone formation response to mechano-transduction signals was increased in cortical bone in mice treated with cathepsin K functional inhibitors or in cathepsin K−deficient mice (Bonnet et al., 2017). In a commensurate way, the mechanotransduction response was blocked in periostin-deficient mice. These results indicate that periostin may play a positive role in regulating growth and remodeling of cortical bone during development, e.g., growth in the width of long bones. It is highly likely that the ability of periostin to bind to multiple extracellular matrix proteins (fibronectin, laminin, collagens I and V, tenascin, and lysyl oxidase) contributes to its capacity to influence the transmission of mechanotransduction signals in bone. Further work is necessary to assess whether the actions of periostin on skeletal stem cells within the periosteum also contribute to this growth (Duchamp de Lageneste et al., 2018).

Osteonectin (SPARC, culture shock protein, and BM40)

With the development of procedures to demineralize and extract bone matrix proteins without the use of degradative enzymes, osteonectin was one of the first proteins isolated in intact form. This molecule was so named owing to its ability to bind to Ca^{2+}, hydroxyapatite, and collagen and to nucleate hydroxyapatite deposition (Termine et al., 1981a,b). Osteonectin is commonly referred to as SPARC (secreted protein acidic and rich in cysteine). It was one of the first extracellular proteins to be characterized as a "matricellular" protein by Sage and Bornstein (Sage and Bornstein, 1991). The osteonectin molecule contains several different structural features, the most notable of which is the presence of two EF-hand high-affinity calcium-binding sites. These structures are usually found in intracellular proteins, such as calmodulin, that function in calcium metabolism (Bhattacharya et al., 2004).

Although osteonectin is highly enriched in bone, it is also expressed in a variety of other connective tissues at specific points during development, maturation, or repair processes in vivo. It was identified after induction by cAMP in terato-carcinoma cells and was found to be produced at very early stages of embryogenesis. Interestingly, if osteonectin is inactivated by the use of blocking antibodies during tadpole development, there is a disruption of somite formation and subsequent malformations in the head and trunk (Purcell et al., 1993). Mice that are deficient in osteonectin present with severe cataracts (Bassuk et al., 1999) and develop severe osteopenia characterized by decreased trabecular connectivity, decreased mineral content, but increased apatite crystal size (Mansergh et al., 2007).

Tetranectin

This tetrameric protein has been identified in woven bone and in tumors undergoing mineralization (Wewer et al., 1994). This protein shares sequence homologies with globular domains of aggrecan and asialoprotein receptor. Mice deficient in tetranectin develop spinal deformities (Iba et al., 2001), but the specific functional role that tetranectin plays in osteogenesis is unknown.

RGD-containing glycoproteins

Some of the major glycoproteins in bone matrix (collagens, thrombospondin (TSP), fibronectin, vitronectin, fibrillins, osteoadherin, osteopontin (OPN), bone sialoprotein (BSP), dentin matrix protein 1 (DMP1), and proteins derived from the

dentin sialophosphoprotein gene) contain the amino acid sequence RGD, which conveys the ability of the extracellular matrix protein to bind to the integrin class of cell surface receptors (Table 15.3). This binding is the basis of many cell attachment activities that have been identified by in vitro analysis; however, it should be noted that in many cases it is not clear how this in vitro activity translates into in vivo physiology.

TABLE 15.3 Glycoproteins in bone matrix, continued: RGD-containing glycoproteins.

Molecule	Structural characteristics	Gene ontology biological processes
Thrombospondins	450-kDa molecule; three identical disulfide-linked subunits of 150–180 kDa; homologies to fibrinogen, properdin, EGF, collagen, von Willebrand Factor , *Plasmodium falciparum*, and calmodulin; RGD at the C-terminal globular domain	Apoptosis-related network due to altered Notch3 in ovarian cancer; bladder cancer; focal adhesion; inflammatory response pathway; microRNA targets in ECM and membrane receptors; senescence and autophagy in cancer; syndecan-4-mediated signaling events; TGFβ receptor signaling; TGFβ signaling pathway
Fibronectin	400 kDa with two nonidentical subunits of 200 kDa, composed of type I, II, and III repeats; RGD in the 11th type III repeat 2/3 from the N terminus	MicroRNA targets in ECM and membrane receptors; nanoparticle-mediated activation of receptor signaling overview of nanoparticle effects; Rac1/Pak1/p38/MMP-2 pathway; regulation of actin cytoskeleton; senescence and autophagy in cancer; simplified interaction map between LOXL4 and oxidative stress pathway; syndecan-2-mediated signaling events; syndecan-4-mediated signaling events; TGFβ signaling in thyroid cells for epithelial–mesenchymal transition; TGFβ signaling pathway; VEGFR3 signaling in lymphatic endothelium
Irisin	24-kDa protein with fibronectin III domain, N-glycosylated, extracellular domain is membrane cleaved	Biological process; regulation of receptor activity; response to muscle activity; positive regulation of brown fat cell differentiation
Vitronectin	Cell attachment protein, terminus, homology to somatomedin B, rich in cysteines, sulfated, phosphorylated	αMβ2 integrin signaling; focal adhesion; FOXA1 transcription factor network inflammatory response pathway; integrins in angiogenesis; primary focal segmental glomerulosclerosis; senescence and autophagy in cancer
Fibrillin1	350 kDa, EGF-like domains, RGD, cysteine motifs	Integrin binding; hormone activity; ECM structural constituent; calcium ion binding; protein binding; heparin binding; ECM constituent conferring elasticity; protein complex binding; identical protein binding
Osteopontin	44–75 kDa, polyaspartyl stretches, no disulfide bonds, glycosylated, phosphorylated, RGD located 2/3 from the N terminus	Brain-derived neurotrophic factor signaling pathway; direct *p*53 effectors; endochondral ossification; FGF signaling pathway; focal adhesion; integrins in angiogenesis; lung fibrosis; osteoclast signaling; osteopontin signaling; osteopontin-mediated events; TGFβ receptor signaling; Toll-like receptor signaling pathway
Bone sialoprotein	46–75 kDa, polyglutamyl stretches, no disulfide bonds, 50% carbohydrate, tyrosine-sulfated, RGD near the C terminus	Focal adhesion; interleukin-11 signaling pathway; osteoblast signaling
Matrix extracellular phosphoglycoprotein	58 kDa	Skeletal system development; biomineral tissue development; posttranslational protein modification; cellular protein metabolic process
BAG-75	75 kDa; sequence homologies to dentin matrix protein-1, osteopontin, and bone sialoprotein; 7% sialic acid, 8% phosphate, 29% acidic amino acid content	Binds large number of calcium ions/mole, may act as a cell attachment protein (RGD sequence not yet confirmed), may regulate bone resorption

ECM, extracellular matrix; *EGF*, epidermal growth factor; *FGF*, fibroblast growth factor; *FOXA1*, forkhead box A1; *LOXL4*, lysyl oxidase-like 4; *MMP-2*, matrix metalloproteinase 2; *TGFβ*, transforming growth factor β; *VEGFR3*, vascular endothelial growth factor receptor 3.
Gene ontologies listed are derived in large part from one of two on-line sources: www.informatics.jax.org/vocab/gene_ontology or www.genecards.org/search/keyword.

Thrombospondins

TSPs are a family of five multidomain, matricellular proteins. TSP-1 was first identified as the most abundant protein in platelet alpha granules, but is found in many tissues during development, including bone, where it is highly expressed (Robey et al., 1989). Subsequently, four other members have been described, including COMP (cartilage oligomeric matrix protein) as TSP-5 (reviewed in Adams, 2004). In bone, all five proteins are present, synthesized by different cell types at different stages of maturation and development (Carron et al., 1999), but TSP-1 and TSP-2 are the most highly expressed by osteoblast lineage cells and the best characterized TSP proteins in bone. TSP-1 and TSP-2 are trimeric proteins, whereas TSP-3 to 5 are pentameric. TSP-1 and 2 are able to bind to a variety of cell surface receptors, including CD36, CD47, LRP1, and integrins, but in addition can bind to other matrix proteins, matrix metalloproteinases (MMPs), and growth factors, particularly TGFβ. The bone phenotype of TSP-2-deficient mice has been extensively characterized. These mice exhibit an increase in osteoblast progenitors, but have defective mineralization. Cortical bone is thicker, but the bones are reduced in periosteal diameter. Manley et al. have shown that cells deficient in TSP-2 are unable to effectively process collagen and the mice have a brittle bone phenotype (Manley et al., 2015). Mice deficient in TSP-2 also show accelerated bone regeneration characterized by reduced chondrogenesis and accelerated intramembranous bone formation. This phenotype is linked to the well-described role of TSPs in regulating vascularization.

Fibronectin

Fibronectin is synthesized by virtually all connective tissue cells and is a major component of serum. There are a large number of different mRNA splice variants such that the number of potential forms is quite high. Consequently, bone matrix could contain fibronectin that originates from exogenous as well as endogenous sources (Pankov and Yamada, 2002). The precise form that is present in cells of the osteoblastic lineage is unknown. Fibronectin is produced during early stages of bone formation and has been found to be highly upregulated in the osteoblastic cell layer. Interestingly, bone cell attachment to fibronectin in vitro takes place in an RGD-independent fashion (Grzesik and Robey, 1994). However, this correlates well with the expression of the fibronectin receptor α4β1, which binds to a sequence other than RGD in the fibronectin molecule and is also expressed by some osteoblastic cells. Cell−matrix interactions mediated by fibronectin receptor−α4β1 binding may play a role in the maturation sequence of cells in the osteoblastic lineage.

In 2017, Lee et al. showed that mutations in fibronectin cause a subtype of spondylometaphyseal dysplasia (SMD) with "corner fractures" at metaphyses. SMDs are often characterized by growth plate abnormalities, short stature, and vertebral problems. Comparisons of the exomes of three individuals with SMD with corner fractures yielded fibronectin mutations in highly conserved residues. The functional consequences of these mutations were examined by expressing the three missense variants into a recombinant secreted N-terminal 70-kDa fragment and into full-length fibronectin. While wild-type forms were secreted into the culture medium as expected, all mutant proteins were either not secreted or secreted only at dramatically lower amounts (Lee et al., 2017). Thus, SMD with corner fractures is caused by defective fibronectin secretion and reinforces the importance of fibronectin in cartilage and bone, two tissues whose structure is altered with functional consequences.

Irisin (FRCP2, fibronectin type III domain−containing protein 5)

Irisin is encoded by a distinct gene that generates several different transcripts produced by alternative splicing. Fibronectin type III domain−containing protein 5 (FNDC5)/irisin, a novel secreted energy-regulating hormone, has been associated with bone lipid and carbohydrate metabolism. Expressed at high levels by muscle, particularly when exercised, irisin has been implicated in muscle−bone cross-talk signalling reactions. Several specific examples illustrate this point.

For one, the use of models of mechanical unloading (hindlimb unloading and sciatic neurectomy) reduce both tibial trabecular bone mineral and surrounding muscle volume. Interestingly, *irisin* mRNA in soleus muscle correlated positively with bone BMD in respective controls and in unloaded mice (Kawao et al., 2018). Since irisin also negatively correlated with RANKL mRNA levels in bone of control and hindlimb-unloaded mice, these authors suggested that irisin is directly implicated in the suppression of osteoclasts and osteoclastic bone resorption, particularly in situations where mechanical stress regulates muscle and bone structure. Using similar mechanical-unloading models in mice, Colaianni et al. showed also that irisin was able not only to prevent but also to restore bone and muscle loss (Colaianni et al., 2017). Treatment maintained muscle volume as well as fiber cross-sectional area and myosin type II composition. These data followed up on earlier pioneering work showing that irisin had positive effects on anabolic bone formation in vivo in mice (Colaianni et al., 2015). Finally, intraperitoneal injection of irisin has also been shown to increase trabecular and cortical bone volume in mice, a result mimicked by intraperitoneal FNDC5.

Vitronectin

This serum protein, first identified as S-protein because of its cell-spreading activity, is found at low levels in mineralized matrix (Grzesik and Robey, 1994). Its cell surface receptor, αVβ3, is distributed broadly throughout bone tissue. In addition to cell attachment activity, it also binds to and affects the activity of plasminogen activator inhibitor (Schvartz et al., 1999). Osteoclasts utilize vitronectin as a cell adhesion substrate when bound to bone.

Fibrillins

In addition to their RGD sequences, fibrillin-1 and fibrillin-2 are glycoproteins that also contain multiple EGF-like repeats. Although generally minor constituents of skeletal tissues in terms of mass, fibrillins are major components of microfibrils, and mutations in these genes lead to Marfan's syndrome and congenital contractural arachnodactyly, which exhibit abnormalities in bone growth (reviewed in Ramirez and Dietz, 2007). Fibrillin-1 and fibrillin-2 associate with LTBP (latent TGFβ-binding protein) in microfibrils and regulate TGFβ bioactivity (Chaudhry et al., 2007). Deletion of fibrillin-1 with Prx1 Cre leads to abnormal mesenchymal stem cell differentiation with resultant bone loss (Smaldone et al., 2016). Work also demonstrates that fibrillin-2 exhibits a special capacity to regulate BMP-7 activity during limb patterning (Nistala et al., 2010). In addition, both fibrillin-1 and fibrillin-2 regulate commitment and differentiation of bone marrow skeletal stem cells (Smaldone et al., 2016). Taken together, the data show that fibrillins function as critical components of the extracellular matrix where, in combination with activin growth and differentiation factors, they regulate the differentiation of skeletal stem cells directly and hemopoietic stem cells indirectly.

Bone acidic glycoprotein-75

The identity of bone acidic glyprotein-75 (BAG-75) relies upon its detection and recognition with three different antibodies, e.g., a monoclonal antibody (HTP IV-#1), a rabbit polyclonal antibody (#704), and an anti-peptide #3−13 antibody against its N-terminal sequence, and its unique N-terminal sequence as well as accumulated internal peptide sequences totaling about 100 residues (Gorski and Shimizu, 1988; Gorski et al., 1990; Wang et al., 2009) (J.P. Gorski, personal communication). Functionally, direct comparisons with OPN and BSP revealed that BAG-75 bound more calcium ions per mole (139 atoms/molecule) than either of the other bone glycoproteins (Chen et al., 1992). When added to osteoclast cultures, BAG-75 was also able to block resorption, presumably by blocking or interfering with the adhesion of osteoclasts with mineralized bone matrix (Sato et al., 1992). Finally, an intriguing property of BAG-75 remains its capacity to identify matrix sites within developing primary bone or in osteoblastic cultures that will be subsequently mineralized (Gorski et al., 2004; Midura et al., 2004). In this sense, it remains an unusual biomarker of sites that are about to become calcified.

Small integrin-binding ligands with N-linked glycosylation

Several bone matrix proteins are characterized not only by the inclusion of RGD within their sequences, but also by the presence of relatively large amounts of sialic acid. Interestingly, they are clustered at a distinct gene locus, 4q21−q23 and appear to have arisen by gene duplication. For this reason, the family has been termed SIBLINGs (small integrin-binding ligands with N-linked glycosylation) (Fisher and Fedarko, 2003) (Table 15.3). The family includes OPN and BSP, the two best characterized proteins of the family; along with DMP1, dentin sialoprotein, and dentin phosphoprotein, which are coded for by the same gene, now termed dentin sialophosphoprotein; matrix extracellular phosphoglycoprotein (MEPE); and the more distantly related protein, enamelin. Although the SIBLINGs were initially thought to be specific for mineralized tissues, it is now apparent that many of them are expressed in metabolically active epithelial cells (Ogbureke and Fisher, 2005). Interestingly, three of the family members bind to and activate specific MMPs (BSP−MMP-2, OPN−MMP-3, and DMP1−MMP-9) (Fedarko et al., 2004).

Osteopontin (spp, BSP-I)

This sialoprotein was first identified in bone matrix extracts, but it was also identified as the primary protein induced by cellular transformation. In bone, it is produced at late stages of osteoblastic maturation corresponding to stages of matrix formation just prior to mineralization. In vitro, it mediates the attachment of many cell types, including osteoclasts. In osteoclasts, it has also been reported to induce intracellular signaling pathways as well. In addition to the RGD sequence, it also contains stretches of polyaspartic acid and it has a fairly high capacity for binding Ca^{2+}ions; however, it does not appear to nucleate hydroxyapatite formation in several different assays. The OPN-deficient mouse develops normally, but

has increased mineral content, although the crystals are smaller than normal. The role of OPN in skeletal homeostasis is covered elsewhere in this volume, and there are numerous reviews available for its role in cancer and immune function (for example, Scatena et al., 2007).

Bone sialoprotein (BSP-II)

The other major sialoprotein is BSP, composed of 50% carbohydrate (12% is sialic acid) and stretches of polyglutamic acid (as opposed to polyaspartic acid in OPN). The RGD sequence is located at the carboxy terminus of the molecule, whereas it is located centrally in OPN. The sequence is also characterized by multiple tyrosine sulfation consensus sequences found throughout the molecule, in particular, in regions flanking the RGD (Fisher et al., 1990). Sulfated BSP has been isolated in a number of animal species, but the levels appear to be variable.

BSP exhibits a more limited pattern of expression than OPN. In general, its expression is tightly associated with mineralization phenomena (although there are exceptions). In the skeleton, it is found at low levels in chondrocytes, in hypertrophic cartilage, in a subset of osteoblasts at the onset of matrix mineralization, and in osteoclasts (Bianco et al., 1991). Consequently, BSP expression marks a late stage of osteoblastic differentiation and an early stage of matrix mineralization. Outside of the skeleton, BSP is found in trophoblasts in placental membranes, which in late stages of gestation fuse and form mineralized foci.

BSP may be multifunctional in osteoblastic metabolism. It is very clear that it plays a role in matrix mineralization as supported by the timing of its appearance in relationship to the appearance of mineral and its Ca^{2+}-binding properties. BSP has a high capacity for binding calcium ions. The polyglutamyl stretches were thought to be solely responsible for this property; however, studies using recombinant peptides suggest that although the polyglutamyl stretches are required, they are not the sole determinants (Stubbs et al., 1997). Unlike OPN, BSP does nucleate hydroxyapatite deposition in a variety of in vitro assays.

It is also clear from in vitro assays that BSP is capable of mediating cell attachment, most likely through interaction with the somewhat ubiquitous $\alpha V\beta 3$ (vitronectin) receptor. Bone cells attach to the intact molecule in an RGD-dependent fashion. However, when BSP is fragmented, either endogenously by cells or using commercially available enzymes, the fragment most active in cell attachment does not contain the RGD sequence (Mintz et al., 1993). Studies indicate that the sequence upstream from the RGD mediates attachment (in an RGD-independent fashion) and suggest that the integrin-binding site is more extended than had been envisioned previously. Sequences flanking the RGD site are often tyrosine sulfated. However, it is not known how sulfation influences BSP activity, as in vitro, unsulfated BSP appears to be equivalent in its activity. Once again, it is not clear if currently available in vitro assays are sufficiently sophisticated to determine what influence post-translational modifications, such as sulfation, have on the biological activity. In addition to sulfation, conformation of the RGD site may also influence the activity of the protein. Although the RGD region in fibronectin is found in a looped-out region that is stabilized by disulfide bonding, there are no disulfide bonds in BSP. However, the flanking sequences most likely influence the conformation of the region. The cyclic conformations also appear to have a higher affinity for cell surface receptors than linear sequences (van der Pluijm et al., 1996).

BSP-knockout mice have been extensively studied by the Malaval laboratory (Bouleftour et al., 2016). Initial studies of the knockout mouse clearly implicate BSP in playing an important role in mineralization and cortical or primary bone formation, but not endochondral bone formation (Bouleftour et al., 2014). More recent studies have demonstrated that BSP can also influence hematopoiesis and vascularization (Granito et al., 2015). Interestingly, in the absence of BSP, OPN is upregulated and it is speculated that some aspects of the BSP-deficient phenotype may be secondary to upregulation of OPN (Granito et al., 2015; Bouleftour et al., 2016)

Dentin matrix protein 1

Although DMP1 was originally thought to be specific to dentin, it was subsequently found to be synthesized by osteoblasts as well (D'Souza et al., 1997). However, its function in bone metabolism is not known as of this writing. The DMP1-deficient mouse has craniofacial and growth plate abnormalities, along with rickets and osteomalacia owing to increased secretion of the phosphate-regulating hormone FGF23. The overproduction of FGF23 is hypothesized to be caused by abnormal osteocyte function (Feng et al., 2006). Mutations in *DMP1* have been identified in patients with dentinogenesis imperfecta (OMIM: 600980) and in forms of autosomal recessive hypophosphatemic rickets (OMIM: 241520). *DMP1* is well recognized as a gene highly expressed by early osteocytes.

Matrix extracellular phosphoglycoprotein

MEPE is expressed in bone and bone marrow, but also at high levels in the brain and low levels in the lung, kidney, and placenta. This protein is also highly expressed by tumors that induce osteomalacia, and it has been regarded as a potential phosphate-regulating hormone (Rowe et al., 2000). It is thought that the C-terminal portion of MEPE (ASARM), together

with PHEX, regulates mineralization and renal phosphate metabolism (Rowe, 2004). Conversely, animals deficient in MEPE have significantly increased bone mass owing to increased numbers of trabeculae and increased cortical thickness (Gowen et al., 2003).

γ-Carboxyglutamic acid-containing proteins

In bone matrix, there are three proteins that undergo γ-carboxylation via vitamin K-dependent enzymes: matrix γ-carboxyglutamic acid (Gla) protein (MGP) (Price et al., 1983) and osteocalcin (Gla protein) (Price et al., 1976), both of which are made by bone cells, and protein S (made primarily in the liver but also made by osteogenic cells) (Maillard et al., 1992) (Table 15.4). The presence of dicarboxylic glutamyl residues confers low-affinity calcium-binding properties to these proteins.

Matrix Gla protein

MGP is found in many connective tissues and is highly expressed in cartilage. It appears that the physiological role of MGP is to act as an inhibitor of mineral deposition. Similar to secreted proteins in other calcium-rich environments, e.g., casein, MGP possesses three highly conserved phosphorylation sequence motifs (Ser-X-Glu/Ser(P)) within its N-terminal region (Price et al., 1994). MGP-deficient mice develop calcification in extraskeletal sites such as in the aorta (Luo et al., 1997). Interestingly, the vascular calcification proceeds via transition of vascular smooth muscle cells into chondrocytes, which subsequently hypertrophy (El-Maadawy et al., 2003). In humans, mutations in *MGP* have also been associated with excessive cartilage calcification (Keutel syndrome, OMIM: 245150). And it has been reported that deficiency of MGP in mice closely mimics the phenotype of patients with Keutel syndrome (Marulanda et al., 2017). A 2017 meta-analysis of 23 different case−control studies now shows that there is a significant association between the *MGP* gene rs1800801 polymorphism and vascular calcification and atherosclerotic disease, particularly in the Caucasian subgroup (Sheng et al., 2017).

Functionally, MGP is an antagonist of BMPs and is highly expressed by vascular endothelial cells. However, another consequence of deletion of *MGP* in mice is the dysregulation of endothelial cell differentiation from mouse embryonic stem cells (Yao et al., 2016). These authors have subsequently shown that this effect may have broader downstream effects,

TABLE 15.4 Characteristics of γ-carboxyglutamic acid−containing proteins in bone matrix.

Molecule	Structural characteristics	Gene ontology biological processes
Matrix Gla protein	15 kDa, five Gla residues, one disulfide bridge, phosphoserine residues	Cartilage condensation; ossification; multicellular organism development; cell differentiation; regulation of bone mineralization; cartilage development
Osteocalcin	5 kDa, one disulfide bridge, Gla residues located in α-helical region	Skeletal system development; ossification; osteoblast differentiation; osteoblast development; signal peptide processing; ER-to-Golgi vesicle-mediated transport; cell adhesion; aging; cell aging; response to mechanical stimulus; response to gravity; response to inorganic substance; response to zinc ion; response to organic cyclic compound; response to activity; peptidylglutamic acid carboxylation; bone mineralization; regulation of bone mineralization; biomineral tissue development; response to nutrient levels; response to vitamin K; response to vitamin D; response to testosterone; response to hydroxyisoflavone; odontogenesis; response to drug; response to estrogen; regulation of bone resorption; response to ethanol; regulation of osteoclast differentiation; response to glucocorticoid; bone development; cellular response to vitamin D; cellular response to growth factor stimulus
Protein S	75 kDa	Platelet degranulation; signal peptide processing; ER-to-Golgi vesicle-mediated transport; blood coagulation; hemostasis; negative regulation of endopeptidase activity; peptidylglutamic acid carboxylation; negative regulation of blood coagulation; regulation of complement activation; fibrinolysis; leukocyte migration

ER, endoplasmic reticulum.
Gene ontologies listed are derived in large part from one of two on-line sources: www.informatics.jax.org/vocab/gene_ontology or www.genecards.org/search/keyword.

since dysregulated *MGP*-deficient endothelial cells were subsequently shown to stimulate epithelial cell precursors in the lung toward a hepatic rather than pulmonary phenotype via altered cross-talk signaling (Yao et al., 2016). Finally, MGP has been suggested to act as an inhibitor of BMPs. While not providing mechanistic details, the work of Malhotra et al. (2015) demonstrates that BMPs play a key role in the signal transduction pathway regulating medial vascular aortic calcification in MGP-deficient mice. Specifically, two separate BMP inhibitors lowered calcification by 80% and prolonged life span compared with vehicle controls (Malhotra et al., 2015).

Osteocalcin

Whereas MGP is broadly expressed, osteocalcin is somewhat bone specific, although mRNA has been found in platelets and megakaryocytes (Thiede et al., 1994). Osteocalcin-deficient mice were first reported to have increased BMD compared with normal controls (Ducy et al., 1996). In human bone, it is concentrated in osteocytes, and its release may be a signal in the bone-turnover cascade (Kasai et al., 1994). Osteocalcin measurements in serum have proved valuable as a marker of bone turnover in metabolic disease states.

Importantly, it has been demonstrated that osteocalcin also acts as a bone-derived hormone that influences energy metabolism by muscle and fat cells, and, that regulates male reproductive function (Lee et al., 2007; Karsenty and Mera, 2017). This topic is considered in detail in Chapter 86. By specifically binding to the G-coupled receptor Gprc6a (Pi and Quarles, 2012), decarboxylated osteocalcin increases insulin secretion by pancreatic cells, promotes glucose homeostasis by muscle and fat tissues, and stimulates testosterone synthesis by Leydig cells of the testis (Ferron et al., 2012; Karsenty and Oury, 2014; Oury et al., 2015). These data provide clear evidence that bone can act as an endocrine organ, regulating systemic functions via receptor-mediated signaling pathways in metabolically active tissues such as bone, muscle, pancreas, fat, and testis. It is expected that new discoveries will help further define the detailed regulatory loops and feedback networks that are likely to exist among and between these skeletal tissues.

Serum proteins

The presence of hydroxyapatite in the bone matrix accounts for the adsorption of a large number of proteins that are synthesized elsewhere and brought in contact with bone via the circulation (Delmas et al., 1984). Most of these proteins are synthesized in the liver and hematopoietic tissue and represent classes of immunoglobulins, carrier proteins, cytokines, chemokines, and growth factors. Interestingly, some of these proteins are also synthesized endogenously by cells of the osteoblastic lineage. It is not known if the origin of a particular factor (and hence proteins with potentially different post-translational modifications) affects its function.

Although serum proteins are not synthesized locally, they may have a significant impact on bone metabolism (Table 15.5). Albumin, which is synthesized by the liver, is concentrated in bone severalfold above levels found in the

TABLE 15.5 Characteristics of serum proteins found in bone matrix.

Molecule	Structural characteristics	Gene ontology biological processes
Albumin	69 kDa, nonglycosylated, one sulfhydryl, 17 disulfide bonds, high-affinity hydrophobic binding pocket	Retina homeostasis; platelet degranulation; receptor-mediated endocytosis; cellular response to starvation; bile acid and bile salt transport; hemolysis by symbiont of host erythrocytes; high-density lipoprotein particle remodeling; negative regulation of apoptotic process; negative regulation of programmed cell death; sodium-independent organic anion transport; posttranslational protein modification; cellular protein metabolic process; maintenance of mitochondrion location; cellular oxidant detoxification
α_2-HS-glycoprotein	Precursor protein of fetuin, cleaved to form A and B chains that are disulfide linked, Ala-Ala and Pro-Pro repeat sequences, N-linked oligosaccharides, cystatin-like domains	Skeletal system development; ossification; platelet degranulation; pinocytosis; acute-phase response; negative regulation of endopeptidase activity; regulation of bone mineralization; negative regulation of bone mineralization; negative regulation of phosphorylation; neutrophil degranulation; post-translational protein modification; cellular protein metabolic process; negative regulation of insulin receptor signaling pathway; regulation of inflammatory response; positive regulation of phagocytosis; negative regulation of biomineral tissue development

Gene ontologies listed are derived in large part from one of two on-line sources: www.informatics.jax.org/vocab/gene_ontology or www.genecards.org/search/keyword.

circulation. It is not known whether it plays a structural role in bone matrix formation but it does have an influence on hydroxyapatite formation. In in vitro assays, albumin inhibits hydroxyapatite growth by binding to several faces of the seed crystal (Garnett and Dieppe, 1990). In addition to this inhibitory activity, it also inhibits crystal aggregation.

Another serum protein, α_2-HS-glycoprotein, is even more highly concentrated in bone than albumin (up to 100 times more concentrated). It is known that α_2-HS-glycoprotein is the human analog of bovine fetuin (Ohnishi et al., 1993). This protein is synthesized as a precursor that contains a disulfide bond linking the amino- and carboxy-terminal regions. Subsequently, the midregion is cleaved and removed from the molecule, yielding the A and B peptides (much in the same way that insulin is processed). In rat, the midregion is not removed and the molecule consists of a single polypeptide. This protein also contains cystatin-like domains (disulfide-linked loop regions) and another member of this family has been identified in bone matrix extracts.

α_2-HS-glycoprotein has many proposed functions that may also be operative in bone cell metabolism. It is a chemoattractant for monocytic cells, and consequently, it may influence the influx of osteoclastic precursor cells into a particular area (Nakamura et al., 1999). Furthermore, it is a TGFβ type II receptor mimic and cytokine antagonist (Demetriou et al., 1996). Fetuin, the bovine homolog, has been found to be a major growth-promoting factor in serum, and results in vitro suggest that fetuin, along with TGFβ, inhibits osteogenesis (Binkert et al., 1999). Interestingly, deletion of the fetuin gene in mice leads to widespread ectopic calcification throughout the body (Jahnen-Dechent et al., 1997). Consequently, this protein may play a very important role in bone cell metabolism irrespective of whether or not it is synthesized locally.

Other proteins

In addition to the proteins already described, there are representatives of many other classes of proteins in the bone matrix, including proteolipids, enzymes and their inhibitors (including metalloproteinases and tissue inhibitors of metalloproteinase, plasminogen activator and plasminogen activator inhibitor, matrix phosphoprotein kinases, and lysosomal enzymes), morphogenetic proteins, and growth factors (Zu et al., 2007). Although their influence on bone cell metabolism is highly significant and they may cause important alterations of the major structural elements of bone matrix, they are not necessarily part of the bone matrix (with the possible exception of proteolipids). Important aspects of many of these classes of proteins are reviewed elsewhere.

Control of gene expression

Even a cursory analysis of noncollagenous protein expression reveals a complex regulatory pathway of interacting environmental, hormonal, and nuclear factors by which cells of the osteoblastic lineage secrete these factors in a temporal and distribution-sensitive manner to produce biomechanically functional mineralized bone (Stein et al., 1996; Wu et al., 2014).

Bone matrix glycoproteins and ectopic calcifications

The development of sensitive radiographic techniques, in addition to histological observations, has led to the description of ectopic calcifications in many different pathological disorders. Although dystrophic mineralization has long been noted, it was not thought that bone matrix proteins played a role in generating this type of mineralization. Dystrophic mineralization (such as in traumatic muscle injury) is brought about by cell death (perhaps in the form of apoptosis) and not by the physiological pathways mediated by collagen or matrix vesicles. However, bone matrix proteins have been identified in mineralized foci in several different pathological states. Osteonectin, OPN, and BSP have been found in mineralized foci in primary breast cancer (Bellahcene and Castronovo, 1997). BSP has also been found in other cancers, such as prostate, thyroid, and lung (Bellahcene et al., 1997; Bellahcene et al., 1998; Waltregny et al., 1998). Although it is possible that, in some cases, the area mineralizes dystrophically and bone matrix proteins are adsorbed from the circulation because of their affinity to hydroxyapatite, mRNAs for the bone matrix proteins are expressed and it appears that the proteins are actually synthesized by resident cells that have been triggered by factors that have yet to be identified.

Given the fact that bone matrix proteins are expressed by a number of different cancers, the obvious question is why. The processes by which cancer cells invade the surrounding normal tissue, gain entry into the circulation, and metastasize to other tissues are complex, but members of the SIBLING family have emerged as active players in tumorigenesis and metastasis. SIBLINGs and their proteolytic fragments, along with their partner MMPs (for BSP, OPN, and DMP1, at least), may modulate a tumor cell's adhesion via specific integrins, matrix degradation, and migration (reviewed in Bellahcene et al., 2008).

Another example of ectopic calcification is seen in atherosclerosis, again, associated with the production of bone matrix proteins (Bini et al., 1999). Unlike dystrophic calcification, vascular calcification appears to form in a regulated fashion similar to what is seen in bone formation in the skeleton. As mentioned earlier in relationship to the *MGP*-deficient mouse, it appears that vascular smooth muscle cells are emerging as the culprit. Factors that stimulate the expression of bone matrix proteins are not yet known but may include changes in cell−cell interactions, serum lipid composition, and phosphate concentrations, and apoptosis of vascular smooth muscle cells may initiate the process (Johnson et al., 2007). It may also be that there exists a population of stem cells that are normally quiescent, but then are induced to become osteogenic again, by factors that are not known. The aorta has its own vasculature, which may harbor these stem cells. Supporting this hypothesis, pericytes from the retinal vasculature have been shown to undergo bone formation in vitro and in vivo (Canfield et al., 2000).

Summary

Bone matrix proteoglycans and glycoproteins are proportionally the most abundant constituents of the noncollagenous proteins in bone matrix. Proteoglycans with protein cores composed of the LRR sequences (decorin, biglycan, fibromodulin, and osteoadherin) are the predominant form found in mineralized matrix, although hyaluronan-binding forms (in particular, versican) are present during early stages of osteogenesis. They participate in matrix organization and in regulating growth factor activity. Glycoproteins such as alkaline phosphatase, osteonectin, RGD-containing proteins (osteoadherin, TSP, fibronectin, vitronectin, OPN, and BSP), irisin, fibrillin, and tetranectin are produced at different stages of osteoblastic maturation. They exhibit a broad array of functions ranging from control of cell proliferation to cell−matrix interactions, mediation of hydroxyapatite deposition, and bone−muscle/adipocyte cross-talk signaling. Finally, sclerostin and DMP1 are preferentially expressed by osteocytic cells in bone where they regulate osteogenesis by feeding back to osteoblastic cells and (together with PHEX) regulate phosphate metabolism via FGF23 production by osteocytes, respectively. The ectopic expression of bone cell secreted noncollagenous proteins may also play a significant role in, normal systemic regulation of glucose and energy metabolism, and of male reproductive function, as well as in pathological processes such as bone metastasis and in atherosclerosis.

References

Adams, J.C., 2004. Functions of the conserved thrombospondin carboxy-terminal cassette in cell-extracellular matrix interactions and signaling. Int. J. Biochem. Cell Biol. 36 (6), 1102−1114.

Ameye, L., Young, M.F., 2002. Mice deficient in small leucine-rich proteoglycans: novel in vivo models for osteoporosis, osteoarthritis, Ehlers-Danlos syndrome, muscular dystrophy, and corneal diseases. Glycobiology 12 (9), 107R−116R.

Arikawa-Hirasawa, E., Watanabe, H., Takami, H., Hassell, J.R., Yamada, Y., 1999. Perlecan is essential for cartilage and cephalic development. Nat. Genet. 23 (3), 354−358.

Barallobre-Barreiro, J., Gupta, S.K., Zoccarato, A., Kitazume-Taneike, R., Fava, M., Yin, X., Werner, T., Hirt, M.N., Zampetaki, A., Viviano, A., Chong, M., Bern, M., Kourliouros, A., Domenech, N., Willeit, P., Shah, A.M., Jahangiri, M., Schaefer, L., Fischer, J.W., Iozzo, R.V., Viner, R., Thum, T., Heineke, J., Kichler, A., Otsu, K., Mayr, M., 2016. Glycoproteomics reveals decorin peptides with anti-myostatin activity in human atrial fibrillation. Circulation 134 (11), 817−832.

Bassuk, J.A., Birkebak, T., Rothmier, J.D., Clark, J.M., Bradshaw, A., Muchowski, P.J., Howe, C.C., Clark, J.I., Sage, E.H., 1999. Disruption of the Sparc locus in mice alters the differentiation of lenticular epithelial cells and leads to cataract formation. Exp. Eye Res. 68 (3), 321−331.

Bellahcene, A., Albert, V., Pollina, L., Basolo, F., Fisher, L.W., Castronovo, V., 1998. Ectopic expression of bone sialoprotein in human thyroid cancer. Thyroid 8 (8), 637−641.

Bellahcene, A., Castronovo, V., 1997. Expression of bone matrix proteins in human breast cancer: potential roles in microcalcification formation and in the genesis of bone metastases. Bull. Cancer 84 (1), 17−24.

Bellahcene, A., Maloujahmoum, N., Fisher, L.W., Pastorino, H., Tagliabue, E., Menard, S., Castronovo, V., 1997. Expression of bone sialoprotein in human lung cancer. Calcif. Tissue Int. 61 (3), 183−188.

Bhattacharya, S., Bunick, C.G., Chazin, W.J., 2004. Target selectivity in EF-hand calcium binding proteins. Biochim. Biophys. Acta 1742 (1−3), 69−79.

Bhattacharya, S., Pal, S., Chattopadhyay, N., 2018. Targeted inhibition of sclerostin for post-menopausal osteoporosis therapy: a critical assessment of the mechanism of action. Eur. J. Pharmacol. 826, 39−47.

Bianco, P., Fisher, L.W., Young, M.F., Termine, J.D., Robey, P.G., 1990. Expression and localization of the two small proteoglycans biglycan and decorin in developing human skeletal and non-skeletal tissues. J. Histochem. Cytochem. 38 (11), 1549−1563.

Bianco, P., Fisher, L.W., Young, M.F., Termine, J.D., Robey, P.G., 1991. Expression of bone sialoprotein (BSP) in developing human tissues. Calcif. Tissue Int. 49 (6), 421−426.

Bini, A., Mann, K.G., Kudryk, B.J., Schoen, F.J., 1999. Noncollagenous bone matrix proteins, calcification, and thrombosis in carotid artery atherosclerosis. Arterioscler. Thromb. Vasc. Biol. 19 (8), 1852−1861.

Binkert, C., Demetriou, M., Sukhu, B., Szweras, M., Tenenbaum, H.C., Dennis, J.W., 1999. Regulation of osteogenesis by fetuin. J. Biol. Chem. 274 (40), 28514–28520.

Bonewald, L.F., 2006. Mechanosensation and transduction in osteocytes. BoneKEy Osteovision 3 (10), 7–15.

Bonnet, N., Brun, J., Rousseau, J.C., Duong, L.T., Ferrari, S.L., 2017. Cathepsin K controls cortical bone formation by degrading periostin. J. Bone Miner. Res. 32 (7), 1432–1441.

Bouleftour, W., Boudiffa, M., Wade-Gueye, N.M., Bouet, G., Cardelli, M., Laroche, N., Vanden-Bossche, A., Thomas, M., Bonnelye, E., Aubin, J.E., Vico, L., Lafage-Proust, M.H., Malaval, L., 2014. Skeletal development of mice lacking bone sialoprotein (BSP)–impairment of long bone growth and progressive establishment of high trabecular bone mass. PLoS One 9 (5), e95144.

Bouleftour, W., Juignet, L., Bouet, G., Granito, R.N., Vanden-Bossche, A., Laroche, N., Aubin, J.E., Lafage-Proust, M.H., Vico, L., Malaval, L., 2016. The role of the SIBLING, Bone Sialoprotein in skeletal biology - contribution of mouse experimental genetics. Matrix Biol. 52–54, 60–77.

Brunkow, M.E., Gardner, J.C., Van Ness, J., Paeper, B.W., Kovacevich, B.R., Proll, S., Skonier, J.E., Zhao, L., Sabo, P.J., Fu, Y., Alisch, R.S., Gillett, L., Colbert, T., Tacconi, P., Galas, D., Hamersma, H., Beighton, P., Mulligan, J., 2001. Bone dysplasia sclerosteosis results from loss of the SOST gene product, a novel cystine knot-containing protein. Am. J. Hum. Genet. 68 (3), 577–589.

Canfield, A.E., Doherty, M.J., Kelly, V., Newman, B., Farrington, C., Grant, M.E., Boot-Handford, R.P., 2000. Matrix Gla protein is differentially expressed during the deposition of a calcified matrix by vascular pericytes. FEBS Lett. 487 (2), 267–271.

Carron, J.A., Bowler, W.B., Wagstaff, S.C., Gallagher, J.A., 1999. Expression of members of the thrombospondin family by human skeletal tissues and cultured cells. Biochem. Biophys. Res. Commun. 263 (2), 389–391.

Chakravarti, S., Paul, J., Roberts, L., Chervoneva, I., Oldberg, A., Birk, D.E., 2003. Ocular and scleral alterations in gene-targeted lumican-fibromodulin double-null mice. Investig. Ophthalmol. Vis. Sci. 44 (6), 2422–2432.

Chaudhry, S.S., Cain, S.A., Morgan, A., Dallas, S.L., Shuttleworth, C.A., Kielty, C.M., 2007. Fibrillin-1 regulates the bioavailability of TGFbeta1. J. Cell Biol. 176 (3), 355–367.

Chen, Y., Bal, B.S., Gorski, J.P., 1992. Calcium and collagen binding properties of osteopontin, bone sialoprotein, and bone acidic glycoprotein-75 from bone. J. Biol. Chem. 267 (34), 24871–24878.

Choocheep, K., Hatano, S., Takagi, H., Watanabe, H., Kimata, K., Kongtawelert, P., Watanabe, H., 2010. Versican facilitates chondrocyte differentiation and regulates joint morphogenesis. J. Biol. Chem. 285 (27), 21114–21125.

Colaianni, G., Cuscito, C., Mongelli, T., Pignataro, P., Buccoliero, C., Liu, P., Lu, P., Sartini, L., Di Comite, M., Mori, G., Di Benedetto, A., Brunetti, G., Yuen, T., Sun, L., Reseland, J.E., Colucci, S., New, M.I., Zaidi, M., Cinti, S., Grano, M., 2015. The myokine irisin increases cortical bone mass. Proc. Natl. Acad. Sci. U. S. A. 112 (39), 12157–12162.

Colaianni, G., Mongelli, T., Cuscito, C., Pignataro, P., Lippo, L., Spiro, G., Notarnicola, A., Severi, I., Passeri, G., Mori, G., Brunetti, G., Moretti, B., Tarantino, U., Colucci, S.C., Reseland, J.E., Vettor, R., Cinti, S., Grano, M., 2017. Irisin prevents and restores bone loss and muscle atrophy in hind-limb suspended mice. Sci. Rep. 7 (1), 2811.

Corsi, A., Xu, T., Chen, X.D., Boyde, A., Liang, J., Mankani, M., Sommer, B., Iozzo, R.V., Eichstetter, I., Robey, P.G., Bianco, P., Young, M.F., 2002. Phenotypic effects of biglycan deficiency are linked to collagen fibril abnormalities, are synergized by decorin deficiency, and mimic Ehlers-Danlos-like changes in bone and other connective tissues. J. Bone Miner. Res. 17 (7), 1180–1189.

D'Souza, R.N., Cavender, A., Sunavala, G., Alvarez, J., Ohshima, T., Kulkarni, A.B., MacDougall, M., 1997. Gene expression patterns of murine dentin matrix protein 1 (Dmp1) and dentin sialophosphoprotein (DSPP) suggest distinct developmental functions in vivo. J. Bone Miner. Res. 12 (12), 2040–2049.

Danielson, K.G., Baribault, H., Holmes, D.F., Graham, H., Kadler, K.E., Iozzo, R.V., 1997. Targeted disruption of decorin leads to abnormal collagen fibril morphology and skin fragility. J. Cell Biol. 136 (3), 729–743.

Delmas, P.D., Tracy, R.P., Riggs, B.L., Mann, K.G., 1984. Identification of the noncollagenous proteins of bovine bone by two-dimensional gel electrophoresis. Calcif. Tissue Int. 36 (3), 308–316.

Demetriou, M., Binkert, C., Sukhu, B., Tenenbaum, H.C., Dennis, J.W., 1996. Fetuin/alpha2-HS glycoprotein is a transforming growth factor-beta type II receptor mimic and cytokine antagonist. J. Biol. Chem. 271 (22), 12755–12761.

Duchamp de Lageneste, O., Julien, A., Abou-Khalil, R., Frangi, G., Carvalho, C., Cagnard, N., Cordier, C., Conway, S.J., Colnot, C., 2018. Periosteum contains skeletal stem cells with high bone regenerative potential controlled by Periostin. Nat. Commun. 9 (1), 773.

Ducy, P., Desbois, C., Boyce, B., Pinero, G., Story, B., Dunstan, C., Smith, E., Bonadio, J., Goldstein, S., Gundberg, C., Bradley, A., Karsenty, G., 1996. Increased bone formation in osteocalcin-deficient mice. Nature 382 (6590), 448–452.

El-Maadawy, S., Kaartinen, M.T., Schinke, T., Murshed, M., Karsenty, G., McKee, M.D., 2003. Cartilage formation and calcification in arteries of mice lacking matrix Gla protein. Connect. Tissue Res. 44 (Suppl. 1), 272–278.

El Shafey, N., Guesnon, M., Simon, F., Deprez, E., Cosette, J., Stockholm, D., Scherman, D., Bigey, P., Kichler, A., 2016. Inhibition of the myostatin/Smad signaling pathway by short decorin-derived peptides. Exp. Cell Res. 341 (2), 187–195.

Falconi, D., Aubin, J.E., 2007. LIF inhibits osteoblast differentiation at least in part by regulation of HAS2 and its product hyaluronan. J. Bone Miner. Res. 22 (8), 1289–1300.

Fedarko, N.S., Jain, A., Karadag, A., Fisher, L.W., 2004. Three small integrin binding ligand N-linked glycoproteins (SIBLINGs) bind and activate specific matrix metalloproteinases. FASEB J. 18 (6), 734–736.

Fedarko, N.S., Vetter, U.K., Weinstein, S., Robey, P.G., 1992. Age-related changes in hyaluronan, proteoglycan, collagen, and osteonectin synthesis by human bone cells. J. Cell. Physiol. 151 (2), 215–227.

Feng, J.Q., Ward, L.M., Liu, S., Lu, Y., Xie, Y., Yuan, B., Yu, X., Rauch, F., Davis, S.I., Zhang, S., Rios, H., Drezner, M.K., Quarles, L.D., Bonewald, L.F., White, K.E., 2006. Loss of DMP1 causes rickets and osteomalacia and identifies a role for osteocytes in mineral metabolism. Nat. Genet. 38 (11), 1310–1315.

Ferron, M., McKee, M.D., Levine, R.L., Ducy, P., Karsenty, G., 2012. Intermittent injections of osteocalcin improve glucose metabolism and prevent type 2 diabetes in mice. Bone 50 (2), 568–575.

Fisher, L.W., Fedarko, N.S., 2003. Six genes expressed in bones and teeth encode the current members of the SIBLING family of proteins. Connect. Tissue Res. 44 (Suppl. 1), 33–40.

Fisher, L.W., McBride, O.W., Termine, J.D., Young, M.F., 1990. Human bone sialoprotein. Deduced protein sequence and chromosomal localization. J. Biol. Chem. 265 (4), 2347–2351.

Fisher, L.W., Termine, J.D., Young, M.F., 1989. Deduced protein sequence of bone small proteoglycan I (biglycan) shows homology with proteoglycan II (decorin) and several nonconnective tissue proteins in a variety of species. J. Biol. Chem. 264 (8), 4571–4576.

Garnett, J., Dieppe, P., 1990. The effects of serum and human albumin on calcium hydroxyapatite crystal growth. Biochem. J. 266, 863–868.

Gleghorn, L., Ramesar, R., Beighton, P., Wallis, G., 2005. A mutation in the variable repeat region of the aggrecan gene (AGC1) causes a form of spondyloepiphyseal dysplasia associated with severe, premature osteoarthritis. Am. J. Hum. Genet. 77 (3), 484–490.

Gong, Y., Slee, R.B., Fukai, N., Rawadi, G., Roman-Roman, S., Reginato, A.M., Wang, H., Cundy, T., Glorieux, F.H., Lev, D., Zacharin, M., Oexle, K., Marcelino, J., Suwairi, W., Heeger, S., Sabatakos, G., Apte, S., Adkins, W.N., Allgrove, J., Arslan-Kirchner, M., Batch, J.A., Beighton, P., Black, G.C., Boles, R.G., Boon, L.M., Borrone, C., Brunner, H.G., Carle, G.F., Dallapiccola, B., De Paepe, A., Floege, B., Halfhide, M.L., Hall, B., Hennekam, R.C., Hirose, T., Jans, A., Juppner, H., Kim, C.A., Keppler-Noreuil, K., Kohlschuetter, A., LaCombe, D., Lambert, M., Lemyre, E., Letteboer, T., Peltonen, L., Ramesar, R.S., Romanengo, M., Somer, H., Steichen-Gersdorf, E., Steinmann, B., Sullivan, B., Superti-Furga, A., Swoboda, W., van den Boogaard, M.J., Van Hul, W., Vikkula, M., Votruba, M., Zabel, B., Garcia, T., Baron, R., Olsen, B.R., Warman, M.L., 2001. LDL receptor-related protein 5 (LRP5) affects bone accrual and eye development. Cell 107 (4), 513–523.

Gorski, J.P., 2011. Biomineralization of bone: a fresh view of the roles of non-collagenous proteins. Front. Biosci. 17, 2598–2621.

Gorski, J.P., Griffin, D., Dudley, G., Stanford, C., Thomas, R., Huang, C., Lai, E., Karr, B., Solursh, M., 1990. Bone acidic glycoprotein-75 is a major synthetic product of osteoblastic cells and localized as 75- and/or 50-kDa forms in mineralized phases of bone and growth plate and in serum. J. Biol. Chem. 265 (25), 14956–14963.

Gorski, J.P., Shimizu, K., 1988. Isolation of new phosphorylated glycoprotein from mineralized phase of bone that exhibits limited homology to adhesive protein osteopontin. J. Biol. Chem. 263 (31), 15938–15945.

Gorski, J.P., Wang, A., Lovitch, D., Law, D., Powell, K., Midura, R.J., 2004. Extracellular bone acidic glycoprotein-75 defines condensed mesenchyme regions to be mineralized and localizes with bone sialoprotein during intramembranous bone formation. J. Biol. Chem. 279 (24), 25455–25463.

Gowen, L.C., Petersen, D.N., Mansolf, A.L., Qi, H., Stock, J.L., Tkalcevic, G.T., Simmons, H.A., Crawford, D.T., Chidsey-Frink, K.L., Ke, H.Z., McNeish, J.D., Brown, T.A., 2003. Targeted disruption of the osteoblast/osteocyte factor 45 gene (OF45) results in increased bone formation and bone mass. J. Biol. Chem. 278 (3), 1998–2007.

Granito, R.N., Bouleftour, W., Sabido, O., Lescale, C., Thomas, M., Aubin, J.E., Goodhardt, M., Vico, L., Malaval, L., 2015. Absence of bone sialoprotein (BSP) alters profoundly hematopoiesis and upregulates osteopontin. J. Cell. Physiol. 230 (6), 1342–1351.

Grzesik, W.J., Robey, P.G., 1994. Bone matrix RGD glycoproteins: immunolocalization and interaction with human primary osteoblastic bone cells in vitro. J. Bone Miner. Res. 9 (4), 487–496.

Hedbom, E., Heinegard, D., 1993. Binding of fibromodulin and decorin to separate sites on fibrillar collagens. J. Biol. Chem. 268 (36), 27307–27312.

Henry, S.P., Takanosu, M., Boyd, T.C., Mayne, P.M., Eberspaecher, H., Zhou, W., de Crombrugghe, B., Hook, M., Mayne, R., 2001. Expression pattern and gene characterization of asporin. a newly discovered member of the leucine-rich repeat protein family. J. Biol. Chem. 276 (15), 12212–12221.

Herring, G.M., Ashton, B.A., 1974. The isolation of soluble proteins, glycoproteins, and proteoglycans from bone. Prep. Biochem. 4 (2), 179–200.

Iba, K., Durkin, M.E., Johnsen, L., Hunziker, E., Damgaard-Pedersen, K., Zhang, H., Engvall, E., Albrechtsen, R., Wewer, U.M., 2001. Mice with a targeted deletion of the tetranectin gene exhibit a spinal deformity. Mol. Cell Biol. 21 (22), 7817–7825.

Jahnen-Dechent, W., Schinke, T., Trindl, A., Muller-Esterl, W., Sablitzky, F., Kaiser, S., Blessing, M., 1997. Cloning and targeted deletion of the mouse fetuin gene. J. Biol. Chem. 272 (50), 31496–31503.

Johnson, W.E., Li, C., Rabinovic, A., 2007. Adjusting batch effects in microarray expression data using empirical Bayes methods. Biostatistics 8 (1), 118–127.

Karsenty, G., Mera, P., 2017. Molecular bases of the crosstalk between bone and muscle. Bone 115, 43–49.

Karsenty, G., Oury, F., 2014. Regulation of male fertility by the bone-derived hormone osteocalcin. Mol. Cell. Endocrinol. 382 (1), 521–526.

Kasai, R., Bianco, P., Robey, P.G., Kahn, A.J., 1994. Production and characterization of an antibody against the human bone GLA protein (BGP/osteocalcin) propeptide and its use in immunocytochemistry of bone cells. Bone Miner. 25 (3), 167–182.

Kawao, N., Moritake, A., Tatsumi, K., Kaji, H., 2018. Roles of irisin in the linkage from muscle to bone during mechanical unloading in mice. Calcif. Tissue Int. 103 (1), 24–34.

Kram, V., Kilts, T.M., Bhattacharyya, N., Li, L., Young, M.F., 2017. Small leucine rich proteoglycans, a novel link to osteoclastogenesis. Sci. Rep. 7 (1), 12627.

Lamoureux, F., Baud'huin, M., Duplomb, L., Heymann, D., Redini, F., 2007. Proteoglycans: key partners in bone cell biology. Bioessays 29 (8), 758–771.

Lee, C.S., Fu, H., Baratang, N., Rousseau, J., Kumra, H., Sutton, V.R., Niceta, M., Ciolfi, A., Yamamoto, G., Bertola, D., Marcelis, C.L., Lugtenberg, D., Bartuli, A., Kim, C., Hoover-Fong, J., Sobreira, N., Pauli, R., Bacino, C., Krakow, D., Parboosingh, J., Yap, P., Kariminejad, A., McDonald, M.T., Aracena, M.I., Lausch, E., Unger, S., Superti-Furga, A., Lu, J.T., Baylor-Hopkins Center for Mendelian, G., Cohn, D.H., Tartaglia, M., Lee, B.H., Reinhardt, D.P., Campeau, P.M., 2017. Mutations in fibronectin cause a subtype of spondylometaphyseal dysplasia with "corner fractures". Am. J. Hum. Genet. 101 (5), 815–823.

Lee, N.K., Sowa, H., Hinoi, E., Ferron, M., Ahn, J.D., Confavreux, C., Dacquin, R., Mee, P.J., McKee, M.D., Jung, D.Y., Zhang, Z., Kim, J.K., Mauvais-Jarvis, F., Ducy, P., Karsenty, G., 2007. Endocrine regulation of energy metabolism by the skeleton. Cell 130 (3), 456–469.

Luo, G., Ducy, P., McKee, M.D., Pinero, G.J., Loyer, E., Behringer, R.R., Karsenty, G., 1997. Spontaneous calcification of arteries and cartilage in mice lacking matrix GLA protein. Nature 386 (6620), 78–81.

Maccarana, M., Svensson, R.B., Knutsson, A., Giannopoulos, A., Pelkonen, M., Weis, M., Eyre, D., Warman, M., Kalamajski, S., 2017. Asporin-deficient mice have tougher skin and altered skin glycosaminoglycan content and structure. PLoS One 12 (8), e0184028.

Maillard, C., Berruyer, M., Serre, C.M., Dechavanne, M., Delmas, P.D., 1992. Protein-S, a vitamin K-dependent protein, is a bone matrix component synthesized and secreted by osteoblasts. Endocrinology 130 (3), 1599–1604.

Malhotra, R., Burke, M.F., Martyn, T., Shakartzi, H.R., Thayer, T.E., O'Rourke, C., Li, P., Derwall, M., Spagnolli, E., Kolodziej, S.A., Hoeft, K., Mayeur, C., Jiramongkolchai, P., Kumar, R., Buys, E.S., Yu, P.B., Bloch, K.D., Bloch, D.B., 2015. Inhibition of bone morphogenetic protein signal transduction prevents the medial vascular calcification associated with matrix Gla protein deficiency. PLoS One 10 (1), e0117098.

Manley Jr., E., Perosky, J.E., Khoury, B.M., Reddy, A.B., Kozloff, K.M., Alford, A.I., 2015. Thrombospondin-2 deficiency in growing mice alters bone collagen ultrastructure and leads to a brittle bone phenotype. J. Appl. Physiol. (1985) 119 (8), 872–881.

Mansergh, F.C., Wells, T., Elford, C., Evans, S.L., Perry, M.J., Evans, M.J., Evans, B.A., 2007. Osteopenia in Sparc (osteonectin)-deficient mice: characterization of phenotypic determinants of femoral strength and changes in gene expression. Physiol. Genom. 32 (1), 64–73.

Mansouri, R., Jouan, Y., Hay, E., Blin-Wakkach, C., Frain, M., Ostertag, A., Le Henaff, C., Marty, C., Geoffroy, V., Marie, P.J., Cohen-Solal, M., Modrowski, D., 2017. Osteoblastic heparan sulfate glycosaminoglycans control bone remodeling by regulating Wnt signaling and the crosstalk between bone surface and marrow cells. Cell Death Dis. 8 (6), e2902.

Markmann, A., Hausser, H., Schonherr, E., Kresse, H., 2000. Influence of decorin expression on transforming growth factor-beta-mediated collagen gel retraction and biglycan induction. Matrix Biol. 19 (7), 631–636.

Marulanda, J., Eimar, H., McKee, M.D., Berkvens, M., Nelea, V., Roman, H., Borras, T., Tamimi, F., Ferron, M., Murshed, M., 2017. Matrix Gla protein deficiency impairs nasal septum growth, causing midface hypoplasia. J. Biol. Chem. 292 (27), 11400–11412.

Matsumoto, K., Li, Y., Jakuba, C., Sugiyama, Y., Sayo, T., Okuno, M., Dealy, C.N., Toole, B.P., Takeda, J., Yamaguchi, Y., Kosher, R.A., 2009. Conditional inactivation of Has2 reveals a crucial role for hyaluronan in skeletal growth, patterning, chondrocyte maturation and joint formation in the developing limb. Development 136 (16), 2825–2835.

Matsushima, N., Ohyanagi, T., Tanaka, T., Kretsinger, R.H., 2000. Super-motifs and evolution of tandem leucine-rich repeats within the small proteoglycans–biglycan, decorin, lumican, fibromodulin, PRELP, keratocan, osteoadherin, epiphycan, and osteoglycin. Proteins 38 (2), 210–225.

McDonald, M.M., Reagan, M.R., Youlten, S.E., Mohanty, S.T., Seckinger, A., Terry, R.L., Pettitt, J.A., Simic, M.K., Cheng, T.L., Morse, A., Le, L.M.T., Abi-Hanna, D., Kramer, I., Falank, C., Fairfield, H., Ghobrial, I.M., Baldock, P.A., Little, D.G., Kneissel, M., Vanderkerken, K., Bassett, J.H.D., Williams, G.R., Oyajobi, B.O., Hose, D., Phan, T.G., Croucher, P.I., 2017. Inhibiting the osteocyte-specific protein sclerostin increases bone mass and fracture resistance in multiple myeloma. Blood 129 (26), 3452–3464.

McEwan, P.A., Scott, P.G., Bishop, P.N., Bella, J., 2006. Structural correlations in the family of small leucine-rich repeat proteins and proteoglycans. J. Struct. Biol. 155 (2), 294–305.

Midura, R.J., Wang, A., Lovitch, D., Law, D., Powell, K., Gorski, J.P., 2004. Bone acidic glycoprotein-75 delineates the extracellular sites of future bone sialoprotein accumulation and apatite nucleation in osteoblastic cultures. J. Biol. Chem. 279 (24), 25464–25473.

Millan, J.L., Whyte, M.P., 2016. Alkaline phosphatase and hypophosphatasia. Calcif. Tissue Int. 98 (4), 398–416.

Mintz, K.P., Grzesik, W.J., Midura, R.J., Robey, P.G., Termine, J.D., Fisher, L.W., 1993. Purification and fragmentation of nondenatured bone sialoprotein: evidence for a cryptic, RGD-resistant cell attachment domain. J. Bone Miner. Res. 8 (8), 985–995.

Miura, T., Kishioka, Y., Wakamatsu, J., Hattori, A., Hennebry, A., Berry, C.J., Sharma, M., Kambadur, R., Nishimura, T., 2006. Decorin binds myostatin and modulates its activity to muscle cells. Biochem. Biophys. Res. Commun. 340 (2), 675–680.

Myren, M., Kirby, D.J., Noonan, M.L., Maeda, A., Owens, R.T., Ricard-Blum, S., Kram, V., Kilts, T.M., Young, M.F., 2016. Biglycan potentially regulates angiogenesis during fracture repair by altering expression and function of endostatin. Matrix Biol. 52–54, 141–150.

Nakamura, I., Pilkington, M.F., Lakkakorpi, P.T., Lipfert, L., Sims, S.M., Dixon, S.J., Rodan, G.A., Duong, L.T., 1999. Role of alpha(v)beta(3) integrin in osteoclast migration and formation of the sealing zone. J. Cell Sci. 112 (Pt 22), 3985–3993.

Nistala, H., Lee-Arteaga, S., Smaldone, S., Siciliano, G., Carta, L., Ono, R.N., Sengle, G., Arteaga-Solis, E., Levasseur, R., Ducy, P., Sakai, L.Y., Karsenty, G., Ramirez, F., 2010. Fibrillin-1 and -2 differentially modulate endogenous TGF-beta and BMP bioavailability during bone formation. J. Cell Biol. 190 (6), 1107–1121.

Ogbureke, K.U., Fisher, L.W., 2005. Renal expression of SIBLING proteins and their partner matrix metalloproteinases (MMPs). Kidney Int. 68 (1), 155–166.

Ohnishi, T., Nakamura, O., Ozawa, M., Arakaki, N., Muramatsu, T., Daikuhara, Y., 1993. Molecular cloning and sequence analysis of cDNA for a 59 kD bone sialoprotein of the rat: demonstration that it is a counterpart of human alpha 2-HS glycoprotein and bovine fetuin. J. Bone Miner. Res. 8 (3), 367–377.

Ominsky, M.S., Vlasseros, F., Jolette, J., Smith, S.Y., Stouch, B., Doellgast, G., Gong, J., Gao, Y., Cao, J., Graham, K., Tipton, B., Cai, J., Deshpande, R., Zhou, L., Hale, M.D., Lightwood, D.J., Henry, A.J., Popplewell, A.G., Moore, A.R., Robinson, M.K., Lacey, D.L., Simonet, W.S., Paszty, C., 2010. Two doses of sclerostin antibody in cynomolgus monkeys increases bone formation, bone mineral density, and bone strength. J. Bone Miner. Res. 25 (5), 948–959.

Oury, F., Ferron, M., Huizhen, W., Confavreux, C., Xu, L., Lacombe, J., Srinivas, P., Chamouni, A., Lugani, F., Lejeune, H., Kumar, T.R., Plotton, I., Karsenty, G., 2015. Osteocalcin regulates murine and human fertility through a pancreas-bone-testis axis. J. Clin. Investig. 125 (5), 2180.

Pacifici, M., 2017. The pathogenic roles of heparan sulfate deficiency in hereditary multiple exostoses. Matrix Biol. 71–72, 28–39.
Padhi, D., Jang, G., Stouch, B., Fang, L., Posvar, E., 2011. Single-dose, placebo-controlled, randomized study of AMG 785, a sclerostin monoclonal antibody. J. Bone Miner. Res. 26 (1), 19–26.
Pankov, R., Yamada, K.M., 2002. Fibronectin at a glance. J. Cell Sci. 115 (Pt 20), 3861–3863.
Pi, M., Quarles, L.D., 2012. Multiligand specificity and wide tissue expression of GPRC6A reveals new endocrine networks. Endocrinology 153 (5), 2062–2069.
Price, P.A., Otsuka, A.A., Poser, J.W., Kristaponis, J., Raman, N., 1976. Characterization of a gamma-carboxyglutamic acid-containing protein from bone. Proc. Natl. Acad. Sci. U. S. A. 73 (5), 1447–1451.
Price, P.A., Rice, J.S., Williamson, M.K., 1994. Conserved phosphorylation of serines in the Ser-X-Glu/Ser(P) sequences of the vitamin K-dependent matrix Gla protein from shark, lamb, rat, cow, and human. Protein Sci. 3 (5), 822–830.
Price, P.A., Urist, M.R., Otawara, Y., 1983. Matrix Gla protein, a new gamma-carboxyglutamic acid-containing protein which is associated with the organic matrix of bone. Biochem. Biophys. Res. Commun. 117 (3), 765–771.
Primorac, D., Johnson, C.V., Lawrence, J.B., McKinstry, M.B., Stover, M.L., Schanfield, M.S., Andjelinovic, S., Tadic, T., Rowe, D.W., 1999. Premature termination codon in the aggrecan gene of nanomelia and its influence on mRNA transport and stability. Croat. Med. J. 40 (4), 528–532.
Purcell, L., Gruia-Gray, J., Scanga, S., Ringuette, M., 1993. Developmental anomalies of Xenopus embryos following microinjection of SPARC antibodies. J. Exp. Zool. 265 (2), 153–164.
Ramirez, F., Dietz, H.C., 2007. Marfan syndrome: from molecular pathogenesis to clinical treatment. Curr. Opin. Genet. Dev. 17 (3), 252–258.
Reese, S.P., Underwood, C.J., Weiss, J.A., 2013. Effects of decorin proteoglycan on fibrillogenesis, ultrastructure, and mechanics of type I collagen gels. Matrix Biol. 32 (7–8), 414–423.
Rios, H., Koushik, S.V., Wang, H., Wang, J., Zhou, H.M., Lindsley, A., Rogers, R., Chen, Z., Maeda, M., Kruzynska-Frejtag, A., Feng, J.Q., Conway, S.J., 2005. Periostin null mice exhibit dwarfism, incisor enamel defects, and an early-onset periodontal disease-like phenotype. Mol. Cell Biol. 25 (24), 11131–11144.
Robey, P.G., Young, M.F., Fisher, L.W., McClain, T.D., 1989. Thrombospondin is an osteoblast-derived component of mineralized extracellular matrix. J. Cell Biol. 108 (2), 719–727.
Roodman, G.D., 2011. Osteoblast function in myeloma. Bone 48 (1), 135–140.
Rowe, P.S., 2004. The wrickkened pathways of FGF23, MEPE and PHEX. Crit. Rev. Oral Biol. Med. 15 (5), 264–281.
Rowe, P.S., de Zoysa, P.A., Dong, R., Wang, H.R., White, K.E., Econs, M.J., Oudet, C.L., 2000. MEPE, a new gene expressed in bone marrow and tumors causing osteomalacia. Genomics 67 (1), 54–68.
Sage, E.H., Bornstein, P., 1991. Extracellular proteins that modulate cell-matrix interactions. SPARC, tenascin, and thrombospondin. J. Biol. Chem. 266 (23), 14831–14834.
Sato, M., Grasser, W., Harm, S., Fullenkamp, C., Gorski, J.P., 1992. Bone acidic glycoprotein 75 inhibits resorption activity of isolated rat and chicken osteoclasts. FASEB J. 6 (11), 2966–2976.
Scatena, M., Liaw, L., Giachelli, C.M., 2007. Osteopontin: a multifunctional molecule regulating chronic inflammation and vascular disease. Arterioscler. Thromb. Vasc. Biol. 27 (11), 2302–2309.
Schvartz, I., Seger, D., Shaltiel, S., 1999. Vitronectin. Int. J. Biochem. Cell Biol. 31 (5), 539–544.
Scott, P.G., Dodd, C.M., Bergmann, E.M., Sheehan, J.K., Bishop, P.N., 2006. Crystal structure of the biglycan dimer and evidence that dimerization is essential for folding and stability of class I small leucine-rich repeat proteoglycans. J. Biol. Chem. 281 (19), 13324–13332.
Sheng, K., Zhang, P., Lin, W., Cheng, J., Li, J., Chen, J., 2017. Association of Matrix Gla protein gene (rs1800801, rs1800802, rs4236) polymorphism with vascular calcification and atherosclerotic disease: a meta-analysis. Sci. Rep. 7 (1), 8713.
Smaldone, S., Clayton, N.P., del Solar, M., Pascual, G., Cheng, S.H., Wentworth, B.M., Schaffler, M.B., Ramirez, F., 2016. Fibrillin-1 regulates skeletal stem cell differentiation by modulating TGFbeta activity within the marrow Niche. J. Bone Miner. Res. 31 (1), 86–97.
Sommarin, Y., Wendel, M., Shen, Z., Hellman, U., Heinegard, D., 1998. Osteoadherin, a cell-binding keratan sulfate proteoglycan in bone, belongs to the family of leucine-rich repeat proteins of the extracellular matrix. J. Biol. Chem. 273 (27), 16723–16729.
Stein, G.S., Lian, J.B., Stein, J.L., Van Wijnen, A.J., Montecino, M., 1996. Transcriptional control of osteoblast growth and differentiation. Physiol. Rev. 76 (2), 593–629.
Stubbs 3rd, J.T., Mintz, K.P., Eanes, E.D., Torchia, D.A., Fisher, L.W., 1997. Characterization of native and recombinant bone sialoprotein: delineation of the mineral-binding and cell adhesion domains and structural analysis of the RGD domain. J. Bone Miner. Res. 12 (8), 1210–1222.
Termine, J.D., Belcourt, A.B., Christner, P.J., Conn, K.M., Nylen, M.U., 1980. Properties of dissociatively extracted fetal tooth matrix proteins. I. Principal molecular species in developing bovine enamel. J. Biol. Chem. 255 (20), 9760–9768.
Termine, J.D., Belcourt, A.B., Conn, K.M., Kleinman, H.K., 1981a. Mineral and collagen-binding proteins of fetal calf bone. J. Biol. Chem. 256 (20), 10403–10408.
Termine, J.D., Kleinman, H.K., Whitson, S.W., Conn, K.M., McGarvey, M.L., Martin, G.R., 1981b. Osteonectin, a bone-specific protein linking mineral to collagen. Cell 26 (1 Pt 1), 99–105.
Thiede, M.A., Smock, S.L., Petersen, D.N., Grasser, W.A., Thompson, D.D., Nishimoto, S.K., 1994. Presence of messenger ribonucleic acid encoding osteocalcin, a marker of bone turnover, in bone marrow megakaryocytes and peripheral blood platelets. Endocrinology 135 (3), 929–937.
Ujita, M., Shinomura, T., Kimata, K., 1995. Molecular cloning of the mouse osteoglycin-encoding gene. Gene 158 (2), 237–240.
van der Pluijm, G., Vloedgraven, H.J., Ivanov, B., Robey, F.A., Grzesik, W.J., Robey, P.G., Papapoulos, S.E., Lowik, C.W., 1996. Bone sialoprotein peptides are potent inhibitors of breast cancer cell adhesion to bone. Cancer Res. 56 (8), 1948–1955.

Vanhoenacker, F.M., Balemans, W., Tan, G.J., Dikkers, F.G., De Schepper, A.M., Mathysen, D.G., Bernaerts, A., Hul, W.V., 2003. Van Buchem disease: lifetime evolution of radioclinical features. Skeletal Radiol. 32 (12), 708–718.

Vigetti, D., Karousou, E., Viola, M., Deleonibus, S., De Luca, G., Passi, A., 2014. Hyaluronan: biosynthesis and signaling. Biochim. Biophys. Acta 1840 (8), 2452–2459.

Viviano, B.L., Silverstein, L., Pflederer, C., Paine-Saunders, S., Mills, K., Saunders, S., 2005. Altered hematopoiesis in glypican-3-deficient mice results in decreased osteoclast differentiation and a delay in endochondral ossification. Dev. Biol. 282 (1), 152–162.

Waltregny, D., Bellahcene, A., Van Riet, I., Fisher, L.W., Young, M., Fernandez, P., Dewe, W., de Leval, J., Castronovo, V., 1998. Prognostic value of bone sialoprotein expression in clinically localized human prostate cancer. J. Natl. Cancer Inst. 90 (13), 1000–1008.

Wang, C., Wang, Y., Huffman, N.T., Cui, C., Yao, X., Midura, S., Midura, R.J., Gorski, J.P., 2009. Confocal laser Raman microspectroscopy of biomineralization foci in UMR 106 osteoblastic cultures reveals temporally synchronized protein changes preceding and accompanying mineral crystal deposition. J. Biol. Chem. 284 (11), 7100–7113.

Watanabe, H., Kimata, K., Line, S., Strong, D., Gao, L.Y., Kozak, C.A., Yamada, Y., 1994. Mouse cartilage matrix deficiency (cmd) caused by a 7 bp deletion in the aggrecan gene. Nat. Genet. 7 (2), 154–157.

Wewer, U.M., Ibaraki, K., Schjorring, P., Durkin, M.E., Young, M.F., Albrechtsen, R., 1994. A potential role for tetranectin in mineralization during osteogenesis. J. Cell Biol. 127 (6 Pt 1), 1767–1775.

Wight, T.N., 2002. Versican: a versatile extracellular matrix proteoglycan in cell biology. Curr. Opin. Cell Biol. 14 (5), 617–623.

Williams Jr., D.R., Presar, A.R., Richmond, A.T., Mjaatvedt, C.H., Hoffman, S., Capehart, A.A., 2005. Limb chondrogenesis is compromised in the versican deficient hdf mouse. Biochem. Biophys. Res. Commun. 334 (3), 960–966.

Winkler, D.G., Yu, C., Geoghegan, J.C., Ojala, E.W., Skonier, J.E., Shpektor, D., Sutherland, M.K., Latham, J.A., 2004. Noggin and sclerostin bone morphogenetic protein antagonists form a mutually inhibitory complex. J. Biol. Chem. 279 (35), 36293–36298.

Wong, M., Lawton, T., Goetinck, P.F., Kuhn, J.L., Goldstein, S.A., Bonadio, J., 1992. Aggrecan core protein is expressed in membranous bone of the chick embryo. Molecular and biomechanical studies of normal and nanomelia embryos. J. Biol. Chem. 267 (8), 5592–5598.

Wu, H., Whitfield, T.W., Gordon, J.A., Dobson, J.R., Tai, P.W., van Wijnen, A.J., Stein, J.L., Stein, G.S., Lian, J.B., 2014. Genomic occupancy of Runx2 with global expression profiling identifies a novel dimension to control of osteoblastogenesis. Genome Biol. 15 (3), R52.

Xu, T., Bianco, P., Fisher, L.W., Longenecker, G., Smith, E., Goldstein, S., Bonadio, J., Boskey, A., Heegaard, A.M., Sommer, B., Satomura, K., Dominguez, P., Zhao, C., Kulkarni, A.B., Robey, P.G., Young, M.F., 1998. Targeted disruption of the biglycan gene leads to an osteoporosis-like phenotype in mice. Nat. Genet. 20 (1), 78–82.

Yao, J., Guihard, P.J., Blazquez-Medela, A.M., Guo, Y., Liu, T., Bostrom, K.I., Yao, Y., 2016. Matrix Gla protein regulates differentiation of endothelial cells derived from mouse embryonic stem cells. Angiogenesis 19 (1), 1–7.

Zu, W., Robey, P.G., Boskey, A.L., 2007. The biochemistry of bone. In: Marcus, R., Feldman, D., Nelson, D.A., Rosen, C.J. (Eds.), Osteoporosis. Elsevier Science and Technology, Burlington, MA, pp. 191–240.

Chapter 16

Bone proteinases

Teruyo Nakatani and Nicola C. Partridge
Department of Basic Science and Craniofacial Biology, New York University College of Dentistry, New York, NY, United States

Chapter outline

Introduction

This chapter surveys our knowledge of the proteinases expressed in bone. Although for a long time the osteoclast had been considered the main producer of proteinases in bone, it became increasingly clear that the osteoblast lineage plays a significant role in the production of many of these proteinases. For example, it is true that the osteoclast secretes abundant lysosomal cysteine proteinases, especially cathepsin K (Vaes, 1988; Xia et al., 1999; Sahara et al., 2003), and produces some of the neutral proteinases, e.g., matrix metalloproteinase-9 (MMP-9; Wucherpfennig et al., 1994; Delaissé et al., 2000). However, osteoblasts and osteocytes, like their related cells, fibroblasts, are able to secrete a host of proteinases, including neutral proteinases such as serine proteinases, plasminogen activators (PAs), and metalloproteinases such as MMP-13, as well as lysosomal proteinases, e.g., cathepsins. Thus, osteoblasts and osteocytes, like fibroblasts, have the capacity not only to synthesize a range of matrix proteins, including type I collagen, but also to remodel their own extracellular matrix via the secretion of a range of proteinases.

Proteinases can be classified into four groups: metalloproteinases, e.g., MMP-13 (also known as collagenase-3); serine proteinases, e.g., PA; cysteine proteinases, e.g., cathepsin K; and aspartic proteinases, e.g., cathepsin D. This subdivision is based on the structure and the catalytic mechanism of the active site involving particular amino acid residues and/or zinc. In the following review of the proteinases synthesized in bone, we deal with each group according to this subdivision in the order just given. For some, much more is known than for others and they have warranted their own section.

Metalloproteinases

MMPs are a family of zinc- and calcium-dependent neutral endoproteinases. MMPs are responsible for remodeling the extracellular matrix (ECM), which is necessary for physiological events such as angiogenesis, wound healing, and bone development (Page-McCaw et al., 2007). Abnormal expression and activation of MMPs lead to the development of diseases such as cirrhosis, cancer, and arthritis (Gong et al., 2014). To maintain homeostasis, MMPs are tightly regulated at the levels of transcription, posttranslational modification, production of the enzymes as inactive zymogens requiring activation, coexpression of tissue inhibitors of metalloproteinases (TIMPs), and receptors to regulate their extracellular abundance (Varghese, 2006; Cerda-Costà and Gomis-Rüth, 2014). At this writing, the MMP family comprises ~24

Principles of Bone Biology. https://doi.org/10.1016/B978-0-12-814841-9.00016-6

structurally and functionally related members in mammals (23 in humans, 22 in mice). According to their structural and functional characteristics, human MMPs can be classified into at least six different subfamilies of closely related members: collagenases (MMP-1, -8, and -13), type IV collagenases (gelatinases, MMP-2, and MMP-9), stromelysins (MMP-3, -10, and -11), matrilysins (MMP-7 and -26), membrane-type MMPs (MT-MMPs; MMP-14, -15, -16, -17, -24, and -25), and other MMPs (MMP-12, -19, -20, -21, -23, -27, and -28) (Matrisian, 1992; Vu and Werb, 2000; Visse and Nagase, 2003). All MMPs are active at neutral pH, require Ca^{2+} for activity, and contain Zn^{2+} in their active site. Mammalian MMPs share a conserved domain structure that consists of a catalytic domain and an autoinhibitory prodomain. The prodomain contains a conserved Cys residue that coordinates the active-site zinc to inhibit catalysis. The catalytic domain of MMPs contains the conserved sequence HEXGH, which is believed to be the zinc-binding site. Metalloproteinases are secreted or inserted into the cell membrane in a latent form caused by the presence of a conserved cysteine residue in the prosegment, which completes the tetrad of zinc bound to three other residues in the active site. Cleavage of this propiece by other proteolytic enzymes (e.g., trypsin, plasmin, cathepsins, or other unknown activators) causes a loss of ~10 kDa of the propiece; this disrupts the cysteine's association with the zinc and results in a conformational change in the enzyme yielding activation. Metalloproteinases all have homology to human fibroblast collagenase (collagenase-1, MMP-1) (Varghese, 2006). It should be noted that MMPs, named "gelatinases" when originally characterized, clearly function as collagenases in vitro, and could potentially function as collagenases in vivo. MMP-2, for example, when free of TIMPs, cleaves native collagens to yield the typical 3/4−1/4 fragments (Ames and Quigley, 1995; Seandel et al., 2001). There are four members of the TIMP family, TIMP-1, -2, -3, and -4, each inhibiting the activities of MMPs with varying efficiency (Gong et al., 2014; Brew et al., 2010).

MMPs play an important role in tissue remodeling associated with various physiological processes; however, abnormal expression and activation of MMPs is implicated in the pathogenesis and pathological progression of multiple diseases, including cirrhosis, arthritis, and cancer (Gong et al., 2014; Fingleton, 2007). The MMPs are promising drug targets in diverse pathologies (Nam et al., 2016). Although many synthetic inhibitors of MMPs (MMPIs) were designed and tested in animal models and in human clinical trials, all of these trials failed (to date, the only approved MMPI is Periostat, for the treatment of chronic periodontal disease). Broad-spectrum MMPIs have failed in clinical trials due to their very strong targeting of the catalytic zinc ion but low specificity (Zucker et al., 2000). In 2017, a novel strategy was used to develop JNJ0966, which binds zymogen and prevents generation of active MMP-9. The agent did not inhibit the production of the mature, active forms of MMP-1, MMP-2, MMP-3, and MMP-14. There is a hope that there will be the development of a next generation of MMP drugs: specific and without off-target effects (Scannevin et al., 2017).

Activation of MMPs can occur via the PA/plasmin pathway. PAs convert plasminogen to plasmin, which subsequently can activate prostromelysin to stromelysin and procollagenase to collagenase. The activated MMPs can then degrade collagens and other ECM proteins. MT-MMP is necessary for MMP-2 activation in fibroblasts (Ruangpanit et al., 2001), and MT-1 MMP (MMP-14)−mediated MMP-2 activation is important for invasion and metastasis of tumors (Mitra et al., 2006).

Apart from the regulation of secretion, activation, and/or inhibition, MMPs are substantially regulated at the transcriptional level (Matrisian, 1992; Crawford and Matrisian, 1996). Several *MMPs* contain specific regulatory elements in their promoter sequences. Human and rat stromelysin-1 and -2 contain activator protein-1 (AP-1)- and polyoma enhancer activator-3 (PEA-3)-binding sites that may be important for basal levels and inducibility. AP-1 and PEA-3 consensus sequences have also been found in human, rabbit, and rat collagenase genes (Brinckerhoff, 1992; Selvamurugan et al., 1998; Tardif et al., 2004). The transcription factors Fos and Jun form heterodimers and act through the AP-1 sequence (Lee et al., 1987; Chiu et al., 1988), whereas c-*ets* family members bind at the PEA-3 sequence (Wasylyk et al., 1993). The urokinase PA gene also contains AP-1- and PEA-3-binding sites and, as a result, agents acting through these sites could lead to coordinate expression of many of these genes (Matrisian, 1992; Hsieh et al., 2007). Moreover, TIMP-1 is controlled by AP-1 transcription factor in brain, and there is a role for AP-1 in regulation of the neuronal *Mmp9* gene (Kaczmarek et al., 2002). Glucocorticoids and retinoids can suppress metalloproteinase synthesis at the transcriptional level (Brinckerhoff, 1992) by forming a complex with AP-1 transcription factors and inhibiting their action (Schroen et al., 1996).

A second transcription factor-binding site was identified in the *Mmp13* (collagenase-3) promoter as well as in bone-specific genes such as osteocalcin (Shah et al., 2004; Selvamurugan et al., 2006). This site is referred to as the runt domain (RD)-binding site or polyomavirus enhancer-binding protein-2A/osteoblast-specific element-2/nuclear matrix protein-2-binding site (Geoffroy et al., 1995; Merriman et al., 1995). Members of the core-binding factor (CBF) protein family (renamed Runx by the Human Genome Organization), such as the osteoblastic transcription factor Runx2 (Cbfa1), bind to these RD sites (Kagoshima et al., 1993). Runx proteins are capable of binding to DNA as monomers, but can also heterodimerize with CBF subunit B, a ubiquitously expressed nuclear factor (Kanno et al., 1998). Runx2 is essential for the maturation of osteoblasts, and targeted disruption of the *Runx2* gene in mice produces skeletal defects

that are essentially identical to those found in human cleidocranial dysplasia (Banerjee et al., 1997; Ducy et al., 1997; Mundlos et al., 1997; Otto et al., 1997).

Stromelysin

Stromelysin-1 (MMP-3) degrades fibronectin, gelatin, proteoglycans, denatured type I collagen, laminin, and other ECM components (Chin et al., 1985). Mesenchymal cells, such as chondrocytes and fibroblasts, are commonly found to secrete stromelysin-1 (Matrisian, 1992). Transin, the rat homolog of human stromelysin, was originally discovered in fibroblasts transformed with the polyomavirus (Matrisian et al., 1985). One importance of stromelysin comes from its implication in the direct activation of procollagenases, including MMP-1, -8, -9, and -13 (Murphy et al., 1987; Knauper et al., 1993), and the enzyme is thought to play a role, together with collagenases, in the destruction of connective tissues during disease states (Brinckerhoff, 1992; Posthumus et al., 2000). It has also been identified to have a crucial role in MMP-mediated cartilage damage in osteoarthritis, as *Mmp3*-knockout mice were shown to have reduced MMP-mediated cartilage breakdown after induction of osteoarthritis (Blom et al., 2007).

Stromelysin-1 is regulated by growth factors, oncogenes, cytokines, and tumor promoters. Epidermal growth factor (EGF) has been shown to increase stromelysin transcription through the induction of Fos and Jun, which interact at the AP-1 site in the promoter (McDonnell et al., 1990). Platelet-derived growth factor is also important in the induction of stromelysin (Kerr et al., 1988a). The protein kinase C (PKC) activator, phorbol myristate acetate (PMA), is a notable stimulator of stromelysin transcription (Brinckerhoff, 1992; Prontera et al., 1996). Transforming growth factor β (TGFβ), however, causes an inhibition of transin (rat stromelysin) expression (Matrisian et al., 1986; Kerr et al., 1988b) through a TGFβ inhibitory element (Kerr et al., 1990). Other studies have shown that bone morphogenetic protein (BMP-4) represses *Mmp3* and *Mmp13* gene expression, but does not induce adipocyte differentiation in C3H10T1/2 cells (Otto et al., 2007). Interleukin-4 (IL-4) and IL-13 were shown to inhibit MMP-3 synthesis in human conjunctival fibroblasts (Fukuda et al., 2006; Stewart et al., 2007).

In bone, stromelysin-1 has been shown to be produced by normal human osteoblasts (Meikle et al., 1992) after stimulation with parathyroid hormone (PTH) or monocyte-conditioned medium (cytokine-rich). Similarly, Rifas et al. (1994) have shown that two human osteosarcoma cell lines (MG-63 and U2OS) secrete stromelysin and this may be increased by treatment with PMA, IL-1β, and tumor necrosis factor-α (TNFα), but these authors were not able to find the enzyme in medium conditioned by cultured normal human osteoblasts. Mouse osteoblasts and osteoblastic cell lines also produce stromelysin-1 and demonstrate enhanced expression with $1,25(OH)_2D_3$, IL-1, or IL-6 treatment (Thomson et al., 1989; Breckon et al., 1999; Kusano et al., 1998; Le Maitre et al., 2005). There have also been reports that this stromelysin is expressed by osteoclasts (Witty et al., 1992). Despite the many papers on stromelysin-1 it is not clear what its physiological substrate is, nor is its role in physiological and pathophysiological skeletal resorption established.

Type IV collagenases (gelatinases)

Type IV collagenases or gelatinases are neutral metalloproteinases requiring Ca^{2+} for activity and are involved in the proteolysis and disruption of basement membranes by degradation of type IV, type V, and denatured collagens. There are two types of gelatinases, 72-kDa gelatinase (gelatinase A), or MMP-2 (Collier et al., 1988), and 92-kDa gelatinase (gelatinase B), or MMP-9 (Wilhelm et al., 1989). There are very distinct differences between the two gelatinases. The 72-kDa gelatinase has been found complexed to TIMP-2 (Stetler-Stevenson et al., 1989), whereas the 92-kDa gelatinase has been found complexed to TIMP-1 (Wilhelm et al., 1989). Regulation of the two gelatinases is also very distinct. Analysis of the genomic structure and promoter of the 72-kDa gelatinase has revealed that this gene does not have an AP-1 site or a TATA box in the 5′ promoter region as all the other *MMPs* have been shown to have (Huhtala et al., 1990). This enzyme is also not regulated by PMA and, in many cases, seems to be expressed constitutively rather than in a regulated fashion. In contrast, the 92-kDa gelatinase has a promoter very similar to that of the other *MMPs* and is regulated similarly (Huhtala et al., 1991). Nevertheless, expression and activity of both types of gelatinase are markedly stimulated by IL-1 (Kusano et al., 1998).

In bone, as is to be expected, MMP-2 is expressed constitutively by many osteoblastic preparations (Overall et al., 1989; Rifas et al., 1989, 1994; Meikle et al., 1992) and is unchanged by treatment with any of the agents tested. The zymogen form of MMP-2 is also resistant to activation by serine proteases, but MT1-MMP (MMP-14) can initiate the activation of MMP-2 by cleavage of the Asn66−Leu peptide bond (Sato et al., 1994). In 2001, Martignetti et al. (2001) described a form of multicentric osteolysis (Winchester/Torg syndrome) with striking tarsal and carpal bone resorption, accompanied by arthropathy, osteoporosis, subcutaneous nodules, and a distinctive facies in large, consanguineous Saudi

Arabian families. They localized the gene to 16q12−q21 and demonstrated two homoallelic, family-specific, mutations in the region that encodes *MMP2*. Nonsense and missense mutations have been documented that are consistent with decreased levels of MMP-2 (Al-Aqeel, 2005). *Mmp2*-null mice were first reported by Itoh et al. (1997) to have no phenotype except for some shortening of limb bones. Subsequent work by this group documented osteoporosis in older mice as well as altered remodeling of the canalicular system with osteocyte apoptosis, fewer canaliculi, and decreased canalicular connectivity (Inoue et al., 2006). They also described striking defects in formation/maintenance of osteocyte networks and connectivity in collagenase-resistant (r/r) mice; the r/r mice had previously been shown to have osteocyte and osteoblast apoptosis and prominent emptying of osteocyte lacunae (Zhao et al., 2000). We emphasize, however, that although the *Mmp2*-null mice had osteoporosis, the characteristic nodulosis and severe focal osteolysis of the human NAO (nodulosis, arthropathy and osteolysis) syndrome with mutations in *MMP2* were not found in the $Mmp2^{-/-}$ mice. Later, Mosig et al. (2007) reported that *Mmp2*- null mice obtained from Itoh et al. (1997), and described above, display progressive loss of bone mineral density, articular cartilage destruction, and abnormal long bone and craniofacial development. These mice had 50% fewer osteoblasts and osteoclasts compared with control littermates at 4 days, while there was almost no difference after 4 weeks of age. In addition, inhibition of MMP-2 via small interfering RNA in human SaOS2 and murine MC3T3 osteoblast cell lines caused a decrease in cell proliferation rates. These findings imply that MMP-2 is critical for normal skeletal and craniofacial development, as well as bone cell growth and proliferation. Mosig et al. (2007) did not comment on focal osteolysis of the NAO human syndrome in the *Mmp2*-null mice they studied, nor did they examine the canalicular networks using approaches similar to those of Inoue et al. (2006).

$Mmp7^{-/-}$ mice were reported to have several abnormalities, such as decreased intestinal tumorigenesis, but no obvious skeletal defects (Wilson et al., 1997). Later work from this group demonstrated in a prostate cancer model that MMP-7 produced by osteoclasts at the tumor−bone interface has the capacity to process cell-bound receptor activator of NF-κB ligand (RANKL) to a soluble form that further promotes osteoclast activation (Lynch et al., 2005). In *Mmp7*-deficient mice, there was reduced RANKL processing and reduced tumor-induced osteolysis. It appears, however, that $Mmp7^{-/-}$ mice have no physiological abnormality in physiological skeletal remodeling (i.e., no abnormality in the absence of bone metastasis).

The 92-kDa gelatinase (MMP-9) is secreted by three osteosarcoma cell lines (TE-85, U2OS, and MG-63) (Rifas et al., 1994) and, in some of the cell lines, can be stimulated by PMA, IL-1β, and TNFα, analogous to these authors' observations regarding stromelysin. Similarly, they were unable to identify secreted MMP-9 in the media of normal human osteoblasts or the human osteosarcoma cell line SaOS-2, which has been shown to have retained many characteristics of highly differentiated osteoblasts. Likewise, Meikle et al. (1992) found very little immunohistochemical staining for MMP-9 in normal human osteoblasts. In fact, this enzyme has been found to be highly expressed by rabbit and human osteoclasts (Tezuka et al., 1994a; Wucherpfennig et al., 1994; Vu et al., 1998). Indeed, a lack of expression of MMP-9 in mature osteoclasts of c-*fos*-null mice may be one of the reasons the animals exhibit an osteopetrotic phenotype (Grigoriadis et al., 1994). Furthermore, studies of mice with a targeted inactivation of the gene indicate that MMP-9 plays a role in regulating endochondral bone formation, particularly of the primary spongiosa, possibly by mediating capillary invasion. Mice containing a null mutation in the *Mmp9* gene exhibit delays in vascularization, ossification, and apoptosis of the hypertrophic chondrocytes at the skeletal growth plates (Vu et al., 1998). These defects result in an accumulation of hypertrophic cartilage in the growth plate and lengthening of the growth plate. The defects are reversible, and by several months of age the affected mice have an axial skeleton of normal appearance. It was postulated that MMP-9 is somehow involved in releasing angiogenic factors such as vascular endothelial growth factor, which is normally sequestered in the ECM (Gerber et al., 1999). Extracellular galectin-3 could be an endogenous substrate of MMP-9 that acts downstream to regulate hypertrophic chondrocyte death and osteoclast recruitment during endochondral bone formation. Thus, the disruption of growth plate homeostasis in *Mmp9*-null mice links galectin-3 and MMP-9 in the regulation of the clearance of late chondrocytes through regulation of their terminal differentiation (Ortega et al., 2005).

Membrane-type matrix metalloproteinases

While most MMPs are secreted, a subtype called MT-MMPs are inserted into the cell membrane (Sato et al., 1997; Pei, 1999). These proteases contain a single transmembrane domain and an extracellular catalytic domain. Characteristically, MT-MMPs have the potential to be activated intracellularly by furin or furin-like proteases through recognition of a unique amino acid sequence: Arg−Arg−Lys−Arg111 (Sato et al., 1996). To date, six MT-MMPs have been described, four transmembrane proteins (MMP-14, -15, -16, and -24) and two glycosylphosphatidylinositol-anchored ones (MMP-17 and -25). MT1-MMP (MMP-14), MT2-MMP (MMP-15), and MT3-MMP (MMP-16) have been shown to have a wide range of activities against ECM proteins (Pei and Weiss, 1996; Velasco et al., 2000). MT1-MMP is involved in endothelial cell

migration and invasion (Galvez et al., 2000; Collen et al., 2003), and MT2-MMP and MT3-MMP are also involved in cell migration and invasion, depending on the cell type (Hotary et al., 2000; Shofuda et al., 2001). In a collagen-invasion model, MT1-MMP appears to be the critical MMP (Sabeh et al., 2004).

MT4-MMP (MMP-17) has the smallest degree of sequence identity to the other family members and has TNFα convertase activity, but does not activate pro-MMP-2 (Puente et al., 1996; English et al., 2000). Conversely, MT5-MMP (MMP-24) and MT6-MMP (MMP-25) may facilitate tumor progression through their ability to activate pro-MMP-2 at the membrane of cells from tumor tissue (Llano et al., 1999; Velasco et al., 2000). As mentioned earlier, MT1-MMP (MMP-14) serves as a membrane receptor or activator of MMP-2 and possibly other secreted MMPs (Sato et al., 1994). Further, studies indicate that MT1-MMP may also function as a fibrinolytic enzyme in the absence of plasmin and facilitate the angiogenesis of endothelial cells (Hiraoka et al., 1998). MT1-MMP is highly expressed in embryonic skeletal and periskeletal tissues and has been identified in osteoblasts by in situ hybridization and immunohistochemistry (Apte et al., 1997; Kinoh et al., 1996). Targeted inactivation of the *Mmp14* gene in mice produces several skeletal defects that result in osteopenia, craniofacial dysmorphisms, arthritis, and dwarfism (Holmbeck et al., 1999; Zhou et al., 2000). Several of the notable defects in bone formation include delayed ossification of the membranous calvarial bones, persistence of the parietal cartilage vestige, incomplete closure of the sutures, and marked delay in the postnatal development of the epiphyseal ossification centers characterized by impaired vascular invasion. Histological observation suggested that the progressive osteopenia noted in these animals may be attributed to excessive osteoclastic resorption and diminished bone formation. This finding was supported by evidence that osteoprogenitor cells isolated from the bone marrow of these mutant mice demonstrate defective osteogenic activity. A similar human disease of "vanishing bone" was observed in two sisters with mutations in MT1-MMP preventing its membrane localization (Evans et al., 2012). This raises the question of a protective effect in bone exerted by MT1-MMP and/or activation of MMP-2. In contrast, a 2018 paper (Delgado-Calle et al., 2018) has shown that MT1-MMP is stimulated by constitutively active PTH receptor 1 signaling in bone and appears to be partly responsible for the high bone turnover phenotype of these mice. The authors showed that MT1-MMP is, in some way, associated with increases in soluble RANKL production. MT1-MMP is also associated with osteoclast-mediated bone resorption in rheumatoid arthritis (Pap et al., 2000).

Collagenases

Collagenases generally cleave fibrillar native collagens I–III at a single helical site at neutral pH (Matrisian, 1992). The resultant cleavage products denature spontaneously at 37°C and become substrates for many enzymes, particularly gelatinases. The collagenase subfamily of human MMPs consists of three distinct members: fibroblast collagenase-1 (MMP-1), neutrophil collagenase-2 (MMP-8), and collagenase-3 (MMP-13) (Goldberg et al., 1986; Freije et al., 1994). An additional collagenase, called collagenase-4 (initially called MMP-18), was identified in *Xenopus laevis* (Stolow et al., 1996), and a human homolog of this enzyme was identified and was given other names, such as MMP RASI-1, and has now been designated MMP-19. As of this writing, only one rat/mouse interstitial collagenase has been studied thoroughly and shown to be expressed by a range of cells, including osteoblasts and osteocytes. This collagenase has a high degree of homology (86%) to human collagenase-3 and is aptly given the same name (Quinn et al., 1990), and both are now called MMP-13. MMP-13 is secreted by osteoblasts and osteocytes, hypertrophic chondrocytes, smooth muscle cells, and fibroblasts, in proenzyme form at 58 kDa, and is subsequently cleaved to its active form of 48 kDa (Roswit et al., 1983). Two murine orthologs of human collagenase-1 (MMP-1), called murine collagenase-like A (Mcol-A) and murine collagenase-like B (Mcol-B), were first identified by nucleotide sequence similarity to human MMP-1, but only Mcol-A was able to degrade native type I and II collagens, casein, and gelatins (Balbin et al., 2001). In this report, the expression of Mcol-A was limited to early embryos. It should be noted here that studies of mouse and rat tissues that report expression of MMP-1 by immunohistochemistry or in situ hybridization are probably not detecting MMP-1. We also made the mistake of calling rat collagenase-3 (i.e., MMP-13) MMP-1 when the nomenclature of the MMPs was being thrashed out (Omura et al., 1994). A murine ortholog of collagenase-2 (MMP-8) has been identified by two groups (Lawson et al., 1998; Balbin et al., 1998). A role for Mcol-A, Mcol-B, or murine collagenase-2 (MMP-8) in bone cell function has not been demonstrated, although human MMP-8 is expressed in chondrocytes and other skeletal cells. *Mmp8*$^{-/-}$ mice (Balbin et al., 2003) have no skeletal abnormalities during development; skeletal changes in adults have not yet been reported.

As noted previously, it has also been shown that other MMPs (MMP-2 [gelatinase A (GelA or 72-kDa gelatinase)] and MMP-14 [MT1-MMP]) can function as collagenases in vitro (Aimes and Quigley, 1995; Ohuchi et al., 1997). These MMPs (-1, -2, -8, -13, and -14) all cleave each of the triple-helical interstitial collagens at the same locus and therefore must also be considered collagenases.

Collagenase-3/MMP-13

In developing rat calvariae, we have found ample amounts of MMP-13 by immunohistochemistry 14 days after birth (Davis et al., 1998). These are always in select areas, mostly associated with sites of active modeling. At the cellular level, staining is associated with osteocytes and bone-lining cells that have the appearance of osteoblasts. Originally, there was controversy regarding the cellular origin of bone collagenase. The osteoclast was reported to show immunohistochemical staining for collagenase (Delaissé et al., 1993), but it was not determined whether this was a gene product of the osteoclast or was, perhaps, produced by osteoblasts/osteocytes and bound by the osteoclast through a receptor (see later). However, in situ hybridization of 17- to 19-gestational-day rat fetal long bones showed *Mmp13* expression only in chondrocytes, bone surface mononuclear cells, and osteocytes adjacent to osteoclasts; there was no evidence of expression in osteoclasts (Fuller and Chambers, 1995). Similarly, Mattot et al. (1995) showed expression of mouse *Mmp13* in hypertrophic chondrocytes and in cells of forming bone from humeri of mice at the 18th gestational day. In human fetal cartilage and calvaria, *MMP13* transcripts were detected in hypertrophic chondrocytes, osteoblasts, and periosteal cells by in situ hybridization, whereas no expression of *MMP13* was detected in osteoclasts (Johansson et al., 1997). In addition, it has been known for some time that bone explants from osteopetrotic mice (lacking active osteoclasts) continue to produce abundant collagenolytic activity, either unstimulated or stimulated by bone-resorbing hormones (Jilka and Cohn, 1983; Heath et al., 1990). These studies demonstrate that osteoblasts/osteocytes and hypertrophic chondrocytes are the sources of collagenases in skeletal tissue, whereas the osteoclast does not appear to express these genes. It should also be noted that the expression of *Mmp13* assayed by in situ hybridization was strikingly reduced (Lanske et al., 1996) in the distal growth plate and midshafts of bones from *Pthr1*$^{-/-}$ mouse embryos (Lanske et al., 1998).

The remodeling of the fracture callus mimics the developmental process of endochondral bone formation. Excess tissue accumulates as callus prior to endochondral ossification followed by osteoclast repopulation. In collaboration with Dr. Mark Bolander, we demonstrated profuse concentrations of metalloproteinases in the fracture callus of adult rat long bones (Partridge et al., 1993). The predominant cells observed to stain for MMP-13 are hypertrophic chondrocytes during the phase of endochondral ossification, marrow stromal cells (putative osteoblasts) when the primary spongiosa is remodeled, and osteoblasts/osteocytes at a time when newly formed woven bone is being remodeled to lamellar bone. This indicates that the adult long bone has the ability to produce profuse levels of MMP-13, but only when challenged, e.g., by a wound-healing situation or an osteotropic hormone. As well, it was shown that *Mmp13*-null mice have delayed bone fracture healing, characterized by a retarded cartilage response in the fracture callus (Kosaki et al., 2007). The consistent observation here is a role for this enzyme when a collagenous matrix must undergo substantial, rapid remodeling.

Liu et al. (1995) have demonstrated that targeted mutation around the collagenase cleavage site in both alleles of the endogenous mouse type I collagen gene Colla1, which results in resistance to collagenase cleavage, leads to dermal fibrosis and uterine collagenous nodules. These animals are able to develop normally to adulthood, and some of the major abnormalities become apparent only with increasing age. Studies of these mice revealed that homozygous mutant (r/r) mice have diminished PTH-induced bone resorption, diminished PTH-induced calcemic responses, and thicker bones (Zhao et al., 1999). These observations imply that collagenase activity is necessary not only in older animals for rapid collagen turnover, but also for PTH-stimulated bone resorption. In the r/r mice, as early as 2 weeks of age, empty osteocyte lacunae were evident in the calvariae and long bones, with the number of empty lacunae increasing with age, and an increase in apoptosis was observed in osteocytes, as well as periosteal cells (Zhao et al., 2000). Thus, normal osteocytes (and osteoblasts) and osteoclasts might bind to cryptic epitopes that are revealed by the collagenase cleavage of type I collagen by liganding the αVβ3 integrin and, if such signals are not induced (as postulated for the osteoclastic defect in r/r mice), they would undergo apoptosis and their lacunae would empty. Young r/r mice are also observed to develop thickening of the calvariae through the deposition of new bone predominantly at the inner periosteal surface; an increased deposition of endosteal trabecular bone was found in long bones in older r/r mice. Thus, the failure of collagenase to cleave type I collagen in r/r mice was associated with increased osteoblast and osteocyte apoptosis and, paradoxically, increased bone deposition as well.

To elucidate the functional roles of MMP-13 during skeletal development in vivo, Inada et al. (2004) generated *Mmp13*-null mice. These mice were found to have lengthened growth plates, due to an increase in the hypertrophic chondrocyte zone, as well as delayed ossification at the primary centers. Abnormalities of growth plates were apparent in the early stages of embryonic development and persisted throughout adulthood. This abnormality is most likely due to a decrease in degradation of ECM cartilage, as was shown by the significant increase in the area of type X collagen deposition, although an increase in the synthesis of type X collagen also remains a possible cause. These observations suggest that MMP-13 plays a critical role in collagen degradation during growth plate development and endochondral ossification. Similar to these findings, Stickens et al. (2004) found that deletion of MMP-13 caused abnormal endochondral

bone development as a result of impaired ECM remodeling. These *Mmp13*-deficient mice were viable, were fertile, and had a normal life span, with no gross phenotypic abnormalities. However, an increase in the hypertrophic chondrocyte zone of the skeletal growth plate was observed, as a result of the delayed exit of chondrocytes from the growth plate. In addition, unlike the late phenotype of the collagenase-resistant mice, these mice showed an early increase in trabecular bone that persisted for months. This was due to the absence of collagenase expression in osteoblasts, not chondrocytes, as was shown by tissue-specific knockouts. The crucial role of MMP-13 in bone formation and remodeling is further demonstrated by a missense mutation, F56S, in the proregion domain of MMP-13 in a form of chondrodysplasia in humans. This mutation, the substitution of an evolutionarily conserved phenylalanine residue for a serine, causes the Missouri type of spondyloepimetaphyseal dysplasia, an autosomal dominant disorder characterized by defective growth and modeling of vertebrae and long bones (Kennedy et al., 2005). This is thought to be due to intracellular autoactivation and degradation of the mutant enzyme.

Related to work in whole animals, we have shown, together with Drs. Jane Lian and Gary Stein, that *Mmp13* is expressed late in differentiation in in vitro mineralizing rat osteoblast cultures (Shalhoub et al., 1992; Winchester et al., 1999, 2000). The appearance of the enzyme in late differentiated osteoblasts may correlate with a period of remodeling of the collagenous ECM. These observations regarding the differentiation of rat osteoblasts may explain the very low levels of MMP-1 observed in cultures of normal human osteoblasts (Rifas et al., 1989), where mRNAs and proteins were isolated from cells at confluence, but apparently not from mineralized cultures. Alternatively, the cultures may predominantly express MMP-13 (rather than MMP-1), which has been shown to be expressed by osteoblasts, by chondrocytes, and in synovial tissue, particularly in pathological conditions such as osteoarthritis (Johansson et al., 1997; Mitchel et al., 1996; Reboul et al., 1996; Wernicke et al., 1996). At the time that Rifas and colleagues conducted the work on human osteoblasts, human MMP-13 had not been identified.

Canalis's group has conducted considerable research on the hormonal regulation of MMP-13 in rat calvarial osteoblasts, including demonstrating stimulation by retinoic acid (Varghese et al., 1994). They have also demonstrated that triiodothyronine, platelet-derived growth factor, and basic fibroblast growth factor (bFGF) all stimulate *Mmp13* transcription (Pereira et al., 1999; Rydziel et al., 2000; Varghese et al., 2000). Interestingly, they have also shown that insulin-like growth factors (IGFs) inhibit both basal and retinoic-stimulated collagenase expression (Canalis et al., 1995) by these cells. We have shown that TGFβ1 stimulates *Mmp13* expression in the rat osteosarcoma cell line UMR 106-01 (Selvamurugan et al., 2004).

We have conducted many studies with the clonal rat osteosarcoma line UMR 106-01, which has been described as osteoblastic in phenotype (Partridge et al., 1980, 1983). This cell line responds to all of the bone-resorbing hormones by synthesizing MMP-13 (Partridge et al., 1987; Civitelli et al., 1989). In contrast to the physiological regulation of collagenase in fibroblasts (Woessner, 1991), synoviocytes (Brinckerhoff and Harris, 1981), and uterine smooth muscle cells (Wilcox et al., 1994), the control of expression of MMP-13 in bone and osteoblastic cells appears to have some distinct differences. First, it is stimulated by all the bone-resorbing hormones (Partridge et al., 1987; Delaissé et al., 1988), which act through different pathways, including protein kinase A (PKA; PTH and prostaglandins [PGs]), PKC (PTH and PGs), tyrosine phosphorylation (EGF), and direct nuclear action ($1,25(OH)_2D_3$, retinoic acid). Second, glucocorticoids do not inhibit stimulation by PTH (Delaissé et al., 1988; T.J. Connolly, N.C. Partridge, and C.O. Quinn, unpublished observations), whereas retinoic acid stimulates MMP-13 expression rather than inhibiting it (Delaissé et al., 1988; Connolly et al., 1994; Varghese et al., 1994). Last, in rat osteosarcoma cells, PMA is unable to elicit a pronounced stimulatory effect on *Mmp13* gene expression.

Among the bone-resorbing agents tested, PTH is the most effective in stimulating MMP-13 production by UMR cells. A single 10^{-7} M PTH dose significantly stimulates transient MMP-13 secretion, with maximal extracellular enzyme concentrations achieved between 12 and 24 h (Partridge et al., 1987; Civitelli et al., 1989). This level is maintained at 48 h, decreases to 20% of the maximum by 72 h, and is ultimately undetectable by 96 h. We hypothesized that MMP-13 was removed from the medium through a cell-mediated binding process because the enzyme is stable in conditioned medium, and experiments showed that this disappearance was not due to extracellular enzymatic degradation. Binding studies conducted with ^{125}I-MMP-13 revealed a specific receptor with high affinity ($K_d = 5$ nM) for rat MMP-13 (Omura et al., 1994). Further studies showed that binding of MMP-13 in this fashion is responsible for its rapid internalization and degradation. The processing of MMP-13 in this system requires receptor-mediated endocytosis and involves sequential processing by endosomes and lysosomes (Walling et al., 1998). In addition to UMR cells, we identified a very similar MMP-13 receptor on normal, differentiated rat osteoblasts, rat and mouse embryonic fibroblasts, and human and rabbit chondrocytes (Walling et al., 1998; Barmina et al., 1999; Raggatt et al., 2006). These results indicate that the function of these receptors is to limit the extracellular abundance of MMP-13 and, consequently, breakdown of the ECM.

Further investigation of the MMP-13 receptor system led us to conclude that MMP-13 binding and internalization required a two-step mechanism involving both a specific MMP-13 receptor and a member of the low-density lipoprotein (LDL) receptor—related superfamily. Ligand blot analyses demonstrated that ^{125}I-labeled MMP-13 specifically bound two proteins (approximately 170 and 600 kDa) in UMR 106-01 cells (Barmina et al., 1999). Of these two binding proteins, the 170-kDa protein appeared to be a high-affinity primary binding site, and the 600-kDa protein appeared to be the LDL receptor—related protein-1 (LRP-1) responsible for mediating internalization. The LDL receptor superfamily represents a diverse group of receptors, including the LDL receptor; the VLDL receptor; LRP-1; megalin (LRP-2); and LRP-4, -5, and -6 (Herz and Bock, 2002; Pohlkamp et al., 2017). All of these plasma membrane receptors have a single membrane-spanning domain and several stereotyped repeats, ligand-binding type and EGF-precursor-like. Most receptors in this family participate in receptor-mediated endocytosis, whereby the receptor—ligand complex is directed (via an NPXY signal in the receptor) to clathrin-coated pits and then internalized. Ligands of these receptors include LDL, VLDL, urokinase-type PA (uPA)— or tissue-type PA (tPA)—PA inhibitor-1 (PAI-1) complexes, tPA, lactoferrin, activated α_2-macroglobulin/proteinase complexes, apolipoprotein E—enriched β-VLDL, lipoprotein lipase, *Pseudomonas* exotoxin A, Wnts, Wnt inhibitors, BMP-4, vitamin D—binding protein, and vitellogenin (Herz and Bock, 2002; Pohlkamp et al., 2017; Yang and Williams, 2017).

The striking stimulation of MMP-13 secretion by bone-resorbing agents in UMR cells was shown to be paralleled by an even more striking induction of *Mmp13* mRNA. Northern blots showed an ∼180-fold induction of *Mmp13* mRNA 4 h after PTH treatment (Scott et al., 1992), with an initial lag period between 0.5 and 2 h before *Mmp13* mRNA levels rose above basal. Nuclear run-on studies showed a comparable increase in transcription of the gene 2 h after treatment with PTH. The PTH-induced increase in *Mmp13* transcription was completely inhibited by cycloheximide, whereas the transcriptional rate of β-actin was unaffected by inclusion of the protein synthesis inhibitor (Scott et al., 1992). These results demonstrate that the PTH-mediated stimulation of MMP-13 involves transcription and requires de novo synthesis of a protein factor(s), i.e., it is a secondary response gene.

PTH treatment was found to increase the transcription of *Mmp13* in rat osteoblastic osteosarcoma cells primarily by stimulation of the cAMP signal transduction pathway (Scott et al., 1992). Second-messenger analogs were used to test which signal transduction pathway is of primary importance in the PTH-mediated transcriptional induction of the *Mmp13* gene. The cAMP analog 8BrcAMP was capable of inducing *Mmp13* transcription to levels close to those of PTH. In contrast, neither the PKC activator, PMA, nor the calcium ionophore, ionomycin, when used alone, resulted in any increase in *Mmp13* gene transcription similar to that elicited by PTH after 2 h of treatment. Furthermore, this effect requires protein synthesis and a 1- to 1.5-h lag period, suggesting that the transcriptional activation of the *Mmp13* gene may be the result of interactions with immediate early gene products. PTH treatment was also found to transiently increase the mRNA expression of the AP-1 protein subunits c-Fos and c-Jun (Clohisy et al., 1992). Both mRNA species were maximally induced within 30 min, well before the maximal transcription rate at 90 min for *Mmp13*. Later, it was determined that PTH is responsible for phosphorylation of the cAMP response element—binding (CREB) protein at serine 133 (Tyson et al., 1999). Once phosphorylated, the CREB protein binds a cAMP response element in the c-Fos promoter and activates transcription (Pearman et al., 1996).

The *Mmp13* gene has 10 exons (Rajakumar et al., 1993), encoding an mRNA of ∼2.9 kb, which in turn encodes the proenzyme, with a predicted core protein molecular weight of 52 kDa (Quinn et al., 1990). A series of deletion and point mutants of the promoter region was generated to identify the PTH-responsive region and subsequently the primary response factors, which convey the hormonal signal and bind to this region(s) of the *Mmp13* gene. The minimum PTH regulatory region was found to be within 148 bp upstream of the transcriptional start site (Selvamurugan et al., 1998). This region contains several consensus transcription factor recognition sequences, including SBE (Smad binding element), C/EBP (CCAAT enhancer-binding protein site), the RD binding sequence, p53, PEA-3, and AP-1 and -2. The AP-1 site is a major target for the Fos and Jun families of oncogenic transcription factors (Chiu et al., 1988; Lee et al., 1987; Angel and Karin, 1991). The RD site is a target for CBF proteins, specifically Runx2. Mice containing a targeted disruption of the Runx2 gene die at birth and lack both skeletal ossification and mature osteoblasts (Ducy et al., 1997; Komori et al., 1997; Otto et al., 1997). These mutant mice also do not express *Mmp13* during fetal development, indicating that *Mmp13* is one of the target genes regulated by Runx2 (Jimenez et al., 1999).

Additional experiments on the *Mmp13* promoter determined that both native AP-1 and RD sites and their corresponding binding proteins, AP-1 and Runx2-related proteins, are involved in PTH regulation of *Mmp13* transcription. Using gel-shift analysis, we further showed enhanced binding of c-Fos and c-Jun proteins at the AP-1 site upon treatment with PTH (Selvamurugan et al., 1998), although there was no significant change in the level of Runx2 binding to the RD site. We determined that PTH induces PKA-mediated posttranslational modification of Runx2 and leads to enhanced *Mmp13* promoter activity in UMR cells (Selvamurugan et al., 2000b). The binding of members of the AP-1 and Runx

families to their corresponding binding sites in the *Mmp13* promoter also appears to regulate *Mmp13* gene expression during osteoblast differentiation (Winchester et al., 2000). As discussed earlier, MMP-13 expression is regulated by a variety of growth factors, hormones, and cytokines, but the effects of these compounds appear to be cell-type specific. Data obtained in breast cancer and other cell lines suggest that the differential expression of and regulation of MMP-13 in osteoblastic compared with nonosteoblastic cells may depend on the expression of AP-1 factors and posttranslational modifications of Runx2 (Selvamurugan and Partridge, 2000; Selvamurugan et al., 2000a). The close proximity of the AP-1 and RD sites and their cooperative involvement in the activation of the *Mmp13* promoter suggest that the proteins binding to these sites physically interact; Runx2 was found to directly bind c-Fos and c-Jun in both in vitro and in vivo experiments (D'Alonzo et al., 2002). To determine the importance of these regulatory sites in the expression of *Mmp13* in vivo, transgenic mice containing the *Escherichia coli* lacZ reporter fused to either the wild-type *Mmp13* promoter or that with mutated AP-1 and RD sites were generated (Selvamurugan et al., 2006). The wild-type transgenic lines expressed higher levels of bacterial β-galactosidase in bone, teeth, and skin compared with the mutant and transgenic lines. Thus, the AP-1 and RD sites of the promoter most likely regulate and are necessary for gene expression in vivo in bone, as well as teeth and skin.

We have shown that the RD and AP-1 sites in the proximal promoter region are essential for PTH stimulation of *Mmp13* promoter activity (Selvamurugan et al., 1998; Winchester et al., 2000; D'Alonzo et al., 2002). At the *Mmp13* promoter in UMR 106-01 cells, Runx2 binds histone deacetylase 4 (HDAC4) at the RD binding site, resulting in a repression of transcription under basal conditions (Shimizu et al., 2010). After PTH treatment, PKA-dependent phosphorylated HDAC4 dissociates from Runx2, which is then free to recruit histone acetyltransferases, especially p300 and p300/CBP-associated factor, to activate transcription (Boumah et al., 2009, Lee and Partridge, 2010). We also demonstrated that HDAC4 associates with myocyte enhancer factor 2C (MEF2C) and MEF2C participates in PTH-stimulated *Mmp13* gene expression by increased binding to c-Fos at the AP-1 site in the *Mmp13* promoter. As with Runx2, PTH causes release of HDAC4 from MEF2C and p300 is recruited to bind MEF2C (Nakatani and Partridge, 2017).

In vivo, we have found that global $Hdac4^{-/-}$ mice have increased MMP-13 mRNA and protein expression in hypertrophic chondrocytes and trabecular osteoblasts (Shimizu et al., 2010). Global $Hdac4^{-/-}$ mice are runted in size and do not survive to weaning. This phenotype is primarily due to the acceleration of onset of chondrocyte hypertrophy and, as a consequence, inappropriate endochondral mineralization. MMP-13 is thought to be involved in endochondral ossification and bone remodeling. To identify whether the phenotype of $Hdac4^{-/-}$ mice was due to upregulation of MMP-13, we generated *Hdac4/Mmp13* double-knockout mice and determined the ability of deletion of MMP-13 to rescue the $Hdac4^{-/-}$ mouse phenotype (Nakatani et al., 2016). $Mmp13^{-/-}$ mice have normal body size. The double-knockout mice were significantly heavier and larger than $Hdac4^{-/-}$ mice, survived longer, and recovered the thickness of their growth plate zones. Micro-computed tomographic analysis revealed that $Hdac4^{-/-}$ mice had significantly decreased cortical bone area compared with the wild-type mice. In addition, bone porosity was significantly decreased. The double-knockout mice recovered these cortical parameters. Likewise, their trabecular bone recovered toward normal for this age. Taken together, our findings indicate that the phenotype seen in the $Hdac4^{-/-}$ mice is partially derived from elevation of MMP-13 and may be due to a bone remodeling disorder caused by overexpression of this enzyme.

Plasminogen activators

The PA/plasmin pathway is involved in several processes, including tissue inflammation, fibrinolysis, ovulation, tumor invasion, malignant transformation, tissue remodeling, and cell migration. The PA/plasmin pathway is also thought to be involved in bone remodeling by osteoblasts and osteoclasts. The pathway results in the formation of plasmin, another neutral serine proteinase, which degrades fibrin and the ECM proteins fibronectin, laminin, and proteoglycans. In addition, plasmin can convert MMPs, procollagenase, and prostromelysin to their active forms (Eeckhout and Vaes, 1977). Plasminogen has been localized to the cell surface of the human osteosarcoma line MG63, where its activity was enhanced by endogenous cell-bound uPA (Campbell et al., 1994).

The PA/plasmin pathway is regulated by members of the serpin family in addition to various hormones and cytokines. The primary function of this family of inhibitors is to neutralize serine proteinases by specific binding to the target enzyme. Serpins are involved in the regulation of several processes, including fibrinolysis, cell migration, tumor suppression, blood coagulation, and ECM remodeling (Potempa et al., 1994). Members of this pathway involved in the regulation of the PA/plasmin pathway are PAI-1 and PAI-2, which regulate uPA and tPA; protease nexin-1, which regulates thrombin, plasmin, and uPA; and α_2-antiplasmin, which regulates plasmin. Active PAI-1 combines with uPA and tPA, forming an equimolar complex, exerting its inhibition through interactions with the active-site serine. PAI-1 has been detected in media of cultured human fibrosarcoma cells (Andreasen et al., 1986) and primary cultures of rat hepatocytes and hepatoma cells.

PAI-1 was also detected in conditioned medium of rat osteoblast-like cells and rat osteosarcoma cells (Allan et al., 1990). The expression of uPA, tPA, type I receptor for uPA, PAI-1, PAI-2, and the broad-spectrum serine proteinase inhibitor protease nexin-1 is induced by PTH treatment in primary mouse osteoblasts. The regulation of these various enzymes within bone tissue may determine the sites where bone resorption will be initiated (Tumber et al., 2003).

Urokinase-type plasminogen activator

The uPA is secreted as a precursor form of ~55 kDa (Nielsen et al., 1988; Wun et al., 1982). It is activated by cleavage into a 30-kDa heavy chain and a 24-kDa light chain, joined by a disulfide bond, with the active site residing in the 30-kDa fragment. Urokinase has a Kringle domain, a serine proteinase-like active site, and a growth factor domain (GFD). The noncatalytic NH_2-terminal fragment contains the GFD and the Kringle domain and is referred to as the amino-terminal fragment (ATF). The uPA and PAI-1 are involved in regulation of the first steps of angiogenesis (Pepper, 1997). Rabbani et al. (1990) demonstrated that ATF stimulated proliferation and was involved in mitogenic activity in primary rat osteoblasts and the human osteosarcoma cell line SaOS-2. The GFD of the ATF is necessary for the binding of uPA to its specific receptor.

Tissue-type plasminogen activator

The tPA is secreted as a single-chain glycosylated 72-kDa polypeptide. This enzyme has been found in human plasma and various tissue extracts, as well as in normal and malignant cells. The cleavage of tPA forms a 39-kDa heavy chain and a 33-kDa light chain linked by a disulfide bond. The heavy chain has no proteinase activity, but contains two Kringle domains that assist in binding fibrin to plasminogen (Banyai et al., 1983; Pennica et al., 1983). Furthermore, the heavy chain contains a finger domain involved in fibrin binding (van Zonneveld et al., 1986) and a GFD with homology to human and murine EGF. tPA has been shown to be expressed in osteoblastic cells after nicotine or PTH treatment (Katano et al., 2006; Tumber et al., 2003).

Plasminogen activators in bone

PA activity is increased in normal and malignant osteoblasts as well as calvariae by many agents, including PTH, $1,25(OH)_2D_3$, PGE_2, IL-1α, fibroblast growth factor, and EGF (Hamilton et al., 1984, 1985; Thomson et al., 1989; Pfeilschifter et al., 1990; Cheng et al., 1991; Leloup et al., 1991; De Bart et al., 1995). It should be noted that other work suggests that PAs are not necessary for PTH- and $1,25(OH)_2D_3$-induced bone resorption (Leloup et al., 1994). Expression of tPA, uPA, PAI-1 and -2, protease nexin, and urokinase receptor isoform 1 was detected in microdissected mouse osteoclasts (Yang et al., 1997). Deletion of tPA, uPA, PAI-1, and plasminogen genes in mice can lead to fibrin deposition, some growth retardation, and inhibition of the osteoclast's ability to remove noncollagenous proteins in vitro (Carmeliet et al., 1993, 1994; Bugge et al., 1995; Daci et al., 1999). Moreover, lack of both PAs leads to elongation of neonatal bones and increased bone mass. Osteoblast differentiation and formation of a mineralized bone matrix are enhanced in osteoblast cultures derived from $tPA^{-/-}/uPA^{-/-}$ neonatal mice (Daci et al., 2003). In a more recent paper (Kawao et al., 2014) the authors showed that bone repair after a femoral bone defect was significantly delayed in global $tPA^{-/-}$ mice but not in global $uPA^{-/-}$ mice and concluded that this was due to reduced proliferation of osteoblasts. In another study of global $uPA^{-/-}$ mice (Popa et al., 2014), fracture healing was slightly delayed with increased cartilage area and decreased tartrate-resistant acid phosphatase staining, suggesting a role for osteoclastic uPA expression.

There are conflicting data as to whether the increase in osteoblastic PA activity in vitro is due to an increase in the total amount of one or both of the PAs or is due to a decline in the amount of PAI-1. All possible results have been observed, depending on which osteoblastic cell culture system is used or the method of identification of the enzymes. The latter have been difficult to assay categorically because there have not been abundant amounts of specific antibodies available for each of the rat PAs. Similarly, different groups have found the predominant osteoblastic PA to be uPA, whereas others have obtained results indicating it to be tPA.

A range of agents have also been found to inhibit the amount of osteoblastic PA activity. These include glucocorticoids, TGFβ, bFGF, leukemia inhibitory factor, and IGF-1 (Allan et al., 1990, 1991; Cheng et al., 1991; Forbes et al., 2003; Lalou et al., 1994; Pfeilschifter et al., 1990). Where it has been examined, in many of these cases the decline is due to a substantial increase in PAI-1 mRNA and protein. Nevertheless, some of these agents also markedly enhance the abundance of mRNA for the PAs (Allan et al., 1991), although the net effect is a decline in PA activity.

Cysteine proteinases

The major organic constituent of the ECM of bone is fibrillar type I collagen, which is deposited in intimate association with an inorganic calcium/phosphate mineral phase. The presence of the mineral phase protects the collagen not only from thermal denaturation but also from attack by proteolytic enzymes (Glimcher, 1998). The mature osteoclast, the bone-resorbing cell, has the capacity to degrade bone collagen through the production of a unique acid environment adjacent to the ruffled border through the concerted action of a vacuolar proton pump ([V]-type H^+-ATPase) (Chakraborty et al., 1994; Bartkowicz et al., 1995; Teitelbaum, 2000) and a chloride channel of the Cl-7 type (Kornak et al., 2001). Loss-of-function mutations in the genes that encode either this proton pump (Li et al., 1999; Frattini et al., 2000; Kornak et al., 2000) or the chloride channel (Kornak et al., 2001) lead to osteopetrosis. At the low pH in this extracellular space adjacent to the ruffled border, it is possible to leach the mineral phase from the collagen and permit proteinases that act at acid pH to cleave the collagen (Blair et al., 1993). Candidate acid-acting proteinases are cysteine proteinases such as cathepsin K. Cathepsin K is highly expressed in osteoclasts (Drake et al., 1996; Bossard et al., 1996). Cysteine proteinases contain an essential cysteine residue at their active site that is involved in forming a covalent intermediate complex with their substrates (Bond and Butler, 1987). The enzymes are either cytosolic or lysosomal. The latter have an acidic pH optimum and make up the majority of the cathepsins. These enzymes are regulated by a variety of protein inhibitors, including the cystatin superfamily (Turk and Bode, 1991) and α_2-macroglobulin (Barrett, 1986). Their extracellular abundance must consequently be regulated by cell surface receptors for α_2-macroglobulin as well as the lysosomal enzyme targeting mannose-6-phosphate/IGF-2 receptors.

The involvement of lysosomal cysteine proteinases in bone resorption has been indicated by many studies showing that inhibition of these enzymes prevents bone resorption in vitro as well as lowering serum calcium in vivo (Delaissé et al., 1984; Montenez et al., 1994). In particular, cathepsin K (Tezuka et al., 1994b) was found to have substantial effects on bone. Mice containing a targeted disruption of cathepsin K were developed and found to exhibit an osteopetrotic phenotype characterized by excessive trabeculation of the bone marrow space (Saftig et al., 1998, 2000). Cathepsin K−deficient osteoclasts are capable of demineralizing the ECM, but are unable to fully remove the demineralized bone (Gowen et al., 1999). In addition, cathepsin K mutations have been linked to pycnodysostosis, a hereditary bone disorder characterized by osteosclerosis, short stature, and defective osteoclast function (Gelb et al., 1996). Further studies show that the expression of MMP-9, TRACP (tartrate-specific acid phosphatase) for osteoclastic enzymes and osteoblastic proteases (MMP-13, MMP-14), and RANKL is increased in cathepsin K−deficient mice (Kiviranta et al., 2005). Moreover, cathepsin K−deficient osteoclasts compensate for the lack of this enzyme by using MMPs in the resorption of bone matrix (Everts et al., 2006). It has been shown that cathepsin K is responsible for the activation of pro-MMP-9 in acidic environments such as are seen in tumors and during bone resorption (Christensen et al., 2015). Importantly, cathepsin K not only degrades type I collagen, it also degrades periostin, bradykinin, TGFβ1, and IGF-1, among other proteins (Bonnet et al., 2017; Godat et al., 2008; Fuller et al., 2004; Panwar et al., 2016). Cathepsin K inhibition increases periostin levels and bone formation in vivo (Bonnet et al., 2017). Its inhibition also leads to increases in serum TGFβ and evident fibrosis in a number of tissues (Runger et al., 2012).

Cathepsin inhibitors may be therapeutically beneficial in the treatment of osteoporosis and rheumatoid arthritis to stimulate cortical bone formation and inhibit bone resorption (Xiang et al., 2007). However, cathepsin K deficiency reduces atherosclerotic plaque and induces plaque fibrosis (Lutgens et al., 2006a). Use of a cathepsin K inhibitor as a possible therapeutic target for atherosclerosis should have been evaluated with care because cathepsin K inhibition probably leads to a profibrotic, but also to a more lipogenic, plaque phenotype (Lutgens et al., 2006b). In fact, this may have been the reason the cathepsin K active-site inhibitor odanacatinib failed in osteoporosis treatment clinical trials due to strokes and other cardiovascular adverse events (Mullard, 2016). However, other non-active-site inhibitors, ectosteric inhibitors, may be promising alternatives (Panwar et al., 2016) that do not have the off-target effects of odanacatinib, since they appear to inhibit only the cathepsin K−mediated degradation of type I collagen.

Immunohistochemistry revealed that the majority of the cysteine proteinases (cathepsins B, K, and L) and the aminopeptidases (cathepsins C and H) are products of osteoclasts (Ohsawa et al., 1993; Yamaza et al., 1998; Littlewood-Evans et al., 1997), although immunoreactive staining for cathepsins B, C, and H was also seen in osteoblasts and osteocytes. It is notable that the most potent collagenolytic cathepsin at acid pH, cathepsin L, was strongly expressed in osteoclasts and very weakly in osteoblasts. Mathieu et al. (1994), however, have detected both cathepsins B and L as proteins secreted by their immortalized osteogenic stromal cell line MN7. Everts et al. (2006) have shown that cathepsin L is involved in modulating MMP-mediated resorption by calvarial osteoclasts.

There has been work demonstrating that osteocytes produce cathepsin K (Qing et al.,2012), and this may have an important physiological role in osteocytic osteolysis, particularly in the lactating mouse, when serum PTH-related protein

levels are high and demand for calcium for milk production is very high. Presumably, osteocytic cathepsin K also degrades growth factors, or perhaps activates them, and thus, could have an added role in bone turnover. The knowledge that the osteocyte expresses cathepsin K is also a cautionary note in the use of the cathepsin K−Cre mouse, since this is unlikely to be specific for osteoclasts.

Oursler et al. (1993) have also demonstrated that normal human osteoblast-like cells produce cathepsin B and that dexamethasone can increase expression and secretion of this lysosomal enzyme by these cells. Interestingly, they also showed that dexamethasone treatment causes activation of TGFβ and, by the use of lysosomal proteinase inhibitors, ascribed a role for cathepsins B and D in the activation of this growth factor.

Aspartic proteinases

These lysosomal proteinases contain an aspartic acid residue at their active site and act at acid pH. Very little investigation has been conducted on these enzymes in bone cells, except for the observations that cathepsin D, a member of this family, can be found by immunohistochemical staining in osteoblasts and osteocytes (Ohsawa et al., 1993), and expression of this enzyme is increased markedly by dexamethasone treatment of human osteoblasts in culture (Oursler et al., 1993). Cathepsin D is secreted into the resorbing area of human odontoclasts in order to participate in degradation of mineralized tooth matrix (Gotz et al., 2000).

Conclusions

The osteoblast lineage has the ability to produce proteinases of all four classes, but far more is known about their production of collagenase and PAs, at least in vitro. We still do not know the absolute role of any of these osteoblastic enzymes in vivo. Further work with global and conditional knockouts of the respective enzymes is likely to be the only way we will determine their required functions. These roles may not be restricted to assisting in the resorption process but may include functions to regulate bone development. In addition, the osteoclast produces MMP-9 and cathepsin K, which appear to have similar roles in the two diverse processes.

References

Aimes, R.T., Quigley, J.P., 1995. Matrix metalloproteinase-2 is an interstitial collagenase: inhibitor-free enzyme catalyzes the cleavage of collagen fibrils and soluble native type I collagen generating the specific 3/4- and 1/4-length cleavage fragments. J. Biol. Chem. 270, 5872−5876.

Al-Aqeel, A.I., 2005. Al-Aqeel Sewairi syndrome, a new autosomal recessive disorder with multicentric osteolysis, nodulosis and arthropathy. The first genetic defect of matrix metalloproteinase-2 gene. Saudi Med. J. 26, 24−30.

Allan, E.H., Hilton, D.J., Brown, M.A., Evely, R.S., Yumita, S., Medcalf, D., Gough, N.M., Ng, K.W., Nicola, N.A., Martin, T.J., 1990. Osteoblasts display receptors for and responses to leukemia-inhibitory factor. J. Cell. Physiol. 145, 110−119.

Allan, E.H., Zeheb, R., Gelehrter, T.D., Heaton, J.H., Fukumoto, S., Yee, J.A., Martin, T.J., 1991. Transforming growth factor beta inhibits plasminogen activator (PA) activity and stimulates production of urokinase-type PA, PA inhibitor-1 mRNA, and protein in rat osteoblast-like cells. J. Cell. Physiol. 149, 34−43.

Andreasen, P.A., Nielsen, L.S., Kristensen, P., Grondahl-Hansen, J., Skriver, L., Dano, K., 1986. Plasminogen activator inhibitor from human fibrosarcoma cells binds urokinase-type plasminogen activator, but not its proenzyme. J. Biol. Chem. 261, 7644−7651.

Angel, P., Karin, M., 1991. The role of *jun, fos* and the AP-1 complex in cell-proliferation and transformation. Biochim. Biophys. Acta 1072, 129−157.

Apte, S.S., Fukai, N., Beier, D.R., Olsen, B.R., 1997. The matrix metalloproteinase-14 (MMP-14) gene is structurally distinct from other MMP genes and is co-expressed with the TIMP-2 gene during mouse embryogenesis. J. Biol. Chem. 272, 25511−25517.

Balbín, M., Fueyo, A., Knauper, V., Lopez, J.M., Alvarez, J., Sanchez, L.M., Quesada, V., Bordallo, J., Murphy, G., Lopez-Otín, C., 2001. Identification and enzymatic characterization of two diverging murine counterparts of human interstitial collagenase (MMP-1) expressed at sites of embryo implantation. J. Biol. Chem. 276, 10253−10262.

Balbín, M., Fueyo, A., Knauper, V., Pendas, A.M., Lopez, J.M., Jimenez, M.G., Murphy, G., Lopez-Otín, C., 1998. Collagenase 2 (MMP-8) expression in murine tissue-remodeling processes: analysis of its potential role in postpartum involution of the uterus. J. Biol. Chem. 273, 23959−23968.

Balbin, M., Fueyo, A., Tester, A.M., Pendas, A.M., Pitiot, A.S., Astudillo, A., Overall, C.M., Shapiro, S.D., López-Otín, C., 2003. Loss of collagenase-2 confers increased skin tumor susceptibility to male mice. Nat. Genet. 35, 252−257.

Banerjee, C., McCabe, L.R., Choi, J.Y., Hiebert, S.W., Stein, J.L., Stein, G.S., Lian, J.B., 1997. An AML-1 consensus sequence binds an osteoblast-specific complex and transcriptionally activates the osteocalcin gene. J. Cell. Biochem. 66, 1−8.

Banyai, L., Varadi, A., Patthy, L., 1983. Common evolutionary origin of the fibrin-binding structures of fibronectin and tissue-type plasminogen activator. FEBS Lett. 163, 37−41.

Barmina, O.Y., Walling, H.W., Fiacco, G.J., Freije, J.M., López-Otín, C., Jeffrey, J.J., Partridge, N.C., 1999. Collagenase-3 binds to a specific receptor and requires the low density lipoprotein receptor-related protein for internalization. J. Biol. Chem. 274, 30087−30093.

Barrett, A.J., 1986. Physiological inhibitors of the human lysosomal cysteine proteinases. In: Ogawa, H., Lazarus, G.S., Hopsu-Havu, V.K. (Eds.), The Biological Role of Proteinases and Their Inhibitors in Skin. Elsevier, New York, pp. 13–26.

Bartkiewicz, M., Hernando, N., Reddy, S.V., Roodman, G.D., Baron, R., 1995. Characterization of the osteoclast vacuolar H(+)-ATPase B-subunit. Gene 160, 157–164.

Blair, H.D., Teitelbaum, S.L., Grosso, L.E., Lacey, D.L., Tan, H.-L., McCourt, D.W., Jeffrey, J.J., 1993. Extracellular-matrix degradation at acid pH: avian osteoclast acid collagenase isolation and characterization. Biochem. J. 29, 873–874.

Blom, A.B., van Lent, P.L., Libregts, S., Holthuysen, A.E., van der Kraan, P.M., van Rooijen, N., van den Berg, W.B., 2007. Crucial role of macrophages in matrix metalloproteinase-mediated cartilage destruction during experimental osteoarthritis: involvement of matrix metalloproteinase 3. Arthritis Rheum. 56, 147–157.

Bond, J.S., Butler, P.E., 1987. Intracellular proteases. Annu. Rev. Biochem. 56, 333–364.

Bonnet, N., Brun, J., Rousseau, J.-C., Duong, L.T., Ferrari, S.L., 2017. Cathepsin K controls cortical bone formation by degrading periostin. J. Bone Miner. Res. 32, 1432–1441.

Bossard, M.J., Tomaszek, T.A., Thompson, S.K., Amegadzie, B.Y., Hanning, C.R., Jones, C., Kurdyla, J.T., McNulty, D.E., Drake, F.H., Gowen, M., Levey, M.A., 1996. Proteolytic activity of human osteoclast cathepsin K: expression, purification, activation, and substrate identification. J. Biol. Chem. 271, 12517–12524.

Boumah, C.E., Lee, M., Selvamurugan, N., Shimizu, E., Partridge, N.C., 2009. Runx2 recruits p300 to mediate parathyroid hormone's effects on histone acetylation and transcriptional activation of the matrix metalloproteinase-13 gene. Mol. Endocrinol. 23, 1255–1263.

Breckon, J.J., Papaioannou, S., Kon, L.W., Tumber, A., Hembry, R.M., Murphy, G., Reynolds, J.J., Meikle, M.C., 1999. Stromelysin (MMP-3) synthesis is up-regulated in estrogen-deficient mouse osteoblasts in vivo and in vitro. J. Bone Miner. Res. 14, 1880–1890.

Brew, K., Nagase, H., 2010. The tissue inhibitors of metalloproteinases (TIMPs): an ancient family with structural and functional diversity. Biochim. Biophys. Acta 1803, 55–71.

Brinckerhoff, C.E., 1992. Regulation of metalloproteinase gene expression: implications for osteoarthritis. Crit. Rev. Eukaryot. Gene Expr. 2, 145–164.

Brinckerhoff, C.E., Harris Jr., E.D., 1981. Modulation by retinoic acid and corticosteroids of collagenase production by rabbit synovial fibroblasts treated with phorbol myristate acetate or poly(ethylene glycol). Biochem. Biophys. Acta 677, 424–432.

Bugge, T.H., Flick, M.T., Daugherty, C.C., Degen, J.L., 1995. Plasminogen deficiency causes severe thrombosis but is compatible with development and reproduction. Genes Dev. 9, 794–807.

Campbell, P.G., Wines, K., Yanosick, T.B., Novak, J.F., 1994. Binding and activation of plasminogen on the surface of osteosarcoma cells. J. Cell. Physiol. 159, 1–10.

Canalis, E., Rydziel, S., Delany, A.M., Varghese, S., Jeffrey, J.J., 1995. Insulin-like growth factors inhibit interstitial collagenase synthesis in bone cultures. Endocrinology 136, 1348–1354.

Carmeliet, P., Kieckens, L., Schoonjans, L., Ream, B., van Nuffelen, A., Prendergast, G., Cole, M., Bronson, R., Collen, D., Mulligan, R.C., 1993. Plasminogen activator inhibitor-1 gene-deficient mice. I. Generation by homologous recombination and characterization. J. Clin. Investig. 92, 2746–2755.

Carmeliet, P., Schoonjans, L., Kieckens, L., Ream, B., Degen, J., Bronson, R., De Vos, R., van den Oord, J.J., Collen, D., Mulligan, R.C., 1994. Physiological consequences of loss of plasminogen activator gene function in mice. Nature 368, 419–424.

Cerda-Costà, N., Gomis-Rüth, X., 2014. Architecture and function of metallopeptidase catalytic domains. Protein Sci. 23, 123–144.

Chakraborty, M., Chatterjee, D., Gorelick, F.S., Baron, R., 1994. Cell cycle-dependent and kinase-specific regulation of the apical Na/H exchanger and the Na, K-ATPase in the kidney cell line LLC-PK_1 by calcitonin. Proc. Natl. Acad. Sci. U.S.A. 91, 2115–2119.

Cheng, S.-L., Shen, V., Peck, W.A., 1991. Regulation of plasminogen activator and plasminogen activator inhibitor production by growth factors and cytokines in rat calvarial cells. Calcif. Tissue Int. 49, 321–327.

Chin, J.R., Murphy, G., Werb, Z., 1985. Stromelysin, a connective tissue-degrading metalloendopeptidase secreted by stimulated rabbit synovial fibroblasts in parallel with collagenase. J. Biol. Chem. 260, 12367–12376.

Chiu, R., Boyle, W.J., Meek, J., Smeal, T., Hunter, T., Karin, M., 1988. The c-fos protein interacts with c-Jun/AP-1 to stimulate transcription of AP-1 responsive genes. Cell 54, 541–542.

Christensen, J., Shastri, V.P., 2015. Matrix-metalloproteinase-9 is cleaved and activated by cathepsin K. BMC Res. Notes 8, 322.

Civitelli, R., Hruska, K.A., Jeffrey, J.J., Kahn, A.J., Avioli, L.V., Partridge, N.C., 1989. Second messenger signaling in the regulation of collagenase production by osteogenic sarcoma cells. Endocrinology 124, 2928–2934.

Clohisy, J.C., Scott, D.K., Brakenhoff, K.D., Quinn, C.O., Partridge, N.C., 1992. Parathyroid hormone induces *c-fos* and *c-jun* messenger RNA in rat osteoblastic cells. Mol. Endocrinol. 6, 1834–1842.

Collen, A., Hanemaaijer, R., Lupu, F., Quax, P.H., van Lent, N., Grimbergen, J., Peters, E., Koolwijk, P., van Hinsbergh, V.W.M., 2003. Membrane-type matrix metalloproteinase-mediated angiogenesis in a fibrin-collagen matrix. Blood 101, 1810–1817.

Collier, I.E., Wilhelm, S.M., Eisen, A.Z., Marmer, B.L., Grant, G.A., Seltzer, J.L., Kronberger, A., He, C., Bauer, E.A., Goldberg, G.I., 1988. H-ras oncogene-transformed human bronchial epithelial cells (TBE-1) secrete a single metalloprotease capable of degrading basement membrane collagen. J. Biol. Chem. 263, 6579–6587.

Connolly, T.J., Clohisy, J.C., Bergman, K.D., Partridge, N.C., Quinn, C.O., 1994. Retinoic acid stimulates interstitial collagenase mRNA in osteosarcoma cells. Endocrinology 135, 2542–2548.

Crawford, H.C., Matrisian, L.M., 1996. Mechanisms controlling the transcription of matrix metalloproteinase genes in normal and neoplastic cells. Enzyme Protein 49, 20–37.

Daci, E., Udagawa, N., Martin, T.J., Bouillon, R., Carmeliet, G., 1999. The role of the plasminogen system in bone resorption in vitro. J. Bone Miner. Res. 14, 946–952.

Daci, E., Everts, V., Torrekens, S., van Herck, E., Tigchelaar-Gutterr, W., Bouillon, R., Carmeliet, G., 2003. Increased bone formation in mice lacking plasminogen activators. J. Bone Miner. Res. 18, 1167–1176.

D'Alonzo, R.C., Selvamurugan, N., Karsenty, G., Partridge, N.C., 2002. Physical interaction of the activator protein-1 factors c-Fos and c-Jun with Cbfa1 for collagenase promoter activation. J. Biol. Chem. 277, 816–822.

Davis, B.A., Sipe, B., Gershan, L.A., Fiacco, G.J., Lorenz, T.C., Jeffrey, J.J., Partridge, N.C., 1998. Collagenase and tissue plasminogen activator production in developing rat calvariae: normal progression despite fetal exposure to microgravity. Calcif. Tissue Int. 63, 416–422.

De Bart, A.C.W., Quax, P.H.A., Lowik, C.W.G.M., Verheijen, J.H., 1995. Regulation of plasminogen activation, matrix metalloproteinases and urokinase-type plasminogen activator-mediated extracellular matrix degradation in human osteosarcoma cell line MG63 by interleukin-1 alpha. J. Bone Miner. Res. 10, 1374–1384.

Delaissé, J.-M., Eeckhout, Y., Vaes, G., 1984. *In vivo* and *in vitro* evidence for the involvement of cysteine proteinases in bone resorption. Biochem. Biophys. Res. Commun. 125, 441–447.

Delaissé, J.-M., Eeckhout, Y., Vaes, G., 1988. Bone-resorbing agents affect the production and distribution of procollagenase as well as the activity of collagenase in bone tissue. Endocrinology 123, 264–276.

Delaissé, J.-M., Eeckhout, Y., Neff, L., Francois-Gillet, C.H., Henriet, P., Su, Y., Vaes, G., Baron, R., 1993. (Pro) collagenase (matrix metalloproteinase-1) is present in rodent osteoclasts and in the underlying bone-resorbing compartment. J. Cell Sci. 106, 1071–1082.

Delaissé, J.-M., Engsig, M.T., Everts, V., del Carmen Ovejero, M., Ferreras, M., Lund, L., Vu, T.H., Werb, Z., Winding, B., Lochter, A., Karsdal, M.A., Kirkegaard, T., Lenhard, T., Heegaard, A.M., Neff, L., Baron, R., Foged, N.T., 2000. Proteinases in bone resorption: obvious and less obvious roles. Clin. Chim. Acta 291, 223–234.

Delgado-Calle, J., Hancock, B., Likine, E.F., Sato, A.Y., McAndrews, K., Sanudo, C., Bruzzaniti, A., Riancho, J.A., Tonra, J.R., Bellido, T., 2018. MMP14 is a novel target of PTH signaling in osteocytes that controls resorption by regulating soluble RANKL production. FASEB J. 32, 2878–2890.

Drake, F.H., Dodds, R.A., James, I.E., Connor, J.R., Debouck, S., Richardson, E., Lee-Rykaczewski, L., Coleman, D., Rieman, R., Barthlow, G., Gowen, M., 1996. Cathepsin K, but not cathepsin B, L, or S, is abundantly expressed in human osteoclasts. J. Biol. Chem. 271, 12511–12516.

Ducy, P., Zhang, R., Geoffroy, V., Ridall, A.L., Karsenty, G., 1997. Osf2/Cbfal: a transcriptional activator of osteoblast differentiation. Cell 89, 747–754.

Eeckhout, Y., Vaes, G., 1977. Further studies on the activation of procollagenase, the latent precursor of bone collagenase: effects of lysosomal cathepsin B, plasmin and kallikrein and spontaneous activation. Biochem. J. 166, 21–31.

English, W.R., Puente, X.S., Freije, J.M., Knauper, V., Amour, A., Merryweather, A., López-Otín, C., Murphy, G., 2000. Membrane type 4 matrix metalloproteinase (MMP17) has tumor necrosis factor-alpha convertase activity but does not activate pro-MMP2. J. Biol. Chem. 275, 14046–14055.

Evans, B.R., Mosig, R.A., Lobl, M., Martignetti, C.R., Camacho, C., Grum-Tokars, V., Glucksman, M.J., Martignetti, J.A., 2012. Mutation of membrane type-1 metalloproteinase, MT1-MMP, causes the multicentric osteolysis and arthritis disease Winchester syndrome. Am. J. Hum. Genet. 91, 572–576.

Everts, V., Korper, W., Hoeben, K.A., Jansen, I.D., Bromme, D., Cleutiens, K.B., Heeneman, S., Peters, C., Reinheckel, T., Saftig, P., Beertsen, W., 2006. Osteoclastic bone degradation and the role of different cysteine proteinases and matrix metalloproteinases: differences between calvaria and long bone. J. Bone Miner. Res. 21, 1399–1408.

Fingleton, B., 2007. Matrix metalloproteinases as valid clinical target. Curr. Pharmaceut. Des. 13, 333–346.

Forbes, K., Webb, M.A., Sehgal, I., 2003. Growth factor regulation of secreted matrix metalloproteinase and plasminogen activators in prostate cancer cells, normal prostate fibroblasts and normal osteoblasts. Prostate Cancer Prostatic Dis. 6, 148–153.

Frattini, A., Orchard, P.J., Sobacchi, C., Giliani, S., Abinun, M., Matsson, J.P., Kieling, D.J., Andersson, A.K., Wallbrandt, P., Zecca, L., Notarangelo, L.D., Vezzoni, P., Villa, A., 2000. Defects in TCIRG1 subunit of the vacuolar proton pump are responsible for a subset of human autosomal recessive osteopetrosis. Nat. Genet. 25, 343–346.

Freije, J.M.P., Diez-Itza, I., Balbín, M., Sanchez, L.M., Blasco, R., Tolivia, J., López-Otín, C., 1994. Molecular cloning and expression of collagenase-3, a novel human matrix metalloproteinase produced by breast carcinomas. J. Biol. Chem. 269, 16766–16773.

Fuller, K., Chambers, T.J., 1995. Localisation of mRNA for collagenase in osteocytic, bone surface, and chondrocytic cells but not osteoclasts. J. Cell Sci. 108, 2221–2230.

Fuller, K., Lawrence, K.M., Ross, J.L., Grabowska, U.B., Shiroo, M., Samuelsson, B., Chambers, T.J., 2008. Cathepsin K inhibitors prevent matrix-derived growth factor degradation by human osteoclasts. Bone 42, 200–211.

Fukuda, K., Fujitsu, Y., Kumagai, N., Nishida, T., 2006. Inhibition of matrix metalloproteinase-3 synthesis in human conjunctival fibroblasts by interleukin-4 or interleukin-13. Invest Ophthalmol Vis Sci 47, 2857–2864.

Galvez, B.G., Matias-Roman, S., Alber, J.P., Sanchez-Madrid, F., Arroyo, A.G., 2001. Membrane type 1-matrix metalloproteinase is activated during migration of human endothelial cells and modulates endothelial motility and matrix remodeling. J. Biol. Chem. 276, 37491–37500.

Gelb, B.D., Shi, G.P., Chapman, H.A., Desnick, R.J., 1996. Pycnodysostosis, a lysosomal disease caused by cathepsin K deficiency. Science 273, 1236–1238.

Geoffroy, V., Ducy, P., Karsenty, G., 1995. A PEBP2a/AML-1-related factor increases osteocalcin promoter activity through its binding to an osteoblast-specific cis-acting element. J. Biol. Chem. 270, 30973–30979.

Gerber, H.P., Vu, T.H., Ryan, A.M., Kowalski, J., Werb, Z., Ferrara, N., 2000. VEGF couples hypertrophic cartilage remodeling, ossification and angiogenesis during endochondral bone formation. Nat. Med. 5, 623–628.

Glimcher, M.J., 1998. The nature of the mineral component of bone: biological and clinical implications. In: Avioli, L.V., Krane, S.M. (Eds.), Metabolic Bone Disease and Clinically Related Disorders. Academic Press, San Diego, pp. 23–50.

Godat, E., Lecaille, F., Desmazes, C., Duchene, S., Weidauer, E., Saftig, P., Brömme, D., Vandier, C., Lalmanach, G., 2004. Cathepsin K: a cysteine protease with unique kinin-degrading properties. Biochem. J. 383, 501–506.

Goldberg, G.I., Wilhelm, S.M., Kronberger, A., Bauer, E.A., Grant, G.A., Eisen, A.Z., 1986. Human fibroblast collagenase: complete primary structure and homology to an oncogene transformation-induced rat protein. J. Biol. Chem. 261, 6600–6605.

Gotz, W., Quondamatteo, F., Ragotzki, S., Affeldt, J., Jager, A., 2000. Localization of cathepsin D in human odontoclasts. A light and electron microscopical immunocytochemical study. Connect. Tissue Res. 41, 185–194.

Gong, Y., Chippa-Vankata, U.D., Oh, W.K., 2014. Role of matrix metalloproteinases and their natural inhibitor in prostate cancer progression. Cancers 6, 1298–1327.

Grigoriadis, A.E., Wang, Z.-Q., Cecchini, M.G., Hofstetter, W., Felix, R., Fleisch, H.A., Wagner, E.F., 1994. c-Fos: a key regulator of osteoclast-macrophage lineage determination and bone remodeling. Science 266, 443–448.

Gowen, M., Lazner, R., Dodds, R., Kapadia, R., Field, J., Tavaria, M., 1999. Cathepsin K knockout mice develop osteopetrosis due to a deficit in matrix degradation but not demineralization. J. Bone Miner. Res. 14, 1654–1663.

Hamilton, J.A., Lingelbach, S.R., Partridge, N.C., Martin, T.J., 1984. Stimulation of plasminogen activator in osteoblast-like cells by bone resorbing-hormones. Biochem. Biophys. Res. Commun. 122, 230–236.

Hamilton, J.A., Lingelbach, S., Partridge, N.C., Martin, T.J., 1985. Regulation of plasminogen activator production by bone-resorbing hormones in normal and malignant osteoblasts. Endocrinology 116, 2186–2191.

Heath, J.K., Reynolds, J.J., Meikle, M.C., 1990. Osteopetrotic (grey-lethal) bone produces collagenase and TIMP in organ culture: regulation by vitamin A. Biochem. Biophys. Res. Commun. 168, 1171–1176.

Herz, J., Bock, H.H., 2002. Lipoprotein receptors in the nervous system. Annu. Rev. Biochem. 71, 405–434.

Hiraoka, N., Allen, E., Apel, I.J., Gyetko, M.R., Weiss, S.J., 1998. Matrix metalloproteinases regulate neovascularization by acting as pericellular fibrinolysins. Cell 95, 365–377.

Holmbeck, K., Bianco, P., Caterina, J., Yamada, S., Kromer, M., Kuznetsov, S.A., Mankani, M., Robey, P.G., Poole, A.R., Pidoux, I., Ward, J.M., Birkedal-Hansen, H., 1999. MT1-MMP-deficient mice develop dwarfism, osteopenia, arthritis, and connective tissue disease due to inadequate collagen turnover. Cell 99, 81–92.

Hotary, K., Allen, E., Punturieri, A., Yana, I., Weiss, S.J., 2000. Regulation of cell invasion and morphogenesis in a three-dimensional type I collagen matrix by membrane-type matrix metalloproteinases 1, 2, and 3. J. Cell Biol. 149, 1309–1323.

Hsieh, Y.S., Chu, S.C., Yang, S.F., Chen, P.N., Liu, Y.C., Lu, K.H., 2007. Silibinin suppresses human osteosarcoma MG-63 cell invasion by inhibiting the ERK-dependent c-Jun/AP-1 induction of MMP-2. Carcinogenesis 28, 977–987.

Huhtala, P., Chow, L.T., Tryggvason, K., 1990. Structure of the human type IV collagenase gene. J. Biol. Chem. 265, 11077–11082.

Huhtala, P., Tuuttila, A., Chow, L.T., Lohi, J., Keski-Oja, J., Tryggvason, K., 1991. Complete structure of the human gene for 92-kDa type IV collagenase. Divergent regulation of expression for the 92- and 72-kiloDalton enzyme genes in HT-1080 cells. J. Biol. Chem. 266, 16485–16490.

Inada, M., Wang, Y., Byrne, M.H., Rahman, M.U., Miyaura, C., Lopez-Otin, C., Krane, S.M., 2004. Critical roles for collagenase-3 (Mmp-13) in development of growth plate cartilage and in endochondral ossification. Proc. Natl. Acad. Sci. U.S.A. 101, 17192–17197.

Inoue, K., Mikuni-Takagaki, Y., Oikawa, K., Itoh, T., Inada, M., Noguchi, T., Park, J.S., Onodera, T., Krane, S.M., Noda, M., Itohara, S., 2006. A crucial role for matrix metalloproteinase 2 in osteocytic canalicular formation and bone metabolism. J. Biol. Chem. 281, 33814–33824.

Itoh, T., Ikeda, T., Gomi, H., Nakao, S., Suzuki, T., Itohara, S., 1997. Unaltered secretion of beta-amyloid precursor protein in gelatinase A (matrix metalloproteinase 2)-deficient mice. J. Biol. Chem. 272, 22389–22392.

Jilka, R.L., Cohn, D.V., 1983. A collagenolytic response to parathormone, 1,25-dihydroxycholecalciferol D_3, and prostaglandin E_2 in bone of osteopetrotic (mi/mi) mice. Endocrinology 112, 945–950.

Jimenez, M.J.G., Balbín, M., Lopez, J.M., Alvarez, J., Komori, T., López-Otín, C., 1999. Collagenase 3 is a target of Cbfa1, a transcription factor of the runt gene family involved in bone formation. Mol. Cell Biol. 19, 4431–4442.

Johansson, N., Saarialho-Kere, U., Airola, K., Herva, R., Nissinen, L., Westermarck, J., Vuorio, E., Heino, J., Kahari, V.M., 1997. Collagenase-3 (MMP-13) is expressed by hypertrophic chondrocytes, periosteal cells, and osteoblasts during human fetal bone development. Dev. Dynam. 208, 387–397.

Kaczmarek, L., Lapinska-Dzwonek, J., Szymczak, S., 2002. Matrix Metalloproteinases in the adult brain physiology: a link between c-Fos, AP-1 and remodeling of neuronal connections? EMBO J. 21, 6643–6648.

Kagoshima, H., Satake, M., Miyoshi, H., Ohki, M., Pepling, M., Gergen, J.P., Shigesada, K., Ito, Y., 1993. The runt domain identifies a new family of heteromeric transcriptional regulators. Trends Genet. 9, 338–341.

Kanno, T., Kanno, Y., Chen, L.F., Ogawa, E., Kim, W.Y., Ito, Y., 1998. Intrinsic transcriptional activation-inhibition domains of the polyomavirus enhancer binding protein 2/core binding factor alpha subunit revealed in the presence of the beta subunit. Mol. Cell Biol. 18, 2444–2454.

Katono, T., Kawato, T., Tanabe, N., Suzuki, N., Yamanaka, K., Oka, H., Motohashi, M., Maeno, M., 2006. Nicotine treatment induces expression of matrix metalloproteinases in human osteoblastic Saos-2 cells. Acta Biochim. Biophys. Sin. 38, 874–882.

Kawao, N., Tamura, Y., Okumoto, K., Yano, M., Okada, K., Matsuo, O., Kaji, H., 2014. Tissue-type plasminogen activator deficiency delays bone repair: roles of osteoblastic proliferation and vascular endothelial growth factor. Am. J. Physiol. Endocrinol. Metab. 307, E278–E288.

Kennedy, A.M., Inada, M., Krane, S.M., Christie, P.T., Harding, B., Lopez-Otin, C., Sanchez, L.M., Pannett, A.A., Dearlove, A., Hartley, C., Byrne, M.H., Reed, A.A., Nesbit, M.A., Whyte, M.P., Thakker, R.V., 2005. MMP13 mutation causes spondyloepimetaphyseal dysplasia, Missouri type (SEMD(MO). J. Clin. Investig. 115, 2832–2842.

Kerr, L.D., Holt, J.T., Matrisian, L.M., 1988a. Growth factors regulate transin gene expression by c-fos-dependent and c-fos-independent pathways. Science 242, 1424–1427.

Kerr, L.D., Olashaw, N.E., Matrisian, L.M., 1988b. Transforming growth factor β1 and and cAMP inhibit transcription of the epidermal growth factor and oncogene-induced transin RNA. J. Biol. Chem. 263, 16999−17005.

Kerr, L.D., Miller, D.B., Matrisian, L.M., 1990. TGF-β1 inhibition of transin/stromelysin gene expression is mediated through a fos binding sequence. Cell 61, 267−278.

Kinoh, H., Sato, H., Tsunezuka, Y., Takino, T., Kawashima, A., Okada, Y., Seiki, M., 1996. MT-MMP, the cell surface activator of proMMP-2 (pro-gelatinase A), is expressed with its substrate in mouse tissue during embryogenesis. J. Cell Sci. 109, 953−959.

Kiviranta, R., Morko, J., Alartalo, S.L., NicAmhlaoibh, R., Risteli, J., Laitala-Leinonen, T., Vuorio, E., 2005. Impared bone resorption in cathepsin K-deficient mice is partially compensated for by enhanced osteoclastogenesis and increased expression of other proteases via an increased RANKL/OPG ratio. Bone 36, 159−172.

Knauper, V., Wilhelm, S.M., Seperack, P.K., DeClerck, Y.A., Osthues, A., Tschesche, H., 1993. Direct activation of human neutrophil procollagenase by recombinant stromelysin. Biochem. J. 295, 581−586.

Komori, T., Yagi, H., Nomura, S., Yamaguchi, A., Sasaki, K., Deguchi, K., Shimizu, Y., Bronson, R.T., Gao, Y.-H., Inada, M., Sato, M., Okamoto, R., Kitamura, Y., Yoshiki, S., Kishimoto, T., 1997. Targeted disruption of *Cbfa1* results in a complete lack of bone formation owing to maturational arrest of osteoblasts. Cell 89, 755−764.

Kornak, U., Schulz, A., Friedrich, W., Uhlhaas, S., Kremens, B., Voit, T., Hasan, C., Bole, U., Jentsch, T.J., Kubisch, C., 2000. Mutations in the a3 subunit of the vacuolar H^+-ATPase cause infantile malignant osteopetrosis. Hum. Mol. Genet. 9, 2059−2063.

Kornak, U., Kasper, D., Bösl, M.R., Kaiser, E., Schweizer, M., Schulz, A., Friedrich, W., Delling, G., Jentsch, T.J., 2001. Loss of the C1C-7 chloride channel leads to osteopetrosis in mice and man. Cell 104, 205−215.

Kosaki, N., Takaishi, H., Kamekura, S., Kimura, T., Okada, Y., Minqi, L., Amizuka, N., Chung, U.I., Nakamura, K., Kawaguchi, H., Toyama, Y., D'Armiento, J., 2007. Impaired bone fracture healing in matrix metalloproteinase-13 deficient mice. Biochem. Biophys. Res. Commun. 354, 846−851.

Kusano, K., Miyaura, C., Inada, M., Tamura, T., Ito, A., Nagase, H., Kamoi, K., Suda, T., 1998. Regulation of matrix metalloproteinases (MMP-2, -3, -9, and -13) by interleukin-1 and interleukin-6 in mouse calvaria: association of MMP induction with bone resorption. Endocrinology 139, 1338−1345.

Lalou, C., Silve, C., Rosato, R., Segovia, B., Binoux, M., 1994. Interactions between insulin-like growth factor-I (IGF-I) and the system of plasminogen activators and their inhibitors in the control of IGF-binding protein-3 production and proteolysis in human osteosarcoma cells. Endocrinology 135, 2318−2326.

Lanske, B., Divieti, P., Kovacs, C.S., Pirro, A., Landis, W.J., Krane, S.M., Bringhurst, F.R., Kronenberg, H.M., 1998. The parathyroid hormone (PTH)/PTH-related peptide receptor mediates actions of both ligands in murine bone. Endocrinology 139, 5194−5204.

Lanske, B., Karaplis, C.A.C., Lee, K., Luz, A., Vortkamp, A., Pirro, A., Karperien, M., Defize, L.H.K., Ho, C., Mulligan, R.C., Abou-Samra, A.B., Jüppner, H., Segre, G.V., Kronenberg, H.M., 1996. PTH/PTHrP receptor in early development and indian hedgehog-regulated bone growth. Science 273, 663−666.

Lawson, N.D., Khanna-Gupta, A., Berliner, N., 1998. Isolation and characterization of the cDNA for mouse neutrophil collagenase: demonstration of shared negative regulatory pathway neutrophil secondary granule protein gene expression. Blood 91, 2517−2524.

Lee, W., Mitchell, P., Tjian, R., 1987. Purified transcription factor AP-1 interacts with TPA-inducible enhancer elements. Cell 49, 741−752.

Lee, M., Partridge, N.C., 2010. Parathyroid hormone activation of matrix metalloproteinase-13 transcription requires the histone acetyltransferase activity of p300 and PCAF and p300-dependent acetylation of PCAF. J. Biol. Chem. 285, 38014−38022.

Leloup, G., Delaissé, J.-M., Vaes, G., 1994. Relationship of the plasminogen activator/plasmin cascade to osteoclast invasion and mineral resorption in explanted fetal metatarsal bones. J. Bone Miner. Res. 9, 891−902.

Leloup, G., Peeters-Joris, C., Delaissé, J.-M., Opdenakker, G., Vaes, G., 1991. Tissue and urokinase plasminogen activators in bone tissue and their regulation by parathyroid hormone. J. Bone Miner. Res. 6, 1081−1090.

Le Maitre, C.L., Freemont, A.J., Hoyland, J.A., 2005. The role of interleukin-1 in the pathogenesis of human intervertebral disc degradation. Arthritis Res. Ther. 7, R732−R745.

Li, Y.P., Chen, W., Liang, Y., Li, E., Stashenko, P., 1999. Atp6i-deficient mice exhibit severe osteopetrosis due to loss of osteoclast-mediated extracellular acidification. Nat. Genet. 23, 447−451.

Littlewood-Evans, A., Kokubo, T., Ishibashi, O., Inaoka, T., Wlodarski, B., Gallagher, J.A., Bilbe, G., 1997. Localization of cathepsin K in human osteoclasts by in situ hybridization and immunohistochemistry. Bone 20, 81−86.

Liu, X., Wu, H., Byrne, M., Jeffrey, J., Krane, S., Jaenisch, R., 1995. A targeted mutation at the known collagenase cleavage site in mouse type I collagen impairs tissue remodeling. J. Cell Biol. 130, 227−237.

Llano, E., Pendas, A.M., Freije, J.P., Nakano, A., Knauper, V., Murphy, G., López-Otín, C., 1999. Identification and characterization of human MT5-MMP, a new membrane-bound activator of progelatinase a overexpressed in brain tumors. Cancer Res. 59, 2570−2576.

Lutgens, E., Lutgens, S.P., Faber, B.C., Heeneman, S., Gijbels, M.M., de Winther, M.P., Frederik, P., van der Made, I., Daugherty, A., Sijbergs, A.M., Fisher, A., Long, C.J., Saftig, P., Black, D., Daemen, M.J., Cleutjens, K.B., 2006a. Disruption of cathpsin K gene reduces atherosclerosis progression and induces plaque fibrosis but accelerates macrophage foam cell formation. Circulation 113, 98−107.

Lutgens, S.P., Kisters, N., Lutgens, E., van Haaften, R.I., Evelo, C.T., de Winther, M.P., Saftig, P., Daemen, M.J., Heenaman, S., Cleutjens, K.B., 2006b. Gene profiling of cathepsin K deficiency in atherogenesis: profibrotic but lipogenic. J. Pathol. 210, 334−343.

Lynch, C.C., Hikosaka, A., Acuff, H.B., Martin, M.D., Kawai, N., Singh, R.K., Vargo-Gogola, T.C., Begtrup, J.L., Peterson, T.E., Fingleton, B., Shirai, T., Matrisian, L.M., Futakuchi, M., 2005. MMP-7 promotes prostate cancer-induced osteolysis via the solubilization of RANKL. Cancer Cell 5, 485−496.

Martignetti, J.A., Aqeel, A.A., Sewairi, W.A., Boumah, C.E., Kambouris, M., Mayouf, S.A., Sheth, K.V., Eid, W.A., Dowling, O., Harris, J., Glucksman, M.J., Bahabri, S., Meyer, B.F., Desnick, R.J., 2001. Mutation of the matrix metalloproteinase 2 gene (MMP2) causes a multicentric osteolysis and arthritis syndrome. Nat. Genet. 28, 261–265.

Mathieu, E., Meheus, L., Raymackers, J., Merregaert, J., 1994. Characterization of the osteogenic stromal cell line MN7: identification of secreted MN7 proteins using two-dimensional polyacrylamide gel electrophoresis, Western blotting, and microsequencing. J. Bone Miner. Res. 9, 903–913.

Matrisian, L.M., 1992. The matrix-degrading metalloproteinases. Bioessays 14, 455–463.

Matrisian, L.M., Glaichenhaus, N., Gesnel, M.C., Breathnach, R., 1985. Epidermal growth factor and oncogenes induce transcription of the same cellular mRNA in rat fibroblasts. EMBO J. 4, 1435–1440.

Matrisian, L.M., Leroy, P., Ruhlmann, C., Gesnel, M.C., Breathnach, R., 1986. Isolation of the oncogene and epidermal growth factor-induced transin gene: complex control in rat fibroblasts. Mol. Cell Biol. 6, 1679–1686.

Mattot, V., Raes, M.B., Henriet, P., Eeckhout, Y., Stehelin, D., Vandenbunder, B., Desbiens, X., 1995. Expression of *interstitial collagenase* is restricted to skeletal tissue during mouse embryogenesis. J. Cell Sci. 108, 529–535.

McDonnell, S.E., Kerr, L.D., Matrisian, L.M., 1990. Epidermal growth factor stimulation of stromelysin mRNA in rat fibroblasts requires induction of proto-oncogenes c-fos and c-jun and activation of protein kinase C. J. Biol. Chem. 10, 4284–4293.

Meikle, M.C., Bond, S., Hembry, R.M., Compston, J., Croucher, P.I., Reynolds, J.J., 1992. Human osteoblasts in culture synthesize collagenase and other matrix metalloproteinases in response to osteotrophic hormones and cytokines. J. Cell Sci. 103, 1093–1099.

Merriman, H.L., van Wijnen, A.J., Hiebert, S., Bidwell, J.P., Fey, E., Lian, J., Stein, J., Stein, G.S., 1995. The tissue-specific nuclear matrix protein, NMP-2, is a member of the AML/CBF/PEBP2/*runt domain* transcription factor family: interactions with the osteocalcin gene promoter. Biochemistry 34, 13125–13132.

Mitra, A., Charkrabarti, J., Banerji, A., Chatterjee, A., 2006. Cell membrane-associated MT1-MMP dependent activation of MMP-2 in SiHa (human cervical cancer) cells. J. Environ. Pathol. Toxicol. Oncol. 25, 655–666.

Mitchell, P.G., Magna, H.A., Reeves, L.M., Lopresti-Morrow, L.L., Yocum, S.A., Rosner, P.J., Geoghegan, K.F., Hambor, J.E., 1996. Cloning, expression, and type II collagenolytic activity of matrix metalloproteinase-13 from human osteoarthritic cartilage. J. Clin. Investig. 97, 761–768.

Montenez, J.P., Delaissé, J.-M., Tulkens, P.M., Kishore, B.K., 1994. Increased activities of cathepsin B and other lysosomal hydrolases in fibroblasts and bone tissue cultured in the presence of cysteine proteinases inhibitors. Life Sci. 55, 1199–1209.

Mosig, R.A., Dowling, O., Difeo, A., Ramirez, M.C., Parker, I.C., Abe, E., Diouri, J., Ageel, A.A., Wylie, J.D., Oblander, S.A., Madri, J., Bianco, P., Apte, S.S., Zaidi, M., Doty, S.B., Majeska, R.J., Schaffler, M.B., Martignetti, J.A., 2007. Loss of MMP-2 disrupts skeletal and craniofacial development, and results in decreased bone mineralization, joint erosion, and defects in osteoblast and osteoclast growth. Hum. Mol. Genet. 16, 1113–1123.

Mudgett, J.S., Hutchinson, N.I., Chartrain, N.A., Forsyth, A.J., McDonnell, J., Singer, I.I., Bayne, E.K., Flanagan, J., Kawka, D., Shen, C.F., Stevens, K., Chen, H., Trumbauer, M., Visco, D.M., 1998. Susceptibility of stromelysin 1-deficient mice to collagen-induced arthritis and cartilage destruction. Arthritis Rheum. 41, 110–121.

Mullard, A., 2016. Merck &Co. drops osteoporosis drug odanacatib. Nat. Rev. Drug Discov. 15, 669.

Mundlos, S., Otto, F., Mundlos, C., Mulliken, J.B., Aylsworth, A.S., Albright, S., Lindhout, D., Cole, W.G., Henn, W., Knoll, J.H., Owen, M.J., Mertelsmann, R., Zabel, B.U., Olsen, B.R., 1997. Mutations involving the transcription factor CBFA1 cause cleidocranial dysplasia. Cell 89, 773–779.

Murphy, G., Cockett, M.I., Stephens, P.E., Smith, B.J., Docherty, A.J.P., 1987. Stromelysin is an activator of procollagenase. Biochem. J. 248, 265–268.

Nakatani, T., Chen, T., Partridge, N.C., 2016. MMP-13 is one of the critical mediators of the effect of HDAC4 deletion on the skeleton. Bone 90, 142–151.

Nakatani, T., Partridge, N.C., 2017. MEF2C interacts with c-FOS in PTH-stimulated *Mmp13* gene expression in osteoblastic cells. Endocrinology 158, 3778–3791.

Nam, D.H., Rodriguez, C., Remade, A.G., Strongin, A.Y., Ge, X., 2016. Active-site MMP-selective antibody inhibitors discovered from convex paratope synthetic libraries. Proc. Natl. Acad. Sci. U.S.A. 27, 14970–14975.

Nielsen, L.S., Kellerman, G.M., Behrendt, N., Picone, R., Dano, K., Blasi, F., 1988. A 55,000–60,000 Mr receptor protein for urokinase-type plasminogen activator. J. Biol. Chem. 263, 2358–2363.

Ohsawa, Y., Nitatori, T., Higuchi, S., Kominami, E., Uchiyama, Y., 1993. Lysosomal cysteine and aspartic proteinases, acid phosphatase, and endogenous cysteine proteinase inhibitor, cystatin-β, in rat osteoclasts. J. Histochem. Cytochem. 41, 1075–1083.

Ohuchi, E., Imai, K., Fuji, Y., Sato, H., Seiki, M., Okada, Y., 1997. Membrane type 1 matrix metalloproteinase digests interstitial collagens and other extracellular matrix macromolecules. J. Biol. Chem. 272, 2446–2451.

Omura, T.H., Noguchi, A., Johanns, C.A., Jeffrey, J.J., Partridge, N.C., 1994. Identification of a specific receptor for interstitial collagenase on osteoblastic cells. J. Biol. Chem. 269, 24994–24998.

Ortega, N., Behonick, D.J., Colnot, C., Cooper, D.N., Werb, Z., 2005. Galectin-3 is a downstream regulator of matrix metalloproteinase-9 function during endochondral bone formation. Mol. Biol. Cell 16, 3028–3039.

Otto, F., Thornell, A.P., Crompton, T., Denzel, A., Gilmour, K.C., Rosewell, I.R., Stamp, G.W.H., Beddington, R.S.P., Mundlos, S., Olsen, B.R., Selby, P.B., Owen, M.J., 1997. *Cbfa1*, a candidate gene for cleidocranial dysplasia syndrome, is essential for osteoblast differentiation and bone development. Cell 89, 765–771.

Otto, T.C., Bowers, R.R., Lane, M.D., 2007. BMP-4 treatment of C3H10T1/2 stem cells blocks expression of MMP-3 and MMP-13. Biochem. Biophys. Res. Commun. 353, 1097–1104.

Oursler, M.J., Riggs, B.L., Spelsberg, T.C., 1993. Glucocorticoid-induced activation of latent transforming growth factor-β by normal human osteoblast-like cells. Endocrinology 133, 2187–2196.

Overall, C.M., Wrana, J.F., Sodek, J., 1989. Transforming growth factor-β regulation of collagenase, 72 kDa- progelatinase, TIMP and PAI-1 expression in rat bone cell populations and human fibroblasts. Connect. Tissue Res. 20, 289–294.

Page-McCaw, A., Ewald, A.J., Werb, Z., 2007. Matrix metalloproteinases and the regulation of tissue remodeling. Nat. Rev. Mol. Cell Biol. 8, 221–233.

Panwar, P., Soe, K., Guido, R.V., Bueno, R.V., Delaisse, J.M., Bromme, D., 2016. A novel approach to inhibit bone resorption: exosite inhibitors against cathepsin K. Br. J. Pharmacol. 173, 396–410.

Pap, T., Shigeyama, Y., Kuchen, S., Fernihough, J.K., Simmen, B., Gay, R.E., Billingham, M., Gay, S., 2000. Differential expression pattern of membrane-type matrix metalloproteinases in rheumatoid arthritis. Arthritis Rheum. 43, 1226–1232.

Partridge, N.C., Frampton, R.J., Eisman, J.A., Michelangeli, V.P., Elms, E., Bradley, T.R., Martin, T.J., 1980. Receptors for $1,25(OH)_2$-vitamin D_3 enriched in cloned osteoblast-like rat osteogenic sarcoma cells. FEBS Lett. 115, 139–142.

Partridge, N.C., Alcorn, D., Michelangeli, V.P., Ryan, G., Martin, T.J., 1983. Morphological and biochemical characterization of four clonal osteogenic sarcoma cell lines of rat origin. Cancer Res. 43, 4308–4314.

Partridge, N.C., Jeffrey, J.J., Ehlich, L.S., Teitelbaum, S.L., Fliszar, C., Welgus, H.G., Kahn, A.J., 1987. Hormonal regulation of the production of collagenase and a collagenase inhibitor activity by rat osteogenic sarcoma cells. Endocrinology 120, 1956–1962.

Partridge, N.C., Scott, D.K., Gershan, L.A., Omura, T.H., Burke, J.S., Jeffrey, J.J., Bolander, M.E., Quinn, C.O., 1993. Collagenase production by normal and malignant osteoblastic cells. In: Novak, J.F., McMaster, J.H. (Eds.), Frontiers of Osteosarcoma Research. Hogrefe and Huber Publishers, Seattle, pp. 269–276.

Pearman, A.T., Chou, W.Y., Bergman, K.D., Pulumati, M.R., Partridge, N.C., 1996. Parathyroid hormone induces c-fos promoter activity in osteoblastic cells through phosphorylated cAMP response element (CRE)-binding protein binding to the major CRE. J. Biol. Chem. 271, 25715–25721.

Pei, D., 1999. Identification and characterization of the fifth membrane-type matrix metalloproteinase MT5-MMP. J. Biol. Chem. 274, 8925–8932.

Pei, D., Weiss, S.J., 1996. Transmembrane-deletion mutants of the membrane-type matrix metalloproteinase-1 process progelatinase A and express intrinsic matrix-degrading activity. J. Biol. Chem. 271, 9135–9140.

Pennica, D., Holmes, W.E., Kohr, W.T., Harkins, R.N., Vehar, G.A., Ward, C.A., Bennett, W.F., Yelverton, E., Seeburg, P.H., Heyneker, H.L., Goeddel, D.V., Collen, D., 1983. Cloning and expression of human tissue-type plasminogen activator cDNA in *E. coli*. Nature 301, 214–221.

Pepper, M.S., 1997. Manipulating angiogenesis: from basic science to the bedside. Arterioscler. Thromb. Vasc. Biol. 17, 605–619.

Pereira, R.C., Jorgetti, V., Canalis, E., 1999. Triiodothyronine induces collagenase-3 and gelatinase B expression in murine osteoblasts. Am J Physiol 277, E496–504.

Pfeilschifter, J., Erdmann, J., Schmidt, W., Naumann, A., Minne, H.W., Ziegler, R., 1990. Differential regulation of plasminogen activator and plasminogen activator inhibitor by osteotropic factors in primary cultures of mature osteoblasts and osteoblast precursors. Endocrinology 126, 703–711.

Pohlkamp, T., Wasser, C.R., Herz, J., 2017. Functional roles of the interaction of APP and lipoprotein receptors. Front. Mol. Neurosci. 10, 54. https://doi.org/10.3389/fnmol.2017.00054.

Popa, N.L., Wergedal, J.E., Lau, K.H., Mohan, S., Rundle, C.H., 2014. Urokinase plasminogen activator gene deficiency inhibits fracture cartilage remodeling. J. Bone Miner. Metab. 32, 124–135.

Posthumus, M.D., Limburg, P.C., Westra, J., van Leeuwen, M.A., van Rijswijk, M.H., 2000. Serum matrix metalloproteinase 3 in early rheumatoid arthritis is correlated with disease activity and radiological progression. J. Rheumatol. 27, 2761–2768.

Potempa, J., Korzos, E., Travis, J., 1994. The serpin superfamily of proteinase inhibitors: structure, function and regulation. J. Biol. Chem. 269, 15957–15960.

Prontera, C., Crescenzi, G., Rotilio, D., 1996. Inhibition by interleukin-4 of stromelysin expression in human skin fibroblasts: role of PKC. Exp. Cell Res. 224, 183–188.

Puente, X.S., Pendás, A.M., Llano, E., Velasco, G., López-Otín, C., 1996. Molecular cloning of a novel membrane-type matrix metalloproteinase from a human breast carcinoma. Cancer Res. 56, 944–949.

Qing, H., Ardeshirpour, L., Pajevic, P.D., Dusevich, V., Jahn, K., Kato, S., Wysolmerski, J., Bonewald, L.F., 2012. Demonstration of osteocytic perilacunar/canalicular remodeling in mice during lactation. J. Bone Miner. Res. 27, 1018–1029.

Quinn, C.O., Scott, D.K., Brinckerhoff, C.E., Matrisian, L.M., Jeffrey, J.J., Partridge, N.C., 1990. Rat collagenase: cloning, amino acid sequence comparison, and parathyroid hormone regulation in osteoblastic cells. J. Biol. Chem. 265, 22342–22347.

Rabbani, S.A., Desjardins, J., Bell, A.W., Banville, D., Mazar, A., Henkin, J., Goltzman, D., 1990. An amino terminal fragment of urokinase isolated from a prostate cancer cell line (PC-3) is mitogenic for osteoblast-like cells. Biochem. Biophys. Res. Commun. 173, 1058–1064.

Raggatt, L.J., Jefcoat Jr., S.C., Choudhury, I., Williams, S., Tiku, M., Partridge, N.C., 2006. Matrix metalloproteinase-13 influences ERK signalling in articular rabbit chondrocytes. Osteoarthritis Cartilage 14, 680–689.

Rajakumar, R.A., Partridge, N.C., Quinn, C.O., 1993. Transcriptional induction of collagenase in rat osteosarcoma cells is mediated by sequence 5 prime of the gene. J. Bone Miner. Res. 8 (Suppl. 1), S294.

Reboul, P., Pelletier, J.P., Tardif, G., Cloutier, J.M., Martel-Pelletier, J., 1996. The new collagenase, collagenase-3, is expressed and synthesized by human chondrocytes but not by synoviocytes: a role in osteoarthritis. J. Clin. Investig. 97, 2011–2019.

Rifas, L., Halstead, L.R., Peck, W.A., Avioli, L.V., Welgus, H.G., 1989. Human osteoblasts *in vitro* secrete tissue inhibitor of metalloproteinases and gelatinase but not interstitial collagenase as major cellular products. J. Clin. Investig. 84, 686–694.

Rifas, L., Fausto, A., Scott, M.J., Avioli, L.V., Welgus, H.G., 1994. Expression of metalloproteinases and tissue inhibitors of metallopro-teinases in human osteoblast-like cells: differentiation is associated with repression of metalloproteinase biosynthesis. Endocrinology 134, 213–221.

Roswit, W.T., Halme, J., Jeffrey, J.J., 1983. Purification and properties of rat uterine procollagenase. Arch. Biochem. Biophys. 225, 285–295.

Ruangpanit, N., Chan, D., Holmbeck, K., Birkedal-Hansen, H., Polarek, J., Yang, C., Bateman, J.F., Thompson, E.W., 2001. Gelatinase A (MMP-2) activation by skin fibroblasts: dependence on MT-1MMP expression and fibrillar collagen form. Matrix Biol. 20, 193–203.

Runger, T.M., Adami, S., Benhamou, C.L., Czerwinski, E., Farrerons, J., Kendler, D.L., Mindeholm, L., Realdi, G., Roux, C., Smith, V., 2012. Morphea-like skin reactions in patients treated with the cathepsin K inhibitor balicatib. J. Am. Acad. Dermatol. 66, e89–96.

Rydziel, S., Durant, D., Canalis, E., 2000. Platelet-derived growth factor induces collagenase 3 transcription in osteoblasts through the activator protein 1 complex. J. Cell. Physiol. 184, 326–333.

Sabeh, F., Ota, I., Holmbeck, K., Birkedal-Hansen, H., Soloway, P., Balbin, M., Lopez-Otin, C., Shapiro, S., Inada, M., Krane, S., Allen, E., Chung, D., Weiss, S.J., 2004. Tumor cell traffic through the extracellular matrix is controlled by the membrane-anchored collagenase MT1-MMP. J. Cell Biol. 167, 769–781.

Saftig, P., Hunziker, E., Wehmeyer, O., Jones, S., Boyde, A., Rommerskirch, W., Moritz, J.D., Schu, P., von Figura, K., 1998. Impaired osteoclastic bone resorption leads to osteopetrosis in cathepsin-K-deficient mice. Proc. Nat. Acad. Sci. USA 95, 13453–13458.

Saftig, P., Hunziker, E., Everts, V., Jones, S., Boyde, A., Wehmeyer, O., Suter, A., Figura, K., 2000. Functions of cathepsin K in bone resorption: lessons from cathepsin K deficient mice. Adv. Exp. Biol. Med. 477, 293–303.

Sahara, T., Itoh, K., Debari, K., Sasaki, T., 2003. Specific biological functions of vacuolar-type H(+)-ATPase and lysosomal cystein proteinase, cathepsin K, in osteoclasts. Anat Rec A Discov Mol. Cell Evol. Biol. 270, 152–161.

Sato, H., Takino, T., Okada, Y., Cao, J., Shinagawa, A., Yamamoto, E., Seiki, M., 1994. A matrix metalloproteinase expressed on the surface of invasive tumour cells. Nature 370, 61–65.

Sato, H., Kinoshita, T., Takino, T., Nakayama, K., Seiki, M., 1996. Activation of a recombinant membrane type 1-matrix metalloproteinase (MT1-MMP) by furin and its interaction with tissue inhibitor of metalloproteinases (TIMP)-2. FEBS Lett. 393, 101–104.

Sato, H., Okada, Y., Seiki, M., 1997. Membrane-type matrix metalloproteinases (MT-MMPs) in cell invasion. Thromb. Haemostasis 78, 497–500.

Scannevin, R.H., Alexander, R., Mezzasalma, T., Burke, S.L., Singer, M., Huo, C., Zhang, Y.-M., Maguire, D., Spurlino, J., Deckman, I., Carroll, K.I., Lewandowski, F., Devine, E., Dzordzorme, K., Tounge, B., Milligan, C., Bayoumy, S., Williams, R., Schalk-Hihi, C., Leonard, K., Jackson, P., Todd, M., Kuo, L.C., Rhodes, K.J., 2017. Discovery of highly selective chemical inhibitor of matrix metalloproteinase-9 (MMP-9) that allosterically inhibits zymogen activation. J. Biol. Chem. 292, 17963–17974.

Schroen, D.J., Brinckerhoff, C.E., 1996. Nuclear hormone receptors inhibit matrix metalloproteinase (MMP) gene expression through diverse mechanisms. Gene Expr. 6, 197–207.

Scott, D.K., Brakenhoff, K.D., Clohisy, J.C., Quinn, C.O., Partridge, N.C., 1992. Parathyroid hormone induces transcription of collagenase in rat osteoblastic cells by a mechanism using cyclic adenosine 3′,5′-monophosphate and requiring protein synthesis. Mol. Endocrinol. 6, 2153–2159.

Seandel, M., Noack-Kunnmann, K., Zhu, D., Aimes, R.T., Quigley, J.P., 2001. Growth factor-induced angiogenesis in vivo requires specific cleavage of fibrillar type I collagen. Blood 97, 2323–2332.

Selvamurugan, N., Chou, W.Y., Pearman, A.T., Pulumati, M.R., Partridge, N.C., 1998. Parathyroid hormone regulates the rat collagenase-3 promoter in osteoblastic cells through the cooperative interaction of the activator protein-1 site and the runt domain binding sequence. J. Biol. Chem. 273, 10647–10657.

Selvamurugan, N., Brown, R.J., Partridge, N.C., 2000a. Constitutive expression and regulation of collagenase-3 in human breast cancer cells. J. Cell. Biochem. 79, 182–190.

Selvamurugan, N., Pulumati, M.R., Tyson, D.R., Partridge, N.C., 2000b. Parathyroid hormone regulation of the rat collagenase-3 promoter by protein kinase A-dependent transactivation of core binding factor A1. J. Biol. Chem. 275, 5037–5042.

Selvamurugan, N., Kwok, S., Alliston, T., Reiss, M., Partridge, N.C., 2004. Transforming growth factor-beta 1 regulation of collagenase-3 expression in osteoblastic cells by cross-talk between the Smad and MAPK signaling pathways and their components, Smad2 and Runx2. J. Biol. Chem. 279, 19327–19334.

Selvamurugan, N., Jefcoat, S.C., Kwok, S., Kowalewski, R., Tamasi, J.A., Partridge, N.C., 2006. Overexpression of Runx2 directed by the matrix metalloproteinase-13 promoter containing the AP-1 and Runx2/RD/Cbfa sites alters bone remodeling in vivo. J. Cell. Biochem. 99, 545–557.

Selvamurugan, N., Partridge, N.C., 2000. Constitutive expression and regulation of collagenase-3 in human breast cancer cells. Mol Cell Biol Res Commun 3, 218–223.

Shah, R., Alvarez, M., Joes, D.R., Torrungruang, K., Wat, A.J., Selvamurugan, N., Partridge, N.C., Quinn, C.O., Pavalko, F.M., Rhodes, S.J., Bidwell, J.P., 2004. Nmp4/CIZ regulation of matrix metalloproteinase 13 (MMP-13) response to parathyroid hormone in osteoblasts. Am. J. Physiol. Endocrinol. Metab. 287, E289–E296.

Shalhoub, V., Conlon, D., Tassinari, M., Quinn, C., Partridge, N., Stein, G.S., Lian, J.B., 1992. Glucocorticoids promote development of the osteoblast phenotype by selectively modulating expression of cell growth and differentiation associated genes. J. Cell. Biochem. 50, 425–440.

Shimizu, E., Selvamurugan, N., Westendorf, J.J., Olson, E.N., Partridge, N.,C., 2010. HDAC4 represses matrix metalloproteinase-13 transcription in osteoblastic cells, and parathyroid hormone controls this repression. J. Biol. Chem. 285, 9616–9626.

Shofuda, K.I., Hasenstab, D., Kenagy, R., Shofuda, T., Li, Z.Y., Lieber, A., Clowes, A.W., 2001. Membrane-type matrix metalloproteinase-1 and -3 activity in primate smooth muscle cells. FASEB J. 15, 2010–2012.

Stetler-Stevenson, W.G., Krutzsch, H.C., Liotta, L.A., 1989. Tissue inhibitor of metalloproteinase (TIMP-2): a new member of the metalloproteinase family. J. Biol. Chem. 264, 17374–17378.

Stewart, D., Javadi, M., Chambers, M., Gunsolly, C., Gorski, G., Borghaei, R.C., 2007. Interleukin-4 inhibition of interleukin-1-induced expression of matrix metalloproteinase-3 (MMP-3) is independent of lipoxygenase and PPARgamma activation in human gingival fibroblasts. BMC Mol. Biol. 8 (12), 1–13.

Stickens, D., Behonick, D.J., Ortega, N., Heyer, B., Hartenstein, B., Yu, Y., Fosang, A.J., Schorpp-Kistner, M., Angel, P., Werb, Z., 2004. Altered endochondral bone development in matrix metalloproteinase 13-deficient mice. Development 131, 5883–5895.

Stolow, M.A., Bauzon, D.D., Li, J., Sedgwick, T., Liang, V.C., Sang, Q.A., Shi, Y.B., 1996. Identification and characterization of a novel collagenase in *Xenopus laevis:* possible roles during frog development. Mol. Biol. Cell 7, 1471–1483.

Tardif, G., Reboul, P., Pelletier, J.P., Martel-Pelletier, J., 2004. Ten years in the life of an enzyme: the story of the human MMP-13 (collagenase-3). Mod. Rheumatol. 14, 197–204.

Teitelbaum, S.L., 2000. Bone resorption by osteoclasts. Science 289, 1504–1508.

Tezuka, K.-I., Nemoto, K., Tezuka, Y., Sato, T., Ikeda, Y., Kobori, M., Kawashima, H., Eguchi, H., Hakeda, Y., Kumegawa, M., 1994a. Identification of matrix metalloproteinase 9 in rabbit osteoclasts. J. Biol. Chem. 269, 15006–15009.

Tezuka, K.-I., Tezuka, Y., Maejima, A., Sato, T., Nemoto, K., Kamioka, H., Hakeda, Y., Kumegawa, M., 1994b. Molecular cloning of a possible cysteine proteinase predominantly expressed in osteoclasts. J. Biol. Chem. 269, 1106–1109.

Thomson, B.M., Atkinson, S.J., McGarrity, A.M., Hembry, R.M., Reynolds, J.J., Meikle, M.C., 1989. Type I collagen degradation by mouse calvarial osteoblasts stimulated with 1,25-dihydroxyvitamin D-3: evidence for a plasminogen-plasmin-metalloproteinase activation cascade. Biochim. Biophys. Acta 1014, 125–132.

Tumber, A., Papaioannou, S., Breckon, J., Meikle, M.C., Reynolds, J.J., Hill, P.A., 2003. The effects of serine protease inhibitors on bone resorption in vitro. J. Endocrinol. 178, 437–447.

Turk, V., Bode, W., 1991. The cystatins: protein inhibitors of cysteine proteinases. FEBS Lett. 285, 213–219.

Tyson, D.R., Swarthout, J.T., Partridge, N.C., 1999. Increased osteoblastic c-fos expression by parathyroid hormone requires protein kinase A phosphorylation of the cyclic adenosine 3′,5′-monophosphate response element-binding protein at serine 133. Endocrinology 140, 1255–1261.

Vaes, G., 1988. Cellular biology and biochemical mechanism of bone resorption. A review of recent developments on the formation, activation and mode of action of osteoclasts. Clin. Orthop. Relat. Res. 231, 239–271.

van Zonneveld, A.-J., Veerman, H., Pannekoek, H., 1986. On the interaction of the finger and the kringle-2 domain of tissue-type plasminogen activator with fibrin. J. Biol. Chem. 261, 14214–14218.

Varghese, S., Rydziel, S., Jeffrey, J.J., Canalis, E., 1994. Regulation of interstitial collagenase expression and collagen degradation by retinoic acid in bone cells. Endocrinology 134, 2438–2444.

Varghese, S., Rydziel, S., Canalis, E., 2000. Basic fibroblast growth factor stimulates collagenase-3 promoter activity in osteoblasts through an activator protein-1-binding site. Endocrinology 141, 2185–2191.

Varghese, S., 2006. Matrix metalloproteinases and their inhibitors in bone: an overview of regulation and functions. Front. Biosci. 11, 2949–2966.

Velasco, G., Cal, S., Merlos-Suárez, A., Ferrando, A.A., Alvarez, S., Nakano, A., Arribas, J., López-Otín, C., 2000. Human MT6-matrix metalloproteinase: identification, progelatinase A activation, and expression in brain tumors. Cancer Res. 60, 877–882.

Visse, R., Nagase, H., 2003. Matrix metalloproteinases and tissue inhibitors of metalloproteinases. Circ. Res. 92, 827–839.

Vu, T.H., Shipley, J.M., Bergers, G., Berger, J.E., Helms, J.A., Hanahan, D., Shapiro, S.D., Senior, R.M., Werb, Z., 1998. MMP-9/gelatinase B is a key regulator of growth plate angiogenesis and apoptosis of hypertrophic chondrocytes. Cell 93, 411–422.

Vu, T.H., Werb, Z., 2000. Matrix metalloproteinases: effectors of development and normal physiology. Genes Dev. 14, 2123–2133.

Walling, H.W., Chan, P.T., Omura, T.H., Barmina, O.Y., Fiacco, G.J., Jeffrey, J.J., Partridge, N.C., 1998. Regulation of the collagenase-3 receptor and its role in intracellular ligand processing in rat osteoblastic cells. J. Cell. Physiol. 177, 563–574.

Wasylyk, B., Hahn, S.L., Giovane, A., 1993. The Ets family of transcription factors. Eur. J. Biochem. 211, 7–18.

Wernicke, D., Seyfert, C., Hinzmann, B., Gromnica-Ihle, E., 1996. Cloning of collagenase 3 from the synovial membrane and its expression in rheumatoid arthritis and osteoarthritis. J. Rheumatol. 23, 590–595.

Wilcox, B.D., Dumin, J.A., Jeffrey, J.J., 1994. Serotonin regulation of interleukin-1 messenger RNA in rat uterine smooth muscle cells. J. Biol. Chem. 269, 29658–29664.

Wilson, C.L., Heppner, K.J., Labosky, P.A., Hogan, B.L.M., Matrisian, L.M., 1997. Intestinal tumorigenesis is suppressed in mice lacking the metalloproteinase, matrilysin. Proc. Natl. Acad. Sci. U.S.A. 94, 1402–1407.

Wilhelm, S.M., Collier, I.E., Marmer, B.L., Eisen, A.Z., Grant, G.A., Goldberg, G.I., 1989. SV40-transformed human lung fibroblasts secrete a 92-kDa type IV collagenase which is identical to that secreted by normal human macrophages. J. Biol. Chem. 264, 17213–17221.

Winchester, S.K., Bloch, S.R., Fiacco, G.J., Partridge, N.C., 1999. Regulation of expression of collagenase-3 in normal, differentiating rat osteoblasts. J. Cell. Physiol. 181, 479–488.

Winchester, S.K., Selvamurugan, N., D'Alonzo, R.C., Partridge, N.C., 2000. Developmental regulation of collagenase-3 mRNA in normal, differentiating osteoblasts through the activator protein-1 and the runt domain binding sites. J. Biol. Chem. 275, 23310–23318.

Witty, J.P., Matrisian, L., Foster, S., Stern, P.H., 1992. Stromelysin in PTH-stimulated bones *in vitro*. J. Bone Miner. Res. 7 (Suppl. 1), S103.

Woessner Jr., J.F., 1991. Matrix metalloproteinases and their inhibitors in connective tissue remodeling. FASEB J 5, 2145–2154.

Wucherpfennig, A.L., Li, Y.-P., Stetler-Stevenson, W.G., Rosenberg, A.E., Stashenko, P., 1994. Expression of 92 kD type IV collagenase/gelatinase B in human osteoclasts. J. Bone Miner. Res. 9, 549–556.

Wun, T.-C., Ossowski, L., Reich, E., 1982. A proenzyme form of human urokinase. J. Biol. Chem. 257, 7262–7268.

Xia, L., Kilb, J., Wex, H., Li, Z., Lipyansky, A., Breuil, V., Stein, L., Palmer, J.T., Dempster, D.W., Bromme, D., 1999. Localization of rat cathepsin K in osteoclasts and resorption pits: inhibition of bone resorption and cathepsin K-activity by peptidyl vinyl sulfones. Biol. Chem. 380, 679–687.

Xiang, A., Kanematsu, M., Kumar, S., Yamashita, D., Kaise, T., Kikkawa, H., Asano, S., Kinoshita, M., 2007. Changes in micro-CT 3D bone parameters reflect effects of a potent cathepsin K inhibitor (SB-553484) on bone resorption and cortical bone formation in ovariectomized mice. Bone 40, 1231–1237.

Yamaza, T., Goto, T., Kamiya, T., Kobayashi, Y., Sakai, H., Tanaka, T., 1998. Study of immunoelectron microscopic localization of cathepsin K in osteoclasts and other bone cells in the mouse femur. Bone 23, 499–509.

Yang, J.N., Allan, E.H., Anderson, G.I., Martin, T.J., Minkin, C., 1997. Plasminogen activator system in osteoclasts. J. Bone Miner. Res. 12, 761–768.

Yang, T., Williams, B.O., 2017. Low-density lipoprotein receptor-related proteins in skeletal development and disease. Physiol. Rev. 97, 1211–1228.

Zhao, W., Byrne, M.H., Boyce, B.F., Krane, S.M., 1999. Bone resorption induced by parathyroid hormone is strikingly diminished in collagenase-resistant mice. J. Clin. Investig. 103, 517–524.

Zhao, W., Byrne, M.H., Wang, Y., Krane, S.M., 2000. Inability of collagenase to cleave type I collagen *in vivo* is associated with osteocyte and osteoblast apoptosis and excessive bone deposition. J. Clin. Investig. 106, 841–849.

Zhou, Z., Apte, S.S., Soininen, R., Cao, R., Baaklini, G.Y., Rauser, R.W., Wang, J., Cao, Y., Tryggvason, K., 2000. Impaired endochondral ossification and angiogenesis in mice deficient in membrane-type matrix metalloproteinase I. Proc. Natl. Acad. Sci. U.S.A. 97, 4052–4057.

Zucker, S., Cao, J., Chen, W.-T., 2000. Critical appraisal of the use of matrix metalloproteinase inhibitors in cancer treatment. Oncogene 19, 6642–6650.

Chapter 17

Integrins and other cell surface attachment molecules of bone cells

Pierre J. Marie[1] and Anna Teti[2]

[1]UMR-1132 Inserm (Institut national de la Santé et de la Recherche Médicale) and University Paris Diderot, Sorbonne Paris Cité, Paris, France;
[2]Department of Biotechnological and Applied Clinical Sciences, University of L'Aquila, L'Aquila, Italy

Chapter outline

Introduction

Cell adhesion molecules play important roles in bone cell functions and fate. Integrins are a family of cell surface adhesion transmembrane molecules composed of α chains and β chains that assemble noncovalently as heterodimers (Campbell and Humphries, 2011), allowing the attachment of osteoclasts and osteoblasts to the extracellular matrix (ECM). Binding of integrins to ECM proteins is essential for the function of bone cells (Bennett et al., 2001; Horton, 2001), and contributes to activating a number of intracellular signals that govern bone cell fate and activity (Marie et al., 2014a). Cadherins are other attachment molecules that control the functions of bone cells through cell−cell adhesion, interactions with other cell surface molecules, and modulation of intracellular pathways (Marie et al., 2014b). During recent years, progress in cell biology and mouse genetics has led to significant advances in our understanding of the roles of integrins, cadherins, and other cell attachment molecules in the control of bone cell activity in vitro and in vivo, and the mechanisms involved in these functions are now better understood. This chapter updates our knowledge of the role of these molecules in bone cell functions and discusses potential therapeutic strategies that emerged from these findings.

Role of integrins in bone cells

Osteoblasts and osteocytes

Osteoblasts and osteocytes express several integrins, although the pattern of expression varies with the stage of cell differentiation (Clover et al., 1992; Hughes et al., 1993; Hultenby et al., 1993; Grzesik and Robey, 1994). Integrin binds to the Arg−Gly−Asp (RGD) sequence present in bone matrix proteins such as fibronectin, type I collagen, bone sialoprotein, and osteopontin (Gronthos et al., 2001; Grzesik, 1997; Puleo and Bizios, 1991; Schaffner and Dard, 2003). Integrins control cell adherence to the ECM through the assembly of intracellular proteins linked to the cytoskeleton. In addition to allowing

Principles of Bone Biology. https://doi.org/10.1016/B978-0-12-814841-9.00017-8

cell−matrix adherence, integrins play a key role in osteoblast differentiation (Moursi et al., 1997; Jikko et al., 1999; Mizuno et al., 2000), an effect that is mediated by intracellular signals generated by ECM−osteoblast interactions. Integrin−ECM interaction leads to the phosphorylation of focal adhesion kinase (FAK) and subsequent activation of mitogen-activated protein kinase (MAPK) extracellular signal-regulated kinase 1/2 (ERK1/2), phosphatidylinositol 3-kinase (PI3K), or GTPases of the Rho family (Lai et al., 2001; Salasznyk et al., 2007; Khatiwala et al., 2009). These signals converge to promote specific gene expression and osteoblast differentiation. In mesenchymal skeletal cells (MSCs), ERK1/2 phosphorylation induced by ECM−integrin binding leads to RUNX2 activation and osteoblast differentiation (Ge et al., 2012). FAK also activates Wnt/β-catenin signaling (Sun et al., 2016), making the activation of FAK an essential step for osteogenic differentiation (Tamura et al., 2001). In vivo, deletion of FAK in type I collagen-expressing osteoblasts reduced reparative bone formation in mice (Rajshankar et al., 2017). However, the lack of FAK in osteoblasts may be in part compensated for by proline-rich tyrosine kinase 2 (PYK2), a tyrosine kinase highly homologous to FAK, in the focal adhesion sites (Kim et al., 2007). One important regulator of integrin-mediated signaling is integrin-linked kinase (ILK), a linker between integrins and the cytoskeleton. In osteoblasts, ILK-dependent phosphorylation of α-nascent polypeptide−associated complex, a c-JUN transcriptional coactivator, potentiates c-JUN-dependent transcription and osteoblast maturation (Meury et al., 2010). ILK also interacts with Wnt signaling by phosphorylating glycogen synthase kinase-3β, leading to β-catenin− lymphoid enhancer factor transcriptional activity and expression of Wnt target genes (Dejaeger et al., 2017). Data indicate that conditional inactivation of ILK in osteoprogenitors impaired bone formation associated with reduced bone morphogenetic protein (BMP)/Smad and Wnt/β-catenin signaling, showing the important role of this linker between integrins and the cytoskeleton in bone formation (Dejaeger et al., 2017). In addition to control of cell differentiation, osteoblast attachment to the ECM is essential for cell survival (Grigoriou et al., 2005; Triplett and Pavalko, 2006). Disruption of RGD−integrin binding leads to altered osteoblast adhesion in vitro (Gronthos et al., 2001), and conversely integrin−ECM interaction suppresses cell apoptosis through PI3K activation (Frisch and Ruoslahti, 1997). Thus, integrins play an important role in the control of bone formation through activation of signaling mechanisms regulating both osteoblast differentiation and survival (Fig. 17.1).

The specific role of integrins in osteoblast function and fate is now better understood. The β1 integrin is the main adhesion receptor required for adhesion to fibronectin and type I collagen in vitro. In vivo, impairment of β1 integrin in mature osteoblasts led to decreased osteoblast activity, bone formation, and bone mass in growing mice (Zimmerman et al., 2000). Disruption of β1 integrin signaling by overexpression of its cytoplasmic tail resulted in skeletal defects, showing the important role of β1 integrin in osteogenesis (Globus et al., 2005). In support of the role of β1 integrin in bone formation, ablation of the specific β1 integrin regulator ICAP-1 in osteoblasts resulted in defective osteoblast proliferation, differentiation, and function; decreased type I collagen deposition; and delayed bone formation in mice (Bouvard et al., 2007; Brunner et al., 2011). Data showed that conditional β1 integrin deletion in early osteogenic mesenchymal cells or in preosteoblasts caused abnormal skeletal ossification or affected intramembranous and

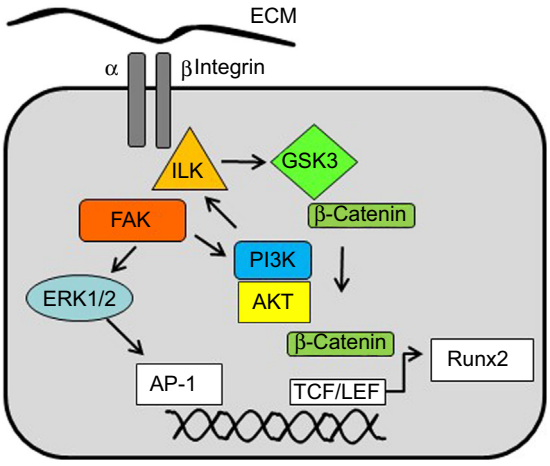

FIGURE 17.1 Role of integrins in osteoblasts. Simplified scheme showing how integrin-mediated signals regulate osteoblast function. Extracellular matrix (*ECM*)−integrin interaction via RGD interacts with integrin-linked kinase (ILK) and activates focal adhesion kinase (FAK), extracellular signal-regulated kinase 1/2 (ERK1/2), and Wnt/β-catenin signaling, leading to Runx2 expression and osteogenic differentiation, and with phosphatidylinositol 3-kinase/protein kinase B (PI3K/AKT) to trigger osteoblast survival (see text for more details). *AP-1*, activator protein 1; *GSK3*, glycogen synthase kinase-3; *TCF/LEF*, T cell factor/lymphoid enhancer factor.

endochondral bone formation in young mice. In contrast, osteocalcin-specific β1 integrin deletion had only minor effects on the skeletal phenotype, indicating that the β1 integrin is essential for early stages of osteogenesis in vivo (Shekaran et al., 2014). In addition to β1, other integrins were shown to control osteoblast function and fate. Early in vitro studies showed that the αVβ3 integrin is involved in dexamethasone- and BMP-2-induced osteoblast differentiation (Cheng et al., 2000, 2001). More recent data indicate that the αVβ3 integrin mediates BMP-2-induced osteoblast differentiation in vitro through activation of the ILK/ERK1/2 signaling pathway (Su et al., 2010). Another integrin, αVβ5, was found to mediate osteoblast attachment to vitronectin in vitro (Lai et al., 2000). The αVβ1 integrin was reported to promote osteoblast differentiation and to inhibit adipocyte differentiation in MSCs through its interaction with RGD present in osteopontin (Chen et al., 2014). Another integrin, α2β1, a major receptor for collagen type 1, is involved in osteoblast differentiation (Takeuchi et al., 1997) by activating ERK signaling and RUNX2 expression in vitro (Xiao et al., 1998). In vivo, α2 integrin deficiency resulted in altered bone properties in mice (Stange et al., 2013). This integrin was found to play a key role in MSC osteogenic differentiation and survival through activation of Rho-associated protein kinase (ROCK) and FAK signaling (Popov et al., 2011; Sens et al., 2017). The α4β1 integrin, which binds to fibronectin, was also found to be involved in MSC homing and osteoblast differentiation in vivo (Kumar and Ponnazhagan, 2007). Both MSCs and osteoblasts express α5β1 integrin, which interacts with fibronectin and is involved in the differentiation of osteoblast precursor cells (Hamidouche et al., 2009). The downregulation of α5 integrin subunit blunts osteoblast differentiation, while its overexpression promotes osteoblast differentiation in MSCs, an effect that is mediated by FAK and ERK1/2 signaling leading to RUNX2 activation (Hamidouche et al., 2009). α5β1 integrin activation also promotes insulin-like growth factor 2 (IGF-2) expression and signaling in MSCs, which contributes to osteogenic differentiation (Hamidouche et al., 2010). In addition, α5β1 integrin activation cross talks with Wnt signaling. α5β1 integrin priming by a monoclonal antibody, or a high-affinity peptide ligand, leads to increased osteogenic differentiation (Hamidouche et al., 2009) in part through activation of PI3K/protein kinase B (AKT) and Wnt/β-catenin signaling, indicating that Wnt/β-catenin signaling is involved in osteoblast differentiation mediated by α5β1 integrin (Saidak et al., 2015). In pluripotent cells, other integrins may be involved in osteogenic differentiation. In vitro data indicate that fibrinogen binds to the α9β1 integrin in human embryonic stem cells to induce pluripotent stem cell osteogenic differentiation mediated by SMAD1/5/8 signaling and *Runx2* expression (Kidwai et al., 2016).

There is ample evidence that integrins are critically involved in the response of osteoblasts and osteocytes to mechanical loading via cytoskeleton−integrin interactions at focal adhesion sites (Katsumi et al., 2004; Bonewald and Johnson, 2008; Turner et al., 2009) and induction of intracellular signaling mechanisms, including FAK, ERK, ROCK, PI3K/AKT, and Wnt signaling (Pommerenke et al., 2002; Wu et al., 2013; Du et al., 2016; Plotkin et al., 2005; Wang et al., 2007; Lee et al., 2010; Chen and Jacobs, 2013; Uda et al., 2017). Several integrins may be involved in the mechanisms mediating mechanotransduction, depending on the context. As expected from the aforementioned important role of β1 integrin in osteoblast differentiation, β1 integrin expressed by osteogenic cells was found to play a major role in mechanotransduction (Iwaniec et al., 2005; Phillips et al., 2008; Litzenberger et al., 2010). In osteocytes, in addition to the β1 integrin, the αVβ3 integrin is required for mechanotransduction (Thi et al., 2013), which involves calcium influx (Miyauchi et al., 2006), IGF-1 expression (Dai et al., 2014), and inhibition of the Wnt inhibitor sclerostin by periostin (Bonnet et al., 2012). In vivo, skeletal unloading in mice decreased αVβ3 integrin expression in osteoblasts, resulting in altered activation of IGF-1 signaling (Bikle, 2008). Skeletal unloading also reduced α5β1 integrin expression in osteoblasts and osteocytes, resulting in decreased PI3K signaling and altered bone formation (Dufour et al., 2007). Conversely, mechanical strain activates α5β1 integrin (Yan et al., 2012) and PI3K/AKT signaling in osteoblasts (Watabe et al., 2011). The activation of α5β1 integrin by mechanical stress in osteoblasts also causes opening of connexin 43 hemichannels and the subsequent release of anabolic factors (Batra et al., 2012). Other integrins were found to be involved in mechanotransduction. In vitro, the α2 integrin subunit is upregulated during induction on stiffer matrices and mediates the osteogenic differentiation of MSCs (Shih et al., 2011). However, mechanosensitivity appears to depend on the ligation between α2 or α5 subunit and ECM proteins to induce FAK activation (Seong et al., 2013), suggesting that specific integrin subunits may mediate mechanosensitivity in osteoblasts. Thus, several mechanisms generated by integrin−ECM interactions in osteoblasts and osteocytes are involved in the bone cell response to mechanotransduction.

The essential role of integrins in both bone formation and mechanotransduction suggests that targeting specific integrins may be an efficient way to promote osteogenic differentiation and bone regeneration. Several strategies were used to target integrins. One example is the ectopic expression of the α4 integrin in MSCs (Kumar and Ponnazhagan, 2007). While the injection of modified MSCs into mice led to increased cell homing in bone and their subsequent differentiation into osteoblasts (Guan et al., 2012), the systemic injection of a peptidomimetic ligand (LLP2A) that binds the α4β1 integrin, conjugated to a bisphosphonate to allow bone binding, led to increased osteoblast differentiation and bone formation in mice with established osteopenia (Guan et al., 2012; Yao et al., 2013). Another strategy is to target the α5β1

integrin (Marie, 2013). Lentiviral-mediated expression of the α5 integrin subunit in human MSCs promoted osteogenic differentiation, bone formation (Hamidouche et al., 2009), and bone repair in critical-size bone defects in mice (Srouji et al., 2012). Moreover, α5 integrin activation by a synthetic cyclic peptide, which activates FAK and ERK1/2−MAPK signaling in osteoprogenitor cells, led to increased osteoblast differentiation and to reduced cell apoptosis in vitro (Fromigué et al., 2012). In vivo, the local injection of an α5 integrin agonist peptide into adult mice increased parietal bone formation, indicating that pharmacological activation of α5 integrin in osteoprogenitor cells is effective in promoting de novo bone formation (Fromigué et al., 2012). An alternative strategy to target integrins may be the use of recombinant NELL-1, a secreted osteoinductive protein that binds to β1 integrin. In vitro, this strategy leads to activation of Wnt/β-catenin signaling and increased osteoblast differentiation. In vivo, delivery of NELL-1 to ovariectomized mice or osteopenic sheep improved bone mineral density (James et al., 2015). These studies showed that targeting integrins may be a promising approach for promoting bone formation and repair in skeletal disorders.

Osteoclasts

Osteoclasts are the multinucleated cells that resorb the bone matrix to promote skeletal modeling and renewal (Soysa and Alles, 2016; Cappariello et al., 2014). They rely on a tight and dynamic mechanism of adhesion to the mineralized matrix, which ensures cell changes indispensable for bone resorption. These are (1) the polarization of the osteoclast and (2) the sealing of the extracellular space between the cell and the bone matrix to be removed, called resorption lacuna (Soysa and Alles, 2016; Cappariello et al., 2014) (Fig. 17.2). The principal integrin involved in the adhesion of osteoclasts to the substrate is the αVβ3 receptor. While αV-deleted mice are embryonically lethal, β3-deleted mice showed a phenotype mimicking Glanzmann thrombasthenia (Morgan et al., 2010) and osteopetrosis (Zou and Teitelbaum, 2015; McHugh et al., 2000). Osteopetrosis is caused by osteoclast dysfunction, and these observations revealed the relevance of the αVβ3 integrin in osteoclast biology. Specifically, β3-null osteoclasts form normally but are prevented from resorbing bone. Their cytoskeletal array is disrupted, adhesion to substrate is reduced, and cell spreading is impeded (McHugh et al., 2000). These results suggest that the αVβ3 integrin is not involved in the molecular mechanisms of osteoclastogenesis, but it rather affects the morphological and molecular changes that make osteoclasts capable of resorbing bone. αVβ3 heterodimers are clustered in specific adhesion areas, called podosomes (Marchisio et al., 1984), that are typical of osteoclasts and other highly motile cells, such as monocytes, macrophages (Calle et al., 2006), and invasive cancer cells, in which they are called invadopodia (Eddy et al., 2017). Compared with classical focal adhesions, podosomes and invadopodia are much more dynamic, with a turnover of a few minutes rather than the hours observed in focal adhesions (Georgess et al., 2014). A typical feature of osteoclast podosomes is their clustering in a continuous peripheral annulus, called actin ring

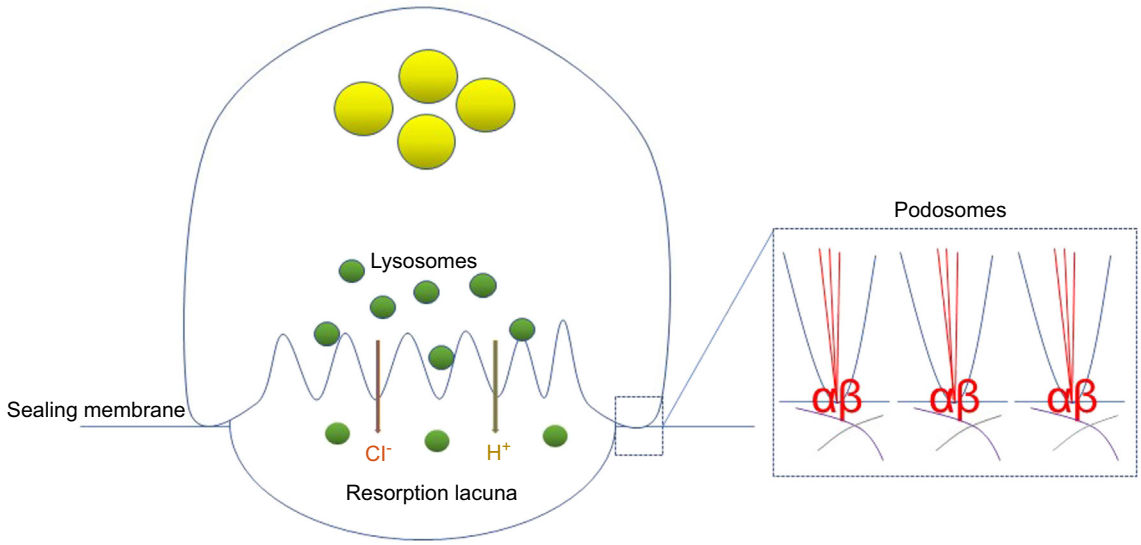

FIGURE 17.2 Role of integrins in osteoclasts. Cartoon showing a polarized osteoclast sitting on the resorption lacuna. Release of protons and chlorides acidifies the lacuna microenvironment, solubilizing the hydroxyapatite and allowing the degradation of the organic matrix by lysosomal enzymes therein secreted. Adhesion to the mineralized matrix occurs through podosomes located in the sealing membrane, which establish contacts with the extracellular molecules through integrin receptors (see text for more details).

(Cappariello et al., 2014), representing the sealing zone of the apical membrane. Here, the number of podosomes and the extension of the acting ring are proportional to the activity of the osteoclasts, reaching the maximum development during bone resorption, when multiple actin rings/osteoclast can be observed (Cappariello et al., 2014). For their high dynamism, podosomes and their associated αVβ3 integrins change rapidly in terms of number and distribution, contributing not only to the sealing of the resorption lacuna and the subsequent organization of the inner irregular domain of the apical membrane lodging the molecular mechanisms of bone resorption, called the ruffled border, but also to the osteoclast motility on the mineralized matrix during and between the bone resorption cycles (Cappariello et al., 2014; Rucci and Teti, 2016). In osteoclast podosomes, the αVβ3 integrin is largely represented and concentrated in a circular podosomal area of membrane adhesion to substrate, whose cytosolic center lodges a core of microfilaments; actin-binding proteins, including α-actinin; and actin-branching proteins, including cortactin, the ARP2/3 complex, and WASP and WASP-interacting protein (Georgess et al., 2014; Rucci and Teti, 2016). The αVβ3 integrin circular "rosette" that surrounds this microfilament core is associated with several intracellular adhesion proteins, such as vinculin, talin, paxillin and tensin, that link the integrins to the microfilaments (Saltel et al., 2008; Correia et al., 1999; Evans and Matsudaira, 2006; Marchisio et al., 1988; Akisaka et al., 2001). Importantly, this complex structure includes microfilament-severing proteins (gelsolin and cofilin) (Ory et al., 2008), as well as the small GTP-binding protein RHO (Teitelbaum, 2011) and the guanine exchange factors DOCK5 and VAV3, which provide rapid podosome remodeling indispensable for their dynamism (Purev et al., 2009). This is also ensured by the localization in podosomes of the large GTP-binding protein dynamin, which regulates E3 ubiquitin ligase c-CBL-dependent degradation or receptors and signaling factors (Bruzzaniti et al., 2005). GTPase activity of dynamin is enhanced by GRB2, which also increases WASP-mediated ARP2/3-dependent actin nucleation (Spinardi and Marchisio, 2006). Along with the microfilament-severing function of gelsolin and cofilin, this molecular cascade ensures rapid microfilament turnover and podosome disassembly and reassembly (Luxenburg et al., 2012). Moreover, ubiquitin ligases, including c-CBL and CBL-b (Horne et al., 2005), phosphoinositide kinases such as PI3K (Chellaiah et al., 2001), nonreceptor tyrosine kinases such as c-SRC and PYK2 (Duong et al., 1998; Destaing et al., 2008), ABL and FAK (Ray et al., 2012), and phosphatases, including PTPα, PTPε, and SHP2 (Granot-Attas and Elson, 2008), associate with the αVβ3 integrin complex to further regulate osteoclast adhesion and podosome dynamics.

Genetic studies have been instrumental in demonstrating the relevance of the αVβ3 receptor signaling in osteoclast activity. The analysis of *c-Src* deletion in mice showed that osteoclasts were not able to polarize and became immotile (Lowe et al., 1993). They exhibited a severe osteopetrotic phenotype, which was observed, in milder form, also in *Pyk2*- and *c-Cbl*-null mice (Gil-Henn et al., 2007; Tanaka et al., 1996). c-SRC coprecipitates with the αVβ3 integrin and through its c-CBL tyrosine phosphorylation activity, promotes substrate ubiquitination and prolonged cell survival (Horne et al., 2005). Furthermore, c-SRC contributes to the metabolism of PYK2 and p130CAS, involved in the organization of the sealing membrane (Nakamura et al., 1998). Therefore, given that c-SRC is upstream of the tyrosine phosphorylation cascade involving PYK2, c-CBL and p130CAS, it is likely that these intracellular signaling molecules act synergistically to determine correct cytoskeletal arrangement, podosome formation, and osteoclast polarization and survival.

On the extracellular side, the osteoclast αVβ3 integrin binds the RGD sequence of a number of matrix proteins that contribute to osteoclast adhesion and outside-in signaling (Rucci and Teti, 2016). Many proteins are recognized by the αVβ3 integrin, including osteopontin, bone sialoprotein 2, vitronectin, fibronectin, and von Willebrand factor (Zou and Teitelbaum, 2010). αVβ3 integrin recognizes also collagen type I but only upon molecular remodeling, the collagen type I RGD sequence being lodged in a cryptic domain. In osteoclasts, osteopontin, bone sialoprotein II, synthetic RGD peptides, echistatin (an RGD-disintegrin peptide extracted from the poison of viper venom), and the αvβ3 integrin activating LM609 monoclonal antibody mobilize intracellular calcium through the αVβ3 receptor, albeit with some species specificity. In fact, in rat osteoclasts, αVβ3 integrin activation triggers intracellular calcium transients and cell retraction (Shankar et al., 1993), while in chicken osteoclasts it induces a calmodulin/Ca^{2+}-ATPase-dependent calcium efflux and intracellular reduction (Miyauchi et al., 1991). The molecular mechanisms underlying these opposite events have not been investigated, leaving this question still open. Finally, in mouse osteoclasts, osteopontin induces RGD-dependent nuclear translocation of nuclear factor of activated T cells 1 (NFATc1), a transcription factor essential for osteoclastogenesis (Tanabe et al., 2011), whose activation is triggered by calcium oscillations (Negishi-Koga and Takayanagi, 2009). The αVβ3 integrin is relatively infrequent in the organism, and osteoclasts are among the cells mostly enriched in these receptors. The αVβ3 integrin has been considered a pharmacological target to combat cancer-induced osteolytic lesions, osteoporosis, and rheumatoid arthritis (Desgrosellier and Cheresh, 2010; Schneider et al., 2011; Tian et al., 2015). αVβ3 integrin targeting molecules include cyclic peptides carrying the αVβ3 integrin binding site (Auzzas et al., 2010), neutralizing antibodies (Hsu et al., 2007) and nonpeptide antagonists (Hsu et al., 2007; Sheldrake and Patterson, 2014). Several of them have been tested in preclinical studies, and one has been tested in clinical trials to treat cancer (Danhier et al., 2012).

Other integrin members are also expressed by osteoclasts. αVβ1, αMβ2, and αVβ5 receptors are expressed by osteoclast mononuclear precursors and switch to αVβ3 during preosteoclast maturation in polykarya (Inoue et al., 1998). The α2β1 integrin is engaged in the binding to collagen type I. It does not recognize vitronectin, fibronectin, or fibrinogen and promotes migration and fusion of precursors into mature cells (Townsend et al., 1999). However, these integrins have not been investigated any further and their relevance in osteoclast biology is probably underestimated.

Chondrocytes

Chondrocytes express a panel of at least seven integrin heterodimers recognizing molecules of the basal lamina and the territorial cartilage matrix. α5β1, αNβ3, and αNβ5 are fibronectin receptors expressed by chondrocytes, which, along with the α6β1 receptor recognizing laminin, and the α1β1, α2β1 and α10β1 integrins binding collagen, ensure tight chondrocyte interaction with the substrate (Loeser, 2002; Aszodi et al., 2003). The dominant integrin subunit in chondrocytes is the β1 chain (Woods et al., 2007a). Consequently, conditional chondrocyte knockout (KO) of *β1 integrin* resulted in a severe cartilage phenotype (Woods et al., 2007a). Typical chondrodysplasia malformations were noticed in these mice, with shorter long bones and reduced growth plate hypertrophic zone. No vascularization of the primary ossification centers was observed, with vessel present only in the periosteum. The growth plate appeared broadened, the chondrocyte columnar array was disrupted, and the hypertrophic zone mineralization was reduced and patchy (Woods et al., 2007a). Given the broad presence of the β1 chain in at least five chondrocyte integrin receptors, such a severe cartilage phenotype is not surprising. Furthermore, a similar outcome was observed in conditional *Il1*-null chondrocytes in mice (Grashoff et al., 2003; Terpstra et al., 2003).

The expression of chondrocyte β1 integrins is regulated by mechanical forces. Tension forces stimulate their expression with a mechanism that appears to be mediated by FAK, and this effect leads to inhibition of chondrogenesis, especially through α2β1 and α5β1 receptors (Takahashi et al., 2003; Onodera et al., 2005). This result is rather surprising and while it is confirmed by the observation that plating mesenchymal stem cells on integrin-activating RGD peptides results in their reduced commitment to chondrogenesis (Connelly et al., 2007), it is contradicted by the discovery that inhibition of β1 integrin activity reduces chondrogenesis and cartilage production (Shakibaei, 1998). These results suggest that integrins have dual roles in cartilage development, inhibiting or inducing chondrogenesis in unlike contexts and in response to different environmental regulations. Functionally, Wang and Kirsch (Wang and Kirsch, 2006) showed that β1 and β5 integrins promote cell survival, while their deletion or blockage by neutralizing antibodies reduces hypertrophic differentiation (Hirsch et al., 1997). Proliferative and hypertrophic chondrocytes of the growth plate express the highest levels of α5β1 receptors, and neutralization of this integrin results in impairment of chondrocyte proliferation (Enomoto-Iwamoto et al., 1997). The α5β1 integrin is also important for the development of the appendicular skeleton and joints. For instance, premature formation of prehypertrophic chondrocyte and joint fusion were observed when *α5β1 integrin* was misexpressed (Garciadiego-Cázares et al., 2004). Finally, deletion of *α10β1 integrin* caused dysfunctions of the growth plate, inducing growth retardation (Bengtsson et al., 2005), with increased apoptosis and altered chondrocyte morphology. Instead deletion of the α1 chain caused osteoarthritis but not growth defects (Zemmyo et al., 2003).

In addition to integrins, the adhesion of chondrocytes to the cartilage matrix is ensured by other types of molecules. The discoidin domain receptor, *Ddr2*, is highly expressed by articular chondrocytes in osteoarthritis, and its conditional deficiency in growth plate chondrocytes was associated with decreased chondrocyte proliferation and subsequent dwarfism (Labrador et al., 2001). Annexin V instead mediates adhesion to the N telopeptide of collagen II in articular cartilage and growth plate, where it appears to regulate apoptosis and matrix mineralization (Wang and Kirsch, 2006; Jennings et al., 2001; Kirsch, 2005). Finally, CD44, an important membrane glycoprotein receptor recognizing collagens and hyaluronic acid, increases during chondrogenesis and contributes to the organization of the territorial matrix and the regulation of chondrocyte survival (Nicoll et al., 2002; Knudson, 2003).

Role of cadherins in bone cells

Osteoblasts and osteocytes

Cadherins are transmembrane glycoproteins that mediate calcium-dependent cell−cell adhesion through homophilic interactions of their extracellular domains (Gumbiner, 2005). The intracellular domain of cadherins interacts with cytoskeletal proteins at adherens junction sites and with signaling molecules such as vinculin, α- and β-catenin, and other molecules involved in cellular signaling processes (Nelson and Nusse, 2004). Osteoblasts express Cadh1 (E-cadherin), Cadh2 (N-cadherin), Cadh3 (P-cadherin), and Cadh11 (“osteoblast cadherin”) (Cheng et al., 1998; Goomer et al., 1998;

Ferrari et al., 2000; Lemonnier et al., 2000; Kawaguchi et al., 2001a), although the expression of these cadherins changes with the stage of osteoblast differentiation. Cadh2 expression initially increases during osteogenic differentiation in vitro but declines thereafter (Ferrari et al., 2000; Greenbaum et al., 2012), whereas Cadh11 is upregulated throughout the osteoblast differentiation program (Kawaguchi et al., 2001b; Shin et al., 2000). In vivo, *Cadh2* is expressed in lining cells but not in osteocytes (Shin et al., 2000). In vitro and in vivo studies suggest that cadherins may control precursor cell lineage determination (Marie et al., 2014a). Both *Cadh2* and *Cadh11* are downregulated with commitment of mesenchymal progenitors to adipogenesis in vitro (Kawaguchi et al., 2001b; Shin et al., 2000). Adult *Cadh11*-KO mice showed increased number of adipogenic precursors and adipogenic differentiation in vitro, suggesting that Cadh11 blocks adipogenesis (Di Benedetto et al., 2010). However, deletion of *Cadh11* does not result in a major skeletal defect in adult mice (Di Benedetto et al., 2010) and causes only modest osteopenia in young mice (Castro et al., 2004), presumably due to compensation by Cadh2. Indeed, ablation of one *Cadh2* allele in *Cadh11*-null mice resulted in severe osteopenia associated with reduced bone strength (Di Benedetto et al., 2010). Consistent with a role for Cadh2 in osteogenesis, overexpression of a dominant-negative *Cadh2* mutant in mature osteoblasts using the osteocalcin promoter resulted in reduced osteoblast differentiation, bone formation, and bone mass (Castro et al., 2004). However, *Cadh2* haploinsufficiency, or conditional deletion of *Cadh2*, in osteoblasts led to increased differentiation of bone marrow stromal cells in vitro, suggesting that Cadh2 may inhibit terminal osteoblast differentiation. Thus, although Cadh2 and Cadh11 contribute to early stages of osteoblast differentiation, Cadh2, but not Cadh11, downregulation is required for terminal differentiation.

How do cadherins control osteoblast differentiation and fate? As they behave as adhesive molecules, cadherins can control osteoblast precursor cell fate in part through cell−cell adhesion (Haÿ et al., 2000). Blocking Cadh2-mediated cell−cell adhesion using specific peptides or antibody reduces osteoblast differentiation in vitro (Ferrari et al., 2000; Haÿ et al., 2000). However, overexpression of *Cadh2* in osteoblasts driven by the Col1A1 promoter reduced osteoblast activity and peak bone mass, indicating that Cadh2 controls bone formation through other mechanisms than cell−cell adhesion (Haÿ et al., 2009a). Cadherins are known modulators of intracellular signaling related to Wnt signaling (Heuberger and Birchmeier, 2010). Cadherins can bind to β-catenin, which leads to increased stabilization of the adhesion structure. Conversely, the release of β-catenin from cadherins destabilizes the adhesion complex and allows cell mobility (Gottardi and Gumbiner, 2001). In addition, cell−cell adhesion mediated by cadherins promotes β-catenin phosphorylation and inactivation of Wnt/β-catenin signaling (Lilien and Balsamo, 2005). Furthermore, cadherins can sequestrate β-catenin at the cell membrane, resulting in decreased β-catenin pool availability for nuclear translocation (Gottardi and Gumbiner, 2001). In osteoblasts, several interactions between cadherins and Wnt signaling molecules were shown to control osteogenic differentiation (Lilien and Balsamo, 2005). The decreased β-catenin abundance at cell−cell contacts induced by deletion of *Cadh2* or *Cadh11* led to decreased cell−cell adhesion with a negative effect on osteoblastogenesis (Di Benedetto et al., 2010). In addition to this mechanism, Cadh2 can bind to low-density lipoprotein receptor−related protein (LRP) 5 or LRP6 via Axin, leading to LRP5/6 sequestration at the cell membrane, reduced LRP5/6 availability, and decreased Wnt/β-catenin signaling (Haÿ et al., 2009a). Cadh2/Axin/LRP5/6 interaction in osteoblasts also reduces ERK1/2 and PI3K/AKT signaling, resulting in decreased osteoblast proliferation, differentiation, and survival (Marie et al., 2014a). Furthermore, Cadh2/LRP5/6 interaction in osteogenic cells causes decreased endogenous Wnt3a expression, which contributes to reduced Wnt signaling and osteoblastogenesis (Marie et al., 2014a). The resulting effect of the negative interaction of Cadh2 overexpression on Wnt signaling in osteogenic cells is to decrease bone formation and delay peak bone mass in young mice (Haÿ et al., 2009a). Consistent with the finding that Cadh2 negatively regulates Wnt/β-catenin signaling in osteoblasts (Marie et al., 2014a; Haÿ et al., 2009a), Cadh2 was found to restrain the bone anabolic action of intermittent parathyroid hormone (iPTH). In vitro, the ablation of *Cadh2* in osteogenic cells results in increased LRP6/PTHR1 interaction and enhanced iPTH-induced protein kinase-dependent Wnt/β-catenin signaling. In mice, conditional *Cadh2* deletion in osteoprogenitor cells led to a greater than normal osteoblast activity and bone mass in response to iPTH, indicating that Cadh2−LRP6 interaction restrains PTH-induced β-catenin signaling (Haÿ et al., 2009b). Consistently, overexpression of *Cadh2* blunted the suppressive effect of PTH on sclerostin/SOST expression in vitro and in vivo, further indicating that Cadh2 expression influences the anabolic effect of iPTH in mice (Revollo et al., 2015). However, the influence of Cadh2 on Wnt signaling and osteogenic cell commitment and differentiation varies with aging. While Cadh2 overexpression in osteoblasts decreased osteoblast differentiation and increased bone marrow adipocyte differentiation in young mice, this phenotype was fully reversed with aging (Yang et al., 2016), which is consistent with the downregulation of Cadh2 during osteoblast maturation. This phenotype was linked to reversal with age of endogenous Wnt5a and Wnt10b signals that are key factors controlling osteogenic cell lineage commitment (Yang et al., 2016). In addition to aging, the negative effect of Cadh2 on Wnt/β-catenin signaling depends on the osteogenic cell differentiation stage. Conditional deletion of *Cadh2* in osteoprogenitors at embryonic and perinatal age was detrimental to bone accrual, whereas loss of *Cadh2* in osteolineage cells in adult mice favored bone formation (Haÿ et al., 2014), indicating that Wnt/β-catenin

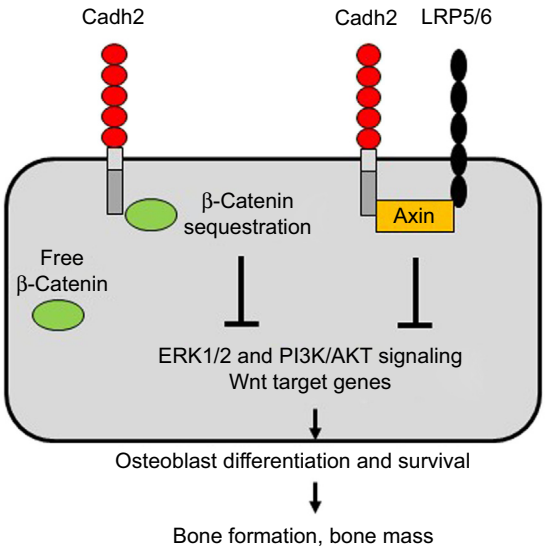

FIGURE 17.3 Role of cadherins in osteoblasts. Cadherin 2 (*Cadh2*) can interact with β-catenin at the cell surface, resulting in β-catenin sequestration, decreased free β-catenin, and reduced Wnt signaling. Cadh2 can also interact with the Wnt coreceptors low-density lipoprotein receptor–related protein 5 (*LRP5*) and *LRP6*, resulting in reduction of Wnt/β-catenin signaling and other signaling pathways that control osteoblast function and survival, bone formation, and bone mass (see text for more details). *ERK1/2*, extracellular signal-regulated kinase 1/2; *PI3K/AKT*, phosphatidylinositol 3-kinase/protein kinase B.

signaling, bone formation, and bone mass are directly influenced by the level of expression of Cadh2 at all stages of the osteoblast lineage. Cadherins also modulate Wnt/β-catenin signaling induced in response to mechanotransduction in bone cells. Mechanical stimulation induced by oscillatory fluid flow in osteoblastic cells leads to reduced Cadh2/β-catenin binding at the cell membrane, resulting in β-catenin nuclear translocation and osteogenic differentiation (Fontana et al., 2017). In addition to the impact on Wnt signaling, Cadh2 interacts with PI3K signaling in osteoblastic cells. Cadh2-mediated adherens junctions activate the PI3K signaling cascade in osteoblasts, which contributes to osteoblast differentiation and osteogenesis in the perichondrium (Arnsdorf et al., 2009). Conversely, *Cadh2* overexpression in osteoblasts reduced Wnt-dependent PI3K/AKT signaling, resulting in decreased osteoblast survival in mice (Marie et al., 2014a; Haÿ et al., 2009a). Thus, cadherins control bone formation through multiple mechanisms that are directly or indirectly linked to Wnt/β-catenin signaling (Fig. 17.3).

Based on the finding that Cadh2 interacts with LRP5/6 to reduce β-catenin/Wnt signaling and osteoblast function (Haÿ et al., 2009a), therapeutic approaches targeting Cadh2/LRP5/6 interaction were developed for promoting bone formation (Guntur et al., 2012). In vitro, deletion of the Cadh2 domain interacting with Axin and LRP5/6 leads to promotion of Wnt/β-catenin signaling and osteoblast differentiation (Fiorino and Harrison, 2016). Moreover, disruption of the Cadh2/LRP5/6 interaction using a competitor peptide that binds to the Cadh2/Axin-interacting domain of LRP5/6 results in enhanced Wnt/β-catenin signaling and osteoblast function in vitro, and increased calvaria bone formation in mice (Marie and Haÿ, 2013). In senescent osteopenic mice, blocking the Cadh2/LRP5/6 interaction led to increased endogenous Wnt5a and Wnt10b expression, osteogenic differentiation, bone formation, and bone mass (Haÿ et al., 2012), suggesting a therapeutic approach targeting the Cadh2/LRP5/6 interaction for promoting bone formation in the aging skeleton.

Osteoclasts

Osteoclasts have been investigated for cadherin expression, especially to understand the mechanisms underlying the fusion process of mononuclear precursors into polykarya (Mbalaviele et al., 1995). Osteoclasts express Cadh1, while they are negative for Cadh2 and Cadh3. Interestingly, Cadh1 expression peaks at the time of preosteoclast fusion, a process that is largely inhibited by Cadh1-neutralizing antibodies. Cadh1 inhibition blocks migration of osteoclast precursors, which is essential for mononuclear cell clustering and fusion of their plasma membranes (Fiorino and Harrison, 2016). In contrast, neutralization of Cadh1 fails to affect proliferation of precursors or adhesion to substrate, confirming a specific role of this cell adhesion molecule in the maturation of polykarya (Mbalaviele et al., 1995). In osteoclast precursors, Cadh1 is localized in areas of membrane protrusions (Fiorino and Harrison, 2016) that are distributed throughout the entire cell surface, but its

expression dramatically declines in mature multinucleated osteoclasts. Cadh1 engagement in osteoclast precursors activates gene expression, and several osteoclast genes are under the control of the Cadh1 pathway. Blocking Cadh1 function, before the preosteoclasts fuse into polykarya, retards the expression of the osteoclast transcription factor NFATc1, the fusion protein dendritic cell-specific transmembrane protein, and the osteoclast enzymes cathepsin K and tartrate-resistant acid phosphatase. Since these genes are essential for osteoclast multinucleation and maturation, these observations highlight the important role of Cadh1 in the late stage of osteoclastogenesis. Conversely, overexpression of *Cadh1* in osteoclast precursors brought forward the activation of NFATc1, which translocates to the nucleus earlier than in control cells (Fiorino and Harrison, 2016). Given that the studies on osteoclast cadherins are scanty, we have no specific clues on the signals induced by these molecules during osteoclastogenesis. However, Cadh1 is implicated in the maturation of a number of other macrophage subtypes. For instance, it is involved in the differentiation and motility of Langerhans cells and regulates the activity of dendritic cells via cooperation of the Wnt/β-catenin signaling (Van den Bossche et al., 2012). Because of the tight interaction of Cadh1 with β-catenin and the role of Wnt/β-catenin signaling in osteoclast formation (Kobayashi et al., 2015), it is likely that these two pathways cooperate for the regulation of osteoclastogenesis as well. Another cadherin isoform identified in osteoclasts is Cadh6/2 (Mbalaviele et al., 1998). Dominant negative or antisense *Cadh6/2* prevents osteoclast precursors from interacting with ST2 cells, known to support osteoclastogenesis, suggesting this cell adhesion molecule is involved in heterotypic interaction between these two cell types, leading to full maturation of the osteoclasts (Mbalaviele et al., 1998). Unfortunately, there are no other data supporting this observation; therefore the underlying molecular mechanisms remain elusive.

Chondrocytes

The most prominent cadherin in chondrocytes is Cadh2. It is strongly expressed during mesenchymal condensation, which allows the formation of the primordial tissue from which limb cartilage originates (Oberlender and Tuan, 1994). This process can be impaired using Cadh2 blocking antibody, which prevents mesenchymal condensation and subsequent chondrogenesis. Cadh2 was upregulated in an in vitro model of chondrocyte differentiation. It was detected in prechondrogenic cells and transiently increased during cell aggregation, disappearing in hypertrophic chondrocytes (Tavella et al., 1994). Cadh2 appears to be essential for cellular condensation (Woodward and Tuan, 1999). Using high-density micromass cultures, Woodward and Tuan (Woodward and Tuan, 1999) induced chick limb mesenchymal cell condensation by ion cross-links promoted by poly-L-lysine. This condition unveiled a time-dependent increase in Cadh2, while its neutralization by a specific antibody inhibited the effect of poly-L-lysine on chondrogenesis. Forced overexpression of *Cadh2* induced precartilage cellular condensation and enhanced chondrogenesis in vitro, with a mechanism that required both extracellular and intracellular domains of Cadh2 (Delise and Tuan, 2002). Cadh2 also appears to be a target for the antichondrogenic effect of retinoic acid. Retinoic acid inhibits the progression of condensed precartilage tissue to cartilage nodules. This progression occurs upon suppression of Cadh2 expression, which is prevented by retinoic acid along with the downregulation of the associated α- and β-catenins. This effect of retinoic acid is blocked by cytochalasin D, a molecule that disrupts the microfilaments implicated in the Cadh2 adhesion function (Cho et al., 2003).

Another important regulator of chondrogenesis that requires Cadh2 is transforming growth factor β (TGFβ). TGFβ induces chondrogenesis through activation of MAPKs, especially p38 and ERK1. These signaling kinases transiently upregulate Cadh2 to allow cellular condensation, followed by its downregulation to induce progression toward chondrogenesis (Tuli et al., 2003). Cellular condensation is also regulated by the small GTP-binding protein RAC1, which triggers upregulation of Cadh2 as well (Woods et al., 2007b). TGFβ also induces the expression of Wnt7. Chondrogenesis is regulated by the Wnt pathway and Wnt7a is a lead chondrogenic signaling t that acts in concert with Cadh2. Using the chick limb mesenchymal cell micromass cultures, Tufan et al. (Tufan et al., 2002) investigated the role of *Chfz-1* and *Chfz-7*, which are members of the Wnt pathway encoded by the Frizzled genes. While CHFZ-1 surrounded the nascent cartilage rudiment, CHFZ-7 was expressed in the area of cell condensation, with progressive downregulation toward the peripheral area. This pattern of expression was similar to the expression of Cadh2, and misexpression of *Chfz-7* impaired chondrogenesis at the early stage of formation of the precartilage aggregates. Notably, *Cadh2* expression was downregulated by *Chfz-7* misexpression, suggesting a functional link between Cadh2 and the Wnt pathway during mesenchymal condensation and subsequent chondrogenesis (Tufan et al., 2002).

To induce chondrogenesis, Cadh2 must be cleaved by ADAM10. Cadh2 cleavage mutants failed to induce cartilage formation, impeding the organization of cartilage aggregates as well as the synthesis of proteoglycans. Furthermore, overexpression of these mutants downregulated type II collagen, aggrecan, and type X collagen (Nakazora et al., 2010), confirming a pivotal role for enzymatic cleavage in the activation of cartilage matrix production. Another factor involved in chondrogenesis that affects Cadh2 is the C-type natriuretic peptide. Treatment of micromass cultures of chick limb

mesenchymal cells with this factor upregulated *Cadh2* along with collagen type X and glycosaminoglycans, ending up with enhanced chondrogenesis (Alan and Tufan, 2008). Despite these striking observations, *Cadh2*-null mice have no skeletal alterations. Given the redundant functions of cadherins, it was hypothesized that, in this mouse model, *Cadh2* deficiency is compensated for by the activity of Cadh11 in cartilage development. *Cadh11* is strongly upregulated in response to chondrogenic conditions and is expressed in normal and osteoarthritic articular cartilage (Stokes et al., 2002). In the growth plate, *Cadh11* is expressed in the late hypertrophic zone. Knockdown of *Cadh11* inhibited the formation of calcified nodules in a growth plate–derived chondrocyte cell line (Matsusaki et al., 2006). The function of Cadh11 has been investigated during the differentiation of mesenchymal stem cells. Kii et al. (Kii et al., 2004) observed that teratomas derived from embryonic stem cells transfected with *Cadh11* formed preferentially bone and cartilage. Using tridimensional hanging drop cultures, it was noticed that *Cadh11*-transfected cells formed sheetlike aggregates, as opposed to *Cadh2*-overexpressing cells, which formed spherical structures, suggesting independent and nonoverlapping functions of Cadh11 and Cadh2 in this context (Kii et al., 2004).

Roles of other attachment molecules in bone cells

Syndecans

Cell surface proteoglycans are composed of a membrane-associated core protein to which glycosaminoglycan (heparan sulfate [HS] or chondroitin sulfate) chains are covalently attached. HS chains can bind several proteins, including growth factors, signaling proteins, membrane receptors, and ECM proteins (Bishop et al., 2007; Bernfield et al., 1999), thus allowing regulation of the availability and function of signaling proteins (Mitsou et al., 2017; Billings and Pacifici, 2015). Notably, binding of extracellular ligands on HS chains increases the probability for ligands to interact with their high-affinity receptors (Billings and Pacifici, 2015). In the growth plate, HS proteoglycans (HSPGs) bind members of the hedgehog, BMP, fibroblast growth factor (FGF), and Wnt protein families (Huegel et al., 2013). Syndecans are an HSPG family composed of four members (syndecan-1 to -4) (Dews and Mackenzie, 2007). In bone, syndecan-1 is expressed transiently during mesenchymal condensation, syndecan-2 is expressed by mesenchymal cells and persists during bone development and osteoblast differentiation, syndecan-3 is mainly expressed in cartilage, whereas syndecan-4 expression is more ubiquitous (David et al., 1993). In osteoblasts, syndecan-2 is strongly associated with FGF/FGFRs (Molténi et al., 1999a; Song et al., 2007) and granulocyte/macrophage colony-stimulating factor (Modrowski et al., 2000), and contributes to the activity of these ligands. Syndecan-2 expression is regulated by Runx2, Wnts, FGF, and TGFβ in osteoblastic cells (Teplyuk et al., 2009; Worapamorn et al., 2002; Dieudonné et al., 2010). BMP-2 increases the synthesis of syndecans (Gutierrez et al., 2006) and interacts with HS complexes to regulate osteoblast differentiation in mesenchymal stromal cells (Manton et al., 2007). In osteogenic cells, syndecan-2 acts as a coreceptor for FGFRs, which is essential for the response to FGF2 (Molténi et al., 1999b; Steinfeld et al., 1996). FGF binding to HS chains results in growth factor dimerization and formation of a tertiary complex with FGFR (Matsuo and Kimura-Yoshida, 2013). Syndecans also interact with Wnt molecules via HS chains to modulate Wnt signaling (Baeg et al., 2001). This leads to the modulation of Wnt molecule concentration at the cell surface, which stabilizes the signaling activity (Fuerer et al., 2010). In bone, syndecan-2 controls the extracellular availability of Wnt effectors and modulates intracellular signals linked to Wnt signaling (Mansouri et al., 2015). Transgenic mice overexpressing *syndecan-2* in osteoblasts showed decreased osteogenesis associated with increased mesenchymal osteoprogenitor cell apoptosis. This phenotype results from inhibition of Wnt/β-catenin signaling and decreased production of Wnt ligands, supporting a role of syndecan-2/Wnt signaling interaction in the control of osteoblastogenesis in vivo (Mansouri et al., 2017). In addition to interacting with signaling factors that regulate osteoblasts, syndecans interact with fibronectin to facilitate cell adhesion through fibronectin–transglutaminase complexes induced by syndecan-4-dependent activation of protein kinase Cα (Wang et al., 2010). This complex supports osteoblast adhesion and rescues from cell death by anoikis in a syndecan- and β1 integrin-dependent manner (Wang et al., 2011). Thus, syndecans control osteoblast adhesion and response to exogenous factors by interacting with both ECM and signaling factors, resulting in the modulation of intracellular factors controlling cell fate.

Glypicans and perlecan

Glypicans are other cell surface proteoglycans expressed in bone. The glycosaminoglycan-bearing perlecan domain I interacts with ligands such as BMP, FGF, hedgehog, and Wnt proteins (Dwivedi et al., 2013) and thereby supports early chondrogenesis (Farach-Carson et al., 2008). In vitro, glypican-3 is involved in osteogenic commitment, as reduced *glypican-3* expression leads to decreased *Runx2* expression and osteoblast differentiation in murine osteoblastic cells

(Haupt et al., 2009). In vivo, *glypican*-KO mice showed decreased trabecular bone mass and delayed endochondral ossification due to reduced osteoclastogenesis, indicating that this HSPG plays a role in bone growth (Viviano et al., 2005). Another HSPG, perlecan, interacts with the ECM, growth factors, and receptors and influences cellular signaling (Whitelock et al., 2008). In bone, perlecan is expressed in cartilage and strongly potentiates chondrogenic differentiation in vitro (French et al., 1999). Perlecan promotes chondrocyte attachment to the matrix (SundarRaj et al., 1995) and is involved in chondrogenic differentiation in vitro (Gomes Jr et al., 2006; French et al., 2002). In vivo, *perlecan*-KO mice showed defective endochondral ossification due to decreased proliferation of chondrocytes and reduced prehypertrophic zone (Arikawa-Hirasawa et al., 1999). Consistent with a role of perlecan in growth plate development, reduced perlecan secretion resulted in achondroplasia in mice (Rodgers et al., 2007). Mechanistically, perlecan binds to FGF2 by its HS chains and enhances FGF2 binding to FGFR-1 and FGFR-3 receptors in the growth plate (Smith et al., 2007). Perlecan may also be involved in the control of osteoblastogenesis and bone formation (Lowe et al., 2014). In the bone marrow, cell-derived ECM that contains perlecan, among other matrix molecules, preserves the ability of mesenchymal stromal cells to differentiate into osteoblasts or adipocytes (Chen et al., 2007). In addition, exogenous perlecan suppresses adipogenic differentiation and promotes osteogenic differentiation of mesenchymal stem cells in vitro (Nakamura et al., 2014). This may be due in part to enhanced interaction with BMP-2, leading to increased BMP-2 bioactivity (Decarlo et al., 2012). At a later stage of osteoblast differentiation, perlecan is localized in the pericellular space of osteocytes in the lacunocanalicular system in cortical bone (Thompson et al., 2011), where it regulates solute transport and mechanosensing within the osteocyte lacunar–canalicular system (Wang et al., 2014). These studies support the notion that, in addition to being involved in cell attachment to the ECM, HSPGs control bone cell functions by interacting with signaling proteins involved in the response to extracellular signals.

CD44

CD44 is a cellular surface adhesion molecule involved in various processes. CD44 binds to hyaluronan (HA), osteopontin, fibronectin, and collagen type I and thereby may regulate bone cell function (Goodison et al., 1999). As noted earlier, CD44 is involved in chondrocyte survival (Nicoll et al., 2002; Knudson, 2003). Osteoclasts express CD44 (Nakamura et al., 1995; Suzuki et al., 2002), and the interaction of CD44 with HA or osteopontin induces intracellular signals in preosteoclasts, leading to osteoclast formation (Spessotto et al., 2002; Chellaiah et al., 2003; Chellaiah and Hruska, 2003). In vitro, osteopontin signals through calcium and NFATc in osteoclasts (Tanabe et al., 2011). Consistently, *CD44* deficiency led to inhibition of osteoclast activity and function by downregulating NF-κB/NFATc1-mediated signaling (Li et al., 2015). Moreover, receptor activator of NF-κB ligand (RANKL) induces *CD44* expression, and CD44 promotes the activation of RANKL–RANK–NF-κB-mediated signaling during osteoclastogenesis (Li et al., 2015). In vivo, *CD44*-KO mice showed normal trabecular bone volume but increased cortical thickness, suggesting a site-specific effect of *CD44* deficiency (Cao et al., 2005). Accordingly, the reduced osteoclastogenesis and osteoclast function induced by *CD44* deficiency counteracts the cortical, but not trabecular, bone loss induced by hindlimb unloading in mice (Li et al., 2015). In contrast to osteoclasts, a role of CD44 in osteoblast function is not firmly established. In vitro, galectin-9 binding to CD44 was reported to induce the formation of a CD44/BMP receptor complex, leading to Smad1/5/8 phosphorylation and osteoblast differentiation (Tanikawa et al., 2010). However, *CD44* deficiency inhibited osteoclast but not osteoblast function in hindlimb-unloading-induced bone loss in mice (Li et al., 2015), suggesting a role of CD44 in bone resorption rather than in bone formation.

Immunoglobulin superfamily members

Neural cell adhesion molecule**,** a member of the immunoglobulin superfamily, is a cell surface molecule expressed transiently during osteoblast lineage (Haÿ et al., 2000; Tanikawa et al., 2010), and its expression is associated with the osteogenic phenotype (Rundus et al., 1998). Activated leukocyte cell adhesion molecule (ALCAM or CD166) is another immunoglobulin member expressed by osteoblasts. *CD166*-deficient mice show increased osteoblast differentiation and bone formation with no change in bone resorption, suggesting that CD166 regulates bone formation (Hooker et al., 2015). Osteoblasts also express intercellular adhesion molecule (ICAM-1) and vascular cell adhesion molecule 1 (VCAM-1), and the cross talk of these molecules induces interleukin-6 (IL-6) secretion by osteoblasts, suggesting that these adhesion molecules transduce activation signals that induce the production of bone-resorbing cytokines (Tanaka et al., 1995). In addition, ICAM-1 and VCAM-1 mediate cell–cell adhesion between osteoclastic precursors and bone marrow stromal cells or osteoblasts, which controls osteoclastogenesis. Neutralization of VCAM-1 in bone marrow stromal cells inhibits the formation of osteoclasts in vitro, indicating that VCAM-1 expression by stromal cells is required for osteoclastogenesis

(Feuerbach and Feyen, 1997). A fraction of osteoblasts that highly express ICAM-1 strongly adhere to osteoclast precursors, resulting in multinuclear osteoclast-like cell formation, indicating that a subpopulation of ICAM-1-expressing osteoblasts controls osteoclastogenesis (Tanaka et al., 2000). Consistent with a role of ICAM-1 in osteoclastogenesis, ICAM-1-mediated cell-to-cell adhesion of osteoblasts and osteoclast precursors was involved in RANKL-dependent osteoclast maturation stimulated by 1,25-dihydroxyvitamin D, PTH, and IL-1α (Okada et al., 2002).

Osteoactivin

Osteoactivin is a glycoprotein expressed by osteoblasts and its expression upregulates osteoblast differentiation in vitro (Abdelmagid et al., 2008). Mice with a loss-of-function mutation in *Gpnmb*, which encodes osteoactivin, showed decreased trabecular bone mass due to reduced osteoblast differentiation, confirming the positive role of osteoactivin in bone formation (Abdelmagid et al., 2014). Osteoactivin is also expressed in osteoclasts and acts as a negative regulator of osteoclast differentiation and survival, but not function (Abdelmagid et al., 2015). Consistent with these findings, transgenic mice overexpressing *osteoactivin* under the cytomegalovirus promoter showed increased trabecular bone mass and bone formation, and decreased bone resorption (Frara et al., 2016). Mechanistically, osteoactivin can bind to CD44 in osteoclasts, leading to inhibition of ERK phosphorylation and RANKL-induced osteolysis (Sondag et al., 2016). In murine osteoblastic cells, recombinant osteoactivin stimulates cell adhesion and spreading through its binding to αVβ1 integrin and HSPGs at the cell surface. This interaction results in FAK and ERK activation and osteoblast differentiation, suggesting a mechanism by which osteoactivin may control osteoblast differentiation (Moussa et al., 2014).

Chondroadherin

Chondroadherin belongs to the family of leucine-rich repeat proteins and was identified in the cartilage matrix, where it promotes attachment of chondrocytes (Larsson et al., 1991). Chondroadherin localizes near the cell surface and is highly expressed in the proliferative and hypertrophic zones of the growth plate. It is a small molecule of 38 kDa molecular weight, containing 359 amino acids. Relevant domains of chondroadherin are a putative signal peptide, a cysteine-rich region at the N-terminal tail, 11 leucine-rich repeats, and a double cysteine loop in the C-terminal tail. Among the members of the leucine-rich repeat protein family, chondroadherin exhibits the unique feature of no posttranslational glycosylation (Neam et al., 1994). The very C terminus of the protein includes a heparin-binding consensus sequence that allows its interaction with heparin (Haglund et al., 2013). This heparin-binding domain recognizes cell surface syndecans and triggers ERK1/2 phosphorylation (Haglund et al., 2013). Chondroadherin is also recognized by the α2β1 integrin expressed by chondrocytes (Camper et al., 1997). The α2β1 integrin binding site was identified in the region carrying the amino acid residues 306−318 at the C terminus of the protein. By affinity purification procedure, α2β1 integrin was confirmed to bind the chondroadherin CQLRGLRRWLEAK^{318} peptide. A longer chondroadherin peptide, spanning amino acid residues 306−326 (CQLRGLRRWEKLAASRPDATC^{326}) was made cyclic and stable through a disulfide bond occurring between the two terminal cysteines and was largely used to investigate the functional role of chondroadherin in vitro and in vivo. The peptide was confirmed to induce cell adhesion and spreading in an α2β1 integrin-dependent manner, activating ERK1/2 phosphorylation (Haglund et al., 2011).

Chondroadherin is expressed also by osteoblasts. It was found to be 50% less expressed in bone biopsies of relatively young female osteoporotic patients (ages between 50 and 65 years), and in ovariectomized mice, a model of estrogen deficiency-induced osteoporosis (Capulli et al., 2014). The cyclic CQLRGLRRWEKLAASRPDATC^{326} peptide was inactive on osteoblasts, but strongly impaired osteoclastogenesis at the late stage of the process. Specifically, the major effect was exerted by the cyclic peptide on migration of osteoclast precursors, which is mandatory for cell clustering and fusion into mature polykarya. The underlying molecular mechanism involved the decreased expression of migfilin and vasodilator-stimulated phosphoprotein (VASP) (Capulli et al., 2014). Migfilin is associated with adhesion sites and binds filamins, VASP, kindling-2 and the transcription factor CSX/NKX2-5, recruiting acting cytoskeleton and promoting cell adhesion, shape modulation, motility and gene expression (Tu et al., 2003). *Migfilin* inactivation in mice induced a severe osteopenic phenotype (Xiao et al., 2012). However, this effect was mostly due to reduced osteoblast differentiation with a parallel increase in the proosteoclastogenic cytokine RANKL, which exacerbated osteoclast differentiation. VASP is known to induce monomeric actin recruitment to the barbed end of microfilaments, preventing capping and regulating filament bundling (Krause et al., 2003). It is implicated in cell motility, adhesion, and sensory capacity, localizing in the tips of filopodia and in adhesion structures (Tokuo and Ikebe, 2004). In osteoclasts, VASP is associated with the αVβ3 integrin and is activated by NO, which promotes osteoclast motility. Consistently, knockdown of *Vasp* reduced osteoclast migration on substrate (Yaroslavskiy et al., 2005). Interestingly, cyclic chondroadherin downregulated NO synthase (*Nos2*)

in osteoclasts, and treatment with an α2β1 integrin blocking antibody increased osteoclast *Nos2* expression, suggesting an inhibitory role of the α2β1 integrin on *Nos2* triggered by chondroadherin (Capulli et al., 2014). Overall, the results obtained using the cyclic α2β1 integrin-binding domain of chondroadherin suggest that this ECM component affects osteoclastogenesis via transcriptional downregulation of *Nos2* and decreased NO, which regulates migfilin and *Vasp* expression and is required for preosteoclast migration, clustering, and fusion into multinucleated osteoclasts.

Cyclic chondroadherin peptide showed also the ability to impair osteoclastogenesis in vivo. Mice injected with cyclic chondroadherin showed enhanced bone mass and reduced osteoclast variables, while osteoblasts and bone formation were not affected (Capulli et al., 2014). This effect was evident both in normal mice and in mice subjected to ovariectomy. In this circumstance, cyclic chondroadherin blocked the increase in serum level of bone resorption biomarkers and prevented bone loss induced by estrogen deficiency, with an improvement of bone quality. These effects were observed in young and old mice and were mimicked by treatment with the NOS2 activity inhibitor (L-N^6-(1-iminoethyl)lysine dihydrochloride). Furthermore, cyclic chondroadherin was effective not only in preventative treatment started at the time of ovariectomy, but also in a curative setting, with the treatment started 5 weeks after ovariectomy, a time at which the osteoporotic phenotype was overt (Capulli et al., 2014). Given the positive response of the bone to treatment with cyclic chondroadherin, the peptide was also tested against bone metastasis-induced osteolysis, which is caused by exacerbated osteoclast activity (Rucci et al., 2015). The results of this study complemented the observations on ovariectomized mice, showing a beneficial effect of the peptide in mice injected intracardiacally or orthotopically with osteotropic breast cancer cells. The peptide reduced the in vitro motility of tumor cells and in vivo tumor growth. It also inhibited the process of tumor-induced osteoclast formation, with consequent reduction of bone resorption, development of osteolytic lesions, and cachexia. Interestingly, cyclic chondroadherin synergistically enhanced the antitumoral effect of the chemotherapeutic doxorubicin, which achieved maximal efficacy at half of the effective dose when administered alone (Rucci et al., 2015). The cyclic chondroadherin−doxorubicin treatment affected tumor cells also in vitro, confirming a synergistic impairment of cell motility at lower doses. Taken together, these results demonstrated that chondroadherin is an important regulator of cell migration, exerting this effect by binding to the α2β1 integrin and impairing the late stage of osteoclast formation and the development of metastatic osteolysis.

Conclusion

Multiple in vitro and in vivo studies have shown that integrins, cadherins, and several other adhesion molecules control bone cell function and fate during chondrogenesis, osteoblastogenesis, and osteoclastogenesis. Genetic studies in mice confirmed the importance of some of these adhesion molecules in the control of bone resorption and formation in vivo. These effects are mediated by complex interactions of these adhesion molecules with bone matrix proteins or cell surface molecules, leading to the modulation of intracellular signaling pathways controlling bone cell differentiation, function, and survival. Studies have revealed that the signaling pathways mediated by integrins, cadherins, and other cell adhesion molecules can cross talk with Wnt/β-catenin signaling to regulate osteogenic differentiation and mechanotransduction, and with other signaling mechanisms to control osteoclastogenesis. These advances led to a more comprehensive view of the role of these adhesion molecules in the signaling mechanisms controlling bone cell recruitment and function. Future studies will have to confirm that targeting specific adhesion molecules and their downstream signals may have potential therapeutic implications in reducing bone resorption or promoting bone formation in skeletal disorders.

Acknowledgments

The authors thank all collaborators who contributed to the work reviewed in this chapter. This work was supported by the Institut National de la Recherche Médicale (Inserm), the Agence Nationale de la Recherche, and the European Commission FP6 and FP7 programs (P.J.M.), and by the Telethon, the Italian Association of Cancer Research, the PRIN-MIUR, and the European Commission FP6, FP7, and H2020 programs (A.T.).

References

Abdelmagid, S.M., Barbe, M.F., Rico, M.C., Salihoglu, S., Arango-Hisijara, I., Selim, A.H., et al., 2008. Osteoactivin, an anabolic factor that regulates osteoblast differentiation and function. Exp. Cell Res. 314, 2334−2351.

Abdelmagid, S.M., Belcher, J.Y., Moussa, F.M., Lababidi, S.L., Sondag, G.R., Novak, K.M., et al., 2014. Mutation in osteoactivin decreases bone formation in vivo and osteoblast differentiation in vitro. Am. J. Pathol. 184, 697−713.

Abdelmagid, S.M., Sondag, G.R., Moussa, F.M., Belcher, J.Y., Yu, B., Stinnett, H., et al., 2015. Mutation in osteoactivin promotes receptor activator of NFκB ligand (RANKL)-mediated osteoclast differentiation and survival but inhibits osteoclast function. J. Biol. Chem. 290, 20128−20146.

Akisaka, T., Yoshida, H., Inoue, S., Shimizu, 2001. Organization of cytoskeletal F-actin, G-actin, and gelsolin in the adhesion structures in cultured osteoclast. J. Bone Miner. Res. 16, 1248−1255.

Alan, T., Tufan, A.C., 2008. C-type natriuretic peptide regulation of limb mesenchymal chondrogenesis is accompanied by altered N-cadherin and collagen type X-related functions. J. Cell. Biochem. 105, 227−235.

Arikawa-Hirasawa, E., Watanabe, H., Takami, H., Hassell, J.R., Yamada, Y., 1999. Perlecan is essential for cartilage and cephalic development. Nat. Genet. 23, 354−358.

Arnsdorf, E.J., Tummala, P., Jacobs, C.R., 2009. Non-canonical Wnt signaling and N-cadherin related beta-catenin signaling play a role in mechanically induced osteogenic cell fate. PLoS One 4, e5388.

Aszodi, A., Hunziker, E.B., Brakebusch, C., Fässler, R., 2003. Beta1 integrins regulate chondrocyte rotation, G1 progression, and cytokinesis. Genes Dev. 17, 2465−2479.

Auzzas, L., Zanardi, F., Battistini, L., Burreddu, P., Carta, P., Rassu, G., et al., 2010. Targeting alphavbeta3 integrin: design and applications of mono- and multifunctional RGD-based peptides and semipeptides. Curr. Med. Chem. 17, 1255−1299.

Baeg, G.H., Lin, X., Khare, N., Baumgartner, S., Perrimon, N., 2001. Heparan sulfate proteoglycans are critical for the organization of the extracellular distribution of Wingless. Development 128, 87−94.

Batra, N., Burra, S., Siller-Jackson, A.J., Gu, S., Xia, X., Weber, G.F., et al., 2012. Mechanical stress-activated integrin α5β1 induces opening of connexin 43 hemichannels. Proc. Natl. Acad. Sci. U. S. A. 109, 3359−3364.

Bengtsson, T., Aszodi, A., Nicolae, C., Hunziker, E.B., Lundgren-Akerlund, E., Fässler, R., 2005. Loss of alpha10beta1 integrin expression leads to moderate dysfunction of growth plate chondrocytes. J. Cell Sci. 118, 929−936.

Bennett, J.H., Moffatt, S., Horton, M., 2001. Cell adhesion molecules in human osteoblasts: structure and function. Histol. Histopathol. 16, 603−611.

Bernfield, M., Götte, M., Park, P.W., Reizes, O., Fitzgerald, M.L., Lincecum, J., et al., 1999. Functions of cell surface heparan sulfate proteoglycans. Annu. Rev. Biochem. 68, 729−777.

Bikle, D.D., 2008. Integrins, insulin like growth factors, and the skeletal response to load. Osteoporos. Int. 19, 1237−1246.

Billings, P.C., Pacifici, M., 2015. Interactions of signaling proteins, growth factors and other proteins with heparan sulfate: mechanisms and mysteries. Connect. Tissue Res. 56, 272−280.

Bishop, J.R., Schuksz, M., Esko, J.D., 2007. Heparan sulphate proteoglycans fine-tune mammalian physiology. Nature 446, 1030−1037.

Bonewald, L.F., Johnson, M.L., 2008. Osteocytes, mechanosensing and Wnt signaling. Bone 42, 606−615.

Bonnet, N., Conway, S.J., Ferrari, S.L., 2012. Regulation of beta catenin signaling and parathyroid hormone anabolic effects in bone by the matricellular protein periostin. Proc. Natl. Acad. Sci. U. S. A. 109, 15048−15053.

Bouvard, D., Aszodi, A., Kostka, G., Block, M.R., Albigès-Rizo, C., Fässler, R., 2007. Defective osteoblast function in ICAP-1-deficient mice. Development 134, 2615−2625.

Brunner, M., Millon-Frémillon, A., Chevalier, G., Nakchbandi, I.A., Mosher, D., Block, M.R., et al., 2011. Osteoblast mineralization requires beta1 integrin/ICAP-1-dependent fibronectin deposition. J. Cell Biol. 194, 307−322.

Bruzzaniti, A., Neff, L., Sanjay, A., Horne, W.C., De Camilli, P., Baron, R., 2005. Dynamin forms a Src kinase-sensitive complex with Cbl and regulates podosomes and osteoclast activity. Mol. Biol. Cell 16, 3301−3313.

Calle, Y., Burns, S., Thrasher, A.J., Jones, G.E., 2006. The leukocyte podosome. Eur. J. Cell Biol. 85, 151−157.

Campbell, I.D., Humphries, M.J., 2011. Integrin structure, activation, and interactions. Cold Spring Harb Perspect Biol 3 (3).

Camper, L., Heinegard, D., Lundgren-Åkerlund, E., 1997. Integrin alpha2beta1 is a receptor for the cartilage matrix protein chondroadherin. J. Cell Biol. 138, 1159−1167.

Cao, J.J., Singleton, P.A., Majumdar, S., Boudignon, B., Burghardt, A., Kurimoto, P., et al., 2005. Hyaluronan increases RANKL expression in bone marrow stromal cells through CD44. J. Bone Miner. Res. 20, 30−40.

Cappariello, A., Maurizi, A., Veeriah, V., Teti, A., 2014. The great beauty of the osteoclast. Arch. Biochem. Biophys. 558, 70−78.

Capulli, M., Olstad, O.K., Önnerfjord, P., Tillgren, V., Muraca, M., Gautvik, K.M., et al., 2014. The C-terminal domain of chondroadherin: a new regulator of osteoclast motility counteracting bone loss. J. Bone Miner. Res. 29, 1833−1846.

Castro, C.H., Shin, C.S., Stains, J.P., Cheng, S.L., Sheikh, S., Mbalaviele, G., et al., 2004. Targeted expression of a dominant-negative N-cadherin in vivo delays peak bone mass and increases adipogenesis. J. Cell Sci. 117, 2853−2864.

Chellaiah, M.A., Hruska, K.A., 2003. The integrin alpha(v)beta(3) and CD44 regulate the actions of osteopontin on osteoclast motility. Calcif. Tissue Int. 72, 197−205.

Chellaiah, M.A., Biswas, R.S., Yuen, D., Alvarez, U.M., Hruska, K.A., 2001. Phosphatidylinositol 3,4,5-trisphosphate directs association of Src homology 2-containing signaling proteins with gelsolin. J. Biol. Chem. 276, 47434−47444.

Chellaiah, M.A., Kizer, N., Biswas, R., Alvarez, U., Strauss-Schoenberger, J., Rifas, L., et al., 2003. Osteopontin deficiency produces osteoclast dysfunction due to reduced CD44 surface expression. Mol. Biol. Cell 14, 173−189.

Chen, J.C., Jacobs, C.R., 2013. Mechanically induced osteogenic lineage commitment of stem cells. Stem Cell Res. Ther. 4, 107.

Chen, X.D., Dusevich, V., Feng, J.Q., Manolagas, S.C., Jilka, R.L., 2007. Extracellular matrix made by bone marrow cells facilitates expansion of marrow-derived mesenchymal progenitor cells and prevents their differentiation into osteoblasts. J. Bone Miner. Res. 22, 1943−1956.

Chen, Q., Shou, P., Zhang, L., Xu, C., Zheng, C., Han, Y., Li, W., et al., 2014. An osteopontin-integrin interaction plays a critical role in directing adipogenesis and osteogenesis by mesenchymal stem cells. Stem Cell. 32, 327−337.

Cheng, S.L., Lecanda, F., Davidson, M.K., Warlow, P.M., Zhang, S.F., Zhang, L., et al., 1998. Human osteoblasts express a repertoire of cadherins, which are critical for BMP-2-induced osteogenic differentiation. J. Bone Miner. Res. 13, 633−644.

Cheng, S.L., Lai, C.F., Fausto, A., Chellaiah, M., Feng, X., McHugh, K.P., et al., 2000. Regulation of alphaVbeta3 and alphaVbeta5 integrins by dexamethasone in normal human osteoblastic cells. J. Cell. Biochem. 77, 265–276.

Cheng, S.L., Lai, C.F., Blystone, S.D., Avioli, L.V., 2001. Bone mineralization and osteoblast differentiation are negatively modulated by integrin alpha(v)beta3. J. Bone Miner. Res. 16, 277–288.

Cho, S.H., Oh, C.D., Kim, S.J., Kim, I.C., Chun, J.S., 2003. Retinoic acid inhibits chondrogenesis of mesenchymal cells by sustaining expression of N-cadherin and its associated proteins. Cell Biochem 89, 837–847.

Clover, J., Dodds, R.A., Gowen, M., 1992. Integrin subunit expression by human osteoblasts and osteoclasts in situ and in culture. J. Cell Sci. 103, 267–271.

Connelly, J.T., García, A.J., Levenston, M.E., 2007. Inhibition of in vitro chondrogenesis in RGD-modified three-dimensional alginate gels. Biomaterials 28, 1071–1083.

Correia, I., Chu, D., Chou, Y.H., Goldman, R.D., Matsudaira, P., 1999. Integrating the actin and vimentin cytoskeletons. Adhesion dependent formation of fimbrin–vimentin complexes in macrophages. J. Cell Biol. 146, 831–842.

Dai, Z., Guo, F., Wu, F., Xu, H., Yang, C., Li, J., et al., 2014. Integrin αvβ3 mediates the synergetic regulation of core-binding factor α1 transcriptional activity by gravity and insulin-like growth factor-1 through phosphoinositide 3-kinase signaling. Bone 69, 126–132.

Danhier, F., Le Breton, A., Préat, V., 2012. RGD-based strategies to target alpha(v) beta(3) integrin in cancer therapy and diagnosis. Mol. Pharm. 9, 2961–2973.

David, G., Bai, X.M., Van der Schueren, B., Marynen, P., Cassiman, J.J., Van den Berghe, H., 1993. Spatial and temporal changes in the expression of fibroglycan (syndecan-2) during mouse embryonic development. Development 119, 841–854.

Decarlo, A.A., Belousova, M., Ellis, A.L., Petersen, D., Grenett, H., Hardigan, P., et al., 2012. Perlecan domain 1 recombinant proteoglycan augments BMP-2 activity and osteogenesis. BMC Biotechnol. 12, 60.

Dejaeger, M., Böhm, A.M., Dirckx, N., Devriese, J., Nefyodova, E., Cardoen, R., et al., 2017. Integrin-linked kinase regulates bone formation by controlling cytoskeletal organization and modulating BMP and Wnt signaling in osteoprogenitors. J. Bone Miner. Res. 32, 2087–2102.

Delise, A.M., Tuan, R.S., 2002. Analysis of N-cadherin function in limb mesenchymal chondrogenesis in vitro. Dev. Dynam. 225, 195–204.

Desgrosellier, J.S., Cheresh, D.A., 2010. Integrins in cancer: biological implications and therapeutic opportunities. Nat. Rev. Canc. 10, 9–22.

Destaing, O., Sanjay, A., Itzstein, C., Horne, W.C., Toomre, D., De Camilli, P., et al., 2008. The tyrosine kinase activity of c-Src regulates actin dynamics and organization of podosomes in osteoclasts. Mol. Biol. Cell 19, 394–404.

Dews, I.C., Mackenzie, K.R., 2007. Transmembrane domains of the syndecan family of growth factor coreceptors display a hierarchy of homotypic and heterotypic interactions. Proc. Natl. Acad. Sci. U. S. A. 104, 20782–20787.

Di Benedetto, A., Watkins, M., Grimston, S., Salazar, V., Donsante, C., Mbalaviele, G., et al., 2010. N-cadherin and cadherin 11 modulate postnatal bone growth and osteoblast differentiation by distinct mechanisms. J. Cell Sci. 123, 2640–2648.

Dieudonné, F.X., Marion, A., Haÿ, E., Marie, P.J., Modrowski, D., 2010. High Wnt signaling represses the proapoptotic proteoglycan syndecan-2 in osteosarcoma cells. Cancer Res. 70, 5399–5408.

Du, J., Zu, Y., Li, J., Du, S., Xu, Y., Zhang, L., et al., 2016. Extracellular matrix stiffness dictates Wnt expression through integrin pathway. Sci. Rep. 6, 20395.

Dufour, C., Holy, X., Marie, P.J., 2007. Skeletal unloading induces osteoblast apoptosis and targets alpha5beta1-PI3K-Bcl-2 signaling in rat bone. Exp. Cell Res. 313, 394–403.

Duong, L.T., Lakkakorpi, P.T., Nakamura, I., Machwate, M., Nagy, R.M., Rodan, G.A., 1998. PYK2 in osteoclasts is an adhesion kinase, localized in the sealing zone, activated by ligation of alpha(v)beta3 integrin, and phosphorylated by src kinase. J. Clin. Investig. 102, 881–892.

Dwivedi, P.P., Lam, N., Powell, B.C., 2013. Boning up on glypicans-Opportunities for new insights into bone biology. Cell Biochem. Funct. 31, 91–114.

Eddy, R.J., Weidmann, M.D., Sharma, V.P., Condeelis, J.S., 2017. Tumor cell invadopodia: invasive protrusions that orchestrate metastasis. Trends Cell Biol. 27, 595–607.

Enomoto-Iwamoto, M., Iwamoto, M., Nakashima, K., Mukudai, Y., Boettiger, D., Pacifici, M., et al., 1997. Involvement of alpha5beta1 integrin in matrix interactions and proliferation of chondrocytes. J. Bone Miner. Res. 12, 1124–1132.

Evans, J.G., Matsudaira, P., 2006. Structure and dynamics of macrophage podosomes. Eur. J. Cell Biol. 85, 145–149.

Farach-Carson, M.C., Brown, A.J., Lynam, M., Safran, J.B., Carson, D.D., 2008. A novel peptide sequence in perlecan domain IV supports cell adhesion, spreading and FAK activation. Matrix Biol. 27, 150–160.

Ferrari, S.L., Traianedes, K., Thorne, M., Lafage-Proust, M.H., Genever, P., Cecchini, M.G., et al., 2000. A role for N-cadherin in the development of the differentiated osteoblastic phenotype. J. Bone Miner. Res. 15, 198–208.

Feuerbach, D., Feyen, J.H., 1997. Expression of the cell-adhesion molecule VCAM-1 by stromal cells is necessary for osteoclastogenesis. FEBS Lett. 402, 21–24.

Fiorino, C., Harrison, R.E., 2016. E-cadherin is important for cell differentiation during osteoclastogenesis. Bone 86, 106–118.

Fontana, F., Hickman-Brecks, C.L., Salazar, V.S., Revollo, L., Abou-Ezzi, G., Grimston, S.K., et al., 2017. N-cadherin regulation of bone growth and homeostasis is osteolineage stage-specific. J. Bone Miner. Res. 32, 1332–1342.

Frara, N., Abdelmagid, S.M., Sondag, G.R., Moussa, F.M., Yingling, V.R., Owen, T.A., et al., 2016. Transgenic expression of osteoactivin/gpnmb enhances bone formation in vivo and osteoprogenitor differentiation ex vivo. J. Cell. Physiol. 231, 72–83.

French, M.M., Smith, S.E., Akanbi, K., Sanford, T., Hecht, J., Farach-Carson, M.C., et al., 1999. Expression of the heparan sulfate proteoglycan, perlecan, during mouse embryogenesis and perlecan chondrogenic activity in vitro. J. Cell Biol. 145, 1103–1115.

French, M.M., Gomes Jr., R.R., Timpl, R., Höök, M., Czymmek, K., Farach-Carson, M.C., et al., 2002. Chondrogenic activity of the heparan sulfate proteoglycan perlecan maps to the N-terminal domain I. J. Bone Miner. Res. 17, 48–55.

Frisch, S.M., Ruoslahti, E., 1997. Integrins and anoikis. Curr. Opin. Cell Biol. 9, 701–706.

Fromigué, O., Brun, J., Marty, C., Da Nascimento, S., Sonnet, P., Marie, P.J., 2012. Peptide-based activation of alpha5 integrin for promoting osteogenesis. J. Cell. Biochem. 113, 3029–3038.

Fuerer, C., Habib, S.J., Nusse, R., 2010. A study on the interactions between heparan sulfate proteoglycans and Wnt proteins. Dev. Dynam. 239, 184–190.

Garciadiego-Cázares, D., Rosales, C., Katoh, M., Chimal-Monroy, J., 2004. Coordination of chondrocyte differentiation and joint formation by alpha5beta1 integrin in the developing appendicular skeleton. Development 131, 4735–4742.

Ge, C., Yang, Q., Zhao, G., Yu, H., Kirkwood, K.L., Franceschi, R.T., 2012. Interactions between extracellular signal-regulated kinase 1/2 and P38 MAP kinase pathways in the control of RUNX2 phosphorylation and transcriptional activity. J. Bone Miner. Res. 27, 538–551.

Georgess, D., Machuca-Gayet, I., Blangy, A., Jurdic, P., 2014. Podosome organization drives osteoclast-mediated bone resorption. Cell Adhes. Migrat. 8, 191–204.

Gil-Henn, H., Destaing, O., Sims, N.A., Aoki, K., Alles, N., Neff, L., et al., 2007. Defective microtubule-dependent podosome organization in osteoclasts leads to increased bone density in Pyk2(-/-) mice. J. Cell Biol. 178, 1053–1064.

Globus, R.K., Amblard, D., Nishimura, Y., Iwaniec, U.T., Kim, J.B., Almeida, E.A., et al., 2005. Skeletal phenotype of growing transgenic mice that express a function-perturbing form of beta1 integrin in osteoblasts. Calcif. Tissue Int. 76, 39–49.

Gomes Jr., R.R., Joshi, S.S., Farach-Carson, M.C., Carson, D.D., 2006. Ribozyme-mediated perlecan knockdown impairs chondrogenic differentiation of C3H10T1/2 fibroblasts. Differentiation 74, 53–63.

Goodison, S., Urquidi, V., Tarin, D., 1999. CD44 cell adhesion molecules. Mol. Pathol. 52, 189–196.

Goomer, R.S., Maris, T., Amiel, D., 1998. Age-related changes in the expression of cadherin-11, the mesenchyme specific calcium-dependent cell adhesion molecule. Calcif. Tissue Int. 62, 532–537.

Gottardi, C.J., Gumbiner, B.M., 2001. Adhesion signaling: how beta-catenin interacts with its partners. Curr. Biol. 11, R792–R794.

Granot-Attas, S., Elson, A., 2008. Protein tyrosine phosphatases in osteoclast differentiation, adhesion, and bone resorption. Eur. J. Cell Biol. 87, 479–490.

Grashoff, C., Aszódi, A., Sakai, T., Hunziker, E.B., Fässler, R., 2003. Integrin-linked kinase regulates chondrocyte shape and proliferation. EMBO Rep. 4, 432–438.

Greenbaum, A.M., Revollo, L.D., Woloszynek, J.R., Civitelli, R., Link, D.C., 2012. N-cadherin in osteolineage cells is not required for maintenance of hematopoietic stem cells. Blood 120, 295–302.

Grigoriou, V., Shapiro, I.M., Cavalcanti-Adam, E.A., Composto, R.J., Ducheyne, P., Adams, C.S., 2005. Apoptosis and survival of osteoblast-like cells are regulated by surface attachment. J. Biol. Chem. 280, 1733–1739.

Gronthos, S., Simmons, P.J., Graves, S.E., Robey, P.G., 2001. Integrin-mediated interactions between human bone marrow stromal precursor cells and the extracellular matrix. Bone 28, 174–178.

Grzesik, W.J., Robey, P.G., 1994. Bone matrix RGD glycoproteins: immunolocalization and interaction with human primary osteoblastic bone cells in vitro. J. Bone Miner. Res. 9, 487–496.

Grzesik, W.J., 1997. Integrins and bone–cell adhesion and beyond. Arch. Immunol. Ther. Exp. 45, 271–275.

Guan, M., Yao, W., Liu, R., Lam, K.S., Nolta, J., Jia, J., et al., 2012. Directing mesenchymal stem cells to bone to augment bone formation and increase bone mass. Nat. Med. 18, 456–462.

Gumbiner, B.M., 2005. Regulation of cadherin-mediated adhesion in morphogenesis. Nat. Rev. Mol. Cell Biol. 6, 622–634.

Guntur, A.R., Rosen, C.J., Naski, M.C., 2012. N-cadherin adherens junctions mediate osteogenesis through PI3K signaling. Bone 50, 54–62.

Gutierrez, J., Osses, N., Brandan, E., 2006. Changes in secreted and cell associated proteoglycan synthesis during conversion of myoblasts to osteoblasts in response to bone morphogenetic protein-2: role of decorin in cell response to BMP-2. J. Cell. Physiol. 206, 58–67.

Haglund, L., Tillgren, V., Addis, L., Wenglén, C., Recklies, A., Heinegård, D., 2011. Identification and characterization of the integrin $\alpha 2\beta 1$ binding motif in chondroadherin mediating cell attachment. J. Biol. Chem. 286, 3925–3934.

Haglund, L., Tillgren, V., Önnerfjord, P., Heinegård, D., 2013. The C-terminal peptide of chondroadherin modulate cellular activity by selectively binding to heparan sulfate chains. J. Biol. Chem. 288, 995–1008.

Hamidouche, Z., Fromigué, O., Ringe, J., Häupl, T., Vaudin, P., Pagès, J.C., et al., 2009. Priming integrin alpha5 promotes human mesenchymal stromal cell osteoblast differentiation and osteogenesis. Proc. Natl. Acad. Sci. U. S. A. 106, 18587–18591.

Hamidouche, Z., Fromigué, O., Ringe, J., Häupl, T., Marie, P.J., 2010. Crosstalks between integrin alpha 5 and IGF2/IGFBP2 signalling trigger human bone marrow-derived mesenchymal stromal osteogenic differentiation. BMC Cell Biol. 11, 44.

Haupt, L.M., Murali, S., Mun, F.K., Teplyuk, N., Mei, L.F., Stein, G.S., et al., 2009. The heparan sulfate proteoglycan (HSPG) glypican-3 mediates commitment of MC3T3-E1 cells toward osteogenesis. J. Cell. Physiol. 220, 780–791.

Haÿ, E., Lemonnier, J., Modrowski, D., Lomri, A., Lasmoles, F., Marie, P.J., 2000. N- and E-cadherin mediate early human calvaria osteoblast differentiation promoted by bone morphogenetic protein-2. J. Cell. Physiol. 183, 117–128.

Haÿ, E., Laplantine, E., Geoffroy, V., Frain, M., Kohler, T., Muller, R., et al., 2009a. N-cadherin interacts with axin and LRP5 to negatively regulate Wnt/beta-catenin signaling, osteoblast function, and bone formation. Mol. Cell Biol. 29, 953–964.

Haÿ, E., Nouraud, A., Marie, P.J., 2009b. N-cadherin negatively regulates osteoblast proliferation and survival by antagonizing Wnt, ERK and PI3K/Akt signalling. PLoS One 4, e8284.

Haÿ, E., Buczkowski, T., Marty, C., Da Nascimento, S., Sonnet, P., Marie, P.J., 2012. Peptide-based mediated disruption of N-cadherin-LRP5/6 interaction promotes Wnt signaling and bone formation. J. Bone Miner. Res. 27, 1852–1863.

Haÿ, E., Dieudonné, F.X., Saidak, Z., Marty, C., Brun, J., Da Nascimento, S., et al., 2014. N-cadherin/Wnt interaction controls bone marrow mesenchymal cell fate and bone mass during aging. J. Cell. Physiol. 229, 1765–1767.

Heuberger, J., Birchmeier, W., 2010. Interplay of cadherin-mediated cell adhesion and canonical Wnt signaling. Cold Spring Harb. Perspect. Biol. 2, a002915.

Hirsch, M.S., Lunsford, L.E., Trinkaus-Randall, V., Svoboda, K.K., 1997. Chondrocyte survival and differentiation in situ are integrin mediated. Dev. Dynam. 210, 249–263.

Hooker, R.A., Chitteti, B.R., Egan, P.H., Cheng, Y.H., Himes, E.R., Meijome, T., et al., 2015. Activated leukocyte cell adhesion molecule (ALCAM or CD166) modulates bone phenotype and hematopoiesis. J. Musculoskelet. Neuronal Interact. 15, 83–94.

Horne, W.C., Sanjay, A., Bruzzaniti, A., Baron, R., 2005. The role(s) of Src kinase and Cbl proteins in the regulation of osteoclast differentiation and function. Immunol. Rev. 208, 106–125.

Horton, M.A., 2001. Integrin antagonists as inhibitors of bone resorption: implications for treatment. Proc. Nutr. Soc. 60, 275–281.

Hsu, A.R., Veeravagu, A., Cai, W., Hou, L.C., Tse, V., Chen, X., 2007. Integrin alpha v beta 3 antagonists for anti-angiogenic cancer treatment. Recent Pat. Anti-Cancer Drug Discov. 2, 143–158.

Huegel, J., Sgariglia, F., Enomoto-Iwamoto, M., Koyama, E., Dormans, J.P., Pacifici, M., 2013. Heparan sulfate in skeletal development, growth, and pathology: the case of hereditary multiple exostoses. Dev. Dynam. 242, 1021–1032.

Hughes, D.E., Salter, D.M., Dedhar, S., Simpson, R., 1993. Integrin expression in human bone. J. Bone Miner. Res. 8, 527–533.

Hultenby, K., Reinholt, F.P., Heinegård, D., 1993. Distribution of integrin subunits on rat metaphyseal osteoclasts and osteoblasts. Eur. J. Cell Biol. 62, 86–93.

Inoue, M., Namba, N., Chappel, J., Teitelbaum, S.L., Ross, F.P., 1998. Granulocyte macrophage-colony stimulating factor reciprocally regulates alphav-associated integrins on murine osteoclast precursors. Mol. Endocrinol. 12, 1955–1962.

Iwaniec, U.T., Wronski, T.J., Amblard, D., Nishimura, Y., van der Meulen, M.C., Wade, C.E., et al., 2005. Effects of disrupted beta1-integrin function on the skeletal response to short-term hindlimb unloading in mice. J. Appl. Physiol. 98, 690–696.

James, A.W., Shen, J., Zhang, X., Asatrian, G., Goyal, R., Kwak, J.H., et al., 2015. NELL-1 in the treatment of osteoporotic bone loss. Nat. Commun. 6, 7362.

Jennings, L., Wu, L., King, K.B., Hämmerle, H., Cs-Szabo, G., Mollenhauer, J., 2001. The effects of collagen fragments on the extracellular matrix metabolism of bovine and human chondrocytes. Connect. Tissue Res. 42, 71–86.

Jikko, A., Harris, S.E., Chen, D., Mendrick, D.L., Damsky, C.H., 1999. Collagen integrin receptors regulate early osteoblast differentiation induced by BMP-2. J. Bone Miner. Res. 14, 1075–1083.

Katsumi, A., Orr, A.W., Tzima, E., Schwartz, M.A., 2004. Integrins in mechanotransduction. J. Biol. Chem. 279, 12001–12004.

Kawaguchi, J., Kii, I., Sugiyama, Y., Takeshita, S., Kudo, A., 2001a. The transition of cadherin expression in osteoblast differentiation from mesenchymal cells: consistent expression of cadherin-11 in osteoblast lineage. J. Bone Miner. Res. 16, 260–269.

Kawaguchi, J., Kii, I., Sugiyama, Y., Takeshita, S., Kudo, A., 2001b. The transition of cadherin expression in osteoblast differentiation from mesenchymal cells: consistent expression of cadherin-11 in osteoblast lineage. J. Bone Miner. Res. 16, 260, 26.

Khatiwala, C.B., Kim, P.D., Peyton, S.R., Putnam, A.J., 2009. ECM compliance regulates osteogenesis by influencing MAPK signaling downstream of RhoA and ROCK. J. Bone Miner. Res. 24, 886–898.

Kidwai, F., Edwards, J., Zou, L., Kaufman, D.S., 2016. Fibrinogen induces Runx2 activity and osteogenic development from human pluripotent stem cells. Stem Cell. 34, 2079–2089.

Kii, I., Amizuka, N., Shimomura, J., Saga, Y., Kudo, A., 2004. Cell-cell interaction mediated by cadherin-11 directly regulates the differentiation of mesenchymal cells into the cells of the osteo-lineage and the chondro-lineage. J. Bone Miner. Res. 19, 1840–1849.

Kim, J.B., Leucht, P., Luppen, C.A., Park, Y.J., Beggs, H.E., Damsky, C.H., et al., 2007. Reconciling the roles of FAK in osteoblast differentiation, osteoclast remodeling, and bone regeneration. Bone 41, 39–51.

Kirsch, T., 2005. Annexins – their role in cartilage mineralization. Front. Biosci. 10, 576–581.

Knudson, C.B., 2003. Hyaluronan and CD44: strategic players for cell-matrix interactions during chondrogenesis and matrix assembly. Birth Defects Res C Embryo Today 69, 174–196.

Kobayashi, Y., Uehara, S., Koide, M., Takahashi, N., 2015. The regulation of osteoclast differentiation by Wnt signals. Bonekey Rep. 4, 713.

Krause, M., Dent, E.W., Bear, J.E., Loureiro, J.J., Gertler, F.B., 2003. Ena/VASP proteins: regulators of the actin cytoskeleton and cell migration. Annu. Rev. Cell Dev. Biol. 19, 541–564.

Kumar, S., Ponnazhagan, S., 2007. Bone homing of mesenchymal stem cells by ectopic alpha 4 integrin expression. FASEB J. 21, 3917–3927.

Labrador, J.P., Azcoitia, V., Tuckermann, J., Lin, C., Olaso, E., Mañes, S., et al., 2001. The collagen receptor DDR2 regulates proliferation and its elimination leads to dwarfism. EMBO Rep. 2, 446–452.

Lai, C.F., Feng, X., Nishimura, R., Teitelbaum, S.L., Avioli, L.V., Ross, F.P., et al., 2000. Transforming growth factor-beta up-regulates the beta 5 integrin subunit expression via Sp1 and Smad signaling. J. Biol. Chem. 275, 36400–36406.

Lai, C.F., Chaudhary, L., Fausto, A., Halstead, L.R., Ory, D.S., Avioli, L.V., et al., 2001. Erk is essential for growth, differentiation, integrin expression, and cell function in human osteoblastic cells. J. Biol. Chem. 276, 14443–14450.

Larsson, T., Sommarin, Y., Paulsson, M., Antonsson, P., Hedbom, E., Wendel, M., et al., 1991. Cartilage matrix proteins. A basic 36-kDa protein with a restricted distribution to cartilage and bone. J. Biol. Chem. 266, 20428–20433.

Lee, Y.S., Chuong, C.M., 1992. Adhesion molecules in skeletogenesis: I. Transient expression of neural cell adhesion molecules (NCAM) in osteoblasts during endochondral and intramembranous ossification. J. Bone Miner. Res. 7, 1435–1446.

Lee, D.Y., Li, Y.S., Chang, S.F., Zhou, J., Ho, H.M., Chiu, J.J., et al., 2010. Oscillatory flow-induced proliferation of osteoblast-like cells is mediated by alphavbeta3 and beta1 integrins through synergistic interactions of focal adhesion kinase and Shc with phosphatidylinositol 3-kinase and the Akt/mTOR/p70S6K pathway. J. Biol. Chem. 285, 30–42.

Lemonnier, J., Delannoy, P., Hott, M., Lomri, A., Modrowski, D., Marie, P.J., 2000. The Ser252Trp fibroblast growth factor receptor-2 (FGFR-2) mutation induces PKC-independent downregulation of FGFR-2 associated with premature calvaria osteoblast differentiation. Exp. Cell Res. 256, 158–167.

Li, Y., Zhong, G., Sun, W., Zhao, C., Zhang, P., Song, J., et al., 2015. CD44 deficiency inhibits unloading-induced cortical bone loss through down-regulation of osteoclast activity. Sci. Rep. 5, 16124.

Lilien, J., Balsamo, J., 2005. The regulation of cadherin-mediated adhesion by tyrosine phosphorylation/dephosphorylation of beta-catenin. Curr. Opin. Cell Biol. 17, 459–465.

Litzenberger, J.B., Kim, J.B., Tummala, P., Jacobs, C.R., 2010. Beta1 integrins mediate mechanosensitive signaling pathways in osteocytes. Calcif. Tissue Int. 86, 325–332.

Loeser, R.F., 2002. Integrins and cell signaling in chondrocytes. Biorheology 39, 119–124.

Lowe, C., Yoneda, T., Boyce, B.F., Chen, H., Mundy, G.R., Soriano, P., 1993. Osteopetrosis in Src-deficient mice is due to an autonomous defect of osteoclasts. Proc. Natl. Acad. Sci. U. S. A. 90, 4485–4489.

Lowe, D.A., Lepori-Bui, N., Fomin, P.V., Sloofman, L.G., Zhou, X., Farach-Carson, M.C., et al., 2014. Deficiency in perlecan/HSPG2 during bone development enhances osteogenesis and decreases quality of adult bone in mice. Calcif. Tissue Int. 95, 29–38.

Luxenburg, C., Winograd-Katz, S., Addadi, L., Geiger, B., 2012. Involvement of actin polymerization in podosome dynamics. J. Cell Sci. 125, 1666–1672.

Mansouri, R., Haÿ, E., Marie, P.J., Modrowski, D., 2015. Role of syndecan-2 in osteoblast biology and pathology. Bonekey Rep. 4, 666.

Mansouri, R., Jouan, Y., Haÿ, E., Blin-Wakkach, C., Frain, M., Ostertag, A., et al., 2017. Osteoblastic heparan sulfate glycosaminoglycans control bone remodeling by regulating Wnt signaling and the crosstalk between bone surface and marrow cells. Cell Death Dis. 8, e2902.

Manton, K.J., Leong, D.F., Cool, S.M., Nurcombe, V., 2007. Disruption of heparan and chondroitin sulfate signaling enhances mesenchymal stem cell-derived osteogenic differentiation via bone morphogenetic protein signaling pathways. Stem Cell. 25 (11), 2845–2854.

Marchisio, P.C., Cirillo, D., Naldini, L., Primavera, M.V., Teti, A., Zambonin-Zallone, A., 1984. Cell-substratum interaction of cultured avian osteoclasts is mediated by specific adhesion structures. J. Cell Biol. 99, 1696–1705.

Marchisio, P.C., Bergui, L., Corbascio, G.C., Cremona, O., D'Urso, N., Schena, M., et al., 1988. Vinculin, talin, and integrins are localized at specific adhesion sites of malignant B lymphocytes. Blood 66, 830–838.

Marie, P.J., Haÿ, E., 2013. Cadherins and Wnt signalling: a functional link controlling bone formation. Bonekey Rep. 2, 330.

Marie, P.J., Haÿ, E., Saidak, Z., 2014a. Integrin and cadherin signaling in bone : role and potential therapeutic targets. Trends Endocrinol. Metabol. 25, 567–575.

Marie, P.J., Haÿ, E., Modrowski, D., Revollo, L., Mbalaviele, G., Civitelli, R., 2014b. Cadherin-mediated cell-cell adhesion and signaling in the skeleton. Calcif. Tissue Int. 94, 46–54.

Marie, P.J., 2013. Targeting integrins to promote bone formation and repair. Nat. Rev. Endocrinol. 9, 288–295.

Matsuo, I., Kimura-Yoshida, C., 2013. Extracellular modulation of Fibroblast Growth Factor signaling through heparan sulfate proteoglycans in mammalian development. Curr. Opin. Genet. Dev. 23, 399–407.

Matsusaki, T., Aoyama, T., Nishijo, K., Okamoto, T., Nakayama, T., Nakamura, T., et al., 2006. Expression of the cadherin-11 gene is a discriminative factor between articular and growth plate chondrocytes. Osteoarthritis Cartilage 14, 353–366.

Mbalaviele, G., Chen, H., Boyce, B.F., Mundy, G.R., Yoneda, T., 1995. The role of cadherin in the generation of multinucleated osteoclasts from mononuclear precursors in murine marrow. J. Clin. Investig. 95, 2757–2765.

Mbalaviele, G., Nishimura, R., Myoi, A., Niewolna, M., Reddy, S.V., Chen, D., et al., 1998. Cadherin-6 mediates the heterotypic interactions between the hemopoietic osteoclast cell lineage and stromal cells in a murine model of osteoclast differentiation. J. Cell Biol. 141, 1467–1476.

McHugh, K.P., Hodivala-Dilke, K., Zheng, M.H., Namba, N., Lam, J., Novack, D., et al., 2000. Mice lacking beta3 integrins are osteosclerotic because of dysfunctional osteoclasts. J. Clin. Investig. 105, 433–440.

Meury, T., Akhouayri, O., Jafarov, T., Mandic, V., St-Arnaud, R., 2010. Nuclear alpha NAC influences bone matrix mineralization and osteoblast maturation in vivo. Mol. Cell Biol. 30, 43–53.

Mitsou, I., Multhaupt, H.A.B., Couchman, J.R., 2017. Proteoglycans, ion channels and cell-matrix adhesion. Biochem. J. 474, 1965–1979.

Miyauchi, A., Alvarez, J., Greenfield, E.M., Teti, A., Grano, M., Colucci, S., et al., 1991. Recognition of osteopontin and related peptides by an alpha v beta 3 integrin stimulates immediate cell signals in osteoclasts. J. Biol. Chem. 266, 20369–20374.

Miyauchi, A., Gotoh, M., Kamioka, H., Notoya, K., Sekiya, H., Takagi, Y., et al., 2006. AlphaVbeta3 integrin ligands enhance volume-sensitive calcium influx in mechanically stretched osteocytes. J. Bone Miner. Metab. 24, 498–504.

Mizuno, M., Fujisawa, R., Kuboki, Y., 2000. Type I collagen-induced osteoblastic differentiation of bone-marrow cells mediated by collagen-alpha2beta1 integrin interaction. J. Cell. Physiol. 184, 207–213.

Modrowski, D., Baslé, M., Lomri, A., Marie, P.J., 2000. Syndecan-2 is involved in the mitogenic activity and signaling of granulocyte-macrophage colony-stimulating factor in osteoblasts. J. Biol. Chem. 275, 9178–9185.

Molténi, A., Modrowski, D., Hott, M., Marie, P.J., 1999a. Differential expression of fibroblast growth factor receptor-1, -2, and -3 and syndecan-1, -2, and -4 in neonatal rat mandibular condyle and calvaria during osteogenic differentiation in vitro. Bone 24, 337–347.

Molténi, A., Modrowski, D., Hott, M., Marie, P.J., 1999b. Alterations of matrix- and cell-associated proteoglycans inhibit osteogenesis and growth response to fibroblast growth factor-2 in cultured rat mandibular condyle and calvaria. Cell Tissue Res. 295, 523–536.

Morgan, E.A., Schneider, J.G., Baroni, T.E., Uluçkan, O., Heller, E., Hurchla, M.A., et al., 2010. Dissection of platelet and myeloid cell defects by conditional targeting of the beta3-integrin subunit. FASEB J. 24, 1117–1127.

Moursi, A.M., Globus, R.K., Damsky, C.H., 1997. Interactions between integrin receptors and fibronectin are required for calvarial osteoblast differentiation in vitro. J. Cell Sci. 110, 2187–2196.

Moussa, F.M., Hisijara, I.A., Sondag, G.R., Scott, E.M., Frara, N., Abdelmagid, S.M., et al., 2014. Osteoactivin promotes osteoblast adhesion through HSPG and αvβ1 integrin. J. Cell. Biochem. 115, 1243–1253.

Nakamura, H., Kenmotsu, S., Sakai, H., Ozawa, H., 1995. Localization of CD44, the hyaluronate receptor, on the plasma membrane of osteocytes and osteoclasts in rat tibiae. Cell Tissue Res. 280, 225–233.

Nakamura, I., Jimi, E., Duong, L.T., Sasaki, T., Takahashi, N., Rodan, G.A., et al., 1998. Tyrosine phosphorylation of p130Cas is involved in actin organization in osteoclasts. J. Biol. Chem. 273, 11144–11149.

Nakamura, R., Nakamura, F., Fukunaga, S., 2014. Contrasting effect of perlecan on adipogenic and osteogenic differentiation of mesenchymal stem cells in vitro. Anim. Sci. J. 85, 262–270.

Nakazora, S., Matsumine, A., Iino, T., Hasegawa, M., Kinoshita, A., Uemura, K., et al., 2010. The cleavage of N-cadherin is essential for chondrocyte differentiation. Biochem. Biophys. Res. Commun. 400, 493–499.

Neam, P.J., Sommarin, Y., Boynton, R.E., Heinegård, D., 1994. The structure of a 38-kDa leucine-rich protein (chondroadherin) isolated from bovine cartilage. J. Biol. Chem. 269, 21547–21554.

Negishi-Koga, T., Takayanagi, H., 2009. Ca2+-NFATc1 signaling is an essential axis of osteoclast differentiation. Immunol. Rev. 231, 241–256.

Nelson, W.J., Nusse, R., 2004. Convergence of Wnt, beta-catenin, and cadherin pathways. Science 303, 1483–1487.

Nicoll, S.B., Barak, O., Csóka, A.B., Bhatnagar, R.S., Stern, R., 2002. Hyaluronidases and CD44 undergo differential modulation during chondrogenesis. Biochem. Biophys. Res. Commun. 292, 819–825.

Oberlender, S.A., Tuan, R.S., 1994. Expression and functional involvement of N-cadherin in embryonic limb chondrogenesis. Development 120, 177–187.

Okada, Y., Morimoto, I., Ura, K., Watanabe, K., Eto, S., Kumegawa, M., et al., 2002. Cell-to-Cell adhesion via intercellular adhesion molecule-1 and leukocyte function-associated antigen-1 pathway is involved in 1alpha,25(OH)2D3, PTH and IL-1alpha-induced osteoclast differentiation and bone resorption. Endocr. J. 49, 483–495.

Onodera, K., Takahashi, I., Sasano, Y., Bae, J.W., Mitani, H., Kagayama, M., et al., 2005. Stepwise mechanical stretching inhibits chondrogenesis through cell-matrix adhesion mediated by integrins in embryonic rat limb-bud mesenchymal cells. Eur. J. Cell Biol. 84, 45–58.

Ory, S., Brazier, H., Pawlak, G., Blangy, A., 2008. Rho-GTPases I osteoclasts: orchestrators of podosome arrangement. Eur. J. Cell Biol. 87, 469–477.

Phillips, J.A., Almeida, E.A., Hill, E.L., Aguirre, J.I., Rivera, M.F., Nachbandi, I., et al., 2008. Role for beta1 integrins in cortical osteocytes during acute musculoskeletal disuse. Matrix Biol. 27, 609–618.

Plotkin, L.I., Mathov, I., Aguirre, J.I., Parfitt, A.M., Manolagas, S.C., Bellido, T., 2005. Mechanical stimulation prevents osteocyte apoptosis: requirement of integrins, Src kinases, and ERKs. Am. J. Physiol. Cell Physiol. 289, C633–C643.

Pommerenke, H., Schmidt, C., Dürr, F., Nebe, B., Lüthen, F., Muller, P., et al., 2002. The mode of mechanical integrin stressing controls intracellular signaling in osteoblasts. J. Bone Miner. Res. 17, 603–611.

Popov, C., Radic, T., Haasters, F., Prall, W.C., Aszodi, A., Gullberg, D., Schieker, M., et al., 2011. Integrins alpha2beta1 and alpha11beta1 regulate the survival of mesenchymal stem cells on collagen I. Cell Death Dis. 2, e186.

Puleo, D.A., Bizios, R., 1991. RGDS tetrapeptide binds to osteoblasts and inhibits fibronectin-mediated adhesion. Bone 12, 271–276.

Purev, E., Neff, L., Horne, W.C., Baron, R., 2009. c-Cbl and Cbl-b act redundantly to protect osteoclasts from apoptosis and to displace HDAC6 from beta-tubulin, stabilizing microtubules and podosomes. Mol. Biol. Cell 20, 4021–4030.

Rajshankar, D., Wang, Y., McCulloch, C.A., 2017. Osteogenesis requires FAK-dependent collagen synthesis by fibroblasts and osteoblasts. FASEB J. 31, 937–953.

Ray, B.J., Thomas, K., Huang, C.S., Gutknecht, M.F., Botchwey, E.A., Bouton, A.H., 2012. Regulation of osteoclast structure and function by FAK family kinases. J. Leukoc. Biol. 92, 1021–1028.

Revollo, L., Kading, J., Jeong, S.Y., Li, J., Salazar, V., Mbalaviele, G., et al., 2015. N-cadherin restrains PTH activation of Lrp6/β-catenin signaling and osteoanabolic action. J. Bone Miner. Res. 30, 274–285.

Rodgers, K.D., Sasaki, T., Aszodi, A., Jacenko, O., 2007. Reduced perlecan in mice results in chondrodysplasia resembling Schwartz-Jampel syndrome. Hum. Mol. Genet. 16, 515–528.

Rucci, N., Teti, A., 2016. The "love-hate" relationship between osteoclasts and bone matrix. Matrix Biol. 52–54, 176–190.

Rucci, N., Capulli, M., Olstad, O.K., Önnerfjord, P., Tillgren, V., Gautvik, K.M., Heinegård, D., Teti, A., 2015. The α2β1 binding domain of chondroadherin inhibits breast cancer-induced bone metastases and impairs primary tumour growth: a preclinical study. Cancer Lett. 358, 67–75.

Rundus, V.R., Marshall, G.B., Parker, S.B., Bales, E.S., Hertzberg, E.L., Minkoff, R., 1998. Association of cell and substrate adhesion molecules with connexin43 during intramembranous bone formation. Histochem. J. 30, 879–896.

Saidak, Z., Le Henaff, C., Azzi, S., Marty, C., Da Nascimento, S., Sonnet, P., et al., 2015. Wnt/β-catenin signaling mediates osteoblast differentiation triggered by peptide-induced α5β1 integrin priming in mesenchymal skeletal cells. J. Biol. Chem. 290, 6903–6912.

Salasznyk, R.M., Klees, R.F., Boskey, A., Plopper, G.E., 2007. Activation of FAK is necessary for the osteogenic differentiation of human mesenchymal stem cells on laminin-5. J. Cell. Biochem. 100, 499–514.

Saltel, F., Chabadel, A., Bonnelye, E., Jurdic, P., 2008. Actin cytoskeletal organisation in osteoclasts: a model to decipher transmigration and matrix degradation. Eur. J. Cell Biol. 87, 459–468.

Schaffner, P., Dard, M.M., 2003. Structure and function of RGD peptides involved in bone biology. Cell. Mol. Life Sci. 60, 119–132.

Schneider, J.G., Amend, S.R., Weilbaecher, K.N., 2011. Integrins and bone metastasis: integrating tumor cell and stromal cell interactions. Bone 48, 54–65.

Sens, C., Huck, K., Pettera, S., Uebel, S., Wabnitz, G., Moser, M., et al., 2017. Fibronectins containing extradomain A or B enhance osteoblast differentiation via distinct integrins. J. Biol. Chem. 292, 7745–7760.

Seong, J., Tajik, A., Sun, J., Guan, J.L., Humphries, M.J., Craig, S.E., et al., 2013. Distinct biophysical mechanisms of focal adhesion kinase mechanoactivation by different extracellular matrix proteins. Proc. Natl. Acad. Sci. U. S. A. 110, 19372–19377.

Shakibaei, M., 1998. Inhibition of chondrogenesis by integrin antibody in vitro. Exp. Cell Res. 240, 95–106.

Shankar, G., Davison, I., Helfrich, M.H., Mason, W.T., Horton, M.A., 1993. Integrin receptor-mediated mobilisation of intranuclear calcium in rat osteoclasts. J. Cell Sci. 105, 61–68.

Shekaran, A., Shoemaker, J.T., Kavanaugh, T.E., Lin, A.S., LaPlaca, M.C., Fan, Y., et al., 2014. The effect of conditional inactivation of beta 1 integrins using twist 2 Cre, Osterix Cre and osteocalcin Cre lines on skeletal phenotype. Bone 68, 131–141.

Sheldrake, H.M., Patterson, L.H., 2014. Strategies to inhibit tumor associated integrin receptors: rationale for dual and multiantagonists. J. Med. Chem. 57, 6301–6315.

Shih, Y.R., Tseng, K.F., Lai, H.Y., Lin, C.H., Lee, O.K., 2011. Matrix stiffness regulation of integrin-mediated mechanotransduction during osteogenic differentiation of human mesenchymal stem cells. J. Bone Miner. Res. 26, 730–738.

Shin, C.S., Lecanda, F., Sheikh, S., Weitzmann, L., Cheng, S.L., Civitelli, R., 2000. Relative abundance of different cadherins defines differentiation of mesenchymal precursors into osteogenic, myogenic, or adipogenic pathways. J. Cell. Biochem. 78, 566–577.

Smith, S.M., West, L.A., Govindraj, P., Zhang, X., Ornitz, D.M., Hassell, J.R., 2007. Heparan and chondroitin sulfate on growth plate perlecan mediate binding and delivery of FGF-2 to FGF receptors. Matrix Biol. 26, 175–184.

Sondag, G.R., Mbimba, T.S., Moussa, F.M., Novak, K., Yu, B., Jaber, F.A., et al., 2016. Osteoactivin inhibition of osteoclastogenesis is mediated through CD44-ERK signaling. Exp. Mol. Med. 48, e257.

Song, S.J., Cool, S.M., Nurcombe, V., 2007. Regulated expression of syndecan-4 in rat calvaria osteoblasts induced by fibroblast growth factor-2. J. Cell. Biochem. 100, 402–411.

Soysa, N.S., Alles, N., 2016. Osteoclast function and bone-resorbing activity: an overview. Biochem. Biophys. Res. Commun. 476, 115–120.

Spessotto, P., Rossi, F.M., Degan, M., Di Francia, R., Perris, R., Colombatti, A., et al., 2002. Hyaluronan-CD44 interaction hampers migration of osteoclast-like cells by down-regulating MMP-9. J. Cell Biol. 158, 1133–1144.

Spinardi, L., Marchisio, P.C., 2006. Podosomes as smart regulators of cellular adhesion. Eur. J. Cell Biol. 85, 191–194.

Srouji, S., Ben-David, D., Fromigué, O., Vaudin, P., Kuhn, G., Müller, R., et al., 2012. Lentiviral-mediated integrin α5 expression in human adult mesenchymal stromal cells promotes bone repair in mouse cranial and long-bone defects. Hum. Gene Ther. 23, 167–172.

Stange, R., Kronenberg, D., Timmen, M., Everding, J., Hidding, H., Eckes, B., et al., 2013. Age-related bone deterioration is diminished by disrupted collagen sensing in integrin α2β1 deficient mice. Bone 56, 48–54.

Steinfeld, R., Van Den Berghe, H., David, G., 1996. Stimulation of fibroblast growth factor receptor-1 occupancy and signaling by cell surface-associated syndecans and glypican. J. Cell Biol. 133, 405–416.

Stokes, D.G., Liu, G., Coimbra, I.B., Piera-Velazquez, S., Crowl, R.M., Jiménez, S.A., 2002. Assessment of the gene expression profile of differentiated and dedifferentiated human fetal chondrocytes by microarray analysis. Arthritis Rheum. 46, 404–419.

Su, J.L., Chiou, J., Tang, C.H., Zhao, M., Tsai, C.H., Chen, P.S., et al., 2010. CYR61 regulates BMP-2-dependent osteoblast differentiation through the {alpha}v{beta}3 integrin/integrin-linked kinase/ERK pathway. J. Biol. Chem. 285, 31325–31336.

Sun, C., Yuan, H., Wang, L., Wei, X., Williams, L., Krebsbach, P.H., et al., 2016. FAK promotes osteoblast progenitor cell proliferation and differentiation by enhancing Wnt signaling. J. Bone Miner. Res. 31, 2227–2238.

SundarRaj, N., Fite, D., Ledbetter, S., Chakravarti, S., Hassell, J.R., 1995. Perlecan is a component of cartilage matrix and promotes chondrocyte attachment. J. Cell Sci. 108, 2663–2672.

Suzuki, K., Zhu, B., Rittling, S.R., Denhardt, D.T., Goldberg, H.A., McCulloch, C.A., et al., 2002. Colocalization of intracellular osteopontin with CD44 is associated with migration, cell fusion, and resorption in osteoclasts. J. Bone Miner. Res. 17, 1486–1497.

Takahashi, I., Onodera, K., Sasano, Y., Mizoguchi, I., Bae, J.W., Mitani, H., et al., 2003. Effect of stretching on gene expression of beta1 integrin and focal adhesion kinase and on chondrogenesis through cell-extracellular matrix interactions. Eur. J. Cell Biol. 82, 182–192.

Takeuchi, Y., Suzawa, M., Kikuchi, T., Nishida, E., Fujita, T., Matsumoto, T., 1997. Differentiation and transforming growth factor-beta receptor down-regulation by collagen-alpha2beta1 integrin interaction is mediated by focal adhesion kinase and its downstream signals in murine osteoblastic cells. J. Biol. Chem. 14 (272), 29309–29316.

Tamura, Y., Takeuchi, Y., Suzawa, M., Fukumoto, S., Kato, M., Miyazono, K., et al., 2001. Focal adhesion kinase activity is required for bone morphogenetic protein-Smad1 signaling and osteoblastic differentiation in murine MC3T3-E1 cells. J. Bone Miner. Res. 16, 1772–1779.

Tanabe, N., Wheal, B.D., Kwon, J., Chen, H.H., Shugg, R.P., Sims, S.M., et al., 2011. Osteopontin signals through calcium and nuclear factor of activated T cells (NFAT) in osteoclasts: a novel RGD-dependent pathway promoting cell survival. J. Biol. Chem. 286, 39871–39881.

Tanaka, Y., Morimoto, I., Nakano, Y., Okada, Y., Hirota, S., Nomura, S., et al., 1995. Osteoblasts are regulated by the cellular adhesion through ICAM-1 and VCAM-1. J. Bone Miner. Res. 10, 1462–1469.

Tanaka, S., Amling, M., Neff, L., Peyman, A., Uhlmann, E., Levy, J.B., et al., 1996. c-Cbl is downstream of c-Src in a signalling pathway necessary for bone resorption. Nature 383, 528–531.

Tanaka, Y., Maruo, A., Fujii, K., Nomi, M., Nakamura, T., Eto, S., et al., 2000. Intercellular adhesion molecule 1 discriminates functionally different populations of human osteoblasts: characteristic involvement of cell cycle regulators. J. Bone Miner. Res. 15, 1912–1923.

Tanikawa, R., Tanikawa, T., Hirashima, M., Yamauchi, A., Tanaka, Y., 2010. Galectin-9 induces osteoblast differentiation through the CD44/Smad signaling pathway. Biochem. Biophys. Res. Commun. 394, 317–322.

Tavella, S., Raffo, P., Tacchetti, C., Cancedda, R., Castagnola, P., 1994. N-CAM and N-cadherin expression during in vitro chondrogenesis. Exp. Cell Res. 215, 354–362.

Teitelbaum, S.L., 2011. The osteoclast and its unique cytoskeleton. Ann NY Acad Sci 1240, 14–17.

Teplyuk, N.M., Haupt, L.M., Ling, L., Dombrowski, C., Mun, F.K., Nathan, S.S., et al., 2009. The osteogenic transcription factor Runx2 regulates components of the fibroblast growth factor/proteoglycan signaling axis in osteoblasts. J. Cell. Biochem. 107, 144–154.

Terpstra, L., Prud'homme, J., Arabian, A., Takeda, S., Karsenty, G., Dedhar, S., et al., 2003. Reduced chondrocyte proliferation and chondrodysplasia in mice lacking the integrin-linked kinase in chondrocytes. J. Cell Biol. 162, 139–148.

Thi, M.M., Suadicani, S.O., Schaffler, M.B., Weinbaum, S., Spray, D.C., 2013. Mechanosensory responses of osteocytes to physiological forces occur along processes and not cell body and require αVβ3 integrin. Proc. Natl. Acad. Sci. U. S. A. 110, 21012–21017.

Thompson, W.R., Modla, S., Grindel, B.J., Czymmek, K.J., Kirn-Safran, C.B., Wang, L., et al., 2011. Perlecan/Hspg2 deficiency alters the pericellular space of the lacunocanalicular system surrounding osteocytic processes in cortical bone. J. Bone Miner. Res. 26, 618–629.

Tian, J., Zhang, F.J., Lei, G.H., 2015. Role of integrins and their ligands in osteoarthritic cartilage. Rheumatol. Int. 35, 787–798.

Tokuo, H., Ikebe, M., 2004. Myosin X transports Mena/VASP to the tip of filopodia. Biochem. Biophys. Res. Commun. 319, 214–220.

Townsend, P.A., Villanova, I., Teti, A., Horton, M.A., 1999. Beta1 integrin antisense oligodeoxy-nucleotides: utility in controlling osteoclast function. Eur. J. Cell Biol. 78, 485–496.

Triplett, J.W., Pavalko, F.M., 2006. Disruption of alpha-actinin-integrin interactions at focal adhesions renders osteoblasts susceptible to apoptosis. Am. J. Physiol. Cell Physiol. 291, C909–C921.

Tu, S., Wu, S., Shi, X., Chen, K., Wu, C., 2003. Migfilin and Mig-2 link focal adhesions to filamin and the actin cytoskeleton and function in cell shape modulation. Cell 113, 37–47.

Tufan, A.C., Daumer, K.M., Tuan, R.S., 2002. Frizzled-7 and limb mesenchymal chondrogenesis: effect of misexpression and involvement of N-cadherin. Dev. Dynam. 223, 241–253.

Tuli, R., Tuli, S., Nandi, S., Huang, X., Manner, P.A., Hozack, W.J., et al., 2003. Transforming growth factor-beta-mediated chondrogenesis of human mesenchymal progenitor cells involves N-cadherin and mitogen-activated protein kinase and Wnt signaling cross-talk. J. Biol. Chem. 278, 41227–41236.

Turner, C.H., Warden, S.J., Bellido, T., Plotkin, L.I., Kumar, N., Jasiuk, I., et al., 2009. Mechanobiology of the skeleton. Sci. Signal. 2, pt.3.

Uda, Y., Azab, E., Sun, N., Shi, C., Pajevic, P.D., 2017. Osteocyte mechanobiology. Curr. Osteoporos. Rep. 15, 318–332.

Van den Bossche, J., Malissen, B., Mantovani, A., De Baetselier, P., Van Ginderachter, J.A., 2012. Regulation and function of the E-cadherin/catenin complex in cells of the monocyte-macrophage lineage and DCs. Blood 119, 1623–1633.

Viviano, B.L., Silverstein, L., Pflederer, C., Paine-Saunders, S., Mills, K., Saunders, S., 2005. Altered hematopoiesis in glypican-3-deficient mice results in decreased osteoclast differentiation and a delay in endochondral ossification. Dev. Biol. 282, 152–162.

Wang, W., Kirsch, T., 2006. Annexin V/beta5 integrin interactions regulate apoptosis of growth plate chondrocytes. J. Biol. Chem. 281, 30848–30856.

Wang, Y., McNamara, L.M., Schaffler, M.B., Weinbaum, S., 2007. A model for the role of integrins in flow induced mechanotransduction in osteocytes. Proc. Natl. Acad. Sci. U. S. A. 104, 15941–15946.

Wang, Z., Collighan, R.J., Gross, S.R., Danen, E.H., Orend, G., Telci, D., et al., 2010. RGD-independent cell adhesion via a tissue transglutaminase-fibronectin matrix promotes fibronectin fibril deposition and requires syndecan-4/2 alpha5beta1 integrin co-signaling. J. Biol. Chem. 285, 40212–40229.

Wang, Z., Telci, D., Griffin, M., 2011. Importance of syndecan-4 and syndecan -2 in osteoblast cell adhesion and survival mediated by a tissue transglutaminase-fibronectin complex. Exp. Cell Res. 317, 367–381.

Wang, B., Lai, X., Price, C., Thompson, W.R., Li, W., Quabili, T.R., et al., 2014. Perlecan-containing pericellular matrix regulates solute transport and mechanosensing within the osteocyte lacunar-canalicular system. J. Bone Miner. Res. 29, 878–891.

Watabe, H., Furuhama, T., Tani-Ishii, N., Mikuni-Takagaki, Y., 2011. Mechanotransduction activates $\alpha_5\beta_1$ integrin and PI3K/Akt signaling pathways in mandibular osteoblasts. Exp. Cell Res. 317, 2642–2649.

Whitelock, J.M., Melrose, J., Iozzo, R.V., 2008. Diverse cell signaling events modulated by perlecan. Biochemistry 47, 11174–11183.

Woods, A., Wang, G., Beier, F., 2007a. Regulation of chondrocyte differentiation by the actin cytoskeleton and adhesive interactions. J. Cell. Physiol. 213, 1–8.

Woods, A., Wang, G., Dupuis, H., Shao, Z., Beier, F., 2007b. Rac1 signaling stimulates N-cadherin expression, mesenchymal condensation, and chondrogenesis. J. Biol. Chem. 282, 23500–23508.

Woodward, W.A., Tuan, R.S., 1999. N-Cadherin expression and signaling in limb mesenchymal chondrogenesis: stimulation by poly-L-lysine. Dev. Genet. 24, 178–187.

Worapamorn, W., Tam, S.P., Li, H., Haase, H.R., Bartold, P.M., 2002. Cytokine regulation of syndecan-1 and -2 gene expression in human periodontal fibroblasts and osteoblasts. J. Periodontal. Res. 37, 273–278.

Wu, D., Schaffler, M.B., Weinbaum, S., Spray, D.C., 2013. Matrix-dependent adhesion mediates network responses to physiological stimulation of the osteocyte cell process. Proc. Natl. Acad. Sci. U. S. A. 110, 12096–12101.

Xiao, G., Wang, D., Benson, M.D., Karsenty, G., Franceschi, R.T., 1998. Role of the alpha2-integrin in osteoblast-specific gene expression and activation of the Osf2 transcription factor. J. Biol. Chem. 273, 32988–32994.

Xiao, G., Cheng, H., Cao, H., Chen, K., Tu, Y., Yu, S., et al., 2012. Critical role of filamin-binding LIM protein 1 (FBLP-1)/migfilin in regulation of bone remodeling. J. Biol. Chem. 287, 21450–21460.

Yan, Y.X., Gong, Y.W., Guo, Y., Lv, Q., Guo, C., Zhuang, Y., et al., 2012. Mechanical strain regulates osteoblast proliferation through integrin-mediated ERK activation. PLoS One 7, e35709.

Yang, H., Dong, J., Xiong, W., Fang, Z., Guan, H., Li, F., 2016. N-cadherin restrains PTH repressive effects on sclerostin/SOST by regulating LRP6-PTH1R interaction. Ann. N. Y. Acad. Sci. 1385, 41–52.

Yao, W., Guan, M., Jia, J., Dai, W., Lay, Y.A., Amugongo, S., et al., 2013. Reversing bone loss by directing mesenchymal stem cells to bone. Stem Cell. 31, 2003–2014.

Yaroslavskiy, B.B., Zhang, Y., Kalla, S.E., García Palacios, V., Sharrow, A.C., Li, Y., et al., 2005. NO-dependent osteoclast motility: reliance on cGMP-dependent protein kinase I and VASP. J. Cell Sci. 118, 5479–5487.

Zemmyo, M., Meharra, E.J., Kühn, K., Creighton-Achermann, L., Lotz, M., 2003. Accelerated, aging-dependent development of osteoarthritis in alpha1 integrin-deficient mice. Arthritis Rheum. 48, 2873–2880.

Zimmerman, D., Jin, F., Leboy, P., Hardy, S., Damsky, C., 2000. Impaired bone formation in transgenic mice resulting from altered integrin function in osteoblasts. Dev. Biol. 220, 2–15.

Zou, W., Teitelbaum, S.L., 2010. Integrins, growth factors, and the osteoclast cytoskeleton. Ann. N. Y. Acad. Sci. 1192, 27–31.

Zou, W., Teitelbaum, S.L., 2015. Absence of Dap12 and the αvβ3 integrin causes severe osteopetrosis. J. Cell Biol. 208, 125–136.

Chapter 18

Intercellular junctions and cell–cell communication in the skeletal system

Joseph P. Stains[1], Francesca Fontana[2] and Roberto Civitelli[2]

[1]*Department of Orthopaedics, University of Maryland School of Medicine, Baltimore, MD, United States;* [2]*Washington University in St. Louis, Department of Medicine, Division of Bone and Mineral Diseases, St. Louis, MO, United States*

Chapter outline

Introduction

The organization of cells in tissues and organs is controlled by molecular programs that afford cells the ability to recognize other cells and the extracellular matrix and to communicate with their neighbors. Adhesive interactions are essential not only in embryonic development, but also in the differentiation and maintenance of tissue architecture and cell polarity, the immune response and the inflammatory process, cell division and death, and tumor progression and metastases. Cell–cell and cell–matrix adhesion is mediated by four major groups of molecules: cadherins, immunoglobulin-like molecules, integrins, and selectins. Cadherins are an integral part of *adherens junctions*, which anchor cells to one another by linking their cytoskeletons. Thus, along with tight junctions and desmosomes, adherens junctions constitute the so-called anchoring junctions (Halbleib and Nelson, 2006). A different type of intercellular junction is the *gap junction*, which does not provide cell anchorage but allows direct communication via specialized intercellular channels formed by connexins (Goodenough et al., 1996).

In the adult skeleton, bone remodeling occurs via repeated sequences of bone resorptive and formative cycles, which require continuous recruitment and differentiation of bone marrow precursors. The cooperative nature of bone remodeling requires efficient means of intercellular recognition, adhesion, and communication that allow cells to sort and migrate, synchronize their activity, equalize hormonal responses, and diffuse locally generated signals. This chapter reviews current knowledge about the role of direct cell–cell interactions in the development and remodeling of the skeletal tissue, focusing on cell–cell adhesion via cadherins and cell–cell communication via gap junctions.

Adherens junctions and the cadherin superfamily of cell adhesion molecules

Cadherins are transmembrane glycoproteins that mediate calcium-dependent cell–cell adhesion through homophilic interactions (Harris and Tepass, 2010; Pokutta et al., 1994). In mammals, there are over 80 members of this large

Principles of Bone Biology. https://doi.org/10.1016/B978-0-12-814841-9.00018-X

superfamily, which also includes protocadherins, desmocollins, and desmogleins (Harris and Tepass, 2010; Cavallaro and Dejana, 2011). Classic cadherins are composed of five repeats of a calcium-binding extracellular domain (EC), a single transmembrane domain, and a cytoplasmic C-terminal region containing two catenin-binding domains (Ishiyama et al., 2010; Obata et al., 1998) (Fig. 18.1). Classical cadherins are further categorized as type I cadherins, including E-, M-, and N-cadherin and cadherin-4 (the human ortholog of mouse R-cadherin), and type II cadherins, comprising cadherin-5 through -12 and VE-cadherin. Typical of type I, but not type II, cadherins is a HAV (His-Ala-Val) motif in the EC1 domain (Blaschuk et al., 1990; Patel et al., 2006), which is important for their adhesive function. At the interface between the five EC domains, four Ca^{2+}-binding pockets allow classical cadherins to assume a rodlike conformation in the presence of Ca^{2+}, thus forming *cis*-dimers (through EC1−2) with adjacent cadherins and *trans*-dimers with cadherins on opposing cells (Pertz et al., 1999). *Trans*-dimerization is necessary for cell−cell adhesion, and it occurs by "strand exchange" or "β-strand swapping" between the EC1 of opposing cadherins (Vendome et al., 2011; Harrison et al., 2005). This interaction requires calcium and docking of a highly conserved Trp residue into the complementary hydrophobic pocket of the opposing cadherin (Vendome et al., 2011; Harrison et al., 2005): for type I cadherins Trp2 mediates the swap, while in type II cadherins both Trp2 and Trp4 are swapped (Patel et al., 2006; Brasch et al., 2012). Accordingly, type I and type II cadherins do not usually engage in heterotypic binding (Patel et al., 2006), while heterotypic dimerization can occur between members of the same cadherin type, for example, between N- and E-cadherin (Katsamba et al., 2009). While *trans*-dimerization is responsible for the relatively weak binding between individual cadherins on opposing cells (Harris and Tepass, 2010), *cis*-interactions account for the assembly of multiple cadherin molecules at sites of cell−cell contact (Brasch et al., 2012), thus creating cadherin clusters that are further stabilized by linkage to the cytoskeleton (Harris and Tepass, 2010; Troyanovsky, 1999).

Cadherins are linked to the cytoskeleton via binding to catenins, specifically, α-, β-, and γ-catenin (the last also known as plakoglobin) and $p120^{ctn}$, which links cadherins to actin filaments at their intracellular cytoplasmic tail. In the classic view, the cadherin intracellular domain binds to β-catenin and plakoglobin, which in turn bind to α-catenin, either directly or through other proteins, including actinin, vinculin, or zonula occludens-1 (ZO-1) (Yamada and Geiger, 1997). Importantly, α-catenin binding either to the cadherin/β-catenin complex or to actin filaments each excludes the other (Drees et al., 2005), implying that the connection between the adhesion structure and the cytoskeleton is dynamic rather than static (Yamada et al., 2005). Studies also suggest that a minimal cadherin−catenin complex, in which both α- and β-catenin can participate, can directly bind filamentous actin upon mechanical strain (Buckley et al., 2014), and that tissue-specific

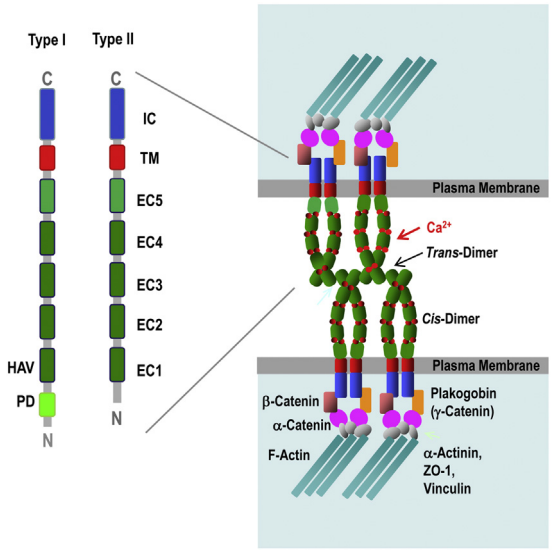

FIGURE 18.1 Cadherins and the adherens junction. (Right) Cadherins are shown with their cytoplasmic (IC), transmembrane (*TM*), and five extracellular domains (*EC1−5*). Small circles between the EC domains symbolize calcium ions. Two complete cadherin *cis*-dimers are shown side by side. These engage in binding with similar complexes from an apposing cell, thus forming *trans*-dimers. The alignment of EC1 domains forms the so-called "zipper" structure of the adhesion complex. Through their CT domain, cadherins bind to β-catenin and plakoglobin, which in turn tether the complex to the actin cytoskeleton via α-catenin and other interacting proteins, including α-actinin, zonula occludens-1 (*ZO-1*), and vinculin. Binding to $p120^{ctn}$ also contributes to stabilizing the cadherin-based adhesion structure. (Left) Enlarged schematic structure of a type I (left) and a type II (right) cadherin. Type I cadherins, such as N-cadherin, have a consensus HAV domain in EC1 important for cell−cell adhesion, and a cadherin-like prodomain (*PD*) at the extreme N terminus. Type II cadherins, such as cadherin-11, engage in cell−cell adhesion via different domains.

catenin isoforms such as αT-catenin may constitutively bind actin (Wickline et al., 2016). Other proteins, such as Lima-1 (Abe and Takeichi, 2008) and ZO-1, can mediate binding of cadherin−catenin complexes to the cytoskeleton (Itoh et al., 1997). The adhesion properties of cadherins are also dependent on the binding of $p120^{ctn}$ to other proteins, such as Rho-family GTPases (Grosheva et al., 2001), which affect membrane dynamics, signaling, and stability of the cadherin complex (Wildenberg et al., 2006). The assembly of cadherins and their associated cytoskeletal elements forms the junctional structures known as adherens junctions (Gumbiner, 2005) (Fig. 18.1).

In addition to their role in cell adhesion, catenins are also components of a signaling system, a function that may evolutionarily predate the appearance of cadherins, as catenin complexes determine cell polarity in *Dictyostelium discoideum* (Dickinson et al., 2011). As detailed later, β-catenin, plakoglobin, and $p120^{ctn}$ modulate the activity of nuclear transcription factors primarily involved in canonical Wnt signaling, a key regulator of osteolineage cell differentiation, function, and bone formation (Krishnan et al., 2006).

Cadherins in commitment and differentiation of chondro-osteogenic cells

Skeletal cells and their precursors express class I and class II cadherins, though their expression levels and functions vary according to developmental stage, lineage, and phase of cell differentiation (Marie et al., 2014; Mbalaviele et al., 2006). During mesenchyme condensation, N-cadherin (gene: *Cdh2*) and cadherin-11 (gene: *Cdh11*) are both expressed in the developing limb buds; and N-cadherin expression increases during chondrogenic differentiation, promoting cell−cell contacts and mesenchymal condensation. N-cadherin then decreases to allow chondrogenic differentiation to proceed (DeLise and Tuan, 2002). These changes in N-cadherin expression during early chondrogenesis are probably modulated by Sox9 (Panda et al., 2001) and bone morphogenetic protein-2 (BMP-2) signaling (Haas and Tuan, 1999). In vitro, inhibition of N-cadherin adhesive functions disrupts mesenchymal condensation in micromass culture and chick limb development, and a dominant-negative N-cadherin mutant is sufficient to impair BMP-2-dependent chondrogenesis (Haas and Tuan, 1999). *Cdh2*-null limb bud cultures, however, do not show major anomalies in chondrogenesis and maintain membrane-bound catenin complexes, suggesting that other cadherins—such as cadherin-11—could be compensating for N-cadherin adhesive function (Luo et al., 2005). Regulation of Wnt signaling by N-cadherin is important in chondrogenesis and in osteogenesis, as detailed later (Modarresi et al., 2005). Indeed, N-cadherin-functionalized hydrogels promote chondrogenesis from human mesenchymal precursors by favoring micromass formation and reducing Wnt signaling via decreased nuclear β-catenin translocation, transcriptional regulation of Wnt receptors, and activating kinases (Li et al., 2017).

Early osteogenic precursors express a broader range of cadherins, including P-cadherin, K-cadherin, E-cadherin, N-cadherin, and cadherin-11 (Cheng et al., 1998; Turel and Rao, 1998; Kawaguchi et al., 2001a; Shin et al., 2005; Hay et al., 2000). Upon osteogenic differentiation, R-cadherin is rapidly downregulated (Cheng et al., 1998), while cadherin-11 is upregulated and maintained through full differentiation (Cheng et al., 1998; Kawaguchi et al., 2001a; Shin et al., 2000). In fact, *Cdh11* was initially cloned in mouse osteoblasts and osteogenic cell lines (Okazaki et al., 1994) and provisionally named OB-cadherin, but it is present in multiple adult and embryonic tissues of mesenchymal origin (Alimperti and Andreadis, 2015). Supporting cadherin-11 proosteogenic action, teratomas originating from cells overexpressing *Cdh11* form preferentially bone and cartilage tissue (Kawaguchi et al., 2001a). As they differentiate into adipocytes, undifferentiated precursors downregulate both *Cdh2* and *Cdh11*, which are absent in adipocytes (Kawaguchi et al., 2001a; Shin et al., 2005), suggesting that coexpression of *Cdh2* and *Cdh11* may be permissive of commitment to osteogenic differentiation while hindering adipogenesis. After the initial increase, N-cadherin is downregulated upon in vitro osteoblast differentiation (Greenbaum et al., 2012), and it is undetectable in osteocytic cells (Kawaguchi et al., 2001a). Accordingly, in histologic sections N-cadherin is present on cells in the bone surface in both humans and rodents (Cheng et al., 1998; Hay et al., 2000; Shin et al., 2000; Castro et al., 2004), but it is absent in osteocytes (Greenbaum et al., 2012). Indeed, for the osteogenic program to proceed to terminal differentiation *Cdh2* must be downregulated (Greenbaum et al., 2012). These observations highlight partially overlapping but distinct functions of *Cdh2* and *Cdh11* at different stages of osteogenesis. Similarly, dental bud stem cells express N-cadherin and cadherin-11, whose expression is modulated during odontogenic differentiation, and they also maintain a low but stable expression of E-cadherin and P-cadherin (Di Benedetto et al., 2015). Cadherin expression in the osteogenic lineage is regulated by local and hormonal factors. BMP-2 and parathyroid hormone (PTH) upregulate both *Cdh2* (Cheng et al., 1998; Hay et al., 2000; Ferrari et al., 2000) and *Cdh11* (Cheng et al., 1998; Yao et al., 2014). *Cdh2* expression is also stimulated by fibroblast growth factor 2 (FGF2) receptor activation via protein kinase Cα (PKCα) in osteoblasts (Delannoy et al., 2001; Debiais et al., 2001), as it occurs in Apert syndrome, where FGFR2 is constitutively activated (Lemonnier et al., 2001). Conversely, stimuli that inhibit osteogenesis, such as dexamethasone, inhibit both *Cdh2* and *Cdh11* (Lecanda et al., 2000a), while proinflammatory cytokines downregulate *Cdh2* only (Tsutsumimoto et al., 1999; Tsuboi et al., 1999).

The function of N-cadherin in osteoblasts also extends to mediating interactions with tumor cells. Indeed, N-cadherin is the hallmark of epithelial-to-mesenchymal transition, which favors tumor growth and metastasis (Tran et al., 1999). Accordingly, N-cadherin has been proposed as a key factor for the establishment of the "preosteolytic" micrometastasis; and inhibition of N-cadherin in tumor cells reduces metastasis in xenograft models (Wang et al., 2015). Preliminary data from our group suggest that the action of N-cadherin in bone cells is actually inhibitory for cancer growth, and it occurs via paracrine and systemic effects (Fontana et al., 2017a). It seems likely that this "niche" function of N-cadherin might also be used for therapeutic targeting.

Cadherins in skeletal development, growth, and maintenance

Mouse models have helped establish the relevance of cadherins in bone formation and homeostasis. Germ-line deletion of *Cdh2* is lethal by day 10 of gestation, with mutant embryos displaying small and irregularly shaped somites and cardiac dysfunction (Radice et al., 1997). Heterozygous $Cdh2^{-/+}$ mice have normal skeletal morphology, but upon ovariectomy they undergo accentuated bone loss with reduced bone formation (Lai et al., 2006). Despite strong in vitro evidence of a proosteogenic action, *Cdh11*-null mice are morphologically normal, except for some widening of calvarial sutures and metaphyseal osteopenia (Kawaguchi et al., 2001b), suggesting some degree of redundancy among cadherins in osteogenesis. Indeed, heterozygous loss of *Cdh2* in a *Cdh11*-null background results in severely reduced trabecular bone, smaller and shorter diaphyses, severe osteopenia, and increased bone fragility (Di Benedetto et al., 2010). Tissue-specific overexpression and deletion models have provided more detailed evidence of the role of *Cdh2* in bone. Conditional ablation of *Cdh2* in osteogenic precursors and committed osteoblasts, using *Osx-Cre*, *Prx-Cre*, and *Col1a1-Cre* consistently results in smaller bones and reduced trabecular bone mineral density (Greenbaum et al., 2012; Di Benedetto et al., 2010; Fontana et al., 2017b), suggesting that N-cadherin has an overall positive role in the osteolineage. However, *Cdh2* overexpression in differentiation osteoblasts using *Bglap-Cre* also leads to low bone mass and delayed bone mass acquisition (Hay et al., 2009a). Work has contributed to resolving this apparent paradox by demonstrating a dual role of N-cadherin in the osteolineage: while N-cadherin supports osteogenic precursor number early in osteogenic differentiation, it also restrains progression through the osteogenic program, a function that can be linked to Wnt signaling inhibition, as discussed later. Further supporting this model, delaying *Cdh2* ablation in osteogenic cells until the postnatal stage using the *tet*-suppressible *Osx-Cre* model prevents the low-bone-mass phenotype, actually leading to expanded metaphyseal trabecularization (Fontana et al., 2017b). Indeed, transgenic mice overexpressing *Cdh2* in osteoblasts exhibit increased osteoprogenitor numbers and bone formation with aging (Hay et al., 2014), despite low bone mass in juvenile animals (Hay et al., 2009a). This observation shows that interference with N-cadherin in the adult skeleton could be targeted to enhance bone formation without potential effects on growth.

In vitro studies corroborate the model of a dual action of N-cadherin in osteogenic differentiation. Interference with N-cadherin-mediated cell−cell adhesion using a HAV inhibitory peptide (specific for type I cadherins, thus not interfering with cadherin-11 adhesion), neutralizing antibodies, antisense oligonucleotides, or transfection of a *Cdh2* mutant with dominant-negative action reduces osteoblast differentiation in vitro, probably via reduced cell−cell adhesion. Cadherin adhesive function might be important for keeping osteoprogenitors in a niche environment and preventing commitment to a lineage (Hay et al., 2000; Ferrari et al., 2000; Cheng et al., 2000). On the other hand, bone marrow stromal cells and calvaria cells isolated from *Cdh2*-haploinsufficient mice or from conditionally osteoblast/osteocyte *Cdh2*-deleted mice differentiate faster in vitro (Greenbaum et al., 2012; Fang et al., 2006); however, the number of osteoprogenitors is decreased in *Cdh2*-haploinsufficient or osteoblast *Cdh2*-deficient mice (Di Benedetto et al., 2010; Fang et al., 2006), consistent with a dual function of N-cadherin in supporting osteoprogenitor number but restraining full osteogenic differentiation (Fig. 18.2). More recent data have confirmed that the number of bone marrow $Sca1^{+}PDGF\alpha^{+}CD45^{-}Ter113^{-}$ cells, representing mesenchymal stem and progenitor cells, is very low in conditionally *Cdh2*-ablated mice. However, delaying *Osx-Cre*-driven *Cdh2* recombination until after weaning, when only committed osteoblasts are targeted (Mizoguchi et al., 2014), prevents such a decrease and associated stunted growth (Fontana et al., 2017b).

N-cadherin modulation of Wnt/β-catenin signaling in osteoblastogenesis and osteoanabolic responses

In addition to their function in the adherens junction, cadherins interfere with intracellular signaling pathways in several cell types (Knudsen and Soler, 2000; Wheelock and Johnson, 2003). Indeed, cadherins may retain signaling functions even after modifications that abrogate their adhesive properties by cleavage, shedding, or mutations (Cavallaro and Dejana, 2011). It is rather intuitive that cadherins may affect the Wnt pathway simply because cadherins bind to β-catenin, a key

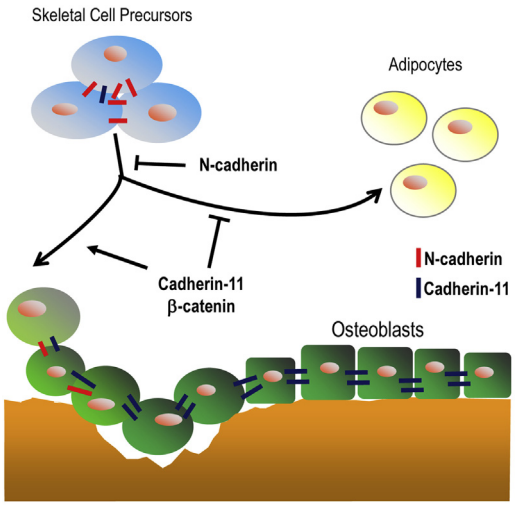

FIGURE 18.2 Cadherins in the osteogenic lineage. In their undifferentiated stage, skeletal cell precursors express a relatively wide repertoire of cadherins, including N-cadherin, cadherin-11, and R-cadherin, with the first being the most abundant. Precursor cells are held together, presumably in a niche, to which N-cadherin is an important contributor. Differentiation of precursors requires downregulation of N-cadherin, which acts as an inhibitor of lineage commitment. By contrast, upregulation of cadherin-11 favors osteogenesis, while adipogenesis is associated with downregulation of cadherin-11. Loss of N-cadherin in the chondro-osteogenic lineage leads to loss of uncommitted precursors. The switch in cadherin expression may allow more β-catenin to become available for transcriptional regulation, thus contributing to osteogenesis and anti-adipogenesis.

component of the canonical Wnt signaling pathway (Daugherty and Gottardi, 2007; Heuberger and Birchmeier, 2010). The Wnt/β-catenin pathway is activated by binding of Wnt ligands to low-density lipoprotein receptor–related protein (LRP) 5/6 and Frizzled coreceptors, followed by recruitment of a complex of Axin/Frat1/adenomatous polyposis coli/glycogen synthase kinase-3β (GSK-3β). This is turn leads to inhibition of GSK-3β, decreased β-catenin phosphorylation at specific sites near its N terminus that prevents β-catenin proteasomal degradation, cytoplasmic accumulation of β-catenin, and subsequent translocation to the nucleus where it binds T cell factor/lymphoid enhancer factor transcription factors to activate gene transcription (Logan and Nusse, 2004). Association of β-catenin with cadherins contributes to stabilizing the adhesion structure (Lilien and Balsamo, 2005), and cell–cell adhesion via cadherins promotes β-catenin phosphorylation and inactivation (Maher et al., 2009). Conversely, release of β-catenin from cadherins destabilizes the adhesion complex, thus facilitating cell movement (Nelson and Nusse, 2004). Thus, an inverse relationship exists between cell adhesion and Wnt/β-catenin signaling. More recent data demonstrate that the interplay between cadherins and signaling is more complex than predicted by a simple interaction with β-catenin at the adherens junction. Certainly, increased cadherin abundance on the cell surface results in decreased β-catenin nuclear translocation and transcriptional activity (Nelson and Nusse, 2004; Gottardi and Gumbiner, 2001; Rhee et al., 2007). As already noted, overexpression of a dominant-negative *Cdh2* mutant in differentiated osteoblasts sequesters β-catenin at the cell surface and decreases bone formation (Castro et al., 2004), as does *Cdh2* overexpression in differentiated osteoblasts (Hay et al., 2012). By contrast, deletion of either *Cdh2* or *Cdh11* or both reduces β-catenin abundance at cell–cell contacts and cell–cell adhesion with a negative effect on osteoblastogenesis and bone growth (Di Benedetto et al., 2010). N-cadherin/β-catenin association can also be modulated by mechanical stimuli, as oscillatory fluid flow releases β-catenin from adherens junctions, resulting in nuclear translocation and transcriptional activation, in turn contributing to osteogenic differentiation (Arnsdorf et al., 2009).

Skeletal biology studies have disclosed an alternative mechanism of N-cadherin interaction with Wnt signaling components via interaction with Lrp5 or Lrp6 (Hay et al., 2009a). Specifically, N-cadherin forms a complex with Lrp5/6 via Axin, thus preventing Lrp5/6 activation of β-catenin, which is instead targeted for proteasomal degradation. This results in decreased Wnt signaling and reduced osteogenic differentiation, function, and bone formation (Marie et al., 2014; Hay et al., 2009a). N-cadherin–Lrp5/6 interaction controls osteoblast differentiation and survival also by reducing endogenous Wnt3a expression and by inhibiting Wnt-dependent phosphatidylinositol 3-kinase (PI3K)/protein kinase B (Akt) signaling (Hay et al., 2009b). Indeed, N-cadherin-mediated adhesion has been linked to activation of PI3K signaling in osteogenic cells (Guntur et al., 2012). Considering the negative action of N-cadherin on Wnt/β-catenin signaling, interference with N-cadherin/Axin/Lrp5/6 binding could potentially lead to osteogenesis by facilitating canonical Wnt signaling. Indeed, deletion of the N-cadherin domain interacting with Axin and Lrp5/6 promotes Wnt/β-catenin signaling and osteoblast differentiation without affecting cell–cell adhesion (Hay et al., 2012). And peptides that bind to the

N-cadherin/Axin-interacting domain of Lrp5 disrupt N-cadherin−Lrp5/6 interaction, enhance Wnt/β-catenin signaling, stimulate osteoblast function in vitro, and promote calvaria bone formation in vivo (Hay et al., 2012).

N-cadherin restraining action on Wnt signaling and its potential for therapeutic targeting to stimulate bone anabolism has been further refined. Our group has reported that the bone anabolic action of PTH is enhanced in mice lacking *Cdh2* in Osterix (Osx)-targeted cells, an effect linked to "noncanonical" β-catenin activation by PTH via the protein kinase A (PKA) pathway and increased Lrp6 association with the PTH/PTH-related protein receptor (Revollo et al., 2015). Enhanced PTH anabolism was reproduced by another group using *DMP1-Cre* to ablate *Cdh2* (Yang et al., 2016a), but was not noted in a study in which *Col1a1-Cre* was used (Bromberg et al., 2012). The reasons for such discrepancies remain unclear, but in vitro work supports a restraining effect of N-cadherin on PTH-induced activation of Wnt signaling (Revollo et al., 2015). More recently, an enhanced osteoanabolic effect of an antibody against Dkk1 was observed in *Col1a1-Cre*-driven *Cdh2*-ablated mice (Fontana et al., 2017b). In the same study, the presence of a Dkk1- and sclerostin-insensitive *Lrp5* mutant in conditional *Cdh2*-ablated mice prevented development of osteopenia but not delayed growth, further supporting the notion that regulation of bone mass accrual, but not longitudinal bone growth, by N-cadherin in young mice is dependent on Wnt signaling (Fontana et al., 2017b). If these data can be corroborated and translated to humans, they would further expand the N-cadherin biologic role in bone-forming cells and further prove that cadherins represent legitimate targets for pharmacological intervention (Fig. 18.3).

Connexins and gap-junctional intercellular communication

The need to maintain tissue integrity during skeletal remodeling demands the temporal and spatial control of bone formation and resorption. Direct intercellular communication through gap junctions allows osteoblasts, osteoprogenitors, and osteocytes to share and amplify signals that permit coordinated function. Gap junctions are intercellular channels that link the cytoplasm of adjacent cells and permit the exchange of second messengers, small molecules, ions, and metabolites that are less than about 1 kDa in molecular mass. In addition, gap junctions can also allow sharing of microRNAs among communicating cells (Valiunas et al., 2005; Plotkin et al., 2017; Zong et al., 2016; Liu et al., 2015). The monomeric subunits of a gap junction are connexins, an evolutionarily conserved family of proteins. There are 21 human connexin genes of which at least four are expressed in bone cells. Osteoblast lineage cells express connexin43 (gene: *Gja1*), connexin45 (*Gjc1*), connexin37 (*Gja4*), and connexin40 (*Gja5*). Of these, connexin43 is the most abundant. On the other hand, osteoclast lineage cells express both connexin43 and connexin37. Mutations or deletions of any these connexins in human or mouse skeletal tissue result in diseases with skeletal manifestations (see later). Pannexins (*Panx1*, *Panx2*, and *Panx3*) are a family of structurally closely related proteins that form a direct channel between the cytoplasm and the extracellular fluid, rather than between two cells. Despite their structural similarities and common sensitivity to pharmacological inhibitors, the mechanisms of action, regulation, and biological role of pannexins in bone are distinct from those of connexins (Plotkin; Stains, 2015; Plotkin et al., 2016; Ishikawa et al., 2016; Ishikawa and Yamada, 2017), thus they will not be reviewed here.

Connexin monomers have a common structure, with four transmembrane-spanning domains, two extracellular loops, an intracellular loop, and both the N and the C termini on the cytoplasmic side of the plasma membrane (Fig. 18.4). Hexamers of connexins form connexons, also called "hemichannels," which dock with connexons on adjacent cells to form an aqueous gap junction channel linking the cytoplasmic compartment of coupled cells. Under some circumstances, undocked hemichannels can also function as a plasma membrane channel that permits exchange of small molecules, such as ATP, between the cytoplasm and the extracellular fluid, acting similar to pannexins. Notably, gap junction channels aggregate into large plaques composed of up to thousands of gap junctions at cell−cell junctions. Thus, the capacity for direct intercellular exchange of small molecules can be quite large.

The size and charge permeability of gap junctions are determined by the connexin composition of a gap junction channel. For example, connexin43 permits the passage of molecules up to 1.2 kDa with a preference for negatively charged molecules (Kanaporis et al., 2011; Harris, 2009). By contrast, connexin45 permits the passage of molecules smaller than 0.3 kDa with a preference for positively charged molecules (Kanaporis et al., 2011). Connexin40 forms gap junctions of size selectivity similar to that of connexin45, while connexin37 is even more restrictive in its size exclusion limit (Kanaporis et al., 2011; Weber et al., 2004). Connexons can be composed of multiple connexin monomeric units (heteromeric gap junctions), and connexins of one type can dock with connexins of a different type, forming a heterotypic gap junction (Fig. 18.4). This variety of heterotypic and heteromeric channels can confer unique biophysical properties to the resulting channel. As most cells express multiple connexins, pairing of different heteromeric channels can tune the resultant gap junction through a wide range of molecular permeabilities. Thus, the composition of a gap junction channel directly regulates its permeability. Similarly, connexins can bind a diverse interactome of

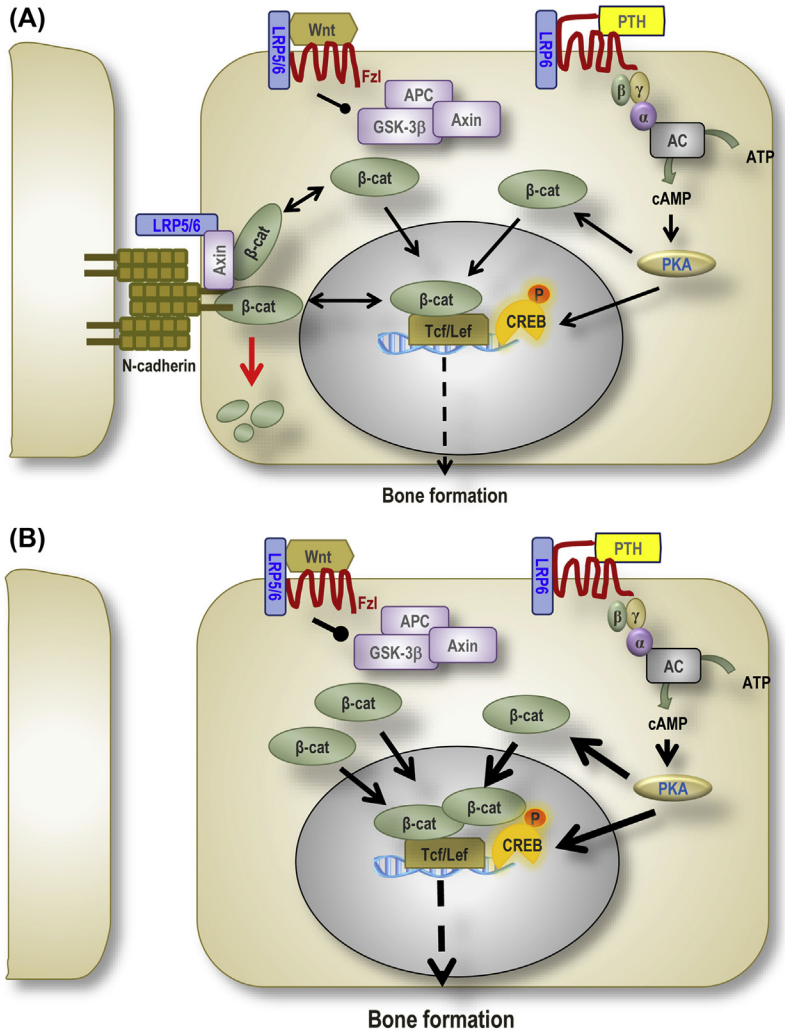

FIGURE 18.3 Cadherins and the Wnt signaling system. (A) Upon Wnt agonist activation of the LRP5/6−Fzl coreceptor complex, GSK-3β is inhibited by binding in an APC/Axin/GSK-3β complex, thus allowing β-catenin nuclear translocation and transcriptional activation. Stabilization of β-catenin can also occur by direct, "noncanonical" phosphorylation at non-GSK-3β sites by PKA, as occurs with PTH binding to PTHR1. PTHR1 can also bind LRP6, presumably also activating the canonical Wnt pathway. Binding to the adherens junction complex keeps β-catenin away from transcriptionally active pools, thus reducing signaling. Another β-catenin pool is kept on the cell surface by binding to N-cadherin via an Axin bridge, which facilitates proteasomal degradation. (B) Absence of N-cadherin releases the system from an inhibitory control mechanism, resulting in increased abundance of active β-catenin and enhanced transcriptional activity. Lack of N-cadherin also releases Lrp5/6 from inactive pools, making more of these coreceptors available for binding to Fzl or PTHR1, and in turn leading to increased β-catenin signaling. In osteogenic cells, this results in proliferation and increased bone-forming activity, in addition to inhibition of osteoclastogenesis. *AC*, adenylyl cyclase; *APC*, adenomatous polyposis coli; *β-cat*, β-catenin; *CREB*, cyclic-AMP response element binding protein; *Fzl*, frizzled; *GSK-3β*, glycogen synthase kinase-3β; *LRP5/6*, low-density lipoprotein receptor−related protein 5/6; *PKA*, protein kinase A; *PTH*, parathyroid hormone; *PTHR1*, PTH/parathyroid hormone related peptide receptor-1; *Tcf/Lef*, T-cell factor/lymphoid enhancer factor.

structural and signaling proteins, which can be connexin specific and can influence downstream signaling (Herve et al., 2012; Moorer and Stains, 2017; Leithe et al., 2018). Thus, the size, number, and composition of a gap junction channel or plaque can lend great plasticity to the ability of the cells to exchange small molecules, thus affecting their function.

Connexin diseases affecting the skeleton

Bone cells are extensively coupled by gap junctions (Yellowley et al., 2000; Doty, 1981; Civitelli et al., 1993; Wang et al., 2016). This permits rapid and efficient exchange of signals via direct intercellular communication among all cells of the bone network, thus providing a key biological mechanism for regulation of bone as a tissue (Fujita et al., 2014;

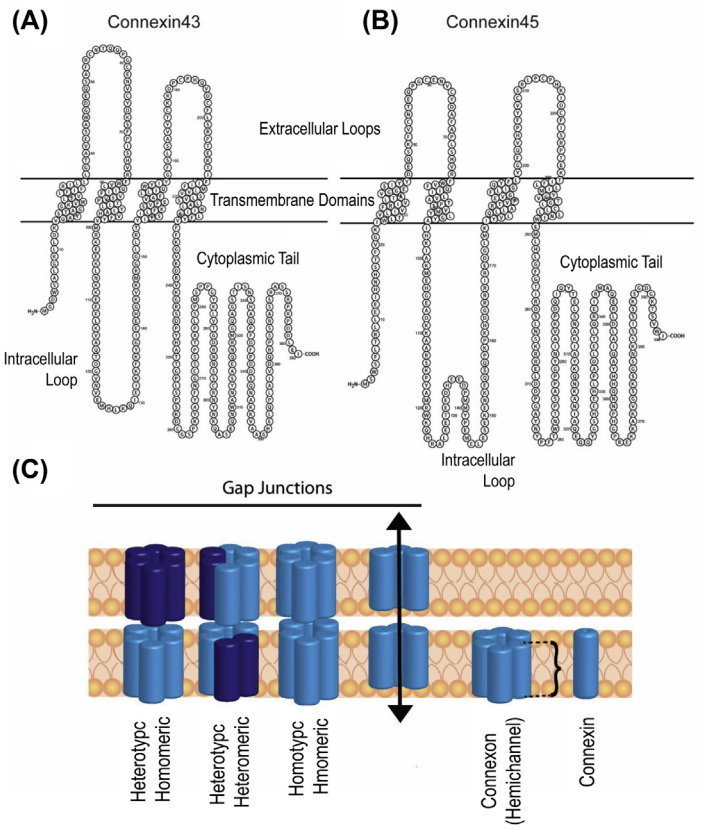

FIGURE 18.4 Connexins and gap junctions. Structure of (A) connexin43 and (B) connexin45, showing conserved topology including four transmembrane spanning domains, two extracellular loops, an intracellular loop, and both the N and C-termini on the cytoplasmic side of the plasma membrane. Images generated using Protter version 1.0 software. (C) Gap junction hemichannels can be formed by hexameric arrays of the same connexin (homomeric) or by mixed connexin hexamers (heteromeric). Likewise, hemichannels in the plasma membrane of one cell can pair with a hemichannel composed of the same (homotypic) or different connexin composition (heterotypic) in an adjacent cell. These combinations can alter the biophysical properties of the resultant gap junction channel.

Nishikawa et al., 2015; Vazquez et al., 2014; Suswillo et al., 2017). The consequences of disrupting this intercellular communication network can be profound. In humans, numerous distinct point mutations in *GJA1* (>62 reported) can lead to the pleiotropic, predominantly autosomal dominant disorder oculodentodigital dysplasia (ODDD) (Paznekas et al., 2009). Skeletal manifestations are prevalent in this disorder and include craniofacial abnormalities (pointed nose, microphthalmia), dental abnormalities (enamel hypoplasia), missing phalanges, syndactyly or camptodactyly, and broad, tubular long bones (Paznekas et al., 2009). These mutations in most cases are dominant negative for connexin43 function, resulting in abnormal gap junction channel function and impaired intercellular communication (Gong et al., 2007; McLachlan et al., 2008). Mice carrying a *Gja1* G60S missense mutation phenocopy many aspects of human ODDD, including cardiac dysfunction, craniofacial abnormalities, syndactyly, tooth enamel hypoplasia, and an alteration in the geometry of the long bones with a broader cross-sectional area at the mid-diaphysis. In addition, these mice display decreased trabecular bone volume fraction (Flenniken et al., 2005; Zappitelli et al., 2013), a feature not reported in ODDD patients, who instead have an osteosclerotic skull (Kjaer et al., 2004). Such discrepancy may reflect species differences or an effect of aging. The changes in skeletal geometry and bone mass are autonomous to the osteoblast lineage, as tissue-specific expression of a *Gja1* G138R mutant, causative of ODDD, in mice reproduces these skeletal features, except, again, the thickened skull (Dobrowolski et al., 2008; Watkins et al., 2011).

A missense mutation in the cytoplasmic tail of the human connexin43 gene (*GJA1* R239Q) has been found in patients with recessive craniometaphyseal dysplasia (CMD), a condition sharing several skeletal manifestations with ODDD, including cranial hyperostosis and widening of long bones with metaphyseal flaring (Hu et al., 2013), but lacking the syndactyly and ocular and dental abnormalities observed in ODDD. Intriguingly, the less rare dominant form of CMD is caused by mutation of a different gene, *Ank*, which encodes the progressive ankylosis protein (ANK), an inorganic pyrophosphate transporter, raising the intriguing possibility that cell−cell diffusion or secretion of pyrophosphate via

hemichannels may contribute to the mechanism of connexin43 regulation of bone cell function. In any case, because of their phenotypic and genetic similarities, ODDD and recessive CMD probably represent two manifestations of the spectrum of connexin43 disease, whose main features are a cortical modeling defect leading to metaphyseal and diaphyseal widening and craniofacial malformations. It is tempting to speculate that the more subtle phenotypic differences between ODDD and recessive CMD may be linked to selective interference by the different mutations with either gap junction channel or signaling, the two main functions of connexins.

A loss-of-function mutation (R75H) in the connexin45 gene (*GJC1*) has been linked to cardiac atrial conduction defects and severe arrhythmias, but also to skeletal manifestations, including clinodactyly and camptodactyly and dental and craniofacial abnormalities (Seki et al., 2017). Thus, despite the different biophysical properties of the gap junctions they form (Kanaporis et al., 2011), there is clear overlap in skeletal features between ODDD-causing *GJA1* mutations and the *GJC1* R75H mutation. These similarities could be related to the existence of heteromeric/heterotypic channels formed by connexin43 and connexin45 in bone cells. Hence, loss of one of the connexins would be sufficient to alter the biophysical properties of such heteromeric/heterotypic gap junctions. Ongoing studies should clarify the relative roles of the two connexins in the skeleton.

Connexins in the skeleton across the life span

As anticipated by human genetics, deletion of *Gja1* results in substantial skeletal abnormalities in mice. Germ-line *Gja1* ablation ($Gja1^{-/-}$) is postnatally lethal, but newborn mice have delayed intramembranous and endochondral ossification; brittle, misshapen ribs; and skull abnormalities that include a hypomineralized cranial vault and open parietal foramen (Lecanda et al., 2000b). These defects are consequent to a cell-autonomous defect in osteoblast differentiation with significant delays in the expression of most osteoblast genes (Lecanda et al., 2000b). Likewise, conditional deletion of *Gja1* in the osteoblast lineage leads to changes in cortical bone geometry, including an expansion of the marrow cavity with a corresponding increase in periosteal and endocortical perimeters, resulting in decreased cortical bone cross-sectional thickness (Stains et al., 2014; Grimston et al., 2013). This skeletal phenotype is more severe the earlier in the osteoblast lineage that *Gja1* is deleted in vivo (Stains et al., 2014). Hence, *Gja1* deletion in chondro-osteoblast progenitors using *Dermo1/Twist2-Cre* results in the most severe cortical bone phenotype, with a 40% greater cross-sectional area at the femoral mid-diaphysis (Watkins et al., 2011). Early lineage deletion of *Gja1* is also accompanied by increased number of endocortical osteoclasts, which are responsible for the expanded marrow cavity, but also for cortical porosity and cortical thinning. Enhanced periosteal bone formation only partially compensates for cortical thinning. Similar alterations in cortical bone are present when *Osx-Cre* is used to delete *Gja1* (Hashida et al., 2014). In contrast, deletion of *Gja1* in late osteoblasts and osteocytes using *Bglap-Cre* or *Dmp1-Cre* results a milder skeletal phenotype with only a 20%–25% increase in middiaphyseal cross-sectional area and little or no change in cortical thickness or cortical porosity (Bivi et al., 2012a,b; Zhang et al., 2011). Compromised bone strength and material properties are also common features of *Gja1* ablation models, demonstrating that connexin43 expression throughout the lineage is crucial for maintaining bone quality (Flenniken et al., 2005; Watkins et al., 2011; Bivi et al., 2012b). Accordingly, loss-of-function *Gja1* mutations phenocopy quite well the skeletal abnormalities of connexin43 diseases, with the exception of the craniofacial changes. Aging is associated with loss of osteocyte network connectivity, as the numbers of viable osteocytes and osteocyte processes and connexin43 expression decrease (Davis et al., 2017; Tiede-Lewis et al., 2017). Not surprisingly, the changes in bone architecture during aging closely resemble those seen in *Gja1* deletion or mutation (Zappitelli et al., 2013; Watkins et al., 2011; Davis et al., 2017).

Far less is known about the role of other connexins in skeletal biology. Genetic association studies have evidenced polymorphisms in *Gja4* segregating with bone mineral density in both humans (Yamada et al., 2007) and mice (Xiong et al., 2009). In mice, germ-line *Gja4* deletion results in increased trabecular bone volume, though connexin37 seems to act directly on the osteoclast rather than the osteoblast lineage, as lack of connexin37 decreases osteoclast number in vivo and impairs osteoclast fusion in vitro (Pacheco-Costa et al., 2014). A subtle and paradoxical defect in cortical bone is also observed in these *Gja4*-knockout mice, which exhibit higher cortical bone strength despite decreased cortical bone thickness. This may result from increased mineralization in a low-turnover state, or from changes in the bone extracellular matrix (Pacheco-Costa et al., 2017). As noted earlier, in humans a loss-of-function mutation of *GJC1* results in skeletal phenotypic features resembling, in part, those of *GJA1*-linked mutations (Seki et al., 2017), suggesting either overlapping function or a dominant-negative action of connexin45 on connexin43, presumably in heteromeric or heterotypic channels. However, a preliminary finding on a mouse model of osteolineage-specific *Gjc1* ablation reveals a surprising high trabecular bone mass but no modeling defects, which would suggest distinct functions of the two connexins in bone and support the notion that the overlapping skeletal features of the connexin45 mutant may be related to a dominant-negative action on connexin43 (Watkins et al., 2014). While a full report has yet to be published, these results support a role of

connexin45 in bone homeostasis. Finally, connexin40 is expressed early in the developing skeleton, where it participates in endochondral bone development; germ-line deletion or haploinsufficiency of *Gja5* results in bony fusions in the forelimbs, elongated metacarpals and phalanges, and malformations of the sternum (Pizard et al., 2005). However, the role of connexin40 in postnatal bone is less clear.

Function of connexin43 in bone cells

Gap junctions propagate signals through the osteoblast and osteocyte network to disseminate, coordinate, and equilibrate their function throughout the skeletal tissue. Indeed, a primary function of gap junctions is to help groups of cells integrate signals from various stimuli to enhance the signal-to-noise ratio (Ellison et al., 2016). The biologic effects of gap junction–communicated signals across the osteogenic lineage are multiple, including coordinating osteogenic differentiation and function, modulating osteoclastogenesis, maintaining osteocyte viability, and processing, organizing, and orienting collagen in the bone extracellular matrix (Fig. 18.5). Indeed, even small changes in this cell network connectivity can have a profound impact on the tissue level response to regulatory cues. A computer simulation of the osteocyte and bone-lining cell network predicted that a 5% loss of gap junction–coupled osteocytes in the network may reduce maximum signaling to the bone surface by 25% (Jahani et al., 2012). Connexin43 is functionally involved in the entire osteogenic program; lack of connexin43 disrupts the expression of most osteoblast genes and reduces mineralization capacity (Lecanda et al., 1998, 2000; Li et al., 1999; Gramsch et al., 2001; Schiller et al., 2001). These actions of connexin43 have been established by multiple models of *Gja1* ablation, or by induction of an ODDD-causing mutation (G138R) in mesenchymal progenitor cells. Mice carrying such mutations have defective osteogenic differentiation (McLachlan et al., 2008; Mikami et al., 2015; Talbot et al., 2018; Wagner et al., 2017; Damaraju et al., 2015; Esseltine et al., 2017), associated with a reciprocal increase in cell proliferation and expansion of the osteoblast progenitor pool, resulting in the accumulation of immature osteoblasts (Watkins et al., 2011; Moorer et al., 2017; Buo et al., 2017). Expansion of immature osteoblasts and consequent production of an abnormal matrix may contribute to increased periosteal bone formation, but also to poor bone quality and material properties despite enhanced osteoblast activity (Watkins et al., 2011; Bivi et al., 2012a,b; Zhang et al., 2011; Moorer et al., 2017). Indeed, the organic matrix of conditional *Gja1*-ablated mice exhibits a highly disorganized fibrillar collagen network, associated with altered expression of collagen-modifying genes, such as lysyl oxidase (*Lox*) and SerpinH1 (*Hsp47*) (Watkins et al., 2011; Bivi et al., 2012b; Moorer et al., 2017; Pacheco-Costa et al., 2016). Among the broad range of osteogenic cell activities regulated by

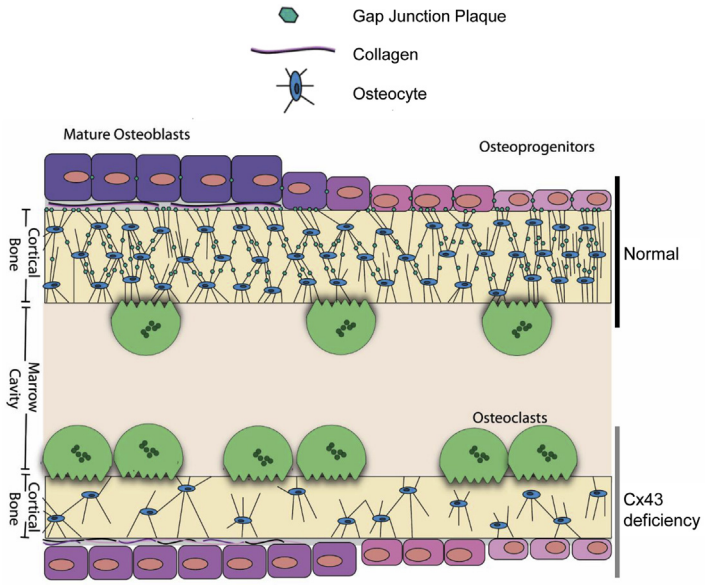

FIGURE 18.5 Connexin43 in bone. Gap junctions formed by connexin43 (*Cx43*) are abundantly present between osteoblasts and their progenitors on the bone surface, between osteoblasts and osteocytes, and at the intersection of osteocytic processes. The presence of connexin43 gap junctions within the osteoblast–osteocyte network is crucial for regulation of osteoblast differentiation, processing and organization of collagen in the bone extracellular matrix, control of osteoclastogenesis, and maintenance of osteocyte viability (top of cartoon). In the absence of connexin43 (bottom of cartoon), osteoblast differentiation is delayed with an expansion of earlier precursors, resulting in production of a disorganized and less mature collagen matrix. Osteocyte viability is reduced, leading to reduced osteocyte number. Endocortical osteoclast number is increased, resulting in expansion of the marrow cavity and thinning of cortical bone.

connexin43 is paracrine regulation of osteoclastogenesis, an action that is primarily responsible for connexin43 modulation of cortical modeling. In vivo and in vitro evidence demonstrates that connexin43 upregulates osteoprotegerin (OPG) (*Tnfrsf11b*) and downregulates receptor activator of NF-κB ligand (RANKL) (*Tnfsf11*) gene expression, resulting in higher RANKL relative to OPG and enhanced osteoclastogenesis (Zappitelli et al., 2013; Watkins et al., 2011; Zhang et al., 2011; Davis et al., 2017; Moorer et al., 2017; Lloyd et al., 2013). The reason why enhanced bone resorption in vivo occurs primarily on the endocortical surfaces, despite broad expression of connexin43 in the trabecular compartment (Watkins et al., 2011), remains to be determined. Increased osteocytic osteolysis (Lloyd et al., 2014a) and osteocyte apoptosis following *Gja1* ablation (Bivi et al., 2012a; Davis et al., 2017; Lloyd et al., 2013; Xu et al., 2015) may contribute to increased osteoclast recruitment and bone resorption, though these effects have not been universally observed. Furthermore, in adult mice, cortical thinning and low bone mass can be corrected by administration of bisphosphonates (Watkins et al., 2012), corroborating the notion that enhanced endocortical bone resorption is indeed the main mechanism causing the cortical abnormalities in conditional connexin43-deficient mice.

Cortical widening, thinning, and porosity present in *Gja1*-deficient bones recapitulate the changes in cortical bone architecture and geometry that develop in disuse osteoporosis and aging (Grimston et al., 2011; Peres-Ueno et al., 2017; Lloyd et al., 2014b). While this phenotype would suggest that connexin43 is involved in elaboration of bone anabolic signals in response to mechanical load, in vivo studies reveal a more complex mechanism. Skeletal mechanical loading by axial tibial compression or cantilever bending consistently shows that lack of connexin43 at different stages of the osteoblast lineage enhances periosteal bone apposition (Zhang et al., 2011; Bivi et al., 2013; Grimston et al., 2012) and accentuates the load-induced decrease of endocortical bone formation (Grimston et al., 2008, 2012). These results can be interpreted as suggesting that absence of connexin43 alters mechanosensing, so that bone-forming cells perceive normal mechanical loading as a disuse scenario, resulting in accentuated endocortical bone resorption, expansion of the marrow cavity, and cortical thinning. This view is further supported by attenuation of the bone-catabolic effects of experimentally induced skeletal unloading by either muscle paralysis or hindlimb suspension in conditional *Gja1*-ablated mice (Lloyd et al., 2012, 2013; Grimston et al., 2011), a finding consistent with the notion that these mice are insensitive to unloading, presumably because endocortical bone resorption is already hyperactivated as an adaptation to abnormal mechanosensing under normal loading conditions in connexin43 deficiency. Further support for this hypothesis is provided by the observation that the cortical modeling abnormalities develop postnatally, after the animal has been able to begin autonomous life (Grimston et al., 2013). Mechanistically, it has been proposed that the accentuated cortical expansion and thinning may be linked to dysregulated sclerostin expression and aberrant Wnt/β-catenin signaling, consistently observed in osteolineage-specific *Gja1*-knockout mice (Watkins et al., 2011; Bivi et al., 2012a; Lloyd et al., 2012, 2013). In support of a role of Wnt/β-catenin signaling in connexin43 action, inhibition of GSK-3β and consequent β-catenin activation improves fracture healing (Loiselle et al., 2013). However, in a genetic interaction study, double *Gja1/Sost* heterozygous mice did not show the cortical phenotype seen in *Gja1*-deficient mice, arguing against a strong interaction between *Sost* and *Gja1* in driving cortical modeling, at least under normal mechanical stimulation (Grimston et al., 2017). Other potential mechanisms may emerge from in vitro studies on mechanically activated osteocytes or osteoblasts, which suggest that multiple paracrine mediators might be involved in connexin43-mediated mechanotransduction (Vazquez et al., 2014; Suswillo et al., 2017; Romanello & D'Andrea, 2001; Genetos et al., 2007; Cherian et al., 2005).

Expression of connexin43 is also required for the bone anabolic action of PTH (Pacheco-Costa et al., 2016; Chung et al., 2006). Intriguingly, *Gja1* gene deletion driven by the 2.3-kb *Col1a1* promoter fully abrogates the anabolic action of PTH, while deletion of *Gja1* using the *Dmp1* promoter does not (Pacheco-Costa et al., 2016; Chung et al., 2006), suggesting that the osteoanabolic effect of PTH is dependent on connexin43 at earlier stages of osteogenesis, perhaps during commitment of undifferentiated precursors. This premise would be consistent with connexin43 key action at the Runx2/Osx transition, as discussed later. Similarly, the C-terminal domain of connexin43 is important for modulating the PTH response of bone cells, as such domain binds to and sequesters β-arrestin to promote PKA-dependent signaling (Bivi et al., 2011). Furthermore, the *Gja1* K258Stop mouse—a model of connexin43 C terminus truncation—failed to increase endocortical bone formation or bone strength in response to anabolic PTH administration (Pacheco-Costa et al., 2015).

Although much less studied, connexins are present and biologically relevant in the osteoclast lineage. Pharmacologic disruption of connexin43 in cell culture reduces fusion of osteoclast progenitors and bone resorption activity (Schilling et al., 2008; Glenske et al., 2014; Kylmaoja et al., 2013; Hobolt-Pedersen et al., 2014; Ransjo et al., 2003; Ilvesaro et al., 2001). However, as of this writing, connexin43 direct action in osteoclasts or their precursors has not been tested in vivo. On the other hand, connexin37 (*Gja4*) does have a function in osteoclasts, as germ-line *Gja4*-null mice have a high bone mass phenotype driven almost exclusively by a defect in osteoclastogenesis (Pacheco-Costa et al., 2014). Accordingly, all osteoclast lineage markers, including RANK, TRAP, cathepsin K, NFATc1, and DC-STAMP, are reduced in connexin37-deficient osteoclasts, as are osteoclast fusion and activity (Pacheco-Costa et al., 2014).

Mechanisms of connexin43 control of bone cell function

Connexin43 expression increases during osteoblast differentiation (Schiller et al., 2001; Donahue et al., 2000), and modulates the activity of the early osteoblast transcription factors Runx2 (Talbot et al., 2018; Lima et al., 2009; Niger et al., 2012; Li et al., 2015; Yang et al., 2016b) and Osx, indirectly (Niger et al., 2011; Stains et al., 2003), resulting in downregulation of downstream genes (Watkins et al., 2011). Functional interaction between connexin43 and Runx2 has been corroborated by in vivo studies, demonstrating that mice heterozygous for both *Gja1* and *Runx2* null mutations ($Gja^{-/+}$;$Runx2^{-/+}$) exhibit both an exacerbated cleidocranial dysplasia-like phenotype than Runx2-/+ mice and a skeletal phenotype that closely resembles that of osteoblast-lineage-specific *Gja1*-knockout mice, including increased middiaphyseal cross-sectional area with periosteal and endocortical expansion, increased endocortical osteoclast number, cortical thinning and porosity, defective osteoblastogenesis, and increased progenitor proliferation (Buo et al., 2017). Hence, connexin43-dependent signals that converge on Runx2 activation are a key mechanism by which gap junctions regulate skeletal homeostasis. Exemplifying such notion, connexin43-dependent parallel activation of the extracellular signal-regulated kinase 1/2 (ERK1/2) and PKCδ pathways converge on regulating Runx2 transcriptional activity and drive osteoblast lineage progression, an effect partly dependent on intercellular diffusion of inositol polyphosphates (Lima et al., 2009; Niger et al., 2012, 2013). Gap junctions also permit intercellular exchange of other second messengers, such as cAMP, Ca^{2+} ions, and ATP, as well as microRNAs (Davis et al., 2017; Romanello & D'Andrea, 2001; Genetos et al., 2007; Gupta et al., 2016; Ishihara et al., 2013; Guo et al., 2006; Jorgensen et al., 2003). These gap junction–communicated second messengers modulate numerous signaling pathways, including ERK1/2, Src, PI3K, 14-3-3θ, PKA, PKCδ, and β-catenin, in osteoblasts and osteocytes (Moorer et al., 2017; Loiselle et al., 2013; Bivi et al., 2011; Gupta et al., 2016; Batra et al., 2012, 2014; Plotkin et al., 2002; Tu et al., 2016). These pathways in turn affect diverse functions, from cell differentiation and survival to fracture healing and expression of paracrine regulators (Watkins et al., 2011; Lecanda et al., 2000b; Bivi et al., 2012a; Lecanda et al., 1998; Loiselle et al., 2013; Cherian et al., 2005; Chung et al., 2006; Stains et al., 2003; Gupta et al., 2016; Plotkin et al., 2002; Plotkin et al., 2008; Stains and Civitelli, 2005; Saunders & et al., 2003; Li et al., 2013; York et al., 2016). Notably, there is dynamic reciprocity, in that stimuli that signal through gap junctions also regulate the expression of gap junction proteins. For example, PTH, prostaglandin E_2 (PGE_2), mechanical load, vitamin D_3, and neuropeptides all increase connexin43 protein abundance (Donahue et al., 1995; Civitelli et al., 1998; Cheng et al., 2001; Cherian et al., 2003; Ziambaras et al., 1998; Schiller et al., 1992; Shen et al., 1986; Saunders et al., 2001; Schirrmacher and Bingmann, 1998; Ma et al., 2013). Conversely, glucocorticoids and 17β-estradiol, as well as aging, decrease connexin43 expression (Davis et al., 2017; Schirrmacher and Bingmann, 1998; Joiner et al., 2014; Roforth et al., 2015; Massas et al., 1998; Gao et al., 2016; Shen et al., 2016). In addition to small molecules, gap junctions formed by connexin43 can transmit microRNAs from cell to cell. In osteocytes, lack of connexin43 decreases the abundance of miR-21, a prosurvival signal that suppresses PTEN-Akt activity (Davis et al., 2017). The resultant increase in osteocyte apoptosis leads to enhanced osteoclastogenesis via increased RANKL/OPG ratio; extracellular release of the high-mobility-group box 1 protein, a pro-osteoclastogenic factor; and consequent bone loss (Davis et al., 2017; Zhou et al., 2008; Yang et al., 2008).

Connexin43 function is not limited to forming transcellular channels; its biologic action is in part mediated by direct interaction with components of cell signaling systems. More than 40 proteins can interact directly or indirectly with the C-terminal tail domain of the connexin43 monomer (Herve et al., 2012; Leithe et al., 2018; Laird, 2006). In bone, PKCδ, ERK1/2, β-catenin, β-arrestin, α5β1 integrin, and Src are part of the characterized connexin43 interactome, where they contribute to regulation of osteoblast signaling processes (Moorer et al., 2017; Bivi et al., 2011, 2013; Batra et al., 2012; Plotkin et al., 2002; Hebert and Stains, 2013; Niger et al., 2010). The assembly of signaling molecules at the gap junction plaque permits efficient modulation of the downstream signaling response to intracellularly communicated signals (Moorer et al., 2017; Batra et al., 2012; Hebert and Stains, 2013). In vivo experiments have confirmed the functional relevance of the C-terminal domain of connexin43 in bone. Genetic deletion of the last 124 amino acids at the connexin43 C-terminal domain (*Gja1* K258Stop) in male mice recapitulates key aspects of *Gja1* gene ablation in bone, including a reciprocal increase in osteoblast proliferation and decrease in osteoblast differentiation, exuberant periosteal osteoblast activity with poorly organized collagenous matrix, increased endocortical osteoclast number, decreased cortical thickness, increased cortical porosity, and widened marrow area (Moorer et al., 2017). Importantly, this C-terminal truncation is associated with a failure to recruit signaling molecules, such as PKCδ, ERK1/2, and β-catenin, to the mutant connexin43, consistent with the notion that the connexin43 C-terminal domain serves as a docking platform for efficient signal transduction (Moorer et al., 2017; Hebert and Stains, 2013). Interestingly, a distinct skeletal phenotype is observed in *Gja1* K258Stop female mice, which exhibit reduced trabecular bone mass (Moorer et al., 2017; Pacheco-Costa et al., 2015; Hammond et al., 2016), although subtle changes in cortical geometry, bone strength, mineral crystallinity, and collagen spacing are also present

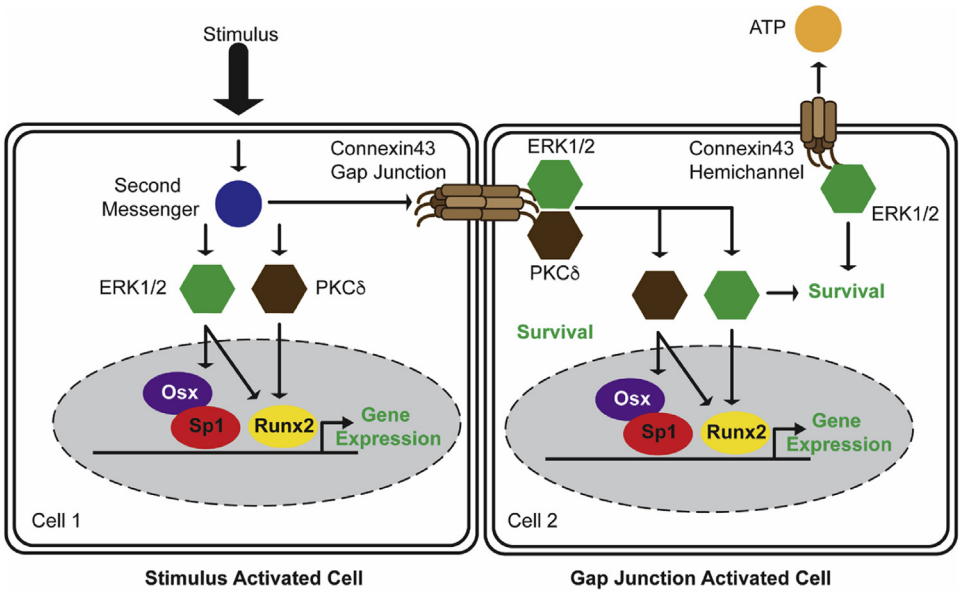

FIGURE 18.6 Intercellular communication and signaling among bone cells. Connexin43-containing gap junctions permit cells that may not be activated by a stimulus to respond as a result of second-messenger diffusion through gap junction channels. There, locally recruited signaling molecules, such as extracellular signal-regulated kinase 1/2 (*ERK1/2*) and protein kinase Cδ (*PKCδ*), are activated by the communicated second messenger resulting in activation of specific signaling cascades, which in turn regulate osteoblast gene expression by modulating the transcriptional activity of specific transcription factors, notably, Runx2, Osterix (*Osx*), and Sp-family members, and by promoting cell survival. Under certain conditions (mechanical strain), connexin43 hemichannels may open and activate signaling independent of gap-junctional communication.

(Moorer et al., 2017; Hammond et al., 2016). These data strongly support the notion that the signal modulation function of connexin43 is necessary for skeletal modeling and homeostasis, independent of or in addition to, gap junction channel function (Fig. 18.6). It should be noted that this biologic model may not apply to all systems and organs; for example, the cardiovascular malformations present in *Gja1*-null mice (*Gja1*$^{-/-}$) are not present in a C-terminus *Gja1*-truncated mutant, although lethal arrhythmias develop (Lubkemeier et al., 2013).

In cultured osteocytes, unpaired connexin43 hemichannels, which form a direct channel between the cytoplasm and the extracellular compartment of a cell, open in response to fluid shear stress and result in PGE_2 and ATP release into the extracellular fluid (Romanello & D'Andrea, 2001; Genetos et al., 2007; Cherian et al., 2005; Plotkin and Bellido, 2001; Riquelme et al., 2015). This process requires an interaction between connexin43 and α5β1 integrin, triggered by mechanical forces and activation of the Akt pathway (Batra et al., 2012). The subsequent actions of extracellular ATP and PGE_2 then regulate osteocyte responses to mechanical load (Blackwell et al., 2010; Kitase et al., 2010; Lenertz et al., 2015; Orriss et al., 2010; Agrawal and Gartland, 2015). However, there is some controversy as to whether the release of extracellular ATP from mechanically activated bone cells is indeed mediated by connexin43 hemichannels or instead by pannexins, a closely related family of proteins. In vitro, both gap junctions and pannexin channels can conduct ATP and are sensitive to the same pharmacologic inhibitors (Thi et al., 2012; Cheung et al., 2016). In any case, connexin43 hemichannels, but not gap junctions, seem to be required for an antiapoptotic effect of bisphosphonates and protection from oxidative stress in osteocytes (Plotkin et al., 2002, 2005, 2008; Kar et al., 2013). Transgenic mice overexpressing either a *Gja1* mutant that exhibits dominant-negative interference with endogenous gap-junctional communication but not hemichannel activity (R76W) or a *Gja1* mutant that exhibits dominant-negative interference with both functions (Δ130−136) have been developed to test the role of connexin43 hemichannels in vivo (Xu et al., 2015). While Δ130−136-expressing mice mimicked the skeletal phenotype observed in models of connexin43 deficiency, cortical modeling defects were less obvious in connexin43 R76W transgenic mice, suggesting that hemichannels, rather than gap-junctional communication, mediate connexin43 action on cortical modeling (Xu et al., 2015). However, these data are in sharp contrast with the evidence of a full skeletal phenotype, with cortical expansion, thinning, and increased endocortical bone resorption, in mice in which one *Gja1* allele was replaced by the G138R *Gja1* ODDD mutant (Watkins et al., 2011). Since this mutant abolishes gap junction function but allows extracellular ATP release (Dobrowolski et al., 2008), the results support the conclusion that gap-junctional communication is a key driver of the skeletal phenotype. Furthermore, ATP can be released by the opening of pannexin channels, but mice with a germ-line null mutation of *Pnx3*, which is highly

expressed in bone cells, show no cortical phenotype (Caskenette et al., 2016). Overall, data from these gene replacement or ablation models argue against a role of ATP release via either connexin43 hemichannels or pannexin channels in the genesis of the cortical modeling defect. Interference with multiple connexins or connexin-binding partners by over-expressed connexin43 mutants may complicate interpretation of the contrasting data emerging from the Δ130−136 transgenic mice.

Conclusions

The unraveling of many of the molecular mechanisms by which cadherins and connexins control skeletal biology has established the importance of direct cell−cell interactions for the achievement of adequate bone mass and maintenance of bone quality. While the necessity of an interconnected cellular communication network in bone is established, much remains to be discovered about the context-specific signals and the modulatory action of cadherins and connexins in elaborating hormonal, paracrine, and physical factors that drive bone modeling and homeostasis. Key questions about how cadherins in osteogenic cells maintain the skeletal stem cell niche, in normal homeostasis and in tumor metastases, and how N-cadherin and cadherin-11 can be leveraged as potential therapeutic targets remain to be addressed. Likewise, the mechanisms underlying mechanotransduction by connexin43, and its exquisite action on cortical modeling, via differential regulation of endocortical and periosteal bone modeling; the role of other connexins in skeletal homeostasis; and the sexual dysmorphism of some connexin actions remain exciting areas of investigation. Defining the signals communicated by gap junction networks adds a new dimension to our understanding of bone modeling and remodeling at the tissue level, opening new avenues for therapeutic intervention to affect bone quality.

Acknowledgments

Part of the work described in this chapter was supported by the National Institute for Musculoskeletal and Skin Diseases, National Institutes of Health (grants AR041255 and AR055913 to R.C., AR063631 and AR071614 to J.P.S.). R.C. receives grant support from Mereo BioPharma and Amgen, and owns stock in Amgen, Eli-Lilly, and Merck & Co. The other authors have no conflicts to disclose.

References

Abe, K., Takeichi, M., 2008. EPLIN mediates linkage of the cadherin catenin complex to F-actin and stabilizes the circumferential actin belt. Proc. Natl. Acad. Sci. U. S. A. 105 (1), 13−19.

Agrawal, A., Gartland, A., 2015. P2X7 receptors: role in bone cell formation and function. J. Mol. Endocrinol. 54 (2), R75−R88.

Alimperti, S., Andreadis, S.T., 2015. CDH2 and CDH11 act as regulators of stem cell fate decisions. Stem Cell Res. 14 (3), 270−282.

Arnsdorf, E.J., Tummala, P., Jacobs, C.R., 2009. Non-canonical Wnt signaling and N-cadherin related beta-catenin signaling play a role in mechanically induced osteogenic cell fate. PLoS One 4 (4), e5388.

Batra, N., et al., 2012. Mechanical stress-activated integrin alpha5beta1 induces opening of connexin43 hemichannels. Proc. Natl. Acad. Sci. U. S. A. 109 (9), 3359−3364.

Batra, N., et al., 2014. 14-3-3theta facilitates plasma membrane delivery and function of mechanosensitive connexin43 hemichannels. J. Cell Sci. 127 (Pt 1), 137−146.

Bivi, N., et al., 2011. Connexin43 interacts with betaarrestin: a pre-requisite for osteoblast survival induced by parathyroid hormone. J. Cell. Biochem. 112 (10), 2920−2930.

Bivi, N., et al., 2012a. Cell autonomous requirement of connexin43 for osteocyte survival: consequences for endocortical resorption and periosteal bone formation. J. Bone Miner. Res. 27 (2), 374−389.

Bivi, N., et al., 2012b. Deletion of Cx43 from osteocytes results in defective bone material properties but does not decrease extrinsic strength in cortical bone. Calcif. Tissue Int. 91 (3), 215−224.

Bivi, N., et al., 2013. Absence of Cx43 selectively from osteocytes enhances responsiveness to mechanical force in mice. J. Orthop. Res. 31 (7), 1075−1081.

Blackwell, K.A., Raisz, L.G., Pilbeam, C.C., 2010. Prostaglandins in bone: bad cop, good cop? Trends Endocrinol. Metabol. 21 (5), 294−301.

Blaschuk, O.W., et al., 1990. Identification of a cadherin cell adhesion recognition sequence. Dev. Biol. 139 (1), 227−229.

Brasch, J., et al., 2012. Thinking outside the cell: how cadherins drive adhesion. Trends Cell Biol. 22 (6), 299−310.

Bromberg, O., et al., 2012. Osteoblastic N-cadherin is not required for microenvironmental support and regulation of hematopoietic stem and progenitor cells. Blood 120 (2), 303−313.

Buckley, C.D., et al., 2014. Cell adhesion. The minimal cadherin-catenin complex binds to actin filaments under force. Science 346 (6209), 1254211.

Buo, A.M., et al., 2017. Connexin43 and Runx2 interact to affect cortical bone geometry, skeletal development, and osteoblast and osteoclast function. J. Bone Miner. Res. 32 (8), 1727−1738.

Caskenette, D., et al., 2016. Global deletion of Panx3 produces multiple phenotypic effects in mouse humeri and femora. J. Anat. 228 (5), 746−756.

Castro, C.H., et al., 2004. Targeted expression of a dominant-negative N-cadherin in vivo delays peak bone mass and increases adipogenesis. J. Cell Sci. 117 (Pt 13), 2853–2864.

Cavallaro, U., Dejana, E., 2011. Adhesion molecule signalling: not always a sticky business. Nat. Rev. Mol. Cell Biol. 12 (3), 189–197.

Cheng, S.L., et al., 1998. Human osteoblasts express a repertoire of cadherins, which are critical for BMP-2-induced osteogenic differentiation. J. Bone Miner. Res. 13 (4), 633–644.

Cheng, S.L., et al., 2000. A dominant negative cadherin inhibits osteoblast differentiation. J. Bone Miner. Res. 15 (12), 2362–2370.

Cheng, B., et al., 2001. PGE(2) is essential for gap junction-mediated intercellular communication between osteocyte-like MLO-Y4 cells in response to mechanical strain. Endocrinology 142 (8), 3464–3473.

Cherian, P.P., et al., 2003. Effects of mechanical strain on the function of Gap junctions in osteocytes are mediated through the prostaglandin EP2 receptor. J. Biol. Chem. 278 (44), 43146–43156.

Cherian, P.P., et al., 2005. Mechanical strain opens connexin43 hemichannels in osteocytes: a novel mechanism for the release of prostaglandin. Mol. Biol. Cell 16 (7), 3100–3106.

Cheung, W.Y., et al., 2016. Pannexin-1 and P2X7-receptor are required for apoptotic osteocytes in fatigued bone to trigger RANKL production in neighboring bystander osteocytes. J. Bone Miner. Res. 31 (4), 890–899.

Chung, D.J., et al., 2006. Low peak bone mass and attenuated anabolic response to parathyroid hormone in mice with an osteoblast-specific deletion of connexin43. J. Cell Sci. 119 (Pt 20), 4187–4198.

Civitelli, R., et al., 1993. Connexin43 mediates direct intercellular communication in human osteoblastic cell networks. J. Clin. Investig. 91 (5), 1888–1896.

Civitelli, R., et al., 1998. Regulation of connexin43 expression and function by prostaglandin E2 (PGE2) and parathyroid hormone (PTH) in osteoblastic cells. J. Cell. Biochem. 68 (1), 8–21.

Damaraju, S., et al., 2015. The role of gap junctions and mechanical loading on mineral formation in a collagen-I scaffold seeded with osteoprogenitor cells. Tissue Eng. 21 (9–10), 1720–1732.

Daugherty, R.L., Gottardi, C.J., 2007. Phospho-regulation of Beta-catenin adhesion and signaling functions. Physiology 22, 303–309.

Davis, H.M., et al., 2017. Disruption of the Cx43/miR21 pathway leads to osteocyte apoptosis and increased osteoclastogenesis with aging. Aging Cell 16 (3), 551–563.

Debiais, F., et al., 2001. Fibroblast growth factor-2 (FGF-2) increases N-cadherin expression through protein kinase C and Src-kinase pathways in human calvaria osteoblasts. J. Cell. Biochem. 81 (1), 68–81.

Delannoy, P., et al., 2001. Protein kinase C-dependent upregulation of N-cadherin expression by phorbol ester in human calvaria osteoblasts. Exp. Cell Res. 269 (1), 154–161.

DeLise, A.M., Tuan, R.S., 2002. Alterations in the spatiotemporal expression pattern and function of N-cadherin inhibit cellular condensation and chondrogenesis of limb mesenchymal cells in vitro. J. Cell. Biochem. 87 (3), 342–359.

Di Benedetto, A., et al., 2010. N-cadherin and cadherin 11 modulate postnatal bone growth and osteoblast differentiation by distinct mechanisms. J. Cell Sci. 123 (Pt 15), 2640–2648.

Di Benedetto, A., et al., 2015. Osteogenic differentiation of mesenchymal stem cells from dental bud: role of integrins and cadherins. Stem Cell Res. 15 (3), 618–628.

Dickinson, D.J., Nelson, W.J., Weis, W.I., 2011. A polarized epithelium organized by beta- and alpha-catenin predates cadherin and metazoan origins. Science 331 (6022), 1336–1339.

Dobrowolski, R., et al., 2008. The conditional connexin43G138R mouse mutant represents a new model of hereditary oculodentodigital dysplasia in humans. Hum. Mol. Genet. 17 (4), 539–554.

Donahue, H.J., et al., 1995. Cell-to-cell communication in osteoblastic networks: cell line-dependent hormonal regulation of gap junction function. J. Bone Miner. Res. 10 (6), 881–889.

Donahue, H.J., et al., 2000. Differentiation of human fetal osteoblastic cells and gap junctional intercellular communication. Am. J. Physiol. Cell Physiol. 278 (2), C315–C322.

Doty, S.B., 1981. Morphological evidence of gap junctions between bone cells. Calcif. Tissue Int. 33 (5), 509–512.

Drees, F., et al., 2005. Alpha-catenin is a molecular switch that binds E-cadherin-beta-catenin and regulates actin-filament assembly. Cell 123 (5), 903–915.

Ellison, D., et al., 2016. Cell-cell communication enhances the capacity of cell ensembles to sense shallow gradients during morphogenesis. Proc. Natl. Acad. Sci. U. S. A. 113 (6), E679–E688.

Esseltine, J.L., et al., 2017. Connexin43 mutant patient-derived induced pluripotent stem cells exhibit altered differentiation potential. J. Bone Miner. Res. 32 (6), 1368–1385.

Fang, L.C., et al., 2006. Accentuated ovariectomy induced bone loss and altered osteogenesis in hyeterozygous N-cadherin null mice. J. Bone Miner. Res. 21 (12), 1897–1906.

Ferrari, S.L., et al., 2000. A role for N-cadherin in the development of the differentiated osteoblastic phenotype. J. Bone Miner. Res. 15 (2), 198–208.

Flenniken, A.M., et al., 2005. A Gja1 missense mutation in a mouse model of oculodentodigital dysplasia. Development 132 (19), 4375–4386.

Fontana, F., et al., 2017a. N-cadherin in extra-skeletal osterix (Osx) positive cells modulates tumor growth independently of cell-cell adhesion. J. Bone Miner. Res. 32 (S1).

Fontana, F., et al., 2017b. N-cadherin regulation of bone growth and homeostasis is osteolineage stage-specific. J. Bone Miner. Res. 32 (6), 1332–1342.

Fujita, K., et al., 2014. Mutual enhancement of differentiation of osteoblasts and osteocytes occurs through direct cell-cell contact. J. Cell. Biochem. 115 (11), 2039–2044.
Gao, J., et al., 2016. Glucocorticoid impairs cell-cell communication by autophagy-mediated degradation of connexin43 in osteocytes. Oncotarget 7 (19), 26966–26978.
Genetos, D.C., et al., 2007. Oscillating fluid flow activation of gap junction hemichannels induces ATP release from MLO-Y4 osteocytes. J. Cell. Physiol. 212 (1), 207–214.
Glenske, K., et al., 2014. Bioactivity of xerogels as modulators of osteoclastogenesis mediated by connexin43. Biomaterials 35 (5), 1487–1495.
Gong, X.Q., et al., 2007. Differential potency of dominant negative connexin43 mutants in oculodentodigital dysplasia. J. Biol. Chem. 282 (26), 19190–19202.
Goodenough, D.A., Goliger, J.A., Paul, D.L., 1996. Connexins, connexons, and intercellular communication. Annu. Rev. Biochem. 65, 475–502.
Gottardi, C.J., Gumbiner, B.M., 2001. Adhesion signaling: how beta-catenin interacts with its partners. Curr. Biol. 11 (19), R792–R794.
Gramsch, B., et al., 2001. Enhancement of connexin43 expression increases proliferation and differentiation of an osteoblast-like cell line. Exp. Cell Res. 264 (2), 397–407.
Greenbaum, A.M., et al., 2012. N-cadherin in osteolineage cells is not required for maintenance of hematopoietic stem cells. Blood 120 (2), 295–302.
Grimston, S.K., et al., 2008. Attenuated response to in vivo mechanical loading in mice with conditional osteoblast ablation of the connexin43 gene (Gja1). J. Bone Miner. Res. 23 (6), 879–886.
Grimston, S.K., et al., 2011. Connexin43 deficiency reduces the sensitivity of cortical bone to the effects of muscle paralysis. J. Bone Miner. Res. 26 (9), 2151–2160.
Grimston, S.K., et al., 2012. Enhanced periosteal and endocortical responses to axial tibial compression loading in conditional connexin43 deficient mice. PLoS One 7 (9), e44222.
Grimston, S.K., et al., 2013. Connexin43 modulates post-natal cortical bone modeling and mechano-responsiveness. BoneKEy Rep. 2, 446.
Grimston, S.K., et al., 2017. Heterozygous deletion of both sclerostin (Sost) and connexin43 (Gja1) genes in mice is not sufficient to impair cortical bone modeling. PLoS One 12 (11), e0187980.
Grosheva, I., et al., 2001. p120 catenin affects cell motility via modulation of activity of Rho-family GTPases: a link between cell-cell contact formation and regulation of cell locomotion. J. Cell Sci. 114 (Pt 4), 695–707.
Gumbiner, B.M., 2005. Regulation of cadherin-mediated adhesion in morphogenesis. Nat. Rev. Mol. Cell Biol. 6 (8), 622–634.
Guntur, A.R., Rosen, C.J., Naski, M.C., 2012. N-cadherin adherens junctions mediate osteogenesis through PI3K signaling. Bone 50 (1), 54–62.
Guo, X.E., et al., 2006. Intracellular calcium waves in bone cell networks under single cell nanoindentation. Mol. Cell. BioMech. 3 (3), 95–107.
Gupta, A., et al., 2016. Communication of cAMP by connexin43 gap junctions regulates osteoblast signaling and gene expression. Cell. Signal. 28 (8), 1048–1057.
Haas, A.R., Tuan, R.S., 1999. Chondrogenic differentiation of murine C3H10T1/2 multipotential mesenchymal cells: II. Stimulation by bone morphogenetic protein-2 requires modulation of N-cadherin expression and function. Differentiation 64 (2), 77–89.
Halbleib, J.M., Nelson, W.J., 2006. Cadherins in development: cell adhesion, sorting, and tissue morphogenesis. Genes Dev. 20 (23), 3199–3214.
Hammond, M.A., et al., 2016. Removing or truncating connexin43 in murine osteocytes alters cortical geometry, nanoscale morphology, and tissue mechanics in the tibia. Bone 88, 85–91.
Harris, T.J., Tepass, U., 2010. Adherens junctions: from molecules to morphogenesis. Nat. Rev. Mol. Cell Biol. 11 (7), 502–514.
Harris, A.L.L.,D., 2009. Permeability of connexin channels. In: Harris, A.L.L. (Ed.), Connexins: A Guide. Humana Press, pp. 165–206.
Harrison, O.J., et al., 2005. The mechanism of cell adhesion by classical cadherins: the role of domain 1. J. Cell Sci. 118 (Pt 4), 711–721.
Hashida, Y., et al., 2014. Communication-dependent mineralization of osteoblasts via gap junctions. Bone 61, 19–26.
Hay, E., et al., 2000. N- and E-cadherin mediate early human calvaria osteoblast differentiation promoted by bone morphogenetic protein-2. J. Cell. Physiol. 183 (1), 117–128.
Hay, E., et al., 2009a. N-cadherin interacts with axin and LRP5 to negatively regulate Wnt/beta-catenin signaling, osteoblast function, and bone formation. Mol. Cell Biol. 29 (4), 953–964.
Hay, E., et al., 2012. Peptide-based mediated disruption of N-cadherin-LRP5/6 interaction promotes Wnt signaling and bone formation. J. Bone Miner. Res. 27 (9), 1852–1863.
Hay, E., et al., 2014. N-cadherin/wnt interaction controls bone marrow mesenchymal cell fate and bone mass during aging. J. Cell. Physiol. 229 (11), 1765–1775.
Hay, E., Nouraud, A., Marie, P.J., 2009b. N-cadherin negatively regulates osteoblast proliferation and survival by antagonizing Wnt, ERK and PI3K/Akt signalling. PLoS One 4 (12), e8284.
Hebert, C., Stains, J.P., 2013. An intact connexin43 is required to enhance signaling and gene expression in osteoblast-like cells. J. Cell. Biochem. 114 (11), 2542–2550.
Herve, J.C., et al., 2012. Gap junctional channels are parts of multiprotein complexes. Biochim. Biophys. Acta 1818 (8), 1844–1865.
Heuberger, J., Birchmeier, W., 2010. Interplay of cadherin-mediated cell adhesion and canonical Wnt signaling. Cold Spring Harb Perspect Biol 2 (2), a002915.
Hobolt-Pedersen, A.S., Delaisse, J.M., Soe, K., 2014. Osteoclast fusion is based on heterogeneity between fusion partners. Calcif. Tissue Int. 95 (1), 73–82.
Hu, Y., et al., 2013. A novel autosomal recessive GJA1 missense mutation linked to Craniometaphyseal dysplasia. PLoS One 8 (8), e73576.
Ilvesaro, J., Tavi, P., Tuukkanen, J., 2001. Connexin-mimetic peptide Gap 27 decreases osteoclastic activity. BMC Muscoskelet. Disord. 2, 10.

Ishihara, Y., et al., 2013. Ex vivo real-time observation of Ca(2+) signaling in living bone in response to shear stress applied on the bone surface. Bone 53 (1), 204–215.
Ishikawa, M., et al., 2016. Pannexin 3 and connexin43 modulate skeletal development through their distinct functions and expression patterns. J. Cell Sci. 129 (5), 1018–1030.
Ishikawa, M., Yamada, Y., 2017. The role of pannexin 3 in bone biology. J. Dent. Res. 96 (4), 372–379.
Ishiyama, N., et al., 2010. Dynamic and static interactions between p120 catenin and E-cadherin regulate the stability of cell-cell adhesion. Cell 141 (1), 117–128.
Itoh, M., et al., 1997. Involvement of ZO-1 in cadherin-based cell adhesion through its direct binding to alpha catenin and actin filaments. J. Cell Biol. 138 (1), 181–192.
Jahani, M., et al., 2012. The effect of osteocyte apoptosis on signalling in the osteocyte and bone lining cell network: a computer simulation. J. Biomech. 45 (16), 2876–2883.
Joiner, D.M., et al., 2014. Aged male rats regenerate cortical bone with reduced osteocyte density and reduced secretion of nitric oxide after mechanical stimulation. Calcif. Tissue Int. 94 (5), 484–494.
Jorgensen, N.R., et al., 2003. Activation of L-type calcium channels is required for gap junction-mediated intercellular calcium signaling in osteoblastic cells. J. Biol. Chem. 278 (6), 4082–4086.
Kanaporis, G., Brink, P.R., Valiunas, V., 2011. Gap junction permeability: selectivity for anionic and cationic probes. Am. J. Physiol. Cell Physiol. 300 (3), C600–C609.
Kar, R., et al., 2013. Connexin43 channels protect osteocytes against oxidative stress-induced cell death. J. Bone Miner. Res. 28 (7), 1611–1621.
Katsamba, P., et al., 2009. Linking molecular affinity and cellular specificity in cadherin-mediated adhesion. Proc. Natl. Acad. Sci. U. S. A. 106 (28), 11594–11599.
Kawaguchi, J., et al., 2001a. The transition of cadherin expression in osteoblast differentiation from mesenchymal cells: consistent expression of cadherin-11 in osteoblast lineage. J. Bone Miner. Res. 16 (2), 260–269.
Kawaguchi, J., et al., 2001b. Targeted disruption of cadherin-11 leads to a reduction in bone density in calvaria and long bone metaphyses. J. Bone Miner. Res. 16 (7), 1265–1271.
Kitase, Y., et al., 2010. Mechanical induction of PGE2 in osteocytes blocks glucocorticoid-induced apoptosis through both the beta-catenin and PKA pathways. J. Bone Miner. Res. 25 (12), 2657–2668.
Kjaer, K.W., et al., 2004. Novel Connexin43 (GJA1) mutation causes oculo-dento-digital dysplasia with curly hair. Am. J. Med. Genet. 127A (2), 152–157.
Knudsen, K.A., Soler, A.P., 2000. Cadherin-mediated cell-cell interactions. Methods Mol. Biol. 137, 409–440.
Krishnan, V., Bryant, H.U., Macdougald, O.A., 2006. Regulation of bone mass by Wnt signaling. J. Clin. Investig. 116 (5), 1202–1209.
Kylmaoja, E., et al., 2013. Osteoclastogenesis is influenced by modulation of gap junctional communication with antiarrhythmic peptides. Calcif. Tissue Int. 92 (3), 270–281.
Lai, C.F., et al., 2006. Accentuated ovariectomy-induced bone loss and altered osteogenesis in heterozygous N-cadherin null mice. J. Bone Miner. Res. 21 (12), 1897–1906.
Laird, D.W., 2006. Life cycle of connexins in health and disease. Biochem. J. 394 (Pt 3), 527–543.
Lecanda, F., et al., 1998. Gap junctional communication modulates gene expression in osteoblastic cells. Mol. Biol. Cell 9 (8), 2249–2258.
Lecanda, F., et al., 2000a. Connexin43 deficiency causes delayed ossification, craniofacial abnormalities, and osteoblast dysfunction. J. Cell Biol. 151 (4), 931–944.
Lecanda, F., et al., 2000b. Differential regulation of cadherins by dexamethasone in human osteoblastic cells. J. Cell. Biochem. 77 (3), 499–506.
Leithe, E., Mesnil, M., Aasen, T., 2018. The connexin43 C-terminus: a tail of many tales. Biochim. Biophys. Acta 1860 (1), 48–64.
Lemonnier, J., et al., 2001. Role of N-cadherin and protein kinase C in osteoblast gene activation induced by the S252W fibroblast growth factor receptor 2 mutation in Apert craniosynostosis. J. Bone Miner. Res. 16 (5), 832–845.
Lenertz, L.Y., et al., 2015. Control of bone development by P2X and P2Y receptors expressed in mesenchymal and hematopoietic cells. Gene 570 (1), 1–7.
Li, Z., et al., 1999. Inhibiting gap junctional intercellular communication alters expression of differentiation markers in osteoblastic cells. Bone 25 (6), 661–666.
Li, X., et al., 2013. Connexin43 is a potential regulator in fluid shear stress-induced signal transduction in osteocytes. J. Orthop. Res. 31 (12), 1959–1965.
Li, S., et al., 2015. Connexin43 and ERK regulate tension-induced signal transduction in human periodontal ligament fibroblasts. J. Orthop. Res. 33 (7), 1008–1014.
Li, R., et al., 2017. Self-assembled N-cadherin mimetic peptide hydrogels promote the chondrogenesis of mesenchymal stem cells through inhibition of canonical Wnt/beta-catenin signaling. Biomaterials 145, 33–43.
Lilien, J., Balsamo, J., 2005. The regulation of cadherin-mediated adhesion by tyrosine phosphorylation/dephosphorylation of beta-catenin. Curr. Opin. Cell Biol. 17 (5), 459–465.
Lima, F., et al., 2009. Connexin43 potentiates osteoblast responsiveness to fibroblast growth factor 2 via a protein kinase C-delta/Runx2-dependent mechanism. Mol. Biol. Cell 20 (11), 2697–2708.
Liu, S., et al., 2015. Connexin43 mediated delivery of ADAMTS5 targeting siRNAs from mesenchymal stem cells to synovial fibroblasts. PLoS One 10 (6), e0129999.
Lloyd, S.A., et al., 2012. Connexin43 deficiency attenuates loss of trabecular bone and prevents suppression of cortical bone formation during unloading. J. Bone Miner. Res. 27 (11), 2359–2372.

Lloyd, S.A., et al., 2013. Connexin43 deficiency desensitizes bone to the effects of mechanical unloading through modulation of both arms of bone remodeling. Bone 57 (1), 76–83.

Lloyd, S.A., et al., 2014a. Evidence for the role of connexin43-mediated intercellular communication in the process of intracortical bone resorption via osteocytic osteolysis. BMC Muscoskelet. Disord. 15, 122.

Lloyd, S.A., et al., 2014b. Interdependence of muscle atrophy and bone loss induced by mechanical unloading. J. Bone Miner. Res. 29 (5), 1118–1130.

Logan, C.Y., Nusse, R., 2004. The Wnt signaling pathway in development and disease. Annu. Rev. Cell Dev. Biol. 20, 781–810.

Loiselle, A.E., et al., 2013. Inhibition of GSK-3beta rescues the impairments in bone formation and mechanical properties associated with fracture healing in osteoblast selective connexin43 deficient mice. PLoS One 8 (11), e81399.

Lubkemeier, I., et al., 2013. Deletion of the last five C-terminal amino acid residues of connexin43 leads to lethal ventricular arrhythmias in mice without affecting coupling via gap junction channels. Basic Res. Cardiol. 108 (3), 348.

Luo, Y., Kostetskii, I., Radice, G.L., 2005. N-cadherin is not essential for limb mesenchymal chondrogenesis. Dev. Dynam. 232 (2), 336–344.

Ma, W., et al., 2013. Neuropeptides stimulate human osteoblast activity and promote gap junctional intercellular communication. Neuropeptides 47 (3), 179–186.

Maher, M.T., et al., 2009. Activity of the beta-catenin phosphodestruction complex at cell-cell contacts is enhanced by cadherin-based adhesion. J. Cell Biol. 186 (2), 219–228.

Marie, P.J., et al., 2014. Cadherin-mediated cell-cell adhesion and signaling in the skeleton. Calcif. Tissue Int. 94 (1), 46–54.

Massas, R., Korenstein, R., Benayahu, D., 1998. Estrogen modulation of osteoblastic cell-to-cell communication. J. Cell. Biochem. 69 (3), 282–290.

Mbalaviele, G., Shin, C.S., Civitelli, R., 2006. Cell-cell adhesion and signaling through cadherins: connecting bone cells in their microenvironment. J. Bone Miner. Res. 21 (12), 1821–1827.

McLachlan, E., et al., 2008. ODDD-linked Cx43 mutants reduce endogenous Cx43 expression and function in osteoblasts and inhibit late stage differentiation. J. Bone Miner. Res. 23 (6), 928–938.

Mikami, Y., et al., 2015. Osteogenic gene transcription is regulated via gap junction-mediated cell-cell communication. Stem Cell. Dev. 24 (2), 214–227.

Mizoguchi, T., et al., 2014. Osterix marks distinct waves of primitive and definitive stromal progenitors during bone marrow development. Dev. Cell 29 (3), 340–349.

Modarresi, R., et al., 2005. N-cadherin mediated distribution of beta-catenin alters MAP kinase and BMP-2 signaling on chondrogenesis-related gene expression. J. Cell. Biochem. 95 (1), 53–63.

Moorer, M.C., et al., 2017. Defective signaling, osteoblastogenesis and bone remodeling in a mouse model of connexin43 C-terminal truncation. J. Cell Sci. 130 (3), 531–540.

Moorer, M.C., Stains, J.P., 2017. Connexin43 and the intercellular signaling network regulating skeletal remodeling. Curr. Osteoporos. Rep. 15 (1), 24–31.

Nelson, W.J., Nusse, R., 2004. Convergence of Wnt, beta-catenin, and cadherin pathways. Science 303 (5663), 1483–1487.

Niger, C., et al., 2011. The transcriptional activity of osterix requires the recruitment of Sp1 to the osteocalcin proximal promoter. Bone 49 (4), 683–692.

Niger, C., et al., 2012. ERK acts in parallel to PKCdelta to mediate the connexin43-dependent potentiation of Runx2 activity by FGF2 in MC3T3 osteoblasts. Am. J. Physiol. Cell Physiol. 302 (7), C1035–C1044.

Niger, C., et al., 2013. The regulation of runt-related transcription factor 2 by fibroblast growth factor-2 and connexin43 requires the inositol polyphosphate/protein kinase Cdelta cascade. J. Bone Miner. Res. 28 (6), 1468–1477.

Niger, C., Hebert, C., Stains, J.P., 2010. Interaction of connexin43 and protein kinase C-delta during FGF2 signaling. BMC Biochem. 11, 14.

Nishikawa, Y., et al., 2015. Osteocytes up-regulate the terminal differentiation of pre-osteoblasts via gap junctions. Biochem. Biophys. Res. Commun. 456 (1), 1–6.

Obata, S., et al., 1998. A common protocadherin tail: multiple protocadherins share the same sequence in their cytoplasmic domains and are expressed in different regions of brain. Cell Adhes. Commun. 6 (4), 323–333.

Okazaki, M., et al., 1994. Molecular cloning and characterization of OB-cadherin, a new member of cadherin family expressed in osteoblasts. J. Biol. Chem. 269 (16), 12092–12098.

Orriss, I.R., Burnstock, G., Arnett, T.R., 2010. Purinergic signalling and bone remodelling. Curr. Opin. Pharmacol. 10 (3), 322–330.

Pacheco-Costa, R., et al., 2014. High bone mass in mice lacking Cx37 because of defective osteoclast differentiation. J. Biol. Chem. 289 (12), 8508–8520.

Pacheco-Costa, R., et al., 2015. Defective cancellous bone structure and abnormal response to PTH in cortical bone of mice lacking Cx43 cytoplasmic C-terminus domain. Bone 81, 632–643.

Pacheco-Costa, R., et al., 2016. Osteocytic connexin43 is not required for the increase in bone mass induced by intermittent PTH administration in male mice. J. Musculoskelet. Neuronal Interact. 16 (1), 45–57.

Pacheco-Costa, R., et al., 2017. Connexin37 deficiency alters organic bone matrix, cortical bone geometry, and increases Wnt/beta-catenin signaling. Bone 97, 105–113.

Panda, D.K., et al., 2001. The transcription factor SOX9 regulates cell cycle and differentiation genes in chondrocytic CFK2 cells. J. Biol. Chem. 276 (44), 41229–41236.

Patel, S.D., et al., 2006. Type II cadherin ectodomain structures: implications for classical cadherin specificity. Cell 124 (6), 1255–1268.

Paznekas, W.A., et al., 2009. GJA1 mutations, variants, and connexin43 dysfunction as it relates to the oculodentodigital dysplasia phenotype. Hum. Mutat. 30 (5), 724–733.

Peres-Ueno, M.J., et al., 2017. Model of hindlimb unloading in adult female rats: characterizing bone physicochemical, microstructural, and biomechanical properties. PLoS One 12 (12), e0189121.

Pertz, O., et al., 1999. A new crystal structure, Ca2+ dependence and mutational analysis reveal molecular details of E-cadherin homoassociation. EMBO J. 18 (7), 1738–1747.

Pizard, A., et al., 2005. Connexin40, a target of transcription factor Tbx5, patterns wrist, digits, and sternum. Mol. Cell Biol. 25 (12), 5073–5083.

Plotkin, L.I., Bellido, T., 2001. Bisphosphonate-induced, hemichannel-mediated, anti-apoptosis through the Src/ERK pathway: a gap junction-independent action of connexin43. Cell Commun. Adhes. 8 (4–6), 377–382.

Plotkin, L.I., et al., 2005. Bisphosphonates and estrogens inhibit osteocyte apoptosis via distinct molecular mechanisms downstream of extracellular signal-regulated kinase activation. J. Biol. Chem. 280 (8), 7317–7325.

Plotkin, L.I., et al., 2008. Connexin43 is required for the anti-apoptotic effect of bisphosphonates on osteocytes and osteoblasts in vivo. J. Bone Miner. Res. 23 (11), 1712–1721.

Plotkin, L.I., Stains, J.P., 2015. Connexins and pannexins in the skeleton: gap junctions, hemichannels and more. Cell. Mol. Life Sci. 72 (15), 2853–2867.

Plotkin, L.I., Manolagas, S.C., Bellido, T., 2002. Transduction of cell survival signals by connexin-43 hemichannels. J. Biol. Chem. 277 (10), 8648–8657.

Plotkin, L.I., Laird, D.W., Amedee, J., 2016. Role of connexins and pannexins during ontogeny, regeneration, and pathologies of bone. BMC Cell Biol. 17 (Suppl. 1), 19.

Plotkin, L.I., Pacheco-Costa, R., Davis, H.M., 2017. microRNAs and connexins in bone: interaction and mechanisms of delivery. Curr Mol Biol Rep 3 (2), 63–70.

Pokutta, S., et al., 1994. Conformational changes of the recombinant extracellular domain of E-cadherin upon calcium binding. Eur. J. Biochem. 223 (3), 1019–1026.

Radice, G.L., et al., 1997. Developmental defects in mouse embryos lacking N-cadherin. Dev. Biol. 181 (1), 64–78.

Ransjo, M., Sahli, J., Lie, A., 2003. Expression of connexin43 mRNA in microisolated murine osteoclasts and regulation of bone resorption in vitro by gap junction inhibitors. Biochem. Biophys. Res. Commun. 303 (4), 1179–1185.

Revollo, L., et al., 2015. N-cadherin restrains PTH activation of Lrp6/beta-catenin signaling and osteoanabolic action. J. Bone Miner. Res. 30 (2), 274–285.

Rhee, J., et al., 2007. Cables links Robo-bound Abl kinase to N-cadherin-bound beta-catenin to mediate Slit-induced modulation of adhesion and transcription. Nat. Cell Biol. 9 (8), 883–892.

Riquelme, M.A., et al., 2015. Mitogen-activated protein kinase (MAPK) activated by prostaglandin E2 phosphorylates connexin43 and closes osteocytic hemichannels in response to continuous flow shear stress. J. Biol. Chem. 290 (47), 28321–28328.

Roforth, M.M., et al., 2015. Global transcriptional profiling using RNA sequencing and DNA methylation patterns in highly enriched mesenchymal cells from young versus elderly women. Bone 76, 49–57.

Romanello, M., D'Andrea, P., 2001. Dual mechanism of intercellular communication in HOBIT osteoblastic cells: a role for gap-junctional hemichannels. J. Bone Miner. Res. 16 (8), 1465–1476.

Saunders, M.M., et al., 2001. Gap junctions and fluid flow response in MC3T3-E1 cells. Am. J. Physiol. Cell Physiol. 281 (6), C1917–C1925.

Saunders, M.M., et al., 2003. Fluid flow-induced prostaglandin E2 response of osteoblastic ROS 17/2.8 cells is gap junction-mediated and independent of cytosolic calcium. Bone 32 (4), 350–356.

Schiller, P.C., et al., 1992. Hormonal regulation of intercellular communication: parathyroid hormone increases connexin43 gene expression and gap-junctional communication in osteoblastic cells. Mol. Endocrinol. 6 (9), 1433–1440.

Schiller, P.C., et al., 2001. Gap-junctional communication is required for the maturation process of osteoblastic cells in culture. Bone 28 (4), 362–369.

Schilling, A.F., et al., 2008. Gap junctional communication in human osteoclasts in vitro and in vivo. J. Cell Mol. Med. 12 (6A), 2497–2504.

Schirrmacher, K., Bingmann, D., 1998. Effects of vitamin D3, 17beta-estradiol, vasoactive intestinal peptide, and glutamate on electric coupling between rat osteoblast-like cells in vitro. Bone 23 (6), 521–526.

Seki, A., et al., 2017. Progressive atrial conduction defects associated with bone malformation caused by a connexin45 mutation. J. Am. Coll. Cardiol. 70 (3), 358–370.

Shen, V., et al., 1986. Prostaglandins change cell shape and increase intercellular gap junctions in osteoblasts cultured from rat fetal calvaria. J. Bone Miner. Res. 1 (3), 243–249.

Shen, C., et al., 2016. Glucocorticoid suppresses connexin43 expression by inhibiting the Akt/mTOR signaling pathway in osteoblasts. Calcif. Tissue Int. 99 (1), 88–97.

Shin, C.S., et al., 2000. Relative abundance of different cadherins defines differentiation of mesenchymal precursors into osteogenic, myogenic, or adipogenic pathways. J. Cell. Biochem. 78 (4), 566–577.

Shin, C.S., et al., 2005. Dominant negative N-cadherin inhibits osteoclast differentiation by interfering with beta-catenin regulation of RANKL, independent of cell-cell adhesion. J. Bone Miner. Res. 20 (12), 2200–2212.

Stains, J.P., Civitelli, R., 2005. Gap junctions regulate extracellular signal-regulated kinase signaling to affect gene transcription. Mol. Biol. Cell 16 (1), 64–72.

Stains, J.P., et al., 2003. Gap junctional communication modulates gene transcription by altering the recruitment of Sp1 and Sp3 to connexin-response elements in osteoblast promoters. J. Biol. Chem. 278 (27), 24377–24387.

Stains, J.P., et al., 2014. Molecular mechanisms of osteoblast/osteocyte regulation by connexin43. Calcif. Tissue Int. 94 (1), 55–67.

Suswillo, R.F., et al., 2017. Strain uses gap junctions to reverse stimulation of osteoblast proliferation by osteocytes. Cell Biochem. Funct. 35 (1), 56–65.

Talbot, J., et al., 2018. Connexin43 intercellular communication drives the early differentiation of human bone marrow stromal cells into osteoblasts. J. Cell. Physiol. 233 (2), 946–957.

Thi, M.M., et al., 2012. Connexin43 and pannexin1 channels in osteoblasts: who is the "hemichannel"? J. Membr. Biol. 245 (7), 401–409.
Tiede-Lewis, L.M., et al., 2017. Degeneration of the osteocyte network in the C57BL/6 mouse model of aging. Aging 9 (10), 2190–2208.
Tran, N.L., et al., 1999. N-Cadherin expression in human prostate carcinoma cell lines. An epithelial-mesenchymal transformation mediating adhesion withStromal cells. Am. J. Pathol. 155 (3), 787–798.
Troyanovsky, S.M., 1999. Mechanism of cell-cell adhesion complex assembly. Curr. Opin. Cell Biol. 11 (5), 561–566.
Tsuboi, M., et al., 1999. Tumor necrosis factor-alpha and interleukin-1beta increase the Fas-mediated apoptosis of human osteoblasts. J. Lab. Clin. Med. 134 (3), 222–231.
Tsutsumimoto, T., et al., 1999. TNF-alpha and IL-1beta suppress N-cadherin expression in MC3T3-E1 cells. J. Bone Miner. Res. 14 (10), 1751–1760.
Tu, B., et al., 2016. Inhibition of connexin43 prevents trauma-induced heterotopic ossification. Sci. Rep. 6, 37184.
Turel, K.R., Rao, S.G., 1998. Expression of the cell adhesion molecule E-cadherin by the human bone marrow stromal cells and its probable role in CD34(+) stem cell adhesion. Cell Biol. Int. 22 (9–10), 641–648.
Valiunas, V., et al., 2005. Connexin-specific cell-to-cell transfer of short interfering RNA by gap junctions. J. Physiol. 568 (Pt 2), 459–468.
Vazquez, M., et al., 2014. A new method to investigate how mechanical loading of osteocytes controls osteoblasts. Front. Endocrinol. 5, 208.
Vendome, J., et al., 2011. Molecular design principles underlying beta-strand swapping in the adhesive dimerization of cadherins. Nat. Struct. Mol. Biol. 18 (6), 693–700.
Wagner, A.S., et al., 2017. Osteogenic differentiation capacity of human mesenchymal stromal cells in response to extracellular calcium with special regard to connexin43. Ann. Anat. 209, 18–24.
Wang, H., et al., 2015. The osteogenic niche promotes early-stage bone colonization of disseminated breast cancer cells. Cancer Cell 27 (2), 193–210.
Wang, Z., et al., 2016. Alternation in the gap-junctional intercellular communication capacity during the maturation of osteocytes in the embryonic chick calvaria. Bone 91, 20–29.
Watkins, M., et al., 2011. Osteoblast connexin43 modulates skeletal architecture by regulating both arms of bone remodeling. Mol. Biol. Cell 22 (8), 1240–1251.
Watkins, M.P., et al., 2012. Bisphosphonates improve trabecular bone mass and normalize cortical thickness in ovariectomized, osteoblast connexin43 deficient mice. Bone 51 (4), 787–794.
Watkins, M.G., Wang, S., Zhang, B., Civitelli, R., 2014. Connexin45 is involved in cancellous but not cortical bone homeostasis. J. Bone Miner. Res. 29 (Suppl. 1).
Weber, P.A., et al., 2004. The permeability of gap junction channels to probes of different size is dependent on connexin composition and permeant-pore affinities. Biophys. J. 87 (2), 958–973.
Wheelock, M.J., Johnson, K.R., 2003. Cadherin-mediated cellular signaling. Curr. Opin. Cell Biol. 15 (5), 509–514.
Wickline, E.D., et al., 2016. alphaT-catenin is a constitutive actin-binding alpha-catenin that directly couples the Cadherin.Catenin complex to actin filaments. J. Biol. Chem. 291 (30), 15687–15699.
Wildenberg, G.A., et al., 2006. p120-catenin and p190RhoGAP regulate cell-cell adhesion by coordinating antagonism between Rac and Rho. Cell 127 (5), 1027–1039.
Xiong, Q., et al., 2009. Quantitative trait loci, genes, and polymorphisms that regulate bone mineral density in mouse. Genomics 93 (5), 401–414.
Xu, H., et al., 2015. Connexin43 channels are essential for normal bone structure and osteocyte viability. J. Bone Miner. Res. 30 (3), 436–448.
Yamada, S., et al., 2005. Deconstructing the cadherin-catenin-actin complex. Cell 123 (5), 889–901.
Yamada, K.M., Geiger, B., 1997. Molecular interactions in cell adhesion complexes. Curr. Opin. Cell Biol. 9 (1), 76–85.
Yamada, Y., Ando, F., Shimokata, H., 2007. Association of candidate gene polymorphisms with bone mineral density in community-dwelling Japanese women and men. Int. J. Mol. Med. 19 (5), 791–801.
Yang, J., et al., 2008. HMGB1 is a bone-active cytokine. J. Cell. Physiol. 214 (3), 730–739.
Yang, H., et al., 2016a. Connexin43 affects osteogenic differentiation of the posterior longitudinal ligament cells via regulation of ERK activity by stabilizing Runx2 in ossification. Cell. Physiol. Biochem. 38 (1), 237–247.
Yang, H., et al., 2016b. N-cadherin restrains PTH repressive effects on sclerostin/SOST by regulating LRP6-PTH1R interaction. Ann. N. Y. Acad. Sci. 1385 (1), 41–52.
Yao, H., et al., 2014. Parathyroid hormone enhances hematopoietic expansion via upregulation of cadherin-11 in bone marrow mesenchymal stromal cells. Stem Cell. 32 (8), 2245–2255.
Yellowley, C.E., et al., 2000. Functional gap junctions between osteocytic and osteoblastic cells. J. Bone Miner. Res. 15 (2), 209–217.
York, S.L., Sethu, P., Saunders, M.M., 2016. Impact of gap junctional intercellular communication on MLO-Y4 sclerostin and soluble factor expression. Ann. Biomed. Eng. 44 (4), 1170–1180.
Zappitelli, T., et al., 2013. The G60S connexin43 mutation activates the osteoblast lineage and results in a resorption-stimulating bone matrix and abrogation of old-age-related bone loss. J. Bone Miner. Res. 28 (11), 2400–2413.
Zhang, Y., et al., 2011. Enhanced osteoclastic resorption and responsiveness to mechanical load in gap junction deficient bone. PLoS One 6 (8), e23516.
Zhou, Z., et al., 2008. HMGB1 regulates RANKL-induced osteoclastogenesis in a manner dependent on RAGE. J. Bone Miner. Res. 23 (7), 1084–1096.
Ziambaras, K., et al., 1998. Cyclic stretch enhances gap junctional communication between osteoblastic cells. J. Bone Miner. Res. 13 (2), 218–228.
Zong, L., et al., 2016. Gap junction mediated miRNA intercellular transfer and gene regulation: a novel mechanism for intercellular genetic communication. Sci. Rep. 6, 19884.

Chapter 19

Histomorphometric analysis of bone remodeling

Carolina A. Moreira[1] and David W. Dempster[2,3]

[1]Bone Unit of Endocrine Division of Federal University of Parana, Laboratory PRO, Section of Bone Histomorphometry, Pro Renal Foundation, Curitiba, Parana, Brazil; [2]Regional Bone Center, Helen Hayes Hospital, West Haverstraw, NY, United States; [3]Department of Pathology and Cell Biology, College of Physicians and Surgeons, Columbia University, New York, NY, United States

Chapter outline

Introduction

Bone histomorphometry is a gold standard technique for evaluation of bone remodeling. It has provided great information about the metabolic bone diseases, including the changes on bone structure and remodeling following treatment.

Tetracycline labeling and the surgical procedure

Prelabeling the patient with tetracycline prior to biopsy allows the histomorphometrist to quantify precisely the rate of bone formation at the time of the biopsy (Frost, 1983). About 3 weeks prior to the biopsy, the patient is given a 3-day course of tetracycline. This is followed by 12 drug-free days and then another 3-day course of tetracycline. This is termed a 3:12:3 sequence. The biopsy should not be performed until at least 5 days after the last tetracycline dose to prevent the last label from leaching out during the processing of the biopsy. This is often denoted as a 3:12:3:5 sequence. The tetracycline binds irreversibly to recently formed hydroxyapatite crystals at sites undergoing new deposition. When the histomorphometrist cuts and visualizes thin sections of the biopsy in a microscope equipped with ultraviolet illumination, the tetracycline fluoresces to label the sites of new bone formation (Fig. 19.1). The labels can be either double labels, if bone formation at that site is continuous throughout the labeling sequence, or single labels, if formation starts after the first or stops before the second label is administered. Demeclocycline, tetracycline, and oxytetracycline can all be used as fluorochrome labels. In

Principles of Bone Biology. https://doi.org/10.1016/B978-0-12-814841-9.00019-1

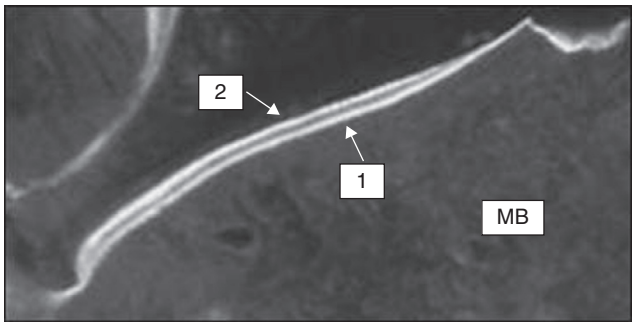

FIGURE 19.1 Double tetracycline label in an iliac crest bone biopsy. The patient was labeled with demeclocycline in a 3:12:3 sequence. *1*, label 1; *2*, label 2; *MB*, mineralized bone.

our laboratory, our preference is for demeclocycline, 600 mg/day (4 × 150-mg tablets), taken on an empty stomach. Dairy products and antacids containing aluminum, calcium, or magnesium should be avoided because they impair absorption. Tetracyclines can cause nausea, vomiting, and diarrhea in some patients, and all patients should be cautioned to avoid excessive exposure to sunlight and UV light because tetracyclines can cause skin phototoxicity. Tetracyclines should not be given to children less than 8 years of age or to pregnant women because, just as it is incorporated into bones, it is incorporated into growing teeth and discolors them.

Although the original site for bone biopsy was the rib, it is now performed exclusively at the anterior iliac crest, which is easily accessible, and the biopsy can be performed with minimal complications. This site also allows one to sample both cancellous and cortical bone in a single biopsy (Figs. 19.2 and 19.3). The structure and cellular activity at this site have been well characterized in a number of laboratories and have been shown to correlate with other clinically relevant skeletal sites, such as the spine and the hip (Bordier et al., 1964; Parfitt, 1983a; Rao, 1983; Dempster, 1988).

The biopsy generally is performed with a standard trephine with an internal diameter of at least 8 mm to obtain sufficient tissue and to minimize damage to the sample (Bordier et al., 1964; Rao, 1983). Immediately before the procedure, the patient should be sedated, usually with intravenous meperidine hydrochloride (Demerol) and diazepam (Valium). The skin, subcutaneous tissue, muscle, and, in particular, the periosteum covering both the lateral and the medial aspects of the

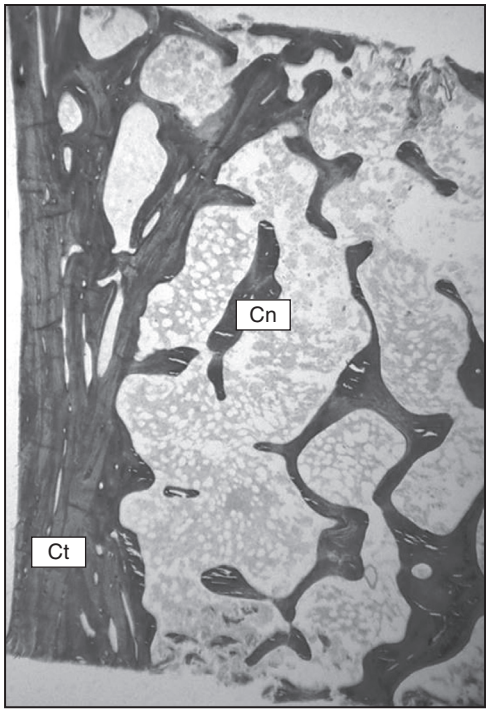

FIGURE 19.2 Low-power photomicrograph of an iliac crest bone biopsy section showing cancellous (*Cn*) and cortical (*Ct*) bone.

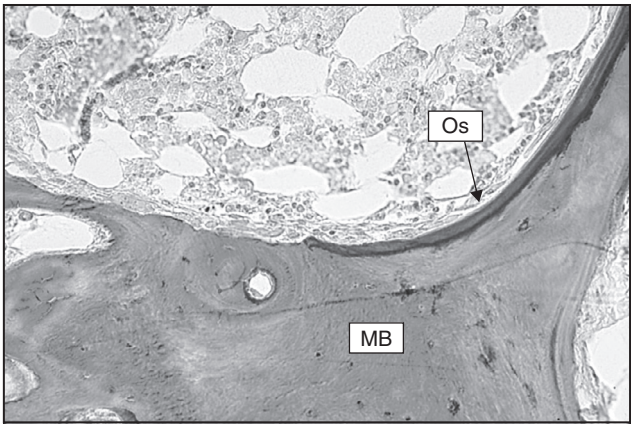

FIGURE 19.3 Photomicrograph of an iliac crest bone biopsy section showing an osteoid seam (*Os*) on the surface of mineralized bone (*MB*).

ilium, should be thoroughly anesthetized with local anesthetic. Access to the iliac crest is achieved through a 2- to 3-cm skin incision made at a point 2 cm posterior and 2 cm inferior to the anterior superior iliac spine. It is important to locate this site carefully because there is considerable variation in bone structure around this location. To avoid damage to the biopsy, which could render it uninterpretable, the trephine should be rotated back and forth with gentle but firm pressure so that it cuts rather than pushes through the ilium. The patient should refrain from excessive activity for 24 h after the procedure and a mild analgesic may be required. Significant complications from transiliac bone biopsy are rare. In an international multicenter study involving 9131 transiliac biopsies, complications were recorded in 64 patients (0.7%) (Rao, 1983). The most common complications were hematoma and pain at the biopsy site that persisted for more than 7 days; rarer complications included wound infection, fracture through the iliac crest, and osteomyelitis.

Sample preparation and analysis

The biopsy should be fixed in 70% ethanol because more aqueous fixatives may leach the tetracycline from the bone. After a fixation period of 4−7 days, the biopsy is dehydrated in ethanol, cleared in toluene, and embedded in methyl methacrylate without decalcification. The polymerized methyl methacrylate allows good-quality, thin (5−10 μm) sections to be cut on a heavy-duty microtome. The sections are then stained with a variety of dyes to allow good discrimination between mineralized and unmineralized bone matrix, which is termed "osteoid" (Figs. 19.4 and 19.5), and clear visualization of the cellular components of bone and marrow (see Fig. 19.7). Unstained sections are also mounted to allow observation of the tetracycline labels by fluorescence microscopy (see Fig. 19.1) (Baron et al., 1983a,b; Weinstein, 2002). The sections are subjected to morphometric analysis, according to standard stereological principles, using either simple "point-counting" techniques or computer-aided image analysis (Parfitt, 1983b; Malluche and Faugere, 1987; Compston, 1997).

Routine histomorphometric variables

A large number of histomorphometric variables can be measured or derived. Because the morphometric analysis is extremely time consuming, the number of variables evaluated depends on whether the biopsy specimen is being analyzed for diagnostic or research purposes. Listed next are eight indices of trabecular bone that are of particular clinical relevance. For a detailed account of more theoretical aspects of bone biopsy analysis, see Parfitt (1983a) and Frost (1983).

More recently, increased attention has been given to cortical bone, as it comprises 80% of the human skeleton and its failure contributes significantly to the nonvertebral fracture burden.

It is conventional to divide histomorphometric parameters into two categories. Static variables yield information on the amount of bone present and the proportion of bone surface engaged in the different phases of the remodeling cycle. Dynamic variables provide information on the rate of cell-mediated processes involved in remodeling. This category can be evaluated only in tetracycline-labeled biopsies. By measuring the extent of tetracycline-labeled surface and the distance between double tetracycline labels, the bone formation rate can be computed directly in a single biopsy. Conversely, the resorption rate can be calculated only indirectly, using certain indices of bone formation, in a single biopsy specimen or from two sequential biopsy specimens (Frost, 1983; Eriksen, 1986).

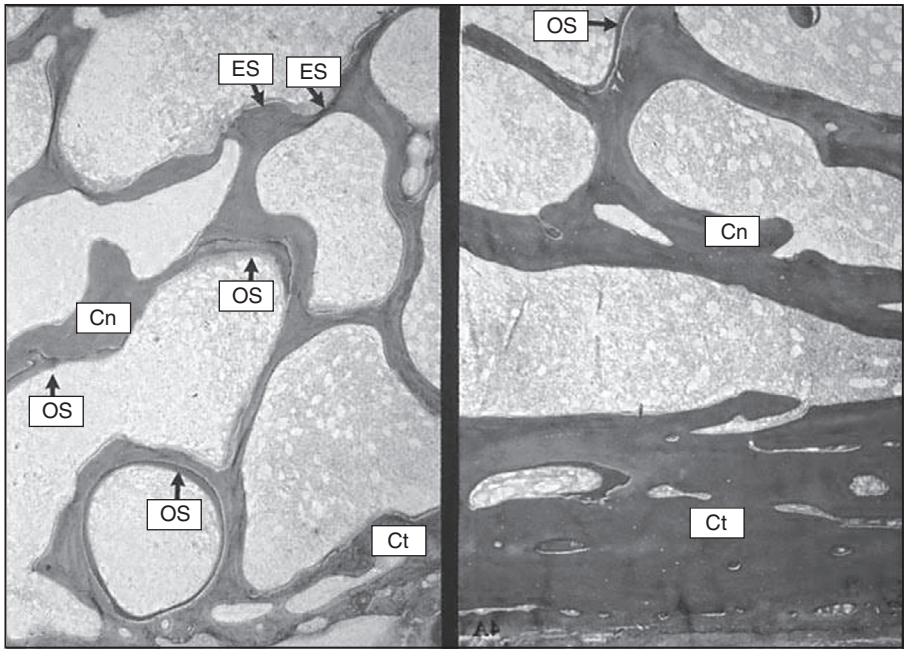

FIGURE 19.4 Photomicrographs of iliac bone biopsy sections from a subject with primary hyperparathyroidism (PHPT) (left), compared with a control subject (right). Note preservation of cancellous bone (*Cn*) and loss of cortical bone (*Ct*) in the subject with PHPT. Also note the marked extension of eroded surface (*ES*) and osteoid surface (*OS*) in PHPT.

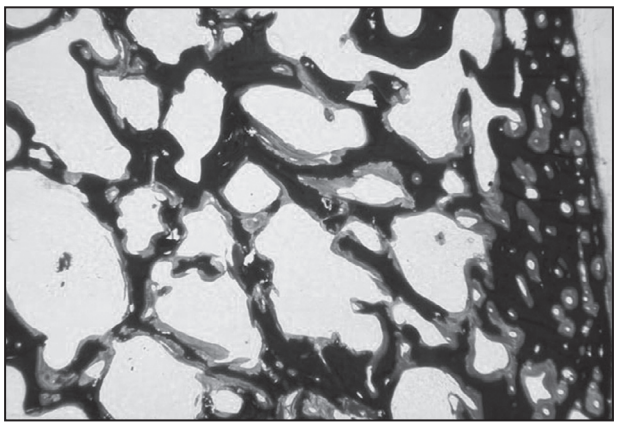

FIGURE 19.5 Photomicrograph of a bone biopsy section from a patient with severe osteomalacia. Note the dramatic extension of osteoid surface (stained *light gray*) and the increase in osteoid thickness.

Static parameters

A list of five commonly used static variables is given here. The terms and abbreviations for all histomorphometric variables have been standardized by the Histomorphometry Nomenclature Committee of the American Society for Bone and Mineral Research, whose recommendations have been widely adopted (Parfitt et al., 1987; Dempster et al., 2013).

Cancellous bone volume (Cn-BV/TV, %) is the fraction of a given volume of whole cancellous bone tissue (i.e., bone + bone marrow) that consists of mineralized and nonmineralized bone.
Osteoid volume (OV/BV, %) is the fraction of a given volume of bone tissue (mineralized bone + osteoid) that is osteoid (i.e., unmineralized matrix).
Osteoid surface (OS/BS, %) is the fraction of the entire trabecular surface that is covered by osteoid seams.

Osteoid thickness (O.Th, μm) is the average thickness of osteoid seams.
Eroded surface (ES/BS, %) is the fraction of the entire trabecular surface that is occupied by resorption bays (Howship lacunae), including both those with and those without osteoclasts.

The main cortical bone parameters are as follows.

Cortical area (Ct.Ar) is the total area of cortical bone, including inner and outer cortices.
Cortical width (Ct.Wi) is the average width of both inner and outer cortices. In growing individuals, however, in whom there are differences in bone cell activity at the internal and external cortices, they are recorded separately.
Cortical porosity number (Ct.Po.N) is the total number of pores of both inner and outer cortices.
Cortical porosity area (Ct.Po.Ar) is the total area of pores.

Dynamic parameters

Following is a list of commonly used dynamic parameters.

Mineral apposition rate (MAR, μm/day): this is calculated by dividing the average distance between the first and the second tetracycline label by the time interval (e.g., 15 days) separating them. It is a measure of linear rate of production of calcified bone matrix by the osteoblasts.
Mineralizing surface (MS/BS, %): this is the fraction of trabecular surface bearing double tetracycline label plus one-half of the singly labeled surface. It is a measure of the proportion of bone surface on which new mineralized bone was being deposited at the time of tetracycline labeling.
Bone formation rate (BFR/BS, $\mu m^3/\mu m^2$ per day): this is the volume of mineralized bone made per unit surface of trabecular bone per year. It is calculated by multiplying the mineralizing surface by the mineral apposition rate.
Many of these static and dynamic parameters described for the cancellous envelope can also be measured in the other three bone envelopes: endocortical, intracortical, and periosteal (Dempster et al., 2012, 2016b).

In the following section, we will briefly review the remodeling process in normal bone and the changes that occur in a number of common disease states, as assessed by bone histomorphometry (Table 19.1).

Normal bone

Bone undergoes a continuous process of renewal, with approximately 25% of trabecular bone and 3% of cortical bone being replaced annually. This remodeling process is referred to as a quantum phenomenon because it occurs in discrete units or "packets." Osteoclasts resorb the old bone and osteoblasts replace it. The group of cells that work cooperatively to create one new packet of bone is called a bone remodeling unit. In normal trabecular bone, approximately 900 bone remodeling units are initiated each day. In cortical bone, about 180 remodeling units are initiated per day (Frost, 1973; Parfitt, 1983a, 1988; Dempster, 2002).

Hyperparathyroidism

Increased circulating parathyroid hormone (PTH) levels increase the activation frequency of bone remodeling units, resulting in increased osteoclast and osteoblast numbers. As a result, histomorphometric analysis of a biopsy from a patient with either primary or secondary hyperparathyroidism reveals increases in eroded surface, osteoid surface, and mineralizing surface (see Fig. 19.4) (Melsen et al., 1983; Malluche and Faugere, 1987; Parisien et al., 1990; Silverberg et al., 1990). Mineralizing surface is increased, but mineral apposition rate is slightly reduced. However, the increased mineralizing surface overcompensates for the decrease in mineral apposition rate, so that the bone formation rate, the product of these two variables, is increased. Bone turnover is higher in hyperparathyroid patients with vitamin D insufficiency (Silverberg et al., 1990). Cancellous bone volume and trabecular connectivity are preserved in primary hyperparathyroidism (Parisien et al., 1992). The elevated bone turnover is often accompanied by increased deposition of immature (woven) bone and marrow fibrosis, in particular, in cases of severe secondary hyperparathyroidism. In cortical bone, there is an increase in cortical porosity and a decrease in cortical width (Fig. 19.4).

Because the biopsy reflects the long-term effects of excessive remodeling activity (e.g., increased eroded surface) it can be a sensitive indicator of parathyroid gland hyperactivity, especially when this is mild or intermittent. However, examination of the biopsy alone does not allow one to distinguish between primary and secondary hyperparathyroidism.

TABLE 19.1 Bone biopsy variables in a variety of disease states.[a]

Disease state	Cancellous bone volume	Osteoid volume	Osteoid surface	Osteoid thickness	Eroded surface	Mineral apposition rate	Mineralizing surface	Bone formation rate
Hyperparathyroidism[b]	N or ↑	↑	↑	N	↑	↓	↑	↑
Osteomalacia[c]	N	↑	↑	↑	↑	↓	↓	↓
Renal osteodystrophy/dialysis[d]	↓ or ↑	↓ or ↑	↓ or ↑	↓ or ↑	↑	↓ or ↑	↓ or ↑	↓ or ↑
Postmenopausal or senile osteoporosis[e]	↓ or N	N or ↑	N or ↑	N or ↓	N or ↑	N or ↓	N, ↑, or ↓	N, ↑, or ↓
Cushing syndrome and corticosteroid-induced osteoporosis[f]	↓ or N	N	↑	↓	↑	↓	↓	↓
Paget disease[g]	↑	↑	↑	↓	↑	↑	↑	↑
Thyrotoxicosis[h]	↓	↑	↑	↓	↑	↑	↑	↑
Hypothyroidism[h]	N	↓	N	↓	N	↓	↓	↓
Medullary thyroid carcinoma[h]	N	↑	↑	N	↑	↓	↑	N
Multiple myeloma[i]	N, ↑, or ↓	↑	↑	↓	↑	↓	↑	↑
Osteogenesis imperfect tarda[j]	↓	N	↑	↓	↑ or N	↓	N	↓

[a] N, *normal*; ↑, *increased*; ↓, *decreased*.
[b] *Melsen et al. (1983), Malluche and Faugere (1987), Parisien et al. (1990), 1992, Silverberg et al. (1990).*
[c] *Teitelbaum (1980), Jaworski (1983), Malluche and Faugere (1987), Siris et al. (1987).*
[d] *Malluche et al. (1976), Boyce et al. (1982), Hodsman et al. (1982), Charhon et al. (1985), Dunstan et al. (1985), Parisien et al. (1988), Salusky et al. (1988), Felsenfeld et al. (1991), Sherrard et al. (1993), Coburn and Salusky (2001), Slatopolsky and Delmez (2002).*
[e] *Meunier et al. (1981), Parfitt et al. (1982), Whyte et al. (1982), Civitelli et al. (1988), Meunier (1988), Garcia Carasco et al., 1989, Arlot et al. (1990), Eriksen et al. (1990), Kimmel et al. (1990), Steiniche et al. (1994), Dempster (2000).*
[f] *Bressot et al. (1979), Dempster (1989).*
[g] *Meunier et al. (1980).*
[h] *Melsen et al. (1983).*
[i] *Valentin-Opran et al. (1982).*
[j] *Baron et al. (1983), Ste-Marie et al. (1984).*

Osteomalacia

The hallmark of osteomalacia, regardless of the underlying pathogenetic mechanism, is inhibition of bone mineralization. Although mineralization is inhibited, the osteoblasts continue to synthesize and secrete organic matrix, leading to an accumulation of osteoid (see Fig. 19.5). Although the cancellous bone volume is normal in osteomalacia, the amount of mineralized bone is actually reduced.

Careful analysis of the dynamic parameters is called for in suspected cases of osteomalacia. At some formation sites, mineral is still deposited, but at a reduced rate, resulting in low values for mineral apposition rate. At other sites, mineralization may be completely inhibited, resulting in reduced mineralizing surface. The decrease in both these variables markedly reduces bone formation rate. The accumulation of osteoid is reflected in increased osteoid thickness, osteoid surface, and osteoid volume. If PTH secretion is elevated, the activation frequency of bone remodeling units is enhanced and the biopsy may show an increase in eroded surface. However, as osteoid surface increases, eroded surface often declines, because osteoid is resistant to osteoclastic resorption. An elevated activation frequency, when accompanied by mineralization failure, will enhance the rate at which osteoid is deposited (Teitelbaum, 1980; Jaworski, 1983; Malluche and Faugere, 1987; Siris et al., 1987).

Renal osteodystrophy

Chronic renal failure is usually accompanied by phosphate retention and hyperphosphatemia, which leads to a reciprocal decrease in serum ionized calcium concentration and secondary hyperparathyroidism. Furthermore, as functional renal mass decreases, the plasma 1,25-dihydroxyvitamin D level falls, leading to impaired intestinal calcium absorption, which exacerbates hypocalcemia and ultimately may impair bone mineralization. As a result of these marked disturbances in metabolism, it is perhaps not surprising that the bone biopsy findings in renal osteodystrophy are heterogeneous (Malluche et al., 1976, 2011; Boyce et al., 1982; Hodsman et al., 1982; Charhon et al., 1985; Dunstan et al., 1985; Parisien et al., 1988; Salusky et al., 1988; Moriniere et al., 1989; Felsenfeld et al., 1991; Hercz et al., 1993; Sherrard et al., 1993; Coburn and Salusky, 2001; Slatopolsky and Delmez, 2002). Indeed, in allowing a better understanding of the skeletal status in patients with chronic renal failure, the bone biopsy continues to play an important role in the management of this disease (Ketteler et al., 2017). Thus, renal osteodystrophy has been subdivided into two broad types, primarily on the basis of histomorphometric features. One type is characterized by normal or high bone turnover and a second is characterized by low bone turnover.

The most frequently observed biopsy changes in patients with end-stage renal disease are the result of chronic excess PTH secretion on the skeleton. These are classified as normal/high turnover, and include osteitis fibrosa, mild hyperparathyroidism, and mixed bone disease (Fig. 19.6). These features are characterized histomorphometrically by increased eroded surface, osteoid surface, and mineralizing surface. In osteitis fibrosa, however, woven osteoid is often present and there are variable amounts of peritrabecular marrow fibrosis in contrast to the minimal or absent fibrosis observed in mild

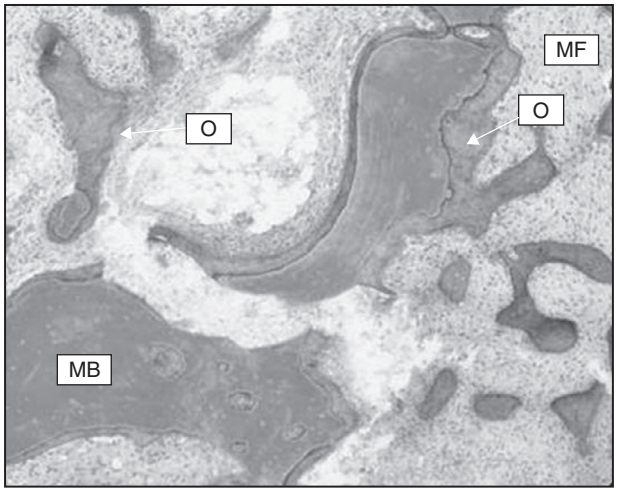

FIGURE 19.6 Photomicrograph of an iliac crest bone biopsy section from a patient with "mixed" renal osteodystrophy. Note deposition of woven osteoid (*O*) and marrow fibrosis (*MF*). *MB*, mineralized bone.

hyperparathyroidism. On the other end of the spectrum, low bone turnover is frequently observed in patients undergoing dialysis, albeit less often than high-turnover disease. The low-turnover states are classified as osteomalacia and aplastic or adynamic bone disease. Patients with osteomalacia have evidence of reduced values for dynamic variables accompanied by the accumulation of excess osteoid, whereas patients with aplastic or adynamic disease have a reduced tetracycline-based bone formation rate, but normal or reduced osteoid volume. In the 1970s and 1980s, most symptomatic patients with osteomalacia or adynamic bone disease showed evidence of aluminum accumulation, with more than 25% of surfaces displaying aluminum stain. They were considered to have aluminum-related bone disease (Boyce et al., 1982; Hodsman et al., 1982; Dunstan et al., 1985; Parisien et al., 1988). The aluminum was primarily derived from aluminum-containing phosphate binders used to control hyperphosphatemia and dialysis solutions that were contaminated with aluminum. Like tetracycline, aluminum accumulates at sites of new bone formation, where it may directly inhibit mineralization, which is manifested in an increase in osteoid thickness and osteoid surface. However, aluminum also is toxic to osteoblasts and may impair their ability both to synthesize and to mineralize bone matrix, resulting in a decrease in mineral apposition rate and the mineralizing surface. However, if matrix production is also reduced, osteoid thickness will not be elevated. With appreciation of the sources of aluminum contamination and increased use of calcium-containing phosphate binders, aluminum-related bone disease has become much less common in recent years.

Another form of low-turnover bone disease has been described that is not accompanied by significant aluminum accumulation. This is called idiopathic aplastic or adynamic bone disease. Its pathogenesis is unclear but may be related to various therapeutic maneuvers designed to prevent or reverse hyperparathyroidism in patients undergoing dialysis, including the use of dialysates with higher calcium concentrations (3.0−3.5 mEq/L), large doses of calcium-containing phosphate binders, and calcitriol therapy. As a rule, these patients have few symptoms of bone disease, and this "disease" ultimately may prove to be a histological rather than a clinically relevant form of bone disorder. However, it is unknown whether patients with adynamic bone disease are at increased risk of the development of skeletal problems in the future.

A 2011 large study by Malluche et al. (2011) provided histomorphometric data on 635 adult patients with chronic kidney disease stage 5 on dialysis. The authors employed the so-called TMV classification (turnover [T], mineralization [M], and volume [V]), which they had previously proposed (Malluche and Monier-Faugere, 2006). They reported that a mineralization defect was observed in only 3% of the subjects. This is probably due to the lower use of aluminum-containing phosphate binders nowadays, compared with the aforementioned earlier studies. The authors also noted distinct racial differences. For example, 62% of white subjects exhibited low turnover, whereas high turnover was observed in 68% of black subjects.

Osteoporosis

The classic feature of bone biopsies in osteoporosis is the reduction in cancellous bone volume. Approximately 80% of patients with vertebral crush fractures have values that are lower than normal. In postmenopausal osteoporosis the reduction in cancellous bone volume is primarily caused by the loss of entire trabeculae and, to a lesser degree, by the thinning of those that remain (Fig. 19.7) (Meunier et al., 1981; Parfitt et al., 1982; Whyte et al., 1982; Meunier, 1988; Dempster, 2000).

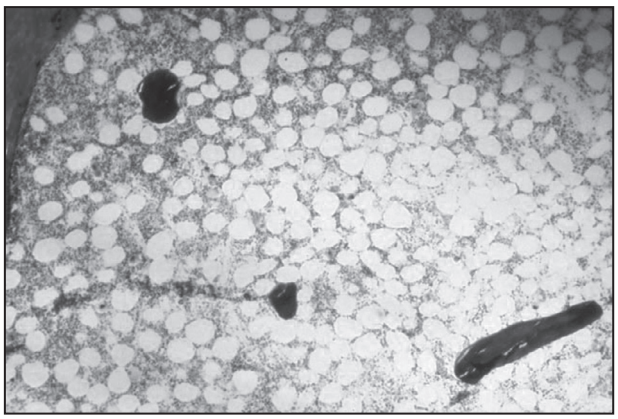

FIGURE 19.7 Photomicrograph of an iliac crest bone biopsy section from a patient with severe osteoporosis. Note marked reduction in cancellous bone volume in isolated trabecular profiles (*arrowheads*), which are cross sections of thin, rodlike structures in three dimensions.

With respect to the changes in the other static and dynamic variables in osteoporosis, there has been debate over whether patients can be stratified into high-, normal-, or low-turnover groups. Even if they can, the pathogenetic and clinical significance of this so-called histological heterogeneity in patients with osteoporosis is unclear. In a study of 50 postmenopausal women with untreated osteoporosis, two subsets of patients were identified: one with normal turnover and one with high turnover, with the high turnover representing 30% of the cases (Arlot et al., 1990). However, this conclusion was based on the finding of a bimodal distribution in the static parameter osteoid surface. The tetracycline-based bone formation rate, a dynamic measure of turnover rate, displayed a normal distribution. Based on the interval between the 10th percentile and the 90th percentile for calculated bone resorption rate in a group of normal postmenopausal women, another study classified 30% of women with untreated postmenopausal osteoporosis as having high turnover, whereas 64% and 6% had normal and low turnover, respectively (Eriksen et al., 1990). When bone formation rate was used as the discriminant variable, 19% were classified as having high turnover, 72% as having normal turnover, and 9% as having low turnover. On the other hand, in two studies of postmenopausal women with osteoporosis and their normal counterparts, the same wide variation in turnover indices was found in both groups, leading the investigators to conclude that there were no important subsets of patients with osteoporosis (Garcia Carasco et al., 1989; Kimmel et al., 1990). These studies, however, confirmed earlier observations that some patients with osteoporosis show profoundly depressed formation with little or no tetracycline uptake (Whyte et al., 1982).

From a clinical viewpoint, the desire to classify patients with osteoporosis according to their turnover status stems from the notion that the turnover rate may influence the response to particular therapeutic agents. For example, patients with high turnover rates may respond better to anticatabolic treatments. There was early evidence that this was the case for calcitonin (Civitelli et al., 1988). However, in clinical practice, the biopsy is an impractical way to determine turnover status. It was once believed that biochemical markers of bone resorption and formation would be useful in this regard, but this has yet to materialize.

Note that, in most cases, bone biopsy is performed when the disease is severe, with multiple fractures having already occurred. It is probable that, in many cases, the disturbances in bone metabolism that led to the reduction in bone mass and strength took place several years before the time of the biopsy and are no longer evident (Steiniche et al., 1994). Another confounding factor is that most patients who undergo biopsy for osteoporosis have already received treatment with one or more pharmaceutical agents.

Clinical indications for bone biopsy

In general, a bone biopsy is helpful only in metabolic bone diseases. Only rarely is a biopsy indicated in patients with localized skeletal disease such as Paget disease of bone, primary bone tumors, or bone metastases involving the iliac crest. The biopsy usually does not provide significantly greater insight into the disease process in postmenopausal women with osteoporosis. However, bone biopsy can be useful in patients who are less frequently affected by osteoporosis, such as young men and premenopausal women. Patients with osteopenia or women with postmenopausal osteoporosis should not have biopsies simply to measure cancellous bone volume to confirm the diagnosis of osteoporosis. The intraindividual and interindividual variability in cancellous bone volume is too great, and there is too much overlap between cancellous bone volume in patients with clinical osteoporosis and normal subjects to make this useful. However, bone biopsy is useful to exclude subclinical osteomalacia. In one study, 5% of patients with vertebral fractures displayed definitive evidence of osteomalacia on biopsy despite normal biochemical and radiological findings (Meunier, 1981). Moreover, the biopsy can be useful in identifying more precisely the probable cause of bone loss in individual patients with osteoporosis. For example, if the biopsy reveals or confirms a high bone turnover rate, it would be important to rule out endocrine disorders, such as hyperthyroidism and hyperparathyroidism. Finally, the biopsy is the best available way to evaluate the effect of various therapeutic maneuvers on bone cell function (e.g., Holland et al., 1994a,b; Marcus et al., 2000). This is discussed in detail in the context of therapies for osteoporosis in the following section.

As noted earlier, the bone biopsy can be extremely useful in patients with renal osteodystrophy (Ketteler et al., 2017), although the large number of patients with renal disease precludes its use in every case. In general, if a symptomatic patient has biochemical evidence of secondary hyperparathyroidism (hyperphosphatemia, hypocalcemia, and markedly elevated intact PTH levels), biopsy is not necessary because one can predict with reasonable certainty that it would reveal osteitis fibrosa. However, patients with renal disease who have bone pain and fractures without the biochemical profile of secondary hyperparathyroidism should undergo biopsy to determine whether they have osteomalacia or idiopathic, aplastic bone disease. Although aluminum accumulation is much less common nowadays, the biopsy will also permit the physician to determine whether it is a significant contributory factor. Although the biopsy can be useful in the clinical management of certain patients with bone disease, its principal use today is as a research tool.

Histomorphometric studies of the effects of osteoporosis drugs

In this section we will review what histomorphometry has revealed about the effects of drugs used to treat osteoporosis. The drugs will be covered under the headings of their two principal mechanisms of action: anticatabolic, also known as antiresorptive, and anabolic (Riggs and Parfitt, 2005).

Anticatabolic agents

Calcitonin

Intranasal calcitonin is approved to reduce the risk of vertebral fractures, but its efficacy in nonvertebral fractures has not been established (Silverman, 2003). There have been several histomorphometric studies of the effects of calcitonin in subjects with osteoporosis or with rheumatoid arthritis (Gruber et al., 1984, 2000; Marie and Caulin, 1986; Alexandre et al., 1988; Palmieri et al., 1989; Kroger et al., 1992; Pepene et al., 2004; Chesnut et al., 2005). In cancellous bone, calcitonin treatment reduced eroded surface (Kroger et al., 1982; Gruber et al., 1984) and active resorption surface (Alexandre et al., 1988) and mean resorption rate (Chesnut et al., 2005), with no observed decrease in osteoclasts (Marie and Caulin, 1986; Palmieri et al., 1989; Gruber et al., 2000). Most studies failed to reveal any differences in bone formation parameters, e.g., osteoblast number and perimeter, osteoid perimeter and thickness, mineralized perimeter, or mineral apposition rate (Gruber et al., 1984; Marie and Caulin, 1986; Alexandre et al., 1988; Chesnut et al., 2005). However, one report (Gruber et al., 2000) suggested that bone formation was not reduced to the same extent as resorption. Cancellous bone volume was shown to be unchanged (Alexandre et al., 1988; Gruber et al., 2000; Chesnut et al., 2005) or increased (Gruber et al., 1984; Alexandre et al., 1988; Palmieri et al., 1989; Marie and Caulin, 1986; Kroger et al., 1992).

Hormone therapy

Bone histomorphometry has been used by several investigators to assess the effects of hormone therapy (HT) on both cancellous and, in some studies, cortical bone of the ilium (Steiniche et al., 1989; Lufkin et al., 1992; Holland et al., 1994a,b; Eriksen et al., 1999; Vedi and Compston, 1996, Vedi et al., 2003). One of the most interesting studies was by Eriksen et al. (1999), who showed that 2 years of HT decreased resorption parameters, reducing bone formation at the basic multicellular unit level. Cancellous wall thickness was similar in treated and placebo groups, but there was a significant reduction in resorption rate in the HT group. This was in contrast to the placebo group, which showed a significant increase in erosion depth and a modest increase in resorption rate. The reduction in the size of the resorption cavity with HT was confirmed in a later study (Vedi and Compston, 1996), although that study also demonstrated a compensatory decrease in the wall width of trabecular bone packets. These findings were not replicated in a study (Steiniche et al., 1989) in which HT was given for only 1 year.

Estrogen treatment has been shown to stimulate bone formation in animal models (Chow et al., 1992a, 1992b; Edwards et al., 1992), but this remains controversial in humans (Steiniche et al., 1989; Lufkin et al., 1992; Holland et al., 1994a,b; Vedi and Compston, 1996; Wahab et al., 1997; Eriksen et al., 1999; Patel et al., 1999; Vedi et al., 1999, 2003). Standard doses of HT reduce osteoid and mineralizing surfaces and bone formation rate, with no change or a decrease in wall width (Steiniche et al., 1989; Lufkin et al., 1992; Holland et al., 1994a,b; Vedi and Compston, 1996; Eriksen et al., 1999; Patel et al., 1999; Vedi et al., 2003). On the other hand, long-term, high-dose HT was reported to increase cancellous wall width and to decrease eroded cavity area. Similarly, 6 years of subcutaneous HT increased cancellous bone volume with an increment in trabecular thickness and number as well as wall width (Khastgir et al., 2001a,b). Such anabolic actions of HT have also been reported in Turner syndrome treated with HT (Khastgir et al., 2003). The improvements in bone structure demonstrated by two-dimensional histomorphometric analysis are supported by micro-computed tomography findings of a higher ratio of plate- to rodlike structures (Jiang et al., 2005). In addition to these changes in histomorphometric variables, HT has also been shown to increase the degree of collagen cross-linking and bone mineralization, consistent with its primary action to lower bone turnover (Walters and Eyre, 1980; Holland et al., 1994a,b; Rey et al., 1995; Yamauchi, 1996; Khastgir et al., 2001a,b; Boivin and Meunier, 2002; Burr et al., 2003; Paschalis et al., 2003; Boivin et al., 2005).

Selective estrogen receptor modulators

Selective estrogen receptor modulators (SERMs) bind to the estrogen receptor and exhibit agonist actions in some tissues, such as bone, and antagonist actions in others, such as breast (Lindsay et al., 1997a,b). Bone histomorphometry studies are primarily limited to raloxifene. Two years of raloxifene treatment in the MORE trial (Ettinger et al., 1999) decreased the

bone formation rate, without changes in eroded surface or osteoclast number at the 60-mg dose, whereas the dose of 120 mg also decreased the bone formation rate and showed a trend toward a decrease in eroded surface and osteoclast number (Ott et al., 2000). Cancellous bone volume, trabecular thickness, and cortical width were unchanged compared with baseline and the placebo group (Ott et al., 2000). A significant decrease in activation frequency was observed with a higher dose (150 mg) of raloxifene (Weinstein et al., 2003). In that study, raloxifene was shown to have effects similar to those of HT. However, a 6-month treatment with 60 mg of raloxifene did not suppress activation frequency and bone formation rate to the same extent as HT (Prestwood et al., 2000). Reductions in activation frequency, bone formation rate, and resorption cavity area have also been demonstrated for another SERM, tamoxifen (Wright et al., 1994). In contrast to HT, raloxifene had little effect on mineralization density as assessed by quantitative microradiography of the biopsy sections (Boivin et al., 2003).

Bisphosphonates

The bisphosphonates have been the mainstay of osteoporosis therapy and will continue to be so for some time to come (Fleisch, 1998). The effects of alendronate, the first bisphosphonate to be approved in the United States, have been investigated in patients with postmenopausal osteoporosis (Bone et al., 1997; Chavassieux et al., 1997; Arlot et al., 2005), as well as in patients with glucocorticoid-induced osteoporosis (Chavassieux et al., 2000). Alendronate reduced osteoid surface and thickness, mineralizing surface, bone formation rate, and activation frequency. The mineral apposition rate was unchanged (Bone et al., 1997; Chavassieux et al., 1997; Arlot et al., 2005). Although the primary target of bisphosphonates is the osteoclast, alendronate, like other anticatabolic agents, had little, if any effect on histomorphometric variables of bone resorption, including eroded surface and volume, osteoclast number, and erosion depth. This is inconsistent with the marked reductions seen in biochemical markers of bone resorption. The discrepancy is most likely explained by the fact that histomorphometric indices of bone resorption are static parameters, in contrast to bone formation indices, which are dynamic. In one study (Chavassieux et al., 1997), wall thickness of trabecular bone packets was increased after 2 years of treatment, but this effect was not observed after 3 years. Histomorphometric studies failed to show an improvement in cancellous bone microarchitecture compared with placebo-treated subjects, but such an effect has been reported for three-dimensional structural parameters obtained by micro-computed tomography (Recker et al., 2005), with the assumption that alendronate prevented the loss of structural integrity experienced by the placebo-treated patients. Consistent with its primary action to reduce the activation frequency, alendronate increased the degree of mineralization of the matrix (Meunier and Boivin, 1997; Boivin et al., 2000; Hernandez et al., 2001; Roschger et al., 1997, 2001).

There have also been extensive studies of the effects of risedronate on the bone biopsy. Here, a paired biopsy design was employed, with biopsies being obtained before and after treatment in the same subjects (Eriksen et al., 2002; Dufresne et al., 2003; Borah et al., 2004, 2005, 2006; Seeman and Delmas, 2006; Zoehrer et al., 2006). Like alendronate, 3 years of risedronate treatment decreased mineralizing surface, bone formation rate, and activation frequency (Eriksen et al., 2002). Again, no significant change was noted in eroded surface and depth, but there was a significant decrease in resorption rate after risedronate treatment, with a significant increase in erosion depth in placebo-treated subjects. Also similar to alendronate's effects, risedronate preserved cancellous microarchitecture, as assessed by micro-computed tomography (Dufresne et al., 2003; Borah et al., 2004, 2005). No significant changes were seen in three-dimensional structural variables compared with baseline in risedronate-treated women, whereas trabecular microstructure deteriorated significantly in a subset of placebo-treated women who exhibited higher bone turnover at baseline (Borah et al., 2004). Furthermore, the degree of structural deterioration was positively correlated with the bone turnover, confirming that high turnover has a deleterious effect on bone structure. Similar results were reported for early postmenopausal women who were treated for just 1 year with risedronate (Dufresne et al., 2003). The reduction in bone turnover was associated with an increase in bone mineralization density, but there was no evidence of an abnormally high degree of mineralization, even when treatment was extended to 5 years (Borah et al., 2006; Durchschlag et al., 2006; Seeman and Delmas, 2006; Zoehrer et al., 2006).

There are a number of other studies on the effects of different bisphosphonates, such as zoledronate and ibandronate, on iliac bone (Recker et al., 2004, 2008). In general, the data obtained in patients with osteoporosis treated with these bisphosphonates are similar to those obtained with alendronate and risedronate (Recker et al., 2004, 2008). It should also be noted that there is evidence of dramatic improvements in bone structure and turnover in children with osteogenesis imperfecta treated with bisphosphonates (Munns et al., 2005).

Denosumab

Bone histomorphometry substudies in the FREEDOM trial have demonstrated the potent antiresorptive mechanism of action of denosumab. Denosumab is a human monoclonal antibody against receptor activator of NF-κB ligand, which

reversibly inhibits osteoclast-mediated bone resorption. Its effects on bone histomorphometry were published for the first time by Reid et al. (2010) after 24 and/or 36 months of treatment with denosumab in postmenopausal women with osteoporosis. The results demonstrated a significant reduction in eroded surface by more than 80%, whereas osteoclasts were absent from more than 50% of biopsies in the denosumab group. Double labeling in trabecular bone was observed in 19% of those treated with denosumab, while it was present in 94% of the placebo group. Bone-formation rate was reduced by 97% in the denosumab group (Reid, 2010). However, even with this important reduction at bone remodeling, the qualitative histologic evaluation of biopsies was unremarkable, showing normally mineralized lamellar bone. Furthermore, bone biopsies after denosumab treatment were compared with biopsies of subjects after treatment with alendronate in the STAND trial. In this study, dynamic indices of bone turnover tended to be lower in the denosumab group than in the alendronate group. The presence of double labeling in trabecular bone was seen in 20% of the denosumab biopsies and in 90% of the alendronate samples, suggesting that the antiresorptive action of denosumab is more potent than that of the bisphosphonate.

Data from the FREEDOM extension trial after 5 or 10 years of denosumab treatment demonstrated that long-term treatment with denosumab maintained normal bone histology and structure (Brown et al., 2014; Bone et al., 2018), Furthermore, denosumab continued to induce a low turnover state, consistent with its mechanism of action.

Osteoanabolic therapies

Bone histomorphometry has confirmed that the mechanism of action of anabolic agents is fundamentally different from that of anticatabolic drugs (Riggs and Parfitt, 2005). Rather than reducing the activation frequency of bone remodeling, anabolic agents elevate it with a positive bone balance. In each bone remodeling unit, more bone is formed than was resorbed. Bone formation is increased prior to the increase in bone resorption. Consequently, anabolic agents are able to improve, rather than simply preserve, cancellous and cortical bone microarchitecture.

PTH(1−34) and PTH(1−84)

The first bone biopsy studies of the effects of PTH(1−34) (teriparatide) were conducted in postmenopausal women with osteoporosis who were treated concurrently with PTH(1−34) and HT for 6 or 12 months (Reeve et al., 1980, 1991; Bradbeer et al., 1992). Hodsman et al. (1993, 2000) also used bone biopsy to study the effects of a cyclical regimen of 28 days of PTH(1−34) every 3 months, with or without sequential calcitonin, for 2 years. Dempster et al. (2001) and Misof et al. (2003) performed paired biopsies in men with osteoporosis treated with PTH(1−34) for 18 months, as well as in postmenopausal women treated with a combination of PTH(1−34) and HT for 3 years. Biopsy studies of the effects of monotherapy with PTH(1−34) were completed as part of a multinational fracture trial (Neer et al., 2001; Jiang et al., 2003; Dobnig et al., 2005; Paschalis et al., 2005; Ma et al., 2006). Arlot et al. (2005) compared the effects of PTH(1−34) with those of alendronate in postmenopausal women with osteoporosis. The effects of the two agents on activation frequency and bone formation rate were diametrically opposed. Compared with appropriate reference ranges (Arlot et al., 1990; Chavassieux et al., 1997), the bone formation rate was 10% of normal in the alendronate-treated group and 150% higher than normal in the PTH(1−34)-treated group. The higher activation frequency in the PTH(1−34) group led to an increase in cortical porosity, which may explain observations of transient reductions in bone mineral density following treatment with PTH(1−34) (Neer et al., 2001; Finkelstein et al., 2003; Ettinger et al., 2004). A novel labeling regimen, quadruple tetracycline, has been perform in a longitudinal study in order to evaluate of the early effects of teriparatide treatment on bone formation. Within 4 weeks of treatment, PTH(1−34) increased mineralized perimeter, mineral apposition rate, and bone formation rate (Hodsman et al., 1993, 2000; Lindsay et al., 2006). The study of Lindsay et al. (2006) suggested that PTH(1−34) stimulates osteoblastic activity in preexisting remodeling units. This could be accomplished by a variety of mechanisms, including an increase in the work rate of preexisting osteoblasts, enhanced recruitment of new osteoblasts, or a prolongation of osteoblast life span (Jilka et al., 1999). Regardless of the mechanism, one noteworthy feature of PTH(1−34) is its ability to extend formation to quiescent surfaces surrounding the original remodeling unit (Fig. 19.8) (Lindsay et al., 2006). Bone-remodeling indices were increased after 1 month (Holland et al., 1994b), 2 months (Chow et al., 1992b), and 6 months (Reeve et al., 1980; Arlot et al., 2005) of treatment, and they returned toward baseline between 12 (Reeve et al., 1991) and 36 months of continuous treatment (Hodsman et al., 2000; Dempster et al., 2001). This temporal sequence of remodeling activation and deactivation, derived from biopsy studies, is confirmed by parallel changes in bone markers (Lindsay et al., 1997a,b; Kurland et al., 2000; Cosman et al., 2001; Arlot et al., 2005; McClung et al., 2005).

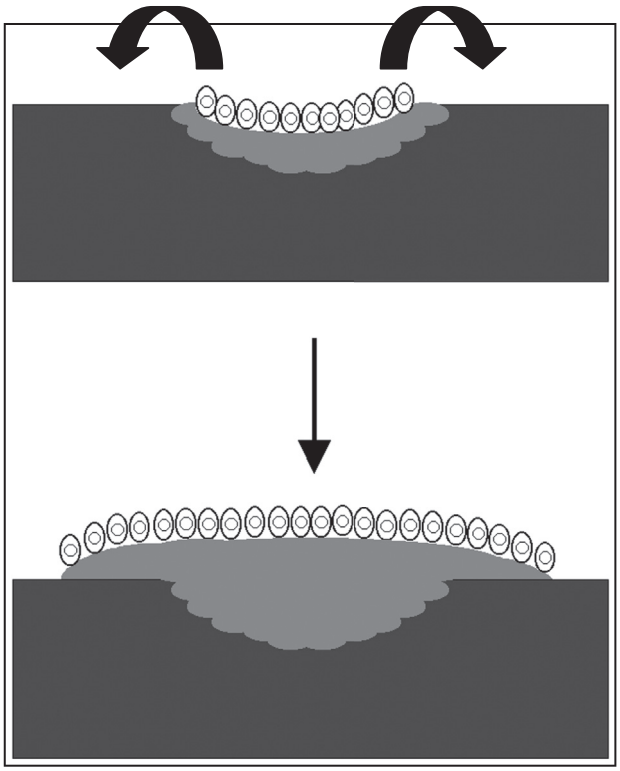

FIGURE 19.8 Proposed mechanism whereby PTH(1−34) could extend bone formation beyond the limits of the remodeling unit to annex the surrounding bone surface. *Reproduced with permission from Lindsay, R., Cosman, F., Zhou, H., Bostrom, M.P., Shen, V.W., Cruz, J.D., Nieves, J.W., Dempster, D.W., 2006. A novel tetracycline labeling schedule for longitudinal evaluation of the short-term effects of anabolic therapy with a single iliac crest bone biopsy: early actions of teriparatide. J. Bone Miner. Res. 21 (3), 366−373.*

The striking stimulation of bone formation by PTH(1−34) provides a mechanism for the reported increases in wall thickness of bone packets on cancellous and endocortical surfaces (Bradbeer et al., 1992; Hodsman et al., 2000; Dempster et al., 2001; Ma et al., 2006), which in turn leads to improvements in cancellous bone mass, trabecular connectivity, and cortical thickness (Dempster et al., 2001; Jiang et al., 2003) (Figs. 19.9 and 19.10). These improvements in cancellous bone structure were correlated with the early increases in bone formation markers (Dobnig et al., 2005). The deposition of new bone brought about an increase in the proportion of bone matrix with lower mineralization, mineral crystallinity, and collagen cross-link ratio (Misof et al., 2003; Paschalis et al., 2005).

The first study of the effects of PTH(1−34) raised the specter that the improvement in cancellous bone mass and structure may have been gained at the expense of cortical bone (Reeve et al., 1980). This was not confirmed in animal models in which cortical thickness and diameter were improved by PTH(1−34) treatment (Hirano et al., 1999, 2000; Jerome et al., 1999; Burr et al., 2001; Mashiba et al., 2001). Histomorphometric and micro-computed tomographic studies in humans revealed an increase in cortical thickness at the iliac crest, which was accompanied by stimulation of bone formation on the endosteal surface (see Figs. 19.9 and 19.10) (Dempster et al., 2001; Jiang et al., 2003; Lindsay et al., 2006). However, whether PTH(1−34) is able to stimulate periosteal bone formation in humans as it does in animals is not yet clear. Noninvasive techniques have yielded conflicting data on the effects of PTH(1−34) on bone diameter in humans (Zanchetta et al., 2003; Uusi-Rasi et al., 2005). However, biopsy studies suggest that PTH(1−34) can enhance periosteal bone formation (Ma et al., 2006; Lindsay et al., 2007). Although there are few data as of this writing, the effects of PTH(1−84) on the human ilium appear to be broadly similar to those of PTH(1−34) (Fox et al., 2005).

Abaloparatide

Abaloparatide (ABL) is a peptide designed with amino acid sequence identical to that of PTH-related peptide in the first 20 amino acids, with strategic insertions of different amino acids between residues 22 and 34 (Hattersley et al., 2016). The resulting peptide is a selective activator of the PTH type 1 receptor signaling pathway with the ability to produce anabolic

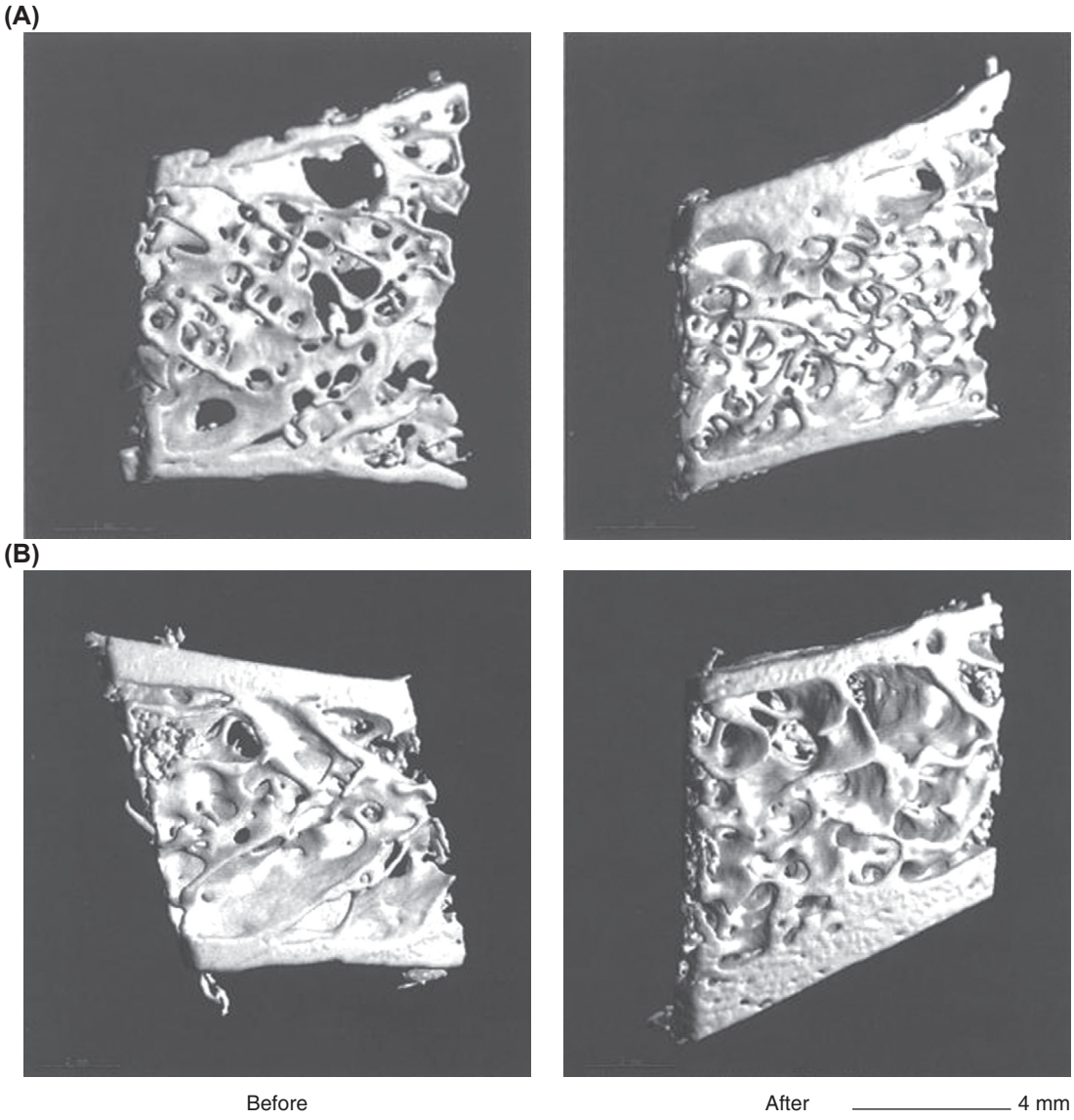

FIGURE 19.9 Micro-computed tomographic images of paired biopsies before (left) and after (right) treatment with PTH(1−34) in a 64-year-old woman (A) and a 47-year-old man (B). Note improvement in cancellous and cortical bone structure after treatment. *Reproduced with permission from Dempster, D.W., Cosman, F., Kurland, E.S., Zhou, H., Nieves, J., Woelfert, L., Shane, E., Plavetic, K., Muller, R., Bilezikian, J., Lindsay, R., 2001. Effects of daily treatment with parathyroid hormone on bone microarchitecture and turnover in patients with osteoporosis: a paired biopsy study. J. Bone Miner. Res. 16 (10), 1846−1853.*

effects with modest stimulation of bone resorption compared with PTH(1−34). In fact, ABL binds to the PTH type 1 receptor with different affinity for the R0 confirmation in comparison to PTH(1−34), resulting in less stimulation of bone resorption and formation. The Abaloparatide-SC Comparator Trial in Vertebral Endpoints (ACTIVE) was a comparative phase III, randomized, double-blind, placebo-controlled, multicenter, international study (Miller et al., 2016). Postmenopausal women were randomized to receive, blinded, daily subcutaneous injections of placebo or ABL 80 μg or open-label teriparatide 20 μg for 18 months.

Iliac bone biopsies were obtained in a subset of patients treated with placebo (n = 35), ABL(n = 36), or teriparatide (n = 34) for between 12 and 18 months.

Histological analysis revealed normal lamellar bone with normal microstructure and bone cell morphology in all three treatment groups (Moreira et al., 2016). There was no evidence of mineralization abnormality, excess woven bone or osteoid, marrow fibrosis, or marrow abnormalities. Histomorphometric analysis was performed on 78 (74.3%) of the 105 specimens. The remaining specimens were not evaluable due to significant damage or fragmentation that occurred in the

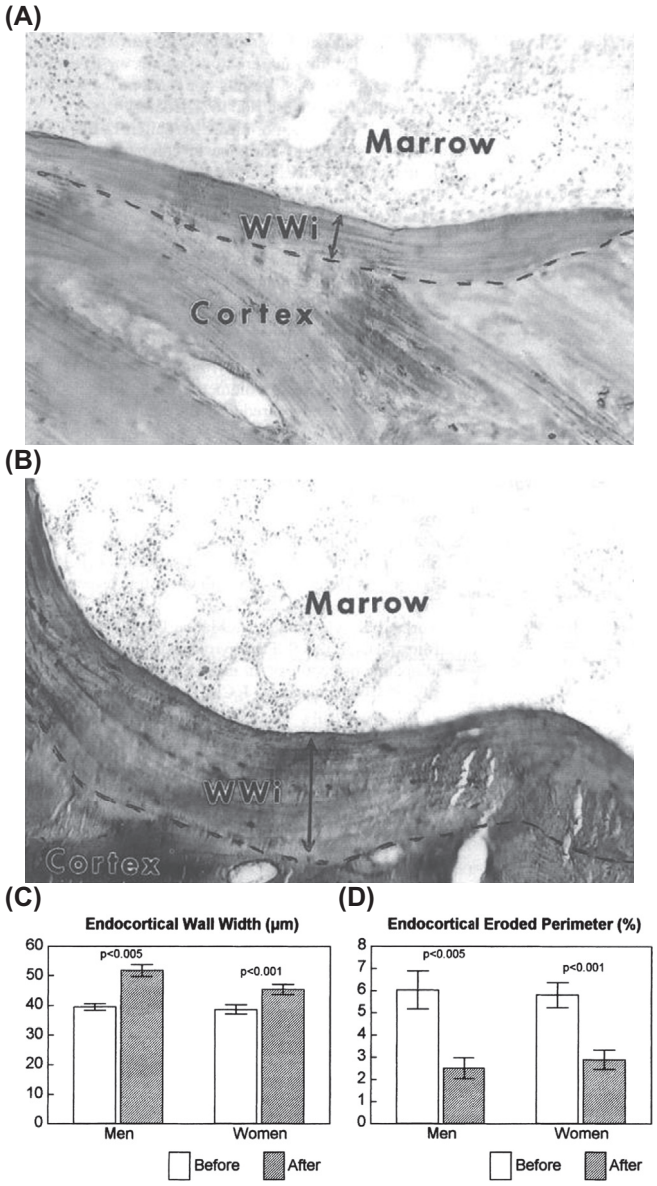

FIGURE 19.10 Bone packets on the endocortical surface of a 52-year-old man before (A) and after (B) 18 months of treatment with PTH(1−34). Note that after treatment the packet is almost twice as wide as the one before treatment. (C and D) Endocortical wall width and eroded perimeter before and after treatment of men and women with teriparatide. Note the increase in wall width and reduction in eroded perimeter after treatment. *WWi*, wall width. *Reproduced with permission from Dempster, D.W., Cosman, F., Kurland, E.S., Zhou, H., Nieves, J., Woelfert, L., Shane, E., Plavetic, K., Muller, R., Bilezikian, J., Lindsay, R., 2001. Effects of daily treatment with parathyroid hormone on bone microarchitecture and turnover in patients with osteoporosis: a paired biopsy study. J. Bone Miner. Res. 16 (10), 1846−1853.*

process of obtaining the biopsy. All specimens displayed tetracycline labels; however, double labels were not observed in three, five, and four specimens in the placebo, ABL, and teriparatide groups, respectively. There were only a few significant differences among the three groups. MAR was significantly higher in the teriparatide-treated group than in the placebo-treated group. The eroded surface was lower in the ABL-treated group than in the placebo group, suggesting a lower resorption rate. This was consistent with the biochemical marker data wherein the increase in carboxy-terminal collagen crosslinks (s-CTX) was less pronounced with ABL than with teriparatide, as well as with the lower incidence of hypercalcemia with ABL compared with teriparatide. Cortical porosity was significantly higher in both treated groups compared to placebo.

Surprisingly, activation frequency and bone formation rate were not different among the three groups, despite the fact that bone mineral density increased in the two treated groups relative to baseline and placebo in the bone biopsy cohort.

One explanation for this result was the timing of the bone biopsies that were obtained after at least 12 months of treatment. Previous histomorphometric studies with similar duration of teriparatide treatment have also not shown increases in bone turnover parameters. In fact, the largest increases in cancellous bone formation rate with teriparatide treatment have been seen with biopsies taken earlier in the course of treatment (Arlot et al., 2005; Lindsay et al., 2006). Furthermore, skeletal sites that exhibit a robust response to anabolic agents, namely the endocortical, intracortical, and periosteal envelopes (Lindsay et al., 2006; Dempster et al., 2012, 2016a), were not analyzed in this study.

Romosozumab

Romosozumab is a sclerostin antibody that has an anabolic effect (Chavassieux et al., 2017). The phase III FRAME study enrolled 7180 postmenopausal women at high risk of fracture and compared the effects of romosozumab with placebo at 12 months and after transition to denosumab at 24 months (Cosman et al., 2017). Vertebral fractures were significantly reduced in the romosozumab compared with the placebo arm at 12 months. At this writing, bone histomorphometry data following romosozumab treatment have not yet been published; however, some results have been presented (Chavassieux et al., 2017). In quadruple-labeled biopsies taken at 2 months, the bone formation rate was dramatically increased compared with pretreatment levels. However, in biopsies taken at 12 months with conventional double labeling, bone formation rate was reduced compared with placebo treatment. If the quadruple-labeling protocol had not been employed, it would have been difficult to explain the large increments in bone mineral density, cancellous bone volume, trabecular connectivity, and cortical thickness achieved by romosozumab treatment.

Comparative studies of anabolic and anticatabolic drugs

SHOTZ

The Skeletal Histomorphometry in Patients on Teriparatide or Zoledronic Acid Therapy study (SHOTZ) assessed the progressive effects of 2 years of treatment with teriparatide 20 μg/day and zoledronic acid 5 mg/year on bone remodeling in the cancellous, endocortical, intracortical, and periosteal envelopes in postmenopausal women with osteoporosis (Dempster et al., 2012, 2016b). Bone biopsies from both groups were performed at 6 and 24 months. A marked difference in the mechanism of action of these two drugs was observed, whereby teriparatide demonstrated higher bone formation indices than zoledronic acid in all four bone envelopes at both early and later time points. In the intracortical envelope, higher cortical porosity rate was observed with teriparatide compared with zoledronic acid, which is attributed to a higher intracortical remodeling rate with the pro-remodeling anabolic agent. However, the 24-month biopsies showed that haversian systems that were open at 6 months were completely filled with new bone at 24 months. In addition, the increase at BFR/BS with teriparatide seen on periosteal and, to a greater extent, on endocortical envelopes at 24 months provides a mechanistic basis for the reported increase in cortical thickness with this drug (Dempster et al., 2001; Jiang et al., 2003).

This study was able to show longitudinal changes within treatment groups with paired biopsies. In the teriparatide group, for example, dynamic indices declined from month 6 to month 24 only in the endocortical envelope. However, the median values for MS/BS and BFR/BS in the endocortical and intracortical envelopes were greater or similar to the values observed in the cancellous envelopes at both time points. Indeed, these results suggest that the anabolic effect of teriparatide is highest in the endocortical and intracortical envelopes and that the anabolic actions continue through 24 months of therapy.

In contrast to the teriparatide group, the low bone formation rate seen at month 6 in the zoledronic acid group persisted through 24 months. In fact, no difference in bone histomorphometry parameters were seen within individual bone envelopes in the zoledronic acid group over time. The only exception was noted in the intracortical envelope, where the median values for MS/BS and BFR/BS were higher compared with the cancellous envelope. This finding suggests that zoledronic acid may have limited access to the intracortical envelope, unlike teriparatide and denosumab as described earlier.

More recently, the SHOTZ study confirmed earlier studies (Lindsay et al., 2006; Ma et al., 2006) showing that teriparatide increases modeling-based formation as well as remodeling-based formation (Dempster et al., 2018). This effect was most prominent during the early course of treatment. In contrast, very little modeling-based formation was seen with zoledronic acid treatment.

AVA study: differential effects of teriparatide and denosumab on intact parathyroid hormone and bone formation indices

This open-label study was designed to evaluate whether denosumab-induced increases in endogenous PTH are able to exert some anabolic effect at the tissue level and on bone-turnover markers. The study included 69 postmenopausal women with osteoporosis and employed quadruple tetracycline labeling to enable longitudinal assessment of bone formation parameters in a single biopsy sample, which was taken at 3 months (Dempster, 2016a). Patients were randomized to teriparatide 20 μg daily for 6 months or denosumab 60 mg in a single infusion. Histomorphometric indices in all four envelopes were analyzed, as well as bone-turnover markers and endogenous intact PTH at baseline and 1, 3, and 6 months.

The results demonstrated that, while denosumab treatment resulted in a significant and prolonged increase in endogenous PTH levels, bone formation indices were decreased. By contrast, teriparatide decreased endogenous PTH but stimulated bone formation indices. These effects were reflected in the changes in bone-turnover markers, which increased with teriparatide and decreased with denosumab treatment. As in the SHOTZ study, stimulation of modeling-based formation accounted for a significant proportion of the total amount of new bone formation induced by teriparatide treatment (Dempster et al., 2017a). On the other hand, the small amount of modeling-based formation seen at baseline in the denosumab group was not affected by treatment, with the exception of a small but significant increase in the cancellous envelope.

Conclusion

Iliac crest bone biopsy and histomorphometry remains a powerful research tool, providing unique information on bone structure and remodeling activity at the tissue level. It is still the single most useful tool for understanding the mechanism of action (MOA) of bone active agents. Although it is rarely used as a diagnostic tool nowadays, a key exception is in the evaluation of renal osteodystrophy.

References

Alexandre, C., Chappard, D., Caulin, F., Bertrand, A., Palle, S., Riffat, G., 1988. Effects of a one-year administration of phosphate and intermittent calcitonin on bone-forming and bone-resorbing cells in involutional osteoporosis: a histomorphometric study. Calcif. Tissue Int. 42 (6), 345–350.

Arlot, M.E., Delmas, P.D., Chappard, D., Meunier, P.J., 1990. Trabecular and endocortical bone remodeling in postmenopausal osteoporosis: comparison with normal postmenopausal women. Osteoporos. Int. 1, 41.

Arlot, M., Meunier, P.J., Boivin, G., Haddock, L., Tamayo, J., Correa-Rotter, R., Jasqui, S., Donley, D.W., Dalsky, G.P., Martin, J.S., Eriksen, E.F., 2005. Differential effects of teriparatide and alendronate on bone remodeling in postmenopausal women assessed by histomorphometric parameters. J. Bone Miner. Res. 20 (7), 1244–1253.

Baron, R., Gertner, J.M., Lang, R., Vignery, A., 1983a. Increased bone turnover with decreased bone formation by osteoblasts in children with osteogenesis imperfect tarda. Pediatr. Res. 17, 204.

Baron, R., Vignery, A., Neff, L., et al., 1983b. Processing of undecalcified bone specimens for bone histomorphometry. In: Recker, R.R. (Ed.), Bone Histomorphometry: Techniques and Interpretation. CRC Press, Boca Raton, FL, p. 13.

Boivin, G., Meunier, P.J., 2002. The degree of mineralization of bone tissue measured by computerized quantitative contact microradiography. Calcif. Tissue Int. 70, 503–511.

Boivin, G.Y., Chavassieux, P.M., Santora, A.C., Yates, J., Meunier, P.J., 2000. Alendronate increases bone strength by increasing the mean degree of mineralization of bone tissue in osteoporotic women. Bone 27 (5), 687–694.

Boivin, G., Lips, P., Ott, S.M., Harper, K.D., Sarkar, S., Pinette, K.V., Meunier, P.J., 2003. Contribution of raloxifene and calcium and vitamin D3 supplementation to the increase of the degree of mineralization of bone in postmenopausal women. J. Clin. Endocrinol. Metab. 88 (9), 4199–4205.

Boivin, G., Vedi, S., Purdie, D.W., Compston, J.E., Meunier, P.J., 2005. Influence of estrogen therapy at conventional and high doses on the degree of mineralization of iliac bone tissue: a quantitative microradiographic analysis in postmenopausal women. Bone 36 (3), 562–567.

Bone, H.G., Downs Jr., R.W., Tucci, J.R., Harris, S.T., Weinstein, R.S., Licata, A.A., McClung, M.R., Kimmel, D.B., Gertz, B.J., Hale, E., Polvino, W.J., 1997. Dose-response relationships for alendronate treatment in osteoporotic elderly women. Alendronate Elderly Osteoporosis Study Centers. J. Clin. Endocrinol. Metab. 82 (1), 265–274.

Bone, H.G., Wagman, R.B., Brandi, M.L., Brown, J.P., Chapurlat, R., Cummings, S.R., Czerwiński, E., Fahrleitner-Pammer, A., Kendler, D.L., Lippuner, K., Reginster, J.Y., Roux, C., Malouf, J., Bradley, M.N., Daizadeh, N.S., Wang, A., Dakin, P., Pannacciulli, N., Dempster, D.W., Papapoulos, S., July 2017. 10 Years of denosumab treatment in postmenopausal women with osteoporosis:results from the phase 3 randomised FREEDOM trial and open-label extension. Lancet Diabetes Endocrinol. 5 (7), 513–523.

Borah, B., Dufresne, T.E., Chmielewski, P.A., Johnson, T.D., Chines, A., Manhart, M.D., 2004. Risedronate preserves bone architecture in postmenopausal women with osteoporosis as measured by three-dimensional microcomputed tomography. Bone 34 (4), 736–746.

Borah, B., Ritman, E.L., Dufresne, T.E., Jorgensen, S.M., Liu, S., Sacha, J., Phipps, R.J., Turner, R.T., 2005. The effect of risedronate on bone mineralization as measured by micro-computed tomography with synchrotron radiation: correlation to histomorphometric indices of turnover. Bone 37 (1), 1–9.

Borah, B., Dufresne, T.E., Ritman, E.L., Jorgensen, S.M., Liu, S., Chmielewski, P.A., Phipps, R.J., Zhou, X., Sibonga, J.D., Turner, R.T., 2006. Long-term risedronate treatment normalizes mineralization and continues to preserve trabecular architecture: sequential triple biopsy studies with micro-computed tomography. Bone 39, 345–352.

Bordier, P., Matrajt, H., Miravet, B., Hioco, D., 1964. Mesure histologique de la masse et de la résorption des través osseuse. Pathol. Biol. 12, 1238.

Boyce, B.F., Fell, G.S., Elder, H.Y., et al., 1982. Hypercalcemic osteomalacia due to aluminum toxicity. Lancet 2, 1009.

Bradbeer, J.N., Arlot, M.E., Meunier, P.J., Reeve, J., 1992. Treatment of osteoporosis with parathyroid peptide (hPTH 1–34) and oestrogen: increase in volumetric density of iliac cancellous bone may depend on reduced trabecular spacing as well as increased thickness of packets of newly formed bone. Clin. Endocrinol. 37 (3), 282–289.

Bressot, C., Meunier, P.J., Chapuy, M.C., et al., 1979. Histomorphometric profile, pathophysiology and reversibility of corticosteroid-induced osteoporosis. Metab. Bone Dis. Relat. Res. 1, 1303.

Brown [1], J.P., Reid, I.R., Wagman, R.B., Kendler, D., Miller, P.D., Jensen, J.E., Bolognese, M.A., Daizadeh, N., Valter, I., Zerbini, C.A., September 2014. Dempster DW Effects of up to 5 years of denosumab treatment on bone histology and histomorphometry: the FREEDOM study extension. J. Bone Miner. Res. 29 (9), 2051–2056.

Burr, D., Hirano, T., Turner, C., Hotchkiss, C., Brommage, R., Hock, J., 2001. Intermittently administered human parathyroid hormone (1–34) treatment increases intracortical bone turnover and porosity without reducing bone strength in the humerus of ovariectomized cynomolgus monkeys. J. Bone Miner. Res. 16, 157–165.

Burr, D.B., Miller, L., Grynpas, M., Li, J., Boyde, A., Mashia, T., Hirano, T., Johnston, C.C., 2003. Tissue mineralization is increased following 1-year treatment with high doses of bisphosphonates in dogs. Bone 33 (6), 960–969.

Charhon, S.A., Berland, Y.F., Olmer, M.J., et al., 1985. Effects of parathyroidectomy on bone formation and mineralization in hemodialized patients. Kidney Int. 27, 426.

Chavassieux, P.M., Arlot, M.E., Reda, C., Wei, L., Yates, A.J., Meunier, P.J., 1997. Histomorphometric assessment of the long-term effects of alendronate on bone quality and remodeling in patients with osteoporosis. J. Clin. Invest. 100 (6), 1475–1480.

Chavassieux, P.M., Arlot, M.E., Roux, J.P., Portero, N., Daifotis, A., Yates, A.J., Hamdy, N.A., Malice, M.P., Freedholm, D., Meunier, P.J., 2000. Effects of alendronate on bone quality and remodeling in glucocorticoid-induced osteoporosis: a histomorphometric analysis of transiliac biopsies. J. Bone Miner. Res. 15 (4), 754–762.

Chavassieux, P., Chapurlat, R., Portero-Muzy, N., Brown, J.P., Horlait, S., Libinati, C., Boyce, R., Wang, A., Grauer, A., September 2017. Effects of romozosumab in postmenopausal women with osteoporosis after 2 and 12 months: Bone histomorphometry substudy. In: ASBMR abstract no. 1072, ASBMR Meeting, Denver, CO.

Chesnut III, C.H., Majumdar, S., Newitt, D.C., Shields, A., Van Pelt, J., Laschansky, E., Azria, M., Kriegman, A., Olson, M., Eriksen, E.F., Mindeholm, L., 2005. Effects of salmon calcitonin on trabecular microarchitecture as determined by magnetic resonance imaging: results from the QUEST study. J. Bone Miner. Res. 20 (9), 1548–1561.

Chow, J., Tobias, J.H., Colston, K.W., Chambers, T.J., 1992a. Estrogen maintains trabecular bone volume in rats not only by suppression of resorption but also by stimulation of bone formation. J. Clin. Invest. 89, 74–78.

Chow, J.W.M., Lean, J.M., Chambers, T.J., 1992b. 17β-Estradiol stimulates cancellous bone formation in female rats. Endocrinology 130, 3025–3032.

Civitelli, R., Gonnelli, S., Zacchei, F., et al., 1988. Bone turnover in postmenopausal osteoporosis. Effect of calcitonin treatment. J. Clin. Invest. 82, 1268.

Coburn, J.W., Salusky, I.B., 2001. Renal bone diseases: clinical features, diagnosis, and management. In: Bilezikian, J.P., Marcus, R., Levine, M.A. (Eds.), The Parathyroids. Basic and Clinical Concepts, second ed. Academic Press, New York, p. 635.

Compston, J., 1997. Bone histomorphometry. In: Arnett, T.R., Henderson, B. (Eds.), Methods in Bone Biology. Chapman and Hall, London, p. 177.

Cosman, F., Nieves, J., Woelfert, L., Formica, C., Gordon, S., Shen, V., Lindsay, R., 2001. Parathyroid hormone added to established hormone therapy: effects on vertebral fracture and maintenance of bone mass after parathyroid hormone withdrawal. J. Bone Miner. Res. 16, 925–931.

Cosman, F., Crittenden, D.B., Adachi, J.D., Binkley, N., Czerwinski, E., Ferrari, S., Hofbauer, L.C., Lau, E., Lewiecki, E.M., Miyauchi, A., Zerbini, C.A., Milmont, C.E., Chen, L., Maddox, J., Meisner, P.D., Libanati, C., Grauer, A., October 20, 2016. Romosozumab treatment in postmenopausal women with osteoporosis. N. Engl. J. Med. 375 (16), 1532–1543.

Dempster, D.W., 1988. The relationship between the iliac crest bone biopsy and other skeletal sites. In: Kleerekoper, M., Krane, S. (Eds.), Clinical Disorders of Bone and Mineral Metabolism. Mary Ann Liebert, Inc., New York, p. 247.

Dempster, D.W., 1989. Bone histomorphometry in glucocorticoid-induced osteoporosis. J. Bone Miner. Res. 4, 137.

Dempster, D.W., 2000. The contribution of trabecular architecture to cancellous bone quality. J. Bone Miner. Res. 15, 20.

Dempster, D.W., 2002. Bone remodeling. In: Coe, F.L., Favus, M.J. (Eds.), Disorders of Bone and Mineral Metabolism, second ed. Lippincott Williams & Wilkins, New York.

Dempster, D.W., Cosman, F., Kurland, E.S., Zhou, H., Nieves, J., Woelfert, L., Shane, E., Plavetic, K., Muller, R., Bilezikian, J., Lindsay, R., 2001. Effects of daily treatment with parathyroid hormone on bone microarchitecture and turnover in patients with osteoporosis: a paired biopsy study. J. Bone Miner. Res. 16 (10), 1846–1853.

Dempster, D.W., Zhou, H., Recker, R.R., Brown, J.P., Bolognese, M.A., Recknor, C.P., Kendler, D.L., Lewiecki, E.M., Hanley, D.A., Rao, D.S., Miller, P.D., Woodson 3rd, G.C., Lindsay, R., Binkley, N., Wan, X., Ruff, V.A., Janos, B., Taylor, K.A., August 2012. Skeletal histomorphometry in subjects on teriparatide or zoledronic acid therapy (SHOTZ) study: a randomized controlled trial. J. Clin. Endocrinol. Metab. 97 (8), 2799–2808.

Dempster, D.W., Compston, J.E., Drezner, M.K., Glorieux, F.H., Kanis, J.A., Malluche, H., Meunier, P.J., Ott, S.M., Recker, R.R., Parfitt, A.M., January 2013. Standardized nomenclature, symbols, and units for bone histomorphometry: a 2012 update of the report of the ASBMR Histomorphometry Nomenclature Committee. J. Bone Miner. Res. 28 (1), 2−17.

Dempster, D.W., Zhou, H., Recker, R.R., Brown, J.P., Recknor, C.P., Lewiecki, E.M., Miller, P.D., Rao, S.D., Kendler, D.L., Lindsay, R., Krege, J.H., Alam, J., Taylor, K.A., Janos, B., Ruff, V.A., 2016a. Differential effects of teriparatide and denosumab on intact PTH and bone formation indices: AVA osteoporosis study. J. Clin. Endocrinol. Metab. 101 (4), 1353−1363.

Dempster, D.W., Zhou, H., Recker, R.R., Brown, J.P., Bolognese, M.A., Recknor, C.P., Kendler, D.L., Lewiecki, E.M., Hanley, D.A., Rao, S.D., Miller, P.D., Woodson 3rd, G.C., Lindsay, R., Binkley, N., Alam, J., Ruff, V.A., Gallagher, E.R., Taylor, K.A., 2016b. A longitudinal study of skeletal histomorphometry at 6 and 24 Months across four bone envelopes in postmenopausal women with osteoporosis receiving teriparatide or zoledronic acid in the SHOTZ trial. J. Bone Miner. Res. 31 (7), 1429−1439.

Dempster, D.W., Zhou, H., Ruff, V.A., Melby, T.E., Alam, J., Taylor, K.A., 2017. Longitudinal effects of teriparatide or zoledronic acid on bone modeling- and remodeling-based formation in the SHOTZ study. J. Bone Miner. Res. https://doi.org/10.1002/jbmr.3350 [Epub ahead of print] PubMed PMID: 29194749.

Dempster, D.W., Zhou, H., Recker, R.R., Brown, J.P., Recknor, C.P., Lewiecki, E.M., Miller, P.D., Rao, S.D., Kendler, D.L., Lindsay, R., Krege, J.H., Alam, J., Taylor, K.A., Melby, T.E., Ruff, V.A., February 2018. Remodeling- and modeling-based bone formation with teriparatide versus denosumab:A longitudinal analysis from baseline to 3 months in the AVA study. J. Bone Miner. Res. 33 (2), 298−306.

Dobnig, H., Sipos, A., Jiang, Y., Fahrleitner-Pammer, A., Ste-Marie, L.G., Gallagher, J.C., Pavo, I., Wang, J., Eriksen, E.F., 2005. Early changes in biochemical markers of bone formation correlate with improvements in bone structure during teriparatide therapy. J. Clin. Endocrinol. Metab. 90 (7), 3970−3977.

Dufresne, T.E., Chmielewski, P.A., Manhart, M.D., Johnson, T.D., Borah, B., 2003. Risedronate preserves bone architecture in early postmenopausal women in 1 year as measured by three-dimensional microcomputed tomography. Calcif. Tissue Int. 73 (5), 423−432.

Dunstan, C.R., Hills, E., Norman, A., et al., 1985. The pathogenesis of renal osteodystrophy: role of vitamin D, aluminum, parathyroid hormone, calcium and phosphorus. Q. J. Med. 55, 127.

Durchschlag, E., Paschalis, E.P., Zoehrer, R., Roschger, P., Fratzl, P., Recker, R., Phipps, R., Klaushofer, K., 2006. Bone material properties in trabecular bone from human iliac crest biopsies after 3- and 5-year treatment with risedronate. J. Bone Miner. Res. 21, 1581−1590.

Edwards, M.W., Bain, S.D., Bailey, M.C., Lantry, M.M., Howard, G.A., 1992. 17β-Estradiol stimulation of endosteal bone formation in the ovarietomised mouse: an animal model for the evaluation of bone -targeted estrogens. Bone 13, 29−34.

Eriksen, E.F., 1986. Normal and pathological remodeling of human trabecular bone: three dimensional reconstruction of the remodeling sequence in normals and metabolic bone disease. Endocr. Rev. 7, 379.

Eriksen, E.F., Hodgson, S.F., Eastell, R., et al., 1990. Cancellous bone remodeling in type I (postmenopausal) osteoporosis: quantitative assessment of rates of formation, resorption, and bone loss at tissue and cellular levels. J. Bone Miner. Res. 5, 311.

Eriksen, E.F., Langdahl, B., Vesterby, A., Rungby, J., Kassem, M., 1999. Hormone replacement therapy prevents osteoclastic hyperactivity: a histomorphometric study in early postmenopausal women. J. Bone Miner. Res. 14 (7), 1217−1221.

Eriksen, E.F., Melsen, F., Sod, E., Barton, I., Chines, A., 2002. Effects of long-term risedronate on bone quality and bone turnover in women with postmenopausal osteoporosis. Bone 31 (5), 620−625.

Ettinger, B., Black, D.M., Mitlak, B.H., Knickerbocker, R.K., Nickelsen, T., Genant, H.K., Christiansen, C., Delmas, P.D., Zanchetta, J.R., Stakkestad, J., Gluer, C.C., Krueger, K., Cohen, F.J., Eckert, S., Ensrud, K.E., Avioli, L.V., Lips, P., Cummings, S.R., 1999. Reduction of vertebral fracture risk in postmenopausal women with osteoporosis treated with raloxifene. J. Am. Med. Assoc. 282, 637−645.

Ettinger, B., San Martin, J., Crans, G., Pavo, I., 2004. Differential effects of teriparatide on BMD after treatment with raloxifene or alendronate. J. Bone Miner. Res. 19 (5), 745−751.

Felsenfeld, A.J., Rodriguez, M., Dunlay, R., Llach, F., 1991. A comparison of parathyroid gland function in hemodialysis patients with different forms of renal osteodystrophy. Nephrol. Dial. Transplant. 6, 244.

Finkelstein, J.S., Hayes, A., Hunzelman, J.L., Wyland, J.J., Lee, H., Neer, R.M., 2003. The effects of parathyroid hormone, alendronate, or both in men with osteoporosis. N. Engl. J. Med. 349 (13), 1216−1226.

Fleisch, H., 1998. Bisphosphonates: mechanism of action. Endocr. Rev. 19, 80−100.

Fox, J., Miller, M.A., Recker, R.R., Bare, S.P., Smith, S.Y., Moreau, I., 2005. Treatment of postmenopausal osteoporotic women with parathyroid hormone 1-84 for 18 months increases cancellous bone formation and improves cancellous architecture: a study of iliac crest biopsies using histomorphometry and microcomputed tomography. J. Musculoskelet. Neuronal Interact. 5, 356−357.

Frost, H.M., 1973. Bone Remodeling and Its Relationship to Metabolic Bone Diseases. Charles C Thomas, Springfield, IL.

Frost, H.M., 1983a. Bone histomorphometry: analysis of trabecular bone dynamics. In: Recker, R.R. (Ed.), Bone Histomorphometry: Techniques and Interpretation. CRC Press, Boca Raton, FL, p. 109.

Frost, H.M., 1983b. Bone histomorphometry: choice of marking agent and labeling schedule. In: Recker, R.R. (Ed.), Bone Histomorphometry: Techniques and Interpretation. CRC Press, Boca Raton, FL, p. 37.

Garcia Carasco, M., de Vernejoul, M.C., Sterkers, Y., et al., 1989. Decreased bone formation in osteoporotic patients compared with age-matched controls. Calcif. Tissue Int. 44, 173.

Gruber, H.E., Ivey, J.L., Baylink, D.J., Matthews, M., Nelp, W.B., Sisom, K., Chesnut III, C.H., 1984. Long-term calcitonin therapy in postmenopausal osteoporosis. Metabolism 33 (4), 295−303.

Gruber, H.E., Grigsby, J., Chesnut III, C.H., 2000. Osteoblast numbers after calcitonin therapy: a retrospective study of paired biopsies obtained during long-term calcitonin therapy in postmenopausal osteoporosis. Calcif. Tissue Int. 66 (1), 29–34.

Hattersley, G., Dean, T., Corbin, B.A., Bahar, H., Gardella, T.J., January 2016. Binding selectivity of abaloparatide for PTH-type-1-receptor conformations and effects on downstream signaling. Endocrinology 157 (1), 141–149.

Hercz, F., Pei, Y., Greenwood, C., et al., 1993. Low turnover osteodystrophy without aluminum; the role of "suppressed" parathyroid function. Kidney Int. 44, 860.

Hernandez, C.J., Beaupre, G.S., Marcus, R., Carter, D.R., 2001. A theoretical analysis of the contributions of remodeling space, mineralization, and bone balance to changes in bone mineral density during alendronate treatment. Bone 29 (6), 511–516.

Hirano, T., Burr, D.B., Turner, C.H., Sato, M., Cain, R.L., Hock, J.M., 1999. Anabolic effects of human biosynthetic parathyroid hormone fragment (1-34), LY333334, on remodeling and mechanical properties of cortical bone in rabbits. J. Bone Miner. Res. 14, 536–545.

Hirano, T., Burr, D.B., Cain, R.L., Hock, J.M., 2000. Changes in geometry and cortical porosity in adult, ovary-intact rabbits after 5 months treatment with LY333334 (hPTH 1–34). Calcif. Tissue Int. 66, 456–460.

Hodsman, A.B., Sherrard, D.J., Alfrey, A.C., et al., 1982. Bone aluminum and histomorphometric features of renal osteodystrophy. J. Clin. Endocrinol. Metab. 54, 539.

Hodsman, A.B., Fraher, L.J., Ostbye, T., Adachi, J.D., Steer, B.M., 1993. An evaluation of several biochemical markers for bone formation and resorption in a protocol utilizing cyclical parathyroid hormone and calcitonin therapy for osteoporosis. J. Clin. Invest. 91 (3), 1138–1148.

Hodsman, A.B., Kisiel, M., Adachi, J.D., Fraher, L.J., Watson, P.H., 2000. Histomorphometric evidence for increased bone turnover without change in cortical thickness or porosity after 2 years of cyclical hPTH(1–34) therapy in women with severe osteoporosis. Bone 27 (2), 311–318.

Holland, E.F.N., Studd, J.W.W., Mansell, J.P., Leather, A.T., Bailey, A.J., 1994a. Changes in collage composition and cross-links in bone and skin of osteoporosis postmenopausal women treated with percutaneous estradiol implants. Obstet. Gynecol. 83, 180–183.

Holland, E.F.N., Chow, J.W.M., Studd, J.W.W., Leather, A.T., Chambers, T.J., 1994b. Histomorphometric changes in the skeleton of postmenopausal women with low bone mineral density treated with percutaneous estradiol implants. Obstet. Gynecol. 83 (3), 387–391.

Jaworski, Z.F.G., 1983. Histomorphometric characteristics of metabolic bone disease. In: Recker, R.R. (Ed.), Bone Histomorphometry: Techniques and Interpretation. CRC Press, Boca Raton, FL, p. 241.

Jerome, C.P., Johnson, C.S., Vafai, H.T., Kaplan, K.C., Bailey, J., Capwell, B., Fraser, F., Hansen, L., Ramsay, H., Shadoan, M., Lees, C.J., Thomsen, J.S., Mosekilde, L., 1999. Effect of treatment for 6 months with human parathyroid hormone (1-34) peptide in ovariectomized cynomolgus monkeys (*Macaca fascicularis*). Bone 25, 301–309.

Jiang, Y., Zhao, J.J., Mitlak, B.H., Wang, O., Genant, H.K., Eriksen, E.F., 2003. Recombinant human parathyroid hormone (1-34) [teriparatide] improves both cortical and cancellous bone structure. J. Bone Miner. Res. 18 (11), 1932–1941.

Jiang, Y., Zhao, J., Liao, E.Y., Dai, R.C., Wu, X.P., Genant, H.K., 2005. Application of micro-CT assessment of 3-D bone microstructure in preclinical and clinical studies. J. Bone Miner. Metab. 23 (Suppl. l), 122–131.

Jilka, R.L., Weinstein, R.S., Bellido, T., Roberson, P., Parfitt, A.M., Manolagas, S.C., 1999. Increased bone formation by prevention of osteoblast apoptosis with parathyroid hormone. J. Clin. Invest. 104 (4), 439–446.

Ketteler, M., Block, G.A., Evenepoel, P., Fukagawa, M., Herzog, C.A., McCann, L., Moe, S.M., Shroff, R., Tonelli, M.A., Toussaint, N.D., Vervloet, M.G., Leonard, M.B., February 20, 2018. Diagnosis, evaluation, prevention, and treatment of chronic kidney disease-mineral and bone disorder: synopsis of the kidney disease: improving global outcomes 2017 clinical practice guideline update. Ann. Intern. Med. https://doi.org/10.7326/M17-2640 [Epub ahead of print] PubMed PMID: 29459980.

Khastgir, G., Studd, J., Holland, N., Alaghband-Zadeh, J., Fox, S., Chow, J., 2001a. Anabolic effect of estrogen replacement on bone in postmenopausal women with osteoporosis: histomorphometric evidence in a longitudinal study. J. Clin. Endocrinol. Metab. 86 (1), 289–295.

Khastgir, G., Studd, J., Holland, N., Alaghband-Zadeh, J., Sims, T.J., Bailey, A.J., 2001b. Anabolic effect of long-term estrogen replacement on bone collagen in elderly postmenopausal women with osteoporosis. Osteoporos. Int. 12 (6), 465–470.

Khastgir, G., Studd, J.W., Fox, S.W., Jones, J., Alaghband-Zadeh, J., Chow, J.W., 2003. A longitudinal study of the effect of subcutaneous estrogen replacement on bone in young women with Turner's syndrome. J. Bone Miner. Res. 18 (5), 925–932.

Kimmel, D.B., Recker, R.R., Gallagher, J.C., et al., 1990. A comparison of iliac bone histomorphometric data in post-menopausal osteoporotic and normal subjects. Bone Miner. 11, 217.

Kroger, H., Arnala, I., Alhava, E.M., 1992. Effect of calcitonin on bone histomorphometry and bone metabolism in rheumatoid arthritis. Calcif. Tissue Int. 50 (1), 11–13.

Kurland, E.S., Cosman, F., McMahon, D.J., Rosen, C.J., Lindsay, R., Bilezikian, J.P., 2000. Parathyroid hormone as a therapy for idiopathic osteoporosis in men: effects on bone mineral density and bone markers. J. Clin. Endocrinol. Metab. 85, 3069–3076.

Lindsay, R., Dempster, D.W., Jordan, C.V. (Eds.), 1997a. Estrogens and Anti-estrogens: Basic and Clinical Aspects. Lipincott-Raven Publishers, Philadelphia.

Lindsay, R., Nieves, J., Formica, C., Henneman, E., Woelfert, L., Shen, V., Dempster, D., Cosman, F., 1997b. Randomised controlled study of effect of parathyroid hormone on vertebral-bone mass and fracture incidence among postmenopausal women on oestrogen with osteoporosis. Lancet 350, 550–555.

Lindsay, R., Cosman, F., Zhou, H., Bostrom, M.P., Shen, V.W., Cruz, J.D., Nieves, J.W., Dempster, D.W., 2006. A novel tetracycline labeling schedule for longitudinal evaluation of the short-term effects of anabolic therapy with a single iliac crest bone biopsy: early actions of teriparatide. J. Bone Miner. Res. 21 (3), 366–373.

Lindsay, R., Zhou, H., Cosman, F., Nieves, J., Dempster, D.W., Hodsman, A.B., 2007. Effects of a one-month treatment with parathyroid hormone (1-34) on bone formation on cancellous, endocortical and periosteal surfaces of the human ilium. J. Bone Miner. Res. 22, 495−502.

Lufkin, E.G., Wahner, H.W., O'Fallon, W.M., Hodgson, S.F., Kotowicz, M.A., Lane, A.W., Judd, H.L., Caplan, R.H., Riggs, B.L., 1992. Treatment of postmenopausal osteoporosis with transdermal estrogen. Ann. Intern. Med. 117 (1), 1−9.

Ma, Y.L., Zeng, Q., Donley, D.W., Ste-Marie, L.G., Gallagher, J.C., Dalsky, G.P., Marcus, R., Eriksen, E.F., 2006. Teriparatide increases bone formation in modeling and remodeling osteons and enhances IGF-II immunoreactivity in postmenopausal women with osteoporosis. J. Bone Miner. Res. 21, 855−864.

Malluche, H.H., Faugere, M.-C., 1987. Atlas of Mineralized Bone Histology. Karger, Basel.

Malluche, H.H., Monier-Faugere, M.C., April 2006. Renal osteodystrophy: what's in a name? Presentation of a clinically useful new model to interpret bone histologic findings. Clin. Nephrol. 65 (4), 235−242.

Malluche, H.H., Ritz, E., Lange, H.P., et al., 1976. Bone histology in incipient and advanced renal failure. Kidney Int. 9, 355−362.

Malluche, H.H., Mawad, H.W., Monier-Faugere, M.C., June 2011. Renal osteodystrophy in the first decade of the new millennium: analysis of 630 bone biopsies in black and white patients. J. Bone Miner. Res. 26 (6), 1368−1376. Erratum, 2011 Erratum in: J. Bone Miner. Res. 2011 Nov; 26 (11), 2793.

Marcus, R., Leary, D., Schneider, D.L., et al., 2000. The contribution of testosterone to skeletal development and maintenance: lessons from the androgen insensitivity syndrome. J. Clin. Endocrinol. Metab. 85, 1032.

Marie, P.J., Caulin, F., 1986. Mechanisms underlying the effects of phosphate and calcitonin on bone histology in postmenopausal osteoporosis. Bone 7 (1), 17−22.

Mashiba, T., Burr, D.B., Turner, C.H., Sato, M., Cain, R.L., HockJ, M., 2001. Effects of human parathyroid hormone (1-34), LY333334, on bone mass, remodeling, and mechanical properties of cortical bone during the first remodeling cycle in rabbits. Bone 28, 538−547.

McClung, M.R., San Martin, J., Miller, P.D., Civitelli, R., Bandeira, F., Omizo, M., Donley, D.W., Dalsky, G.P., Eriksen, E.F., 2005. Opposite bone remodeling effects of teriparatide and alendronate in increasing bone mass. Arch. Intern. Med. 165, 1762−1768.

Melsen, F., Mosekilde, L., Kragstrup, J., 1983. Metabolic bone diseases as evaluated by bone histomorphometry. In: Recker, R.R. (Ed.), Bone Histomorphometry: Techniques and Interpretation. CRC Press, Boca Raton, FL, p. 265.

Meunier, P.J., 1981. Bone biopsy in diagnosis of metabolic bone disease. In: Cohn, T.V., Talmage, R., Matthews, J.L. (Eds.), "Hormonal Control of Calcium Metabolism," Proceedings of the Seventh International Conference on Calcium Regulating Hormones. Excerpta Medica, Amsterdam, p. 109.

Meunier, P.J., 1988. Assessment of bone turnover by histomorphometry in osteoporosis. In: Riggs, B.L., Melton III, L.J. (Eds.), Osteporosis: Etiology, Diagnosis, and Management. Raven Press, New York, p. 317.

Meunier, P.J., Boivin, G., 1997. Bone mineral reflects bone mass but also the degree of mineralization of bone: therapeutic implications. Bone 21, 373−377.

Meunier, P.J., Coindre, J.M., Edouard, C.M., Arlot, M.E., 1980. Bone histomorphometry in Paget's disease quantitative and dynamic analysis of pagetic and non-pagetic bone tissue. Arthritis Rheum. 23, 1095.

Meunier, P.J., Sellami, S., Briancon, D., Edouard, C., 1981. Histological heterogeneity of apparently idiopathic osteoporosis. In: Deluca, H.F., Frost, H.M., Jee, W.S.S., et al. (Eds.), Osteoporosis, Recent Advances in Pathogenesis and Treatment. University Park Press, Baltimore, p. 293.

Miller, P.D., Hattersley, G., Riis, B.J., Williams, G.C., Lau, E., Russo, L.A., Alexandersen, P., Zerbini, C.A., Hu, M.Y., Harris, A.G., Fitzpatrick, L.A., Cosman, F., Christiansen, C., August 16, 2016. ACTIVE study investigators. Effect of abaloparatide vs placebo on new vertebral fractures in postmenopausal women with osteoporosis: a randomized clinical trial. J. Am. Med. Assoc. 316 (7), 722−733.

Misof, B.M., Roschger, P., Cosman, F., Kurland, E.S., Tesch, W., Messmer, P., Dempster, D.W., Nieves, J., Shane, E., Fratzl, P., Klaushofer, K., Bilezikian, J., Lindsay, R., 2003. Effects of intermittent parathyroid hormone administration on bone mineralization density in iliac crest biopsies from patients with osteoporosis: a paired study before and after treatment. J. Clin. Endocrinol. Metab. 88 (3), 1150−1156.

Moreira, C.A., Fitzpatrick, L.A., Wang, Y., Recker, R.R., April 2017. Effects of abaloparatide-SC (BA058) on bone histology and histomorphometry: the ACTIVE phase 3 trial. Bone 97, 314−319.

Moriniere, P., Cohen-Solal, M., Belbrik, S., et al., 1989. Disappearance of aluminic bone disease in a long-term asymptomatic dialysis population restricting Al(OH)3 intake: emergence of an idiopathic adynamic bone disease not related to aluminum. Nephron 53, 975.

Munns, C.F., Rauch, F., Travers, R., Glorieux, F.H., 2005. Effects of intravenous pamidronate treatment in infants with osteogenesis imperfecta: clinical and histomorphometric outcome. J. Bone Miner. Res. 20 (7), 1235−1243.

Neer, R.M., Arnaud, C.D., Zanchetta, J.R., Prince, R., Gaich, G.A., Reginster, J.Y., Hodsman, A.B., Eriksen, E.F., Ish-Shalom, S., Genant, H.K., Wang, O., Mitlak, B.H., 2001. Effect of parathyroid hormone (1-34) on fractures and bone mineral density in postmenopausal women with osteoporosis. N. Engl. J. Med. 344 (19), 1434−1441.

Ott, S.M., Oleksik, A., Lu, Y., Harper, K., Lips, P., 2002. Bone histomorphometric and biochemical marker results of a 2-year placebo-controlled trial of raloxifene in postmenopausal women. J. Bone Miner. Res. 17 (2), 341−348.

Palmieri, G.M., Pitcock, J.A., Brown, P., Karas, J.G., Roen, L.J., 1989. Effect of calcitonin and vitamin D in osteoporosis. Calcif. Tissue Int. 45 (3), 137−141.

Parfitt, A.M., 1983a. Stereological basis of bone histomorphometry: theory of quantitative microscopy and reconstruction of the third dimension. In: Recker, R.R. (Ed.), Bone Histomorphometry: Techniques and Interpretation. CRC Press, Boca Raton, FL, p. 53.

Parfitt, A.M., 1983b. The physiological and clinical significance of bone histomorphometric data. In: Recker, R.R. (Ed.), Bone Histomorphometry: Techniques and Interpretation. CRC Press, Boca Raton, FL, p. 143.

Parfitt, A.M., 1988. Bone remodeling: relationship to the amount and structure of bone, and the pathogenesis and prevention of fractures. In: Riggs, B.L., Melton III, L.J. (Eds.), Osteoporosis: Etiology, Diagnoses, and Management. Raven Press, New York, p. 45.

Parfitt, A.M., Matthews, C.H.E., Villanueva, A.R., et al., 1982. Relationships between surface, volume and thickness of iliac trabecular bone in aging and in osteoporosis. Implications for the microanatomic and cellular mechanisms of bone loss. J. Clin. Invest. 72, 1396.

Parfitt, A.M., Drezner, M.K., Glorieux, F.H., et al., 1987. Bone histomorphometry: standardization of nomenclature, symbols, and units. J. Bone Miner. Res. 2, 595.

Parisien, M., Charhon, S.A., Mainetti, E., et al., 1988. Evidence for a toxic effect of aluminum on ostetoblasts: a histomorphometric study in hemodialysis patients with aplastic bone disorder. J. Bone Miner. Res. 3, 259.

Parisien, M., Silverberg, S.J., Shane, E., et al., 1990. The histomorphometry of bone in primary hyperparathyroidism: preservation of cancellous bone structure. J. Clin. Endocrinol. Metab. 70, 930.

Parisien, M.V., Mellish, R.W.E., Silverberg, S.J., et al., 1992. Maintenance of cancellous bone connectivity in primary hyperparathyroidism: trabecular strut analysis. J. Bone Miner. Res. 7, 913.

Paschalis, E.P., Boskey, A.L., Kassem, M., Eriksen, E.F., 2003. Effect of hormone replacement therapy on bone quality in early postmenopausal women. J. Bone Miner. Res. 18 (6), 955–959.

Paschalis, E.P., Glass, E.V., Donley, D.W., Eriksen, E.F., 2005. Bone mineral and collagen quality in iliac crest biopsies of patients given teriparatide: new results from the fracture prevention trial. J. Clin. Endocrinol. Metab. 90 (8), 4644–4649.

Patel, S., Pazianas, M., Tobias, J., Chambers, T.J., Fox, S., Chow, J., 1999. Early effects of hormone replacement therapy on bone. Bone 24, 245–248.

Pepene, C.E., Seck, T., Diel, I., Minne, H.W., Ziegler, R., Pfeilschifter, J., 2004. Influence of fluor salts, hormone replacement therapy and calcitonin on the concentration of insulin-like growth factor (IGF)-I, IGF-II and transforming growth factor-beta 1 in human iliac crest bone matrix from patients with primary osteoporosis. Eur. J. Endocrinol. 150 (1), 81–91.

Prestwood, K.M., Gunness, M., Muchmore, D.B., Lu, Y., Wong, M., Raisz, L.G., 2000. A comparison of the effects of raloxifene and estrogen on bone in postmenopausal women. J. Clin. Endocrinol. Metab. 85 (6), 2197–2202.

Rao, D.S., 1983. Practical approach to bone biopsy. In: Recker, R.R. (Ed.), Bone Histomorphometry: Techniques and Interpretation. CRC Press, Boca Raton, FL, p. 3.

Recker, R.R., Weinstein, R.S., Chesnut III, C.H., Schimmer, R.C., Mahoney, P., Hughes, C., Bonvoisin, B., Meunier, P.J., 2004. Histomorphometric evaluation of daily and intermittent oral ibandronate in women with postmenopausal osteoporosis: results from the BONE study. Osteoporos. Int. 15 (3), 231–237.

Recker, R., Masarachia, P., Santora, A., Howard, T., Chavassieux, P., Arlot, M., Rodan, G., Wehren, L., Kimmel, D., 2005. Trabecular bone microarchitecture after alendronate treatment of osteoporotic women. Curr. Med. Res. Opin. 21 (2), 185–194.

Recker, R.R., Delmas, P.D., Halse, J., Reid, I.R., Boonen, S., García-Hernandez, P.A., Supronik, J., Lewiecki, E.M., Ochoa, L., Miller, P., Hu, H., Mesenbrink, P., Hartl, F., Gasser, J., Eriksen, E.F., 2008. Effects of intravenous zoledronic acid once yearly on bone remodeling and bone structure. J. Bone Miner. Res. 23, 6–16.

Reeve, J., Meunier, P.J., Parsons, J.A., Bernat, M., Bijvoet, O.L., Courpron, P., Edouard, C., Klenerman, L., Neer, R.M., Renier, J.C., Slovik, D., Vismans, F.J., Potts Jr., J.T., 1980. Anabolic effect of human parathyroid hormone fragment on trabecular bone in involutional osteoporosis: a multicentre trial. Br. Med. J. 280, 1340–1344.

Reeve, J., Bradbeer, J.N., Arlot, M., Davies, U.M., Green, J.R., Hampton, L., Edouard, C., Hesp, R., Hulme, P., Ashby, J.P., Zanelli, J.M., Meunier, P.J., 1991. hPTH 1–34 treatment of osteoporosis with added hormone replacement therapy: biochemical, kinetic and histological responses. Osteoporos. Int. 1 (3), 162–170.

Reid [1], I.R., Miller, P.D., Brown, J.P., Kendler, D.L., Fahrleitner-Pammer, A., Valter, I., Maasalu, K., Bolognese, M.A., Woodson, G., Bone, H., Ding, B., Wagman, R.B., San Martin, J., Ominsky, M.S., Dempster, D.W., October 2010. Effects of denosumab on bone histomorphometry: the FREEDOM and STAND studies. J. Bone Miner. Res. 25 (10), 2256–2265.

Rey, C., Hina, A., Glimcher, M.J., 1995. Maturation of poorly crystalline apatites: chemical and structural aspects in vivo and in vitro. Cells Mater 5, 345–356.

Riggs, B.L., Parfitt, A.M., 2005. Drugs used to treat osteoporosis: the critical need for a uniform nomenclature based on their action on bone remodeling. J. Bone Miner. Res. 20 (2), 177–184.

Roschger, P., Fratzl, P., Klaushofer, K., Rodan, G., 1997. Mineralization of cancellous bone after alendronate and sodium fluoride treatment: a quantitative backscattered electron imaging study on minipig ribs. Bone 20, 393–397.

Roschger, P., Rinnerthaler, S., Yates, J., Rodan, G.A., Fratzl, P., Klaushofer, K., 2001. Alendronate increases degree and uniformity of mineralization in cancellous bone and decreases the porosity in cortical bone of osteoporotic women. Bone 29, 185–191.

Salusky, I.B., Coburn, J.W., Brill, J., et al., 1988. Bone disease in pediatric patients undergoing dialysis with CAPD or CCPD. Kidney Int. 33, 975.

Seeman, E., Delmas, P.D., 2006. Bone quality—the material and structural basis of bone strength and fragility. N. Engl. J. Med. 354, 2250–2261.

Sherrard, D.J., Hercz, G., Pei, Y., et al., 1993. The spectrum of bone disease in end-stage renal failure—an evolving disorder. Kidney Int. 43, 435.

Silverberg, S.J., Shane, E., Dempster, D.W., Bilezikian, J.P., 1990. The effects of vitamin D insufficiency in patients with primary hyperparathyroidism. Am. J. Med. 107, 561.

Silverman, S.L., 2003. Calcitonin. Endocrinol. Metab. Clin. North Am. 32 (1), 273–284.

Siris, E.S., Clemens, T.L., Dempster, D.W., et al., 1987. Tumor-induced osteomalacia. Kinetics of calcium, phosphorus, and vitamin D metabolism and characteristics of bone histomorphometry. Am. J. Med. 82, 307.

Slatopolsky, E., Delmez, J., 2002. Bone disease in chronic renal failure and after renal transplantation. In: Coe, F.L., Favus, M.J. (Eds.), Disorders of Bone and Mineral Metabolism, second ed. Lippincott Williams & Wilkins, New York, p. 865.

Ste-Marie, L.G., Charhon, S.A., Edouard, C., et al., 1984. Iliac bone histomorphometry in adults and children with osteogenesis imperfecta. J. Clin. Pathol. 37, 1801.

Steiniche, T., Hasling, C., Charles, P., Eriksen, E.F., Mosekilde, L., Melsen, F., 1989. A randomized study on the effects of estrogen/gestagen or high dose oral calcium on trabecular bone remodeling in postmenopausal osteoporosis. Bone 10 (5), 313–320.

Steiniche, T., Christiansen, P., Vesterby, A., et al., 1994. Marked changes in iliac crest bone structure in postmenopausal women without any signs of disturbed bone remodeling or balance. Bone 15, 73.

Teitelbaum, S.L., 1980. Pathological manifestations of osteomalacia and rickets. J. Clin. Endocrinol. Metab. 9, 43.

Uusi-Rasi, K., Semanick, L.M., Zanchetta, J.R., Bogado, C.E., Eriksen, E.F., Sato, M., Beck, T.J., 2005. Effects of teriparatide [rhPTH (1-34)] treatment on structural geometry of the proximal femur in elderly osteoporotic women. Bone 36, 948–958.

Valentin-Opran, A., Charhon, S.A., Meunier, P.J., et al., 1982. Quantitative histology of myeloma-induced bone changes. Br. J. Haematol. 52, 601.

Vedi, S., Compston, J.E., 1996. The effects of long-term hormone replacement therapy on bone remodeling in postmenopausal women. Bone 19 (5), 535–539.

Vedi, S., Purdie, D.W., Ballard, P., Bord, S., Cooper, A.C., Compston, J.E., 1999. Bone remodeling and structure in postmenopausal women treated with long-term, high-dose estrogen therapy. Osteoporos. Int. 10 (1), 52–58.

Vedi, S., Bell, K.L., Loveridge, N., Garrahan, N., Purdie, D.W., Compston, J.E., 2003. The effects of hormone replacement therapy on cortical bone in postmenopausal women. A histomorphometric study. Bone 33 (3), 330–334.

Wahab, M., Ballard, P., Purdie, D.W., Cooper, A., Willson, J.C., 1997. The effect of long term oestradiol implantation on bone mineral density in postmenopausal women who have undergone hysterectomy and bilateral oophorectomy. Br. J. Obstet. Gynaecol. 104, 728–731.

Walters, C., Eyre, D.R., 1980. Collagen crosslinks in human dentin: increasing content of hydroxypyridinum residues with age. Calcif. Tissue Int. 35, 401–405.

Weinstein, R.S., 2002. Clinical use of bone biopsy. In: Coe, F.L., Favus, M.J. (Eds.), Disorders of Bone and Mineral Metabolism, second ed. Lippincott Williams & Wilkins, New York, p. 448.

Weinstein, R.S., Parfitt, A.M., Marcus, R., Greenwald, M., Crans, G., Muchmore, D.B., 2003. Effects of raloxifene, hormone replacement therapy, and placebo on bone turnover in postmenopausal women. Osteoporos. Int. 14 (10), 814–822.

Whyte, M.P., Bergfeld, M.A., Murphy, W.A., et al., 1982. Postmenopausal osteoporosis; a heterogeneous disorder as assessed by histomorphometric analysis of iliac crest bone from untreated patients. Am. J. Med. 72, 183.

Wright, C.D., Garrahan, N.J., Stanton, M., Gazet, J.C., Mansell, R.E., Compston, J.E., 1994. Effect of long-term tamoxifen therapy on cancellous bone remodeling and structure in women with breast cancer. J. Bone Miner. Res. 9 (2), 153–159.

Yamauchi, M., 1996. Collagen: the major matrix molecule in mineralized tissues. In: Anderson, J.J.B., Garner, S.C. (Eds.), Calcium and Phosphorus in Health and Disease. CRC Press, New York, pp. 127–141.

Zanchetta, J.R., Bogado, C.E., Ferretti, J.L., Wang, O., Wilson, M.G., Sato, M., Gaich, G.A., Dalsky, G.P., Myers, S.L., 2003. Effects of teriparatide [recombinant human parathyroid hormone (1-34)] on cortical bone in postmenopausal women with osteoporosis. J. Bone Miner. Res. 18, 539–543.

Zoehrer, R., Roschger, P., Paschalis, E.P., Hofstaetter, J.G., Durchschlag, E., Fratzl, P., Phipps, R., Klaushofer, K., 2006. Effects of 3- and 5-year treatment with risedronate on bone mineralization density distribution in triple biopsies of the iliac crest in postmenopausal women. J. Bone Miner. Res. 21, 1106–1119.

Chapter 20

Phosphorus homeostasis and related disorders

Thomas O. Carpenter, Clemens Bergwitz and Karl L. Insogna
Departments of Pediatrics and Internal Medicine, Yale University School of Medicine, New Haven, CT, United States

Chapter outline

Introduction

Phosphorus is critical to life as we know it. In mammalian tissues, phosphorus is one of the most abundant components; it has critical roles in growth and development and is a major structural component of bone. Physiologic functions at the organism level include its ability to serve as a buffer in acid—base regulation and multiple roles in cellular metabolism. Inorganic phosphorus exists primarily as phosphate (PO_4), a stable, divalent anionic complex with four oxygen atoms. Phosphate is a requisite component of hydroxyapatite ($Ca_{10}(PO_4)_6(OH)_2$), which crystallizes to form the mineral basis of the vertebrate skeleton. At the molecular level, phosphate provides the molecular backbone of DNA. The chemical bonding of two phosphate molecules creates pyrophosphate (PPi; P_2O_7), a potent inhibitor of bone mineralization, and an intricate balance between local phosphate/PPi balance regulates mineralization. The chemical nature of phosphate—phosphate bonds allows for storage of biological energy as adenosine triphosphate (ATP). In addition, phosphorus influences a variety of enzymatic reactions (e.g., glycolysis) and protein functions (e.g., the oxygen-carrying capacity of hemoglobin by regulation of 2,3-diphosphoglycerate synthesis). Phosphorus influences both the storage and the release of the principal

Principles of Bone Biology. https://doi.org/10.1016/B978-0-12-814841-9.00020-8

carbohydrate energy source, glucose, as glucose is phosphorylated prior to storage as glycogen, and that same phosphorylation step is reversed during glycogenolysis. Finally, bonding (or removal) of phosphorus at specific amino acid residues in proteins provides for highly evolved signaling cascades, as phosphorylation or dephosphorylation of many proteins activates or deactivates a variety of pathways.

Individuals eating a Western diet consume roughly 20 mg/kg of dietary phosphorus daily, varying somewhat by age and sex (Calvo et al., 2014). However, this estimate does not capture the large amount of phosphorus contained in food additives. The majority of phosphorus in the body is contained in mineralized tissue (600−700 g), with the remainder in soft tissues (100−200 g). Less than 1% of the total phosphorus in the body is in extracellular fluids. The plasma contains approximately 12 mg of phosphorus, the majority of which (8 mg) is contained in phospholipids, while only a small amount circulates as inorganic phosphate, either as monohydrogen phosphate or dihydrogen phosphate. The relative concentrations of these two moieties generally favor the monohydrogenated compound (4:1).

The terms "serum phosphorus" and "serum phosphate" are generally used interchangeably when referring to plasma inorganic phosphorus concentrations, because plasma inorganic phosphorus is nearly all in the form of the PO_4 ion. It should be noted that this terminology can be confusing when using mass units (i.e., mg/dL) when the weight of the phosphorus content of the phosphate is reported, yet the term "serum phosphate" is often used in the clinical setting. When using molar units the concentrations of the phosphate and of the phosphorus are equivalent, and less confusion may arise.

In adult humans, most phosphorus is found in bone (600−700 g), whereas the remainder is generally in soft tissue (100−200 g). The plasma contains 11−12 mg/dL of total phosphorus (in both organic and inorganic states) in adults. Inorganic phosphorus is largely in the form of phosphate (PO_4) and is the fraction typically measured in clinical settings. The plasma or serum concentration of phosphorus averages 3.0−4.5 mg/dL in older children and adults, but is greater in infants and younger children. Plasma phosphorus can often be as high as 8 mg/dL in small infants, gradually declining through the first year of life and then further as childhood progresses to adult values.

Rapid shifts in extracellular phosphate can occur during a variety of physiologic processes and pathologic disturbances. For example, the phosphorylation of glucose after it enters the cell explains the rapid depletion of extracellular phosphate with exogenous administration of insulin. Rapid bone remineralization ("hungry bone syndrome") can also cause rapid depletion of extracellular phosphate. Phosphorus deprivation (as occurs with the administration of phosphate-binding resins) can lead to hypophosphatemia. Furthermore, insulin induces shifts of phosphate into cells as is seen in refeeding hypophosphatemia and with the correction of diabetic ketoacidosis. Profound and sustained declines in extracellular phosphate can result in impaired muscle, leukocyte, and platelet function; rhabdomyolysis; and even cardiopulmonary compromise.

Despite the paramount importance of phosphate in mammalian physiology, the local and systemic regulation of phosphate homeostasis is poorly understood. It was not until 2000/2001 that the hormone now recognized as having a critical role in regulating the concentration of extracellular phosphate, fibroblast growth factor 23 (FGF23), was identified. That discovery, while representing a major advance in understanding phosphate homeostatic mechanisms, also highlights a crucial, and as yet unanswered, question: how do osteocytes, the cells that produce FGF23, sense extracellular phosphate and thereby regulate production of FGF23?

Phosphate transporters are present throughout the body and are the portals for entry of phosphate into cells, but their regulation and/or modulation by extracellular phosphate remains to be explored. A better understanding of the regulation of, as well as interactions between, extra- and intracellular phosphate will lead to improved insights into human physiology and better therapies for disorders of phosphate homeostasis.

Regulation of phosphate metabolism

Overview

To provide for these various functions, organisms have developed elaborate mechanisms for regulating supply and intercompartmental transport of phosphate. Various regulatory mechanisms permit modulation based on metabolic phosphorus need and exogenous phosphorus supply. This adaptive homeostatic system primarily adjusts gastrointestinal absorption and renal excretion to control total body stores, while maintaining extracellular concentration of phosphorus within a relatively narrow range. The identification of several hormones (e.g., parathyroid hormone [PTH], FGF23) and transporter proteins (e.g., NPT2, PIT) that are integral to the system has markedly increased our understanding of phosphate homeostasis, but the sensory system underlying regulation of phosphorus balance remains incompletely understood. The majority of ingested phosphate is absorbed in the small intestine, where active transport is mediated by sodium-dependent transporter proteins, and sodium-independent phosphate transport also occurs. The kidney, however, is

thought to be the dominant organ involved in the regulation of phosphorus balance, as renal tubular reabsorption of filtered phosphate is adjusted in response to various regulatory factors. Finally, in the setting of severe phosphorus deprivation, the phosphate contained in bone mineral provides a source of phosphorus for the metabolic needs of the organism. The specific roles that the intestine, kidney, and bone play in this complex process are discussed in detail in the following sections.

Hormonal regulators

Parathyroid hormone

PTH was long considered the predominant hormonal effector of phosphate homeostasis. Effects of PTH on proximal tubular phosphate transport can be mediated by both cAMP−protein kinase A (PKA) and phospholipase C−protein kinase C (PKC) signal transduction pathways, although the PKA pathway is the more important pathway in this regard. After interaction with the PTH receptor 1 (PTHR1), PTH effects a rapid removal of the inorganic phosphate transporters NPT2a and NPT2c from proximal tubular apical membranes. Stabilization of NPT2a is mediated by the sodium/hydrogen exchange regulatory cofactor NHERF1, which is phosphorylated by PTH's activation of the PKA and PKC pathways. Overall, PTH appears to serve as a regulator of renal sodium/phosphate cotransport in an acute time frame, and the regulation is determined by changes in the abundance of NPT2 proteins in the renal brush border membrane (Forster et al., 2006). Certain aspects of phosphate homeostasis at the renal level, however, are not explained by actions of PTH. For instance, after removal of the parathyroid glands, regulation of renal phosphate transport by dietary phosphorus content persists, implying that other mediators of this process are at work.

Fibroblast growth factor 23

FGF23 is the most recently identified important physiologic regulator of renal phosphate excretion (Farrow and White, 2010). This novel member of the FGF family is produced by osteocytes and, to some extent, osteoblasts, thus providing a mechanism by which skeletal mineral demands can be communicated to the kidney and thereby influence the phosphate economy of the entire organism. In rodents and humans, after days of dietary phosphate loading, circulating FGF23 levels increase, and similarly, with dietary phosphorus deprivation, FGF23 levels decrease (Antoniucci et al., 2006). FGF23 activates FGF receptors (FGFRs) on the basolateral membrane of renal tubules, resulting in removal of type II sodium-dependent phosphate transporters from the apical surface of the tubular cell by a NHERF1-dependent process, similar to the previously described mechanism for PTH. However, in contrast to PTH, FGF23 actions are mediated by activation of extracellular signal-regulated kinase 1/2 (ERK1/2) rather than the PTH-driven PKA-dependent pathway. Evidence also exists for decreased expression of type II sodium-dependent phosphate transporters via genomic mechanisms. FGF23 interacts with its receptor via a mechanism now identified as characteristic of the endocrine FGFs. FGF23 recognizes its cognate FGFR only in the presence of the coreceptor α-klotho (Urakawa et al., 2006). Activation of this complex results in downstream ERK phosphorylation and subsequently reduced expression of NPT2a and NPT2c, and *CYP27B1* (encoding the vitamin D 1α-hydroxylase), with an increase in expression of *CYP24A1* (encoding the vitamin D 24-hydroxylase). This mechanism of signaling is apparent for the endocrine FGFs, FGF19 and FGF21, which require a separate member of the klotho family (β-klotho) for tissue-specific activation of FGFRs (for a detailed review, see Belov and Mohammadi, 2013).

FGF23 contains a unique C-terminal domain, thought to be the site of the interaction with klotho. The crystal structure of the FGF23/FGFR1c/α-klotho complex has been solved (Chen et al., 2018), confirming this prediction (Fig. 20.1). The C-terminal tail of FGF23 binds both the klotho 1 and the klotho 2 domains of α-klotho, and the FGF-like domain, which is N-terminal to the RXXR furin/subtilisin protease recognition site, binds to the FGFR. α-Klotho is able to associate with "c" isoforms of FGFR1 and FGFR3, and also FGFR4 (Urakawa et al., 2006); renal signaling is thought to primarily occur via FGFR1c. The actions of FGF23 and other related proteins as mediators of disease are discussed in detail later in the section on X-linked hypophosphatemia (XLH).

The role of osteocytes

Osteocytes are the most abundant cell in cortical bone, distributed in an organized array with interconnecting canaliculi (for review, see Dallas et al., 2013). Cellular processes extending from the cell body of the osteocyte tunnel through these canaliculi and communicate with other cells and bony surfaces. The osteocyte produces several proteins involved in phosphate regulation, including: (1) PHEX (phosphate-regulating gene with homologies to endopeptidases on the X chromosome), which regulates FGF23 secretion, with loss of function resulting in elevated circulating FGF23; (2) DMP1 (dentin matrix protein 1), a SIBLING (small integrin-binding ligand N-linked glycoprotein) protein, of which loss of

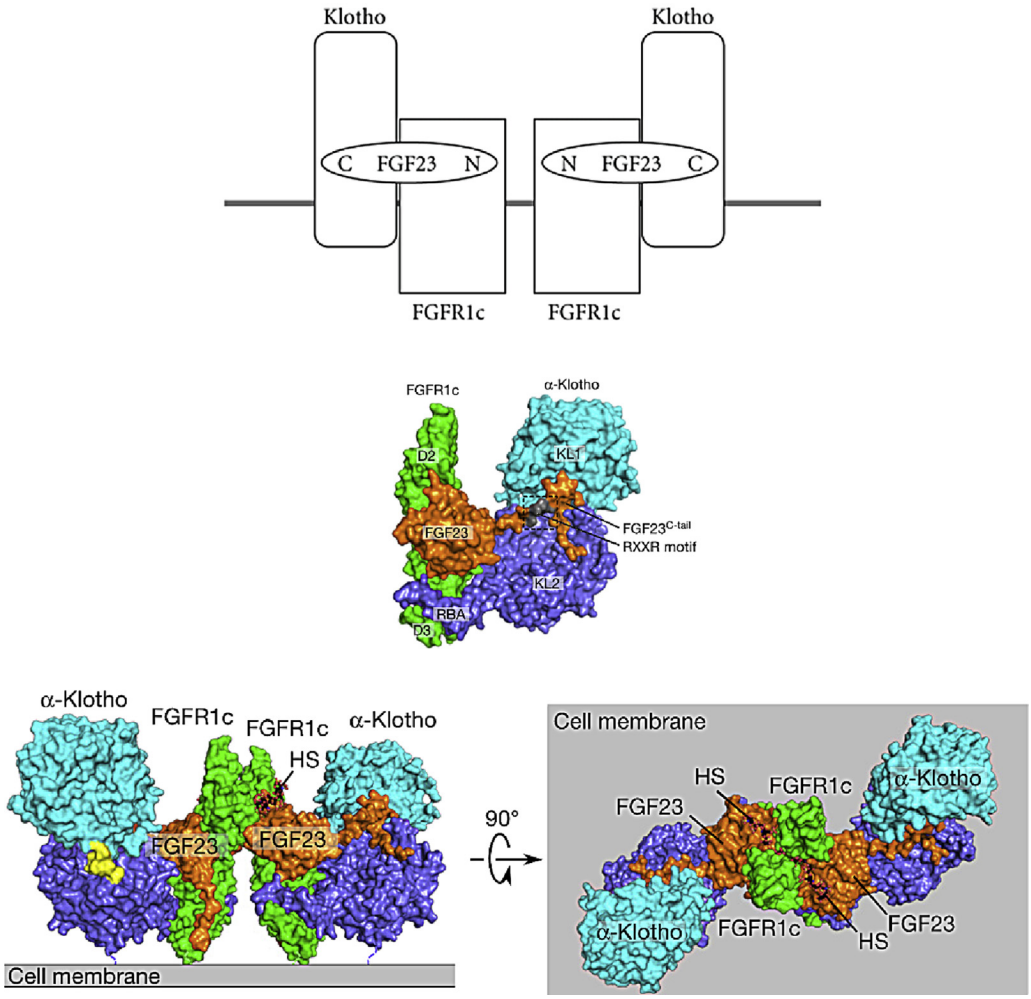

FIGURE 20.1 Schematic and crystal structure of the FGF23-FGFR1c-α-klotho complex. (Top) Schematic diagram of the membrane orientation of fibroblast growth factor 23 (FGF23)—receptor complex. The N terminus (N) binds to the extracellular domain of FGF receptor 1c (FGFR1c) and the C terminus (C) to α-klotho, in a dimerized configuration. (Middle) Surface topology of the ternary structure of this complex: α-klotho is shown in *cyan* (KL1 domain) and *purple* (KL2 domain), with FGF23 in *brown*, with the C terminus (*FGF23*$^{C\text{-}tail}$) bound to α-klotho and the N terminus to FGFR1c, shown in *green*. FGF23 is inactivated by cleavage at the protease recognition site (RXXR). (Bottom) Views of the complex in its dimer formation, stabilized by heparan sulfate (HS), parallel to the cell membrane (left) and looking down on the membrane (right). Colors are as noted for the middle; in *yellow* is the linker between the KL1 and KL2 domains of α-klotho. *Lower and middle images from Chen et al., 2018, with permission.*

function also results in elevated circulating FGF23; (3) FGF23 itself; and (4) FGFR1, which appears to be activated in osteocytes, resulting in elevated FGF23 expression. These observations have led to the consideration that osteocytes may directly respond to phosphate nutritional status, and ultimately relay, via production of FGF23, the mineral demands for bone maintenance to the kidney, where phosphate conservation is regulated. The osteocyte's response to phosphate status does not appear to be an acute process, as is observed with the extracellular calcium-sensing receptor system that regulates PTH secretion in parathyroid glands. It follows that genetic disruption of this pathway may result in the profound systemic disturbances observed in the diseases discussed herein.

In summary, the body's phosphorus status is largely adjusted at the kidney. Phosphate reabsorption is increased under conditions of greater need (rapid growth, pregnancy, lactation, and dietary restriction) and decreased during slow growth, chronic renal failure, or dietary excess. Changes in NPT2 protein abundance parallel these changes and are mediated by FGF23 and other possible factors. Removal of NPT2 cotransporters from the apical membrane of renal tubular cells is an acute process, mediated by PTH. The interaction of PTH and FGF23 in the overall process may also be important. Indeed, ablation of PTH in a murine model of excess FGF23 abrogates hypophosphatemia. Likewise, suppression of PTH may reduce phosphate losses even with persistence of high FGF23 (Bai et al., 2007; Carpenter et al., 2014), suggesting an interaction between the two pathways (Lanske and Razzaque, 2014).

Nutritional and gastrointestinal considerations

Whole-body phosphorus economy is summarized in Fig. 20.2. Dietary phosphorus is estimated at approximately 20 mg/kg/day, when not considering the phosphorus content of food additives. Based on NHANES data, dietary phosphorus intake in adults between the ages of 19 and 70 ranges from 1500 to 1700 mg/day for men and 1000 to 1200 mg/day for women (Calvo et al., 2014). Of the ingested phosphorus there is a net absorption of approximately 13 mg/kg; 16 mg/kg is unidirectionally absorbed, while 3 mg/kg is lost in endogenous gut secretions. The steady-state transit of phosphorus in and out of the skeletal compartment is balanced at roughly 3 mg/kg/day such that the daily urine phosphorus excretion largely reflects net gut absorption. The majority of the body's phosphorus (approximately 85%) is stored as hydroxyapatite in mineralized tissue. Roughly 14% is in soft tissues and only 1% is in the circulation or in the extracellular space. Eight-five percent of circulating phosphorus is ultrafilterable, the remainder is bound to serum proteins. The average woman in the United States has approximately 400 g of phosphorus stored in skeletal tissue, and men have approximately 500 g (Aloia et al., 1984).

The Western diet is awash in phosphorus, and dietary phosphorus estimates do not adequately capture the large amount of phosphorus in food additives. Estimates indicate that, at all ages, the typical phosphorus intake in the United States considerably exceeds the recommended dietary allowance by 1.5- to 2-fold (Calvo et al., 2014). This large phosphorus load may have deleterious consequences that are only now being studied. In a small clinical study, feeding healthy individuals a diet containing 1000 mg of phosphorus to which were added foods containing phosphorus additives resulted in increased circulating levels of FGF23, osteopontin, and osteocalcin, compared with the same diet with no food additives, suggesting the possibility that food additives in the context of the usual dietary phosphorus intakes could alter skeletal homeostasis (Gutierrez et al., 2015). Using NHANES data, a multiply adjusted association between high dietary phosphorus intake and all-cause mortality has been observed, with an inflection point at approximately 1400 mg/day of ingested phosphorus (Chang et al., 2014). It is noteworthy that men in the United States are estimated to have phosphorus intakes that often exceed 1400 mg/day (Calvo et al., 2014).

Intestinal phosphate absorption is highest in infancy and childhood and declines with age, but remains robust at approximately 50%–70% of bioavailable phosphorus. The majority of phosphate is absorbed in the small bowel by two pathways: the first is a passive paracellular pathway, in which phosphate moves through tight junction complexes formed by molecules, such as occludins and claudins. The second pathway is sodium-dependent phosphate cotransport, mediated by the type II sodium-dependent transporter NPT2b (encoded by *SLC34A2*) and, to a lesser extent, by the type III sodium-dependent transporter PIT1. The important role of NPT2b in intestinal phosphate absorption is highlighted by the impaired intestinal phosphate absorption in mice with genetic disruption of the gene (Sabbagh et al., 2009). The contributions of these two pathways to overall intestinal phosphate absorption vary, depending on the type and amount of dietary phosphate

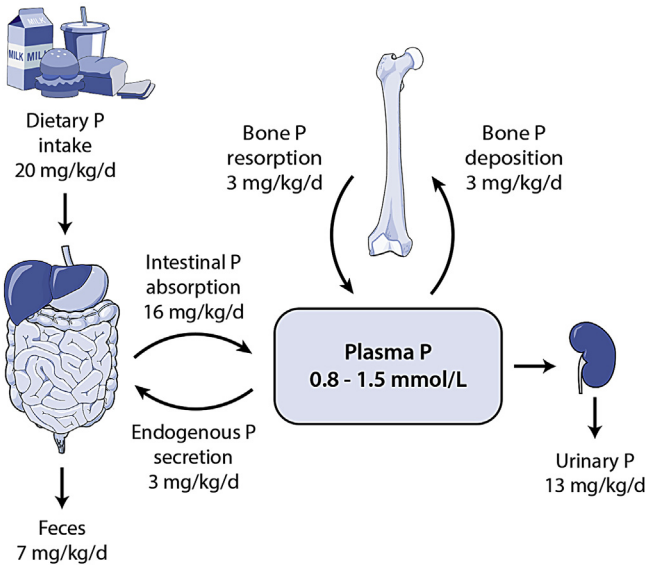

FIGURE 20.2 Summary of whole-body phosphorus economy. *From Figure 8.1, O'Brien, Kerstetter, Insogna. Chapter 8: Phosphorus; in Modern Nutrition in Health and Disease, 11th Edition. A. Ross, B. Caballero, R. Cousin, K. Tucker, T. Ziegler, eds. Lippincott, Williams and Williams. Baltimore, MD. pp 150–158. Reproduced with permission.*

presented to the gut. In experimental animals, it has been estimated that these two pathways contribute roughly equally to intestinal phosphate absorption (Lee and Marks, 2015). However, earlier estimates suggest that the paracellular pathway is the major mechanism for phosphate absorption. Both transcriptional and posttranscriptional regulation of Npt2b has been reported. For example, 1,25-dihydroxyvitamin D ($1,25(OH)_2D$) induces expression of Npt2b via a transcriptional mechanism, while low dietary phosphorus increases the activity of this transporter by posttranscriptional mechanisms. Whether changes in dietary phosphate absorption can lead to rapid changes in renal phosphate handling via as yet uncharacterized pathways that do not involve FGF23 or vitamin D remains an intriguing, but unproven, hypothesis. An early report suggested that this might be the case and, in particular, experimentally induced changes in duodenal phosphate absorption in rats led to rapid changes in renal phosphate handling without changes in systemic mineral homeostasis, suggesting novel "direct" gut/bone communication (Berndt et al., 2007). However, no similar observations have been reported nor have there been any further studies to characterize this pathway.

Finally, a novel interaction between the gut microbiota and FGF23 has been reported in an experimental model. Germ-free mice were found to have elevated circulating levels of FGF23 in the setting of low levels of 25-hydroxyvitamin D (25-OHD) and $1,25(OH)_2D$. Conventionalization of the germ-free mice (with the microbiome of normal mice) resulted in a fall in FGF23 levels and normalization in circulating levels of 25-OHD and $1,25(OH)_2D$. The authors posited that an inflammatory pathway, mediated by gut microbiota, leads to suppression of FGF23 expression. Whether changes in gut microbiota influence systemic phosphorus homeostasis through this pathway in humans remains unclear (Bora et al., 2018).

Phosphate and bone mineralization

The principal form of mineral in bone, hydroxyapatite ($Ca_{10}(PO_4)_6(OH)_2$), contains six atoms of phosphorus per crystal unit (each composed of two molecules). When the extracellular phosphorus supply is chronically deficient, mineralization is disrupted, resulting in the clinical conditions of rickets in children and osteomalacia in adults. Mineralization is essential during growth, when new bone is formed (modeling), as well as after epiphyseal closure, when replacing old bone and repairing damaged bone requires an orchestrated series of cellular events in which discrete packets of bone are removed and replaced (remodeling). Normal mineralization of bone requires the action of osteoblasts and hypertrophic chondrocytes, which secrete matrix vesicles (MVs). MVs have the ability to rapidly induce hydroxyapatite crystal formation in the presence of sufficient concentrations of extracellular calcium and phosphate (Bottini et al., 2018). Phosphate, liberated by the phosphatase PHOSPHO1 from phosphocholine, is then imported into the vesicle via the PIT1 transporter. The ambient extracellular phosphate concentration in bone is regulated by tissue nonspecific alkaline phosphatase (TNAP), which is abundant in MVs. TNAP cleaves PPi generating 2 phosphate molecules, resulting in a phosphate/PPi (Pi/PPi) ratio that favors mineralization. The process of mineralization is critically dependent on this ratio. Hydroxyapatite crystals initially form within MVs but are subsequently propagated onto the collagen matrix through as yet unclear mechanisms. The protein matrix that is eventually mineralized is composed primarily of collagen, but includes many other proteins, such as fibronectin, osteopontin, and osteocalcin.

There is currently intense interest in PPi as a central regulator of mineralization (Bottini et al., 2018; Bonucci, 2012; Zhou et al., 2012; Kim et al., 2010). In addition to TNAP, the extracellular concentration of PPi is regulated by several other proteins, including ENPP1 (ectonucleotide pyrophosphatase/phosphodiesterase 1), an exoenzyme that cleaves ATP to AMP and PPi. With genetic loss of function of ENPP1, extracellular concentrations of PPi are low, leading to rapid and aberrant mineralization of tissues, including the vasculature, a rare but devastating syndrome termed generalized arterial calcification of infancy (GACI) (Ferreira et al., 1993). Conversely, in the genetic absence of TNAP function, high PPi concentrations in the bone microenvironment prevent skeletal mineralization, resulting in the syndrome of hypophosphatasia, which in its most severe form is lethal around the time of birth (Whyte, 2017). ANKH (progressive ankylosis protein homolog) exports intracellular PPi and also plays a role in regulating the Pi/PPi ratio. Mutations in ANKH are associated with rare familial syndromes of calcium PPi deposition disease as well as autosomal dominant craniometaphyseal dysplasia (Pendleton et al., 2002; Nurnberg et al., 2001). Adding further complexity to this process is the fact that the hepatic-specific transporter ABCC6 (ATP binding cassette subfamily C member 6) also supports the extracellular concentration of PPi, since loss-of-function mutations are the basis for the syndrome pseudoxanthoma elasticum, in which serum PPi levels are low and heterotopic calcification, including in vascular tissue, can occur (Kranenburg et al., 2017). The fact that vascular calcification occurs in the genetic absence of both ENPP1 and ABCC6 points to the critical role of PPi in regulating heterotopic mineralization, particularly in the vascular tree. How these proteins modulate tissue mineralization in sites other than bone and vascular tissue remains to be fully explored.

Phosphorus also plays a critical role in chondrocyte maturation. The growth plate is a tightly regulated structure in which cells progress from resting to proliferating chondrocytes and then become prehypertrophic and finally hypertrophic chondrocytes that ultimately apoptose and are replaced by mineralized tissue. The concentration of extracellular phosphate is a key apoptotic signal for hypertrophic chondrocytes (Sabbagh et al., 2005). In the setting of low extracellular phosphate, chondrocytes fail to apoptose, which is part of the pathogenesis of the abnormal growth plate seen in hypophosphatemic rachitic disorders such as XLH. Since hypophosphatemia is also seen with nutritional rickets, the same pathology applies to that condition. A detailed molecular pathway involving ERK1/2−Raf signaling has been described as mediating the proapoptotic effect of phosphate in chondrocytes that, interestingly, is opposed by PTH-related protein, a cytokine that slows chondrocyte apoptosis (Papaioannou et al., 2017; Liu et al., 2014).

A fourth major participant in the regulation of mineralization is the hormone FGF23, which controls extracellular phosphate concentrations. Excess FGF23 levels cause systemic hypophosphatemia and impaired mineralization as described elsewhere in this chapter. In addition, it has been reported that FGF23 directly suppresses TNAP in osteocytes, allowing local concentrations of PPi to rise (Murali et al., 2016). This is another potential mechanism by which FGF23 could impair bone mineralization.

Finally, while the control of circulating levels of phosphorus by systemic hormones like FGF23, PTH, and $1,25(OH)_2D$, coupled with metabolism of PPi by TNAP, ENPP1, ANKH, and ABCC6, seems to be the major regulator of mineralization, other potential mechanisms that interact with phosphorus metabolism have been reported. Thus, the SIBLING proteins, such as osteopontin, as well as peptides derived from their incomplete metabolism in the absence of PHEX, called ASARM (acidic serine aspartate-rich MEPE-associated motif) peptides, have been reported to directly regulate phosphate metabolism and local bone mineralization (David et al., 2011; Boukpessi et al., 2017; Yuan et al., 2014). For this, the reader is referred to a discussion of the SIBLING proteins and ASARM peptides in the section of this chapter devoted to XLH.

Intracellular/extracellular compartmentalization

After absorption from the diet in the gut, phosphate is stored together with calcium as hydroxyapatite in the skeleton, and it is excreted in urine (for reviews see Forster et al., 2006; Prie et al., 2004; Liu and Quarles, 2007; Miyamoto et al., 2007; Shaikh et al., 2008; Strom and Juppner, 2008; White et al., 2006; Kurosu & Kuro-o, 2008) (Fig. 20.3). Phosphate typically moves between the intracellular and the extracellular compartments under the control of transporter proteins. The type III transporters PIT1 (*SLC20A1*) and PIT2 (*SLC20A2*) are ubiquitously expressed and are considered housekeeping transporters that mediate cellular uptake of phosphate to meet the needs of cell metabolism in many tissues. This metabolic uptake of phosphate into muscle, bone, and other tissues is regulated by various factors, such as phosphate itself (Chien et al., 1997; Wang et al., 2001), epinephrine (Suzuki et al., 2001), platelet-derived growth factor (PDGF) (Zhen et al., 1997), insulin and insulin-like growth factor 1 (Polgreen et al., 1994), basic FGF (Suzuki et al., 2000), and transforming growth factor-β (Palmer et al., 2000).

Upregulation of phosphate transporters by insulin, causing sequestration of phosphate into cells and hypophosphatemia, is encountered during refeeding in nutritionally deprived individuals following intravenous glucose infusion or oral carbohydrate intake (Petersen et al., 2005; Price et al., 1996; Butterworth and Younus, 1993; Kemp et al., 1993). Hypophosphatemia can also occur in the setting of high cellular demand for phosphate, for example, during rapid cell growth in hematological malignancies (Liamis and Elisaf, 2000; Milionis et al., 1999) or following hepatic resection (Keushkerian and Wade, 1984; Nafidi et al., 2007). In general, the circulating phosphate concentration is determined by phosphorus absorption from the intestine, excretion in urine, and balance between the intracellular and the extracellular compartments.

Mechanisms of phosphate transport

Transporter-mediated cellular absorption of dietary phosphate (Hilfiker et al., 1998), which is regulated in a $1,25(OH)_2D$-dependent manner (Wilz et al., 1979), accounts for 30% of intestinal phosphate absorption. The remaining 70% is absorbed through a poorly defined paracellular mechanism. The type II cotransporters NPT2a and NPT2c are expressed exclusively at the renal brush border membrane of the proximal tubules, where the bulk of filtered phosphate is reabsorbed (Segawa et al., 2002; Murer et al., 2004; Miyamoto et al., 2004; Shimada et al., 2004a). Based on data obtained in mice and rats, Npt2c is predicted to contribute about 15%−20% to total proximal tubular reabsorption of phosphate (TRP) (Segawa et al., 2002; Ohkido et al., 2003). Npt2c is thought to be rate-limiting only during weaning, with minimal contribution to total sodium/phosphate cotransport in adult rats (Segawa et al., 2002). The type III transporters, Pit1 and Pit2, are ubiquitously

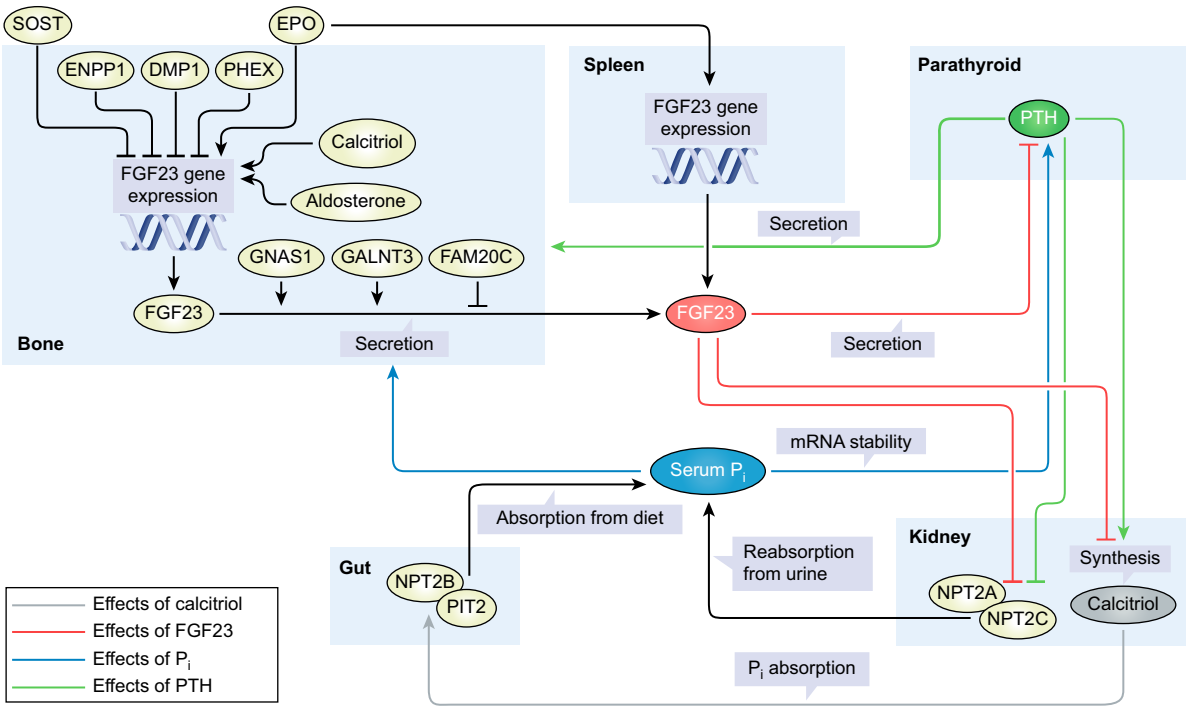

FIGURE 20.3 Regulation of phosphate homeostasis. Endocrine regulation of Pi homeostasis (originally published in Chande and Bergwitz, 2018). Serum phosphate (Pi) stimulates secretion of bioactive fibroblast growth factor 23 (FGF23) in osteoblasts and osteocytes (*blue arrow* (dark grey in print versions)), which directly or indirectly acts at the proximal tubule of the kidneys to inhibit synthesis of calcitriol and the function of NPT2A and NPT2C (*red arrows* (light grey in print versions)). Inhibition of calcitriol reduces absorption of Pi from the diet in the gut (*gray arrow*) and mobilization of Pi from bone mineral. Downregulation of NPT2A and NPT2C reduces renal phosphate reabsorption (*black arrows*). The net effect of FGF23 action is to lower blood levels of Pi. Similar to FGF23, parathyroid hormone (*PTH*) downregulates NPT2A and NPT2B and reduces renal phosphate reabsorption (*green arrows*(grey in print versions)). However, different from FGF23, PTH induces calcitriol and bone turnover, which increase blood Pi (*green arrows*). However, the net effect of PTH is to lower blood levels of Pi. Although not completely understood, golgi associated secretory pathway kinase (FAM20C), DMP1, ENPP1, and PHEX reduce FGF23 expression or secretion, whereas phosphate, iron deficiency, erythropoietin (EPO), GALNT3, and guanine nucleotide binding protein (G protein), alpha stimulating activity polypeptide 1 (GNAS1) stimulate it (*black arrows*). In addition, sclerostin (SOST) seems to negatively regulate FGF23 (*black arrows*). Furthermore, EPO might directly upregulate FGF23 gene expression in myeloid lineage stem cells of the spleen, providing a link to iron homeostasis (*black arrows*). PTH is suppressed by FGF23 in rodents but not in humans (*red arrow*). DMP1, dentin matrix acidic phosphoprotein 1; ENPP1, ectonucleotide pyrophosphatase/phosphodiesterase 1; GALNT3, UDP-*N*-acetyl-α-D-galactosamine:polypeptide *N*-acetylgalactosaminyltransferase, isoform 3; NPT2, solute carrier family 34 (type II) sodium/phosphate cotransporters (with "A", "B", and "C" species); PHEX, phosphate-regulating gene with homologies to endopeptidases on the X chromosome; PIT2, solute carrier family 20 (type III) sodium/phosphate cotransporter ("2" species).

expressed yet account for less than 1% of the mRNAs encoding the various renal sodium/phosphate cotransporters (Tenenhouse et al., 1998). All of these transporter classes utilize the transepithelial sodium gradient to transport phosphate against its electrochemical gradient into cells.

Intestinal phosphate transport

Intestinal uptake of phosphate occurs primarily by passive paracellular diffusion, while only 30% occurs via Na^+-dependent, carrier-mediated transcellular transport (Murer et al., 2000, 2004; Eto et al., 2006; Berndt & Kumar, 2009). The molecular mechanism of the former is unclear; the latter is mediated by the type IIb sodium/phosphate cotransporter NPT2b and the type III sodium/phosphate cotransporter PIT2 (Sabbagh et al., 2011; Giral et al., 2009; Xu et al., 2002, 2003, 2005; Yeh and Aloia, 1987). $1,25(OH)_2D$ and dietary phosphorus depletion are thought to be the most important physiological stimuli of intestinal phosphate absorption and act by increasing the abundance of NPT2b protein (Hattenhauer et al., 1999). Glucocorticoids (Yeh and Aloia, 1987) and estrogen (Xu et al., 2003) increase, and nicotinamide (Eto et al., 2005) decreases, intestinal phosphate transport, but the mechanism is unknown. There is no known direct effect of FGF23 or PTH on intestinal phosphate transporters (Tomoe et al., 2010), but intestine may release a factor(s) that

signals dietary phosphate availability to the kidney (Berndt et al., 2007). Evaluation of *Npt2b* (Sabbagh et al., 2009; Knöpfel et al., 2017) conditional knockout (KO) mice suggests that this transporter is probably the primary transepithelial intestinal phosphate transporter. Ablation of *Npt2b* attenuates the rise in blood phosphate seen in the setting of adenine-induced chronic kidney disease (CKD) (Schiavi et al., 2012; Sabbagh and Schiavi, 2014; Ohi et al., 2011). Furthermore, chronic adaptation to a low-phosphate diet in wild-type mice appears to go along with upregulation of *Npt2b* in the duodenum and upregulation of *Npt2a* in the proximal tubules (Giral et al., 2009). However, chronic adaptation in $Npt2b^{+/-}$ (Ohi et al., 2011), conditional $Npt2a^{-/-}$ mice (Schiavi et al., 2012), and, in our experience, $Npt2a^{-/-}$ mice (Pesta et al., 2016) suggests additional transport mechanisms.

Renal phosphate transport

Three classes of sodium/phosphate cotransporters are expressed in the kidney: the type I cotransporter, NPT1 (*SLC17A1*); the type II cotransporters, NPT2a (*SLC34A1*) and NPT2c (*SLC34A3*); and the type III cotransporter PIT2 (*SLC20A2*). Reabsorption of phosphate from the urine in the renal proximal tubules via NPT2a and NPT2c plays a key role in maintaining phosphate homeostasis, while other tubule segments are believed to be of less importance, and there are no known excretory mechanisms for phosphate. The NPT2a and NPT2c transporters preferentially transport divalent phosphate (HPO_4^{2-}) (Biber et al., 2013). Immunohistochemical analysis shows the localization of NPT2a to the apical membrane of renal proximal tubule cells (S1−S3 segments of the proximal tubule) in rodents (Murer et al., 2000, 2004; Berndt et al., 2005). Conversely, NPT2c in rodents appears to be expressed along with PIT2 only in segment 1 of the proximal tubules (Wagner et al., 2017). The NPT2c transporter, which shares approximately 54% amino acid identity with NPT2a, is not electrogenic and mediates cotransport at a ratio of 2 Na^+/1 HPO_4^{2-}. Renal expression of NPT2c in human kidneys was found to resemble the distribution seen in mice (Ohkido et al., 2007) and the response of these individuals to oral phosphorus therapy based on cross-sectional evaluation appears to resemble that described in Npt2a-KO and Npt2a;Npt2c-double-KO (DKO) mice.

Constitutive mouse KO models of Npt2a and Npt2c suggest that Npt2a mediates the bulk of renal reabsorption of phosphate, whereas the contribution of Npt2c to this process is minor and probably restricted to young mice (Miyamoto et al., 2007; Murer et al., 2000, 2004; Berndt et al., 2005; Segawa et al., 2009). Furthermore, rickets or osteomalacia is absent in both mouse models. However, Npt2a;Npt2c DKO suggest that both transporters have nonredundant roles, since these mice exhibit reduced body weight and expansion of the late hypertrophic zone in the bone, which is a characteristic feature of rickets, along with severe hypophosphatemia, hypercalciuria, and renal calcification, which can be reversed by a high-phosphorus diet (Segawa et al., 2009; Tomoe et al., 2009). In contrast to Npt2c-KO mice, humans with homozygous or compound-heterozygous loss-of-function mutations in NPT2c develop hypophosphatemic rickets in the first decade of life. These observations suggest that there may be important differences in renal phosphate handling between mice and humans.

FGF23 reduces reabsorption of phosphate by reducing expression of NPT2a and NPT2c (Yan et al., 2005). FGF23 binds to FGFR1c and its coreceptor klotho (Urakawa et al., 2006; Kuro-o, 2006) with activation of ERK1/2 at the distal convoluted tubules (Farrow et al., 2009). Alternatively, FGF23 may bind to FGFRs in the proximal tubule, leading to phosphorylation of NHERF1 via Sgk1 (Andrukhova et al., 2012). Also, a direct regulation of NPT2a activity by klotho without FGF23 has been demonstrated, whereby klotho causes cleavage and inactivation of NPT2a in the brush border membrane and subsequent internalization (Hu et al., 2010). Internalization of NPT2a from the apical membrane occurs as with receptor-mediated endocytosis (Bacic et al., 2006; Bachmann et al., 2004). Consequently, NPT2a is routed to lysosomes for degradation (Keusch et al., 1998; Pfister et al., 1998; Inoue et al., 2004). The regulation of NPT2c has been studied in less detail: in response to high phosphate, NPT2c downregulation occurs but is slower than for NPT2a (Miyamoto et al., 2007; Picard et al., 2010). Proximal TRP, to a lesser extent, is regulated by insulin, hormones of the somatotropic pituitary axis (Bringhurst and Leder, 2006), FGF7 (Carpenter et al., 2005), and possibly matrix extracellular phosphoglycoprotein (MEPE) and secreted Frizzled-related protein 4 (sFRP4) (White et al., 2006). The signaling mechanisms whereby insulin, growth hormone/IGF-1, FGF7, MEPE, and sFRP4 regulate NPT2a and NPT2c are unknown. The original description of Npt2c suggests that this transporter is exclusively expressed in mouse and rat kidney (Segawa et al., 2002). However, public RNA-sequencing expression databases (GTEx Consortium, 2013) and a qRT-PCR tissue expression analysis (Nishimura and Naito, 2008) suggest low-level expression of NPT2c in many tissues. Furthermore, data from a kidney-specific and inducible Npt2c-deficient mouse Npt2c (CKO) model (Myakala et al., 2014) suggest a role of extrarenal Npt2c in calcium homeostasis. However, the significance of widespread expression of Npt2c outside of the kidneys for human phosphorus and calcium metabolism requires further investigation.

Ubiquitous metabolic phosphate transporters

The PIT transporters serve as "housekeeping" transporters in most tissues (Kavanaugh and Kabat, 1996). Furthermore phosphate activates ERK1/2 in most cell types, and is blocked by pharmacological or genetic ablation of type III transporters (Wittrant et al., 2009). Since PIT1 is able to compensate for the loss of PIT2, intracellular phosphate may be what is "sensed" to activate ERK1/2. However, PIT transporters also bind and signal extracellular phosphate independent of phosphate transport, as shown in HeLa and vascular smooth muscle cells expressing a transporter-deficient mutation, [E70K]PIT1 (Chavkin et al., 2015; Beck et al., 2009). Furthermore, functional cooperation between PIT1 and FGFR1 appears to exist based on in vitro (Yamazaki et al., 2010) and in vivo (Xiao et al., 2014) reports. In addition to ERK1/2, the yeast second messenger inositol heptakisphosphate (IP7) (Azevedo and Saiardi, 2017; Saiardi, 2012) was found to be synthesized by inositol hexakisphosphate kinase 2 in various human cell lines, including HCT116 (colon) and U2OS (bone) cells (Koldobskiy et al., 2010). Furthermore, the highly conserved IP7 binding domain SPX is found in the xenotropic retroviral receptor 1 (XPR1) (Wild et al., 2016). Loss of function of XPR1 causes renal Fanconi syndrome in mice (Ansermet et al., 2017) and primary familial brain calcification (PFBC) in humans (Azevedo and Saiardi, 2017). These findings suggest a role for ERK1/2 and IP7 in metabolic phosphate effects, although details as to the mechanism and whether these second messengers regulate PTH, FGF23, or $1,25(OH)_2D$ remain unknown (Chande and Bergwitz, 2018).

As noted earlier intracellular phosphate may be sequestered into subcellular compartments. PIT1 can localize to the endoplasmic reticulum (ER) and contribute to regulation of ER stress in growth plate chondrocytes (Couasnay et al., 2019). The mitochondrial phosphate carrier PIC (SLC25A3) is part of a multiprotein complex, the mitochondrial permeability transition pore (MPTP), which regulates mitochondrial membrane potential and mitochondrial apoptosis (Pauleau et al., 2008), as well as being important in skeletal and cardiac muscle function (Seifert et al., 2015). The related dicarboxylate carrier (SLC25A10) (Fiermonte et al., 1999) catalyzes transport of dicarboxylates such as malate and succinate across the mitochondrial membrane in exchange for phosphate, sulfate, and thiosulfate.

Surprisingly mild bone and mineral metabolism phenotypes of the individual Pit1- and Pit2-KO mice suggest a high degree of redundance of these generally coexpressed transporters, and bone-selective ablation of Pit1 and Pit2 individually and in combination will likely shed a better light on their metabolic and endocrine functions. For example, acute chondrocyte-specific deletion of Pit1 in mice using a tamoxifen-inducible annexin-Cre in the first 2 days postnatally results in pronounced cell death, possibly as a result of phosphate-transport-independent ER stress (Couasnay et al., 2019), which in hindsight is consistent with earlier reported mildly reduced femur length in Pit1 hypomorphic mice (Bourgine et al., 2013) and the MV mineral defect observed in *collagen2a1*-Cre in Pit1;PHOSPHO1-DKO mice (Yadav et al., 2016).

Primary disorders of phosphate homeostasis

Fibroblast growth factor 23–mediated hypophosphatemic disorders

X-linked hypophosphatemia (OMIM: 307800)

In 1936, Fuller Albright reported a case of rickets unresponsive to vitamin D treatment, and thus termed the condition "vitamin D-resistant rickets "(Albright et al., 1936). In the late 1950s the cardinal feature of renal phosphate wasting, together with an X-linked dominant inheritance pattern, was recognized (Hsia et al., 1959). Subsequent studies in the *Hyp* mouse, a murine model of XLH, demonstrated defective renal tubular phosphate transport (Glorieux and Scriver, 1972; Bell et al., 1988), and decreased expression of renal sodium/phosphate cotransporters in the renal tubules (Tenenhouse et al., 1994; Collins and Ghishan, 1994). In 1974 the observation of persistent hypophosphatemia following renal transplantation in a man with classical XLH raised the consideration that the disease was due to a humoral factor rather than an intrinsic renal defect (Morgan et al., 1974). This concept was substantiated by Meyer and Meyer, who demonstrated that a normal mouse joined in parabiosis to a *Hyp* mouse became hypophosphatemic (Meyer Jr. et al., 1989).

In 1995, loss-of-function mutations in PHEX, a neutral endopeptidase, were shown to be responsible for XLH (HYP-Consortium, 1995). In 2000/2001, a circulating factor responsible for tumor-induced osteomalacia (TIO) and autosomal dominant hypophosphatemic rickets (ADHR) was identified as FGF23, a novel member of the FGF family (ADHR Consortium T, 2000; Shimada et al., 2001). It was quickly realized that FGF23 was overproduced in XLH, establishing that disorder as a classic endocrine syndrome due to overproduction of a hormone (Jonsson et al., 2003; Yamazaki et al., 2002). In XLH, FGF23 is overproduced by osteocytes (Feng et al., 2006), where PHEX is primarily expressed, but how PHEX regulates the production of FGF23 remains unclear.

Pathophysiology

FGF23 directs the kidney to excrete phosphate upon exposure to an excessive phosphate load. Its production is stimulated by increases in extracellular phosphate (and also by $1,25(OH)_2D$) but this axis is perturbed in XLH, such that FGF23 is overproduced, despite the ambient hypophosphatemia. Consequent suppression of transcription of the renal sodium/phosphate cotransporters NPT2a and NPT2c (Shimada et al., 2004b, 2004a; Erben, 2016), as well as their removal from the apical surface of the proximal renal tubule cell (Murali et al., 2016), results in reduced phosphate reclamation. FGF23 also decreases circulating $1,25(OH)_2D$, resulting in impaired intestinal calcium and phosphate absorption.

Abnormal metabolism of bone-derived extracellular matrix proteins may also contribute to the pathophysiology of XLH. Substrates for PHEX may include SIBLING proteins (osteopontin, bone sialoprotein, DMP1, dentin sialophosphoprotein, and MEPE). In vitro evidence suggests that these proteins can be metabolized by PHEX, and in the absence of normal metabolism, protein fragments—ASARM peptides—accumulate, resulting in inhibition of bone mineralization in vitro and renal phosphate wasting in vivo (David et al., 2011; Barros et al., 2013; Addison et al., 2010). Moreover, work has identified increased osteopontin in the osteomalacic osteoid of Hyp mice, and less extensive osteomalacia in the osteopontin null/Hyp (DKO mouse) compared with Hyp littermates (Hoac et al., 2018).

Prevalence

The exact prevalence of XLH is estimated as between 1 in 20,000 live births (United States and Denmark) and 1 in 60,000 (Norway) (Ruppe; Beck-Nielsen et al., 2009; Rafaelsen et al., 2016). As many as 25% of cases appear to be sporadic (Beck-Nielsen et al., 2012; Whyte et al., 1996).

Clinical manifestations

XLH causes rickets in children manifest as bowed lower extremities, short stature, and radiographically abnormal epiphyses. Both children and adults with XLH suffer from the early appearance and persistent recurrence of dental abscesses. These are associated with structural abnormalities in the tooth, including abnormal mineralization of dentin, less abundant cementum, impaired tooth attachment, and increased risk of periodontal disease (Antoniucci et al., 2006; Coyac, 2017). Pulp chambers appear to be enlarged while enamel is largely unaffected (Turan et al., 2010). How these changes relate to the pathogenesis of dental abscesses is not clear. Tooth fragility is often also reported by patients, including fracturing of teeth with normal mastication. Finally, craniosynostosis with associated Chiari malformations are not infrequent occurrences in XLH (Rothenbuhler et al., 2018).

Skeletal disease in XLH was once thought to quiesce following epiphyseal closure, but in fact, adults experience some of the worst complications of the disease. Nearly all affected adults have osteomalacia and poor bone quality leading to increased risks of clinical fracture and insufficiency fractures with little or no trauma, occurring most often in the lower extremities. Abnormal biomechanics (persisting from deformities acquired in childhood) contribute to the high incidence and early onset of osteoarthritis. Osteophytes and calcification of tendons and ligaments at insertion sites (entheses) occur, and can severely limit of range of motion, particularly of the hips, elbows, and shoulders (Liang et al., 2009; Connor et al., 2015). Degenerative changes in the spine may lead to restricted range of motion and chronic low back pain. Calcification of the spinal longitudinal ligaments can occur (Hirao et al., 2016; Forrest et al., 2016; Shiba et al., 2015), as well as spinal stenosis, result in neurologic deficits requiring surgical intervention (Chesher et al., 2018). Scoliosis is common, and hearing loss occurs (Fishman et al., 2004).

Both children and adults with XLH complain of weakness and diminished endurance, which may in part relate to impaired muscle function. Indeed, hypophosphatemia is associated with impaired ATP flux in skeletal muscle, which improves with correction of the hypophosphatemia (Pesta et al., 2016).

Therapy

Medical treatment for XLH historically included phosphate supplements with vitamin D used as a cotherapy. Limited efficacy, secondary hyperparathyroidism, and vitamin D intoxication were not infrequent. In 1980, Glorieux et al. published a landmark study comparing phosphate alone with combined therapy with ergocalciferol and phosphate and with calcitriol and phosphate (Glorieux et al., 1980). Histomorphometric improvement in osteomalacia with calcitriol and phosphate was superior to that of the other two regimens, serum phosphorus levels were improved to a greater extent, and radiographic healing of rickets was superior as well. This work led to a fundamental change in the treatment for XLH, and until 2018, calcitriol and phosphate therapy was the standard medical treatment for children. The therapy, however, does require careful monitoring to avoid hypercalcemia, hypercalciuria, and secondary hyperparathyroidism. Frequent dose adjustments are required as the skeleton grows, necessitating careful monitoring, usually every 3–6 months during rapid

growth (Carpenter et al., 2011). Adherence is particularly difficult, as multiple doses of phosphate and two doses of calcitriol daily are usually employed. Phosphate supplementation has frequent gastrointestinal side effects, such as nausea and diarrhea, which further complicate compliance. With good adherence and careful monitoring, and when initiated early in life (i.e., less than 2 years of age), linear growth is improved, and there are fewer rachitic deformities.

Despite these effects, *surgical treatment* is often additionally required in XLH. Correction of genu valgus or genu varum of the lower extremities has traditionally required osteotomies and rodding of the long bones of the lower extremities (Eyres et al., 1993). More recently, when identified early in childhood, and when the bowing deformities are mild−moderate, epiphysiodesis can be used as a less invasive approach to guide growth at the distal femur or tibial growth plates (Ghanem et al., 2011). Children with cranial stenosis sometimes have severe headaches that require surgical treatment.

Growth hormone has been used as an adjunct to standard therapy in children with XLH, with mixed results. Some studies suggest improved linear growth, while others report little long-term benefit and potential worsening of disproportion between upper and lower body segments (Baroncelli et al., 2001; Haffner et al., 2004; Zivicnjak et al., 2011).

In contrast, therapy for adults has remained less widely employed; however, calcitriol and phosphate have been shown to have efficacy in adults: calcitriol and phosphate led to a 50% healing in osteomalacia (over 4 years) and a subjective improvement in pain in an open-label trial (Sullivan et al., 1992). In that study the daily dose of calcitriol and phosphorous ranged between 1.0 and 2.0 μg/day and 1.0 and 1.5 g/day, respectively. Other cross-sectional studies have demonstrated that therapy with calcitriol and phosphate during adult life is associated with less severe dental disease (Connor et al., 2015).

Conventional therapy does prevent enthesopathy, or hearing loss. Even when initiated early in childhood the therapy does not result in a normal adult height. Male sex and obesity portend worse enthesopathy and, importantly, in a cross-sectional study, persistent secondary hyperparathyroidism tended to be associated with worse enthesopathy (Connor et al., 2015). The latter point is highlighted by a study in which paricalcitol was used to suppress PTH in patients with XLH and secondary hyperparathyroidism (Carpenter et al., 2014). Despite the expected rise in FGF23 when paricalcitol was added to conventional therapy, the renal phosphate threshold improved, and bone-specific alkaline phosphatase fell. These data suggest that PTH contributes to the renal pathophysiology in XLH and is a major driver of skeletal turnover. Whether an increase in skeletal turnover contributes to enthesopathy remains unclear, and requires further study.

In 2018, a fully humanized monoclonal blocking antibody to FGF23, burosumab, was approved for treatment of XLH in children and adults in the United States and Canada and in children in the European Union. The drug binds to FGF23, and thereby inhibits the activity of the elevated circulating levels, essentially reversing the major pathophysiologic element of the disease. Renal phosphate reclamation improves and $1,25(OH)_2D$ production is restored, limiting the tendency for PTH oversecretion. In open-label clinical trials in 5- to 12-year-old children (90% of whom were treated with conventional therapy for ~7 years) the serum phosphorus levels corrected and were maintained in the low normal range in more than 90% of the study subjects (Wolfgang et al., 2018), with accompanying improvements in rickets (Carpenter et al., 2018). More recently, in a head-to-head comparison with conventional therapy, burosumab administered every 2 weeks showed more impressive improvements in serum phosphorus, alkaline phosphatase, and radiographic healing of rickets (Imel et al., 2018). Complications in children have been thus far limited to local injection site reactions and rare occurrences of urticaria. In adults, a double-blind, placebo-controlled, 24-week trial showed that monthly administration of burosumab (1 mg/kg) improved serum phosphorus and $1,25(OH)_2D$ levels, with over 90% of patients normalizing serum phosphorus at the dose cycle midpoint (2 weeks after dosing) (Insogna et al., 2018). Stiffness was significantly improved. Comprehensive imaging identified numerous extant fractures and pseudofractures at baseline; subjects treated with burosumab had a 17-fold greater likelihood of healing fractures and pseudofractures than those receiving placebo (Insogna et al., 2018). Preliminary data from a second year of treatment support continued efficacy of the drug in adults (Portale et al., 2018). Treatment of adults with burosumab demonstrated greater than 50% healing of osteomalacia (Insogna et al., 2018) after 1 year of therapy, comparable to that seen after 4½ years in the previously mentioned open-label trial of calcitriol and phosphate. The safety profile of burosumab was good, with restless leg syndrome and local injection site reactions being the only adverse events of note. Importantly, there has not been any evidence of development of nephrocalcinosis or worsening of existing nephrocalcinosis with burosumab, and no evidence for heterotopic cardiac calcification.

Early treatment of XLH in children has been advantageous, and conventional therapy has generally been applied by 6 months of age. It is recommended that treatment of affected children with burosumab be initiated as soon as possible after the first birthday until safety and dosing parameters in infants less than one year of age is established. It is unclear which children should discontinue currently applied conventional therapy and begin treatment with burosumab. Longer term follow-up may provide important guidance in that regard, but thus far, it appears that burosumab is likely to be safer, more convenient, and more effective than conventional therapy. Importantly, adherence is likely to be far better with the parenteral, less frequent dosing regimen. One barrier to the use of burosumab is its high expense, although the

manufacturer's program to assist patients while negotiating insurance coverage for the drug has been operational in many settings. In contrast to children, there is no consensus on indications for treatment of any kind for adults with XLH. Suggested indications for treating adults with conventional therapy have been published, although these are not strictly evidenced based and largely represent recommendations from a group of experienced clinicians (Carpenter et al., 2011). Nonetheless they could serve as initial indications for burosumab. They include (1) spontaneous insufficiency fractures, (2) pending orthopedic procedures, (3) biochemical evidence of significant osteomalacia (specifically a significantly elevated bone-specific alkaline phosphatase), and (4) disabling skeletal pain.

Autosomal dominant hypophosphatemic rickets (OMIM: 193100)

Although occurring with far less frequency, ADHR is a disorder with a clinical presentation essentially identical to that of XLH, but occurring in the setting of autosomal dominant inheritance. Patients with an XLH-like phenotype in families with male-to-male transmission should be suspected as having this disorder (Harrison and Harrison, 1979; Econs and McEnery, 1997). Like XLH, hypophosphatemia secondary to renal phosphate wasting occurs, with lower extremity deformities, and rickets/osteomalacia. Affected patients also demonstrate normal serum 25-OHD levels, with inappropriately normal serum concentrations of $1,25(OH)_2D$, all hallmarks of XLH (Table 20.1). PTH levels are normal. Long-term studies indicate that a few of the affected female patients demonstrate delayed penetrance of clinically apparent disease and an increased tendency to fracture, features that appear to be less common in XLH. In addition, among patients with the expected biochemical features documented in childhood, some patients, albeit rarely, have been reported to lose the renal phosphate wasting defect after puberty. Specific missense mutations in FGF23 that result in the substitution of an arginine residue at amino acid residue 176 or 179 are present in patients with ADHR (ADHR Consortium, 2000). These mutations disrupt an RXXR subtilisin/furin protease recognition site, and the resultant mutant molecule is thereby protected from proteolysis, and resultant accumulation of unprocessed FGF23 results in elevated circulating intact FGF23 levels.

Circulating FGF23 levels can vary and reflect the activity of disease status (Imel et al., 2007). Exploration of the waxing/waning severity of disease in ADHR has indicated that iron may play a significant role in the regulation of circulating FGF23 (Imel et al., 2011). It is now evident that iron deficiency is able to upregulate FGF23 expression, and in normal individuals the unrestricted processing of the intact protein to its inactive N- and C-terminal fragments is able to compensate for the increased intact FGF23 production observed in the setting of iron deficiency. Therefore normal individuals who become iron deficient maintain normal circulating levels of intact FGF23 despite an increase in production. However, in ADHR, inefficient processing of FGF23, due to the impaired recognition of the protease site, may not be able to compensate for increased FGF23 synthesis during periods of iron deficiency, resulting in elevated active FGF23 accumulation in the circulation with the subsequent renal effects on phosphate excretion. It appears that the waxing and waning clinical severity observed in some cases of ADHR may be amenable to iron supplementation and provide a straightforward approach to therapy. Correction of serum iron levels to high normal levels allowed for discontinuation of conventional rickets medications in one report (Kapelari et al., 2015).

Autosomal recessive hypophosphatemic rickets

Autosomal recessive hypophosphatemic rickets type 1 (ARHR1; OMIM: 241520). Another gene identified as causal to FGF23-mediated hypophosphatemia is *DMP1*, which encodes the SIBLING protein dentin matrix protein 1, yet another product of the osteocyte. Biallelic loss of function mutations in *DMP1* can result in autosomal recessive phosphate wasting rickets due to excess circulating FGF23 levels. The same constellation of progressive rachitic deformities seen in both XLH and ADHR (Feng et al., 2006; Lorenz-Depiereux et al., 2006a) occurs, along with the features of hypophosphatemia, excess urinary phosphate loss and aberrant vitamin D metabolism (normal circulating 25-OHD and $1,25(OH)_2D$ levels, despite ambient hypophosphatemia), observed in XLH and ADHR. In addition to the expected phenotypic features consequential to excess FGF23, and in contrast to XLH, spinal radiographs of patients with ARHR reveal noticeably sclerotic vertebral bodies and sclerosis of the skull. The clinical diagnosis of a novel sclerosing dysplasia in adulthood led to the investigation of the causes of osteopetrosis in one recently reported family, but genetic investigation revealed *DMP1* mutations (Gannage-Yared et al., 2014). Mild hypophosphatemia was present. In addition to the enlarged pulp chamber characteristic of teeth in individuals with XLH, enamel hypoplasia can be evident in heterozygotes. Experience with long-term follow-up is not widespread in ARHR and therapeutic response or guidelines have not been definitively established, although severe adult complications of disease such as enthesopathy have been documented (Gannage-Yared et al., 2014; Karaplis et al., 2012). One 2016 study in a *DMP1*-KO animal model of the disease found that an anti-sclerostin antibody improved osteomalacia with little effect on the serum phosphorus or FGF23 levels (Ren et al., 2016).

TABLE 20.1 Human genetic disorders of phosphate homeostasis.

Disorder	Abbreviation	Inheritance	Gene	Mechanism	OMIM No.	Reference
Hyperphosphatemic disorders						
Hyperphosphatemic familial tumoral calcinosis type 1 and the allelic variant Hyperostosis–hyperphosphatemia syndrome	HFTC HSS	AR AR	GALNT3	FGF23 deficiency	211900 610233	(Topaz et al., 2004; Frishberg et al., 2004)
Hyperphosphatemic familial tumoral calcinosis type 2	HFTC	AR	FGF23	FGF23 deficiency	211900	(Ichikawa et al., 2006; Benet-Pages et al., 2005)
Hyperphosphatemic familial tumoral calcinosis type 3	HFTC	AR	KL	FGF23 resistance	211900	Ichikawa et al. (2007)
Pseudohypoparathyroidism	PHP1A PHP1B	AD AD	GNAS GNAS or up-stream regulatory region	PTH resistance FGF23 independent	103580 603233	(Weinstein et al., 1992; Juppner et al., 1998)
Familial isolated hypoparathyroidism	FIH	AD or AR	CaR GCMB PTH	PTH deficiency; FGF23 independent	146200	(Arnold et al., 1990; Pollak et al., 1994; Ding et al., 2001)
Blomstrand disease	BOCD	AR	PTHR1	PTH resistance; FGF23 independent	215045	(Zhang et al., 1998; Karperien et al., 1999)
Hypophosphatemic disorders						
X-linked hypophosphatemia	XLH	X-linked	PHEX	FGF23 dependent	307800	HYP-Consortium (1995)
Autosomal dominant hypophosphatemic rickets	ADHR	AD	FGF23	FGF23 dependent	193100	ADHR Consortium T (2000)
Autosomal dominant hypophosphatemic rickets with hyperparathyroidism	ADHR	AD	KL	FGF23 dependent	612089	Brownstein et al. (2008).
Autosomal recessive hypophosphatemia	ARHP	AR	DMP1	FGF23 dependent	241520	Lorenz-Depiereux et al. (2006)
Hereditary hypophosphatemic rickets with hypercalciuria	HHRH	AR	SLC34A3	Proximal tubular Pi wasting, FGF23 independent	241530	(Bergwitz et al., 2006; Lorenz-Depiereux et al., 2006b)

Vitamin-resistant rickets type 1	VDDR1	AR	CYP27B1	$1,25(OH)_2D$ deficiency, FGF23 independent	264700	Kitanaka et al. (1998)
Vitamin-resistant rickets type 2	VDDR2	AR	VDR	$1,25(OH)_2D$ resistance, FGF23 independent	277440	Hughes et al. (1988)
Familial hypocalciuric hypercalcemia/ neonatal severe hyperparathyroidism	FHH NSHPT	AD/AR	CaR	PTH excess, FGF23 independent	145980 239200	Pollak et al. (1993)
Jansen disease		AD	PTHR1	Constitutively active PTHR1; FGF23 dependent	156400	(Schipani et al., 1995), (Brown et al., 2009)
Normophosphatemic disorders						
Pulmonary alveolar microlithiasis	PAM	AR	SLC34A2	Reduced alveolar epithelial Pi uptake	265100	Sabbagh et al. (2009)
Normophosphatemic familial tumoral calcinosis	NFTC	AR	SAMD9	Unknown	610455	Topaz et al. (2006)
Muscular dystrophy and cardiomyopathy	MDC	AR	SLC25A3	Reduced mitochondrial Pi uptake	610773	(Bhoj et al., 2015; Mayr et al., 2011)
Primary familial basal ganglial calcification type 1	PFBC1	AR	PIT2	Reduced microglial Pi uptake	213600	Lemos et al. (2015)
Primary familial basal ganglial calcification type 6	PFBC6	AR	XPR1	Reduced vascular Pi export	616413	Legati et al. (2015)
Primary familial basal ganglial calcification type 3	PFBC4	AR	PDGFBR	Reduced PIT2 expression	615007	Keller et al. (2013)
Primary familial basal ganglial calcification type 4	PFBC5	AR	PDGFB	Reduced PIT2 expression	615483	Keller et al. (2013)

$1,25(OH)_2D$, 1,25-dihydroxyvitamin D; *AD*, autosomal dominant; *AR*, autosomal recessive; *FGF23*, fibroblast growth factor 23; *Pi*, phosphate; *PIT2*, solute carrier family 20 (type III) sodium/phosphate cotransporter 2; *PTH*, parathyroid hormone.

ARHR2 (OMIM: 613312). Another rare variant of hypophosphatemic rickets with renal phosphate wasting, ARHR2, occurs in association with GACI (Levy-Litan et al., 2010; Lorenz-Depiereux et al., 2010; Rutsch et al., 2003). ARHR2 and GACI are attributed to homozygous loss-of-function mutations of ENPP1. Loss of function of ENPP1 results in the inability to generate the mineralization inhibitor PPi, thereby disrupting the restriction of heterotopic (e.g., vascular) mineralization. GACI is often fatal, but hypophosphatemia, identified in the setting of elevated FGF23 levels in an adult with a homozygous ENPP1 mutation, raised this consideration of rickets in survivors of GACI (Lorenz-Depiereux et al., 2010). Moreover the patient's son was affected with both GACI and hypophosphatemia. The mechanism by which this enzyme influences renal tubular phosphate wasting is not evident, and further study is necessary to understand this intriguing problem. One speculated mechanism may reflect a bone cell response to a relatively hypermineralized (or high phosphate/low PPi) milieu, which results in a compensatory, prolonged secretion of FGF23. Such a mechanism may effectively signal the kidney to reduce the body's mineral load, but apparently cannot be downregulated to protect against excessive phosphate losses. Although there has been concern that the treatment of rickets in patients affected with GACI may promote worsening of vascular calcification (Rutsch et al., 2008), no evidence to sustain this concern has emerged, and one long-term observational report suggests that treatment does not worsen this finding (Ferreira et al., 2016).

Tumor-induced osteomalacia

TIO is a rare paraneoplastic syndrome caused by difficult-to-localize, usually benign tumors that secrete a circulating factor causing renal phosphate wasting. Many of the biochemical features of TIO mimic those seen in XLH, as the secreted factor in most tumors is FGF23, as occurs with XLH. TIO has been reviewed in detail and the reader is referred to that summary for additional details (Chong et al., 2011).

The differential diagnosis of TIO includes other FGF-dependent phosphate wasting disorders, which are often genetic in origin, such that a family history and documentation of time of onset of disease are useful in differentiating these conditions from TIO. Genetic testing may be useful. Among the most important clinical findings in TIO is profound weakness. Despite equivalent degrees of fasting hypophosphatemia, and often a similar extent of histologic osteomalacia, patients with lifelong hypophosphatemia, as in XLH, seem to function much better than patients with TIO, who usually acquire hypophosphatemia later in life. Patients with TIO are not infrequently crippled by their disease, with severe skeletal pain and obvious muscle weakness, manifested by difficulty with ambulation or rising from the floor or chair. Bone pain in TIO is due to the osteomalacia and resulting pseudofractures, which result from chronic phosphate wasting. Fractures occur most often in ribs and in weight-bearing bones such the spine and pelvis, femurs (included the femoral neck), and feet. The muscle weakness is presumably due to a hypophosphatemic myopathy. Correction of the hypophosphatemia often results in improvement in muscle function considerably before healing of the osteomalacia. Since the correct diagnosis is often missed for years, patients with TIO frequently suffer with poor quality of life for extended periods of time (Sanders, 2018).

TIO-causing tumors, categorized as phosphaturic mesenchymal tumors—mixed connective tissue variant (PMTs—MCT) (Folpe et al., 2004), have a varied histologic appearance, frequently with bland, spindle-shaped cells in a myxoid matrix and occasionally osteoclast-like giant cells. A microvascular component is often present. PMTs—MCT can occur in any tissue but frequently arise in soft tissues such as muscle or fat or in skeletal tissues, including bone, cartilage, and tendons. Rarely, tumors other than PMTs—MCT can cause TIO, including myeloma and prostate cancer (Narvaez et al., 2005; Nakahama et al., 1995).

As with XLH, hypophosphatemia occurs with renal phosphate wasting, circulating $1,25(OH)_2D$ levels are low, and 25-OHD levels are normal or low normal, excluding vitamin D deficiency as the cause of the patient's symptoms. PTH levels are usually normal, as is serum calcium. If the clinical index of suspicion is high and biochemical features are consistent, then measuring circulating FGF23 is an appropriate confirmatory study. Rarely, other circulating factors have been associated with TIO, including FGF7, FRP4, and MEPE (Carpenter et al., 2005; Chong et al., 2011; Jan de Beur et al., 2002). Interestingly, nearly 40% of TIO tumors have a chromosome rearrangement resulting in expression of a fusion protein in which a fibronectin molecule is fused with the FGFR1 (Lee et al., 2015). Although no direct experimental evidence has yet been reported, it has been speculated that TIO results, in part, from a feed-forward circuit in which tumor-secreted FGF23 activates this hybrid molecule and induces further FGF23 production.

Localizing the offending tumor can be challenging. A careful physical examination, focused on the head, neck, and oral pharynx, with palpation all soft tissues, can sometimes identify a PMT—MCT. Newer imaging technologies have greatly improved tumor localization. Among these is indium-111-labeled octreotide scintigraphy combined with single-photon-emission computed tomography (SPECT/CT) scanning, which allows for 3D visualization as well as taking advantage of the fact that TIO tumors often express somatostatin receptor subtype 2. Fluorodeoxyglucose positron emission tomography (FDG—PET)/CT is increasingly used to localized tumors in patients with TIO, particularly those that are not octreotide

avid or are very small. The extreme sensitivity of FDG−PET/CT, however, can lead to false positive results. 1,4,7,10-Tetraazacyclododecane-1,4,7,10-tetraacetic acid (DOTA) (and its derivatives DOTANOC and DOTATATE) PET/CT addresses the "nonspecificity" of conventional FDG−PET/CT by employing a bifunctional chelator that binds gallium and the type 2 somatostatin receptor with high affinity (DOTA NaI^3-octreotide) (Wild et al., 2005; Hesse et al., 2007a; El-Maouche et al., 2016). Reports indicate that this approach may be more sensitive than conventional octreotide SPECT/CT (von Falck et al., 2008). Since the cranial/facial area, as well as distal extremities, can harbor TIO-inducing tumors, it is important to include the entire body in these scan images. In the past, venous sampling has been used in an effort to identify tumors, but the aforementioned imaging studies have largely supplanted the need for that more invasive diagnostic approach.

Effective treatment for TIO is complete surgical resection of the tumor when possible. Generally, these tumors are benign and slow growing with a low mitotic index. Occasionally TIO tumors can arise in a surgically inaccessible site or can be locally invasive, making complete resection impossible. We encountered such a patient, with a cervical vertebral tumor and extensive involvement of paraspinal soft tissues. Rarely TIO tumors can be frankly malignant and metastasize. In patients in whom the tumor cannot be completely resected or identified, medical management can provide significant symptomatic improvement. At this writing, treatment with calcitriol and supplemental phosphorus represents the best medical therapy for TIO. Conventional doses of calcitriol and phosphorus, in the range of 1−3 μg/day calcitriol and 1−3 g/day phosphorus in divided doses, are usually effective. Unlike in XLH, secondary hyperparathyroidism is less often encountered in TIO when using calcitriol/phosphorus, but hypercalciuria and even hypercalcemia can occur, so blood and urine calcium, in addition to serum phosphorus, needs to be monitored during treatment to avoid overreplacement. Unlike in XLH, where FGF23 levels are usually modestly elevated, in TIO FGF23 levels are also often very elevated, despite which conventional therapy seems to provide symptomatic improvement.

The use of a blocking antibody to FGF23 (burosumab) has shown promising results in the treatment of TIO. In an open-label trial, patients with TIO had significant improvement in their hypophosphatemia and marked symptomatic improvement with monthly administration of the drug at doses up to 1 mg/kg (Jan de Beur et al., 2018). A selective FGFR inhibitor (NVP-BGJ398) has, in preliminary studies, been reported to cause dramatic symptomatic improvement in a patient with metastatic TIO. In this patient the drug also caused tumor regression (Collins et al., 2015). Finally, radiofrequency ablation has been used to treat TIO tumors where a non-invasive approach was preferred (Hesse et al., 2007b).

Other FGF23-mediated hypophosphatemic syndromes

In widespread fibrous dysplasia of bone (due to mosaic-activating mutations in GNAS, as part of the McCune−Albright syndrome) (OMIM: 174800), hypophosphatemic osteomalacia/rickets can be a result of elevated circulating FGF23 levels. Indeed, variable degrees of decreased renal tubular phosphate reabsorption, as assessed by tubular maximum reabsorption of phosphate/glomerular filtration rate (TmP/GFR), occur in patients with fibrous dysplasia of bone. Of note, given that activation of GNAS in the renal proximal tubule would be expected to result in phosphaturia, it had long been considered that the mechanism of reduced renal TRP was due to a surmised renal distribution of the mosaic-activating GNAS mutation. The studies of Rimunucci et al. identified elevated circulating FGF23 levels in this condition and that the greater burden of skeletal disease is associated with more impressive hypophosphatemia. Whether the bone affected with fibrous dysplasia or normal bone under other systemic influences accounts for the increased FGF23 secretion has not been clearly settled.

Somatic mutations in HRAS and NRAS appear to generate a mechanism by which mutated skin or bone can increase secretion of FGF23, a condition known as epidermal nevus syndrome (OMIM: 162900), or more recently cutaneous skeletal hypophosphatemia syndrome (Lim et al., 2014; Ovejero et al., 2016).

Other primary skeletal disorders in which elevated FGF23 levels have been reported include osteoglophonic dysplasia (due to mutations in FGFR1) (OMIM: 166250) (White et al., 2005), Jansen metaphyseal chondrodysplasia (due to activating mutations of the PTH1 receptor) (OMIM: 156400) (Brown et al., 2009), neurofibromatosis (OMIM: 162200), and FAM20C mutations (e.g., Raine syndrome, OMIM: 259775) (Rafaelsen et al., 2013). This condition has also been referred to as autosomal recessive hypophosphatemic rickets type 3 (ARHR3). The mechanism(s) by which elevations in FGF23 occur in these settings is not certain at this time. There is evidence to support the finding that FAM20C alters phosphorylation of FGF23, thereby affecting O-glycosylation and allowing for diminished degradation (Tagliabracci et al., 2014). Alternatively, data have shown direct increases in FGF23 secretion with loss of function of FAM20C (Liu et al., 2018). Likewise, loss of function of Nuclear Factor 1 may play a role in the skeletal disease seen in neurofibromatosis by increasing FGF23 production (Kamiya et al., 2017).

Fibroblast growth factor 23–independent hypophosphatemic disorders

Hereditary hypophosphatemic rickets with hypercalciuria (OMIM: 241530)

Hereditary hypophosphatemic rickets with hypercalciuria (HHRH) is a rare autosomal recessive disorder first described in 1985 in a large consanguineous Bedouin kindred (Tieder et al., 1985). HHRH is distinct from the more common XLH (HYP-Consortium, 1995; Holm et al., 1997) with respect to mode of inheritance, and distinct biochemical features associated with increased synthesis and serum levels of $1,25(OH)_2D$, particularly hypercalciuria (Tieder et al., 1985, 1987; Gazit et al., 1991).

Epidemiology

HHRH has been described in all races, although most reports describe cases of Caucasian and Middle Eastern origin. More than 40 different mutations in *SLC34A3* affecting over 35 kindreds have been reported (Rafaelsen et al., 2016; Daga et al., 2018; Pronicka et al., 2017; Schlingmann et al., 2016; Dhir et al., 2017; Dasgupta et al., 2014; Chi et al., 2014; Ichikawa et al., 2014). Based on the allele frequency of 0.002 for proven pathogenic *SLC34A3* mutations, HHRH has a predicted prevalence of 1:250,000 (Wagner et al., 2017), although the true prevalence is not known. Therefore, HHRH is approximately 10-fold less frequent than the most common inherited disorder of phosphate homeostasis, XLH (1:20,000; Burnett et al., 1964). The predicted prevalence of idiopathic hypercalciuria associated with heterozygous mutation of *SLC34A* is 1:500.

Cloning and identification of human mutations in NPT2c

The genetic defect in HHRH was identified in a combined genome-wide search for linkage and homozygosity mapping using genomic DNA from the original Bedouin kindred (Tieder et al., 1985, 1987). A homozygous deletion SLC34A3.c.228delC was found in all affected individuals, which is predicted to result in complete loss of function of NPT2c (Bergwitz et al., 2006). Different genetic mutations in the same gene were subsequently reported (Rafaelsen et al., 2016; Daga et al., 2018; Pronicka et al., 2017; Schlingmann et al., 2016; Dhir et al., 2017; Dasgupta et al., 2014; Ichikawa et al., 2014; Bhoj et al., 2015) and include missense mutations, mutations affecting potential splice sites, and smaller and larger deletions causing premature stop codons with expression of a truncated transporter protein (Fig. 20.4). Some of these mutations have been functionally characterized in vitro using opossum kidney cells and *Xenopus* oocyte expression systems (Haito-Sugino et al., 2012; Shiozaki et al., 2015; Jaureguiberry et al., 2008).

Pathophysiology

The consequence for human carriers of *SLC34A3*/NPT2c loss-of-function mutations on one or two alleles is isolated proximal tubular phosphate wasting. Renal Fanconi syndrome has not been described for carriers of *SLC34A3*/NPT2c mutations, as occurs with *SLC34A1*/NPT2a mutations. To date no genotype–phenotype correlation has been described, and there is no evidence for dominant negative effects of mutant transporters. Of interest would also be to determine whether loss of NPT2c has consequences for other proximal tubular functions such as CYP24A1 activity, sodium excretion, urine anion gap, and osteopontin and PPi levels (Tenenhouse et al., 2001; Caballero et al., 2017a,b; Li et al., 2017), all of which, together with the characteristic hypercalciuria, may contribute to formation of renal mineral deposits in HHRH and idiopathic hypercalciuria (IH). Haploinsufficiency of NPT2c can cause mild hypophosphatemia, reduced TmP/GFR, and elevations in $1,25(OH)_2D$ and/or urinary calcium excretion (Tieder et al., 1985, 1987; Bergwitz et al., 2006), but, with the exception of one report (Yamamoto et al., 2007), does not generally cause bone disease.

Clinical presentation and diagnostic evaluation

Laboratory findings and genetic testing The clinical assessment of phosphate homeostasis can be challenging: serum phosphorus concentrations are influenced by the time of day, meals, and age. Clinical methods for determination of tubular reabsorption are imprecise. To determine the cause of abnormal serum phosphorus levels in a patient with normal parathyroid and renal function, we first assess TRP (Fig. 20.5) based on the measurement of phosphorus and creatinine in a 2- to 3-h urine collection along with the corresponding serum parameters. TRP, TmP/GFR (Walton and Bijvoet, 1975), or TP/GFR, which provides a more accurate assessment of renal phosphate handling in children (Alon and Hellerstein, 1994), is then calculated. Inappropriately low %TRP in the setting of hypophosphatemia is suggestive of a proximal renal tubular defect. With respect to HHRH, further confirmation can be aided by measurement of circulating $1,25(OH)_2D$ levels. The combined reduction in both TRP and $1,25(OH)_2D$ levels suggests excess FGF23 action, whereas elevated $1,25(OH)_2D$

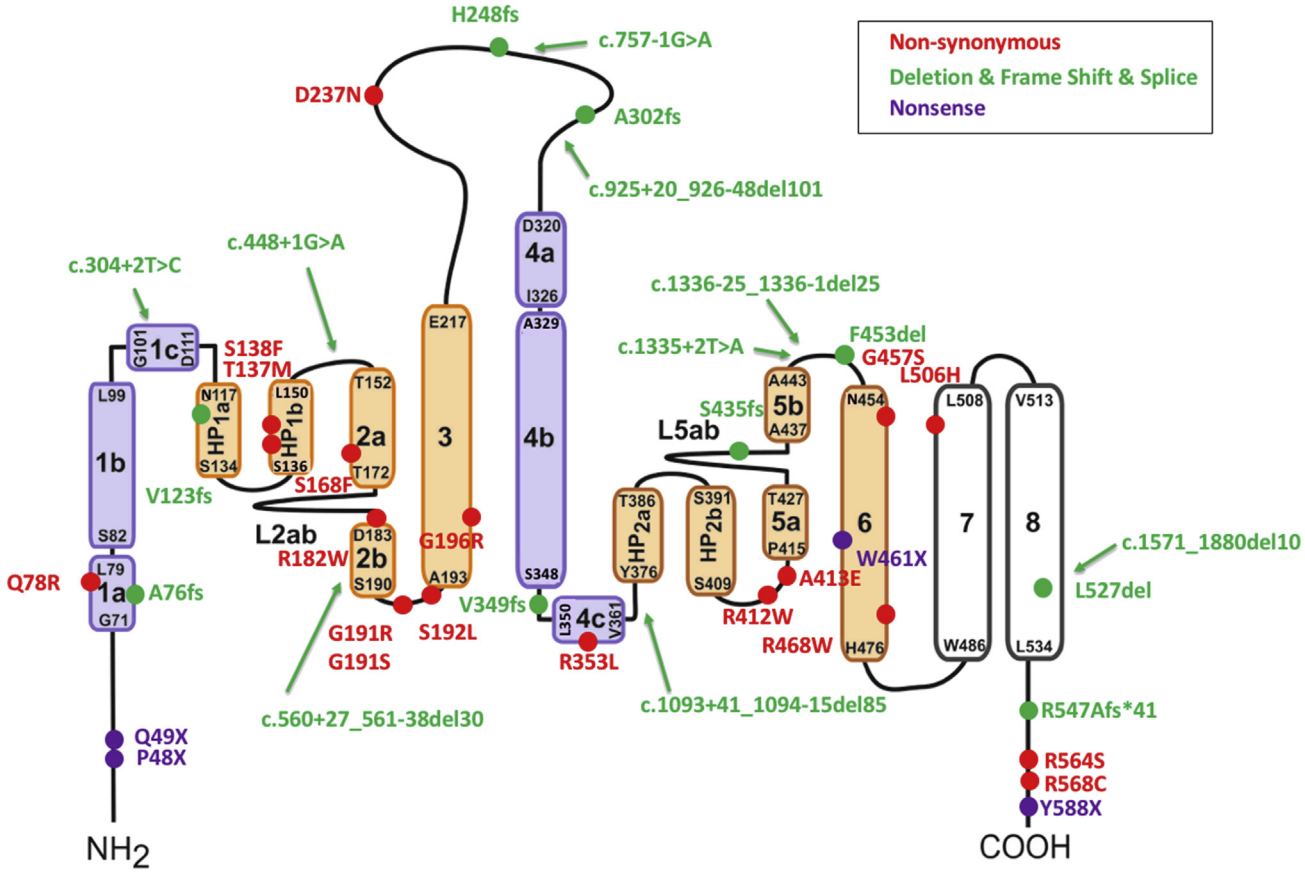

FIGURE 20.4 Reported human mutations in NPT2c. Predicted models of *SLC34A3*/NPT2c (Wagner et al., 2017) and localization of mutations identified in patients. (*Red*, missense mutations; *green*, frameshift, deletion, and splice-site mutations; *purple*, nonsense mutations). The scaffold domain is represented in lavender and the transport domain in orange as in. (Forster and Wagner, 2018; Bergwitz and Miyamoto, 2019). *For details on mutations and references see Rafaelsen, S., Johansson, S., Raeder, H., Bjerknes, R., 2016. Hereditary hypophosphatemia in Norway: a retrospective population-based study of genotypes, phenotypes, and treatment complications. Eur. J. Endocrinol. 174, 125–136 DOI 10.1530/EJE-15-0515; Daga, A., Majmundar, A.J., Braun, D.A., Gee, H.Y., Lawson, J.A., Shril, S., Jobst-Schwan, T., Vivante, A., Schapiro, D., Tan, W., Warejko, J.K., Widmeier, E., Nelson, C.P., Fathy, H.M., Gucev, Z., Soliman, N.A., Hashmi, S., Halbritter, J., Halty, M., Kari, J.A., El-Desoky, S., Ferguson, M.A., Somers, M.J.G., Traum, A.Z., Stein, D.R., Daouk, G.H., Rodig, N.M., Katz, A., Hanna, C., Schwaderer, A.L., Sayer, J.A., Wassner, A.J., Mane, S., Lifton, R.P., Milosevic, D., Tasic, V., Baum, M.A., Hildebrandt, F., 2018. Whole exome sequencing frequently detects a monogenic cause in early onset nephrolithiasis and nephrocalcinosis. Kidney Int. 93, 204–213. DOI S0085-2538(17)30494-5 [pii] 10.1016/j.kint.2017.06.025; Pronicka, E., Ciara, E., Halat, P., Janiec, A., Wojcik, M., Rowinska, E., Rokicki, D., Pludowski, P., Wojciechowska, E., Wierzbicka, A., Ksiazyk, J.B., Jacoszek, A., Konrad, M., Schlingmann, K.P., Litwin, M. 2017. Biallelic mutations in CYP24A1 or SLC34A1 as a cause of infantile idiopathic hypercalcemia (IIH) with vitamin D hypersensitivity: molecular study of 11 historical IIH cases. J. Appl. Genet. 58, 349–353. DOI 10.1007/s13353-017-0397-2 10.1007/s13353-017-0397-2; Schlingmann, K.P., Ruminska, J., Kaufmann, M., Dursun, I., Patti, M., Kranz, B., Pronicka, E., Ciara, E., Akcay, T., Bulus, D., Cornelissen, EAM., Gawlik, A., Sikora, P., Patzer, L., Galiano, M., Boyadzhiev, V., Dumic, M., Vivante, A., Kleta, R., Dekel, B., Levtchenko, E., Bindels, R.J., Rust, S., Forster, I.C., Hernando, N., Jones, G., Wagner, C.A., Konrad, M. 2016. Autosomal-recessive mutations in SLC34A1 encoding sodium-phosphate cotransporter 2A cause idiopathic infantile hypercalcemia. J. Am. Soc. Nephrol. 27, 604–614. DOI 10.1681/asn.2014101025; Dhir, G., Li, D., Hakonarson, H., Levine, M.A. 2017. Late-onset hereditary hypophosphatemic rickets with hypercalciuria (HHRH) due to mutation of SLC34A3/NPT2c. Bone 97, 15–19 DOI S8756-3282(16)30363-5 [pii] 10.1016/j.bone.2016.12.001); Dasgupta, D., Wee, M.J., Reyes, M., Li, Y., Simm, P.J., Sharma, A., Schlingmann, K.P., Janner, M., Biggin, A., Lazier, J., Gessner, M., Chrysis, D., Tuchman, S., Baluarte, H.J., Levine, M.A., Tiosano, D., Insogna, K., Hanley, D.A., Carpenter, T.O., Ichikawa, S., Hoppe, B., Konrad, M., Savendahl, L., Munns, C.F., Lee, H., Juppner, H., Bergwitz, C. 2014. Mutations in SLC34A3/NPT2c are associated with kidney stones and nephrocalcinosis. J. Am. Soc. Nephrol. 25, 2366–2375. DOI 10.1681/ASN.2013101085 ASN, 2013101085 ASN.2013101085; Chi, Y., Zhao, Z., He, X., Sun, Y., Jiang, Y., Li, M., Wang, O., Xing, X., Sun, A.Y., Zhou, X., Meng, X., Xia, W., 2014. A compound heterozygous mutation in SLC34A3 causes hereditary hypophosphatemic rickets with hypercalciuria in a Chinese patient. Bone 59, 114–121. DOI 10.1016/j.bone.2013.11.008 S8756-3282(13)00444-4; Ichikawa, S., Tuchman, S., Padgett, L.R., Gray, A.K., Baluarte, H.J., Econs, M.J., 2014. Intronic deletions in the SLC34A3 gene: a cautionary tale for mutation analysis of hereditary hypophosphatemic rickets with hypercalciuria. Bone 59, 53–56 DOI 10.1016/j.bone.2013.10.018 S8756-3282(13)00428-6; Acar, S., BinEssa, H.A., Demir, K., Al-Rijjal, R.A., Zou, M., Catli, G., Anik, A., Al-Enezi, A.F., Ozisik, S., Al-Faham, M.S.A., Abaci, A., Dundar, B., Kattan, W.E., Alsagob, M., Kavukcu, S., Tamimi, H.E., Meyer, B.F., Bober, E., Shi, Y. 2018. Clinical and genetic characteristics of 15 families with hereditary hypophosphatemia: novel Mutations in PHEX and SLC34A3. PLoS One 13, e0193388. DOI 10.1371/journal.pone.0193388 PONE-D-17-39524.*

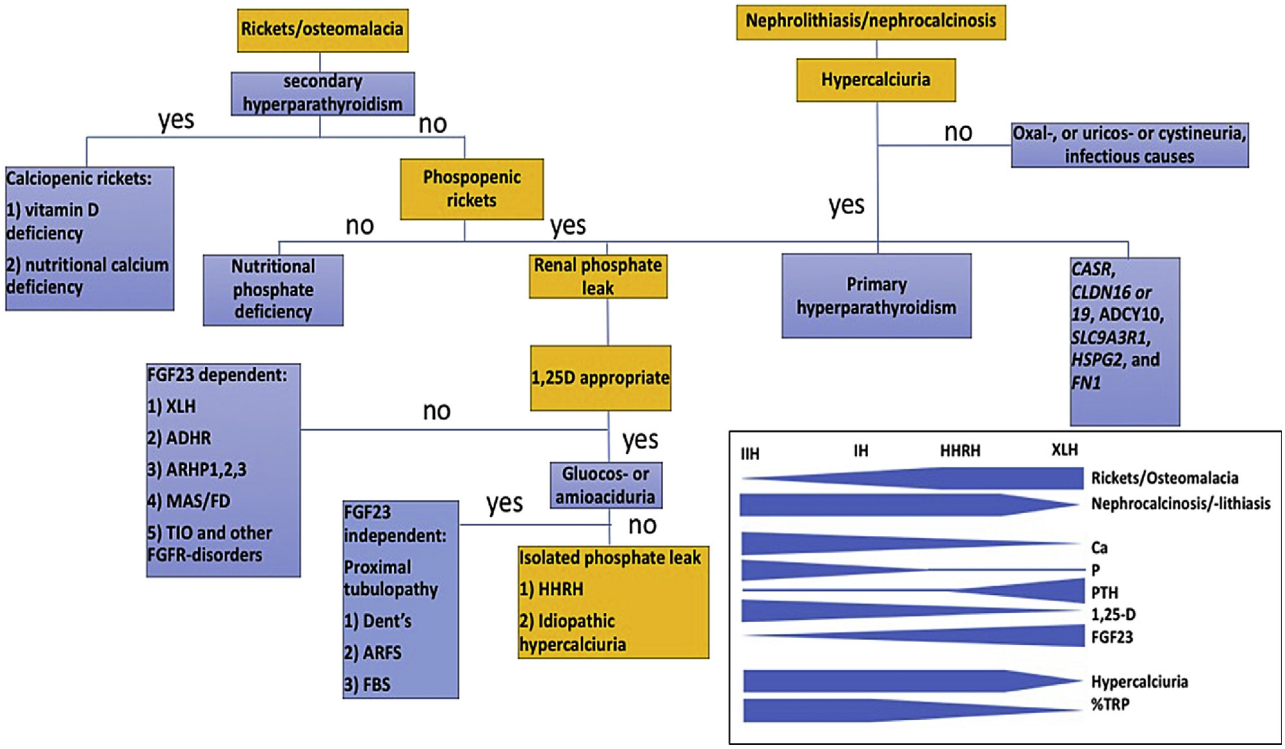

FIGURE 20.5 Differential diagnosis of hypophosphatemic disorders with and without nephrocalcinosis/nephrolithiasis. HHRH may present initially with bone disease or renal calcifications and bone disease is generally missing in heterozygous carriers of *SLC34A3*/NPT2c mutations. Presence of additional symptoms in *orange* further supports the diagnosis, while symptoms in *blue* argue against it. *ADHR*, autosomal dominant hypophosphatemic rickets; *ARFS*, autosomal recessive Fanconi syndrome; *ARHP1,2,3*, autosomal recessive hypophosphatemia type 1, 2, or 3; *FBS*, Fanconi–Bickel syndrome; *FGF23*, fibroblast growth factor 23; *FGFR*, FGF receptor; *HHRH*, hereditary hypophosphatemic rickets with hypercalciuria; *MAS/FD*, McCune–Albright syndrome/fibrous dysplasia; *PTH*, parathyroid hormone; *TIO*, tumor-induced osteomalacia; *%TRP*, percentage tubular reabsorption of phosphate; *XLH*, X-linked dominant hypophosphatemia. For gene names see text. *Originally published in Bergwitz, C., Miyamoto, K.I., 2019. Hereditary hypophosphatemic rickets with hypercalciuria: pathophysiology, clinical presentation, diagnosis and therapy. Pflügers Archiv 471, 149–163. https://doi.org/10.1007/s00424-018-2184-2.*

levels in the context of a low TRP suggest an FGF23-independent process, as would be seen in HHRH. Excess production of $1,25(OH)_2D$ may lead to increased absorption of calcium in the gut, resulting in hypercalciuria and some degree of suppression of PTH production (Tieder et al., 1985). Vitamin D deficiency may mask these findings and needs to be corrected before the aforementioned testing (Kremke et al., 2009). Circulating FGF23 levels can be determined using several commercially available enzyme-linked immunometric assays (Yamazaki et al., 2002). The C-terminal FGF23 assay (Immutopics, Inc., San Clemente, CA, USA) uses antibodies directed against two distinct epitopes within the C-terminal region of FGF23 (Larsson et al., 2005) and, as of this writing, is the only CLIA-certified assay in the United States. This assay in our experience returns FGF23 levels in the low normal range in FGF23-independent hypophosphatemic disorders such as HHRH or renal Fanconi syndrome.

Genetic testing employing whole-exome sequence analysis of leukocyte DNA is increasingly performed, allowing for screening of a panel of genes. Some centers (including the Yale Clinical Genome Research Center) employ techniques with sufficient coverage of intronic sequence to permit detection of the known intronic deletions (Daga et al., 2018; Ma et al., 2015). Single-gene sequencing may be required to detect deletions in 5′ and 3′ UTRs or in the larger intron 12, which, at this writing, is offered only by research laboratories. Fig. 20.4 indicates the locations of known mutations. More detailed information on the type and location of specific mutations is provided at several freely accessible websites: Online Mendelian Inheritance in Man (OMIM) (http://www.ncbi.nlm.nih.gov/omim/), the Exome Variant Server (http://evs.gs.washington.edu/EVS/), and the National Center for Biotechnology Information (NCBI) SNP (http://www.ncbi.nlm.nih.gov/projects/SNP/). Since compound heterozygous loss-of-function mutations in *SLC34A3*/NPT2c have been identified in HHRH (Bergwitz et al., 2006; Lorenz-Depiereux et al., 2006b), genetic evaluation of one parent may be useful to permit allele assignment when heterozygous mutations are discovered.

Musculoskeletal findings Rickets, bowing, and short stature in children and osteopenia/osteoporosis in adults are the most commonly observed features in individuals with classic HHRH. Bone pain is often present (Narchi et al., 2001; Francis and Selby, 1997). The radiological findings of rickets are evident at growth plates, and osteomalacia (undermineralization of the osteoid) may blur the trabecular architecture. Clinical consequences of these lesions include bone pain and impaired biomechanical properties, which can result in bowing, and insufficiency fractures. Swollen wrists and knees may occur due to growth plate abnormality (Donohue & Demay, 2002). The primary biochemical marker for rickets and osteomalacia is elevated total or bone-specific alkaline phosphatase (Narchi et al., 2001; Francis and Selby, 1997). Bone biopsy has shown increased accumulation of osteoid, compatible with osteomalacia, responsive to oral phosphorus supplementation (Yamamoto et al., 2007; Chen et al., 1989). Interestingly, hypomineralized periosteocytic lesions typical of XLH were absent (Yamamoto et al., 2007). Furthermore, osteoblast surface was increased, while osteoclast number was decreased (Chen et al., 1989). Rickets or osteomalacia occur in many hypophosphatemic disorders, but subtle differences can guide diagnostic and therapeutic decisions. Enthesopathy (painful or indolent mineral deposition of tendon and ligament insertion sites) occurs with XLH, ADHR, and ARHR1, but has not been reported in HHRH (Econs et al., 1994). Likewise, dental cysts, craniosynostosis, midfacial hypoplasia, frontal bossing, scaphocephaly, and Chiari I malformation, all reported in XLH (Jones et al., 2001; Tenenhouse and Econs, 2001), are not present in HHRH, possibly because of the absence of elevated FGF23 in HHRH (Econs et al., 1994; DiMeglio and Econs, 2001). Whether HHRH predisposes to accelerated bone loss in adulthood as may occur with NPT2a or NHERF1 mutations is not known (Prie et al., 2002; Karim et al., 2008).

The mechanism of muscle weakness caused by hypophosphatemia is not well understood and may be related to the role of phosphorus in intracellular signal transduction, phosphocreatine recovery (Clarke et al., 1990; Sinha et al., 2013), and/or ATP synthesis (Pesta et al., 2016; Sinha et al., 2013; Smith et al., 1984; Aono et al., 2011). Sarcopenia may develop in HHRH due to chronic hypophosphatemia. In contrast to the hypophosphatemic myopathy seen in XLH or vitamin D deficiency, HHRH presents with increased calcium, increased $1,25(OH)_2D$, and low FGF23, making this disorder uniquely suited to study of the effects of hypophosphatemia per se on muscle metabolism.

Renal findings None of the originally described HHRH patients were reported to have renal calcifications and kidney stones (Tieder et al., 1985, 1987), but subsequent investigation has revealed that renal complications are common with compound heterozygous or homozygous NPT2c mutations (Kremke et al., 2009; Ichikawa et al., 2006; Page et al., 2008; Phulwani et al., 2011; Mejia-Gaviria et al., 2010; Tencza et al., 2009). Renal calcifications are the only presenting sign in 16% of individuals with HHRH, where concomitant bone disease is not described (Romero et al., 2010; Schissel and Johnson, 2011). Even heterozygous carriers of *SLC34A3*/NPT2c mutations show an approximately threefold higher incidence of renal calcifications, probably related to their intermediate biochemical profile. Therefore, all affected individuals and their first-degree relatives should be examined for renal calcifications. It is unknown whether loss of NPT2c can cause additional proximal tubular phenotypes, such as Fanconi syndrome, as described in two patients with homozygous NPT2a mutations (Magen et al., 2004) who developed CKD later in life. Genome-wide association studies for uric acid nephrolithiasis (Tore et al., 2011), serum phosphorus levels (Kestenbaum et al., 2010), and CKD (Gudbjartsson et al., 2010) have not supported an association of hypercalciuric stone disease with the *SLC34A3*/NPT2c locus, whereas renal calcifications and impaired renal function are so associated (Arcidiacono et al., 2014; Taguchi et al., 2017; Boger et al., 2011; Pattaro et al., 2016). Our meta-analysis clearly suggests that *SLC34A3* should be added to the list of hypercalciuric stone disease genes (Dasgupta et al., 2014).

Therapy and resources

Standard therapy It is important to establish the correct diagnosis of HHRH, as patients require long-term medical therapy with phosphorus supplements (Tieder et al., 1985, 1987), and *not* supplementation with vitamin D, as in nutritional rickets (Reginato and Coquia, 2003). When HHRH is mistaken for XLH, active vitamin D analogs (i.e., calcitriol) are used with oral phosphorus (White et al., 2011), often leading to hypercalcemia, hypercalciuria, nephrocalcinosis, and potentially renal insufficiency (Jaureguiberry et al., 2008; Kremke et al., 2009). When correctly treated with oral phosphorus supplementation only, the rachitic bone disease in HHRH improves quickly. However, the long-term safety of this therapy is unknown with respect to renal calcifications, or the development of hyperparathyroidism or enthesopathy, as occurs in XLH (HYP-Consortium, 1995). Finally, genetic and biochemical data may predict risk for renal calcifications and inform management of oral phosphorus therapy. Serum phosphorus levels, urinary phosphate excretion, and serum $1,25(OH)_2D$ merit further evaluation as predictors of renal calcifications. Our studies in NPT2a-KO mice (Li et al., 2017) suggest that phosphorus can be harmful under certain conditions, suggesting that patients may need to be carefully monitored to avoid

renal calcifications despite resolution of hypercalciuria while receiving supplemental phosphorus therapy. Serum $1,25(OH)_2D$ may remain elevated long after initiation of phosphorus supplementation and thus it is not clear how suitable this measure is for assessing compliance with oral phosphorus therapy in the short term… (Yu et al., 2012).

Dent's disease (X-linked recessive hypophosphatemic rickets) (OMIM: 300009)

The initial description of X-linked recessive hypophosphatemic rickets involved a family in which males presented with rickets or osteomalacia, hypophosphatemia, and a reduced threshold for renal phosphate reabsorption (Wrong et al., 1994). In contrast to XLH, affected subjects usually exhibit hypercalciuria, elevated serum $1,25(OH)_2D$ levels, and proteinuria of up to 3 g/day. Nephrolithiasis and nephrocalcinosis with progressive renal failure occur in early adulthood. Female (heterozygous) carriers are normophosphatemic and lack biochemical abnormalities other than hypercalciuria. Three other independently reported syndromes, X-linked recessive nephrolithiasis with renal failure, Dent's disease, and low-molecular-weight proteinuria with hypercalciuria and nephrocalcinosis, have an overall similar phenotype, but manifest differences in degree of proximal tubular reabsorptive defects, nephrolithiasis, nephrocalcinosis, progressive renal insufficiency, and, in some cases, rickets or osteomalacia. Identification of mutations in the voltage-gated chloride channel gene *CLCN5*, in all four syndromes, has established that these disorders are phenotypic variants of a single disease (Lloyd et al., 1996; Thakker, 2000). The varied manifestations associated with mutations in *CLCN5*, particularly hypophosphatemia and rickets/osteomalacia, emphasize the role of environmental differences, diet, and/or modifying genetic backgrounds on phenotypic expression.

Hypophosphatemia with osteoporosis and nephrolithiasis due to SLC34A1 (OMIM: 612286) and NHERF1 mutations (OMIM: 604990)

Prie et al. investigated a heterogeneous group of patients with idiopathic hypercalciuria, osteoporosis, and renal stones. Using a candidate gene approach they found 2/20 individuals heterozygous for nonsynonymous single-nucleotide polymorphisms (SNPs) in *SLC34A1*/NPT2a (Prie et al., 2002) and 7/94 individuals heterozygous for nonsynonymous SNPs in *SLC9A3R1*/NHERF1 (Karim et al., 2008). Potential dominant negative effects of the *SLC34A1*/NPT2a mutations on proximal renal tubular phosphate reabsorption remain controversial (Virkki et al., 2003), and some of the identified NHERF1 alterations are listed in the NCBI dbSNP database as low-frequency polymorphisms (Bergwitz and Bastepe, 2008). Further study is thus required to prove that these NPT2a or NHERF1 mutations are disease-causing ones. In contrast to HHRH there is generally no history of childhood rickets in individuals with NPT2a mutations.

Autosomal recessive Fanconi syndrome (OMIM: 613388)

In 1988, Tieder et al. described a consanguineous Arab kindred with childhood rickets and defective proximal tubular handing of phosphate, amino acids, and glucose consistent with renal Fanconi syndrome (Tieder et al., 1988). Distinct from other forms of Fanconi, their patients also had elevated $1,25(OH)_2D$ levels and absorptive hypercalciuria. In 2010, homozygosity mapping of this kindred showed linkage of the disease to chromosome 5q35.1−q35.3, and subsequent sequence analysis of the *SLC34A1*/NPT2a gene in the linked interval revealed a homozygous duplication, g.2061_2081dup (p.I154V160dup) (Magen et al., 2010). Expression of the mutant NPT2a protein in *Xenopus* oocytes and opossum kidney cells showed complete loss of function and lack of membrane insertion, respectively. The two patients described in the 1988 report, who at this writing are 39 and 43 years of age, continue to have low TmP/GFR, and their FGF23 and PTH levels were recently shown to be low normal (despite impaired renal function), suggesting that their hypophosphatemia is FGF23 and PTH independent. However, their previously documented absorptive hypercalciuria due to increased $1,25(OH)_2D$ levels had normalized in the setting of vitamin D deficiency. Although symptoms of rickets were present in childhood, both patients have been relatively asymptomatic during adulthood and discontinued phosphorus supplementation. Both developed CKD stage 2−3 renal failure in their 30s, which is in contrast to the other *SLC34A1*- and *SLC34A3*-related disorders described earlier. Heterozygous carriers had normal renal function and no evidence of proximal tubulopathy, arguing against dominant negative effects of the mutant NPT2a.

Fanconi−Bickel syndrome (OMIM: 227810)

Fanconi−Bickel syndrome is a rare autosomal recessive disorder of hepatorenal glycogen accumulation, proximal renal tubular dysfunction, and impaired utilization of glucose and galactose (Santer et al., 1997, 2002), first described in 1949 and caused by defects in the facilitative glucose transporter 2 (*SLC2A2*/GLUT2) (Santer et al., 1997). Patients present early

in life with rickets and hepatomegaly. By 2 years of age enlarged kidneys are evident. Fasting hypoglycemia and postprandial hyperglycemia and hypergalactosemia, as well as hyperlipidemia, may be present. Some cases have presented with isolated but variable increases in urinary phosphate excretion (Mannstadt et al., 2012).

Intestinal malabsorption of phosphate

Primary disorders of intestinal phosphate absorption have not been reported to occur in widespread fashion. However, we have encountered a worrisome pattern of phosphate malabsorption in children with complex disorders associated with intestinal compromise. These children were fed amino acid–based elemental formulas, particularly certain Neocate products (Gonzalez Ballesteros et al., 2017). Associated tube-feeding and use of antacid medications appear to be risk factors for the development of this syndrome, and the phenomenon does not appear to occur when the formulas are used for the labeled indication of milk protein allergy in children who are otherwise healthy (Harvey et al., 2017). Without suspicion of this finding, routine monitoring of biochemical predictors of the condition are generally not monitored until overt skeletal consequences are evident, particularly rickets and fractures. Hypophosphatemia, low-to-undetectable urinary phosphate excretion, and elevated serum alkaline phosphatase levels represent the usually observed biochemical findings. We have recommended that serum phosphorus levels be monitored periodically with the use of such formulas. The disorder can be managed with either phosphate supplementation or transition to alternative formulas. We caution that the transition to an alternative formula should be done gradually, using slowly decreasing percentages of the offending formula (i.e., over 1–2 weeks), as the physiologic adaptation to phosphate deprivation will have probably resulted in marked upregulation of intestinal and renal transporters. Thus hyperabsorption of phosphate, as well as renal retention, is likely to occur initially as abundant phosphate is provided, resulting in hyperphosphatemia and a reciprocal acute hypocalcemia. The problem generally resolves in several days or a few weeks as the system is restored to a normal phosphate-handling equilibrium.

Hyperphosphatemic syndromes

Hyperphosphatemia may result from a variety of physiologic perturbations, such as phosphate loading, tumor lysis syndrome, and CKD, as discussed earlier. This section is focused on FGF23-dependent hyperphosphatemia, of interest as it provides a physiologic example of a symmetrical contrast to the hypophosphatemia seen with excess FGF23 activity.

Tumoral calcinosis

The converse pathophysiology of excess FGF23 can arise with the disorder familial hyperphosphatemic tumoral calcinosis (FHTC) (Folsom and Imel, 2015). This rare disorder is most frequently inherited in an autosomal recessive manner, presenting with findings of ectopic calcifications, often at extensor surfaces and in the pelvis, and in other locations, which appear to be amorphous calcium phosphate precipitates. The precipitates may generate the findings of chronic inflammation at their anatomic location as well (Ramnitz et al., 2016). The biochemical findings in these syndromes are the converse of those seen in XLH, with elevated TmP/GFR, consequent hyperphosphatemia, and normal or elevated $1,25(OH)_2D$ levels.

The disorder is due to deficient FGF23 activity and inherited in an autosomal recessive manner. Most reported cases are due to loss-of-function mutations in *GALNT3* (encoding UDP-*N*-acetyl-α-D-galactosamine:polypeptide *N*-acetylgalactosaminyltransferase 3) (HTC1, OMIM: 211900), resulting in impaired O-glycosylation of FGF23. The consequences of the mutation are increased proteolysis, occurring in the Golgi apparatus, before secretion into the circulation (Topaz et al., 2004). Therefore fragments are the dominant species found in the circulation, such that FGF23 levels will vary dependent on the nature of the immunoassay employed: FGF23 measured using an intact FGF23 assay is usually low, yet high values are detected when employing assays that recognize only the C terminus of the protein. FGF23 mRNA is overexpressed, indicating an intact feedback loop, presumably as the osteocyte responds to the ambient hyperphosphatemia. The disorder has variable effects on the skeleton and has been also described as a hyperostosis/hyperphosphatemia syndrome (Ramnitz et al., 2016). Dental findings may include short, blunt roots and pulpal obliteration (Vieira et al., 2015). We have identified a patient with back pain and intervertebral disc calcifications who has the biochemical phenotype of FHTC, with biallelic *GALNT3* mutations (Lee et al., 2018).

Recessive loss-of-function mutations in FGF23 itself may cause FHTC (HTC2, OMIM: 617993), with mutations evident in conserved residues of the molecule. Presumably, proteolysis is also affected, resulting in the discordance in FGF23 levels depending on the use of intact or C-terminal assays. Finally, FHTC has been reported in one patient who has

loss-of-function mutations in α-klotho, the coreceptor for FGF23 (HTC3, OMIM: 617994) (Ichikawa et al., 2007). This individual demonstrated increased levels of intact FGF23 indicating the expected resistance in the setting of the deficient coreceptor. One case of autoimmune HTC has been described, in which high titers of antibodies directed toward FGF23 resulted in resistance to FGF23 action and elevated levels of circulating FGF23 in both intact and C-terminal assays (Roberts et al., 2018). Finally, tumoral calcinosis in the absence of hyperphosphatemia has been described as secondary to CKD and in the setting of loss-of-function mutations in *SAMD9* (OMIM: 610455) (Topaz et al., 2006).

Treatment of the condition has been variably successful with low-phosphorus diet, sevelamer (or other phosphate binders), and acetazolamide. Combinations of these approaches are sometimes attempted. A 2016 report suggests the potential of topical sodium thiosulfate for this difficult to manage clinical situation (Jost et al., 2016).

Other non-FGF23-mediated hyperphosphatemic syndromes, related to hypoparathyroidism, and various forms of resistance to PTH are listed in Table 20.1. These disorders are discussed at length elsewhere (Weinstein et al., 1992; Juppner et al., 1998; Arnold et al., 1990; Pollak et al., 1994; Ding et al., 2001; Zhang et al., 1998; Karperien et al., 1999). Finally, the hyperphosphatemia is well known to increase through increasing stages of CKD, in association with reduction in serum $1,25(OH)_2D$ levels and markedly elevated circulating levels of FGF23.

Normophosphatemic disorders of cellular phosphorus metabolism

Given the widespread role of phosphate in energy metabolism, signaling, protein function, and bone matrix, disorders of phosphate homeostasis impair the function of many organ systems. The majority of disorders of phosphate homeostasis primarily alter extracellular phosphate; however, disorders that primarily change intracellular phosphate have been described. Since extracellular phosphate and intracellular phosphate are intimately related, symptoms of these disorders may overlap. For example, excess phosphate uptake into cells may result in hypophosphatemia and rickets, while reduced phosphate uptake into cells may result in hyperphosphatemia and matrix calcifications. In addition, some transporters have cell-autonomous and systemic functions. For example, loss-of-function mutations in NPT2a may reduce intracellular phosphate and stimulate renal synthesis of $1,25(OH)_2D$ thereby causing hyperabsorption of calcium and phosphate in the gut. However, the net effect of NPT2a loss-of-function mutations can be infantile hypercalcemia with hypercalciuric nephrocalcinosis, while hypophosphatemic rickets are more commonly encountered in the setting of NPT2c loss-of-function mutations.

Individuals with hypertrophic cardiomyopathy muscular dystrophy and lactic acidosis (Bhoj et al., 2015; Mayr et al., 2011) were found to carry loss-of-function mutations in PIC (*SLC25A3*), which mediates uptake of phosphate by the mitochondria. These findings suggest that phosphate is important for the function of the mitochondrial respiratory chain and ATP synthesis as has been reported by us (Pesta et al., 2016) and others (Sinha et al., 2013; Smith et al., 1984; Brown et al., 1985; Choi et al., 2008; Maldonado and Lemasters, 2014). PIC is also a component of the MPTP, which requires the presence of phosphate to permit influx of calcium into the mitochondrial matrix (Seifert et al., 2015). Detailed evaluation of the hearts in a mouse model with an inducible and cardiac-specific deletion of the *SLC25A3* gene (Kwong et al., 2014) showed reduced MPTP opening in response to calcium challenge. PIC therefore also has phosphate transport−independent roles in mitochondrial function.

Loss-of-function mutations in PIT2 (Lemos et al., 2015) and XPR1 (Legati et al., 2015) were reported in individuals suffering from PFBC or Fahr syndrome (OMIM: 213600). These individuals develop vascular calcifications in the basal ganglia of their brain, leading to seizures. Inhibition of phosphate uptake into microglia due to loss of function in PIT2 or inhibition of phosphate export from vascular smooth muscle cells due to loss of function in XPR1 may stimulate formation of calcium phosphate deposits inside these cells (Legati et al., 2015; Anheim et al., 2016). A similar phenotype was observed in human individuals and mouse models with loss-of-function mutations in the PDGFB receptor (PDGFBR) and PDGFB (Keller et al., 2013). Along with reports of a physical interaction of XPR1 with PDGFBR in mice (Yao et al., 2017), these reports suggest that PDGFB, PDGFBR, and phosphate transporters functionally interact. Interestingly, Pit2-KO mice have increased cerebrospinal fluid phosphate levels, which may suggest a role for this transporter in phosphate homeostasis of cerebrospinal fluid (Jensen et al., 2016).

Summary

Advances since the end of the 20th century have led to the identification of intricate mechanisms by which phosphorus is regulated in the whole organism. An improved understanding of P transport processes, the distribution and function of transporters, and the overall hormonal control of this process has emerged. In particular, the FGF23-mediated bone−renal phosphate axis has markedly expanded our conceptual framework for mineral homeostasis. The related disorders of

phosphate homeostasis are now better understood, allowing for new molecular targets for treatment of disease, yet raising a multitude of further questions waiting to be explored.

Patient information/web resources:

Orphanet: http://www.orpha.net
OMIM: http://omim.org
NORD: https://rarediseases.org
The XLH Network: http://www.xlhnetwork.org

Key term/acronym	Definition
ATP	Adenosine triphosphate
PPi	Pyrophosphate
PTH	Parathyroid hormone
NPT2	Solute carrier family 34 (type II) sodium/phosphate cotransporters (with "a", "b", and "c" species)
PIT	Solute carrier family 20 (type III) sodium/phosphate cotransporters (with "1" and "2" species)
PKA	Protein kinase A
PKC	Protein kinase C
NHERF1	Sodium/hydrogen exchange regulatory cofactor
GALNT3	UDP-*N*-acetyl-α-D-galactosamine:polypeptide *N*-acetylgalactosaminyltransferase, isoform 3
FGF23	Fibroblast growth factor 23
KL	α-Klotho
PHEX	Phosphate-regulating gene with homologies to endopeptidases on the X chromosome
MV	Matrix vesicle
DMP1	Dentin matrix protein 1
PXE	Pseudoxanthoma elasticum
MEPE	Matrix extracellular phosphoglycoprotein
SIBLING	Small integrin-binding ligand N-linked glycoprotein
FGFR	Fibroblast growth factor receptor
ENPP1	Ectonucleotide pyrophosphatase/phosphodiesterase 1
ANKH	Progressive ankylosis protein homolog
ABCC6	ATP binding cassette subfamily C member 6
ARHR	Autosomal recessive hypophosphatemic rickets
ASARM	Acidic serine aspartate-rich MEPE-associated motif
HHRH	Hereditary hypophosphatemic rickets with hypercalciuria
PTHR1	PTH/PTHrP receptor
VDR	Vitamin D receptor, forms heterodimer with RXR
HFTC	Hyperphosphatemic familial tumoral calcinosis
TNAP	Tissue nonspecific alkaline phosphatase
XLH	X-linked dominant hypophosphatemia
ADHR	Autosomal dominant hypophosphatemic rickets
SLC34	Solute carrier family 34 (sodium/phosphate cotransporter); members 1 and 3 are expressed in the proximal renal tubule, member 2 is expressed in the intestine
CYP27B1	Vitamin D 1-α-hydroxylase
CYP24A1	Vitamin D 24-hydroxylase
GACI	Generalized arterial calcification of infancy
TRPV	Transient receptor potential cation channel, subfamily V; members 5 and 6 are calcium selective
PMCA	Plasma membrane Ca^{2+} ATPase
VDDR1	Vitamin D–dependent rickets type 1

VDDR2	Vitamin D−dependent rickets type 2
FRP4	Frizzled-related protein 4
PFBC	Primary familial brain calcification
MPTP	Mitochondrial permeability transition pore
PIC	Mitochondrial phosphate carrier
PMT−MCT	Phosphaturic mesenchymal tumor−mixed connective tissue variant
TIO	Tumor-induced osteomalacia
PDGF	Platelet-derived growth factor

References

Addison, W.N., Masica, D.L., Gray, J.J., McKee, M.D., 2010. Phosphorylation-dependent inhibition of mineralization by osteopontin ASARM peptides is regulated by PHEX cleavage. J. Bone Miner. Res. 25, 695−705. https://doi.org/10.1359/jbmr.090832.

Acar, S., BinEssa, H.A., Demir, K., Al-Rijjal, R.A., Zou, M., Catli, G., Anik, A., Al-Enezi, A.F., Ozisik, S., Al-Faham, M.S.A., Abaci, A., Dundar, B., Kattan, W.E., Alsagob, M., Kavukcu, S., Tamimi, H.E., Meyer, B.F., Bober, E., Shi, Y., 2018. Clinical and genetic characteristics of 15 families with hereditary hypophosphatemia: novel Mutations in PHEX and SLC34A3. PLoS One 13, e0193388. https://doi.org/10.1371/journal.pone.0193388 pii:PONE-D-17-39524.

ADHR Consortium T, 2000. Autosomal dominant hypophosphataemic rickets is associated with mutations in FGF23. Nat. Genet. 26, 345−348. https://doi.org/10.1038/81664.

Albright, F.B., Allan, M., Bloomberg, E., 1936. Rickets resistant to vitamin D therapy. Am. J. Dis. Child. 9, 529−547.

Aloia, J.F., Vaswani, A., Yeh, J.K., Ellis, K., Cohn, S.H., 1984. Total body phosphorus in postmenopausal women. Miner. Electrolyte Metab. 10, 73−76.

Alon, U., Hellerstein, S., 1994. Assessment and interpretation of the tubular threshold for phosphate in infants and children. Pediatr. Nephrol. 8, 250−251.

Andrukhova, O., Zeitz, U., Goetz, R., Mohammadi, M., Lanske, B., Erben, R.G., 2012. FGF23 acts directly on renal proximal tubules to induce phosphaturia through activation of the ERK1/2-SGK1 signaling pathway. Bone 51, 621−628. https://doi.org/10.1016/j.bone.2012.05.015.

Anheim, M., López-Sánchez, U., Giovannini, D., Richard, A.-C., Touhami, J., N'Guyen, L., Rudolf, G., Thibault-Stoll, A., Frebourg, T., Hannequin, D., Campion, D., Battini, J.-L., Sitbon, M., Nicolas, G., 2016. XPR1 mutations are a rare cause of primary familial brain calcification. J. Neurol. 263, 1559−1564. https://doi.org/10.1007/s00415-016-8166-4.

Ansermet, C., Moor, M.B., Centeno, G., Auberson, M., Hu, D.Z., Baron, R., Nikolaeva, S., Haenzi, B., Katanaeva, N., Gautschi, I., Katanaev, V., Rotman, S., Koesters, R., Schild, L., Pradervand, S., Bonny, O., Firsov, D., 2017. Renal Fanconi syndrome and hypophosphatemic rickets in the absence of xenotropic and polytropic retroviral receptor in the nephron. J. Am. Soc. Nephrol. 28, 1073−1078. https://doi.org/10.1681/ASN.2016070726.

Antoniucci, D.M., Yamashita, T., Portale, A.A., 2006. Dietary phosphorus regulates serum fibroblast growth factor-23 concentrations in healthy men. J. Clin. Endocrinol. Metab. 91, 3144−3149. https://doi.org/10.1210/jc.2006-0021.

Aono, Y., Hasegawa, H., Yamazaki, Y., Shimada, T., Fujita, T., Yamashita, T., Fukumoto, S., 2011. Anti-FGF-23 neutralizing antibodies ameliorate muscle weakness and decreased spontaneous movement of Hyp mice. J. Bone Miner. Res. 26, 803−810. https://doi.org/10.1002/jbmr.275.

Arcidiacono, T., Mingione, A., Macrina, L., Pivari, F., Soldati, L., Vezzoli, G., 2014. Idiopathic calcium nephrolithiasis: a review of pathogenic mechanisms in the light of genetic studies. Am. J. Nephrol. 40, 499−506. https://doi.org/10.1159/000369833.

Arnold, A., Horst, S.A., Gardella, T.J., Baba, H., Levine, M.A., Kronenberg, H.M., 1990. Mutation of the signal peptide-encoding region of the pre-proparathyroid hormone gene in familial isolated hypoparathyroidism. J. Clin. Investig. 86, 1084−1087.

Azevedo, C., Saiardi, A., 2017. Eukaryotic phosphate homeostasis: the inositol pyrophosphate perspective. Trends Biochem. Sci. 42, 219−231. https://doi.org/10.1016/j.tibs.2016.10.008.

Bachmann, S., Schlichting, U., Geist, B., Mutig, K., Petsch, T., Bacic, D., Wagner, C.A., Kaissling, B., Biber, J., Murer, H., Willnow, T.E., 2004. Kidney-specific inactivation of the megalin gene impairs trafficking of renal inorganic sodium phosphate cotransporter (NaPi-IIa). J. Am. Soc. Nephrol. 15, 892−900.

Bacic, D., Lehir, M., Biber, J., Kaissling, B., Murer, H., Wagner, C.A., 2006. The renal Na+/phosphate cotransporter NaPi-IIa is internalized via the receptor-mediated endocytic route in response to parathyroid hormone. Kidney Int. 69, 495−503. https://doi.org/10.1038/sj.ki.5000148 pii:S0085-2538(15)51522-6.

Bai, X., Miao, D., Goltzman, D., Karaplis, A.C., 2007. Early lethality in Hyp mice with targeted deletion of Pth gene. Endocrinology 148, 4974−4983. https://doi.org/10.1210/en.2007-0243.

Baroncelli, G.I., Bertelloni, S., Ceccarelli, C., Saggese, G., 2001. Effect of growth hormone treatment on final height, phosphate metabolism, and bone mineral density in children with X-linked hypophosphatemic rickets. J. Pediatr. 138, 236−243. https://doi.org/10.1067/mpd.2001.108955.

Barros, N.M., Hoac, B., Neves, R.L., Addison, W.N., Assis, D.M., Murshed, M., Carmona, A.K., McKee, M.D., 2013. Proteolytic processing of osteopontin by PHEX and accumulation of osteopontin fragments in Hyp mouse bone, the murine model of X-linked hypophosphatemia. J. Bone Miner. Res. 28, 688−699. https://doi.org/10.1002/jbmr.1766.

Beck, L., Leroy, C., Salaun, C., Margall-Ducos, G., Desdouets, C., Friedlander, G., 2009. Identification of a novel function of PiT1 critical for cell proliferation and independent of its phosphate transport activity. J. Biol. Chem. 284, e99959.

Beck-Nielsen, S.S., Brock-Jacobsen, B., Gram, J., Brixen, K., Jensen, T.K., 2009. Incidence and prevalence of nutritional and hereditary rickets in southern Denmark. Eur. J. Endocrinol. 160, 491–497. https://doi.org/10.1530/EJE-08-0818.

Beck-Nielsen, S.S., Brixen, K., Gram, J., Brusgaard, K., 2012. Mutational analysis of PHEX, FGF23, DMP1, SLC34A3 and CLCN5 in patients with hypophosphatemic rickets. J. Hum. Genet. 57, 453–458. https://doi.org/10.1038/jhg.2012.56.

Bell, C.L., Tenenhouse, H.S., Scriver, C.R., 1988. Primary cultures of renal epithelial cells from X-linked hypophosphatemic (Hyp) mice express defects in phosphate transport and vitamin D metabolism. Am. J. Hum. Genet. 43, 293–303.

Belov, A.A., Mohammadi, M., 2013. Molecular mechanisms of fibroblast growth factor signaling in physiology and pathology. Cold Spring Harb Perspect Biol 5 (6). https://doi.org/10.1101/cshperspect.a015958. Online publication: https://cshperspectives.cshlp.org/content/5/6/a015958.long.

Benet-Pages, A., Orlik, P., Strom, T.M., Lorenz-Depiereux, B., 2005. An FGF23 missense mutation causes familial tumoral calcinosis with hyperphosphatemia. Hum. Mol. Genet. 14, 385–390.

Bergwitz, C., Bastepe, M., 2008. NHERF1 mutations and responsiveness of renal parathyroid hormone. NEJM 359, 2615–2617.

Bergwitz, C., Miyamoto, K.I., 2019. Hereditary hypophosphatemic rickets with hypercalciuria: pathophysiology, clinical presentation, diagnosis and therapy. Pflügers Archiv 471, 149–163. https://doi.org/10.1007/s00424-018-2184-2.

Bergwitz, C., Roslin, N.M., Tieder, M., Loredo-Osti, J.C., Bastepe, M., Abu-Zahra, H., Frappier, D., Burkett, K., Carpenter, T.O., Anderson, D., Garabedian, M., Sermet, I., Fujiwara, T.M., Morgan, K., Tenenhouse, H.S., Juppner, H., 2006. SLC34A3 mutations in patients with hereditary hypophosphatemic rickets with hypercalciuria predict a key role for the sodium-phosphate cotransporter NaPi-IIc in maintaining phosphate homeostasis. Am. J. Hum. Genet. 78, 179–192. https://doi.org/10.1086/499409 pii:S0002-9297(07)62351-9.

Berndt, T., Kumar, R., 2009. Novel mechanisms in the regulation of phosphorus homeostasis. Physiology 24, 17–25.

Berndt, T.J., Schiavi, S., Kumar, R., 2005. "Phosphatonins" and the regulation of phosphorus homeostasis. Am. J. Physiol. Renal. Physiol. 289, F1170–F1182.

Berndt, T., Thomas, L.F., Craig, T.A., Sommer, S., Li, X., Bergstralh, E.J., Kumar, R., 2007. Evidence for a signaling axis by which intestinal phosphate rapidly modulates renal phosphate reabsorption. Proc. Natl. Acad. Sci. U. S. A. 104, 11085–11090. https://doi.org/10.1073/pnas.0704446104.

Bhoj, E.J., Li, M., Ahrens-Nicklas, R., Pyle, L.C., Wang, J., Zhang, V.W., Clarke, C., Wong, L.J., Sondheimer, N., Ficicioglu, C., Yudkoff, M., 2015. Pathologic variants of the mitochondrial phosphate carrier SLC25A3: two new patients and expansion of the cardiomyopathy/skeletal myopathy phenotype with and without lactic acidosis. JIMD Rep 19, 59–66. https://doi.org/10.1007/8904_2014_364.

Biber, J., Hernando, N., Forster, I., 2013. Phosphate transporters and their function. Annu. Rev. Physiol. 75, 535–550. https://doi.org/10.1146/annurev-physiol-030212-183748.

Boger, C.A., Gorski, M., Li, M., Hoffmann, M.M., Huang, C., Yang, Q., Teumer, A., Krane, V., O'Seaghdha, C.M., Kutalik, Z., Wichmann, H.E., Haak, T., Boes, E., Coassin, S., Coresh, J., Kollerits, B., Haun, M., Paulweber, B., Kottgen, A., Li, G., Shlipak, M.G., Powe, N., Hwang, S.J., Dehghan, A., Rivadeneira, F., Uitterlinden, A., Hofman, A., Beckmann, J.S., Kramer, B.K., Witteman, J., Bochud, M., Siscovick, D., Rettig, R., Kronenberg, F., Wanner, C., Thadhani, R.I., Heid, I.M., Fox, C.S., Kao, W.H., Consortium, C.K., 2011. Association of eGFR-related loci identified by GWAS with incident CKD and ESRD. PLoS Genet. 7, e1002292. https://doi.org/10.1371/journal.pgen.1002292 pii:PGENETICS-D-11-00374.

Bonucci, E., 2012. Bone mineralization. Front. Biosci. 17, 100–128.

Bora, S.A., Kennett, M.J., Smith, P.B., Patterson, A.D., Cantorna, M.T., 2018. The gut microbiota regulates endocrine vitamin D metabolism through fibroblast growth factor 23. Front. Immunol. 9, 408. https://doi.org/10.3389/fimmu.2018.00408.

Bottini, M., Mebarek, S., Anderson, K.L., Strzelecka-Kiliszek, A., Bozycki, L., Simao, A.M.S., Bolean, M., Ciancaglini, P., Pikula, J.B., Pikula, S., Magne, D., Volkmann, N., Hanein, D., Millan, J.L., Buchet, R., 2018. Matrix vesicles from chondrocytes and osteoblasts: their biogenesis, properties, functions and biomimetic models. Biochim. Biophys. Acta Gen. Subj. 1862, 532–546. https://doi.org/10.1016/j.bbagen.2017.11.005.

Boukpessi, T., Hoac, B., Coyac, B.R., Leger, T., Garcia, C., Wicart, P., Whyte, M.P., Glorieux, F.H., Linglart, A., Chaussain, C., McKee, M.D., 2017. Osteopontin and the dento-osseous pathobiology of X-linked hypophosphatemia. Bone 95, 151–161. https://doi.org/10.1016/j.bone.2016.11.019.

Bourgine, A., Pilet, P., Diouani, S., Sourice, S., Lesoeur, J., Beck-Cormier, S., Khoshniat, S., Weiss, P., Friedlander, G., Guicheux, J., Beck, L., 2013. Mice with hypomorphic expression of the sodium-phosphate cotransporter PiT1/Slc20a1 have an unexpected normal bone mineralization. PLoS One 8, e65979. https://doi.org/10.1371/journal.pone.0065979 pii:PONE-D-12-23346.

Bringhurst, F.R., Leder, B.Z., 2006. Regulation of calcium and phosphate homeostasis. In: DeGroot, L.J., Jameson, J.L. (Eds.), Endocrinology. W.B. Saunders Co., Philadelphia, pp. 805–843.

Brown, B.J., Robinson, A.E., Brogdon, B.G., 1985. Radiographic findings in hydantoin toxicity. Ala. J. Med. Sci. 22, 428–430.

Brown, W.W., Juppner, H., Langman, C.B., Price, H., Farrow, E.G., White, K.E., McCormick, K.L., 2009. Hypophosphatemia with elevations in serum fibroblast growth factor 23 in a child with Jansen's metaphyseal chondrodysplasia. J. Clin. Endocrinol. Metab. 94, 17–20. https://doi.org/10.1210/jcem.94.2.9988, 10.1210/jc.2008-0220.

Brownstein, C.A., Adler, F., Nelson-Williams, C., Iijima, J., Li, P., Imura, A., Nabeshima, Y., Reyes-Mugica, M., Carpenter, T.O., Lifton, R.P., 2008. A translocation causing increased alpha-klotho level results in hypophosphatemic rickets and hyperparathyroidism. Proc. Natl. Acad. Sci. U. S. A. 105, 3455–3460. https://doi.org/10.1073/pnas.0712361105.

Burnett, C.H., Dent, C.E., Harper, C., Warland, B.J., 1964. Vitamin D-resistant rickets. Analysis of twenty-four pedigrees with hereditary and sporadic cases. Am. J. Med. 36, 222–232.

Butterworth, P.J., Younus, M.J., 1993. Uptake of phosphate by rat hepatocytes in primary culture: a sodium-dependent system that is stimulated by insulin. Biochim. Biophys. Acta 1148, 117–122.

Caballero, D., Li, Y., Fetene, J., Ponsetto, J., Chen, A., Zhu, C., Braddock, D.T., Bergwitz, C., 2017a. Intraperitoneal pyrophosphate treatment reduces renal calcifications in Npt2a null mice. PLoS One 12, e0180098. https://doi.org/10.1371/journal.pone.0180098.

Caballero, D., Li, Y., Ponsetto, J., Zhu, C., Bergwitz, C., 2017b. Impaired urinary osteopontin excretion in Npt2a−/− mice. Am. J. Physiol. Renal. Physiol. 312, F77−F83. https://doi.org/10.1152/ajprenal.00367.2016.

Calvo, M.S., Moshfegh, A.J., Tucker, K.L., 2014. Assessing the health impact of phosphorus in the food supply: issues and considerations. Adv Nutr 5, 104−113. https://doi.org/10.3945/an.113.004861.

Carpenter, T.O., Ellis, B.K., Insogna, K.L., Philbrick, W.M., Sterpka, J., Shimkets, R., 2005. Fibroblast growth factor 7: an inhibitor of phosphate transport derived from oncogenic osteomalacia-causing tumors. J. Clin. Endocrinol. Metab. 90, 1012−1020. https://doi.org/10.1210/jc.2004-0357.

Carpenter, T.O., Imel, E.A., Holm, I.A., Jan de Beur, S.M., Insogna, K.L., 2011. A clinician's guide to X-linked hypophosphatemia. J. Bone Miner. Res. 26, 1381−1388. https://doi.org/10.1002/jbmr.340.

Carpenter, T.O., Olear, E.A., Zhang, J.H., Ellis, B.K., Simpson, C.A., Cheng, D., Gundberg, C.M., Insogna, K.L., 2014. Effect of paricalcitol on circulating parathyroid hormone in X-linked hypophosphatemia: a randomized, double-blind, placebo-controlled study. J. Clin. Endocrinol. Metab. 99, 3103−3111. https://doi.org/10.1210/jc.2014-2017.

Carpenter, T.O., Whyte, M.P., Imel, E.A., Boot, A.M., Hogler, W., Linglart, A., Padidela, R., Van't Hoff, W., Mao, M., Chen, C.Y., Skrinar, A., Kakkis, E., San Martin, J., Portale, A.A., 2018. Burosumab therapy in children with X-linked hypophosphatemia. N. Engl. J. Med. 378, 1987−1998. https://doi.org/10.1056/NEJMoa1714641.

Chande, S., Bergwitz, C., 2018. Role of phosphate sensing in bone and mineral metabolism. Nat. Rev. Endocrinol. 14, 637−655. https://doi.org/10.1038/s41574-018-0076-3.

Chang, A.R., Lazo, M., Appel, L.J., Gutierrez, O.M., Grams, M.E., 2014. High dietary phosphorus intake is associated with all-cause mortality: results from NHANES III. Am. J. Clin. Nutr. 99, 320−327. https://doi.org/10.3945/ajcn.113.073148.

Chavkin, N.W., Chia, J.J., Crouthamel, M.H., Giachelli, C.M., 2015. Phosphate uptake-independent signaling functions of the type III sodium-dependent phosphate transporter, PiT-1, in vascular smooth muscle cells. Exp. Cell Res. 333, 39−48. https://doi.org/10.1016/j.yexcr.2015.02.002.

Chen, C., Carpenter, T., Steg, N., Baron, R., Anast, C., 1989. Hypercalciuric hypophosphatemic rickets, mineral balance, bone histomorphometry, and therapeutic implications of hypercalciuria. Pediatrics 84, 276−280.

Chen, G., Liu, Y., Goetz, R., Fu, L., Jayaraman, S., Hu, M.C., Moe, O.W., Liang, G., Li, X., Mohammadi, M., 2018. alpha-Klotho is a non-enzymatic molecular scaffold for FGF23 hormone signalling. Nature 553, 461−466. https://doi.org/10.1038/nature25451.

Chesher, D., Oddy, M., Darbar, U., Sayal, P., Casey, A., Ryan, A., Sechi, A., Simister, C., Waters, A., Wedatilake, Y., Lachmann, R.H., Murphy, E., 2018. Outcome of adult patients with X-linked hypophosphatemia caused by PHEX gene mutations. J. Inherit. Metab. Dis. 41, 865−876. https://doi.org/10.1007/s10545-018-0147-6.

Chi, Y., Zhao, Z., He, X., Sun, Y., Jiang, Y., Li, M., Wang, O., Xing, X., Sun, A.Y., Zhou, X., Meng, X., Xia, W., 2014. A compound heterozygous mutation in SLC34A3 causes hereditary hypophosphatemic rickets with hypercalciuria in a Chinese patient. Bone 59, 114−121. https://doi.org/10.1016/j.bone.2013.11.008 pii:S8756-3282(13)00444-4.

Chien, M.L., Foster, J.L., Douglas, J.L., Garcia, J.V., 1997. The amphotropic murine leukemia virus receptor gene encodes a 71-kilodalton protein that is induced by phosphate depletion. J. Virol. 71, 4564−4570.

Choi, C.S., Befroy, D.E., Codella, R., Kim, S., Reznick, R.M., Hwang, Y.J., Liu, Z.X., Lee, H.Y., Distefano, A., Samuel, V.T., Zhang, D., Cline, G.W., Handschin, C., Lin, J., Petersen, K.F., Spiegelman, B.M., Shulman, G.I., 2008. Paradoxical effects of increased expression of PGC-1alpha on muscle mitochondrial function and insulin-stimulated muscle glucose metabolism. Proc. Natl. Acad. Sci. U. S. A. 105, 19926−19931. https://doi.org/10.1073/pnas.0810339105.

Chong, W.H., Molinolo, A.A., Chen, C.C., Collins, M.T., 2011. Tumor-induced osteomalacia. Endocr. Relat. Cancer 18, R53−R77. https://doi.org/10.1530/ERC-11-0006.

Clarke, G.D., Kainer, G., Conway, W.F., Chan, J.C., 1990. Intramyocellular phosphate metabolism in X-linked hypophosphatemic rickets. J. Pediatr. 116, 288−292.

Collins, J.F., Ghishan, F.K., 1994. Molecular cloning, functional expression, tissue distribution, and in situ hybridization of the renal sodium phosphate (Na+/Pi) transporter in the control and hypophosphatemic mouse. FASBJ 8, 862−868.

Collins, M., Bergwitz, C., Aitcheson, G., Blau, J., Boyce, A., Gafni, R., Guthrie, L., Miranda, F., Slosberg, E., Graus-Porta, D., Hopmann, C., Welaya, K., Isaacs, R., Miller, C., 2015. Striking response of tumor-induced osteomalacia to the FGFR inhibitor NVP-BGJ398. J. Bone Miner. Res. 30 (Suppl. 1) available at: http://www.asbmr.org/education/AbstractDetail?aid=c5464be6-d873-49f3-bb71-719e2198867e.

Connor, J., Olear, E.A., Insogna, K.L., Katz, L., Baker, S., Kaur, R., Simpson, C.A., Sterpka, J., Dubrow, R., Zhang, J.H., Carpenter, T.O., 2015. Conventional therapy in adults with X-linked hypophosphatemia: effects on enthesopathy and dental disease. J. Clin. Endocrinol. Metab. 100, 3625−3632. https://doi.org/10.1210/JC.2015-2199.

Couasnay, G., Bon, N., Devignes, C.S., Sourice, S., Bianchi, A., Veziers, J., Weiss, P., Elefteriou, F., Provot, S., Guicheux, J., Beck-Cormier, S., Beck, L., 2019. PiT1/Slc20a1 is required for endoplasmic reticulum homeostasis, chondrocyte survival, and skeletal development. J. Bone Miner. Res. 34 (2), 387−398. https://doi.org/10.1002/jbmr.3609 (Epub 2018).

Coyac, B.R., 2017. Tissue-specific mineralization defects in the periodontium of the Hyp mouse model of X-linked hypophosphatemia. Bone 103, 334−346.

Daga, A., Majmundar, A.J., Braun, D.A., Gee, H.Y., Lawson, J.A., Shril, S., Jobst-Schwan, T., Vivante, A., Schapiro, D., Tan, W., Warejko, J.K., Widmeier, E., Nelson, C.P., Fathy, H.M., Gucev, Z., Soliman, N.A., Hashmi, S., Halbritter, J., Halty, M., Kari, J.A., El-Desoky, S., Ferguson, M.A., Somers, M.J.G., Traum, A.Z., Stein, D.R., Daouk, G.H., Rodig, N.M., Katz, A., Hanna, C., Schwaderer, A.L., Sayer, J.A., Wassner, A.J., Mane, S.,

Lifton, R.P., Milosevic, D., Tasic, V., Baum, M.A., Hildebrandt, F., 2018. Whole exome sequencing frequently detects a monogenic cause in early onset nephrolithiasis and nephrocalcinosis. Kidney Int. 93, 204–213. https://doi.org/10.1016/j.kint.2017.06.025 pii:S0085-2538(17)30494-5.

Dallas, S.L., Prideaux, M., Bonewald, L.F., 2013. The osteocyte: an endocrine cell … and more. Endocr. Rev. 34, 658–690. https://doi.org/10.1210/er.2012-1026.

Dasgupta, D., Wee, M.J., Reyes, M., Li, Y., Simm, P.J., Sharma, A., Schlingmann, K.P., Janner, M., Biggin, A., Lazier, J., Gessner, M., Chrysis, D., Tuchman, S., Baluarte, H.J., Levine, M.A., Tiosano, D., Insogna, K., Hanley, D.A., Carpenter, T.O., Ichikawa, S., Hoppe, B., Konrad, M., Savendahl, L., Munns, C.F., Lee, H., Juppner, H., Bergwitz, C., 2014. Mutations in SLC34A3/NPT2c are associated with kidney stones and nephrocalcinosis. J. Am. Soc. Nephrol. 25, 2366–2375. https://doi.org/10.1681/ASN.2013101085.

David, V., Martin, A., Hedge, A.M., Drezner, M.K., Rowe, P.S., 2011. ASARM peptides: PHEX-dependent and -independent regulation of serum phosphate. Am. J. Physiol. Renal. Physiol. 300, F783–F791. https://doi.org/10.1152/ajprenal.00304.2010.

Dhir, G., Li, D., Hakonarson, H., Levine, M.A., 2017. Late-onset hereditary hypophosphatemic rickets with hypercalciuria (HHRH) due to mutation of SLC34A3/NPT2c. Bone 97, 15–19. https://doi.org/10.1016/j.bone.2016.12.001 pii:S8756-3282(16)30363-5.

DiMeglio, L.A., Econs, M.J., 2001. Hypophosphatemic rickets. Rev. Endocr. Metab. Disord. 2, 165–173.

Ding, C., Buckingham, B., Levine, M.A., 2001. Familial isolated hypoparathyroidism caused by a mutation in the gene for the transcription factor GCMB. J. Clin. Investig. 108, 1215–1220.

Donohue, M.M., Demay, M.B., 2002. Rickets in VDR null mice is secondary to decreased apoptosis of hypertrophic chondrocytes. Endocrinology 143, 3691–3694.

Econs, M.J., McEnery, P.T., 1997. Autosomal dominant hypophosphatemic rickets/osteomalacia: clinical characterization of a novel renal phosphate-wasting disorder. J. Clin. Endocrinol. Metab. 82, 674–681. https://doi.org/10.1210/jcem.82.2.3765.

Econs, M.J., Samsa, G.P., Monger, M., Drezner, M.K., Feussner, J.R., 1994. X-Linked hypophosphatemic rickets: a disease often unknown to affected patients. Bone Miner. 24, 17–24.

El-Maouche, D., Sadowski, S.M., Papadakis, G.Z., Guthrie, L., Cottle-Dellisle, C., Merkel, R., Milo, C., Chen, C.C., Kebebew, E., Collins, M.T., 2016. 68Ga-DOTATATE for tumor localization in tumor-induced osteomalacia. J. Clin. Endocrinol. Metab. 101, 3575–3581.

Erben, R.G., 2016. Update on FGF23 and klotho signaling. Mol. Cell. Endocrinol. 432, 56–65. https://doi.org/10.1016/j.mce.2016.05.008.

Eto, N., Miyata, Y., Ohno, H., Yamashita, T., 2005. Nicotinamide prevents the development of hyperphosphataemia by suppressing intestinal sodium-dependent phosphate transporter in rats with adenine-induced renal failure. Nephrol. Dial. Transplant. 20, 1378–1384. https://doi.org/10.1093/ndt/gfh781 pii:gfh781.

Eto, N., Tomita, M., Hayashi, M., 2006. NaPi-mediated transcellular permeation is the dominant route in intestinal inorganic phosphate absorption in rats. Drug Metab. Pharmacokinet. 21, 217–221.

Eyres, K.S., Brown, J., Douglas, D.L., 1993. Osteotomy and intramedullary nailing for the correction of progressive deformity in vitamin D-resistant hypophosphataemic rickets. J. R. Coll. Surg. Edinb. 38, 50–54.

Farrow, E.G., White, K.E., 2010. Recent advances in renal phosphate handling. Nat. Rev. Nephrol. 6, 207–217. https://doi.org/10.1038/nrneph.2010.17.

Farrow, E.G., Davis, S.I., Ward, L.M., Summers, L.J., Bubbear, J.S., Keen, R., Stamp, T.C., Baker, L.R., Bonewald, L.F., White, K.E., 2009. Molecular analysis of DMP1 mutants causing autosomal recessive hypophosphatemic rickets. Bone 44, 287–294.

Feng, J.Q., Ward, L.M., Liu, S., Lu, Y., Xie, Y., Yuan, B., Yu, X., Rauch, F., Davis, S.I., Zhang, S., Rios, H., Drezner, M.K., Quarles, L.D., Bonewald, L.F., White, K.E., 2006. Loss of DMP1 causes rickets and osteomalacia and identifies a role for osteocytes in mineral metabolism. Nat. Genet. 38, 1310–1315. https://doi.org/10.1038/ng1905.

Ferreira, C., Ziegler, S., Gahl, W.A., 1993. Generalized arterial calcification of infancy. In: Adam, M.P., Ardinger, H.H., Pagon, R.A., Wallace, S.E., Bean, L.J.H., Stephens, K., Amemiya, A. (Eds.), GeneReviews((R)). Seattle (WA).

Ferreira, C.R., Ziegler, S.G., Gupta, A., Groden, C., Hsu, K.S., Gahl, W.A., 2016. Treatment of hypophosphatemic rickets in generalized arterial calcification of infancy (GACI) without worsening of vascular calcification. Am. J. Med. Genet. A 170 (5), 1308–1311. https://doi.org/10.1002/ajmg.a.37574.

Fiermonte, G., Dolce, V., Arrigoni, R., Runswick, M.J., Walker, J.E., Palmieri, F., 1999. Organization and sequence of the gene for the human mitochondrial dicarboxylate carrier: evolution of the carrier family. Biochem. J. 344 (Pt 3), 953–960.

Fishman, G., Miller-Hansen, D., Jacobsen, C., Singhal, V.K., Alon, U.S., 2004. Hearing impairment in familial X-linked hypophosphatemic rickets. Eur. J. Pediatr. 163, 622–623. https://doi.org/10.1007/s00431-004-1504-z.

Folpe, A.L., Fanburg-Smith, J.C., Billings, S.D., Bisceglia, M., Bertoni, F., Cho, J.Y., Econs, M.J., Inwards, C.Y., Jan de Beur, S.M., Mentzel, T., Montgomery, E., Michal, M., Miettinen, M., Mills, S.E., Reith, J.D., O'Connell, J.X., Rosenberg, A.E., Rubin, B.P., Sweet, D.E., Vinh, T.N., Wold, L.E., Wehrli, B.M., White, K.E., Zaino, R.J., Weiss, S.W., 2004. Most osteomalacia-associated mesenchymal tumors are a single histopathologic entity: an analysis of 32 cases and a comprehensive review of the literature. Am. J. Surg. Pathol. 28, 1–30.

Folsom, L.J., Imel, E.A., 2015. Hyperphosphatemic familial tumoral calcinosis: genetic models of deficient FGF23 action. Curr. Osteoporos. Rep. 13, 78–87. https://doi.org/10.1007/s11914-015-0254-3.

Forrest, G., German, J., Giuffrida, A., Luidens, M., Dowling, J., 2016. Hereditary x-linked hypophosphatemia and thoracic myelopathy. Aace Clin. Case Rep. 2, e244–e246.

Forster, I., Wagner, A., 2018. SLC34. In: Choi, S. (Ed.), Encyclopedia of Signalling Molecules. Springer, pp. 5013–5022.

Forster, I.C., Hernando, N., Biber, J., Murer, H., 2006. Proximal tubular handling of phosphate: a molecular perspective. Kidney Int. 70, 1548–1559. https://doi.org/10.1038/sj.ki.5001813.

Francis, R.M., Selby, P.L., 1997. Osteomalacia. Baillieres Clin Endocrinol Metab 11, 145–163.

Frishberg, Y., Araya, K., Rinat, C., Topaz, O., Yamazaki, Y., Feinstein, Y., Navon-Elkan, P., Becker-Cohen, R., Yamashita, T., Igarashi, T., Sprecher, E., 2004. Hyperostosis-hyperphosphatemia syndrome caused by mutations in GALNT3 and associated with augmented processing of FGF-23. Philadelphia, pp. F-P0937 Am. Soc. Nephrol.

Gannage-Yared, M.H., Makrythanasis, P., Chouery, E., Sobacchi, C., Mehawej, C., Santoni, F.A., Guipponi, M., Antonarakis, S.E., Hamamy, H., Megarbane, A., 2014. Exome sequencing reveals a mutation in DMP1 in a family with familial sclerosing bone dysplasia. Bone 68, 142−145. https://doi.org/10.1016/j.bone.2014.08.014.

Gazit, D., Tieder, M., Liberman, U.A., Passi-Even, L., Bab, I.A., 1991. Osteomalacia in hereditary hypophosphatemic rickets with hypercalciuria: a correlative clinical-histomorphometric study. J. Clin. Endocrinol. Metab. 72, 229−235.

Ghanem, I., Karam, J.A., Widmann, R.F., 2011. Surgical epiphysiodesis indications and techniques: update. Curr. Opin. Pediatr. 23, 53−59. https://doi.org/10.1097/MOP.0b013e32834231b3.

Giral, H., Caldas, Y., Sutherland, E., Wilson, P., Breusegem, S., Barry, N., Blaine, J., Jiang, T., Wang, X.X., Levi, M., 2009. Regulation of rat intestinal Na-dependent phosphate transporters by dietary phosphate. Am. J. Physiol. Renal. Physiol. 297, F1466−F1475. https://doi.org/10.1152/ajprenal.00279.2009.

Glorieux, F., Scriver, C.R., 1972. Loss of a parathyroid hormone-sensitive component of phosphate transport in X-linked hypophosphatemia. Science 175, 997−1000.

Glorieux, F.H., Marie, P.J., Pettifor, J.M., Delvin, E.E., 1980. Bone response to phosphate salts, ergocalciferol, and calcitriol in hypophosphatemic vitamin D-resistant rickets. N. Engl. J. Med. 303, 1023−1031. https://doi.org/10.1056/NEJM198010303031802.

Gonzalez Ballesteros, L.F., Ma, N.S., Gordon, R.J., Ward, L., Backeljauw, P., Wasserman, H., Weber, D.R., DiMeglio, L.A., Gagne, J., Stein, R., Cody, D., Simmons, K., Zimakas, P., Topor, L.S., Agrawal, S., Calabria, A., Tebben, P., Faircloth, R., Imel, E.A., Casey, L., Carpenter, T.O., 2017. Unexpected widespread hypophosphatemia and bone disease associated with elemental formula use in infants and children. Bone 97, 287−292. https://doi.org/10.1016/j.bone.2017.02.003.

GTEx Consortium, T., 2013. The genotype-tissue expression (GTEx) project. Nat. Genet. 45, 580−585. https://doi.org/10.1038/ng.2653.

Gudbjartsson, D.F., Holm, H., Indridason, O.S., Thorleifsson, G., Edvardsson, V., Sulem, P., de Vegt, F., d'Ancona, F.C., den Heijer, M., Wetzels, J.F., Franzson, L., Rafnar, T., Kristjansson, K., Bjornsdottir, U.S., Eyjolfsson, G.I., Kiemeney, L.A., Kong, A., Palsson, R., Thorsteinsdottir, U., Stefansson, K., 2010. Association of variants at UMOD with chronic kidney disease and kidney stones-role of age and comorbid diseases. PLoS Genet. 6, e1001039. https://doi.org/10.1371/journal.pgen.1001039.

Gutierrez, O.M., Luzuriaga-McPherson, A., Lin, Y., Gilbert, L.C., Ha, S.W., Beck Jr., G.R., 2015. Impact of phosphorus-based food additives on bone and mineral metabolism. J. Clin. Endocrinol. Metab. 100, 4264−4271. https://doi.org/10.1210/jc.2015-2279.

Haffner, D., Nissel, R., Wuhl, E., Mehls, O., 2004. Effects of growth hormone treatment on body proportions and final height among small children with X-linked hypophosphatemic rickets. Pediatrics 113, e593−e596.

Haito-Sugino, S., Ito, M., Ohi, A., Shiozaki, Y., Kangawa, N., Nishiyama, T., Aranami, F., Sasaki, S., Mori, A., Kido, S., Tatsumi, S., Segawa, H., Miyamoto, K., 2012. Processing and stability of type IIc sodium-dependent phosphate cotransporter mutations in patients with hereditary hypophosphatemic rickets with hypercalciuria. Am. J. Physiol. Cell Physiol. 302, C1316−C1330. https://doi.org/10.1152/ajpcell.00314.2011.

Harrison, H.E., Harrison, H.C., 1979. Disorders of calcium and phosphate metabolism in childhood and adolescence. Major Probl. Clin. Pediatr. 20, 1−314.

Harvey, B.M., Eussen, S., Harthoorn, L.F., Burks, A.W., 2017. Mineral intake and status of cow's milk allergic infants consuming an amino acid-based formula. J. Pediatr. Gastroenterol. Nutr. 65, 346−349. https://doi.org/10.1097/MPG.0000000000001655.

Hattenhauer, O., Traebert, M., Murer, H., Biber, J., 1999. Regulation of small intestinal Na-P(i) type IIb cotransporter by dietary phosphate intake. Am. J. Physiol. 277, G756−G762.

Hesse, E., Moessinger, E., Rosenthal, H., Laenger, F., Brabant, G., Petrich, T., Gratz, K.F., Bastian, L., 2007a. Oncogenic osteomalacia: exact tumor localization by co-registration of positron emission and computed tomography. J. Bone Miner. Res. 22, 158−162. https://doi.org/10.1359/jbmr.060909.

Hesse, E., Rosenthal, H., Bastian, L., 2007b. Radiofrequency ablation of a tumor causing oncogenic osteomalacia. N. Engl. J. Med. 357, 422−424. https://doi.org/10.1056/NEJMc070347.

Hilfiker, H., Kvietikova, I., Hartmann, C.M., Stange, G., Murer, H., 1998. Characterization of the human type II Na/Pi-cotransporter promoter. Pflügers Archiv 436, 591−598.

Hirao, Y., Chikuda, H., Oshima, Y., Matsubayashi, Y., Tanaka, S., 2016. Extensive ossification of the paraspinal ligaments in a patient with vitamin D-resistant rickets: case report with literature review. Int. J. Surg. Case Rep. 27, 125−128.

Hoac, B., Boukpessi, T., Buss, D.J., Chaussain, C., Murshed, M., McKee, M.D., 2018. Ablation of osteopontin in osteomalacic Hyp mice partially rescues the deficient mineralization without correcting hypophosphatemia. In: American Society for Bone and Mineral Research Annual Meeting. Montreal.

Holm, I.A., Huang, X., Kunkel, L.M., 1997. Mutational analysis of the PEX gene in patients with X-linked hypophosphatemic rickets. Am. J. Hum. Genet. 60, 790−797.

Hsia, D.Y., Kraus, M., Samuels, J., 1959. Genetic studies on vitamin D resistant rickets (familial hypophosphatemia). Am. J. Hum. Genet. 11, 156−165.

Hu, M.C., Shi, M., Zhang, J., Pastor, J., Nakatani, T., Lanske, B., Shawkat Razzaque, M., Rosenblatt, K.P., Baum, M.G., Kuro, O.M., Moe, O.W., 2010. Klotho: a novel phosphaturic substance acting as an autocrine enzyme in the renal proximal tubule. FASEB J. 24, 3438−3450.

Hughes, M.R., Malloy, P.J., Kieback, D.G., Kesterson, R.A., Pike, J.W., Feldman, D., O'Malley, B.W., 1988. Point mutations in the human vitamin D receptor gene associated with hypocalcemic rickets. Science 242, 1702−1705.

HYP-Consortium, 1995. A gene (PEX) with homologies to endopeptidases is mutated in patients with X-linked hypophosphatemic rickets. Nat. Genet. 11, 130–136.

Ichikawa, S., Sorenson, A.H., Imel, E.A., Friedman, N.E., Gertner, J.M., Econs, M.J., 2006. Intronic deletions in the SLC34A3 gene cause hereditary hypophosphatemic rickets with hypercalciuria. J. Clin. Endocrinol. Metab. 91, 4022–4027. https://doi.org/10.1210/jc.2005-2840.

Ichikawa, S., Imel, E.A., Kreiter, M.L., Yu, X., Mackenzie, D.S., Sorenson, A.H., Goetz, R., Mohammadi, M., White, K.E., Econs, M.J., 2007. A homozygous missense mutation in human KLOTHO causes severe tumoral calcinosis. J. Clin. Investig. 117, 2684–2691. https://doi.org/10.1172/JCI31330.

Ichikawa, S., Tuchman, S., Padgett, L.R., Gray, A.K., Baluarte, H.J., Econs, M.J., 2014. Intronic deletions in the SLC34A3 gene: a cautionary tale for mutation analysis of hereditary hypophosphatemic rickets with hypercalciuria. Bone 59, 53–56. https://doi.org/10.1016/j.bone.2013.10.018 pii:S8756-3282(13)00428-6.

Imel, E.A., Hui, S.L., Econs, M.J., 2007. FGF23 concentrations vary with disease status in autosomal dominant hypophosphatemic rickets. J. Bone Miner. Res. 22, 520–526. https://doi.org/10.1359/jbmr.070107.

Imel, E.A., Peacock, M., Gray, A.K., Padgett, L.R., Hui, S.L., Econs, M.J., 2011. Iron modifies plasma FGF23 differently in autosomal dominant hypophosphatemic rickets and healthy humans. J. Clin. Endocrinol. Metab. 96, 3541–3549. https://doi.org/10.1210/jc.2011-1239.

Imel, E., Whyte, M., Munns, C., Portale, A., Ward, L., Nilsson, O., Simmons, J., Padidela, R., Namba, N., Cheong, H., Mao, M., Chen, C.-Y., Skrinar, A., San Martin, J., Glorieux, F., 2018. Burosumab improved rickets, phosphate metabolism, and clinical outcomes compared to conventional therapy in children with XLH. J. Bone Miner. Res. 33 (Suppl. 1).

Inoue, M., Digman, M.A., Cheng, M., Breusegem, S.Y., Halaihel, N., Sorribas, V., Mantulin, W.W., Gratton, E., Barry, N.P., Levi, M., 2004. Partitioning of NaPi cotransporter in cholesterol-, sphingomyelin-, and glycosphingolipid-enriched membrane domains modulates NaPi protein diffusion, clustering, and activity. J. Biol. Chem. 279, 49160–49171. https://doi.org/10.1074/jbc.M408942200.

Insogna, K., Rauch, F., Kamenický, P., Ito, N., Takuo Kubota, T., Nakamura, A., Zhang, L., Mealiffe, M., San Martin, J., Portale, A., 2018. The effect of burosumab (KRN23), a fully human anti-FGF23 monoclonal antibody, on osteomalacia in adults with X-linked hypophosphatemia (XLH). J. Bone Miner. Res. 33 (Suppl. 1).

Insogna, K.L., Briot, K., Imel, E.A., Kamenicky, P., Ruppe, M.D., Portale, A.A., Weber, T., Pitukcheewanont, P., Cheong, H.I., Jan de Beur, S., Imanishi, Y., Ito, N., Lachmann, R.H., Tanaka, H., Perwad, F., Zhang, L., Chen, C.Y., Theodore-Oklota, C., Mealiffe, M., San Martin, J., Carpenter, T.O., Investigators, A., 2018. A randomized, double-blind, placebo-controlled, phase 3 trial evaluating the efficacy of burosumab, an anti-FGF23 antibody, in adults with X-linked hypophosphatemia: week 24 primary analysis. J. Bone Miner. Res. 33, 1383–1393. https://doi.org/10.1002/jbmr.3475.

Jan de Beur, S.M., Finnegan, R.B., Vassiliadis, J., Cook, B., Barberio, D., Estes, S., Manavalan, P., Petroziello, J., Madden, S.L., Cho, J.Y., Kumar, R., Levine, M.A., Schiavi, S.C., 2002. Tumors associated with oncogenic osteomalacia express genes important in bone and mineral metabolism. J. Bone Miner. Res. 17, 1102–1110. https://doi.org/10.1359/jbmr.2002.17.6.1102.

Jan de Beur, S., Miller, P.D., Weber, T.J., Peacock, M., Insogna, K.L., Kumar, R., Rauch, F., Luca, D., Theodore-Oklota, C., Lampl, K., San Martin, J., Carpenter, T.O., 2018. Burosumab improved serum phosphorus, osteomalacia, mobility, and fatigue in the 48-week, phase 2 study in adults with tumor-induced osteomalacia syndrome, 2018 J Bone Min Res J. Bone Miner. Res. 33 (Suppl. 1). available at: http://www.asbmr.org/ItineraryBuilder/PresentationDetail.aspx?pid=d311f659-4f63-4aad-9cd4-6f548bc700d3&ptag=WebItinerarySearch.

Jaureguiberry, G., Carpenter, T.O., Forman, S., Juppner, H., Bergwitz, C., 2008. A novel missense mutation in SLC34A3 that causes hereditary hypophosphatemic rickets with hypercalciuria in humans identifies threonine 137 as an important determinant of sodium-phosphate cotransport in NaPi-IIc. Am. J. Physiol. Renal. Physiol. 295, F371–F379. https://doi.org/10.1152/ajprenal.00090.2008.

Jensen, N., Autzen, J.K., Pedersen, L., 2016. Slc20a2 is critical for maintaining a physiologic inorganic phosphate level in cerebrospinal fluid. Neurogenetics 17, 125–130. https://doi.org/10.1007/s10048-015-0469-6.

Jones, A., Tzenova, J., Frappier, D., Crumley, M., Roslin, N., Kos, C., Tieder, M., Langman, C., Proesmans, W., Carpenter, T., Rice, A., Anderson, D., Morgan, K., Fujiwara, T., Tenenhouse, H., 2001. Hereditary hypophosphatemic rickets with hypercalciuria is not caused by mutations in the Na/Pi cotransporter NPT2 gene. J. Am. Soc. Nephrol. 12, 507–514.

Jonsson, K.B., Zahradnik, R., Larsson, T., White, K.E., Sugimoto, T., Imanishi, Y., Yamamoto, T., Hampson, G., Koshiyama, H., Ljunggren, O., Oba, K., Yang, I.M., Miyauchi, A., Econs, M.J., Lavigne, J., Juppner, H., 2003. Fibroblast growth factor 23 in oncogenic osteomalacia and X-linked hypophosphatemia. N. Engl. J. Med. 348, 1656–1663. https://doi.org/10.1056/NEJMoa020881.

Jost, J., Bahans, C., Courbebaisse, M., Tran, T.A., Linglart, A., Benistan, K., Lienhardt, A., Mutar, H., Pfender, E., Ratsimbazafy, V., Guigonis, V., 2016. Topical sodium thiosulfate: a treatment for calcifications in hyperphosphatemic familial tumoral calcinosis? J. Clin. Endocrinol. Metab. 101, 2810–2815. https://doi.org/10.1210/jc.2016-1087.

Juppner, H., Schipani, E., Bastepe, M., Cole, D.E., Lawson, M.L., Mannstadt, M., Hendy, G.N., Plotkin, H., Koshiyama, H., Koh, T., Crawford, J.D., Olsen, B.R., Vikkula, M., 1998. The gene responsible for pseudohypoparathyroidism type Ib is paternally imprinted and maps in four unrelated kindreds to chromosome 20q13.3. Proc. Natl. Acad. Sci. U. S. A. 95, 11798–11803.

Kamiya, N., Yamaguchi, R., Aruwajoye, O., Kim, A.J., Kuroyanagi, G., Phipps, M., Adapala, N.S., Feng, J.Q., Kim, H.K., 2017. Targeted disruption of NF1 in osteocytes increases FGF23 and osteoid with osteomalacia-like bone phenotype. J. Bone Miner. Res. 32, 1716–1726. https://doi.org/10.1002/jbmr.3155.

Kapelari, K., Kohle, J., Kotzot, D., Hogler, W., 2015. Iron supplementation associated with loss of phenotype in autosomal dominant hypophosphatemic rickets. J. Clin. Endocrinol. Metab. 100, 3388–3392. https://doi.org/10.1210/jc.2015-2391.

Karaplis, A.C., Bai, X., Falet, J.P., Macica, C.M., 2012. Mineralizing enthesopathy is a common feature of renal phosphate-wasting disorders attributed to FGF23 and is exacerbated by standard therapy in hyp mice. Endocrinology 153, 5906−5917. https://doi.org/10.1210/en.2012-1551.

Karim, Z., Gerard, B., Bakouh, N., Alili, R., Leroy, C., Beck, L., Silve, C., Planelles, G., Urena-Torres, P., Grandchamp, B., Friedlander, G., Prie, D., 2008. NHERF1 mutations and responsiveness of renal parathyroid hormone. N. Engl. J. Med. 359, 1128−1135.

Karperien, M.C., van der Harten, H.J., van Schooten, R., Farih-Sips, H., den Hollander, N.S., Kneppers, A.L.J., Nijweide, P., Papapoulos, S.E., Löwik, C.W., 1999. A frame-shift mutation in the type I parathyroid hormone/parathyroid hormone-related peptide receptor causing Blomstrand lethal osteochondrodysplasia. J. Clin. Endocrinol. Metab. 84, 3713−3720.

Kavanaugh, M.P., Kabat, D., 1996. Identification and characterization of a widely expressed phosphate transporter/retrovirus receptor family. Kidney Int. 49, 959−963.

Keller, A., Westenberger, A., Sobrido, M.J., García-Murias, M., Domingo, A., Sears, R.L., Lemos, R.R., Ordoñez-Ugalde, A., Nicolas, G., da Cunha, J.E.G., Rushing, E.J., Hugelshofer, M., Wurnig, M.C., Kaech, A., Reimann, R., Lohmann, K., Dobričić, V., Carracedo, A., Petrović, I., Miyasaki, J.M., Abakumova, I., Mäe, M.A., Raschperger, E., Zatz, M., Zschiedrich, K., Klepper, J., Spiteri, E., Prieto, J.M., Navas, I., Preuss, M., Dering, C., Janković, M., Paucar, M., Svenningsson, P., Saliminejad, K., Khorshid, H.R.K., Novaković, I., Aguzzi, A., Boss, A., Le Ber, I., Defer, G., Hannequin, D., Kostić, V.S., Campion, D., Geschwind, D.H., Coppola, G., Betsholtz, C., Klein, C., Oliveira, J.R.M., 2013. Mutations in the gene encoding PDGF-B cause brain calcifications in humans and mice. Nat. Genet. 45, 1077. https://doi.org/10.1038/ng.2723. https://www.nature.com/articles/ng.2723#supplementary-information.

Kemp, G.J., Land, J.M., Coppack, S.W., Frayn, K.N., 1993. Skeletal muscle phosphate uptake during euglycemic-hyperinsulinemic clamp. Clin. Chem. 39, 170−171.

Kestenbaum, B., Glazer, N.L., Kottgen, A., Felix, J.F., Hwang, S.J., Liu, Y., Lohman, K., Kritchevsky, S.B., Hausman, D.B., Petersen, A.K., Gieger, C., Ried, J.S., Meitinger, T., Strom, T.M., Wichmann, H.E., Campbell, H., Hayward, C., Rudan, I., de Boer, I.H., Psaty, B.M., Rice, K.M., Chen, Y.D., Li, M., Arking, D.E., Boerwinkle, E., Coresh, J., Yang, Q., Levy, D., van Rooij, F.J., Dehghan, A., Rivadeneira, F., Uitterlinden, A.G., Hofman, A., van Duijn, C.M., Shlipak, M.G., Kao, W.H., Witteman, J.C., Siscovick, D.S., Fox, C.S., 2010. Common genetic variants associate with serum phosphorus concentration. J. Am. Soc. Nephrol. 21, 1223−1232. https://doi.org/10.1681/ASN.2009111104.

Keusch, I., Traebert, M., Lotscher, M., Kaissling, B., Murer, H., Biber, J., 1998. Parathyroid hormone and dietary phosphate provoke a lysosomal routing of the proximal tubular Na/Pi-cotransporter type II. Kidney Int. 54, 1224−1232. https://doi.org/10.1046/j.1523-1755.1998.00115.x pii:S0085-2538(15)30744-4.

Keushkerian, S., Wade, T., 1984. Hypophosphatemia after major hepatic resection. Curr. Surg. 41, 12−14.

Kim, H.J., Delaney, J.D., Kirsch, T., 2010. The role of pyrophosphate/phosphate homeostasis in terminal differentiation and apoptosis of growth plate chondrocytes. Bone 47, 657−665. https://doi.org/10.1016/j.bone.2010.06.018.

Kitanaka, S., Takeyama, K., Murayama, A., Sato, T., Okumura, K., Nogami, M., Hasegawa, Y., Niimi, H., Yanagisawa, J., Tanaka, T., Kato, S., 1998. Inactivating mutations in the 25-hydroxyvitamin D3 1alpha-hydroxylase gene in patients with pseudovitamin D-deficiency rickets. N. Engl. J. Med. 338, 653−661.

Knöpfel, T., Pastor-Arroyo, E.M., Schnitzbauer, U., Kratschmar, D.V., Odermatt, A., Pellegrini, G., Hernando, N., Wagner, C.A., 2017. The intestinal phosphate transporter NaPi-IIb (Slc34a2) is required to protect bone during dietary phosphate restriction. Sci. Rep. 7, 11018. https://doi.org/10.1038/s41598-017-10390-2.

Koldobskiy, M.A., Chakraborty, A., Werner, J.K., Snowman, A.M., Juluri, K.R., Vandiver, M.S., Kim, S., Heletz, S., Snyder, S.H., 2010. p53-mediated apoptosis requires inositol hexakisphosphate kinase-2. Proc. Natl. Acad. Sci. Unit. States Am. 107, 20947−20951. https://doi.org/10.1073/pnas.1015671107.

Kranenburg, G., de Jong, P.A., Mali, W.P., Attrach, M., Visseren, F.L., Spiering, W., 2017. Prevalence and severity of arterial calcifications in pseudoxanthoma elasticum (PXE) compared to hospital controls. Novel insights into the vascular phenotype of PXE. Atherosclerosis 256, 7−14. https://doi.org/10.1016/j.atherosclerosis.2016.11.012.

Kremke, B., Bergwitz, C., Ahrens, W., Schutt, S., Schumacher, M., Wagner, V., Holterhus, P.M., Juppner, H., Hiort, O., 2009. Hypophosphatemic rickets with hypercalciuria due to mutation in SLC34A3/NaPi-IIc can be masked by vitamin D deficiency and can be associated with renal calcifications. Exp. Clin. Endocrinol. Diabetes 117, 49−56. https://doi.org/10.1055/s-2008-1076716.

Kuro-o, M., 2006. Klotho as a regulator of fibroblast growth factor signaling and phosphate/calcium metabolism. Curr. Opin. Nephrol. Hypertens. 15, 437−441.

Kurosu, H., Kuro-o, M., 2008. The Klotho gene family and the endocrine fibroblast growth factors. Curr. Opin. Nephrol. Hypertens. 17, 368−372.

Kwong, J.Q., Davis, J., Baines, C.P., Sargent, M.A., Karch, J., Wang, X., Huang, T., Molkentin, J.D., 2014. Genetic deletion of the mitochondrial phosphate carrier desensitizes the mitochondrial permeability transition pore and causes cardiomyopathy. Cell Death Differ. 21, 1209−1217. https://doi.org/10.1038/cdd.2014.36.

Lanske, B., Razzaque, M.S., 2014. Molecular interactions of FGF23 and PTH in phosphate regulation. Kidney Int. 86, 1072−1074. https://doi.org/10.1038/ki.2014.316.

Larsson, T., Davis, S.I., Garringer, H.J., Mooney, S.D., Draman, M.S., Cullen, M.J., White, K.E., 2005. Fibroblast growth factor-23 mutants causing familial tumoral calcinosis are differentially processed. Endocrinology 146, 3883−3891.

Lee, G.J., Marks, J., 2015. Intestinal phosphate transport: a therapeutic target in chronic kidney disease and beyond? Pediatr. Nephrol. 30, 363−371. https://doi.org/10.1007/s00467-014-2759-x.

Lee, J.C., Jeng, Y.M., Su, S.Y., Wu, C.T., Tsai, K.S., Lee, C.H., Lin, C.Y., Carter, J.M., Huang, J.W., Chen, S.H., Shih, S.R., Marino-Enriquez, A., Chen, C.C., Folpe, A.L., Chang, Y.L., Liang, C.W., 2015. Identification of a novel FN1-FGFR1 genetic fusion as a frequent event in phosphaturic mesenchymal tumour. J. Pathol. 235, 539–545. https://doi.org/10.1002/path.4465.

Lee, G.S., Brownstein, C.M., Carpenter, T.O., 2018. In: Case Report of a Patient with Hyperphosphatemia and a Novel Mutation in GALNT3Annual Meeting of the Endocrine Society. Chicago.

Legati, A., Giovannini, D., Nicolas, G., Lopez-Sanchez, U., Quintans, B., Oliveira, J.R., Sears, R.L., Ramos, E.M., Spiteri, E., Sobrido, M.J., Carracedo, A., Castro-Fernandez, C., Cubizolle, S., Fogel, B.L., Goizet, C., Jen, J.C., Kirdlarp, S., Lang, A.E., Miedzybrodzka, Z., Mitarnun, W., Paucar, M., Paulson, H., Pariente, J., Richard, A.C., Salins, N.S., Simpson, S.A., Striano, P., Svenningsson, P., Tison, F., Unni, V.K., Vanakker, O., Wessels, M.W., Wetchaphanphesat, S., Yang, M., Boller, F., Campion, D., Hannequin, D., Sitbon, M., Geschwind, D.H., Battini, J.L., Coppola, G., 2015. Mutations in XPR1 cause primary familial brain calcification associated with altered phosphate export. Nat. Genet. 47, 579–581. https://doi.org/10.1038/ng.3289.

Lemos, R.R., Ramos, E.M., Legati, A., Nicolas, G., Jenkinson, E.M., Livingston, J.H., Crow, Y.J., Campion, D., Coppola, G., Oliveira, J.R.M., 2015. Update and mutational analysis of SLC20A2: a major cause of primary familial brain calcification. Hum. Mutat. 36, 489–495. https://doi.org/10.1002/humu.22778.

Levy-Litan, V., Hershkovitz, E., Avizov, L., Leventhal, N., Bercovich, D., Chalifa-Caspi, V., Manor, E., Buriakovsky, S., Hadad, Y., Goding, J., Parvari, R., 2010. Autosomal-recessive hypophosphatemic rickets is associated with an inactivation mutation in the ENPP1 gene. Am. J. Hum. Genet. 86, 273–278. https://doi.org/10.1016/j.ajhg.2010.01.010.

Li, Y., Caballero, D., Ponsetto, J., Chen, A., Zhu, C., Guo, J., Demay, M., Jüppner, H., Bergwitz, C., 2017. Response of Npt2a knockout mice to dietary calcium and phosphorus. PLoS One 12, e0176232. https://doi.org/10.1371/journal.pone.0176232.

Liamis, G., Elisaf, M., 2000. Hypokalemia, hypophosphatemia and hypouricemia due to proximal renal tubular dysfunction in acute myeloid leukemia. Eur. J. Haematol. 64, 277–278.

Liang, G., Katz, L.D., Insogna, K.L., Carpenter, T.O., Macica, C.M., 2009. Survey of the enthesopathy of X-linked hypophosphatemia and its characterization in Hyp mice. Calcif. Tissue Int. 85, 235–246. https://doi.org/10.1007/s00223-009-9270-6.

Lim, Y.H., Ovejero, D., Sugarman, J.S., Deklotz, C.M., Maruri, A., Eichenfield, L.F., Kelley, P.K., Juppner, H., Gottschalk, M., Tifft, C.J., Gafni, R.I., Boyce, A.M., Cowen, E.W., Bhattacharyya, N., Guthrie, L.C., Gahl, W.A., Golas, G., Loring, E.C., Overton, J.D., Mane, S.M., Lifton, R.P., Levy, M.L., Collins, M.T., Choate, K.A., 2014. Multilineage somatic activating mutations in HRAS and NRAS cause mosaic cutaneous and skeletal lesions, elevated FGF23 and hypophosphatemia. Hum. Mol. Genet. 23, 397–407. https://doi.org/10.1093/hmg/ddt429.

Liu, S., Quarles, L.D., 2007. How fibroblast growth factor 23 works. J. Am. Soc. Nephrol. 18, 1637–1647.

Liu, E.S., Zalutskaya, A., Chae, B.T., Zhu, E.D., Gori, F., Demay, M.B., 2014. Phosphate interacts with PTHrP to regulate endochondral bone formation. Endocrinology 155, 3750–3756. https://doi.org/10.1210/en.2014-1315.

Liu, C., Zhou, N., Wang, Y., Zhang, H., Jani, P., Wang, X., Lu, Y., Li, N., Xiao, J., Qin, C., 2018. Abrogation of Fam20c altered cell behaviors and BMP signaling of immortalized dental mesenchymal cells. Exp. Cell Res. 363, 188–195. https://doi.org/10.1016/j.yexcr.2018.01.004.

Lloyd, S.E., Pearce, S.H., Fisher, S.E., Steinmeyer, K., Schwappach, B., Scheinman, S.J., Harding, B., Bolino, A., Devoto, M., Goodyer, P., Rigden, S.P., Wrong, O., Jentsch, T.J., Craig, I.W., Thakker, R.V., 1996. A common molecular basis for three inherited kidney stone diseases. Nature 379, 445–449. https://doi.org/10.1038/379445a0.

Lorenz-Depiereux, B., Bastepe, M., Benet-Pages, A., Amyere, M., Wagenstaller, J., Muller-Barth, U., Badenhoop, K., Kaiser, S.M., Rittmaster, R.S., Shlossberg, A.H., Olivares, J.L., Loris, C., Ramos, F.J., Glorieux, F., Vikkula, M., Juppner, H., Strom, T.M., 2006a. DMP1 mutations in autosomal recessive hypophosphatemia implicate a bone matrix protein in the regulation of phosphate homeostasis. Nat. Genet. 38, 1248–1250. https://doi.org/10.1038/ng1868.

Lorenz-Depiereux, B., Benet-Pages, A., Eckstein, G., Tenenbaum-Rakover, Y., Wagenstaller, J., Tiosano, D., Gershoni-Baruch, R., Albers, N., Lichtner, P., Schnabel, D., Hochberg, Z., Strom, T.M., 2006b. Hereditary hypophosphatemic rickets with hypercalciuria is caused by mutations in the sodium-phosphate cotransporter gene SLC34A3. Am. J. Hum. Genet. 78, 193–201. https://doi.org/10.1086/499410 pii:S0002-9297(07)62352-0.

Lorenz-Depiereux, B., Schnabel, D., Tiosano, D., Hausler, G., Strom, T.M., 2010. Loss-of-function ENPP1 mutations cause both generalized arterial calcification of infancy and autosomal-recessive hypophosphatemic rickets. Am. J. Hum. Genet. 86, 267–272. https://doi.org/10.1016/j.ajhg.2010.01.006.

Ma, S.L., Vega-Warner, V., Gillies, C., Sampson, M.G., Kher, V., Sethi, S.K., Otto, E.A., 2015. Whole exome sequencing reveals novel PHEX splice site mutations in patients with hypophosphatemic rickets. PLoS One 10, e0130729. https://doi.org/10.1371/journal.pone.0130729 pii:PONE-D-15-04157.

Magen, D., Adler, L., Mandel, H., Efrati, E., Zelikovic, I., 2004. Autosomal recessive renal proximal tubulopathy and hypercalciuria: a new syndrome. Am. J. Kidney Dis. 43, 600–606.

Magen, D., Berger, L., Coady, M.J., Ilivitzki, A., Militianu, D., Tieder, M., Selig, S., Lapointe, J.Y., Zelikovic, I., Skorecki, K., 2010. A loss-of-function mutation in NaPi-IIa and renal Fanconi's syndrome. N. Engl. J. Med. 362, 1102–1109.

Maldonado, E.N., Lemasters, J.J., 2014. ATP/ADP ratio, the missed connection between mitochondria and the Warburg effect. Mitochondrion 19 (Pt A), 78–84. https://doi.org/10.1016/j.mito.2014.09.002.

Mannstadt, M., Magen, D., Segawa, H., Stanley, T., Sharma, A., Sasaki, S., Bergwitz, C., Mounien, L., Boepple, P., Thorens, B., Zelikovic, I., Juppner, H., 2012. Fanconi-Bickel syndrome and autosomal recessive proximal tubulopathy with hypercalciuria (ARPTH) are allelic variants caused by GLUT2 mutations. J. Clin. Endocrinol. Metab. 97, E1978–E1986. https://doi.org/10.1210/jc.2012-1279.

Mayr, J.A., Zimmermann, F.A., Horvath, R., Schneider, H.C., Schoser, B., Holinski-Feder, E., Czermin, B., Freisinger, P., Sperl, W., 2011. Deficiency of the mitochondrial phosphate carrier presenting as myopathy and cardiomyopathy in a family with three affected children. Neuromuscul. Disord. 21, 803–808. https://doi.org/10.1016/j.nmd.2011.06.005.

Mejia-Gaviria, N., Gil-Pena, H., Coto, E., Perez-Menendez, T.M., Santos, F., 2010. Genetic and clinical peculiarities in a new family with hereditary hypophosphatemic rickets with hypercalciuria: a case report. Orphanet J. Rare Dis. 5, 1. https://doi.org/10.1186/1750-1172-5-1.

Meyer Jr., R.A., Meyer, M.H., Gray, R.W., 1989. Parabiosis suggests a humoral factor is involved in X-linked hypophosphatemia in mice. J. Bone Miner. Res. 4, 493–500. https://doi.org/10.1002/jbmr.5650040407.

Milionis, H., Pritsivelis, N., Elisaf, M., 1999. Marked hypophosphatemia in a patient with acute leukemia. Nephron 83, 173.

Miyamoto, K., Segawa, H., Ito, M., Kuwahata, M., 2004. Physiological regulation of renal sodium-dependent phosphate cotransporters. Jpn. J. Physiol. 54, 93–102.

Miyamoto, K., Ito, M., Tatsumi, S., Kuwahata, M., Segawa, H., 2007. New aspect of renal phosphate reabsorption: the type IIc sodium-dependent phosphate transporter. Am. J. Nephrol. 27, 503–515. https://doi.org/10.1159/000107069.

Morgan, J.M., Hawley, W.L., Chenoweth, A.I., Retan, W.J., Diethelm, A.G., 1974. Renal transplantation in hypophosphatemia with vitamin D-resistant rickets. Arch. Intern. Med. 134, 549–552.

Murali, S.K., Andrukhova, O., Clinkenbeard, E.L., White, K.E., Erben, R.G., 2016. Excessive osteocytic Fgf23 secretion contributes to pyrophosphate accumulation and mineralization defect in hyp mice. PLoS Biol. 14, e1002427. https://doi.org/10.1371/journal.pbio.1002427.

Murer, H., Hernando, N., Forster, I., Biber, J., 2000. Proximal tubular phosphate reabsorption: molecular mechanisms. Physiol. Rev. 80, 1373–1409. https://doi.org/10.1152/physrev.2000.80.4.1373.

Murer, H., Forster, I., Biber, J., 2004. The sodium phosphate cotransporter family SLC34. Pflügers Archiv 447, 763–767.

Myakala, K., Motta, S., Murer, H., Wagner, C.A., Koesters, R., Biber, J., Hernando, N., 2014. Renal-specific and inducible depletion of NaPi-IIc/Slc34A3, the cotransporter mutated in HHRH, does not affect phosphate or calcium homeostasis in mice. Am. J. Physiol. Renal. Physiol. https://doi.org/10.1152/ajprenal.00133.2013.

Nafidi, O., Lepage, R., Lapointe, R.W., D'Amour, P., 2007. Hepatic resection-related hypophosphatemia is of renal origin as manifested by isolated hyperphosphaturia. Ann. Surg. 245, 1000–1002.

Nakahama, H., Nakanishi, T., Uno, H., Takaoka, T., Taji, N., Uyama, O., Kitada, O., Sugita, M., Miyauchi, A., Sugishita, T., et al., 1995. Prostate cancer-induced oncogenic hypophosphatemic osteomalacia. Urol. Int. 55, 38–40. https://doi.org/10.1159/000282746.

Narchi, H., El Jamil, M., Kulaylat, N., 2001. Symptomatic rickets in adolescence. Arch. Dis. Child. 84, 501–503.

Narvaez, J., Domingo-Domenech, E., Narvaez, J.A., Nolla, J.M., Valverde, J., 2005. Acquired hypophosphatemic osteomalacia associated with multiple myeloma. Joint Bone Spine 72, 424–426. https://doi.org/10.1016/j.jbspin.2004.10.012.

Nishimura, M., Naito, S., 2008. Tissue-specific mRNA expression profiles of human solute carrier transporter superfamilies. Drug Metab. Pharmacokinet. 23, 22–44. JST.JSTAGE/dmpk/23.22.

Nurnberg, P., Thiele, H., Chandler, D., Hohne, W., Cunningham, M.L., Ritter, H., Leschik, G., Uhlmann, K., Mischung, C., Harrop, K., Goldblatt, J., Borochowitz, Z.U., Kotzot, D., Westermann, F., Mundlos, S., Braun, H.S., Laing, N., Tinschert, S., 2001. Heterozygous mutations in ANKH, the human ortholog of the mouse progressive ankylosis gene, result in craniometaphyseal dysplasia. Nat. Genet. 28, 37–41. https://doi.org/10.1038/88236.

Ohi, A., Hanabusa, E., Ueda, O., Segawa, H., Horiba, N., Kaneko, I., Kuwahara, S., Mukai, T., Sasaki, S., Tominaga, R., Furutani, J., Aranami, F., Ohtomo, S., Oikawa, Y., Kawase, Y., Wada, N.A., Tachibe, T., Kakefuda, M., Tateishi, H., Matsumoto, K., Tatsumi, S., Kido, S., Fukushima, N., Jishage, K., Miyamoto, K., 2011. Inorganic phosphate homeostasis in sodium-dependent phosphate cotransporter Npt2b(+)/(-) mice. Am. J. Physiol. Renal. Physiol. 301, F1105–F1113. https://doi.org/10.1152/ajprenal.00663.2010.

Ohkido, I., Segawa, H., Yanagida, R., Nakamura, M., Miyamoto, K., 2003. Cloning, gene structure and dietary regulation of the type-IIc Na/Pi cotransporter in the mouse kidney. Pflügers Archiv 446, 106–115.

Ohkido, I., Hara, S., Segawa, H., Yokoyama, K., Yamamoto, H., Miyamoto, K., Kawaguchi, H., Hosoya, T., 2007. Localization of sodium-phosphate cotransporter NaPi-IIa and -IIc in human proximal renal and distal TubulesRENAL WEEK 2006. J. Am. Soc. Nephrol. San Francisco, pp. abstract SU-PO704.

Ovejero, D., Lim, Y.H., Boyce, A.M., Gafni, R.I., McCarthy, E., Nguyen, T.A., Eichenfield, L.F., DeKlotz, C.M., Guthrie, L.C., Tosi, L.L., Thornton, P.S., Choate, K.A., Collins, M.T., 2016. Cutaneous skeletal hypophosphatemia syndrome: clinical spectrum, natural history, and treatment. Osteoporos. Int. 27, 3615–3626. https://doi.org/10.1007/s00198-016-3702-8.

Page, K., Bergwitz, C., Jaureguiberry, G., Harinarayan, C.V., Insogna, K., 2008. A patient with hypophosphatemia, a femoral fracture, and recurrent kidney stones: report of a novel mutation in SLC34A3. Endocr. Pract. 14, 869–874. https://doi.org/10.4158/EP.14.7.869 pii:K344465V44550341.

Palmer, G., Guicheux, J., Bonjour, J.P., Caverzasio, J., 2000. Transforming growth factor-beta stimulates inorganic phosphate transport and expression of the type III phosphate transporter Glvr-1 in chondrogenic ATDC5 cells. Endocrinology 141, 2236–2243. https://doi.org/10.1210/endo.141.6.7495.

Papaioannou, G., Petit, E.T., Liu, E.S., Baccarini, M., Pritchard, C., Demay, M.B., 2017. Raf kinases are essential for phosphate induction of ERK1/2 phosphorylation in hypertrophic chondrocytes and normal endochondral bone development. J. Biol. Chem. 292, 3164–3171. https://doi.org/10.1074/jbc.M116.763342.

Pattaro, C., Teumer, A., Gorski, M., Chu, A.Y., Li, M., Mijatovic, V., Garnaas, M., Tin, A., Sorice, R., Li, Y., Taliun, D., Olden, M., Foster, M., Yang, Q., Chen, M.H., Pers, T.H., Johnson, A.D., Ko, Y.A., Fuchsberger, C., Tayo, B., Nalls, M., Feitosa, M.F., Isaacs, A., Dehghan, A., d'Adamo, P., Adeyemo, A., Dieffenbach, A.K., Zonderman, A.B., Nolte, I.M., van der Most, P.J., Wright, A.F., Shuldiner, A.R., Morrison, A.C., Hofman, A., Smith, A.V., Dreisbach, A.W., Franke, A., Uitterlinden, A.G., Metspalu, A., Tonjes, A., Lupo, A., Robino, A., Johansson, A., Demirkan, A.,

Kollerits, B., Freedman, B.I., Ponte, B., Oostra, B.A., Paulweber, B., Kramer, B.K., Mitchell, B.D., Buckley, B.M., Peralta, C.A., Hayward, C., Helmer, C., Rotimi, C.N., Shaffer, C.M., Muller, C., Sala, C., van Duijn, C.M., Saint-Pierre, A., Ackermann, D., Shriner, D., Ruggiero, D., Toniolo, D., Lu, Y., Cusi, D., Czamara, D., Ellinghaus, D., Siscovick, D.S., Ruderfer, D., Gieger, C., Grallert, H., Rochtchina, E., Atkinson, E.J., Holliday, E.G., Boerwinkle, E., Salvi, E., Bottinger, E.P., Murgia, F., Rivadeneira, F., Ernst, F., Kronenberg, F., Hu, F.B., Navis, G.J., Curhan, G.C., Ehret, G.B., Homuth, G., Coassin, S., Thun, G.A., Pistis, G., Gambaro, G., Malerba, G., Montgomery, G.W., Eiriksdottir, G., Jacobs, G., Li, G., Wichmann, H.E., Campbell, H., Schmidt, H., Wallaschofski, H., Volzke, H., Brenner, H., Kroemer, H.K., Kramer, H., Lin, H., Mateo Leach, I., Ford, I., Guessous, I., Rudan, I., Prokopenko, I., Borecki, I., Heid, I.M., Kolcic, I., Persico, I., Jukema, J.W., Wilson, J.F., Felix, J.F., Divers, J., Lambert, J.C., Stafford, J.M., Gaspoz, J.M., Smith, J.A., Faul, J.D., Wang, J.J., Ding, J., Hirschhorn, J.N., Attia, J., Whitfield, J.B., Chalmers, J., Viikari, J., Coresh, J., Denny, J.C., Karjalainen, J., Fernandes, J.K., Endlich, K., Butterbach, K., Keene, K.L., Lohman, K., Portas, L., Launer, L.J., Lyytikainen, L.P., Yengo, L., Franke, L., Ferrucci, L., Rose, L.M., Kedenko, L., Rao, M., Struchalin, M., Kleber, M.E., Cavalieri, M., Haun, M., Cornelis, M.C., Ciullo, M., Pirastu, M., de Andrade, M., McEvoy, M.A., Woodward, M., Adam, M., Cocca, M., Nauck, M., Imboden, M., Waldenberger, M., Pruijm, M., Metzger, M., Stumvoll, M., Evans, M.K., Sale, M.M., Kahonen, M., Boban, M., Bochud, M., Rheinberger, M., Verweij, N., Bouatia-Naji, N., Martin, N.G., Hastie, N., Probst-Hensch, N., Soranzo, N., Devuyst, O., Raitakari, O., Gottesman, O., Franco, O.H., Polasek, O., Gasparini, P., Munroe, P.B., Ridker, P.M., Mitchell, P., Muntner, P., Meisinger, C., Smit, J.H., Consortium I, Consortium A, Cardiogram, Group CH-HF, Consortium EC, Kovacs, P., Wild, P.S., Froguel, P., Rettig, R., Magi, R., Biffar, R., Schmidt, R., Middelberg, R.P., Carroll, R.J., Penninx, B.W., Scott, R.J., Katz, R., Sedaghat, S., Wild, S.H., Kardia, S.L., Ulivi, S., Hwang, S.J., Enroth, S., Kloiber, S., Trompet, S., Stengel, B., Hancock, S.J., Turner, S.T., Rosas, S.E., Stracke, S., Harris, T.B., Zeller, T., Zemunik, T., Lehtimaki, T., Illig, T., Aspelund, T., Nikopensius, T., Esko, T., Tanaka, T., Gyllensten, U., Volker, U., Emilsson, V., Vitart, V., Aalto, V., Gudnason, V., Chouraki, V., Chen, W.M., Igl, W., Marz, W., Koenig, W., Lieb, W., Loos, R.J., Liu, Y., Snieder, H., Pramstaller, P.P., Parsa, A., O'Connell, J.R., Susztak, K., Hamet, P., Tremblay, J., de Boer, I.H., Boger, C.A., Goessling, W., Chasman, D.I., Kottgen, A., Kao, W.H., Fox, C.S., 2016. Genetic associations at 53 loci highlight cell types and biological pathways relevant for kidney function. Nat. Commun. 7, 10023. https://doi.org/10.1038/ncomms10023.

Pauleau, A.L., Galluzzi, L., Scholz, S.R., Larochette, N., Kepp, O., Kroemer, G., 2008. Unexpected role of the phosphate carrier in mitochondrial fragmentation. Cell Death Differ. 15, 616. https://doi.org/10.1038/sj.cdd.4402295. https://www.nature.com/articles/4402295#supplementary-information.

Pendleton, A., Johnson, M.D., Hughes, A., Gurley, K.A., Ho, A.M., Doherty, M., Dixey, J., Gillet, P., Loeuille, D., McGrath, R., Reginato, A., Shiang, R., Wright, G., Netter, P., Williams, C., Kingsley, D.M., 2002. Mutations in ANKH cause chondrocalcinosis. Am. J. Hum. Genet. 71, 933−940. https://doi.org/10.1086/343054.

Pesta, D.H., Tsirigotis, D.N., Befroy, D.E., Caballero, D., Jurczak, M.J., Rahimi, Y., Cline, G.W., Dufour, S., Birkenfeld, A.L., Rothman, D.L., Carpenter, T.O., Insogna, K., Petersen, K.F., Bergwitz, C., Shulman, G.I., 2016. Hypophosphatemia promotes lower rates of muscle ATP synthesis. FASEB J. 30, 3378−3387. https://doi.org/10.1096/fj.201600473R.

Petersen, K.F., Dufour, S., Shulman, G.I., 2005. Decreased insulin-stimulated ATP synthesis and phosphate transport in muscle of insulin-resistant offspring of type 2 diabetic parents. PLoS Med. 2, e233. https://doi.org/10.1371/journal.pmed.0020233. 05-PLME-RA-0003R2.

Pfister, M.F., Ruf, I., Stange, G., Ziegler, U., Lederer, E., Biber, J., Murer, H., 1998. Parathyroid hormone leads to the lysosomal degradation of the renal type II Na/Pi cotransporter. Proc. Natl. Acad. Sci. U. S. A. 95, 1909−1914.

Phulwani, P., Bergwitz, C., Jaureguiberry, G., Rasoulpour, M., Estrada, E., 2011. Hereditary hypophosphatemic rickets with hypercalciuria and nephrolithiasis-identification of a novel SLC34A3/NaPi-IIc mutation. Am. J. Med. Genet. 155A, 626−633. https://doi.org/10.1002/ajmg.a.33832.

Picard, N., Capuano, P., Stange, G., Mihailova, M., Kaissling, B., Murer, H., Biber, J., Wagner, C.A., 2010. Acute parathyroid hormone differentially regulates renal brush border membrane phosphate cotransporters. Pflügers Archiv 460, 677−687. https://doi.org/10.1007/s00424-010-0841-1.

Polgreen, K.E., Kemp, G.J., Leighton, B., Radda, G.K., 1994. Modulation of Pi transport in skeletal muscle by insulin and IGF-1. Biochim. Biophys. Acta 1223, 279−284.

Pollak, M.R., Brown, E.M., WuChou, Y.H., Hebert, S.C., Marx, S.J., Steinmann, B., Levi, T., Seidman, C.E., Seidman, J.G., 1993. Mutations in the human Ca^{2+}-sensing receptor gene cause familial hypocalciuric hypercalcemia and neonatal severe hyperparathyroidism. Cell 75, 1297−1303.

Pollak, M.R., Brown, E.M., Estep, H.L., McLaine, P.N., Kifor, O., Park, J., Hebert, S.C., Seidman, C.E., Seidman, J.G., 1994. Autosomal dominant hypocalcaemia caused by a Ca^{2+}-sensing receptor gene mutation. Nat. Genet. 8, 303−307.

Portale, A.A.I., Karl, L., Briot, K., Imel, E., Kamenicky, P., Weber, T., Pitukcheewanont, P., Cheong, H.I., Jan de Beur, S., Imanishi, Y., Ito, N., Lachmann, R., Tanaka, H., Perwad, F., Zhang, L., Theodore-Oklota, C., Mealiffe, M., San Martin, J., Carpenter, T.O., 2018. Continued improvement in clinical outcomes in the phase 3 randomized, double-blind, placebo-controlled study of burosumab, an anti-FGF23 antibody, in adults with X-linked hypophosphatemia (XLH). J. Bone Miner. Res. 33 (Suppl. 1).

Price, T.B., Perseghin, G., Duleba, A., Chen, W., Chase, J., Rothman, D.L., Shulman, R.G., Shulman, G.I., 1996. NMR studies of muscle glycogen synthesis in insulin-resistant offspring of parents with non-insulin-dependent diabetes mellitus immediately after glycogen-depleting exercise. Proc. Natl. Acad. Sci. U. S. A. 93, 5329−5334.

Prie, D., Huart, V., Bakouh, N., Planelles, G., Dellis, O., Gerard, B., Hulin, P., Benque-Blanchet, F., Silve, C., Grandchamp, B., Friedlander, G., 2002. Nephrolithiasis and osteoporosis associated with hypophosphatemia caused by mutations in the type 2a sodium-phosphate cotransporter. N. Engl. J. Med. 347, 983−991.

Prie, D., Beck, L., Friedlander, G., Silve, C., 2004. Sodium-phosphate cotransporters, nephrolithiasis and bone demineralization. Curr. Opin. Nephrol. Hypertens. 13, 675−681.

Pronicka, E., Ciara, E., Halat, P., Janiec, A., Wojcik, M., Rowinska, E., Rokicki, D., Pludowski, P., Wojciechowska, E., Wierzbicka, A., Ksiazyk, J.B., Jacoszek, A., Konrad, M., Schlingmann, K.P., Litwin, M., 2017. Biallelic mutations in CYP24A1 or SLC34A1 as a cause of infantile idiopathic

hypercalcemia (IIH) with vitamin D hypersensitivity: molecular study of 11 historical IIH cases. J. Appl. Genet. 58, 349–353. https://doi.org/10.1007/s13353-017-0397-2.

Rafaelsen, S.H., Raeder, H., Fagerheim, A.K., Knappskog, P., Carpenter, T.O., Johansson, S., Bjerknes, R., 2013. Exome sequencing reveals FAM20c mutations associated with fibroblast growth factor 23-related hypophosphatemia, dental anomalies, and ectopic calcification. J. Bone Miner. Res. 28, 1378–1385. https://doi.org/10.1002/jbmr.1850.

Rafaelsen, S., Johansson, S., Raeder, H., Bjerknes, R., 2016. Hereditary hypophosphatemia in Norway: a retrospective population-based study of genotypes, phenotypes, and treatment complications. Eur. J. Endocrinol. 174, 125–136. https://doi.org/10.1530/EJE-15-0515.

Ramnitz, M.S., Gourh, P., Goldbach-Mansky, R., Wodajo, F., Ichikawa, S., Econs, M.J., White, K.E., Molinolo, A., Chen, M.Y., Heller, T., Del Rivero, J., Seo-Mayer, P., Arabshahi, B., Jackson, M.B., Hatab, S., McCarthy, E., Guthrie, L.C., Brillante, B.A., Gafni, R.I., Collins, M.T., 2016. Phenotypic and genotypic characterization and treatment of a cohort with familial tumoral calcinosis/hyperostosis-hyperphosphatemia syndrome. J. Bone Miner. Res. 31, 1845–1854. https://doi.org/10.1002/jbmr.2870.

Reginato, A.J., Coquia, J.A., 2003. Musculoskeletal manifestations of osteomalacia and rickets. Best Pract. Res. Clin. Rheumatol. 17, 1063–1080.

Ren, Y., Han, X., Jing, Y., Yuan, B., Ke, H., Liu, M., Feng, J.Q., 2016. Sclerostin antibody (Scl-Ab) improves osteomalacia phenotype in dentin matrix protein 1(Dmp1) knockout mice with little impact on serum levels of phosphorus and FGF23. Matrix Biol. 52–54, 151–161. https://doi.org/10.1016/j.matbio.2015.12.009.

Roberts, M.S., Burbelo, P.D., Egli-Spichtig, D., Perwad, F., Romero, C.J., Ichikawa, S., Farrow, E., Econs, M.J., Guthrie, L.C., Collins, M.T., Gafni, R.I., 2018. Autoimmune hyperphosphatemic tumoral calcinosis in a patient with FGF23 autoantibodies. J. Clin. Investig. 128, 5368–5373. https://doi.org/10.1172/JCI122004 122004.

Romero, V., Akpinar, H., Assimos, D.G., 2010. Kidney stones: a global picture of prevalence, incidence, and associated risk factors. Rev. Urol. 12, e86–96.

Rothenbuhler, A., Fadel, N., Debza, Y., Bacchetta, J., Diallo, M.T., Adamsbaum, C., Linglart, A., Di Rocco, F., 2018. High incidence of cranial synostosis and Chiari I malformation in children with X-linked hypophosphatemic rickets (XLHR). J. Bone Miner. Res. https://doi.org/10.1002/jbmr.3614.

Ruppe MD X-linked hypophosphatemia. In: Pagon RA, Adam MP, Ardinger HH, al e (eds) Gene Reviews.

Rutsch, F., Ruf, N., Vaingankar, S., Toliat, M.R., Suk, A., Hohne, W., Schauer, G., Lehmann, M., Roscioli, T., Schnabel, D., Epplen, J.T., Knisely, A., Superti-Furga, A., McGill, J., Filippone, M., Sinaiko, A.R., Vallance, H., Hinrichs, B., Smith, W., Ferre, M., Terkeltaub, R., Nurnberg, P., 2003. Mutations in ENPP1 are associated with 'idiopathic' infantile arterial calcification. Nat. Genet. 34, 379–381. https://doi.org/10.1038/ng1221.

Rutsch, F., Boyer, P., Nitschke, Y., Ruf, N., Lorenz-Depierieux, B., Wittkampf, T., Weissen-Plenz, G., Fischer, R.J., Mughal, Z., Gregory, J.W., Davies, J.H., Loirat, C., Strom, T.M., Schnabel, D., Nurnberg, P., Terkeltaub, R., Group, G.S., 2008. Hypophosphatemia, hyperphosphaturia, and bisphosphonate treatment are associated with survival beyond infancy in generalized arterial calcification of infancy. Circ Cardiovasc Genet 1, 133–140. https://doi.org/10.1161/CIRCGENETICS.108.797704.

Sabbagh, Y., Schiavi, S.C., 2014. Role of NPT2b in health and chronic kidney disease. Curr. Opin. Nephrol. Hypertens. 23, 377–384. https://doi.org/10.1097/01.mnh.0000447015.44099.5f.

Sabbagh, Y., Carpenter, T.O., Demay, M.B., 2005. Hypophosphatemia leads to rickets by impairing caspase-mediated apoptosis of hypertrophic chondrocytes. Proc. Natl. Acad. Sci. U. S. A. 102, 9637–9642. https://doi.org/10.1073/pnas.0502249102.

Sabbagh, Y., O'Brien, S.P., Song, W., Boulanger, J.H., Stockmann, A., Arbeeny, C., Schiavi, S.C., 2009. Intestinal npt2b plays a major role in phosphate absorption and homeostasis. J. Am. Soc. Nephrol. 20, 2348–2358. https://doi.org/10.1681/ASN.2009050559.

Sabbagh, Y., Giral, H., Caldas, Y., Levi, M., Schiavi, S.C., 2011. Intestinal phosphate transport. Adv. Chron. Kidney Dis. 18, 85–90. https://doi.org/10.1053/j.ackd.2010.11.004.

Saiardi, A., 2012. How inositol pyrophosphates control cellular phosphate homeostasis? Adv Biol Regul 52, 351–359. https://doi.org/10.1016/j.jbior.2012.03.002.

Sanders, L., 2018. Bone Basics: she was a runner who fractured her foot . It healed but the pain wouldn't subside. Why? N. Y. Times Sunday Magazine, 20.

Santer, R., Schneppenheim, R., Dombrowski, A., Gotze, H., Steinmann, B., Schaub, J., 1997. Mutations in GLUT2, the gene for the liver-type glucose transporter, in patients with Fanconi-Bickel syndrome. Nat. Genet. 17, 324–326. https://doi.org/10.1038/ng1197-324.

Santer, R., Steinmann, B., Schaub, J., 2002. Fanconi-Bickel syndrome–a congenital defect of facilitative glucose transport. Curr. Mol. Med. 2, 213–227.

Schiavi, S.C., Tang, W., Bracken, C., O'Brien, S.P., Song, W., Boulanger, J., Ryan, S., Phillips, L., Liu, S., Arbeeny, C., Ledbetter, S., Sabbagh, Y., 2012. Npt2b deletion attenuates hyperphosphatemia associated with CKD. J. Am. Soc. Nephrol. 23, 1691–1700. https://doi.org/10.1681/ASN.2011121213.

Schipani, E., Kruse, K., Juppner, H., 1995. A constitutively active mutant PTH-PTHrP receptor in Jansen-type metaphyseal chondrodysplasia. Science 268, 98–100.

Schissel, B.L., Johnson, B.K., 2011. Renal stones: evolving epidemiology and management. Pediatr. Emerg. Care 27, 676–681. https://doi.org/10.1097/PEC.0b013e3182228f10 pii:00006565-201107000-00024.

Schlingmann, K.P., Ruminska, J., Kaufmann, M., Dursun, I., Patti, M., Kranz, B., Pronicka, E., Ciara, E., Akcay, T., Bulus, D., Cornelissen, E.A.M., Gawlik, A., Sikora, P., Patzer, L., Galiano, M., Boyadzhiev, V., Dumic, M., Vivante, A., Kleta, R., Dekel, B., Levtchenko, E., Bindels, R.J., Rust, S., Forster, I.C., Hernando, N., Jones, G., Wagner, C.A., Konrad, M., 2016. Autosomal-recessive mutations in SLC34A1 encoding sodium-phosphate cotransporter 2A cause idiopathic infantile hypercalcemia. J. Am. Soc. Nephrol. 27, 604–614. https://doi.org/10.1681/asn.2014101025.

Segawa, H., Kaneko, I., Takahashi, A., Kuwahata, M., Ito, M., Ohkido, I., Tatsumi, S., Miyamoto, K., 2002. Growth-related renal type II Na/Pi cotransporter. J. Biol. Chem. 277, 19665–19672.

Segawa, H., Onitsuka, A., Furutani, J., Kaneko, I., Aranami, F., Matsumoto, N., Tomoe, Y., Kuwahata, M., Ito, M., Matsumoto, M., Li, M., Amizuka, N., Miyamoto, K., 2009. Npt2a and Npt2c in mice play distinct and synergistic roles in inorganic phosphate metabolism and skeletal development. Am. J. Physiol. Renal. Physiol. 297, F671–F678.

Seifert, E.L., Ligeti, E., Mayr, J.A., Sondheimer, N., Hajnoczky, G., 2015. The mitochondrial phosphate carrier: role in oxidative metabolism, calcium handling and mitochondrial disease. Biochem. Biophys. Res. Commun. 464, 369–375. https://doi.org/10.1016/j.bbrc.2015.06.031.

Shaikh, A., Berndt, T., Kumar, R., 2008. Regulation of phosphate homeostasis by the phosphatonins and other novel mediators. Pediatr. Nephrol. 23, 1203–1210.

Shiba, M., Mizuno, M., Kuraishi, K., Suzuki, H., 2015. Cervical ossification of posterior longitudinal ligament in x-linked hypophosphatemic rickets revealing homogeneously increased vertebral bone density. Asian Spine J 9, 106–109. https://doi.org/10.4184/asj.2015.9.1.106.

Shimada, T., Mizutani, S., Muto, T., Yoneya, T., Hino, R., Takeda, S., Takeuchi, Y., Fujita, T., Fukumoto, S., Yamashita, T., 2001. Cloning and characterization of FGF23 as a causative factor of tumor-induced osteomalacia. Proc. Natl. Acad. Sci. U. S. A. 98, 6500–6505. https://doi.org/10.1073/pnas.101545198.

Shimada, T., Hasegawa, H., Yamazaki, Y., Muto, T., Hino, R., Takeuchi, Y., Fujita, T., Nakahara, K., Fukumoto, S., Yamashita, T., 2004a. FGF-23 is a potent regulator of vitamin D metabolism and phosphate homeostasis. J. Bone Miner. Res. 19, 429–435.

Shimada, T., Kakitani, M., Yamazaki, Y., Hasegawa, H., Takeuchi, Y., Fujita, T., Fukumoto, S., Tomizuka, K., Yamashita, T., 2004b. Targeted ablation of Fgf23 demonstrates an essential physiological role of FGF23 in phosphate and vitamin D metabolism. J. Clin. Investig. 113, 561–568. https://doi.org/10.1172/JCI19081.

Shiozaki, Y., Segawa, H., Ohnishi, S., Ohi, A., Ito, M., Kaneko, I., Kido, S., Tatsumi, S., Miyamoto, K., 2015. Relationship between sodium-dependent phosphate transporter (NaPi-IIc) function and cellular vacuole formation in opossum kidney cells. J. Med. Investig. 62, 209–218. https://doi.org/10.2152/jmi.62.209.

Sinha, A., Hollingsworth, K.G., Ball, S., Cheetham, T., 2013. Improving the vitamin D status of vitamin D deficient adults is associated with improved mitochondrial oxidative function in skeletal muscle. J. Clin. Endocrinol. Metab. 98, E509–E513. https://doi.org/10.1210/jc.2012-3592.

Smith, R., Newman, R.J., Radda, G.K., Stokes, M., Young, A., 1984. Hypophosphataemic osteomalacia and myopathy: studies with nuclear magnetic resonance spectroscopy. Clin. Sci. (Lond.) 67, 505–509.

Strom, T.M., Juppner, H., 2008. PHEX, FGF23, DMP1 and beyond. Curr. Opin. Nephrol. Hypertens. 17, 357–362.

Sullivan, W., Carpenter, T., Glorieux, F., Travers, R., Insogna, K., 1992. A prospective trial of phosphate and 1,25-dihydroxyvitamin D3 therapy in symptomatic adults with X-linked hypophosphatemic rickets. J. Clin. Endocrinol. Metab. 75, 879–885. https://doi.org/10.1210/jcem.75.3.1517380.

Suzuki, A., Palmer, G., Bonjour, J.P., Caverzasio, J., 2000. Stimulation of sodium-dependent phosphate transport and signaling mechanisms induced by basic fibroblast growth factor in MC3T3-E1 osteoblast-like cells. J. Bone Miner. Res. 15, 95–102. https://doi.org/10.1359/jbmr.2000.15.1.95.

Suzuki, A., Palmer, G., Bonjour, J.P., Caverzasio, J., 2001. Stimulation of sodium-dependent inorganic phosphate transport by activation of Gi/o-protein-coupled receptors by epinephrine in MC3T3-E1 osteoblast-like cells. Bone 28, 589–594 pii:S8756328201004598.

Tagliabracci, V.S., Engel, J.L., Wiley, S.E., Xiao, J., Gonzalez, D.J., Nidumanda Appaiah, H., Koller, A., Nizet, V., White, K.E., Dixon, J.E., 2014. Dynamic regulation of FGF23 by Fam20C phosphorylation, GalNAc-T3 glycosylation, and furin proteolysis. Proc. Natl. Acad. Sci. U. S. A. 111, 5520–5525. https://doi.org/10.1073/pnas.1402218111.

Taguchi, K., Yasui, T., Milliner, D.S., Hoppe, B., Chi, T., 2017. Genetic risk factors for idiopathic urolithiasis: a systematic review of the literature and causal Network analysis. Eur Urol Focus 3, 72–81. https://doi.org/10.1016/j.euf.2017.04.010 pii:S2405-4569(17)30116-5.

Tencza, A.L., Ichikawa, S., Dang, A., Kenagy, D., McCarthy, E., Econs, M.J., Levine, M.A., 2009. Hypophosphatemic rickets with hypercalciuria due to mutation in SLC34A3/type IIc sodium-phosphate cotransporter: presentation as hypercalciuria and nephrolithiasis. J. Clin. Endocrinol. Metab. 94, 4433–4438. https://doi.org/10.1210/jc.2009-1535.

Tenenhouse, H.S., Econs, M.J., 2001. Mendelian hypophosphatemias. In: Scriver, C.R., Beaudet, A.L., Valle, D., Sly, W.S., Vogelstein, B., Childs, B., Kinzler, K.W. (Eds.), The Metabolic and Molecular Bases of Inherited Diseases. McGraw-Hill, New York, pp. 5039–5067.

Tenenhouse, H.S., Werner, A., Biber, J., Ma, S., Martel, J., Roy, S., Murer, H., 1994. Renal Na(+)-phosphate cotransport in murine X-linked hypophosphatemic rickets. Molecular characterization. J. Clin. Investig. 93, 671–676. https://doi.org/10.1172/JCI117019.

Tenenhouse, H.S., Roy, S., Martel, J., Gauthier, C., 1998. Differential expression, abundance, and regulation of Na+-phosphate cotransporter genes in murine kidney. Am. J. Physiol. 275, F527–F534.

Tenenhouse, H.S., Martel, J., Gauthier, C., Zhang, M.Y., Portale, A.A., 2001. Renal expression of the sodium/phosphate cotransporter gene, Npt2, is not required for regulation of renal 1 alpha-hydroxylase by phosphate. Endocrinology 142, 1124–1129.

Thakker, R.V., 2000. Pathogenesis of Dent's disease and related syndromes of X-linked nephrolithiasis. Kidney Int. 57, 787–793.

Tieder, M., Modai, D., Samuel, R., Arie, R., Halabe, A., Bab, I., Gabizon, D., Liberman, U.A., 1985. Hereditary hypophosphatemic rickets with hypercalciuria. N. Engl. J. Med. 312, 611–617.

Tieder, M., Modai, D., Shaked, U., Samuel, R., Arie, R., Halabe, A., Maor, J., Weissgarten, J., Averbukh, Z., Cohen, N., et al., 1987. Idiopathic" hypercalciuria and hereditary hypophosphatemic rickets. Two phenotypical expressions of a common genetic defect. N. Engl. J. Med. 316, 125–129.

Tieder, M., Arie, R., Modai, D., Samuel, R., Weissgarten, J., Liberman, U.A., 1988. Elevated serum 1,25-dihydroxyvitamin D concentrations in siblings with primary Fanconi's syndrome. N. Engl. J. Med. 319, 845–849.

Tomoe, Y., Segawa, H., Kaneko, I., Furutani, J., Aranami, F., Kuwahara, S., Tominaga, R., Hanabusa, E., Ito, M., Miyamoto, K-i, 2009. Effect of fibroblast growth factor (FGF)23 on Npt2a-/-, Npt2c-/- double-knockout (WKO). Mice J. Am. Soc. Nephrol. Philadelphia, pp. [SA-PO2780].

Tomoe, Y., Segawa, H., Shiozawa, K., Kaneko, I., Tominaga, R., Hanabusa, E., Aranami, F., Furutani, J., Kuwahara, S., Tatsumi, S., Matsumoto, M., Ito, M., Miyamoto, K., 2010. Phosphaturic action of fibroblast growth factor 23 in Npt2 null mice. Am. J. Physiol. Renal. Physiol. 298, F1341–F1350. https://doi.org/10.1152/ajprenal.00375.2009.

Topaz, O., Shurman, D.L., Bergman, R., Indelman, M., Ratajczak, P., Mizrachi, M., Khamaysi, Z., Behar, D., Petronius, D., Friedman, V., Zelikovic, I., Raimer, S., Metzker, A., Richard, G., Sprecher, E., 2004. Mutations in GALNT3, encoding a protein involved in O-linked glycosylation, cause familial tumoral calcinosis. Nat. Genet. 36, 579. https://doi.org/10.1038/ng1358.

Topaz, O., Indelman, M., Chefetz, I., Geiger, D., Metzker, A., Altschuler, Y., Choder, M., Bercovich, D., Uitto, J., Bergman, R., Richard, G., Sprecher, E., 2006. A deleterious mutation in SAMD9 causes normophosphatemic familial tumoral calcinosis. Am. J. Hum. Genet. 79, 759–764.

Tore, S., Casula, S., Casu, G., Concas, M.P., Pistidda, P., Persico, I., Sassu, A., Maestrale, G.B., Mele, C., Caruso, M.R., Bonerba, B., Usai, P., Deiana, I., Thornton, T., Pirastu, M., Forabosco, P., 2011. Application of a new method for GWAS in a related case/control sample with known pedigree structure: identification of new loci for nephrolithiasis. PLoS Genet. 7, e1001281. https://doi.org/10.1371/journal.pgen.1001281.

Turan, S., Aydin, C., Bereket, A., Akcay, T., Guran, T., Yaralioglu, B.A., Bastepe, M., Juppner, H., 2010. Identification of a novel dentin matrix protein-1 (DMP-1) mutation and dental anomalies in a kindred with autosomal recessive hypophosphatemia. Bone 46, 402–409. https://doi.org/10.1016/j.bone.2009.09.016.

Urakawa, I., Yamazaki, Y., Shimada, T., Iijima, K., Hasegawa, H., Okawa, K., Fujita, T., Fukumoto, S., Yamashita, T., 2006. Klotho converts canonical FGF receptor into a specific receptor for FGF23. Nature 444, 770–774. https://doi.org/10.1038/nature05315.

Vieira, A.R., Lee, M., Vairo, F., Loguercio Leite, J.C., Munerato, M.C., Visioli, F., D'Avila, S.R., Wang, S.K., Choi, M., Simmer, J.P., Hu, J.C., 2015. Root anomalies and dentin dysplasia in autosomal recessive hyperphosphatemic familial tumoral calcinosis (HFTC). Oral Surg. Oral Med. Oral Pathol. Oral Radiol. 120, e235–e239. https://doi.org/10.1016/j.oooo.2015.05.006 pii:S2212-4403(15)00918-9.

Virkki, L.V., Forster, I.C., Hernando, N., Biber, J., Murer, H., 2003. Functional characterization of two naturally occurring mutations in the human sodium-phosphate cotransporter type IIa. J. Bone Miner. Res. 18, 2135–2141. https://doi.org/10.1359/jbmr.2003.18.12.2135.

von Falck, C., Rodt, T., Rosenthal, H., Langer, F., Goesling, T., Knapp, W.H., Galanski, M., 2008. (68)Ga-DOTANOC PET/CT for the detection of a mesenchymal tumor causing oncogenic osteomalacia. Eur. J. Nucl. Med. Mol. Imaging 35, 1034. https://doi.org/10.1007/s00259-008-0755-8.

Wagner, C.A., Rubio-Aliaga, I., Hernando, N., 2017. Renal phosphate handling and inherited disorders of phosphate reabsorption: an update. Pediatr. Nephrol. https://doi.org/10.1007/s00467-017-3873-3.

Walton, R.J., Bijvoet, O.L., 1975. Nomogram for derivation of renal threshold phosphate concentration. Lancet 2, 309–310.

Wang, D., Canaff, L., Davidson, D., Corluka, A., Liu, H., Hendy, G.N., Henderson, J.E., 2001. Alterations in the sensing and transport of phosphate and calcium by differentiating chondrocytes. J. Biol. Chem. 276, 33995–34005. https://doi.org/10.1074/jbc.M007757200.

Weinstein, L.S., Gejman, P.V., de Mazancourt, P., American, N., Spiegel, A.M., 1992. A heterozygous 4-bp deletion mutation in the Gs alpha gene (GNAS1) in a patient with Albright hereditary osteodystrophy. Genomics 13, 1319–1321.

White, K.E., Cabral, J.M., Davis, S.I., Fishburn, T., Evans, W.E., Ichikawa, S., Fields, J., Yu, X., Shaw, N.J., McLellan, N.J., McKeown, C., Fitzpatrick, D., Yu, K., Ornitz, D.M., Econs, M.J., 2005. Mutations that cause osteoglophonic dysplasia define novel roles for FGFR1 in bone elongation. Am. J. Hum. Genet. 76, 361–367. https://doi.org/10.1086/427956.

White, K.E., Larsson, T.E., Econs, M.J., 2006. The roles of specific genes implicated as circulating factors involved in normal and disordered phosphate homeostasis: frizzled related protein-4, matrix extracellular phosphoglycoprotein, and fibroblast growth factor 23. Endocr. Rev. 27, 221–241.

White, A.J., Northcutt, M.J., Rohrback, S.E., Carpenter, R.O., Niehaus-Sauter, M.M., Gao, Y., Wheatly, M.G., Gillen, C.M., 2011. Characterization of sarcoplasmic calcium binding protein (SCP) variants from freshwater crayfish *Procambarus clarkii*. Comp. Biochem. Physiol. B Biochem. Mol. Biol. 160 (8–14) https://doi.org/10.1016/j.cbpb.2011.04.003 pii:S1096-4959(11)00080-7.

Whyte, M.P., 2017. Hypophosphatasia: an overview for 2017. Bone 102, 15–25. https://doi.org/10.1016/j.bone.2017.02.011.

Whyte, M.P., Schranck, F.W., Armamento-Villareal, R., 1996. X-linked hypophosphatemia: a search for gender, race, anticipation, or parent of origin effects on disease expression in children. J. Clin. Endocrinol. Metab. 81, 4075–4080. https://doi.org/10.1210/jcem.81.11.8923863.

Wild, D., Macke, H.R., Waser, B., Reubi, J.C., Ginj, M., Rasch, H., Muller-Brand, J., Hofmann, M., 2005. 68Ga-DOTANOC: a first compound for PET imaging with high affinity for somatostatin receptor subtypes 2 and 5. Eur. J. Nucl. Med. Mol. Imaging 32, 724. https://doi.org/10.1007/s00259-004-1697-4.

Wild, R., Gerasimaite, R., Jung, J.Y., Truffault, V., Pavlovic, I., Schmidt, A., Saiardi, A., Jessen, H.J., Poirier, Y., Hothorn, M., Mayer, A., 2016. Control of eukaryotic phosphate homeostasis by inositol polyphosphate sensor domains. Science 352, 986–990. https://doi.org/10.1126/science.aad9858.

Wilz, D.R., Gray, R.W., Dominguez, J.H., Lemann Jr., J., 1979. Plasma 1,25-(OH)2-vitamin D concentrations and net intestinal calcium, phosphate, and magnesium absorption in humans. Am. J. Clin. Nutr. 32, 2052–2060.

Wittrant, Y., Bourgine, A., Khoshniat, S., Alliot-Licht, B., Masson, M., Gatius, M., Rouillon, T., Weiss, P., Beck, L., Guicheux, J., 2009. Inorganic phosphate regulates Glvr-1 and -2 expression: role of calcium and ERK1/2. Biochem. Biophys. Res. Commun. 381, 259–263. https://doi.org/10.1016/j.bbrc.2009.02.034.

Wolfgang, C.T.O., Imel, E., Portale, A.A., Boot, A., Linglart, A., Padidela, R., van't Hoff, W., Gottesman, G.S., Mao, M., Skrinar, A., San Martin, J., Whyte, M.P., 2018. Sustained efficacy and safety of burosumab, an anti-FGF23 monoclonal antibody, for 88 Weeks in children and early adolescents with X-linked hypophosphatemia (XLH). J. Bone Miner. Res. 33 (Suppl. 1).

Wrong, O.M., Norden, A.G., Feest, T.G., 1994. Dent's disease; a familial proximal renal tubular syndrome with low-molecular-weight proteinuria, hypercalciuria, nephrocalcinosis, metabolic bone disease, progressive renal failure and a marked male predominance. QJM 87, 473–493.

Xiao, Z., Huang, J., Cao, L., Liang, Y., Han, X., Quarles, L.D., 2014. Osteocyte-specific deletion of Fgfr1 suppresses FGF23. PLoS One 9, e104154. https://doi.org/10.1371/journal.pone.0104154.

Xu, H., Bai, L., Collins, J.F., Ghishan, F.K., 2002. Age-dependent regulation of rat intestinal type IIb sodium-phosphate cotransporter by 1,25-(OH)(2) vitamin D(3). Am. J. Physiol. Cell Physiol. 282, C487–C493.

Xu, H., Uno, J.K., Inouye, M., Xu, L., Drees, J.B., Collins, J.F., Ghishan, F.K., 2003. Regulation of intestinal NaPi-IIb cotransporter gene expression by estrogen. Am. J. Physiol. Gastrointest. Liver Physiol. 285, G1317–G1324.

Xu, H., Uno, J.K., Inouye, M., Collins, J.F., Ghishan, F.K., 2005. NF1 transcriptional factor(s) is required for basal promoter activation of the human intestinal NaPi-IIb cotransporter gene. Am. J. Physiol. Gastrointest. Liver Physiol. 288, G175–G181.

Yadav, M.C., Bottini, M., Cory, E., Bhattacharya, K., Kuss, P., Narisawa, S., Sah, R.L., Beck, L., Fadeel, B., Farquharson, C., Millan, J.L., 2016. Skeletal mineralization deficits and impaired biogenesis and function of chondrocyte-derived matrix vesicles in Phospho1(-/-) and phospho1/pi t1 double-knockout mice. J. Bone Miner. Res. 31, 1275–1286. https://doi.org/10.1002/jbmr.2790.

Yamamoto, T., Michigami, T., Aranami, F., Segawa, H., Yoh, K., Nakajima, S., Miyamoto, K., Ozono, K., 2007. Hereditary hypophosphatemic rickets with hypercalciuria: a study for the phosphate transporter gene type IIc and osteoblastic function. J. Bone Miner. Metab. 25, 407–413.

Yamazaki, Y., Okazaki, R., Shibata, M., Hasegawa, Y., Satoh, K., Tajima, T., Takeuchi, Y., Fujita, T., Nakahara, K., Yamashita, T., Fukumoto, S., 2002. Increased circulatory level of biologically active full-length FGF-23 in patients with hypophosphatemic rickets/osteomalacia. J. Clin. Endocrinol. Metab. 87, 4957–4960. https://doi.org/10.1210/jc.2002-021105.

Yamazaki, M., Ozono, K., Okada, T., Tachikawa, K., Kondou, H., Ohata, Y., Michigami, T., 2010. Both FGF23 and extracellular phosphate activate Raf/MEK/ERK pathway via FGF receptors in HEK293 cells. J. Cell. Biochem. 111, 1210–1221. https://doi.org/10.1002/jcb.22842.

Yan, X., Yokote, H., Jing, X., Yao, L., Sawada, T., Zhang, Y., Liang, S., Sakaguchi, K., 2005. Fibroblast growth factor 23 reduces expression of type IIa Na+/Pi co-transporter by signaling through a receptor functionally distinct from the known FGFRs in opossum kidney cells. Genes Cells 10, 489–502.

Yao, X.-P., Zhao, M., Wang, C., Guo, X.-X., Su, H.-Z., Dong, E.-L., Chen, H.-T., Lai, J.-H., Liu, Y.-B., Wang, N., Chen, W.-J., 2017. Analysis of gene expression and functional characterization of XPR1: a pathogenic gene for primary familial brain calcification. Cell Tissue Res. 370, 267–273. https://doi.org/10.1007/s00441-017-2663-3.

Yeh, J.K., Aloia, J.F., 1987. Effect of glucocorticoids on the passive transport of phosphate in different segments of the intestine in the rat. Bone Miner. 2, 11–19.

Yu, Y., Sanderson, S.R., Reyes, M., Sharma, A., Dunbar, N., Srivastava, T., Juppner, H., Bergwitz, C., 2012. Novel NaPi-IIc mutations causing HHRH and idiopathic hypercalciuria in several unrelated families: long-term follow-up in one kindred. Bone 50, 1100–1106. https://doi.org/10.1016/j.bone.2012.02.015 pii:S8756-3282(12)00071-3.

Yuan, Q., Jiang, Y., Zhao, X., Sato, T., Densmore, M., Schuler, C., Erben, R.G., McKee, M.D., Lanske, B., 2014. Increased osteopontin contributes to inhibition of bone mineralization in FGF23-deficient mice. J. Bone Miner. Res. 29, 693–704. https://doi.org/10.1002/jbmr.2079.

Zhang, P., Jobert, A.S., Couvineau, A., Silve, C., 1998. A homozygous inactivating mutation in the parathyroid hormone/parathyroid hormone-related peptide receptor causing Blomstrand chondrodysplasia. J. Clin. Endocrinol. Metab. 83, 3365–3368.

Zhen, X., Bonjour, J.P., Caverzasio, J., 1997. Platelet-derived growth factor stimulates sodium-dependent Pi transport in osteoblastic cells via phospholipase Cgamma and phosphatidylinositol 3' -kinase. J. Bone Miner. Res. 12, 36–44. https://doi.org/10.1080/14041049709409113.

Zhou, X., Cui, Y., Zhou, X., Han, J., 2012. Phosphate/pyrophosphate and MV-related proteins in mineralisation: discoveries from mouse models. Int. J. Biol. Sci. 8, 778–790. https://doi.org/10.7150/ijbs.4538.

Zivicnjak, M., Schnabel, D., Staude, H., Even, G., Marx, M., Beetz, R., Holder, M., Billing, H., Fischer, D.C., Rabl, W., Schumacher, M., Hiort, O., Haffner, D., Hypophosphatemic Rickets Study, Group of the Arbeitsgemeinschaft fur Padiatrische E, Gesellschaft fur Padiatrische N, 2011. Three-year growth hormone treatment in short children with X-linked hypophosphatemic rickets: effects on linear growth and body disproportion. J. Clin. Endocrinol. Metab. 96, E2097–E2105. https://doi.org/10.1210/jc.2011-0399.

Chapter 21

Magnesium homeostasis

Karl P. Schlingmann and Martin Konrad

Department of General Pediatrics, University Children's Hospital Münster, Münster, Germany

Chapter outline

Introduction

Mg^{2+} is the most prevalent intracellular divalent cation and the fourth most abundant cation in the body. The human body contains approximately 24 g (1000 mmol) of Mg^{2+}, of which 50%−60% is present in bone, while most of the rest is stored in soft tissues. Less than 1% of total body Mg^{2+} is present in blood. Studies on body Mg^{2+} kinetics have already been conducted in the 1960s with the radioactive isotope ^{28}Mg. Avioli and Berman proposed a multicompartmental model of exchangeable Mg^{2+} pools: (1) a Mg^{2+} pool with a relatively fast turnover, comprising ∼15% of the estimated body content representing primarily the extracellular fluid, and (2) a slow-turnover intracellular pool comprising >70% of total body Mg^{2+} (Avioli and Berman, 1966).

Therefore, the assessment of Mg^{2+} status represents a difficult task. The most commonly used method for assessing Mg^{2+} status is the measurement of serum Mg^{2+} concentrations. Under physiologic conditions, serum levels are maintained at almost constant values, with a normal serum Mg^{2+} ranging between 0.75 and 1.05 mmol/L. Hypomagnesemia is usually defined as a serum Mg^{2+} level less than 0.75 mmol/L. Unfortunately, there is little correlation with specific tissue concentrations or total body Mg^{2+} stores, and normomagnesemia does not necessarily reflect a sufficient body Mg^{2+} content. Mg^{2+} deficiency and hypomagnesemia often remain asymptomatic. Clinical symptoms are mostly nonspecific and Mg^{2+} deficiency might be associated with additional electrolyte abnormalities, especially hypocalcemia and hypokalemia. Moreover, symptoms do not necessarily correlate with serum Mg^{2+} concentrations. Therefore, additional diagnostic measures have been evaluated to diagnose clinically relevant Mg^{2+} deficiency in the face of normomagnesemia. Examples for such complementary methods, which are usually not available in routine clinical practice, comprise serum ionized Mg^{2+} or erythrocyte Mg^{2+} concentrations.

Mg^{2+} homeostasis primarily depends on the balance between intestinal absorption and renal excretion. Therefore, deficiency can result from reduced dietary intake, intestinal malabsorption or losses, or renal Mg^{2+} wasting. Within physiologic limits, a diminished dietary Mg^{2+} intake is balanced by enhanced Mg^{2+} absorption in the intestine and reduced renal excretion.

In 1964, analyzing a large number of balance studies, Seelig concluded that the intake of Mg^{2+} for a healthy adult required to maintain balance is around 0.25 mmol or 6 mg/kg body weight per day (Seelig, 1964). Actually, the US Food and Nutrition Board recommends a daily intake of Mg^{2+} of 420 mg for men and 320 mg for women (Institutes of Medicine, 1997). However, NHANES data indicate that almost half of the US population consumes considerably lower amounts of Mg^{2+} from daily food (Mosfegh et al., 2006). A reduced nutritional Mg^{2+} intake does not necessarily lead to

Principles of Bone Biology. https://doi.org/10.1016/B978-0-12-814841-9.00021-X

symptomatic Mg^{2+} depletion. However, latent or subclinical hypomagnesemia is relatively frequent, with an estimated prevalence of around 14% in the general population (Schimatschek and Rempis, 2001). This is especially alarming as there is growing evidence of an association of Mg^{2+} deficiency with common chronic diseases such as hypertension, coronary heart disease, metabolic syndrome, or diabetes mellitus (Maier, 2003; Sontia and Touyz, 2007; Ford et al., 2007; Guerrero-Romero and Rodríguez-Morán, 2002; Song et al., 2004; Kieboom et al., 2016).

Magnesium physiology

Under physiologic conditions, around 30%–40% of nutritional Mg^{2+} is absorbed in the small intestine, with smaller amounts taken up in the colon (Quamme, 2008). Intestinal Mg^{2+} absorption occurs via two different transport pathways: (1) a saturable, active transcellular pathway and (2) a nonsaturable, passive paracellular pathway (Kerstan and Quamme., 2002). Whereas at low intraluminal concentrations Mg^{2+} is absorbed primarily via the active transcellular route, the passive paracellular pathway is increasingly used with rising intraluminal concentrations, yielding a curvilinear function for total intestinal Mg^{2+} absorption (Fig. 21.1). The discovery of *TRPM6* mutations in patients with hypomagnesemia with secondary hypocalcemia (HSH) has substantially expanded our understanding of intestinal Mg^{2+} absorption (Quamme, 2008; Schlingmann et al., 2002). The *TRPM6* gene encodes a member of the TRP (transient receptor potential) family of ion channels that is involved in the formation of the apical Mg^{2+}-permeable ion channel in intestinal epithelia as well as in kidney. Therefore, HSH patients, next to an impaired renal Mg^{2+} conservation (see later), exhibit a primary defect in intestinal Mg^{2+} absorption. However, the impaired active transcellular transport can be compensated for by increasing nutritional Mg^{2+} and intraluminal Mg^{2+} concentrations in the intestine, promoting passive paracellular Mg^{2+} uptake. Therefore, HSH patients are able to achieve at least subnormal serum Mg^{2+} levels with high-dose oral Mg^{2+} supplementation. Common acquired causes of hypomagnesemia due to a decreased intestinal absorption include malabsorption syndromes, short bowel syndrome, severe vomiting, diarrhea, or steatorrhea (Hoorn and Zietse, 2013).

The control of body Mg^{2+} homeostasis primarily resides in the kidney. Approximately 80% of total serum Mg^{2+} is filtered in the glomeruli. Thereafter, 95%–97% of filtered Mg^{2+} is reabsorbed along the kidney tubule so that under physiologic, normomagnesemic conditions, 3%–5% of filtered Mg^{2+} is finally excreted in the urine (Fig. 21.2). Fifteen to twenty percent of filtered Mg^{2+} is already reabsorbed in the proximal tubule. The majority of filtered Mg^{2+} (~70%) is reabsorbed in the thick ascending limb (TAL) of Henle's loop. Mg^{2+} reabsorption in the TAL is passive and paracellular in

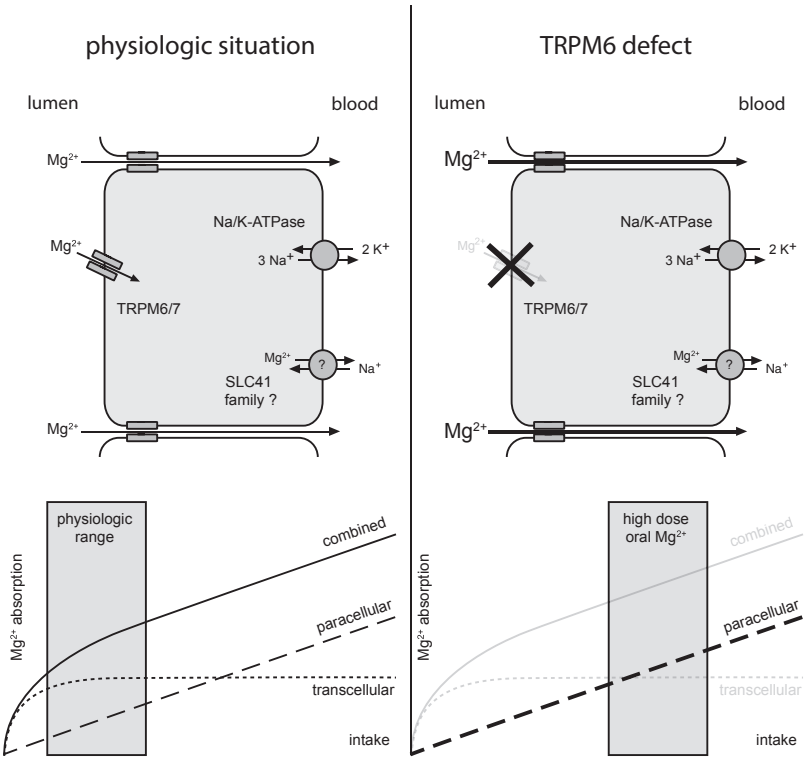

FIGURE 21.1 Intestinal Mg^{2+} absorption in health and disease. Saturable active transcellular transport (*dotted line*), which predominates at low intraluminal Mg^{2+} concentrations, and passive paracellular transport (*dashed line*), which linearly rises with increasing intraluminal Mg^{2+}, result in a curvilinear kinetic profile (left). Transient receptor potential, subfamily M, 6 (*TRPM6*) is a component of the active transcellular pathway. Hypomagnesemia with secondary hypocalcemia patients are able to compensate for TRPM6 deficiency by increasing passive paracellular absorption with high oral Mg^{2+} intake (right). *SLC41*, solute carrier 41 family.

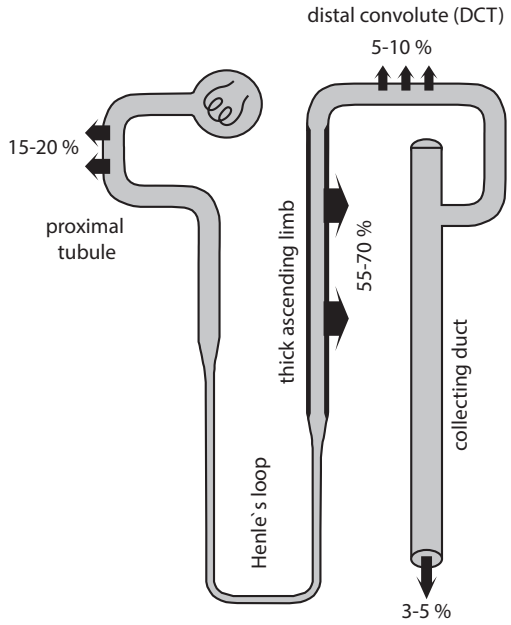

FIGURE 21.2 Renal tubular magnesium reabsorption. Approximately 80% of total serum Mg^{2+} is filtered in the glomeruli, of which 95%–97% is reabsorbed along the kidney tubule. Fifteen to twenty percent of filtered Mg^{2+} is already reabsorbed in the proximal tubule. The majority of filtered Mg^{2+} (~70%) is reabsorbed in the thick ascending limb of Henle's loop (TAL). Mg^{2+} reabsorption in the TAL is passive and paracellular in nature. Thereafter, 5%–10% of filtered Mg^{2+} is reabsorbed in the distal convoluted tubule (*DCT*) by an active and transcellular process consisting of an apical entry into the DCT cell and a basolateral extrusion into the interstitium. Finally, 3%–5% of the filtered Mg^{2+} is excreted in the urine.

nature and occurs together with calcium (Ca^{2+}) through the intercellular space. Here, specialized tight junctions composed of a specific set of proteins of the claudin family seal the paracellular space for water and electrolytes, but, on the other hand, allow for the selective passage of ions. Paracellular Ca^{2+} and Mg^{2+} transport in the TAL is driven by a lumen-positive transepithelial electric gradient that is generated by active transcellular salt reabsorption (Fig. 21.3). It is negatively regulated by the basolaterally located Ca^{2+}-sensing receptor (CaSR) (Houillier, 2013). The CaSR senses extracellular Ca^{2+} as well as Mg^{2+} concentrations in the distal nephron as well as in other tissues and thereby plays an essential role in Ca^{2+} and Mg^{2+} homeostasis (Brown et al., 1995).

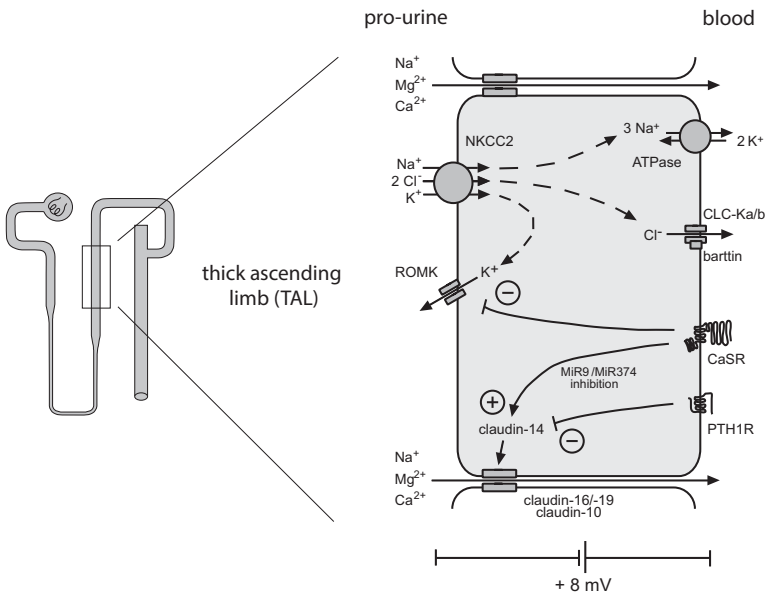

FIGURE 21.3 Mg^{2+} reabsorption in the thick ascending limb of Henle's loop. Mg^{2+} reabsorption is passive and occurs through the paracellular pathway together with Ca^{2+}. The driving force is the lumen-positive transepithelial voltage generated by active transcellular salt reabsorption. Paracellular Ca^{2+} and Mg^{2+} reabsorption occurs through specialized tight junctions. It is negatively regulated by the action of the basolateral Ca^{2+}-sensing receptor (*CaSR*) as well as the parathyroid hormone receptor (*PTH1R*), both influencing the expression of claudin-14, a tight junction protein that seals the paracellular space for both divalent cations.

Finally, 5%−10% of filtered Mg^{2+} is reabsorbed in the distal convoluted tubule (DCT), which defines the final urinary Mg^{2+} excretion as there is no significant reabsorption of Mg^{2+} in the collecting duct. Mg^{2+} reabsorption in the DCT is an active and transcellular process consisting of an apical entry into the DCT cell through a specific and regulated Mg^{2+}-permeable ion channel and a basolateral extrusion into the interstitium. The molecular nature of the apical Mg^{2+} channel was resolved by genetic studies in patients with HSH that identified TRPM6 (see later) (Schlingmann et al., 2002). Unfortunately, the molecular components involved in basolateral Mg^{2+} export are still not completely resolved. Most physiologic studies have favored a Na^{+}-dependent exchange mechanism for basolateral Mg^{2+} extrusion (Quamme, 1997); more recent data point to an involvement of Mg^{2+} transporters of the solute carrier 41 (SLC41) family (Kolisek et al., 2012). Apical Mg^{2+} entry is driven by a favorable transmembrane voltage and represents the rate-limiting step and site of regulation (Dai et al., 2001). Finally, 3%−5% of the filtered Mg^{2+} is excreted in the urine.

For the determination of renal Mg^{2+} conservation and the diagnosis of Mg^{2+} deficiency, the parallel determination of serum and urine Mg^{2+} concentrations is critical. In hypomagnesemic patients, the determination of urinary Mg^{2+} excretions allows for a differentiation between renal Mg^{2+} wasting and extrarenal losses. In the presence of hypomagnesemia, the 24-h Mg^{2+} excretion is expected to be below 1 mmol (Sutton and Domrongkitchaiporn, 1993). In contrast, a decreased 24-h Mg^{2+} excretion might indicate Mg^{2+} deficiency in normomagnesemic individuals, presuming an intact renal Mg^{2+} conservation. Similarly, Mg^{2+}/creatinine ratios and fractional Mg^{2+} excretions calculated from spot urine samples might be useful (Elisaf et al., 1997; Tang et al., 2000). Finally, the parenteral Mg^{2+} loading test (MLT) remains the gold standard for the evaluation of body Mg^{2+} status (Elin, 1994; Hébert et al., 1997). It determines the retention of a defined intravenous Mg^{2+} load as a sensitive index of Mg^{2+} deficiency. Several protocols have been published (Ryzen et al., 1985; Gullestad et al., 1994). A short-term MLT using an infusion of 0.1 mmol Mg^{2+} per kilogram body weight given over 1 h was proposed as a less elaborate alternative to the 8-h standard, yielding comparable results (Rob et al., 1996). Usually, an excretion of less than 70% of the infused Mg^{2+} is considered indicative of Mg^{2+} deficiency (Hébert et al., 1997). Moreover, the MLT can be successfully applied to differentiate between renal and extrarenal Mg^{2+} losses in hypomagnesemic patients to uncover a renal Mg^{2+} leak that becomes evident only at higher serum Mg^{2+} concentrations (Walder et al., 2002).

Hereditary disorders of magnesium homeostasis

Advances in molecular genetics identified a number of genes and their encoded proteins involved in epithelial Mg^{2+} transport (de Baaij et al., 2015b). Knowledge of the underlying genetic defects allows the definition of a growing spectrum of clinical entities underlying hereditary disorders of Mg^{2+} homeostasis. Moreover, the clarification of the molecular structures and of the pathophysiology of hypomagnesemic disorders enables an understanding of disturbances in Mg^{2+} metabolism as a frequent side effect of common drug treatments and raises the alertness of the clinician for the prevention and treatment of acquired hypomagnesemia in their patients.

Disturbed Mg^{2+} reabsorption in the thick ascending limb

In the TAL, the paracellular reabsorption pathway for divalent cations is composed of specialized tight junctions comprising different proteins of the claudin family (i.e., claudin-3, -10, -11, -14, -16, -19). Paracellular transport of divalent cations is passive in nature, driven by the lumen positive transepithelial potential. Patients with genetic defects in *CLDN16* (encoding claudin-16) and *CLDN19* genes (encoding claudin-19) suffer from an autosomal-recessive disease named familial hypomagnesemia with hypercalciuria and nephrocalcinosis (FHHNC; MIM: 248250) (Simon et al., 1999; Konrad et al., 2006). Due to excessive renal Ca^{2+} and Mg^{2+} wasting, patients develop the characteristic triad of hypomagnesemia, hypercalciuria, and nephrocalcinosis. FHHNC patients usually present during childhood with recurrent urinary tract infections, polyuria/polydipsia, nephrolithiasis, and/or failure to thrive. Signs of profound hypomagnesemia such as cerebral seizures or muscular tetany are observed less frequently. An additional ocular involvement (including severe myopia, nystagmus, or chorioretinitis) is common in patients with *CLDN19* mutations (Konrad et al., 2006). Additional laboratory findings include elevated intact parathyroid hormone (iPTH) levels before the onset of renal failure, an incomplete distal tubular acidosis, hypocitraturia, and hyperuricemia present in the majority of patients (Weber et al., 2001). The clinical course of FHHNC patients is often complicated by a continuous decline in renal function leading to end-stage renal disease (ESRD) early in life. A significant number of patients exhibit a marked decline in glomerular filtration rate (GFR) already at the time of diagnosis, and about one-third of patients develop ESRD during adolescence (Konrad et al., 2008). Hypomagnesemia may completely disappear with the decline of GFR. In addition to oral Mg^{2+} supplementation, therapy aims at a reduction in renal Ca^{2+} excretions to prevent the progression of nephrocalcinosis and kidney stone formation, as the

extent of renal calcifications has been correlated with the progression of chronic renal failure (Praga et al., 1995). Supportive therapy is critical for the protection of kidney function, including sufficient fluid uptake and an effective treatment of bacterial infections and kidney stone disease. Data on bone mineral density or an additional bone phenotype in patients with FHHNC are sparse. A potential defect in bone mineralization caused by renal Ca^{2+} and Mg^{2+} wasting and early elevations of iPTH might overlap with renal osteodystrophy that develops with the decline in renal function. However, there are recent data on a primary defect in amelogenesis in patients with *CLDN16* mutations (Bardet et al., 2016; Yamaguti et al., 2017). Finally, there is evidence for a heterozygote effect in carriers of *CLDN16* mutations who may present with hypercalciuria, nephrolithiasis, and/or nephrocalcinosis (Weber et al., 2001; Praga et al., 1995). Another study also reported mild hypomagnesemia in family members with heterozygous *CLDN16* mutations (Blanchard et al., 2001). Thus, one might speculate that *CLDN16* mutations could be involved in idiopathic hypercalciuric stone formation.

Interestingly, physiologic data indicate that claudin-16 and claudin-19 do not just facilitate paracellular Mg^{2+} and Ca^{2+} transport (Hou et al., 2008). Rather, the authors suggest that claudin-16 also critically influences paracellular sodium (Na^+) permeability, while claudin-19 seals the paracellular space for chloride (Cl^-). Another study points to the existence of spatially distinct sets of tight junction strands that allow for the permeation of either monovalent or divalent cations (Milatz et al., 2017). In line with these findings are the observations made in mice with a deletion of claudin-10 (*cldn10*), which is thought to form a paracellular Na^+ pore (Breiderhoff et al., 2012). These mice display a decreased paracellular Na^+ permeability but an increase in paracellular Mg^{2+} and Ca^{2+} transport that phenotypically leads to hypermagnesemia and nephrocalcinosis. Similarly, patients with recessive *CLDN10* mutations exhibit a Bartter-like salt wasting phenotype with hypokalemic alkalosis and display serum Ca^{2+} and Mg^{2+} levels that are in the upper normal range or elevated (Bongers et al., 2017; Hadj-Rabia et al., 2018). Finally, the additional knockout of *cldn10* corrects the Mg^{2+} and Ca^{2+} wasting phenotype of *cldn16*-deficient mice (Breiderhoff et al., 2018). Data on bone mineralization have not been reported as of this writing for either patients or mice.

Another claudin that is expressed at tight junctions in the TAL is claudin-14 (*CLDN14*) (Gong et al., 2012). *CLDN14* has been identified in a genome-wide association study (GWAS) as a major risk gene for hypercalciuric nephrolithiasis and a reduced bone mineral density (Thorleifsson et al., 2009). The association of *CLDN14* with bone mineral density was subsequently replicated in two independent studies (Zhang et al., 2014; Tang et al., 2016). Moreover, a variant in the *CLDN14* promotor has been associated with pediatric-onset hypercalciuria and kidney stones (Ure et al., 2017). Claudin-14 interacts with claudin-16 and diminishes paracellular cation permeability in vitro (Gong et al., 2012). Under physiologic conditions, expression of claudin-14 is suppressed via a microRNA pathway (Gong et al., 2015). By activation of the CaSR, extracellular Ca^{2+} is able to relieve this suppression, induce claudin-14 expression, and inhibit paracellular divalent cation reabsorption (Hou et al., 2013). Moreover, claudin-14 expression and therefore paracellular cation transport are critically influenced by parathyroid hormone (PTH) via PTH receptor (PTH1R) signaling (Fig. 21.3). Accordingly, the TAL-specific inactivation of the PTH1R in mice leads to hypercalciuria and diminished serum Ca^{2+} levels, while expression of claudin-14 is significantly increased (Sato et al., 2017). In contrast, the deletion of *cldn14* in mice provokes hypermagnesemia, hypomagnesiuria, and hypocalciuria under a high-Ca^{2+} diet (Gong et al., 2012).

Basolaterally expressed CaSR negatively regulates Mg^{2+} and Ca^{2+} reabsorption in the TAL (Fig. 21.3) (Houillier, 2013). The CaSR senses extracellular Ca^{2+} as well as Mg^{2+} concentrations in the distal nephron (Brown, 2013). In the parathyroid, the CaSR is responsible for adjusting the rate of PTH synthesis and release to the extracellular levels of both divalent cations (Hebert and Brown, 1995). Two different hereditary disorders result from either activating or inactivating CaSR mutations. Heterozygous activating mutations lead to autosomal-dominant hypocalcemia (ADH; MIM: 601198) (Pollak et al., 1994). Patients present with hypocalcemic seizures or muscle spasms. In addition, a significant number of affected patients also exhibit hypomagnesemia (Pearce et al., 1996). Moreover, patients may develop significant renal salt wasting due to parallel inhibition of active transcellular NaCl reabsorption in the TAL (Watanabe et al., 2002). Inappropriately low iPTH levels due to the activation of the CaSR in the parathyroid gland often lead to the diagnosis of primary hypoparathyroidism. In ADH, supplementation with vitamin D and Ca^{2+} should be reserved for symptomatic patients as it may increase calciuria and renal complications (Hannan and Thakker, 2013).

In contrast, inactivating mutations on one or two *CASR* alleles result in familial hypocalciuric hypercalcemia (FHH1; MIM:145980) and neonatal severe hyperparathyroidism (NSHPT; MIM 239200), respectively (Pollak et al., 1993). FHH patients normally present with mild-to-moderate hypercalcemia, accompanied by few if any symptoms, and usually do not require treatment. Urinary excretion rates for Ca^{2+} and Mg^{2+} are markedly reduced, and affected individuals may also exhibit mild hypermagnesemia (Marx et al., 1981). In contrast, NSHPT patients with two mutant *CASR* alleles present in early infancy with severe symptomatic hypercalcemia. If untreated, hyperparathyroidism and hypercalcemia result in diffuse bone demineralization, fractures, and skeletal deformities. Traditionally, partial-to-total parathyroidectomy within the first weeks of life has been propagated and still represents the treatment of choice for most patients (Cole et al., 1997;

Mayr et al., 2016). More recent data indicate that cinacalcet, a calcimimetic drug enhancing CaSR function, may exert positive effects in a subset of patients, while a lack of effect was demonstrated in others (Atay et al., 2014; Gannon et al., 2014). As in symptomatic hypercalcemia of different origin, pamidronate has been shown to effectively lower serum Ca^{2+} levels (Waller et al., 2004). Data on Mg^{2+} metabolism in patients with NSHPT are scarce; however, elevations of serum Mg^{2+} levels to around 50% above the upper normal limit have been reported (Cole et al., 1997). The bone phenotype resulting from inactivating Casr mutations has been extensively studied in mice (Ho et al., 1995; Garner et al., 2001; Liu et al., 2011). $Casr^{-/-}$ mice exhibit markedly elevated iPTH levels, parathyroid hyperplasia, severe hypercalcemia, severe skeletal growth retardation, and premature death (Ho et al., 1995). Garner et al. performed a detailed skeletal analysis in $Casr^{-/-}$ mice and described a rickets phenotype with impaired growth plate calcification and decreased mineralization of metaphyseal bone (Garner et al., 2001).

Disturbed Mg^{2+} reabsorption in the distal convoluted tubule

Genetic studies in patients with inherited hypomagnesemia have identified numerous genes that are involved in active transcellular Mg^{2+} reabsorption in the DCT (Fig. 21.4). Mg^{2+} enters the DCT cell through a specific Mg^{2+}-permeable ion channel. As intraluminal and intracellular Mg^{2+} concentrations are of the same magnitude, the intracellularly negative membrane voltage represents the major driving force for apical Mg^{2+} entry.

Genetic studies in patients with HSH (HOMG1; MIM: 602014) led to the identification of TRPM6 as a critical component of apically located Mg^{2+}-permeable ion channels (Schlingmann et al., 2002; Walder et al., 2002; Chubanov et al., 2004). Recessive loss-of-function mutations in *TRPM6* result in the development of severe hypomagnesemia, cerebral seizures, or other symptoms of increased neuromuscular excitability during infancy as first described in 1968 (Paunier et al., 1968). Delayed diagnosis or noncompliance with treatment can even be fatal or result in permanent neurological damage. In addition to hypomagnesemia, patients exhibit suppressed iPTH levels and consecutive hypocalcemia. The hypocalcemia observed in HSH is resistant to treatment with Ca^{2+} or vitamin D. Relief of clinical symptoms, normocalcemia, and normalization of iPTH levels can be achieved only by administration of high doses of Mg^{2+} (Shalev et al., 1998). The suppression of PTH is thought to result from an inhibition of PTH synthesis and secretion in the presence of profound hypomagnesemia (Anast et al., 1972). The paradoxical block of the parathyroid gland caused by severe Mg^{2+} depletion involves intracellular signaling pathways of the CaSR with an increase in the activity of inhibitory Gα subunits (Quitterer et al., 2001). In addition, profound hypomagnesemia might result in an end organ resistance to PTH as intracellular Mg^{2+} is a cofactor for adenylate cyclase (Mori et al., 1992; Mihara et al., 1995). Finally, hypomagnesemia results in a reduction in PTH-induced release of Ca^{2+} from bone, which contributes to the development of secondary hypocalcemia (Freitag et al., 1979). The *TRPM6* gene encodes a member of the TRP family of cation channels. The TRPM6 protein is highly homologous to TRPM7, another Ca^{2+}- and Mg^{2+}-permeable ion channel regulated by Mg-ATP (Nadler et al., 2001). TRPM6 is expressed along the entire gastrointestinal tract as well as in kidney in the DCT, supporting the assumption of HSH being a combined gastrointestinal and renal Mg^{2+} wasting disorder (Voets et al., 2004).

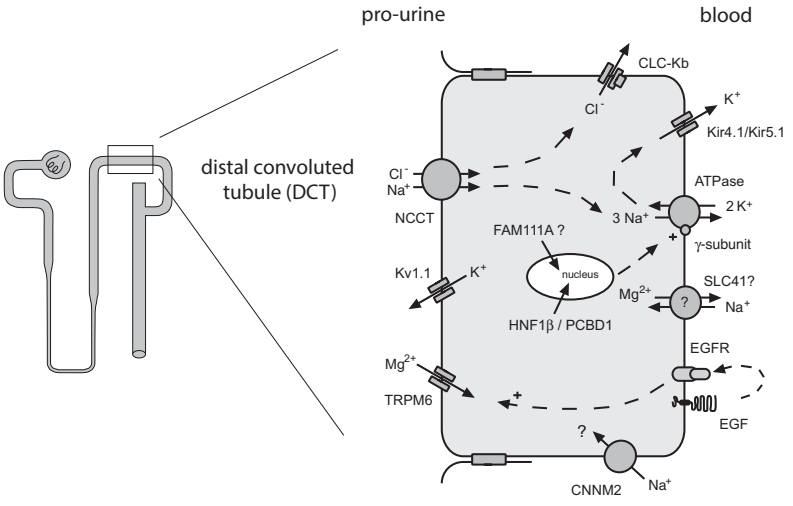

FIGURE 21.4 Mg^{2+} reabsorption in the distal convoluted tubule. Mg^{2+} transport is active and transcellular in nature. Mg^{2+} entry through transient receptor potential, subfamily M, 6 (*TRPM6*) ion channels is dependent on the negative membrane potential. The molecular identity of the basolateral Mg^{2+} extrusion mechanism is still unknown but might involve Na^+/Mg^{2+} exchangers of the solute carrier 41 (*SLC41*) family. Mg^{2+} transport is critically influenced by transcellular salt reabsorption, potassium recycling, and the paracrine action of epidermal growth factor (*EGF*), as well as the transcriptional activity of hepatocyte nuclear factor 1β (*HNF1β*). *CNNM2* might represent a basolaterally expressed Mg^{2+} sensor.

The functional characterization of TRPM6 in different overexpression systems yielded contradictory results. Voets et al. were able to express functional TRPM6 monomers and could demonstrate striking similarities to TRPM7 with respect to gating mechanisms and ion-selectivity profiles, as TRPM6 was shown to be regulated by intracellular Mg^{2+} levels and to be permeable for Mg^{2+} as well as for Ca^{2+} (Voets et al., 2004). Permeation characteristics with currents almost exclusively carried by divalent cations with a higher affinity for Mg^{2+} than for Ca^{2+} supported the role of TRPM6 as the apical Mg^{2+} influx pathway. In contrast, Chubanov and coworkers observed that TRPM6 was present at the cell surface only when associating with TRPM7 (Chubanov et al., 2004). Electrophysiological data in the *Xenopus* oocyte expression system indicated that coexpression of TRPM6 results in a significant amplification of TRPM7-induced currents (Chubanov et al., 2004). The idea of a heteromultimerization of TRPM6 with TRPM7 was also confirmed by another independent group that demonstrated that TRPM6 and TRPM7 are functionally not redundant, but that both proteins can influence each other's biological activity (Schmitz et al., 2005). This group showed that TRPM6 is able to phosphorylate TRPM7, thereby modulating its function.

The most common inherited disorder affecting magnesium conservation in the DCT is the Gitelman syndrome (GS; MIM: 263800), a primary renal salt wasting disorder with an estimated prevalence of approximately 1:40,000. GS is caused by recessive mutations in *SLC12A3* encoding the thiazide-sensitive NaCl cotransporter NCCT (Simon et al., 1996). In contrast to other forms of the Bartter syndrome spectrum, urinary-concentration ability typically is not affected and the extent of renal salt wasting is rather mild. Nevertheless, salt craving is a common clinical feature. Patients usually present at school age or in later life with muscular weakness, cramps, or fatigue. Also, a significant percentage of affected individuals are diagnosed while searching medical consultation because of growth retardation, constipation, or enuresis. Furthermore, many so-called "asymptomatic" patients have been reported, or GS is diagnosed incidentally after the assessment of serum electrolytes for other reasons. Nevertheless, it has been demonstrated that GS should not be considered a mild disorder, since none of the studied patients was truly asymptomatic (Cruz et al., 2001). Salt craving, nycturia, and paresthesia were the most frequent symptoms, all of them significantly affecting the quality of life.

Laboratory examinations in GS patients show the typical constellation of metabolic alkalosis, hypokalemia, and hypomagnesemia; urine analyses reveal hypocalciuria (Bettinelli et al., 1992). The dissociation of renal Ca^{2+} and Mg^{2+} handling was initially considered pathognomonic for GS; however, it has been observed in a number of hypomagnesemic disorders (see later). Mg^{2+} depletion causes neuromuscular irritability and tetany. Decreased renal Ca^{2+} elimination together with Mg^{2+} deficiency favors deposition of mineral Ca^{2+} as demonstrated by increased bone density as well as chondrocalcinosis (Nicolet-Barousse et al., 2005; Ea et al., 2005). Family studies demonstrated that electrolyte imbalances are present from infancy on, although the affected infants remain clinically asymptomatic. Of note, the combination of hypokalemia and hypomagnesemia exerts an exceptionally unfavorable effect on cardiac excitability, which puts these patients at high risk for cardiac arrhythmias (Foglia et al., 2004). Substitution of K^+ and Mg^{2+} represents the central treatment of this disorder. Avoidance of factors that in addition to hypokalemia and hypomagnesemia might affect cardiac excitability (in particular, QT-time prolonging drugs) is mandatory to prevent life-threatening cardiac arrhythmias (Blanchard et al., 2017). Unfortunately, the exact mechanisms compromising Mg^{2+} reabsorption while favoring reabsorption of Ca^{2+} are not yet completely understood. Studies in *Trpv5*-knockout mice with disrupted Ca^{2+} reabsorption in the DCT that were treated with thiazides to inhibit NCCT pointed to an increase in passive Ca^{2+} reabsorption in the proximal tubule underlying hypocalciuria (Nijenhuis et al., 2005). The same study demonstrated a downregulation of TRPM6 in NCC-knockout mice as well as thiazide-treated mice in parallel to the development of hypomagnesemia.

In 2009, a novel clinical syndrome with autosomal-recessive inheritance combining epilepsy, ataxia, sensorineural deafness, and renal NaCl wasting was described under the acronym EAST or SeSAME syndrome (SESAMES; MIM: 612780) (Bockenhauer et al., 2009; Scholl et al., 2009). While in early life, neurological symptoms predominate, renal salt wasting is typically recognized only later during the course of the disease. As in GS, the renal phenotype includes hypokalemic alkalosis, hypomagnesemia, and hypocalciuria. EAST/SeSAME syndrome is caused by loss-of-function mutations in *KCNJ10* encoding the K^+ channel Kir4.1 (Reichold et al., 2010). The expression pattern of Kir4.1 fits the disease phenotype with highest expression in brain, the stria vascularis of the inner ear, and the DCT. Here, Kir4.1 is thought to mediate K^+ recycling over the basolateral membrane and thereby to maintain activity and function of Na/K-ATPase (Fig. 21.4) (Bockenhauer et al., 2009). Accordingly, loss of Kir4.1 function leads to depolarization of the basolateral membrane and therefore to a reduction in the driving force for basolateral Na^+-coupled exchangers. By this mechanism, Kir4.1 defects putatively affect the proposed Na^+/Mg^{2+} exchanger, which possibly explains the Mg^{2+} wasting observed in EAST/SeSAME syndrome.

An impairment of basolateral Na/K-ATPase function had already been implicated in renal Mg^{2+} wasting when Meij et al. in 1999 discovered a mutation in *FXYD2* in two related families with isolated dominant hypomagnesemia (IDH; MIM: 154020) (Meij et al., 2000). *FXYD2* encodes an accessory γ subunit of Na/K-ATPase that is expressed in a tissue-

specific manner (Arystarkhova et al., 2002b). FXYD2 increases the apparent affinity of Na/K-ATPase for ATP while decreasing its Na^+ affinity (Arystarkhova et al., 2002a). Thus, it might provide a mechanism for balancing energy utilization and maintaining appropriate salt gradients. Expression studies of the identified mutant p.G41R γ-subunit in mammalian renal tubule cells revealed a dominant-negative effect of the mutation leading to a retention of the γ-subunit within the cell (Cairo et al., 2008). A possible explanation for the resulting defect in Mg^{2+} reabsorption is based on changes in intracellular Na^+ and K^+ levels: in addition to the presumed effect on basolateral Na^+/Mg^{2+} exchange, Meij et al. suggested that diminished intracellular K^+ might depolarize the apical membrane, resulting in a decrease in Mg^{2+} uptake (Meij et al., 2003). The index patients had presented with cerebral seizures, and laboratory analyses demonstrated profound hypomagnesemia (Geven et al., 1987). Systematic serum Mg^{2+} measurements performed in additional family members revealed hypomagnesemia in numerous additional, apparently healthy individuals. Urine analyses indicated renal Mg^{2+} wasting. Interestingly, urinary Ca^{2+} excretion rates were reduced in all hypomagnesemic individuals, a finding reminiscent of GS patients (mentioned earlier). However, no other associated biochemical abnormalities were reported, especially no hypokalemic alkalosis. Meanwhile, the identical *FXYD2* mutation has been identified in two additional families from the Netherlands and Belgium with dominant hypomagnesemia, substantiating the initial findings (de Baaij et al., 2015a). Several affected family members suffered from muscle cramps and cerebral seizures. Serum Mg^{2+} levels were found to be severely low. Interestingly, two patients exhibited hypokalemia in addition, possibly pointing to a disturbance in cellular Na^+ and K^+ handling with consecutive stimulation of the renin−angiotensin−aldosterone system. Like in the original family, urine analyses demonstrated hypocalciuria in all affected individuals (de Baaij et al., 2015a). This finding without apparent volume depletion potentially contradicts the aforementioned experimental data that favored an increase in proximal tubular Ca^{2+} reabsorption due to volume depletion in GS (Nijenhuis et al., 2005).

Another hereditary defect possibly resulting in defective apical uptake of Mg^{2+} in the DCT was discovered by Glaudemans et al. The authors described a dominant-negative missense mutation in *KCNA1* encoding the voltage-gated potassium (K^+) channel Kv1.1 in a large Brazilian family with hypomagnesemia (EA1; MIM: 176260 - 160120) (Glaudemans et al., 2009). Kv1.1 colocalizes with TRPM6 in the apical DCT cell membrane. These findings for the first time demonstrated a dependency between renal Mg^{2+} and K^+ handling at the molecular level linking Mg^{2+} reabsorption to K^+ secretion. The authors proposed a model in which Kv1.1 contributes to the establishment of a negative apical membrane potential as a prerequisite for TRPM6-mediated Mg^{2+} entry (Fig. 21.4) (Glaudemans et al., 2009). The clinical phenotype of affected patients included muscle cramps, tetanic episodes, tremor, and muscle weakness starting in infancy. Laboratory analyses demonstrated a renal Mg^{2+} leak without alterations in renal Ca^{2+} handling (see later). Interestingly, *KCNA1* mutations had previously been identified in patients with episodic ataxia with myokymia, a neurologic disorder characterized by a periodic appearance of incoordination and imbalance as well as myokymia, an involuntary, spontaneous, and localized trembling of muscles (Browne et al., 1994). Similar clinical findings were also present in members of the kindred studied by Glaudemans et al. with hypomagnesemia (Glaudemans et al., 2009).

Studying a consanguineous family with two affected sisters with isolated recessive hypomagnesemia (HOMG3; MIM: 248250), Groenestege et al. identified a homozygous missense mutation in the *EGF* gene encoding the pro−epidermal growth factor (EGF) protein (Groenestege et al., 2007). The two affected girls initially presented with cerebral seizures during infancy. Unfortunately, a delay in diagnosis resulted in significant neurodevelopmental deficits in both patients. A thorough clinical and laboratory workup at 4 and 8 years of age, respectively, revealed serum Mg^{2+} levels around 0.5−0.6 mmol/L without other associated electrolyte abnormalities. A ^{28}Mg retention study in one patient as well as renal Mg^{2+} excretion rates of 3 to 6 mmol per day in the presence of hypomagnesemia pointed to a primary renal defect, while intestinal Mg^{2+} uptake appeared to be preserved. In contrast, renal Ca^{2+} excretion rates were within the normal range.

Pro-EGF is a small peptide hormone expressed in various tissues, including the DCT in kidney (Groenestege et al., 2007). It has a single transmembrane segment that is inserted in both the luminal and the basolateral membrane of polarized epithelia. After membrane insertion it is processed into active EGF peptide by cleavage from the transmembrane section. EGF activates specialized EGF receptors (EGFRs) that are expressed in the basolateral membrane of DCT cells (Fig. 21.4). This activation was shown to lead to an increase in TRPM6 membrane trafficking and increased Mg^{2+} reabsorption (Thebault et al., 2009). The identified mutation disrupts the basolateral sorting motif in pro-EGF. Hence, the activation of EGFRs in the basolateral membrane is compromised, ultimately leading to reduced Mg^{2+} reabsorption. Despite acting in a paracrine fashion in the DCT, the authors also speculated about a role for EGF as a novel selectively acting magnesiotropic hormone (Groenestege et al., 2007).

Interestingly, renal Mg^{2+} wasting is observed as a common side effect of anti-cancer treatment with EGFR-targeting antibodies (i.e., cetuximab), supporting a critical role of the EGFR signaling pathway in regulating Mg^{2+} reabsorption in

the DCT (Tejpar et al., 2007). Inhibitors of EGFR tyrosine kinase (i.e., erlotinib) were shown to have a less pronounced effect on TRPM6 trafficking and function and renal Mg^{2+} conservation in a mouse model (Dimke et al., 2010).

Another form of hereditary hypomagnesemia has been linked to mutations in *CNNM2* (HOMGSMR1; MIM: 613882) (Stuiver et al., 2011). The authors identified heterozygous *CNNM2* mutations in two families in which the affected patients presented with a clinical spectrum ranging from seizures in early childhood to muscle weakness, vertigo, and headache during adolescence. Additional heterozygous mutation carriers from both families even remained asymptomatic. Other than hypomagnesemia, serum electrolytes were within normal ranges. There are no definitive data concerning renal Ca^{2+} conservation and the presence of hypocalciuria. Of note, a neurological phenotype was not reported in any of the four affected family members. Previously, *CNNM2*, next to its homologs *CNNM3* and *CNNM4*, as well as *TRPM6*, had already been associated with serum Mg^{2+} levels in a large GWAS (Meyer et al., 2010). The *CNNM2* gene codes for cyclin M2, a transmembrane protein that is expressed in kidney at the basolateral membranes of TAL and DCT, but also in other organs, especially in brain (Stuiver et al., 2011; de Baaij et al., 2012). Whereas a truncating frameshift mutation was identified in one of the described families, affected individuals of the second family carried a missense mutation leading to a nonconservative amino acid exchange (Stuiver et al., 2011). Contrasting the initial patient cohort, Arjona et al. identified mutations in the *CNNM2* gene in hypomagnesemic patients who presented with seizures and displayed an impaired neurological development despite adequate treatment (Arjona et al., 2014). In addition, patients showed features of autism spectrum disorder, and two affected girls demonstrated severe obesity. *CNNM2* mutations were predominantly identified in the heterozygous state and occurred de novo. Finally, two siblings from a family with suspected parental consanguinity who developed seizures already in the neonatal period and displayed a severe degree of intellectual disability were found to be carriers of a homozygous *CNNM2* mutation. Magnetic resonance imaging (MRI) in these two patients demonstrated an abnormal brain morphology, whereas MRI findings in heterozygous patients were without obvious pathological findings (Arjona et al., 2014). Clearly, the neurological phenotype, i.e., seizure severity and frequency, in these patients appeared to be independent of serum Mg^{2+} levels, suggesting a primary disturbance of brain development or function. In accordance with the human phenotype, heterozygous *Cnnm2*-knockout mice display hypomagnesemia, but in addition show significantly decreased arterial blood pressure (Funato et al., 2017).

Functional studies using overexpression of *CNNM2* in HEK293 cells demonstrated an impaired cellular uptake of Mg^{2+} for mutant in comparison with wild-type CNNM2, pointing to a loss-of-function character of identified *CNNM2* mutations (Arjona et al., 2014). Biotinylation assays demonstrated a lack of cell surface expression at least for a subset of mutated CNNM2 proteins. Yet many questions concerning the cellular localization and function of CNNM2 remain unanswered. Data point to a role for CNNM2 as a potential Mg^{2+} sensor or regulatory factor rather than as a Mg^{2+} transporter, as the authors could not detect CNNM2-mediated Mg^{2+} influx nor efflux (Sponder et al., 2016). Furthermore, the Mg^{2+} uptake stimulated by CNNM2 overexpression is not dependent on extracellular Na^{+} but is abolished by 2-aminoethoxydiphenyl borate, a known inhibitor of TRPM7 ion channels, pointing to a functional coupling of CNNM2 with Mg^{2+}-permeable ion channels (Arjona and de Baaij, 2018). The role of CNNM2 in Mg^{2+} homeostasis and human physiology will be an intriguing topic of future research, as recent GWASs have identified potential links between CNNM2 and body mass index, hypertension, and coronary artery disease, as well as schizophrenia and bipolar disorders (Lv et al., 2017; Takeuchi et al., 2010; Grigoroiu-Serbanescu et al., 2015).

Hepatocyte nuclear factor 1β (*HNF1B*; *TCF2*) is a transcription factor involved in the development of kidney and pancreas. Heterozygous *HNF1B/TCF2* mutations were implicated in a subtype of maturity-onset diabetes of the young (MODY5) before an association with developmental kidney disease was reported (Horikawa et al., 1997). The renal phenotype is highly variable, including enlarged hyperechogenic kidneys, multicystic kidney disease, renal agenesis, renal hypoplasia, and cystic dysplasia, as well as hyperuricemic nephropathy (Heidet et al., 2010). The association with both symptom complexes led to the denomination "renal cysts and diabetes syndrome" (RCAD; MIM: 137920). However, this term was later replaced by the more general description as HNF1B nephropathy because the renal cystic phenotype and the development of diabetes are not uniform clinical findings. Interestingly, approximately half of affected patients present with hypomagnesemia due to renal Mg^{2+} wasting (Adalat et al., 2009). Again, the defect in renal Mg^{2+} conservation is accompanied by hypocalciuria. HNF1B regulates the expression of numerous renal genes, including the *FXYD2* gene, which bears several HNF1B-binding sites in its promoter region (Adalat et al., 2009). Therefore, defective *FXYD2* transcription and diminished expression of the γ-subunit of Na/K-ATPase represent a putative mechanism explaining the renal Mg^{2+} wasting in patients with *HNF1B* mutations.

A similar renal phenotype comprising urinary Mg^{2+} loss has been demonstrated in patients affected with transient neonatal hyperphenylalaninemia due to recessive mutations in *PCBD1* (MIM: 264070) (Ferre et al., 2014). *PCBD1* encodes a bifunctional protein that acts in the salvage pathway for the regeneration of tetrahydrobiopterin, but also as a binding partner of the HNF1B transcription factor. Functional studies demonstrated a dimerization with HNF1B that leads

to a stimulation of the *FXYD2* promotor in the DCT (Ferre et al., 2014). Interestingly, a MODY-type diabetes was also observed in two of the described patients.

Kenny−Caffey syndrome type 2 (MIM: 127000) is clinically characterized by severe short stature, small hands and feet, craniofacial anomalies, delayed closure of the anterior fontanelle, and the occurrence of cerebral convulsions. Radiologic studies reveal a cortical thickening and medullary stenosis of tubular bones. Seizures are secondary to severe hypoparathyroidism and resulting hypocalcemia. In addition, patients may develop severe hypomagnesemia. Early manifestations in infancy with profound hypomagnesemia, hypocalcemia, and undetectable serum PTH have been described, resembling the clinical picture of HSH due to *TRPM6* mutations (Isojima et al., 2014). As magnesium repletion was able to correct the hypoparathyroidism, the authors suggested a paradoxical block in PTH synthesis and/or secretion similar to that observed in HSH (see earlier) (Abraham et al., 2017). Kenny−Caffey syndrome type 2 is caused by heterozygous mutations in the *FAM111A* gene that mostly occur de novo (Unger et al., 2013). *FAM111A* codes for an intracellular protein with homology to trypsin-like peptidases with yet undefined function. It is primarily expressed in bone and parathyroid gland and a complex role in the regulation of bone formation as well as parathyroid gland development was suggested (Abraham et al., 2017).

Finally, the clinical and biochemical evaluation of a large Caucasian family in which affected individuals presented with hypomagnesemia, hypercholesterolemia, and hypertension established another entity, termed "metabolic or mitochondrial hypomagnesemia" (MIM: 500005) (Wilson et al., 2004). The transmission of the phenotype exclusively by females suggested mitochondrial inheritance. Genetic studies identified a mutation in the mitochondrial-coded isoleucine tRNA gene, $tRNA^{Ile}$ or MTTI.

The majority of genetically affected family members exhibited at least one of the mentioned symptoms; approximately half showed a combination of two or more symptoms, and around 1/6 had all three features. Serum Mg^{2+} levels of family members in the maternal lineage greatly varied, ranging from ∼0.8 to ∼2.5 mg/dL (equivalent to ∼0.3−∼1.0 mmol/L) with approximately 50% of individuals being hypomagnesemic (serum Mg^{2+} <1.8 mg/dL). These hypomagnesemic individuals exhibited higher fractional Mg^{2+} excretions than their normomagnesemic relatives in the maternal lineage, clearly pointing to a renal Mg^{2+} leak. Interestingly, hypomagnesemia was accompanied by decreased urinary Ca^{2+} levels, a finding pointing to the DCT as the affected tubular segment.

The mitochondrial mutation affects the $tRNA^{Ile}$ gene *MTTI* and is located directly adjacent to the anticodon triplet. This position is highly conserved and critical for codon−anticodon recognition. However, the functional link between the tRNA defect and mitochondrial function remains to be elucidated in detail. As ATP consumption along the kidney tubule is highest in the DCT, the authors speculate on an impaired energy metabolism of DCT cells, which in turn could lead to disturbed transcellular Mg^{2+} reabsorption (Wilson et al., 2004).

Acquired hypomagnesemia

Cisplatin and carboplatin

The cytostatic agents cisplatin and carboplatin are widely used in various protocols for anti-cancer treatment of solid tumors. Among various side effects, nephrotoxicity receives the most attention as it represents a major dose-limiting factor. Carboplatin has been reported to have less severe side effects than cisplatin (Boulikas and Vougiouka, 2004; English et al., 1999; Goren, 2003). Hypomagnesemia due to renal Mg^{2+} wasting is regularly observed in patients treated with cisplatin (Goren, 2003; Lajer and Daugaard, 1999). The incidence of Mg^{2+} deficiency is greater than 30% but increases to over 70% with longer usage and greater accumulated doses. Interestingly, cisplatin-induced renal Mg^{2+} wasting is relatively selective (Goren, 2003). Hypocalcemia and hypokalemia may be observed but only with prolonged and severe Mg^{2+} deficiency (Mavichak et al., 1988). The effects of cisplatin may persist for months or years, long after the inorganic platinum has disappeared from the renal tissue (Bianchetti et al., 1991; Markmann et al., 1991).

Studies in cisplatin-treated rats demonstrated a downregulation of TRPM6 as well as EGF expression (van Angelen et al., 2013; Ledeganck et al., 2013). In contrast, the expression of other genes and proteins involved in tubular Mg^{2+} reabsorption remained stable or was even upregulated (*cldn16, cldn19*), potentially reflecting compensatory mechanisms (Ledeganck et al., 2013). Therefore, a defect in EGF-mediated stimulation of TRPM6 in the DCT is suggested to represent the underlying cause of renal Mg^{2+} wasting. Interestingly, cotreatment with Mg^{2+} ameliorated the cisplatin-induced downregulation of TRPM6 and hypomagnesemia and prevented a decline in renal function observed after administration of cisplatin alone (Saito et al., 2017).

Aminoglycosides

Aminoglycosides such as gentamicin induce renal impairment in a significant number of patients, depending on dose and duration of administration. Furthermore, aminoglycosides cause renal Mg^{2+} as well as Ca^{2+} wasting (Shah and Kirschenbaum, 1991). These effects occur soon after onset of therapy; they are dose dependent and reversible upon withdrawal of the drug (Elliott et al., 2000). The combined renal loss of Ca^{2+} and Mg^{2+} suggests that aminoglycosides might affect divalent cation transport in the TAL. As gentamicin is a polyvalent cation it was postulated that it may have its effects on the CaSR (Dai et al., 2001; Ward et al., 2002). As in patients with a constitutive activation of the CaSR (see earlier; Watanabe et al., 2002), a more complex, Bartter-like phenotype consisting of hypokalemic metabolic alkalosis, hypocalcemia, hypomagnesemia, and polyuria has been observed (Singh et al., 2016). In line with the assumption of a TAL defect, studies in mice demonstrated that within hours of gentamicin administration the expression of genes involved in transcellular Ca^{2+} and Mg^{2+} reabsorption in the DCT (Trpv5, Trpv6, Trpm6) is upregulated as a potential compensatory mechanism preventing further electrolyte losses (Lee et al., 2012).

Calcineurin inhibitors

The calcineurin inhibitors cyclosporine and tacrolimus (FK506) are widely used as immunosuppressants in organ transplant recipients and in patients with numerous immunologic disorders. However, patients are at high risk of developing acute and chronic renal injury, including tubular dysfunction with subsequent disturbances in mineral metabolism. Both drugs commonly lead to renal Mg^{2+} wasting and hypomagnesemia (Rob et al., 1996). Calcineurin inhibitor therapy has been shown to be associated with inappropriately high fractional excretion rates for Mg^{2+}, suggesting a distal tubular reabsorption defect (Lote et al., 2000). For tacrolimus, a downregulation of Ca^{2+} and Mg^{2+} transport proteins, including TRPV5 and TRPM6, in the DCT was demonstrated (Nijenhuis et al., 2004). It was speculated that FK506-binding proteins, which are known to regulate Ca^{2+}-permeable TRP-like cation channels, might be involved (Goel et al., 2001). More recent studies in mice demonstrated that cyclosporine downregulates TRPM6 ion channels as well as the NaCl cotransporter NCCT (Ledeganck et al., 2014). The same group also described decreased urinary EGF levels in hypomagnesemic cyclosporine-treated renal transplant patients, pointing to the involvement of the EGF axis in disturbed TRPM6 expression and function (Ledeganck et al., 2014).

Mg^{2+} deficiency has also been implicated as a contributor to calcineurin inhibitor—related nephrotoxicity and arterial hypertension. These adverse effects were shown to depend on dietary salt intake in the rat and may be prevented by oral Mg^{2+} supplementation (Mervaala et al., 1999; Miura et al., 2002).

Proton pump inhibitors

Proton pump inhibitors (PPIs) used for the reduction of gastric acidity have emerged as one of the most widely used classes of drugs worldwide. A small, but significant number of patients receiving PPIs develop moderate to severe hypomagnesemia clinically apparent as muscle cramps, tetany, or even cerebral convulsions (Cundy and Mackay, 2011). In a substantially larger number of patients receiving PPIs, hypomagnesemia or the connection between PPI use and Mg^{2+} deficiency may remain unrecognized. In their review, Cundy and Mackay summarize the data from previous publications revealing severely low serum Mg^{2+} levels of less than 0.4 mmol/L with concomitant hypocalcemia, a finding reminiscent of HSH patients with genetic TRPM6 defects (see earlier) (Cundy and Mackay, 2011). Suppressed PTH levels with consecutive hypocalcemia had already been described before in hypomagnesemic patients receiving PPIs (Epstein et al., 2006). Unfortunately, the mechanism underlying the hypomagnesemia in PPI has not been clarified in detail. As renal Mg^{2+} excretion rates have been reported to be normal or even low, a defective intestinal Mg^{2+} absorption has been suggested (William and Danziger, 2016). However, whether the proposed effects of PPIs on intestinal Mg^{2+} absorption involve the pH-sensitive regulation of TRPM6 ion channels apically located on intestinal brush border cells or other proteins involved in intestinal Mg^{2+} uptake remains to be investigated.

At any rate, it is recommended to closely monitor serum Mg^{2+} levels in patients receiving PPIs, particularly those with concomitant cardiac disease and risk for arrhythmia. The other way around, attention should be drawn to the medication of patients presenting with severe hypomagnesemia and suppressed PTH.

References

Adalat, S., Woolf, A.S., Johnstone, K.A., Wirsing, A., Harries, L.W., Long, D.A., Hennekam, R.C., Ledermann, S.E., Rees, L., van't Hoff, W., Marks, S.D., Trompeter, R.S., Tullus, K., Winyard, P.J., Cansick, J., Mushtaq, I., Dhillon, H.K., Bingham, C., Edghill, E.L., Shroff, R., Stanescu, H., Ryffel, G.U., Ellard, S., Bockenhauer, D., 2009. HNF1B mutations associate with hypomagnesemia and renal magnesium wasting. J. Am. Soc. Nephrol. 20 (5), 1123−1131.

Abraham, M.B., Li, D., Tang, D., O'Connell, S.M., McKenzie, F., Lim, E.M., Hakonarson, H., Levine, M.A., Choong, C.S., 2017. Short stature and hypoparathyroidism in a child with Kenny-Caffey syndrome type 2 due to a novel mutation in FAM111A gene. Int. J. Pediatr. Endocrinol. 2017.

Anast, C.S., Mohs, J.M., Kaplan, S.L., Burns, T.W., 1972. Evidence for parathyroid failure in magnesium deficiency. Science 177 (4049), 606−608.

Arjona, F.J., de Baaij, J.H.F., 2018. CrossTalk opposing view: CNNM proteins are not Na(+)/Mg(2+) exchangers but Mg(2+) transport regulators playing a central role in transepithelial Mg(2+) (re)absorption. J. Physiol. 596 (5), 747−750.

Arjona, F.J., de Baaij, J.H., Schlingmann, K.P., Lameris, A.L., van Wijk, E., Flik, G., Regele, S., Korenke, G.C., Neophytou, B., Rust, S., Reintjes, N., Konrad, M., Bindels, R.J., Hoenderop, J.G., 2014. CNNM2 mutations cause impaired brain development and seizures in patients with hypomagnesemia. PLoS Genet. 10 (4) e1004267.

Arystarkhova, E., Donnet, C., Asinovski, N.K., Sweadner, K.J., 2002a. Differential regulation of renal Na,K-ATPase by splice variants of the gamma subunit. J. Biol. Chem. 277 (12), 10162−10172.

Arystarkhova, E., Wetzel, R.K., Sweadner, K.J., 2002b. Distribution and oligomeric association of splice forms of Na(+)-K(+)-ATPase regulatory gamma-subunit in rat kidney. Am. J. Physiol. Renal. Physiol. 282 (3), F393−F407.

Atay, Z., Bereket, A., Haliloglu, B., Abali, S., Ozdogan, T., Altuncu, E., Canaff, L., Vilaca, T., Wong, B.Y., Cole, D.E., Hendy, G.N., Turan, S., 2014. Novel homozygous inactivating mutation of the calcium-sensing receptor gene (CASR) in neonatal severe hyperparathyroidism-lack of effect of cinacalcet. Bone 64, 102−107.

Avioli, L.V., Berman, M., 1966. Mg28 kinetics in man. J. Appl. Physiol. 21 (6), 1688−1694.

Bardet, C., Courson, F., Wu, Y., Khaddam, M., Salmon, B., Ribes, S., Thumfart, J., Yamaguti, P.M., Rochefort, G.Y., Figueres, M.L., Breiderhoff, T., Garcia-Castano, A., Vallee, B., Le Denmat, D., Baroukh, B., Guilbert, T., Schmitt, A., Masse, J.M., Bazin, D., Lorenz, G., Morawietz, M., Hou, J., Carvalho-Lobato, P., Manzanares, M.C., Fricain, J.C., Talmud, D., Demontis, R., Neves, F., Zenaty, D., Berdal, A., Kiesow, A., Petzold, M., Menashi, S., Linglart, A., Acevedo, A.C., Vargas-Poussou, R., Muller, D., Houillier, P., Chaussain, C., 2016. Claudin-16 deficiency impairs tight junction function in ameloblasts, leading to abnormal enamel formation. J. Bone Miner. Res. 31 (3), 498−513.

Bettinelli, A., Bianchetti, M.G., Girardin, E., Caringella, A., Cecconi, M., Appiani, A.C., Pavanello, L., Gastaldi, R., Isimbaldi, C., Lama, G., et al., 1992. Use of calcium excretion values to distinguish two forms of primary renal tubular hypokalemic alkalosis: Bartter and Gitelman syndromes. J. Pediatr. 120 (1), 38−43.

Bianchetti, M.G., Kanaka, C., Ridolfi-Lüthy, A., Hirt, A., Wagner, H.P., Oetliker, O.H., 1991. Persisting renotubular sequelae after cisplatin in children and adolescents. Am. J. Nephrol. 11 (2), 127−130.

Blanchard, A., Jeunemaitre, X., Coudol, P., Dechaux, M., Froissart, M., May, A., Demontis, R., Fournier, A., Paillard, M., Houillier, P., 2001. Paracellin-1 is critical for magnesium and calcium reabsorption in the human thick ascending limb of Henle. Kidney Int. 59 (6), 2206−2215.

Blanchard, A., Bockenhauer, D., Bolignano, D., Calo, L.A., Cosyns, E., Devuyst, O., Ellison, D.H., Karet Frankl, F.E., Knoers, N.V., Konrad, M., Lin, S.H., Vargas-Poussou, R., 2017. Gitelman syndrome: consensus and guidance from a kidney disease: improving global outcomes (KDIGO) controversies conference. Kidney Int. 91 (1), 24−33.

Bockenhauer, D., Feather, S., Stanescu, H.C., Bandulik, S., Zdebik, A.A., Reichold, M., Tobin, J., Lieberer, E., Sterner, C., Landoure, G., Arora, R., Sirimanna, T., Thompson, D., Cross, J.H., van't Hoff, W., Al Masri, O., Tullus, K., Yeung, S., Anikster, Y., Klootwijk, E., Hubank, M., Dillon, M.J., Heitzmann, D., Arcos-Burgos, M., Knepper, M.A., Dobbie, A., Gahl, W.A., Warth, R., Sheridan, E., Kleta, R., 2009. Epilepsy, ataxia, sensorineural deafness, tubulopathy, and KCNJ10 mutations. N. Engl. J. Med. 360 (19), 1960−1970.

Bongers, E., Shelton, L.M., Milatz, S., Verkaart, S., Bech, A.P., Schoots, J., Cornelissen, E.A.M., Bleich, M., Hoenderop, J.G.J., Wetzels, J.F.M., Lugtenberg, D., Nijenhuis, T., 2017. A novel hypokalemic-alkalotic salt-losing tubulopathy in patients with CLDN10 mutations. J. Am. Soc. Nephrol. 28 (10), 3118−3128.

Boulikas, T., Vougiouka, M., 2004. Recent clinical trials using cisplatin, carboplatin and their combination chemotherapy drugs (review). Oncol. Rep. 11 (3), 559−595.

Breiderhoff, T., Himmerkus, N., Stuiver, M., Mutig, K., Will, C., Meij, I.C., Bachmann, S., Bleich, M., Willnow, T.E., Muller, D., 2012. Deletion of claudin-10 (Cldn10) in the thick ascending limb impairs paracellular sodium permeability and leads to hypermagnesemia and nephrocalcinosis. Proc. Natl. Acad. Sci. U.S.A. 109 (35), 14241−14246.

Breiderhoff, T., Himmerkus, N., Drewell, H., Plain, A., Gunzel, D., Mutig, K., Willnow, T.E., Muller, D., Bleich, M., 2018. Deletion of claudin-10 rescues claudin-16-deficient mice from hypomagnesemia and hypercalciuria. Kidney Int. 93 (3), 580−588.

Brown, E.M., 2013. Role of the calcium-sensing receptor in extracellular calcium homeostasis. Best Pract. Res. Clin. Endocrinol. Metabol. 27 (3), 333−343.

Brown, E.M., Pollak, M., Chou, Y.H., Seidman, C.E., Seidman, J.G., Hebert, S.C., 1995. Cloning and functional characterization of extracellular Ca(2+)-sensing receptors from parathyroid and kidney. Bone 17 (2 Suppl. l), 7S−11S.

Browne, D.L., Gancher, S.T., Nutt, J.G., Brunt, E.R., Smith, E.A., Kramer, P., Litt, M., 1994. Episodic ataxia/myokymia syndrome is associated with point mutations in the human potassium channel gene, KCNA1. Nat. Genet. 8 (2), 136−140.

Cairo, E.R., Friedrich, T., Swarts, H.G., Knoers, N.V., Bindels, R.J., Monnens, L.A., Willems, P.H., De Pont, J.J., Koenderink, J.B., 2008. Impaired routing of wild type FXYD2 after oligomerisation with FXYD2-G41R might explain the dominant nature of renal hypomagnesemia. Biochim. Biophys. Acta 1778 (2), 398−404.

Chubanov, V., Waldegger, S., Mederos y Schnitzler, M., Vitzthum, H., Sassen, M.C., Seyberth, H.W., Konrad, M., Gudermann, T., 2004. Disruption of TRPM6/TRPM7 complex formation by a mutation in the TRPM6 gene causes hypomagnesemia with secondary hypocalcemia. Proc. Natl. Acad. Sci. U.S.A. 101 (9), 2894−2899.

Cole, D.E., Janicic, N., Salisbury, S.R., Hendy, G.N., 1997. Neonatal severe hyperparathyroidism, secondary hyperparathyroidism, and familial hypocalciuric hypercalcemia: multiple different phenotypes associated with an inactivating Alu insertion mutation of the calcium-sensing receptor gene. Am. J. Med. Genet. 71 (2), 202−210.

Cruz, D.N., Shaer, A.J., Bia, M.J., Lifton, R.P., Simon, D.B., 2001. Gitelman's syndrome revisited: an evaluation of symptoms and health-related quality of life. Kidney Int. 59 (2), 710−717.

Cundy, T., Mackay, J., 2011. Proton pump inhibitors and severe hypomagnesaemia. Curr. Opin. Gastroenterol. 27 (2), 180−185.

Dai, L.J., Ritchie, G., Kerstan, D., Kang, H.S., Cole, D.E., Quamme, G.A., 2001. Magnesium transport in the renal distal convoluted tubule. Physiol. Rev. 81 (1), 51−84.

de Baaij, J.H., Stuiver, M., Meij, I.C., Lainez, S., Kopplin, K., Venselaar, H., Muller, D., Bindels, R.J., Hoenderop, J.G., 2012. Membrane topology and intracellular processing of cyclin M2 (CNNM2). J. Biol. Chem. 287 (17), 13644−13655.

de Baaij, J.H., Dorresteijn, E.M., Hennekam, E.A., Kamsteeg, E.J., Meijer, R., Dahan, K., Muller, M., van den Dorpel, M.A., Bindels, R.J., Hoenderop, J.G., Devuyst, O., Knoers, N.V., 2015a. Recurrent FXYD2 p.Gly41Arg mutation in patients with isolated dominant hypomagnesaemia. Nephrol. Dial. Transplant. 30 (6), 952−957.

de Baaij, J.H., Hoenderop, J.G., Bindels, R.J., 2015b. Magnesium in man: implications for health and disease. Physiol. Rev. 95 (1), 1−46.

Dimke, H., van der Wijst, J., Alexander, T.R., Meijer, I.M., Mulder, G.M., van Goor, H., Tejpar, S., Hoenderop, J.G., Bindels, R.J., 2010. Effects of the EGFR inhibitor erlotinib on magnesium handling. J. Am. Soc. Nephrol. 21 (8), 1309−1316.

Ea, H.K., Blanchard, A., Dougados, M., Roux, C., 2005. Chondrocalcinosis secondary to hypomagnesemia in Gitelman's syndrome. J. Rheumatol. 32 (9), 1840−1842.

Elin, R.J., 1994. Magnesium: the fifth but forgotten electrolyte. Am. J. Clin. Pathol. 102 (5), 616−622.

Elisaf, M., Panteli, K., Theodorou, J., Siamopoulos, K.C., 1997. Fractional excretion of magnesium in normal subjects and in patients with hypomagnesemia. Magnes. Res. 10 (4), 315−320.

Elliott, C., Newman, N., Madan, A., 2000. Gentamicin effects on urinary electrolyte excretion in healthy subjects. Clin. Pharmacol. Ther. 67 (1), 16−21.

English, M.W., Skinner, R., Pearson, A.D., Price, L., Wyllie, R., Craft, A.W., 1999. Dose-related nephrotoxicity of carboplatin in children. Br. J. Canc. 81 (2), 336−341.

Epstein, M., McGrath, S., Law, F., 2006. Proton-pump inhibitors and hypomagnesemic hypoparathyroidism. N. Engl. J. Med. 355 (17), 1834−1836.

Ferre, S., de Baaij, J.H., Ferreira, P., Germann, R., de Klerk, J.B., Lavrijsen, M., van Zeeland, F., Venselaar, H., Kluijtmans, L.A., Hoenderop, J.G., Bindels, R.J., 2014. Mutations in PCBD1 cause hypomagnesemia and renal magnesium wasting. J. Am. Soc. Nephrol. 25 (3), 574−586.

Foglia, P.E., Bettinelli, A., Tosetto, C., Cortesi, C., Crosazzo, L., Edefonti, A., Bianchetti, M.G., 2004. Cardiac work up in primary renal hypokalaemia-hypomagnesaemia (Gitelman syndrome). Nephrol. Dial. Transplant. 19 (6), 1398−1402.

Ford, E.S., Li, C., McGuire, L.C., Mokdad, A.H., Liu, S., 2007. Intake of dietary magnesium and the prevalence of the metabolic syndrome among U.S. adults. Obesity 15 (5), 1139−1146.

Freitag, J.J., Martin, K.J., Conrades, M.B., Bellorin-Font, E., Teitelbaum, S., Klahr, S., Slatopolsky, E., 1979. Evidence for skeletal resistance to parathyroid hormone in magnesium deficiency. Studies in isolated perfused bone. J. Clin. Investig. 64 (5), 1238−1244.

Funato, Y., Yamazaki, D., Miki, H., 2017. Renal function of cyclin M2 Mg2+ transporter maintains blood pressure. J. Hypertens. 35 (3), 585−592.

Gannon, A.W., Monk, H.M., Levine, M.A., 2014. Cinacalcet monotherapy in neonatal severe hyperparathyroidism: a case study and review. J. Clin. Endocrinol. Metab. 99 (1), 7−11.

Garner, S.C., Pi, M., Tu, Q., Quarles, L.D., 2001. Rickets in cation-sensing receptor-deficient mice: an unexpected skeletal phenotype. Endocrinology 142 (9), 3996−4005.

Geven, W.B., Monnens, L.A., Willems, H.L., Buijs, W.C., ter Haar, B.G., 1987. Renal magnesium wasting in two families with autosomal dominant inheritance. Kidney Int. 31 (5), 1140−1144.

Glaudemans, B., van der Wijst, J., Scola, R.H., Lorenzoni, P.J., Heister, A., van der Kemp, A.W., Knoers, N.V., Hoenderop, J.G., Bindels, R.J., 2009. A missense mutation in the Kv1.1 voltage-gated potassium channel-encoding gene KCNA1 is linked to human autosomal dominant hypomagnesemia. J. Clin. Investig. 119 (4), 936−942.

Goel, M., Garcia, R., Estacion, M., Schilling, W.P., 2001. Regulation of Drosophila TRPL channels by immunophilin FKBP59. J. Biol. Chem. 276 (42), 38762−38773.

Gong, Y., Renigunta, V., Himmerkus, N., Zhang, J., Renigunta, A., Bleich, M., Hou, J., 2012. Claudin-14 regulates renal Ca(+)(+) transport in response to CaSR signalling via a novel microRNA pathway. EMBO J. 31 (8), 1999−2012.

Gong, Y., Himmerkus, N., Plain, A., Bleich, M., Hou, J., 2015. Epigenetic regulation of microRNAs controlling CLDN14 expression as a mechanism for renal calcium handling. J. Am. Soc. Nephrol. 26 (3), 663−676.

Goren, M.P., 2003. Cisplatin nephrotoxicity affects magnesium and calcium metabolism. Med. Pediatr. Oncol. 41 (3), 186−189.

Grigoroiu-Serbanescu, M., Diaconu, C.C., Heilmann-Heimbach, S., Neagu, A.I., Becker, T., 2015. Association of age-of-onset groups with GWAS significant schizophrenia and bipolar disorder loci in Romanian bipolar I patients. Psychiatr. Res. 230 (3), 964−967.

Groenestege, W.M., Thébault, S., van der Wijst, J., van den Berg, D., Janssen, R., Tejpar, S., van den Heuvel, L.P., van Cutsem, E., Hoenderop, J.G., Knoers, N.V., Bindels, R.J., 2007. Impaired basolateral sorting of pro-EGF causes isolated recessive renal hypomagnesemia. J. Clin. Investig. 117 (8), 2260–2267.

Guerrero-Romero, F., Rodríguez-Morán, M., 2002. Low serum magnesium levels and metabolic syndrome. Acta Diabetol. 39 (4), 209–213.

Gullestad, L., Midtvedt, K., Dolva, L.O., Norseth, J., Kjekshus, J., 1994. The magnesium loading test: reference values in healthy subjects. Scand. J. Clin. Lab. Invest. 54 (1), 23–31.

Hadj-Rabia, S., Brideau, G., Al-Sarraj, Y., Maroun, R.C., Figueres, M.L., Leclerc-Mercier, S., Olinger, E., Baron, S., Chaussain, C., Nochy, D., Taha, R.Z., Knebelmann, B., Joshi, V., Curmi, P.A., Kambouris, M., Vargas-Poussou, R., Bodemer, C., Devuyst, O., Houillier, P., El-Shanti, H., 2018. Multiplex epithelium dysfunction due to CLDN10 mutation: the HELIX syndrome. Genet. Med. 20 (2), 190–201.

Hannan, F.M., Thakker, R.V., 2013. Calcium-sensing receptor (CaSR) mutations and disorders of calcium, electrolyte and water metabolism. Best Pract. Res. Clin. Endocrinol. Metabol. 27 (3), 359–371.

Hebert, S.C., Brown, E.M., 1995. The extracellular calcium receptor. Curr. Opin. Cell Biol. 7 (4), 484–492.

Hébert, P., Mehta, N., Wang, J., Hindmarsh, T., Jones, G., Cardinal, P., 1997. Functional magnesium deficiency in critically ill patients identified using a magnesium-loading test. Crit. Care Med. 25 (5), 749–755.

Heidet, L., Decramer, S., Pawtowski, A., Morinière, V., Bandin, F., Knebelmann, B., Lebre, A.S., Faguer, S., Guigonis, V., Antignac, C., Salomon, R., 2010. Spectrum of HNF1B mutations in a large cohort of patients who harbor renal diseases. Clin. J. Am. Soc. Nephrol. 5 (6), 1079–1090.

Ho, C., Conner, D.A., Pollak, M.R., Ladd, D.J., Kifor, O., Warren, H.B., Brown, E.M., Seidman, J.G., Seidman, C.E., 1995. A mouse model of human familial hypocalciuric hypercalcemia and neonatal severe hyperparathyroidism. Nat. Genet. 11 (4), 389–394.

Hoorn, E.J., Zietse, R., 2013. Disorders of calcium and magnesium balance: a physiology-based approach. Pediatr. Nephrol. 28 (8), 1195–1206.

Horikawa, Y., Iwasaki, N., Hara, M., Furuta, H., Hinokio, Y., Cockburn, B.N., Lindner, T., Yamagata, K., Ogata, M., Tomonaga, O., Kuroki, H., Kasahara, T., Iwamoto, Y., Bell, G.I., 1997. Mutation in hepatocyte nuclear factor-1 beta gene (TCF2) associated with MODY. Nat. Genet. 17 (4), 384–385.

Hou, J., Renigunta, A., Konrad, M., Gomes, A.S., Schneeberger, E.E., Paul, D.L., Waldegger, S., Goodenough, D.A., 2008. Claudin-16 and claudin-19 interact and form a cation-selective tight junction complex. J. Clin. Investig. 118 (2), 619–628.

Hou, J., Rajagopal, M., Yu, A.S., 2013. Claudins and the kidney. Annu. Rev. Physiol. 75, 479–501.

Houillier, P., 2013. Calcium-sensing in the kidney. Curr. Opin. Nephrol. Hypertens. 22 (5), 566–571.

Institutes of Medicine, 1997. Dietary Reference Intakes for Calcium, Phosphorus, Magnesium, Vitamin D, and Fluoride.

Isojima, T., Doi, K., Mitsui, J., Oda, Y., Tokuhiro, E., Yasoda, A., Yorifuji, T., Horikawa, R., Yoshimura, J., Ishiura, H., Morishita, S., Tsuji, S., Kitanaka, S., 2014. A recurrent de novo FAM111A mutation causes Kenny-Caffey syndrome type 2. J. Bone Miner. Res. 29 (4), 992–998.

Kerstan, D., Quamme, G., 2002. Physiology and pathophysiology of intestinal absorption of magnesium. In: Massry, S.G., M, H., Nishizawa, Y. (Eds.), Calcium in Internal Medicine. Springer-Verlag, Surry, UK, pp. 171–183.

Kieboom, B.C., Niemeijer, M.N., Leening, M.J., van den Berg, M.E., Franco, O.H., Deckers, J.W., Hofman, A., Zietse, R., Stricker, B.H., Hoorn, E.J., 2016. Serum magnesium and the risk of death from coronary heart disease and sudden cardiac death. J Am Heart Assoc 5 (1).

Kolisek, M., Nestler, A., Vormann, J., Schweigel-Rontgen, M., 2012. Human gene SLC41A1 encodes for the Na+/Mg(2)+ exchanger. Am. J. Physiol. Cell Physiol. 302 (1), C318–C326.

Konrad, M., Schaller, A., Seelow, D., Pandey, A.V., Waldegger, S., Lesslauer, A., Vitzthum, H., Suzuki, Y., Luk, J.M., Becker, C., Schlingmann, K.P., Schmid, M., Rodriguez-Soriano, J., Ariceta, G., Cano, F., Enriquez, R., Juppner, H., Bakkaloglu, S.A., Hediger, M.A., Gallati, S., Neuhauss, S.C., Nurnberg, P., Weber, S., 2006. Mutations in the tight-junction gene claudin 19 (CLDN19) are associated with renal magnesium wasting, renal failure, and severe ocular involvement. Am. J. Hum. Genet. 79 (5), 949–957.

Konrad, M., Hou, J., Weber, S., Dötsch, J., Kari, J.A., Seeman, T., Kuwertz-Bröking, E., Peco-Antic, A., Tasic, V., Dittrich, K., Alshaya, H.O., von Vigier, R.O., Gallati, S., Goodenough, D.A., Schaller, A., 2008. CLDN16 genotype predicts renal decline in familial hypomagnesemia with hypercalciuria and nephrocalcinosis. J. Am. Soc. Nephrol. 19 (1), 171–181.

Lajer, H., Daugaard, G., 1999. Cisplatin and hypomagnesemia. Cancer Treat Rev. 25 (1), 47–58.

Ledeganck, K.J., Boulet, G.A., Bogers, J.J., Verpooten, G.A., De Winter, B.Y., 2013. The TRPM6/EGF pathway is downregulated in a rat model of cisplatin nephrotoxicity. PLoS One 8 (2) e57016.

Ledeganck, K.J., De Winter, B.Y., Van den Driessche, A., Jurgens, A., Bosmans, J.L., Couttenye, M.M., Verpooten, G.A., 2014. Magnesium loss in cyclosporine-treated patients is related to renal epidermal growth factor downregulation. Nephrol. Dial. Transplant. 29 (5), 1097–1102.

Lee, C.T., Chen, H.C., Ng, H.Y., Lai, L.W., Lien, Y.H., 2012. Renal adaptation to gentamicin-induced mineral loss. Am. J. Nephrol. 35 (3), 279–286.

Liu, J., Lv, F., Sun, W., Tao, C., Ding, G., Karaplis, A., Brown, E., Goltzman, D., Miao, D., 2011. The abnormal phenotypes of cartilage and bone in calcium-sensing receptor deficient mice are dependent on the actions of calcium, phosphorus, and PTH. PLoS Genet. 7 (9) e1002294.

Lote, C.J., Thewles, A., Wood, J.A., Zafar, T., 2000. The hypomagnesaemic action of FK506: urinary excretion of magnesium and calcium and the role of parathyroid hormone. Clin. Sci. (Lond.) 99 (4), 285–292.

Lv, W.Q., Zhang, X., Zhang, Q., He, J.Y., Liu, H.M., Xia, X., Fan, K., Zhao, Q., Shi, X.Z., Zhang, W.D., Sun, C.Q., Deng, H.W., 2017. Novel common variants associated with body mass index and coronary artery disease detected using a pleiotropic cFDR method. J. Mol. Cell. Cardiol. 112, 1–7.

Maier, J.A., 2003. Low magnesium and atherosclerosis: an evidence-based link. Mol. Aspect. Med. 24 (1–3), 137–146.

Markmann, M., Rothman, R., Reichman, B., Hakes, T., Lewis, J.L., Rubin, S., Jones, W., Almadrones, L., Hoskins, W., 1991. Persistent hypomagnesemia following cisplatin chemotherapy in patients with ovarian cancer. J. Cancer Res. Clin. Oncol. 117 (2), 89–90.

Marx, S.J., Attie, M.F., Levine, M.A., Spiegel, A.M., Downs, R.W., Lasker, R.D., 1981. The hypocalciuric or benign variant of familial hypercalcemia: clinical and biochemical features in fifteen kindreds. Medicine (Baltim.) 60 (6), 397−412.

Mavichak, V., Coppin, C.M., Wong, N.L., Dirks, J.H., Walker, V., Sutton, R.A., 1988. Renal magnesium wasting and hypocalciuria in chronic cis-platinum nephropathy in man. Clin. Sci. (Lond.) 75 (2), 203−207.

Mayr, B., Schnabel, D., Dorr, H.G., Schofl, C., 2016. Genetics in endocrinology: gain and loss of function mutations of the calcium-sensing receptor and associated proteins: current treatment concepts. Eur. J. Endocrinol. 174 (5), R189−R208.

Meij, I.C., Koenderink, J.B., van Bokhoven, H., Assink, K.F., Groenestege, W.T., de Pont, J.J., Bindels, R.J., Monnens, L.A., van den Heuvel, L.P., Knoers, N.V., 2000. Dominant isolated renal magnesium loss is caused by misrouting of the Na(+), K(+)-ATPase gamma-subunit. Nat. Genet. 26 (3), 265−266.

Meij, I.C., Koenderink, J.B., De Jong, J.C., De Pont, J.J., Monnens, L.A., Van Den Heuvel, L.P., Knoers, N.V., 2003. Dominant isolated renal magnesium loss is caused by misrouting of the Na+,K+-ATPase gamma-subunit. Ann. N.Y. Acad. Sci. 986, 437−443.

Mervaala, E.M., Müller, D.N., Park, J.K., Schmidt, F., Löhn, M., Breu, V., Dragun, D., Ganten, D., Haller, H., Luft, F.C., 1999. Monocyte infiltration and adhesion molecules in a rat model of high human renin hypertension. Hypertension 33 (1 Pt 2), 389−395.

Meyer, T.E., Verwoert, G.C., Hwang, S.J., Glazer, N.L., Smith, A.V., van Rooij, F.J., Ehret, G.B., Boerwinkle, E., Felix, J.F., Leak, T.S., Harris, T.B., Yang, Q., Dehghan, A., Aspelund, T., Katz, R., Homuth, G., Kocher, T., Rettig, R., Ried, J.S., Gieger, C., Prucha, H., Pfeufer, A., Meitinger, T., Coresh, J., Hofman, A., Sarnak, M.J., Chen, Y.D., Uitterlinden, A.G., Chakravarti, A., Psaty, B.M., van Duijn, C.M., Kao, W.H., Witteman, J.C., Gudnason, V., Siscovick, D.S., Fox, C.S., Köttgen, A., Consortium, G. F. f. O., Consortium, M. A. o. G. a. I. R. T., 2010. Genome-wide association studies of serum magnesium, potassium, and sodium concentrations identify six Loci influencing serum magnesium levels. PLoS Genet. 6 (8).

Mihara, M., Kamikubo, K., Hiramatsu, K., Itaya, S., Ogawa, T., Sakata, S., 1995. Renal refractoriness to phosphaturic action of parathyroid hormone in a patient with hypomagnesemia. Intern. Med. 34 (7), 666−669.

Milatz, S., Himmerkus, N., Wulfmeyer, V.C., Drewell, H., Mutig, K., Hou, J., Breiderhoff, T., Muller, D., Fromm, M., Bleich, M., Gunzel, D., 2017. Mosaic expression of claudins in thick ascending limbs of Henle results in spatial separation of paracellular Na^{+} and Mg^{2+} transport. Proc. Natl. Acad. Sci. U.S.A. 114 (2), E219−e227.

Miura, K., Nakatani, T., Asai, T., Yamanaka, S., Tamada, S., Tashiro, K., Kim, S., Okamura, M., Iwao, H., 2002. Role of hypomagnesemia in chronic cyclosporine nephropathy. Transplantation 73 (3), 340−347.

Mori, S., Harada, S., Okazaki, R., Inoue, D., Matsumoto, T., Ogata, E., 1992. Hypomagnesemia with increased metabolism of parathyroid hormone and reduced responsiveness to calcitropic hormones. Intern. Med. 31 (6), 820−824.

Mosfegh, A., Goldman, J., Ahuja, J., Rhodes, D., LaComb, R., 2006. What We Eat in America, NHANES 2005−2006: Usual Nutrient Intakes from Food and Water Compared to 1997 Dietary Reference for Vitamin D, Calcium, Phosphorus, and Magnesium, p. 24.

Nadler, M.J., Hermosura, M.C., Inabe, K., Perraud, A.L., Zhu, Q., Stokes, A.J., Kurosaki, T., Kinet, J.P., Penner, R., Scharenberg, A.M., Fleig, A., 2001. LTRPC7 is a Mg.ATP-regulated divalent cation channel required for cell viability. Nature 411 (6837), 590−595.

Nicolet-Barousse, L., Blanchard, A., Roux, C., Pietri, L., Bloch-Faure, M., Kolta, S., Chappard, C., Geoffroy, V., Morieux, C., Jeunemaitre, X., Shull, G.E., Meneton, P., Paillard, M., Houillier, P., De Vernejoul, M.C., 2005. Inactivation of the Na-Cl co-transporter (NCC) gene is associated with high BMD through both renal and bone mechanisms: analysis of patients with Gitelman syndrome and Ncc null mice. J. Bone Miner. Res. 20 (5), 799−808.

Nijenhuis, T., Hoenderop, J.G., Bindels, R.J., 2004. Downregulation of Ca(2+) and Mg(2+) transport proteins in the kidney explains tacrolimus (FK506)-induced hypercalciuria and hypomagnesemia. J. Am. Soc. Nephrol. 15 (3), 549−557.

Nijenhuis, T., Vallon, V., van der Kemp, A.W., Loffing, J., Hoenderop, J.G., Bindels, R.J., 2005. Enhanced passive Ca^{2+} reabsorption and reduced Mg^{2+} channel abundance explains thiazide-induced hypocalciuria and hypomagnesemia. J. Clin. Investig. 115 (6), 1651−1658.

Paunier, L., Radde, I.C., Kooh, S.W., Conen, P.E., Fraser, D., 1968. Primary hypomagnesemia with secondary hypocalcemia in an infant. Pediatrics 41 (2), 385−402.

Pearce, S.H., Williamson, C., Kifor, O., Bai, M., Coulthard, M.G., Davies, M., Lewis-Barned, N., McCredie, D., Powell, H., Kendall-Taylor, P., Brown, E.M., Thakker, R.V., 1996. A familial syndrome of hypocalcemia with hypercalciuria due to mutations in the calcium-sensing receptor. N. Engl. J. Med. 335 (15), 1115−1122.

Pollak, M.R., Brown, E.M., Chou, Y.H., Hebert, S.C., Marx, S.J., Steinmann, B., Levi, T., Seidman, C.E., Seidman, J.G., 1993. Mutations in the human Ca(2+)-sensing receptor gene cause familial hypocalciuric hypercalcemia and neonatal severe hyperparathyroidism. Cell 75 (7), 1297−1303.

Pollak, M.R., Brown, E.M., Estep, H.L., McLaine, P.N., Kifor, O., Park, J., Hebert, S.C., Seidman, C.E., Seidman, J.G., 1994. Autosomal dominant hypocalcaemia caused by a Ca(2+)-sensing receptor gene mutation. Nat. Genet. 8 (3), 303−307.

Praga, M., Vara, J., González-Parra, E., Andrés, A., Alamo, C., Araque, A., Ortiz, A., Rodicio, J.L., 1995. Familial hypomagnesemia with hypercalciuria and nephrocalcinosis. Kidney Int. 47 (5), 1419−1425.

Quamme, G.A., 1997. Renal magnesium handling: new insights in understanding old problems. Kidney Int. 52 (5), 1180−1195.

Quamme, G.A., 2008. Recent developments in intestinal magnesium absorption. Curr. Opin. Gastroenterol. 24 (2), 230−235.

Quitterer, U., Hoffmann, M., Freichel, M., Lohse, M.J., 2001. Paradoxical block of parathormone secretion is mediated by increased activity of G alpha subunits. J. Biol. Chem. 276 (9), 6763−6769.

Reichold, M., Zdebik, A.A., Lieberer, E., Rapedius, M., Schmidt, K., Bandulik, S., Sterner, C., Tegtmeier, I., Penton, D., Baukrowitz, T., Hulton, S.A., Witzgall, R., Ben-Zeev, B., Howie, A.J., Kleta, R., Bockenhauer, D., Warth, R., 2010. KCNJ10 gene mutations causing EAST syndrome (epilepsy, ataxia, sensorineural deafness, and tubulopathy) disrupt channel function. Proc. Natl. Acad. Sci. U.S.A. 107 (32), 14490−14495.

Rob, P.M., Lebeau, A., Nobiling, R., Schmid, H., Bley, N., Dick, K., Weigelt, I., Rohwer, J., Gobel, Y., Sack, K., Classen, H.G., 1996. Magnesium metabolism: basic aspects and implications of ciclosporine toxicity in rats. Nephron 72 (1), 59–66.

Ryzen, E., Elbaum, N., Singer, F.R., Rude, R.K., 1985. Parenteral magnesium tolerance testing in the evaluation of magnesium deficiency. Magnesium 4 (2–3), 137–147.

Saito, Y., Okamoto, K., Kobayashi, M., Narumi, K., Yamada, T., Iseki, K., 2017. Magnesium attenuates cisplatin-induced nephrotoxicity by regulating the expression of renal transporters. Eur. J. Pharmacol. 811, 191–198.

Sato, T., Courbebaisse, M., Ide, N., Fan, Y., Hanai, J.I., Kaludjerovic, J., Densmore, M.J., Yuan, Q., Toka, H.R., Pollak, M.R., Hou, J., Lanske, B., 2017. Parathyroid hormone controls paracellular Ca(2+) transport in the thick ascending limb by regulating the tight-junction protein Claudin14. Proc. Natl. Acad. Sci. U.S.A. 114 (16), E3344–e3353.

Schimatschek, H.F., Rempis, R., 2001. Prevalence of hypomagnesemia in an unselected German population of 16,000 individuals. Magnes. Res. 14 (4), 283–290.

Schlingmann, K.P., Weber, S., Peters, M., Niemann Nejsum, L., Vitzthum, H., Klingel, K., Kratz, M., Haddad, E., Ristoff, E., Dinour, D., Syrrou, M., Nielsen, S., Sassen, M., Waldegger, S., Seyberth, H.W., Konrad, M., 2002. Hypomagnesemia with secondary hypocalcemia is caused by mutations in TRPM6, a new member of the TRPM gene family. Nat. Genet. 31 (2), 166–170.

Schmitz, C., Dorovkov, M.V., Zhao, X., Davenport, B.J., Ryazanov, A.G., Perraud, A.L., 2005. The channel kinases TRPM6 and TRPM7 are functionally nonredundant. J. Biol. Chem. 280 (45), 37763–37771.

Scholl, U.I., Choi, M., Liu, T., Ramaekers, V.T., Häusler, M.G., Grimmer, J., Tobe, S.W., Farhi, A., Nelson-Williams, C., Lifton, R.P., 2009. Seizures, sensorineural deafness, ataxia, mental retardation, and electrolyte imbalance (SeSAME syndrome) caused by mutations in KCNJ10. Proc. Natl. Acad. Sci. U.S.A. 106 (14), 5842–5847.

Seelig, M.S., 1964. The requirement of magnesium by the normal adult. summary and analysis of published data. Am. J. Clin. Nutr. 14, 242–290.

Shah, G.M., Kirschenbaum, M.A., 1991. Renal magnesium wasting associated with therapeutic agents. Miner. Electrolyte Metab. 17 (1), 58–64.

Shalev, H., Phillip, M., Galil, A., Carmi, R., Landau, D., 1998. Clinical presentation and outcome in primary familial hypomagnesaemia. Arch. Dis. Child. 78 (2), 127–130.

Simon, D.B., Nelson-Williams, C., Bia, M.J., Ellison, D., Karet, F.E., Molina, A.M., Vaara, I., Iwata, F., Cushner, H.M., Koolen, M., Gainza, F.J., Gitleman, H.J., Lifton, R.P., 1996. Gitelman's variant of Bartter's syndrome, inherited hypokalaemic alkalosis, is caused by mutations in the thiazide-sensitive Na-Cl cotransporter. Nat. Genet. 12 (1), 24–30.

Simon, D.B., Lu, Y., Choate, K.A., Velazquez, H., Al-Sabban, E., Praga, M., Casari, G., Bettinelli, A., Colussi, G., Rodriguez-Soriano, J., McCredie, D., Milford, D., Sanjad, S., Lifton, R.P., 1999. Paracellin-1, a renal tight junction protein required for paracellular Mg^{2+} resorption. Science 285 (5424), 103–106.

Singh, J., Patel, M.L., Gupta, K.K., Pandey, S., Dinkar, A., 2016. Acquired Bartter syndrome following gentamicin therapy. Indian J. Nephrol. 26 (6), 461–463.

Song, Y., Manson, J.E., Buring, J.E., Liu, S., 2004. Dietary magnesium intake in relation to plasma insulin levels and risk of type 2 diabetes in women. Diabetes Care 27 (1), 59–65.

Sontia, B., Touyz, R.M., 2007. Role of magnesium in hypertension. Arch. Biochem. Biophys. 458 (1), 33–39.

Sponder, G., Mastrototaro, L., Kurth, K., Merolle, L., Zhang, Z., Abdulhanan, N., Smorodchenko, A., Wolf, K., Fleig, A., Penner, R., Iotti, S., Aschenbach, J.R., Vormann, J., Kolisek, M., 2016. Human CNNM2 is not a Mg(2+) transporter per se. Pflügers Archiv 468 (7), 1223–1240.

Stuiver, M., Lainez, S., Will, C., Terryn, S., Günzel, D., Debaix, H., Sommer, K., Kopplin, K., Thumfart, J., Kampik, N.B., Querfeld, U., Willnow, T.E., Němec, V., Wagner, C.A., Hoenderop, J.G., Devuyst, O., Knoers, N.V., Bindels, R.J., Meij, I.C., Müller, D., 2011. CNNM2, encoding a basolateral protein required for renal Mg^{2+} handling, is mutated in dominant hypomagnesemia. Am. J. Hum. Genet. 88 (3), 333–343.

Sutton, R.A., Domrongkitchaiporn, S., 1993. Abnormal renal magnesium handling. Miner. Electrolyte Metab. 19 (4–5), 232–240.

Takeuchi, F., Isono, M., Katsuya, T., Yamamoto, K., Yokota, M., Sugiyama, T., Nabika, T., Fujioka, A., Ohnaka, K., Asano, H., Yamori, Y., Yamaguchi, S., Kobayashi, S., Takayanagi, R., Ogihara, T., Kato, N., 2010. Blood pressure and hypertension are associated with 7 loci in the Japanese population. Circulation 121 (21), 2302–2309.

Tang, N.L., Cran, Y.K., Hui, E., Woo, J., 2000. Application of urine magnesium/creatinine ratio as an indicator for insufficient magnesium intake. Clin. Biochem. 33 (8), 675–678.

Tang, R., Wei, Y., Li, Z., Chen, H., Miao, Q., Bian, Z., Zhang, H., Wang, Q., Wang, Z., Lian, M., Yang, F., Jiang, X., Yang, Y., Li, E., Seldin, M.F., Gershwin, M.E., Liao, W., Shi, Y., Ma, X., 2016. A common variant in CLDN14 is associated with primary biliary cirrhosis and bone mineral density. Sci. Rep. 6, 19877.

Tejpar, S., Piessevaux, H., Claes, K., Piront, P., Hoenderop, J.G., Verslype, C., Van Cutsem, E., 2007. Magnesium wasting associated with epidermal-growth-factor receptor-targeting antibodies in colorectal cancer: a prospective study. Lancet Oncol. 8 (5), 387–394.

Thebault, S., Alexander, R.T., Tiel Groenestege, W.M., Hoenderop, J.G., Bindels, R.J., 2009. EGF increases TRPM6 activity and surface expression. J. Am. Soc. Nephrol. 20 (1), 78–85.

Thorleifsson, G., Holm, H., Edvardsson, V., Walters, G.B., Styrkarsdottir, U., Gudbjartsson, D.F., Sulem, P., Halldorsson, B.V., de Vegt, F., d'Ancona, F.C., den Heijer, M., Franzson, L., Christiansen, C., Alexandersen, P., Rafnar, T., Kristjansson, K., Sigurdsson, G., Kiemeney, L.A., Bodvarsson, M., Indridason, O.S., Palsson, R., Kong, A., Thorsteinsdottir, U., Stefansson, K., 2009. Sequence variants in the CLDN14 gene associate with kidney stones and bone mineral density. Nat. Genet. 41 (8), 926–930.

Unger, S., Gorna, M.W., Le Bechec, A., Do Vale-Pereira, S., Bedeschi, M.F., Geiberger, S., Grigelioniene, G., Horemuzova, E., Lalatta, F., Lausch, E., Magnani, C., Nampoothiri, S., Nishimura, G., Petrella, D., Rojas-Ringeling, F., Utsunomiya, A., Zabel, B., Pradervand, S., Harshman, K., Campos-Xavier, B., Bonafe, L., Superti-Furga, G., Stevenson, B., Superti-Furga, A., 2013. FAM111A mutations result in hypoparathyroidism and impaired skeletal development. Am. J. Hum. Genet. 92 (6), 990−995.

Ure, M.E., Heydari, E., Pan, W., Ramesh, A., Rehman, S., Morgan, C., Pinsk, M., Erickson, R., Herrmann, J.M., Dimke, H., Cordat, E., Lemaire, M., Walter, M., Alexander, R.T., 2017. A variant in a cis-regulatory element enhances claudin-14 expression and is associated with pediatric-onset hypercalciuria and kidney stones. Hum. Mutat. 38 (6), 649−657.

van Angelen, A.A., Glaudemans, B., van der Kemp, A.W., Hoenderop, J.G., Bindels, R.J., 2013. Cisplatin-induced injury of the renal distal convoluted tubule is associated with hypomagnesaemia in mice. Nephrol. Dial. Transplant. 28 (4), 879−889.

Voets, T., Nilius, B., Hoefs, S., van der Kemp, A.W., Droogmans, G., Bindels, R.J., Hoenderop, J.G., 2004. TRPM6 forms the Mg^{2+} influx channel involved in intestinal and renal Mg^{2+} absorption. J. Biol. Chem. 279 (1), 19−25.

Walder, R.Y., Landau, D., Meyer, P., Shalev, H., Tsolia, M., Borochowitz, Z., Boettger, M.B., Beck, G.E., Englehardt, R.K., Carmi, R., Sheffield, V.C., 2002. Mutation of TRPM6 causes familial hypomagnesemia with secondary hypocalcemia. Nat. Genet. 31 (2), 171−174.

Waller, S., Kurzawinski, T., Spitz, L., Thakker, R., Cranston, T., Pearce, S., Cheetham, T., van't Hoff, W.G., 2004. Neonatal severe hyperparathyroidism: genotype/phenotype correlation and the use of pamidronate as rescue therapy. Eur. J. Pediatr. 163 (10), 589−594.

Ward, D.T., McLarnon, S.J., Riccardi, D., 2002. Aminoglycosides increase intracellular calcium levels and ERK activity in proximal tubular OK cells expressing the extracellular calcium-sensing receptor. J. Am. Soc. Nephrol. 13 (6), 1481−1489.

Watanabe, S., Fukumoto, S., Chang, H., Takeuchi, Y., Hasegawa, Y., Okazaki, R., Chikatsu, N., Fujita, T., 2002. Association between activating mutations of calcium-sensing receptor and Bartter's syndrome. Lancet 360 (9334), 692−694.

Weber, S., Schneider, L., Peters, M., Misselwitz, J., Rönnefarth, G., Böswald, M., Bonzel, K.E., Seeman, T., Suláková, T., Kuwertz-Bröking, E., Gregoric, A., Palcoux, J.B., Tasic, V., Manz, F., Schärer, K., Seyberth, H.W., Konrad, M., 2001. Novel paracellin-1 mutations in 25 families with familial hypomagnesemia with hypercalciuria and nephrocalcinosis. J. Am. Soc. Nephrol. 12 (9), 1872−1881.

William, J.H., Danziger, J., 2016. Proton-pump inhibitor-induced hypomagnesemia: current research and proposed mechanisms. World J. Nephrol. 5 (2), 152−157.

Wilson, F.H., Hariri, A., Farhi, A., Zhao, H., Petersen, K.F., Toka, H.R., Nelson-Williams, C., Raja, K.M., Kashgarian, M., Shulman, G.I., Scheinman, S.J., Lifton, R.P., 2004. A cluster of metabolic defects caused by mutation in a mitochondrial tRNA. Science 306 (5699), 1190−1194.

Yamaguti, P.M., Neves, F.A., Hotton, D., Bardet, C., de La Dure-Molla, M., Castro, L.C., Scher, M.D., Barbosa, M.E., Ditsch, C., Fricain, J.C., de La Faille, R., Figueres, M.L., Vargas-Poussou, R., Houillier, P., Chaussain, C., Babajko, S., Berdal, A., Acevedo, A.C., 2017. Amelogenesis imperfecta in familial hypomagnesaemia and hypercalciuria with nephrocalcinosis caused by CLDN19 gene mutations. J. Med. Genet. 54 (1), 26−37.

Zhang, L., Choi, H.J., Estrada, K., Leo, P.J., Li, J., Pei, Y.F., Zhang, Y., Lin, Y., Shen, H., Liu, Y.Z., Liu, Y., Zhao, Y., Zhang, J.G., Tian, Q., Wang, Y.P., Han, Y., Ran, S., Hai, R., Zhu, X.Z., Wu, S., Yan, H., Liu, X., Yang, T.L., Guo, Y., Zhang, F., Guo, Y.F., Chen, Y., Chen, X., Tan, L., Deng, F.Y., Deng, H., Rivadeneira, F., Duncan, E.L., Lee, J.Y., Han, B.G., Cho, N.H., Nicholson, G.C., McCloskey, E., Eastell, R., Prince, R.L., Eisman, J.A., Jones, G., Reid, I.R., Sambrook, P.N., Dennison, E.M., Danoy, P., Yerges-Armstrong, L.M., Streeten, E.A., Hu, T., Xiang, S., Papasian, C.J., Brown, M.A., Shin, C.S., Uitterlinden, A.G., Deng, H.W., 2014. Multistage genome-wide association meta-analyses identified two new loci for bone mineral density. Hum. Mol. Genet. 23 (7), 1923−1933.

Chapter 22

Metal ion toxicity in the skeleton: lead and aluminum

J. Edward Puzas[1] and Brendan F. Boyce[2]

[1]*Department of Orthopaedics and Rehabilitation, University of Rochester School of Medicine and Dentistry, Rochester, NY, United States;*

[2]*Department of Pathology and Laboratory Medicine, University of Rochester School of Medicine and Dentistry, Rochester, NY, United States*

Chapter outline

Introduction

The skeleton is unique organ system that serves human physiology in many ways. Some of its key functions include mechanical support, protection of vital soft tissue organs, and serving as a reservoir for key minerals such as calcium, phosphorus, protons, and carbonate. The mineral phase of bone is predominantly a crystalline form of hydroxyapatite with the formula $Ca_{10}(PO_4)_6(OH)_2$. However, in actuality, in humans there is extensive substitution of the hydroxyl groups (OH^-) with anions such as fluoride, chloride, and carbonate. About 60% of the volume of bone resides in the mineral phase with about 40% in the organic matrix. And with the skeleton making up about 15% of the total body weight of an average human being, bone can be a very large storage compartment for osseous-seeking elements.

In addition, and with more relevance to this discussion, there can be extensive accumulation of toxic elements that replace calcium in the crystalline structure. These forms of apatite are referred to as "calcium-deficient hydroxyapatites." Approximately 60 cations and anions have been identified as osteotropic elements with avid bone-seeking affinities. About 20 are present in higher quantities with the rest existing in trace amounts. This affinity of charged molecules for hydroxyapatites is a common characteristic of a material with a high charge density. In fact, in the case of hydroxyapatite, its ionic properties have been exploited as a scaffold for the chromatographic partitioning of complex molecules. Thus, it is easy to understand that extending this physical chemistry to the mineral phases in the skeleton provides a large and avid reservoir for an array of molecules and ions.

Research into bone-seeking toxic elements

Surprisingly, it was during the era of the development of the atomic bomb in 1942 that the study of how heavy metals affected bone and other human tissues began in earnest. Literally dozens of elemental by-products were produced by an atomic explosion, but little to nothing was known about how they affected human tissues. The United States dealt with this problem with the launch of a large and sophisticated project known as the Manhattan Project. The project had two major

Principles of Bone Biology. https://doi.org/10.1016/B978-0-12-814841-9.00022-1

scientific directions. The first was centered in the physics laboratories studying the development of the bomb that was carried out in secret atomic energy facilities in Oak Ridge, Tennessee; Los Alamos, New Mexico; and Hanford, Washington. The second direction was devoted to studying how radioactive elements were harbored by specific organs and how they affected tissue function. And as expected, the properties of the skeleton provided a large and high-affinity reservoir for bone-seeking metals such as polonium, plutonium, uranium, thorium, radium, cadmium, cobalt, aluminum, and lead. These investigations were carried out in Rochester, New York, and were the impetus for the growth and development of a world-renowned bone research group in the following decades. The program in Rochester morphed into an Atomic Energy Commission−supported facility in 1947.

After World War II and with the expansion in manufacturing, most of the heavy metal toxins entering the environment were from industrial pollution (Jaishankar, 2014; Nagajyoti, 2010). Heavy metals in wastewater originated from natural sources, soil erosion, natural weathering, and, most importantly, human activities such as mining, industrial effluents, and farming control agents (Morais, 2012).

The most common metals that affect the skeleton are lead and aluminum. Both of these toxic elements contribute to well-recognized bone diseases. The exposure source for lead is generally known to be from the environment and for aluminum is known to be from the environment as well as inadvertent human dosing during clinical procedures such as renal dialysis. Other environmental trace elements that have been identified in bone include cadmium, mercury, and iron, in addition to elements such as cobalt entering humans through injudicious clinical use of orthopedic implants containing mixed metal alloys (Rebolledo, 2011).

Of the key elements that seek the hydroxyapatite of bone, two have been identified as the agents responsible for most of the toxicological pathologies. They are lead and aluminum, with lead being identified as the most dangerous to skeletal metabolism at the present time.

Lead

Much is known regarding the toxicity of lead in neural, renal, and hematopoietic development (reviewed in Wani et al., 2015). Its effects are uniformly devastating to the normal physiology of not only these well-studied tissues but virtually every organ system in the body. However, what has been underappreciated since the 1970's is that bone is also a key target for lead toxicity. This is due to two important features related to how lead interacts with the skeleton; they are the sequestering of lead in bone and the slow turnover and long half-life of lead in the mineral phase of bone.

Virtually all of the lead (94%−97%) in adult humans resides in the skeleton, with the remaining sites being (in order of content) red blood cells, liver, skeletal muscle, skin, kidney, lung, and brain (and other soft tissues) (Barry, 1975). The half-life of lead in bodily tissues is known. It is approximately 1 month in blood, approximately 2 months in soft tissues, and 25−30 years in bone (ATSDR, 2007).

Consider the implications of these facts. Essentially any individual who has been exposed to lead either from the environment or from occupational sources will carry a significant portion of that burden for his or her entire lifetime. In fact, once a person is no longer exposed to a lead source, blood and soft tissue levels may decline to low levels, but skeletal lead can remain unacceptably high and continue to adversely affect cells in the bone compartment.

The reason the skeletal half-life for lead is so long is due to two key properties of bone. First, lead is incorporated into the crystal lattice structure of hydroxyapatite by displacing calcium ions. Its affinity for the mineral phases of bone is very high, such that when lead ions are mobilized through bone resorption, they can redistribute to other mineral sites and not leave the bone compartment. Second, skeletal turnover in humans is slow. Estimates indicate that the entire skeleton turns over at a rate of approximately 10% per year, with cortical bone averaging 4% per year and trabecular bone averaging 28% per year (Manolagas, 2000). Thus, there is little opportunity to decrease the level of lead in osseous tissues through normal metabolism. Also, as might be expected, the accumulation and release of lead levels in cortical and trabecular bone follow the general metabolic activity of their particular compartments. That is, (1) acute lead exposure will lead to a more rapid rise in trabecular bone than cortical bone and (2) lead release from the skeleton will occur first from trabecular bone and later from cortical bone.

Another feature of the long half-life of lead in bone is that the skeleton can continue to dose the blood and soft tissues throughout life. That is, in low-skeletal-turnover states lead remains in the bone compartment, but in high-turnover states it is released into the circulation. This accounts for the long-standing finding that blood lead levels rise in all females during and after the menopause due to enhanced skeletal turnover upon the loss of estrogen (Silbergeld et al., 1988; Potula, 2006). In fact, any acceleration in skeletal turnover (i.e., calcium deficiency, fracture, hyperparathyroidism, pregnancy, lactation, etc.) will lead to elevated blood lead levels (ATSDR, 2007).

Measurement of lead in bone

The measurement of lead levels in a human skeleton can be performed either with invasive or with noninvasive techniques. Invasive measurements are, as one might expect, limited to situations in which an actual sample of bone can be obtained from a living subject undergoing surgery or from a cadaveric specimen. The "pros" to using a specimen of bone are (1) the quantification methods (using atomic absorption spectrometry or mass spectrometry) are highly accurate and (2) different compartments of bone (i.e., cortical vs. trabecular) can be measured separately. The "cons" to using specimens of bone are the invasiveness of the specimen procurement and the unfeasibility of making longitudinal measurements in any one person.

Interestingly, it is possible to measure lead levels in the skeleton in a noninvasive, safe way utilizing an X-ray fluorescence technique. This method was first described in 1976 by Ahlgren et al. (Ahlgren, 1976) and later perfected by the physicists at McMaster University, Hamilton, Ontario (Chettle, 1991).

The principle behind this method depends on the use of an exciting isotope (^{109}Cd) and a sensitive X-ray detection system. ^{109}Cd emits characteristic energies of gamma rays that when directed toward a bone (close to the surface of the skin) can excite an inner shell (i.e., K-shell) electron in lead atoms. Upon deexcitation of the activated lead atom, specific and characteristic X-rays are emitted and detected by the detection sensors. The magnitude of this fluorescence decay is proportional to the number of lead atoms activated by the ^{109}Cd. The system is calibrated with lead-doped samples and after the appropriate calculations are made, a value of micrograms of lead/gram of bone can be made. The "pros" for this method are that (1) it is noninvasive, (2) longitudinal measurements can be made in a single subject, and (3) the radiation dose is extremely low, with little safety concern. The "cons" are (1) accuracy of the measurements in bones with a low lead content is low, (2) the subject must remain in the scanner for 30–45 min for one measurement, and (3) there are no commercially available systems; each system must be constructed from specialty equipment. Nevertheless, the ability to make noninvasive measurements led to a flurry of activity in the 1990s using K-shell X-ray fluorescence to measure many different cohorts of people (reviewed in Hu, 1998).

Lead as an unrecognized risk factor in osteoporosis

An unexpected technical discrepancy in measuring bone mineral density (BMD) by dual-energy X-ray absorptiometry (DXA) prevented clinicians and investigators from recognizing that lead exposure could cause osteopenia and contribute to the genesis of osteoporosis. This technical anomaly occurred in the early years when first-generation DXA scanners were first being used in the diagnosis of osteoporosis. It appears that the presence of lead in bone created an artifactually elevated estimate of bone density. The reason for this is not entirely clear but might be related to the very high atomic mass of lead. Reports in the literature bore out this finding. Escribano and colleagues (1997) showed in an animal study that lead exposure in rats led to a marked decrease in the histomorphometric parameters of trabecular bone volume, number, and thickness. But when these same animals were evaluated with early models of densitometers (i.e., dual-photon absorptiometers) the rat bones showed significant elevations in bone density.

A qualitatively similar result was described by Laraque et al. (1990). In this report, the investigators showed that children with elevated blood lead levels showed a significantly higher bone mineral content (BMC) than a control cohort available at that time. The BMC measurements were made with a single-photon absorptiometer.

To definitively document these discrepancies, it would be best to make a direct comparison of bone density using both the older and the newer-generation technologies. Fortuitously, while upgrading densitometers, our research group had the opportunity to perform a direct comparison between a pencil-beam dual-photon absorptiometer (Lunar DPX-L) and a fan-beam dual X-ray absorptiometer (Lunar Prodigy). In this experiment, bovine bone was doped with known trace amounts of lead and then measured in both scanners. The (unpublished) data are shown in Fig. 22.1. The addition of "micrograms" of lead to "grams" of bone (i.e., parts per million) should not have changed the total mass of the bone sample to any measurable degree. Yet, the DPX-L scanner showed a clear increase in BMD with added lead. If this measurement were being made in a human it would have increased the patient's T score by 0.5–1.0 standard deviations. The Prodigy scanner was also affected by lead in the sample; however, the effect was not evident until a level near 1000 μg Pb/g bone was reached. A level of 1000 μg Pb/g bone is at least 100 times what an exposed human would be expected to have and has never been reported. Discrepancies in the detection and calculations for BMD between dual-photon scanners and dual-X-ray scanners have been documented in the literature (Huffman, 2005).

Two important points can be derived from these observations. First, many years ago lead exposure and its sequestration in the skeleton probably was overlooked as a risk factor for low bone density and osteoporosis. This was due to the apparent interference by lead in the photon-based methods used in bone densitometers. Second, new-generation scanners

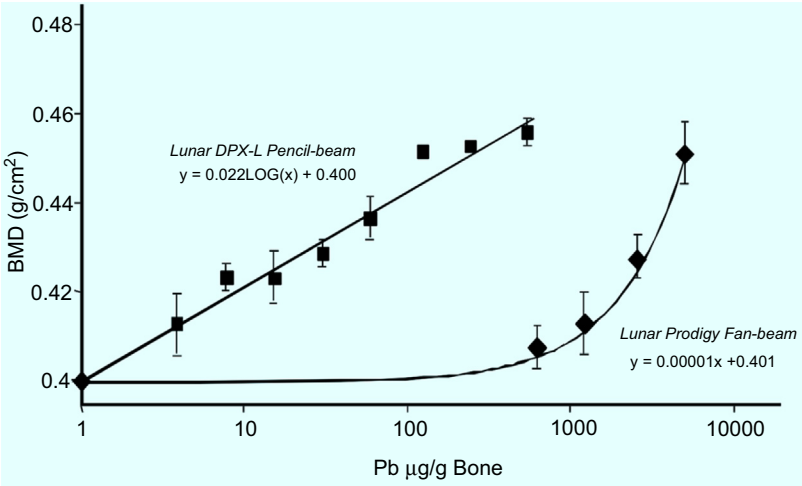

FIGURE 22.1 Bone densitometry in specimens containing measured amounts of lead. Two grams of pulverized bovine bone containing graded amounts of lead salts was scanned with a Lunar Dual-Photon DPX-L densitometer or a GE/Lunar Dual-Energy X-ray absorptiometer. The bone specimens were contained in tissue culture wells (area = 2.0 cm^2). The data are presented as areal density, i.e., "grams of mineralized bone/cm^2 versus micrograms of elemental lead per gram of bone." The bovine bone specimens were not incubated to dryness prior to making the measurements and thus their "weight percent" was approximately 40% mineral and 60% organic matrix + water. Lead (in the parts per million range) affected the bone mineral density (*BMD*) measurement at as little as 5.0 µg/g bone when scanned with the dual-photon densitometer. The dual-energy X-ray densitometer did not detect the added lead until the levels reached supratoxicological levels (approximately 1000 µg/g bone).

with the different mechanisms for generating X-rays and with different calculation algorithms do not appear to be affected by skeletal lead in the range seen in the human population.

How does lead cause low bone density?

In an adult skeleton, bone mass is controlled through regulation of bone-forming activities (by osteoblasts) and bone-resorbing activities (by osteoclasts). When these two cellular processes are in balance with each other, bone mass is maintained at a healthy, steady-state level. However, when these two processes are no longer balanced bone mass can be pathologically increased (i.e., osteopetrosis) or, more commonly, pathologically decreased (i.e., osteoporosis). The skeleton maintains an exquisite series of check and balances to prevent large swings in bone mass. This was recognized many years ago when Harris and Heaney described the kinetically coupled activities of bone-forming and bone-resorbing cells (Harris, 1969). Thus, for an agent such as lead to alter bone mass, it must disrupt the balance between osteoblastic and osteoclastic cellular activities. The question that arises is, which process is the target of lead toxicity in the skeleton?

Given the observation that lead can be easily mobilized in high-turnover states in the skeleton (as mentioned earlier) and that basic science investigations do not show any major effects on osteoclastic bone resorption (Carmouche, 2005), it seems that the important cellular target for lead toxicity is the osteoblast.

Osteoblasts and their progenitor cells residing in the bone compartment can be exposed to locally high concentrations of lead. Assuming conservative values of the lead content of the skeleton (i.e., 5 µg/g bone), the amount of bone resorbed by an osteoclast (i.e., 1 µg), and the diffusion of lead into a radius of 100 µm around a lacuna, an approximate estimate of the lead concentration at a remodeling site can be on the order of 1−10 µM. From basic science investigations, this concentration of lead is sufficient to have profound inhibitory effects on osteoblast function (Beier et al., 2015).

As expected, the in vitro effects of lead manifest themselves in whole-animal models as a decrease in bone quantity and bone quality. Exposing mice (which happen to be an excellent model for lead-induced bone loss) to lead in their drinking water will induce an osteoporotic-like phenotype (Beier et al., 2013). By altering the concentration of lead acetate in the animals' drinking water it is possible to achieve virtually any relevant concentration of the metal ion in blood and bone in 3−6 weeks (Carmouche, 2005; Beier et al., 2013). Interestingly, animals display no difficulty in drinking the water, as the addition of lead confers a pleasant sweet taste. (Unfortunately, this also occurs in human infants around lead-contaminated

materials.) After 6 weeks of exposure at 55 ppm lead in water, micro-computed tomographic and histological analyses demonstrate significant changes. They are:

- decrease in skeletal bone volume/total volume
- decrease in volumetric BMD
- decrease in trabecular number
- increase in trabecular separation
- decrease in bone apposition rate
- no change in osteoclast number

The β-catenin/sclerostin axis: is it the mechanism for lead toxicity in osteoblasts?

The *SOST* gene encodes a protein known as sclerostin. The gene is located on chromosome 17q12−q21. Osteocytes were one of the first cells shown to express sclerostin; however, it now appears that the cells from at least four tissues can produce this molecule. They include uterus, kidney, tissues of tooth development, and, most importantly, osteoblasts (Maeda, 2007; Blish, 2008; Murashima-Suginami, 2008; Tanaka, 2008; Rutger, 2005). Sclerostin is a very potent inhibitor of bone formation. It represses osteoblast function and number and can induce apoptotic pathways in these cells. The mechanism of action of sclerostin appears to occur through the Wnt/β-catenin pathway. Data suggest that sclerostin binds to low-density lipoprotein receptor−related protein 5/6, preventing association with the Wnt receptor, Frizzled. This interference blocks Wnt binding and depresses osteoblastic bone formation (van Bezooijen, 2004; Li, 2005).

What is most remarkable regarding this intracellular pathway is that when osteoblasts are exposed to lead there is a manifold upregulation of both the mRNA and the protein for sclerostin (Beier et al., 2015). This stimulation is observed in vitro (with qPCR and western blot assays) and in vivo (with immunohistochemical quantification). Thus, it is likely that during remodeling of lead-containing bone, excess sclerostin expression uncouples osteoblastic bone formation from resorption and an inadequate amount of new bone is deposited. Over many remodeling cycles this would lead to a decrease in skeletal mass.

Mechanism of action of lead: stimulation of sclerostin expression

How can a heavy metal divalent cation specifically affect a key gene in osteoblasts? This is a question that is not yet fully answered; however, the work of Beier (Beier et al. 2013, 2014, 2015) and Holz (Holz, 2012) provides some clues. Lead ion is known to interact with a number of kinase enzymes that utilize ATPase reactions to drive phosphorylation (protein kinase C, calmodulin, Na/K-ATPase, Ca-ATPase) (Flora et al, 2008; Murakami, 1993; Kramer, 1986). One of these kinases is the type 2 transforming growth factor β (TGFβ) receptor, responsible for the phosphorylation of Smad3, and thus it would be expected that lead can block Smad3 reporter activity, decrease phospho-Smad3 intracellular protein levels, and prevent phosphorylation of Smad3 in a cell-free system (Beier et al., 2015). The relevance of these observations lies in the fact that through TGFβ/Smad3 signaling, gene expression of sclerostin is repressed (Beier et al., 2015) and thus, any mechanism that interferes with phospho-Smad3 formation would derepress *SOST* gene activation and stimulate sclerostin levels. A diagrammatic representation of this regulatory pathway is presented in Fig. 22.2.

A clinical opportunity

From a clinical perspective, it may be possible to directly treat lead-induced osteoporosis with a pharmaceutical agent that was recommended in January 2019 for approval by the US FDA Advisory Panel (AMG 785, romosozumab). This humanized blocking antibody inhibits sclerostin activity. If the effect of lead in humans is mediated, even in small part, by upregulation of sclerostin, then this therapeutic agent could be extremely effective in treating the low bone mass. This is a real possibility given that romosozumab has shown very promising results in stimulating bone formation in a large phase III clinical trial (i.e., the ARCH study, Saag, 2017).

Aluminum

Aluminum (Al) toxicity-induced osteomalacia was a common complication of hemodialysis for some patients with chronic renal failure in the 1970s and 1980s, until it was discovered that high levels of aluminum in the tap water used to make the dialysis fluid was the main cause. High serum Al levels (100−800 μg/L vs. normal values of <35 μg/L) from the contaminated water resulted in so-called "dialysis" dementia as well as osteomalacia and microcytic anemia (Alfrey, 1976;

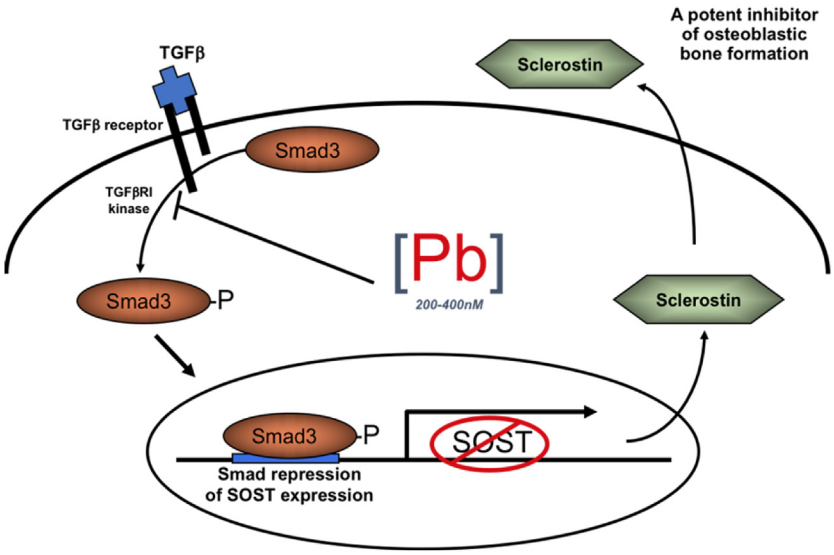

FIGURE 22.2 Intracellular mechanism by which lead induces sclerostin synthesis. Lead, in the 200−400 nM range, can block the phosphorylation of Smad3. Under normal conditions phospho-Smad3 resides in the nucleus and binds to a DNA-response element that represses *SOST* gene expression and sclerostin synthesis. However, in the presence of lead phospho-Smad3 levels are decreased and *SOST* gene activation is "derepressed," evoking a large increase in sclerostin production. *TGFβ*, transforming growth factor β.

Parkinson, 1979; Ellis, 1979; Boyce, 1982), and most patients with this dementia died of it before the cause was discovered. Aluminum is the most common metal in the earth's crust and it can be leached from surface rocks by rain, particularly acid rain (Krewski, 2007). This leaching can lead to high Al levels occurring naturally in water in some reservoirs. Thus, depending upon local conditions, levels of Al in the tap water used in dialysis units or for home dialysis can vary significantly around the world, from <30 μg/L (normal and acceptable) to ~100 μg/L (Boyce, 1982) or >200 μg/L (Krewski, 2007), which is the upper limit of the US Environmental Protection Agency's secondary maximum contaminant level for total Al in water and above which water becomes colored (Willhite, 2012).

Importantly, however, the highest levels of Al were found in water from reservoirs to which Al had been added by water authorities in the form of aluminum sulfate to cause aggregation (flocculation) and subsequent precipitation of suspended particles that discolored the water (Krewski, 2007). This fulfilled legal mandates that tap water must be clear, but it led to Al levels in water from some reservoirs being >1000 μg/L (Boyce, 1982). The Al passed directly from the dialysis fluid into patients' bloodstreams, resulting in cumulative toxicity with each dialysis, typically three per week, because Al is excreted normally by the kidneys, and the lack of renal function in dialysis patients compounded the damage (Alfrey, 1980).

After the cause of the dementia and osteomalacia was identified, Al was removed from contaminated tap water by passing it through reverse osmosis and/or deionization units before being used for dialysis. However, this did not prevent recurrence of the toxicity in all cases until it was fully appreciated that these units needed to be serviced regularly and that Al levels had to be measured in the water flowing from them to confirm that they were working efficiently. This is particularly necessary in home dialysis settings in towns where Al levels are very high as a result of the addition of aluminum sulfate and where monitoring of water Al levels in each home is the responsibility of local authorities.

The identification of aluminum toxicity as a cause of dementia then led to studies to determine if lifelong exposure to aluminum in drinking water and from other sources could be a cause of Alzheimer's disease. Some studies reported Al deposits in brains of Alzheimer's patients (Crapper, 1973; Perl, 1980) and these reports led to numerous epidemiologic studies. Although Al concentrations increase in brain and bone (Hellstrom, 2005) with age in humans, other investigators did not confirm these findings in neuritic plaques in brains from Alzheimer's patients (Landsberg, 1992). Nevertheless, improvement in cognitive function has been reported in some Alzheimer's patients given treatment to reduce blood and tissue levels of aluminum, supporting the "aluminum/dementia hypothesis" (Davenward, 2013). Overall, however, a potential causative role for Al in the pathogenesis of Alzheimer's disease remains controversial (Exley, 2014).

Aluminum toxicity can also occur as a consequence of ingestion of aluminum-containing phosphate-binding drugs given to patients with chronic renal failure to help reduce absorption of phosphate from the intestinal tract (Kaehny et al., 1977a). Serum phosphate levels are high in these patients because they are unable to excrete phosphate through their

dysfunctional kidneys. Initially, it was thought that aluminum in phosphate binders, such as aluminum hydroxide, was not absorbed from the gastrointestinal tract. However, this was proven to be wrong by the finding of high serum aluminum levels not only in patients with renal failure not yet on dialysis, but also in individuals with normal renal function taking large quantities of aluminum hydroxide as an antacid for indigestion (Kaehny et al., 1977a). Aluminum absorption from the gut is enhanced by acidic fruits, such as oranges and lemons, and orange juice. Aluminum can be leached from aluminum cooking pots and wrapping foil and this can lead to high Al concentrations, for example, in the juice from chickens wrapped and cooked in aluminum foil along with lemons (Krewski, 2007).

Lead, cadmium, and arsenic can also leach out of cooking utensils during food preparation, which may be a more pressing contemporary issue in developing countries (Weidenhamer, 2017). Aluminum was also found to be a contaminant of casein hydrolysate used as the amino acid source in some intravenous preparations for patients receiving total parenteral nutrition in the 1980s (Klein, 1982), with some patients being reported to receive 2−3 mg Al/day (Kaehny et al., 1977b). Aluminum was also found in some albumin solutions used to expand the intravascular volume in patients with acute hypovolemic states and as the replacement fluid used during plasma exchange (Maharaj, 1987). These problems have largely been solved by removal of Al from medical fluids given to patients.

Patients with end-stage chronic renal failure typically develop hypocalcemia as a consequence of inadequate phosphate excretion and calcium reabsorption in their damaged kidneys, coupled with their inability to 1-hydroxylate 25(OH) vitamin D_3 because their renal tubular cells become deficient in 1α-hydroxylase (Goodman, 2008). Consequently, they develop secondary hyperparathyroidism with associated increased bone remodeling, which can be accompanied by vitamin D deficiency-related osteomalacia unless they are given appropriate treatment to prevent these (Sherrad, 1993). These treatments include dietary phosphate restriction, phosphate binders, calcimimetics, calcitriol, or vitamin D analogs, or a combination of calcimimetics with calcitriol or vitamin D analogs, and addition of calcium to dialysis fluid (KDIGO, 2017; Jamai, 2013; Cocchiara, 2017; Vestergaard, 2011). If patients are exposed to sufficiently high levels of Al, mineralization will be inhibited because the aluminum gets deposited along the mineralization front between osteoid and calcified matrix where it prevents calcification and leads to osteomalacia (Ellis, 1979; Boyce, 1981, 1982, 1992). Al-related osteomalacia became recognized as an entity distinct from vitamin D deficiency-related osteomalacia because of its association with dementia, microcytic anemia, myopathy, fractures, and a tendency to develop hypercalcemia (Boyce, 1982). These were accompanied by a characteristic focal distribution of thickened osteoid seams on trabecular surfaces (Fig. 22.3) (Boyce, 1982) compared with the typical extensive distribution of thickened osteoid seams in vitamin D deficiency-related osteomalacia (Fig. 22.4). The fact that osteoid seams were much thicker than those seen in biopsy specimens from patients with secondary hyperparathyroidism and osteoid seams of normal thickness indicates that aluminum does not inhibit the formation and deposition of osteoid matrix by osteoblasts in vivo in many patients. Some studies have reported aluminum staining along osteoid surfaces associated with normal osteoid thickness in addition to reduced bone formation rates and osteoblast surfaces, suggesting that aluminum may inhibit mineralization and bone formation in some patients

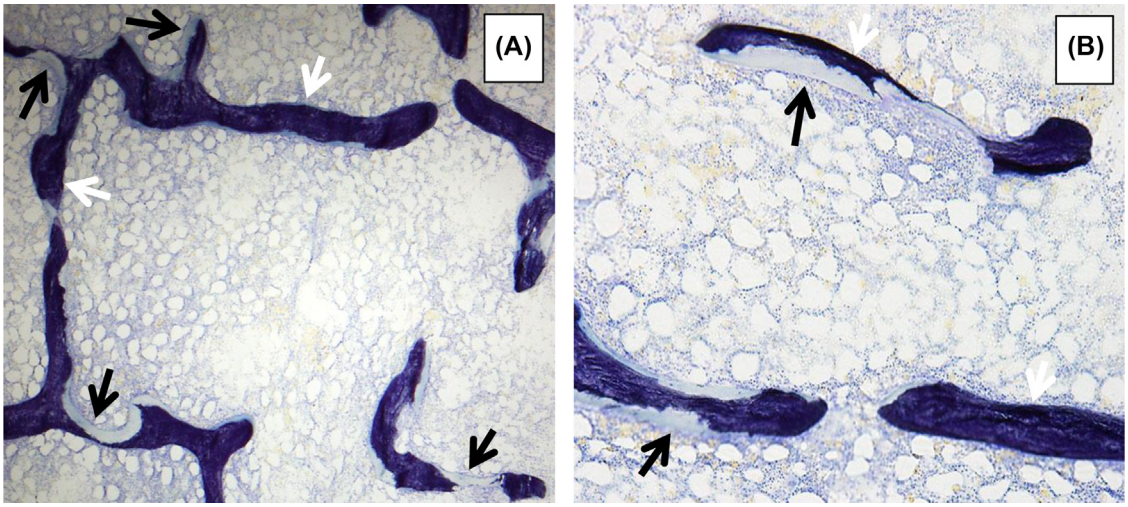

FIGURE 22.3 Undecalcified sections of an iliac crest bone biopsy specimen from a dialysis patient with chronic renal failure and aluminum-induced osteomalacia. Note the characteristic focal distribution of thickened osteoid seams (*black arrows*) on the trabecular surfaces, much of which is fully calcified (*white arrows*). Toluidine blue staining. (A) ×4 original magnification, (B) ×10 original magnification.

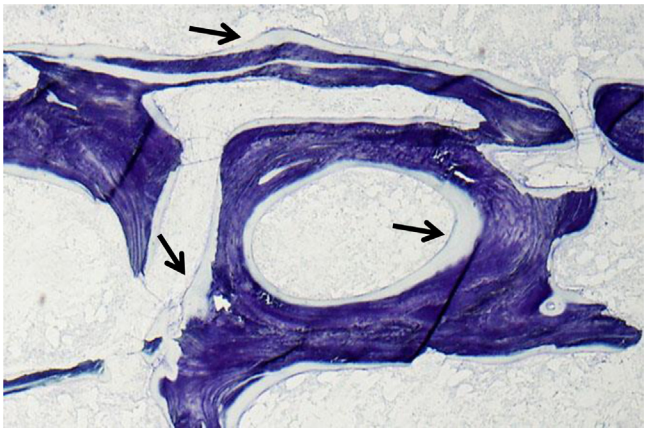

FIGURE 22.4 Undecalcified section of an iliac crest bone biopsy specimen from a patient with alcoholic cirrhosis and vitamin D deficiency–induced osteomalacia. Thickened osteoid seams (*black arrows*) are present on most of the trabecular surfaces. Toluidine blue staining, ×4 original magnification.

(de Vernejoul, 1985; Dunstan, 1984; Parisien, 1988). Indeed, inhibitory effects of aluminum have been reported on osteoblasts and mineralization in vitro (Sprague, 1993; Sun, 2016). Aluminum can be incorporated into mineralizing bone without inhibiting calcification (Chappard, 2016) and interestingly, the thickened osteoid seams can mineralize after Al sources have been removed (Boyce, 1992). The hypercalcemia in aluminum toxicity developed as a consequence of treatment with calcitriol, which enhanced the intestinal absorption of calcium, and the addition of calcium to dialysis fluid (Boyce, 1982). This hypercalcemia sometimes led to unnecessary and potentially fatal parathyroidectomy in patients who were mistakenly diagnosed with tertiary hyperparathyroidism. Aluminum toxicity has also been implicated in the pathogenesis of so-called aplastic or low-turnover renal osteodystrophy (Sherrard, 1996). In this condition, bone turnover is suppressed and osteoid seams are typically thin, and in some of these cases aluminum has been detected along mineralization fronts. It is associated with low bone mass and increased risk of fractures (Cannata-Andia, 2013). Although high concentrations of Al can be toxic to osteoblasts cultured in vitro, the cause of this low-turnover osteodystrophy in renal failure remains poorly understood.

Bone biopsy became the gold standard for the diagnosis and management of Al-induced osteodystrophy in renal failure in many academic nephrology departments in the 1970s through the 1990s. However, as water contamination with Al became more generally recognized as the cause of the osteodystrophy, and water purification measures kept dialysis water Al levels low, and Al-containing phosphate binders were replaced by others containing calcium, bone biopsy became redundant in most dialysis centers. Today, few centers use biopsy to help manage patients with chronic renal failure. Consequently, few nephrologists know how to perform the technique or have the special 6- to 8-mm-wide biopsy needles used typically to get specimens, which were taken from the iliac crest. These biopsy specimens also required special processing and embedding undecalcified in plastic. This allowed osteoid to be distinguished from calcified matrix and bone mineralization and formation rates to be measured in patients given prior double tetracycline labeling. This is not possible when specimens are decalcified and embedded in paraffin, which is how most bone samples are handled in pathology laboratories. Special heavy-duty microtomes are also required to cut sections from the plastic blocks. Most pathology departments do not have these microtomes or technicians who know how to prepare sections using them, nor do they have pathologists trained to interpret sections of undecalcified bone. There are a small number of physicians and scientists in the world today who know how to interpret undecalcified human bone biopsy specimen slides, and most are nearing or have passed retirement age. Thus, it is possible that Al toxicity remains a problem for patients with chronic renal failure and for others exposed to additional sources of Al (Chappard, 2016) but that it is going undetected.

Summary

Metal ion toxicity is an underinvestigated and underappreciated issue in skeletal biology. With the continued accumulation of environmental and industrial agents in our ecosystem that may have an adverse effect on osseous tissues, it might be expected that research on this topic would be an important and well-studied area. However, it seems that among clinicians and scientists in the musculoskeletal field there is little interest in the world of toxicological science, and in the fields of environmental health science there is little interest in bones and joints. Given the fact that human biology must cope with changes in the environment, this lack of interest is unfortunate. As discussed in this treatise, the skeleton can be an avid

reservoir for toxins, especially heavy metals. Two of these metals, lead and aluminum, are at the forefront of scientific awareness. It is now time that other skeletal health-modifying environmental compounds be researched.

References

Ahlgren, L., Liden, K., Mattsson, S., Tejning, S., 1976. X-ray fluorescence analysis of lead in human skeleton in vivo. Scand. J. Work. Environ. Health 2, 82−86.

Alfrey, A.C., 1980. Aluminum metabolism in uremia. Neurotoxicology 1, 43−53.

Alfrey, A.C., LeGendre, G.R., Kaehny, W.D., 1976. The dialysis encephalopathy syndrome. Possible aluminum intoxication. N. Engl. J. Med. 294, 184−188.

ATDSR (Agency for Toxic Substance and Disease Registry), 2007. Toxicological Profile for Lead-Update. U.S. Department of Health & Human Services, Public Health Service, Atlanta.

Barry, P.S.I., 1975. A comparison of concentrations of lead in human tissue. Br. J. Ind. Med. 32, 119−139.

Beier, E.E., Maher, J.R., Sheu, T.J., Cory-Slechta, D.A., Berger, A.J., Zuscik, M.J., Puzas, J.E., 2013. Heavy metal lead exposure, osteoporotic-like phenotype in an animal model, and depression of Wnt Signaling. Envion. Health Perspect. 121 (1), 97−104.

Beier, E.E., Sheu, T.J., Buckley, T., Yukata, K., O'Keefe, R.J., Zuscik, M.J., Puzas, J.E., 2014. Inhibition of beta-catenin signaling by Pb leads to incomplete fracture healing. J. Orthoptera Res. 32 (11), 1397−1405.

Beier, E.E., Sheu, T.J., Dang, D., Holz, J.D., Ubayawardena, R., Babij, P., Puzas, J.E., 2015. Heavy metal ion regulation of gene expression: mechanisms by which lead inhibits osteoblastic bone forming activity through modulation of the Wnt/β-catenin signaling pathway. J. Biol. Chem. 290 (29), 18216−18226.

Blish, K.R., Wang, W., Willingham, M.C., Du, W., Birse, C.E., Krishnan, S.R., Brown, J.C., Hawkins, G.A., Garvin, A.J., D'Agostino Jr., R.B., Torti, F.M., Torti, S.V., 2008. A human bone morphogenetic protein antagonist is down-regulated in renal cancer. Mol. Biol. Cell 19 (2), 457−464. PMC2230586.

Boyce, B.F., Elder, H.Y., Fell, G.S., Nicholson, W.A.P., Smith, G.D., Dempster, D.W., Gray, C.C., Boyle, I.T., 1981. Quantitation and localization of aluminium in human cancellous bone in renal osteodystrophy. Scanning Electron. Microsc. 3, 329−337.

Boyce, B.F., Fell, G.S., Elder, H.Y., Junor, B.J., Elliot, H.L., Beastall, G., Fogelman, I., Boyle, I.T., 1982. Hypercalcaemic osteomalacia due to aluminum toxicity. Lancet 2 (8306), 1009−1013.

Boyce, B.F., Byars, J., McWilliams, S., Mocan, M.Z., Elder, H.Y., Boyle, I.T., Junor, B.J., 1992. Histological and electron microprobe studies of mineralization in aluminium-related osteomalacia. J. Clin. Pathol. 45, 502−508.

Cannata-Andía, J.B., Rodriguez-García, M., Gómez-Alonso, C., 2013. Osteoporosis and adynamic bone in chronic kidney disease. J. Nephrol. 26, 73−80.

Carmouche, J.J., Puzas, J.E., Zhang, X., Tiyapatanaputi, P., Cory-Slechta, D.A., Gelein, R., Zuscik, M., Rosier, R.N., Boyce, B.F., O'Keefe, R.J., Schwarz, E.M., 2005. Lead exposure inhibits fracture healing and is associated with increased chondrogenesis, delay in cartilage mineralization, and a decrease in osteoprogenitor frequency. Environ. Health Perspect. 113, 749−755.

Chappard, D., Bizot, P., Mabilleau, G., Hubert, L., 2016. Aluminum and bone: review of new clinical circumstances associated with Al(3+) deposition in the calcified matrix of bone. Morphologie 100, 95−105.

Chettle, D.R., Scott, M.C., Somervaile, L.J., 1991. Lead in bone: sampling and quantitation using K X-rays excited by ^{109}Cd. Environ. Health Perspect. 91, 49−55.

Cocchiara, G., Fazzotta, S., Palumbo, V.D., Damiano, G., Cajozzo, M., Maione, C., Buscemi, S., Spinelli, G., Ficarella, S., Maffongelli, A., Caternicchia, F., Ignazio Lo Monte, A., Buscemi, G., 2017. The medical and surgical treatment in secondary and tertiary hyperparathyroidism. Review. Clin Ter 168, 158−167.

Crapper, D.R., Krishnan, S.S., Dalton, A.J., May 4, 1973. Brain aluminum distribution in Alzheimer's disease and experimental neurofibrillary degeneration. Science 180 (4085), 511−513.

Davenward, S., Bentham, P., Wright, J., et al., 2013. Silicon-rich mineral water as a non-invasive test of the 'aluminium hypothesis' in Alzheimer's disease. J. Alzheimer's Dis. 33 (2), 423−430.

de Vernejoul, M.C., Belenguer, R., Halkidou, H., Buisine, A., Bielakoff, J., Miravet, L., 1985. Histomorphometric evidence of deleterious effect of aluminum on osteoblasts. Bone 6, 15−20.

Dunstan, C.R., Evans, R.A., Hills, E., Wong, S.Y., Alfrey, A.C., 1984. Effect of aluminum and parathyroid hormone on osteoblasts and bone mineralization in chronic renal failure. Calcif. Tissue Int. 36, 133−138.

Ellis, H.A., McCarthy, J.H., Herrington, J., 1979. Bone aluminum in haemodialysed patients and in rats injected with aluminum chloride: relationship to impaired bone metabolism. J. Clin. Pathol. 32, 832−844.

Escribano, A., Revilla, M., Hernandez, E.R., Seco, C., Gonzalez-Riola, J., Villa, L.F., Rico, H., 1997. Effect of lead on bone development and bone mass: a morphometric, densitometric, and histomorphometric study in growing rats. Calcif. Tissue Int. 60, 200−203.

Exley, C., June 2014. What is the risk of aluminium as a neurotoxin? Expert Rev. Neurother. 14 (6), 589−591.

Flora, S.J., Mittal, M., Mehta, A., 2008. Heavy metal induced oxidative stress & its possible reversal by chelation therapy. Indian J. Med. Res. 128 (4), 501−523.

Goodman, W.G., Quarles, L.D., 2008. Development and progression of secondary hyperparathyroidism in chronic kidney disease: lessons from molecular genetics. Kidney Int 74 (3), 276−288.

Harris, W.H., Heaney, R.P., 1969. Skeletal renewal and metabolic bone disease. N. Engl. J. Med. 280 (4), 193−202.

Hellstrom, H.O., Mjoberg, B., Mallmin, H., Michaelsson, K., 2005. The aluminum content of bone increases with age, but is not higher in hip fracture cases with and without dementia compared to controls. Osteoporos. Int. 16, 1982e−1988.

Holz, J.D., Beier, E., Sheu, T.J., Ubayawardena, R., Wang, M., Sampson, E.R., Rosier, R.N., Zuscik, M., Puzas, J.E., 2012. Lead induces an osteoarthritis-like phenotype in articular chondrocytes through disruption of TGF-β signaling. J. Orthop. Res. 30 (11), 1760−1766.

Hu, H., August 1998. Bone lead as a new biologic marker of lead dose: recent findings and implications for public health. Environ. Health Perspect. 106 (Suppl. 4), 961−967.

Huffman, D.M., Niamh, M.A., Landy, M., Potter, E., Nagy, T.R., Gower, B.A., January 1, 2005. Comparison of the Lunar DPX-L and Prodigy dual-energy X-ray absorptiometers for assessing total and regional body composition. Int. J. Body Compos. Res. 3 (1), 25−30.

Jaishankar, M., Mathew, B.B., Shah, M.S., Gowda, K.R.S., 2014. Biosorption of few heavy metal ions using agricultural wastes. J. Environ. Pollution Human Health 2 (1), 1−6.

Jamal, S.A.1, Miller, P.D., 2013 . Secondary and tertiary hyperparathyroidism. J. Clin. Densitom. 16 (1), 64−68.

Kaehny, W.D., Hegg, A.P., Alfrey, A.C., 1977a. Gastrointestinal absorption of aluminum from aluminum-containing antacids. N. Engl. J. Med. 296, 1389−1390.

Kaehny, W.D., Alfrey, A.C., Holman, R.E., et al., 1977b. Aluminum transfer during hemodialysis. Kidney Int. 12, 361−365.

KDIGO, 2017. Clinical practice guideline update for the diagnosis, evaluation, prevention, and treatment of chronic kidney disease−mineral and bone disorder (CKD-MBD). Kidney Int. Suppl. 7, 1−59.

Klein, G.L., Alfrey, A.C., Miller, N.L., et al., 1982. Aluminum loading during total parenteral nutrition. Am. J. Clin. Nutr. 35, 1425−1429.

Kramer, H.J., Gonick, C., Lu, E., 1986. In vitro inhibition of Na-K-ATPase by trace metals: relation to renal and cardiovascular damage. Nephron 44, 329−336.

Krewski, D., et al., 2007. Human health risk assessment for aluminum, aluminum oxide and aluminum hydroxide. J. Toxicol. Environ. Health B Crit. Rev. 10 (Suppl. 1), 1−269.

Landsberg, J.P., McDonald, B., Watt, F., November 5, 1992. Absence of aluminium in neuritic plaque cores in Alzheimer's disease. Nature 360 (6399), 65−68.

Laraque, D., Arena, L., Karp, J., Gruskay, D., 1990. Bone mineral content in black preschoolers: normative data using single photon absorptiometry. Pediatr. Radiol. 20, 461−463.

Li, X., 2005. Sclerostin binds to LRP5/6 and antagonizes canonical Wnt signaling. J. Biol. Chem. 280, 19883−19887.

Maeda, K., Lee, D.S., Yanagimoto Ueta, Y., Suzuki, H., 2007. Expression of uterine sensitization-associated gene-1 (USAG-1) in the mouse uterus during the peri-implantation period. J. Reprod. Dev. 53 (4), 931−936.

Maharaj, D., Fell, G.S., Boyce, B.F., Ng, J.P., Smith, G.D., Boulton-Jones, J.M., Cumming, R.L., Davidson, J.F., 1987. Aluminum bone disease in patients receiving plasma exchange with contaminated albumin. Br. Med. J. 295, 693−696.

Manolagas, S.C., April 2000. Birth and death of bone cells: basic regulatory mechanisms and implications for the pathogenesis and treatment of osteoporosis. Endocr. Rev. 21 (2), 115−137.

Morais, S., Costa, F.G., Pereira, M.L., 2012. Heavy metals and human health. In: Oosthuizen, J. (Ed.), Environmental Health − Emerging Issues and Practice. InTech, pp. 227−246.

Murakami, K., Feng, G., Chen, S.G., February 1993. Inhibition of brain protein kinase C subtypes by lead. J. Pharmacol. Exp. Therap. 264 (2), 757−761.

Murashima-Suginami, A., Takahashi, K., Sakata, T., Tsukamoto, H., Sugai, M., Yanagita, M., Shimizu, A., Sakurai, T., Slavkin, H.C., Bessho, K., 2008. Enhanced BMP signaling results in supernumerary tooth formation in USAG-1 deficient mouse. Biochem. Biophys. Res. Commun. 369 (4), 1012−1016.

Nagajyoti, P.C., Lee, K.D., Sreekanth, T.V.M., 2010. Heavy metals, occurrence and toxicity for plants: a review. Environ. Chem. Lett. 8 (3), 199−216.

Parisien, M., Charhon, S.A., Arlot, M., Mainetti, E., Chavassieux, P., Chapuy, M.C., Meunier, P.J., 1988. Evidence for a toxic effect of aluminum on osteoblasts: a histomorphometric study in hemodialysis patients with aplastic bone disease. J. Bone Miner. Res. 3, 259−267.

Parkinson, I.S., Ward, M.K., Feest, T.G., et al., 1979. Fracturing dialysis osteodystrophy and dialysis encephalopathy. An epidemiological survey. Lancet 1, 406−409.

Perl, D.P., Brody, A.R., April 18, 1980. Alzheimer's disease: X-ray spectrometric evidence of aluminum accumulation in neurofibrillary tangle-bearing neurons. Science 208 (4441), 297−299. PMID: 7367858.

Potula, V.1, Kaye, W., March 2006. The impact of menopause and lifestyle factors on blood and bone lead levels among female former smelter workers: the Bunker Hill Study. Am. J. Ind. Med. 49 (3), 143−152.

Rebolledo, J., Fierens, S., Versporten, A., et al., 2011. Human biomonitoring on heavy metals in Ath: methodological aspects. Arch. Public Health 69, 10.

Rutger, L., van Bezooijena, R.L., 2005. *SOST*/sclerostin, an osteocyte-derived negative regulator of bone formation. Cytokine Growth Factor Rev. 16, 319−327.

Saag, K.G., Petersen, J., Brandi, M.L., Karaplis, A.C., Lorentzon, M., Thomas, T., Maddox, J., Fan, M., Meisner, P.D., Grauer, A., 2017. Romosozumab or alendronate for fracture prevention in women with osteoporosis. N. Engl. J. Med. 377 (15), 1417−1427.

Sherrard, D.J., Hercz, G., Pei, Y., et al., 1993. The spectrum of bone disease in endstage renal failure − an evolving disorder. Kidney Int. 43, 436−442.

Sherrard, D.J., Hercz, G., Pei, Y., Segre, G., 1996. The aplastic form of renal osteodystrophy. Nephrol. Dial. Transplant. 11 (Suppl. 3), 29−31.

Silbergeld, E.K., Schwartz, J., Mahaffey, K., 1988. Lead and osteoporosis: mobilization of lead from bone in postmenopausal women. Environ Res. 47 (1), 79−94.

Sprague, S.M., Krieger, N.S., Bushinsky, D.A., 1993. Aluminum inhibits bone nodule formation and calcification in vitro. Am. J. Physiol. 264, 882−890.

Sun, X., Cao, Z., Zhang, Q., Li, M., Han, L., Li, Y., 2016. Aluminum trichloride inhibits osteoblast mineralization via TGF-β1/Smad signaling pathway. Chem. Biol. Interact. 25 (244), 9−15.

Tanaka, M., Endo, S., Okuda, T., Economides, A.N., Valenzuela, D.M., Murphy, A.J., Robertson, E., Sakurai, T., Fukatsu, A., Yancopoulos, G.D., Kita, T., Yanagita, M., 2008. Expression of BMP-7 and USAG-1 (a BMP antagonist) in kidney development and injury. Kidney Int. 73 (2), 181−191.

van Bezooijen, R.L., 2004. Sclerostin is an osteocyte-expressed negative regulator of bone formation, but not a classical BMP antagonist. J. Exp. Med. 199, 805−814.

Vestergaard, P., Thomsen, S., 2011. Medical treatment of primary, secondary, and tertiary hyperparathyroidism. Curr. Drug Saf. 6, 108−113.

Wani, A.L., Ara, A., Usmani, J.A., June 2015. Lead toxicity: a review. Interdiscip. Toxicol. 8 (2), 55−64.

Weidenhamer, J.D., Fitzpatrick, M.P., Biro, A.M., Kobunski, P.A., Hudson, M.R., Corbin, R.W., Gottesfeld, P., February 1, 2017. Metal exposures from aluminum cookware: an unrecognized public health risk in developing countries. Sci. Total Environ. 579, 805−813.

Willhite, C.C., Ball, G.L., McLellan, C.J., May 2012. Total allowable concentrations of monomeric inorganic aluminum and hydrated aluminum silicates in drinking water. Crit. Rev. Toxicol. 42 (5), 358−442.

Chapter 23

Biology of the extracellular calcium-sensing receptor

Chia-Ling Tu, Wenhan Chang and Dolores M. Shoback

Endocrine Research Unit, Department of Veterans Affairs Medical Center, Department of Medicine, University of California, San Francisco, CA, United States

Chapter outline

Introduction

Extracellular calcium $\left(Ca_o^{2+}\right)$ serves as a versatile modulator of numerous physiological processes including hormone secretion, muscle contraction, blood clotting, cell adhesion, and neuronal excitability (Brown, 1991). In mammals, the level of Ca_o^{2+} is maintained within a narrow range (1.1−1.3 mM) by a homeostatic mechanism involving endocrine factors such as the parathyroid hormone (PTH) and the active metabolite of vitamin D, 1,25-dihydroxyvitamin D3 ($1,25(OH)_2D_3$) (Brown, 2013). When circulating $[Ca^{2+}]$ is low, parathyroid chief cells secrete PTH, which acts on bone, kidney, and intestine to mobilize skeletal Ca^{2+}, enhance renal Ca^{2+} reabsorption, and increase intestinal Ca^{2+} absorption, respectively, and to restore normocalcemia; conversely, PTH release decreases with hypercalcemia. In parathyroid cells, there is a very steep inverse sigmoidal relationship between PTH secretion and Ca_o^{2+} concentration (Brent et al., 1988; Rudberg et al., 1982), and the response curves suggest a positive cooperativity by various agonists that could account for the narrow range of Ca_o^{2+} regulating PTH secretion (Brown et al., 1989). In addition, changes in Ca_o^{2+} levels affect several intracellular signaling pathways including cyclic AMP (cAMP)-dependent protein kinase A (PKA) (Chen et al., 1989), phospholipase C (Kifor and Brown, 1988), and inositol phosphate generation (Nemeth and Scarpa, 1987; Shoback et al., 1988) in parathyroid cells. These initial findings supported the hypothesis of an extracellular Ca^{2+}-sensitive surface receptor regulating PTH secretion by coupling to multiple G-protein-dependent pathways (Brown, 1991; Fitzpatrick et al., 1986).

The cloning and characterization of the Ca_o^{2+}-sensing receptor (CaSR), a plasma membrane G-protein-coupled receptor (GPCR), from bovine parathyroid tissue by Brown et al. confirmed the role of Ca^{2+} as an extracellular first messenger in

Principles of Bone Biology. https://doi.org/10.1016/B978-0-12-814841-9.00023-3

controlling parathyroid function and confirmed that other di-, tri- and polyvalent cations mimic the effects of Ca^{2+} (Brown et al., 1993). Functional clones of the CaSR were subsequently isolated from human parathyroid (Garrett et al., 1995a), kidney (Aida et al., 1995b; Riccardi et al., 1995), and thyroid C cells (Garrett et al., 1995b). CaSRs in these tissues function as the "calciostat" to coordinate Ca^{2+} homeostasis by adjusting PTH and calcitonin secretion or renal cation handling. The importance of the CaSR in systemic Ca^{2+} homeostasis is highlighted by the pathological conditions in which inactivating and activating mutations in *CASR* cause hypercalcemia and hypocalcemia, respectively. These disorders include familial hypocalciuric hypercalcemia (FHH) type 1 (FHH1), neonatal severe hyperparathyroidism (NSHPT), and autosomal dominant hypocalcemia (ADH) type 1 (ADH1) (Brown, 2013; Hannan and Thakker, 2013).

Furthermore, CaSRs are widely expressed in cells and tissues not directly involved in regulating systemic mineral ion homeostasis, such as brain (Ruat et al., 1995), liver (Canaff et al., 2001), lung (Finney et al., 2008), vasculature (Alam et al., 2009), and skin (Oda et al., 2000). In addition to Ca^{2+}, the CaSR responds to an assorted array of stimuli that instigate different intracellular signaling pathways regulating a diverse range of biological processes such as hormone secretion (Yano et al., 2004b), gene expression (Yasukawa et al., 2017), ion channel activity (Parkash and Asotra, 2011; Ye et al., 2004), inflammation (Rossol et al., 2012), and cellular proliferation and differentiation (Diez-Fraile et al., 2013; Tu et al., 2011; Zhang X. et al., 2014).

Structural and biochemical properties of the calcium-sensing receptor

The CaSR is a member of a subfamily (family C) of GPCRs that includes eight subtypes of metabotropic glutamate receptors (mGluRs), mGluR1 to mGluR8; two type B γ-aminobutyric acid receptors (GABAB-Rs), GABAB-R1 and GABAB-R2; the promiscuous L-amino acid receptor; three taste receptors; several pheromone receptors; and five orphan receptors (Brauner-Osborne et al., 2007). All these receptors have small molecules as their ligands and share similar structural features: a large extracellular ligand-binding domain (ECD) including a Venus flytrap (VFT) module in the amino-terminal portion of the receptor, a seven-helix transmembrane domain (TMD) characteristic of GPCRs, and a sizable carboxyl-terminal (C-) tail.

The human CaSR cDNA sequence predicts a 120-kDa protein with 11 potential N-linked glycosylation sites in glycosylated ECD (Bai et al., 1996), of which 8 are glycosylated and 3 are not (Ray et al., 1998). While N-glycosylation may not be essential for signal transduction (Brown and MacLeod, 2001), it is critical for normal cell surface expression of the receptor (Ray et al., 1998). An altered CaSR glycosylation pattern has been observed in some forms of FHH (Bai et al., 1996). The CaSR is expressed on the cell surface in the form of disulfide-tethered homodimer (Bai et al., 1998a; Ward et al., 1998). Dimerization occurs in the endoplasmic reticulum during biosynthesis through two disulfide bonds between the cysteine 129 and 131 of each CaSR monomer (Ray et al., 1999), but noncovalent interactions also contribute to receptor dimerization (Jiang et al., 2004). The observation that the coexpression of CaSR monomers carrying inactivating mutations in different functional domains (e.g., the ECD and tail) can reconstitute considerable biological activity suggests intimate functional interactions between the monomeric CaSR subunits in a dimer (Bai et al., 1999). Furthermore, the CaSR can heterodimerize with mGluRs (Gama et al., 2001) and GABAB-Rs (Chang et al., 2007) through disulfide and noncovalent linkages. These heterodimeric interactions alter the protein trafficking, surface expression, and signal transduction properties of the CaSR (Gama et al., 2001) (Chang et al., 2007).

The CaSR ECD is connected to the TMD by a cysteine-rich domain (CRD) that contains nine cysteine residues forming four disulfide bridges within the CRD (Hu et al., 2000). They are critical for maintaining receptor structure, expression, and function (Fan et al., 1998; Hu et al., 2000). The CaSR VFT is formed by two lobes (LB1 and LB2) separated by a cleft representing the ligand-binding site (Silve et al., 2005). It was hypothesized that the binding of ligand in the cleft between the two lobes causes the lobes to close on each other, which directly or indirectly modifies the conformation of the TMD, leading to receptor activation (Hendy et al., 2013). The VFT module is probably evolved from the family of periplasmic binding proteins in bacteria (Felder et al., 1999), which serve as receptors responding to a wide variety of small ligands (e.g., ions, amino acids, and other nutrients) to promote bacterial chemotaxis toward and cellular uptake of environmental nutrients (Tam and Saier, 1993). Studies using CaSR-mGluR chimeric receptor constructs and mutagenesis have predicted five potential Ca^{2+}-binding sites in each monomeric ECD in the hinge region between the lobes of the VFT (site 1) (Huang Y. et al., 2009; Huang Y. et al., 2007; Silve et al., 2005). Functional studies and computational simulation suggested that the interactions between other Ca^{2+}-binding sites in ECD and the ones in site 1 are essential in tuning functionally positive homotropic cooperativity of CaSR activity induced by Ca_o^{2+} (Zhang C. et al., 2014). Other studies showed that L-amino acids could increase the sensitivity of the CaSR toward Ca^{2+} (Conigrave et al., 2007a). A potential L-phenylalanine-binding pocket was identified in the VFT near site 1 (Mun et al., 2004, 2005; Zhang et al., 2002), and mutational studies indicate its importance for positive heterotropic cooperativity between Ca^{2+} and L-amino acids in CaSR-mediated

signaling (Zhang C. et al., 2014). Recent X-ray crystallographic study of the CaSR ECD revealed that the interlobe cleft of VFT, the canonical agonist-binding site (Geng et al., 2013; Kunishima et al., 2000; Muto et al., 2007), is empty in the resting state and surprisingly is occupied solely by an L-tryptophan in the active state (Geng et al., 2016). Binding of an L-amino acid closes the interlobe groove in the VFT module, thereby inducing the formation of a novel homodimer interface by LB2 and CRD between subunits (Geng et al., 2016). Four novel Ca^{2+}-binding sites were identified in each protomer in the active structure, and Ca^{2+} stabilizes the active state by enhancing homodimer interactions to fully activate the receptor (Geng et al., 2016). While the presence of Ca_o^{2+} above a threshold level was required for amino acid−mediated CaSR activation, mutations of L-tryptophan-binding residues completely blocked Ca^{2+}-induced intracellular Ca^{2+} mobilization (Conigrave et al., 2007b; Geng et al., 2016), indicating that L-amino acid and Ca^{2+} are coagonists of the CaSR. Furthermore, four anion-binding sites were identified in the interlobe cleft and LB2 in the inactive and active CaSR ECD structures; and anion, such as PO_4^{3-} , may have a negative allosteric effect on receptor activity by stabilizing inactive conformation (Geng et al., 2016).

The structural similarity between CaSR TMD and those of the rhodopsin GPCR family suggests that these receptors share a common mechanism of G protein coupling (Pin et al., 2003) via TMD. The amino acid residues in the second and third intracellular loops are involved in CaSR coupling to G-protein-mediated signaling (Chang et al., 2000). Two cysteine residues, Cys677 and Cys765, within the first and second extracellular loops are critical for maintaining conformation of the CaSR (Ray et al., 2004). A chimeric receptor with the rhodopsin ECD linking with the TMD and tail of CaSR responds to Ca^{2+} in the presence of NPS-R568, a positive CaSR allosteric modulator (Hauache et al., 2000). Computational modeling and mutagenesis studies indicated that extracellular loops 2 and 3 contain additional binding sites for Ca^{2+} and allosteric modulators. Selective positive (calcimimetics) and negative (calcilytics) allosteric modulators bind to distinct but overlapping regions of the TMD (Hu et al., 2002; Petrel et al., 2004). A recent study of specific heterodimers of two loss-of-function CaSR mutants showed that one functional allosteric site per CaSR dimer was sufficient for obtaining the modulatory effects (Jacobsen et al., 2017). In addition to its role in signal transduction, CaSR TMD may also be involved in receptor dimerization through noncovalent interactions (Zhang et al., 2001).

Unlike the ECD and TMD, very few naturally occurring mutations have been identified in the intracellular tail of the CaSR; however, it contains three common polymorphisms, A986S, R990G, and Q1011E, associated with abnormal blood Ca^{2+} levels (Scillitani et al., 2004). A membrane proximal region (residues 863−925) has been shown to be essential to the cell surface expression and biological activity of the receptor (Chang et al., 2001; Goolam et al., 2014; Ray et al., 1997), as a large PEST-like sequence motif may direct lysosomal degradation of the receptor and regulate cell surface receptor level (Zhuang et al., 2012). In addition, a region comprising amino acids 960−984 is involved in binding to accessory proteins (Hjalm et al., 2001). Within its intracellular loops and C tail, the human CaSR harbors five predicted protein kinase C (PKC) and two predicted PKA phosphorylation sites (Garrett et al., 1995a; Hofer and Brown, 2003). Studies utilizing site-directed mutagenesis have demonstrated that phosphorylation of a single key PKC site at Thr888 inhibited most CaSR-mediated stimulation of PLC (Bai et al., 1998b; Davies et al., 2007; Jiang et al., 2002). Phosphorylation of Thr888 was increased by Ca_o^{2+} or calcimimetic and inhibited by calcilytics (Davies et al., 2007). Therefore, PKC-induced phosphorylation of Thr888 at the CaSR tail confers a negative feedback regulation to limit further activation of the PLC pathway. PKA phosphorylation per se plays a minor role in the regulation of CaSR, although one study found that PKA and PKC synergistically inhibited CaSR-mediated activation of PLC (Bosel et al., 2003).

Agonists, antagonists, and modulators of the calcium-sensing receptor

Cationic agonists of the calcium-sensing receptor

The CaSR has a broad spectrum of ligands in addition to Ca^{2+} and other di- and trivalent cations (Be^{2+}, Sr^{2+}, Ni^{2+}, Mn^{2+} Mg^{2+}, Ba^{2+}, Gd^{3+}, and La^{3+}) that bind at the orthosteric site within the interlobe crevice of the VFT module. Organic polycations including polyamines (i.e., spermine, spermidine, and putrescine), aminoglycoside antibiotics (e.g., neomycin, gentamycin), β-amyloid peptides, and basic polypeptides (e.g., polylysine and polyarginine) have been found to bind unidentified sites in VFT (Quinn et al., 1997; Saidak et al., 2009b). Cations and polyamine with higher positive charge density have higher potency as CaSR agonists (Quinn et al., 1997; Riccardi, 2002). All CaSR polycation agonists have been shown to potentiate one another's stimulatory effects on the receptor. In addition to the ECD of the receptor, studies using chimeric receptors indicated that the extracellular loops in TMD may contain binding sites for Ca^{2+} and allosteric modulators (Hammerland et al., 1999; Hauache et al., 2000).

Among these polycation agonists, however, only Ca^{2+}, Mg^{2+}, and spermine are thought to be physiological CaSR agonists. Mg^{2+} behaves as a partial agonist, as it is about twofold less potent than Ca^{2+} on a molar basis in activating the

CaSR (Butters et al., 1997). In the presence of physiological Ca_o^{2+} levels, $Mg^{2+}{}_o$ positively modulates CaSR function (Ruat et al., 1996). Mg^{2+}, in addition to Ca^{2+}, inhibits Ca^{2+} reabsorption in renal cortical thick ascending limb cells (de Rouffignac and Quamme, 1994). Persons with hypercalcemia due to heterozygous or homozygous inactivating mutations of the CaSR (e.g., FHH and NSHPT) manifest varied degrees of hypermagnesemia (Aida et al., 1995a). Conversely, patients with moderate to severe hypomagnesemia also exhibit impaired PTH secretion and develop hypocalcemia (Brown et al., 1999).

Allosteric modulators

Allosteric modulators bind outside of the orthosteric site, most likely changing the three-dimensional receptor conformation and thus affecting receptor affinity and/or ligand-binding efficacy (Hu, 2008). Positive allosteric modulators (PAMs) and negative allosteric modulators respectively increase and decrease CaSR agonist sensitivity. Well-known natural PAMs include aromatic L-amino acids (L-Phe, L-Tyr, L-His, and L-Trp) and short aliphatic amino acids (L-Thr and L-Ala) (Conigrave et al., 2000), which bind at or adjacent to the orthosteric site within the VFT module (Geng et al., 2016; Mun et al., 2005; Zhang et al., 2002). Activation of the CaSR by L-amino acids requires a threshold Ca_o^{2+} level of 1 mM (Conigrave et al., 2000). Acute elevations of amino acid concentrations stimulate Ca_i^{2+} mobilization and suppress PTH secretion in human parathyroid cells in vitro by enhancing the sensitivity of the CaSR to Ca_o^{2+} (Conigrave et al., 2004). These observations support that the CaSR not only is a Ca^{2+}- (and probably an Mg^{2+}-) receptor but also functions as a general "nutrient" sensor. Coordinating mineral ion and protein metabolism might be particularly relevant in the gastrointestinal tract. Indeed, the CaSR has been clearly identified in transgenic mouse studies as an L-amino acid sensor regulating macronutrient-dependent hormone secretion (Brennan et al., 2014).

Polypeptides such as polyarginine, polylysine, protamine (Ruat et al., 1996), and γ-glutamyl peptides (Broadhead et al., 2011; Wang et al., 2006), as well as β-amyloid peptide (Ye et al., 1997), which is excessively produced in the brain of patients with Alzheimer's disease, and polyvalent aminoglycoside antibiotics (McLarnon et al., 2002), are positive modulators that bind in the receptor's VFT domain. Interestingly, the CaSR was found to be activated by glutathione (γ-Glu-Cys-Gly) and its analog γ-Glu-Val-Gly, which can elicit the kokumi taste response and sapid compound denatonium (Maruyama et al., 2012; Rogachevskaja et al., 2011). Coinciding with the fact that these taste-enhancing substances have a positive allosteric effect on the receptor, functional CaSRs have recently been identified in mammalian taste cells (Bystrova et al., 2010; San Gabriel et al., 2009). Glutathione and its analogs may also act as neuromodulators by activating CaSRs on neurons and/or glial cells in the central nervous system (Conigrave and Hampson, 2010).

The CaSR is negatively modulated by pH and ionic strength (e.g., alterations in the concentration of NaCl). Elevated ionic strength suppresses Ca_o^{2+} sensitivity, and reduced ionic strength enhances it (Quinn et al., 1998). On the other hand, raised pH enhances Ca_o^{2+} sensitivity while reduced pH suppresses it (Quinn et al., 2004). Ion strength may have an impact on the binding efficacies of polyvalent cations to CaSR, thereby changing the responsiveness of the receptor to agonists (Quinn et al., 1998). The alterations in CaSR agonist sensitivity by pH are thought to result from changes in the ionization of the charges on CaSR agonists and changes in the conformation of the receptor (Quinn et al., 2004). The impact of changing ionic strength and pH on the responsiveness of the CaSR to divalent cations may be especially relevant in particular microenvironments where ionic strength and pH can vary greatly (Quinn et al., 1998). For instance, Ca_o^{2+}-induced CaSR-mediated acid secretion from intercalated cells in the distal convoluted tubule may be attenuated as local pH falls (Tyler Miller, 2013), and CaSR expression in the subfornical organ may contribute to the ionic strength-dependent regulation of vasopressin secretion and blood pressure (Yano et al., 2004a). Furthermore, anions have a negative allosteric effect on the receptor, as the CaSR ECD contains four anion-binding sites, and the binding of anions, such as SO_4^{2-} and PO_4^{3-}, stabilizes inactive conformation (Geng et al., 2016). SO_4^{2-} decreases Ca_o^{2+}-stimulated IP accumulation in CaSR-expressing HEK-293 cells (Geng et al., 2016). It is assumed that polycation agonists could compete with positively charged residues at anion-binding sites to bind to anions, thereby promoting the dissociation of anions from CaSR ECD and releasing their inhibitory effect on the receptor. This would drive the CaSR toward its active-state conformation (Geng et al., 2016).

Synthetic modulators

Several pharmacological agents that positively modulate CaSR signaling (calcimimetics) or negatively modulate CaSR signaling (calcilytics) (Nemeth, 2002; Nemeth et al., 1998) have been developed. In contrast to cationic agonists that bind to the ECD (Hammerland et al., 1999), selective calcimimetics and calcilytics bind to distinct but overlapping regions in the extracellular loops of the CaSR TMD (Hu, 2008; Petrel et al., 2004). Besides modulating CaSR activity, calcimimetics

and calcilytics have been shown to increase and decrease the level of receptor expression by controlling the susceptibility of the receptor to endoplasmic reticulum (ER)-associated degradation (Huang and Breitwieser, 2007).

Calcimimetics such as NPS R-467 and NPS R-568 are small hydrophobic derivatives of phenylalkylamines that activate the CaSR by increasing its affinity for Ca^{2+} (Nemeth et al., 1998). One calcimimetic compound, cinacalcet, has been approved for the treatment of primary hyperparathyroidism in patients with parathyroid carcinoma and the treatment of secondary hyperparathyroidism in patients on dialysis for end-stage renal disease (Nemeth et al., 1998). Cinacalcet targets the parathyroid CaSR and effectively lowers circulating PTH levels, reduces serum phosphorus and FGF23 concentrations, improves bone histopathology, and may diminish skeletal fracture rates and the need for parathyroidectomy (Nemeth and Shoback, 2013). Recent studies demonstrated that a novel therapeutic regimen combining calcimimetics and PTH produced more robust anabolic effects on bones than those resulting from intermittent PTH treatment (Santa Maria et al., 2016). Because CaSRs expressed in chondrocytes, osteoblasts, and osteoclasts have nonredundant roles in modulating the recruitment, proliferation, survival, and differentiation of these cells (Chang et al., 2008), it was hypothesized that calcimimetics in the presence of elevated local $Ca^{2+}{}_o$ levels induced by PTH activate endogenous CaSRs in the skeletal tissues, resulting in increased osteoblastic functions and reduced osteoclast-mediated bone resorption (Santa Maria et al., 2016).

Calcilytics, including NPS 2143 and Calhex 231, are CaSR antagonists that stimulate the secretion of PTH and have been tested for the treatment of osteoporosis (Nemeth and Shoback, 2013). Calcilytics might achieve the same osteoanabolic effects as those of intermittent PTH by suppressing parathyroid CaSR activation and producing a "pulse" of endogenous PTH secretion (Gowen et al., 2000; Kumar et al., 2010). Although several calcilytic compounds were evaluated as orally active anabolic therapies for postmenopausal osteoporosis, clinical development has stopped due to lack of efficacy. Calcilytics may be adapted for the treatment of ADH1 or potentially other disorders (Nemeth and Goodman, 2016).

Ligand-biased signaling

"Biased signaling" is the phenomenon by which distinct ligands stabilize distinct receptor conformational states that activate preferred signaling pathways (Leach et al., 2015). The CaSR is subject to biased signaling in response to its endogenous ligands. Aromatic amino acids such as L-Phe have a greater influence on CaSR-mediated mobilization of Ca_i^{2+} (Conigrave et al., 2000, 2004) than on the activation of PI-PLC (Rey et al., 2005), extracellular-signal-regulated kinases (ERKs) 1/2 (Lee et al., 2007), and CREB (Avlani et al., 2013). Similarly, small-molecule drugs such as the calcimimetics NPS-R568 and cinacalcet, and the calcilytic NPS-2143, instigate biased signaling that prefers $Ca^{2+}{}_i$ mobilization to ERK1/2 phosphorylation in CaSR-expressing HEK-293 cells (Davey et al., 2012). Certain CaSR mutants underlying disorders of calcium homeostasis also manifest altered biased signaling (Leach et al., 2012). Thus, biased signaling from the CaSR may have important pathophysiological and therapeutic implications.

Calcium-sensing receptor intracellular signaling

Calcium-sensing receptor–mediated signaling

The CaSR activates signaling pathways downstream through three main groups of heterotrimeric G proteins, $G_{q/11}$, $G_{i/o}$, and $G_{12/13}$, and in certain circumstances also activates G_s (see Fig. 23.1). The CaSR's second and third intracellular loops (Chang et al., 2000) and its proximal C-terminus (Chang et al., 2001; Ray et al., 1997) provide key interaction sites with its associated heterotrimeric G proteins—i.e., $G_{q/11}$. CaSR activation in parathyroid cells and other systems elicits $G_{q/11}$-mediated activation of PI-PLCβ, and with the breakdown of membrane phospholipid PIP_2 to IP_3 and diacylglycerol, induces Ca_i^{2+} mobilization and the activation of various isoforms of PKC (Bai et al., 1998b; Brown et al., 1993). The importance of this mechanism for CaSR-mediated inhibition of PTH secretion was demonstrated by the finding that mice with parathyroid-specific deletion of the α-subunit of G_q on a global G_{11} α-subunit-null background developed severe hyperparathyroidism (Wettschureck et al., 2007) similar to that seen in global CaSR exon 5–null mice (Ho et al., 1995) and humans with NSHPT (Pollak et al., 1994).

Besides PLC, the CaSR is able to activate two other phospholipases, phospholipase D (PLD) and phospholipase A2 (PLA2) (Kifor et al., 1997). Studies using specific inhibitors show that PKC and Rho are involved in CaSR-mediated PLD activation (Huang et al., 2004; Kifor et al., 1997). The CaSR primarily modulates PLA2 activity by increasing Ca_i^{2+} levels via activation of the G_q–PLC pathway (Handlogten et al., 2001). The increase in Ca_i^{2+} activates calmodulin and calmodulin-dependent protein kinases, leading to activation of cytosolic PLA2 (Handlogten et al., 2001) and generation of

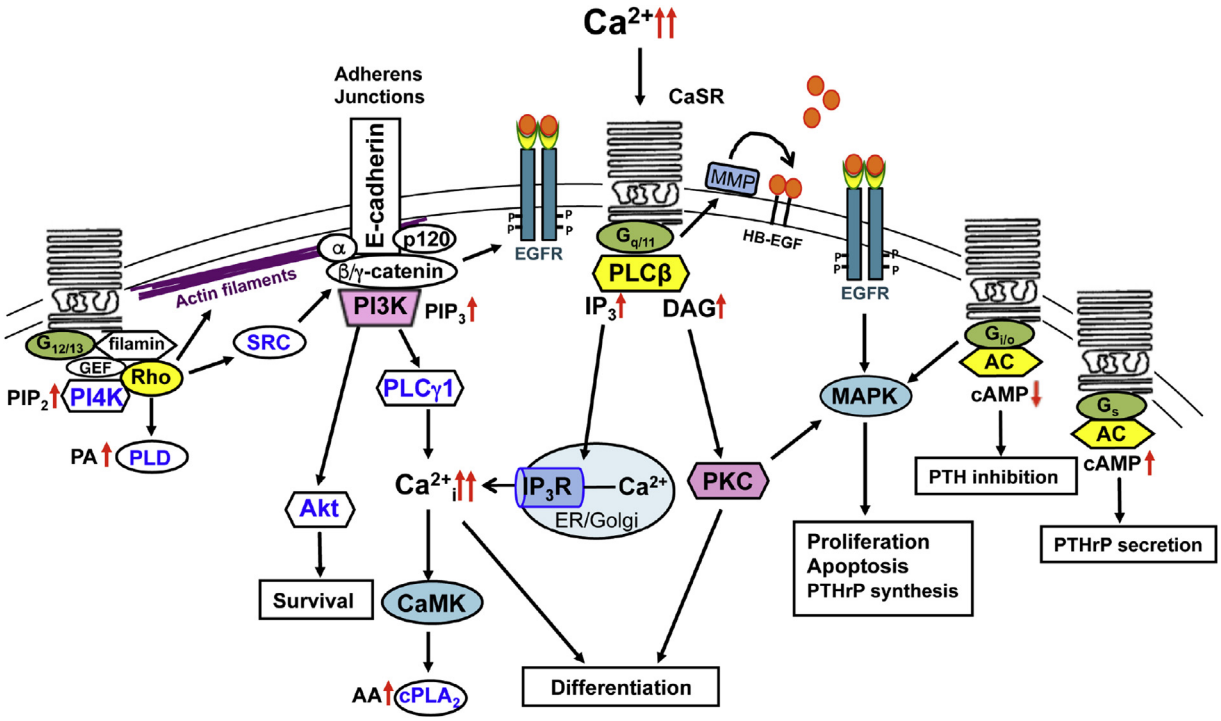

FIGURE 23.1 Schematic representation of calcium-sensing receptor—mediated intracellular signaling. The calcium-sensing receptor (CaSR) typically interacts with three heterotrimeric G protein subfamilies, $G_{q/11}$, $G_{i/o}$, and $G_{12/13}$, and in certain cancer cell types, G_s. Activation of $G_{q/11}$ induces phospholipase C (PLC)-mediated Ca^{2+} mobilization from intracellular stores and protein kinase C (PKC) activation. The increased $Ca^{2+}{}_i$ activates Ca^{2+}/calmodulin-dependent protein kinases (CaMKs) and cytoplasmic phospholipase A2 ($cPLA_2$). Instigating $G_{12/13}$ stimulates Rho-mediated activation of phosphatidylinositol 4-kinase (PI4K) to generate PIP_2, phosphatidylinositol 3-kinase (PI3K) to produce PIP_3 and to activate the downstream effectors Akt and PLCγ1, and cytoskeleton reorganization to promote the formation of stress fibers, cadherin/catenin adhesion complexes, and membrane ruffling. CaSR-mediated activation of phospholipase D (PLD), producing phosphatidic acid, also involves Rho and PKC. Adenylyl cyclase is inhibited by $G_{i/o}$ but activated by G_s in breast cancer cell lines, resulting in decreased or increased cytoplasmic cyclic AMP (cAMP) concentrations, respectively. Activation of the mitogen-activated protein kinase (MAPK) extracellular-signal-related kinases (ERKs) 1/2 involves transactivation of the epidermal growth factor receptor (EGFR) either via liberation of EGF-like ligands by extracellular matrix metalloproteinases (MMPs) or through an E-cadherin-mediated ligand-independent EGFR recruitment and activation. Activation of ERK1/2 also involves PKC and Gi/o-mediated signaling.

second messengers such as arachidonic acid. In kidney, this PLA2 signaling axis mediates the effects of hypercalcemia. However, CaSR-induced activation of PKC and ERK may also contribute to the phosphorylation and activation of PLA2 (Handlogten et al., 2001; Kifor et al., 2001).

In CaSR-expressing HEK-293 cells, elevating Ca_o^{2+} induces sinusoidal oscillations in Ca_i^{2+} (Szekely et al., 2009; Young and Rozengurt, 2002). The repetitive oscillations result from the dynamic phosphorylation and dephosphorylation of a key residue, T888, the primary PKC phosphorylation site of the CaSR located in the proximal intracellular domain (Bai et al., 1998b; Davies et al., 2007; McCormick et al., 2010; Young et al., 2002). Ligand-induced activation of PKC leads to phosphorylation of T888 to uncouple the receptor from $G\alpha_{q/11}$-induced PLC activation and Ca_i^{2+} mobilization (Bai et al., 1998b; Jiang et al., 2002). PKC activation by phorbol esters overcomes the inhibitory effect of high Ca_o^{2+} and increases PTH secretion, whereas disruption of the T888 PKC phosphorylation site increases receptor Ca_o^{2+} sensitivity (Brown et al., 1992; Membreno et al., 1989). The naturally occurring CaSR mutant T888M has been linked to sustained CaSR-mediated suppression of PTH secretion at low Ca_o^{2+} levels causing ADH (Lazarus et al., 2011), demonstrating that the T888 residue and its regulation by PKC are critical for physiological CaSR function in vivo. The phosphorylation state of CaSR T888 depends not only on PKC but also on the dynamic activity of PP2A, a phosphatase that induces dephosphorylation (McCormick et al., 2010). Also, the PLC/Ca_i^{2+}-mediated control of chemotaxis of preosteoblasts to sites of bone resorption may involve a G_{12}-dependent mechanism that sustains Ca_i^{2+} elevations via the activation of PP2A and dephosphorylation of T888 (Godwin and Soltoff, 2002; Zhu et al., 2004, 2007).

Elevated Ca_o^{2+} typically suppresses cAMP levels in CaSR-expressing cells via pertussis toxin-sensitive $G_{i/o}$, which suppresses the activity of various isoforms of adenylyl cyclase. $G_{i/o}$ is responsible for mediating the inhibitory control of

PTH and PTH-related protein (PTHrP) secretion by various CaSR ligands including Ca_o^{2+} (Fitzpatrick et al., 1986; Mamillapalli and Wysolmerski, 2010). Nevertheless, CaSR-mediated activation of PI-PLC provides a $G_{i/o}$-independent mechanism for the inhibition of cAMP synthesis via Ca_i^{2+}-dependent inhibition of adenylyl cyclase isoforms 5, 6, and/or 9 or via phosphodiesterase isoform-1, which breaks down cAMP in response to elevated Ca_i^{2+}/calmodulin (Brown and MacLeod, 2001). This pathway supports Ca_o^{2+}-induced suppression of renin secretion from renal juxtaglomerular cells (Atchison and Beierwaltes, 2013; Beierwaltes, 2010) and vasopressin-induced aquaporin-2 expression in water-reabsorbing principal cells of the collecting ducts (CDs) (Procino et al., 2012). However, the CaSR stimulates rather than inhibits adenylyl cyclase in certain cancers (e.g., breast cancer cells) (Mamillapalli et al., 2008) and in At-T20 pituitary cells, which secrete adrenocorticotropic hormone and PTHrP (Mamillapalli and Wysolmerski, 2010). In normal mammary epithelial cells, CaSR preferably couples to $G_{i/o}$, but the receptor-dependent coupling is switched to G_s in breast cancer cells (Mamillapalli et al., 2008). In contrast, Ca_o^{2+}-induced activation of adenylyl cyclase isoforms 1 and 8 may provide an alternative mechanism for the CaSR-mediated elevation of cAMP (Cooper, 2003).

$G_{12/13}$ modulate receptor-mediated control of shape change, cell migration, and gene expression through the activation of Rho kinase and phosphorylation of serum-response factor (Siehler, 2009). Ca_o^{2+} and the calcimimetic NPS R-467, but not L-amino acids, induced Rho kinase-dependent formation of actin stress fibers in CaSR-expressing HEK-293 cells (Davies et al., 2006); yet G_{12} and Rho are required for L-amino acid-induced Ca_i^{2+} mobilization (Rey et al., 2005). $G_{12/13}$-mediated pathways promote osteoblast differentiation through Wnt3a-β-catenin signaling (Rybchyn et al., 2011) and inhibit osteoclastogenesis by suppressing the expression of receptor activator of nuclear factor kappa-B ligand (RANKL) and promoting the expression of osteoprotegerin (Brennan et al., 2009). $G_{12/13}$ also activates adenylyl cyclase isoform-7 (Jiang et al., 2008), and this pathway may contribute to $Ca^{2+}{}_o$-stimulated cAMP synthesis in primary mouse osteoblasts (Choudhary et al., 2004).

Calcium-sensing receptor–associated intracellular signaling effectors

CaSR activation is linked to proproliferative stimuli in many cell systems, involving the activation of mitogen-activated protein kinases (MAPKs) including ERK1/2, p38, and JNK (Brennan and Conigrave, 2009; Magno et al., 2011b). Ca_o^{2+}-induced ERK1/2 is typically activated through the CaSR–Src–Ras–Raf–MEK–ERK pathway (Hobson et al., 2000). Nevertheless, pertussis toxin, the PLC inhibitor U73122, and PKC inhibitor GF109203X all have been shown to partially inhibit Ca_o^{2+}-induced ERK1/2 phosphorylation in bovine parathyroid and HEK-293 cells expressing the CaSR (Holstein et al., 2004; Kifor et al., 2001). These findings indicate that the CaSR can activate tyrosine kinases and stimulate ERK activity through the $G_{q/11}$–PLC–PKC pathway and by coupling to G_i (Kifor et al., 2001). CaSR-mediated activation of ERK1/2 via G_i requires dynamin/β-arrestin-dependent receptor internalization (Holstein et al., 2004). In addition, CaSR-mediated ERK phosphorylation can occur through a transactivation mechanism in which CaSR stimulates matrix metalloproteinase-mediated release of membrane-bound epidermal growth factor (EGF)-like peptide, which in turn activates EGF receptor (EGFR) and downstream Ras–Raf–MEK–ERK signaling (MacLeod et al., 2004; Yano et al., 2004b). This pathway drives CaSR-mediated cell proliferation in human MCF-7 breast cancer cells (El Hiani et al., 2009b) and PTHrP secretion in human PC-3 prostate cancer cells (Yano et al., 2004b). Furthermore, the engagement of E-cadherin in newly formed cell contacts provides an alternate mechanism for the recruitment and sensitization of EGFR to allow $Ca^{2+}{}_o$ to activate downstream MAPK and Rac1 signaling cascades, together supporting epithelial proliferation (Betson et al., 2002) (Fedor-Chaiken et al., 2003) (Pece and Gutkind, 2000). CaSR-mediated ERK activation in CaSR-expressing HEK-293 cells and ovarian surface epithelial cells may involve the phosphatidylinositol 3-kinase (PI3K) (Hobson et al., 2003). The mouse osteoblastic cell line, MC3T3- E1, responds to CaSR agonists with increased phosphorylation of p38 MAPK (Yamaguchi et al., 2000). CaSR-mediated p38 MAPK signaling modulates the release of PTHrP in CaSR-expressing HEK-293 cells and rat H-500 Leydig cancer cells (MacLeod et al., 2003; Tfelt-Hansen et al., 2003) and regulates vitamin D receptor (VDR) expression in a proximal tubule human kidney epithelial cell line, HK-2G (Maiti et al., 2008). JNK has been shown to control CaSR-mediated proliferation in rat calvarial osteoblasts (Chattopadhyay et al., 2004). JNK and p38 MAPK have also been implicated in other CaSR-mediated pathways regulating proliferation and apoptosis (Corbetta et al., 2000).

In addition to MAPK cascades, CaSR controls cell survival, proliferation, and differentiation through multiple distal effectors. Activation of the CaSR stimulates the expression of Fos, Egr-1, and cyclin-D to promote G1/S cell cycle transition (Chattopadhyay et al., 2004). CaSR-mediated signaling via the PI3K pathway stimulates phosphorylation and activation of the antiapoptotic protein kinase Akt in fetal rat calvarial cells (Dvorak et al., 2004) and opossum kidney cells (Ward et al., 2005). Conversely, CaSR stimulates NF- κB activation and promotes expression of cell death genes such as p53, c-Myc, and Bcl-2 in mature rabbit osteoclasts (Mentaverri et al., 2006). CaSR-mediated apoptosis is induced by $Ca^{2+}{}_i$

overload and activation of the mitochondrial apoptotic pathways and involves the upregulation of caspase-3 and cytochrome *c* as well as Fas/FasL expression (Xing et al., 2011; Zheng et al., 2011). Moreover, CaSR promotes cell differentiation in keratinocytes and colonic epithelial cells (Chakrabarty et al., 2005; Tu et al., 2008, 2011). Stimulating the CaSR increased the expression of E-cadherin in colon carcinoma cells and concomitantly reduced the activation of β-catenin/T-cell factor and suppression of tumor malignancy (Chakrabarty et al., 2005). In keratinocytes, physical interactions between the CaSR, filamin A, and RhoA stimulate E-cadherin-mediated recruitment and the activation of downstream kinases, and also facilitate cell differentiation (Tu et al., 2011). CaSR activators induce the secretion of Wnt5a and expression of Wnt5a receptor Ror2, leading to the inhibition of canonical Wnt/β-catenin signaling and stimulation of cell differentiation in colonic epithelial cells and keratinocytes (Macleod, 2013; Popp et al., 2014).

In kidney, CaSR is coupled to the metabolism of arachidonic acid by cytochrome P450 (Ferreri et al., 2012) and regulates renal calcium excretion in the thick ascending limb independently of PTH by modulating the calcineurin−NFAT1c−microRNA−claudin 14 signaling axis (Toka, 2014). In thyroid C cells, the CaSR controls calcitonin secretion through the activation of voltage-gated Ca^{2+} channels (Freichel et al., 1996). The CaSR has been shown to form signaling complexes with integrins to facilitate cell migration and differentiation in neurons (Tharmalingam et al., 2016). CaSR activation stimulates cyclooxygenase pathways in osteoblasts via a G_i- and PKA-dependent mechanism (Choudhary et al., 2004). Additionally, the CaSR plays a significant role in bone metastasis in renal carcinoma, breast cancer, and prostate cancer (Breuksch et al., 2016). CaSR-mediated activation of ERK1/2, Akt, and PLC signaling determines the tumor cells' ability to proliferate, migrate (Liao et al., 2006; Saidak et al., 2009a), and secrete PTHrP (Mamillapalli and Wysolmerski, 2010), which in turn increases the expression of RANKL in immature osteoblasts and stimulates osteoclastogenesis (Chirgwin and Guise, 2000). These processes promote osteoclast-mediated osteolysis, resulting in the enhanced secretion of growth factors and calcium, again activating tumor cells (Breuksch et al., 2016; Tfelt-Hansen et al., 2003).

Calcium-sensing receptor interacting proteins

The CaSR is a GPCR that operates in the constant presence of agonists, sensing small changes with minimal functional desensitization. Resistance to desensitization requires the maintenance of a functional receptor pool at the cell surface and persistent coupling of the receptor to its heterotrimeric G proteins and downstream signaling pathways. CaSR cell surface expression is maintained by an unusual phenomenon termed agonist-driven insertional signaling (ADIS) (Breitwieser, 2013), in which CaSR activation drives its own trafficking to the plasma membrane. ADIS has potential therapeutic implications for disorders of Ca^{2+} homeostasis in which CaSR expression is impaired due to loss-of-function mutations in the *CASR* gene found in FHH1 and NSHPT (Hannan and Thakker, 2013). However, CaSR-associated disorders can also be caused by different mechanisms. Recent studies revealed that FHH or ADH phenotypes can be associated with mutations on partner proteins associated with CaSR-mediated signaling—e.g., loss-of-function mutations of the sigma subunit of adaptor protein-2 (AP2) and mutations on G protein subunit-α11(GNA11) (Nesbit et al., 2013b; Rogers et al., 2014). A number of molecular binding partners of the CaSR are involved in controlling receptor trafficking to the cell surface and its desensitization, degradation, and signaling (Grant et al., 2011; Huang and Miller, 2007; Ray, 2015).

Once synthesized in the ER, improperly folded CaSR proteins will be moved toward the proteasome for degradation, a process involving osteosarcoma-9 protein, which targets immature CaSRs (Ward et al., 2018). Receptors passing the quality control process will traffic to the plasma membrane or other cellular compartments via interaction with chaperones and small GTP-binding proteins (Breitwieser, 2014). Several proteins interact with the CaSR when the receptor exits the ER. P24A (Strating and Martens, 2009), Sar1 (Zhuang et al., 2010), receptor activity-modifying proteins (Bouschet et al., 2012), and Rab1 (Zhuang et al., 2010) are found to facilitate CaSR trafficking from the ER to the Golgi and increase its plasma membrane expression. On the other hand, the 14-3-3 proteins are predicted to interact with the arginine-rich domain (amino acids 890−898) of the CaSR C-terminal tail and may lead to the retention of the CaSR in the ER (Arulpragasam et al., 2012; Grant et al., 2011). The surface expression of CaSR is also influenced by the interaction of calmodulin (CaM) at residues 871−898 at the C-terminal tail of CaSR, a region involved in phosphorylation and biased signaling (Davey et al., 2012; Leach et al., 2012). CaM binding may stabilize the CaSR on the cell membrane via modulation of anterograde trafficking and thus increase the potency of its functional activity (Bai et al., 1998b; Huang et al., 2010). In addition, dimerization of the CaSR is essential, although not sufficient, for membrane trafficking and full receptor function (Bai et al., 1999).

After CaSRs are inserted into plasma membrane, their interactions with a variety of proteins direct them to different subcellular localizations. Caveolin binds to CaSR intracellular loops 1 and 3 and keeps the receptor highly enriched in invaginations of the plasma membrane, called caveolae, in parathyroid chief cells and cardiac myocytes (Kifor et al., 1998; Sun and Murphy, 2010). Filamin A, an actin-binding scaffold/adaptor protein with the ability to bind various components

in MAPK and Rho-GTPase-mediated signaling cascades, interacts with the C-terminal tail of the CaSR (Awata et al., 2001; Hjalm et al., 2001; Pi et al., 2002). Filamin A potentiates CaSR expression in parathyroid cells by protecting the receptor from degradation (Zhang and Breitwieser, 2005). CaSR-dependent activation of downstream ERK1/2 and Rho also relies, in part, on its physical interaction with filamin A (Pi et al., 2002; Rey et al., 2005; Tu et al., 2011). In keratinocytes, disruption of the CaSR−filamin interaction prevents Ca_o^{2+}-induced RhoA activation and the formation of E-cadherin−catenin adhesion complex on the cell membrane, thereby impairing cell−cell adhesion (Tu et al., 2011; Tu and You, 2014). In addition, the CaSR modulates cell adhesion and migration via direct interactions with integrins in developing cerebellum granule cell precursors and medullary thyroid carcinoma cells (Tharmalingam et al., 2011, 2016). Heterodimerization of CaSR with mGluR (Gama et al., 2001) and subunits of GABAB-R (Kim et al., 2014) is found in certain regions of bovine and rat brains. These interactions affect trafficking and surface expression of CaSR as well as receptor signaling to the PLC/IP_3 pathway (Chang et al., 2007; Gama et al., 2001). Testin, a focal adhesion protein, binds to the intracellular tail of the CaSR and positively modulates CaSR-stimulated Rho kinase (Magno et al., 2011a). The binding of hypoxia-induced mitogenic factor to the membrane proximal region in the CaSR tail enhances CaSR-mediated Ca_i^{2+} signaling and hypoxia-evoked proliferation of pulmonary artery smooth cells, leading to the development of pulmonary vascular remodeling and pulmonary hypertension. Additionally, the CaSR's C-terminal tail has been shown to interact directly with two potassium channels, Kir4.1 and Kir4.2, an interaction that inhibits the activities of these channels in the renal thick ascending limb (Huang C. et al., 2007).

Surface-expressed CaSR may undergo endocytosis initiated through phosphorylation by GPCR kinases or PKC (Lorenz et al., 2007; Pi et al., 2005). β-arrestin subsequently binds to the phosphorylated receptor to decrease its capacity to activate G proteins (Lorenz et al., 2007). Endocytosis of CaSR is facilitated by Rab7, Rab11a (Reyes-Ibarra et al., 2007), and AP2 (Nesbit et al., 2013b; Zhuang et al., 2012). The endocytosed receptors are either recycled to the cell membrane, thereby contributing to receptor resensitization, or translocated to lysosomes for degradation (Ray, 2015). Two mechanisms are involved in degradation of the CaSR: (1) CaSR proteins are targeted to the proteasome after being ubiquitinated by the E3 ubiquitin ligase, dorfin, via binding to the C-terminal tail (Huang et al., 2006; Zhuang et al., 2012), or (2) they are degraded in lysosomes, elicited by the binding of AMSH, a deubiquitinating enzyme, to the PEST-like sequence in the C-terminal tail of the CaSR (Herrera-Vigenor et al., 2006; Zhuang et al., 2012). Furthermore, CaSR proteins are sensitive to m-calpain-dependent destruction, adding an additional mechanism for regulating CaSR protein expression (Kifor et al., 2003). These mentioned secretory pathways and endocytosis mechanisms work collaboratively in the continuous presence of agonist stimulation, resulting in a net increase in CaSR expressed on the plasma membrane (Breitwieser, 2013).

Regulation of calcium-sensing receptor gene expression

The human *CASR* gene is located on chromosome 3q13.3−21, and rat and mouse *Casr* genes reside on chromosomes 11 and 16, respectively (Janicic et al., 1995). The *CASR* gene has seven exons (Pearce et al., 1995): Exon 1 contains two alternative promoters for transcription (Chikatsu et al., 2000; Garrett et al., 1995a). Exon 2 encodes a common upstream untranslated region (5′-UTR) and the translation initiation codon ATG. Exons 2 to 6 encode various regions of the ECD, while exon 7 encodes the entire TMD and the C-terminus tail. *CASR* transcripts may have different 3′-untranslated regions (3′-UTRs) derived from two alternative polyadenylation signal sequences in exon 7 (Aida et al., 1995b; Garrett et al., 1995a). Like the human *CASR* gene, mouse and rat genes are organized in a similar manner and have at least two promoters (Hendy et al., 2013). Promoter P1 has TATA and CCAAT boxes upstream to the initiation site, and promoter P2 has Sp1/3 motif at the transcriptional start site; both promoters drive significant levels of basal activity, with P2 more active than P1 (Canaff and Hendy, 2002). Direct analyses of transcripts revealed that transcripts from P2 are expressed at much higher levels than for P1-derived transcripts in human parathyroid, thyroid C cells, and renal proximal tubular cells (Canaff and Hendy, 2002; Mizobuchi et al., 2009). Transcripts from the P1 promoter are reduced in parathyroid adenomas and colorectal carcinomas (Chikatsu et al., 2000; Kallay et al., 2003a). Several factors including active vitamin D, proinflammatory cytokines, and the transcription factors glial cells missing-2 (GCM2) and thyroid transcription factor 1 (TTF1) control *CASR* transcription, and functional cis-elements in *CASR* promoters responsive to these modulators have been characterized (Hendy et al., 2013; Suzuki et al., 1998). Studies of colon carcinomas and neuroblastomas have indicated that epigenetic changes, such as histone deacetylation and promoter hypermethylation of the GC-rich P2 (Casala et al., 2013; Fetahu et al., 2014; Hizaki et al., 2011), contribute to reduced *CASR* expression in these tumors. Although the increased expression of several microRNAs has been proposed as a cause for *CASR* silencing in colorectal tumors (Fetahu et al., 2016; Singh and Chakrabarty, 2013), direct involvement of microRNA in regulating receptor gene expression has not been confirmed.

Alternative spliced *CASR* transcripts have been reported. An exon 3−deleted variant, in which fusion of exons 2 and 4 produces a truncated receptor protein unable to reach the cell surface, is found in placental cytotrophoblast (Bradbury et al., 1998) and parathyroid, thyroid, and kidney tissues (D'Souza-Li et al., 2001). A mouse model of human FHH1 and NSHPT (Ho et al., 1995) in which exon 5 of the *Casr* gene is deleted unexpectedly generates an alternatively spliced *Casr* variant lacking exon 5 in the skin, kidney, and growth plate (Oda et al., 1998; Rodriguez et al., 2005). Although this variant encodes a protein with a 77-amino acid in-frame deletion in the exodomain and exerts a dominant-negative effect on the full-length receptor, reducing its response to Ca_o^{2+} in vitro (Oda et al., 1998), it apparently compensates for the absence of the full-length receptor in bone and cartilage (Rodriguez et al., 2005).

High levels of both Ca_o^{2+} and $1,25(OH)_2D_3$ upregulate CaSR expression in certain cell types. High Ca_o^{2+} increases the expression of the CaSR in mouse pituitary AtT-20 cells (Emanuel et al., 1996) and rat parathyroid glands (Mizobuchi et al., 2004), whereas administration of $1,25(OH)_2D_3$ elevates *CASR* mRNA levels in vivo in kidney and parathyroid gland in rat (Brown et al., 1996; Canaff and Hendy, 2002; Yao et al., 2005). Upregulation of CaSR in the parathyroid gland by $1,25(OH)_2D_3$ increases the responsiveness of the gland to Ca_o^{2+}, thereby reinforcing the negative action of Ca_o^{2+} on PTH synthesis and secretion and parathyroid cell proliferation. Conversely, kidney CaSR expression is downregulated in VDR-null mice and in *Cyp27*$^{-/-}$ mice lacking the 25-hydroxyvitamin D-1α-hydroxylase enzyme (Li et al., 2003). Likewise, reduced CaSR expression in patients with chronic kidney disease could result in part from a concomitant decrease in circulating levels of $1,25(OH)_2D_3$ (Williams et al., 2009). Modulation of the activity of *CASR* promoters by Ca_o^{2+} was shown in vitro by transfecting promoter-reporter constructs in human kidney proximal tubule cells and mouse distal convoluted tubule cells (Hendy and Canaff, 2016). $1,25(OH)_2D_3$ has been shown to potentiate CaSR-mediated antineoplastic effects in differentiated human colon carcinoma cells (Aggarwal et al., 2016). Although functional vitamin D response elements are present in both promoters in the *CASR* gene (Canaff and Hendy, 2002; Klein et al., 2016), Ca_o^{2+} and $1,25(OH)_2D_3$ additively stimulate transcription from promoter P2 but not P1 (Chakrabarty et al., 2005).

GCM2 is a transcription factor essential for the development of the parathyroid gland in terrestrial vertebrates (Okabe and Graham, 2004). The expression of CaSRs in parathyroid cells correlated with GCM2 levels, and the inactivating mutations of *GCM2* gene cause familial isolated hypoparathyroidism (Mannstadt et al., 2008; Okabe and Graham, 2004). GCM2 transactivates the *CASR* gene via GCM2 response elements in promoters P1 and P2 (Canaff et al., 2009). In adenomatous tissue from patients with primary hyperparathyroidism, reduced CaSR expression may be attributed to underexpression of the *GCM2* gene (Correa et al., 2002). TTF1 is present in rat thyroid C cells and parathyroid cells, and it is expressed inversely with the CaSR. TTF1 suppresses the promoter activity of the *Casr* gene via interactions with specific elements on the 5′-flanking regions (Suzuki et al., 1998). However, the regulation of CaSR expression by TTF1 is modulated by $Ca^{2+}{}_i$ levels and may involve other transcription factors (Suzuki et al., 1998).

Expression of the CaSR is regulated physiologically and pathologically at the gene level. CaSR is highly expressed in the developing fetus, with the highest expression levels found in the central and peripheral nervous systems, heart, lung, and cartilage (Riccardi et al., 2009). CaSR plays important roles in neuronal growth (Vizard et al., 2008), lung morphogenesis (Finney et al., 2008), and skeletal development (Chang et al., 2008). In the adult, CaSR expression has been detected in a myriad of cells and tissues. It regulates cellular fate in the parathyroid gland, bone, kidney, blood, and skin as well as in reproductive, cardiovascular, and gastrointestinal tissues (Diez-Fraile et al., 2013). Altered expression of the CaSR has been associated with various disorders in humans. In atherosclerosis, the loss of CaSR expression in vascular smooth muscle cells (VSMCs) leads to vascular calcification (Alam et al., 2009). Animal models of renal insufficiency (Mathias et al., 1998; Toka et al., 2012) show that deficiency of renal CaSR causes PTH-independent hypocalciuria, as the reduction of renal CaSR increases tubular Ca^{2+} reabsorption (Brown and MacLeod, 2001). In genetic forms of hypercalciuria, dysregulation of CaSR expression by vitamin D metabolites may be a critical factor for kidney stone formation. In a rat model of hypercalciuric nephrolithiasis, renal VDR and CaSR levels are elevated and renal Ca^{2+} reabsorption is reduced (Bai and Favus, 2006; Yao et al., 2005). Activation of CaSR inhibits cell proliferation in parathyroid cells, keratinocytes (Tu et al., 2001), and cells of the colon crypts (Rey et al., 2010). CaSR expression is reduced or absent in parathyroid glands of patients with primary or severe uremic secondary hyperparathyroidism (Cetani et al., 2000; Corbetta et al., 2000; Kifor et al., 1996) and in many colon cancers (Bhagavathula et al., 2005; Kallay et al., 2003b). Impaired Ca_o^{2+}-sensing may increase cell proliferation and contribute to parathyroid neoplasia and colorectal tumors. In contrast, the CaSR is overexpressed in breast and prostate cancers with high bone metastatic potential (Liao et al., 2006; Mihai et al., 2006; Saidak et al., 2009a). CaSR activation promotes cancer progression by stimulating secretion of PTHrP, thus contributing to osteolytic bone destruction (Guise et al., 2005; Liao et al., 2006). Moreover, the CaSR is found to be overexpressed in the hippocampus neurons of mice sustaining traumatic or ischemic brain injury (Kim et al., 2011, 2014) and in a model of Alzheimer's disease (Gardenal et al., 2017), leading to calcium overload and neuronal death in brain. The

administration of calcilytics, allosteric CaSR inhibitors, renders neuroprotection against the detrimental effects of CaSR overactivation in these pathological conditions (Chiarini et al., 2017; Kim et al., 2013, 2014).

Roles of calcium-sensing receptor in calciotropic tissues

Calcium-sensing receptor in parathyroid glands

CaSRs coevolved with the parathyroid glands in terrestrial vertebrates to maintain systemic Ca^{2+} homeostasis via the close control of the secretion of PTH—the hormone that ultimately controls Ca^{2+} handling by the intestine, kidney, and bone. PTH therefore balances the uptake, storage in bone, and excretion of Ca^{2+} in the body according to systemic needs.

CaSRs enable parathyroid cells to respond to supra- and subphysiological Ca_o^{2+} levels by respectively suppressing and enhancing PTH secretion (Brown, 2013). These critical actions of the parathyroid CaSR are established by the identification of inactivating and activating mutations of the *CASR* in humans with FHH1 and autosomal dominant hypoparathyroidism type 1 (ADH1), respectively (Hannan et al., 2018; Vargas-Poussou et al., 2016). This idea is further supported by the observation that there is a right-shifted Ca_o^{2+}/PTH secretion set point in parathyroid glands cultured from mice with *Casr* deficiency (Cheng et al., 2013). How CaSR activation inversely couples to PTH secretion remains unclear. The ability of homomeric CaSRs to stimulate $G_{q/11}$ proteins and downstream signaling cascades is thought to result from major pathways suppressing PTH secretion at high Ca_o^{2+} concentrations (Conigrave and Ward, 2013). This concept is supported by the development of a phenotype of severe hyperparathyroidism in mice with parathyroid cell-targeted *Gnaq* and *Gna11* double-gene knockouts (Wettschureck et al., 2007) and the association of inactivating and activating *GNA11* mutations in patients afflicted with FHH type 2 (Hannan et al., 2018) and ADH type 2 (Nesbit et al., 2013a) (Howles et al., 2016; Roszko et al., 2016). The linkage of loss-of-function mutations of the sigma subunit of the adapter protein 2 with FHH type 3 (Hovden et al., 2017) further indicates roles for clathrin-mediated endocytosis, receptor trafficking, and receptor reinsertion into the membrane in mediating normal CaSR function in physiological states (Gorvin et al., 2017; Hannan et al., 2016). In contrast, the ability of CaSR to stimulate intracellular Ca^{2+} mobilization can be blunted by the overexpression of regulator of G protein signaling 5 (RGS5) (Balenga et al., 2019), whose expression levels are increased in parathyroid tumors (Koh et al., 2011), indicating an inhibitory action of RGS5 on CaSR signaling. In addition to regulation of acute PTH secretion, CaSR activation suppresses transcription of the PTH gene (Garrett et al., 1995a) and cell growth. The latter is well demonstrated by the presence of significant parathyroid cellular hyperplasia in mice with global knockout of both alleles of *Casr* (Ho et al., 1995) as well as the ability of calcimimetics to prevent parathyroid hyperplasia in rats subjected to the induction of chronic kidney disease (Colloton et al., 2005; Wada et al., 1998). Klotho has also recently been shown to be involved in cross talk with CaSR signaling to suppress PTH synthesis and glandular growth in parathyroid tissue in mice (Fan et al., 2018), implicating a role of FGF23 signaling in mediating parathyroid function.

The ability of parathyroid cells to sense changes in extracellular levels of Ca^{2+} is fundamentally important for skeletal development and maintenance. Deletion of both *Casr* alleles in the parathyroid glands of mice retards perinatal skeletal development in these $^{PTC}Casr^{-/-}$ mice (Chang et al., 2008). While $^{PTC}Casr^{-/-}$ mice recapitulate most biochemical (severe hyperparathyroidism, hypercalcemia, and hypophosphatemia) and skeletal (expansion of growth plate, osteopenia, osteiod accumulation, and excess fractures with poor healing) phenotypes of NSHPT in patients and in mice with global *Casr* knockout ($Casr^{-/-}$ mice) (Ho et al., 1995), they manifest hypercalciuria, in contrast to hypocalciuria in $Casr^{-/-}$ mice. This is because normal CaSRs are still functioning in the kidney to promote Ca^{2+} excretion in response to the marked hypercalcemia of this conditional knockout mouse ($^{PTC}Casr^{-/-}$ mice).

Given that *Casr* genes are unaltered outside of PTCs in $^{PTC}Casr^{-/-}$ mice, severe PTH excess appears to be sufficient to cause skeletal defects regardless of the status of CaSR function in other tissues. In contrast to severe PTH excess, milder forms of hyperparathyroidism studied in $^{PTC}Casr^{\pm}$ mice with heterozygous *Casr* gene knockout targeted specifically to the parathyroid are anabolic to trabecular bone by protecting the bones from aging-induced bone loss (Cheng et al., 2013). However, these protective effects are at the expense of cortical thinning and demineralization, indicating differential responses of osteoblasts and osteocytes to mild PTH elevations. Given that $^{PTC}Casr^{\pm}$ mice also manifest hypercalcemia, the direct activation of CaSR in osteoblasts, osteocytes, and/or osteoclasts in their skeletons cannot be ruled out as a secondary effect of hyperparathyroidism that contributes to skeletal changes.

Calcium-sensing receptor in the kidney

Molecular mechanisms responsive to changes in the need for Ca^{2+} conservation and the excretion of Ca^{2+} when in excess were postulated to be present in different segments of the kidney long before CaSR cDNA was identified in the parathyroid

(Brown et al., 1993) and later in kidney (Riccardi et al., 1995). This was because evidence had accumulated, from a large body of in vitro and in vivo animal studies, on the many effects that divalent cations (Ca^{2+} and Mg^{2+}) were known to have on renal function, water and solute handling, and ion transport. Aberrant perception of ambient serum Ca^{2+} concentration in the human disorders of FHH and NSHPT lent further support to the critical importance of renal Ca^{2+}- (and Mg^{2+}-) sensing mechanisms operating in human physiology and altered in disease states. Patients with FHH had notable hypocalciuria despite hypercalcemia and normal or even mildly elevated PTH levels (Marx, 2018). This phenotype, when it became clearly evident in the 1970s and 1980s (Attie et al., 1983) (Marx et al., 1978a, 1978b, 1981a, 1981b, 1982a, 1982b, 1985), along with the typical autosomal dominant mode of inheritance of FHH, predicted the condition to be due to a genetic defect with a high degree of penetrance. The phenotypic features further predicted that the responsible gene would be strongly expressed in both parathyroid and renal cells. The fact that many individuals with FHH also had mild hypermagnesemia emphasized that the Ca_o^{2+}-sensing defect of FHH also involved defective Mg_o^{2+}-sensing. The diagnosis of FHH is assessed for clinically by the use of the Ca^{2+}—creatinine clearance ratio, which directly reflects the handling of Ca^{2+} by the kidney in relation to renal function and serum Ca^{2+} levels, and this clearance calculation is widely used (Christensen et al., 2008).

Fluctuations in $[Ca^{2+}]_o$ can exert several different effects on renal function. Increased levels of Ca_o^{2+} promote renal Ca^{2+} excretion, and this response occurs in the absence of PTH. It was observed that patients with FHH who underwent total parathyroidectomy to treat their hypercalcemia continued to demonstrate hypocalciuria, indicating that this was an intrinsic property of the kidney and not a PTH-dependent phenomenon (Attie et al., 1983).

Renal sensitivity to Ca_o^{2+} involves many functions and locations in the kidney (Riccardi and Valenti, 2016). Areas in the nephron and renal functions include (1) Ca^{2+} transport in the thick ascending limb of the loop of Henle (TAL), which is the main site of abnormal Ca^{2+} handling in individuals with FHH (Attie et al., 1983); (2) proximal tubule; (3) CD; (4) distal convoluted tubule; and (5) juxtaglomerular apparatus (JGA).

Where exactly and to what extent CaSR mRNA and protein are expressed within different segments of the nephron have been controversial topics over the years (Riccardi and Valenti, 2016). A lack of reliable reagents for definitively identifying and quantifying the often-low levels of CaSR expression has hindered the development of a clear picture of the sites where CaSRs are expressed. Expression of CaSRs in the TAL is widely accepted and is among the strongest in the kidney. The renal CD is another site where water handling and urinary concentration occur and where CaSRs are prominently expressed. Other sites of CaSR expression include the glomerulus (in podocytes and mesangial cells) and in proximal tubular cells.

Extensive studies have been done in various renal cell systems and mouse models. In cultured mesangial cells, CaSR activation stimulated inositol trisphosphate production and $Ca^{2+}{}_i$ mobilization, similar to the signaling pathways activated by high Ca_o^{2+} and Mg_o^{2+} concentrations and calcimimetics in parathyroid cells (Brown et al., 1993; Riccardi and Valenti, 2016). CaSR activation is also linked to the opening of the transient receptor potential channels (TRPCs) TRPC3 and TRPC6 in these cells (Oh et al., 2011).

The JGA is the principal source of renin release, which is negatively regulated (suppressed) by high Ca_o^{2+} levels but positively regulated by many other important physiological factors. Similar to the signaling pathways activated by high Ca_o^{2+} levels in parathyroid cells, CaSR activation involves Ca_i^{2+} mobilization (via a Gq mechanism) in modulating renin secretion as well as inhibition of cyclic AMP accumulation and adenyl cyclase activity (Beierwaltes, 2010).

Several functions of proximal tubular cells are Ca^{2+}-regulated. One such critical function is phosphate reabsorption. PTH, through its receptor (PTH1R), is a key regulator of phosphate reabsorption. When the PTH1R is stimulated, phosphate excretion increases. CaSR activation by high Ca_o^{2+} or calcimimetic can blunt the ability of PTH to stimulate phosphaturia. This has been used to advantage with the calcimimetic cinacalcet in treating disorders of phosphate wasting such as tumor-induced osteomalacia. High Ca_o^{2+} concentrations also inhibit proximal tubular 1-alpha hydroxylase activity and thereby dampen the production of $1,25(OH)_2D_3$, which will ultimately lower serum Ca^{2+} levels. Acute PTH administration can also reduce CaSR expression in that region of the kidney (Riccardi and Valenti, 2016). Other actions of CaSR signaling in the proximal tubule include luminal acidification and fluid reabsorption (Riccardi and Valenti, 2016). $1,25(OH)_2D_3$ can modulate CaSR expression in the distal tubule, where this hormone promotes Ca^{2+} transport and thereby contributes to the raising of serum Ca^{2+} levels.

A great number of mechanistic studies have been done to clarify the pathways by which CaSRs modulate Ca^{2+} reabsorption in the TAL (Riccardi and Valenti, 2016). PTH stimulates Ca^{2+} reabsorption by increasing Ca^{2+} permeability. CaSRs in the cortical TAL are involved in the actions of hormone-mediated cAMP accumulation such as that due to calcitonin or vasopressin. Decreased cAMP accumulation in these cells will reduce overall Ca^{2+} permeability and thereby Ca^{2+} transport and reabsorption. Ca^{2+} permeability in this portion of the nephron requires NaCl uptake across the lumen of the nephron segment. The transepithelial K^+ gradient that ultimately becomes established in this segment is the driving

force of the reabsorption of Ca^{2+}, Mg^{2+}, and Na^{+}. Paracellular Ca^{2+} permeability in the TAL is importantly regulated by various members of the family of claudin proteins. Human disorders of Ca_o^{2+}-sensing also shed light on the role of CaSRs in Ca^{2+} reabsorption by the kidney and in Ca^{2+} excretion. Individuals with germline-activating mutations in the CaSR (ADH1) may have hypercalciuria as a result of their activated renal CaSRs. Renal-specific *Casr* deletion in a mouse model (Toka et al., 2012) produces hypocalciuria along with normal serum Ca^{2+} and PTH levels. This is evidence that renal CaSRs operate to control renal Ca^{2+} excretion independently of changes in PTH in vivo.

The distal convoluted tubule also plays a role in Ca^{2+} reabsorption (Riccardi and Valenti, 2016), and multiple membrane channels and transporters play essential parts in that process. An especially prominent role is played by transient receptor potential cation channel (TRPV) 5, which moves Ca^{2+} across the apical membrane of the distal tubular cell. Other ion transport mechanisms cooperatively participate in Ca^{2+} reabsorption thereafter.

CaSRs are strongly expressed along the CD (Riccardi and Valenti, 2016). In that nephron segment, if high $[Ca^{2+}]_o$ is present, there is urinary acidification due to the activation of an H^{+}-ATPase. CaSRs are also expressed in this nephron segment along with aquaporin 2 water channels. Both CaSRs and aquaporin 2 channels are colocated within the same vesicles in the CD. In this portion of the nephron, the activation of CaSRs is thought to inhibit vasopressin-mediated insertion of aquaporin 2 water channels into the membrane and thereby reduce water reabsorption. This yields water diuresis and "resistance" to the effects of vasopressin when increased levels of CaSR activation are present. The interrelationships between CaSR activity and vasopressin action in this portion of the kidney are thought to underlie the nephrogenic diabetes insipidus commonly seen in individuals with significant hypercalcemia. Thus, there are multiple areas of the kidney where CaSR activation plays a central role in transport and/or permeability to water, Ca^{2+}, Mg^{2+} phosphate, acid, and other ions. CaSR activation also modulates kidney responses to critically important hormones that modulate its function including vasopressin, calcitonin, and others. Human disorders of Ca_o^{2+}-sensing help to underscore the importance of specific physiological pathways and integrate them into in vivo responses.

Calcium-sensing receptor in bone cells

Long before the CaSR cDNA was identified in 1993 by Brown and colleagues (Brown et al., 1993) with an expression cloning strategy using parathyroid gland cRNA in *Xenopus laevis* oocytes, it was clear that changes in the extracellular concentration of Ca^{2+} had significant effects on the function of several different cell types in bone (Dvorak et al., 2004) (Chang et al., 2008; Goltzman and Hendy, 2015). These studies were largely in vitro in cell culture systems of transformed osteosarcoma cell lines and often required higher-than-physiological $[Ca^{2+}]_o$ to achieve effects on signaling pathway activation, Ca_i^{2+} mobilization, or functional or biochemical outcomes (mitogenesis, mineralization, and so forth). The pharmacology of these responses led to controversy in the field as to whether the putative parathyroid Ca_o^{2+}-sensing mechanism responsible for mediating the effects of Ca_o^{2+} on PTH secretion (in a tight physiological range) was the same molecular mechanism operating in different bone cell populations. Once the CaSR cDNA became available, along with highly specific antibodies directed against CaSR epitopes, it became clear, by immunocytochemistry and in situ hybridization, that CaSRs were present in osteoblasts, osteocytes, osteoclasts, marrow mononuclear cells, and macrophages (Chang et al., 1999; Dvorak et al., 2004). Speculations from earlier studies were subsequently supported by strong evidence that CaSRs were playing critical roles in bone and were responsible for the effects of changes in $[Ca^{2+}]_o$ on the activation of signaling responses, alterations in gene expression, and mineralization in bone cell systems (Chang et al., 2008; Dvorak et al., 2004; Goltzman and Hendy, 2015; Rybchyn et al., 2011). Furthermore, the receptor was implicated in regulating bone development and mass in vivo (Chang et al., 2008; Dvorak et al., 2007; Dvorak-Ewell et al., 2011).

The phenotype of global *Casr* knockout mice, $Casr^{-/-}$, generated by Ho et al. (Ho et al., 1995) confirmed the critical role of CaSRs in mediating the control of PTH secretion by Ca_o^{2+}. These mice showed severe hyperparathyroidism, hypercalcemia, and hypophosphatemia and died at 2–3 weeks of age. Dramatic skeletal demineralization was present along with growth retardation and failure to thrive. Given the severe mineral and hormonal disturbances in these mice, it was difficult to ascertain what role bone CaSRs might be playing in the skeletal aspects of their phenotype, because the hyperparathyroidism and serum Ca^{2+} and phosphate derangements in these mice can alone have profound effects on bone growth, development, and mineralization. Knockout mouse models in which the *Pth* gene was deleted on the background of this global $Casr^{-/-}$ mouse (i.e., a double-knockout, $Pth^{-/-}/Casr^{-/-}$) had relatively normal-appearing bone by histology; however, these animals had markedly low PTH levels (Goltzman and Hendy, 2015; Kantham et al., 2009). Similarly, when PTH was eliminated by creating a double-knockout using $Gcm2^{-/-}$ mice in whom parathyroid glands did not develop on the background of this global $Casr^{-/-}$ mouse (i.e., $Gcm2^{-/-}/Casr^{-/-}$), a similarly normal skeletal histology was noted (Tu et al., 2003). This led investigators to surmise that CaSRs were not critical to skeletal development. Thus, it

became necessary to generate and assess conditional knockout mice with *Casr* deletion selectively targeted to specific bone cell populations without the complicating features of hypo- or hyperparathyroidism present in the prior models.

The most compelling data for Ca^{2+} as a ligand and CaSR activation as an anabolic pathway in bone emerged from conditional knockout mouse models (Chang et al., 2008). When CaSRs were deleted across the osteoblastic lineage in mice (under control of the 2.3 or 3.6 kb type 1 collagen [Col1] promoter-driven Cre recombinase), the bone phenotypes were dramatic (Chang et al., 2008; Dvorak-Ewell et al., 2011). These bone-specific conditional knockout mice (e.g., $^{2.3Col1}Casr^{-/-}$ and $^{3.6Col1}Casr^{-/-}$ mice) showed growth retardation, spontaneous fractures, low trabecular and cortical bone mass, undermineralized bone, osteoblast and osteocyte apoptosis, and gene expression profiles indicative of arrested osteoblast differentiation (Chang et al., 2008; Dvorak-Ewell et al., 2011). When the conditional knockout of *Casr* was restricted to mature osteoblasts and osteocytes using a *Cre* mouse in which Cre expression was driven by the osteocalcin promoter, markers of osteoblast gene expression were delayed and trabecular bone mass and microarchitecture were reduced (Chang et al., 2008; Dvorak-Ewell et al., 2011), but the phenotype was much milder. These observations in vivo are supported by work in osteoblast cell lines by many labs (Chang et al., 2008; Goltzman and Hendy, 2015; Santa Maria et al., 2016), confirming that CaSR activation by agonists (e.g., high $[Ca^{2+}]_o$) is critical for osteoblast proliferation and differentiation and the maintenance of bone mass.

CaSR activation also modifies the function of mature osteoclasts and other cells within the osteoclastic lineage (monocytes and macrophages) (Goltzman and Hendy, 2015). In osteoclast lineage cells, CaSR activation suppresses resorptive function, expression of markers of osteoclast differentiation, and cell survival (Goltzman and Hendy, 2015; Kameda et al., 1998; Kanatani et al., 1999; Olszak et al., 2000; Santa Maria et al., 2016; Yamaguchi et al., 1998). High $[Ca^{2+}]_o$ also inhibits the resorption of mature osteoclasts. The concentrations of Ca_o^{2+} at which these phenomena are observed are in general much higher than those in the circulation but are ones likely to be present in the bone microenvironment and in the vicinity of resorbing osteoclasts (Datta et al., 1989; Malgaroli et al., 1989; Moonga et al., 1990; Zaidi et al., 1991). Osteoclasts also undergo apoptosis in response to high concentrations of Ca_o^{2+}, and the pathway responsible involves phospholipase C and NF-kappa B (Mentaverri et al., 2006). That a dominant-negative *Casr* construct interferes with these effects is highly supportive of CaSRs as involved in these events in osteoclasts. However, calcimimetics, which stimulate CaSRs and suppress PTH secretion, and calcilytics, which block CaSRs and enhance PTH secretion, do not have the effects predicted of straightforward CaSR activation and inhibition in osteoclasts (Shalhoub et al., 2003) (Gowen et al., 2000).

Observations from certain single-knockout and double-knockout mouse models have shed further light on the interaction of CaSRs with other key molecules involved in Ca^{2+} homeostasis such as PTH and PTH1R and $1,25(OH)_2D_3$. CaSR activation is key in the full actions of PTH on bone compartments. PTH-induced cortical bone demineralization is reduced in $Pth^{-/-}/Casr^{-/-}$ mice compared with $Pth^{-/-}$ mice (Xue et al., 2012), indicating that intact CaSRs are important in the actions of PTH-mediated bone resorption. In addition, the hypercalcemic actions of $1,25(OH)_2D_3$ are at least in part mediated by CaSRs, because deletion of *Casr* in mice on the background of *Cyp27b1* knockout produces less hypercalcemia (Richard et al., 2010). Isolated marrow cells from $Pth^{-/-}/Casr^{-/-}$ mice showed reduced RANKL expression and osteoclastogenesis in response to PTH versus responses in marrow cells from $Pth^{-/-}$ mice (Xue et al., 2012). These studies indicate that in addition to the effects of solitary CaSR activation in bone, there are cooperative effects of CaSR signaling in mediating the actions of PTH and PTH1R and $1,25(OH)_2D_3$, and likely its receptor as well.

Calcium-sensing receptor in the breast

Mammary CaSR plays pivotal roles in modulating maternal Ca^{2+} metabolism and neonatal bone development during lactation. CaSR levels are low during postnatal mammary gland development through late pregnancy but increase to a peak during lactation (VanHouten et al., 2004), when the receptor is expressed primarily on the basolateral surface of ductal epithelial and alveolar cells (Cheng et al., 1998; VanHouten et al., 2004, 2007). During milk production, the mammary gland synthesizes and secretes PTHrP into milk and into the circulation, where it activates bone resorption to mobilize skeletal calcium (Wysolmerski, 2012). Delivery of Ca^{2+} to the mammary gland induces the plasma membrane Ca^{2+}-ATPase 2 (PMCA2) to transport Ca^{2+} from breast epithelial cells across the apical membrane and into the acinar lumen (Reinhardt et al., 2004) (VanHouten and Wysolmerski, 2007). Although the CaSR does not have a dominant role in regulating morphological development or differentiation in the normal mammary gland (Kim and Wysolmerski, 2016), the CaSR adjusts transcellular Ca^{2+} transport, overall milk secretion, and PTHrP production in response to Ca^{2+} availability in the maternal circulation during milk production (Mamillapalli et al., 2013; Vanhouten and Wysolmerski, 2013). The mammary CaSR adjusts milk PTHrP levels in a manner inverse to milk Ca^{2+} content to coordinate maternal and neonatal bone and Ca^{2+} metabolism. In normal mammary epithelial cells, CaSR activation increases milk Ca^{2+} content by

stimulating Ca^{2+} pumping and ATPase activity of PMCA2 (VanHouten et al., 2007) while it suppresses PTHrP production via coupling to Gαi to decrease cAMP production by adenylate cyclase and subsequent PKA activation (Mamillapalli et al., 2008). Systemic hypocalcemia reduces overall milk production and Ca^{2+} content and decreases the skeletal Ca^{2+} accrual of suckling pups (Ardeshirpour et al., 2006; VanHouten et al., 2004) but increases PTHrP production, an effect that can be prevented by treatment with a calcimimetic (VanHouten et al., 2004).

The CaSR is overexpressed by many breast cancers; however, CaSR signaling seems to have opposing effects on proliferation and cell death in breast cancer cells. Certain studies have shown that increasing $Ca^{2+}{}_o$ concentration above the physiological range inhibits proliferation, invasion, and anchorage-independent growth of breast cancer cells and that the CaSR mediates growth-inhibitory effects by downregulating the expression of survivin, an antiapoptotic factor (Liu et al., 2009; Promkan et al., 2011). On the contrary, other studies have shown that activation of CaSR promotes cell proliferation and the migration of breast cancer cells via stimulation of PLC, ERK1/2, and EGFR activation, upregulation of phosphocholine and cytokine production, and activation of TRPC1 (El Hiani et al., 2009a; El Hiani et al., 2009b; Hernandez-Bedolla et al., 2015; Huang C. et al., 2009; Saidak et al., 2009a). Knocking out the *Casr* gene or treating breast cancer cells with calcilytic has been shown to inhibit tumor cell proliferation and increase Ca^{2+}-mediated cell death (Kim et al., 2016). Furthermore, CaSR expression was correlated directly with PTHrP protein levels in human breast cancers (Kim et al., 2016; Mu et al., 2012; VanHouten et al., 2010). Unlike normal breast cells, activation of the CaSR in breast cancer cells with Ca_o^{2+}, spermine, aminoglycoside antibiotics, or allosteric calcimimetics upregulates PTHrP secretion through the stimulation of cAMP production (Mamillapalli et al., 2008; Sanders et al., 2000). A switch in G protein usage, by which the CaSR couples to Gαs instead of Gαi, underlies the opposing effects of the CaSR on PTHrP expression in malignant and normal breast cells (Mamillapalli et al., 2008). Nuclear PTHrP stimulates cell proliferation by decreasing the levels of the cell cycle inhibitor p27 kip1 and protects against Ca_o^{2+}-mediated cell death by preventing the nuclear accumulation of apoptosis-inducing factor (Kim et al., 2016). The alteration in PTHrP production has important consequences for the progression of bone metastases (Mihai et al., 2006). Increased PTHrP secretion in response to high Ca_o^{2+} levels acts in a paracrine fashion to accelerate osteolysis (Mamillapalli et al., 2008; Wysolmerski, 2012). As a result of bone resorption, release of growth factors such as TGF-β, IGFs, and FGFs from the bone matrix further stimulates the growth of bone-metastasizing tumors and increases PTHrP production, developing a vicious cycle of osteolysis (Patel et al., 2011; Theriault and Theriault, 2012).

Noncalciotropic roles of the calcium-sensing receptor

Calcium-sensing receptor in the pancreas

CaSR is expressed in the endocrine and exocrine pancreas including β-islet cells, α-cells, duct cells, acinar cells, and various nonexocrine cells such as intrapancreatic nerves and blood vessels (Bruce et al., 1999) (Gray et al., 2006; Racz et al., 2002), whereas somatostatin-secreting δ-cells do not express the CaSR (Squires, 2000). Activation of the CaSR in α-cells stimulates glucagon secretion from human islets (Gray et al., 2006). Within the islet, glucagon can increase insulin secretion despite its counteracting effect on energy homeostasis.

CaSR regulates glucose-evoked insulin secretion by β-cells (Jones et al., 2007; Rybczynska et al., 2017). Elevation of plasma glucose concentration leads to an increase in the ATP/ADP ratio mediated by glucokinase, which closes ATP-dependent K^+ channels, depolarizing the cell membrane and opening voltage-dependent Ca^{2+} channels (VDCCs) to increase Ca_i^{2+} levels and induce insulin release (Squires, 2000). In human islets and insulin-secreting MIN6 cell lines, activation of the CaSR by elevating Ca_o^{2+} induced transient MAPK activation and insulin secretion (Devis et al., 1975; Gray et al., 2006; Squires, 2000). Calcimimetic activation of the CaSR not only enhanced the maximal secretory response to glucose in human and rodent β-cells, but also transiently increased insulin secretion in the absence of an increase in associated nutrient stimulation (Gray et al., 2006). CaSR may modulate insulin secretory responses through the stimulation of β-cell proliferation and cell−cell communication (Hills et al., 2012). Calcimimetic activation of the CaSR in MIN6 increased the expression of E-cadherin and L-type VDCCs and stimulated MAPK-mediated cell proliferation, thereby augmenting cell−cell adhesion and β-cell function to promote the insulin secretion of neighboring cells (Hills et al., 2012; Kitsou-Mylona et al., 2008). Colocalization and spatial interactions between the CaSR and L-type VDCCs may also enhance glucose-induced secretion of insulin (Parkash, 2011). Conversely, cell turnover and glucose-evoked insulin secretion in MIN6 pseudoislets was reduced when CaSR expression was knocked down (Kitsou-Mylona et al., 2008). CaSR-dependent regulation of insulin secretion involves complex signaling cascades including ERK1/2, PLC/IP_3/intracellular Ca^{2+}, and CAMKII (Gray et al., 2006). However, persistent activation of CaSR in human β-cells has been shown to inhibit insulin secretion (Squires et al., 2000). Mice with gain-of-function CaSR mutations manifested hypocalcemia in

association with impaired glucose tolerance and insulin secretion (Babinsky et al., 2017; Dong et al., 2015). In one ADH1 mouse model, pancreas islet mass was reduced, and both α-cell and β-cell functions were impaired (Babinsky et al., 2017). The rectification of glucose intolerance and hypoinsulinemia in these mice by a calcilytic highlighted a potential therapeutic application of these compounds for disordered glucose metabolism (Babinsky et al., 2017; Dong et al., 2015).

CaSR is highly expressed in pancreatic duct cells and regulates their proliferation (Racz et al., 2002). It has been reported that the activation of CaSR in the rat pancreas duct luminal membrane increased ductal HCO_3^- secretion (Bruce et al., 1999). These observations suggest that CaSR is able to monitor and regulate Ca^{2+} concentration in pancreatic juice by triggering ductal electrolyte and fluid secretion, and this could reduce the risk of calcium carbonate stone formation and progression to pancreatitis (Racz et al., 2002). Clinical genetic linkage studies have identified that mutations in the CaSR gene and the pancreatic secretory trypsin inhibitor gene in patients with FHH are associated with susceptibility to acute and/or chronic pancreatitis (Felderbauer et al., 2006; Muddana et al., 2008).

Calcium-sensing receptor in the gastrointestinal system

The CaSR is present along the gastrointestinal tract and plays key roles in glandular and fluid secretion and in the occurrence of digestive disease. CaSRs are expressed in the stratified squamous esophageal epithelium (Justinich et al., 2008) and regulate the proliferation, differentiation, cell−cell adhesion, and cytoskeletal organization of epithelial cells (Abdulnour-Nakhoul et al., 2015). Activation of CaSR in the esophageal epithelial cell line HET-1A increases Ca_i^{2+} mobilization and activates MAPK (ERK1/2) signaling pathways to stimulate the secretion of cytokine IL-8 (Justinich et al., 2008). CaSR is implicated in the proliferative response to injury and the pathogenesis of esophagitis, as CaSR expression is increased in eosinophilic esophagitis and Barrett's adenocarcinoma (Abdulnour-Nakhoul et al., 2015). Under the condition of esophagitis, CaSR can be activated by eosinophil-released major basic protein to stimulate FGF9 secretion and activate downstream proliferation-related genes in esophageal epithelial cells (Mulder et al., 2009).

In the stomach, the CaSR is expressed on the basolateral membrane of parietal cells and on both the basolateral and the apical surface on gastrin-releasing G-cells (Cheng et al., 1999). The CaSR is considered a key modulator of gastric acid secretion and gastric luminal pH because it can be activated by the same dietary components (amino acids, amines, calcium) that activate gastrin release from G-cells. Activation of basolateral CaSR by agonists (e.g., Ca^{2+}, Gd^{3+}, and L-type amino acids) stimulates H+ and K+ ATPase and results in the increased production and secretion of gastric acid (Buchan et al., 2001; Busque et al., 2005; Dufner et al., 2005). In contrast, $Casr^{-/-}$ animals cannot respond to high intraluminal calcium and L-type amino acid concentrations with gastrin secretion (Feng et al., 2010). The intracellular signal cascades underlying CaSR-mediated H+ and K + ATPase induction include Ca_i^{2+}, PLC, MAPK, and PKC (Kopic et al., 2012; Remy et al., 2007).

Low pH in the gastric lumen produces ionized Ca^{2+} to be absorbed by the small intestine. CaSR participates in the regulation of intestinal secretion and absorption of Ca^{2+} in cooperation with 1,25-dihydroxy vitamin D_3 (Favus et al., 1980, 1981). CaSR is predominantly expressed on both apical and basolateral membranes of colonic crypts in the intestine brush border (Alfadda et al., 2014) and is also localized on the neuronal plexuses, Meissner and Auerbach (Cheng, 2012). Activation of the apical receptor by high luminal Ca^{2+} results in an increase in NaCl, water, and Ca^{2+} absorption. Consequently, elevated levels of blood Ca^{2+} activate intestinal basolateral CaSR to inhibit the absorption, forming a negative feedback loop (Alfadda et al., 2014). CaSR also acts as an important regulator of intestinal enteroendocrine activity in response to nutrient and nonnutrient stimuli. CaSR is involved in the L-amino acid stimulation of gut peptide secretion by K-cell and L-cell in the rat small intestine (Mace et al., 2012) and cholecystokinin secretion in isolated intestinal I cells (Liou et al., 2011). Furthermore, the CaSR plays a central role in intestinal fluid transport. Activation of the colonic CaSR by Ca^{2+}, Gd^{3+}, polyamines, or neomycin induces a rapid increase in $Ca^{2+}{}_i$ levels in both surface and crypt cells and reduces the stimulatory effect of forskolin on net fluid secretion in perfused crypts (Cheng et al., 2002, 2004). While secretagogues such as forskolin and cholera toxin could induce fluid secretion by increasing cyclic nucleotides, activation of either the luminal or the basolateral CaSR by Ca^{2+} and spermine can reverse forskolin-stimulated fluid secretion via facilitation of the destruction of cAMP and cGMP, inhibiting Cl^- secretion and stimulating Na^+ absorption (Geibel et al., 2006). CaSR deficiency in the intestinal epithelium induced a proinflammatory immune response, compromised intestinal barrier function, and altered the composition of the microbiota (Cheng et al., 2014). These findings suggest that CaSR activator and CaSR-based nutrients might provide an effective treatment for disorders such as inflammatory bowel disease, enterocolitis, and secretory diarrhea (Cheng, 2016; Owen et al., 2016).

CaSR negatively modulates colonic epithelial growth and the inactivation of CaSR due to promoter hypermethylation, and defective histone acetylation (Fetahu et al., 2014) plays a key role in colorectal tumorigenesis (Rogers et al., 2012; Singh et al., 2013). High dietary Ca^{2+} intake promotes colonic mucosal epithelial cell differentiation, decreases cell

growth, and reduces risk for the development of colorectal cancer (Lamprecht and Lipkin, 2001). Conditional knockout of CaSR in intestinal epithelial cells increases nuclear β-catenin localization, enhances cell proliferation, and diminishes the differentiation of colonic crypts (Rey et al., 2012). Activation of the CaSR by raising Ca_o^{2+} in Caco-2 cells leads to a decrease in c-Myc proto-oncogene expression and abrogates its proproliferative effect (Kallay et al., 1997). Activation of the CaSR in human carcinoma cell lines by elevating Ca_o^{2+} levels decreases cell growth and promotes cell differentiation in correspondence with increased E-cadherin expression and suppressed β-catenin activation (Chakrabarty et al., 2003; Van Aken et al., 2001; Wong and Pignatelli, 2002). Increased E-cadherin stimulated by CaSR can interact with β-catenin to enhance cell−cell and cell−matrix adhesion via remodeling of the actin-cytoskeleton (Brembeck et al., 2006). Meanwhile, the activation of CaSR also prevents nuclear translocation of β-catenin, thereby reducing the formation of β-catenin−TCF4 complex and downregulating c-Myc and cyclin D1 expression (Chakrabarty et al., 2003). In addition, activation of CaSR stimulates the noncanonical Wnt pathway (Wnt5a/Ror2) to inhibit overly active Wnt signaling in colon cancer cell lines (MacLeod et al., 2007) and to decrease the risk of colitis-associated colon cancer by suppressing NFκ-B activity and reducing TNFα secretion and TNFR1 expression (Kelly et al., 2011) (Macleod, 2013). Restoration of CaSR expression in colorectal cancer cells reduces proliferation and increases differentiation and apoptotic potential (Aggarwal et al., 2015) and results in the concurrent reversal of stem cell markers, drug resistance, and epithelial−mesenchymal transition-related transcription factors (Singh and Chakrabarty, 2013). Taken together, these data support a role of CaSR as a tumor suppressor.

Calcium-sensing receptor in the peripheral vascular system

Although arterial blood pressure is regulated by the centrally located circulatory centers in the medulla oblongata, long-term blood pressure is controlled primarily by the volume balance of blood vessels. In addition to the central control mechanisms mediated by vegetative neuronal innervation and hormone secretion, blood vessels are able to independently control their perfusion locally via the actions of the CaSR (Smajilovic et al., 2011). CaSR expression is found in several cell types in vasculature including the endothelium (Ziegelstein et al., 2006), VSMCs (Schepelmann et al., 2016), and the perivascular nerve (Bukoski et al., 1997). The activation of CaSR in rat mesenteric branch arteries induced neuronal release of cannabinoid, causing endothelium-independent hyperpolarization of VSMCs and subsequent relaxation of the arteries (Ishioka and Bukoski, 1999). The CaSR of endothelial cells participates in Ca^{2+}-induced vasorelaxation by two mechanisms, endothelial hyperpolarization and nitric oxide release (Weston et al., 2005) (Greenberg et al., 2016). In mesenteric arteries, activation of CaSR by Ca_o^{2+} or calcimimetic led to the opening of the Ca^{2+}-sensitive K^+ channel, which induced hyperpolarization of endothelium and VSMCs (Greenberg et al., 2016). In the human aorta, activation of CaSR by spermine induced an increase in $Ca^{2+}{}_i$ concentration and nitric oxide (NO) production, resulting in decreased vascular tone (Loot et al., 2013; Ziegelstein et al., 2006). It was suggested that the heteromeric TRPV4/TRPC1 channels in vascular endothelial cells play a role in CaSR-induced NO production and vasorelaxation (Ma et al., 2011) (Greenberg et al., 2017). On the other hand, rises in Ca_o^{2+} induced endothelium-independent contractility in the aorta and mesenteric artery (Schepelmann et al., 2016; Wonneberger et al., 2000). Ablation of CaSR in VSMCs led to lower diastolic and mean arterial blood pressures in *Casr* knockout mice (Schepelmann et al., 2016). Activation of the CaSR of smooth muscle cells induced ERK1/2 phosphorylation and a subsequent increase in proliferation with no elevation in the IP_3 level (Smajilovic et al., 2006). Thus, vascular CaSR plays a dual role in controlling blood vessel tone and heart rate with prorelaxing actions in the endothelium (Lopez-Fernandez et al., 2015) and procontractile effects in vascular smooth muscle (Schepelmann et al., 2016). Nonetheless, a recent study revealed another mechanism for the CaSR to control regional blood flow and blood pressure. Lee et al. emonstrated that activating the CaSR in the olfactory epithelium of rat with Ca_o^{2+} or CaSR agonists increased sympathetic efferent nerve activities and arterial blood pressure and subsequently decreased renal blood flow and renal, hepatic, and enteral microcirculation (Lee et al., 2019). In addition, the suppressive effect on renal perfusion was antagonized by calcilytic NPS-2143 and abolished by mechanic denervation (Lee et al., 2019), supporting a direct coupling between CaSR activation and increased peripheral vascular resistance by sympathetic excitation.

Reduced vasorelaxation by low CaSR expression or function has been linked to the complications of diabetic vasculopathy (Loot et al., 2013). Decreased expression of CaSR is also associated with the development of cardiovascular calcification in individuals with advanced chronic kidney disease (London et al., 2005). In vitro studies show that calcimimetic treatment increases CaSR expression and reduces vascular mineralization (Alam et al., 2009) (Henaut et al., 2014; Molostvov et al., 2015). Additionally, calcimimetic treatments were shown to exert antihypertensive effects in patients with chronic kidney disease (Zitt et al., 2011) and reduced the risk of cardiovascular events in elderly hemodialysis patients (Parfrey et al., 2015; Sumida et al., 2013), possibly because of their ability to restore CaSR expression levels in the vasculature (Henaut et al., 2014).

Calcium-sensing receptor in the lung

CaSR is expressed in both epithelium and smooth muscle in developing fetal lungs (Riccardi et al., 2013). The CaSR has been identified as an important regulator of intraluminal pressure and lung development. A crucial part of lung development is branching morphogenesis during the pseudoglandular stage. Exposure of isolated fetal lung buds to increased Ca_o^{2+} or calcimimetic induced elevations in Ca_i^{2+} and had a suppressive effect on branching because of the inhibition of cell proliferation (Finney et al., 2008). This CaSR-mediated suppression of the lung branching program requires PLC-dependent Ca_i^{2+} release and the activation of PI3K (Finney et al., 2008). Furthermore, higher Ca_o^{2+} or calcimimetic induced lumen distension by increasing luminal fluid volume and stimulating transepithelial fluid transport (Finney et al., 2008). CaSR is also found in the neuroepithelial bodies of the postnatal mouse lung and is implicated in coordinating intercellular communication through Ca_i^{2+} signaling in this intrapulmonary airway stem cell niche (Lembrechts et al., 2013).

Greater expression and function of CaSR in pulmonary arterial smooth muscle cells has been linked with the onset of idiopathic pulmonary arterial hypertension (PAH) (Yamamura et al., 2012) and the development of asthma (Yarova et al., 2015). Unlike the largely protective properties of CaSR in the peripheral vascular system, CaSR is involved in hypoxic vasoconstriction in the pulmonary vasculature and in vascular remodeling during the development and progression of PAH (Peng et al., 2014; Tang et al., 2016; Zhang et al., 2012). Nonetheless, recent work demonstrated that calcilytics can significantly improve the remodeling process of lung vessels in cases of PAH (Yamamura et al., 2015, 2016).

Asthma is characterized by airway accumulation of a group of polycationic proteins, particularly eosinophilic cationic proteins and major basic proteins, due to chronic inflammation (Kurosawa et al., 1992; North et al., 2013). Activation of CaSR by polycations increases Ca_i^{2+} levels and cell proliferation in airway smooth muscle cells, leading to airway hyperresponsiveness, bronchoconstriction, and inflammation in allergic asthma. It was postulated that CaSR may also control the recruitment and activation of inflammatory cells, which in turn release cytokines that subsequently elevate CaSR expression, thus creating a positive feedback loop in asthma (Yarova et al., 2015). These effects, however, could be ameliorated by CaSR ablation from the airway smooth muscle or prevented by nebulized calcilytics (Yarova et al., 2015). The protective effects of nebulized calcilytics are mediated by preventing Ca_i^{2+} increases and by abrogating the signaling pathways associated with airway contractility, such as ERK1/2, p38 MAPK, and PI3K/Akt (Yarova et al., 2015).

Calcium-sensing receptor in the epidermis

The epidermis consists of multiple layers of keratinocytes that differentiate and produce a permeability barrier that provides protection against desiccation, xenobiotic infection, and other environmental insults. Ca_o^{2+} is essential for initiating keratinocyte differentiation and maintaining epidermal functions. Activating CaSR by raising Ca_o^{2+} levels increases Ca_i^{2+} levels through coupling to the $G_{q/11}$/PLC pathway (Bikle et al., 2012) and induces cell−cell adhesion by stimulating the formation of the E-cadherin−catenin protein complex via the activation of Rho small GTPases and Src family tyrosine kinase signaling pathways (Calautti et al., 1998, 2002). The E-cadherin−catenin adhesion complexes in the cell membrane recruit and activate PI3K, Akt, PLCγ1, and EGFR, important regulators of cell proliferation, survival, and differentiation (Calautti et al., 2005; Tu et al., 2018; Xie and Bikle, 2007).

The CaSR is expressed throughout all keratinocyte layers in the epidermis (Komuves et al., 2002) with predominant intracellular perinuclear localization (Tu et al., 2001). Fluorescence immunostaining and coimmunoprecipitation studies revealed that CaSR colocalized and formed a protein complex with PLCγ1, IP_3R, and SPCA1 in the *trans*-Golgi (Tu et al., 2007). Inactivation of CaSR in keratinocytes profoundly reduced releasable Ca_i^{2+} pools (Tu et al., 2007), suggesting that the CaSR may coordinate Ca^{2+} release and the replenishment of stores and Ca^{2+} entry through membrane channels via direct interactions with $Ca^{2+}{}_i$ modulators such as PLC and Ca^{2+}-ATPase. Besides the initial Ca^{2+} release via PLC activation, the CaSR sustains increases in Ca_i^{2+} levels via E-cadherin-mediated signaling (Tu et al., 2008). Ca_o^{2+} stimulates interactions among the CaSR, filamin A, Rho-GEF Trio, RhoA, and E-cadherin at the cell membrane and facilitates CaSR signaling through the Rho and E-cadherin pathways (Tu et al., 2011; Tu and You, 2014). In Casr-deficient keratinocytes, the ability of Ca_o^{2+} to stimulate Ca_i^{2+} mobilization is severely inhibited, and the ineffectual Rho signaling fails to stabilize the E-cadherin−catenin adhesion complex and activate PI3K and PLCγ1, resulting in decreased basal Ca_i^{2+} level, impaired intercellular adhesion, increased cell apoptosis, and reduced differentiation (Tu et al., 2008, 2011). Additionally, depleting CaSRs suppresses keratinocyte proliferation by downregulating the E-cadherin/EGFR/MAPK signaling axis (Tu et al., 2018). Furthermore, the control of keratinocyte proliferation and differentiation by CaSR may involve activation of the Wnt/β-catenin signaling cascade (Popp et al., 2014; Turksen and Troy, 2003).

The physiological importance of CaSR in epidermal development and maintenance is made clear by animal models in which the CaSR gene has been overexpressed or deleted. The skin of keratinocyte-specific CaSR knockout ($^{Epid}Casr^{-/-}$) mice exhibits the loss of an innate epidermal Ca^{2+} gradient, aberrant keratinocyte differentiation, and retarded epidermal repair after injury due to impaired Ca_i^{2+}- and E-cadherin-mediated signaling (Tu et al., 2012, 2018). CaSR abrogation also delays the formation of the permeability barrier during prenatal development and impairs skin barrier function in adults (Tu et al., 2012). On the other hand, transgenic mice with constitutive expression of CaSR in basal keratinocytes manifest advanced differentiation and epidermal permeability barrier formation during embryologic development as well as accelerated hair growth at birth (Turksen and Troy, 2003). These changes in epidermal differentiation may be attributed to enhanced cross talk between CaSR and the Wnt/β-catenin signaling pathway in the CaSR transgenic epidermis (Turksen and Troy, 2003). Similarly, stimulating endogenous epidermal CaSR with calcimimetic NPS-R568 accelerated wound reepithelialization through enhancing of the epidermal $Ca^{2+}{}_i$ signals and E-cadherin membrane expression (Tu et al., 2018). These findings demonstrated a critical role for the CaSR in epidermal homeostasis and the therapeutic potential of calcimimetics for improving skin wound repair.

References

Abdulnour-Nakhoul, S., Brown, K.L., Rabon, E.C., Al-Tawil, Y., Islam, M.T., Schmieg, J.J., et al., 2015. Cytoskeletal changes induced by allosteric modulators of calcium-sensing receptor in esophageal epithelial cells. Phys. Rep. 3 (11).

Aggarwal, A., Hobaus, J., Tennakoon, S., Prinz-Wohlgenannt, M., Graca, J., Price, S.A., et al., 2016. Active vitamin D potentiates the anti-neoplastic effects of calcium in the colon: a cross talk through the calcium-sensing receptor. J. Steroid Biochem. Mol. Biol. 155 (Pt B), 231–238.

Aggarwal, A., Prinz-Wohlgenannt, M., Tennakoon, S., Hobaus, J., Boudot, C., Mentaverri, R., et al., 2015. The calcium-sensing receptor: a promising target for prevention of colorectal cancer. Biochim. Biophys. Acta 1853 (9), 2158–2167.

Aida, K., Koishi, S., Inoue, M., Nakazato, M., Tawata, M., Onaya, T., 1995a. Familial hypocalciuric hypercalcemia associated with mutation in the human $Ca^{(2+)}$-sensing receptor gene. J. Clin. Endocrinol. Metab. 80 (9), 2594–2598.

Aida, K., Koishi, S., Tawata, M., Onaya, T., 1995b. Molecular cloning of a putative $Ca^{(2+)}$-sensing receptor cDNA from human kidney. Biochem. Biophys. Res. Commun. 214 (2), 524–529.

Alam, M.U., Kirton, J.P., Wilkinson, F.L., Towers, E., Sinha, S., Rouhi, M., et al., 2009. Calcification is associated with loss of functional calcium-sensing receptor in vascular smooth muscle cells. Cardiovasc. Res. 81 (2), 260–268.

Alfadda, T.I., Saleh, A.M., Houillier, P., Geibel, J.P., 2014. Calcium-sensing receptor 20 years later. Am. J. Physiol. Cell Physiol. 307 (3), C221–C231.

Ardeshirpour, L., Dann, P., Pollak, M., Wysolmerski, J., VanHouten, J., 2006. The calcium-sensing receptor regulates PTHrP production and calcium transport in the lactating mammary gland. Bone 38 (6), 787–793.

Arulpragasam, A., Magno, A.L., Ingley, E., Brown, S.J., Conigrave, A.D., Ratajczak, T., et al., 2012. The adaptor protein 14-3-3 binds to the calcium-sensing receptor and attenuates receptor-mediated Rho kinase signalling. Biochem. J. 441 (3), 995–1006.

Atchison, D.K., Beierwaltes, W.H., 2013. The influence of extracellular and intracellular calcium on the secretion of renin. Pflügers Archiv 465 (1), 59–69.

Attie, M.F., Gill Jr., J.R., Stock, J.L., Spiegel, A.M., Downs Jr., R.W., Levine, M.A., et al., 1983. Urinary calcium excretion in familial hypocalciuric hypercalcemia. Persistence of relative hypocalciuria after induction of hypoparathyroidism. J. Clin. Investig. 72 (2), 667–676.

Avlani, V.A., Ma, W., Mun, H.C., Leach, K., Delbridge, L., Christopoulos, A., et al., 2013. Calcium-sensing receptor-dependent activation of CREB phosphorylation in HEK293 cells and human parathyroid cells. Am. J. Physiol. Endocrinol. Metab. 304 (10), E1097–E1104.

Awata, H., Huang, C., Handlogten, M.E., Miller, R.T., 2001. Interaction of the calcium-sensing receptor and filamin, a potential scaffolding protein. J. Biol. Chem. 276 (37), 34871–34879.

Babinsky, V.N., Hannan, F.M., Ramracheya, R.D., Zhang, Q., Nesbit, M.A., Hugill, A., et al., 2017. Mutant mice with calcium-sensing receptor activation have hyperglycemia that is rectified by calcilytic therapy. Endocrinology 158 (8), 2486–2502.

Bai, M., Quinn, S., Trivedi, S., Kifor, O., Pearce, S.H., Pollak, M.R., et al., 1996. Expression and characterization of inactivating and activating mutations in the human Ca^{2+}o-sensing receptor. J. Biol. Chem. 271 (32), 19537–19545.

Bai, M., Trivedi, S., Brown, E.M., 1998a. Dimerization of the extracellular calcium-sensing receptor (CaR) on the cell surface of CaR-transfected HEK293 cells. J. Biol. Chem. 273 (36), 23605–23610.

Bai, M., Trivedi, S., Kifor, O., Quinn, S.J., Brown, E.M., 1999. Intermolecular interactions between dimeric calcium-sensing receptor monomers are important for its normal function. Proc. Natl. Acad. Sci. U. S. A. 96 (6), 2834–2839.

Bai, M., Trivedi, S., Lane, C.R., Yang, Y., Quinn, S.J., Brown, E.M., 1998b. Protein kinase C phosphorylation of threonine at position 888 in Ca^{2+}o-sensing receptor (CaR) inhibits coupling to Ca^{2+} store release. J. Biol. Chem. 273 (33), 21267–21275.

Bai, S., Favus, M.J., 2006. Vitamin D and calcium receptors: links to hypercalciuria. Curr. Opin. Nephrol. Hypertens. 15 (4), 381–385.

Balenga, N., Koh, J., Azimzadeh, P., Hogue, J., Gabr, M., Stains, J.P., et al., 2019 Jan 28. Parathyroid-targeted overexpression of Regulator of G-Protein Signaling 5 (R GS5) causes hyperparathyroidism in transgenic mice. J. Bone Miner. Res. https://doi.org/10.1002/jbmr.3674 [Epub ahead of print].

Beierwaltes, W.H., 2010. The role of calcium in the regulation of renin secretion. Am. J. Physiol. Renal. Physiol. 298 (1), F1–F11.

Betson, M., Lozano, E., Zhang, J., Braga, V.M., 2002. Rac activation upon cell-cell contact formation is dependent on signaling from the epidermal growth factor receptor. J. Biol. Chem. 277 (40), 36962–36969.

Bhagavathula, N., Kelley, E.A., Reddy, M., Nerusu, K.C., Leonard, C., Fay, K., et al., 2005. Upregulation of calcium-sensing receptor and mitogen-activated protein kinase signalling in the regulation of growth and differentiation in colon carcinoma. Br. J. Canc. 93 (12), 1364–1371.

Bikle, D.D., Xie, Z., Tu, C.L., 2012. Calcium regulation of keratinocyte differentiation. Expert Rev. Endocrinol. Metab. 7 (4), 461–472.

Bosel, J., John, M., Freichel, M., Blind, E., 2003. Signaling of the human calcium-sensing receptor expressed in HEK293-cells is modulated by protein kinases A and C. Exp. Clin. Endocrinol. Diabetes 111 (1), 21–26.

Bouschet, T., Martin, S., Henley, J.M., 2012. Regulation of calcium sensing receptor trafficking by RAMPs. Adv. Exp. Med. Biol. 744, 39–48.

Bradbury, R.A., Sunn, K.L., Crossley, M., Bai, M., Brown, E.M., Delbridge, L., et al., 1998. Expression of the parathyroid $Ca^{(2+)}$-sensing receptor in cytotrophoblasts from human term placenta. J. Endocrinol. 156 (3), 425–430.

Brauner-Osborne, H., Wellendorph, P., Jensen, A.A., 2007. Structure, pharmacology and therapeutic prospects of family C G-protein coupled receptors. Curr. Drug Targets 8 (1), 169–184.

Breitwieser, G.E., 2013. The calcium sensing receptor life cycle: trafficking, cell surface expression, and degradation. Best Pract. Res. Clin. Endocrinol. Metabol. 27 (3), 303–313.

Breitwieser, G.E., 2014. Pharmacoperones and the calcium sensing receptor: exogenous and endogenous regulators. Pharmacol. Res. 83, 30–37.

Brembeck, F.H., Rosario, M., Birchmeier, W., 2006. Balancing cell adhesion and Wnt signaling, the key role of beta-catenin. Curr. Opin. Genet. Dev. 16 (1), 51–59.

Brennan, S.C., Conigrave, A.D., 2009. Regulation of cellular signal transduction pathways by the extracellular calcium-sensing receptor. Curr. Pharmaceut. Biotechnol. 10 (3), 270–281.

Brennan, S.C., Davies, T.S., Schepelmann, M., Riccardi, D., 2014. Emerging roles of the extracellular calcium-sensing receptor in nutrient sensing: control of taste modulation and intestinal hormone secretion. Br. J. Nutr. 111 (Suppl. 1), S16–S22.

Brennan, T.C., Rybchyn, M.S., Green, W., Atwa, S., Conigrave, A.D., Mason, R.S., 2009. Osteoblasts play key roles in the mechanisms of action of strontium ranelate. Br. J. Pharmacol. 157 (7), 1291–1300.

Brent, G.A., LeBoff, M.S., Seely, E.W., Conlin, P.R., Brown, E.M., 1988. Relationship between the concentration and rate of change of calcium and serum intact parathyroid hormone levels in normal humans. J. Clin. Endocrinol. Metab. 67 (5), 944–950.

Breuksch, I., Weinert, M., Brenner, W., 2016. The role of extracellular calcium in bone metastasis. J Bone Oncol. 5 (3), 143–145.

Broadhead, G.K., Mun, H.C., Avlani, V.A., Jourdon, O., Church, W.B., Christopoulos, A., et al., 2011. Allosteric modulation of the calcium-sensing receptor by gamma-glutamyl peptides: inhibition of PTH secretion, suppression of intracellular cAMP levels, and a common mechanism of action with L-amino acids. J. Biol. Chem. 286 (11), 8786–8797.

Brown, A.J., Zhong, M., Finch, J., Ritter, C., McCracken, R., Morrissey, J., et al., 1996. Rat calcium-sensing receptor is regulated by vitamin D but not by calcium. Am. J. Physiol. 270 (3 Pt 2), F454–F460.

Brown, E.M., 1991. Extracellular Ca^{2+} sensing, regulation of parathyroid cell function, and role of Ca^{2+} and other ions as extracellular (first) messengers. Physiol. Rev. 71 (2), 371–411.

Brown, E.M., 2013. Role of the calcium-sensing receptor in extracellular calcium homeostasis. Best Pract. Res. Clin. Endocrinol. Metabol. 27 (3), 333–343.

Brown, E.M., Butters, R., Katz, C., Kifor, O., Fuleihan, G.E., 1992. A comparison of the effects of concanavalin-A and tetradecanoylphorbol acetate on the modulation of parathyroid function by extracellular calcium and neomycin in dispersed bovine parathyroid cells. Endocrinology 130 (6), 3143–3151.

Brown, E.M., Chen, C.J., LeBoff, M.S., Kifor, O., Oetting, M.H., el-Hajj, G., 1989. Mechanisms underlying the inverse control of parathyroid hormone secretion by calcium. Soc. Gen. Physiol. 44, 251–268.

Brown, E.M., Gamba, G., Riccardi, D., Lombardi, M., Butters, R., Kifor, O., et al., 1993. Cloning and characterization of an extracellular $Ca^{(2+)}$-sensing receptor from bovine parathyroid. Nature 366 (6455), 575–580.

Brown, E.M., MacLeod, R.J., 2001. Extracellular calcium sensing and extracellular calcium signaling. Physiol. Rev. 81 (1), 239–297.

Brown, E.M., Vassilev, P.M., Quinn, S., Hebert, S.C., 1999. G-protein-coupled, extracellular $Ca^{(2+)}$-sensing receptor: a versatile regulator of diverse cellular functions. Vitam. Horm. 55, 1–71.

Bruce, J.I., Yang, X., Ferguson, C.J., Elliott, A.C., Steward, M.C., Case, R.M., et al., 1999. Molecular and functional identification of a Ca^{2+} (polyvalent cation)-sensing receptor in rat pancreas. J. Biol. Chem. 274 (29), 20561–20568.

Buchan, A.M., Squires, P.E., Ring, M., Meloche, R.M., 2001. Mechanism of action of the calcium-sensing receptor in human antral gastrin cells. Gastroenterology 120 (5), 1128–1139.

Bukoski, R.D., Bian, K., Wang, Y., Mupanomunda, M., 1997. Perivascular sensory nerve Ca^{2+} receptor and Ca^{2+}-induced relaxation of isolated arteries. Hypertension 30 (6), 1431–1439.

Busque, S.M., Kerstetter, J.E., Geibel, J.P., Insogna, K., 2005. L-type amino acids stimulate gastric acid secretion by activation of the calcium-sensing receptor in parietal cells. Am. J. Physiol. Gastrointest. Liver Physiol. 289 (4), G664–G669.

Butters Jr., R.R., Chattopadhyay, N., Nielsen, P., Smith, C.P., Mithal, A., Kifor, O., et al., 1997. Cloning and characterization of a calcium-sensing receptor from the hypercalcemic New Zealand white rabbit reveals unaltered responsiveness to extracellular calcium. J. Bone Miner. Res. 12 (4), 568–579.

Bystrova, M.F., Romanov, R.A., Rogachevskaja, O.A., Churbanov, G.D., Kolesnikov, S.S., 2010. Functional expression of the extracellular- Ca^{2+}-sensing receptor in mouse taste cells. J. Cell Sci. 123 (Pt 6), 972–982.

Calautti, E., Cabodi, S., Stein, P.L., Hatzfeld, M., Kedersha, N., Paolo Dotto, G., 1998. Tyrosine phosphorylation and src family kinases control keratinocyte cell-cell adhesion. J. Cell Biol. 141 (6), 1449–1465.

Calautti, E., Grossi, M., Mammucari, C., Aoyama, Y., Pirro, M., Ono, Y., et al., 2002. Fyn tyrosine kinase is a downstream mediator of Rho/PRK2 function in keratinocyte cell-cell adhesion. J. Cell Biol. 156 (1), 137–148.

Calautti, E., Li, J., Saoncella, S., Brissette, J.L., Goetinck, P.F., 2005. Phosphoinositide 3-kinase signaling to Akt promotes keratinocyte differentiation versus death. J. Biol. Chem. 280 (38), 32856–32865.

Canaff, L., Hendy, G.N., 2002. Human calcium-sensing receptor gene. Vitamin D response elements in promoters P1 and P2 confer transcriptional responsiveness to 1,25-dihydroxyvitamin D. J. Biol. Chem. 277 (33), 30337–30350.

Canaff, L., Petit, J.L., Kisiel, M., Watson, P.H., Gascon-Barre, M., Hendy, G.N., 2001. Extracellular calcium-sensing receptor is expressed in rat hepatocytes. coupling to intracellular calcium mobilization and stimulation of bile flow. J. Biol. Chem. 276 (6), 4070–4079.

Canaff, L., Zhou, X., Mosesova, I., Cole, D.E., Hendy, G.N., 2009. Glial cells missing-2 (GCM2) transactivates the calcium-sensing receptor gene: effect of a dominant-negative GCM2 mutant associated with autosomal dominant hypoparathyroidism. Hum. Mutat. 30 (1), 85–92.

Casala, C., Gil-Guinon, E., Ordonez, J.L., Miguel-Queralt, S., Rodriguez, E., Galvan, P., et al., 2013. The calcium-sensing receptor is silenced by genetic and epigenetic mechanisms in unfavorable neuroblastomas and its reactivation induces ERK1/2-dependent apoptosis. Carcinogenesis 34 (2), 268–276.

Cetani, F., Picone, A., Cerrai, P., Vignali, E., Borsari, S., Pardi, E., et al., 2000. Parathyroid expression of calcium-sensing receptor protein and in vivo parathyroid hormone-$Ca^{(2+)}$ set-point in patients with primary hyperparathyroidism. J. Clin. Endocrinol. Metab. 85 (12), 4789–4794.

Chakrabarty, S., Radjendirane, V., Appelman, H., Varani, J., 2003. Extracellular calcium and calcium sensing receptor function in human colon carcinomas: promotion of E-cadherin expression and suppression of beta-catenin/TCF activation. Cancer Res. 63 (1), 67–71.

Chakrabarty, S., Wang, H., Canaff, L., Hendy, G.N., Appelman, H., Varani, J., 2005. Calcium sensing receptor in human colon carcinoma: interaction with $Ca^{(2+)}$ and 1,25-dihydroxyvitamin D(3). Cancer Res. 65 (2), 493–498.

Chang, W., Chen, T.H., Pratt, S., Shoback, D., 2000. Amino acids in the second and third intracellular loops of the parathyroid Ca^{2+}-sensing receptor mediate efficient coupling to phospholipase C. J. Biol. Chem. 275 (26), 19955–19963.

Chang, W., Pratt, S., Chen, T.H., Bourguignon, L., Shoback, D., 2001. Amino acids in the cytoplasmic C terminus of the parathyroid Ca^{2+}-sensing receptor mediate efficient cell-surface expression and phospholipase C activation. J. Biol. Chem. 276 (47), 44129–44136.

Chang, W., Tu, C., Chen, T.H., Bikle, D., Shoback, D., 2008. The extracellular calcium-sensing receptor (CaSR) is a critical modulator of skeletal development. Sci. Signal. 1 (35), ra1.

Chang, W., Tu, C., Chen, T.H., Komuves, L., Oda, Y., Pratt, S.A., et al., 1999. Expression and signal transduction of calcium-sensing receptors in cartilage and bone. Endocrinology 140 (12), 5883–5893.

Chang, W., Tu, C., Cheng, Z., Rodriguez, L., Chen, T.H., Gassmann, M., et al., 2007. Complex formation with the Type B gamma-aminobutyric acid receptor affects the expression and signal transduction of the extracellular calcium-sensing receptor. Studies with HEK-293 cells and neurons. J. Biol. Chem. 282 (34), 25030–25040.

Chattopadhyay, N., Yano, S., Tfelt-Hansen, J., Rooney, P., Kanuparthi, D., Bandyopadhyay, S., et al., 2004. Mitogenic action of calcium-sensing receptor on rat calvarial osteoblasts. Endocrinology 145 (7), 3451–3462.

Chen, C.J., Barnett, J.V., Congo, D.A., Brown, E.M., 1989. Divalent cations suppress 3',5'-adenosine monophosphate accumulation by stimulating a pertussis toxin-sensitive guanine nucleotide-binding protein in cultured bovine parathyroid cells. Endocrinology 124 (1), 233–239.

Cheng, I., Klingensmith, M.E., Chattopadhyay, N., Kifor, O., Butters, R.R., Soybel, D.I., et al., 1998. Identification and localization of the extracellular calcium-sensing receptor in human breast. J. Clin. Endocrinol. Metab. 83 (2), 703–707.

Cheng, I., Qureshi, I., Chattopadhyay, N., Qureshi, A., Butters, R.R., Hall, A.E., et al., 1999. Expression of an extracellular calcium-sensing receptor in rat stomach. Gastroenterology 116 (1), 118–126.

Cheng, S.X., 2012. Calcium-sensing receptor inhibits secretagogue-induced electrolyte secretion by intestine via the enteric nervous system. Am. J. Physiol. Gastrointest. Liver Physiol. 303 (1), G60–G70.

Cheng, S.X., 2016. Calcium-sensing receptor: a new target for therapy of diarrhea. World J. Gastroenterol. 22 (9), 2711–2724.

Cheng, S.X., Geibel, J.P., Hebert, S.C., 2004. Extracellular polyamines regulate fluid secretion in rat colonic crypts via the extracellular calcium-sensing receptor. Gastroenterology 126 (1), 148–158.

Cheng, S.X., Lightfoot, Y.L., Yang, T., Zadeh, M., Tang, L., Sahay, B., et al., 2014. Epithelial CaSR deficiency alters intestinal integrity and promotes proinflammatory immune responses. FEBS Lett. 588 (22), 4158–4166.

Cheng, S.X., Okuda, M., Hall, A.E., Geibel, J.P., Hebert, S.C., 2002. Expression of calcium-sensing receptor in rat colonic epithelium: evidence for modulation of fluid secretion. Am. J. Physiol. Gastrointest. Liver Physiol. 283 (1), G240–G250.

Cheng, Z., Liang, N., Chen, T.H., Li, A., Santa Maria, C., You, M., et al., 2013. Sex and age modify biochemical and skeletal manifestations of chronic hyperparathyroidism by altering target organ responses to Ca^{2+} and parathyroid hormone in mice. J. Bone Miner. Res. 28 (5), 1087–1100.

Chiarini, A., Armato, U., Gardenal, E., Gui, L., Dal Pra, I., 2017. Amyloid beta-exposed human astrocytes overproduce phospho-tau and overrelease it within exosomes, effects suppressed by calcilytic NPS 2143-further implications for alzheimer's therapy. Front. Neurosci. 11, 217.

Chikatsu, N., Fukumoto, S., Takeuchi, Y., Suzawa, M., Obara, T., Matsumoto, T., et al., 2000. Cloning and characterization of two promoters for the human calcium-sensing receptor (CaSR) and changes of CaSR expression in parathyroid adenomas. J. Biol. Chem. 275 (11), 7553–7557.

Chirgwin, J.M., Guise, T.A., 2000. Molecular mechanisms of tumor-bone interactions in osteolytic metastases. Crit. Rev. Eukaryot. Gene Expr. 10 (2), 159–178.

Choudhary, S., Kumar, A., Kale, R.K., Raisz, L.G., Pilbeam, C.C., 2004. Extracellular calcium induces COX-2 in osteoblasts via a PKA pathway. Biochem. Biophys. Res. Commun. 322 (2), 395–402.

Christensen, S.E., Nissen, P.H., Vestergaard, P., Heickendorff, L., Brixen, K., Mosekilde, L., 2008. Discriminative power of three indices of renal calcium excretion for the distinction between familial hypocalciuric hypercalcaemia and primary hyperparathyroidism: a follow-up study on methods. Clin. Endocrinol. 69 (5), 713–720.

Colloton, M., Shatzen, E., Miller, G., Stehman-Breen, C., Wada, M., Lacey, D., et al., 2005. Cinacalcet HCl attenuates parathyroid hyperplasia in a rat model of secondary hyperparathyroidism. Kidney Int. 67 (2), 467–476.

Conigrave, A.D., Hampson, D.R., 2010. Broad-spectrum amino acid-sensing class C G-protein coupled receptors: molecular mechanisms, physiological significance and options for drug development. Pharmacol. Ther. 127 (3), 252–260.

Conigrave, A.D., Mun, H.C., Brennan, S.C., 2007a. Physiological significance of L-amino acid sensing by extracellular Ca(2+)-sensing receptors. Biochem. Soc. Trans. 35 (Pt 5), 1195–1198.

Conigrave, A.D., Mun, H.C., Delbridge, L., Quinn, S.J., Wilkinson, M., Brown, E.M., 2004. L-amino acids regulate parathyroid hormone secretion. J. Biol. Chem. 279 (37), 38151–38159.

Conigrave, A.D., Mun, H.C., Lok, H.C., 2007b. Aromatic L-amino acids activate the calcium-sensing receptor. J. Nutr. 137 (6 Suppl. 1), 1524S-7S; discussion 48S.

Conigrave, A.D., Quinn, S.J., Brown, E.M., 2000. L-amino acid sensing by the extracellular Ca2+-sensing receptor. Proc. Natl. Acad. Sci. U. S. A. 97 (9), 4814–4819.

Conigrave, A.D., Ward, D.T., 2013. Calcium-sensing receptor (CaSR): pharmacological properties and signaling pathways. Best Pract. Res. Clin. Endocrinol. Metabol. 27 (3), 315–331.

Cooper, D.M., 2003. Molecular and cellular requirements for the regulation of adenylate cyclases by calcium. Biochem. Soc. Trans. 31 (Pt 5), 912–915.

Corbetta, S., Mantovani, G., Lania, A., Borgato, S., Vicentini, L., Beretta, E., et al., 2000. Calcium-sensing receptor expression and signalling in human parathyroid adenomas and primary hyperplasia. Clin. Endocrinol. 52 (3), 339–348.

Correa, P., Akerstrom, G., Westin, G., 2002. Underexpression of Gcm2, a master regulatory gene of parathyroid gland development, in adenomas of primary hyperparathyroidism. Clin. Endocrinol. 57 (4), 501–505.

D'Souza-Li, L., Canaff, L., Janicic, N., Cole, D.E., Hendy, G.N., 2001. An acceptor splice site mutation in the calcium-sensing receptor (CASR) gene in familial hypocalciuric hypercalcemia and neonatal severe hyperparathyroidism. Hum. Mutat. 18 (5), 411–421.

Datta, H.K., MacIntyre, I., Zaidi, M., 1989. The effect of extracellular calcium elevation on morphology and function of isolated rat osteoclasts. Biosci. Rep. 9 (6), 747–751.

Davey, A.E., Leach, K., Valant, C., Conigrave, A.D., Sexton, P.M., Christopoulos, A., 2012. Positive and negative allosteric modulators promote biased signaling at the calcium-sensing receptor. Endocrinology 153 (3), 1232–1241.

Davies, S.L., Gibbons, C.E., Vizard, T., Ward, D.T., 2006. Ca2+-sensing receptor induces Rho kinase-mediated actin stress fiber assembly and altered cell morphology, but not in response to aromatic amino acids. Am. J. Physiol. Cell Physiol. 290 (6), C1543–C1551.

Davies, S.L., Ozawa, A., McCormick, W.D., Dvorak, M.M., Ward, D.T., 2007. Protein kinase C-mediated phosphorylation of the calcium-sensing receptor is stimulated by receptor activation and attenuated by calyculin-sensitive phosphatase activity. J. Biol. Chem. 282 (20), 15048–15056.

de Rouffignac, C., Quamme, G., 1994. Renal magnesium handling and its hormonal control. Physiol. Rev. 74 (2), 305–322.

Devis, G., Somers, G., Malaisse, W.J., 1975. Stimulation of insulin release by calcium. Biochem. Biophys. Res. Commun. 67 (2), 525–529.

Diez-Fraile, A., Lammens, T., Benoit, Y., D'Herde, K.G., 2013. The calcium-sensing receptor as a regulator of cellular fate in normal and pathological conditions. Curr. Mol. Med. 13 (2), 282–295.

Dong, B., Endo, I., Ohnishi, Y., Kondo, T., Hasegawa, T., Amizuka, N., et al., 2015. Calcilytic ameliorates abnormalities of mutant calcium-sensing receptor (CaSR) knock-in mice mimicking autosomal dominant hypocalcemia (ADH). J. Bone Miner. Res. 30 (11), 1980–1993.

Dufner, M.M., Kirchhoff, P., Remy, C., Hafner, P., Muller, M.K., Cheng, S.X., et al., 2005. The calcium-sensing receptor acts as a modulator of gastric acid secretion in freshly isolated human gastric glands. Am. J. Physiol. Gastrointest. Liver Physiol. 289 (6), G1084–G1090.

Dvorak, M.M., Chen, T.H., Orwoll, B., Garvey, C., Chang, W., Bikle, D.D., et al., 2007. Constitutive activity of the osteoblast Ca2+-sensing receptor promotes loss of cancellous bone. Endocrinology 148 (7), 3156–3163.

Dvorak, M.M., Siddiqua, A., Ward, D.T., Carter, D.H., Dallas, S.L., Nemeth, E.F., et al., 2004. Physiological changes in extracellular calcium concentration directly control osteoblast function in the absence of calciotropic hormones. Proc. Natl. Acad. Sci. U. S. A. 101 (14), 5140–5145.

Dvorak-Ewell, M.M., Chen, T.H., Liang, N., Garvey, C., Liu, B., Tu, C., et al., 2011. Osteoblast extracellular Ca^{2+} -sensing receptor regulates bone development, mineralization, and turnover. J. Bone Miner. Res. 26 (12), 2935–2947.

El Hiani, Y., Ahidouch, A., Lehen'kyi, V., Hague, F., Gouilleux, F., Mentaverri, R., et al., 2009a. Extracellular signal-regulated kinases 1 and 2 and TRPC1 channels are required for calcium-sensing receptor-stimulated MCF-7 breast cancer cell proliferation. Cell. Physiol. Biochem. 23 (4–6), 335–346.

El Hiani, Y., Lehen'kyi, V., Ouadid-Ahidouch, H., Ahidouch, A., 2009b. Activation of the calcium-sensing receptor by high calcium induced breast cancer cell proliferation and TRPC1 cation channel over-expression potentially through EGFR pathways. Arch. Biochem. Biophys. 486 (1), 58–63.

Emanuel, R.L., Adler, G.K., Kifor, O., Quinn, S.J., Fuller, F., Krapcho, K., et al., 1996. Calcium-sensing receptor expression and regulation by extracellular calcium in the AtT-20 pituitary cell line. Mol. Endocrinol. 10 (5), 555–565.

Fan, G.F., Ray, K., Zhao, X.M., Goldsmith, P.K., Spiegel, A.M., 1998. Mutational analysis of the cysteines in the extracellular domain of the human Ca^{2+} receptor: effects on cell surface expression, dimerization and signal transduction. FEBS Lett. 436 (3), 353–356.

Fan, Y., Liu, W., Bi, R., Densmore, M.J., Sato, T., Mannstadt, M., et al., 2018. Interrelated role of Klotho and calcium-sensing receptor in parathyroid hormone synthesis and parathyroid hyperplasia. Proc. Natl. Acad. Sci. U. S. A. 115 (16), E3749–E3758.

Favus, M.J., Kathpalia, S.C., Coe, F.L., 1981. Kinetic characteristics of calcium absorption and secretion by rat colon. Am. J. Physiol. 240 (5), G350–G354.

Favus, M.J., Kathpalia, S.C., Coe, F.L., Mond, A.E., 1980. Effects of diet calcium and 1,25-dihydroxyvitamin D3 on colon calcium active transport. Am. J. Physiol. 238 (2), G75–G78.

Fedor-Chaiken, M., Hein, P.W., Stewart, J.C., Brackenbury, R., Kinch, M.S., 2003. E-cadherin binding modulates EGF receptor activation. Cell Commun. Adhes. 10 (2), 105–118.

Felder, C.B., Graul, R.C., Lee, A.Y., Merkle, H.P., Sadee, W., 1999. The Venus flytrap of periplasmic binding proteins: an ancient protein module present in multiple drug receptors. AAPS PharmSci 1 (2), E2.

Felderbauer, P., Klein, W., Bulut, K., Ansorge, N., Dekomien, G., Werner, I., et al., 2006. Mutations in the calcium-sensing receptor: a new genetic risk factor for chronic pancreatitis? Scand. J. Gastroenterol. 41 (3), 343–348.

Feng, J., Petersen, C.D., Coy, D.H., Jiang, J.K., Thomas, C.J., Pollak, M.R., et al., 2010. Calcium-sensing receptor is a physiologic multimodal chemosensor regulating gastric G-cell growth and gastrin secretion. Proc. Natl. Acad. Sci. U. S. A. 107 (41), 17791–17796.

Ferreri, N.R., Hao, S., Pedraza, P.L., Escalante, B., Vio, C.P., 2012. Eicosanoids and tumor necrosis factor-alpha in the kidney. Prostag. Other Lipid Mediat. 98 (3–4), 101–106.

Fetahu, I.S., Hobaus, J., Aggarwal, A., Hummel, D.M., Tennakoon, S., Mesteri, I., et al., 2014. Calcium-sensing receptor silencing in colorectal cancer is associated with promoter hypermethylation and loss of acetylation on histone 3. Int. J. Cancer 135 (9), 2014–2023.

Fetahu, I.S., Tennakoon, S., Lines, K.E., Groschel, C., Aggarwal, A., Mesteri, I., et al., 2016. miR-135b- and miR-146b-dependent silencing of calcium-sensing receptor expression in colorectal tumors. Int. J. Cancer 138 (1), 137–145.

Finney, B.A., del Moral, P.M., Wilkinson, W.J., Cayzac, S., Cole, M., Warburton, D., et al., 2008. Regulation of mouse lung development by the extracellular calcium-sensing receptor, CaR. J. Physiol. 586 (24), 6007–6019.

Fitzpatrick, L.A., Brandi, M.L., Aurbach, G.D., 1986. Calcium-controlled secretion is effected through a guanine nucleotide regulatory protein in parathyroid cells. Endocrinology 119 (6), 2700–2703.

Freichel, M., Zink-Lorenz, A., Holloschi, A., Hafner, M., Flockerzi, V., Raue, F., 1996. Expression of a calcium-sensing receptor in a human medullary thyroid carcinoma cell line and its contribution to calcitonin secretion. Endocrinology 137 (9), 3842–3848.

Gama, L., Wilt, S.G., Breitwieser, G.E., 2001. Heterodimerization of calcium sensing receptors with metabotropic glutamate receptors in neurons. J. Biol. Chem. 276 (42), 39053–39059.

Gardenal, E., Chiarini, A., Armato, U., Dal Pra, I., Verkhratsky, A., Rodriguez, J.J., 2017. Increased calcium-sensing receptor immunoreactivity in the Hippocampus of a triple transgenic mouse model of alzheimer's disease. Front. Neurosci. 11, 81.

Garrett, J.E., Capuano, I.V., Hammerland, L.G., Hung, B.C., Brown, E.M., Hebert, S.C., et al., 1995a. Molecular cloning and functional expression of human parathyroid calcium receptor cDNAs. J. Biol. Chem. 270 (21), 12919–12925.

Garrett, J.E., Tamir, H., Kifor, O., Simin, R.T., Rogers, K.V., Mithal, A., et al., 1995b. Calcitonin-secreting cells of the thyroid express an extracellular calcium receptor gene. Endocrinology 136 (11), 5202–5211.

Geibel, J., Sritharan, K., Geibel, R., Geibel, P., Persing, J.S., Seeger, A., et al., 2006. Calcium-sensing receptor abrogates secretagogue- induced increases in intestinal net fluid secretion by enhancing cyclic nucleotide destruction. Proc. Natl. Acad. Sci. U. S. A. 103 (25), 9390–9397.

Geng, Y., Bush, M., Mosyak, L., Wang, F., Fan, Q.R., 2013. Structural mechanism of ligand activation in human GABA(B) receptor. Nature 504 (7479), 254–259.

Geng, Y., Mosyak, L., Kurinov, I., Zuo, H., Sturchler, E., Cheng, T.C., et al., 2016. Structural mechanism of ligand activation in human calcium-sensing receptor. Elife 5.

Godwin, S.L., Soltoff, S.P., 2002. Calcium-sensing receptor-mediated activation of phospholipase C-gamma1 is downstream of phospholipase C-beta and protein kinase C in MC3T3-E1 osteoblasts. Bone 30 (4), 559–566.

Goltzman, D., Hendy, G.N., 2015. The calcium-sensing receptor in bone–mechanistic and therapeutic insights. Nat. Rev. Endocrinol. 11 (5), 298–307.

Goolam, M.A., Ward, J.H., Avlani, V.A., Leach, K., Christopoulos, A., Conigrave, A.D., 2014. Roles of intraloops-2 and -3 and the proximal C-terminus in signalling pathway selection from the human calcium-sensing receptor. FEBS Lett. 588 (18), 3340–3346.

Gorvin, C.M., Rogers, A., Stewart, M., Paudyal, A., Hough, T.A., Teboul, L., et al., 2017. N-ethyl-N-nitrosourea-Induced adaptor protein 2 sigma subunit 1 (Ap2s1) mutations establish Ap2s1 loss-of-function mice. JBMR Plus 1 (1), 3–15.

Gowen, M., Stroup, G.B., Dodds, R.A., James, I.E., Votta, B.J., Smith, B.R., et al., 2000. Antagonizing the parathyroid calcium receptor stimulates parathyroid hormone secretion and bone formation in osteopenic rats. J. Clin. Investig. 105 (11), 1595–1604.

Grant, M.P., Stepanchick, A., Cavanaugh, A., Breitwieser, G.E., 2011. Agonist-driven maturation and plasma membrane insertion of calcium-sensing receptors dynamically control signal amplitude. Sci. Signal. 4 (200), ra78.

Gray, E., Muller, D., Squires, P.E., Asare-Anane, H., Huang, G.C., Amiel, S., et al., 2006. Activation of the extracellular calcium-sensing receptor initiates insulin secretion from human islets of Langerhans: involvement of protein kinases. J. Endocrinol. 190 (3), 703–710.

Greenberg, H.Z., Shi, J., Jahan, K.S., Martinucci, M.C., Gilbert, S.J., Vanessa Ho, W.S., et al., 2016. Stimulation of calcium-sensing receptors induces endothelium-dependent vasorelaxations via nitric oxide production and activation of IKCa channels. Vasc. Pharmacol. 80, 75–84.

Greenberg, H.Z.E., Carlton-Carew, S.R.E., Khan, D.M., Zargaran, A.K., Jahan, K.S., Vanessa Ho, W.S., et al., 2017. Heteromeric TRPV4/TRPC1 channels mediate calcium-sensing receptor-induced nitric oxide production and vasorelaxation in rabbit mesenteric arteries. Vasc. Pharmacol. 96–98, 53–62.

Guise, T.A., Kozlow, W.M., Heras-Herzig, A., Padalecki, S.S., Yin, J.J., Chirgwin, J.M., 2005. Molecular mechanisms of breast cancer metastases to bone. Clin. Breast Canc. 5 (Suppl. l(2)), S46–S53.

Hammerland, L.G., Krapcho, K.J., Garrett, J.E., Alasti, N., Hung, B.C., Simin, R.T., et al., 1999. Domains determining ligand specificity for Ca^{2+} receptors. Mol. Pharmacol. 55 (4), 642–648.

Handlogten, M.E., Huang, C., Shiraishi, N., Awata, H., Miller, R.T., 2001. The Ca^{2+}-sensing receptor activates cytosolic phospholipase A2 via a Gqalpha -dependent ERK-independent pathway. J. Biol. Chem. 276 (17), 13941–13948.

Hannan, F.M., Babinsky, V.N., Thakker, R.V., 2016. Disorders of the calcium-sensing receptor and partner proteins: insights into the molecular basis of calcium homeostasis. J. Mol. Endocrinol. 57 (3), R127–R142.

Hannan, F.M., Kallay, E., Chang, W., Brandi, M.L., Thakker, R.V., 2018. The calcium-sensing receptor in physiology and in calcitropic and non-calcitropic diseases. Nat. Rev. Endocrinol. 15 (1), 33–51.

Hannan, F.M., Thakker, R.V., 2013. Calcium-sensing receptor (CaSR) mutations and disorders of calcium, electrolyte and water metabolism. Best Pract. Res. Clin. Endocrinol. Metabol. 27 (3), 359–371.

Hauache, O.M., Hu, J., Ray, K., Xie, R., Jacobson, K.A., Spiegel, A.M., 2000. Effects of a calcimimetic compound and naturally activating mutations on the human Ca2+ receptor and on Ca2+ receptor/metabotropic glutamate chimeric receptors. Endocrinology 141 (11), 4156–4163.

Henaut, L., Boudot, C., Massy, Z.A., Lopez-Fernandez, I., Dupont, S., Mary, A., et al., 2014. Calcimimetics increase CaSR expression and reduce mineralization in vascular smooth muscle cells: mechanisms of action. Cardiovasc. Res. 101 (2), 256–265.

Hendy, G.N., Canaff, L., 2016. Calcium-sensing receptor gene: regulation of expression. Front. Physiol. 7, 394.

Hendy, G.N., Canaff, L., Cole, D.E., 2013. The CASR gene: alternative splicing and transcriptional control, and calcium-sensing receptor (CaSR) protein: structure and ligand binding sites. Best Pract. Res. Clin. Endocrinol. Metabol. 27 (3), 285–301.

Hernandez-Bedolla, M.A., Carretero-Ortega, J., Valadez-Sanchez, M., Vazquez-Prado, J., Reyes-Cruz, G., 2015. Chemotactic and proangiogenic role of calcium sensing receptor is linked to secretion of multiple cytokines and growth factors in breast cancer MDA-MB-231 cells. Biochim. Biophys. Acta 1853 (1), 166–182.

Herrera-Vigenor, F., Hernandez-Garcia, R., Valadez-Sanchez, M., Vazquez-Prado, J., Reyes-Cruz, G., 2006. AMSH regulates calcium-sensing receptor signaling through direct interactions. Biochem. Biophys. Res. Commun. 347 (4), 924–930.

Hills, C.E., Younis, M.Y., Bennett, J., Siamantouras, E., Liu, K.K., Squires, P.E., 2012. Calcium-sensing receptor activation increases cell-cell adhesion and beta-cell function. Cell. Physiol. Biochem. 30 (3), 575–586.

Hizaki, K., Yamamoto, H., Taniguchi, H., Adachi, Y., Nakazawa, M., Tanuma, T., et al., 2011. Epigenetic inactivation of calcium-sensing receptor in colorectal carcinogenesis. Mod. Pathol. 24 (6), 876–884.

Hjalm, G., MacLeod, R.J., Kifor, O., Chattopadhyay, N., Brown, E.M., 2001. Filamin-A binds to the carboxyl-terminal tail of the calcium-sensing receptor, an interaction that participates in CaR-mediated activation of mitogen-activated protein kinase. J. Biol. Chem. 276 (37), 34880–34887.

Ho, C., Conner, D.A., Pollak, M.R., Ladd, D.J., Kifor, O., Warren, H.B., et al., 1995. A mouse model of human familial hypocalciuric hypercalcemia and neonatal severe hyperparathyroidism. Nat. Genet. 11 (4), 389–394.

Hobson, S.A., McNeil, S.E., Lee, F., Rodland, K.D., 2000. Signal transduction mechanisms linking increased extracellular calcium to proliferation in ovarian surface epithelial cells. Exp. Cell Res. 258 (1), 1–11.

Hobson, S.A., Wright, J., Lee, F., McNeil, S.E., Bilderback, T., Rodland, K.D., 2003. Activation of the MAP kinase cascade by exogenous calcium-sensing receptor. Mol. Cell. Endocrinol. 200 (1–2), 189–198.

Hofer, A.M., Brown, E.M., 2003. Extracellular calcium sensing and signalling. Nat. Rev. Mol. Cell Biol. 4 (7), 530–538.

Holstein, D.M., Berg, K.A., Leeb-Lundberg, L.M., Olson, M.S., Saunders, C., 2004. Calcium-sensing receptor-mediated ERK1/2 activation requires Galphai2 coupling and dynamin-independent receptor internalization. J. Biol. Chem. 279 (11), 10060–10069.

Hovden, S., Rejnmark, L., Ladefoged, S.A., Nissen, P.H., 2017. AP2S1 and GNA11 mutations - not a common cause of familial hypocalciuric hypercalcemia. Eur. J. Endocrinol. 176 (2), 177–185.

Howles, S.A., Hannan, F.M., Babinsky, V.N., Rogers, A., Gorvin, C.M., Rust, N., et al., 2016. Cinacalcet for symptomatic hypercalcemia caused by AP2S1 mutations. N. Engl. J. Med. 374 (14), 1396–1398.

Hu, J., 2008. Allosteric modulators of the human calcium-sensing receptor: structures, sites of action, and therapeutic potentials. Endocr. Metab. Immune Disord. - Drug Targets 8 (3), 192–197.

Hu, J., Hauache, O., Spiegel, A.M., 2000. Human Ca^{2+} receptor cysteine-rich domain. Analysis of function of mutant and chimeric receptors. J. Biol. Chem. 275 (21), 16382–16389.

Hu, J., Reyes-Cruz, G., Chen, W., Jacobson, K.A., Spiegel, A.M., 2002. Identification of acidic residues in the extracellular loops of the seven-transmembrane domain of the human Ca^{2+} receptor critical for response to Ca2+ and a positive allosteric modulator. J. Biol. Chem. 277 (48), 46622–46631.

Huang, C., Hujer, K.M., Wu, Z., Miller, R.T., 2004. The Ca^{2+}-sensing receptor couples to Galpha12/13 to activate phospholipase D in Madin-Darby canine kidney cells. Am. J. Physiol. Cell Physiol. 286 (1), C22–C30.

Huang, C., Hydo, L.M., Liu, S., Miller, R.T., 2009a. Activation of choline kinase by extracellular Ca^{2+} is $Ca(^{2+})$-sensing receptor, Galpha12 and Rho-dependent in breast cancer cells. Cell. Signal. 21 (12), 1894–1900.

Huang, C., Miller, R.T., 2007. The calcium-sensing receptor and its interacting proteins. J. Cell Mol. Med. 11 (5), 923–934.

Huang, C., Sindic, A., Hill, C.E., Hujer, K.M., Chan, K.W., Sassen, M., et al., 2007a. Interaction of the Ca^{2+}-sensing receptor with the inwardly rectifying potassium channels Kir4.1 and Kir4.2 results in inhibition of channel function. Am. J. Physiol. Renal. Physiol. 292 (3), F1073–F1081.

Huang, Y., Breitwieser, G.E., 2007. Rescue of calcium-sensing receptor mutants by allosteric modulators reveals a conformational checkpoint in receptor biogenesis. J. Biol. Chem. 282 (13), 9517–9525.

Huang, Y., Niwa, J., Sobue, G., Breitwieser, G.E., 2006. Calcium-sensing receptor ubiquitination and degradation mediated by the E3 ubiquitin ligase dorfin. J. Biol. Chem. 281 (17), 11610−11617.

Huang, Y., Zhou, Y., Castiblanco, A., Yang, W., Brown, E.M., Yang, J.J., 2009b. Multiple $Ca^{(2+)}$-binding sites in the extracellular domain of the $Ca^{(2+)}$-sensing receptor corresponding to cooperative $Ca^{(2+)}$ response. Biochemistry 48 (2), 388−398.

Huang, Y., Zhou, Y., Wong, H.C., Castiblanco, A., Chen, Y., Brown, E.M., et al., 2010. Calmodulin regulates Ca^{2+}-sensing receptor-mediated Ca^{2+} signaling and its cell surface expression. J. Biol. Chem. 285 (46), 35919−35931.

Huang, Y., Zhou, Y., Yang, W., Butters, R., Lee, H.W., Li, S., et al., 2007b. Identification and dissection of $Ca^{(2+)}$-binding sites in the extracellular domain of $Ca^{(2+)}$-sensing receptor. J. Biol. Chem. 282 (26), 19000−19010.

Ishioka, N., Bukoski, R.D., 1999. A role for N-arachidonylethanolamine (anandamide) as the mediator of sensory nerve-dependent Ca^{2+}-induced relaxation. J. Pharmacol. Exp. Ther. 289 (1), 245−250.

Jacobsen, S.E., Gether, U., Brauner-Osborne, H., 2017. Investigating the molecular mechanism of positive and negative allosteric modulators in the calcium-sensing receptor dimer. Sci. Rep. 7, 46355.

Janicic, N., Soliman, E., Pausova, Z., Seldin, M.F., Riviere, M., Szpirer, J., et al., 1995. Mapping of the calcium-sensing receptor gene (CASR) to human chromosome 3q13.3-21 by fluorescence in situ hybridization, and localization to rat chromosome 11 and mouse chromosome 16. Mamm. Genome 6 (11), 798−801.

Jiang, L.I., Collins, J., Davis, R., Fraser, I.D., Sternweis, P.C., 2008. Regulation of cAMP responses by the G12/13 pathway converges on adenylyl cyclase VII. J. Biol. Chem. 283 (34), 23429−23439.

Jiang, Y., Minet, E., Zhang, Z., Silver, P.A., Bai, M., 2004. Modulation of interprotomer relationships is important for activation of dimeric calcium-sensing receptor. J. Biol. Chem. 279 (14), 14147−14156.

Jiang, Y.F., Zhang, Z., Kifor, O., Lane, C.R., Quinn, S.J., Bai, M., 2002. Protein kinase C (PKC) phosphorylation of the Ca^{2+} o-sensing receptor (CaR) modulates functional interaction of G proteins with the CaR cytoplasmic tail. J. Biol. Chem. 277 (52), 50543−50549.

Jones, P.M., Kitsou-Mylona, I., Gray, E., Squires, P.E., Persaud, S.J., 2007. Expression and function of the extracellular calcium-sensing receptor in pancreatic beta-cells. Arch. Physiol. Biochem. 113 (3), 98−103.

Justinich, C.J., Mak, N., Pacheco, I., Mulder, D., Wells, R.W., Blennerhassett, M.G., et al., 2008. The extracellular calcium-sensing receptor (CaSR) on human esophagus and evidence of expression of the CaSR on the esophageal epithelial cell line (HET-1A). Am. J. Physiol. Gastrointest. Liver Physiol. 294 (1), G120−G129.

Kallay, E., Bonner, E., Wrba, F., Thakker, R.V., Peterlik, M., Cross, H.S., 2003a. Molecular and functional characterization of the extracellular calcium-sensing receptor in human colon cancer cells. Oncol. Res. 13 (12), 551−559.

Kallay, E., Kifor, O., Chattopadhyay, N., Brown, E.M., Bischof, M.G., Peterlik, M., et al., 1997. Calcium-dependent c-myc proto-oncogene expression and proliferation of Caco-2 cells: a role for a luminal extracellular calcium-sensing receptor. Biochem. Biophys. Res. Commun. 232 (1), 80−83.

Kallay, E., Wrba, F., Cross, H.S., 2003b. Dietary calcium and colon cancer prevention. Forum Nutr. 56, 188−190.

Kameda, T., Mano, H., Yamada, Y., Takai, H., Amizuka, N., Kobori, M., et al., 1998. Calcium-sensing receptor in mature osteoclasts, which are bone resorbing cells. Biochem. Biophys. Res. Commun. 245 (2), 419−422.

Kanatani, M., Sugimoto, T., Kanzawa, M., Yano, S., Chihara, K., 1999. High extracellular calcium inhibits osteoclast-like cell formation by directly acting on the calcium-sensing receptor existing in osteoclast precursor cells. Biochem. Biophys. Res. Commun. 261 (1), 144−148.

Kantham, L., Quinn, S.J., Egbuna, O.I., Baxi, K., Butters, R., Pang, J.L., et al., 2009. The calcium-sensing receptor (CaSR) defends against hypercalcemia independently of its regulation of parathyroid hormone secretion. Am. J. Physiol. Endocrinol. Metab. 297 (4), E915−E923.

Kelly, J.C., Lungchukiet, P., Macleod, R.J., 2011. Extracellular calcium-sensing receptor inhibition of intestinal EpithelialTNF signaling requires CaSR-mediated Wnt5a/Ror2 interaction. Front. Physiol. 2, 17.

Kifor, O., Brown, E.M., 1988. Relationship between diacylglycerol levels and extracellular Ca^{2+} in dispersed bovine parathyroid cells. Endocrinology 123 (6), 2723−2729.

Kifor, O., Diaz, R., Butters, R., Brown, E.M., 1997. The Ca^{2+}-sensing receptor (CaR) activates phospholipases C, A2, and D in bovine parathyroid and CaR-transfected, human embryonic kidney (HEK293) cells. J. Bone Miner. Res. 12 (5), 715−725.

Kifor, O., Diaz, R., Butters, R., Kifor, I., Brown, E.M., 1998. The calcium-sensing receptor is localized in caveolin-rich plasma membrane domains of bovine parathyroid cells. J. Biol. Chem. 273 (34), 21708−21713.

Kifor, O., Kifor, I., Moore Jr., F.D., Butters Jr., R.R., Brown, E.M., 2003. m-Calpain colocalizes with the calcium-sensing receptor (CaR) in caveolae in parathyroid cells and participates in degradation of the CaR. J. Biol. Chem. 278 (33), 31167−31176.

Kifor, O., MacLeod, R.J., Diaz, R., Bai, M., Yamaguchi, T., Yao, T., et al., 2001. Regulation of MAP kinase by calcium-sensing receptor in bovine parathyroid and CaR-transfected HEK293 cells. Am. J. Physiol. Renal. Physiol. 280 (2), F291−F302.

Kifor, O., Moore Jr., F.D., Wang, P., Goldstein, M., Vassilev, P., Kifor, I., et al., 1996. Reduced immunostaining for the extracellular Ca^{2+}-sensing receptor in primary and uremic secondary hyperparathyroidism. J. Clin. Endocrinol. Metab. 81 (4), 1598−1606.

Kim, J.Y., Ho, H., Kim, N., Liu, J., Tu, C.L., Yenari, M.A., et al., 2014. Calcium-sensing receptor (CaSR) as a novel target for ischemic neuroprotection. Ann Clin Transl Neurol 1 (11), 851−866.

Kim, J.Y., Kim, N., Yenari, M.A., Chang, W., 2011. Mild hypothermia suppresses calcium-sensing receptor (CaSR) induction following forebrain ischemia while increasing GABA-B receptor 1 (GABA-B-R1) expression. Transl Stroke Res 2 (2), 195−201.

Kim, J.Y., Kim, N., Yenari, M.A., Chang, W., 2013. Hypothermia and pharmacological regimens that prevent overexpression and overactivity of the extracellular calcium-sensing receptor protect neurons against traumatic brain injury. J. Neurotrauma 30 (13), 1170−1176.

Kim, W., Takyar, F.M., Swan, K., Jeong, J., VanHouten, J., Sullivan, C., et al., 2016. Calcium-sensing receptor promotes breast cancer by stimulating intracrine actions of parathyroid hormone-related protein. Cancer Res. 76 (18), 5348–5360.

Kim, W., Wysolmerski, J.J., 2016. Calcium-sensing receptor in breast physiology and cancer. Front. Physiol. 7, 440.

Kitsou-Mylona, I., Burns, C.J., Squires, P.E., Persaud, S.J., Jones, P.M., 2008. A role for the extracellular calcium-sensing receptor in cell-cell communication in pancreatic islets of langerhans. Cell. Physiol. Biochem. 22 (5–6), 557–566.

Klein, G.L., Castro, S.M., Garofalo, R.P., 2016. The calcium-sensing receptor as a mediator of inflammation. Semin. Cell Dev. Biol. 49, 52–56.

Koh, J., Dar, M., Untch, B.R., Dixit, D., Shi, Y., Yang, Z., et al., 2011. Regulator of G protein signaling 5 is highly expressed in parathyroid tumors and inhibits signaling by the calcium-sensing receptor. Mol. Endocrinol. 25 (5), 867–876.

Komuves, L., Oda, Y., Tu, C.L., Chang, W.H., Ho-Pao, C.L., Mauro, T., et al., 2002. Epidermal expression of the full-length extracellular calcium-sensing receptor is required for normal keratinocyte differentiation. J. Cell. Physiol. 192 (1), 45–54.

Kopic, S., Wagner, M.E., Griessenauer, C., Socrates, T., Ritter, M., Geibel, J.P., 2012. Vacuolar-type H+-ATPase-mediated proton transport in the rat parietal cell. Pflügers Archiv 463 (3), 419–427.

Kumar, S., Matheny, C.J., Hoffman, S.J., Marquis, R.W., Schultz, M., Liang, X., et al., 2010. An orally active calcium-sensing receptor antagonist that transiently increases plasma concentrations of PTH and stimulates bone formation. Bone 46 (2), 534–542.

Kunishima, N., Shimada, Y., Tsuji, Y., Sato, T., Yamamoto, M., Kumasaka, T., et al., 2000. Structural basis of glutamate recognition by a dimeric metabotropic glutamate receptor. Nature 407 (6807), 971–977.

Kurosawa, M., Shimizu, Y., Tsukagoshi, H., Ueki, M., 1992. Elevated levels of peripheral-blood, naturally occurring aliphatic polyamines in bronchial asthmatic patients with active symptoms. Allergy 47 (6), 638–643.

Lamprecht, S.A., Lipkin, M., 2001. Cellular mechanisms of calcium and vitamin D in the inhibition of colorectal carcinogenesis. Ann. N. Y. Acad. Sci. 952, 73–87.

Lazarus, S., Pretorius, C.J., Khafagi, F., Campion, K.L., Brennan, S.C., Conigrave, A.D., et al., 2011. A novel mutation of the primary protein kinase C phosphorylation site in the calcium-sensing receptor causes autosomal dominant hypocalcemia. Eur. J. Endocrinol. 164 (3), 429–435.

Leach, K., Conigrave, A.D., Sexton, P.M., Christopoulos, A., 2015. Towards tissue-specific pharmacology: insights from the calcium-sensing receptor as a paradigm for GPCR (patho)physiological bias. Trends Pharmacol. Sci. 36 (4), 215–225.

Leach, K., Wen, A., Davey, A.E., Sexton, P.M., Conigrave, A.D., Christopoulos, A., 2012. Identification of molecular phenotypes and biased signaling induced by naturally occurring mutations of the human calcium-sensing receptor. Endocrinology 153 (9), 4304–4316.

Lee, H.J., Mun, H.C., Lewis, N.C., Crouch, M.F., Culverston, E.L., Mason, R.S., et al., 2007. Allosteric activation of the extracellular Ca^{2+}-sensing receptor by L-amino acids enhances ERK1/2 phosphorylation. Biochem. J. 404 (1), 141–149.

Lee, S.P., Wu, W.Y., Hsiao, J.K., Zhou, J.H., Chang, H.H., Chien, C.T., 2019. Aromatherapy: activating olfactory calcium-sensing receptors impairs renal hemodynamics via sympathetic nerve-mediated vasoconstriction. Acta Physiol. 225 (1), e13157.

Lembrechts, R., Brouns, I., Schnorbusch, K., Pintelon, I., Kemp, P.J., Timmermans, J.P., et al., 2013. Functional expression of the multimodal extracellular calcium-sensing receptor in pulmonary neuroendocrine cells. J. Cell Sci. 126 (Pt 19), 4490–4501.

Li, X., Zheng, W., Li, Y.C., 2003. Altered gene expression profile in the kidney of vitamin D receptor knockout mice. J. Cell. Biochem. 89 (4), 709–719.

Liao, J., Schneider, A., Datta, N.S., McCauley, L.K., 2006. Extracellular calcium as a candidate mediator of prostate cancer skeletal metastasis. Cancer Res. 66 (18), 9065–9073.

Liou, A.P., Sei, Y., Zhao, X., Feng, J., Lu, X., Thomas, C., et al., 2011. The extracellular calcium-sensing receptor is required for cholecystokinin secretion in response to L-phenylalanine in acutely isolated intestinal I cells. Am. J. Physiol. Gastrointest. Liver Physiol. 300 (4), G538–G546.

Liu, G., Hu, X., Chakrabarty, S., 2009. Calcium sensing receptor down-regulates malignant cell behavior and promotes chemosensitivity in human breast cancer cells. Cell Calcium 45 (3), 216–225.

London, G.M., Marchais, S.J., Guerin, A.P., Metivier, F., 2005. Arteriosclerosis, vascular calcifications and cardiovascular disease in uremia. Curr. Opin. Nephrol. Hypertens. 14 (6), 525–531.

Loot, A.E., Pierson, I., Syzonenko, T., Elgheznawy, A., Randriamboavonjy, V., Zivkovic, A., et al., 2013. Ca^{2+}-sensing receptor cleavage by calpain partially accounts for altered vascular reactivity in mice fed a high-fat diet. J. Cardiovasc. Pharmacol. 61 (6), 528–535.

Lopez-Fernandez, I., Schepelmann, M., Brennan, S.C., Yarova, P.L., Riccardi, D., 2015. The calcium-sensing receptor: one of a kind. Exp. Physiol. 100 (12), 1392–1399.

Lorenz, S., Frenzel, R., Paschke, R., Breitwieser, G.E., Miedlich, S.U., 2007. Functional desensitization of the extracellular calcium-sensing receptor is regulated via distinct mechanisms: role of G protein-coupled receptor kinases, protein kinase C and beta-arrestins. Endocrinology 148 (5), 2398–2404.

Ma, X., Cheng, K.T., Wong, C.O., O'Neil, R.G., Birnbaumer, L., Ambudkar, I.S., et al., 2011. Heteromeric TRPV4-C1 channels contribute to store-operated $Ca^{(2+)}$ entry in vascular endothelial cells. Cell Calcium 50 (6), 502–509.

Mace, O.J., Schindler, M., Patel, S., 2012. The regulation of K- and L-cell activity by GLUT2 and the calcium-sensing receptor CasR in rat small intestine. J. Physiol. 590 (12), 2917–2936.

Macleod, R.J., 2013. CaSR function in the intestine: hormone secretion, electrolyte absorption and secretion, paracrine non-canonical Wnt signaling and colonic crypt cell proliferation. Best Pract. Res. Clin. Endocrinol. Metabol. 27 (3), 385–402.

MacLeod, R.J., Chattopadhyay, N., Brown, E.M., 2003. PTHrP stimulated by the calcium-sensing receptor requires MAP kinase activation. Am. J. Physiol. Endocrinol. Metab. 284 (2), E435–E442.

MacLeod, R.J., Hayes, M., Pacheco, I., 2007. Wnt5a secretion stimulated by the extracellular calcium-sensing receptor inhibits defective Wnt signaling in colon cancer cells. Am. J. Physiol. Gastrointest. Liver Physiol. 293 (1), G403–G411.

MacLeod, R.J., Yano, S., Chattopadhyay, N., Brown, E.M., 2004. Extracellular calcium-sensing receptor transactivates the epidermal growth factor receptor by a triple-membrane-spanning signaling mechanism. Biochem. Biophys. Res. Commun. 320 (2), 455–460.

Magno, A.L., Ingley, E., Brown, S.J., Conigrave, A.D., Ratajczak, T., Ward, B.K., 2011a. Testin, a novel binding partner of the calcium-sensing receptor, enhances receptor-mediated Rho-kinase signalling. Biochem. Biophys. Res. Commun. 412 (4), 584–589.

Magno, A.L., Ward, B.K., Ratajczak, T., 2011b. The calcium-sensing receptor: a molecular perspective. Endocr. Rev. 32 (1), 3–30.

Maiti, A., Hait, N.C., Beckman, M.J., 2008. Extracellular calcium-sensing receptor activation induces vitamin D receptor levels in proximal kidney HK-2G cells by a mechanism that requires phosphorylation of p38alpha MAPK. J. Biol. Chem. 283 (1), 175–183.

Malgaroli, A., Meldolesi, J., Zallone, A.Z., Teti, A., 1989. Control of cytosolic free calcium in rat and chicken osteoclasts. The role of extracellular calcium and calcitonin. J. Biol. Chem. 264 (24), 14342–14347.

Mamillapalli, R., VanHouten, J., Dann, P., Bikle, D., Chang, W., Brown, E., et al., 2013. Mammary-specific ablation of the calcium-sensing receptor during lactation alters maternal calcium metabolism, milk calcium transport, and neonatal calcium accrual. Endocrinology 154 (9), 3031–3042.

Mamillapalli, R., VanHouten, J., Zawalich, W., Wysolmerski, J., 2008. Switching of G-protein usage by the calcium-sensing receptor reverses its effect on parathyroid hormone-related protein secretion in normal versus malignant breast cells. J. Biol. Chem. 283 (36), 24435–24447.

Mamillapalli, R., Wysolmerski, J., 2010. The calcium-sensing receptor couples to Galpha(s) and regulates PTHrP and ACTH secretion in pituitary cells. J. Endocrinol. 204 (3), 287–297.

Mannstadt, M., Bertrand, G., Muresan, M., Weryha, G., Leheup, B., Pulusani, S.R., et al., 2008. Dominant-negative GCMB mutations cause an autosomal dominant form of hypoparathyroidism. J. Clin. Endocrinol. Metab. 93 (9), 3568–3576.

Maruyama, Y., Yasuda, R., Kuroda, M., Eto, Y., 2012. Kokumi substances, enhancers of basic tastes, induce responses in calcium-sensing receptor expressing taste cells. PLoS One 7 (4), e34489.

Marx, S.J., 2018. Familial hypocalciuric hypercalcemia as an atypical form of primary hyperparathyroidism. J. Bone Miner. Res. 33 (1), 27–31.

Marx, S.J., Attie, M.F., Levine, M.A., Spiegel, A.M., Downs Jr., R.W., Lasker, R.D., 1981a. The hypocalciuric or benign variant of familial hypercalcemia: clinical and biochemical features in fifteen kindreds. Medicine (Baltim.) 60 (6), 397–412.

Marx, S.J., Attie, M.F., Spiegel, A.M., Levine, M.A., Lasker, R.D., Fox, M., 1982a. An association between neonatal severe primary hyperparathyroidism and familial hypocalciuric hypercalcemia in three kindreds. N. Engl. J. Med. 306 (5), 257–264.

Marx, S.J., Attie, M.F., Stock, J.L., Spiegel, A.M., Levine, M.A., 1981b. Maximal urine-concentrating ability: familial hypocalciuric hypercalcemia versus typical primary hyperparathyroidism. J. Clin. Endocrinol. Metab. 52 (4), 736–740.

Marx, S.J., Fraser, D., Rapoport, A., 1985. Familial hypocalciuric hypercalcemia. Mild expression of the gene in heterozygotes and severe expression in homozygotes. Am. J. Med. 78 (1), 15–22.

Marx, S.J., Spiegel, A.M., Brown, E.M., Koehler, J.O., Gardner, D.G., Brennan, M.F., et al., 1978a. Divalent cation metabolism. Familial hypocalciuric hypercalcemia versus typical primary hyperparathyroidism. Am. J. Med. 65 (2), 235–242.

Marx, S.J., Spiegel, A.M., Brown, E.M., Windeck, R., Gardner, D.G., Downs Jr., R.W., et al., 1978b. Circulating parathyroid hormone activity: familial hypocalciuric hypercalcemia versus typical primary hyperparathyroidism. J. Clin. Endocrinol. Metab. 47 (6), 1190–1197.

Marx, S.J., Spiegel, A.M., Levine, M.A., Rizzoli, R.E., Lasker, R.D., Santora, A.C., et al., 1982b. Familial hypocalciuric hypercalcemia: the relation to primary parathyroid hyperplasia. N. Engl. J. Med. 307 (7), 416–426.

Mathias, R.S., Nguyen, H.T., Zhang, M.Y., Portale, A.A., 1998. Reduced expression of the renal calcium-sensing receptor in rats with experimental chronic renal insufficiency. J. Am. Soc. Nephrol. 9 (11), 2067–2074.

McCormick, W.D., Atkinson-Dell, R., Campion, K.L., Mun, H.C., Conigrave, A.D., Ward, D.T., 2010. Increased receptor stimulation elicits differential calcium-sensing receptor(T888) dephosphorylation. J. Biol. Chem. 285 (19), 14170–14177.

McLarnon, S., Holden, D., Ward, D., Jones, M., Elliott, A., Riccardi, D., 2002. Aminoglycoside antibiotics induce pH-sensitive activation of the calcium-sensing receptor. Biochem. Biophys. Res. Commun. 297 (1), 71–77.

Membreno, L., Chen, T.H., Woodley, S., Gagucas, R., Shoback, D., 1989. The effects of protein kinase-C agonists on parathyroid hormone release and intracellular free Ca2+ in bovine parathyroid cells. Endocrinology 124 (2), 789–797.

Mentaverri, R., Yano, S., Chattopadhyay, N., Petit, L., Kifor, O., Kamel, S., et al., 2006. The calcium sensing receptor is directly involved in both osteoclast differentiation and apoptosis. FASEB J. 20 (14), 2562–2564.

Mihai, R., Stevens, J., McKinney, C., Ibrahim, N.B., 2006. Expression of the calcium receptor in human breast cancer–a potential new marker predicting the risk of bone metastases. Eur. J. Surg. Oncol. 32 (5), 511–515.

Mizobuchi, M., Hatamura, I., Ogata, H., Saji, F., Uda, S., Shiizaki, K., et al., 2004. Calcimimetic compound upregulates decreased calcium-sensing receptor expression level in parathyroid glands of rats with chronic renal insufficiency. J. Am. Soc. Nephrol. 15 (10), 2579–2587.

Mizobuchi, M., Ritter, C.S., Krits, I., Slatopolsky, E., Sicard, G., Brown, A.J., 2009. Calcium-sensing receptor expression is regulated by glial cells missing-2 in human parathyroid cells. J. Bone Miner. Res. 24 (7), 1173–1179.

Molostvov, G., Hiemstra, T.F., Fletcher, S., Bland, R., Zehnder, D., 2015. Arterial expression of the calcium-sensing receptor is maintained by physiological pulsation and protects against calcification. PLoS One 10 (10), e0138833.

Moonga, B.S., Moss, D.W., Patchell, A., Zaidi, M., 1990. Intracellular regulation of enzyme secretion from rat osteoclasts and evidence for a functional role in bone resorption. J. Physiol. 429, 29–45.

Mu, L., Tuck, D., Katsaros, D., Lu, L., Schulz, V., Perincheri, S., et al., 2012. Favorable outcome associated with an IGF-1 ligand signature in breast cancer. Breast Canc. Res. Treat. 133 (1), 321–331.

Muddana, V., Lamb, J., Greer, J.B., Elinoff, B., Hawes, R.H., Cotton, P.B., et al., 2008. Association between calcium sensing receptor gene polymorphisms and chronic pancreatitis in a US population: role of serine protease inhibitor Kazal 1type and alcohol. World J. Gastroenterol. 14 (28), 4486–4491.

Mulder, D.J., Pacheco, I., Hurlbut, D.J., Mak, N., Furuta, G.T., MacLeod, R.J., et al., 2009. FGF9-induced proliferative response to eosinophilic inflammation in oesophagitis. Gut 58 (2), 166–173.

Mun, H.C., Culverston, E.L., Franks, A.H., Collyer, C.A., Clifton-Bligh, R.J., Conigrave, A.D., 2005. A double mutation in the extracellular Ca^{2+}-sensing receptor's venus flytrap domain that selectively disables L-amino acid sensing. J. Biol. Chem. 280 (32), 29067–29072.

Mun, H.C., Franks, A.H., Culverston, E.L., Krapcho, K., Nemeth, E.F., Conigrave, A.D., 2004. The Venus Fly Trap domain of the extracellular Ca^{2+}-sensing receptor is required for L-amino acid sensing. J. Biol. Chem. 279 (50), 51739–51744.

Muto, T., Tsuchiya, D., Morikawa, K., Jingami, H., 2007. Structures of the extracellular regions of the group II/III metabotropic glutamate receptors. Proc. Natl. Acad. Sci. U. S. A. 104 (10), 3759–3764.

Nemeth, E.F., 2002. The search for calcium receptor antagonists (calcilytics). J. Mol. Endocrinol. 29 (1), 15–21.

Nemeth, E.F., Goodman, W.G., 2016. Calcimimetic and calcilytic drugs: feats, flops, and futures. Calcif. Tissue Int. 98 (4), 341–358.

Nemeth, E.F., Scarpa, A., 1987. Rapid mobilization of cellular Ca^{2+} in bovine parathyroid cells evoked by extracellular divalent cations. Evidence for a cell surface calcium receptor. J. Biol. Chem. 262 (11), 5188–5196.

Nemeth, E.F., Shoback, D., 2013. Calcimimetic and calcilytic drugs for treating bone and mineral-related disorders. Best Pract. Res. Clin. Endocrinol. Metabol. 27 (3), 373–384.

Nemeth, E.F., Steffey, M.E., Hammerland, L.G., Hung, B.C., Van Wagenen, B.C., DelMar, E.G., et al., 1998. Calcimimetics with potent and selective activity on the parathyroid calcium receptor. Proc. Natl. Acad. Sci. U. S. A. 95 (7), 4040–4045.

Nesbit, M.A., Hannan, F.M., Howles, S.A., Babinsky, V.N., Head, R.A., Cranston, T., et al., 2013a. Mutations affecting G-protein subunit alpha11 in hypercalcemia and hypocalcemia. N. Engl. J. Med. 368 (26), 2476–2486.

Nesbit, M.A., Hannan, F.M., Howles, S.A., Reed, A.A., Cranston, T., Thakker, C.E., et al., 2013b. Mutations in AP2S1 cause familial hypocalciuric hypercalcemia type 3. Nat. Genet. 45 (1), 93–97.

North, M.L., Grasemann, H., Khanna, N., Inman, M.D., Gauvreau, G.M., Scott, J.A., 2013. Increased ornithine-derived polyamines cause airway hyperresponsiveness in a mouse model of asthma. Am. J. Respir. Cell Mol. Biol. 48 (6), 694–702.

Oda, Y., Tu, C.L., Chang, W., Crumrine, D., Komuves, L., Mauro, T., et al., 2000. The calcium sensing receptor and its alternatively spliced form in murine epidermal differentiation. J. Biol. Chem. 275 (2), 1183–1190.

Oda, Y., Tu, C.L., Pillai, S., Bikle, D.D., 1998. The calcium sensing receptor and its alternatively spliced form in keratinocyte differentiation. J. Biol. Chem. 273 (36), 23344–23352.

Oh, J., Beckmann, J., Bloch, J., Hettgen, V., Mueller, J., Li, L., et al., 2011. Stimulation of the calcium-sensing receptor stabilizes the podocyte cytoskeleton, improves cell survival, and reduces toxin-induced glomerulosclerosis. Kidney Int. 80 (5), 483–492.

Okabe, M., Graham, A., 2004. The origin of the parathyroid gland. Proc. Natl. Acad. Sci. U. S. A. 101 (51), 17716–17719.

Olszak, I.T., Poznansky, M.C., Evans, R.H., Olson, D., Kos, C., Pollak, M.R., et al., 2000. Extracellular calcium elicits a chemokinetic response from monocytes in vitro and in vivo. J. Clin. Investig. 105 (9), 1299–1305.

Owen, J.L., Cheng, S.X., Ge, Y., Sahay, B., Mohamadzadeh, M., 2016. The role of the calcium-sensing receptor in gastrointestinal inflammation. Semin. Cell Dev. Biol. 49, 44–51.

Parfrey, P.S., Drueke, T.B., Block, G.A., Correa-Rotter, R., Floege, J., Herzog, C.A., et al., 2015. The effects of cinacalcet in older and younger patients on hemodialysis: the evaluation of cinacalcet HCl therapy to lower cardiovascular events (EVOLVE) trial. Clin. J. Am. Soc. Nephrol. 10 (5), 791–799.

Parkash, J., 2011. Glucose-mediated spatial interactions of voltage dependent calcium channels and calcium sensing receptor in insulin producing beta-cells. Life Sci. 88 (5–6), 257–264.

Parkash, J., Asotra, K., 2011. L-histidine sensing by calcium sensing receptor inhibits voltage-dependent calcium channel activity and insulin secretion in beta-cells. Life Sci. 88 (9–10), 440–446.

Patel, L.R., Camacho, D.F., Shiozawa, Y., Pienta, K.J., Taichman, R.S., 2011. Mechanisms of cancer cell metastasis to the bone: a multistep process. Future Oncol. 7 (11), 1285–1297.

Pearce, S.H., Trump, D., Wooding, C., Besser, G.M., Chew, S.L., Grant, D.B., et al., 1995. Calcium-sensing receptor mutations in familial benign hypercalcemia and neonatal hyperparathyroidism. J. Clin. Investig. 96 (6), 2683–2692.

Pece, S., Gutkind, J.S., 2000. Signaling from E-cadherins to the MAPK pathway by the recruitment and activation of epidermal growth factor receptors upon cell-cell contact formation. J. Biol. Chem. 275 (52), 41227–41233.

Peng, X., Li, H.X., Shao, H.J., Li, G.W., Sun, J., Xi, Y.H., et al., 2014. Involvement of calcium-sensing receptors in hypoxia-induced vascular remodeling and pulmonary hypertension by promoting phenotypic modulation of small pulmonary arteries. Mol. Cell. Biochem. 396 (1–2), 87–98.

Petrel, C., Kessler, A., Dauban, P., Dodd, R.H., Rognan, D., Ruat, M., 2004. Positive and negative allosteric modulators of the Ca^{2+}-sensing receptor interact within overlapping but not identical binding sites in the transmembrane domain. J. Biol. Chem. 279 (18), 18990–18997.

Pi, M., Oakley, R.H., Gesty-Palmer, D., Cruickshank, R.D., Spurney, R.F., Luttrell, L.M., et al., 2005. Beta-arrestin- and G protein receptor kinase-mediated calcium-sensing receptor desensitization. Mol. Endocrinol. 19 (4), 1078–1087.

Pi, M., Spurney, R.F., Tu, Q., Hinson, T., Quarles, L.D., 2002. Calcium-sensing receptor activation of rho involves filamin and rho-guanine nucleotide exchange factor. Endocrinology 143 (10), 3830–3838.

Pin, J.P., Galvez, T., Prezeau, L., 2003. Evolution, structure, and activation mechanism of family 3/C G-protein-coupled receptors. Pharmacol. Ther. 98 (3), 325–354.

Pollak, M.R., Chou, Y.H., Marx, S.J., Steinmann, B., Cole, D.E., Brandi, M.L., et al., 1994. Familial hypocalciuric hypercalcemia and neonatal severe hyperparathyroidism. Effects of mutant gene dosage on phenotype. J. Clin. Investig. 93 (3), 1108–1112.

Popp, T., Steinritz, D., Breit, A., Deppe, J., Egea, V., Schmidt, A., et al., 2014. Wnt5a/beta-catenin signaling drives calcium-induced differentiation of human primary keratinocytes. J. Investig. Dermatol. 134 (8), 2183–2191.

Procino, G., Mastrofrancesco, L., Tamma, G., Lasorsa, D.R., Ranieri, M., Stringini, G., et al., 2012. Calcium-sensing receptor and aquaporin 2 interplay in hypercalciuria-associated renal concentrating defect in humans. An in vivo and in vitro study. PLoS One 7 (3), e33145.

Promkan, M., Liu, G., Patmasiriwat, P., Chakrabarty, S., 2011. BRCA1 suppresses the expression of survivin and promotes sensitivity to paclitaxel through the calcium sensing receptor (CaSR) in human breast cancer cells. Cell Calcium 49 (2), 79–88.

Quinn, S.J., Bai, M., Brown, E.M., 2004. pH Sensing by the calcium-sensing receptor. J. Biol. Chem. 279 (36), 37241–37249.

Quinn, S.J., Kifor, O., Trivedi, S., Diaz, R., Vassilev, P., Brown, E., 1998. Sodium and ionic strength sensing by the calcium receptor. J. Biol. Chem. 273 (31), 19579–19586.

Quinn, S.J., Ye, C.P., Diaz, R., Kifor, O., Bai, M., Vassilev, P., et al., 1997. The Ca^{2+}-sensing receptor: a target for polyamines. Am. J. Physiol. 273 (4 Pt 1), C1315–C1323.

Racz, G.Z., Kittel, A., Riccardi, D., Case, R.M., Elliott, A.C., Varga, G., 2002. Extracellular calcium sensing receptor in human pancreatic cells. Gut 51 (5), 705–711.

Ray, K., 2015. Calcium-sensing receptor: trafficking, endocytosis, recycling, and importance of interacting proteins. Prog Mol Biol Transl Sci 132, 127–150.

Ray, K., Clapp, P., Goldsmith, P.K., Spiegel, A.M., 1998. Identification of the sites of N-linked glycosylation on the human calcium receptor and assessment of their role in cell surface expression and signal transduction. J. Biol. Chem. 273 (51), 34558–34567.

Ray, K., Fan, G.F., Goldsmith, P.K., Spiegel, A.M., 1997. The carboxyl terminus of the human calcium receptor. Requirements for cell-surface expression and signal transduction. J. Biol. Chem. 272 (50), 31355–31361.

Ray, K., Ghosh, S.P., Northup, J.K., 2004. The role of cysteines and charged amino acids in extracellular loops of the human $Ca^{(2+)}$ receptor in cell surface expression and receptor activation processes. Endocrinology 145 (8), 3892–3903.

Ray, K., Hauschild, B.C., Steinbach, P.J., Goldsmith, P.K., Hauache, O., Spiegel, A.M., 1999. Identification of the cysteine residues in the amino-terminal extracellular domain of the human $Ca^{(2+)}$ receptor critical for dimerization. Implications for function of monomeric $Ca^{(2+)}$ receptor. J. Biol. Chem. 274 (39), 27642–27650.

Reinhardt, T.A., Lippolis, J.D., Shull, G.E., Horst, R.L., 2004. Null mutation in the gene encoding plasma membrane Ca^{2+}-ATPase isoform 2 impairs calcium transport into milk. J. Biol. Chem. 279 (41), 42369–42373.

Remy, C., Kirchhoff, P., Hafner, P., Busque, S.M., Mueller, M.K., Geibel, J.P., et al., 2007. Stimulatory pathways of the Calcium-sensing receptor on acid secretion in freshly isolated human gastric glands. Cell. Physiol. Biochem. 19 (1–4), 33–42.

Rey, O., Chang, W., Bikle, D., Rozengurt, N., Young, S.H., Rozengurt, E., 2012. Negative cross-talk between calcium-sensing receptor and beta-catenin signaling systems in colonic epithelium. J. Biol. Chem. 287 (2), 1158–1167.

Rey, O., Young, S.H., Jacamo, R., Moyer, M.P., Rozengurt, E., 2010. Extracellular calcium sensing receptor stimulation in human colonic epithelial cells induces intracellular calcium oscillations and proliferation inhibition. J. Cell. Physiol. 225 (1), 73–83.

Rey, O., Young, S.H., Yuan, J., Slice, L., Rozengurt, E., 2005. Amino acid-stimulated Ca^{2+} oscillations produced by the Ca^{2+}-sensing receptor are mediated by a phospholipase C/inositol 1,4,5-trisphosphate-independent pathway that requires G12, Rho, filamin-A, and the actin cytoskeleton. J. Biol. Chem. 280 (24), 22875–22882.

Reyes-Ibarra, A.P., Garcia-Regalado, A., Ramirez-Rangel, I., Esparza-Silva, A.L., Valadez-Sanchez, M., Vazquez-Prado, J., et al., 2007. Calcium-sensing receptor endocytosis links extracellular calcium signaling to parathyroid hormone-related peptide secretion via a Rab11a-dependent and AMSH-sensitive mechanism. Mol. Endocrinol. 21 (6), 1394–1407.

Riccardi, D., 2002. Wellcome Prize Lecture. Cell surface, ion-sensing receptors. Exp. Physiol. 87 (4), 403–411.

Riccardi, D., Brennan, S.C., Chang, W., 2013. The extracellular calcium-sensing receptor, CaSR, in fetal development. Best Pract. Res. Clin. Endocrinol. Metabol. 27 (3), 443–453.

Riccardi, D., Finney, B.A., Wilkinson, W.J., Kemp, P.J., 2009. Novel regulatory aspects of the extracellular Ca^{2+}-sensing receptor, CaR. Pflügers Archiv 458 (6), 1007–1022.

Riccardi, D., Park, J., Lee, W.S., Gamba, G., Brown, E.M., Hebert, S.C., 1995. Cloning and functional expression of a rat kidney extracellular calcium/polyvalent cation-sensing receptor. Proc. Natl. Acad. Sci. U. S. A. 92 (1), 131–135.

Riccardi, D., Valenti, G., 2016. Localization and function of the renal calcium-sensing receptor. Nat. Rev. Nephrol. 12 (7), 414–425.

Richard, C., Huo, R., Samadfam, R., Bolivar, I., Miao, D., Brown, E.M., et al., 2010. The calcium-sensing receptor and 25-hydroxyvitamin D-1alpha-hydroxylase interact to modulate skeletal growth and bone turnover. J. Bone Miner. Res. 25 (7), 1627–1636.

Rodriguez, L., Tu, C., Cheng, Z., Chen, T.H., Bikle, D., Shoback, D., et al., 2005. Expression and functional assessment of an alternatively spliced extracellular Ca^{2+}-sensing receptor in growth plate chondrocytes. Endocrinology 146 (12), 5294–5303.

Rogachevskaja, O.A., Churbanov, G.D., Bystrova, M.F., Romanov, R.A., Kolesnikov, S.S., 2011. Stimulation of the extracellular $Ca^{(2+)}$-sensing receptor by denatonium. Biochem. Biophys. Res. Commun. 416 (3–4), 433–436.

Rogers, A., Nesbit, M.A., Hannan, F.M., Howles, S.A., Gorvin, C.M., Cranston, T., et al., 2014. Mutational analysis of the adaptor protein 2 sigma subunit (AP2S1) gene: search for autosomal dominant hypocalcemia type 3 (ADH3). J. Clin. Endocrinol. Metab. 99 (7), E1300–E1305.

Rogers, A.C., Hanly, A.M., Collins, D., Baird, A.W., Winter, D.C., 2012. Review article: loss of the calcium-sensing receptor in colonic epithelium is a key event in the pathogenesis of colon cancer. Clin. Colorectal Cancer 11 (1), 24−30.

Rossol, M., Pierer, M., Raulien, N., Quandt, D., Meusch, U., Rothe, K., et al., 2012. Extracellular Ca^{2+} is a danger signal activating the NLRP3 inflammasome through G protein-coupled calcium sensing receptors. Nat. Commun. 3, 1329.

Roszko, K.L., Bi, R.D., Mannstadt, M., 2016. Autosomal dominant hypocalcemia (hypoparathyroidism) types 1 and 2. Front. Physiol. 7, 458.

Ruat, M., Molliver, M.E., Snowman, A.M., Snyder, S.H., 1995. Calcium sensing receptor: molecular cloning in rat and localization to nerve terminals. Proc. Natl. Acad. Sci. U. S. A. 92 (8), 3161−3165.

Ruat, M., Snowman, A.M., Hester, L.D., Snyder, S.H., 1996. Cloned and expressed rat Ca^{2+}-sensing receptor. Differential cooperative responses to calicum and magnesium. J. Biol. Chem. 271 (11), 5972−5975.

Rudberg, C., Akerstrom, G., Ljunghall, S., Grimelius, L., Johansson, H., Pertoft, H., et al., 1982. Regulation of parathyroid hormone release in primary and secondary hyperparathyroidism − studies in vivo and in vitro. Acta Endocrinol. 101 (3), 408−413.

Rybchyn, M.S., Slater, M., Conigrave, A.D., Mason, R.S., 2011. An Akt-dependent increase in canonical Wnt signaling and a decrease in sclerostin protein levels are involved in strontium ranelate-induced osteogenic effects in human osteoblasts. J. Biol. Chem. 286 (27), 23771−23779.

Rybczynska, A., Marchwinska, A., Dys, A., Boblewski, K., Lehmann, A., Lewko, B., 2017. Activity of the calcium-sensing receptor influences blood glucose and insulin levels in rats. Pharmacol. Rep. 69 (4), 709−713.

Saidak, Z., Boudot, C., Abdoune, R., Petit, L., Brazier, M., Mentaverri, R., et al., 2009a. Extracellular calcium promotes the migration of breast cancer cells through the activation of the calcium sensing receptor. Exp. Cell Res. 315 (12), 2072−2080.

Saidak, Z., Brazier, M., Kamel, S., Mentaverri, R., 2009b. Agonists and allosteric modulators of the calcium-sensing receptor and their therapeutic applications. Mol. Pharmacol. 76 (6), 1131−1144.

San Gabriel, A., Uneyama, H., Maekawa, T., Torii, K., 2009. The calcium-sensing receptor in taste tissue. Biochem. Biophys. Res. Commun. 378 (3), 414−418.

Sanders, J.L., Chattopadhyay, N., Kifor, O., Yamaguchi, T., Butters, R.R., Brown, E.M., 2000. Extracellular calcium-sensing receptor expression and its potential role in regulating parathyroid hormone-related peptide secretion in human breast cancer cell lines. Endocrinology 141 (12), 4357−4364.

Santa Maria, C., Cheng, Z., Li, A., Wang, J., Shoback, D., Tu, C.L., et al., 2016. Interplay between CaSR and PTH1R signaling in skeletal development and osteoanabolism. Semin. Cell Dev. Biol. 49, 11−23.

Schepelmann, M., Yarova, P.L., Lopez-Fernandez, I., Davies, T.S., Brennan, S.C., Edwards, P.J., et al., 2016. The vascular Ca^{2+}-sensing receptor regulates blood vessel tone and blood pressure. Am. J. Physiol. Cell Physiol. 310 (3), C193−C204.

Scillitani, A., Guarnieri, V., De Geronimo, S., Muscarella, L.A., Battista, C., D'Agruma, L., et al., 2004. Blood ionized calcium is associated with clustered polymorphisms in the carboxyl-terminal tail of the calcium-sensing receptor. J. Clin. Endocrinol. Metab. 89 (11), 5634−5638.

Shalhoub, V., Grisanti, M., Padagas, J., Scully, S., Rattan, A., Qi, M., et al., 2003. In vitro studies with the calcimimetic, cinacalcet HCl, on normal human adult osteoblastic and osteoclastic cells. Crit. Rev. Eukaryot. Gene Expr. 13 (2−4), 89−106.

Shoback, D.M., Membreno, L.A., McGhee, J.G., 1988. High calcium and other divalent cations increase inositol trisphosphate in bovine parathyroid cells. Endocrinology 123 (1), 382−389.

Siehler, S., 2009. Regulation of RhoGEF proteins by G12/13-coupled receptors. Br. J. Pharmacol. 158 (1), 41−49.

Silve, C., Petrel, C., Leroy, C., Bruel, H., Mallet, E., Rognan, D., et al., 2005. Delineating a Ca^{2+} binding pocket within the venus flytrap module of the human calcium-sensing receptor. J. Biol. Chem. 280 (45), 37917−37923.

Singh, N., Chakrabarty, S., 2013. Induction of CaSR expression circumvents the molecular features of malignant CaSR null colon cancer cells. Int. J. Cancer 133 (10), 2307−2314.

Singh, N., Promkan, M., Liu, G., Varani, J., Chakrabarty, S., 2013. Role of calcium sensing receptor (CaSR) in tumorigenesis. Best Pract. Res. Clin. Endocrinol. Metabol. 27 (3), 455−463.

Smajilovic, S., Hansen, J.L., Christoffersen, T.E., Lewin, E., Sheikh, S.P., Terwilliger, E.F., et al., 2006. Extracellular calcium sensing in rat aortic vascular smooth muscle cells. Biochem. Biophys. Res. Commun. 348 (4), 1215−1223.

Smajilovic, S., Yano, S., Jabbari, R., Tfelt-Hansen, J., 2011. The calcium-sensing receptor and calcimimetics in blood pressure modulation. Br. J. Pharmacol. 164 (3), 884−893.

Squires, P.E., 2000. Non-Ca^{2+}-homeostatic functions of the extracellular Ca^{2+}-sensing receptor (CaR) in endocrine tissues. J. Endocrinol. 165 (2), 173−177.

Squires, P.E., Harris, T.E., Persaud, S.J., Curtis, S.B., Buchan, A.M., Jones, P.M., 2000. The extracellular calcium-sensing receptor on human beta-cells negatively modulates insulin secretion. Diabetes 49 (3), 409−417.

Strating, J.R., Martens, G.J., 2009. The p24 family and selective transport processes at the ER-Golgi interface. Biol. Cell 101 (9), 495−509.

Sumida, K., Nakamura, M., Ubara, Y., Marui, Y., Tanaka, K., Takaichi, K., et al., 2013. Cinacalcet upregulates calcium-sensing receptors of parathyroid glands in hemodialysis patients. Am. J. Nephrol. 37 (5), 405−412.

Sun, J., Murphy, E., 2010. Calcium-sensing receptor: a sensor and mediator of ischemic preconditioning in the heart. Am. J. Physiol. Heart Circ. Physiol. 299 (5), H1309−H1317.

Suzuki, K., Lavaroni, S., Mori, A., Okajima, F., Kimura, S., Katoh, R., et al., 1998. Thyroid transcription factor 1 is calcium modulated and coordinately regulates genes involved in calcium homeostasis in C cells. Mol. Cell Biol. 18 (12), 7410−7422.

Szekely, D., Brennan, S.C., Mun, H.C., Conigrave, A.D., Kuchel, P.W., 2009. Effectors of the frequency of calcium oscillations in HEK-293 cells: wavelet analysis and a computer model. Eur. Biophys. J. 39 (1), 149−165.

Tam, R., Saier Jr., M.H., 1993. Structural, functional, and evolutionary relationships among extracellular solute-binding receptors of bacteria. Microbiol. Rev. 57 (2), 320–346.

Tang, H., Yamamura, A., Yamamura, H., Song, S., Fraidenburg, D.R., Chen, J., et al., 2016. Pathogenic role of calcium-sensing receptors in the development and progression of pulmonary hypertension. Am. J. Physiol. Lung Cell Mol. Physiol. 310 (9), L846–L859.

Tfelt-Hansen, J., MacLeod, R.J., Chattopadhyay, N., Yano, S., Quinn, S., Ren, X., et al., 2003. Calcium-sensing receptor stimulates PTHrP release by pathways dependent on PKC, p38 MAPK, JNK, and ERK1/2 in H-500 cells. Am. J. Physiol. Endocrinol. Metab. 285 (2), E329–E337.

Tharmalingam, S., Daulat, A.M., Antflick, J.E., Ahmed, S.M., Nemeth, E.F., Angers, S., et al., 2011. Calcium-sensing receptor modulates cell adhesion and migration via integrins. J. Biol. Chem. 286 (47), 40922–40933.

Tharmalingam, S., Wu, C., Hampson, D.R., 2016. The calcium-sensing receptor and integrins modulate cerebellar granule cell precursor differentiation and migration. Dev Neurobiol 76 (4), 375–389.

Theriault, R.L., Theriault, R.L., 2012. Biology of bone metastases. Cancer Control 19 (2), 92–101.

Toka, H.R., 2014. New functional aspects of the extracellular calcium-sensing receptor. Curr. Opin. Nephrol. Hypertens. 23 (4), 352–360.

Toka, H.R., Al-Romaih, K., Koshy, J.M., DiBartolo 3rd, S., Kos, C.H., Quinn, S.J., et al., 2012. Deficiency of the calcium-sensing receptor in the kidney causes parathyroid hormone-independent hypocalciuria. J. Am. Soc. Nephrol. 23 (11), 1879–1890.

Tu, C.L., Celli, A., Mauro, T., Chang, W., 2018. The calcium-sensing receptor regulates epidermal intracellular $Ca^{(2+)}$ signaling and re-epithelialization after wounding. J. Investig. Dermatol.

Tu, C.L., Chang, W., Bikle, D.D., 2001. The extracellular calcium-sensing receptor is required for calcium-induced differentiation in human keratinocytes. J. Biol. Chem. 276 (44), 41079–41085.

Tu, C.L., Chang, W., Bikle, D.D., 2007. The role of the calcium sensing receptor in regulating intracellular calcium handling in human epidermal keratinocytes. J. Investig. Dermatol. 127 (5), 1074–1083.

Tu, C.L., Chang, W., Bikle, D.D., 2011. The calcium-sensing receptor-dependent regulation of cell-cell adhesion and keratinocyte differentiation requires Rho and filamin A. J. Investig. Dermatol. 131 (5), 1119–1128.

Tu, C.L., Chang, W., Xie, Z., Bikle, D.D., 2008. Inactivation of the calcium sensing receptor inhibits E-cadherin-mediated cell-cell adhesion and calcium-induced differentiation in human epidermal keratinocytes. J. Biol. Chem. 283 (6), 3519–3528.

Tu, C.L., Crumrine, D.A., Man, M.Q., Chang, W., Elalieh, H., You, M., et al., 2012. Ablation of the calcium-sensing receptor in keratinocytes impairs epidermal differentiation and barrier function. J. Investig. Dermatol. 132 (10), 2350–2359.

Tu, C.L., You, M., 2014. Obligatory roles of filamin A in E-cadherin-mediated cell-cell adhesion in epidermal keratinocytes. J. Dermatol. Sci. 73 (2), 142–151.

Tu, Q., Pi, M., Karsenty, G., Simpson, L., Liu, S., Quarles, L.D., 2003. Rescue of the skeletal phenotype in CasR-deficient mice by transfer onto the Gcm2 null background. J. Clin. Investig. 111 (7), 1029–1037.

Turksen, K., Troy, T.C., 2003. Overexpression of the calcium sensing receptor accelerates epidermal differentiation and permeability barrier formation in vivo. Mech. Dev. 120 (6), 733–744.

Tyler Miller, R., 2013. Control of renal calcium, phosphate, electrolyte, and water excretion by the calcium-sensing receptor. Best Pract. Res. Clin. Endocrinol. Metabol. 27 (3), 345–358.

Van Aken, E., De Wever, O., Correia da Rocha, A.S., Mareel, M., 2001. Defective E-cadherin/catenin complexes in human cancer. Virchows Arch. 439 (6), 725–751.

VanHouten, J., Dann, P., McGeoch, G., Brown, E.M., Krapcho, K., Neville, M., et al., 2004. The calcium-sensing receptor regulates mammary gland parathyroid hormone-related protein production and calcium transport. J. Clin. Investig. 113 (4), 598–608.

VanHouten, J., Sullivan, C., Bazinet, C., Ryoo, T., Camp, R., Rimm, D.L., et al., 2010. PMCA2 regulates apoptosis during mammary gland involution and predicts outcome in breast cancer. Proc. Natl. Acad. Sci. U. S. A. 107 (25), 11405–11410.

VanHouten, J.N., Neville, M.C., Wysolmerski, J.J., 2007. The calcium-sensing receptor regulates plasma membrane calcium adenosine triphosphatase isoform 2 activity in mammary epithelial cells: a mechanism for calcium-regulated calcium transport into milk. Endocrinology 148 (12), 5943–5954.

VanHouten, J.N., Wysolmerski, J.J., 2007. Transcellular calcium transport in mammary epithelial cells. J. Mammary Gland Biol. Neoplasia 12 (4), 223–235.

Vanhouten, J.N., Wysolmerski, J.J., 2013. The calcium-sensing receptor in the breast. Best Pract. Res. Clin. Endocrinol. Metabol. 27 (3), 403–414.

Vargas-Poussou, R., Mansour-Hendili, L., Baron, S., Bertocchio, J.P., Travers, C., Simian, C., et al., 2016. Familial hypocalciuric hypercalcemia types 1 and 3 and primary hyperparathyroidism: similarities and differences. J. Clin. Endocrinol. Metab. 101 (5), 2185–2195.

Vizard, T.N., O'Keeffe, G.W., Gutierrez, H., Kos, C.H., Riccardi, D., Davies, A.M., 2008. Regulation of axonal and dendritic growth by the extracellular calcium-sensing receptor. Nat. Neurosci. 11 (3), 285–291.

Wada, M., Ishii, H., Furuya, Y., Fox, J., Nemeth, E.F., Nagano, N., 1998. NPS R-568 halts or reverses osteitis fibrosa in uremic rats. Kidney Int. 53 (2), 448–453.

Wang, M., Yao, Y., Kuang, D., Hampson, D.R., 2006. Activation of family C G-protein-coupled receptors by the tripeptide glutathione. J. Biol. Chem. 281 (13), 8864–8870.

Ward, B.K., Rea, S.L., Magno, A.L., Pedersen, B., Brown, S.J., Mullin, S., et al., 2018. The endoplasmic reticulum-associated protein, OS-9, behaves as a lectin in targeting the immature calcium-sensing receptor. J. Cell. Physiol. 233 (1), 38–56.

Ward, D.T., Brown, E.M., Harris, H.W., 1998. Disulfide bonds in the extracellular calcium-polyvalent cation-sensing receptor correlate with dimer formation and its response to divalent cations in vitro. J. Biol. Chem. 273 (23), 14476–14483.

Ward, D.T., Maldonado-Perez, D., Hollins, L., Riccardi, D., 2005. Aminoglycosides induce acute cell signaling and chronic cell death in renal cells that express the calcium-sensing receptor. J. Am. Soc. Nephrol. 16 (5), 1236–1244.

Weston, A.H., Absi, M., Ward, D.T., Ohanian, J., Dodd, R.H., Dauban, P., et al., 2005. Evidence in favor of a calcium-sensing receptor in arterial endothelial cells: studies with calindol and Calhex 231. Circ. Res. 97 (4), 391–398.

Wettschureck, N., Lee, E., Libutti, S.K., Offermanns, S., Robey, P.G., Spiegel, A.M., 2007. Parathyroid-specific double knockout of Gq and G11 alpha-subunits leads to a phenotype resembling germline knockout of the extracellular Ca^{2+}-sensing receptor. Mol. Endocrinol. 21 (1), 274–280.

Williams, S., Malatesta, K., Norris, K., 2009. Vitamin D and chronic kidney disease. Ethn. Dis. 19 (4 Suppl. 5). S5-8-11.

Wong, N.A., Pignatelli, M., 2002. Beta-catenin–a linchpin in colorectal carcinogenesis? Am. J. Pathol. 160 (2), 389–401.

Wonneberger, K., Scofield, M.A., Wangemann, P., 2000. Evidence for a calcium-sensing receptor in the vascular smooth muscle cells of the spiral modiolar artery. J. Membr. Biol. 175 (3), 203–212.

Wysolmerski, J.J., 2012. Parathyroid hormone-related protein: an update. J. Clin. Endocrinol. Metab. 97 (9), 2947–2956.

Xie, Z., Bikle, D.D., 2007. The recruitment of phosphatidylinositol 3-kinase to the E-cadherin-catenin complex at the plasma membrane is required for calcium-induced phospholipase C-gamma1 activation and human keratinocyte differentiation. J. Biol. Chem. 282 (12), 8695–8703.

Xing, W.J., Kong, F.J., Li, G.W., Qiao, K., Zhang, W.H., Zhang, L., et al., 2011. Calcium-sensing receptors induce apoptosis during simulated ischaemia-reperfusion in Buffalo rat liver cells. Clin. Exp. Pharmacol. Physiol. 38 (9), 605–612.

Xue, Y., Xiao, Y., Liu, J., Karaplis, A.C., Pollak, M.R., Brown, E.M., et al., 2012. The calcium-sensing receptor complements parathyroid hormone-induced bone turnover in discrete skeletal compartments in mice. Am. J. Physiol. Endocrinol. Metab. 302 (7), E841–E851.

Yamaguchi, T., Chattopadhyay, N., Kifor, O., Sanders, J.L., Brown, E.M., 2000. Activation of p42/44 and p38 mitogen-activated protein kinases by extracellular calcium-sensing receptor agonists induces mitogenic responses in the mouse osteoblastic MC3T3-E1 cell line. Biochem. Biophys. Res. Commun. 279 (2), 363–368.

Yamaguchi, T., Olozak, I., Chattopadhyay, N., Butters, R.R., Kifor, O., Scadden, D.T., et al., 1998. Expression of extracellular calcium (Ca2+o)-sensing receptor in human peripheral blood monocytes. Biochem. Biophys. Res. Commun. 246 (2), 501–506.

Yamamura, A., Guo, Q., Yamamura, H., Zimnicka, A.M., Pohl, N.M., Smith, K.A., et al., 2012. Enhanced $Ca^{(2+)}$-sensing receptor function in idiopathic pulmonary arterial hypertension. Circ. Res. 111 (4), 469–481.

Yamamura, A., Ohara, N., Tsukamoto, K., 2015. Inhibition of excessive cell proliferation by calcilytics in idiopathic pulmonary arterial hypertension. PLoS One 10 (9), e0138384.

Yamamura, A., Yagi, S., Ohara, N., Tsukamoto, K., 2016. Calcilytics enhance sildenafil-induced antiproliferation in idiopathic pulmonary arterial hypertension. Eur. J. Pharmacol. 784, 15–21.

Yano, S., Brown, E.M., Chattopadhyay, N., 2004a. Calcium-sensing receptor in the brain. Cell Calcium 35 (3), 257–264.

Yano, S., Macleod, R.J., Chattopadhyay, N., Tfelt-Hansen, J., Kifor, O., Butters, R.R., et al., 2004b. Calcium-sensing receptor activation stimulates parathyroid hormone-related protein secretion in prostate cancer cells: role of epidermal growth factor receptor transactivation. Bone 35 (3), 664–672.

Yao, J.J., Bai, S., Karnauskas, A.J., Bushinsky, D.A., Favus, M.J., 2005. Regulation of renal calcium receptor gene expression by 1,25-dihydroxyvitamin D3 in genetic hypercalciuric stone-forming rats. J. Am. Soc. Nephrol. 16 (5), 1300–1308.

Yarova, P.L., Stewart, A.L., Sathish, V., Britt Jr., R.D., Thompson, M.A., Lowe, A.P.P., et al., 2015. Calcium-sensing receptor antagonists abrogate airway hyperresponsiveness and inflammation in allergic asthma. Sci. Transl. Med. 7 (284), 284ra60.

Yasukawa, T., Hayashi, M., Tanabe, N., Tsuda, H., Suzuki, Y., Kawato, T., et al., 2017. Involvement of the calcium-sensing receptor in mineral trioxide aggregate-induced osteogenic gene expression in murine MC3T3-E1 cells. Dent. Mater. J. 36 (4), 469–475.

Ye, C., Ho-Pao, C.L., Kanazirska, M., Quinn, S., Rogers, K., Seidman, C.E., et al., 1997. Amyloid-beta proteins activate $Ca^{(2+)}$-permeable channels through calcium-sensing receptors. J. Neurosci. Res. 47 (5), 547–554.

Ye, C.P., Yano, S., Tfelt-Hansen, J., MacLeod, R.J., Ren, X., Terwilliger, E., et al., 2004. Regulation of a Ca^{2+}-activated K^+ channel by calcium-sensing receptor involves p38 MAP kinase. J. Neurosci. Res. 75 (4), 491–498.

Young, S.H., Rozengurt, E., 2002. Amino acids and Ca^{2+} stimulate different patterns of Ca^{2+} oscillations through the Ca^{2+}-sensing receptor. Am. J. Physiol. Cell Physiol. 282 (6), C1414–C1422.

Young, S.H., Wu, S.V., Rozengurt, E., 2002. Ca^{2+}-stimulated Ca^{2+} oscillations produced by the Ca^{2+}-sensing receptor require negative feedback by protein kinase C. J. Biol. Chem. 277 (49), 46871–46876.

Zaidi, M., Kerby, J., Huang, C.L., Alam, T., Rathod, H., Chambers, T.J., et al., 1991. Divalent cations mimic the inhibitory effect of extracellular ionised calcium on bone resorption by isolated rat osteoclasts: further evidence for a "calcium receptor". J. Cell. Physiol. 149 (3), 422–427.

Zhang, C., Huang, Y., Jiang, Y., Mulpuri, N., Wei, L., Hamelberg, D., et al., 2014a. Identification of an L-phenylalanine binding site enhancing the cooperative responses of the calcium-sensing receptor to calcium. J. Biol. Chem. 289 (8), 5296–5309.

Zhang, J., Zhou, J., Cai, L., Lu, Y., Wang, T., Zhu, L., et al., 2012. Extracellular calcium-sensing receptor is critical in hypoxic pulmonary vasoconstriction. Antioxid. Redox Signal 17 (3), 471–484.

Zhang, M., Breitwieser, G.E., 2005. High affinity interaction with filamin A protects against calcium-sensing receptor degradation. J. Biol. Chem. 280 (12), 11140–11146.

Zhang, X., Zhang, T., Wu, J., Yu, X., Zheng, D., Yang, F., et al., 2014b. Calcium sensing receptor promotes cardiac fibroblast proliferation and extracellular matrix secretion. Cell. Physiol. Biochem. 33 (3), 557–568.

Zhang, Z., Qiu, W., Quinn, S.J., Conigrave, A.D., Brown, E.M., Bai, M., 2002. Three adjacent serines in the extracellular domains of the CaR are required for L-amino acid-mediated potentiation of receptor function. J. Biol. Chem. 277 (37), 33727–33735.

Zhang, Z., Sun, S., Quinn, S.J., Brown, E.M., Bai, M., 2001. The extracellular calcium-sensing receptor dimerizes through multiple types of intermolecular interactions. J. Biol. Chem. 276 (7), 5316–5322.

Zheng, H., Liu, J., Liu, C., Lu, F., Zhao, Y., Jin, Z., et al., 2011. Calcium-sensing receptor activating phosphorylation of PKCdelta translocation on mitochondria to induce cardiomyocyte apoptosis during ischemia/reperfusion. Mol. Cell. Biochem. 358 (1–2), 335–343.

Zhu, D., Kosik, K.S., Meigs, T.E., Yanamadala, V., Denker, B.M., 2004. Galpha12 directly interacts with PP2A: evidence FOR Galpha12-stimulated PP2A phosphatase activity and dephosphorylation of microtubule-associated protein, tau. J. Biol. Chem. 279 (53), 54983–54986.

Zhu, D., Tate, R.I., Ruediger, R., Meigs, T.E., Denker, B.M., 2007. Domains necessary for Galpha12 binding and stimulation of protein phosphatase-2A (PP2A): is Galpha12 a novel regulatory subunit of PP2A? Mol. Pharmacol. 71 (5), 1268–1276.

Zhuang, X., Adipietro, K.A., Datta, S., Northup, J.K., Ray, K., 2010. Rab1 small GTP-binding protein regulates cell surface trafficking of the human calcium-sensing receptor. Endocrinology 151 (11), 5114–5123.

Zhuang, X., Northup, J.K., Ray, K., 2012. Large putative PEST-like sequence motif at the carboxyl tail of human calcium receptor directs lysosomal degradation and regulates cell surface receptor level. J. Biol. Chem. 287 (6), 4165–4176.

Ziegelstein, R.C., Xiong, Y., He, C., Hu, Q., 2006. Expression of a functional extracellular calcium-sensing receptor in human aortic endothelial cells. Biochem. Biophys. Res. Commun. 342 (1), 153–163.

Zitt, E., Woess, E., Mayer, G., Lhotta, K., 2011. Effect of cinacalcet on renal electrolyte handling and systemic arterial blood pressure in kidney transplant patients with persistent hyperparathyroidism. Transplantation 92 (8), 883–889.

Chapter 24

Parathyroid hormone molecular biology

Tally Naveh-Many[1], Justin Silver[1] and Henry M. Kronenberg[2]

[1]Minerva Center for Calcium and Bone Metabolism, Nephrology Services, Hadassah University Hospital, Hebrew University School of Medicine, Jerusalem, Israel; [2]Endocrine Unit, Massachusetts General Hospital, Harvard Medical School, Boston, MA, United States

Chapter outline

The parathyroid hormone gene

Organization of the parathyroid hormone gene

The human parathyroid hormone (PTH) gene is localized on the short arm of chromosome 11 at 11p15 (Antonarakis et al., 1983; Zabel et al., 1985). The human and bovine genes have two functional TATA transcription start sites, and the rat has only one. The two homologous TATA sequences flanking the human PTH gene direct the synthesis of two human PTH gene transcripts, both in normal parathyroid glands and in parathyroid adenomas (Igarashi et al., 1986; Kronenberg et al., 1986). The PTH genes in all species that have been cloned have two introns or intervening sequences and three exons (Kronenberg et al., 1986). Strikingly, even though fish do not have discrete parathyroid glands, they do synthesize PTH using two distinct genes that resemble mammalian PTH and that share the same exon–intron pattern found in tetrapod PTH genes (Danks et al., 2003; Gensure et al., 2004). Fish, as well as other vertebrates except mammals, also express a PTH-like gene (PTH4 or PTH-L) that bears some resemblance to PTH-related protein (PTHrP) and may contribute to calcium homeostasis as well (Suarez-Bregua et al., 2017). The elephant shark, which is a jawed cartilaginous fish, has at least two Pth genes and one Pthrp gene. The expression of several Pth gene family members in the elephant shark suggests that the Pthrp and Pth genes evolved in a common ancestor of jawed vertebrates even before the development of bone (Liu et al., 2010).

Principles of Bone Biology. https://doi.org/10.1016/B978-0-12-814841-9.00024-5

Intron A splits the 5′ untranslated sequence of the mRNA five nucleotides before the initiator methionine codon (Bell et al., 2005a,b,c). Intron B splits the fourth codon of the region that codes for the pro sequence of prepro-PTH. The three exons that result are roughly divided into three functional domains. Exon I contains the 5′ untranslated region (UTR). Exon II codes for the pre sequence, or signal peptide, and most of the pro sequence and exon III codes for PTH as well as the 3′ UTR. The structure of the PTH gene is thus consistent with the proposal that exons represent functional domains of the mRNA (Bell et al., 2005a,b,c; Kemper, 1986). Although the introns are at the same location, the large intron A in human is about twice as large as those in the rat and bovine. It is interesting that the human gene is considerably longer in both intron A and the 3′ UTR of the cDNA compared with bovine, rat, and mouse. Both introns have the characteristic splice-site elements. The second exon, containing 106 and 121 nucleotides in the human and bovine pre-mRNA, is much smaller and more homologous in size among the genes than intron A. Of interest, the elephant shark Pth1 and Pth2 genes both contain introns in the 5′ UTR and in the coding region at identical positions that are totally conserved in Pth genes from other vertebrates (Liu et al., 2010). The genes for human PTH and PTHrP are located at similar positions on sibling chromosomes 11 and 12. It is therefore likely that they arose from a common precursor by chromosomal duplication.

Promoter sequences

Regions upstream of the transcribed structural gene often determine tissue specificity and contain many of the regulatory sequences for the gene. For PTH, analysis of this region has been hampered by the lack of a parathyroid cell line. The 5 kb of DNA upstream of the start site of the human PTH gene was able to direct parathyroid gland-specific expression in transgenic mice (Hosokawa and Leahy, 1997). Computer analysis of the human PTH promoter region identified a number of consensus sequences (Kel et al., 2005). These include a sequence resembling the canonical cAMP-responsive element (CRE) 5′-TGACGTCA-3′ at position −81 with a single residue deviation. This element was fused to a reporter gene (chloramphenicol acetyltransferase, or CAT) and then transfected into different cell lines. Pharmacological agents that increase cAMP led to an increased expression of the CAT gene, suggesting a functional role for the CRE. The role of this putative CRE in the PTH gene in the parathyroid remains to be established. Specificity protein (Sp) and the nuclear factor-Y (NF-Y) complex are ubiquitously expressed transcription factors associated with basal expression of a host of gene products. Sp family members and NF-Y can cooperatively enhance transcription of a target gene. A highly conserved Sp1 DNA element present in mammalian PTH promoters has been identified and characterized (Alimov et al., 2005; Koszewski et al., 2004). Coexpression of Sp proteins and NF-Y complex leads to synergistic transactivation of the human PTH promoter, with alignment of the Sp1 DNA element essential for full activation (Alimov et al., 2005). A similar arrangement of DNA-response elements and synergism is present in the bovine PTH promoter, suggesting that this may be a conserved mechanism to enhance transcription of the PTH gene.

Several groups have identified DNA sequences that may mediate the negative regulation of PTH gene transcription by 1,25-dihydroxyvitamin D_3 ($1,25(OH)_2D_3$). Demay et al. (1992) identified DNA sequences in the human PTH gene that bind the $1,25(OH)_2D_3$ receptor (VDR). Nuclear extracts containing the VDR were examined for binding to sequences in the 5′ flanking region of the human PTH gene. A 25-bp oligonucleotide containing sequences from −125 to −101 from the start of exon I bound nuclear proteins that were recognized by monoclonal antibodies against the VDR. The sequences in this region contained a single copy of a motif (AGGTTCA) that is homologous to the motifs repeated in the upregulatory $1,25(OH)_2D_3$-response element of the osteocalcin gene. When placed upstream of a heterologous viral promoter, the sequences contained in this 25-bp oligonucleotide mediated transcriptional repression in response to $1,25(OH)_2D_3$ in GH4C1 cells but not in ROS 17/2.8 cells. Therefore, this downregulatory element differs from upregulatory elements both in sequence composition and in the requirement for particular cellular factors other than the VDR for repressing PTH transcription (Demay et al., 1992). Russell et al. (1999) have shown that there are two negative vitamin D-response elements (VDREs) in the rat PTH gene, with different binding affinities to a VDR/RXR heterodimer. Transfection studies with VDRE−CAT constructs showed that they had an additive effect. Liu et al. (Alon et al., 2008; Liu et al., 1996) have identified such sequences in the chicken PTH gene and demonstrated their functionality after transfection into an opossum kidney cell line. They converted the negative activity imparted by the PTH VDRE to a positive transcriptional response through selective mutations introduced into the element. They showed that there was a p160 protein that specifically interacted with a heterodimer complex bound to the wild-type VDRE, but was absent from complexes bound to response elements associated with positive transcriptional activity.

The parathyroid hormone mRNA

Complementary DNAs encoding human, bovine, rat, mouse, pig, chicken, dog, cat, horse, macaque, fugu fish, and zebrafish PTH have all been cloned. The PTH gene is a typical eukaryotic gene with consensus sequences for initiation of RNA synthesis, RNA splicing, and polyadenylation. The primary RNA transcript consists of RNA transcribed from both

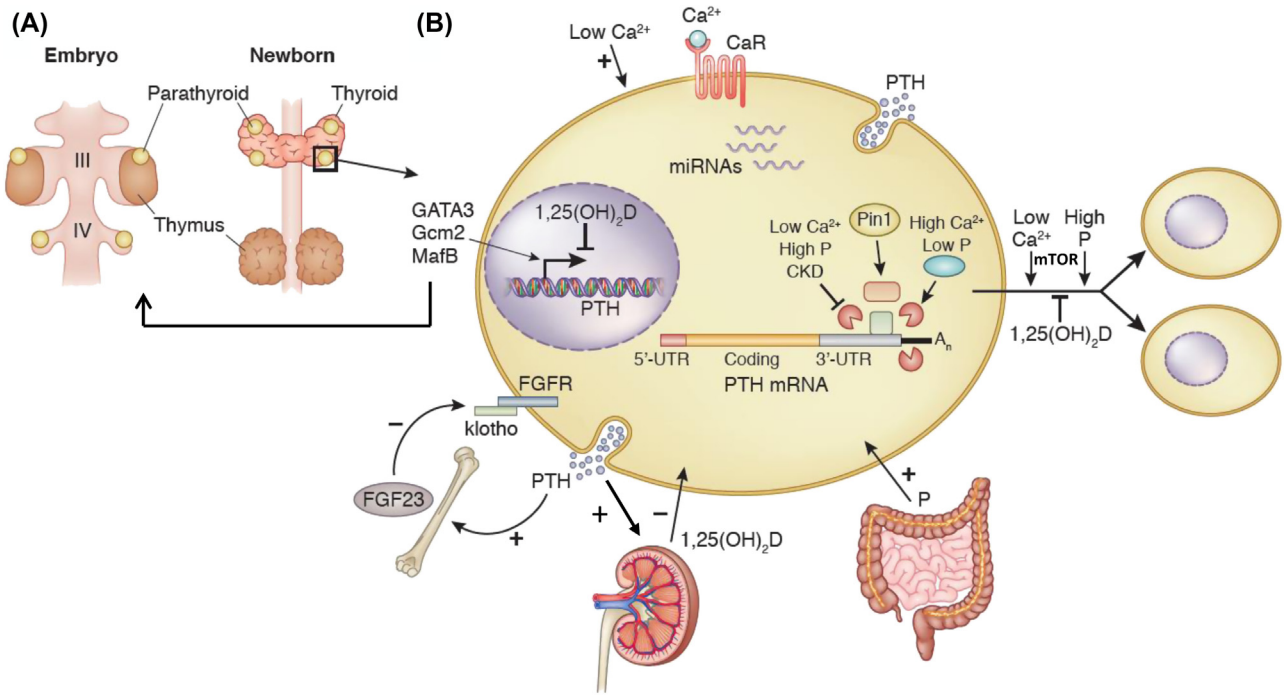

FIGURE 24.1 Parathyroid embryonic development and the regulators of PTH expression and parathyroid cell proliferation. (A) Diagram of the third and fourth pharyngeal pouches showing the embryonic location of the parathyroid- and thymus-fated domains in humans and the postnatal position of the parathyroids adjacent to the thyroid glands. (B) Schematic presentation of a parathyroid cell and daughter cells. The different regulators of PTH gene expression, secretion, and parathyroid cell proliferation are shown. Calcium, 1,25(OH)$_2$D$_3$, the high phosphate of uremia, and FGF23 all regulate PTH secretion and PTH gene expression through transcriptional and posttranscriptional mechanisms. In prolonged hypocalcemia and uremia, there is also parathyroid cell proliferation mediated by mTOR signaling, as shown by the two small cells on the right. miRNAs are also essential for the activation of the parathyroid in secondary hyperparathyroidism. Among the factors affecting parathyroid organogenesis, GATA3, Gcm2, and MafB are all essential for normal gland development and physically interact to activate the PTH gene promoter postnatally. *1,25(OH)$_2$D*, 1,25-dihydroxyvitamin D$_3$; *CaR*, calcium-sensing receptor; *CKD*, chronic kidney disease; *FGF23*, fibroblast growth factor 23; *FGFR*, fibroblast growth factor receptor; *miRNAs*, microRNAs; *PTH*, parathyroid hormone; *UTR*, untranslated region; *mTOR*, mammalian target of rapamycin. *Modified with permission from* Kidney International *(Naveh-Many, T., Silver, J., 2018. Transcription factors that determine parathyroid development power PTH expression. Kidney Int. 93 (1), 7–9).*

introns and exons, and then RNA sequences derived from the introns are spliced out. The product of this RNA processing, which represents the exons, is the mature PTH mRNA, which will then be translated into prepro-PTH (Figs. 24.1 and 24.2). There is considerable identity among mammalian PTH genes, which is reflected in an 85% identity between human and bovine proteins and 75% identity between human and rat proteins. There is less identity in the 3′ noncoding region. The initiator ATG codons for the human and bovine have been identified by sequencing in vitro translation products of the mRNAs (Habener et al., 1975; Kemper et al., 1976). In the bovine sequence, the first ATG codon is the initiator codon, in accord with many other eukaryotic mRNAs (Kozak, 1991). The human and rat sequences have ATG triplets prior to the probable initiator ATG, which are present 10 nucleotides before the initiation codon and are immediately followed by a termination codon. The termination codon immediately following the codon for glutamine at position 84 of PTH indicates that there are no additional precursors of PTH with peptide extensions at the carboxyl position. A more extensive review of the structure and sequences of the PTH gene has been published elsewhere (Bell et al., 2005a,b,c).

Mutations in the parathyroid hormone gene

Rare patients have been found with abnormal PTH genes that result in hypoparathyroidism (Gafni and Levine, 2005). The PTH gene of a patient with familial isolated hypoparathyroidism (Ahn et al., 1986) has been studied by Arnold et al. (1990), and a point mutation in the hydrophobic core of the signal peptide–encoding region of prepro-PTH was identified. This T-to-C point mutation changed the codon for position 18 of the 31-amino-acid prepro sequence from cysteine to arginine, and in functional studies the mutant protein was processed inefficiently. The mutation impaired interaction of the nascent protein with signal recognition particles and the translocation machinery, and cleavage of the mutant signal sequence by solubilized signal peptidase was slow (Karaplis et al., 1995). A novel mutation of the signal peptide of the

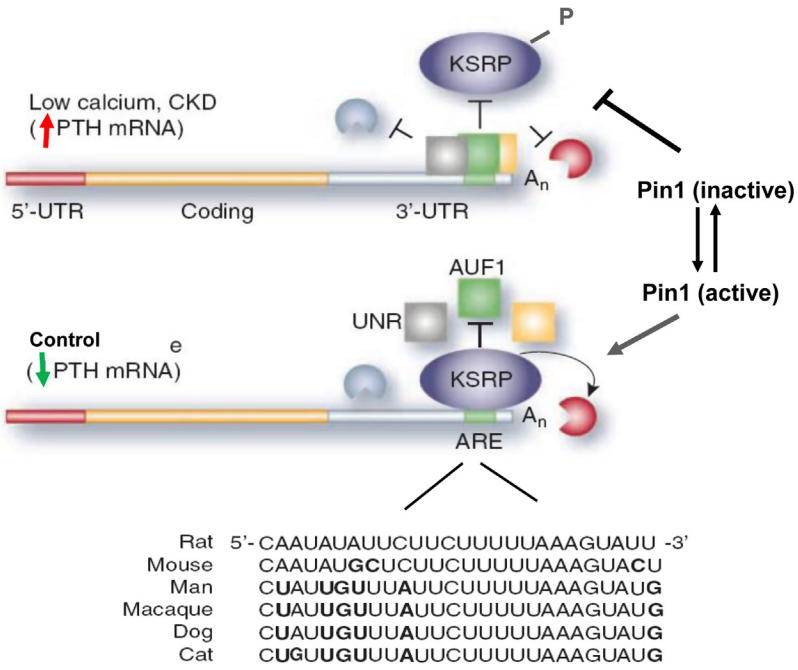

FIGURE 24.2 Model for the regulation of parathyroid hormone (*PTH*) mRNA stability by changes in calcium and kidney failure. A schematic representation of the PTH mRNA and binding proteins and the nucleotide sequence of the 26-nucleotide *cis* element in different species. Nucleotides that differ from the rat sequence are in *bold*. AU-rich binding factor (*AUF1*) and upstream of NRAS (UNR) stabilize and K-homology splicing regulator protein (*KSRP*) destabilizes PTH mRNA. Pin1 is upstream of KSRP and leads to KSRP dephosphorylation and activation. In hypocalcemic and experimental chronic kidney disease (*CKD*) rats, the enzymatic activity of the peptidyl-prolyl *cis/trans* isomerase Pin1 is reduced. As a result, KSRP is phosphorylated and hence less active. The stabilizing proteins AUF1 and UNR then bind the PTH mRNA 3′ UTR AU-rich element (*ARE*) with a greater affinity leading to increased PTH mRNA stability and levels. *Modification of a model shown in* Endocrinology *(Naveh-Many, T., 2010. Minireview: the play of proteins on the parathyroid hormone messenger ribonucleic acid regulates its expression. Endocrinology 151 (4), 1398−1402).*

prepro-PTH gene was associated with autosomal recessive familial isolated hypoparathyroidism (Sunthornthepvarakul et al., 1999). The affected members in this family presented with neonatal hypocalcemic seizures. Their intact PTH levels were undetectable during severe hypocalcemia. A replacement of thymine with a cytosine was found in the first nucleotide of position 23 in the 25-amino-acid signal peptide. This results in the replacement of the normal Ser (TCG) with a Pro (CCG). Only affected family members were homozygous for the mutant allele, whereas the parents were heterozygous, supporting autosomal recessive inheritance. Because this mutation is at the −3 position in the signal peptide of the prepro-PTH gene, the authors hypothesized that the prepro-PTH mutant might not be cleaved by signal peptidase at the normal position and might be degraded in the rough endoplasmic reticulum. The only mutation discovered in the coding region of secreted human PTH is an arginine-to-cysteine mutation at residue 25 of mature PTH(1−84). This ligand has a decreased affinity for the PTH receptor and fails to stimulate hypercalcemia when infused into mice (Lee et al., 2015). Parkinson et al. (Parkinson and Thakker, 1992) studied one kindred with autosomal recessive isolated hypoparathyroidism and identified a G-to-C substitution in the first nucleotide of intron B of the PTH gene. Restriction enzyme cleavage revealed that the patients were homozygous for mutant alleles, unaffected relatives were heterozygous, and unrelated normals were homozygous for the wild-type alleles. Defects in mRNA splicing were investigated by the detection of illegitimate transcription of the PTH gene in lymphoblastoid cells. The mutation resulted in exon skipping with a loss of exon II, which encodes the initiation codon and the signal peptide, thereby causing PTH deficiency. Goswami et al. (2004) studied 51 patients with sporadic idiopathic hypoparathyroidism. Neither the clinical manifestations nor the biochemical indexes of the disease were related to the occurrence of mutations or single-nucleotide polymorphisms in the PTH gene. Autosomal dominant hypocalcemia type 1 and type 2 are genetically distinct disorders that were found to be associated with germ-line gain-of-function mutations of CaR and G11α proteins, respectively (Hannan et al., 2016; Nesbit et al., 2013).

Development of the parathyroid

The parathyroid glands develop from a shared initial organ primordium together with the thymus. Both organs arise from the third pharyngeal pouch endoderm and surrounding neural crest cells. Humans have two additional superior parathyroid

glands that develop from the fourth pouch. In mice, the third pouch forms during embryonic days (E) 9−10.5. A transcriptional network involving Hoxa3, Pax1/Pax9, Eya1, Tbx1, Sox3, and Six1/Six4 controls early pouch patterning and formation of the parathyroid/thymus common primordium (Han et al., 2015; Chojnowski et al., 2014). After third pouch formation, it becomes subdivided into two molecularly distinct domains. The parathyroid-destined domain can be distinguished from E10.5 by the expression of the transcription factor Gcm2 (glial cells missing 2), which is required for parathyroid differentiation and survival (Liu et al., 2007). Foxn1 (Forkhead box N1) expression marks the thymus domain. Each primordium separates into a single parathyroid gland and a thymic lobe at E12.5−13.5. The parathyroids are "dragged" along by the migrating thymus lobes until the separation process is complete and then move to their eventual adult locations by about E14.5, adjacent to or embedded in the thyroid glands (Kamitani-Kawamoto et al., 2011; Manley, 2015) (Fig. 24.1). Mice that lack Hoxa3, Pax1/9, Eya1, and Six1/4 have normal initial pouch formation, but then fail to form or have hypoplastic parathyroids and thymus. *Hoxa3*$^{-/-}$ mutants fail to initiate the formation of the parathyroid/thymus primordia. In these mutants, Gcm2 is expressed in its normal domain, but at very low levels, indicating that Hoxa3 upregulates Gcm2 expression. Eya1 and Six1/4 are also required for Gcm2 expression, and mutations result in the loss of parathyroid precursor cells through apoptosis. As loss of Gcm2 itself is sufficient to cause apoptosis, it is possible that the effects of all of these genes, either individually or as a pathway, are mediated by their effect on Gcm2 expression (Manley, 2015).

The DiGeorge syndrome is a human genetic condition resulting from deletion of contiguous genes. The specific gene causing the hypoparathyroidism found in DiGeorge syndrome and the closely related CATCH-22 syndrome (cardiac defects, abnormal facies, thymic hypoplasia, cleft palate, hypocalcemia, associated with chromosome 22 microdeletion) is likely to be Tbx1 (Lindsay et al., 2001). In the DiGeorge syndrome, malformations include absence of the parathyroid glands and thymus as well as the heart outflow tract, and most DiGeorge syndrome patients are hemizygous for a 1.5- to 3.0-Mb region of 22q11. In mice, deletion of one copy of Tbx1 (in the equivalent genetic region in the mouse) affects the development of the fourth pharyngeal arch arteries, whereas homozygous mutation severely disrupts the pharyngeal arch artery system (Lindsay et al., 2001; Merscher et al., 2001). These data in mice suggest that Tbx1 has a major role in the molecular etiology of the DiGeorge syndrome phenotype.

Gata3 (GATA-binding protein 3), Gcm2, and MafB (transcriptional activator v-maf musculoaponeurotic fibrosarcoma oncogene homolog B) transcription factors constitute a genetic cascade regulating parathyroid development and PTH expression (Han et al., 2015). GATA3 haploinsufficiency results in congenital hypoparathyroidism, deafness, and renal dysplasia syndrome in humans. *Gata3*$^{-/-}$ embryos lack Gcm2 expression and exhibit gross defects in the third and fourth pharyngeal pouches, including absent parathyroid−thymus primordia (Grigorieva et al., 2010). *Gata3*$^{+/-}$ mice are viable and have apparently normal parathyroid glands. However, when fed a low calcium and vitamin D diet, plasma PTH levels and calcium concentrations are lower than those in wild-type mice, indicating partial parathyroid dysfunction in the *Gata3*$^{+/-}$ mice (Grigorieva et al., 2010). Gata3 directly binds and regulates Gcm2 expression. Gcm2 is expressed predominately in the pharyngeal pouches and, at later stages, in the developing and mature parathyroid glands. Once the parathyroid domain is established, upregulation of Gcm2 expression is necessary and sufficient for parathyroid differentiation and survival (Manley, 2015). Mutations of the *GCM2* gene in humans lead to familial isolated hypoparathyroidism. Genetic ablation of *Gcm2* in mice results in parathyroid agenesis and hypoparathyroidism. Without Gcm2 function, parathyroid precursor cells fail to differentiate and then undergo apoptosis by E12, resulting in the aparathyroid phenotype (Manley, 2015). Serum PTH levels were low or undetectable in *Gcm2*-knockout mice. In conditional *Gcm2*-knockout mice, immunoreactive PTH was identified within a few thymus cells in wild-type and homozygous knockout mice, consistent with the proposal that expression of PTH in medullary thymic epithelial cells provides a source of self-antigen for negative selection. Work has excluded the thymus as a source of circulating PTH in humans and mice (Yuan et al., 2014). It is possible that the normal process of parathyroid organogenesis in both mice and humans leads to the generation of multiple small parathyroid clusters in addition to the main parathyroid glands (Manley, 2015).

MafB is a basic leucine zipper transcription factor expressed in the developing parathyroid after E11.5 and postnatally. MafB expression is lost in the parathyroid primordium of *Gcm2*-null mice. The parathyroid glands of *MafB*$^{+/-}$ mice are mislocalized between the thymus and the thyroid. In *MafB*$^{-/-}$ mice, the parathyroids do not separate from the thymus during embryological development (Kamitani-Kawamoto et al., 2011). Therefore, MafB regulates later steps of parathyroid development, the separation from the thymus, and migration toward the thyroid.

Among Gata3, Gcm2, and MafB transcription factors, Gata3 is the most upstream, followed by Gcm2, and then MafB, which is the most downstream in parathyroid development (Han et al., 2015). This cascade is critical for parathyroid development. However, expression of Gata3, Gcm2, and MafB persists after parathyroid morphogenesis (Kamitani-Kawamoto et al., 2011), suggesting that they are components of a gene regulatory program that governs parathyroid-specific gene expression and function. Gata3, Gcm2, and MafB form a transcriptional complex that mediates

parathyroid-specific PTH expression. Recent in vitro analyses in heterologous cells revealed that Gata3, Gcm2, and MafB physically interact and synergistically activate the *PTH* gene promoter (Han et al., 2015). The in vivo functions of Gata3 and Gcm2 and MafB in parathyroid physiology and disease have been shown. Morito et al. (2018) showed a role for MafB in experimental secondary hyperparathyroidism. Deletion of MafB had no effect on serum PTH levels or mineral metabolism under normal conditions, but decreased serum PTH levels at postnatal day 0 in $MafB^{-/-}$ mice (Kamitani-Kawamoto et al., 2011). Stimulation of the parathyroid by prolonged uremia in $MafB^{+/-}$ mice resulted in an impaired increase in serum PTH, PTH mRNA, and parathyroid cell proliferation. Both PTH and cyclin D2, but not cyclin D1, expression was blunted in $MafB^{+/-}$ uremic mice, suggesting that MafB contributes to the increased PTH and cyclin D2 expression in secondary hyperparathyroidism. Acute hypocalcemia-induced PTH secretion and PTH mRNA were also impaired in $MafB^{+/-}$ and in global *MafB*-knockout mice. Therefore, MafB plays a role in regulation of PTH secretion but this effect may be less important than its role in controlling the development and differentiation of the parathyroid gland. It is intriguing that transcription factors that affect parathyroid morphogenesis are expressed and functional in parathyroid physiology (Fig. 24.1).

Okabe and Graham (2004) have performed elegant studies that demonstrate a role for Gcm2 even in fish, which do not have discrete parathyroid glands. They showed that the parathyroid gland of tetrapods and the gills of fish both express Gcm2 and require this gene for their formation. They also showed that the gill region expresses mRNA encoding the two PTH genes found in fish, as well as mRNA encoding the calcium-sensing receptor (CaR). The conserved role of Gcm2 in forming pharyngeal structures is established, but the relationship between Gcm2 and PTH-producing cells in fish is not clear.

Regulation of parathyroid hormone gene expression

1,25-Dihydroxyvitamin D_3

PTH regulates serum concentrations of calcium and phosphate, which, in turn, regulate the synthesis and secretion of PTH. $1,25(OH)_2D_3$ has independent effects on calcium and phosphate levels and also participates in a well-defined feedback loop between $1,25(OH)_2D_3$ and PTH.

PTH increases the renal synthesis of $1,25(OH)_2D_3$. $1,25(OH)_2D_3$ then increases blood calcium largely by increasing the efficiency of intestinal calcium absorption. $1,25(OH)_2D_3$ also potently decreases transcription of the PTH gene. This action was first demonstrated in vitro in bovine parathyroid cells in primary culture, where $1,25(OH)_2D_3$ led to a marked decrease in PTH mRNA levels (Silver et al., 1985; Russell et al., 1984) and a consequent decrease in PTH secretion (Cantley et al., 1985; Karmali et al., 1989; Chan et al., 1986). The physiological relevance of these findings was established by in vivo studies in rats (Silver et al., 1986). The localization of VDR mRNA to parathyroids was demonstrated by in situ hybridization studies of the thyroparathyroid and duodenum. VDR mRNA was localized to the parathyroids in the same concentration as in the duodenum, the classic target organ of $1,25(OH)_2D_3$ (Naveh-Many and Silver, 1990). Rats injected with amounts of $1,25(OH)_2D_3$ that did not increase serum calcium had marked decreases in PTH mRNA levels, reaching $<4\%$ of control at 48 h (Fig. 24.1). This effect was shown to be transcriptional in both in vivo studies in rats (Silver et al., 1986) and in vitro studies with primary cultures of bovine parathyroid cells (Russell et al., 1986). When 684 bp of the 5′ flanking region of the human PTH gene was linked to a reporter gene and transfected into a rat pituitary cell line (GH4C1), gene expression was lowered by $1,25(OH)_2D_3$ (Okazaki et al., 1988). These studies suggest that $1,25(OH)_2D_3$ decreases PTH transcription by acting on the 5′ flanking region of the PTH gene. The effect of $1,25(OH)_2D_3$ may involve heterodimerization with the retinoic acid receptor. This is because 9-*cis*-retinoic acid, which binds to the retinoic acid receptor, when added to bovine parathyroid cells in primary culture, led to a decrease in PTH mRNA levels. Moreover, combined treatment with retinoic acid and $1,25(OH)_2D_3$ decreased PTH secretion and prepro-PTH mRNA more effectively than either compound alone (Macdonald et al., 1994). Alternatively, retinoic acid receptors might synergize with VDRs through actions on distinct sequences.

A further level at which $1,25(OH)_2D_3$ may regulate the PTH gene would be at the level of the VDR. $1,25(OH)_2D_3$ acts on its target tissues by binding to the VDR, which regulates the transcription of genes with the appropriate recognition sequences. Concentration of the VDR in $1,25(OH)_2D_3$ target sites could allow a modulation of the $1,25(OH)_2D_3$ effect, with an increase in receptor concentration leading to an amplification of its effect and a decrease in receptor concentration dampening the $1,25(OH)_2D_3$ effect. Naveh-Many and Silver (1990) injected $1,25(OH)_2D_3$ into rats and measured the levels of VDR mRNA and PTH mRNA in the thyroparathyroid tissue. They showed that $1,25(OH)_2D_3$ in physiologically relevant doses led to an increase in VDR mRNA levels in the parathyroid glands in contrast to the decrease in PTH mRNA levels. This increase in VDR mRNA occurred after a time lag of 6 h, and a dose response showed a peak at 25 pmol.

Weanling rats fed a diet deficient in calcium were markedly hypocalcemic at 3 weeks and had very high serum $1,25(OH)_2D_3$ levels. Despite the chronically high serum $1,25(OH)_2D_3$ levels, there was no increase in VDR mRNA levels; furthermore, PTH mRNA levels did not fall and were increased markedly. The low calcium in the bloodstream may have prevented the increase in parathyroid VDR levels, which may partially explain PTH mRNA suppression. Whatever the mechanism, the lack of suppression of PTH synthesis in the setting of hypocalcemia and increased serum $1,25(OH)_2D_3$ is crucial physiologically because it allows an increase in both PTH and $1,25(OH)_2D_3$ at a time of chronic hypocalcemic stress. Russell et al. (1993) studied the parathyroids of chicks with vitamin D deficiency and confirmed that $1,25(OH)_2D_3$ regulates PTH and VDR gene expression in the avian parathyroid gland. Brown et al. (1995) studied vitamin D-deficient rats and confirmed that $1,25(OH)_2D_3$ upregulated parathyroid VDR mRNA. Rodriguez et al. (2007) showed that administration of the calcimimetic R568 resulted in increased VDR expression in parathyroid tissue. In vitro studies of the effect of R568 on VDR mRNA and protein were conducted in cultures of whole rat parathyroid glands. Incubation of rat parathyroid glands in vitro with R568 resulted in a dose-dependent decrease in PTH secretion and an increase in VDR expression. Together with previous work on the effect of extracellular calcium to increase parathyroid VDR mRNA in vitro (Garfia et al., 2002), they concluded that activation of the CaR upregulates the parathyroid VDR mRNA.

All these studies show that $1,25(OH)_2D_3$, and calcium in certain circumstances, increases the expression of the VDR gene in the parathyroid gland, which would result in increased VDR protein synthesis and increased binding of $1,25(OH)_2D_3$. This ligand-dependent receptor upregulation would lead to an amplified effect of $1,25(OH)_2D_3$ on the PTH gene and might help explain the dramatic effect of $1,25(OH)_2D_3$ on the PTH gene.

Vitamin D may also amplify its effect on the parathyroid by increasing the activity of the calcium receptor (CaR). Canaff et al. (Canaff and Hendy, 2002) showed that in fact there are VDREs in the human CaR promoter. The CaR, expressed in parathyroid chief cells, thyroid C cells, and cells of the kidney tubule, is essential for maintenance of calcium homeostasis. They showed that parathyroid, thyroid, and kidney CaR mRNA levels increased twofold at 15 h after intraperitoneal injection of $1,25(OH)_2D_3$ in rats. Human thyroid C-cell (TT) and kidney proximal tubule cell (HKC) CaR gene transcription increased approximately twofold at 8 and 12 h after $1,25(OH)_2D_3$ treatment. The human CaR gene has two promoters yielding alternative transcripts containing either exon IA or exon IB 5′ UTR sequences that splice to exon II some 242 bp before the ATG translation start site. $1,25(OH)_2D_3$ stimulated P1 activity 2-fold and P2 activity 2.5-fold. VDREs, in which the half-sites (6 bp) are separated by three nucleotides, were identified in both promoters and shown to confer $1,25(OH)_2D_3$ responsiveness to a heterologous promoter. This responsiveness was lost when the VDREs were mutated. In electrophoretic mobility-shift assays specific protein−DNA complexes were formed in the presence of $1,25(OH)_2D_3$ on oligonucleotides representing the P1 and P2 VDREs. In summary, functional VDREs have been identified in the CaR gene and probably provide the mechanism whereby $1,25(OH)_2D_3$ upregulates parathyroid, thyroid C-cell, and kidney CaR expression.

The use of $1,25(OH)_2D_3$ is limited by its hypercalcemic effect, and therefore a number of $1,25(OH)_2D_3$ analogs have been synthesized that are biologically active but are less hypercalcemic than $1,25(OH)_2D_3$ (Brown, 2005). These analogs usually involve modifications of the $1,25(OH)_2D_3$ side chain, such as 22-oxa-$1,25(OH)_2D_3$, which is the chemical modification in oxacalcitriol (Nishii et al., 1991), or a cyclopropyl group at the end of the side chain in calcipotriol (Kissmeyer and Binderup, 1991). However, detailed in vivo dose−response studies showed that in vivo $1,25(OH)_2D_3$ is the most effective analog for decreasing PTH mRNA levels, even at doses that do not cause hypercalcemia (Naveh-Many and Silver, 1993). The marked activity of $1,25(OH)_2D_3$ analogs in vitro compared with their modest hypercalcemic actions in vivo probably reflects their rapid clearance from the circulation (Bouillon et al., 1991).

The ability of $1,25(OH)_2D_3$ to decrease PTH gene transcription is used therapeutically in the management of patients with chronic renal failure. They are treated with $1,25(OH)_2D_3$, or its prodrug 1α(OH)-vitamin D_3, to prevent the secondary hyperparathyroidism of chronic renal failure. The poor response in some patients may well result from poor control of serum phosphate, decreased VDR concentration in the patients' parathyroids (Fukuda et al., 1993), an inhibitory effect of a uremic toxin(s) on VDR−VDRE binding (Patel and Rosenthal, 1985), or tertiary hyperparathyroidism with monoclonal parathyroid tumors (Arnold et al., 1995).

Another possible level at which $1,25(OH)_2D_3$ may regulate PTH gene expression involves calreticulin. Calreticulin is a calcium-binding protein present in the endoplasmic reticulum of the cell and may have an additional nuclear function. It regulates gene transcription via its ability to bind a protein motif in the DNA-binding domain of nuclear hormone receptors of sterol hormones. It has been shown to prevent vitamin D's binding and action on the osteocalcin gene in vitro (Wheeler et al., 1995). Sela-Brown et al. (1998) showed that calreticulin inhibits the action of vitamin D on the PTH gene. Hypocalcemic rats had increased levels of calreticulin protein in their parathyroid nuclear fraction, which may explain why hypocalcemia leads to increased PTH gene expression, despite high serum $1,25(OH)_2D_3$ levels.

Calcium

In vitro studies

A remarkable characteristic of the parathyroid is its sensitivity to small changes in serum calcium, which leads to large changes in PTH secretion. This remarkable sensitivity of the parathyroid to increase hormone secretion after small decreases in serum calcium levels is unique to the parathyroid. All other endocrine glands increase hormone secretion after exposure to high extracellular calcium. Calcium sensing also regulates PTH gene expression and parathyroid cell proliferation (Fig. 24.1). In vitro and in vivo data agree that calcium regulates PTH mRNA levels, but data differ in important ways. In vitro studies with bovine parathyroid cells in primary culture showed that calcium regulated PTH mRNA levels (Russell et al., 1983; Brookman et al., 1986), with an effect mainly of high calcium to decrease PTH mRNA. These effects were most pronounced after more prolonged incubations, such as 72 h. The physiologic correlates of these studies in tissue culture are hard to ascertain, as the parathyroid calcium sensor may well have decreased over the time period of the experiment (Mithal et al., 1995). This may explain why the dose response differs from in vivo data, but the dramatic difference in time course suggests that in vivo data reflect something not seen in cultured cells.

In vivo studies

Calcium and phosphate both have marked effects on the levels of PTH mRNA and secretion in vivo. The major effect is for low calcium to increase PTH mRNA levels and low phosphate to decrease PTH mRNA levels. Naveh-Many et al. (1989) showed that a small decrease in serum calcium from 2.6 to 2.1 mmol/L led to large increases in PTH mRNA levels, reaching threefold that of controls at 1 and 6 h. A high serum calcium had no effect on PTH mRNA levels even at concentrations as high as 6.0 mmol/L. Interestingly, in these same thyroparathyroid tissue RNA extracts, calcium had no effect on the expression of the calcitonin gene (Naveh-Many et al., 1989, 1992a,b). Thus, while high calcium is a secretagogue for calcitonin, it does not regulate calcitonin gene expression. Yamamoto et al. (Yamamoto et al., 1989) also studied the in vivo effect of calcium on PTH mRNA levels in rats. They showed that hypocalcemia induced by a calcitonin infusion for 48 h led to a sevenfold increase in PTH mRNA levels. Rats made hypercalcemic (2.9−3.4 mM) for 48 h had the same PTH mRNA levels as controls that had received no infusion (2.5 mM); these levels were modestly lower than those found in rats that had received a calcium-free infusion. In further studies, Naveh-Many et al. (1992a,b) transplanted Walker carcinosarcoma 256 cells into rats. Serum calcium levels increased to 18 mg/dL at day 10 after transplantation. There was no change in PTH mRNA levels in these rats with marked chronic hypercalcemia (Naveh-Many et al., 1992a,b). Differences between in vivo and in vitro results probably reflect the instability of the in vitro system. Nevertheless, the physiological conclusion is that common causes of hypercalcemia in vivo do not importantly decrease PTH mRNA levels; these results emphasize that the gland is geared to respond to hypocalcemia and not hypercalcemia.

The mechanism whereby calcium regulates PTH gene expression is particularly interesting. Changes in extracellular calcium are sensed by a calcium sensor that then regulates PTH secretion (Brown et al., 1993; Yano and Brown, 2005). Signal transduction from the CaR involves activation of phospholipase C, D, and A_2 enzymes (Kifor et al., 1997). It is not known what mechanism transduces the message of changes in extracellular calcium leading to changes in PTH mRNA. However, it has been shown that the response to changes in serum calcium involves the protein phosphatase type 2B, calcineurin (Bell et al., 2005a,b,c). In vivo and in vitro studies demonstrated that inhibition of calcineurin by genetic manipulation or pharmacologic agents affected the response of PTH mRNA levels to changes in extracellular calcium (Bell et al., 2005a,b,c).

Okazaki et al. (1992) identified a negative calcium regulatory element (nCaRE) in the atrial natriuretic peptide gene, with a homologous sequence in the PTH gene. They identified a redox factor protein (ref1), which bound a putative nCaRE, and the level of ref1 mRNA and protein were elevated by an increase in extracellular calcium concentration. They suggested that ref1 had transcription repressor activity in addition to its function as a transcriptional auxiliary protein (Okazaki et al., 1992). Because no parathyroid cell line is available, these studies were performed in nonparathyroid cells, so their relevance to physiologic PTH gene regulation remains to be established.

Moallem et al. (1998) have performed in vivo studies on the effect of hypocalcemia on PTH gene expression. The effect is posttranscriptional in vivo and involves protein−RNA interactions at the 3′ UTR of the PTH mRNA (Moallem et al., 1998). A similar mechanism is involved in the effect of phosphate on PTH gene expression so the mechanisms involved will be discussed later in this chapter.

Phosphate

The demonstration of a direct effect of high phosphate on the parathyroid, independent of calcium and $1,25(OH)_2D_3$, has been difficult. One of the reasons is that the various maneuvers used to increase or decrease serum phosphate invariably lead to a change in the ionized calcium concentration. In moderate renal failure, phosphate clearance decreases and serum phosphate increases; this increase becomes an important problem in severe renal failure. Hyperphosphatemia has always been considered central to the pathogenesis of secondary hyperparathyroidism, but it has been difficult to separate the effects of hyperphosphatemia from those of the attendant hypocalcemia and decrease in serum $1,25(OH)_2D_3$ levels. In the 1970s, Slatopolsky and Bricker (1973) showed in dogs with experimental chronic renal failure that dietary phosphate restriction prevented secondary hyperparathyroidism. Clinical studies demonstrated that phosphate restriction in patients with chronic renal insufficiency is effective in preventing the increase in serum PTH levels (Lucas et al., 1986; Portale et al., 1984; Aparicio et al., 1994; Lafage et al., 1992; Combe and Aparicio, 1994; Combe et al., 1995). The mechanism of this effect was not clear, although at least part of it was considered to be due to changes in serum $1,25(OH)_2D_3$ concentrations. In vitro (Tanaka and DeLuca, 1973; Condamine et al., 1994) and in vivo (Portale et al., 1984, 1989) phosphate directly regulates the production of $1,25(OH)_2D_3$. A raised serum phosphate decreases serum $1,25(OH)_2D_3$ levels, which then leads to decreased calcium absorption from the diet and eventually a low serum calcium. The raised phosphate complexes calcium, which is then deposited in bone and soft tissues and decreases serum calcium. However, a number of careful clinical and experimental studies suggested that the effect of phosphate on serum PTH levels was independent of changes in both serum calcium and $1,25(OH)_2D_3$ levels. In experimental chronic renal failure in dogs, phosphate increased parathyroid cell activity by a mechanism independent of its effect on serum $1,25(OH)_2D_3$ and calcium levels (Lopez-Hilker et al., 1990). Therefore, phosphate plays a central role in the pathogenesis of secondary hyperparathyroidism, by its effects on both serum $1,25(OH)_2D_3$ and serum calcium levels and possibly independently. A raised serum phosphate also stimulates the secretion of fibroblast growth factor 23 (FGF23), which in turn decreases PTH gene expression and serum PTH levels. This effect would act as a counterbalance to the stimulatory effect of phosphate on the parathyroid and is discussed separately in this chapter.

Kilav et al. (1995) were the first to establish in vivo that the effects of serum phosphate on PTH gene expression and serum PTH levels were independent of any changes in serum calcium or $1,25(OH)_2D_3$ (Fig. 24.1). They bred second-generation vitamin D-deficient rats and then placed the weanling vitamin D-deficient rats on a diet with no vitamin D, low calcium, and low phosphate. After one night of this diet, serum phosphate had decreased markedly with no changes in serum calcium or $1,25(OH)_2D_3$. These rats with isolated hypophosphatemia had marked decreases in PTH mRNA levels and serum PTH (Kilav et al., 1995). To establish that the effect of serum phosphate on the parathyroid was indeed a direct effect, in vitro confirmation was needed, which was provided by three groups. Rodriguez et al. showed that increased phosphate levels increased PTH secretion from isolated parathyroid glands in vitro; the effect required maintenance of tissue architecture (Almaden et al., 1996). The effect was found in whole glands or tissue slices but not in isolated cells. This result was confirmed by Slatopolsky et al. (1996). Olgaard's laboratory provided elegant further evidence of the importance of cell−cell communication in mediating the effect of phosphate on PTH secretion (Nielsen et al., 1996). The requirement for intact tissue suggests either that the sensing mechanism for phosphate is damaged during the preparation of isolated cells or that the intact gland structure is important to the phosphate response.

The parathyroid responds to changes in serum phosphate at the level of secretion, gene expression, and cell proliferation, although the signaling involved is unknown. The effect of high phosphate to increase PTH secretion may be mediated by phospholipase A_2-activated signal transduction. Bourdeau et al. (1992, 1994) showed that arachidonic acid and its metabolites inhibit PTH secretion. Almaden et al. (2000) showed in vitro that a high-phosphate medium increased PTH secretion, which was prevented by the addition of arachidonic acid.

Protein−PTH mRNA interactions determine the posttranscriptional regulation of PTH gene expression by calcium, phosphate, and uremia

Diet-induced hypocalcemia and adenine/high phosphorus−induced chronic kidney disease (CKD) increase PTH mRNA levels, and diet-induced hypophosphatemia decreases PTH mRNA levels (Fig. 24.1). In both instances, the effect is posttranscriptional, as shown by nuclear transcript run-on experiments (Moallem et al., 1998; Kilav et al., 2005). Parathyroid cytosolic proteins bind in vitro-transcribed PTH mRNA. Interestingly, this binding was increased with parathyroid proteins from hypocalcemic and CKD rats (with increased PTH mRNA levels) and decreased with parathyroid proteins from hypophosphatemic rats (with decreased PTH mRNA levels). Proteins from other tissues bound to PTH mRNA, but

only parathyroid proteins bound PTH mRNA in a way that was regulated by calcium and phosphate. Intriguingly, binding required the presence of the terminal 60 nucleotides of the PTH transcript.

An in vitro degradation assay showed that the effects of hypocalcemic and hypophosphatemic parathyroid proteins on PTH mRNA stability reproduced the differences in PTH mRNA levels observed in vivo (Moallem et al., 1998). Moreover, the difference in RNA stability stimulated by the parathyroid extracts was dependent on an intact 3′ UTR and, in particular, on the terminal 60 nucleotides. Proteins from other tissues in these rats subjected to hypocalcemia, hypophosphatemia, or uremia did not affect PTH mRNA stability in this in vitro assay. Therefore, calcium, phosphate, and CKD change the properties of parathyroid cytosolic proteins, which bind specifically to the PTH mRNA 3′ UTR and determine its stability (Fig. 24.2). What are these proteins?

A conserved sequence in the PTH mRNA 3′ UTR binds parathyroid cytosolic proteins and determines mRNA stability

We have identified the minimal sequence for protein binding in the PTH mRNA 3′ UTR and determined its functionality (Fig. 24.2) (Kilav et al., 2001). A minimum sequence of 26 nucleotides was sufficient for PTH RNA−protein binding. To study the functionality of the sequence in the context of another RNA, a 63-bp cDNA PTH sequence consisting of the 26-nucleotide and flanking regions was fused to growth hormone cDNA. The conserved PTH RNA protein-binding region was necessary and sufficient for responsiveness to calcium and phosphate and determines PTH mRNA stability and levels (Kilav et al., 2001).

The PTH mRNA 3′-UTR-binding element is AU rich and is a type III AU-rich element (ARE). Sequence analysis of the PTH mRNA 3′ UTR of different species revealed a preservation of the 26-nucleotide protein-binding element in rat, murine, human, macaque, feline, and canine 3′ UTRs (Fig. 24.2) (Kilav et al., 2001; Bell et al., 2005a,b,c). In contrast to protein coding sequences that are highly conserved, UTRs are less conserved. The conservation of the protein-binding element in the PTH mRNA 3′ UTR suggests that this element represents a functional unit that has been evolutionarily conserved. The *cis*-acting element is at the 3′ distal end in all species in which it is expressed.

The PTH mRNA 3′-UTR-binding proteins that determine PTH mRNA stability

AU-rich binding factor

Affinity chromatography using the PTH RNA 3′ UTR identified AU-rich-binding factor (AUF1) as a PTH mRNA-binding protein (Sela-Brown et al., 2000; Brewer, 1991). Added recombinant AUF1 stabilized the PTH transcript in the in vitro degradation assay. Therefore, AUF1 is a protein that binds to the PTH mRNA 3′ UTR and stabilizes the PTH transcript. The regulation of protein−PTH mRNA binding involves posttranslational modification of AUF1 (Bell et al., 2005a,b,c; Sela-Brown et al., 2000; Levi et al., 2006). The balance between the stabilizing and the destabilizing proteins determines mRNA levels in response to physiological stimuli (Fig. 24.2) (Brewer, 1991; Naveh-Many, 2010; Nechama et al., 2008; Barreau et al., 2006).

K-homology splicing regulator protein

The mRNA decay-promoting protein K-homology splicing regulator protein (KSRP) binds to PTH mRNA in intact parathyroid glands and in transfected cells (Nechama et al., 2008, 2009; Nechama et al., 2009a,b,c; Gherzi et al., 2004). This binding of KSRP is decreased in glands from calcium-depleted or experimental uremic rats in which PTH mRNA is more stable, compared with parathyroid glands from control and phosphorus-depleted rats in which PTH mRNA is less stable. The differences in KSRP−PTH mRNA binding counter those of AUF1. PTH mRNA decay depends on the KSRP-recruited exosome in parathyroid extracts. In transfected cells, KSRP overexpression and knockdown experiments showed that KSRP decreases PTH mRNA stability and steady-state levels through the PTH mRNA ARE. Overexpression of the PTH mRNA-stabilizing protein AUF1 blocks KSRP−PTH mRNA binding and partially prevents the KSRP-mediated decrease in PTH mRNA levels (Nechama et al., 2008). Therefore, calcium or phosphorus depletion, as well as CKD, regulates the interaction of KSRP and AUF1 with PTH mRNA and its half-life. The balance between the stabilizing and the destabilizing proteins determines PTH mRNA levels in response to physiological stimuli (Fig. 24.2).

Most patients with CKD develop secondary hyperparathyroidism with disabling systemic complications. Calcimimetic agents are effective tools in the management of secondary hyperparathyroidism, acting through allosteric modification of the CaR on the parathyroid gland to decrease PTH secretion and parathyroid cell proliferation. R568 decreased both PTH mRNA and serum PTH levels in adenine/high phosphorus-induced uremia (Nechama et al., 2009a,b,c). The effect of the calcimimetic, similar to that of uremia on PTH gene expression, was posttranscriptional and correlated with differences in

protein−RNA binding and posttranslational modifications of AUF1 in the parathyroid. AUF1 modifications were reversed compared with those of normal rats by treatment with R568. Therefore, uremia and activation of the CaR mediated by calcimimetics modify AUF1 posttranslationally. These modifications in AUF1 correlate with changes in protein−PTH mRNA binding and PTH mRNA levels (Nechama et al., 2009a,b,c). In addition, KSRP−PTH mRNA binding was decreased in parathyroids from rats with adenine-induced CKD, a condition in which PTH mRNA is more stable. KSRP−PTH mRNA binding was increased by treatment with R568, correlating with decreased PTH gene expression. This destabilizing effect of R568 was dependent on KSRP and the PTH mRNA 3′ UTR. Therefore, the calcimimetic R568 decreases PTH mRNA levels by altering the balance between KSRP and AUF binding to the PTH mRNA 3′ UTR.

The peptidyl-prolyl isomerase Pin1 determines parathyroid hormone mRNA stability and levels in secondary hyperparathyroidism

Pin1 activity is decreased in parathyroid protein extracts from hypocalcemic and uremic rats. Pharmacologic inhibition of Pin1 increases PTH mRNA levels posttranscriptionally in vivo in the parathyroid and in transfected cells (Nechama et al., 2009a,b,c). Pin1 regulates PTH mRNA stability and levels through the PTH mRNA 3′ UTR *cis*-acting element. Pin1 interacts with the PTH mRNA destabilizing protein, KSRP, and leads to KSRP dephosphorylation and activation. In the parathyroid, Pin1 inhibition in secondary hyperparathyroidism decreases KSRP−PTH mRNA interaction that contributes to the increased PTH gene expression. Furthermore, *Pin1*$^{-/-}$ mice had increased serum PTH and PTH mRNA levels. Therefore, Pin1 determines basal PTH expression in vivo and in vitro, and decreased Pin1 activity correlates with increased PTH mRNA levels in CKD and hypocalcemic rats (Nechama et al., 2009a,b,c). These results demonstrate that Pin1 is a key mediator of PTH mRNA stability and indicate a role for Pin1 in the pathogenesis of the secondary hyperparathyroidism of CKD (Fig. 24.2) (Naveh-Many, 2010; Nechama et al., 2009a,b,c; Kumar, 2009).

Dynein light-chain M_r 8000 binds the PTH mRNA 3′ untranslated region and mediates its association with microtubules

mRNA expression cloning identified dynein light-chain M_r 8000 (LC8) as a 3′-UTR PTH mRNA-binding protein. LC8 is part of the cytoplasmic dynein complexes that function as molecular motors that translocate along microtubules. Recombinant LC8 bound the PTH mRNA 3′ UTR as assessed by RNA mobility-shift assay. PTH mRNA colocalized with polymerized microtubules in the parathyroid gland, as well as with a purified microtubule preparation from calf brain, and this was mediated by LC8 (Epstein et al., 2000). This was the first report of a dynein complex protein binding an mRNA and acting as a motor for the transport and localization of mRNAs in the cytoplasm and the subsequent asymmetric distribution of translated proteins in the cell.

MicroRNA in the parathyroid

Parathyroid-specific deletion of Dicer-dependent microRNA

A further level of posttranscriptional regulation of PTH gene expression is by microRNA (miRNA). miRNAs downregulate gene expression and have vital roles in biology but their functions in the parathyroid have been unexplored. The final step in miRNA maturation is cleavage by Dicer protein in the cytoplasm (Lee et al., 2003). We generated parathyroid-specific Dicer 1-knockout (PT-*Dicer*$^{-/-}$) mice, in which parathyroid miRNA maturation is blocked only in the parathyroid (Shilo et al., 2015). Despite normal basal PTH, under conditions of stress, deletion of Dicer and the subsequent absence of mature miRNA in the mouse parathyroid had surprising effects on parathyroid function. Remarkably, the PT-*Dicer*$^{-/-}$ mice did not increase serum PTH in response to acute hypocalcemia compared with the greater than fivefold increase in controls. PT-*Dicer*$^{-/-}$ glands cultured in low-calcium medium secreted fivefold less PTH at 1.5 h than controls. Chronic hypocalcemia increased serum PTH greater than fourfold less in PT-*Dicer*$^{-/-}$ mice compared with control mice, with no increase in PTH mRNA levels and parathyroid cell proliferation compared with the two- to threefold increase in hypocalcemic controls (Shilo et al., 2015). The importance of our findings is highlighted by the fact that uremic PT-*Dicer*$^{-/-}$ mice with normal serum calcium had an impaired increase in serum PTH similar to their failure to respond to hypocalcemia (Shilo et al., 2015). Therefore, parathyroid miRNAs are necessary for the development of secondary hyperparathyroidism not only of chronic hypocalcemia but also of CKD (Holmes, 2015) (Fig. 24.3). In contrast to the impaired increase in PTH by hypocalcemia and uremia, the PT-*Dicer*$^{-/-}$ mice decreased serum PTH as expected after activation of the parathyroid CaR by both hypercalcemia and a calcimimetic, demonstrating that these processes that suppress PTH secretion are dicer independent. In conclusion, miRNAs are essential for activation of the parathyroid by both acute and chronic hypocalcemia and uremia, the major stimuli for PTH secretion (Shilo et al., 2015, 2016) (Fig. 24.3).

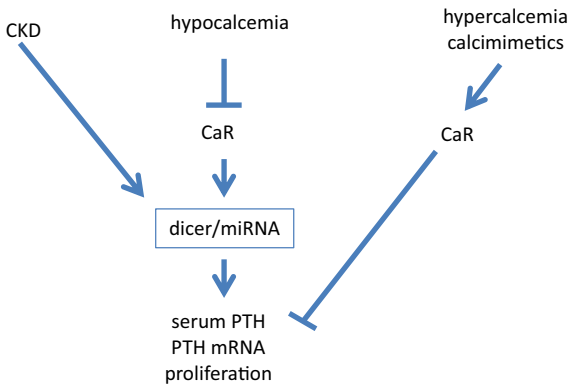

FIGURE 24.3 Model for the role of microRNAs (*miRNA*) in stimulation of the parathyroid by hypocalcemia and chronic kidney disease (*CKD*) but not in suppression of the parathyroid by hypercalcemia or a calcimimetic. Parathyroid miRNAs are essential for the increase in parathyroid gland activity by acute and chronic hypocalcemia and uremia, mediating the increase in parathyroid hormone (*PTH*) mRNA levels, PTH secretion, and parathyroid cell proliferation. Suppression of parathyroid activity by hypercalcemia or a calcimimetic is miRNA independent. *CaR*, calcium-sensing receptor. *With permission from* Current Opinion in Nephrology and Hypertension *(Shilo, V., Silver, J., Naveh-Many, T., 2016. Micro-RNAs in the parathyroid: a new portal in understanding secondary hyperparathyroidism. Curr. Opin. Nephrol. Hypertens. 25 (4), 271–277).*

Let-7 and miRNA-148 regulate parathyroid hormone levels in secondary hyperparathyroidism

miRNA profiling of parathyroid glands from mice and rats with experimental CKD and dialysis patients by miRNA deep sequencing showed that human and rodent parathyroids share similar profiles (Shilo et al., 2017). Parathyroids from uremic and normal rats segregated on the basis of their miRNA expression profiles, and a similar finding was observed in humans. There were several parathyroid miRNAs that were dysregulated in experimental secondary hyperparathyroidism, including miR-29, miR-21, miR-148, miR-30, and miR-141 (upregulated) and miR-10, miR-125, and miR-25 (downregulated). Inhibition of the abundant let-7 family increased PTH secretion in normal and CKD rats, as well as in mouse parathyroid organ cultures. Conversely, inhibition of the upregulated miR-148 family prevented the increase in serum PTH level in CKD rats and decreased levels of secreted PTH in parathyroid cultures. The evolutionary conservation of abundant miRNAs in normal parathyroid glands and the regulation of these miRNAs in secondary hyperparathyroidism indicate their importance for parathyroid function and the development of hyperparathyroidism. Specifically, let-7 and miR-148 antagonism modified PTH secretion in vivo and in vitro, implying roles for these specific miRNAs in the parathyroid (Shilo et al., 2017).

Sex steroids

PTH is anabolic to bone and is an effective means of treating postmenopausal osteoporosis. In postmenopausal women with osteoporosis, time series analysis has shown that there is a loss in the periodicity of PTH secretion (Prank et al., 1995; Fraser et al., 1998). This suggests that estrogens may have an effect on the parathyroid. Estradiol and progesterone both increased the secretion of PTH from bovine parathyroid cells in primary culture (Greenberg et al., 1987). However, transdermal estrogen did not increase serum PTH levels in postmenopausal patients (Prince et al., 1990). Estrogen receptors were not detected in parathyroid tissue by a hormone-binding method (Prince et al., 1991), but were detected by immunohistochemistry and PCR for the estrogen receptor mRNA (Naveh-Many et al., 1992a,b). Moreover, in vivo in ovariectomized rats, both estrogen and progestins regulated PTH gene expression (Naveh-Many et al., 1992a,b).

Further studies were performed on the effects of progestins on PTH gene expression (Epstein et al., 1995). The 19-nor progestin R5020 given to weanling rats or mature ovariectomized rats led to a twofold increase in thyroparathyroid PTH mRNA levels. In addition, in vitro, in primary cultures of bovine parathyroid cells, progesterone increased PTH mRNA levels. The progesterone receptor mRNA was demonstrated in rat parathyroid tissue by in situ hybridization and in human parathyroid adenoma by immunohistochemistry. PTH mRNA levels varied during the rat estrous cycle (Epstein et al., 1995). These results confirm that the parathyroid gland is a target organ for the ovarian sex steroids estrogen and progesterone and they are of physiological relevance, as shown by the changes during estrus. In a rat model of CKD with ovariectomy, estrogen treatment decreased PTH mRNA and serum levels, unlike the increase after estrogen in control rats (Epstein et al., 1995; Carrillo-López et al., 2009). In the CKD rats, estrogens significantly increased FGF23 mRNA and serum levels, suggesting that estrogens may regulate PTH indirectly through FGF23 (Carrillo-López et al., 2009).

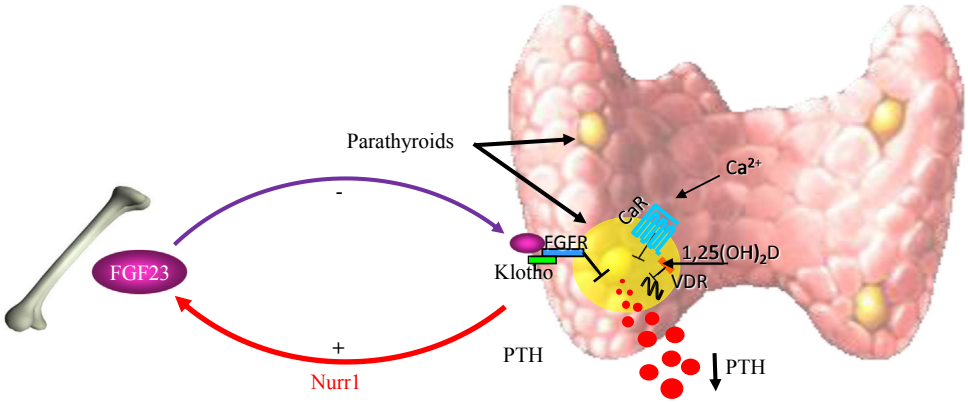

FIGURE 24.4 A bone–parathyroid endocrine loop of fibroblast growth factor 23 (*FGF23*) and parathyroid hormone (*PTH*). Parathyroid function is decreased by calcium through the calcium sensing receptor (*CaR*) and $1,25(OH)_2D_3$ through the vitamin D receptor (*VDR*). FGF23 is secreted by bone and acts on the parathyroid to also decrease PTH synthesis, secretion, and parathyroid cell proliferation by acting on the parathyroid klotho–FGFR1c receptor. PTH in turn increases FGF23 expression by activating the Nurr1 transcription factor in osteoblasts and osteocytes. *Modified from* Kidney International *with permission (Silver, J., Naveh-Many, T., 2009. Phosphate and the parathyroid. Kidney Int. 75 (9), 898–905).*

Fibroblast growth factor 23

Fibroblast growth factor 23 decreases parathyroid hormone expression

Phosphate homeostasis is maintained by a counterbalance between efflux from the kidney and influx from intestine and bone. FGF23 is a bone-derived phosphaturic hormone that acts on the kidney to increase phosphate excretion and suppress biosynthesis of $1,25(OH)_2D_3$. FGF23 signals through FGF receptors (FGFRs) bound by the transmembrane protein klotho (Kurosu et al., 2006; Urakawa et al., 2006). Klotho protein is expressed not only in the kidney but also in the parathyroid, pituitary, and sinoatrial node (Takeshita et al., 2004). Ben Dov et al. (2007) identified the parathyroid as a target organ for FGF23 in rats (Fig. 24.4). The parathyroid gland expressed klotho and FGFRs. The administration of recombinant FGF23 led to an increase in parathyroid klotho levels. In addition, FGF23 activated the mitogen-activated protein kinase (MAPK) pathway in the parathyroid through extracellular signal-regulated kinase 1/2 phosphorylation and increased Egr1 (early growth response) mRNA levels. FGF23 suppressed PTH secretion and PTH gene expression both in vivo in rats and in vitro in parathyroid cultures (Ben Dov et al., 2007). These data indicate that FGF23 acts directly on the parathyroid through the MAPK pathway to decrease serum PTH. Krajisnik et al. (2007) showed similar results using bovine parathyroid cells in primary culture. Interestingly, they also showed that FGF23 led to a dose-dependent increase in the expression of the 1α-hydroxylase enzyme in the parathyroid (Krajisnik et al., 2007). The increased $1,25(OH)_2D_3$ may then act in an autocrine manner to decrease PTH gene transcription. In addition, PTH increases FGF23 expression in bone (Lavi-Moshayoff et al., 2010). PTH increases the levels of the orphan nuclear receptor, Nurr1, in osteocytes and osteoblasts in vivo and in osteoblast-like UMR106 cells, which then acts on the FGF23 promoter to increase FGF23 transcription (Meir et al., 2014). The bone–parathyroid endocrine feedback loop of PTH and FGF23 adds a new dimension to the understanding of mineral homeostasis (Fig. 24.4).

Resistance of the parathyroid to FGF23 in chronic kidney disease

In CKD both serum FGF23 and serum PTH levels are increased. Several studies have shown that a decrease in klotho–FGFR1 expression and signal transduction may explain the resistance of the parathyroid to FGF23 in CKD. In experimental CKD, quantitative immunohistochemistry and qRT-PCR using laser capture microscopy showed that klotho and FGFR1 protein and mRNA levels were decreased in parathyroid sections of rats with adenine diet–induced advanced CKD (Galitzer et al., 2010). Similar results have been shown using the parathyroids from patients with advanced CKD (Komaba et al., 2010). Moreover, in parathyroids of rats with advanced CKD, recombinant FGF23 failed to decrease serum PTH or activate the MAPK pathway. In rat parathyroid organ culture, FGF23 decreased secreted PTH and PTH mRNA levels in control or early CKD rats but not in rats with advanced CKD (Galitzer et al., 2010). Therefore, in advanced experimental CKD, there is a decrease in parathyroid klotho and FGFR1 mRNA and protein levels in rats and in patients with CKD. This decrease corresponds with the resistance of the parathyroid to FGF23 in vivo, which is sustained in parathyroid organ culture in vitro. The increased levels of FGF23 do not decrease PTH levels in established CKD because

of a downregulation of its receptor heterodimer complex klotho−FGFR1c. Olauson et al. (2013) showed by genetic and functional studies that a klotho-independent, calcineurin-mediated FGF23 signaling pathway in parathyroid glands can mediate suppression of PTH in the absence of klotho. The presence of klotho-independent FGF23 effects in a klotho-expressing target organ represents a paradigm shift in the conceptualization of FGF23 endocrine action and suggests the centrality of the suppression of FGFR1 more than that of klotho in the resistance to FGF23 in renal failure (Olauson et al., 2013).

Parathyroid cell proliferation and mammalian target of rapamycin

Phosphorylation of ribosomal protein S6 mediates mammalian target of rapamycin−induced parathyroid cell proliferation in secondary hyperparathyroidism

Secondary hyperparathyroidism is characterized by increases in PTH expression and parathyroid cell proliferation (Naveh-Many et al., 1995; Denda et al., 1996; Cozzolino et al., 2005; Silver and Naveh-Many, 2013). Decreased expression of the calcium, $1,25(OH)_2D_3$, and FGF23 receptors contributes to the increased parathyroid cell proliferation in uremia (Garfia et al., 2002; Galitzer et al., 2010; Lewin et al., 2002). Expression of transforming growth factor-α and its receptor, the epidermal growth factor (EGF) receptor (EGFR), is increased in uremic rats and patients (Cozzolino et al., 2005; Gogusev et al., 1996; Drueke, 2000). A dominant negative EGFR gene expressed specifically in the parathyroid glands prevented the activation of endogenous EGFR and the increase in parathyroid gland enlargement and serum PTH (Arcidiacono et al., 2008, 2015; Dusso et al., 2010). Other cell cycle regulators such as cyclin D1 also induce parathyroid cell proliferation, as shown in transgenic mice overexpressing cyclin D1 only in the parathyroid (Imanishi et al., 2001).

Mammalian target of rapamycin (mTOR) integrates signaling pathways to regulate cell growth and proliferation. mTOR is regulated by binding partners found in two complexes, mTOR complex 1 (mTORC1) and mTORC2. Rapamycin inhibits mTORC1 and proliferation in many cell types (Shimobayashi and Hall, 2014; Xu et al., 2015). Different stimuli activate mTORC1 through Akt phosphorylation. 4E-binding protein 1 and the ribosomal protein S6 kinase 1 (S6K1) are mTORC1 targets (Shahbazian et al., 2006). S6K1 phosphorylates ribosomal protein S6 (rpS6) on a cluster of five serine residues at the carboxy terminus. Knock-in mice encoding a mutant rpS6 harboring alanine substitutions at all five phosphorylation sites ($rpS6^{P-/-}$ mice) have reduced size, glucose intolerance, muscle weakness, and impaired renal hypertrophy after uninephrectomy (Ruvinsky et al., 2005, 2009). Volovelsky et al. (2016) have shown that the mTOR pathway is activated in the parathyroid of rats with secondary hyperparathyroidism induced by either chronic hypocalcemia or CKD, as measured by increased phosphorylation of rpS6, a downstream target of the mTOR pathway (Fig. 24.5). This

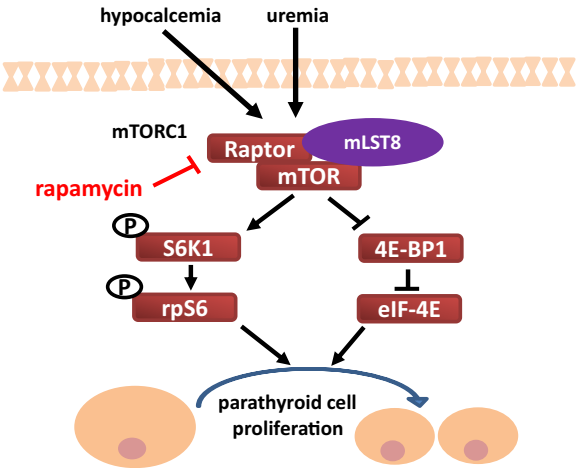

FIGURE 24.5 Mammalian target of rapamycin (*mTOR*) complex 1 (*mTORC1*) induces parathyroid cell proliferation in secondary hyperparathyroidism (SHP) through ribosomal protein S6 (*rpS6*) phosphorylation. The mTOR pathway is activated in the parathyroids of rats and mice with SHP induced by either chronic hypocalcemia or uremia. On activation, mTORC1 phosphorylates and activates S6 kinase 1 (*S6K1*), which then phosphorylates rpS6. mTORC1 also disinhibits eukaryotic translation initiation factor-4E (*eIF-4E*) by inhibiting 4E-binding protein 1 (*4E-BP1*). rpS6 phosphorylation is necessary for the increased parathyroid cell proliferation of SHP. Inhibition of mTORC1 by rapamycin decreases and prevents parathyroid cell proliferation in SHP. *With permission from* Journal of the American Society of Nephrology *(Volovelsky, O., Cohen, G., Kenig, A., Wasserman, G., Dreazen, A., Meyuhas, O., et al., 2016. Phosphorylation of ribosomal protein S6 mediates mammalian target of rapamycin complex 1-induced parathyroid cell proliferation in secondary hyperparathyroidism. J. Am. Soc. Nephrol. 27 (4), 1091−1101).*

activation correlated with increased parathyroid cell proliferation. Inhibition of mTORC1 by rapamycin decreased or prevented parathyroid cell proliferation in rats with secondary hyperparathyroidism and in vitro in uremic rat parathyroid glands in organ culture. Knock-in $rpS6^{p-/-}$ mice, in which rpS6 cannot be phosphorylated, had impaired PTH secretion after experimental uremia. Uremic $rpS6^{p-/-}$ mice had no increase in parathyroid cell proliferation compared with a marked increase in uremic wild-type mice. These results highlight the importance of mTOR activation and rpS6 phosphorylation for the pathogenesis of secondary hyperparathyroidism and indicate that mTORC1 is a significant regulator of parathyroid cell proliferation through rpS6 (Fig. 24.5) (Volovelsky et al., 2016). mTORC1 responds to growth factors, such as insulin, IGF-1, and EGF. The EGFR also activates the Akt−mTORC1 pathway (Huse and Holland, 2010). Therefore, the mTORC1 and EGFR pathways may act together to stimulate parathyroid cell proliferation in secondary hyperparathyroidism.

Summary

The PTH mRNA consists of three exons that are roughly divided into the 5′ UTR, the signal peptide sequence and PTH, and the 3′ UTR. The parathyroid glands develop from a shared initial organ primordium together with the thymus. A transcriptional network determines the embryological development of the parathyroid. $1,25(OH)_2D_3$ decreases PTH gene transcription. The major regulator of the parathyroid is hypocalcemia. Hypocalcemia regulates PTH gene expression in vivo by increasing PTH mRNA levels, and this is mainly posttranscriptional. Phosphate also regulates PTH gene expression, and this effect is independent of the effect of phosphate on serum calcium and $1,25(OH)_2D_3$. The effects of phosphate and uremia are also posttranscriptional. *Trans*-acting parathyroid cytosolic proteins bind to a defined *cis* element in the PTH mRNA 3′ UTR. This binding determines the degradation of PTH mRNA and thereby the PTH mRNA half-life. Changes in the balance of stabilizing and degrading factors on PTH mRNA determine the posttranscriptional effects of calcium, phosphate, and uremia on PTH gene expression. Pin1 regulates protein−PTH mRNA interactions, leading to more rapid PTH mRNA decay. In secondary hyperparathyroidism, Pin1 is less active and is associated with an increase in PTH mRNA stability and levels and thus increased PTH secretion. A further level of the posttranscriptional regulation of PTH gene expression is through miRNAs that are necessary for the increased PTH in acute and chronic hypocalcemia and uremia. mTOR is activated in secondary hyperparathyroidism, correlating with the increase in parathyroid cell proliferation. Inhibition of mTOR decreases parathyroid cell proliferation in both chronic hypocalcemia and CKD. FGF23 acts on its receptor, the klotho−FGFR1c receptor, to decrease PTH mRNA levels and secretion. In advanced CKD there is resistance of the parathyroid to the high FGF23 levels due to downregulation of the FGF23 receptor. $1,25(OH)_2D_3$, hypercalcemia, calcimimetics, hypophosphatemia, and rapamycin all decrease PTH gene expression and parathyroid cell proliferation (Fig. 24.1).

Acknowledgments

This work was supported in part by grants from the National Institutes of Health and the Israel Academy of Sciences (grant 642/16).

References

Alimov, A.P., Park-Sarge, O.K., Sarge, K.D., Malluche, H.H., Koszewski, N.J., 2005. Transactivation of the parathyroid hormone promoter by specificity proteins and the nuclear factor Y complex. Endocrinology 146 (8), 3409−3416.

Ahn, T.G., Antonarakis, S.E., Kronenberg, H.M., Igarashi, T., Levine, M.A., 1986. Familial isolated hypoparathyroidism: a molecular genetic analysis of 8 families with 23 affected persons. Medicine 65, 73−81.

Almaden, Y., Canalejo, A., Hernandez, A., Ballesteros, E., Garcia-Navarro, S., Torres, A., et al., 1996. Direct effect of phosphorus on parathyroid hormone secretion from whole rat parathyroid glands in vitro. J. Bone Miner. Res. 11, 970−976.

Almaden, Y., Canalejo, A., Ballesteros, E., Anon, G., Rodriguez, M., 2000. Effect of high extracellular phosphate concentration on arachidonic acid production by parathyroid tissue in vitro. J. Am. Soc. Nephrol. 11 (9), 1712−1718.

Alon, U.S., Levy-Olomucki, R., Moore, W.V., Stubbs, J., Liu, S., Quarles, L.D., 2008. Calcimimetics as an adjuvant treatment for familial hypophosphatemic rickets. Clin. J. Am. Soc. Nephrol. 3 (3), 658−664.

Antonarakis, S.E., Phillips, J.A., Mallonee, R.L., Kazazian, H.H.J., Fearon, E.R., Waber, P.G., et al., 1983. Beta-globin locus is linked to the parathyroid hormone (PTH) locus and lies between the insulin and PTH loci in man. Proc. Natl. Acad. Sci. U.S.A. 80, 6615−6619.

Aparicio, M., Combe, C., Lafage, M.H., De Precigout, V., Potaux, L., Bouchet, J.L., 1994. In advanced renal failure, dietary phosphorus restriction reverses hyperparathyroidism independent of the levels of calcitriol. Nephron 63, 122−123.

Arcidiacono, M.V., Sato, T., Alvarez-Hernandez, D., Yang, J., Tokurl, M., Gonzalez-Suarez, I., et al., 2008. EGFR activation increases parathyroid hyperplasia and calcitriol resistance in kidney disease. J. Am. Soc. Nephrol. 19 (2), 310−320.

Arcidiacono, M.V., Yang, J., Fernandez, E., Dusso, A., 2015. Parathyroid-specific epidermal growth factor-receptor inactivation prevents uremia-induced parathyroid hyperplasia in mice. Nephrol. Dial. Transplant. 30 (3), 434–440.

Arnold, A., Horst, S.A., Gardella, T.J., Baba, H., Levine, M.A., Kronenberg, H.M., 1990. Mutation of the signal peptide-encoding region of the pre-proparathyroid hormone gene in familial isolated hypoparathyroidism. J. Clin. Investig. 86, 1084–1087.

Arnold, A., Brown, M.F., Urena, P., Gaz, R.D., Sarfati, E., Drueke, T.B., 1995. Monoclonality of parathyroid tumors in chronic renal failure and in primary parathyroid hyperplasia. J. Clin. Investig. 95, 2047–2053.

Barreau, C., Paillard, L., Osborne, H.B., 2006. AU-rich elements and associated factors: are there unifying principles? Nucleic Acids Res. 33 (22), 7138–7150.

Bell, O., Gaberman, E., Kilav, R., Levi, R., Cox, K.B., Molkentin, J.D., et al., 2005a. The protein phosphatase calcineurin determines basal parathyroid hormone gene expression. Mol. Endocrinol. 19, 516–526.

Bell, O., Silver, J., Naveh-Many, T., 2005b. Identification and characterization of *cis*-acting elements in the human and bovine parathyroid hormone mRNA 3'-untranslated region. J. Bone Miner. Res. 20, 858–866.

Bell, O., Silver, J., Naveh-Many, T., 2005c. Parathyroid hormone, from gene to protein. In: Naveh-Many, T. (Ed.), Molecular Biology of the Parathyroid. Molecular Biology Intelligence Unit, first ed. Landes Bioscience and Kluwer Academic/Plenum Publishers, New York, pp. 8–28.

Ben Dov, I.Z., Galitzer, H., Lavi-Moshayoff, V., Goetz, R., Kuro-o, M., Mohammadi, M., et al., 2007. The parathyroid is a target organ for FGF23 in rats. J. Clin. Investig. 117 (12), 4003–4008.

Bouillon, R., Allewaert, K., Xiang, D.Z., Tan, B.K., van-Baelen, H., 1991. Vitamin D analogs with low affinity for the vitamin D binding protein: enhanced in vitro and decreased in vivo activity. J. Bone Miner. Res. 6, 1051–1057.

Bourdeau, A., Souberbielle, J.-C., Bonnet, P., Herviaux, P., Sachs, C., Lieberherr, M., 1992. Phospholipase-A_2 action and arachidonic acid in calcium-mediated parathyroid hormone secretion. Endocrinology 130, 1339–1344.

Bourdeau, A., Moutahir, M., Souberbielle, J.C., Bonnet, P., Herviaux, P., Sachs, C., et al., 1994. Effects of lipoxygenase products of arachidonate metabolism on parathyroid hormone secretion. Endocrinology 135, 1109–1112.

Brewer, G., 1991. An A + U-rich element RNA-binding factor regulates c-myc mRNA stability in vitro. Mol. Cell Biol. 11 (5), 2460–2466.

Brookman, J.J., Farrow, S.M., Nicholson, L., O'Riordan, J.L., Hendy, G.N., 1986. Regulation by calcium of parathyroid hormone mRNA in cultured parathyroid tissue. J. Bone Miner. Res. 1, 529–537.

Brown, A.J., 2005. Vitamin D analogs for the treatment of secondary hyperparathyroidsim in chronic renal failure. In: Naveh-Many, T. (Ed.), Molecular Biology of the Parathyoid. Molecular Biology Intelligence Unit, first ed. Landes Bioscience and Kluwer Academic/Plenum Publishers, New York, pp. 95–112.

Brown, E.M., Gamba, G., Riccardi, D., Lombardi, M., Butters, R., Kifor, O., et al., 1993. Cloning and characterization of an extracellular Ca^{2+} -sensing receptor from bovine parathyroid. Nature 366, 575–580.

Brown, A.J., Zhong, M., Finch, J., Ritter, C., Slatopolsky, E., 1995. The roles of calcium and 1,25-dihydroxyvitamin D3 in the regulation of vitamin D receptor expression by rat parathyroid glands. Endocrinology 136, 1419–1425.

Canaff, L., Hendy, G.N., 2002. Human calcium-sensing receptor gene. Vitamin D response elements in promoters P1 and P2 confer transcriptional responsiveness to 1,25-dihydroxyvitamin D. J. Biol. Chem. 277 (33), 30337–30350.

Cantley, L.K., Ontjes, D.A., Cooper, C.W., Thomas, C.G., Leight, G.S., Wells, S.A.J., 1985. Parathyroid hormone secretion from dispersed human hyperparathyroid cells: increased secretion in cells from hyperplastic glands versus adenomas. J. Clin. Endocrinol. Metab. 60, 1032–1037.

Carrillo-López, N., Román-García, P., Rodríguez-Rebollar, A., Fernández-Martín, J.L., Naves-Díaz, M., Cannata-Andía, J.B., 2009. Indirect regulation of PTH by estrogens may require FGF23. J. Am. Soc. Nephrol. 20 (9), 2009–2017.

Chan, Y.L., McKay, C., Dye, E., Slatopolsky, E., 1986. The effect of 1,25 dihydroxycholecalciferol on parathyroid hormone secretion by monolayer cultures of bovine parathyroid cells. Calcif. Tissue Int. 38, 27–32.

Chojnowski, J.L., Masuda, K., Trau, H.A., Thomas, K., Capecchi, M., Manley, N.R., 2014. Multiple roles for HOXA3 in regulating thymus and parathyroid differentiation and morphogenesis in mouse. Development 141 (19), 3697–3708.

Combe, C., Aparicio, M., 1994. Phosphorus and protein restriction and parathyroid function in chronic renal failure. Kidney Int. 46, 1381–1386.

Combe, C., Morel, D., de-Precigout, V., Blanchetier, V., Bouchet, J.L., Potaux, L., et al., 1995. Long-term control of hyperparathyroidism in advanced renal failure by low-phosphorus low-protein diet supplemented with calcium (without changes in plasma calcitriol). Nephron 70, 287–295.

Condamine, L., Vztovsnik, F., Friedlander, G., Menaa, C., Garabedian, M., 1994. Local action of phosphate depletion and insulin-like growth factor 1 on in vitro production of 1,25-dihydroxyvitamin D by cultured mammalian kidney cells. J. Clin. Investig. 94, 1673–1679.

Cozzolino, M., Lu, Y., Sato, T., Yang, J., Suarez, I.G., Brancaccio, D., et al., 2005. A critical role for enhanced TGF-alpha and EGFR expression in the initiation of parathyroid hyperplasia in experimental kidney disease. Am. J. Physiol. Renal. Physiol. 289 (5), F1096–F1102.

Danks, J.A., Ho, P.M., Notini, A.J., Katsis, F., Hoffmann, P., Kemp, B.E., et al., 2003. Identification of a parathyroid hormone in the fish Fugu rubripes. J. Bone Miner. Res. 18 (7), 1326–1331.

Demay, M.B., Kiernan, M.S., DeLuca, H.F., Kronenberg, H.M., 1992. Sequences in the human parathyroid hormone gene that bind the l,25-dihydroxyvitamin D-3 receptor and mediate transcriptional repression in response to l,25-dihydroxyvitamin D-3. Proc. Natl. Acad. Sci. U.S.A. 89, 8097–8101.

Denda, M., Finch, J., Slatopolsky, E., 1996. Phosphorus accelerates the development of parathyroid hyperplasia and secondary hyperparathyroidism in rats with renal failure. Am. J. Kidney Dis. 28 (4), 596–602.

Drueke, T.B., 2000. Cell biology of parathyroid gland hyperplasia in chronic renal failure. J. Am. Soc. Nephrol. 11 (6), 1141–1152.

Dusso, A., Arcidiacono, M.V., Yang, J., Tokumoto, M., 2010. Vitamin D inhibition of TACE and prevention of renal osteodystrophy and cardiovascular mortality. J. Steroid Biochem. Mol. Biol. 121 (1−2), 193−198.

Epstein, E., Silver, J., Almogi, G., Livni, N., Naveh-Many, T., 1995. Parathyroid hormone mRNA levels are increased by progestins and vary during the rat estrous cycle. Am. J. Physiol. 33, E158−E163.

Epstein, E., Sela-Brown, A., Ringel, I., Kilav, R., King, S.M., Benashski, S.E., et al., 2000. Dynein light chain (M_r *8000)* binds the parathyroid hormone mRNA 3'-untranslated region and mediates its association with microtubules. J. Clin. Investig. 105, 505−512.

Fraser, W.D., Logue, F.C., Christie, J.P., Gallacher, S.J., Cameron, D., OqReilly, D.S., et al., 1998. Alteration of the circadian rhythm of intact parathyroid hormone and serum phosphate in women with established postmenopausal osteoporosis. Osteoporos. Int. 8 (2), 121−126.

Fukuda, N., Tanaka, H., Tominaga, Y., Fukagawa, M., Kurokawa, K., Seino, Y., 1993. Decreased 1,25-dihydroxyvitamin D3 receptor density is associated with a more severe form of parathyroid hyperplasia in chronic uremic patients. J. Clin. Investig. 92, 1436−1443.

Gafni, R.I., Levine, M.A., 2005. Genetic causes of hypoparathyroidism. In: Naveh-Many, T. (Ed.), Molecular Biology of the Parathyoid. Molecular Biology Intelligence Unit, first ed. Landes Bioscience and Kluwer Academic/Plenum Publishers, New York, pp. 159−178.

Galitzer, H., Ben Dov, I.Z., Silver, J., Naveh-Many, T., 2010. Parathyroid cell resistance to fibroblast growth factor 23 in secondary hyperparathyroidism of chronic kidney disease. Kidney Int. 77 (3), 211−218.

Garfia, B., Canadillas, S., Canalejo, A., Luque, F., Siendones, E., Quesada, M., et al., 2002. Regulation of parathyroid vitamin d receptor expression by extracellular calcium. J. Am. Soc. Nephrol. 13 (12), 2945−2952.

Gensure, R.C., Ponugoti, B., Gunes, Y., Papasani, M.R., Lanske, B., Bastepe, M., et al., 2004. Identification and characterization of two parathyroid hormone-like molecules in zebrafish. Endocrinology 145 (4), 1634−1639.

Gherzi, R., Lee, K.Y., Briata, P., Wegmuller, D., Moroni, C., Karin, M., et al., 2004. A KH domain RNA binding protein, KSRP, promotes ARE-directed mRNA turnover by recruiting the degradation machinery. Mol. Cell 14 (5), 571−583.

Gogusev, J., Duchambon, P., Stoermann-Chopard, C., Giovannini, M., Sarfati, E., Drueke, T.B., 1996. De novo expression of transforming growth factor-alpha in parathyroid gland tissue of patients with primary or secondary uraemic hyperparathyroidism. Nephrol. Dial. Transplant. 11 (11), 2155−2162.

Goswami, R., Mohapatra, T., Gupta, N., Rani, R., Tomar, N., Dikshit, A., et al., 2004. Parathyroid hormone gene polymorphism and sporadic idiopathic hypoparathyroidism. J. Clin. Endocrinol. Metab. 89 (10), 4840−4845.

Greenberg, C., Kukreja, S.C., Bowser, E.N., Hargis, G.K., Henderson, W.J., Williams, G.A., 1987. Parathyroid hormone secretion: effect of estradiol and progesterone. Metabolism 36, 151−154.

Grigorieva, I.V., Mirczuk, S., Gaynor, K.U., Nesbit, M.A., Grigorieva, E.F., Wei, Q., et al., 2010. Gata3-deficient mice develop parathyroid abnormalities due to dysregulation of the parathyroid-specific transcription factor Gcm2. J. Clin. Investig. 120 (6), 2144−2155.

Habener, J.F., Kamper, B., Potts, J.T.J., Rich, A., 1975. Preproparathyroid hormone identified by cell-free translation of messenger RNA from hyperplastic human parathyroid tissue. J. Clin. Investig. 56, 1328−1333.

Han, S.I., Tsunekage, Y., Kataoka, K., 2015. Gata3 cooperates with Gcm2 and MafB to activate parathyroid hormone gene expression by interacting with SP1. Mol. Cell. Endocrinol. 411, 113−120.

Hannan, F.M., Babinsky, V.N., Thakker, R.V., 2016. Disorders of the calcium-sensing receptor and partner proteins: insights into the molecular basis of calcium homeostasis. J. Mol. Endocrinol. 57 (3), R127−R142.

Holmes, D., 2015. Parathyroid function: key role for dicer-dependent miRNAs. Nat. Rev. Endocrinol. 11 (8), 445.

Hosokawa, Y.A., Leahy, J.L., 1997. Parallel reduction of pancreas insulin content and insulin secretion in 48-h tolbutamide-infused normoglycemic rats. Diabetes 46 (5), 808−813.

Huse, J.T., Holland, E.C., 2010. Targeting brain cancer: advances in the molecular pathology of malignant glioma and medulloblastoma. Nat. Rev. Canc. 10 (5), 319−331.

Igarashi, T., Okazaki, T., Potter, H., Gaz, R., Kronenberg, H.M., 1986. Cell-specific expression of the human parathyroid hormone gene in rat pituitary cells. Mol. Cell Biol. 6, 1830−1833.

Imanishi, Y., Hosokawa, Y., Yoshimoto, K., Schipani, E., Mallya, S., Papanikolaou, A., et al., 2001. Dual abnormalities in cell proliferation and hormone regulation caused by cyclin D1 in a murine model of hyperparathyroidism. J. Clin. Investig. 107, 1093−1102.

Kamitani-Kawamoto, A., Hamada, M., Moriguchi, T., Miyai, M., Saji, F., Hatamura, I., et al., 2011. MafB interacts with Gcm2 and regulates parathyroid hormone expression and parathyroid development. J. Bone Miner. Res. 26 (10), 2463−2472.

Karaplis, A.C., Lim, S.K., Baba, H., Arnold, A., Kronenberg, H.M., 1995. Inefficient membrane targeting, translocation, and proteolytic processing by signal peptidase of a mutant preproparathyroid hormone protein. J. Biol. Chem. 270, 1629−1635.

Karmali, R., Farrow, S., Hewison, M., Barker, S., O'Riordan, J.L., 1989. Effects of 1,25-dihydroxyvitamin D3 and cortisol on bovine and human parathyroid cells. J. Endocrinol. 123, 137−142.

Kel, A., Scheer, M., Mayer, H., 2005. In silico analysis of regulatory sequences in the human parathyroid hormone gene. In: Naveh-Many, T. (Ed.), Molecular Biology of the Parathyroid. Molecular Biology Intelligence Unit, first ed. Landes Bioscience and Kluwer Academic/Plenum Publishers, New York, pp. 68−83.

Kemper, B., 1986. Molecular biology of parathyroid hormone. CRC Crit. Rev. Biochem. 19, 353−379.

Kemper, B., Habener, J.F., Ernst, M.D., Potts Jr., J.T., Rich, A., 1976. Pre-proparathyroid hormone: analysis of radioactive tryptic peptides and amino acid sequence. Biochemistry 15 (1), 15−19.

Kifor, O., Diaz, R., Butters, R., Brown, E.M., 1997. The Ca2+-sensing receptor (CaR) activates phospholipases C, A2, and D in bovine parathyroid and CaR-transfected, human embryonic kidney (HEK293) cells. J. Bone Miner. Res. 12 (5), 715−725.

Kilav, R., Silver, J., Naveh-Many, T., 1995. Parathyroid hormone gene expression in hypophosphatemic rats. J. Clin. Investig. 96, 327−333.

Kilav, R., Silver, J., Naveh-Many, T., 2001. A conserved cis-acting element in the parathyroid hormone 3'-untranslated region is sufficient for regulation of RNA stability by calcium and phosphate. J. Biol. Chem. 276, 8727–8733.

Kilav, R., Silver, J., Naveh-Many, T., 2005. Regulation of parathyroid hormone mRNA stability by calcium and phosphate. In: Naveh-Many, T. (Ed.), Molecular Biology of the Parathyroid. Molecular Biology Intelligence Unit, first ed. Landes Bioscience and Kluwer Academic/Plenum Publishers, New York, pp. 57–67.

Kissmeyer, A.M., Binderup, L., 1991. Calcipotriol (MC 903): pharmacokinetics in rats and biological activities of metabolites. A comparative study with 1,25(OH)2D3. Biochem. Pharmacol. 41, 1601–1606.

Komaba, H., Goto, S., Fujii, H., Hamada, Y., Kobayashi, A., Shibuya, K., et al., 2010. Depressed expression of Klotho and FGF receptor 1 in hyperplastic parathyroid glands from uremic patients. Kidney Int. 77, 232–238.

Koszewski, N.J., Alimov, A.P., Park-Sarge, O.K., Malluche, H.H., 2004. Suppression of the human parathyroid hormone promoter by vitamin D involves displacement of NF-Y binding to the vitamin D response element. J. Biol. Chem. 279 (41), 42431–42437.

Kozak, M., 1991. Structural features in eukaryotic mRNAs that modulate the initiation of translation. J. Biol. Chem. 266 (30), 19867–19870.

Krajisnik, T., Bjorklund, P., Marsell, R., Ljunggren, O., Akerstrom, G., Jonsson, K.B., et al., 2007. Fibroblast growth factor-23 regulates parathyroid hormone and 1alpha-hydroxylase expression in cultured bovine parathyroid cells. J. Endocrinol. 195 (1), 125–131.

Kronenberg, H.M., Igarashi, T., Freeman, M.W., Okazaki, T., Brand, S.J., Wiren, K.M., et al., 1986. Structure and expression of the human parathyroid hormone gene. Recent Prog. Horm. Res. 42, 641–663.

Kumar, R., 2009. Pin1 regulates parathyroid hormone mRNA stability. J. Clin. Investig. 119 (10), 2887–2891.

Kurosu, H., Ogawa, Y., Miyoshi, M., Yamamoto, M., Nandi, A., Rosenblatt, K.P., et al., 2006. Regulation of fibroblast growth factor-23 signaling by klotho. J. Biol. Chem. 281 (10), 6120–6123.

Lafage, M.H., Combe, C., Fournier, A., Aparicio, M., 1992. Ketodiet, physiological calcium intake and native vitamin D improve renal osteodystrophy. Kidney Int. 42, 1217–1225.

Lavi-Moshayoff, V., Wasserman, G., Meir, T., Silver, J., Naveh-Many, T., 2010. PTH increases FGF23 gene expression and mediates the high-FGF23 levels of experimental kidney failure: a bone parathyroid feedback loop. Am. J. Physiol. Renal. Physiol. 299 (4), F882–F889.

Lee, Y., Ahn, C., Han, J.J., Choi, H., Kim, J., Yim, J., et al., 2003. The nuclear RNase III Drosha initiates microRNA processing. Nature 425 (6956), 415–419.

Lee, S., Mannstadt, M., Guo, J., Kim, S.M., Yi, H.-S., Khatri, A., et al., 2015. A homozygous [Cys25]PTH(1-84) mutation that impairs PTH/PTHrP receptor activation defines a novel form of hypoparathyroidism. J. Bone Miner. Res. 30 (10), 1803–1813.

Levi, R., Ben Dov, I.Z., Lavi-Moshayoff, V., Dinur, M., Martin, D., Naveh-Many, T., et al., 2006. Increased parathyroid hormone gene expression in secondary hyperparathyroidism of experimental uremia is reversed by calcimimetics: correlation with posttranslational modification of the trans acting factor AUF1. J. Am. Soc. Nephrol. 17 (1), 107–112.

Lewin, E., Garfia, B., Recio, F.L., Rodriguez, M., Olgaard, K., 2002. Persistent downregulation of calcium-sensing receptor mRNA in rat parathyroids when severe secondary hyperparathyroidism is reversed by an isogenic kidney transplantation. J. Am. Soc. Nephrol. 13 (8), 2110–2116.

Lindsay, E.A., Vitelli, F., Su, H., Morishima, M., Huynh, T., Pramparo, T., et al., 2001. Tbx1 haploinsufficiency in the DiGeorge syndrome region causes aortic arch defects in mice. Nature 410 (6824), 97–101.

Liu, M., Lee, M.H., Cohen, M., Bommakanti, M., Freedman, L.P., 1996. Transcriptional activation of the Cdk inhibitor p21 by vitamin D3 leads to the induced differentiation of the myelomonocytic cell line U937. Genes Dev. 10, 142–153.

Liu, Z., Yu, S., Manley, N.R., 2007. Gcm2 is required for the differentiation and survival of parathyroid precursor cells in the parathyroid/thymus primordia. Dev. Biol. 305 (1), 333–346.

Liu, Y., Ibrahim, A.S., Tay, B.-H., Richardson, S.J., Bell, J., Walker, T.I., et al., 2010. Parathyroid hormone gene family in a cartilaginous fish, the elephant shark (*Callorhinchus milii*). J. Bone Miner. Res. 25 (12), 2613–2623.

Lopez-Hilker, S., Dusso, A.S., Rapp, N.S., Martin, K.J., Slatopolsky, E., 1990. Phosphorus restriction reverses hyperparathyroidism in uremia independent of changes in calcium and calcitriol. Am. J. Physiol. 259, F432–F437.

Lucas, P.A., Brown, R.C., Woodhead, J.S., Coles, G.A., 1986. 1,25-dihydroxycholecalciferol and parathyroid hormone in advanced chronic renal failure: effects of simultaneous protein and phosphorus restriction. Clin. Nephrol. 25, 7–10.

Macdonald, L.E., Durbin, R.K., Dunn, J.J., McAllister, W.T., 1994. Characterization of two types of termination signal for bacteriophage T7 RNA polymerase. J. Mol. Biol. 238 (2), 145–158.

Manley, N.R., 2015. Embryology of the parathyroid glands. In: Brandi, M.L., Brown, E.M. (Eds.), Hypoparathyroidism. Springer Milan, Milano, pp. 11–18.

Meir, T., Durlacher, K., Pan, Z., Amir, G., Richards, W.G., Silver, J., et al., 2014. Parathyroid hormone activates the orphan nuclear receptor Nurr1 to induce FGF23 transcription. Kidney Int. 86 (6), 1106–1115.

Merscher, S., Funke, B., Epstein, J.A., Heyer, J., Puech, A., Lu, M.M., et al., 2001. TBX1 is responsible for cardiovascular defects in velo-cardio-facial/DiGeorge syndrome. Cell 104 (4), 619–629.

Mithal, A., Kifor, O., Kifor, I., Vassilev, P., Butters, R., Krapcho, K., et al., 1995. The reduced responsiveness of cultured bovine parathyroid cells to extracellular Ca^{2+} is associated with marked reduction in the expression of extracellular Ca^{2+}-sensing receptor messenger ribonucleic acid and protein. Endocrinology 136, 3087–3092.

Moallem, E., Silver, J., Kilav, R., Naveh-Many, T., 1998. RNA protein binding and post-transcriptional regulation of PTH gene expression by calcium and phosphate. J. Biol. Chem. 273, 5253–5259.

Morito, N., Yoh, K., Usui, T., Oishi, H., Ojima, M., Fujita, A., et al., 2018. Transcription factor MafB may play an important role in secondary hyperparathyroidism. Kidney Int. 93 (1), 54–68.

Naveh-Many, T., 2010. Minireview: the play of proteins on the parathyroid hormone messenger ribonucleic acid regulates its expression. Endocrinology 151 (4), 1398–1402.

Naveh-Many, T., Silver, J., 1990. Regulation of parathyroid hormone gene expression by hypocalcemia, hypercalcemia, and vitamin D in the rat. J. Clin. Investig. 86, 1313–1319.

Naveh-Many, T., Silver, J., 1993. Effects of calcitriol, 22-oxacalcitriol and calcipotriol on serum calcium and parathyroid hormone gene expression. Endocrinology 133, 2724–2728.

Naveh-Many, T., Silver, J., 2018. Transcription factors that determine parathyroid development power PTH expression. Kidney Int. 93 (1), 7–9.

Naveh-Many, T., Friedlander, M.M., Mayer, H., Silver, J., 1989. Calcium regulates parathyroid hormone messenger ribonucleic acid (mRNA), but not calcitonin mRNA in vivo in the rat. Endocrinology 125, 275–280.

Naveh-Many, T., Almogi, G., Livni, N., Silver, J., 1992a. Estrogen receptors and biologic response in rat parathyroid tissue and C-cells. J. Clin. Investig. 90, 2434–2438.

Naveh-Many, T., Raue, F., Grauer, A., Silver, J., 1992b. Regulation of calcitonin gene expression by hypocalcemia, hypercalcemia, and vitamin D in the rat. J. Bone Miner. Res. 7, 1233–1237.

Naveh-Many, T., Rahamimov, R., Livni, N., Silver, J., 1995. Parathyroid cell proliferation in normal and chronic renal failure rats: the effects of calcium, phosphate and vitamin D. J. Clin. Investig. 96, 1786–1793.

Nechama, M., Ben Dov, I.Z., Briata, P., Gherzi, R., Naveh-Many, T., 2008. The mRNA decay promoting factor K-homology splicing regulator protein post-transcriptionally determines parathyroid hormone mRNA levels. FASEB J. 22, 3458–3468.

Nechama, M., Ben Dov, I.Z., Silver, J., Naveh-Many, T., 2009a. Regulation of PTH mRNA stability by the calcimimetic R568 and the phosphorus binder lanthanum carbonate in CKD. Am. J. Physiol. Renal. Physiol. 296 (4), F795–F800.

Nechama, M., Peng, Y., Bell, O., Briata, P., Gherzi, R., Schoenberg, D.R., et al., 2009b. KSRP-PMR1-exosome association determines parathyroid hormone mRNA levels and stability in transfected cells. BMC Cell Biol. 10, 70–81.

Nechama, M., Uchida, T., Yosef-Levi, I.M., Silver, J., Naveh-Many, T., 2009c. The peptidyl-prolyl isomerase Pin1 determines parathyroid hormone mRNA levels and stability in rat models of secondary hyperparathyroidism. J. Clin. Investig. 119 (10), 3102–3114.

Nesbit, M.A., Hannan, F.M., Howles, S.A., Babinsky, V.N., Head, R.A., Cranston, T., et al., 2013. Mutations affecting G-protein subunit α(11) in hypercalcemia and hypocalcemia. N. Engl. J. Med. 368 (26), 2476–2486.

Nielsen, P.K., Feldt-Rasmusen, U., Olgaard, K., 1996. A direct effect of phosphate on PTH release from bovine parathyroid tissue slices but not from dispersed parathyroid cells. Nephrol. Dial. Transplant. 11, 1762–1768.

Nishii, Y., Abe, J., Mori, T., Brown, A.J., Dusso, A.S., Finch, J., et al., 1991. The noncalcemic analogue of vitamin D, 22-oxacalcitriol, suppresses parathyroid hormone synthesis and secretion. Contrib. Nephrol. 91, 123–128.

Okabe, M., Graham, A., 2004. The origin of the parathyroid gland. Proc. Natl. Acad. Sci. U.S.A. 101 (51), 17716–17719.

Okazaki, T., Igarashi, T., Kronenberg, H.M., 1988. 5'-flanking region of the parathyroid hormone gene mediates negative regulation by 1,25-(OH)2 vitamin D3. J. Biol. Chem. 263, 2203–2208.

Okazaki, T., Ando, K., Igarashi, T., Ogata, E., Fujita, T., 1992. Conserved mechanism of negative gene regulation by extracellular calcium. J. Clin. Investig. 89, 1268–1273.

Olauson, H., Lindberg, K., Amin, R., Sato, T., Jia, T., Goetz, R., et al., 2013. Parathyroid-specific deletion of klotho unravels a novel calcineurin-dependent FGF23 signaling pathway that regulates PTH secretion. PLoS Genet. 9 (12).

Parkinson, D.B., Thakker, R.V., 1992. A donor splice site mutation in the parathyroid hormone gene is associated with autosomal recessive hypoparathyroidism. Nat. Genet. 1, 149–152.

Patel, S., Rosenthal, J.T., 1985. Hypercalcemia in carcinoma of prostate. Its cure by orchiectomy. Urology 25, 627–629.

Portale, A.A., Booth, B.E., Halloran, B.P., Morris, R.C.J., 1984. Effect of dietary phosphorus on circulating concentrations of 1,25-dihydroxyvitamin D and immunoreactive parathyroid hormone in children with moderate renal insufficiency. J. Clin. Investig. 73, 1580–1589.

Portale, A.A., Halloran, B.P., Curtis Morris, J., 1989. Physiologic regulation of the serum concentration of l,25-dihydroxyvitamin D by phosphorus in normal men. J. Clin. Investig. 83, 1494–1499.

Prank, K., Nowlan, S.J., Harms, H.M., Kloppstech, M., Brabant, G., Hesch, R.-D., et al., 1995. Time series prediction of plasma hormone concentration. Evidence for differences in predictability of parathyroid hormone secretion between osteoporotic patients and normal controls. J. Clin. Investig. 95, 2910–2919.

Prince, R.L., Dick, I., Garcia-Webb, P., Retallack, R.W., 1990. The effects of the menopause on calcitriol and parathyroid hormone: responses to a low dietary calcium stress test. J. Clin. Endocrinol. Metab. 70, 1119–1123.

Prince, R.L., MacLaughlin, D.T., Gaz, R.D., Neer, R.M., 1991. Lack of evidence for estrogen receptors in human and bovine parathyroid tissue. J. Clin. Endocrinol. Metab. 72, 1226–1228.

Rodriguez, M.E., Almaden, Y., Canadillas, S., Canalejo, A., Siendones, E., Lopez, I., et al., 2007. The calcimimetic R-568 increases vitamin D receptor expression in rat parathyroid glands. AJP Renal Physiol. 292, F1390–F1395.

Russell, J., Lettieri, D., Sherwood, L.M., 1983. Direct regulation by calcium of cytoplasmic messenger ribonucleic acid coding for pre-proparathyroid hormone in isolated bovine parathyroid cells. J. Clin. Investig. 72, 1851–1855.

Russell, J., Silver, J., Sherwood, L.M., 1984. The effects of calcium and vitamin D metabolites on cytoplasmic mRNA coding for pre-proparathyroid hormone in isolated parathyroid cells. Trans. Assoc. Am. Physicians 97, 296–303.

Russell, J., Lettieri, D., Sherwood, L.M., 1986. Suppression by $1,25(OH)_2D_3$ of transcription of the pre-proparathyroid hormone gene. Endocrinology 119, 2864–2866.

Russell, J., Bar, A., Sherwood, L.M., Hurwitz, S., 1993. Interaction between calcium and 1,25-dihydroxyvitamin D3 in the regulation of preproparathyroid hormone and vitamin D receptor messenger ribonucleic acid in avian parathyroids. Endocrinology 132, 2639–2644.

Russell, J., Ashok, S., Koszewski, N.J., 1999. Vitamin D receptor interactions with the rat parathyroid hormone gene: synergistic effects between two negative vitamin D response elements. J. Bone Miner. Res. 14 (11), 1828–1837.

Ruvinsky, I., Sharon, N., Lerer, T., Cohen, H., Stolovich-Rain, M., Nir, T., et al., 2005. Ribosomal protein S6 phosphorylation is a determinant of cell size and glucose homeostasis. Genes Dev. 19 (18), 2199–2211.

Ruvinsky, I., Katz, M., Dreazen, A., Gielchinsky, Y., Saada, A., Freedman, N., et al., 2009. Mice deficient in ribosomal protein S6 phosphorylation suffer from muscle weakness that reflects a growth defect and energy deficit. PLoS One 4 (5).

Sela-Brown, A., Russell, J., Koszewski, N.J., Michalak, M., Naveh-Many, T., Silver, J., 1998. Calreticulin inhibits vitamin D's action on the PTH gene *in vitro* and may prevent vitamin D's effect *in vivo* in hypocalcemic rats. Mol. Endocrinol. 12, 1193–1200.

Sela-Brown, A., Silver, J., Brewer, G., Naveh-Many, T., 2000. Identification of AUF1 as a parathyroid hormone mRNA 3'-untranslated region binding protein that determines parathyroid hormone mRNA stability. J. Biol. Chem. 275 (10), 7424–7429.

Shahbazian, D., Roux, P.P., Mieulet, V., Cohen, M.S., Raught, B., Taunton, J., et al., 2006. The mTOR/PI3K and MAPK pathways converge on eIF4B to control its phosphorylation and activity. EMBO J. 25 (12), 2781–2791.

Shilo, V., Ben Dov, I.Z., Nechama, M., Silver, J., Naveh-Many, T., 2015. Parathyroid-specific deletion of dicer-dependent microRNAs abrogates the response of the parathyroid to acute and chronic hypocalcemia and uremia. FASEB J. 29 (9), 3964–3976.

Shilo, V., Silver, J., Naveh-Many, T., 2016. Micro-RNAs in the parathyroid: a new portal in understanding secondary hyperparathyroidism. Curr. Opin. Nephrol. Hypertens. 25 (4), 271–277.

Shilo, V., Mor-Yosef Levi, I., Abel, R., Mihailovic, A., Wasserman, G., Naveh-Many, T., et al., 2017. Let-7 and MicroRNA-148 regulate parathyroid hormone levels in secondary hyperparathyroidism. J. Am. Soc. Nephrol. 28 (8), 2353–2363.

Shimobayashi, M., Hall, M.N., 2014. Making new contacts: the mTOR network in metabolism and signalling crosstalk. Nat. Rev. Mol. Cell Biol. 15 (3), 155–162.

Silver, J., Naveh-Many, T., 2009. Phosphate and the parathyroid. Kidney Int. 75 (9), 898–905.

Silver, J., Naveh-Many, T., 2013. FGF-23 and secondary hyperparathyroidism in chronic kidney disease. Nat. Rev. Nephrol. 9 (11), 641–649.

Silver, J., Landau, H., Bab, I., Shvil, Y., Friedlaender, M.M., Rubinger, D., et al., 1985. Vitamin D-dependent rickets types I and II. Diagnosis and response to therapy. Isr. J. Med. Sci. 21, 53–56.

Silver, J., Naveh-Many, T., Mayer, H., Schmelzer, H.J., Popovtzer, M.M., 1986. Regulation by vitamin D metabolites of parathyroid hormone gene transcription in vivo in the rat. J. Clin. Investig. 78, 1296–1301.

Slatopolsky, E., Bricker, N.S., 1973. The role of phosphorus restriction in the prevention of secondary hyperparathyroidism in chronic renal disease. Kidney Int. 4, 141–145.

Slatopolsky, E., Finch, J., Denda, M., Ritter, C., Zhong, A., Dusso, A., et al., 1996. Phosphate restriction prevents parathyroid cell growth in uremic rats. High phosphate directly stimulates PTH secretion in vitro. J. Clin. Investig. 97, 2534–2540.

Suarez-Bregua, P., Cal, L., Cañestro, C., Rotllant, J., 2017. PTH reloaded: a new evolutionary perspective. Front. Physiol. 8, 776.

Sunthornthepvarakul, T., Churesigaew, S., Ngowngarmratana, S., 1999. A novel mutation of the signal peptide of the preproparathyroid hormone gene associated with autosomal recessive familial isolated hypoparathyroidism. J. Clin. Endocrinol. Metab. 84 (10), 3792–3796.

Takeshita, K., Fujimori, T., Kurotaki, Y., Honjo, H., Tsujikawa, H., Yasui, K., et al., 2004. Sinoatrial node dysfunction and early unexpected death of mice with a defect of klotho gene expression. Circulation 109 (14), 1776–1782.

Tanaka, Y., DeLuca, H.F., 1973. The control of vitamin D by inorganic phosphorus. Arch. Biochem. Biophys. 154, 566–570.

Urakawa, I., Yamazaki, Y., Shimada, T., Iijima, K., Hasegawa, H., Okawa, K., et al., 2006. Klotho converts canonical FGF receptor into a specific receptor for FGF23. Nature 444 (7120), 770–774.

Volovelsky, O., Cohen, G., Kenig, A., Wasserman, G., Dreazen, A., Meyuhas, O., et al., 2016. Phosphorylation of ribosomal protein S6 mediates mammalian target of rapamycin complex 1-induced parathyroid cell proliferation in secondary hyperparathyroidism. J. Am. Soc. Nephrol. 27 (4), 1091–1101.

Wheeler, D.G., Horsford, J., Michalak, M., White, J.H., Hendy, G.N., 1995. Calreticulin inhibits vitamin D3 signal transduction. Nucleic Acids Res. 23, 3268–3274.

Xu, J., Chen, J., Dong, Z., Meyuhas, O., Chen, J.K., 2015. Phosphorylation of ribosomal protein S6 mediates compensatory renal hypertrophy. Kidney Int. 87 (3), 543–556.

Yamamoto, M., Igarashi, T., Muramatsu, M., Fukagawa, M., Motokura, T., Ogata, E., 1989. Hypocalcemia increases and hypercalcemia decreases the steady-state level of parathyroid hormone messenger RNA in the rat. J. Clin. Investig. 83, 1053–1056.

Yano, S., Brown, E.M., 2005. The calcium sensing receptor. In: Naveh-Many, T. (Ed.), Molecular Biology of the Parathyroid. Molecular Biology Intelligence Unit, first ed. Landes Bioscience and Kluwer Academic/Plenum Publishers, New York, pp. 44–56.

Yuan, Z., Opas, E.E., Vrikshajanani, C., Libutti, S.K., Levine, M.A., 2014. Generation of mice encoding a conditional null allele of Gcm2. Transgenic Res. 23 (4), 631–641.

Zabel, B.U., Kronenberg, H.M., Bell, G.I., Shows, T.B., 1985. Chromosome mapping of genes on the short arm of human chromosome 11: parathyroid hormone gene is at 11p15 together with the genes for insulin, c-Harvey-ras 1, and beta-hemoglobin. Cytogenet. Cell Genet. 39, 200–205.

Chapter 25

Paracrine parathyroid hormone–related protein in bone: physiology and pharmacology

T. John Martin and Natalie A. Sims

St. Vincent's Institute of Medical Research, Melbourne, Australia; Department of Medicine at St. Vincent's Hospital, The University of Melbourne, Melbourne, Australia

Chapter outline

Introduction: discovery of parathyroid hormone–related protein

When he carried out 650 autopsies on patients with breast cancer, the English surgeon Stephen Paget noted the remarkable frequency of secondary growths in bone, especially at the ends of the femora and in the skull (Paget, 1889). This led him to write: "in cancer of the breast, the bones suffer in a special way, which cannot be explained by any theory of embolism alone. Some bones suffer more than others, the disease has its seats of election." In that series, he also reported six subjects with breast cancer who had no bone metastases, but who appeared to have a generalized susceptibility of the skeleton to fracture. No explanation of the findings of Paget was forthcoming, but some decades later, the discovery of parathyroid hormone–related protein (PTHrP) as the cause of hypercalcemia in many patients with cancer provided new insights into the pathogenesis of the skeletal complications of malignancy (Suva et al., 1987). Two other chapters (Chapter 54, Goltzman; Chapter 55, Sterling) will consider this topic in more depth, but it is appropriate to introduce the topic of PTHrP in bone with some relevant background.

When Fuller Albright in 1941 was discussing a patient with hypercalcemia accompanying a hypernephroma that had metastasized to the ilium, he suggested that the hypercalcemia might be due to production by the cancer of parathyroid hormone (PTH) (Albright, 1941). This was an influential comment that played a part in the adoption within the next years of the concept of "ectopic" production of PTH by tumors. This became a commonly used explanation through the 1960s and into the 1970s for hypercalcemia in cancer with no or minimal bone metastases (Lafferty, 1966). This seemed at that time to fit with a more general concept of ectopic production of hormones by cancers, for example, with adrenocorticotropic hormone production resulting in hypercorticolism in certain patients with cancer (Meador et al., 1962).

Principles of Bone Biology. https://doi.org/10.1016/B978-0-12-814841-9.00025-7

The first radioimmunoassays for PTH appeared to support this view, with apparently elevated circulating levels of PTH in unselected patients with bronchogenic carcinoma (Berson and Yalow, 1966). When further assays were developed whose specificities were better defined (Riggs et al., 1971), the observations were made that PTH levels in cancer hypercalcemia were lower than those in primary hyperparathyroid subjects with the same degree of elevation of calcium and, furthermore, that immunoreactivity of cancer hypercalcemia samples differed from PTH in that it was nonparallel to PTH standards (Melick et al., 1972; Benson et al., 1974). These findings suggested that the circulating and tumor-derived activity measured in some patients with hypercalcemia in cancer differed immunochemically from authentic PTH itself. Strong support for this was provided by a study in which immunoreactive PTH could not be detected in plasma or tumor extracts from a number of patients whose tumor extracts resorbed bone in vitro (Powell et al., 1973), despite the use of several antibodies of differing specificities. Thus, the term "humoral hypercalcemia of malignancy" (HHM) was used to describe patients with cancer and hypercalcemia without bone metastases (Martin and Atkins, 1979).

A defining step in progress was made with three clinical studies each showing that in patients with HHM the mimicry of PTH action extended beyond the calcium and phosphorus effects to increased excretion of cyclic AMP (cAMP) (Kukreja et al., 1980; Rude et al., 1980; Stewart et al., 1980). This consolidated the view that the tumor activity resembled PTH biologically, resulting in even greater interest in the pathogenesis. By that time rapid, sensitive assays of PTH-like activity that made use of cAMP responses in osteosarcoma (OS) cells had been developed (Majeska et al., 1980; Partridge et al., 1981). These were applied to cancer cell cultures and to tumor extracts from patients with HHM, and resulted in the purification, sequencing, and cloning of what came to be called PTHrP (Moseley et al., 1987; Suva et al., 1987). This newly identified molecule, related to PTH by an evolutionary gene duplication event (Mangin et al., 1990), was recognized as a potent bone-resorbing agent in vivo and in vitro, providing an explanation for the pathogenesis of hypercalcemia in HHM through its actions on bone and kidney. Subsequent to this, PTHrP production by cancer cells was found to favor the establishment and growth of secondary cancer deposits in bone (Powell et al., 1991; Guise et al., 1996), illustrating its behavior as a paracrine agent, analogous with its physiological paracrine/autocrine roles in many normal tissues, including bone.

From its discovery in cancer as a result of its PTH-like actions, PTHrP soon emerged as a paracrine/autocrine mediator of essential processes in endochondral bone formation during skeletal development, and in bone remodeling in the adult skeleton. This chapter will discuss those roles, beginning by considering the unique structural features of PTHrP that equip it to exert biological activities, not only through the common G-protein-coupled receptor that it shares with PTH, but also through other unique recognizable domains within the molecule.

Primary structure, active domains, processing, and secretion

Whereas PTH consists of 84 amino acids, molecular cloning predicted human PTHrP to have three alternatively spliced products of 139, 141, and 173 amino acids (Mangin et al., 1988; Thiede et al., 1988; Yasuda et al., 1989). While the human PTHrP gene undergoes alternative 3′ splicing, the rat and mouse PTHrP genes have a much simpler structure and produce only one form of PTHrP cDNA (Mangin et al., 1990). PTH and PTHrP have identical amino acids in 8 of their first 13 residues, but other similarities within the sequences are no more than would be expected by chance (Martin, 2016). The marked conservation of the PTHrP amino acid sequence in human, rat, mouse, chicken, and canine up to position 111 indicates that important functions are likely to reside in this region.

PTHrP promotes bone resorption, in a manner identical to that of PTH, by acting upon the receptor it shares with PTH (PTHR1). From the time of its discovery, the structural requirements within PTHrP that activate the PTHR1 were recognized to be the same as those required with PTH (Tregear and Potts, 1975; Kemp et al., 1987). Biological assay showed that recombinant PTHrP and synthetic shorter amino-terminal forms were equipotent on a molar basis with one another and with PTH(1−34) in generating cAMP in osteoblast-like cells (Hammonds et al., 1989). They were also recognized equally on a molar basis when measured in a radioimmunoassay directed at the amino terminus of PTHrP (Grill et al., 1991), indicating that the N-terminal region, with high homology to PTH, activates cAMP formation.

Despite their equal ability to activate cAMP via PTHR1, it was clear from the earliest work, even with peptides up to the first 14 residues of PTHrP, that highly specific antibodies that discriminate between PTH and PTHrP could be generated (Moseley et al., 1987). Such antibodies against PTHrP that neutralized its effects in promoting cAMP production completely in vitro, without any detectable neutralizing effect on PTH, were used to prevent and treat hypercalcemia in nude mice bearing xenografts of PTHrP-secreting human cancers (Kukreja et al. 1988, 1990).

PTHrP can be divided into different domains on the basis of its primary amino acid sequence (Fig. 25.1). Intracellular "pre-pro" and "pro" precursors of the mature peptide, essential for intracellular trafficking, are encoded by the first 36 amino acids (−36 to −1); this domain is cleaved from the molecule when it is secreted. The next domain includes the first

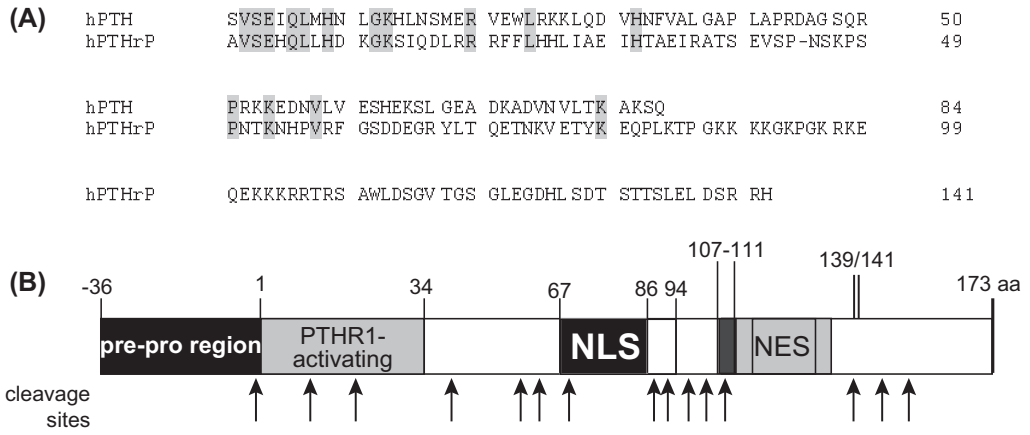

FIGURE 25.1 Protein structure of parathyroid hormone–related protein (PTHrP). (A) Amino acid alignment of the secreted portions of human PTH (*hPTH*) and human PTHrP (*hPTHrP*). Amino acid homologies are marked in *gray*. *Boxes* indicate the common PTH receptor (*PTHR1*)-activating region and the unique nuclear localization sequence (*NLS*) of PTHrP. (B) Protein structure of PTHrP including the amino acid numbers and approximate locations of cleavage sites. Structural domains described in the text are shown, including the pre-pro region, required for PTHrP secretion; the PTHR1-activating region that has high homology with PTH; the NLS; and the nuclear export sequence (*NES*).

13 residues of the mature protein showing the sequence homology with PTH. This domain is critical for most of the agonist effects of PTH and PTHrP on their shared PTHR1 receptor (Kemp et al., 1987). The following residues, PTHrP(14–36), although having almost no homology with PTH, appear to be critical for binding of PTHrP to PTHR1 (Juppner et al., 1991).

Molecular details of the actions of amino acids 36–139/141, including the nuclear localization sequence (NLS), are less well established. The midmolecule portion, between residues 35 and 84, has been shown to be responsible for promoting placental calcium transport, making calcium available for fetal skeletal development (Rodda et al., 1988; Abbas et al., 1989; Kovacs et al., 1996). Residues 107–111 have been reported to inhibit osteoclast activity and bone resorption in vitro (Fenton et al., 1991a; Fenton et al., 1991b) and in vivo (Cornish et al., 1997), and to be mitogenic for osteoblasts (Cornish et al., 1999).

The final tail region of PTHrP, amino acids 142–173, is found only in humans and is encoded by only one of the three human PTHrP mRNA isoforms. Its significance in terms of tissue distribution, processing, or function is unknown, although immunoreactivity for PTHrP(141–173) has been reported in plasma (Burtis et al., 1990) and in amnion (Bruns et al., 1995). It is presumed that the actions ascribed to regions of the molecule beyond the N-terminal 34 amino acids are mediated by non-receptor-mediated actions, or by unique PTHrP receptors, although these have yet to be discovered.

The realization that PTHrP was probably an important paracrine regulator in many tissues directed attention to mechanisms of PTHrP secretion and the nature of the secreted molecule. This topic has increased in interest with the advent of therapeutic approaches for osteoporosis aimed at mimicking PTHrP local action as a skeletal anabolic agent (Neer et al., 2001; Miller et al., 2016).

Two secretory pathways exist in eukaryotic cells: the regulated pathway whereby the proteins are packaged into secretory granules and the constitutive pathway through which the secreted proteins are found in the endoplasmic reticulum (Burgess and Kelly, 1987); PTHrP makes use of both these pathways depending on the cell type. In neuroendocrine cells, PTHrP is secreted via the regulated pathway. PTHrP is a neuroendocrine protein in the sense that it undergoes extensive posttranslational processing in a fashion analogous to that of chromogranin A or somatostatin, and it is a product of a broad variety of neuroendocrine cell types (e.g., pancreatic islet cells, parathyroid cells, adrenal medullary cells, pituitary cells, central nervous system neurons, etc.) (Philbrick et al., 1996; Matsushita et al., 1997; Martin, 2016). In these cells, PTHrP is packaged into secretory granules.

PTHrP is also produced by a broad range of constitutively secreting cell types (e.g., vascular smooth muscle cells, hepatocytes, osteoblasts, osteocytes, keratinocytes, chondrocytes, and renal tubular cells). In these cells, which do not contain the neuroendocrine machinery, PTHrP would be expected to be secreted in a constitutive fashion, analogous to the cytokines and growth factors whose actions it resembles. Indeed, secretion of PTHrP by the constitutive pathway was shown in nonendocrine cell types by Plawner et al. (Plawner et al., 1995), but in that study the nature of the secreted form was not defined, although three region-specific immunoradiometric assays detected secreted products. The first study to define the nature of PTHrP secreted by nonendocrine cells was carried out in osteocytes, of the osteoblast lineage, showing

secretion of full-length PTHrP, with no evidence of secretion of any shorter biologically active form (Ansari et al., 2017). This will be discussed later in further detail ("PTH and PTHrP in adult bone: PTHrP in physiology and PTH in pharmacology").

Interaction with parathyroid hormone receptor 1

The discovery of PTHrP was possible because of its very similar biological action compared with that of PTH, in that it promotes adenylyl cyclase activity in cells known to be targets of PTH. The sequencing and cloning data, followed by synthesis of active peptides (Kemp et al., 1987), confirmed this, showing that the structural features within the amino-terminal PTHrP that were required for activation of PTHR1 were closely similar to those in PTH, and that PTH and PTHrP shared actions upon a common receptor, PTHR1 (Juppner et al., 1991), a member of the B class of G-protein-coupled receptors.

Sequence similarity between PTHrP and PTH is contained within the first half of the N-terminal domain (Fig. 25.1), in which 8 of the first 13 residues are identical between the two. Structural studies have helped explain the similar actions of PTHrP and PTH at the receptor, with nuclear magnetic resonance data indicating that there is a relatively stable α-helical portion within amino acids 15−34 of each peptide (Gardella and Vilardaga, 2015). With the use of mutant receptors and altered ligands, a model of interaction of ligand with PTHR1 has been proposed, in which the carboxy-terminal portion of the (1−34) peptide binds to the extracellular domain of the receptor, and then the amino-terminal portion interacts with the receptor's transmembrane domain to induce the conformational change that results in intracellular signaling (Gardella and Vilardaga, 2015). Although the (15−34) sequences of PTH and PTHrP are quite different, in the absence of evidence to the contrary, it must be assumed that the conformation of this portion of PTHrP is sufficiently similar to that in PTH to confer receptor binding capability upon it. Later chapters will consider details of the interaction with PTHR1 (Chapter 28, Gardella and Potts) and postreceptor signaling pathways (Chapter 27, Friedman).

The dominant signaling pathway mediating responses to PTHrP and PTH is the cAMP/protein kinase A (PKA) pathway, with activation by either PTH or PTHrP resulting in coupling of PTHR1 predominantly to Gαs/adenylyl cyclase/cAMP/PKA signaling (Fig. 25.2). Chapter 27 (Bisello and Friedman) considers these activation mechanisms in detail as well as the involvement of other PTHR1-mediated pathways. Downstream effectors include the cAMP-response element binding protein (CREB) and activator protein 1 transcription factors. By using peptide analogs, it has been concluded that cAMP signaling plays the major role in mediating the renal phosphaturic (Nagai et al., 2011) and anabolic responses in bone through the PTHR1 (Yang et al., 2007a).

In light of these very similar actions through the PTHR1, it was not surprising that the effects of pharmacologic PTHrP administration in vitro and in vivo were similar to those of PTH. Thus, addition of exogenous PTHrP(1−34) promoted

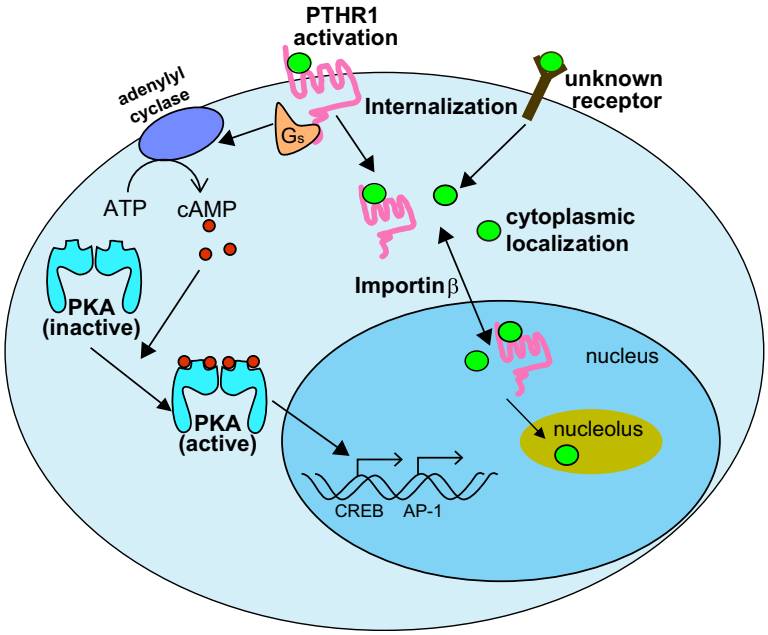

FIGURE 25.2 Multiple known pathways of parathyroid hormone−related protein (PTHrP) action. (1) PTHrP (green (grey in print versions) circle) acts through the G-protein-coupled PTH receptor (*PTHR1*), and via G_s protein, activates adenylyl cyclase to generate cyclic AMP (*cAMP*) from ATP. cAMP activates protein kinase A (*PKA*), which then induces transcription of cAMP-response element binding protein (*CREB*)- and activator protein 1 (*AP-1*)-responsive genes in the nucleus. (2) PTHrP is also internalized by the cell through mechanisms either dependent on the PTHR1 or that make use of an alternative, unknown receptor. PTHrP is also localized within the cytoplasm. PTHrP, both bound to the receptor and unbound, is transported into the nucleus via importin β and can be transported out of the nucleus and into the nucleolus.

bone resorption in organ culture (Kemp et al., 1987), although its lesser potency compared with PTH(1−34) probably reflected its greater susceptibility to proteolytic inactivation in these 48-h cultures (see Fig. 25.1B). Similar effects were observed with amino-terminal PTHrP peptides up to full-length PTHrP (Pilbeam et al., 1993), again with significantly less potency than with PTH(1−34). Such peptides also stimulated osteoclast formation in cocultures of osteoblasts with hemopoietic cells, and both PTHrP(1−34) and the full-length molecule promoted phosphate excretion in the rat when administered intravenously (Kemp et al., 1987; Zhou et al., 1989).

The first demonstration of an anabolic effect of amino-terminal PTHrP in vivo was obtained in the ovariectomized rat, where a dose-dependent anabolic effect of treatment with PTHrP(1−34) was clearly established, but PTHrP(1−34) potency was approximately 25% that of PTH(1−34) in the same experiment (Hock et al., 1989). Lesser potency in vivo of amino-terminal PTHrP peptides was found in virtually all studies (Horwitz et al. 2006, 2013). It might relate to the very marked susceptibility of PTHrP to proteolytic degradation (Diefenbach-Jagger et al., 1995), with the result that when dosage schedules the same as those with PTH are used, less of the injected PTHrP will reach the target cells having avoided degradation. This will be discussed in more detail in a later section ("PTHrP analogs in pharmacology: could this change the approach to skeletal anabolic therapy?"). Comparison of the activities of synthetic and recombinant peptides of various lengths have shown consistently that PTHrP(1−141), (1−84), (1−108), (1−36), and (1−34) are equally potent on a molar basis with one another and with PTH(1−34) in promoting cAMP formation in target cells (Kemp et al., 1987; Hammonds et al., 1989; Li et al., 2012). These assays measure cell responses that are sufficiently rapid that peptide inactivation plays little or no part, unlike prolonged organ culture responses or in vivo effects. These matters need to be taken into consideration in light of the finding that the form of PTHrP released locally, at least by osteocytes, is the full-length molecule (Ansari et al., 2017) (*vide infra*), without any evidence of any shorter forms capable of action through PTHR1. Thus, the form of PTHrP presenting locally as a physiological paracrine/autocrine agent is likely to be the full molecule.

PTHrP tissue distribution and function as a cytokine: the vascular tissue example

It soon became recognized that, apart from its role as a cancer cell product, PTHrP is produced in many tissues throughout the body. The common receptor, PTHR1, is also expressed in these many tissues, often in the same cells as those expressing PTHrP, or closely adjacent to them. Such colocalization was considered consistent with the function of PTHrP as a paracrine/autocrine factor in the developing embryo, particularly in epithelia at many locations and in a number of adult tissues, and raised the possibility that PTHrP is a multifunction cytokine whose actions might influence cell growth and differentiation (Martin et al., 1997; Philbrick, 1998). A body of evidence, particularly in epithelial cells, cancer cells, smooth muscle cells, and osteoblasts, supported this notion, although precise roles are not established in all these cell types.

PTHrP mRNA or protein has been detected in the following human tissues: adrenal, bone, brain, heart, intestine, kidney, liver, lung, mammary gland, ovary, parathyroid, placenta, prostate, skeletal muscle, skin, spleen, stomach, and smooth muscle (Moseley and Gillespie, 1995). PTHrP protein was identified immunologically in normal human and rat fetal bone and cartilage (Moseley et al., 1991; Guenther et al., 1995; Tsukazaki et al., 1995; Suda et al., 1996) and in fetal rat long bones in culture (Nijs-de Wolf et al., 1991), and PTHrP mRNA was detected by RT-PCR in human and rat osteogenic sarcoma cell lines (Rodan et al., 1989; Suda et al., 1996). In situ hybridization analyses localized PTHrP mRNA to active osteoblasts on the bone surface of newborn rat calvarial sections (Suda et al., 1996) and also to spindle-shaped cells of the periosteum, which may represent immature preosteoblasts (Lee et al., 1996; Suda et al., 1996; Rihani-Basharat and Lewinson, 1997). In areas of endochondral bone formation, PTHrP mRNA was detected by in situ hybridization in the perichondrium and maturing chondrocytes in a cell-type and stage-specific manner during fetal rat development (Lee et al., 1996). In a model of intramembranous bone formation in the rabbit, PTHrP mRNA and protein were strongly expressed in osteoblastic cells throughout the bone formation process, including in mature, actively synthetic osteoblasts and in osteocytes (Kartsogiannis et al., 1997).

The vasodilatory effect of PTHrP interacting with PTHR1 on smooth muscle (Roca-Cusachs et al., 1991; Maeda et al., 1996; Massfelder et al., 1998) is instructive in illustrating PTHrP as a physiological paracrine regulator of smooth muscle tone. Decades before the discovery of PTHrP it was known that PTH injection in several animal species resulted in dilatation of vascular beds, increased total blood flow, and decreased blood pressure (Charbon, 1968; Charbon and Hulstaert, 1974; Wang et al., 1984; Mok et al., 1989). These were puzzling observations, not fitting with the accepted role of PTH in regulating blood calcium levels.

The finding that vasoconstrictors such as angiotensin II induced a rapid rise in PTHrP production (Pirola et al., 1993) suggested that vasoconstriction is physiologically limited or reversed through the relaxant action of PTHrP on vascular smooth muscle. For example, in cultured aortic smooth muscle cells subject to stretch, PTHrP responsiveness to angiotensin II was greatly increased and accompanied by increased secretion of PTHrP protein (Noda et al., 1994). In human

coronary arteries, the level of PTHrP mRNA expression by smooth muscle cells has been correlated with the degree of coronary atherosclerosis (Nakayama et al., 1994). In coronary arteries restenosing after angioplasty, expression of PTHrP was greatly increased (Ozeki et al., 1996), consistent with a role for PTHrP in the pathogenesis of vascular stenosis. A physiological role of PTHrP was indicated when mice with transgenic overexpression of PTHrP in vascular smooth muscle cells exhibited low blood pressure (Qian et al., 1999). A less conclusive outcome came from conditional knockdown of PTHrP in vascular smooth muscle in mice; no change in blood pressure was found, but renal blood flow was decreased in targeted mice, particularly with saline volume expansion (Raison et al., 2013).

Thus, the discovery of PTHrP and its production and action in vascular smooth muscle provided an explanation for the long-recognized pharmacological response to PTH injection. Despite evidence of a role for PTHrP as a cardiac hormone, a vasodilatory agent, and a local paracrine regulator of smooth muscle tone, PTHrP-null mutant mice develop normal cardiovascular systems (Karaplis et al., 1994). Although this might indicate that PTHrP is not essential for cardiovascular development, any functions for PTHrP in vascular remodeling, local regulation of vascular flow, and vascular response to injury in adult animals might remain undefined, because the animals die at birth of skeletal defects (see "PTHrP in fetus: early development and endochondral ossification").

Nuclear import of parathyroid hormone–related protein

In addition to its actions through the PTHR1, there is evidence that PTHrP also has intracellular signaling capacities (Fig. 25.2). The first evidence of this was the identification of nuclear and nucleolar localization of PTHrP in chondrocytes (Henderson et al., 1995), where its translocation was dependent upon a highly basic region of PTHrP(87–107) homologous to known NLSs within human retroviral regulatory proteins (Truant and Cullen, 1999). Nuclear localization was essential for the ability of PTHrP to confer enhanced survival on the chondrocytes following serum starvation (Henderson et al., 1995). Although the evidence for translocation of PTHrP to the nucleus in both malignant and normal cells is compelling, the molecular mechanisms by which PTHrP acts in the nucleus remain unclear.

The NLS of PTHrP was defined by Lam and colleagues as between residues 67 and 94 (Lam et al. 1999, 2000) (see Fig. 25.1); however there was debate over the precise region required. Others proposed that PTHrP has a bipartite NLS (Massfelder et al., 1998) (Massfelder et al., 1998; Massfelder et al., 1998) and that residues 87–107 include a second NLS that is required for nuclear localization (Henderson et al., 1995). The region 67–94 was found to include the residues necessary for efficient binding to the nuclear transport factor importin β1 (Lam et al. 1999, 2000), rather than to the conventional NLS-binding importin α subunit. In support of this, importin β1 and the monomeric GTP-binding protein Ran were shown to mediate the nuclear import of PTHrP in vitro via the nuclear pore complex in the absence of importin α (Lam et al., 1999). Further, deletion of the basic residues of the NLS resulted in complete cytoplasmic localization of PTHrP. Studies using a series of alanine-mutated PTHrP constructs and truncated importin β1 derivatives showed that PTHrP residues 83–93 are absolutely essential for importin β1 recognition, with residues 71–82 additionally required for high-affinity binding (Lam et al., 2001). The region of 67–94 also includes a candidate nucleus (CcN) motif and a nucleolus-localizing motif. A CcN motif is a type of nuclear localization signal regulated by dual phosphorylation. When its CK2 substrate site is phosphorylated, the rate of NLS-dependent nuclear import is elevated, and when the cdc2 kinase substrate site is phosphorylated, nuclear transport is inhibited. The CcN motif in PTHrP is similar to that described for the archetypal CcN-containing protein, SV40 T-antigen (Jans et al., 1991; Jans, 1995), and for the N-terminal domain of prointerleukin-16 (pro-IL-16) (Wilson et al., 2002) and pro-IL-1α (Stevenson et al., 1997), comprising also in each case consensus protein kinase CK2 and confirmed cyclin-dependent kinase phosphorylation sites. In the case of PTHrP, a threonine residue at amino acid 85 in PTHrP functions as a p34cdc2 kinase phosphorylation site, with its phosphorylation status determining the nuclear localization of PTHrP (Lam et al., 1999).

Most importantly, support for this region of PTHrP as the NLS comes from the crystal structure of importin β bound to PTHrP(67–94), which identified the specific binding sequence within importin β (Cingolani et al., 2002). It remains possible that there may be more than one contributing segment to nuclear translocation. This could even include the triple-arginine motif at position 19–21, which is highly conserved across species (Fig. 25.1A) and which could mediate nuclear trafficking of a recently identified circulating PTHrP(12–48) isoform (Washam et al., 2013).

Nuclear actions: intracrine and autocrine

In studying how PTHrP gains access to the nucleus it was found that when PTHrP(1–141) was transiently expressed in COS-1 cells, it could be detected in cytoplasm and nucleus as well as at the cell membrane (Aarts et al., 1999a,b). This raised the possibility of intracrine actions of PTHrP, for which evidence then came from studies showing that initiation of

translation downstream of the methionine initiation site gave rise to forms of PTHrP that could not be secreted, but would be available for nuclear transport (Nguyen et al., 2001). Such a mechanism had been proposed for a second eukaryotic protein, fibroblast growth factor 3 (FGF3), which initiates translation at both a classic AUG codon and an upstream CUG site. For both FGF3 and PTHrP, if the AUG codon is used, the protein may follow the secretory pathway, whereas if the CUG codon is used, the protein may be translocated first to the cytosol and then the nucleus, without secretion (Massfelder et al., 1997; Amizuka et al., 2000; Nguyen et al., 2001). This introduced a new biological concept. Having been discovered as a hormone in cancer, PTHrP was then realized to be an autocrine/paracrine factor in normal physiology, with a nuclear role that could be either autocrine (action by PTHrP is secreted and then internalized) or intracrine (by PTHrP that acts within the cell without requiring secretion).

In vascular smooth muscle cells, nuclear PTHrP localization increased cell proliferation, whereas extracellular PTHrP treatment decreased cell proliferation and enhanced muscle relaxation in the same cells by acting through PTHR1 (Massfelder et al., 1997; de Miguel et al., 2001). This indicates a striking dichotomy of outcome that depends on the mode of delivery of PTHrP to the cell, and needs to be kept in mind when considering any organ in which PTHrP acts in an autocrine/paracrine manner. Perhaps even more remarkably, the increased mitogenesis in vascular smooth muscle cells resulting from PTHrP transfection was found to require not only the NLS, but also the C-terminal 108−139 domain of the molecule (de Miguel et al., 2001), suggesting that additional nonnuclear actions are involved in the intracrine action of PTHrP. The importance of the NLS was illustrated further by the finding that adenoviral delivery at angioplasty of PTHrP lacking the NLS markedly inhibited vascular smooth muscle proliferation and cell cycle progression (Fiaschi-Taesch et al., 2009). The importance of C-terminal intracrine actions has yet to be elucidated.

There are at least two mechanisms by which autocrine PTHrP may gain entry to the nucleus from outside the cell: PTHR1 dependent and PTHR1 independent. Internalization and nuclear localization of fluorescein isothiocyanate-labeled PTHrP(1−108) in keratinocytes required PTHR1 expression (Lam et al., 1999). Similarly, in a study using PTHrP mutant constructs in the MC3T3-E1 osteoblastic cell line, it was concluded that PTHrP needs to be secreted and then internalized via the PTHR1 for NLS-mediated shuttling to the nucleus (Garcia-Martin et al., 2014). In other work though, PTHrP gained entry into chondrocytes independent of PTHR1, with PTHrP(1−141) being transported to the nucleus after binding to the cell surface; this mechanism was dependent on the presence of an intact NLS (Aarts et al., 1999a,b). This effect was abrogated by pretreatment with PTHrP(74−113) alone; since it does not bind to PTHR1, this that indicates endocytosis-dependent nucleolar translocation does not involve PTHR1, but an as-yet undefined cell surface receptor.

In cells in which PTHR1-dependent nuclear translocation of PTHrP is used, if the mechanism is similar to that operating with IL-5, growth hormone (Jans et al., 1997), and vascular endothelial growth factor (Liu et al., 2012), the PTHR1 should be found in the nucleus. There is some evidence for that, with the PTHR1 being found by immunostaining in the nucleus of some cells of all tissues examined in the rat—kidney, liver, small intestine, uterus, and ovary—with PTHrP mRNA protein and mRNA localized in the same or adjacent cells (Watson et al., 2000; Watson et al., 2000). Nuclear localization of PTHR1 was also observed in UMR106, ROS 17.2/8, MC3T3-E1, and SaOS-2 cells (Watson et al., 2000; Watson et al., 2000). Furthermore, the cytoplasmic tail of the PTHR1 at residues 471−488 has a putative NLS similar to that of PTHrP, though whether this is required for nuclear transport has not been shown (Patterson et al., 2007).

In vascular smooth muscle cells (Okano et al., 1995) and keratinocytes (Lam et al., 1997), PTHrP expression was found to be cell cycle dependent. In keratinocytes the highest levels of PTHrP mRNA appeared in response to mitogenic factors only at the G_1 phase of the cell cycle, during which PTHrP localized to the nucleolus (Lam et al., 1997). The possession of a CcN motif and cell cycle regulation of kinases by PTHrP are consistent with a role for PTHrP in cell cycle regulation and/or cell proliferation. This has been the case with a number of other proteins containing CcN motifs, e.g., SV40 T-antigen, nucleoplasmin, interferon-inducible nuclear factor, γ-interferon-inducible protein 16, and p53 (Jans et al., 1991; Robbins et al., 1991; Briggs et al., 2001). Although clearly implicated in delaying apoptosis and promoting proliferation in certain cell types, the precise role of PTHrP in the nucleus/nucleolus remains unclear, and has not been investigated in the osteoblast. RNA has been shown to bind PTHrP (Aarts et al., 1999a,b) through a distinct motif in the nucleolar targeting sequence (Pache et al., 2006), and PTHrP inhibits rRNA synthesis (Aarts et al., 2001). This might indicate a role, perhaps in conjunction with other proteins, as a nuclear export factor for RNA. This would be consistent with the ability of PTHrP to shuttle between nuclear/nucleolar and cytoplasmic compartments. Among the most important tasks will be to identify nuclear binding partners for PTHrP, including the possibility that it could bind DNA directly as a transcription factor.

Several lines of evidence therefore converge to indicate that PTHrP is likely to exert many functions from within the cell: (1) the finding of the CcN motif, (2) the redistribution within the cell as a result of phosphorylation at T85, (3) the striking cell cycle dependence of PTHrP location, (4) the identification of nuclear localization of exogenously supplied PTHrP, (5) the participation of the PTHrP NLS with importin β in a specific, regulated nuclear import process, and (6) the involvement of other sequences within PTHrP in intracrine action. In the many tissues in which PTHrP plays a potent local role,

including bone and cartilage, these observations need to be studied further, rather than assuming all local actions of PTHrP can be ascribed to its effects through PTHR1. The fact that PTHrP nuclear localization is integral to its function in any cell studied so far implies that strategies to block PTHrP nuclear localization could have important effects on target cell function.

C-terminal PTHrP and osteostatin

The concept that PTHrP has actions that do not involve signaling through the PTHR1 developed early with the finding that PTHrP promoted the transport of calcium from mother to fetus, making it available for mineralization of the fetal skeleton (Rodda et al., 1988; Kovacs et al., 1996). This action was ascribed to a midmolecule domain of PTHrP when calcium transport could be achieved by placental perfusion with PTHrP(67−86) (Care et al., 1990) or PTHrP(38−94) (Wu et al., 1996). The placental calcium transport data were strongly suggestive of a receptor for PTHrP other than PTHR1. This has not been identified, but a 2014 comprehensive review by Kovacs summarizes the role of PTHrP in the process (Kovacs, 2014).

An alternative receptor for PTHrP has also been long suggested from the outcome of pharmacological experiments using its C-terminal portion. Up to residue 111 a remarkable degree of conservation of PTHrP primary sequence is maintained among human, rat, mouse, dog, cow, and rabbit, with some significant divergence in the remainder of the molecule (Martin, 2016). Interest in the C-terminal domain began with the finding that PTHrP(107−139) inhibited osteoclast activity and bone resorption by isolated rat osteoclasts in vitro. That effect was exerted by the pentapeptide TRSAW (residues 107−111), which was then named "osteostatin" (Fenton et al., 1991; Fenton et al. 1991; Fenton et al. 1993). Similar equipotent inhibitory effects were observed in osteoclasts from embryonic chickens using human or chicken PTHrP(107−139), and the human (TRSAW) and chicken (ARSAW) pentapeptides (Fenton et al., 1994). Although injection of PTHrP(107−139) over the calvariae in mice was found to inhibit bone resorption (Cornish et al., 1997), the antiresorptive effect of TRSAW in organ culture has been controversial, with some investigators not finding this effect in vitro (Sone et al., 1992; Kaji et al., 1995; Murrills et al., 1995).

Although no receptor has yet been identified, both TRSAW and PTHrP(107−139) increased protein kinase C activity in rat splenocytes at low picomolar concentrations (Whitfield et al., 1994), with similar actions in ROS 17.2/8 OS cells (Gagnon et al., 1993). The same group of authors reported protein kinase C activation in OS cells by PTH(28−34) and PTHrP(28−34) (Jouishomme et al., 1992; Gagnon et al., 1993). The actions of these peptides on osteoblasts have been difficult to interpret, since in UMR106 OS cells PTHrP(107−139) and TRSAW inhibited proliferation (Valin et al., 1997), whereas both increased proliferation of fetal rat osteoblasts (Cornish et al., 1999). Others reported that PTHrP(107−139) enhanced human osteoblast differentiation (Alonso et al., 2008) and survival (de Gortazar et al., 2006) through interaction with the vascular endothelial growth factor receptor-2.

In addition to these many in vitro observations, some biological effects of TRSAW and PTHrP(107−139) on bone have been reported in vivo. When neonatal mouse bones were labeled with [^{3}H]tetracycline, TRSAW treatment inhibited PTHrP(1−34)-induced bone resorption, indicated by the release of radioactivity (Rihani-Basharat and Lewinson, 1997). Treatment of streptozotocin-diabetic mice with PTHrP(107−139) promoted bone healing after marrow ablation (Lozano et al., 2011), and perhaps most surprising of all these phenomena and very difficult to explain, high doses of PTHrP(1−34) and PTHrP(107−139) were claimed to be similarly effective in treating mice after initiation of ovariectomy-induced bone loss (de Castro et al., 2012).

Among these reported pharmacologic effects of C-terminal PTHrP(107−139) and TRSAW, many of the in vitro findings were dose dependent and made use of control peptides, but the problems remain that there has still been no receptor identified for any such actions, no non-receptor-mediated internalization mechanism described, nor any signaling pathway that could be held responsible. Furthermore, in most of these studies reported in various species, the C-terminal peptide used was predominantly human PTHrP(107−139). The C-terminal domain is the least conserved among species, with only TRSAW being conserved among mammals. It should be noted that in many of the cited studies, the TRSAW peptide reproduced faithfully the effects of PTHrP(107−139). Thus, this short sequence seems likely to be the most important contributor to the host of pharmacologic effects reported, in which case it could provide a pathway to receptor identification. Although there can be no certainty of any physiological implications, possible roles for the C-terminal domain should continue to be sought, and this would include studies in bone.

PTHrP in fetus: early development and endochondral ossification

Studies using immunohistochemistry, in situ hybridization, or northern blot analyses revealed that PTHrP production took place in the early embryo in mouse (van de Stolpe et al., 1993), chicken (Schermer et al., 1991), rat (Senior et al., 1991), and human (Moseley et al., 1991; Dunne et al., 1994).

In the mouse, the temporal and spatial distribution of PTHrP expression has been described in fetal and adult skeletal and extraskeletal tissues such as brain, kidney, lung, heart, liver, small intestine, skin, and skeletal muscle (Kartsogiannis et al., 1997). Similarly, an extensive range of tissue in the rat expressed PTHrP (Campos et al., 1991; Senior et al., 1991; Lee et al., 1995). Analogous profiles of PTHrP expression were also reported in the human fetus (Moniz et al., 1990; Moseley et al., 1991; Dunne et al., 1994). In the fetus at 7−8 weeks of gestation, ectodermal structures strongly positive for PTHrP expression include the epidermis, the otic placode, and the tooth bud (Dunne et al., 1994). PTHrP-expressing tissues of endodermal origin include the lung, liver, pancreas, stomach, intestine, and hindgut, while those of mesodermal origin include the perichondrium and the developing skeleton. In most of these tissues, PTHrP protein seems to be confined to the epithelial layer, while the mRNA is sometimes seen in mesenchymal components (Moseley et al., 1991; Dunne et al., 1994). Later in embryonic development (18−20 weeks of gestation), PTHrP expression is also apparent in cardiac and skeletal muscle, vascular smooth muscle, neural tissues, and areas of both endochondral and intramembranous osteogenesis in the limb buds and calvariae, respectively (Moniz et al., 1990; Moseley et al., 1991; Dunne et al., 1994). The expression of PTHrP was highest in tissues where active growth and differentiation were occurring, thus favoring the idea that PTHrP may be closely associated with the regulation of fetal, and perhaps neonatal, cellular growth and differentiation.

The spatial and temporal distribution of PTHrP associates strongly with that of the PTHR1 (Karperien et al., 1994). The relative expression levels of PTHrP and its receptor are often inversely correlated within a tissue or in certain locales along a border of apposition. Such a tight inverse coupling of expression would seem to imply either feedback downregulation of the receptor or a precise coordinated regulation of the two genes during the course of fetal development (Lee et al., 1996).

With such evidence of production of PTHrP in many tissues throughout fetal life in a number of species, it was perhaps to be expected that functional evidence of a role for PTHrP and its receptor in mammalian fetal development might come from studies of animals that are transgenic or have gene-targeted knockouts; these models, including later cell-specific models, are summarized in Table 25.1. The first evidence of a physiological role for PTHrP came soon after the discovery of PTHrP, with a dramatic phenotype in mice null for the *Pthlh* gene following homologous recombination (Amizuka et al., 1994; Karaplis et al., 1994; Karaplis and Kronenberg, 1996; Lee et al., 1996). Neonatal mice homozygous for *Pthlh* gene ablation exhibited severe skeletal abnormalities at birth and died within 24 h, with their abnormal ribcage development not allowing adequate respiration and this respiratory distress accentuated by reduced surfactant production and impaired type II alveolar cell development. Whereas the nonskeletal organs and tissues of the *Pthlh* homozygous mutant mice appeared grossly normal, the mice at birth had a domed skull, short snout and mandible, protruding tongue, and disproportionately short limbs. Phenotypic abnormalities were evident throughout the endochondral skeleton (axial as well as appendicular), while, in contrast, no abnormality was noted in skeletal structures that develop entirely by intramembranous ossification.

In the growth plates of $Pthlh^{-/-}$ mutant mice there was a marked reduction in the height of the resting and proliferating chondrocyte zones. This resulted from decreased cell division, and was associated with disorganization of the cartilage columns in the hypertrophic zone and altered deposition of matrix molecules such as type II collagen (Karaplis and Kronenberg, 1996). PTHrP thus proved to be necessary for normal chondrocyte proliferation, and the premature maturation of the skeleton was presumably a consequence of the reduced proliferation and accelerated differentiation/premature hypertrophy and apoptosis of growth plate chondrocytes. These findings were substantiated by a study in which transgenic mice overexpressing PTHrP in chondrocytes (using the mouse collagen type II promoter) were found to have an opposing form of short-limbed dwarfism, in which endochondral ossification was significantly delayed as a result of persistent chondrocyte proliferation and spatially and temporally abnormal chondrocyte hypertrophy (Weir et al., 1996). The delay in endochondral ossification was initially so profound that mice were born with cartilaginous endochondral skeletons. However, by 7 weeks of age in the mice overexpressing *Pthlh* in chondrocytes, this delay in chondrocyte differentiation and ossification was largely corrected, leaving foreshortened and misshapen but histologically near-normal bones.

The alterations in chondrocyte differentiation at the growth plate and ultimate histological healing noted in mice transgenically overexpressing PTHrP in chondrocytes (Weir et al., 1996) are reminiscent of those seen in patients with Jansen's metaphyseal chondrodysplasia, a condition arising from constitutive activation of the PTHR1 (Schipani et al. 1995, 1996, 1997) and in transgenic mice with expression of a constitutively active PTHR1 targeted to the growth plate (Schipani et al., 1997). In the latter study, targeted expression of constitutively active PTHR1 corrected at birth the growth plate abnormalities of $Pthlh^{-/-}$ mice and allowed for their prolonged survival. These "rescued" animals lacked tooth eruption and showed premature epiphyseal closure, indicating the requirement of PTHrP in both processes. Therefore, overexpression of *Pthlh* or constitutive activation of the PTHR1 in the growth plate ultimately result in a similar pattern of abnormalities in endochondral bone formation. Even further evidence for the part played by the PTHrP/PTHR1 signaling pathway comes from the study of Blomstrand's chondrodysplasia, a rare syndrome resulting from loss-of-function

TABLE 25.1 Skeletal phenotypes in mouse models of parathyroid hormone (PTH)–related protein and PTH receptor 1 deficiency.

Targeted gene	Manipulation	Lethality	Bone length	Trabecular bone mass	Osteoblasts	Osteoclasts/ resorption	Marrow adipocytes	Cortical bone	Serum calcium	References
Pthlh	*Global deletion*	Neonatal	Short	Low	Normal	High	—	Normal	—	Amizuka et al. (1994); Karaplis et al. (1994)
	Global haploinsufficiency	Viable	—	Low (12 weeks old)	Low	Low	High	Normal	—	Amizuka et al. (1996); Miao et al. (2005)
	Col1Cre	Viable	—	Low (6 weeks old)	Low	Low	Normal	Normal	Normal	Miao et al. (2005)
	Dmp1(10kb)Cre	Viable	Normal	Low (12 weeks old)	Low	Normal	Normal	Size normal, low strength	Normal	Ansari et al. (2017)
Pth1r	*Global deletion*	Embryonic/neonatal (strain dependent)	Short	Less	More	—	—	Thickened	—	Lanske et al. (1996, 1999)
	Col2Cre	—	Short	—	—	—	—	Thickened	Low	Hirai et al. (2015)
	Prrx1Cre	Viable, impaired survival rate	Short	Less (long bones only)	Less	—	—	Thin, less mineralized	Normal	Fan et al. (2016)
	Osx1Cre	Viable	—	—	—	—	—	—	—	Ono et al. (2016)
	Bglap1Cre	Viable	—	—	—	—	—	—	—	Ono et al. (2016)
	Dmp1(8kb)Cre	Viable	—	High	Normal	Low (variable)	—	Normal	—	Delgado-Calle et al. (2017)
	Dmp1(10kb)Cre	Viable	—	High (12 weeks old)	Low?	Low?	—	Thickened (12 weeks old)	—	Saini et al. (2013)

—, not reported; results with question mark indicate that changes were reported to occur, but were not statistically significant.

mutations within the *PTH1R* gene, in which the human syndrome is recapitulated in mice rendered null for *Pth1r* (Wysolmerski et al., 2001).

It was noted that, just as PTHrP and the PTHR1 localize to the growth plate region of long bones, so too does Indian hedgehog (Ihh) (Lanske et al., 1996; Vortkamp et al., 1996). Ihh belongs to the hedgehog family of genes (McMahon, 2000), which is involved in the regulation of *Drosophila* segment polarity and regulates embryonic patterning during development in many organisms (Goodrich et al., 1996; Iwamoto et al., 1999). Overexpression of *Ihh* in developing chick limbs blocked chondrocyte differentiation in a manner similar to that seen with overexpression of *Pthlh* in chondrocytes. The findings of Lanske et al. (Lanske et al., 1996) and Vortkamp et al. (Vortkamp et al., 1996) showed that PTHrP and the PTHR1 form a negative feedback loop with the Ihh pathway to establish the correct spatial and temporal progression of chondrocyte differentiation and thereby determine the rate and extent of long bone formation. In this instance, the role of PTHrP is a paracrine one, making use of activation of the PTHR1 by locally generated PTHrP. Indeed genetically altered mice with PTHR1 deletion targeted to chondrocytes and their progeny using *Col2Cre* or *Prx1Cre* resulted in a similar shortened bone/accelerated chondrocyte differentiation phenotype compared with the global knockout (Hirai et al., 2015; Fan et al., 2016) (see Table 25.1 for comparison). There has been no investigation of possible actions in chondrocyte differentiation of other functional domains of PTHrP or non-PTHR1-mediated actions, since the comparison of these genetically altered mouse models provides substantial evidence that PTHrP regulates chondrocyte differentiation through the PTHR1.

PTHrP in bone after endochondral ossification

The discovery of the crucial part played by PTHrP in endochondral bone formation in development was a dramatic outcome of the earliest mouse genetic studies. Much more was to come though, when the recognition of widespread production of PTHrP led to evidence of its production in bone (Moseley and Gillespie, 1995) (*vide supra).* In this respect, genetically altered mouse models have again played a critical role in identifying stage-specific roles of PTHrP during osteoblast differentiation in regulating bone formation and resorption (Table 25.1, Fig. 25.3).

Major insights into the role of PTHrP in bone were obtained from further studies carried out in heterozygous $Pthlh^{+/-}$ mice. Although homozygous $Pthlh^{-/-}$ mice died soon after birth (Amizuka et al., 1994), heterozygous $Pthlh^{+/-}$ mice survived and, although phenotypically normal at birth, by 3 months of age exhibited a markedly lower trabecular thickness and connectivity, and histomorphometry revealed low bone formation rate and osteoclast surface (Amizuka et al., 1996). In $Pthlh^{+/-}$ mice the number of apoptotic osteoblasts was greater than in controls, and ex vivo culture of bone marrow cells

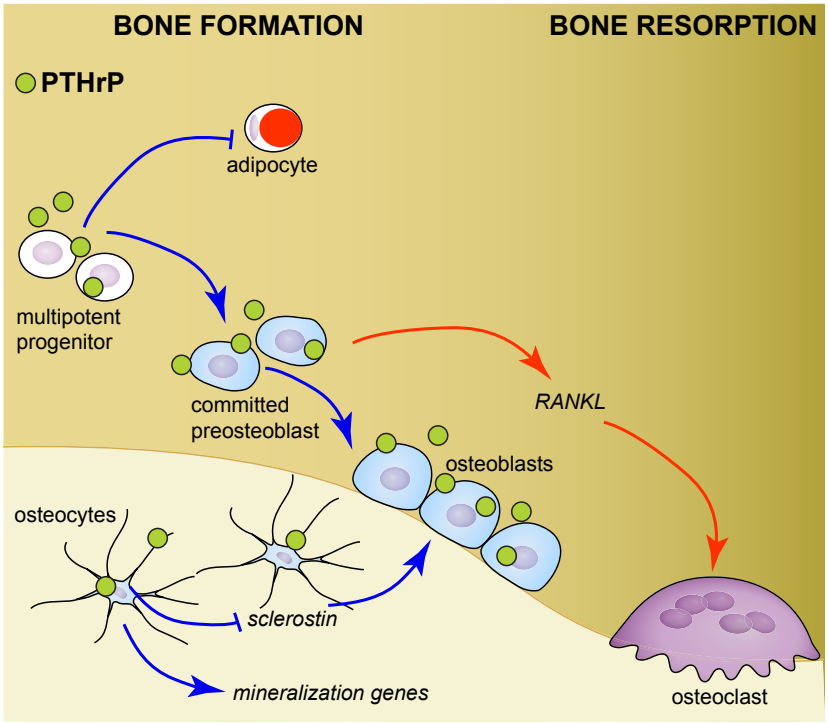

FIGURE 25.3 Stage-specific actions of parathyroid hormone–related protein (*PTHrP*) on the osteoblast and related cell lineages. (1) PTHrP is produced at all stages of osteoblast differentiation. (2) PTHrP acts on multipotent progenitors to inhibit adipogenic differentiation and promote osteoblast differentiation. (3) PTHrP acts on committed osteoblast precursors to promote their continued differentiation to osteoblasts, and promotes their expression of receptor activator of NF-κB ligand (*RANKL*), thereby indirectly stimulating the differentiation of osteoclast precursors to form bone-resorbing osteoclasts. (4) PTHrP acts on mature, bone-forming osteoblasts to promote their bone-forming activity and inhibit their apoptosis. (5) PTHrP acts on osteocytes, resulting in signals that promote bone formation by osteoblasts and signals that maintain mineralization of the bone matrix.

resulted in markedly fewer alkaline phosphatase−positive colonies, indicating impairment of osteogenic cell recruitment and survival. Moreover, *Pthlh*$^{+/-}$ bone marrow contained an abnormally high number of adipocytes. Since the same pluripotent stromal cells in the bone marrow compartment can give rise to adipocytes and osteoprogenitor cells (Owen, 1971), the increased number of adipocytes and osteopenia in these mice could be attributed to preferential development of adipocytes rather than osteoblasts as a consequence of PTHrP haploinsufficiency. Further investigations of the PTHrP mutant mice provided evidence that PTHrP is equally important for the orderly commitment of precursor cells toward the osteogenic lineage and their subsequent maturation and/or function (see Fig. 25.3). In the *Pthlh*$^{+/-}$ mice, osteoblastic progenitor cells (as with chondrocytes) were observed to contain inappropriate accumulations of glycogen, indicative of a defect in cells of the osteogenic lineage arising as a consequence of PTHrP deficiency (Amizuka et al., 1994). The overall conclusion was that PTHrP haploinsufficiency resulted in a low-bone-turnover state with low bone mass resulting from impaired bone formation.

The finding of an osteopenic phenotype in the *Pthlh*$^{+/-}$ mice was sufficiently intriguing to prompt the preparation of mice with osteoblast-specific knockout of *Pthlh* to determine whether it was locally derived PTHrP that was responsible for the low bone mass phenotype. *Col1(2.3kb).Cre* mice were crossed with *Pthlh* floxed mice, resulting in generation of mice that closely reproduced the low-bone-mass phenotype of the earlier *Pthlh*$^{+/-}$ (Miao et al., 2005). Higher levels of osteoblast apoptosis occurred in *Col1(2.3kb).Cre.Pthlh*$^{fl/fl}$ mice than in controls, and histomorphometry showed a low mineral apposition rate, osteoblast number, and osteoid volume, and few osteoclasts. Ex vivo studies showed that precursor cells from these mice were markedly less able to generate osteoblasts. Differences noted between the *Pthlh*$^{+/-}$ and the *Col1(2.3kb).Cre.Pthlh*$^{fl/fl}$ mice were that the latter lacked a marrow adiposity phenotype (Table 25.1). This difference could be explained by the fact that genetic deficiency in the *Pthlh*$^{+/-}$ mice was operative throughout cellular development, whereas in the targeted knockout it came into play at a later stage, after stromal cells had already committed to the osteoblast lineage. The findings in these genetic experiments gave much impetus to the view that locally derived PTHrP, produced by cells in the osteoblast lineage, acts within the lineage to inhibit apoptosis and promote differentiation of committed precursors to become osteoblasts capable of forming bone, and promotes support of osteoclastogenesis by the osteoblast lineage (Fig. 25.3).

The fact that PTHrP protein and mRNA had been noted in osteocytes (Suda et al., 1996; Kartsogiannis et al., 1997), together with the increased awareness of the importance of osteocytes, led to studies that revealed a role for osteocyte-derived PTHrP in bone remodeling, and confirmed suspicions that this might be achieved through autocrine/paracrine mechanisms. First, the effect of disruption of PTHR1 signaling was investigated in *Dmp1Cre.Pth1r*$^{fl/fl}$ mice. This was carried out using two different Cre models: *Dmp1(8kb)Cre* (Delgado-Calle et al., 2017) and *Dmp1(10kb)Cre* (Saini et al., 2013). In contrast to PTHrP deletion, both these PTHR1-deficient models had greater trabecular bone mass than control mice. This phenotype may result from a mild osteopetrosis since both osteoblast and osteoclast surfaces were slightly, but not significantly, lower in the *Dmp1(10kb)Cre.Pth1r* model, and the resorption marker Ctx1 was significantly lower in *Dmp1(8kb)Cre.Pth1r* mice; it does not appear to relate to a high level of bone formation. Furthermore, while both mice showed a blunted anabolic response to intermittent PTH treatment, induction of high circulating PTH levels in the *Dmp1(10kb)Cre.Pth1r* mice by dietary calcium restriction still markedly increased osteoclast formation despite the lack of PTH1R expression in osteocytes. This is consistent with a view that receptor activator of NF-κB ligand (RANKL) production induced through PTHR1 action in less mature osteoblast lineage cells, rather than mature osteoblasts or osteocytes, contributes to osteoclast formation.

The phenotype arising from the osteocyte-specific knockout of PTHrP was strikingly different from the receptor knockout. This was addressed using *Dmp1Cre.Pthlh*$^{f/f}$ mice prepared with the *Dmp1(10kb)Cre*. The mice with PTHrP-deficient osteocytes had low trabecular bone mass with low osteoblast numbers and mineralizing surface, as well as impaired cortical bone strength, indicating a material change in cortical bone matrix (Ansari et al., 2017). This phenotype differed in two important ways from that of *Col1(2.3kb).Cre.Pthlh*$^{fl/fl}$ (Table 25.1). First, the *Dmp1Cre.Pthlh*$^{f/f}$ phenotype was not evident at 6 weeks, but was so at 12 weeks of age, suggesting that while osteoblast-derived PTHrP may play a role in the development of the trabecular network, osteocyte-derived PTHrP is important later in life, when it has a role in remodeling the young adult skeleton. Second, the lack of osteoclast phenotype in the osteocyte-null mice indicated a lesser role for osteocytes in supporting osteoclastogenesis than that for cells earlier in the osteoblast lineage. In addition, the bones from the *Dmp1Cre.Pthlh*$^{f/f}$ mice had impaired bone material strength despite normal size, indicating a role for osteocyte-derived PTHrP in regulating bone composition. PTHrP knockdown, treatment, and overexpression studies in the Ocy454 osteocyte cell line showed that osteocyte-derived PTHrP suppresses sclerostin expression and modifies production of genes known to regulate bone mineralization (*Dmp1*, *Mepe)* (Ansari et al., 2017). This suggests that osteocyte-derived PTHrP not only is physiologically required to promote osteoblast differentiation, but also may regulate the process of bone mineralization, thereby controlling not only bone mass, but also bone strength (Fig. 25.3).

The difference in phenotypes between the high-bone-mass phenotype of the *Dmp1Cre*-driven PTH1R-deficient mice and the low-bone-mass phenotype in *Dmp1Cre*-driven PTHrP ligand−deficient mice suggests that PTHrP could have effects in the osteocyte that are mediated by non-PTH1R-mediated actions. Such noncanonical PTHrP signaling pathways acting in autocrine or paracrine ways have been noted in other cell types, as discussed earlier. The actions of these regions of PTHrP in bone remain poorly defined. Low bone mass, retarded growth, and early senescence (Miao et al., 2008; Toribio et al., 2010) have been reported in knock-in mice expressing PTHrP lacking both its NLS and its C-terminal regions, but retaining the PTHR1-activating N terminus. This provides evidence that these regions are physiologically important. However, the extreme defects in bone growth and development in that model make it difficult to discern their roles in the mature adult skeleton.

Parathyroid hormone−related protein and osteosarcoma

Given the evidence that PTHrP has important roles in osteoblast biology and bone formation, it might have been predicted that it would feature in the pathology of OS. This tumor of the osteoblast lineage is the fifth most common cancer in children and has become a focus of attention, since an improved understanding could lead to new pathways of treatment. We now have evidence from studies of genetically induced OS in the mouse that tumor-derived PTHrP acts in an autocrine/paracrine way in OS to drive its establishment and progression.

Induction of OS in rats with radio-phosphorus injection yielded transplantable tumors that exhibited sensitive dose responsiveness of adenylyl cyclase to PTH activation. PTH-responsive clonal cell lines from those tumors (UMR106 cells) (Partridge et al., 1981) and from a similar rat osteogenic sarcoma (Ros17.2/8 cells) (Majeska et al., 1980) have been used widely in studies of hormone and cytokine actions upon osteoblast-like cells. In that early work, removing the source of PTH by parathyroidectomy had no influence on the growth or on any other aspect of this transplantable OS (Ingleton et al., 1977). These findings came many years before PTHrP was discovered. Subsequent studies in OS cell lines from several species, including human, established that PTHR1 expression is a common, if not universal, feature of OS (e.g., Goerdeladze et al., 1993). Consistent with a pathogenic role for PTHR1 in OS, higher expression of PTHR1 mRNA was detected in metastatic or relapsed human OS samples compared with primary sites, and overexpression of PTHR1 in an OS cell line increased its proliferation and invasion (Yang et al., 2007b).

Although these findings suggested that activation of PTHR1 in OS may promote tumor invasion and proliferation, the role of the receptor signaling or of PTHrP has never been clearly defined. Studies in genetically induced mouse models of OS have pointed to an important pathogenetic role of activation of the cAMP/PKA/CREB pathway in osteoblast lineage cells, driven by autocrine PTHrP acting through the PTHR1 (Ho et al., 2014; Walia et al., 2016). Evidence obtained from human OS is also consistent with this possibility. Although a diverse mutational pattern of single-nucleotide variations has been reported in human OS (Chen et al., 2014), when we compared these proteins known to interact with the cAMP pathway the data suggested that recurrent and enriched changes in the cAMP/CREB pathway occur in osteogenic sarcoma (Walia et al., 2016).

Murine models have been long established for OS, developed from the knockout of genes associated with familial predisposition to OS (such as $p53^{-/-}$; Jacks et al., 1994) or from phenotyping in mutant or transgenic mice (Wang et al., 1995). However, not all cases of murine/rodent OS have proven to be applicable to human OS, with the murine OSs induced by *Nf2* and *Notch1* mutations being key examples (Engin et al., 2008; Mutsaers and Walkley, 2014; Tao et al., 2014; Walia et al., 2018). However, high-fidelity models recapitulating the mutational pattern and phenotypes of human OS have been developed by mesenchymal- and osteoblast-targeted conditional mutant alleles of *p53* and *Rb1,* the key genes implicated in familial OS (Berman et al., 2008; Walkley et al., 2008; Lin et al., 2009; Mutsaers et al., 2013; Quist et al., 2015). These murine models reproduce the cardinal features of the common forms of human OS, where osteoblastic OS is the most common clinical subtype (60%), with fibroblastic and chondroblastic OS comprising about 15% each (Walkley et al., 2008; Mutsaers et al., 2013). The *Osx*-Cre $p53^{fl/fl}pRb^{fl/fl}$ model (osteoblast lineage deletion of *p53*) yields a fibroblastic OS characterized by predominant areas of relatively poorly differentiated (Berman et al., 2008) histology with cells on the surface that appear to be immature osteoblasts (Walkley et al., 2008; Mutsaers et al., 2013). The *Osx*-Cre TRE_shp53.1224$pRb^{fl/fl}$ model (short hairpin RNA [shRNA] knockdown of *p53*) histologically resembles osteoblastic OS, with large mineralized areas and a cell surface phenotype of mature osteoblasts (Mutsaers et al., 2013). The early passage cells from both models have genetic and pharmacological sensitivities comparable to those of primary human patient-derived OS cultures (Baker et al., 2015; Gupte et al., 2015).

In these models of fibroblastic and osteoblastic OS, the primary and metastatic tumors from either subtype all express functional PTHR1. The cultures derived from those models all express PTHrP and PTHR1, and responded to treatment with either PTH or PTHrP with increased adenylyl cyclase activity and consequent increased expression of CREB pathway

genes (Mutsaers et al., 2013; Ho et al., 2014; Walia et al., 2016). Conversely, knockdown of PTHR1 in murine OS (fibroblastic) reduced PTHR1 activation, cAMP responses, and tumor cell invasion in vitro (Ho et al., 2014). Although PTHR1 knockdown resulted in greatly reduced proliferation, the tumor was more mineralized in vivo. PTHrP was present intracellularly in OS cells, but was very low as a secreted protein in culture media.

Osteoblastic OS cells expressed high levels of *Pthlh* transcript (Walia et al., 2016), consistent with our previous data identifying substantial levels of intracellular PTHrP in OS cells (Ho et al., 2014). We showed that PTHrP was an OS autocrine ligand by treating cells with phosphodiesterase inhibitor without adding exogenous PTHrP, thus assaying the cAMP induced by an endogenous ligand(s) of the OS cells. This was confirmed when neutralizing anti-PTHrP antibody reduced cAMP formation, and when shRNAs against *Pthlh* reduced cAMP accumulation by >50%. This indicated that OS-derived PTHrP is an endogenous ligand promoting cAMP accumulation in an autocrine/paracrine manner (Fig. 25.4).

An early consequence of p53 deletion in osteoblastic cells was increased cAMP levels, PTHrP production, and autocrine activation of cAMP signaling via PTHrP (Walia et al., 2016). Activation of the PTHrP/cAMP/CREB1 axis was required for the hyperproliferative phenotype of p53-deficient osteoblasts and the maintenance of established OS, identifying this as a tractable pathway for therapeutic inhibition in OS. In support of this, knockdown of *Pthlh* reduced cell proliferation, reduced CREB phosphorylation and transcription of known CREB target genes, and induced apoptosis (Walia et al., 2016). In vivo, two different fibroblastic OS lines infected with sh-*Pthlh* showed reduced tumor growth that

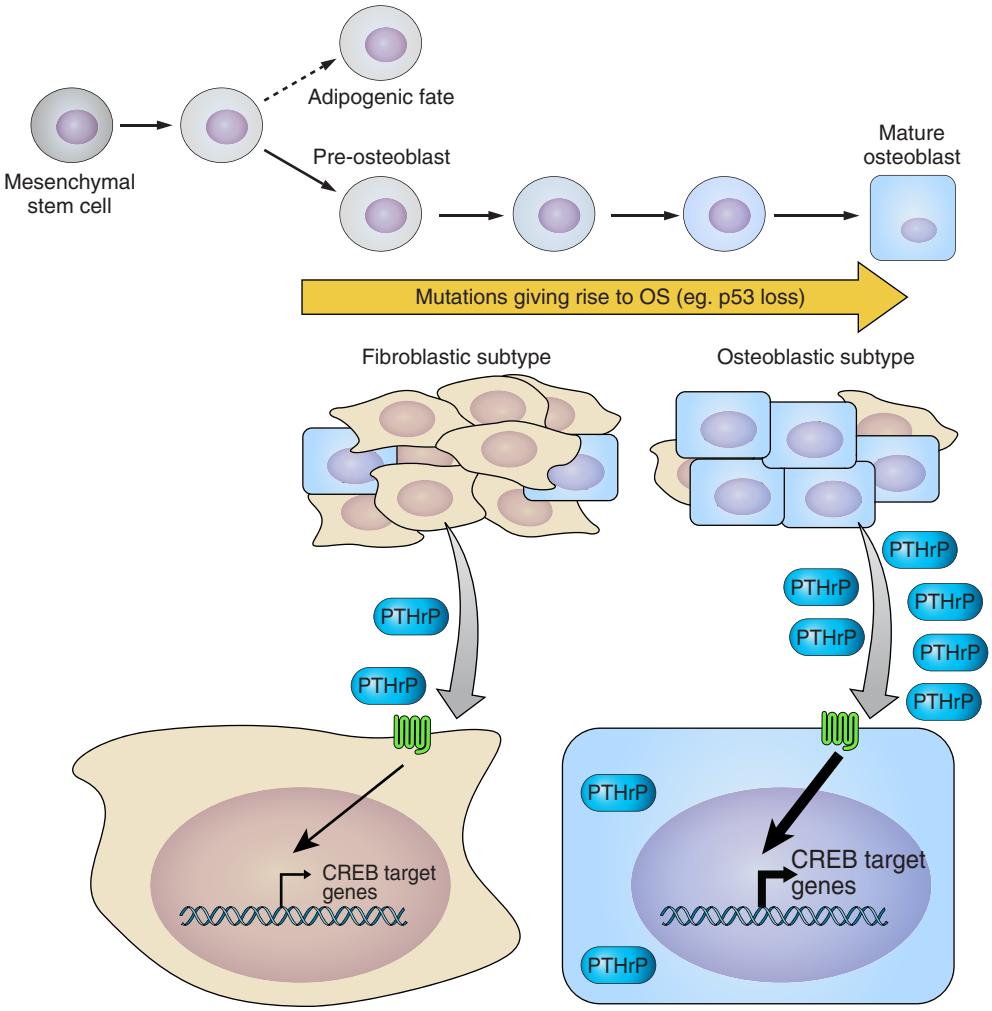

FIGURE 25.4 Actions of parathyroid hormone–related protein (*PTHrP*) in osteosarcoma (*OS*). Mutations giving rise to OS in committed pre-osteoblasts lead to the development of OS of a fibroblastic subtype, which expresses low levels of PTHrP that act through the PTH transmembrane receptor to promote low levels of cAMP-responsive element binding protein (*CREB*) target gene expression. When these mutations occur in more differentiated osteoblasts, this leads to an osteoblastic subtype of OS, which produces high levels of both secreted and intracellular PTHrP, acting in an autocrine/paracrine manner leading to higher levels of CREB target gene expression.

was comparable to the effects of *Pthr1* knockdown in the same OS lines (Ho et al., 2014), providing additional support for the concept that PTHrP is the tumor-derived ligand that promotes PTHR1-dependent OS growth (Fig. 25.4).

The identification of the PTHrP → PTHR1 → CREB-dependent mechanism for OS development may provide an explanation for data showing OS caused by enhanced PKA activity (Molyneux et al., 2010), and suggests that PTHrP → PTHR1 may be an upstream effector of such a pathway (Walia et al., 2016). Such a role extends the involvement of PTHrP in cancer, but in quite a different way compared with that in which it was discovered, as a bone-resorbing factor produced by certain cancers and resulting in hypercalcemia, and possibly also as a paracrine factor contributing to bone metastasis formation.

These data may also have relevance to the high incidence of OS in rats in long-term toxicology studies of any agonist of the PTHR1 (Tashjian and Chabner, 2002). This has resulted in a warning label accompanying these anabolic therapies for bone (Tashjian and Goltzman, 2008). The mechanism of tumor induction in these circumstances is not known. The toxicology study involved daily treatment of Fisher rats from soon after birth to 2 years of age. The high incidence of OS was obtained in rats treated with PTH(1−34) (Vahle et al., 2002), PTH(1−84) (Jolette et al., 2006), and abaloparatide (Jolette et al., 2017). It is conceivable that OS development is related to prolonged stimulation of the PKA/CREB pathway in an animal that might be susceptible to tumor development with such a treatment, but establishing this would require much further work.

Distinct roles of PTH and PTHrP in fetal and postnatal bone

All that has been available in anabolic therapy for the skeleton has been teriparatide (hPTH(1−34)), in use for some years, and now abaloparatide (Tymlos), which is a modified form of PTHrP(1−34) that has been approved by the US FDA. We might make better use of this anabolic pathway if we were to understand better how physiology and pharmacology meet.

A central question of the relative roles of PTH and PTHrP in the regulation of bone remodeling is: to what extent does the hormone PTH contribute to bone remodeling, either directly or indirectly? Further insights into this question came from a series of studies using *Pthlh*, *Pth*, and compound knockout mice.

When *Pth* was ablated in mice, trabecular bone mass in the fetal metaphysis was low compared with controls; in the postnatal state this phenotype reversed, and *Pth*-null mice exhibited high metaphyseal bone mass (Miao et al., 2002). Although this was at first puzzling, a low trabecular bone mass phenotype was then observed when the mice were rendered PTHrP deficient by crossing *Pth*-null mice with $Pthlh^{+/-}$ mice (Miao et al., 2004). In this case PTHrP deficiency prevented the high trabecular bone mass of postnatal PTH-deficient mice, even though the mice were still hypoparathyroid with low serum calcium and high serum phosphate. It was concluded that the PTH-null phenotype of high trabecular bone mass was caused by increased local production of PTHrP; this provided the first indication in vivo for a local role of PTHrP in promoting bone formation.

A comparable series of experiments in older mice provided further insights into the relative roles of PTH and PTHrP in osteogenesis. A model of bone marrow ablation was used (Zhu et al., 2013), in which de novo bone formation precedes resorption during recovery (Suva et al., 1993). When this was carried out in *Pth*-null mice, both osteogenesis and osteoclast formation were delayed and impaired, and *Pthlh* expression in osteoblasts was increased (Zhu et al., 2013). When a similar experiment was carried out in *Pth*-null mice crossed with *Pthlh*-haploinsufficient mice, the response to bone marrow ablation generated fewer osteoblasts, less bone formation, and fewer osteoclasts than in *Pth*-null mice (Zhu et al., 2013). These data suggest a role for PTH in recruiting osteoblast progenitor cells, with locally generated PTHrP being necessary both for further differentiation of osteoblast progenitors to bone-forming osteoblasts and for the generation of osteoclasts.

These genetic experiments point to specific roles for PTH and PTHrP that change between fetal and postnatal environments (Fig. 25.5). In the fetus, ambient calcium is dependent on maternal supply promoted by PTHrP placental action. In the fetus, when PTH promotes osteogenesis, the major function of PTHrP appears to be in directing the sequential controlled proliferation and differentiation of chondrocytes for growth plate development. In the immediate postnatal period, with the major environmental change and the source of nutrient calcium switching from the placenta to the diet, PTH secretion is regulated by extracellular fluid calcium levels, and its action on bone serves primarily to provide calcium to the body by promoting bone resorption. The aforementioned study provided evidence that the other major change in function after birth is that PTHrP becomes the major endogenous stimulus of bone formation, and it does this in a paracrine and possibly an autocrine manner. This is achieved at least partly by action through the PTHR1, but possibly also through actions promoted by other active domains within PTHrP (*vide supra*).

Thus, the anabolic physiological roles of PTH and PTHrP are development and environment dependent. PTH has not been shown to exert a direct physiological anabolic role in the adult animal, where its physiological function rather is the regulation of calcium homeostasis postnatally and in the fetus, and in the latter case is essential in providing calcium for

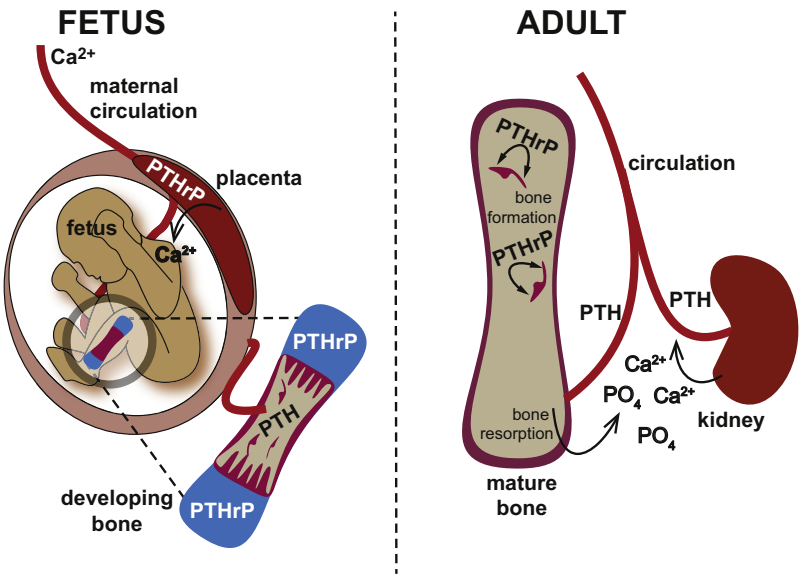

FIGURE 25.5 Roles of parathyroid hormone–related protein (*PTHrP*) and PTH in fetus and adult. Fetal calcium is predominantly provided by the placental action of PTHrP, which is also essential for chondrogenesis. PTH promotes osteogenesis. Postnatally, functions change, with the hormone PTH responsible for calcium homeostasis through actions on the kidney to restrict excretion and through generation of osteoclasts to provide calcium to the extracellular fluid. The bone-forming function is physiologically ascribed to locally generated PTHrP.

mineralization of bone. A hypothesis embracing the relative roles of PTH and PTHrP is that the hormone, PTH, governs osteogenesis through PTHR1 in the fetus and newborn, while PTHrP governs chondrocyte differentiation. The paracrine/autocrine action of PTHrP on bone becomes important when remodeling supervenes sometime after birth, and this role is maintained in the mature skeleton.

PTH and PTHrP in adult bone: PTHrP in physiology and PTH in pharmacology

The observation that physiological functions of PTHrP are carried out by local generation and action made it important to understand the nature of PTHrP released locally in bone and thus available for autocrine and paracrine actions. In discussing processing of PTHrP in an earlier section (*vide supra*) we reviewed early work in neuroendocrine cells that showed PTHrP is subject to the regulated secretory pathway, thereby generating PTHrP(1–36), midterminal peptides, and a C-terminal sequence. Although that might be true of cells that are capable of using the regulated secretory pathway, it would not be expected of mesenchymal cells such as those within the osteoblast lineage.

Accordingly, in studying the role of osteocyte-derived PTHrP, we used knockdown of PTHrP in the immortalized osteocyte cell line Ocy454 to show that PTHrP derived from those cells acts upon PTHR1 in the same cells in an autocrine/paracrine manner to activate adenylyl cyclase and modify gene expression (Ansari et al., 2017). In the same series of experiments full-length and mutant constructs of PTHrP were expressed in the osteocytes, secretion of biologically active PTHrP was established, and a combination of bioassay, radioimmunoassay, and chromatographic and electrophoretic separation methods was used to show that the only protein released from those cells and able to act through PTHR1 was PTHrP of full length. This might not be surprising, given the mesenchymal origin of cells of the osteoblast lineage, which would be expected to use the constitutive pathway of secretion, without the packaging and processing ability inherent in the regulated secretory pathway.

The importance of the observations, though, is that they identify full-length PTHrP as the most likely locally active material released in bone and available to act on the same or nearby cells. Among the questions that this leads to are: (1) does full-length PTHrP interact with the receptor PTHR1 in any unique way that distinguishes it from shorter forms used pharmacologically, (2) do other domains within the PTHrP molecule contribute to actions locally in bone, and (3) what significance might this have for the pharmacological use of peptide analogs that are based to some extent on PTHrP?

The discovery of the role of paracrine/autocrine PTHrP in bone remodeling underlies the thought that has been harbored for some time, that the anabolic action of intermittent (daily) treatment with PTH for osteoporosis mimics pharmacologically the physiological action of PTHrP. That anabolic action is predominantly remodeling based (Lindsay et al., 2006; Ma et al., 2006), with the effect of therapeutic PTH being to promote the recruitment of new basic multicellular units (BMUs) and enhance the activity of those already in progress (Fig. 25.6). Overfilling of BMUs (Compston, 2007), and perhaps also some effect on modeling through activation of lining cells (Kim et al., 2012), results in increased bone

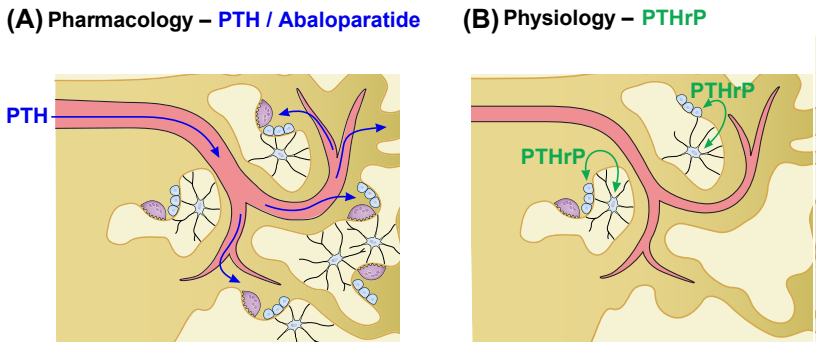

FIGURE 25.6 Physiological actions of parathyroid hormone–related protein (*PTHrP*) versus pharmacologic actions of PTH (teriparatide) and abaloparatide. (A) Pharmacologic administration of intermittent injections of PTH (teriparatide) or abaloparatide provide brief bursts of high systemic levels of these agents that act through the PTH receptor to stimulate bone remodeling at multiple basic multicellular units (BMUs) throughout the skeleton. (B) Physiologically, PTHrP is not provided through the bloodstream, but is provided locally, and stimulates active BMUs at those sites at which they are needed and active.

mass. The cellular actions of exogenous PTH administration are to promote osteoblast differentiation, prevent osteoblast and osteocyte apoptosis, and reduce osteocyte production of the bone formation inhibitor, sclerostin (Jilka, 2007; Martin, 2016). Although PTH promotes bone resorption by stimulating RANKL expression in osteoblasts, in the context of intermittent administration, PTH action on osteoclasts is probably confined to the recruitment of osteoclasts for the initiation of new BMUs, because of the brief exposure of cells to PTH. In contrast, prolonged activation of PTHR1 results in a net greater effect on osteoclast formation and activity. Early experimental evidence for this was obtained in rats using treatment with several different intermittent PTH(1−34) injection schedules and continuous infusion (Frolik et al., 2003). The pharmacokinetic profile and outcome data showed that an anabolic outcome required a short period of elevation of plasma PTH, whereas a catabolic outcome was associated with prolonged elevation of PTH levels.

It is easy to see how PTH given pharmacologically by intermittent injection can mimic the effects of local PTHrP to promote bone formation that take place through the PTH1R, since all these effects of anabolic PTH have been ascribed to locally generated PTHrP (Fig. 25.6). Nevertheless, if the anabolic action of PTHrP is modified in any way, or mediated in part by non-receptor-mediated actions in addition to PTHR1-mediated actions, some differences might be expected. In that case discovering how noncanonical actions might signal through osteoblastic cells could provide ways to optimize PTH-based therapies.

A question related to this concerns the interpretation of experimental data obtained by the treatment of cells in vitro with PTHR1 agonists. Over decades there have been very many published effects of treatment of cells in vitro with PTH, e.g., on gene expression and/or protein production. Although these are often taken to indicate that such pharmacological actions reflect physiological actions of PTH in vivo, evidence for such a physiological role is invariably lacking. In such circumstances, the possibility should be considered that such effects might reflect physiological roles of PTHrP. Some examples in which this might be considered are the PTH promotion of glycolysis in osteoblast lineage cells (Esen et al., 2015), PTH inhibition of salt-induced kinase in osteocytes (Wein et al., 2016), and the finding in osteoblast precursor lineage tracing experiments in mice that PTHR1 is required for the PTH-mediated increase and suppression of apoptosis in early osteoblast precursors without any effect on their rate of proliferation (Balani et al., 2017). If these effects are also induced by physiological PTHrP, this provides further information on how this protein functions in the normal adult skeleton.

Since bone remodeling takes place asynchronously throughout the skeleton at sites where it is needed to replace old or damaged bone and to respond to loading and unloading, it is obvious that the control of remodeling needs to be very local. It might be argued that local PTHrP release would need to be very tightly regulated so that in bone remodeling it is presented only briefly to its target cells so that bone formation is promoted, rather than stimulating both bone formation and resorption. Excessive osteoclast formation in response to PTHrP is unlikely in the context of normal physiological remodeling, where (1) BMUs are active at any one time only in those places in which they are required (Fig. 25.6) and (2) where only osteoblast-derived, and not osteocyte-derived, PTHrP promotes osteoclast formation, as evidenced by the comparison of the cell-specific PTHrP-null mice (see earlier and Table 25.1).

Can changes in the level of the circulating hormone, PTH, exert any fine controlling influence upon these processes that take place asynchronously, scattered throughout the skeleton in virtually a stochastic manner? There have been studies that suggest that circulating PTH levels vary in a circadian manner in human subjects. The changes in circulating levels of PTH in those studies were consistently at a maximum of about 40% and within the normal circulation range of 2−6 pmol/L (Fraser et al., 1998; Rejnmark et al., 2002; Joseph et al., 2007). In one such study (Logue et al., 1989) the late night/early morning increase in plasma PTH rose in parallel with nephrogenous cAMP, suggesting the change in PTH may be sufficient to produce an appropriate response in the kidney target. It remains difficult to envisage how such changes in

circulating PTH could bring about initiation of BMUs at sites of need scattered throughout the skeleton. These comments do not apply to situations of PTH excess. Persistent elevation of circulating PTH resulting from primary hyperparathyroidism, from prolonged PTH treatment, or from transgenic overexpression in mice results in a generalized activation of remodeling sites and therefore increased resorption.

PTHrP analogs in pharmacology: could this change the approach to skeletal anabolic therapy?

Studies of the anabolic effect of PTHrP(1−36) in human subjects had their origin in the view that amino-terminal PTHrP is the paracrine ligand for PTHR1 in bone (Wu et al., 1996). The susceptibility of full-length protein to proteolysis (Orloff et al., 1989; Diefenbach-Jagger et al., 1995) precluded its use for this application, so preclinical experiments tested several truncated forms as anabolic agents, including PTHrP(1−34), PTHrP(1−36), and PTHrP(1−74). From the earliest of these studies in the rat (Hock et al., 1989) it was evident that these PTHrP preparations exerted anabolic effects, but were significantly less potent in vivo than PTH, although the two are equally active in promoting cAMP production in vitro. Such a lesser potency in vivo could be anticipated because even these truncated forms of PTHrP have many target sequences that are susceptible to proteolysis (Fig. 25.1). The anabolic action of PTHrP(1−36) in human subjects has been investigated extensively by Stewart and colleagues (Horwitz et al. 2003, 2006, 2010, 2011, 2013; Augustine and Horwitz, 2013). The daily dose of PTHrP(1−36) in human subjects required to increase bone formation markers was manifold higher than the dose of teriparatide needed to achieve these marker levels (Augustine and Horwitz, 2013; Horwitz et al., 2013), probably due to the proteolytic cleavage described earlier. The higher dose requirements might be due to a difference in pharmacokinetics, with PTHrP(1−36) degraded more rapidly following injection, and thus not so widely distributed to activate BMUs. The result would be that lesser amounts of active agonist would be available to the receptor.

Early studies by Stewart and colleagues suggested that PTHrP(1−36) action was relatively free of a resorptive effect as determined by measuring serum biochemical markers of bone formation and resorption. Similar claims have been made for abaloparatide (Leder et al., 2015; Miller et al., 2016), which is a 34-amino-acid peptide in which the first 21 residues are identical with PTHrP. Abaloparatide also contains a number of substitutions that were planned to improve stability (Dong et al., 2001; Hattersley et al., 2016), though the most susceptible of the PTHrP cleavage sites ($-R_{19}R_{20}R_{21}-$) is located within both PTHrP(1−36) and abaloparatide. Abaloparatide (80 μg per day) and teriparatide (20 μg per day) have been reported to have comparable anti-fracture efficacy in the vertebrae, with claims based on biochemical marker data of a greater net bone formation due to a lesser effect on bone resorption marker with abaloparatide than with teriparatide (Dong et al., 2001; Leder et al., 2015; Hattersley et al., 2016). In the same data, the formation marker level was also less with abaloparatide (Dong et al., 2001), so the claim of a lesser effect on resorption might not be soundly based. There remains no information on the cellular basis by which PTHrP(1−36) or abaloparatide could have a lesser effect on bone resorption than formation.

The structural features of abaloparatide have led to it being called a PTHrP analog that is a selective activator of the PTHR1 receptor (Dong et al., 2001; Leder et al., 2015; Hattersley et al., 2016), with adenylyl cyclase assay data showing it to be equipotent with teriparatide. Despite this equivalence, when PTH(1−34) and PTHrP(1−36) were compared for their initial receptor interaction mechanisms, the action of PTHrP(1−36) was restricted to the cell surface, while PTHrP(1−34) was more readily internalized and brought about a somewhat more prolonged increase in cAMP in the target cells through continued endosomal signaling (Ferrandon et al., 2009) (Gardella and Vilardaga, 2015). Similar findings were obtained with abaloparatide (Hattersley et al., 2016), leading to this being suggested as a mechanism by which PTHrP(1−36) and abaloparatide might lead to a lesser resorption response than that with PTH(1−34). These in vitro findings of differing initial interactions of the peptides with receptor have not been taken beyond the stage of cAMP generation. It is difficult to extrapolate them to explain the purportedly different in vivo effects on bone resorption given the lack of evidence of differences in cellular effects beyond cAMP generation in vitro, e.g., on gene expression.

Without information to the contrary it might be assumed that any anabolic action of abaloparatide is through a mechanism shared with teriparatide—predominantly activation of remodeling sites. The possibility of either PTHrP(1−36) or abaloparatide being anabolic and resorption sparing would be an intriguing one, if very difficult to explain. Given that resorption is an inescapable first phase of BMU-based bone remodeling, it is not easy to see how an anabolic effect equivalent to that of teriparatide could be obtained while sparing resorption. The nature of the question is such that it could be resolved only by the use of histomorphometry such as that used to show the predominantly modeling effect of teriparatide when used as an anabolic agent (Lindsay et al., 2006; Ma et al., 2006). A more likely explanation might lie in the pharmacokinetics, with a lesser potency of abaloparatide in vivo because of proteolytic degradation, and less of the agonist being presented to the receptor.

Abaloparatide offers an interesting new approach to anabolic therapy that merits much further understanding of mechanisms. If it can be regarded as a "PTHrP analog," it might be instructive in revealing aspects of the actions of the PTHrP N-terminal domain on target bone cells. The findings indicating full-length PTHrP as the locally generated secreted product highlight the need to consider also the possibility of other PTHrP actions in bone, especially through noncanonical pathways. It has always been assumed that all that is required of PTHrP is that it exerts its activity through acting on the PTHR1. That might not be so, however, in light of the increasing awareness of noncanonical actions of PTHrP.

Conclusion

We have been learning since the 1980s how PTH and PTHrP share a common receptor in many tissues. The current concept is that the hormone PTH regulates calcium homeostasis in development and maturity. PTHrP provides calcium to the developing fetus through its placental calcium transport action, and its local expression directs growth plate development by controlling chondrocyte proliferation and differentiation. Postnatally, PTH assumes the role of supplying calcium by stimulating bone resorption, while PTHrP is the main factor generated locally in bone and controls bone remodeling, without normally contributing to the maintenance of serum calcium. In maturity calcium homeostasis is the sole domain of PTH. Whether PTH physiologically regulates bone formation in maturity remains to be established in human subjects. These views have developed largely as a result of the insights provided from mouse genetic experiments, but much is owed also to pharmacological studies in animals and to the therapeutic efficacy of PTH in the treatment of osteoporosis.

The susceptibility of PTHrP to posttranslational processing is a striking feature of the molecule that results in the generation of a number of peptide components, some of which have been shown to have biological activities that do not require the PTHR1, leading it to be considered as a polyfunctional cytokine. The search for the presumed receptors of these peptides and the identification of the circulating peptide isoforms obviously needs to continue. Such investigation provides attractive challenges, as does the aim of determining the function of nuclear PTHrP. The nuclear role(s) and the susceptibility of PTHrP to proteolysis, together with the lability of PTHrP mRNA and the multiple splice forms, may be the result of evolutionary pressures that equip PTHrP to function as a paracrine agent, as it does in so many tissues.

When used as a skeletal anabolic therapy, PTH appears simply to be reproducing the local physiologic action of PTHrP. The great susceptibility of PTHrP to proteolytic degradation makes it unsuitable as a therapy itself. The possibility is raised in this chapter that domains of PTHrP other than that acting through PTHR1 might contribute to the action on bone. If that were so, the signaling pathways involved could be of interest therapeutically. In the meantime, the use of analogs of PTH and PTHrP that act through PTHR1 are the subject of attention, and much can be learned of the anabolic process through their use.

Acknowledgments

The authors acknowledge research support from the National Health and Medical Research Council (Australia) and the Victorian Government OIS Program.

References

Aarts, M.M., Davidson, D., Corluka, A., Petroulakis, E., Guo, J., Bringhurst, F.R., Galipeau, J., Henderson, J.E., 2001. Parathyroid hormone-related protein promotes quiescence and survival of serum-deprived chondrocytes by inhibiting rRNA synthesis. J. Biol. Chem. 276 (41), 37934–37943.

Aarts, M.M., Levy, D., He, B., Stregger, S., Chen, T., Richard, S., Henderson, J.E., 1999a. Parathyroid hormone-related protein interacts with RNA. J. Biol. Chem. 274 (8), 4832–4838.

Aarts, M.M., Rix, A., Guo, J., Bringhurst, R., Henderson, J.E., 1999b. The nucleolar targeting signal (NTS) of parathyroid hormone related protein mediates endocytosis and nucleolar translocation. J. Bone Miner. Res. 14 (9), 1493–1503.

Abbas, S.K., Pickard, D.W., Rodda, C.P., Heath, J.A., Hammonds, R.G., Wood, W.I., Caple, I.W., Martin, T.J., Care, A.D., 1989. Stimulation of ovine placental calcium transport by purified natural and recombinant parathyroid hormone-related protein (PTHrP) preparations. Q. J. Exp. Physiol. 74 (4), 549–552.

Albright, F., 1941. Case records of the Massachisetts general hospital – case 39061. N. Engl. J. Med. 225, 789–796.

Alonso, V., de Gortazar, A.R., Ardura, J.A., Andrade-Zapata, I., Alvarez-Arroyo, M.V., Esbrit, P., 2008. Parathyroid hormone-related protein (107–139) increases human osteoblastic cell survival by activation of vascular endothelial growth factor receptor-2. J. Cell. Physiol. 217 (3), 717–727.

Amizuka, N., Fukushi-Irie, M., Sasaki, T., Oda, K., Ozawa, H., 2000. Inefficient function of the signal sequence of PTHrP for targeting into the secretory pathway. Biochem. Biophys. Res. Commun. 273 (2), 621–629.

Amizuka, N., Karaplis, A.C., Henderson, J.E., Warshawsky, H., Lipman, M.L., Matsuki, Y., Ejiri, S., Tanaka, M., Izumi, N., Ozawa, H., Goltzman, D., 1996. Haploinsufficiency of parathyroid hormone-related peptide (PTHrP) results in abnormal postnatal bone development. Dev. Biol. 175 (1), 166–176.

Amizuka, N., Warshawsky, H., Henderson, J.E., Goltzman, D., Karaplis, A.C., 1994. Parathyroid hormone-related peptide-depleted mice show abnormal epiphyseal cartilage development and altered endochondral bone formation. J. Cell Biol. 126 (6), 1611–1623.

Ansari, N., Ho, P., Crimeen-Irwin, B., Poulton, I.J., Brunt, A.R., Forwoof, M.R., VDivieti Pajevic, P., Gooi, J., Martin, T.J., Sims, N.A., 2017. Autocrine and paracrine regulation of the murine skeleton by osteocyte -derived parathyroid hormone-related protein. J. Bone Miner. Res. https://doi.org/10.1002/jbmr.3291.

Augustine, M., Horwitz, M.J., 2013. Parathyroid hormone and parathyroid hormone-related protein analogs as therapies for osteoporosis. Curr. Osteoporos. Rep. 11 (4), 400–406.

Baker, E.K., Taylor, S., Gupte, A., Sharp, P.P., Walia, M., Walsh, N.C., Zannettino, A.C., Chalk, A.M., Burns, C.J., Walkley, C.R., 2015. BET inhibitors induce apoptosis through a MYC independent mechanism and synergise with CDK inhibitors to kill osteosarcoma cells. Sci. Rep. 5, 10120.

Balani, D.H., Ono, N., Kronenberg, H.M., 2017. Parathyroid hormone regulates fates of murine osteoblast precursors in vivo. J. Clin. Investig. 127 (9), 3327–3338.

Benson Jr., R.C., Riggs, B.L., Pickard, B.M., Arnaud, C.D., 1974. Immunoreactive forms of circulating parathyroid hormone in primary and ectopic hyperparathyroidism. J. Clin. Investig. 54 (1), 175–181.

Berman, S.D., Calo, E., Landman, A.S., Danielian, P.S., Miller, E.S., West, J.C., Fonhoue, B.D., Caron, A., Bronson, R., Bouxsein, M.L., Mukherjee, S., Lees, J.A., 2008. Metastatic osteosarcoma induced by inactivation of Rb and p53 in the osteoblast lineage. Proc. Natl. Acad. Sci. U.S.A. 105 (33), 11851–11856.

Berson, S.A., Yalow, R.S., 1966. Parathyroid hormone in plasma in adenomatous hyperparathyroidism, uremia, and bronchogenic carcinoma. Science 154 (3751), 907–909.

Briggs, L.J., Johnstone, R.W., Elliot, R.M., Xiao, C.Y., Dawson, M., Trapani, J.A., Jans, D.A., 2001. Novel properties of the protein kinase CK2-site-regulated nuclear- localization sequence of the interferon-induced nuclear factor IFI 16. Biochem. J. 353 (Pt 1), 69–77.

Bruns, M.E., Ferguson 2nd, J.E., Bruns, D.E., Burton, D.W., Brandt, D.W., Juppner, H., Segre, G.V., Deftos, L.J., 1995. Expression of parathyroid hormone-related peptide and its receptor messenger ribonucleic acid in human amnion and chorion-decidua: implications for secretion and function. Am. J. Obstet. Gynecol. 173 (3 Pt 1), 739–746.

Burgess, T.L., Kelly, R.B., 1987. Constitutive and regulated secretion of proteins. Annu. Rev. Cell Biol. 3, 243–293.

Burtis, W.J., Brady, T.G., Orloff, J.J., Ersbak, J.B., Warrell Jr., R.P., Olson, B.R., Wu, T.L., Mitnick, M.E., Broadus, A.E., Stewart, A.F., 1990. Immunochemical characterization of circulating parathyroid hormone-related protein in patients with humoral hypercalcemia of cancer. N. Engl. J. Med. 322 (16), 1106–1112.

Campos, R.V., Asa, S.L., Drucker, D.J., 1991. Immunocytochemical localization of parathyroid hormone-like peptide in the rat fetus. Cancer Res. 51 (23 Pt 1), 6351–6357.

Care, A.D., Abbas, S.K., Pickard, D.W., Barri, M., Drinkhill, M., Findlay, J.B., White, I.R., Caple, I.W., 1990. Stimulation of ovine placental transport of calcium and magnesium by mid-molecule fragments of human parathyroid hormone-related protein. Exp. Physiol. 75 (4), 605–608.

Charbon, G.A., 1968. A rapid and selective vasodialtor effect of parathyroid hormone. Eur. J. Pharmacol. 3 (3), 275–278.

Charbon, G.A., Hulstaert, P.F., 1974. Augmentation of arterial hepatic and renal flow by extracted and synthetic parathyroid hormone. Endocrinology 96 (2), 621–626.

Chen, X., Bahrami, A., Pappo, A., Easton, J., Dalton, J., Hedlund, E., Ellison, D., Shurtleff, S., Wu, G., Wei, L., Parker, M., Rusch, M., Nagahawatte, P., Wu, J., Mao, S., Boggs, K., Mulder, H., Yergeau, D., Lu, C., Ding, L., Edmonson, M., Qu, C., Wang, J., Li, Y., Navid, F., Daw, N.C., Mardis, E.R., Wilson, R.K., Downing, J.R., Zhang, J., Dyer, M.A., P. St Jude Children's Research Hospital-Washington University Pediatric Cancer Genome, 2014. Recurrent somatic structural variations contribute to tumorigenesis in pediatric osteosarcoma. Cell Rep. 7 (1), 104–112.

Cingolani, G., Bednenko, J., Gillespie, M.T., Gerace, L., 2002. Molecular basis for the recognition of a nonclassical nuclear localization signal by importin beta. Mol. Cell 10 (6), 1345–1353.

Compston, J.E., 2007. Skeletal actions of intermittent parathyroid hormone: effects on bone remodelling and structure. Bone 40 (6), 1447–1452.

Cornish, J., Callon, K.E., Lin, C., Xiao, C., Moseley, J.M., Reid, I.R., 1999. Stimulation of osteoblast proliferation by C-terminal fragments of parathyroid hormone-related protein. J. Bone Miner. Res. 14 (6), 915–922.

Cornish, J., Callon, K.E., Nicholson, G.C., Reid, I.R., 1997. Parathyroid hormone-related protein-(107-139) inhibits bone resorption in vivo. Endocrinology 138 (3), 1299–1304.

de Castro, L.F., Lozano, D., Portal-Nunez, S., Maycas, M., De la Fuente, M., Caeiro, J.R., Esbrit, P., 2012. Comparison of the skeletal effects induced by daily administration of PTHrP (1-36) and PTHrP (107-139) to ovariectomized mice. J. Cell. Physiol. 227 (4), 1752–1760.

de Gortazar, A.R., Alonso, V., Alvarez-Arroyo, M.V., Esbrit, P., 2006. Transient exposure to PTHrP (107-139) exerts anabolic effects through vascular endothelial growth factor receptor 2 in human osteoblastic cells in vitro. Calcif. Tissue Int. 79 (5), 360–369.

de Miguel, F., Fiaschi-Taesch, N., Lopez-Talavera, J.C., Takane, K.K., Massfelder, T., Helwig, J.J., Stewart, A.F., 2001. The C-terminal region of PTHrP, in addition to the nuclear localization signal, is essential for the intracrine stimulation of proliferation in vascular smooth muscle cells. Endocrinology 142 (9), 4096–4105.

Delgado-Calle, J., Tu, X., Pacheco-Costa, R., McAndrews, K., Edwards, R., Pellegrini, G.G., Kuhlenschmidt, K., Olivos, N., Robling, A., Peacock, M., Plotkin, L.I., Bellido, T., 2017. Control of bone anabolism in response to mechanical loading and PTH by distinct mechanisms downstream of the PTH receptor. J. Bone Miner. Res. 32 (3), 522–535.

Diefenbach-Jagger, H., Brenner, C., Kemp, B.E., Baron, W., McLean, J., Martin, T.J., Moseley, J.M., 1995. Arg21 is the preferred kexin cleavage site in parathyroid-hormone-related protein. Eur. J. Biochem. 229 (1), 91–98.

Dong, J., Shen, Y., Culler, M., JE, C.-W., Woon, J.-J., Legrand, B., Morgan, M., Chorev, M., Rosenblatt, Nakamoto, C., Moreau, J., 2001. Highly potent analogs of human parathyroid hormone and human parathyroid hormone-related protein. In: Houghten, M.L.a.R. (Ed.), Peptides: The Wave of the Future. American Peptide Society, USA, pp. 668–669.

Dunne, F.P., Ratcliffe, W.A., Mansour, P., Heath, D.A., 1994. Parathyroid hormone related protein (PTHrP) gene expression in fetal and extra-embryonic tissues of early pregnancy. Hum. Reprod. 9 (1), 149–156.

Engin, F., Yao, Z., Yang, T., Zhou, G., Bertin, T., Jiang, M.M., Chen, Y., Wang, L., Zheng, H., Sutton, R.E., Boyce, B.F., Lee, B., 2008. Dimorphic effects of Notch signaling in bone homeostasis. Nat. Med. 14 (3), 299–305.

Esen, E., Lee, S.Y., Wice, B.M., Long, F., 2015. PTH promotes bone anabolism by stimulating aerobic glycolysis via IGF signaling. J. Bone Miner. Res. 30 (11), 1959–1968.

Fan, Y., Bi, R., Densmore, M.J., Sato, T., Kobayashi, T., Yuan, Q., Zhou, X., Erben, R.G., Lanske, B., 2016. Parathyroid hormone 1 receptor is essential to induce FGF23 production and maintain systemic mineral ion homeostasis. FASEB J. 30 (1), 428–440.

Fenton, A.J., Kemp, B.E., Hammonds Jr., R.G., Mitchelhill, K., Moseley, J.M., Martin, T.J., Nicholson, G.C., 1991a. A potent inhibitor of osteoclastic bone resorption within a highly conserved pentapeptide region of parathyroid hormone-related protein; PTHrP[107-111]. Endocrinology 129 (6), 3424–3426.

Fenton, A.J., Kemp, B.E., Kent, G.N., Moseley, J.M., Zheng, M.H., Rowe, D.J., Britto, J.M., Martin, T.J., Nicholson, G.C., 1991b. A carboxyl-terminal peptide from the parathyroid hormone-related protein inhibits bone resorption by osteoclasts. Endocrinology 129 (4), 1762–1768.

Fenton, A.J., Martin, T.J., Nicholson, G.C., 1993. Long-term culture of disaggregated rat osteoclasts: inhibition of bone resorption and reduction of osteoclast-like cell number by calcitonin and PTHrP[107-139]. J. Cell. Physiol. 155 (1), 1–7.

Fenton, A.J., Martin, T.J., Nicholson, G.C., 1994. Carboxyl-terminal parathyroid hormone-related protein inhibits bone resorption by isolated chicken osteoclasts. J. Bone Miner. Res. 9 (4), 515–519.

Ferrandon, S., Feinstein, T.N., Castro, M., Wang, B., Bouley, R., Potts, J.T., Gardella, T.J., Vilardaga, J.P., 2009. Sustained cyclic AMP production by parathyroid hormone receptor endocytosis. Nat. Chem. Biol. 5 (10), 734–742.

Fiaschi-Taesch, N., Sicari, B., Ubriani, K., Cozar-Castellano, I., Takane, K.K., Stewart, A.F., 2009. Mutant parathyroid hormone-related protein, devoid of the nuclear localization signal, markedly inhibits arterial smooth muscle cell cycle and neointima formation by coordinate up-regulation of p15Ink4b and p27kip1. Endocrinology 150 (3), 1429–1439.

Fraser, W.D., Logue, F.C., Christie, J.P., Gallacher, S.J., Cameron, D., O'Reilly, D.S., Beastall, G.H., Boyle, I.T., 1998. Alteration of the circadian rhythm of intact parathyroid hormone and serum phosphate in women with established postmenopausal osteoporosis. Osteoporos. Int. 8 (2), 121–126.

Frolik, C.A., Black, E.C., Cain, R.L., Satterwhite, J.H., Brown-Augsburger, P.L., Sato, M., Hock, J.M., 2003. Anabolic and catabolic bone effects of human parathyroid hormone (1-34) are predicted by duration of hormone exposure. Bone 33 (3), 372–379.

Gagnon, L., Jouishomme, H., Whitfield, J.F., Durkin, J.P., MacLean, S., Neugebauer, W., Willick, G., Rixon, R.H., Chakravarthy, B., 1993. Protein kinase C-activating domains of parathyroid hormone-related protein. J. Bone Miner. Res. 8 (4), 497–503.

Garcia-Martin, A., Ardura, J.A., Maycas, M., Lozano, D., Lopez-Herradon, A., Portal-Nunez, S., Garcia-Ocana, A., Esbrit, P., 2014. Functional roles of the nuclear localization signal of parathyroid hormone-related protein (PTHrP) in osteoblastic cells. Mol. Endocrinol. 28 (6), 925–934.

Gardella, T.J., Vilardaga, J.P., 2015. International Union of Basic and Clinical Pharmacology. XCIII. The parathyroid hormone receptors-family B G protein-coupled receptors. Pharmacol. Rev. 67 (2), 310–337.

Goerdeladze, J., Jablonski, G., Paulssen, R., Mortensen, B., Gutvik, K., Haug, E., Rian, E., Jemtland, R., Friedman, E., Bruland, O., 1993. In: Frontiers in osteosarcoma research, Novak, J.F., McMaster, J.H. (Eds.), G-protein Coupled Signaling in Osteosarcoma Cell Lines. Hogref and Huber, Seattle, Toronto, pp. 297–308.

Goodrich, L.V., Johnson, R.L., Milenkovic, L., McMahon, J.A., Scott, M.P., 1996. Conservation of the hedgehog/patched signaling pathway from flies to mice: induction of a mouse patched gene by Hedgehog. Genes Dev. 10 (3), 301–312.

Grill, V., Ho, P., Body, J.J., Johanson, N., Lee, S.C., Kukreja, S.C., Moseley, J.M., Martin, T.J., 1991. Parathyroid hormone-related protein: elevated levels in both humoral hypercalcemia of malignancy and hypercalcemia complicating metastatic breast cancer. J. Clin. Endocrinol. Metab. 73 (6), 1309–1315.

Guenther, H.L., Hofstetter, W., Moseley, J.M., Gillespie, M.T., Suda, N., Martin, T.J., 1995. Evidence for the synthesis of parathyroid hormone-related protein (PTHrP) by nontransformed clonal rat osteoblastic cells in vitro. Bone 16 (3), 341–347.

Guise, T.A., Yin, J.J., Taylor, S.D., Kumagai, Y., Dallas, M., Boyce, B.F., Yoneda, T., Mundy, G.R., 1996. Evidence for a causal role of parathyroid hormone-related protein in the pathogenesis of human breast cancer-mediated osteolysis. J. Clin. Investig. 98 (7), 1544–1549.

Gupte, A., Baker, E.K., Wan, S.S., Stewart, E., Loh, A., Shelat, A.A., Gould, C.M., Chalk, A.M., Taylor, S., Lackovic, K., Karlstrom, A., Mutsaers, A.J., Desai, J., Madhamshettiwar, P.B., Zannettino, A.C., Burns, C., Huang, D.C., Dyer, M.A., Simpson, K.J., Walkley, C.R., 2015. Systematic screening identifies dual PI3K and mTOR inhibition as a conserved therapeutic vulnerability in osteosarcoma. Clin. Cancer Res. 21 (14), 3216–3229.

Hammonds Jr., R.G., McKay, P., Winslow, G.A., Diefenbach-Jagger, H., Grill, V., Glatz, J., Rodda, C.P., Moseley, J.M., Wood, W.I., Martin, T.J., et al., 1989. Purification and characterization of recombinant human parathyroid hormone-related protein. J. Biol. Chem. 264 (25), 14806–14811.

Hattersley, G., Dean, T., Corbin, B.A., Bahar, H., Gardella, T.J., 2016. Binding selectivity of abaloparatide for PTH-type-1-receptor conformations and effects on downstream signaling. Endocrinology 157 (1), 141–149.

Henderson, J.E., Amizuka, N., Warshawsky, H., Biasotto, D., Lanske, B.M., Goltzman, D., Karaplis, A.C., 1995. Nucleolar localization of parathyroid hormone-related peptide enhances survival of chondrocytes under conditions that promote apoptotic cell death. Mol. Cell Biol. 15 (8), 4064–4075.

Hirai, T., Kobayashi, T., Nishimori, S., Karaplis, A.C., Goltzman, D., Kronenberg, H.M., 2015. Bone is a major target of PTH/PTHrP receptor signaling in regulation of fetal blood calcium homeostasis. Endocrinology 156 (8), 2774−2780.

Ho, P.W., Goradia, A., Russell, M.R., Chalk, A.M., Milley, K.M., Baker, E.K., Danks, J.A., Slavin, J.L., Walia, M., Crimeen-Irwin, B., Dickins, R.A., Martin, T.J., Walkley, C.R., 2014. Knockdown of PTHR1 in osteosarcoma cells decreases invasion and growth and increases tumor differentiation in vivo. Oncogene 34, 2922−2933, 2015.

Hock, J.M., Fonseca, J., Gunness-Hey, M., Kemp, B.E., Martin, T.J., 1989. Comparison of the anabolic effects of synthetic parathyroid hormone-related protein (PTHrP) 1-34 and PTH 1-34 on bone in rats. Endocrinology 125 (4), 2022−2027.

Horwitz, M.J., Augustine, M., Khan, L., Martin, E., Oakley, C.C., Carneiro, R.M., Tedesco, M.B., Laslavic, A., Sereika, S.M., Bisello, A., Garcia-Ocana, A., Gundberg, C.M., Cauley, J.A., Stewart, A.F., 2013. A comparison of parathyroid hormone-related protein (1-36) and parathyroid hormone (1-34) on markers of bone turnover and bone density in postmenopausal women: the PrOP study. J. Bone Miner. Res. 28 (11), 2266−2276.

Horwitz, M.J., Tedesco, M.B., Garcia-Ocana, A., Sereika, S.M., Prebehala, L., Bisello, A., Hollis, B.W., Gundberg, C.M., Stewart, A.F., 2010. Parathyroid hormone-related protein for the treatment of postmenopausal osteoporosis: defining the maximal tolerable dose. J. Clin. Endocrinol. Metab. 95 (3), 1279−1287.

Horwitz, M.J., Tedesco, M.B., Sereika, S.M., Garcia-Ocana, A., Bisello, A., Hollis, B.W., Gundberg, C., Stewart, A.F., 2006. Safety and tolerability of subcutaneous PTHrP(1-36) in healthy human volunteers: a dose escalation study. Osteoporos. Int. 17 (2), 225−230.

Horwitz, M.J., Tedesco, M.B., Sereika, S.M., Hollis, B.W., Garcia-Ocana, A., Stewart, A.F., 2003. Direct comparison of sustained infusion of human parathyroid hormone-related protein-(1-36) [hPTHrP-(1-36)] versus hPTH-(1-34) on serum calcium, plasma 1,25-dihydroxyvitamin D concentrations, and fractional calcium excretion in healthy human volunteers. J. Clin. Endocrinol. Metab. 88 (4), 1603−1609.

Horwitz, M.J., Tedesco, M.B., Sereika, S.M., Prebehala, L., Gundberg, C.M., Hollis, B.W., Bisello, A., Garcia-Ocana, A., Carneiro, R.M., Stewart, A.F., 2011. A 7-day continuous infusion of PTH or PTHrP suppresses bone formation and uncouples bone turnover. J. Bone Miner. Res. 26 (9), 2287−2297.

Ingleton, P.M., Underwood, J.C., Hunt, N.H., Atkins, D., Giles, B., Coulton, L.A., Martin, T.J., 1977. Radiation induced osteogenic sarcoma in the rat as a model of hormone-responsive differentiated cancer. Lab. Anim. Sci. 27 (5 Pt 2), 748−756.

Iwamoto, M., Enomoto-Iwamoto, M., Kurisu, K., 1999. Actions of hedgehog proteins on skeletal cells. Crit. Rev. Oral Biol. Med. 10 (4), 477−486.

Jacks, T., Remington, L., Williams, B.O., Schmitt, E.M., Halachmi, S., Bronson, R.T., Weinberg, R.A., 1994. Tumor spectrum analysis in p53-mutant mice. Curr. Biol. 4 (1), 1−7.

Jans, D.A., 1995. The regulation of protein transport to the nucleus by phosphorylation. Biochem. J. 311 (Pt 3), 705−716.

Jans, D.A., Ackermann, M.J., Bischoff, J.R., Beach, D.H., Peters, R., 1991. p34cdc2-mediated phosphorylation at T124 inhibits nuclear import of SV-40 T antigen proteins. J. Cell Biol. 115 (5), 1203−1212.

Jans, D.A., Briggs, L.J., Gustin, S.E., Jans, P., Ford, S., Young, I.G., 1997. The cytokine interleukin-5 (IL-5) effects cotransport of its receptor subunits to the nucleus in vitro. FEBS Lett. 410 (2−3), 368−372.

Jilka, R.L., 2007. Molecular and cellular mechanisms of the anabolic effect of intermittent PTH. Bone 40 (6), 1434−1446.

Jolette, J., Attalla, B., Varela, A., Long, G.G., Mellal, N., Trimm, S., Smith, S.Y., Ominsky, M.S., Hattersley, G., 2017. Comparing the incidence of bone tumors in rats chronically exposed to the selective PTH type 1 receptor agonist abaloparatide or PTH(1-34). Regul. Toxicol. Pharmacol. 86, 356−365.

Jolette, J., Wilker, C.E., Smith, S.Y., Doyle, N., Hardisty, J.F., Metcalfe, A.J., Marriott, T.B., Fox, J., Wells, D.S., 2006. Defining a noncarcinogenic dose of recombinant human parathyroid hormone 1-84 in a 2-year study in Fischer 344 rats. Toxicol. Pathol. 34 (7), 929−940.

Joseph, F., Chan, B.Y., Durham, B.H., Ahmad, A.M., Vinjamuri, S., Gallagher, J.A., Vora, J.P., Fraser, W.D., 2007. The circadian rhythm of osteoprotegerin and its association with parathyroid hormone secretion. J. Clin. Endocrinol. Metab. 92 (8), 3230−3238.

Jouishomme, H., Whitfield, J.F., Chakravarthy, B., Durkin, J.P., Gagnon, L., Isaacs, R.J., MacLean, S., Neugebauer, W., Willick, G., Rixon, R.H., 1992. The protein kinase-C activation domain of the parathyroid hormone. Endocrinology 130 (1), 53−60.

Juppner, H., Abou-Samra, A.B., Freeman, M., Kong, X.F., Schipani, E., Richards, J., Kolakowski Jr., L.F., Hock, J., Potts Jr., J.T., Kronenberg, H.M., et al., 1991. A G protein-linked receptor for parathyroid hormone and parathyroid hormone-related peptide. Science 254 (5034), 1024−1026.

Kaji, H., Sugimoto, T., Kanatani, M., Fukase, M., Chihara, K., 1995. Carboxyl-terminal peptides from parathyroid hormone-related protein stimulate osteoclast-like cell formation. Endocrinology 136 (3), 842−848.

Karaplis, A.C., Kronenberg, H.M., 1996. Physiological roles for parathyroid hormone-related protein: lessons from gene knockout mice. Vitam. Horm. 52, 177−193.

Karaplis, A.C., Luz, A., Glowacki, J., Bronson, R.T., Tybulewicz, V.L., Kronenberg, H.M., Mulligan, R.C., 1994. Lethal skeletal dysplasia from targeted disruption of the parathyroid hormone-related peptide gene. Genes Dev. 8 (3), 277−289.

Karperien, M., van Dijk, T.B., Hoeijmakers, T., Cremers, F., Abou-Samra, A.B., Boonstra, J., de Laat, S.W., Defize, L.H., 1994. Expression pattern of parathyroid hormone/parathyroid hormone related peptide receptor mRNA in mouse postimplantation embryos indicates involvement in multiple developmental processes. Mech. Dev. 47 (1), 29−42.

Kartsogiannis, V., Moseley, J., McKelvie, B., Chou, S.T., Hards, D.K., Ng, K.W., Martin, T.J., Zhou, H., 1997. Temporal expression of PTHrP during endochondral bone formation in mouse and intramembranous bone formation in an in vivo rabbit model. Bone 21 (5), 385−392.

Kemp, B.E., Moseley, J.M., Rodda, C.P., Ebeling, P.R., Wettenhall, R.E., Stapleton, D., Diefenbach-Jagger, H., Ure, F., Michelangeli, V.P., Simmons, H.A., et al., 1987. Parathyroid hormone-related protein of malignancy: active synthetic fragments. Science 238 (4833), 1568−1570.

Kim, S.W., Pajevic, P.D., Selig, M., Barry, K.J., Yang, J.Y., Shin, C.S., Baek, W.Y., Kim, J.E., Kronenberg, H.M., 2012. Intermittent parathyroid hormone administration converts quiescent lining cells to active osteoblasts. J. Bone Miner. Res. 27 (10), 2075−2084.

Kovacs, C.S., 2014. Bone development and mineral homeostasis in the fetus and neonate: roles of the calciotropic and phosphotropic hormones. Physiol. Rev. 94 (4), 1143–1218.

Kovacs, C.S., Lanske, B., Hunzelman, J.L., Guo, J., Karaplis, A.C., Kronenberg, H.M., 1996. Parathyroid hormone-related peptide (PTHrP) regulates fetal-placental calcium transport through a receptor distinct from the PTH/PTHrP receptor. Proc. Natl. Acad. Sci. U.S.A. 93 (26), 15233–15238.

Kukreja, S.C., Rosol, T.J., Wimbiscus, S.A., Shevrin, D.H., Grill, V., Barengolts, E.I., Martin, T.J., 1990. Tumor resection and antibodies to parathyroid hormone-related protein cause similar changes on bone histomorphometry in hypercalcemia of cancer. Endocrinology 127 (1), 305–310.

Kukreja, S.C., Shemerdiak, W.P., Lad, T.E., Johnson, P.A., 1980. Elevated nephrogenous cyclic AMP with normal serum parathyroid hormone levels in patients with lung cancer. J. Clin. Endocrinol. Metab. 51 (1), 167–169.

Kukreja, S.C., Shevrin, D.H., Wimbiscus, S.A., Ebeling, P.R., Danks, J.A., Rodda, C.P., Wood, W.I., Martin, T.J., 1988. Antibodies to parathyroid hormone-related protein lower serum calcium in athymic mouse models of malignancy-associated hypercalcemia due to human tumors. J. Clin. Investig. 82 (5), 1798–1802.

Lafferty, F.W., 1966. Pseudohyperparathyroidism. Medicine (Baltim.) 45 (3), 247–260.

Lam, M.H., House, C.M., Tiganis, T., Mitchelhill, K.I., Sarcevic, B., Cures, A., Ramsay, R., Kemp, B.E., Martin, T.J., Gillespie, M.T., 1999. Phosphorylation at the cyclin-dependent kinases site (Thr85) of parathyroid hormone-related protein negatively regulates its nuclear localization. J. Biol. Chem. 274 (26), 18559–18566.

Lam, M.H., Hu, W., Xiao, C.Y., Gillespie, M.T., Jans, D.A., 2001. Molecular dissection of the importin beta1-recognized nuclear targeting signal of parathyroid hormone-related protein. Biochem. Biophys. Res. Commun. 282 (2), 629–634.

Lam, M.H., Olsen, S.L., Rankin, W.A., Ho, P.W., Martin, T.J., Gillespie, M.T., Moseley, J.M., 1997. PTHrP and cell division: expression and localization of PTHrP in a keratinocyte cell line (HaCaT) during the cell cycle. J. Cell. Physiol. 173 (3), 433–446.

Lam, M.H., Thomas, R.J., Martin, T.J., Gillespie, M.T., Jans, D.A., 2000. Nuclear and nucleolar localization of parathyroid hormone-related protein. Immunol. Cell Biol. 78 (4), 395–402.

Lanske, B., Amling, M., Neff, L., Guiducci, J., Baron, R., Kronenberg, H.M., 1999. Ablation of the PTHrP gene or the PTH/PTHrP receptor gene leads to distinct abnormalities in bone development. J. Clin. Investig. 104 (4), 399–407.

Lanske, B., Karaplis, A.C., Lee, K., Luz, A., Vortkamp, A., Pirro, A., Karperien, M., Defize, L.H., Ho, C., Mulligan, R.C., Abou-Samra, A.B., Juppner, H., Segre, G.V., Kronenberg, H.M., 1996. PTH/PTHrP receptor in early development and Indian hedgehog-regulated bone growth. Science 273 (5275), 663–666.

Leder, B.Z., O'Dea, L.S., Zanchetta, J.R., Kumar, P., Banks, K., McKay, K., Lyttle, C.R., Hattersley, G., 2015. Effects of abaloparatide, a human parathyroid hormone-related peptide analog, on bone mineral density in postmenopausal women with osteoporosis. J. Clin. Endocrinol. Metab. 100 (2), 697–706.

Lee, K., Deeds, J.D., Segre, G.V., 1995. Expression of parathyroid hormone-related peptide and its receptor messenger ribonucleic acids during fetal development of rats. Endocrinology 136 (2), 453–463.

Lee, K., Lanske, B., Karaplis, A.C., Deeds, J.D., Kohno, H., Nissenson, R.A., Kronenberg, H.M., Segre, G.V., 1996. Parathyroid hormone-related peptide delays terminal differentiation of chondrocytes during endochondral bone development. Endocrinology 137 (11), 5109–5118.

Li, J., Dong, S., Townsend, S.D., Dean, T., Gardella, T.J., Danishefsky, S.J., 2012. Chemistry as an expanding resource in protein science: fully synthetic and fully active human parathyroid hormone-related protein (1-141). Angew Chem. Int. Ed. Engl. 51 (49), 12263–12267.

Lin, P.P., Pandey, M.K., Jin, F., Raymond, A.K., Akiyama, H., Lozano, G., 2009. Targeted mutation of p53 and Rb in mesenchymal cells of the limb bud produces sarcomas in mice. Carcinogenesis 30 (10), 1789–1795.

Lindsay, R., Cosman, F., Zhou, H., Bostrom, M.P., Shen, V.W., Cruz, J.D., Nieves, J.W., Dempster, D.W., 2006. A novel tetracycline labeling schedule for longitudinal evaluation of the short-term effects of anabolic therapy with a single iliac crest bone biopsy: early actions of teriparatide. J. Bone Miner. Res. 21 (3), 366–373.

Liu, Y., Berendsen, A.D., Jia, S., Lotinun, S., Baron, R., Ferrara, N., Olsen, B.R., 2012. Intracellular VEGF regulates the balance between osteoblast and adipocyte differentiation. J. Clin. Investig. 122 (9), 3101–3113.

Logue, F.C., Fraser, W.D., O'Reilly, D.S., Beastall, G.H., 1989. The circadian rhythm of intact parathyroid hormone (1-84) and nephrogenous cyclic adenosine monophosphate in normal men. J. Endocrinol. 121 (1), R1–R3.

Lozano, D., Fernandez-de-Castro, L., Portal-Nunez, S., Lopez-Herradon, A., Dapia, S., Gomez-Barrena, E., Esbrit, P., 2011. The C-terminal fragment of parathyroid hormone-related peptide promotes bone formation in diabetic mice with low-turnover osteopaenia. Br. J. Pharmacol. 162 (6), 1424–1438.

Ma, Y.L., Zeng, Q., Donley, D.W., Ste-Marie, L.G., Gallagher, J.C., Dalsky, G.P., Marcus, R., Eriksen, E.F., 2006. Teriparatide increases bone formation in modeling and remodeling osteons and enhances IGF-II immunoreactivity in postmenopausal women with osteoporosis. J. Bone Miner. Res. 21 (6), 855–864.

Maeda, S., Wu, S., Juppner, H., Green, J., Aragay, A.M., Fagin, J.A., Clemens, T.L., 1996. Cell-specific signal transduction of parathyroid hormone (PTH)-related protein through stably expressed recombinant PTH/PTHrP receptors in vascular smooth muscle cells. Endocrinology 137 (8), 3154–3162.

Majeska, R.J., Rodan, S.B., Rodan, G.A., 1980. Parathyroid hormone-responsive clonal cell lines from rat osteosarcoma. Endocrinology 107 (5), 1494–1503.

Mangin, M., Ikeda, K., Broadus, A.E., 1990. Structure of the mouse gene encoding parathyroid hormone-related peptide. Gene 95 (2), 195–202.

Mangin, M., Ikeda, K., Dreyer, B.E., Milstone, L., Broadus, A.E., 1988. Two distinct tumor-derived, parathyroid hormone-like peptides result from alternative ribonucleic acid splicing. Mol. Endocrinol. 2 (11), 1049–1055.

Martin, T.J., 2016. Parathyroid hormone-related protein, its regulation of cartilage and bone development, and role in treating bone diseases. Physiol. Rev. 96 (3), 831–871.

Martin, T.J., Atkins, D., 1979. Biochemical regulators of bone resorption and their significance in cancer. Essays Med. Biochem. 4, 49–82.

Martin, T.J., Moseley, J.M., Williams, E.D., 1997. Parathyroid hormone-related protein: hormone and cytokine. J. Endocrinol. 154 (Suppl. l), S23–S37.

Massfelder, T., Dann, P., Wu, T.L., Vasavada, R., Helwig, J.J., Stewart, A.F., 1997. Opposing mitogenic and anti-mitogenic actions of parathyroid hormone-related protein in vascular smooth muscle cells: a critical role for nuclear targeting. Proc. Natl. Acad. Sci. U.S.A. 94 (25), 13630–13635.

Massfelder, T., Fiaschi-Taesch, N., Stewart, A.F., Helwig, J.J., 1998. Parathyroid hormone-related peptide–a smooth muscle tone and proliferation regulatory protein. Curr. Opin. Nephrol. Hypertens. 7 (1), 27–32.

Matsushita, H., Usui, M., Hara, M., Shishiba, Y., Nakazawa, H., Honda, K., Torigoe, K., Kohno, K., Kurimoto, M., 1997. Co-secretion of parathyroid hormone and parathyroid-hormone-related protein via a regulated pathway in human parathyroid adenoma cells. Am. J. Pathol. 150 (3), 861–871.

McMahon, A.P., 2000. More surprises in the Hedgehog signaling pathway. Cell 100 (2), 185–188.

Meador, C.K., Liddle, G.W., Island, D.P., Nicholson, W.E., Lucas, C.P., Nuckton, J.G., Luetscher, J.A., 1962. Cause of Cushing's syndrome in patients with tumors arising from "nonendocrine" tissue. J. Clin. Endocrinol. Metab. 22, 693–703.

Melick, R.A., Martin, T.J., Hicks, J.D., 1972. Parathyroid hormone production and malignancy. Br. Med. J. 2 (5807), 204–205.

Miao, D., He, B., Jiang, Y., Kobayashi, T., Soroceanu, M.A., Zhao, J., Su, H., Tong, X., Amizuka, N., Gupta, A., Genant, H.K., Kronenberg, H.M., Goltzman, D., Karaplis, A.C., 2005. Osteoblast-derived PTHrP is a potent endogenous bone anabolic agent that modifies the therapeutic efficacy of administered PTH 1-34. J. Clin. Investig. 115 (9), 2402–2411.

Miao, D., He, B., Karaplis, A.C., Goltzman, D., 2002. Parathyroid hormone is essential for normal fetal bone formation. J. Clin. Investig. 109 (9), 1173–1182.

Miao, D., Li, J., Xue, Y., Su, H., Karaplis, A.C., Goltzman, D., 2004. Parathyroid hormone-related peptide is required for increased trabecular bone volume in parathyroid hormone-null mice. Endocrinology 145 (8), 3554–3562.

Miao, D., Su, H., He, B., Gao, J., Xia, Q., Zhu, M., Gu, Z., Goltzman, D., Karaplis, A.C., 2008. Severe growth retardation and early lethality in mice lacking the nuclear localization sequence and C-terminus of PTH-related protein. Proc. Natl. Acad. Sci. U.S.A. 105 (51), 20309–20314.

Miller, P.D., Hattersley, G., Riis, B.J., Williams, G.C., Lau, E., Russo, L.A., Alexandersen, P., Zerbini, C.A., Hu, M.Y., Harris, A.G., Fitzpatrick, L.A., Cosman, F., Christiansen, C., Investigators, A.S., 2016. Effect of abaloparatide vs placebo on new vertebral fractures in postmenopausal women with osteoporosis: a randomized clinical trial. J. Am. Med. Assoc. 316 (7), 722–733.

Mok, L.L., Nickols, G.A., Thompson, J.C., Cooper, C.W., 1989. Parathyroid hormone as a smooth muscle relaxant. Endocr. Rev. 10 (4), 420–436.

Molyneux, S.D., Di Grappa, M.A., Beristain, A.G., McKee, T.D., Wai, D.H., Paderova, J., Kashyap, M., Hu, P., Maiuri, T., Narala, S.R., Stambolic, V., Squire, J., Penninger, J., Sanchez, O., Triche, T.J., Wood, G.A., Kirschner, L.S., Khokha, R., 2010. Prkar1a is an osteosarcoma tumor suppressor that defines a molecular subclass in mice. J. Clin. Investig. 120 (9), 3310–3325.

Moniz, C., Burton, P.B., Malik, A.N., Dixit, M., Banga, J.P., Nicolaides, K., Quirke, P., Knight, D.E., McGregor, A.M., 1990. Parathyroid hormone-related peptide in normal human fetal development. J. Mol. Endocrinol. 5 (3), 259–266.

Moseley, J.M., Gillespie, M.T., 1995. Parathyroid hormone-related protein. Crit. Rev. Clin. Lab. Sci. 32 (3), 299–343.

Moseley, J.M., Hayman, J.A., Danks, J.A., Alcorn, D., Grill, V., Southby, J., Horton, M.A., 1991. Immunohistochemical detection of parathyroid hormone-related protein in human fetal epithelia. J. Clin. Endocrinol. Metab. 73 (3), 478–484.

Moseley, J.M., Kubota, M., Diefenbach-Jagger, H., Wettenhall, R.E., Kemp, B.E., Suva, L.J., Rodda, C.P., Ebeling, P.R., Hudson, P.J., Zajac, J.D., et al., 1987. Parathyroid hormone-related protein purified from a human lung cancer cell line. Proc. Natl. Acad. Sci. U.S.A. 84 (14), 5048–5052.

Murrills, R.J., Stein, L.S., Dempster, D.W., 1995. Lack of significant effect of carboxyl-terminal parathyroid hormone-related peptide fragments on isolated rat and chick osteoclasts. Calcif. Tissue Int. 57 (1), 47–51.

Mutsaers, A.J., Ng, A.J., Baker, E.K., Russell, M.R., Chalk, A.M., Wall, M., Liddicoat, B.J., Ho, P.W., Slavin, J.L., Goradia, A., Martin, T.J., Purton, L.E., Dickins, R.A., Walkley, C.R., 2013. Modeling distinct osteosarcoma subtypes in vivo using Cre:lox and lineage-restricted transgenic shRNA. Bone 55 (1), 166–178.

Mutsaers, A.J., Walkley, C.R., 2014. Cells of origin in osteosarcoma: mesenchymal stem cells or osteoblast committed cells? Bone 62, 56–63.

Nagai, S., Okazaki, M., Segawa, H., Bergwitz, C., Dean, T., Potts Jr., J.T., Mahon, M.J., Gardella, T.J., Juppner, H., 2011. Acute down-regulation of sodium-dependent phosphate transporter NPT2a involves predominantly the cAMP/PKA pathway as revealed by signaling-selective parathyroid hormone analogs. J. Biol. Chem. 286 (2), 1618–1626.

Nakayama, T., Ohtsuru, A., Enomoto, H., Namba, H., Ozeki, S., Shibata, Y., Yokota, T., Nobuyoshi, M., Ito, M., Sekine, I., et al., 1994. Coronary atherosclerotic smooth muscle cells overexpress human parathyroid hormone-related peptides. Biochem. Biophys. Res. Commun. 200 (2), 1028–1035.

Neer, R.M., Arnaud, C.D., Zanchetta, J.R., Prince, R., Gaich, G.A., Reginster, J.Y., Hodsman, A.B., Eriksen, E.F., Ish-Shalom, S., Genant, H.K., Wang, O., Mitlak, B.H., 2001. Effect of parathyroid hormone (1-34) on fractures and bone mineral density in postmenopausal women with osteoporosis. N. Engl. J. Med. 344 (19), 1434–1441.

Nguyen, M., He, B., Karaplis, A., 2001. Nuclear forms of parathyroid hormone-related peptide are translated from non-AUG start sites downstream from the initiator methionine. Endocrinology 142 (2), 694–703.

Nijs-de Wolf, N., Pepersack, T., Corvilain, J., Karmali, R., Bergmann, P., 1991. Adenylate cyclase stimulating activity immunologically similar to parathyroid hormone-related peptide can be extracted from fetal rat long bones. J. Bone Miner. Res. 6 (9), 921–927.

Noda, M., Katoh, T., Takuwa, N., Kumada, M., Kurokawa, K., Takuwa, Y., 1994. Synergistic stimulation of parathyroid hormone-related peptide gene expression by mechanical stretch and angiotensin II in rat aortic smooth muscle cells. J. Biol. Chem. 269 (27), 17911–17917.

Okano, K., Pirola, C.J., Wang, H.M., Forrester, J.S., Fagin, J.A., Clemens, T.L., 1995. Involvement of cell cycle and mitogen-activated pathways in induction of parathyroid hormone-related protein gene expression in rat aortic smooth muscle cells. Endocrinology 136 (4), 1782–1789.

Ono, W., Sakagami, N., Nishimori, S., Ono, N., Kronenberg, H.M., 2016. Parathyroid hormone receptor signalling in osterix-expressing mesenchymal progenitors is essential for tooth root formation. Nat. Commun. 7, 11277.

Orloff, J.J., Wu, T.L., Stewart, A.F., 1989. Parathyroid hormone-like proteins: biochemical responses and receptor interactions. Endocr. Rev. 10 (4), 476–495.

Owen, M., 1971. Cellular Dynamics of Bone. Academic Press, New York, N.Y.

Ozeki, S., Ohtsuru, A., Seto, S., Takeshita, S., Yano, H., Nakayama, T., Ito, M., Yokota, T., Nobuyoshi, M., Segre, G.V., Yamashita, S., Yano, K., 1996. Evidence that implicates the parathyroid hormone-related peptide in vascular stenosis. Increased gene expression in the intima of injured carotid arteries and human restenotic coronary lesions. Arterioscler. Thromb. Vasc. Biol. 16 (4), 565–575.

Pache, J.C., Burton, D.W., Deftos, L.J., Hastings, R.H., 2006. A carboxyl leucine-rich region of parathyroid hormone-related protein is critical for nuclear export. Endocrinology 147 (2), 990–998.

Paget, S., 1889. The distribution of secondary growths in cancer of the breast. Lancet 1, 571–573.

Partridge, N.C., Alcorn, D., Michelangeli, V.P., Kemp, B.E., Ryan, G.B., Martin, T.J., 1981. Functional properties of hormonally responsive cultured normal and malignant rat osteoblastic cells. Endocrinology 108 (1), 213–219.

Patterson, E.K., Watson, P.H., Hodsman, A.B., Hendy, G.N., Canaff, L., Bringhurst, F.R., Poschwatta, C.H., Fraher, L.J., 2007. Expression of PTH1R constructs in LLC-PK1 cells: protein nuclear targeting is mediated by the PTH1R NLS. Bone 41 (4), 603–610.

Philbrick, W.M., 1998. Parathyroid hormone-related protein is a developmental regulatory molecule. Eur. J. Oral Sci. 106 (Suppl. 1), 32–37.

Philbrick, W.M., Wysolmerski, J.J., Galbraith, S., Holt, E., Orloff, J.J., Yang, K.H., Vasavada, R.C., Weir, E.C., Broadus, A.E., Stewart, A.F., 1996. Defining the roles of parathyroid hormone-related protein in normal physiology. Physiol. Rev. 76 (1), 127–173.

Pilbeam, C.C., Alander, C.B., Simmons, H.A., Raisz, L.G., 1993. Comparison of the effects of various lengths of synthetic human parathyroid hormone-related peptide (hPTHrP) of malignancy on bone resorption and formation in organ culture. Bone 14 (5), 717–720.

Pirola, C.J., Wang, H.M., Kamyar, A., Wu, S., Enomoto, H., Sharifi, B., Forrester, J.S., Clemens, T.L., Fagin, J.A., 1993. Angiotensin II regulates parathyroid hormone-related protein expression in cultured rat aortic smooth muscle cells through transcriptional and post-transcriptional mechanisms. J. Biol. Chem. 268 (3), 1987–1994.

Plawner, L.L., Philbrick, W.M., Burtis, W.J., Broadus, A.E., Stewart, A.F., 1995. Cell type-specific secretion of parathyroid hormone-related protein via the regulated versus the constitutive secretory pathway. J. Biol. Chem. 270 (23), 14078–14084.

Powell, D., Singer, F.R., Murray, T.M., Minkin, C., Potts Jr., J.T., 1973. Nonparathyroid humoral hypercalcemia in patients with neoplastic diseases. N. Engl. J. Med. 289 (4), 176–181.

Powell, G.J., Southby, J., Danks, J.A., Stillwell, R.G., Hayman, J.A., Henderson, M.A., Bennett, R.C., Martin, T.J., 1991. Localization of parathyroid hormone-related protein in breast cancer metastases: increased incidence in bone compared with other sites. Cancer Res. 51 (11), 3059–3061.

Qian, J., Lorenz, J.N., Maeda, S., Sutliff, R.L., Weber, C., Nakayama, T., Colbert, M.C., Paul, R.J., Fagin, J.A., Clemens, T.L., 1999. Reduced blood pressure and increased sensitivity of the vasculature to parathyroid hormone-related protein (PTHrP) in transgenic mice overexpressing the PTH/PTHrP receptor in vascular smooth muscle. Endocrinology 140 (4), 1826–1833.

Quist, T., Jin, H., Zhu, J.F., Smith-Fry, K., Capecchi, M.R., Jones, K.B., 2015. The impact of osteoblastic differentiation on osteosarcomagenesis in the mouse. Oncogene 34 (32), 4278–4284.

Raison, D., Coquard, C., Hochane, M., Steger, J., Massfelder, T., Moulin, B., Karaplis, A.C., Metzger, D., Chambon, P., Helwig, J.J., Barthelmebs, M., 2013. Knockdown of parathyroid hormone related protein in smooth muscle cells alters renal hemodynamics but not blood pressure. Am. J. Physiol. Renal. Physiol. 305 (3), F333–F342.

Rejnmark, L., Lauridsen, A.L., Vestergaard, P., Heickendorff, L., Andreasen, F., Mosekilde, L., 2002. Diurnal rhythm of plasma 1,25-dihydroxyvitamin D and vitamin D-binding protein in postmenopausal women: relationship to plasma parathyroid hormone and calcium and phosphate metabolism. Eur. J. Endocrinol. 146 (5), 635–642.

Riggs, B.L., Arnaud, C.D., Reynolds, J.C., Smith, L.H., 1971. Immunologic differentiation of primary hyperparathyroidism from hyperparathyroidism due to nonparathyroid cancer. J. Clin. Investig. 50 (10), 2079–2083.

Rihani-Basharat, S., Lewinson, D., 1997. PTHrP(107-111) inhibits in vivo resorption that was stimulated by PTHrP(1-34) when applied intermittently to neonatal mice. Calcif. Tissue Int. 61 (5), 426–428.

Robbins, J., Dilworth, S.M., Laskey, R.A., Dingwall, C., 1991. Two interdependent basic domains in nucleoplasmin nuclear targeting sequence: identification of a class of bipartite nuclear targeting sequence. Cell 64 (3), 615–623.

Roca-Cusachs, A., DiPette, D.J., Nickols, G.A., 1991. Regional and systemic hemodynamic effects of parathyroid hormone-related protein: preservation of cardiac function and coronary and renal flow with reduced blood pressure. J. Pharmacol. Exp. Ther. 256 (1), 110–118.

Rodan, S.B., Wesolowski, G., Ianacone, J., Thiede, M.A., Rodan, G.A., 1989. Production of parathyroid hormone-like peptide in a human osteosarcoma cell line: stimulation by phorbol esters and epidermal growth factor. J. Endocrinol. 122 (1), 219–227.

Rodda, C.P., Kubota, M., Heath, J.A., Ebeling, P.R., Moseley, J.M., Care, A.D., Caple, I.W., Martin, T.J., 1988. Evidence for a novel parathyroid hormone-related protein in fetal lamb parathyroid glands and sheep placenta: comparisons with a similar protein implicated in humoral hypercalcaemia of malignancy. J. Endocrinol. 117 (2), 261–271.

Rude, R.K., Bethune, J.E., Singer, F.R., 1980. Renal tubular maximum for magnesium in normal, hyperparathyroid, and hypoparathyroid man. J. Clin. Endocrinol. Metab. 51 (6), 1425–1431.

Saini, V., Marengi, D.A., Barry, K.J., Fulzele, K.S., Heiden, E., Liu, X., Dedic, C., Maeda, A., Lotinun, S., Baron, R., Pajevic, P.D., 2013. Parathyroid hormone (PTH)/PTH-related peptide type 1 receptor (PPR) signaling in osteocytes regulates anabolic and catabolic skeletal responses to PTH. J. Biol. Chem. 288 (28), 20122–20134.

Schermer, D.T., Chan, S.D., Bruce, R., Nissenson, R.A., Wood, W.I., Strewler, G.J., 1991. Chicken parathyroid hormone-related protein and its expression during embryologic development. J. Bone Miner. Res. 6 (2), 149–155.

Schipani, E., Kruse, K., Juppner, H., 1995. A constitutively active mutant PTH-PTHrP receptor in Jansen-type metaphyseal chondrodysplasia. Science 268 (5207), 98–100.

Schipani, E., Langman, C.B., Parfitt, A.M., Jensen, G.S., Kikuchi, S., Kooh, S.W., Cole, W.G., Juppner, H., 1996. Constitutively activated receptors for parathyroid hormone and parathyroid hormone-related peptide in Jansen's metaphyseal chondrodysplasia. N. Engl. J. Med. 335 (10), 708–714.

Schipani, E., Lanske, B., Hunzelman, J., Luz, A., Kovacs, C.S., Lee, K., Pirro, A., Kronenberg, H.M., Juppner, H., 1997. Targeted expression of constitutively active receptors for parathyroid hormone and parathyroid hormone-related peptide delays endochondral bone formation and rescues mice that lack parathyroid hormone-related peptide. Proc. Natl. Acad. Sci. U.S.A. 94 (25), 13689–13694.

Senior, P.V., Heath, D.A., Beck, F., 1991. Expression of parathyroid hormone-related protein mRNA in the rat before birth: demonstration by hybridization histochemistry. J. Mol. Endocrinol. 6 (3), 281–290.

Sone, T., Kohno, H., Kikuchi, H., Ikeda, T., Kasai, R., Kikuchi, Y., Takeuchi, R., Konishi, J., Shigeno, C., 1992. Human parathyroid hormone-related peptide-(107-111) does not inhibit bone resorption in neonatal mouse calvariae. Endocrinology 131 (6), 2742–2746.

Stevenson, F.T., Turck, J., Locksley, R.M., Lovett, D.H., 1997. The N-terminal propiece of interleukin 1 alpha is a transforming nuclear oncoprotein. Proc. Natl. Acad. Sci. U.S.A. 94 (2), 508–513.

Stewart, A.F., Horst, R., Deftos, L.J., Cadman, E.C., Lang, R., Broadus, A.E., 1980. Biochemical evaluation of patients with cancer-associated hypercalcemia: evidence for humoral and nonhumoral groups. N. Engl. J. Med. 303 (24), 1377–1383.

Suda, N., Gillespie, M.T., Traianedes, K., Zhou, H., Ho, P.W., Hards, D.K., Allan, E.H., Martin, T.J., Moseley, J.M., 1996. Expression of parathyroid hormone-related protein in cells of osteoblast lineage. J. Cell. Physiol. 166 (1), 94–104.

Suva, L.J., Seedor, J.G., Endo, N., Quartuccio, H.A., Thompson, D.D., Bab, I., Rodan, G.A., 1993. Pattern of gene expression following rat tibial marrow ablation. J. Bone Miner. Res. 8 (3), 379–388.

Suva, L.J., Winslow, G.A., Wettenhall, R.E., Hammonds, R.G., Moseley, J.M., Diefenbach-Jagger, H., Rodda, C.P., Kemp, B.E., Rodriguez, H., Chen, E.Y., et al., 1987. A parathyroid hormone-related protein implicated in malignant hypercalcemia: cloning and expression. Science 237 (4817), 893–896.

Tao, J., Jiang, M.M., Jiang, L., Salvo, J.S., Zeng, H.C., Dawson, B., Bertin, T.K., Rao, P.H., Chen, R., Donehower, L.A., Gannon, F., Lee, B.H., 2014. Notch activation as a driver of osteogenic sarcoma. Cancer Cell 26 (3), 390–401.

Tashjian Jr., A.H., Chabner, B.A., 2002. Commentary on clinical safety of recombinant human parathyroid hormone 1-34 in the treatment of osteoporosis in men and postmenopausal women. J. Bone Miner. Res. 17 (7), 1151–1161.

Tashjian Jr., A.H., Goltzman, D., 2008. On the interpretation of rat carcinogenicity studies for human PTH(1-34) and human PTH(1-84). J. Bone Miner. Res. 23 (6), 803–811.

Thiede, M.A., Strewler, G.J., Nissenson, R.A., Rosenblatt, M., Rodan, G.A., 1988. Human renal carcinoma expresses two messages encoding a parathyroid hormone-like peptide: evidence for the alternative splicing of a single-copy gene. Proc. Natl. Acad. Sci. U.S.A. 85 (13), 4605–4609.

Toribio, R.E., Brown, H.A., Novince, C.M., Marlow, B., Hernon, K., Lanigan, L.G., Hildreth 3rd, B.E., Werbeck, J.L., Shu, S.T., Lorch, G., Carlton, M., Foley, J., Boyaka, P., McCauley, L.K., Rosol, T.J., 2010. The midregion, nuclear localization sequence, and C terminus of PTHrP regulate skeletal development, hematopoiesis, and survival in mice. FASEB J. 24 (6), 1947–1957.

Tregear, G.W., Potts Jr., J.T., 1975. Synthetic analogues of residues 1-34 of human parathyroid hormone: influence of residue number 1 on biological potency in vitro. Endocr. Res. Commun. 2 (8), 561–570.

Truant, R., Cullen, B.R., 1999. The arginine-rich domains present in human immunodeficiency virus type 1 Tat and Rev function as direct importin beta-dependent nuclear localization signals. Mol. Cell Biol. 19 (2), 1210–1217.

Tsukazaki, T., Ohtsuru, A., Enomoto, H., Yano, H., Motomura, K., Ito, M., Namba, H., Iwasaki, K., Yamashita, S., 1995. Expression of parathyroid hormone-related protein in rat articular cartilage. Calcif. Tissue Int. 57 (3), 196–200.

Vahle, J.L., Sato, M., Long, G.G., Young, J.K., Francis, P.C., Engelhardt, J.A., Westmore, M.S., Linda, Y., Nold, J.B., 2002. Skeletal changes in rats given daily subcutaneous injections of recombinant human parathyroid hormone (1-34) for 2 years and relevance to human safety. Toxicol. Pathol. 30 (3), 312–321.

Valin, A., Garcia-Ocana, A., De Miguel, F., Sarasa, J.L., Esbrit, P., 1997. Antiproliferative effect of the C-terminal fragments of parathyroid hormone-related protein, PTHrP-(107-111) and (107-139), on osteoblastic osteosarcoma cells. J. Cell. Physiol. 170 (2), 209–215.

van de Stolpe, A., Karperien, M., Lowik, C.W., Juppner, H., Segre, G.V., Abou-Samra, A.B., de Laat, S.W., Defize, L.H., 1993. Parathyroid hormone-related peptide as an endogenous inducer of parietal endoderm differentiation. J. Cell Biol. 120 (1), 235–243.

Vortkamp, A., Lee, K., Lanske, B., Segre, G.V., Kronenberg, H.M., Tabin, C.J., 1996. Regulation of rate of cartilage differentiation by Indian hedgehog and PTH-related protein. Science 273 (5275), 613–622.

Walia, M., Castillo-Tandozo, W., Mutsaers, A.J., Martin, T.J., Walkley, C.R., 2018. Murine models of osteosarcoma: a piece of the translational puzzle. J. Cell. Biochem. in press.

Walia, M.K., Ho, P.M., Taylor, S., Ng, A.J., Gupte, A., Chalk, A.M., Zannettino, A.C., Martin, T.J., Walkley, C.R., 2016. Activation of PTHrP-cAMP-CREB1 signaling following p53 loss is essential for osteosarcoma initiation and maintenance. Elife 5.

Walkley, C.R., Qudsi, R., Sankaran, V.G., Perry, J.A., Gostissa, M., Roth, S.I., Rodda, S.J., Snay, E., Dunning, P., Fahey, F.H., Alt, F.W., McMahon, A.P., Orkin, S.H., 2008. Conditional mouse osteosarcoma, dependent on p53 loss and potentiated by loss of Rb, mimics the human disease. Genes Dev. 22 (12), 1662–1676.

Wang, H.H., Drugge, E.D., Yen, Y.C., Blumenthal, M.R., Pang, P.K., 1984. Effects of synthetic parathyroid hormone on hemodynamics and regional blood flows. Eur. J. Pharmacol. 97 (3–4), 209–215.

Wang, Z.Q., Liang, J., Schellander, K., Wagner, E.F., Grigoriadis, A.E., 1995. c-fos-induced osteosarcoma formation in transgenic mice: cooperativity with c-jun and the role of endogenous c-fos. Cancer Res. 55 (24), 6244–6251.

Washam, C.L., Byrum, S.D., Leitzel, K., Ali, S.M., Tackett, A.J., Gaddy, D., Sundermann, S.E., Lipton, A., Suva, L.J., 2013. Identification of PTHrP(12-48) as a plasma biomarker associated with breast cancer bone metastasis. Cancer Epidemiol. Biomark. Prev. 22 (5), 972–983.

Watson, P.H., Fraher, L.J., Hendy, G.N., Chung, U.I., Kisiel, M., Natale, B.V., Hodsman, A.B., 2000a. Nuclear localization of the type 1 PTH/PTHrP receptor in rat tissues. J. Bone Miner. Res. 15 (6), 1033–1044.

Watson, P.H., Fraher, L.J., Natale, B.V., Kisiel, M., Hendy, G.N., Hodsman, A.B., 2000b. Nuclear localization of the type 1 parathyroid hormone/parathyroid hormone-related peptide receptor in MC3T3-E1 cells: association with serum-induced cell proliferation. Bone 26 (3), 221–225.

Wein, M.N., Liang, Y., Goransson, O., Sundberg, T.B., Wang, J., Williams, E.A., O'Meara, M.J., Govea, N., Beqo, B., Nishimori, S., Nagano, K., Brooks, D.J., Martins, J.S., Corbin, B., Anselmo, A., Sadreyev, R., Wu, J.Y., Sakamoto, K., Foretz, M., Xavier, R.J., Baron, R., Bouxsein, M.L., Gardella, T.J., Divieti-Pajevic, P., Gray, N.S., Kronenberg, H.M., 2016. SIKs control osteocyte responses to parathyroid hormone. Nat. Commun. 7, 13176.

Weir, E.C., Philbrick, W.M., Amling, M., Neff, L.A., Baron, R., Broadus, A.E., 1996. Targeted overexpression of parathyroid hormone-related peptide in chondrocytes causes chondrodysplasia and delayed endochondral bone formation. Proc. Natl. Acad. Sci. U.S.A. 93 (19), 10240–10245.

Whitfield, J.F., Isaacs, R.J., Chakravarthy, B.R., Durkin, J.P., Morley, P., Neugebauer, W., Williams, R.E., Willick, G., Rixon, R.H., 1994. C-terminal fragments of parathyroid hormone-related protein, PTHrP-(107-111) and (107-139), and the N-terminal PTHrP-(1-40) fragment stimulate membrane-associated protein kinase C activity in rat spleen lymphocytes. J. Cell. Physiol. 158 (3), 518–522.

Wilson, K.C., Cruikshank, W.W., Center, D.M., Zhang, Y., 2002. Prointerleukin-16 contains a functional CcN motif that regulates nuclear localization. Biochemistry 41 (48), 14306–14312.

Wu, T.L., Vasavada, R.C., Yang, K., Massfelder, T., Ganz, M., Abbas, S.K., Care, A.D., Stewart, A.F., 1996. Structural and physiologic characterization of the mid-region secretory species of parathyroid hormone-related protein. J. Biol. Chem. 271 (40), 24371–24381.

Wysolmerski, J.J., Cormier, S., Philbrick, W.M., Dann, P., Zhang, J.P., Roume, J., Delezoide, A.L., Silve, C., 2001. Absence of functional type 1 parathyroid hormone (PTH)/PTH-related protein receptors in humans is associated with abnormal breast development and tooth impaction. J. Clin. Endocrinol. Metab. 86 (4), 1788–1794.

Yang, D., Singh, R., Divieti, P., Guo, J., Bouxsein, M.L., Bringhurst, F.R., 2007a. Contributions of parathyroid hormone (PTH)/PTH-related peptide receptor signaling pathways to the anabolic effect of PTH on bone. Bone 40 (6), 1453–1461.

Yang, R., Hoang, B.H., Kubo, T., Kawano, H., Chou, A., Sowers, R., Huvos, A.G., Meyers, P.A., Healey, J.H., Gorlick, R., 2007b. Over-expression of parathyroid hormone Type 1 receptor confers an aggressive phenotype in osteosarcoma. Int. J. Cancer 121 (5), 943–954.

Yasuda, T., Banville, D., Hendy, G.N., Goltzman, D., 1989. Characterization of the human parathyroid hormone-like peptide gene. Functional and evolutionary aspects. J. Biol. Chem. 264 (13), 7720–7725.

Zhou, H., Leaver, D.D., Moseley, J.M., Kemp, B., Ebeling, P.R., Martin, T.J., 1989. Actions of parathyroid hormone-related protein on the rat kidney in vivo. J. Endocrinol. 122 (1), 229–235.

Zhu, Q., Zhou, X., Zhu, M., Wang, Q., Goltzman, D., Karaplis, A., Miao, D., 2013. Endogenous parathyroid hormone-related protein compensates for the absence of parathyroid hormone in promoting bone accrual in vivo in a model of bone marrow ablation. J. Bone Miner. Res. 28 (9), 1898–1911.

Chapter 26

Cardiovascular actions of parathyroid hormone/parathyroid hormone–related protein signaling

Sasan Mirfakhraee and Dwight A. Towler

The University of Texas Southwestern Medical Center, Department of Internal Medicine, Endocrine Division, Dallas, TX, United Sates

Chapter outline

Introduction

All osteotropic hormones have vasculotropic actions (Thompson and Towler, 2012b; Towler, 2017a). This pithy statement of fact most certainly holds true for the prototypic bone anabolic polypeptides parathyroid hormone (PTH) and parathyroid hormone–related protein (PTHrP) (aka PTHLH). The cardiovascular actions of PTH were first identified in 1925, when Collip and Clark injected anesthetized Dog 164 with intravenous parathyroid extract and documented hypotensive actions (Collip and Clark, 1925; Rambausek et al., 1982). However, only since the end of the 20th century has the fundamental role of PTH/PTHrP receptor (PTH1R) signaling in cardiovascular development, physiology, and disease been fully vetted—but this is not yet widely appreciated (Bilezikian et al., 2015; Tomaschitz et al., 2013). For example, PTH1R signaling is required for normal aortic valve (Gray et al., 2013) and myocardial (Qian et al., 2003) development. Paracrine vascular smooth muscle PTHrP/PTH1R signaling has emerged as important in the homeostatic regulation of renovascular blood flow (Raison et al., 2013), while endothelial PTH1R actions convey the endocrine regulation of blood flow to bone in response to PTH (Benson et al., 2016). In addition to its bone anabolic actions, intermittent pharmacological dosing with PTH(1–34) mitigates the endothelial dysfunction associated with aging (Guers et al., 2017) and suppresses arteriosclerotic responses to dysmetabolic states such as diabetes (Cheng et al., 2010). These observations, among others, provide a second "bookend" that, with Collip and Clark's early observation, serves to brace the first century of PTH/PTHrP research—a century that has *continuously* pointed to cardiovascular actions of the PTH family of ligands. Thus, a fundamental understanding of PTH/PTHrP biology must encompass a better understanding of actions within and upon the cardiovascular system (Cheng et al., 2010).

In this chapter, we build upon our recent reviews (Bilezikian et al., 2015; Thompson and Towler, 2012b; Towler, 2014a) to help highlight once again the importance of PTH/PTHrP to cardiovascular biology and disease. While

Principles of Bone Biology. https://doi.org/10.1016/B978-0-12-814841-9.00026-9

mammalian PTHrP is a dedicated PTH1R ligand, PTH can activate both human PTH1R and human PTH2R (Hoare and Usdin, 2001). Therefore, we also briefly discuss PTH2R and tuberoinfundibular peptide of 39 residues (TIP39), the dedicated PTH2R ligand, as relevant to cardiovascular biology. Finally, we reflect upon chronic kidney disease−mineral and bone disorder (CKD−MBD) as a "perfect storm" of cardiometabolic risk arising in significant part from perturbed PTH1R signaling. We use this discussion as a framework to detail physiologically important interconnections of PTH/PTHrP signaling within the emerging bone−vascular axis (Fadini et al., 2012; Thompson and Towler, 2012a; Towler, 2011). The reader is referred to recent editions of *The Parathyroids* for a more comprehensive historical review (Bilezikian et al., 2015).

PTH/PTHrP in cardiovascular development

Some of the earliest evidence that PTH/PTHrP signaling might contribute to cardiovascular development arose in Buck Strewler's group; they identified expression of PTHrP in the chicken embryonic heart as well as in other mesodermally derived tissues (Schermer et al., 1991). Descriptive studies in the rat revealed that mesenchymal PTH1R expression lay adjacent to epithelial or endothelial sources of PTHrP (Lee et al., 1995). Inductive, paracrine epithelial-to-mesenchymal signals mediated by PTHrP were inferred from the spatial relationship between *PTHrP* ligand and *PTH1R* expression as revealed by these in situ hybridization studies. In dogs, PTH1R was also identified early on as being expressed in heart and aorta, albeit at levels much lower than those observed in kidney and bone (Smock et al., 2001). However, the important role of PTH/PTHrP in cardiovascular development was not truly appreciated until Hank Kronenberg, Tom Clemens, and colleagues began their systematic analyses as to why mice globally lacking the PTH1R exhibit prenatal lethality (Qian et al., 2003). They demonstrated that, as in other vertebrate species, the murine *PTH1R* gene was abundantly expressed in developing mouse cardiomyocytes, but then went on to show that mice genetically lacking PTH1R abruptly die between embryonic day (E) 11.5 and E12.5 due to massive cardiomyocyte apoptosis (Qian et al., 2003). The primary abnormalities in cardiomyocyte mitochondrial morphology and pump function that arise with myocardial PTH1R deficiency were followed by secondary hepatic injury and tissue necrosis (presumptively due to cardiogenic circulatory congestion). The mechanisms whereby PTH1R signaling regulates mitochondrial metabolism to prevent apoptotic cell death in the cardiomyocyte have yet to be fully explored, but based upon recent studies will probably converge on protein kinase A-dependent inhibition of the mitochondrial fission protein Drp1 (Monterisi et al., 2017). Skeletal PTH1R activation has been shown to inhibit apoptosis in several cell types, including in osteoblasts challenged with glucocorticoids (O'Brien et al., 2008) or chondrocytes treated with tumor necrosis factor (Okoumassoun et al., 2007). Thus, PTH1R expression and signaling represent a fundamental component of cardiomyocyte cell physiology. A better understanding of the prosurvival mechanisms afforded by PTH1R signaling in the heart may prove useful in therapeutic approaches to ischemic heart disease as well as cardiotoxicity associated with a subset of chemotherapeutics (Babiker et al., 2018).

Other vertebrate models have confirmed the important role of PTH/PTHrP signaling in cardiovascular development. In zebrafish, a total of three PTH receptors (*pth1r*, *pth2r*, *pth3r*) are expressed (Gray et al., 2013). Knockdown of either *pth1r* or the selective zebrafish *pth1r/pth2r* ligand *pthrp* results in morphants with aortic coarctation defects. Because of the important role for *notch* in mammalian aortic valve development (van den Akker et al., 2012), Chico and colleagues wondered whether *notch* signaling might be perturbed and, indeed, demonstrated that restoration of *notch* signaling in *pth1r*-targeted morphants prevented the aortic defects (Gray et al., 2013). Thus, the variable penetrance for preductal aortic coarctation in lethal Blomstrand chondrodysplasia—a rare disorder due to loss-of-function mutations in the human *PTH1R* (Hoogendam et al., 2007)—may in fact relate to variable compensatory changes in Notch coregulatory pathways that partially compensate for PTH1R deficiency during development. PTH1R and Notch play vital roles in both bone and vascular biology, including vascular endothelial growth factor (VEGF)-dependent processes such as tip-cell selection (Blanco and Gerhardt, 2013). Thus, the cross talk between these morphogenetic signaling systems is likely to help juxtaposition microvascular supply to sites of bone formation in the basic multicellular unit in response to PTH anabolic actions (Prisby et al., 2011).

PTH receptor signaling in arterial biology: vascular smooth muscle cell and endothelial responses to PTH and PTHrP

The acute vasodilatory actions of PTH administration were recognized in the very earliest studies of the hormone's physiological response (Collip and Clark, 1925). Following Collip and Clark's lead, Pang et al. confirmed that bovine PTH(1−34) reduced blood pressure in anesthetized dogs and rats (Pang et al., 1980). Imai and colleagues demonstrated

coronary vasodilation in response to PTH that same year (Hashimoto et al., 1981). Ex vivo, human and bovine middle cerebral arteries were identified to undergo vasodilatation as well (Suzuki et al., 1983). These observations prompted additional work that demonstrated vasodilatory PTH responses in multiple vertebrate tissue beds, but responses varied widely in potency and efficacy (Crass et al., 1987; Nickols et al., 1986). Tissue-specific expression of PDZ domain-containing coadapters markedly influences the capacity of the PTH1R to access protein kinase A, phospholipase C, and extracellular signal-regulated kinase (ERK) signaling mediators that shape these responses (Romero et al., 2011). As of this writing, the molecular mechanisms conveying temporal and spatial differences in PTH1R-dependent vasodilation have not been delineated. Of note, in 1986 the salutary actions of PTH in a preclinical model of myocardial ischemia were reported; enhanced collateral blood flow was thought to represent the primary mechanism of benefit (see later) (Feola and Crass, 1986). However, since PTH1R signaling exerts direct antiapoptotic actions within fetal cardiomyocytes (*vide supra*), this response may also contribute to postnatal PTH1R benefits in the setting of ischemia.

Nickols, Barthelmebs, Jean-Jacques Helwig, and colleagues went on to confirm a widespread vasodilatory reaction to PTHrP (Musso et al., 1989; Roca-Cusachs et al., 1991). Endothelial NO production in response to PTH1R activation certainly contributes to vasodilatory PTH/PTHrP actions, as Prisby and colleagues have elegantly demonstrated in bone (Benson et al., 2016) (Fig. 26.1). However, direct PTH1R signaling in arterial vascular smooth muscle cells (VSMC) conveys many beneficial functions in other large conduit vessels. Coronary artery vasodilation is only partly dependent upon endothelial NO release due to direct actions of PTHrP/PTH1R signaling in coronary VSMC that drive vasorelaxation; the latter is dependent upon cAMP-mediated reductions in cytosolic calcium (Ishikawa et al., 1994; Nyby et al., 1995). However, as discussed earlier, this varies with vascular venue. Rhonda Prisby and colleagues identified that the endothelium was vital to PTH actions enhancing blood flow to the skeleton in studies of the femoral principal nutrient artery (Prisby et al., 2013). Whether age-dependent increases in vascular sensitivity to pressors combine with altered nutrient artery endothelial PTH1R signaling to compromise bone health remains to be fully explored.

Bilezikian et al. first established that PTH exerts acute inotropic actions in the isolated perfused heart, dependent upon coronary vasodilatation and independent of direct chronotropy (Ogino et al., 1995). In mechanisms that resemble the epithelial−mesenchymal induction effects of paracrine PTHrP during development (*vide supra*), subsets of endothelial cells appear to provide important sources of PTHrP tone that maintains myocardial function and coronary blood flow. Schlüter determined that coronary endothelial cells produce PTHrP under ischemic conditions to enhance both myocardial inotropy (contraction velocity) and lusitropy (relaxation velocity) (Lutteke et al., 2005; Schluter et al., 2000). Consistent with this, Feola and Crass demonstrated that administration of PTH(1−34) 30 min after the initiation of myocardial ischemia preserved left ventricular function and prevented cardiogenic shock in a canine model of myocardial infarction

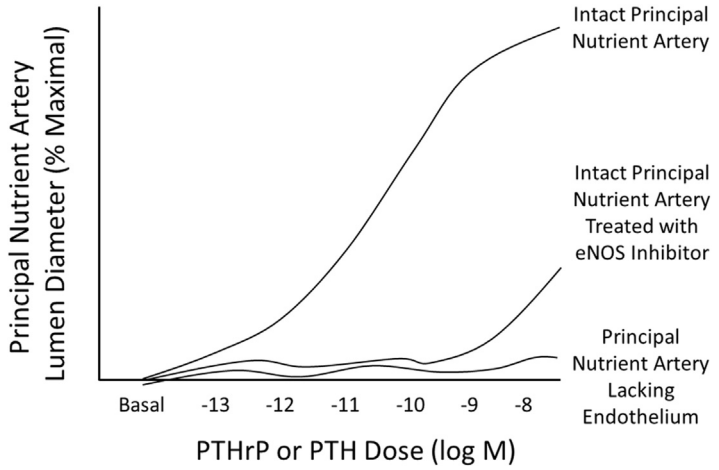

FIGURE 26.1 Parathyroid hormone (*PTH*) and parathyroid hormone−related protein (*PTHrP*) vasodilation of rat femoral nutrient arteries requires intact endothelial nitric oxide synthase (*eNOS*) signaling (Benson et al., 2016). Prisby and colleagues demonstrated that, in addition to aligning the marrow microvasculature closer to the bone multicellular unit as necessary for bone formation (Prisby et al., 2011), PTH/PTHrP signaling also increases blood flow to bone. In elegant ex vivo studies, they demonstrated that PTHrP and PTH induced vasodilation (increased lumen diameter) in the principal nutrient artery supplying rat femurs. This required an intact endothelium (Benson et al., 2016). Inhibition of eNOS with $_L N^G$-nitroarginine methyl ester (L-NAME) also significantly inhibited the vasodilatory responses to either PTH or PTHrP. Importantly, Gohin et al. (2016) have shown that L-NAME inhibits PTH-stimulated increases in bone formation as well. *Graphic representation/summary of results from Benson, T., Menezes, T., Campbell, J., Bice, A., Hood, B., Prisby, R., 2016. Mechanisms of vasodilation to PTH 1-84, PTH 1-34, and PTHrP 1-34 in rat bone resistance arteries. Osteoporos. Int. 27, 1817−1826.*

(Feola and Crass, 1986). However, others have reported direct inotropic effects of PTH(1−34) using isolated cardiomyocytes studied in culture (Tastan et al., 2009). This suggests that pharmacological mimicry of these PTHrP-mediated paracrine endothelial-to-mesenchymal (e.g., coronary smooth muscle, myocardium) signals may hold therapeutic potential in human cardiovascular disease.

Vascular smooth muscle-derived PTHrP has emerged as a stretch-inducible paracrine vasodilator, important for homeostatic roles of PTH1R signaling that control tissue perfusion via regional arterial tone (Noda et al., 1994; Pirola et al., 1994; Takahashi et al., 1995). Clemens's group first established that augmenting local PTHrP/PTH1R signaling has an impact on blood pressure and vascular contractility; sustained reductions in blood pressure and increases in volume-dependent renal tissue perfusion were obtained in novel VSMC-specific transgenic mice expressing either PTHrP or the PTH1R (Noonan et al., 2003). Moreover, pressor responses to angiotensin II were significantly reduced in transgenic animals versus nontransgenic siblings. Wild-type PTH1R activation is ligand dependent; thus, these data strongly suggest that endogenous paracrine PTHrP production—modulated by mechanical, inflammatory, and endocrine cues—locally regulates tissue perfusion (Noonan et al., 2003).

However, it was a seminal study published a decade later by Raison et al. that elegantly confirmed and refined this working model (Raison et al., 2013). Using mice possessing floxed PTHrP alleles and implementing a smooth muscle cell transgene driving tamoxifen-inducible Cre recombinase, postnatal conditional deletion of VSMC PTHrP was achieved in adult mice, thus permitting an assessment of effects on renal blood flow (Raison et al., 2013). Compared with control mice, mice lacking PTHrP in VSMCs (viz., transgenic smooth muscle ERT2-Cre;PTHrP(flox/flox) treated with tamoxifen) exhibited increased renal vascular resistance with concomitant reductions in kidney perfusion and glomerular filtration (Raison et al., 2013). Importantly, renovascular perfusion in response to mechanical stimulation with saline volume expansion (SVE) was also impaired. While normal mice increase renal plasma flow with subsequent diuresis in response to SVE—indices of renovascular vasodilation (see Fig. 26.2)—mice lacking VSMC PTHrP were unable to do so. Interestingly, no change in systemic blood pressure was noted in these VSMC-specific PTHrP-knockout mice even though *pharmacological* dosing with PTHrP simultaneously reduced blood pressure while increasing renal plasma flow (Raison et al., 2013). Thus, endogenous VSMC PTHrP production is required to enable regulated renal perfusion in response to hemodynamic challenge without overt changes in baseline blood pressure.

At first glance, this emerging physiology appears paradoxical when viewed against the backdrop of the cardiovascular disease burden that accrues with primary hyperparathyroidism (HPT) (Yu et al., 2010, 2011, 2013) or the secondary HPT of CKD. Hypertension, arteriosclerosis, valve and vascular calcification, and cardiovascular mortality are all increased with HPT (Carrelli et al., 2013; Fitzpatrick et al., 2008; Iwata et al., 2012; Rubin et al., 2005; Silverberg et al., 2009; Walker

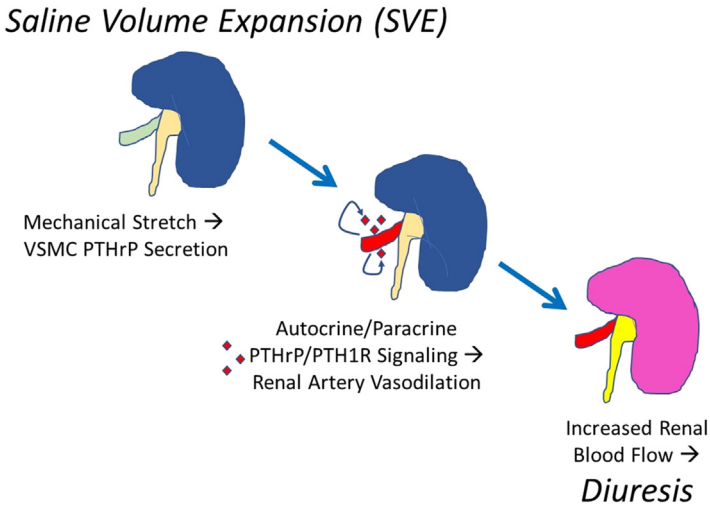

FIGURE 26.2 Saline volume expansion (*SVE*) activates vasodilatory vascular smooth muscle cell (*VSMC*) parathyroid hormone−related protein (*PTHrP*) actions that regulate renal blood flow. Barthelmebs and colleagues demonstrated that increases in renal blood flow in response to SVE require VSMC PTHrP expression (Raison et al., 2013). Unlike the model depicted for wild-type mice, conditional deletion of PTHrP in adult VSMCs abrogates physiological increases in renovascular perfusion and diuresis in response to SVE. Interestingly, no change in systemic blood pressure was noted with genetic VSMC PTHrP deficiency, even though *pharmacological* dosing with PTHrP simultaneously reduces blood pressure while increasing renal plasma flow (Raison et al., 2013). *Graphic representation/summary of results from Raison, D., Coquard, C., Hochane, M., Steger, J., Massfelder, T., Moulin, B., Karaplis, A.C., Metzger, D., Chambon, P., Helwig, J.J., et al. 2013. Knockdown of parathyroid hormone related protein in smooth muscle cells alters renal hemodynamics but not blood pressure. Am. J. Physiol. Renal. Physiol. 305, F333−F342.*

et al., 2009, 2010; Walker and Silverberg, 2008; Yu et al., 2010). Vascular desensitization to the aforementioned paracrine PTHrP cues is likely to be one explanation—arising from sustained elevation in circulating PTH with HPT and the inhibitory PTH fragments that accrue in CKD (Friedman and Goodman, 2006; Langub et al., 2003; Nyby et al., 1995). Vascular tissue PTH1R signaling exhibits tachyphylaxis, becoming rapidly refractory to PTH1R-dependent vasorelaxation in response to PTH or PTHrP exposure (Nyby et al., 1995). By studying rat femoral artery segments contracted with norepinephrine ex vivo, Brickman and colleagues demonstrated that vasodilatory responses to either PTHrP or PTH were markedly diminished, by >50%, following 40 min of prior exposure to either of these PTH1R ligands (Nyby et al., 1995) (Fig. 26.3). Similarly, isolated rat VSMCs exhibit tachyphylaxis within 30 min of exposure by using cAMP production as an assay of PTH1R activation (Nyby et al., 1995). Of note, renovascular tachyphylaxis to PTH has been independently documented in the isolated perfused rabbit kidney model (Massfelder et al., 1996). Finally, in otherwise healthy adult humans, while singular administration lowers blood pressure, sustained PTH administration over a period of 12 days actually increases blood pressure (Hulter et al., 1986)—consistent with data from these preclinical disease models (see also "PTH1R activation and the renin–angiotensin–aldosterone axis: a feed-forward vicious cycle"). The precise molecular mechanisms are poorly characterized with respect to the cardiovascular PTH1R; however, as observed in other tissues, modulation of PTH1R actions by PDZ adapter proteins, β-arrestins, and G-protein-receptor kinases certainly contributes to arterial responsivity (Dicker et al., 1999; Peterson and Luttrell, 2017; Romero et al., 2011; Smith and Rajagopal, 2016; Song et al., 2010). Thus, the vasculopathy of primary and secondary HPT will relate in part to arterial desensitization to the important paracrine, PTHrP-dependent regulation of vascular tone and cellular function (Nyby et al., 1995; Raison et al., 2013) (Figs. 26.2 and 26.3). In this model, sustained exposure to PTH and antagonistic PTH degradation fragments can downregulate PTH1R signals regulated by paracrine PTHrP actions that serve homeostatic roles in cardiovascular health (Fig. 26.4) (Friedman and Goodman, 2006; Thompson and Towler, 2012a).

No clinically useful test of *cardiovascular* PTH1R signaling has been developed or validated as of this writing—a clear shortcoming. However, by implementing histomorphometry to quantify the *skeletal* anabolic state (osteoblast surface, mineralizing surfaces) coupled with simultaneous measurements of the prevailing intact PTH level, London and colleagues (London et al., 2015) created an index that reflects an individual's *skeletal* responsiveness to PTH (Towler, 2015) (Fig. 26.5). The investigative team then demonstrated that as a cohort, those dialysis patients with lower ankle–brachial index (ABI)—an index of peripheral arterial disease—exhibit impaired skeletal PTH1R responsiveness (lower osteoblast surface, reduced bone mineralization) compared with dialysis patients with normal ABI (London et al., 2015) (Fig. 26.5). Vascular responses to PTH are important to bone physiology, increasing not only NO-dependent blood flow to bone, but also VEGF-dependent juxtaposition of microvasculature to bone-forming surfaces (Fig. 26.6) (Benson et al., 2016; Guers et al., 2017; Prisby et al., 2011, 2013; Prisby, 2017). Gohin demonstrated that PTH administration increases hindlimb

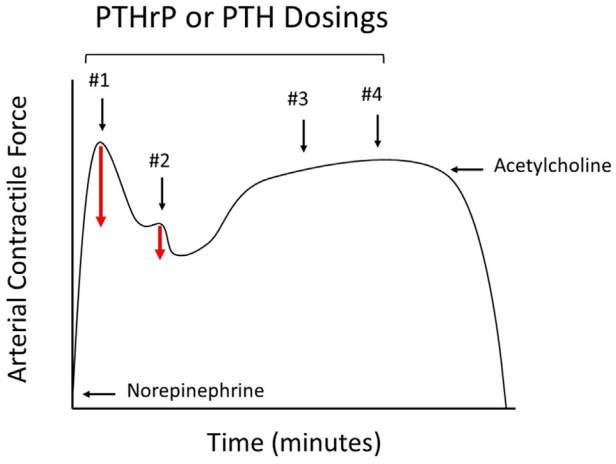

FIGURE 26.3 Arterial desensitization to the vasodilatory actions of parathyroid hormone–related protein (*PTHrP*) or parathyroid hormone (*PTH*). Brickman and colleagues established that following maximal contraction of isolated rat femoral artery segments with the pressor norepinephrine, the initial vasodilatory responses observed with PTH or PTHrP dosing are rapidly lost (Nyby et al., 1995). Compared with the first dose (#1) of either PTH or PTHrP, which resulted in vasorelaxation, subsequent dosing over the next tens of minutes exhibited either blunted (#2) or no (#3, #4) response, indicating tachyphylaxis. However, response to other vasodilators remained intact, as exhibited by preserved vasorelaxation to acetylcholine. *Downward red arrows*, magnitude of vasorelaxation in response to PTHrP or PTH dosing. See text for details. *Graphic representation/summary of results from Nyby, M.D., Hino, T., Berger, M.E., Ormsby, B.L., Golub, M.S., Brickman, A.S., 1995. Desensitization of vascular tissue to parathyroid hormone and parathyroid hormone-related protein. Endocrinology 136, 2497–2504.*

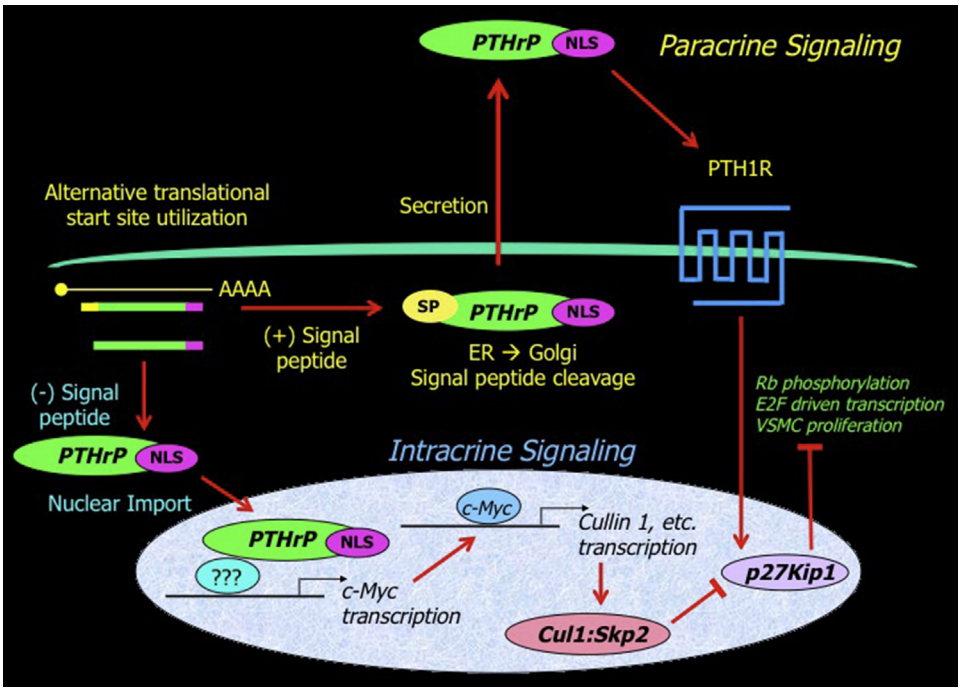

FIGURE 26.4 Paracrine versus intracrine parathyroid hormone–related protein (*PTHrP*) signaling. Translation of the full-length PTHrP protein results in signal peptide (*SP*)-dependent secretion of PTHrP(1–141). Paracrine PTHrP signaling in vascular smooth muscle cells (*VSMCs*), via the G-protein-coupled plasma membrane receptor *PTH1R*, reduces cellular proliferation, promotes vasodilation, and mitigates procalcific signals. Since prior exposure to PTH1R ligands impairs subsequent vasodilatory responses to agonists such as PTHrP (tachyphylaxis; see Fig. 26.3), primary or secondary hyperparathyroidism is predicted to impair the paracrine PTHrP signals important in the hemodynamic regulation of tissue perfusion (e.g., kidney, Fig. 26.2). The nuclear localization signal (*NLS*), although present, is not required for this paracrine activity. Of note, the initiation of PTHrP translation at an alternative internal start site results in a truncated PTHrP protein lacking the N-terminal SP. This nonsecreted PTHrP protein is directed to the nucleus via the NLS encoded at residues 88–106. Nuclear PTHrP activates the c-Myc promoter via this intracrine mechanism, directing expression of programs that enhance Skp2/Cul1-dependent p27Kip1 degradation and promote Cdk2-dependent cellular proliferation. The antagonistic paracrine versus intracrine PTHrP signals differentially regulate p27Kip1— and this emerges as a relevant nodal point in the reciprocal control of VSMC proliferation. Nullification of the paracrine PTHrP actions, as arises with desensitization to chronic PTH exposure (see Fig. 26.3), is predicted to result in unchecked intracrine PTHrP signaling. *ER*, endoplasmic reticulum; *???*, unidentified DNA-binding coregulators of nuclear PTHrP actions. *Reprinted with permission from Towler, D.A., 2014b. The role of PTHrP in vascular smooth muscle. Clin. Rev. Bone Miner. Metabol. 12, 190–196.*

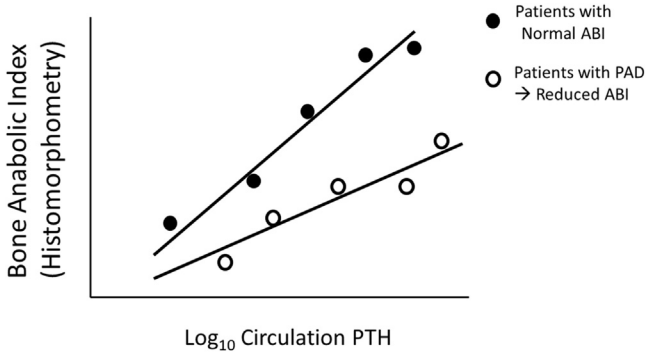

FIGURE 26.5 Histomorphometric evidence of skeletal resistance to parathyroid hormone (*PTH*) in chronic kidney disease patients with peripheral arterial disease (*PAD*). PAD can be identified using a measurement called the ankle–brachial index, or *ABI*. London and colleagues established that, compared with those patients without PAD, patients with PAD exhibit a regression relationship between osteoblast anabolic functions (*y* axis; double-labeled surface or osteoblast surface with bone surface referent) and intact PTH (*x* axis) that characterizes a reduced PTH sensitivity (London et al., 2015). *Graphic representation of the results of London, G.M., Marchais, S.J., Guerin, A.P., de Vernejoul, M.C. 2015. Ankle-brachial index and bone turnover in patients on dialysis. J. Am. Soc. Nephrol. 26, 476-483; Towler, D.A. 2015. Arteriosclerosis, bone biology, and calciotropic hormone signaling: learning the ABCs of disease in the bone-vascular axis. J. Am. Soc. Nephrol. 26, 243–245.*

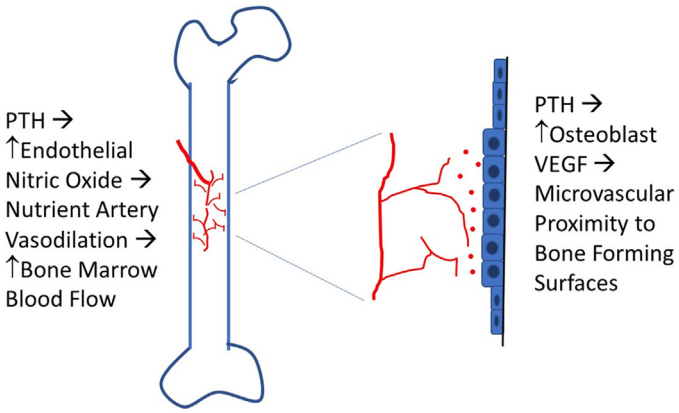

FIGURE 26.6 Parathyroid hormone (*PTH*) actions on skeletal microvasculature are important contributors to anabolic responses. Prisby and colleagues have demonstrated that PTH enhances nutrient artery vasodilation and marrow blood flow in part via endothelial nitric oxide generation by endothelial NO synthase (Prisby et al., 2011) (see also Fig. 26.1). These PTH-induced increases in hindlimb blood flow are important in endocortical bone formation responses (Gohin et al., 2016). Moreover, PTH also increases osteoblast production of vascular endothelial growth factor (*VEGF*; depicted as *red dots*). The paracrine VEGF signaling promotes the juxtaposition of marrow microvasculature to active bone-forming surfaces (Prisby et al., 2011).

blood flow by ca. 30% within 10 min following dosing: a response that is required for PTH-stimulated cortical bone formation (Gohin et al., 2016). Perhaps not surprisingly, then, the vascular dysfunction of arteriosclerosis reduces hip bone mass in humans (Collins et al., 2009) and skeletal perfusion in mice (Shao et al., 2011). However, it remains to be shown that impaired *skeletal* PTH1R signaling is a reliable surrogate for impaired *cardiovascular* PTH1R signaling. Nevertheless, London's important paper (London et al., 2015) highlights that a human metabolic milieu associated with impaired PTH1R signaling exhibits simultaneous reductions in bone and vascular health.

Like CKD, type 2 diabetes and the metabolic syndrome increase the incidence and prevalence of arteriosclerosis, vascular calcification, and conduit vessel stiffness (Stabley and Towler, 2017; Towler, 2017a). This arteriosclerotic vascular stiffness conveys risk for cognitive impairment, stroke, myocardial infarction, heart failure, progression of CKD, and lower extremity amputation (Stabley and Towler, 2017; Thompson and Towler, 2012b; Towler, 2017a). In 2010, our group began to directly assess the potential benefits of cell-autonomous arterial smooth muscle PTH1R signaling in a preclinical model of diabetic arteriosclerosis. We did this by generating a transgenic mouse expressing a constitutively active PTH1R transgene, *PTH1R(H223R)*, in vascular smooth muscle of LDLR$^{-/-}$ mice using the SM22 promoter as a delivery module (Cheng et al., 2010). The PTH1R(H223R) Jansen metaphyseal chondrodysplasia variant is ligand-independent, constitutively active PTH1R that does not undergo homologous desensitization/tachyphylaxis (Schipani et al., 1995). In the LDLR-deficient mouse model of diet-induced diabetic arteriosclerosis, we showed that the VSMC *PTH1R(H223R)* transgene significantly reduced aortic calcification and fibrosis while maintaining arterial compliance (Cheng et al., 2010). This occurred in part via PTH1R-dependent inhibition of arterial prosclerotic Wnt signaling and arterial oxidative stress in VSMCs. Furthermore, intermittent dosing with PTH(1−34) was also shown to reduce vascular osteogenic programs, mineralization, and oxidative stress (Cheng et al., 2010; Shao et al., 2003, 2005). Of note, similar responses have been reported by Morii and colleagues in vitro using cultured primary VSMCs treated with PTHrP (Jono et al., 1997). In vivo, Friedman and coworkers subsequently showed that intermittent PTH(1−34) administration reduces vascular calcification in uremic rats (Sebastian et al., 2008). Likewise, Prisby, Lennon-Edwards, and colleagues showed that intermittent PTH(1−34) administration restores endothelial nitric oxide synthase (NOS) levels and endothelium-dependent arterial vasorelaxation impaired with advanced age in rats (Guers et al., 2017). In collaborative studies that are still ongoing at the time of writing, we have shown that conditional deletion of the PTH1R in VSMCs increases arterial fibrosis in diabetic LDLR$^{-/-}$ mice (Cheng et al., 2016). This confirms and extends our previous results demonstrating that enhancing vascular smooth muscle PTH1R actions reduces arteriosclerosis in this diet-induced murine arteriosclerotic disease model (Cheng et al., 2010). Thus, data from multiple laboratories converge to reveal that maintenance of vascular PTH1R signaling tone helps mitigate the arteriosclerotic responses to diabetes, dyslipidemia, uremia, and aging. However, the precise pharmacokinetic−pharmacodynamic (PK−PD) relationships, including the healthy homeostatic "set point" for cardiovascular PTH1R signaling, remain to be determined.

Of note, a novel intracellular signaling system has been identified for PTHrP actions in both VSMCs and the skeleton that differs dramatically from classical PTH1R activation, and actually antagonizes many of the latter's actions (Fig. 26.4) (Clemens et al., 2001; Miao et al., 2008; Towler, 2014b). This mechanism needs to be recognized in any detailed

understanding of PTHrP biology, molecular genetics, and perturbations in circulating PTH levels. The PTHrP gene can encode a transcript wherein translation generates an N-terminal truncation lacking the signal peptide for secretion (Nguyen et al., 2001; Wysolmerski, 2012). A nuclear localization sequence within PTHrP targets the protein to the nucleus where suppression of p27Kip1 expression promotes cell proliferation and neointima formation (Fiaschi-Taesch et al., 2004, 2006, 2009; Fiaschi-Taesch and Stewart, 2003; Massfelder et al., 1997). This intracrine PTHrP/p27Kip1 suppression pathway exerts actions in contradistinction to those elicited by paracrine (secreted) PTHrP/PTH1R signal transduction that suppress proliferation. Thus, when sensitization of the paracrine PTHrP/PTH1R pathway occurs from prior exogenous ligand exposure (Fig. 26.3), the intracrine VSMC PTHrP signaling remains unchecked (Fig. 26.4). The spectrum of nucleoprotein complexes mediating nuclear PTHrP responses involves retinoblastoma-regulated E2F transcriptional pathways (Fiaschi-Taesch et al., 2004; MacLean et al., 2004) and p53 expression (Zhang et al., 2018), but is incompletely characterized.

Thus, strategies that selectively preserve the *paracrine* PTHrP/PTH1R pathway are predicted to exert cardiovascular benefits with respect to enhanced tissue perfusion, reduced arteriosclerotic calcification and vascular stiffness, and restricted neointimal proliferation; these actions, in sum, help to preserve arterial structure, cardiac pump functions, and tissue perfusion. Therefore, in addition to alterations in circulating calcium phosphate levels, the physiology of direct cardiovascular PTH1R signaling and actions deserves full consideration. This concept is very important to embrace as we seek to better define medical and surgical strategies to combat cardiovascular disease in the settings of primary HPT and CKD (Shroff, 2011). As briefly mentioned earlier, no clinically validated metric yet exists to monitor the healthy cardiovascular PTH1R signaling set point. This is all the more difficult since beneficial actions of paracrine PTHrP signaling will be influenced by endocrine PTH tone and circulating inhibitory fragments that accumulate with CKD (Friedman and Goodman, 2006). Moreover, as highlighted (Bilezikian et al., 2015), because variable posttranslational oxidation occurs at residues Met-8 and Met-18 of intact PTH that alters bioactivity, establishing these relationships in certain disease states (CKD, diabetes) may require implementation of an even newer generation of PTH assays (Hocher et al., 2012).

PTH2R signaling in vascular pharmacology

PTH and TIP39 are both agonists for the human PTH2R, while TIP39 is selective for PTH2R and PTHrP is selective for PTH1R activation (Hoare and Usdin, 2001). Compared with PTH1R, far less is known concerning PTH2R signaling and cardiovascular physiology and function. At this early stage of investigation, available data suggest that endogenous TIP39 actions relevant to cardiovascular physiology are likely to be mediated through the central nervous system (CNS). Functional TIP39 protein in peripheral tissues has yet to be unambiguously established; however, since mice transgenic for chondrocyte-specific expression of its cognate receptor PTH2R exhibit skeletal defects, the *TIP39* expression noted in the hypertrophic zone is likely to be functional (Panda et al., 2012). Strategies that rigorously probe *endogenous* TIP39/PTH2R signaling in cardiovascular biology have not yet been pursued. Most relevant studies have pursued pharmacological approaches. In the CNS, intracerebroventricular injection of TIP39 causes a fall in blood pressure in rats (Sugimura et al., 2003). Presynaptic augmentation of glutamatergic autonomic outflow in the hypothalamus (Dimitrov et al., 2011; Dobolyi et al., 2012) and/or arginine vasopressin release may also be important. Of interest, though, TIP39 mRNA has been detected in intrarenal arteries and aorta by RT-PCR (Eichinger et al., 2002).

The *pharmacological* actions of TIP39 administration have been implemented as a strategy to explore contributions of the peripheral PTH2R to cardiovascular physiology. Like the PTH1R, the PTH2R is expressed in endothelial cells, smooth muscle cells, and cardiomyocytes (Potthoff et al., 2011; Ross et al., 2005). Coronary artery flow reserve as modulated by TIP39/PTH2R signaling has been studied in the Langendorff-perfusion isolated rat heart model (Ross et al., 2007). TIP39 treatment exerted little activity in vessels precontracted with phenylephrine. Curiously, precontraction followed by pretreatment with the PTH1R-selective agonist PTHrP enabled vasodilatory response to subsequent TIP39/PTH2R activation (Ross et al., 2007). In vivo, prior cardiac ischemia provided sufficient stimulus for sustained release of endogenous PTHrP from the heart (Monego et al., 2009), and thus potentially enabled the subsequent vasodilatory response to PTH2R ligands. The mechanisms and kinetics of PTH1R−PTH2R cross talk have yet to be fully elucidated, and while TIP39 expression has been detected in the heart and coronary endothelium (Papasani et al., 2004; Ross et al., 2005), endogenous role and regulation therein are virtually unexplored. However, because inducible NOS activity was required for TIP39-mediated dilatation, the coronary endothelium is likely to participate in this complex pharmacology (Ross et al., 2007). Of note, TIP39/PTH2R signaling profoundly reduces the contractility of *isolated* cardiomyocytes in culture (Ross et al., 2005). Thus, as Ross et al. note (Ross et al., 2007), as a dual PTH1R/PTH2R agonist, in some settings human PTH could theoretically exhibit direct negative inotropic actions in vivo via the PTH2R— actions that are countermanded by NOS

release via PTH1R. However, this notion contrasts profoundly with in vivo cardiac PTHrP/PTH1R responses; inotropy is augmented with a net positive impact dependent upon endothelial NO release in vivo (Ogino et al., 1995; Schreckenberg et al., 2009). Nevertheless, it remains possible that PTH1R-selective agonists, compared with dual PTH1R/PTH2R agonists, may differ substantially in any putative cardiovascular actions in human subjects.

By deploying newly available murine genetic models in studies of skin biology, TIP39/PTH2R receptor signaling has been shown to support expression of type I collagen and the small proteoglycan decorin as necessary for robust wound healing in the skin (Sato et al., 2017). Since these very same extracellular matrix molecules are also vital to the integrity of large conduit vessels such as aorta (Faarvang et al., 2016; Farb et al., 2004), PTH2R signaling may potentially play a role in cardiovascular tissue matrix remodeling and repair.

In humans, the complex interplay between actions of PTH as an agonist for both PTH1R and PTH2R has yet to be integrated with the kinetics of PTH1R versus PTH2R desensitization (Bisello et al., 2004); this integration will be necessary to provide a unifying model with respect to the PK−PD for PTH1R signaling in cardiovascular health and disease (Thompson and Towler, 2012a). Since PTH binds to both human PTH1R and human PTH2R and can induce tachyphylaxis in PTH1R—and PTH1R downregulation enables cardiovascular PTH2R vasodilation (Ross et al., 2007)—the kinetics of impaired PTH1R versus PTH2R signaling in HPT will matter. Based upon the current data, HPT is predicted to inhibit coronary flow reserve (CFR; discussed later) as supported by either PTH1R or PTH2R, with loss in PTH1R tone exerting the greater impact. Furthermore, the potential relationships between central actions of TIP39 with respect to peripheral PTH/PTHrP biology have yet to be vetted in detail. It is important to note that centrally administered PTHrP (Yamamoto et al., 1998) and TIP39 (Sugimura et al., 2003) differentially regulate arginine vasopressin release (increased by the former, decreased by the latter), which is relevant to cardiovascular pressor/volume homeostasis. Moreover, in contradistinction to peripheral actions, central actions of PTHrP provide a pressor response that is dependent upon CNS-regulated sympathetic outflow (Nagao et al., 1998), while CNS administration of TIP39 reduces blood pressure (Sugimura et al., 2003). Thus, pharmacology targeting the PTH family of ligands must be cognizant that any peripherally administered compounds that cross the blood−brain barrier may exhibit mixed cardiovascular responses.

Parathyroid hormone, hyperparathyroidism, and calcific aortic valve disease

Another vascular structure affected by PTH signaling is the aortic valve (Iwata et al., 2012). As of this writing, the role of PTH/PTHrP signaling in cardiac valve physiology is very poorly understood. As mentioned, knockdown in zebrafish of either *pth1r* or *pthrp* = *pthlh* ligand impairs aortic valve morphogenesis, dependent upon downstream *notch* actions (Gray et al., 2013). In humans, calcific aortic valve disease (CAVD) is prevalent, afflicting approximately 2% of our population over age 60, with up to half of these possessing previously unappreciated bicuspid aortic valves (Yutzey et al., 2014). By age 75 or older, 15% of individuals will have moderate to severe calcific aortic stenosis. Intriguingly, *NOTCH1* mutations in humans convey valve malformations, CAVD, and Notch1 expression inhibits aortic valve interstitial cell calcification in culture (Acharya et al., 2011). For those with valve stenosis and symptoms, surgical intervention is required to mitigate the very high cardiovascular mortality observed in this setting. Several epidemiological studies indicate that primary HPT is associated with CAVD (Iwata et al., 2012; Linhartova et al., 2008; Stefenelli et al., 1997), and genetic variation in the *PTH* gene has been suggested to be a contributor (Gaudreault et al., 2011; Schmitz et al., 2009). Moreover, elevated PTH and hypertension are both risk factors associated with accelerated clinical progression of CAVD in patients with CKD (Iwata et al., 2013). Because the annulus of the heart valve is rich in chondrocytes and chondrocyte progenitors (Lincoln et al., 2006)—cellular targets of PTH1R signaling in the endochondral skeleton (Hirai et al., 2011; Kronenberg, 2006)—the aortic valve response to PTH1R signaling is likely to be quite complex, and in some instances more akin to the tissue response of endochondral bone (Yutzey et al., 2014). With advanced CAVD, true ectopic woven bone formation—replete with marrow elements and osteoclast-dependent bone remodeling—is observed in 13% of specimens (Fuery et al., 2018; Mohler et al., 2001). Medical therapies targeting cholesterol metabolism have failed to have a significant impact on CAVD (Rajamannan et al., 2011), potentially because oxidized phospholipids and lysophosphatidic acid carried by Lp(a) appear much more important (briefly reviewed in Towler, 2017b). Once valve mineralization is advanced, surgical or endovascular strategies for aortic valve replacement are required (Unger et al., 2016). Should surgical treatment of asymptomatic primary HPT (Yu et al., 2010) prove to mitigate risk for future development of clinically significant CAVD (Iwata et al., 2012) in at-risk individuals (e.g., bicuspid valve, high Lp(a) levels, sclerosis without calcinosis on echocardiography), this would (1) provide additional rationale for integrating cardiovascular phenotyping into indications for surgical treatment and (2) potentially alter the age-specific cutoff for recommending surgery (e.g., to age < 60 in lieu of < 50) (Bilezikian, 2018)

Impaired vascular PTH1R signaling and cardiovascular disease: the impact of hyperparathyroidism on cardiovascular mortality, coronary flow reserve, and vascular stiffness

Numerous observational studies have supported the relationship between primary HPT and cardiovascular disease (Walker and Silverberg, 2008). However, one large study of 2.99 million person-years of follow-up in 5735 patients with mild primary HPT presents a clinically compelling epidemiological data set for this pathophysiological relationship (Yu et al., 2010). This study is called PEARS, the Parathyroid Epidemiology and Audits Research Study. PEARS is a retrospective, population-based outcomes study that investigated patients diagnosed with mild primary HPT in Tayside, Scotland, between 1997 and 2006 (Yu et al., 2010). In the 1683 subjects identified with mild primary HPT (2/3rd female), age- and gender-correlated cardiovascular mortality was increased 2.7-fold (Yu et al., 2010). Baseline PTH levels, not calcium, predict long-term outcomes in untreated primary HPT (Yu et al., 2013). The HEALTH ABC cohort, focused on individuals in Memphis and Pittsburgh, confirmed increases in cardiovascular mortality with elevated PTH; elevation conveyed a 1.8-fold increased risk, independent of serum calcium and 25-hydroxyvitamin D levels (Kritchevsky et al., 2012). As discussed before, preclinical models evaluating PTH/PTHrP actions have long indicated the role of the cardiovascular system as a physiologically relevant target, with mechanisms relevant to disease biology rapidly emerging from genetically and pharmacologically manipulated animals (Cheng et al., 2010, 2016; Qian et al., 2003; Raison et al., 2013). However, it is the physiological studies of human subjects that have confirmed and extended these observations in important ways that are likely to alter our recommendations for treatment of HPT in otherwise "asymptomatic" patients (Silverberg et al., 2009).

Macrovascular compliance and conduit functions, known as Windkessel physiology (Safar and Boudier, 2005; Westerhof et al., 2009), are impaired by HPT (Briet et al., 2012; Rubin et al., 2005; Walker et al., 2009). With every heartbeat, part of the energy of each systolic pulse is stored as potential energy within the rubbery elasticity of conduit vessels via systole-induced circumferential stretching of large arteries (Westerhof et al., 2009). During diastole, this energy is released to provide smooth perfusion of the coronary arteries, myocardium, and distal tissues (Thompson and Towler, 2012a). Moreover, with arterial stiffening, retrograde pulse wave reflections arising at vessel branch points travel faster; rather than supporting early diastole, these omnipresent reflections now sum with the orthograde pulse waves of late systole to increase systolic blood pressure (Safar and Boudier, 2005; Soldatos et al., 2011; Westerhof et al., 2009). Thus, with arterial stiffening, not only does perfusion during diastole become more erratically pulsatile, but the workload placed upon the heart increases due to systolic hypertension. Silverberg, Bilezikian, and colleagues established that arterial stiffening is increased in patients with mild HPT. Using the augmentation index (AIx), a measure of the retrograde wave reflection that characterizes vascular stiffening, they uncovered a positive linear relationship between PTH and AIx after adjusting for heart rate, height, gender, blood pressure, age, diabetes mellitus, smoking, and hyperlipidemia (Rubin et al., 2005). Smith and colleagues reported similar responses in their smaller patient cohort (Smith et al., 2000). Importantly, in patients with preexisting cardiovascular abnormalities, parathyroidectomy improves indices of cardiovascular/carotid stiffness (Walker et al., 2012), indicating reversibility. Of note, Prisby and colleagues noted a protective action of intermittent PTH administration on endothelial NOS expression and conduit vessel endothelial function with aging marrow in rodents (Lee et al., 2018). While not studied in great detail, a few small longitudinal studies of primary HPT patients pre− and post−curative parathyroidectomy have shown that the circadian, pulsatile nature of diurnal PTH secretion is normalized as well (Lobaugh et al., 1989).

CFR is a physiological index of epicardial conduit function. CFR assesses not only the significance of any coronary stenosis present, but also the presence of downstream microvascular dysfunction (Bianco and Alpert, 1997). When myocardial oxygen demand downstream of a conduit artery segment cannot be met by vasodilation, CFR is deemed to be compromised (Bianco and Alpert, 1997). Importantly, reduced CFR portends adverse cardiovascular outcomes in men and women (Cortigiani et al., 2012; Pepine et al., 2010). CFR was initially evaluated by angiography following intracoronary administration of vasodilators coupled with Doppler imaging (Pepine et al., 2010); however, transthoracic Doppler echocardiography (Cortigiani et al., 2012) has now been implemented, with peripheral adenosine vasodilator administration, as a mechanism for noninvasively assessing CFR (Caiati et al., 1999; Montisci et al., 2006).

In 2012, Osto and colleagues performed a highly important, longitudinal analysis of CFR in 100 primary HPT patients with solitary adenomas. These patients were studied before and after adenoma resection, comparing CFR results in that population to 50 gender- and age-matched controls (Osto et al., 2012). In this landmark study, they established that PTH, age, and heart rate were the only major variables altering CFR— and that CFR changes with HPT were independent of serum calcium. Moreover, in the 27 primary HPT patients with clearly abnormal CFR ($\leq$2.5 following adenosine

infusion), all of these individuals exhibited normal CFR (>2.5) following curative adenoma resection (Osto et al., 2012). Deploying an independent method for CFR measurement—viz., nuclear perfusion imaging—Marini and colleagues also demonstrated improvement of CFR in primary HPT undergoing surgical treatment (Marini et al., 2010). In a clinically important way, these two studies confirmed and extended the previous work of Kosch et al. (Kosch et al., 2000); they had shown that brachial artery flow-mediated vasodilation, an index of endothelial function and NOS activation, is impaired in primary HPT but reversed following surgical treatment (Kosch et al., 2000). The impaired flow-mediated dilation in patients with primary HPT undergoing medical observation has only recently been confirmed by others (Colak et al., 2017). Thus, primary HPT is consistently associated with reversible alterations in coronary and peripheral artery endothelial function that improve following surgical intervention. The improvements in CFR following surgery for HPT have significant implications as the risks versus benefits of parathyroidectomy in otherwise asymptomatic HPT are considered.

Chronic kidney disease–mineral and bone disorder: the metabolic "perfect storm" of cardiovascular risk

CKD is a highly significant cardiovascular risk factor, synergizing with diabetes to increase morbidity and mortality at least 5- to 10-fold (Chang et al., 2013; Debella et al., 2011). While cholesterol-lowering therapies have an impact, reducing nonfatal cardiovascular events by ca. 20% in predialysis CKD, no significant reduction in cardiovascular mortality has been achieved with this strategy in CKD patients on dialysis (Baigent et al., 2011; Baigent and Landry, 2003). This appears to be in large part due to the contributions of perturbed calcium phosphate metabolism to cardiovascular risk (Block et al., 2013) and the bone-derived hormone FGF23 (Moe et al., 2015). Indeed, the CKD–mineral and bone disorder designation was created as an imperfect mechanism meant to capture the implications of this clinical setting (Kidney Disease: Improving Global Outcomes, 2009; Moe et al., 2007).

In the setting of CKD, serum phosphate exerts a stepwise increase in cardiovascular mortality (Eddington et al., 2010). Vascular toxicity is mediated in part via arterial calcification (Shao et al., 2010), and cardiovascular mortality tracks the presence and extent of vascular mineralization (Blacher et al., 2001; London, 2003; London et al., 2003). Phosphate-dependent activation of sodium phosphate cotransporter signaling in VSMCs drives osteogenic mineralization programs (Liu et al., 2013) and proapoptotic responses that perturb mineralizing matrix vesicle clearance, thus augmenting vascular calcium load (Shroff et al., 2008, 2010, 2013). However, at every level of renal function, serum phosphate is a cardiovascular risk factor (Tonelli et al., 2005, 2009) and PTH is a key defense against hyperphosphatemia (Martin and Gonzalez, 2011). PTH directly induces renal phosphate excretion when renal function is intact, recruits osteoblast-derived FGF23 to assist in these phosphaturic actions, and maintains bone formation even in the setting of CKD—a state of variable skeletal resistance to PTH (London et al., 2004; Martin et al., 2012; Quarles, 2013). Thus, actions of PTH play an important role along with FGF23 in mitigating phosphate-dependent vascular toxicity when renal function is intact and normal bone turnover is maintained (London et al., 2004; Martin et al., 2012; Quarles, 2013). Extremes of bone turnover—too high or too low—are likely to negatively influence serum phosphate homeostasis in the setting of CKD (Barreto et al., 2008; Goodman, 2004; London et al., 2004). This may in part explain the bimodal relationship between PTH levels and mortality in dialysis patients (Durup et al., 2012). However, the specific relationship between bone formation (potentially functioning as a "buffer" mitigating vascular phosphate toxicity), changes in PTH tone with declining renal function, and maintaining healthy norms of serum phosphate homeostasis with respect to vascular physiology has not yet been established (Block et al., 2013; Maeda et al., 2007).

Gerard London and colleagues have provided the most important insights into the relationship between PTH, arterial calcification, and bone formation in the setting of CKD (London et al., 2004). Implementing an ultrasound-based method for scoring calcification in the common carotid arteries, the abdominal aorta, the iliofemoral axis, and the lower extremities, his group related the extent of arterial calcification with dynamic histomorphometric assessment of cellular bone functions to circulating PTH. In this important study, they established that patients with the lowest levels of PTH (with or without prior parathyroid surgery) exhibited low-turnover bone disease and the most extensive vascular calcification (London et al., 2004). The relationship between low PTH values and increased coronary artery calcification was subsequently confirmed by others (Kim et al., 2011). Interestingly, similar observations were made by Chertow and colleagues upon comparison of the relationships between bone mineral density, vascular calcium load, and PTH levels in patients treated with calcium-based phosphate binders versus sevelamer (does not contain calcium) (Raggi et al., 2005). Suppression of PTH levels in those subjects given calcium-based binders was associated with lower bone mass and increased vascular calcium load.

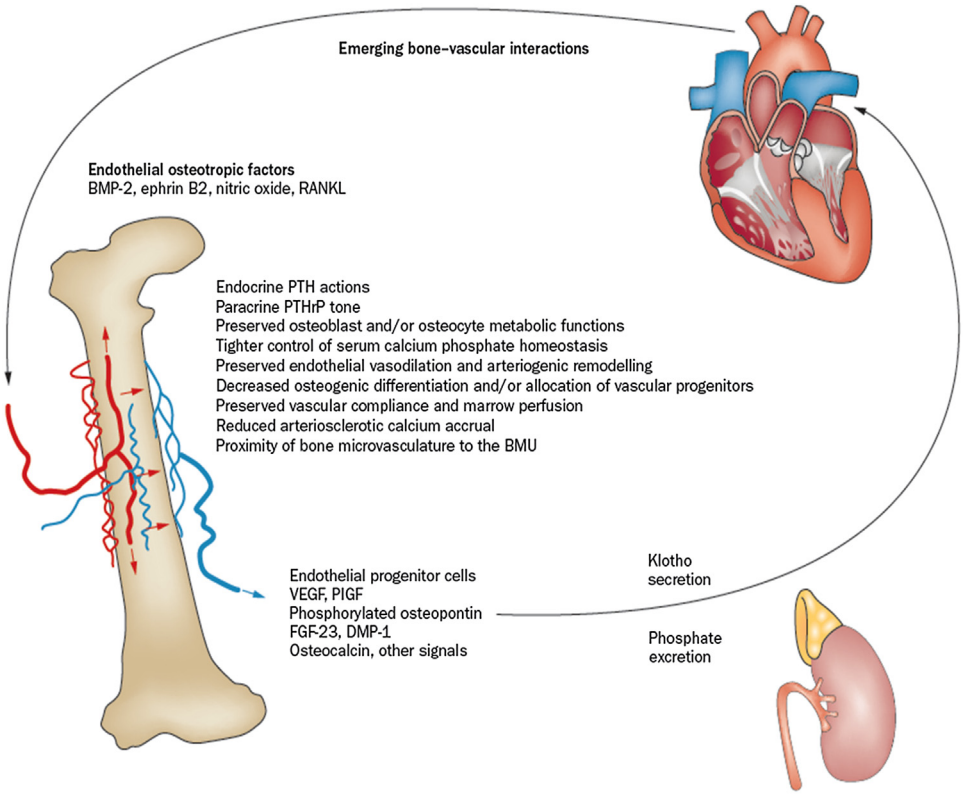

FIGURE 26.7 An emerging bone–vascular axis is connected by calcium, phosphate, hormonal, and cellular signals in cardiovascular health and disease. The skeleton is a parathyroid hormone (*PTH*) receptor 1 (PTH1R)-regulated source/repository of hormones, electrolytes, and cellular elements that profoundly influence cardiovascular health. The kidney plays a pivotal role in modulating this axis by mediating phosphate excretion and by providing additional hormonal relays. The vasculature is also a direct target of PTH actions via both PTH1R and PTH2R in humans. Perturbation of this axis creates the chronic kidney disease–mineral and bone disorder. *BMP-2*, bone morphogenetic protein; *BMU*, basic multicellular unit; *DMP-1*, dentin matrix protein 1; *FGF-23*, fibroblast growth factor 23; *PlGF*, placental growth factor; *PTHrP*, PTH-related protein; *RANKL*, receptor activator of NF-κB ligand; *VEGF*, vascular endothelial growth factor. *See text for details, reprinted with permission from Thompson, B., Towler, D.A. 2012a. Arterial calcification and bone physiology: role of the bone-vascular axis. Nat. Rev. Endocrinol.*

Basal PTH tone most likely exerts beneficial actions via maintenance of bone formation (London et al., 2004). As discussed (Demer and Tintut, 2010; Fadini et al., 2012; Thompson and Towler, 2012a; Zoppellaro et al., 2012), it has become increasingly clear that skeletal maintenance of hematopoiesis, regulation of calcium phosphate exchange, and skeletal production of phosphaturic hormones such as FGF23 play important roles in vascular health (Fig. 26.7; see also discussion of EVOLVE results later). Surgery is the standard of care for severe primary and severe secondary/tertiary HPT (Silverberg et al., 2009). However, surgery is not the first-line approach to the vast majority of patients with significant secondary HPT in CKD because of the clinical need to "titrate" PTH levels to maintain bone formation (London et al., 2004). In the setting of uremia, circulating fragments of PTH and uremic toxins give rise to a skeletal resistance to PTH (Friedman and Goodman, 2006). Based on dynamic histomorphometry performed in patients with CKD5 and on dialysis, PTH levels between 150 and 300 pg/mL were associated with maintenance of normal bone turnover in this setting. However, similar analyses have not been performed in CKD patients prior to the initiation of renal replacement therapy. Moreover, the specific PTH assay used to establish this treatment goal is no longer available, calling into question how one coregisters these prior guidelines with current-generation PTH assays. Hence, current KDIGO (Kidney Disease Improving Global Outcomes) guidelines recommend levels of PTH between two and nine times the upper limit of normal in any given assay, although not strictly coregistered with skeletal or cardiovascular indices of health (London et al., 2010).

Nevertheless, striving to achieve this skeletally defined set point also appears to improve cardiovascular disease risk; and the cardiovascular benefits of pharmacological management of HPT were first established in the setting of CKD5 on dialysis. Treatment with injectable calcitriol or paricalcitol to maintain PTH levels to approximately two to four times the upper limit of normal reduces cardiovascular mortality (Teng et al., 2003, 2005) and points once again to the importance of calciotropic hormones as key modulators of cardiovascular disease in this setting. This biology and pharmacology is likely

to be relevant to improving the care of the many aging individuals with CKD3 or worse who do not require renal replacement therapy (30 million individuals estimated in the United States alone). The Systolic Blood Pressure Intervention Trial (SPRINT) noted that predialysis patients with CKD3 or worse and high PTH levels accrued less cardiovascular benefit from intensive blood pressure therapy (Ginsberg et al., 2018). It will be important to determine if normalizing PTH levels in CKD3/CKD4 with novel oral extended-release formulations of calcifediol (Sprague et al., 2017) will restore the cardiovascular benefits of intensive blood pressure control (Ginsberg et al., 2018).

As a type II calcium-sensing receptor mimetic with a short half-life, cinacalcet successfully reduces circulating PTH levels and enables facile titration to goal. Cinacalcet is very effective in treating primary and secondary HPT, but its actions on cardiovascular and fracture risks are still emerging (Verheyen et al., 2013). A meta-analysis of four studies suggested reductions in both hip fracture and cardiovascular hospitalization rates with cinacalcet (Cunningham et al., 2005). In EVOLVE (Evaluation of Cinacalcet Hydrochloride Therapy to Lower Cardiovascular Events), a prospective study to treat secondary HPT in dialysis patients with CKD5, cinacalcet failed to achieve significant reductions in cardiovascular mortality ($P = .11$) in the unadjusted intention-to-treat analysis (Investigators et al., 2012). However, in a second prespecified analysis, older patients on hemodialysis with moderate to severe secondary HPT did accrue cardiovascular benefit with cinacalcet-mediated reductions in PTH (Parfrey et al., 2015). The milieu of CKD5 and dialysis represents a metabolic "perfect storm" for cardiovascular disease; in this setting, secondary HPT is but one important contributor that must be addressed (Towler, 2013). Moving forward, the multifactorial high-risk metabolic and genetic milieu of CKD must be prospectively embraced as strategies targeting PTH biology are evaluated for mitigating cardiovascular risk. Recall that PTH controls FGF23 release from the osteocyte (Rhee et al., 2011). Upon stratification of secondary reductions in FGF23 also achievable by cinacalcet dosing (64% vs. 28% placebo), the EVOLVE trial was able to demonstrate reduced cardiovascular mortality in those patients that exhibited a 30% or greater reduction in FGF23 (Moe et al., 2015). The improvement was achieved via reductions in nonatherosclerotic cardiovascular events, and mechanisms segregating responders from nonresponders have yet to be determined, but may reflect unknown features of the PTH-regulated bone−vascular axis (Fig. 26.7).

Of note, the relationship between bone turnover, PTH, and vascular risk may not hold with respect to the calciphylaxis syndrome, aka calcific uremic arteriolopathy (Shao et al., 2010). This distinct clinical entity involves fibroproliferative calcification of smaller-diameter arterioles in dermal adipose, lung, and mesentery. It is seen most frequently in obese diabetic patients with CKD on warfarin anticoagulation and can be associated with severe HPT (Matsuoka et al., 2005; Rogers et al., 2007). The pathobiology of this important and lethal entity is still poorly understood (Nigwekar et al., 2015).

PTH/PTHrP signaling and the bone−vascular axis

As Scadden, Kronenberg, and colleagues have established, the PTH1R controls the size of the bone marrow hematopoietic niche via its osteotropic actions (Adams et al., 2007; Calvi et al., 2003). This is a critically important concept to consider particularly in the setting of CKD−MBD; circulating hematopoietic progenitors and endothelial progenitor cells derived from the bone marrow niche contribute to both healthy and pathological injury responses in distant venues (Eghbali-Fatourechi et al., 2005, 2007; Fadini et al., 2012). Cognizant of this, Zaruba et al. (Brunner et al., 2008; Zaruba et al., 2008) and Napoli and colleagues (Napoli et al., 2008) examined the impact of PTH(1−34) in models of myocardial and critical limb ischemia, respectively. Zaruba demonstrated that survival following occlusion of the left anterior descending artery in mice was increased from 40% to 60% by postischemia dosing with PTH(1−34). While the relative contributions of vasodilation, angiogenesis, and apoptosis were not examined, survival tracked PTH(1−34)-induced increases in myocardial VEGF expression, neovascularization, and $CD31^+$ and $CD34^+/CD45^+$ cell populations (Zaruba et al., 2008). Border zone cardiomyocyte apoptosis was reduced, with concomitant improvement in cardiac output. Using unilateral femoral artery ligation to model critical limb ischemia, Napoli et al. demonstrated that preligation dosing with PTH(1−34) followed by postischemic granulocyte colony-stimulating factor mobilization of marrow progenitors simultaneously increased limb blood flow and viability and $CD34^+$ stem cell recruitment to and capillary density in ischemic limb skeletal muscle (Napoli et al., 2008).

Thus, an emerging bone−vascular axis has been proposed wherein circulating progenitor cells dependent upon PTH1R bioactivity can favorably influence cardiovascular health (Fig. 26.7). Since circulating endothelial progenitor cell subtypes are differentially altered in patients with peripheral arterial disease, coronary syndromes, or diabetes (Flammer et al., 2012a, 2012b, endothelial progenitor cell quality and character will be extremely important to consider (Gossl et al., 2010). Whether this axis can be productively harnessed with PTH/PTHrP signaling to have an impact on cardiovascular disease burden in humans remains to be explored.

PTH1R activation and the renin–angiotensin–aldosterone axis: a feed-forward vicious cycle

As mentioned before, the relationships between HPT and hypertension are well appreciated (Tomaschitz et al., 2012). In otherwise healthy adults, while singular administration lowers blood pressure, sustained PTH administration over a period of 12 days actually increases blood pressure in humans (Hulter et al., 1986). In addition to the aforementioned PTH1R desensitization mechanisms (Nyby et al., 1995) that impair paracrine PTHrP-mediated vasorelaxation (Maeda et al., 1999; Raison et al., 2013), PTH may have direct effects on aldosterone biosynthesis (Tomaschitz et al., 2012). However, PTH1R-dependent signals in the juxtaglomerular apparatus also support renin production (Saussine et al., 1993a, 1993b). Following surgery for HPT, renin and aldosterone levels fall (Kovacs et al., 1998), albeit with variable improvements in blood pressure and cardiac hypertrophy (Agarwal et al., 2013; Broulik et al., 2011; Ishay et al., 2011; Kovacs et al., 1998; Persson et al., 2011; Vazquez-Diaz et al., 2009). Conversely, it has become clear that angiotensin II augments circulating PTH levels in part via aldosterone/mineralocorticoid receptor signaling pathways in humans (Brown et al., 2013). Thus, a "feed-forward" vicious cycle may exist between dysregulated PTH and the renin–angiotensin–aldosterone (RAA) axis that promotes cardiovascular disease arising from the metabolic derangements of aging, declining renal function, and HPT (Tomaschitz et al., 2013). Of note, the risk for CAVD progression in the Japanese Aortic Stenosis Study tracked with absence of angiotensin receptor blocker therapy in early-stage disease (Yamamoto et al., 2010). While PTH levels were not assessed, it is intriguing to speculate that modulating both arms of the prosclerotic PTH–RAA cycle might help mitigate CAVD risk with aging and uremia (Rajamannan et al., 2011). This potential relationship has yet to be tested in either preclinical or clinical research settings. The use of RAA inhibitors does indeed reduce PTH levels in humans (Brown et al., 2015).

Summary, conclusions, and future directions

The cardiovascular actions of PTH have been known for almost a century (Collip and Clark, 1925). However, the clinical and pharmacological implications of altered PTH/PTHrP signaling with respect to cardiovascular endocrinology have been underappreciated except in the settings of extreme excess with severe hypercalcemia or calciphylaxis. In addition to mild primary HPT, secondary HPT associated with advancing age and/or declining renal function is increasingly prevalent. In addition to the uremic milieu of CKD (Friedman and Goodman, 2006), dyslipidemia also induces a state of PTH/PTHrP resistance (Li et al., 2014; Sage et al., 2011). As such, perturbations in PTH/PTHrP physiology are emerging as one of the most prevalent endocrinopathies affecting human health and health care today. Heart disease remains the No. 1 cause of mortality worldwide and is a growing burden (Gaziano et al., 2006). Given the contributions of PTH/PTHrP signaling in cardiovascular health and disease—and the prevalence of perturbed PTH endocrine physiology—it remains stunning that so very little is known about the fundamentals of PTH/PTHrP biology within the vasculature. The specific protein–protein interactions and signaling cascades conveying PTH1R/PTH2R actions in VSMCs, endothelial cells, and interstitial/adventitial cell populations need to be defined for each relevant vascular bed. Coronary, renal, and iliofemoral vessels may represent the most clinically relevant with respect to cardiovascular and metabolic bone diseases. The mechanisms controlling paracrine PTHrP bioactivities have yet to be identified and fully integrated with the mechanical and neuroendocrine cues that together coordinate tissue perfusion. Most importantly, tissue-specific biomarkers and functional imaging methods are required to quantify cardiovascular PTH/PTHrP actions as a first step toward establishing the healthy set point for signaling tone and dynamics. Because posttranslational modifications and dysmetabolic states induce PTH/PTHrP resistance in the very settings where this biology becomes most clinically significant (Demer and Tintut, 2010; Thompson and Towler, 2012a), titration to a single circulating PTH value range will probably prove to be inadequate. Moreover, whereas surgery is a standard of care in primary HPT that yields reductions in hip fracture risk, renal disease, and hypercalcemic crises (Silverberg et al., 2009; VanderWalde et al., 2006), the impact of parathyroid surgery on cardiovascular morbidity has yet to be firmly established for mild or asymptomatic disease. However, beneficial changes with curative surgery in important cardiovascular parameters, such as vascular stiffness (Walker et al., 2012) and CFR (Osto et al., 2012), are truly compelling. It remains unclear whether surgical and pharmacological interventions for treatment of HPT are functionally equivalent with respect to cardiovascular outcomes. As occurred during the history of the cholesterol controversy, discovery and implementation of clearly effective pharmacotherapy will be important (Steinberg, 2006). Clearly, detailed examination of cardiovascular physiology as regulated by the PTH superfamily will continue to yield important new insights, and will be necessary to devise novel therapeutic strategies that better treat our patients afflicted with cardiometabolic and mineral metabolism disorders.

Acknowledgments

D.A.T. is supported by grants from the National Institutes of Health (HL069229, HL114806) and the American Diabetes Association, the J.D. and Maggie E. Wilson Distinguished Chair in Biomedical Research, and the Louis V. Avioli Professorship in Mineral Metabolism Research.

References

Acharya, A., Hans, C.P., Koenig, S.N., Nichols, H.A., Galindo, C.L., Garner, H.R., Merrill, W.H., Hinton, R.B., Garg, V., 2011. Inhibitory role of Notch1 in calcific aortic valve disease. PLoS One 6, e27743.

Adams, G.B., Martin, R.P., Alley, I.R., Chabner, K.T., Cohen, K.S., Calvi, L.M., Kronenberg, H.M., Scadden, D.T., 2007. Therapeutic targeting of a stem cell niche. Nat. Biotechnol. 25, 238–243.

Agarwal, G., Nanda, G., Kapoor, A., Singh, K.R., Chand, G., Mishra, A., Agarwal, A., Verma, A.K., Mishra, S.K., Syal, S.K., 2013. Cardiovascular dysfunction in symptomatic primary hyperparathyroidism and its reversal after curative parathyroidectomy: results of a prospective case control study. Surgery 154, 1394–1404.

Babiker, H.M., McBride, A., Newton, M., Boehmer, L.M., Drucker, A.G., Gowan, M., Cassagnol, M., Camenisch, T.D., Anwer, F., Hollands, J.M., 2018. Cardiotoxic effects of chemotherapy: a review of both cytotoxic and molecular targeted oncology therapies and their effect on the cardiovascular system. Crit. Rev. Oncol. Hematol. 126, 186–200.

Baigent, C., Landray, M.J., Reith, C., Emberson, J., Wheeler, D.C., Tomson, C., Wanner, C., Krane, V., Cass, A., Craig, J., et al., 2011. The effects of lowering LDL cholesterol with simvastatin plus ezetimibe in patients with chronic kidney disease (Study of Heart and Renal Protection): a randomised placebo-controlled trial. Lancet 377, 2181–2192.

Baigent, C., Landry, M., 2003. Study of heart and renal protection (SHARP). Kidney Int. Suppl. S207–S210.

Barreto, D.V., Barreto Fde, C., Carvalho, A.B., Cuppari, L., Draibe, S.A., Dalboni, M.A., Moyses, R.M., Neves, K.R., Jorgetti, V., Miname, M., et al., 2008. Association of changes in bone remodeling and coronary calcification in hemodialysis patients: a prospective study. Am. J. Kidney Dis. 52, 1139–1150.

Benson, T., Menezes, T., Campbell, J., Bice, A., Hood, B., Prisby, R., 2016. Mechanisms of vasodilation to PTH 1-84, PTH 1-34, and PTHrP 1-34 in rat bone resistance arteries. Osteoporos. Int. 27, 1817–1826.

Bianco, J.A., Alpert, J.S., 1997. Physiologic and clinical significance of myocardial blood flow quantitation: what is expected from these measurements in the clinical ward and in the physiology laboratory? Cardiology 88, 116–126.

Bilezikian, J.P., 2018. Primary hyperparathyroidism. J. Clin. Endocrinol. Metab. 103, 3993–4004.

Bilezikian, J.P., Marcus, R., Levine, M.A., Marococci, C., Silverberg, S.J., Potts, J.T., 2015. The Parathyroids: Basic and Clinical Concepts. Elsevier/AP, Academic Press is an imprint of Elsevier, Amsterdam, Boston.

Bisello, A., Manen, D., Pierroz, D.D., Usdin, T.B., Rizzoli, R., Ferrari, S.L., 2004. Agonist-specific regulation of parathyroid hormone (PTH) receptor type 2 activity: structural and functional analysis of PTH- and tuberoinfundibular peptide (TIP) 39-stimulated desensitization and internalization. Mol. Endocrinol. 18, 1486–1498.

Blacher, J., Guerin, A.P., Pannier, B., Marchais, S.J., London, G.M., 2001. Arterial calcifications, arterial stiffness, and cardiovascular risk in end-stage renal disease. Hypertension 38, 938–942.

Blanco, R., Gerhardt, H., 2013. VEGF and Notch in tip and stalk cell selection. Cold Spring Harb. Perspect. Med. 3, a006569.

Block, G.A., Ix, J.H., Ketteler, M., Martin, K.J., Thadhani, R.I., Tonelli, M., Wolf, M., Juppner, H., Hruska, K., Wheeler, D.C., 2013. Phosphate homeostasis in CKD: report of a scientific symposium sponsored by the National Kidney Foundation. Am. J. Kidney Dis. 62, 457–473.

Briet, M., Pierre, B., Laurent, S., London, G.M., 2012. Arterial stiffness and pulse pressure in CKD and ESRD. Kidney Int. 82, 388–400.

Broulik, P.D., Broulikova, A., Adamek, S., Libansky, P., Tvrdon, J., Broulikova, K., Kubinyi, J., 2011. Improvement of hypertension after parathyroidectomy of patients suffering from primary hyperparathyroidism. Int. J. Endocrinol. 2011, 309068.

Brown, J., de Boer, I.H., Robinson-Cohen, C., Siscovick, D.S., Kestenbaum, B., Allison, M., Vaidya, A., 2015. Aldosterone, parathyroid hormone, and the use of renin-angiotensin-aldosterone system inhibitors: the multi-ethnic study of atherosclerosis. J. Clin. Endocrinol. Metab. 100, 490–499.

Brown, J.M., Williams, J.S., Luther, J.M., Garg, R., Garza, A.E., Pojoga, L.H., Ruan, D.T., Williams, G.H., Adler, G.K., Vaidya, A., 2013. Human interventions to characterize novel relationships between the renin-angiotensin-aldosterone system and parathyroid hormone. Hypertension.

Brunner, S., Zaruba, M.M., Huber, B., David, R., Vallaster, M., Assmann, G., Mueller-Hoecker, J., Franz, W.M., 2008. Parathyroid hormone effectively induces mobilization of progenitor cells without depletion of bone marrow. Exp. Hematol. 36, 1157–1166.

Caiati, C., Montaldo, C., Zedda, N., Bina, A., Iliceto, S., 1999. New noninvasive method for coronary flow reserve assessment: contrast-enhanced transthoracic second harmonic Echo Doppler. Circulation 99, 771–778.

Calvi, L.M., Adams, G.B., Weibrecht, K.W., Weber, J.M., Olson, D.P., Knight, M.C., Martin, R.P., Schipani, E., Divieti, P., Bringhurst, F.R., et al., 2003. Osteoblastic cells regulate the haematopoietic stem cell niche. Nature 425, 841–846.

Carrelli, A.L., Walker, M.D., Di Tullio, M.R., Homma, S., Zhang, C., McMahon, D.J., Silverberg, S.J., 2013. Endothelial function in mild primary hyperparathyroidism. Clin. Endocrinol. 78, 204–209.

Chang, Y.T., Wu, J.L., Hsu, C.C., Wang, J.D., Sung, J.M., 2013. Diabetes and end-stage renal disease synergistically contribute to increased incidence of cardiovascular events: a nation-wide follow-up study during 1998–2009. Diabetes Care.

Cheng, S.L., Behrmann, A.S., Mead, M., Ramachandran, B., Kapoor, K., Perera, R., Kronenberg, H.M., Towler, D.A., 2016. Abstract 219: vascular PTH1R signaling limits aortic collagen deposition in diabetic LDLR-/- mice. Arterioscler. Thromb. Vasc. Biol. 36. Abstract 219.

Cheng, S.L., Shao, J.S., Halstead, L.R., Distelhorst, K., Sierra, O., Towler, D.A., 2010. Activation of vascular smooth muscle parathyroid hormone receptor inhibits Wnt/beta-catenin signaling and aortic fibrosis in diabetic arteriosclerosis. Circ. Res. 107, 271−282.

Clemens, T.L., Cormier, S., Eichinger, A., Endlich, K., Fiaschi-Taesch, N., Fischer, E., Friedman, P.A., Karaplis, A.C., Massfelder, T., Rossert, J., et al., 2001. Parathyroid hormone-related protein and its receptors: nuclear functions and roles in the renal and cardiovascular systems, the placental trophoblasts and the pancreatic islets. Br. J. Pharmacol. 134, 1113−1136.

Colak, S., Aydogan, B.I., Gokcay Canpolat, A., Tulunay Kaya, C., Sahin, M., Corapcioglu, D., Uysal, A.R., Emral, R., 2017. Is primary hyperparathyroidism a cause of endothelial dysfunction? Clin. Endocrinol. 87, 459−465.

Collins, T.C., Ewing, S.K., Diem, S.J., Taylor, B.C., Orwoll, E.S., Cummings, S.R., Strotmeyer, E.S., Ensrud, K.E., 2009. Peripheral arterial disease is associated with higher rates of hip bone loss and increased fracture risk in older men. Circulation 119, 2305−2312.

Collip, J.B., Clark, E.P., 1925. Further studies on the physiological action of a parathyroid hormone. J. Biol. Chem. 64, 485−507.

Cortigiani, L., Rigo, F., Gherardi, S., Bovenzi, F., Molinaro, S., Picano, E., Sicari, R., 2012. Coronary flow reserve during dipyridamole stress echocardiography predicts mortality. JACC Cardiovasc. Imag. 5, 1079−1085.

Crass 3rd, M.F., Jayaseelan, C.L., Darter, T.C., 1987. Effects of parathyroid hormone on blood flow in different regional circulations. Am. J. Physiol. 253, R634−R639.

Cunningham, J., Danese, M., Olson, K., Klassen, P., Chertow, G.M., 2005. Effects of the calcimimetic cinacalcet HCl on cardiovascular disease, fracture, and health-related quality of life in secondary hyperparathyroidism. Kidney Int. 68, 1793−1800.

Debella, Y.T., Giduma, H.D., Light, R.P., Agarwal, R., 2011. Chronic kidney disease as a coronary disease equivalent–a comparison with diabetes over a decade. Clin. J. Am. Soc. Nephrol. 6, 1385−1392.

Demer, L., Tintut, Y., 2010. The bone-vascular axis in chronic kidney disease. Curr. Opin. Nephrol. Hypertens. 19, 349−353.

Dicker, F., Quitterer, U., Winstel, R., Honold, K., Lohse, M.J., 1999. Phosphorylation-independent inhibition of parathyroid hormone receptor signaling by G protein-coupled receptor kinases. Proc. Natl. Acad. Sci. U. S. A. 96, 5476−5481.

Dimitrov, E.L., Kim, Y.Y., Usdin, T.B., 2011. Regulation of hypothalamic signaling by tuberoinfundibular peptide of 39 residues is critical for the response to cold: a novel peptidergic mechanism of thermoregulation. J. Neurosci. 31, 18166−18179.

Dobolyi, A., Dimitrov, E., Palkovits, M., Usdin, T.B., 2012. The neuroendocrine functions of the parathyroid hormone 2 receptor. Front. Endocrinol. 3, 121.

Durup, D., Jorgensen, H.L., Christensen, J., Schwarz, P., Heegaard, A.M., Lind, B., 2012. A reverse J-shaped association of all-cause mortality with serum 25-hydroxyvitamin D in general practice: the CopD study. J. Clin. Endocrinol. Metab. 97, 2644−2652.

Eddington, H., Hoefield, R., Sinha, S., Chrysochou, C., Lane, B., Foley, R.N., Hegarty, J., New, J., O'Donoghue, D.J., Middleton, R.J., et al., 2010. Serum phosphate and mortality in patients with chronic kidney disease. Clin. J. Am. Soc. Nephrol. 5, 2251−2257.

Eghbali-Fatourechi, G.Z., Lamsam, J., Fraser, D., Nagel, D., Riggs, B.L., Khosla, S., 2005. Circulating osteoblast-lineage cells in humans. N. Engl. J. Med. 352, 1959−1966.

Eghbali-Fatourechi, G.Z., Modder, U.I., Charatcharoenwitthaya, N., Sanyal, A., Undale, A.H., Clowes, J.A., Tarara, J.E., Khosla, S., 2007. Characterization of circulating osteoblast lineage cells in humans. Bone 40, 1370−1377.

Eichinger, A., Fiaschi-Taesch, N., Massfelder, T., Fritsch, S., Barthelmebs, M., Helwig, J.J., 2002. Transcript expression of the tuberoinfundibular peptide (TIP)39/PTH2 receptor system and non-PTH1 receptor-mediated tonic effects of TIP39 and other PTH2 receptor ligands in renal vessels. Endocrinology 143, 3036−3043.

Faarvang, A.S., Rordam Preil, S.A., Nielsen, P.S., Beck, H.C., Kristensen, L.P., Rasmussen, L.M., 2016. Smoking is associated with lower amounts of arterial type I collagen and decorin. Atherosclerosis 247, 201−206.

Fadini, G.P., Rattazzi, M., Matsumoto, T., Asahara, T., Khosla, S., 2012. Emerging role of circulating calcifying cells in the bone-vascular axis. Circulation 125, 2772−2781.

Farb, A., Kolodgie, F.D., Hwang, J.Y., Burke, A.P., Tefera, K., Weber, D.K., Wight, T.N., Virmani, R., 2004. Extracellular matrix changes in stented human coronary arteries. Circulation 110, 940−947.

Feola, M., Crass 3rd, M.F., 1986. Parathyroid hormone reduces acute ischemic injury of the myocardium. Surg. Gynecol. Obstet. 163, 523−530.

Fiaschi-Taesch, N., Sicari, B., Ubriani, K., Cozar-Castellano, I., Takane, K.K., Stewart, A.F., 2009. Mutant parathyroid hormone-related protein, devoid of the nuclear localization signal, markedly inhibits arterial smooth muscle cell cycle and neointima formation by coordinate up-regulation of p15Ink4b and p27kip1. Endocrinology 150, 1429−1439.

Fiaschi-Taesch, N., Sicari, B.M., Ubriani, K., Bigatel, T., Takane, K.K., Cozar-Castellano, I., Bisello, A., Law, B., Stewart, A.F., 2006. Cellular mechanism through which parathyroid hormone-related protein induces proliferation in arterial smooth muscle cells: definition of an arterial smooth muscle PTHrP/p27kip1 pathway. Circ. Res. 99, 933−942.

Fiaschi-Taesch, N., Takane, K.K., Masters, S., Lopez-Talavera, J.C., Stewart, A.F., 2004. Parathyroid-hormone-related protein as a regulator of pRb and the cell cycle in arterial smooth muscle. Circulation 110, 177−185.

Fiaschi-Taesch, N.M., Stewart, A.F., 2003. Minireview: parathyroid hormone-related protein as an intracrine factor–trafficking mechanisms and functional consequences. Endocrinology 144, 407−411.

Fitzpatrick, L.A., Bilezikian, J.P., Silverberg, S.J., 2008. Parathyroid hormone and the cardiovascular system. Curr. Osteoporos. Rep. 6, 77−83.

Flammer, A.J., Gossl, M., Li, J., Matsuo, Y., Reriani, M., Loeffler, D., Simari, R.D., Lerman, L.O., Khosla, S., Lerman, A., 2012a. Patients with an HbA1c in the prediabetic and diabetic range have higher numbers of circulating cells with osteogenic and endothelial progenitor cell markers. J. Clin. Endocrinol. Metab. 97, 4761−4768.

Flammer, A.J., Gossl, M., Widmer, R.J., Reriani, M., Lennon, R., Loeffler, D., Shonyo, S., Simari, R.D., Lerman, L.O., Khosla, S., et al., 2012b. Osteocalcin positive CD133+/CD34-/KDR+ progenitor cells as an independent marker for unstable atherosclerosis. Eur. Heart J. 33, 2963−2969.

Friedman, P.A., Goodman, W.G., 2006. PTH(1-84)/PTH(7-84): a balance of power. Am. J. Physiol. Renal. Physiol. 290, F975–F984.

Fuery, M.A., Liang, L., Kaplan, F.S., Mohler 3rd, E.R., 2018. Vascular ossification: pathology, mechanisms, and clinical implications. Bone 109, 28–34.

Gaudreault, N., Ducharme, V., Lamontagne, M., Guauque-Olarte, S., Mathieu, P., Pibarot, P., Bossé, Y., 2011. Replication of genetic association studies in aortic stenosis in adults. Am. J. Cardiol. 108 (9), 1305–1310.

Gaziano, T., Reddy, K.S., Paccaud, F., Horton, S., Chaturvedi, V., 2006. Cardiovascular disease. In: Jamison, D.T., Breman, J.G., Measham, A.R., Alleyne, G., Claeson, M., Evans, D.B., Jha, P., Mills, A., Musgrove, P. (Eds.), Disease Control Priorities in Developing Countries. Washington (DC).

Ginsberg, C., Craven, T.E., Chonchol, M.B., Cheung, A.K., Sarnak, M.J., Ambrosius, W.T., Killeen, A.A., Raphael, K.L., Bhatt, U.Y., Chen, J., et al., 2018. PTH, FGF23, and intensive blood pressure lowering in chronic kidney disease participants in SPRINT. Clin. J. Am. Soc. Nephrol. 13, 1816–1824.

Gohin, S., Carriero, A., Chenu, C., Pitsillides, A.A., Arnett, T.R., Marenzana, M., 2016. The anabolic action of intermittent parathyroid hormone on cortical bone depends partly on its ability to induce nitric oxide-mediated vasorelaxation in BALB/c mice. Cell Biochem. Funct. 34, 52–62.

Goodman, W.G., 2004. The consequences of uncontrolled secondary hyperparathyroidism and its treatment in chronic kidney disease. Semin. Dial. 17, 209–216.

Gossl, M., Modder, U.I., Gulati, R., Rihal, C.S., Prasad, A., Loeffler, D., Lerman, L.O., Khosla, S., Lerman, A., 2010. Coronary endothelial dysfunction in humans is associated with coronary retention of osteogenic endothelial progenitor cells. Eur. Heart J. 31, 2909–2914.

Gray, C., Bratt, D., Lees, J., daCosta, M., Plant, K., Watson, O.J., Solaymani-Kohal, S., Tazzyman, S., Serbanovic-Canic, J., Crossman, D.C., et al., 2013. Loss of function of parathyroid hormone receptor 1 induces Notch-dependent aortic defects during zebrafish vascular development. Arterioscler. Thromb. Vasc. Biol. 33, 1257–1263.

Guers, J.J., Prisby, R.D., Edwards, D.G., Lennon-Edwards, S., 2017. Intermittent parathyroid hormone administration attenuates endothelial dysfunction in old rats. J. Appl. Physiol. 122, 76–81.

Hashimoto, K., Nakagawa, Y., Shibuya, T., Satoh, H., Ushijima, T., Imai, S., 1981. Effects of parathyroid hormone and related polypeptides on the heart and coronary circulation of dogs. J. Cardiovasc. Pharmacol. 3, 668–676.

Hirai, T., Chagin, A.S., Kobayashi, T., Mackem, S., Kronenberg, H.M., 2011. Parathyroid hormone/parathyroid hormone-related protein receptor signaling is required for maintenance of the growth plate in postnatal life. Proc. Natl. Acad. Sci. U. S. A. 108 (1), 191–196.

Hoare, S.R., Usdin, T.B., 2001. Molecular mechanisms of ligand recognition by parathyroid hormone 1 (PTH1) and PTH2 receptors. Curr. Pharmaceut. Des. 7, 689–713.

Hocher, B., Armbruster, F.P., Stoeva, S., Reichetzeder, C., Gron, H.J., Lieker, I., Khadzhynov, D., Slowinski, T., Roth, H.J., 2012. Measuring parathyroid hormone (PTH) in patients with oxidative stress–do we need a fourth generation parathyroid hormone assay? PLoS One 7, e40242.

Hoogendam, J., Farih-Sips, H., Wynaendts, L.C., Lowik, C.W., Wit, J.M., Karperien, M., 2007. Novel mutations in the parathyroid hormone (PTH)/PTH-related peptide receptor type 1 causing Blomstrand osteochondrodysplasia types I and II. J. Clin. Endocrinol. Metab. 92, 1088–1095.

Hulter, H.N., Melby, J.C., Peterson, J.C., Cooke, C.R., 1986. Chronic continuous PTH infusion results in hypertension in normal subjects. J. Clin. Hypertens. 2, 360–370.

Investigators, E.T., Chertow, G.M., Block, G.A., Correa-Rotter, R., Drueke, T.B., Floege, J., Goodman, W.G., Herzog, C.A., Kubo, Y., London, G.M., et al., 2012. Effect of cinacalcet on cardiovascular disease in patients undergoing dialysis. N. Engl. J. Med. 367, 2482–2494.

Ishay, A., Herer, P., Luboshitzky, R., 2011. Effects of successful parathyroidectomy on metabolic cardiovascular risk factors in patients with severe primary hyperparathyroidism. Endocr. Pract. 17, 584–590.

Ishikawa, M., Ouchi, Y., Han, S.Z., Akishita, M., Kozaki, K., Toba, K., Namiki, A., Yamaguchi, T., Orimo, H., 1994. Parathyroid hormone-related protein reduces cytosolic free Ca2+ level and tension in rat aortic smooth muscle. Eur. J. Pharmacol. 269, 311–317.

Iwata, S., Hyodo, E., Yanagi, S., Hayashi, Y., Nishiyama, H., Kamimori, K., Ota, T., Matsumura, Y., Homma, S., Yoshiyama, M., 2013. Parathyroid hormone and systolic blood pressure accelerate the progression of aortic valve stenosis in chronic hemodialysis patients. Int. J. Cardiol. 163 (3), 256–259.

Iwata, S., Walker, M.D., Di Tullio, M.R., Hyodo, E., Jin, Z., Liu, R., Sacco, R.L., Homma, S., Silverberg, S.J., 2012. Aortic valve calcification in mild primary hyperparathyroidism. J. Clin. Endocrinol. Metab. 97, 132–137.

Jono, S., Nishizawa, Y., Shioi, A., Morii, H., 1997. Parathyroid hormone-related peptide as a local regulator of vascular calcification. Its inhibitory action on in vitro calcification by bovine vascular smooth muscle cells. Arterioscler. Thromb. Vasc. Biol. 17, 1135–1142.

Kidney Disease: Improving Global Outcomes, C.K.D.M.B.D.W.G, 2009. KDIGO clinical practice guideline for the diagnosis, evaluation, prevention, and treatment of Chronic Kidney Disease-Mineral and Bone Disorder (CKD-MBD). Kidney Int. Suppl. S1–S130.

Kim, S.C., Kim, H.W., Oh, S.W., Yang, H.N., Kim, M.G., Jo, S.K., Cho, W.Y., Kim, H.K., 2011. Low iPTH can predict vascular and coronary calcifications in patients undergoing peritoneal dialysis. Nephron Clin. Pract. 117, c113–119.

Kosch, M., Hausberg, M., Vormbrock, K., Kisters, K., Gabriels, G., Rahn, K.H., Barenbrock, M., 2000. Impaired flow-mediated vasodilation of the brachial artery in patients with primary hyperparathyroidism improves after parathyroidectomy. Cardiovasc. Res. 47, 813–818.

Kovacs, L., Goth, M.I., Szabolcs, I., Dohan, O., Ferencz, A., Szilagyi, G., 1998. The effect of surgical treatment on secondary hyperaldosteronism and relative hyperinsulinemia in primary hyperparathyroidism. Eur. J. Endocrinol. 138, 543–547.

Kritchevsky, S.B., Tooze, J.A., Neiberg, R.H., Schwartz, G.G., Hausman, D.B., Johnson, M.A., Bauer, D.C., Cauley, J.A., Shea, M.K., Cawthon, P.M., et al., 2012. 25-Hydroxyvitamin D, parathyroid hormone, and mortality in black and white older adults: the health ABC study. J. Clin. Endocrinol. Metab. 97, 4156–4165.

Kronenberg, H.M., 2006. PTHrP and skeletal development. Ann. N Y Acad. Sci. 1068, 1–13.

Langub, M.C., Monier-Faugere, M.C., Wang, G., Williams, J.P., Koszewski, N.J., Malluche, H.H., 2003. Administration of PTH-(7-84) antagonizes the effects of PTH-(1-84) on bone in rats with moderate renal failure. Endocrinology 144, 1135–1138.

Lee, K., Deeds, J.D., Segre, G.V., 1995. Expression of parathyroid hormone-related peptide and its receptor messenger ribonucleic acids during fetal development of rats. Endocrinology 136, 453–463.

Lee, S., Bice, A., Hood, B., Ruiz, J., Kim, J., Prisby, R.D., 2018. Intermittent PTH 1-34 administration improves the marrow microenvironment and endothelium-dependent vasodilation in bone arteries of aged rats. J. Appl. Physiol. 124, 1426–1437.

Li, X., Garcia, J., Lu, J., Iriana, S., Kalajzic, I., Rowe, D., Demer, L.L., Tintut, Y., 2014. Roles of parathyroid hormone (PTH) receptor and reactive oxygen species in hyperlipidemia-induced PTH resistance in preosteoblasts. J. Cell. Biochem. 115, 179–188.

Lincoln, J., Lange, A.W., Yutzey, K.E., 2006. Hearts and bones: shared regulatory mechanisms in heart valve, cartilage, tendon, and bone development. Dev. Biol. 294 (2), 292–302.

Linhartová, K., Veselka, J., Sterbáková, G., Racek, J., Topolcan, O., Cerbák, R., 2008. Parathyroid hormone and vitamin D levels are independently associated with calcific aortic stenosis. Circ. J. 72 (2), 245–250.

Liu, L., Sanchez-Bonilla, M., Crouthamel, M., Giachelli, C., Keel, S., 2013. Mice lacking the sodium-dependent phosphate import protein, PiT1 (SLC20A1), have a severe defect in terminal erythroid differentiation and early B cell development. Exp. Hematol. 41, 432–443 e437.

Lobaugh, B., Neelon, F.A., Oyama, H., Buckley, N., Smith, S., Christy, M., Leight Jr., G.S., 1989. Circadian rhythms for calcium, inorganic phosphorus, and parathyroid hormone in primary hyperparathyroidism: functional and practical considerations. Surgery 106, 1009–1016 discussion 1016-1007.

London, G., Coyne, D., Hruska, K., Malluche, H.H., Martin, K.J., 2010. The new kidney disease: improving global outcomes (KDIGO) guidelines – expert clinical focus on bone and vascular calcification. Clin. Nephrol. 74, 423–432.

London, G.M., 2003. Cardiovascular calcifications in uremic patients: clinical impact on cardiovascular function. J. Am. Soc. Nephrol. 14, S305–S309.

London, G.M., Guerin, A.P., Marchais, S.J., Metivier, F., Pannier, B., Adda, H., 2003. Arterial media calcification in end-stage renal disease: impact on all-cause and cardiovascular mortality. Nephrol. Dial. Transplant. 18, 1731–1740.

London, G.M., Marchais, S.J., Guerin, A.P., de Vernejoul, M.C., 2015. Ankle-brachial index and bone turnover in patients on dialysis. J. Am. Soc. Nephrol. 26, 476–483.

London, G.M., Marty, C., Marchais, S.J., Guerin, A.P., Metivier, F., de Vernejoul, M.C., 2004. Arterial calcifications and bone histomorphometry in end-stage renal disease. J. Am. Soc. Nephrol. 15, 1943–1951.

Lutteke, D., Ross, G., Abdallah, Y., Schafer, C., Piper, H.M., Schluter, K.D., 2005. Parathyroid hormone-related peptide improves contractile responsiveness of adult rat cardiomyocytes with depressed cell function irrespectively of oxidative inhibition. Basic Res. Cardiol. 100, 320–327.

MacLean, H.E., Guo, J., Knight, M.C., Zhang, P., Cobrinik, D., Kronenberg, H.M., 2004. The cyclin-dependent kinase inhibitor p57(Kip2) mediates proliferative actions of PTHrP in chondrocytes. J. Clin. Investig. 113, 1334–1343.

Maeda, H., Tokumoto, M., Yotsueda, H., Taniguchi, M., Tsuruya, K., Hirakata, H., Iida, M., 2007. Two cases of calciphylaxis treated by parathyroidectomy: importance of increased bone formation. Clin. Nephrol. 67, 397–402.

Maeda, S., Sutliff, R.L., Qian, J., Lorenz, J.N., Wang, J., Tang, H., Nakayama, T., Weber, C., Witte, D., Strauch, A.R., et al., 1999. Targeted overexpression of parathyroid hormone-related protein (PTHrP) to vascular smooth muscle in transgenic mice lowers blood pressure and alters vascular contractility. Endocrinology 140, 1815–1825.

Marini, C., Giusti, M., Armonino, R., Ghigliotti, G., Bezante, G., Vera, L., Morbelli, S., Pomposelli, E., Massollo, M., Gandolfo, P., et al., 2010. Reduced coronary flow reserve in patients with primary hyperparathyroidism: a study by G-SPECT myocardial perfusion imaging. Eur. J. Nucl. Med. Mol. Imaging 37, 2256–2263.

Martin, A., David, V., Quarles, L.D., 2012. Regulation and function of the FGF23/klotho endocrine pathways. Physiol. Rev. 92, 131–155.

Martin, K.J., Gonzalez, E.A., 2011. Prevention and control of phosphate retention/hyperphosphatemia in CKD-MBD: what is normal, when to start, and how to treat? Clin. J. Am. Soc. Nephrol. 6, 440–446.

Massfelder, T., Dann, P., Wu, T.L., Vasavada, R., Helwig, J.J., Stewart, A.F., 1997. Opposing mitogenic and anti-mitogenic actions of parathyroid hormone-related protein in vascular smooth muscle cells: a critical role for nuclear targeting. Proc. Natl. Acad. Sci. U. S. A. 94, 13630–13635.

Massfelder, T., Stewart, A.F., Endlich, K., Soifer, N., Judes, C., Helwig, J.J., 1996. Parathyroid hormone-related protein detection and interaction with NO and cyclic AMP in the renovascular system. Kidney Int. 50, 1591–1603.

Matsuoka, S., Tominaga, Y., Uno, N., Goto, N., Sato, T., Katayama, A., Haba, T., Uchida, K., Kobayashi, K., Nakao, A., 2005. Calciphylaxis: a rare complication of patients who required parathyroidectomy for advanced renal hyperparathyroidism. World J. Surg. 29, 632–635.

Miao, D., Su, H., He, B., Gao, J., Xia, Q., Zhu, M., Gu, Z., Goltzman, D., Karaplis, A.C., 2008. Severe growth retardation and early lethality in mice lacking the nuclear localization sequence and C-terminus of PTH-related protein. Proc. Natl. Acad. Sci. U. S. A. 105, 20309–20314.

Moe, S.M., Chertow, G.M., Parfrey, P.S., Kubo, Y., Block, G.A., Correa-Rotter, R., Drueke, T.B., Herzog, C.A., London, G.M., Mahaffey, K.W., et al., 2015. Cinacalcet, fibroblast growth factor-23, and cardiovascular disease in hemodialysis: the evaluation of cinacalcet HCl therapy to lower cardiovascular events (EVOLVE) trial. Circulation 132, 27–39.

Moe, S.M., Drueke, T., Lameire, N., Eknoyan, G., 2007. Chronic kidney disease-mineral-bone disorder: a new paradigm. Adv. Chron. Kidney Dis. 14, 3–12.

Mohler, E.R., 3rd., Gannon, F., Reynolds, C., Zimmerman, R., Keane, M.G., Kaplan, F.S., 2001. Bone formation and inflammation in cardiac valves. Circulation 103 (11), 1522–1528.

Monego, G., Arena, V., Pasquini, S., Stigliano, E., Fiaccavento, R., Leone, O., Arpesella, G., Potena, L., Ranelletti, F.O., Di Nardo, P., et al., 2009. Ischemic injury activates PTHrP and PTH1R expression in human ventricular cardiomyocytes. Basic Res. Cardiol. 104, 427–434.

Monterisi, S., Lobo, M.J., Livie, C., Castle, J.C., Weinberger, M., Baillie, G., Surdo, N.C., Musheshe, N., Stangherlin, A., Gottlieb, E., et al., 2017. PDE2A2 regulates mitochondria morphology and apoptotic cell death via local modulation of cAMP/PKA signalling. Elife 6.

Montisci, R., Chen, L., Ruscazio, M., Colonna, P., Cadeddu, C., Caiati, C., Montisci, M., Meloni, L., Iliceto, S., 2006. Non-invasive coronary flow reserve is correlated with microvascular integrity and myocardial viability after primary angioplasty in acute myocardial infarction. Heart 92, 1113–1118.

Musso, M.J., Plante, M., Judes, C., Barthelmebs, M., Helwig, J.J., 1989. Renal vasodilatation and microvessel adenylate cyclase stimulation by synthetic parathyroid hormone-like protein fragments. Eur. J. Pharmacol. 174, 139–151.

Nagao, S., Seto, S., Kitamura, S., Akahoshi, M., Kiriyama, T., Yano, K., 1998. Central pressor effect of parathyroid hormone-related protein in conscious rats. Brain Res. 785, 75–79.

Napoli, C., William-Ignarro, S., Byrns, R., Balestrieri, M.L., Crimi, E., Farzati, B., Mancini, F.P., de Nigris, F., Matarazzo, A., D'Amora, M., et al., 2008. Therapeutic targeting of the stem cell niche in experimental hindlimb ischemia. Nat. Clin. Pract. Cardiovasc. Med. 5, 571–579.

Nguyen, M., He, B., Karaplis, A., 2001. Nuclear forms of parathyroid hormone-related peptide are translated from non-AUG start sites downstream from the initiator methionine. Endocrinology 142, 694–703.

Nickols, G.A., Metz, M.A., Cline Jr., W.H., 1986. Vasodilation of the rat mesenteric vasculature by parathyroid hormone. J. Pharmacol. Exp. Ther. 236, 419–423.

Nigwekar, S.U., Kroshinsky, D., Nazarian, R.M., Goverman, J., Malhotra, R., Jackson, V.A., Kamdar, M.M., Steele, D.J., Thadhani, R.I., 2015. Calciphylaxis: risk factors, diagnosis, and treatment. Am. J. Kidney Dis. 66, 133–146.

Noda, M., Katoh, T., Takuwa, N., Kumada, M., Kurokawa, K., Takuwa, Y., 1994. Synergistic stimulation of parathyroid hormone-related peptide gene expression by mechanical stretch and angiotensin II in rat aortic smooth muscle cells. J. Biol. Chem. 269, 17911–17917.

Noonan, W.T., Qian, J., Stuart, W.D., Clemens, T.L., Lorenz, J.N., 2003. Altered renal hemodynamics in mice overexpressing the parathyroid hormone (PTH)/PTH-related peptide type 1 receptor in smooth muscle. Endocrinology 144, 4931–4938.

Nyby, M.D., Hino, T., Berger, M.E., Ormsby, B.L., Golub, M.S., Brickman, A.S., 1995. Desensitization of vascular tissue to parathyroid hormone and parathyroid hormone-related protein. Endocrinology 136, 2497–2504.

O'Brien, C.A., Plotkin, L.I., Galli, C., Goellner, J.J., Gortazar, A.R., Allen, M.R., Robling, A.G., Bouxsein, M., Schipani, E., Turner, C.H., et al., 2008. Control of bone mass and remodeling by PTH receptor signaling in osteocytes. PLoS One 3, e2942.

Ogino, K., Burkhoff, D., Bilezikian, J.P., 1995. The hemodynamic basis for the cardiac effects of parathyroid hormone (PTH) and PTH-related protein. Endocrinology 136, 3024–3030.

Okoumassoun, L., Averill-Bates, D., Denizeau, F., Henderson, J.E., 2007. Parathyroid hormone related protein (PTHrP) inhibits TNFalpha-induced apoptosis by blocking the extrinsic and intrinsic pathways. J. Cell. Physiol. 210, 507–516.

Osto, E., Fallo, F., Pelizzo, M.R., Maddalozzo, A., Sorgato, N., Corbetti, F., Montisci, R., Famoso, G., Bellu, R., Luscher, T.F., et al., 2012. Coronary microvascular dysfunction induced by primary hyperparathyroidism is restored after parathyroidectomy. Circulation 126, 1031–1039.

Panda, D.K., Goltzman, D., Karaplis, A.C., 2012. Defective postnatal endochondral bone development by chondrocyte-specific targeted expression of parathyroid hormone type 2 receptor. Am. J. Physiol. Endocrinol. Metab. 303, E1489–E1501.

Pang, P.K., Tenner Jr., T.E., Yee, J.A., Yang, M., Janssen, H.F., 1980. Hypotensive action of parathyroid hormone preparations on rats and dogs. Proc. Natl. Acad. Sci. U. S. A. 77, 675–678.

Papasani, M.R., Gensure, R.C., Yan, Y.L., Gunes, Y., Postlethwait, J.H., Ponugoti, B., John, M.R., Juppner, H., Rubin, D.A., 2004. Identification and characterization of the zebrafish and fugu genes encoding tuberoinfundibular peptide 39. Endocrinology 145, 5294–5304.

Parfrey, P.S., Drueke, T.B., Block, G.A., Correa-Rotter, R., Floege, J., Herzog, C.A., London, G.M., Mahaffey, K.W., Moe, S.M., Wheeler, D.C., et al., 2015. The effects of cinacalcet in older and younger patients on hemodialysis: the evaluation of cinacalcet HCl therapy to lower cardiovascular events (EVOLVE) trial. Clin. J. Am. Soc. Nephrol. 10, 791–799.

Pepine, C.J., Anderson, R.D., Sharaf, B.L., Reis, S.E., Smith, K.M., Handberg, E.M., Johnson, B.D., Sopko, G., Bairey Merz, C.N., 2010. Coronary microvascular reactivity to adenosine predicts adverse outcome in women evaluated for suspected ischemia results from the National Heart, Lung and Blood Institute WISE (Women's Ischemia Syndrome Evaluation) study. J. Am. Coll. Cardiol. 55, 2825–2832.

Persson, A., Bollerslev, J., Rosen, T., Mollerup, C.L., Franco, C., Isaksen, G.A., Ueland, T., Jansson, S., Caidahl, K., Group, S.S., 2011. Effect of surgery on cardiac structure and function in mild primary hyperparathyroidism. Clin. Endocrinol. 74, 174–180.

Peterson, Y.K., Luttrell, L.M., 2017. The diverse roles of arrestin scaffolds in G protein-coupled receptor signaling. Pharmacol. Rev. 69, 256–297.

Pirola, C.J., Wang, H.M., Strgacich, M.I., Kamyar, A., Cercek, B., Forrester, J.S., Clemens, T.L., Fagin, J.A., 1994. Mechanical stimuli induce vascular parathyroid hormone-related protein gene expression in vivo and in vitro. Endocrinology 134, 2230–2236.

Potthoff, S.A., Janus, A., Hoch, H., Frahnert, M., Tossios, P., Reber, D., Giessing, M., Klein, H.M., Schwertfeger, E., Quack, I., et al., 2011. PTH-receptors regulate norepinephrine release in human heart and kidney. Regul. Pept. 171, 35–42.

Prisby, R., Guignandon, A., Vanden-Bossche, A., Mac-Way, F., Linossier, M.T., Thomas, M., Laroche, N., Malaval, L., Langer, M., Peter, Z.A., et al., 2011. Intermittent PTH(1-84) is osteoanabolic but not osteoangiogenic and relocates bone marrow blood vessels closer to bone-forming sites. J. Bone Miner. Res. 26, 2583–2596.

Prisby, R., Menezes, T., Campbell, J., 2013. Vasodilation to PTH (1-84) in bone arteries is dependent upon the vascular endothelium and is mediated partially via VEGF signaling. Bone 54, 68–75.

Prisby, R.D., 2017. Mechanical, hormonal and metabolic influences on blood vessels, blood flow and bone. J. Endocrinol. 235, R77–R100.

Qian, J., Colbert, M.C., Witte, D., Kuan, C.Y., Gruenstein, E., Osinska, H., Lanske, B., Kronenberg, H.M., Clemens, T.L., 2003. Midgestational lethality in mice lacking the parathyroid hormone (PTH)/PTH-related peptide receptor is associated with abrupt cardiomyocyte death. Endocrinology 144, 1053–1061.

Quarles, L.D., 2013. A systems biology preview of the relationships between mineral and metabolic complications in chronic kidney disease. Semin. Nephrol. 33, 130–142.

Raggi, P., James, G., Burke, S.K., Bommer, J., Chasan-Taber, S., Holzer, H., Braun, J., Chertow, G.M., 2005. Decrease in thoracic vertebral bone attenuation with calcium-based phosphate binders in hemodialysis. J. Bone Miner. Res. 20, 764–772.

Raison, D., Coquard, C., Hochane, M., Steger, J., Massfelder, T., Moulin, B., Karaplis, A.C., Metzger, D., Chambon, P., Helwig, J.J., et al., 2013. Knockdown of parathyroid hormone related protein in smooth muscle cells alters renal hemodynamics but not blood pressure. Am. J. Physiol. Renal. Physiol. 305, F333–F342.

Rajamannan, N.M., Evans, F.J., Aikawa, E., Grande-Allen, K.J., Demer, L.L., Heistad, D.D., Simmons, C.A., Masters, K.S., Mathieu, P., O'Brien, K.D., et al., 2011. Calcific aortic valve disease: not simply a degenerative process: a review and agenda for research from the National Heart and Lung and Blood Institute Aortic Stenosis Working Group. Executive summary: calcific aortic valve disease-2011 update. Circulation 124, 1783–1791.

Rambausek, M., Ritz, E., Rascher, W., Kreusser, W., Mann, J.F., Kreye, V.A., Mehls, O., 1982. Vascular effects of parathyroid hormone (PTH). Adv. Exp. Med. Biol. 151, 619–632.

Rhee, Y., Bivi, N., Farrow, E., Lezcano, V., Plotkin, L.I., White, K.E., Bellido, T., 2011. Parathyroid hormone receptor signaling in osteocytes increases the expression of fibroblast growth factor-23 in vitro and in vivo. Bone 49, 636–643.

Roca-Cusachs, A., DiPette, D.J., Nickols, G.A., 1991. Regional and systemic hemodynamic effects of parathyroid hormone-related protein: preservation of cardiac function and coronary and renal flow with reduced blood pressure. J. Pharmacol. Exp. Ther. 256, 110–118.

Rogers, N.M., Teubner, D.J., Coates, P.T., 2007. Calcific uremic arteriolopathy: advances in pathogenesis and treatment. Semin. Dial. 20, 150–157.

Romero, G., von Zastrow, M., Friedman, P.A., 2011. Role of PDZ proteins in regulating trafficking, signaling, and function of GPCRs: means, motif, and opportunity. Adv. Pharmacol. 62, 279–314.

Ross, G., Engel, P., Abdallah, Y., Kummer, W., Schluter, K.D., 2005. Tuberoinfundibular peptide of 39 residues: a new mediator of cardiac function via nitric oxide production in the rat heart. Endocrinology 146, 2221–2228.

Ross, G., Heinemann, M.P., Schluter, K.D., 2007. Vasodilatory effect of tuberoinfundibular peptide (TIP39): requirement of receptor desensitization and its beneficial effect in the post-ischemic heart. Peptides 28, 878–886.

Rubin, M.R., Maurer, M.S., McMahon, D.J., Bilezikian, J.P., Silverberg, S.J., 2005. Arterial stiffness in mild primary hyperparathyroidism. J. Clin. Endocrinol. Metab. 90, 3326–3330.

Safar, M.E., Boudier, H.S., 2005. Vascular development, pulse pressure, and the mechanisms of hypertension. Hypertension 46, 205–209.

Sage, A.P., Lu, J., Atti, E., Tetradis, S., Ascenzi, M.G., Adams, D.J., Demer, L.L., Tintut, Y., 2011. Hyperlipidemia induces resistance to PTH bone anabolism in mice via oxidized lipids. J. Bone Miner. Res. 26, 1197–1206.

Sato, E., Zhang, L.J., Dorschner, R.A., Adase, C.A., Choudhury, B.P., Gallo, R.L., 2017. Activation of parathyroid hormone 2 receptor induces decorin expression and promotes wound repair. J. Investig. Dermatol. 137, 1774–1783.

Saussine, C., Judes, C., Massfelder, T., Musso, M.J., Simeoni, U., Hannedouche, T., Helwig, J.J., 1993a. Stimulatory action of parathyroid hormone on renin secretion in vitro: a study using isolated rat kidney, isolated rabbit glomeruli and superfused dispersed rat juxtaglomerular cells. Clin. Sci. (Lond.) 84, 11–19.

Saussine, C., Massfelder, T., Parnin, F., Judes, C., Simeoni, U., Helwig, J.J., 1993b. Renin stimulating properties of parathyroid hormone-related peptide in the isolated perfused rat kidney. Kidney Int. 44, 764–773.

Schermer, D.T., Chan, S.D., Bruce, R., Nissenson, R.A., Wood, W.I., Strewler, G.J., 1991. Chicken parathyroid hormone-related protein and its expression during embryologic development. J. Bone Miner. Res. 6, 149–155.

Schipani, E., Kruse, K., Juppner, H., 1995. A constitutively active mutant PTH-PTHrP receptor in Jansen-type metaphyseal chondrodysplasia. Science 268, 98–100.

Schmitz, F., Ewering, S., Zerres, K., Klomfass, S., Hoffmann, R., 2009. Ortlepp JR Parathyroid hormone gene variant and calcific aortic stenosis. J. Heart Valve Dis. 18 (3), 262–267.

Schluter, K., Katzer, C., Frischkopf, K., Wenzel, S., Taimor, G., Piper, H.M., 2000. Expression, release, and biological activity of parathyroid hormone-related peptide from coronary endothelial cells. Circ. Res. 86, 946–951.

Schreckenberg, R., Wenzel, S., da Costa Rebelo, R.M., Rothig, A., Meyer, R., Schluter, K.D., 2009. Cell-specific effects of nitric oxide deficiency on parathyroid hormone-related peptide (PTHrP) responsiveness and PTH1 receptor expression in cardiovascular cells. Endocrinology 150, 3735–3741.

Sebastian, E.M., Suva, L.J., Friedman, P.A., 2008. Differential effects of intermittent PTH(1-34) and PTH(7-34) on bone microarchitecture and aortic calcification in experimental renal failure. Bone 43, 1022–1030.

Shao, J.S., Cheng, S.L., Charlton-Kachigian, N., Loewy, A.P., Towler, D.A., 2003. Teriparatide (human parathyroid hormone (1-34)) inhibits osteogenic vascular calcification in diabetic low density lipoprotein receptor-deficient mice. J. Biol. Chem. 278, 50195–50202.

Shao, J.S., Cheng, S.L., Pingsterhaus, J.M., Charlton-Kachigian, N., Loewy, A.P., Towler, D.A., 2005. Msx2 promotes cardiovascular calcification by activating paracrine Wnt signals. J. Clin. Investig. 115, 1210–1220.

Shao, J.S., Cheng, S.L., Sadhu, J., Towler, D.A., 2010. Inflammation and the osteogenic regulation of vascular calcification: a review and perspective. Hypertension 55, 579–592.

Shao, J.S., Sierra, O.L., Cohen, R., Mecham, R.P., Kovacs, A., Wang, J., Distelhorst, K., Behrmann, A., Halstead, L.R., Towler, D.A., 2011. Vascular calcification and aortic fibrosis: a bifunctional role for osteopontin in diabetic arteriosclerosis. Arterioscler. Thromb. Vasc. Biol.

Shroff, R., 2011. Dysregulated mineral metabolism in children with chronic kidney disease. Curr. Opin. Nephrol. Hypertens. 20, 233–240.

Shroff, R., Long, D.A., Shanahan, C., 2013. Mechanistic insights into vascular calcification in CKD. J. Am. Soc. Nephrol. 24, 179–189.

Shroff, R.C., McNair, R., Figg, N., Skepper, J.N., Schurgers, L., Gupta, A., Hiorns, M., Donald, A.E., Deanfield, J., Rees, L., et al., 2008. Dialysis accelerates medial vascular calcification in part by triggering smooth muscle cell apoptosis. Circulation 118, 1748–1757.

Shroff, R.C., McNair, R., Skepper, J.N., Figg, N., Schurgers, L.J., Deanfield, J., Rees, L., Shanahan, C.M., 2010. Chronic mineral dysregulation promotes vascular smooth muscle cell adaptation and extracellular matrix calcification. J. Am. Soc. Nephrol. 21, 103–112.

Silverberg, S.J., Lewiecki, E.M., Mosekilde, L., Peacock, M., Rubin, M.R., 2009. Presentation of asymptomatic primary hyperparathyroidism: proceedings of the third international workshop. J. Clin. Endocrinol. Metab. 94, 351–365.

Smith, J.C., Page, M.D., John, R., Wheeler, M.H., Cockcroft, J.R., Scanlon, M.F., Davies, J.S., 2000. Augmentation of central arterial pressure in mild primary hyperparathyroidism. J. Clin. Endocrinol. Metab. 85, 3515–3519.

Smith, J.S., Rajagopal, S., 2016. The beta-arrestins: multifunctional regulators of G protein-coupled receptors. J. Biol. Chem. 291, 8969–8977.

Smock, S.L., Vogt, G.A., Castleberry, T.A., Lu, B., Owen, T.A., 2001. Molecular cloning and functional characterization of the canine parathyroid hormone/parathyroid hormone related peptide receptor (PTH1). Mol. Biol. Rep. 28, 235–243.

Soldatos, G., Jandeleit-Dahm, K., Thomson, H., Formosa, M., D'Orsa, K., Calkin, A.C., Cooper, M.E., Ahimastos, A.A., Kingwell, B.A., 2011. Large artery biomechanics and diastolic dysfunctionin patients with Type 2 diabetes. Diabet. Med. 28, 54–60.

Song, G.J., Barrick, S., Leslie, K.L., Sicari, B., Fiaschi-Taesch, N.M., Bisello, A., 2010. EBP50 inhibits the anti-mitogenic action of the parathyroid hormone type 1 receptor in vascular smooth muscle cells. J. Mol. Cell. Cardiol. 49, 1012–1021.

Sprague, S.M., Strugnell, S.A., Bishop, C.W., 2017. Extended-release calcifediol for secondary hyperparathyroidism in stage 3-4 chronic kidney disease. Expert Rev. Endocrinol. Metab. 12, 289–301.

Stabley, J.N., Towler, D.A., 2017. Arterial calcification in diabetes mellitus: preclinical models and translational implications. Arterioscler. Thromb. Vasc. Biol. 37, 205–217.

Stefenelli, T., Abela, C., Frank, H., Koller-Strametz, J., Niederle, B., 1997. Time course of regression of left ventricular hypertrophy after successful parathyroidectomy. Surgery 121 (2), 157–161.

Steinberg, D., 2006. Thematic review series: the pathogenesis of atherosclerosis. An interpretive history of the cholesterol controversy, Part V: the discovery of the statins and the end of the controversy. J. Lipid Res. 47, 1339–1351.

Sugimura, Y., Murase, T., Ishizaki, S., Tachikawa, K., Arima, H., Miura, Y., Usdin, T.B., Oiso, Y., 2003. Centrally administered tuberoinfundibular peptide of 39 residues inhibits arginine vasopressin release in conscious rats. Endocrinology 144, 2791–2796.

Suzuki, Y., Lederis, K., Huang, M., LeBlanc, F.E., Rorstad, O.P., 1983. Relaxation of bovine, porcine and human brain arteries by parathyroid hormone. Life Sci. 33, 2497–2503.

Takahashi, K., Inoue, D., Ando, K., Matsumoto, T., Ikeda, K., Fujita, T., 1995. Parathyroid hormone-related peptide as a locally produced vasorelaxant: regulation of its mRNA by hypertension in rats. Biochem. Biophys. Res. Commun. 208, 447–455.

Tastan, I., Schreckenberg, R., Mufti, S., Abdallah, Y., Piper, H.M., Schluter, K.D., 2009. Parathyroid hormone improves contractile performance of adult rat ventricular cardiomyocytes at low concentrations in a non-acute way. Cardiovasc. Res. 82, 77–83.

Teng, M., Wolf, M., Lowrie, E., Ofsthun, N., Lazarus, J.M., Thadhani, R., 2003. Survival of patients undergoing hemodialysis with paricalcitol or calcitriol therapy. N. Engl. J. Med. 349, 446–456.

Teng, M., Wolf, M., Ofsthun, M.N., Lazarus, J.M., Hernan, M.A., Camargo Jr., C.A., Thadhani, R., 2005. Activated injectable vitamin D and hemodialysis survival: a historical cohort study. J. Am. Soc. Nephrol. 16, 1115–1125.

Thompson, B., Towler, D.A., 2012a. Arterial calcification and bone physiology: role of the bone-vascular axis. Nat. Rev. Endocrinol.

Thompson, B., Towler, D.A., 2012b. Arterial calcification and bone physiology: role of the bone-vascular axis. Nat. Rev. Endocrinol. 8, 529–543.

Tomaschitz, A., Ritz, E., Pieske, B., Fahrleitner-Pammer, A., Kienreich, K., Horina, J.H., Drechsler, C., Marz, W., Ofner, M., Pieber, T.R., et al., 2012. Aldosterone and parathyroid hormone: a precarious couple for cardiovascular disease. Cardiovasc. Res. 94, 10–19.

Tomaschitz, A., Ritz, E., Pieske, B., Rus-Machan, J., Kienreich, K., Verheyen, N., Gaksch, M., Grubler, M., Fahrleitner-Pammer, A., Mrak, P., et al., 2013. Aldosterone and parathyroid hormone interactions as mediators of metabolic and cardiovascular disease. Metabolism.

Tonelli, M., Curhan, G., Pfeffer, M., Sacks, F., Thadhani, R., Melamed, M.L., Wiebe, N., Muntner, P., 2009. Relation between alkaline phosphatase, serum phosphate, and all-cause or cardiovascular mortality. Circulation 120, 1784–1792.

Tonelli, M., Sacks, F., Pfeffer, M., Gao, Z., Curhan, G., Cholesterol, and Recurrent Events Trial, I., 2005. Relation between serum phosphate level and cardiovascular event rate in people with coronary disease. Circulation 112, 2627–2633.

Towler, D.A., 2011. Skeletal anabolism, PTH, and the bone-vascular axis. J. Bone Miner. Res. 26, 2579–2582.

Towler, D.A., 2013. Chronic kidney disease: the "perfect storm" of cardiometabolic risk illuminates genetic diathesis in cardiovascular disease. J. Am. Coll. Cardiol. 62, 799–801.

Towler, D.A., 2014a. Physiological actions of PTH and PTHrP IV: vascular, cardiovascular, and CNS biology. In: Bilezikian, J.P. (Ed.), The Parathyroids: Basic and Clinical Concepts. Academic Press in press.

Towler, D.A., 2014b. The role of PTHrP in vascular smooth muscle. Clin. Rev. Bone Miner. Metabol. 12, 190–196.

Towler, D.A., 2015. Arteriosclerosis, bone biology, and calciotropic hormone signaling: learning the ABCs of disease in the bone-vascular axis. J. Am. Soc. Nephrol. 26, 243–245.

Towler, D.A., 2017a. Commonalities between vasculature and bone: an osseocentric view of arteriosclerosis. Circulation 135, 320–322.

Towler, D.A., 2017b. Lipoprotein(a): a taxi for autotaxin takes a toll in calcific aortic valve disease. JACC Basic Transl Sci 2, 241−243.

Unger, P., Clavel, M.A., Lindman, B.R., Mathieu, P., Pibarot, P., 2016. Pathophysiology and management of multivalvular disease. Nat. Rev. Cardiol. 13, 429−440.

van den Akker, N.M., Caolo, V., Molin, D.G., 2012. Cellular decisions in cardiac outflow tract and coronary development: an act by VEGF and NOTCH. Differentiation 84, 62−78.

VanderWalde, L.H., Liu, I.L., O'Connell, T.X., Haigh, P.I., 2006. The effect of parathyroidectomy on bone fracture risk in patients with primary hyperparathyroidism. Arch. Surg. 141, 885−889 discussion 889-891.

Vazquez-Diaz, O., Castillo-Martinez, L., Orea-Tejeda, A., Orozco-Gutierrez, J.J., Asensio-Lafuente, E., Reza-Albarran, A., Silva-Tinoco, R., Rebollar-Gonzalez, V., 2009. Reversible changes of electrocardiographic abnormalities after parathyroidectomy in patients with primary hyperparathyroidism. Cardiol. J. 16, 241−245.

Verheyen, N., Pilz, S., Eller, K., Kienreich, K., Fahrleitner-Pammer, A., Pieske, B., Ritz, E., Tomaschitz, A., 2013. Cinacalcet hydrochloride for the treatment of hyperparathyroidism. Expert Opin. Pharmacother. 14, 793−806.

Walker, M.D., Fleischer, J., Rundek, T., McMahon, D.J., Homma, S., Sacco, R., Silverberg, S.J., 2009. Carotid vascular abnormalities in primary hyperparathyroidism. J. Clin. Endocrinol. Metab. 94, 3849−3856.

Walker, M.D., Fleischer, J.B., Di Tullio, M.R., Homma, S., Rundek, T., Stein, E.M., Zhang, C., Taggart, T., McMahon, D.J., Silverberg, S.J., 2010. Cardiac structure and diastolic function in mild primary hyperparathyroidism. J. Clin. Endocrinol. Metab. 95, 2172−2179.

Walker, M.D., Rundek, T., Homma, S., DiTullio, M., Iwata, S., Lee, J.A., Choi, J., Liu, R., Zhang, C., McMahon, D.J., et al., 2012. Effect of parathyroidectomy on subclinical cardiovascular disease in mild primary hyperparathyroidism. Eur. J. Endocrinol. 167, 277−285.

Walker, M.D., Silverberg, S.J., 2008. Cardiovascular aspects of primary hyperparathyroidism. J. Endocrinol. Investig. 31, 925−931.

Westerhof, N., Lankhaar, J.W., Westerhof, B.E., 2009. The arterial Windkessel. Med. Biol. Eng. Comput. 47, 131−141.

Wysolmerski, J.J., 2012. Parathyroid hormone-related protein: an update. J. Clin. Endocrinol. Metab. 97, 2947−2956.

Yamamoto, K., Yamamoto, H., Yoshida, K., Kisanuki, A., Hirano, Y., Ohte, N., Akasaka, T., Takeuchi, M., Nakatani, S., Ohtani, T., et al., 2010. Prognostic factors for progression of early- and late-stage calcific aortic valve disease in Japanese: The Japanese Aortic Stenosis Study (JASS) retrospective analysis. Hypertens. Res. 33, 269−274.

Yamamoto, S., Morimoto, I., Zeki, K., Ueta, Y., Yamashita, H., Kannan, H., Eto, S., 1998. Centrally administered parathyroid hormone (PTH)-related protein(1-34) but not PTH(1-34) stimulates arginine-vasopressin secretion and its messenger ribonucleic acid expression in supraoptic nucleus of the conscious rats. Endocrinology 139, 383−388.

Yu, N., Donnan, P.T., Flynn, R.W., Murphy, M.J., Smith, D., Rudman, A., Leese, G.P., 2010. Increased mortality and morbidity in mild primary hyperparathyroid patients. The Parathyroid Epidemiology and Audit Research Study (PEARS). Clin. Endocrinol. 73, 30−34.

Yu, N., Donnan, P.T., Leese, G.P., 2011. A record linkage study of outcomes in patients with mild primary hyperparathyroidism: the Parathyroid Epidemiology and Audit Research Study (PEARS). Clin. Endocrinol. 75, 169−176.

Yu, N., Leese, G.P., Donnan, P.T., 2013. What predicts adverse outcomes in untreated primary hyperparathyroidism? The Parathyroid Epidemiology and Audit Research Study (PEARS). Clin. Endocrinol. 79, 27−34.

Yutzey, K.E., Demer, L.L., Body, S.C., Huggins, G.S., Towler, D.A., Giachelli, C.M., Hofmann-Bowman, M.A., Mortlock, D.P., Rogers, M.B., Sadeghi, M.M., et al., 2014. Calcific aortic valve disease: a consensus summary from the alliance of investigators on calcific aortic valve disease. Arterioscler. Thromb. Vasc. Biol. 34, 2387−2393.

Zaruba, M.M., Huber, B.C., Brunner, S., Deindl, E., David, R., Fischer, R., Assmann, G., Herbach, N., Grundmann, S., Wanke, R., et al., 2008. Parathyroid hormone treatment after myocardial infarction promotes cardiac repair by enhanced neovascularization and cell survival. Cardiovasc. Res. 77, 722−731.

Zhang, Y., Chen, G., Gu, Z., Sun, H., Karaplis, A., Goltzman, D., Miao, D., 2018. DNA damage checkpoint pathway modulates the regulation of skeletal growth and osteoblastic bone formation by parathyroid hormone-related peptide. Int. J. Biol. Sci. 14, 508−517.

Zoppellaro, G., Faggin, E., Puato, M., Pauletto, P., Rattazzi, M., 2012. Fibroblast growth factor 23 and the bone-vascular axis: lessons learned from animal studies. Am. J. Kidney Dis. 59, 135−144.

Chapter 27

Parathyroid hormone and parathyroid hormone–related protein actions on bone and kidney

Alessandro Bisello and Peter A. Friedman

Department of Pharmacology and Chemical Biology, Laboratory for GPCR Biology, University of Pittsburgh School of Medicine, Pittsburgh, PA, United States

Chapter outline

Principles of Bone Biology. https://doi.org/10.1016/B978-0-12-814841-9.00027-0

Introduction

Bone and kidney form a mineral-ion storage depot and regulatory axis that assures normal skeletal growth and development. Parathyroid hormone−related protein (PTHrP) is a major hormonal regulator of bone formation, while PTH (parathyroid hormone) contributes to postnatal skeletal integrity and extracellular mineral-ion homeostasis. PTHrP effects on the kidney are associated with controlling vascular tone, whereas PTH regulates phosphate and calcium absorption and the biosynthesis of vitamin D. Despite these distinct actions and tissue effects, PTH and the type I PTH/PTHrP receptor (PTHR) operate through a single canonical PTH/PTHrP receptor. This chapter reviews both well-accepted and recent advances in our understanding of PTH and PTHrP actions and considers controversial and unsettled elements of their effects.

Receptors and second-messenger systems for parathyroid hormone and parathyroid hormone−related protein

Most PTH and PTHrP effects in bone are mediated by the PTHR (Abou-Samra et al., 1992; Juppner et al., 1991). This family B G-protein-coupled receptor (GPCR) recognizes PTH and PTHrP as well as their biologically active N-terminal peptides PTH(1−34) and (1−36) and PTHrP(1−36). The PTHR binds PTH and PTHrP with equal affinity (although some differences in the affinity for G-protein-coupled and uncoupled states have been reported (Dean et al., 2008)), and in response, ligand binding signals through various cellular effector systems. Signal transduction by the PTHR is primarily mediated by G_s, $G_{q/11}$, G_i, and G_{12}/G_{13} heterotrimeric G proteins (Gardella and Vilardaga, 2015) (see alsoChapters 24, 25, and 28). The particular coupling mechanism for distinct G proteins depends on the cell type in a manner that remains incompletely understood (Abou-Samra et al., 1992; Civitelli et al., 1989, 1990; Juppner et al., 1991; Pines et al., 1996). Studies of the PDZ adapter protein Na^+/H^+ exchange-regulatory factor 1 (NHERF1) revealed that it serves as a switch to control signaling by G_s, $G_{q/11}$, and G_i (Mahon et al., 2002; Wang et al., 2010).

Important effects of the PTHR on mitogen-activated protein kinases (MAPKs), especially the extracellular signaling-related kinases (ERKs) ERK1 and ERK2, have been described (Cole, 1999; Miao et al., 2001; Sneddon et al., 2000, 2007; Swarthout et al., 2001; Syme et al., 2005). The mechanisms of activation of MAPK signaling by the PTHR are complex and involve Src. This nonreceptor tyrosine kinase interacts with the PTHR and its activity contributes to PTH-mediated ERK activation (Rey et al., 2006). In addition, ERK activation may arise from EGFR transactivation (Syme et al., 2005). Polyubiquitination of specific lysine residues in the C-terminal tail of the PTHR also regulates MAPK signaling, specifically activation of ERK1/2 and p38 (Zhang et al., 2018).

More recently, a newer paradigm of PTHR signaling via Gs/cAMP has emerged that differentiates the signaling activities of PTH and PTHrP (and related analogs) (Cheloha et al., 2015). Studies in cell systems show that in response to PTHrP, the PTHR at the cell membrane generates short-lived cAMP signals. PTH also elicits membrane signals via Gs. However, PTH also stimulates the recruitment of β-arrestins by the PTHR followed by its internalization in endosomes. Here, the PTHR assembles a functional complex with β-arrestin and Gs to produce sustained cAMP signaling (Ferrandon et al., 2009). In endosomes, β-arrestin promotes cAMP signaling, contrary to its typical function at the cell membrane, which terminates cAMP signaling. This action involves stimulation of ERK1/2 leading to inhibition of phosphodiesterases, in particular PDE4, and diminished cAMP degradation (Wehbi et al., 2013). Subsequent studies in animals show that this temporally discrete pattern of signaling by PTH and PTHrP results in markedly distinct calcemic responses (Shimizu et al., 2016). Thus, the induction of hypercalcemia by PTHrP is significantly lower than that elicited by PTH. These observations are consistent with studies in humans showing that PTHrP and its modified analog abaloparatide elicit significantly less hypercalcemia than does PTH (Horwitz et al., 2005, 2006; Leder et al., 2015).

The magnitude of physiological responses mediated by the PTHR is tightly linked to the balance between signal generation and termination. The receptor normally behaves in a cyclical pattern of activation and inactivation, where PTHR desensitization guards cells against excessive stimulation, and resensitization protects cells against prolonged hormone resistance. Rapid attenuation of PTHR signaling is mediated by receptor desensitization and internalization, while protracted reductions in responsiveness are due to downregulation and diminished receptor biosynthesis. Desensitization and internalization of the PTHR, as with other G-protein-coupled receptors, is generally thought to be regulated primarily by phosphorylation and arrestins. Ligand binding to the PTHR promotes receptor phosphorylation both by G protein receptor kinases (GRKs) and by two second-messenger-dependent protein kinases, protein kinase A (PKA) and protein kinase C (PKC) (Blind et al., 1996; Dicker et al., 1999; Flannery and Spurney, 2001). GRK2, and to a lesser extent by PKC, mediates phosphorylation of serine residues in the PTHR (Castro et al., 2002; Dicker et al., 1999; Malecz et al., 1998). GRK2 preferentially phosphorylates the distal sites of the intracellular PTHR tail, whereas PKC phosphorylates more

upstream residues (Blind et al., 1996). Mice harboring a phosphorylation-resistant PTHR, where serine residues at positions 489, 491, 492, 493, 495, 501, and 504 were mutated to alanine, exhibit essentially normal anabolic responses (Datta et al., 2012), suggesting that PTHR phosphorylation does not importantly affect PTHR internalization or bone anabolism.

Following activation, the PTHR rapidly recruits β-arrestins at the plasma membrane, an event that initiates dynamin-dependent endocytosis. Interestingly, PTHR phosphorylation is not required for the interaction of the receptor with β-arrestins or for receptor internalization (Dicker et al., 1999; Ferrari et al., 1999; Malecz et al., 1998; Sneddon et al., 2003). However, receptor phosphorylation may stabilize the receptor–arrestin complex. As described previously, although the interaction with β-arrestins dampens acute cAMP generation at the plasma membrane, the PTHR, in complex with β-arrestins, remains active in endosomes and induces prolonged cAMP signaling. Although the PTHR lacks a canonical NPXXY internalization motif, other endocytotic signals have been identified within the carboxy terminus. Detailed analysis of the intracellular tail of the PTHR revealed bipartite sequences that negatively or positively regulate receptor endocytosis (Huang et al., 1995). An endocytic signal was detected within residues 475–494 of the opossum kidney PTHR (corresponding to D482-S501 of the human PTHR). Mutations or deletions within this region result in diminished PTH-induced receptor endocytosis (Huang et al., 1995).

In addition to governing PTHR signaling, NHERF1 is importantly involved in determining receptor endocytosis. The interaction of NHERF1 with the PTHR is disrupted by mutating its carboxy-terminal PDZ-binding motif; mutating NHERF1; or depolymerizing the actin cytoskeleton, all of which cause important alterations in PTHR endocytosis (Sneddon et al., 2003). Notably, in the absence of NHERF1, both PTH(1–34) and PTH(7–34) (along with their corresponding full-length peptides) promoted efficient PTHR sequestration. In the presence of NHERF1, however, PTH(1–34)-induced receptor internalization was unaffected, whereas PTH(7–34)-initiated endocytosis was largely inhibited (Sneddon et al., 2003). NHERF1 contains two tandem PDZ domains and an ezrin-binding domain (EBD). PDZ core-binding domains and the NHERF1 EBD domain are required for the inhibition of endocytosis (Wang et al., 2007a).

Expression and actions of parathyroid hormone receptor in bone

The PTHR is expressed widely in cells of the osteoblast lineage. Receptor expression is greater in more differentiated cells such as mature osteoblasts on the trabecular, endosteal, and periosteal surfaces (Fermor and Skerry, 1995; Lee et al., 1993) and osteocytes (Fermor and Skerry, 1995; van der Plas et al., 1994). PTHRs are also expressed in marrow stromal cells near the bone surface (Amizuka et al., 1996), a putatively preosteoblast cell population shown to bind radiolabeled PTH (Rouleau et al., 1988, 1990). However, PTHR is virtually absent in STRO-1–positive alkaline phosphatase-negative marrow stromal cells (Gronthos et al., 1999; Stewart et al., 1999), which are thought to represent relatively early osteoblast precursors. Indeed, PTHR expression can be induced by the differentiation of stromal cells, MC3T3 cells, or C3H10T1/2 cells with dexamethasone, ascorbic acid, or bone morphogenetic proteins (Feuerbach et al., 1997; Hicok et al., 1998; Liang et al., 1999; Stewart et al., 1999; Wang et al., 1999; Yamaguchi et al., 1987). Other data suggest that PTH receptors are limited to a relatively mature population of osteoprogenitor cells that express the osteocalcin gene (Bos et al., 1996).

Whether receptors for PTH or PTHrP are expressed on the osteoclast is controversial. Initial studies using receptor autoradiography failed to demonstrate them (Rouleau et al., 1990; Silve et al., 1982), and other studies have not identified PTHR mRNA or protein on mature osteoclasts (Amizuka et al., 1996; Lee et al., 1993, 1995). However, PTHRs are reportedly present on normal human osteoclasts (Dempster et al., 2005) and osteoclasts from patients with renal failure (Langub et al., 2001). Also, relatively low-affinity binding of radiolabeled PTH peptides to osteoclasts or preosteoclasts has been reported (Teti et al., 1991). The functional importance of such putative receptors is unclear.

PTH and PTHrP have additional receptors besides the PTHR. The PTH2R, which recognizes the amino terminal domain of PTH but not of PTHrP, is a GPCR closely related to the PTHR (Usdin et al., 1995) (Chapter 28). The endogenous ligand for the PTH2R is likely to be tuberoinfundibular peptide of 39 amino acids (TIP39). The PTH2R and TIP39 are expressed predominantly in brain, vasculature, and pancreas (Dobolyi et al., 2003; Eichinger et al., 2002; Usdin et al., 1996, 1999). TIP39 and PTH2R are expressed in distinct areas of the growth plate of newborn mice. Whereas the PTH2R localizes to the resting zone, TIP39 is restricted to prehypertrophic and hypertrophic chondrocytes. In chondrocytes, the TIP39/PTH2R system inhibits proliferation and differentiation (Panda et al., 2009). These findings were expanded to postnatal mice with chondrocyte-specific expression of the PTH2R (Panda et al., 2012). Targeted PTH2R expression in chondrocytes resulted in delayed formation of the secondary ossification center and reduced trabecular bone. Consistent with the finding in cell systems, these mice have attenuated expression of numerous markers of chondrocyte proliferation and differentiation including Sox9, Gdf5, Wdr5, and β-catenin.

A large body of evidence exists for the presence of specific receptor(s) for carboxyl-terminal PTH peptides on osteoblasts (Divieti et al., 2005; Inomata et al., 1995; Nguyen-Yamamoto et al., 2001) and osteocytes (Divieti et al., 2001), and evidence for actions of carboxyl-terminal PTH peptides on bone has been presented (Murray et al., 1989, 1991; Nakamoto et al., 1993; Sutherland et al., 1994). Such a carboxyl-terminal PTHR has thus far eluded molecular cloning.

PTHrP is expressed and secreted by osteoblast-like osteosarcoma cells (Rodan et al., 1989; Suda et al., 1996) and by rat long-bone explants in vitro (Bergmann et al., 1990). Messenger RNA for PTHrP is detected in periosteal cells of fetal rat bones (Karmali et al., 1992). *In situ* hybridization and immunohistochemistry localized PTHrP mRNA and protein to mature osteoblasts on the bone surface of fetal and adult bones from mice and rats (Amizuka et al., 1996; Lee et al., 1995) and to flattened bone-lining cells and some superficial osteocytes (Amizuka et al., 1996) in postnatal mice. In addition, the PTHrP gene is expressed in preosteoblast cells in culture, and in some studies its expression is reduced as preosteoblasts undergo differentiation (Kartsogiannis et al., 1997; Oyajobi et al., 1999; Suda et al., 1996).

As discussed in Chapter 25, PTHrP is cleaved to produce a set of peptides: those that contain the amino terminus (such as PTHrP(1−36)) activate the PTHR, and additional peptides representing the midregion and carboxyl terminus of PTHrP appear to have distinct biological actions mediated by their own receptors (Philbrick et al., 1996; Wysolmerski and Stewart, 1998). Receptors that are specific for amino-terminal PTHrP and do not recognize PTH have been identified in brain (Yamamoto et al., 1997) and other tissues (Gaich et al., 1993; Orloff et al., 1992; Valin et al., 2001), and midregion peptides of PTHrP have actions on placental calcium transport that imply a distinct receptor (Care et al., 1990; Kovacs et al., 1996), but there is presently no evidence for either receptor in bone. Carboxyl-terminal PTHrP fragments [e.g., PTHrP(107−139)] reportedly inhibit bone resorption (Cornish et al., 1997; Fenton et al., 1991a, 1991b, 1993) and stimulate (Goltzman and Mitchell, 1985) or inhibit (Martinez et al., 1997) osteoblast growth and function (Esbrit et al., 2000; Gray et al., 1999), and it is thus likely that a specific receptor for this peptide is present on osteoblasts and conceivably also on osteoclasts.

Effects of parathyroid hormone and parathyroid hormone−related protein on bone cells

Molecular mechanisms of action in osteoblasts

Transcription factors

A major effect of PTH and PTHrP in osteoblasts is directed at modulating the expression and/or function of a number of transcription factors important in bone metabolism. Among these, the most prominent are the cAMP response element binding protein (CREB) (Brindle and Montminy, 1992; Papavassiliou, 1994), the immediate early gene of activator protein-1 (AP-1) family members *c-fos* (c-fos, fra-1, fra-2) and *c-jun* (c-jun, junD) (Clohisy et al., 1992; Lee et al., 1994; McCauley et al., 1997, 2001; Stanislaus et al., 2000a), and Runx2 (Komori, 2002).

PTH induces *c-fos* transcription in a fashion that does not require protein synthesis and is mediated by the transcription factor CREB. Binding and phosphorylation of CREB to cAMP responsive elements within the *c-fos* promoter (Evans et al., 1996; Pearman et al., 1996; Tyson et al., 1999) are required to activate transcription. These events are stimulated by PTH through its ability to activate PKA, whereas the PKC signaling pathway is not involved in this response (Evans et al., 1996; McCauley et al., 1997). Activation of AP-1 transcription factors is important for osteoblast function because the *collagenase-3* (MMP-13) promoter contains AP-1 binding sites (Pendas et al., 1997; Selvamurugan et al., 1998).

One member of the runt-domain transcription factor family, viz. Runx2 (also called cbfa1 and OSF2), is a specific osteoblast transcriptional activator and is required for determination of the osteoblast phenotype (Ducy et al., 1997; Komori, 2002). Runx2 stimulates transcription of a number of key osteoblastic genes such as osteocalcin, osteopontin, collagenase-3, and collagens α1 and α2 (Banerjee et al., 2001; Porte et al., 1999; Selvamurugan et al., 1998). The importance of Runx2 for osteoblast formation and bone metabolism has been established with in vitro and in vivo models (Ducy et al., 1997, 1999; Komori et al., 1997; Otto et al., 1997). Brief PTH treatment stimulates rapid and transient increases of Runx2 mRNA and protein both in osteoblastic cell cultures and in mice (Krishnan et al., 2003). In addition, PTH, likely via cAMP/PKA activation, stimulates Runx2 activity (Selvamurugan et al., 2000; Winchester et al., 2000). In contrast, long-term treatment with PTH reduces Runx2 levels (Bellido et al., 2003). The dual effect of PTH on Runx2 levels and activity is particularly interesting. As will be discussed later, PTH promotes osteoblast survival in part by increasing Runx2 activity and consequently inducing expression of the survival gene *Bcl2*. However, PTH also induces proteasomal degradation of Runx2 through a mechanism involving Smurf2. Therefore, the ability of PTH to either increase or decrease Runx2 levels in osteoblasts in a fashion dependent on the administration schedule may provide one of the possible (and likely many) mechanisms to explain the complex effect of PTH on bone formation and resorption.

Osterix is a zinc finger domain transcription factor expressed specifically in osteoblasts (Nakashima et al., 2002). Its function is necessary for full osteoblastic differentiation and maturation (Nakashima et al., 2002), and studies in cells (Nishio et al., 2006) and genetically modified mice (Nakashima et al., 2002) have established that osterix lies downstream of Runx2. Similar to Runx2, PTH rapidly stimulates expression of osterix both in cell cultures (Wang et al., 2006) and in vivo (Tanaka et al., 2004).

Finally, PTH injection stimulates rapid and transient increases in the expression of at least three members of the nerve growth factor-inducible factor B (NR4A/NGFI-B) family of orphan nuclear receptors: Nurr1, Nur77, and NOR-1 (Pirih et al., 2005). Nurr1 mediates PTH-stimulated activation of the *osteopontin* (Lammi et al., 2004) and *osteocalcin* (Nervina et al., 2006; Pirih et al., 2004) promoters.

Clearly, PTH has profound effects on gene expression during bone remodeling. The complexity of this regulation is further illustrated by studies showing that PTH induces epigenetic modifications via histone deacetylating enzymes (HDACs). These epigenetic events profoundly impact PTH-mediated regulation of important genes including MMP13, Runx2, RANKL, and sclerostin. In osteoblastic cells, PTH signaling induces PKA-dependent phosphorylation of HDAC4 that in turn regulates expression of MMP13 via Runx2 (Shimizu et al., 2014). In contrast, in calvarial cells PTH elicits polyubiquitylation and degradation of HDAC4, an event that promotes RANKL (Obri et al., 2014). Further understanding of the complex mechanisms by which PTH regulates HDACs comes from studies in osteocytes (Wein et al., 2016, 2017). In these cells, the salt-inducible kinases (SIKs) maintain HDAC4/5 phosphorylated and outside the nucleus. Activation of the PTHR induces PKA-mediated phosphorylation of SIK2, which inhibits its activity. This causes nuclear translocation of HDAC4/5, inhibition of sclerostin transcription, and bone formation. By a similar mechanism, PTH controls the localization of the cAMP-regulated transcriptional coactivators CRTC2. When dephosphorylated, CRTC2 translocates to the nucleus, where it potentiates CREB-dependent transcription of RANKL, thus inducing bone resorption. Collectively, these observations highlight the critical contribution of epigenetic modification to the dual actions of PTH on bone formation and resorption.

The HDAC Sirt1 inhibits PTH-induced MMP13 transcription (Fei et al., 2015) in osteoblastic cells. Other studies show that PTH induces nuclear translocation of HDAC5 with attendant reduction in sclerostin expression, whereas HDAC2 and HDAC3 appear to induce constitutive *SOST* transcription in osteoblastic cells (Baertschi et al., 2014).

Growth factors and cytokines

Insulin-like growth factors. PTH stimulates synthesis and secretion of insulin-like growth factors (IGFs) IGF-I and IGF-II in bone. IGF-I and IGF-II are expressed in the rat (McCarthy et al., 1989) and mouse (Linkhart and Mohan, 1989; Watson et al., 1995). A PTH-dependent increase of IGF requires activation of the cAMP/PKA pathway because its effects are mimicked by cAMP analogs or agents that increase cAMP but not by stimulation of calcium signals or PKC (McCarthy et al., 1990).

IGF-I exerts proliferative and antiapoptotic actions in osteoblasts (Gray et al., 2003), and a number of observations support the requirement of IGF-I as a mediator of the anabolic action of PTH. First, treatment with PTH under conditions where it has an anabolic effect on bone leads to an increase in IGF-I mRNA (Watson et al., 1995) and the bone matrix content of IGF-I. Second, daily PTH injection failed to stimulate bone formation in mice lacking IGF-I (Bikle et al., 2002). Third, a similar absence of an anabolic effect of PTH was observed in mice lacking insulin receptor substrate-1 (Yamaguchi et al., 2005), the key intracellular mediator of IGF-I receptor signaling.

Additionally, both PTH and PTHrP affect the secretion in bone of IGF-binding proteins (IGFBPs), in particular IGFBP-4 (LaTour et al., 1990) and IGFBP-5 (Conover et al., 1993). The role of IGFBPs on IGF function is complex, since they can exert both inhibitory (IGFBP-4) and stimulatory (IGFBP-5) effects on IGF action in a cell- and context-specific manner. Moreover, some IGFBPs have been proposed to have effects independent of IGF (Conover, 2008). Thus, the role of IGFBPs on PTH action remains mostly to be defined.

Fibroblast growth factor-2 (FGF-2). Like IGF-I, FGF-2 is a potent mitogen (Ling et al., 2006), induces differentiation (Woei Ng et al., 2007), and exerts antiapoptotic actions on osteoblasts (Chaudhary and Hruska, 2001; Debiais et al., 2004). PTH rapidly increases FGF-2 and FGF receptor expression in both primary and clonal osteoblastic cells (Hurley et al., 1999). Stimulation of bone formation by PTH is impaired in mice null for FGF-2 (Hurley et al., 2006), and bone marrow cultures from these mice produce fewer osteoclasts in response to PTH (Okada et al., 2003). Collectively, these observations provide evidence that FGF-2 participates in the skeletal actions of PTH in vivo.

Amphiregulin. Recent studies demonstrated an important role for amphiregulin (AR), a member of the epidermal growth factor (EGF) family, as a mediator of PTH action. PTH stimulates AR expression in osteoblastic cells in a cAMP/PKA-dependent manner (Qin and Partridge, 2005). The increase in AR mRNA is mediated by phosphorylation of CREB and binding to a conserved CRE site in the AR promoter. AR appears to be important for bone metabolism because mice

lacking AR have decreased trabecular bone (Qin et al., 2005b). In addition, AR stimulates rapid increases in *c-fos* and *c-jun* expression (Qin et al., 2005b). Treatment of primary calvarial cultures in vitro with AR stimulated cell proliferation and concomitant inhibition of osteoblastic differentiation, suggesting a role for AR on preosteoblastic mesenchymal stem cells (Qin and Partridge, 2005; Qin et al., 2005b). It is also notable that PTH stimulates the release of heparin-bound EGF, which belongs to the same family of membrane-bound and releasable EGF receptor agonists as AR, by activation of ADAM proteins in osteoblasts (Ahmed et al., 2003). This process leads to the activation of EGF receptor in an autocrine and paracrine fashion. It is therefore likely that PTH may induce not only the expression of AR in osteoblasts but also its release via a similar mechanism.

Transforming growth factor-β. All three TGF-β isoforms are detected in bone, with TGF-β1 being the most abundant (Hering et al., 2001; Seyedin et al., 1985). TGF-β1 is secreted by bone cells and stored in the extracellular matrix. TGF-β is a potent mitogen for osteoprogenitors (Hock et al., 1990) and has varied effects on differentiation and mineralization. Intermittent PTH treatment of rats increases the bone matrix content of TGF-β1 (Pfeilschifter et al., 1995; Watson et al., 1995) and the expression of TGF-β in osteoblasts (Oursler et al., 1991; Pfeilschifter and Mundy, 1987; Wu and Kumar, 2000). Moreover, PTH and PTHrP increase the secretion of TGF-β by osteoblast-like bone cells (Wu and Kumar, 2000), TGF-β1 activity (Pfeilschifter and Mundy, 1987; Sowa et al., 2003) and the release of TGF-β from bone matrix. Collectively, these observations suggest that TGF-β may contribute to the anabolic effects of intermittent PTH administration.

RANK ligand and osteoprotegerin. The regulation of these molecules by PTH and PTHrP is now recognized as the most prominent mechanism linking PTHR-mediated actions in osteoblasts (and possibly stromal cells) and osteoclastogenesis. RANK ligand (RANKL)[1] is a member of the TNF family of cytokines that is expressed on the osteoblast and stromal cell surface. Its receptor, called receptor activator of NFkB (RANK), is expressed in osteoclast precursors and mature osteoclasts, and its activation by RANKL stimulates osteoclast formation, activity, and survival (Burgess et al., 1999; Fuller et al., 1998; Hofbauer et al., 2000; Lacey et al., 1998). A second component of this system, expressed and secreted by osteoblasts, is osteoprotegerin (OPG) (Simonet et al., 1997; Yasuda et al., 1998), a released protein that binds and sequesters RANKL, preventing its actions on RANK. Therefore, it is the balance between RANKL and OPG (in other words the ratio RANKL:OPG) that ultimately determines the extent of osteoclast formation and function.

PTH and PTHrP regulate the expression of RANKL and OPG. It is interesting to note that the frequency of administration of PTH affects the RANKL:OPG ratio differently. Thus, prolonged exposure to PTH in rats causes sustained stimulation of RANKL expression while inhibiting OPG expression (Huang et al., 2004; Kondo et al., 2002; Lee and Lorenzo, 1999; Ma et al., 2001), with the final effect being an overall stimulation of osteoclast number and resorptive capacity. In contrast, intermittent PTH treatment affected RANKL and OPG only transiently (Ma et al., 2001). Exposure to PTH increases the expression of RANKL in murine bone marrow cultures, cultured osteoblasts, and mouse calvariae (Hofbauer et al., 2000; Lee and Lorenzo, 1999; Tsukii et al., 1998) as well as simultaneously decreasing the expression of OPG (Lee and Lorenzo, 1999). In addition, studies using primary cultures indicate that the effect of PTH on RANKL expression is more pronounced in differentiated osteoblasts, whereas the inhibition of OPG occurs at all differentiation stages (Huang et al., 2004). Notably, the stimulation of osteoclastic differentiation by RANKL requires the presence of macrophage-colony stimulating factor M-CSF, which is also upregulated by PTH (Horowitz et al., 1989; Weir et al., 1989).

Strong evidence supports the key role of the RANK/RANKL/OPG system in the activation of bone resorption upon prolonged exposure to PTH and PTHrP. Stimulation of osteoclastogenesis by PTH is blocked by antibodies to RANKL (Tsukii et al., 1998) or by OPG (Lacey et al., 1998; Yasuda et al., 1998), and OPG inhibits the hypercalcemic response to PTH and PTHrP (Morony et al., 1999; Oyajobi et al., 2001).

Wnt/β-catenin/sclerostin. The Wnt/β-catenin signaling pathway is recognized as an important regulator of bone mass. This is a complex signaling system comprising a number of members. Canonical Wnt signaling is mediated by a receptor complex formed by a Frizzled (a seven-transmembrane domain GPCR) and a lipoprotein-receptor-related protein 5 or 6 (LRP5/6) coreceptor. Upon engagement by Wnt, this complex activates the cytoplasmic protein disheveled (Dvl) followed by the accumulation of unphosphorylated β-catenin. As a result, β-catenin translocates to the nucleus and regulates gene transcription. Moreover, cells secrete proteins such as Dickkopf-1 that interact with the coreceptors LRP5/6 and inhibit Wnt signaling (Baron and Rawadi, 2007). All the key elements of this pathway are expressed in bone cells and osteoblastic cultures and regulated by PTH (Kulkarni et al., 2005). Treatment of rats with PTH increased Frizzled-1 and β-catenin levels and decreased DKK-1, with resulting activation of Wnt responses (Kulkarni et al., 2005). Sclerostin, the product of the *Sost* gene, is also a secreted Wnt inhibitor that binds LRP5 and LRP6 (Li et al., 2005; Semenov et al., 2005), and its

1. RANKL is also called osteoprotegerin ligand (OPGL), osteoclast differentiation factor (ODF), and TNF-related activation-induced cytokine (TRANCE).

level in osteocytes is dramatically reduced by continuous PTH treatment (Bellido, 2006; Bellido et al., 2005). It is interesting that sclerostin appears to inhibit osteoblast differentiation (van Bezooijen et al., 2004, 2007), thereby providing a functional link between osteocytes and osteoblasts. The profound effects of the Wnt signaling complex on bone metabolism are well described by a number of genetic studies in both human and animal models (Baron and Rawadi, 2007), and the observation that PTH engages this pathway in bone cells is indeed of great interest.

Adaptor proteins

G-protein-coupled receptor kinase 2 and β-arrestins. These two ubiquitously expressed proteins play important roles in the regulation of several G-protein-coupled receptors including the PTHR. It is not surprising that alterations in their expression or activity impact the function of osteoblasts and their responsiveness to PTH. G-protein-coupled receptor kinase 2 (GRK2) phosphorylates agonist-occupied PTHR and promotes the binding of β-arrestins (Dicker et al., 1999; Ferrari et al., 1999; Flannery and Spurney, 2001; Vilardaga et al., 2001). These combined actions result in decreased signaling at the cell membrane (Bisello et al., 2002; Dicker et al., 1999; Ferrari and Bisello, 2001). As mentioned earlier, prolonged PTHR signaling in endosomes is promoted by β-arrestins through the inhibition of PDE4 and reduction in cAMP degradation (Gardella, Vilardaga) (Cheloha et al., 2015).

Targeted overexpression of GRK2 in osteoblasts promotes bone loss (Wang et al., 2005a). In contrast, inhibition of GRK2 activity by expression of a dominant negative mutant increases PTH-stimulated cAMP, and mice overexpressing Grk2 have increased bone remodeling with a net gain in bone content (Spurney et al., 2002). Similarly, intermittent PTH increased the number of osteoblasts in mice null for β-arrestin2 (Ferrari et al., 2005). However, no net increase in bone mass was observed, likely due to the intense stimulation of osteoclastogenesis. Another regulator of G-protein-coupled receptor signaling, the regulator of G protein signaling-2 (RGS2), which increases the rate of hydrolysis of GTP bound to G proteins, thereby terminating signaling, has also been implicated in PTHR actions on bone cells. RGS2 mRNA is rapidly and transiently increased by PTH in rat bones as well as osteoblast cultures (Miles et al., 2000b), and its expression in bone cells resulted in decreased PTH-stimulated cAMP production (Thirunavukkarasu et al., 2002). Interestingly, RGS2 upregulation was also observed in cells overexpressing Runx2 (Thirunavukkarasu et al., 2002), suggesting the possibility that mechanisms limiting PTHR signaling by G proteins may be activated upon differentiation of cells along the osteoblastic lineage.

Na^+/H^+ exchange-regulatory factor 1 (NHERF1). NHERF1 is a PDZ-domain scaffolding protein that interacts with the PTHR and regulates various functions including preferential G-protein coupling, membrane retention, and trafficking. Little information exists concerning the role of NHERF1 in regulating the PTH-mediated effect in bone cells. NHERF1 is expressed in active mineralizing osteoblasts, where it regulates PTHR expression during differentiation (Liu et al., 2012). Indeed, when cultured in differentiating medium, mesenchymal stem cells from NHERF1$^{-/-}$ mice show a dramatic reduction in PTHR mRNA accompanied by preferential differentiation to adipocyte. NHERF1 is required for osteoblast differentiation and matrix synthesis, but whether this is directly due to alterations in PTHR signaling is yet unknown. NHERF1-null mice and humans with NHERF1 polymorphisms display osteopenia and increased skeletal fractures (Karim et al., 2008; Morales et al., 2004; Shenolikar et al., 2002). Proliferating osteoblasts express Npt2a and Npt2b, PTHR, and NHERF1 (Wang et al., 2013). In cells from wild-type mice, PTH inhibits phosphate uptake, but this effect was not observed in cells from NHERF1$^{-/-}$ mice. In contrast, PTH increases phosphate uptake in differentiated osteoblasts, and this effect depends on NHERF1 expression.

Effects on gap junctions

PTH increases intercellular communication of bone cells by increasing connexin-43 gene expression (Schiller et al., 1992) and opening gap junctions (Donahue et al., 1995; Schiller et al., 1992). The reduction of connexin-43 levels by transfection of antisense cDNA markedly inhibited the cAMP response to PTH (Vander Molen et al., 1996) and blocked the effect of PTH on mineralization by osteoblast-like cells (Schiller et al., 2001). These effects appear to significantly impair the anabolic action of PTH because increases in bone mineral content in response to intermittent PTH administration were significantly decreased in mice with targeted deletion of connexin43 in osteoblasts (Chung et al., 2006).

Effects on bone matrix proteins and alkaline phosphatase

PTH regulates the expression of a number of bone matrix proteins including type I collagen, osteocalcin, osteopontin, bone sialoprotein, osteonectin, and alkaline phosphatase. In most cases, these genes (with the exception of osteocalcin) are

downregulated by continuous exposure to PTH (Wang et al., 2005b), whereas intermittent administration of PTH has inhibitory and stimulatory effects on different genes.

Type I collagen is the most abundant bone matrix protein. PTH and PTHrP acutely inhibit collagen synthesis in vitro (Kream et al., 1980, 1986; Partridge et al., 1989; Pines et al., 1990). Similar inhibition is observed upon infusion of PTH in humans (Simon et al., 1988). However, anabolic PTH treatment can stimulate type I collagen expression (Canalis et al., 1990; Opas et al., 2000), an effect that is likely mediated by increases in IGF-I (Canalis et al., 1989). Intermittent treatment of mouse bone marrow cells with PTH modestly increased collagen expression (Locklin et al., 2003). Similarly, PTH treatment inhibits osteopontin (Noda et al., 1988) and osteonectin (Termine et al., 1981) expression.

The osteocalcin gene is also importantly regulated by PTH (Noda et al., 1988; Towler and Rodan, 1995; Yu and Chandrasekhar, 1997). However, in contrast to the effect on type I collagen, expression of osteocalcin is stimulated by chronic administration of PTH or PTHrP, whereas the acute effect of these hormones is inhibitory (Gundberg et al., 1995).

Finally, the effect of PTH on the expression of bone sialoprotein can be either stimulatory (Ogata et al., 2000; Yang and Gerstenfeld, 1997) or inhibitory (Ma et al., 2001; Wang et al., 2000).

The reported actions of PTH on the expression of alkaline phosphatase are inconsistent. PTH can either stimulate or inhibit secretion of alkaline phosphatase from bone cells (Jongen et al., 1993; Kano et al., 1994; Majeska and Rodan, 1982; McPartlin et al., 1978; Yee, 1985) and may not be particularly indicative of PTH-specific actions. Indeed, although anabolic therapy with PTH generally increases the circulating levels of alkaline phosphatase (Finkelstein et al., 1998), this effect is likely due to an increase in osteoblast number rather than an increase in protein expression.

Effects on bone proteases

PTH stimulates the secretion of a number of matrix metalloproteases (MMPs) in bone cells (see Chapter 16) that are involved in bone remodeling. These include collagenase-3 (MMP-13) (Partridge et al., 1987; Quinn et al., 1990; Scott et al., 1992; Winchester et al., 1999, 2000), stromelysin-1 (Meikle et al., 1992), gelatinase B (Meikle et al., 1992), and the disintegrin and metalloprotease with thrombospondin repeats (Miles et al., 2000a). Bone proteases, in particular collagenase-3 and gelatinase B, partially mediate the stimulation of bone resorption by PTH (Witty et al., 1996). As described above, stimulation of the MMP-13 promoter by PTH requires the combined action of AP-1 transcription factors and Runx2, effects that are mediated by cAMP-dependent activation of CREB (Porte et al., 1999; Selvamurugan et al., 1998, 2000). All of these events are stimulated by PTH. PTH treatment also increases secretion of the tissue inhibitor of matrix metalloproteins (TIMP-1) by osteoblasts (Meikle et al., 1992). This is relevant to the action of PTH because mice overexpressing TIMP-1 in osteoblasts responded to intermittent PTH with increases in bone mineral density higher than those in normal mice (Merciris et al., 2007). This was also accompanied by decreased osteoclastic differentiation (Geoffroy et al., 2004; Merciris et al., 2007).

Effects of parathyroid hormone and parathyroid hormone–related protein on bone cell proliferation

Continuous exposure to relatively high concentrations of PTH(1–34) or PTHrP(1–34) inhibits proliferation of virtually every osteoblastic cell line including UMR 106–01, MC3T3-E1, SaOS-2, and calvarial primary cultures (Civitelli et al., 1990; Kano et al., 1991; Onishi et al., 1997; Qin et al., 2005a). This effect is mediated by changes in the expression levels of several components of the cell cycle, ultimately resulting in arresting cells in the G1 phase. PTH treatment decreases expression of cyclin D1 while increasing the levels of $p21^{Cip1}$ and $p27^{Kipl}$ (Onishi et al., 1997; Qin et al., 2005a), with evident cell cycle arrest.

In contrast, some in vitro studies demonstrated that in certain circumstances PTH stimulates the proliferation of osteoblastic cells (Finkelman et al., 1992; Onishi et al., 1997; Somjen et al., 1990). In particular, very low concentrations of PTH (Swarthout et al., 2001) and brief exposure to PTH (Scutt et al., 1994) resulted in increased cell proliferation. In the preosteoblast cell line TE-85, PTH stimulated proliferation by increasing expression of the cyclin-dependent kinase cdc2 (Onishi et al., 1997).

The effects of PTH and PTHrP on the cell cycle in osteoblastic cells have important consequences in vivo. Several studies indicate that intermittent injections of PTH increase the number of osteoblasts (Kostenuik et al., 1999; Nishida et al., 1994), and this contributes to the stimulation of bone formation. However, this effect does not appear to be related to direct stimulation of osteoblast mitogenesis. Indeed, although intermittent PTH administration in rats greatly increased osteoblast number and function, osteoblast proliferation was not detected (Dobnig and Turner, 1995; Onyia et al., 1995, 1997). It is possible that the increase in osteoblast number produced by intermittent treatment with PTH is due to the

activation of bone-lining cells to osteoblasts (Dobnig and Turner, 1995), a process that does not require mitosis. These findings are compatible with the conclusion that PTH inhibits cell cycle progression of committed osteoprogenitors, thereby permitting their maturation.

Effects of parathyroid hormone and parathyroid hormone–related protein on bone cell differentiation

PTH and PTHrP profoundly influence the differentiation program of bone marrow cells to form osteoblasts (Fig. 27.1). Several studies indicate that anabolic administration of PTH stimulates rapid changes in histomorphometry and gene expression, which have been interpreted as resulting from cell differentiation (Hodsman and Steer, 1993; Onyia et al., 1995). The effects of PTH and PTHrP on cell differentiation in culture are also well documented and appear to depend on both the duration and the frequency of PTH exposure. Early, transient PTH treatment enhances the commitment of progenitor cells and increases osteoblast differentiation (Wang et al., 2007b). In vitro, primary osteoblasts briefly (1 h every 48 h) exposed to PTH showed inhibited expression of alkaline phosphatase activity and bone nodule formation (Ishizuya et al., 1997). In contrast, intermittent PTH treatment for 6 h every 2 days stimulated osteoblastic differentiation and formation of mineralized nodules (Ishizuya et al., 1997). Similarly, transient PTH treatment of calvarial osteoblasts inhibited initial osteoblast differentiation but ultimately resulted in increased mineralized nodules and osteoblastic differentiation (Wang et al., 2007b). In cultured murine marrow cells, intermittent PTH treatment increases the expression of osteoblast differentiation markers (such as Runx2, alkaline phosphatase, and type I collagen) (Locklin et al., 2003). In all cases, however, continuous exposure to PTH strongly inhibits osteoblast differentiation (Ishizuya et al., 1997; Wang et al., 2007b). In this respect, it is interesting to note that in humoral hypercalcemia of malignancy (HHM), PTHrP is continuously secreted by tumors and results in the virtual absence of mature osteoblasts (Stewart et al., 1982). In contrast, elevated PTH levels observed in hyperparathyroidism do not have the same effect: indeed, hyperparathyroidism is characterized by increased bone remodeling (i.e., higher formation and resorption) with complex effects on bone (Bilezikian, 2012) (Chapter 54). Although the mechanisms of this difference remain to be fully elucidated, one possible underlying basis is the pulsatile secretion of PTH by the parathyroids in hyperparathyroidism versus the continuous, unregulated secretion of PTHrP in HHM.

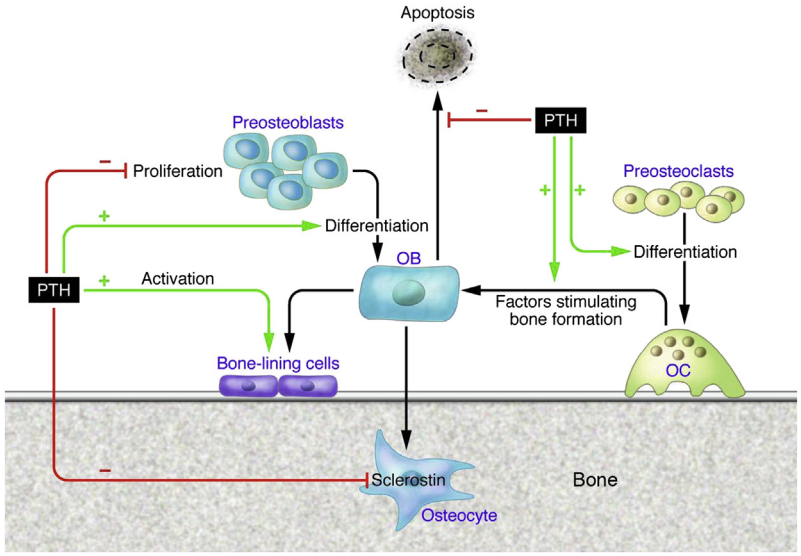

FIGURE 27.1 Cellular effects of PTH on bone. *Bone resorption*. PTH stimulates differentiation and activation of osteoclasts by increasing RANKL and possibly decreasing OPG production by stromal cells and osteoblasts. *Bone formation*. PTH decreases proliferation of preosteoblasts and stimulates their differentiation. PTH decreases osteoblast apoptosis and can activate bone-lining cells into functioning osteoblasts. These combined actions result in increased numbers of osteoblast. Moreover, PTH suppresses the production of the Wnt inhibitor sclerostin by osteocytes, thereby increasing β-catenin signaling in osteoblasts. *From Khosla, S., Westendorf, J.J., Oursler, M.J. 2008. Building bone to reverse osteoporosis and repair fractures. J. Clin. Investig. 118, 421–428.*

Effects of parathyroid hormone and parathyroid hormone–related protein on bone cells

Survival

Cell culture studies show that PTH rapidly stimulates transcription of the prosurvival gene *Bcl-2* while increasing the inactivation of the apoptotic protein Bad (Bellido et al., 2003; Jilka et al., 1998), suggesting that activation of the PTHR in osteoblasts may inhibit apoptosis. Indeed, various studies showed that PTH reduces the apoptotic effects of etoposide, dexamethasone, and serum deprivation in osteoblastic cultures (Bellido et al., 2003; Chen et al., 2002; Jilka et al., 1998). The effect of PTH on the expression of survival proteins appears to require the action of CREB and Runx2 (Bellido et al., 2003). Considering the disparate effects of PTH on Runx2 stability discussed previously, it is therefore possible that the timing and frequency of PTH stimulation may be key determinants for its prosurvival action. Thus, although some studies in mice demonstrated a significant decrease in apoptotic osteoblasts following daily PTH administration (Bellido et al., 2003; Jilka et al., 1999), a study in rats reported an actual increase in apoptotic osteoblasts by intermittent PTH (Stanislaus et al., 2000b). An additional complexity results from the observation that daily administration of PTH in post-menopausal women resulted in increased osteoblast apoptosis (Lindsay et al., 2007). Finally, it should be noted that differences have been observed in the effect of PTH on osteoblast apoptosis at different skeletal sites (cortical and trabecular) and possibly between primary and secondary spongiosa (Jilka et al., 1999; Stanislaus et al., 2000b).

Effects of parathyroid hormone and parathyroid hormone–related protein on bone

Bone resorption

Cellular basis of parathyroid hormone action

PTH and PTHrP increase bone resorption by stimulating osteoclastogenesis and activating the mature osteoclast. These effects require the participation of classical PTH target cells including stromal cells and osteoblasts (Akatsu et al., 1989; McSheehy and Chambers, 1986). Moreover, as described earlier, osteoclasts seemingly do not express high-affinity PTHR (Amizuka et al., 1996; Rouleau et al., 1990; Silve et al., 1982). The identification of the central role of the RANK/RANKL system in osteoclast formation and function, and the appreciation that PTH and PTHrP affect the expression of RANKL and OPG in stromal cells and osteoblasts, provide a molecular basis for understanding PTH-stimulated bone resorption. The precise target cell in the osteoblast lineage responsible for mediating the bone-resorbing effects of PTH and PTHrP, if any, has not been identified, but various marrow stromal cell lines suffice in vitro (Aubin and Bonnelye, 2000), and bone resorption is still active when mature osteoblasts have been ablated (Corral et al., 1998). By binding to its cognate receptor, RANK, on osteoclast precursors and mature osteoclasts, RANKL stimulates osteoclastogenesis and the activity of mature osteoclasts. Therefore, increased RANKL expression mediated the acute and chronic actions of PTH on bone resorption. The major difference in the two effects is likely related to the stronger suppression of the decoy receptor OPG upon prolonged exposure to PTH (Huang et al., 2004). Osteoclast activation by RANKL is apparently responsible for bone resorption at the cellular level and for hypercalcemia, as both are blocked by the decoy receptor OPG (Morony et al., 1999; Yamamoto et al., 1998).

The bone-resorbing effects of amino-terminal PTH and PTHrP are essentially indistinguishable when studied using isolated osteoclasts (Evely et al., 1991; Murrills et al., 1990), bone explant systems (Raisz et al., 1990; Yates et al., 1988), or infusion into the intact animal (Kitazawa et al., 1991; Thompson et al., 1988). In contrast, PTHrP is considerably less potent than PTH in inducing hypercalcemia in humans (Horwitz et al., 2006). This difference is most likely due to lower induction of renal $1.25(OH)_2D_3$ by PTHrP compared with PTH (Horwitz et al., 2003b), though recent findings regarding the persistent noncanonical signaling of cAMP by PTH but not PTHrP described earlier provide a compelling alternative explanation (Cheloha et al., 2015; Ferrandon et al., 2009). Notably, studies in humans showed that intermittent administration of PTHrP(1–36) over 3 months stimulated bone formation without attendant increases in markers of bone resorption (Horwitz et al., 2003b).

As discussed in Chapter 3, PTHrP is a polyhormone, the precursor of multiple biologically active peptides. Carboxy-terminal peptides predicted to arise from cleavage of PTHrP in the polybasic region PTHrP(102–106) have been synthesized and shown to inhibit bone resorption in several explant systems (Fenton et al., 1991a, 1993) and in vivo (Cornish et al., 1997). On this basis, the minimal peptide that inhibits bone resorption, PTHrP(107–111), has been identified and called osteostatin.

Effects of parathyroid hormone and parathyroid hormone–related protein on bone

Bone formation

The mechanisms by which PTH increases bone formation are complex. As described before, PTH and PTHrP exert a variety of effects on osteoblasts. The increase in bone formation in response to intermittent administration of PTH and PTHrP correlates with marked increases in the number of active osteoblasts (Boyce et al., 1996; Dempster et al., 1999; Shen et al., 1993).

It is evident from the previous discussion that every aspect of the osteoblast existence is affected by PTH, and all of these cellular actions may contribute to the increase in osteoblast number observed in the stimulation of bone formation. First, activation of the PTHR produces various actions on the cell cycle of osteoblasts and their precursors. It is clear that in most circumstances PTH and PTHrP cause cell cycle arrest in osteoblasts and preosteoblasts, and this may be a prerequisite to induce further differentiation and activation. Most in vivo evidence does not support a direct proliferative effect of PTH on mature osteoblasts (Dobnig and Turner, 1995; Onyia et al., 1995, 1997). However, PTH and PTHrP increase the expression and release of a number of potent mitogens including IGF-I, TGFβ, and amphiregulin, which may act in a paracrine fashion to expand the pool of osteoprogenitors (Gray et al., 2003; Hock et al., 1990; Qin and Partridge, 2005). Second, intermittent PTH administration stimulates transcription factors, such as Runx2 and osterix, which in turn stimulate differentiation. This effect is accompanied by increases in osteoblastic differentiation markers (Hodsman and Steer, 1993; Onyia et al., 1995; Wang et al., 2007b). Third, some rapid histomorphometric changes observed upon anabolic administration of PTH may derive from stimulation of bone-lining cells to become active osteoblasts (Dobnig and Turner, 1995). Fourth, intermittent PTH administration exerts antiapoptotic actions in osteoblasts and osteocytes (Bellido et al., 2003; Jilka et al., 1999). Obviously, prolonging the life span of osteoblasts would enhance the number of mature osteoblasts. It is interesting that Runx2, a key molecule mediating PTH effects on osteoblast survival, is also involved in the stimulation of osteoblastic differentiation.

The relative contribution of each of these mechanisms to the anabolic action of PTH has not been completely established. It seems likely that the remarkable increases of bone formation in response to intermittent administration of PTH and PTHrP arise from a combination of these effects. Moreover, it is possible that PTH and PTHrP may not have the same effect under all circumstances and in the presence of other treatments affecting bone metabolism.

Finally, it has long been thought that the anabolic actions of PTH and PTHrP are substantially equivalent because most of their cellular effects in vitro and activities in animal models are quite similar. However, it has recently become apparent that some basic differences exist in the action of these two hormones in humans. Intermittent administration of PTHrP(1–36) for 2 weeks (Plotkin et al., 1998) and 3 months (Horwitz et al., 2003a), for instance, leads to increases in biochemical markers of bone formation without changing markers of bone resorption, suggesting that PTHrP(1–36) may uncouple bone formation and resorption.

Parathyroid hormone actions on kidney

PTH regulates renal tubular absorption of phosphate and calcium and synthesis of $1.25(OH)_2D_3$, thereby controlling plasma levels and urinary excretion of these mineral ions and vitamin D (calcitriol) Fig. 27.2). Renal tubular responses to PTH deficiency, PTH or PTHrP excess, and defects in function of the PTHR lead to alterations in blood calcium, phosphate, or vitamin D that are the hallmarks of numerous clinical disorders described later in this volume. Here we review the mechanisms of PTH and PTHrP control of renal tubular calcium and phosphate absorption. The narrative focuses principally on PTH because distinct or unique PTHrP actions on tubular ion transport are not well delineated despite their displaying distinct signaling dynamics (Ferrandon et al., 2009). Because the amino termini of both ligands are similarly recognized by the PTHR, it is likely that PTHrP shares the effects of PTH, though the differences in signaling noted and described earlier may translate to different patterns of dynamic actions. Expression and specific renal actions of PTHrP are associated with regulation of renovascular hemodynamics and may have important effects on hypertension or preeclampsia (Massfelder et al., 1998; Massfelder and Helwig, 1999; Yadav et al., 2014).

Although biologically important, serum magnesium levels do not appear to be significantly regulated by PTH and PTHrP and therefore are not discussed here. Reviews of renal magnesium transport can be found elsewhere (Blaine et al., 2015; Houillier, 2014; Schaffers et al., 2018).

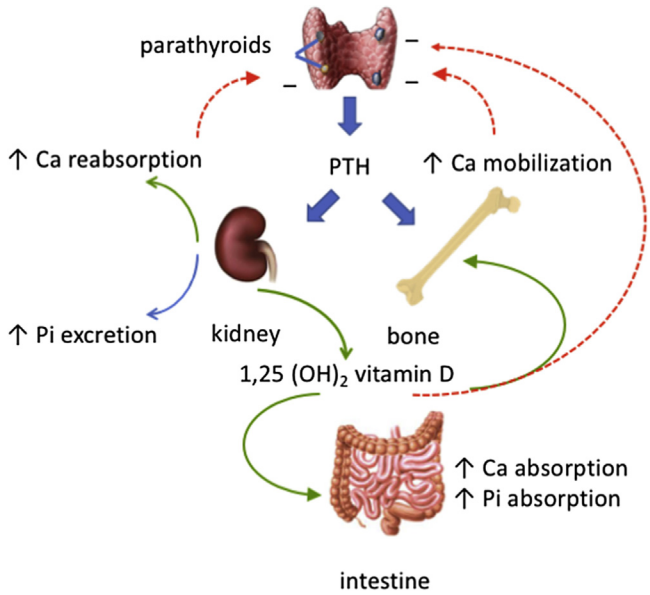

FIGURE 27.2 Parathyroid hormone (PTH) regulation of calcium homeostasis. PTH regulates extracellular calcium homeostasis through a negative feedback scheme. Decreases of extracellular calcium trigger PTH release. PTH in turn stimulates renal calcium reabsorption and mobilizes surface calcium from bone to inhibit further PTH release (dashed lines). PTH also promotes phosphate excretion and stimulates 1α-hydroxylase activity in kidney mitochondria leading to the production of 1,25-dihydroxyvitamin D (calcitriol). Calcitriol, the biologically active metabolite of vitamin D, increases intestinal calcium and phosphate absorption, and calcium mobilization in bone.

Calcium and phosphate homeostasis

Calcium chemistry

Calcium participates in a variety of structural and functional roles in animal cells and tissues. The physical qualities of the calcium ion are especially well suited to the tasks it performs. At first glance, calcium would seem to be an unlikely choice to subserve such diverse functions as an integral macromolecular constituent of bone and at the same time be a primary element in micromolecular signaling. Extracellular concentrations of unbound calcium are roughly 1 mM, whereas its intracellular free concentration under resting conditions is about 0.1 μM—i.e., four orders of magnitude lower. Such extreme differences between intra- and extracellular concentrations place severe constraints and demands on plasma membrane transport proteins to safeguard the integrity of the intracellular milieu. To extrude calcium from the cell, for instance, a prodigious adverse electrochemical gradient must be overcome. Simultaneously, extracellular calcium must be fastidiously regulated. What makes calcium so biologically apt that a variety of evolutionarily taxing developments emerged to accommodate its superior aspects? Some of these structural virtues have been summarized by Williams (1976). For example, calcium, in contrast to magnesium, exhibits a particularly adaptable coordination sphere that facilitates binding to the irregular geometry of proteins. The ability to cross-link two proteins requires an ion with a high coordination number (which dictates the number of electron pairs that can be formed) and is generally six to eight for calcium (Williams, 1976). Such cross-linking of osseous structural proteins is facilitated at the high calcium concentrations found in extracellular fluid. At the same time, the variable bond length of calcium permits formation of the more extensive cross-linking involved in membrane stabilization by facilitating lipid polymorphism and formation of hexagonal arrays. Moreover, unlike disulfide or sugar-peptide cross-links, calcium linking is readily reversible. Despite these virtues, if intracellular free calcium ($[Ca^{2+}]_i$) was similar to its extracellular concentration, the proper functioning of a variety of proteins and macromolecules would be impaired. Thus, there seems to be some evolutionary rationale for maintaining the intracellular concentration of calcium at rather low levels. What benefits, then, result from maintaining low intracellular calcium?

The corollary of the benefits of the physical characteristics of calcium at high extracellular concentrations defines a nearly ideal set of attributes that are desirable at submicromolar intracellular concentrations. By virtue of its low cytoplasmic levels, changes of calcium activity can function as first or second messengers to activate effector targets. The fact that calcium can be rapidly bound and released, together with the high affinity and selectivity of many proteins for calcium, would seem to enhance its ability to serve as a trigger or rapid on/off signaling switch. Another advantage of low free

intracellular calcium concentrations is that microcrystallization and precipitation of calcium phosphate is avoided. Circumventing these processes, it has been speculated (396), favors the evolution of high-energy phosphate compounds, which serve as the energy source for a host of biological reactions.

Serum calcium

Calcium may be measured in serum or plasma. As discussed later, this makes little practical difference. Clinical laboratories typically analyze and report results for total calcium; free calcium requires an additional order. Insofar as much circulating calcium is bound either to proteins or as small chemical complexes, the determination of free, or ionized, calcium is useful. Moreover, because pathological conditions including liver disease or kidney failure may change protein levels. Thus, discrepancies between total and ionized calcium may arise but can go undetected without knowing both total and free calcium.

Total calcium concentrations fluctuate with age (Fig. 27.3), averaging 9.5 mg/dL (2.4 mmol/L) (Table 27.1) in adults. Calcium in plasma is present to varying extents in protein-bound, complexed, and ionized forms. Approximately 45% percent of calcium is bound to plasma proteins, mostly to albumin. Smaller amounts of calcium are bound to globulins and a negligible portion to fibrin. Therefore, serum and plasma calcium concentrations are generally indistinguishable (Miles et al., 2004). Another 45% of calcium is ionized (or "free"). The remaining 10% of calcium is associated with small polyvalent anions such as bicarbonate, phosphate, and sulfate. Such ion pairs, e.g., calcium bicarbonate, that arise by electrostatic forces are called "calcium complexes." Together, ionized and complexed calcium are referred to as "diffusible" because only these forms are (1) filtered at the glomerulus and (2) able to cross cell membranes.

Ultrafilterable and ionized fractions of calcium are affected by changes in the total serum calcium concentration, blood pH, plasma protein concentration, and the abundance of complexing anions. Increases in total serum calcium are usually

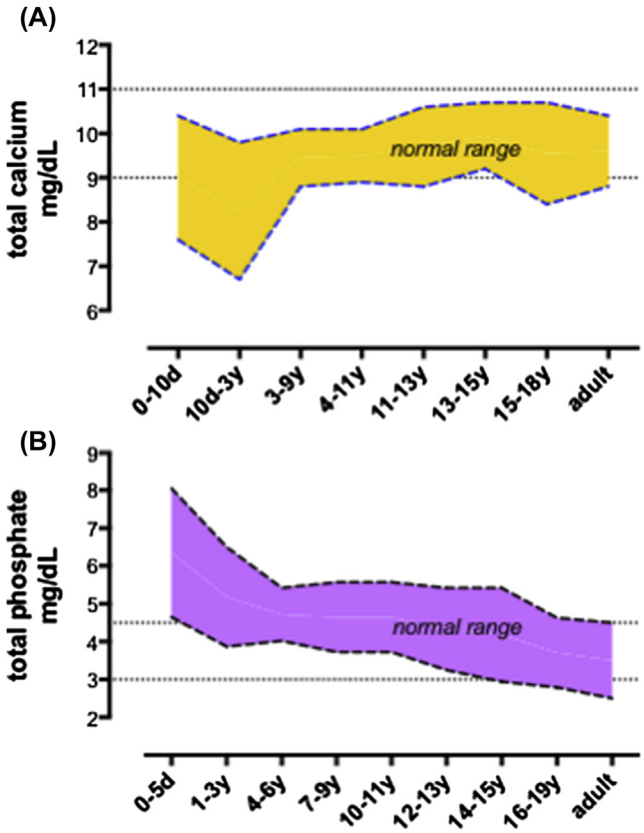

FIGURE 27.3 Total serum calcium (A) and phosphate (B) concentrations during growth and in adults. The normal ranges are highlighted. *Values compiled from various sources Fischbach, F.T., Dunning, M.B. 2015. A manual of laboratory and diagnostic tests. ninth ed. Wolters Kluwer Health, Philadelphia; Meites, S. 1989. Pediatric clinical chemistry: reference (Normal) values. third ed. AACC Press, Washington, DC.*

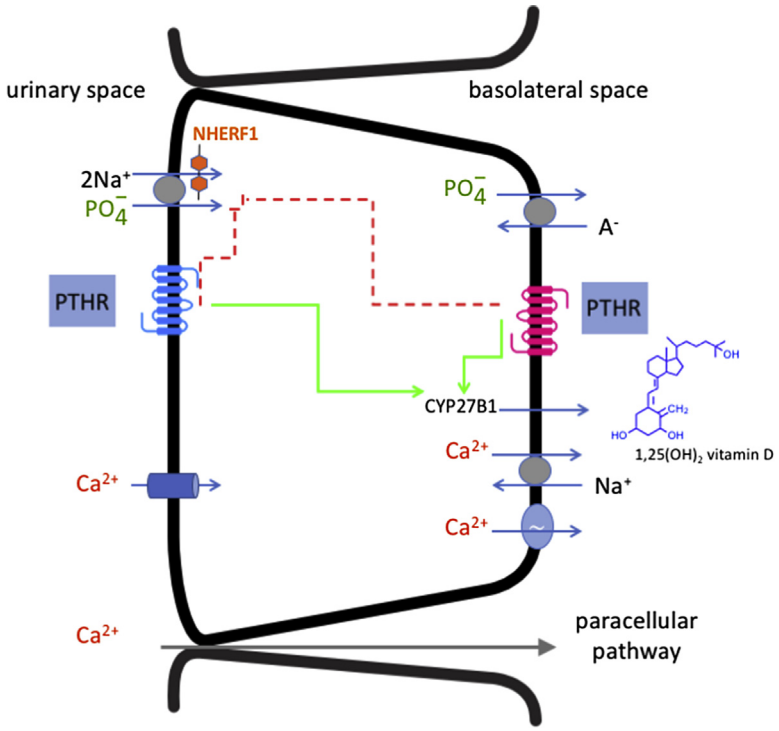

FIGURE 27.4 Phosphate and calcium transport in proximal tubules. Proximal tubule Na-Pi cotransport is mediated principally by apical membrane Npt2a. Two sodium ions are taken up together with a single phosphate molecule. Npt2a is inhibited by PTH as described in the accompanying text. NHERF1 is required for this activity. The mechanism of basolateral PO_4 extrusion is uncertain and is illustrated here as proceeding by a nonspecified anion (A^-) exchanger. Calcium absorption by proximal tubules is largely, if not entirely, a passive process that proceeds through the paracellular pathway of the lateral intercellular spaces (dashed line). Evidence for apical membrane Ca^{2+} entry and basolateral efflux has been described but it is uncertain whether these single processes contribute to transcellular calcium absorption or subserve intracellular calcium homeostasis. PTHR is shown on apical and basolateral cell membranes. Emerging evidence along with published findings suggest the preferential regulation of Npt2a by apical PTHR and induction of CYP27B1 and vitamin D formation by basolateral PTHR.

accompanied by concomitant elevations of ultrafilterable calcium to a total of about 4 mM (Edwards et al., 1974; Le Grimellec et al., 1974). This upper limit of calcium ultrafiltration with hypercalcemia has been postulated to result from the formation of insoluble $[Ca_3(PO_4)_2^-$ −protein] complexes. This idea is supported by the finding that the ultrafilterable phosphate concentration also declines (Cuche et al., 1976). Conversely, hypocalcemia is generally associated with a decline of calcium ultrafiltration (Terepka et al., 1957).

Changes in the concentration of serum proteins are accompanied by parallel alterations of total serum calcium concentration. However, the ultrafilterable fraction generally remains constant. In severe hypoproteinemia, however, the ultrafilterable fraction increases.

TABLE 27.1 Serum calcium (Fischbach and Dunning, 2015).

	mg/dL	mEq/L	mM
Adults			
Total calcium	8.8–10.4	4.4–5.2	2.2–2.6
Ionized calcium	4.6–5.3	2.3–2.6	1.16–1.32
Children			
Total calcium (10d–3yr)	6.7–9.8	3.4–4.9	4.80–5.52
Ionized calcium (1–18yr)	2.24–2.75	1.1–1.4	1.2–1.4

Normal ranges vary between laboratories and depend on applied measurement technology and assay conditions.

In contrast to the parallel relation between total calcium and serum protein, ionized Ca^{2+} levels vary inversely with blood pH. Acidosis increases ionized Ca^{2+} because H^+ ions displace Ca^{2+} from serum proteins. Conversely and for the same reason, alkalosis decreases Ca^{2+} (Hopkins et al., 1952; Loeb, 1926; Peterson et al., 1961). Thus, in these settings the fraction of ionized calcium changes without affecting total calcium. Ionized Ca^{2+} concentrations also change inversely with variations of serum anions. For instance, elevation of phosphate, citrate, sulfate, or bicarbonate increases the serum-free Ca^{2+} secondary to augmented formation of calcium complexes (Walser, 1973).

Symptoms of hypocalcemia vary in relation to the ionized serum calcium concentration. Mild reductions of plasma calcium are associated with paresthesia and muscle cramps; more severe decreases of calcium may induce seizures. Hypercalcemia, on the other hand, has been implicated in the attenuation of the renal effects of PTH, the antidiuretic action of vasopressin, and reduced renal concentrating capacity (Gill and Bartter, 1961; Takaichi and Kurokawa, 1986). The calcium concentration in the extracellular fluid represents a dynamic balance between intestinal absorption, renal reabsorption, and skeletal resorption. Assuming a daily dietary calcium intake of 1000 mg, net intestinal absorption amounts to about 200 mg with the remaining 800 mg excreted in the feces. When in balance, net intestinal absorption is matched by urinary excretion, while calcium accretion and loss from bone are equal. Thus, approximately 200 mg of calcium are excreted daily. In adults, net calcium balance is effectively zero, suggesting that in the absence of a calcium challenge such as lactation, the kidneys represent the dominant regulatory site of calcium metabolism (Peacock et al., 1969).

Phosphate chemistry

Terrestrial mammals are characterized by their avidity for calcium and equally keen mechanisms to eliminate phosphorous. Elemental phosphorous (P) exists in organic and inorganic (Pi) forms. Organic forms include phospholipids and various organic esters. The bulk of phosphate in extracellular fluid exists as the inorganic forms, Na_2HPO_4 and NaH_2PO_4. The Henderson relation determines the ratio of the two:

$$\frac{HPO_4^{2-}}{H_2PO_4^{-}} = 10^{pH-pKa} \tag{27.1}$$

The dissociation constant, pKa, for phosphate is 6.8. Thus, at pH 7.4, the ratio is essentially 4:1, and the plasma phosphate thus has an intermediate valence of 1.8.[2]

Serum phosphate

Serum phosphate is generally expressed as milligrams per deciliter because concentration in millimolar units can vary with acid–base status as outlined previously. Serum Pi averages between 3 and 4.5 mg/dL and decreases with age (Fig. 27.3B). As with calcium, serum Pi circulates in both free and protein-bound forms. However, some 90% of Pi, whether ionized or complexed with Ca, Mg, or Na, is filtered at the glomerulus. Although it is commonly stated that Pi is freely and completely filtered at the glomerulus, this is incorrect. Ten percent of plasma Pi is bound to protein and not filtered. However, the reduction in ultrafilterable Pi is counterbalanced by an opposite Gibbs–Donnan effect that raises the Pi concentration in the ultrafiltrate. Correcting the volume occupied by plasma proteins (7%) raises the ultrafiltrate Pi concentration by an additional 7.5%, mitigating the reduction of protein-bound Pi. Indeed, both in vivo and in vitro measurements show that the ratio of ultrafilterable Pi to total plasma Pi is close to unity (Harris et al., 1974). Ultrafilterable Pi decreases with the elevation of Ca or Pi, presumably because of formation of high-molecular-weight protein complexes.

Parathyroid hormone actions on mineral-ion homeostasis

By regulating renal tubular absorption of calcium and phosphate and the synthesis of $1.25(OH)_2D_3$, PTH controls the urinary excretion and intestinal absorption of these mineral ions and thereby plays a prominent role in setting their blood levels. Renal tubular responses to PTH deficiency, PTH or PTHrP excess, and defects in PTHR function lead to alterations in blood calcium, phosphate, or $1.25(OH)_2D_3$ that are the hallmarks of numerous clinical disorders, described later in this volume. This chapter reviews current understanding of the mechanisms whereby PTH and PTHrP control renal tubular epithelial function. Because PTH and PTHrP actions in kidney and bone are mediated by the PTHR, its expression, signaling, and trafficking are presented first as a foundation for understanding hormone actions. Although PTH and PTHrP

2. The net valence is calculated from the total number of negative charges, $2 \times 4 + 1$, divided by the number of molecules, $4 + 1$, as determined by the Henderson relation, viz., $9/5 = 1.8$. Thus, at pH 7.4, 1 mmol of phosphorous = 1.8 mEq.

receptors distinct from the PTHR have been described (see Chapter 28), their role, if any, in normal renal physiology is unknown. While not unequivocally proven in each case, it is likely that the effects of PTH and PTHrP described here are mediated by the canonical PTHR.

Parathyroid hormone receptor expression, signaling, and regulation in the kidney

Renal PTHR in is expressed on tubular epithelial cells and vascular endothelial cells. PTHR expression along the nephron is associated with regulatory actions on mineral-ion homeostasis, whereas expression on capillary endothelial cells and glomerular podocytes mediates PTH effects on vascular tone and GFR.

The response to PTHR activation observed in individual renal cells depends upon several factors including (1) receptor location and abundance; (2) the expression of cell-specific adapter proteins that modify PTHR signaling; (3) the array of PTHR-inducible genes; (4) effector proteins including enzymes, ion channels, and transporters; (5) the local concentration of PTH or PTHrP; (6) exposure to other agents that heterologously regulate PTHR function; and (7) the history of recent exposure to PTH or PTHrP, which affects the state of receptor desensitization.

Parathyroid hormone receptor expression

The prominent actions of infused PTH on phosphate and calcium absorption pointed to proximal and distal tubules, respectively, as the principal sites of PTHR expression. These deductions were confirmed as molecular biological tools and antibodies became available. We now recognize PTHR expression at the glomerulus, proximal convoluted and straight tubules, cortical ascending limbs, and distal convoluted tubules. Unexpectedly, detailed examination revealed PTHR localization in proximal tubules on both basolateral and apical cell membranes (Amizuka et al., 1997; Ba et al., 2003; Kaufmann et al., 1994). Possible roles of apical membrane PTHRs are discussed later.

Considerable evidence supports the bilateral expression of PTHR on apical and basolateral surfaces of proximal tubules. Moreover, PTH actions are asymmetrical (Quamme et al., 1989; Reshkin et al., 1990, 1991). Such biased actions suggest differential PTHR coupling to G proteins on apical and basolateral membranes; the presence of adapter proteins such as the PDZ proteins NHERF1 and SCRIBBLE; or A-kinase-anchoring proteins that modify or specify second messenger signaling. The possibility of differential G protein expression seems unlikely because G_s is abundant in brush border membrane vesicles (Brunskill et al., 1991; Stow et al., 1991; Zhou et al., 1990). Interestingly, inhibitory G_i isoforms are found only on apical and not basolateral proximal tubule cells (Stow et al., 1991). Nonetheless, PTH triggers greater cAMP formation when added to the serosal than to the mucosal compartment of cells grown on filter barriers (Reshkin et al., 1991). This finding is compatible with other results showing that apical membrane receptors appear not to be coupled tightly, if at all, to adenylyl cyclase (Kaufmann et al., 1994; Shlatz et al., 1975).

Apical membrane expression of PTHR in proximal tubules was unexpected. The conspicuous presence of apical PTHR raises the question of the nature and function of PTH peptides in the urine. Full-length PTH(1−84) has a molecular weight of 9.4 kDa, is filtered at the glomerulus, and is found in urine (Bethune and Turpin, 1968; Norden et al., 2001). The role of urinary PTH fragments has largely been ignored because of the absence of a conceptual framework meriting their examination, the attendant problems of bioassay and immunometric PTH determinations that have been applied to these assays, and the overriding view that PTHR functionality stems from its expression at basolateral surfaces facing the vasculature. The demonstrable effects of PTH peptides applied to the apical surface of isolated kidney tubules or cultured proximal tubule cells, however, supports the view that PTH may differentially regulate phosphate transport from apical and basolateral surfaces (Kaufmann et al., 1994; Reshkin et al., 1990; Traebert et al., 2000)}.

The *PTHR* gene harbors multiple promoters and 5′-untranslated exons and is thereby capable of generating various transcripts by alternative promoter usage and different RNA splicing patterns (Amizuka et al., 1997; Bettoun et al., 1998; Jobert et al., 1996; Joun et al., 1997; McCuaig et al., 1995). P1 promoters in mouse and P3 in human seem to be used exclusively in kidney cells, whereas the P2 promoter is employed to generate PTHR mRNAs that are widely expressed in extrarenal tissues and organs (Amizuka et al., 1997; Bettoun et al., 1998; Joun et al., 1997). It is presently unknown whether these differences simply reflect opportunities for tissue-specific gene regulation or lead to expression of structurally different forms of the PTHR (Jobert et al., 1996; Joun et al., 1997).

Parathyroid hormone receptor signal transduction in kidney tubular cells

PTH administration promptly increases urinary excretion of cAMP, referred to as nephrogenous cAMP. This effect has been employed clinically to distinguish between primary and secondary hyperparathyroidism, wherein nephrogenous

cAMP is elevated in primary but not secondary hyperparathyroidism due to impaired kidney function in the latter condition (Broadus, 1979; Llach and Massry, 1985). Practically speaking, cAMP formation in the nephron originates exclusively from proximal tubules because of the extensive mass of this portion of the nephron compared with other nephron segments. Further, although PTH-induced nephrogenous cAMP is a robust index of the phosphaturic action of PTH, it fails to disclose the effects of PTH on calcium absorption by distal tubules. This too stems from the profusion of proximal tubules compared with distal tubules, possible differences in receptor abundance on the two cell types, the presence of modifying proteins that alter the coupling of the PTHR to G_s, and the signaling array employed.

PTH stimulates adenylyl cyclase with attendant formation of cAMP and activation of PKA in kidney epithelial and vascular cells. PLC may also or alternatively be activated with consequent generation of inositol phosphates and diacylglycerol, release of intracellular calcium, and activation of PKCs, phospholipase A_2, and phospholipase D (PLD). Other signaling mechanisms may participate in mediating PTHR actions in renal cells. For example, PTH-induced stimulation of MAPKs in renal epithelial cells may be triggered by GPCRs, proceeding by activation of nonreceptor tyrosine kinases and transactivation of EGF receptors. MAPK, through PTHR and the FGFR1 fibroblast growth factor receptor, participates in mediating PTH and FGF23 effects, respectively, on phosphate transport (Sneddon et al., 2016). In heterologous cell expression systems, PTHR activation of MAPK occurs by transactivation and PTHR internalization (Syme et al., 2005).

Different patterns of PTHR signaling are present along the nephron. For example, PTH provokes rapid and transient elevations of Ca_i^{2+} in proximal tubule cells (Filburn and Harrison, 1990; Friedman et al., 1999; Hruska et al., 1986, 1987; Tanaka et al., 1995). This response is characteristic of PLC activation, as opposed to calcium influx that produces a more sustained increase of intracellular calcium, which results from the formation of inositol trisphosphate and calcium release from endoplasmic reticulum. Distal tubule cells, in contrast, exhibit a delayed and sustained elevation of Ca_i^{2+} in response to PTH. This effect is due to apical membrane Ca^{2+} entry (Bacskai and Friedman, 1990; Hoenderop et al., 1999). Furthermore, PTH-stimulated calcium transport in distal tubule cells involves PLC-independent PKC activation (Friedman et al., 1996), which is mediated by phospholipase D (Garrido et al., 2009).

More recent characterization of PTHR signaling offers additional and alternative interpretations of cAMP signaling and function. Refined analysis of PTHR activation in single cells using FRET revealed that PTH but not PTHrP promoted sustained elevation of cAMP. Similar findings subsequently were described for other GPCRs (Calebiro et al., 2009; Feinstein et al., 2013; Inda et al., 2016; Kuna et al., 2013; Merriam et al., 2013; Pavlos and Friedman, 2017). In the case of PTHR, sustained cAMP signaling originating at basolateral surfaces may induce 25-hydroxyvitamin D-hydroxylase (*CYP27B1)* transcription, CREB phosphorylation, and 1.25$(OH)_2$vitamin D_3 formation.

Regulation of parathyroid hormone receptor signaling in tubular epithelial cells

As described before, the expression of PTHRs on the surface of kidney cells is controlled by the interaction with adaptor proteins. However, PTHR expression is also controlled by the rate of PTHR gene transcription, though current understanding of this process is incomplete. Hypoparathyroidism, induced by parathyroidectomy or dietary phosphate depletion, upregulates PTHR mRNA levels in rat renal cortex (Kilav et al., 1995a). However, high concentrations of PTH have no detectable effect on PTHR mRNA (Kilav et al., 1995b; Ureña et al., 1994). Renal PTHR mRNA expression is reduced in rats with renal failure, but this apparently is due to some aspect of uremia or renal disease (Disthabanchong et al., 2004) other than secondary hyperparathyroidism per se, as it is not prevented by parathyroidectomy (Largo et al., 1999; Urena et al., 1994; Ureña et al., 1995). In rats with secondary hyperparathyroidism due to vitamin D deficiency, renal cortical PTHR mRNA levels were found to be twice as high as normal and could not be corrected by normalizing serum calcium (Turner et al., 1995). These results suggest that vitamin D impairs PTHR gene transcription in proximal tubules. However, in immortalized distal convoluted tubule cells, PTHR expression was upregulated severalfold by 1.25$(OH)_2D_3$ (Sneddon et al., 1998). In opossum kidney (OK) cells, TGFβ1 diminished PTHR mRNA expression (Law et al., 1994). The physiologic significance of this effect has not been clarified. PTHR mRNA expression was not affected by the mild secondary hypoparathyroidism induced by ovariectomy in rats nor by subsequent estrogen treatment (Cros et al., 1998).

A critical insight to PTHR regulation was achieved with the discovery that the receptor interacts with the cytoplasmic scaffolding proteins Na/H exchanger regulatory factors NHERF1 NHERF2 (NHERF1/2; known also as EBP50 and E3KARP, respectively), which govern certain aspects of signaling and trafficking (Mahon et al., 2002). NHERF1/2 consist of two tandem PSD95/Discs Large/ZO-1 (PDZ) domains and an EBD. The PTHR binds to either PDZ domain through a recognition sequence at its carboxy-terminus. This Glu-Thr-Val-Met sequence corresponds to a canonical PDZ ligand that takes the form D/E–S/T-X-Φ, where X is any amino acid and Φ is a hydrophobic residue—generally L/I/V, but it can also be M (Broadbent et al., 2017). Mutation of any residue of the PDZ sequence of the PTHR, other than the permissive

position, abrogates interaction with NHERF1/2 (Mahon et al., 2002; Sneddon et al., 2003). In pivotal work, Mahon and Segre found that NHERF1/2 switched PTHR signaling from adenylyl cyclase to PLC. NHERF1 also regulates mitogen-activated ERK signaling (Wang et al., 2008). NHERF1 is abundantly expressed on proximal tubule apical membranes (Wade et al., 2001). Mouse proximal tubules expresses both NHERF1 and NHERF2 (Wade et al., 2003). NHERF1 is strongly expressed in microvilli, whereas NHERF2 is detected only weakly in microvilli. However, it is expressed predominantly at the base of the microvilli in the vesicle-rich domain. Notably, neither NHERF1 nor NHERF2 is found in distal tubules. Human and mouse kidneys exhibit comparable NHERF1 localization (Shenolikar et al., 2002; Wade et al., 2001, 2003; Weinman et al., 2002). As will be discussed in greater detail later, NHERF1 is expressed in the proximal nephron, where it importantly regulates PTH-dependent phosphate absorption.

Calcium absorption and excretion

The kidneys are responsible for controlling extracellular calcium balance by controlling the amount of calcium retained by the nephron or excreted in the urine. Renal calcium regulation occurs by a series of sequential events as the incipient urine passes through the nephron. The bulk of the filtered calcium is absorbed by proximal tubules, with progressively smaller fractions recovered as the urine passes through downstream tubule segments. Most calcium absorption is not subject to hormone regulation because it proceeds in upstream sites through passive mechanisms that are not regulated by hormones. Hormonal and pharmacological regulation of calcium absorption is achieved by fine-tuning the final few percent of calcium transport in distal nephron segments.

PTH participates importantly in maintaining extracellular calcium homeostasis. Early observations in animals and patients with hypo- or hyperparathyroidism clearly implicated renal calcium handling in PTH abnormalities (Carney, 1996; Gley, 1893; Hackett and Kauffman, 2004; Sandström, 1879−1880).

Renal calcium absorption

PTH reduces renal calcium excretion. Although calcium is absorbed throughout the nephron, the calcium-sparing action of PTH occurs primarily in distal tubule (Friedman, 2008; Sutton and Dirks, 1975). The sites of renal calcium absorption and mechanism of PTH action are summarized here. Extensive descriptions of this older work are available elsewhere (Friedman, 2008; Ko, 2017).

Approximately 20%−25% of the calcium filtered at the glomerulus is absorbed by medullary and cortical thick ascending limbs. In contrast to proximal tubules, calcium movement in thick ascending limbs occurs by parallel transcellular and paracellular calcium transport pathways. Passive paracellular calcium absorption is driven by the favorable lumen-positive transepithelial voltage. In this setting, the rate and magnitude of calcium transport are parallel and proportional to those of sodium. Physiological responses and interventions that enhance sodium absorption increase voltage, thereby augmenting calcium absorption (Hoover et al., 2015). Conversely, maneuvers that decrease sodium absorption concomitantly reduce calcium absorption. Such interventions typically involve the use of diuretics such as furosemide or bumetanide that inhibit sodium absorption by thick ascending limbs and increase calcium excretion. Less commonly, mutations of the Na−K−2Cl cotransporter (*SLC12A1*), as well as the ROMK apical K^+ channel and basolateral ClC−K2 basolateral Cl^- channel associated with the different forms of Bartter's syndrome, are accompanied by hypercalciuria, underscoring the parallel nature of sodium and calcium absorption by thick ascending limbs. PTH stimulates active calcium absorption by cortical thick limbs (Friedman, 2000).

Distal convoluted tubules display a third pattern of transepithelial calcium recovery. Two important features characterize this process (Fig. 27.5). First, calcium transport occurs only by a transcellular mechanism and second, calcium and sodium movement are inversely related. Here, decreased sodium absorption enhances calcium recovery; likewise, increased sodium absorption is accompanied by diminished calcium transport. This inverse relationship has important consequences for calcium economy. For example, thiazide diuretics, which increase sodium excretion, diminish that of calcium. Patients with Gitelman's syndrome further exemplify the inverse association of sodium and calcium movement. This inherited disorder is due to inactivating mutations of the Na−Cl cotransporter (NCC; *SLC12A3*) that mediates sodium absorption by distal convoluted tubules. Patients (Bettinelli et al., 1992; Gitelman et al., 1966) and experimental animals (Schultheis et al., 1998) with Na−Cl cotransporter mutations exhibit characteristic natriuresis accompanied by hypocalciuria, thus exemplifying the inverse relations between sodium and calcium absorption in distal tubules.

Cortical and medullary collecting tubules contribute minimally if at all to renal calcium conservation, and PTH exerts no detectable action on calcium movement by these nephron sites (Bernardo and Friedman, 2013; Friedman, 2014).

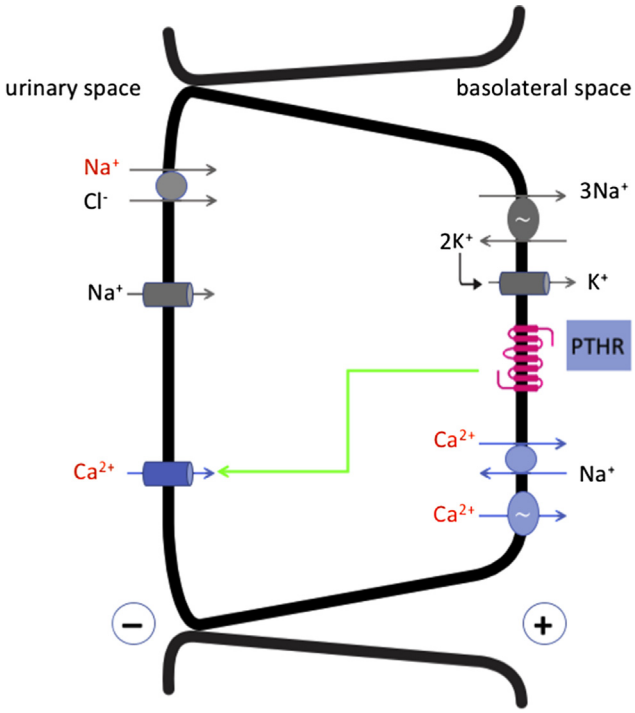

FIGURE 27.5 Calcium absorption by distal convoluted tubules. Two features distinguish distal tubule calcium absorption. First, calcium transport proceeds exclusively through a cellular pathway. Because of the substantial adverse electrochemical barrier, calcium movement is negligible in the absence of PTH (Costanzo and Windhager, 1980). Second, calcium and sodium movement in distal convoluted tubules are inversely related. Thus, thiazide diuretics, which block sodium transport, augment calcium absorption (Gesek and Friedman, 1992). The cell model shows two apical membrane sodium entry mechanisms, the thiazide-diuretic-inhibitable NaCl cotransporter and the amiloride-blockable epithelial Na channel, ENaC. Amiloride also stimulates calcium transport by distal tubule cells (Friedman and Gesek, 1995). Calcium enters the cell across apical membranes through dihydropyridine-sensitive calcium channels. PTHR expressed on basolateral membranes stimulates apical membrane calcium entry that is accompanied by efflux across basolateral membranes. Basolateral calcium efflux is mediated by the plasma membrane Ca^{2+}-ATPase (shown as the energy-dependent [∼] process), and the Na^{+}/Ca^{2+} exchanger as discussed in detail in the text and elsewhere (Ko, 2017; Moe, 2016).

Parathyroid hormone regulation of renal calcium absorption

PTH is the most important hormone regulating renal tubular calcium transport. PTH increases renal calcium reabsorption and lowers urinary calcium excretion. In the complete absence of the hormone or in PTH deficiency states, diminished tubular reabsorption is accompanied by frank hypercalciuria. The stimulatory effect of PTH on calcium transport is limited to distal nephron segments. Paradoxically, PTH decreases calcium absorption by proximal tubules; the calcium-sparing action is due to its effects on distal convoluted tubules, and to a limited extent actions on cortical thick ascending limbs. In some species, the calcium-sparing action proceeds in connecting tubules.

Parathyroid hormone effects on proximal tubule calcium transport

The primary action of PTH on proximal tubule mineral-ion transport is to inhibit Na^{+}-dependent phosphate (Na^{+}-Pi) absorption (see below). It is uncertain whether PTH exerts significant or even specific actions on proximal calcium transport. PTH has been reported to increase (234), decrease (5), or not change (150, 251) proximal tubule calcium absorption. Studies showing that PTH alters intracellular free calcium, $[Ca^{2+}]_i$, irrespective of whether it increased or decreased (123, 146, 179, 213, 214, 368), should not be construed as evidence for an effect of PTH on calcium entry, much less on net calcium absorption. Although the aforementioned findings may be associated with net calcium absorption, they may also represent the aggregate of intracellular calcium release, and perhaps individual calcium entry and exit steps that support constitutive cellular activities and intracellular homeostasis. The reason for this is that PTH exerts a host of biochemical effects on proximal tubules such as activation of 25-hydroxyvitamin D-1α-hydroxylase, gluconeogenesis, or ammoniagenesis as well as transport effects on Na^{+}-Pi absorption, Na^{+}/H^{+} exchange, and Na^{+}/Ca^{2+} exchange that may involve calcium signaling but do not entail effects on net calcium absorption.

Parathyroid hormone effects on distal tubule calcium transport

Substantial evidence supports the view that PTH increases active transcellular calcium absorption by distal convoluted tubules (Ko, 2017; Moe, 2016). The distal action of PTH may be accompanied by decreased sodium absorption and diuresis (Ko et al., 2011).

PTH potently induces apical calcium entry in distal convoluted tubule cells (165). PTH-stimulated calcium entry in distal convoluted tubules is mediated by the TRPV5/Trpv5 calcium channels (van Goor et al., 2017b). This action is mediated by PKA (de Groot et al., 2009). PKA-induced phosphorylation of TrpV5 Thr^{709} increases open-channel probability (de Groot et al., 2009). Other studies point to a role (Hoenderop et al., 1999) or requirement for combined PKA and PKC action (Friedman et al., 1994).

PTH may further dissociate calcium and sodium absorption by distal convoluted tubules. PTH depresses Slc12a3, the electroneutral NaCl cotransporter, and its surface expression (Ko et al., 2011). Thus, reducing Na^+ entry while enhancing calcium absorption supports the inverse relation between basal and hormone-stimulated calcium transport.

Phosphate excretion

Extracellular phosphate homeostasis is regulated primarily by controlling its renal excretion, where it is absorbed mostly by proximal tubules. The prompt phosphaturia caused by PTH was one of the earliest recognized and best studied actions of PTH (Albright et al., 1929; Greenwald and Gross, 1925). Fibroblast growth factor 23 (FGF23) plays an equally important role in phosphate balance. FGF23 is discussed in Chapter 65 and its renal actions reviewed elsewhere (Erben, 2017; Hu et al., 2013). One point worth emphasizing here is that although PTH and FGF23 exert parallel inhibitory actions on renal phosphate absorption, they display opposing effects on vitamin D metabolism, with PTH increasing vitamin D levels and FGF23 lowering them. The underlying basis for these diverse actions is not known.

NPT2a (SLC9A3R1) and NPT2c (SLC9A3R3) mediate renal Na-Pi cotransport[3] (Table 27.2). Npt2a is found throughout the proximal tubule, with expression decreasing from S1 to S2 and then to S3 segments (Picard et al., 2010; Segawa et al., 2007). Npt2c is found only in the S1 portion of proximal tubules. NPT2b is expressed by intestines, where it participates in phosphate absorption.

Mechanisms of proximal tubular phosphate absorption

Apical phosphate entry is rate-limiting for cellular phosphate absorption and is the major site of its regulation. Phosphate enters the cell across apical brush border membranes against a steep electrochemical gradient established primarily by the strongly negative intracellular voltage. This electrochemical barrier is overcome by NaP_i cotransporters that couple phosphate influx to the favorable dissipative entry of Na^+ (Fig. 27.4).

Type I and type IIa NaP_i cotransporters are localized on apical brush border membranes of proximal convoluted tubule cells. Nonspecific type I transporters exert a variety of functions unrelated to phosphate absorption and are not regulated by PTH or FGF23. Type II cotransporters are structurally and genetically distinct from type I transporters, sharing only 20% identity. As alluded to above, NPT2a and NPT2c are expressed in kidney proximal tubules, whereas NPT2b, an isoform of Npt2a, is expressed exclusively in intestine (Hilfiker et al., 1998). Type III NaP_i cotransporters, originally identified as cell surface virus receptors Glvr-1 and Ram-1, are widely expressed within and outside the kidney (Kavanaugh and Kabat, 1996). Type III cotransporters, found on basolateral cell membranes, are regulated by extracellular phosphate deprivation and PTH (Ohkido et al., 2003; Segawa et al., 2007). Type II cotransporters may also be expressed by distal convoluted tubule cells and may thus be involved in phosphate absorption by both proximal and distal nephrons (Collins et al., 2004; Tenenhouse et al., 1998). Npt1, Npt2a, and Npt3 account for 15%, 84%, and 0.5% of Na-Pi-cotransporter mRNAs (Murer et al., 2003). Type II cotransporters are 80−90-kDa glycoproteins predicted to span the membrane eight times with both their amino and carboxyl termini in the cytoplasm (Murer and Biber, 1997). Recent work shows two variant transcripts of the mouse Npt2a gene, Npt2a-v1 and Npt2a-v2 (Yamamoto et al., 2005). These are characterized by the presence of alternative first exons (either exon 1A or exon 1B). Npt2a-v2 is important for $1.25(OH)_2D_3$-dependent renal cell-specific activation. Npt2a cotransporters are electrogenic and transport Na^+ and $H_2PO^-_4$ at a molar ratio of 3:1 (Murer and Biber, 1997). Expression and activity of NPT2a/Npt2a are strongly regulated by parathyroid status and dietary phosphate (and FGF23) (Keusch et al., 1998; Lotscher et al., 1999; Pfister et al., 1997; Ritthaler et al., 1999; Takahashi et al., 1998). PTH regulation of serum phosphate and tubular NaP_i absorption is lost in mice lacking Npt2a (Zhao and Tenenhouse, 2000).

3. Human genes and gene products are designated by uppercase italics, whereas nonhuman forms are shown in lowercase.

TABLE 27.2 Sodium phosphate transporter family.

Type	GenBank	Function	Reference
NPT1	*SLC17A1*	Modulator of organic and inorganic anion transport	Busch et al. (1996)
NPT2A	*SLC34A1*	3:1 electrogenic BBM proximal tubule Pi uptake	Murer et al. (2000)
NPT2B	*SLC34A2*	Intestinal Pi transport	Hilfiker et al. (1998)
NPT2C	*SLC34A3*	2:1 electroneutral BBM proximal tubule Pi uptake	Bacconi et al. (2005); Bergwitz et al. (2006); Madjdpour et al. (2004); Segawa et al. (2002); Tenenhouse et al. (2003)
NPT3	*SLC20A1*, *SLC20A2*	Pi transporter in bone. Broadly expressed.	Suzuki et al. (2001, 2006)

Npt2c/NPT2c is expressed in rat and human kidneys (Ohkido et al., 2003). Npt2c accounts for approximately 30% of Na/Pi cotransport in kidneys of phosphate-deprived adult mice (Ohkido et al., 2003). Npt2a activity is the principal mechanism whereby PTH controls phosphate absorption in proximal convoluted tubules, at least in rodents. In humans, however, NPT2c plays an important role in phosphate economy. NPT2c mutations are associated with hereditary hypophosphatemic rickets with hypercalciuria, kidney stones, and nephrocalcinosis (Christov and Juppner, 2013; Dasgupta et al., 2014).

Parathyroid hormone regulation of renal phosphate absorption

PTH promptly elevates urinary phosphate elimination. Early studies revealed that this action is involved reduction of Na-Pi cotransport and that restoration of maximal phosphate absorption required microtubules and new protein synthesis (Dousa et al., 1976; Malmström and Murer, 1987).

Functional and immunohistochemical analyses of Npt2 in intact kidneys and cultured cells revealed that PTH induces rapid (15 min) removal of Npt2 from the apical membrane into the subapical endocytic apparatus, followed by microtubule-dependent delivery to lysosomes and proteolytic degradation (Bacic et al., 2006; Kempson et al., 1995; Keusch et al., 1998; Lötscher et al., 1999; Pfister et al., 1997; Zhang et al., 1999). It had been assumed that PTH inhibited Na-Pi cotransport through phosphorylation or other action that would control the kinetics or driving force. This turned out not to be the case. Instead, PTH and FGF23 inhibit Na-Pi cotransport by initiating internalization and downregulation of Npt2a. Though Npt2a phosphorylation apparently is not involved, PTH and FGF23 lead to phosphorylation of NHERF1 (Andrukhova et al., 2012; Deliot et al., 2005; Weinman et al., 2007). It is also worth noting that PTH and FGF23 maximally inhibit only 50%–60% of phosphate transport. It is not known if the balance is subject to hormonal or other regulatory control.

Hypoparathyroidism and hypophosphatemia increase PTHR, Npt2a mRNA, and protein, showing the proteins mediating PTH effects on renal phosphate transport that are coordinately regulated (Kilav et al., 1995a). PTH does not acutely reduce Npt2 mRNA expression, although parathyroidectomy leads to a severalfold increase of apical Npt2a protein and mRNA (Kilav et al., 1995a; Saxena et al., 1995; Takahashi et al., 1998).

Parathyroid hormone receptor signal transduction in the regulation of calcium and phosphate excretion

As described earlier and discussed in Chapter 28, the PTHR mediates its actions through multiple signaling pathways. Signaling is both ligand- and cell type-specific. PTH exerts physiologically distinct and temporospatially separated effects on the kidney. In proximal tubules, PTH inhibits Na-Pi cotransport and Na/H exchange, increases Na^+/Ca^{2+} exchange (Fig. 27.4), and activates CYP27B1 while suppressing 24-hydroxylase activity to increase circulating vitamin D levels. PTH also inhibits Na^+,K^+-ATPase activity, stimulates gluconeogenesis and ammoniagenesis. Complex but precise individual control over these multiple physiological activities assures that all are not simultaneously engaged in response to changing levels of PTH. Just how this is accomplished is far from understood. However, important insights have been gained into PTH-dependent regulation of renal calcium and phosphate transport by identifying cytoplasmic scaffolding proteins that specifically modulate individual PTH actions (Mahon, 2012; Pavlos and Friedman, 2017).

Parathyroid hormone signaling of renal calcium transport

The primary action of PTH is to stimulate renal calcium conservation. This related process proceeds principally in distal tubules. The portion of the distal tubule where this occurs differs somewhat between species. In most species including humans, the rat, the mouse, and the dog, distal convoluted tubules are the primary site of PTH-dependent calcium absorption. This has been demonstrated directly or can be inferred from the localization of the PTHR or the presence of PTH-stimulated adenylyl cyclase activity (Chabardès et al., 1980; Friedman and Gesek, 1993). In the rabbit, connecting tubules are the site of PTH-stimulated calcium transport (Shimizu et al., 1990).

Ca^{2+} entry across apical cell membranes of distal convoluted tubule cells is mediated by TrpV5/TRPV5 calcium channels (Mensenkamp et al., 2007; Na and Peng, 2014). Although activating PKA purportedly accounts for PTH actions on calcium absorption (de Groot et al., 2009), we think it likely that this action involves both PKA and PKC insofar as activation of omnipresent β_2-adrenergic receptors, which are well expressed by distal tubules, fails to augment calcium recovery (Gesek and White, 1997). This suggests that PTH-sensitive calcium transport requires activating both PKA and PKC. Such effects have been reported (Cha et al., 2008; de Groot et al., 2009; Hoover et al., 2015). Some interspecies differences of PKA-sensitive PTH activation of TRPV5 have been noted between rabbit and rodent and human, which behave similarly (van Goor et al., 2017a).

Cellular calcium efflux is mediated by the NCX1 Na^+/Ca^{2+} exchanger and PMCA1 and PMCA4 plasma membrane Ca^{2+}-ATPases (van der Hagen et al., 2014; van Loon et al., 2016), which are expressed on distal tubule cell basolateral membranes (Magyar et al., 2002; White et al., 1997). Although opinions differ regarding the relative contribution of NCX1 and PMCA1/4 to net calcium absorption, we think it likely that Ca^{2+}-ATPase mediates the bulk of Ca^{2+} efflux because the electrochemical driving force for Ca^{2+} extrusion by Na^+/Ca^{2+} exchange is insufficient to account for more than basal calcium transport levels (Friedman, 1998). How these two processes are regulated and synchronized so as to coordinate apical calcium entry with basolateral extrusion is unknown.

Parathyroid hormone signaling of renal phosphate transport

Early experiments in vivo or with isolated renal membranes indicated that regulation of phosphate absorption was mediated by cAMP. The evidence marshaled in support of this conclusion was based, inter alia, on the observation that cAMP analogs and phosphodiesterase inhibitors mimicked the phosphaturic action of PTH (Agus et al., 1973; Coulson and Scheinman, 1989; Gmaj and Murer, 1986; Hammerman, 1986). Indeed, the excretion of urinary cAMP in response to PTH administration, so-called nephrogenic cAMP, reflects virtually exclusively the action of PTH on proximal tubule phosphate absorption (and not distal tubule Ca absorption) and is a direct index of PTHR sensitivity or refractoriness (Besarab and Swanson, 1984). Although these conclusions are solid, the mechanisms by which PTH inhibits renal phosphate transport are complex and incompletely resolved. The intricacy stems from the recognition that the PTHR activates multiple signaling paths. The possibility that differentially expressed PTHR types (Pun et al., 1988) or isoforms account for the heterogeneity of action can be excluded. The first studies profiling the effect of PTH on inositol phosphate and Ca^{2+}-signaling, in fact, preceded the cloning of the PTHR (Bidot-López et al., 1981; Meltzer et al., 1982). PTH stimulation of inositol phosphate and diacylglycerol accumulation is independent of cAMP formation (Hruska et al., 1987) and occurs in parallel (Friedman et al., 1996).

The involvement of specific PTHR-generated signals in regulating Na-P_i cotransport has been pursued extensively in vitro using immortalized OK cells, which exhibit a proximal tubule-like phenotype that includes expression of the Npt2a NaP_i cotransporter and the PTHR (Jüppner et al., 1991; Rabito, 1986). Considerable evidence supports cAMP/PKA-mediated signaling, while other observations point to an important contribution of inositol phosphates/PKC. The extensive body of work on this subject has been reviewed elsewhere (Muff et al., 1992; Murer et al., 2000; Pfister et al., 1999) and described in the previous edition of this text (Bringhurst and Strewler, 2002). Recent incisive work and the discovery of cytoplasmic binding partners for the PTHR and Npt2a have largely reconciled the apparently disparate views. The salient features of PTHR signaling of proximal tubule phosphate transport can be summarized as follows.

PTHRs, as noted earlier, are expressed at both apical and basolateral surfaces of proximal tubule cell membranes (Amizuka et al., 1997; Ba et al., 2003; Traebert et al., 2000). Both PTH(1−34) and PTH(3−34), thought to be a relatively PKC-selective agonist, induced rapid removal of apical NaP_i proteins when selectively applied to apical surfaces of perfused murine proximal tubules or proximal-like OK cells (Pfister et al., 1999; Traebert et al., 2000). Only PTH(1−34) promoted Npt2a endocytosis when added at basolateral surfaces. Two conclusions can be drawn from these findings. First, they are consistent with the expression of PTHRs at both membrane domains. Second, they are compatible with the view that apical PTHR activates both PKA and PKC, whereas basolateral PTHRs couple primarily to PKA. The biological

significance of these findings may relate to the dynamics of PTHR signaling and the duration of the phosphaturic action of PTH. Short-term, acute regulation of phosphate absorption is mediated mainly by the PKA pathway, whereas long-term, persistent actions are signaled by PKC (Guo et al., 2013; Nagai et al., 2011).

Independent studies uncovered a likely molecular basis for the polarized PTH action and asymmetric effects and signaling of PKC and PKA. The explanation stems from the localized expression of the adapter protein NHERF1. NHERF1 is a PDZ protein that binds to both the PTHR and Npt2a (Hernando et al., 2002; Mahon et al., 2002; Wade et al., 2003). In the absence of NHERF1, mice exhibit a phosphate-wasting phenotype (Shenolikar et al., 2002). NHERF1 is abundantly expressed at proximal tubule brush border membranes in the rat, and is also detected in the cytoplasm and on basolateral membranes (Wade et al., 2001). In mice, NHERF1 is found exclusively on proximal tubule brush border microvilli (Wade et al., 2003). In OK/H cells, which lack NHERF1, PTH fails to inhibit Na-Pi cotransport, and this defect can be surmounted by overexpressing NHERF1 (Mahon et al., 2003).

According to presently accepted views, PTHR signals through PKA in the absence of NHERF1 and by means of PKC in its presence (Mahon et al., 2002). Thus, at basolateral membranes, where NHERF1 is absent, PTH would be expected to signal through adenylyl cyclase and PKA. At apical (i.e., luminal or mucosal) cell membranes, signaling would be predicted to be mediated by PLC and PKC because of the coupling between the PTHR and PLC (Mahon and Segre, 2004). These predictions are compatible with the observations that PTH(1–34) evoked Npt2a sequestration when added to either cell surface, whereas PTH(3–34), which activates PKC but not PKA, induced Npt2a internalization only when applied to the luminal surface (Traebert et al., 2000). Consistent with this scheme, more recent studies reveal that PTH(3–34) was unable to promote Npt2a internalization from proximal tubule brush border membranes prepared from NHERF1-null mice (Capuano et al., 2006). Activation of PLC by PTH was impaired; bypassing this defect by directly activating PKC with a diacylglycerol analog caused Npt2a internalization in proximal tubules of both wild-type and NHERF1-null mice. Although these are elegant and compelling observations, their relevance to the regulation of phosphate transport under physiological and pathophysiological conditions is unsettled. Complicating this picture, metabolism of cAMP involves nucleotide degradation to adenosine by brush border membrane ectoenzymes such as ecto-5′-nucleotidase. PTH(1–34) augmented ecto-5′-nucleotidase activity in apical membranes of OK cells (Siegfried et al., 1995). This effect was mimicked by PTH(3–34) but not by forskolin. Both PTH fragments increased cytoplasmic Ca^{2+} and stimulated PKC activity. Conversely, stimulation of ecto-5′-nucleotidase activity was blocked by inhibitors of PKC. Thus, PKC-mediated stimulation of 5′-nucleotidase thereby bolsters the effects transduced by PKA.

PTHRs present on proximal tubule luminal membranes are presumably activated by PTH peptides that are filtered at the glomerulus and appear in the luminal fluid. Most of these peptides or smaller fragments are absorbed (Kau and Maack, 1977), internalized (Hilpert et al., 1999), and metabolized (Brown et al., 1991; Daugaard et al., 1994; Yamaguchi et al., 1994) during their passage through the nephron. However, given the increased generation and accumulation of amino-truncated PTH peptides during kidney disease and other pathological settings, it is likely that significant amounts of biologically active PTH reach luminal brush border membranes and would be expected to elicit Npt2a/NPT2a internalization with attendant elevation of urinary phosphate excretion. Such actions might represent an adaptive response to the elevation of plasma phosphate in chronic kidney disease. By contrast, in distal tubules, which lack NHERF1, no such effect would be anticipated.

Not covered here and only partially understood are the convergent actions of PTH and FGF23 on NPT2A and phosphate transport. PTHR and FGFR1, through distinct signaling pathways, both require NHERF1 for their inhibitory effects (Sneddon et al., 2016). The details of how a G-protein-coupled receptor and a receptor tyrosine kinase produce convergent effects to phosphorylate the same critical residue on NHERF1 remains to be defined.

Sodium and hydrogen excretion

Beyond its effects on mineral-ion metabolism, PTH is involved in acid–base balance through its actions on Na/H exchange in proximal tubules. Acute (Ellsworth and Nicholson, 1935; Hellman et al., 1965; Kleeman and Cooke, 1951; Nordin, 1960) or chronic (Hulter and Peterson, 1985) increases in PTH exert a prompt alkalotic response attended by elevated bicarbonate excretion. This action stems from PKA-dependent acute inhibition of NHE3. Chronic exposure to elevated PTH downregulates NHE3 expression (Lee et al., 2017). PTH actions on NHE3 involve and require NHERF1 (Cunningham et al., 2010). Sporadic case reports notwithstanding, primary hyperparathyroidism is generally not attended by consistent or remarkable changes in serum pH and is largely asymptomatic (Bilezikian, 2012; Coe, 1974).

PTH inhibits acidification by suppressing the NHE3, the Na^+/H^+ exchanger. This involves activating adenylyl cyclase, NHERF1, which serves as a scaffold to assemble PKA and NHE3, followed by phosphorylation and inhibition of NHE3

(Moe et al., 1995; Weinman et al., 1998, 2005). Notably, the inhibitory effect of PTH on proximal tubules does not necessarily result in increased bicarbonate excretion (Bank and Aynedjian, 1976; Puschett et al., 1976) and is not accompanied by appreciable reductions in serum bicarbonate (Hulter, 1985). These results suggest that distal tubule compensatory bicarbonate absorption (Bichara et al., 1986) and acidification by downstream tubule segments in response to PTH (Paillard and Bichara, 1989) mitigate the upstream actions of PTH. Secondary actions of PTH to mobilize bicarbonate from bone also contribute to the absence of an effect on systemic pH (Hulter and Peterson, 1985). More important than its modest effects on net bicarbonate balance or pH homeostasis, however, is the permissive action of bicarbonate to facilitate PTH-dependent distal tubule calcium absorption (Marone et al., 1983; Mori et al., 1992; Sutton et al., 1979), a primary function of PTH.

Na^+/H^+ exchange mediates most proximal tubule sodium absorption (Palmer and Schnermann, 2015). Although PTH inhibits Na^+/H^+ exchange and proximal sodium absorption, PTH has a negligible effect on net sodium excretion because of compensatory absorption by downstream tubule segments (Harris et al., 1979). Natriuretic actions of PTH, however, have been described in experimental animals (Bichara et al., 1986; Hellman et al., 1965) and humans (Jespersen et al., 1997).

The fundamental mechanism whereby PTH inhibits Na^+/H^+ exchange differs from its action on Na-Pi cotransport. Whereas PTH decreases Na-Pi cotransport by sequestering Npt2a from brush border membranes, PTH acutely regulates Na^+/H^+ exchange by PKA-dependent NHE3 phosphorylation (Hamm et al., 2008). Decreased NHE3 activity is followed several hours later by reduced brush border membrane NHE3 abundance (Fan et al., 1999). Details of this process and the involvement of NHERF1 are detailed in the next section.

Na^+/H^+ exchange is a dissipative—i.e., secondary active—transport process that depends on the continuous extrusion of Na across basolateral cell membranes. This is accomplished by the ATP-dependent Na^+,K^+-ATPase. Data showing that PTH inhibits the Na^+,K^+-ATPase have been published (Ribeiro and Mandel, 1992; Zhang et al., 1999). An inhibitory action of PTH on Na^+,K^+-ATPase would certainly contribute to, or explain, reduced Na^+/H^+ exchange. However, such an action would be expected to have profound effects on proximal tubule ion transport and all Na-coupled transport processes such as those mediating glucose (Na-glucose) and amino acid (Na-amino acid) cotransport, and perhaps Na-Pi cotransport. Moreover, the inhibitory action of PTH should extend to virtually all cells expressing PTHR including the distal tubule. In this setting, blockade of the Na^+,K^+-ATPase would be expected to reduce Na^+/Ca^{2+} exchange and decrease net calcium absorption, when in fact just the opposite occurs. The described actions of PTH seem remarkably specific for the proximal tubule Na^+,K^+-ATPase and for Na^+/H^+ exchange. A rational explication of these findings awaits further clarification.

Parathyroid hormone regulation of proximal tubular sodium and hydrogen excretion

Efficient bicarbonate absorption by proximal tubules requires NHERF1. Targeted disruption of NHERF1 virtually eliminates PTH- and forskolin-inhibited Na^+/H^+ exchange in proximal tubule cells (Cunningham et al., 2004). This defect could be restored by infecting the cells with an adenovirus containing NHERF1. Interestingly, cAMP generation and PKC activation were equivalent in proximal tubule cells from wild-type mice and NHERF1-null animals. This result seemingly contrasts with the paradigm of the PTH "signaling switch" advanced by Mahon and Segre (Mahon et al., 2002), where PTHR signaling proceeds through cAMP in the presence of NHERF1 but by PKC in its absence. However, mouse proximal tubules express both NHERF1 and NHERF2, and NHERF2 expression is normal in NHERF1-null mice (Cunningham et al., 2008; Shenolikar et al., 2002). Alternate PDZ proteins such as PDZK1 could also compensate for the lack of NHERF1 (Ardura and Friedman, 2011; Yeruva et al., 2015). Thus, it is entirely possible that NHERF2 compensates for the absence of NHERF1, binds the PTH receptor and directs appropriate signaling and cell functions. Notably, OK cells express NHERF1 but not NHERF2 (Wade et al., 2001). Rats too express only NHERF1 on proximal tubule brush border membranes. Thus, OK cells are more of a model for the rat proximal tubule than for that of humans or mice, where both NHERF1 and NHERF2 are expressed (Wade et al., 2003). Thus, results of studies conducted with OK cells demonstrating an absolute role of NHERF1 in PTHR mediated inhibition of Na-Pi cotransport (Mahon et al., 2003) may have fortuitously benefited from the absence of NHERF2.

The majority of PTH effects appear to be mediated by PKA, and to a lesser extent by PKC. However, recent evidence uncovered an alternative pathway that involves cAMP but utilizes exchange protein directly activated by cAMP (EPAC) rather than PKA as an effector (Fujita et al., 2002). Studies employing proximal tubule cells derived from wild-type and NHERF1-null mice revealed a role for EPAC in mediating Na^+/H^+ exchange (Murtazina et al., 2007).

Following secretion of H^+ in exchange for one Na^+ ion by the apical cell membrane Na^+/H^+ exchanger, OH^- is generated within the cell. This is converted to HCO_3^- which is extruded across basolateral cell membranes. This is accomplished by Na^+-dependent-HCO_3^- (NBC1-4, SLC4A4) cotransporters (Boron, 2006; Romero et al., 2004; Soleimani

and Burnham, 2001). The possibility that PTH inhibits bicarbonate absorption by an action on basolateral HCO_3^- exit was uncertain and this action was attributed to an effect on the Na^+,K^+-ATPase. More recent studies reveal direct effects of PTH on NBC activity through multiple signaling pathways (Ruiz et al., 1996). This action requires NHERF1 (Bernardo et al., 1999; Weinman et al., 2001). NHE3 is a target for PKA-mediated phosphorylation (Zhao et al., 1999). A role for PKC on PTH-regulated NHE3 is uncertain. Apical PTHR stimulation preferentially activates PKC. PTH induces phosphorylation of multiple serine residues within the cytoplasmic tail of NHE3 (Collazo et al., 2000). Phosphorylation is maximal within 5 min and associated with a reduction in NHE3 activity but not surface expression.

By way of summary, PTH regulates Na^+/H^+ exchange primarily by an immediate inhibitory action that depends upon phosphorylation and requires the presence of NHERF1. PKA and PKC phosphorylate NHE3 (Lee et al., 2017). Following the initial inhibition of membrane-associated NHE3, the protein is withdrawn from the membrane but unlike NPT2A is not degraded or downregulated. Thus, following dephosphorylation the transporter likely is recycled to the plasma membrane.

Vitamin D metabolism

The biologically active form of vitamin D, $1.25(OH)_2D_3$, is synthesized by a cascade of multiorgan processes, the penultimate step of which is 1α hydroxylation that proceeds in proximal renal tubules and is regulated by PTH and the CaSR calcium-sensing receptor (Nolin and Friedman, 2018).

Parathyroidectomy reduces $1.25(OH)_2D_3$ synthesis, whereas PTH administration increases renal 1α-hydroxylase activity (Armbrecht et al., 2003; Fraser and Kodicek, 1973; Walker et al., 1990). Increased synthesis of *CYP27B1*, the $25(OH)D_3$ 1α-hydroxylase gene, results from kidney-specific regulated expression, where the promoter is rapidly induced in response to PTH (Christakos, 2017; Meyer et al., 2017)}. Positive actions of PTH on 1α-hydroxylase expression and $1.25(OH)_2D_3$ biosynthesis are counterregulated by the CaSR (Maiti and Beckman, 2007; Maiti et al., 2008).

PTH not only promotes $1.25(OH)_2D_3$ synthesis but also regulates its degradation. 24-hydroxylation of $1.25(OH)_2D_3$ is the first step in the catabolic inactivation of $1.25(OH)_2D_3$ (Carpenter, 2017; Zierold et al., 2003). It was thought that only proximal renal tubules expressed 24-hydroxylase. Distal tubules, however, take up $1.25(OH)_2D_3$, express the vitamin D receptor, and possess vitamin D-dependent calcium-binding proteins. 24-hydroxylase message, protein, and activity have been demonstrated in distal tubule cells (Yang et al., 1999) and human distal tubules (Blomberg Jensen et al., 2010). Whereas PTH reduces 24-hydroxylase activity in proximal tubule cells, PTH and cAMP augment 24-hydroxylase activity in murine distal tubule cells (Yang et al., 1999). Oppositely oriented actions of PTH on 24-hydroxylase activity suggest differential regulation of 24-hydroxylase expression in proximal and distal tubules.

The signaling pathways employed by the PTHR to increase $1.25(OH)_2D_3$ synthesis have been examined extensively in vivo and in vitro. Involvement of cAMP is suggested by the fact that the PTH effect can be mimicked by cAMP analogs, forskolin, and phosphodiesterase inhibitors (Armbrecht et al., 1984; Henry, 1985; Horiuchi et al., 1977; Korkor et al., 1987; Larkins et al., 1974; Rost et al., 1981; Shigematsu et al., 1986). PTH- or forskolin-stimulated transcriptional induction of 1α-hydroxylase occurred and was blocked by the PKA inhibitor H89 (Murayama et al., 1999). A role for PKC in regulating 1α-hydroxylation has been identified from studies of the effects of PTH on isolated proximal tubules (Janulis et al., 1992, 1993). PKC activation produced rapid (30–60 min) increases of $1.25(OH)_2D_3$ synthesis (PKC and $1.25(OH)_2D_3$ synthesis correlated with PTH concentrations 100-fold to 1000-fold lower than those required for the activation of PKA). Moreover, inhibition of PKC blocked $1.25(OH)_2D_3$ synthesis, and amino-truncated PTH fragments that stimulate PKC but not PKA likewise enhanced $1.25(OH)_2D_3$ formation. Taken together, the results suggest a predominant effect of PKA on transcriptional regulation of *CYP27B1* gene expression and a more rapid posttranscriptional action of PKC on 1α-hydroxylase enzymatic activity.

Other renal effects of parathyroid hormone

PTH exerts a variety of additional described, but far less well understood, effects on ion transport, such as activation of apical Cl^- channels (Suzuki et al., 1991) and metabolism.

The kidney contributes importantly to systemic gluconeogenesis (Friedman and Torretti, 1978; Schoolwerth et al., 1988), although this is not normally apparent because of balancing by renal medullary glycolysis. PTH-dependent renal gluconeogenesis is attended by segmental and internephron heterogeneity. PTH increases gluconeogenesis (Chobanian and Hammerman, 1988), ammoniagenesis (Wang and Kurokawa, 1984), and phosphoenolpyruvate carboxykinase (Watford and Mapes, 1990) mRNA expression in proximal tubules. PTH primarily stimulates gluconeogenesis in cortical S1 and S2

proximal tubules (Wang and Kurokawa, 1984). Although juxtamedullary S1 proximal tubules exhibit the highest rate of gluconeogenesis, it is unaffected by PTH.

Gluconeogenesis is linked to ammoniagenesis because both are stimulated by acidosis and by PTH. Moreover, L-glutamine, which is the major gluconeogenic precursor, is also a substrate for ammoniagenesis. Thus, there may be some metabolic interdependence of PTH actions on gluconeogenesis and ammoniagenesis.

PTH also exerts conspicuous morphological effects causing rapid microvillus shortening (Hruska et al., 1986). This action appears to be specific for proximal tubule cells. Emerging observations suggest that this cell-specific effect may be due to prominent brush border expression of NHERF1 in proximal tubule cells and its absence from distal tubule cells.

It is not known if PTH regulation of Na-Pi cotransport, Na^+/H^+ exchange or Na^+/Ca^{2+} exchange, or its metabolic actions on 25-hydroxyvitamin D-1α-hydroxylase, gluconeogenesis, and ammoniagenesis, involves more complicated second messenger signaling. Notably, PTH receptors activate additional signaling pathways involving phospholipase A_2 (Mandel and Derrickson, 1997; Ribeiro et al., 1994), PLD (Garrido et al., 2009; Somermeyer et al., 1983), and MAPK (Quamme et al., 1994; Swarthout et al., 1997; Verheijen and Defize, 1997). Thus, subtle differences in regulatory control or changes in signaling may arise in pathological settings.

Renal expression and actions of parathyroid hormone–related protein

PTHrP is expressed by glomeruli, distal tubules, and collecting ducts of fetal kidneys and by proximal convoluted tubules, distal convoluted tubules, and glomeruli of adult kidneys (Aya et al., 1999; Philbrick et al., 1996). In rat kidneys, PTHrP mRNA is found in glomeruli, proximal convoluted tubules, and macula densa but not in cortical ascending limbs, medullary ascending limbs, distal convoluted tubules, or collecting ducts (Yang et al., 1997), whereas other studies reported PTHrP transcripts in glomerular mesangial cells and proximal and distal tubules (Soifer et al., 1993). Although PTHrP is critical for normal cardiovascular and bone development, the kidneys of PTHrP-null mice appear histologically normal (Karmali et al., 1992) and a physiological role for PTHrP on the kidney is uncertain (Mundy and Edwards, 2008).

Amino-terminal fragments of PTHrP exhibit renal actions including stimulation of cAMP production, regulation of Na-Pi cotransport, and calcium excretion that are largely indistinguishable from those of PTH (Everhart-Caye et al., 1996; Horiuchi et al., 1987; Horwitz et al., 2003b; Pizurki et al., 1988; Scheinman et al., 1990; Yates et al., 1988). Some differences may be discerned. In distal tubule cells, for instance, PTHrP(1–34) and PTHrP(1–74) were more potent than equimolar concentrations of PTH(1–34) and PTH(1–84) in stimulating adenylyl cyclase (Friedman et al., 1989). In contrast, PTHrP(1–36) has a markedly lower effect at raising serum $1.25(OH)_2D_3$ levels (a consequence of its action on proximal tubules) in human volunteers than does comparable administration of PTH(1–34) (Horwitz et al., 2003b).

PTHrP possesses mid- and carboxy-terminal regions that have distinct biological actions (Clemens et al., 2001; Philbrick et al., 1996). Longer PTHrP fragments may exhibit unique renal properties. For example, bicarbonate excretion in perfused rat kidneys was enhanced equivalently by PTHrP(1–34) and PTH(1–34), whereas PTHrP(1–84), PTHrP(1–108), and PTHrP(1–141) were each less active than PTH(1–34) (Ellis et al., 1990). As discussed in Chapter 25, the PTHrP gene can generate multiple transcripts and protein products, some of which may undergo unique nuclear localization. It is therefore possible that locally expressed PTHrP exerts actions in the kidney that are not shared with PTH.

A possible role for locally produced PTHrP in the renal response to insufficient vascular perfusion has been suggested by findings that PTHrP expression is induced by ischemia or following recovery from ATP depletion (García-Ocaña et al., 1999; Largo et al., 1999; Soifer et al., 1993). PTHrP is expressed by the intima and media of human renal microvessels and in the macula densa (Massfelder et al., 1996). PTHrP (like PTH) increases renin release from the juxtaglomerular apparatus and also stimulates cAMP in renal afferent and efferent arterioles, leading to vasodilation and enhanced renal blood flow (Endlich et al., 1995; Helwig et al., 1991; Musso et al., 1989; Saussine et al., 1993). Both cAMP and nitric oxide have been implicated in PTHrP-induced in vitro vasorelaxation (Massfelder et al., 1996). Thus, enhanced local PTHrP production induced by inadequate renal perfusion or ischemia may be involved in local and systemic autoregulatory mechanisms. According to this view, direct local vasodilatory actions are supplemented by the systemic activation of angiotensinogen, which increases arterial pressure and further sustains renal blood flow.

PTHrP promotes fibrogenesis and is upregulated in experimental nephropathy (Funk, 2001; Ortega et al., 2005, 2006). Locally produced PTHrP may contribute to the proinflammatory effect by activating NF-KB and ERKs (Ramila et al., 2008). The incidence of renal hypertrophy is greater in diabetic mice overexpressing PTHrP than in control animals, suggesting that constitutive PTHrP overexpression may elicit adaptive responses such as nitric oxide production to mitigate against renal damage (Izquierdo et al., 2006).

ACKNOWLEDGMENTS

Original cited work was supported by National Institutes of Health (NIH) awards R01 DK105811-A1, R01 DK111427-A1 (PAF), and R01 HL136382 (AB).

References

Abou-Samra, A.B., Juppner, H., Force, T., Freeman, M.W., Kong, X.F., Schipani, E., Urena, P., Richards, J., Bonventre, J.V., Potts Jr., J.T., et al., 1992. Expression cloning of a common receptor for parathyroid hormone and parathyroid hormone-related peptide from rat osteoblast-like cells: a single receptor stimulates intracellular accumulation of both cAMP and inositol trisphosphates and increases intracellular free calcium. Proc. Natl. Acad. Sci. U. S. A. 89, 2732–2736.

Agus, Z.S., Gardner, L.B., Beck, L.H., Goldberg, M., 1973. Effects of parathyroid hormone on renal tubular reabsorption of calcium, sodium, and phosphate. Am. J. Physiol. 224, 1143–1148.

Ahmed, I., Gesty-Palmer, D., Drezner, M.K., Luttrell, L.M., 2003. Transactivation of the epidermal growth factor receptor mediates parathyroid hormone and prostaglandin F2 alpha-stimulated mitogen-activated protein kinase activation in cultured transgenic murine osteoblasts. Mol. Endocrinol. 17, 1607–1621.

Akatsu, T., Takahashi, N., Udagawa, N., Sato, K., Nagata, N., Moseley, J.M., Martin, T.J., Suda, T., 1989. Parathyroid hormone (PTH)-related protein is a potent stimulator of osteoclast-like multinucleated cell formation to the same extent as PTH in mouse marrow cultures. Endocrinology 125, 20–27.

Albright, F., Bauer, W., Ropes, M., Aub, J.C., 1929. Studies of calcium and phosphorus metabolism: IV. The effect of the parathyroid hormone. J. Clin. Investig. 7, 139–181.

Amizuka, N., Karaplis, A.C., Henderson, J.E., Warshawsky, H., Lipman, M.L., Matsuki, Y., Ejiri, S., Tanaka, M., Izumi, N., Ozawa, H., Goltzman, D., 1996. Haploinsufficiency of parathyroid hormone-related peptide (PTHrP) results in abnormal postnatal bone development. Dev. Biol. 175, 166–176.

Amizuka, N., Lee, H.S., Kwan, M.Y., Arazani, A., Warshawsky, H., Hendy, G.N., Ozawa, H., White, J.H., Goltzman, D., 1997. Cell-specific expression of the parathyroid hormone (PTH)/PTH-related peptide receptor gene in kidney from kidney-specific and ubiquitous promoters. Endocrinology 138, 469–481.

Andrukhova, O., Zeitz, U., Goetz, R., Mohammadi, M., Lanske, B., Erben, R.G., 2012. FGF23 acts directly on renal proximal tubules to induce phosphaturia through activation of the ERK1/2-SGK1 signaling pathway. Bone 51, 621–628.

Ardura, J.A., Friedman, P.A., 2011. Regulation of G protein-coupled receptor function by Na^+/H^+ exchange regulatory factors. Pharmacol. Rev. 63, 882–900.

Armbrecht, H.J., Boltz, M.A., Hodam, T.L., 2003. PTH increases renal $25(OH)D_3$-1α-hydroxylase (CYP1α) mRNA but not renal $1,25(OH)_2D_3$ production in adult rats. Am. J. Physiol. Renal. Physiol. 284, F1032–F1036.

Armbrecht, H.J., Wongsurawat, N., Zenser, T.V., Davis, B.B., 1984. Effect of PTH and $1,25(OH)_2D_3$ on renal $25(OH)D_3$ metabolism, adenylate cyclase, and protein kinase. Am. J. Physiol. Endocrinol. Metab. 246, E102–E107.

Aubin, J.E., Bonnelye, E., 2000. Osteoprotegerin and its ligand: a new paradigm for regulation of osteoclastogenesis and bone resorption. Osteoporos. Int. 11, 905–913.

Aya, K., Tanaka, H., Ichinose, Y., Kobayashi, M., Seino, Y., 1999. Expression of parathyroid hormone-related peptide messenger ribonucleic acid in developing kidney. Kidney Int. 55, 1696–1703.

Ba, J., Brown, D., Friedman, P.A., 2003. Calcium-sensing receptor regulation of PTH-inhibitable proximal tubule phosphate transport. Am. J. Physiol. Renal. Physiol. 285, F1233–F1243.

Bacconi, A., Virkki, L.V., Biber, J., Murer, H., Forster, I.C., 2005. Renouncing electroneutrality is not free of charge: switching on electrogenicity in a Na^+-coupled phosphate cotransporter. Proc. Natl. Acad. Sci. U. S. A. 102, 12606–12611.

Bacic, D., Lehir, M., Biber, J., Kaissling, B., Murer, H., Wagner, C.A., 2006. The renal Na^+/phosphate cotransporter NaPi-IIa is internalized via the receptor-mediated endocytic route in response to parathyroid hormone. Kidney Int. 69, 495–503.

Bacskai, B.J., Friedman, P.A., 1990. Activation of latent Ca^{2+} channels in renal epithelial cells by parathyroid hormone. Nature 347, 388–391.

Baertschi, S., Baur, N., Lueders-Lefevre, V., Voshol, J., Keller, H., 2014. Class I and IIa histone deacetylases have opposite effects on sclerostin gene regulation. J. Biol. Chem. 289, 24995–25009.

Banerjee, C., Javed, A., Choi, J.Y., Green, J., Rosen, V., van Wijnen, A.J., Stein, J.L., Lian, J.B., Stein, G.S., 2001. Differential regulation of the two principal Runx2/Cbfa1 n-terminal isoforms in response to bone morphogenetic protein-2 during development of the osteoblast phenotype. Endocrinology 142, 4026–4039.

Bank, N., Aynedjian, H.S., 1976. A micropuncture study of the effect of parathyroid hormone on renal bicarbonate reabsorption. J. Clin. Investig. 58, 336–344.

Baron, R., Rawadi, G., 2007. Targeting the Wnt/beta-catenin pathway to regulate bone formation in the adult skeleton. Endocrinology 148, 2635–2643.

Bellido, T., 2006. Downregulation of SOST/sclerostin by PTH: a novel mechanism of hormonal control of bone formation mediated by osteocytes. J. Musculoskelet. Neuronal Interact. 6, 358–359.

Bellido, T., Ali, A.A., Gubrij, I., Plotkin, L.I., Fu, Q., O'Brien, C.A., Manolagas, S.C., Jilka, R.L., 2005. Chronic elevation of parathyroid hormone in mice reduces expression of sclerostin by osteocytes: a novel mechanism for hormonal control of osteoblastogenesis. Endocrinology 146, 4577–4583.

Bellido, T., Ali, A.A., Plotkin, L.I., Fu, Q., Gubrij, I., Roberson, P.K., Weinstein, R.S., O'Brien, C.A., Manolagas, S.C., Jilka, R.L., 2003. Proteasomal degradation of Runx2 shortens parathyroid hormone-induced anti-apoptotic signaling in osteoblasts. A putative explanation for why intermittent administration is needed for bone anabolism. J. Biol. Chem. 278, 50259–50272.

Bergmann, P., Nijs-De Wolf, N., Pepersack, T., Corvilain, J., 1990. Release of parathyroid hormonelike peptides by fetal rat long bones in culture. J. Bone Miner. Res. 5, 741−753.

Bergwitz, C., Roslin, N.M., Tieder, M., Loredo-Osti, J.C., Bastepe, M., Abu-Zahra, H., Frappier, D., Burkett, K., Carpenter, T.O., Anderson, D., Garabedian, M., Sermet, I., Fujiwara, T.M., Morgan, K., Tenenhouse, H.S., Juppner, H., 2006. *SLC34A3* mutations in patients with hereditary hypophosphatemic rickets with hypercalciuria predict a key role for the sodium-phosphate Cotransporter NaPi-IIc in maintaining phosphate homeostasis. Am. J. Hum. Genet. 78, 179−192.

Bernardo, A.A., Kear, F.T., Santos, A.V., Ma, J., Steplock, D., Robey, R.B., Weinman, E.J., 1999. Basolateral Na^+/HCO_3^- cotransport activity is regulated by the dissociable Na^+/H^+ exchanger regulatory factor. J. Clin. Investig. 104, 195−201.

Bernardo, J.F., Friedman, P.A., 2013. Renal calcium metabolism. In: Alpern, R.J., Caplan, M.J., Moe, O.W. (Eds.), Seldin and Giebisch's the Kidney: Physiology and Pathophysiology. Academic Press, San Diego, pp. 2225−2247.

Besarab, A., Swanson, J.W., 1984. Tachyphylaxis to PTH in the isolated perfused rat kidney: resistance of anticalciuria. Am. J. Physiol. Renal. Physiol. 247, F240−F245.

Bethune, J.E., Turpin, R.A., 1968. A study of urinary excretion of parathyroid hormone in man. J. Clin. Investig. 47, 1583−1589.

Bettinelli, A., Bianchetti, M.G., Girardin, E., Caringella, A., Cecconi, M., Appiani, A.C., Pavanello, L., Gastaldi, R., Isimbaldi, C., Lama, G., et al., 1992. Use of calcium excretion values to distinguish two forms of primary renal tubular hypokalemic alkalosis: Bartter and Gitelman syndromes. J. Pediatr. 120, 38−43.

Bettoun, J.D., Minagawa, M., Hendy, G.N., Alpert, L.C., Goodyer, C.G., Goltzman, D., White, J.H., 1998. Developmental upregulation of human parathyroid hormone (PTH)/PTH-related peptide receptor gene expression from conserved and human-specific promoters. J. Clin. Investig. 102, 958−967.

Bichara, M., Mercier, O., Paillard, M., Leviel, F., 1986. Effects of parathyroid hormone on urinary acidification. Am. J. Physiol. Renal. Physiol. 251, F444−F453.

Bidot-López, P., Farese, R.V., Sabir, M.A., 1981. Parathyroid hormone and adenosine-3',5'-monophosphate acutely increase phospholipids of the phosphatidate-polyphosphoinositide pathway in rabbit kidney cortex tubules *in vitro* by a cycloheximide-sensitive process. Endocrinology 108, 2078−2081.

Bikle, D.D., Sakata, T., Leary, C., Elalieh, H., Ginzinger, D., Rosen, C.J., Beamer, W., Majumdar, S., Halloran, B.P., 2002. Insulin-like growth factor I is required for the anabolic actions of parathyroid hormone on mouse bone. J. Bone Miner. Res. 17, 1570−1578.

Bilezikian, J.P., 2012. Primary hyperparathyroidism. Endocr. Pract. 18, 781−790.

Bisello, A., Chorev, M., Rosenblatt, M., Monticelli, L., Mierke, D.F., Ferrari, S.L., 2002. Selective ligand-induced stabilization of active and desensitized parathyroid hormone type 1 receptor conformations. J. Biol. Chem. 277, 38524−38530.

Blaine, J., Chonchol, M., Levi, M., 2015. Renal control of calcium, phosphate, and magnesium homeostasis. Clin. J. Am. Soc. Nephrol. 10, 1257−1272.

Blind, E., Bambino, T., Huang, Z., Bliziotes, M., Nissenson, R.A., 1996. Phosphorylation of the cytoplasmic tail of the PTH/PTHrP receptor. J. Bone Miner. Res. 11, 578−586.

Blomberg Jensen, M., Andersen, C.B., Nielsen, J.E., Bagi, P., Jorgensen, A., Juul, A., Leffers, H., 2010. Expression of the vitamin D receptor, 25-hydroxylases, 1alpha-hydroxylase and 24-hydroxylase in the human kidney and renal clear cell cancer. J. Steroid Biochem. Mol. Biol. 121, 376−382.

Boron, W.F., 2006. Acid-base transport by the renal proximal tubule. J. Am. Soc. Nephrol. 17, 2368−2382.

Bos, M.P., van der Meer, J.M., Feyen, J.H., Herrmann-Erlee, M.P., 1996. Expression of the parathyroid hormone receptor and correlation with other osteoblastic parameters in fetal rat osteoblasts. Calcif. Tissue Int. 58, 95−100.

Boyce, R.W., Paddock, C.L., Franks, A.F., Jankowsky, M.L., Eriksen, E.F., 1996. Effects of intermittent hPTH(1-34) alone and in combination with $1,25(OH)_2D_3$ or risedronate on endosteal bone remodeling in canine cancellous and cortical bone. J. Bone Miner. Res. 11, 600−613.

Brindle, P.K., Montminy, M.R., 1992. The CREB family of transcription activators. Curr. Opin. Genet. Dev. 2, 199−204.

Bringhurst, F.R., Strewler, G.J., 2002. Renal and skeletal actions of parathyroid hormone (PTH) and PTH-related protein. In: Bilezikian, J.P., Raisz, L.G., Rodan, G.A. (Eds.), Principles of Bone Biology, 2 ed. Academic Press, San Diego, pp. 483−514.

Broadbent, D., Ahmadzai, M.M., Kammala, A.K., Yang, C., Occhiuto, C., Das, R., Subramanian, H., 2017. Roles of NHERF family of PDZ-binding proteins in regulating GPCR functions. Adv. Immunol. 136, 353−385.

Broadus, A.E., 1979. Nephrogenous cyclic AMP as a parathyroid function test. Nephron 23, 136−141.

Brown, R.C., Silver, A.C., Woodhead, J.S., 1991. Binding and degradation of NH_2-terminal parathyroid hormone by opossum kidney cells. Am. J. Physiol. Endocrinol. Metab. 260, E544−E552.

Brunskill, N., Bastani, B., Hayes, C., Morrissey, J., Klahr, S., 1991. Localization and polar distribution of several G-protein subunits along nephron segments. Kidney Int. 40, 997−1006.

Burgess, T.L., Qian, Y., Kaufman, S., Ring, B.D., Van, G., Capparelli, C., Kelley, M., Hsu, H., Boyle, W.J., Dunstan, C.R., Hu, S., Lacey, D.L., 1999. The ligand for osteoprotegerin (OPGL) directly activates mature osteoclasts. J. Cell Biol. 145, 527−538.

Busch, A.E., Schuster, A., Waldegger, S., Wagner, C.A., Zempel, G., Broer, S., Biber, J., Murer, H., Lang, F., 1996. Expression of a renal type I sodium/phosphate transporter (NaPi-1) induces a conductance in Xenopus oocytes permeable for organic and inorganic anions. Proc. Natl. Acad. Sci. U. S. A. 93, 5347−5351.

Calebiro, D., Nikolaev, V.O., Gagliani, M.C., de Filippis, T., Dees, C., Tacchetti, C., Persani, L., Lohse, M.J., 2009. Persistent cAMP-signals triggered by internalized G-protein-coupled receptors. PLoS Biol. 7, e1000172.

Canalis, E., Centrella, M., Burch, W., McCarthy, T.L., 1989. Insulin-like growth factor I mediates selective anabolic effects of parathyroid hormone in bone cultures. J. Clin. Investig. 83, 60−65.

Canalis, E., McCarthy, T.L., Centrella, M., 1990. Differential effects of continuous and transient treatment with parathyroid hormone related peptide (PTHrp) on bone collagen synthesis. Endocrinology 126, 1806–1812.

Capuano, P., Bacic, D., Roos, M., Gisler, S.M., Stange, G., Biber, J., Kaissling, B., Weinman, E.J., Shenolikar, S., Wagner, C.A., Murer, H., 2006. Defective coupling of apical PTH receptors to phospholipase C prevents internalization of the Na^+/phosphate cotransporter NaPi-IIa in NHERF1 deficient mice. Am. J. Physiol. Cell Physiol. 292, C927–C934.

Care, A.D., Abbas, S.K., Pickard, D.W., Barri, M., Drinkhill, M., Findlay, J.B., White, I.R., Caple, I.W., 1990. Stimulation of ovine placental transport of calcium and magnesium by mid-molecule fragments of human parathyroid hormone-related protein. Exp. Physiol. 75, 605–608.

Carney, J.A., 1996. The glandulae parathyroideae of Ivar Sandstrom. Contributions from two continents. Am. J. Surg. Pathol. 20, 1123–1144.

Carpenter, T.O., 2017. CYP24A1 loss of function: clinical phenotype of monoallelic and biallelic mutations. J. Steroid Biochem. Mol. Biol. 173, 337–340.

Castro, M., Dicker, F., Vilardaga, J.P., Krasel, C., Bernhardt, M., Lohse, M.J., 2002. Dual regulation of the parathyroid hormone (PTH)/PTH-related peptide receptor signaling by protein kinase C and β-arrestins. Endocrinology 143, 3854–3865.

Cha, S.K., Wu, T., Huang, C.L., 2008. Protein kinase C inhibits caveolae-mediated endocytosis of TRPV5. Am. J. Physiol. Renal. Physiol. 294, F1212–F1221.

Chabardès, D., Gagnan-Brunette, M., Imbert-Teboul, M., Gontcharevskaia, O., Montégut, M., Clique, A., Morel, F., 1980. Adenylate cyclase responsiveness to hormones in various portions of the human nephron. J. Clin. Investig. 65, 439–448.

Chaudhary, L.R., Hruska, K.A., 2001. The cell survival signal Akt is differentially activated by PDGF-BB, EGF, and FGF-2 in osteoblastic cells. J. Cell. Biochem. 81, 304–311.

Cheloha, R.W., Gellman, S.H., Vilardaga, J.P., Gardella, T.J., 2015. PTH receptor-1 signalling-mechanistic insights and therapeutic prospects. Nat. Rev. Endocrinol. 11, 712–724.

Chen, H.L., Demiralp, B., Schneider, A., Koh, A.J., Silve, C., Wang, C.Y., McCauley, L.K., 2002. Parathyroid hormone and parathyroid hormone-related protein exert both pro- and anti-apoptotic effects in mesenchymal cells. J. Biol. Chem. 277, 19374–19381.

Chobanian, M.C., Hammerman, M.R., 1988. Parathyroid hormone stimulates ammoniagenesis in canine renal proximal tubular segments. Am. J. Physiol. Renal. Physiol. 255, F847–F852.

Christakos, S., 2017. In search of regulatory circuits that control the biological activity of vitamin D. J. Biol. Chem. 292, 17559–17560.

Christov, M., Juppner, H., 2013. Insights from genetic disorders of phosphate homeostasis. Semin. Nephrol. 33, 143–157.

Chung, D.J., Castro, C.H., Watkins, M., Stains, J.P., Chung, M.Y., Szejnfeld, V.L., Willecke, K., Theis, M., Civitelli, R., 2006. Low peak bone mass and attenuated anabolic response to parathyroid hormone in mice with an osteoblast-specific deletion of connexin43. J. Cell Sci. 119, 4187–4198.

Civitelli, R., Hruska, K.A., Shen, V., Avioli, L.V., 1990. Cyclic AMP-dependent and calcium-dependent signals in parathyroid hormone function. Exp. Gerontol. 25, 223–231.

Civitelli, R., Martin, T.J., Fausto, A., Gunsten, S.L., Hruska, K.A., Avioli, L.V., 1989. Parathyroid hormone-related peptide transiently increases cytosolic calcium in osteoblast-like cells: comparison with parathyroid hormone. Endocrinology 125, 1204–1210.

Clemens, T.L., Cormier, S., Eichinger, A., Endlich, K., Fiaschi-Taesch, N., Fischer, E., Friedman, P.A., Karaplis, A.C., Massfelder, T., Rossert, J., Schluter, K.D., Silve, C., Stewart, A.F., Takane, K., Helwig, J.J., 2001. Parathyroid hormone-related protein and its receptors: nuclear functions and roles in the renal and cardiovascular systems, the placental trophoblasts and the pancreatic islets. Br. J. Pharmacol. 134, 1113–1136.

Clohisy, J.C., Scott, D.K., Brakenhoff, K.D., Quinn, C.O., Partridge, N.C., 1992. Parathyroid hormone induces c-fos and c-jun messenger RNA in rat osteoblastic cells. Mol. Endocrinol. 6, 1834–1842.

Coe, F.L., 1974. Magnitude of metabolic acidosis in primary hyperparathyroidism. Arch. Intern. Med. 134, 262–265.

Cole, J.A., 1999. Parathyroid hormone activates mitogen-activated protein kinase in opossum kidney cells. Endocrinology 140, 5771–5779.

Collazo, R., Fan, L.Z., Hu, M.C., Zhao, H., Wiederkehr, M.R., Moe, O.W., 2000. Acute regulation of Na^+/H^+ exchanger NHE3 by parathyroid hormone via NHE3 phosphorylation and dynamin-dependent endocytosis. J. Biol. Chem. 275, 31601–31608.

Collins, J.F., Bai, L., Ghishan, F.K., 2004. The SLC20 family of proteins: dual functions as sodium-phosphate cotransporters and viral receptors. Pflügers Archiv 447, 647–652.

Conover, C.A., 2008. Insulin-like growth factor-binding proteins and bone metabolism. Am. J. Physiol. Endocrinol. Metab. 294, E10–E14.

Conover, C.A., Bale, L.K., Clarkson, J.T., Torring, O., 1993. Regulation of insulin-like growth factor binding protein-5 messenger ribonucleic acid expression and protein availability in rat osteoblast-like cells. Endocrinology 132, 2525–2530.

Cornish, J., Callon, K.E., Nicholson, G.C., Reid, I.R., 1997. Parathyroid hormone-related protein-(107-139) inhibits bone resorption in vivo. Endocrinology 138, 1299–1304.

Corral, D.A., Amling, M., Priemel, M., Loyer, E., Fuchs, S., Ducy, P., Baron, R., Karsenty, G., 1998. Dissociation between bone resorption and bone formation in osteopenic transgenic mice. Proc. Natl. Acad. Sci. U. S. A. 95, 13835–13840.

Costanzo, L.S., Windhager, E.E., 1980. Effects of PTH, ADH, and cyclic AMP on distal tubular Ca and Na reabsorption. Am. J. Physiol. 239, F478–F485.

Coulson, R., Scheinman, S.J., 1989. Xanthine effects on renal proximal tubular function and cyclic AMP metabolism. J. Pharmacol. Exp. Ther. 248, 589–595.

Cros, M., Silve, C., Graulet, A.M., Morieux, C., Ureña, P., De Vernejoul, M.C., Bouizar, Z., 1998. Estrogen stimulates PTHrP but not PTH/PTHrP receptor gene expression in the kidney of ovariectomized rat. J. Cell. Biochem. 70, 84–93.

Cuche, J.L., Ott, C.E., Marchand, G.R., Diaz-Buxo, J.A., Knox, F.G., 1976. Intrarenal calcium in phosphate handling. Am. J. Physiol. 230, 790–796.

Cunningham, R., Biswas, R., Steplock, D., Shenolikar, S., Weinman, E.J., 2010. Role of NHERF and scaffolding proteins in proximal tubule transport. Urol. Res. 38, 257–262.

Cunningham, R., Steplock, D., Wang, F., Huang, H., E, X., Shenolikar, S., Weinman, E.J., 2004. Defective PTH regulation of NHE3 activity and phosphate adaptation in cultured NHERF-$1^{-/-}$ renal proximal tubule cells. J. Biol. Chem. 279, 37815–37821.

Cunningham, R.M., Esmaili, A., Brown, E., Biswas, R.S., Murtazina, R., Donowitz, M., Dijkman, H.B., van der Vlag, J., Hogema, B.M., De Jonge, H.R., Shenolikar, S., Wade, J.B., Weinman, E.J., 2008. Urine electrolyte, mineral, and protein excretion in NHERF-2 and NHERF-1 null mice. Am. J. Physiol. Renal. Physiol. 294, F1001–F1007.

Dasgupta, D., Wee, M.J., Reyes, M., Li, Y., Simm, P.J., Sharma, A., Schlingmann, K.P., Janner, M., Biggin, A., Lazier, J., Gessner, M., Chrysis, D., Tuchman, S., Baluarte, H.J., Levine, M.A., Tiosano, D., Insogna, K., Hanley, D.A., Carpenter, T.O., Ichikawa, S., Hoppe, B., Konrad, M., Savendahl, L., Munns, C.F., Lee, H., Juppner, H., Bergwitz, C., 2014. Mutations in SLC34A3/NPT2c are associated with kidney stones and nephrocalcinosis. J. Am. Soc. Nephrol. 25, 2366–2375.

Datta, N.S., Samra, T.A., Abou-Samra, A.B., 2012. Parathyroid hormone induces bone formation in phosphorylation-deficient PTHR1 knockin mice. Am. J. Physiol. Endocrinol. Metab. 302, E1183–E1188.

Daugaard, H., Egfjord, M., Lewin, E., Olgaard, K., 1994. Metabolism of N-terminal and C-terminal parathyroid hormone fragments by isolated perfused rat kidney and liver. Endocrinology 134, 1373–1381.

de Groot, T., Lee, K., Langeslag, M., Xi, Q., Jalink, K., Bindels, R.J., Hoenderop, J.G., 2009. Parathyroid hormone activates TRPV5 via PKA-dependent phosphorylation. J. Am. Soc. Nephrol. 20, 1693–1704.

Dean, T., Vilardaga, J.P., Potts Jr., J.T., Gardella, T.J., 2008. Altered selectivity of parathyroid hormone (PTH) and PTH-related protein (PTHrP) for distinct conformations of the PTH/PTHrP receptor. Mol. Endocrinol. 22, 156–166.

Debiais, F., Lefevre, G., Lemonnier, J., Le Mee, S., Lasmoles, F., Mascarelli, F., Marie, P.J., 2004. Fibroblast growth factor-2 induces osteoblast survival through a phosphatidylinositol 3-kinase-dependent, -β-catenin-independent signaling pathway. Exp. Cell Res. 297, 235–246.

Deliot, N., Hernando, N., Horst-Liu, Z., Gisler, S.M., Capuano, P., Wagner, C.A., Bacic, D., O'Brien, S., Biber, J., Murer, H., 2005. Parathyroid hormone treatment induces dissociation of type IIa Na^+-P_i cotransporter-Na^+/H^+ exchanger regulatory factor-1 complexes. Am. J. Physiol. Cell Physiol. 289, C159–C167.

Dempster, D.W., Hughes-Begos, C.E., Plavetic-Chee, K., Brandao-Burch, A., Cosman, F., Nieves, J., Neubort, S., Lu, S.S., Iida-Klein, A., Arnett, T., Lindsay, R., 2005. Normal human osteoclasts formed from peripheral blood monocytes express PTH type 1 receptors and are stimulated by PTH in the absence of osteoblasts. J. Cell. Biochem. 95, 139–148.

Dempster, D.W., Parisien, M., Silverberg, S.J., Liang, X.G., Schnitzer, M., Shen, V., Shane, E., Kimmel, D.B., Recker, R., Lindsay, R., Bilezikian, J.P., 1999. On the mechanism of cancellous bone preservation in postmenopausal women with mild primary hyperparathyroidism. J. Clin. Endocrinol. Metab. 84, 1562–1566.

Dicker, F., Quitterer, U., Winstel, R., Honold, K., Lohse, M.J., 1999. Phosphorylation-independent inhibition of parathyroid hormone receptor signaling by G protein-coupled receptor kinases. Proc. Natl. Acad. Sci. U. S. A. 96, 5476–5481.

Disthabanchong, S., Hassan, H., McConkey, C.L., Martin, K.J., Gonzalez, E.A., 2004. Regulation of PTH1 receptor expression by uremic ultrafiltrate in UMR 106-01 osteoblast-like cells. Kidney Int. 65, 897–903.

Divieti, P., Geller, A.I., Suliman, G., Juppner, H., Bringhurst, F.R., 2005. Receptors specific for the carboxyl-terminal region of parathyroid hormone on bone-derived cells: determinants of ligand binding and bioactivity. Endocrinology 146, 1863–1870.

Divieti, P., Inomata, N., Chapin, K., Singh, R., Juppner, H., Bringhurst, F.R., 2001. Receptors for the carboxyl-terminal region of PTH(1-84) are highly expressed in osteocytic cells. Endocrinology 142, 916–925.

Dobnig, H., Turner, R.T., 1995. Evidence that intermittent treatment with parathyroid hormone increases bone formation in adult rats by activation of bone lining cells. Endocrinology 136, 3632–3638.

Dobolyi, A., Palkovits, M., Usdin, T.B., 2003. Expression and distribution of tuberoinfundibular peptide of 39 residues in the rat central nervous system. J. Comp. Neurol. 455, 547–566.

Donahue, H.J., McLeod, K.J., Rubin, C.T., Andersen, J., Grine, E.A., Hertzberg, E.L., Brink, P.R., 1995. Cell-to-cell communication in osteoblastic networks: cell line-dependent hormonal regulation of gap junction function. J. Bone Miner. Res. 10, 881–889.

Dousa, T.P., Duarte, C.G., Knox, F.G., 1976. Effect of colchicine on urinary phosphate and regulation by parathyroid hormone. Am. J. Physiol. 231, 61–65.

Ducy, P., Starbuck, M., Priemel, M., Shen, J., Pinero, G., Geoffroy, V., Amling, M., Karsenty, G., 1999. A Cbfa1-dependent genetic pathway controls bone formation beyond embryonic development. Genes Dev. 13, 1025–1036.

Ducy, P., Zhang, R., Geoffroy, V., Ridall, A.L., Karsenty, G., 1997. Osf2/Cbfa1: a transcriptional activator of osteoblast differentiation. Cell 89, 747–754.

Edwards, B.R., Sutton, R.A.L., Dirks, J.H., 1974. Effect of calcium infusion on renal tubular reabsorption in the dog. Am. J. Physiol. 227, 13–18.

Eichinger, A., Fiaschi-Taesch, N., Massfelder, T., Fritsch, S., Barthelmebs, M., Helwig, J.J., 2002. Transcript expression of the tuberoinfundibular peptide (TIP)39/PTH2 receptor system and non-PTH1 receptor-mediated tonic effects of TIP39 and other PTH2 receptor ligands in renal vessels. Endocrinology 143, 3036–3043.

Ellis, A.G., Adam, W.R., Martin, T.J., 1990. Comparison of the effects of parathyroid hormone (PTH) and recombinant PTH-related protein on bicarbonate excretion by the isolated perfused rat kidney. J. Endocrinol. 126, 403–408.

Ellsworth, R., Nicholson, W.M., 1935. Further observations upon the changes in the electrolytes of the urine following the injection of parathyroid extract. J. Clin. Investig. 14, 823–827.

Endlich, K., Massfelder, T., Helwig, J.J., Steinhausen, M., 1995. Vascular effects of parathyroid hormone and parathyroid hormone-related protein in the split hydronephrotic rat kidney. J. Physiol. 483, 481–490.

Erben, R.G., 2017. Pleiotropic actions of FGF23. Toxicol. Pathol. https://doi.org/10.1177/0192623317737469.

Esbrit, P., Alvarez-Arroyo, M.V., De Miguel, F., Martin, O., Martinez, M.E., Caramelo, C., 2000. C-terminal parathyroid hormone-related protein increases vascular endothelial growth factor in human osteoblastic cells. J. Am. Soc. Nephrol. 11, 1085–1092.

Evans, D.B., Hipskind, R.A., Bilbe, G., 1996. Analysis of signaling pathways used by parathyroid hormone to activate the c-fos gene in human SaOS2 osteoblast-like cells. J. Bone Miner. Res. 11, 1066–1074.

Evely, R.S., Bonomo, A., Schneider, H.G., Moseley, J.M., Gallagher, J., Martin, T.J., 1991. Structural requirements for the action of parathyroid hormone-related protein (PTHrP) on bone resorption by isolated osteoclasts. J. Bone Miner. Res. 6, 85–93.

Everhart-Caye, M., Inzucchi, S.E., Guinness-Henry, J., Mitnick, M.A., Stewart, A.F., 1996. Parathyroid hormone (PTH)-related protein(1-36) is equipotent to PTH(1-34) in humans. J. Clin. Endocrinol. Metab. 81, 199–208.

Fan, L., Wiederkehr, M.R., Collazo, R., Wang, H., Crowder, L.A., Moe, O.W., 1999. Dual mechanisms of regulation of Na/H exchanger NHE-3 by parathyroid hormone in rat kidney. J. Biol. Chem. 274, 11289–11295.

Fei, Y., Shimizu, E., McBurney, M.W., Partridge, N.C., 2015. Sirtuin 1 is a negative regulator of parathyroid hormone stimulation of matrix metalloproteinase 13 expression in osteoblastic cells: role of sirtuin 1 in the action of PTH on osteoblasts. J. Biol. Chem. 290, 8373–8382.

Feinstein, T.N., Yui, N., Webber, M.J., Wehbi, V.L., Stevenson, H.P., King Jr., J.D., Hallows, K.R., Brown, D., Bouley, R., Vilardaga, J.P., 2013. Noncanonical control of vasopressin receptor type 2 signaling by retromer and arrestin. J. Biol. Chem. 288, 27849–27860.

Fenton, A.J., Kemp, B.E., Hammonds Jr., R.G., Mitchelhill, K., Moseley, J.M., Martin, T.J., Nicholson, G.C., 1991a. A potent inhibitor of osteoclastic bone resorption within a highly conserved pentapeptide region of parathyroid hormone-related protein; PTHrP[107-111]. Endocrinology 129, 3424–3426.

Fenton, A.J., Kemp, B.E., Kent, G.N., Moseley, J.M., Zheng, M.H., Rowe, D.J., Britto, J.M., Martin, T.J., Nicholson, G.C., 1991b. A carboxyl-terminal peptide from the parathyroid hormone-related protein inhibits bone resorption by osteoclasts. Endocrinology 129, 1762–1768.

Fenton, A.J., Martin, T.J., Nicholson, G.C., 1993. Long-term culture of disaggregated rat osteoclasts: inhibition of bone resorption and reduction of osteoclast-like cell number by calcitonin and PTHrP[107-139]. J. Cell. Physiol. 155, 1–7.

Fermor, B., Skerry, T.M., 1995. PTH/PTHrP receptor expression on osteoblasts and osteocytes but not resorbing bone surfaces in growing rats. J. Bone Miner. Res. 10, 1935–1943.

Ferrandon, S., Feinstein, T.N., Castro, M., Wang, B., Bouley, R., Potts, J.T., Gardella, T.J., Vilardaga, J.P., 2009. Sustained cyclic AMP production by parathyroid hormone receptor endocytosis. Nat. Chem. Biol. 5, 734–742.

Ferrari, S.L., Behar, V., Chorev, M., Rosenblatt, M., Bisello, A., 1999. Endocytosis of ligand-human parathyroid hormone receptor 1 complexes is protein kinase C-dependent and involves ß-arrestin2. Real-time monitoring by fluorescence microscopy. J. Biol. Chem. 274, 29968–29975.

Ferrari, S.L., Bisello, A., 2001. Cellular distribution of constitutively active mutant parathyroid hormone (PTH)/PTH-related protein receptors and regulation of cyclic adenosine 3',5'-monophosphate signaling by β-arrestin2. Mol. Endocrinol. 15, 149–163.

Ferrari, S.L., Pierroz, D.D., Glatt, V., Goddard, D.S., Bianchi, E.N., Lin, F.T., Manen, D., Bouxsein, M.L., 2005. Bone response to intermittent parathyroid hormone is altered in mice null for β-arrestin2. Endocrinology 146, 1854–1862.

Feuerbach, D., Loetscher, E., Buerki, K., Sampath, T.K., Feyen, J.H., 1997. Establishment and characterization of conditionally immortalized stromal cell lines from a temperature-sensitive T-Ag transgenic mouse. J. Bone Miner. Res. 12, 179–190.

Filburn, C.R., Harrison, S., 1990. Parathyroid hormone regulation of cytosolic Ca^{2+} in rat proximal tubules. Am. J. Physiol. Renal. Physiol. 258, F545–F552.

Finkelman, R.D., Mohan, S., Linkhart, T.A., Abraham, S.M., Boussy, J.P., Baylink, D.J., 1992. PTH stimulates the proliferation of TE-85 human osteosarcoma cells by a mechanism not involving either increased cAMP or increased secretion of IGF-I, IGF-II or TGFβ. Bone Miner. 16, 89–100.

Finkelstein, J.S., Klibanski, A., Arnold, A.L., Toth, T.L., Hornstein, M.D., Neer, R.M., 1998. Prevention of estrogen deficiency-related bone loss with human parathyroid hormone-(1-34): a randomized controlled trial. J. Am. Med. Assoc. 280, 1067–1073.

Fischbach, F.T., Dunning, M.B., 2015. A Manual of Laboratory and Diagnostic Tests, ninth ed. Wolters Kluwer Health, Philadelphia.

Flannery, P.J., Spurney, R.F., 2001. Domains of the parathyroid hormone (PTH) receptor required for regulation by G protein-coupled receptor kinases (GRKs). Biochem. Pharmacol. 62, 1047–1058.

Fraser, D.R., Kodicek, E., 1973. Regulation of 25-hydroxycholecalciferol-1-hydroxylase activity in kidney by parathyroid hormone. Nat. New Biol. 241, 163–166.

Friedman, P.A., 1998. Codependence of renal calcium and sodium transport. Annu. Rev. Physiol. 60, 179–197.

Friedman, P.A., 2000. Mechanisms of calcium transport. Exp. Nephrol. 8, 343–350.

Friedman, P.A., 2008. Renal calcium metabolism. In: Alpern, R.J., Hebert, S.C. (Eds.), Seldin and Giebisch's the Kidney: Physiology and Pathophysiology, 4 ed. Elsevier, San Diego, pp. 1851–1890.

Friedman, P.A., 2014. Physiological actions of PTH II: renal actions. In: Bilezikian, J.P., Marcus, R., Silverberg, S.J., Marcocci, C., Levine, M.A., Potts Jr., J.T. (Eds.), The Parathyroids, third ed. Elsevier, San Diego, pp. 153–164.

Friedman, P.A., Coutermarsh, B.A., Kennedy, S.M., Gesek, F.A., 1996. Parathyroid hormone stimulation of calcium transport is mediated by dual signaling mechanisms involving PKA and PKC. Endocrinology 137, 13–20.

Friedman, P.A., Coutermarsh, B.A., Kennedy, S.M., Pizzonia, J.H., 1989. Differential stimulation of cAMP formation in renal distal convoluted tubule and cortical thick ascending limb cells by PTH and by PTH-like peptides. J. Bone Miner. Res. 4, S346.

Friedman, P.A., Gesek, F.A., 1993. Calcium transport in renal epithelial cells. Am. J. Physiol. Renal. Physiol. 264, F181–F198.

Friedman, P.A., Gesek, F.A., 1995. Stimulation of calcium transport by amiloride in mouse distal convoluted tubule cells. Kidney Int. 48, 1427–1434.
Friedman, P.A., Gesek, F.A., Coutermarsh, B.A., Kennedy, S.M., 1994. PKA and PKC activation is required for PTH-stimulated calcium uptake by distal convoluted tubule cells. J. Am. Soc. Nephrol. 5, 715.
Friedman, P.A., Gesek, F.A., Morley, P., Whitfield, J.F., Willick, G.E., 1999. Cell-specific signaling and structure-activity relations of parathyroid hormone analogs in mouse kidney cells. Endocrinology 140, 301–309.
Friedman, P.A., Torretti, J., 1978. Regional glucose metabolism in the cat kidney in vivo. Am. J. Physiol. Renal. Physiol. 234, F415–F423.
Fujita, T., Meguro, T., Fukuyama, R., Nakamuta, H., Koida, M., 2002. New signaling pathway for parathyroid hormone and cyclic AMP action on extracellular-regulated kinase and cell proliferation in bone cells. Checkpoint of modulation by cyclic AMP. J. Biol. Chem. 277, 22191–22200.
Fuller, K., Wong, B., Fox, S., Choi, Y., Chambers, T.J., 1998. TRANCE is necessary and sufficient for osteoblast-mediated activation of bone resorption in osteoclasts. J. Exp. Med. 188, 997–1001.
Funk, J.L., 2001. A role for parathyroid hormone-related protein in the pathogenesis of inflammatory/autoimmune diseases. Int. Immunopharmacol. 1, 1101–1121.
Gaich, G., Orloff, J.J., Atillasoy, E.J., Burtis, W.J., Ganz, M.B., Stewart, A.F., 1993. Amino-terminal parathyroid hormone-related protein: specific binding and cytosolic calcium responses in rat insulinoma cells. Endocrinology 132, 1402–1409.
García-Ocaña, A., Galbraith, S.C., Van Why, S.K., Yang, K., Golovyan, L., Dann, P., Zager, R.A., Stewart, A.F., Siegel, N.J., Orloff, J.J., 1999. Expression and role of parathyroid hormone-related protein in human renal proximal tubule cells during recovery from ATP depletion. J. Am. Soc. Nephrol. 10, 238–244.
Gardella, T.J., Vilardaga, J.-P., 2015. International Union of Basic and Clinical Pharmacology. XCIII. The parathyroid hormone receptors—family B G Protein–coupled receptors. Pharmacol. Rev. 67, 310–337.
Garrido, J.L., Wheeler, D., Vega, L.L., Friedman, P.A., Romero, G., 2009. Role of phospholipase D in parathyroid hormone receptor type 1 signaling and trafficking. Mol. Endocrinol. 23, 2048–2059.
Geoffroy, V., Marty-Morieux, C., Le Goupil, N., Clement-Lacroix, P., Terraz, C., Frain, M., Roux, S., Rossert, J., de Vernejoul, M.C., 2004. In vivo inhibition of osteoblastic metalloproteinases leads to increased trabecular bone mass. J. Bone Miner. Res. 19, 811–822.
Gesek, F.A., Friedman, P.A., 1992. Mechanism of calcium transport stimulated by chlorothiazide in mouse distal convoluted tubule cells. J. Clin. Investig. 90, 429–438.
Gesek, F.A., White, K.E., 1997. Molecular and functional identification of β-adrenergic receptors in distal convoluted tubule cells. Am. J. Physiol. Renal. Physiol. 272, F712–F720.
Gill Jr., J.R., Bartter, F.C., 1961. On the impairment of renal concentrating ability in prolonged hypercalcemia and hypercalciuria in man. J. Clin. Investig. 40, 716–722.
Gitelman, H.J., Graham, J.B., Welt, L.G., 1966. A new familial disorder characterized by hypokalemia and hypomagnesemia. Trans. Assoc. Am. Phys. 79, 221–235.
Gley, E., 1893. Glande et glandules thyroides du chien. C. R. Seances Soc. Biol. Fil. 45, 217–219.
Gmaj, P., Murer, H., 1986. Cellular mechanisms of inorganic phosphate transport in kidney. Physiol. Rev. 66, 36–70.
Goltzman, D., Mitchell, J., 1985. Interaction of calcitonin and calcitonin gene-related peptide at receptor sites in target tissues. Science 227, 1343–1345.
Greenwald, I., Gross, J.B., 1925. The effect of the administration of a potent parathyroid extract upon the excretion of nitrogen, phosphorus, calcium, and magnesium, with some remarks on the solubility of calcium phosphate in serum and on the pathogenesis of tetany. J. Biol. Chem. 66, 217–227.
Grey, A., Chen, Q., Xu, X., Callon, K., Cornish, J., 2003. Parallel phosphatidylinositol-3 kinase and p42/44 mitogen-activated protein kinase signaling pathways subserve the mitogenic and antiapoptotic actions of insulin-like growth factor I in osteoblastic cells. Endocrinology 144, 4886–4893.
Grey, A., Mitnick, M.A., Masiukiewicz, U., Sun, B.H., Rudikoff, S., Jilka, R.L., Manolagas, S.C., Insogna, K., 1999. A role for interleukin-6 in parathyroid hormone-induced bone resorption in vivo. Endocrinology 140, 4683–4690.
Gronthos, S., Zannettino, A.C., Graves, S.E., Ohta, S., Hay, S.J., Simmons, P.J., 1999. Differential cell surface expression of the STRO-1 and alkaline phosphatase antigens on discrete developmental stages in primary cultures of human bone cells. J. Bone Miner. Res. 14, 47–56.
Gundberg, C.M., Fawzi, M.I., Clough, M.E., Calvo, M.S., 1995. A comparison of the effects of parathyroid hormone and parathyroid hormone-related protein on osteocalcin in the rat. J. Bone Miner. Res. 10, 903–909.
Guo, J., Song, L., Liu, M., Segawa, H., Miyamoto, K.I., Bringhurst, F.R., Kronenberg, H.M., Juppner, H., 2013. Activation of a non-cAMP/PKA signaling pathway downstream of the PTH/PTHrP receptor is essential for a sustained hypophosphatemic response to PTH infusion in male mice. Endocrinology 154, 1680–1689.
Hackett, D.A., Kauffman Jr., G.L., 2004. Historical perspective of parathyroid disease. Otolaryngol. Clin. 37, 689–700.
Hamm, L.L., Alpern, R.J., Preisig, P.A., 2008. Cellular mechanisms of renal tubular acidification. In: Alpern, R.J., Hebert, S.C. (Eds.), Seldin and Giebisch's the Kindey. Physiology and Pathophysiology. Academic Press, San Diego, pp. 1539–1585.
Hammerman, M.R., 1986. Phosphate transport across renal proximal tubular cell membranes. Am. J. Physiol. Renal. Physiol. 251, F385–F398.
Harris, C.A., Baer, P.G., Chirito, E., Dirks, J.H., 1974. Composition of mammalian glomerular filtrate. Am. J. Physiol. 227, 972–976.
Harris, C.A., Burnatowska, M.A., Seely, J.F., Sutton, R.A.L., Quamme, G.A., Dirks, J.H., 1979. Effects of parathyroid hormone on electrolyte transport in the hamster nephron. Am. J. Physiol. Renal. Physiol. 236, F342–F348.
Hellman, D.E., Au, W.Y., Bartter, F.C., 1965. Evidence for a direct effect of parathyroid hormone on urinary acidification. Am. J. Physiol. 209, 643–650.
Helwig, J.-J., Musso, M.-J., Judes, C., Nickols, G.A., 1991. Parathyroid hormone and calcium: interactions in the control of renin secretion in the isolated, nonfiltering rat kidney. Endocrinology 129, 1233–1242.

Henry, H.L., 1985. Parathyroid hormone modulation of 25-hydroxyvitamin D_3 metabolism by cultured chick kidney cells is mimicked and enhanced by forskolin. Endocrinology 116, 503–510.

Hering, S., Isken, E., Knabbe, C., Janott, J., Jost, C., Pommer, A., Muhr, G., Schatz, H., Pfeiffer, A.F., 2001. TGFβ1 and TGFβ2 mRNA and protein expression in human bone samples. Exp. Clin. Endocrinol. Diabetes 109, 217–226.

Hernando, N., Deliot, N., Gisler, S.M., Lederer, E., Weinman, E.J., Biber, J., Murer, H., 2002. PDZ-domain interactions and apical expression of type IIa Na/P_i cotransporters. Proc. Natl. Acad. Sci. U. S. A. 99, 11957–11962.

Hicok, K.C., Thomas, T., Gori, F., Rickard, D.J., Spelsberg, T.C., Riggs, B.L., 1998. Development and characterization of conditionally immortalized osteoblast precursor cell lines from human bone marrow stroma. J. Bone Miner. Res. 13, 205–217.

Hilfiker, H., Hattenhauer, O., Traebert, M., Forster, I., Murer, H., Biber, J., 1998. Characterization of a murine type II sodium-phosphate cotransporter expressed in mammalian small intestine. Proc. Natl. Acad. Sci. U. S. A. 95, 14564–14569.

Hilpert, J., Nykjaer, A., Jacobsen, C., Wallukat, G., Nielsen, R., Moestrup, S.K., Haller, H., Luft, F.C., Christensen, E.I., Willnow, T.E., 1999. Megalin antagonizes activation of the parathyroid hormone receptor. J. Biol. Chem. 274, 5620–5625.

Hock, J.M., Canalis, E., Centrella, M., 1990. Transforming growth factor-β stimulates bone matrix apposition and bone cell replication in cultured fetal rat calvariae. Endocrinology 126, 421–426.

Hodsman, A.B., Steer, B.M., 1993. Early histomorphometric changes in response to parathyroid hormone therapy in osteoporosis: evidence for de novo bone formation on quiescent cancellous surfaces. Bone 14, 523–527.

Hoenderop, J.G., De Pont, J.J., Bindels, R.J., Willems, P.H., 1999. Hormone-stimulated Ca^{2+} reabsorption in rabbit kidney cortical collecting system is cAMP-independent and involves a phorbol ester-insensitive PKC isotype. Kidney Int. 55, 225–233.

Hofbauer, L.C., Khosla, S., Dunstan, C.R., Lacey, D.L., Boyle, W.J., Riggs, B.L., 2000. The roles of osteoprotegerin and osteoprotegerin ligand in the paracrine regulation of bone resorption. J. Bone Miner. Res. 15, 2–12.

Hoover, R.S., Tomilin, V., Hanson, L.N., Pochynyuk, O., Ko, B., 2015. PTH modulation of NCC activity regulates TRPV5 calcium reabsorption. Am. J. Physiol. Renal. Physiol. 310, F144–F151.

Hopkins, T., Howard, J.E., Eisenberg, H., 1952. Ultrafiltration studies on calcium and phosphorous in human serum. Bull. Johns Hopkins Hosp. 91, 1–21.

Horiuchi, N., Caulfield, M.P., Fisher, J.E., Goldman, M.E., McKee, R.L., Reagan, J.E., Levy, J.J., Nutt, R.F., Rodan, S.B., Schofield, T.L., 1987. Similarity of synthetic peptide from human tumor to parathyroid hormone in vivo and in vitro. Science 238, 1566–1568.

Horiuchi, N., Suda, T., Takahashi, H., Shimazawa, E., Ogata, E., 1977. In vivo evidence for the intermediary role of 3',5'-cyclic AMP in parathyroid hormone-induced stimulation of 1α,25-dihydroxyvitamin D_3 synthesis in rats. Endocrinology 101, 969–974.

Horowitz, M.C., Coleman, D.L., Flood, P.M., Kupper, T.S., Jilka, R.L., 1989. Parathyroid hormone and lipopolysaccharide induce murine osteoblast-like cells to secrete a cytokine indistinguishable from granulocyte-macrophage colony-stimulating factor. J. Clin. Investig. 83, 149–157.

Horwitz, M.J., Tedesco, M.B., Gundberg, C., Garcia-Ocana, A., Stewart, A.F., 2003a. Short-term, high-dose parathyroid hormone-related protein as a skeletal anabolic agent for the treatment of postmenopausal osteoporosis. J. Clin. Endocrinol. Metab. 88, 569–575.

Horwitz, M.J., Tedesco, M.B., Sereika, S.M., Garcia-Ocana, A., Bisello, A., Hollis, B.W., Gundberg, C., Stewart, A.F., 2006. Safety and tolerability of subcutaneous PTHrP(1-36) in healthy human volunteers: a dose escalation study. Osteoporos. Int. 17, 225–230.

Horwitz, M.J., Tedesco, M.B., Sereika, S.M., Hollis, B.W., Garcia-Ocana, A., Stewart, A.F., 2003b. Direct comparison of sustained infusion of human parathyroid hormone-related protein-(1-36) [hPTHrP-(1-36)] versus hPTH-(1-34) on serum calcium, plasma 1,25-dihydroxyvitamin D concentrations, and fractional calcium excretion in healthy human volunteers. J. Clin. Endocrinol. Metab. 88, 1603–1609.

Horwitz, M.J., Tedesco, M.B., Sereika, S.M., Syed, M.A., Garcia-Ocana, A., Bisello, A., Hollis, B.W., Rosen, C.J., Wysolmerski, J.J., Dann, P., Gundberg, C., Stewart, A.F., 2005. Continuous PTH and PTHrP infusion causes suppression of bone formation and discordant effects on 1,25(OH)2 vitamin D. J. Bone Miner. Res. 20, 1792–1803.

Houillier, P., 2014. Mechanisms and regulation of renal magnesium transport. Annu. Rev. Physiol. 76, 411–430.

Hruska, K.A., Goligorsky, M.S., Scoble, J., Tsutsumi, M., Westbrook, S., Moskowitz, D., 1986. Effects of parathyroid hormone on cytosolic calcium in renal proximal tubular primary cultures. Am. J. Physiol. Renal. Physiol. 251, F188–F198.

Hruska, K.A., Moskowitz, D., Esbrit, P., Civitelli, R., Westbrook, S., Huskey, M., 1987. Stimulation of inositol trisphosphate and diacylglycerol production in renal tubular cells by parathyroid hormone. J. Clin. Investig. 79, 230–239.

Hu, M.C., Shiizaki, K., Kuro, O.M., Moe, O.W., 2013. Fibroblast growth factor 23 and klotho: physiology and pathophysiology of an endocrine network of mineral metabolism. Annu. Rev. Physiol. 75, 503–533.

Huang, J.C., Sakata, T., Pfleger, L.L., Bencsik, M., Halloran, B.P., Bikle, D.D., Nissenson, R.A., 2004. PTH differentially regulates expression of RANKL and OPG. J. Bone Miner. Res. 19, 235–244.

Huang, Z., Chen, Y., Nissenson, R.A., 1995. The cytoplasmic tail of the G-protein-coupled receptor for parathyroid hormone and parathyroid hormone-related protein contains positive and negative signals for endocytosis. J. Biol. Chem. 270, 151–156.

Hulter, H.N., 1985. Effects and interrelationships of PTH, Ca^{2+}, vitamin D, and Pi in acid-base homeostasis. Am. J. Physiol. Renal. Physiol. 248, F739–F752.

Hulter, H.N., Peterson, J.C., 1985. Acid-base homeostasis during chronic PTH excess in humans. Kidney Int. 28, 187–192.

Hurley, M.M., Okada, Y., Xiao, L., Tanaka, Y., Ito, M., Okimoto, N., Nakamura, T., Rosen, C.J., Doetschman, T., Coffin, J.D., 2006. Impaired bone anabolic response to parathyroid hormone in Fgf2-/- and Fgf2+/- mice. Biochem. Biophys. Res. Commun. 341, 989–994.

Hurley, M.M., Tetradis, S., Huang, Y.F., Hock, J., Kream, B.E., Raisz, L.G., Sabbieti, M.G., 1999. Parathyroid hormone regulates the expression of fibroblast growth factor-2 mRNA and fibroblast growth factor receptor mRNA in osteoblastic cells. J. Bone Miner. Res. 14, 776–783.

Inda, C., Dos Santos Claro, P.A., Bonfiglio, J.J., Senin, S.A., Maccarrone, G., Turck, C.W., Silberstein, S., 2016. Different cAMP sources are critically involved in G protein-coupled receptor CRHR1 signaling. J. Cell Biol. 214, 181–195.

Inomata, N., Akiyama, M., Kubota, N., Juppner, H., 1995. Characterization of a novel parathyroid hormone (PTH) receptor with specificity for the carboxyl-terminal region of PTH-(1-84). Endocrinology 136, 4732–4740.

Ishizuya, T., Yokose, S., Hori, M., Noda, T., Suda, T., Yoshiki, S., Yamaguchi, A., 1997. Parathyroid hormone exerts disparate effects on osteoblast differentiation depending on exposure time in rat osteoblastic cells. J. Clin. Investig. 99, 2961–2970.

Izquierdo, A., Lopez-Luna, P., Ortega, A., Romero, M., Guitierrez-Tarres, M.A., Arribas, I., Alvarez, M.J., Esbrit, P., Bosch, R.J., 2006. The parathyroid hormone-related protein system and diabetic nephropathy outcome in streptozotocin-induced diabetes. Kidney Int. 69, 2171–2177.

Janulis, M., Tembe, V., Favus, M.J., 1992. Role of PKC in parathyroid hormone stimulation of renal 1,25-dihydroxyvitamin D_3 secretion. J. Clin. Investig. 90, 2278–2283.

Janulis, M., Wong, M.S., Favus, M.J., 1993. Structure-function requirements of parathyroid hormone for stimulation of 1,25-dihydroxyvitamin D_3 production by rat renal proximal tubules. Endocrinology 133, 713–719.

Jespersen, B., Randlov, A., Abrahamsen, J., Fogh-Andersen, N., Kanstrup, I.L., 1997. Effects of PTH(1-34) on blood pressure, renal function, and hormones in essential hypertension: the altered pattern of reactivity may counteract raised blood pressure. Am. J. Hypertens. 10, 1356–1367.

Jilka, R.L., Weinstein, R.S., Bellido, T., Parfitt, A.M., Manolagas, S.C., 1998. Osteoblast programmed cell death (apoptosis): modulation by growth factors and cytokines. J. Bone Miner. Res. 13, 793–802.

Jilka, R.L., Weinstein, R.S., Bellido, T., Roberson, P., Parfitt, A.M., Manolagas, S.C., 1999. Increased bone formation by prevention of osteoblast apoptosis with parathyroid hormone. J. Clin. Investig. 104, 439–446.

Jobert, A.S., Fernandes, I., Turner, G., Coureau, C., Prie, D., Nissenson, R.A., Friedlander, G., Silve, C., 1996. Expression of alternatively spliced isoforms of the parathyroid hormone (PTH)/PTH-related peptide receptor messenger RNA in human kidney and bone cells. Mol. Endocrinol. 10, 1066–1076.

Jongen, J.W., Bos, M.P., van der Meer, J.M., Herrmann-Erlee, M.P., 1993. Parathyroid hormone-induced changes in alkaline phosphatase expression in fetal calvarial osteoblasts: differences between rat and mouse. J. Cell. Physiol. 155, 36–43.

Joun, H., Lanske, B., Karperien, M., Qian, F., Defize, L., Abou-Samra, A., 1997. Tissue-specific transcription start sites and alternative splicing of the parathyroid hormone (PTH)/PTH-related peptide (PTHrP) receptor gene: a new PTH/PTHrP receptor splice variant that lacks the signal peptide. Endocrinology 138, 1742–1749.

Juppner, H., Abou-Samra, A.B., Freeman, M., Kong, X.F., Schipani, E., Richards, J., Kolakowski Jr., L.F., Hock, J., Potts Jr., J.T., Kronenberg, H.M., et al., 1991. A G protein-linked receptor for parathyroid hormone and parathyroid hormone-related peptide. Science 254, 1024–1026.

Kano, J., Sugimoto, T., Fukase, M., Chihara, K., 1994. Direct involvement of cAMP-dependent protein kinase in the regulation of alkaline phosphatase activity by parathyroid hormone (PTH) and PTH-related peptide in osteoblastic UMR-106 cells. Biochem. Biophys. Res. Commun. 199, 271–276.

Kano, J., Sugimoto, T., Fukase, M., Fujita, T., 1991. The activation of cAMP-dependent protein kinase is directly linked to the inhibition of osteoblast proliferation (UMR-106) by parathyroid hormone-related protein. Biochem. Biophys. Res. Commun. 179, 97–101.

Karim, Z., Gerard, B., Bakouh, N., Alili, R., Leroy, C., Beck, L., Silve, C., Planelles, G., Urena-Torres, P., Grandchamp, B., Friedlander, G., Prie, D., 2008. NHERF1 mutations and responsiveness of renal parathyroid hormone. N. Engl. J. Med. 359, 1128–1135.

Karmali, R., Schiffmann, S.N., Vanderwinden, J.M., Hendy, G.N., Nys-DeWolf, N., Corvilain, J., Bergmann, P., Vanderhaeghen, J.J., 1992. Expression of mRNA of parathyroid hormone-related peptide in fetal bones of the rat. Cell Tissue Res. 270, 597–600.

Kartsogiannis, V., Moseley, J., McKelvie, B., Chou, S.T., Hards, D.K., Ng, K.W., Martin, T.J., Zhou, H., 1997. Temporal expression of PTHrP during endochondral bone formation in mouse and intramembranous bone formation in an in vivo rabbit model. Bone 21, 385–392.

Kau, S.T., Maack, T., 1977. Transport and catabolism of parathyroid hormone in isolated rat kidney. Am. J. Physiol. Renal. Physiol. 233, F445–F454.

Kaufmann, M., Muff, R., Stieger, B., Biber, J., Murer, H., Fischer, J.A., 1994. Apical and basolateral parathyroid hormone receptors in rat renal cortical membranes. Endocrinology 134, 1173–1178.

Kavanaugh, M.P., Kabat, D., 1996. Identification and characterization of a widely expressed phosphate transporter/retrovirus receptor family. Kidney Int. 49, 959–963.

Kempson, S.A., Lötscher, M., Kaissling, B., Biber, J., Murer, H., Levi, M., 1995. Parathyroid hormone action on phosphate transporter mRNA and protein in rat renal proximal tubules. Am. J. Physiol. Renal. Physiol. 268, F784–F791.

Keusch, I., Traebert, M., Lotscher, M., Kaissling, B., Murer, H., Biber, J., 1998. Parathyroid hormone and dietary phosphate provoke a lysosomal routing of the proximal tubular Na/Pi-cotransporter type II. Kidney Int. 54, 1224–1232.

Khosla, S., Westendorf, J.J., Oursler, M.J., 2008. Building bone to reverse osteoporosis and repair fractures. J. Clin. Investig. 118, 421–428.

Kilav, R., Silver, J., Biber, J., Murer, H., Naveh-Many, T., 1995a. Coordinate regulation of rat renal parathyroid hormone receptor mRNA and Na-Pi cotransporter mRNA and protein. Am. J. Physiol. Renal. Physiol. 268, F1017–F1022.

Kilav, R., Silver, J., Naveh-Many, T., 1995b. Parathyroid hormone gene expression in hypophosphatemic rats. J. Clin. Investig. 96, 327–333.

Kitazawa, R., Imai, Y., Fukase, M., Fujita, T., 1991. Effects of continuous infusion of parathyroid hormone and parathyroid hormone-related peptide on rat bone in vivo: comparative study by histomorphometry. Bone Miner. 12, 157–166.

Kleeman, C.R., Cooke, R.E., 1951. The acute effects of parathyroid hormone on the metabolism of endogenous phosphate. J. Lab. Clin. Med. 38, 112–127.

Ko, B., 2017. Parathyroid hormone and the regulation of renal tubular calcium transport. Curr. Opin. Nephrol. Hypertens. 26, 405–410.

Ko, B., Cooke, L.L., Hoover, R.S., 2011. Parathyroid hormone (PTH) regulates the sodium chloride cotransporter via Ras guanyl releasing protein 1 (Ras-GRP1) and extracellular signal-regulated kinase (ERK)1/2 mitogen-activated protein kinase (MAPK) pathway. Transl. Res. 158, 282–289.

Komori, T., 2002. Runx2, a multifunctional transcription factor in skeletal development. J. Cell. Biochem. 87, 1–8.

Komori, T., Yagi, H., Nomura, S., Yamaguchi, A., Sasaki, K., Deguchi, K., Shimizu, Y., Bronson, R.T., Gao, Y.H., Inada, M., Sato, M., Okamoto, R., Kitamura, Y., Yoshiki, S., Kishimoto, T., 1997. Targeted disruption of Cbfa1 results in a complete lack of bone formation owing to maturational arrest of osteoblasts. Cell 89, 755–764.

Kondo, H., Guo, J., Bringhurst, F.R., 2002. Cyclic adenosine monophosphate/protein kinase A mediates parathyroid hormone/parathyroid hormone-related protein receptor regulation of osteoclastogenesis and expression of RANKL and osteoprotegerin mRNAs by marrow stromal cells. J. Bone Miner. Res. 17, 1667–1679.

Korkor, A.B., Gray, R.W., Henry, H.L., Kleinman, J.G., Blumenthal, S.S., Garancis, J.C., 1987. Evidence that stimulation of $1,25(OH)_2D_3$ production in primary cultures of mouse kidney cells by cyclic AMP requires new protein synthesis. J. Bone Miner. Res. 2, 517–524.

Kostenuik, P.J., Harris, J., Halloran, B.P., Turner, R.T., Morey-Holton, E.R., Bikle, D.D., 1999. Skeletal unloading causes resistance of osteoprogenitor cells to parathyroid hormone and to insulin-like growth factor-I. J. Bone Miner. Res. 14, 21–31.

Kovacs, C.S., Lanske, B., Hunzelman, J.L., Guo, J., Karaplis, A.C., Kronenberg, H.M., 1996. Parathyroid hormone-related peptide (PTHrP) regulates fetal-placental calcium transport through a receptor distinct from the PTH/PTHrP receptor. Proc. Natl. Acad. Sci. U. S. A. 93, 15233–15238.

Kream, B.E., Rowe, D., Smith, M.D., Maher, V., Majeska, R., 1986. Hormonal regulation of collagen synthesis in a clonal rat osteosarcoma cell line. Endocrinology 119, 1922–1928.

Kream, B.E., Rowe, D.W., Gworek, S.C., Raisz, L.G., 1980. Parathyroid hormone alters collagen synthesis and procollagen mRNA levels in fetal rat calvaria. Proc. Natl. Acad. Sci. U. S. A. 77, 5654–5658.

Krishnan, V., Moore, T.L., Ma, Y.L., Helvering, L.M., Frolik, C.A., Valasek, K.M., Ducy, P., Geiser, A.G., 2003. Parathyroid hormone bone anabolic action requires Cbfa1/Runx2-dependent signaling. Mol. Endocrinol. 17, 423–435.

Kulkarni, N.H., Halladay, D.L., Miles, R.R., Gilbert, L.M., Frolik, C.A., Galvin, R.J., Martin, T.J., Gillespie, M.T., Onyia, J.E., 2005. Effects of parathyroid hormone on Wnt signaling pathway in bone. J. Cell. Biochem. 95, 1178–1190.

Kuna, R.S., Girada, S.B., Asalla, S., Vallentyne, J., Maddika, S., Patterson, J.T., Smiley, D.L., DiMarchi, R.D., Mitra, P., 2013. Glucagon-like peptide-1 receptor-mediated endosomal cAMP generation promotes glucose-stimulated insulin secretion in pancreatic β-cells. Am. J. Physiol. Endocrinol. Metab. 305, E161–E170.

Lacey, D.L., Timms, E., Tan, H.L., Kelley, M.J., Dunstan, C.R., Burgess, T., Elliott, R., Colombero, A., Elliott, G., Scully, S., Hsu, H., Sullivan, J., Hawkins, N., Davy, E., Capparelli, C., Eli, A., Qian, Y.X., Kaufman, S., Sarosi, I., Shalhoub, V., Senaldi, G., Guo, J., Delaney, J., Boyle, W.J., 1998. Osteoprotegerin ligand is a cytokine that regulates osteoclast differentiation and activation. Cell 93, 165–176.

Lammi, J., Huppunen, J., Aarnisalo, P., 2004. Regulation of the osteopontin gene by the orphan nuclear receptor NURR1 in osteoblasts. Mol. Endocrinol. 18, 1546–1557.

Langub, M.C., Monier-Faugere, M.C., Qi, Q., Geng, Z., Koszewski, N.J., Malluche, H.H., 2001. Parathyroid hormone/parathyroid hormone-related peptide type 1 receptor in human bone. J. Bone Miner. Res. 16, 448–456.

Largo, R., Gomez-Garre, D., Santos, S., Penaranda, C., Blanco, J., Esbrit, P., Egido, J., 1999. Renal expression of parathyroid hormone-related protein (PTHrP) and PTH/PTHrP receptor in a rat model of tubulointerstitial damage. Kidney Int. 55, 82–90.

Larkins, R.G., MacAuley, S.J., Rapoport, A., Martin, T.J., Tulloch, B.R., Byfield, P.G., Matthews, E.W., MacIntyre, I., 1974. Effects of nucleotides, hormones, ions, and 1,25-dihydroxycholecalciferon on 1,25-dihydroxycholecalciferol production in isolated chick renal tubules. Clin. Sci. Mol. Med. 46, 569–582.

LaTour, D., Mohan, S., Linkhart, T.A., Baylink, D.J., Strong, D.D., 1990. Inhibitory insulin-like growth factor-binding protein: cloning, complete sequence, and physiological regulation. Mol. Endocrinol. 4, 1806–1814.

Law, F., Bonjour, J.P., Rizzoli, R., 1994. Transforming growth factor-beta: a down-regulator of the parathyroid hormone-related protein receptor in renal epithelial cells. Endocrinology 134, 2037–2043.

Le Grimellec, C., Roinel, N., Morel, F., 1974. Simultaneous Mg, Ca, P, K, Na and Cl analysis in rat tubular fluid. III. During acute Ca plasma loading. Pflügers Archiv 346, 171–188.

Leder, B.Z., O'Dea, L.S., Zanchetta, J.R., Kumar, P., Banks, K., McKay, K., Lyttle, C.R., Hattersley, G., 2015. Effects of abaloparatide, a human parathyroid hormone-related peptide analog, on bone mineral density in postmenopausal women with osteoporosis. J. Clin. Endocrinol. Metab. 100, 697–706.

Lee, J.J., Plain, A., Beggs, M.R., Dimke, H., Alexander, R.T., 2017. Effects of phospho- and calciotropic hormones on electrolyte transport in the proximal tubule. F1000Res 6, 1797.

Lee, K., Deeds, J.D., Bond, A.T., Juppner, H., Abou-Samra, A.B., Segre, G.V., 1993. In situ localization of PTH/PTHrP receptor mRNA in the bone of fetal and young rats. Bone 14, 341–345.

Lee, K., Deeds, J.D., Chiba, S., Un-No, M., Bond, A.T., Segre, G.V., 1994. Parathyroid hormone induces sequential c-fos expression in bone cells in vivo: in situ localization of its receptor and c-fos messenger ribonucleic acids. Endocrinology 134, 441–450.

Lee, K., Deeds, J.D., Segre, G.V., 1995. Expression of parathyroid hormone-related peptide and its receptor messenger ribonucleic acids during fetal development of rats. Endocrinology 136, 453–463.

Lee, S.K., Lorenzo, J.A., 1999. Parathyroid hormone stimulates TRANCE and inhibits osteoprotegerin messenger ribonucleic acid expression in murine bone marrow cultures: correlation with osteoclast-like cell formation. Endocrinology 140, 3552–3561.

Li, X., Zhang, Y., Kang, H., Liu, W., Liu, P., Zhang, J., Harris, S.E., Wu, D., 2005. Sclerostin binds to LRP5/6 and antagonizes canonical Wnt signaling. J. Biol. Chem. 280, 19883–19887.

Liang, J.D., Hock, J.M., Sandusky, G.E., Santerre, R.F., Onyia, J.E., 1999. Immunohistochemical localization of selected early response genes expressed in trabecular bone of young rats given hPTH 1-34. Calcif. Tissue Int. 65, 369–373.

Lindsay, R., Zhou, H., Cosman, F., Nieves, J., Dempster, D.W., Hodsman, A.B., 2007. Effects of a one-month treatment with PTH(1-34) on bone formation on cancellous, endocortical, and periosteal surfaces of the human ilium. J. Bone Miner. Res. 22, 495–502.

Ling, L., Murali, S., Dombrowski, C., Haupt, L.M., Stein, G.S., van Wijnen, A.J., Nurcombe, V., Cool, S.M., 2006. Sulfated glycosaminoglycans mediate the effects of FGF2 on the osteogenic potential of rat calvarial osteoprogenitor cells. J. Cell. Physiol. 209, 811–825.

Linkhart, T.A., Mohan, S., 1989. Parathyroid hormone stimulates release of insulin-like growth factor-I (IGF-I) and IGF-II from neonatal mouse calvaria in organ culture. Endocrinology 125, 1484–1491.

Liu, L., Alonso, V., Guo, L., Tourkova, I., Henderson, S.E., Almarza, A.J., Friedman, P.A., Blair, H.C., 2012. Na+/H+ exchanger regulatory factor 1 (NHERF1) directly regulates osteogenesis. J. Biol. Chem. 287, 43312–43321.

Llach, F., Massry, S.G., 1985. On the mechanism of secondary hyperparathyroidism in moderate renal insufficiency. J. Clin. Endocrinol. Metab. 61, 601–606.

Locklin, R.M., Khosla, S., Turner, R.T., Riggs, B.L., 2003. Mediators of the biphasic responses of bone to intermittent and continuously administered parathyroid hormone. J. Cell. Biochem. 89, 180–190.

Loeb, R.F., 1926. The effect of pure protein solutions and of blood serum on the diffusibility of calcium. J. Gen. Physiol. 8, 451–461.

Lötscher, M., Scarpetta, Y., Levi, M., Halaihel, N., Wang, H.M., Zajicek, H.K., Biber, J., Murer, H., Kaissling, B., 1999. Rapid downregulation of rat renal Na/P_i cotransporter in response to parathyroid hormone involves microtubule rearrangement. J. Clin. Investig. 104, 483–494.

Ma, Y.L., Cain, R.L., Halladay, D.L., Yang, X., Zeng, Q., Miles, R.R., Chandrasekhar, S., Martin, T.J., Onyia, J.E., 2001. Catabolic effects of continuous human PTH (1–38) in vivo is associated with sustained stimulation of RANKL and inhibition of osteoprotegerin and gene-associated bone formation. Endocrinology 142, 4047–4054.

Madjdpour, C., Bacic, D., Kaissling, B., Murer, H., Biber, J., 2004. Segment-specific expression of sodium-phosphate cotransporters NaPi-IIa and -IIc and interacting proteins in mouse renal proximal tubules. Pflügers Archiv 448, 402–410.

Magyar, C.E., White, K.E., Rojas, R., Apodaca, G., Friedman, P.A., 2002. Plasma membrane Ca^{2+}-ATPase and NCX1 Na^+/Ca^{2+} exchanger expression in distal convoluted tubule cells. Am. J. Physiol. Renal. Physiol. 283, F29–F40.

Mahon, M.J., 2012. The parathyroid hormone receptorsome and the potential for therapeutic intervention. Curr. Drug Targets 13, 116–128.

Mahon, M.J., Cole, J.A., Lederer, E.D., Segre, G.V., 2003. Na^+/H^+ exchanger-regulatory factor 1 mediates Inhibition of phosphate transport by parathyroid hormone and second messengers by acting at multiple sites in opossum kidney cells. Mol. Endocrinol. 17, 2355–2364.

Mahon, M.J., Donowitz, M., Yun, C.C., Segre, G.V., 2002. Na^+/H^+ exchanger regulatory factor 2 directs parathyroid hormone 1 receptor signalling. Nature 417, 858–861.

Mahon, M.J., Segre, G.V., 2004. Stimulation by parathyroid hormone of a NHERF-1-assembled complex consisting of the parathyroid hormone I receptor, PLCß, and actin increases intracellular calcium in opossum kidney cells. J. Biol. Chem. 279, 23550–23558.

Maiti, A., Beckman, M.J., 2007. Extracellular calcium is a direct effecter of VDR levels in proximal tubule epithelial cells that counter-balances effects of PTH on renal Vitamin D metabolism. J. Steroid Biochem. Mol. Biol. 103, 504–508.

Maiti, A., Hait, N.C., Beckman, M.J., 2008. Extracellular calcium sensing receptor activation induces vitamin D receptor levels in proximal kidney HK-2G cells by a mechanism that requires phosphorylation of p38α MAPK. J. Biol. Chem. 283, 175–183.

Majeska, R.J., Rodan, G.A., 1982. Alkaline phosphatase inhibition by parathyroid hormone and isoproterenol in a clonal rat osteosarcoma cell line. Possible mediation by cyclic AMP. Calcif. Tissue Int. 34, 59–66.

Malecz, N., Bambino, T., Bencsik, M., Nissenson, R.A., 1998. Identification of phosphorylation sites in the G protein-coupled receptor for parathyroid hormone. Receptor phosphorylation is not required for agonist-induced internalization. Mol. Endocrinol. 12, 1846–1856.

Malmström, K., Murer, H., 1987. Parathyroid hormone regulates phosphate transport in OK cells via an irreversible inactivation of a membrane protein. FEBS Lett. 216, 257–260.

Mandel, L.J., Derrickson, B.H., 1997. Parathyroid hormone inhibits Na^+-K^+ ATPase through G_q/G_{11} and the calcium-independent phospholipase A_2. Am. J. Physiol. Renal. Physiol. 272, F781–F788.

Marone, C.C., Wong, N.L., Sutton, R.A., Dirks, J.H., 1983. Effects of metabolic alkalosis on calcium excretion in the conscious dog. J. Lab. Clin. Med. 101, 264–273.

Martinez, M.E., Garcia-Ocana, A., Sanchez, M., Medina, S., del Campo, T., Valin, A., Sanchez-Cabezudo, M.J., Esbrit, P., 1997. C-terminal parathyroid hormone-related protein inhibits proliferation and differentiation of human osteoblast-like cells. J. Bone Miner. Res. 12, 778–785.

Massfelder, T., Fiaschi-Taesch, N., Stewart, A.F., Helwig, J.J., 1998. Parathyroid hormone-related peptide–a smooth muscle tone and proliferation regulatory protein. Curr. Opin. Nephrol. Hypertens. 7, 27–32.

Massfelder, T., Helwig, J.J., 1999. Parathyroid hormone-related protein in cardiovascular development and blood pressure regulation. Endocrinology 140, 1507–1510.

Massfelder, T., Stewart, A.F., Endlich, K., Soifer, N., Judes, C., Helwig, J.J., 1996. Parathyroid hormone-related protein detection and interaction with NO and cyclic AMP in the renovascular system. Kidney Int. 50, 1591–1603.

McCarthy, T.L., Centrella, M., Canalis, E., 1989. Parathyroid hormone enhances the transcript and polypeptide levels of insulin-like growth factor I in osteoblast-enriched cultures from fetal rat bone. Endocrinology 124, 1247–1253.

McCarthy, T.L., Centrella, M., Canalis, E., 1990. Cyclic AMP induces insulin-like growth factor I synthesis in osteoblast-enriched cultures. J. Biol. Chem. 265, 15353–15356.

McCauley, L.K., Koh, A.J., Beecher, C.A., Rosol, T.J., 1997. Proto-oncogene c-fos is transcriptionally regulated by parathyroid hormone (PTH) and PTH-related protein in a cyclic adenosine monophosphate-dependent manner in osteoblastic cells. Endocrinology 138, 5427–5433.

McCauley, L.K., Koh-Paige, A.J., Chen, H., Chen, C., Ontiveros, C., Irwin, R., McCabe, L.R., 2001. Parathyroid hormone stimulates fra-2 expression in osteoblastic cells in vitro and in vivo. Endocrinology 142, 1975–1981.

McCuaig, K.A., Lee, H.S., Clarke, J.C., Assar, H., Horsford, J., White, J.H., 1995. Parathyroid hormone/parathyroid hormone related peptide receptor gene transcripts are expressed from tissue-specific and ubiquitous promoters. Nucleic Acids Res. 23, 1948–1955.

McPartlin, J., Skrabanek, P., Powell, D., 1978. Early effects of parathyroid hormone on rat calvarian bone alkaline phosphatase. Endocrinology 103, 1573–1578.

McSheehy, P.M., Chambers, T.J., 1986. Osteoblastic cells mediate osteoclastic responsiveness to parathyroid hormone. Endocrinology 118, 824–828.

Meikle, M.C., Bord, S., Hembry, R.M., Compston, J., Croucher, P.I., Reynolds, J.J., 1992. Human osteoblasts in culture synthesize collagenase and other matrix metalloproteinases in response to osteotropic hormones and cytokines. J. Cell Sci. 103 (Pt 4), 1093–1099.

Meites, S., 1989. Pediatric Clinical Chemistry: Reference (Normal) Values, third ed. AACC Press, Washington, DC.

Meltzer, V., Weinreb, S., Bellorin-Font, E., Hruska, K.A., 1982. Parathyroid hormone stimulation of renal phosphoinositide metabolism is a cyclic nucleotide-independent effect. Biochim. Biophys. Acta 712, 258–267.

Mensenkamp, A.R., Hoenderop, J.G., Bindels, R.J., 2007. TRPV5, the gateway to Ca^{2+} homeostasis. Handb. Exp. Pharmacol. 207–220.

Merciris, D., Schiltz, C., Legoupil, N., Marty-Morieux, C., de Vernejoul, M.C., Geoffroy, V., 2007. Over-expression of TIMP-1 in osteoblasts increases the anabolic response to PTH. Bone 40, 75–83.

Merriam, L.A., Baran, C.N., Girard, B.M., Hardwick, J.C., May, V., Parsons, R.L., 2013. Pituitary adenylate cyclase 1 receptor internalization and endosomal signaling mediate the pituitary adenylate cyclase activating polypeptide-induced increase in Guinea pig cardiac neuron excitability. J. Neurosci. 33, 4614–4622.

Meyer, M.B., Benkusky, N.A., Kaufmann, M., Lee, S.M., Onal, M., Jones, G., Pike, J.W., 2017. A kidney-specific genetic control module in mice governs endocrine regulation of the cytochrome P450 gene Cyp27b1 essential for vitamin D3 activation. J. Biol. Chem. 292, 17541–17558.

Miao, D., Tong, X.K., Chan, G.K., Panda, D., McPherson, P.S., Goltzman, D., 2001. Parathyroid hormone-related peptide stimulates osteogenic cell proliferation through protein kinase C activation of the Ras/mitogen-activated protein kinase signaling pathway. J. Biol. Chem. 276, 32204–32213.

Miles, R.R., Roberts, R.F., Putnam, A.R., Roberts, W.L., 2004. Comparison of serum and heparinized plasma samples for measurement of chemistry analytes. Clin. Chem. 50, 1704–1706.

Miles, R.R., Sluka, J.P., Halladay, D.L., Santerre, R.F., Hale, L.V., Bloem, L., Thirunavukkarasu, K., Galvin, R.J., Hock, J.M., Onyia, J.E., 2000a. ADAMTS-1: a cellular disintegrin and metalloprotease with thrombospondin motifs is a target for parathyroid hormone in bone. Endocrinology 141, 4533–4542.

Miles, R.R., Sluka, J.P., Santerre, R.F., Hale, L.V., Bloem, L., Boguslawski, G., Thirunavukkarasu, K., Hock, J.M., Onyia, J.E., 2000b. Dynamic regulation of RGS2 in bone: potential new insights into parathyroid hormone signaling mechanisms. Endocrinology 141, 28–36.

Moe, O.W., Amemiya, M., Yamaji, Y., 1995. Activation of protein kinase A acutely inhibits and phosphorylates Na/H exchanger NHE-3. J. Clin. Investig. 96, 2187–2194.

Moe, S.M., 2016. Calcium homeostasis in health and in kidney disease. Comp. Physiol. 6, 1781–1800.

Morales, F.C., Takahashi, Y., Kreimann, E.L., Georgescu, M.M., 2004. Ezrin-radixin-moesin (ERM)-binding phosphoprotein 50 organizes ERM proteins at the apical membrane of polarized epithelia. Proc. Natl. Acad. Sci. U. S. A. 101, 17705–17710.

Mori, Y., Machida, T., Miyakawa, S., Bomsztyk, K., 1992. Effects of amiloride on distal renal tubule sodium and calcium absorption: dependence on luminal pH. Pharmacol. Toxicol. 70, 201–204.

Morony, S., Capparelli, C., Lee, R., Shimamoto, G., Boone, T., Lacey, D.L., Dunstan, C.R., 1999. A chimeric form of osteoprotegerin inhibits hypercalcemia and bone resorption induced by IL-β, TNF-α, PTH, PTHrP, and 1, $25(OH)_2D_3$. J. Bone Miner. Res. 14, 1478–1485.

Muff, R., Fischer, J.A., Biber, J., Murer, H., 1992. Parathyroid hormone receptors in control of proximal tubule function. Annu. Rev. Physiol. 54, 67–79.

Mundy, G.R., Edwards, J.R., 2008. PTH-related peptide (PTHrP) in hypercalcemia. J. Am. Soc. Nephrol. 19, 672–675.

Murayama, A., Takeyama, K., Kitanaka, S., Kodera, Y., Kawaguchi, Y., Hosoya, T., Kato, S., 1999. Positive and negative regulations of the renal 25-hydroxyvitamin D_3 1α-hydroxylase gene by parathyroid hormone, calcitonin, and $1\alpha,25(OH)_2D_3$ in intact animals. Endocrinology 140, 2224–2231.

Murer, H., Biber, J., 1997. A molecular view of proximal tubular inorganic phosphate (P_i) reabsorption and of its regulation. Pflügers Archiv 433, 379–389.

Murer, H., Hernando, N., Forster, I., Biber, J., 2000. Proximal tubular phosphate reabsorption: molecular mechanisms. Physiol. Rev. 80, 1373–1409.

Murer, H., Hernando, N., Forster, I., Biber, J., 2003. Regulation of Na/Pi transporter in the proximal tubule. Annu. Rev. Physiol. 65, 531–542.

Murray, T.M., Rao, L.G., Muzaffar, S.A., 1991. Dexamethasone-treated ROS 17/2.8 rat osteosarcoma cells are responsive to human carboxylterminal parathyroid hormone peptide hPTH (53-84): stimulation of alkaline phosphatase. Calcif. Tissue Int. 49, 120–123.

Murray, T.M., Rao, L.G., Muzaffar, S.A., Ly, H., 1989. Human parathyroid hormone carboxyterminal peptide (53-84) stimulates alkaline phosphatase activity in dexamethasone-treated rat osteosarcoma cells in vitro. Endocrinology 124, 1097–1099.

Murrills, R.J., Stein, L.S., Fey, C.P., Dempster, D.W., 1990. The effects of parathyroid hormone (PTH) and PTH-related peptide on osteoclast resorption of bone slices in vitro: an analysis of pit size and the resorption focus. Endocrinology 127, 2648–2653.

Murtazina, R., Kovbasnjuk, O., Zachos, N.C., Li, X., Chen, Y., Hubbard, A., Hogema, B.M., Steplock, D., Seidler, U., Hoque, K.M., Tse, C.M., De Jonge, H.R., Weinman, E.J., Donowitz, M., 2007. Tissue-specific regulation of sodium/proton exchanger isoform 3 activity in Na^+/H^+ exchanger regulatory factor 1 (NHERF1) null mice. cAMP inhibition is differentially dependent on NHERF1 and exchange protein directly activated by cAMP in ileum versus proximal tubule. J. Biol. Chem. 282, 25141–25151.

Musso, M.J., Barthelmebs, M., Imbs, J.L., Plante, M., Bollack, C., Helwig, J.J., 1989. The vasodilator action of parathyroid hormone fragments on isolated perfused rat kidney. Naunyn-Schmiedeberg's Arch. Pharmacol. 340, 246–251.

Na, T., Peng, J.B., 2014. TRPV5: a Ca^{2+} channel for the fine-tuning of Ca^{2+} reabsorption. Handb. Exp. Pharmacol. 222, 321–357.

Nagai, S., Okazaki, M., Segawa, H., Bergwitz, C., Dean, T., Potts Jr., J.T., Mahon, M.J., Gardella, T.J., Juppner, H., 2011. Acute down-regulation of sodium-dependent phosphate transporter NPT2a involves predominantly the cAMP/PKA pathway as revealed by signaling-selective parathyroid hormone analogs. J. Biol. Chem. 286, 1618–1626.

Nakamoto, C., Baba, H., Fukase, M., Nakajima, K., Kimura, T., Sakakibara, S., Fujita, T., Chihara, K., 1993. Individual and combined effects of intact PTH, amino-terminal, and a series of truncated carboxyl-terminal PTH fragments on alkaline phosphatase activity in dexamethasone-treated rat osteoblastic osteosarcoma cells, ROS 17/2.8. Acta Endocrinol. 128, 367–372.

Nakashima, K., Zhou, X., Kunkel, G., Zhang, Z., Deng, J.M., Behringer, R.R., de Crombrugghe, B., 2002. The novel zinc finger-containing transcription factor osterix is required for osteoblast differentiation and bone formation. Cell 108, 17–29.

Nervina, J.M., Magyar, C.E., Pirih, F.Q., Tetradis, S., 2006. PGC-1alpha is induced by parathyroid hormone and coactivates Nurr1-mediated promoter activity in osteoblasts. Bone 39, 1018–1025.

Nguyen-Yamamoto, L., Rousseau, L., Brossard, J.H., Lepage, R., D'Amour, P., 2001. Synthetic carboxyl-terminal fragments of parathyroid hormone (PTH) decrease ionized calcium concentration in rats by acting on a receptor different from the PTH/PTH-related peptide receptor. Endocrinology 142, 1386–1392.

Nishida, S., Yamaguchi, A., Tanizawa, T., Endo, N., Mashiba, T., Uchiyama, Y., Suda, T., Yoshiki, S., Takahashi, H.E., 1994. Increased bone formation by intermittent parathyroid hormone administration is due to the stimulation of proliferation and differentiation of osteoprogenitor cells in bone marrow. Bone 15, 717–723.

Nishio, Y., Dong, Y., Paris, M., O'Keefe, R.J., Schwarz, E.M., Drissi, H., 2006. Runx2-mediated regulation of the zinc finger Osterix/Sp7 gene. Gene 372, 62–70.

Noda, M., Yoon, K., Rodan, G.A., 1988. Cyclic AMP-mediated stabilization of osteocalcin mRNA in rat osteoblast-like cells treated with parathyroid hormone. J. Biol. Chem. 263, 18574–18577.

Nolin, T.D., Friedman, P.A., 2018. Agents affecting mineral ion homeostasis and bone turnover. In: Brunton, L.L., Knollman, B., Hilal-Dandan, R. (Eds.), Goodman & Gilman's the Pharmacological Basis of Therapeutics, 13 ed. McGraw Hill, New York, pp. 887–906.

Norden, A.G., Lapsley, M., Lee, P.J., Pusey, C.D., Scheinman, S.J., Tam, F.W., Thakker, R.V., Unwin, R.J., Wrong, O., 2001. Glomerular protein sieving and implications for renal failure in Fanconi syndrome. Kidney Int. 60, 1885–1892.

Nordin, B.E., 1960. The effect of intravenous parathyroid extract on urinary pH, bicarbonate and electrolyte excretion. Clin. Sci. 19, 311–319.

Obri, A., Makinistoglu, M.P., Zhang, H., Karsenty, G., 2014. HDAC4 integrates PTH and sympathetic signaling in osteoblasts. J. Cell Biol. 205, 771–780.

Ogata, Y., Nakao, S., Kim, R.H., Li, J.J., Furuyama, S., Sugiya, H., Sodek, J., 2000. Parathyroid hormone regulation of bone sialoprotein (BSP) gene transcription is mediated through a pituitary-specific transcription factor-1 (Pit-1) motif in the rat BSP gene promoter. Matrix Biol. 19, 395–407.

Ohkido, I., Segawa, H., Yanagida, R., Nakamura, M., Miyamoto, K., 2003. Cloning, gene structure and dietary regulation of the type-IIc Na/Pi cotransporter in the mouse kidney. Pflügers Archiv 446, 106–115.

Okada, Y., Montero, A., Zhang, X., Sobue, T., Lorenzo, J., Doetschman, T., Coffin, J.D., Hurley, M.M., 2003. Impaired osteoclast formation in bone marrow cultures of Fgf2 null mice in response to parathyroid hormone. J. Biol. Chem. 278, 21258–21266.

Onishi, T., Zhang, W., Cao, X., Hruska, K., 1997. The mitogenic effect of parathyroid hormone is associated with E2F-dependent activation of cyclin-dependent kinase 1 (cdc2) in osteoblast precursors. J. Bone Miner. Res. 12, 1596–1605.

Onyia, J.E., Bidwell, J., Herring, J., Hulman, J., Hock, J.M., 1995. In vivo, human parathyroid hormone fragment (hPTH 1-34) transiently stimulates immediate early response gene expression, but not proliferation, in trabecular bone cells of young rats. Bone 17, 479–484.

Onyia, J.E., Miller, B., Hulman, J., Liang, J., Galvin, R., Frolik, C., Chandrasekhar, S., Harvey, A.K., Bidwell, J., Herring, J., Hock, J.M., 1997. Proliferating cells in the primary spongiosa express osteoblastic phenotype in vitro. Bone 20, 93–100.

Opas, E.E., Gentile, M.A., Rossert, J.A., de Crombrugghe, B., Rodan, G.A., Schmidt, A., 2000. Parathyroid hormone and prostaglandin E2 preferentially increase luciferase levels in bone of mice harboring a luciferase transgene controlled by elements of the pro-alpha1(I) collagen promoter. Bone 26, 27–32.

Orloff, J.J., Ganz, M.B., Ribaudo, A.E., Burtis, W.J., Reiss, M., Milstone, L.M., Stewart, A.F., 1992. Analysis of PTHRP binding and signal transduction mechanisms in benign and malignant squamous cells. Am. J. Physiol. Endocrinol. Metab. 262, E599–E607.

Ortega, A., Ramila, D., Ardura, J.A., Esteban, V., Ruiz-Ortega, M., Barat, A., Gazapo, R., Bosch, R.J., Esbrit, P., 2006. Role of parathyroid hormone-related protein in tubulointerstitial apoptosis and fibrosis after folic acid-induced nephrotoxicity. J. Am. Soc. Nephrol. 17, 1594–1603.

Ortega, A., Ramila, D., Izquierdo, A., Gonzalez, L., Barat, A., Gazapo, R., Bosch, R.J., Esbrit, P., 2005. Role of the renin-angiotensin system on the parathyroid hormone-related protein overexpression induced by nephrotoxic acute renal failure in the rat. J. Am. Soc. Nephrol. 16, 939–949.

Otto, F., Thornell, A.P., Crompton, T., Denzel, A., Gilmour, K.C., Rosewell, I.R., Stamp, G.W., Beddington, R.S., Mundlos, S., Olsen, B.R., Selby, P.B., Owen, M.J., 1997. Cbfa1, a candidate gene for cleidocranial dysplasia syndrome, is essential for osteoblast differentiation and bone development. Cell 89, 765–771.

Oursler, M.J., Cortese, C., Keeting, P., Anderson, M.A., Bonde, S.K., Riggs, B.L., Spelsberg, T.C., 1991. Modulation of transforming growth factor-β production in normal human osteoblast-like cells by 17 β-estradiol and parathyroid hormone. Endocrinology 129, 3313–3320.

Oyajobi, B.O., Anderson, D.M., Traianedes, K., Williams, P.J., Yoneda, T., Mundy, G.R., 2001. Therapeutic efficacy of a soluble receptor activator of nuclear factor kappaB-IgG Fc fusion protein in suppressing bone resorption and hypercalcemia in a model of humoral hypercalcemia of malignancy. Cancer Res. 61, 2572–2578.

Oyajobi, B.O., Lomri, A., Hott, M., Marie, P.J., 1999. Isolation and characterization of human clonogenic osteoblast progenitors immunoselected from fetal bone marrow stroma using STRO-1 monoclonal antibody. J. Bone Miner. Res. 14, 351–361.

Paillard, M., Bichara, M., 1989. Peptide hormone effects on urinary acidification and acid-base balance: PTH, ADH, and glucagon. Am. J. Physiol. Renal. Physiol. 256, F973–F985.

Palmer, L.G., Schnermann, J., 2015. Integrated control of Na transport along the nephron. Clin. J. Am. Soc. Nephrol. 10, 676–687.

Panda, D., Goltzman, D., Juppner, H., Karaplis, A.C., 2009. TIP39/parathyroid hormone type 2 receptor signaling is a potent inhibitor of chondrocyte proliferation and differentiation. Am. J. Physiol. Endocrinol. Metab. 297, E1125–E1136.

Panda, D.K., Goltzman, D., Karaplis, A.C., 2012. Defective postnatal endochondral bone development by chondrocyte-specific targeted expression of parathyroid hormone type 2 receptor. Am. J. Physiol. Endocrinol. Metab. 303, E1489–E1501.

Papavassiliou, A.G., 1994. The CREB/ATF family of transcription factors: modulation by reversible phosphorylation. Anticancer Res. 14, 1801–1805.

Partridge, N.C., Dickson, C.A., Kopp, K., Teitelbaum, S.L., Crouch, E.C., Kahn, A.J., 1989. Parathyroid hormone inhibits collagen synthesis at both ribonucleic acid and protein levels in rat osteogenic sarcoma cells. Mol. Endocrinol. 3, 232–239.

Partridge, N.C., Jeffrey, J.J., Ehlich, L.S., Teitelbaum, S.L., Fliszar, C., Welgus, H.G., Kahn, A.J., 1987. Hormonal regulation of the production of collagenase and a collagenase inhibitor activity by rat osteogenic sarcoma cells. Endocrinology 120, 1956–1962.

Pavlos, N.J., Friedman, P.A., 2017. GPCR Signaling and Trafficking: the long and short of it. Trends Endocrinol. Metabol. 28, 213–226.

Peacock, M., Robertson, W.G., Nordin, B.E.C., 1969. Relation between serum and urinary calcium with particular reference to parathyroid activity. Lancet 1, 384–386.

Pearman, A.T., Chou, W.Y., Bergman, K.D., Pulumati, M.R., Partridge, N.C., 1996. Parathyroid hormone induces c-fos promoter activity in osteoblastic cells through phosphorylated cAMP response element (CRE)-binding protein binding to the major CRE. J. Biol. Chem. 271, 25715–25721.

Pendas, A.M., Balbin, M., Llano, E., Jimenez, M.G., Lopez-Otin, C., 1997. Structural analysis and promoter characterization of the human collagenase-3 gene (MMP13). Genomics 40, 222–233.

Peterson, N.A., Feigen, G.A., Crimson, J.M., 1961. Effect of pH on interaction of calcium ions with serum proteins. Am. J. Physiol. 201, 386–392.

Pfeilschifter, J., Laukhuf, F., Muller-Beckmann, B., Blum, W.F., Pfister, T., Ziegler, R., 1995. Parathyroid hormone increases the concentration of insulin-like growth factor-I and transforming growth factor beta 1 in rat bone. J. Clin. Investig. 96, 767–774.

Pfeilschifter, J., Mundy, G.R., 1987. Modulation of type β transforming growth factor activity in bone cultures by osteotropic hormones. Proc. Natl. Acad. Sci. U. S. A. 84, 2024–2028.

Pfister, M.F., Forgo, J., Ziegler, U., Biber, J., Murer, H., 1999. cAMP-dependent and -independent downregulation of type IINa-P_i cotransporters by PTH. Am. J. Physiol. Renal. Physiol. 276, F720–F725.

Pfister, M.F., Lederer, E., Forgo, J., Ziegler, U., Lötscher, M., Quabius, E.S., Biber, J., Murer, H., 1997. Parathyroid hormone-dependent degradation of type II Na^+/P_i cotransporters. J. Biol. Chem. 272, 20125–20130.

Philbrick, W.M., Wysolmerski, J.J., Galbraith, S., Holt, E., Orloff, J.J., Yang, K.H., Vasavada, R.C., Weir, E.C., Broadus, A.E., Stewart, A.F., 1996. Defining the roles of parathyroid hormone-related protein in normal physiology. Physiol. Rev. 76, 127–173.

Picard, N., Capuano, P., Stange, G., Mihailova, M., Kaissling, B., Murer, H., Biber, J., Wagner, C.A., 2010. Acute parathyroid hormone differentially regulates renal brush border membrane phosphate cotransporters. Pflügers Archiv 460, 677–687.

Pines, M., Fukayama, S., Costas, K., Meurer, E., Goldsmith, P.K., Xu, X., Muallem, S., Behar, V., Chorev, M., Rosenblatt, M., Tashjian Jr., A.H., Suva, L.J., 1996. Inositol 1-,4-,5-trisphosphate-dependent Ca2+ signaling by the recombinant human PTH/PTHrP receptor stably expressed in a human kidney cell line. Bone 18, 381–389.

Pines, M., Granot, I., Hurwitz, S., 1990. Cyclic AMP-dependent inhibition of collagen synthesis in avian epiphyseal cartilage cells: effect of chicken and human parathyroid hormone and parathyroid hormone-related peptide. Bone Miner. 9, 23–33.

Pirih, F.Q., Aghaloo, T.L., Bezouglaia, O., Nervina, J.M., Tetradis, S., 2005. Parathyroid hormone induces the NR4A family of nuclear orphan receptors in vivo. Biochem. Biophys. Res. Commun. 332, 494–503.

Pirih, F.Q., Tang, A., Ozkurt, I.C., Nervina, J.M., Tetradis, S., 2004. Nuclear orphan receptor Nurr1 directly transactivates the osteocalcin gene in osteoblasts. J. Biol. Chem. 279, 53167–53174.

Pizurki, L., Rizzoli, R., Moseley, J., Martin, T.J., Caverzasio, J., Bonjour, J.P., 1988. Effect of synthetic tumoral PTH-related peptide on cAMP production and Na-dependent Pi transport. Am. J. Physiol. Renal. Physiol. 255, F957–F961.

Plotkin, H., Gundberg, C., Mitnick, M., Stewart, A.F., 1998. Dissociation of bone formation from resorption during 2-week treatment with human parathyroid hormone-related peptide-(1-36) in humans: potential as an anabolic therapy for osteoporosis. J. Clin. Endocrinol. Metab. 83, 2786–2791.

Porte, D., Tuckermann, J., Becker, M., Baumann, B., Teurich, S., Higgins, T., Owen, M.J., Schorpp-Kistner, M., Angel, P., 1999. Both AP-1 and Cbfa1-like factors are required for the induction of interstitial collagenase by parathyroid hormone. Oncogene 18, 667–678.

Pun, K.K., Arnaud, C.D., Nissenson, R.A., 1988. Parathyroid hormone receptors in human dermal fibroblasts: structural and functional characterization. J. Bone Miner. Res. 3, 453–460.

Puschett, J.B., Zurbach, P., Sylk, D., 1976. Acute effects of parathyroid hormone on proximal bicarbonate transport in the dog. Kidney Int. 9, 501–510.

Qin, L., Li, X., Ko, J.K., Partridge, N.C., 2005a. Parathyroid hormone uses multiple mechanisms to arrest the cell cycle progression of osteoblastic cells from G1 to S phase. J. Biol. Chem. 280, 3104–3111.

Qin, L., Partridge, N.C., 2005. Stimulation of amphiregulin expression in osteoblastic cells by parathyroid hormone requires the protein kinase A and cAMP response element-binding protein signaling pathway. J. Cell. Biochem. 96, 632–640.

Qin, L., Tamasi, J., Raggatt, L., Li, X., Feyen, J.H., Lee, D.C., Dicicco-Bloom, E., Partridge, N.C., 2005b. Amphiregulin is a novel growth factor involved in normal bone development and in the cellular response to parathyroid hormone stimulation. J. Biol. Chem. 280, 3974–3981.

Quamme, G., Pelech, S., Biber, J., Murer, H., 1994. Abnormalities of parathyroid hormone-mediated signal transduction mechanisms in opossum kidney cells. Biochim. Biophys. Acta 1223, 107–116.

Quamme, G., Pfeilschifter, J., Murer, H., 1989. Parathyroid hormone inhibition of Na^+/phosphate cotransport in OK cells: generation of second messengers in the regulatory cascade. Biochem. Biophys. Res. Commun. 158, 951–957.

Quinn, C.O., Scott, D.K., Brinckerhoff, C.E., Matrisian, L.M., Jeffrey, J.J., Partridge, N.C., 1990. Rat collagenase. Cloning, amino acid sequence comparison, and parathyroid hormone regulation in osteoblastic cells. J. Biol. Chem. 265, 22342–22347.

Rabito, C.A., 1986. Sodium cotransport processes in renal epithelial cell lines. Miner. Electrolyte Metab. 12, 32–41.

Raisz, L.G., Simmons, H.A., Vargas, S.J., Kemp, B.E., Martin, T.J., 1990. Comparison of the effects of amino-terminal synthetic parathyroid hormone-related peptide (PTHrP) of malignancy and parathyroid hormone on resorption of cultured fetal rat long bones. Calcif. Tissue Int. 46, 233–238.

Ramila, D., Ardura, J.A., Esteban, V., Ortega, A., Ruiz-Ortega, M., Bosch, R.J., Esbrit, P., 2008. Parathyroid hormone-related protein promotes inflammation in the kidney with an obstructed ureter. Kidney Int. 73, 835–847.

Reshkin, S.J., Forgo, J., Murer, H., 1990. Functional asymmetry in phosphate transport and its regulation in opossum kidney cells: parathyroid hormone inhibition. Pflueg. Arch. Eur. J. Physiol. 416, 624–631.

Reshkin, S.J., Forgo, J., Murer, H., 1991. Apical and basolateral effects of PTH in OK cells: transport inhibition, messenger production, effects of pertussis toxin, and interaction with a PTH analog. J. Membr. Biol. 124, 227–237.

Rey, A., Manen, D., Rizzoli, R., Caverzasio, J., Ferrari, S.L., 2006. Proline-rich motifs in the parathyroid hormone (PTH)/PTH-related protein receptor C terminus mediate scaffolding of c-Src with β-arrestin2 for ERK1/2 activation. J. Biol. Chem. 281, 38181–38188.

Ribeiro, C.P., Dubay, G.R., Falck, J.R., Mandel, L.J., 1994. Parathyroid hormone inhibits Na^+-K^+-ATPase through a cytochrome *P*-450 pathway. Am. J. Physiol. Renal. Physiol. 266, F497–F505.

Ribeiro, C.P., Mandel, L.J., 1992. Parathyroid hormone inhibits proximal tubule Na^+-K^+-ATPase activity. Am. J. Physiol. Renal. Physiol. 262, F209–F216.

Ritthaler, T., Traebert, M., Lötscher, M., Biber, J., Murer, H., Kaissling, B., 1999. Effects of phosphate intake on distribution of type II Na/Pi cotransporter mRNA in rat kidney. Kidney Int. 55, 976–983.

Rodan, S.B., Wesolowski, G., Ianacone, J., Thiede, M.A., Rodan, G.A., 1989. Production of parathyroid hormone-like peptide in a human osteosarcoma cell line: stimulation by phorbol esters and epidermal growth factor. J. Endocrinol. 122, 219–227.

Romero, M.F., Fulton, C.M., Boron, W.F., 2004. The SLC4 family of HCO_3^- transporters. Pflueg. Arch. Eur. J. Physiol. 447, 495–509.

Rost, C.R., Bikle, D.D., Kaplan, R.A., 1981. In vitro stimulation of 25-hydroxycholecalciferol 1α-hydroxylation by parathyroid hormone in chick kidney slices: evidence for a role for adenosine 3',5'-monophosphate. Endocrinology 108, 1002–1006.

Rouleau, M.F., Mitchell, J., Goltzman, D., 1988. In vivo distribution of parathyroid hormone receptors in bone: evidence that a predominant osseous target cell is not the mature osteoblast. Endocrinology 123, 187–191.

Rouleau, M.F., Mitchell, J., Goltzman, D., 1990. Characterization of the major parathyroid hormone target cell in the endosteal metaphysis of rat long bones. J. Bone Miner. Res. 5, 1043–1053.

Ruiz, O.S., Qiu, Y.Y., Wang, L.J., Arruda, J.A.L., 1996. Regulation of the renal Na-HCO_3 cotransporter: V. Mechanism of the inhibitory effect of parathyroid hormone. Kidney Int. 49, 396–402.

Sandström, I., 1879-1880. Om en ny körtel hos menniskan och àtskilliga däggdjur. Upsala Läkareförening Forhandlingar 15, 441–471.

Saussine, C., Massfelder, T., Parnin, F., Judes, C., Simeoni, U., Helwig, J.-J., 1993. Renin stimulating properties of parathyroid hormone-related peptide in the isolated perfused rat kidney. Kidney Int. 44, 764–773.

Saxena, S., Dansby, L., Allon, M., 1995. Adaptation to phosphate depletion in opossum kidney cells. Biochem. Biophys. Res. Commun. 216, 141–147.

Schaffers, O.J.M., Hoenderop, J.G.J., Bindels, R.J.M., de Baaij, J.H.F., 2018. The rise and fall of novel renal magnesium transporters. Am. J. Physiol. Renal. Physiol. 314, F1027–F1033.

Scheinman, S.J., Mitnick, M.E., Stewart, A.F., 1990. Quantitative evaluation of anticalciuretic effects of synthetic parathyroid hormone like peptides. J. Bone Miner. Res. 5, 653–658.

Schiller, P.C., D'Ippolito, G., Balkan, W., Roos, B.A., Howard, G.A., 2001. Gap-junctional communication mediates parathyroid hormone stimulation of mineralization in osteoblastic cultures. Bone 28, 38–44.

Schiller, P.C., Mehta, P.P., Roos, B.A., Howard, G.A., 1992. Hormonal regulation of intercellular communication: parathyroid hormone increases connexin 43 gene expression and gap-junctional communication in osteoblastic cells. Mol. Endocrinol. 6, 1433–1440.

Schoolwerth, A.C., Smith, B.C., Culpepper, R.M., 1988. Renal gluconeogenesis. Miner. Electrolyte Metab. 14, 347–361.

Schultheis, P.J., Lorenz, J.N., Meneton, P., Nieman, M.L., Riddle, T.M., Flagella, M., Duffy, J.J., Doetschman, T., Miller, M.L., Shull, G.E., 1998. Phenotype resembling Gitelman's syndrome in mice lacking the apical Na^+- Cl^- cotransporter of the distal convoluted tubule. J. Biol. Chem. 273, 29150–29155.

Scott, D.K., Brakenhoff, K.D., Clohisy, J.C., Quinn, C.O., Partridge, N.C., 1992. Parathyroid hormone induces transcription of collagenase in rat osteoblastic cells by a mechanism using cyclic adenosine 3',5'-monophosphate and requiring protein synthesis. Mol. Endocrinol. 6, 2153–2159.

Scutt, A., Duvos, C., Lauber, J., Mayer, H., 1994. Time-dependent effects of parathyroid hormone and prostaglandin E2 on DNA synthesis by periosteal cells from embryonic chick calvaria. Calcif. Tissue Int. 55, 208–215.

Segawa, H., Kaneko, I., Takahashi, A., Kuwahata, M., Ito, M., Ohkido, I., Tatsumi, S., Miyamoto, K., 2002. Growth-related renal type II Na/Pi cotransporter. J. Biol. Chem. 277, 19665–19672.

Segawa, H., Yamanaka, S., Onitsuka, A., Tomoe, Y., Kuwahata, M., Ito, M., Taketani, Y., Miyamoto, K.I., 2007. Parathyroid hormone dependent endocytosis of renal type IIc Na/Pi cotransporter. Am. J. Physiol. Renal. Physiol. 292, F395–F403.

Selvamurugan, N., Chou, W.Y., Pearman, A.T., Pulumati, M.R., Partridge, N.C., 1998. Parathyroid hormone regulates the rat collagenase-3 promoter in osteoblastic cells through the cooperative interaction of the activator protein-1 site and the runt domain binding sequence. J. Biol. Chem. 273, 10647–10657.

Selvamurugan, N., Pulumati, M.R., Tyson, D.R., Partridge, N.C., 2000. Parathyroid hormone regulation of the rat collagenase-3 promoter by protein kinase A-dependent transactivation of core binding factor alpha1. J. Biol. Chem. 275, 5037–5042.

Semenov, M., Tamai, K., He, X., 2005. SOST is a ligand for LRP5/LRP6 and a Wnt signaling inhibitor. J. Biol. Chem. 280, 26770–26775.

Seyedin, S.M., Thomas, T.C., Thompson, A.Y., Rosen, D.M., Piez, K.A., 1985. Purification and characterization of two cartilage-inducing factors from bovine demineralized bone. Proc. Natl. Acad. Sci. U. S. A. 82, 2267–2271.

Shen, V., Dempster, D.W., Birchman, R., Xu, R., Lindsay, R., 1993. Loss of cancellous bone mass and connectivity in ovariectomized rats can be restored by combined treatment with parathyroid hormone and estradiol. J. Clin. Investig. 91, 2479–2487.

Shenolikar, S., Voltz, J.W., Minkoff, C.M., Wade, J.B., Weinman, E.J., 2002. Targeted disruption of the mouse NHERF-1 gene promotes internalization of proximal tubule sodium-phosphate cotransporter type IIa and renal phosphate wasting. Proc. Natl. Acad. Sci. U. S. A. 99, 11470–11475.

Shigematsu, T., Horiuchi, N., Ogura, Y., Miyahara, T., Suda, T., 1986. Human parathyroid hormone inhibits renal 24-hydroxylase activity of 25-hydroxyvitamin D_3 by a mechanism involving adenosine 3',5'-monophosphate in rats. Endocrinology 118, 1583–1589.

Shimizu, E., Nakatani, T., He, Z., Partridge, N.C., 2014. Parathyroid hormone regulates histone deacetylase (HDAC) 4 through protein kinase A-mediated phosphorylation and dephosphorylation in osteoblastic cells. J. Biol. Chem. 289, 21340–21350.

Shimizu, M., Joyashiki, E., Noda, H., Watanabe, T., Okazaki, M., Nagayasu, M., Adachi, K., Tamura, T., Potts Jr., J.T., Gardella, T.J., Kawabe, Y., 2016. Pharmacodynamic actions of a long-acting PTH analog (LA-PTH) in thyroparathyroidectomized (TPTX) rats and normal monkeys. J. Bone Miner. Res. 31, 1405–1412.

Shimizu, T., Yoshitomi, K., Nakamura, M., Imai, M., 1990. Effects of PTH, calcitonin, and cAMP on calcium transport in rabbit distal nephron segments. Am. J. Physiol. Renal. Physiol. 259, F408–F414.

Shlatz, L.J., Schwartz, I.L., Kinne-Saffran, E., Kinne, R., 1975. Distribution of parathyroid hormone-stimulated adenylate cyclase in plasma membranes of cells of the kidney cortex. J. Membr. Biol. 24, 131–144.

Siegfried, G., Vrtovsnik, F., Prie, D., Amiel, C., Friedlander, G., 1995. Parathyroid hormone stimulates ecto-5'-nucleotidase activity in renal epithelial cells: role of protein kinase-C. Endocrinology 136, 1267–1275.

Silve, C.M., Hradek, G.T., Jones, A.L., Arnaud, C.D., 1982. Parathyroid hormone receptor in intact embryonic chicken bone: characterization and cellular localization. J. Cell Biol. 94, 379–386.

Simon, L.S., Slovik, D.M., Neer, R.M., Krane, S.M., 1988. Changes in serum levels of type I and III procollagen extension peptides during infusion of human parathyroid hormone fragment (1-34). J. Bone Miner. Res. 3, 241–246.

Simonet, W.S., Lacey, D.L., Dunstan, C.R., Kelley, M., Chang, M.S., Luthy, R., Nguyen, H.Q., Wooden, S., Bennett, L., Boone, T., Shimamoto, G., DeRose, M., Elliott, R., Colombero, A., Tan, H.L., Trail, G., Sullivan, J., Davy, E., Bucay, N., Renshaw-Gegg, L., Hughes, T.M., Hill, D., Pattison, W., Campbell, P., Sander, S., Van, G., Tarpley, J., Derby, P., Lee, R., Boyle, W.J., 1997. Osteoprotegerin: a novel secreted protein involved in the regulation of bone density. Cell 89, 309–319.

Sneddon, W.B., Barry, E.L.R., Coutermarsh, B.A., Gesek, F.A., Liu, F., Friedman, P.A., 1998. Regulation of renal parathyroid hormone receptor expression by 1,25-dihydroxyvitamin D_3 and retinoic acid. Cell. Physiol. Biochem. 8, 261–277.

Sneddon, W.B., Liu, F., Gesek, F.A., Friedman, P.A., 2000. Obligate mitogen-activated protein kinase activation in parathyroid hormone stimulation of calcium transport but not calcium signaling. Endocrinology 141, 4185–4193.

Sneddon, W.B., Ruiz, G.W., Gallo, L.I., Xiao, K., Zhang, Q., Rbaibi, Y., Weisz, O.A., Apodaca, G.L., Friedman, P.A., 2016. Convergent signaling pathways regulate parathyroid hormone and fibroblast growth factor-23 action on NPT2A-mediated phosphate transport. J. Biol. Chem. 291, 18632–18642.

Sneddon, W.B., Syme, C.A., Bisello, A., Magyar, C.E., Weinman, E.J., Rochdi, M.D., Parent, J.L., Abou-Samra, A.B., Friedman, P.A., 2003. Activation-independent parathyroid hormone receptor internalization is regulated by NHERF1 (EBP50). J. Biol. Chem. 278, 43787–43796.

Sneddon, W.B., Yang, Y., Ba, J., Harinstein, L.M., Friedman, P.A., 2007. Extracellular signal-regulated kinase activation by parathyroid hormone in distal tubule cells. Am. J. Physiol. Renal. Physiol. 292, F1028–F1034.

Soifer, N.E., Van Why, S.K., Ganz, M.B., Kashgarian, M., Siegel, N.J., Stewart, A.F., 1993. Expression of parathyroid hormone-related protein in the rat glomerulus and tubule during recovery from renal ischemia. J. Clin. Investig. 92, 2850–2857.

Soleimani, M., Burnham, C.E., 2001. Na^+:HCO_3^- cotransporters (NBC): cloning and characterization. J. Membr. Biol. 183, 71–84.

Somermeyer, M.G., Knauss, T.C., Weinberg, J.M., Humes, H.D., 1983. Characterization of Ca^{2+} transport in rat renal brush-border membranes and its modulation by phosphatidic acid. Biochem. J. 214, 37–46.

Somjen, D., Binderman, I., Schluter, K.D., Wingender, E., Mayer, H., Kaye, A.M., 1990. Stimulation by defined parathyroid hormone fragments of cell proliferation in skeletal-derived cell cultures. Biochem. J. 272, 781–785.

Sowa, H., Kaji, H., Iu, M.F., Tsukamoto, T., Sugimoto, T., Chihara, K., 2003. Parathyroid hormone-Smad3 axis exerts anti-apoptotic action and augments anabolic action of transforming growth factor β in osteoblasts. J. Biol. Chem. 278, 52240–52252.

Spurney, R.F., Flannery, P.J., Garner, S.C., Athirakul, K., Liu, S., Guilak, F., Quarles, L.D., 2002. Anabolic effects of a G protein-coupled receptor kinase inhibitor expressed in osteoblasts. J. Clin. Investig. 109, 1361–1371.

Stanislaus, D., Devanarayan, V., Hock, J.M., 2000a. In vivo comparison of activated protein-1 gene activation in response to human parathyroid hormone (hPTH)(1-34) and hPTH(1-84) in the distal femur metaphyses of young mice. Bone 27, 819–826.

Stanislaus, D., Yang, X., Liang, J.D., Wolfe, J., Cain, R.L., Onyia, J.E., Falla, N., Marder, P., Bidwell, J.P., Queener, S.W., Hock, J.M., 2000b. In vivo regulation of apoptosis in metaphyseal trabecular bone of young rats by synthetic human parathyroid hormone (1-34) fragment. Bone 27, 209–218.

Stewart, A.F., Vignery, A., Silverglate, A., Ravin, N.D., LiVolsi, V., Broadus, A.E., Baron, R., 1982. Quantitative bone histomorphometry in humoral hypercalcemia of malignancy: uncoupling of bone cell activity. J. Clin. Endocrinol. Metab. 55, 219–227.

Stewart, K., Walsh, S., Screen, J., Jefferiss, C.M., Chainey, J., Jordan, G.R., Beresford, J.N., 1999. Further characterization of cells expressing STRO-1 in cultures of adult human bone marrow stromal cells. J. Bone Miner. Res. 14, 1345–1356.

Stow, J.L., Sabolic, I., Brown, D., 1991. Heterogeneous localization of G protein α-subunits in rat kidney. Am. J. Physiol. Renal. Physiol. 261, F831–F840.

Suda, N., Gillespie, M.T., Traianedes, K., Zhou, H., Ho, P.W., Hards, D.K., Allan, E.H., Martin, T.J., Moseley, J.M., 1996. Expression of parathyroid hormone-related protein in cells of osteoblast lineage. J. Cell. Physiol. 166, 94–104.

Sutherland, M.K., Rao, L.G., Wylie, J.N., Gupta, A., Ly, H., Sodek, J., Murray, T.M., 1994. Carboxyl-terminal parathyroid hormone peptide (53-84) elevates alkaline phosphatase and osteocalcin mRNA levels in SaOS-2 cells. J. Bone Miner. Res. 9, 453–458.

Sutton, R.A.L., Dirks, J.H., 1975. The renal excretion of calcium: a review of micropuncture data. Can. J. Physiol. Pharmacol. 53, 979–988.

Sutton, R.A.L., Wong, N.L.M., Dirks, J.H., 1979. Effects of metabolic acidosis and alkalosis on sodium and calcium transport in the dog kidney. Kidney Int. 15, 520–533.

Suzuki, A., Ghayor, C., Guicheux, J., Magne, D., Quillard, S., Kakita, A., Ono, Y., Miura, Y., Oiso, Y., Itoh, M., Caverzasio, J., 2006. Enhanced expression of the inorganic phosphate transporter Pit-1 is involved in BMP-2-induced matrix mineralization in osteoblast-like cells. J. Bone Miner. Res. 21, 674–683.

Suzuki, A., Palmer, G., Bonjour, J.P., Caverzasio, J., 2001. Stimulation of sodium-dependent inorganic phosphate transport by activation of Gi/o-protein-coupled receptors by epinephrine in MC3T3-E1 osteoblast-like cells. Bone 28, 589–594.

Suzuki, M., Morita, T., Hanaoka, K., Kawaguchi, Y., Sakai, O., 1991. A Cl^- channel activated by parathyroid hormone in rabbit renal proximal tubule cells. J. Clin. Investig. 88, 735–742.

Swarthout, J.T., Doggett, T.A., Lemker, J.L., Partridge, N.C., 2001. Stimulation of extracellular signal-regulated kinases and proliferation in rat osteoblastic cells by parathyroid hormone is protein kinase C-dependent. J. Biol. Chem. 276, 7586–7592.

Swarthout, J.T., Lemker, J.F., Wilhelm, D., Dieckmann, A., Angel, P., Partridge, N.C., 1997. Parathyroid hormone regulation of mitogen activated protein kinases in osteoblastic cells. J. Bone Miner. Res. 12, S162.

Syme, C.A., Friedman, P.A., Bisello, A., 2005. Parathyroid hormone receptor trafficking contributes to the activation of extracellular signal-regulated kinases but is not required for regulation of cAMP signaling. J. Biol. Chem. 280, 11281–11288.

Takahashi, F., Morita, K., Katai, K., Segawa, H., Fujioka, A., Kouda, T., Tatsumi, S., Nii, T., Taketani, Y., Haga, H., Hisano, S., Fukui, Y., Miyamoto, K.I., Takeda, E., 1998. Effects of dietary Pi on the renal Na^+-dependent Pi transporter NaPi-2 in thyroparathyroidectomized rats. Biochem. J. 333 (Pt 1), 175–181.

Takaichi, K., Kurokawa, K., 1986. High Ca^{2+} inhibits peptide hormone-dependent cAMP production specifically in thick ascending limbs of Henle. Miner. Electrolyte Metab. 12, 342–346.

Tanaka, H., Smogorzewski, M., Koss, M., Massry, S.G., 1995. Pathways involved in PTH-induced rise in cytosolic Ca^{2+} concentration of rat renal proximal tubule. Am. J. Physiol. Renal. Physiol. 268, F330–F337.

Tanaka, S., Sakai, A., Tanaka, M., Otomo, H., Okimoto, N., Sakata, T., Nakamura, T., 2004. Skeletal unloading alleviates the anabolic action of intermittent PTH(1-34) in mouse tibia in association with inhibition of PTH-induced increase in c-fos mRNA in bone marrow cells. J. Bone Miner. Res. 19, 1813–1820.

Tenenhouse, H.S., Gauthier, C., Martel, J., Gesek, F.A., Coutermarsh, B.A., Friedman, P.A., 1998. Na^+-phosphate cotransport in mouse distal convoluted tubule cells: evidence for *Glvr-1* and *Ram-1* Gene Expression. J. Bone Miner. Res. 13, 590–597.

Tenenhouse, H.S., Martel, J., Gauthier, C., Segawa, H., Miyamoto, K.I., 2003. Differential effects of Npt2a gene ablation and the X-linked Hyp mutation on renal expression of type IIc Na/Pi cotransporter. Am. J. Physiol. Renal. Physiol. 285, F1271–F1278.

Terepka, A.R., Dewey, P.A., Toribara, T.Y., 1957. The ultrafiltrable calcium of human serum. II. Variations is disease states and under experimental conditions. J. Clin. Investig. 37, 87–98.

Termine, J.D., Kleinman, H.K., Whitson, S.W., Conn, K.M., McGarvey, M.L., Martin, G.R., 1981. Osteonectin, a bone-specific protein linking mineral to collagen. Cell 26, 99–105.

Teti, A., Rizzoli, R., Zambonin Zallone, A., 1991. Parathyroid hormone binding to cultured avian osteoclasts. Biochem. Biophys. Res. Commun. 174, 1217–1222.

Thirunavukkarasu, K., Halladay, D.L., Miles, R.R., Geringer, C.D., Onyia, J.E., 2002. Analysis of regulator of G-protein signaling-2 (RGS-2) expression and function in osteoblastic cells. J. Cell. Biochem. 85, 837–850.

Thompson, D.D., Seedor, J.G., Fisher, J.E., Rosenblatt, M., Rodan, G.A., 1988. Direct action of the parathyroid hormone-like human hypercalcemic factor on bone. Proc. Natl. Acad. Sci. U. S. A. 85, 5673–5677.

Towler, D.A., Rodan, G.A., 1995. Identification of a rat osteocalcin promoter 3',5'-cyclic adenosine monophosphate response region containing two PuGGTCA steroid hormone receptor binding motifs. Endocrinology 136, 1089–1096.

Traebert, M., Völkl, H., Biber, J., Murer, H., Kaissling, B., 2000. Luminal and contraluminal action of 1-34 and 3-34 PTH peptides on renal type IIa Na-P_i cotransporter. Am. J. Physiol. Renal. Physiol. 278, F792–F798.

Tsukii, K., Shima, N., Mochizuki, S., Yamaguchi, K., Kinosaki, M., Yano, K., Shibata, O., Udagawa, N., Yasuda, H., Suda, T., Higashio, K., 1998. Osteoclast differentiation factor mediates an essential signal for bone resorption induced by 1 alpha,25-dihydroxyvitamin D3, prostaglandin E2, or parathyroid hormone in the microenvironment of bone. Biochem. Biophys. Res. Commun. 246, 337–341.

Turner, G., Coureau, C., Rabin, M.R., Escoubet, B., Hruby, M., Walrant, O., Silve, C., 1995. Parathyroid hormone (PTH)/PTH-related protein receptor messenger ribonucleic acid expression and PTH response in a rat model of secondary hyperparathyroidism associated with vitamin D deficiency. Endocrinology 136, 3751–3758.

Tyson, D.R., Swarthout, J.T., Partridge, N.C., 1999. Increased osteoblastic c-fos expression by parathyroid hormone requires protein kinase A phosphorylation of the cyclic adenosine 3',5'-monophosphate response element-binding protein at serine 133. Endocrinology 140, 1255–1261.

Ureña, P., Iida-Klein, A., Kong, X.-F., Jüppner, H., Kronenberg, H.M., Abou-Samra, A.B., Segre, G.V., 1994. Regulation of parathyroid hormone (PTH)/PTH-related peptide receptor messenger ribonucleic acid by glucocorticoids and PTH in ROS 17/2.8 and OK cells. Endocrinology 134, 451–456.

Urena, P., Kubrusly, M., Mannstadt, M., Hruby, M., Trinh, M.M., Silve, C., Lacour, B., Abou-Samra, A.B., Segre, G.V., Drueke, T., 1994. The renal PTH/PTHrP receptor is down-regulated in rats with chronic renal failure. Kidney Int. 45, 605–611.

Ureña, P., Mannstadt, M., Hruby, M., Ferreira, A., Schmitt, F., Silve, C., Ardaillou, R., Lacour, B., Abou-Samra, A.B., Segre, G.V., Drüeke, T., 1995. Parathyroidectomy does not prevent the renal PTH/PTHrP receptor down-regulation in uremic rats. Kidney Int. 47, 1797–1805.

Usdin, T.B., Bonner, T.I., Harta, G., Mezey, E., 1996. Distribution of parathyroid hormone-2 receptor messenger ribonucleic acid in rat. Endocrinology 137, 4285–4297.

Usdin, T.B., Gruber, C., Bonner, T.I., 1995. Identification and functional expression of a receptor selectively recognizing parathyroid hormone, the PTH2 receptor. J. Biol. Chem. 270, 15455–15458.

Usdin, T.B., Hilton, J., Vertesi, T., Harta, G., Segre, G., Mezey, E., 1999. Distribution of the parathyroid hormone 2 receptor in rat: immunolocalization reveals expression by several endocrine cells. Endocrinology 140, 3363–3371.

Valin, A., Guillen, C., Esbrit, P., 2001. C-terminal parathyroid hormone-related protein (PTHrP) (107-139) stimulates intracellular Ca(2+) through a receptor different from the type 1 PTH/PTHrP receptor in osteoblastic osteosarcoma UMR 106 cells. Endocrinology 142, 2752–2759.

van Bezooijen, R.L., Roelen, B.A., Visser, A., van der Wee-Pals, L., de Wilt, E., Karperien, M., Hamersma, H., Papapoulos, S.E., ten Dijke, P., Lowik, C.W., 2004. Sclerostin is an osteocyte-expressed negative regulator of bone formation, but not a classical BMP antagonist. J. Exp. Med. 199, 805–814.

van Bezooijen, R.L., Svensson, J.P., Eefting, D., Visser, A., van der Horst, G., Karperien, M., Quax, P.H., Vrieling, H., Papapoulos, S.E., ten Dijke, P., Lowik, C.W., 2007. Wnt but not BMP signaling is involved in the inhibitory action of sclerostin on BMP-stimulated bone formation. J. Bone Miner. Res. 22, 19–28.

van der Hagen, E.A., Lavrijsen, M., van Zeeland, F., Praetorius, J., Bonny, O., Bindels, R.J., Hoenderop, J.G., 2014. Coordinated regulation of TRPV5-mediated Ca^{2+} transport in primary distal convolution cultures. Pflügers Archiv 466, 2077–2087.

van der Plas, A., Aarden, E.M., Feijen, J.H., de Boer, A.H., Wiltink, A., Alblas, M.J., de Leij, L., Nijweide, P.J., 1994. Characteristics and properties of osteocytes in culture. J. Bone Miner. Res. 9, 1697–1704.

van Goor, M.K., Verkaart, S., van Dam, T.J., Huynen, M.A., van der Wijst, J., 2017a. Interspecies differences in PTH-mediated PKA phosphorylation of the epithelial calcium channel TRPV5. Pflügers Archiv.

van Goor, M.K.C., Hoenderop, J.G.J., van der Wijst, J., 2017b. TRP channels in calcium homeostasis: from hormonal control to structure-function relationship of TRPV5 and TRPV6. Biochim. Biophys. Acta 1864, 883–893.

van Loon, E.P., Little, R., Prehar, S., Bindels, R.J., Cartwright, E.J., Hoenderop, J.G., 2016. Calcium extrusion pump PMCA4: a new player in renal calcium handling? PLoS One 11, e0153483.

Vander Molen, M.A., Rubin, C.T., McLeod, K.J., McCauley, L.K., Donahue, H.J., 1996. Gap junctional intercellular communication contributes to hormonal responsiveness in osteoblastic networks. J. Biol. Chem. 271, 12165–12171.

Verheijen, M.H.G., Defize, L.H.K., 1997. Parathyroid hormone activates mitogen-activated protein kinase via a cAMP-mediated pathway independent of Ras. J. Biol. Chem. 272, 3423–3429.

Vilardaga, J.P., Frank, M., Krasel, C., Dees, C., Nissenson, R.A., Lohse, M.J., 2001. Differential conformational requirements for activation of G proteins and the regulatory proteins arrestin and G protein-coupled receptor kinase in the G protein-coupled receptor for parathyroid hormone (PTH)/PTH-related protein. J. Biol. Chem. 276, 33435–33443.

Wade, J.B., Liu, J., Coleman, R.A., Cunningham, R., Steplock, D.A., Lee-Kwon, W., Pallone, T.L., Shenolikar, S., Weinman, E.J., 2003. Localization and interaction of NHERF isoforms in the renal proximal tubule of the mouse. Am. J. Physiol. Cell Physiol. 285, C1494–C1503.

Wade, J.B., Welling, P.A., Donowitz, M., Shenolikar, S., Weinman, E.J., 2001. Differential renal distribution of NHERF isoforms and their colocalization with NHE3, ezrin, and ROMK. Am. J. Physiol. Cell Physiol. 280, C192–C198.

Walker, A.T., Stewart, A.F., Korn, E.A., Shiratori, T., Mitnick, M.A., Carpenter, T.O., 1990. Effect of parathyroid hormone-like peptides on 25-hydroxyvitamin D-1a-hydroxylase activity in rodents. Am. J. Physiol. Endocrinol. Metab. 258, E297–E303.

Walser, M., 1973. Divalent cations: physicochemical state in glomerular filtrate and urine and renal excretion. In: Orloff, J., Berliner, R.W. (Eds.), Handbook of Physiology, Section 8: Renal Physiology, first ed. American Physiological Society, Washington, D.C., pp. 555–586

Wang, A., Martin, J.A., Lembke, L.A., Midura, R.J., 2000. Reversible suppression of in vitro biomineralization by activation of protein kinase A. J. Biol. Chem. 275, 11082–11091.

Wang, B., Ardura, J.A., Romero, G., Yang, Y., Hall, R.A., Friedman, P.A., 2010. Na/H exchanger regulatory factors control PTH receptor signaling by differential activation of Gα protein subunits. J. Biol. Chem. 285, 26976−26986.

Wang, B., Bisello, A., Yang, Y., Romero, G.G., Friedman, P.A., 2007a. NHERF1 regulates parathyroid hormone receptor membrane retention without affecting recycling. J. Biol. Chem. 282, 36214−36222.

Wang, B., Yang, Y., Friedman, P.A., 2008. Na/H Exchange regulator factor 1, a novel Akt-associating protein, regulates extracellular signal-related signaling through a B-Raf-mediated pathway. Mol. Biol. Cell 19, 1637−1645.

Wang, B., Yang, Y., Liu, L., Blair, H.C., Friedman, P.A., 2013. NHERF1 regulation of PTH-dependent bimodal Pi transport in osteoblasts. Bone 52, 268−277.

Wang, B.L., Dai, C.L., Quan, J.X., Zhu, Z.F., Zheng, F., Zhang, H.X., Guo, S.Y., Guo, G., Zhang, J.Y., Qiu, M.C., 2006. Parathyroid hormone regulates osterix and Runx2 mRNA expression predominantly through protein kinase A signaling in osteoblast-like cells. J. Endocrinol. Investig. 29, 101−108.

Wang, D., Christensen, K., Chawla, K., Xiao, G., Krebsbach, P.H., Franceschi, R.T., 1999. Isolation and characterization of MC3T3-E1 preosteoblast subclones with distinct in vitro and in vivo differentiation/mineralization potential. J. Bone Miner. Res. 14, 893−903.

Wang, L., Liu, S., Quarles, L.D., Spurney, R.F., 2005a. Targeted overexpression of G protein-coupled receptor kinase-2 in osteoblasts promotes bone loss. Am. J. Physiol. Endocrinol. Metab. 288, E826−E834.

Wang, M.-S., Kurokawa, K., 1984. Renal gluconeogenesis: axial and internephron heterogeneity and the effect of parathyroid hormone. Am. J. Physiol. Renal. Physiol. 246, F59−F66.

Wang, Y.H., Liu, Y., Buhl, K., Rowe, D.W., 2005b. Comparison of the action of transient and continuous PTH on primary osteoblast cultures expressing differentiation stage-specific GFP. J. Bone Miner. Res. 20, 5−14.

Wang, Y.H., Liu, Y., Rowe, D.W., 2007b. Effects of transient PTH on early proliferation, apoptosis, and subsequent differentiation of osteoblast in primary osteoblast cultures. Am. J. Physiol. Endocrinol. Metab. 292, E594−E603.

Watford, M., Mapes, R.E., 1990. Hormonal and acid-base regulation of phosphoenolpyruvate carboxykinase mRNA levels in rat kidney. Arch. Biochem. Biophys. 282, 399−403.

Watson, P., Lazowski, D., Han, V., Fraher, L., Steer, B., Hodsman, A., 1995. Parathyroid hormone restores bone mass and enhances osteoblast insulin-like growth factor I gene expression in ovariectomized rats. Bone 16, 357−365.

Wehbi, V.L., Stevenson, H.P., Feinstein, T.N., Calero, G., Romero, G., Vilardaga, J.P., 2013. Noncanonical GPCR signaling arising from a PTH receptor-arrestin-Gβγ complex. Proc. Natl. Acad. Sci. U. S. A. 110, 1530−1535.

Wein, M.N., Liang, Y., Goransson, O., Sundberg, T.B., Wang, J., Williams, E.A., O'Meara, M.J., Govea, N., Beqo, B., Nishimori, S., Nagano, K., Brooks, D.J., Martins, J.S., Corbin, B., Anselmo, A., Sadreyev, R., Wu, J.Y., Sakamoto, K., Foretz, M., Xavier, R.J., Baron, R., Bouxsein, M.L., Gardella, T.J., Divieti-Pajevic, P., Gray, N.S., Kronenberg, H.M., 2016. SIKs control osteocyte responses to parathyroid hormone. Nat. Commun. 7, 13176.

Wein, M.N., Liang, Y., Goransson, O., Sundberg, T.B., Wang, J., Williams, E.A., O'Meara, M.J., Govea, N., Beqo, B., Nishimori, S., Nagano, K., Brooks, D.J., Martins, J.S., Corbin, B., Anselmo, A., Sadreyev, R., Wu, J.Y., Sakamoto, K., Foretz, M., Xavier, R.J., Baron, R., Bouxsein, M.L., Gardella, T.J., Divieti-Pajevic, P., Gray, N.S., Kronenberg, H.M., 2017. Corrigendum: SIKs control osteocyte responses to parathyroid hormone. Nat. Commun. 8, 14745.

Weinman, E.J., Biswas, R.S., Peng, G., Shen, L., Turner, C.L., E, X., Steplock, D., Shenolikar, S., Cunningham, R., 2007. Parathyroid hormone inhibits renal phosphate transport by phosphorylation of serine 77 of sodium-hydrogen exchanger regulatory factor-1. J. Clin. Investig. 117, 3412−3420.

Weinman, E.J., Cunningham, R., Wade, J.B., Shenolikar, S., 2005. The role of NHERF-1 in the regulation of renal proximal tubule sodium-hydrogen exchanger 3 and sodium-dependent phosphate cotransporter 2a. J. Physiol. 567, 27−32.

Weinman, E.J., Evangelista, C.M., Steplock, D., Liu, M.Z., Shenolikar, S., Bernardo, A., 2001. Essential role for NHERF in cAMP-mediated inhibition of the Na^+-HCO^-_3 co-transporter in BSC-1 cells. J. Biol. Chem. 276, 42339−42346.

Weinman, E.J., Lakkis, J., Akom, M., Wali, R.K., Drachenberg, C.B., Coleman, R.A., Wade, J.B., 2002. Expression of NHERF-1, NHERF-2, PDGFR-a, and PDGFR-ß in normal human kidneys and in renal transplant rejection. Pathobiology 70, 314−323.

Weinman, E.J., Steplock, D., Tate, K., Hall, R.A., Spurney, R.F., Shenolikar, S., 1998. Structure-function of recombinant Na/H exchanger regulatory factor (NHE-RF). J. Clin. Investig. 101, 2199−2206.

Weir, E.C., Insogna, K.L., Horowitz, M.C., 1989. Osteoblast-like cells secrete granulocyte-macrophage colony-stimulating factor in response to parathyroid hormone and lipopolysaccharide. Endocrinology 124, 899−904.

White, K.E., Gesek, F.A., Nesbitt, T., Drezner, M.K., Friedman, P.A., 1997. Molecular dissection of Ca^{2+} efflux in immortalized proximal tubule cells. J. Gen. Physiol. 109, 217−228.

Williams, R.J.P., 1976. Calcium chemistry and its relation to biological function. Symp. Soc. Exp. Biol. 30, 1−17.

Winchester, S.K., Bloch, S.R., Fiacco, G.J., Partridge, N.C., 1999. Regulation of expression of collagenase-3 in normal, differentiating rat osteoblasts. J. Cell. Physiol. 181, 479−488.

Winchester, S.K., Selvamurugan, N., D'Alonzo, R.C., Partridge, N.C., 2000. Developmental regulation of collagenase-3 mRNA in normal, differentiating osteoblasts through the activator protein-1 and the runt domain binding sites. J. Biol. Chem. 275, 23310−23318.

Witty, J.P., Foster, S.A., Stricklin, G.P., Matrisian, L.M., Stern, P.H., 1996. Parathyroid hormone-induced resorption in fetal rat limb bones is associated with production of the metalloproteinases collagenase and gelatinase B. J. Bone Miner. Res. 11, 72−78.

Woei Ng, K., Speicher, T., Dombrowski, C., Helledie, T., Haupt, L.M., Nurcombe, V., Cool, S.M., 2007. Osteogenic differentiation of murine embryonic stem cells is mediated by fibroblast growth factor receptors. Stem Cell. Dev. 16, 305−318.

Wu, Y., Kumar, R., 2000. Parathyroid hormone regulates transforming growth factor β and β synthesis in osteoblasts via divergent signaling pathways. J. Bone Miner. Res. 15, 879–884.

Wysolmerski, J.J., Stewart, A.F., 1998. The physiology of parathyroid hormone-related protein: an emerging role as a developmental factor. Annu. Rev. Physiol. 60, 431–460.

Yadav, S., Yadav, Y.S., Goel, M.M., Singh, U., Natu, S.M., Negi, M.P., 2014. Calcitonin gene- and parathyroid hormone-related peptides in normotensive and preeclamptic pregnancies: a nested case-control study. Arch. Gynecol. Obstet. 290, 897–903.

Yamaguchi, D.T., Hahn, T.J., Iida-Klein, A., Kleeman, C.R., Muallem, S., 1987. Parathyroid hormone-activated calcium channels in an osteoblast-like clonal osteosarcoma cell line. cAMP-dependent and cAMP-independent calcium channels. J. Biol. Chem. 262, 7711–7718.

Yamaguchi, M., Ogata, N., Shinoda, Y., Akune, T., Kamekura, S., Terauchi, Y., Kadowaki, T., Hoshi, K., Chung, U.I., Nakamura, K., Kawaguchi, H., 2005. Insulin receptor substrate-1 is required for bone anabolic function of parathyroid hormone in mice. Endocrinology 146, 2620–2628.

Yamaguchi, T., Fukase, M., Kido, H., Sugimoto, T., Katunuma, N., Chihara, K., 1994. Meprin is predominantly involved in parathyroid hormone degradation by the microvillar membranes of rat kidney. Life Sci. 54, 381–386.

Yamamoto, H., Tani, Y., Kobayashi, K., Taketani, Y., Sato, T., Arai, H., Morita, K., Miyamoto, K., Pike, J.W., Kato, S., Takeda, E., 2005. Alternative promoters and renal cell-specific regulation of the mouse type IIa sodium-dependent phosphate cotransporter gene. Biochim. Biophys. Acta 1732, 43–52.

Yamamoto, M., Murakami, T., Nishikawa, M., Tsuda, E., Mochizuki, S., Higashio, K., Akatsu, T., Motoyoshi, K., Nagata, N., 1998. Hypocalcemic effect of osteoclastogenesis inhibitory factor/osteoprotegerin in the thyroparathyroidectomized rat. Endocrinology 139, 4012–4015.

Yamamoto, S., Morimoto, I., Yanagihara, N., Zeki, K., Fujihira, T., Izumi, F., Yamashita, H., Eto, S., 1997. Parathyroid hormone-related peptide-(1-34) [PTHrP-(1-34)] induces vasopressin release from the rat supraoptic nucleus in vitro through a novel receptor distinct from a type I or type II PTH/PTHrP receptor. Endocrinology 138, 2066–2072.

Yang, R., Gerstenfeld, L.C., 1997. Structural analysis and characterization of tissue and hormonal responsive expression of the avian bone sialoprotein (BSP) gene. J. Cell. Biochem. 64, 77–93.

Yang, T.X., Hassan, S., Huang, Y.N.G., Smart, A.M., Briggs, J.P., Schnermann, J.B., 1997. Expression of PTHrP, PTH/PTHrP receptor, and Ca^{2+}-sensing receptor mRNAs along the rat nephron. Am. J. Physiol. Renal. Physiol. 272, F751–F758.

Yang, W., Friedman, P.A., Siu-Caldera, M.-L., Reddy, G.S., Kumar, R., Christakos, S., 1999. Expression of $25(OH)D_3$ 24-hydroxylase in the distal nephron: coordinate regulation by $1,25(OH)_2D_3$ and or PTH. Am. J. Physiol. Endocrinol. Metab. 276, E793–E805.

Yasuda, H., Shima, N., Nakagawa, N., Mochizuki, S.I., Yano, K., Fujise, N., Sato, Y., Goto, M., Yamaguchi, K., Kuriyama, M., Kanno, T., Murakami, A., Tsuda, E., Morinaga, T., Higashio, K., 1998. Identity of osteoclastogenesis inhibitory factor (OCIF) and osteoprotegerin (OPG): a mechanism by which OPG/OCIF inhibits osteoclastogenesis in vitro. Endocrinology 139, 1329–1337.

Yates, A.J.P., Guttierrez, G.E., Smolens, P., Travis, P.S., Katz, M.S., Aufdemorte, T.B., Boyce, B.F., Hymer, T.K., Poser, J.W., Mundy, G.R., 1988. Effects of a synthetic peptide of a parathyroid hormone-related protein on calcium homeostasis, renal tubular calcium reabsorption, and bone metabolism in vivo and in vitro in rodents. J. Clin. Investig. 81, 932–938.

Yee, J.A., 1985. Stimulation of alkaline phosphatase activity in cultured neonatal mouse calvarial bone cells by parathyroid hormone. Calcif. Tissue Int. 37, 530–538.

Yeruva, S., Chodisetti, G., Luo, M., Chen, M., Cinar, A., Ludolph, L., Lunnemann, M., Goldstein, J., Singh, A.K., Riederer, B., Bachmann, O., Bleich, A., Gereke, M., Bruder, D., Hagen, S., He, P., Yun, C., Seidler, U., 2015. Evidence for a causal link between adaptor protein PDZK1 downregulation and Na^+/H^+ exchanger NHE3 dysfunction in human and murine colitis. Pflügers Archiv 467, 1795–1807.

Yu, X.P., Chandrasekhar, S., 1997. Parathyroid hormone (PTH 1-34) regulation of rat osteocalcin gene transcription. Endocrinology 138, 3085–3092.

Zhang, Q., Xiao, K., Liu, H., Song, L., McGarvey, J.C., Sneddon, W.B., Bisello, A., Friedman, P.A., 2018. Site-specific polyubiquitination differentially regulates parathyroid hormone receptor-initiated MAPK signaling and cell proliferation. J. Biol. Chem. 293, 5556–5571.

Zhang, Y.B., Norian, J.M., Magyar, C.E., Holstein-Rathlou, N.H., Mircheff, A.K., McDonough, A.A., 1999. In vivo PTH provokes apical NHE3 and NaPi2 redistribution and Na-K-ATPase inhibition. Am. J. Physiol. Renal. Physiol. 276, F711–F719.

Zhao, N, Tenenhouse, H.S., 2000. Npt2 gene disruption confers resistance to the inhibitory action of parathyroid hormone on renal sodium-phosphate cotransport. Endocrinology 141, 2159–2165.

Zhao, H., Wiederkehr, M.R., Fan, L., Collazo, R.L., Crowder, L.A., Moe, O.W., 1999. Acute inhibition of Na/H exchanger NHE-3 by cAMP. Role of protein kinase a and NHE-3 phosphoserines 552 and 605. J. Biol. Chem. 274, 3978–3987.

Zhou, J., Sims, C., Chang, C.H., Berti-Mattera, L., Hopfer, U., Douglas, J., 1990. Proximal tubular epithelial cells possess a novel 42-kilodalton guanine nucleotide-binding regulatory protein. Proc. Natl. Acad. Sci. U. S. A. 87, 7532–7535.

Zierold, C., Mings, J.A., DeLuca, H.F., 2003. Regulation of 25-hydroxyvitamin D3-24-hydroxylase mRNA by 1,25-dihydroxyvitamin D3 and parathyroid hormone. J. Cell. Biochem. 88, 234–237.

Chapter 28

Receptors for parathyroid hormone and parathyroid hormone–related protein

Thomas J. Gardella, Harald Jüppner and John T. Potts, Jr.

Endocrine Unit, Department of Medicine and Pediatric Nephrology, MassGeneral Hospital for Children, Massachusetts General Hospital and Harvard Medical School, Boston, MA, United States

Chapter outline

Introduction

Parathyroid hormone (PTH) and PTH-related protein (PTHrP) mediate their principal biological actions by acting on a single cell-surface receptor, the type-1 PTH/PTHrP receptor, or PTHR1. The PTHR1 thus stands as a key regulatory molecule that is essential for normal physiology at all stages of life. The biological situation is somewhat unique in that the one receptor responds to two endogenous ligands to thereby control two disparate physiological processes: the maintenance of blood calcium and phosphate homeostasis via PTH and the timing of cell differentiation events in the developing skeleton and other tissues via PTHrP. The PTHR1 also holds interest as a prospective drug target, as pharmacologic agents that specifically modulate its activity can potentially be used to treat disturbances of bone and calcium metabolism that occur in a variety of pathologic conditions, such as osteoporosis.

The endogenous PTH and PTHrP ligands are polypeptide chains of 84 and 141 amino acids, respectively, with the first 34 amino acids containing sufficient information for high-affinity binding to the PTHR1 and potent activation of downstream signaling responses. Thus synthetic PTH(1–34) and PTHrP(1–34) peptides can generally mimic most of the biological actions of the full-length molecules. Nevertheless, certain functional activities have been reported for peptides derived from the C-terminal portions of PTH and PTHrP, which has led to the notion that other receptors, distinct from the PTHR1, might exist that bind the C-terminal portion of the ligands, although no such receptor has so far been identified. For the PTHR1, much effort has been directed at elucidating the mechanisms by which the ligands PTH and PTHrP engage the receptor and stimulate signal transduction. These studies generally reveal that PTH(1–34) and PTHrP(1–34) interact

Principles of Bone Biology. https://doi.org/10.1016/B978-0-12-814841-9.00028-2

with the PTHR1 in highly similar, yet not identical, fashions. Consistent with this, the primary structures of the ligands exhibit considerable amino acid sequence homology in the amino-terminal region, particularly at the N-terminal 1−14 portion, which is critical for receptor activation, with eight amino acid identities, while the 15−34 portion, which contributes to binding affinity, shows only a moderate level of homology, with three identities. As discussed later in this chapter, studies suggest that differences can indeed be discerned in the binding modes utilized by PTH(1−34) and PTHrP(1−34) and that such differences can lead to differences in functional effects, particularly in the duration of the signaling responses induced. Such findings further support the notion that the capacity of the PTHR1 to regulate the aforementioned two disparate types of physiological processes—the endocrine control of mineral ion homeostasis and the paracrine control of tissue development—is at least partly based on differences in the mechanisms by which the two respective ligands engage the receptor.

Early work conducted prior to the cloning of the PTHR1 in 1991 and which used canine or bovine renal membrane preparations or cell lines derived from bone or kidney gave initial clues as to the basic pharmacology of PTH ligand binding to endogenous receptor binding sites and the downstream signaling responses that could be activated. This work was made possible in large part by the development of peptide synthesis technology and its early application to PTH (Potts et al., 1971), which yielded most notably the PTH(1−34) peptide, as well as radioiodinated derivatives that enabled direct characterization of the binding sites used (Segre et al., 1979). Such studies further revealed that residues in both the N- and the C-terminal region were important for overall binding affinity (Nussbaum et al., 1980). Parallel studies revealed that PTH peptides induced rapid and robust increases in intracellular cAMP, and that the N-terminal residues of the ligand were critical for activating this response. That this response was mediated by a cell-surface G-protein-coupled receptor (GPCR) was indeed borne out in 1991 by the cloning of the cDNA encoding the PTHR1 from kidney- and bone-derived cell lines (Juppner et al., 1991), which revealed the seven membrane-spanning-domain protein architecture that defines all 800 or so members of the GPCR superfamily. A key goal now is to elucidate the specific mechanisms by which the PTHR1 uniquely recognizes its two specific ligands, PTH and PTHrP, and activates selected intracellular effectors in different target cells. Progress toward this goal has been made via the application of a number of molecular and pharmacological approaches, such as the use of receptor mutagenesis coupled with peptide analog design strategies to reveal sites of specific intermolecular contact and clues about conformational changes involved in activation. The use of genetically modified mice engineered so as to have a specific alteration in a selected component of the ligand−receptor response system have also helped make possible a level of analysis at the whole-animal physiological level. These experimental systems ultimately help reveal the involvement of the PTHR1 and its ligands in skeletal and mineral ion physiology as well in diseases, such that they could lead to the development of new forms of therapy targeted to the PTHR1. Broader views of the roles that the PTHR1 and its ligands play in the systemic control of metabolic processes in bone and kidney, and developing tissue, as well as the downstream processes that the receptor controls within target cells, are discussed in detail in other chapters (see Chapters 24−27, 32, and 52). This chapter then focuses on the molecular properties of the PTHR1 per se, and principally on the mechanisms by which PTH and PTHrP ligands, via their N-terminal portions, interact with this receptor and induce signal transduction processes. It will also discuss findings on the so-called type-2 PTH receptor, or PTHR2, and its endogenous ligand, tuberoinfundibular peptide of 39 residues (TIP39), as well as the possibility that other, as yet unidentified, receptors exist that can bind and potentially respond to the carboxy-terminal portion of the endogenous PTH and PTHrP ligands, which appear not to be contributing to interactions with the PTHR1.

The PTHR1 is a class B G-protein-coupled receptor

The PTHR1 exhibits the general protein architecture seen in each of the class B GPCRs and thus is a single-chain integral membrane protein containing a relatively long amino-terminal extracellular domain (ECD) of ∼170 amino acids (after removal of residues 1−22, which act as the signal sequence), a transmembrane domain (TMD) or core region comprising the seven membrane-spanning α helices (TMs 1−7) and their interconnecting extracellular and intracellular loops (ECLs 1−3 and ICLs 1−3), and a C-terminal tail extending from the base of TM7 (∼Cys452) to the C terminus (Met593) (Fig. 28.1A). As a class B GPCR, the PTHR1 contains none of the hallmark amino acid residues and sequence motifs that define the three other main classes of GPCRs: the class A receptors represented by the β_2Ar, the class C GPCRs represented by the calcium-sensing receptor, and class F receptors, as represented by the Frizzled receptors (Fredriksson et al., 2003). Instead, the PTHR1 exhibits a distinct pattern of amino acids that is conserved in each of the 14 or so other class B GPCRs, which include the receptors for calcitonin, secretin, glucagon, glucagon-like peptide-1 (GLP1), corticotropin-releasing factor (CRF), and several other peptide hormone ligands (Segre and Goldring, 1993). Nevertheless, comparison of the three-dimensional structures obtained for GPCR representatives from each of the main GPCR families reveals

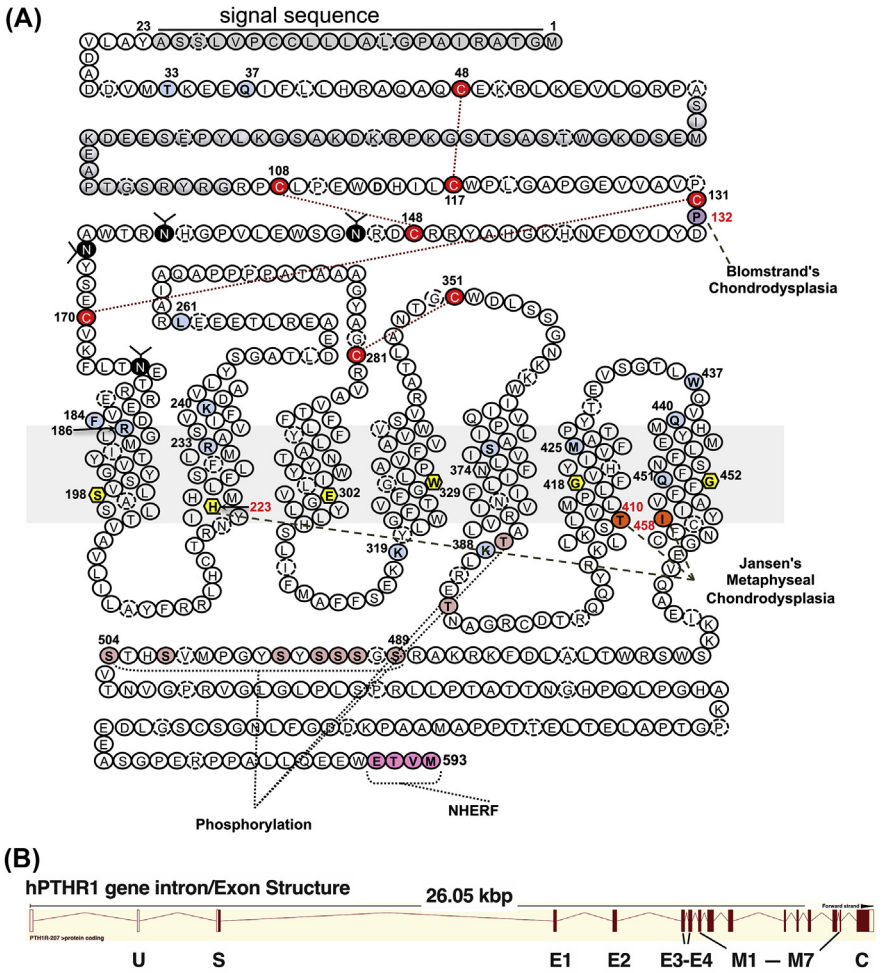

FIGURE 28.1 Primary structure of the human parathyroid hormone receptor type 1 protein and corresponding gene organization. (A) The human parathyroid hormone receptor type 1 (*hPTHR1*) protein is displayed to illustrate the domain organization and locations of selected key residues, including the eight extracellular cysteines involved in a disulfide bond network (*connecting dotted lines*); the four glycosylated extracellular asparagines; Pro132, at which loss-of-function mutations occur in Blomstrand's chondrodysplasia (compound homozygous) and in failed tooth eruption (heterozygous); His223, Thr410, and Ile458, at which activating mutations occur in Jansen's metaphyseal chondrodysplasia; cytoplasmic sites of serine and threonine phosphorylation; the four C-terminal residues involved in PDZ-domain interactions with Na^+/H^+ exchange regulatory factor 1 (*NHERF*) proteins; and a number of residues shown by mutagenesis and/or cross-linking studies to be involved in ligand interaction (*filled shaded circles* with position numbers). Also shown is the residue in each transmembrane domain helix that is the most conserved among the class B G-protein-coupled receptors (*filled hexagons*). (B) The intron/exon structure of the hPTHR1 gene with coding and noncoding exons indicated as *filled* and *open boxes*, respectively.

similarities not only in the basic seven-TMD protein fold that is shared across all GPCR classes, but also in some of the key interhelical contact points that occur within the hepta-helical bundle and are thought to mediate key mechanistic steps of activation (Cvicek et al., 2016). At least some aspects of function are thus likely preserved, at least topologically, between the PTHR1 and perhaps most of the 800 or so other GPCRs encoded in the human genome.

While each class B GPCR responds to a peptide ligand of moderate size—about 30–40 amino acids in length—the PTHR1 is the only class B GPCR for which the endogenous ligands extend more C-terminally, as PTH is 84 amino acids in length and PTHrP is 141 amino acids. Such C-terminal extensions are absent in the ligands identified in the genomes of fish and other nonmammalian species (Rubin and Jüppner, 1999; Mirabeau and Joly, 2013), and thus appear to be modifications that occurred later in vertebrate evolution. In any event, most if not all of the available data indicate that only the first 34 amino acids or so of PTH and PTHrP participate in binding to the PTHR1, such that PTH(1–34) and PTHrP(1–34) peptides exhibit nearly the same affinities and signaling potencies on the PTHR1 as the corresponding full-length polypeptides (Li et al., 2012; Dong et al., 2012).

Parathyroid hormone receptor gene structure and evolution

Structure of the PTHR1 gene

The gene encoding the human PTHR1 resides on chromosome 3 (locus 3p22−p21.1) and spans ∼26 kb of DNA (Fig. 28.1B) (McCuaig et al., 1994; Kong et al., 1994). The predicted transcript consists of 14 coding exons and 2 noncoding exons, ranging in size from 42 bp for exon M7 encoding a portion of transmembrane helix 7 to more than 400 bp for exon T encoding the C-terminal tail. The introns vary in size from 81 bp between exons M6 and M6/7 to more than 10 kb between exon S encoding the signal sequence and exon E1 encoding the N-terminal portion of the mature receptor. Three promoter regions have been identified for the gene and shown to be active at different levels in different tissues (Minagawa et al., 2001; Bettoun et al., 1997; Amizuka et al., 1997). Expression of PTHR1 mRNA can be detected in a variety of fetal and adult tissues, including the adrenals, placenta, fat, brain, spleen, liver, lung, and cardiac muscle, with strongest signals observed in adult bone and kidney (Urena et al., 1993; Tian et al., 1993; Uhlen et al., 2015). The genes for the other class B GPCRs generally exhibit a similar intron/exon organization, which is consistent with their evolution from a common ancestor gene and utilization of a similar protein design for engaging their cognate peptide ligands (Hwang et al., 2013).

Evolution of the parathyroid hormone receptor−ligand system

Bioinformatics-based investigations of PTH receptor as well as PTH and PTHrP ligand coding sequences present in the genomes of species representing various stages of evolution have yielded clues about how the PTH ligand and receptor system first emerged and evolved over time to provide the complex developmental and adaptive capacities established in the mammalian species. These studies suggest that PTH receptors and ligands emerged before the evolution of the first vertebrates, as apparent orthologs of the receptor as well as PTH-like ligands have been detected in the genomes of early vertebrates, such as the elephant shark and sea lamprey, as well as some invertebrates, such as the tunicate *Ciona intestinalis* and the amphioxus *Branchiostoma floridae*, which are thought to be representative of early chordates (Fig. 28.2) (Kamesh et al., 2008; Pinheiro et al., 2012; Mirabeau and Joly, 2013; On et al., 2015; Cardoso et al., 2006; Hwang et al., 2013). Sequences with at least some homology (∼69% amino acid similarity) have also been identified in the genomes of several insects, such as the red flour beetle (*Tribolium castaneum*) and honeybee (*Apis mellifera*), but not in the fruit fly (*Drosophila melanogaster*) (Li et al., 2013; Cardoso et al., 2014). The biological function of any such invertebrate PTH receptor−like sequence remains unknown.

Genome studies also suggest that chromosomal rearrangements contributed to the diversification of the PTH ligand−receptor system. At least two copies of a PTH receptor gene family member are thus found in the haploid genomes of most vertebrate species, and these can be attributed, in part, to two rounds of whole-genome duplication that are thought to have occurred during the early phases of vertebrate evolution (Fig. 28.2) (Hwang et al., 2013; On et al., 2015; Pinheiro et al., 2012; Cardoso et al., 2006, 2014). These early duplications were followed by other gene duplications as well as deletion events that occurred at different points along the evolutionary paths leading to the divergent animal groups. The genomes of teleost fish, as represented by the zebrafish, *Danio rerio*, thus encode three receptors, the PTHR1, PTHR2, and PTHR3, but lack a PTHR4 gene as a putative partner to the PTHR2, apparently due to a deletion event that happened in early fish evolution (Rubin and Juppner, 1999; Hwang et al., 2013). Bird genomes encode PTHR1 and PTHR3, and lack PTHR2 and PTHR4, while mammals encode PTHR1 and PTHR2, and lack PTHR3 and PTHR4. The absence of a PTHR2 in birds and a PTHR3 in primates apparently reflects separate gene deletion events that occurred at distinct times during the evolution of these two vertebrate groups. The peptide ligands, as represented in humans by PTH, PTHrP, and TIP39, the last a ligand for the PTHR2 as discussed further in a later section, are presumed to have evolved in parallel with their receptors, and thus to have stemmed from some precursor peptide ligand that emerged at or about the time that the first chordates appeared, as indeed, PTH- and/or TIP39-like coding sequences are found in the genomes of early fish, as well as amphioxus and *C. intestinalis* (Rubin and Juppner, 1999, Yan et al., 2012; Pinheiro et al., 2012; Trivett et al., 2005; Liu et al., 2010). These findings are consistent with the notion that the PTH ligand−receptor system is an evolutionarily ancient adaption that emerged in some precursor form before the appearance of the first vertebrates and evolved over time so as to contribute importantly not only to the successful adaption of the animal to changing environments but also to the development of higher-order organ systems, such as the skeleton (Hogan et al., 2005; Suzuki et al., 2011; Trivett et al., 2005).

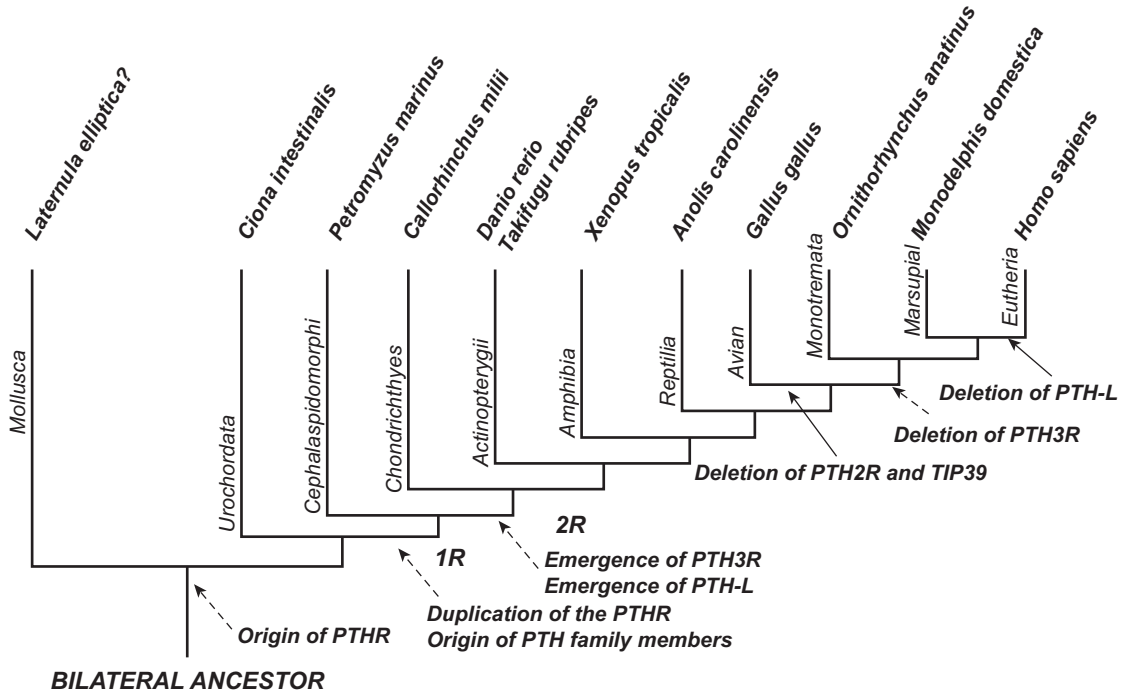

FIGURE 28.2 Evolutionary model for parathyroid hormone receptors. Shown is a tree diagram to depict that the ancestral parathyroid hormone receptor (*PTHR*) sequence probably originated before the appearance of the first chordates, as represented by the tunicate *Ciona intestinalis*, and that two rounds of whole-genome duplication (*1*R and *2R*) occurred before the emergence of the terrestrial vertebrates to result in three receptor subtypes—PTHR1, PTHR2, and PTHR3—with the expected fourth subtype lost by an early gene deletion event. The PTHR2 and PTHR3 subtypes were probably lost by later gene deletion events occurring with the radiations leading to birds and mammals, respectively. *Reproduced pending permission from Pinheiro, P. L., Cardoso, J. C., Power, D. M., Canario, A. V. 2012. Functional characterization and evolution of PTH/PTHrP receptors: insights from the chicken. BMC Evol. Biol. 12, 110.*

Mechanisms of ligand recognition and activation by parathyroid hormone receptors

Basic structural properties of the PTHR1

As in all class B GPCRs, the ECD contains six highly conserved cysteine residues that form a disulfide network (Fig. 28.1A) that maintains the tertiary fold of the ECD, which follows a tripartite helix–β sheet–helix pattern (Pioszak et al., 2008). The ECD contains four asparagines that are glycosylated during intracellular processing and transported to the plasma membrane. A feature of the ECD that is seen only in the mammalian PTHR1s, and not in the mammalian PTHR2s or any other class B GPCR, is a 44-amino-acid segment—Ser61–Gly105 in the human PTHR1—located between the first and the second cysteine. This segment is encoded by a separate exon, called E2, and appears not to contribute to function, as assessed by site-directed mutagenesis strategies and pharmacological analyses in transfected cells (Lee et al., 1994).

Other than the general seven membrane-spanning helical architecture, the class B receptors share no obvious homology with receptors from the other main GPCR subgroups, including the class A GPCRs, which comprise the largest GPCR subgroup and include the β-adrenergic receptor and rhodopsin as well-studied representatives. Nevertheless, the high-resolution structures now available for a number of GPCRs from each main class, including several class B GPCRs, suggest that certain relationships of structure and function might be preserved in all GPCRs, particularly in the intramolecular interaction networks that are located within the TMD bundle and mediate processes of receptor activation and G protein coupling (Bortolato et al., 2014; Cvicek et al., 2016). Within the class B GPCRs there are about 45 amino acid residues that are strongly conserved. These conserved residues are dispersed in the seven TM helices and in the ECD and probably help define the basic three-dimensional scaffold structure of the receptor and as well may participate more directly in basic mechanisms of activation, while other more divergent residues are likely to provide the specific recognition determinants used for selective binding of the appropriate peptide ligand.

Binding of a PTH agonist peptide ligand, such as PTH(1–34), to the extracellular surface of the PTHR1 induces a conformational change in the receptor that leads to G protein coupling and activation of downstream signaling responses (see Chapters 32 and 52 for an in-depth discussion of downstream signaling responses). In most target cells the PTHR1

couples strongly to G proteins containing the GαS subunit, and thus activates the adenylyl cyclase/cAMP/protein kinase A (PKA) signaling system. The agonist-stimulated PTHR1 can also activate other signaling systems, including the Gαq/phospholipase C (PLC)/IP3/iCa^{2+} pathway, the Gα12/DAG/PLD pathway, and the arrestin/ERK1/2 pathway, depending potentially on the type of target cell and PTH or PTHrP ligand analog used (Gesty-Palmer et al., 2006, 2013). PTHR1 signaling is generally thought to be a highly regulated process and thus to terminate relatively soon after initial binding via mechanisms involving receptor phosphorylation and internalization (Bisello et al., 2002; Malecz et al., 1998; Qian et al., 1998), but variations on this theme now seem possible, as discussed in a later section. It is now becoming clear that ligands with different structures can bind to a receptor in different modalities so as to induce different biological outcomes in target cells, in terms of type of pathway activated as well as the duration of the response, a concept generally referred to as biased agonism (Luttrell et al., 2015). This concept has particular relevance for the PTHR1, as it may help explain, at least in part, certain differences in biological actions that have been observed for PTH and PTHrP peptides (Horwitz et al., 2003) and, moreover, could provide a strategic basis for developing new ligand analogs for the PTHR1 that have therapeutic utility.

Two-site model of ligand binding to the PTHR1

Clues regarding the overall mechanism of ligand binding and agonist-induced activation used by the PTHR1 were initially obtained from receptor mutagenesis and photoaffinity cross-linking studies, but more recently have come from the successful application of X-ray crystallography and cryo-electron microscopy (cryo-EM) approaches to the analysis of several other class B GPCRs, either as intact receptors or as the isolated ECD or TMD. Such structural information for the PTHR1, however, is so far reported only for the isolated ECD in complex with PTH(15−34) or PTHrP(12−34) peptides (Pioszak et al., 2008, 2009). The emerging structural data combined are providing valuable insights into the basic mechanisms by which the class B GPCRs engage their cognate peptide ligand and activate signal transduction. The earlier studies on binding mechanisms for the PTHR1 performed in parallel by several groups led to the so-called "two-site" model of ligand−receptor interaction. According to the model, the ligand, such as PTH(1−34), first docks to the receptor via the binding of the C-terminal domain of the ligand, approximately residues 15−34, to the ECD of the receptor. Then the amino-terminal portion of the ligand, approximately residues 1−14, engages the extracellular surface of the TMD portion of the receptor to yield the intact ligand−receptor complex (Fig. 28.3). The ECD component of the interaction contributes predominantly to the overall binding affinity of the complex, while the TMD component mediates the process of receptor activation and G protein coupling. The experimental findings that led to this model came from studies employing, often in parallel, the two complementary approaches of receptor mutagenesis and photoaffinity cross-linking. By the former approach, receptors altered at specific residues or defined regions were generated and analyzed in pharmacologic binding and signaling assays for interaction with various peptide ligand analogs with defined structural modifications such that they could be used as functional probes of specific contact sites or regions. For example, a receptor chimera strategy based on the weaker binding of PTH(7−34) to the rat versus the human PTH receptor was used to establish that the ECD of the receptor was the major site of binding for the C-terminal portion of the ligand (Juppner et al., 1994). A similar chimera strategy based on the capacity of the analog Arg2-PTH(1−34), in which the highly conserved valine-2 is replaced by a bulky arginine, to function as an antagonist on the rat PTHR1 and an agonist on the opossum PTHR1 led to the finding that residue 370 at the extracellular end of TM5, alanine and serine in the opossum and rat receptors, respectively, is a key determinant of ligand-induced activation (Goltzman et al., 1975). Other such mutagenesis studies that followed, extending also to the PTHR2, further supported the two-domain model (Bergwitz et al., 1996, 1997; Turner et al., 1998). The second approach involving the use of photoaffinity cross-linking strategies provided more direct biophysical analyses of ligand and receptor sites in close intermolecular proximity. The method involved ligands modified at a selected position with an amino acid analog containing a photolabile side chain, typically benzophenylalanine (BPA) (Zhou et al., 1997). After binding to the receptor, the complex is UV irradiated, causing the BPA group to covalently link to a site in the target protein chain within a radius of a few angstroms. Initially BPA was thought to react rather nonselectively, but was later discovered to have a propensity to react with methionines (Wittelsberger et al., 2006b). In any event, the strategy resulted in the identification of a number of cross-links that could be mapped to specific receptor residues, including between positions 1 and 2 in the ligand and Met425 at the extracellular end of TM6 (Bisello et al., 1998; Gensure et al., 2001a), between ligand residue 13 and Arg186 at the extracellular end of TM1 (Adams et al., 1998), and between ligand position 23 and Thr33 and/or Gln27 at the N-terminal end of the receptor (Mannstadt et al., 1998). A number of other contacts involving residues in the middle or C-terminal region of PTH(1−34) or PTHrP(1−36) and various sites in the receptor were also mapped, although not always to specific receptor residues (Gensure et al., 2001b, 2003; Greenberg et al., 2000; Wittelsberger et al., 2006a). The information gained from these cross-linking studies provided distance constraints that enabled development of initial molecular models of the PTHR1·PTH ligand complex (Greenberg et al., 2000; Gensure

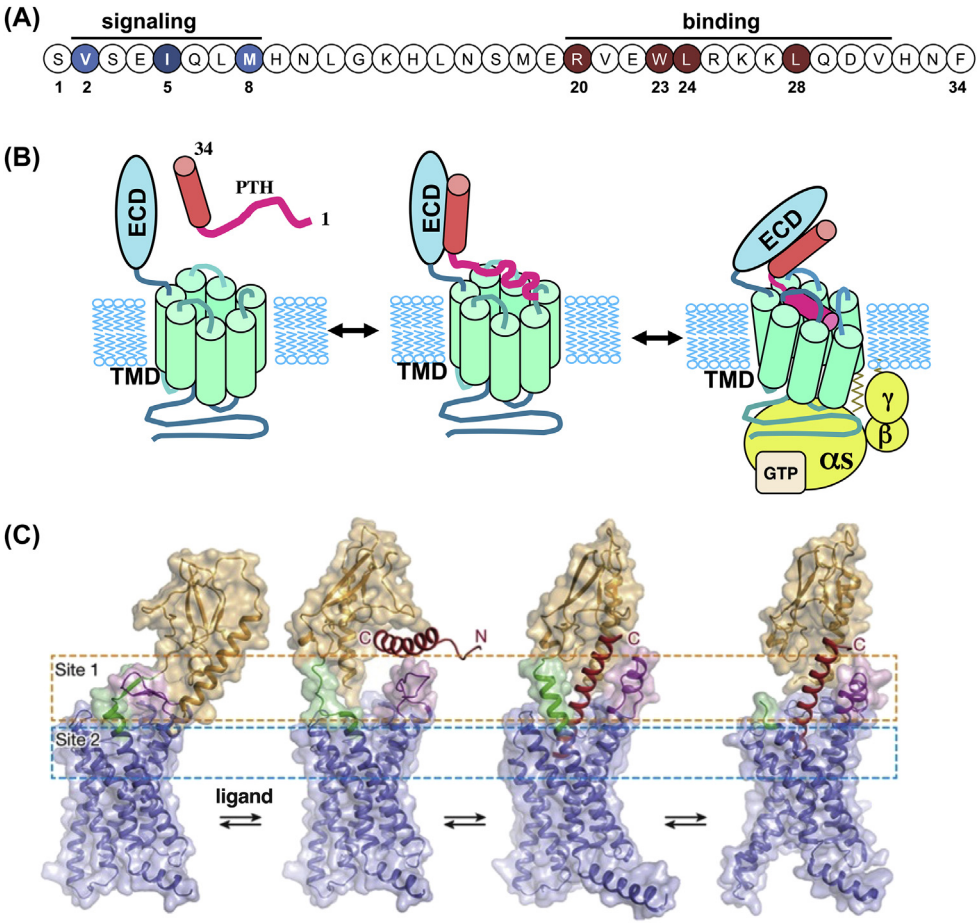

FIGURE 28.3 Ligand binding mechanisms at the parathyroid hormone receptor 1. (A) Sequence of PTH(1−34) highlighting the N-terminal residues Val2, Ile5, and Met8, which play critical roles in receptor activation, and the C-terminal residues Arg20, Trp23, Leu24, and Leu28, which play critical roles in receptor binding. (B) The two-domain model of ligand binding and activation at the PTHR1, as developed by cross-linking and mutagenesis data obtained for the parathyroid hormone receptor 1 (PTHR1): the C-terminal portion of PTH(1−34) first docks to the amino-terminal extracellular domain (*ECD*) of the receptor to provide affinity interactions, and then the amino-terminal portion of the ligand engages the transmembrane domain (*TMD*) of the receptor to induce conformational changes that enable G protein coupling. (C) Refinement of the two-domain model based on high-resolution X-ray crystal and cryo-electron microscopy structures of the glucagon receptor and GLP1 receptor, which are class B GPCRs structurally related to the PTHR1. The ligand, shown in *red*, binds as a nearly linear α helix and makes extensive contacts with exposed extracellular surfaces in both the ECD and the TMD receptor regions. Ligand binding results in an outward movement of the cytoplasmic termini of several of the TM helices, particularly TM6, to thus open a cavity that will accommodate the G protein. *(C) Reproduced pending permission from Zhang, H., Qiao, A., Yang, L., Van Eps, N., Frederiksen, K. S., Yang, D., Dai, A., Cai, X., Zhang, H., Yi, C., Cao, C., He, L., Yang, H., Lau, J., Ernst, O. P., Hanson, M. A., Stevens, R. C., Wang, M. W., Reedtz-Runge, S., Jiang, H., Zhao, Q., Wu, B. 2018a. Structure of the glucagon receptor in complex with a glucagon analogue. Nature 553, 106−110.*

et al., 2003; Wittelsberger et al., 2006a; Piserchio et al., 2002), although the incomplete nature of the input data left a fair amount of uncertainty.

The two-site model was also found to be relevant for most if not all of the other class B GPCRs and their cognate peptide ligands, as elucidated using similar functional and cross-linking-based approaches by other groups (Parthier et al., 2009). This basic model has now been confirmed and refined by high-resolution structural data that have been obtained using X-ray crystallography or cryo-EM approaches for several of the other class B GPCRs, including the CRFR1, the glucagon receptor, and the GLP1 receptor, although not yet for the PTHR1 (de Graaf et al., 2017). A key modification used in the crystallography work, and a potential limitation in terms of data interpretation, is the introduction of thermostabilizing point mutations and insertions of heterologous protein segments known to promote crystallization at dispersed positions in the receptor TMD, which generally tends to be conformationally dynamic. One set of findings from the functional studies that helped define the TMD component of the two-domain model for the PTHR1 was that short amino-terminal PTH fragment peptides, such as PTH(1−14) and PTH(1−11), which as unmodified peptides are inert for binding

and signaling due to a lack of stabilizing interactions with the ECD, could act as potent agonists when modified with certain helix-stabilizing and affinity enhancing substitutions. Furthermore, they could stimulate signaling via a PTHR1 construct that lacks most of the ECD (up to Glu182), about as potently as PTH(1−34) does on the intact PTHR1 (Shimizu et al., 2001). These findings highlight the functional autonomy of the N-terminal region of the ligand and the TMD of the receptor, and also suggested that ligands much smaller than PTH(1−34) that target the functionally critical TMD and thus act as potent PTH mimetics could be developed. Native PTH and PTHrP peptides are thought to bind to the PTHR1 via a sequential process that involves initial ligand interactions with the ECD followed by interactions with the TMD and the conformational rearrangements involved in activation (Fig. 28.3) (Hoare and Usdin, 2001). The nature of these conformational changes and the extent to which they may involve a higher-order folding of the complex, for example, a movement of the ECD relative to the TMD, remains an area of uncertainty, but the new class B GPCR structures now available provide clues as to the types of changes that might be possible for the PTHR1−PTH complex.

The crystal structures of the isolated ECD protein in complex with the PTH(15−34) or PTHrP(12−34) fragment suggest that the two ligands bind to the ECD via similar, though not identical, mechanisms (Pioszak et al., 2009). Each peptide thus is bound to the ECD as an α helix and fits into a groove that runs along the center of the ECD. Key hydrophobic interactions occur between Trp23, Leu24, and Leu 28 in the ligand, which align along an apolar face of the helix, and complementary apolar surfaces in the receptor-binding groove. The side chain of Arg20 in the ligand makes extensive interactions with a ring of polar residues located at one end of the ECD. Residues Arg20, Trp23, Leu24, and Leu28 are well conserved in PTH and PTHrP ligands, while residues on the opposite helix face are less well conserved, are mostly polar in character, and can be mutated with relatively little effect on binding. Compared with the PTH(15−34)·ECD structure, the PTHrP helix bends modestly at about Leu24 such that the C-terminal portions of the two helices make distinct contacts, and the C-terminal residue is offset by a few angstroms in the two structures (Pioszak et al., 2009).

Interactions that occur between the N-terminal portion of the ligand, as contained in the PTH(1−14) segment, and the receptor's TMD are of key interest as they are critically involved in receptor activation. There is no direct structural data available for the PTHR1 TMD. The aforementioned mutagenesis and cross-linking data are consistent with the ligand making multiple contacts with an extensive, solvent-exposed surface area that involves the extracellular ends of the TMD helices and the extracellular loops. In the crystal and cryo-EM structures of the TMDs of the other class B GPCRs, the extracellularly exposed surface of the TMD bundle forms a relatively large pocket that accommodates the N-terminal portion of the ligand (Liang et al., 2017; de Graaf et al., 2017). In the intact GLP1R−GLP1 (Zhang et al., 2017, 2018a) and CTR−calcitonin structures, the full-length peptides are bound as linear α helices that extend along the ECD, which is positioned above the TMD, and enter into the TMD bundle such that the N-terminal residues of the ligand helix project into the bundle such that they can trigger the conformational rearrangements involved in receptor activation (Zhang et al., 2018a) (Fig. 28.3C). It is reasonable to suggest that PTH(1−34) binds to the PTHR1 in a fashion similar to that seen for glucagon and calcitonin, but direct confirmation of any such interaction mode for PTH and the PTHR1 remains to be established by direct high-resolution methods.

Mechanism of ligand-induced activation at the PTHR1

Previous mutagenesis and biophysical cross-linking data suggest that substantial conformational changes occur within the TMD bundle of the PTHR1 during agonist-induced activation (Gardella et al., 1996; Gensure et al., 2001a; Thomas et al., 2008). Insights into the types of specific changes that might occur can be inferred by comparing the active- versus inactive-state structures obtained for the several other class B GPCRs. Such comparisons suggest that during the agonist binding and receptor activation process, the ECD of the complex rotates in a counterclockwise direction, relative to the vertical axis of the TMD bundle, by nearly 90 degrees (Zhang et al., 2018a). In addition, two segments at the extracellular ends of the TM1 and TM2 helices isomerize from β-strand conformations to α-helical conformations. Interestingly, whereas the two β strands in the inactive state receptor pair together to form a cover over the ligand-binding pocket of the TMD bundle, the induced α-helical segments extend upward and contact the midregion of the bound ligand helix to thus help stabilize the ligand and guide the N-terminal segment into the TMD pocket (Zhang et al., 2018a). The structural studies on the class B GPCRs also reveal a cluster of highly conserved polar residues within the core of the TMD bundle that form a network of H-bond and electrostatic interactions and thus act to constrain the bundle in a closed, inactive conformation. Agonist interactions within the TMD core trigger a rearrangement of this network to release the constraints and promote the outward movement of the cytoplasmic ends of several of the TM helices, particularly TM6. These movements result in a cavity on the cytoplasmic surface of the receptor that accommodates the G protein (Fig. 28.3C) (Zhang et al., 2017; Yin et al., 2017).

While any such mechanism remains to be assessed for the PTHR1, the studies provide clues as to the types of conformational changes that are likely to occur during the PTHR1 activation process. It is worth noting that several PTHR1 residues that are located at least in the vicinity of the predicted cytoplasmic cavity used by G proteins have been implicated by mutagenesis methods to be involved in G protein interaction. These include Lys319, Val384, and Leu385 for Gαq coupling; Thr387 for Gαs coupling; and Lys388 for Gαs and Gαq coupling (Iida-Klein et al., 1997; Huang et al., 1996). Of further note, these studies led to the generation of the "DSEL" knock-in mouse in which the normal PTH receptor allele is replaced by a PTHR1 mutant having the Glu–Lys–Lys–Tyr sequence at positions 317–320 replaced by Asp–Ser–Glu–Leu and which is thus selectively impaired for Gαq/PLC signaling; the relatively modest effect of the mutant allele on the skeletons of these mice suggests that the Gαq/PLC signaling pathway does not play a critical role in PTH receptor–mediated control of endochondral bone formation (Guo et al., 2002).

Conformational selectivity and temporal bias at the PTHR1

Two high-affinity PTH receptor conformational states, R^0 and RG

The aforementioned structural models are consistent with the notion that structurally distinct ligands for the PTHR1 can stabilize or induce different receptor conformations so as to result in different types of signal transduction responses. The notion that variation in receptor conformation could play an important role in determining the affinity with which certain ligands bind to the PTHR1 emerged from a series of PTH radioligand binding studies that utilized membranes from cells transfected to express the PTHR1 and were performed under conditions to favor either the G-protein-uncoupled receptor conformation or the G-protein-coupled conformation (Hoare et al., 1999b). To promote the G-protein-uncoupled state, the binding reactions were conducted in the presence of GTPγS, which binds to the G protein α subunit and causes it to dissociate from the receptor. To promote the G-protein-coupled state, the binding reactions were conducted using membranes from cells transfected to express excess Gαs, typically a mutant form that binds the receptor with high affinity. The conceptual basis came from early pharmacologic studies performed on the β_2-adrenergic receptor and other such prototypic GPCRs that bind small catecholamine ligands. These studies led to the classical ternary complex model of GPCR action that posits that G protein coupling promotes a high-affinity receptor conformation, while G protein uncoupling, which occurs upon GDP–GTP exchange or GTPγS binding, causes the receptor to relax to a low-affinity state and thus release the bound agonist (De Lean et al., 1980). It was thus surprisingly found that certain ligands for the PTHR1, including PTH(1–34), bound with high affinity even in the presence of GTPγS, while others, such as PTHrP(1–36) and the modified N-terminal PTH fragment M-PTH(1–14), behaved in a fashion more consistent with the classical model and dissociated rapidly upon addition of GTPγS (Hoare et al., 2001; Dean et al., 2006, 2008). The findings thus suggested that the PTHR1 could exist in two distinct high-affinity conformations, depending on the type of ligand bound: one high-affinity conformation, as bound by PTH(1–34), could exist even in the absence of a bound G protein, while the other conformation, as bound by PTHrP(1–36) and M-PTH(1–14), required G protein coupling. Consequently, the two high-affinity states, G protein uncoupled and G protein coupled, were termed R^0 and RG, respectively.

Conformation-based differences in signaling responses to PTH and PTHrP ligands

While the initial findings on distinct affinity PTHR1 conformations came from biochemical studies performed in cell membranes, subsequent studies in intact cells as well as animals supported a biological significance. Thus, cAMP time-course studies performed in PTHR1-expressing cells, in which various ligands were allowed to bind to the receptor typically for 15–30 min and then all unbound ligand was removed by washout, revealed that Gαs/cAMP signaling as induced by R^0-selective ligands such as PTH(1–34) persisted for extended durations after washout. In contrast, cAMP signaling induced by RG-selective ligands such as PTHrP(1–36) or M-PTH(1–14) terminated more rapidly after washout (Okazaki et al., 2007; Dean et al., 2008). The results thus revealed a difference in the mode of binding and hence biological action for the structurally distinct ligands, including for PTH(1–34) and PTHrP(1–36), which until then were thought to bind to and activate the PTHR1 in similar if not identical fashions (Nissenson et al., 1988; Jüppner et al., 1988). However, an intriguing deficiency for stimulation of vitamin D synthesis was suggested for PTHrP(1–36) relative to PTH(1–34) in a human infusion study (Horwitz et al., 2003). The kinetic washout approaches thus enabled differences in modes of binding and signaling to be revealed for different PTH and PTHrP ligands. The kinetic assays initially used were performed in multiwell plate formats and involved measurement of cAMP either by radioimmunoassay of cell lysates or by a luciferase-based Glo sensor reporter that enables the nearly continuous detection of intracellular cAMP in live cells over time (Okazaki et al., 2007; Dean et al., 2008; Maeda et al., 2013). Such studies were subsequently complemented by highly

sensitive optical methods of fluorescence resonance energy transfer (FRET) microscopy, which enabled assessment of near-instantaneous changes in intracellular cAMP production at the single-cell level (Ferrandon et al., 2009; Feinstein et al., 2011). The findings also suggest a possible mechanistic basis for the distinct biological roles that PTH and PTHrP play in biology. Thus, a sustained mode of action, as occurs with PTH, would provide a suitable means to maintain blood calcium at the levels needed for normal physiological processes, while a more transient mode of signaling, as occurs with PTHrP, would provide a more suitable means to achieve the precise temporal control of cell differentiation that is required during tissue development, as for example in the skeletal growth plates, in which a precisely timed program of chondrocyte differentiation is required for proper elongation and shape formation of the long bones (Chagin and Kronenberg, 2014; Kronenberg, 2003).

The structural basis for the different modes of binding and hence signaling observed for PTH and PTHrP ligands in these studies is not completely known, but several amino acids that differ in the two ligands have been implicated. Most notably is the divergence at position 5, which is Ile in PTH and His in PTHrP, as it was thus found that the Ile5-PTHrP(1−36) analog binds with higher affinity to the R^0 conformation and exhibits more prolonged cAMP responses after washout than does PTHrP(1−36) (Dean et al., 2008). The divergences in the C-terminal (15−34) regions of the two ligands, which probably result in moderately altered modes of binding to the ECD (Pioszak et al., 2009), could also contribute to the differences in binding modes detected for the two ligands in the functional assays. The PTHrP(12−34) fragment was in fact shown to bind to the isolated ECD of the PTHR1 with an affinity about twofold higher than that of PTH(15−34), which supports an altered mode of binding, although the difference in affinity is opposite to that seen for the N-terminally intact ligands and the intact receptor (Dean et al., 2008). In any case, the findings on conformational selectivity for the PTHR1 provide insights into the mechanisms controlling the duration of ligand-induced signaling at the PTHR1, and furthermore have potential implications for the development of new PTHR1-based therapeutics. These two aspects are discussed in the following sections.

Endosomal signaling and signal termination at the PTHR1

Termination of G protein signaling at most GPCRs has generally been thought to occur relatively soon after initial binding of the agonist ligand and coincident with internalization of the receptor into endosomes (Drake et al., 2006). Findings on the PTHR1, as well as several other GPCRs, however, indicate that G-protein-mediated signaling can continue after most if not all of the receptor has moved into the endosomal domain. According to classical GPCR models, the process of signal termination involves a sequence of biochemical steps that include the phosphorylation of the receptor at serine and threonine residues located on exposed portions of the receptor's C-terminal tail and intracellular loops, the recruitment of β-arrestin proteins to the phosphorylated receptor with a coincident displacement of the G protein, the assembly of the β-arrestin-associated receptor into clathrin-coated pits that then pinch off from the membrane to form vesicles, and the trafficking of the vesicles containing the receptor and ligand as cargo through the endosomal sorting system. The last step directs the cargo to pathways of degradation as mediated by lysosomes and/or the proteasome system or recycles the receptor back to the cell surface (Drake et al., 2006). Many studies provide data generally consistent with this general scenario for the PTHR1. Thus, the agonist-activated PTHR1 is indeed rapidly phosphorylated on at least seven serine and two threonine residues, as well as being ubiquitinated on at least two lysines in the C-terminal tail and intracellular loops; β-arrestin proteins are recruited, the receptor moves into endosomal vesicles and internalizes, and it can be at least partially recycled back to the cell surface (Rey et al., 2006; Tawfeek et al., 2002; Vilardaga et al., 2002; Chauvin et al., 2002; Zhang et al., 2018b). The PTHR1 also engages with certain intracellular scaffolding proteins, particularly members of the Na^+/H^+ exchange regulatory factor family of proteins via PDZ-domain-based anchoring to the receptor's C-terminal tail (Mahon et al., 2003; Mamonova et al., 2012), which further are thought to contribute to the trafficking and signal termination events that occur following agonist binding and activation (see Chapter 27 for further information on PTHR1 trafficking events related to actions in the kidney).

The initial evidence suggesting that PTHR1 could deviate from the classical model of GPCR signal termination came from studies on M-PTH(1−34) and M-PTH(1−28) analogs that contained the same set of affinity- and potency-enhancing modifications as contained in the M-PTH(1−14) analogs mentioned earlier (Okazaki et al., 2008). These M-PTH(1−34) analogs were thus found to mediate cAMP responses in PTHR1-expressing cells that lasted for as long as several hours after washout, and thus for much longer times than those induced by PTH(1−34). Microscopy studies using fluorescent PTH analogs, typically modified with tetramethylrhodamine attached to the ε-amino function of lysine-13, revealed that within 15 min of initial binding, most, if not all, of the ligand was located in cytoplasmic vessels and not on the cell surface. There was thus a spatiotemporal correlation between persistent signaling and location in vesicles, which raised the novel possibility that the agonist-activated PTHR1, at least when bound by certain modified ligands, could mediate

prolonged Gαs-mediated cAMP responses from the endosomal compartment. It was further observed that upon injection into mice, such M-PTH(1–34) and related analogs induced elevations in blood calcium that persisted for much longer durations than those induced by PTH(1–34). Importantly, the prolonged calcium responses could not be explained by a simple plasma pharmacokinetic effect, as the modified ligands disappeared from the blood, if anything, more rapidly than did PTH(1–34). The results thus suggested that the modified ligands were rapidly sequestered by binding to receptors in target cells of bone and kidney and thus continued to signal from the endosomal compartment (Okazaki et al., 2008).

Parallel studies by Vilardaga and colleagues using fluorescence microscopy and FRET-based kinetic approaches to track ligand–receptor complexes in real-time in live HEK293 cells supported a novel mechanism, and also identified some of the key cytoplasmic effector proteins involved. These data thus confirmed that the ligand–receptor complexes were translocated rapidly from the plasma membrane to internalized endosomes where they remained associated with the G protein as well as adenylyl cyclase (Ferrandon et al., 2009). Prolonged signaling at the PTHR1 thus clearly correlated not only with binding to a distinct high-affinity state of the receptor, R^0, but also with the formation of signaling complexes that remained stable and presumably active in endosomes. Evidence of such endosomal signaling has now been reported for a number of other GPCRs, including the calcitonin receptor (Andreassen et al., 2014), the calcium-sensing receptor, a class C GPCR (Gorvin et al., 2018), and a number of class A receptors (Godbole et al., 2017; Thomsen et al., 2016).

The concept of endosomal signaling could have implications for understanding the basic processes for how these receptors function. PTHrP(1–36) was found to bind more selectively to the RG conformation of the PTHR1 and thus induces more transient cAMP responses compared with PTH(1–34) or the more strongly R^0-selective analogs, such as M-PTH(1–34) (Dean et al., 2008). Live-cell fluorescence tracking studies in HEK293 cells revealed that PTHrP(1–36) did not colocalize with the PTHR1 in intracellular vesicles (Ferrandon et al., 2009). The findings thus suggested that PTHrP and presumably other RG-selective ligands follow a subcellular trafficking path distinct from that used by PTH(1–34) and the longer-acting analogs and which thus involves differences in processes of signal termination. A key step in the signal termination process for the PTHR1, as induced by PTH(1–34), was thus found to be the association of the internalized receptor with a macromolecular assembly called the retromer complex (Feinstein et al., 2011), which acts at the later stages of endosomal maturation to sort vesicle cargo along pathways of either recycling or degradation. Retromer-mediated signal termination for the PTHR1 was found to be dependent on the constituent proteins, VPS26, VPS35, and SNX27, the last of which binds to the PTHR1 C tail via a PDZ-domain-directed interaction (McGarvey et al., 2016; Chan et al., 2016; Feinstein et al., 2011). The biological relevance for this PTHR1–retromer interaction, initially revealed in HEK293 cells, is supported by studies showing that targeted reduction of VP35 expression in osteoblastic MC3T3 cells prolongs the cAMP signaling response to PTH(1–34), and that mice genetically ablated for VPS35 in osteoblasts exhibit a mild osteoporotic phenotype and an enhanced anabolic response to intermittent PTH(1–34) (Xiong et al., 2016). These studies also revealed that PPP1R14C, which acts to inhibit the PP1 phosphatase, can associate with VPS35 or the internalized PTHR1 to thus result in changes in the phosphorylation status of downstream effectors, including phosphorylated cAMP-responsive element binding protein (CREB). It is thus intriguing to consider that endosomal signaling provides a means for the PTHR1 to activate specific target effectors in defined subcellular compartments so as to achieve efficient control of downstream responses; for example, the phosphorylation of a transcriptional activator such as CREB in the immediate vicinity of the nucleus to thus facilitate its access to the genome.

A second mechanistic aspect of subcellular trafficking and signal termination for the PTHR1 revealed in these studies concerns the role of endosomal acidification. In general, the endosomal interior progressively acidifies from an initial pH of ~7.4 to a low pH of ~4.5, at which most biological ligand–receptor complexes dissociate. This acidification is mediated by the vacuolar ATPase proton pumps, which are activated by cAMP/PKA-dependent phosphorylation. PTH(1–34)-induced cAMP/PKA signaling was thus found to promote vesicle acidification and hence the dissociation of the PTH·PTHR1 complexes, leading to signal termination. Thus PTHR1 signaling appears to be regulated at the level of the endosome by a negative feedback system of acidification (Gidon et al., 2014). These findings further suggest the possibility that structurally distinct ligands might bind to the PTHR1 in different fashions so as to form complexes that have differential sensitivities to endosomal acidification and hence can signal for different durations.

Ligand-directed temporal bias and therapeutic implications

The profound differences in the duration of signaling now seen to be clearly possible for structurally distinct ligand analogs via binding to distinct PTHR1 conformations are consistent with the emerging GPCR concept of ligand-directed temporal bias (Grundmann and Kostenis, 2017). Thus, for the PTHR1, ligands that bind mainly to the G-protein-dependent conformation, RG, mediate transient signaling responses because the ligand–receptor complexes dissociate soon after the first round of G protein activation, hastened by endosomal acidification, whereas ligands that bind with high affinity to the

G-protein-independent conformation, R^0, mediate prolonged signaling responses as the ligand−receptor complexes remain intact upon G protein uncoupling and endosomal acidification and hence can activate multiple G protein coupling cycles (Okazaki et al., 2008). Such temporal bias for the PTHR1, as it relates to distinct PTH and PTHrP analog ligands, has relevance to strategies aimed at the development of new PTHR1-based therapeutics, as the duration of signaling at the PTHR1 can have a profound impact on physiological outcomes, particularly those relating to the balanced processed of bone anabolism and catabolism (Martin et al., 2006).

Ligand-dependent temporal bias at the PTHR1 holds relevance for two key diseases that are treatable with PTHR1-targeted ligands: osteoporosis and hypoparathyroidism. Because of the distinct pathophysiological mechanisms underlying these two diseases—an imbalance in the coupled processes of bone formation bone and resorption leading to an inadequate bone structure in osteoporosis, and a deficiency of PTH production by the parathyroid glands leading to a condition of chronic hypocalcemia in hypoparathyroidism—distinct PTH ligand modes of action and hence pharmacodynamic profiles are needed to achieve effective treatment. Thus, a pulsatile mode of action is needed for osteoporosis, while a more sustained mode of action is needed for hypoparathyroidism (see Chapters 10, 23, and 70 for more detailed information on underlying mechanisms and modes of treatment for these diseases). The concept of temporal bias thus suggests that a short-acting RG-selective ligand, such as PTHrP(1−36), could have utility for osteoporosis, whereas a longer-acting R^0-selective ligand, such as those in the M-PTH(1−34) series of peptides and the long-acting analog LA-PTH, discussed in the next section, could have utility for hypoparathyroidism (Okazaki et al., 2008).

LA-PTH, a long-acting PTH/PTHrP analog for hypoparathyroidism

Based on the initial findings with M-PTH(1−34), efforts were made to develop even longer-acting analogs that could potentially be useful for hypoparathyroidism. One new long-acting analog derived, called LA-PTH, is a hybrid peptide in which the M-PTH(1−14) portion also present in the M-PTH(1−34) is joined to a modified C-terminal 15−36 portion of PTHrP(1−36). This unique structure results in high-affinity binding to the PTHR1 R^0 conformation, and hence markedly prolonged calcemic responses (Fig. 28.4A−D) (Maeda et al., 2013). The functional properties of LA-PTH suggested that it could have therapeutic utility for hypoparathyroidism, a disease for which PTH(1−34) as delivered especially by pump (Winer et al., 2014) and PTH(1−84) by subcutaneous injection by which it exhibits a prolonged pharmacokinetic profile (Mannstadt et al., 2013) have proven to be efficacious, with the latter now available as the drug Natpara. As a potentially improved form of therapy, LA-PTH was tested in several rodent models of the disease in which the parathyroid glands were either surgically removed or, in mice, ablated by diphtheria toxin treatment (Fig. 28.4D), and the results revealed that indeed the analog could normalize blood calcium levels more effectively and for longer periods of time after a single injection than could at least severalfold higher doses of PTH(1−34) or PTH(1−84) (Shimizu et al., 2016; Bi et al., 2016). The observed prolonged pharmacodynamic effects were again not explained by a prolonged pharmacokinetic profile, as the analog was cleared from the circulation if anything more rapidly than PTH(1−34). LA-PTH thus stands as a promising preclinical candidate as a new therapeutic option for hypoparathyroidism.

It should be noted that several other PTH(1−34)-based analogs have been reported to induce sustained pharmacodynamic actions in animals via distinct mechanisms. These mechanisms include the prolongation of the pharmacokinetic profile, as is achieved via fusion of the C terminus of the PTH(1−34) peptide to either the fragment crystallizable (Fc) portion of IgG (Kostenuik et al., 2007) or a 20-kDa polyethylene glycol (PEG) chain (Guo et al., 2017), each of which acts to impede the rate of glomerular filtration, or, in a third analog, via a combination of modifications (Nle8, Lys27, and a C-terminal 2-kDa PEG group) that results apparently in a prolonged retention of the peptide on the cell surface due to impairment of β-arrestin-mediated receptor internalization (Krishnan et al., 2018). Such analogs could also lead to new modes of treatment for hypoparathyroidism. Whether such analogs designed to induce prolonged actions in vivo via distinct mechanisms elicit different types of downstream responses, as, for example, in the specific gene sets regulated, remains to be determined.

Abaloparatide: a PTHrP analog for osteoporosis

Based on the dogma that a pulsatile administration and hence action of PTH is required to achieve an optimal increase in bone structure and strength while avoiding an excess of bone resorption, which typically occurs with a more continuous administration and action of the peptide, it was postulated that a PTHR1 ligand analog that binds selectively to the RG PTHR1 conformation, and thus induces signaling responses of short duration, would be more effective at building new

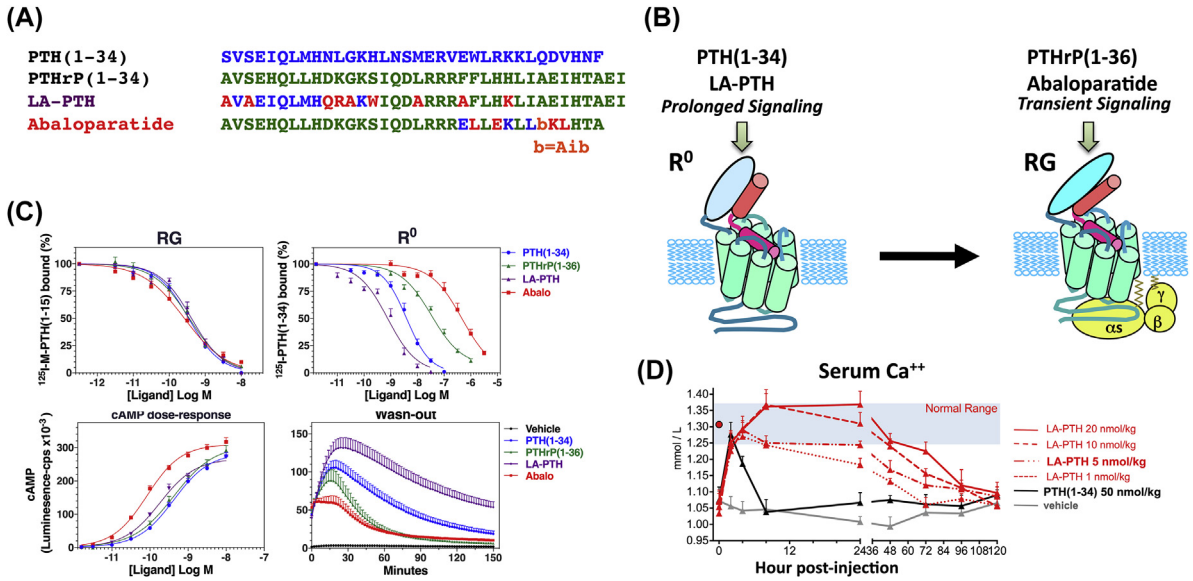

FIGURE 28.4 Conformational selectivity and temporal bias at the parathyroid hormone receptor 1. (A) Ligands that exhibit altered modes of conformational selectivity and temporal bias at the parathyroid hormone receptor 1 (PTHR1). (B) Proposed mechanism of temporal bias. A ligand that binds with high affinity to the G-protein-independent conformation, R^0, mediates prolonged signaling since the complex is stable and can interconvert over time to the biologically active G-protein-coupled conformation, RG; a ligand that binds selectively to RG induces only transient signaling since the ligand dissociates after G protein activation. (C) In HEK293 membranes and cells expressing the human PTHR1, LA-PTH binds with high affinity to R^0 and thus mediates prolonged cAMP signaling responses after washout, whereas abaloparatide binds preferentially to RG and induces more transient cAMP responses. PTH(1–34) and PTHrP(1–36) exhibit intermediate selectivity profiles. (D) In a parathyroidectomized mouse model of hypoparathyroidism, a single injection of LA-PTH, assessed at several doses, results in an extended elevation in serum calcium, whereas PTH(1–34) at an even higher dose results in a more transient elevation. *(C) Reproduced pending permission from Hattersley, G., Dean, T., Corbin, B. A., Bahar, H. & Gardella, T. J. 2016. Binding selectivity of abaloparatide for PTH-type-1-receptor conformations and effects on downstream signaling. Endocrinology 157, 141–149; (D) Reproduced pending permission from Bi, R., Fan, Y., Lauter, K., Hu, J., Watanabe, T., Cradock, J., Yuan, Q., Gardella, T. & Mannstadt, M. 2016. Diphtheria toxin- and GFP-based mouse models of acquired hypoparathyroidism and treatment with a long-acting parathyroid hormone analog. J. Bone Miner. Res. 31, 975–984.*

bone than would an analog that binds selectively to the R^0 conformation and thus induces prolonged responses. Moreover, because excess bone resorption, as occurs with continuous PTHR1 signaling, gives rise to hypercalcemia, an RG-selective analog might provide a reduced risk of this adverse event, which probably was a factor that limited the final dose approved by the US FDA to 20 μg per day rather than 40 μg, even though the latter was more effective at reducing fracture risk (Neer et al., 2001). The newer PTHrP(1–34) analog, called abaloparatide, formerly called BA058, which was approved by the FDA in 2016 as an alternative anabolic treatment for osteoporosis, is thus of interest as data from preclinical and human clinical studies suggest that it increases bone mass at least as effectively as PTH(1–34) but causes less bone resorption and hence hypercalcemia (Miller et al., 2016). Abaloparatide is administered by subcutaneous injection at a dose of 80 μg per day. As both peptide drugs act by binding to the same target PTHR1, the differences in clinical outcomes suggested the possibility that their modes of action on the receptor might not be equivalent. Abaloparatide was found to bind with relatively high selectively to the RG PTHR1 conformation and thus induce more transient cAMP signaling responses in PTHR1-expressing HEK293 cells than PTH(1–34) (Hattersley et al., 2016) (Fig. 28.4A–C). These studies thus revealed a conformation-based mode of temporal bias for abaloparatide that was distinct from that of PTH(1–34), and hence provided at least a plausible mechanism to help explain the distinct effects that the two ligands have on bone metabolism, as seen in the clinical and preclinical testing (Makino et al., 2018).

PTHR1 mutations in disease

The full spectrum of diseases associated with PTHR1 mutations and their biological and clinical aspects are discussed in Chapter 58. The following sections focus on how the disease-associated mutations relate to the structure and functional properties of the receptor, particularly as they are assessed in cell and mouse model systems.

Jansen's metaphyseal chondrodysplasia

Jansen's metaphyseal chondrodysplasia (JMC) is a rare disease associated with skeletal abnormalities, dwarfism, and hypercalcemia, and is caused by heterozygous dominant activating mutations in the PTHR1 (Ohishi et al., 2012; Schipani et al., 1995). Five different PTHR1-activating mutations have been identified in patients with JMC. These mutations occur at the cytoplasmic termini of TM2 (Arg233 → His), TM6 (Thr410 → Pro/Arg), and TM7 (Ile458 → Arg/Lys) (Fig. 28.1A), and each results in agonist-independent cAMP signaling. Strikingly, the mutations each occur at or, in the case of the Ile458 mutations, adjacent to a residue that is involved in the conserved polar network that is present in all class B GPCRs and operates to control receptor activation and deactivation processes and particularly the outward movements of the TMD helices that allow G protein coupling (Yin et al., 2017). Several PTH and PTHrP antagonist ligand analogs, such as [Leu^{11}, D-Trp^{12}]PTHrP(7−34), behave as inverse agonists on the mutant receptors and thus depress their basal signaling activities (Carter et al., 2001, 2015). The mechanism by which these ligands achieve their inverse effect on the receptor's conformational status is unknown, although the Gly12 → D-Trp substitution is required for the effect. In any case, the functional properties of the analogs suggest possible paths toward therapy for JMC, which potentially can be tested in the transgenic models of JMC that have been developed to express the PTHR1-H223R allele in osteoblasts or osteocytes, which leads to marked increases in bone mass (O'Brien et al., 2008; Calvi et al., 2001).

Other diseases linked to PTHR1 mutations

Enchondromatosis (Ollier disease/Maffucci syndrome) is a rare disease characterized by cartilage tumors of the bone, and has been associated with four PTHR1 mutations, Gly121 → Glu, Ala122 → Thr, Arg150 → Cys, and Arg255 → His, each located in the ECD or ECL1 portion of the receptor. One study on the Arg150 → His mutant expressed in COS-7 cells intriguingly suggested a moderately elevated rate of basal cAMP signaling when corrected for a reduced cell-surface expression level (Hopyan et al., 2002), while another study suggested that each of the four mutations causes a loss-of-function phenotype due to effects on expression and/or binding affinity (Couvineau et al., 2008). The mechanism by which these mutations result in cartilage tumors in bone thus remains unclear, but certainly effects on the extracellular scaffold structure seem possible. Blomstrand's chondrodysplasia is a neonatal lethal condition of markedly accelerated bone mineralization that is caused by homozygous loss-of-function mutations in the PTHR1. One coding mutation has been identified, Pro132 → Leu, which affects a conserved site in the core ECD scaffold (Zhang et al., 1998; Karaplis et al., 1998). Eiken syndrome is a very rare skeletal dysplasia that has been associated with a homozygous recessive nonsense mutation in the PTHR1, Arg485 → Stop, that leads to a shortened C-terminal tail (Duchatelet et al., 2005). The phenotype is markedly delayed ossification of the skeleton, which is opposite that of Blomstrand's disease and seems consistent with a gain-of-function effect, albeit a mild one, since the heterozygous mutation is not associated with disease and the homozygous phenotype is distinct from that of JMC. In any case, it seems possible that the mutation leads to altered interactions with cytoplasmic effectors or scaffolding proteins, and hence diversions in subcellular trafficking and signaling, but this remains to be determined. A number of heterozygous loss-of-function mutations have been identified in individuals with defects in tooth eruption (Roth et al., 2014), which is consistent with studies in mice that show that PTHR1 signaling, as induced by PTHrP, is required for proper tooth formation (Ono et al., 2016). Among the mutations found in patients with tooth eruption defects is the Pro132 → Leu also found in Blomstrand's disease, but in that disease the mutation is in a compound-heterozygous arrangement.

Nonpeptide mimetic ligands for the PTHR1

The capacity for PTH agonists to effectively treat osteoporosis and hypoparathyroidism raises interest in the goal of developing orally available nonpeptide mimetics for this receptor. So far two such small-molecule PTHR1 agonists have been reported. The first, AH3960, was tested only in cells and shown to stimulate cAMP formation at doses of about 10 μM or higher (Rickard et al., 2006). More recently, PCO371 was reported and shown to stimulate cAMP formation in cells at concentrations in the low-micromolar range and, moreover, to effectively raise blood calcium levels in TPTX rats (Tamura et al., 2016). Due to an unexpectedly prolonged calcium response, possibly attributable to a prolonged pharmacokinetic profile, PCO371 is under development for hypoparathyroidism, rather than osteoporosis, as treatment of the latter disease requires a transient pharmacodynamic response to avoid excess bone catabolism, whereas treatment of the former disease requires a more sustained pharmacodynamic profile to mimic the effects of the missing hormone. Several nonpeptide antagonist compounds have also been identified for the PTHR1. SW106, discovered by screening a compound library for agents that could inhibit the binding of a radiolabeled PTH(1−14) peptide analog, binds to the PTHR1 with

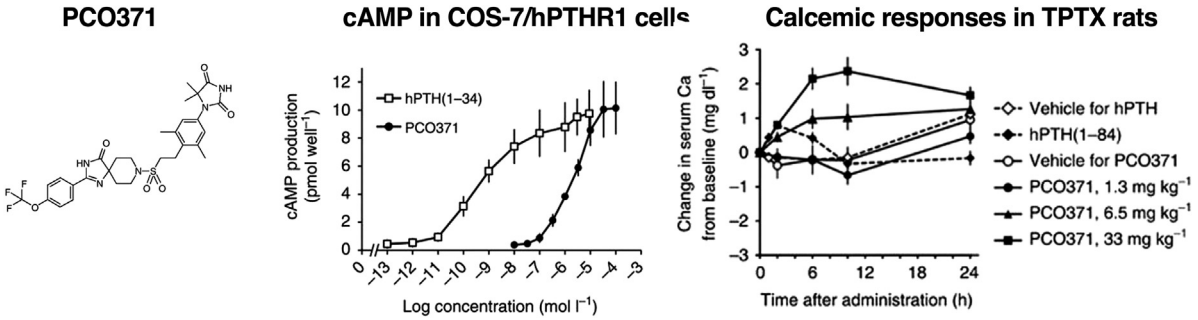

FIGURE 28.5 Small-molecule agonist for the PTHR1. The compound PCO371 was developed from a lead compound identified in a high-throughput screen for parathyroid hormone receptor 1 (*PTHR1*) agonist ligands. In COS-7 cells expressing the human PTHR1, PCO371 is a full agonist for cAMP signaling, albeit its potency is about 3 log-orders weaker than that of PTH(1−34). In TPTX rats, PCO371 induces elevations in serum calcium that are sustained, relative to the effects of PTH(1−34), presumably because of a prolonged pharmacokinetic profile. Consequently, PCO371 is reported to be in development for hypoparathyroidism. *Reproduced pending permission from Tamura, T., Noda, H., Joyashiki, E., Hoshino, M., Watanabe, T., Kinosaki, M., Nishimura, Y., Esaki, T., Ogawa, K., Miyake, T., Arai, S., Shimizu, M., Kitamura, H., Sato, H. & Kawabe, Y. 2016. Identification of an orally active small-molecule PTHR1 agonist for the treatment of hypoparathyroidism. Nat. Commun. 7, 13384.*

micromolar affinity and behaves as a competitive antagonist (Carter et al., 2007, 2015). A broad set of antagonist compounds was reported by a different group, and the most effective of these antagonized the cAMP-stimulating actions of PTH(1−34) in HEK293 cells transfected with the human PTHR1, with inhibitory constants in the 10 nM range, although studies in vivo were not reported (McDonald et al., 2007). Mechanistic studies performed on SW106 and AH3960 (Carter et al., 2015), as well as on PCO371 (Tamura et al., 2016), show that each of these compounds interacts with the TMD region of the receptor, as they exhibit the same effectiveness on the PTHR1 construct that lacks the ECD as they do on the intact PTHR1. Moreover, PCO371 was found to be inactive on the human PTHR2, specifically due to a single divergent residue corresponding to proline-415 in the PTHR1, which is replaced by leucine in the PTHR2. Pro415 is otherwise highly conserved in the class B GPCRs and is located in the middle of TM6, where it is predicted to play a pivotal role in receptor activation (Zhang et al., 2017). Whether PCO371 directly binds to Pro415 or to a site within the extracellularly exposed orthosteric pocket used by the peptide ligand remains to be determined. In any event, it is now clear that small-molecule ligands, both agonists and antagonists, can be developed for the PTHR1, and ultimately might lead to more effective therapies for PTHR1-related diseases (Fig. 28.5).

Other receptors for parathyroid hormone and related ligands

PTHR2 and PTHR3 subtypes

There continues to be appropriate interest in other receptors for the PTH family of ligands. Two apparent receptor subtypes distinct from the PTHR1 have been identified, as discussed in the earlier section on the evolution of this receptor/ligand family. The PTHR3 is present in vertebrate evolution as late as the avian radiation, but its function is not yet clarified or studied extensively, partly because it has been lost from the genome of higher mammals, including humans. Some cell-based tests suggest that it can function in a fashion similar to that of the PTHR1, at least in terms of ligand recognition and response properties (Rubin and Juppner, 1999; Pinheiro et al., 2012). The apparent absence of the PTHR3 in the higher vertebrates leaves open the question of biological importance. On the other hand, the PTHR2 is present in humans and other mammals, and has been characterized sufficiently to suggest a distinct ligand and biological role profile (Dimitrov et al., 2013), although it has been apparently lost in the avian lineage (Pinheiro et al., 2012).

The PTHR2 was initially identified through hybridization-based screening of a human brain cDNA library for PTHR1-related sequences. The identified receptor was thus found to share 51% amino acid identity with the human PTHR1 (Usdin et al., 1995), but to respond weakly to PTH and not at all to PTHrP, while the rat PTHR2 responded to neither (Hoare et al., 1999a). The search for a cognate ligand in bovine hypothalamic extracts yielded the new bioactive peptide called TIP39 (Usdin et al., 1999). TIP39 binds only weakly to the PTHR1 and lacks agonist activity. Nevertheless, TIP39 exhibits some structural homology with PTH and PTHrP (Piserchio et al., 2000), and N-terminally truncated analogs such as TIP9(7−39) bind with improved affinity such that they act as PTHR1 inhibitors (Hoare and Usdin, 2000; Jonsson et al., 2001). Continuing studies with the PTHR2 and TIP39 system since the initial discovery have emphasized its principal role in the central nervous system, with evidence suggesting that it functions to modify behavior, such as combating excessive fear

reactions, modifying pain sensations, and playing a role in positive maternal behavior, as studied in suckling rodents, perhaps by stimulating oxytocin release (Cservenak et al., 2017; Usdin et al., 2003). Distinctive other functions include a critical role in spermatid production and fertility through receptors in testicular tissue (Usdin et al., 2008). Other studies indicate the presence of TIP39 and the PTHR2 in skin with a role for keratinocyte differentiation and regulation of extracellular matrix formation and wound repair (Sato et al., 2016). There is no/little evidence to suggest a role in calcium or bone metabolism.

Possible receptors for C-terminal PTH and PTHrP

Other receptors with actions on bone and calcium have been postulated to interact with the carboxyl regions of PTH and PTHrP that lie beyond the amino-terminal (1−34) segment. Indirect evidence for such a possibility is suggested by the moderate degree of sequence homology maintained in the middle and carboxy-terminal regions of ligands from human and related mammalian species and even in chicken for the PTHrP molecule and also, but to a slightly lesser, extent for PTH. Added to this is the awareness that the overall peptide length of these two molecules is considerably greater than that noted for the ligands that activate other members of the class B receptor class, raising the possibility that the C-terminal extensions of PTH and PTHrP were acquired or preserved biologically during evolution. Experimental support for a C-terminal receptor for PTH comes from the capacity of the PTH(39−84) fragment to bind and cross-link to a 90-kDa protein on the surface of ROS17-2.8 cells (Inomata et al., 1995; Takasu et al., 1996), and that the fragment also induced apoptosis in a mouse osteocytic cell line ablated for the PTHR1 (Divieti et al., 2001). For PTHrP, there is evidence from in vivo studies that the mid- or C-terminal region contributes to effects on placental calcium transport as well as tissue development, the latter involving a nuclear localization mechanism (Kovacs et al., 1996; Wu et al., 1996; Gu et al., 2012; Toribio et al., 2010; Lam et al., 1999). On the other hand, genetic data support the view that the actions of PTH and PTHrP on bone are largely attributable to actions through the PTHR1. Thus, homozygous ablation of the PTHR1 in mice gives rise to a neonatal lethal skeletal dysplasia similar to that seen with homozygous ablation of PTHrP (Lanske et al., 1996). In addition, in the very rare human disorder Blomstrand's chondrodysplasia with homozygous loss-of-function PTHR1 alleles there is a similar lethal skeletal chondrodysplasia. Heterozygous loss-of-function mutations of PTHrP in humans give rise to brachydactyly type E (Bae et al., 2018), and such mutations of the PTHR1 give rise to failures in tooth eruption (Ono et al., 2016; Roth et al., 2014), both of which are consistent with a defect in bone development as controlled by the PTHR1. For PTH, conditions of hypoparathyroidism can be sufficiently corrected with PTH(1−34) administration (Winer et al., 2012), while the related condition of pseudohypoparathyroidism results from deficiencies in Gαs (Juppner, 2015), the primary mediator of PTHR1 signaling. In any event, there remains considerable interest in the possibility of such C-terminal receptors, as potential roles in calcium and bone biology have been supported by biological data in studies extending back several decades. However, despite much effort, such putative receptors have not been cloned and therefore the molecular identities not characterized.

Conclusions

Mechanisms of ligand binding and signal transduction at the PTHR1 are becoming increasingly better understood, with the high-resolution X-ray crystal and cryo-EM structures obtained for several related class B GPCRs providing particularly valuable new information. Ligand binding is thus seen to occur via the basic two-site model initially revealed by mutagenesis and cross-linking studies, but to further involve significant conformational rearrangements and molecular movements that ultimately lead to G protein coupling and activation. Structurally distinct PTH and PTHrP ligand analogs can induce or stabilize different PTHR1 conformations to thereby mediate different modes of signaling, with some ligands inducing particularly prolonged cAMP signaling responses, probably from within endosomes, while others induce more transient responses, presumably from the cell surface. Such conformation-based temporal bias for the PTHR1 suggests new approaches for the development of therapies for diseases such as hypoparathyroidism and osteoporosis. Insights into key sites in the receptor involved in function are also provided by PTHR1 mutations identified in certain skeletal disorders, including loss-of-function mutations in cases of failed tooth eruption and gain-of-function mutations in JMC. Mutations of the latter disease reveal the importance of a conserved polar network located at the base of the TMD helical bundle in controlling receptor activation and deactivation. As the views provided by such insights continue to deepen and refine, so should the capacity to design new ligand analogs for the PTHR1 that offer improved efficacy as treatments for diseases of bone and mineral metabolism.

References

Adams, A., Bisello, A., Chorev, M., Rosenblatt, M., Suva, L., 1998. Arginine 186 in the extracellular N-terminal region of the human parathyroid hormone 1 receptor is essential for contact with position 13 of the hormone. Mol. Endocrinol. 12, 1673−1683.

Amizuka, N., Lee, H.S., Kwan, M.Y., Arazani, A., Warshawsky, H., Hendy, G.N., Ozawa, H., White, J.H., Goltzman, D., 1997. Cell-specific expression of the parathyroid hormone (PTH)/PTH-related peptide receptor gene in kidney from kidney-specific and ubiquitous promoters. Endocrinology 138, 469−481.

Andreassen, K.V., Hjuler, S.T., Furness, S.G., Sexton, P.M., Christopoulos, A., Nosjean, O., Karsdal, M.A., Henriksen, K., 2014. Prolonged calcitonin receptor signaling by salmon, but not human calcitonin, reveals ligand bias. PLoS One 9, e92042.

Bae, J., Choi, H., Park, S., Lee, D.-E., Lee, S., 2018. Novel mutation in PTHLH related to brachydactyly type E2 initially confused with unclassical Pseudopseudohypoparathyroidism. Endocrinol. Metab. On-line, 1-8.

Bergwitz, C., Gardella, T.J., Flannery, M.R., Potts, J.T., Kronenberg, H.M., Goldring, S.R., Juppner, H., 1996. Full activation of chimeric receptors by hybrids between parathyroid hormone and calcitonin − evidence for a common pattern of ligand-receptor interaction. J. Biol. Chem. 271, 26469−26472.

Bergwitz, C., Jusseaume, S., Luck, M., Jüppner, H., Gardella, T., 1997. Residues in the membrane-spanning and extracellular loop regions of the PTH-2 receptor determine signaling selectivity for PTH and PTH-related peptide. J. Biol. Chem. 272, 28861−28868.

Bettoun, J.D., Minagawa, M., Kwan, M.Y., Lee, H.S., Yasuda, T., Hendy, G.N., Goltzman, D., White, J.H., 1997. Cloning and characterization of the promoter regions of the human parathyroid hormone (PTH)/PTH-related peptide receptor gene: analysis of deoxyribonucleic acid from normal subjects and patients with pseudohypoparathyroidism type 1b. J. Clin. Endocrinol. Metab. 82, 1031−1040.

Bi, R., Fan, Y., Lauter, K., Hu, J., Watanabe, T., Cradock, J., Yuan, Q., Gardella, T., Mannstadt, M., 2016. Diphtheria toxin- and GFP-based mouse models of acquired hypoparathyroidism and treatment with a long-acting parathyroid hormone analog. J. Bone Miner. Res. 31, 975−984.

Bisello, A., Adams, A.E., Mierke, D., Pellegrini, M., Rosenblatt, M., Suva, L., Chorev, M., 1998. Parathyroid hormone-receptor interactions identified directly by photocross-linking and molecular modeling studies. J. Biol. Chem. 273, 22498−22505.

Bisello, A., Chorev, M., Rosenblatt, M., Monticelli, L., Mierke, D.F., Ferrari, S.L., 2002. Selective ligand-induced stabilization of active and desensitized parathyroid hormone type 1 receptor conformations. J. Biol. Chem. 277, 38524−38530.

Bortolato, A., Dore, A.S., Hollenstein, K., Tehan, B.G., Mason, J.S., Marshall, F.H., 2014. Structure of Class B GPCRs: new horizons for drug discovery. Br. J. Pharmacol. 171, 3132−3145.

Calvi, L.M., Sims, N.A., Hunzelman, J.L., Knight, M.C., Giovannetti, A., Saxton, J.M., Kronenberg, H.M., Baron, R., Schipani, E., 2001. Activated parathyroid hormone/parathyroid hormone-related protein receptor in osteoblastic cells differentially affects cortical and trabecular bone. J. Clin. Investig. 107, 277−286.

Cardoso, J.C., Felix, R.C., Power, D.M., 2014. Nematode and arthropod genomes provide new insights into the evolution of class 2 B1 GPCRs. PLoS One 9, e92220.

Cardoso, J.C., Pinto, V.C., Vieira, F.A., Clark, M.S., Power, D.M., 2006. Evolution of secretin family GPCR members in the metazoa. BMC Evol. Biol. 6, 1−16.

Carter, P.H., Dean, T., Bhayana, B., Khatri, A., Rajur, R., Gardella, T.J., 2015. Actions of the small molecule ligands SW106 and AH-3960 on the type-1 parathyroid hormone receptor. Mol. Endocrinol. 29, 307−321.

Carter, P.H., Liu, R.Q., Foster, W.R., Tamasi, J.A., Tebben, A.J., Favata, M., Staal, A., Cvijic, M.E., French, M.H., Dell, V., Apanovitch, D., Lei, M., Zhao, Q., Cunningham, M., Decicco, C.P., Trzaskos, J.M., Feyen, J.H., 2007. Discovery of a small molecule antagonist of the parathyroid hormone receptor by using an N-terminal parathyroid hormone peptide probe. Proc. Natl. Acad. Sci. U. S. A. 104, 6846−6851.

Carter, P.H., Petroni, B.D., Gensure, R.C., Schipani, E., Potts Jr., J.T., Gardella, T.J., 2001. Selective and nonselective inverse agonists for constitutively active type-1 parathyroid hormone receptors: evidence for altered receptor conformations. Endocrinology 142, 1534−1545.

Chagin, A.S., Kronenberg, H.M., 2014. Role of G-proteins in the differentiation of epiphyseal chondrocytes. J. Mol. Endocrinol. 53, R39−R45.

Chan, A.S., Clairfeuille, T., LANDAO-Bassonga, E., Kinna, G., Ng, P.Y., Loo, L.S., Cheng, T.S., Zheng, M., Hong, W., Teasdale, R.D., Collins, B.M., Pavlos, N.J., 2016. Sorting nexin 27 couples PTHR trafficking to retromer for signal regulation in osteoblasts during bone growth. Mol. Biol. Cell 27, 1367−1382.

Chauvin, S., Bencsik, M., Bambino, T., Nissenson, R.A., 2002. Parathyroid hormone receptor recycling: role of receptor dephosphorylation and beta-arrestin. Mol. Endocrinol. 16, 2720−2732.

Couvineau, A., Wouters, V., Bertrand, G., Rouyer, C., Gerard, B., Boon, L.M., Grandchamp, B., Vikkula, M., Silve, C., 2008. PTHR1 mutations associated with Ollier disease result in receptor loss of function. Hum. Mol. Genet. 17, 2766−2775.

Cservenak, M., Keller, D., Kis, V., Fazekas, E.A., Ollos, H., Leko, A.H., Szabo, E.R., Renner, E., Usdin, T.B., Palkovits, M., Dobolyi, A., 2017. A thalamo-hypothalamic pathway that activates oxytocin neurons in social contexts in female rats. Endocrinology 158, 335−348.

Cvicek, V., Goddard 3rd, W.A., Abrol, R., 2016. Structure-based sequence alignment of the transmembrane domains of all human GPCRs: Phylogenetic, structural and functional implications. PLoS Comput. Biol. 12, e1004805.

De Graaf, C., Song, G., Cao, C., Zhao, Q., Wang, M.W., Wu, B., Stevens, R.C., 2017. Extending the structural view of class B GPCRs. Trends Biochem. Sci. 42, 946−960.

De Lean, A., Stadel, J., Lefkowitz, R., 1980. A ternary complex model explains the agonist-specific binding properties of the adenylate cyclase-coupled b-adrenergic receptor. J. Biol. Chem. 255, 7108−7117.

Dean, T., Linglart, A., Mahon, M.J., Bastepe, M., Juppner, H., Potts Jr., J.T., Gardella, T.J., 2006. Mechanisms of ligand binding to the parathyroid hormone (PTH)/PTH-related protein receptor: selectivity of a modified PTH(1-15) radioligand for GalphaS-coupled receptor conformations. Mol. Endocrinol. 20, 931–943.

Dean, T., Vilardaga, J.P., Potts Jr., J.T., Gardella, T.J., 2008. Altered selectivity of parathyroid hormone (PTH) and PTH-related protein (PTHrP) for distinct conformations of the PTH/PTHrP receptor. Mol. Endocrinol. 22, 156–166.

Dimitrov, E.L., Kuo, J., Kohno, K., Usdin, T.B., 2013. Neuropathic and inflammatory pain are modulated by tuberoinfundibular peptide of 39 residues. Proc. Natl. Acad. Sci. U. S. A. 110, 13156–13161.

Divieti, P., Inomata, N., Chapin, K., Singh, R., Juppner, H., Bringhurst, F.R., 2001. Receptors for the carboxyl-terminal region of pth(1-84) are highly expressed in osteocytic cells. Endocrinology 142, 916–925.

Dong, S., Shang, S., Li, J., Tan, Z., Dean, T., Maeda, A., Gardella, T.J., Danishefsky, S.J., 2012. Engineering of therapeutic polypeptides through chemical synthesis: early lessons from human parathyroid hormone and analogues. J. Am. Chem. Soc. 134, 15122–15129.

Drake, M.T., Shenoy, S.K., Lefkowitz, R.J., 2006. Trafficking of G protein-coupled receptors. Circ. Res. 99, 570–582.

Duchatelet, S., Ostergaard, E., Cortes, D., Lemainque, A., Julier, C., 2005. Recessive mutations in PTHR1 cause contrasting skeletal dysplasias in Eiken and Blomstrand syndromes. Hum. Mol. Genet. 14, 1–5.

Feinstein, T.N., Wehbi, V.L., Ardura, J.A., Wheeler, D.S., Ferrandon, S., Gardella, T.J., Vilardaga, J.P., 2011. Retromer terminates the generation of cAMP by internalized PTH receptors. Nat. Chem. Biol. 7, 278–284.

Ferrandon, S., Feinstein, T.N., Castro, M., Wang, B., Bouley, R., Potts, J.T., Gardella, T.J., Vilardaga, J.P., 2009. Sustained cyclic AMP production by parathyroid hormone receptor endocytosis. Nat. Chem. Biol. 5, 734–742.

Fredriksson, R., Lagerstrom, M.C., Lundin, L.G., Schioth, H.B., 2003. The G-protein-coupled receptors in the human genome form five main families. Phylogenetic analysis, paralogon groups, and fingerprints. Mol. Pharmacol. 63, 1256–1272.

Gardella, T.J., Luck, M.D., Fan, M.H., Lee, C., 1996. Transmembrane residues of the parathyroid hormone (PTH)/PTH-related peptide receptor that specifically affect binding and signaling by agonist ligands. J. Biol. Chem. 271, 12820–12825.

Gensure, R., Carter, P., Petroni, B., Juppner, H., Gardella, T., 2001a. Identification of determinants of inverse agonism in a constitutively active parathyroid hormone/parathyroid hormone related peptide receptor by photoaffinity cross linking and mutational analysis. J. Biol. Chem. 276, 42692–42699.

Gensure, R., Gardella, T., Juppner, H., 2001b. Multiple sites of contact between the carboxyl terminal binding domain of PTHrP (1 36) analogs and the amino terminal extracellular domain of the PTH/PTHrP receptor identified by photoaffinity cross linking. J. Biol. Chem. 276, 28650–28658.

Gensure, R.C., Shimizu, N., Tsang, J., Gardella, T.J., 2003. Identification of a contact site for residue 19 of parathyroid hormone (PTH) and PTH-related protein analogs in transmembrane domain two of the type 1 PTH receptor. Mol. Endocrinol. 17, 2647–2658.

Gesty-Palmer, D., Chen, M., Reiter, E., Ahn, S., Nelson, C.D., Wang, S., Eckhardt, A.E., Cowan, C.L., Spurney, R.F., Luttrell, L.M., Lefkowitz, R.J., 2006. Distinct beta-arrestin- and G protein-dependent pathways for parathyroid hormone receptor-stimulated ERK1/2 activation. J. Biol. Chem. 281, 10856–10864.

Gesty-Palmer, D., Yuan, L., Martin, B., Wood 3rd, W.H., Lee, M.H., Janech, M.G., Tsoi, L.C., Zheng, W.J., Luttrell, L.M., Maudsley, S., 2013. Beta-arrestin-selective G protein-coupled receptor agonists engender unique biological efficacy in vivo. Mol. Endocrinol. 27, 296–314.

Gidon, A., AL-Bataineh, M.M., Jean-Alphonse, F.G., Stevenson, H.P., Watanabe, T., Louet, C., Khatri, A., Calero, G., Pastor-Soler, N.M., Gardella, T.J., Vilardaga, J.P., 2014. Endosomal GPCR signaling turned off by negative feedback actions of PKA and v-ATPase. Nat. Chem. Biol. 10, 707–709.

Godbole, A., Lyga, S., Lohse, M.J., Calebiro, D., 2017. Internalized TSH receptors en route to the TGN induce local Gs-protein signaling and gene transcription. Nat. Commun. 8, 443.

Goltzman, D., Peytremann, A., Callahan, E., Tregear, G.W., Potts Jr., J.T., 1975. Analysis of the requirements for parathyroid hormone action in renal membranes with the use of inhibiting analogues. J. Biol. Chem. 250, 3199–3203.

Gorvin, C.M., Rogers, A., Hastoy, B., Tarasov, A.I., Frost, M., Sposini, S., Inoue, A., Whyte, M.P., Rorsman, P., Hanyaloglu, A.C., Breitwieser, G.E., Thakker, R.V., 2018. AP2? Mutations impair calcium-sensing receptor trafficking and signaling, and show an endosomal pathway to spatially direct G-protein selectivity. Cell Rep. 22, 1054–1066.

Greenberg, Z., Bisello, A., Mierke, D., Rosenblatt, M., Chorev, M., 2000. Mapping the bimolecular interface of the parathyroid hormone (PTH) PTH1 receptor complex: spatial proximity between Lys(27) (of the hormone principal binding domain) and Leu(261) (of the first extracellular loop) of the human PTH1 receptor. Biochemistry 39, 8142–8152.

Grundmann, M., Kostenis, E., 2017. Temporal bias: time-encoded dynamic GPCR signaling. Trends Pharmacol. Sci. 38, 1110–1124.

Gu, Z., Liu, Y., Zhang, Y., Jin, S., Chen, Q., Goltzman, D., Karaplis, A., Miao, D., 2012. Absence of PTHrP nuclear localization and carboxyl terminus sequences leads to abnormal brain development and function. PLoS One 7, e41542.

Guo, J., Chung, U.I., Kondo, H., Bringhurst, F.R., Kronenberg, H.M., 2002. The PTH/PTHrP receptor can delay chondrocyte hypertrophy in vivo without activating phospholipase C. Dev. Cell 3, 183–194.

Guo, J., Khatri, A., Maeda, A., Potts Jr., J.T., Juppner, H., Gardella, T.J., 2017. Prolonged pharmacokinetic and pharmacodynamic actions of a Pegylated parathyroid hormone (1-34) peptide fragment. J. Bone Miner. Res. 32, 86–98.

Hattersley, G., Dean, T., Corbin, B.A., Bahar, H., Gardella, T.J., 2016. Binding selectivity of abaloparatide for PTH-type-1-receptor conformations and effects on downstream signaling. Endocrinology 157, 141–149.

Hoare, S., Usdin, T., 2001. Molecular mechanisms of ligand-recognition by parathyroid hormone 1 (PTH1) and PTH2 receptors. Curr. Pharmaceut. Des. 7, 689–713.

Hoare, S.R., Bonner, T.I., Usdin, T.B., 1999a. Comparison of rat and human parathyroid hormone 2 (PTH2) receptor activation: PTH is a low potency partial agonist at the rat PTH2 receptor. Endocrinology 140, 4419–4425.

Hoare, S.R., DE Vries, G., Usdin, T.B., 1999b. Measurement of agonist and antagonist ligand-binding parameters at the human parathyroid hormone type 1 receptor: evaluation of receptor states and modulation by guanine nucleotide. J. Pharmacol. Exp. Ther. 289, 1323–1333.

Hoare, S.R., Gardella, T.J., Usdin, T.B., 2001. Evaluating the signal transduction mechanism of the parathyroid hormone 1 receptor. Effect of receptor-G-protein interaction on the ligand binding mechanism and receptor conformation. J. Biol. Chem. 276, 7741–7753.

Hoare, S.R., Usdin, T.B., 2000. Tuberoinfundibular peptide (7-39) [TIP(7-39)], a novel, selective, high-affinity antagonist for the parathyroid hormone-1 receptor with no detectable agonist activity. J. Pharmacol. Exp. Ther. 295, 761–770.

Hogan, B.M., Danks, J.A., Layton, J.E., Hall, N.E., Heath, J.K., Lieschke, G.J., 2005. Duplicate zebrafish pth genes are expressed along the lateral line and in the central nervous system during embryogenesis. Endocrinology 146, 547–551.

Hopyan, S., Gokgoz, N., Poon, R., Gensure, R.C., Yu, C., Cole, W.G., Bell, R.S., Juppner, H., Andrulis, I.L., Wunder, J.S., Alman, B.A., 2002. A mutant PTH/PTHrP type I receptor in enchondromatosis. Nat. Genet. 30, 306–310.

Horwitz, M.J., Tedesco, M.B., Sereika, S.M., Hollis, B.W., Garcia-Ocana, A., Stewart, A.F., 2003. Direct comparison of sustained infusion of human parathyroid hormone-related protein-(1-36) [hPTHrP-(1-36)] versus hPTH-(1-34) on serum calcium, plasma 1,25-dihydroxyvitamin D concentrations, and fractional calcium excretion in healthy human volunteers. J. Clin. Endocrinol. Metab. 88, 1603–1609.

Huang, Z., Chen, Y., Pratt, S., Chen, T.-H., Bambino, T., Nissenson, R., Shoback, D., 1996. The N-terminal region of the third intracellular loop of the parathyroid hormone (PTH)/PTH-related peptide receptor is critical for coupling to cAMP and inositol phosphate/Ca^{2++} signal transduction pathways. J. Biol. Chem. 271, 33382–33389.

Hwang, J.I., Moon, M.J., Park, S., Kim, D.K., Cho, E.B., Ha, N., Son, G.H., Kim, K., Vaudry, H., Seong, J.Y., 2013. Expansion of secretin-like G protein-coupled receptors and their peptide ligands via local duplications before and after two rounds of whole-genome duplication. Mol. Biol. Evol. 30, 1119–1130.

Iida-Klein, A., Guo, J., Takemura, M., Drake, M.T., Potts Jt, J.R., Abou-Samra, A., Bringhurst, F.R., Segre, G.V., 1997. Mutations in the second cytoplasmic loop of the rat parathyroid hormone (PTH)/PTH-related protein receptor result in selective loss of PTH-stimulated phospholipase C activity. J. Biol. Chem. 272, 6882–6889.

Inomata, N., Akiyama, M., Kubota, N., Juppner, H., 1995. Characterization of a novel parathyroid hormone (PTH) receptor with specificity for the carboxyl terminal region of PTH (1-84). Endocrinology 136, 4732–4740.

Jonsson, K.B., John, M.R., Gensure, R.C., Gardella, T.J., Juppner, H., 2001. Tuberoinfundibular peptide 39 binds to the parathyroid hormone (PTH)/PTH-related peptide receptor, but functions as an antagonist. Endocrinology 142, 704–709.

Juppner, H., 2015. Genetic and epigenetic defects at the GNAS locus cause different forms of pseudohypoparathyroidism. Ann. Endocrinol. 76, 92–97.

Juppner, H., ABOU-Samra, A.B., Freeman, M., Kong, X.F., Schipani, E., Richards, J., Kolakowski Jr., L.F., Hock, J., Potts Jr., J.T., Kronenberg, H.M., et al., 1991. A G protein-linked receptor for parathyroid hormone and parathyroid hormone-related peptide. Science 254, 1024–1026.

Jüppner, H., Abou-Samra, A.B., Uneno, S., Gu, W.X., Potts Jr., J.T., Segre, G.V., 1988. The parathyroid hormone-like peptide associated with humoral hypercalcemia of malignancy and parathyroid hormone bind to the same receptor on the plasma membrane of ROS 17/2.8 cells. J. Biol. Chem. 263, 8557–8560.

Juppner, H., Schipani, E., Bringhurst, F.R., Mcclure, I., Keutmann, H.T., Potts, J.T., Kronenberg, H.M., Abousamra, A.B., Segre, G.V., Gardella, T.J., 1994. The extracellular amino-terminal region of the parathyroid-hormone (PTH)/PTH-Related peptide receptor determines the binding-affinity for carboxyl-terminal fragments of PTH-(1-34). Endocrinology 134, 879–884.

Kamesh, N., Aradhyam, G.K., Manoj, N., 2008. The repertoire of G protein-coupled receptors in the sea squirt *Ciona intestinalis*. BMC Evol. Biol. 8, 129.

Karaplis, A.C., He, B., Nguyen, M.T., Young, I.D., Semeraro, D., Ozawa, H., Amizuka, N., 1998. Inactivating mutation in the human parathyroid hormone receptor type 1 gene in Blomstrand chondrodysplasia. Endocrinology 139, 5255–5258.

Kong, X.F., Schipani, E., Lanske, B., Joun, H., Karperien, M., Defize, L.H., Juppner, H., Potts Jr., J.T., Segre, G.V., Kronenberg, H.M., et al., 1994. The rat, mouse and human genes encoding the receptor for parathyroid hormone and parathyroid hormone-related peptide are highly homologous. Biochem. Biophys. Res. Commun. 200, 1290–1299.

Kostenuik, P.J., Ferrari, S., Pierroz, D., Bouxsein, M., Morony, S., Warmington, K.S., Adamu, S., Geng, Z., Grisanti, M., Shalhoub, V., Martin, S., Biddlecome, G., Shimamoto, G., Boone, T., Shen, V., Lacey, D., 2007. Infrequent delivery of a long-acting PTH-Fc fusion protein has potent anabolic effects on cortical and cancellous bone. J. Bone Miner. Res. 22, 1534–1547.

Kovacs, C.S., Lanske, B., Hunzelman, J.L., Guo, J., Karaplis, A.C., Kronenberg, H.M., 1996. Parathyroid hormone-related peptide (PTHrP) regulates fetal placental calcium transport through a receptor distinct from the PTH/PTHrP receptor. Proc. Natl. Acad. Sci. U.S.A. 93, 15233–15238.

Krishnan, V., Ma, Y.L., Chen, C.Z., Thorne, N., Bullock, H., Tawa, G., Javella-Cauley, C., Chu, S., Li, W., Kohn, W., Adrian, M.D., Benson, C., Liu, L., Sato, M., Zheng, W., Pilon, A.M., Yang, N.N., Bryant, H.U., 2018. Repurposing a novel parathyroid hormone analogue to treat hypoparathyroidism. Br. J. Pharmacol. 175, 262–271.

Kronenberg, H.M., 2003. Developmental regulation of the growth plate. Nature 423, 332–336.

Lam, M., Briggs, L., Hu, W., Martin, T., Gillespie, M., Jans, D., 1999. Importin beta recognizes parathyroid hormone related protein with high affinity and mediates its nuclear import in the absence of importin alpha. J. Biol. Chem. 274, 7391–7398.

Lanske, B., Karaplis, A., Lee, K., Luz, A., Vortkamp, A., Pirro, A., Karperien, M., Defize, L., Ho, C., Mulligan, R., Abou-Samra, A., Jüppner, H., Segre, G., Kronenberg, H., 1996. PTH/PTHrP receptor in early development and indian hedgehog-regulated bone growth. Science 273, 663–666.

Lee, C.W., Gardella, T.J., Abousamra, A.B., Nussbaum, S.R., Segre, G.V., Potts, J.T., Kronenberg, H.M., Juppner, H., 1994. Role of the extracellular regions of the parathyroid-hormone (PTH) PTH-related peptide receptor in hormone-binding. Endocrinology 135, 1488–1495.

Li, C., Chen, M., Sang, M., Liu, X., Wu, W., Li, B., 2013. Comparative genomic analysis and evolution of family-B G protein-coupled receptors from six model insect species. Gene 519, 1−12.

Li, J., Dong, S., Townsend, S.D., Dean, T., Gardella, T.J., Danishefsky, S.J., 2012. Chemistry as an expanding resource in protein science: fully synthetic and fully active human parathyroid hormone-related protein (1-141). Angew Chem. Int. Ed. Engl. 51, 12263−12267.

Liang, Y.L., Khoshouei, M., Radjainia, M., Zhang, Y., Glukhova, A., Tarrasch, J., Thal, D.M., Furness, S.G.B., Christopoulos, G., Coudrat, T., Danev, R., Baumeister, W., Miller, L.J., Christopoulos, A., Kobilka, B.K., Wootten, D., Skiniotis, G., Sexton, P.M., 2017. Phase-plate cryo-EM structure of a class B GPCR-G-protein complex. Nature 546, 118−123.

Liu, Y., Ibrahim, A.S., Tay, B.H., Richardson, S.J., Bell, J., Walker, T.I., Brenner, S., Venkatesh, B., Danks, J.A., 2010. Parathyroid hormone gene family in a cartilaginous fish, the elephant shark (*Callorhinchus milii*). J. Bone Miner. Res. 25, 2613−2623.

Luttrell, L.M., Maudsley, S., Bohn, L.M., 2015. Fulfilling the promise of "biased" G protein-coupled receptor agonism. Mol. Pharmacol. 88, 579−588.

Maeda, A., Okazaki, M., Baron, D.M., Dean, T., Khatri, A., Mahon, M., Segawa, H., ABOU-Samra, A.B., Jueppner, H., Bloch, K.D., Potts Jr., J.T., Gardella, T.J., 2013. Critical role of parathyroid hormone (PTH) receptor-1 phosphorylation in regulating acute responses to PTH. Proc. Natl. Acad. Sci. U.S.A. 110, 5864−5869.

Mahon, M.J., Cole, J.A., Lederer, E.D., Segre, G.V., 2003. Na+/H+ exchanger-regulatory factor 1 mediates inhibition of phosphate transport by parathyroid hormone and second messengers by acting at multiple sites in opossum kidney cells. Mol. Endocrinol. 17, 2355−2364.

Makino, A., Takagi, H., Takahashi, Y., Hase, N., Sugiyama, H., Yamana, K., Kobayashi, T., 2018. Abaloparatide exerts bone anabolic effects with less stimulation of bone resorption-related factors: a comparison with teriparatide. Calcif. Tissue Int. 103, 289−297.

Malecz, N., Bambino, T., Bencsik, M., Nissenson, R., 1998. Identification of phosphorylation sites in the G protein-coupled receptor for parathyroid hormone. receptor phosphorylation is not required for agonist-induced internalization. Mol. Endocrinol. 12, 1846−1856.

Mamonova, T., Kurnikova, M., Friedman, P.A., 2012. Structural basis for NHERF1 PDZ domain binding. Biochemistry 51, 3110−3120.

Mannstadt, M., Clarke, B.L., Vokes, T., Brandi, M.L., Ranganath, L., Fraser, W.D., Lakatos, P., Bajnok, L., Garceau, R., Mosekilde, L., Lagast, H., Shoback, D., Bilezikian, J.P., 2013. Efficacy and safety of recombinant human parathyroid hormone (1-84) in hypoparathyroidism (REPLACE): a double-blind, placebo-controlled, randomised, phase 3 study. Lancet Diabetes Endocrinol. 1, 275−283.

Mannstadt, M., Luck, M.D., Gardella, T.J., Juppner, H., 1998. Evidence for a ligand interaction site at the amino-terminus of the parathyroid hormone (PTH)/PTH-related protein receptor from cross-linking and mutational studies. J. Biol. Chem. 273, 16890−16896.

Martin, T.J., Quinn, J.M., Gillespie, M.T., Ng, K.W., Karsdal, M.A., Sims, N.A., 2006. Mechanisms involved in skeletal anabolic therapies. Ann. N. Y. Acad. Sci. 1068, 458−470.

Mccuaig, K.A., Clarke, J.C., White, J.H., 1994. Molecular cloning of the gene encoding the mouse parathyroid hormone/parathyroid hormone-related peptide receptor. Proc. Natl. Acad. Sci. U. S. A. 91, 5051−5055.

Mcdonald, I.M., Austin, C., Buck, I.M., Dunstone, D.J., Gaffen, J., Griffin, E., Harper, E.A., Hull, R.A., Kalindjian, S.B., Linney, I.D., Low, C.M., Patel, D., Pether, M.J., Raynor, M., Roberts, S.P., Shaxted, M.E., Spencer, J., Steel, K.I., Sykes, D.A., Wright, P.T., Xun, W., 2007. Discovery and characterization of novel, potent, non-peptide parathyroid hormone-1 receptor antagonists. J. Med. Chem. 50, 4789−4792.

Mcgarvey, J.C., Xiao, K., Bowman, S.L., Mamonova, T., Zhang, Q., Bisello, A., Sneddon, W.B., Ardura, J.A., Jean-Alphonse, F., Vilardaga, J.P., Puthenveedu, M.A., Friedman, P.A., 2016. Actin-sorting nexin 27 (SNX27)-Retromer complex mediates rapid parathyroid hormone receptor recycling. J. Biol. Chem. 291, 10986−11002.

Miller, P.D., Hattersley, G., Riis, B.J., Williams, G.C., Lau, E., Russo, L.A., Alexandersen, P., Zerbini, C.A., Hu, M.Y., Harris, A.G., Fitzpatrick, L.A., Cosman, F., Christiansen, C., Investigators, A.S., 2016. Effect of abaloparatide vs placebo on new vertebral fractures in postmenopausal women with osteoporosis: a randomized clinical trial. J. Am. Med. Assoc. 316, 722−733.

Minagawa, M., Watanabe, T., Kohno, Y., Mochizuki, H., Hendy, G.N., Goltzman, D., White, J.H., Yasuda, T., 2001. Analysis of the P3 promoter of the human parathyroid hormone (PTH)/PTH-related peptide receptor gene in pseudohypoparathyroidism type 1b. J. Clin. Endocrinol. Metab. 86, 1394−1397.

Mirabeau, O., Joly, J.S., 2013. Molecular evolution of peptidergic signaling systems in bilaterians. Proc. Natl. Acad. Sci. U. S. A. 110, E2028−E2037.

Neer, R.M., Arnaud, C.D., Zanchetta, J.R., Prince, R., Gaich, G.A., Reginster, J.Y., Hodsman, A.B., Eriksen, E.F., ISH-Shalom, S., Genant, H.K., Wang, O.H., Mitlak, B.H., 2001. Effect of parathyroid hormone (1-34) on fractures and bone mineral density in postmenopausal women with osteoporosis. N. Engl. J. Med. 344, 1434−1441.

Nissenson, R.A., Diep, D., Strewler, G.J., 1988. Synthetic peptides comprising the amino-terminal sequence of a parathyroid hormone-like protein from human malignancies. Binding to parathyroid hormone receptors and activation of adenylate cyclase in bone cells and kidney. J. Biol. Chem. 263, 12866−12871.

Nussbaum, S.R., Rosenblatt, M., Potts Jr., J.T., 1980. Parathyroid hormone/renal receptor interactions: demonstration of two receptor-binding domains. J. Biol. Chem. 255, 10183−10187.

O'brien, C.A., Plotkin, L.I., Galli, C., Goellner, J.J., Gortazar, A.R., Allen, M.R., Robling, A.G., Bouxsein, M., Schipani, E., Turner, C.H., Jilka, R.L., Weinstein, R.S., Manolagas, S.C., Bellido, T., 2008. Control of bone mass and remodeling by PTH receptor signaling in osteocytes. PLoS One 3, e2942.

Ohishi, M., Ono, W., Ono, N., Khatri, R., Marzia, M., Baker, E.K., Root, S.H., Wilson, T.L., Iwamoto, Y., Kronenberg, H.M., Aguila, H.L., Purton, L.E., Schipani, E., 2012. A novel population of cells expressing both hematopoietic and mesenchymal markers is present in the normal adult bone marrow and is augmented in a murine model of marrow fibrosis. Am. J. Pathol. 180, 811−818.

Okazaki, M., Ferrandon, S., Vilardaga, J.P., Bouxsein, M.L., Potts Jr., J.T., Gardella, T.J., 2008. Prolonged signaling at the parathyroid hormone receptor by peptide ligands targeted to a specific receptor conformation. Proc. Natl. Acad. Sci. U. S. A. 105, 16525−16530.

Okazaki, M., Nagai, S., Dean, T., Potts, J.J., Gardella, T., 2007. Analysis of PTH-PTH receptor interaction mechanisms using a new, long-acting PTH(1-28) analog reveals selective binding to distinct PTH receptor conformations and biological consequences in vivo. J. Bone Miner. Res. 22 (Suppl. l). Abstract 1190.

On, J.S., Chow, B.K., Lee, L.T., 2015. Evolution of parathyroid hormone receptor family and their ligands in vertebrate. Front. Endocrinol. 6, 28.

Ono, W., Sakagami, N., Nishimori, S., Ono, N., Kronenberg, H.M., 2016. Parathyroid hormone receptor signalling in osterix-expressing mesenchymal progenitors is essential for tooth root formation. Nat. Commun. 7, 11277.

Parthier, C., Reedtz-Runge, S., Rudolph, R., Stubbs, M.T., 2009. Passing the baton in class B GPCRs: peptide hormone activation via helix induction? Trends Biochem. Sci. 34, 303–310.

Pinheiro, P.L., Cardoso, J.C., Power, D.M., Canario, A.V., 2012. Functional characterization and evolution of PTH/PTHrP receptors: insights from the chicken. BMC Evol. Biol. 12, 110.

Pioszak, A.A., Parker, N.R., Gardella, T.J., Xu, H.E., 2009. Structural basis for parathyroid hormone-related protein binding to the parathyroid hormone receptor and design of conformation-selective peptides. J. Biol. Chem. 284, 28382–28391.

Pioszak, A.A., Parker, N.R., Suino-Powell, K., Xu, H.E., 2008. Molecular recognition of corticotropin-releasing factor by its G-protein-coupled receptor CRFR1. J. Biol. Chem. 283, 32900–32912.

Piserchio, A., Shimizu, N., Gardella, T.J., Mierke, D.F., 2002. Residue 19 of the parathyroid hormone: structural consequences. Biochemistry 41, 13217–13223.

Piserchio, A., Usdin, T., Mierke, D., 2000. Structure of tuberoinfundibular peptide of 39 residues. J. Biol. Chem. 275, 27284–27290.

Potts Jr., J.T., Tregear, G.W., Keutmann, H.T., Niall, H.D., Sauer, R., Deftos, L.J., Dawson, B.F., Hogan, M.L., Aurbach, G.D., 1971. Synthesis of a biologically active N-terminal tetratriacontapeptide of parathyroid hormone. Proc. Natl. Acad. Sci. U.S.A. 68, 63–67.

Qian, F., Leung, A., Abou-Samra, A., 1998. Agonist-dependent phosphorylation of the parathyroid hormone/parathyroid hormone-related peptide receptor. Biochemistry 37, 6240–6246.

Rey, A., Manen, D., Rizzoli, R., Caverzasio, J., Ferrari, S.L., 2006. Proline-rich motifs in the parathyroid hormone (PTH)/PTH-related protein receptor C terminus mediate scaffolding of c-Src with beta-arrestin2 for ERK1/2 activation. J. Biol. Chem. 281, 38181–38188.

Rickard, D.J., Wang, F.L., Rodriguez-Rojas, A.M., Wu, Z., Trice, W.J., Hoffman, S.J., Votta, B., Stroup, G.B., Kumar, S., Nuttall, M.E., 2006. Intermittent treatment with parathyroid hormone (PTH) as well as a non-peptide small molecule agonist of the PTH1 receptor inhibits adipocyte differentiation in human bone marrow stromal cells. Bone 39, 1361–1372.

Roth, H., Fritsche, L.G., Meier, C., Pilz, P., Eigenthaler, M., Meyer-Marcotty, P., Stellzig-Eisenhauer, A., Proff, P., Kanno, C.M., Weber, B.H., 2014. Expanding the spectrum of PTH1R mutations in patients with primary failure of tooth eruption. Clin. Oral Investig. 18, 377–384.

Rubin, D.A., Juppner, H., 1999. Zebrafish express the common parathyroid hormone/parathyroid hormone-related peptide receptor (PTH1R) and a novel receptor (PTH3R) that is preferentially activated by mammalian and fugufish parathyroid hormone-related peptide. J. Biol. Chem. 274, 28185–28190.

Sato, E., Muto, J., Zhang, L.J., Adase, C.A., Sanford, J.A., Takahashi, T., Nakatsuji, T., Usdin, T.B., Gallo, R.L., 2016. The parathyroid hormone second receptor PTH2R and its ligand tuberoinfundibular peptide of 39 residues TIP39 regulate intracellular calcium and influence keratinocyte differentiation. J. Investig. Dermatol. 136, 1449–1459.

Schipani, E., Kruse, K., Jüppner, H., 1995. A constitutively active mutant PTH-PTHrP receptor in Jansen-type metaphyseal chondrodysplasia. Science 268, 98–100.

Segre, G.V., Goldring, S.R., 1993. Receptors for secretin, calcitonin, parathyroid hormone (PTH)/PTH-related peptide, vasoactive intestinal peptide, glucagonlike peptide 1, growth hormone-releasing hormone, and glucagon belong to a newly discovered G-protein-linked receptor family. Trends Endocrinol. Metabol. 4, 309–314.

Segre, G.V., Rosenblatt, M., Reiner, B.L., Mahaffey, J.E., Potts Jr., J.T., 1979. Characterization of parathyroid hormone receptors in canine renal cortical plasma membranes using a radioiodinated sulfur-free hormone analogue. correlation of binding with adenylate cyclase activity. J. Biol. Chem. 254, 6980–6986.

Shimizu, M., Carter, P., Khatri, A., Potts, J., Gardella, T., 2001. Enhanced activity in parathyroid hormone (1–14) and (1–11): novel peptides for probing the ligand-receptor interaction. Endocrinology 142, 3068–3074.

Shimizu, M., Joyashiki, E., Noda, H., Watanabe, T., Okazaki, M., Nagayasu, M., Adachi, K., Tamura, T., Potts Jr., J.T., Gardella, T.J., Kawabe, Y., 2016. Pharmacodynamic actions of a long-acting PTH analog (LA-PTH) in thyroparathyroidectomized (TPTX) rats and normal monkeys. J. Bone Miner. Res. 7, 1405–1412.

Suzuki, N., Danks, J.A., Maruyama, Y., Ikegame, M., Sasayama, Y., Hattori, A., Nakamura, M., Tabata, M.J., Yamamoto, T., Furuya, R., Saijoh, K., Mishima, H., Srivastav, A.K., Furusawa, Y., Kondo, T., Tabuchi, Y., Takasaki, I., Chowdhury, V.S., Hayakawa, K., Martin, T.J., 2011. Parathyroid hormone 1 (1–34) acts on the scales and involves calcium metabolism in goldfish. Bone 48, 1186–1193.

Takasu, H., Baba, H., Inomata, N., Uchiyama, Y., Kubota, N., Kumaki, K., Matsumoto, A., Nakajima, K., Kimura, T., Sakakibara, S., Fujita, T., Chihara, K., Nagai, I., 1996. The 69-84 amino acid region of the parathyroid hormone molecule is essential for the interaction of the hormone with the binding sites with carboxyl terminal specificity. Endocrinology 137, 5537–5543.

Tamura, T., Noda, H., Joyashiki, E., Hoshino, M., Watanabe, T., Kinosaki, M., Nishimura, Y., Esaki, T., Ogawa, K., Miyake, T., Arai, S., Shimizu, M., Kitamura, H., Sato, H., Kawabe, Y., 2016. Identification of an orally active small-molecule PTHR1 agonist for the treatment of hypoparathyroidism. Nat. Commun. 7, 13384.

Tawfeek, H.A.W., Qian, F., Abou-Samra, A.B., 2002. Phosphorylation of the receptor for PTH and PTHrP is required for internalization and regulates receptor signaling. Mol. Endocrinol. 16, 1–13.

Thomas, B.E., Sharma, S., Mierke, D.F., Rosenblatt, M., 2008. Parathyroid hormone (PTH) and PTH antagonist induce different conformational changes in the PTHR1 receptor. J. Bone Miner. Res. 5, 925−934.

Thomsen, A.R., Plouffe, B., Cahill 3rd, T.J., Shukla, A.K., Tarrasch, J.T., Dosey, A.M., Kahsai, A.W., Strachan, R.T., Pani, B., Mahoney, J.P., Huang, L., Breton, B., Heydenreich, F.M., Sunahara, R.K., Skiniotis, G., Bouvier, M., Lefkowitz, R.J., 2016. GPCR-G protein-beta-arrestin super-complex mediates sustained G protein signaling. Cell 166, 907−919.

Tian, J., Smogorzewski, M., Kedes, L., Massry, S.G., 1993. Parathyroid hormone-parathyroid hormone related protein receptor messenger RNA is present in many tissues besides the kidney. Am. J. Nephrol. 13, 210−213.

Toribio, R.E., Brown, H.A., Novince, C.M., Marlow, B., Hernon, K., Lanigan, L.G., Hildreth 3rd, B.E., Werbeck, J.L., Shu, S.T., Lorch, G., Carlton, M., Foley, J., Boyaka, P., Mccauley, L.K., Rosol, T.J., 2010. The midregion, nuclear localization sequence, and C terminus of PTHrP regulate skeletal development, hematopoiesis, and survival in mice. FASEB J. 24, 1947−1957.

Trivett, M.K., Potter, I.C., Power, G., Zhou, H., Macmillan, D.L., Martin, T.J., Danks, J.A., 2005. Parathyroid hormone-related protein production in the lamprey *Geotria australis*: developmental and evolutionary perspectives. Dev. Gene. Evol. 215, 553−563.

Turner, P.R., Mefford, S., Bambino, T., Nissenson, R.A., 1998. Transmembrane residues together with the amino terminus limit the response of the parathyroid hormone (PTH) 2 receptor to PTH-related peptide. J. Biol. Chem. 273, 3830−3837.

Uhlen, M., Fagerberg, L., Hallstrom, B.M., Lindskog, C., Oksvold, P., Mardinoglu, A., Sivertsson, A., Kampf, C., Sjostedt, E., Asplund, A., Olsson, I., Edlund, K., Lundberg, E., Navani, S., Szigyarto, C.A., Odeberg, J., Djureinovic, D., Takanen, J.O., Hober, S., Alm, T., Edqvist, P.H., Berling, H., Tegel, H., Mulder, J., Rockberg, J., Nilsson, P., Schwenk, J.M., Hamsten, M., VON Feilitzen, K., Forsberg, M., Persson, L., Johansson, F., Zwahlen, M., VON Heijne, G., Nielsen, J., Ponten, F., 2015. Proteomics. Tissue-based map of the human proteome. Science 347, 1260419.

Urena, P., Kong, X.F., ABOU-Samra, A.B., Juppner, H., Kronenberg, H.M., Potts Jr., J.T., Segre, G.V., 1993. Parathyroid hormone (PTH)/PTH-related peptide receptor messenger ribonucleic acids are widely distributed in rat tissues. Endocrinology 133, 617−623.

Usdin, T., Gruber, C., Bonner, T., 1995. Identification and functional expression of a receptor selectively recognizing parathyroid hormone, the PTH2 receptor. J. Biol. Chem. 270, 15455−15458.

Usdin, T.B., Dobolyi, A., Ueda, H., Palkovits, M., 2003. Emerging functions for tuberoinfundibular peptide of 39 residues. Trends Endocrinol. Metabol. 14, 14−19.

Usdin, T.B., Hoare, S.R., Wang, T., Mezey, E., Kowalak, J.A., 1999. TIP39: a new neuropeptide and PTH2-receptor agonist from hypothalamus. Nat. Neurosci. 2, 941−943.

Usdin, T.B., Paciga, M., Riordan, T., Kuo, J., Parmelee, A., Petukova, G., Camerini-Otero, R.D., Mezey, E., 2008. Tuberoinfundibular Peptide of 39 residues is required for germ cell development. Endocrinology 149, 4292−4300.

Vilardaga, J.P., Krasel, C., Chauvin, S., Bambino, T., Lohse, M.J., Nissenson, R.A., 2002. Internalization determinants of the parathyroid hormone receptor differentially regulate beta-arrestin/receptor association. J. Biol. Chem. 277, 8121−8129.

Winer, K.K., Fulton, K.A., Albert, P.S., Cutler Jr., G.B., 2014. Effects of pump versus twice-daily injection delivery of synthetic parathyroid hormone 1-34 in children with severe congenital hypoparathyroidism. J. Pediatr. 165, 556-563 e1.

Winer, K.K., Zhang, B., Shrader, J.A., Peterson, D., Smith, M., Albert, P.S., Cutler Jr., G.B., 2012. Synthetic human parathyroid hormone 1-34 replacement therapy: a randomized crossover trial comparing pump versus injections in the treatment of chronic hypoparathyroidism. J. Clin. Endocrinol. Metab. 97, 391−399.

Wittelsberger, A., Corich, M., Thomas, B.E., Lee, B.K., Barazza, A., Czodrowski, P., Mierke, D.F., Chorev, M., Rosenblatt, M., 2006a. The mid-region of parathyroid hormone (1-34) serves as a functional docking domain in receptor activation. Biochemistry 45, 2027−2034.

Wittelsberger, A., Thomas, B.E., Mierke, D.F., Rosenblatt, M., 2006b. Methionine acts as a "magnet" in photoaffinity crosslinking experiments. FEBS Lett. 580, 1872−1876.

Wu, T.L., Vasavada, R.C., Yang, K., Massfelder, T., Ganz, M., Abbas, S.K., Care, A.D., Stewart, A.F., 1996. Structural and physiologic characterization of the mid-region secretory species of parathyroid hormone-related protein. J. Biol. Chem. 271, 24371−24381.

Xiong, L., Xia, W.F., Tang, F.L., Pan, J.X., Mei, L., Xiong, W.C., 2016. Retromer in osteoblasts interacts with protein phosphatase 1 regulator subunit 14c, terminates parathyroid hormone's signaling, and promotes its catabolic response. EBioMedicine 9, 45−60.

Yan, Y.L., Bhattacharya, P., He, X.J., Ponugoti, B., Marquardt, B., Layman, J., Grunloh, M., Postlethwait, J.H., Rubin, D.A., 2012. Duplicated zebrafish co-orthologs of parathyroid hormone-related peptide (PTHrp, Pthlh) play different roles in craniofacial skeletogenesis. J. Endocrinol. 214, 421−435.

Yin, Y., DE Waal, P.W., He, Y., Zhao, L.H., Yang, D., Cai, X., Jiang, Y., Melcher, K., Wang, M.W., Xu, H.E., 2017. Rearrangement of a polar core provides a conserved mechanism for constitutive activation of class B G protein-coupled receptors. J. Biol. Chem. 292, 9865−9881.

Zhang, H., Qiao, A., Yang, L., Van Eps, N., Frederiksen, K.S., Yang, D., Dai, A., Cai, X., Zhang, H., Yi, C., Cao, C., He, L., Yang, H., Lau, J., Ernst, O.P., Hanson, M.A., Stevens, R.C., Wang, M.W., Reedtz-Runge, S., Jiang, H., Zhao, Q., Wu, B., 2018a. Structure of the glucagon receptor in complex with a glucagon analogue. Nature 553, 106−110.

Zhang, P., Jobert, A.S., Couvineau, A., Silve, C., 1998. A homozygous inactivating mutation in the parathyroid hormone/parathyroid hormone-related peptide receptor causing Blomstrand chondrodysplasia. J. Clin. Endocrinol. Metab. 83, 3365−3368.

Zhang, Q., Xiao, K., Liu, H., Song, L., Mcgarvey, J.C., Sneddon, W.B., Bisello, A., Friedman, P.A., 2018b. Site-specific polyubiquitination differentially regulates parathyroid hormone receptor-initiated MAPK signaling and cell proliferation. J. Biol. Chem. 293, 5556−5571.

Zhang, Y., Sun, B., Feng, D., Hu, H., Chu, M., Qu, Q., Tarrasch, J.T., Li, S., Sun Kobilka, T., Kobilka, B.K., Skiniotis, G., 2017. Cryo-EM structure of the activated GLP-1 receptor in complex with a G protein. Nature 546, 248−253.

Zhou, A., Bessalle, R., Bisello, A., Nakamoto, C., Rosenblatt, M., Suva, L.J., Chorev, M., 1997. Direct mapping of an agonist-binding domain within the parathyroid hormone/parathyroid hormone-related protein receptor by photoaffinity crosslinking. Proc. Natl. Acad. Sci. U.S.A. 94, 3644−3649.

Chapter 29

Structure and function of the vitamin D-binding proteins

Daniel D. Bikle

VA Medical Center and University of California San Francisco, San Francisco, California, United States

Chapter outline

Introduction

Vitamin D is obtained by the body either from its production in the skin or through absorption from the intestine. In either case vitamin D must be transported to tissues such as the liver where it is metabolized to its major circulating form, 25-hydroxyvitamin D (25(OH)D), by a number of 25-hydroxylases, the most important of which is Cyp2r1. 25(OH)D is then transported to tissues such as the kidney where it undergoes further metabolism to its major hormonal form 1,25-dihydroxyvitamin D ($1,25(OH)_2D$) by the mitochondrial-based Cyp27b1. Vitamin D-binding protein (DBP) is the key transport protein and, at least in some cells such as the kidney, participates in the transport of 25(OH)D into the cell. However, as will be discussed, DBP has a number of functions independent of its role as a vitamin D transport protein. Within at least some cells the 25(OH)D entering from the blood appears to be shuttled to mitochondria for this enzymatic reaction by what was originally called intracellular vitamin D-binding protein, later identified as the heat shock protein Hsp70, a known chaperone. Hsp70 in some cells may also facilitate the movement of $1,25(OH)_2D$ into the nucleus where it provides the activating ligand for the vitamin D receptor (VDR). The VDR is responsible for all the known genomic actions of vitamin D, most of which require $1,25(OH)_2D$ and its heterodimer partner RXR. However, VDR also has a nongenomic role in the membrane where it responds to a different conformation of ligands in activating a different set of signaling pathways. The membrane VDR shares this role with another protein initially called membrane-associated rapid response steroid (MARRS)-binding protein, more recently known as thioredoxin-like protein (GRP58), endoplasmic reticulum protein 57/60 (ERp57 or 60), or protein disulfide isomerase family A, member 3 (Pdia3). Thus, there is a series of vitamin D-binding proteins that sequentially provide for the transport of vitamin D from its point of origin (skin or gut) to tissues involved with its metabolism to its hormonal form, which mediate the handling of these metabolites within the cells

Principles of Bone Biology. https://doi.org/10.1016/B978-0-12-814841-9.00029-4

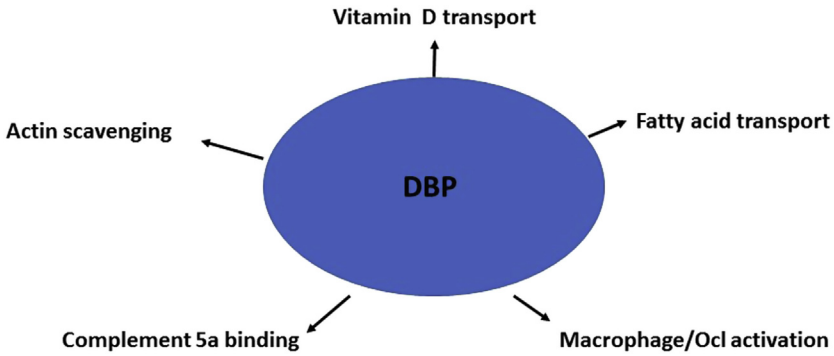

FIGURE 29.1 The multiple functions of vitamin D-binding protein. In addition to being the major transport protein for the vitamin D metabolites, vitamin D-binding protein (*DBP*) along with gelsolin participates in actin scavenging, fatty acid transport, and binding of complement 5a to neutrophils regulating their chemotaxis, and when the Gc1F and Gc1S variants are deglycosylated to form macrophage-activating factor, *DBP*—MAF can activate macrophages and osteoclasts (*Ocl*).

and ultimately to the proteins that initiate the biologic response, genomic and nongenomic. In this chapter aspects of the structures of these proteins relevant to their function and the mechanisms by which these proteins function will be reviewed. Given that vitamin D signaling affects nearly all if not all cells in the body, specific cellular responses will not be reviewed except as they illustrate these mechanisms.

Vitamin D-binding protein

Although the best known function of DBP is the transport of vitamin D metabolites from their source of production to their target tissues, DBP has a number of other functions, including actin scavenging, fatty acid binding, complement 5a (C5a)-binding regulation of neutrophil migration and chemotaxis, and, by way of its conversion to DBP—macrophage-activating factor (DBP—MAF), the regulation of osteoclast activity, immune function, and cancer growth (Fig. 29.1). These functions will be discussed in turn, including their clinical significance and the influence of the different polymorphisms on these functions.

Genomic regulation

The human *DBP* gene is located on chromosome 4q12—q13. It is 35 kb in length and comprises 13 exons encoding 474 amino acids, including a 16-amino-acid leader sequence, which is cleaved before release. The region of the chromosome where *DBP* is located also contains the homologous genes for albumin, α-fetoprotein, and afamin, with which it shares some properties, leading to speculation that this gene cluster arose from gene duplications. However, the transcription of *DBP* goes in the direction opposite that of the other genes in this cluster and it is separated by about 1500 kb (White and Cooke, 2000; Song et al., 1999). Expression of DBP is widespread, but the vast majority originates from the liver (Cooke et al., 1991). The proximal promoter of the *DBP* gene contains three hepatocyte nuclear factor 1 (HNF1) binding sites within 2 kb of the transcription start site (TSS). HNF1 is expressed as the α or β isoform and binds to its response element as a dimer. HNF1α is an activator, whereas HNF1β is inhibitory. In the liver, levels of HNF1α are high, resulting in increased expression of DBP, whereas in the kidney the β form exists, thus suppressing expression, and in the brain, little HNF1 is present (White and Cooke, 2000). The expression of DBP is increased by estrogen (Hagenfeldt et al., 1991) as is well illustrated with the rise in DBP during pregnancy (Moller et al., 2012; Zhang et al., 2014) and with oral contraceptive utilization (Moller et al., 2013). However, whether this is a direct action on the *DBP* gene via the estrogen receptor is not clear. Androgens, on the other hand, do not appear to affect DBP expression (Hagenfeldt et al., 1991). Dexamethasone and certain cytokines such as interleukin-6 (IL-6) also increase DBP production, whereas transforming growth factor β is inhibitory (Guha et al., 1995). As for estrogen, the mechanism underlying such regulation is unclear. However, from a clinical perspective these factors are likely to contribute to the increase in DBP production following trauma (Dahl et al., 2001a) and acute liver failure (Schiodt, 2008), which will be discussed subsequently. Primary hyperparathyroidism, on the other hand, is associated with a reduction in DBP levels, probably contributing to the lower 25(OH)D levels in these patients, as the free 25(OH)D is not reduced (Wang et al., 2017). Vitamin D itself or any of its metabolites does not regulate DBP production.

Structure and polymorphisms

The mature human DBP is 58 kDa in size, although differences in glycosylation of the protein alter the actual size. DBP is composed of three structurally similar domains. The first domain has an α-helical arrangement and is the binding site for the vitamin D metabolites (aa 35−49). Fatty acid binding demonstrates a single high-affinity site for both palmitic acid and arachidonic acid, but only arachidonic acid competes with 25(OH)D for binding, suggesting that the binding of fatty acids is not competitive for the vitamin D binding site in domain 1, but is due to alterations in DBP conformation (Calvo and Ena, 1989; Bouillon et al., 1992). The actin binding site is located in aa 373−403, spanning parts of domains 2 and 3, but part of domain 1 is also involved (Haddad et al., 1992; Head et al., 2002). The C5a/C5a des Arg binding site is to aa 130−149 (Zhang and Kew, 2004). Membrane binding sites have been identified in aa 150−172 and 379−402 (Wilson et al., 2015). DBP is the most polymorphic gene known. Over 120 variants have been described based on electrophoretic properties (Cleve and Constans, 1988), with 1242 polymorphisms listed in the NCBI database as of this writing (Chun, 2012). Of these variants, the Gc1F and Gc1S (rs7041) and Gc2 (rs4588) are the most common (Fig. 29.2). Gc1F and Gc1S involve two polymorphisms, one at aa 432 (416 in the mature DBP) and one at aa 436 (420 in the mature DBP). The 1F allele encodes the sequence of amino acids between 432 and 436 as **D**ATPT; the 1S allele encodes the sequence **E**ATPT. This subtle difference in charge makes GcF run faster and GcS slower during electrophoresis. The Gc2 allele encodes DATP**K**, which runs slower still**.** Glycosylation further distinguishes the Gc1 variants from the Gc2 variant. The threonine (T) in Gc1 binds *N*-acetylgalactosamine to which galactose and sialic acid bind in tandem. The lysine (K) in the comparable position in Gc2 does not bind these residues (Malik et al., 2013; Nagasawa et al., 2005). This affects the conversion of DBP to DBP−MAF, which involves a partial deglycosylation, removing the galactose and sialic acid by the sequential action of sialidase and β-galactosidase, by T and B cells (Uto et al., 2012).

Biologic function

Binding to and transport of vitamin D metabolites

DBP was discovered by Hirschfeld in 1959 (Hirschfeld, 1959), and was originally called group-specific component (Gc-globulin), and not until 1975 was its function as a carrier of vitamin D metabolites realized (Daiger et al., 1975). This is the function that gives DBP its name, although only about 5% of DBP is required for this purpose. In serum samples from normal individuals, ∼85% of circulating vitamin D metabolites are bound to DBP, whereas albumin with its substantially lower binding affinity binds only ∼15% of these metabolites despite its 10-fold higher concentration compared with DBP. Approximately 0.4% of total $1,25(OH)_2D_3$ and 0.03% of total $25(OH)D_3$ is free in serum from normal nonpregnant individuals. The affinity of DBP for the vitamin D_2 metabolites is lower (Armas et al., 2004), such that the free fraction would be expected to be higher, but this has not been directly determined. The "bioavailable" vitamin D metabolite comprises the free vitamin D metabolite and the amount bound to albumin, thus measuring around 15% in normal individuals (reviewed in Bikle et al., 2017a). At this point there is little evidence that the albumin fraction is truly bioavailable, and several studies indicate that albumin-bound vitamin D metabolites are not available to cells, at least under static conditions (Bikle and Gee, 1989). However, because the albumin−hormone complexes generally dissociate rapidly this fraction may be more bioavailable in a dynamically perfused tissue (Mendel, 1990). The free hormone hypothesis postulates that only the unbound fraction (the free fraction) of hormones that otherwise circulate in blood bound to their carrier proteins is able to enter cells and exert its biologic effects (Fig. 29.3). Examples include the vitamin D metabolites, about which we are concerned in this chapter; sex steroids; cortisol; and thyroid hormone. These are lipophilic hormones assumed to cross the plasma membrane by diffusion and not by an active transport mechanism. However, at least for some tissues, a transport system has been identified that takes up the 25(OH)D (and presumably other vitamin D metabolites) attached to DBP. That system involves megalin and cubilin. The importance of megalin for vitamin D metabolism was first

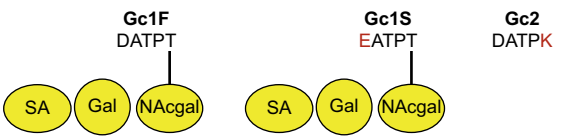

FIGURE 29.2 Major vitamin D-binding protein variants. Gc1F, Gc1S, and Gc2 are the major vitamin D-binding protein (DBP) variants. They differ in the sequence of amino acids from 432 to 436 as shown. DATPT of Gc1F represents Asp−Ala−Thr−Pro−Thr. In Gc1S the aspartate is mutated to glutamate. In Gc2, the threonine is mutated to lysine. The glycosylation at the threonine in Gc1F and Gc1S enables these forms to be converted to DBP−macrophage-activating factor by removal of the *N*-acetylgalactosamine (*NAcgal*) and galactose (*Gal*), leaving sialic acid (*SA*).

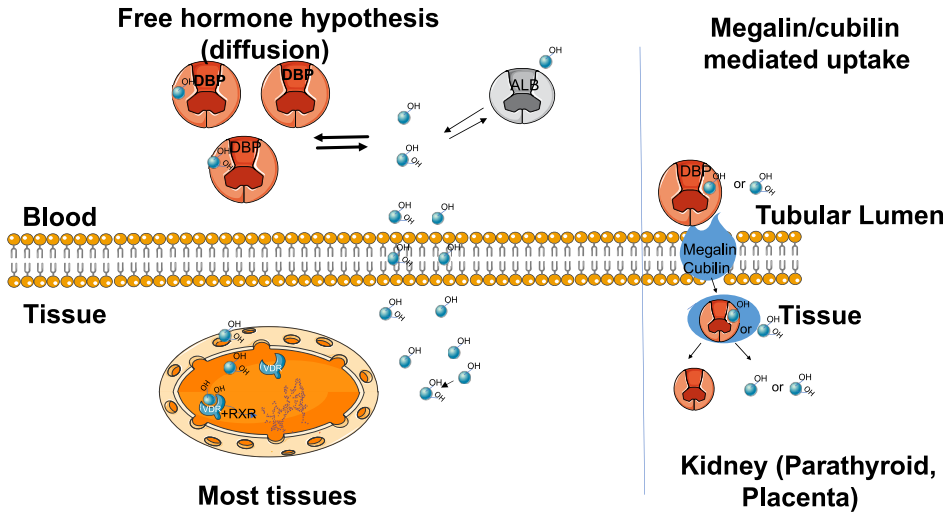

FIGURE 29.3 Free hormone hypothesis. For most cells the vitamin D metabolites are thought to diffuse into the cells in the unbound or free form. However, for some cells, such as the kidney, megalin and cubilin transport the vitamin D into the cell bound to vitamin D-binding protein (*DBP*).

noted by Nykjaer et al. (Nykjaer et al., 1999), who found in the megalin-knockout mouse extensive loss of DBP and 25(OH)D in the urine with the development of bone disease. These mice have very poor survival, but subsequently a kidney-specific knockout of megalin was developed with good survival, enabling the clear demonstration of decreased levels of the vitamin D metabolites, hypocalcemia, and osteomalacia in these mice (Leheste et al., 2003). While megalin has a transcellular domain that is necessary for its endocytosis, cubilin does not, but associates directly with megalin to enable the uptake of DBP and other ligands into the cell (reviewed in Christensen and Birn, 2002). A substantial number of tissues express the megalin/cubilin complex, including the parathyroid gland, choroid plexus, placenta, thyroid, type II pneumocytes, and endometrium, but the role of this complex with respect to its importance for vitamin D metabolism has been best studied in the kidney (Christensen and Birn, 2002), and its role in other tissues with respect to vitamin D metabolite transport into cells is unclear. Although the megalin/cubilin transport system is the best understood mechanism by which DBP-bound 25(OH)D is transported into cells, activated monocytes and the Raji cell line (human B cell lymphoma cell line) have also been reported to accumulate DBP by a mechanism apparently independent of megalin (Chun et al., 2010; Esteban et al., 1992). This mechanism has received little further study.

The knockout of megalin is fruitfully compared with the knockout of DBP in attempting to distinguish the respective roles of DBP and megalin/cubilin with respect to vitamin D entry into cells. In DBP-knockout mice the vitamin D metabolites are presumably all free and/or bioavailable. Unlike the megalin-knockout mice, mice lacking DBP do not show evidence of vitamin D deficiency unless placed on a vitamin D-deficient diet, despite having very low levels of serum 25(OH)D and $1,25(OH)_2D$ and losses of these metabolites in the urine (Safadi et al., 1999). However, on a vitamin D deficient-diet they rapidly develop hyperparathyroidism indicative of vitamin D deficiency. On the other hand, the DBP-knockout mice resisted the development of vitamin D toxicity (renal calcifications) when large doses of vitamin D were administered. In subsequent studies tissue levels of $1,25(OH)_2D$ were found to be normal in the DBP-knockout mice, as was the expression of markers of vitamin D action, such as intestinal transient receptor potential cation channel subfamily V member 6 (TRPV6), calbindin 9k, PMCA1b, and renal TRPV5. Moreover, injection of $1,25(OH)_2D$ into these DBP knockouts showed a more rapid increase in the expression of cytochrome P450 family 24 subfamily A member 1 (Cyp24A1), TRPV5, and TRPV6 (Zella et al., 2008). These studies support the concept that although the megalin/cubilin complex is critical for transporting 25(OH)D−DBP into some tissues such as the kidney, DBP is not necessary for getting the vitamin D metabolites into other cells, thus supporting the free hormone hypothesis for those cells. However, DBP clearly serves as a critical reservoir for the vitamin D metabolites, reducing the risk of vitamin D deficiency when intake or epidermal production is transiently reduced. Further support for this concept comes from studies in cell culture. In keratinocytes, only the free fraction of $1,25(OH)_2D$ was capable of inducing Cyp24A1 under varying conditions of DBP and albumin (Bikle and Gee, 1989). These results were subsequently supported by the observation that serum from DBP-knockout mice enabled the induction of Cyp24A1 by $1,25(OH_2)D$ in MC3T3 cells (Zella et al., 2008) and the induction by 25(OH)D and $1,25(OH)_2D$ of both Cyp24A1 and cathelicidin in monocytes (Chun et al., 2010) better than serum from control mice. These results indicate that DBP and albumin restricted the entry of the vitamin D metabolites into these cells.

To address the free hormone hypothesis, a method to measure the free concentration needed to be developed. This was originally performed by centrifugal ultrafiltration developed by the author to directly determine the free levels of 25(OH)D and 1,25$(OH)_2$D (Bikle et al., 1984, 1986a) in various clinical situations. However, this method is quite labor intensive and has been replaced, at least for free 25(OH)D, by a two-step enzyme-linked immunosorbent assay (ELISA) that directly measures free 25(OH)D (Future Diagnostics Solutions B.V., Wijchen, The Netherlands) using monoclonal antibodies from DIAsource ImmunoAssays (Louvain-la-Neuve, Belgium). This newer assay is dependent on the quality of the antibody used to bind the free 25(OH)D. The antibody in the current assay does not recognize 25$(OH)D_2$ as well as 25$(OH)D_3$ (77% of the 25$(OH)D_3$ value) so it underestimates the free 25$(OH)D_2$. However, in most situations where the predominant vitamin D metabolite is 25$(OH)D_3$, the data compare quite well with those obtained from similar populations using the centrifugal ultrafiltration assay (Bikle et al., 2017b; Schwartz et al., 2014a).

The centrifugal ultrafiltration method was utilized for the determination of the affinity constants for DBP and albumin binding to 25(OH)D and 1,25$(OH)_2$D. These affinity constants were measured in serum from a healthy young adult (the author) and demonstrated an affinity constant (K_a) of DBP for 1,25$(OH)_2$D of $3.7-4.2 \times 10^7\ M^{-1}$ and for 25(OH)D of $7-9 \times 10^8\ M^{-1}$, with a K_a of albumin for 1,25$(OH)_2$D of $5.4 \times 10^4\ M^{-1}$ and for 25(OH)D of $6 \times 10^5\ M^{-1}$ (Bikle et al., 1985, 1986b). Using these affinity constants along with measurements of DBP, albumin, and total vitamin D metabolite of interest permitted the free concentration to be calculated according to the following formula:

$$\text{free vitamin D metabolite} = \frac{\text{total vitamin D metabolite}}{1 + (\text{Ka}_{\text{alb}} * \text{albumin}) + (\text{Ka}_{\text{DBP}} * \text{DBP})}.$$

In sera from normal healthy younger individuals, the calculated values using DBP measured with polyclonal antibodies and the calculated values of free 25(OH)D and 1,25$(OH)_2$D correlate well with the directly measured free levels.

When applied to clinical populations with altered DBP levels during either physiologic (e.g., pregnancy) or pathologic (e.g., liver disease) conditions, however, the calculated values no longer are consistent with those measured directly by either centrifugal ultrafiltration or the newly developed ELISA (Schwartz et al., 2014b). There are a number of reasons for this. As noted earlier, calculation of free vitamin D metabolite levels depends on the accurate measurement of total vitamin D metabolite, DBP, and albumin and the affinity constants between DBP and albumin for the vitamin D metabolite whose free concentration is being measured. Although measurement of albumin is considered well standardized, that of the vitamin D metabolites is less so (Fuleihan Gel et al., 2015); although with major efforts to encourage laboratories to use well-defined standards and more advanced technology such as mass spectroscopy, this is improving (Muller and Volmer, 2015; Binkley and Carter, 2017). However, the measurement of DBP has not been standardized, and the results vary substantially between laboratories. One widely used monoclonal assay underestimates the Gc1F allele of DBP, leading to the conclusion that individuals expressing this allele, primarily African Americans, had lower DBP levels than Caucasians (Powe et al., 2013). On the other hand, Nielson et al. (Nielson et al., 2016a,b) subsequently reported their results measuring DBP levels with four different assays, three of which involved polyclonal assays and one the aforementioned monoclonal assay used by Powe et al. (Powe et al., 2013). The monoclonal antibody-based assay resulted in a 54% lower concentration of DBP in African Americans expressing the Gc1F allele, compared with Caucasians, with minimal differences in DBP levels among these groups using the three polyclonal assays. Similarly, mass spectrometry measurements of DBP by Hoofnagle et al. (Hoofnagle et al., 2015) failed to show a major difference in DBP levels with the various alleles, although the results with mass spectroscopy tended to be lower than those with the polyclonal assays. That said, assays using polyclonal assays or mass spectroscopy have consistently demonstrated a modest reduction in the Gc2 variant of DBP compared with the Gc1 variants (Hoofnagle et al., 2015; Lauridsen et al., 2001; Carpenter et al., 2013; Santos et al., 2013). A 2010 genome-wide association study demonstrated that rs2282679, an intronic polymorphism in the DBP gene, was likewise associated with lower 25(OH)D and DBP levels (Wang et al., 2010). This observation has been confirmed in several other populations (Leong et al., 2014; Cheung et al., 2013).

The clinical significance of these allelic differences is unclear. Individuals with the Gc2 variant have been shown to respond to vitamin D supplementation with a more robust increase in 25(OH)D (Fu et al., 2009).

Nevertheless, differences in these alleles were not found to contribute to a difference in fracture rate in a large study including African Americans and Caucasians (Takiar et al., 2015) or in other calcemic and cardiometabolic diseases in the Canadian Multicentre Osteoporosis Study (Leong et al., 2014). However, as reviewed by Malik et al. (Malik et al., 2013) and Speeckaert et al (Speeckaert et al., 2006), a large number of chronic diseases, including types 1 and 2 diabetes (Hirai et al., 1998; Baier et al., 1998; Ye et al., 2001), osteoporosis (Lauridsen et al., 2004; Papiha et al., 1999; Ezura et al., 2003), chronic obstructive lung disease (Chishimba et al., 2010), endometriosis (Faserl et al., 2011), inflammatory bowel disease (Eloranta et al., 2011), some cancers (Abbas et al., 2008; Dimopoulos et al., 1984; Zhou et al., 2012; Poynter et al., 2010)

(although see Poynter et al., 2010; McCullough et al., 2007; Ahn et al., 2009), and tuberculosis (Martineau et al., 2010) have been associated with various DBP variants.

A third major problem in attempting to calculate the free fraction of vitamin D metabolites is the assumption that all DBP alleles have the same affinity for the vitamin D metabolites, and that this is invariant under varying clinical conditions. Although differences in the affinity constants for the different DBP alleles have been reported, with Gc1F having the highest affinity and Gc2 the lowest among the common alleles (Arnaud and Constans, 1993), results from other laboratories have not confirmed these differences (Bouillon et al., 1980; Boutin et al., 1989). However, in a more recent study evaluating the half-life of 25(OH)D in serum, subjects homozygous for the Gc1F allele were found to have the shortest half-life, indicating reduced affinity (Jones et al., 2014). On the other hand, serum containing the Gc1F variant of DBP reduced the ability of 25(OH)D and $1,25(OH)_2D$ to induce cathelicidin in monocytes more than serum with the Gc2 allele, suggesting the opposite order of affinity (Chun et al., 2010). Regardless, these potential differences in measured affinity do not begin to explain the large differences between the calculated and the directly measured free metabolite levels in various disease states. Although there are statistically significant correlations between calculated and directly measured free 25(OH)D, the relationship accounts for only 13% of the variation. Calculated free 25(OH)D concentrations are consistently higher than directly measured concentrations in a variety of studies, such as those performed during the third trimester of pregnancy and in patients with liver disease and cystic fibrosis (Schwartz et al., 2014b; Nielson et al., 2016a,b; Lee et al., 2015; Sollid et al., 2016). These studies suggest changes in the affinity of 25(OH)D to DBP independent of allelic variations in at least these clinical conditions.

Studies of normal populations using direct methods of determining free 25(OH)D concentrations have shown good correlations with total 25(OH)D concentrations. The free levels have been reported to be between 0.02% and 0.09% of total 25(OH)D concentrations. Concentrations generally range from 1.2 to 7.9 pg/mL. However, in a study of normal individuals in which DBP alleles and total and free 25(OH)D were measured, those with the Gc2/2 variant had lower DBP and lower total 25(OH)D levels than those with Gc1 alleles, but the differences in directly measured free 25(OH)D levels were nearly the same, unlike the calculated free 25(OH)D levels (Sollid et al., 2016). Parathyroid hormone (PTH) is generally found to be negatively correlated with free 25(OH)D as well as total 25(OH)D, whereas serum C-terminal telopeptide of type I collagen has been reported to have a moderate positive correlation with total and free 25(OH)D (Aloia et al., 2015).

Thus in normal individuals, total 25(OH)D provides a reasonable assessment of vitamin D status. However, this is not the case in conditions in which DBP levels and/or affinities for the vitamin D metabolites are altered. Obesity is associated with reductions in total and free 25(OH)D but not DBP or half-life measurements of 25(OH)D (Walsh et al., 2016). On the other hand, bioavailable 25(OH)D correlated with bone mineral density but total 25(OH)D did not in one study (Powe et al., 2011). Similarly, in hemodialysis patients bioavailable 25(OH)D correlated negatively with PTH and positively with serum calcium, unlike total 25(OH)D. In the nephrotic syndrome, DBP is lost in the urine along with 25(OH)D, reducing the levels of both total and bioavailable 25(OH)D. However, like in the hemodialysis patients, bone mineral density correlated positively and PTH negatively with bioavailable 25(OH)D but not with total 25(OH)D (Aggarwal et al., 2016). In a study of patients with acute kidney injury, bioavailable 25(OH)D but not total 25(OH)D correlated inversely with mortality (Leaf et al., 2013). In acromegaly, DBP levels were observed to be increased, whereas 25(OH)D levels were not, resulting in a reduction in the calculated free 25(OH)D (Altinova et al., 2016) that may contribute to some of the alterations in bone and mineral metabolism in this condition. In a study of HIV^+ patients on triple antiviral therapy, the DBP levels were increased but not the total 25(OH)D, and these changes were associated with an increase in bone turnover markers and PTH, suggesting a fall in free 25(OH)D (which was not measured) (Hsieh et al., 2016). With vitamin D or 25(OH)D supplementation, free 25(OH)D concentrations rise in concert with total 25(OH)D concentrations (Sollid et al., 2016; Aloia et al., 2015; Alzaman et al., 2016; Schwartz et al., 2016; Liu et al., 2006), rising more steeply with D_3 supplementation compared with D_2 (Shieh et al., 2016) and even faster with $25(OH)D_3$ (Shieh et al., 2017). With high-dose D supplementation the changes in PTH were significantly related to changes in free 25(OH)D but not to changes in total 25(OH)D or changes in total $1,25(OH)_2D$ (Shieh et al., 2016), suggesting that free 25(OH)D might be a better marker of the biologically available fraction. In the third trimester of pregnancy, directly measured free 25(OH)D tends to be higher, and free $1,25(OH)_2D$ is substantially higher in pregnant women versus comparator groups of women (Bikle et al., 1984; Schwartz et al., 2014b). These results suggest that the affinity of DBP for the vitamin D metabolites is decreased during pregnancy, perhaps compensating for increased DBP concentrations and the needs of both the mother and the fetus for calcium. Directly measured free 25(OH)D and $1,25(OH)_2D$ tend to be higher in outpatients with cirrhosis compared with other groups (Bikle et al., 1986a; Schwartz et al., 2014b), despite lower total vitamin D metabolite concentrations. The relationship between free 25(OH)D and total 25(OH)D is both steeper and more variable in patients with liver disease than in healthy people, indicating altered affinity of DBP for 25(OH)D in these patients. Those with the most severe cirrhosis

and protein synthesis dysfunction have a higher percentage of free 25(OH)D compared with cirrhotics without protein synthesis dysfunction, but free 25(OH)D concentrations are similar due to the presence of both lower total 25(OH)D concentrations and lower DBP. In a vitamin D dose-titration study (Schwartz et al., 2016) of nursing home residents, who are older and likely to have more medical problems and receive more medications than younger people or community-dwelling elderly, free 25(OH)D levels rose along with increases in total 25(OH)D, but responses appeared to be steeper than those of normal subjects, younger outpatients, diabetics, or HIV-infected patients, suggesting altered affinity of 25(OH)D for DBP in this group of individuals. Additional support for the free hormone hypothesis comes from animal studies comparing the effects of vitamin D_2 with vitamin D_3 on calcium metabolism. In one such study mice were raised on a diet containing only vitamin D_2 or vitamin D_3 postweaning. These mice had comparable 25(OH)D levels 8 weeks later, but the D_2-raised mice had higher free 25(OH)D levels with increased numbers of osteoclasts and increased indices of both bone resorption and formation (Chun et al., 2016). These studies, clinical and translational, support the free hormone hypothesis and argue that measurement of the free vitamin D metabolite concentration provides information concerning the vitamin D status of the individual over and above that of the total vitamin D metabolite measurements.

Actin scavenging

A major function of DBP that has received considerably less study than that of vitamin D metabolite binding is its role in actin scavenging. Following trauma (Dahl et al., 2001a), sepsis (Wang et al., 2008; Dahl et al., 2003; Kempker et al., 2012), liver trauma (Schiodt, 2008; Gressner et al., 2009; Schiodt et al., 1997), acute lung injury (Lind et al., 1988), preeclampsia (Tannetta et al., 2014), surgery (Speeckaert et al., 2010; Dahl et al., 2001b), and burn injuries (Koike et al., 2002), large amounts of actin are released from the damaged cells, forming polymerized filamentous F-actin that in combination with coagulation factor Va can lead to disseminated intravascular coagulation and multiorgan failure unless cleared (Meier et al., 2006). The actin scavenging system consists of gelsolin and DBP. Gelsolin depolymerizes F-actin to G (globular)-actin. DBP with its high affinity for G-actin ($K_d = 10$ nM) prevents repolymerization and clears it from the blood (Vasconcellos and Lind, 1993; Mc Leod et al., 1989). There does not appear to be a difference among the major DBP variants for binding to G-actin (Speeckaert et al., 2006). The DBP−actin complexes are rapidly cleared (half-life in blood approximately 30 min) (Dahl et al., 2001b), primarily by the liver, lungs, and spleen, which express receptors for the DBP−actin complexes (Dueland et al., 1991). The immediate result is a drop in DBP levels, potentially altering the bioavailability of the vitamin D metabolites (Schiodt, 2008; Madden et al., 2015; Waldron et al., 2013), but a rise in the DBP−actin complexes (Dahl et al., 2001a; Wang et al., 2008; Schiodt et al., 1997; Lind et al., 1988). The ability of the organism to respond to the insult by increasing DBP production is correlated to survival (Dahl et al., 2001a; Schiodt, 2008; Leaf et al., 2013), and has led to consideration of the use of DBP therapeutically (Pihl et al., 2010; Gomme and Bertolini, 2004).

Neutrophil recruitment and migration with complement 5a binding

Neutrophil activation during inflammation increases their binding sites for DBP (DiMartino et al., 2007), and DBP binding to these sites facilitates C5a-induced chemotaxis (Binder et al., 1999). This role of DBP is not limited to C5a but includes other chemoattractants such as CXCL1 during inflammation (Trujillo et al., 2013). DBP by itself does not promote chemotaxis, nor does the DBP−actin complex discussed before (Ge et al., 2014). The interaction with C5a involves residues 130−149 of DBP, a region that is common to all major DBP alleles (Zhang and Kew, 2004), and no difference in these alleles has been found with respect to their promotion of C5a-mediated chemotaxis (Binder et al., 1999). Binding of $1,25(OH)_2D$ blocks the promotion by DBP of the C5a activity, although 25(OH)D does not (Shah et al., 2006). CD44 and annexin A2 are thought to be part of the DBP cell surface binding site, which also appears to involve cell surface ligands such as chondroitin sulfate proteoglycans, and are involved in C5a chemotaxis (DiMartino et al., 2001; DiMartino and Kew, 1999; McVoy and Kew, 2005). The binding of DBP to its receptor is not altered by and does not alter the affinity of C5a for its receptor (Zhang et al., 2010; Perez, 1994), but does increase the amount of binding of C5a des Arg to the C5a receptor (Perez, 1994).

Fatty acid binding

Like albumin, DBP binds fatty acids but with lower affinity ($K_a = 10^5-10^6 M^{-1}$) and a single binding site (Calvo and Ena, 1989; Swamy and Ray, 2008). Most of the fatty acids binding to DBP are monounsaturated or saturated, with only 5% polyunsaturated. However, only polyunsaturated fatty acids such as arachidonic acid and linoleic acid compete with vitamin D metabolites for DBP binding (Bouillon et al., 1992; Ena et al., 1989), suggesting that the different fatty acids

alter the configuration of DBP, which influences binding of the vitamin D metabolites, rather than directly competing with the vitamin D metabolites for their binding site. The role of DBP in fatty acid transport is not clear given its relatively minor participation in fatty acid transport in blood.

Formation of vitamin D-binding protein–macrophage-activating factor and its functions

DBP–MAF is formed from certain alleles of DBP by removal of galactose by membrane-bound β-galactosidase induced in B cells during inflammation by lysophosphatidylcholine, followed by removal of sialic acid by membrane-bound sialidase on T cells (Yamamoto and Homma, 1991). These deglycosylation steps are required for its role in macrophage activation (Uto et al., 2012), but further removal of the *N*-acetylgalactosamine (NAcgal) reduces this activity (Yamamoto et al., 1991). Swamy et al. (Swamy et al., 2001) demonstrated the ability of DBP–MAF to activate osteoclasts, and this activity was independent of its 25(OH)D-binding function. The presence of the NAcgal moiety on DBP–MAF is essential for its ability to activate osteoclasts. DBP–MAF has been shown to stimulate bone resorption in two models of osteopetrosis (Schneider et al., 1995): the osteopetrosis (OP) and the incisor absent (IA) rat. The OP rat lacks osteoclasts, whereas the IA rat has nonfunctional osteoclasts. When given DBP–MAF the OP rats showed increased numbers of osteoclasts, whereas the IA rats showed improved osteoclast function. DBP–MAF has shown efficacy in a number of tumor models. The mouse SCCVII tumor model of squamous cell carcinoma was used to demonstrate that DBP–MAF enhanced the curative effect of photodynamic treatment (Korbelik et al., 1997). The survival time of mice bearing Ehrlich ascites tumors was prolonged by DBP–MAF (Koga et al., 1999). Kister et al. (Kisker et al., 2003) showed that DBP–MAF had antiangiogenic activity and inhibited the growth of pancreatic cancer in SCID mice, which on histologic exam also showed an increase in macrophages with decreased vascularity. Removal of NAcgal by α-NAcgalase blocks DBP–MAF formation, contributing to the loss of immunosuppression in cancer patients (Yamamoto et al., 1996). α-NAcgalase is produced in the liver, and appears to be directly related to tumor burden (Yamamoto et al., 1997). Preparations of DBP–MAF may have therapeutic potential (Nagasawa et al., 2005).

Intracellular trafficking of vitamin D metabolites: role of heat shock protein 70 and hnRNPC1/C2

The role of DBP is to get the vitamin D metabolites to and, for some cells, into the cell. However, a protein originally called intracellular DBP, identified subsequently as Hsp70 (Gacad et al., 1997), was found to promote the intracellular uptake and distribution of the vitamin D metabolites within the cell (Wu et al., 2000). This observation was originally made in New World monkeys, which were resistant to $1,25(OH)_2D$ (Gacad and Adams, 1993), but expressed a lot of this protein compared with Old World monkeys. Overexpression of this protein in cells from Old World monkeys increased the amount of 25(OH)D in these cells, promoted synthesis of $1,25(OH)_2D$, and increased the genomic actions of $1,25(OH)_2D$, such as the induction of Cyp24A1 (Adams et al., 2004). Antisense constructs to Hsp70 blocked these actions. The concept is that Hsp70 functions to transport 25(OH)D to the mitochondria where Cyp27B1 (the 1-hydroxylase) is located, and then transport the product of Cyp27B1, $1,25(OH)_2D$, to the nucleus where it binds the VDR for its genomic actions. The affinities of these proteins favor this trafficking, with higher affinity of Hsp70 for 25(OH)D than DBP and lower affinity of Hsp70 for $1,25(OH)_2D$ than VDR. However, there is an additional intracellular protein that was discovered in New World monkeys that better explains their hormone resistance (Arbelle et al., 1996), and that was subsequently found in a human with vitamin D resistance (Hewison et al., 1993; Chen et al., 2003). This protein, originally called VDRE-BP, is now known to be hnRPC1/C2 protein (Chen et al., 2006). Its overexpression blocks $1,25(OH)_2D$ transcriptional activity. This protein normally sits on the VDRE (vitamin D response element), but is displaced by $1,25(OH)_2D$, allowing the liganded VDR to initiate transcription (Chen et al., 2006).

The vitamin D receptor

The VDR was first discovered as a chromatin-associated $1,25(OH)_2D$-binding protein in 1974 (Brumbaugh & Haussler, 1974, 1975). Although initially identified in the intestine, the site of the best studied actions of vitamin D at the time and the tissue from which it was originally cloned and sequenced (McDonnell et al., 1987), the VDR has subsequently been found in essentially all tissues in which it has been sought (Stumpf et al., 1979; Berger et al., 1988). Even in tissues such as the liver and muscle, low levels of the VDR have been identified. In the liver VDR is primarily expressed in the stellate cells, and not in the more abundant parenchymal cells (Ding et al., 2013). In skeletal muscle the VDR is more highly expressed during development such that in adult tissue the levels are quite low, making it difficult to detect by standard

methods (Girgis et al., 2014). Moreover, vitamin D has an impact on many cellular processes. In a 2015 ontology analysis 11,031 putative VDR target genes were identified, of which 43% were involved with metabolism, 19% with cell and tissue morphology, 10% with cell junction and adhesion, 10% with differentiation and development, 9% with angiogenesis, and 5% with epithelial-to-mesenchymal transition (Saccone et al., 2015). Furthermore, VDR can regulate various microRNAs and long noncoding RNAs, regulating the expression of numerous other proteins indirectly (Khanim et al., 2004; Wang et al., 2009; Jiang and Bikle, 2014). As a result of the appreciation that the VDR has such universal distribution and that vitamin D-metabolizing enzymes such as Cyp27B1 (that produces the active metabolite $1,25(OH)_2D$) and Cyp24A1 (that catabolizes 25(OH)D and $1,25(OH)_2D$ to less active forms) are also widely distributed (Bikle, 2014), interest in understanding the role of vitamin D and the VDR in tissues not obviously participating in the classic target tissues regulating calcium and phosphate homeostasis has been substantial. Over 4000 publications regarding vitamin D have appeared each year since 2014, most focused on the nonclassical actions of vitamin D. The remarkable aspect of this widespread distribution of the VDR is how many and yet how specific the actions of VDR are for any given cell. Although we have clues on how this specificity comes about, and these clues will be discussed in this chapter, we have much more to discover. Moreover, although most actions of VDR involve its role as a transcription factor within the nucleus (Carlberg, 2017; Pike et al., 2017), the VDR has also been shown to have nongenomic actions via its location in the membrane (Haussler et al., 2011) and perhaps even in mitochondria (Silvagno and Pescarmona, 2017). In this chapter I will not be dealing with actions of VDR signaling in specific tissues except as they illustrate more general points regarding VDR function, as tissue-specific aspects of VDR function have been well covered in several reviews (Bikle, 2014, 2016; Christakos et al., 2016).

Genomic location, protein structure, and regulation

The human *VDR* is located on chromosome 12. It spans 75 kb of DNA, and comprises nine exons, although the 5′ end is complex, with a number of potential minor TSSs 5′ of the major start site immediately upstream of exon 1a, resulting in alternatively spliced forms (Baker et al., 1988; Crofts et al., 1998; Sunn et al., 2001). Exon 2 contains the translation start site and the nucleotide sequence encoding the short A/B domain (24 aa), to which transcription factors such as TFIIB bind, and the first zinc finger of the DNA-binding domain (DBD) (65 aa). Exon 3 encodes the second zinc finger of the DBD. Exons 4–6 encode the hinge region (143 aa). Exons 7–9 encode part of the hinge region, the entire ligand-binding domain (LBD; E/F) (195 aa) including the AF2 domain, and the extensive 3′ untranslated region (UTR) (Fig. 29.4). A polymorphism (FokI restriction site) is found in the human *VDR*, changing an ATG to an ACG and shifting the translation start site by 3 aa, shifting the total length from 427 to 424 aa. The shorter form may be more transcriptionally active (Jurutka et al., 2000). Numerous other polymorphisms have been described in untranslated regions of the *VDR* gene, to which associations with various diseases have been made, but generally such studies suffer from small numbers and/or lack of reproducibility (Iqbal and Khan, 2017; Bizzaro et al., 2017; Rai et al., 2017) and will not be discussed further. Amino acids 49 and 50 between the two zinc fingers and 102–104 C terminal to the zinc fingers appear to provide the nuclear localization signal (Hsieh et al., 1998; Luo et al., 1994).

The DBD is composed of two zinc fingers held in a tetrahedral configuration by four cysteine residues. The first zinc finger directs DNA binding in the major groove of the DNA binding site. The second zinc finger provides a dimerization interface for its primary partner RXR. A short C-terminal extension from the second zinc finger participates in this dimerization interface (Wan et al., 2015a). The LBD is composed of 12 α helices (H1–H12) as shown in the original crystal structures (Rochel et al., 2000). The terminal H12 provides the essence of the mousetrap model for binding of

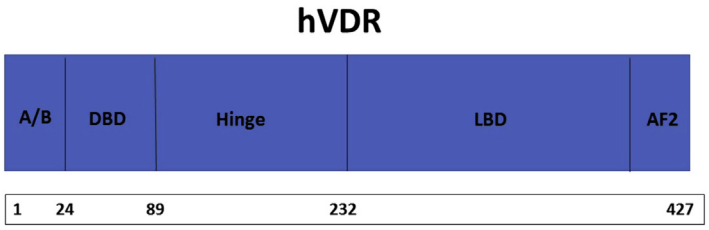

FIGURE 29.4 The structure of the human vitamin D receptor. The major domains of the human vitamin D receptor (*hVDR*) are depicted. The N-terminal A/B or AF2 domain is short in the VDR. It plays a role in TFII binding. The DNA-binding domain (*DBD*) comes next and is the site of the two zinc fingers that directly bind to DNA. The second zinc finger participates in binding to RXR, the major heterodimer partner for VDR. The hinge region also participates in RXR binding. The ligand-binding domain (*LBD*) is the site of binding for $1,25(OH)_2D$ and other ligands, as well as corepressors. When VDR binds to its ligand, AF2 on the C-terminal end undergoes a major conformational change to both enclose the ligand and provide docking for coactivators such as steroid receptor coactivators and Med1 of the Mediator complex.

$1,25(OH)_2D$ to the VDR in that in the nonliganded VDR H12 is open, but with ligand binding H12 moves over the ligand, enclosing it in the ligand-binding pocket (Rochel et al., 2000). This results in very tight binding (K_d approximately 10^{-10} M) (Mellon and DeLuca, 1979). In the closed position H12 along with H3 and H4 provides the interface for coactivators such as the steroid receptor coactivators (SRCs) and mediator complexes, which bind to H12 via their NR boxes containing the LxxLL sequence of amino acids (L for leucine, x any amino acid) (McInerney et al., 1998). The ligand-binding pocket is actually quite large and accommodates a number of ligands, including lithocholic acid. $1,25(OH)_2D$ fits into this pocket in an extended configuration, with its A ring in the β-chair configuration and the 1α group in an equatorial position (6-S *trans* conformation). Thirty-six residues line the ligand pocket, of which six make direct hydrogen bonds with the ligand (Wan et al., 2015b). H9 and H10 along with the second zinc finger provide the heterodimerization site for RXR (Whitfield et al., 1996). The structure of the full human RXR/VDR heterodimer complex with its DR3 DNA binding site has been revealed by cryo-electron microscopy (Orlov et al., 2012). This structure confirms the binding of the DBDs of both RXR and VDR to its major binding site on DNA (a direct repeat element with two hexanucleotide DNA sequences separated by a three-nucleotide spacer) with the RXR DBD binding to the 5′ half-site and the VDR to the 3′ half-site. Their LBDs project perpendicular to the DNA in an open confirmation, enabling binding by coregulators. The membrane VDR accepts a different configuration (6-S *cis* conformation), which led Mizwicki et al. (Mizwicki et al., 2004) to propose an alternative pocket for ligand binding, but this structure has not been confirmed by crystallography.

Amino acid residues critical for the structure/function of the VDR have been well demonstrated by mutations in the VDR in either the human or the mouse gene (reviewed in Malloy and Feldman, 2012). Approximately 45 different mutations in 100 patients have been described as of this writing. Mutations in the DBD block all functions of the VDR. Mutations at aa 274 in the LBD alter the affinity of the VDR for $1,25(OH)_2D$ by affecting the amino acid forming a hydrogen bond with the 1α group. Similarly, mutation at aa 305 alters the hydrogen bond with the 25(OH) group, likewise reducing affinity for the ligand. Mutation of 391 affects the dimerization domain at H9 and H10, reducing transactivation. Mutations of aa 420 in H12 alter coactivator binding. Mutations in the DBD and dimerization domain lead to alopecia as well as rickets, whereas those in the LBD that affect only the affinity for $1,25(OH)_2D$ or the coactivators result in rickets, but not alopecia, indicating that ligand binding is not essential for hair follicle cycling.

The regulation of VDR expression is quite cell specific. For example, $1,25(OH)_2D$ autoregulates VDR expression in bone cells but not in the intestine (Lee et al., 2014; Wood et al., 1998). Moreover, ligand binding to VDR stabilizes it, increasing its levels (Wiese et al., 1992). Many factors, including $1,25(OH)_2D$ itself, have been shown to regulate VDR expression. These include growth factors such as fibroblast growth factor, epidermal growth factor, insulin-like growth factor, and insulin, as well as PTH, glucocorticoids, estrogen, and retinoic acid. A variety of transcription factors have been identified that may mediate their regulation of VDR expression, including activator protein-1 (AP-1), specificity protein-1, CCAAT/enhancer binding protein (C/EBP), and caudal-type homeobox 2 (CDX2). For example, several enhancer elements have been found in the *VDR* gene that bind VDR. These enhancer elements are associated with binding sites for other transcription factors such as C/EBPβ, Runx2, cyclic AMP response element binding protein (CREB), retinoic acid receptor (RAR), and glucocorticoid receptor (Zella et al., 2010). Similarly, calcium upregulates VDR expression in the parathyroid gland presumably through its calcium-sensing receptor (Canadillas et al., 2010). On the other hand, SNAIL1 and SNAIL2 (SLUG) downregulate VDR expression in a number of cancer cell lines (Palmer et al., 2004; Mittal et al., 2008). MicroRNAs have also been shown to regulate VDR levels. miR-125b binds to the 3′ UTR to decrease VDR levels (Mohri et al., 2009; Gu et al., 2011), in the latter study in response to UVB treatment of psoriatic epidermis (Gu et al., 2011). Similarly miR-298 and miR-27b have been shown to bind to the 3′ UTR of VDR to reduce its expression (Pan et al., 2009). In addition the *VDR* promoter may also be hypermethylated by various methylases and methyltransferases, reducing its expression (Chandel et al., 2013).

Vitamin D receptor mechanism of action: genomic

Vitamin D binding sites in the genome

Combining data from chromatin immunoprecipitation sequencing studies of the entire genome from several different cell lines, Carlberg (Carlberg, 2017) reported that the human genome contained over 23,000 VDR binding sites, 70% of which occurred in only one cell type (Tuoresmaki et al., 2014). Only a small percentage of these binding sites can be clearly identified with a target gene (Ramagopalan et al., 2010). Moreover, within a given genome, the number of binding sites varied with the duration of exposure to ligand. Most of these binding sites were ligand dependent, but a substantial number of sites did not require $1,25(OH)_2D$ for VDR binding to occur, although the addition of ligand altered the location of these

sites (Heikkinen et al., 2011). For example, in LS180 colon cancer cells 262 VDR binding sites were identified without ligand, but following $1,25(OH)_2D$ 2209 binding sites were found, 71% in intergenic regions, 27% in introns, and only a small number near the TSS (Meyer et al., 2012). Similarly the addition of $1,25(OH)_2D$ also markedly enhances the number of RXR binding sites, a substantial percentage of which colocalized with the VDR binding sites (Meyer et al., 2010). Although the DR3 was the most common binding sequence, it occurred in only a minority of binding sites, albeit the ones with the highest affinity for VDR. An ER9 VDRE (everted repeats with nine spacing nucleotides) has been documented in a number of genes (Schrader et al., 1995, 1997), and a DR6, which incorporated RAR rather than RXR as the heterodimer partner with VDR, was identified in the phospholipase Cγ (PLCγ) promoter (Xie and Bikle, 1997). However, no obvious consensus DNA sequences have emerged for most other binding sites. The DR3, as noted earlier, refers to a DNA sequence with two hexanucleotide half-sites separated by a three-nucleotide spacer. Other nuclear hormone receptors have a similar DNA binding site, but the half-sites are separated by different numbers of nucleotides (Kliewer et al., 1992; Perlmann et al., 1993). The consensus sequence of the half sites is A/G G G/T T C/G A.

The VDR binding sites can be thousands of bases away from the TSS of the genes they regulate, and genes generally have multiple VDR binding sites, the activity of which may vary in different cells and different species. The likely explanation is that the DNA can be looped to bring the relevant regulatory elements adjacent to the TSS. This function is performed by CCCTC-binding factors (CTCFs), which define genomic insulator regions, although not all CTCF sites are involved in insulator actions. Genomic loops of hundreds to thousands of bases can be looped into topologically associating domains (TADs), organizing the genome into several thousand such domains (Dixon et al., 2012). In human monocytes $1,25(OH)_2D$ stimulated CTCF binding to approximately 1300 sites, 50% of which marked the anchors for TADs containing at least one VDR binding site and a $1,25(OH)_2D$ target gene (Neme et al., 2016). An informative example of how this might work in different cells is the regulation of the receptor activator of NF-κB ligand (RANKL) gene (*Tnfsf11*) (Fig. 29.5). This gene is regulated by PTH and $1,25(OH)_2D$ in osteoblasts, but by activators of c-fos in activated T cells. The Pike laboratory identified seven VDR binding sites in this gene up to 88 kb upstream of the TSS, of which the −75 kb site proved most active in the mouse gene (Kim et al., 2006; Martowicz et al., 2011), whereas the proximal site was most active in the human gene (Nerenz et al., 2008). However, in activated T cells, three additional sites even farther

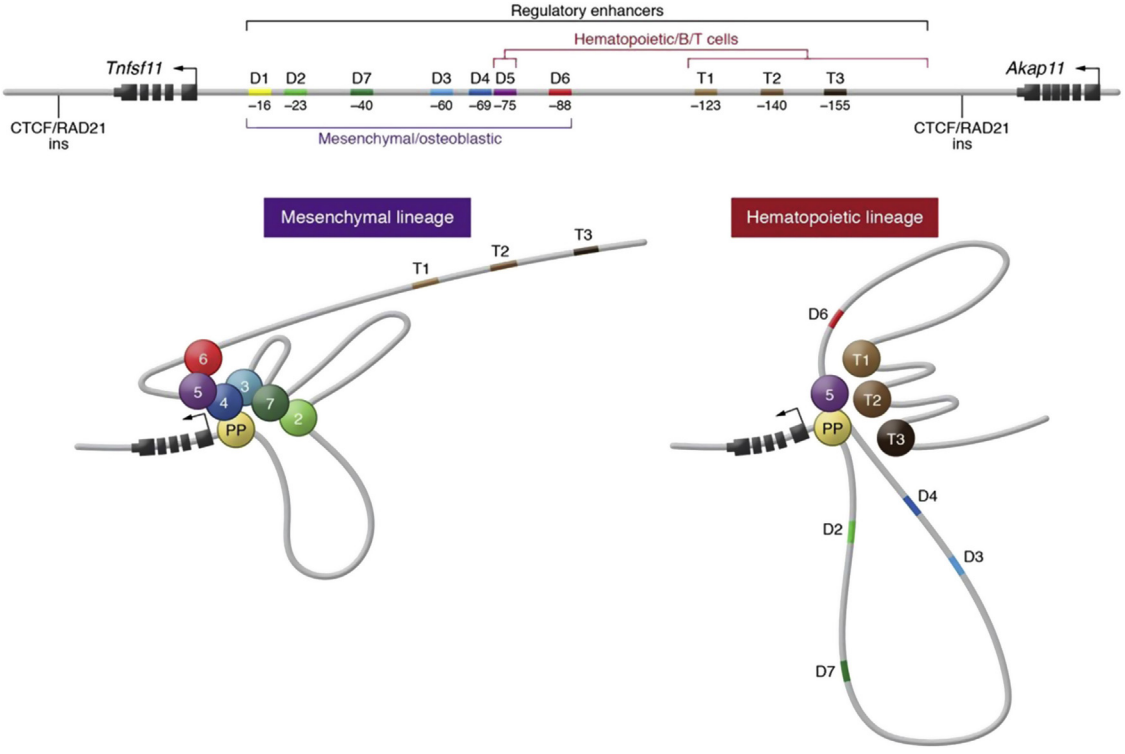

FIGURE 29.5 Theoretical schematic of the *Tnfsf11* (RANKL) gene as it might be configured in osteoblasts or T cells. These two configurations of the gene bring different response elements to the transcription site by alternate forms of looping, illustrating the potential for different means of regulating the same gene in different cellular contexts. The CCCTC-binding factor (*CTCF*) sites demarcate the gene. *Reproduced from Pike et al. Fig. 29.2, J Clin Invest 127:1148, 2017 permission pending.*

upstream of the TSS have been identified as sites of RANKL induction by c-fos (Bishop et al., 2011). CTCF binding sites separate the RANKL gene from adjacent genes, but also separate the VDR binding sites from the more upstream c-fos binding site active in T cells, potentially enabling different looping in these two types of cells (Pike et al., 2017; Bishop et al., 2011). A similar example can be found for Cyp27B1, the enzyme that produces $1,25(OH)_2D$. This gene is negatively regulated by its product in the kidney, as will be discussed later, but not in other tissues (Bikle, 2016b). Pike et al. demonstrated tissue-specific binding of VDR to response elements for this gene, showing differences between that in the kidney and that in other tissues (Meyer et al., 2017).

The VDR binding sites are generally situated in a region with other transcription factors that may share regulation of that gene. The RANKL gene is again a good example, as the −75 kb VDR binding region contains several CREB sites responsible for PTH regulation of this gene (Fu et al., 2006; Kim et al., 2007). Many genes regulated by $1,25(OH)_2D$ in bone cells also have Runx2 and C/EBPβ binding sites in the same regions as the VDR binding sites and influence VDR activity (Meyer et al., 2014). In intestinal cells the VDR binding sites have been colocalized with C/EBPβ, AP-1, CDX2, and T cell factor-4 (TCF4) (Meyer et al., 2012). Other transcription factors found in the vicinity of VDR binding sites that affect its transcriptional activity include ras-activated Ets transcription factors (Dwivedi et al., 2000) and YY1 (Guo et al., 1997; Raval-Pandya et al., 2001). Pu.1 has been hypothesized to serve as a pioneer factor preceding VDR binding, and has been found associated with a number of VDR binding sites in monocytes (Seuter et al., 2017). Changes in VDR binding sites as can occur during differentiation of the cell can affect the binding of these other transcription factors in similar fashion (Meyer et al., 2015, 2016). In osteoblasts such changes probably account for the ability of $1,25(OH)_2D$ to inhibit the early stages of osteoblast differentiation while promoting the later stages (Bikle, 2012a).

Coregulators and epigenetic changes regulating VDR function

The sites of active transcription are marked by epigenetic changes in both the gene itself and the histones that regulate access of the transcriptional machinery to the gene (reviewed in Long et al., 2015). For example, H3K4me3 (histone 3 in which lysine 4 is triply methylated) is found in sites of active transcription, whereas H3K9 is associated with silent promoter regions. H3K27me is associated with active enhancers, whereas H3K27me is associated with gene suppression. $1,25(OH)_2D$ can increase or decrease the expression of these methylases (Pereira et al., 2012). Sites of epigenetic gene suppression are also generally marked by methylation of cytosine in CpG islands (reviewed in Fetahu et al., 2014) in association with the epigenetic changes in the aforementioned histones (Esteller, 2008). The *VDR* promoter has three CpG islands in its promoter in exon 1a, which in breast cancer are hypermethylated, reducing VDR expression (Marik et al., 2010). Similar effects are seen in HIV-infected T cells (Chandel et al., 2013). $1,25(OH)_2D$ reduces the methylation of the E-cadherin promoter (Lopes et al., 2012), increasing its expression, but may promote methylation of other promoters (Doig et al., 2013). Methylases (amine oxidases or jumonji C domain-containing proteins JmJC) can be activators or suppressors. $1,25(OH)_2D$ regulates these epigenetic changes by affecting the binding of coregulators to the VDR, whether coactivators with histone acetyltransferase activity (HATs) or cosuppressors with histone deacetylase activity (HDACs).

There are over 250 published coregulators interacting with nuclear hormone receptors (McKenna et al., 2009). The best studied coactivators with respect to the VDR are the steroid hormone receptor coactivators (SRCs 1−3) (Xu and O'Malley, 2002) and the Mediator complex (Rachez and Freedman, 2001). Phosphorylation of serine 208 in the VDR following dimerization with RXR enhances their binding (Barletta et al., 2002; Arriagada et al., 2007) The SRCs have three NR boxes containing the LxxLL motif described earlier to which they bind the nuclear hormone receptors (Heery et al., 1997), but VDR binding is primarily to the third NR box (Teichert et al., 2009). Med1, the principal component of the Mediator complex binding to VDR and other nuclear hormone receptors, has two NR boxes, the second NR box being the one binding to VDR (Teichert et al., 2009). SRCs recruit HATs to the VDR, in particular CREB binding protein, CBP/p300 (Ogryzko et al., 1996) and the CBP/p300-associated factor p/CAF (Yang et al., 1996). The Med complex does not contain HAT activity but binds directly to RNA polymerase II to help form the preinitiation complex along with basal transcription factors such as TFIIB and several TAT-binding proteins (Yin and Wang, 2014). The peroxisome proliferator-activated γ coactivator-1α interacts with VDR to regulate genes involved in muscle development and energy metabolism (Narvaez et al., 2009). The VDR also binds histone methyltransferases that can synergize with SRCs in terms of regulation (Koh et al., 2001). These coactivators all bind to the AF2 domain (H12). NCoA62/SKIP does not bind to the AF2 domain but binds to the VDR/RXR heterodimer to increase transcription with SRC, but could also coordinate with corepressors NCoR/SMRT to suppress transcription (Baudino et al., 1998; Leong et al., 2004). WINAC is a member of the SWI/SNF subfamily which is an ATP-dependent chromatin remodeling complex involved in DNA replication and transcriptional elongation (Kitagawa et al., 2003). This complex includes the Williams syndrome transcription factor (WSTF) that when mutated results in Williams syndrome, a developmental disorder manifesting as hypercalcemia and disordered vitamin D

metabolism (Morris and Mervis, 2000). This complex plays a central role in the suppression by $1,25(OH)_2D$ of its own production by Cyp27B1, at least in the kidney as will be discussed further (Kim et al., 2007). Meningioma-1 is expressed in osteoblasts, where it enhances $1,25(OH)_2D$/VDR transcription (Sutton et al., 2005).

The best studied corepressors are the SMRT and NCoR complexes (Perissi et al., 1999; Tagami et al., 1998). They have HDAC activity. These corepressors bind to nuclear hormone receptors via their CoRNR boxes, analogous to the NR boxes of the SRC family but with the sequence LxxH/IxxxI/L (Hu and Lazar, 1999). These corepressors do not bind to the AF2 domain (H12) but to H3−H5 in the absence of ligand. In the presence of $1,25(OH)_2D$ and the conformational change with H12, these corepressors are displaced, enabling the coactivators to bind to their sites on H12. Hairless is a corepressor of VDR expressed primarily in the brain and skin (Xie et al., 2006). It binds to the central region of the LBD of VDR, as do NCoR/SMRT to two ϕxxϕϕ hydrophobic sites (ϕ = hydrophobic amino acid) (Hsieh et al., 2003), but also to H12 via its LxxLL motif, similar to SRC and Med1 (Teichert et al., 2009). The role of Hairless is complex in that it represses ligand-dependent VDR functions with respect to epidermal differentiation (Xie et al., 2006) but appears to be required for ligand-independent VDR regulation of hair follicle cycling (Wang et al., 2007). Alien binds to VDR and inhibits transcription by increasing HDAC activity and nucleosome assembly (Polly et al., 2000; Eckey et al., 2007). SUG1 is a proteasomal component that binds to the AF2 domain of VDR and may be involved in VDR degradation (Masuyama and MacDonald, 1998).

Negative vitamin D response elements

The general (and oversimplified) cycling model for the mechanism by which these coregulators control VDR transcription is that $1,25(OH)_2D$, by enhancing the conformational change in VDR, enhances its dimerization to RXR, strengthening the affinity of the complex for specific sites (e.g., DR3) in the DNA, displacing corepressors, and enabling the binding of the VDR/RXR heterodimer to coactivators. SRCs with their HAT activity are hypothesized to be the first to bind to the VDR, enzymatically altering the histones to open up the site for access to transcription factors. Med1 binding follows, which, by recruiting RNA polymerase II to the gene, facilitates the transcription process (Kim et al., 2005). This cycling model (Carlberg, 2010) does not explain situations such as the differentiation process in the epidermis where Med1 predominates in the early stages of differentiation, whereas SRCs 2 and 3 predominate in the more differentiated keratinocytes, each regulating a different profile of genes (Bikle, 2012b; Oda et al., 2003, 2009; Hawker et al., 2007). Moreover, this model does not explain the role of $1,25(OH)_2D$/VDR as an inhibitor of transcription. In microarray analyses genes downregulated by $1,25(OH)_2D$ are nearly as numerous as upregulated genes (White, 2004), but the mechanisms by which such inhibition takes place are unclear, as the VDR binding sites generally demonstrate no clear nucleotide sequence and may not involve direct binding of the VDR to the DNA. In the PTH and PTH-related protein genes inhibition has been reported to involve either half-sites of a DR3 (Demay et al., 1992) or a full DR3-like sequence (Falzon, 1996), but may also involve the binding of VDR to a vitamin D-interacting repressor (VDIR) that binds to DNA at E-box-like motifs (CANNTG, where N can be any nucleotide) (Kim et al., 2007; Murayama et al., 2004). The Kato lab (Kitagawa et al., 2003; Kato et al., 2004) has studied how $1,25(OH)_2D$ represses its own production in kidney cells through this mechanism. Such suppression appears to be restricted to kidney cells as Cyp27B1 expression in other cells does not show this suppression by $1,25(OH)_2D$ (Xie et al., 2002)). Their studies led them to propose that WSTF in the WINAC complex recruits the ligand-bound VDR to the VDIR sitting on the E-box-like negative VDRE, recruiting corepressors with HDAC activity as well as DNA methyltransferases and a methyl-CpG-binding protein (MBD4) that silences the Cyp27B1 promoter (Kim et al., 2009). PTH stimulated the phosphorylation of MBD4, which promoted demethylation by the glycosylase activity of MBD4, relieving the suppression, thus activating gene expression.

Interaction of VDR with β-catenin signaling

The interaction between VDR and β-catenin in terms of their complementary and opposing transcriptional activities has been well studied in the skin, bone, and intestine. β-Catenin binds to VDR in the AF2 domain (Shah et al., 2006) in a $1,25(OH)_2D$-dependent fashion. Such binding can promote ligand-dependent VDR transcriptional activity and promote cell fate determination (Shah et al., 2006; Palmer et al., 2008), but can also result in inhibition of β-catenin's transcriptional activity with respect to cell proliferation by preventing its interaction with T cell factors/lymphoid enhancer factors (TCFs/LEFs) in the nucleus and increasing its binding to the E-cadherin complex in the membrane (Palmer et al., 2001). VDR and calcium are essential for the formation of the E-cadherin complex (Bikle et al., 2012; Bikle, 2011). Palmer et al. (Palmer et al., 2008) evaluated the interaction between VDR and β-catenin in transcriptional regulation, and identified putative response elements for VDR and β-catenin/LEF in a number of genes, including *Shh*, *Ptch1* and *Ptch2*, and *Gli1* and *Gli2*,

members of the Hedgehog signaling pathway. For some genes the interaction is positive. An example of this was shown in TE-85 osteosarcoma cells in a ligand-independent fashion (Haussler et al., 2010). For other genes such as c-myc (where the region showing colocalization of VDR/RXR and β-cateninTCF4 is 335 kb away from the TSS) (Meyer et al., 2012) and cyclin D, $1,25(OH)_2D$/VDR suppresses β-catenin transcriptional activity (Sancho et al., 2004; Salehi-Tabar et al., 2012). The type of β-catenin transcriptional complex also plays a role in that β-catenin/LEF1 increases VDR induction of osteopontin, whereas β-catenin/TCF4 reduces the induction (Xu et al., 2009). Furthermore, the ability of β-catenin overexpression to induce trichofolliculomas (a benign tumor of the hair follicle) was blocked by an analog of $1,25(OH)_2D$, but in the absence of VDR, basal cell carcinomas were induced rather than trichofolliculomas. In the hair follicle and intestinal crypt cells, β-catenin signaling is essential for stem cell activation and their proliferation through a process that, at least in hair follicle stem cells, is dependent on the presence of the VDR (Sancho et al., 2004; Lisse et al., 2014; Cianferotti et al., 2007). In the epidermis β-catenin plays a critical role in cell migration and differentiation during wound repair as part of the E-cadherin/catenin complex in the membrane, which as noted is regulated by vitamin D signaling.

Vitamin D receptor mechanism of action: nongenomic

$1,25(OH)_2D$ exerts rapid effects on cells that cannot readily be explained by its better understood genomic actions. The first description of such rapid actions was that of rapid increases in intestinal calcium transport following $1,25(OH)_2D$ administration, called transcaltachia (Nemere et al., 1984). However, these rapid actions have subsequently been identified in a number of other cells, including chondrocytes, osteoblasts, keratinocytes, and fibroblasts as well as intestinal cells. A variety of signaling pathways are regulated by these rapid effects of $1,25(OH)_2D$, including PLC, phospholipase A_2 ,the tyrosine kinase Src, phosphatidylinositol-3-kinase (PI3K), Wnt5a, and p21ras, opening up calcium and chloride channels, with the generation of second messengers such as calcium, cyclic AMP, fatty acids, phosphatidylinositol 3,4,5-triphosphate activating downstream protein kinases A and C, src, mitogen-activated protein kinases, and calmodulin kinase II (reviewed in Hii and Ferrante, 2016; Doroudi et al., 2015). Two receptors for $1,25(OH)_2D$, both in the membrane, have been identified as mediating these rapid actions. The first receptor isolated from the chick intestinal membrane was initially called MARRS-binding protein (Nemere et al., 1994), which was subsequently shown to be the same protein as GRP58, ERp57 or 60, and Pdia3 (Khanal and Nemere, 2007). The second receptor is the VDR itself, but in its membrane location it is activated by $1,25(OH)_2D$ analogs with a different configuration (6-S *cis*) compared with those that activate the genomic actions of VDR (6-S *trans*), as mentioned earlier (Dormanen et al., 1994; Norman, 2006). In osteoblasts and epidermal fibroblasts both receptors have been shown to be involved in selected nongenomic actions of $1,25(OH)_2D$ (Chen et al., 2013; Sequeira et al., 2012). Moreover, these receptors can be found together with caveolin-1 in caveolae (Chen et al., 2013), where at least in skin fibroblasts they physically interact (Sequeira et al., 2012). Caveolin can provide a scaffold for other signaling molecules with which these nongenomic receptors may interact (Doroudi et al., 2015).

The interaction between the membrane VDR and the nuclear VDR has been suggested, but the mechanism is not totally clear. In kidney cells and the intestinal cell line Caco2 the rapid activation of extracellular signal-regulated kinase 1/2 (ERK1/2), JNK1/2, PKC, PI3K, and p21ras all has been shown to regulate $1,25(OH)_2D$ induction of Cyp24A1, a genomic action of VDR (Dwivedi et al., 2002; Nutchey et al., 2005; Cui et al., 2009). These studies indicated that the rapid activation of ERK1/2 and ERK5 affected $1,25(OH)_2D$ induction of Cyp24A1 by phosphorylating RXRα and Ets-1, respectively, thus modulating the environment of the VDREs in the Cyp24A1 promoter (Dwivedi et al., 2002). In Caco2 cells ERK1/2 activation did not alter VDR binding to its VDRE in the Cyp24A1 promoter but enhanced its transcription by helping recruit the coregulator Med1. On the other hand ERK1/2 activation did not influence another $1,25(OH)_2D$-induced gene, TRPV6, and did not alter the recruitment of Med1 to the VDR in the TRPV6 promoter (Cui et al., 2009). In human embryonic kidney 293T cells, JNK but not ERK1/2 activation facilitated $1,25(OH)_2D$ induction of Cyp24A1 (Nutchey et al., 2005). Rapid activation of PI3K by $1,25(OH)_2D$ also appears to enhance $1,25(OH)_2D$ induction of Cyp24A1 by mediating $1,25(OH)_2D$ activation of PKCζ and its phosphorylation of SP1, influencing its binding to the GC box in the Cyp24A1 promoter region (Dwivedi et al., 2010). In keratinocytes, activation of ERK1/2 promotes the ability of liganded VDR to induce the antimicrobial peptide cathelicidin (Peric et al., 2009).

VDR also alters the actions of other transcription factors in a nongenomic fashion. For example, the liganded VDR interacts directly with IκB kinase to block NF-κB signaling (Chen et al., 2013), and the liganded MARRS/ERp57/PIA3 has been shown to interact directly with NF-κB, with translocation of the complex into the nucleus where it appears to participate in the differentiation of NB4 leukemia cells (Wu et al., 2010). In T cells VDR/RXR prevents the formation of the NFATc1/AP-1 complex, suppressing the induction of IL-2 and IL-17A (reviewed in Wei and Christakos, 2015).VDR in the absence of $1,25(OH)_2D$ bound Stat1, inhibiting its action (Lange et al., 2014). $1,25(OH)_2D$ plus interferon-α (IFN-α) released this binding, enabling the binding of phosphorylated Stat1 to IFN-α DNA target genes, increasing their expression

(Lange et al., 2014). In some cancer cells nonliganded VDR can block arsenite-induced cell death by binding to and blocking c-jun (Li et al., 2007).

Conclusions

In this chapter I have reviewed three vitamin D-binding proteins: DBP, the protein that transports the vitamin D metabolites between and, in some cases, into cells; the intracellular DBP, otherwise known as Hsp70, that ferries the vitamin D metabolites between the relevant intracellular organelles; and VDR, which mediates the actions of the active vitamin D metabolite, $1,25(OH)_2D$, both in the nucleus for its genomic actions and in the membrane for its nongenomic actions. However, these proteins serve other functions that are not dependent on their binding to the vitamin D metabolites. DBP is an important actin scavenger, binds fatty acids, fixes C5a to neutrophils regulating chemotaxis, and when deglycosylated forms the DBP−MAF, which plays a role in osteoclast activation, macrophage function, and anticancer activity. Hsp70 serves as a chaperone role for other proteins. VDR has functions both genomic and nongenomic that do not require and may be inhibited by its binding to $1,25(OH)_2D$. Regulation of hair follicle cycling is one clear example of this ligand-independent action. Although we have learned much about the structure and function of these vitamin D-binding proteins, there is much more to learn. That said, the huge surge in vitamin D-related publications since 2008 indicates that research in this area will continue to produce new knowledge by which the roles of these proteins in both physiology and pathophysiology will be better understood.

References

Abbas, S., Linseisen, J., Slanger, T., Kropp, S., Mutschelknauss, E.J., Flesch-Janys, D., et al., 2008. The Gc2 allele of the vitamin D binding protein is associated with a decreased postmenopausal breast cancer risk, independent of the vitamin D status. Cancer Epidemiol. Biomark. Prev. 17 (6), 1339−1343.

Adams, J.S., Chen, H., Chun, R., Gacad, M.A., Encinas, C., Ren, S., et al., 2004. Response element binding proteins and intracellular vitamin D binding proteins: novel regulators of vitamin D trafficking, action and metabolism. J. Steroid Biochem. Mol. Biol. 89−90 (1−5), 461−465.

Aggarwal, A., Yadav, A.K., Ramachandran, R., Kumar, V., Kumar, V., Sachdeva, N., et al., 2016. Bioavailable vitamin D levels are reduced and correlate with bone mineral density and markers of mineral metabolism in adults with nephrotic syndrome. Nephrology 21 (6), 483−489.

Ahn, J., Albanes, D., Berndt, S.I., Peters, U., Chatterjee, N., Freedman, N.D., et al., 2009. Vitamin D-related genes, serum vitamin D concentrations and prostate cancer risk. Carcinogenesis 30 (5), 769−776.

Aloia, J., Dhaliwal, R., Mikhail, M., Shieh, A., Stolberg, A., Ragolia, L., et al., 2015. Free 25(OH)D and calcium absorption, PTH, and markers of bone turnover. J. Clin. Endocrinol. Metab. 100 (11), 4140−4145.

Altinova, A.E., Ozkan, C., Akturk, M., Gulbahar, O., Yalcin, M., Cakir, N., et al., 2016. Vitamin D-binding protein and free vitamin D concentrations in acromegaly. Endocrine 52 (2), 374−379.

Alzaman, N.S., Dawson-Hughes, B., Nelson, J., D'Alessio, D., Pittas, A.G., 2016. Vitamin D status of black and white Americans and changes in vitamin D metabolites after varied doses of vitamin D supplementation. Am. J. Clin. Nutr. 104 (1), 205−214.

Arbelle, J.E., Chen, H., Gaead, M.A., Allegretto, E.A., Pike, J.W., Adams, J.S., 1996. Inhibition of vitamin D receptor-retinoid X receptor-vitamin D response element complex formation by nuclear extracts of vitamin D-resistant New World primate cells. Endocrinology 137 (2), 786−789.

Armas, L.A., Hollis, B.W., Heaney, R.P., 2004. Vitamin D2 is much less effective than vitamin D3 in humans. J. Clin. Endocrinol. Metab. 89 (11), 5387−5391.

Arnaud, J., Constans, J., 1993. Affinity differences for vitamin D metabolites associated with the genetic isoforms of the human serum carrier protein (DBP). Hum. Genet. 92 (2), 183−188.

Arriagada, G., Paredes, R., Olate, J., van Wijnen, A., Lian, J.B., Stein, G.S., et al., 2007. Phosphorylation at serine 208 of the 1alpha,25-dihydroxy Vitamin D3 receptor modulates the interaction with transcriptional coactivators. J. Steroid Biochem. Mol. Biol. 103 (3−5), 425−429.

Baier, L.J., Dobberfuhl, A.M., Pratley, R.E., Hanson, R.L., Bogardus, C., 1998. Variations in the vitamin D-binding protein (Gc locus) are associated with oral glucose tolerance in nondiabetic Pima Indians. J. Clin. Endocrinol. Metab. 83 (8), 2993−2996.

Baker, A.R., McDonnell, D.P., Hughes, M., Crisp, T.M., Mangelsdorf, D.J., Haussler, M.R., et al., 1988. Cloning and expression of full-length cDNA encoding human vitamin D receptor. Proc. Natl. Acad. Sci. U.S.A. 85 (10), 3294−3298.

Barletta, F., Freedman, L.P., Christakos, S., 2002. Enhancement of VDR-mediated transcription by phosphorylation: correlation with increased interaction between the VDR and DRIP205, a subunit of the VDR-interacting protein coactivator complex. Mol. Endocrinol. 16 (2), 301−314.

Baudino, T.A., Kraichely, D.M., Jefcoat Jr., S.C., Winchester, S.K., Partridge, N.C., MacDonald, P.N., 1998. Isolation and characterization of a novel coactivator protein, NCoA-62, involved in vitamin D-mediated transcription. J. Biol. Chem. 273 (26), 16434−16441.

Berger, U., Wilson, P., McClelland, R.A., Colston, K., Haussler, M.R., Pike, J.W., et al., 1988. Immunocytochemical detection of 1,25-dihydroxyvitamin D receptors in normal human tissues. J. Clin. Endocrinol. Metab. 67 (3), 607−613.

Bikle, D.D., Gee, E., 1989. Free, and not total, 1,25-dihydroxyvitamin D regulates 25-hydroxyvitamin D metabolism by keratinocytes. Endocrinology 124 (2), 649−654.

Bikle, D.D., Gee, E., Halloran, B., Haddad, J.G., 1984. Free 1,25-dihydroxyvitamin D levels in serum from normal subjects, pregnant subjects, and subjects with liver disease. J. Clin. Investig. 74 (6), 1966–1971.

Bikle, D.D., Siiteri, P.K., Ryzen, E., Haddad, J.G., 1985. Serum protein binding of 1,25-dihydroxyvitamin D: a reevaluation by direct measurement of free metabolite levels. J. Clin. Endocrinol. Metab. 61 (5), 969–975.

Bikle, D.D., Halloran, B.P., Gee, E., Ryzen, E., Haddad, J.G., 1986a. Free 25-hydroxyvitamin D levels are normal in subjects with liver disease and reduced total 25-hydroxyvitamin D levels. J. Clin. Investig. 78 (3), 748–752.

Bikle, D.D., Gee, E., Halloran, B., Kowalski, M.A., Ryzen, E., Haddad, J.G., 1986b. Assessment of the free fraction of 25-hydroxyvitamin D in serum and its regulation by albumin and the vitamin D-binding protein. J. Clin. Endocrinol. Metab. 63 (4), 954–959.

Bikle, D.D., Xie, Z., Tu, C.L., 2012. Calcium regulation of keratinocyte differentiation. Expert Rev. Endocrinol. Metabol. 7 (4), 461–472.

Bikle, D.D., Malmstroem, S., Schwartz, J., 2017a. Current controversies: are free vitamin metabolite levels a more accurate assessment of vitamin D status than total levels? Endocrinol Metab. Clin. N. Am. 46 (4), 901–918.

Bikle, D., Bouillon, R., Thadhani, R., Schoenmakers, I., 2017b. Vitamin D metabolites in captivity? Should we measure free or total 25(OH)D to assess vitamin D status? J. Steroid Biochem. Mol. Biol. 173, 105–116.

Bikle, D.D., 2011. The vitamin D receptor: a tumor suppressor in skin. Discov. Med. 11 (56), 7–17.

Bikle, D.D., 2012a. Vitamin D and bone. Curr. Osteoporos. Rep. 10 (2), 151–159.

Bikle, D.D., 2012b. Vitamin D and the skin: physiology and pathophysiology. Rev. Endocr. Metab. Disord. 13 (1), 3–19.

Bikle, D.D., 2014. Vitamin D metabolism, mechanism of action, and clinical applications. Chem. Biol. 21 (3), 319–329.

Bikle, D.D., 2016a. Extraskeletal actions of vitamin D. Ann. N. Y. Acad. Sci. 1376 (1), 29–52.

Bikle, D.D., 2016b. The endocrine society centennial: extrarenal production of 1,25 dihyroxyvitamin D is now proven. Endocrinology 157 (5), 1717–1718.

Binder, R., Kress, A., Kan, G., Herrmann, K., Kirschfink, M., 1999. Neutrophil priming by cytokines and vitamin D binding protein (Gc-globulin): impact on C5a-mediated chemotaxis, degranulation and respiratory burst. Mol. Immunol. 36 (13–14), 885–892.

Binkley, N., Carter, G.D., 2017. Toward clarity in clinical vitamin D status assessment: 25(OH)D assay standardization. Endocrinol Metab. Clin. N. Am. 46 (4), 885–899.

Bishop, K.A., Coy, H.M., Nerenz, R.D., Meyer, M.B., Pike, J.W., 2011. Mouse Rankl expression is regulated in T cells by c-Fos through a cluster of distal regulatory enhancers designated the T cell control region. J. Biol. Chem. 286 (23), 20880–20891.

Bizzaro, G., Antico, A., Fortunato, A., Bizzaro, N., 2017. Vitamin D and autoimmune diseases: is vitamin D receptor (VDR) polymorphism the culprit? Isr. Med. Assoc. J. 19 (7), 438–443.

Bouillon, R., van Baelen, H., de Moor, P., 1980. Comparative study of the affinity of the serum vitamin D-binding protein. J. Steroid Biochem. 13 (9), 1029–1034.

Bouillon, R., Xiang, D.Z., Convents, R., Van Baelen, H., 1992. Polyunsaturated fatty acids decrease the apparent affinity of vitamin D metabolites for human vitamin D-binding protein. J. Steroid Biochem. Mol. Biol. 42 (8), 855–861.

Boutin, B., Galbraith, R.M., Arnaud, P., 1989. Comparative affinity of the major genetic variants of human group-specific component (vitamin D-binding protein) for 25-(OH) vitamin D. J. Steroid Biochem. 32 (1A), 59–63.

Brumbaugh, P.F., Haussler, M.R., 1974. 1 Alpha,25-dihydroxycholecalciferol receptors in intestine. I. Association of 1 alpha,25-dihydroxycholecalciferol with intestinal mucosa chromatin. J. Biol. Chem. 249 (4), 1251–1257.

Brumbaugh, P.F., Haussler, M.R., 1975. Specific binding of 1alpha,25-dihydroxycholecalciferol to nuclear components of chick intestine. J. Biol. Chem. 250 (4), 1588–1594.

Calvo, M., Ena, J.M., 1989. Relations between vitamin D and fatty acid binding properties of vitamin D-binding protein. Biochem. Biophys. Res. Commun. 163 (1), 14–17.

Canadillas, S., Canalejo, R., Rodriguez-Ortiz, M.E., Martinez-Moreno, J.M., Estepa, J.C., Zafra, R., et al., 2010. Upregulation of parathyroid VDR expression by extracellular calcium is mediated by ERK1/2-MAPK signaling pathway. Am. J. Physiol. Renal. Physiol. 298 (5), F1197–F1204.

Carlberg, C., 2010. The impact of transcriptional cycling on gene regulation. Transcription 1 (1), 13–16.

Carlberg, C., 2017. Molecular endocrinology of vitamin D on the epigenome level. Mol. Cell. Endocrinol. 453, 14–21.

Carpenter, T.O., Zhang, J.H., Parra, E., Ellis, B.K., Simpson, C., Lee, W.M., et al., 2013. Vitamin D binding protein is a key determinant of 25-hydroxyvitamin D levels in infants and toddlers. J. Bone Miner. Res. 28 (1), 213–221.

Chandel, N., Husain, M., Goel, H., Salhan, D., Lan, X., Malhotra, A., et al., 2013. VDR hypermethylation and HIV-induced T cell loss. J. Leukoc. Biol. 93 (4), 623–631.

Chen, H., Hewison, M., Hu, B., Adams, J.S., 2003. Heterogeneous nuclear ribonucleoprotein (hnRNP) binding to hormone response elements: a cause of vitamin D resistance. Proc. Natl. Acad. Sci. U.S.A. 100 (10), 6109–6114.

Chen, H., Hewison, M., Adams, J.S., 2006. Functional characterization of heterogeneous nuclear ribonuclear protein C1/C2 in vitamin D resistance: a novel response element-binding protein. J. Biol. Chem. 281 (51), 39114–39120.

Chen, J., Doroudi, M., Cheung, J., Grozier, A.L., Schwartz, Z., Boyan, B.D., 2013. Plasma membrane Pdia3 and VDR interact to elicit rapid responses to 1alpha,25(OH)(2)D(3). Cell. Signal. 25 (12), 2362–2373.

Chen, Y., Zhang, J., Ge, X., Du, J., Deb, D.K., Li, Y.C., 2013. Vitamin D receptor inhibits nuclear factor kappaB activation by interacting with IkappaB kinase beta protein. J. Biol. Chem. 288 (27), 19450–19458.

Cheung, C.L., Lau, K.S., Sham, P.C., Tan, K.C., Kung, A.W., 2013. Genetic variant in vitamin D binding protein is associated with serum 25-hydroxyvitamin D and vitamin D insufficiency in southern Chinese. J. Hum. Genet. 58 (11), 749–751.

Chishimba, L., Thickett, D.R., Stockley, R.A., Wood, A.M., 2010. The vitamin D axis in the lung: a key role for vitamin D-binding protein. Thorax 65 (5), 456–462.

Christakos, S., Dhawan, P., Verstuyf, A., Verlinden, L., Carmeliet, G., 2016. Vitamin D: metabolism, molecular mechanism of action, and pleiotropic effects. Physiol. Rev. 96 (1), 365–408.

Christensen, E.I., Birn, H., 2002. Megalin and cubilin: multifunctional endocytic receptors. Nat. Rev. Mol. Cell Biol. 3 (4), 256–266.

Chun, R.F., Lauridsen, A.L., Suon, L., Zella, L.A., Pike, J.W., Modlin, R.L., et al., 2010. Vitamin D-binding protein directs monocyte responses to 25-hydroxy- and 1,25-dihydroxyvitamin D. J. Clin. Endocrinol. Metab. 95 (7), 3368–3376.

Chun, R.F., Hernandez, I., Pereira, R., Swinkles, L., Huijs, T., Zhou, R., et al., 2016. Differential responses to vitamin D2 and vitamin D3 are associated with variations in free 25-hydroxyvitamin D. Endocrinology 157 (9), 3420–3430.

Chun, R.F., 2012. New perspectives on the vitamin D binding protein. Cell Biochem. Funct. 30 (6), 445–456.

Cianferotti, L., Cox, M., Skorija, K., Demay, M.B., 2007. Vitamin D receptor is essential for normal keratinocyte stem cell function. Proc. Natl. Acad. Sci. U.S.A. 104 (22), 9428–9433.

Cleve, H., Constans, J., 1988. The mutants of the vitamin-D-binding protein: more than 120 variants of the GC/DBP system. Vox Sang. 54 (4), 215–225.

Cooke, N.E., McLeod, J.F., Wang, X.K., Ray, K., 1991. Vitamin D binding protein: genomic structure, functional domains, and mRNA expression in tissues. J. Steroid Biochem. Mol. Biol. 40 (4–6), 787–793.

Crofts, L.A., Hancock, M.S., Morrison, N.A., Eisman, J.A., 1998. Multiple promoters direct the tissue-specific expression of novel N-terminal variant human vitamin D receptor gene transcripts. Proc. Natl. Acad. Sci. U.S.A. 95 (18), 10529–10534.

Cui, M., Zhao, Y., Hance, K.W., Shao, A., Wood, R.J., Fleet, J.C., 2009. Effects of MAPK signaling on 1,25-dihydroxyvitamin D-mediated CYP24 gene expression in the enterocyte-like cell line, Caco-2. J. Cell. Physiol. 219 (1), 132–142.

Dahl, B., Schiodt, F.V., Gehrchen, P.M., Ramlau, J., Kiaer, T., Ott, P., 2001a. Gc-globulin is an acute phase reactant and an indicator of muscle injury after spinal surgery. Inflamm. Res. 50 (1), 39–43.

Dahl, B., Schiodt, F.V., Rudolph, S., Ott, P., Kiaer, T., Heslet, L., 2001b. Trauma stimulates the synthesis of Gc-globulin. Intensive Care Med. 27 (2), 394–399.

Dahl, B., Schiodt, F.V., Ott, P., Wians, F., Lee, W.M., Balko, J., et al., 2003. Plasma concentration of Gc-globulin is associated with organ dysfunction and sepsis after injury. Crit. Care Med. 31 (1), 152–156.

Daiger, S.P., Schanfield, M.S., Cavalli-Sforza, L.L., 1975. Group-specific component (Gc) proteins bind vitamin D and 25-hydroxyvitamin D. Proc. Natl. Acad. Sci. U.S.A. 72 (6), 2076–2080.

Demay, M.B., Kiernan, M.S., DeLuca, H.F., Kronenberg, H.M., 1992. Sequences in the human parathyroid hormone gene that bind the 1,25-dihydroxyvitamin D3 receptor and mediate transcriptional repression in response to 1,25-dihydroxyvitamin D3. Proc. Natl. Acad. Sci. U.S.A. 89 (17), 8097–8101.

DiMartino, S.J., Kew, R.R., 1999. Initial characterization of the vitamin D binding protein (Gc-globulin) binding site on the neutrophil plasma membrane: evidence for a chondroitin sulfate proteoglycan. J. Immunol. 163 (4), 2135–2142.

DiMartino, S.J., Shah, A.B., Trujillo, G., Kew, R.R., 2001. Elastase controls the binding of the vitamin D-binding protein (Gc-globulin) to neutrophils: a potential role in the regulation of C5a co-chemotactic activity. J. Immunol. 166 (4), 2688–2694.

DiMartino, S.J., Trujillo, G., McVoy, L.A., Zhang, J., Kew, R.R., 2007. Upregulation of vitamin D binding protein (Gc-globulin) binding sites during neutrophil activation from a latent reservoir in azurophil granules. Mol. Immunol. 44 (9), 2370–2377.

Dimopoulos, M.A., Germenis, A., Savides, P., Karayanis, A., Fertakis, A., Dimopoulos, C., 1984. Genetic markers in carcinoma of the prostate. Eur. Urol. 10 (5), 315–316.

Ding, N., Yu, R.T., Subramaniam, N., Sherman, M.H., Wilson, C., Rao, R., et al., 2013. A vitamin D receptor/SMAD genomic circuit gates hepatic fibrotic response. Cell 153 (3), 601–613.

Dixon, J.R., Selvaraj, S., Yue, F., Kim, A., Li, Y., Shen, Y., et al., 2012. Topological domains in mammalian genomes identified by analysis of chromatin interactions. Nature 485 (7398), 376–380.

Doig, C.L., Singh, P.K., Dhiman, V.K., Thorne, J.L., Battaglia, S., Sobolewski, M., et al., 2013. Recruitment of NCOR1 to VDR target genes is enhanced in prostate cancer cells and associates with altered DNA methylation patterns. Carcinogenesis 34 (2), 248–256.

Dormanen, M.C., Bishop, J.E., Hammond, M.W., Okamura, W.H., Nemere, I., Norman, A.W., 1994. Nonnuclear effects of the steroid hormone 1 alpha,25(OH)2-vitamin D3: analogs are able to functionally differentiate between nuclear and membrane receptors. Biochem. Biophys. Res. Commun. 201 (1), 394–401.

Doroudi, M., Olivares-Navarrete, R., Boyan, B.D., Schwartz, Z., 2015. A review of 1alpha,25(OH)2D3 dependent Pdia3 receptor complex components in Wnt5a non-canonical pathway signaling. J. Steroid Biochem. Mol. Biol. 152, 84–88.

Dueland, S., Nenseter, M.S., Drevon, C.A., 1991. Uptake and degradation of filamentous actin and vitamin D-binding protein in the rat. Biochem. J. 274 (Pt 1), 237–241.

Dwivedi, P.P., Omdahl, J.L., Kola, I., Hume, D.A., May, B.K., 2000. Regulation of rat cytochrome P450C24 (CYP24) gene expression. Evidence for functional cooperation of Ras-activated Ets transcription factors with the vitamin D receptor in 1,25-dihydroxyvitamin D(3)-mediated induction. J. Biol. Chem. 275 (1), 47–55.

Dwivedi, P.P., Hii, C.S., Ferrante, A., Tan, J., Der, C.J., Omdahl, J.L., et al., 2002. Role of MAP kinases in the 1,25-dihydroxyvitamin D3-induced transactivation of the rat cytochrome P450C24 (CYP24) promoter. Specific functions for ERK1/ERK2 and ERK5. J. Biol. Chem. 277 (33), 29643–29653.

Dwivedi, P.P., Gao, X.H., Tan, J.C., Evdokiou, A., Ferrante, A., Morris, H.A., et al., 2010. A role for the phosphatidylinositol 3-kinase–protein kinase C zeta–Sp1 pathway in the 1,25-dihydroxyvitamin D3 induction of the 25-hydroxyvitamin D3 24-hydroxylase gene in human kidney cells. Cell. Signal. 22 (3), 543−552.

Eckey, M., Hong, W., Papaioannou, M., Baniahmad, A., 2007. The nucleosome assembly activity of NAP1 is enhanced by Alien. Mol. Cell Biol. 27 (10), 3557−3568.

Eloranta, J.J., Wenger, C., Mwinyi, J., Hiller, C., Gubler, C., Vavricka, S.R., et al., 2011. Association of a common vitamin D-binding protein polymorphism with inflammatory bowel disease. Pharmacogenetics Genom. 21 (9), 559−564.

Ena, J.M., Esteban, C., Perez, M.D., Uriel, J., Calvo, M., 1989. Fatty acids bound to vitamin D-binding protein (DBP) from human and bovine sera. Biochem. Int. 19 (1), 1−7.

Esteban, C., Geuskens, M., Ena, J.M., Mishal, Z., Macho, A., Torres, J.M., et al., 1992. Receptor-mediated uptake and processing of vitamin D-binding protein in human B-lymphoid cells. J. Biol. Chem. 267 (14), 10177−10183.

Esteller, M., 2008. Epigenetics in cancer. N. Engl. J. Med. 358 (11), 1148−1159.

Ezura, Y., Nakajima, T., Kajita, M., Ishida, R., Inoue, S., Yoshida, H., et al., 2003. Association of molecular variants, haplotypes, and linkage disequilibrium within the human vitamin D-binding protein (DBP) gene with postmenopausal bone mineral density. J. Bone Miner. Res. 18 (9), 1642−1649.

Falzon, M., 1996. DNA sequences in the rat parathyroid hormone-related peptide gene responsible for 1,25-dihydroxyvitamin D3-mediated transcriptional repression. Mol. Endocrinol. 10 (6), 672−681.

Faserl, K., Golderer, G., Kremser, L., Lindner, H., Sarg, B., Wildt, L., et al., 2011. Polymorphism in vitamin D-binding protein as a genetic risk factor in the pathogenesis of endometriosis. J. Clin. Endocrinol. Metab. 96 (1), E233−E241.

Fetahu, I.S., Hobaus, J., Kallay, E., 2014. Vitamin D and the epigenome. Front. Physiol. 5, 164.

Fu, Q., Manolagas, S.C., O'Brien, C.A., 2006. Parathyroid hormone controls receptor activator of NF-kappaB ligand gene expression via a distant transcriptional enhancer. Mol. Cell Biol. 26 (17), 6453−6468.

Fu, L., Yun, F., Oczak, M., Wong, B.Y., Vieth, R., Cole, D.E., 2009. Common genetic variants of the vitamin D binding protein (DBP) predict differences in response of serum 25-hydroxyvitamin D [25(OH)D] to vitamin D supplementation. Clin. Biochem. 42 (10−11), 1174−1177.

Fuleihan Gel, H., Bouillon, R., Clarke, B., Chakhtoura, M., Cooper, C., McClung, M., et al., 2015. Serum 25-hydroxyvitamin D levels: variability, knowledge gaps, and the concept of a desirable range. J. Bone Miner. Res. 30 (7), 1119−1133.

Gacad, M.A., Adams, J.S., 1993. Identification of a competitive binding component in vitamin D-resistant New World primate cells with a low affinity but high capacity for 1,25-dihydroxyvitamin D3. J. Bone Miner. Res. 8 (1), 27−35.

Gacad, M.A., Chen, H., Arbelle, J.E., LeBon, T., Adams, J.S., 1997. Functional characterization and purification of an intracellular vitamin D-binding protein in vitamin D-resistant new world primate cells. Amino acid sequence homology with proteins in the hsp-70 family. J. Biol. Chem. 272 (13), 8433−8440.

Ge, L., Trujillo, G., Miller, E.J., Kew, R.R., 2014. Circulating complexes of the vitamin D binding protein with G-actin induce lung inflammation by targeting endothelial cells. Immunobiology 219 (3), 198−207.

Girgis, C.M., Mokbel, N., Cha, K.M., Houweling, P.J., Abboud, M., Fraser, D.R., et al., 2014. The vitamin D receptor (VDR) is expressed in skeletal muscle of male mice and modulates 25-hydroxyvitamin D (25OHD) uptake in myofibers. Endocrinology 155 (9), 3227−3237.

Gomme, P.T., Bertolini, J., 2004. Therapeutic potential of vitamin D-binding protein. Trends Biotechnol. 22 (7), 340−345.

Gressner, O.A., Gao, C., Siluschek, M., Kim, P., Gressner, A.M., 2009. Inverse association between serum concentrations of actin-free vitamin D-binding protein and the histopathological extent of fibrogenic liver disease or hepatocellular carcinoma. Eur. J. Gastroenterol. Hepatol. 21 (9), 990−995.

Gu, X., Nylander, E., Coates, P.J., Nylander, K., 2011. Effect of narrow-band ultraviolet B phototherapy on p63 and microRNA (miR-21 and miR-125b) expression in psoriatic epidermis. Acta Dermato-Venereologica. 91 (4), 392−397.

Guha, C., Osawa, M., Werner, P.A., Galbraith, R.M., Paddock, G.V., 1995. Regulation of human Gc (vitamin D–binding) protein levels: hormonal and cytokine control of gene expression in vitro. Hepatology 21 (6), 1675−1681.

Guo, B., Aslam, F., van Wijnen, A.J., Roberts, S.G., Frenkel, B., Green, M.R., et al., 1997. YY1 regulates vitamin D receptor/retinoid X receptor mediated transactivation of the vitamin D responsive osteocalcin gene. Proc. Natl. Acad. Sci. U.S.A. 94 (1), 121−126.

Haddad, J.G., Hu, Y.Z., Kowalski, M.A., Laramore, C., Ray, K., Robzyk, P., et al., 1992. Identification of the sterol- and actin-binding domains of plasma vitamin D binding protein (Gc-globulin). Biochemistry 31 (31), 7174−7181.

Hagenfeldt, Y., Carlstrom, K., Berlin, T., Stege, R., 1991. Effects of orchidectomy and different modes of high dose estrogen treatment on circulating "free" and total 1,25-dihydroxyvitamin D in patients with prostatic cancer. J. Steroid Biochem. Mol. Biol. 39 (2), 155−159.

Haussler, M.R., Haussler, C.A., Whitfield, G.K., Hsieh, J.C., Thompson, P.D., Barthel, T.K., et al., 2010. The nuclear vitamin D receptor controls the expression of genes encoding factors which feed the "Fountain of Youth" to mediate healthful aging. J. Steroid Biochem. Mol. Biol. 121 (1−2), 88−97.

Haussler, M.R., Jurutka, P.W., Mizwicki, M., Norman, A.W., 2011. Vitamin D receptor (VDR)-mediated actions of 1alpha,25(OH)(2)vitamin D(3): genomic and non-genomic mechanisms. Best Prac. Res. Clin. Endocrinol. Metabol. 25 (4), 543−559.

Hawker, N.P., Pennypacker, S.D., Chang, S.M., Bikle, D.D., 2007. Regulation of human epidermal keratinocyte differentiation by the vitamin D receptor and its coactivators DRIP205, SRC2, and SRC3. J. Investig. Dermatol. 127 (4), 874−880.

Head, J.F., Swamy, N., Ray, R., 2002. Crystal structure of the complex between actin and human vitamin D-binding protein at 2.5 A resolution. Biochemistry 41 (29), 9015−9020.

Heery, D.M., Kalkhoven, E., Hoare, S., Parker, M.G., 1997. A signature motif in transcriptional co-activators mediates binding to nuclear receptors. Nature 387 (6634), 733–736.

Heikkinen, S., Vaisanen, S., Pehkonen, P., Seuter, S., Benes, V., Carlberg, C., 2011. Nuclear hormone 1alpha,25-dihydroxyvitamin D3 elicits a genome-wide shift in the locations of VDR chromatin occupancy. Nucleic Acids Res. 39 (21), 9181–9193.

Hewison, M., Rut, A.R., Kristjansson, K., Walker, R.E., Dillon, M.J., Hughes, M.R., et al., 1993. Tissue resistance to 1,25-dihydroxyvitamin D without a mutation of the vitamin D receptor gene. Clin. Endocrinol. 39 (6), 663–670.

Hii, C.S., Ferrante, A., 2016. The non-genomic actions of vitamin D. Nutrients 8 (3), 135.

Hirai, M., Suzuki, S., Hinokio, Y., Chiba, M., Kasuga, S., Hirai, A., et al., 1998. Group specific component protein genotype is associated with NIDDM in Japan. Diabetologia 41 (6), 742–743.

Hirschfeld, J., 1959. Immune-electrophoretic demonstration of qualitative differences in human sera and their relation to the haptoglobins. Acta Pathol. Microbiol. Scand. 47, 160–168.

Hoofnagle, A.N., Eckfeldt, J.H., Lutsey, P.L., 2015. Vitamin D-binding protein concentrations quantified by mass spectrometry. N. Engl. J. Med. 373 (15), 1480–1482.

Hsieh, J.C., Shimizu, Y., Minoshima, S., Shimizu, N., Haussler, C.A., Jurutka, P.W., et al., 1998. Novel nuclear localization signal between the two DNA-binding zinc fingers in the human vitamin D receptor. J. Cell. Biochem. 70 (1), 94–109.

Hsieh, J.C., Sisk, J.M., Jurutka, P.W., Haussler, C.A., Slater, S.A., Haussler, M.R., et al., 2003. Physical and functional interaction between the vitamin D receptor and hairless corepressor, two proteins required for hair cycling. J. Biol. Chem. 278 (40), 38665–38674.

Hsieh, E., Fraenkel, L., Han, Y., Xia, W., Insogna, K.L., Yin, M.T., et al., 2016. Longitudinal increase in vitamin D binding protein levels after initiation of tenofovir/lamivudine/efavirenz among individuals with HIV. AIDS 30 (12), 1935–1942.

Hu, X., Lazar, M.A., 1999. The CoRNR motif controls the recruitment of corepressors by nuclear hormone receptors. Nature 402 (6757), 93–96.

Iqbal, M.U.N., Khan, T.A., 2017. Association between vitamin D receptor (Cdx2, Fok1, Bsm1, Apa1, Bgl1, Taq1, and poly (a)) gene polymorphism and breast cancer: a systematic review and meta-analysis. Tumour Biol 39 (10), 1010428317731280.

Jiang, Y.J., Bikle, D.D., 2014. LncRNA: a new player in 1alpha, 25(OH)(2) vitamin D(3)/VDR protection against skin cancer formation. Exp. Dermatol. 23 (3), 147–150.

Jones, K.S., Assar, S., Harnpanich, D., Bouillon, R., Lambrechts, D., Prentice, A., et al., 2014. 25(OH)D2 half-life is shorter than 25(OH)D3 half-life and is influenced by DBP concentration and genotype. J. Clin. Endocrinol. Metab. 99 (9), 3373–3381.

Jurutka, P.W., Remus, L.S., Whitfield, G.K., Thompson, P.D., Hsieh, J.C., Zitzer, H., et al., 2000. The polymorphic N terminus in human vitamin D receptor isoforms influences transcriptional activity by modulating interaction with transcription factor IIB. Mol. Endocrinol. 14 (3), 401–420.

Kato, S., Fujiki, R., Kitagawa, H., 2004. Vitamin D receptor (VDR) promoter targeting through a novel chromatin remodeling complex. J. Steroid Biochem. Mol. Biol. 89–90 (1–5), 173–178.

Kempker, J.A., Tangpricha, V., Ziegler, T.R., Martin, G.S., 2012. Vitamin D in sepsis: from basic science to clinical impact. Crit. Care 16 (4), 316.

Khanal, R.C., Nemere, I., 2007. The ERp57/GRp58/1,25D3-MARRS receptor: multiple functional roles in diverse cell systems. Curr. Med. Chem. 14 (10), 1087–1093.

Khanim, F.L., Gommersall, L.M., Wood, V.H., Smith, K.L., Montalvo, L., O'Neill, L.P., et al., 2004. Altered SMRT levels disrupt vitamin D3 receptor signalling in prostate cancer cells. Oncogene 23 (40), 6712–6725.

Kim, S., Shevde, N.K., Pike, J.W., 2005. 1,25-Dihydroxyvitamin D3 stimulates cyclic vitamin D receptor/retinoid X receptor DNA-binding, co-activator recruitment, and histone acetylation in intact osteoblasts. J. Bone Miner. Res. 20 (2), 305–317.

Kim, S., Yamazaki, M., Zella, L.A., Shevde, N.K., Pike, J.W., 2006. Activation of receptor activator of NF-kappaB ligand gene expression by 1,25-dihydroxyvitamin D3 is mediated through multiple long-range enhancers. Mol. Cell Biol. 26 (17), 6469–6486.

Kim, S., Yamazaki, M., Shevde, N.K., Pike, J.W., 2007. Transcriptional control of receptor activator of nuclear factor-kappaB ligand by the protein kinase A activator forskolin and the transmembrane glycoprotein 130-activating cytokine, oncostatin M, is exerted through multiple distal enhancers. Mol. Endocrinol. 21 (1), 197–214.

Kim, M.S., Fujiki, R., Murayama, A., Kitagawa, H., Yamaoka, K., Yamamoto, Y., et al., 2007. 1Alpha,25(OH)2D3-induced transrepression by vitamin D receptor through E-box-type elements in the human parathyroid hormone gene promoter. Mol. Endocrinol. 21 (2), 334–342.

Kim, M.S., Kondo, T., Takada, I., Youn, M.Y., Yamamoto, Y., Takahashi, S., et al., 2009. DNA demethylation in hormone-induced transcriptional derepression. Nature 461 (7266), 1007–1012.

Kisker, O., Onizuka, S., Becker, C.M., Fannon, M., Flynn, E., D'Amato, R., et al., 2003. Vitamin D binding protein-macrophage activating factor (DBP-maf) inhibits angiogenesis and tumor growth in mice. Neoplasia 5 (1), 32–40.

Kitagawa, H., Fujiki, R., Yoshimura, K., Mezaki, Y., Uematsu, Y., Matsui, D., et al., 2003. The chromatin-remodeling complex WINAC targets a nuclear receptor to promoters and is impaired in Williams syndrome. Cell 113 (7), 905–917.

Kliewer, S.A., Umesono, K., Mangelsdorf, D.J., Evans, R.M., 1992. Retinoid X receptor interacts with nuclear receptors in retinoic acid, thyroid hormone and vitamin D3 signalling. Nature 355 (6359), 446–449.

Koga, Y., Naraparaju, V.R., Yamamoto, N., 1999. Antitumor effect of vitamin D-binding protein-derived macrophage activating factor on Ehrlich ascites tumor-bearing mice. Proc. Soc. Exp. Biol. Med. 220 (1), 20–26.

Koh, S.S., Chen, D., Lee, Y.H., Stallcup, M.R., 2001. Synergistic enhancement of nuclear receptor function by p160 coactivators and two coactivators with protein methyltransferase activities. J. Biol. Chem. 276 (2), 1089–1098.

Koike, K., Shinozawa, Y., Yamazaki, M., Endo, T., Nomura, R., Aiboshi, J., et al., 2002. Recombinant human interleukin-1alpha increases serum albumin, Gc-globulin, and alpha1-antitrypsin levels in burned mice. Tohoku J. Exp. Med. 198 (1), 23–29.

Korbelik, M., Naraparaju, V.R., Yamamoto, N., 1997. Macrophage-directed immunotherapy as adjuvant to photodynamic therapy of cancer. Br. J. Canc. 75 (2), 202–207.

Lange, C.M., Gouttenoire, J., Duong, F.H., Morikawa, K., Heim, M.H., Moradpour, D., 2014. Vitamin D receptor and Jak-STAT signaling crosstalk results in calcitriol-mediated increase of hepatocellular response to IFN-alpha. J. Immunol. 192 (12), 6037–6044.

Lauridsen, A.L., Vestergaard, P., Nexo, E., 2001. Mean serum concentration of vitamin D-binding protein (Gc globulin) is related to the Gc phenotype in women. Clin. Chem. 47 (4), 753–756.

Lauridsen, A.L., Vestergaard, P., Hermann, A.P., Moller, H.J., Mosekilde, L., Nexo, E., 2004. Female premenopausal fracture risk is associated with gc phenotype. J. Bone Miner. Res. 19 (6), 875–881.

Leaf, D.E., Waikar, S.S., Wolf, M., Cremers, S., Bhan, I., Stern, L., 2013. Dysregulated mineral metabolism in patients with acute kidney injury and risk of adverse outcomes. Clin. Endocrinol. 79 (4), 491–498.

Lee, S.M., Bishop, K.A., Goellner, J.J., O'Brien, C.A., Pike, J.W., 2014. Mouse and human BAC transgenes recapitulate tissue-specific expression of the vitamin D receptor in mice and rescue the VDR-null phenotype. Endocrinology 155 (6), 2064–2076.

Lee, M.J., Kearns, M.D., Smith, E.M., Hao, L., Ziegler, T.R., Alvarez, J.A., et al., 2015. Free 25-hydroxyvitamin D concentrations in cystic fibrosis. Am. J. Med. Sci. 350 (5), 374–379.

Leheste, J.R., Melsen, F., Wellner, M., Jansen, P., Schlichting, U., Renner-Muller, I., et al., 2003. Hypocalcemia and osteopathy in mice with kidney-specific megalin gene defect. FASEB J. 17 (2), 247–249.

Leong, G.M., Subramaniam, N., Issa, L.L., Barry, J.B., Kino, T., Driggers, P.H., et al., 2004. Ski-interacting protein, a bifunctional nuclear receptor coregulator that interacts with N-CoR/SMRT and p300. Biochem. Biophys. Res. Commun. 315 (4), 1070–1076.

Leong, A., Rehman, W., Dastani, Z., Greenwood, C., Timpson, N., Langsetmo, L., et al., 2014. The causal effect of vitamin D binding protein (DBP) levels on calcemic and cardiometabolic diseases: a Mendelian randomization study. PLoS Med. 11 (10), e1001751.

Li, Q.P., Qi, X., Pramanik, R., Pohl, N.M., Loesch, M., Chen, G., 2007. Stress-induced c-Jun-dependent Vitamin D receptor (VDR) activation dissects the non-classical VDR pathway from the classical VDR activity. J. Biol. Chem. 282 (3), 1544–1551.

Lind, S.E., Smith, D.B., Janmey, P.A., Stossel, T.P., 1988. Depression of gelsolin levels and detection of gelsolin-actin complexes in plasma of patients with acute lung injury. Am. Rev. Respir. Dis. 138 (2), 429–434.

Lisse, T.S., Saini, V., Zhao, H., Luderer, H.F., Gori, F., Demay, M.B., 2014. The vitamin D receptor is required for activation of cWnt and hedgehog signaling in keratinocytes. Mol. Endocrinol. 28 (10), 1698–1706.

Liu, P.T., Stenger, S., Li, H., Wenzel, L., Tan, B.H., Krutzik, S.R., et al., 2006. Toll-like receptor triggering of a vitamin D-mediated human antimicrobial response. Science 311 (5768), 1770–1773.

Long, M.D., Sucheston-Campbell, L.E., Campbell, M.J., 2015. Vitamin D receptor and RXR in the post-genomic era. J. Cell. Physiol. 230 (4), 758–766.

Lopes, N., Carvalho, J., Duraes, C., Sousa, B., Gomes, M., Costa, J.L., et al., 2012. 1Alpha,25-dihydroxyvitamin D3 induces de novo E-cadherin expression in triple-negative breast cancer cells by CDH1-promoter demethylation. Anticancer Res. 32 (1), 249–257.

Luo, Z., Rouvinen, J., Maenpaa, P.H., 1994. A peptide C-terminal to the second Zn finger of human vitamin D receptor is able to specify nuclear localization. Eur. J. Biochem. 223 (2), 381–387.

Madden, K., Feldman, H.A., Chun, R.F., Smith, E.M., Sullivan, R.M., Agan, A.A., et al., 2015. Critically ill children have low vitamin D-binding protein, influencing bioavailability of vitamin D. Ann. Am. Thorac. Soc. 12 (11), 1654–1661.

Malik, S., Fu, L., Juras, D.J., Karmali, M., Wong, B.Y., Gozdzik, A., et al., 2013. Common variants of the vitamin D binding protein gene and adverse health outcomes. Crit. Rev. Clin. Lab. Sci. 50 (1), 1–22.

Malloy, P.J., Feldman, D., 2012. Genetic disorders and defects in vitamin D action. Rheum. Dis. Clin. N. Am. 38 (1), 93–106.

Marik, R., Fackler, M., Gabrielson, E., Zeiger, M.A., Sukumar, S., Stearns, V., et al., 2010. DNA methylation-related vitamin D receptor insensitivity in breast cancer. Cancer Biol. Ther. 10 (1), 44–53.

Martineau, A.R., Leandro, A.C., Anderson, S.T., Newton, S.M., Wilkinson, K.A., Nicol, M.P., et al., 2010. Association between Gc genotype and susceptibility to TB is dependent on vitamin D status. Eur. Respir. J. 35 (5), 1106–1112.

Martowicz, M.L., Meyer, M.B., Pike, J.W., 2011. The mouse RANKL gene locus is defined by a broad pattern of histone H4 acetylation and regulated through distinct distal enhancers. J. Cell. Biochem. 112 (8), 2030–2045.

Masuyama, H., MacDonald, P.N., 1998. Proteasome-mediated degradation of the vitamin D receptor (VDR) and a putative role for SUG1 interaction with the AF-2 domain of VDR. J. Cell. Biochem. 71 (3), 429–440.

Mc Leod, J.F., Kowalski, M.A., Haddad Jr., J.G., 1989. Interactions among serum vitamin D binding protein, monomeric actin, profilin, and profilactin. J. Biol. Chem. 264 (2), 1260–1267.

McCullough, M.L., Stevens, V.L., Diver, W.R., Feigelson, H.S., Rodriguez, C., Bostick, R.M., et al., 2007. Vitamin D pathway gene polymorphisms, diet, and risk of postmenopausal breast cancer: a nested case-control study. Breast Cancer Res. 9 (1), R9.

McDonnell, D.P., Mangelsdorf, D.J., Pike, J.W., Haussler, M.R., O'Malley, B.W., 1987. Molecular cloning of complementary DNA encoding the avian receptor for vitamin D. Science 235 (4793), 1214–1217.

McInerney, E.M., Rose, D.W., Flynn, S.E., Westin, S., Mullen, T.M., Krones, A., et al., 1998. Determinants of coactivator LXXLL motif specificity in nuclear receptor transcriptional activation. Genes Dev. 12 (21), 3357–3368.

McKenna, N.J., Cooney, A.J., DeMayo, F.J., Downes, M., Glass, C.K., Lanz, R.B., et al., 2009. Minireview: evolution of NURSA, the nuclear receptor signaling atlas. Mol. Endocrinol. 23 (6), 740–746.

McVoy, L.A., Kew, R.R., 2005. CD44 and annexin A2 mediate the C5a chemotactic cofactor function of the vitamin D binding protein. J. Immunol. 175 (7), 4754–4760.

Meier, U., Gressner, O., Lammert, F., Gressner, A.M., 2006. Gc-globulin: roles in response to injury. Clin. Chem. 52 (7), 1247–1253.

Mellon, W.S., DeLuca, H.F., 1979. An equilibrium and kinetic study of 1,25-dihydroxyvitamin D3 binding to chicken intestinal cytosol employing high specific activity 1,25-dehydroxy[3H-26, 27] vitamin D3. Arch. Biochem. Biophys. 197 (1), 90–95.

Mendel, C.M., 1990. Rates of dissociation of sex steroid hormones from human sex hormone-binding globulin: a reassessment. J. Steroid Biochem. Mol. Biol. 37 (2), 251–255.

Meyer, M.B., Goetsch, P.D., Pike, J.W., 2010. Genome-wide analysis of the VDR/RXR cistrome in osteoblast cells provides new mechanistic insight into the actions of the vitamin D hormone. J. Steroid Biochem. Mol. Biol. 121 (1–2), 136–141.

Meyer, M.B., Goetsch, P.D., Pike, J.W., 2012. VDR/RXR and TCF4/beta-catenin cistromes in colonic cells of colorectal tumor origin: impact on c-FOS and c-MYC gene expression. Mol. Endocrinol. 26 (1), 37–51.

Meyer, M.B., Benkusky, N.A., Lee, C.H., Pike, J.W., 2014. Genomic determinants of gene regulation by 1,25-dihydroxyvitamin D3 during osteoblast-lineage cell differentiation. J. Biol. Chem. 289 (28), 19539–19554.

Meyer, M.B., Benkusky, N.A., Pike, J.W., 2015. Selective distal enhancer control of the Mmp13 gene identified through clustered regularly interspaced short palindromic repeat (CRISPR) genomic deletions. J. Biol. Chem. 290 (17), 11093–11107.

Meyer, M.B., Benkusky, N.A., Sen, B., Rubin, J., Pike, J.W., 2016. Epigenetic plasticity drives adipogenic and osteogenic differentiation of marrow-derived mesenchymal stem cells. J. Biol. Chem. 291 (34), 17829–17847.

Meyer, M.B., Benkusky, N.A., Kaufmann, M., Lee, S.M., Onal, M., Jones, G., et al., 2017. A kidney-specific genetic control module in mice governs endocrine regulation of the cytochrome P450 gene Cyp27b1 essential for vitamin D3 activation. J. Biol. Chem. 292 (42), 17541–17558.

Mittal, M.K., Myers, J.N., Misra, S., Bailey, C.K., Chaudhuri, G., 2008. In vivo binding to and functional repression of the VDR gene promoter by SLUG in human breast cells. Biochem. Biophys. Res. Commun. 372 (1), 30–34.

Mizwicki, M.T., Keidel, D., Bula, C.M., Bishop, J.E., Zanello, L.P., Wurtz, J.M., et al., 2004. Identification of an alternative ligand-binding pocket in the nuclear vitamin D receptor and its functional importance in 1alpha,25(OH)2-vitamin D3 signaling. Proc. Natl. Acad. Sci. U.S.A. 101 (35), 12876–12881.

Mohri, T., Nakajima, M., Takagi, S., Komagata, S., Yokoi, T., 2009. MicroRNA regulates human vitamin D receptor. Int. J. Cancer 125 (6), 1328–1333.

Moller, U.K., Streym, S., Heickendorff, L., Mosekilde, L., Rejnmark, L., 2012. Effects of 25OHD concentrations on chances of pregnancy and pregnancy outcomes: a cohort study in healthy Danish women. Eur. J. Clin. Nutr. 66 (7), 862–868.

Moller, U.K., Streym, S., Jensen, L.T., Mosekilde, L., Schoenmakers, I., Nigdikar, S., et al., 2013. Increased plasma concentrations of vitamin D metabolites and vitamin D binding protein in women using hormonal contraceptives: a cross-sectional study. Nutrients 5 (9), 3470–3480.

Morris, C.A., Mervis, C.B., 2000. Williams syndrome and related disorders. Annu. Rev. Genom. Hum. Genet. 1, 461–484.

Muller, M.J., Volmer, D.A., 2015. Mass spectrometric profiling of vitamin D metabolites beyond 25-hydroxyvitamin D. Clin. Chem. 61 (8), 1033–1048.

Murayama, A., Kim, M.S., Yanagisawa, J., Takeyama, K., Kato, S., 2004. Transrepression by a liganded nuclear receptor via a bHLH activator through co-regulator switching. EMBO J. 23 (7), 1598–1608.

Nagasawa, H., Uto, Y., Sasaki, H., Okamura, N., Murakami, A., Kubo, S., et al., 2005. Gc protein (vitamin D-binding protein): gc genotyping and GcMAF precursor activity. Anticancer Res. 25 (6A), 3689–3695.

Narvaez, C.J., Matthews, D., Broun, E., Chan, M., Welsh, J., 2009. Lean phenotype and resistance to diet-induced obesity in vitamin D receptor knockout mice correlates with induction of uncoupling protein-1 in white adipose tissue. Endocrinology 150 (2), 651–661.

Neme, A., Seuter, S., Carlberg, C., 2016. Vitamin D-dependent chromatin association of CTCF in human monocytes. Biochim. Biophys. Acta 1859 (11), 1380–1388.

Nemere, I., Yoshimoto, Y., Norman, A.W., 1984. Calcium transport in perfused duodena from normal chicks: enhancement within fourteen minutes of exposure to 1,25-dihydroxyvitamin D3. Endocrinology 115 (4), 1476–1483.

Nemere, I., Dormanen, M.C., Hammond, M.W., Okamura, W.H., Norman, A.W., 1994. Identification of a specific binding protein for 1 alpha,25-dihydroxyvitamin D3 in basal-lateral membranes of chick intestinal epithelium and relationship to transcaltachia. J. Biol. Chem. 269 (38), 23750–23756.

Nerenz, R.D., Martowicz, M.L., Pike, J.W., 2008. An enhancer 20 kilobases upstream of the human receptor activator of nuclear factor-kappaB ligand gene mediates dominant activation by 1,25-dihydroxyvitamin D3. Mol. Endocrinol. 22 (5), 1044–1056.

Nielson, C.M., Jones, K.S., Bouillon, R., Osteoporotic Fractures in Men Research, G., Chun, R.F., Jacobs, J., et al., 2016a. Role of assay type in determining free 25-hydroxyvitamin D levels in diverse populations. N. Engl. J. Med. 374 (17), 1695–1696.

Nielson, C.M., Jones, K.S., Chun, R.F., Jacobs, J.M., Wang, Y., Hewison, M., et al., 2016b. Free 25-hydroxyvitamin D: impact of vitamin D binding protein assays on racial-genotypic associations. J. Clin. Endocrinol. Metab. 101 (5), 2226–2234.

Norman, A.W., 2006. Minireview: vitamin D receptor: new assignments for an already busy receptor. Endocrinology 147 (12), 5542–5548.

Nutchey, B.K., Kaplan, J.S., Dwivedi, P.P., Omdahl, J.L., Ferrante, A., May, B.K., et al., 2005. Molecular action of 1,25-dihydroxyvitamin D3 and phorbol ester on the activation of the rat cytochrome P450C24 (CYP24) promoter: role of MAP kinase activities and identification of an important transcription factor binding site. Biochem. J. 389 (Pt 3), 753–762.

Nykjaer, A., Dragun, D., Walther, D., Vorum, H., Jacobsen, C., Herz, J., et al., 1999. An endocytic pathway essential for renal uptake and activation of the steroid 25-(OH) vitamin D3. Cell 96 (4), 507–515.

Oda, Y., Sihlbom, C., Chalkley, R.J., Huang, L., Rachez, C., Chang, C.P., et al., 2003. Two distinct coactivators, DRIP/mediator and SRC/p160, are differentially involved in vitamin D receptor transactivation during keratinocyte differentiation. Mol. Endocrinol. 17 (11), 2329–2339.

Oda, Y., Uchida, Y., Moradian, S., Crumrine, D., Elias, P.M., Bikle, D.D., 2009. Vitamin D receptor and coactivators SRC2 and 3 regulate epidermis-specific sphingolipid production and permeability barrier formation. J. Investig. Dermatol. 129 (6), 1367–1378.

Ogryzko, V.V., Schiltz, R.L., Russanova, V., Howard, B.H., Nakatani, Y., 1996. The transcriptional coactivators p300 and CBP are histone acetyltransferases. Cell 87 (5), 953–959.

Orlov, I., Rochel, N., Moras, D., Klaholz, B.P., 2012. Structure of the full human RXR/VDR nuclear receptor heterodimer complex with its DR3 target DNA. EMBO J. 31 (2), 291–300.

Palmer, H.G., Gonzalez-Sancho, J.M., Espada, J., Berciano, M.T., Puig, I., Baulida, J., et al., 2001. Vitamin D(3) promotes the differentiation of colon carcinoma cells by the induction of E-cadherin and the inhibition of beta-catenin signaling. J. Cell Biol. 154 (2), 369–387.

Palmer, H.G., Larriba, M.J., Garcia, J.M., Ordonez-Moran, P., Pena, C., Peiro, S., et al., 2004. The transcription factor SNAIL represses vitamin D receptor expression and responsiveness in human colon cancer. Nat. Med. 10 (9), 917–919.

Palmer, H.G., Anjos-Afonso, F., Carmeliet, G., Takeda, H., Watt, F.M., 2008. The vitamin D receptor is a wnt effector that controls hair follicle differentiation and specifies tumor type in adult epidermis. PLoS One 3 (1), e1483.

Pan, Y.Z., Gao, W., Yu, A.M., 2009. MicroRNAs regulate CYP3A4 expression via direct and indirect targeting. Drug Metab. Dispos. 37 (10), 2112–2117.

Papiha, S.S., Allcroft, L.C., Kanan, R.M., Francis, R.M., Datta, H.K., 1999. Vitamin D binding protein gene in male osteoporosis: association of plasma DBP and bone mineral density with (TAAA)(n)-Alu polymorphism in DBP. Calcif. Tissue Int. 65 (4), 262–266.

Pereira, F., Barbachano, A., Singh, P.K., Campbell, M.J., Munoz, A., Larriba, M.J., 2012. Vitamin D has wide regulatory effects on histone demethylase genes. Cell Cycle 11 (6), 1081–1089.

Perez, H.D., 1994. Gc globulin (vitamin D-binding protein) increases binding of low concentrations of C5a des Arg to human polymorphonuclear leukocytes: an explanation for its cochemotaxin activity. Inflammation 18 (2), 215–220.

Peric, M., Koglin, S., Dombrowski, Y., Gross, K., Bradac, E., Ruzicka, T., et al., 2009. VDR and MEK-ERK dependent induction of the antimicrobial peptide cathelicidin in keratinocytes by lithocholic acid. Mol. Immunol. 46 (16), 3183–3187.

Perissi, V., Staszewski, L.M., McInerney, E.M., Kurokawa, R., Krones, A., Rose, D.W., et al., 1999. Molecular determinants of nuclear receptor-corepressor interaction. Genes Dev. 13 (24), 3198–3208.

Perlmann, T., Rangarajan, P.N., Umesono, K., Evans, R.M., 1993. Determinants for selective RAR and TR recognition of direct repeat HREs. Genes Dev. 7 (7B), 1411–1422.

Pihl, T.H., Jorgensen, C.S., Santoni-Rugiu, E., Leifsson, P.S., Hansen, E.W., Laursen, I., et al., 2010. Safety pharmacology, toxicology and pharmacokinetic assessment of human Gc globulin (vitamin D binding protein). Basic Clin. Pharmacol. Toxicol. 107 (5), 853–860.

Pike, J.W., Meyer, M.B., Lee, S.M., Onal, M., Benkusky, N.A., 2017. The vitamin D receptor: contemporary genomic approaches reveal new basic and translational insights. J. Clin. Investig. 127 (4), 1146–1154.

Polly, P., Herdick, M., Moehren, U., Baniahmad, A., Heinzel, T., Carlberg, C., 2000. VDR-Alien: a novel, DNA-selective vitamin D(3) receptor-corepressor partnership. FASEB J. 14 (10), 1455–1463.

Powe, C.E., Ricciardi, C., Berg, A.H., Erdenesanaa, D., Collerone, G., Ankers, E., et al., 2011. Vitamin D-binding protein modifies the vitamin D-bone mineral density relationship. J. Bone Miner. Res. 26 (7), 1609–1616.

Powe, C.E., Evans, M.K., Wenger, J., Zonderman, A.B., Berg, A.H., Nalls, M., et al., 2013. Vitamin D-binding protein and vitamin D status of black Americans and white Americans. N. Engl. J. Med. 369 (21), 1991–2000.

Poynter, J.N., Jacobs, E.T., Figueiredo, J.C., Lee, W.H., Conti, D.V., Campbell, P.T., et al., 2010. Genetic variation in the vitamin D receptor (VDR) and the vitamin D-binding protein (GC) and risk for colorectal cancer: results from the Colon Cancer Family Registry. Cancer Epidemiol. Biomark. Prev. 19 (2), 525–536.

Rachez, C., Freedman, L.P., 2001. Mediator complexes and transcription. Curr. Opin. Cell Biol. 13 (3), 274–280.

Rai, V., Abdo, J., Agrawal, S., Agrawal, D.K., 2017. Vitamin D receptor polymorphism and cancer: an update. Anticancer Res. 37 (8), 3991–4003.

Ramagopalan, S.V., Heger, A., Berlanga, A.J., Maugeri, N.J., Lincoln, M.R., Burrell, A., et al., 2010. A ChIP-seq defined genome-wide map of vitamin D receptor binding: associations with disease and evolution. Genome Res. 20 (10), 1352–1360.

Raval-Pandya, M., Dhawan, P., Barletta, F., Christakos, S., 2001. YY1 represses vitamin D receptor-mediated 25-hydroxyvitamin D(3)24-hydroxylase transcription: relief of repression by CREB-binding protein. Mol. Endocrinol. 15 (6), 1035–1046.

Rochel, N., Wurtz, J.M., Mitschler, A., Klaholz, B., Moras, D., 2000. The crystal structure of the nuclear receptor for vitamin D bound to its natural ligand. Mol. Cell 5 (1), 173–179.

Saccone, D., Asani, F., Bornman, L., 2015. Regulation of the vitamin D receptor gene by environment, genetics and epigenetics. Gene 561 (2), 171–180.

Safadi, F.F., Thornton, P., Magiera, H., Hollis, B.W., Gentile, M., Haddad, J.G., et al., 1999. Osteopathy and resistance to vitamin D toxicity in mice null for vitamin D binding protein. J. Clin. Investig. 103 (2), 239–251.

Salehi-Tabar, R., Nguyen-Yamamoto, L., Tavera-Mendoza, L.E., Quail, T., Dimitrov, V., An, B.S., et al., 2012. Vitamin D receptor as a master regulator of the c-MYC/MXD1 network. Proc. Natl. Acad. Sci. U.S.A. 109 (46), 18827–18832.

Sancho, E., Batlle, E., Clevers, H., 2004. Signaling pathways in intestinal development and cancer. Annu. Rev. Cell Dev. Biol. 20, 695–723.

Santos, B.R., Mascarenhas, L.P., Boguszewski, M.C., Spritzer, P.M., 2013. Variations in the vitamin D-binding protein (DBP) gene are related to lower 25-hydroxyvitamin D levels in healthy girls: a cross-sectional study. Hormone Res. Paediatr. 79, 162–168.

Schiodt, F.V., Ott, P., Bondesen, S., Tygstrup, N., 1997. Reduced serum Gc-globulin concentrations in patients with fulminant hepatic failure: association with multiple organ failure. Crit. Care Med. 25 (8), 1366–1370.

Schiodt, F.V., 2008. Gc-globulin in liver disease. Dan. Med. Bull. 55 (3), 131–146.

Schneider, G.B., Benis, K.A., Flay, N.W., Ireland, R.A., Popoff, S.N., 1995. Effects of vitamin D binding protein-macrophage activating factor (DBP-MAF) infusion on bone resorption in two osteopetrotic mutations. Bone 16 (6), 657–662.

Schrader, M., Nayeri, S., Kahlen, J.P., Muller, K.M., Carlberg, C., 1995. Natural vitamin D3 response elements formed by inverted palindromes: polarity-directed ligand sensitivity of vitamin D3 receptor-retinoid X receptor heterodimer-mediated transactivation. Mol. Cell Biol. 15 (3), 1154–1161.

Schrader, M., Kahlen, J.P., Carlberg, C., 1997. Functional characterization of a novel type of 1 alpha,25-dihydroxyvitamin D3 response element identified in the mouse c-fos promoter. Biochem. Biophys. Res. Commun. 230 (3), 646–651.

Schwartz, J.B., Lai, J., Lizaola, B., Kane, L., Weyland, P., Terrault, N.A., et al., 2014a. Variability in free 25(OH) vitamin D levels in clinical populations. J. Steroid Biochem. Mol. Biol. 144 (Pt A), 156–158.

Schwartz, J.B., Lai, J., Lizaola, B., Kane, L., Markova, S., Weyland, P., et al., 2014b. A comparison of measured and calculated free 25(OH) vitamin D levels in clinical populations. J. Clin. Endocrinol. Metab. 99 (5), 1631–1637.

Schwartz, J.B., Kane, L., Bikle, D., 2016. Response of vitamin D concentration to vitamin D3 administration in older adults without sun exposure: a randomized double-blind trial. J. Am. Geriatr. Soc. 64 (1), 65–72.

Sequeira, V.B., Rybchyn, M.S., Tongkao-On, W., Gordon-Thomson, C., Malloy, P.J., Nemere, I., et al., 2012. The role of the vitamin D receptor and ERp57 in photoprotection by 1alpha,25-dihydroxyvitamin D3. Mol. Endocrinol. 26 (4), 574–582.

Seuter, S., Neme, A., Carlberg, C., Epigenomic, P.U., 2017. 1-VDR crosstalk modulates vitamin D signaling. Biochim. Biophys. Acta 1860 (4), 405–415.

Shah, A.B., DiMartino, S.J., Trujillo, G., Kew, R.R., 2006. Selective inhibition of the C5a chemotactic cofactor function of the vitamin D binding protein by 1,25(OH)2 vitamin D3. Mol. Immunol. 43 (8), 1109–1115.

Shah, S., Islam, M.N., Dakshanamurthy, S., Rizvi, I., Rao, M., Herrell, R., et al., 2006. The molecular basis of vitamin D receptor and beta-catenin crossregulation. Mol. Cell 21 (6), 799–809.

Shieh, A., Chun, R.F., Ma, C., Witzel, S., Meyer, B., Rafison, B., et al., 2016. Effects of high-dose vitamin D2 versus D3 on total and free 25-hydroxyvitamin D and markers of calcium balance. J. Clin. Endocrinol. Metab. 101 (8), 3070–3078.

Shieh, A., Ma, C., Chun, R.F., Witzel, S., Rafison, B., Contreras, H.T.M., et al., 2017. Effects of cholecalciferol vs calcifediol on total and free 25-hydroxyvitamin D and parathyroid hormone. J. Clin. Endocrinol. Metab. 102 (4), 1133–1140.

Silvagno, F., Pescarmona, G., 2017. Spotlight on vitamin D receptor, lipid metabolism and mitochondria: some preliminary emerging issues. Mol. Cell. Endocrinol. 450, 24–31.

Sollid, S.T., Hutchinson, M.Y., Berg, V., Fuskevag, O.M., Figenschau, Y., Thorsby, P.M., et al., 2016. Effects of vitamin D binding protein phenotypes and vitamin D supplementation on serum total 25(OH)D and directly measured free 25(OH)D. Eur. J. Endocrinol. 174 (4), 445–452.

Song, Y.H., Naumova, A.K., Liebhaber, S.A., Cooke, N.E., 1999. Physical and meiotic mapping of the region of human chromosome 4q11-q13 encompassing the vitamin D binding protein DBP/Gc-globulin and albumin multigene cluster. Genome Res. 9 (6), 581–587.

Speeckaert, M., Huang, G., Delanghe, J.R., Taes, Y.E., 2006. Biological and clinical aspects of the vitamin D binding protein (Gc-globulin) and its polymorphism. Clin. Chim. Acta 372 (1–2), 33–42.

Speeckaert, M.M., Wehlou, C., De Somer, F., Speeckaert, R., Van Nooten, G.J., Delanghe, J.R., 2010. Evolution of vitamin D binding protein concentration in sera from cardiac surgery patients is determined by triglyceridemia. Clin. Chem. Lab. Med. 48 (9), 1345–1350.

Stumpf, W.E., Sar, M., Reid, F.A., Tanaka, Y., DeLuca, H.F., 1979. Target cells for 1,25-dihydroxyvitamin D3 in intestinal tract, stomach, kidney, skin, pituitary, and parathyroid. Science 206 (4423), 1188–1190.

Sunn, K.L., Cock, T.A., Crofts, L.A., Eisman, J.A., Gardiner, E.M., 2001. Novel N-terminal variant of human VDR. Mol. Endocrinol. 15 (9), 1599–1609.

Sutton, A.L., Zhang, X., Ellison, T.I., Macdonald, P.N., 2005. The 1,25(OH)2D3-regulated transcription factor MN1 stimulates vitamin D receptor-mediated transcription and inhibits osteoblastic cell proliferation. Mol. Endocrinol. 19 (9), 2234–2244.

Swamy, N., Ray, R., 2008. Fatty acid-binding site environments of serum vitamin D-binding protein and albumin are different. Bioorg. Chem. 36 (3), 165–168.

Swamy, N., Ghosh, S., Schneider, G.B., Ray, R., 2001. Baculovirus-expressed vitamin D-binding protein-macrophage activating factor (DBP-maf) activates osteoclasts and binding of 25-hydroxyvitamin D(3) does not influence this activity. J. Cell. Biochem. 81 (3), 535–546.

Tagami, T., Lutz, W.H., Kumar, R., Jameson, J.L., 1998. The interaction of the vitamin D receptor with nuclear receptor corepressors and coactivators. Biochem. Biophys. Res. Commun. 253 (2), 358–363.

Takiar, R., Lutsey, P.L., Zhao, D., Guallar, E., Schneider, A.L., Grams, M.E., et al., 2015. The associations of 25-hydroxyvitamin D levels, vitamin D binding protein gene polymorphisms, and race with risk of incident fracture-related hospitalization: twenty-year follow-up in a bi-ethnic cohort (the ARIC Study). Bone 78, 94–101.

Tannetta, D.S., Redman, C.W., Sargent, I.L., 2014. Investigation of the actin scavenging system in pre-eclampsia. Eur. J. Obstet. Gynecol. Reprod. Biol. 172, 32–35.

Teichert, A., Arnold, L.A., Otieno, S., Oda, Y., Augustinaite, I., Geistlinger, T.R., et al., 2009. Quantification of the vitamin D receptor-coregulator interaction. Biochemistry 48 (7), 1454–1461.

Trujillo, G., Habiel, D.M., Ge, L., Ramadass, M., Cooke, N.E., Kew, R.R., 2013. Neutrophil recruitment to the lung in both C5a- and CXCL1-induced alveolitis is impaired in vitamin D-binding protein-deficient mice. J. Immunol. 191 (2), 848–856.

Tuoresmaki, P., Vaisanen, S., Neme, A., Heikkinen, S., Carlberg, C., 2014. Patterns of genome-wide VDR locations. PLoS One 9 (4), e96105.

Uto, Y., Yamamoto, S., Mukai, H., Ishiyama, N., Takeuchi, R., Nakagawa, Y., et al., 2012. beta-Galactosidase treatment is a common first-stage modification of the three major subtypes of Gc protein to GcMAF. Anticancer Res. 32 (6), 2359–2364.

Vasconcellos, C.A., Lind, S.E., 1993. Coordinated inhibition of actin-induced platelet aggregation by plasma gelsolin and vitamin D-binding protein. Blood 82 (12), 3648–3657.

Waldron, J.L., Ashby, H.L., Cornes, M.P., Bechervaise, J., Razavi, C., Thomas, O.L., et al., 2013. Vitamin D: a negative acute phase reactant. J. Clin. Pathol. 66 (7), 620–622.

Walsh, J.S., Evans, A.L., Bowles, S., Naylor, K.E., Jones, K.S., Schoenmakers, I., et al., 2016. Free 25-hydroxyvitamin D is low in obesity, but there are no adverse associations with bone health. Am. J. Clin. Nutr. 103 (6), 1465–1471.

Wan, L.Y., Zhang, Y.Q., Chen, M.D., Liu, C.B., Wu, J.F., 2015a. Relationship of structure and function of DNA-binding domain in vitamin D receptor. Molecules 20 (7), 12389–12399.

Wan, L.Y., Zhang, Y.Q., Chen, M.D., Du, Y.Q., Liu, C.B., Wu, J.F., 2015b. Relationship between structure and conformational change of the vitamin D receptor ligand binding domain in 1alpha,25-dihydroxyvitamin D3 signaling. Molecules 20 (11), 20473–20486.

Wang, J., Malloy, P.J., Feldman, D., 2007. Interactions of the vitamin D receptor with the corepressor hairless: analysis of hairless mutants in atrichia with papular lesions. J. Biol. Chem. 282 (35), 25231–25239.

Wang, H., Cheng, B., Chen, Q., Wu, S., Lv, C., Xie, G., et al., 2008. Time course of plasma gelsolin concentrations during severe sepsis in critically ill surgical patients. Crit. Care 12 (4), R106.

Wang, X., Gocek, E., Liu, C.G., Studzinski, G.P., 2009. MicroRNAs181 regulate the expression of p27Kip1 in human myeloid leukemia cells induced to differentiate by 1,25-dihydroxyvitamin D3. Cell Cycle 8 (5), 736–741.

Wang, T.J., Zhang, F., Richards, J.B., Kestenbaum, B., van Meurs, J.B., Berry, D., et al., 2010. Common genetic determinants of vitamin D insufficiency: a genome-wide association study. Lancet 376 (9736), 180–188.

Wang, X., Shapses, S.A., Al-Hraishawi, H., 2017. Free and bioavailable 25-hydroxyvitamin D levels in patients with primary hyperparathyroidism. Endocr. Pract. 23 (1), 66–71.

Wei, R., Christakos, S., 2015. Mechanisms underlying the regulation of innate and adaptive immunity by vitamin D. Nutrients 7 (10), 8251–8260.

White, P., Cooke, N., 2000. The multifunctional properties and characteristics of vitamin D-binding protein. Trends Endocrinol. Metabol. 11 (8), 320–327.

White, J.H., 2004. Profiling 1,25-dihydroxyvitamin D3-regulated gene expression by microarray analysis. J. Steroid Biochem. Mol. Biol. 89–90 (1–5), 239–244.

Whitfield, G.K., Selznick, S.H., Haussler, C.A., Hsieh, J.C., Galligan, M.A., Jurutka, P.W., et al., 1996. Vitamin D receptors from patients with resistance to 1,25-dihydroxyvitamin D3: point mutations confer reduced transactivation in response to ligand and impaired interaction with the retinoid X receptor heterodimeric partner. Mol. Endocrinol. 10 (12), 1617–1631.

Wiese, R.J., Uhland-Smith, A., Ross, T.K., Prahl, J.M., DeLuca, H.F., 1992. Up-regulation of the vitamin D receptor in response to 1,25-dihydroxyvitamin D3 results from ligand-induced stabilization. J. Biol. Chem. 267 (28), 20082–20086.

Wilson, R.T., Bortner Jr., J.D., Roff, A., Das, A., Battaglioli, E.J., Richie Jr., J.P., et al., 2015. Genetic and environmental influences on plasma vitamin D binding protein concentrations. Transl. Res. 165 (6), 667–676.

Wood, R.J., Fleet, J.C., Cashman, K., Bruns, M.E., Deluca, H.F., 1998. Intestinal calcium absorption in the aged rat: evidence of intestinal resistance to 1,25(OH)2 vitamin D. Endocrinology 139 (9), 3843–3848.

Wu, S., Ren, S., Chen, H., Chun, R.F., Gacad, M.A., Adams, J.S., 2000. Intracellular vitamin D binding proteins: novel facilitators of vitamin D-directed transactivation. Mol. Endocrinol. 14 (9), 1387–1397.

Wu, W., Beilhartz, G., Roy, Y., Richard, C.L., Curtin, M., Brown, L., et al., 2010. Nuclear translocation of the 1,25D3-MARRS (membrane associated rapid response to steroids) receptor protein and NFkappaB in differentiating NB4 leukemia cells. Exp. Cell Res. 316 (7), 1101–1108.

Xie, Z., Bikle, D.D., 1997. Cloning of the human phospholipase C-gamma1 promoter and identification of a DR6-type vitamin D-responsive element. J. Biol. Chem. 272 (10), 6573–6577.

Xie, Z., Munson, S.J., Huang, N., Portale, A.A., Miller, W.L., Bikle, D.D., 2002. The mechanism of 1,25-dihydroxyvitamin D(3) autoregulation in keratinocytes. J. Biol. Chem. 277 (40), 36987–36990.

Xie, Z., Chang, S., Oda, Y., Bikle, D.D., 2006. Hairless suppresses vitamin D receptor transactivation in human keratinocytes. Endocrinology 147 (1), 314–323.

Xu, J., O'Malley, B.W., 2002. Molecular mechanisms and cellular biology of the steroid receptor coactivator (SRC) family in steroid receptor function. Rev. Endocr. Metab. Disord. 3 (3), 185–192.

Xu, H., McCann, M., Zhang, Z., Posner, G.H., Bingham, V., El-Tanani, M., et al., 2009. Vitamin D receptor modulates the neoplastic phenotype through antagonistic growth regulatory signals. Mol. Carcinog. 48 (8), 758–772.

Yamamoto, N., Homma, S., 1991. Vitamin D3 binding protein (group-specific component) is a precursor for the macrophage-activating signal factor from lysophosphatidylcholine-treated lymphocytes. Proc. Natl. Acad. Sci. U.S.A. 88 (19), 8539–8543.

Yamamoto, N., Homma, S., Millman, I., 1991. Identification of the serum factor required for in vitro activation of macrophages. Role of vitamin D3-binding protein (group specific component, Gc) in lysophospholipid activation of mouse peritoneal macrophages. J. Immunol. 147 (1), 273–280.

Yamamoto, N., Naraparaju, V.R., Asbell, S.O., 1996. Deglycosylation of serum vitamin D3-binding protein leads to immunosuppression in cancer patients. Cancer Res. 56 (12), 2827–2831.

Yamamoto, N., Naraparaju, V.R., Urade, M., 1997. Prognostic utility of serum alpha-N-acetylgalactosaminidase and immunosuppression resulted from deglycosylation of serum Gc protein in oral cancer patients. Cancer Res. 57 (2), 295–299.

Yang, X.J., Ogryzko, V.V., Nishikawa, J., Howard, B.H., Nakatani, Y., 1996. A p300/CBP-associated factor that competes with the adenoviral oncoprotein E1A. Nature 382 (6589), 319–324.

Ye, W.Z., Dubois-Laforgue, D., Bellanne-Chantelot, C., Timsit, J., Velho, G., 2001. Variations in the vitamin D-binding protein (Gc locus) and risk of type 2 diabetes mellitus in French Caucasians. Metab. Clin. Exp. 50 (3), 366–369.

Yin, J.W., Wang, G., 2014. The Mediator complex: a master coordinator of transcription and cell lineage development. Development 141 (5), 977–987.

Zella, L.A., Shevde, N.K., Hollis, B.W., Cooke, N.E., Pike, J.W., 2008. Vitamin D-binding protein influences total circulating levels of 1,25-dihydroxyvitamin D3 but does not directly modulate the bioactive levels of the hormone in vivo. Endocrinology 149 (7), 3656–3667.

Zella, L.A., Meyer, M.B., Nerenz, R.D., Lee, S.M., Martowicz, M.L., Pike, J.W., 2010. Multifunctional enhancers regulate mouse and human vitamin D receptor gene transcription. Mol. Endocrinol. 24 (1), 128–147.

Zhang, J., Kew, R.R., 2004. Identification of a region in the vitamin D-binding protein that mediates its C5a chemotactic cofactor function. J. Biol. Chem. 279 (51), 53282–53287.

Zhang, J., Habiel, D.M., Ramadass, M., Kew, R.R., 2010. Identification of two distinct cell binding sequences in the vitamin D binding protein. Biochim. Biophys. Acta 1803 (5), 623–629.

Zhang, J.Y., Lucey, A.J., Horgan, R., Kenny, L.C., Kiely, M., 2014. Impact of pregnancy on vitamin D status: a longitudinal study. Br. J. Nutr. 112 (7), 1081–1087.

Zhou, L., Zhang, X., Chen, X., Liu, L., Lu, C., Tang, X., et al., 2012. GC Glu416Asp and Thr420Lys polymorphisms contribute to gastrointestinal cancer susceptibility in a Chinese population. Int. J. Clin. Exp. Med. 5 (1), 72–79.

Chapter 30

Vitamin D gene regulation

Sylvia Christakos[1] and J. Wesley Pike[2]

[1]Department of Microbiology, Biochemistry and Molecular Genetics, Rutgers, New Jersey Medical School, Newark, NJ, United States; [2]Department of Biochemistry, University of Wisconsin—Madison, Madison, WI, United States

Chapter outline

Vitamin D metabolism

Vitamin D is a principal factor required for the development and maintenance of bone as well as for maintaining normal calcium and phosphorus homeostasis. In addition, evidence has indicated the involvement of vitamin D in a number of diverse cellular processes, including effects on differentiation and cell proliferation, cancer progression, and the immune system (DeLuca, 2016; Christakos et al., 2016). For vitamin D to affect mineral metabolism as well as numerous other systems, it must first be metabolized to its active form. Vitamin D, which is taken in from the diet or is synthesized in the skin from 7-dehydrocholesterol in a reaction catalyzed by ultraviolet irradiation, is transported in the blood by the vitamin D-binding protein (DBP) to the liver. In the liver, vitamin D is hydroxylated at the carbon 25 position, resulting in the formation of 25-hydroxyvitamin D$_3$ (25(OH)D$_3$), the major circulating form of vitamin D, which is one of the most reliable biomarkers of vitamin D status (Bikle et al., 2013). The synthesis of 25(OH)D$_3$ has not been reported to be highly regulated (DeLuca, 2008). Cytochrome P450 2R1 (CYP2R1) is probably the key vitamin D 25-hydroxylase responsible for the conversion of vitamin D to 25(OH)D$_3$ based in part on genetic evidence that patients with a mutation in *CYP2R1* have vitamin D dysfunction (Cheng et al., 2004). However, in studies in *Cyp2r1*-null mice, 25(OH)D$_3$ levels were markedly reduced but not abolished, suggesting that other hydroxylases may also be involved (Zhu et al., 2013). 25-Hydroxyvitamin D proceeds to the kidney via the serum DBP. Megalin, a member of the low-density lipoprotein receptor superfamily, plays an essential role in the renal uptake of 25(OH)D$_3$ (Nykjaer et al., 1999). Cubilin and disabled 2 also work in conjunction with megalin for the cellular uptake of DBP/25(OH)D$_3$ (Nykjaer et al., 2001; Morris et al., 2002). In the proximal convoluted and straight tubules of the kidney nephron, 25(OH)D$_3$ is hydroxylated at the position of carbon 1 of the A ring

Principles of Bone Biology. https://doi.org/10.1016/B978-0-12-814841-9.00030-0

through the action of mitochondrial 25(OH)D 1α-hydroxylase (CYP27B1), resulting in the formation of the hormonally active form of vitamin D, 1,25-dihydroxyvitamin D_3 ($1,25(OH)_2D_3$) (Fig. 30.1). Mutations in the *CY27B1* gene result in vitamin D-dependent rickets (VDDR) type I, indicating the importance of the *CYP27B1* enzyme (Kitanaka et al., 1998). *Cyp27b1*-null mice have provided a model of VDDR type I (undetectable $1,25(OH)_2D_3$, low serum calcium, and secondary hyperparathyroidism) (Panda et al., 2001; Dardenne et al., 2001). The kidney can also produce 24,25-dihydroxyvitamin D_3 ($24,25(OH)_2D_3$). CYP24A1 has been reported to be capable of hydroxylating the 24 position of both $25(OH)D_3$ and $1,25(OH)_2D_3$ (Omdahl et al., 2003; Jones et al., 2014; Veldurthy et al., 2016) (see Fig. 30.1). It has been suggested that the preferred substrate for CYP24A1 in vivo is $1,25(OH)_2D_3$ rather than $25(OH)D_3$ (Shinki et al., 1992). Studies using mice with a targeted inactivating mutation of the *Cyp24a1* gene (*Cyp24a1*-null-mutant mice) provided the first direct in vivo evidence for a role for CYP24A1 in the catabolism of $1,25(OH)_2D_3$ (St-Arnaud et al., 2000). Both chronic and acute treatment with $1,25(OH)_2D_3$ resulted in an inability of *Cyp24a1*-deficient mice to clear $1,25(OH)_2D_3$ from their bloodstream. CYP24A1 limits the amount of $1,25(OH)_2D_3$ by catalyzing the conversion of $1,25(OH)_2D_3$ into 24-hydroxylated products targeted for excretion. In addition, production of $24,25(OH)_2D_3$ by CYP24A1 decreases the pool of $25(OH)D_3$ available for 1-hydroxylation. CYP24A1 can also catalyze the C23 oxidation pathway, resulting in the formation of $1,25(OH)_2D_3$ 26,23-lactone from $1,25(OH)_2D_3$ and $25(OH)D_3$ 26,23-lactone from $25(OH)D_3$ (Jones et al., 2014). CYP24A1 is present not only in kidney but also in all cells that contain the vitamin D receptor (VDR). Thus CYP24A1 not only regulates circulating $1,25(OH)_2D_3$ concentrations, but may also modulate the amount of $1,25(OH)_2D_3$ in target tissues, resulting in an appropriate cellular response. Inactivating mutations in CYP24A1 have been found in young children with idiopathic infantile hypercalcemia and in adults (Schlingmann et al., 2011; Dinour et al., 2013). In adults, patients were characterized by hypercalcemia, hypercalciuria, and recurring kidney stones (Dinour et al., 2013). These findings provide evidence for a critical role of CYP24A1 in the regulation of $1,25(OH)_2D_3$ in humans.

The production of $1,25(OH)_2D_3$ and $24,25(OH)_2D_3$ is under stringent control. Calcium and phosphorus deprivation results in enhanced production of $1,25(OH)_2D_3$ (Omdahl et al., 2003; Jones et al., 2014). Elevated parathyroid hormone (PTH) resulting from calcium deprivation may be the primary signal mediating the calcium regulation of $1,25(OH)_2D_3$ synthesis (Boyle et al., 1971; Henry, 1985). PTH has been reported to stimulate *CYP27B1* (Brezna and DeLuca, 2000; Meyer et al., 2017). $1,25(OH)_2D_3$ also regulates its own production by inhibiting *CYP27B1* (Brenza and DeLuca, 2000; Meyer et al., 2017). The synthesis of $24,25(OH)_2D_3$ has been reported to be reciprocally regulated compared with the synthesis of $1,25(OH)_2D_3$ (stimulated by $1,25(OH)_2D_3$, and inhibited by low calcium and PTH) (Shinki et al., 1992; Omdahl et al., 2003; Jones et al., 2014) (Fig. 30.1). Fibroblast growth factor 23 (FGF23), which promotes renal phosphate excretion and requires klotho, a transmembrane protein, has also been identified as a physiological regulator of vitamin D metabolism, which suppresses the expression of *CYP27B1* (Shimada et al., 2004; Hu et al., 2013) (Fig. 30.1). Low dietary phosphate intake results in decreased FGF23 levels and a corresponding increase in *CYP27B1* activity (Perwad et al.,

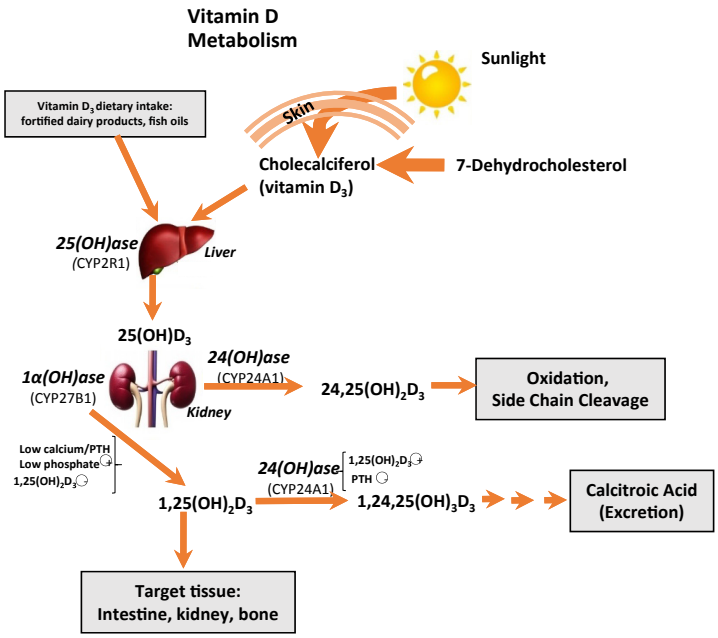

FIGURE 30.1 The pathway of vitamin D metabolism. Cytochrome P450 2R1 (*CYP2R1*) has been identified as a key vitamin D 25-hydroxylase. Parathyroid hormone (*PTH*), fibroblast growth factor 23/α-klotho, and serum calcium and phosphate act together to maintain optimal $1,25(OH)_2D_3$ levels (Dhawan et al., 2017).

2005). FGF23 requires the transmembrane receptor α-klotho (a multifunctional protein involved in phosphate and calcium homeostasis and in aging that binds to FGF receptors) to activate FGF signaling (Hu et al., 2013). Studies by Meyer et al. (2017) identified a kidney-specific control module generated by a renal cell−specific chromatin structure located distal to *Cyp27b1* that mediates PTH, FGF23, and $1,25(OH)_2D_3$ regulation of *Cyp27b1* expression, which will be discussed later in this chapter. In addition to the kidney, *CYP27B1* is also expressed during pregnancy in placenta (Zehnder et al., 2002). Extrarenal production by macrophages of CYP27B1 has also been convincingly demonstrated in patients with sarcoidosis (Barbour et al., 1981; Adams et al., 1983). Other immune cells also can produce $1,25(OH)_2D_3$ (Ooi et al., 2014). In addition, cancer cells have been shown to express *CYP27B1* (Hobaus et al., 2013). Although *CYP27B1* expression has been noted in a number of tissues (Bikle, 2009), whether there is a functional impact of *CYP27B1* activity in vivo in tissues other than the kidney and placenta under normal physiological conditions remains to be determined.

Serum $1,25(OH)_2D_3$ levels and the capacity of the kidney to hydroxylate $25(OH)D_3$ to $1,25(OH)_2D_3$ have been reported to decline with age (Armbrecht et al., 1980). In addition, an increase in renal *CYP24A1* gene expression and an increase in the clearance of $1,25(OH)_2D_3$ with aging have been reported (Matkovits and Christakos, 1995; Wada et al., 1992). These findings have implications concerning the etiology of osteoporosis and suggest that the combined effect of a decline in the ability of the kidney to synthesize $1,25(OH)_2D_3$ and an increase in the renal metabolism of $1,25(OH)_2D_3$ may contribute to age-related bone loss. Whether there is an interrelationship between the decline of sex steroids with age and age-related changes in *CYP27B1* and *CYP24A1* remains to be determined.

Role of $1,25(OH)_2D_3$ in classical target tissues

Bone

Exactly how $1,25(OH)_2D_3$ affects mineral homeostasis is a subject of continuing investigation. It has been suggested that the antirachitic action of $1,25(OH)_2D_3$ is indirect and the result of increased intestinal absorption of calcium and phosphorus by $1,25(OH)_2D_3$, thus resulting in their increased availability for incorporation into bone (Underwood and DeLuca, 1984; Weinstein et al., 1984). Studies using VDR-ablated mice (VDR-null mice) also suggest that a principal role of the VDR in skeletal homeostasis is its role in intestinal calcium absorption (Li et al., 1997; Yoshizawa et al., 1997; Amling et al., 1999). When VDR-null mice were fed a calcium/phosphorus/lactose-enriched diet, serum-ionized calcium levels were normalized, the development of hyperparathyroidism was prevented, and the animals did not develop rickets or osteomalacia, although alopecia was still observed. In addition, transgenic expression of VDR in the intestine of VDR-null mice results in normalization of serum calcium, bone density, and bone volume (Xue and Fleet, 2009). Thus, it was suggested that skeletal consequences of VDR ablation are due primarily to impaired intestinal calcium absorption. In vitro studies, however, have shown that $1,25(OH)_2D_3$ can resorb bone (Raisz et al., 1972). Although $1,25(OH)_2D_3$ stimulates the formation of bone-resorbing osteoclasts, receptors for $1,25(OH)_2D_3$ are not present in osteoclasts but rather in osteoblasts (Wang et al., 2014). Stimulation of osteoclast formation by $1,25(OH)_2D_3$ requires cell-to-cell contact between osteoblastic cells and osteoclast precursors and involves upregulation by $1,25(OH)_2D_3$ in osteoblastic cells of osteoprotegerin ligand or receptor activator of nuclear factor-κB ligand (RANKL; Takeda et al., 1999; Yasuda et al., 1998a, 1998b). RANKL is induced by $1,25(OH)_2D_3$ (Kim et al., 2007; Nerenz et al., 2008) as well as by PTH in osteoblasts/stromal cells. In *Cyp27a1*-null mice and in VDR-null mice, although PTH levels are markedly elevated, osteoclast numbers are not increased, indicating that both $1,25(OH)_2D_3$ and VDR are necessary for PTH production of osteoclasts (Amling et al., 1999; Panda et al., 2001). RANKL is a member of the membrane-associated tumor necrosis factor ligand family that enhances osteoclast formation by mediating direct interactions between osteoblasts/stromal cells and osteoclast precursor cells. Osteoclastogenesis-inhibitory factor/osteoprotegerin, a member of the tumor necrosis factor receptor family, is a soluble decoy receptor for RANKL that antagonizes RANKL function, thus blocking osteoclastogenesis. Osteoprotegerin is downregulated by $1,25(OH)_2D_3$ (Yasuda et al., 1998a).

In addition to increasing the availability of calcium and phosphorus for incorporation into bone and stimulating osteoclast formation, direct effects of $1,25(OH)_2D_3$ on bone cells have also been demonstrated (Bikle, 2012). For example, $1,25(OH)_2D_3$ has been reported to stimulate the synthesis of the calcium-binding proteins osteocalcin (OC) (Price and Baukol, 1980; Demay et al., 1990; Kerner et al., 1989) and osteopontin (OPN) (Prince and Butler, 1987; Noda et al., 1990; Shen and Christakos, 2005) in osteoblastic cells. OPN, a major noncollagenous bone protein, has been reported to inhibit bone matrix mineralization (Boskey et al., 1993). $1,25(OH)_2D_3$ suppresses mineralization by increasing the expression of mineralization inhibitors in osteoblasts in addition to OPN, including *Ennp1* and *Ennp3* (ectonucleotide pyrophosphastase phosphodiesterase 1 and 3) (Lieben et al., 2012). Thus during a negative calcium balance $1,25(OH)_2D_3$ can promote increased bone resorption and reduced matrix mineralization to maintain normal serum calcium levels at the expense of

skeletal integrity (Lieben et al., 2012). Direct effects of $1,25(OH)_2D_3$ on bone cells have also been demonstrated in osteocytes. $1,25(OH)_2D_3$ stimulates FGF23 production from osteocytes, resulting in renal modulation of phosphate levels (Lanske et al., 2014). Collectively these studies support a direct effect of $1,25(OH)_2D_3$ on bone as well as an indirect role through stimulation of intestinal calcium absorption.

Intestine

The major defect in VDR-null mice is in intestinal calcium absorption indicating that a principal action of $1,25(OH)_2D_3$ is to maintain calcium homeostasis via increasing efficiency of intestinal calcium absorption (Li et al., 1997; Yoshizawa et al., 1997; Amling et al., 1999). In addition, when patients with hereditary $1,25(OH)_2D_3$-resistant rickets (HVDRR) are treated with intravenous or high-dose oral calcium the skeletal phenotype of the patients is reversed (Hochberg et al., 1992). Although these studies indicate the importance of the intestine in $1,25(OH)_2D_3$ regulation of intestinal calcium absorption, the mechanisms involved are still incompletely understood. When the demand for calcium increases due to a diet deficient in calcium, demand for skeletal growth, or pregnancy or lactation, synthesis of $1,25(OH)_2D_3$ increases and intestinal calcium absorption occurs predominantly by an active transcellular process (Wasserman and Fullmer, 1995). In the transcellular process $1,25(OH)_2D_3$ has been reported to act by regulating (1) calcium entry through the apical calcium channel transient receptor potential cation channel subfamily V member 6 (TRPV6), (2) transcellular movement of calcium by binding to the calcium-binding protein calbindin, and (3) extrusion of calcium from the cell by the plasma membrane calcium ATPase (PMCA1b). Studies in TRPV6-null and calbindin-D-null mice have challenged this traditional view. There are no phenotypic differences between calbindin-D_{9k}-null mice and TRPV6-null mice and wild-type mice when dietary calcium is normal (Benn et al., 2008; Kutuzova et al., 2006; Kutuzova et al., 2008). However, studies in TRPV6/calbindin-D_{9k} double-null mice under conditions of low dietary calcium have shown that intestinal calcium absorption is least efficient in the absence of both proteins (compared with single-null mice and wild-type mice), suggesting that TRPV6 and calbindin can act together in certain aspects of the absorptive process (Benn et al., 2008). Findings in the single-null mice under adequate calcium conditions suggest that calbindin-D_{9k} and TRPV6 are redundant for intestinal calcium absorption and suggest compensation by other channels or proteins yet to be identified (Benn et al., 2008; Kutuzova et al, 2006, 2008; Christakos, 2012). Although other apical membrane transporters may compensate for the loss of TRPV6, intestine-specific transgenic expression of TRPV6 has been shown to result in a marked increase in intestinal calcium absorption and bone density in VDR-null mice, indicating a direct role for TRPV6 in the calcium absorptive process and that a primary defect in VDR-null mice is low apical membrane calcium uptake (Cui et al., 2012). It should also be noted that although the duodenum has been the focus of research related to $1,25(OH)_2D_3$ regulation of calcium absorption, it is the distal intestine where most of the ingested calcium is absorbed. Studies have shown that transgenic expression of VDR specifically in ileum, cecum, and colon can prevent abnormal calcium homeostasis and rickets in VDR-null mice (Dhawan et al., 2017a, 2017b). These findings indicate that, although calcium is absorbed more rapidly in the duodenum, the distal segments of the intestine contribute significantly to vitamin D regulation of calcium homeostasis. Studies related to mechanisms involved in $1,25(OH)_2D_3$ regulation of calcium absorption in the distal intestine may suggest new strategies to increase the efficiency of calcium absorption in individuals at risk for bone loss due to aging, bariatric surgery, or inflammatory bowel disease.

Kidney

In addition to bone and intestine, a third target tissue involved in the regulation by $1,25(OH)_2D_3$ of mineral homeostasis is the kidney. Although most of the filtered calcium is reabsorbed by a passive, paracellular path in the proximal renal tubule that is independent of $1,25(OH)_2D_3$, 10%−15% of the filtered calcium is reabsorbed in the distal convoluted tubule and connecting tubule and is regulated by PTH and $1,25(OH)_2D_3$ (Boros et al., 2009). $1,25(OH)_2D_3$ has been reported to enhance the stimulatory effect of PTH on calcium transport in the distal nephron in part by increasing PTH receptor mRNA and binding activity in distal tubule cells (Sneddon et al., 1998). Similar to studies in the intestine, $1,25(OH)_2D_3$ regulates an active transcellular process in the distal portion of the nephron by inducing the apical calcium channel TRPV5 (which shows 73.4% sequence homology with TPRV6) and by inducing the calbindins (both calbindin-D_{9k} [9000 M_r] and calbindin-D_{28k} [28,000 M_r] are present in mouse kidney and only calbindin-D_{28k} is present in rat and human kidney) (Boros et al., 2009; Rhoten et al., 1985; Christakos et al., 1989; Christakos, 1995). Calcium is extruded via PMCA1b and the Na^+/Ca^{2+} exchanger (Boros et al., 2009). Mice lacking TRPV5 display diminished calcium reabsorption in the distal tubule, hypercalciuria, and disturbances in bone structure, supporting the suggested role for TRPV5 in renal calcium handling (Hoenderop et al., 2003). Another important effect of $1,25(OH)_2D_3$ in the kidney is inhibition of *CYP27B1* and

stimulation of *CYP24A1* (Ohyama et al., 1996; Shinki et al., 1992; Kerry et al., 1996; Zierold et al., 1995; Meyer et al., 2010a, 2010b). In addition to effects on calcium transport in the distal nephron and modulation of the hydroxylases, effects of $1,25(OH)_2D_3$ on renal phosphate reabsorption have also been suggested. $1,25(OH)_2D_3$ may regulate phosphate homeostasis by increasing FGF23 expression in osteocytes and by inducing klotho expression in the distal tubule (Lanske et al., 2014; Forster et al., 2011).

Parathyroid glands

$1,25(OH)_2D_3$ and its analogs markedly decrease parathyroid hormone expression (Zella et al., 2014). $1,25(OH)_2D_3$ upregulates the calcium receptor, which is a major regulator of PTH (Canaff and Hendy, 2002). Parathyroid-specific VDR-null mice showed only a modest increase in PTH levels (Mier et al., 2009). In contrast, deletion of the calcium receptor in parathyroid resulted in severe hyperparathyroidism and the condition was lethal (Wettschureck et al., 2007). These findings suggest that a principal function of $1,25(OH)_2D_3$ is to sensitize the parathyroid gland to calcium inhibition by upregulating the calcium receptor. Direct action of $1,25(OH)_2D_3$ on the prepro-PTH gene has also been reported (Demay et al., 1992).

Nonclassical actions of $1,25(OH)_2D_3$

In addition to the regulation of calcium homeostasis, many additional biological processes are regulated by $1,25(OH)_2D_3$, including cellular proliferation and differentiation, inhibition of cancer progression, regulation of adaptive and innate immunity, and effects on cardiovascular function (for review see Christakos et al., 2016; Christakos and DeLuca, 2011). Convincing evidence for extraskeletal effects of $1,25(OH)_2D_3$ has been obtained through studies in cells and animal models. Understanding $1,25(OH)_2D_3$ extraskeletal biological responses may suggest similar pathways in humans that could lead to the development of new therapies to prevent and treat disease.

Transcriptional regulation by $1,25(OH)_2D_3$

The vitamin D receptor

The VDR mediates the genomic mechanism of action of $1,25(OH)_2D_3$ and was first discovered in the chicken intestine in 1974 and shortly thereafter in other tissues, including the parathyroid glands, kidney, and bone (Brumbaugh and Haussler, 1974a, 1974b; Brumbaugh et al., 1975). The protein's biochemical features, including its retention in chromatin (Haussler et al., 1968) and its ability to bind to DNA (Pike and Haussler, 1979), suggested that it was similar to other receptors for known steroid hormones and that it probably played a role in transcriptional regulation. However, it was the cloning of the chicken *VDR* gene (McDonnell et al., 1987) and then the human (Baker et al., 1988) and rat (Burmester et al., 1988) versions that ushered in a new era of defining the mechanisms through which vitamin D operated to control gene expression. Aside from the development of unique experimental probes, the cloning of the VDR enabled studies of the domain structure of the receptor that confirmed that it was a bona fide member of the steroid receptor gene family (Evans, 1988; Jin et al., 1996; McDonnell et al., 1989). Equally important, the cloning and structural analysis of the VDR's human chromosomal gene that followed (Hughes et al., 1988; Miyamoto et al., 1997) led ultimately to the identification of a series of mutations within the gene itself that were responsible for the syndrome of HVDRR (Brooks et al., 1978; Hughes et al., 1991; Malloy et al., 1990; Ritchie et al., 1989; Sone et al., 1989). This syndrome had been identified in 1978 (Brooks et al., 1978) and its etiology suggested at the time that it could be due to a defect(s) in the mechanism through which vitamin D exerted its actions (Eil et al., 1981; Lin et al., 1996; Pike et al., 1984; Sone et al., 1990), a hypothesis that was extended during the intervening years (Malloy et al., 2014). The discovery of mutations in the *VDR* gene solidified the essential role of the VDR as the sole mediator of the activities of the vitamin D hormone. This conclusion was eventually confirmed and extended through studies that recapitulated features of the disease phenotype through deletion of the VDR from the mouse genome.

General features of VDR action

Sites of DNA binding

Initial studies suggested that $1,25(OH)_2D_3$ activated gene expression programs in a wide variety of cell types and identified numerous gene candidates for further investigation. Most prominent among these were tissues that expressed the vitamin D-dependent calcium-binding proteins (calbindins) (Christakos et al., 1989; Gill and Christakos, 1993), OC (Lian et al.,

1989; Price and Baukol, 1980), OPN (Prince and Butler, 1987), and CYP24A1 (Haussler et al., 1980), although numerous others emerged during the following several decades as well. The cloning of many of the genes for these proteins and identification of their structural organization also prompted exploration of the mechanisms through which $1,25(OH)_2D_3$ and its receptor promoted their regulation. These studies, first with human *BGLP* (OC) (Kerner et al., 1989; Ozono et al., 1990) and subsequently with *Spp1* (OPN) (Noda et al., 1990), *Cyp24a1* (Ohyama et al., 1994, 1996; Zierold et al., 1994, 1995) and others (Carlberg, 2003), suggested that the VDR bound to a 15-bp vitamin D-responsive DNA element (VDRE) comprising two directly repeated consensus AGGTCA hexanucleotide half-sites separated by 3 bp that was generally located within a kilobase or so of the promoters for these genes (Ozono et al., 1990). These features were similar, but not identical, to those for other nuclear receptors. $1,25(OH)_2D_3$ also strongly suppressed the expression of numerous genes, most notably that of *PTH* and *CYP27B1*, but also in more recent studies that of the interleukin-17 (*IL-17*) gene. Repression of IL-17 transcription by $1,25(OH)_2D_3$ is thought to involve, in part, dissociation of histone acetylase activity, recruitment of deacetylase, and VDR/retinoid X receptor (RXR) binding to NFAT sites (Joshi et al., 2011). While some progress has been made, additional details of the mechanisms of suppression for these and other downregulated genes have yet to be fully understood but are almost certain to be highly diverse. Nevertheless, some progress has been made relative to the suppression of *Cyp27b1* by $1,25(OH)_2D_3$, and will be considered in specific detail later in this chapter. Although the presence of unique "negative VDREs" has been suggested at negatively regulated genes such as the PTH gene, this type of mechanism has yet to be substantiated (Demay et al., 1992).

Heterodimer formation with retinoid X receptors

The discovery of the first VDREs enabled the important subsequent finding that VDR binding to these specific DNA sequences was dependent upon an unknown nuclear factor (Liao et al., 1990; Sone et al., 1991a, 1991b). The identity of this protein was revealed shortly thereafter when it was found that RXRs, also members of the steroid receptor family, were capable of forming heterodimeric complexes with the VDR as well as other members of the steroid receptor class (Mangelsdorf and Evans, 1995). Importantly, $1,25(OH)_2D_3$ was found to promote heterodimer formation between VDR and RXR, although the precise cellular location where this interaction occurs between the two remains unclear (Kliewer et al., 1992). It has been suggested that in addition to its contribution to DNA binding, RXR may participate in the transcriptional activation process (Pathrose et al., 2002; Thompson et al., 2001); structural studies suggest otherwise (Orlov et al., 2012).

The vitamin D receptor functions to recruit coregulatory complexes that mediate gene regulation

Early studies revealed that transcription factor binding near promoters leads to an interaction with basal transcriptional machinery that enhances gene output. It is now known, however, that the activity of most DNA-binding transactivators involves the recruitment of additional coregulatory complexes by this protein class that function to modulate chromatin in a highly specific fashion. Overcoming and/or restoring the inherent repressive state of chromatin requires the presence of this complex regulatory machinery, which is able to shift and/or displace nucleosomes (chromatin remodeling), alter the condensation state and therefore the local architecture of chromatin (histone modifications), create or restrict novel binding sites for additional coregulatory complexes (epigenetic sites), and/or facilitate the entry of RNA polymerase II (RNA pol II) at appropriate times and sites. Three complexes that participate in these activities that are known to be recruited by the VDR include (1) vertebrate ATPase-containing homologs of the yeast SWI/SNF complex that utilize the energy of ATP to remodel and reposition nucleosomes (Carlson and Laurent, 1994); (2) complexes that contain either histone acetyltransferases (HATs) or methyltransferases and deacetyltransferases (HDACs) or histone demethylases, which function to modify the lysine- or arginine-containing tails of histone 3 and/or histone 4 at specific locations (Rachez and Freedman, 2000; Smith and O'Malley, 2004); and (3) the Mediator complex, believed to facilitate the entry of RNA pol II into the general transcriptional apparatus and perhaps to play a role in transcriptional reinitiation (Lewis and Reinberg, 2003) (Fig. 30.2). The activities of each of these complexes may be essential for the downstream activity of almost all DNA-binding proteins. Several classes of regulatory transferase complexes comprise components of dynamic and highly active mechanisms that are epigenetic in nature, and involve the coordinated integration of expression of gene networks (Arrowsmith et al., 2012). These programs are widely responsible for development, differentiation, and mature cell function (Gifford et al., 2013; Xie et al., 2013). HATs and their reciprocal HDACs, for example, regulate the level of epigenetic histone H3 and H4 marks, controlling the degree to which chromatin is condensed and therefore the DNA accessible for transcription factor binding (Ho and Crabtree, 2010). The recruitment of these large chromatin regulatory complexes is frequently coordinated by factors such as the p160 family steroid receptor coactivator 1 (SRC1), SRC2, and

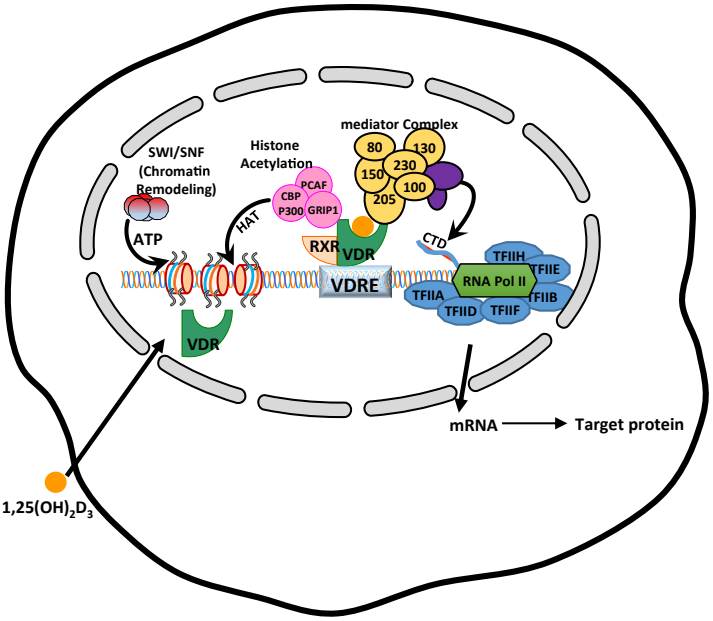

FIGURE 30.2 Mechanism of action of $1,25(OH)_2D_3$ in target cells. $1,25(OH)_2D_3$ regulates gene transcription in target cells by binding to its nuclear receptor, *VDR*. Activated VDR heterodimerizes with retinoid X receptor (*RXR*) and binds to vitamin D-response elements (*VDREs*) in and around target genes. In addition to basal transcription factors, VDR interacts with steroid receptor coactivator 2 (SRC2; also known as *GRIP1*), which has histone acetylase (HAT) activity as a primary coactivator. SRC2 can recruit proteins as secondary coactivators, such as CBP/P300 (which also have HAT activity). VDR also interacts with the Mediator complex, which facilitates the activation of the RNA polymerase II (*RNA Pol II*) holoenzyme through its C-terminal domain (*CTD*), thus promoting the formation of the preinitiation complex. The SWI/SNF complex, which remodels chromatin using the energy of ATP hydrolysis, also contributes to activation by VDR (Dhawan et al., 2017).

SRC3; the HATs CBP and p300; and the corepressor SMRT or NCoR, as well as any one of the many HDACs that interact directly with transcription factors such as the VDR to suppress activity (Smith and O'Malley, 2004). Importantly, activation of the VDR with $1,25(OH)_2D_3$ leads to the creation of a binding site on the VDR protein that mediates the link between the receptor and these coregulatory complexes (McInerney et al., 1998; Perissi et al., 1999; Westin et al., 1998). It is important to note, however, that many of these coregulatory factors are frequently prebound to sites of regulatory action by $1,25(OH)_2D_3$ as a result of their prior recruitment through additional DNA-binding proteins that co-interact at sites of VDR binding. Studies show that the ability of the VDR to recruit several of these coregulatory factors results in striking changes in epigenetic histone marks that facilitate altered gene output (Martowicz et al., 2011; Meyer et al., 2007; Zella et al., 2010). Thus, it is clear that, like other DNA-binding proteins, the function of the VDR is simply to focus and/or modulate the recruitment of transcriptionally active complexes to gene subsets that are then responsible for vitamin D hormone response. Considerable crystallographic information has now accrued to support not only the structural organization of the VDR/RXR heterodimer, but also its association with DNA and its recruitment of coregulators (Orlov et al., 2012). Many of these interactions are prompted by $1,25(OH)_2D_3$, and may well be differentially affected in the present of analogs of the vitamin D hormone. These differential interactions are proposed to account for the concept of analog selectivity in vivo, although this remains unproven and is highly controversial at this writing.

Applying emerging methodologies to study vitamin D receptor action on a genome-wide scale

The study of transcription has been revitalized since 2010, in part as a result of the coupling of chromatin immunoprecipitation (ChIP) to next-generation DNA sequence (ChIP-seq) analysis, providing new methodologies that are now capable of revealing unprecedented mechanistic detail on a genome-wide scale (Ernst and Kellis, 2010; Ernst et al., 2011; Hoffman et al., 2013). Using these methodologies many new principles have emerged, particularly when paired with transcriptomic measurements using RNA-sequencing analysis (Wang et al., 2009). In the following we will highlight the results of some of these collective studies, which have provided important new insights into the transcriptional mechanism of action of $1,25(OH)_2D_3$.

Overarching principles of VDR interaction at target cell genomes in bone cells

A compelling advantage of ChIP-seq analysis is the ability of this approach to identify VDR binding sites and other features of gene regulation in an unbiased manner on a genome-wide scale. Thus, although studies using traditional methods correctly pinpointed the regulatory regions of a few vitamin D target genes located near promoters, including *OC*,

OPN, *Cyp24a1*, and others (Kim et al., 2005), subsequent studies using ChIP-chip and ChIP-seq analyses not only confirmed many of these findings but also provided a broader overarching, genome-wide perspective on binding sites for the VDR in cells in general (see Table 30.1). In osteoblasts, we could detect approximately 1000 residual binding sites for the VDR in the absence of $1,25(OH)_2D_3$ using ChIP-chip analysis, which was increased to approximately 7000−8000 in the presence of $1,25(OH)_2D_3$ (Meyer et al., 2010b). This collection of binding sites has been termed a cellular cistrome and supports the idea that VDR DNA binding is largely hormone dependent (Meyer et al., 2014a). Importantly, similar analyses of binding sites for RXR revealed a more extensive collection of sites that was only modestly increased through $1,25(OH)_2D_3$ activation, emphasizing that RXR is a heterodimer partner not only for the VDR but also for several additional nuclear receptors (Mangelsdorf and Evans, 1995). Interestingly, RXR was frequently prebound at potential VDR binding sites in the absence of $1,25(OH)_2D_3$, suggesting that it might mark potential sites of VDR interaction on DNA. Each of these findings was confirmed in additional studies in mesenchymal stem cells, osteoblasts, osteocytes, and adipocytes, and revealed that while overlap was present, DNA sites for the VDR differed significantly across the genome depending on the cell type and stage examined (Meyer et al., 2014b, 2016; St John et al., 2014). Studies of VDR binding in EB-immortalized human B cells, primary B cells and monocytes (Ramagopalan et al., 2010), and THP-1 monocytes (Heikkinen et al., 2011) confirmed these conclusions. Importantly, although genome-wide ChIP-seq analyses demonstrate binding sites for the VDR near the promoters of genes such as OC, OPN, *Cyp24a1*, and a few others (Meyer et al., 2014b), this technique was unable to confirm a promoter-proximal VDR element for many genes, suggesting that regulatory elements were likely to be located elsewhere. Despite this, however, de novo motif finding analyses of the most common DNA sequence elements found in thousands of identified VDR binding sites confirm that most contain the originally postulated VDRE motif composed of AGGTCA xxg AGGTCA (Meyer et al., 2012, 2014b). Thus, the consensus VDRE initially identified in the human OC gene (Kerner et al., 1989; Ozono et al., 1990) remains the most representative of the DNA sequences with which the VDR interacts in mammalian genomes.

Interestingly, the unbiased and distance-unrestricted nature of ChIP-seq analysis also provided a number of surprising and unexpected insights of major significance (Ong and Corces, 2011). Perhaps most important, although traditional studies of $1,25(OH)_2D_3$ action identified regions immediately upstream of transcriptional start sites as indicated earlier, unbiased ChIP-seq analyses revealed that regulatory regions for the vitamin D hormone and its receptor are more commonly located in clusters within introns or in intergenic regions tens if not hundreds of kilobases upstream or downstream of regulated genes (Meyer et al., 2012, 2014b, 2016). Examples of such distal elements for the VDR abound, but can be found in many of the genes whose putative promoter proximal elements were undetectable by ChIP-seq analysis. They include the mouse *Tnfsf11* (RANKL) gene in bone cells, where at least five intergenic regulatory regions for the VDR are located (Kim et al., 2006); the *Cyp24a1* gene in numerous cell types, including bone cells, where in addition to the well-known promoter proximal element discussed before, a complex downstream cluster of regulatory elements exists in both the mouse and the human genes (Meyer et al., 2010a); the *Vdr* gene in bone cells, where both upstream regulatory regions and several intronic elements are present, a topic to be considered later (Lee et al., 2015a; Zella

TABLE 30.1 Overarching principles of vitamin D action in target cells.

Active transcription unit for induction: the VDR/RXR heterodimer
VDR binding sites (the VDR cistrome): 2000−8000 $1,25(OH)_2D_3$-sensitive binding sites per genome whose number and location are chromatin dependent and a function of cell type
Mode of DNA binding: predominantly, but not exclusively, $1,25(OH)_2D_3$ dependent
VDR/RXR binding site sequence (VDRE): induction mediated by classic hexameric half-sites (AGGTCA) separated by 3 bp; repression mediated by divergent sites
Distal binding site locations: dispersed across the genome in *cis*-regulatory modules (CRMs, or enhancers); located in a cell-type-specific manner near promoters, but preferentially within introns and distal intergenic regions; frequently located in clusters of elements
Epigenetic CRM signatures: defined by dynamically regulated posttranslational histone H3 and H4 modifications
Modular features of CRMs: contain binding sites for multiple transcription factors that facilitate either independent or synergistic interaction and mediate integration
VDR cistromes: dynamic alterations in the cellular epigenome during differentiation, maturation, and disease provoke changes to the VDR cistrome that qualitatively and quantitatively affect the vitamin D-regulated transcriptome

RXR, retinoid X receptor; *VDR*, vitamin D receptor.

et al., 2010); the *TRPV6* gene in intestinal cells, which contains multiple upstream elements (Lee et al., 2015b; Meyer et al., 2006); the *S100g* and PMCA2b (*Atp2b1*) genes in the intestine, which also contain multiple upstream elements (Lee et al., 2015b); and many target genes such as *c-FOS* and *c-MYC* and others in human colorectal cancer cells as well (Meyer et al., 2012). Indeed, enhancers for other transcription factors have been identified more than a megabase from the genes they are known to regulate, although at present the most distal VDR binding site is located 335 kb upstream of the human *c-MYC* promoter. It is important to clarify, however, that the linear/distal nature of regulatory elements for genes is illusionary, as distances do not take into account DNA packaging and looping events imposed on DNA that bring key regulatory segments into the proximity of a gene's promoter region (Deng and Blobel, 2010, 2014; 2017; Deng et al., 2012; Whalen et al., 2016). It is also worth indicating that of the tens of thousands of "putative" VDRE-like sequences that occur across the genome based purely on in silico analyses alone, only a small proportion of these elements mediate vitamin D action due to chromatin restriction (Kellis et al., 2014). An additional observation, as indicated earlier, is the finding through ChIP-seq analysis that most genes are regulated by more than one distal enhancer and, in some cases, by multiple regulatory regions. Recent ENCODE (Encyclopedia of DNA Elements) estimates suggest that genes on a genome-wide scale are regulated by an average of 10 independent enhancers (Kellis et al., 2014).

Modularity comprises an additional important regulatory feature of genes. Thus, individual enhancers often contain organized arrays of linear DNA sequences capable of assembling distinct, nonrandom DNA-binding transcription factor complexes that can function uniquely to regulate the gene with which they are linked. Therefore, it is interesting to note that over 42% of VDR-binding sites in bone cells are located in enhancers that contain prebound CCAAT/enhancer binding protein β (C/EBPβ) and the master regulator RUNX2 (Meyer et al., 2014a, 2014b). Indeed, these factors assemble in a highly organized fashion relative to each other, a nucleoprotein structure we have termed an osteoblast enhancer complex. Not surprisingly, both RUNX2 and C/EBPβ in this configuration can positively and perhaps negatively influence the overall regulatory activity of $1,25(OH)_2D_3$ and its receptor. An alternative and dispersed arrangement has also been identified in bone cells as highlighted in the *Mmp13* gene. Here, binding sites for the VDR, C/EBPβ, and RUNX2 are located across three separate upstream enhancers (Meyer et al., 2015a, 2015b). The activities of these three regions do not function independently, however, but rather influence one another's activity in an overall hierarchical manner to modulate the expression of *Mmp13*. It is known that many other genes contain this or similar arrangements as well. A collective summary of many of the newly acquired features of vitamin D-mediated gene regulation obtained via genome-wide analyses is provided in Table 30.1.

Genome-wide coregulatory recruitment to target genes via the vitamin D receptor

The primary function of the VDR is to recruit chromatin-active coregulatory complexes that facilitate in turn the modulation of gene output. Numerous studies at single-gene levels support the capacity of the VDR to recruit these complexes, and ChIP-seq analyses support the presence of these complexes on a genome-wide scale as well. Thus, for example, the VDR was found to recruit coactivators such as SRC1, CBP, and MED1 as well as the corepressors NCoR and SMRT in colorectal LS180 cells (Meyer and Pike, 2013). This recruitment was correlated with VDR binding sites linked to genes that are modulated directly by $1,25(OH)_2D_3$, although not preferentially to either induced or suppressed genes, as might be expected, suggesting that the roles of coregulators are not limited specifically to activation or repression and that their activities may be gene-context driven. On the other hand, studies in liver stellate cells suggest that $1,25(OH)_2D_3$-mediated repression of a profibrotic gene expression program induced by transforming growth factor β (TGFβ) does not involve the apparent recruitment of corepressors SMRT and NCoR (Ding et al., 2013). In addition to SRC1, CBP, and MED1, Brahma-related gene 1 (BRG1), an ATPase that is a component of the SWI/SNF chromatin remodeling complex, also plays a fundamental role in $1,25(OH)_2D_3$-induced transcription (Seth-Vollenweider et al., 2014). In previous studies cooperative effects between the C/EBP family of transcription factors and the VDR in $1,25(OH)_2D_3$-induced *CYP24A1* transcription were noted (Dhawan et al., 2005). C/EBP and BRG1 were subsequently found to be components of the same complex that are recruited to the C/EBP site of the *CYP24A1* gene by $1,25(OH)_2D_3$, resulting in activation of *CYP24A1* transcription (Seth-Vollenweider et al., 2014). PRMT5, a type II protein arginine methyltransferase that interacts with BRG1, represses $1,25(OH)_2D_3$-induced *CYP24A1* transcription via its methylation of H3R8 and H4R3 Seth-Vollenweider et al. (2014). Thus, the SWI/SNF complex can play a role in the silencing as well as in the activation of VDR mediated transcription.

Identifying underlying early mechanistic outcomes in response to VDR/RXR binding

The ability of the VDR to recruit epigenetically active coregulatory complexes such as HATs, HDACs, and a variety of histone methyltransferases that regulate chromatin structure suggests that $1,25(OH)_2D_3$ may influence the levels of distinct

epigenetic marks imposed by these chromatin modifiers as a means of regulating gene output. Importantly, many such epigenetic marks on histones H3 and H4 are enriched in regions within gene loci that are uniquely active (Ernst and Kellis, 2010; Ernst et al., 2011; Meyer et al., 2015c; Pike et al., 2015). Perhaps of most importance are changes in the levels of acetylation at H4K5 (H4K5ac), H3K9 (H3K9ac), and H3K27 (H3K27ac) that reflect alterations in the transcriptional activity of the genes with which they are linked; these modifications generally occur within enhancers that regulate these genes, although they can also occur at locations within genes as well. Regulatory regions that are marked by both genetic and epigenetic information at gene loci are frequently termed variable chromatin modulators (Deplancke et al., 2016). An increase in several of these acetylation marks occurs at specific sites of VDR binding in genes such as *Opn* and *Cyp24a1*, *Lrp5*, *Tnfsf11*, and *Vdr* following $1,25(OH)_2D_3$ stimulation (Pike et al., 2014, 2015, 2016) and can be used to define sites of action of $1,25(OH)_2D_3$ even in the absence of evidence of VDR occupancy. Overall, histone modification analyses suggest that $1,25(OH)_2D_3$ promotes VDR/RXR binding at sites on cellular genomes that are marked by acetylated H3K9, H3K27, and H4K5, and that these interactions frequently result in an upregulation of acetylation that facilitates enhanced levels of gene expression. These studies provide a global perspective on the actions of vitamin D in several cell types, indicating that the primary role of the VDR is to facilitate the recruitment of chromatin modifiers such as acetyltransferases and deacetyltransferases that function to impose epigenetic histone changes within the enhancers of some but not all vitamin D-sensitive target genes.

The dynamic impact of cellular differentiation and disease on vitamin D receptor cistromes and transcriptional outcomes

Perhaps the most important observation made on a genome-wide scale has been the discovery that cellular differentiation exerts a dramatic quantitative and qualitative impact on sites of genomic VDR binding, an effect that correlates directly with the hormone's ability to regulate the differentiating cell's transcriptome in a highly dynamic manner (Meyer et al., 2014b; St John et al., 2014). This process is probably responsible for the cell-type-specific nature of VDR binding and thus transcriptional outcomes at diverse sets of genes that can be measured in different tissues. A general change in the cellular RNA profile in response to $1,25(OH)_2D_3$ is perhaps not surprising, given the fact that the overall effects of $1,25(OH)_2D_3$ on osteoblast lineage cells are known to differ significantly depending upon the state of bone cell differentiation. This concept of differentiation-induced changes in VDR binding and transcriptional integrity is aptly illustrated through a detailed examination of the differential expression of several genes, including *Mmp13*, in osteoblast precursors and mature mineralizing osteoblasts (Meyer et al., 2015a).

With respect to disease processes, Evans and colleagues have demonstrated that these can affect VDR cistromes as well (Ding et al., 2013). The activation of hepatic stellate cells via the upregulation of TGFβ in the liver induces the expression of a collagen program that causes hepatic fibrosis and can induce cirrhosis of the liver. This disease progression can be ameliorated by simultaneous treatment in vivo with an analog of vitamin D. The authors show that the VDR cistrome, which functions normally to suppress the program of collagen expression, is altered as a result of TGFβ action, redirecting VDR binding to alternative sites of action away from collagen genes, thereby blunting opposing sites of vitamin D action. Interestingly, while these findings identify an important action of the VDR to prevent liver fibrosis, they also highlight the role of the VDR in the disease-potentiating activation of stellate cells, a process that could be considered analogous to that of differentiation. Further studies of this system identify the role of the chromatin regulator BRD4 in this activity, and suggest that direct inhibition of this downstream factor by a small-molecule epigenetic regulator can bypass the positive effects of a vitamin D analog (Ding et al., 2015).

New approaches to the study of vitamin D-mediated gene regulation in vitro and in vivo

Although ChIP-seq analyses are able to identify transcription factor sites of occupancy and the epigenetic landscape that characterizes these regions, the frequently distal nature of these regulatory sites prevents direct identification of the genes with which they are functionally linked (Ong and Corces, 2008; Whalen et al., 2016). It has therefore become a requirement to study genes in the endogenous genomic environment in which they are located, whether in cells in culture or in tissues in vivo. One approach has been to create large minigenes that not only span the transcription unit of interest, but also contain all the putative regulatory regions identified surrounding the gene of interest (Meyer et al., 2010a). A second and perhaps more robust strategy is to create individual enhancer deletions within the context of the genome itself, a homologous recombination approach that is highly amenable to studies in the mouse in vivo (Galli et al., 2008; Onal et al., 2015, 2016a, 2016b). A third approach represents a modification of the second: introducing mutations into genomes using RNA-directed CRISPR/Cas9 nuclease methods, which create precise genomic deletions, insertions, and/or mutations at

specific gene locations both in vitro and in vivo (Meyer et al., 2015a, 2015b). In the last two approaches, the phenotypic consequences of specific enhancer deletion can be assessed directly in cells or tissues at the level of the putative target gene's expression as well as at the levels of the gene product's biological function. This loss-of-function approach enables a determination of the functional relationship between a distal enhancer and its target gene and, as importantly, facilitates assessment of the biological function of the enhancer in question through phenotyping. Studies of this nature have been conducted for a number of genes, including *Tnfsf11* (RANKL), *Mmp13*, *Lrp5*, *Sost*, *Cdon*, *Boc*, *TRPV6*, and *VDR* itself. The location and distribution of enhancers that have been identified as responsible for the regulation of VDR gene expression by $1,25(OH)_2D_3$ and other hormones in bone and other cell types are described in Lee et al. (2015a, 2017). As can be seen, these sites of regulation are located near the promoter, within several introns, and at multiple intergenic locations many kilobases upstream of the VDR gene itself. Most importantly, these sites have been validated functionally not only in cell-based studies, but in target tissues in the mouse as well, thereby illustrating many of the overarching principles documented in Table 30.1.

Defining the regulatory sites of action of $1,25(OH)_2D_3$, PTH, and FGF23 in the *Cyp27b1* and *Cyp24a1* genes in the kidney

As discussed in an earlier section of this review, vitamin D is metabolized sequentially in the liver by *Cyp2R1* to $25(OH)D_3$ and then in the kidney by *Cyp27b1* to $1,25(OH)_2D_3$, the active hormonal form of vitamin D_3. Its circulating levels are similarly regulated through degradation in the kidney by *Cyp24a1*. Ironically, while it has long been known that $1,25(OH)_2D_3$ suppresses the expression of the *Cyp27b1* gene in the kidney and that PTH induces the gene's expression in this tissue as well, neither the sites of action of these hormones at the *Cyp27b1* gene nor their mechanisms have emerged. A similar commentary can be made for the observed suppression of *Cyp27b1* in the kidney by FGF23, the more recently discovered phosphaturic hormone. Interestingly, these same hormones reciprocally regulate *Cyp24a1* as well, although aside from $1,25(OH)_2D_3$, the mechanisms underlying this regulation also remain obscure (Meyer et al., 2010a). However, a series of experiments conducted using ChIP-seq and other genomic analyses of kidney tissue and loss-of-function enhancer deletion studies in the mouse in vivo have revealed these sites of hormonal regulatory action (Meyer et al., 2017). Indeed, ChIP-seq analysis identified sites of VDR binding within the *Cyp27b1* gene locus in response to $1,25(OH)_2D_3$, while cAMP-responsive element−binding protein (CREB) binding sites were identified in response to PTH. That these sites represented bona fide regulatory regions was confirmed through the presence of regulated epigenetic histone signatures as well as the presence of DNase I sites in these regions reflective of true enhancers. Although not surprising, given the earlier narrative with regard to the frequent distal locations of enhancers relative to the genes they regulate, a single colocalized VDR and CREB site was located within an intron of the upstream neighboring gene *Mettl1*, and three sites for both factors were located within a large intron of *Mettl21b* located even farther upstream and adjacent to *Mettl1*, while no evidence was found for regulatory activity immediately proximal to the *Cyp27b1* promoter.

Deletion of the *Mettl1* intronic site in the mouse in vivo (loss-of-function analysis) resulted in a striking decrease in *Cyp27b1* expression in the kidney due to loss of sensitivity to PTH, the consequence of which was hypocalcemia, hypophosphatemia, elevated blood PTH, absent FGF23, highly reduced levels of $1,25(OH)_2D_3$, and severe skeletal and other aberrations. Sensitivity to FGF23 and $1,25(OH)_2D_3$ suppression was unaltered. On the other hand, although deletion of the *Mettl21b* intron in the mouse also led to a significant decrease in basal expression of *Cyp27b1*, PTH response was retained, while FGF23 response was lost. In these animals, $1,25(OH)_2D_3$ levels were generally normal and the systemic and skeletal phenotype was near normal. Coincident with the reduction in *Cyp27b1* levels in both enhancer-deleted mouse strains was a coordinated reduction in renal *Cyp24a1* expression levels due to aberrant PTH and FGF23 levels, which limited the turnover of $1,25(OH)_2D_3$ in the blood, thereby enabling higher sustained levels of blood $1,25(OH)_2D_3$ than would ordinarily have been suspected. Interestingly, the expression of *Cyp27b1* in nonrenal target tissues such as skin, immune cells, and bone, expression that is largely insensitive to PTH, FGF23, or $1,25(OH)_2D_3$ and has been suggested to account for local production of $1,25(OH)_2D_3$ as a function of $25(OH)D_3$, was unaffected by these enhancer deletions and at the same time retained broad sensitivity to the inflammatory modulator lipopolysaccharide. These results suggest that key genomic elements within the *Cyp27b1* locus, but not immediately upstream of the gene, have been identified that mediate basal and PTH, FGF23, and $1,25(OH)_2D_3$ regulation in the kidney in vivo, and that this collective regulatory module is structurally and functionally unique to the kidney (Fig. 30.3). Similar features are resident at the *Cyp24a1* gene, where PTH suppresses and both FGF23 and $1,25(OH)_2D_3$ induce this gene in the kidney. Further studies will be necessary to define the mechanisms through which PTH/CREB, $1,25(OH)_2D_3$/VDR, and FGF23/(transcription factor unknown) actually modulate the reciprocal expression of *Cyp27b1* and *Cyp24a1* in the kidney. Regardless of this, however, these studies of the two key genes involved in the activation and degradation of vitamin D continue to highlight the utility of

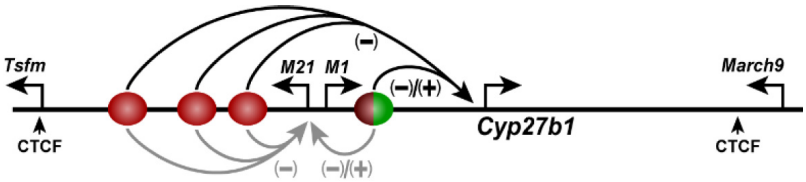

FIGURE 30.3 Schematic diagram of the kidney-specific endocrine regulatory module that controls renal *Cyp27b1* expression. The single enhancer submodule in the *Mettl1* intron and the triple components of the enhancer submodule in the *Mettl21b* intron are shown as *circles*. *Arrows* from each enhancer component are directed to the *Cyp27b1* gene as well as to the *Mettl21b* gene; both are regulated by parathyroid hormone (PTH), fibroblast growth factor 23 (FGF23), and $1,25(OH)_2D_3$. *Green* indicates a positive regulator (PTH) and *red* indicates negative regulators ($1,25(OH)_2D_3$ and FGF23). The active sites of the two hormonal suppressors have not been resolved functionally within the *Mettl21b* intron. *Arrows* above the line indicate transcriptional start sites for the *Tsfm*, *Mettl21b* (*M21*), *Mettl1* (*M1*), *Cyp27b1*, and *March9* genes. March9 is a member of the March family of membrane-bound E3 ubiquitin protein ligases. The *March9* gene is immediately downstream of *Cyp27b1*. Active CCCTC-binding factor (CTCF) sites are indicated below the line.

emerging genomic principles that are consistent with the mechanisms of action of $1,25(OH)_2D_3$ (and other hormones) at many of its target genes.

Future directions

New target genes and new factors involved in vitamin D-mediated transcription will undoubtedly be identified in numerous different systems that are known to be affected by $1,25(OH)_2D_3$. The new methodology that has enabled the study of these transcriptional mechanisms in unprecedented detail in cells and animal models will lead to new insights into mechanisms through which $1,25(OH)_2D_3$ controls calcium homeostasis and also modulates cell-specific biological processes in numerous extraskeletal systems. In addition to studies concerning the mechanisms involved in mediating the genomic actions of $1,25(OH)_2D_3$, further studies related to the physiological significance of target proteins using null-mutant mice and transgenic mice are needed. Although the principal function of vitamin D is intestinal calcium absorption, the mechanisms involved are still incompletely understood. To identify new therapeutic approaches to sustain calcium balance, mechanisms by which $1,25(OH)_2D_3$ acts at both the proximal and the distal segments of the intestine need to be defined. In vivo studies addressing physiological significance combined with studies related to the molecular mechanisms involved in $1,25(OH)_2D_3$ action are needed to provide new insight into the role of $1,25(OH)_2D_3$ in calcium homoeostasis and extraskeletal health, which could lead to the development of vitamin D therapeutics with selective modulation of responses in bone and other target tissues.

References

Adams, J.S., Sharma, O.P., Gacad, M.A., Singer, F.R., 1983. Metabolism of 25-hydroxyvitamin D3 by cultured pulmonary alveolar macrophages in sarcoidosis. J. Clin. Invest. 72 (5), 1856–1860.

Amling, M., Priemel, M., Holzmann, T., Chapin, K., Rueger, J.M., Baron, R., Demay, M.B., 1999. Rescue of the skeletal phenotype of vitamin D receptor-ablated mice in the setting of normal mineral ion homeostasis: formal histomorphometric and biomechanical analyses. Endocrinology 140, 4982–4987.

Armbrecht, H.J., Zenser, T.V., Davis, B.B., 1980. Effect of age on the conversion of 25-hydroxyvitamin D3 to 1,25-dihydroxyvitamin D3 by kidney of rat. J. Clin. Invest. 66, 1118–1123.

Arrowsmith, C.H., Bountra, C., Fish, P.V., Lee, K., Schapira, M., 2012. Epigenetic protein families: a new frontier for drug discovery. Nat. Rev. Drug Discov. 11 (5), 384–400.

Baker, A.R., McDonnell, D.P., Hughes, M., Crisp, T.M., Mangelsdorf, D.J., Haussler, M.R., et al., 1988. Cloning and expression of full-length cDNA encoding human vitamin D receptor. Proc. Natl. Acad. Sci. U.S.A. 85 (10), 3294–3298.

Barbour, G.L., Coburn, J.W., Slatopolsky, E., Norman, A.W., Horst, R.L., 1981. Hypercalcemia in an anephric patient with sarcoidosis: evidence for extrarenal generation of 1,25-dihydroxyvitamin D. N. Engl. J. Med. 305 (8), 440–443.

Benn, B.S., Ajibade, D., Porta, A., Dhawan, P., Hediger, M., Peng, J.B., Jiang, Y., Oh, G.T., Jeung, E.B., Lieben, L., Bouillon, R., Carmeliet, G., Christakos, S., 2008. Active intestinal calcium transport in the absence of transient receptor vanilloid type 6 and calbindin-D9k. Endocrinology 149, 2196–3205.

Bikle, D.D., 2009. Extra renal synthesis of 1, 25-dihydroxyvitamin D and it's health implications. Clin. Rev. Bone Miner. Metab. 7, 114–125.

Bikle, D.D., Adams, J., Christakos, S., 2013. Vitamin D: production, metabolism and clinical requirements. In: Rosen, C. (Ed.), Primer Metab Bone Dis. Wiley, Hoboken, NJ, pp. 235–245.

Bikle, D.D., 2012. Vitamin D and bone. Curr. Osteoporos. Rep. 10 (2), 151–159.

Boros, S., Bindels, R.J., Hoenderop, J.G., 2009. Active Ca(2+) reabsorption in the connecting tubule. Pflugers Arch. 458 (1), 99–109.

Boskey, A.L., Maresca, M., Ullrich, W., Doty, S.B., Butler, W.T., Prince, C.W., 1993. Osteopontin-hydroxyapatite interactions in vitro: inhibition of hydroxyapatite formation and growth in a gelatin-gel. Bone Miner. 22 (2), 147–159.

Boyle, I.T., Gray, R.W., DeLuca, H.F., 1971. Regulation by calcium of in vitro synthesis of 1,25-dihdroxycholecalciferol and 24,25-dihdroxycholecalciferol. Proc. Natl. Acad. Sci. U.S.A. 68, 2131–2135.

Brenza, H.L., DeLuca, H.F., 2000. Regulation of 25-hydroxyvitamin D3 1alpha-hydroxylase gene expression by parathyroid hormone and 1,25-dihydroxyvitamin D3. Arch. Biochem. Biophys. 381, 143–152.

Brooks, M.H., Bell, N.H., Love, L., Stern, P.H., Orfei, E., Queener, S.F., et al., 1978. Vitamin-D-dependent rickets type II. Resistance of target organs to 1,25-dihydroxyvitamin D. N. Engl. J. Med. 298 (18), 996–999.

Brumbaugh, P., Haussler, M., 1974a. 1 Alpha,25-dihydroxycholecalciferol receptors in intestine. I. Association of 1 alpha,25-dihydroxycholecalciferol with intestinal mucosa chromatin. J. Biol. Chem. 249 (4), 1251–1257.

Brumbaugh, P.F., Haussler, M.R., 1974b. 1a,25-dihydroxycholecalciferol receptors in intestine. II. Temperature-dependent transfer of the hormone to chromatin via a specific cytosol receptor. J. Biol. Chem. 249 (4), 1258–1262.

Brumbaugh, P.F., Hughes, M.R., Haussler, M.R., 1975. Cytoplasmic and nuclear binding components for 1a25-dihydroxyvitamin D3 in chick parathyroid glands. Proc. Natl. Acad. Sci. U.S.A. 72 (12), 4871–4875.

Burmester, J.K., Maeda, N., DeLuca, H.F., 1988. Isolation and expression of rat 1,25-dihydroxyvitamin D3 receptor cDNA. Proc. Natl. Acad. Sci. U.S.A. 85 (4), 1005–1009.

Canaff, L., Hendy, G.N., 2002. Human calcium-sensing receptor gene. Vitamin D response elements in promoters P1 and P2 confer transcriptional responsiveness to 1,25-dihydroxyvitamin D. J. Biol. Chem. 277 (33), 30337–30350.

Carlberg, C., 2003. Molecular basis of the selective activity of vitamin D analogues. J. Cell. Biochem. 88 (2), 274–281.

Carlson, M., Laurent, B.C., 1994. The SNF/SWI family of global transcriptional activators. Curr. Opin. Cell Biol. 6 (3), 396–402.

Cheng, J.B., Levine, M.A., Bell, N.H., Mangelsdorf, D.J., Russell, D.W., 2004. Genetic evidence that the human CYP2R1 enzyme is a key vitamin D 25-hydroxylase. Proc. Natl. Acad. Sci. U.S.A. 101 (20), 7711–7715.

Christakos, S., 1995. Vitamin D-dependent calcium-binding proteins: chemistry distribution, functional considerations, and molecular biology: update 1995. Endocr. Rev. Monogr. 4, 108–110.

Christakos, S., 2012. Recent advances in our understanding of 1,25-dihydroxyvitamin D(3) regulation of intestinal calcium absorption. Arch. Biochem. Biophys. 523 (1), 73–76.

Christakos, S., DeLuca, H.F., 2011. Minireview: vitamin D: is there a role in extraskeletal health? Endocrinology 152 (8), 2930–2936.

Christakos, S., Dhawan, P., Verstuyf, A., Verlinden, L., Carmeliet, G., 2016. Vitamin D: metabolism, molecular mechanism of action, and pleiotropic effects. Physiol. Rev. 96 (1), 365–408.

Christakos, S., Gabrielides, C., Rhoten, W.B., 1989. Vitamin D-dependent calcium binding proteins: chemistry, distribution, functional considerations, and molecular biology. Endocr. Rev. 10 (1), 3–26.

Cui, M., Li, Q., Johnson, R., Fleet, J.C., 2012. Villin promoter-mediated transgenic expression of transient receptor potential cation channel, subfamily V, member 6 (TRPV6) increases intestinal calcium absorption in wild-type and vitamin D receptor knockout mice. J. Bone Miner. Res. 27 (10), 2097–2107.

Dardenne, O., Prud'homme, J., Arabian, A., Glorieux, F.H., St-Arnaud, R., 2001. Targeted inactivation of the 25-hydroxyvitamin D(3)-1(alpha)-hydroxylase gene (CYP27B1) creates an animal model of pseudovitamin D-deficiency rickets. Endocrinology 142 (7), 3135–3141.

DeLuca, H.F., 2008. Evolution of our understanding of vitamin D. Nutr. Rev. 66 (10 Suppl. 2), S73–S87.

DeLuca, H.F., 2016. Vitamin D: historical overview. Vitam. Horm. 100, 1–20.

Demay, M.B., Gerardi, J.M., DeLuca, H.F., Kronenberg, H.M., 1990. DNA sequences in the rat osteocalcin gene that bind the 1,25-dihydroxyvitamin D3 receptor and confer responsiveness to 1,25-dihydroxyvitamin D3. Proc. Natl. Acad. Sci. U.S.A. 87, 369–373.

Demay, M.B., Kiernan, M.S., DeLuca, H.F., Kronenberg, H.M., 1992. Sequences in the human parathyroid hormone gene that bind the 1,25-dihydroxyvitamin D3 receptor and mediate transcriptional repression in response to 1,25-dihydroxyvitamin D3. Proc. Natl. Acad. Sci. U.S.A. 89 (17), 8097–8101.

Deng, W., Blobel, G.A., 2010. Do chromatin loops provide epigenetic gene expression states? Curr. Opin. Genet. Dev. 20 (5), 548–554.

Deng, W., Blobel, G.A., 2014. Manipulating nuclear architecture. Curr. Opin. Genet. Dev. 25, 1–7.

Deng, W., Blobel, G.A., 2017. Detecting long-range enhancer-promoter interactions by quantitative chromosome conformation capture. Methods Mol. Biol. 1468, 51–62.

Deng, W., Lee, J., Wang, H., Miller, J., Reik, A., Gregory, P.D., et al., 2012. Controlling long-range genomic interactions at a native locus by targeted tethering of a looping factor. Cell 149 (6), 1233–1244.

Deplancke, B., Alpern, D., Gardeux, V., 2016. The genetics of transcription factor DNA binding variation. Cell 166 (3), 538–554.

Dhawan, P., Peng, X., Sutton, A.L., MacDonald, P.N., Croniger, C.M., Trautwein, C., Centrella, M., McCarthy, T.L., Christakos, S., 2005. Functional cooperation between CCAAT/enhancer-binding proteins and the vitamin D receptor in regulation of 25-hydroxyvitamin D3 24-hydroxylase. Mol. Cell Biol. 25, 472–487.

Dhawan, P., Veldurthy, V., Yehia, G., Hsaio, C., Porta, A., Kim, K.I., Patel, N., Lieben, L., Verlinden, L., Carmeliet, G., Christakos, S., 2017a. Transgenic expression of the vitamin D receptor restricted to the ileum, cecum, and colon of vitamin D receptor knockout mice rescues vitamin D receptor-dependent rickets. Endocrinology 158 (11), 3792–3804.

Dhawan, P., Wei, R., Veldurthy, V., Christakos, S., 2017b. New developments in our understanding of the regulation of calcium homeostasis by vitamin D. In: Collins, J. (Ed.), Molecular, Genetic and Nutritional Aspects of Major and Trace Minerals. Elsevier Inc., pp. 27–34.

Ding, N., Hah, N., Yu, R.T., Sherman, M.H., Benner, C., Leblanc, M., et al., 2015. BRD4 is a novel therapeutic target for liver fibrosis. Proc. Natl. Acad. Sci. U.S.A. 112 (51), 15713–15718.

Ding, N., Yu, R.T., Subramaniam, N., Sherman, M.H., Wilson, C., Rao, R., et al., 2013. A vitamin D receptor/SMAD genomic circuit gates hepatic fibrotic response. Cell 153 (3), 601–613.

Dinour, D., Beckerman, P., Ganon, L., Tordjman, K., Eisenstein, Z., Holtzman, E.J., 2013. Loss-of-function mutations of CYP24A1, the vitamin D 24-hydroxylase gene, cause long-standing hypercalciuric nephrolithiasis and nephrocalcinosis. J. Urol. 190 (2), 552–557.

Eil, C., Liberman, U.A., Rosen, J.F., Marx, S.J., 1981. A cellular defect in hereditary vitamin-D-dependent rickets type II: defective nuclear uptake of 1,25-dihydroxyvitamin D in cultured skin fibroblasts. N. Engl. J. Med. 304 (26), 1588–1591.

Ernst, J., Kellis, M., 2010. Discovery and characterization of chromatin states for systematic annotation of the human genome. Nat. Biotechnol. 28 (8), 817–825.

Ernst, J., Kheradpour, P., Mikkelsen, T.S., Shoresh, N., Ward, L.D., Epstein, C.B., et al., 2011. Mapping and analysis of chromatin state dynamics in nine human cell types. Nature 473 (7345), 43–49.

Evans, R.M., 1988. The steroid and thyroid hormone receptor superfamily. Science 240 (4854), 889–895.

Forster, R.E., Jurutka, P.W., Hsieh, J.C., Haussler, C.A., Lowmiller, C.L., Kaneko, I., et al., 2011. Vitamin D receptor controls expression of the anti-aging klotho gene in mouse and human renal cells. Biochem. Biophys. Res. Commun. 414 (3), 557–562.

Galli, C., Zella, L.A., Fretz, J.A., Fu, Q., Pike, J.W., Weinstein, R.S., et al., 2008. Targeted deletion of a distant transcriptional enhancer of the receptor activator of nuclear factor-kappaB ligand gene reduces bone remodeling and increases bone mass. Endocrinology 149 (1), 146–153.

Gifford, C.A., Ziller, M.J., Gu, H., Trapnell, C., Donaghey, J., Tsankov, A., et al., 2013. Transcriptional and epigenetic dynamics during specification of human embryonic stem cells. Cell 153 (5), 1149–1163.

Gill, R.K., Christakos, S., 1993. Identification of sequence elements in mouse calbindin-D28k gene that confer 1,25-dihydroxyvitamin D3- and butyrate-inducible responses. Proc. Natl. Acad. Sci. U.S.A. 90 (7), 2984–2988.

Haussler, M.R., Chandler, J.S., Pike, J.W., Brumbaugh, P.F., Speer, D.P., Pitt, M.J., 1980. Physiological importance of vitamin D metabolism. Prog. Biochem. Pharmacol. 17, 134–142.

Haussler, M.R., Myrtle, J.F., Norman, A.W., 1968. The association of a metabolite of vitamin D3 with intestinal mucosa chromatin in vivo. J. Biol. Chem. 243 (15), 4055–4064.

Heikkinen, S., Väisänen, S., Pehkonen, P., Seuter, S., Benes, V., Carlberg, C., 2011. Nuclear hormone 1α,25-dihydroxyvitamin D3 elicits a genome-wide shift in the locations of VDR chromatin occupancy. Nucleic Acids Res. 39 (21), 9181–9193.

Henry, H., 1985. Parathyroid modulation of 25-hydroxyvitamin D3 metabolism by cultured chick kidney cells is mimicked and enhanced by forskolin. Endocrinology 116, 503–510.

Ho, L., Crabtree, G.R., 2010. Chromatin remodelling during development. Nature 463 (7280), 474–484.

Hobaus, J., Thiem, U., Hummel, D.M., Kallay, E., 2013. Role of calcium, vitamin D, and the extrarenal vitamin D hydroxylases in carcinogenesis. Anti Cancer Agents Med. Chem. 13 (1), 20–35.

Hochberg, Z., Tiosano, D., Even, L., 1992. Calcium therapy for calcitriol-resistant rickets. J. Pediatr. 121 (5 Pt 1), 803–808.

Hoenderop, J.G., van Leeuwen, J.P., van der Eerden, B.C., Kersten, F.F., van der Kemp, A.W., Merillat, A.M., Waarsing, J.H., Rossier, B.C., Vallon, V., Hummler, E., Bindels, R.J., 2003. Renal Ca21 wasting, hyperabsorption, and reduced bone thickness in mice lacking TRPV5. J. Clin. Invest. 112, 1906–1914.

Hoffman, M.M., Ernst, J., Wilder, S.P., Kundaje, A., Harris, R.S., Libbrecht, M., et al., 2013. Integrative annotation of chromatin elements from ENCODE data. Nucleic Acids Res. 41 (2), 827–841.

Hu, M.C., Shiizaki, K., Kuro-o, M., Moe, O.W., 2013. Fibroblast growth factor 23 and Klotho: physiology and pathophysiology of an endocrine network of mineral metabolism. Annu. Rev. Physiol. 75, 503–533.

Hughes, M.R., Malloy, P.J., Kieback, D.G., Kesterson, R.A., Pike, J.W., Feldman, D., O'Malley, B.W., 1988. Point mutations in the human vitamin D receptor gene associated with hypocalcemic rickets. Science 242 (4886), 1702–1705.

Hughes, M., Malloy, P., O'Malley, B., Pike, J., Feldman, D., 1991. Genetic defects of the 1,25-dihydroxyvitamin D3 receptor. J. Recept. Res. 11 (1–4), 699–716.

Jin, C.H., Kerner, S.A., Hong, M.H., Pike, J.W., 1996. Transcriptional activation and dimerization functions in the human vitamin D receptor. Mol. Endocrinol. 10 (8), 945–957.

Jones, G., Prosser, D.E., Kaufmann, M., 2014. Cytochrome P450-mediated metabolism of vitamin D. J. Lipid Res. 55 (1), 13–31.

Joshi, S., Pantalena, L.C., Liu, X.K., Gaffen, S.L., Liu, H., Rohowsky-Kochan, C., Ichiyama, K., Yoshimura, A., Steinman, L., Christakos, S., Youssef, S., 2011. 1,25-Dihydroxyvitamin D(3) ameliorates Th17 autoimmunity via transcriptional modulation of interleukin-17A. Mol. Cell Biol. 31 (17), 3653–3669.

Kellis, M., Wold, B., Snyder, M.P., Bernstein, B.E., Kundaje, A., Marinov, G.K., Ward, L.D., Birney, E., Crawford, G.E., Dekker, J., Dunham, I., Elnitski, L.L., Farnham, P.J., Feingold, E.A., Gerstein, M., Giddings, M.C., Gilbert, D.M., Gineras, T.R., Green, E.D., Guigo, R., Hubbard, T., Kent, J., Lieb, J.D., Myers, R.M., Pazin, M.J., Ren, B., Stamatoyannopoulos, J.A., Weng, Z., White, K.P., Hardison, R.C., 2014. Defining functional DNA elements in the human genome. Proc. Natl. Acad. Sci. U.S.A. 111 (17), 6131–6138.

Kerner, S.A., Scott, R.A., Pike, J.W., 1989. Sequence elements in the human osteocalcin gene confer basal activation and inducible response to hormonal vitamin D3. Proc. Natl. Acad. Sci. U.S.A. 86 (12), 4455–4459.

Kerry, D.M., Dwivedi, P.P., Hahn, C.N., Morris, H.A., Omdahl, J.L., May, B.K., 1996. Transcriptional synergism between vitamin D-responsive elements in the rat 25-hydroxyvitamin D3 24-hydroxylase (CYP24) promoter. J. Biol. Chem. 271, 29715−29721.

Kim, S., Shevde, N., Pike, J., 2005. 1,25-Dihydroxyvitamin D3 stimulates cyclic vitamin D receptor/retinoid X receptor DNA-binding, co-activator recruitment, and histone acetylation in intact osteoblasts. J. Bone Miner. Res. 20 (2), 305−317.

Kim, S., Yamazaki, M., Shevde, N.K., Pike, J.W., 2007. Transcriptional control of receptor activator of nuclear factor-kappaB ligand by the protein kinase A activator forskolin and the transmembrane glycoprotein 130-activating cytokine, oncostatin M, is exerted through multiple distal enhancers. Mol. Endocrinol. 21, 197−214.

Kim, S., Yamazaki, M., Zella, L., Shevde, N., Pike, J., 2006. Activation of receptor activator of NF-kappaB ligand gene expression by 1,25-dihydroxyvitamin D3 is mediated through multiple long-range enhancers. Mol. Cell Biol. 26 (17), 6469−6486.

Kitanaka, S., Takeyama, K., Murayama, A., Sato, T., Okumura, K., Nogami, M., et al., 1998. Inactivating mutations in the 25-hydroxyvitamin D3 1alpha-hydroxylase gene in patients with pseudovitamin D-deficiency rickets. N. Engl. J. Med. 338 (10), 653−661.

Kliewer, S.A., Umesono, K., Mangelsdorf, D.J., Evans, R.M., 1992. Retinoid X receptor interacts with nuclear receptors in retinoic acid, thyroid hormone and vitamin D3 signalling. Nature 355 (6359), 446−449.

Kutuzova, G.D., Akhter, S., Christakos, S., Vanhooke, J., Kimmel-Jehan, C., Deluca, H.F., 2006. Calbindin D(9k) knockout mice are indistinguishable from wild-type mice in phenotype and serum calcium level. Proc. Natl. Acad. Sci. U.S.A. 103 (33), 12377−12381.

Kutuzova, G.D., Sundersingh, F., Vaughan, J., Tadi, B.P., Ansay, S.E., Christakos, S., Deluca, H.F., 2008. TRPV6 is not required for 1alpha,25-dihydroxyvitamin D3-induced intestinal calcium absorption in vivo. Proc. Natl. Acad. Sci. U.S.A. 105 (50), 19655−19659.

Lanske, B., Densmore, M.J., Erben, R.G., 2014. Vitamin D endocrine system and osteocytes. Bonekey Rep. 3, 494.

Lee, S.M., Meyer, M.B., Benkusky, N.A., O'Brien, C.A., Pike, J.W., 2015a. Mechanisms of enhancer-mediated hormonal control of vitamin D receptor gene expression in target cells. J. Biol. Chem. 290 (51), 30573−30586.

Lee, S.M., Meyer, M.B., Benkusky, N.A., O'Brien, C.A., Pike, J.W., 2017. The impact of VDR expression and regulation in vivo. J. Steroid Biochem. Mol. Biol. 177, 36−45.

Lee, S.M., Riley, E.M., Meyer, M.B., Benkusky, N.A., Plum, L.A., DeLuca, H.F., Pike, J.W., 2015b. 1,25-Dihydroxyvitamin D3 controls a cohort of vitamin D receptor target genes in the proximal intestine that is enriched for calcium-regulating components. J. Biol. Chem. 290 (29), 18199−18215.

Lewis, B.A., Reinberg, D., 2003. The mediator coactivator complex: functional and physical roles in transcriptional regulation. J. Cell Sci. 116 (Pt 18), 3667−3675.

Li, Y.C., Pirro, A.E., Amling, M., Delling, G., Baron, R., Bronson, R., Demay, M.B., 1997. Targeted ablation of the vitamin D receptor: an animal model of vitamin D-dependent rickets type II with alopecia. Proc. Natl. Acad. Sci. U.S.A. 94, 9831−9835.

Lian, J.B., Stein, G.S., Stewart, C., Puchacz, E., Mackowiak, S., Aronow, M., et al., 1989. Osteocalcin: characterization and regulated expression of the rat gene. Connect. Tissue Res. 21 (1−4), 61−68 discussion 69.

Liao, J., Ozono, K., Sone, T., McDonnell, D., Pike, J., 1990. Vitamin D receptor interaction with specific DNA requires a nuclear protein and 1,25-dihydroxyvitamin D3. Proc. Natl. Acad. Sci. U.S.A. 87 (24), 9751−9755.

Lieben, L., Masuyama, R., Torrekens, S., Van Looveren, R., Schrooten, J., Baatsen, P., et al., 2012. Normocalcemia is maintained in mice under conditions of calcium malabsorption by vitamin D-induced inhibition of bone mineralization. J. Clin. Invest. 122 (5), 1803−1815.

Lin, N., Malloy, P., Sakati, N., al-Ashwal, A., Feldman, D., 1996. A novel mutation in the deoxyribonucleic acid-binding domain of the vitamin D receptor causes hereditary 1,25-dihydroxyvitamin D-resistant rickets. J. Clin. Endocrinol. Metab. 81 (7), 2564−2569.

Malloy, P.J., Tasic, V., Taha, D., Tóthóncóler, F., Ying, G.S., Yin, L.K., et al., 2014. Vitamin D receptor mutations in patients with hereditary 1,25-dihydroxyvitamin D-resistant rickets. Mol. Genet. Metab. 111 (1), 33−40.

Malloy, P., Hochberg, Z., Tiosano, D., Pike, J., Hughes, M., Feldman, D., 1990. The molecular basis of hereditary 1,25-dihydroxyvitamin D3 resistant rickets in seven related families. J. Clin. Invest. 86 (6), 2071−2079.

Mangelsdorf, D.J., Evans, R.M., 1995. The RXR heterodimers and orphan receptors. Cell 83 (6), 841−850.

Martowicz, M.L., Meyer, M.B., Pike, J.W., 2011. The mouse RANKL gene locus is defined by a broad pattern of histone H4 acetylation and regulated through distinct distal enhancers. J. Cell. Biochem. 112 (8), 2030−2045.

Matkovits, T., Christakos, S., 1995. Variable in vivo regulation of rat vitamin D dependent genes (osteopontin, Ca,Mg-Adenosine Triphosphatase, and 25-hydroxyvitamin D3 24-hydroxylase): implications for differing mechanisms of regulation and involvement of multiple factors. Endocrinology 136, 3971−3982.

McDonnell, D.P., Mangelsdorf, D.J., Pike, J.W., Haussler, M.R., O'Malley, B.W., 1987. Molecular cloning of complementary DNA encoding the avian receptor for vitamin D. Science 235 (4793), 1214−1217.

McDonnell, D., Scott, R., Kerner, S., O'Malley, B., Pike, J., 1989. Functional domains of the human vitamin D3 receptor regulate osteocalcin gene expression. Mol. Endocrinol. 3 (4), 635−644.

McInerney, E.M., Rose, D.W., Flynn, S.E., Westin, S., Mullen, T.M., Krones, A., et al., 1998. Determinants of coactivator LXXLL motif specificity in nuclear receptor transcriptional activation. Genes Dev. 12 (21), 3357−3368.

Meir, T., Levi, R., Lieben, L., Libutti, S., Carmeliet, G., Bouillon, R., et al., 2009. Deletion of the vitamin D receptor specifically in the parathyroid demonstrates a limited role for the receptor in parathyroid physiology. Am. J. Physiol. Renal. Physiol. 297 (5), F1192−F1198.

Meyer, M.B., Pike, J.W., 2013. Corepressors (NCoR and SMRT) as well as coactivators are recruited to positively regulated 1α,25-dihydroxyvitamin D3-responsive genes. J. Steroid Biochem. Mol. Biol. 136, 120−124.

Meyer, M.B., Benkusky, N.A., Pike, J.W., 2014a. The RUNX2 cistrome in osteoblasts: characterization, down-regulation following differentiation, and relationship to gene expression. J. Biol. Chem. 289 (23), 16016−16031.

Meyer, M.B., Benkusky, N.A., Pike, J.W., 2015c. Profiling histone modifications by chromatin immunoprecipitation coupled to deep sequencing in skeletal cells. Methods Mol. Biol. 1226, 61–70.

Meyer, M.B., Benkusky, N.A., Pike, J.W., 2015a. Selective distal enhancer control of the Mmp13 gene identified through clustered regularly interspaced short palindromic repeat (CRISPR) genomic deletions. J. Biol. Chem. 290 (17), 11093–11107.

Meyer, M.B., Benkusky, N.A., Kaufmann, M., Lee, S.M., Onal, M., Jones, G., Pike, J.W., 2017. A kidney-specific genetic control module in mice governs endocrine regulation of the cytochrome P450 gene Cyp27b1 essential for vitamin D3 activation. J. Biol. Chem. 292 (42), 17541–17558.

Meyer, M.B., Benkusky, N.A., Lee, C.H., Pike, J.W., 2014b. Genomic determinants of gene regulation by 1,25-dihydroxyvitamin D3 during osteoblast-lineage cell differentiation. J. Biol. Chem. 289 (28), 19539–19554.

Meyer, M.B., Benkusky, N.A., Onal, M., Pike, J.W., 2015b. Selective regulation of Mmp13 by 1,25(OH)2D3, PTH, and Osterix through distal enhancers. J. Steroid Biochem. Mol. Biol. 164, 258–264.

Meyer, M.B., Benkusky, N.A., Sen, B., Rubin, J., Pike, J.W., 2016. Epigenetic plasticity drives adipogenic and osteogenic differentiation of marrow-derived mesenchymal stem cells. J. Biol. Chem. 291 (34), 17829–17847.

Meyer, M.B., Goetsch, P.D., Pike, J.W., 2010a. A downstream intergenic cluster of regulatory enhancers contributes to the induction of CYP24A1 expression by 1alpha,25-dihydroxyvitamin D3. J. Biol. Chem. 285 (20), 15599–15610.

Meyer, M.B., Goetsch, P.D., Pike, J.W., 2010b. Genome-wide analysis of the VDR/RXR cistrome in osteoblast cells provides new mechanistic insight into the actions of the vitamin D hormone. J. Steroid Biochem. Mol. Biol. 121 (1–2), 136–141.

Meyer, M.B., Goetsch, P.D., Pike, J.W., 2012. VDR/RXR and TCF4/β-catenin cistromes in colonic cells of colorectal tumor origin: impact on c-FOS and c-MYC gene expression. Mol. Endocrinol. 26 (1), 37–51.

Meyer, M.B., Watanuki, M., Kim, S., Shevde, N.K., Pike, J.W., 2006. The human transient receptor potential vanilloid type 6 distal promoter contains multiple vitamin D receptor binding sites that mediate activation by 1,25-dihydroxyvitamin D3 in intestinal cells. Mol. Endocrinol. 20 (6), 1447–1461.

Meyer, M.B., Zella, L.A., Nerenz, R.D., Pike, J.W., 2007. Characterizing early events associated with the activation of target genes by 1,25-dihydroxyvitamin D3 in mouse kidney and intestine in vivo. J. Biol. Chem. 282 (31), 22344–22352.

Miyamoto, K., Kesterson, R., Yamamoto, H., Taketani, Y., Nishiwaki, E., Tatsumi, S., et al., 1997. Structural organization of the human vitamin D receptor chromosomal gene and its promoter. Mol. Endocrinol. 11 (8), 1165–1179.

Morris, S.M., Tallquist, M.D., Rock, C.O., Cooper, J.A., 2002. Dual roles for the Dab2 adaptor protein in embryonic development and kidney transport. EMBO J. 21 (7), 1555–1564.

Nerenz, R.D., Martowicz, M.L., Pike, J.W., 2008. An enhancer 20 kilobases upstream of the human receptor activator of nuclear factor-kappaB ligand gene mediates dominant activation by 1,25-dihydroxyvitamin D3. Mol. Endocrinol. 22 (5), 1044–1056.

Noda, M., Vogel, R.L., Craig, A.M., Prahl, J., DeLuca, H.F., Denhardt, D.T., 1990. Identification of a DNA sequence responsible for binding of the 1,25-dihydroxyvitamin D3 receptor and 1,25-dihydroxyvitamin D3 enhancement of mouse secreted phosphoprotein 1 (SPP-1 or osteopontin) gene expression. Proc. Natl. Acad. Sci. U.S.A. 87 (24), 9995–9999.

Nykjaer, A., Dragun, D., Walther, D., Vorum, H., Jacobsen, C., Herz, J., Melsen, F., Christensen, E.I., Willnow, T.E., 1999. An endocytic pathway essential for renal uptake and activation of the steroid 25-(OH) vitamin D3. Cell 96, 507–515.

Nykjaer, A., Fyfe, J.C., Kozyraki, R., Leheste, J.R., Jacobsen, C., Nielsen, M.S., et al., 2001. Cubilin dysfunction causes abnormal metabolism of the steroid hormone 25(OH) vitamin D(3). Proc. Natl. Acad. Sci. U.S.A. 98 (24), 13895–13900.

Ohyama, Y., Ozono, K., Uchida, M., Shinki, T., Kato, S., Suda, T., et al., 1994. Identification of a vitamin D-responsive element in the 5′-flanking region of the rat 25-hydroxyvitamin D3 24-hydroxylase gene. J. Biol. Chem. 269 (14), 10545–10550.

Ohyama, Y., Ozono, K., Uchida, M., Yoshimura, M., Shinki, T., Suda, T., Yamamoto, O., 1996. Functional assessment of two vitamin D-responsive elements in the rat 25-hydroxyvitamin D3 24-hydroxylase gene. J. Biol. Chem. 271 (48), 30381–30385.

Omdahl, J.L., Bobrovnikova, E.V., Annalora, A., Chen, P., Serda, R., 2003. Expression, structure-function, and molecular modeling of vitamin D P450s. J. Cell. Biochem. 88, 356–362.

Onal, M., Bishop, K.A., St John, H.C., Danielson, A.L., Riley, E.M., Piemontese, M., et al., 2015. A DNA segment spanning the mouse Tnfsf11 transcription unit and its upstream regulatory domain rescues the pleiotropic biologic phenotype of the RANKL null mouse. J. Bone Miner. Res. 30 (5), 855–868.

Onal, M., St John, H.C., Danielson, A.L., Pike, J.W., 2016a. Deletion of the distal Tnfsf11 RL-D2 enhancer that contributes to PTH-mediated RANKL expression in osteoblast lineage cells results in a high bone mass phenotype in mice. J. Bone Miner. Res. 31 (2), 416–429.

Onal, M., St John, H.C., Danielson, A.L., Markert, J.W., Riley, E.M., Pike, J.W., 2016b. Unique distal enhancers linked to the mouse Tnfsf11 gene direct tissue-specific and inflammation-induced expression of RANKL. Endocrinology 157 (2), 482–496.

Ong, C.T., Corces, V.G., 2008. Modulation of CTCF insulator function by transcription of a noncoding RNA. Dev. Cell 15 (4), 489–490.

Ong, C.T., Corces, V.G., 2011. Enhancer function: new insights into the regulation of tissue-specific gene expression. Nat. Rev. Genet. 12 (4), 283–293.

Ooi, J.H., McDaniel, K.L., Weaver, V., Cantorna, M.T., 2014. Murine $CD8^+$ T cells but not macrophages express the vitamin D 1alpha-hydroxylase. J. Nutr. Biochem. 25 (1), 58–65.

Orlov, I., Rochel, N., Moras, D., Klaholz, B.P., 2012. Structure of the full human RXR/VDR nuclear receptor heterodimer complex with its DR3 target DNA. EMBO J. 31 (2), 291–300.

Ozono, K., Liao, J., Kerner, S.A., Scott, R.A., Pike, J.W., 1990. The vitamin D-responsive element in the human osteocalcin gene. Association with a nuclear proto-oncogene enhancer. J. Biol. Chem. 265 (35), 21881–21888.

Panda, D.K., Miao, D., Tremblay, M.L., Sirois, J., Farookhi, R., Hendy, G.N., Goltzman, D., 2001. Targeted ablation of the 25-hydroxyvitamin D 1alpha-hydroxylase enzyme: evidence for skeletal, reproductive, and immune dysfunction. Proc. Natl. Acad. Sci. U.S.A. 98, 7498–7503.

Pathrose, P., Barmina, O., Chang, C.Y., McDonnell, D.P., Shevde, N.K., Pike, J.W., 2002. Inhibition of 1,25-dihydroxyvitamin D3-dependent transcription by synthetic LXXLL peptide antagonists that target the activation domains of the vitamin D and retinoid X receptors. J. Bone Miner. Res. 17 (12), 2196–2205.

Perissi, V., Staszewski, L.M., McInerney, E.M., Kurokawa, R., Krones, A., Rose, D.W., et al., 1999. Molecular determinants of nuclear receptor-corepressor interaction. Genes Dev. 13 (24), 3198–3208.

Perwad, F., Azam, N., Zhang, M.Y., Yamashita, T., Tenenhouse, H.S., Portale, A.A., 2005. Dietary and serum phosphorus regulate fibroblast growth factor 23 expression and 1,25-dihydroxyvitamin D metabolism in mice. Endocrinology 146, 5358–5364.

Pike, J.W., Haussler, M.R., 1979. Purification of chicken intestinal receptor for 1,25-dihydroxyvitamin D. Proc. Natl. Acad. Sci. U.S.A. 76 (11), 5485–5489.

Pike, J.W., Lee, S.M., Meyer, M.B., 2014. Regulation of gene expression by 1,25-dihydroxyvitamin D3 in bone cells: exploiting new approaches and defining new mechanisms. Bonekey Rep. 3, 482.

Pike, J.W., Meyer, M.B., Benkusky, N.A., Lee, S.M., St John, H., Carlson, A., et al., 2016. Genomic determinants of vitamin D-regulated gene expression. Vitam. Horm. 100, 21–44.

Pike, J.W., Meyer, M.B., St John, H.C., Benkusky, N.A., 2015. Epigenetic histone modifications and master regulators as determinants of context dependent nuclear receptor activity in bone cells. Bone 81, 757–764.

Pike, J., Dokoh, S., Haussler, M., Liberman, U., Marx, S., Eil, C., 1984. Vitamin D3-resistant fibroblasts have immunoassayable 1,25-dihydroxyvitamin D3 receptors. Science 224 (4651), 879–881.

Price, P.A., Baukol, S.A., 1980. 1,25-Dihydroxyvitamin D3 increases synthesis of the vitamin K-dependent bone protein by osteosarcoma cells. J. Biol. Chem. 255 (24), 11660–11663.

Prince, C.W., Butler, W.T., 1987. 1,25-Dihydroxyvitamin D3 regulates the biosynthesis of osteopontin, a bone-derived cell attachment protein, in clonal osteoblast-like osteosarcoma cells. Coll. Relat. Res. 7 (4), 305–313.

Rachez, C., Freedman, L.P., 2000. Mechanisms of gene regulation by vitamin D(3) receptor: a network of coactivator interactions. Gene 246 (1–2), 9–21.

Raisz, L.G., Trammel, C.L., Holick, M.F., DeLuca, H.F., 1972. 1,25-Dihydroxyvitamin D3: a potent stimulator of bone resorption in tissue culture. Science 175, 768–769.

Ramagopalan, S.V., Heger, A., Berlanga, A.J., Maugeri, N.J., Lincoln, M.R., Burrell, A., et al., 2010. A ChIP-seq defined genome-wide map of vitamin D receptor binding: associations with disease and evolution. Genome Res. 20 (10), 1352–1360.

Rhoten, W.B., Bruns, M.E., Christakos, S., 1985. Presence and localization of two vitamin D-dependent calcium-binding proteins in kidneys of higher vertebrates. Endocrinology 117, 674–683.

Ritchie, H., Hughes, M., Thompson, E., Malloy, P., Hochberg, Z., Feldman, D., et al., 1989. An ochre mutation in the vitamin D receptor gene causes hereditary 1,25-dihydroxyvitamin D3-resistant rickets in three families. Proc. Natl. Acad. Sci. U.S.A. 86 (24), 9783–9787.

Schlingmann, K.P., Kaufmann, M., Weber, S., Irwin, A., Goos, C., John, U., et al., 2011. Mutations in CYP24A1 and idiopathic infantile hypercalcemia. N. Engl. J. Med. 365 (5), 410–421.

Seth-Vollenweider, T., Joshi, S., Dhawan, P., Sif, S., Christakos, S., 2014. Novel mechanism of negative regulation of 1,25-dihydroxyvitamin D3-induced 25-hydroxyvitamin D3 24-hydroxylase (Cyp24a1) Transcription: epigenetic modification involving cross-talk between protein-arginine methyltransferase 5 and the SWI/SNF complex. J. Biol. Chem. 289 (49), 33958–33970.

Shen, Q., Christakos, S., 2005. The vitamin D receptor, Runx2, and the Notch signaling pathway cooperate in the transcriptional regulation of osteopontin. J. Biol. Chem. 280, 40589–40598.

Shimada, T., Kakitani, M., Yamazaki, Y., Hasegawa, H., Takeuchi, Y., Fujita, T., Fukumoto, S., Tomizuka, K., Yamashita, T., 2004. Targeted ablation of Fgf23 demonstrates an essential physiological role of FGF23 in phosphate and vitamin D metabolism. J. Clin. Invest. 113, 561–568.

Shinki, T., Jin, C.H., Nishimura, A., Nagai, Y., Ohyama, Y., Noshiro, M., Okuda, K., Suda, T., 1992. Parathyroid hormone inhibits 25-hydroxyvitamin D3-24-hydroxylase mRNA expression stimulated by 125-dihydroxyvitamin D3 in rat kidney but not in intestine. J. Biol. Chem. 267, 13757–13762.

Smith, C.L., O'Malley, B.W., 2004. Coregulator function: a key to understanding tissue specificity of selective receptor modulators. Endocr. Rev. 25 (1), 45–71.

Sneddon, W.B., Barry, E.L., Coutermarsh, B.A., Gesek, F.A., Liu, F., Friedman, P.A., 1998. Regulation of renal parathyroid hormone receptor expression by 1,25-dihydroxyvitamin D3 and retinoic acid. Cell. Physiol. Biochem. 8, 261–277.

Sone, T., Kerner, S., Pike, J.W., 1991a. Vitamin D receptor interaction with specific DNA. Association as a 1,25-dihydroxyvitamin D3-modulated heterodimer. J. Biol. Chem. 266 (34), 23296–23305.

Sone, T., Marx, S., Liberman, U., Pike, J., 1990. A unique point mutation in the human vitamin D receptor chromosomal gene confers hereditary resistance to 1,25-dihydroxyvitamin D3. Mol. Endocrinol. 4 (4), 623–631.

Sone, T., Ozono, K., Pike, J.W., 1991b. A 55-kilodalton accessory factor facilitates vitamin D receptor DNA binding. Mol. Endocrinol. 5 (11), 1578–1586.

Sone, T., Scott, R., Hughes, M., Malloy, P., Feldman, D., O'Malley, B., Pike, J., 1989. Mutant vitamin D receptors which confer hereditary resistance to 1,25-dihydroxyvitamin D3 in humans are transcriptionally inactive in vitro. J. Biol. Chem. 264 (34), 20230–20234.

St John, H.C., Bishop, K.A., Meyer, M.B., Benkusky, N.A., Leng, N., Kendziorski, C., et al., 2014. The osteoblast to osteocyte transition: epigenetic changes and response to the vitamin D3 hormone. Mol. Endocrinol. 28 (7), 1150–1165.

St-Arnaud, R., Arabian, A., Travers, R., Barletta, F., Raval-Pandya, M., Chapin, K., Depovere, J., Mathieu, C., Christakos, S., Demay, M.B., Glorieux, F.H., 2000. Deficient mineralization of intramembranous bone in vitamin D-24-hydroxylase-ablated mice is due to elevated 1,25-dihydroxyvitamin D and not to the absence of 24, 25-dihydroxyvitamin D. Endocrinology 141, 2658–2666.

Takeda, S., Yoshizawa, T., Nagai, Y., Yumato, H., Fukumoto, S., Sekine, K., Kato, S., Matsumoto, T., Fujita, T., 1999. Stimulation of osteoclast formation by 1,25−dihydroxyvitamin D requires its binding to vitamin D receptor (VDR) in osteoblastic cells: studies using VDR knockout mice. Endocrinology 140, 1005−1008.

Thompson, P.D., Remus, L.S., Hsieh, J.C., Jurutka, P.W., Whitfield, G.K., Galligan, M.A., et al., 2001. Distinct retinoid X receptor activation function-2 residues mediate transactivation in homodimeric and vitamin D receptor heterodimeric contexts. J. Mol. Endocrinol. 27 (2), 211−227.

Underwood, J.L., DeLuca, H.F., 1984. Vitamin D is not directly necessary for bone growth and mineralization. Am. J. Physiol. 246, E493−eE498.

Veldurthy, V., Wei, R., Campbell, M., Lupicki, K., Dhawan, P., Christakos, S., 2016. 25-Hydroxyvitamin D(3) 24-hydroxylase: a key regulator of 1,25(OH)(2)D(3) catabolism and calcium homeostasis. Vitam. Horm. 100, 137−150.

Wada, L., Daly, R., Kern, D., Halloran, B., 1992. Kinetics of 1,25-dihydroxyvitamin D metabolism in the aging rat. Am. J. Physiol. 262, E906−eE910.

Wang, Y., Zhu, J., DeLuca, H.F., 2014. Identification of the vitamin D receptor in osteoblasts and chondrocytes but not osteoclasts in mouse bone. J. Bone Miner. Res. 29 (3), 685−692.

Wang, Z., Gerstein, M., Snyder, M., 2009. RNA-Seq: a revolutionary tool for transcriptomics. Nat. Rev. Genet. 10 (1), 57−63.

Wasserman, R.H., Fullmer, C.S., 1995. Vitamin D and intestinal calcium transport: facts, speculations, and hypotheses. J. Nutr. 125, 1971S−1979S.

Weinstein, R.S., Underwood, J.L., Hutson, M.S., DeLuca, H.F., 1984. Bone histomorphometry in vitamin D-deficient rats infused with calcium and phosphorus. Am. J. Physiol. 246, E499−E505.

Westin, S., Kurokawa, R., Nolte, R.T., Wisely, G.B., McInerney, E.M., Rose, D.W., et al., 1998. Interactions controlling the assembly of nuclear-receptor heterodimers and co-activators. Nature 395 (6698), 199−202.

Wettschureck, N., Lee, E., Libutti, S.K., Offermanns, S., Robey, P.G., Spiegel, A.M., 2007. Parathyroid specific double knockout of Gq and G11 a subunits leads to a pheyotype resembling germline knockout of the extracellular Ca^{2+} sending receptor. Mol. Endocrinol. 21, 274−280.

Whalen, S., Truty, R.M., Pollard, K.S., 2016. Enhancer-promoter interactions are encoded by complex genomic signatures on looping chromatin. Nat. Genet. 48 (5), 488−496.

Xie, W., Schultz, M.D., Lister, R., Hou, Z., Rajagopal, N., Ray, P., et al., 2013. Epigenomic analysis of multilineage differentiation of human embryonic stem cells. Cell 153 (5), 1134−1148.

Xue, Y., Fleet, J.C., 2009. Intestinal vitamin D receptor is required for normal calcium and bone metabolism in mice. Gastroenterology 136 (4), 1317−1327 e1311−1312.

Yasuda, H., Shima, N., Nakagawa, N., Mochizuki, S.I., Yano, K., Fujise, N., Sato, Y., Goto, M., Yamaguchi, K., Kuriyama, M., Kanno, T., Murakami, A., Tsuda, E., Morinaga, T., Higashio, K., 1998a. Identity of osteoclastogenesis inhibitory factor (OCIF) and osteoprotegerin (OPG): a mechanism by which OPG/OCIF inhibits osteoclastogenesis in vitro. Endocrinology 139, 1329−1337.

Yasuda, H., Shima, N., Nakagawa, N., Yamaguchi, K., Kinosaki, M., Mochizuki, S.I., Tomoyasu, A., Yano, K., Goto, M., Murakami, A., Tsuda, E., Morinaga, T., Higashio, K., Udagawa, N., Takahashi, N., Suda, T., 1998b. Osteoclast differentiation factor is a ligand for osteoprotegerin/osteoclastogenesis-inhibitory factor and is identical to TRANCE/RANKL. Proc. Natl. Acad. Sci. U.S.A. 95, 3597−3602.

Yoshizawa, T., Handa, Y., Uematsu, Y., Takeda, S., Sekine, K., Yoshihara, Y., Kawakami, T., Arioka, K., Sato, H., Uchiyama, Y., Masushige, S., Fukamizu, A., Matsumoto, T., Kato, S., 1997. Mice lacking the vitamin D receptor exhibit impaired bone formation, uterine hypoplasia and growth retardation after weaning. Nat. Genet. 16, 391−396.

Zehnder, D., Evans, K.N., Kilby, M.D., Bulmer, J.N., Innes, B.A., Stewart, P.M., Hewison, M., 2002. The ontogeny of 25-hydroxyvitamin D(3) 1alpha-hydroxylase expression in human placenta and decidua. Am. J. Pathol. 161 (1), 105−114.

Zella, J.B., Plum, L.A., Plowchalk, D.R., Potochoiba, M., Clagett-Dame, M., DeLuca, H.F., 2014. Novel, selective vitamin D analog suppresses parathyroid hormone in uremic animals and postmenopausal women. Am. J. Nephrol. 39 (6), 476−483.

Zella, L.A., Meyer, M.B., Nerenz, R.D., Lee, S.M., Martowicz, M.L., Pike, J.W., 2010. Multifunctional enhancers regulate mouse and human vitamin D receptor gene transcription. Mol. Endocrinol. 24 (1), 128−147.

Zhu, J.G., Ochalek, J.T., Kaufmann, M., Jones, G., Deluca, H.F., 2013. CYP2R1 is a major, but not exclusive, contributor to 25-hydroxyvitamin D production in vivo. Proc. Natl. Acad. Sci. U.S.A. 110 (39), 15650−15655.

Zierold, C., Darwish, H.M., DeLuca, H.F., 1994. Identification of a vitamin D-response element in the rat calcidiol (25-hydroxyvitamin D3) 24-hydroxylase gene. Proc. Natl. Acad. Sci. U.S.A. 91 (3), 900−902.

Zierold, C., Darwish, H.M., DeLuca, H.F., 1995. Two vitamin D response elements function in the rat 1,25-dihydroxyvitamin D 24-hydroxylase promoter. J. Biol. Chem. 270 (4), 1675−1678.

Further Reading

Hoenderop, J.G., van der Kemp, A.W., Hartog, A., van de Graaf, S.F., Van Os, C.H., Willems, P.H., Bindels, R.J., 1999. Molecular identification of the apical Ca21 channel in 1,25-dihydroxyvitamin D-responsive epithelia. J. Biol. Chem. 274, 8375−8378.

Maurano, M.T., Wang, H., John, S., Shafer, A., Canfield, T., Lee, K., Stamatoyannopoulos, J.A., 2015. Role of DNA methylation in modulating transcription factor occupancy. Cell Rep. 12 (7), 1184−1195.

Chapter 31

Nonskeletal effects of vitamin D: current status and potential paths forward

Neil Binkley[1], Daniel D. Bikle[2], Bess Dawson-Hughes[3], Lori Plum[4], Chris Sempos[5] and Hector F. DeLuca[4]

[1]University of Wisconsin School of Medicine and Public Health, Madison, Wisconsin, United States; [2]VA Medical Center and University of California San Francisco, San Francisco, California, United States; [3]Jean Mayer USDA Human Nutrition Research Center on Aging at Tufts University, Boston, Massachusetts, United States; [4]Department of Biochemistry, University of Wisconsin–Madison, Madison, Wisconsin, United States; [5]Vitamin D Standardization Program, Havre de Grace, MD, United States

Chapter outline

Introduction

It is widely assumed that hypovitaminosis D is highly prevalent worldwide (Palacios and Gonzalez, 2014). This is reasonable as humans historically obtained vitamin D via cutaneous production upon UVB exposure, and sun avoidance is now common and widely advocated (USDDH, 2014). Vitamin D deficiency could potentially have widespread adverse health consequences (Holick, 2017). As many tissues possess both the vitamin D receptor and the 1-hydroxylase, it can be hypothesized that active vitamin D (i.e., $1,25(OH)_2D$) is produced locally, i.e., that vitamin D has autocrine/paracrine effects in addition to the classic endocrine effects on calcium homeostasis (Holick, 2008). The effects of vitamin D deficiency on the musculoskeletal system are well established. However, it is reasonable that vitamin D inadequacy could, potentially, compromise the functions of multiple organs and systems (in addition to the musculoskeletal system) and thereby, ultimately, lead to dysfunction leading to acute and chronic disease (Holick, 2011). Consistent with this, hypovitaminosis D, generally defined as low circulating 25-hydroxyvitamin D (25(OH)D), has been associated with a multitude of human diseases, e.g., muscular dysfunction, cardiovascular disease (CVD), cancer, immune function, hypertension, obesity, diabetes mellitus, and many, many others (Holick, 2017; Wang et al., 2017). If these associational studies are reflective of causality, i.e., if vitamin D inadequacy is contributing in a causal way to a multitude of human diseases with

Principles of Bone Biology. https://doi.org/10.1016/B978-0-12-814841-9.00031-2

immense impact upon quality of life, mortality, and health care expense, then widespread screening for this deficiency is needed and societal efforts such as food supplementation are needed. Indeed, vitamin D inadequacy (using the Institute of Medicine guidance) is present in over 30% of Americans (Looker et al., 2011). This prevalence is comparable to those of obesity, hypertension, and hyperlipidemia, other widely recognized contributors to chronic diseases for which widespread public health efforts to manage exist. Alternatively, it could be hypothesized that the association of low vitamin D status with the multitude of human conditions is nothing more than the use of circulating 25(OH)D to identify those with poor nutritional status and/or suboptimal health, thereby reducing the likelihood of sun exposure. If this is true, widespread 25(OH)D measurement and supplementation is an unnecessary waste of limited health care resources and must cease. Clearly, it is essential to determine whether vitamin D inadequacy does, or does not, contribute to nonskeletal disease.

As such, it is not surprising that a plethora of observational and prospective studies evaluating the association of vitamin D status with many diseases has been and is being performed and published. As systematic reviews of randomized trials are considered the highest level of evidence-based medicine (Sackett et al., 1996), it is expected that meta-analyses relating vitamin D to nonskeletal disease are often being performed. Indeed, a PubMed search in March 2018 found that 747 vitamin D-related meta-analyses were performed from 2013 through 2017, an average of approximately three every week. Moreover, a number of authoritative reviews have evaluated the potential role of vitamin D in nonskeletal conditions (Autier et al., 2017; Rejnmark et al., 2017; Rosen et al., 2012). To succinctly summarize these reviews, it remains unclear what role, if any, vitamin D inadequacy plays in causing nonskeletal diseases. We believe this state of uncertainty reflects deficiencies in assessment of vitamin D status and clinical trial design as is discussed later. As such, this chapter will not replicate recent reviews. However, as examples of existing data suggesting a potential importance in human disease, we will briefly overview data relating vitamin D status to cancer, immune function, falls, and CVD. These conditions were selected as they cause immense morbidity, mortality, and health care cost worldwide.

Vitamin D and immunity

There are many extensive reviews that explore the possible role of vitamin D in the immune system (Colotta et al., 2017; Hayes et al., 2015; Peelen et al., 2011). Certainly, the vitamin D receptor (VDR) is found in activated T cells and macrophages (Wang et al., 2012c). In vitamin D deficiency the VDR is either low or absent from T cells but is present in macrophages. The receptor quickly appears in T cells following vitamin D administration. B cells lack the VDR in our hands, while others claim its presence in these cells. By autoradiography, Stumpf et al. demonstrated that titrated $1,25(OH)_2D_3$ is found in the nuclei of thymus, spleen, lymph nodes, and macrophages, but interestingly not in lymphocytes (Stumpf et al., 1990; Stumpf and Downs, 1987). There is little doubt vitamin D plays a role in immunity; however, there is much debate and little agreement on how vitamin D is involved in immunity.

A great deal of information has been generated, primarily by in vitro methods, on cytokine levels in T cells, with concentrations of $1,25(OH)_2D_3$ higher than found in vivo. Although arguments that these levels can be achieved locally have been made, no such in vivo demonstration has appeared. Further, rarely has true vitamin D deficiency through dietary means been achieved, and most studies examine the effect of supplemental vitamin D above normal. In this brief review an attempt will be made to present the effects of vitamin D deficiency versus sufficiency in animal models when available. Unfortunately, consistent information on whether vitamin D deficiency has any impact on innate or acquired immunity in animals or humans is unavailable.

On the other hand, some information is available in situations in which the adaptive immune system fails, or autoimmunity, in animals. One example is in type 1 diabetes. Vitamin D deficiency accelerated both the onset and the severity of the disease in the NOD mouse (Zella et al., 2003). In this circumstance a major consideration is that the insulin-producing islet cells have a high concentration of the VDR (Wang et al., 2012b). While vitamin D through its active form suppresses the disease (Zella et al., 2003), the suppression could be a result of $1,25(OH)_2D_3$ action on the islet cell rather than an action on cells of the immune system. A combination of cellular targets is also possible, as specific T cell populations show small alterations in NOD mice when the VDR is eliminated (Gysemans et al., 2008). However, the consequences of these changes are not clear.

The opposite impact of vitamin D status is found in the case of experimental autoimmune encephalomyelitis (EAE), a model of multiple sclerosis (MS). Quite unexpected is the finding from our group (DeLuca and Plum, 2011), and independently by a group in France (Fernandes de Abreu et al., 2010), that vitamin D deficiency suppresses EAE instead of exacerbating disease. Thus, vitamin D is required and functions in some manner to program T cells and/or macrophages to attack the spinal cord, precipitating EAE, a widely accepted model of MS. Originally Lemire and Archer reported that

$1,25(OH)_2D_3$ could suppress EAE, a finding that was repeated in other laboratories (Lemire and Archer, 1991; VanAmerongen et al., 2004). In our group the suppression of EAE by $1,25(OH)_2D_3$ is accompanied by hypercalcemia (Cantorna et al., 1996). When dietary calcium was reduced to 0.02%, the effectiveness of $1,25(OH)_2D_3$ to suppress EAE was severely limited (Cantorna et al., 1999). Further hypercalcemia itself suppresses EAE (Meehan et al., 2005). Therefore, the suppression of EAE by $1,25(OH)_2D_3$ is linked to dietary and perhaps serum calcium. Consistent with the removal of vitamin D from the diet, the ablation of VDR also blocks the development of EAE (Wang et al., 2012b). Thus, in contrast to type 1 diabetes, vitamin D is required for the development of the disease, reducing the likelihood vitamin D might be used to suppress MS. Results from meta-analyses of the clinical trials done to test the use of vitamin D to suppress MS seem to confirm this idea (Cashman et al., 2016b; Hempel et al., 2017; Zheng et al., 2018).

Distinct from this finding, a narrow band of UV light (295−315 nm) suppresses EAE by a mechanism not involving vitamin D. Although this may provide an explanation of the low incidence of MS in high-sunlight areas, its mechanism is largely unknown.

Another disease that involves the immune system is inflammatory bowel disease, which has been extensively studied by Cantorna et al. (Bora and Cantorna, 2017). Their results are similar to those observed in animal models of type 1 diabetes, i.e., that VDR and ligand deficiency both exacerbate the disease. The intestinal epithelium possesses large amounts of the VDR and it is unclear whether the effect of the vitamin D is directly on immune cells or through its action on the intestinal villi. It is clear that subsets of T cells, i.e., invariant natural killer T cells as well as CD8aa populations, are significantly reduced in the gastrointestinal tract of mice lacking VDR (Bora and Cantorna, 2017). Whether the decrease in these populations can explain the reduction of disease is unclear.

In conclusion, the presence of the VDR and its ligand in cells of the immune system strongly suggests a role for vitamin D in immunity. However, little in vivo evidence is available on the role of vitamin D in the immune system. Vitamin D deficiency and/or a lack of the VDR does suppress the animal model of MS (EAE). Quite differently, 1,25-dihydroxyvitamin D, the active form of vitamin D, suppresses type 1 diabetes in NOD mice, while vitamin D deficiency exacerbates the disease. A similar relationship is found in the case of inflammatory bowel disease. Although these effects of vitamin D are clear, the underlying mechanisms remain unknown.

Vitamin D and muscle performance, balance, and falls

Physiology

VDRs are present in many tissues, including muscle, but their role in muscle is not entirely clear. The number of VDRs in muscle (Bischoff-Ferrari et al., 2004) and the number of type 2 muscle fibers (Vandervoort, 2002) decline with aging, and preliminary evidence indicates that similar changes may occur in vitamin D deficiency (Ceglia et al., 2013). In a small study of 21 older women with a low mean serum 25(OH)D level of 18.4 ng/mL, daily supplementation with 4000 IU of vitamin D_3 for 4 months increased the intramyonuclear VDR number and the cross-sectional area of type 2 muscle fibers compared with placebo (Ceglia et al., 2013). No significant changes in muscle performance were documented.

With aging, the number of motor neurons enervating muscle declines (Brown, 1972), as does balance. There is limited evidence that vitamin D deficiency may adversely affect motor neurons. Skaria documented reduced nerve conduction velocities as well as myopathy in patients with osteomalacia (Skaria et al., 1975). However, treatment with vitamin D reversed the myopathy but did not improve nerve conduction velocity in these patients, leaving open the possibility that the patients had unrelated peripheral neuropathies (Skaria et al., 1975). Irani (1976) observed no nerve conduction abnormalities in patients with osteomalacia.

Clinical studies of muscle performance and balance

Based on the histomorphometric muscle changes seen in severe vitamin D deficiency, many investigators have hypothesized that supplementation with vitamin D may reduce muscle wasting and improve muscle performance in older adults with milder degrees of vitamin D deficiency. A 2014 meta-analysis of 30 randomized controlled clinical trials (RCTs) involving 5615 older adults examined the impact of vitamin D supplementation on muscle strength, mass, and power (Beaudart et al., 2014). In 29 of these trials, supplemental vitamin D significantly increased a global index of strength comprising mainly grip and leg strength. Subset analyses indicated that benefit was greater for participants with 25(OH)D levels <12 ng/mL, and that leg strength but not grip strength improved significantly with supplementation. In the trials that

measured muscle mass (N = 6) and power (N = 5), no significant effect of vitamin D was observed (Beaudart et al., 2014). Several subsequent trials have found no impact of supplemental vitamin D on muscle function in older adults (Hansen et al., 2015; Levis and Gomez-Marin, 2017; Uusi-Rasi et al., 2015), possibly because the study participants were not vitamin D deficient (see "Clinical studies"). In contrast, a study by Cangussu et al. reported improved chair rise performance with vitamin D supplementation over 9 months in postmenopausal women with a mean serum 25(OH)D level of 15 ng/mL (Cangussu et al., 2015).

The role of vitamin D in muscle mass and performance in young adults is less extensively studied. In a large clinical trial in school girls with a mean serum 25(OH)D level of 14 ng/mL, vitamin D supplementation for 1 year increased lean tissue mass (and bone mass) but had no effect on grip strength (El-Hajj Fuleihan et al., 2006). Similarly, in a study of young women, mean age 21 years, with a low mean 25(OH)D level of 9.3 ng/mL, treatment over 6 months increased serum 25(OH)D to near 30 ng/mL but had no significant effect on grip strength (Goswami et al., 2012). Thus current evidence indicates that supplementation modestly increases muscle mass and bone mass, but does not improve muscle strength.

Several trials conducted in older adults have reported vitamin D treatment to improve balance, measured under static conditions by body sway, compared with placebo (Cangussu et al., 2016; Pfeifer et al., 2009). The impact of vitamin D on dynamic balance (a complex process involving sensory information, selection of the appropriate response to maintain balance, and efficient activation of the muscles that respond to a balance disturbance) is unknown, but it may be inferred by the effect of vitamin D on risk of falling (see the next section).

Vitamin D and falls

Prevention of falls is a public health priority because 1%–2% of falls lead to hip fractures, falls are independent determinants of functional decline, and falls lead to 40% of all nursing home admissions (Tinetti and Williams, 1997). Moreover, falls are a substantial and increasing cause of mortality in the very old (Hartholt et al., 2018).

The role of vitamin D in preventing falls has been studied extensively and clinical trials have produced mixed findings. Two meta-analyses published in 2009 and 2011 found that vitamin D supplementation had a modest beneficial effect on fall risk in older adults (Bischoff-Ferrari et al., 2009; Murad et al., 2011). One of these papers suggested that fall risk reduction with supplementation may be more effective in individuals with low 25(OH)D levels (Murad et al., 2011). In 2014, a meta-analysis concluded that the effect estimate for vitamin D with or without calcium on falls did not alter the relative risk by 15% or more (Bolland et al., 2014). A 2015 meta-analysis found vitamin D supplementation to be more effective in elders with low 25(OH)D levels (LeBlanc and Chou, 2015). Since this most recent meta-analysis (LeBlanc and Chou, 2015), several large, placebo-controlled trials have been published that collectively appear to fit the pattern that only vitamin D-insufficient elders are responsive to supplementation with vitamin D. Hansen et al. treated postmenopausal women with a mean serum 25(OH)D level of 21 ng/mL with 50,000 IU of vitamin D_3 twice monthly or 800 IU daily for 1 year and observed no effect on falls (Hansen et al., 2015). Similarly, the Vitamin D Assessment (ViDA) Study found no effect of treatment for 3.4 years with 100,000 IU of vitamin D_3 per month on fall risk in older adults with a mean serum 25(OH)D level of 25 ng/mL (Khaw et al., 2017). In contrast, in postmenopausal women with a very low mean 25(OH)D level of 15 ng/mL, treatment with 1000 IU of vitamin D_3 per day for 9 months reduced fall risk by about 50% (Cangussu et al., 2016).

In summary, available evidence indicates that elders with low 25(OH)D levels are most likely to benefit from supplementation with vitamin D and the degree of fall risk reduction may be proportional to the degree of insufficiency. The results of a large ongoing trial (as of this writing) testing several doses of vitamin D in elders with 25(OH)D levels in the range of 10–29 ng/mL should provide a more precise estimate of the segment of the elderly population that is likely to benefit from supplementation and the optimal replacement dose(s) (NCT02166333).

Several studies have indicated that supplementation under certain circumstances can increase risk of falling. This was first noted by Sanders et al., who found that a large annual oral dose of 500,000 IU of vitamin D increased risk of falls (and fractures) in elders (Sanders et al., 2010). An increase in fall risk was also seen in a trial administering an oral dose of 60,000 IU of vitamin D_3 monthly (Bischoff-Ferrari et al., 2016). In long-term care residents, treatment with 100,000 IU of vitamin D_3 per month, compared with standard dosing, significantly increased fall risk (secondary end point), while significantly lowering the risk of developing an acute respiratory infection (primary outcome) (Ginde et al., 2017). A common feature of these trials is that they employed high intermittent doses of vitamin D. But treatment with 100,000 IU per month does not always increase risk of falls; this dose administered in the ViDA study had no significant effect on the fall rate (Khaw et al., 2017). Nonetheless, there is sufficient evidence for risk that daily or weekly dosing is preferred to higher intermittent dosing.

Vitamin D and cancer

The antiproliferative, prodifferentiating effects of vitamin D signaling on many, if not all, cell types have raised the hope that vitamin D, $1,25(OH)_2D$, or one or more of its analogs would prove useful in the prevention and/or treatment of cancer. Although the cellular and animal studies have been promising, and at least for some cancers epidemiologic evidence is suggestive, to date the RCTs are less compelling. That said, a number of mechanisms by which $1,25(OH)_2D$ and its analogs might alter tumor development and progression have been documented, at least in the cellular and animal studies as reviewed in 2016 (Bikle, 2016).

Cellular mechanisms

Vitamin D metabolism

Most tumors express the VDR and often express cytochrome P450 27B1 (CYP27B1), the enzyme that converts 25(OH)D to $1,25(OH)_2D$, thus producing the ligand for VDR. Their expression is often lost as the tumor undergoes progressive dedifferentiation (Brozek et al., 2012; Matusiak and Benya, 2007; Santagata et al., 2014). On the other hand CYP24A1 expression is also often increased in tumors, and is associated with resistance to $1,25(OH)_2D$ (Brozek et al., 2012; Tannour-Louet et al., 2014). These changes in vitamin D metabolism and responsiveness reduce the ability of $1,25(OH)_2D$ to control the proliferation and differentiation of these tumors.

MicroRNA

A number of microRNAs that alter tumor proliferation have been identified as being regulated by $1,25(OH)_2D$ (Christakos et al., 2016). This includes increased expression of miR-145, which blocks the expression of E2F3, a key regulator of proliferation (Chang et al., 2015), and miR-32, which blocks the proapoptotic protein Bim, protecting the cell (human myeloid leukemia) from AraC-induced apoptosis (Gocek et al., 2011).

Cell cycle regulation and proliferation

$1,25(OH)_2D$ typically causes arrest at the G0/G1 and/or G1/S transition in the cell cycle, associated with a decrease in cyclins and an increase in the inhibitors of the cyclin-dependent kinases such as p21cip1 and p27kip1 (Hager et al., 2001; Palmer et al., 2003). The family of Forkhead box O proteins blocks proliferation. $1,25(OH)_2D$ promotes their interaction with the VDR as well as their regulation by Sirt1 and protein phosphatase 1, maintaining these proteins in the transcriptionally active dephosphorylated state (An et al., 2010). On the other hand $1,25(OH)_2D$ reduces the expression of proproliferative genes such Myc, Fos, and Jun (Meyer et al., 2012), while stimulating the expression of insulin-like growth factor (IGF)-binding protein 3 (IGFBP3) in prostate and breast cancer (BCa) cells. The increased expression of IGFBP3 would bind the IGFs, blocking their ability to stimulate proliferation (Colston et al., 1998; Huynh et al., 1998). In epithelial cells $1,25(OH)_2D$ stimulates the expression of transforming growth factor β2, which is antiproliferative in these cells (Peehl et al., 2004; Swami et al., 2003; Yang et al., 2001) and suppresses components of the Hedgehog pathway, which when overexpressed result in basal cell carcinomas (BCCs) (Aszterbaum et al., 1998; Teichert et al., 2011). $1,25(OH)_2D$ inhibits the proliferative effects of epidermal growth factor by inhibiting the expression of its receptor in breast cell lines (McGaffin and Chrysogelos, 2005). Constitutive activation of the Wnt/β-catenin pathway is the cause of most colorectal cancers (CRCs). When activated, β-catenin enters the nucleus, where it binds to T cell factor/lymphoid enhancer-binding factor (TCF/LEF) sites in genes promoting proliferation (e.g., cyclin D1). VDR, on binding to its ligand, blocks this pathway both by binding to β-catenin, limiting its access to the TCF/LEF sites in the nucleus, and by stimulating the formation of the E-cadherin/catenin complex in the cell membrane to which β-catenin is bound, limiting its translocation to the nucleus (Byers et al., 2012). Moreover, $1,25(OH)_2D$ can increase the expression of the Wnt inhibitor dickkopf (Dkk)-1 (Aguilera et al., 2007) while inhibiting that of the Wnt activator Dkk-4 (Pendas-Franco et al., 2008) in colon cancer cells.

Apoptosis

$1,25(OH)_2D$ stimulates the expression of a number of proapoptotic genes, such as GOS2 (G0/G1 switch gene 2) (Palmer et al., 2003), Bax (Kizildag et al., 2010), DAP (death-associated protein)-3, CFKAR (caspase 8 apoptosis-related cysteine peptidase), FADD (Fas-associated death domain), and caspases (e.g., caspases 3, 4, 6, and 8) (Swami et al., 2003) in a variety of cell lines, while suppressing the expression of proapoptotic genes such as Bcl2 and Bcl-XL in these and other cell lines (Kizildag et al., 2010; Weitsman et al, 2003, 2005).

Animal studies

Animal studies demonstrating the efficacy of $1,25(OH)_2D$ in preventing or slowing the progression of various tumors are numerous, with those of the colorectum (CRC), breast, prostate, and skin being most studied. Below are selected examples.

Colorectal cancer

Diets that are low in calcium and vitamin D (Western diet) fed to mice increase the risk of CRC for these mice. This risk can be reversed by diets supplemented with calcium and vitamin D (Newmark et al., 2009). The administration of vitamin D metabolites to mice in which CRC was induced by azoxymethane and dextran sulfate incorporated into the diet is at least partially protective (Murillo et al., 2010). Activation of the Wnt/β-catenin pathway caused by mutations in adenomatous polyposis coli (APCmin) results in tumor formation much faster when the mice are placed on a low-calcium, low-vitamin-D Western diet (Yang et al., 2008) or on a vitamin D-deficient diet (Xu et al., 2010). Similarly, these tumors develop faster when these mice are bred with VDR-null mice (Zheng et al., 2012).

Breast cancer

BCa induced by dimethylbenzanthracene (DMBA) are increased in number when rats are fed the low-calcium, low-vitamin-D Western diet (Lipkin and Newmark, 1999) or when VDR-null mice are administered DMBA (Zinser and Welsh, 2004). The growth of BCa xenografts can be prevented by vitamin D analogs (VanWeelden et al., 1998).

Prostate cancer

Vitamin D analogs can also inhibit the growth of prostate cancer (PCa) regardless of androgen receptor status (Bhatia et al., 2009). A vitamin D-deficient diet will promote the growth of PC3 PCa cells in bone (Zheng et al., 2011). Breeding the transgenic prostate tumor model LPB-Tag with VDR-null mice stimulates the growth of these tumors (Mordan-McCombs et al., 2010). The development of tumors in the TRAMP (transgenic adenocarcinoma of the mouse prostate) model of PCa can be prevented with high doses of $1,25(OH)_2D$ (Krishnan et al., 2010).

Skin

The most common skin cancers are squamous cell carcinomas (SCCs) and BCCs. VDR-null mice develop skin tumors when exposed to DMBA (with or without topical application of phorbol myristate acetate (TPA)) or after chronic exposure to UVB at a rate far greater than that of their wild-type controls (Ellison et al., 2008; Teichert et al., 2011). Topical $1,25(OH)_2D$ is protective at least from the early effects of UVB on markers of DNA damage such as cyclobutane pyrimidine dimers (Gupta et al., 2007), although extended studies to determine whether topical application of $1,25(OH)_2D$ is protected in UVB-induced tumor formation have not been done.

Clinical studies

The inverse relationship between solar exposure and cancer mortality in North America was first noted by Apperly (1941) in 1941, and then popularized and linked to vitamin D by the Garland brothers (Garland and Garland, 1980) in 1980 in their epidemiologic studies with colon cancer. With the exception of skin cancer, this inverse relationship between solar exposure and cancer has been reported for many types of cancer (van der Rhee et al., 2006). More recent studies have examined the association of vitamin D intake or serum levels of 25(OH)D, generally using case−control and cohort studies. RCTs have generally been smaller, and often do not support the positive associations between sunlight, dietary vitamin D, or 25(OH)D levels and cancer prevention found in the epidemiologic studies. As for animal studies, most data come from studies of colorectal, breast, prostate, and skin cancer.

Colorectal cancer

In meta-analyses of nine studies (eight cohort, one nested case−control; 6466 subjects) evaluating the relationship of vitamin D intake and CRC and nine studies (seven cohort, two case−control; 2764 cases, 3948 controls) evaluating serum levels of 25(OH)D and CRC, Ma et al. (2011) found an overall relative risk (RR) of 0.88 (CI 0.8−0.96) comparing the highest with the lowest categories of vitamin D intake and an RR of 0.67 (CI 0.54−0.80) for the highest to lowest 25(OH)D levels. When dietary calcium was taken into account (higher calcium is better) the risk reduction was enhanced. These

meta-analyses confirm previous results from the American Cancer Society cohort study (120,000 men and women) (Cho et al., 2004) and the National Institutes of Health (NIH; 16,000 participants) (Carroll et al., 2010). Thus, at least for CRC, there is a reasonably consistent set of epidemiologic data supporting the protective effect of vitamin D (and calcium) with respect to CRC incidence. However, RCTs have been disappointing. The Women's Health Initiative (WHI), in which 400 IU of vitamin D daily was assessed, failed to show protection against CRC (Wactawski-Wende et al., 2006). The low dose of vitamin D used in this trial may have limited the likelihood of observing an effect. However, a study of 1000 IU vitamin D daily for 3−5 years also failed to show a benefit in the reduction of colon adenomas and colon cancer even in a high-risk population (Baron et al., 2015). Perhaps vitamin D supplementation over short time spans relative to the time required for cancer to manifest is a limiting factor.

Breast cancer

In a large case−control study from Italy (Rossi et al., 2009) a 34% decrease in BCa was found in those ingesting the highest level of vitamin D (>194 IU/day) versus those ingesting the lowest level (<60 IU/day). The largest cohort studies (Lin et al., 2007; Shin et al., 2002) (Nurses Health Study with 88,891 participants and WHI with 31,487 participants) showed a reduction in risk (RR 0.72, CI 0.55−0.94, and RR 0.65, CI 0.42−1.00, respectively) in those ingesting the highest amount of vitamin D, but only in the premenopausal women. Chlebowski (2011) reviewed 10 case−control and 10 cohort studies with respect to vitamin D intake and BCa and four case−control and six nested case−control studies with respect to 25(OH)D levels and BCa. Only when premenopausal/perimenopausal women were included in the analysis was a significant negative association between increased vitamin D intake and BCa incidence found (RR 0.83, CI 0.73−0.95) (Chen et al., 2010). Of the six nested case−control studies assessing the relationship of serum 25(OH)D and BCa, only one showed a significant negative association between high 25(OH)D levels and incidence of BCa. In a separate meta-analysis by Gandini et al. (2011) an RR of 0.89 (0.82−0.98) for a 10 ng/mL increase in 25(OH)D was found when all studies were included and an RR of 0.83 (0.79−0.87) when only case−control studies were pooled. As for CRC, the WHI did not show a protective role for vitamin D in BCa. Thus the epidemiologic data tend to support a protective role for vitamin D against BCa, but the data are not as consistent as for CRC.

Prostate cancer

In contrast to CRC, the role of vitamin D in PCa is decidedly mixed. In a summary of 14 prospective studies (not RCTs) examining the association between 25(OH)D levels and the development of PCa, van der Rhee et al. (2006) found that 11 studies showed no association, and one study (Ahn et al., 2008) showed a positive association with PCa aggressiveness, although this was not seen in other studies (Gilbert et al., 2011). In particular, a meta-analysis of six cohort/nested case−control studies (8722 cases) examining the association of dietary vitamin D intake with PCa found an RR of 1.14 (CI 0.99−1.31) for an increase in dietary vitamin D of 1000 IU (Gilbert et al., 2011). Similarly, a meta-analysis of 14 cohort/nest case−control studies, including 4353 cases, examining the association of serum 25(OH)D and PCa found an RR of 1.04 (CI 0.99−1.1) for a 10 ng/mL increase in 25(OH)D for all PCas (Gilbert et al., 2011). Although an initial phase I clinical trial (ASCENT I) with high dose of $1,25(OH)_2D$ and docetaxol seemed to show promise in the treatment of castration-resistant PCa, this initial success could not be repeated in a larger phase II trial (ASCENT II) potentially flawed by differences in the dose of docetaxol between the calcitriol plus docetaxol arm and that with docetaxol alone (Scher et al., 2011). These trials did establish the safety of using high doses of calcitriol in the treatment of cancer when administered under controlled conditions. Nevertheless, the clinical evidence weighs against vitamin D being beneficial in the prevention or treatment of PCa.

Skin cancer

Skin cancer, in particular nonmelanoma skin cancer (NMSC), is by far the most common cancer, with over 1 million skin cancers occurring annually in the United States. Of these, 96% are NMSC (80% BCC, 16% SCC), with melanomas making up the remaining 4%. Because UVB is the major etiologic agent for NMSC, but is also the major means by which the body makes vitamin D, it has been difficult to separate out the beneficial effects of vitamin D on NMSC from the deleterious effects of UVB exposure. Moreover, most national registries do not include NMSC, leaving no easily accessible database with which to track the development of these cancers. That said, a few epidemiologic studies have been published. An earlier study on vitamin D intake found no association between vitamin D and BCC risk (Hunter et al., 1992). However, some clinical studies of BCC patients show a potential beneficial role for vitamin D. In a nested case−control study of 178 elderly men with NMSC compared with 930 without skin cancer enrolled in the Osteoporotic Fractures in Men (MrOS)

study, men with the highest baseline serum 25(OH)D levels (30 ng/mL) had 47% lower odds of NMSC (CI 0.3−0.93) compared with those with the lowest baseline 25(OH)D levels (Tang et al., 2010). However, this observation has not been confirmed in other studies, which have shown a positive correlation between 25(OH)D levels and BCC (Asgari et al., 2010; Eide et al., 2011). In an analysis of 36,282 postmenopausal women in the WHI, no difference was found in the incidence of melanoma between women receiving 400 IU vitamin D plus calcium (1000 mg) supplementation compared with placebo over a follow-up period of 7 years, although a subgroup analysis of women at high risk based on a previous history of NMSC showed a reduction in the incidence of melanoma in those receiving calcium and vitamin D supplementation (Tang et al., 2011).

Vitamin D and cardiovascular disease

In observational studies, low circulating 25(OH)D concentrations have been associated with increased risk of CVD. Although these associations are not seen in all studies, there is no evidence that higher 25(OH)D levels are associated with greater CVD risk (Nemerovski et al., 2009). As such, it is plausible that vitamin D is indeed causally related to CVD. Importantly, both blood vessels and cardiac myocytes have been reported to possess VDRs and CYP27B1, the 1α-hydroxylase enzyme (Tishkoff et al., 2008).

Low vitamin D status has been hypothesized to potentially cause CVD by multiple, not exclusive, mechanisms, including regulation of calcium flux altering vascular and myocardial calcification, mediation of inflammation/cell proliferation, and interactions producing antiatherosclerotic effects (among others) (Norman and Powell, 2014; Cashman, 2014; Pilz et al., 2010). For example, it is plausible that the relationship of 25(OH)D with parathyroid hormone (PTH) might be involved in CVD, as elevated PTH is associated with increased blood pressure, which, if sustained, could lead to cardiac hypertrophy and ultimately to heart failure (Rostand and Drueke, 1999). In addition, chronically high inflammation is positively associated with CVD, and $1,25(OH)_2D$ may downregulate proinflammatory and upregulate antiinflammatory cytokines (Cardus et al., 2009; Chen et al., 2013; Helming et al., 2005). Consistent with a potential effect in CVD, a 2018 meta-analysis of six vitamin D supplementation RCTs in adults with heart failure found vitamin D supplementation to lower tumor necrosis factor α (Rodriguez et al., 2018). Other potential linkages of vitamin D status with CVD include potential effects on the functions of endothelial cells (Dong et al., 2012; Merke et al., 1989) and cardiac myocytes (Pilz et al., 2010; Tishkoff et al., 2008).

Epidemiologic evidence supports a potential relationship of low vitamin D status with CVD. For example, over ∼8 years of follow-up, the hazard ratios for heart failure death and sudden cardiac death for those whose 25(OH)D was <10 ng/mL were 2.8 and 5.1, respectively, compared with those with a 25(OH)D of ≥30 ng/mL (Pilz et al., 2008). Similarly, in an NHANES cohort, a composite CVD index (stroke, myocardial infarction, and angina) found that the prevalence of circulating 25(OH)D at <20 ng/mL was higher (29%) in those with CVD than those without (21%) (Kendrick et al., 2009). Moreover, a Framingham Offspring cohort study found circulating 25(OH)D levels below 15 ng/mL to be associated with increased risk of cardiovascular events, with the 5-year rate being double in those with vitamin D deficiency compared with those with higher concentrations (Wang et al., 2008). Importantly, low vitamin D status is associated with increased risk of death due to heart failure, sudden cardiac event, and CVD all-cause mortality. This was demonstrated in the Ludwigshafen Risk and Cardiovascular Health (LURIC) cohort after a median follow-up of 7.7 years. Heart failure and sudden cardiac events were increased in those with 25(OH)D of <10 ng/mL (Pilz et al., 2008) and CVD all-cause mortality was increased in subjects with lower 25(OH)D (Dobnig et al., 2008) even after adjustment for many traditional CVD risk factors. Multiple other observational studies with generally similar results exist and will not be reviewed here; overall, a 2012 meta-analysis of prospective studies relating 25(OH)D with CVD risk found an inverse relationship between 25(OH)D and CVD risk (Wang et al., 2012a).

Issues in existing data and paths forward to resolve the role of vitamin D deficiency in nonskeletal disease

As noted in the introduction, immense interest, clinical trials, publications, and meta-analyses related to vitamin D have been and are currently being published without adequate clarification of the potential role of vitamin D in nonskeletal diseases. As an oversimplification, we believe this reflects two major issues in vitamin D research: inadequate measurement of vitamin D status and limitations in clinical trial design.

Vitamin D status assessment

It is widely accepted that measurement of the circulating total 25-hydroxyvitamin D (25(OH)D) concentration—i.e., the sum of $25(OH)D_3$ and $25(OH)D_2$—is the best way to define vitamin D status (Scientific Advisory Committee on Nutrition (SACN), 2016; Holick et al. 2011; Institute of Medicine, 2010). However, substantial variability in "25(OH)D" results has existed, and continues to exist (Binkley et al., 2004; Carter et al., 2004; de la Hunty et al., 2010; Le Goff et al., 2015; Wallace et al., 2010). This variability confounds in a major way all efforts to clarify a potential role of vitamin D in nonskeletal disease and moreover to develop clinical and public health guidelines. It seems self-evident that use of different "25(OH)D" values could lead to differences in the definition of vitamin D inadequacy. Indeed, the use of differing 25(OH)D assays yields differing estimates of the prevalence of vitamin D inadequacy; retrospective standardization documents that prevalence can increase or decrease based on whether the initial assay was negatively or positively biased (Cashman et al, 2013, 2015a, 2016a; Sarafin et al., 2015; Schleicher et al., 2016). As such, failure to standardize 25(OH)D measurement standardization could be considered the major issue contributing to the "chaos" that continues to surround vitamin D (Binkley et al., 2017b).

Historically, no reference measurement procedure or reference materials existed to allow 25(OH)D measurement standardization. As such, 25(OH)D assay standardization is essential for clinical, research, and public health recommendation clarity. The Vitamin D Standardization Program (VDSP) was developed in an attempt to rectify this situation (Sempos et al., 2012).

Detailed review of the VDSP is beyond the scope of this chapter. Briefly, the VDSP coordinates the international effort to standardize serum 25(OH)D measurement to gold standard reference assays that have been developed (Mineva et al., 2015; Phinney et al., 2017; Stockl et al., 2009; Tai et al., 2017). In addition, guidance for retrospective standardization of previously published research for which stored specimens exist has been published (Durazo-Arvizu et al., 2017). Thus, VDSP approaches exist to allow performance and reporting of standardized 25(OH)D results (Sempos et al., 2017). Such an approach is essential if 25(OH)D data are to be pooled in meta-analyses.

Moreover, we believe that the NIH and other grant-funding agencies around the world should require grant applicants to demonstrate the procedures they will use to standardize 25(OH)D measurement before funding of a vitamin D-related study is approved. In addition, as certain automated immunoassays may not function properly in some patient populations due to altered vitamin D-binding protein levels, e.g., pregnant women and intensive care unit patients, researchers need to demonstrate that the assay can function in the patient populations to be studied (Apperly, 1941). Finally, we suggest that standardization of 25(OH)D data be a requirement for research study publication. Indeed, the Endocrine Society journals have updated their author instructions to require detailed description of hormone assay requirements. Appropriately, these instructions specifically note "…a requirement for traceability of an assay to a certified standard is not yet available for all steroid hormones, but is an important goal" (Wierman et al., 2014). The VDSP has published guidance that allows researchers to meet this goal (Sempos et al., 2017). Such a requirement for 25(OH)D data would allow pooling of results in meta-analyses; failure to implement this requirement will facilitate continuation of chaos regarding the role of vitamin D in health and disease.

Is 25(OH)D measurement enough?

A multitude of vitamin D metabolites exist, some of which may possess physiologic effects. As such, it is appropriate to consider whether the current approach of measuring only 25(OH)D is adequate to define an individual's vitamin D status. Indeed, it is plausible that considering a compilation of all vitamin D metabolites that possess a physiologic effect should be done to define vitamin D deficiency (Jones and Kaufmann, 2016). Such metabolites might include free 25(OH)D, $1,25(OH)_2D_3$, $24,25(OH)_2D_3$, and cholecalciferol, among others (Herrmann et al., 2017; Hollis and Wagner, 2013). Ultimately, low vitamin D status must be defined based on measurement of vitamin D-related metabolites that best predict health outcomes. As of this writing, the importance of these other metabolites, if any, in defining vitamin D status remains to be determined (Scientific Advisory Committee on Nutrition (SACN), 2016; Bouillon, 2017; Holick et al., 2011; Institute on Medicine, 2010). However, the ratio of $24,25(OH)_2D_3$ to 25(OH)D appears to be a promising potential advance as it may be predictive of response to vitamin D supplementation and provide additional insights into vitamin D status (Cashman et al., 2015b; Graeff-Armas et al., 2018; Jones and Schlingmann, 2018; Kaufmann et al., 2014; Molin et al., 2015; Wagner et al., 2011). Further work is clearly needed.

As part of the VDSP effort, the National Institute of Standards and Technology (NIST), with support from the NIH Office of Dietary Supplements, has developed reference methods and materials for standardizing the measurement of 3-epi-25(OH)D_3 and 24,25$(OH)_2D_3$. NIST is also working on a reference method for vitamin D-binding protein, PTH, and 1,25$(OH)_2D_3$. Efforts such as these are essential; it must be emphasized that if and when it becomes established that additional vitamin D metabolite measurements contribute to the definition of hypovitaminosis D, standardization or harmonization of such assays (where tools to do so exist) will be essential to avoid repeating the history of chaos seen with 25(OH)D measurement (Krishnan et al., 2010). Moreover, efforts to develop assays that simultaneously measure multiple vitamin D metabolites should, as a requirement, include steps to standardize measurements of these metabolites (Jones and Kaufmann, 2016).

Clinical and preclinical studies

Animal research and small clinical studies are essential precursors to successful large RCTs. Appropriate animal models are essential in studying vitamin D's role in the pathophysiology of complex human disease. We need to ask: are we using the appropriate animal models? Mouse models are superb for evaluating vitamin D metabolism using targeted knockout mouse models; are they the best and most appropriate surrogates of human physiology? Should additional studies be performed in Old World primates?

Small clinical studies can play a key role in moving toward large RCTs, as they are useful in evaluating potential treatment regimens, including evaluating possible doses and treatment regimens. Finally, has the vitamin D field moved too quickly to large RCTs? In the past, large clinical trials were not begun, generally, unless there was solid evidence from in vivo research, animal studies, and small clinical studies that a large trial was likely to be successful. The rationale was that we should not subject humans to clinical trials unless and until there were good data to support a result consistent with the hypothesis. Not knowing the answer to a question should not be sufficient criteria to expose humans to potential risks associated with large clinical trials without extensive data from in vivo, animal, and small clinical research indicating that the trial is likely to support the hypothesis being tested. It could be argued that the vitamin D field has not adequately followed this logical approach before embarking on large-scale RCTs.

Nonetheless, if vitamin D supplementation has beneficial effects on nonskeletal disease, it is reasonable to expect that RCTs should demonstrate such effects. However, despite multiple RCTs being conducted, with various vitamin D doses, regimens, durations, and end points, clarity regarding nonskeletal effects remains elusive. Why this is the case was noted by Heaney, who emphasized RCT failure to consider the "dose–response relation that vitamin D shares with most nutrients" (Heaney, 2012). To state this slightly differently, nutrients are not drugs. This concept is depicted in Fig. 31.1,

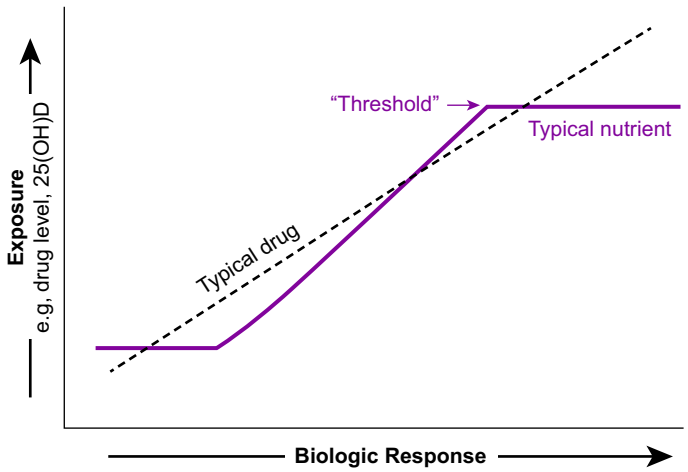

FIGURE 31.1 The sigmoidal relationship of nutrient status ("exposure") to biologic response. Nutrients behave different from drugs; with nutrients a threshold is reached when the individual has an adequate amount of the nutrient. Going above this level does not produce additional beneficial biologic response and could only, potentially, produce toxicity. Failure to consider baseline vitamin D status, specifically, failure to require it to be low as an inclusion criterion for vitamin D supplementation studies, biases such research to a negative conclusion.

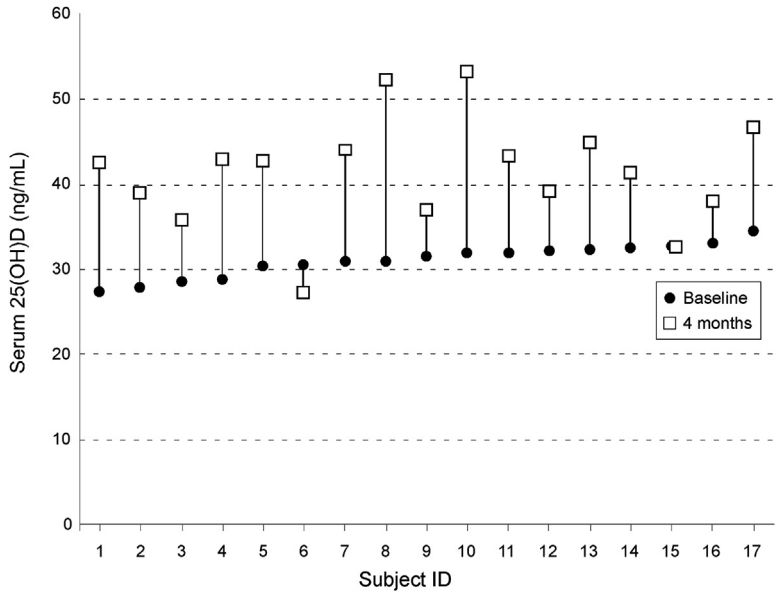

FIGURE 31.2 Variability in 25(OH)D response to a fixed daily supplementation dose. These data demonstrate a substantial variability in the 25(OH)D increase following provision of a fixed supplementation dose. Presented here are 25(OH)D data from postmenopausal women who received 1800 IU of vitamin D_3 daily for 4 months (Binkley et al., 2017a). Among these women, the serum 25(OH)D change ranged from −3.3 ng/mL to +21.4 ng/mL. This variability does not appear to reflect compliance; in this cohort the mean compliance with the daily supplement was 100.3% and ranged from 96% to 105%. Failure to consider such variable response confounds virtually all randomized trials of vitamin D supplementation.

upon review of which it is clear that an adequate dose must be given to individuals who are deficient in the nutrient in question (in this case vitamin D).

Failure to provide a dose that substantially increases 25(OH)D could not be expected to have any beneficial effect. Nonetheless, the vast majority of RCTs simply randomize to a predetermined vitamin D dose without consideration of whether the study subject achieves adequacy. Importantly, between-individual variation in 25(OH)D response to a fixed dose of oral vitamin D supplementation is dramatic (see Fig. 31.2).

Thus, even if a study included only vitamin D-deficient subjects, providing a single dose may not achieve adequacy in all. Perhaps a "treat to target" strategy should be considered in vitamin D supplementation studies (Binkley et al., 2015). Finally, vitamin D supplementation studies have employed various dosing approaches, e.g., daily, weekly, monthly, or less frequently. It has been suggested that daily dosing more closely replicates cutaneous production in circulating cholecalciferol levels (Heaney and Armas, 2015). Indeed, it is plausible that high cholecalciferol concentrations achieved with bolus dosing may induce 24-hydroxylation (Vieth, 2009); a concept supported by work demonstrating that a single vitamin D_3 dose of 150,000 IU led to greater $24,25(OH)_2D$ than daily dosing of 5000 IU for 1 month (Ketha et al., 2018). At a minimum, the possibility that daily and intermittent dosing may have different effects on vitamin D metabolism raises the question of whether these supplementation approaches should be considered equivalent in RCTs.

Of at least equal importance is that nutrients reach a "threshold"; once adequacy is achieved the provision of additional vitamin D could have no beneficial effect and only potentially lead to toxicity (Heaney, 2014). Studies including only those who are deficient in vitamin D could be expected to have a beneficial effect (if one indeed exists), whereas studies of those who are already replete would show no effect. It would seem self-evident that giving "more" vitamin D to a cohort of study subjects who already have "enough" would not inform a potential role of vitamin D in nonskeletal diseases. Nonetheless, the vast majority of vitamin D supplementation RCTs have not required documentation of inadequacy at study baseline. Performing meta-analyses of RCTs conducted without consideration of baseline status or individual response to supplementation should not be expected to clarify whether vitamin D is, or is not, important in nonskeletal disease. Indeed, as Heaney stated, "The question of how much vitamin D is enough is likely to remain muddled as long as meta-analyses focus on trial methodology rather than on biology" (Heaney, 2012). Guidance for the conduct of nutrient supplementation trials have been published and include measurement and use of basal nutrient status as an inclusion criterion, use of a supplementation dose adequate to produce an effect, and documentation of a change in nutrient status (Heaney, 2014). Such guidance must be followed to define what constitutes vitamin D inadequacy.

Conclusion and paths forward

Physiologic rationale combined with in vitro/in vivo preclinical studies and abundant observational data suggest that vitamin D deficiency could contribute to a multitude of human diseases. Unfortunately, despite immense amounts of clinical research and multiple meta-analyses of existing data, we do not know if, or for which nonskeletal diseases, vitamin D deficiency is relevant. This must be resolved. Improvements in clinical trial design and in laboratory measurements to define vitamin D status are needed to clarify what constitutes vitamin D inadequacy and the role, if any, that it plays in nonskeletal disease.

References

Aguilera, O., Pena, C., Garcia, J.M., Larriba, M.J., Ordonez-Moran, P., Navarro, D., Barbachano, A., Lopez de Silanes, I., Ballestar, E., Fraga, M.F., Esteller, M., Gamallo, C., Bonilla, F., Gonzalez-Sancho, J.M., Munoz, A., 2007. The Wnt antagonist DICKKOPF-1 gene is induced by 1alpha,25-dihydroxyvitamin D3 associated to the differentiation of human colon cancer cells. Carcinogenesis 28, 1877–1884.

Ahn, J., Peters, U., Albanes, D., Purdue, M.P., Abnet, C.C., Chatterjee, N., Horst, R.L., Hollis, B.W., Huang, W.Y., Shikany, J.M., Hayes, R.B., 2008. Serum vitamin D concentration and prostate cancer risk: a nested case-control study. J. Natl. Cancer Inst. 100, 796–804.

An, B.S., Tavera-Mendoza, L.E., Dimitrov, V., Wang, X., Calderon, M.R., Wang, H.J., White, J.H., 2010. Stimulation of Sirt1-regulated FoxO protein function by the ligand-bound vitamin D receptor. Mol. Cell. Biol. 30, 4890–4900.

Apperly, F.L., 1941. The relation of solar radiation to cancer mortality in North America. Cancer Res. 1, 191–195.

Asgari, M.M., Tang, J., Warton, M.E., Chren, M.M., Quesenberry Jr., C.P., Bikle, D., Horst, R.L., Orentreich, N., Vogelman, J.H., Friedman, G.D., 2010. Association of prediagnostic serum vitamin D levels with the development of basal cell carcinoma. J. Invest. Dermatol. 130, 1438–1443.

Aszterbaum, M., Rothman, A., Johnson, R.L., Fisher, M., Xie, J., Bonifas, J.M., Zhang, X., Scott, M.P., Epstein Jr., E.H., 1998. Identification of mutations in the human PATCHED gene in sporadic basal cell carcinomas and in patients with the basal cell nevus syndrome. J. Invest. Dermatol. 110, 885–888.

Autier, P., Mullie, P., Macacu, A., Dragomir, M., Boniol, M., Coppens, K., Pizot, C., Boniol, M., 2017. Effect of vitamin D supplementation on non-skeletal disorders: a systematic review of meta-analyses and randomised trials. Lancet Diabetes Endocrinol 5, 986–1004.

Baron, J.A., Barry, E.L., Mott, L.A., Rees, J.R., Sandler, R.S., Snover, D.C., Bostick, R.M., Ivanova, A., Cole, B.F., Ahnen, D.J., Beck, G.J., Bresalier, R.S., Burke, C.A., Church, T.R., Cruz-Correa, M., Figueiredo, J.C., Goodman, M., Kim, A.S., Robertson, D.J., Rothstein, R., Shaukat, A., Seabrook, M.E., Summers, R.W., 2015. A trial of calcium and vitamin D for the prevention of colorectal adenomas. N. Engl. J. Med. 373, 1519–1530.

Beaudart, C., Buckinx, F., Rabenda, V., Gillain, S., Cavalier, E., Slomian, J., Petermans, J., Reginster, J.Y., Bruyere, O., 2014. The effects of vitamin D on skeletal muscle strength, muscle mass, and muscle power: a systematic review and meta-analysis of randomized controlled trials. J. Clin. Endocrinol. Metab. 99, 4336–4345.

Bhatia, V., Saini, M.K., Shen, X., Bi, L.X., Qiu, S., Weigel, N.L., Falzon, M., 2009. EB1089 inhibits the parathyroid hormone-related protein-enhanced bone metastasis and xenograft growth of human prostate cancer cells. Mol. Cancer Ther. 8, 1787–1798.

Bikle, D.D., 2016. Extraskeletal actions of vitamin D. Ann. N.Y. Acad. Sci. 1376, 29–52.

Binkley, N., Borchardt, G., Siglinsky, E., Krueger, D., 2017a. Does vitamin D metabolite measurement help predict 25(OH)D change following vitamin D supplementation? Endocr. Pract. 23, 432–441.

Binkley, N., Dawson-Hughes, B., Durazo-Arvizu, R., Thamm, M., Tian, L., Merkel, J.M., Jones, J.C., Carter, G.D., Sempos, C.T., 2017b. Vitamin D measurement standardization: the way out of the chaos. J. Steroid Biochem. Mol. Biol. 173, 117–121.

Binkley, N., Krueger, D., Cowgill, C.S., Plum, L., Lake, E., Hansen, K.E., DeLuca, H.F., Drezner, M.K., 2004. Assay variation confounds the diagnosis of hypovitaminosis D: a call for standardization. J. Clin. Endocrinol. Metab. 89, 3152–3157.

Binkley, N., Lappe, J., Singh, R.J., Khosla, S., Krueger, D., Drezner, M.K., Blank, R.D., 2015. Can vitamin D metabolite measurements facilitate a "treat-to-target" paradigm to guide vitamin D supplementation? Osteoporos. Int. 26, 1655–1660.

Bischoff-Ferrari, H.A., Borchers, M., Gudat, F., Durmuller, U., Stahelin, H.B., Dick, W., 2004. Vitamin D receptor expression in human muscle tissue decreases with age. J. Bone Miner. Res. 19, 265–269.

Bischoff-Ferrari, H.A., Dawson-Hughes, B., Orav, E.J., Staehelin, H.B., Meyer, O.W., Theiler, R., Dick, W., Willett, W.C., Egli, A., 2016. Monthly high-dose vitamin D treatment for the prevention of functional decline: a randomized clinical trial. JAMA Intern. Med. 176, 175–183.

Bischoff-Ferrari, H.A., Dawson-Hughes, B., Staehelin, H.B., Orav, J.E., Stuck, A.E., Theiler, R., Wong, J.B., Egli, A., Kiel, D.P., Henschkowski, J., 2009. Fall prevention with supplemental and active forms of vitamin D: a meta-analysis of randomised controlled trials. Br. Med. J. 339, b3692.

Bolland, M.J., Grey, A., Gamble, G.D., Reid, I.R., 2014. Vitamin D supplementation and falls: a trial sequential meta-analysis. Lancet Diabetes Endocrinol. 2, 573–580.

Bora, S., Cantorna, M.T., 2017. The role of UVR and vitamin D on T cells and inflammatory bowel disease. Photochem. Photobiol. Sci. 16, 347–353.

Bouillon, R., 2017. Comparative analysis of nutritional guidelines for vitamin D. Nat. Rev. Endocrinol. 13, 466–479.

Brown, W.F., 1972. A method for estimating the number of motor units in thenar muscles and the changes in motor unit count with ageing. J. Neurol. Neurosurg. Psychiatry 35, 845–852.

Brozek, W., Manhardt, T., Kallay, E., Peterlik, M., Cross, H.S., 2012. Relative expression of vitamin D hydroxylases, CYP27B1 and CYP24A1, and of cyclooxygenase-2 and heterogeneity of human colorectal cancer in relation to age, gender, tumor location, and malignancy: results from factor and cluster analysis. Cancers 4, 763−776.

Byers, S.W., Rowlands, T., Beildeck, M., Bong, Y.S., 2012. Mechanism of action of vitamin D and the vitamin D receptor in colorectal cancer prevention and treatment. Rev. Endocr. Metab. Disord. 13, 31−38.

Cangussu, L.M., Nahas-Neto, J., Orsatti, C.L., Bueloni-Dias, F.N., Nahas, E.A., 2015. Effect of vitamin D supplementation alone on muscle function in postmenopausal women: a randomized, double-blind, placebo-controlled clinical trial. Osteoporos. Int. 26, 2413−2421.

Cangussu, L.M., Nahas-Neto, J., Orsatti, C.L., Poloni, P.F., Schmitt, E.B., Almeida-Filho, B., Nahas, E.A., 2016. Effect of isolated vitamin D supplementation on the rate of falls and postural balance in postmenopausal women fallers: a randomized, double-blind, placebo-controlled trial. Menopause 23, 267−274.

Cantorna, M.T., Hayes, C.E., DeLuca, H.F., 1996. 1, 25-dihydroxyvitamin D3 reversibly blocks the progression of relapsing encephalomyelitis, a model of multiple sclerosis. Proc. Natl. Acad. Sci. U.S.A. 93, 7861−7864.

Cantorna, M.T., Humpal-Winter, J., DeLuca, H.F., 1999. Dietary calcium is a major factor in 1,25-dihydroxycholecalciferol suppression of experimental autoimmune encephalomyelitis in mice. J. Nutr. 129, 1966−1971.

Cardus, A., Panizo, S., Encinas, M., Dolcet, X., Gallego, C., Aldea, M., Fernandez, E., Valdivielso, J.M., 2009. 1,25-dihydroxyvitamin D3 regulates VEGF production through a vitamin D response element in the VEGF promoter. Atherosclerosis 204, 85−89.

Carroll, C., Cooper, K., Papaioannou, D., Hind, D., Pilgrim, H., Tappenden, P., 2010. Supplemental calcium in the chemoprevention of colorectal cancer: a systematic review and meta-analysis. Clin. Ther. 32, 789−803.

Carter, G.D., Carter, R., Jones, J., Berry, J., 2004. How accurate are assays for 25-hydroxyvitamin D? Date from the international vitamin D external quality assessment scheme. Clin. Chem. 50, 2195−2197.

Cashman, K.D., 2014. A review of vitamin D status and CVD. Proc. Nutr. Soc. 73, 65−72.

Cashman, K.D., Dowling, K.G., Skrabakova, Z., Gonzalez-Gross, M., Valtuena, J., De Henauw, S., Moreno, L., Damsgaard, C.T., Michaelsen, K.F., Molgaard, C., Jorde, R., Grimnes, G., Moschonis, G., Mavrogianni, C., Manios, Y., Thamm, M., Mensink, G.B., Rabenberg, M., Busch, M.A., Cox, L., Meadows, S., Goldberg, G., Prentice, A., Dekker, J.M., Nijpels, G., Pilz, S., Swart, K.M., van Schoor, N.M., Lips, P., Eiriksdottir, G., Gudnason, V., Cotch, M.F., Koskinen, S., Lamberg-Allardt, C., Durazo-Arvizu, R.A., Sempos, C.T., Kiely, M., 2016a. Vitamin D deficiency in Europe: pandemic? Am. J. Clin. Nutr. 103, 1033−1044.

Cashman, K.D., Dowling, K.G., Skrabakova, Z., Kiely, M., Lamberg-Allardt, C., Durazo-Arvizu, R.A., Sempos, C.T., Koskinen, S., Lundqvist, A., Sundvall, J., Linneberg, A., Thuesen, B., Husemoen, L.L., Meyer, H.E., Holvik, K., Gronborg, I.M., Tetens, I., Andersen, R., 2015a. Standardizing serum 25-hydroxyvitamin D data from four Nordic population samples using the vitamin D standardization program protocols: shedding new light on vitamin D status in Nordic individuals. Scand. J. Clin. Lab. Invest. 75, 549−561.

Cashman, K.D., Hayes, A., Galvin, K., Merkel, J., Jones, G., Kaufmann, M., Hoofnagle, A.N., Carter, G.D., Durazo-Arvizu, R.A., Sempos, C.T., 2015b. Significance of serum 24,25-dihydroxyvitamin D in the assessment of vitamin D status: a double-edged sword? Clin. Chem. 61, 636−645.

Cashman, K.D., Kiely, M., Kinsella, M., Durazo-Arvizu, R.A., Tian, L., Zhang, Y., Lucey, A., Flynn, A., Gibney, M.J., Vesper, H.W., Phinney, K.W., Coates, P.M., Picciano, M.F., Sempos, C.T., 2013. Evaluation of vitamin D standardization program protocols for standardizing serum 25-hydroxyvitamin D data: a case study of the program's potential for national nutrition and health surveys. Am. J. Clin. Nutr. 97, 1235−1242.

Cashman, K.D., Kiely, M., Seamans, K.M., Urbain, P., 2016b. Effect of ultraviolet light-exposed mushrooms on vitamin D status: liquid chromatography-tandem mass spectrometry reanalysis of biobanked sera from a randomized controlled trial and a systematic review plus meta-analysis. J. Nutr. 146, 565−575.

Ceglia, L., Niramitmahapanya, S., da Silva Morais, M., Rivas, D.A., Harris, S.S., Bischoff-Ferrari, H., Fielding, R.A., Dawson-Hughes, B., 2013. A randomized study on the effect of vitamin D(3) supplementation on skeletal muscle morphology and vitamin D receptor concentration in older women. J. Clin. Endocrinol. Metab. 98, E1927−E1935.

Chang, S., Gao, L., Yang, Y., Tong, D., Guo, B., Liu, L., Li, Z., Song, T., Huang, C., 2015. miR-145 mediates the antiproliferative and gene regulatory effects of vitamin D3 by directly targeting E2F3 in gastric cancer cells. Oncotarget 6, 7675−7685.

Chen, P., Hu, P., Xie, D., Qin, Y., Wang, F., Wang, H., 2010. Meta-analysis of vitamin D, calcium and the prevention of breast cancer. Breast Canc. Res. Treat. 121, 469−477.

Chen, Y., Liu, W., Sun, T., Huang, Y., Wang, Y., Deb, D.K., Yoon, D., Kong, J., Thadhani, R., Li, Y.C., 2013. 1,25-Dihydroxyvitamin D promotes negative feedback regulation of TLR signaling via targeting microRNA-155-SOCS1 in macrophages. J. Immunol. 190, 3687−3695.

Chlebowski, R.T., 2011. Vitamin D and breast cancer: interpreting current evidence. Breast Cancer Res. 13, 217.

Cho, E., Smith-Warner, S.A., Spiegelman, D., Beeson, W.L., van den Brandt, P.A., Colditz, G.A., Folsom, A.R., Fraser, G.E., Freudenheim, J.L., Giovannucci, E., Goldbohm, R.A., Graham, S., Miller, A.B., Pietinen, P., Potter, J.D., Rohan, T.E., Terry, P., Toniolo, P., Virtanen, M.J., Willett, W.C., Wolk, A., Wu, K., Yaun, S.S., Zeleniuch-Jacquotte, A., Hunter, D.J., 2004. Dairy foods, calcium, and colorectal cancer: a pooled analysis of 10 cohort studies. J. Natl. Cancer Inst. 96, 1015−1022.

Christakos, S., Dhawan, P., Verstuyf, A., Verlinden, L., Carmeliet, G., 2016. Vitamin D: metabolism, molecular mechanism of action, and pleiotropic effects. Physiol. Rev. 96, 365−408.

Colotta, F., Jansson, B., Bonelli, F., 2017. Modulation of inflammatory and immune responses by vitamin D. J. Autoimmun. 85, 78−97.

Colston, K.W., Perks, C.M., Xie, S.P., Holly, J.M., 1998. Growth inhibition of both MCF-7 and Hs578T human breast cancer cell lines by vitamin D analogues is associated with increased expression of insulin-like growth factor binding protein-3. J. Mol. Endocrinol. 20, 157−162.

de la Hunty, A., Wallace, A.M., Gibson, S., Viljakainen, H., Lamberg-Allardt, C., Ashwell, M., 2010. UK foods standards agency workshop consensus report: the choice of method for measuring 25-hydroxyvitamin D to estimate vitamin D status for the UK National Diet and Nutrition Survey. Br. J. Nutr. 104, 612–619.

DeLuca, H.F., Plum, L.A., 2011. Vitamin D deficiency diminishes the severity and delays onset of experimental autoimmune encephalomyelitis. Arch. Biochem. Biophys. 513, 140–143.

Dobnig, H., Pilz, S., Scharnagl, H., Renner, W., Seelhorst, U., Wellnitz, B., Kinkeldei, J., Boehm, B.O., Weihrauch, G., Maerz, W., 2008. Independent association of low serum 25-hydroxyvitamin D and 1, 25-dihydroxyvitamin D levels with all-cause and cardiovascular mortality. Arch. Intern. Med. 168, 1340–1349.

Dong, J., Wong, S.L., Lau, C.W., Lee, H.K., Ng, C.F., Zhang, L., Yao, X., Chen, Z.Y., Vanhoutte, P.M., Huang, Y., 2012. Calcitriol protects renovascular function in hypertension by down-regulating angiotensin II type 1 receptors and reducing oxidative stress. Eur. Heart J. 33, 2980–2990.

Durazo-Arvizu, R.A., Tian, L., Brooks, S.P.J., Sarafin, K., Cashman, K.D., Kiely, M., Merkel, J., Myers, G.L., Coates, P.M., Sempos, C.T., 2017. The vitamin D standardization program (VDSP) manual for retrospective laboratory standardization of serum 25-hydroxyvitamin D data. J. AOAC Int. 100, 1234–1243.

Eide, M.J., Johnson, D.A., Jacobsen, G.R., Krajenta, R.J., Rao, D.S., Lim, H.W., Johnson, C.C., 2011. Vitamin D and nonmelanoma skin cancer in a health maintenance organization cohort. Arch. Dermatol. 147, 1379–1384.

El-Hajj Fuleihan, G., Nabulsi, M., Tamim, H., Maalouf, J., Salamoun, M., Khalife, H., Choucair, M., Arabi, A., Vieth, R., 2006. Effect of vitamin D replacement on musculoskeletal parameters in school children: a randomized controlled trial. J. Clin. Endocrinol. Metab. 91, 405–412.

Ellison, T.I., Smith, M.K., Gilliam, A.C., MacDonald, P.N., 2008. Inactivation of the vitamin D receptor enhances susceptibility of murine skin to UV-induced tumorigenesis. J. Invest. Dermatol. 128, 2508–2517.

Fernandes de Abreu, D.A., Ibrahim, E.C., Boucraut, J., Khrestchatisky, M., Feron, F., 2010. Severity of experimental autoimmune encephalomyelitis is unexpectedly reduced in mice born to vitamin D-deficient mothers. J. Steroid Biochem. Mol. Biol. 121, 250–253.

Gandini, S., Boniol, M., Haukka, J., Byrnes, G., Cox, B., Sneyd, M.J., Mullie, P., Autier, P., 2011. Meta-analysis of observational studies of serum 25-hydroxyvitamin D levels and colorectal, breast and prostate cancer and colorectal adenoma. Int. J. Cancer 128, 1414–1424.

Garland, C.F., Garland, F.C., 1980. Do sunlight and vitamin D reduce the likelihood of colon cancer? Int. J. Epidemiol. 9, 227–231.

Gilbert, R., Martin, R.M., Beynon, R., Harris, R., Savovic, J., Zuccolo, L., Bekkering, G.E., Fraser, W.D., Sterne, J.A., Metcalfe, C., 2011. Associations of circulating and dietary vitamin D with prostate cancer risk: a systematic review and dose-response meta-analysis. Cancer Causes Control 22, 319–340.

Ginde, A.A., Blatchford, P., Breese, K., Zarrabi, L., Linnebur, S.A., Wallace, J.I., Schwartz, R.S., 2017. High-dose monthly vitamin D for prevention of acute respiratory infection in older long-term care residents: a randomized clinical trial. J. Am. Geriatr. Soc. 65, 496–503.

Gocek, E., Wang, X., Liu, X., Liu, C.G., Studzinski, G.P., 2011. MicroRNA-32 upregulation by 1,25-dihydroxyvitamin D3 in human myeloid leukemia cells leads to Bim targeting and inhibition of AraC-induced apoptosis. Cancer Res. 71, 6230–6239.

Goswami, R., Vatsa, M., Sreenivas, V., Singh, U., Gupta, N., Lakshmy, R., Aggarwal, S., Ganapathy, A., Joshi, P., Bhatia, H., 2012. Skeletal muscle strength in young Asian Indian females after vitamin D and calcium supplementation: a double-blind randomized controlled clinical trial. J. Clin. Endocrinol. Metab. 97, 4709–4716.

Graeff-Armas, L.A., Kaufmann, M., Lyden, E., Jones, G., 2018. Serum 24,25-dihydroxyvitamin D3 response to native vitamin D2 and D3 Supplementation in patients with chronic kidney disease on hemodialysis. Clin. Nutr. 37, 1041–1045.

Gupta, R., Dixon, K.M., Deo, S.S., Holliday, C.J., Slater, M., Halliday, G.M., Reeve, V.E., Mason, R.S., 2007. Photoprotection by 1,25 dihydroxyvitamin D3 is associated with an increase in p53 and a decrease in nitric oxide products. J. Invest. Dermatol. 127, 707–715.

Gysemans, C., van Etten, E., Overbergh, L., Giulietti, A., Eelen, G., Waer, M., Verstuyf, A., Bouillon, R., Mathieu, C., 2008. Unaltered diabetes presentation in NOD mice lacking the vitamin D receptor. Diabetes 57, 269–275.

Hager, G., Formanek, M., Gedlicka, C., Thurnher, D., Knerer, B., Kornfehl, J., 2001. 1,25(OH)2 vitamin D3 induces elevated expression of the cell cycle-regulating genes P21 and P27 in squamous carcinoma cell lines of the head and neck. Acta Otolaryngol. 121, 103–109.

Hansen, K.E., Johnson, R.E., Chambers, K.R., Johnson, M.G., Lemon, C.C., Vo, T.N., Marvdashti, S., 2015. Treatment of vitamin D insufficiency in postmenopausal women: a randomized clinical trial. JAMA Intern. Med. 175, 1612–1621.

Hartholt, K.A., van Beeck, E.F., van der Cammen, T.J.M., 2018. Mortality from falls in Dutch adults 80 Years and older, 2000-2016. J. Am. Med. Assoc. 319, 1380–1382.

Hayes, C.E., Hubler, S.L., Moore, J.R., Barta, L.E., Praska, C.E., Nashold, F.E., 2015. Vitamin D actions on CD4(+) T cells in autoimmune disease. Front. Immunol. 6, 100.

Heaney, R.P., 2012. Vitamin D–baseline status and effective dose. N. Engl. J. Med. 367, 77–78.

Heaney, R.P., 2014. Guidelines for optimizing design and analysis of clinical studies of nutrient effects. Nutr. Rev. 72, 48–54.

Heaney, R.P., Armas, L.A., 2015. Quantifying the vitamin D economy. Nutr. Rev. 73, 51–67.

Helming, L., Bose, J., Ehrchen, J., Schiebe, S., Frahm, T., Geffers, R., Probst-Kepper, M., Balling, R., Lengeling, A., 2005. 1alpha,25-Dihydroxyvitamin D3 is a potent suppressor of interferon gamma-mediated macrophage activation. Blood 106, 4351–4358.

Hempel, S., Graham, G.D., Fu, N., Estrada, E., Chen, A.Y., Miake-Lye, I., Miles, J.N., Shanman, R., Shekelle, P.G., Beroes, J.M., Wallin, M.T., 2017. A systematic review of the effects of modifiable risk factor interventions on the progression of multiple sclerosis. Mult. Scler. 23, 513–524.

Herrmann, M., Farrell, C.L., Pusceddu, I., Fabregat-Cabello, N., Cavalier, E., 2017. Assessment of vitamin D status – a changing landscape. Clin. Chem. Lab. Med. 55, 3–26.

Holick, M.F., 2008. The vitamin D deficiency pandemic and consequences for nonskeletal health: mechanisms of action. Mol. Aspects Med. 29, 361–368.

Holick, M.F., 2011. Vitamin D: evolutionary, physiological and health perspectives. Curr. Drug Targets 12, 4–18.

Holick, M.F., 2017. The vitamin D deficiency pandemic: approaches for diagnosis, treatment and prevention. Rev. Endocr. Metab. Disord. 18, 153–165.

Holick, M.F., Binkley, N., Bischoff-Ferrari, H.A., Gordon, C.M., Hanley, D.A., Heaney, R.P., Murad, M.H., Weaver, C.M., 2011. Evaluation, treatment, and prevention of vitamin D deficiency: an endocrine society clinical practice guideline. J. Clin. Endocrinol. Metab. 96, 1911–1930.

Hollis, B.W., Wagner, C.L., 2013. Clinical review: the role of the parent compound vitamin D with respect to metabolism and function: why clinical dose intervals can affect clinical outcomes. J. Clin. Endocrinol. Metab. 98, 4619–4628.

Hunter, D.J., Colditz, G.A., Stampfer, M.J., Rosner, B., Willett, W.C., Speizer, F.E., 1992. Diet and risk of basal cell carcinoma of the skin in a prospective cohort of women. Ann. Epidemiol. 2, 231–239.

Huynh, H., Pollak, M., Zhang, J.C., 1998. Regulation of insulin-like growth factor (IGF) II and IGF binding protein 3 autocrine loop in human PC-3 prostate cancer cells by vitamin D metabolite 1,25(OH)2D3 and its analog EB1089. Int. J. Oncol. 13, 137–143.

Institute of Medicine, 2010. Dietary Reference Intakes for Calcium and Vitamin D. Available online: http://www.iom.edu/Reports/2010/Dietary-Reference-Intakes-for-Calcium-and-Vitamin-D/Report-Brief.aspx?page=1.

Irani, P.F., 1976. Electromyography in nutritional osteomalacic myopathy. J. Neurol. Neurosurg. Psychiatry 39, 686–693.

Jones, G., Kaufmann, M., 2016. Vitamin D metabolite profiling using liquid chromatography-tandem mass spectrometry (LC-MS/MS). J. Steroid Biochem. Mol. Biol. 164, 110–114.

Jones, G., Schlingmann, K.-P., 2018. Hypercalcemic states associated with abnormalities in vitamin D metabolism. In: Giustina, A., Bilezikian, J.P. (Eds.), Vitamin D in Clinical Medicine, Frontiers of Hormone Research. Karger, Basal, Switzerland, pp. 89–113.

Kaufmann, M., Gallagher, C., Peacock, M., Schlingmann, K.P., Konrad, M., Deluca, H.F., Sigueiro, R., Lopez, B., Mourino, A., Maestro, M., St-Arnaud, R., Finkelstein, J., Cooper, D.P., Jones, G., 2014. Clinical utility of simultaneous quantitation of 25-hydroxyvitamin D & 24,25-dihydroxyvitamin D by LC-MS/MS involving derivatization with DMEQ-TAD. J. Clin. Endocrinol. Metab. 99, 2567–2574.

Kendrick, J., Targher, G., Smits, G., Chonchol, M., 2009. 25-Hydroxyvitamin D deficiency is independently associated with cardiovascular disease in the Third National Health and Nutrition Examination Survey. Atherosclerosis 205, 255–260.

Ketha, H., Thacher, T.D., Oberhelman, S.S., Fischer, P.R., Singh, R.J., Kumar, R., 2018. Comparison of the effect of daily versus bolus dose maternal vitamin D3 supplementation on the 24,25-dihydroxyvitamin D3 to 25-hydroxyvitamin D3 ratio. Bone 110, 321–325.

Khaw, K.T., Stewart, A.W., Waayer, D., Lawes, C.M.M., Toop, L., Camargo Jr., C.A., Scragg, R., 2017. Effect of monthly high-dose vitamin D supplementation on falls and non-vertebral fractures: secondary and post-hoc outcomes from the randomised, double-blind, placebo-controlled ViDA trial. Lancet Diabetes Endocrinol 5, 438–447.

Kizildag, S., Ates, H., Kizildag, S., 2010. Treatment of K562 cells with 1,25-dihydroxyvitamin D3 induces distinct alterations in the expression of apoptosis-related genes BCL2, BAX, BCLXL, and p21. Ann. Hematol. 89, 1–7.

Krishnan, A.V., Trump, D.L., Johnson, C.S., Feldman, D., 2010. The role of vitamin D in cancer prevention and treatment. Endocrinol. Metab. Clin. North Am. 39, 401–418 (table of contents).

Le Goff, C., Cavalier, E., Souberbielle, J.-C., Gonzalez-Antuna, A., Delvin, E., 2015. Measurement of circulating 25-hydroxyvitamin D: a historical review. Pract. Lab. Med. 2, 1–14.

LeBlanc, E.S., Chou, R., 2015. Vitamin D and falls-fitting new data with current guidelines. JAMA Intern. Med. 175, 712–713.

Lemire, J.M., Archer, D.C., 1991. 1,25-dihydroxyvitamin D3 prevents the in vivo induction of murine experimental autoimmune encephalomyelitis. J. Clin. Invest. 87, 1103–1107.

Levis, S., Gomez-Marin, O., 2017. Vitamin D and physical function in sedentary older men. J. Am. Geriatr. Soc. 65, 323–331.

Lin, J., Manson, J.E., Lee, I.M., Cook, N.R., Buring, J.E., Zhang, S.M., 2007. Intakes of calcium and vitamin D and breast cancer risk in women. Arch. Intern. Med. 167, 1050–1059.

Lipkin, M., Newmark, H.L., 1999. Vitamin D, calcium and prevention of breast cancer: a review. J. Am. Coll. Nutr. 18, 392S–397S.

Looker, A.C., Johnson, C.L., Lacher, D.A., Pfeiffer, C.M., Schleicher, R.L., Sempos, C.T., 2011. Vitamin D status: United States, 2001–2006. NCHS Data Brief 1–8.

Ma, Y., Zhang, P., Wang, F., Yang, J., Liu, Z., Qin, H., 2011. Association between vitamin D and risk of colorectal cancer: a systematic review of prospective studies. J. Clin. Oncol. 29, 3775–3782.

Matusiak, D., Benya, R.V., 2007. CYP27A1 and CYP24 expression as a function of malignant transformation in the colon. J. Histochem. Cytochem. 55, 1257–1264.

McGaffin, K.R., Chrysogelos, S.A., 2005. Identification and characterization of a response element in the EGFR promoter that mediates transcriptional repression by 1,25-dihydroxyvitamin D3 in breast cancer cells. J. Mol. Endocrinol. 35, 117–133.

Meehan, T.F., Vanhooke, J., Prahl, J., Deluca, H.F., 2005. Hypercalcemia produced by parathyroid hormone suppresses experimental autoimmune encephalomyelitis in female but not male mice. Arch. Biochem. Biophys. 442, 214–221.

Merke, J., Milde, P., Lewicka, S., Hugel, U., Klaus, G., Mangelsdorf, D.J., Haussler, M.R., Rauteerberg, E.W., Ritz, E., 1989. Identification and regulation of 1, 25-dihydroxyvitamin D3 receptor activity and biosynthesis of 1, 25-dihydroxyvitamin D3: studies in cultured bovine aortic endothelial cells and human dermal capillaries. J. Clin. Invest. 83, 1903–1915.

Meyer, M.B., Goetsch, P.D., Pike, J.W., 2012. VDR/RXR and TCF4/beta-catenin cistromes in colonic cells of colorectal tumor origin: impact on c-FOS and c-MYC gene expression. Mol. Endocrinol. 26, 37–51.

Mineva, E.M., Schleicher, R.L., Chaudhary-Webb, M., Maw, K.L., Botelho, J.C., Vesper, H.W., et al., 2015. A candidate reference measurement procedure for quantifying serum concentrations of 25-hydroxyvitamin D(3) and 25-hydroxyvitamin D(2) using isotope-dilution liquid chromatography-tandem mass spectrometry. Anal. Bioanal. Chem. 407 (19), 5615−5624.

Molin, A., Baudoin, R., Kaufmann, M., Souberbielle, J.C., Ryckewaert, A., Vantyghem, M.C., Eckart, P., Bacchetta, J., Deschenes, G., Kesler-Roussey, G., Coudray, N., Richard, N., Wraich, M., Bonafiglia, Q., Tiulpakov, A., Jones, G., Kottler, M.L., 2015. CYP24A1 mutations in a cohort of hypercalcemic patients: evidence for a recessive trait. J. Clin. Endocrinol. Metab. 100, E1343−E1352.

Mordan-McCombs, S., Brown, T., Wang, W.L., Gaupel, A.C., Welsh, J., Tenniswood, M., 2010. Tumor progression in the LPB-Tag transgenic model of prostate cancer is altered by vitamin D receptor and serum testosterone status. J. Steroid Biochem. Mol. Biol. 121, 368−371.

Murad, M.H., Elamin, K.B., Elnour, N.O.A., Elamin, M.B., Alkatib, A.A., Fatourechi, M.M., Almandoz, J.P., Mullan, R.J., Lane, M.A., Liu, H., Erwin, P.J., Hensrud, D.D., Montori, V.M., 2011. The effect of vitamin D on falls: a systematic review and meta-analysis. J. Clin. Endocrinol. Metab. 96, 2997−3006.

Murillo, G., Nagpal, V., Tiwari, N., Benya, R.V., Mehta, R.G., 2010. Actions of vitamin D are mediated by the TLR4 pathway in inflammation-induced colon cancer. J. Steroid Biochem. Mol. Biol. 121, 403−407.

Nemerovski, C.W., Dorsch, M.P., Simpson, R.U., Bone, H.G., Aaronson, K.D., Bleske, B.E., 2009. Vitamin D and cardiovascular disease. Pharmacotherapy 29, 691−708.

Newmark, H.L., Yang, K., Kurihara, N., Fan, K., Augenlicht, L.H., Lipkin, M., 2009. Western-style diet-induced colonic tumors and their modulation by calcium and vitamin D in C57Bl/6 mice: a preclinical model for human sporadic colon cancer. Carcinogenesis 30, 88−92.

Norman, P.E., Powell, J.T., 2014. Vitamin D and cardiovascular disease. Circ. Res. 114, 379−393.

Palacios, C., Gonzalez, L., 2014. Is vitamin D deficiency a major global public health problem? J. Steroid Biochem. Mol. Biol. 144 (Pt A), 138−145.

Palmer, H.G., Sanchez-Carbayo, M., Ordonez-Moran, P., Larriba, M.J., Cordon-Cardo, C., Munoz, A., 2003. Genetic signatures of differentiation induced by 1alpha,25-dihydroxyvitamin D3 in human colon cancer cells. Cancer Res. 63, 7799−7806.

Peehl, D.M., Shinghal, R., Nonn, L., Seto, E., Krishnan, A.V., Brooks, J.D., Feldman, D., 2004. Molecular activity of 1,25-dihydroxyvitamin D3 in primary cultures of human prostatic epithelial cells revealed by cDNA microarray analysis. J. Steroid Biochem. Mol. Biol. 92, 131−141.

Peelen, E., Knippenberg, S., Muris, A.H., Thewissen, M., Smolders, J., Tervaert, J.W., Hupperts, R., Damoiseaux, J., 2011. Effects of vitamin D on the peripheral adaptive immune system: a review. Autoimmun. Rev. 10, 733−743.

Pendas-Franco, N., Garcia, J.M., Pena, C., Valle, N., Palmer, H.G., Heinaniemi, M., Carlberg, C., Jimenez, B., Bonilla, F., Munoz, A., Gonzalez-Sancho, J.M., 2008. DICKKOPF-4 is induced by TCF/beta-catenin and upregulated in human colon cancer, promotes tumour cell invasion and angiogenesis and is repressed by 1alpha,25-dihydroxyvitamin D3. Oncogene 27, 4467−4477.

Pfeifer, M., Begerow, B., Minne, H.W., Suppan, K., Fahrleitner-Pammer, A., Dobnig, H., 2009. Effects of a long-term vitamin D and calcium supplementation on falls and parameters of muscle function in community-dwelling older individuals. Osteoporos. Int. 20, 315−322.

Phinney, K.W., Tai, S.S., Bedner, M., Camara, J.E., Chia, R.R.C., Sander, L.C., et al., 2017. Development of an Improved Standard Reference Material for Vitamin D Metabolites in Human Serum. Anal. Chem. 89 (9), 4907−4913.

Pilz, S., Marz, W., Wellnitz, B., Seelhorst, U., Fahrleitner-Pammer, A., Dimai, H.P., Boehm, B.O., Dobnig, H., 2008. Association of vitamin D deficiency with heart failure and sudden cardiac death in a large cross-sectional study of patients referred for coronary angiography. J. Clin. Endocrinol. Metab. 93, 3927−3935.

Pilz, S., Tomaschitz, A., Drechsler, C., Dekker, J.M., Marz, W., 2010. Vitamin D deficiency and myocardial diseases. Mol. Nutr. Food Res. 54, 1103−1113.

Rejnmark, L., Bislev, L.S., Cashman, K.D., Eiriksdottir, G., Gaksch, M., Grubler, M., Grimnes, G., Gudnason, V., Lips, P., Pilz, S., van Schoor, N.M., Kiely, M., Jorde, R., 2017. Non-skeletal health effects of vitamin D supplementation: a systematic review on findings from meta-analyses summarizing trial data. PLoS One 12, e0180512.

Rodriguez, A.J., Mousa, A., Ebeling, P.R., Scott, D., de Courten, B., 2018. Effects of vitamin D supplementation on inflammatory markers in heart failure: a systematic review and meta-analysis of randomized controlled trials. Sci. Rep. 8, 1169.

Rosen, C.J., Adams, J.S., Bikle, D.D., Black, D.M., Demay, M.B., Manson, J.E., Murad, M.H., Kovacs, C.S., 2012. The nonskeletal effects of vitamin D: an Endocrine Society scientific statement. Endocr. Rev. 33, 456−492.

Rossi, M., McLaughlin, J.K., Lagiou, P., Bosetti, C., Talamini, R., Lipworth, L., Giacosa, A., Montella, M., Franceschi, S., Negri, E., La Vecchia, C., 2009. Vitamin D intake and breast cancer risk: a case-control study in Italy. Ann. Oncol. 20, 374−378.

Rostand, S.G., Drueke, T.B., 1999. Parathyroid hormone, vitamin D, and cardiovascular disease in chronic renal failure. Kidney Int. 56, 383−392.

Sackett, D.L., Rosenberg, W.M., Gray, J.A., Haynes, R.B., Richardson, W.S., 1996. Evidence based medicine: what it is and what it isn't. BMJ 312, 71−72.

Sanders, K.M., Stuart, A.L., Williamson, E.J., Simpson, J.A., Kotowicz, M.A., Young, D., Nicholson, G.C., 2010. Annual high-dose oral vitamin D and falls and fractures in older women. J. Am. Med. Assoc. 303, 1815−1822.

Santagata, S., Thakkar, A., Ergonul, A., Wang, B., Woo, T., Hu, R., Harrell, J.C., McNamara, G., Schwede, M., Culhane, A.C., Kindelberger, D., Rodig, S., Richardson, A., Schnitt, S.J., Tamimi, R.M., Ince, T.A., 2014. Taxonomy of breast cancer based on normal cell phenotype predicts outcome. J. Clin. Invest. 124, 859−870.

Sarafin, K., Durazo-Arvizu, R., Tian, L., Phinney, K.W., Tai, S., Camara, J.E., Merkel, J., Green, E., Sempos, C.T., Brooks, S.P., 2015. Standardizing 25-hydroxyvitamin D values from the Canadian health measures survey. Am. J. Clin. Nutr. 102, 1044−1050.

Scher, H.I., Jia, X., Chi, K., de Wit, R., Berry, W.R., Albers, P., Henick, B., Waterhouse, D., Ruether, D.J., Rosen, P.J., Meluch, A.A., Nordquist, L.T., Venner, P.M., Heidenreich, A., Chu, L., Heller, G., 2011. Randomized, open-label phase III trial of docetaxel plus high-dose calcitriol versus docetaxel plus prednisone for patients with castration-resistant prostate cancer. J. Clin. Oncol. 29, 2191–2198.

Schleicher, R.L., Sternberg, M.R., Lacher, D.A., Sempos, C.T., Looker, A.C., Durazo-Arvizu, R.A., Yetley, E.A., Chaudhary-Webb, M., Maw, K.L., Pfeiffer, C.M., Johnson, C.L., 2016. The vitamin D status of the US population from 1988 to 2010 using standardized serum concentrations of 25-hydroxyvitamin D shows recent modest increases. Am. J. Clin. Nutr. 104, 454–461.

Scientific Advisory Committee on Nutrition (SACN), 2016. SACN vitamin D and health report. In: England, P.H. (Ed.), SACN: Reports and Position Statements. Public Health England.

Sempos, C.T., Betz, J.M., Camara, J.E., Carter, G.D., Cavalier, E., Clarke, M.W., Dowling, K.G., Durazo-Arvizu, R.A., Hoofnagle, A.N., Liu, A., Phinney, K.W., Sarafin, K., Wise, S.A., Coates, P.M., 2017. General steps to standardize the laboratory measurement of serum total 25-hydroxyvitamin D. J. AOAC Int. 100, 1230–1233.

Sempos, C.T., Vesper, H.W., Phinney, K.W., Thienpont, L.M., Coates, P.M., 2012. Vitamin D status as an international issue: national surveys and the problem of standardization. Scand. J. Clin. Lab. Invest. 72, 32–40.

Shin, M.H., Holmes, M.D., Hankinson, S.E., Wu, K., Colditz, G.A., Willett, W.C., 2002. Intake of dairy products, calcium, and vitamin d and risk of breast cancer. J. Natl. Cancer Inst. 94, 1301–1311.

Skaria, J., Katiyar, B.C., Srivastava, T.P., Dube, B., 1975. Myopathy and neuropathy associated with osteomalacia. Acta Neurol. Scand. 51, 37–58.

Stockl, D., Sluss, P.M., Thienpont, L.M., 2009. Specifications for trueness and precision of a reference measurement system for serum/plasma 25-hydroxyvitamin D analysis. Clin. Chim. Acta. 408 (1-2), 8–13.

Stumpf, W.E., Bidmon, H.J., Murakami, R., Heiss, C., Mayerhofer, A., Bartke, A., 1990. Sites of action of soltriol (vitamin D) in hamster spleen, thymus, and lymph node, studied by autoradiography. Histochemistry 94, 121–125.

Stumpf, W.E., Downs, T.W., 1987. Nuclear receptors for 1,25(OH)2 vitamin D3 in thymus reticular cells studied by autoradiography. Histochemistry 87, 367–369.

Swami, S., Raghavachari, N., Muller, U.R., Bao, Y.P., Feldman, D., 2003. Vitamin D growth inhibition of breast cancer cells: gene expression patterns assessed by cDNA microarray. Breast Canc. Res. Treat. 80, 49–62.

Tai, S., Nelson, M., Bedner, M., Lang, B., Phinney, K., Sander, L., et al., 2017. Development of Standard Reference Material (SRM) 2973 Vitamin D Metabolites in Frozen Human Serum (High Level). J AOAC Int. 100 (5), 1294–1303.

Tang, J.Y., Fu, T., Leblanc, E., Manson, J.E., Feldman, D., Linos, E., Vitolins, M.Z., Zeitouni, N.C., Larson, J., Stefanick, M.L., 2011. Calcium plus vitamin D supplementation and the risk of nonmelanoma and melanoma skin cancer: post hoc analyses of the women's health initiative randomized controlled trial. J. Clin. Oncol. 29, 3078–3084.

Tang, J.Y., Parimi, N., Wu, A., Boscardin, W.J., Shikany, J.M., Chren, M.M., Cummings, S.R., Epstein Jr., E.H., Bauer, D.C., 2010. Inverse association between serum 25(OH) vitamin D levels and non-melanoma skin cancer in elderly men. Cancer Causes Control 21, 387–391.

Tannour-Louet, M., Lewis, S.K., Louet, J.F., Stewart, J., Addai, J.B., Sahin, A., Vangapandu, H.V., Lewis, A.L., Dittmar, K., Pautler, R.G., Zhang, L., Smith, R.G., Lamb, D.J., 2014. Increased expression of CYP24A1 correlates with advanced stages of prostate cancer and can cause resistance to vitamin D3-based therapies. FASEB J. 28, 364–372.

Teichert, A.E., Elalieh, H., Elias, P.M., Welsh, J., Bikle, D.D., 2011. Overexpression of hedgehog signaling is associated with epidermal tumor formation in vitamin D receptor-null mice. J. Invest. Dermatol. 131, 2289–2297.

Tinetti, M.E., Williams, C.S., 1997. Falls, injuries due to falls, and the risk of admission to a nursing home. N. Engl. J. Med. 337, 1279–1284.

Tishkoff, D.X., Nibbelink, K.A., Holmberg, K.H., Dandu, L., Simpson, R.U., 2008. Functional vitamin D receptor (VDR) in the t-tubules of cardiac myocytes: VDR knockout cardiomyocyte contractility. Endocrinology 149, 558–564.

Uusi-Rasi, K., Patil, R., Karinkanta, S., Kannus, P., Tokola, K., Lamberg-Allardt, C., Sievanen, H., 2015. Exercise and vitamin D in fall prevention among older women: a randomized clinical trial. JAMA Intern. Med. 175, 703–711.

USDHHS, 2014. The Surgeon General's Call to Action to Prevent Skin Cancer (Washington, DC).

van der Rhee, H.J., de Vries, E., Coebergh, J.W., 2006. Does sunlight prevent cancer? A systematic review. Eur. J. Cancer 42, 2222–2232.

VanAmerongen, B.M., Dijkstra, C.D., Lips, P., Polman, C.H., 2004. Multiple sclerosis and vitamin D: an update. Eur. J. Clin. Nutr. 58, 1095–1109.

Vandervoort, A.A., 2002. Aging of the human neuromuscular system. Muscle Nerve 25, 17–25.

VanWeelden, K., Flanagan, L., Binderup, L., Tenniswood, M., Welsh, J., 1998. Apoptotic regression of MCF-7 xenografts in nude mice treated with the vitamin D3 analog, EB1089. Endocrinology 139, 2102–2110.

Vieth, R., 2009. How to optimize vitamin D supplementation to prevent cancer, based on cellular adaptation and hydroxylase enzymology. Anticancer Res. 29, 3675–3684.

Wactawski-Wende, J., Kotchen, J.M., Anderson, G.L., Assaf, A.R., Brunner, R.L., O'Sullivan, M.J., Margolis, K.L., Ockene, J.K., Phillips, L., Pottern, L., Prentice, R.L., Robbins, J., Rohan, T.E., Sarto, G.E., Sharma, S., Stefanick, M.L., Van Horn, L., Wallace, R.B., Whitlock, E., Bassford, T., Beresford, S.A., Black, H.R., Bonds, D.E., Brzyski, R.G., Caan, B., Chelebowski, R.T., Cochrane, B., Garland, C., Gass, M., Hays, J., Heiss, G., Hendrix, S.L., Howard, B.V., Hsia, J., Hubbell, F.A., Jackson, R.D., Johnson, K.C., Judd, H., Kooperberg, C.L., Kuller, L.H., LaCroix, A.Z., Lane, D.S., Langer, R.D., Lasser, N.L., Lewis, C.E., Limacher, M.C., Manson, J.E., 2006. Calcium plus vitamin D supplementation and the risk of colorectal cancer. N. Engl. J. Med. 354, 684–696.

Wagner, D., Hanwell, H.E., Schnabl, K., Yazdanpanah, M., Kimball, S., Fu, L., Sidhom, G., Rousseau, D., Cole, D.E.C., Vieth, R., 2011. The ratio of serum 24, 25-dihydroxyvitamin D3 to serum 25-hydroxyvitamin D3 is predictive of 25-hydroxyvitamin D3 response to vitamin D3 supplementation. J. Steroid Biochem. Mol. Biol. 126, 72–77.

Wallace, A.M., Gibson, S., de la Hunty, A., Lamberg-Allardt, C., Ashwell, M., 2010. Measurement of 25-hydroxyvitamin D in the clinical laboratory: current procedures, performance characteristics and limitations. Steroids 75, 477−488.

Wang, H., Chen, W., Li, D., Yin, X., Zhang, X., Olsen, N., Zheng, S.G., 2017. Vitamin D and chronic diseases. Aging Dis 8, 346−353.

Wang, L., Song, Y., Manson, J.E., Pilz, S., Marz, W., Michaelsson, K., Lundqvist, A., Jassal, S.K., Barrett-Connor, E., Zhang, C., Eaton, C.B., May, H.T., Anderson, J.L., Sesso, H.D., 2012a. Circulating 25-hydroxy-vitamin D and risk of cardiovascular disease: a meta-analysis of prospective studies. Circ. Cardiovasc. Qual. Outcomes 5, 819−829.

Wang, T.J., Pencina, M.J., Booth, S.L., Jacques, P.F., Ingelsson, E., Lanier, K., Benjamin, E.J., D'Agostino, R.B., Wolf, M., Vasan, R.S., 2008. Vitamin D deficiency and risk of cardiovascular disease. Circulation 117, 503−511.

Wang, Y., Marling, S.J., Zhu, J.G., Severson, K.S., DeLuca, H.F., 2012b. Development of experimental autoimmune encephalomyelitis (EAE) in mice requires vitamin D and the vitamin D receptor. Proc. Natl. Acad. Sci. U.S.A. 109, 8501−8504.

Wang, Y., Zhu, J., DeLuca, H.F., 2012c. Where is the vitamin D receptor? Arch. Biochem. Biophys. 523, 123−133.

Weitsman, G.E., Koren, R., Zuck, E., Rotem, C., Liberman, U.A., Ravid, A., 2005. Vitamin D sensitizes breast cancer cells to the action of H2O2: mitochondria as a convergence point in the death pathway. Free Radic. Biol. Med. 39, 266−278.

Weitsman, G.E., Ravid, A., Liberman, U.A., Koren, R., 2003. Vitamin D enhances caspase-dependent and independent TNF-induced breast cancer cell death: the role of reactive oxygen species. Ann. N.Y. Acad. Sci. 1010, 437−440.

Wierman, M.E., Auchus, R.J., Haisenleder, D.J., Hall, J.E., Handelsman, D., Hankinson, S., Rosner, W., Singh, R.J., Sluss, P.M., Stanczyk, F.Z., 2014. Editorial: the new instructions to authors for the reporting of steroid hormone measurements. J. Clin. Endocrinol. Metab. 99, 4375.

Xu, H., Posner, G.H., Stevenson, M., Campbell, F.C., 2010. Apc(MIN) modulation of vitamin D secosteroid growth control. Carcinogenesis 31, 1434−1441.

Yang, K., Lamprecht, S.A., Shinozaki, H., Fan, K., Yang, W., Newmark, H.L., Kopelovich, L., Edelmann, W., Jin, B., Gravaghi, C., Augenlicht, L., Kucherlapati, R., Lipkin, M., 2008. Dietary calcium and cholecalciferol modulate cyclin D1 expression, apoptosis, and tumorigenesis in intestine of adenomatous polyposis coli1638N/+ mice. J. Nutr. 138, 1658−1663.

Yang, L., Yang, J., Venkateswarlu, S., Ko, T., Brattain, M.G., 2001. Autocrine TGFbeta signaling mediates vitamin D3 analog-induced growth inhibition in breast cells. J. Cell. Physiol. 188, 383−393.

Zella, J.B., McCary, L.C., DeLuca, H.F., 2003. Oral administration of 1,25-dihydroxyvitamin D3 completely protects NOD mice from insulin-dependent diabetes mellitus. Arch. Biochem. Biophys. 417, 77−80.

Zheng, C., He, L., Liu, L., Zhu, J., Jin, T., 2018. The efficacy of vitamin D in multiple sclerosis: a meta-analysis. Mult. Scler. Relat. Disord. 23, 56−61.

Zheng, W., Wong, K.E., Zhang, Z., Dougherty, U., Mustafi, R., Kong, J., Deb, D.K., Zheng, H., Bissonnette, M., Li, Y.C., 2012. Inactivation of the vitamin D receptor in APC(min/+) mice reveals a critical role for the vitamin D receptor in intestinal tumor growth. Int. J. Cancer 130, 10−19.

Zheng, Y., Zhou, H., Ooi, L.L., Snir, A.D., Dunstan, C.R., Seibel, M.J., 2011. Vitamin D deficiency promotes prostate cancer growth in bone. Prostate 71, 1012−1021.

Zinser, G.M., Welsh, J., 2004. Effect of Vitamin D3 receptor ablation on murine mammary gland development and tumorigenesis. J. Steroid Biochem. Mol. Biol. 89−90, 433−436.

Chapter 32

Cellular actions of parathyroid hormone on bone

Elena Ambrogini[1,2] and Robert L. Jilka[1,2]

[1]Center for Osteoporosis and Metabolic Bone Diseases, University of Arkansas for Medical Sciences Division of Endocrinology and Metabolism, Little Rock, AR, United States; [2]Central Arkansas Veterans Healthcare System, Little Rock, AR, United States

Chapter outline

Introduction

Parathyroid hormone (PTH) maintains serum Ca homeostasis by direct actions on the kidney and on bone. A fall in serum Ca enhances the activity of the Ca-sensing receptor of parathyroid glands, which immediately increases the secretion of PTH into the circulation. The rise in PTH enhances tubular reabsorption of Ca and the synthesis of 1,25-dihydroxyvitamin D3 in the kidney, which in turn stimulates intestinal Ca absorption. PTH also enhances the release of Ca from bone by increasing osteoclastic bone resorption. The cumulative impact is a rise in serum Ca which then lowers the secretion of PTH, leading to reduced tubular Ca reabsorption, Ca absorption from the gut, and osteoclastic bone resorption.

In adults, bone resorption only takes place at sites of bone remodeling (Parfitt, 1996). This process is carried out by anatomically discrete teams of osteoclasts and osteoblasts, which along with an associated capillary are called basic multicellular units (BMUs). PTH drives the assembly and maintenance of BMUs. Remodeling replaces old or damaged bone with new. In the ilium of postmenopausal women, BMUs remodel 18% of the trabecular bone surface per year and 34% of the endocortical surface. BMUs arise within Haversian canals and tunnel through the cortex to remodel 6% of the cortical bone volume per year (Parfitt, 2002). Trabecular and endocortical surfaces undergo remodeling in laboratory rodents, but in these small mammals the Haversian system is absent (Piemontese et al., 2017). PTH may also stimulate osteocytes to degrade their surrounding lacunar bone (Baud and Boivin, 1978; Tazawa et al., 2004). The high demand for Ca during lactation may be met by PTHrP-stimulated osteocytic osteolysis in rodents (Kovacs, 2017), but the role of this phenomenon in day-to-day Ca homeostasis has not been established. In contrast to the role of PTH in Ca homeostasis, daily injections of exogenous PTH (aka intermittent administration) increase bone mass. This latter feature of PTH function has been employed for the therapy of osteoporosis (Hodsman et al., 2005). This chapter focuses on the cellular mechanisms underlying the diverse effects of PTH on bone.

Principles of Bone Biology. https://doi.org/10.1016/B978-0-12-814841-9.00032-4

The regulation of bone remodeling by parathyroid hormone

Osteoclasts initiate bone remodeling by adhering to the bone surface and forming a tightly sealed pocket into which they pump HCl and secrete lysosomes that dissolve the hydroxyapatite and degrade the collagenous and other proteinaceous components of the matrix. The degraded proteins are packaged into endosomes, transcytosed to the apical surface, and released into the extracellular space (Salo et al., 1997). Bone formation is temporally and spatially linked to this resorptive activity within the BMU in a process called coupling, which ensures that sufficient bone matrix is made to replace the one removed by osteoclasts (Sims and Martin, 2014). Mesenchymal precursors of the osteoblast lineage are recruited to the previously resorbed surface where they intermingle with some of the osteoclasts to form a "reversal-resorption" surface (Lassen et al., 2017). The mesenchymal cells deposit a thin layer of glycosaminoglycan-containing matrix that marks the limit of bone resorption. These mesenchymal cells and/or other recruited progenitors differentiate into osteoblasts and elaborate a matrix consisting of type I collagen, a variety of noncollagenous proteins, and growth factors. The matrix is then calcified. During matrix deposition, some osteoblasts differentiate into osteocytes. Osteocytes are embedded into the matrix and form connections with each other and with the bone surface. Osteoblasts eventually cease matrix production and become the very thin lining cells that cover the quiescent surface of bone.

The dependence of bone formation on bone resorption is the "sine qua non" feature of remodeling. If coupling is defective, the thickness and connectivity of trabecular bone declines. Cortical bone becomes thinner because of endosteal bone loss and more porous because the Haversian canals become wider. If excessive matrix is deposited during coupling, trabecular bone mass increases, and cortical bone becomes thicker.

In addition to remodeling, bone also undergoes modeling. As opposed to bone remodeling, bone modeling is a process carried out by osteoclasts and osteoblasts that operate independently of each other. The purpose of modeling is to sculpt the skeleton during growth and adapt it to the prevailing mechanical strains at different sites.

The function of the BMU can be measured using histologic approaches that quantify the rate of resorption and formation (Dempster et al., 2013) (see Box 32.1). The life span of BMUs in humans is 6–9 months, but the life span of osteoclasts is 1 week or so, and the life span of osteoblasts is a few months (Manolagas, 2000). All osteoclasts and the majority of osteoblasts die by apoptosis (Jilka et al., 2007, 2008). Thus, the function of the BMU requires a continuous supply of new osteoclasts and osteoblasts derived from local or circulating progenitors and the timely death of these cells (Manolagas, 2000). Recent advances in the genetic manipulation of mice has permitted more rigorous examination of the origination and fate of cells of the osteoblast lineage (Ono and Kronenberg, 2015). The important role of the timely death of osteoblasts and perhaps osteoblast progenitors by apoptosis has been illustrated by the increased trabecular bone in mice with osteoblast lineage cells lacking Bax and Bak, two proteins critical for apoptosis (Jilka et al., 2014).

BOX 32.1 Histologic measurements of bone modeling and remodeling.

Term	Description
Mineralizing surface	Bone surface undergoing mineralization as visualized by fluorochromes labeling.
Mineral apposition rate	Distance between fluorochromes labels divided by the labeling interval.
Bone formation rate	Product of mineralizing surface and mineral apposition rate.
Activation frequency	Probability that a remodeling event will be initiated on the bone surface.
Cement line	Thin line of toluidine blue staining that marks the boundary between resorption and formation in remodeled bone, or new bone formation in modeled bone.
Wall width	Amount of bone formed during remodeling by a team of osteoblasts. Measured by the average distance between scalloped cement lines and quiescent bone surface.
Eroded surface	Osteoclast surface plus the reversal-osteoclast surface.
Erosion depth	Average depth of active resorption lacunae.

The generation and Maintenance of basic multicellular units Is governed by parathyroid hormone

Bone turnover is primarily influenced by circulating levels of PTH. In hypoparathyroidism, bone remodeling and the number of BMUs is severely reduced (Rubin et al., 2008; Clarke, 2014; Langdahl et al., 1996). The length of the resorption and formation period of each BMU is prolonged, and the resorption depth and the wall thickness is reduced, as is osteoid width, mineral apposition rate, and bone formation rate (see Box 32.1). Nevertheless, cancellous bone volume is increased due to increased trabecular thickness, likely due to reduced erosion depth combined with a reduced proportion of the surface undergoing remodeling. In mice, deletion of the PTH gene has similar effects (Miao et al., 2004).

Hyperparathyroidism increases bone remodeling. In mild primary hyperparathyroidism there is a 50% increase in the activation frequency of the BMUs and increased formation and resorption surfaces (Christiansen et al., 1992; Dempster et al., 1999; Parisien et al., 2001). In cortical bone, increased remodeling is seen at both the endocortical and intracortical surfaces. The result of the increased intracortical remodeling is larger Haversian canals accounting for increased cortical porosity, and "trabecularization" of the endocortical surface (Vu et al., 2013; Stein et al., 2013). Periosteal surfaces are usually unaffected. In severe primary hyperparathyroidism, bone remodeling is dramatically increased. This is manifested by skeletal deformities, pathological fractures, subperiosteal bone erosion, "brown tumors," and peritrabecular bone marrow fibrosis, also called osteitis fibrosa.

Parathyroid hormone regulates factors that govern the assembly and maintenance of basic multicellular units

Osteoclast differentiation and life span

Under normal physiologic conditions, PTH drives the development of osteoclasts. Osteoclastogenesis requires extravasation of monocytic progenitors from capillaries near the bone targeted for renewal or from locally produced progenitors in the bone marrow. Osteoclast differentiation requires macrophage-colony stimulating factor (M-CSF) which stimulates the replication of these progenitors, and receptor activator of NF-kB ligand (RANKL) which promotes differentiation into multinucleated bone resorptive cells (Boyle et al., 2003). Mice lacking either of these two cytokines are osteopetrotic and practically devoid of osteoclasts. RANKL also maintains the viability of osteoclasts. Administration of osteoprotegerin (OPG), a soluble receptor antagonist of RANKL, causes a decline in osteoclast number coincident with the appearance of apoptotic fragments of osteoclasts as early as 6h after administration (Lacey et al., 2000). OPG also reduces osteoblast number and bone formation rate, directly demonstrating the coupling of bone formation to bone resorption (Jilka et al., 2010; Piemontese et al., 2017).

RANKL is produced by many cell types including cells of the osteoblast lineage, T and B lymphocytes, synovial fibroblasts, adipocytes, and hypertrophic chondrocytes (O'Brien et al., 2013). PTH stimulates the production of RANKL by osteoblastic cells (Rodan and Martin, 1981; Lee and Lorenzo, 1999; Yasuda et al., 1998; Fu et al., 2002; McSheehy and Chambers, 1986). These effects are mediated by activation of a distal enhancer located 76 kb from the transcriptional start site of the RANKL gene (Galli et al., 2008; Fu et al., 2006). The osteopetrotic phenotype of mice lacking a functional RANKL gene can be rescued by a 220-Kb transgene containing the RANKL gene and its upstream regulatory domains (Onal et al., 2015). Targeted deletion of RANKL in osteoblasts/osteocytes using DMP1-Cre, or in osteocytes using Sost-Cre, causes a reduction in osteoclast number and an increase in trabecular bone mass (Xiong et al., 2011, 2014, 2015; Nakashima et al., 2011). These changes are apparent as early as 5 weeks of age, indicating that osteocytes represent the main source of RANKL when skeletal growth and modeling begins to slow, and osteoclasts are needed only for remodeling. In contrast, global deletion of RANKL causes osteopetrosis that is evident from birth (Kong et al., 1999). Thus, other cell types produce the RANKL required for the formation of osteoclasts needed for skeletal development, for example resorption of calcified cartilage in the growth plate (Gebhard et al., 2008).

Conditional deletion of RANKL in osteoblasts/osteocytes with DMP1-Cre attenuates the increase in osteoclast number and the bone loss caused by dietary Ca deficiency in adult mice (Xiong et al., 2014). Osteocytes vastly outnumber osteoblasts, making the former cell type the most likely source of RANKL. Moreover, mice lacking PTHR1 in osteoblast/osteocyte fail to exhibit the increase in RANKL and the loss of bone caused by chronic elevation of PTH (Saini et al., 2013). These findings show that the stimulatory effects of chronic elevation of PTH on osteoclast number and bone remodeling are primarily mediated by direct actions of the hormone on RANKL production by osteocytes. Consistent with this contention, expression of a constitutively active PTHR1 mutant in osteocytes (using the DMP1 promoter) increases RANKL and bone remodeling (O'Brien et al., 2008; Ben-Awadh et al., 2014). RANKL is initially expressed as a

transmembrane protein on the cell surface. Following cleavage by extracellular endopeptidases, it is released in soluble form (sRANKL). Mice expressing endopeptidase[HYPHEN]resistant RANKL exhibit normal bone development. However, osteoclasts are reduced and trabecular bone is increased in adult mice, indicating that sRANKL contributes to physiological bone remodeling (Xiong et al., 2018). The circulating levels of sRANKL increase in patients with mild primary hyperparathyroidism and correlate with the level of circulating markers of bone resorption and the rate of femoral bone loss (Nakchbandi et al., 2008). However, the level of circulating sRANKL is too low to be biologically relevant, indicating that local production of the cytokine is responsible for the induction and maintenance of BMUs.

PTH exerts a negative effect on the production of OPG (Fu et al., 2002; Onyia et al., 2000). Since bone mass is severely reduced and osteoclast number is dramatically increased in OPG null mice (Bucay et al., 1998), this cytokine must play a fundamental role in the regulation of osteoclast differentiation and survival in physiological circumstances. In parathyroidectomized patients, bone exhibits a decrease in the ratio of RANKL to OPG transcripts (Stilgren et al., 2004), demonstrating that PTH increases the RANKL/OPG ratio. Surprisingly, however, little is known about the underlying genetic regulatory mechanism or the cellular source(s) of OPG.

PTH affects several other factors with proosteoclastogenic properties. The expression of monocyte chemoattractant protein 1 (MCP-1), a cytokine that promotes osteoclast multinucleation, is strongly induced by PTH in cultured osteoblastic cells (Li et al., 2007). Mice with global deletion of MCP-1 have normal bone mass and osteoclast number, but infusion of PTH fails to cause the expected cortical or trabecular bone loss (Siddiqui et al., 2017). PTH also stimulates the production of IL-11 (Walker et al., 2012), which stimulates osteoclastogenesis in ex-vivo cultures of bone marrow cells (Girasole et al., 1994), by stimulating RANKL synthesis (Horwood et al., 1998; Palmqvist et al., 2002). Moreover, global deletion of the IL-11R reduces osteoclast number (Sims et al., 2005). In vitro and in vivo studies show that PTH also stimulates the synthesis of IL-6, which can increase osteoclast number by promoting the replication of monocytic progenitors (Greenfield et al., 1996; Walker et al., 2012; O'Brien et al., 2005). However, mice lacking IL-6 have normal bone (Fattori et al., 1994; Sims et al., 2005); and studies with these mice show that IL-6 is dispensable for the increased RANKL, osteoclast number, and bone loss caused by secondary hyperparathyroidism (O'Brien et al., 2005).

Matrix metalloproteinase 13 (MMP-13) is involved in collagen turnover in many tissues including bone (Stickens et al., 2004). PTH stimulates the synthesis of MMP-13 in osteoblastic cells (Winchester et al., 2000). Moreover, PTH-induced osteoclastogenesis in calvaria is attenuated in mice bearing a mutation that causes resistance of type I collagen to MMP-13 (Zhao et al., 1999). Unexpectedly, MMP-13 may also act as a cytokine, as indicated by the finding that formation of multinucleated osteoclasts is dramatically accelerated in vitro by a catalytically inactive mutant of MMP-13 (Fu et al., 2016).

T cells bear PTH receptors, and conditional deletion of PTHR1 in these cells. Using Lck-Cre has no effect on bone mass or osteoclast number (Tawfeek et al., 2010). Infusion of PTH, however, increases T cell production of tumor necrosis factor (TNF), which may potentiate RANKL synthesis. Moreover, TNF stimulates proinflammatory T helper cells (Th17 cells) to produce IL-17A, which may also stimulate RANKL expression (Li et al., 2015). Work with an IL-17A neutralizing antibody indicates that an IL17-/RANKL cascade contributes to the bone effects of hyperparathyroidism (Li et al., 2015).

Osteoblast differentiation and the coupling of bone formation to bone resorption

Osteoblasts originate from multipotential progenitors in the bone marrow, many of which are associated with the vasculature (Bianco et al., 2013). The commitment of these progenitors to the osteoblast lineage and their development into matrix synthesizing cells, is orchestrated by locally produced growth factors like insulin-like growth factor-I (IGF-1), bone morphogenetic proteins (BMPs), transforming growth factor-β (TGFβ), and wingless-related integration site (Wnt) ligands. Osteoblastogenesis critically depends on a variety of transcription regulators including β-catenin, runt related transcription factor 2 (Runx2), and Osterix 1(Osx1). Wnt ligands bind to frizzled (FZD)\lipoprotein related protein 5 (LRP5) or FZD\LRP6 co-receptor complexes to increase proosteogenic β-catenin mediated transcription (Baron and Kneissel, 2013). Wnt signaling is suppressed by sclerostin, which is produced exclusively by osteocytes, as well as by Dkk1 and both block activation of the Wnt receptors LRP5/6. Sost null mice exhibit high bone mass, illustrating the critical role of sclerostin as a brake on bone formation under physiologic circumstances.

Release of proosteoblastogenic factors from osteoclasts, or from the bone matrix during resorption, contribute to the temporal and spatial linkage of bone formation to bone resorption within the BMU (Fuller et al., 2008; Sims and Martin, 2014). Matrix-derived TGFβ (Tang et al., 2009) and IGF-1 (Crane and Cao, 2014) are released during bone resorption and recruit osteoblast progenitors to sites of bone remodeling (Tang et al., 2009; Xian et al., 2012). Osteoclasts themselves also secrete a variety of proosteogenic factors (Sims, 2016). Among these, sphingosine-1-phosphate (S1P) (Lotinun et al., 2013; Sartawi et al., 2017; Keller et al., 2014), and leukemia inhibitory factor LIF (Koide et al., 2017) have received attention.

Importantly, osteoclast-derived LIF may suppress the expression of sclerostin by osteocytes, thus removing a brake on Wnt signaling in the microenvironment of the BMU (Koide et al., 2017). Consistent with this evidence, deletion of gp130, a subunit of the LIF receptor, in osteoblasts/osteocytes reduces osteoblast number and bone mass without altering osteoclast number, consistent with diminished coupling (Johnson et al., 2014).

Osteoclast-independent factors also contribute to coupling. In a study comparing infused RANKL and infused PTH on trabecular bone remodeling in mice (Jilka et al., 2010), both treatments increased osteoclast and osteoblast number and bone formation rate. However, osteogenic indices and bone mass were lower in RANKL-treated mice compared with PTH-treated mice. The increase in osteoblasts in mice infused with RANKL provides functional evidence for the osteoclast-derived proosteogenic signals mentioned above. However, these signals are evidently insufficient for full replacement of the previously resorbed matrix. PTH-stimulated Wnt signaling may play an additive role. This Wnt signaling is independent of osteoclasts since OPG did not affect PTH-stimulated expression of several established Wnt target genes.

PTH stimulates proosteoblastogenic Wnt signaling via several mechanisms. One is suppression of the constitutive synthesis of the Wnt signaling inhibitor sclerostin (Bellido et al., 2005; Keller and Kneissel, 2005). Indeed, the level of circulating sclerostin is decreased or increased in hyperparathyroidism and hypoparathyroidism, respectively (Costa et al., 2011; van Lierop et al., 2010). PTH also suppresses the expression of the Wnt antagonist Dkk1; and mice overexpressing Dkk1 have low bone mass (Guo et al., 2010). Importantly, continuous elevation of PTH does not increase bone formation or cause peritrabecular fibrosis in Dkk-overexpressing mice, presumably because PTH cannot reduce the Dkk transgene in this model. Mice expressing a constitutively active PTHR1 in osteoblasts and osteocytes, on the other hand, have increased bone mass and high remodeling. These changes are associated with suppression of sclerostin and increased Wnt signaling, which were attenuated by deletion of LRP5 (O'Brien et al., 2008). Finally, in vitro evidence indicates that PTH may stimulate Wnt signaling directly by inducing the association of PTH1R with LRP6, and thereby increasing β-catenin (Wan et al., 2008).

Despite increased Wnt signaling and production of other growth factors, bone mass decreases in hyperparathyroidism. This is probably due to excessive genesis and prolongation of the life span of osteoclasts secondary to increased RANKL and other PTH-regulated cytokines. Osteoblast apoptosis is unaffected in hyperparathyroidism (Bellido et al., 2003), but high levels of PTH have a negative impact on osteoblastogenesis. Indeed, the peritrabecular fibroblasts that characterize severe hyperparathyroidism likely represent osteoblastic cells arrested at a late stage of differentiation. Thus, experiments in mice receiving PTH demonstrate rapid development of these cells, and cessation of PTH administration results in their conversion to bone-forming osteoblasts (Lotinun et al., 2005). Excessive levels of PDGFa may be responsible (Lowry et al., 2008). Another cause of arrested osteoblast differentiation may be accelerated proteasomal degradation of essential transcription factors like Runx2 (Bellido et al., 2003).

The elucidation of the cellular mechanisms responsible for PTH-regulated BMU function helps explain the "hungry bone" syndrome that can be seen after parathyroidectomy (Mallette, 1994). In these patients, because of the rapid decline in PTH, RANKL levels fall, leading to premature osteoclast death, thereby reducing Ca release from bone. However, serum Ca continues to be deposited into bone by osteoblasts already assembled in the BMUs that had been generated prior to surgery and by. New osteoblasts generated upon release of progenitors from the direct or indirect inhibitory effects of PTH.

The bone anabolic effects of intermittent parathyroid hormone

Stimulation of anabolic remodeling and modeling

In contrast to hyperparathyroidism, intermittent (usually daily) injections of PTH (iPTH) increase bone mass in animals and humans. Modified amino terminal versions of hPTH(1−34) (Forteo) and hPTHrP(1−36) (Abaloparatide) increase BMD and reduce the incidence of fractures (Jiang et al., 2003; Hodsman et al., 2005; Miller et al., 2016; Doyle et al., 2018; Finkelstein et al., 2003; Orwoll et al., 2003). Anabolism is confined to trabecular, endocortical, and periosteal surfaces. In contrast, iPTH tends to increase cortical porosity (Zebaze et al., 2017; Moreira et al., 2017; Sato et al., 2004; Burr et al., 2001; Doyle et al., 2018; Fox et al., 2007a). The magnitude of the increase in bone mass declines with time with modest if any benefit after 2 years of treatment (Finkelstein et al., 2009; Dempster et al., 2018a).

Injection of a therapeutic dose of 20 μg of hPTH(1−34) increases levels of this peptide to ∼150 pg/mL after 30 min, which is 2- to 10-fold higher than the normal circulating level of 15−65 pg/mL of endogenous PTH. The exogenous peptide has a half-life of ∼1 h (Satterwhite et al., 2010). The magnitude of the change in circulating PTH required for anabolism is far beyond the ∼20%−30% variation that occurs in a diurnal manner (El Hajj et al., 1997). In rodents the

minimum effective interval between bouts of PTH administration is 6 h, with smaller intervals resulting in the histologic changes and bone loss characteristic of hyperparathyroidism. Thus, both a substantial rise and rapid decline in the level of PTH are required for the anabolic effect of the hormone.

Intermittent PTH increases bone remodeling secondary to a transient increase of RANKL. However, the increase in osteoblast number is much higher and occurs rapidly (Jilka et al., 1999; Iida-Klein et al., 2002; Bellido et al., 2003; Lindsay et al., 2006; Ma et al., 2006). Administration of fluorochromes to identify sites of bone formation prior to and following daily PTH injections in postmenopausal women have allowed for more detailed investigation of the cellular events involved. (Lindsay et al., 2006). As illustrated in Fig. 32.1, the location of each label with respect to the shape of the underlying cement lines was used to distinguish new bone made during remodeling, new bone made by overflow of osteoblasts outside the boundaries of the BMU, and new bone made by modeling. Intermittent iPTH clearly elevated remodeling on cancellous, endocortical, and intracortical surfaces after 1 month of therapy (Lindsay et al., 2006). More importantly, iPTH induced overflow labeling and modeling, both of which were rare or absent at baseline. These responses occurred in trabecular and endosteal bone but not in Haversian canals. Increased modeling was reported in another study, based on similar labeling criteria (Ma et al., 2006). iPTH also stimulated modeling-based bone formation on the periosteal surface in about half of the subjects. Increased remodeling, overfill, and modeling were also observed after 6 months of treatment, but after 24 months, overfill- and modeling-based bone formation had practically ceased (Lindsay et al., 2007;

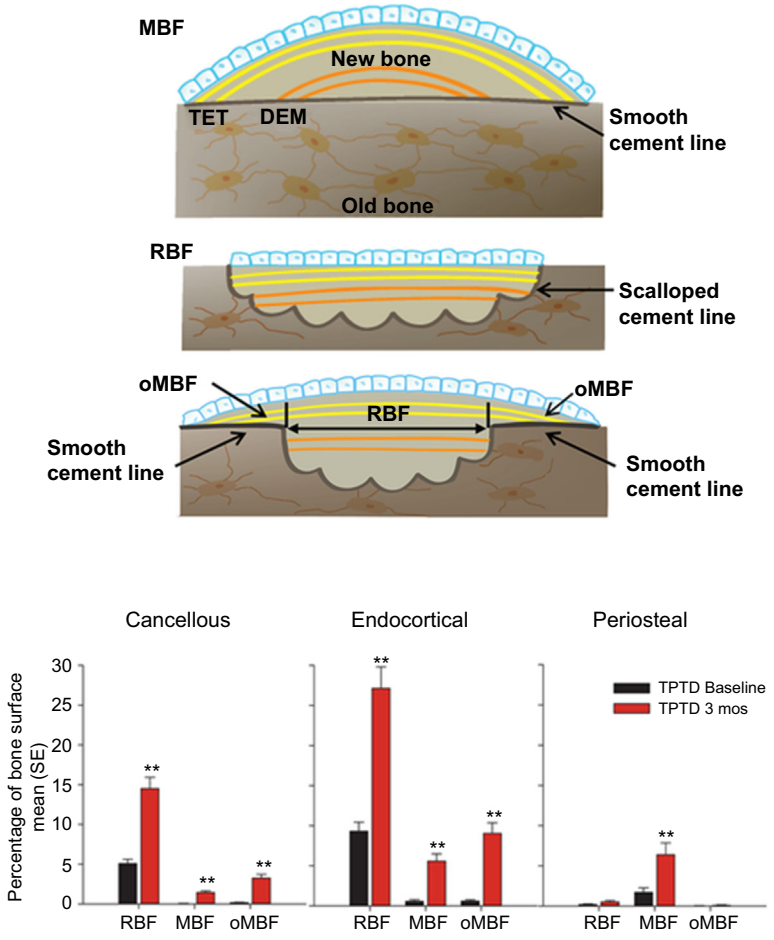

FIGURE 32.1 Cellular basis of the effect of anabolic effect of iPTH. Top. Illustration of modeling-based bone formation (MBF) marked by fluorochrome labeling overlying smooth cement lines; remodeling-based bone formation (RBF) marked by labeling on top of scalloped cement lines that mark the extent of previous osteoclastic bone resorption; and overflow-modeling-based bone formation (oMBF) taking place on smooth cement lines adjacent to scalloped cement lines. Bottom: Effect of 3 months of iPTH on different types of bone formation on cancellous, endocortical, and periosteal surface measured in the same patient using quadrupole fluorochrome labeling. Note absence of MBF and oMBF in cancellous and endocortical bone at baseline. *Reproduced from Dempster, D.W., Zhou, H., Recker, R.R., Brown, J.P., Recknor, C.P., Lewiecki, E.M., Miller, P.D., Rao, S.D., Kendler, D.L., Lindsay, R., Krege, J.H., Alam, J., Taylor, K.A., Melby, T.E., Ruff, V.A. 2018a. Remodeling- and modeling-based bone formation with teriparatide versus denosumab: a longitudinal analysis from baseline to 3 Months in the AVA study. J. Bone Miner. Res. 33, 298–306, with permission.*

Dempster et al., 2018a, 2018b). This coincides with the decline in the stimulatory effect of iPTH on BMD. Moreover, after 24 months, the magnitude of remodeling-based bone formation on cancellous and endocortical surfaces declined two- to threefold from its level at 6 months (Dempster et al., 2018b).

The increased Haversian remodeling in response to intermittent PTH is associated with increased porosity (Dempster et al., 2016; Cohen et al., 2013; Lindsay et al., 2006; Cosman et al., 2016; Ma et al., 2014). This effect is also evident following administration of PTH for 4 months to hypoparathyroid patients (Sikjaer et al., 2012). Increased porosity may be partly due to the formation of new BMUs—i.e., an increase in intracortical remodeling space. Moreover, iPTH fails to arrest ovariectomy-induced development of cortical porosity in non-human primates (Fox et al., 2007b). At a higher dose, iPTH increases cortical porosity even further in this model; yet the anabolic effect in trabecular bone is still present.

Mechanisms underlying overfill of resorption cavities in response to injections of parathyroid hormone

Improved coupling of bone formation to bone resorption at sites of remodeling, resulting from increased osteoblast number within each BMU, most likely accounts for the overfilling of resorption cavities with iPTH. In mice, the anabolic effect of iPTH is attenuated by conditional deletion of the PTHR1 in multipotent osteoblast progenitors (Balani et al., 2017), osteoblasts and osteocytes (Saini et al., 2013; Delgado-Calle et al., 2017) and in T cells (Bedi et al., 2012), suggesting that several interdependent mechanisms are responsible.

Early studies indicated that iPTH increases the number of osteoblast progenitors in the bone marrow (Nishida et al., 1994). Lineage tracing studies in mice have elucidated the underlying mechanisms. In this work the authors utilize mice bearing a floxed gene encoding a fluorescent protein, as well as a transgene consisting of a tamoxifen-inducible Sox9 promoter (known to be expressed in early multipotent mesenchymal cells) driving Cre recombinase (Balani et al., 2017). Administration of tamoxifen for 1 week caused appearance of fluorescence-labeled Sox9+ progenitors within the bone marrow. These progenitors were the source of osteoblasts needed for remodeling, because fluorescent osteoblasts and osteocytes were evident for several months after tamoxifen injection. Intermittent PTH increased the number of fluorescent Sox9+ progenitors as well as the number of fluorescent osteoblasts and osteocytes. FACS analysis of the Sox9+ cells showed that iPTH did not stimulate their replication. This finding is consistent with earlier nucleotide labeling studies (Dobnig and Turner, 1995; Jilka et al., 2009) and evidence that PTH modulates the expression of cell cycle-regulating proteins in cultured osteoblastic cells, resulting in their exit from the cell cycle (summarized in Jilka, 2007). Instead, iPTH increased the number of osteoblast progenitors by attenuating their apoptosis. Moreover, deletion of PTHR1 in Sox9+ cells abrogated the increase in progenitors, as well as the anabolic effect, suggesting that this response depends on direct actions of the hormone on Sox9+ progenitors and/or their progeny. Cessation of iPTH caused the expected loss of anabolism, but interestingly also resulted in an increase in adipocytes that were descended from labeled Sox9+ progenitors.

Besides osteoblast progenitors, intermittent PTH reduces the number of apoptotic osteoblasts in trabecular bone (Jilka et al., 1999; Bellido et al., 2003). PTH-induced survival signaling depends on CREB- and Runx2-mediated transcription, increased expression of the antiapoptotic genes like Bcl-2, and phosphorylation and thereby inactivation of the antiapoptotic protein Bad. The duration of PTH-stimulated antiapoptotic signals is about 6 h in vitro. This is probably because of a separate effect of PTH on stimulating Smurf1-mediated proteosomal proteolysis of the Runx2 required for suppression of apoptosis. This may be the reason that osteoblast apoptosis is unaffected in hyperparathyroidism.

Intermittent PTH modulates the synthesis of autocrine/paracrine factors that accelerate osteoblast differentiation. LRP6 but not LRP5 (Iwaniec et al., 2007) is required for iPTH anabolism, consistent with direct activation of LPR6 by the hormone (Wan et al., 2008). Following injection of PTH, the expression of the Wnt signaling inhibitor sclerostin in osteocytes is transiently suppressed, coinciding with the rise and fall in the circulating level of the injected hormone (Bellido et al., 2005; Keller and Kneissel, 2005). A critical role of the decrease in sclerostin in the effects of iPTH has been suggested by the attenuation of the anabolic effect of iPTH in mice with global deletion of sclerostin (Robling et al., 2011). Moreover, PTH-induced bone formation is attenuated by increasing the dosage of the Sost gene (Kramer et al., 2010). Mice over-expressing sclerostin under the control of the DMP-1 promoter, however, still respond to iPTH (Delgado-Calle et al., 2017). This seeming discrepancy could be explained by the fact that, in the latter studies, sclerostin was overexpressed in both osteocytes and osteoblasts; as opposed to normal mice in which sclerostin is expressed only in osteocytes. Intermittent PTH-stimulated production of Wnt10b by T cells may also contribute to Wnt signaling and bone

anabolism (Bedi et al., 2012; Terauchi et al., 2009), but for reasons that are unclear, this mechanism is only relevant to trabecular bone.

Of the many proosteogenic cytokines and growth factors stimulated by PTH, IGF-1 (Bikle et al., 2002; Miyakoshi et al., 2001), FGF2 (Hurley et al., 2006), or ephrinB2 (Tonna et al., 2014) are required for the full anabolic response to iPTH. However, it is unclear whether the IGF-I- and FGF2-dependent anabolism by iPTH reflects increased release from the bone matrix or locally increased biosynthetic actions of the hormone. IGF-I increases glucose uptake and oxidative phosphorylation during osteoblast differentiation, which is critical for the development of the high biosynthetic and secretory capacity of these cells (Esen et al., 2015). Deletion of gp130 — the common co-receptor for IL-6 type cytokines - in osteoblasts/osteocytes attenuates the anabolic effect of iPTH (Standal et al., 2014). This might be explained by a dependence on osteoclast-derived LIF, which can suppress sclerostin as discussed above. Notch signaling normally suppresses osteoblast differentiation, and PTH antagonizes this pathway (Zanotti and Canalis, 2017). Accordingly, mice with conditional deletion of the Notch ligand Jagged 1 in mesenchymal stem cells exhibit increased femoral cancellous bone mass. Moreover, iPTH increases trabecular bone in these mice, perhaps because of loss of Jagged1-dependent limits on osteoblast differentiation (Lawal et al., 2017).

Stimulation of bone modeling by osteoblasts in response to injections of parathyroid hormone

In adults, the periosteum contains a reservoir of osteoblast progenitors that facilitate fracture repair and the slow deposition of periosteal bone that occurs via modeling. Lineage tracing studies in growing mice using tamoxifen-inducible DMP1-Cre transgene showed that some periosteal cells are former osteoblasts (Kim et al., 2012). More important, iPTH reactivated these marked lining cells to resume their matrix-synthesizing function.

Trabecular bone surfaces have lining cells descended from osteoblasts (Kim et al., 2012). Previous morphologic studies had suggested that iPTH rapidly converts these cells into osteoblasts (Leaffer et al., 1995; Dobnig and Turner, 1995), but this has not yet been confirmed using the lineage tracing approach. Nevertheless, administration of an antisclerostin antibody did reactivate trabecular lining cells marked with either DMP1-Cre or OCN-Cre on trabecular and periosteal surfaces (Kim et al., 2012). This anabolic response was short lived, probably because most of the reactivated postmitotic osteoblasts were incorporated into the bone matrix as osteocytes or died; only a minority returned to their former life as lining cells. Thus, the constitutive production of sclerostin by osteocytes may serve an antiproosteoblastogenic role on most skeletal surfaces by suppressing Wnt signaling that would otherwise be induced by locally produced Wnt ligands. Sequestration of sclerostin by the antibody unleashes Wnt signaling throughout the skeleton. Similarly, lining cells may be reactivated by periodic suppression of sclerostin by iPTH.

Unresolved issues

Why does iPTH fail to overfill of BMUs and to reactivate lining cells in Haversian canals? There may be an inhibitory effect of the capillary, since anabolism in Haversian canals has the potential to closing the canal and blocking cortical circulation. Fundamental differences in BMU and lining cell characteristics in Haversian surfaces versus other sites is also possible.

Why does PTH-stimulated BMU overfill and PTH-stimulated modeling wane with time? It is possible that activation of negative feedback pathways on osteoblastogenesis and on reactivation of lining cells is responsible. The new BMUs generated during the later stages of therapy may also have excessive bone resorption. Given the complexity of the cellular response and the absence of anabolism at sites of intracortical remodeling, as reviewed herein, studies of changes in circulating markers of osteoclast and osteoblast function are not very informative (Seeman and Martin, 2015).

References

Balani, D.H., Ono, N., Kronenberg, H.M., 2017. Parathyroid hormone regulates fates of murine osteoblast precursors in vivo. J. Clin. Investig. 127, 3327–3338.

Baron, R., Kneissel, M., 2013. WNT signaling in bone homeostasis and disease: from human mutations to treatments. Nat. Med. 19, 179–192.

Baud, C.A., Boivin, G., 1978. Effects of hormones on osteocyte function and perilacunar wall structure. Clin. Orthop. Relat. Res. 270–281.

Bedi, B., Li, J.Y., Tawfeek, H., Baek, K.H., Adams, J., Vangara, S.S., Chang, M.K., Kneissel, M., Weitzmann, M.N., Pacifici, R., 2012. Silencing of parathyroid hormone (PTH) receptor 1 in T cells blunts the bone anabolic activity of PTH. Proc. Natl. Acad. Sci. Unit. States Am. 109, E725–E733.

Bellido, T., Ali, A.A., Gubrij, I., Plotkin, L.I., Fu, Q., O'brien, C.A., Manolagas, S.C., Jilka, R.L., 2005. Chronic elevation of parathyroid hormone in mice reduces expression of sclerostin by osteocytes: a novel mechanism for hormonal control of osteoblastogenesis. Endocrinology 146, 4577–4583.

Bellido, T., Ali, A.A., Plotkin, L.I., Fu, Q., Gubrij, I., Roberson, P.K., Weinstein, R.S., O'brien, C.A., Manolagas, S.C., Jilka, R.L., 2003. Proteasomal degradation of Runx2 shortens parathyroid hormone-induced anti-apoptotic signaling in osteoblasts: a putative explanation for why intermittent administration is needed for bone anabolism. J. Biol. Chem. 278, 50259–50272.

Ben-Awadh, A.N., Delgado-Calle, J., Tu, X., Kuhlenschmidt, K., Allen, M.R., Plotkin, L.I., Bellido, T., 2014. Parathyroid hormone receptor signaling induces bone resorption in the adult skeleton by directly regulating the RANKL gene in osteocytes. Endocrinology 155, 2797–2809.

Bianco, P., Cao, X., Frenette, P.S., Mao, J.J., Robey, P.G., Simmons, P.J., Wang, C.Y., 2013. The meaning, the sense and the significance: translating the science of mesenchymal stem cells into medicine. Nat. Med. 19, 35–42.

Bikle, D.D., Sakata, T., Leary, C., Elalieh, H., Ginzinger, D., Rosen, C.J., Beamer, W., Majumdar, S., Halloran, B.P., 2002. Insulin-like growth factor I is required for the anabolic actions of parathyroid hormone on mouse bone. J. Bone Miner. Res. 17, 1570–1578.

Boyle, W.J., Simonet, W.S., Lacey, D.L., 2003. Osteoclast differentiation and activation. Nature 423, 337–342.

Bucay, N., Sarosi, I., Dunstan, C.R., Morony, S., Tarpley, J., Capparelli, C., Scully, S., Tan, H.L., Xu, W.L., Lacey, D.L., Boyle, W.J., Simonet, W.S., 1998. *Osteoprotegerin*-deficient mice develop early onset osteoporosis and arterial calcification. Genes Dev. 12, 1260–1268.

Burr, D.B., Hirano, T., Turner, C.H., Hotchkiss, C., Brommage, R., Hock, J.M., 2001. Intermittently administered human parathyroid hormone (1-34) treatment increases intracortical bone turnover and porosity without reducing bone strength in the humerus of ovariectomized cynomolgus monkeys. J. Bone Miner. Res. 16, 157–165.

Christiansen, P., Steiniche, T., Vesterby, A., Mosekilde, L., Hessov, I., Melsen, F., 1992. Primary hyperparathyroidism: iliac crest trabecular bone volume, structure, remodeling, and balance evaluated by histomorphometric methods. Bone 13, 41–49.

Clarke, B.L., 2014. Bone disease in hypoparathyroidism. Arq. Bras. Endocrinol. Metabol. 58, 545–552.

Cohen, A., Stein, E.M., Recker, R.R., Lappe, J.M., Dempster, D.W., Zhou, H., Cremers, S., Mcmahon, D.J., Nickolas, T.L., Muller, R., Zwahlen, A., Young, P., Stubby, J., Shane, E., 2013. Teriparatide for idiopathic osteoporosis in premenopausal women: a pilot study. J. Clin. Endocrinol. Metab. 98, 1971–1981.

Cosman, F., Dempster, D.W., Nieves, J.W., Zhou, H., Zion, M., Roimisher, C., Houle, Y., Lindsay, R., Bostrom, M., 2016. Effect of teriparatide on bone formation in the human femoral neck. J. Clin. Endocrinol. Metab. 101, 1498–1505.

Costa, A.G., Cremers, S., Rubin, M.R., Mcmahon, D.J., Sliney, J., Lazaretti-Castro, M., Silverberg, S.J., Bilezikian, J.P., 2011. Circulating sclerostin in disorders of parathyroid gland function. J. Clin. Endocrinol. Metab. 96, 3804–3810.

Crane, J.L., Cao, X., 2014. Function of matrix IGF-1 in coupling bone resorption and formation. J. Mol. Med. 92, 107–115.

delgado-Calle, J., Tu, X., Pacheco-Costa, R., Mcandrews, K., Edwards, R., Pellegrini, G.G., Kuhlenschmidt, K., Olivos, N., Robling, A., Peacock, M., Plotkin, L.I., Bellido, T., 2017. Control of bone anabolism in response to mechanical loading and PTH by distinct mechanisms downstream of the PTH receptor. J. Bone Miner. Res. 32, 522–535.

Dempster, D.W., Compston, J.E., Drezner, M.K., Glorieux, F.H., Kanis, J.A., Malluche, H., Meunier, P.J., Ott, S.M., Recker, R.R., Parfitt, A.M., 2013. Standardized nomenclature, symbols, and units for bone histomorphometry: a 2012 update of the report of the ASBMR Histomorphometry Nomenclature Committee. J. Bone Miner. Res. 28, 2–17.

Dempster, D.W., Parisien, M., Silverberg, S.J., Liang, X.G., Schnitzer, M., Shen, V., Shane, E., Kimmel, D.B., Recker, R., Lindsay, R., Bilezikian, J.P., 1999. On the mechanism of cancellous bone preservation in postmenopausal women with mild primary hyperparathyroidism. J. Clin. Endocrinol. Metab. 84, 1562–1566.

Dempster, D.W., Zhou, H., Recker, R.R., Brown, J.P., Bolognese, M.A., Recknor, C.P., Kendler, D.L., Lewiecki, E.M., Hanley, D.A., Rao, S.D., Miller, P.D., Woodson 3rd, G.C., Lindsay, R., Binkley, N., Alam, J., Ruff, V.A., Gallagher, E.R., Taylor, K.A., 2016. A longitudinal study of skeletal histomorphometry at 6 and 24 months across four bone envelopes in postmenopausal women with osteoporosis receiving teriparatide or zoledronic acid in the SHOTZ trial. J. Bone Miner. Res. 31, 1429–1439.

Dempster, D.W., Zhou, H., Recker, R.R., Brown, J.P., Recknor, C.P., Lewiecki, E.M., Miller, P.D., Rao, S.D., Kendler, D.L., Lindsay, R., Krege, J.H., Alam, J., Taylor, K.A., Melby, T.E., Ruff, V.A., 2018a. Remodeling- and modeling-based bone formation with teriparatide versus denosumab: a longitudinal analysis from baseline to 3 Months in the AVA study. J. Bone Miner. Res. 33, 298–306.

Dempster, D.W., Zhou, H., Ruff, V.A., Melby, T.E., Alam, J., Taylor, K.A., 2018b. Longitudinal effects of teriparatide or zoledronic acid on bone modeling- and remodeling-based formation in the SHOTZ study. J. Bone Miner. Res. 33, 627–633.

Dobnig, H., Turner, R.T., 1995. Evidence that intermittent treatment with parathyroid hormone increases bone formation in adult rats by activation of bone lining cells. Endocrinology 136, 3632–3638.

Doyle, N., Varela, A., Haile, S., Guldberg, R., Kostenuik, P.J., Ominsky, M.S., Smith, S.Y., Hattersley, G., 2018. Abaloparatide, a novel PTH receptor agonist, increased bone mass and strength in ovariectomized cynomolgus monkeys by increasing bone formation without increasing bone resorption. Osteoporos. Int. 29, 685–697.

EL Hajj, F.G., Klerman, E.B., Brown, E.N., Choe, Y., Brown, E.M., Czeisler, C.A., 1997. The parathyroid hormone circadian rhythm is truly endogenous–a general clinical research center study. J. Clin. Endocrinol. Metab. 82, 281–286.

Esen, E., Lee, S.Y., Wice, B.M., Long, F., 2015. PTH promotes bone anabolism by stimulating aerobic glycolysis via IGF signaling. J. Bone Miner. Res. 30, 1959–1968.

Fattori, E., Cappelletti, M., Costa, P., Sellitto, C., Cantoni, L., Carelli, M., Faggioni, R., Fantuzzi, G., Ghezzi, P., Poli, V., 1994. Defective inflammatory response in interleukin 6-deficient mice. J. Exp. Med. 180, 1243–1250.

Finkelstein, J.S., Hayes, A., Hunzelman, J.L., Wyland, J.J., Lee, H., Neer, R.M., 2003. The effects of parathyroid hormone, alendronate, or both in men with osteoporosis. N. Engl. J. Med. 349, 1216–1226.

Finkelstein, J.S., Wyland, J.J., Leder, B.Z., Burnett-Bowie, S.A., Lee, H., Juppner, H., Neer, R.M., 2009. Effects of teriparatide retreatment in osteoporotic men and women. J. Clin. Endocrinol. Metab. 94, 2495–2501.

Fox, J., Miller, M.A., Newman, M.K., Recker, R.R., Turner, C.H., Smith, S.Y., 2007a. Effects of daily treatment with parathyroid hormone 1–84 for 16 months on density, architecture and biomechanical properties of cortical bone in adult ovariectomized rhesus monkeys. Bone 41, 321–330.

Fox, J., Miller, M.A., Recker, R.R., Turner, C.H., Smith, S.Y., 2007b. Effects of treatment of ovariectomized adult rhesus monkeys with parathyroid hormone 1–84 for 16 months on trabecular and cortical bone structure and biomechanical properties of the proximal femur. Calcif. Tissue Int. 81, 53–63.

Fu, J., Li, S., Feng, R., Ma, H., Sabeh, F., Roodman, G.D., Wang, J., Robinson, S., Guo, X.E., Lund, T., Normolle, D., Mapara, M.Y., Weiss, S.J., Lentzsch, S., 2016. Multiple myeloma-derived MMP-13 mediates osteoclast fusogenesis and osteolytic disease. J. Clin. Investig. 126, 1759–1772.

Fu, Q., Jilka, R.L., Manolagas, S.C., O'brien, C.A., 2002. Parathyroid hormone stimulates receptor activator of NFkappa B ligand and inhibits osteoprotegerin expression via protein kinase A activation of cAMP-response element-binding protein. J. Biol. Chem. 277, 48868–48875.

Fu, Q., Manolagas, S.C., O'brien, C.A., 2006. Parathyroid hormone controls receptor activator of NF-κB ligand gene expression via a distant transcriptional enhancer. Mol. Cell Biol. 26, 6453–6468.

Fuller, K., Lawrence, K.M., Ross, J.L., Grabowska, U.B., Shiroo, M., Samuelsson, B., Chambers, T.J., 2008. Cathepsin K inhibitors prevent matrix-derived growth factor degradation by human osteoclasts. Bone 42, 200–211.

Galli, C., Zella, L.A., Fretz, J.A., Fu, Q., Pike, J.W., Weinstein, R.S., Manolagas, S.C., O'brien, C.A., 2008. Targeted deletion of a distant transcriptional enhancer of the receptor activator of nuclear factor-kappaB ligand gene reduces bone remodeling and increases bone mass. Endocrinology 149, 146–153.

Gebhard, S., Hattori, T., Bauer, E., Schlund, B., Bosl, M.R., de Crombrugghe, B., von der Mark, K., 2008. Specific expression of Cre recombinase in hypertrophic cartilage under the control of a BAC-Col10a1 promoter. Matrix Biol. 27, 693–699.

Girasole, G., Passeri, G., Jilka, R.L., Manolagas, S.C., 1994. Interleukin-11: a new cytokine critical for osteoclast development. J. Clin. Investig. 93, 1516–1524.

Greenfield, E.M., Horowitz, M.C., Lavish, S.A., 1996. Stimulation by parathyroid hormone of interleukin-6 and leukemia inhibitory factor expression in osteoblasts is an immediate-early gene response induced by cAMP signal transduction. J. Biol. Chem. 271, 10984–10989.

Guo, J., Liu, M., Yang, D., Bouxsein, M.L., Saito, H., Galvin, S., Kuhstoss, S.A., Thomas, C.C., Schipani, E., Baron, R., Bringhurst, F.R., Kronenberg, H.M., 2010. Suppression of Wnt signaling by Dkk1 attenuates PTH-mediated stromal cell response and new bone formation. Cell Metabol. 11, 161–171.

Hodsman, A.B., Bauer, D.C., Dempster, D., Dian, L., Hanley, D.A., Harris, S.T., Kendler, D., Mcclung, M.R., Miller, P.D., Olszynski, W.P., Orwoll, E., Yuen, C.K., 2005. Parathyroid hormone and teriparatide for the treatment of osteoporosis: a review of the evidence and suggested guidelines for its use. Endocr. Rev. 26, 688–703.

Horwood, N.J., Elliott, J., Martin, T.J., Gillespie, M.T., 1998. Osteotropic agents regulate the expression of osteoclast differentiation factor and osteoprotegerin in osteoblastic stromal cells. Endocrinology 139, 4743–4746.

Hurley, M.M., Okada, Y., Xiao, L., Tanaka, Y., Ito, M., Okimoto, N., Nakamura, T., Rosen, C.J., Doetschman, T., Coffin, J.D., 2006. Impaired bone anabolic response to parathyroid hormone in Fgf2−/− and Fgf2+/− mice. Biochem. Biophys. Res. Commun. 341, 989–994.

IIDA-Klein, A., Zhou, H., Lu, S.S., Levine, L.R., Ducayen-Knowles, M., Dempster, D.W., Nieves, J., Lindsay, R., 2002. Anabolic action of parathyroid hormone is skeletal site specific at the tissue and cellular levels in mice. J. Bone Miner. Res. 17, 808–816.

Iwaniec, U.T., Wronski, T.J., Liu, J., Rivera, M.F., Arzaga, R.R., Hansen, G., Brommage, R., 2007. PTH stimulates bone formation in mice deficient in Lrp5. J. Bone Miner. Res. 22, 394–402.

Jiang, Y., Zhao, J.J., Mitlak, B.H., Wang, O., Genant, H.K., Eriksen, E.F., 2003. Recombinant human parathyroid hormone (1–34) [teriparatide] improves both cortical and cancellous bone structure. J. Bone Miner. Res. 18, 1932–1941.

Jilka, R.L., 2007. Molecular and cellular mechanisms of the anabolic effect of intermittent PTH. Bone 40, 1434–1446.

Jilka, R.L., Bellido, T., Almeida, M., Plotkin, L.I., O'brien, C., Weinstein, R.S., Manolagas, S.C., 2008. Apoptosis of bone cells. In: Bilezikian, J., Raisz, L., Martin, T. (Eds.), Principles of Bone Biology, third ed. Academic Press.

Jilka, R.L., O'brien, C.A., Ali, A.A., Roberson, P.K., Weinstein, R.S., Manolagas, S.C., 2009. Intermittent PTH stimulates periosteal bone formation by actions on post-mitotic preosteoblasts. Bone 44, 275–286.

Jilka, R.L., O'brien, C.A., Bartell, S.M., Weinstein, R.S., Manolagas, S.C., 2010. Continuous elevation of PTH increases the number of osteoblasts via both osteoclast-dependent and - independent mechanisms. J. Bone Miner. Res. 25, 2427–2437.

Jilka, R.L., O'brien, C.A., Roberson, P.K., Bonewald, L.F., Weinstein, R.S., Manolagas, S.C., 2014. Dysapoptosis of osteoblasts and osteocytes increases cancellous bone formation but exaggerates bone porosity with age. J. Bone Miner. Res. 29, 103–117.

Jilka, R.L., Weinstein, R.S., Bellido, T., Roberson, P., Parfitt, A.M., Manolagas, S.C., 1999. Increased bone formation by prevention of osteoblast apoptosis with parathyroid hormone. J. Clin. Investig. 104, 439–446.

Jilka, R.L., Weinstein, R.S., Parfitt, A.M., Manolagas, S.C., 2007. Quantifying osteoblast and osteocyte apoptosis: challenges and rewards. J. Bone Miner. Res. 22, 1492–1501.

Johnson, R.W., Brennan, H.J., Vrahnas, C., Poulton, I.J., Mcgregor, N.E., Standal, T., Walker, E.C., Koh, T.T., Nguyen, H., Walsh, N.C., Forwood, M.R., Martin, T.J., Sims, N.A., 2014. The primary function of gp130 signaling in osteoblasts is to maintain bone formation and strength, rather than promote osteoclast formation. J. Bone Miner. Res. 29, 1492–1505.

Keller, H., Kneissel, M., 2005. SOST is a target gene for PTH in bone. Bone 37, 148–158.

Keller, J., Catala-Lehnen, P., Huebner, A.K., Jeschke, A., Heckt, T., Lueth, A., Krause, M., Koehne, T., Albers, J., Schulze, J., Schilling, S., Haberland, M., Denninger, H., Neven, M., Hermans-Borgmeyer, I., Streichert, T., Breer, S., Barvencik, F., Levkau, B., Rathkolb, B., Wolf, E., Calzada-Wack, J., Neff, F., Gailus-Durner, V., Fuchs, H., De Angelis, M.H., Klutmann, S., Tsourdi, E., Hofbauer, L.C., Kleuser, B., Chun, J., Schinke, T., Amling, M., 2014. Calcitonin controls bone formation by inhibiting the release of sphingosine 1-phosphate from osteoclasts. Nat. Commun. 5.

Kim, S.W., Pajevic, P.D., Selig, M., Barry, K.J., Yang, J.Y., Shin, C.S., Baek, W.Y., Kim, J.E., Kronenberg, H.M., 2012. Intermittent parathyroid hormone administration converts quiescent lining cells to active osteoblasts. J. Bone Miner. Res. 27, 2075–2084.

Koide, M., Kobayashi, Y., Yamashita, T., Uehara, S., Nakamura, M., Hiraoka, B.Y., Ozaki, Y., Iimura, T., Yasuda, H., Takahashi, N., Udagawa, N., 2017. Bone formation is coupled to resorption via suppression of sclerostin expression by osteoclasts. J. Bone Miner. Res. 32, 2074–2086.

Kong, Y.Y., Yoshida, H., Sarosi, I., Tan, H.L., Timms, E., Capparelli, C., Morony, S., Oliveira, D.S., Van, G., Itie, A., Khoo, W., Wakeham, A., Dunstan, C.R., Lacey, D.L., Mak, T.W., Boyle, W.J., Penninger, J.M., 1999. OPGL is a key regulator of osteoclastogenesis, lymphocyte development and lymph-node organogenesis. Nature 397, 315–323.

Kovacs, C.S., 2017. The skeleton is a storehouse of mineral that is plundered during lactation and (fully?) replenished afterwards. J. Bone Miner. Res. 32, 676–680.

Kramer, I., Loots, G.G., Studer, A., Keller, H., Kneissel, M., 2010. Parathyroid hormone (PTH) induced bone gain is blunted in SOST overexpressing and deficient mice. J. Bone Miner. Res. 25, 178–189.

Lacey, D.L., Tan, H.L., Lu, J., Kaufman, S., Van, G., Qiu, W., Rattan, A., Scully, S., Fletcher, F., Juan, T., Kelley, M., Burgess, T.L., Boyle, W.J., Polverino, A.J., 2000. Osteoprotegerin ligand modulates murine osteoclast survival in vitro and in vivo. Am. J. Pathol. 157, 435–448.

Langdahl, B.L., Mortensen, L., Vesterby, A., Eriksen, E.F., Charles, P., 1996. Bone histomorphometry in hypoparathyroid patients treated with vitamin D. Bone 18, 103–108.

Lassen, N.E., Andersen, T.L., Ploen, G.G., Soe, K., Hauge, E.M., Harving, S., Eschen, G.E.T., Delaisse, J.M., 2017. Coupling of bone resorption and formation in real time: new knowledge gained from human Haversian BMUs. J. Bone Miner. Res. 32, 1395–1405.

Lawal, R.A., Zhou, X., Batey, K., Hoffman, C.M., Georger, M.A., Radtke, F., Hilton, M.J., Xing, L., Frisch, B.J., Calvi, L.M., 2017. The Notch ligand Jagged1 regulates the osteoblastic lineage by maintaining the osteoprogenitor pool. J. Bone Miner. Res. 32, 1320–1331.

Leaffer, D., Sweeney, M., Kellerman, L.A., Avnur, Z., Krstenansky, J.L., Vickery, B.H., Caulfield, J.P., 1995. Modulation of osteogenic cell ultrastructure by RS-23581, an analog of human parathyroid hormone (PTH)-related peptide- (1–34), and bovine PTH-(1–34). Endocrinology 136, 3624–3631.

Lee, S.K., Lorenzo, J.A., 1999. Parathyroid hormone stimulates TRANCE and inhibits osteoprotegerin messenger ribonucleic acid expression in murine bone marrow cultures: correlation with osteoclast-like cell formation. Endocrinology 140, 3552–3561.

Li, J.Y., D'amelio, P., Robinson, J., Walker, L.D., Vaccaro, C., Luo, T., Tyagi, A.M., Yu, M., Reott, M., Sassi, F., Buondonno, I., Adams, J., Weitzmann, M.N., Isaia, G.C., Pacifici, R., 2015. IL-17A is increased in humans with primary hyperparathyroidism and mediates PTH-induced bone loss in mice. Cell Metabol. 22, 799–810.

Li, X., Qin, L., Bergenstock, M., Bevelock, L.M., Novack, D.V., Partridge, N.C., 2007. Parathyroid hormone stimulates osteoblastic expression of MCP-1 to recruit and increase the fusion of pre/osteoclasts. J. Biol. Chem. 282, 33098–33106.

Lindsay, R., Cosman, F., Zhou, H., Bostrom, M.P., Shen, V.W., Cruz, J.D., Nieves, J.W., Dempster, D.W., 2006. A novel tetracycline labeling schedule for longitudinal evaluation of the short-term effects of anabolic therapy with a single iliac crest bone biopsy: early actions of teriparatide. J. Bone Miner. Res. 21, 366–373.

Lindsay, R., Zhou, H., Cosman, F., Nieves, J., Dempster, D.W., Hodsman, A.B., 2007. Effects of a one-month treatment with parathyroid hormone (1–34) on bone formation on cancellous, endocortical and periosteal surfaces of the human ilium. J. Bone Miner. Res. 22, 495–502.

Lotinun, S., Kiviranta, R., Matsubara, T., Alzate, J.A., Neff, L., Luth, A., Koskivirta, I., Kleuser, B., Vacher, J., Vuorio, E., Horne, W.C., Baron, R., 2013. Osteoclast-specific cathepsin K deletion stimulates S1P-dependent bone formation. J. Clin. Investig. 123, 666–681.

Lotinun, S., Sibonga, J.D., Turner, R.T., 2005. Evidence that the cells responsible for marrow fibrosis in a rat model for hyperparathyroidism are pre-osteoblasts. Endocrinology 146, 4074–4081.

Lowry, M.B., Lotinun, S., Leontovich, A.A., Zhang, M., Maran, A., Shogren, K.L., Palama, B.K., Marley, K., Iwaniec, U.T., Turner, R.T., 2008. Osteitis fibrosa is mediated by platelet-derived growth factor-A via a phosphoinositide 3-kinase-dependent signaling pathway in a rat model for chronic hyperparathyroidism. Endocrinology 149, 5735–5746.

Ma, Y.L., Zeng, Q., Donley, D.W., Ste-Marie, L.G., Gallagher, J.C., Dalsky, G.P., Marcus, R., Eriksen, E.F., 2006. Teriparatide increases bone formation in modeling and remodeling osteons and enhances IGF-II immunoreactivity in postmenopausal women with osteoporosis. J. Bone Miner. Res. 21, 855–864.

Ma, Y.L., Zeng, Q.Q., Chiang, A.Y., Burr, D., Li, J., Dobnig, H., Fahrleitner-Pammer, A., Michalska, D., Marin, F., Pavo, I., Stepan, J.J., 2014. Effects of teriparatide on cortical histomorphometric variables in postmenopausal women with or without prior alendronate treatment. Bone 59, 139–147.

Mallette, L.E., 1994. The functional and pathological spectrum of parathyroid abnormalities in hyperparathyroidism (Chapter 25). In: Bilezikian, J.P., Levine, M., Marcus, R. (Eds.), The Parathyroids. Raven Press Ltd. New York, pp. 423–455.

Manolagas, S.C., 2000. Birth and death of bone cells: basic regulatory mechanisms and implications for the pathogenesis and treatment of osteoporosis. Endocr. Rev. 21, 115–137.

Mcsheehy, P.M., Chambers, T.J., 1986. Osteoblast-like cells in the presence of parathyroid hormone release soluble factor that stimulates osteoclastic bone resorption. Endocrinology 119, 1654–1659.

Miao, D., Li, J., Xue, Y., Su, H., Karaplis, A.C., Goltzman, D., 2004. Parathyroid hormone-related peptide is required for increased trabecular bone volume in parathyroid hormone-null mice. Endocrinology 145, 3554–3562.

Miller, P.D., Hattersley, G., Riis, B.J., Williams, G.C., Lau, E., Russo, L.A., Alexandersen, P., Zerbini, C.A., Hu, M.Y., Harris, A.G., Fitzpatrick, L.A., Cosman, F., Christiansen, C., Investigators, A.S., 2016. Effect of abaloparatide vs placebo on new vertebral fractures in postmenopausal women with osteoporosis: a randomized clinical trial. J. Am. Med. Assoc. 316, 722–733.

Miyakoshi, N., Kasukawa, Y., Linkhart, T.A., Baylink, D.J., Mohan, S., 2001. Evidence that anabolic effects of PTH on bone require IGF-I in growing mice. Endocrinology 142, 4349–4356.

Moreira, C.A., Fitzpatrick, L.A., Wang, Y., Recker, R.R., 2017. Effects of abaloparatide-SC (BA058) on bone histology and histomorphometry: the ACTIVE phase 3 trial. Bone 97, 314–319.

Nakashima, T., Hayashi, M., Fukunaga, T., Kurata, K., OH-Hora, M., Feng, J.Q., Bonewald, L.F., Kodama, T., Wutz, A., Wagner, E.F., Penninger, J.M., Takayanagi, H., 2011. Evidence for osteocyte regulation of bone homeostasis through RANKL expression. Nat. Med. 17, 1231–1234.

Nakchbandi, I.A., Lang, R., Kinder, B., Insogna, K.L., 2008. The role of the receptor activator of nuclear factor-κb ligand/osteoprotegerin cytokine system in primary hyperparathyroidism. J. Clin. Endocrinol. Metab. 93, 967–973.

Nishida, S., Yamaguchi, A., Tanizawa, T., Endo, N., Mashiba, T., Uchiyama, Y., Suda, T., Yoshiki, S., Takahashi, H.E., 1994. Increased bone formation by intermittent parathyroid hormone administration is due to the stimulation of proliferation and differentiation of osteoprogenitor cells in bone marrow. Bone 15, 717–723.

O'brien, C.A., Jilka, R.L., Fu, Q., Stewart, S., Weinstein, R.S., Manolagas, S.C., 2005. IL-6 is not required for parathyroid hormone stimulation of RANKL expression, osteoclast formation, and bone loss in mice. Am. J. Physiol. Endocrinol. Metab. 289, E784–E793.

O'brien, C.A., Nakashima, T., Takayanagi, H., 2013. Osteocyte control of osteoclastogenesis. Bone 54, 258–263.

O'brien, C.A., Plotkin, L.I., Galli, C., Goellner, J.J., Gortazar, A.R., Allen, M.R., Robling, A., Bouxsein, M., Schipani, E., Turner, C.H., Jilka, R.L., Weinstein, R.S., Manolagas, S.C., Bellido, T., 2008. Control of bone mass and remodeling by PTH receptor signaling in osteocytes. PLoS One 3, e2942. https://doi.org/10.1371/journal.pone.0002942.

Onal, M., Bishop, K.A., ST John, H.C., Danielson, A.L., Riley, E.M., Piemontese, M., Xiong, J., Goellner, J.J., O'brien, C.A., Pike, J.W., 2015. A DNA segment spanning the mouse Tnfsf11 transcription unit and its upstream regulatory domain rescues the pleiotropic biologic phenotype of the RANKL null mouse. J. Bone Miner. Res. 30, 855–868.

Ono, N., Kronenberg, H.M., 2015. Mesenchymal progenitor cells for the osteogenic lineage. Curr. Mol. Biol. Rep. 1, 95–100.

Onyia, J.E., Miles, R.R., Yang, X., Halladay, D.L., Hale, J., Glasebrook, A., Mcclure, D., Seno, G., Churgay, L., Chandrasekhar, S., Martin, T.J., 2000. In vivo demonstration that human parathyroid hormone 1-38 inhibits the expression of osteoprotegerin in bone with the kinetics of an immediate early gene. J. Bone Miner. Res. 15, 863–871.

Orwoll, E.S., Scheele, W.H., Paul, S., Adami, S., Syversen, U., Diez-Perez, A., Kaufman, J.M., Clancy, A.D., Gaich, G.A., 2003. The effect of teriparatide [human parathyroid hormone (1–34)] therapy on bone density in men with osteoporosis. J. Bone Miner. Res. 18, 9–17.

Palmqvist, P., Persson, E., Conaway, H.H., Lerner, U.H., 2002. IL-6, leukemia inhibitory factor, and oncostatin M stimulate bone resorption and regulate the expression of receptor activator of NF-kappa B ligand, osteoprotegerin, and receptor activator of NF-kappa B in mouse calvariae. J. Immunol. 169, 3353–3362.

Parfitt, A.M., 1996. Skeletal heterogeneity and the purposes of bone remodeling/Implications for the understanding of osteoporosis. In: Marcus, R., Feldman, D., Kelsey, J. (Eds.), Osteoporosis. Academic Press, San Diego, CA.

Parfitt, A.M., 2002. Misconceptions (2): turnover is always higher in cancellous than in cortical bone. Bone 30, 807–809.

Parisien, M., Dempster, D.W., Shane, E., Bilezikian, J.P., 2001. Histomorphometric analysis of bone in primary hyperparathyroidism. In: Bilezikian, J.P., Marcus, R., Levine, M.A. (Eds.), The Parathyroids. Basic and Clinical Concepts. Academic Press, San Diego.

Piemontese, M., Almeida, M., Robling, A.G., Kim, H.N., Xiong, J., Thostenson, J.D., Weinstein, R.S., Manolagas, S.C., O'brien, C.A., Jilka, R.L., 2017. Old age causes de novo intracortical bone remodeling and porosity in mice. JCI Insight 2.

Robling, A.G., Kedlaya, R., Ellis, S.N., Childress, P.J., Bidwell, J.P., Bellido, T., Turner, C.H., 2011. Anabolic and catabolic regimens of human parathyroid hormone 1–34 elicit bone- and envelope-specific attenuation of skeletal effects in sost-deficient mice. Endocrinology 152, 2963–2975.

Rodan, G.A., Martin, T.J., 1981. Role of osteoblasts in hormonal control of bone resorption - a hypothesis. Calcif. Tissue Int. 33, 349–351.

Rubin, M.R., Dempster, D.W., Zhou, H., Shane, E., Nickolas, T., Sliney, J., Silverberg, S.J., Bilezikian, J.P., 2008. Dynamic and structural properties of the skeleton in hypoparathyroidism. J. Bone Miner. Res. 23, 2018–2024.

Saini, V., Marengi, D.J., Barry, K.J., Fulzele, K.S., Heiden, E., Liu, X., Dedic, C., Maeda, A., Lotinun, S., Baron, R., Pajevic, P.D., 2013. Parathyroid hormone (PTH)/PTH-related peptide type 1 receptor (PPR) signaling in osteocytes regulates anabolic and catabolic skeletal responses to PTH. J. Biol. Chem. 288, 20122–20134.

Salo, J., Lehenkari, P., Mulari, M., Metsikkö, K., Väänänen, H.K., 1997. Removal of osteoclast bone resorption products by transcytosis. Science 276, 270–273.

Sartawi, Z., Schipani, E., Ryan, K.B., Waeber, C., 2017. Sphingosine 1-phosphate (S1P) signalling: role in bone biology and potential therapeutic target for bone repair. Pharmacol. Res. 125, 232–245.

Sato, M., Westmore, M., Ma, Y.L., Schmidt, A., Zeng, Q.Q., Glass, E.V., Vahle, J., Brommage, R., Jerome, C.P., Turner, C.H., 2004. Teriparatide [PTH(1–34)] strengthens the proximal femur of ovariectomized nonhuman primates despite increasing porosity. J. Bone Miner. Res. 19, 623–629.

Satterwhite, J., Heathman, M., Miller, P.D., Marin, F., Glass, E.V., Dobnig, H., 2010. Pharmacokinetics of teriparatide (rhPTH[1–34]) and calcium pharmacodynamics in postmenopausal women with osteoporosis. Calcif. Tissue Int. 87, 485–492.

Seeman, E., Martin, T.J., 2015. Co-administration of antiresorptive and anabolic agents: a missed opportunity. J. Bone Miner. Res. 30, 753–764.

Siddiqui, J.A., Johnson, J., LE Henaff, C., Bitel, C.L., Tamasi, J.A., Partridge, N.C., 2017. Catabolic effects of human PTH (1−34) on bone: requirement of monocyte chemoattractant protein-1 in murine model of hyperparathyroidism. Sci. Rep. 7, 15300.

Sikjaer, T., Rejnmark, L., Thomsen, J.S., Tietze, A., Bruel, A., Andersen, G., Mosekilde, L., 2012. Changes in 3-dimensional bone structure indices in hypoparathyroid patients treated with PTH(1−84): a randomized controlled study. J. Bone Miner. Res. 27, 781−788.

Sims, N.A., 2016. Cell-specific paracrine actions of IL-6 family cytokines from bone, marrow and muscle that control bone formation and resorption. Int. J. Biochem. Cell Biol. 79, 14−23.

Sims, N.A., Jenkins, B.J., Nakamura, A., Quinn, J.M., Li, R., Gillespie, M.T., Ernst, M., Robb, L., Martin, T.J., 2005. Interleukin-11 receptor signaling is required for normal bone remodeling. J. Bone Miner. Res. 20, 1093−1102.

Sims, N.A., Martin, T., 2014. Coupling the activities of bone formation and resorption: a multitude of signals within the basic multicellular unit. BoneKEy Rep. 3.

Standal, T., Johnson, R.W., Mcgregor, N.E., Poulton, I.J., Ho, P.W., Martin, T.J., Sims, N.A., 2014. gp130 in late osteoblasts and osteocytes is required for PTH-induced osteoblast differentiation. J. Endocrinol. 223, 181−190.

Stein, E.M., Silva, B.C., Boutroy, S., Zhou, B., Wang, J., Udesky, J., Zhang, C., Mcmahon, D.J., Romano, M., Dworakowski, E., Costa, A.G., Cusano, N., Irani, D., Cremers, S., Shane, E., Guo, X.E., Bilezikian, J.P., 2013. Primary hyperparathyroidism is associated with abnormal cortical and trabecular microstructure and reduced bone stiffness in postmenopausal women. J. Bone Miner. Res. 28, 1029−1040.

Stickens, D., Behonick, D.J., Ortega, N., Heyer, B., Hartenstein, B., Yu, Y., Fosang, A.J., Schorpp-Kistner, M., Angel, P., Werb, Z., 2004. Altered endochondral bone development in matrix metalloproteinase 13-deficient mice. Development 131, 5883−5895.

Stilgren, L.S., Rettmer, E., Eriksen, E.F., Hegedüs, L., Beck-Nielsen, H., Abrahamsen, B., 2004. Skeletal changes in osteoprotegerin and receptor activator of nuclear factor-κb ligand mRNA levels in primary hyperparathyroidism: effect of parathyroidectomy and association with bone metabolism. Bone 35, 256−265.

Tang, Y., Wu, X., Lei, W., Pang, L., Wan, C., Shi, Z., Zhao, L., Nagy, T.R., Peng, X., Hu, J., Feng, X., Van Hul, W., Wan, M., Cao, X., 2009. TGF-β1-induced migration of bone mesenchymal stem cells couples bone resorption with formation. Nat. Med. 15, 757−765.

Tawfeek, H., Bedi, B., Li, J.Y., Adams, J., Kobayashi, T., Weitzmann, M.N., Kronenberg, H.M., Pacifici, R., 2010. Disruption of PTH receptor 1 in T cells protects against PTH-induced bone loss. PLoS One 5, e12290.

Tazawa, K., Hoshi, K., Kawamoto, S., Tanaka, M., Ejiri, S., Ozawa, H., 2004. Osteocytic osteolysis observed in rats to which parathyroid hormone was continuously administered. J. Bone Miner. Metab. 22, 524−529.

Terauchi, M., Li, J.Y., Bedi, B., Baek, K.H., Tawfeek, H., Galley, S., Gilbert, L., Nanes, M.S., Zayzafoon, M., Guldberg, R., Lamar, D.L., Singer, M.A., Lane, T.F., Kronenberg, H.M., Weitzmann, M.N., Pacifici, R., 2009. T lymphocytes amplify the anabolic activity of parathyroid hormone through Wnt10b signaling. Cell Metabol. 10, 229−240.

Tonna, S., Takyar, F.M., Vrahnas, C., Crimeen-Irwin, B., Ho, P.W.M., Poulton, I.J., Brennan, H.J., Mcgregor, N.E., Allan, E.H., Nguyen, H., Forwood, M.R., Tatarczuch, L., Mackie, E.J., Martin, T.J., Sims, N.A., 2014. EphrinB2 signaling in osteoblasts promotes bone mineralization by preventing apoptosis. FASEB J. 28, 4482−4496.

Van Lierop, A.H., Witteveen, J.E., Hamdy, N.A., Papapoulos, S.E., 2010. Patients with primary hyperparathyroidism have lower circulating sclerostin levels than euparathyroid controls. Eur. J. Endocrinol. 163, 833−837.

Vu, T.D., Wang, X.F., Wang, Q., Cusano, N.E., Irani, D., Silva, B.C., Ghasem-Zadeh, A., Udesky, J., Romano, M.E., Zebaze, R., Jerums, G., Boutroy, S., Bilezikian, J.P., Seeman, E., 2013. New insights into the effects of primary hyperparathyroidism on the cortical and trabecular compartments of bone. Bone 55, 57−63.

Walker, E.C., Poulton, I.J., Mcgregor, N.E., Ho, P.W., Allan, E.H., Quach, J.M., Martin, T.J., Sims, N.A., 2012. Sustained RANKL response to parathyroid hormone in oncostatin M receptor-deficient osteoblasts converts anabolic treatment to a catabolic effect in vivo. J. Bone Miner. Res. 27, 902−912.

Wan, M., Yang, C., Li, J., Wu, X., Yuan, H., Ma, H., He, X., Nie, S., Chang, C., Cao, X., 2008. Parathyroid hormone signaling through low-density lipoprotein-related protein 6. Genes Dev. 22, 2968−2979.

Winchester, S.K., Selvamurugan, N., D'alonzo, R.C., Partridge, N.C., 2000. Developmental regulation of collagenase-3 mRNA in normal, differentiating osteoblasts through the activator protein-1 and the runt domain binding sites. J. Biol. Chem. 275, 23310−23318.

Xian, L., Wu, X., Pang, L., Lou, M., Rosen, C.J., Qiu, T., Crane, J., Frassica, F., Zhang, L., Rodriguez, J.P., Jia, X., Yakar, S., Xuan, S., Efstratiadis, A., Wan, M., Cao, X., 2012. Matrix IGF-1 maintains bone mass by activation of mTOR in mesenchymal stem cells. Nat. Med. 18, 1095−1101.

Xiong, J., Cawley, K., Piemontese, M., Fujiwara, Y., Zhao, H., Goellner, J.J., O'Brien, C.A., 2018 Jul 25. Soluble RANKL contributes to osteoclast formation in adult mice but not ovariectomy-induced bone loss. Nat Comm 9 (1), 2909.

Xiong, J., Onal, M., Jilka, R.L., Weinstein, R.S., Manolagas, S.C., O'brien, C.A., 2011. Matrix-embedded cells control osteoclast formation. Nat. Med. 17, 1235−1241.

Xiong, J., Piemontese, M., Onal, M., Campbell, J., Goellner, J.J., Dusevich, V., Bonewald, L., Manolagas, S.C., O'brien, C.A., 2015. Osteocytes, not osteoblasts or lining cells, are the main source of the RANKL required for osteoclast formation in remodeling bone. PLoS One 10, e0138189.

Xiong, J., Piemontese, M., Thostenson, J.D., Weinstein, R.S., Manolagas, S.C., O'brien, C.A., 2014. Osteocyte-derived RANKL is a critical mediator of the increased bone resorption caused by dietary calcium deficiency. Bone 66, 146−154.

Yasuda, H., Shima, N., Nakagawa, N., Yamaguchi, K., Kinoshaki, M., Mochizuki, S., Tomoyasu, A., Yano, K., Goto, M., Murakami, A., Tsuda, E., Morinaga, T., Higashio, K., Udagawa, N., Takahashi, N., Suda, T., 1998. Osteoclast differentiation factor is a ligand for osteoprotegerin/osteoclastogenesis-inhibitory factor and is identical to TRANCE/RANKL. Proc. Natl. Acad. Sci. Unit. States Am. 95, 3597−3602.

Zanotti, S., Canalis, E., 2017. Parathyroid hormone inhibits Notch signaling in osteoblasts and osteocytes. Bone 103, 159−167.

Zebaze, R., Takao-Kawabata, R., Peng, Y., Zadeh, A.G., Hirano, K., Yamane, H., Takakura, A., Isogai, Y., Ishizuya, T., Seeman, E., 2017. Increased cortical porosity is associated with daily, not weekly, administration of equivalent doses of teriparatide. Bone 99, 80−84.

Zhao, W., Byrne, M.H., Boyce, B.F., Krane, S.M., 1999. Bone resorption induced by parathyroid hormone is strikingly diminished in collagenase-resistant mutant mice. J. Clin. Investig. 103, 517−524.

Chapter 33

Calcitonin peptides

Dorit Naot*, **David S. Musson and Jillian Cornish**
Department of Medicine, University of Auckland, Auckland, New Zealand

Chapter outline

Introduction

The peptide hormone calcitonin was discovered as the active component in extracts from the thyroid gland that acutely lowered the concentration of circulating calcium (Copp et al., 1962; Copp and Cheney, 1962). Over the years, several peptides with structural similarity to calcitonin have been discovered and became recognized as the "calcitonin family," which includes the calcitonin gene-related peptides (αCGRP and βCGRP), amylin, adrenomedullin, and adrenomedullin 2. The peptides of the calcitonin family signal through related receptors; calcitonin itself binds to the calcitonin receptor, a seven-transmembrane domain G-protein coupled receptor (GPCR), while all other family members require receptor heterodimers that include a GPCR and receptor-activity-modifying protein (RAMP). The calcitonin family peptides have been investigated extensively; in addition to studies of the biochemistry, pharmacology, and physiological activities of the peptides, a large body of literature describes the development of these peptides, their analogues and their antagonists for clinical use. This chapter provides a general introduction to the calcitonin family and summarizes the current knowledge of the skeletal activities of calcitonin, CGRP, and amylin.

Calcitonin-family gene and peptide structure

Calcitonin and αCGRP are generated by alternative splicing of mRNA transcribed from the *CALCA* gene, which in humans is located on the short arm of chromosome 11. The *CALCA* gene contains six exons: exons I–IV are included in the mRNA for the precursor of calcitonin, preprocalcitonin, whereas preproCGRP is encoded by exons I–III and V–IV (Fig. 33.1A). The alternative splicing of *CALCA* mRNA is tissue specific—calcitonin mRNA is produced mainly in parafollicular

* Contributor retains copyright for images.

Principles of Bone Biology. https://doi.org/10.1016/B978-0-12-814841-9.00033-6

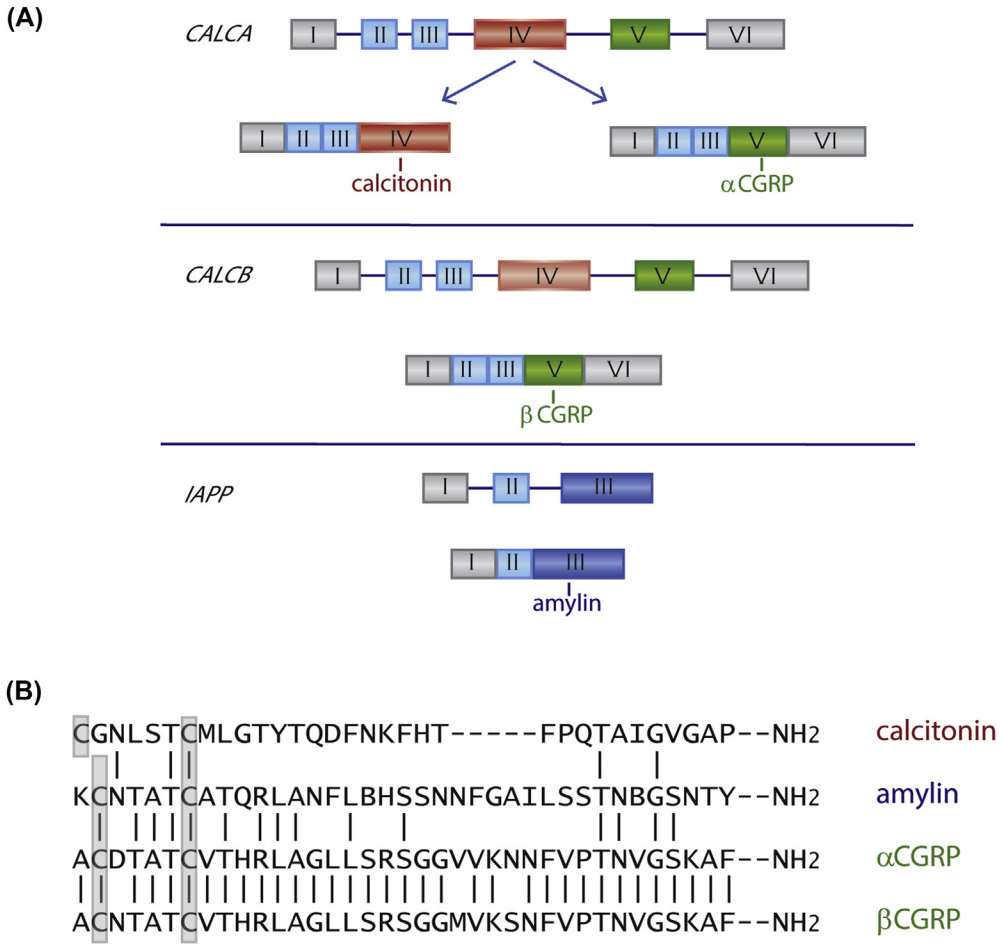

FIGURE 33.1 Genes, mRNA, and peptides of four members of the human calcitonin family: calcitonin, αCGRP, βCGRP, and amylin. (A) The *CALCA* primary transcript is processed through alternative splicing. Calcitonin mRNA contains exons I, II, III, and IV, whereas αCGRP mRNA contains exons I, II, III, V, and VI. Each mRNA is translated into a precursor protein that undergoes proteolytic cleavage to produce the mature peptides. Exon IV encodes the mature calcitonin peptide and exon V encodes the mature αCGRP. βCGRP is the only mature peptide encoded by *CALCB*. The *IAPP* gene contains only three exons, with exon III encoding the mature amylin peptide. (B) Amino acid sequences of the human peptides. All four peptides are amidated at the C terminal. The cysteine residues connected by a disulfide bond in each peptide are shaded, and identical amino acids are indicated by vertical lines.

cells of the thyroid, whereas in the nervous system, αCGRP mRNA is the predominant form (Breimer et al., 1988). In nonmammalian species—birds, fish and reptiles—calcitonin is derived from the ultimobranchial body. Salmon calcitonin (sCT), which shares only 50% sequence identity with the human peptide, has a much higher biological potency in humans than human calcitonin itself (Niall et al., 1969). A second CGRP peptide, βCGRP, which in humans differs from αCGRP by three amino acids, is encoded by *CALCB*, a separate gene located on the short arm of chromosome 11. Human amylin (also called island amyloid polypeptide) is encoded by *IAPP*, a gene that includes three exons and is located on the short arm of chromosome 12. Like calcitonin and CGRP, amylin is synthesized as a prepropeptide, which is processed by proteolytic cleavage to the mature amylin peptide. Amylin is produced mainly in β islet cells of the pancreas but has also been detected in the gastrointestinal tract as well as lung and neuronal tissues. The amino acid sequences of the mature calcitonin, αCGRP, βCGRP, and amylin in humans are presented in Fig. 33.1B. Mature calcitonin is a 32 amino-acid peptide, whereas CGRPs and amylin contain 37 amino acids. All the calcitonin family peptides have an amino acid ring structure at the N terminal created by a disulfide bond between cysteine residues at positions 2 and 7 in CGRP and amylin, and positions 1 and 7 in calcitonin, and all are amidated at the C terminal. These structural elements are shared by the additional members of the calcitonin family, adrenomedullin and adrenomedullin 2, which are not discussed further in this chapter.

Extraskeletal actions of calcitonin-family peptides

Calcitonin

Calcitonin was initially identified as a hormone that induces hypocalcemia through a rapid and potent inhibition of bone resorption by osteoclasts. The great majority of studies of calcitonin have focused on its skeletal activity and its effect on

calcium homeostasis. The scientific literature includes a large number of clinical studies of the skeletal effects of sCT, as sCT has been in wide clinical use for a number of years, mainly for patients with Paget's bone disease and osteoporosis (Chesnut 3rd et al., 2008; Henriksen et al., 2016). Although recent studies (discussed later in the chapter) indicate that calcitonin regulates bone formation during development, the physiological role of calcitonin has not yet been clearly established, and it has been suggested that calcitonin might not have a major role in mammals under normal physiological conditions (Davey and Findlay, 2013). Calcium metabolism and bone mineral density (BMD) are unaffected in patients with medullary thyroid carcinoma, who have long-term excess of endogenous calcitonin levels, or who have undergone thyroidectomy and have undetectable circulating calcitonin (Hurley et al., 1987; Wuster et al., 1992). The current understanding is that the main significance of calcitonin appears to be the conservation of body calcium stores in situations of calcium stress, including rapid growth, pregnancy, and lactation.

Outside the skeleton, calcitonin transiently enhances calcium excretion through the inhibition of tubular calcium resorption. In addition, calcitonin was found to increase the urinary excretion rate of sodium, potassium, phosphorus, chloride, and magnesium (Findlay and Sexton, 2004). Calcitonin is also involved in the regulation of vitamin D processing, enhancing the 1-hydroxylation of 25-hydroxyvitamin D in the proximal straight tubule of the kidney. Another target tissue of calcitonin is the central nervous system. Calcitonin receptors are highly expressed in the central nervous system, and calcitonin administration has been shown to affect the pituitary and the hypothalamus. In rats, intracerebral injection of calcitonin reduced food and water intake and changed the pattern of secretion of growth hormone. In humans, high concentrations of sCT reduced the circulating levels of hormones including LH, FSH, and testosterone. Calcitonin has an analgesic effect on chronic bone pain and pain associated with osteoporotic fracture (Silverman and Azria, 2002).

Calcitonin gene-related peptide

CGRP is mainly expressed in the central and peripheral nervous systems. It is stored in large, dense-core vesicles within sensory nerve terminals and is commonly colocalized with substance P. The circulating levels of CGRP are low, and it is suggested that the major effects of CGRP are exerted locally. CGRP is recognized as a potent microvascular vasodilator, and its physiological activity is largely dependent on its release from perivascular nerves (Russell et al., 2014). Interestingly, injections of CGRP antagonists to healthy individuals have no significant effects on blood pressure, suggesting that CGRP has no major role in the control of physiological systemic blood pressure. CGRP-containing nerve fibers are also present in the heart vasculature, where CGRP release produces both positive inotropic and positive chronotropic effects and is thought to play a cardioprotective role (Russell et al., 2014).

CGRP also affects energy metabolism. In skeletal muscle, CGRP inhibits glycogen synthesis and stimulates glycogenolysis, while in the liver it increases gluconeogenesis and glucose output (Lima et al., 2017). A number of animal studies have found that CGRP administration reduces food intake, with CGRP inducing anorexia through activation of the cAMP/protein kinase A pathway. Mice deficient of αCGRP were protected from obesity induced by a high-fat diet. In comparison with wild-type controls, the αCGRP knockout mice had higher metabolic rate, increased energy expenditure, and raised body temperature (Russell et al., 2014).

CGRP is involved in neuronal regulation of the immune system. It has been shown to mediate a host of immune regulatory responses, and in different experimental systems CGRP was found to have either proinflammatory or antiinflammatory effects. CGRP promotes neurogenic inflammation, and its release from nerve terminals causes local vasodilation, edema formation, increased blood flow, and recruitment of inflammatory cells. On the other hand, in murine dendritic cells, CGRP inhibited TLR-stimulated production of the inflammatory mediators tumor necrosis factor (TNFα) and C−C motif chemokine ligand 4 (CCL4), an effect that was dependent on the cAMP/protein kinase A signaling pathway (Harzenetter et al., 2007).

A large number of investigations of CGRP in recent years have focused on its involvement in the pathophysiology of migraines (Iyengar et al., 2017). Raised levels of CGRP are observed both peripherally and centrally in migraine patients. CGRP is released from trigeminal afferent nerve fibers during a migraine attack, causing vasodilatation and neurogenic inflammation. The maintenance of a sensitized, hyperresponsive neuronal state is considered a central underlying mechanism in migraine. CGRP facilitates nociceptive transmission and contributes to the development and maintenance of a sensitized state in peripheral sensory neurons as well as neurons within the central nervous system. Four monoclonal antibodies are currently in development for migraine prevention, three against CGRP itself and one against the CGRP receptor. Results from phase III trials suggest comparable efficacy, safety, and tolerability of all four antibodies (Paemeleire & MaassenVanDenBrink, 2018).

Amylin

Amylin was purified from pancreatic deposits of patients with type 2 diabetes and from human insulinoma and was found to be predominantly expressed in β cells of the islets of Langerhans in the pancreas (Cooper et al., 1987; Westermark et al., 1987). In these cells, amylin is stored in secretory granules together with insulin, and it is cosecreted with insulin in response to changes in circulating glucose levels; hyperglycemia stimulates amylin secretion, whereas hypoglycemia inhibits it. Human amylin monomers are soluble, but aggregate to form pancreatic amyloid in patients with type 2 diabetes as well as spontaneously in vitro, in a concentration-dependent manner (Konarkowska et al., 2006). The role of amylin aggregates in the development of β-cell lesions in type 2 diabetes is not entirely clear, although there is evidence that they contribute to the progressive failure and eventually to the death of islet β-cells (Lorenzo et al., 1994; Zhang et al., 2016).

The main physiological role of amylin is the regulation of energy homeostasis (Hay et al., 2015). Eating leads to a rapid increase in circulating levels of amylin, which produces satiation signals and thus controls ingested meal size. Administration of exogenous amylin into animals reduces eating within minutes, an effect that could be reproduced by amylin analogues and blocked by amylin antagonists. Mechanisms involved in the activity of amylin as a satiety signal include delayed gastric emptying, which leads to satiation and prevents further food intake, and central signaling of amylin in specific areas of the brain stem. In addition to the short-term effect on satiety, amylin is also one of a group of hormones secreted in proportion to body adiposity, and is considered an adiposity signal that has a long-term effect to reduce eating by enhancing satiety. In obese rats, basal plasma levels of amylin were higher in comparison with lean controls, and peripheral or central administration of amylin led to decreased body weight as well as fat gain. In addition to short- and long-term effects on food intake, central administration of amylin increases energy expenditure (Hay et al., 2015).

In recent years, studies have demonstrated the importance of interactions between amylin and leptin, an adipokine secreted predominantly from white fat tissue, in the control of energy homeostasis (Levin and Lutz, 2017; Lutz, 2012). Similar to amylin and insulin, leptin provides negative, catabolic feedback to the brain when body adiposity is increased. Circulating leptin levels are generally elevated in obesity, and obese individuals can become leptin-resistant. Amylin was shown to act as an endogenous leptin sensitizer, and cross talk between leptin and amylin was suggested by the observation that leptin-deficient mice have reduced expression of amylin in the hypothalamus, which could be normalized by exogenous leptin (Li et al., 2015). Moreover, infusion of the amylin antagonist AC187 acutely reduced the anorectic effect of leptin.

The synthetic analogue of human amylin, pramlintide, is currently in clinical use for diabetes as an adjunctive therapy to mealtime insulin (Qiao et al., 2017; Singh-Franco et al., 2007). Multiple clinical studies in patients with type 1 and type 2 diabetes have shown that pramlintide in combination with insulin improved overall glycemic control in comparison with insulin alone, possibly by providing a more physiologically balanced therapeutic approach. Pramlintide was found to reduce body weight in patients with insulin-treated diabetes, suggesting a potential use as an antiobesity agent (Hay et al., 2015; Qiao et al., 2017; Singh-Franco et al., 2007). Clinical studies of pramlintide for weight reduction in obese subjects have so far produced promising results (Boyle et al., 2017).

Receptors for calcitonin-family peptides

Calcitonin receptor (CTR) belongs to the type II seven-transmembrane GPCRs and was cloned initially from porcine (Lin et al., 1991) and subsequently from rat, human, and other species. In most species, calcitonin receptor RNA is alternatively spliced, resulting in the expression of several isoforms (Gorn et al., 1995; Sexton et al., 1993). The various isoforms differ from each other structurally, as well as in their tissue distribution, affinity for ligands and the downstream signaling pathways activated by these ligands. The second GPCR that binds calcitonin-family ligands is calcitonin receptor-like receptor (CRLR), which was identified as a protein that shares about 55% amino acid sequence homology with CTR (Chang et al., 1993; Njuki et al., 1993). In contrast to CTR, CRLR itself is not transported to the cell membrane, and in order to form a functional receptor it requires the coexpression of one of three of the receptor activity-modifying proteins (RAMP1—RAMP3) (McLatchie et al., 1998). These single-transmembrane domain proteins interact with the seven-transmembrane domain GPCRs, and regulate their activity through a number of mechanisms: (1) RAMPs modify the binding specificities of the GPCRs to their ligands. (2) Receptor trafficking—RAMPs act as chaperones, directing CRLR to the cell membrane. (3) Receptor desensitization—following ligand binding, the complexes of CTR-RAMP are internalized by the cell. The RAMPs appear to determine whether the complex will be directed to degradative pathways or recycled back to the cell surface (Bomberger et al., 2005; Klein et al., 2016). (4) Signaling—studies of amylin receptors (AMY1-3) found that downstream signaling pathways of intracellular calcium production depend on the specific interacting RAMP (Morfis et al., 2008). A recent study of the pharmacology of CRLR-RAMP receptor complex demonstrated that the receptors display both ligand- and RAMP-dependent signaling bias among the downstream Gα subunit activation (Weston et al., 2016).

TABLE 33.1 Receptors for the calcitonin-family peptides

Receptor name	Subunits		Ligands
	GPCR	RAMP	
CTR	CTR	-	Calcitonin
AMY_1	CTR	RAMP1	Amylin, CGRP
AMY_2	CTR	RAMP2	Amylin
AMY_3	CTR	RAMP3	Amylin
CGRP	CRLR	RAMP1	CGRP
AM_1	CRLR	RAMP2	Adrenomedullin
AM_2	CRLR	RAMP3	Adrenomedullin, Adrenomedullin2

GPCR; G-protein coupled receptor, RAMP; receptor activity-modifying protein,

It has been well-established that specific combinations of CTR and CRLR with RAMPs produce the receptors for all peptides of the calcitonin family. Thus, while calcitonin is the ligand of CTR, heterodimerization of the CTR with either of the three RAMPs produces receptors with high affinity for amylin, the combination of CRLR with RAMP1 creates a CGRP receptor, and CRLR with either RAMP2 or RAMP3 acts as an adrenomedullin receptor (Lerner, 2006; Poyner et al., 2002) (Table 33.1). Pharmacological studies have shown that each of the receptor combinations typically binds one or two of the calcitonin-family peptides with high affinity, while other members of the family can bind to the same receptor dimer with lower affinities (Bower and Hay, 2016). The cross-reactivity of members of the calcitonin family with the various receptor combinations presents a challenge when interpreting experimental results, as deficiency in one specific component can be masked by interactions of the remaining members of the peptide and receptor families.

Peptide access to the bone microenvironment

The access of calcitonin and amylin to the bone environment is mainly through the circulation. Amylin is secreted from the islets of Langerhans of the pancreas and can be found in the circulation at 5 pmol/L in fasting state, rising to 15−25 pmol/L following a meal (Hay et al., 2015). Amylin secretion is pulsatile, with peaks occurring at about 5-min intervals (Juhl et al., 2000). Increased levels of circulating amylin are found in individuals with obesity or hypertension. In early stages of type 2 diabetes, along with the development of insulin resistance, circulating levels of insulin and amylin are high, whereas at later stages the secretion of both amylin and insulin becomes deficient (Zhang et al., 2016). Calcitonin, secreted predominantly from the C cells of the thyroid, circulates at low concentrations of about 3 pmol/L (Findlay and Sexton, 2004). The release of calcitonin is stimulated by a fall in blood calcium and inhibited by elevated calcium levels. Circulating levels of CT are increased in some pathological states, for example, in patients with medullary thyroid carcinoma.

Different studies determined the concentration of CGRP in circulation within the range of 1−40 pmol/L (Born et al., 1991; Schifter, 1991). Circulating concentrations are increased by sex hormone replacement therapy in postmenopausal women (Spinetti et al., 1997). However, local nerve terminals are the most important source of CGRP in the bone environment, and in certain situations local concentrations are likely to be much higher than those found in the circulation. Sensory nerve fibers containing CGRP are widely distributed in bone and bone marrow, with the richest innervation found at the epiphysis and periosteum (Bjurholm, 1991; Hill and Elde, 1991; Irie et al., 2002). Immuno-staining of CGRP-containing nerve fibers in bone tissue demonstrated changes in distribution during bone development and regeneration (Irie et al., 2002). When bone defects are created surgically, the development of CGRP-containing nerves is noted several days later, often in association with new blood vessels (Aoki et al., 1994), suggesting a role in callus formation and bone healing. Similar responses are seen following fractures (Hukkanen et al., 1993).

Effects on osteoclasts

The osteoclast has been recognized as a main target cell for calcitonin, central to its activity in lowering circulating calcium levels. Following the discovery of other members of the calcitonin family, their activities in osteoclasts have also been studied in detail. Mature osteoclasts express CTR, CRLR, and RAMP1-3 and are therefore a potential target for direct activity by all peptides of the calcitonin family.

Calcitonin

Bone-resorbing osteoclasts become polarized and form specialized structures that attach to the bone surface: the ruffled border, where protons and proteases are secreted to demineralize and degrade the bone matrix; and the surrounding sealing zone, produced by a dense ring of actin-rich podosomes. These structure are highly dynamic and allow continuous resorption while the osteoclast is moving along the bone surface. Early studies have shown that mature osteoclasts express high-affinity calcitonin receptors, and that calcitonin binding causes the immediate arrest of bone resorption (Chambers et al., 1984; Chambers and Magnus, 1982). Within 1 min of binding, calcitonin causes arrest of cell motility, which is then followed by the disruption of the podosomes and ruffled border and detachment of the osteoclast from the bone surface. Interestingly, the effects of calcitonin on osteoclast motility and attachment are mediated via two different signaling pathways: arrest of motility is cAMP-dependent, whereas retraction and disruption of the ruffled border and sealing zone are mediated through intracellular calcium signaling (Zaidi et al., 2002) (Fig. 33.2). Detachment of the sealing zone is mediated through the phosphorylation and changes in the intracellular distribution of Src and by the tyrosine kinase Pyk2, which is highly expressed in osteoclasts and localized mainly in the sealing zone (Shyu et al., 2007; Zhang et al., 2002). In addition to the key effects on mature osteoclast motility and attachment, the antiresorptive activity of calcitonin appears to be mediated by inhibition of early stages of osteoclast differentiation. In murine bone marrow cultures, calcitonin decreased the number of tartrate-resistant acid phosphatase (TRAP)-positive multinucleated cells and reduced the ratio of TRAP-positive multinucleated to mono- and binucleated cells, indicating an inhibitory effect on the fusion of osteoclast precursors (Cornish et al., 2001). Similar results were found in cultures of mouse spleen cells and in bone marrow macrophages induced to differentiate into osteoclasts, where sCT inhibited the formation of TRAP-positive multinucleated cells and the number of resorption pits formed on bone slices (Granholm et al., 2007). The inhibitory effect was reproduced by activation of protein kinase A and cAMP. The presence of a large number of TRAP-positive mono nucleated cells suggested that expression of early osteoclastogenesis markers was not disrupted, but further differentiation and cell fusion were inhibited.

The effect of calcitonin on osteoclast activity is transient, and within 48 h of continuous or repetitive calcitonin treatment the inhibitory effect is lost (Wener et al., 1972). This desensitization of osteoclasts was named the "escape phenomenon," and further investigations have shown that the cells become unresponsive due to a ligand-induced internalization of the calcitonin receptor as well as inhibition of receptor synthesis (Takahashi et al., 1995; Wada et al., 1996). More recent studies examined whether the escape phenomenon is unique to calcitonin or shared by other members of the calcitonin family. Initially, amylin was shown to produce a transient inhibitory effect on bone resorption in neonatal mouse calvaria, and subsequently all members of the calcitonin family were found to downregulate the expression of CTR mRNA and therefore to induce desensitization of osteoclasts to further treatment (Granholm et al., 2011).

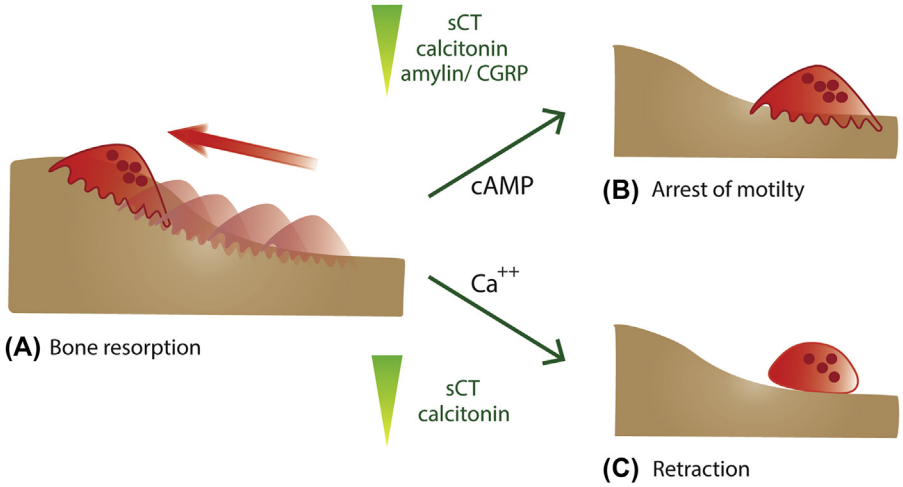

FIGURE 33.2 Inhibition of osteoclast activity by calcitonin-family peptides. (A) Actively resorbing osteoclasts attach to the bone surface through a ruffled border and a surrounding sealing zone, two highly dynamic structures that allow continuous resorption while the osteoclast is moving along the bone surface. (B) Calcitonin, CGRP. and amylin arrest the movement of osteoclast along the bone surface through a cAMP-dependent mechanism. (C) Calcitonin induces the retraction of osteoclasts from the bone surface, an effect that is mediated through intracellular calcium signaling and is not shared by the other members of the calcitonin family. This additional mechanism used by calcitonin may explain its greater potency in inhibiting osteoclast activity in comparison with the other peptides. The peptides are listed in order of potency, which is also indicated by the triangle color gradient. sCT, salmon calcitonin; CGRP, calcitonin gene-related peptide.

Interestingly, CGRP and adrenomedullin, which signal through CRLR-RAMP dimers and not through CTR, were also shown to downregulate the expression of CTR. In contrast to CTR, CRLR is not internalized following the binding of its ligands to the receptor dimers, and its levels remain unchanged.

Calcitonin gene-related peptide

Shortly after the discovery of CGRP, its injection into rats and rabbits was found to produce a calcitonin-like effect, lowering circulating calcium concentrations (Tippins et al., 1984). In rabbits, CGRP was approximately equipotent with calcitonin, whereas concentrations of two to three orders of magnitude higher than those of calcitonin were required to produce hypocalcemia in rats. A number of groups used calvariae organ cultures to study the effect of CGRP in greater detail. In this experimental system, the release of ^{45}Ca from prelabeled neonatal mouse or rat calvariae is used as a quantitative measure of bone resorption. Yamamoto et al. (Yamamoto et al., 1986) have shown that human CGRP produces a comparable level of inhibition of both basal and parathyroid hormone-stimulated resorption, but the half-maximal concentration of CGRP was 500-fold higher than that of human calcitonin. Similar studies in bone organ cultures have confirmed the antiresorptive activity of CGRP, which blocked the stimulation of bone resorption produced by different osteolytic factors (D'Souza et al., 1986; Roos et al., 1986). In cell cultures of neonatal rat osteoclasts, both αCGRP and βCGRP were found to directly inhibit bone resorption, although their potency was three orders of magnitude lower than that of human calcitonin (Zaidi et al., 1987a,b).

Further characterization of CGRP activity in osteoclasts found that it inhibits cell motility but not cell retraction. The inhibition of cell motility is mediated by increase in cAMP levels and could be blocked by the inhibitory analog CGRP(8-37), whereas CGRP had no effect on intracellular calcium levels (Alam et al., 1993a,b; Alam et al., 1991). cAMP production was also demonstrated in osteoclast-like multinucleated cells formed in cocultures of mouse osteoblasts and bone marrow cells in the presence of calcitriol (Tamura et al., 1992). It appears that the consistent lower potency of CGRP in inhibiting bone resorption, compared with calcitonin, results from its selective activation of cAMP and the downstream inhibition of motility and its lack of effect on intracellular calcium, which is linked to the downstream inhibitory effect on cell retraction (Fig. 33.2).

In addition to its activity on mature osteoclasts, evidence suggests that CGRP also affects osteoclast precursors. Specific binding of CGRP to mouse bone marrow cells and macrophages has been demonstrated, and CGRP was found to inhibit the development of osteoclasts in macrophage-osteoblast cocultures (Mullins et al., 1993; Owan and Ibaraki, 1994). In cultures of mouse bone marrow, CGRP inhibited the formation of TRAP-positive mononuclear cells as well as the subsequent fusion of these cells to form multinucleated osteoclasts (Cornish et al., 2001). Studies of the effect of CGRP on the differentiation and activity of osteoclasts in mouse bone marrow cultures found that a 100-fold higher concentration of CGRP is required for an inhibitory effect on differentiation than is required to inhibit pit formation, suggesting that the main effect of CGRP is in inhibiting osteoclast activity rather than formation (Wang et al., 2010).

In recent years, new aspects of CGRP as an inhibitor of bone resorption have come into focus. With the recognition that CGRP is released locally from sensory nerves that innervate the skeleton, a putative protective role for CGRP in the process of particle-induced osteolysis has been suggested. One of the common complications of joint arthroplasty is the formation of wear particles that induce inflammation and the release of cytokines that activate local bone resorption and can lead to aseptic loosening and eventually to early implant failure. The observation that CGRP nerve fibers are present adjacent to sites of periprosthetic osteolysis led to the hypothesis that CGRP acts locally to inhibit osteolysis. Ultra-high-molecular-weight polyethylene (UHMWPE) particles are common prosthetic wear debris and were studied in vitro in primary human osteoblasts and in the human osteosarcoma cell line MG-63 (Kauther et al., 2011; Xu et al., 2010). UHMWPE particles induced RANKL expression and inhibited the expression of OPG, while CGRP reduced UHMWPE-induced RANKL expression, suggesting an indirect inhibition of particle-induced bone resorption. CGRP was also shown to inhibit the secretion of osteolysis-associated proinflammatory cytokines and therefore could have additional beneficial effects on prevention of prosthesis loosening (Jablonski et al., 2015).

Amylin

Injection of amylin into laboratory animals strongly induced hypocalcemia with a potency that was either equal to or lower than that of human calcitonin (Datta et al., 1989; Wimalawansa, 1997; Zaidi et al., 1990). Amylin inhibits bone resorption by mature osteoclasts as determined by the reduced number of resorptive pits per TRAP-positive multinucleated cell in bone marrow cells cultured on bone slices (Cornish et al., 2001). Like CGRP, amylin inhibits the motility of mature osteoclasts in a cAMP-dependent mechanism but has no effect on cell retraction (Fig. 33.2). In organ cultures of neonatal

mouse calvariae, where bone resorption was stimulated by 1,25(OH)2D3, amylin increased cAMP levels and reduced both basal and PTH-stimulated resorption (Cornish et al., 1998b; Pietschmann et al., 1993). Fragments of amylin tested in this experimental system had no effect, and an intact amylin molecule was required in order to inhibit bone resorption. This is in contrast to the osteoblast activity of amylin tested in vitro, where a peptide fragment of the eight amino acids of the N-terminal (amylin(1-8)) acts as an agonist, and the fragment amylin(8-37) acts as an antagonist (Cornish et al., 1998a,b). Amylin was also shown to inhibit bone resorption in organ cultures of fetal mouse long bones, where its potency was similar to that of CGRP but 60-fold less than that of human calcitonin (Tamura et al., 1992). In addition to inhibiting the activity of osteoclasts, amylin has been shown to inhibit their differentiation. In mouse bone marrow cultures that were stimulated to generate osteoclasts by 1,25(OH)2D3, amylin inhibited the formation of TRAP-positive mono- and bi-nuclear cells as well as the fusion of these cells and the formation of multinucleated osteoclast-like cells (Cornish et al., 2001). Amylin inhibition of osteoclast differentiation was mediated via ERK1/2 signaling, and the expression of a negative dominant form of ERK1/2 blocked amylin's inhibitory effect (Dacquin et al., 2004). Amylin had no effect on bone marrow cell proliferation, and in the presence of amylin osteoclasts were smaller and contained fewer nuclei. Results from in vitro studies of amylin should be interpreted in light of its marked propensity to adhere to the surfaces of laboratory plasticware (Young et al., 1992), suggesting that the actual concentrations of amylin in all in vitro experiments may be one to two orders of magnitude less than the amount added to the media. Thus, both osteoclast and calvariae studies imply that amylin may regulate bone resorption at physiological concentrations.

Effects on osteoblasts

Calcitonin

A large number of studies have shown that calcitonin receptor is not expressed in osteoblasts, strongly indicating that calcitonin cannot affect these cells directly (Naot and Cornish, 2008). Consistent with this observation, calcitonin had no effect on the proliferation of osteoblasts in vitro, and when injected locally over the calvaria of adult mice, indices of bone formation were not different from those of vehicle-injected control mice (Cornish et al., 1995, 2000). However, a small number of studies found evidence for calcitonin activity in osteoblasts. These studies have shown that calcitonin stimulates the proliferation of primary osteoblasts and osteoblastic cell lines in vitro and increases bone matrix synthesis ex vivo in an organ culture system (Farley et al., 1988; Villa et al., 2003). An earlier study, using subcutaneously implanted demineralized bone matrix in rats, found that administration of calcitonin soon after the implantation stimulated osteoblast proliferation and bone formation, whereas administration of calcitonin after the initiation of bone formation had the reverse, inhibitory effect (Weiss et al., 1981). One possible explanation for the observed activity of calcitonin in osteoblasts in these experiments is that the effects were in fact indirect, mediated via osteoclasts, in a mechanism that has been discovered more recently and will be discussed in detail below (Keller et al., 2014). In addition, given the cross-reactivity of members of the calcitonin family and their receptors, a low-affinity interaction of calcitonin with receptors other than CTR might have contributed to the observed activity.

Calcitonin gene-related peptide

The activity of CGRP in osteoblasts is likely to be mediated by the high-affinity receptor complex CRLR-RAMP1, as genes encoding for these two receptor components are highly expressed in osteoblasts (Naot and Cornish, 2008). Early studies demonstrated binding of CGRP to cells of rat calvaria, and increased cAMP levels in the UMR-106 rat osteosarcoma cell line following CGRP treatment, while the cells were not responsive to calcitonin (Michelangeli et al., 1986). Subsequent studies in bone cell cultures obtained by sequential digestion of neonatal chicken, rat, and mouse calvariae again demonstrated a cAMP response to CGRP with no response to calcitonin (Michelangeli et al., 1989). Several other intracellular signaling pathways are activated by CGRP in osteoblast-like cells. In UMR-106 cells, CGRP stimulated Na+/H+ exchange and induced a transient twofold increase in intracellular calcium concentrations by mobilization of calcium from intracellular stores (Gupta and Schwiening, 1994; Kawase et al., 1995). Detailed analysis of the changes in intracellular calcium in the human osteosarcoma cell line MG-63 found a two-phase response to CGRP: a rapid transient calcium discharge from intracellular stores in a cAMP-independent mechanism followed by a secondary sustained calcium influx into the cell in a cAMP-dependent manner (Burns et al., 2004). In the osteosarcoma cell line OHS-4, CGRP increased intracellular calcium concentrations but had no detectable effect on cAMP, suggesting that in these cells

the initial cAMP-independent stage predominates (Drissi et al., 1999). CGRP was also shown to stimulate potassium efflux, inducing membrane hyperpolarization that results in rapid changes in cell morphology in UMR-106 cells (Kawase and Burns, 1998). Structure−function studies of CGRP in preosteoblast KS-4 cells found that cAMP response was greatly reduced with truncation of either the C-terminal amino acids or the disulfide bridge at the N-terminal (Thiebaud et al., 1991).

Studying the effect of CGRP on osteoblast proliferation, Cornish et al. (Cornish et al., 1995) showed a small increase in proliferation in primary rat osteoblast-like cells in response to CGRP, although the potency of CGRP was much lower than that of amylin. CGRP also stimulated proliferation in primary cultures of human osteoblast-like cells, and neither CGRP(8-37) nor amylin (8-37) inhibited this effect (Villa et al., 2000).

CGRP can activate the differentiation of precursor cells into osteoblasts. This has been demonstrated in bone marrow stromal cells derived from either healthy or ovariectomized (OVX) rats, where CGRP induced the formation of mineralizing osteoblasts in vitro (Liang et al., 2015). The effect of CGRP on bone marrow stromal cell differentiation was mediated via the Wnt/β-catenin pathway, and could be inhibited by either CGRP(8-37) or the Wnt pathway antagonist secreted frizzled-related protein (Zhou et al., 2016). The Wnt/β-catenin pathway was also found to mediate the activity of CGRP as a survival factor in human osteoblast-like primary cultures, where CGRP inhibited the apoptosis induced by serum depravation or dexamethasone (Mrak et al., 2010). Another pathway that may be involved in mediating the effect of CGRP in osteoblasts is the BMP-signaling pathway. BMP2 expression was induced by CGRP in MG-63 osteosarcoma cells and contributed to the activity of CGRP to promote osteogenic differentiation, while the proliferative effect of CGRP in these cells appeared to be BMP-independent (Tian et al., 2013).

The positive effect of CGRP on osteoblasts and its potential to enhance bone formation have been studied in the context of orthopedic implants and tissue engineering. In a recent study, Zhang et al. (Zhang et al., 2016) investigated the mechanisms underlying the effect of implants containing biodegradable magnesium to improve fracture healing. Using a fracture repair model in rats, they have shown that implant-derived magnesium increases neuronal CGRP in both the peripheral cortex of the femur and the ipsilateral dorsal root ganglia. CGRP released from sensory neurons was shown to induce local osteogenic differentiation of periosteum-derived stem cells and accelerate healing (Zhang et al., 2016). In other studies, CGRP was added to bone graft substitutes and scaffold materials, and its potential to promote local bone formation and healing was tested. Bio-Oss is a scaffold material prepared by removal of the organic component form bovine bone, and is used as bone graft that allows osteogenic cell migration (Li et al., 2017). CGRP loaded onto Bio-Oss surface was shown to enhance proliferation and differentiation of primary osteoblasts in vitro. CGRP was also shown to promote proliferation and osteogenic differentiation of rabbit adipose-derived stem cells cultured within calcium alginate gel, and a potential use of these constructs in tissue engineering has been suggested (Huang et al., 2015).

While early studies investigated the potential general role of CGRP in regulation of bone remodeling and found that it promotes osteoblast differentiation and only weakly induces proliferation, in later years the focus has shifted, and the activity of CGRP in osteoblasts is mainly studied in the context of bone healing. Thus, the role of CGRP released from nerve endings at sites of fracture or bone lesions, as well as the potential of CGRP as a bone anabolic factor added to bone scaffold materials, are areas of research that are likely to generate important novel findings in the near future.

Amylin

Shortly after its discovery, amylin was shown to stimulate cAMP production in a preosteoblastic cell line, in primary fetal rat osteoblasts and primary human osteoblasts (Tamura et al., 1992; Cornish et al., 1995; Millet and Vignery, 1997; Villa et al., 1997). These studies have shown that amylin stimulated the proliferation of primary osteoblasts from rats and humans at concentrations as low as 10 pmol/L. In rat primary osteoblastic cells, the mitogenic effect of amylin was mediated via the phosphorylation of ERK1/2, most likely through activation of Gi proteins, and was blocked by the specific inhibitor of this pathway, PD-98059 (Cornish et al., 2004). It is not clear which receptor mediates the activity of amylin in osteoblasts, as the three receptors $AMY_{1\text{-}3}$ include CTR, which is not expressed in these cells. It is possible that amylin affects osteoblasts through interaction with one of the other receptors for the calcitonin-family peptides. Surprisingly, the proliferative effect of amylin in osteoblasts required the presence of IGF1 receptor, despite the fact there was no direct binding of amylin to IGF1 receptor, nor was there a paracrine effect of osteoblast-derived IGF1. Stimulation of osteoblast proliferation in vitro was also produced by the N-terminal octapeptide fragment amylin(1-8), although its half-maximal effective concentration was 10-fold higher than that of the intact peptide (Cornish et al., 1998a,b).

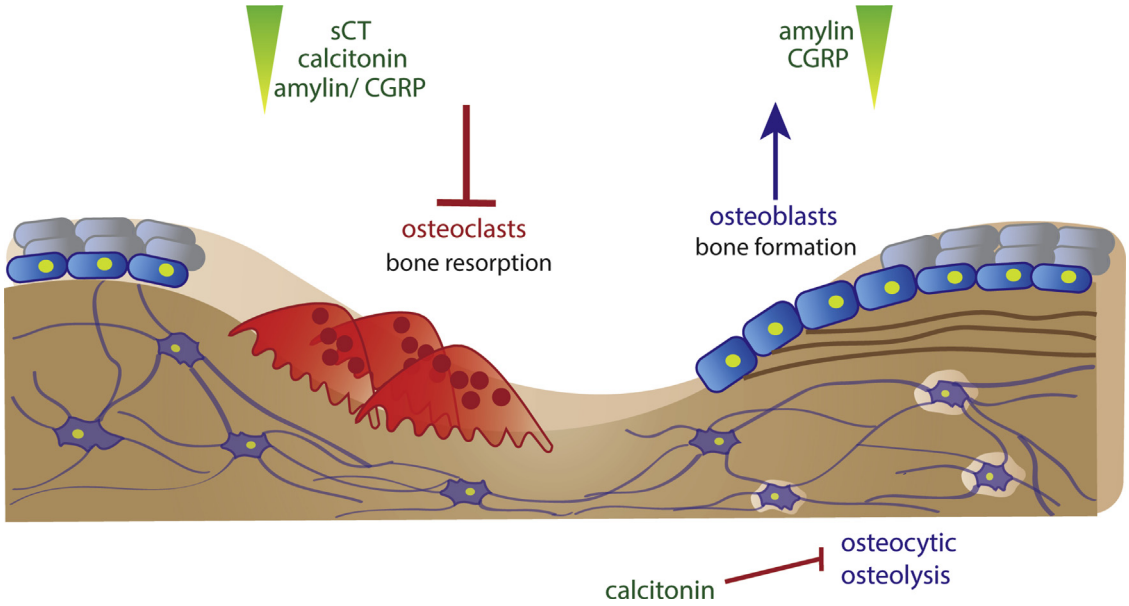

FIGURE 33.3 The effects of calcitonin-family peptides on bone cells. In vitro studies have established an overall positive effect of the calcitonin-family peptides in bone. Calcitonin, CGRP, and amylin are inhibitory to osteoclasts, and CGRP and amylin also promote osteoblast formation and activity. The osteocyte appears to be a target cell for calcitonin, as studies in genetically modified mice suggested a protective role for calcitonin in osteocytic osteolysis. The peptides are listed in order of potency, which is also indicated by the color gradient. sCT, salmon calcitonin; CGRP, calcitonin gene-related peptide.

The activities of calcitonin, CGRP and amylin in bone cells, as determined by in vitro studies, are summarized in Fig. 33.3.

Effects of local and systemic peptide administration into laboratory animals

Skeletal effects

OVX rats that were given daily subcutaneous injections of CGRP for 28 days had decreased bone resorption and a modest reduction in postovariectomy bone loss from 60% to 46% (Valentijn et al., 1997). In contrast, injection of CGRP over the calvariae of adult mice detected no significant effects on either bone resorption or formation (Cornish et al., 1995; Cornish and Reid, 1999). A different approach to determining the effect of CGRP on bone mass was used by Hill et al. (Hill et al., 1991). Reasoning that most of the CGRP that gains access to bone does so via sensory nerves, they studied the effect of sensory denervation using capsaicin treatment in rats. This intervention produced no change in cortical or medullary area, or periosteal apposition rate in tibiae, but the osteoclast surface in the mandible was decreased. In a more recent study, Offley et al. showed that capsaicin treatment destroyed the unmyelinated sensory axons containing CGRP, and the reduced CGRP signaling was associated with a decrease in bone mass (Offley et al., 2005).

Local injection of amylin over the calvariae of adult mice produced a substantial decrease in bone resorption, an increase in bone formation, and in mineralized bone area after only five daily injections (Cornish et al., 1995). Systemic administration of amylin to adult mice over 4 weeks produced a 70% increase in total bone volume in the proximal tibia (Fig. 33.4) as well as increased cortical width, tibial growth plate width, and tibial length along with increased body weight and fat mass (Cornish et al., 1998a,b). Structure–function studies identified amylin(1-8) as potentially retaining the beneficial effects in bone but devoid of amylin's activity on energy and carbohydrate metabolism. Thus, administration of amylin(1-8) by local injection over the calvariae of female mice produced a positive effect on bone formation, which was greater than that of an equimolar dose of hPTH-(1–34). Daily systemic administration of amylin (1-8) to sexually mature male mice for 4 weeks produced a near twofold increase in histomorphometric indices of osteoblast activity and resulted in increased bone strength as determined by three-point bending (Cornish et al., 2000). In contrast, amylin(1-8) administration to OVX rats had no effect on parameters of bone formation (Ellegaard et al., 2010). In rats, systemic administration of amylin for 18 days increased trabecular bone volume of the proximal tibia by 25%, although there were no changes in histomorphometric indices of formation or resorption (Romero et al., 1995). In a study of OVX rats, systemic administration of amylin increased bone formation and inhibited bone resorption as determined by analysis of the bone

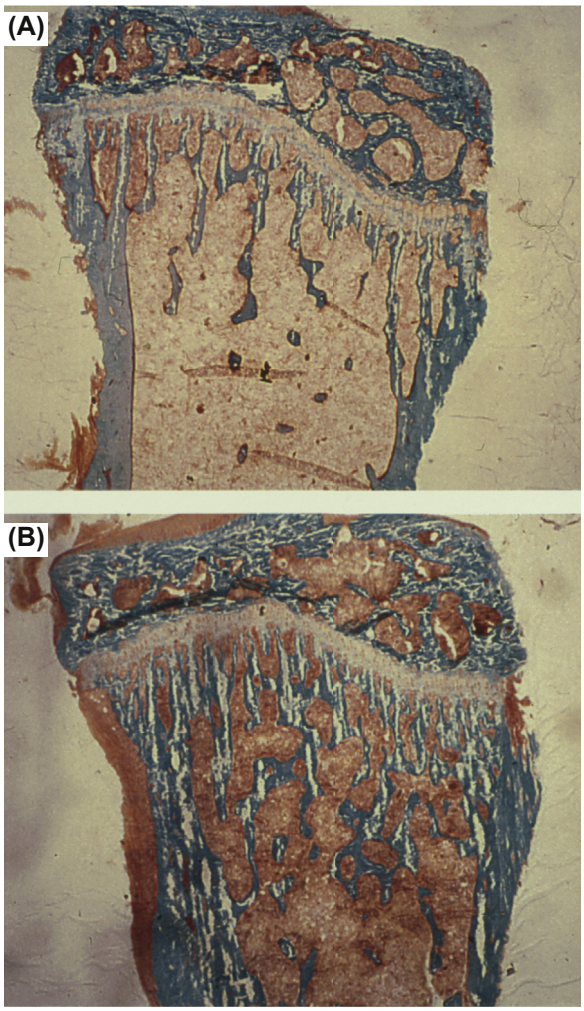

FIGURE 33.4 Increases bone volume induced by systemic administration of amylin. Photomicrographs of proximal tibiae of mice treated systemically with (A) vehicle or (B) amylin (10 μg/day) for 4 weeks. Trabecular bone volume is increased by 70% in amylin-treated animals. *Reprinted from Cornish et al., 1998a, with permission.*

turnover markers: plasma osteocalcin and urinary deoxypyridinoline. Distal metaphyseal and total femoral bone densities were higher in the OVX animals treated with amylin in comparison with untreated controls (Horcajada-Molteni et al., 2000). Interestingly, amylin infusion has also produced osteogenic effects in diabetic rat models, although its efficacy varied depending on the model (Gutierrez-Rojas et al., 2013).

In summary, the great majority of studies found that amylin administration increases bone formation and inhibits bone resorption, producing an overall positive skeletal effects. The investigations of amylin(1-8) produced less consistent results, with increased bone formation seen in a local and systemic administration models but no protective effect found against OVX-induced bone loss. In light of the recent findings regarding the mechanisms of action of calcitonin in bone, as discussed below (Keller et al., 2014), it is possible that the increase in bone formation measured in the animal models results from indirect activity of amylin through cells other than osteoblasts.

Effects on calcium metabolism

The most apparent effect of the injection of amylin or CGRP to laboratory animal is the induction of hypocalcemia. In fasted rats that were given a single intravenous bolus injections of amylin or CGRP, the decrease in total plasma calcium concentration was similar for both peptides (Young et al., 1993). Although the hypocalcemic effect is largely attributable to inhibition of osteoclastic bone resorption, amylin, like calcitonin, may have a direct calciuretic effect on the kidney. Rat amylin bound to receptors in porcine kidney with an affinity comparable to that of porcine calcitonin itself, and induced

cAMP production (Sexton et al., 1994). In rat renal tubular membranes, CGRP and amylin stimulated cAMP production with comparable half-maximal concentrations, and the effects of both peptides were blocked by CGRP(8-37) (Osajima et al., 1995). Consistent with these findings, amylin infusion doubled urinary calcium excretion in dogs (Miles et al., 1994). However, the increased urinary loss of calcium accounted for less than 10% of the fall in serum calcium, suggesting that reduced osteoclastic resorption was the principal contributor to the hypocalcemic effect. These changes were accompanied by a doubling of PTH levels, whereas circulating calcitonin concentrations remained unchanged.

The skeletal effects of calcitonin, calcitonin gene-related peptide, and amylin: lessons from genetically modified mice

Calcitonin and calcitonin gene-related peptide

In one of the early studies that examined the skeletal effects of the calcitonin-family peptides in genetically modified mice, CGRP was introduced under the osteocalcin promoter, directing its overexpression specifically to the osteoblast lineage (Ballica et al., 1999). The transgenic mice had increased bone formation rate, as well as higher trabecular bone density and volume in comparison with wild-type (WT) littermate controls, suggesting a positive effect of CGRP in osteoblasts. Later studies used mostly knockout mice to investigate the skeletal effects of the calcitonin family peptides. Mice deficient of the *Calca* gene, missing both calcitonin and αCGRP, were the first knockout model created (Hoff et al., 2002). Based on previous in vitro and in vivo studies of calcitonin activity in bone, the *Calca*-KO mice were expected to display an osteoporotic phenotype due to accelerated bone resorption in the absence of calcitonin. However, the mice had no changes in osteoclast number or bone resorption markers in comparison with WT controls, and surprisingly, had higher bone volume and trabecular number with decreased trabecular spacing. Double calcein-labeling showed the high bone volume was a result of a significant increase in bone formation (Hoff et al., 2002). *Calca*-KO mice were less sensitive to ovariectomy; while WT mice lost about one-third of their bone mass over 2 months after ovariectomy, the *Calca*-KO mice had no change in bone mass. Overall, the unexpected skeletal phenotype of the *Calca*-KO mice suggested that calcitonin or αCGRP inhibited bone formation. A second knockout mouse model, which was only deficient of αCGRP, was generated in order to differentiate between the contributions of the deficiency in calcitonin and that of αCGRP to the increased bone formation seen in the *Calca*-KO mice (Schinke et al., 2004). αCGRP-KO mice had normal levels of circulating calcitonin and unlike the *Calca*-KO, had reduced bone formation rate and developed osteopenia. This phenotype was consistent with the earlier study that demonstrated increased bone formation in mice over-expressing αCGRP (Ballica et al., 1999). A subsequent long-term study of the bone phenotype of the knockout animals showed that the osteopenia displayed by the αCGRP-KO mice was also evident at 6, 12, and 18 months of age (Huebner et al., 2006). In the *Calca*-KO mice the bone phenotype developed with age, and at 12 and 18 months, along with the increased bone formation, there was evidence for increased bone resorption. The high bone turnover resulted in a substantial increase of trabecular structures that lead to trabecularization of cortical bone, and in addition, 20% of the *Calca*-deficient mice had hyperostotic lesions. A number of common potential secondary mechanisms that cause increased bone resorption have been investigated and excluded, as the *Calca*-KO mice had normal histologic appearance of several organs and the absence of hyperparathyroidism and hypogonadism (Huebner et al., 2006). The analyses of the two mice strains, *Calca*-KO and αCGRP-KO, are confounded by the presence of an intact *Calcb* gene that encodes for βCGRP. However, a study of the bone phenotype of *Calcb* -KO mice found no differences between these mice and control WT mice, suggesting that βCGRP does not play an important role in the regulation of bone remodeling (Huebner et al., 2008).

Taken together, the studies of genetically modified mice strains imply that in vivo, αCGRP is a physiological inducer of bone formation, whereas calcitonin inhibits osteoblast activity and bone formation, at least in young animals. Our current understanding of the physiological activity of calcitonin in bone is still incomplete, and a clear understanding of the unusual histological appearance of cortical trabecularization and hyperostotic lesions in the older *Calca*-KO mice is still missing. It is possible that some unanswered questions could be resolved by examining the bone phenotype of mice deficient of calcitonin only, with functional αCGRP. However, this animal model has not yet been described.

Amylin

The phenotype of amylin-deficient mice was described by Dacquin et al (Dacquin et al., 2004). The mice had normal food intake, body weight, and glucose metabolism. At the age of 24 weeks, amylin-deficient mice had a typical osteoporotic phenotype, showing decreased bone density of long bones, low bone mass, and a 50% decrease in trabecular bone volume.

The number of osteoblasts as well as the bone formation rate, assessed by double calcein injection, were similar between amylin-deficient mice and WT controls, suggesting that the osteoporotic phenotype was not a result of a defect in bone formation. In contrast, the amylin-deficient mice had an increased number of osteoclasts and an increase in degradation products of collagen in the urine, suggestive of accelerated bone resorption. Further studies of amylin-deficient mice demonstrated that the bone-effects were sex-dependent. Amylin-deficient males showed increased trabecular thickness at 4 and 6 weeks of age and increased femoral length at 26 weeks, whereas female mice were no different than the wild type (Davey et al., 2006). The role of CTR in mediating the bone-effects of amylin was investigated in a compound hemizygous mouse model: CTR (*Calcr* +/−) and amylin (*Iapp* +/−) (Dacquin et al., 2004). These mice displayed a combination of abnormalities identified in each of the individual hemizygous knockout, leading the authors to conclude that CTR is unlikely to be mediating amylin bone effects.

Calcitonin receptor

The contribution of CTR to skeletal physiology has been studied in three different strains of genetically modified mice. Since global deletion of CTR was embryonic lethal, the skeletal phenotype was initially studied in hemizygote CTR-KO mice (*Calcr*+/-), whose level of expression of CTR in osteoclasts was half that found in the WT mice, providing a model for the study of CTR haploinsufficiency (Dacquin et al., 2004). *Calcr* +/- mice had high bone mass due to increased bone formation, whereas no changes were identified in measures of bone resorption. These observations were consistent with the phenotype of the *Calca*-KO mice, providing further evidence for a physiological role of calcitonin as an inhibitor of bone formation, and indicating its activity is mediated via CTR. A second viable animal model was generated by incomplete deletion of the CTR gene, leaving a low residual level of expression (Davey et al., 2008). In this animal model only male mice had a small increase in bone formation rate, indicating that CTR plays a minor role in the physiological regulation of bone and calcium homeostasis in the basal state. More recently, employing a modified technique to knockout the expression of CTR, viable mice with global deletion of *Calcr* have been generated (Keller et al., 2014). The *Calcr*-KO mice had high bone mass due to increased bone formation, a phenotype that was then reproduced in mice that had the gene deletion restricted to the osteoclast lineage. The study further investigated the underlying mechanisms of the activity of calcitonin, signaling via CTR, to inhibit bone formation. The loss of CTR in osteoclasts has been shown to increase the levels of SPINSTER2, an exporter protein required for the secretion of sphingosine-1-phosphate (S1P), a potent inducer of bone formation. Therefore, the study suggests that calcitonin inhibits bone formation indirectly, through interaction with the osteoclast-expressed CTR (Keller et al., 2014).

Taken together, while pharmacological studies found that calcitonin inhibits of bone resorption, studies of genetically modified animals determined that calcitonin's physiological role is to inhibit bone formation. A similar discrepancy was identified in studies of the effect of PTH in bone; as PTH is a physiological stimulator of bone resorption that stimulates bone formation in pharmacological use (Martin and Sims, 2015).

The role of calcitonin and calcitonin receptor in situations of calcium stress

The roles of calcitonin and calcitonin receptor in situations of calcium stress were investigated in the genetically modified mice models. When hypercalcemia was induced in *Calcr*-KO mice by $1,25(OH)_2D_3$, the peak levels of total serum calcium were significantly higher in the KO mice in comparison with the WT controls, suggesting that in these conditions CTR is important for calcium homeostasis (Davey et al., 2008). The underlying mechanism for calcitonin activity appears to be the inhibition of osteoclast activity, as a similar impaired response to hypercalcemia was later identified in a mouse model in which CTR was specifically missing in osteoclasts (Turner et al., 2011). A physiological condition of calcium stress is also present during lactation, as the maternal skeleton rapidly demineralizes in order to supply calcium to the milk. In the *Calca*-KO model, deficient in both calcitonin and CGRP, spine BMC dropped during lactation by over 50%, whereas in the WT controls the drop was only of 23.6% (Woodrow et al., 2006). After weaning, spine BMC was slower to return to baseline values in the *Calca*-KO in comparison with WT mice. Injection of sCT normalized the bone parameters, whereas CGRP was without effect, indicating that calcitonin is the peptide that plays an important role in calcium balance and preservation of the maternal skeleton during lactation and its recovery after weaning (Woodrow et al., 2006). Another mechanism that mobilizes calcium from skeletal stores during lactation is osteolytic osteolysis. Interestingly, osteocytes have been shown to express a number of genes in common with osteoclasts and to resorb bone locally. Histomorphometric analysis of the femurs at the end of lactation found that osteocyte lacunar area in *Calcr*-KO mice were larger than in WT, suggesting a role for calcitonin in inhibition of osteocytic osteolysis and protection of the maternal skeleton during lactation (Clarke et al., 2015).

Calcitonin, calcitonin gene-related peptide, and amylin—relevance to human bone physiology

The roles of the three peptides—calcitonin, CGRP, and amylin—in human physiology and pathophysiology have been studied extensively. The current understating is that calcitonin plays an important role in situations of calcium stress, regulating calcium homeostasis mainly through skeletal effects and perhaps through activity in the kidney during rapid growth, pathological hypercalcemia, pregnancy, and lactation. In contrast, the main physiological effects of CGRP and amylin appear not to be related directly to bone, with CGRP being a most potent microvascular vasodilator and contributing to pain especially in migraine, while amylin appears to be primarily important for energy homeostasis, inducing satiety, and increasing energy expenditure. Nevertheless, the peptides are likely to play at least a secondary role in bone metabolism.

It has been hypothesized that amylin secretion following a meal directs the absorbed calcium and protein from the meal into new bone synthesis by increasing bone growth at a time when the substrates are available (MacIntyre, 1989; Zaidi et al., 1993). Amylin may also contribute to the relationship between body mass and bone density. Body mass, and particularly fat mass, is the principal determinant of bone density in women (Reid et al., 1992a,b). A number of factors contribute to the fat−bone relationship; including the effect of weight on skeletal load bearing and adipocyte production of estrogen and adipokines (Naot and Cornish, 2014; Reid, 2002). In addition, the increased circulating levels of amylin and insulin in obesity are likely to have positive effects in bone and thus contribute to the fat mass−bone mass relationship. In fact, insulin levels were found to directly relate to bone density in normal postmenopausal women, and because amylin is cosecreted with insulin, it would seem likely that a similar relationship for this peptide exists (Reid et al., 1993). Pramlintide is a synthetic analog of amylin that is currently approved for the treatment of type 1 and type 2 diabetes, and might be in wider use in the future due to its effect on fat reduction. However, so far the effect of pramlintide on bone metabolism in humans has not been studied extensively. In a study of 23 patients with type 1 diabetes, 12 months of pramlintide treatment had no significant effects on markers on bone turnover or BMD (Chandran, 2017). As in vitro and animal studies determined an overall positive effect of amylin in bone, it would be of great interest to assess the impact of pramlintide treatment on long-term bone health and fracture risk.

Because CGRP access to bone is mainly via sensory innervation, the current understanding is that the bone activity of CGRP is predominantly localized. Evidence suggests that CGRP plays a role in the local bone response to different stimuli, including exercise, injury and the presence of metal implants. Given that monoclonal antibodies against CGRP are likely to be approved for clinical use for migraine prevention in the near future, it will be important to monitor the effects of their long-term use on bone physiology and healing.

References

Alam, A.S., Moonga, B.S., Bevis, P.J., Huang, C.L., Zaidi, M., 1991. Selective antagonism of calcitonin-induced osteoclastic quiescence (Q effect) by human calcitonin gene-related peptide-(Val8Phe37). Biochem. Biophys. Res. Commun. 179 (1), 134−139.

Alam, A.S., Bax, C.M., Shankar, V.S., Bax, B.E., Bevis, P.J., Huang, C.L., et al., 1993a. Further studies on the mode of action of calcitonin on isolated rat osteoclasts: pharmacological evidence for a second site mediating intracellular $Ca2^{+}$ mobilization and cell retraction. J. Endocrinol. 136 (1), 7−15.

Alam, A.S., Moonga, B.S., Bevis, P.J., Huang, C.L., Zaidi, M., 1993b. Amylin inhibits bone resorption by a direct effect on the motility of rat osteoclasts. Exp. Physiol. 78 (2), 183−196.

Aoki, M., Tamai, K., Saotome, K., 1994. Substance P- and calcitonin gene-related peptide-immunofluorescent nerves in the repair of experimental bone defects. Int. Orthop. 18 (5), 317−324.

Ballica, R., Valentijn, K., Khachatryan, A., Guerder, S., Kapadia, S., Gundberg, C., et al., 1999. Targeted expression of calcitonin gene-related peptide to osteoblasts increases bone density in mice. J. Bone Miner. Res. 14 (7), 1067−1074.

Bjurholm, A., 1991. Neuroendocrine peptides in bone. Int. Orthop. 15 (4), 325−329.

Bomberger, J.M., Parameswaran, N., Hall, C.S., Aiyar, N., Spielman, W.S., 2005. Novel function for receptor activity-modifying proteins (RAMPs) in post-endocytic receptor trafficking. J. Biol. Chem. 280 (10), 9297−9307.

Born, W., Beglinger, C., Fischer, J.A., 1991. Diagnostic relevance of the amino-terminal cleavage peptide of procalcitonin (PAS-57), calcitonin and calcitonin gene-related peptide in medullary thyroid carcinoma patients. Regul. Pept. 32 (3), 311−319.

Bower, R.L., Hay, D.L., 2016. Amylin structure-function relationships and receptor pharmacology: implications for amylin mimetic drug development. Br. J. Pharmacol. 173 (12), 1883−1898.

Boyle, C.N., Lutz, T.A., Le Foll, C., 2017. Amylin − its role in the homeostatic and hedonic control of eating and recent developments of amylin analogs to treat obesity. Mol Metab 8, 203−210.

Breimer, L.H., MacIntyre, I., Zaidi, M., 1988. Peptides from the calcitonin genes: molecular genetics, structure and function. Biochem. J. 255 (2), 377−390.

Burns, D.M., Stehno-Bittel, L., Kawase, T., 2004. Calcitonin gene-related peptide elevates calcium and polarizes membrane potential in MG-63 cells by both cAMP-independent and -dependent mechanisms. Am. J. Physiol. Cell Physiol. 287 (2), C457–C467.

Chambers, T.J., Magnus, C.J., 1982. Calcitonin alters behaviour of isolated osteoclasts. J. Pathol. 136 (1), 27–39.

Chambers, T.J., Athanasou, N.A., Fuller, K., 1984. Effect of parathyroid hormone and calcitonin on the cytoplasmic spreading of isolated osteoclasts. J. Endocrinol. 102 (3), 281–286.

Chandran, M., 2017. Diabetes drug effects on the skeleton. Calcif. Tissue Int. 100 (2), 133–149.

Chang, C.P., Pearse 2nd, R.V., O'Connell, S., Rosenfeld, M.G., 1993. Identification of a seven transmembrane helix receptor for corticotropin-releasing factor and sauvagine in mammalian brain. Neuron 11 (6), 1187–1195.

Chesnut 3rd, C.H., Azria, M., Silverman, S., Engelhardt, M., Olson, M., Mindeholm, L., 2008. Salmon calcitonin: a review of current and future therapeutic indications. Osteoporos. Int. 19 (4), 479–491.

Clarke, M.V., Russell, P.K., Findlay, D.M., Sastra, S., Anderson, P.H., Skinner, J.P., et al., 2015. A role for the calcitonin receptor to limit bone loss during lactation in female mice by inhibiting osteocytic osteolysis. Endocrinology 156 (9), 3203–3214.

Cooper, G.J., Willis, A.C., Clark, A., Turner, R.C., Sim, R.B., Reid, K.B., 1987. Purification and characterization of a peptide from amyloid-rich pancreases of type 2 diabetic patients. Proc. Natl. Acad. Sci. U. S. A. 84 (23), 8628–8632.

Copp, D.H., Cheney, B., 1962. Calcitonin-a hormone from the parathyroid which lowers the calcium-level of the blood. Nature 193, 381–382.

Copp, D.H., Cameron, E.C., Cheney, B.A., Davidson, A.G., Henze, K.G., 1962. Evidence for calcitonin–a new hormone from the parathyroid that lowers blood calcium. Endocrinology 70, 638–649.

Cornish, J., Reid, I.R., 1999. Skeletal effects of amylin and related peptides. Endocrinololgist 9, 183–189.

Cornish, J., Callon, K.E., Cooper, G.J., Reid, I.R., 1995. Amylin stimulates osteoblast proliferation and increases mineralized bone volume in adult mice. Biochem. Biophys. Res. Commun. 207 (1), 133–139.

Cornish, J., Callon, K.E., King, A.R., Cooper, G.J., Reid, I.R., 1998a. Systemic administration of amylin increases bone mass, linear growth, and adiposity in adult male mice. Am. J. Physiol. 275 (4 Pt 1), E694–E699.

Cornish, J., Callon, K.E., Lin, C.Q., Xiao, C.L., Mulvey, T.B., Coy, D.H., et al., 1998b. Dissociation of the effects of amylin on osteoblast proliferation and bone resorption. Am. J. Physiol. 274 (5 Pt 1), E827–E833.

Cornish, J., Callon, K.E., Gasser, J.A., Bava, U., Gardiner, E.M., Coy, D.H., et al., 2000. Systemic administration of a novel octapeptide, amylin-(1-8), increases bone volume in male mice. Am. J. Physiol. Endocrinol. Metab. 279 (4), E730–E735.

Cornish, J., Callon, K.E., Bava, U., Kamona, S.A., Cooper, G.J., Reid, I.R., 2001. Effects of calcitonin, amylin, and calcitonin gene-related peptide on osteoclast development. Bone 29 (2), 162–168.

Cornish, J., Grey, A., Callon, K.E., Naot, D., Hill, B.L., Lin, C.Q., et al., 2004. Shared pathways of osteoblast mitogenesis induced by amylin, adrenomedullin, and IGF-1. Biochem. Biophys. Res. Commun. 318 (1), 240–246.

Dacquin, R., Davey, R.A., Laplace, C., Levasseur, R., Morris, H.A., Goldring, S.R., et al., 2004. Amylin inhibits bone resorption while the calcitonin receptor controls bone formation in vivo. J. Cell Biol. 164 (4), 509–514.

Datta, H.K., Zaidi, M., Wimalawansa, S.J., Ghatei, M.A., Beacham, J.L., Bloom, S.R., et al., 1989. In vivo and in vitro effects of amylin and amylin-amide on calcium metabolism in the rat and rabbit. Biochem. Biophys. Res. Commun. 162 (2), 876–881.

Davey, R.A., Findlay, D.M., 2013. Calcitonin: physiology or fantasy? J. Bone Miner. Res. 28 (5), 973–979.

Davey, R.A., Moore, A.J., Chiu, M.W., Notini, A.J., Morris, H.A., Zajac, J.D., 2006. Effects of amylin deficiency on trabecular bone in young mice are sex-dependent. Calcif. Tissue Int. 78 (6), 398–403.

Davey, R.A., Turner, A.G., McManus, J.F., Chiu, W.S., Tjahyono, F., Moore, A.J., et al., 2008. Calcitonin receptor plays a physiological role to protect against hypercalcemia in mice. J. Bone Miner. Res. 23 (8), 1182–1193.

Drissi, H., Lieberherr, M., Hott, M., Marie, P.J., Lasmoles, F., 1999. Calcitonin gene-related peptide (CGRP) increases intracellular free $Ca2^{+}$ concentrations but not cyclic AMP formation in CGRP receptor-positive osteosarcoma cells (OHS-4). Cytokine 11 (3), 200–207.

D'Souza, S.M., MacIntyre, I., Girgis, S.I., Mundy, G.R., 1986. Human synthetic calcitonin gene-related peptide inhibits bone resorption in vitro. Endocrinology 119 (1), 58–61.

Ellegaard, M., Thorkildsen, C., Petersen, S., Petersen, J.S., Jorgensen, N.R., Just, R., et al., 2010. Amylin(1-8) is devoid of anabolic activity in bone. Calcif. Tissue Int. 86 (3), 249–260.

Farley, J.R., Tarbaux, N.M., Hall, S.L., Linkhart, T.A., Baylink, D.J., 1988. The anti-bone-resorptive agent calcitonin also acts in vitro to directly increase bone formation and bone cell proliferation. Endocrinology 123 (1), 159–167.

Findlay, D.M., Sexton, P.M., 2004. Calcitonin. Growth Factors. 22 (4), 217–224.

Gorn, A.H., Rudolph, S.M., Flannery, M.R., Morton, C.C., Weremowicz, S., Wang, T.Z., et al., 1995. Expression of two human skeletal calcitonin receptor isoforms cloned from a giant cell tumor of bone. The first intracellular domain modulates ligand binding and signal transduction. J. Clin. Investig. 95 (6), 2680–2691.

Granholm, S., Lundberg, P., Lerner, U.H., 2007. Calcitonin inhibits osteoclast formation in mouse haematopoetic cells independently of transcriptional regulation by receptor activator of NF-{kappa}B and c-Fms. J. Endocrinol. 195 (3), 415–427.

Granholm, S., Henning, P., Lerner, U.H., 2011. Comparisons between the effects of calcitonin receptor-stimulating peptide and intermedin and other peptides in the calcitonin family on bone resorption and osteoclastogenesis. J. Cell. Biochem. 112 (11), 3300–3312.

Gupta, A., Schwiening, C.J., 1994. Boron WF. Effects of CGRP, forskolin, PMA, and ionomycin on pHi dependence of Na-H exchange in UMR-106 cells. Am. J. Physiol. 266 (4 Pt 1), C1088–C1092.

Gutierrez-Rojas, I., Lozano, D., Nuche-Berenguer, B., Moreno, P., Acitores, A., Ramos-Alvarez, I., et al., 2013. Amylin exerts osteogenic actions with different efficacy depending on the diabetic status. Mol. Cell. Endocrinol. 365 (2), 309−315.

Harzenetter, M.D., Novotny, A.R., Gais, P., Molina, C.A., Altmayr, F., Holzmann, B., 2007. Negative regulation of TLR responses by the neuropeptide CGRP is mediated by the transcriptional repressor ICER. J. Immunol. 179 (1), 607−615.

Hay, D.L., Chen, S., Lutz, T.A., Parkes, D.G., Roth, J.D., 2015. Amylin: pharmacology, physiology, and clinical potential. Pharmacol. Rev. 67 (3), 564−600.

Henriksen, K., Byrjalsen, I., Andersen, J.R., Bihlet, A.R., Russo, L.A., Alexandersen, P., et al., 2016. A randomized, double-blind, multicenter, placebo-controlled study to evaluate the efficacy and safety of oral salmon calcitonin in the treatment of osteoporosis in postmenopausal women taking calcium and vitamin D. Bone 91, 122−129.

Hill, E.L., Elde, R., 1991. Distribution of CGRP-, VIP-, D beta H-, SP-, and NPY-immunoreactive nerves in the periosteum of the rat. Cell Tissue Res. 264 (3), 469−480.

Hill, E.L., Turner, R., Elde, R., 1991. Effects of neonatal sympathectomy and capsaicin treatment on bone remodeling in rats. Neuroscience 44 (3), 747−755.

Hoff, A.O., Catala-Lehnen, P., Thomas, P.M., Priemel, M., Rueger, J.M., Nasonkin, I., et al., 2002. Increased bone mass is an unexpected phenotype associated with deletion of the calcitonin gene. J. Clin. Investig. 110 (12), 1849−1857.

Horcajada-Molteni, M.N., Davicco, M.J., Lebecque, P., Coxam, V., Young, A.A., Barlet, J.P., 2000. Amylin inhibits ovariectomy-induced bone loss in rats. J. Endocrinol. 165 (3), 663−668.

Huang, C.Z., Yang, X.N., Liu, D.C., Sun, Y.G., Dai, X.M., 2015. Calcitonin gene-related peptide-induced calcium alginate gel combined with adipose-derived stem cells differentiating to osteoblasts. Cell Biochem. Biophys. 73 (3), 609−617.

Huebner, A.K., Schinke, T., Priemel, M., Schilling, S., Schilling, A.F., Emeson, R.B., et al., 2006. Calcitonin deficiency in mice progressively results in high bone turnover. J. Bone Miner. Res. 21 (12), 1924−1934.

Huebner, A.K., Keller, J., Catala-Lehnen, P., Perkovic, S., Streichert, T., Emeson, R.B., et al., 2008. The role of calcitonin and alpha-calcitonin gene-related peptide in bone formation. Arch. Biochem. Biophys. 473 (2), 210−217.

Hukkanen, M., Konttinen, Y.T., Santavirta, S., Paavolainen, P., Gu, X.H., Terenghi, G., et al., 1993. Rapid proliferation of calcitonin gene-related peptide-immunoreactive nerves during healing of rat tibial fracture suggests neural involvement in bone growth and remodelling. Neuroscience 54 (4), 969−979.

Hurley, D.L., Tiegs, R.D., Wahner, H.W., Heath 3rd, H., 1987. Axial and appendicular bone mineral density in patients with long-term deficiency or excess of calcitonin. N. Engl. J. Med. 317 (9), 537−541.

Irie, K., Hara-Irie, F., Ozawa, H., Yajima, T., 2002. Calcitonin gene-related peptide (CGRP)-containing nerve fibers in bone tissue and their involvement in bone remodeling. Microsc. Res. Tech. 58 (2), 85−90.

Iyengar, S., Ossipov, M.H., Johnson, K.W., 2017. The role of calcitonin gene-related peptide in peripheral and central pain mechanisms including migraine. Pain 158 (4), 543−559.

Jablonski, H., Kauther, M.D., Bachmann, H.S., Jager, M., Wedemeyer, C., 2015. Calcitonin gene-related peptide modulates the production of pro-inflammatory cytokines associated with periprosthetic osteolysis by THP-1 macrophage-like cells. Neuroimmunomodulation 22 (3), 152−165.

Juhl, C.B., Porksen, N., Sturis, J., Hansen, A.P., Veldhuis, J.D., Pincus, S., et al., 2000. High-frequency oscillations in circulating amylin concentrations in healthy humans. Am. J. Physiol. Endocrinol. Metab. 278 (3), E484−E490.

Kauther, M.D., Bachmann, H.S., Neuerburg, L., Broecker-Preuss, M., Hilken, G., Grabellus, F., et al., 2011. Calcitonin substitution in calcitonin deficiency reduces particle-induced osteolysis. BMC Muscoskelet. Disord. 12, 186.

Kawase, T., Burns, D.M., 1998. Calcitonin gene-related peptide stimulates potassium efflux through adenosine triphosphate-sensitive potassium channels and produces membrane hyperpolarization in osteoblastic UMR106 cells. Endocrinology 139 (8), 3492−3502.

Kawase, T., Howard, G.A., Roos, B.A., Burns, D.M., 1995. Diverse actions of calcitonin gene-related peptide on intracellular free $Ca2^{+}$ concentrations in UMR 106 osteoblastic cells. Bone 16 (4 Suppl. l), 379S−384S.

Keller, J., Catala-Lehnen, P., Huebner, A.K., Jeschke, A., Heckt, T., Lueth, A., et al., 2014. Calcitonin controls bone formation by inhibiting the release of sphingosine 1-phosphate from osteoclasts. Nat. Commun. 5, 5215.

Klein, K.R., Matson, B.C., Caron, K.M., 2016. The expanding repertoire of receptor activity modifying protein (RAMP) function. Crit. Rev. Biochem. Mol. Biol. 51 (1), 65−71.

Konarkowska, B., Aitken, J.F., Kistler, J., Zhang, S., Cooper, G.J., 2006. The aggregation potential of human amylin determines its cytotoxicity towards islet beta-cells. FEBS J. 273 (15), 3614−3624.

Lerner, U.H., 2006. Deletions of genes encoding calcitonin/alpha-CGRP, amylin and calcitonin receptor have given new and unexpected insights into the function of calcitonin receptors and calcitonin receptor-like receptors in bone. J. Musculoskelet. Neuronal Interact. 6 (1), 87−95.

Levin, B.E., Lutz, T.A., 2017. Amylin and leptin: Co-regulators of energy homeostasis and neuronal development. Trends Endocrinol. Metabol. 28 (2), 153−164.

Li, Z., Kelly, L., Gergi, I., Vieweg, P., Heiman, M., Greengard, P., et al., 2015. Hypothalamic amylin acts in concert with leptin to regulate food intake. Cell Metabol. 22 (6), 1059−1067.

Li, Y., Yang, L., Zheng, Z., Li, Z., Deng, T., Ren, W., et al., 2017. Bio-Oss((R)) modified by calcitonin gene-related peptide promotes osteogenesis in vitro. Exp Ther Med 14 (5), 4001−4008.

Liang, W., Zhuo, X., Tang, Z., Wei, X., Li, B., 2015. Calcitonin gene-related peptide stimulates proliferation and osteogenic differentiation of osteoporotic rat-derived bone mesenchymal stem cells. Mol. Cell. Biochem. 402 (1−2), 101−110.

Lima, W.G., Marques-Oliveira, G.H., da Silva, T.M., Chaves, V.E., 2017. Role of calcitonin gene-related peptide in energy metabolism. Endocrine 58 (1), 3–13.

Lin, H.Y., Harris, T.L., Flannery, M.S., Aruffo, A., Kaji, E.H., Gorn, A., et al., 1991. Expression cloning and characterization of a porcine renal calcitonin receptor. Trans. Assoc. Am. Phys. 104, 265–272.

Lorenzo, A., Razzaboni, B., Weir, G.C., Yankner, B.A., 1994. Pancreatic islet cell toxicity of amylin associated with type-2 diabetes mellitus. Nature 368 (6473), 756–760.

Lutz, T.A., 2012. Control of energy homeostasis by amylin. Cell. Mol. Life Sci. 69 (12), 1947–1965.

MacIntyre, I., 1989. Amylinamide, bone conservation, and pancreatic beta cells. Lancet 2 (8670), 1026–1027.

Martin, T.J., Sims, N.A., 2015. Calcitonin physiology, saved by a lysophospholipid. J. Bone Miner. Res. 30 (2), 212–215.

McLatchie, L.M., Fraser, N.J., Main, M.J., Wise, A., Brown, J., Thompson, N., et al., 1998. RAMPs regulate the transport and ligand specificity of the calcitonin-receptor-like receptor. Nature 393 (6683), 333–339.

Michelangeli, V.P., Findlay, D.M., Fletcher, A., Martin, T.J., 1986. Calcitonin gene-related peptide (CGRP) acts independently of calcitonin on cyclic AMP formation in clonal osteogenic sarcoma cells (UMR 106-01). Calcif. Tissue Int. 39 (1), 44–48.

Michelangeli, V.P., Fletcher, A.E., Allan, E.H., Nicholson, G.C., Martin, T.J., 1989. Effects of calcitonin gene-related peptide on cyclic AMP formation in chicken, rat, and mouse bone cells. J. Bone Miner. Res. 4 (2), 269–272.

Miles, P.D., Deftos, L.J., Moossa, A.R., Olefsky, J.M., 1994. Islet amyloid polypeptide (amylin) increases the renal excretion of calcium in the conscious dog. Calcif. Tissue Int. 55 (4), 269–273.

Millet, I., Vignery, A., 1997. The neuropeptide calcitonin gene-related peptide inhibits TNF-alpha but poorly induces IL-6 production by fetal rat osteoblasts. Cytokine 9 (12), 999–1007.

Morfis, M., Tilakaratne, N., Furness, S.G., Christopoulos, G., Werry, T.D., Christopoulos, A., et al., 2008. Receptor activity-modifying proteins differentially modulate the G protein-coupling efficiency of amylin receptors. Endocrinology 149 (11), 5423–5431.

Mrak, E., Guidobono, F., Moro, G., Fraschini, G., Rubinacci, A., Villa, I., 2010. Calcitonin gene-related peptide (CGRP) inhibits apoptosis in human osteoblasts by beta-catenin stabilization. J. Cell. Physiol. 225 (3), 701–708.

Mullins, M.W., Ciallella, J., Rangnekar, V., McGillis, J.P., 1993. Characterization of a calcitonin gene-related peptide (CGRP) receptor on mouse bone marrow cells. Regul. Pept. 49 (1), 65–72.

Naot, D., Cornish, J., 2008. The role of peptides and receptors of the calcitonin family in the regulation of bone metabolism. Bone 43 (5), 813–818.

Naot, D., Cornish, J., 2014. Cytokines and hormones that contribute to the positive association between fat and bone. Front. Endocrinol. 5, 70.

Niall, H.D., Keutmann, H.T., Copp, D.H., Potts Jr., J.T., 1969. Amino acid sequence of salmon ultimobranchial calcitonin. Proc. Natl. Acad. Sci. U. S. A. 64 (2), 771–778.

Njuki, F., Nicholl, C.G., Howard, A., Mak, J.C., Barnes, P.J., Girgis, S.I., et al., 1993. A new calcitonin-receptor-like sequence in rat pulmonary blood vessels. Clin. Sci. 85 (4), 385–388.

Offley, S.C., Guo, T.-Z., Wei, T., Clark, J.D., Vogel, H., Lindsey, D.P., et al., 2005. Capsaicin-sensitive sensory neurons contribute to the maintenance of trabecular bone integrity. J. Bone Miner. Res. 20 (2), 257–267.

Osajima, A., Mutoh, Y., Uezono, Y., Kawamura, M., Izumi, F., Takasugi, M., et al., 1995. Adrenomedullin increases cyclic AMP more potently than CGRP and amylin in rat renal tubular basolateral membranes. Life Sci. 57 (5), 457–462.

Owan, I., Ibaraki, K., 1994. The role of calcitonin gene-related peptide (CGRP) in macrophages: the presence of functional receptors and effects on proliferation and differentiation into osteoclast-like cells. Bone Miner. 24 (2), 151–164.

Paemeleire, K., MaassenVanDenBrink, A., 2018. Calcitonin-gene-related peptide pathway mAbs and migraine prevention. Curr. Opin. Neurol. 31 (3), 274–280.

Pietschmann, P., Farsoudi, K.H., Hoffmann, O., Klaushofer, K., Horandner, H., Peterlik, M., 1993. Inhibitory effect of amylin on basal and parathyroid hormone-stimulated bone resorption in cultured neonatal mouse calvaria. Bone 14 (2), 167–172.

Poyner, D.R., Sexton, P.M., Marshall, I., Smith, D.M., Quirion, R., Born, W., et al., 2002. International Union of Pharmacology. XXXII. The mammalian calcitonin gene-related peptides, adrenomedullin, amylin, and calcitonin receptors. Pharmacol. Rev. 54 (2), 233–246.

Qiao, Y.C., Ling, W., Pan, Y.H., Chen, Y.L., Zhou, D., Huang, Y.M., et al., 2017. Efficacy and safety of pramlintide injection adjunct to insulin therapy in patients with type 1 diabetes mellitus: a systematic review and meta-analysis. Oncotarget 8 (39), 66504–66515.

Reid, I.R., Ames, R., Evans, M.C., Sharpe, S., Gamble, G., France, J.T., et al., 1992a. Determinants of total body and regional bone mineral density in normal postmenopausal women–a key role for fat mass. J. Clin. Endocrinol. Metab. 75 (1), 45–51.

Reid, I.R., Plank, L.D., Evans, M.C., 1992b. Fat mass is an important determinant of whole body bone density in premenopausal women but not in men. J. Clin. Endocrinol. Metab. 75 (3), 779–782.

Reid, I.R., Evans, M.C., Cooper, G.J., Ames, R.W., Stapleton, J., 1993. Circulating insulin levels are related to bone density in normal postmenopausal women. Am. J. Physiol. 265 (4 Pt 1), E655–E659.

Reid, I.R., 2002. Relationships among body mass, its components, and bone. Bone 31 (5), 547–555.

Romero, D.F., Bryer, H.P., Rucinski, B., Isserow, J.A., Buchinsky, F.J., Cvetkovic, M., et al., 1995. Amylin increases bone volume but cannot ameliorate diabetic osteopenia. Calcif. Tissue Int. 56 (1), 54–61.

Roos, B.A., Fischer, J.A., Pignat, W., Alander, C.B., Raisz, L.G., 1986. Evaluation of the in vivo and in vitro calcium-regulating actions of noncalcitonin peptides produced via calcitonin gene expression. Endocrinology 118 (1), 46–51.

Russell, F.A., King, R., Smillie, S., Kodji, X., Brain, S.D., 2014. Calcitonin gene-related peptide: physiology and pathophysiology. Physiol. Rev. 94 (4), 1099–1142.

Schifter, S., 1991. Circulating concentrations of calcitonin gene-related peptide (CGRP) in normal man determined with a new, highly sensitive radioimmunoassay. Peptides 12 (2), 365–369.

Schinke, T., Liese, S., Priemel, M., Haberland, M., Schilling, A.F., Catala-Lehnen, P., et al., 2004. Decreased bone formation and osteopenia in mice lacking alpha-calcitonin gene-related peptide. J. Bone Miner. Res. 19 (12), 2049–2056.

Sexton, P.M., Houssami, S., Hilton, J.M., O'Keeffe, L.M., Center, R.J., Gillespie, M.T., et al., 1993. Identification of brain isoforms of the rat calcitonin receptor. Mol. Endocrinol. 7 (6), 815–821.

Sexton, P.M., Houssami, S., Brady, C.L., Myers, D.E., Findlay, D.M., 1994. Amylin is an agonist of the renal porcine calcitonin receptor. Endocrinology 134 (5), 2103–2107.

Shyu, J.F., Shih, C., Tseng, C.Y., Lin, C.H., Sun, D.T., Liu, H.T., et al., 2007. Calcitonin induces podosome disassembly and detachment of osteoclasts by modulating Pyk2 and Src activities. Bone 40 (5), 1329–1342.

Silverman, S.L., Azria, M., 2002. The analgesic role of calcitonin following osteoporotic fracture. Osteoporos. Int. 13 (11), 858–867.

Singh-Franco, D., Robles, G., Gazze, D., 2007. Pramlintide acetate injection for the treatment of type 1 and type 2 diabetes mellitus. Clin. Ther. 29 (4), 535–562.

Spinetti, A., Margutti, A., Bertolini, S., Bernardi, F., BiFulco, G., degli Uberti, E.C., et al., 1997. Hormonal replacement therapy affects calcitonin gene-related peptide and atrial natriuretic peptide secretion in postmenopausal women. Eur. J. Endocrinol. 137 (6), 664–669.

Takahashi, S., Goldring, S., Katz, M., Hilsenbeck, S., Williams, R., Roodman, G.D., 1995. Downregulation of calcitonin receptor mRNA expression by calcitonin during human osteoclast-like cell differentiation. J. Clin. Investig. 95 (1), 167–171.

Tamura, T., Miyaura, C., Owan, I., Suda, T., 1992. Mechanism of action of amylin in bone. J. Cell. Physiol. 153 (1), 6–14.

Thiebaud, D., Akatsu, T., Yamashita, T., Suda, T., Noda, T., Martin, R.E., et al., 1991. Structure-activity relationships in calcitonin gene-related peptide: cyclic AMP response in a preosteoblast cell line (KS-4). J. Bone Miner. Res. 6 (10), 1137–1142.

Tian, G., Zhang, G., Tan, Y.H., 2013. Calcitonin gene-related peptide stimulates BMP-2 expression and the differentiation of human osteoblast-like cells in vitro. Acta Pharmacol. Sin. 34 (11), 1467–1474.

Tippins, J.R., Morris, H.R., Panico, M., Etienne, T., Bevis, P., Girgis, S., et al., 1984. The myotropic and plasma-calcium modulating effects of calcitonin gene-related peptide (CGRP). Neuropeptides 4 (5), 425–434.

Turner, A.G., Tjahyono, F., Chiu, W.S., Skinner, J., Sawyer, R., Moore, A.J., et al., 2011. The role of the calcitonin receptor in protecting against induced hypercalcemia is mediated via its actions in osteoclasts to inhibit bone resorption. Bone 48 (2), 354–361.

Valentijn, K., Gutow, A.P., Troiano, N., Gundberg, C., Gilligan, J.P., Vignery, A., 1997. Effects of calcitonin gene-related peptide on bone turnover in ovariectomized rats. Bone 21 (3), 269–274.

Villa, I., Rubinacci, A., Ravasi, F., Ferrara, A.F., Guidobono, F., 1997. Effects of amylin on human osteoblast-like cells. Peptides 18 (4), 537–540.

Villa, I., Melzi, R., Pagani, F., Ravasi, F., Rubinacci, A., Guidobono, F., 2000. Effects of calcitonin gene-related peptide and amylin on human osteoblast-like cells proliferation. Eur. J. Pharmacol. 409 (3), 273–278.

Villa, I., Dal Fiume, C., Maestroni, A., Rubinacci, A., Ravasi, F., Guidobono, F., 2003. Human osteoblast-like cell proliferation induced by calcitonin-related peptides involves PKC activity. Am. J. Physiol. Endocrinol. Metab. 284 (3), E627–E633.

Wada, S., Udagawa, N., Nagata, N., Martin, T.J., Findlay, D.M., 1996. Calcitonin receptor down-regulation relates to calcitonin resistance in mature mouse osteoclasts. Endocrinology 137 (3), 1042–1048.

Wang, L., Shi, X., Zhao, R., Halloran, B.P., Clark, D.J., Jacobs, C.R., et al., 2010. Calcitonin-gene-related peptide stimulates stromal cell osteogenic differentiation and inhibits RANKL induced NF-kappaB activation, osteoclastogenesis and bone resorption. Bone 46 (5), 1369–1379.

Weiss, R.E., Singer, F.R., Gorn, A.H., Hofer, D.P., Nimni, M.E., 1981. Calcitonin stimulates bone formation when administered prior to initiation of osteogenesis. J. Clin. Investig. 68 (3), 815–818.

Wener, J.A., Gorton, S.J., Raisz, L.G., 1972. Escape from inhibition or resorption in cultures of fetal bone treated with calcitoninand parathyroid hromone. Endocrinology 90 (3), 752–759.

Westermark, P., Wernstedt, C., Wilander, E., Hayden, D.W., O'Brien, T.D., Johnson, K.H., 1987. Amyloid fibrils in human insulinoma and islets of Langerhans of the diabetic cat are derived from a neuropeptide-like protein also present in normal islet cells. Proc. Natl. Acad. Sci. U. S. A. 84 (11), 3881–3885.

Weston, C., Winfield, I., Harris, M., Hodgson, R., Shah, A., Dowell, S.J., et al., 2016. Receptor activity-modifying protein-directed G protein signaling specificity for the calcitonin gene-related peptide family of receptors. J. Biol. Chem. 291 (42), 21925–21944.

Wimalawansa, S.J., 1997. Amylin, calcitonin gene-related peptide, calcitonin, and adrenomedullin: a peptide superfamily. Crit. Rev. Neurobiol. 11 (2–3), 167–239.

Woodrow, J.P., Sharpe, C.J., Fudge, N.J., Hoff, A.O., Gagel, R.F., Kovacs, C.S., 2006. Calcitonin plays a critical role in regulating skeletal mineral metabolism during lactation. Endocrinology 147 (9), 4010–4021.

Wuster, C., Raue, F., Meyer, C., Bergmann, M., Ziegler, R., 1992. Long-term excess of endogenous calcitonin in patients with medullary thyroid carcinoma does not affect bone mineral density. J. Endocrinol. 134 (1), 141–147.

Xu, J., Kauther, M.D., Hartl, J., Wedemeyer, C., 2010. Effects of alpha-calcitonin gene-related peptide on osteoprotegerin and receptor activator of nuclear factor-kappaB ligand expression in MG-63 osteoblast-like cells exposed to polyethylene particles. J. Orthop. Surg. Res. 5, 83.

Yamamoto, I., Kitamura, N., Aoki, J., Shigeno, C., Hino, M., Asonuma, K., et al., 1986. Human calcitonin gene-related peptide possesses weak inhibitory potency of bone resorption in vitro. Calcif. Tissue Int. 38 (6), 339–341.

Young, A.A., Gedulin, B., Wolfe-Lopez, D., Greene, H.E., Rink, T.J., Cooper, G.J., 1992. Amylin and insulin in rat soleus muscle: dose responses for cosecreted noncompetitive antagonists. Am. J. Physiol. 263 (2 Pt 1), E274–E281.

Young, A.A., Rink, T.J., Wang, M.W., 1993. Dose response characteristics for the hyperglycemic, hyperlactemic, hypotensive and hypocalcemic actions of amylin and calcitonin gene-related peptide-I (CGRP alpha) in the fasted, anaesthetized rat. Life Sci. 52 (21), 1717−1726.

Zaidi, M., Chambers, T.J., Gaines Das, R.E., Morris, H.R., MacIntyre, I., 1987a. A direct action of human calcitonin gene-related peptide on isolated osteoclasts. J. Endocrinol. 115 (3), 511−518.

Zaidi, M., Fuller, K., Bevis, P.J., GainesDas, R.E., Chambers, T.J., MacIntyre, I., 1987b. Calcitonin gene-related peptide inhibits osteoclastic bone resorption: a comparative study. Calcif. Tissue Int. 40 (3), 149−154.

Zaidi, M., Datta, H.K., Bevis, P.J., Wimalawansa, S.J., MacIntyre, I., 1990. Amylin-amide: a new bone-conserving peptide from the pancreas. Exp. Physiol. 75 (4), 529−536.

Zaidi, M., Shankar, V.S., Huang, C.L.H., Pazianas, M., Bloom, S.R., 1993. Amylin in bone conservation: current evidence and hypothetical considerations. Trends Endocrinol. Metabol. 4, 255−259.

Zaidi, M., Inzerillo, A.M., Moonga, B.S., Bevis, P.J., Huang, C.L., 2002. Forty years of calcitonin–where are we now? A tribute to the work of Iain Macintyre. FRS. Bone. 30 (5), 655−663.

Zhang, Z., Neff, L., Bothwell, A.L., Baron, R., Horne, W.C., 2002. Calcitonin induces dephosphorylation of Pyk2 and phosphorylation of focal adhesion kinase in osteoclasts. Bone 31 (3), 359−365.

Zhang, X.X., Pan, Y.H., Huang, Y.M., Zhao, H.L., 2016. Neuroendocrine hormone amylin in diabetes. World J. Diabetes 7 (9), 189−197.

Zhang, Y., Xu, J., Ruan, Y.C., Yu, M.K., O'Laughlin, M., Wise, H., et al., 2016. Implant-derived magnesium induces local neuronal production of CGRP to improve bone-fracture healing in rats. Nat. Med. 22 (10), 1160−1169.

Zhou, R., Yuan, Z., Liu, J., Liu, J., 2016. Calcitonin gene-related peptide promotes the expression of osteoblastic genes and activates the WNT signal transduction pathway in bone marrow stromal stem cells. Mol. Med. Rep. 13 (6), 4689−4696.

Chapter 34

Regulation of bone remodeling by central and peripheral nervous signals

Patricia Ducy

Department of Pathology & Cell Biology, Columbia University, College of Physicians & Surgeons, New York, NY, United States

Chapter outline

Introduction

Hints of a connection between the nervous system and the regulation of bone mass have long been present in the literature. For instance, osteoporosis is a known complication of spinal cord injury and experimental models of sensory or sympathetic denervation have shown that these two neuronal systems could be involved in bone development and remodeling (Chenu, 2004; Jiang et al., 2006). Likewise, major depression is associated with low bone mass and increased incidence of osteoporotic fractures, as is the use of several types of central nervous system-active drugs such as anticonvulsants and opioids (Kinjo et al., 2005). These examples all point at a regulation of bone mass by the nervous system—i.e., at signals efferent from the brain (or nerves) to bone cells. This might explain why most of the earlier studies have focused on peripherally produced neuromediators (Chenu, 2002; Spencer et al., 2007). More recently, however, afferent signals that influence the brain's control of bone mass have been identified, and a comprehensive understanding of their central mode of action has emerged. Overall, the identification of these pathways illustrates the investigative power of mouse genetics and can be viewed as an archetype of the current effort of integrative biology. More importantly, this rapidly evolving field of bone neurobiology has shed light on perplexing clinical observations and may therefore become critical in developing novel concepts in drug development.

Principles of Bone Biology. https://doi.org/10.1016/B978-0-12-814841-9.00034-8

Afferent signals regulating bone remodeling via the central nervous system

At the present time there are two signals known, in vivo, to affect bone mass via a central nervous system (CNS) relay. Remarkably, they both originate from adipocytes, suggesting a preferential relationship between the regulation of energy metabolism and bone homeostasis. One signal is leptin, a 16 kDa peptide hormone that was originally identified by positional cloning of the mutation present in *ob/ob* mice, a natural mutant presenting morbid obesity and sterility (Zhang et al., 1994). The other one is adiponectin, a secreted molecule previously known for its insulin-sensitizing ability in animals fed a high-fat diet (Maeda et al., 2002; Kadowaki and Yamauchi, 2005). Subsequent analysis of their respective central mode of action has identified a significant overlap in their ability to influence bone remodeling.

Negative regulation of bone remodeling by leptin

Mice harboring an inactivating mutation in the leptin-encoding gene (*ob/ob* mice) or in the gene encoding Lepr, its only known receptor (*db/db* mice), are obese and hypogonadic (Zhang et al., 1994; Tartaglia et al., 1995; Ahima, 2004). Given the negative effect of sex steroid hormone depletion on bone mass, they should therefore exhibit a low-bone-mass phenotype. Instead, these two mutant strains display a high-bone-mass phenotype when analyzed by histomorphometry, which given this mice obesity, allows the most objective evaluation of bone parameters as its results do not need to be adjusted for differences of lean/fat mass (Ducy et al., 2000; Baldock et al., 2005). This increased bone mass, which appears limited to cancellous bone, is also observed in genetically engineered *Lepr* knockout rats (Vaira et al., 2012; Solomon et al., 2014) and in transgenic lipodystrophic mice (b-ZIP mice) (Ducy et al., 2000). The latter observation is consistent with the advanced bone age observed in patients with lipodystrophy, a condition associated with a severe deficiency in serum leptin (Westvik, 1996; Elefteriou et al., 2004). Conversely, expression of a leptin transgene and intracerebroventricular infusion (ICV) of leptin can correct the high-bone-mass phenotype of respectively lipodystrophic and *ob/ob* mice, and mice expressing a gain-of-function of the leptin receptor (*l/l* mice) have decreased bone mass (Elefteriou et al., 2004; Shi et al., 2008).

The high-bone-mass phenotype of leptin-signaling deficient mice is due to an increase in bone formation rate that is already present in fat-restricted 1-month-old *ob/ob* mice and heterozygote *ob/+* mice, which are not obese, indicating that it is the absence of leptin not an increase in fat mass that is responsible for this phenotype (Ducy et al., 2000). Consistent with their hypogonadism, *ob/ob* and *db/db* mice have an increase in bone resorption (Ducy et al., 2000). It is, however, milder than their innate and permanent sex steroid depletion would have predicted, because by itself leptin deficiency has a negative effect on bone resorption through its action on the sympathetic tone (see below).

Studies using peripheral injections of pharmacological doses of leptin (over 40 μg/day; i.e., 700-fold the amount used in ICV studies) (Steppan et al., 2000; Cornish et al., 2002; Turner et al., 2013) have reported a beneficial effect on bone mass accrual, and proposed that leptin could act directly on osteoblasts. However, several arguments argue against a direct action on bone cells. First, gene expression in bone tissue or isolated osteoblasts as well as lineage-tracing studies using a Leptin receptor reporter transgene (*Lepr-YFP*) have failed to detect it in osteoblasts (Ducy et al., 2000; Ding et al., 2012). Second, osteoblasts derived from *db/db* mice proliferate and differentiate normally when cultured ex vivo (Ducy et al., 2000). Third, neither transgenic expression of leptin in osteoblasts nor the conditional inactivation of *Lepr* specifically in osteoblasts causes a bone phenotype in mice (Takeda et al., 2002; Shi et al., 2008). In contrast, inactivating *Lepr* in neurons induces the same high-bone-mass phenotype than the one observed in *db/db* mice (Shi et al., 2008; Yadav et al., 2009). The positive effect on bone mass observed upon leptin injections at high doses could in fact be explained by the well-known leptin resistance that centrally occurs when its serum concentration becomes too high, for example due to obesity (Könner and Brüning, 2012; Motyl and Rosen, 2012; Mark, 2013). Since leptin centrally affects bone mass accrual at a lower threshold than it affects body weight, the effect of leptin on bone remodeling is likely to be more quickly impacted by a leptin-resistance mechanism (Elefteriou et al., 2004; Shi et al., 2008). Hence, supraphysiological doses of this hormone injected peripherally could still cause weight loss, as some of the above mentioned studies reported, while already eliciting a central leptin resistance that will cause a gain of bone mass similar to the one observed in the absence of leptin signaling.

Dual action of adiponectin on bone remodeling

Analysis of mice deficient in adiponectin has identified both central and peripheral effects of this hormone on bone mass accrual. Young adult *Adiponectin−/−* mice display a high-bone-mass phenotype that is due to an increase in the number of osteoblasts and bone formation rate (Kajimura et al., 2013). Genetic and in vitro studies attributed this effect to adiponectin's ability to regulate proliferation and apoptosis of osteoblasts in a FoxO1-dependent manner via PI3 kinase activation.

This early high-bone-mass phenotype, however, cannot be observed in older mice that, instead, show a decreased bone mass characterized by a lesser number and proliferation ability of osteoblasts and an increase in bone resorption parameters (Kajimura et al., 2013; Wu et al., 2014). This phenotype is consistent with the observation that injection of an adiponectin-expressing adenovirus increases bone mass by suppressing osteoclastogenesis while activating osteoblastogenesis (Oshima et al., 2005).

The observations mentioned above indicate that the adipocyte secretes two hormones exerting opposite influences on the same physiological functions in adult mice. The fact that b-ZIP lipodystrophic mice have a high-bone-mass phenotype despite lacking both these hormones (Ducy et al., 2000), however, suggests that lack of leptin is dominant over the absence of adiponectin.

Central and efferent regulators of bone remodeling

Leptin's action on bone remodeling is mediated by brain serotonin signaling and the sympathetic nervous system

Leptin's action on appetite and reproduction depends on its binding to a specific receptor expressed by brain neurons (Ahima and Flier, 2000; Ahima, 2004). In agreement with this central mode of action, ICV infusion of low doses of leptin in *ob/ob* mice, at a rate that does not result in any detectable leak of leptin in the general circulation, corrects their high-bone-mass phenotype (Ducy et al., 2000). This rescue is complete and occurs even at minimal doses that do not influence body weight (Elefteriou et al., 2004). Likewise, low doses of leptin administered by ICV infusion in wild-type animals induce a potent antiosteogenic effect resulting in severe bone loss within 1 month (Ducy et al., 2000).

Chemical lesioning experiments identified the ventromedial hypothalamus (VMH) as the relay of the leptin antiosteogenic effect in the brain (Takeda et al., 2002). Yet deletion of the leptin receptor in these same neurons does not cause a bone phenotype (Balthasar et al., 2004; Yadav et al., 2009). This apparent contradiction is explained by the fact that leptin uses a serotonin relay to act on the VMH neurons of the hypothalamus (Yadav et al., 2009; Ducy and Karsenty, 2010; Oury and Karsenty, 2011). Indeed, leptin signals to neurons of the dorsal and median raphe nuclei in the brain stem to blunt the production of brain serotonin that itself is a positive regulator of bone mass accrual (Yadav et al., 2009) (Fig. 34.1). In support of this mechanism, *Tph2*-deficient mice, which lack brain serotonin, show a low-bone-mass phenotype mirroring the one observed in *ob/ob* mice, and normalizing the brain content of the *ob/ob* mice by inactivating one allele of *Tph2* corrects their bone phenotype (Yadav et al., 2009). Conversely, inactivation of *LepR* in the *Tph2*-expressing neurons of the brain stem causes a bone phenotype similar to the one presented by *db/db* mice (Yadav et al., 2009). The negative influence of a deficit in brain serotonin signaling on bone mass explains the bone loss observed upon chronic use of selective serotonin reuptake inhibitors (SSRIs) as well as in a mouse model of Alzheimer's disease (Dengler-Crish et al., 2016; Ortuno et al., 2016).

Consistent with the lesioning experiments that identified the VMH nuclei as mediating leptin antiosteogenic action, dextran anterograde and retrograde neuron tracing studies showed that serotonergic neurons project from the brain stem to the VMH nuclei (Yadav et al., 2009). Serotonin then signals to VMH neurons via the Htr2c receptor to regulate CREB phosphorylation on Ser133 via Ca^{2+} as a second messenger and a CaMKKβ/CaMKIV cascade (Oury et al., 2010). This osteogenic pathway was demonstrated in vivo as mice with an inactivation of *Creb* in VMH neurons (*Creb* $_{VHM}$*−/−*) or heterozygous compound for *Creb* and *Htr2c* (*Creb* $_{VHM}$*−/−*; *Htr2c+/−)* or for *Creb* and *CaMKIV* (*Creb* $_{VHM}$*+/−*; *CaMKIV* $_{VHM}$ *+/−)* in VMH neurons all show a low-bone-mass phenotype characterized by decreased bone formation and increased bone resorption (Oury et al., 2010). Thus, leptin negatively regulates bone mass by inhibiting brain stem serotonergic neurons, which normally signal to VMH neurons via an Htr2c → CaMKKβ → CaMKIV → CREB cascade to increased bone formation and decrease bone resorption (Fig. 34.1).

A recurrent feature of the mouse models mentioned above is an increase in sympathetic tone, as evidenced by high *Ucp1* expression in brown adipose tissue and urinary levels of epinephrine (Oury et al., 2010). In contrast, *ob/ob* mice are known to exhibit low sympathetic activity (Bray and York, 1998) that, when corrected by treatment with an adrenergic agonist, leads to a dramatic decrease in bone mass (Takeda et al., 2002). The role of the sympathetic nervous system (SNS) as an antiosteogenic activity is supported by the observation that mice deficient in dopamine β-hydroxylase (DBH), an enzyme necessary to produce norepinephrine and epinephrine (the catecholamine ligands produced by the SNS), have a high-bone-mass phenotype (Takeda et al., 2002). Also consistent with this notion is the existence of a high-bone-mass phenotype associated with both an increase in bone formation and a decrease in bone resorption in mice deficient globally or only in osteoblasts for the β2 adrenergic receptor, the main adrenergic receptor expressed in these cells (Takeda et al., 2002; Kajimura et al., 2011). Importantly, the bone phenotype observed in Adrβ2-deficient mice cannot be rescued by

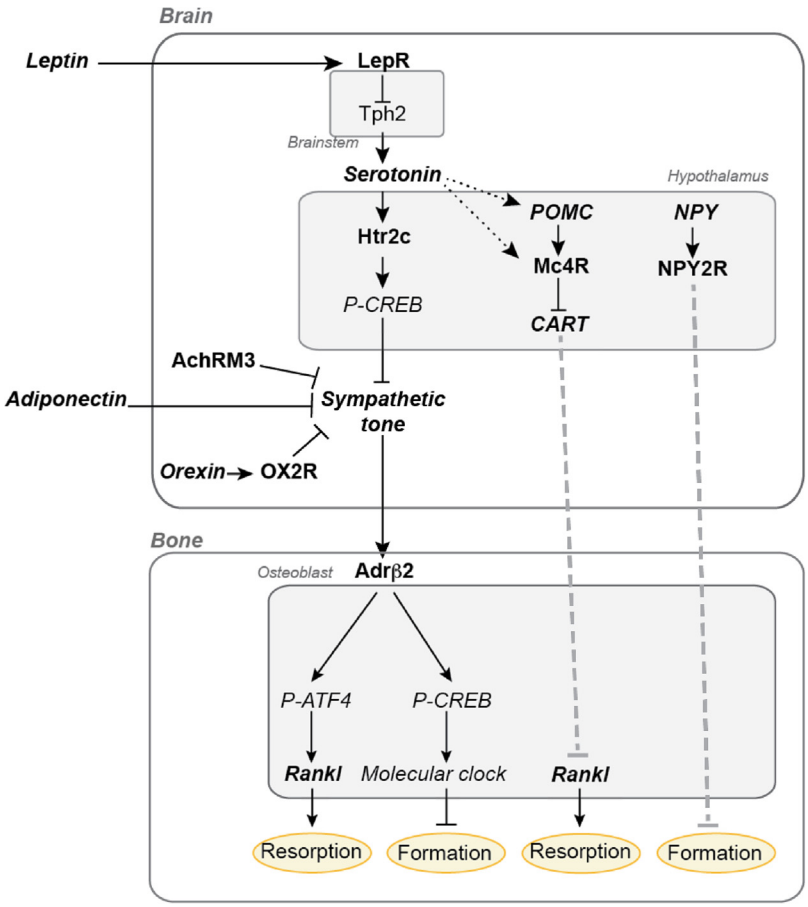

FIGURE 34.1 Central regulation of bone remodeling in mice. Secreted molecules are shown in bold Italics, receptors are shown in bold letters and intracellular effectors are shown in italics. *Black dotted lines* indicate regulation that are most likely to exist but have not yet been demonstrated formally. *Dashed gray lines* indicate mode of actions that have not yet been identified.

leptin ICV infusion demonstrating that the sympathetic nervous system, via Adrβ2 mediates leptin regulation of bone mass (Takeda et al., 2002; Elefteriou et al., 2005). Pharmacologic experiments have confirmed the genetic demonstration of an effect of the SNS on bone mass. Treatment of ovariectomized mice or rats with low doses of propranolol, a nonselective β-blocker, inhibits bone loss and preserves mechanical properties (Takeda et al., 2002; Bonnet et al., 2008; Khajuria et al., 2013). Similar improvements have been observed in a rat model of hypertension associated with bone fragility using low doses of butoxamine, a selective Adrβ2 antagonist (Arai et al., 2013).

At the molecular level, sympathetic signaling acts in osteoblasts through a dual mechanism (Fig. 34.1). It impairs osteoblast proliferation through phosphorylation of CREB, the molecular clock, type D cyclins, and *AP-1* gene expression (Fu et al., 2005; Kajimura et al., 2011). It also promotes *Rankl* expression in osteoblast progenitor cells following protein kinase A phosphorylation of ATF4, a cell-specific CREB-related transcription factor essential (Yang et al., 2004; Elefteriou et al., 2005; Kajimura et al., 2011).

Counterregulation of sympathetic nervous system control of bone remodeling by the parasympathetic nervous system and adiponectin

The low-bone-mass phenotype observed in aged adiponectin-deficient mice, which is due to the conjunction of a decrease in bone formation and an increase in bone resorption parameters is caused by an increase in sympathetic activity. Indeed, infusing adiponectin centrally or removing one allele of *Dbh* from *Adiponectin−/−* mice normalizes *Ucp1* expression in brown fat, norepinephrine content in the brain and urinary epinephrine elimination. and triggers an increase in bone mass secondary to an increase in osteoblast numbers and bone formation rate (Kajimura et al., 2013; Wu et al., 2014). The regulation of SNS output by adiponectin is mediated by its activity on the neurons of the locus coeruleus (LC), the site of *Dbh* expression in the brain stem. Indeed, *Adiponectin−/−* mice lacking only in neurons of the LC one allele of *FoxO1,* which encodes an intracellular effector of adiponectin signaling, have normal sympathetic activity as measured by *Ucp1*

expression in brown fat and a significant increase in bone mass, osteoblast number, and bone formation rate while osteoclast number, *Rankl* expression, and serum CTx levels are decreased compared with *Adiponectin−/−* mice (Kajimura et al., 2013).

Signaling through the muscarinic receptor 3 (AchRM3) is another mechanism counteracting the SNS control of bone remodeling. Muscarinic receptors (AchRM1-4) bind acetylcholine, the main neurotransmitter used by the PNS. While inactivation of *AchRM1*, *AchRM2*, or *AchRM4* does not significantly affect bone mass, mice lacking AchRM3 either globally or only in neurons have a low-bone-mass phenotype associated with increased bone resorption and decreased bone formation (Shi et al., 2010). This phenotype can be attributed to the negative action of the SNS, since it is associated with elevated levels of epinephrine in the urine and is corrected when catecholamine signaling is normalized through coinactivation of one allele of *Adrβ2* (*AchRM3−/−; Adrβ2+/−* mice) (Shi et al., 2010). *AchRM3* being expressed in the noradrenergic neurons of the LC but not in the VMH of the hypothalamus or in sympathetic chain ganglia (Shi et al., 2010) suggests a direct effect on central sympathetic output similar to the one described for adiponectin signaling (Fig. 34.1). Whether these two effectors indeed mechanistically overlap still needs to be defined.

Other regulators of sympathetic nervous system control of bone remodeling

NeuromedinU

NeuromedinU (NMU) is a neuropeptide produced by nerve cells in the small intestine and in the brain (Brighton et al., 2004). It is generally assumed that NMU regulates various aspects of physiology including appetite, stress response, and SNS activation (Brighton et al., 2004). NMU-deficient mice present a high-bone-mass phenotype associated with an increase in bone formation similar to the one displayed by *ob/ob* mice (Sato et al., 2007). This phenotype is not cell autonomous, as NMU-deficient osteoblasts in culture are indistinguishable from wild-type osteoblasts and treatment of wild-type osteoblasts with NMU do not affect their proliferation or differentiation. In contrast, ICV infusion of NMU in wild-type, NMU−/− and *ob/ob* mice decreases bone formation and bone volume (Sato et al., 2007). However, ICV infusion of leptin in NMU−/− mice cannot decrease bone mass, indicating that NMU is a mediator for leptin's action on bone formation (Sato et al., 2007). Accordingly, NMU affects the leptin-dependent negative regulation of bone formation by the molecular clock and it was thus proposed that the high-bone-mass phenotype of the NMU−/− mice is caused by their resistance to the antiosteogenic activity of the SNS (Sato et al., 2007). Yet the basis of this mechanism of action still remains incompletely understood.

Endocannabinoid signaling

Endocannabinoids are lipid mediators that regulate analgesia, energy balance, and appetite by binding to the G protein-coupled receptors CB1 and CB2. CB1 is predominantly expressed in the brain and peripheral neurons, where it is responsible for the psychotropic action of cannabinoids, but it is also expressed in peripheral tissues including immune cells as well as the reproductive system, gastrointestinal tract, and lungs (Di Marzo et al., 2004). Global and conditional inactivation of *CB1* in noradrenergic and adrenergic neurons of the central and peripheral nervous system up-regulates bone formation and bone mass while decreasing bone resorption in adult male mice (Idris et al., 2005; Tam et al., 2006; Deis et al., 2018). Although skeletal levels of norepinephrine are not changed in the conditional knockout mice, expression of *Adrβ2* is increased (Deis et al., 2018). Whether this increase explains their bone phenotype and the molecular basis of this observation remain to be defined. In contrast, *CB2* is not expressed in the brain but is mainly expressed by immune cells (Di Marzo et al., 2004). It is also expressed at lower levels in osteoblasts and osteoclasts and CB2-deficient mice have a low-bone-mass phenotype most likely of peripheral origin (Ofek et al., 2006).

Orexin signaling

Orexins are neuropeptides expressed in the lateral hypothalamus, stimulating multiple behaviors including wakefulness and feeding by binding to two receptors OX1R and OX2R. In the absence of orexin, mice develop a low-bone-mass phenotype caused by a decrease in bone formation (Wei et al., 2014). Analysis of mice lacking the orexin receptors identified an underlying complexity to this phenotype (Wei et al., 2014). Indeed, inactivation of OX1R is associated with increased bone formation and bone mass while bone resorption and *Rankl* expression are decreased. This phenotype appears to be caused by a peripheral effect involving signaling in osteoblasts by Ghrelin, a peptide predominantly expressed in stomach that binds to receptors expressed in osteoblasts to regulate their differentiation and function (Delhanty et al., 2014; Ma et al., 2015). In contrast, absence of OX2R is associated with decreased bone formation and

bone mass, and this phenotype is centrally mediated since it can be reproduced by ICV injection of an OX2R-selective antagonist (Wei et al., 2014). Orexin's central effect could be achieved through modulation of the sympathetic tone, since *Ucp1* expression in brown adipose tissue is increased in OX2R−/− mice (Wei et al., 2014), and the densest extrahypothalamic projection of orexin-positive neurons extends to the noradrenergic LC (Peyron et al., 1998) (Fig. 34.1). Such a mechanism, however, stills needs to be formally demonstrated.

Regulation of bone resorption by melanocortin receptor 4 and cocaine- and amphetamine-regulated transcript

In addition to the SNS-related pathway mentioned above, the absence of brain serotonin causes a sharp increase in the expression of the melanocortin receptor 4 gene (*Mc4R*) (Yadav et al., 2009). Melanocortins, a family of peptides produced by posttranslational processing of proopiomelanocortin (POMC), regulate food intake and energy expenditure via binding to two melanocortin receptors expressed in the central nervous system (Mc3R and Mc4R). While these receptors show a widespread presence in the rodent brain (Mountjoy et al., 1994; Kishi et al., 2003), POMC has a limited distribution, being described in only two neuronal populations: one in the arcuate nucleus of the hypothalamus (ARC) and the other in the nucleus of the tractus solitarius (NTS) of the brain stem (Palkovits et al., 1987; Bronstein et al., 1992). The POMC neurons of the ARC are known to be responsive to leptin and MC4R has thus been implicated in leptin's control of appetite (Cheung et al., 1997; Cone, 1999). It was first reported that patients lacking Mc4R have high bone mineral density (BMD) and advanced bone age (Farooqi et al., 2000). Subsequently, *Mc4r−/−* mice were shown to have an increase in bone mass caused by an isolated decrease in osteoclast number and function consistent with decreased *Rankl* expression (Elefteriou et al., 2005). The same decrease in bone resorption activity was also noted in MC4R-deficient patients (Ahn et al., 2006).

This high-bone-mass/low-resorption phenotype has been explained by an increase in CART signaling. CART is a neuropeptide encoded by a gene expressed in hypothalamic neurons among other parts of the nervous system and in peripheral organs such as the pancreas and the adrenal glands but not in bone cells (Couceyro et al., 1997; Elias et al., 1998; Wierup et al., 2004; Elefteriou et al., 2005). That *Cart* expression is virtually undetectable in hypothalamic neurons of *ob/ob* mice suggested that it is positively regulated by leptin and could therefore act as a mediator of its functions (Douglass et al., 1995; Kristensen et al., 1998). Yet Cart-deficient mice do not present a body weight or reproduction phenotype (Asnicar et al., 2001). Instead they display a late-onset low-bone-mass phenotype (Elefteriou et al., 2005). Osteoblast numbers and bone formation rates are normal in these mice, but the osteoclast surface and number are nearly doubled, leading to a significant increase in urinary Dpd elimination. Given the absence of *Cart* central expression in *ob/ob* mice, this negative regulation of bone resorption by CART explains, at least in part, the increase in bone resorption observed in these mice.

The action of CART on bone resorption is peripheral, as ICV infusion of recombinant CART in *Cart−/−* mice does not correct their low-bone-mass phenotype while transgenic mice harboring a twofold increase in CART circulating level display high bone mass due to an isolated decrease in osteoclast number. Moreover, this same transgene can rescue the low-bone-mass phenotype of the *Cart−/−* mice (Singh et al., 2008). The *Cart−/−* phenotype is not bone cells autonomous as Cart-deficient bone marrow macrophages differentiate normally into osteoclasts and Cart-deficient bone marrow stromal cells can normally support osteoclastogenesis in coculture experiments (Elefteriou et al., 2005). *Rankl* expression is increased in *Cart−/−* bones, suggesting that Cart regulates bone resorption by ultimately modulating Rankl signaling (Elefteriou et al., 2005; Ahn et al., 2006). In the absence of any identified CART receptor, however, one can only speculate whether this factor acts directly on osteoblasts or uses one or several relays to signal to bone cells.

Mc4r inactivation in mice causes an increase in hypothalamic *Cart* expression, and serum CART levels are significantly elevated in patients heterozygous for inactivating mutations of Mc4R (Elefteriou et al., 2005; Ahn et al., 2006). Moreover, inactivation of one or two copies of the *Cart* gene in Mc4r-deficient mice normalizes their bone resorption parameters, *Rankl* expression, and thereby their bone mass (Ahn et al., 2006). Thus, in addition to the SNS pathway, leptin also controls bone resorption via an MC4R/CART pathway (Fig. 34.1). Although likely, whether this regulation also occurs via a brain serotonin relay remains to be genetically confirmed.

Y receptor signaling

The Y signaling system is complex, consisting of at least five receptors (NPY1R, NPY2R, NPY4R, NPY5R, and NPY6R in mouse) with different binding profiles and sites of expression in the central nervous system and the periphery as well as multiple endogenous ligands: neuropeptide Y (NPY), peptide YY (PYY), and pancreatic polypeptide (PP) (Lin et al., 2004). NPY is widely expressed in the central and peripheral nervous system, and NPY fibers project from the ARC nuclei,

which are known to participate in the control of appetite (Hokfelt et al., 1998). The related family members PYY and PP are produced in the small intestine and colon or in the pancreas, respectively (Hazelwood, 1993), where they affect gut motility in addition to pancreatic and gall bladder secretion. PYY is also expressed in a subset of brain stem neurons (Glavas et al., 2008). PYY and PP can signal to specific Y receptors in the hypothalamus and the brain stem to further influence pancreatic and gastric secretion. NPY and PYY have identical affinity for all known Y receptors, and PP binds preferentially to the Y4 receptor (Larhammar 1996).

While *PP−/−* mice do not show a bone phenotype, both PYY-deficient and NPY-deficient mice show an increase in bone mass (Wortley et al., 2007; Baldock et al., 2009; Wong et al., 2012), suggesting that the latter two peptides are negative regulators of bone remodeling. Evidence from overexpressing mice and studies of genetically engineered models suggests that only NPY may exert such activity via central signaling (in addition to direct effects on bone cells) (Matic et al., 2012; Wong et al., 2012) (Fig. 34.1). Indeed, overexpression of NPY in the hypothalamus decreases bone mass by inhibiting bone formation, and this activity can, even if partly, normalize bone mass in the *NPY−/−* mice (Baldock et al., 2005; Baldock et al., 2009). This central activity is most likely mediated by the NPY2R receptor, as its hypothalamus-specific depletion causes an increase in cancellous bone volume by increasing bone formation (Baldock et al., 2002; Baldock et al., 2006; Shi et al., 2010), while the peripheral activity of NPY depends on NPY1R (Baldock et al., 2007). An opposite role has been recently proposed for the Y6 receptor, which is expressed in brain but not in bone and whose global inactivation is associated with reduced bone mass, decreased bone formation, and increased osteoclast number (Khor et al., 2016). This central role, however, awaits to be confirmed via brain-specific inactivation experiments.

Brain-derived neurotrophic factor

Brain-derived neurotrophic factor (BDNF) is a member of the nerve growth factor family of proteins that binds to the tyrosine kinase receptor type B (Trkb). It is expressed in the CNS as well as the peripheral nervous system and is known to affect memory, cognition, and behavior including feeding. Specific inactivation of *Bdnf* in the brain of mice causes a high-bone-mass phenotype associated with decreased osteoclast number, at least in females (Camerino et al., 2012). These mice do not show changes in sympathetic activity or serotonin levels suggesting another, yet unidentified, mode of action.

Interleukin-1

IL-1 is a polypeptide product that mediates several components of acute-phase response to infection and injury. Its main sites of expression are the peripheral immune system and bone cells as well as glia and neuron cells in the CNS (Lorenzo et al., 1990; Dinarello, 1997). When injected subcutaneously, IL-1 is a potent stimulator of bone resorption, and IL-1R-deficient mice do not lose bone after ovariectomy (Sabatini et al., 1988; Lorenzo et al., 1998). Targeted overexpression in the CNS of mice of human IL-1Ra, a natural IL-1 receptor antagonist, results in a low-bone-mass phenotype caused by a doubling of osteoclast numbers (Bajayo et al., 2005). However, the cellular and molecular bases of this central activity are still unknown.

Evidence of central/neuronal regulations of bone mass in human

While genetic engineering in mice has been a powerful tool in identifying many central and neuron-related factors controlling bone remodeling, human genetic evidence confirming these findings is still limited. One possible explanation for this paucity of data stems from the fact that most of the factors identified have major roles regulating other key functions in the body such as feeding, energy metabolism, reproduction, ad behavior, and it is therefore difficult to assess effects on bone mass independently of these other consequences in patients. For example, correcting for body weight or body mass index (BMI) may weaken correlations, since they could be inherent to the trait analyzed and therefore legitimately associated with it but also may simply reflect lifestyle differences. Another issue could come from the exclusion (or absence of exclusion) of patients using medications (yet) considered unrelated to bone health but that are designed to address other activities of these pleiotropic factors. Given these limitations, as much as a positive genetic evidence can be considered a validation of the findings made in rodents, an absence of evidence should be interpreted cautiously.

In addition to the limitations mentioned above, association studies based on the quantification of these factors' blood levels or on therapeutic interventions related to their role in other diseases can be biased by the technical difficulty to accurately extrapolate neuron-produced levels of neuromediators from blood to bone and by the specificity (or lack thereof), dose, effect, and side effects of the drugs evaluated. In that respect, their conclusions should be taken with even more reservation than genetic associations.

Leptin

An association with increased circulating levels of leptin and incidence of osteoporosis has been reported in patients harboring specific alleles at two polymorphism sites of the leptin receptor gene (rs1137100 and rs1137101, both G variants) (Ye and Lu, 2013). Although these variants were not associated with obesity in this particular population, suggesting that they do not cause a receptor loss-of-function, their impact on leptin signaling has not been elucidated, and these data should therefore be interpreted carefully. In contrast, a patient harboring a known obesity-inducing inactivating mutation of the leptin gene was shown to display high bone mass, more definitely indicating that leptin fulfills a role in humans similar to the one it plays in rodents (Elefteriou et al., 2004). Other, although indirect, evidence of such a role is the advanced bone age and presence of osteosclerotic lesions in lipodystrophic patients, whose serum leptin levels are extremely low due to the absence of adipocytes (Westvik, 1996; Elefteriou et al., 2004).

Multiple studies have also assessed a correlation between leptin serum levels and bone mass. However, especially in the case of leptin, one must be cautious when reporting the results of clinical studies including obese participants since their blood leptin levels are expected to be high, but they may be experiencing central leptin resistance. The mere fact that obese individuals are overweight despite high levels of serum leptin most likely demonstrates such a leptin loss-of-function effect. In this case, finding a positive association of leptin levels with BMD would be an expected outcome. In contrast, when leptin levels are moderately elevated and body weight remains within the normal range, negative correlations between serum leptin levels and bone mass have been observed. For instance, an early study noted an inverse association between serum leptin levels adjusted for fat mass and BMD in a group of 221 Japanese men (Sato et al., 2001). Likewise, in a large cohort of young men (the Gothenburg Osteoporosis and Obesity Determinants cohort), leptin was found to be a negative independent predictor of areal BMD at several measured sites, and of cortical bone size at both non−weight-loaded bones (radius) and weight-loaded bones (tibia) (Lorentzon et al., 2006). Importantly, this study was performed on a primarily healthy population with normal body mass indexes sparing the need to adjust BMD readings for differences in lean and fat mass. In another population of healthy subjects without difference on body weight or body mass index, serum levels of leptin were significantly associated with reduced total body, hip, femoral neck, femoral shaft, and total femur BMD (Wu et al., 2009). Other cross-sectional studies have failed to show such a negative association between serum leptin levels and areal BMD (Goulding and Taylor, 1998; Martini et al., 2001; Thomas et al., 2001; Papadopoulou et al., 2004). Most likely, some of the differences between these and other studies can be attributed to the way data are evaluated and are presented, either adjusted or unadjusted for body weight. For instance, in a large North American population-based study including a high representation of the elderly, non-Hispanic blacks, and Mexican Americans, BMD increases with increasing leptin concentration in men. However, after adjustment for BMI and other bone-related factors, an inverse association emerged, being most evident in men younger than 60 years (Ruhl and Everhart, 2002). Similarly, in a few recent studies in men, leptin was inversely correlated to aBMD, an association that became apparent only after adjustment of aBMD for body weight (Sato et al., 2001; Morberg et al., 2003). Lastly, in a small population of middle-age (non-pre-menopausal) Japanese subjects, significant negative correlations were observed between cortical bone thickness and both blood leptin levels and sympathetic activity, as assessed by quantification of heart rate variability, while a positive correlation existed between leptin levels and sympathetic activity (Kuriyama et al., 2017).

Adrenergic signaling

Multiple nongenomic evidence indicates that the SNS function on bone mass is conserved in humans. For instance, patients with reflex sympathetic dystrophy, a disease characterized by localized high sympathetic activity, develop a severe and localized osteoporosis that can be treated by β-blockers (Kurvers, 1998). Likewise, short sleep, which causes an increase in SNS activity, is associated with bone loss; pheochromocytomas, which cause an increase in catecholamine levels, are associated with an increase in bone resorption that can be normalized by adrenalectomy; and sympathetic activity, quantified by microneurography, was found inversely associated with bone volume, trabecular thickness, and bone strength at the distal radius in women (Farr et al., 2012; Veldhuis-Vlug et al., 2012; Kuriyama et al., 2017). Genetic evidence, however, has not been conclusive. While the risk of osteoporosis at the femoral neck was associated with a polymorphism in the *ADRβ2* gene (rs1042713, AG and GG genotypes) in a medium-sized population of postmenopausal Korean women, no correlation could be found with BMD and fracture risk in case-control and meta-analysis studies of populations of European origin (Lee et al., 2014; Veldhuis-Vlug et al., 2015). Additional studies are needed that analyze polymorphisms at this locus in different populations but also in genes encoding other adrenergic receptors, as in humans those may contribute to the effect of the SNS on osteoblasts.

From a pharmacological standpoint, beneficial effects of β-blocker administration on BMD and/or fracture risk in women have been reported by multiple epidemiologic studies. In postmenopausal women (Geelong Osteoporosis Study), higher BMD at the total hip and ultradistal forearm as well as a decreased fracture risk and serum CTx levels were associated with β-blocker use (Pasco et al. 2004, 2005). Likewise, in a large cohort of elderly men (Concord Health and Aging in Men Project, CHAMP), age-related loss of BMD was found attenuated by the use of β-blockers (Bleicher et al., 2013). Analysis of the Dubbo Osteoporosis Epidemiology Study (DOES) cohort also showed that both men and women using β-blockers had higher BMD at the femoral neck and spine as well as lower fracture risk than those not treated (Yang et al., 2011) Case-control studies also showed that the use of β-blockers decreases the odds ratio for facture and was associated with a higher BMD at the spine, femoral neck, and proximal femur (Schlienger et al., 2004; Bonnet et al., 2007). Two prospective case-control studies respectively in elderly and severely burned patients showed that BMD was significantly improved in β-blocker users (Turker et al., 2006; Herndon et al., 2012). More generally, meta-analyses have identified an association between use of β-blockers (but not α-blockers) and a statistically significant protection against all fractures, with protection against hip fractures being stronger (Wiens et al., 2006; Yang et al., 2012).

A few studies also reported less conclusive evidence of a beneficial effect of β-blockers on bone mass in human patients. For instance, in US women enrolled in the Study of Osteoporotic Fractures, total hip BMD was greater among β-blocker users, but adjustment for body weight or other parameters eliminated the difference. Nevertheless, there was a protective effect of β-blockers against hip fracture (hazard ratio for hip fracture associated with β-blocker use was 0.76 [95% CI 0.58−0.99]) (Reid et al., 2005). Analysis of a large cohort of Medicare beneficiaries treated with antihypertensive agents also did not observe a protective effect of β-blockers on the incidence of bone fractures identified based on diagnosis and procedure codes, but in the absence of radiographs and BMD data (Solomon et al., 2011). The discrepancy between the results of these and the studies cited above could have many origins. One of them could relate to the absence of specificity of the β-blocker used, a parameter that is usually not taken into account. As a matter of fact, many studies have been performed on populations using β-blockers following a diagnosis of hypertension and therefore most likely to be treated with β_1-blockers, which are cardioselective. Although a lower risk of fracture was associated with usage of this class of drugs in the Korean Health Insurance Review and Assessment Service database (Song et al., 2012), their biological effect on bone cells is not clear, since studies in mice have suggested that the Adrβ1 receptor could counteract the effect of Adrβ2 on bone remodeling (Elefteriou et al., 2005; Pierroz et al., 2012). Perhaps even more critical, the length of treatment and dose of β-blockers could be other significant factors of variability within and between studies. At least in ovariectomized rats the best preventive effect against bone loss was obtained with the lowest dose of propranolol, the highest dose being ineffective, while the opposite was observed for cardiac hemodynamic functions (Bonnet et al., 2006). Given that most patients analyzed in studies using β-blockers were prescribed these drugs to treat hypertension, it is thus possible that a significant proportion of them may be taking doses inappropriate to achieve a positive effect on bone mass.

Brain serotonin and neuromedinU

Variants of human *TPH2* linked to serotonin deficiency have been reported as associated with a spectrum of neuropsychiatric disorders such as major depression or bipolar disorder, and these conditions are also associated with bone loss and/or increased risk of fractures (Misra et al., 2004; McKinney et al., 2009; Hsu et al., 2016). Although this observation is suggestive of a link between these variants and bone health, specific studies are needed to confirm this hypothesis. Another indication that brain serotonin plays a role in the control of bone mass in human stems from the bone loss observed in patients chronically using SSRIs (Wu et al., 2009; Haney et al., 2010; Rizzoli et al., 2012; Zhou et al., 2018). This same effect can be reproduced in rodents, and molecular studies have shown that it is mediated by a decrease of brain serotonin signaling leading to increased sympathetic output (Warden et al., 2005; Bonnet et al., 2007; Warden et al., 2008; Ortuno et al., 2016). Accordingly, it could be prevented by cotreatment with a β-blocker (Ortuno et al., 2016). This latter observation also awaits confirmation by clinical studies.

In contrast, the contribution of NeuromedinU to the central regulation of bone mass has already been assessed in humans. Analysis of a large population of European children (IDEFICS cohort) has associated variants of the *NMU* gene with bone strength (C variant of both rs6827359 and rs12500837 as well as homozygosity of the C variant of rs9999653) (Gianfagna et al., 2013). Interestingly, this study also reported a synergistic effect between NMU and ADRB2 variants (*NMU* rs6827359, CC variant and *ADRB2* rs1042713, GG variant), confirming the functional link observed in mouse models (Sato et al., 2007).

Melanocortin receptor 4 and cocaine- and amphetamine-regulated transcript

As mentioned above, inactivating mutations in one allele of MC4R are linked to advanced bone age, assessed by radiography of the wrist, in children and a high-bone-mass phenotype in adults (Farooqi et al., 2000). This phenotype is associated with an increase in circulating CART levels and a decrease in the resorption biomarker CTx (Ahn et al., 2006). In addition, a polymorphism in the CART gene (rs2239670, AG variant) was found associated with a higher BMD at the lumbar spine (Chun et al., 2015) in Korean postmenopausal women while a significant association between another one (rs7379701, TC and CC variants) and forearm BMD was reported in Caucasian postmenopausal women (Guerardel et al., 2006).

Neuropeptide Y, brain-derived neurotrophic factor, and cannabinoid receptor 2

A small longitudinal substudy of early postmenopausal women (Kuopio Osteoporosis Risk Factor and Prevention population) has shown that a gain-of-function polymorphism in the *NPY* gene (rs16139, variant C) associates with a better maintenance of femoral neck BMD after 5 years (Heikkinen et al., 2004, Ding et al., 2005) and analysis of a population of Afro-Caribbean men (Tobago Bone Health Study) has identified two single nucleotide polymorphisms (SNPs) in the *NPY* gene associated with higher total-hip BMD (rs16135 and rs16123, G variants) (Goodrich et al., 2009). However, the other variant of the latter polymorphism (rs16123, CC variant), along with another NPY SNP (rs17149106, GG variant), was associated with increased odds ratio for osteoporosis at the lumbar spine (although there was no significant difference in BMD) in postmenopausal Korean women (Chun et al., 2015). This discrepancy may reflect sex-based differences, a trend that was also observed in mouse models (Baldock et al., 2009). Lastly, in this same population of women, the combination of two polymorphisms in the *NPY2R* gene (TT variants of both rs2880415 and rs6857715) was also associated with a higher rate of osteoporosis at the lumber spine (Chun et al., 2015). Altogether, these results support an involvement of NPY signaling in the regulation of bone mass in human.

While the analysis of four SNPs in human *CB1* did not find a statistically significant correlation with bone health, in a small population of postmenopausal women, several *CB2* SNPs, alone or in combination, show a significant increase in the odds ratio for osteoporosis (Karsak et al., 2005). These results are consistent with an involvement of at least the *CB2* locus in human osteoporosis.

Lastly, two studies have shown a link between BDNF and bone mass. A genome-wide search for phospho-SNP associated with BMD at the hip and spine identified a BDNF variant (rs6265, V66M) in both Caucasian and Chinese populations (Deng et al., 2013). This variant, which impairs the phosphorylation of BDNF by the CHEK2 kinase at amino-acid T62, also associates with multiple mental disorders (Gratacos et al., 2007; Deng et al., 2013). In addition, an integrative analysis that combined four genome-wide association study datasets identified two *BDNF* SNPs (rs7124442, 3′UTR variant and rs11030119, intron variant) with spine BMD and osteoporotic fractures (Guo et al., 2016).

Conclusions and perspective

Since the identification of leptin's central regulation of bone remodeling in mice, the past 2 decades have seen a large number of studies revealing the complexity and potential biomedical importance of the neuronal control of bone mass. The pleiotropic nature of these pathways as well as the technical difficulty in measuring central or even peripheral neuromediator levels or activity in patients have somewhat hampered their validation in human physiology, but many elements have also emerged that confirm findings made using animal models. Whether some or most of these regulations take place in humans, they represent potential targets for designing new diagnostic and therapeutic tools that should be further explored to predict or treat bone health disorders.

References

Ahima, R.S., 2004. Body fat, leptin, and hypothalamic amenorrhea. N. Engl. J. Med. 351 (10), 959–962.

Ahima, R.S., Flier, J.S., 2000. Leptin. Annu. Rev. Physiol. 62, 413–437.

Ahn, J.D., Dubern, B., Lubrano-Berthelier, C., Clement, K., Karsenty, G., 2006. Cart overexpression is the only identifiable cause of high bone mass in melanocortin 4 receptor deficiency. Endocrinology 147 (7), 3196–3202.

Arai, M., Sato, T., Takeuchi, S., Goto, S., Togari, A., 2013. Dose effects of butoxamine, a selective beta2-adrenoceptor antagonist, on bone metabolism in spontaneously hypertensive rat. Eur. J. Pharmacol. 701 (1–3), 7–13.

Asnicar, M.A., Smith, D.P., Yang, D.D., Heiman, M.L., Fox, N., Chen, Y.F., Hsiung, H.M., Koster, A., 2001. Absence of cocaine- and amphetamine-regulated transcript results in obesity in mice fed a high caloric diet. Endocrinology 142 (10), 4394–4400.

Bajayo, A., Goshen, I., Feldman, S., Csernus, V., Iverfeldt, K., Shohami, E., Yirmiya, R., Bab, I., 2005. Central IL-1 receptor signaling regulates bone growth and mass. Proc. Natl. Acad. Sci. U. S. A. 102 (36), 12956–12961.

Baldock, P.A., Allison, S., McDonald, M.M., Sainsbury, A., Enriquez, R.F., Little, D.G., Eisman, J.A., Gardiner, E.M., Herzog, H., 2006. Hypothalamic regulation of cortical bone mass: opposing activity of Y2 receptor and leptin pathways. J. Bone Miner. Res. 21 (10), 1600–1607.

Baldock, P.A., Allison, S.J., Lundberg, P., Lee, N.J., Slack, K., Lin, E.J., Enriquez, R.F., McDonald, M.M., Zhang, L., During, M.J., Little, D.G., Eisman, J.A., Gardiner, E.M., Yulyaningsih, E., Lin, S., Sainsbury, A., Herzog, H., 2007. Novel role of Y1 receptors in the coordinated regulation of bone and energy homeostasis. J. Biol. Chem. 282 (26), 19092–19102.

Baldock, P.A., Lee, N.J., Driessler, F., Lin, S., Allison, S., Stehrer, B., Lin, E.J., Zhang, L., Enriquez, R.F., Wong, I.P., McDonald, M.M., During, M., Pierroz, D.D., Slack, K., Shi, Y.C., Yulyaningsih, E., Aljanova, A., Little, D.G., Ferrari, S.L., Sainsbury, A., Eisman, J.A., Herzog, H., 2009. Neuropeptide Y knockout mice reveal a central role of NPY in the coordination of bone mass to body weight. PLoS One 4 (12), e8415.

Baldock, P.A., Sainsbury, A., Allison, S., Lin, E.J., Couzens, M., Boey, D., Enriquez, R., During, M., Herzog, H., Gardiner, E.M., 2005. Hypothalamic control of bone formation: distinct actions of leptin and y2 receptor pathways. J. Bone Miner. Res. 20 (10), 1851–1857.

Baldock, P.A., Sainsbury, A., Couzens, M., Enriquez, R.F., Thomas, G.P., Gardiner, E.M., Herzog, H., 2002. Hypothalamic Y2 receptors regulate bone formation. J. Clin. Investig. 109 (7), 915–921.

Balthasar, N., Coppari, R., McMinn, J., Liu, S.M., Lee, C.E., Tang, V., Kenny, C.D., McGovern, R.A., Chua Jr., S.C., Elmquist, J.K., Lowell, B.B., 2004. Leptin receptor signaling in POMC neurons is required for normal body weight homeostasis. Neuron 42 (6), 983–991.

Bleicher, K., Cumming, R.G., Naganathan, V., Seibel, M.J., Blyth, F.M., Le Couteur, D.G., Handelsman, D.J., Creasey, H.M., Waite, L.M., 2013. Predictors of the rate of BMD loss in older men: findings from the CHAMP study. Osteoporos. Int. 24 (7), 1951–1963.

Bonnet, N., Benhamou, C.L., Malaval, L., Goncalves, C., Vico, L., Eder, V., Pichon, C., Courteix, D., 2008. Low dose beta-blocker prevents ovariectomy-induced bone loss in rats without affecting heart functions. J. Cell. Physiol. 217 (3), 819–827.

Bonnet, N., Bernard, P., Beaupied, H., Bizot, J.C., Trovero, F., Courteix, D., Benhamou, C.L., 2007a. Various effects of antidepressant drugs on bone microarchitecture, mechanical properties and bone remodeling. Toxicol. Appl. Pharmacol. 221 (1), 111–118.

Bonnet, N., Gadois, C., McCloskey, E., Lemineur, G., Lespessailles, E., Courteix, D., Benhamou, C.L., 2007b. Protective effect of beta blockers in postmenopausal women: influence on fractures, bone density, micro and macroarchitecture. Bone 40 (5), 1209–1216.

Bonnet, N., Laroche, N., Vico, L., Dolleans, E., Benhamou, C.L., Courteix, D., 2006. Dose effects of propranolol on cancellous and cortical bone in ovariectomized adult rats. J. Pharmacol. Exp. Ther. 318 (3), 1118–1127.

Bray, G.A., York, D.A., 1998. The MONA LISA hypothesis in the time of leptin. Recent Prog. Horm. Res. 53, 95–117.

Brighton, P.J., Szekeres, P.G., Willars, G.B., 2004. Neuromedin U and its receptors: structure, function, and physiological roles. Pharmacol. Rev. 56 (2), 231–248.

Bronstein, D.M., Schafer, M.K., Watson, S.J., Akil, H., 1992. Evidence that beta-endorphin is synthesized in cells in the nucleus tractus solitarius: detection of POMC mRNA. Brain Res. 587 (2), 269–275.

Camerino, C., Zayzafoon, M., Rymaszewski, M., Heiny, J., Rios, M., Hauschka, P.V., 2012. Central depletion of brain-derived neurotrophic factor in mice results in high bone mass and metabolic phenotype. Endocrinology 153 (11), 5394–5405.

Chenu, C., 2002. Glutamatergic regulation of bone remodeling. J. Musculoskelet. Neuronal Interact. 2 (3), 282–284.

Chenu, C., 2004. Role of innervation in the control of bone remodeling. J. Musculoskelet. Neuronal Interact. 4 (2), 132–134.

Cheung, C.C., Clifton, D.K., Steiner, R.A., 1997. Proopiomelanocortin neurons are direct targets for leptin in the hypothalamus. Endocrinology 138 (10), 4489–4492.

Chun, E.H., Kim, H., Suh, C.S., Kim, J.H., Kim, D.Y., Kim, J.G., 2015. Polymorphisms in neuropeptide genes and bone mineral density in Korean postmenopausal women. Menopause 22 (11), 1256–1263.

Cone, R.D., 1999. The central melanocortin system and energy homeostasis. Trends Endocrinol. Metabol. 10 (6), 211–216.

Cornish, J., Callon, K.E., Bava, U., Lin, C., Naot, D., Hill, B.L., Grey, A.B., Broom, N., Myers, D.E., Nicholson, G.C., Reid, I.R., 2002. Leptin directly regulates bone cell function in vitro and reduces bone fragility in vivo. J. Endocrinol. 175 (2), 405–415.

Couceyro, P.R., Koylu, E.O., Kuhar, M.J., 1997. Further studies on the anatomical distribution of CART by in situ hybridization. J. Chem. Neuroanat. 12 (4), 229–241.

Deis, S., Srivastava, R.K., Ruiz de Azua, I., Bindila, L., Baraghithy, S., Lutz, B., Bab, I., Tam, J., 2018. Age-related regulation of bone formation by the sympathetic cannabinoid CB1 receptor. Bone 108, 34–42.

Delhanty, P.J., van der Velde, M., van der Eerden, B.C., Sun, Y., Geminn, J.M., van der Lely, A.J., Smith, R.G., van Leeuwen, J.P., 2014. Genetic manipulation of the ghrelin signaling system in male mice reveals bone compartment specificity of acylated and unacylated ghrelin in the regulation of bone remodeling. Endocrinology 155 (11), 4287–4295.

Deng, F.Y., Tan, L.J., Shen, H., Liu, Y.J., Liu, Y.Z., Li, J., Zhu, X.Z., Chen, X.D., Tian, Q., Zhao, M., Deng, H.W., 2013. SNP rs6265 regulates protein phosphorylation and osteoblast differentiation and influences BMD in humans. J. Bone Miner. Res. 28 (12), 2498–2507.

Dengler-Crish, C.M., Smith, M.A., Wilson, G.N., 2016. Early evidence of low bone density and decreased serotonergic synthesis in the dorsal raphe of a tauopathy model of Alzheimer's disease. J. Alzheimer's Dis. 55 (4), 1605–1619.

Di Marzo, V., Bifulco, M., De Petrocellis, L., 2004. The endocannabinoid system and its therapeutic exploitation. Nat. Rev. Drug Discov. 3 (9), 771–784.

Dinarello, C.A., 1997. Interleukin-1. Cytokine Growth Factor Rev. 8 (4), 253–265.

Ding, B., Kull, B., Liu, Z., Mottagui-Tabar, S., Thonberg, H., Gu, H.F., Brookes, A.J., Grundemar, L., Karlsson, C., Hamsten, A., Arner, P., Ostenson, C.G., Efendic, S., Monne, M., von Heijne, G., Eriksson, P., Wahlestedt, C., 2005. Human neuropeptide Y signal peptide gain-of-function polymorphism is associated with increased body mass index: possible mode of function. Regul. Pept. 127 (1–3), 45–53.

Ding, L., Saunders, T.L., Enikolopov, G., Morrison, S.J., 2012. Endothelial and perivascular cells maintain haematopoietic stem cells. Nature 481 (7382), 457–462.

Douglass, J., McKinzie, A.A., Couceyro, P., 1995. PCR differential display identifies a rat brain mRNA that is transcriptionally regulated by cocaine and amphetamine. J. Neurosci. 15 (3 Pt 2), 2471–2481.

Ducy, P., Amling, M., Takeda, S., Priemel, M., Schilling, A.F., Beil, F.T., Shen, J., Vinson, C., Rueger, J.M., Karsenty, G., 2000. Leptin inhibits bone formation through a hypothalamic relay: a central control of bone mass. Cell 100 (2), 197–207.

Ducy, P., Karsenty, G., 2010. The two faces of serotonin in bone biology. J. Cell Biol. 191 (1), 7–13.

Elefteriou, F., Ahn, J.D., Takeda, S., Starbuck, M., Yang, X., Liu, X., Kondo, H., Richards, W.G., Bannon, T.W., Noda, M., Clement, K., Vaisse, C., Karsenty, G., 2005. Leptin regulation of bone resorption by the sympathetic nervous system and CART. Nature 434 (7032), 514–520.

Elefteriou, F., Takeda, S., Ebihara, K., Magre, J., Patano, N., Kim, C.A., Ogawa, Y., Liu, X., Ware, S.M., Craigen, W.J., Robert, J.J., Vinson, C., Nakao, K., Capeau, J., Karsenty, G., 2004. Serum leptin level is a regulator of bone mass. Proc. Natl. Acad. Sci. U. S. A. 101 (9), 3258–3263.

Elias, C.F., Lee, C., Kelly, J., Aschkenasi, C., Ahima, R.S., Couceyro, P.R., Kuhar, M.J., Saper, C.B., Elmquist, J.K., 1998. Leptin activates hypothalamic CART neurons projecting to the spinal cord. Neuron 21 (6), 1375–1385.

Farooqi, I.S., Yeo, G.S., Keogh, J.M., Aminian, S., Jebb, S.A., Butler, G., Cheetham, T., O'Rahilly, S., 2000. Dominant and recessive inheritance of morbid obesity associated with melanocortin 4 receptor deficiency. J. Clin. Investig. 106 (2), 271–279.

Farr, J.N., Charkoudian, N., Barnes, J.N., Monroe, D.G., McCready, L.K., Atkinson, E.J., Amin, S., Melton 3rd, L.J., Joyner, M.J., Khosla, S., 2012. Relationship of sympathetic activity to bone microstructure, turnover, and plasma osteopontin levels in women. J. Clin. Endocrinol. Metab. 97 (11), 4219–4227.

Fu, L., Patel, M.S., Bradley, A., Wagner, E.F., Karsenty, G., 2005. The molecular clock mediates leptin-regulated bone formation. Cell 122 (5), 803–815.

Gianfagna, F., Cugino, D., Ahrens, W., Bailey, M.E.S., Bammann, K., Herrmann, D., Koni, A.C., Kourides, Y., Marild, S., Molnár, D., Moreno, L.A., Pitsiladis, Y.P., Russo, P., Siani, A., Sieri, S., Sioen, I., Veidebaum, T., Iacoviello, L., I. c. on behalf of the, 2013. Understanding the links among neuromedin U gene, beta2-adrenoceptor gene and bone health: an observational study in European children. PLoS One 8 (8), e70632.

Glavas, M.M., Grayson, B.E., Allen, S.E., Copp, D.R., Smith, M.S., Cowley, M.A., Grove, K.L., 2008. Characterization of brainstem peptide YY (PYY) neurons. J. Comp. Neurol. 506 (2), 194–210.

Goodrich, L.J., Yerges-Armstrong, L.M., Miljkovic, I., Nestlerode, C.S., Kuipers, A.L., Bunker, C.H., Patrick, A.L., Wheeler, V.W., Zmuda, J.M., 2009. Molecular variation in neuropeptide Y and bone mineral density among men of African Ancestry. Calcif. Tissue Int. 85 (6), 507.

Goulding, A., Taylor, R.W., 1998. Plasma leptin values in relation to bone mass and density and to dynamic biochemical markers of bone resorption and formation in postmenopausal women. Calcif. Tissue Int. 63 (6), 456–458.

Gratacos, M., Gonzalez, J.R., Mercader, J.M., de Cid, R., Urretavizcaya, M., Estivill, X., 2007. Brain-derived neurotrophic factor Val66Met and psychiatric disorders: meta-analysis of case-control studies confirm association to substance-related disorders, eating disorders, and schizophrenia. Biol. Psychiatry 61 (7), 911–922.

Guerardel, A., Tanko, L.B., Boutin, P., Christiansen, C., Froguel, P., 2006. Obesity susceptibility CART gene polymorphism contributes to bone remodeling in postmenopausal women. Osteoporos. Int. 17 (1), 156–157.

Guo, Y., Dong, S.S., Chen, X.F., Jing, Y.A., Yang, M., Yan, H., Shen, H., Chen, X.D., Tan, L.J., Tian, Q., Deng, H.W., Yang, T.L., 2016. Integrating Epigenomic elements and GWASs identifies BDNF gene affecting bone mineral density and osteoporotic fracture risk. Sci. Rep. 6, 30558.

Haney, E.M., Warden, S.J., Bliziotes, M.M., 2010. Effects of selective serotonin reuptake inhibitors on bone health in adults: time for recommendations about screening, prevention and management? Bone 46 (1), 13–17.

Hazelwood, R.L., 1993. The pancreatic polypeptide (PP-fold) family: gastrointestinal, vascular, and feeding behavioral implications. Proc. Soc. Exp. Biol. Med. 202 (1), 44–63.

Heikkinen, A.-M., Niskanen, L.K., Salmi, J.A., Koulu, M., Pesonen, U., Uusitupa, M.I.J., Komulainen, M.H., Tuppurainen, M.T., Kröger, H., Jurvelin, J., Saarikoski, S., 2004. Leucine7 to proline7 polymorphism in prepro-NPY gene and femoral neck bone mineral density in postmenopausal women. Bone 35 (3), 589–594.

Herndon, D.N., Rodriguez, N.A., Diaz, E.C., Hegde, S., Jennings, K., Mlcak, R.P., Suri, J.S., Lee, J.O., Williams, F.N., Meyer, W., Suman, O.E., Barrow, R.E., Jeschke, M.G., Finnerty, C.C., 2012. Long-term propranolol use in severely burned pediatric patients: a randomized controlled study. Ann. Surg. 256 (3), 402–411.

Hokfelt, T., Broberger, C., Zhang, X., Diez, M., Kopp, J., Xu, Z., Landry, M., Bao, L., Schalling, M., Koistinaho, J., DeArmond, S.J., Prusiner, S., Gong, J., Walsh, J.H., 1998. Neuropeptide Y: some viewpoints on a multifaceted peptide in the normal and diseased nervous system. Brain Res. Brain Res. Rev. 26 (2–3), 154–166.

Hsu, C.C., Hsu, Y.C., Chang, K.H., Lee, C.Y., Chong, L.W., Wang, Y.C., Hsu, C.Y., Kao, C.H., 2016. Increased risk of fracture in patients with bipolar disorder: a nationwide cohort study. Soc. Psychiatr. Psychiatr. Epidemiol. 51 (9), 1331–1338.

Idris, A.I., van 't Hof, R.J., Greig, I.R., Ridge, S.A., Baker, D., Ross, R.A., Ralston, S.H., 2005. Regulation of bone mass, bone loss and osteoclast activity by cannabinoid receptors. Nat. Med. 11 (7), 774–779.

Jiang, S.D., Jiang, L.S., Dai, L.Y., 2006. Mechanisms of osteoporosis in spinal cord injury. Clin. Endocrinol. 65 (5), 555–565.

Kadowaki, T., Yamauchi, T., 2005. Adiponectin and adiponectin receptors. Endocr. Rev. 26 (3), 439–451.

Kajimura, D., Hinoi, E., Ferron, M., Kode, A., Riley, K.J., Zhou, B., Guo, X.E., Karsenty, G., 2011. Genetic determination of the cellular basis of the sympathetic regulation of bone mass accrual. J. Exp. Med. 208 (4), 841–851.

Kajimura, D., Lee, H.W., Riley, K.J., Arteaga-Solis, E., Ferron, M., Zhou, B., Clarke, C.J., Hannun, Y.A., DePinho, R.A., Guo, E.X., Mann, J.J., Karsenty, G., 2013. Adiponectin regulates bone mass via opposite central and peripheral mechanisms through FoxO1. Cell Metabol. 17 (6), 901–915.

Karsak, M., Cohen-Solal, M., Freudenberg, J., Ostertag, A., Morieux, C., Kornak, U., Essig, J., Erxlebe, E., Bab, I., Kubisch, C., de Vernejoul, M.C., Zimmer, A., 2005. Cannabinoid receptor type 2 gene is associated with human osteoporosis. Hum. Mol. Genet. 14 (22), 3389–3396.

Khajuria, D.K., Razdan, R., Mahapatra, D.R., Bhat, M.R., 2013. Osteoprotective effect of propranolol in ovariectomized rats: a comparison with zoledronic acid and alfacalcidol. J. Orthop. Sci. 18 (5), 832–842.

Khor, E.C., Yulyaningsih, E., Driessler, F., Kovacic, N., Wee, N.K.Y., Kulkarni, R.N., Lee, N.J., Enriquez, R.F., Xu, J., Zhang, L., Herzog, H., Baldock, P.A., 2016. The y6 receptor suppresses bone resorption and stimulates bone formation in mice via a suprachiasmatic nucleus relay. Bone 84, 139–147.

Kinjo, M., Setoguchi, S., Schneeweiss, S., Solomon, D.H., 2005. Bone mineral density in subjects using central nervous system-active medications. Am. J. Med. 118 (12), 1414.

Kishi, T., Aschkenasi, C.J., Lee, C.E., Mountjoy, K.G., Saper, C.B., Elmquist, J.K., 2003. Expression of melanocortin 4 receptor mRNA in the central nervous system of the rat. J. Comp. Neurol. 457 (3), 213–235.

Könner, A.C., Brüning, J.C., 2012. Selective insulin and leptin resistance in metabolic disorders. Cell Metabol. 16 (2), 144–152.

Kristensen, P., Judge, M.E., Thim, L., Ribel, U., Christjansen, K.N., Wulff, B.S., Clausen, J.T., Jensen, P.B., Madsen, O.D., Vrang, N., Larsen, P.J., Hastrup, S., 1998. Hypothalamic CART is a new anorectic peptide regulated by leptin. Nature 393 (6680), 72–76.

Kuriyama, N., Inaba, M., Ozaki, E., Yoneda, Y., Matsui, D., Hashiguchi, K., Koyama, T., Iwai, K., Watanabe, I., Tanaka, R., Omichi, C., Mizuno, S., Kurokawa, M., Horii, M., Niwa, F., Iwasa, K., Yamada, S., Watanabe, Y., 2017. Association between loss of bone mass due to short sleep and leptin-sympathetic nervous system activity. Arch. Gerontol. Geriatr. 70, 201–208.

Kurvers, H.A., 1998. Reflex sympathetic dystrophy: facts and hypotheses. Vasc. Med. 3 (3), 207–214.

Larhammar, D., 1996. Structural diversity of receptors for neuropeptide Y, peptide YY and pancreatic polypeptide. Regul. Pept. 65 (3), 165–174.

Lee, H.J., Kim, H., Ku, S.Y., Choi, Y.M., Kim, J.H., Kim, J.G., 2014. Association between polymorphisms in leptin, leptin receptor, and beta-adrenergic receptor genes and bone mineral density in postmenopausal Korean women. Menopause 21 (1), 67–73.

Lin, S., Boey, D., Herzog, H., 2004. NPY and Y receptors: lessons from transgenic and knockout models. Neuropeptides 38 (4), 189–200.

Lorentzon, M., Landin, K., Mellstrom, D., Ohlsson, C., 2006. Leptin is a negative independent predictor of areal BMD and cortical bone size in young adult Swedish men. J. Bone Miner. Res. 21 (12), 1871–1878.

Lorenzo, J.A., Naprta, A., Rao, Y., Alander, C., Glaccum, M., Widmer, M., Gronowicz, G., Kalinowski, J., Pilbeam, C.C., 1998. Mice lacking the type I interleukin-1 receptor do not lose bone mass after ovariectomy. Endocrinology 139 (6), 3022–3025.

Lorenzo, J.A., Sousa, S.L., Van den Brink-Webb, S.E., Korn, J.H., 1990. Production of both interleukin-1 alpha and beta by newborn mouse calvarial cultures. J. Bone Miner. Res. 5 (1), 77–83.

Ma, C., Fukuda, T., Ochi, H., Sunamura, S., Xu, C., Xu, R., Okawa, A., Takeda, S., 2015. Genetic determination of the cellular basis of the ghrelin-dependent bone remodeling. Mol. Metabol. 4 (3), 175–185.

Maeda, N., Shimomura, I., Kishida, K., Nishizawa, H., Matsuda, M., Nagaretani, H., Furuyama, N., Kondo, H., Takahashi, M., Arita, Y., Komuro, R., Ouchi, N., Kihara, S., Tochino, Y., Okutomi, K., Horie, M., Takeda, S., Aoyama, T., Funahashi, T., Matsuzawa, Y., 2002. Diet-induced insulin resistance in mice lacking adiponectin/ACRP30. Nat. Med. 8 (7), 731–737.

Mark, A.L., 2013. Selective leptin resistance revisited. Am. J. Physiol. Regul. Integr. Comp. Physiol. 305 (6), R566–R581.

Martini, G., Valenti, R., Giovani, S., Franci, B., Campagna, S., Nuti, R., 2001. Influence of insulin-like growth factor-1 and leptin on bone mass in healthy postmenopausal women. Bone 28 (1), 113–117.

Matic, I., Matthews, B.G., Kizivat, T., Igwe, J.C., Marijanovic, I., Ruohonen, S.T., Savontaus, E., Adams, D.J., Kalajzic, I., 2012. Bone-specific overexpression of NPY modulates osteogenesis. J. Musculoskelet. Neuronal Interact. 12 (4), 209–218.

McKinney, J.A., Turel, B., Winge, I., Knappskog, P.M., Haavik, J., 2009. Functional properties of missense variants of human tryptophan hydroxylase 2. Hum. Mutat. 30 (5), 787–794.

Misra, M., Papakostas, G.I., Klibanski, A., 2004. Effects of psychiatric disorders and psychotropic medications on prolactin and bone metabolism. J. Clin. Psychiatry 65 (12), 1607–1618 quiz 1590, 1760–1601.

Morberg, C.M., Tetens, I., Black, E., Toubro, S., Soerensen, T.I., Pedersen, O., Astrup, A., 2003. Leptin and bone mineral density: a cross-sectional study in obese and nonobese men. J. Clin. Endocrinol. Metab. 88 (12), 5795–5800.

Motyl, K.J., Rosen, C.J., 2012. Understanding leptin-dependent regulation of skeletal homeostasis. Biochimie 94 (10), 2089–2096.

Mountjoy, K.G., Mortrud, M.T., Low, M.J., Simerly, R.B., Cone, R.D., 1994. Localization of the melanocortin-4 receptor (MC4-R) in neuroendocrine and autonomic control circuits in the brain. Mol. Endocrinol. 8 (10), 1298–1308.

Ofek, O., Karsak, M., Leclerc, N., Fogel, M., Frenkel, B., Wright, K., Tam, J., Attar-Namdar, M., Kram, V., Shohami, E., Mechoulam, R., Zimmer, A., Bab, I., 2006. Peripheral cannabinoid receptor, CB2, regulates bone mass. Proc. Natl. Acad. Sci. U. S. A. 103 (3), 696–701.

Ortuno, M.J., Robinson, S.T., Subramanyam, P., Paone, R., Huang, Y.Y., Guo, X.E., Colecraft, H.M., Mann, J.J., Ducy, P., 2016. Serotonin-reuptake inhibitors act centrally to cause bone loss in mice by counteracting a local anti-resorptive effect. Nat. Med. 22 (10), 1170–1179.

Oshima, K., Nampei, A., Matsuda, M., Iwaki, M., Fukuhara, A., Hashimoto, J., Yoshikawa, H., Shimomura, I., 2005. Adiponectin increases bone mass by suppressing osteoclast and activating osteoblast. Biochem. Biophys. Res. Commun. 331 (2), 520–526.

Oury, F., Karsenty, G., 2011. Towards a serotonin-dependent leptin roadmap in the brain. Trends Endocrinol. Metabol. 22 (9), 382–387.

Oury, F., Yadav, V.K., Wang, Y., Zhou, B., Liu, X.S., Guo, X.E., Tecott, L.H., Schutz, G., Means, A.R., Karsenty, G., 2010. CREB mediates brain serotonin regulation of bone mass through its expression in ventromedial hypothalamic neurons. Genes Dev. 24 (20), 2330–2342.

Palkovits, M., Mezey, E., Eskay, R.L., 1987. Pro-opiomelanocortin-derived peptides (ACTH/beta-endorphin/alpha-MSH) in brainstem baroreceptor areas of the rat. Brain Res. 436 (2), 323–338.

Papadopoulou, F., Krassas, G.E., Kalothetou, C., Koliakos, G., Constantinidis, T.C., 2004. Serum leptin values in relation to bone density and growth hormone-insulin like growth factors axis in healthy men. Arch. Androl. 50 (2), 97–103.

Pasco, J.A., Henry, M.J., Nicholson, G.C., Schneider, H.G., Kotowicz, M.A., 2005. Beta-blockers reduce bone resorption marker in early postmenopausal women. Ann. Hum. Biol. 32 (6), 738–745.

Pasco, J.A., Henry, M.J., Sanders, K.M., Kotowicz, M.A., Seeman, E., Nicholson, G.C., 2004. Beta-adrenergic blockers reduce the risk of fracture partly by increasing bone mineral density: geelong osteoporosis study. J. Bone Miner. Res. 19 (1), 19–24.

Peyron, C., Tighe, D.K., van den Pol, A.N., de Lecea, L., Heller, H.C., Sutcliffe, J.G., Kilduff, T.S., 1998. Neurons containing hypocretin (orexin) project to multiple neuronal systems. J. Neurosci. 18 (23), 9996–10015.

Pierroz, D.D., Bonnet, N., Bianchi, E.N., Bouxsein, M.L., Baldock, P.A., Rizzoli, R., Ferrari, S.L., 2012. Deletion of β-adrenergic receptor 1, 2, or both leads to different bone phenotypes and response to mechanical stimulation. J. Bone Miner. Res. 27 (6), 1252–1262.

Reid, I.R., Gamble, G.D., Grey, A.B., Black, D.M., Ensrud, K.E., Browner, W.S., Bauer, D.C., 2005. Beta-blocker use, BMD, and fractures in the study of osteoporotic fractures. J. Bone Miner. Res. 20 (4), 613–618.

Rizzoli, R., Cooper, C., Reginster, J.Y., Abrahamsen, B., Adachi, J.D., Brandi, M.L., Bruyère, O., Compston, J., Ducy, P., Ferrari, S., Harvey, N.C., Kanis, J.A., Karsenty, G., Laslop, A., Rabenda, V., Vestergaard, P., 2012. Antidepressant medications and osteoporosis. Bone 51 (3), 606–613.

Ruhl, C.E., Everhart, J.E., 2002. Relationship of serum leptin concentration with bone mineral density in the United States population. J. Bone Miner. Res. 17 (10), 1896–1903.

Sabatini, M., Boyce, B., Aufdemorte, T., Bonewald, L., Mundy, G.R., 1988. Infusions of recombinant human interleukins 1 alpha and 1 beta cause hypercalcemia in normal mice. Proc. Natl. Acad. Sci. U. S. A. 85 (14), 5235–5239.

Sato, M., Takeda, N., Sarui, H., Takami, R., Takami, K., Hayashi, M., Sasaki, A., Kawachi, S., Yoshino, K., Yasuda, K., 2001. Association between serum leptin concentrations and bone mineral density, and biochemical markers of bone turnover in adult men. J. Clin. Endocrinol. Metab. 86 (11), 5273–5276.

Sato, S., Hanada, R., Kimura, A., Abe, T., Matsumoto, T., Iwasaki, M., Inose, H., Ida, T., Mieda, M., Takeuchi, Y., Fukumoto, S., Fujita, T., Kato, S., Kangawa, K., Kojima, M., Shinomiya, K.I., Takeda, S., 2007. Central control of bone remodeling by neuromedin U. Nat. Med. 10, 1234–1240.

Schlienger, R.G., Kraenzlin, M.E., Jick, S.S., Meier, C.R., 2004. Use of beta-blockers and risk of fractures. JAMA 292 (11), 1326–1332.

Shi, Y., Oury, F., Yadav, V.K., Wess, J., Liu, X.S., Guo, X.E., Murshed, M., Karsenty, G., 2010. Signaling through the M(3) muscarinic receptor favors bone mass accrual by decreasing sympathetic activity. Cell Metabol. 11 (3), 231–238.

Shi, Y., Yadav, V.K., Suda, N., Liu, X.S., Guo, X.E., Myers Jr., M.G., Karsenty, G., 2008. Dissociation of the neuronal regulation of bone mass and energy metabolism by leptin in vivo. Proc. Natl. Acad. Sci. U. S. A 105 (51), 20529–20533.

Shi, Y.C., Lin, S., Wong, I.P., Baldock, P.A., Aljanova, A., Enriquez, R.F., Castillo, L., Mitchell, N.F., Ye, J.M., Zhang, L., Macia, L., Yulyaningsih, E., Nguyen, A.D., Riepler, S.J., Herzog, H., Sainsbury, A., 2010. NPY neuron-specific Y2 receptors regulate adipose tissue and trabecular bone but not cortical bone homeostasis in mice. PLoS One 5 (6), e11361.

Singh, M.K., Elefteriou, F., Karsenty, G., 2008. Cocaine and amphetamine-regulated transcript may regulate bone remodeling as a circulating molecule. Endocrinology 149 (8), 3933–3941.

Solomon, D.H., Mogun, H., Garneau, K., Fischer, M.A., 2011. Risk of fractures in older adults using antihypertensive medications. J. Bone Miner. Res. 26 (7), 1561–1567.

Solomon, G., Atkins, A., Shahar, R., Gertler, A., Monsonego-Ornan, E., 2014. Effect of peripherally administered leptin antagonist on whole body metabolism and bone microarchitecture and biomechanical properties in the mouse. Am. J. Physiol. Endocrinol. Metab. 306 (1), E14–E27.

Song, H.J., Lee, J., Kim, Y.-J., Jung, S.-Y., Kim, H.J., Choi, N.-K., Park, B.-J., 2012. β1 selectivity of β-blockers and reduced risk of fractures in elderly hypertension patients. Bone 51 (6), 1008–1015.

Spencer, G.J., McGrath, C.J., Genever, P.G., 2007. Current perspectives on NMDA-type glutamate signalling in bone. Int. J. Biochem. Cell Biol. 39 (6), 1089–1104.

Steppan, C.M., Crawford, D.T., Chidsey-Frink, K.L., Ke, H., Swick, A.G., 2000. Leptin is a potent stimulator of bone growth in ob/ob mice. Regul. Pept. 92 (1–3), 73–78.

Takeda, S., Elefteriou, F., Levasseur, R., Liu, X., Zhao, L., Parker, K.L., Armstrong, D., Ducy, P., Karsenty, G., 2002. Leptin regulates bone formation via the sympathetic nervous system. Cell 111 (3), 305–317.

Tam, J., Ofek, O., Fride, E., Ledent, C., Gabet, Y., Muller, R., Zimmer, A., Mackie, K., Mechoulam, R., Shohami, E., Bab, I., 2006. Involvement of neuronal cannabinoid receptor CB1 in regulation of bone mass and bone remodeling. Mol. Pharmacol. 70 (3), 786–792.

Tartaglia, L.A., Dembski, M., Weng, X., Deng, N., Culpepper, J., Devos, R., Richards, G.J., Campfield, L.A., Clark, F.T., Deeds, J., et al., 1995. Identification and expression cloning of a leptin receptor, OB-R. Cell 83 (7), 1263–1271.

Thomas, T., Burguera, B., Melton 3rd, L.J., Atkinson, E.J., O'Fallon, W.M., Riggs, B.L., Khosla, S., 2001. Role of serum leptin, insulin, and estrogen levels as potential mediators of the relationship between fat mass and bone mineral density in men versus women. Bone 29 (2), 114–120.

Turker, S., Karatosun, V., Gunal, I., 2006. Beta-blockers increase bone mineral density. Clin. Orthop. Relat. Res. 443, 73–74.

Turner, R.T., Kalra, S.P., Wong, C.P., Philbrick, K.A., Lindenmaier, L.B., Boghossian, S., Iwaniec, U.T., 2013. Peripheral leptin regulates bone formation. J. Bone Miner. Res. 28 (1), 22–34.

Vaira, S., Yang, C., McCoy, A., Keys, K., Xue, S., Weinstein, E.J., Novack, D.V., Cui, X., 2012. Creation and preliminary characterization of a leptin knockout rat. Endocrinology 153 (11), 5622–5628.

Veldhuis-Vlug, A.G., El Mahdiui, M., Endert, E., Heijboer, A.C., Fliers, E., Bisschop, P.H., 2012. Bone resorption is increased in pheochromocytoma patients and normalizes following adrenalectomy. J. Clin. Endocrinol. Metab. 97 (11), E2093–E2097.

Veldhuis-Vlug, A.G., Oei, L., Souverein, P.C., Tanck, M.W.T., Rivadeneira, F., Zillikens, M.C., Kamphuisen, P.W., Maitland-van der Zee, A.H., de Groot, M.C.H., Hofman, A., Uitterlinden, A.G., Fliers, E., de Boer, A., Bisschop, P.H., 2015. Association of polymorphisms in the beta-2 adrenergic receptor gene with fracture risk and bone mineral density. Osteoporos. Int. 26 (7), 2019−2027.

Warden, S.J., Nelson, I.R., Fuchs, R.K., Bliziotes, M.M., Turner, C.H., 2008. Serotonin (5-hydroxytryptamine) transporter inhibition causes bone loss in adult mice independently of estrogen deficiency. Menopause 15 (6), 1176−1183.

Warden, S.J., Robling, A.G., Sanders, M.S., Bliziotes, M.M., Turner, C.H., 2005. Inhibition of the serotonin (5-hydroxytryptamine) transporter reduces bone accrual during growth. Endocrinology 146 (2), 685−693.

Wei, W., Motoike, T., Krzeszinski, J.Y., Jin, Z., Xie, X.J., Dechow, P.C., Yanagisawa, M., Wan, Y., 2014. Orexin regulates bone remodeling via a dominant positive central action and a subordinate negative peripheral action. Cell Metabol. 19 (6), 927−940.

Westvik, J., 1996. Radiological features in generalized lipodystrophy. Acta Paediatr. Suppl. 13, 44−51.

Wiens, M., Etminan, M., Gill, S.S., Takkouche, B., 2006. Effects of antihypertensive drug treatments on fracture outcomes: a meta-analysis of observational studies. J. Intern. Med. 260 (4), 350−362.

Wierup, N., Kuhar, M., Nilsson, B.O., Mulder, H., Ekblad, E., Sundler, F., 2004. Cocaine- and amphetamine-regulated transcript (CART) is expressed in several islet cell types during rat development. J. Histochem. Cytochem. 52 (2), 169−177.

Wong, I.P.L., Driessler, F., Khor, E.C., Shi, Y.-C., Hörmer, B., Nguyen, A.D., Enriquez, R.F., Eisman, J.A., Sainsbury, A., Herzog, H., Baldock, P.A., 2012. Peptide YY regulates bone remodeling in mice: a link between gut and skeletal biology. PLoS One 7 (7), e40038.

Wortley, K.E., Garcia, K., Okamoto, H., Thabet, K., Anderson, K.D., Shen, V., Herman, J.P., Valenzuela, D., Yancopoulos, G.D., Tschöp, M.H., Murphy, A., Sleeman, M.W., 2007. Peptide YY regulates bone turnover in rodents. Gastroenterology 133 (5), 1534−1543.

Wu, J.Y., Scadden, D.T., Kronenberg, H.M., 2009. Role of the osteoblast lineage in the bone marrow hematopoietic niches. J. Bone Miner. Res. 24 (5), 759−764.

Wu, Q., Magnus, J.H., Liu, J., Bencaz, A.F., Hentz, J.G., 2009. Depression and low bone mineral density: a meta-analysis of epidemiologic studies. Osteoporos. Int. 20 (8), 1309−1320.

Wu, Y., Tu, Q., Valverde, P., Zhang, J., Murray, D., Dong, L.Q., Cheng, J., Jiang, H., Rios, M., Morgan, E., Tang, Z., Chen, J., 2014. Central adiponectin administration reveals new regulatory mechanisms of bone metabolism in mice. Am. J. Physiol. Endocrinol. Metabol. 306 (12), E1418−E1430.

Yadav, V.K., Oury, F., Suda, N., Liu, Z.W., Gao, X.B., Confavreux, C., Klemenhagen, K.C., Tanaka, K.F., Gingrich, J.A., Guo, X.E., Tecott, L.H., Mann, J.J., Hen, R., Horvath, T.L., Karsenty, G., 2009. A serotonin-dependent mechanism explains the leptin regulation of bone mass, appetite, and energy expenditure. Cell 138 (5), 976−989.

Yang, S., Nguyen, N.D., Center, J.R., Eisman, J.A., Nguyen, T.V., 2011. Association between beta-blocker use and fracture risk: the Dubbo osteoporosis Epidemiology study. Bone 48 (3), 451−455.

Yang, S., Nguyen, N.D., Eisman, J.A., Nguyen, T.V., 2012. Association between beta-blockers and fracture risk: a Bayesian meta-analysis. Bone 51 (5), 969−974.

Yang, X., Matsuda, K., Bialek, P., Jacquot, S., Masuoka, H.C., Schinke, T., Li, L., Brancorsini, S., Sassone-Corsi, P., Townes, T.M., Hanauer, A., Karsenty, G., 2004. ATF4 is a substrate of RSK2 and an essential regulator of osteoblast biology; implication for Coffin-Lowry Syndrome. Cell 117 (3), 387−398.

Ye, X.L., Lu, C.F., 2013. Association of polymorphisms in the leptin and leptin receptor genes with inflammatory mediators in patients with osteoporosis. Endocrine 44 (2), 481−488.

Zhang, Y., Proenca, R., Maffei, M., Barone, M., Leopold, L., Friedman, J.M., 1994. Positional cloning of the mouse obese gene and its human homologue. Nature 372, 425−432.

Zhou, C., Fang, L., Chen, Y., Zhong, J., Wang, H., Xie, P., 2018. Effect of selective serotonin reuptake inhibitors on bone mineral density: a systematic review and meta-analysis. Osteoporos. Int. 29 (6), 1243−1251.

Chapter 35

Estrogens and progestins

David G. Monroe and Sundeep Khosla

Department of Medicine, Division of Endocrinology, Mayo Clinic College of Medicine, Rochester, MN, United States; The Robert and Arlene Kogod Center on Aging, Rochester, MN, United States

Chapter outline

Estrogens and estrogen receptors

Osteoporosis, characterized by loss of bone mass and microarchitecture, is an enormous and growing public health concern worldwide. Indeed, one in three women and one in five men will suffer an osteoporotic fracture in their lifetime (Melton 3rd et al., 1998; Kanis et al., 2000). Moreover, this burden in women exceeds the incidence of breast cancer, stroke, and myocardial infarction combined in a given year (Cauley et al., 2008). Although aging is the greatest risk factor for osteoporotic bone loss, estrogen deficiency in women and men is an important determinant for bone loss later in life (Riggs et al., 2002). Interestingly, although menopause is the major life event leading to the reduction in gonadal function in women, increasing evidence demonstrates that gradually declining levels of biologically available estrogens in men also lead to age-related bone loss (Khosla et al., 2008). Therefore, the understanding of how estrogens modulate bone physiology is critical not only from a scientific perspective, but also from a clinical perspective due to the widespread prevalence of osteoporosis.

The general importance of estrogen in the regulation of bone physiology was first recognized by the studies of Fuller Albright in the 1940s, who demonstrated that estrogen deficiency, through either ovariectomy (OVX) or following menopause, caused bone loss that could be effectively reversed through the administration of estradiol (Albright, 1940). Following this seminal discovery, investigators hypothesized that a protein, or receptor, must exist which can bind estrogens and mediate their effects on cellular and/or tissue physiology. The first evidence for an "estrogen receptor" (ER) came from experiments conducted by Gorski and Jensen in the 1960s, where they showed that rat uterus protein extract homogenate bound labeled-17β-estradiol (Gorski et al., 1968; Jensen et al., 1968; Shyamala and Gorski, 1969).

The molecular evidence for a direct effect of estrogens on bone did not occur for another 20 years, when a number of investigators demonstrated that bone was indeed an estrogen-responsive tissue (Chow et al., 1992; Ernst et al., 1989; Spelsberg et al., 1999; Tobias and Chambers, 1991; Tobias et al., 1991; Turner et al., 1993). Two distinct ERs are now recognized as mediating the effects of estrogen. ERα (*ESR1*) was cloned in the 1980s (Greene et al., 1986; Walter et al., 1985), and ERβ (*ESR2*) was cloned about a decade later (Kraus et al., 1995; Mosselman et al., 1996; Onoe et al., 1997). Both receptors share a structural homology with each other as well as with all members of the nuclear hormone superfamily of receptors (Mangelsdorf et al., 1995): (1) a central DNA binding (DBD) and hinge domain exists that mediates the interaction with specific DNA sequence elements and dimerization, (2) a C-terminal ligand binding domain (LBD), which also contains a transcriptional activation function (AF2) that allows specific ligands to bind causing a conformational change in the 12 α-helices necessary for activation of the ERs, and (3) a variable N-terminal domain with a secondary activation function (AF1). The simplified domain structure of human ERα and ERβ, with percent homologies, is shown in

Principles of Bone Biology. https://doi.org/10.1016/B978-0-12-814841-9.00035-X

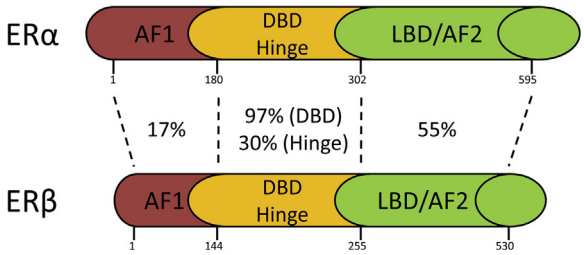

FIGURE 35.1 Structure and amino acid identity between human ERα and ERβ.

Fig. 35.1. ERα is expressed in cells of the osteoblastic (Eriksen et al., 1988; Ikegami et al., 1993) and osteoclastic (Oursler et al., 1991, 1994) lineages. ERβ is also often also coexpressed in these same lineages (Braidman et al., 2001; Vidal et al., 1999; Windahl et al., 2000; Arts et al., 1997; Monroe et al., 2003a).

Since estrogens are steroid molecules and largely hydrophobic, they can easily diffuse into cells from the circulation, where they encounter and bind to the ERs. This complex can directly regulate the transcription of genes under the control of estrogen response elements, called primary response genes, which typically occurs within 30–60 min of estrogen binding. These proteins then can modulate the transcription of further downstream genes (24–48 h later), in a process termed the "cascade model" of steroid hormone action (Landers and Spelsberg, 1992). ERs typically function as dimers, with both homodimers and heterodimers observed in osteoblastic cells. Although ERα and ERβ can regulate some of the same genes, their patterns of expression have been shown to be largely unique in bone cells (Monroe et al., 2003a, 2005). There is also considerable evidence that nongenomic ER pathways exist that are mediated by membrane-bound ERs and activate kinase cascades to elicit very rapid (within minutes) cellular effects (Razandi et al., 1999). These functions have been extensively reviewed (Levin, 2002; Saczko et al., 2017; Kelly and Levin, 2001) and thus will not be discussed in further detail here.

Estrogen receptor mouse models

As described above, the effects of estrogen on bone physiology are largely mediated through two related yet distinct soluble proteins belonging to the nuclear receptor superfamily of transcription factors, termed ERα and ERβ (Mangelsdorf et al., 1995; Monroe et al., 2003b; Almeida et al., 2017). Although more information exists on the role of ERα in bone physiology compared with ERβ, our understanding of the full effects of ERα on bone during growth and aging is far from complete. The first studies conducted on understanding the role of ERα in bone physiology were performed by Sims and colleagues, who examined mice harboring a global deletion (e.g., in all tissues) of ERα (Sims et al., 2002). They found in both males and females that global ERα deletion triggered a complex phenotype, including a decrease in bone turnover, decreased cortical thickness, and an increase in trabecular bone mass. However, the effects were confounded by high circulating estrogen levels in female mice and high testosterone levels in both sexes. Because ER expression has been shown to exhibit a compartment-specific expression pattern (with ERα expression in both cortical and trabecular sites, whereas ERβ expression is only evident in trabecular sites) (Onoe et al., 1997; Bord et al., 2001), these data suggest that high estrogen levels activate ERβ in trabecular bone, leading to a compensatory response at trabecular sites. On the contrary, global deletion of ERβ did not affect circulated steroid levels in either males or females and largely had no effect on bone in males. In females, trabecular bone, periosteal, and endosteal circumference were increased (Windahl et al., 1999, 2000; Sims et al., 2002). Even with the confounding steroid levels in the ERα global knockout mouse models, these studies demonstrated that loss of ERα decreased cortical thickness, that ERβ could compensate for loss of ERα in trabecular bone, and in the setting of intact ERα signaling, ERβ seemed to antagonize ERα action in bone.

Although the data garnered from these global ER knockout mouse models provided some insights into ER function in bone physiology, it was necessary to characterize the functions of these receptors in the various cell types responsible for bone remodeling (i.e., osteoblasts, osteoclasts, osteocytes). Therefore, more conclusive data on the functions of ERs in bone came from utilizing the Cre/LoxP system to achieve cell-specific deletion of ERs. In these systems, a crucial exon in either ERα or ERβ is flanked by loxP recombination sites and crossed into a "driver" mouse model whereby a tissue-specific promoter drives expression of Cre recombinase, thereby triggering a recombination event in which the gene is effectively knocked out in a cell-specific manner. Recently, this system has been used to demonstrate that an important target cell for ERα action is the osteoclast. ERα deletion in the early myeloid lineage using the LysM-Cre model (Martin-Millan et al., 2010) and in the more differentiated osteoclast lineage cells using the Ctsk-Cre model

(Nakamura et al., 2007) led to reduced trabecular bone mass due to increased osteoclast number and bone resorption in female mice. These data suggest that ERα is crucial for the control of osteoclast number and resorption in female mice.

The Cre/LoxP system has also been utilized to examine the role of ERα and ERβ in osteoblasts, using osteoblast lineage-specific Cre mouse drivers. Using Cre drivers that are active in early mesenchymal progenitor cells (Prx1-Cre) (Logan et al., 2002) or in osteoprogenitors (Osx-Cre) (Rodda and McMahon, 2006) to delete ERα resulted in impaired Wnt signaling and impaired optimal cortical bone mass acquisition that was ligand independent (Almeida et al., 2013). No trabecular phenotype was observed in either model. Surprisingly, deletion of ERα using the Col1a1-Cre driver, which is active in fully differentiated osteoblasts, elicited no bone phenotype in either sex up to 26 weeks of age (Almeida et al., 2013). In contrast with these findings, deletion of ERα using an osteocalcin-Cre (Ocn-Cre) model, which also is active in differentiated osteoblasts (although possibly somewhat more mature than the Col1a1 promoter), led to deficits in bone mass at both trabecular and cortical sites in female mice (Maatta et al., 2013; Melville et al., 2014). There was also a deficit in trabecular bone in males, although this phenotype was not apparent until ~6 months of age (whereas the phenotype in females was evident by 3 months of age).

Since the osteocyte has recently been identified as an important controller of bone metabolism (Bonewald, 2017), studies have been conducted in which ERα was conditionally deleted in osteocytes using the osteocyte-dominant Dmp1 promoter-driven Cre (Dmp1-Cre) (Kalajzic et al., 2004). This promoter may slightly overlap with the Ocn-Cre and has yielded somewhat inconsistent results. Windahl and colleagues (Windahl et al., 2013) reported that only male mice exhibited a lowered trabecular bone mass, whereas Kondoh and colleagues (Kondoh et al., 2014) reported the same phenotype but in only female mice. The two studies were consistent in that no cortical phenotype was observed in either sex. Although the true nature of ERα function in osteocytes cannot be cleanly gleaned from these studies, it is clear that ERα signaling is somehow important in late osteoblasts/osteocytes. Future studies will need to be designed to address these discrepant findings.

Studies examining the role of cell-specific deletion of ERβ have begun to shed insight into this molecule as well. Deletion of ERβ in osteoprogenitor (Prx1-Cre) or osteoblasts (Col1a1-Cre) elicited opposite effects to that of ERα deletion, which is an increase in trabecular bone mass with no effect on cortical bone mass in female mice (Nicks et al., 2016). In experiments examining the effects of ERβ deletion using bone marrow stromal cells, an increase in the ratio of colony-forming unit (CFU)-osteoblasts to CFU-fibroblasts was observed, suggesting an increased differentiation capacity of ERβ-negative progenitor cells. Consistent with this, ERβ has been shown to antagonize ERα in other systems (Hall and McDonnell, 1999); it is likely that ERβ plays a similar antagonistic role in bone.

The understanding of how ERα and ERβ function in bone physiology is now becoming more complete and Table 35.1 summarizes the current published knowledge from multiple laboratories concerning the phenotypes of the ER conditional-deletion mouse models. Although certainly discrepancies exist, a general consensus is becoming evident: ERα deletion in osteoclasts leads to reduced trabecular bone but not cortical bone in female (but not male) mice, ERα deletion in later osteoblastic lineages generally leads to reduction in both trabecular and cortical bone mass (although this appears to be somewhat sex-specific in some cases), and that ERβ deletion in osteoblastic lineages leads to increased trabecular bone mass in female mice. However, these data were all collected in mice where the conditional deletion was present from conception onwards and therefore may involve developmental effects of the deletion that may persist into adulthood. In order to understand the specific roles of the receptors in a cell-specific manner in adulthood without the confounding effects of developmental deletion, inducible mouse models in which the deletion can be induced later in life are necessary to further understand and clarify the role of both ERα and ERβ in the adult skeleton.

Estrogens—from a clinical perspective

Over 70 years ago, Fuller Albright demonstrated that estrogen deficiency, achieved through either OVX or menopause, caused a rapid bone loss that estrogen replacement could mitigate (Albright, 1940). This also occurs in men, as it was shown that following the removal of the testes, men also experienced a similar loss of bone (Stepan et al., 1989). Since the major sex steroid in males is testosterone, this at the time led to the generalization that estrogen regulates bone mass in women, and testosterone regulates bone mass in men. This, however, proved to be an oversimplification, and as we will discuss shortly, estrogens prove to be the major sex steroid regulating bone physiology in both sexes. In this section, we will review our understanding of how estrogen regulates bone metabolism in humans in both sexes.

The first crack in the notion that testosterone is the dominant regulator of bone mass in men was the identification of a 28-year old male with homozygous null mutations in the ERα gene (Smith et al., 1994). This man exhibited osteopenia with unfused epiphyses and had a spine bone mineral density (BMD) of 2 standard deviations below the average for normal 15 year-old males. This was followed by two independent reports describing a two males with a complete

TABLE 35.1 Summary of phenotypes for ER and PR conditional mouse knockouts.

Conditional KOs		Female		Male		
Genotype	**Cell type**	**Trabecular bone**	**Cortical bone**	**Trabecular bone**	**Cortical bone**	**References**
ERα/LysM-Cre	Osteoclast	↓	~	~	~	Martin-Millan et al., 2010
ERα/Catk-Cre	Osteoclast	↓	~			Nakamura et al., 2007
ERα/Prx1-Cre	Mesen-Prog	~	↓			Almeida et al., 2013
ERα/Osx1-Cre	Osteo-Prog	~	↓			Almeida et al., 2013
ERα/Col1a1-Cre	Osteoblast	~	~	~	~	Almeida et al., 2013
ERα/Ocn-Cre	Osteoblast	↓	↓	~ then↓	~	Maatta et al., 2013; Melville et al., 2014
ERα/Dmp1-Cre	Osteocyte			↓	~	Windahl et al., 2013
ERα/Dmp1-Cre	Osteocyte	↓	~			Kondoh et al., 2014
ERβ/Prx1-Cre	Mesen-Prog	↑	~			Nicks et al., 2016
ERβ/Col1a1-Cre	Mesen-Prog	↑	~			Nicks et al., 2016
PR/Prx1-Cre	Mesen-Prog	↑	~	↑	~	Zhong et al., 2017
PR/Ocn-Cre	Osteoblast	~	~	~	~	Zhong et al., 2017
PR/Dmp1-Cre	Osteocyte	↑	~	↑	~	Zhong et al., 2017

~ parameter is unchanged; ↓ parameter is decreased; ↑ parameter is increased.

deficiency in the aromatase enzyme, the molecule responsible for the conversion of testosterone to estrogens (Carani et al., 1997; Bilezikian et al., 1998). Interestingly, these males exhibited a virtually indistinguishable bone phenotype for the original ERα-deficient man. These reports demonstrated that estrogens indeed had an important role in both epiphyseal closure and the attainment of peak bone mass that occurs in the late puberty of males. The original ERα-deficient male (Smith et al., 1994) was reanalyzed later in life and a reduction was found in the bone parameters of both trabecular and cortical compartments (Smith et al., 2008), demonstrating that his osteopenia tracked into later life. While the typical forms of osteoporosis, such as in hypogonadal men or estrogen-deficient women, exhibit increased bone turnover (with indices of resorption and formation both increasing), this male had a reduction in both resorption and formation indices. These "experiments of nature" logically lead to an interesting insight into molecular mechanism—that a loss of estrogen (e.g., the ligand) leads to reduced bone mass in a fundamentally different manner than the loss of the receptor. This notion is supported by the presence of many estrogen-independent effects that have been observed in numerous other tissues (Ciana et al., 2003). Interestingly, cultured primary bone cells from the ERα-deficient male exhibited an increase in the ERβ protein, suggesting a compensatory response (Smith et al., 2008). However, when this data is considered in context with the high circulating estrogen levels present in this individual, it suggests that the ERβ pathway cannot adequately compensate for ERα in the regulation of global bone mass. Whether this is due to the loss of ERα itself, the compensatory increase in ERβ protein, changes in transcriptional coregulatory dynamics, or all of the above, is unclear and would warrant further investigation.

In women, a number of observational studies have also substantiated the original observation made by Fuller Albright and further confirm the essential and key role of estrogens in the regulation of bone physiology. The decline in serum estrogens that occurs throughout menopause is tightly associated with an increased in the bone resorption parameter N-telopeptide of type I collagen (Sowers et al., 2013). Since androgen production, albeit at a low level, still continues in the ovaries following menopause, androgen levels are unchanged and argue against their role in estrogen deficiency-mediated bone loss (Handelsman et al., 2016). The radical idea that estrogen regulates BMD in both women and men has been documented in other human observational studies, where serum estradiol levels appear to be more closely correlated to BMD and turnover indices than androgen levels (Khosla et al., 1998).

A number of human interventional studies from various groups have also concluded that estrogen is indeed the dominant sex steroid that regulates bone physiology. The Women's Health Initiative study, which investigated the effects of estrogen/progesterone (vs. placebo) in a large cohort of postmenopausal women, demonstrated that steroid treatment increased BMD at multiple sites and reduced the risk of hip fracture by one-third (Cauley et al., 2003). Another key study compared the effects of estrogen and testosterone treatment in older men (mean age 68 years) where endogenous sex steroid production was pharmacologically eliminated, and exogenously treated with either sex steroid alone or in combination using patches for 3 weeks (Falahati-Nini et al., 2000). Increases in bone resorption indices were prevented by treatment with steroids as well as by the estrogen-replaced group alone. Importantly, the testosterone-replaced group, in which aromatization to estrogens in inhibited, was ineffective in altering bone resorption makers. Using a statistical model, the investigators estimated that 70% of the effect was due to estrogen alone. This notion was confirmed by a similar study that found that testosterone replacement in hypogonadal men (±an aromatase inhibitor) was ineffective in altering serum turnover markers and that estrogen was indeed the major sex steroid involved in the regulation of bone mass in men (Finkelstein et al., 2016). Collectively, these studies provide strong evidence that in both sexes estrogen is the major sex steroid involved in the regulation bone physiology (Khosla, 2015). The function of testosterone in the regulation of bone mass in men appears to be as a precursor for the aromatization to estrogens, although testosterone also likely plays other important roles in periosteal apposition during growth, leading to larger bone size in men versus women (Almeida et al., 2017).

Another important question when considering the effects of estrogens and ERs (ERα and ERβ) is what might be the potential mechanisms and/or mediators of estrogen action in human bone. Based largely on rodent OVX models, genes that encode proinflammatory cytokines have emerged as one class of potential mediators of estrogen action in bone, especially on osteoclast action and bone resorption. Of particular interest, TNFα, IL1α/β, and IL6 have been the most consistent (Weitzmann and Pacifici, 2006). In humans, several interventional studies have addressed the influence of these proinflammatory cytokines on bone health. One study examined a cohort of normal women ranging from 24 to 87 years old and showed that IL6 concentrations correlated highly with age; however, using sophisticated multiple-regression statistical models, no correlation with estrogen status could be established (McKane et al., 1994). To further clarify this issue, a study was designed in which estrogen-withdrawn early postmenopausal women were placed on either an IL1 or TNFα blocker for 3 weeks, and bone resorption indices were analyzed (Charatcharoenwitthaya et al., 2007). They found a reduction in serum resorption markers suggesting that these proinflammatory cytokines mediate in part bone resorption during estrogen deficiency in humans.

Receptor activator of nuclear factor kappa-B ligand (RANKL), which is produced by both osteoblasts and osteocytes in the bone microenvironment, is another key regulator of bone remodeling by influencing the process of osteoclastic differentiation (Xiong and O'Brien, 2012). In one study designed to examine the role of estrogenic regulation of RANKL in bone, RANKL + cells were isolated from premenopausal women (control) and postmenopausal women treated with either vehicle or estradiol (Eghbali-Fatourechi et al., 2003). They found that the number of RANKL + cells increases with age and estrogenic status, and that such increases were reversible with estradiol treatment. These data suggest that loss of estrogens at menopause may contribute to increased bone resorption through the increase in the proosteoclastic factor RANKL. The increased resorption in estrogen-deficient women can be abrogated clinically through treatment with denosumab, a humanized monoclonal antibody to RANKL (Cummings et al., 2009).

Increasing evidence also exists that demonstrates that the secreted Wnt inhibitor, sclerostin, is regulated by estrogen (Drake and Khosla, 2017). Treatment of estrogen-deficient women with estrogen or the select estrogen receptor modulator raloxifene negatively regulates circulating serum sclerostin protein levels (Drake and Khosla, 2017; Chung et al., 2012; Fujita et al., 2014; Modder et al., 2011a,b). Sclerostin mRNA expression, as assessed by RNA sequencing and QPCR analyses, was also decreased in primary bone needle biopsies isolated from postmenopausal women treated with estradiol (Farr et al., 2017). The new therapeutic agent romosozumab (Cosman et al., 2016), which is a humanized monoclonal antibody directed against sclerostin, results in increases in bone formation with a concomitant decrease in bone resorption in postmenopausal women, similar to those changes observed with estrogen treatment (Drake and Khosla, 2017).

Progestins and progesterone receptors in bone biology

Clinically, progesterone has been used in addition to estradiol to treat postmenopausal osteoporosis to minimize the adverse effects of estradiol on the uterus and breast, however the effects of progestins on bone biology have been significantly less studied (Prior et al., 1990). As with estrogen and estrogen receptors, progestins exert their effects via the progesterone receptor (PR), a member of the nuclear receptor superfamily of transcription factors (Mangelsdorf et al., 1995). Activated PR can acts a progesterone response elements to alter gene expression of specific PR target genes, however nongenomic effects have also been observed (Grosse et al., 2000).

In mammals, PRs exists in two related protein isoforms, which arise from the regulated activation of alternative promoters, resulting in the PR-A and PR-B isoforms (Kastner et al., 1990; Giangrande and McDonnell, 1999). Since they are a member of the nuclear receptor superfamily of transcription factors along with ERs (Mangelsdorf et al., 1995), they share the same modular protein structure including a DBD, LBD, and AF domains (Fig. 35.2) (Hill et al., 2012). The two isoforms are identical except for an additional 164 amino acid residues on the N-terminus of PR-B, which contains an additional and unique activation function (AF-3). Interestingly, both PR isoforms are estrogen inducible (Jung-Testas et al., 1991; Harris et al., 1995; Rickard et al., 2002), suggesting cross-talk between the estrogenic and progestin pathways. In general, the PR-B isoform has a more dominant effect on transcriptional regulation, and under certain conditions, the PR-A isoform can act as an antagonist to PR-B function, as can other nuclear hormone receptors such as ERα (Kraus et al., 1995). Expression of both mRNA and protein for PRs has been demonstrated in multiple osteoblastic cell lines (Rickard et al., 2002; Wei et al., 1993; MacNamara et al., 1995, 1998) and in an age-dependent manner in mouse bone tissue (Zhong et al., 2017).

There is considerable in vitro evidence that progestins can affect osteoblast and bone marrow–derived osteoblastic progenitor cells through the regulation of both proliferation and differentiation, although the data are somewhat conflicting. Various reports have demonstrated that progesterone treatment of some osteoblast cell models has shown either an inhibition of proliferation (Canalis and Raisz, 1978), no effect on proliferation when treated alone (Slootweg et al., 1992), or a stimulation of proliferation (Tremollieres et al., 1992; Scheven et al., 1992; Manzi et al., 1994; Verhaar et al., 1994). Although these data are variable, the overall weight of the evidence suggests that progestins indeed stimulate proliferation in certain mouse and rat osteoblast cell models. Using primary rat bone explants, it was shown the progesterone stimulated

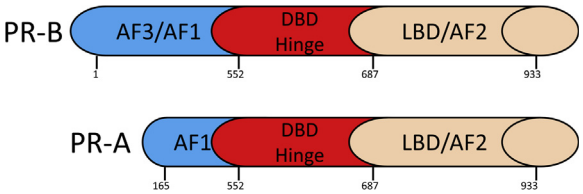

FIGURE 35.2 Structure of human PR-A and PR-B.

the formation of alkaline phosphatase positive (AP+) colonies (Ishida & Heersche, 1997, 1999), suggesting that progesterone may positively influence osteoblast differentiation. In human primary osteoblast cultures and in rat osteosarcoma cells, progesterone treatment stimulated IGF2 secretion (Tremollieres et al., 1992). This regulation of the IGF system was demonstrated to be via activation of IGFBP5, which is known to enhance IGF1/2 activity in osteoblast cultures (Boonyaratanakornkit et al., 1999). In summary, these data support the notion that progesterone positively influences the proliferation and bone-forming activities of osteoblasts.

Initial studies in the 1980s using animal models showed that progesterone has positive effects on bone metabolism in both rats (Burnett and Reddi, 1983) and dogs (Snow and Anderson, 1985). Using an OVX-induced model of bone loss in rats, it was also shown that progesterone replacement had a significant effect on the preservation of bone during sex steroid deficiency (Barengolts et al., 1990, 1996; Bowman and Miller, 1996; Schmidt et al., 2000). However other studies have failed to show an effect on trabecular bone when either treated alone or coadministered with estradiol (Fujimaki et al., 1995; Kalu et al., 1991), creating some uncertainty in the field in regard to the effects of progestins on bone metabolism. Interestingly, the PR antagonist mifepristone (RU486) was also shown to reduce OVX-induced bone loss in rats (Barengolts et al., 1995) and in a patient with Cushing's disease and severe osteoporosis (Newfield et al., 2001), although the latter effects could be due to RU486-mediated antagonism of the glucocorticoid receptor.

Due to these conflicting reports on the effects of progestins on bone metabolism in both animal and human models of osteoporosis, mutant mice have been generated where both PR-A and PR-B have been deleted (the PRKO mouse), in hopes of understanding the true nature of the effects of progestins and PRs in bone physiology. These mice exhibit severe reproductive abnormalities, and the females are infertile (Lydon et al., 1995; Conneely et al., 2001), and also exhibit an increase in trabecular bone mass and bone formation at 12 and 26 weeks of age in female mice (Rickard et al., 2008). Treatment with the PR antagonist RU486 also leads to an increase in trabecular bone mass in young wild-type mice (Yao et al., 2010). Recently, cell-type specific deletions of both PR isoforms using the Cre/LoxP system (the PRcKO mouse) have been made (Zhong et al., 2017). This report confirmed the data from the PRKO knockout mouse and RU486 antagonist data and found a significant increase in trabecular bone mass when PRs were deleted in early mesenchymal progenitor cells (using the Prx1-Cre driver), but not in mature osteoblasts (using the Ocn-Cre driver), and a modest increased trabecular bone mass phenotype following deletion in osteocytes (using the Dmp1-Cre driver). These phenotypes were observed in both sexes (see Table 35.1). Cortical bone mass was unaffected in all models. Taken together, these findings suggest that PR may play a negative role in bone homeostasis. Interestingly, in a specific PR-A mouse knockout model, progesterone had a significantly higher effect on reproductive tissues (Mulac-Jericevic et al., 2000), suggesting that PR-A plays a negative role on the actions of PR-B, although these data need to be confirmed in the skeleton.

Although the data on the effects or progestins in human physiology are somewhat controversial (Waller et al., 1996; De Souza et al., 1997), the bulk of the evidence suggests a role for progestins, albeit modest, in bone physiology. Women who have ovulatory dysfunction due to luteal phase defects have lower bone mass over 1 year compared with normal women (Prior et al., 1990; Prior, 1990), which can be reversed with progesterone replacement therapy (Prior et al., 1994). Additionally, progesterone treatment of women with postmenopausal osteoporosis could protect against further cortical bone loss (Gallagher et al., 1991; Gray et al., 1996; McNeeley Jr. et al., 1991). Although some reports have demonstrated that progesterone treatment of postmenopausal women is as effective as estradiol treatment in preventing further bone loss (Gray et al., 1996; McNeeley Jr. et al., 1991), others have shown a lesser effect when compared to estradiol alone (Prior et al., 1997; PEPI, 1996).

Summary and conclusions

In recent years, many discoveries have advanced our knowledge regarding estrogen action in the bone microenvironment. Although some of the phenotypes of the ERα and ERβ conditional knockout mouse models have been described, it is still unclear the precise mechanism(s) that ERs utilize to regulate bone metabolism, which is especially evident in the role of ERβ itself and ERα/ERβ interactions that may influence bone processes. Given how important estrogen action is for bone, it will be important to continue to define the mechanism(s) that these ERs play, including the role of nonnuclear ERs, to develop novel clinical therapies for aging-related bone diseases such as osteoporosis. It is of interest that two of the new therapies developed for osteoporosis (i.e., denosumab and sclerostin) appear to lie in the estrogen pathway in humans. Therefore, future investigation into how these mechanisms function during aging in bone will be especially important and will help in the improvement of current therapies and in the development of novel therapies for osteoporosis.

CONFLICT OF INTEREST

The authors have declared that no financial conflict of interest exists.

References

Albright, F., 1940. Post-menopausal osteoporosis. Trans. Assoc. Am. Phys. 55, 298–305.

Almeida, M., et al., 2013. Estrogen receptor-alpha signaling in osteoblast progenitors stimulates coritcal bone accrual. J. Clin. Investig. 123, 394–404.

Almeida, M., et al., 2017. Estrogens and androgens in skeletal physiology and pathophysiology. Physiol. Rev. 97, 135–187.

Arts, J., et al., 1997. Differential expression of estrogen receptors alpha and beta mRNA during differentiation of human osteoblast SV-HFO cells. Endocrinology 138, 5067–5070. https://doi.org/10.1210/endo.138.11.5652.

Barengolts, E.I., et al., 1990. Effects of progesterone on postovariectomy bone loss in aged rats. J. Bone Miner. Res. 5, 1143–1147. https://doi.org/10.1002/jbmr.5650051109.

Barengolts, E.I., et al., 1996. Effects of progesterone on serum levels of IGF-1 and on femur IGF-1 mRNA in ovariectomized rats. J. Bone Miner. Res. 11, 1406–1412. https://doi.org/10.1002/jbmr.5650111006.

Barengolts, E.I., Lathon, P.V., Lindh, F.G., 1995. Progesterone antagonist RU 486 has bone-sparing effects in ovariectomized rats. Bone 17, 21–25.

Bilezikian, J.P., Morishima, A., Bell, J., Grumbach, M.M., 1998. Increased bone mass as a result of estrogen therapy in a man with aromatase deficiency. N. Engl. J. Med. 339, 599–603.

Bonewald, L.F., 2017. The role of the osteocyte in bone and nonbone disease. Endocrinol Metab. Clin. N. Am. 46, 1–18. https://doi.org/10.1016/j.ecl.2016.09.003.

Boonyaratanakornkit, V., et al., 1999. Progesterone stimulation of human insulin-like growth factor-binding protein-5 gene transcription in human osteoblasts is mediated by a CACCC sequence in the proximal promoter. J. Biol. Chem. 274, 26431–26438.

Bord, S., Horner, A., Beavan, S., Compston, J., 2001. Estrogen receptors alpha and beta are differentially expressed in developing human bone. J. Clin. Endocrinol. Metab. 86, 2309–2314. https://doi.org/10.1210/jcem.86.5.7513.

Bowman, B.M., Miller, S.C., 1996. Elevated progesterone during pseudopregnancy may prevent bone loss associated with low estrogen. J. Bone Miner. Res. 11, 15–21. https://doi.org/10.1002/jbmr.5650110104.

Braidman, I.P., et al., 2001. Localization of estrogen receptor beta protein expression in adult human bone. J. Bone Miner. Res. 16, 214–220. https://doi.org/10.1359/jbmr.2001.16.2.214.

Burnett, C.C., Reddi, A.H., 1983. Influence of estrogen and progesterone on matrix-induced endochondral bone formation. Calcif. Tissue Int. 35, 609–614.

Canalis, E., Raisz, L.G., 1978. Effect of sex steroids on bone collagen synthesis in vitro. Calcif. Tissue Res. 25, 105–110.

Carani, C., et al., 1997. Effect of testosterone and estradiol in a man with aromatase deficiency. N. Engl. J. Med. 337, 91–95.

Cauley, J.A., et al., 2003. Effects of estrogen plus progestin on risk of fracture and bone mineral density. J. Am. Med. Assoc. 290, 1729–1738.

Cauley, J.A., et al., 2008. Incidence of fractures compared to cardiovascular disease and breast cancer: the Women's Health Initiative Observational Study. Osteoporos. Int. 19, 1717–1723.

Charatcharoenwitthaya, N., Khosla, S., Atkinson, E.J., McCready, L.K., Riggs, B.L., 2007. Effect of blockade of TNF-a and interleukin-1 action on bone resorption in early postmenopausal women. J. Bone Miner. Res. 22, 724–729.

Chow, J.W., Lean, J.M., Chambers, T.J., 1992. 17 beta-estradiol stimulates cancellous bone formation in female rats. Endocrinology 130, 3025–3032. https://doi.org/10.1210/endo.130.5.1572310.

Chung, Y.E., et al., 2012. Long-term treatment with raloxifene, but not bisphosphonates reduces circulating sclerostin levels in postmenopausal women. Osteoporos. Int. 23, 1235–1243.

Ciana, P., et al., 2003. In vivo imaging of transcriptionally active estrogen receptors. Nat. Med. 9, 82–86.

Conneely, O.M., Mulac-Jericevic, B., Lydon, J.P., De Mayo, F.J., 2001. Reproductive functions of the progesterone receptor isoforms: lessons from knock-out mice. Mol. Cell. Endocrinol. 179, 97–103.

Cosman, F., et al., 2016. Romosozumab treatment in postmenopausal women with osteoporosis. N. Engl. J. Med. 375, 1532–1543.

Cummings, S.R., et al., 2009. Denosumab for prevention of fractures in postmenopausal women with osteoporosis. N. Engl. J. Med. 361, 756–765.

De Souza, M.J., et al., 1997. Bone health is not affected by luteal phase abnormalities and decreased ovarian progesterone production in female runners. J. Clin. Endocrinol. Metab. 82, 2867–2876. https://doi.org/10.1210/jcem.82.9.4201.

Drake, M.T., Khosla, S., 2017. Hormomal and systemic regulation of sclerostin. Bone 96, 8–17.

Eghbali-Fatourechi, G., et al., 2003. Role of RANK ligand in mediating increased bone resorption in early postmenopausal women. J. Clin. Investig. 111, 1221–1230.

Eriksen, E.F., et al., 1988. Evidence of estrogen receptors in normal human osteoblast-like cells. Science 241, 84–86.

Ernst, M., Heath, J.K., Schmid, C., Froesch, R.E., Rodan, G.A., 1989. Evidence for a direct effect of estrogen on bone cells in vitro. J. Steroid Biochem. 34, 279–284.

Falahati-Nini, A., et al., 2000. Relative contributions of testosterone and estrogen in regulating bone resorption and formation in normal elderly men. J. Clin. Investig. 106, 1553–1560.

Farr, J.N., et al., 2017. Targeting cellular senescence prevents age-related bone loss in mice. Nat. Med. 23, 1072–1079. https://doi.org/10.1038/nm.4385.

Finkelstein, J.S., et al., 2016. Gonadal steroid-dependent effects on bone turnover and bone mineral density in men. J. Clin. Investig. 126, 1114–1125.

Fujimaki, T., et al., 1995. Effects of progesterone on the metabolism of cancellous bone in young oophorectomized rats. J. Obstet. Gynaecol. 21, 31–36.

Fujita, K., et al., 2014. Effects of estrogen on bone mRNA levels of sclerostin and other genes relevant to bone metabolism in postmenopausal women. J. Clin. Endocrinol. Metab. 99, E81−E88.

Gallagher, J.C., Kable, W.T., Goldgar, D., 1991. Effect of progestin therapy on cortical and trabecular bone: comparison with estrogen. Am. J. Med. 90, 171−178.

Giangrande, P.H., McDonnell, D.P., 1999. The A and B isoforms of the human progesterone receptor: two functionally different transcription factors encoded by a single gene. Recent Prog. Horm. Res. 54, 291−313 discussion 313-294.

Gorski, J., Toft, D., Shyamala, G., Smith, D., Notides, A., 1968. Hormone receptors: studies on the interaction of estrogen with the uterus. Recent Prog. Horm. Res. 24, 45−80.

Greene, G.L., et al., 1986. Sequence and expression of human estrogen receptor complementary DNA. Science 231, 1150−1154.

Grey, A., Cundy, T., Evans, M., Reid, I., 1996. Medroxyprogesterone acetate enhances the spinal bone mineral density response to oestrogen in late postmenopausal women. Clin. Endocrinol. 44, 293−296.

Grosse, B., Kachkache, M., Le Mellay, V., Lieberherr, M., 2000. Membrane signalling and progesterone in female and male osteoblasts. I. Involvement of intracellular Ca(2+), inositol trisphosphate, and diacylglycerol, but not cAMP. J. Cell. Biochem. 79, 334−345.

Hall, J.M., McDonnell, D.P., 1999. The estrogen receptor beta-isoform (ER-beta) of the human estrogen receptor modulates ER-alpha transcriptional activity and is a key regulator of the cellular response to estrogens and antiestrogens. Endocrinology 140, 5566−5578.

Handelsman, D.J., Sikaris, K., Ly, L.P., 2016. Estimating age-specific trends in circulating testosterone and sex hormone-binding globulin in males and females across the lifespan. Ann. Clin. Biochem. 53, 377−384.

Harris, S.A., Enger, R.J., Riggs, B.L., Spelsberg, T.C., 1995. Development and characterization of a conditionally immortalized human fetal osteoblastic cell line. J. Bone Miner. Res. 10, 178−186. https://doi.org/10.1002/jbmr.5650100203.

Hill, K.K., Roemer, S.C., Churchill, M.E., Edwards, D.P., 2012. Structural and functional analysis of domains of the progesterone receptor. Mol. Cell. Endocrinol. 348, 418−429. https://doi.org/10.1016/j.mce.2011.07.017.

Ikegami, A., et al., 1993. Immunohistochemical detection and northern blot analysis of estrogen receptor in osteoblastic cells. J. Bone Miner. Res. 8, 1103−1109. https://doi.org/10.1002/jbmr.5650080911.

Ishida, Y., Heersche, J.N., 1997. Progesterone stimulates proliferation and differentiation of osteoprogenitor cells in bone cell populations derived from adult female but not from adult male rats. Bone 20, 17−25.

Ishida, Y., Heersche, J.N., 1999. Progesterone- and dexamethasone-dependent osteoprogenitors in bone cell populations derived from rat vertebrae are different and distinct. Endocrinology 140, 3210−3218. https://doi.org/10.1210/endo.140.7.6850.

Jensen, E.V., et al., 1968. A two-step mechanism for the interaction of estradiol with rat uterus. Proc. Natl. Acad. Sci. U.S.A. 59, 632−638.

Jung-Testas, I., Renoir, J.M., Gasc, J.M., Baulieu, E.E., 1991. Estrogen-inducible progesterone receptor in primary cultures of rat glial cells. Exp. Cell Res. 193, 12−19.

Kalajzic, I., et al., 2004. Dentin matrix protein 1 expression during osteoblastic differentiation, generation of an osteocyte GFP-transgene. Bone 35, 74−82. https://doi.org/10.1016/j.bone.2004.03.006.

Kalu, D.N., et al., 1991. A comparative study of the actions of tamoxifen, estrogen and progesterone in the ovariectomized rat. Bone Miner. 15, 109−123.

Kanis, J.A., et al., 2000. Long-term risk of osteoporotic fracture in Malmo. Osteoporos. Int. 11, 669−674.

Kastner, P., et al., 1990. Two distinct estrogen-regulated promoters generate transcripts encoding the two functionally different human progesterone receptor forms A and B. EMBO J. 9, 1603−1614.

Kelly, M.J., Levin, E.R., 2001. Rapid actions of plasma membrane estrogen receptors. Trends Endocrinol. Metabol. 12, 152−156.

Khosla, S., et al., 1998. Relationship of serum sex steroid levels and bone turnover markers with bone mineral density in men and women: a key role for bioavailable estrogen. J. Clin. Endocrinol. Metab. 83, 2266−2274.

Khosla, S., Amin, S., Orwoll, E., 2008. Osteoporosis in men. Endocr. Rev. 29, 441−464.

Khosla, S., 2015. New insights into androgen and estrogen receptor regulation of the male skeleton. J. Bone Miner. Res. 30, 1134−1137.

Kondoh, S., et al., 2014. Estrogen receptor α in osteocytes regulates trabecular bone formation in female mice. Bone 60, 68−77.

Kraus, W.L., Weis, K.E., Katzenellenbogen, B.S., 1995. Inhibitory cross-talk between steroid hormone receptors: differential targeting of estrogen receptor in the repression of its transcriptional activity by agonist- and antagonist-occupied progestin receptors. Mol. Cell Biol. 15, 1847−1857.

Landers, J.P., Spelsberg, T.C., 1992. New concepts in steroid hormone action: transcription factors, proto-oncogenes, and the cascade model for steroid regulation of gene expression. Crit. Rev. Eukaryot. Gene Expr. 2, 19−63.

Levin, E.R., 2002. Cellular functions of plasma membrane estrogen receptors. Steroids 67, 471−475.

Logan, M., et al., 2002. Expression of Cre Recombinase in the developing mouse limb bud driven by a Prxl enhancer. Genesis 33, 77−80. https://doi.org/10.1002/gene.10092.

Lydon, J.P., et al., 1995. Mice lacking progesterone receptor exhibit pleiotropic reproductive abnormalities. Genes Dev. 9, 2266−2278.

Maatta, J.A., et al., 2013. Inactivation of estrogen receptor α in bone-forming cells induces bone loss in female mice. FASEB J. 27, 478−488.

MacNamara, P., O'Shaughnessy, C., Manduca, P., Loughrey, H.C., 1995. Progesterone receptors are expressed in human osteoblast-like cell lines and in primary human osteoblast cultures. Calcif. Tissue Int. 57, 436−441.

MacNamara, P., Skillington, J., Loughrey, H.C., 1998. Studies on progesterone receptor expression in human osteoblast cells. Biochem. Soc. Trans. 26, S1.

Mangelsdorf, D.J., et al., 1995. The nuclear receptor superfamily: the second decade. Cell 83, 835−839.

Manzi, D.L., Pilbeam, C.C., Raisz, L.G., 1994. The anabolic effects of progesterone on fetal rat calvaria in tissue culture. J. Soc. Gynecol. Investig. 1, 302−309.

Martin-Millan, M., et al., 2010. The estrogen receptor-alpha in osteoclasts mediates the protective effects of estrogens on cancellous but not cortical bone. Mol. Endocrinol. 24, 323–334.

McKane, W.R., Khosla, S., Peterson, J.M., Egan, K., Riggs, B.L., 1994. Circulating levels of cytokines that modulate bone resorption: effects of age and menopause in women. J. Bone Miner. Res. 9, 1313–1318. https://doi.org/10.1002/jbmr.5650090821.

McNeeley Jr., S.G., Schinfeld, J.S., Stovall, T.G., Ling, F.W., Buxton, B.H., 1991. Prevention of osteoporosis by medroxyprogesterone acetate in postmenopausal women. Int. J. Gynaecol. Obstet. 34, 253–256.

Melton 3rd, L.J., Atkinson, E.J., O'Connor, M.K., O'Fallon, W.M., Riggs, B.L., 1998. Bone density and fracture risk in men. J. Bone Miner. Res. 13, 1915–1923. https://doi.org/10.1359/jbmr.1998.13.12.1915.

Melville, K.M., et al., 2014. Female mice lacking estrogen receptor-alpha in osteoblast have compromised bone mass and strength. J. Bone Miner. Res. 29, 370–379.

Modder, U.I., et al., 2011a. Regulation of circulating sclerostin levels by sex steroids in women and in men. J. Bone Miner. Res. 26, 27–34. https://doi.org/10.1002/jbmr.128.

Modder, U.I., et al., 2011b. Effects of estrogen on osteoprogenitor cells and cytokines/bone-regulatory factors in postmenopausal women. Bone 49, 202–207. https://doi.org/10.1016/j.bone.2011.04.015.

Monroe, D.G., et al., 2003a. Mutual antagonism of estrogen receptors alpha and beta and their preferred interactions with steroid receptor coactivators in human osteoblastic cell lines. J. Endocrinol. 176, 349–357.

Monroe, D.G., et al., 2005. Estrogen receptor alpha and beta heterodimers exert unique effects on estrogen- and tamoxifen-dependent gene expression in human U2OS osteosarcoma cells. Mol. Endocrinol. 19, 1555–1568. https://doi.org/10.1210/me.2004-0381.

Monroe, D.G., Secreto, F.J., Spelsberg, T.C., 2003b. Overview of estrogen action in osteoblasts: role of the ligand, the receptor, and the co-regulators. J. Musculoskelet. Neuronal Interact. 3, 357–362 discussion 381.

Mosselman, S., Polman, J., Dijkema, R., 1996. ER beta: identification and characterization of a novel human estrogen receptor. FEBS Lett. 392, 49–53.

Mulac-Jericevic, B., Mullinax, R.A., DeMayo, F.J., Lydon, J.P., Conneely, O.M., 2000. Subgroup of reproductive functions of progesterone mediated by progesterone receptor-B isoform. Science 289, 1751–1754.

Nakamura, T., et al., 2007. Estrogen prevents bone loss via estrogen receptor alpha and induction of fas ligand in osteoclasts. Cell 130, 811–823.

Newfield, R.S., Spitz, I.M., Isacson, C., New, M.I., 2001. Long-term mifepristone (RU486) therapy resulting in massive benign endometrial hyperplasia. Clin. Endocrinol. 54, 399–404.

Nicks, K.M., et al., 2016. Deletion of estrogen receptor beta in osteoprogenitor cells increases trabecular but not cortical bone mass in female mice. J. Bone Miner. Res. 31, 606–614.

Onoe, Y., Miyaura, C., Ohta, H., Nozawa, S., Suda, T., 1997. Expression of estrogen receptor beta in rat bone. Endocrinology 138, 4509–4512. https://doi.org/10.1210/endo.138.10.5575.

Oursler, M.J., Osdoby, P., Pyfferoen, J., Riggs, B.L., Spelsberg, T.C., 1991. Avian osteoclasts as estrogen target cells. Proc. Natl. Acad. Sci. U.S.A. 88, 6613–6617.

Oursler, M.J., Pederson, L., Fitzpatrick, L., Riggs, B.L., 1994. Human giant cell tumors of the bone (osteoclastomas) are estrogen target cells. Proc. Natl. Acad. Sci. U.S.A. 91, 5227–5231.

PEPI, 1996. Effects of hormone therapy on bone mineral density: results from the postmenopausal estrogen/progestin interventions (PEPI) trial. The Writing Group for the PEPI. J. Am. Med. Assoc. 276, 1389–1396.

Prior, J.C., et al., 1997. Premenopausal ovariectomy-related bone loss: a randomized, double-blind, one-year trial of conjugated estrogen or medroxyprogesterone acetate. J. Bone Miner. Res. 12, 1851–1863. https://doi.org/10.1359/jbmr.1997.12.11.1851.

Prior, J.C., Vigna, Y.M., Schechter, M.T., Burgess, A.E., 1990. Spinal bone loss and ovulatory disturbances. N. Engl. J. Med. 323, 1221–1227. https://doi.org/10.1056/NEJM199011013231801.

Prior, J.C., Vigna, Y.M., Barr, S.I., Rexworthy, C., Lentle, B.C., 1994. Cyclic medroxyprogesterone treatment increases bone density: a controlled trial in active women with menstrual cycle disturbances. Am. J. Med. 96, 521–530.

Prior, J.C., 1990. Progesterone as a bone-trophic hormone. Endocr. Rev. 11, 386–398.

Razandi, M., Pedram, A., Greene, G.L., Levin, E.R., 1999. Cell membrane and nuclear estrogen receptors (ERs) originate from a single transcript: studies of ERalpha and ERbeta expressed in Chinese hamster ovary cells. Mol. Endocrinol. 13, 307–319. https://doi.org/10.1210/mend.13.2.0239.

Rickard, D.J., et al., 2002. Estrogen receptor isoform-specific induction of progesterone receptors in human osteoblasts. J. Bone Miner. Res. 17, 580–592. https://doi.org/10.1359/jbmr.2002.17.4.580.

Rickard, D.J., et al., 2008. Bone growth and turnover in progesterone receptor knockout mice. Endocrinology 149, 2383–2390. https://doi.org/10.1210/en.2007-1247.

Riggs, B.L., Khosla, S., Melton 3rd, L.J., 2002. Sex steroids and the construction and conservation of the adult skeleton. Endocr. Rev. 23, 279–302.

Rodda, S.J., McMahon, A.P., 2006. Distinct roles for Hedgehog and canonical Wnt signaling in specification, differentiation and maintenance of osteoblast progenitors. Development 133, 3231–3244. https://doi.org/10.1242/dev.02480.

Saczko, J., et al., 2017. Estrogen receptors in cell membranes: regulation and signaling. Adv. Anat. Embryol. Cell Biol. 227, 93–105. https://doi.org/10.1007/978-3-319-56895-9_6.

Scheven, B.A., Damen, C.A., Hamilton, N.J., Verhaar, H.J., Duursma, S.A., 1992. Stimulatory effects of estrogen and progesterone on proliferation and differentiation of normal human osteoblast-like cells in vitro. Biochem. Biophys. Res. Commun. 186, 54–60.

Schmidt, I.U., Wakley, G.K., Turner, R.T., 2000. Effects of estrogen and progesterone on tibia histomorphometry in growing rats. Calcif. Tissue Int. 67, 47–52.

Shyamala, G., Gorski, J., 1969. Estrogen receptors in the rat uterus. Studies on the interaction of cytosol and nuclear binding sites. J. Biol. Chem. 244, 1097–1103.

Sims, N.A., et al., 2002. Deletion of estrogen receptors reveals a regulatory role for estrogen receptors beta in bone remodeling in females but not in males. Bone 30, 18–25.

Slootweg, M.C., Ederveen, A.G., Schot, L.P., Schoonen, W.G., Kloosterboer, H.J., 1992. Oestrogen and progestogen synergistically stimulate human and rat osteoblast proliferation. J. Endocrinol. 133, R5–R8.

Smith, E.P., et al., 1994. Estrogen resistance caused by a mutation in the estrogen-receptor gene in a man. N. Engl. J. Med. 331, 1056–1061.

Smith, E.P., et al., 2008. Impact on bone of an estrogen receptor-alpha gene loss of function mutation. J. Clin. Endocrinol. Metab. 93, 3088–3096.

Snow, G.R., Anderson, C., 1985. The effects of continuous progestogen treatment on cortical bone remodeling activity in beagles. Calcif. Tissue Int. 37, 282–286.

Sowers, M.R., et al., 2013. Changes in bone resorption across the menopause transition: effects of reproductive hormones, body size, and ethnicity. J. Clin. Endocrinol. Metab. 98, 2854–2863.

Spelsberg, T.C., Subramaniam, M., Riggs, B.L., Khosla, S., 1999. The actions and interactions of sex steroids and growth factors/cytokines on the skeleton. Mol. Endocrinol. 13, 819–828. https://doi.org/10.1210/mend.13.6.0299.

Stepan, J.J., Lachman, M., Zverina, J., Pacovsky, V., 1989. Castrated men exhibit bone loss: effect of calcitonin treatment on biochemical indices of bone remodeling. J. Clin. Endocrinol. Metab. 69, 523–527.

Tobias, J.H., Chambers, T.J., 1991. The effect of sex hormones on bone resorption by rat osteoclasts. Acta Endocrinol. 124, 121–127.

Tobias, J.H., Chow, J., Colston, K.W., Chambers, T.J., 1991. High concentrations of 17 beta-estradiol stimulate trabecular bone formation in adult female rats. Endocrinology 128, 408–412. https://doi.org/10.1210/endo-128-1-408.

Tremollieres, F.A., Strong, D.D., Baylink, D.J., Mohan, S., 1992. Progesterone and promegestone stimulate human bone cell proliferation and insulin-like growth factor-2 production. Acta Endocrinol. 126, 329–337.

Turner, R.T., Bell, N.H., Gay, C.V., 1993. Evidence that estrogen binding sites are present in bone cells and mediate medullary bone formation in Japanese quail. Poultry Sci. 72, 728–740.

Verhaar, H.J., Damen, C.A., Duursma, S.A., Scheven, B.A., 1994. A comparison of the action of progestins and estrogen on the growth and differentiation of normal adult human osteoblast-like cells in vitro. Bone 15, 307–311.

Vidal, O., Kindblom, L.G., Ohlsson, C., 1999. Expression and localization of estrogen receptor-beta in murine and human bone. J. Bone Miner. Res. 14, 923–929. https://doi.org/10.1359/jbmr.1999.14.6.923.

Waller, K., et al., 1996. Bone mass and subtle abnormalities in ovulatory function in healthy women. J. Clin. Endocrinol. Metab. 81, 663–668. https://doi.org/10.1210/jcem.81.2.8636286.

Walter, P., et al., 1985. Cloning of the human estrogen receptor cDNA. Proc. Natl. Acad. Sci. U.S.A. 82, 7889–7893.

Wei, L.L., Leach, M.W., Miner, R.S., Demers, L.M., 1993. Evidence for progesterone receptors in human osteoblast-like cells. Biochem. Biophys. Res. Commun. 195, 525–532. https://doi.org/10.1006/bbrc.1993.2077.

Weitzmann, M.N., Pacifici, R., 2006. Estrogen deficiency and bone loss: an inflammatory tale. J. Clin. Investig. 116, 1186–1194.

Windahl, S.H., et al., 2013. Estrogen receptor-α in osteocytes is important for trabecular bone formation in male mice. Proc. Natl. Acad. Sci. U.S.A. 110, 2294–2299.

Windahl, S.H., Vidal, O., Andersson, G., Gustafsson, J.A., Ohlsson, C., 1999. Increased cortical bone mineral content but unchanged trabecular bone mineral density in female ERbeta(-/-) mice. J. Clin. Investig. 104, 895–901. https://doi.org/10.1172/JCI6730.

Windahl, S.H., Norgard, M., Kuiper, G.G., Gustafsson, J.A., Andersson, G., 2000. Cellular distribution of estrogen receptor beta in neonatal rat bone. Bone 26, 117–121.

Xiong, J., O'Brien, C.A., 2012. Osteocyte RANKL: new insights into the control of bone remodeling. J. Bone Miner. Res. 27, 499–505. https://doi.org/10.1002/jbmr.1547.

Yao, W., et al., 2010. Inhibition of the progesterone nuclear receptor during the bone linear growth phase increases peak bone mass in female mice. PLoS One 5, e11410. https://doi.org/10.1371/journal.pone.0011410.

Zhong, Z.A., et al., 2017. Sex-dependent, osteoblast stage-specific effects of progesterone receptor on bone acquisition. J. Bone Miner. Res. 32, 1841–1852. https://doi.org/10.1002/jbmr.3186.

Chapter 36

Physiological actions of parathyroid hormone-related protein in epidermal, mammary, reproductive, and pancreatic tissues

Christopher S. Kovacs
Faculty of Medicine, Memorial University of Newfoundland, St. John's, NL, Canada

Chapter outline

Introduction

A substantial breakthrough in the study of parathyroid hormone-related protein (PTHrP) was the development of genetic models that ablated the gene for PTHrP or its receptor, or overexpressed PTHrP within bone cells. These models revealed that PTHrP plays an important role in regulating the terminal differentiation of chondrocytes and the development of the endochondral skeleton; the major findings are reviewed in Chapters 1 and 25. These same models provided insight into PTHrP's previously unknown roles in the development and function of organs and tissues outside the skeleton. The actions of PTHrP in the vascular system and central nervous system are reviewed in Chapter 26, and in bone in Chapter 25. In this chapter we review the known and putative roles of PTHrP in skin, mammary gland, placenta, and other reproductive tissues as well as the islet cells of the pancreas.

Principles of Bone Biology. https://doi.org/10.1016/B978-0-12-814841-9.00036-1

Skin

Parathyroid hormone-related protein and its receptor expression

Normal human keratinocytes were the first nonmalignant cells shown to produce PTHrP (Merendino et al., 1986), and multiple studies have confirmed that rodent and human keratinocytes in tissue culture express the PTHrP gene and secrete bioactive PTHrP (reviewed in Philbrick et al., 1996). PTHrP expression has also been examined in skin in vivo using both immunohistochemistry and in situ hybridization. During fetal development in rats and mice, PTHrP is expressed principally within the epithelial cells of developing hair follicles (Karmali et al., 1992; Lee et al., 1995). In mature skin, the PTHrP gene is also expressed most prominently within hair follicles, and mRNA levels appear to vary with the hair cycle. Cho et al. (2003) found that PTHrP expression increased within the outer root sheath and isthmus of late anagen hair follicles in mice. During catagen and telogen, PTHrP transcripts were abundant within the isthmus, but expression was downregulated during early anagen (Cho et al., 2003). In addition to hair follicles, low levels of PTHrP expression may also be found throughout the interfollicular epidermis from the basal to granular layer. Some studies have suggested that PTHrP is more highly expressed in superbasal keratinocytes (Danks et al., 1989; Hayman et al., 1989), although not all studies have reported this pattern (Atillasoy et al., 1991; Grone et al., 1994). A variety of factors have been reported to regulate PTHrP production by cultured keratinocytes (see Philbrick et al., 1996 for review). For example, glucocorticoids and 1,25-(OH)2D have been shown to suppress PTHrP production, whereas fetal bovine serum, matrigel, and an as-yet-unidentified factor(s) secreted from cultured fibroblasts have been shown to enhance PTHrP production. The upregulation of PTHrP production by fibroblast-conditioned media is particularly interesting, as PTHrP in turn acts back on dermal fibroblasts, suggesting that it may function in a short regulatory loop between keratinocytes and dermal fibroblasts (Shin et al., 1997; Blomme et al., 1999a). Finally, in vivo, PTHrP expression has been shown to be upregulated at the margins of healing wounds in guinea pigs (Blomme et al., 1999b). Interestingly, in this study, PTHrP was also detected in myofibroblasts and macrophages, suggesting that keratinocytes may not be the only source of PTHrP in skin.

The general consensus has been that keratinocytes do not express the type I PTH/PTHrP receptor (PTH1R), but dermal fibroblasts do (Hanafin et al., 1995; Orloff et al., 1995). PTHrP has been shown to bind to skin fibroblasts and elicit biochemical and biological responses in these cells (Shin et al., 1997; Blomme et al., 1999a; Wu et al., 1987). In addition, studies utilizing in situ hybridization in fetal skin have demonstrated that PTH1R mRNA is absent from the epidermis yet abundant in the dermis, especially in those cells adjacent to the keratinocytes (Karmali et al., 1992; Lee et al., 1995; Dunbar et al., 1999). There are fewer data concerning the expression patterns of the PTH1R in more mature skin, but in mice, it appears that the relative amount of PTH1R mRNA in dermal fibroblasts is reduced in adult compared with fetal skin (Cho et al., 2003). As with PTHrP, there also appears to be a hair-cycle-dependent variation in the expression of the PTH1R gene in the connective tissue adjacent to the isthmus of the hair follicles. However, unlike PTHrP mRNA, PTH1R mRNA appears to be most plentiful during early anagen (Cho et al., 2003). In addition to fibroblasts, studies using sensitive PCR-based detection methods have also reported expression of the PTH1R in keratinocytes, although these studies have used cultured cells (Errazahi et al., 2003, 2004). Furthermore, studies have shown that cultured keratinocytes bind and respond to PTHrP by inducing calcium transients, suggesting the presence of PTHrP receptors, either classical PTH1R or nonclassical, alternative PTHrP receptors (Orloff et al., 1992, 1995). However, to date no such alternative receptors have been isolated, so their existence remains uncertain. Furthermore, it is not clear whether PTH1R is expressed on keratinocytes in vivo. Therefore, although the possibility of both paracrine and autocrine signaling exists, no functional studies address the relative importance of either pathway to the biology of PTHrP in skin.

Biochemistry of parathyroid hormone-related protein

As described in Chapter 25, during transcription, the PTHrP gene undergoes alternative splicing to generate multiple mRNAs, which in human cells give rise to three main protein isoforms. In addition, each isoform is subject to posttranslational processing to generate a variety of peptides of varying length. Human keratinocytes have been shown to contain mRNA encoding for each of the three main isoforms, although as in other systems, no clearly defined or unique role has yet emerged for any of the three individual isoforms (Philbrick et al., 1996). Keratinocytes have also been shown to process full-length PTHrP into a variety of smaller peptides, including PTHrP(1−36) and a midregion fragment beginning at amino acid 38 (Soifer et al., 1992). These cells have also been shown to secrete a large (<10 kDa) amino-terminal form that is glycosylated (Wu et al., 1991). There is currently no specific information regarding the secretion of COOH-terminal peptides of PTHrP in skin, but keratinocytes are also likely to produce these peptides.

Function of parathyroid hormone-related protein

Several studies suggest that PTHrP is involved in the regulation of hair growth. As noted earlier, the PTHrP gene in embryonic skin is expressed most prominently in developing hair follicles, and overexpression of PTHrP in the basal keratinocytes of skin in transgenic mice leads to a severe inhibition of ventral hair follicle morphogenesis during fetal development (Wysolmerski et al., 1994). This appears to be the result of an interaction between PTHrP and BMP signaling that normally is involved in the regulation of Msx2 expression, patterning of the mammary mesenchyme, and lateral inhibition of hair follicle development around the nipple (Hens et al., 2007) (see "Mammary Gland"). However, it is unlikely that PTHrP is critical to hair follicle morphogenesis elsewhere, because disruption of the PTHrP or PTH1R genes does not seem to affect hair follicle formation or patterning in mice except for the vicinity of the nipple (Karaplis et al., 1994; Lanske et al., 1996; Foley et al., 1998).

It has also been suggested that PTHrP may participate in the regulation of the hair cycle. Systemic or topical administration of PTH1R antagonists to mice appears to perturb the hair cycle by prematurely terminating telogen, prolonging anagen growth, and inhibiting catagen (Schilli et al., 1997; Safer et al., 2007). In a reciprocal fashion, mice overexpressing PTHrP in their skin (K14-PTHrP mice) demonstrate a delayed emergence of dorsal hair and have shorter hairs, and their hair follicles enter catagen approximately 2 days early (Cho et al., 2003; Diamond et al., 2006). These findings were associated with a lower proliferation rate in the hair matrix and a less well-developed perifollicular vasculature during anagen. Together, these studies imply that PTHrP may regulate the anagen-to-catagen transition, acting to inhibit hair follicle growth by pushing growing hair follicles into the growth-arrested or catagen/telogen phase of the hair cycle. If this hypothesis were correct, one would expect PTHrP knockout mice to exhibit findings similar to PTH1R antagonist-treated mice. However, this does not appear to be the case. In mice that lack PTHrP in their skin, the hair cycle appears to be normal (Foley et al., 1998). In fact, rather than a promotion of hair growth, these mice demonstrate a thinning of their coats over time. These conflicting results are difficult to rationalize at this point, but suggest that although PTHrP may contribute to the regulation of the hair cycle, it is unlikely to be necessary for this process to unfold normally.

PTHrP has also been implicated in the regulation of keratinocyte proliferation and/or differentiation. Data from studies in vitro have suggested that PTHrP promotes the differentiation of keratinocytes (reviewed in Philbrick et al., 1996), but studies in vivo have suggested that PTHrP inhibits keratinocyte differentiation (Foley et al., 1998). A careful comparison of the histology of PTHrP-null and PTHrP-overexpressing skin demonstrated reciprocal changes. In the absence of PTHrP, it appeared that keratinocyte differentiation was accelerated, whereas in skin exposed to PTHrP overexpression, keratinocyte differentiation appeared to be retarded (Foley et al., 1998). Therefore, in a physiological context, PTHrP appears to slow the rate of keratinocyte differentiation and to preserve the proliferative basal compartment. Remarkably, these changes in the rate of keratinocyte differentiation are exactly analogous to those noted for chondrocyte differentiation in the growth plates of mice overexpressing PTHrP compared with PTHrP- and PTH1R-null mice (Philbrick et al., 1996). Again, at present it is difficult to rationalize conflicting data regarding the effects of PTHrP on keratinocyte differentiation, but studies in genetically altered mice indicate that PTHrP participates in the complex regulation of these processes in vivo. Further research will be needed to understand its exact role.

As alluded to previously, an important but still unresolved question is whether the effects of PTHrP on keratinocyte proliferation, differentiation, and hair follicle growth are the result of its effects on keratinocytes directly or via its effects on dermal fibroblasts. At present, more data support the paracrine possibility. PTH1R is expressed on dermal fibroblasts in vivo and in culture (Lee et al., 1995; Hanafin et al., 1995). Dermal fibroblasts have been demonstrated to show biochemical and biological responses to PTHrP (Shin et al., 1997; Blomme et al., 1999a; Wu et al., 1987; Thomson et al., 2003). Furthermore, PTHrP has been shown to induce changes in growth factor and extracellular matrix production that could in turn lead to changes in keratinocyte proliferation and/or differentiation and hair follicle growth (Shin et al., 1997; Blomme et al., 1999a; Insogna et al., 1989). Of course, the autocrine and paracrine signaling pathways are not mutually exclusive, but any direct autocrine effects of PTHrP on keratinocytes would require the presence of PTHrP receptors. An alternative possibility by which PTHrP might have cell autonomous effects on keratinocytes is via an intracrine pathway involving its translocation to the nucleus (Philbrick et al., 1996). Clearly, much research is needed to define the receptors and signaling pathways by which PTHrP acts in skin. Only when this information is available will we be able to understand the mechanisms leading to the skin phenotypes that have been observed in the various transgenic models discussed earlier.

Pathophysiology of parathyroid hormone-related protein

To date, PTHrP has not been clearly implicated in any diseases of the skin. It has been suggested that skin and skin appendage findings in rescued PTHrP-null mice are reminiscent of a series of disorders collectively known as ectodermal

dysplasias (Foley et al., 1998), but PTHrP has not been formally linked to any of these diseases. It has also been noted that psoriatic skin may downregulate PTHrP expression, and a small trial of topically administered PTH suggested that stimulation of the PTH1R might improve the histological abnormalities in psoriatic plaques (Hollick et al., 2003). However, these potentially exciting results have not yet been verified in larger trials. Topical application of PTH1R antagonists may be useful for stimulating hair growth, although no data yet suggest that PTHrP is involved in the pathogenesis of alopecia(s) (Safer et al., 2007; Skrok et al., 2015). The most common tumors causing humoral hypercalcemia of malignancy (HHM) are those of squamous histology, but these tumors rarely arise from skin keratinocytes. In fact, the most common skin tumors, basal cell carcinomas, do not overexpress PTHrP and are not associated with hypercalcemia (Philbrick et al., 1996). Primary hyperparathyroidism, hypoparathyroidism, and pseudohypoparathyroidism have each been sporadically reported to have cutaneous manifestations, but whether such findings are directly the result of abnormal PTH1R signaling, abnormal calcitriol concentrations, or a consequence of hypocalcemia or hypercalcemia remains unknown (Skrok et al., 2015). Although PTHrP appears to participate in the normal physiology of the skin, it is not clear at this juncture whether it is involved in skin pathophysiology.

Mammary gland

Very soon after its discovery, PTHrP was reported to be expressed in mammary tissue and secreted into milk at high concentrations (Thiede and Rodan, 1988; Budayr et al., 1989). In retrospect, it would have been much easier to extract PTHrP from human or cow milk than from the tiny amounts expressed in the tumors from which it was first isolated. It is now appreciated that PTHrP is critically important for the proper development and functioning of the mammary gland throughout life. In addition, it has been implicated as an important modulator of the biological behavior of breast cancer. The mammary gland develops in several discrete stages and only reaches its fully differentiated state during pregnancy and lactation. PTHrP appears to serve different functions during the principle stages of mammary development: embryonic development, adolescent growth, and pregnancy and lactation. For each stage, we will first outline the pertinent developmental events in rodents, as data regarding the function(s) of PTHrP largely come from studies in mice and rats. Next, we will discuss the localization of PTHrP and PTHrP receptors and the regulation of the expression of PTHrP and its receptors. Finally, we will address the function of PTHrP.

Embryonic mammary development

In mice, there are two phases of embryonic mammary development. The first involves the formation of five pairs of mammary buds, each of which consists of a bulb-shaped collection of epithelial cells surrounded by several layers of fibroblasts known as the mammary mesenchyme (Sakakura, 1987). After the formation of these buds, mouse mammary development displays a characteristic pattern of sexual dimorphism. In male embryos, in response to androgens, the mammary mesenchyme destroys the epithelial bud and male mice are left without mammary glands or nipples (Sakakura, 1987). In female embryos, however, the mammary buds remain quiescent until embryonic day 16 (E16), when they undergo a transition into the second step of embryonic development, the formation of the rudimentary ductal tree. This process involves the elongation of the mammary bud, its penetration out of the dermis and into a specialized stromal compartment known as the mammary fat pad, and the initiation of ductal branching morphogenesis. At the time of birth, the gland consists of a simple epithelial ductal tree consisting of 15−20 branched tubes within a fatty stroma (Sakakura, 1987). This initial pattern persists until puberty, at which time the mature virgin gland is formed through a second round of branching morphogenesis regulated by circulating hormones (discussed later).

The PTHrP gene is expressed exclusively within epithelial cells of the mammary bud soon after it begins to form. PTHrP mRNA continues to be localized to mammary epithelial cells during the initial round of branching morphogenesis as the bud grows out into the presumptive mammary fat pad and begins to branch (Dunbar et al., 1998, 1999; Wysolmerski et al., 1998). At some point after birth, PTHrP gene expression is downregulated, and in the adult virgin gland, PTHrP mRNA is found only within specific portions of the duct system (Dunbar et al., 1998). In contrast to the PTHrP gene, the PTH1R gene appears to be expressed within the mesenchyme, but its expression is widespread and is not limited to the developing mammary structures. Transcripts for the PTH1R gene are found within the mammary mesenchyme but also throughout the developing dermis (Dunbar et al., 1999; Wysolmerski et al., 1998). It is not clear when the receptor gene is first expressed within the subepidermal mesenchyme. However, it is already present when the mammary bud begins to form, and it continues to be expressed within fibroblasts surrounding the mammary ducts as they begin to extend and branch (Wysolmerski et al., 1998; Dunbar et al., 1998).

Epithelial expression of PTHrP and mesenchymal expression of the PTH1R are not unique to the developing mammary gland, and this pattern has long led to speculation that PTHrP and its receptor might contribute to the regulation of epithelial−mesenchymal interactions during organogenesis. There is now solid evidence that this is the case during embryonic mammary development, where PTHrP acts as an epithelial signal that influences cell fate decisions within the developing mammary mesenchyme. Data supporting this notion come from studies in several genetically altered mouse models. First, in PTHrP or PTH1R knockout mice, there is a failure of the normal androgen-mediated destruction of the mammary bud owing to the failure of the mammary mesenchyme to differentiate properly and to express androgen receptors (Dunbar et al., 1999). Second, in PTHrP and PTH1R knockout mice, the mammary buds fail to grow out into the fat pad and initiate branching morphogenesis, again due to defects in the mammary mesenchyme (Wysolmerski et al., 1998; Dunbar et al., 1998). Finally, in keratin 14 (K14)-PTHrP transgenic mice that ectopically overexpress PTHrP within all the basal keratinocytes of the developing embryo, subepidermal mesenchymal cells, which should acquire a dermal fate, instead react to the excess PTHrP by becoming mammary mesenchyme (Dunbar et al., 1999).

As demonstrated by these studies, PTHrP signaling is essential for mammary gland formation in rodents. When the mammary gland begins to form, PTH1R is expressed in all of the mesenchymal cells underneath the epidermis, but PTHrP is expressed only within the mammary epithelial buds and not within the epidermis itself (Karmali et al., 1992; Thiede and Rodan, 1988; Wysolmerski et al., 1998). As the mammary bud grows down into the mesenchyme, PTHrP, produced by mammary epithelial cells, interacts over short distances with PTH1R on the immature mesenchymal cells closest to the epithelial bud and triggers these cells to differentiate into mammary mesenchyme. PTHrP accomplishes this, at least in part, by upregulating expression of BMP receptors on the mesenchymal cells and sensitizing them to respond in an autocrine fashion to BMP4 expressed in the ventral surface of the embryo (Hens et al., 2007). In this way, PTHrP acts as a patterning molecule contributing to the formation of small patches of mammary-specific stroma around the mammary buds and within the surrounding sea of presumptive dermis (Fig. 36.1; Foley et al., 2001). The process of differentiation set in motion by PTHrP signaling is critical to the ability of the mammary-specific stroma to direct further morphogenesis of the epithelium and to inhibit hair follicle development in the vicinity of the developing nipple. In the absence of this signaling, the mesenchyme can neither destroy the epithelial bud in response to androgens nor trigger the outgrowth of the bud and the initiation of branching morphogenesis (Dunbar et al., 1998, 1999a; Wysolmerski et al., 1998).

Although the model described earlier was developed from studies in mice, PTHrP is also critical to the formation of breast tissues in human fetuses. Blomstrand's chondrodysplasia is a fatal form of dwarfism caused by null mutations of the PTH1R gene (Jobert et al., 1998) (see Chapter 44). Affected fetuses have skeletal abnormalities similar to those caused by deletion of the PTHrP and PTH1R genes in mice (see Chapter 15) and in addition lack breast tissue and nipples (Wysolmerski et al., 1999). In normal human fetuses, the PTHrP gene is expressed within the mammary epithelial bud, and

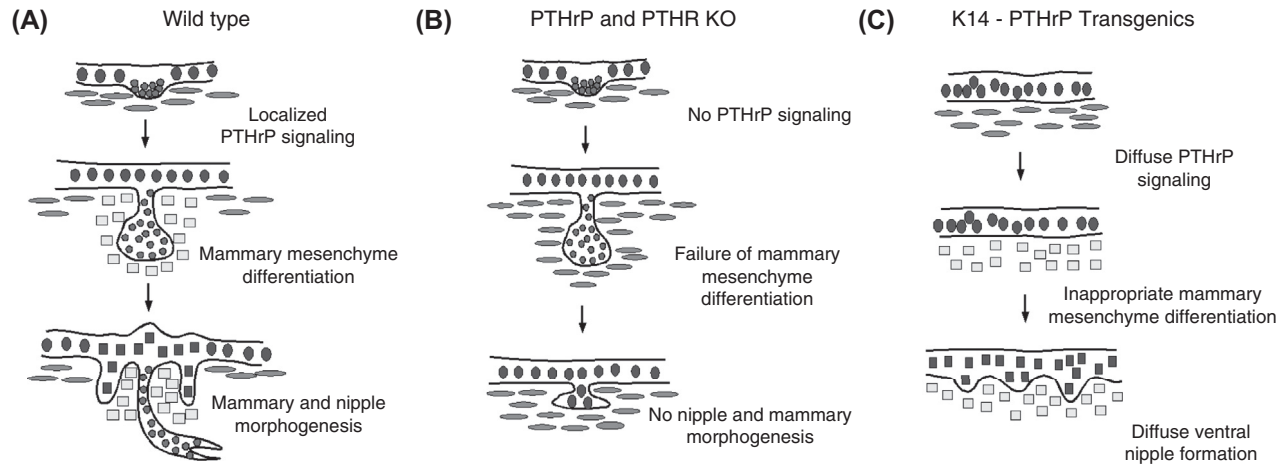

FIGURE 36.1 Model for the regulation of cell fate by PTHrP signaling during mammary gland and nipple development. (A) Normally, the mammary epithelial cells (small circles) express PTHrP after the bud starts to form. PTHrP signals to the dermal mesenchyme (ovals) near the developing bud, and as a result, these cells become mammary mesenchyme (light squares). The mammary mesenchyme maintains the mammary fate of the epithelial cells, triggers their morphogenesis, and induces the overlying epidermis (upright ovals) to become the nipple (dark squares). (B) In the absence of PTHrP signaling, no mammary mesenchyme is formed. Therefore, the mammary epithelial cells revert to an epidermal fate, no morphogenesis occurs, and the nipple does not form. (C) In the presence of diffuse PTHrP signaling, the entire ventral dermis becomes mammary mesenchyme, and the ventral epidermis becomes nipple sheath. *Reproduced from Foley, J., Dann, P., Hong, J., Cosgrove, J., Dreyer, B., Rimm, D., Dunbar, M. E., Philbrick, W., Wysolmerski, J.J., 2001. Parathyroid hormone-related protein maintains mammary epithelial fate and triggers nipple skin differentiation during embryonic mammary development. Development 128, 513−525, with permission.*

the PTH1R gene is expressed in surrounding mesenchyme (Wysolmerski et al., 1999; Cormier et al., 2003). Therefore, in humans as in mice, epithelial-to-mesenchymal PTHrP-to-PTH1R signaling is essential to the formation of the embryonic mammary gland.

Adolescent mammary development

After birth, the murine mammary gland undergoes little development until the onset of puberty. At that point, in response to hormonal changes, the distal ends of the mammary ducts form specialized structures called terminal end buds. These structures serve as sites of cellular proliferation and differentiation during a period of active growth that gives rise to the typical branched duct system of the mature virgin gland (Daniel and Silberstein, 1987). Once formed, the ductal tree remains relatively unchanged until pregnancy when another round of hormonal stimulation induces the formation of the alveolar units that produce milk.

Similar to findings in the embryonic mammary gland, during puberty PTHrP is a product of mammary epithelial cells, and PTH1R is expressed in stromal cells (Dunbar et al., 1998). However, the structure of the pubertal gland is more complex than that of the embryonic gland, and here there are conflicting data regarding the localization of PTHrP and the PTH receptor. Although there is general agreement that PTHrP is expressed in epithelial cells in the postnatal gland, there is some disagreement regarding the specific epithelial compartments in which PTHrP is found. Studies employing in situ hybridization in mice have suggested that after birth, the overall levels of PTHrP gene expression in mammary ducts are reduced except in the terminal end buds during puberty (Dunbar et al., 1998). In these structures, appreciable amounts of PTHrP mRNA were detected in the peripherally located cap cells. In other parts of the gland there was little, if any, specific hybridization for PTHrP. In contrast, studies looking at mature human and canine mammary glands using immunohistochemical techniques have suggested that PTHrP can be found in both luminal epithelial and myoepithelial cells throughout the ducts (Grone et al., 1994; Liapis et al., 1993). Furthermore, studies using cultured cells have suggested that PTHrP is produced by luminal and myoepithelial cells isolated from normal glands (Ferrari et al., 1992; Seitz et al., 1993; Wojcik et al., 1999). Fewer reports have looked at the localization of PTH1R expression in the postnatal mammary gland, but as in embryological development, it is expressed in the mammary stroma (Dunbar et al., 1998). In situ hybridization studies have found the highest concentration of PTH1R mRNA in the stroma immediately surrounding terminal end buds during puberty (Dunbar et al., 1998). This same study found lower levels of PTH1R mRNA distributed generally within the fat pad stroma but very little expression in the dense stroma surrounding the more mature ducts. In addition, these investigators found no evidence of PTH1R mRNA in freshly isolated epithelial cells (Dunbar et al., 1998). In contrast, other studies have suggested that PTH1R is expressed in cultured luminal epithelial and myoepithelial cells (Seitz et al., 1993; Wojcik et al., 1999) as well as in cultured breast cancer cell lines (Birch et al., 1995). In summary, during puberty PTHrP and its receptor are found predominantly within the terminal end buds, with PTHrP localized to the epithelium and PTH1R localized in the stroma. It remains an open and interesting question whether, at some time during mammary ductal development, epithelial cells express low levels of PTH1R.

Studies in transgenic mice have suggested that PTHrP regulates mammary morphogenesis during puberty. Overexpression of PTHrP in mammary epithelial cells using the K14 promoter results in an impairment of ductal branching morphogenesis (Wysolmerski et al., 1995). There are two aspects to the defect. First, the terminal end buds advance through the mammary fat pad at a significantly slower rate than normal. Second, there is a severe reduction in the branching complexity of the ductal tree. As seen in Fig. 36.2, this results in a spare and stunted epithelial duct system. Experiments altering the timing and duration of PTHrP overexpression in the mammary gland using a tetracycline-regulated K14-PTHrP transgene have demonstrated that the two aspects of this pubertal phenotype appear to represent separate functions of PTHrP. The branching (or patterning) defect results from embryonic overexpression of PTHrP, whereas the ductal elongation defect is a function of overexpression of PTHrP during puberty (Dunbar et al., 2001). These effects on ductal patterning provide further evidence of the importance of PTHrP as a regulator of embryonic mammary development. In addition, the localization patterns for PTHrP and PTH1R during puberty, combined with the effects of pubertal overexpression of PTHrP on ductal growth, suggest that PTHrP also functions later in mammary development. During puberty it appears to modulate the epithelial−mesenchymal interactions that govern ductal elongation.

Pregnancy and lactation

Mammary epithelial cells only reach their fully differentiated state during lactation. Under hormonal stimulation during pregnancy, there is a massive wave of epithelial proliferation and morphogenesis that gives rise to multiple terminal ductules and alveolar units. During the later stages of pregnancy, the epithelial cells fully differentiate and then begin to

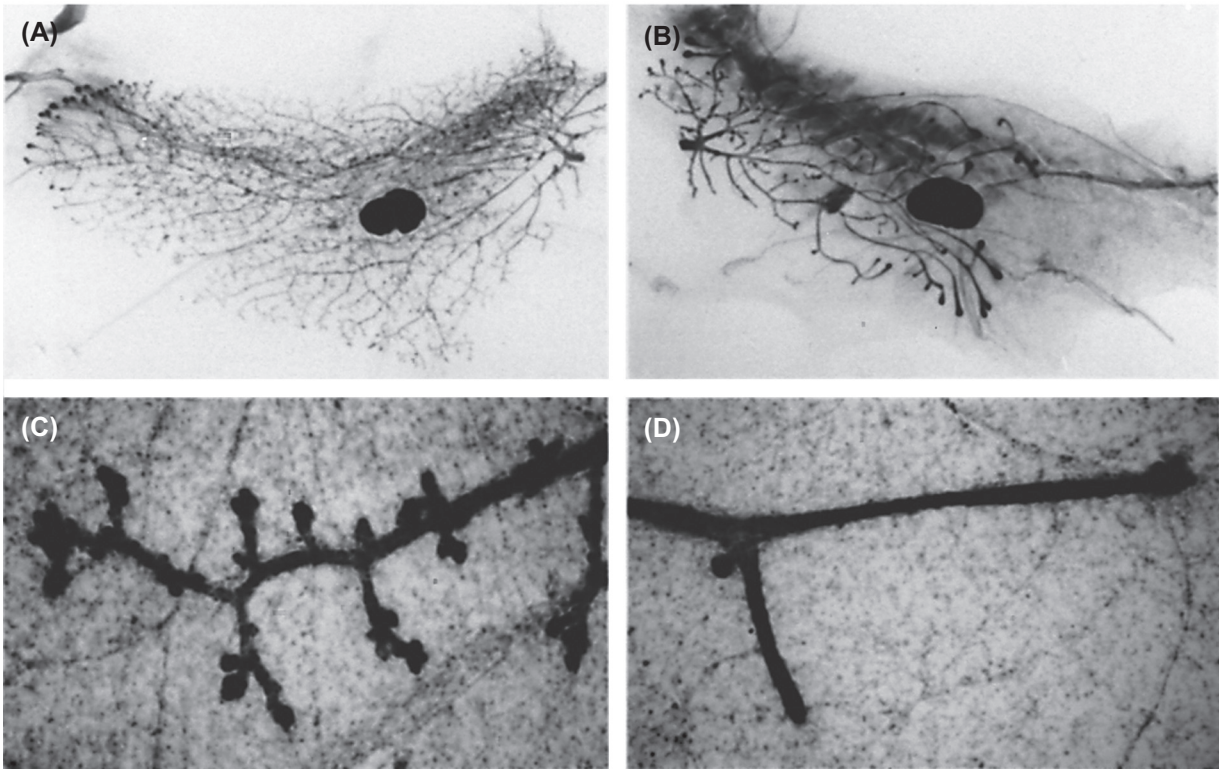

FIGURE 36.2 Overexpression of PTHrP in the mammary gland of K14-PTHrP transgenic mice antagonizes ductal elongation and branching morphogenesis during puberty. **A** and **B** represent typical whole-mount analyses of the fourth inguinal mammary glands from wild-type (A) and K14-PTHrP transgenic mice (B) at 6 weeks of age. The dark oval in the center of each gland is a lymph node. Growth of the ducts during puberty is directional, and each gland is arranged so that the primary duct (the origin of the duct system) is toward the center of the figure. Note that overexpression of PTHrP results in an impairment of the elongation of the ducts through the fat pad as well as a dramatic reduction of the branching complexity of the ductal tree. **C** and **D** represent higher magnifications of a portion of the ducts from the wild-type (C) and transgenic (D) glands demonstrating the reduction in side branching caused by overexpression of PTHrP. *Modified from Wysolmerski, J.J., McCaughern-Carucci, J.F., Daifotis, A.G., Broadus, A.E., Philbrick, W.M., 1995. Overexpression of parathyroid hormone-related protein or parathyroid hormone in transgenic mice impairs branching morphogenesis during mammary gland development. Development 121, 3539–3547 with permission.*

secrete milk during lactation. By the time lactation commences, the fatty stroma of the mammary gland is almost completely replaced by actively secreting alveoli. Upon completion of lactation, widespread apoptosis of the differentiated epithelial cells occurs, and the gland remodels itself into a duct system similar to that of the virgin animal (Daniel and Silberstein, 1987).

Localization studies in humans, rodents, and cows have all noted epithelial cells to be the source of PTHrP in the mammary gland during pregnancy and lactation (Liapis et al., 1993; Wojcik et al., 1998, 1999; Rakopoulos et al., 1992). Based on the assessment of whole-gland RNA, PTHrP expression appears to be upregulated at the start of lactation under the control of both local and systemic factors (Philbrick et al., 1996; Thiede and Rodan, 1988; Thiede, 1989; Thompson et al., 1994; Buch et al., 1992). Thiede and Rodan (1988) and Thiede (1989) originally reported that PTHrP expression in rats is dependent on suckling and on serum prolactin concentrations. However, prolactin must serve only as a permissive factor, for additional studies have shown that the suckling response is a local one and that PTHrP only rises in the milked gland (Thompson et al., 1994). Furthermore, overall PTHrP expression increases gradually over the course of lactation, and in later stages its expression becomes independent of serum prolactin levels (Bucht et al., 1992). Serotonin is now recognized as playing an important role in local control of PTHrP production by mammary tissue (Hernandez et al., 2012; Marshall et al., 2014). It is clear that much of the PTHrP made during lactation ends up in milk, in which levels of PTHrP are up to 10,000-fold higher than in the circulation of normal individuals and 1000-fold higher than in patients suffering from HHM (Philbrick et al., 1996). PTHrP concentrations in milk have generally been found to mirror RNA levels in the gland, increasing over the duration of lactation and rising acutely with suckling (Thompson et al., 1994; Yamamoto et al., 1991; Law et al., 1991; Goff et al., 1991). In addition, evidence shows that PTHrP levels may vary with the calcium content of milk (Yamamoto et al., 1992a; Law et al., 1991; Goff et al., 1991; Uemura et al., 1997; Kovacs and Kronenberg, 1997; Kovacs, 2016). In mice, the

calcium-sensing receptor (CaR) is expressed on the basolateral surface of mammary epithelial cells during lactation and regulates PTHrP production such that increased delivery of calcium to the mammary gland decreases PTHrP production and secretion into milk (VanHouten et al., 2004; Ardeshirpour et al., 2006). Selective ablation of CaR within mammary tissue results in locally increased PTHrP production and increased milk PTHrP content (Mamillapalli et al., 2013). Finally, in mice, PTHrP mRNA levels are promptly downregulated during the early stages of involution and then increase to prelactation levels about a week into the remodeling process (Wysolmerksi et al., 2008).

In contrast to PTHrP, little study has been made of the expression and regulation of PTHrP receptors during pregnancy and lactation. In early pregnancy, the PTH/PTHrP receptor is expressed at low levels in the stroma surrounding the developing alveolar units (Dunbar et al., 1998). Studies using whole-gland RNA demonstrate a reciprocal relationship between PTH1R and PTHrP mRNA levels. That is, as PTHrP expression rises during lactation, PTH1R mRNA levels decrease, and as PTHrP mRNA levels fall during early involution, PTH1R expression increases to its former level (Wysolmerski et al., 2008). This may represent active downregulation of the receptor by PTHrP or may simply reflect the changing amount of stroma within the gland at these different stages. However, in a study of cells isolated from lactating rats, it was suggested that epithelial cells, as well as stromal cells, express this receptor (Wojcik et al., 1999), so the regulation of PTH1R expression during pregnancy and lactation may be complex.

Initial reports of the presence of PTHrP in the mammary gland and milk prompted a great deal of speculation regarding its functions in breast tissue during lactation. These proposals revolved around four general hypotheses that PTHrP may be involved in (1) maternal calcium homeostasis and the mobilization of calcium from the maternal skeleton; (2) regulating vascular and/or myoepithelial tone in the lactating mammary gland; (3) transepithelial calcium transport into milk; and (4) neonatal calcium homeostasis or neonatal gut physiology. As will be discussed, there is support for all four hypotheses. The function of PTHrP in the lactating mammary gland in mice was addressed by disrupting the PTHrP gene solely in mammary epithelial cells during lactation (VanHouten et al., 2003). This experiment has supplied evidence to support the role of PTHrP in regulating maternal and neonatal calcium and bone metabolism and has shown that PTHrP plays an indirect role in mediating calcium transport into milk. This point was made clearer in experiments that used calcimimetic drugs or ablated CaR from mammary epithelial cells and found that this increased the mammary production of PTHrP and milk calcium content. It appears that PTHrP's role during lactation is a systemic one to maintain the supply of calcium to the breast tissue that supports milk production, whereas the transport of calcium into milk is locally controlled by CaR and other factors (VanHouten et al., 2004; Ardeshirpour et al., 2006; Mamillapalli et al., 2013; Kovacs, 2016).

Milk production requires a great deal of calcium, and providing an adequate supply to the mammary gland stresses maternal bone and mineral metabolism (Kovacs and Kronenberg, 1997; Kovacs, 2016). Some of the calcium required for milk comes from the diet, as calcium intake is increased owing to the orexigenic effects of suckling (Smith and Grove, 2002). In addition, renal reabsorption of calcium is increased during lactation so that urinary losses are reduced. Finally, a significant proportion of the calcium transported into milk is derived from the maternal skeleton, through the processes of osteoclast-mediated bone resorption and osteocytic osteolysis (Kovacs, 2016). All three processes (intestinal calcium absorption, renal calcium conservation, and skeletal resorption) are stimulated in part by PTHrP. The interplay between intestinal calcium absorption, renal calcium conservation, and skeletal resorption is best illustrated in the rodent, which requires both increased intestinal calcium absorption *and* increased skeletal resorption in order to provide the calcium needed to milk. Increasing the calcium content of the diet causes increased renal calcium excretion and blunts skeletal resorption, whereas a low-calcium diet causes a marked increase in skeletal resorption and reduced renal calcium excretion (Kovacs, 2016). The combination of a low-calcium diet and the use of an antiresorptive medication to block skeletal resorption leads to reduced milk calcium content, tetany, and sudden death of lactating rodents (Kovacs, 2016). In contrast to rodents, intestinal calcium absorption is normal during lactation in women, and low and high intakes of calcium do not influence the magnitude of skeletal resorption during lactation (Kovacs, 2016). Instead, during human lactation, the extent of skeletal resorption appears to be programmed by the intensity of lactation, which in turn determines the production of PTHrP. Breast milk output predicts the rise in PTHrP, and both parameters predict the magnitude of bone mineral density lost during lactation (Kovacs, 2016).

Overall rates of bone turnover are elevated during lactation, but bone resorption and formation are uncoupled, such that bone resorption outstrips bone formation to cause a rapid decline in bone mass. The average nursing woman loses between 5% and 10% of her bone mass over 6 months, especially from the trabecular spine (Kovacs, 2016), whereas rodents lose up to one-third of their skeletal mass over 21 days of lactation (VanHouten and Wysolmerski, 2003). Mobilization of skeletal calcium during lactation does not rely on any of the established calcium-regulating hormones, PTH, 1,25(OH)2D, or calcitonin (Kovacs and Kronenberg, 1997; Kovacs, 2016). Multiple investigations have confirmed that bone resorption is increased because of the combination of decreased systemic estradiol concentrations and elevated circulating PTHrP levels. Suckling directly inhibits hypothalamic gonadotropin-releasing hormone (GnRH) secretion and induces hypogonadotropic

hypogonadism (Smith and Grove, 2002). Bone loss correlates with the duration of amenorrhea in nursing women; however, the intensity of lactation predicts bone loss and the duration of amenorrhea, and bone loss has been shown to continue in women whose menses resume despite ongoing intense lactation (Kovacs, 2016). Pharmacological treatment with estradiol in lactating mice reduced bone loss by 60% (VanHouten and Wysolmerski, 2003); however, the resulting estradiol levels were fivefold higher than normal and may therefore indicate suppressed bone loss from the known pharmacological effects of estradiol rather than implicating that estradiol deficiency accounts for 60% of the bone loss that normally occurs during lactation.

Many studies have now documented elevated circulating PTHrP levels in lactating humans and rodents (Kovacs and Kronenberg, 1997; Kovacs, 2016), and PTHrP levels correlate directly with biochemical markers of bone resorption and inversely with bone mass in lactating mice (VanHouten and Wysolmerski, 2003). In addition, circulating PTHrP levels have been shown to correlate with bone density changes in lactating humans (Sowers et al., 1996). Furthermore, there have been multiple case reports of pseudohyperparathyroidism during pregnancy and lactation, in which PTHrP secretion by breasts was determined to have caused hypercalcemia with high plasma concentrations of PTHrP (see below) (Kovacs, 2016). In normal lactating women who have been followed longitudinally, the albumin-corrected serum calcium and ionized calcium rise significantly but stay within the normal range, whereas serum phosphorus rises above normal, with these effects implying the release of calcium and phosphorus from bone (Kovacs, 2016). Therefore, the condition of pseudohyperparathyroidism may represent one extreme of the normal physiology of lactation, in which PTHrP's effects to increase bone resorption lead to an increase in the circulating calcium concentration.

When the PTHrP gene was disrupted specifically in the lactating mammary gland in mice, circulating PTHrP levels declined, milk PTHrP became unmeasurable, rates of bone resorption decreased, and bone loss was reduced by 50% (VanHouten et al., 2003). The circulating PTHrP level remained above nonpregnant values; moreover, the mice developed significant secondary hyperparathyroidism, which would have supported ongoing bone resorption despite lower circulating PTHrP. Similarly, loss of the gene encoding calcitonin led to a doubling of bone loss during lactation, increased milk calcium content, increased PTHrP, and marked secondary hyperparathyroidism (Woodrow et al., 2006; Collins et al., 2013; Kovacs, 2016). Thus, it is now clear that the lactating mammary gland secretes PTHrP into both milk and the circulation, and that secondary hyperparathyroidism can contribute to increasing skeletal resorption during lactation when the demand for skeletal calcium is particularly high or PTHrP is absent. Systemic PTHrP from the breast acts together with estrogen deficiency to stimulate bone resorption and cause bone loss during lactation. As noted previously, the production of PTHrP by the lactating breast is decreased by stimulation of the CaR on mammary epithelial cells (VanHouten et al., 2004).

Fig. 36.3 displays the "breast−brain−bone" circuit, a classic endocrine feedback loop during lactation in which the mammary gland functions as an "accessory" parathyroid gland. It uses PTHrP instead of PTH to ensure an adequate flow of calcium from the maternal skeleton to make milk. If calcium delivery to the gland falls, mammary epithelial cells produce more PTHrP, which stimulates increased bone resorption. The delivery of more calcium to the mammary gland from the skeleton then stimulates the CaR and decreases PTHrP production. But milk production is controlled mainly by suckling on demand, which in turn can provoke maternal hypocalcemia (milk fever in animals) and secondary hyperparathyroidism.

Genetic removal of PTHrP from the mammary gland does not alter milk calcium levels, and PTHrP-null mammary epithelial cells are able to transport calcium in vitro at the same rate as wild-type mammary epithelial cells (VanHouten et al., 2003). Thus, unlike the placenta (see later), it does not appear that PTHrP directly contributes to the regulation of transepithelial calcium transport in the mammary gland. However, as mentioned earlier, the marked secondary hyperparathyroidism that developed in that model would have supported calcium delivery to the mammary tissues despite the absence of PTHrP's normal effects, and the circulating PTHrP level was still elevated during lactation over its nonpregnancy values. Multiple human studies have found that milk calcium content correlates with the content of PTHrP, which is consistent with PTHrP's function to supply calcium to mammary tissue, even if it does not directly stimulate pumping of calcium into milk from mammary epithelial cells (Kovacs, 2016).

The function of PTHrP in milk remains an open question. Murine pups that receive PTHrP-deleted milk accrete more skeletal mineral content over the first 12 days after birth (Mamillapalli, 2013), which suggests that PTHrP within milk may modulate either intestinal calcium absorption or skeletal mineral accretion in neonatal mice. Whether PTHrP in milk is absorbed into the neonatal circulation is an unresolved question, but some animal studies have suggested that it is absorbed intact, and might therefore have effects on the skeletal and mineral metabolism in the neonate (Kovacs, 2016). Further work is needed to understand the role of PTHrP in milk.

Another potential function of PTHrP during lactation is the regulation of vascular and/or myoepithelial cell tone. As discussed in Chapter 26, PTHrP has been shown to modulate smooth muscle cell tone in a variety of organs, including the vascular tree, where it acts as a vasodilator. Consistent with these effects, two studies have shown that PTHrP increases

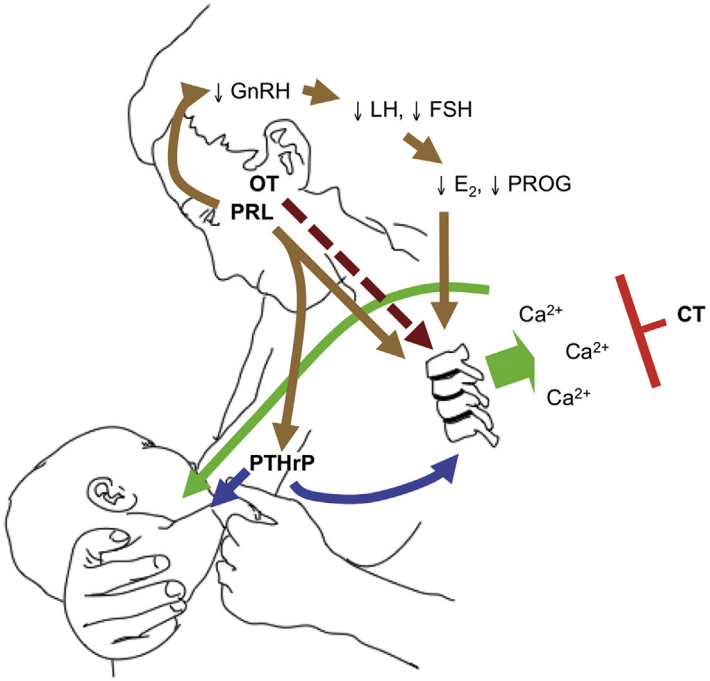

FIGURE 36.3 Breast–Brain–Bone circuit controls lactation. Suckling and prolactin [PRL] both inhibit the hypothalamic GnRH pulse center, which in turn suppresses the gonadotropins (luteinizing hormone [LH] and follicle-stimulating hormone [FSH]), leading to low levels of the ovarian sex steroids (estradiol [E_2] and progesterone [PROG]). Prolactin may also have direct effects on its receptor in bone cells. PTHrP production and release from the breast are stimulated by suckling, prolactin, low estradiol, and the calcium receptor. PTHrP enters the bloodstream and combines with systemically low estradiol levels to markedly upregulate bone resorption and (at least in rodents) osteocytic osteolysis. Increased bone resorption releases calcium and phosphate into the blood stream, which then reaches the breast ducts and is actively pumped into the breast milk. PTHrP also passes into milk at high concentrations, but whether swallowed PTHrP plays a role in regulating calcium physiology of the neonate is uncertain. In addition to stimulating milk ejection, oxytocin may directly affect osteoblast and osteoclast function (dashed line). Calcitonin may inhibit skeletal responsiveness to PTHrP and low estradiol given that mice lacking calcitonin lose twice the amount of bone during lactation as normal mice. Not depicted is that calcitonin may also act on the pituitary to suppress prolactin release, and within breast tissue to reduce PTHrP expression and lower the milk calcium content (see text). *Adapted with kind permission from Kovacs, C.S., 2005a. Calcium and bone metabolism during pregnancy and lactation. J. Mammary Gland Biol. Neoplasia 10 (2), 105–118, © Springer Science and Business Media B.V.*

mammary blood flow during lactation (Davicco et al., 1993; Thiede et al., 1992). The injection of amino-terminal fragments of PTHrP into the mammary artery of dried (nonlactating) ewes was shown to increase mammary blood flow and override the vasoconstrictive effects of endothelin (Davicco et al., 1993). Thiede and colleagues (1992) have demonstrated that the nutrient arteries of the inguinal mammary glands of rats secrete PTHrP and that its production is responsive to suckling and prolactin. Myoepithelial cells in the breast are similar in some ways to vascular smooth muscle cells and are thought to participate in the control of milk ejection by contracting in response to oxytocin (Daniel and Silberstein, 1987). Therefore, it is interesting that myoepithelial cells in culture have been shown to express PTH1R and to respond to PTHrP by elevating intracellular cAMP (Seitz et al., 1993; Wojcik et al., 1999). Furthermore, mirroring the effects of PTHrP on the endothelin-induced contraction of vascular smooth muscle, PTHrP has been shown to block the rise in intracellular calcium normally induced in response to oxytocin in myoepithelial cells (Seitz et al., 1993).

Pathophysiology of parathyroid hormone-related protein in the mammary gland

PTHrP may contribute to pathophysiology in the human breast in several instances. First, as noted previously, fetuses afflicted with Blomstrand's chondrodystrophy lack nipples and breast tissue (Wysolmerski et al., 1999). Second, some cases of PTHrP-mediated hypercalcemia during pregnancy or lactation (pseudohyperparathyroidism) have been reported to be associated with elevations in circulating levels of PTHrP (Khosla et al., 1990; Reid et al., 1992; Kovacs, 2016). Additional cases of pseudohyperparathyroidism have been caused by the placental production of PTHrP; see later. One of these cases was caused by massive breast hyperplasia, and after reduction mammoplasty, the patient's hypercalcemia and elevated PTHrP levels both resolved (Khosla et al., 1990). However, large breasts are not a requirement for pseudohyperparathyroidism to occur. A related aspect is that the production of PTHrP by the lactating mammary gland

leads to normalization of mineral and bone metabolism in hypoparathyroid women who breastfeed (Kovacs, 2016). In some cases, hypercalcemia has developed when exogenous use of calcitriol and calcium supplements has not been stopped in advance of lactation in these hypoparathyroid women. Finally, the area with the greatest potential impact on human health is the relationship of PTHrP production to breast cancer. This is evolving into a complicated topic and will be addressed only briefly here. However, it will be reviewed in more depth in Chapters 55 and 56.

It is well documented that PTHrP is produced by a number of primary breast carcinomas and that this sometimes leads to classical HHM (Isales et al., 1987). A potentially more widespread role may be the involvement of PTHrP in the osteotrophism of breast cancer (Guise et al., 1996; Yin et al., 1999). Animal models have suggested that PTHrP production by breast tumor cells is important to their ability to form skeletal metastases (Guise et al., 1996; Yin et al., 1999). However, there is conflicting evidence as to whether PTHrP production by a primary breast tumor is predictive of bone metastases in patients (Bundred et al., 1996; Henderson et al., 2001, 2006). The largest and most carefully controlled study suggested that PTHrP production by the primary tumor is actually a negative rather than positive predictor of skeletal metastases (Henderson et al., 2006). It may be that PTHrP production does not enable a tumor cell to get into the skeleton, but once there, the ability of tumor cells to upregulate PTHrP production within the bone microenvironment becomes important to their ability to grow in the skeleton (Yin et al., 1999). Several studies suggest that TGF-β released from the bone matrix during bone resorption may be particularly important in stimulating PTHrP production (Kakonen et al., 2002). More PTHrP would in turn be expected to increase osteoclast activity and release more TGF-β, setting up a potential feed-forward vicious cycle that may be important in the pathogenesis of bone destruction around the metastatic tumor.

There is a growing literature suggesting that PTHrP may also be important in controlling breast cancer cell proliferation, apoptosis, migration, and invasion. Although it is unclear whether normal mammary epithelial cells express significant levels of the PTH1R, it appears that many breast cancer cell lines do so (Birch et al., 1995). Some of the effects ascribed to PTHrP appear to be mediated by this receptor, but some appear to be mediated by midregion PTHrP fragments acting either through intracrine mechanisms or perhaps via a specific midregion PTHrP cell-surface receptor (Shen et al., 2004; Kumari et al., 2006; Shen and Falzon, 2006; Dittmer et al., 2006; Sirchia et al., 2007). In either case, the effects of midregion PTHrP apparently require that this portion of the peptide enter the nucleus via a distinct bipartite nuclear localization signal. In particular, several studies have suggested that midregion PTHrP fragments may promote cell migration by regulating α6β4 integrin expression through nuclear effects (Shen et al., 2003; Dittmer et al., 2006; Shen and Falzon, 2006). Despite these intriguing findings, at this point it is not clear whether these effects are artifacts of cell lines or will prove to be clinically relevant. Most studies in cell lines suggest that PTHrP expression by a breast tumor would contribute to increased aggressiveness or a tendency to metastasize.

However, animal models have provided seemingly contradictory data regarding PTHrP's potential influence on breast cancer tumor progression. Deletion of PTHrP promoted tumor progression in the *Neu* mouse model of spontaneous tumor development (Fleming et al., 2009), while deletion of PTHrP in the MMTV-PyMT mouse model had the opposing effect of preventing tumor progression (Li et al., 2011). These mouse studies make it unclear as to whether it would be beneficial or harmful to inhibit PTHrP expression in the primary tumors of patients with breast cancer.

On the other hand, human studies have suggested that expression of PTHrP by the primary breast tumor has beneficial effects on multiple outcomes. In the large prospective clinical study of Henderson and colleagues mentioned previously (Henderson et al., 2001, 2006), in which patients were assessed 5 and 10 years after surgery, PTHrP expression by a primary breast tumor was clearly a marker of a less aggressive course correlating with estrogen and progesterone receptor positive status, increased survival, lower rates of recurrence, and lower rates of all metastases (not just bone metastases). An analysis of the METABRIC dataset within The Cancer Genome Atlas breast cancer dataset revealed that expression of the human PTHrP gene, *PTHLH*, was upregulated (not downregulated) at the mRNA level or amplified in breast cancer patients (R.J. Johnson, A.W. Freeman and T.J. Martin, unpublished, 2018). Furthermore, patients with mRNA upregulation of *PTHLH* had significantly increased overall survival. Similar results have been gleaned from other gene expression surveys in breast cancer (www.oncomine.org; Rhodes et al., 2004). Further in vivo studies are clearly needed, but the available human data suggest that inhibiting PTHrP expression in primary breast cancers may be harmful rather than beneficial.

Reproductive tissues

Parathyroid hormone-related protein and placental calcium transport

Nearly all the calcium, and a large proportion of inorganic phosphate (85%) and magnesium (70%), transferred from mother to fetus is associated with development and mineralization of the fetal skeleton (Grace et al., 1986). The bulk of placental calcium transfer occurs rapidly over a short interval late in gestation, such that 80% occurs in the third trimester in

humans (Givens and Macy, 1933), and 96% occurs in the last 5 days of gestation in the rat (Comar, 1956). The concentrations of both total and ionized Ca in all mammalian fetuses studied during late gestation have been observed to be higher than maternal levels. As a result of studies in which the sheep was used extensively for the study of fetal calcium control, one of the first suggested physiological roles of PTHrP was that of regulating the transport of calcium from mother to fetus in the mammal, thereby making calcium available to the growing fetal skeleton (Rodda et al., 1988).

Immunoreactive PTH levels were found to be low in fetal lambs, whereas PTH-like biological activity in serum was high (Care et al., 1985), suggesting the presence of another PTH-like substance. Similar findings of low PTH and high PTHrP have been demonstrated in multiple studies of fetal mice and human cord blood (Kovacs, 2003, 2016). Parathyroidectomy in the fetal lamb resulted in loss of the calcium gradient that exists between mother and fetus as well as impairment of bone mineralization, implicating parathyroids as the source of the regulatory agent. Crude, partially purified, or recombinant PTHrP, but neither PTH nor maternal parathyroid extract that contained no immunoreactive PTHrP, restored the gradient (Rodda et al., 1988). Thus, PTHrP appeared to be the active component of the fetal parathyroid glands responsible for maintaining fetal calcium levels and suppressing fetal PTH levels. In support of this hypothesis, immunoreactive PTHrP was found to be readily detectable in sheep fetal parathyroids from the time they form (MacIsaac et al., 1991) and was also found in early placenta, suggesting that the latter tissue may be a source of PTHrP for calcium transport early in gestation.

The portion of PTHrP that appears to be responsible for regulating placental calcium transport lies between residues 67 and 86 (Care et al., 1990), but the responsible receptor has not yet been identified. Although syncytiotrophoblasts are believed to be central in the transport of calcium to the fetus, cytotrophoblasts (which differentiate to form the syncytium) are believed to be the calcium-sensing cells, and raising the extracellular calcium concentration has been shown to inhibit PTHrP release from these cells (Hellman et al., 1992). The CaR has been localized to cytotrophoblasts of human placenta (Bradbury et al., 1997), and the work of Kovacs et al. (1998) has implicated it in placental calcium transport. Specifically, ablation of CaR reduced placental calcium transport, and this was accompanied by a reduction in plasma PTHrP (Kovacs et al., 1998). Furthermore, a calreticulin-like calcium-binding protein has been isolated from trophoblast cells, and its expression is increased by treatment with PTHrP(67−84) but not with N-terminal PTHrP (Hershberger and Tuan, 1998).

Although these observations are strongly suggestive of involvement of PTHrP and the CaR, the mechanisms of placental calcium transport are still not fully understood. Support for the role of PTHrP also comes from the PTHrP gene knockout mouse, in which placental calcium transport is severely impaired (Kovacs et al., 1996). In mice homozygous for deletion of the PTHrP gene, fetal plasma calcium and maternal−fetal calcium gradient were significantly reduced. When fetuses were injected in utero with fragments of PTHrP or PTH, calcium transport was significantly restored only by treatment with a midmolecular region of PTHrP that does not act via PTH1R. Furthermore, in mice rendered null for the PTH1R gene, placental calcium transport was increased, and PTH1R-null fetuses had plasma PTHrP levels more than 10 times higher than controls (Kovacs et al., 2001). The circulating PTHrP in the fetal mice was found to be derived from several tissues, including liver and placenta, but parathyroids were excluded as a source of PTHrP in this setting (Kovacs et al., 2001). Additional studies confirmed that mice lacking parathyroid glands or parathyroid hormone did not have an alteration in circulating PTHrP, nor was placental calcium transport reduced, although the absence of fetal PTH was associated with an even greater reversal of the maternal−fetal calcium gradient than that induced by loss of PTHrP (Kovacs et al., 2001; Simmonds et al., 2010). These findings indicate that fetal parathyroids may not be a source of circulating PTHrP and are compatible with an earlier detailed examination of normal fetal rat parathyroids that found no detectable PTHrP by in situ hybridization, RT-PCR, and immunohistochemistry (Tucci et al., 1996).

Additional support for the role of PTHrP is that placental expression of PTHrP was increased in two different models in which the vitamin D receptor is ablated, and in both studies placental calcium transport was also increased (Kovacs, 2005b; Lieben, 2013).

Study of mice lacking the gene encoding PTH enabled the detection of a low level of expression of PTH mRNA in the murine placenta and alterations in the expression of genes involved in cation transport (Simmonds et al., 2010). Exogenous PTH administration also stimulated placental calcium transport in *Pth*-null fetuses but not in WT fetuses within the same litters (Simmonds et al., 2010). Therefore, the placenta appears to be an ectopic site of low-level PTH expression, but whether this has an important influence on fetal−placental mineral homeostasis in normal mice is unknown. Furthermore, whether PTH is expressed at all in the human placenta has not been examined with modern methods.

Overall, conclusions from the murine studies are similar in many respects to those in sheep, namely that PTHrP contributes to fetal skeleton calcium supply by controlling maternal−fetal calcium transport through actions mediated by a midmolecule portion of the PTHrP molecule. The murine and sheep studies differ in that the parathyroids do not appear to be a dominant source of PTHrP in rodents; the placenta may be the relevant source of PTHrP that controls placental calcium transfer and the fetal−placental gradient. Murine data support reduced placental calcium transport when PTHrP is

reduced or absent and increased placental calcium transport when circulating PTHrP concentrations or placental PTHrP expression are increased.

Uterus and extraembryonic tissues

The uterus, both pregnant and nonpregnant, is another of the many sites of production and action of PTHrP. The relaxing effect of PTH on uterine smooth muscle had been long recognized (Shew et al., 1984), and it was not surprising that PTHrP had the same effect (Shew et al., 1991). The finding that expression of mRNA for PTHrP in the myometrium during late gestation in the rat was controlled by intrauterine occupancy by the fetoplacental unit raised the possibility of a role for PTHrP in regulating uterine muscle tone (Thiede et al., 1990).

In studies in rats with or without estrogen treatment, protein and mRNA for PTHrP were localized not only in the myometrium, as had been shown in pregnancy (Thiede et al., 1990), but also in the epithelial cells lining the endometrium and endometrial glands. Indeed, the strongest PTHrP production appeared to be in these sites (Paspaliaris et al., 1992), suggesting that the endometrium and endometrial glands might be the major uterine site of PTHrP production and that PTHrP might be a local regulator of endometrial function and myometrial contractility. Estrogen treatment enhanced uterine production of PTHrP, but most significantly, the relaxing effect of PTHrP on uterine contractility in vitro was enhanced greatly by the pretreatment of noncycling rats with estrogen. In keeping with this observation, uterine horns from cycling rats in proestrous and estrous phases of the cycle showed a greater responsiveness to PTHrP than those from noncycling rats. These findings are consistent with a role for PTHrP as an autocrine and/or paracrine regulator of uterine motility and function. Furthermore, they suggest that PTHrP belongs to a class of other locally acting peptides, such as oxytocin, vasoactive intestinal peptide, and relaxin, for which pretreatment of animals with estrogen increases the response of the uterus (Ottesen et al., 1985; Mercado-Simmen et al., 1982; Fuchs et al., 1982).

Further evidence for a specific and regulated role of PTHrP in the uterus during gestation comes from the observation of a temporal pattern in the relaxation response to PTHrP by longitudinal uterine muscle during pregnancy in the rat, with maximal responses at times when estrogen levels would be high. In contrast, the circular muscle did not respond at any stage during gestation (Williams et al., 1994). The inability of PTHrP to relax uterine muscle in the last stages of gestation does not support a direct role in the onset of parturition. Treatment of pregnant rats with intraperitoneal injections of human PTHrP 1−34 resulted in a significant decrease in the expression of connexin-43 (mRNA and protein) and the oxytocin receptor mRNA in the myometrium, but it did not affect the timing of delivery, progesterone in maternal plasma, or levels of c-fos, fra-2, or PTH1R mRNA on any gestational day. These findings are compatible with the hypothesis that PTHrP may act to keep the myometrium quiescent at a time when progesterone levels are falling, but that the effects of PTHrP signaling are overridden by other factors that dictate the onset of labor (Mitchell et al., 2003). This hypothesis is supported by the demonstration (Thiede et al., 1990) that expression of mRNA was dependent on the presence of the fetus and that levels increased throughout pregnancy and decreased sharply after delivery. It seems likely, therefore, that the observed fall in PTHrP reflects the recontracted state of the uterine muscle, consistent with the observation in the bladder (Yamamoto et al., 1992), and that the level of expression is functionally related to contractility. The temporal expression of PTHrP in endometrial glands and blood vessels (Williams et al., 1994) also supports roles in other regulated functions that might include uterine growth during pregnancy and the regulation of uterine and placental blood flow (Mandsager et al., 1994).

Uterine growth restriction was induced in Wistar−Kyoto rats by ligating uterine vessels, and this resulted in a 15% decrease in fetal weight, a 21% decrease in fetal number, and a 46% decrease in placental PTHrP content, but a 2.5-fold increase in uterine PTHrP content (Wlodek et al., 2005). The increase in uterine PTHrP content may be compensatory to increase uteroplacental blood flow. Other studies have demonstrated that the vasodilatory effect of PTHrP on myometrial blood vessels is dependent upon the presence of functional endothelium, and that the effect is likely mediated by nitric oxide (Meziani et al., 2005). Conversely, treatment of pregnant rats with a PTHrP antagonist (PTHrP 7−34) resulted in evidence of growth restriction (reduced fetal weight and placental weight) and apoptosis within placentas (Thoten et al., 2005). Thus, there is some functional evidence to suggest that PTHrP plays a role in regulating uterine blood flow and growth.

Placenta and fetal membranes

PTHrP mRNA and protein have been detected in rat and human placenta in various cell types (Hellman et al., 1992; Germain et al., 1992; Bowden et al., 1994). In addition, neoplastic cells of placental origin secrete PTHrP, including hydatidiform moles and choriocarcinomas in vitro (Deftos et al., 1994). The presence of PTH/PTHrP receptor mRNA has been demonstrated in rat (Urena et al., 1993), mouse (Kovacs et al., 2002), and human (Curtis et al., 1998) placenta, and infusion of PTHrP(1−34) into isolated human placental lobules stimulates cyclic AMP production (Williams et al., 1991).

Three further sets of observations lend support to the hypothesis that PTHrP is involved in placental/uterine interactions and that its most likely role in the placenta and placental membranes is related to the growth and maintenance of the placenta itself during pregnancy. First, PTHrP production by cultured amniotic cells has been shown to be regulated by prolactin, human placental lactogen, transforming growth factor-β (TGF-β), insulin, insulin-like growth factor, and epidermal growth factor (Dvir et al., 1995). Second, PTHrP has been shown to regulate epidermal growth factor receptor expression in cytotrophoblast cultures (Alsat et al., 1993), an event associated with placental development. Third, studies of vascular reactivity in isolated human placental cotyledons preconstricted with a thromboxane A2 mimetic showed PTHrP to be a very effective vasodilator (Macgill et al., 1997). The narrow concentration range to which the tissue responded, together with the desensitization in response to repeated PTHrP infusions, was consistent with a paracrine and/or an autocrine action of PTHrP in human gestational tissues. Adequacy of the fetoplacental circulation is essential for the nutritional demands of the growing fetus, and both humoral and local factors are likely to be important in its control. It is possible that alterations of the expression, localization, and/or action of PTHrP might contribute to the genesis of conditions such as preeclampsia and intrauterine growth retardation in which placental vascular resistance is increased (Gude et al., 1996). Another related and potentially interacting influence is angiotensin II, known to be a powerful enhancer of PTHrP production in the vasculature and in human placental explants (Li et al., 1998). The ability of angiotensin II to stimulate estradiol production in human placental explants through actions upon its AT1 receptor (Kalenga et al., 1995) provides a further link with PTHrP control.

PTHrP has also been shown to regulate the differentiation of cells explanted from the murine placenta. PTHrP treatment reduced proliferation, inhibited apoptosis, and promoted differentiation into trophoblast giant cells. As well, PTHrP treatment induced the expression of transcription factors known to stimulate giant cell formation (Stra13 and AP-2gamma) and inhibited the formation of other trophoblast cell types by suppressing trophoblast progenitors and spongiotrophoblast-promoting factors (Eomes, Mash-2, and mSNA) (El-Hashashetd et al., 2005). Thus, PTHrP likely plays a role in the differentiation of cells during placentation.

The most likely source of increased amniotic fluid PTHrP concentrations during pregnancy is the amnion itself, because PTHrP mRNA expression is also highest at term and greater in the amnion than in choriodecidua or placenta (Bowden et al., 1994; Ferguson et al., 1992; Wlodek et al., 1996). In tissue from women with full-term pregnancies and not in labor, the concentration of N-terminal PTHrP has been found to be higher in amnion covering the placenta than in the reflected amnion covering the decidua parietalis (Bowden et al., 1994). Nevertheless, the concentration of N-terminal PTHrP in reflected amnion (the layer apposed to the uterus) was inversely related to the interval between rupture of the membranes and delivery. The observation that PTHrP levels in the amnion decrease after rupture of the fetal membranes has led to the proposal that PTHrP derived from the membranes may inhibit uterine contraction and that labor may occur following loss of this inhibition. Plasma levels of PTHrP increase threefold during pregnancy and reach even higher levels postpartum (Bertelloni et al., 1994; Gallacher et al., 1994; Ardawi et al., 1997; Yadav et al., 2014) with the likely sources being placenta and breast, respectively. Human fetal membranes have been shown to inhibit contractions of the rat uterus in vitro (Collins et al., 1993), so this tissue does appear to produce factors that can modulate uterine activity. Furthermore, primary cultures of human amniotic cells secrete PTHrP into the medium (Germain et al., 1992). Thus, although the physiological function(s) of amnion-derived PTHrP is currently unknown, preliminary evidence suggests that it may play a role in regulating the onset of labor. It is also possible that amniotic fluid is a source of PTHrP ingested by the fetus and acts as a growth factor in lung and/or gut development. Consistent with this hypothesis, mice lacking PTHrP have immature lungs associated with arrested type II alveolar cell development and reduced surfactant production in vivo and in vitro (Rubin et al., 2004).

In summary, although many functional studies remain to be completed, potential roles for PTHrP produced by fetal membranes and placenta include transport of calcium across the placenta, accommodation of stretch of membranes, growth and differentiation of fetal and/or maternal tissues, vasoregulation, and regulation of labor.

Implantation and early pregnancy

Some physiological functions other than control of myometrial activity were suggested by findings of Beck et al. (1993), who identified PTHrP mRNA as being limited to epithelial cells of implantation sites. This pregnancy-related expression appeared at day 5.5 in the rat fetus in the antimesometrial uterine epithelium of implantation sites, raising the possibility of a further function of PTHrP playing a part in the localization of implantation or initial decidualization. Decidual cells produced mRNA for PTHrP both in normal gestation and after the induction of deciduomata. Expression of the gene in these cells followed epithelial expression by 48 h. It was concluded from this work that the location of PTHrP gene expression in the uterus, together with the time of its expression, may play a part in implantation of the blastocyst.

Further evidence for a function of PTHrP in the implantation process came from Nowak et al. (1999), who showed that PTHrP and TGF-β were potent stimulators of trophoblast outgrowth by mouse blastocysts cultured in vitro. The TGF-β effect appeared to be mediated by PTHrP, which itself was acting through a mechanism distinct from the PTHR1.

Thus, both the timing and the localization of PTHrP gene expression suggested that it might play a part in the implantation of the blastocyst (Beck et al., 1993). Upon finding substantial levels of immunoreactive PTHrP in the uterine luminal fluid of estrogen-treated immature rats, and because the PTH/PTHrP receptor was known to be expressed in rat uterus (Urena et al., 1993), Williams et al. (1998) investigated the role of PTHrP acting through this receptor in influencing early pregnancy in the rat. Infusion of either a PTHrP antagonist peptide or a monoclonal anti-PTHrP antibody into the uterine lumen during pregnancy resulted in excessive decidualization. The latter appeared to be the result of a decrease in the number of apoptotic decidual cells in the antagonist-infused horn. In pseudopregnant rats, infusion of receptor antagonist into the uterine lumen resulted in increases in wet weight of the infused horn compared with the control side, indicating an effect on deciduoma formation.

These observations suggest that activation of the PTH/PTHrP receptor by locally produced PTHrP might be crucial for normal decidualization during pregnancy in rats, probably not by being involved in the initiation of the decidual reaction but rather in the maintenance of the decidual cell mass.

Pathophysiology of parathyroid hormone-related protein in the placenta

The breasts and placenta contribute PTHrP to maternal circulation during pregnancy, and this occasionally leads to the development of PTHrP-mediated hypercalcemia (pseudohyperparathyroidism) (Kovacs, 2016). This is accompanied by plasma PTHrP concentrations as high as 40 pmol/L and evidence of increased bone resorption. Although uncommon, it suggests that PTHrP production by breasts and placenta may also contribute to the normal regulation of maternal mineral homeostasis during pregnancy, including upregulation of calcitriol production by the maternal kidneys (Kovacs, 2016).

The clinical courses of individual cases of pseudohyperparathyroidism have made evident which of breasts versus placenta were responsible for the excess production of PTHrP. When the breasts (of normal or large size) are the source, the hypercalcemia persists and may worsen postpartum as the onset of lactation induces a further rise in mammary PTHrP production. Breast binders, dopaminergic agents, and weaning usually lead to a prompt resolution of the hypercalcemia, but occasionally it has persisted for months to years or has required a reduction mammoplasty to resolve it (Kovacs, 2016). On the other hand, when the placenta is the source of excess PTHrP, the condition reverses within a few hours of delivery. One pregnant woman with normal-sized breasts developed severe hypercalcemia (5.25 mmol/L) in the third trimester, accompanied by undetectable PTH and a serum PTHrP of 21 pmol/L (Eller-Vainicher et al., 2012). Within 6 hours after an urgent C-section, she was profoundly hypocalcemic, PTHrP had become undetectable, and PTH had risen above the normal range. The rapid reversal from hypercalcemia to hypocalcemia, elevated PTHrP to undetectable PTHrP, and undetectable PTH to high PTH revealed the placenta as the culprit source of excess PTHrP.

Some cases of pseudohyperparathyroidism have presented with vertebral compression fractures during pregnancy or lactation, confirming that the excess production of PTHrP causes marked bone resorption and can temporarily cause skeletal fragility (Kovacs, 2016).

Summary

The multiple roles of PTHrP in the reproductive tissues and cycle, and in the placenta, largely reflect its roles as a paracrine/autocrine/intracrine regulator. Of the many functions it exerts in these systems, probably the only endocrinal one is when PTHrP in the fetal circulation regulates placental calcium transport. There remains much to be learned of the place of PTHrP in reproductive and placental physiology and pathology.

Endocrine pancreas

Parathyroid hormone-related protein and its receptors

The presence of PTHrP in the pancreatic islets became apparent shortly after the identification of PTHrP in 1987. It is expressed as early as day 18 of gestation in the islet cells of fetal rodents (Campos et al., 1991). Asa et al. (1990) demonstrated that PTHrP was present in islet cells and in all 4 cell types, including the α, β, δ, and PP cells. PTHrP mRNA was shown to be present in isolated islet RNA as well (Drucker et al., 1989), demonstrating that the peptide could be produced within the islet. Gaich et al. (1993) confirmed these findings, demonstrating that PTHrP was indeed present in islet cells of all four types and that it was also present in pancreatic ductular epithelial cells. The peptide is not present in

adult pancreatic exocrine cells. Plawner et al. (1995) demonstrated that PTHrP is present in individual beta cells in culture and showed that PTHrP colocalized with insulin in the Golgi apparatus as well as in insulin secretory granules. Interestingly, in a perifusion system employing a beta-cell line, PTHrP was shown to be cosecreted with insulin from beta cells following depolarization of the cell (Plawner et al., 1995). The secreted forms of PTHrP included amino-terminal, midregion, and carboxy-terminal forms of PTHrP (see later).

The PTH1R is expressed throughout the gut epithelium, including the pancreas, from day 9 of development in fetal rodents (Karperien et al., 1994). PTH1R mRNA and protein have been confirmed to be present in adult mouse islet cells by RT-PCR and immunostaining (Fujinaka et al., 2004). There is also functional evidence for PTHrP receptors on the pancreatic beta cell, as it is clear that PTHrP(1−36) elicits prompt and vigorous responses in intracellular calcium in cultured beta-cell lines. For example, Gaich et al. (1993) have demonstrated that PTHrP(1−36) in doses as low as 10−12 M stimulates calcium release from intracellular stores. Interestingly, unlike events observed in bone and renal cell types where PTHrP receptor activation is associated with activation of cAMP/PKA, as well as the PKC/intracellular calcium pathways, only the latter is observed in cultured beta cells in response to PTH or PTHrP(1−36) (Gaich et al., 1993). Whether this reflects the presence of a different type of receptor on beta cells or differential coupling of the PTH1R to subsets of specific G-proteins or catalytic subunits in beta cells compared with bone and renal cells has not been studied.

Regulation of parathyroid hormone-related protein and its receptors

There is little information describing how or to what degree PTHrP or the PTH receptor family is regulated in the pancreatic islet. As will become clear from the sections that follow, there are physiological reasons why such regulation might occur under normal circumstances, but this area remains unexplored.

Biochemistry of parathyroid hormone-related protein

PTHrP undergoes extensive posttranslational processing. Much of what is known or inferred regarding PTHrP processing is derived from studies in the rat insulinoma line, RIN-1038 (Soifer et al., 1992; Yang et al., 1994; Wu et al., 1991). These cells model the processing of PTHrP in the regulated secretory pathway, and have been shown to serve as a model for authentic processing of other human neuroendocrine peptides, such as insulin, proopiomelanocortin, glucagon, and calcitonin. Using a combination of untransfected RIN-1038 cells, RIN-1038 cells overexpressing hPTHrP(1−139), hPTHrP(1−141), or hPTHrP(1−173), and a panel of region-specific radioimmunoassays and immunoradiometric assays, RIN cells have been shown to secrete PTHrP(1−36), PTHrP(38−94), PTHrP(38−95), and PTHrP(38−101) (Soifer et al., 1992; Yang et al., 1994; Wu et al., 1991). In addition, RIN 1038 cells have been shown to secrete a form of PTHrP that is recognized by a PTHrP (109−138) radioimmunoassay (Yang et al., 1994) and another form that is recognized by a PTHrP(139−173) radioimmunoassay (Burtis et al., 1992).

As mentioned, these data derive from rat insulinoma cells that use the regulated secretory pathway for the processing of PTHrP. On the other hand, osteoblasts, chondrocytes, and other cells of mesenchymal origin use the constitutive secretory pathway and would not be expected to use the same processing mechanisms as cells that use the regulated secretory pathway. In accord with that, the only isoform of PTHrP found to be secreted by the Ocy454 osteocyte cell line was full-length PTHrP (Ansari et al., 2018).

As described earlier, PTHrP(1−36) stimulates intracellular calcium increments in cultured beta cells (Gaich et al., 1993). PTHrP(38−94) has also been shown to stimulate intracellular calcium release in these cells (Wu et al., 1991). PTHrP(38−94) does not activate adenylyl cyclase in cultured beta cells, and other PTHrP species have not been explored in beta cells in functional terms.

Function of parathyroid hormone-related protein

Pancreas development in rodents begins at approximately day E9−10, and by day E18−19, clusters of beta cells have begun to coalesce and form immature islets (Edlund, 1998). These islet cell clusters continue to increase in number, size, and density of beta cells in the week after delivery and then decline abruptly in number through a wave of beta-cell apoptosis (Finegood et al., 1995).

The role of PTHrP in pancreatic cell development and function is poorly understood at present. The pancreas of PTHrP-null mice (Karaplis et al., 1994) develops normally in anatomic terms (Vasavada et al., 1998), but nothing is known about the function of these islets. PTHrP-null mice die immediately after delivery, so nothing is known of islet function or development following birth in the absence of PTHrP. “Rescued” PTHrP mice do exist (Wysolmerski et al., 1998),

and they survive to adulthood. These mice have normal-appearing pancreata and islets (Vasavada et al., 1998), but they have dental abnormalities, are undernourished, and grow poorly. Therefore, it is difficult to characterize their islets in functional terms, as islet mass, proliferation, and function are heavily dependent on fuel availability. Streuker and Drucker (1991) have suggested that PTHrP may play a role in beta-cell differentiation because it is upregulated in beta-cell lines in the presence of the islet-differentiating agent, butyrate.

In vitro studies have demonstrated that, similar to the actions of PTH, PTHrP(1−34) and PTHrP(1−86) can enhance glucose-stimulated insulin release from cultured islet cells, and increased insulin mRNA expression and protein content within cultured islets and islet tumor cell lines (Villanueva-Penacarrillo et al., 1999; Sawada et al., 2001). PTHrP has been shown to increase proliferation of cultured islet cells, with the effects varying by cell passage and the ambient glucose concentration (Sawada et al., 2001; Vasavada et al., 2007). Also within cell lines, there is evidence that PTHrP induces cAMP production, raises intracellular calcium through influx of calcium into the cell, and inhibits JNK1/2 activation (Mozar et al., 2014).

In an effort to understand the role of PTHrP in the pancreatic islet, Vasavada and collaborators have developed transgenic mice that overexpress PTHrP under the control of the rat insulin-II promoter (RIP) (Vasavada et al., 1996; Porter et al., 1998). RIP-PTHrP mice display striking degrees of islet hyperplasia and an increase in islet number as well as the size of individual islets. This increased islet mass is associated with increased function; RIP-PTHrP mice are hyperinsulinemic and hypoglycemic compared with their littermates (Vasavada et al., 1996; Porter et al., 1998). They become profoundly and symptomatically hypoglycemic with fasting. Interestingly, RIP-PTHrP mice are also resistant to the diabetogenic effects of the beta-cell toxin, streptozotocin. Following the administration of streptozotocin, normal mice readily develop diabetes, but RIP-PTHrP mice either fail to become diabetic or develop only mild hyperglycemia (Porter et al., 1998).

The mechanism(s) responsible for the increase in islet mass in the RIP-PTHrP mouse remains undefined. There are two levels at which this question can be addressed: identification of the source of the cells responsible for the increase in islet mass and the signaling mechanisms that are responsible for the increase. With respect to the first, islet mass can, in theory, be increased by three pathways: (1) the recruitment of new islets from the pancreatic duct or its branches distributed throughout the exocrine pancreas in a process referred to as “islet neogenesis”; (2) induction of proliferation of existing beta cells within islets; and (3) prolongation of the life span of existing beta cells. Of these options, there is evidence that PTHrP can drive beta-cell replication (Villanueva et al., 1999; Fujinaka et al., 2004), suggesting that beta-cell proliferation may account for at least part of the phenotype. The RIP promoter is restricted to expression in beta cells and therefore unable to influence pancreatic cells prior to their differentiation into beta cells, suggesting that the neogenesis of beta cells from ductal or other precursors is not a likely contributor (Vasavada et al., 1996). Finally, the bulk of evidence would support a dominant role for PTHrP in enhancing beta-cell survival, as occurs in other cell types (Cebrian et al., 2002).

More recently, daily subcutaneous injections of PTHrP(1−36) in adult mice have been shown to increase the proliferation of beta cells and improve glucose tolerance (Williams et al., 2011). Vasavada’s group has shown that after partial pancreatectomy, treatment with PTHrP(1−36) increased beta-cell proliferation over the first 30 days and led to a marked increase in beta cell mass by 90 days (Mozar et al., 2016). Therefore, PTHrP could conceivably be a treatment to improve beta cell mass in patients with diabetes. Further studies are needed.

At the signaling level, little is known regarding the mechanism of action of PTHrP on beta cells. Although it is known that PTHrP can stimulate intracellular calcium in cultured beta-cell lines (Gaich et al., 1993; Wu et al., 1991), it is not known whether this occurs in vivo in normal, nontransformed beta cells within intact islets. Nor is it known whether PTHrP stimulates adenylyl cyclase in normal beta cells in vivo or whether it participates in nuclear or intracrine signaling in beta cells as it appears to in chondrocytes, osteoblasts, vascular smooth muscle cells, or other cell types (Aarts et al., 1999; Massfelder et al., 1997; Lam et al., 1999) (see Chapter 25). These processes, too, are under study.

Pathophysiology of parathyroid hormone-related protein

From the earlier discussion, it is clear that the normal physiological role of PTHrP in the pancreatic islet remains undefined. In contrast, PTHrP plays clear pathophysiological roles in at least some pancreatic islet neoplasms. PTHrP overexpression with resultant development of HHM has been demonstrated on multiple occasions in multiple investigators’ hands (Asa et al., 1990; Stewart et al., 1986; Wu et al., 1997; Skrabanek et al., 1980). In the only large series of malignancy-associated hypercalcemia in which tumors have been fully subdivided based on histology (Skrabanek et al., 1980), islet cell carcinomas, which are not particularly common, produce HHM fully as often as pancreatic adenocarcinomas, a very common neoplasm. Historically, islet tumors were among the first in which PTHrP bioactivity was identified (Stewart et al., 1986; Wu et al., 1997). Furthermore, patients with islet carcinomas regularly demonstrate increases in circulating PTHrP as

determined by radioimmunoassay or immunoradiometric assays (Lanske et al., 1996). When assessed by immunohistochemistry, these tumors also demonstrate increased staining for PTHrP (Asa et al., 1990; Drucker et al., 1989).

The significance of these findings for islet tumor oncogenesis is not known. Is this simply a random derepression of the PTHrP gene or is it a specific upregulation of the PTHrP gene? Is there a pathological role for PTHrP in the development of pancreatic islet tumors, corresponding to the mass enhancing effects of PTHrP in the islets of the RIP-PTHrP mouse? These questions remain interesting but unanswered at present.

Conclusions

Advances in mouse genetics and transgenic technology have been a boon to the study of physiology. This has certainly been the case for the PTHrP field, where studies in genetically altered mice have provided a starting place for the study of the physiology of a protein that was discovered outside its natural context. This chapter has outlined the current state of knowledge regarding the physiological roles of PTHrP in skin, the mammary gland, placenta, uterus, extraembryonic tissues, and pancreas. Much of this information (although not all) has come from studies performed in a variety of transgenic mice. These studies have shown that PTHrP is important to both the development and physiological functioning of these organs. However, at this point, we continue to have as many questions as answers. Many experiments remain to be done before we comprehend all the nuances of the functions of PTHrP at these sites.

Acknowledgments

This chapter has been updated from a prior version cowritten with Drs. Andrew F. Stewart and John J. Wysolmerski. The work was supported by the Canadian Institutes of Health Research (#133413), the Janeway Research Foundation, and both the Discipline of Medicine and Faculty of Medicine of Memorial University of Newfoundland.

References

Aarts, M.M., Levy, D., He, B., Stregger, S., Chen, T., Richard, S., Henderson, J.E., 1999. Parathyroid hormone-related protein interacts with RNA. J. Biol. Chem. 274, 4832−4838.

Alsat, E., Haziza, J., Scippo, M.L., Frankenne, F., Evain Brion, D., 1993. Increase in epidermal growth factor receptor and its mRNA levels by parathyroid hormone (1−34) and parathyroid hormone-related protein (1−34) during differentiation of human trophoblast cells in culture. J. Cell. Physiol. 53, 32−42.

Ansari, N., Ho, P.W., Crimeen-Irwin, B., Poulton, I.J., Brunt, A.R., Forwood, M.R., Divieti Pajevic, P., Gooi, J.H., Martin, T.J., Sims, N.A., 2018. Autocrine and paracrine regulation of the murine skeleton by osteocyte-derived parathyroid hormone0related protein. J. Bone Miner. Res. 33, 137−153.

Ardawi, M.S., Nasrat, H.A., BA'Aqueel, H.S., 1997. Calcium regulating hormones and parathyroid hormone-related peptide in normal human pregnancy and post-partum: a longitudinal study. Eur. J. Endocrinol. 137 (4), 402−409.

Ardeshirpour, L., Dann, P., Pollak, M., Wysolmerski, J., VanHouten, J., 2006. The calcium-sensing receptor regulates PTHrP production and calcium transport in the lactating mammary gland. Bone 38, 787−793.

Asa, S.L., Henderson, J., Goltzman, D., Drucker, D.J., 1990. Parathyroid hormone-related peptide in normal and neoplastic human endocrine tissues. J. Clin. Endocrinol. Metab. 71, 1112−1118.

Atillasoy, E.J., Burtis, W.J., Milstone, L.M., 1991. Immunohisto-chemical localization of parathyroid hormone-related protein (PTHRP) in normal human skin. J. Investig. Dermatol. 96, 277−280.

Beck, F., Tucci, J., Senior, P.V., 1993. Expression of parathyroid hormone-related protein mRNA by uterine tissues and extraembryonic membranes during gestation in rats. J. Reprod. Fertil. 99, 343−352.

Bertelloni, S., Baroncelli, G.I., Pelletti, A., Battini, R., Saggese, G., 1994. Parathyroid hormone related protein in healthy pregnant women. Calcif. Tissue Int. 54, 195−197.

Birch, M.A., Carron, J.A., Scott, M., Fraser, W.D., Gallagher, J.A., 1995. Parathyroid hormone (PTH)/PTH-related protein (PTHrP) receptor expression and mitogenic responses in human breast cancer cell lines. Br. J. Canc. 72, 90−95.

Blomme, E.A., Sugimoto, Y., Lin, Y.C., Capen, C.C., Rosol, T.J., 1999a. Parathyroid hormone-related protein is a positive regulator of keratinocyte growth factor expression by normal dermal fibroblasts. Mol. Cell. Endocrinol. 152, 189−197.

Blomme, E.A., Zhou, H., Kartsogiannis, V., Capen, C.C., Rosol, T.J., 1999b. Spatial and temporal expression of parathyroid hormone-related protein during wound healing. J. Investig. Dermatol. 112, 788−795.

Bowden, S.J., Emly, J.F., Hughes, S.V., Powell, G., Ahmed, A., Whittle, M.J., Ratcliffe, J.G., Ratcliffe, W.A., 1994. Parathyroid hormone-related protein in human term placenta and membranes. J. Endocrinol. 142, 217−224.

Bradbury, R.A., Sunn, K.L., Crossley, M.C., Bai, M., Brown, F.M., Del-bridge, L., Conigrave, A.D., 1997. Expression of the parathyroid Ca21 sensing receptor in cytotrophoblasts from human term placenta. J. Endocrinol. 156, 425−430.

Bucht, E., Carlqvist, M., Hedlund, B., Bremme, K., Torring, O., 1992. Parathyroid hormone-related peptide in human milk measured by a mid-molecule radioimmunoassay. Metab. Clin. Exp. 41, 11–16.

Budayr, A.A., Halloran, B.R., King, J., Diep, D., Nissenson, R.A., Strewler, G.J., 1989. High levels of parathyroid hormone-related protein in milk. Proc. Natl. Acad. Sci. U. S. A 86, 7183–7185.

Bundred, N.J., Walker, R.A., Ratcliffe, W.A., Warwick, J., Morrison, J.M., 1996. Parathyroid hormone related protein and skeletal morbidity in breast cancer. Eur. J. Cancer 28, 690–692.

Burtis, W.J., Debeyssey, M., Philbrick, W.M., Orloff, J.J., Daifotis, A.G., Soifer, N.E., Milstone, L.M., 1992. Evidence for the presence of an extreme carboxy-terminal parathyroid hormone-related peptide in biological specimens. J. Bone Miner. Res. 7 (Suppl. 1), S225.

Campos, R.V., Asa, S.L., Drucker, D.J., 1991. Immunocytochemical localization of parathyroid hormone-like peptide in the rat fetus. Cancer Res. 51, 6351–6357.

Care, A.D., Caple, I.W., Pickard, D.W., 1985. The roles of the parathyroid and thyroid glands on calcium homeostasis in the ovine fetus. In: Jones, C.T., Nathaniels, P.W. (Eds.), The Physiological Development of the Fetus and Newborn. Academic Press, London, pp. 135–140.

Care, A.D., Abbas, S.K., Pickard, D.W., Barri, M., Drinkhill, M., Findlay, J.B.C., White, I.R., Caple, I.W., 1990. Stimulation of ovine placental transport of calcium and magnesium by mid-molecule fragments of human parathyroid hormone-related protein. Exp. Physiol. 75, 605–608.

Cebrian, A., Garcia-Ocaña, A., Takane, K.K., Sipula, D., Stewart, A.F., Vasavada, R.C., 2002. Overexpression of parathyroid hormone-related protein inhibits pancreatic beta cell death in vivo and in vitro. Diabetes 51, 3003–3013.

Cho, Y.M., Woodard, G.L., Dunbar, M., Gocken, T., Jimenez, J.A., Foley, J., 2003. Hair-cycle-dependent expression of parathyroid hormone-related protein and its type I receptor: evidence for regulation at the anagen to catagen transition. J. Investig. Dermatol. 120, 715–727.

Collins, J.N., Kirby, B.J., Woodrow, J.P., Gagel, R.F., Rosen, C.J., Sims, N.A., Kovacs, C.S., 2013. Lactating *Ctcgrp* nulls lose twice normal bone mineral content due to fewer osteoblasts and more osteoclasts, while bone mass is fully restored post-weaning in association with upregulation of Wnt signaling and other novel genes. Endocrinology 154 (4), 1400–1413.

Collins, P.L., Idriss, E., Moore, J.J., 1993. Human fetal membranes inhibit spontaneous uterine contractions. J. Clin. Endocrinol. Metab. 77, 1479–1484.

Comar, C.L., 1956. Radiocalciums studies in pregnancy. Ann. N. Y. Acad. Sci. 64, 281–298.

Cormier, S., Delezoide, A.L., Silve, C., 2003. Expression patterns of parathyroid hormone-related peptide (PTHrP) and parathyroid hormone receptor type 1 (PTHR1) during human development are suggestive of roles specific for each gene that are not mediated through the PTHrP/PTHR1 paracrine signaling pathway. Gene. Expr. Patterns. 3 (1), 59–63.

Curtis, N.E., King, R.G., Moseley, J.M., Ho, P.W., Rice, G.E., Wlodek, M.E., 1998. Intrauterine expression of parathyroid hormone-related protein in normal and pre-eclamptic pregnancies. Placenta 19, 595–601.

Daniel, C.W., Silberstein, G.B., 1987. Postnatal development of the rodent mammary gland. In: Neville, M.C., Daniel, C.W. (Eds.), The Mammary Gland: Development, Regulation and Function. Plenum, New York, pp. 3–36.

Danks, J.A., Ebeling, P.R., Hayman, J., Chou, S.T., Moseley, J.M., Dunlop, J., Kemp, B.E., Martin, T.J., 1989. PTHRP: immunohisto-chemical localization in cancers and in normal skin. J. Bone Miner. Res. 4, 237–238.

Davicco, M., Rouffet, J., Durand, D., Lefaivre, J., Barlet, J.P., 1993. Parathyroid hormone-related peptide may increase mammary blood flow. J. Bone Miner. Res. 8, 1519–1524.

Deftos, L.J., Burton, D.W., Brant, D.W., Pinar, H., Rubin, L.P., 1994. Neoplastic hormone-producing cells of the placenta produce and secrete parathyroid hormone-related protein. Studies by immuno-histology, immunoassay, and polymerase chain reaction. Lab. Invest. 71, 847–852.

Diamond, A.G., Gonterman, R.M., Anderson, A.L., Menon, K., Offutt, C.D., Weaver, C.H., Philbrick, W.M., Foley, J., 2006. Parathyroid hormone-related protein and the PTH receptor regulate angiogenesis of the skin. J. Investig. Dermatol. 126, 2127–2134.

Dittmer, A., Vetter, M., Schunke, D., Span, P.N., Sweep, F., Thomssen, C., Dittmer, J., 2006. Parathyroid hormone-related protein regulates tumor-relevant genes in breast cancer cells. J. Biol. Chem. 281, 14563–14572.

Drucker, D.J., Asa, S.L., Henderson, J., Goltzman, D., 1989. The PTHrP gene is expressed in the normal and neoplastic human endocrine pancreas. Mol. Endocrinol. 3, 1589–1595.

Dunbar, M.E., Young, P., Zhang, J.P., McCaughern-Carucci, J., Lanske, B., Orloff, J., Karaplis, A., Cunha, G., Wysolmerski, J.J., 1998. Stromal cells are critical targets in the regulation of mammary ductal morphogenesis by parathyroid hormone-related protein (PTHrP). Dev. Biol. 203, 75–89.

Dunbar, M.E., Dann, P.R., Robinson, G.W., Hennighausen, L., Zhang, J.P., Wysolmerski, J.J., 1999. Parathyroid hormone-related protein is necessary for sexual dimorphism during embryonic mammary development. Development 126, 3485–3493.

Dunbar, M.E., Dann, P., Brown, C.W., Dreyer, B., Philbrick, W.P., Wysolmerski, J.J., 2001. Temporally-regulated overexpression of PTHrP in the mammary gland reveals distinct fetal and pubertal phenotypes. J. Endocrinol. 171, 403–416.

Dvir, R., Golander, A., Jaccard, N., Yedwab, G., Otremski, I., Spirer, Z., Weisman, Y., 1995. Amniotic fluid and plasma levels of parathyroid hormone-related protein and hormonal modulation of its secretion by amniotic fluid cells. Eur. J. Endocrinol. 133, 277–282.

Edlund, H., 1998. Transcribing pancreas. Diabetes 47, 1817–1823.

El-Hashash, A.H., Esbrit, P., Kimber, S.J., 2005. PTHrP promotes murine secondary trophoblast giant cell differentiation through induction of endocycle, upregulation of giant-cell-promoting transcription factors and suppression of other trophoblast cell types. Differentiation 73 (4), 154–174.

Eller-Vainicher, C., Ossola, M.W., Beck-Peccoz, P., Chiodini, I., 2012. PTHrP-associated hypercalcemia of pregnancy resolved after delivery: a case report. Eur. J. Endocrinol. 166, 753–756.

Errazahi, A., Bouizar, Z., Lieberherr, M., Souil, E., Rizk-Rabin, M., 2003. Functional type I PTH/PTHrP receptor in freshly isolated newborn rat keratinocytes: identification by RT-PCR and immunohistochemistry. J. Bone. Miner. Res. 18 (4), 737–750.

Errazahi, A., Lieberherr, M., Bouizar, Z., Rizk-Rabin, M., 2004. PTH-1R responses to PTHrP and regulation by vitamin D in keratinocytes and adjacent fibroblasts. J. Steroid Biochem. Mol. Biol. 89–90, 381–385.

Ferguson, J.E., Gorman, J.V., Bruns, D.E., Weir, E.C., Burtis, W.J., Martin, T.J., Bruns, M.E., 1992. Abundant expression of parathyroid hormone-related protein in human amnion and its association with labor. Proc. Natl. Acad. Sci. U.S.A. 89, 8384–8388.

Ferrari, S.L., Rizzoli, R., Bonjour, J.P., 1992. Parathyroid hormone-related protein production by primary cultures of mammary epithelial cells. J. Cell. Physiol. 150, 304–411.

Finegood, D.T., Scaglia, L., Bonner-Weir, S., 1995. Perspectives in diabetes. Dynamics of beta-cell mass in the growing rat pancreas. Estimation with a simple mathematical model. Diabetes 44, 249–256.

Fleming, N.I., Trivett, M.K., George, J., Slavin, J.L., Murray, W.K., Moseley, J.M., Anderson, R.L., Thomas, D.M., 2009. Parathyroid hormone-related protein protects against mammary tumor emergence and is associated with monocyte infiltration in ductal carcinoma in situ. Cancer Res. 69 (18), 7473–7479.

Foley, J., Longely, B.J., Wysolmerski, J.J., Dreyer, B.E., Broadus, A.E., Philbrick, W.M., 1998. Regulation of epidermal differentiation by PTHrP: evidence from PTHrP-null and PTHrP-overexpressing mice. J. Investig. Dermatol. 111, 1122–1128.

Foley, J., Dann, P., Hong, J., Cosgrove, J., Dreyer, B., Rimm, D., Dunbar, M.E., Philbrick, W., Wysolmerski, J.J., 2001. Parathyroid hormone-related protein maintains mammary epithelial fate and triggers nipple skin differentiation during embryonic mammary development. Development 128, 513–525.

Fuchs, A.R., Fuchs, F., Husslein, P., Soloff, M.S., Fernstrom, M., 1982. Oxytocin receptors and human parturition: a dual role of oxytocin in the initiation of labor. Science 215, 1396–1398.

Fujinaka, Y., Sipula, D., Garcia-Ocana, A., Vasavada, R.C., 2004. Characterization of mice doubly transgenic for parathyroid hormone-related protein and murine placental lactogen: a novel role for placental lactogen in pancreatic beta-cell survival. Diabetes 53, 3120–3130.

Gaich, G., Orloff, J.J., Atillasoy, E.J., Burtis, W.J., Ganz, M.B., Stewart, A.F., 1993. Amino-terminal parathyroid hormone-related protein: specific binding and cytosolic calcium responses in rat insulinoma cells. Endocrinology 132, 1402–1409.

Gallacher, S.J., Fraser, W.D., Owens, O.J., Dryburgh, F.J., Logue, F.C., Jenkins, A., Kennedy, J., Boyle, I.T., 1994. Changes in calciotrophic hormones and biochemical markers of bone turnover in normal human pregnancy. Eur. J. Endocrinol. 131 (4), 369–374.

Germain, A.M., Attaroglu, H., MacDonald, P.C., Casey, M.L., 1992. Parathyroid hormone-related protein mRNA in avascular human amnion. J. Clin. Endocrinol. Metab. 75, 1173–1175.

Givens, M.H., Macy, I.C., 1933. The chemical composition of the human fetus. J. Biol. Chem. 102, 7–17.

Goff, J.P., Reinhardt, T.A., Lee, S., Hollis, B.W., 1991. Parathyroid hormone-related peptide content of bovine milk and calf blood as assessed by radioimmunoassay and bioassay. Endocrinology 129, 2815–2819.

Grace, N.D., Atkinson, J.H., Martinson, P.L., 1986. Accumulation of minerals by the foetus(es) and conceptus of single and twin-bearing ewes. N. Z. J. Agric. Res. 29, 207–222.

Grone, A., Werkmeister, J.R., Steinmeyer, C.L., Capen, C.C., Rosol, T.J., 1994. Parathyroid hormone-related protein in normal and neo-plastic canine tissues: immunohistochemical localization and biochemical extraction. Vet. Pathol. 31, 308–315.

Gude, N.M., King, R.G., Brennecke, S.P., 1996. Factors regulating placenta hemodynamics. In: Sastry, B.V.R. (Ed.), Placental Pharmacology. CRC Press, Boca Raton, FL, pp. 23–45.

Guise, T.A., Yin, J.J., Taylor, S.D., Kumagai, Y., Dallas, M., Boyce, B., Yoneda, T., Mundy, G.R., 1996. Evidence for a causal role of parathyroid hormone-related protein in the pathogenesis of human breast cancer-mediated osteolysis. J. Clin. Investig. 98, 1544–1549.

Hanafin, N.M., Chen, T.C., Heinrich, G., Segré, G.V., Holick, M.F., 1995. Cultured human fibroblasts and not cultured human keratinocytes express a PTH/PTHrP receptor mRNA. J. Investig. Dermatol. 105, 133–137.

Hayman, J.A., Danks, J.A., Ebeling, P.R., Moseley, J.M., Kemp, B.E., Martin, T.J., 1989. Expression of PTHRP in normal skin and tumors. J. Pathol. 158, 293–296.

Hellman, P., Ridefelt, P., Juhlin, C., Akerstrom, G., Rastad, J., Gylfe, E., 1992. Parathyroid-like regulation of parathyroid-hormone-related protein release and cytoplasmic calcium in cytotrophoblast cells of human placenta. Arch. Biochem. Biophys. 293, 174–180.

Henderson, M.A., Danks, J.A., Moseley, J.M., Slavin, J.L., Harris, T.L., McKinlay, M.R., Hopper, J.L., Martin, T.J., 2001. Parathyroid hormone-related protein production by breast cancers, improved survival, and reduced bone metastases. J. Natl. Cancer Inst. 93, 234–237.

Henderson, M.A., Danks, J.A., Slavin, J.L., Byrnes, G.B., Choong, P.F., Spillane, J.B., Hopper, J.L., Martin, T.J., 2006. Parathyroid hormone-related protein localization in breast cancers predict improved prognosis. Cancer Res. 66 (4), 2250–2256.

Hens, J., Dann, P., Zhang, J.P., Robinson, G., Wysolmerski, J., 2007. BMP4 and PTHrP interact to stimulate ductal outgrowth and inhibit hair follicle induction during embryonic mammary development. Development 134, 1221–1230.

Hernandez, L.L., Gregerson, K.A., Horseman, N.D., 2012. Mammary gland serotonin regulates parathyroid hormone-related protein and other bone-related signals. Am. J. Physiol. Endocrinol. Metab. 302 (8), E1009–E1015.

Hershberger, M.E., Tuan, R.S., 1998. Placental 57-kDa $Ca(2^{1})$-binding protein: regulation of expression and function in trophoblast calcium transport. Dev. Biol. 199, 80–92.

Holick, M.F., Chimeh, F.N., Ray, S., 2003. Topical PTH (1–34) is a novel, safe and effective treatment for psoriasis: a randomized self-controlled trial and an open trial. Br. J. Dermatol. 149, 370–376.

Insogna, K.L., Stewart, A.F., Morris, C.F., Hough, L.M., Milstone, L.M., Centrella, M., 1989. Native and synthetic analogues of the malignancy-associated parathyroid hormone-like protein have in vivo transforming growth factor-like properties. J. Clin. Investig. 83, 1057–1060.

Isales, C., Carcangiu, M.L., Stewart, A.F., 1987. Hypercalcemia in breast cancer: reassessment of the mechanism. Am. J. Med. 82, 1143.

Jobert, A.S., Zhang, P., Couvineau, A., Bonaventure, J., Roume, J., Le Merer, M., Silve, C., 1998. Absence of functional receptors for parathyroid hormone and parathyroid hormone-related peptide in Blomstrand Chondrodysplasia. J. Clin. Investig. 102, 34–40.

Kalenga, M.K., De Gasparo, M., Thomas, K., De Hertogh, R., 1995. Angiotensin-II stimulates estradiol secretion from human placental explants through A_1 receptor activation. J. Clin. Endocrinol. Metab. 80, 1233–1237.

Karaplis, A.C., Luz, A., Glowacki, J., Bronson, R.T., Tybulewicz, V.L.J., Kronenberg, H.M., Mulligan, R.C., 1994. Lethal skeletal dysplasia from targeted disruption of the parathyroid hormone-related peptide gene. Genes Dev. 8, 277–289.

Karmali, R., Schiffman, S.N., Vanderwinden, J.M., Hendy, G.N., Nys-DeWolf, N., Corvilain, J., Bergmann, P., Vanderhaeghen, J.J., 1992. Expression of mRNA of parathyroid hormone-related peptide in fetal bones of the rat. Cell Tissue Res. 270, 597–600.

Karperien, M., van Dijk, T.B., Hoeijmakers, T., et al., 1994. Expression pattern of parathyroid hormone/parathyroid hormone related peptide receptor mRNA in mouse postimplantation embryos indicates involvement in multiple developmental processes. Mech. Dev. 47, 29–42.

Kakonen, S.M.1, Selander, K.S., Chirgwin, J.M., Yin, J.J., Burns, S., Rankin, W.A., Grubbs, B.G., Dallas, M., Cui, Y., Guise, T.A., 2002. Transforming growth factor-beta stimulates parathyroid hormone-related protein and osteolytic metastases via Smad and mitogen-activated protein kinase signaling pathways. J. Biol. Chem. 277 (27), 24571–24578. Epub 2002 Apr 18.

Khosla, S., van Heerden, J.A., Gharib, H., Jackson, I.T., Danks, J., Hayman, J.A., Martin, T.J., 1990. Parathyroid hormone-related protein and hypercalcemia secondary to massive mammary hyperplasia (letter). N. Engl. J. Med. 322, 1157.

Kovacs, C.S., Kronenberg, H.M., 1997. Maternal-fetal calcium and bone metabolism during pregnancy, puerperium, and lactation. Endocr. Rev. 18, 832–872.

Kovacs, C.S., Lanske, B., Hunzelman, J.L., Guo, J., Karaplis, A.C., Kronenberg, H.M., 1996. Parathyroid hormone-related peptide (PTHrP) regulates fetal-placental calcium transport through a receptor distinct from the PTH/PTHrP receptor. Proc. Natl. Acad. Sci. U.S.A. 93, 15233–15238.

Kovacs, C.S., Ho-Pao, C.I., Hunzelman, J.L., Lanske, B., Fox, J., Seidman, J.G., Seidman, C.E., Kronenberg, H.M., 1998. Regulation of murine fetal-placental calcium metabolism by the calcium-sensing receptor. J. Clin. Investig. 101 (28), 12–20.

Kovacs, C.S., Manley, N.R., Moseley, J.M., Martin, T.J., Kronenberg, H.M., 2001. Fetal parathyroids are not required to maintain placental calcium transport. J. Clin. Investig. 107, 1007–1015.

Kovacs, C.S., Chafe, L.L., Woodland, M.L., McDonald, K.R., Fudge, N.J., Wookey, P.J., 2002. Calcitropic gene expression suggests a role for intraplacental yolk sac in maternal-fetal calcium exchange. Am. J. Physiol. Endocrinol. Metab. 282, E721–E732.

Kovacs, C.S., 2003. Fetal mineral homeostasis. In: Glorieux, F.H., Pettifor, J.M., Jüppner, H. (Eds.), Pediatric Bone: Biology and Diseases. Academic Press, San Diego, pp. 271–302.

Kovacs, C.S., 2005a. Calcium and bone metabolism during pregnancy and lactation. J. Mammary Gland Biol. Neoplasia 10 (2), 105–118.

Kovacs, C.S., Woodland, M.L., Fudge, N.J., Friel, J.K., 2005b. The vitamin D receptor is not required for fetal mineral homeostasis or for the regulation of placental calcium transfer in mice. Am. J. Physiol. Endocrinol. Metab. 289 (1), E133–E144.

Kovacs, C.S., 2016. Maternal mineral and bone metabolism during pregnancy, lactation, and post-weaning recovery. Physiol. Rev. 96, 449–547.

Kumari, R., Robertson, J.F., Watson, S.A., 2006. Nuclear targeting of a midregion PTHrP fragment is necessary for stimulating growth in breast cancer cells. Int. J. Cancer 119, 49–59.

Lam, M.H.C., House, C.M., Tiganis, T., Mitchelhill, K.I., Sarcevic, B., Cures, A., Ramsay, R., Kemp, B.E., Martin, T.J., Gillespie, M.T., 1999. Phosphorylation at the cyclin-dependent kinases site (Thr^{85}) of parathyroid hormone-related protein negatively regulates its nuclear localization. J. Biol. Chem. 274, 18559–18566.

Lanske, B., Karaplis, A., Lee, K., Luz, A., Vortkam, A., Pirro, A., Karperien, M., Defize, L., Ho, C., Mulligan, R., Abou-Samra, A., Jüppner, H., Segré, G., Kronenberg, H., 1996. PTH/PTHrP receptor in early development and Indian hedgehog-regulated bone growth. Science 273, 663–666.

Law, F.M.L., Moate, P.J., Leaver, D.D., Dieffenbach, H., Grill, V., Ho, P.W.M., Martin, T.J., 1991. Parathyroid hormone-related protein in milk and its correlation with bovine milk calcium. J. Endocrinol. 128, 21–26.

Li, J., Karaplis, A.C., Huang, D.C., Siegel, P.M., Camirand, A., Yang, X.F., Muller, W.J., Kremer, R., 2011. PTHrP drives breast tumor initiation, progression, and metastasis in mice and is a potential therapy target. J. Clin. Investig. 121 (12), 4655–4669.

Li, X., Shams, M., Zhu, J., Khalig, A., Wilkes, M., Whittle, M., Barnes, N., Ahmed, A., 1998. Cellular localization of ATI receptor mRNA and protein in normal placenta and its reduced expression in intrauterine growth restriction. Angiotensin II stimulates the release of vasorelaxants. J. Clin. Investig. 101, 442–454.

Liapis, H., Crouch, E.C., Grosso, L.E., Kitazawa, S., Wick, M.R., 1993. Expression of parathyroid like protein in normal, proliferative, and neoplastic human breast tissues. Am. J. Pathol. 143, 1169–1178.

Lieben, L., Stockmans, I., Moermans, K., Carmeliet, G., 2013. Maternal hypervitaminosis D reduces fetal bone mass and mineral acquisition and leads to neonatal lethality. Bone 57, 123–131.

Lee, K., Deeds, J.D., Segre, G.V., 1995. Expression of parathyroid hormone-related peptide and its messenger ribonucleic acids during fetal development of rats. Endocrinology 136, 453–463.

Macgill, K., Mosely, J.M., Martin, T.J., Brennecke, S.P., Rice, G.E., Wlodek, M.E., 1997. Vascular effects of PTHrP (1–34) and PTH (1–34) in the human fetal-placental circulation. Placenta 18, 587–592.

MacIsaac, R.J., Heath, J.A., Rodda, C.P., Mosely, J.M., Care, A.D., Martin, T.J., Caple, I.W., 1991. Role of the fetal parathyroid glands and parathyroid hormone-related protein in the regulation of placental transport of calcium, magnesium and inorganic phosphate. Reprod. Fertil. Dev. 3, 447–457.

Mamillapalli, R., VanHouten, J., Dann, P., Bikle, D., Chang, W., Brown, E., Wysolmerski, J., 2013. Mammary-specific ablation of the calcium-sensing receptor during lactation alters maternal calcium metabolism, milk calcium transport, and neonatal calcium accrual. Endocrinology 154, 3031–3042.

Mandsager, N.T., Brewer, A.S., Myatt, L., 1994. Vasodilator effects of parathyroid hormone, parathyroid hormone-related protein, and calcitonin gene-related peptide in the human fetal-placental circulation. J. Soc. Gynecol. Investig. 1, 19–24.

Marshall, A.M., Hernandez, L.L., Horseman, N.D., 2014. Serotonin and serotonin transport in the regulation of lactation. J. Mammary Gland Biol. Neoplasia 19 (1), 139–146.

Massfelder, T., Dann, P., Wu, T.L., Vasavada, R., Helwig, J.-J., Stewart, A.F., 1997. Opposing mitogenic and anti-mitogenic actions of parathyroid hormone-related protein in vascular smooth muscle cells: a critical role for nuclear targeting. Proc. Natl. Acad. Sci. U.S.A. 94, 13630–13635.

Mercado-Simmen, R., Bryant-Greenwood, G.D., Greenwood, F.C., 1982. Relaxin receptor in the rat myometrium: regulation by estrogen and progesterone. Endocrinology 110, 220–226.

Merendino, J.J., Insogna, K.L., Milstone, L.M., Broadus, A.E., Stewart, A.F., 1986. Cultured human keratinocytes, produce a parathyroid hormone-like protein. Science 231, 388–390.

Meziani, F., Van Overloop, B., Schneider, F., Gairard, A., 2005. Parathyroid hormone-related protein-induced relaxation of rat uterine arteries: influence of the endothelium during gestation. J. Soc. Gynecol. Investig. 12 (1), 14–19.

Mitchell, J.A., Ting, T.C., Wong, S., Mitchell, B.F., Lye, S.J., 2003. Parathyroid hormone-related protein treatment of pregnant rats delays the increase in connexin 43 and oxytocin receptor expression in the myometrium. Biol. Reprod. 69 (2), 556–562.

Mozar, A., Guthalu Kondegowda, N.G., Pollack, I., Fenutria, R., Vasavada, R.C., 2014. The role of PTHrP in pancreatic beta-cells and implications for diabetes pathophysiology and treatment. Clin. Rev. Bone Miner. Metabol. 12, 165–177.

Mozar, A., Lin, H., Williams, K., Chin, C., Li, R., Kondegowda, N.G., Stewart, A.F., Garcia-Ocaña, A., Vasavada, R.C., 2016. Parathyroid hormone-related peptide (1–36) enhances beta cell regeneration and increases beta cell mass in a mouse model of partial pancreatectomy. PLoS One 11 (7), e0158414.

Nowak, R.A., Haimovici, F., Biggers, J.D., Erbach, G.T., 1999. Transforming growth factor-beta stimulates mouse blastocyst out-growth through a mechanism involving parathyroid hormone-related protein. Biol. Reprod. 60, 85–93.

Orloff, J.J., Ganz, M.B., Ribaudo, A.E., Burtis, W.J., Reiss, M., Milstone, L.M., Stewart, A.F., 1992. Analysis of parathyroid hormone-related protein binding and signal transduction mechanisms in benign and malignant squamous cells. Am. J. Physiol. 262, E599–E607.

Orloff, J.J., Kats, J., Urena, P., Schipani, E., Vasavada, R.C., Philbrick, W.M., Behal, A., Abou-Samra, A.B., Segre, G.V., Juppner, H., 1995. Further evidence for a novel receptor for amino-terminal PTHrP on keratinocytes and squamous carcinoma cell lines. Endocrinology 136, 3016–3023.

Ottesen, B., Larsen, J.J., Stau-Olsen, P., Gammeltoft, S., Fahrenkrug, J., 1985. Influence of pregnancy and sex steroids on concentration, motor effect and receptor binding on VIP in the rabbit female genital tract. Regul. Pept. 11, 83–92.

Paspaliaris, V., Vargas, S.J., Gillespie, M.T., Williams, E.D., Danks, J.A., Moseley, J.M., Story, M.E., Pennefather, J.N., Leaver, D.D., Martin, T.J., 1992. Oestrogen enhancement of the myometrial response to exogenous parathyroid hormone-related protein (PTHrP), and tissue localization of endogenous PTHrP and its mRNA in the virgin rat uterus. J. Endocrinol. 134, 415–425.

Philbrick, W.M., Wysolmerski, J.J., Galbraith, S., Holt, E., Orloff, J.J., Yang, K.H., Vasavada, R.C., Weir, E.C., Broadus, A.E., Stewart, A.F., 1996. Defining the roles of parathyroid hormone-related protein in normal physiology. Physiol. Rev. 76, 127–173.

Plawner, L.L., Philbrick, W.M., Burtis, W.J., Broadus, A.E., Stewart, A.F., 1995. Secretion of parathyroid hormone-related protein: cell-specific secretion via the regulated vs. the constitutive secretory pathway. J. Biol. Chem. 270, 14078–14084.

Porter, S.E., Sorenson, R.L., Dann, P., Garcia-Ocana, A., Stewart, A.F., Vasavada, R.C., 1998. Progressive pancreatic islet hyperplasia in the islet-targeted, PTH-related protein-overexpressing mouse. Endocrinology 139, 3743–3745.

Rakopoulos, M., Vargas, S.J., Gillespie, M.T., Ho, P.W.M., Diefenbach-Jagger, H., Leaver, D.D., Grill, V., Moseley, J.M., Danks, J.A., Martin, T.J., 1992. Production of parathyroid hormone-related protein by the rat mammary gland in pregnancy and lactation. Am. J. Physiol. 263, E1077–E1085.

Reid, I.R., Wattie, D.J., Evans, M.C., Budayr, A.A., 1992. Postpregnancy osteoporosis associated with hypercalcemia. Clin. Endocrinol. 37, 298–303.

Rhodes, D.R., Yu, J., Shanker, K., Deshpande, N., Varambally, R., Ghosh, D., Barrette, T., Pandey, A., Chinnaiyan, A.M., 2004. Oncomine: a cancer microarray database and integrated data-mining platform. Neoplasia 6, 1–6.

Rodda, C.P., Kubota, M., Heath, J.A., Ebeling, P.R., Mosely, J.M., Care, A.D., Caple, I.W., Martin, T.J., 1988. Evidence for a novel parathyroid hormone-related protein in fetal lamb parathyroid glands and sheep placenta: comparisons with a similar protein implicated in humoral hypercalcemia of malignancy. J. Endocrinol. 117, 261–271.

Rubin, L.P., Kovacs, C.S., Pinar, H., Tsai, S.W., Torday, J.S., Kronenberg, H.M., 2004. Arrested pulmonary alveolar cytodifferentiation and defective surfactant synthesis in mice missing the gene for parathyroid hormone-related protein. Dev. Dynam. 230 (2), 278–289.

Safer, J.D., Ray, S., Holick, M.F., 2007. A topical parathyroid hormone/parathyroid hormone-related peptide receptor antagonist stimulates hair growth in mice. Endocrinology 148, 1167–1170.

Sakakura, T., 1987. Mammary embryogenesis. In: Neville, M.C., Daniel, C.W. (Eds.), The Mammary Gland: Development, Regulation and Function. Plenum, New York, pp. 37–66.

Sawada, Y., Zhang, B., Okajima, F., Izumi, T., Takeuchi, T., 2001. PTHrP increases pancreatic beta-cell-specific functions in well-differentiated cells. Mol. Cell. Endocrinol. 182, 265–275.

Schilli, M.B., Ray, S., Paus, R., Obi-Tabot, E., Holick, M.F., 1997. Control of hair growth with parathyroid hormone (7–34). J. Investig. Dermatol. 108, 928–932.

Seitz, P.K., Cooper, K.M., Ives, K.L., Ishizuka, J., Townsend, C.M., Rajsraman, S., Cooper, C.W., 1993. Parathyroid hormone-related peptide production and action in a myoepithelial cell line derived from normal human breast. Endocrinology 133, 1116–1124.

Shen, X., Falzon, M., 2003. PTH-related protein modulates PC-3 prostate cancer cell adhesion and integrin subunit profile. Mol. Cell. Endocrinol. 199 (1-2), 165–177. PMID: 12581888.

Shen, X., Falzon, M., 2006. PTH-related protein upregulates integrin a6b4 expression and activates Akt in breast cancer cells. Exp. Cell Res. 312, 3822–3834.

Shen, X., Qian, L., Falzon, M., 2004. PTH-related protein enhances MCF-7 breast cancer cell adhesion, migration, and invasion via an intracrine pathway. Exp. Cell. Res. 294 (2), 420–433.

Shew, R.L., Yee, J.A., Pang, P.K.T., 1984. Direct effect of parathyroid hormone on rat uterine contraction. J. Pharmacol. Exp. Ther. 230, 1–6.

Shew, R.L., Yee, J.A., Kliewer, D.B., Keflemariam, Y.J., McNeill, D.L., 1991. Parathyroid hormone-related peptide inhibits stimulated uterine contraction in vitro. J. Bone Miner. Res. 6, 955–960.

Shin, J.H., Ji, C., Casinghino, S., McCarthy, T.L., Centrella, M., 1997. Parathyroid hormone-related protein enhances insulin-like growth factor-I expression by fetal rat dermal fibroblasts. J. Biol. Chem. 272, 23498–23502.

Simmonds, C.S., Karsenty, G., Karaplis, A.C., Kovacs, C.S., 2010. Parathyroid hormone regulates fetal-placental mineral homeostasis. J. Bone Miner. Res. 25 (3), 594–605.

Sirchia, R., Priulla, M., Sciandrello, G., Caradonna, F., Barbata, G., Luparello, C., 2007. Mid-region parathyroid hormone-related protein (PTHrP) binds chromatin of MDA-MB231 breast cancer cells and isolated oligonucleotides "in vitro". Breast Canc. Res. Treat. 105, 105–116.

Skrabanek, P., McPartlin, J., Powell, D.M., 1980. Tumor hypercalcemia and ectopic hyperparathyroidism. Medicine (Baltim.) 59, 262–282.

Skrok, A., Bednarczuk, T., Skwarek, A., ·Popow, M., Rudnicka, L., Olszewska, M., 2015. The effect of parathyroid hormones on hair follicle physiology: implications for treatment of chemotherapy-induced alopecia. Skin Pharmacol. Physiol. 28, 213–225.

Smith, M.S., Grove, K.L., 2002. Integration of the regulation of reproductive function and energy balance: lactation as a model. Front. Neuroendocrinol. 23 (3), 225–256. In review.

Soifer, N.E., Dee, K.E., Insogna, K.L., Burtis, W.J., Matovcik, L.M., Wu, T.L., Milstone, L.M., Broadus, A.E., Philbrick, W.M., Stewart, A.F., 1992. Secretion of a novel mid-region fragment of parathyroid hormone-related protein by three different cell lines in culture. J. Biol. Chem. 267, 18236–18243.

Sowers, M.F., Hollis, B.W., Shapiro, B., Randolph, J., Janney, C.A., Zhang, D., Schork, A., Crutchfield, M., Stanczyk, F., Russell-Aulet, M., 1996. Elevated parathyroid hormone-related peptide associated with lactation and bone density loss. J. Am. Med. Assoc. 276, 549–554.

Stewart, A.F., Insogna, K.L., Burtis, W.J., Aminiafshar, A., Wu, T., Weir, E.C., Broadus, A.E., 1986. Frequency and partial characterization of adenylate cyclase-stimulating activity in tumors associated with humoral hypercalcemia of malignancy. J. Bone Miner. Res. 1, 267–276.

Streuker, C., Drucker, D.J., 1991. Rapid induction of parathyroid hormone-like peptide gene expression by sodium butyrate in a rat islet cell line. Mol. Endocrinol. 5, 703–708.

Thiede, M.A., 1989. The mRNA encoding a parathyroid hormone-like peptide is produced in mammary tissue in response to elevations in serum prolactin. Mol. Endocrinol. 3, 1443–1447.

Thiede, M.A., Rodan, G.A., 1988. Expression of a calcium-mobilizing parathyroid hormone-like peptide in lactating mammary tissue. Science 242, 278–280.

Thiede, M.A., Daifotis, A.G., Weir, E.C., Brines, M.L., Burtis, W.J., Ikeda, K., Dreyer, B.E., Garfield, R.E., Braodus, A.E., 1990. Intrauterine occupancy controls expression of the parathyroid hormone-related peptide gene in preterm rat myometrium. Proc. Natl. Acad. Sci. U.S.A. 87, 6969–6973.

Thiede, M.A., Grasser, W.A., Peterson, D.N., 1992. Regulation of PTHrP in the mammary blood supply supports a role in mammary gland blood flow. Bone Miner. 17, A8 (Abstract).

Thompson, G.E., Ratcliffe, W.A., Hughes, S., Abbas, S.K., Care, A.D., 1994. Local control of parathyroid hormone-related protein secretion by the mammary gland of the goat. Comp. Biochem. Physiol. A108, 485–490.

Thomson, M., McCarrol, J., Bond, J., Gordon-Thomson, C., Williams, E.D., Moore, G.P.M., 2003. Parathyroid hormone-related peptide modulates signal pathways in skin and hair follicle cells. Exp. Dermatol. 12, 389–395.

Thota, C.S., Reed, L.C., Yallampalli, C., 2005. Effects of parathyroid hormone like hormone (PTHLH) antagonist, PTHLH(7–34), on fetoplacental development and growth during midgestation in rats. Biol. Reprod. 73, 1191–1198.

Tucci, J., Russell, A., Senior, P.V., Fernley, R., Ferraro, T., Beck, F., 1996. The expression of parathyroid hormone and parathyroid hormone-related protein in developing rat parathyroid glands. J. Mol. Endocrinol. 17, 149–157.

Urena, P., Kong, X.F., Abou Samra, A.B., Juppner, H., Kronenberg, H.M., Potts, J.T., Segré, G.V., 1993. Parathyroid hormone (PTH) PTH-related peptide receptor messenger ribonucleic acids are widely distributed in rat tissues. Endocrinology 133, 617–623.

Uemura, H., Yasui, T., Yoneda, N., Irahara, M., Aono, T., 1997. Measurement of N- and C-terminal-region fragments of parathyroid hormone-related peptide in milk from lactating women and investigation of the relationship of their concentrations to calcium in milk. J. Endocrinol. 153, 445–451.

VanHouten, J.N., Dann, P., Stewart, A.F., Watson, C.J., Pollak, M., Karaplis, A.C., Wysolmerski, J.J., 2003. Cre-mediated deletion of PTHrP from the mammary gland reduces bone turnover and preserves bone mass during lactation. J. Clin. Investig. 112, 1429–1436.

VanHouten, J.N., Wysolmerski, J.J., 2003. Low estrogen and high PTHrP levels contribute to accelerated bone resorption and bone loss in lactating mice. Endocrinology 144, 5521–5529.

VanHouten, J., Dann, P., McGeoch, G., Brown, E.M., Krapcho, K., Neville, M., Wysolmerski, J.J., 2004. The calcium sensing receptor regulates mammary gland production of PTHrP and calcium transport into milk. J. Clin. Investig. 113, 598–608.

Vasavada, R., Cavaliere, C., D'Ercole, A.J., Dann, P., Burtis, W.J., Madlener, A.L., Zawalich, K., Zawalich, W., Philbrick, W.M., Stewart, A.F., 1996. Overexpression of PTHrP in the pancreatic islets of transgenic mice causes hypoglycemia, hyperinsulinemia and islet hyperplasia. J. Biol. Chem. 271, 1200–1208.

Vasavada, R.C., Garcia-Ocana, A., Massfelder, T., Dann, P., Stewart, A.F., 1998. Parathyroid hormone-related protein in the pancreatic islet and the cardiovascular system. Recent Prog. Horm. Res. 53, 305–338 discussion 338–340.

Vasavada, R.C., Wang, L., Fujinaka, Y., Takane, K.K., Rosa, T., Mellado-Gil, J.M., Garcia-Ocaña, A., 2007. Protein kinase C-zeta activation markedly enhances beta-cell proliferation: an essential role in growth factor mediated beta-cell mitogenesis. Diabetes 56, 2732–2743.

Villanueva-Penacarrillo, M.L., Cancelas, J., de Miguel, F., Redondo, A., Valin, A., Valverde, I., Esbrit, P., 1999. Parathyroid hormone-related peptide stimulates DNA synthesis and insulin secretion in pancreatic islets. J. Endocrinol. 163, 403–408.

Williams, E.D., Leaver, D.D., Danks, J.A., Moseley, J.M., Martin, T.J., 1994. Effect of parathyroid hormone-related protein (PTHrP) on the contractility of the myometrium and localization of PTHrP in the uterus of pregnant rats. J. Reprod. Fertil. 102, 209–214.

Williams, E.D., Major, B.J., Martin, T.J., Moseley, J.M., Leaver, D.D., 1998. Effect of antagonism of the parathyroid hormone (PTH)/PTH-related protein receptor on decidualization in rat uterus. J. Reprod. Fertil. 112, 59–67.

Williams, J.M.A., Abramovich, D.R., Dacke, C.G., Mayhew, T.M., Page, K.R., 1991. Parathyroid hormone (1–34) peptide activates cyclic AMP in the human placenta. Exp. Physiol. 76, 297–300.

Williams, K., Abanquah, D., Joshi-Gokhale, S., Otero, A., Lin, H., Guthalu, N.K., Zhang, X., Mozar, A., Bisello, A., Stewart, A.F., Garcia-Ocaña, A., Vasavada, R.C., 2011. Systemic and acute administration of parathyroid hormone-related peptide (1–36) stimulates endogenous beta cell proliferation while preserving function in adult mice. Diabetologia 54 (11), 2867–2877.

Wlodek, M.E., Ho, P., Rice, G.E., Moseley, J.M., Martin, T.J., Brennecke, S.P., 1996. Parathyroid hormone-related protein (PTHrP) concentrations in human amniotic fluid during gestation and at the time of labour. Reprod. Fertil. Dev. 7, 1509–1513.

Wlodek, M.E., Westcott, K.T., O'Dowd, R., Serruto, A., Wassef, L., Moritz, K.M., Moseley, J.M., 2005. Uteroplacental restriction in the rat impairs fetal growth in association with alterations in placental growth factors including PTHrP. Am. J. Physiol. 288 (6), R1620–R1627.

Wojcik, S.F., Schanbacher, F.L., McCauley, L.K., Zhou, H., Kartsogiannis, V., Capen, C.C., Rosol, T.J., 1998. Cloning of bovine parathyroid hormone-related protein (PTHrP) cDNA and expression of PTHrP mRNA in the bovine mammary gland. J. Mol. Endocrinol. 20, 271–280.

Wojcik, S.F., Capen, C.C., Rosol, T.J., 1999. Expression of PTHrP and the PTH/PTHrP receptor in purified alveolar epithelial cells, myoepithelial cells and stromal fibroblasts derived from the lactating mammary gland. Exp. Cell Res. 248, 415–422.

Woodrow, J.P., Sharpe, C.J., Fudge, N.J., Hoff, A.O., Gagel, R.F., Kovacs, C.S., 2006. Calcitonin plays a critical role in regulating skeletal mineral metabolism during lactation in mice. Endocrinology 147 (9), 4010–4021.

Wu, T.L., Insogna, K.L., Milstone, L., Stewart, A.F., 1987. Skin-derived fibroblasts respond to human PTH-like adenylate cyclase-stimulating proteins. J. Clin. Endocrinol. Metab. 65, 105–109.

Wu, T.L., Soifer, N.E., Burtis, W.J., Milstone, M., Stewart, A.F., 1991. Glycosylation of parathyroid hormone-related peptide secreted by human epidermal keratinocytes. J. Clin. Endocrinol. Metab. 73, 1002–1007.

Wu, T.-J., Lin, C.-L., Taylor, R.L., Kvols, L.K., Kao, P.C., 1997. Increased parathyroid hormone-related peptide in patients with hypercalcemia associated with islet cell carcinoma. Mayo Clin. Proc. 72, 111–115.

Wysolmerski, J.J., Broadus, A.E., Zhou, J., Fuchs, E., Milstone, L.M., Philbrick, W.P., 1994. Overexpression of parathyroid hormone-related protein in the skin of transgenic mice interferes with hair follicle development. Proc. Natl. Acad. Sci. U.S.A. 91, 1133–1137.

Wysolmerski, J.J., McCaughern-Carucci, J.F., Daifotis, A.G., Broadus, A.E., Philbrick, W.M., 1995. Overexpression of parathyroid hormone-related protein or parathyroid hormone in transgenic mice impairs branching morphogenesis during mammary gland development. Development 121, 3539–3547.

Wysolmerski, J.J., Philbrick, W.M., Dunbar, M.E., Lanske, B., Kronenberg, H., Karaplis, A., Broadus, A.E., 1998. Rescue of the parathyroid hormone-related protein knockout mouse demonstrates that parathyroid hormone-related protein is essential for mammary gland development. Development 125, 1285–1294.

Wysolmerski, J.J., Roume, J., Silve, C., 1999. Absence of functional type I PTH/PTHrP receptors in humans is associated with abnormalities in breast and tooth development. J. Bone Miner. Res. 14, S135.

Wysolmerski, J.J., Stewart, A.F., Kovacs, C.S., 2008. Physiological actions of parathyroid hormone (PTH) and PTH-related protein: epidermal, mammary, reproductive, pancreatic tissues. In: Bilezikian, J.P., Raisz, L.G., Martin, T.J. (Eds.), Principles of Bone Biology, third ed. Academic Press, San Diego, pp. 713–731.

Yadav, S., Yadav, Y.S., Goel, M.M., Singh, U., Natu, S.M., Negi, M.P., 2014. Calcitonin gene- and parathyroid hormone-related peptides in normotensive and preeclamptic pregnancies: a nested case-control study. Arch. Gynecol. Obstet. 290, 897–903.

Yang, K.H., dePapp, A.E., Soifer, N.S., Wu, T.L., Porter, S.E., Bellantoni, M., Burtis, W.J., Broadus, A.E., Philbrick, W.M., Stewart, A.F., 1994. Parathyroid hormone-related protein: evidence for transcript- and tissue-specific post-translational processing. Biochemistry 33, 7460–7469.

Yamamoto, M., Duong, L.T., Fisher, J.E., Thiede, M.A., Caulfield, M.P., Rosenblatt, M., 1991. Suckling-mediated increases in urinary phosphate and 3′-5′-cyclic adenosine monophosphate excretion in lactating rats: possible systemic effects of parathyroid hormone-related protein. Endocrinology 129, 2614–2622.

Yamamoto, M., Harm, S.C., Grasser, W.A., Thiede, M.A., 1992. Parathyroid hormone-related protein in the rat urinary bladder: a smooth muscle relaxant produced locally in response to mechanical stretch. Proc. Natl. Acad. Sci. U.S.A. 89, 5326–5330.

Yin, J.J., Selander, K., Chirgwin, J.M., Dallas, M., Grubbs, B.G., Wieser, R., Massague, J., Mundy, G.R., Guise, T.A., 1999. TGF-β signaling blockade inhibits PTHrP secretion by breast cancer cells and bone metastases development. J. Clin. Investig. 103, 197–206.

Chapter 37

The pharmacology of selective estrogen receptor modulators: past and present*

Jasna Markovac[1] and Robert Marcus[2]
[1]California Institute of Technology, Pasadena, CA, United States; [2]Stanford University, Stanford, CA, United States

Chapter outline

Introduction

In the past decade, essentially no new significant information about the skeletal aspects of selective estrogen receptor modulators (SERMs) has appeared. Ten years ago, several promising candidate molecules were making their way through clinical trials. Some of these showed clinical efficacy in reducing vertebral fractures, particularly lasofoxifene and bazedoxifene. However, except for bazedoxifene, side effects stifled continued development. Moreover, as the efficacy and safety profiles of bazedoxifene closely resembled those of raloxifene (EVISTA, Eli Lilly & Co), which had already been available for patient care for more than 2 decades, no clear path for it to succeed as a stand-alone product was evident. Accordingly, bazedoxifene has been combined with conjugated equine estrogens as a dual preparation (DUAVEE, Pfizer, Inc.) that is FDA-approved for use in postmenopausal women for control of vasomotor symptoms and the prevention (but not treatment) of osteoporosis. Thus, raloxifene remains the only approved SERM for both the treatment and the prevention of osteoporosis.

In recent years, the pharmaceutical industry has shown little or no interest in developing other SERMs for skeletal purposes, although some interest persists in the basic science surrounding the determinants of their tissue specificity. Feng and O'Malley (2014) published some of the more current research dealing with the role of nuclear reception modulators and other coregulators in the action of SERMs. In addition, recent studies gave interesting and potentially clinically useful

* Most of this chapter is an edited version of the chapter from the third edition of this book, written by Henry U. Bryant, Eli Lilly and Company, Indianapolis, IN.

Principles of Bone Biology. https://doi.org/10.1016/B978-0-12-814841-9.00037-3

results with SERMs in other therapeutic areas (Mirkin and Pickar, 2015), but discussion of these exceeds the scope of this chapter and of this book.

For this reason, what follows is material little changed from what was published on SERMs in the third edition of this work (2009).

The widespread distribution of estrogen receptors (ERs), and their critical role in normal physiology and various pathophysiological states when estrogen levels decline, indicate the importance of ER-targeted therapies for use in postmenopausal women. Controversy and concern over the use of estrogen replacement therapies created the opportunity to design molecules to selectively modulate estrogen action in those tissues where estrogen agonism is the desired goal while simultaneously producing an estrogen-neutral or estrogen-antagonistic effect in tissues where estrogen-related side effects are a concern. SERMs are in clinical use for the treatment and prevention of osteoporosis (raloxifene), breast cancer prevention (tamoxifen and raloxifene) and treatment (tamoxifen and toremifene), and the induction of ovulation (clomiphene). By 2008, seven different SERMs had reached advanced clinical evaluation for postmenopausal osteoporosis, with three molecules (droloxifene, idoxifene, and levormeloxifene) withdrawn for unfavorable risk/benefit profiles and three additional molecules (lasofoxifene, bazedoxifene, and arzoxifene) in phase 3 status or under regulatory review. Experience with these molecules revealed several key themes for chronic use of SERMs: (1) Each SERM generates a unique complex with the ER that influences cofactor recruitment in estrogen−target tissues responsible for the tissue-selective pharmacological profile, which translates to each SERM generating potentially an entirely unique overall safety and efficacy profile, indicating the need for thorough evaluation of each individual SERM across multiple tissue types for efficacy and safety determination. (2) Uterine safety historically has been the critical safety feature for chronic SERM use in osteoporosis therapy, and careful assessment of the potential for uterine stimulation has been a key element in the consideration of new molecules in this class. (3) The pharmacokinetic and distribution properties of SERMs offered an additional aspect influencing the magnitude of the overall biological response by either improving systemic bioavailability or altering uptake into important estrogen-responsive tissues.

Research in the ER field attracted considerable attention during the 15 years prior to 2009 with significant events ranging from very basic research discoveries, such as resolution of the liganded ER crystal structure and identification of a second ER form (ERβ), to important clinical observations regarding estrogen use in postmenopausal women from the Women's Health Initiative (WHI) trial. Estrogen exhibited a "Jekyll and Hyde" therapeutic profile, as hormone replacement (estrogen 1 progestin) was associated with distinct benefits on the menopausal syndrome including reductions in vasomotor symptoms and fracture incidence as well as other benefits such as a reduction in colon cancer. However, these benefits were offset by significant increases in risk for coronary events (myocardial infarction and stroke) and breast and uterine cancer. In the early 1990s, research around the concept of SERMs—molecules that simultaneously agonized or antagonized estrogen action in different tissue types—offered a new way of looking at ER pharmacology and served to trigger renewed interest in estrogen-related research in the mid-1990s.

Prior to the development of the "SERM-concept," ER ligands were generally thought of as falling into the category of full agonist, partial agonist, or full antagonist across all tissue types (i.e., uterus, mammary, and bone). For example, steroidal hormones such as 17β-estradiol were known to behave as full agonists both in vitro and in vivo across multiple tissue types, whereas compounds such as fulvestrant (ICI-182,780) were known to be complete ER antagonists that bound tightly to the ER but lacked intrinsic activity, and therefore completely blocked the action of full ER agonists like 17β-estradiol. These "pharmacotypes" are depicted in Fig. 37.1A and B, respectively. Conversely, compounds such as tamoxifen were known, in the presence of estrogen, to block estrogen action in estrogen-responsive tissues (i.e., breast cancer cells), but in the absence of estrogen to mimic estrogen in bone and uterus in estrogen-deficient animals and women, thus exhibiting a classical partial-agonist profile (see Fig. 37.1C). Although this profile held some attractive features for use in ER-dependent breast cancer, the profile was prohibitive for chronic use in postmenopausal women for noncancer indications (like osteoporosis), where even the potentially less robust uterine stimulation induced by tamoxifen's partial agonist action produced untenable side effects that created a risk/benefit ratio that was unfavorable for use in diseases such as osteoporosis (Kalu et al., 1991). As a result, virtually no work was being done in the pharmaceutical industry developing novel ER ligands for osteoporosis because the prevailing medical opinion at the time was that any molecule with sufficient estrogen agonism capable of producing a benefit in bone would also generate sufficient agonism (even if a partial agonist) in uterine tissue to create a risk that would unfavorably offset the bone benefit (Feldman et al., 1989).

With the first preclinical and clinical descriptions of the unique profile of raloxifene in estrogen-deficient animals and postmenopausal women (Black et al., 1994; Draper et al., 1997), the SERM concept was born, radically shifting thought around use of ER ligands in postmenopausal women and opening the door for use in chronic diseases such as osteoporosis. Accordingly, the initial goals of SERM-based therapy for osteoporosis required the molecule to have estrogen-like efficacy on bone and concomitant fracture reduction without estrogen-like stimulatory effects on the uterus or mammary tissue. As

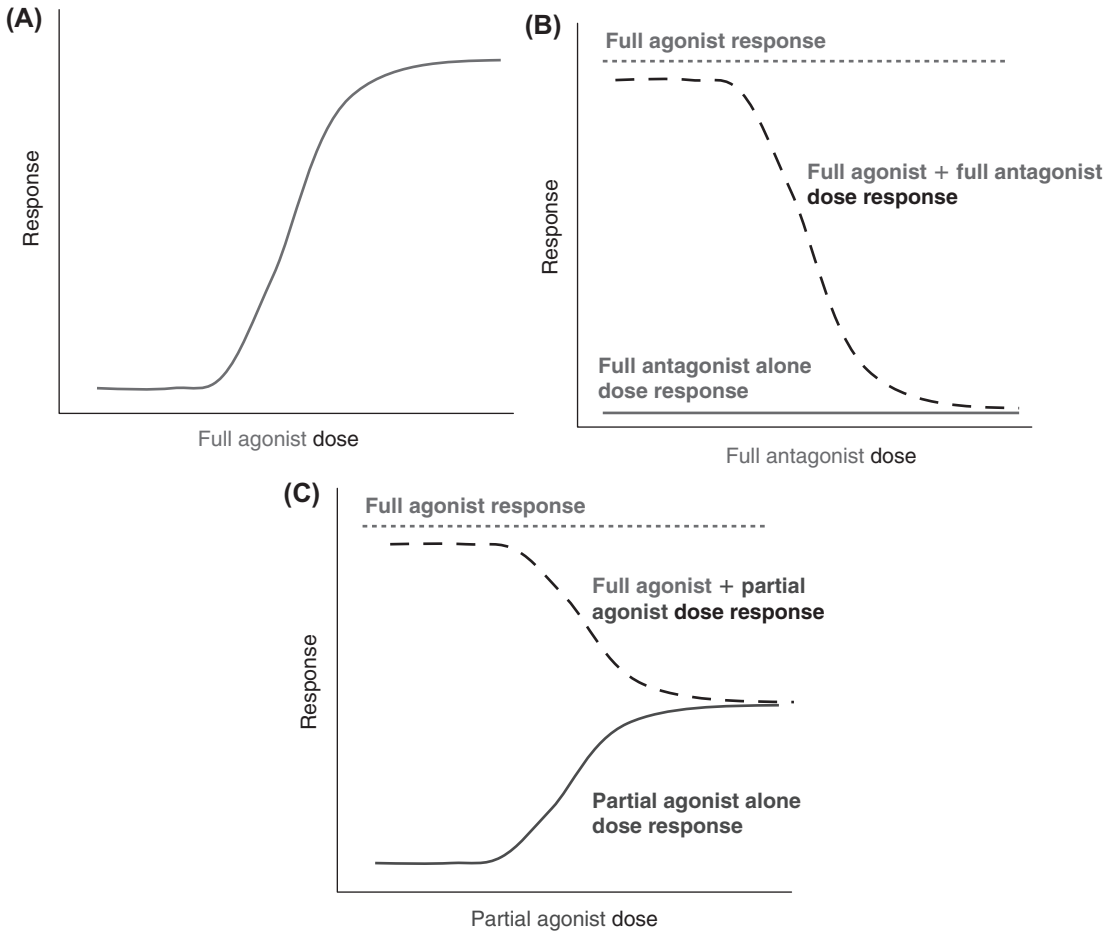

FIGURE 37.1 Potential pharmacotypes resulting from various estrogen receptor–ligand interactions in the form of hypothetical dose–response curves for a full agonist (A), full antagonist (B), and partial agonist (C). (See plate section.)

of the writing of this chapter for the third edition of this book, only four molecules with SERM-like profiles had achieved clinical use (Table 37.1), and only one, raloxifene, had attained approval for use in the treatment and prevention of osteoporosis. However, other molecules had been evaluated clinically for postmenopausal osteoporosis and are reviewed here. In addition, some other SERM applications are presented that could potentially benefit other diseases or disorders in postmenopausal women.

Selective estrogen receptor modulator mechanism

The effects of SERMs on biological systems are predominantly mediated by specific, high-affinity interactions with ERs that are primarily located in target cell nuclei (Nilsson *et al.*, 2001). Their nuclear hormonal action involves the complex interplay of a number of protein and genomic elements that allow SERMs to regulate gene transcription and subsequent protein production by the cell. Three key elements of the SERM mechanism are depicted in Fig. 37.2, which include (1) high-affinity interaction with the ER, (2) ER–ligand dimerization and association with a tissue-specific set of coregulatory proteins, and (3) binding of the ER/adaptor protein complex to specific DNA response elements located in the promoter regions of nuclear target genes and ensuing regulation of gene transcription. Depending on the cellular and promoter context, the DNA-bound receptor can induce or inhibit the transcription of specific genes within the tissue.

The ability to specifically bind to the ER is perhaps the single most important feature of all molecules with a SERM profile. The affinities of several of the more extensively studied SERMs are provided in Table 37.2. An important determinant of the ultimate pharmacological response is the shape of the ligand–ER complex, which is unique with each individual ligand (McDonnell et al., 1995), with different SERMs leading to specific orientation of ER subunits (i.e., raloxifene; Brzozowski et al., 1997). This conformation or shape of the ligand–ER complex then determines the

TABLE 37.1 Selective estrogen receptor modulators currently approved for human use.

SERM	Trade name	Approved indications	Daily dose (mg)
Clomiphene	Clomid	Induction of ovulation	50–100
Raloxifene	EVISTA	Osteoporosis prevention	60
		Osteoporosis treatment	
		Breast cancer risk reduction in postmenopausal osteoporotic women and in high-risk postmenopausal women	
Tamoxifen	Nolvadex	Metastatic breast cancer treatment	20–40
		Adjuvant breast cancer treatment	
		Ductal carcinoma in situ	
		Breast cancer risk reduction in high-risk women	
Toremifene[a]	Fareston	Metastatic breast cancer treatment	60

[a]*Toremifene (Fareston) is currently not approved in the United States but is approved for metastatic breast cancer treatment in Europe.*

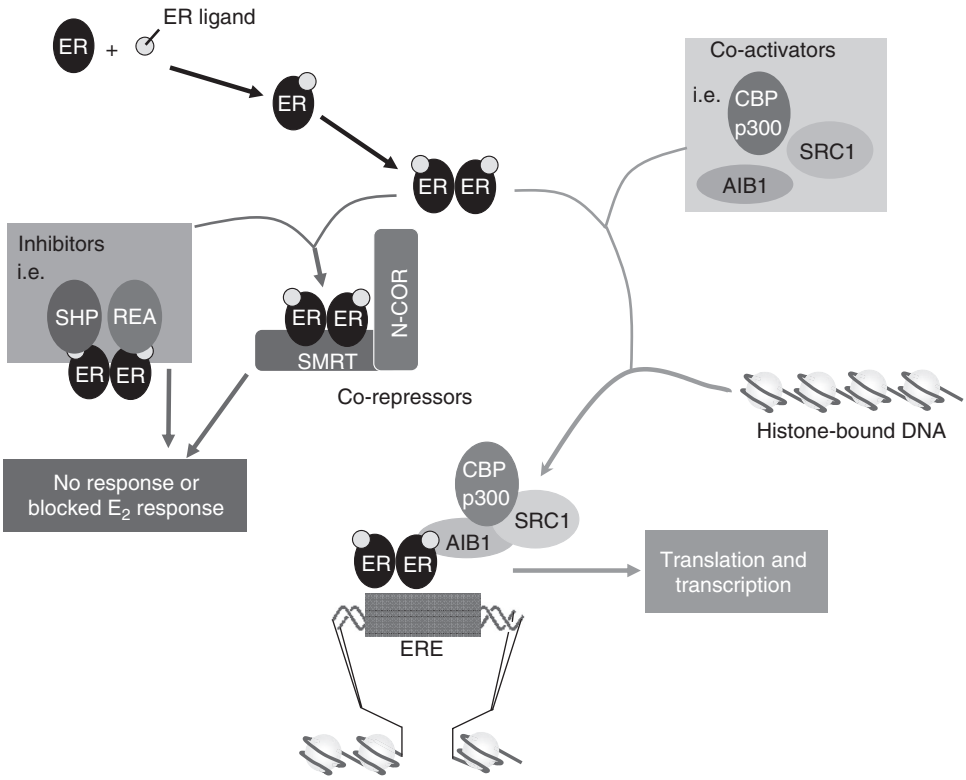

FIGURE 37.2 Selective estrogen receptor (ER) modulator mechanism of action.

subsequent protein–protein interactions that ensue. Herein lies the basis for the wide array of different pharmacological profiles produced by different SERMs, because the confirmation of the ER–SERM complex is distinct for each molecule (McDonnell et al., 1995). It is important to recognize that a second form of ER is known to exist, ERβ (Kuiper et al., 1996). ERα and ERβ display unique patterns of tissue distribution, typically with the expression levels of one subtype dominating (Saunders et al., 1997), although it should be noted that most tissues contain at least small amounts of both subtypes, and with the role of putative α/β heterodimers unknown, it is possible that a low-expression subtype may be a key rate-limiting

TABLE 37.2 Affinities of various SERMs for human estrogen receptors ERα and ERβ.

ER ligand	ERα(IC_{50})	ERβ(IC_{50})
17β-Estradiol	0.3–0.8[a]	0.9–2.5[a]
Tamoxifen	72–138	173–1204
4-Hydroxytamoxifen	0.22–0.98	1.5–2.46
Raloxifene	0.4–1.31	5.6–13.0
Fulvestrant (ICI-182,780)	0.8–1.0	1.12–3.6

[a]*All values are in nM. As binding data often can vary from laboratory to laboratory, and various approaches can be taken to attaining binding affinities, ranges for ERα and ERβ obtained from representative references are presented (Sun et al., 1999; Brady et al., 2001; de Boer et al., 2004; He et al., 2005; Leblanc et al., 2007).*

step in ultimate nuclear activity. All SERMs that have reached advanced clinical evaluation show high affinity for both ERα and ERβ with sufficient circulating and tissue exposure to ensure binding of both subtypes, indicating that for these molecules at least, differential ERα or ERβ activation does not explain the tissue-selective pharmacological effects.

In addition to ERs themselves, a number of other coregulatory proteins, such as coactivators (which enhance transcription) and corepressors (which reduce transcription), play an essential role in determining the ultimate response of an individual cell to liganded ER. A number of coactivators and corepressors that interact with ligand-bound ER have been identified and are reviewed thoroughly elsewhere (Smith, 2006).

The relative tissue expression of the different cofactors and the ability of the ER–ligand complex to interact with those cofactors determine the tissue-selective agonist/antagonist profile of the various SERM molecules. Cofactor tissue expression can also be altered with various pathophysiological states, such as breast cancer (Bautista et al., 1998). The important nature of the tissue-relevant cofactor context was demonstrated by Shang and Brown (2002), who compared the effects of two SERMs, tamoxifen and raloxifene, with estrogen in two tissue contexts, a breast cancer cell line and a uterine endometrial carcinoma cell line. In the mammary cells that proliferate in response to estrogen, 17β-estradiol recruited coactivators leading to increased gene expression. In these same cells, where tamoxifen and raloxifene both display estrogen antagonist pharmacology, the ligand–SERM complex with both molecules recruited corepressors and not the coactivators observed with 17β-estradiol on ER-mediated transcription. However, in a uterine cell line where tamoxifen exhibits estrogen agonist pharmacology and raloxifene is a complete antagonist, tamoxifen was associated with the recruitment of a coactivator protein complex that is expressed at higher levels in uterine cells. The coactivator requirements for estrogen-stimulated gene expression in uterine cells were distinct from those for tamoxifen, indicating multiple signaling mechanisms even for the agonist response. Conversely, raloxifene failed to recruit a coactivator construct and rather induced a corepressor construct in uterine cells (Shang and Brown, 2002). Thus, the relative abundance of ER-associated coactivators and corepressors is an important factor in the tissue-specific pharmacology of SERMs.

In addition to the layers of complexity provided by multiple ER–SERM conformations and tissue-selective cofactor recruitment, the mechanism of tissue selectivity of SERMs is further complicated by the existence of multiple DNA response elements. Many estrogen-responsive genes contain the classical estrogen response element and a number of DNA response elements, such as activator protein-1 and steroidogenic factor-1 response element (Vanacker et al., 1999). The mechanism for SERM activation (or inactivation) of ER-mediated function is further complicated by the presence of novel DNA response elements that are more apparent following formation of the ER–SERM cofactor complex.

Although there have been considerable strides in understanding the molecular biology of SERM action in a general sense, with the critical role of the ER, specific cofactors that are recruited to the transcriptional complex, and the specific DNA response elements activated, it is important to recognize that each SERM has the potential to produce a unique fingerprint of pharmacological activity at the whole-organism level. Contributing to the eventual profile are the molecular mechanisms reviewed earlier as well as other factors, such as absorption, distribution, excretion, and metabolism of the SERM, that add another layer of complexity for ultimate pharmacological response, creating the need to fully characterize the tissue-specific effects of each individual SERM in an in vivo paradigm.

Selective estrogen receptor modulator chemistry

A key element in determining the pharmacological profile of each distinct SERM is influenced heavily by the chemical makeup of the SERM including the basic scaffold, the placement of the hydroxyl moieties, and the positioning and nature of the basic side chain. Crystal structures of various ligands bound to the ER indicate that small molecules can induce a spectrum of receptor conformations. As described previously, the specific SERM−ER conformation has a tremendous impact on cofactor recruitment and ultimate genomic activation or inhibition by the SERM. Chemical scaffolds that have produced SERMs in current clinical use, or at least that have reached phase 3 clinical evaluation in humans, are depicted in Fig. 37.3 and include triphenylethylenes (i.e., tamoxifen, droloxifene, idoxifene, clomiphene, and toremifene), benzothiophenes (raloxifene and arzoxifene), tetrahydronaphthalenes (lasofoxifene and nafoxidine), indoles (bazedoxifene), and benzopyrans (acolbifene and levormeloxifene). Key structural features of these molecules, which are indicated in Fig. 37.4 for raloxifene versus 17β-estradiol, are typical for the entire class, with the most important features being the hydroxyl moieties and the basic side chain, as described thoroughly elsewhere (Grese et al., 1997).

Selective estrogen receptor modulator pharmacology

Given the wide distribution of ER and the pleiotropic nature of estrogen and its multiple metabolites, SERMs should be expected to likewise affect multiple organ systems, and this is indeed the case. Because one area of focus in this volume is skeletal pharmacology, emphasis here will be placed on the pharmacologic effects of SERMs on bone and other tissues that are of relevance to safety in the clinical setting. Accordingly, emphasis is placed on those SERMs where osteoporosis and

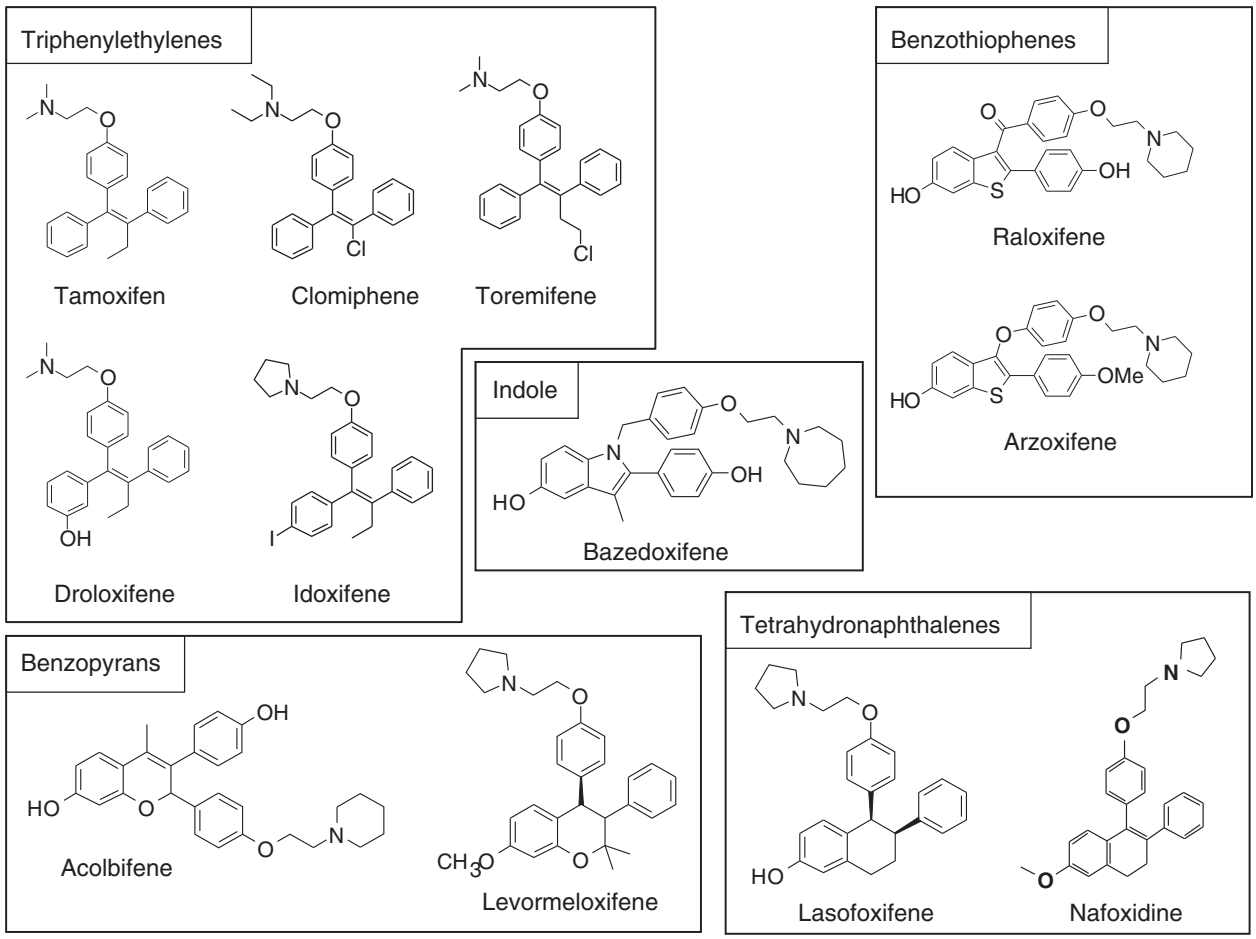

FIGURE 37.3 Structures and chemical classes of selective estrogen receptor modulators currently in clinical use or that have reached phase 3 clinical trials in women.

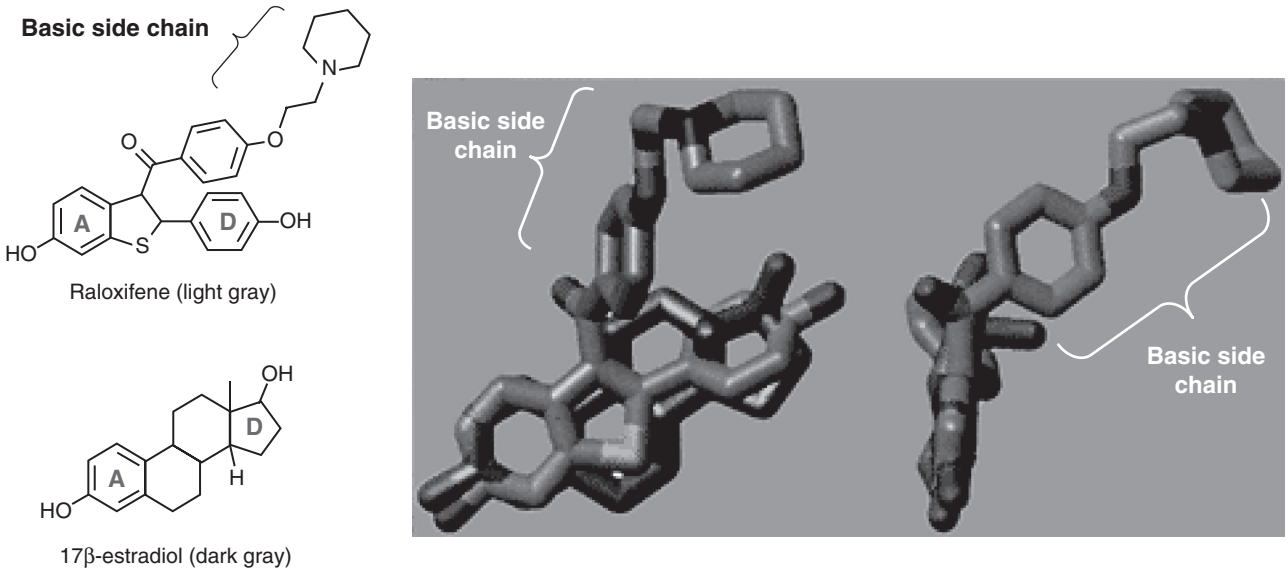

FIGURE 37.4 Key structural features of raloxifene versus 17β-estradiol.

bone have been the primary focus of research. SERMs used primarily for other indications (present or with future potential) will be briefly summarized as well.

Skeletal system

Preclinical studies

Much as in postmenopausal women, estrogen deficiency in ovariectomized (OVX) animals leads to a rapid increase in bone turnover, where excessive osteoclast resorptive activity results in a marked decline in trabecular bone mass and strength with a concomitant increase in fractures. In rats, ovariectomy produces a rapid osteopenic response that can be discerned within 5 weeks. All of the SERMs depicted in Fig. 37.3 have been evaluated in the OVX rat and demonstrate estrogen-like protection from bone loss induced by estrogen deficiency. In the OVX rat model, SERMs like raloxifene (Black et al., 1994), arzoxifene (Sato et al., 1998), tamoxifen (Sato et al., 1996a,b), droloxifene (Ke et al., 1995), idoxifene (Nuttall et al., 1998), clomiphene (Jiminez et al., 1997), bazedoxifene (Komm et al., 2005), lasofoxifene (Ke et al., 1998), levormeloxifene (Galbiati et al., 2002), toremifene (Qu et al., 2000), and acolbifene (Martel et al., 2000) prevent the loss of bone in vertebrae, distal femur, and proximal tibia, all trabecular-rich bone sites. In addition to maintaining bone mass, SERMs also preserve bone strength through improvements in bone microarchitecture (i.e., raloxifene; Turner et al., 1994). For both bone mass and bone strength, the absolute magnitudes of the effects of most SERMs in OVX rats are indistinguishable from those of estrogen and can approach values attained for sham-surgery controls when the SERM is administered in a preventative mode. However, differences in potency for these bone-protective effects can occur, with third-generation SERMs like arzoxifene, bazedoxifene, and lasofoxifene producing efficacy equivalent to that of raloxifene in OVX rat trabecular BMD responses at approximately 10% of the dose (Ke et al., 1998; Sato et al., 1998). There had been preclinical hints of improved efficacy of some of these latter agents as well, for example with arzoxifene, which improves cortical bone strength to a greater degree than observed with maximally effective doses of either estrogen or raloxifene (Sato et al., 1998). Similarly, with bazedoxifene, improved biomechanical properties in trabecular bone were observed relative to estrogen after 1 year of treatment in OVX rats (Komm et al., 2007).

As with estrogen, the primary activity of SERMs that is responsible for the beneficial effect on bone is antiresorptive. Mechanistic studies in vitro demonstrated that raloxifene and estrogen exert their antiresorptive effects primarily as inhibitors of osteoclast differentiation, rather than as direct inhibitors of activated osteoclasts. Raloxifene acts to suppress mediators of osteoclast differentiation, such as the receptor activator of nuclear factor-kappa-β (RANK) and RANK-ligand (Bashir et al., 2005), and increase endogenous antiresorptive factors such as osteoprotegerin (Viereck et al., 2003). Biochemical markers of bone turnover (i.e., serum osteocalcin and urinary collagen cross-links) are suppressed in OVX rats in a manner similar to that observed with estrogen (Frolik et al., 1996). Histomorphometric analysis of bone from raloxifene-treated OVX rats confirmed the antiresorptive mechanism of action for raloxifene (Evans et al., 1994). Similar

studies with the other SERMs discussed here indicate the same antiresorptive mechanism for bone protection. Of likely importance with respect to long-term safety in the skeleton is the finding that SERMs such as raloxifene produce their inhibitory action on bone resorption with minimal suppressive effects on bone formation, leaving bone formation rates at levels comparable to those of sham-operated control animals (Evans et al., 1994). The molecular fingerprint of SERMs in estrogen-deficient rat trabecular bone, as assessed by DNA microarray, is unique for each SERM, although it is clear that some SERMs are less suppressive of bone formation. For example, in OVX rats, raloxifene returned a cluster of genes associated with bone formation to ovary-intact control levels, as opposed to a bisphosphonate (alendronate), estrogen, or even another SERM (acolbifene), which exhibited a greater suppressive effect on bone formation−associated genes (Helvering et al., 2005a,b). The overall SERM profile on bone then represents a sharp distinction from the marked suppression of bone formation that occurs with other bone antiresorptives, such as the bisphosphonates. A final bone cell type that may be of relevance to the skeletal-protective effect of SERMs is the osteocyte. Whereas relatively less work has been done with this bone cell owing to technical challenges, work in MLO-Y4 cells (an osteocyte-like cell line) has indicated that raloxifene prevents oxidative stress−induced apoptosis and inhibits the generation of reactive oxygen species with oxidative insults, such as hydrogen peroxide (Mann et al., 2007).

Clinical studies

The abundance of preclinical information on the effects of SERMs on bone was easily matched by a plethora of long-term clinical trials conducted on a number of different SERM molecules, either as the primary element of registration trials for postmenopausal osteoporosis or as part of the safety assessment for use in breast cancer. Certainly the most extensively studied SERM on the human skeleton has been raloxifene, which has been investigated in nearly 40,000 clinical trial subjects enrolled in prospective, randomized trials (placebo or active comparator) that have ranged in duration from 1 to 8 years. In postmenopausal women, raloxifene (60 mg/day) exhibited an antiresorptive action, as evidenced by reductions in accelerated bone turnover as measured by biochemical markers of bone resorption (Ettinger et al., 1999), while only modestly suppressing bone formation. In calcium tracer kinetic studies in postmenopausal women, Heaney and Draper (1997) showed suppression of bone resorption with raloxifene, whereas bone formation was not affected after 31 weeks of treatment. The observation of resorption inhibition with minimal formation suppression by raloxifene was confirmed by histomorphometric analysis of iliac crest bone biopsies (Ott et al., 2002). This antiresorptive activity is associated with an approximately 2.5% increase in vertebral BMD relative to placebo-treated controls. This increase in spine BMD that occurs following raloxifene treatment in postmenopausal women is less marked than observed with a bisphosphonate (alendronate; Johnell et al., 2002). However, this magnitude of BMD improvement in the spine underestimates the mechanical improvement produced by raloxifene as evidenced by the 55% reduction in new vertebral fractures in women with prevalent fractures (Ettinger et al., 1999), a rate comparable to that produced by bisphosphonates. This observation led to increased attentiveness to the potential effects of raloxifene (and putatively other SERMs in the future) on bone quality. The eventual resistance of bone to fracture was the result of both the content, or mass of the material (i.e., BMD), and the quality of that material, which was likely the result of bone microarchitecture and the nature of the mineralized matrix itself. In animal models, increased trabecular thickness and the maintenance of platelike (vs. rodlike) trabecular structures, both of which correlate with improved biomechanical strength of bone, were observed in OVX mice (Cano et al., 2008). Although BMD is a noninvasive, easily quantifiable parameter in clinical trials, bone quality remains more difficult to quantify because it is primarily revealed by the eventual incidence of fracture. A number of efforts targeted better understanding and quantifying of bone quality in instances where raloxifene had shown some benefits over other antiresorptive therapies such as histomorphometric analyses of trabecular bone architecture and microcrack frequency in bone (Allen et al., 2006; Li et al., 2005). One area where some aspect of bone quality was beginning to be elucidated is the proximal femur, where imaging technologies had been applied to postmenopausal clinical trial subjects to show an increase in resistance to axial and bending stresses in raloxifene-treated women (Uusi-Rasi et al., 2006), indicating improved structural components of bone strength and stability with the SERM. Raloxifene produced positive effects on hip BMD, which increased 2.1% versus placebo after 3 years in postmenopausal women (Ettinger et al., 1999), although without a significant effect on nonvertebral fracture rates (Ettinger et al., 1999). However, an interesting trend was noted in a subset of women who entered the trials with severe vertebral fractures. In this subset of more severely osteoporotic women, raloxifene produced a 50% reduction in nonvertebral fractures (Delmas et al., 2003). Finally, in addition to the reduction of vertebral fractures in osteoporotic women, raloxifene provided fracture risk protection to osteopenic women (Kanis et al., 2003).

A number of other SERMs had attempted unsuccessfully to register for an osteoporosis prevention/treatment indication. The failure of those molecules to achieve regulatory approval for osteoporosis was primarily based on safety and risk/

benefit analysis, as each demonstrated some level of improvement on skeletal parameters in earlier clinical trials. Prior to discontinuation of levormeloxifene phase 3 clinical trials because of gynecological-associated adverse events, phase 2 clinical trials demonstrated positive effects of this SERM on BMD and bone turnover (Alexandersen et al., 2001). Idoxifene, a triphenylethylene also discontinued in phase 3 for uterine-adverse events, produced clinically relevant increases in BMD in osteopenic postmenopausal women (Chesnut et al., 1998). The third-generation molecules, lasofoxifene and bazedoxifene, are both very potent SERMs with relatively high bioavailability (Gardner et al., 2006; Patat et al., 2003) and produced advanced clinical testing results for osteoporosis. In a 2-year trial in 410 postmenopausal women, lasofoxifene at 0.25 or 1 mg/day suppressed bone turnover similarly to raloxifene, but lasofoxifene increased lumbar spine BMD by 3.6% and 3.9% (respectively by dosage), which outpaced the increase observed with raloxifene (McClung et al., 2006). A 2-year BMD trial and 3-year fracture prevention trial demonstrated the skeletal protective effects of bazedoxifene relative to raloxifene. In the 3-year trial, nearly 7500 women were treated with 20 or 40 mg/day bazedoxifene, placebo, or 60 mg/day raloxifene. In this trial, bazedoxifene produced a significant reduction in relative risk for new vertebral fractures of 37% for the higher dose and 42% for the lower dose, with raloxifene producing a comparable 42% reduction in relative risk of new vertebral fractures (Silverman et al., 2007). Mean lumbar spine BMD was significantly improved, relative to placebo, by bazedoxifene with a magnitude of response comparable to raloxifene, and biochemical markers of bone turnover were also significantly lowered with bazedoxifene (Miller et al., 2007).

A number of clinical trials have focused on the bone-sparing effects of two triphenylethylene SERMs used for breast cancer treatment, tamoxifen and toremifene. Although most studies demonstrated a skeletal benefit for these two agents, trials have typically been small and not placebo-controlled in design. A consistent benefit was observed with tamoxifen and toremifene primarily at trabecular bone sites, which was consistent with observations made with raloxifene in postmenopausal women. After 3 years of use, tamoxifen or toremifene in breast cancer patients led to a less-than-expected decline in vertebral BMD (Tiitinen et al., 2004). In shorter trials (1 year), similar effects were observed, with the effect of tamoxifen somewhat stronger than that of toremifene (2% higher BMD with tamoxifen vs. toremifene, which basically prevented age-related decline over the 1-year trial; Marttenun et al., 1998). Although many studies had reported similar benefits on BMD in postmenopausal breast cancer patients, particularly with tamoxifen (e.g., Love et al., 1992), there was at least one indication that the use of tamoxifen in normal premenopausal women was associated with a reduction in bone mineral density (Powles et al., 1996).

Reproductive system

Uterus

Atrophy of the uterus accompanies estrogen deficiency in humans and most animal species, and cessation of menses is a hallmark feature of menopause in women. A major side effect of most current ER-based therapies is stimulation of the uterus resulting in part from estrogen-induced proliferation of uterine endometrial tissue. The cancer concern associated with this proliferative effect and the resumption of menses (when combined with progestin regimens as hormonal replacement therapy) have been major limitations to estrogen replacement therapeutic approaches. These uterine side effects of estrogen are often the primary deterrent in the risk/benefit decision for postmenopausal women to utilize or remain compliant with hormonal estrogen therapies for chronic use with diseases such as osteoporosis. For postmenopausal women, a major and significant advantage of SERMs like raloxifene over hormonal estrogen therapies is the lack of uterine stimulation with the SERM. However, not all SERMs share the same degree of uterine safety observed with raloxifene, and thus effects on the uterus also serve as an important distinguishing feature among various SERMs. In this regard, SERMs that have failed in phase 3 clinical trials have done so primarily because of an untenable degree of uterine stimulation or uterus-related adverse events. The accumulated clinical experience with uterine safety for a number of SERMs helps one determine which preclinical models and parameters provide optimal predictive value for uterine safety. The use of in vitro systems, estrogen-depleted animals, and estrogen-replete animals to assess antagonist potential formed a triangulated approach for the uterine safety assessment of SERMs.

Estrogen agonism in the uterus

Initial indication of the uterine estrogenic potential of SERMs was demonstrated using Ishikawa cells, a human endometrial cancer cell line. Ishikawa cell proliferation is stimulated by 17β-estradiol, tamoxifen, and 4-hydroxytamoxifen (active metabolite of tamoxifen), but not by uterine-sparing SERMs such as raloxifene (Koda et al., 2004). More subtle changes among various SERMs were detected by evaluating their effects on ER-mediated alkaline phosphatase production, creatine kinase production, and expression of progesterone receptor. The more uterine-stimulatory SERMs produced greater

induction of alkaline phosphatase and progesterone receptor expression and were less effective antagonists of 17β-estradiol-stimulated responses in Ishikawa cells (Bramlett et al., 2003). Of note, whereas uterine-safe SERMs like raloxifene failed to stimulate creatine kinase production in Ishikawa cells, raloxifene induced this activity in cell lines with an osteoblast background, consistent with the "SERM" activity profile (Koda et al., 2004).

Lack of biologically meaningful stimulation of the uterus in the estrogen-depleted state (e.g., in postmenopausal women and OVX animals) was the crux of SERM uterine-safety evaluation. The uterine effects of tamoxifen and raloxifene had been thoroughly evaluated in numerous clinical settings as well as in a variety of preclinical models. Raloxifene did not produce estrogen-like stimulatory effects in the uterus of OVX rats (Black et al., 1994). In the OVX rat model, a slight non-dose-related elevation of uterine weight was frequently observed. However, this phenomenon contrasted markedly with the robust dose-related elevation of uterine weight produced by estrogen in these animals. Raloxifene failed to stimulate other estrogen-sensitive markers in the uterus of OVX rats, such as uterine eosinophilia or uterine epithelial cell height (Black et al., 1994). In large-scale clinical trials, after 8 years of chronic use in postmenopausal women, extensive uterine safety evaluation revealed no significant uterine-stimulatory effects of raloxifene in humans (Delmas et al., 1997). Indeed, a significant reduction in endometrial cancer of the uterus was noted in postmenopausal women using raloxifene (Delmas et al., 1997).

As indicated, not all SERMs exhibit the uterine safety profile demonstrated with raloxifene. This is perhaps most evident in the extensive work done with tamoxifen. Studies in the uterus of OVX rats demonstrated robust dose-related stimulatory effects of tamoxifen on uterine weight, uterine epithelial cell height, and uterine eosinophilia (Adrian et al., 1996). Clinical experience with tamoxifen is consistent with these observations, as uterine bleeding and significant elevation of endometrial cancer has been observed in women exposed to tamoxifen in long-term studies (Fisher et al., 1994).

Thus, raloxifene and tamoxifen serve as bookend profiles for uterine safety for chronic SERM use in postmenopausal women, where molecules can be assessed for either a "raloxifene-like" profile of little or no uterine stimulation or a more estrogenic "tamoxifen-like" profile. Several SERMs have advanced to clinical research and corroborated the preclinical observations for those molecules. For example, droloxifene, idoxifene, and levormeloxifene all produced dose-related elevation of uterine weight, uterine epithelial height, and uterine eosinophilia in the OVX rat (Adrian et al., 1996) and were eventually halted in clinical development on the basis of uterine liabilities such as increased bleeding, increased endometrial thickness, and polyps that developed in phase 3 studies for osteoporosis (Silfen et al., 1999). The other triphenylethylenes used clinically, clomiphene and toremifene, also exhibit an overall uterine stimulatory profile in OVX rats (Turner et al., 1998; Carthew, 1999), although uterine safety is less of a concern with acute therapeutic use of clomiphene, and the risk/benefit profile for toremifene use in breast cancer treatment has a different weighting of risk. Mixed effects have been observed with lasofoxifene, which in some preclinical reports produced significant dose-related stimulation of uterine epithelial cell height and uterine eosinophilia (Cole et al., 1997), but not in others (Ke et al., 1998). The outcome of clinical trials with lasofoxifene is incomplete, although initial observations indicate statistically significant uterine stimulation with an approximately 80% increase in endometrial thickness relative to placebo-treated controls and an increased incidence of leukorrhea (McClung et al., 2006). On the other hand, bazedoxifene, arzoxifene, and acolbifene produced very little stimulation of the uterus in OVX rats (Komm et al., 2005; Sato et al., 1998; Martel et al., 2000), and at least with bazedoxifene, studies in postmenopausal women have corroborated the animal work (Adachi et al., 2007).

A significant uterine-related adverse event that emerged in a number of clinical trials is relaxation of the pelvic floor, typically with associated prolapse of the uterus. Estrogen therapy was traditionally thought to improve the structural integrity of pelvic tissue with expected favorable effects on symptoms such as urinary incontinence. However, data from both the WHI trial and the Heart and Estrogen/progestin Replacement Study (HERS) provided evidence for the increased incidence of urinary incontinence in association with estrogen use (Hendrix et al., 2005). Related to this, pelvic organ prolapse was associated with both levormeloxifene and idoxifene within 1 year of therapy (Fleischer et al., 1999; Goldstein et al., 2002). These observations, taken together, suggest that these uterine wall−associated adverse events with idoxifene and levormeloxifene might be due to their more estrogen-like uterine activity. The mechanism by which estrogen and some SERMs compromise the uterine wall in postmenopausal women may be linked to an increase in collagen-degrading enzymes, such as metalloproteinase-2 (MMP-2), based on OVX rat studies. In OVX rats, uterine MMP-2 levels were reduced relative to those of ovary-intact animals. Estrogen, as well as levormeloxifene, produced marked increases in uterine MMP-2 expression (Helvering et al., 2005a,b). Not all SERMs, however, have been associated with pelvic floor problems, because no increase in this adverse event has been related to the chronic use of tamoxifen, toremifene, bazedoxifene, or lasofoxifene (Fisher et al., 1994; Maenpaa et al., 1997; McClung et al., 2006; Adachi et al., 2007). Consistent with its uterine-safe overall profile, the extensive uterine safety evaluations with raloxifene showed no increase in the incidence of problems associated with pelvic floor relaxation. Rather, in at least one report, raloxifene produced benefit

with a significant reduction in the frequency of surgery for pelvic floor relaxation in a population of postmenopausal women (Goldstein et al., 2001).

Estrogen antagonism in the uterus

The final important component in assessing the uterine safety profile of SERMs relied primarily on preclinical data—the ability of SERMs to antagonize the uterine-stimulatory effects of estrogen. Further insight into the uterine activity profile of SERMs was gleaned from effects on the uterus in the presence of estrogen, because this allowed assessment of the uterine estrogen antagonist potential for these compounds. As in the estrogen-deficient state, the various SERMs also produced one of two general activity profiles in estrogen-replete animals: that of either a complete estrogen antagonist or a partial agonist at the ER. In the uterus of either estrogen-treated immature or adult OVX rats, SERMs producing desirable uterine safety profiles in postmenopausal women, such as raloxifene, arzoxifene, and bazedoxifene, produced a complete estrogen antagonistic effect (Adrian et al., 1996; Sato et al., 1998; Komm et al., 2005). This effect is most clearly demonstrated in the estrogen-treated immature rat, a model classically used to determine uterine liability of ligands for the ER. In this model, raloxifene blocks the uterotrophic effects of estrogen with an ED_{50} of 0.3 mg/kg (Silfen et al., 1999), whereas arzoxifene and bazedoxifene completely antagonizes the estrogen response with greater potency (Sato et al., 1998; Komm et al., 2005). A key feature of this antagonistic effect with SERMs like raloxifene in the immature rat uterus is the complete antagonism of the uterotrophic effect of estrogen. That is, the uteri from estrogen-treated immature rats given doses of raloxifene exceeding 3 mg/kg are indistinguishable from those of non-estrogen-treated immature rats (Adrian et al., 1996). This is in dramatic contrast to other SERMs—this is best exemplified by tamoxifen, which behaves as a classical partial agonist in the uterus. That is, tamoxifen does significantly antagonize the effects of estrogen in the immature rat uterus. However, in the case of tamoxifen, the maximal degree of this antagonism is only approximately 50% (Adrian et al., 1996). The primary reason for this incomplete antagonistic effect of tamoxifen is that at higher doses, the inherent uterine stimulatory capacity of tamoxifen limits further suppression of estrogen-induced uterotrophic response. Other triphenylethylene SERMs, as well as levormeloxifene (Adrian et al., 1996), produce partial estrogen agonist profiles in estrogen-stimulated immature rats.

In addition to the usefulness of this parameter for SERM uterine safety assessment, the complete estrogen antagonistic effects of SERMs like raloxifene were utilized successfully in a variety of preclinical models of estrogen-stimulated uterine pathologies with some limited success in clinical studies. For example, in vitro and in vivo models of uterine leiomyoma (fibroids) demonstrated favorable responses to raloxifene (Porter et al., 1998) with some reports of successful use of high-dose raloxifene to prevent the progression of uterine leiomyomas in small groups of premenopausal and postmenopausal women, either alone or in combination with a GnRH agonist (Jirecek et al., 2004; Palomaba et al., 2002b, 2005) via a combined antiproliferative/proapoptotic effect. However, other small clinical trials have failed to detect a benefit of raloxifene on uterine leiomyoma (Palomba et al., 2002a), indicating the need for randomized, well-controlled clinical trials for this indication, which would be necessary to balance the benefit on leiomyoma status versus the additional risk of ovarian stimulation from SERM use in premenopausal women (discussed later; note: raloxifene was not indicated for any uses in premenopausal women). In a rat model of another estrogen-dependent, uterine-related pathology, endometriosis, raloxifene inhibited the estrogen-dependent growth of peritoneal uterine explants (Swisher et al., 1995). In monkeys with spontaneous endometrial lesions, raloxifene eliminated the occurrence of peritoneal endometriosis lesions (Fanning et al., 1996).

The uterine estrogen antagonist effect of SERMs is also of potential benefit in the treatment of endometrial cancer, the most common neoplasm of the female urogenital tract. In many cases, endometrial cancer is susceptible to hormonal-targeted therapies involving both progestin-based and estrogen-depletion strategies. Given the role of estrogens both directly and indirectly via the regulation of progesterone receptor, SERM approaches have been explored. Tamoxifen was evaluated in a small cohort of advanced or recurrent endometrial carcinoma patients with limited success, dissuading the use of tamoxifen as a single agent for this tumor type (Thigpen et al., 2001). Promising efficacy in endometrial cancer treatment was reported with the third-generation SERM, arzoxifene. In early studies in a small number of treatment-refractory endometrial cancer patients, arzoxifene produced a favorable clinical response rate and stabilized the disease in a substantial number of women (Burke and Walker, 2003). In a phase 2 open-label study, ER-positive and progesterone receptor-positive patients with recurrent/advanced endometrial cancer also exhibited a high response rate and duration of response with a favorable side effect profile after administration of arzoxifene (McMeekin et al., 2003).

Mammary

The effects of estrogens on mammary tissue in normal adult animals and women are not typically as clear and robust as those effects observed in the uterus. However, clearly a majority of mammary tumors are ER-positive and respond

favorably to estrogen antagonism (Wakeling et al., 1987). The role of estrogen replacement in the risk of breast cancer continues to be a controversial topic, and clearly the concomitant use of progestins in most hormonal replacement therapy paradigms is confounding. In the WHI trial, a significant increase in breast cancer risk in postmenopausal women was a key finding (Writing Group for WHI Investigators, 2002), contributing to dramatic reductions in the use of estrogen replacement strategies for various postmenopausal indications. The role of progestin in this observation was suggested by a follow-up study of hysterectomized women using unopposed conjugated equine estrogens for more than 7 years, where no increase in breast cancer risk was observed (Stefanick et al., 2006). Although some controversy remains over the exact potential for breast cancer risk with estrogen therapies, it is clear that concern over this risk has limited patient compliance with steroidal estrogen therapies. A major advantage of the SERM class of molecules is the lack of this cancer concern with respect to mammary tissue. Indeed, SERMs as a class have demonstrated a benefit in either treating or preventing breast cancer in animal models and women. The effects of SERMs in normal mammary tissue, as breast cancer therapies and preventatives, will be summarized here.

In normal mammary tissue, the effects of SERMs are largely unnoticeable. Extensive use of tamoxifen in both premenopausal and postmenopausal women for the use of breast cancer risk reduction has not been associated with untoward effects on mammary tissue, although in developing mammary glands in mice, tamoxifen impaired the growth of mammary ducts and increased mammary alveolar development (Hovey et al., 2005). A cautionary note in interpreting animal data with respect to SERMs and mammary tissue is worth mentioning. The rat is unique in that male mammary tissue exhibits a layering of epithelial cells with a somewhat hypertrophic appearance, which is an androgen-dependent phenotype in rats. SERMs with highly effective estrogen antagonism in mammary tissue can sufficiently block estrogen influence on mammary epithelia in rats, permitting the low ambient level of androgen in the female rat to predominate and convert the mammary histological phenotype to resemble that of the male rat (Rudmann et al., 2005), a phenomenon known not to exist in humans. Caution should be taken not to confuse this female/male phenotype conversion in the rat with hypertrophy of mammary tissue.

The antitumor effects of SERMs can be demonstrated readily in mammary tumor cell lines (i.e., MCF-7, T-47D, ZR-75-1) in vitro. Each SERM depicted in Fig. 37.3 is an estrogen antagonist in one or all of these cell lines (Short et al., 1996; Simard et al., 1997; Komm et al., 2005). The MCF-7 human mammary tumor cell line is an excellent, estrogen-dependent, in vitro system for determining antagonism of estrogen-induced proliferative activity of compounds. Most SERMs inhibit estrogen-stimulated proliferation in the 0.2−1 nM range in this assay, although for those triphenylethylene SERMs requiring the formation of active metabolites, such as tamoxifen and toremifene, one must evaluate the active metabolite to see this level of potency. For example, the IC_{50} for tamoxifen in MCF-7 cells is 200, vs. 1.2 nM for 4-hydroxytamoxifen (Suh et al., 2001). Des-methylarzoxifene, a likely active metabolite of arzoxifene, is the most potent inhibitor of MCF-7 proliferation, with an IC_{50} value of 0.05 nM (vs. 0.4 nM IC_{50} for arzoxifene in this cell line; Suh et al., 2001). Also of relevance in the MCF-7 tumor cell line, raloxifene fails to induce proliferation of these cells in the absence of exogenous estrogen, contrasting raloxifene with other SERMs, such as tamoxifen, that produce a low level of MCF-7 proliferation in estrogen-deficient cell culture media (Sato et al., 1995).

Consistent with the mammary tumor cell culture work are the estrogen antagonist effects of SERMs in animal models of estrogen-dependent breast cancer. Various animal models have shown the ability of SERMs such as tamoxifen, toremifene, and raloxifene to blunt the growth of established mammary tumors induced by carcinogens such as dimethylbenzanthracene (Clemens et al., 1983; Robinson et al., 1988) or in breast cancer tumor cell line xenografts in athymic mice (Fuchs-Young et al., 1997; Qu et al., 2000). Tamoxifen, raloxifene, and lasofoxifene are also effective in preventing mammary tumors induced by other chemical carcinogens, such as nitrosomethylurea (Gottardis et al., 1987; Anzano et al., 1996; Cohen et al., 2001). Of great interest is the apparent increase in mammary tumor efficacy that has been demonstrated preclinically for some of the more recently developed SERMs. For example, arzoxifene, a third-generation SERM molecule, produced significantly improved efficacy in preventing mammary tumor growth in vivo (Suh et al., 2001).

With respect to treatment of human breast cancer, numerous options have been in use that employ endocrine-based strategies, with some patients considered suitable for estrogen reduction or antagonism strategies alone (i.e., estrogen-positive tumors) and others using endocrine manipulation approaches as an adjunct to traditional tumor chemotherapy. Two SERMs, tamoxifen and toremifene, are approved for chemo/endocrine treatment in the management of postmenopausal women with node-positive breast cancer. With respect to breast cancer, tamoxifen has been in use the longest of any SERM, with greater than 20 years of clinical use. When used as an adjunct, tamoxifen reduces the risk of recurrent cancer and also decreases the risk of new tumors arising in the other breast. Both tamoxifen and toremifene show similar efficacy in terms of 5-year overall survival and disease-free survival rates (the disease-free rate for tamoxifen is 69%, and for toremifene is 72%) for early-stage breast cancer and also demonstrate similar efficacy as first-line therapy for metastatic breast cancer in postmenopausal women (Cuzick et al., 2002 and 2003). As of 2009, the only other SERM in late-stage

clinical development with clinical assessment of breast cancer treatment potential was arzoxifene, which was evaluated in several phase 2 trials in advanced breast cancer patients, where some benefit in terms of time to progressive disease and clinical benefit rate were observed (Baselga et al., 2003).

The other significant application of SERMs is in breast cancer prevention. A number of environmental and genetic factors are associated with increased risk of developing breast cancer in women including advanced age, family history of breast cancer, and a greater lifetime estrogen exposure (assessed via surrogate indicators such as estradiol levels, use of estrogen therapy, age at menopause, and body mass index). One of the best tools for overall assessment of breast cancer risk is the Gail model, where a risk factor of greater than or equal to 1.67 defines a woman at risk (Costantino et al., 1989). Tamoxifen was the first SERM to show reduced risk of breast cancer through a number of large, placebo-controlled trials. In the Breast Cancer Prevention Trial, tamoxifen was evaluated in a cohort of 13,388 women at increased risk of breast cancer and produced a 49% reduction in the relative risk of invasive breast cancer, with a 69% reduced risk of ER-positive mammary tumors (Fisher et al., 1998). However, despite this substantial reduction in risk and inclusion of breast cancer risk reduction as an approved use for tamoxifen, the clinical use of tamoxifen for this indication has been rather lackluster—primarily owing to a side effects profile that tilts the risk/benefit ratio in a negative direction in the minds of most physicians and women. Side effects profiles will be reviewed in subsequent sections, but for tamoxifen, side effects include endometrial cancer, uterine sarcoma, stroke, venous thrombus events, and cataracts. The increase in endometrial cancer in postmenopausal women likely stems from the uterine stimulatory properties of tamoxifen and represents one area for improvement in other SERMs. In this regard, raloxifene received approval for reducing the risk of invasive breast cancer in postmenopausal women with osteoporosis and in postmenopausal women at high risk for invasive breast cancer. After 8 years of monitoring 4011 postmenopausal women with osteoporosis, a 66% reduction in the incidence of invasive breast cancer was observed with raloxifene use (Martino et al., 2004). In the Study of Tamoxifen and Raloxifene (STAR) trial, a head-to-head comparison of the two SERMs was conducted in 19,000 postmenopausal women at high risk of breast cancer, where tamoxifen and raloxifene were found to produce similar reductions in the incidence of invasive breast cancer (Vogel et al., 2006), with the primary benefit being a reduced risk of ER-positive invasive breast cancers (Barrett-Conner et al., 2006). The most significant differences between raloxifene and tamoxifen in the STAR trial were significantly fewer uterine-associated adverse events with raloxifene (most notably the lack of endometrial cancer), whereas tamoxifen appeared to have a greater effect on noninvasive breast cancer incidence than raloxifene (Vogel et al., 2006). These differences between tamoxifen and raloxifene, although subtle, indicated a difference from preclinical and even early clinical indicators, and as such demonstrated the need for thorough clinical evaluation before accurate therapeutic risk/benefit assessment and approval of indications can be made for human use. In this regard, several SERMs in development, such as acolbifene and bazedoxifene (Labrie et al., 2004; Adachi et al., 2007), had preclinical and early clinical profiles that were promising for potential use in reduction of the risk for breast cancer, but clinical evaluation was needed to predict the ultimate utility of these molecules in this regard.

The mechanism by which SERMs such as tamoxifen, raloxifene, and toremifene inhibit breast cancer development or progression is likely the result of multiple beneficial effects. Direct antagonism of estrogen action at the ER in target cells in breast tissue, as previously described, is a key component of the action of the SERMs, given the strong positive linkage of estrogen exposure to relative risk for developing breast cancer and the fact that SERMs are much more effective versus ER-positive breast cancers. However, it is also likely that antitumor effects that reduce estrogen bioavailability as well as effects independent of estrogen contribute to the ultimate anti—breast cancer effect. Raloxifene is known to elevate levels of sex hormone-binding globulin (Reindollar et al., 2002), which would be expected to reduce bioavailable estrogen levels and thereby further reduce the risk of estrogen-associated breast cancer. Other beneficial indirect SERM effects include (1) modification of signaling proteins with a role in tumor cell biology, as is observed with tamoxifen on protein kinase C, TGFβ, calmodulin, ceramide, and MAP-kinases (Mandlekar and Kong, 2001); (2) induction of apoptosis in mammary tumor cell lines, as with tamoxifen, raloxifene, and toremifene (Mandlekar and Kong, 2001; Diel et al., 2002; Houvinen et al., 1993); and (3) dampening of growth factor systems known to play a role in tumor progression. The effect of growth factors in the pathogenesis of breast cancer continues to attract considerable attention. The insulin-like growth factor (IGF) system, inclusive of signaling factors, IGF receptors, and IGF-binding proteins, has strong connections to the malignant transformation of normal breast epithelium and thus is implicated in the development and progression of breast cancer (Ward et al., 1994). The IGF system protects cancer cells from apoptosis, thus promoting their survival. Beneficial effects of SERMs on the IGF system were demonstrated in postmenopausal women after 2 years of raloxifene treatment. Raloxifene reduced circulating IGF-1 levels and increased IGF-binding protein-3 levels, which would be expected to be associated with reductions in bioavailable IGF-1 (Lasco et al., 2006).

Mammographic density of the breast depends on the contributions of the predominant cell types in the breast: stromal, epithelial (both of which are higher-density tissue types), and fat tissue (which is relatively radiolucent by standard

mammography). Although the role of breast density in the prediction of relative breast cancer risk remains a topic of debate, most investigators agree that breast cancer risk is higher in women with higher-density breast tissue (Boyd et al., 1995). Whether this is related to a protective effect of increased abundance of fatty tissue or simply impedance in detecting small amounts of cancerous tissue in higher-density breast is not clear. However, it is clear that estrogen use is associated with a significant increase in mammographic density (Breendale *et al.*, 1999). Conversely, SERMs, specifically raloxifene and arzoxifene, were associated with a reduction of breast density in postmenopausal women (Lasko et al., 2006; Kimler et al., 2006).

Other

In addition to the uterus and mammary tissue, other components of the female reproductive system are under the direct or indirect control of estrogen and thus are also susceptible to the effects of SERMs. Depending on the patient, those SERM effects may be desirable, undesirable, or neutral.

Ovarian effects

The ovary is an important regulator of cyclicity in the female reproductive system and the predominant source of circulating estrogen, and it is indirectly regulated via estrogen action on the hypothalamic−pituitary−ovarian (HPO) axis. In mice, 15- to 24-month exposure to tamoxifen, toremifene, or raloxifene is associated with ovarian tumors. However, there is no evidence of increased ovarian cancer risk with these agents in women. Careful evaluation of multiple randomized, placebo-controlled studies indicates that raloxifene did not increase ovarian cancer in postmenopausal women compared with placebo (Neven et al., 2002). Thus, the murine observations may be owing to species differences in ovarian responses in terms of tumor development between mice and humans. The endocrine system plays a key role in the production of ovarian tumors in mice, particularly when gonadotropins are sustained at elevated levels for extended periods (Murphy et al., 1973). In this regard, raloxifene produces a sustained, dose-related increase in serum luteinizing hormone (LH) levels and inhibition of ovarian follicle maturation in mice, both effects being reversible upon discontinuation of the SERM (Cohen et al., 2000). In vitro, raloxifene is an antagonist of 17β-estradiol in pituitary gonadotrophs (Ortmann et al., 1988), suggesting that the elevation of LH with SERMs is related to blockade of the feedback-inhibitory properties of estrogen on the HPO axis.

Hormonal effects

In women, the most striking effects of SERMs on ovarian function are primarily through hormonal effects on the HPO axis. Because ovarian function obviously has major differences between the premenopausal and postmenopausal state, the effects of SERMs are likewise different with each state of ovarian function. The HPO axis is a complex endocrine system for which normal physiology requires the interplay of a number of steroid and peptidyl hormones including GnRH from the hypothalamus, follicle-stimulating hormone (FSH), prolactin and LH from the anterior pituitary, and estradiol as a hormone primarily originating from the ovary (although multiple tissue types possess the necessary enzymes to interconvert estrogen and testosterone as well as to generate multiple estrogen metabolites).

In premenopausal women, SERMs predominantly exert a stimulatory effect on the HPO axis and ovulation, with stimulatory effects on GnRH, FSH, and LH and marked increases in serum estradiol levels (Adashi et al., 1996). Depending on the situation, this may be a desired therapeutic goal or an undesirable side effect. This effect has been taken advantage of for more than 40 years with the widespread use of clomiphene for induction of ovulation in women with ovulatory dysfunction who desire pregnancy. For this indication, clomiphene has been used acutely to induce ovulation and increase the number of follicles produced in a given cycle. Use of clomiphene for more than 12 cycles in women who failed to become pregnant has been associated with an increase in ovarian cancer, leading to the recommendation to limit use of this agent to no more than six cycles if a pregnancy does not occur (Rossing et al., 1994). The other two SERMs currently approved for use in premenopausal women are tamoxifen and toremifene, used in the management of breast cancer. In these women, chronic treatment with the SERM results in ovarian-associated adverse effects. Of note are the induction of ovarian cysts and high circulating levels of estradiol that frequently occur with tamoxifen in reproductive-age women (Cook et al., 1995). Although these ovarian cysts can cause discomfort, they rarely require surgical intervention.

By far, the predominant use of SERMs in postmenopausal women has been for osteoporosis treatment or prevention (raloxifene), breast cancer treatment (tamoxifen or toremifene), and breast cancer risk reduction (tamoxifen or raloxifene). After menopause or in estrogen-deficient OVX animals, estrogen levels drop, and the lack of negative feedback provided by estrogen on the hypothalamus-anterior pituitary leads to an increase in FSH and LH levels or pulses. In general, SERMs

exhibit a partial agonist effect on the HPO axis in postmenopausal women. Raloxifene, tamoxifen, and toremifene are associated with reductions in LH and FSH levels in postmenopausal women (Cheng et al. 2004; Ellmen et al., 2003). HPO axis-related adverse effects, such as ovarian cysts, have not been typically seen in postmenopausal women and have been reported only occasionally with tamoxifen use (Shushan et al., 1996).

Another important estrogen-regulated hormonal product of the anterior pituitary is prolactin. In premenopausal women, raloxifene failed to alter circulating prolactin levels (Faupel-Badger et al., 2006). In postmenopausal women, raloxifene (Cheng et al., 2004) and clomiphene (Garas et al., 2006) reduced serum prolactin, operating either directly on lactotropes in the anterior pituitary or via increasing opiatergic tone in the hypothalamus (Lasco et al., 2002).

Vaginal effects

The drop in circulating estradiol levels associated with menopause is responsible for various vaginal-related symptoms including itching, dryness, and dyspareunia. Various forms of estrogen and hormone replacement, via both systemic and local delivery routes, have been widely used to provide relief for postmenopausal women who have these symptoms. SERMs demonstrate a range of profiles on vaginal symptoms of menopause. Most reports in postmenopausal women indicated estrogen-like maturation of vaginal epithelial cells with tamoxifen and toremifene (Ellmen et al., 2003; Friedrich et al., 1998). Conversely, there was some indication for antagonism of estrogen influence on vaginal tissue because both toremifene and tamoxifen produced a fourfold increase in vaginal dryness in postmenopausal women (Marttunen et al., 2001) and toremifene partially antagonized the effect of estrogen on vaginal epithelium in postmenopausal women (Homesley et al., 1993). The background estrogen status of the individual may be an important determinant, because in women with a high estrogenic activity (with respect to hormonal cytology), tamoxifen produced no vaginal estrogen-like effects, whereas women with lower estrogen levels saw an increase in vaginal tissue maturation index (Shiota et al., 2002). Even with these modest estrogen-like effects produced by toremifene and tamoxifen on the vagina, no beneficial or untoward urogenital effects of either agent had been observed in postmenopausal women (Marttunen et al., 2001). Raloxifene use in postmenopausal women was associated with a more neutral profile on vaginal tissue in postmenopausal women because it failed to affect vaginal epithelium in this population (Komi et al., 2005) and was not associated with adverse vaginal symptoms (Davies et al., 1999). Raloxifene also did not antagonize the beneficial effect of vaginal estrogen cream or an estradiol-releasing ring on vaginal atrophy or sexual function in postmenopausal women (Kessel et al., 2003). One SERM that was extensively studied for potential beneficial effects on postmenopausal vaginal-associated symptoms in phase 3 clinical trials is lasofoxifene. In clinical trials, lasofoxifene improved the vaginal epithelium maturation index (as was observed with tamoxifen and toremifene) but also reduced vaginal pH and reduced the incidence of dyspareunia (Portman et al., 2004; Bachmann et al., 2004). These unique effects of lasofoxifene might be related to the increased vaginal mucus formation observed in vaginal tissue from OVX rats treated with lasofoxifene (Wang et al., 2006)—effects that were not observed with raloxifene and tamoxifen.

Cardiovascular system

Menopause is associated with a dramatic increase in cardiovascular disease and characteristic changes in a number of heart disease-associated risk factors, such as an increase in serum cholesterol and specifically LDL-cholesterol, a decline in the cardioprotective HDL-cholesterol, elevated levels of lipoprotein(a) [Lp(a)], and increased insulin resistance and fat mass, resulting in a classic "metabolic syndrome" profile for heart disease risk (Spencer et al., 1997). Unfavorable markers of vascular endothelial damage, such as elevations in homocysteine levels and C-reactive protein (CRP), also accompany declining ovarian function during menopause (Hak et al., 2000). The fact that women enjoy a relatively "cardioprotected" status prior to menopause relative to their male counterparts historically presented the impression that estrogen replacement should be beneficial for reducing cardiovascular disease in postmenopausal women. Certainly, in both estrogen-deficient animal models and postmenopausal women, estrogen produces a number of effects that would be associated with an improvement in risk for cardiovascular disease, such as reduction of total circulating cholesterol levels, LDL-cholesterol in particular, and a concomitant increase in HDL-cholesterol. Accordingly, observational clinical trials suggested a significant reduction of cardiovascular disease in women who used hormone replacement therapy after menopause (i.e., Stampfer and Colditz, 1991). Thus, it was an unanticipated result when randomized clinical trials conducted to confirm the beneficial effects of hormone replacement therapy on the cardiovascular system indicated the opposite effect—an increase in cardiovascular disease associated with estrogen/progestin use. The first trial to indicate this was the HERS trial, where no reduction in coronary heart disease was detected, but an increase in cardiovascular-related deaths in the initial year of therapy was observed (Hulley et al., 1998). Similarly, the WHI trial failed to demonstrate any beneficial effects of estrogen

use, but again an increased risk of adverse cardiovascular outcomes including increased incidence of myocardial infarction and stroke (Manson et al., 2003). Finally, the Women's Estrogen for Stroke Trial (WEST) indicated an early increase in risk of fatal stroke during the first year of estrogen use in women with preexisting cerebrovascular disease (Viscoli et al., 2001). Both observational and randomized, placebo-controlled studies in postmenopausal women indicated a significant increase in the risk of deep venous thrombosis and pulmonary embolism in association with hormone replacement (Manson et al., 2003).

Thus, it is clear that two important considerations related to SERMs needed to be addressed. First, and foremost, the cardiovascular safety profile of SERMs in postmenopausal women has to be thoroughly evaluated based on the risk ascribed to hormone replacement therapy by trials such as HERS, WHI, and WEST. The second consideration revolves around potential beneficial effects on cardiovascular risk factors, which might be instructive in determining the additional benefit of these molecules. However, if we are to learn a lesson from the hormone replacement field, one needs to be careful to rely on randomized, well-controlled trials to make these assessments. The cardiovascular safety of SERMs in clinical use and their potential cardiovascular benefits are discussed here.

Cardiovascular safety of selective estrogen receptor modulators

The primary adverse event associated with every chronically used ER ligand is the occurrence of venous thrombolic events (VTEs), typically as deep vein thromboses or pulmonary emboli. The relative frequency of VTEs with SERMs is typically two- to threefold greater than for placebo when assessed in randomized clinical trials, a rate that is comparable to that observed with the use of oral estrogen replacement therapy (Cosman and Lindsay, 1999). Such an increase in venous thromboses was described with tamoxifen and toremifene use in breast cancer patients (Cuzick et al., 2003; Harvey et al., 2006) and raloxifene use in osteoporotic patients (Duvernoy et al., 2005). Comparable rates of venous thromboses were also reported in the 2- and 3-year phase 3 clinical trials for lasofoxifene and bazedoxifene (Adachi et al., 2007; McClung et al., 2006). The incident rate of VTEs was elevated in postmenopausal women subjected to prolonged periods of inactivity (i.e., extended bed stay during invasive surgical procedures), and as such, SERMs used chronically carry a recommendation to discontinue drug therapy during periods of anticipated immobility of several hours or more (Cuzick et al., 2002; Seeman, 2001). The mechanism for the increased incidence of VTEs with SERMs is not clear, although a number of clinical trials noted procoagulant changes with estrogen replacement, tamoxifen, or raloxifene along with impairment of anticoagulant factors with these three regimens. Although there was some variability in the results of different studies with respect to specific factor changes, such as fibrinogen that is increased by raloxifene in some reports (Sgarabotto et al., 2006) but decreased in others (Walsh et al., 1998), some clear trends have emerged. In a randomized, placebo-controlled trial in healthy postmenopausal women (Cosman et al., 2005), estrogen replacement increased coagulation factor VII and reduced the anticoagulation factors antithrombin and plasminogen activator inhibitor-1 (PAI-1). Tamoxifen generated an overall procoagulant profile, although via an increase in clotting factor VIII, factor IX, and von Willebrand factor on the coagulant side, and decreases in antithrombin, protein C, and PAI-1 on the anticoagulant side. Raloxifene produced a different pattern of changes with some similarity to that of tamoxifen, although without elevation in clotting factor IX or reduction of protein C (Cosman et al., 2005). In a separate study, Dahm et al. (2006) demonstrated that estrogen replacement, tamoxifen, and raloxifene all acted to reduce human endothelial production of tissue factor pathway inhibitor-1 (TFPI), an anticoagulant factor. Thus, some clear trends have emerged as the most critical determinants for VTE occurrence with estrogen or SERMs, those being the reduction of important factors such as antithrombin, PAI-1 and TFPI, all anticoagulant functional proteins. However, this is more of a correlative hypothesis because no chronically used SERM seemed to avoid the 2%−3% rate of VTE occurrence. No preclinical models or predictors are available to predict the relative likelihood for VTEs in humans with SERMs or estrogens.

With respect to the more severe cardiovascular adverse events observed with hormone replacement in the HERS, WHI, and WEST clinical trials, reports were mixed regarding the incidence of stroke or myocardial infarction with various SERMs. Although a coronary heart disease neutral profile was reported initially with tamoxifen in the breast cancer prevention trial, an increased risk for stroke with tamoxifen was eventually observed (Reis et al., 2001). The long-term clinical trials that supported raloxifene approval for osteoporosis indications found no change in the incidence of myocardial infarction relative to placebo (Martino et al., 2005). Analysis on a per-year basis showed no increase in cardiovascular events in the first year of raloxifene use, which contrasts with the pattern reported for estrogen replacement in the HERS and WHI trials (Keech et al., 2005). Cardiovascular events were the primary outcome of the Raloxifene Use for The Heart, or RUTH, trial, where no increase in coronary events or stroke incidence was observed, but a statistically significant increase in stroke-associated mortality was reported (Barrett-Conner et al., 2006).

Potential cardiovascular benefit of selective estrogen receptor modulators

Although the large, randomized, placebo-controlled trials conducted with SERMs did not show a significant reduction in cardiovascular events, smaller trials and subsets of larger placebo-controlled trials demonstrated some favorable trends, leaving open the possibility that SERMs may offer a degree of cardioprotection. With tamoxifen, one clinical study concluded a slight reduction in cardiac death and reduced risk for myocardial infarction (Rutqvist et al., 1993). In the raloxifene osteoporosis registration clinical trial, a positive effect on the incidence of cardiovascular events was observed in a subset of women at high risk for heart disease (Barrett-Connor et al., 2002). Despite the lack of verifiable cardiovascular outcomes with SERMs, most SERMs evaluated in both clinical and preclinical settings showed largely favorable effects on most cardiovascular risk factors for heart disease including lipid metabolism, clotting factors, and vessel wall factors. However, the "fingerprint" of each SERM on the wide array of cardiovascular surrogates is strikingly distinct, suggesting that each SERM needs careful clinical evaluation before a complete assessment of cardiovascular benefit or risk can be ascribed.

The most clear and robust effect observed with SERMs on cardiovascular-relevant parameters in preclinical models was the reduction of serum cholesterol levels (i.e., raloxifene, Black et al., 1994; tamoxifen, Sato et al., 1996a,b; clomiphene, Turner et al., 1998; toremifene, Qu et al., 2000; acolbifene, Martel et al., 2000; lasofoxifene, Ke et al., 1998; bazedoxifene, Komm et al., 2005; arzoxifene, Palkowitz et al., 1997). As with the skeletal responses in OVX rats, all SERMs depicted in Fig. 37.3 were capable of reducing serum cholesterol by roughly the same magnitude, thus mimicking the response to estrogen in this animal model, although differences in potency are evident. This hypocholesterolemic effect of SERMs is mediated by the ER, as demonstrated in the case of raloxifene by a very close correlation of ER-binding affinity and cholesterol-lowering in vivo for a series of raloxifene analogues (Kauffman et al., 1997).

In clinical trials, most of the SERMs depicted in Fig. 37.3 reduced total serum cholesterol and LDL-cholesterol (Reid et al., 2004; Joensuu et al., 2000; McClung et al., 2006) even in hypertriglyceridemic women (Dayspring et al., 2006), with raloxifene and tamoxifen also reducing Lp(a) (Love et al., 1994; Mijatovic et al., 1999)—all effects that are cardioprotective with respect to cardiovascular disease risk factors. Neither tamoxifen nor raloxifene elevated HDL-cholesterol (Love et al., 1994; Walsh et al., 1998), a cardiovascular-beneficial effect of estrogen replacement. Triglyceride elevation, an undesired effect often associated with estrogen replacement, was increased in most clinical trials with tamoxifen, although a triglyceride-neutral profile was observed with raloxifene and toremifene (Walsh et al., 1998; Kusama et al., 2004).

Preclinical models focused on the vessel wall have produced beneficial effects after SERM administration. In rats, neointimal thickening following aortic denudation injury was reduced by either raloxifene or tamoxifen, with both SERMs shown to regulate vascular smooth muscle cell function, indicating a potential benefit against restenosis following percutaneous transluminal coronary angioplasty (Savolainen-Peltonen et al., 2004). Even though SERMs are linked to increases in VTEs in clinical studies, preclinical work has indicated a beneficial effect of raloxifene in a model of carotid artery thrombosis. In OVX mice, estrogen deficiency amplifies thrombosis following carotid photochemical injury. In this model system, raloxifene as well as estrogen significantly reduces intraarterial thrombosis prolonging time to occlusion, likely via a mechanism that involves reduced platelet adhesion and increased expression of COX-2 (Abu-Fanne et al., 2008). Vascular antiinflammatory effects of raloxifene were also linked to vasorelaxant properties (Pinna et al., 2006).

Cardiovascular disease surrogates associated with vessel wall function and inflammation were also generally improved in clinical studies following raloxifene and tamoxifen. CRP, a marker linked to vascular injury that reflects inflammatory activity in the vascular wall, was elevated with estrogen replacement (Cushman et al., 1999) but reduced with raloxifene and tamoxifen (Cushman et al., 2001; Walsh et al., 2000), as was homocysteine (Anker et al., 1995; De Leo et al., 2001), a circulating factor linked to toxicity of vascular endothelial cells. Improved endothelial function with tamoxifen (Stamatelopoulos et al., 2004) and reduction in endothelin-1 (Saitta et al., 2001), an endogenous vasoconstrictor, have also been described.

Clearly, other factors in addition to circulating lipids influence the ultimate potential cardiovascular benefit provided by compounds such as the SERMs. In this regard, direct effects of SERMs on cardiovascular tissue have been investigated extensively, and agents such as raloxifene produced a number of effects of potential cardiovascular benefit. For example, raloxifene produced an antioxidant effect on serum lipoproteins (Zuckerman and Bryan, 1996), inhibited vascular smooth muscle migration (Wiernicki et al., 1996), and elevated vascular endothelial cell nitric oxide production (Saitta et al., 2001). Preclinical studies in models of atherogenesis have provided mixed results. Raloxifene failed to prevent the reduction of the coronary artery intimal area in cholesterol-fed OVX monkeys (Clarkson et al., 1998). However, 6-month exposure to raloxifene did reduce aortic atherogenesis in cholesterol-fed OVX rabbits (Bjarnason et al., 1997) and improved the coronary artery intimal area in OVX sheep (Gaynor et al., 2000). Given that nearly all direct cardiovascular

studies with SERMs in postmenopausal women have been conducted with raloxifene, it is difficult to know whether these particular effects can be generalized across the SERM class or whether, as in the uterus, distinct cardiovascular SERM profiles might emerge. Additional research would be needed.

Central nervous system

The mixed biological results observed with estrogen in the cardiovascular system are paralleled by the profile of estrogen activity in the central nervous system (CNS). Extensive in vitro and animal studies suggest neuroprotective and other beneficial effects of estrogen on central processes ranging from cognition to fine motor control and mood. However, translational work to human neurodegenerative disease has failed to corroborate the preclinical data, and as in the cardiovascular system, suggests potential untoward effects of estrogen on the human CNS.

Clearly, ER is broadly distributed throughout the brain. Original thoughts were that ER was predominantly restricted to the hypothalamus and associated with well-known functions such as regulation of reproductive hormones in the periventricular nucleus and thermoregulation in the lateral hypothalamus. The discovery of the ERβ subtype and improved antibodies for the detection of ERβ, however, led to the reconstruction of ER distribution neuroanatomical charts to include higher brain regions such as the cortex and hippocampus, specifically neurons associated with learning and memory, such as pyramidal cells throughout the CA1 and CA3 regions of the hippocampus and cortex (Shugrue and Merchenthaler, 2001).

Estrogen produces a number of beneficial effects in vitro and in animal models. In neuronal cell culture, 17β-estradiol has neurotrophic effects and inhibits neuronal damage induced by neurotoxicants (O'Neill et al., 2004). In OVX rats, estrogen increases hippocampal choline acetyltransferase activity, which leads to increased levels of acetylcholine, a neurotransmitter associated with cognition (Wu et al., 1999). Estrogen also reduces neural damage after experimental forebrain ischemia (Simpkins et al., 1997) and produces beneficial effects in animal models of Parkinson's disease (Gomez-Mancilla and Bedard, 1992). Estrogen also affects central serotonergic neurotransmission in animal models, leading to increased serotonin production and firing and reduced degradation (Bethea et al., 2002a,b). Dopaminergic neurotransmission in the striatum is influenced by estrogen (Landry et al., 2002), as are glutamate receptors (Cyr et al., 2001).

The preclinical data are consistent in indicating a beneficial effect of estrogen on CNS function. However, clinical data have not supported this conclusion. Certainly, early observational studies suggested up to a 30% reduction in risk of dementia with estrogen use (Yaffe et al., 1998). However, because these trials were not well-controlled prospective studies, there was considerable room for group-related artifacts (e.g., educational status) that may affect data interpretation. In this regard, in large, randomized, placebo-controlled trials, estrogen not only failed to reduce the incidence of dementia but also was associated with increased risk of dementia and stroke (Shumaker et al., 2003). Additional data are clearly needed, because the role of progestin in studies where hormone replacement is employed is a complicating factor—although even with estrogen-only use, a similar profile was observed (Shumaker et al., 2004). Other potential effects of estrogen on the brain (e.g., on mood) are equally controversial. Clearly, in consideration of SERMs, careful attention must be paid not only to potential beneficial effects but also to CNS safety.

Central nervous system safety of selective estrogen receptor modulators

No outwardly neurotoxic effects of tamoxifen, raloxifene, or any SERM depicted in Fig. 37.3 have been reported in neuronal cell culture and animal studies. Some differences among various SERMs have been reported with respect to their ability to antagonize estrogen effects in the brain. For example, tamoxifen blocks the effect of estrogen on serotonin 2A receptor expression in the forebrain or dorsal raphe of rats (Sumner et al., 1999), whereas raloxifene fails to show an antagonist profile on this receptor subtype in these brain regions (Cyr et al., 2000).

In clinical studies, use of tamoxifen for 5 years in women for breast cancer therapy did not alter performance on a series of cognitive tests compared with breast cancer patients who had never used tamoxifen, although an increase in physician visits for memory problems was noted (Paganini-Hill and Clark, 2000b). The confounding variable of ongoing disease state in these women must be considered, though, because studies conducted in elderly women found no differences in mental functional tests or speed of response with tamoxifen use (Ernst et al., 2002). In pilot studies conducted to evaluate the safety of raloxifene on cognitive function in postmenopausal women with osteoporosis, no negative effects on memory function were detected as determined by a number of mental acuity tests (Nickelsen et al., 1999). Follow-up work in more than 7700 postmenopausal women with osteoporosis confirmed the initial observation of no negative effects of raloxifene

on cognitive performance (Yaffe et al., 2001). Consistent with the latter observation, no untoward effects of raloxifene were observed on mood, sexual behavior, or sleep in postmenopausal women.

Central nervous system efficacy of selective estrogen receptor modulators

Much as with estrogen, SERMs are largely associated with preclinical profiles that suggest neuroprotection and an overall positive CNS profile, although certain subtle differences can be observed among different SERMs, further indicating the need to thoroughly evaluate each specific SERM molecule. Positive effects of SERMs can be demonstrated in vitro; as in a neural cell line, raloxifene increased neurite outgrowth in culture (Nilsen et al., 1998). Raloxifene and tamoxifen were neuroprotective in a neuroepithelial cell line by conferring resistance to β-amyloid-induced toxicity via elevation of seladin-1 (Benvenuti et al., 2005), a factor known to be downregulated in brain regions affected by Alzheimer's disease (Greeve et al., 2001).

Neurotransmitter-related changes within the CNS by various SERMs can be similar for some transmitters in some brain regions but differ in other neurotransmitter systems. Much as with estrogen, raloxifene and tamoxifen increase hippocampal choline acetyltransferase activity (Wu et al., 1999). Indicating comparable effect of these two SERMs on the neurotransmission of acetylcholine, a neurotransmitter associated with cognition. Raloxifene and tamoxifen, however, produce different overall profiles on serotonin neurotransmission in the brain. In both rats and monkeys, raloxifene produces a spectrum of changes in the forebrain that are favorable for serotonin neurotransmission, such as increased tryptophan hydroxylase, increased serotonin 2A receptor expression, and reduced serotonin transporter (Cyr et al., 2000; Smith et al., 2004). In contrast, tamoxifen does not affect serotonin transporter and reduces tryptophan hydroxylase activity in the forebrain (Sumner et al., 1999), a profile unfavorable for serotonin neurotransmission. Of note, the SERM arzoxifene produces a pattern of effects on forebrain serotonin neurotransmission that parallels that produced by raloxifene (Bethea et al., 2002a,b). Other differences on neurotransmitter profiles can be observed with dopaminergic systems, as with lateral striatum dopamine receptor expression, which is increased in response to raloxifene but not affected by tamoxifen (Landry et al., 2002).

Distinct SERM efficacy profiles can also be detected in various CNS pathology animal models. Hippocampal neurodegeneration can be induced in rats by systemic injection of kainic acid, which leads to induction of inflammatory astroglia and neural loss that is protected by pretreatment with estrogen. In OVX rats injected with kainic acid, hippocampal neural loss was prevented in each case by tamoxifen, raloxifene, and bazedoxifene without affecting the reactive gliosis component (Ciriza et al., 2004), a profile distinct from that of 17β-estradiol, which was both neuroprotective and antiinflammatory in this model. Again, not all SERMs behaved the same in this model system, as lasofoxifene failed to exhibit a neuroprotective profile (Ciriza et al., 2004). Neuroprotective effects of SERMs in other animal models have also been observed. In separate studies, tamoxifen and arzoxifene reduced neural damage following occlusion of the middle cerebral artery in OVX rats, an experimental model for stroke (Mehta et al., 2003; Rossberg et al., 2000). The mechanism for SERM protection from focal cerebral ischemia in these animal models is unclear, because raloxifene induced a relaxation of rat cerebral arteries in vitro via inhibition of L-type calcium channels (Tsang et al., 2004), although direct effects on cerebral blood flow were ruled out in one study (Rossberg, 2000). Attenuation of excitatory amino acid release and putative antioxidant effects have also been demonstrated as potentially contributing to the neuroprotective effects of tamoxifen and raloxifene (Osuka et al., 2001; Siefer et al., 1994). Finally, neuroprotective effects of tamoxifen and raloxifene were observed in 1-methyl-4-phenyl-1,2,3,6-tetrahydropyridine-induced dopamine depletion in a Parkinsonian model (Obata and Kubota, 2001; Grandbois et al., 2000).

A number of metabolic-based imaging and cognitive performance clinical trials suggested potential CNS benefits with some SERMs. Proton magnetic resonance spectroscopy in elderly women who had taken tamoxifen for at least 2 years for breast cancer treatment demonstrated a reduction in myoinositol, a glial marker that reflects glial proliferation in response to brain injury (Ernst et al., 2002), suggesting a neuroprotective effect of tamoxifen. Although the disease status of these women complicated interpretation of the data, it was interesting to note that in a comparable population of women taking estrogen replacement therapy but without breast cancer, a similar effect on myoinositol was observed (Ernst et al., 2002). Assessment of adverse CNS events in the randomized, placebo-controlled osteoporosis registration studies for raloxifene revealed no negative effects during the course of safety assessment. These studies did suggest some interesting trends for raloxifene-related improvement in cognitive performance, specifically higher verbal memory and attention scores; decreases in these areas are putative harbingers of mild cognitive impairment and Alzheimer's disease (Nickelsen et al., 1999; Yaffe et al., 2001). Women over the age of 70 in particular experienced smaller declines in memory and attention on raloxifene (Yaffe et al., 2005). In studies focused on the risk for Alzheimer's disease in postmenopausal women with osteoporosis, Yaffe and colleagues (2005) reported a one-third reduction in the risk of mild cognitive impairment with a

trend for reduced risk of Alzheimer's disease. In both studies where cognitive improvement was suggested with raloxifene, it is worth noting that the benefit was primarily observed in women receiving 120 mg/day of raloxifene. These benefits of raloxifene were not observed in similar women taking 60 mg/day of raloxifene, the standard and approved daily dose for osteoporosis prevention and treatment and breast cancer risk reduction. The potential requirement for a greater dose of raloxifene to generate meaningful CNS benefits was consistent with preclinical literature, such as increased hippocampal choline acetyltransferase activity, which also requires higher doses of raloxifene than are necessary for the bone effects in OVX rats (Wu et al., 1999), and the recognition that raloxifene has poor penetration of the blood−brain barrier (Bryant et al., 1997). The relative estrogen background may be a complicating factor because women with undetectable circulating estrogen levels prior to administration of raloxifene showed a greater benefit for mild cognitive impairment risk than women with higher circulating estrogen levels at baseline (Yaffe et al., 2005). The precise process of cognitive function that SERMs affect would require additional research. Although executive function/decision-making is the ultimate output of cognitive networks, these activities depend on more basic processes, such as alertness and arousal, to be operational. In this regard, it is interesting to note that in a study conducted in a small cohort of elderly men using functional magnetic resonance imaging, raloxifene improved memory function via increased arousal during initial encoding of information, likely via a neurogenic effect (Goekoop et al., 2006).

The important principle of drug exposure for SERMs will be reviewed in the next section, but particularly germane to the brain, as a central pharmacological tenant, is that for agents to exert their effect on a receptor, they must be available to the receptor. The limited brain exposure with raloxifene predicted by preclinical models is certainly an important factor. ER-binding studies also suggest reduced exposure of tamoxifen in the brain relative to peripheral tissues, such as the uterus (Bowman et al., 1982). Clearly, the functional studies with various SERMs in animal models with raloxifene and tamoxifen argue strongly that there is sufficient exposure to exert a biological response to these SERMs in the brain. However, critical factors such as dose, duration, and agonist/antagonist potential may be severely or subtly affected by the ability of the molecule to penetrate the brain. As a result, dose−response relationships that are expected based on peripheral tissues may not be monitored for effects within the CNS.

General safety profile and other pharmacological considerations

Other safety

In addition to the adverse events already reviewed (i.e., VTEs observed with all SERMs and uterine stimulation observed with some SERMs), SERMs are associated with other untoward effects that should be considered in the risk/benefit decision for each patient. Of these other adverse events observed in clinical trials, leg cramps and the induction of hot flushes were observed in women, to at least some extent, with all the SERM molecules depicted in Fig. 37.3. Hot flushes, or vasomotor symptoms, are a hallmark indicator of menopausal transition occurring in up to 70% of US women. The incidence of hot flushes is likely reflective of declining or changing estrogen status and typically abates when circulating estrogen levels reach their postmenopausal steady-state concentration. However, in a small percentage of women, vasomotor symptoms can be severe and extend well into menopause. Estrogen replacement clearly is effective in relieving postmenopausal hot flushes. With SERM use, however, it is likely that an estrogen withdrawal-like response is initiated, producing a state similar to that experienced by women who are estrogen depleted and have subsequent hot flushes. Although it is unclear whether this phenomenon is caused by the estrogen antagonist or agonist properties of the SERM at the ER in hypothalamic thermoregulatory centers, SERM-induced hot flushes are transient in nature, because with continued use in most cases, this side effect subsides typically within 6 months, likely as the thermoregulatory set point reestablishes (Tataryn et al., 1980). Consistent with this proposed mechanism, proximity to the climacteric state may influence the incident rate and severity of SERM-induced hot flushes. In postmenopausal women over the age of 55, significantly fewer hot flushes were observed in response to raloxifene compared with those observed in younger postmenopausal women. In a similar context, tamoxifen-induced hot flushes tended to be more severe in premenopausal breast cancer patients than in postmenopausal patients.

One problem in the assessment of the incident rate of hot flush induction following SERM administration is the relatively high placebo response rate in the postmenopausal population. In observational studies performed on randomized, placebo-controlled trials, the rate of reported hot flushes in postmenopausal women receiving placebo was 21% over a 30-month trial period (Cohen and Lu, 2000). In this study, the incidence of hot flushes in postmenopausal women using raloxifene was 28%. Others have confirmed an approximately 7% increase in hot flush incidence as a side effect of raloxifene use (Davies et al., 1999). Of note, the hot flushes induced by raloxifene were in the mild to moderate category in terms of severity, as severe hot flushes in postmenopausal women using raloxifene occurred at a rate indistinguishable from

that of placebo controls. Finally, the increase in hot flush incidence with raloxifene was transient, because no differences relative to placebo controls were observed after 6 months (Davies et al., 1999).

The observation of hot flush incidence is typical for other SERM molecules as well. Tamoxifen use in both premenopausal and postmenopausal women for breast cancer treatment has long been associated with hot flushes as a side effect in 10%−20% of patients and is more common in women with higher estrogen levels (Legha, 1988). Toremifene also induces hot flushes at rates equivalent to or slightly greater than that of tamoxifen (Hays et al., 1995). Clomiphene use for induction of ovulation increases hot flushes as well (Derman and Adashi, 1994). Levormeloxifene (Alexanderson et al., 2001), lasofoxifene (McClung et al., 2006), and bazedoxifene (Adachi et al., 2007) also increase hot flush incidence in postmenopausal women.

An interesting note of relevance to hot flushes and SERMs is the potential application of SERMs in combination with estrogen for the treatment of hot flushes. In a small study of postmenopausal women using 17β-estradiol in combination with raloxifene, a significant decrease in hot flushes was observed (compared with raloxifene treatment alone), although signs of endometrial stimulation were detected as well with this combination (Stoval et al., 2007). Large, randomized, placebo-controlled clinical trials have evaluated the combination of bazedoxifene and conjugated equine estrogens as a potential alternative for the treatment of hot flushes (and potentially other menopausal symptoms) without the need to include a progestin for the maintenance of uterine safety. Uterine assessment at 1- and 2-year intervals demonstrated a lack of endometrial hyperplasia for the bazedoxifene/conjugated equine estrogens combination (Pickar et al., 2007), indicating that the SERM had effectively blocked the potent stimulatory action of the estrogenic component of the combination. The combination also produced an increase in lumbar spine BMD in postmenopausal women that was superior to that of both placebo and raloxifene (Lindsay et al., 2007). Full assessment of the risk/benefit ratio of the bazedoxifene/conjugated equine estrogens combination for use in the relief of menopausal symptoms requires full assessment of hot flush and other symptom efficacy as well as effects on other adverse events, such as VTEs.

Other adverse events not already discussed and associated with some triphenylethylene SERMs are those associated with the eye. These ocular-related untoward effects include retinopathy, macular crystal formation, corneal keratopathies, and cataracts. Eye pathologies have been primarily associated with the use of tamoxifen and toremifene, with comparable incidence of 7%−10% (Hays et al., 1995). Visual disturbances were also noted with clomiphene use (Asch and Greenblat, 1976) but were not increased with nontriphenylethylene SERMs, such as with raloxifene use in postmenopausal women (Cohen and Lu, 2000). Length of therapy increased the risk of cataract development with tamoxifen use (Paganini-Hill and Clark, 2000a). One mechanism that has been proposed to address cataract formation with tamoxifen is the blockade of the chloride channels in the lens of the eye, which are important for the maintenance of lens hydration (Zhang et al., 1994). Of importance, this effect of tamoxifen on chloride channels in the lens seems to be independent of interaction with ER, and as such is likely off-target toxicity for certain triphenylethylene SERMs.

Pharmacokinetics

Pharmacokinetic properties of the SERMs are an important consideration in the overall effects of these molecules and served as a focal point for the development of novel and improved agents. For example, the third-generation SERMs arzoxifene, bazedoxifene, and lasofoxifene all have pharmacokinetic properties that represent improvements over raloxifene and tamoxifen. The ultimate advantage of these improvements to patients would require additional research, but as noted earlier in this chapter, much of the research and development has been redirected.

As previously indicated, tamoxifen generates active metabolite(s) with greater affinity and efficacy at the ER (Coezy et al., 1982). After a single oral dose of tamoxifen, maximal plasma levels are reached within several hours with an elimination half-life of 5−7 days (Fromson et al., 1973). Steady-state concentrations are attained within 3−4 weeks of chronic dosing (Adam et al., 1980). The potential for preferential tissue distribution was suggested in animal studies, where greater levels of radioactive tamoxifen were detected in mammary gland, uterus, and liver than in blood (Furr and Jordan, 1984). In humans, elevated uterine levels of tamoxifen with respect to circulating concentrations were observed, with endometrial levels twice those of myometrial or cervical concentrations (Fromson and Sharp, 1974). The primary route of elimination of tamoxifen follows hepatic metabolism, primarily glucuronidation, and subsequent biliary excretion with fairly little of the parent molecule being excreted in the urine and the potential for enterohepatic recirculation suggested in animal studies (Furr and Jordan, 1984).

Toremifene also is a triphenylethylene SERM that generates active metabolites (i.e., deaminohydroxy-toremifene; DeGregorio et al., 2000). Peak plasma concentrations of toremifene occur within 2−4 h after a single oral dose with nearly complete absorption, and plasma levels are linear with dose over a fairly wide dose range (Anttila et al., 1990). The elimination half-life of toremifene is 5 days, and steady-state circulating concentrations are reached within 2−4 weeks of

chronic dosing. There is evidence in animal models for relatively increased tissue distribution of toremifene in some tissues, with mammary gland uptake similar to tamoxifen (Kargas et al., 1989). Toremifene is extensively metabolized in the liver via demethylation, hydroxylation, and side-chain oxidation modifications (Anttila et al., 1990), and the primary route of elimination is fecal elimination following enterohepatic recirculation (Anttilla et al., 1990). Hepatic impairment significantly increases the half-life of toremifene, nearly doubling it (Anttila et al., 1995).

Clomiphene is the only triphenylethylene SERM in current clinical use for which there are no known active metabolites. Clomiphene is a racemic mixture of cis- (zuclomifene) and trans- (enclomiphene) isomers that is rapidly absorbed following oral administration. Peak plasma concentrations are achieved in approximately 6 h, with a half-life of approximately 5 days (Dickey and Holtkamp, 1996), although metabolites have been detected up to 6 weeks after a single dose, suggesting likely enterohepatic recirculation (Kausta et al., 1997). Clomiphene is hepatically metabolized and fecally excreted (Adashi, 1996).

The pharmacokinetics of raloxifene, a benzothiophene SERM, have some features similar to those of triphenylethylenes but also some considerable differences. Like tamoxifen and its relatives, raloxifene is rapidly absorbed from the gastrointestinal tract after oral administration, with peak blood levels attained in approximately 6 h and 60% of the oral dose absorbed (Heringa, 2003). Raloxifene is also highly bound to plasma proteins (approximately 95%; Heringa, 2003). However, in contrast to triphenylethylenes, the elimination half-life of raloxifene is considerably shorter at 28 h, and there are no known active metabolites of raloxifene in humans or rodents. Although there is virtually no P450 metabolism of raloxifene in the liver, it is extensively metabolized by first-pass hepatic glucuronidation, yielding an absolute oral bioavailability of only approximately 2% in humans (Snyder et al., 2000). Raloxifene is widely distributed, and as with triphenylethylenes, very little is excreted in the urine, with the bulk of clearance through biliary excretion and loss in the feces (Knadler et al., 1995).

Relatively less information is available on pharmacokinetic profiles of the third-generation SERMs arzoxifene, bazedoxifene, and lasofoxifene. Lasofoxifene demonstrates improved bioavailability because the molecule was designed to resist intestinal wall glucuronidation (Gennari et al., 2006). The elimination half-life of lasofoxifene is 165 h, and there is a linear relationship between plasma concentrations and dose (Gardner et al., 2006). The primary metabolic route for lasofoxifene is hepatic oxidation and subsequent conjugation (Branson et al., 2006). Bazedoxifene produces an absolute bioavailability of 6.2% following an oral dose, which is about threefold greater than that produced by raloxifene. Bazedoxifene demonstrates kinetic linearity at dose levels of 5−40 mg (Ermer et al., 2003). Maximal circulating concentrations of bazedoxifene are achieved within 1−2 h after oral exposure, and the elimination half-life is approximately 28 h with steady-state circulating levels attained in 7 days (Ermer et al., 2003). As with raloxifene, there is very little P450-mediated metabolism of bazedoxifene, and glucuronidation is the major metabolic route. The primary route of elimination is the feces, with evidence for enterohepatic recirculation (Chandrasekaran et al., 2003). Arzoxifene also exhibits pharmacokinetic advantages over raloxifene. Over a dosage range of 10−100 mg, blood levels of arzoxifene increase linearly with respect to dose, with maximal levels attained at 2−6 h and an elimination half-life of 30−35 h over this dose range (Munster et al., 2001). Arzoxifene is metabolized (demethylated) to desmethylarzoxifene, which is an active metabolite with a high binding affinity for the ER (Rash and Knadler, 1997).

Future directions with selective estrogen receptor modulators

In addition to the use of SERMs for osteoporosis, breast cancer, and the induction of ovulation, the ability of ER-activity-modulating agents to favorably impact other diseases and syndromes, in both women and men, is under discovery and clinical development efforts. The overall scope of these drug discovery efforts is broad, changing rapidly, and beyond the focus of this review.

Summary

SERMs are a diverse class of molecules that affect a broad spectrum of biological systems, with potential therapeutic benefit for a variety of diseases. Current concern over long-term use of estrogen-containing regimens has created an opportunity for the application of SERMs to chronic indications such as osteoporosis treatment or prevention. The unique SERM profile also potentially allows their use in other chronic indications of interest to postmenopausal women, most notably breast cancer risk reduction and treatment. However, safety considerations are very important for SERM use in these chronic indications. The pleiotropic nature of the ER and its role in numerous physiological systems raise the importance of considering potential SERM benefits and/or adverse events in the cardiovascular system and other tissues.

References

Abu-Fanne, R., Brzezinski, A., Golomb, M., Grad, E., Foldes, A.J., Shufaro, Y., Varon, D., Brill, A., Lotan, C., Danenberg, H.D., 2008. Effects of estradiol and raloxifene on arterial thrombosis in ovariectomized mice. Menopause 15. Published online 2007 Nov 19 [Epub ahead of print].

Adachi, J.D., Chesnut, C.H., Brown, J.P., Christiansen, C., Russo, L.A., Fernandes, C.E., Menegoci, J.C., King, A., Chines, A.A., Bessac, L., Chakrabarti, D., 2007. Safety and tolerability of bazedoxifene in postmenopausal women with osteoporosis: results from a 3-year, randomized, placebo- and active-controlled clinical trial. J. Bone Miner. Res. 22 (Suppl. 1), S460.

Adam, H.K., Patterson, J.S., Kemp, J.V., 1980. Studies on the mechanism and pharmacokinetics of tamoxifen in normal volunteers. Cancer Treat. 64, 761–764.

Adashi, E.Y., 1996. Ovulation induction: clomiphene citrate. In: Adahsi, E.Y., Rock, J.A., Rosenwalks, Z. (Eds.), Reproductive Endocrinology, Surgery and Technology. Lippincott-Raven, Philadelphia, pp. 1181–1206.

Adrian, M.D., Cole, H.W., Shetler, P.K., Rowley, E.R., Magee, D.E., Pell, T., Zeng, G., Sato, M., Bryant, H.U., 1996. Comparative pharmacology of a series of selective estrogen receptor modulators. J. Bone Miner. Res. 11 (Suppl. 1), S447.

Alexandersen, P., Riss, B.J., Stakkestad, J.A., Delmas, P.D., Christiansen, C., 2001. Efficacy of levormeloxifene in the prevention of postmenopausal bone loss and on the lipid profile compared to low dose hormone replacement therapy. J. Clin. Endocrinol. Metab. 86, 755–760.

Allen, M.R., Iwata, K., Sato, M., Burr, D.B., 2006. Raloxifene enhances vertebral mechanical properties independent of bone density. Bone 39, 1130–1135.

Anker, G., Lonning, P.E., Ueland, P.M., Refsum, H., Lien, E.A., 1995. Plasma levels of the atherogenic amino acid homocysteine in post-menopausal women with breast cancer treated with tamoxifen. Int. J. Cancer 60, 365–368.

Anttila, M., Valavaara, R., Krivinen, S., Maenpaa, J., 1990. Pharmacokinetics of toremifene. J. Steroid Biochem. 36, 249–252.

Anttila, M., Laakso, S., Nylandern, P., Sotaniemi, E.A., 1995. Pharmacokinetics of the novel antiestrogenic agent toremifene in subjects with altered liver and kidney function. Clin. Pharmacol. Ther. 57, 628–635.

Anzano, M.A., Peer, C.W., Smith, J.M., Mullen, L.T., Schrader, W.M., Logsdon, D.L., Driver, C.L., Brown, C.C., Roberts, A.B., Sporn, M.B., 1996. Chemoprevention of mammary carcinogenesis in the rat: combined use of raloxifene and 9-cis-retinoic acid. J. Natl. Cancer Inst. 88, 23–25.

Asch, R.H., Greenblatt, R.B., 1976. Update on the safety and efficacy of clomiphene citrate as a therapeutic agent. J. Reprod. Med. 17, 175–180.

Bachmann, G.A., Gass, Moffett, A., Portman, D., Symons, J., 2004. Lasofoxifene improves symptoms associated with vaginal atrophy. Menopause 11, 669.

Barrett-Connor, E., Grady, D., Sashegyi, A., Anderson, P.W., Cox, D.A., Hoszowski, K., Rautaharju, P., Harper, K.D., 2002. Raloxifene and cardiovascular events in osteoporotic women: four-year results from MORE (Multiple Outcomes of Raloxifene Evaluation) randomized trial. J. Am. Med. Assoc. 287, 847–857.

Barrett-Connor, E., Mosca, L., Collins, P., Geiger, M.J., Grady, D., Kornitzer, M., McNabb, M., Wenger, N., 2006. Effects of raloxifene on cardiovascular events and breast cancer in postmenopausal women. N. Engl. J. Med. 335, 125–137.

Baselga, J., Llombart-Cussa, A., Bellet, M., Guillem-Porta, V., Enas, N., Krejcy, K., Carrasco, E., Kayitalire, L., Kuta, M., Lluch, A., Vodvarka, P., Kerbrat, P., Namer, M., Petruzelka, L., 2003. Randomized, double-blind, multicenter trial comparing two doses of arzoxifene (LY353381) in hormone-sensitive advanced or metastatic breast cancer patients. Ann. Oncol. 14, 1383–1390.

Bashir, A., Mak, Y.T., Sankaralingam, S., Cheung, J., McGowan, N.W.A., Grigoriadis, A.E., Fogelman, I., Hampson, G., 2005. Changes in RANKL/OPG/RANK gene expression in peripheral mononuclear cells following treatment with estrogen or raloxifene. Steroids 70, 847–855.

Bautista, S., Valles, H., Walker, R.L., Anzick, S., Zellinger, R., Meltzer, P., Theillet, C., 1998. In breast cancer, amplification of the steroid receptor coactivator gene AIB1 is correlated with estrogen and progesterone receptor positivity. Clin. Cancer Res. 4, 2925–2929.

Benvenuti, S., Luciani, P., Vannelli, G.B., Gelmini, S., Franceschi, E., Serio, M., Peri, A., 2005. Estrogen and selective estrogen receptor modulators exert neuroprotective effects and stimulate the expression of Selective Alzheimer's Disease Indicator-1, a recently discovered anti-apoptotic gene, in human neuroblast long-term cell cultures. J. Clin. Endocrinol. Metab. 90, 1775–1782.

Bethea, C.L., Lu, N.Z., Gundlah, C., Streicher, J.M., 2002a. Diverse actions of ovarian steroids in the serotonin neural system. Front. Neuroendocrinol. 23, 41–100.

Bethea, C.L., Mirkes, S.J., Su, A., Michelson, D., 2002b. Effects of oral estrogen, raloxifene and arzoxifene on gene expression in serotonin neurons of macaques. Psychoneuroendocrinology 27, 431–445.

Bjarnason, N.H., Haarbo, J., Byrjalsen, I., Kauffman, R.F., Christiansen, C., 1997. Raloxifene inhibits aortic accumulation of cholesterol in ovariectomized, cholesterol-fed, rabbits. Circulation 96, 1964–1969.

Black, L.J., Rowley, E.R., Bekele, A., Sato, M., Magee, D.E., Williams, D.C., Cullinan, G.J., Bendele, R., Kauffman, R.F., Bensch, W., Frolik, C.A., Termine, J.D., Bryant, H.U., 1994. Raloxifene (LY139482 HCl) prevents bone loss and reduces serum cholesterol without causing uterine hypertrophy in ovariectomized rats. J. Clin. Investig. 93, 63–69.

Bowman, S.P., Leake, A., Morris, I.D., 1982. Hypothalamic, pituitary and uterine cytosolic and nuclear oestrogen receptors and their relationship to the serum concentrations of tamoxifen and its metabolite, 4-hydroxytamoxifen, in the ovariectomized rat. J. Endocrinol. 94, 167–175.

Boyd, N.F., Byng, J.W., Jong, R.A., Fishell, E.K., Little, L.E., Miller, A.B., Lockwood, G.A., Tritchler, D.L., Yaffe, M.J., 1995. Quantitative classification of mammographic densities and breast cancer risk: results from the Canadian National Breast Screening Study. J. Natl. Cancer Inst. 87, 670–675.

Brady, H., Doubleday, M., Gayo-Fung, L.M., Hicman, M., Khammungkhune, S., Kois, A., Lipps, S., Pierce, S., Richard, N., Shevlin, G., Sutherland, M.K., Anderson, D.W., Bhagwat, S.S., Stein, B., 2002. Differential response of estrogen receptors alpha and beta to SP500263, a novel potent selective estrogen receptor modulator. Mol. Pharmacol. 61, 562–568.

Bramson, C., Ouellet, D., Roman, D., Randinitis, E., Gardner, M.J., 2006. A single-dose pharmacokinetic study of lasofoxifene in healthy volunteers and subjects with mild and moderate hepatic impairment. J. Clin. Pharmacol. 46, 29–36.

Bramlett, K.S., Burris, T.P., 2003. Target specificity of selective estrogen receptor modulators within human endometrial cancer cells. Steroid Biochem. Mol. Biol. 86, 27–34.

Bryant, H.U., Bales, K.R., Paul, S.M., Yang, H., Cole, H.W., Walker-Daniels, J., McEwen, R.S., Chow, H., Santerre, R.F., 1997. Estrogen agonist effects of selective estrogen receptor modulators in the ovariectomized rat brain. Soc. Neurosci. Abstr. 23, 2377.

Brzozowski, A.M., Pike, A.C., Dauter, Z., Hubbard, R.E., Bonn, T., Engstrom, O., Ohman, L., Green, G.L., Gustafsson, J.A., 1997. Molecular basis of agonism and antagonism in the estrogen receptor. Nature 389, 753–768.

Burke, T.W., Walker, C.L., 2003. Arzoxifene as therapy for endometrial cancer. Gynecol. Oncol. 90 (Pt 2), S40–S46.

Cano, A., Dapia, S., Noguera, I., Pineda, B., hermenegildo, C., del Val, R., Caeiro, J.R., Garcia-Perez, M.A., 2008 Jun. Comparative effects of 17b-estradiol, raloxifene and genistein on bone 3D microarchitecture and volumetric bone mineral density in the ovariectomized mice. Osteoporos. Int. 19 (6), 793–800.

Carthew, P., Edwards, R.E., Nolan, B.M., Tucker, M.J., Smith, L.L., 1999. Compartmentalized uterotrophic effects of tamoxifen, toremifene and estradiol in the ovariectomized Wistar rat. Toxicol. Sci. 48, 197–205.

Chandrasekaran, A., Ermer, J., McKenad, W., Lee, H., DeMaio, W., Kotake, A., Sullivan, P., Orczyk, G., Scantina, J., 2003. Bazedoxifene acetate metabolic disposition in healthy postmenopausal women. J. Clin. Pharm. Ther. 73, 47.

Cheng, W.C., Yen, M.L., Hsu, S.H., Chen, K.H., Tsai, K.S., 2004. Effects of raloxifene, one of the selective estrogen receptor modulators, on pituitary-ovary axis and prolactin in postmenopausal women. Endocrine 23, 215–218.

Chesnut, C., Weiss, S., Mulder, H., Wasnich, R., Greenwald, R., Eastell, R., Fitts, D., Jensen, C., Haines, A., MacDonald, B., 1998. Idoxifene increases bone mineral density in osteopenic postmenopausal women. Bone 23 (Suppl. l), S389.

Ciriza, I., Carrero, P., Azcoitia, I., Lundeen, S.G., Garcia-Segura, L.M., 2004. Selective estrogen receptor modulators protect hippocampal neurons from kainic acid excitotoxicity: differences with the effect of estradiol. J. Neurobiol. 61, 209–221.

Clarkson, T.B., Anthony, M.S., Jerome, C.P., 1998. Lack of effect of raloxifene on coronary artery atherosclerosis of postmenopausal monkeys. J. Clin. Endocrinol. Metab. 83, 721–726.

Clemens, J.A., Bennett, D.R., Black, L.J., Jones, C.D., 1983. Effects of a new antiestrogen, keoxifene (LY156758), on growth of carcinogen-induced mammary tumors and on LH and prolactin levels. Life Sci. 32, 2869–2875.

Coezy, E., Borgna, J.L., Rochefort, H., 1982. Tamoxifen and metabolites in MCF-7 cells: correlation between binding to estrogen receptor and inhibition of cell growth. Cancer Res. 42, 317–323.

Cohen, F.J., Lu, Y.M., 2000. Characterization of hot flashes reported by healthy postmenopausal women receiving raloxifene or placebo during osteoporosis prevention trials. Maturitas 34, 65–73.

Cohen, I.R., Sims, M.L., Robbins, M.R., Lakshmanan, M.C., Francis, P.C., Long, G.G., 2000. The reversible effects of raloxifene on luteinizing hormone levels and ovarian morphology in mice. Reprod. Toxicol. 14, 37–44.

Cohen, L.A., Pittman, B., Wang, C.X., Aliaga, C., Yu, L., Moyer, J.D., 2001. LAS, a novel selective estrogen receptor modulator with chemopreventative and therapeutic activity in the N-nitroso-N-methylurea-induced rat mammary tumor model. Cancer Res. 61, 8683–8688. I.

Cole, H.W., Adrian, M.D., Shetler, P.K., Sato, M., Rowley, E.R., Glasebrook, A.L., Short, L.L., Grese, T.A., Palkowitz, A.D., Thrasher, K.J., Bryant, H.U., 1997. Comparative pharmacology of high potency selective estrogen receptor modulators: LY353381•HCL and CP-336,156. J. Bone Miner. Res. 12 (Suppl. 1), S349.

Cook, L.S., Weiss, N.S., Schwartz, S.M., White, E., McKnight, B., Moore, D.E., Daling, J.R., 1995. Population-based study of tamoxifen therapy and subsequent ovarian, endometrial, and breast cancers. J. Natl. Cancer Inst. 87, 1259–1364.

Cosman, F., Lindsay, R., 1999. Selective estrogen receptor modulators: clinical spectrum. Endocr. Rev. 20, 418–434.

Cosman, F., Baz-Hecht, M., Cushman, M., Vardy, M.D., Cruz, J.D., Nieves, J.W., Zion, M., Lindsay, R., 2005. Short-term effects of estrogen, tamoxifen and raloxifene on hemostasis: a randomized-controlled study and review of the literature. Thromb. Res. 116, 1–13.

Costantino, J.P., Gail, M.H., Pee, D., Anderson, S., Redmond, C.K., Benichou, J., Wieand, H.S., 1999. Validation studies for models projecting the risk of invasive and total breast cancer incidence. J. Natl. Cancer Inst. 91, 1541–1548.

Cushman, M., Legault, C., Barrett-Connor, E., Stefanick, M.L., Kessler, C., Judd, H.L., Sakkunen, P.A., Tracy, R.P., 1999. Effect of postmenopausal hormones on inflammation-sensitive proteins: the postmenopausal estrogen/progestin interventions (PEPI) study. Circulation 100, 717–722.

Cushman, M., Costantino, J.P., Tracy, R.P., Song, K., Buckle, L., Roberts, J.D., Krag, D.N., 2001. Tamoxifen and cardiac risk factors in healthy women: suggestion of an anti-inflammatory effect. Arterioscler. Thromb. Vasc. Biol. 21, 255–261.

Cuzick, J., Forbes, J., Edwards, R., Baum, M., Cawthorn, S., Contes, A., Hamed, H., Howell, A., Powles, T., 2002. First results from the international breast cancer intervention study (IBIS-I): a randomized prevention trial. Lancet 360, 817–824.

Cuzick, J., Powles, T., Veronesi, U., Forbes, J., Edwards, R., Ashley, S., Boyle, P., 2003. Overview of the main outcomes in breast-cancer prevention trials. Lancet 361, 296–300.

Cyr, M., Landry, M., DiPaolo, T., 2000. Modulation of estrogen receptor directed drugs of 5-hydroxytryptamine-2A receptors in rat brain. Neuropsychopharmacology 23, 69–78.

Cyr, M., Thibault, C., Morissette, M., Landry, M., DiPaolo, T., 2001. Estrogen-like activity of tamoxifen and raloxifene on NMDA receptor binding and expression of its subunits in rat brain. Neuropsychopharmacology 25, 242–257.

Dahm, A.E.A., Iversen, N., Birkenes, B., Ree, A.H., Sandset, P.M., 2006. Estrogens, selective estrogen receptor modulators, and a selective estrogen down-regulator inhibit endothelial production of tissue factor pathway inhibitor I. BMC Cardiovasc. Disord. 6, 40–48.

Davies, G.C., Huster, W.J., Lu, Y., Plouffe, L., Lakshmanan, M., 1999. Adverse events reported by postmenopausal women in controlled trials with raloxifene. Obstet. Gynecol. 93, 558–565.

Dayspring, T., Qu, Y., Keech, C., 2006. Effects of raloxifene on lipid and lipoprotein levels in postmenopausal osteoporotic women with and without hypertriglyceridemia. Metab. Clin. Exp. 55, 972–979.

de Boer, T., Otjens, D., Muntendam, A., Meulman, E., van Oostijen, M., Ensing, K., 2004. Development and validation of fluorescent receptor assays based on the human recombinant estrogen receptor subtypes alpha and beta. J. Pharm. Biomed. Anal. 34, 671–679.

De Leo, V., La Marca, A., Morgante, G., Lanzetta, D., Setaci, C., Petraglia, F., 2001. Randomized control study of the effects of raloxifene on serum lipids and homocysteine in older women. Am. J. Obstet. Gynecol. 184, 350–353.

DeGregoria, M.W., Wurz, G.T., Taras, T.L., Erkkola, R.U., Halonen, K.H., Huupponen, R.K., 2000. Pharmacokinetics of (deaminohydroxy)toremifene in humans: a new, selective estrogen receptor modulator. Eur. J. Clin. Pharmacol. 56, 469–475.

Delmas, P.D., Bjarnason, N.H., Mitlak, B.H., Ravoux, A.-C., Shah, A.S., Huster, W.J., Draper, M., Christiansen, C., 1997. Effects of raloxifene on bone mineral density, serum cholesterol concentrations and uterine endometrium in postemenopausal women. N. Engl. J. Med. 337, 1641–1647.

Delmas, P.D., Genant, H.K., Crans, G.G., Stock, J.L., Wong, M., Siris, E., Adachi, J.C., 2003. Severity of prevalent vertebral fractures and the risk of subsequent vertebral and nonvertebral fractures: results from the MORE trial. Bone 33, 522–532.

Derman, S.G., Adahi, E.Y., 1994. Adverse effects of fertility drugs. Drug Saf. 11, 408–421.

Dickey, R.P., Holtkamp, D.E., 1996. Development, pharmacology and clinical experience with clomiphene citrate. Hum. Reprod. Update 2, 483–506.

Diel, P., Olff, S., Schmidt, S., Michna, H., 2002. Effects of the environmental estrogens bisphenol A, o,p'-DDT, p-tert-octylphenol and coumestrol on apoptosis induction, cell proliferation and the expression of estrogen sensitive molecular parameters in the human breast cancer cell line MCF-7. J. Steroid Biochem. Mol. Biol. 80, 61–70.

Draper, M.W., Flowers, D.E., Huster, W.J., Nield, J.A., Harper, K.D., Arnaud, C., 1997. A controlled trial of raloxifene (LY139481) HCl: impact on bone turnover and serum lipid profile in healthy postmenopausal women. J. Bone Miner. Res. 11, 835–842.

Duvernoy, C.S., Kulkarni, P.M., Dowsett, S.A., Keech, C.A., 2005. Vascular events in the Multiple Outcomes of Raloxifene Evaluation (MORE) trial: incidence, patient characteristics, and effect of raloxifene. Menopause 12, 444–452.

Ellmen, J., Hakulinen, P., Partanen, A., Hayes, D.F., 2003. Estrogenic effects of toremifene and tamoxifen in postmenopausal breast cancer patients. Breast Canc. Res. Treat. 82, 103–111.

Ermer, J., McKeand, W., Sullivan, P., Parker, V., Orczyk, G., 2003. Bazedoxifene acetate dose proportionality in healthy, postmenopausal women. J. Clin. Pharm. Ther. 73, 43.

Ernst, T., Chang, L., Cooray, D., Salvador, C., Jovicich, J., Walot, I., Boone, K., Chlebowski, R., 2002. The effects of tamoxifen and estrogen on brain metabolism in elderly women. J. Natl. Cancer Inst. 94, 592–597.

Ettinger, B., Black, D.M., Mitlak, B.M., Knickerbocker, R.K., Nickelsen, T., Genant, H.K., Christiansen, C., Delmas, P.D., Zanchetta, J.R., Stakkestad, J., Gluer, C.C., Krueger, K., Cohen, F.J., Eckert, S., Ensrud, K.E., Avioli, L.V., Lips, P., Cummings, S.R., 1999. Reduction of vertebral fracture risk in postmenopausal women with osteoporosis treated with raloxifene. J. Am. Med. Assoc. 282, 637–645.

Evans, G., Bryant, H.U., Magee, D., Sato, M., Turner, R.T., 1994. The effects of raloxifene on tibia histomorphometry in ovariectomized rats. Endocrinology 134, 2283–2288.

Fanning, P., Kuehl, T., Lee, R., Pearson, S., Wincek, T., Pliego, J., Spiekeman, A., Bryant, H.U., Rippy, M., 1996. Video mapping to assess efficacy of an antiestrogen (raloxifene) on spontaneous endometriosis in the rhesus monkey, Macaca mulata. In: Juehl, T.J. (Ed.), Bunkley Day Proceedings, vol. 6. Texas A&M University Health Science Centre, Temple TX, pp. 51–61.

Faupel-Badger, J.M., Prindville, S.A., Venzon, D., Vonderhaar, B.K., Zujewski, J.A., Eng-Wong, J., 2006. Effects of raloxifene on circulating prolactin and estradiol levels in premenopausal women at high risk for developing breast cancer. Cancer Epidemiol. Biomark. Prev. 15, 1153–1158.

Feldman, S., Minne, H.W., Parvizi, S., Pfeifer, M., Lempert, U.G., Bauss, F., Ziegler, R., 1989. Antiestrogen and antiandrogen administration reduce bone mass in the rat. Bone Miner. 7, 245–254.

Feng, Q., O'Malley, B.W., 2014. Nuclear receptor modulation-Role of coregulators in selective estrogen receptor (SERM) actions. Steroids 90, 39–43.

Fisher, B., Constantino, J.P., Redmond, C.K., Fisher, E.R., Wickerham, D.L., Cronin, W.M., 1994. Endometrial cancer in tamoxifen treated breast cancer patients: findings from the National surgical adjuvant breast and Bowel Project. J. Natl. Cancer Inst. 86, 527–537.

Fisher, B., Costantino, J.P., Wickerham, D.L., Redmond, C.K., Kavanah, M., Cronin, W.M., Vogel, V., Robidoux, A., Dimitrov, N., Atkins, J., Daly, M., Wieand, S., Tan-Chiu, E., Ford, L., Wolmark, N., 1998. Tamoxifen for prevention of breast cancer: report of the National surgical adjuvant breast and Bowel Project P-1 study. J. Natl. Cancer Inst. 90, 1371–1388.

Fleischer, A.C., Wheeler, J.E., Yeh, I.T., Kravitz, B., Jensen, C., MacDonald, B., 1999. Sonographic assessment of the endometrium in osteopenic postmenopausal women treated with idoxifene. J. Ultrasound Med. 18, 503–512.

Friedrich, M., Mink, D., Villena-Heinsen, C., Woll-Hermann, A., Wagner, S., Schmidt, W., 1998. The influence of tamoxifen on the maturation index of vaginal epithelium. Clin. Exp. Obstet. Gynecol. 25, 121–124.

Frolik, C.A., Bryant, H.U., Black, E.C., Magee, D.E., Chandrasekhar, S., 1996. Time dependent changes in biochemical bone markers and serum cholesterol in ovariectomized rats: effects of raloxifene HCI, tamoxifen, estrogen and alendronate. Bone 18, 621–627.

Fromson, J.M., Sharp, D.S., 1974. The selective uptake of tamoxifen by human uterine tissue. J. Obstet. Gynaecol. Br. Commonw. 81, 321–323.

Fromson, J.M., Pearson, S., Branah, S., 1973. The metabolism of tamoxifen II: in female patients. Xenobiotica 3, 711–714.

Fuchs-Young, R., Iversen, P., Shetler, P., Layman, N., Hale, L., Short, L., Magee, D., Sluka, J., Glasebrook, A., Bryant, H.U., Palkowitz, A., 1997. Preclinical demonstrations of specific and potent inhibition of mammary tumor growth by new selective estrogen receptor modulators. Proc. Am. Assoc. Cancer Res. 38, 573.

Furr, B.J., Jordan, V.C., 1984. The pharmacology and clinical uses of tamoxifen. Pharmacol. Ther. 25, 127–205.

Galbiati, E., Caruso, P.L., Amari, G., Armani, E., Ghirardi, S., Delcanale, M., Civelli, M., 2002. Effects of 3-phenyl-4-[[4-[2-(1-piperidinyl) ethoxy] phenyl]methyl]-2H-1-benzopyran-7-ol (CHF 4056), a novel nonsteroidal estrogen agonist/antagonist, on reproductive and nonreproductive tissue. J. Pharmacol. Exp. Ther. 300, 802–809.

Garas, A., Trypsianis, G., Kallitsaris, G., Milingos, A., Messinis, I.E., 2006. Oestradiol stimulates prolactin secretion in women through oestrogen receptors. Clin. Endocrinol. 65, 638–642.

Gardner, M., Taylor, A., Wei, G., Calcagni, A., Duncan, B., Milton, A., 2006. Clinical pharmacology of multiple doses of lasofoxifene in postmenopausal women. J. Clin. Pharmacol. 46, 52–58.

Gaynor, J.S., Monnet, E., Selzman, C., Parker, D., Kaufman, L., Bryant, H.U., Mallinckrodt, C., Wrigley, R., Whitehill, T., Turner, A.S., 2000. The effect of raloxifene on coronary arteries in aged ovariectomized ewes. J. Vet. Pharmacol. Ther. 23, 175–179.

Gennari, L., Merlotti, D., Martini, G., Nuti, R., 2006. Lasofoxifene: a third-generation selective estrogen receptor modulator for the prevention and treatment of osteoporosis. Expert Opin. Investig. Drugs 15, 1091–1103.

Goldstein, S.R., Nanavati, N., 2002. Adverse events that are associated with the selective estrogen receptor modulator levormeloxifene in an aborted phase III osteoporosis treatment study. Am. J. Obstet. Gynecol. 187, 521–527.

Goekoop, R., Barkhof, F., Duschek, E.J.J., Netlenbos, C., Knol, D.L., Scheltens, P., Rombouts, S.A.R.B., 2006. Raloxifene treatment enhances brain activation during recognition of familiar items: A pharmacologic fMRI study in elderly males. Neuropsychopharmacology 31, 1508–1518.

Goldstein, S.R., Neven, P., Zhou, L., Taylor, Y.L., Ciaccia, A.V., Plouffe, L., 2001. The effect of raloxifene on the frequency of pelvic floor relaxation. Obstet. Gynecol. 98, 91–96.

Gomez-Mancilla, B., Bedard, P.J., 1992. Effect of estrogen and progesterone on L-DOPA induced dyskinesia in MPTP-treated monkeys. Neurosci. Lett. 135, 129–132.

Gottardis, M.M., Jordan, V.C., 1987. Antitumor actions of keoxifene and tamoxifen in the N-nitrosomethylurea induced rat mammary carcinoma model. Cancer Res. 47, 4020–4024.

Grandbois, M., Morissette, M., Callier, S., Di Paolo, T., 2000. Ovarian steroids and raloxifene prevent MPTP-induced dopamine depletion in mice. Neuroreport 11, 343–346.

Greeve, I., Hermans-Borgmeyer, I., Bellinger, C., Kasper, D., Gomez-Isla, T., Behl, C., Levkau, B., Nitsch, R.M., 2001. The human DIMINUTO/DWARF1 homolog seladin-1 confers resistance to Alzheimer's disease-associated neurodegeneration and oxidative stress. J. Neurosci. 20, 7345–7352.

Grese, T.A., Sluka, J.P., Bryant, H.U., Cullinan, G.C., Glasebrook, A.L., Jones, C.D., Matsumoto, K., Palkowitz, A.D., Sato, M., Termine, J.D., Winter, M.A., Yang, N.N., Dodge, J.A., 1997. Molecular determinants of tissue selectivity in estrogen receptor modulators. Proc. Natl. Acad. Sci. U.S.A. 94, 14105–14110.

Hak, A.E., Polderman, K.H., Westendorp, I.C., 2000. Increased plasma homocysteine after menopause. Atherosclerosis 149, 163–168.

Harvey, H.A., Kinura, M., Hajba, A., 2006. Toremifene: an evaluation of its safety profile. Breast 15, 142–157.

Hays, D.F., Van Zyl, J.A., Hacking, A., Goedhals, L., Bezwoda, W.R., Mailliand, J.A., Jones, S.E., Vogel, C.L., Berris, R.F., Shemano, I., 1995. Randomized comparison of tamoxifen and two separate doses of toremifene in postmenopausal patients with metastatic breast cancer. J. Clin. Oncol. 13, 2556–2566.

He, L., Xiang, H., Lu-Yong, Z., Wei-Sheng, T., Hong, H.H., 2005. Novel estrogen receptor ligands and their structure activity relationship evaluated by scintillation proximity assay for high throughput screening. Drug Discov. Res. 64, 203–212.

Heany, R.P., Draper, M.W., 1997. Raloxifene and estrogen: comparative bone-remodelling kinetics. J. Clin. Endocrinol. Metab. 82, 3425–3429.

Helvering, L.M., Adrian, M.D., Geiser, A.G., Estrem, S.T., Wei, T., Huang, S., Chen, P., Dow, E.R., Calley, J.N., Dodge, J.A., Grese, T.A., Jones, S.A., Halladay, D.L., Miles, R.R., Onyia, J.E., Ma, Y.L., Sato, M., Bryant, H.U., 2005a. Differential effects of estrogen and raloxifene on messenger RNA and matrix metalloproteinase 2 activity in the rat uterus. Biol. Reprod. 72, 830–841.

Helvering, L.M., Liu, R., Kulkarni, N.H., Wei, T., Chen, P., Huang, S., Lawrence, F., Halladay, D.L., Miles, R.R., Ambrose, E.M., Sato, M., Ma, Y.L., Frolik, C.A., Dow, E.R., Bryant, H.U., Onyia, J.E., 2005b. Expression profiling of rat femur revealed suppression of bone formation genes by treatment with alendronate and estrogen but not raloxifene. Mol. Pharmacol. 68, 1225–1238.

Hendrix, S.L., Cochrane, B.B., Nygaard, I.E., Handa, V.L., Barnabei, V.M., Iglesia, C., Aragaki, A., Naughton, M.J., Wallace, R.B., McNeely, S.G., 2005. Effects of estrogen with and without progestin on urinary incontinence. J. Am. Med. Assoc. 293, 935–948.

Heringa, M., 2003. Review on raloxifene: profile of a selective estrogen receptor modulator. Int. J. Clin. Pharmacol. Ther. 41, 331–345.

Homesley, H.D., Shemano, I., Gams, R.A., Harry, D.S., Hickox, P.G., Rebar, R.W., Bump, R.C., Mullin, T.J., Wentz, A.C., O'Toole, R.V., Lovelace, J.V., Lyden, C.C.T., 1993. Antiestrogenic potency of toremifene and tamoxifen in postmenopausal women. Am. J. Clin. Oncol. Cancer Clin. Trials 16, 117–122.

Houvinen, R., Warri, A., Collan, Y., 1993. Mitotic activity, apoptosis and TRPM-2 mRNA expression in DMBA-induced rat mammary carcinoma treated with anti-estrogen toremifene. Int. J. Cancer 55, 685–691.

Hovey, R.C., Asai-Sato, M., Warri, A., Terry-Koroma, B., Colyn, N., Ginsburg, E., Vonderhaar, B.K., 2005. Effects of neonatal exposure to diethylstilbesterol, tamoxifen, and toremifene on the BABL/c mouse mammary gland. Biol. Reprod. 72, 423–435.

Hulley, S., Grady, D., Bush, T., Furberf, C., Herrington, D., Riggs, B., Vittinghoff, E., 1998. Randomized trial of estrogen plus progestin for secondary prevention of coronary heart disease in postmenopausal women. Heart and estrogen/progestin replacement study (HERS) research group. J. Am. Med. Assoc. 280, 605–613.

Jimenez, M.A., Magee, D.E., Bryant, H.U., Turner, R.T., 1997. Clomiphene prevents cancellous bone loss from tibia of ovariectomized rats. Endocrinology 138, 1794–1800.

Jirecek, S., Lee, A., Pave, I., Crans, G., Eppel, W., Wenzl, R., 2004. Raloxifene prevents the growth of uterine leiomyomas in premenopausal women. Fertil. Steril. 81, 132–136.

Joensuu, H., Holli, K., Oksanen, H., Valavaara, R., 2000. Serum lipid levels during and after adjuvant toremifene or tamoxifen therapy for breast cancer. Breast Canc. Res. Treat. 63, 225–234.

Johnell, O., Scheele, W.M., Lu, Y., Reginster, J.-Y., Need, A.G., Seeman, E., 2002. Additive effects of raloxifene and alendronate on bone density and biochemical markers of bone remodeling in postmenopausal women with osteoporosis. J. Clin. Endocrinol. Metab. 87, 985–1002.

Kalu, D., Salerno, E., Liu, C.C., Echon, R., Ray, M., Gaza-Zepata, M., Hollis, B.W., 1991. A comparative study of the actions of tamoxifen, estrogen and progesterone in the ovariectomized rat. Bone Miner. 15, 109–124.

Kangas, L., Haaparanta, M., Paul, R., Roeda, D., Sipila, H., 1989. Biodistribution and scintigraphy of 14C-toremifene in rats bearing DMBA-induced mammary carcinoma. Pharmacol. Toxicol. 64, 373–377.

Kauffman, R.F., Bensch, W.R., Roudebush, R.E., Cole, H.W., Bean, J.S., Phillips, D., Monroe, A., Cullinan, G.J., Glasebrook, A.L., Bryant, H.U., 1997. Hypocholesterolemic activity of raloxifene (LY139481): pharmacological characterization as a selective estrogen receptor modulator (SERM). J. Pharmacol. Exp. Ther. 280, 146–153.

Kanis, J.A., Johnell, O., Black, D.M., Downs Jr., R.W., Sarkar, S., Fuerst, T., Secrest, R.J., Pavo, I., 2003. Effect of raloxifene on the risk of new vertebral fracture inpostmenopausal women with osteopenia or osteoporosis: a reanalysis of the Multiple Outcomes of Raloxifene Evaluation trial. Bone 33, 293–300.

Kausta, E., White, D., Franks, S., 1997. Modern use of clomiphene citrate in induction of ovulation. Hum. Reprod. Update 3, 359–365.

Ke, H.Z., Chen, H.K., Qi, H., Pirie, C.M., Simmons, H.A., Ma, Y.F., Jee, W.S.S., Thompson, D.D., 1995. Effects of droloxifene on prevention of cancellous bone loss and bone turnover in the axial skeleton of aged, ovariectomized rats. Bone 17, 491–496.

Ke, H.Z., Paralkar, V.M., Grasser, W.A., Crawford, D.T., Qi, H., Simmons, H.A., Pirie, C.M., Chidsey-Frink, K.L., Owen, T.A., Smock, S.L., Chen, H.K., Jee, W.S., Cameron, K.O., Rosati, R.L., Brown, T.A., Dasilva-Jardine, P., Tompson, D.D., 1998. Effects of CP336,156, a new, nonsteroidal estrogen agonist/antagonist on bone, serum cholesterol, uterus and body composition in rat models. Endocrinology 139, 2068–2076.

Keech, C.A., Sashegyi, A., Barrett-Conner, E., 2005. Year-by-year analysis of cardiovascular events in the multiple outcomes of raloxifene evaluation (MORE) trial. Curr. Med. Res. Opin. 21, 135–140.

Kessel, B., Nachtigall, L., Plouffe, L., Siddhanti, S., Rosen, A., Parsons, A., 2003. Effect of raloxifene on sexual function in postmenopausal women. Climacteric 6, 248–256.

Kimler, B.F., Ursin, C., Fabian, J., Anderson, J.R., Chamberlain, C., Mayo, M.S., O'Shaughnessy, J.A., Lynch, H.T., Johnson, K.A., Browne, D., 2006. Effect of the third generation selective estrogen receptor modulator arzoxifene on mammographic breast density. J. Clin. Oncol. 24 (Suppl. l), 562.

Knadler, M.P., Lantz, R.J., Gillespie, T.A., 1995. The disposition and metabolism of 14C-labelled raloxifene in humans. Pharm. Res. (N. Y.) 12 (Suppl. l), 372.

Koda, M., Jarzabek, K., Haczynski, J., Knapp, P., Sulkowski, S., Woczynski, S., 2004. Differential effects of raloxifene and tamoxifen on the expression of estrogen receptors and antigen Ki-67 in human endometrial adenocarcinoma cell line. Oncol. Rep. 12, 517–521.

Komi, J., Lankinen, K.S., Harkonen, P., DeGregoria, M.W., Voipio, S., Kivinen, S., Tuimala, R., Vihtamaki, T., Vihko, K., Ylikorkala, O., Erkkola, R., 2005. Effects of ospemifene and raloxifene on hormonal status, lipids, genital tract and tolerability in postmenopausal women. Menopause 12, 202–209.

Komm, B.S., Kharode, Y.P., Bodine, P.V., Harris, H.A., Miller, C.P., Lyttle, C.R., 2005. Bazedoxifene acetate: a selective estrogen receptor modulator with improved selectivity. Endocrinology 146, 3999–4008.

Komm, B.S., Bodine, P.V., Minck, D.R., 2007. Effects of bazedoxifene on bone loss: a 12 month study in ovariectomized rats. J. Bone Miner. Res. 22 (Suppl. 1), S206.

Kuiper, G.G.J.M., Enmark, E., Pelto-Huikko, M., Nilsson, S., Gustafsson, J.A., 1996. Cloning of a novel receptor expressed in rat prostate and ovary. Proc. Natl. Acad. Sci. U.S.A. 93, 5925–5930.

Kusama, M., Miyauchi, K., Aoyama, H., Sano, M., Kimura, M., Mitsuyama, S., Komaki, K., Doihara, H., 2004. Effects of toremifene and tamoxifen on serum lipids in postmenopausal patients with breast cancer. Breast Canc. Res. Treat. 88, 1–8.

Labrie, F., Champagne, P., Labrie, C., Roy, J., Laverdiere, J., Provencher, L., Potvin, M., Drolet, Y., Panasci, L., Esperance, B., Dufresne, J., Latreille, J., Robert, J., Samson, B., Jolivet, J., Yelle, L., Cusan, L., Diamond, P., Candas, B., 2004. Activity and safety of the antiestrogen EM-800, the orally active precursor of acolbifene, in tamoxifen -resistant breast cancer. J. Clin. Oncol. 22, 864–871.

Landry, M., Levesqu, D., DiPaolo, T., 2002. Estrogenic properties of raloxifene, but not tamoxifen, on D2 and D3 dopamine receptors in the rat forebrain. Neuroendocrinology 76, 214–222.

Lasco, A., Cannavo, S., Gaudio, A., Morabito, N., Basile, N., Nicita-Mauro, B., Frisina, N., 2002. Raloxifene and pituitary secretion in post-menopausal women. Eur. J. Endocrinol. 147, 461–465.

Lasco, A., Gaudio, A., Morini, E., Morabito, N., Nicita-Mauro, C., Catalano, A., Denuzzo, G., Sansotta, C., Xourafa, A., Macri, I., Frisina, N., 2006. Effect of long-term treatment with raloxifene on mammary density in postmenopausal women. Menopause 13, 787–792.

Leblanc, K., Sexton, E., Parent, S., Belanger, G., Dery, M.-C., Boucehr, V., Asselin, E., 2007. Effects of 4-hydroxytamoxifen, raloxifene and ICI-182,780 on survival of uterine cancer cell lines in the presence and absence of exogenous estrogens. Int. J. Oncol. 30, 477–487.

Legha, S.S., 1988. Tamoxifen in the treatment of breast cancer. Ann. Intern. Med. 109, 219–228.

Li, J., Sato, M., Jerome, C., Turner, C.H., Fan, Z., Burr, D.B., 2005. Microdamage accumulation in the monkey vertebrae does not occur when bone turnover is suppressed by 50% or less with estrogen or raloxifene. J. Bone Miner. Res. 23, 48–54.

Lindsay, R., Rankin, S., Constantine, G., Olivier, S., Pickar, J., 2007. A double-blind, placebo-controlled, phase III study of bazedoxifene/conjugated equine estrogens in postmenopausal women: effects on BMD. In: Endocrine Society Abstracts 89th Meeting. Abstract 126.

Love, R.R., Mazess, R.B., Barden, H.S., Epstein, S., Newcomb, P.A., Jordan, V.C., Carbone, P.P., DeMets, D.L., 1992. Effects of tamoxifen on bone mineral density in postmenopausal women with breast cancer. N. Engl. J. Med. 326, 852–856.

Love, R.R., Wiebe, D.A., Feyzi, J.M., Newcomb, P.A., Chappell, R.J., 1994. Effects of tamoxifen on cardiovascular risk factors in postmenopausal women after 5 years of treatment. J. Natl. Cancer Inst. 86, 1534–1539.

Maenpaa, J.U., Ala-Fossi, S.L., 1997. Toremefine in postmenopausal breast cancer. Efficacy, safety and cost. Drugs Aging 11, 261–270.

Mandlekar, S., Kong, A.N., 2001. Mechanisms of tamoxifen-induced apoptosis. Apoptosis 6, 469–477.

Mann, V., Huber, C., Kogianni, G., Collins, F., Noble, B., 2007. The antioxidant effect of estrogen and selective estrogen receptor modulators in the inhibition of osteocyte apoptosis in vitro. Bone 40, 674–684.

Manson, J.E., Hsia, J., Johnson, K.C., Rossouw, J.E., Assaf, A.R., Lasser, N.L., Trevisan, M., Black, H.R., Heckbert, S.R., Detrano, R., Strickland, O.L., Wong, N.D., Crouse, J.R., Stein, E., 2003. Estrogen plus progestin and the risk of coronary heart disease. N. Engl. J. Med. 349, 523–534.

Martel, C., Picard, S., Belanger, R.V., Labrie, C., Labrie, F., 2000. Prevention of bone loss by EM-800 and raloxifene in the ovariectomized rat. J. Steroid Biochem. Mol. Biol. 74, 45–56.

Martino, S., Cauley, J.A., Barrett-Connor, E., Powles, T.J., Mershon, J., Disch, D., Secrest, R.J., Cummings, S.R., 2004. Continuing Outcomes Relevant to Evista: breast cancer incidence in postmenopausal osteoporotic women in a randomized trial of raloxifene. J. Natl. Cancer Inst. 96, 1751–1761.

Martino, S., Disch, D., Dowsett, S.A., Keech, C.A., Mershon, J., 2005. Safety assessment of raloxifene over eight years in a clinical trial setting. Curr. Med. Res. Opin. 21, 1441–1452.

Marttunen, M.B., Hietanen, P., Tiitinen, A., Ylikorkala, O., 1998. Comparison of effects of tamoxifen and toremifene on bone biochemistry and bone mineral density in postmenopausal breast cancer patients. J. Clin. Endocrinol. Metab. 83, 1158–1162.

Marttunen, M.B., Cacciatore, B., Hietanen, P., Pyrhonen, S., Tiitinen, A., Wahlstrom, T., Ylikorkala, O., 2001. Prospective study on gynaecological effects of two antiestrogens tamoxifen and toremifene in postmenopausal women. Br. J. Canc. 84, 897–902.

McClung, M.R., Siris, E., Cummings, S., Bolognese, M., Ettinger, M., Moffett, A., Emkey, R., Day, W., Somayaji, V., Lee, A., 2006. Prevention of bone loss in postmenopausal women treated with lasofoxifene compared with raloxifene. Menopause 13, 377–386.

McDonnel, D.P., Clemm, D.L., Hermann, T., Goldman, M.E., Pike, J.W., 1995. Analysis of estrogen receptor function in vitro reveals three distinct classes of anti-estrogens. Mol. Endocrinol. 9, 659–669.

McMeekin, D.S., Gordon, A., Fowler, J., Melemed, A., Buller, R., Burke, T., Bloss, J., Sabbatini, P., 2003. A phase II trial of arzoxifene, a selective estrogen receptor modulator, in patients with recurrent or advanced endometrial cancer. Gynecol. Oncol. 90, 49–64.

Mehta, S.H., Dhandapani, K.M., De Sevilla, L.M., Webb, R.C., Mahesh, V.B., Brann, D.W., 2003. Tamoxifen, a selective estrogen receptor modulator reduces ischemic damage caused by middle cerebral artery occlusion in the ovariectomized female rat. Neuroendocrinology 77, 44–50.

Mijatovic, V., van der Mooren, M.J., Kenemans, P., de Valk-de Roo, G.W., Netlenboss, C., 1999. Raloxifene lowers serum lipoprotein (a) in healthy postmenopausal women: a randomized, double-blind, placebo-controlled comparison with conjugated equine estrogens. Menopause 6, 134–137.

Miller, P.D., Christiansen, C., Hoeck, H.C., Kendler, D.L., Lewiecki, E.M., Woodson, G., Ciesielska, M., Chines, A.A., Constantine, G., Delmas, P.D., 2007. Efficacy of bazedoxifene for prevention of postmenopausal osteoporosis: results of a 2-year, phase III, placebo- and active-controlled study. J. Bone Miner. Res. 22 (Suppl. 1), S59.

Mirkin, S., Pickar, J.H., 2015. Selective estrogen receptor modulators (SERMS): a review of clinical data. Maturitas 80, 52–57.

Munster, P.N., Buzdar, A., Dhingra, K., Enas, N., Ni, L., Major, M., Melemed, A., Seidman, A., Booser, D., Theriault, R., Norton, L., Hudis, C., 2001. Phase I study of a third-generation selective estrogen receptor modulator, LY353381. HCl, in metastatic breast cancer. J. Clin. Oncol. 19, 2002–2009.

Murphy, E.D., Beamer, W.G., 1973. Plasma gonadotropin levels during early stages of ovarian tumorigenesis in mice of the Wx-Wu genotype. Cancer Res. 33, 721–723.

Neven, P., Goldstein, S.R., Ciaccia, A.V., Zhou, L., Silfen, S.L., Muram, D., 2002. The effect of raloxifene on the incidence of ovarian cancer in postmenopausal women. Gynecol. Oncol. 85, 388–390.

Nickelsen, T., Lufkin, E.G., Riggs, B.L., Cox, D.A., Crook, T.H., 1999. Raloxifene hydrochloride, a selective estrogen receptor modulator: safety assessment of effects on cognitive function and mood in postmenopausal women. Psychoneuroendocrinology 24, 115–128.

Nilsen, J., Mor, G., Naftolin, F., 1998. Raloxifene induces neurite outgrowth in estrogen receptor positive PC-12 cells. Menopause 5, 211–216.

Nuttall, M.E., Bradbeer, J.N., Stroup, G.B., Nadeau, D.P., Hoffman, S.J., Zhao, H., Rehm, S., Gowen, M., 1998. Idoxifene: a novel selective estrogen receptor modulator prevents bone loss and lowers cholesterol levels in ovariectomized rats and decreases uterine weight in intact rats. Endocrinology 139, 5224–5234.

Obata, T., Kubota, S., 2001. Protective effect of tamoxifen on 1-methyl-4-phenylpyridine-induced hydroxyl radical generation in the rat striatum. Neurosci. Lett. 308, 87–90.

Ortmann, O., Emons, G., Knuppen, R., Catt, K.J., 1988. Inhibitory actions of keoxifene on luteinizing hormone secretion in pituitary gonadotrophs. Endocrinology 123, 962–968.

Osuka, K., Feustel, P.J., Mongin, A.A., Tranmer, B.I., Kimelberg, H.K., 2001. Tamoxifen inhibits nitrotyrosine formation after reversible middle cerebral artery occlusion in the rat. J. Neurochem. 76, 1842–1850.

Ott, S.M., Oleksik, A., Lu, Y., Harper, K.D., Lips, P., 2002. Bone histomorphometric and biochemical marker results of a two year placebo controlled trial of raloxifene in postmenopausal women. J. Bone Miner. Res. 17, 341–348.

O'Neill, K., Chen, S., Brinton, R.D., 2004. Impact of the selective estrogen receptor modulator, raloxifene, on neuronal survival and out-growth following toxic insults associated with aging and Alzheimer's disease. Exp. Neurol. 185, 63–80.

Paganini-Hill, A., Clark, L.J., 2000a. Eye problems in breast cancer patients treated with tamoxifen. Breast Canc. Res. Treat. 60, 167–172.

Paganini-Hill, A., Clark, L.J., 2000b. Preliminary assessment of cognitive function in breast cancer patients treated with tamoxifen. Breast Canc. Res. Treat. 64, 165–176.

Palkowitz, A.L., Glasebrook, A.L., Thrasher, K.J., Hauser, K.L., Short, L.L., Phillips, D.L., Muehl, B.S., Sato, M., Shetler, P.K., Cullinan, G.J., Zeng, G.Q., Pell, T.R., Bryant, H.U., 1997. Discovery and synthesis of 6-hydroxy-3-[4-(1-piperidinyl)-ethoxy-phenoxy]-2-(4-hydroxyphenyl)benzo [b]-thiophene: a novel, highly potent selective estrogen receptor modulator (SERM). J. Med. Chem. 40, 1407–1416.

Palomba, S., Orio, F., Morelli, M., Russo, T., Pellicano, M., Zupi, E., Lombardi, G., Nappi, C., Panici, P.L.B., Zullo, F., 2002a. Raloxifene administration in premenopausal women with uterine leiomyomas: a pilot study. J. Clin. Endocrinol. Metab. 87, 3603–3608.

Palomba, S., Russo, T., Oria, F., Tauchmanova, K., Supi, E., Panici, P.L.B., Nappi, C., Calao, A., Lombardi, G., Zullo, F., 2002b. Effectiveness of combined GnRH analogue plus raloxifene administration in the treatment of uterine leiomyomas: a prospective, randomized, single-blind, placebo-controlled clinical trial. Hum. Reprod. 17, 3213–3219.

Palomba, S., Orio, F., Russo, T., Falbo, A., Tolino, A., Lombardi, G., Climini, V., Zullo, F., 2005. Antiproliferative and proapoptotic effects of raloxifene on uterine leiomyomas in postmenopausal women. Fertil. Steril. 84, 154–161.

Patat, A., McKeand, W., Baird-Bellaire, S., Ermer, J., LeCoz, F., 2003. Absolute/relative bioavailability of bazedoxifene acetate in healthy post-menopausal women. J. Clin. Pharm. Ther. 73, 43.

Pickar, J.H., Archer, D.F., Constantine, G., Ronkin, S., Speroff, L., 2007. SMART-1: a double-blind, placebo-controlled, phase III study of bazedoxifene/conjugate equine estrogens in postmenopausal women—effects on endometrium. In: Endocrine Society Abstracts 89th Meeting. Abstract 246.

Pinna, C., Bolego, C., Sanvito, P., Pelosi, V., Baetta, R., Corsini, A., Gaion, R.M., Cignarella, A., 2006. Raloxifene elicits combined rapid vasorelaxation and long-term anti-inflammatory actions in rat aorta. J. Pharmacol. Exp. Ther. 319, 1444–1451.

Porter, K.B., Tsibris, J.C., Porter, G.W., Fuchs-Young, R., Nicosia, S.V., O'Brien, W.F., Spellacy, W.N., 1998. Effects of raloxifene in a Guinea pig model for leiomyomas. Am. J. Obstet. Gynecol. 170, 1283–1287.

Portman, D., Moffett, A., Kerber, I., Drossman, S., Somayaji, V., Lee, A., 2004. Lasofoxifene, a selective estrogen receptor modulator, improves objective measure of vaginal atrophy. Menopause 11, 675.

Powles, T.J., Hickish, T., Kanis, J.A., Tidy, A., Ashley, S., 1996. Effect of tamoxifen on bone mineral density measured by dual-energy X-ray absorptiometry in healthy premenopausal and postmenopausal women. J. Clin. Oncol. 14, 78–84.

Rash, T., Knadler, M.P., 1997. The disposition and biotransformation of the selective estrogen receptor modulator, LY353381, in femal Fisher 344 rats following a single oral dose. In: Proceedings of the American Association of Pharmaceutical Science. A1223 [Abstract].

Qu, Q., Zheng, H., Dahlund, J., Laine, A., Cockcroft, N., Peng, Z., Koskinen, M., Hemminki, K., Kangas, L., Vaananen, K., Harkonen, P., 2000. Selective estrogenic effects of a novel triphenylethylene compound, FC-1271a on bone, cholesterol level, and reproductive tissue in intact and ovariectomized rats. Endocrinology 141, 809–820.

Reid, I.R., Eastell, R., Fogelman, I., Adachi, J.D., Rosen, A., Netelenbos, C., Watts, N.B., Seeman, E., Ciaccia, A.V., Draper, M.W., 2004. A comparison of the effects of raloxifene and conjugated equine estrogen on bone and lipids in healthy postmenopausal women. Arch. Intern. Med. 164, 871–879.

Reindollar, R., Koltun, W., Parsons, A., Rosen, A., Siddhanti, S., Plouffe, L., 2002. Effects of oral raloxifene on serum estradiol levels and other markers of estrogenicity. Fertil. Steril. 78, 469–472.

Reis, S.E., Costantino, J.P., Wickerham, D.L., Tan-Chiu, E., Wang, J., Kavanah, M., 2001. Cardiovascular effects of tamoxifen in women with and without heart disease: breast cancer prevention trial. National surgical adjuvant breast and Bowel Project breast cancer prevention trial investigators. J. Natl. Cancer Inst. 93, 16–21.

Robinson, S.P., Mauel, D.P., Jordan, V.C., 1988. Antitumor actions of toremifene in 7,12-dimethylbenzanthrocene (DMBA)-induced rat mammary tumor model. J. Cancer Clin. Oncol. 24, 1817–1821.

Rossberg, M.I., Murphy, S.J., Traystman, R.J., Hurn, P.D., 2000. LY353381.HCl, a selective estrogen receptor modulator, and experimental stroke. Stroke 31, 3041–3046.

Rossing, M.A., Daling, J.R., Weiss, N.S., Moore, D.E., Self, S.G., 1994. Ovarian tumors in a cohort of infertile women. N. Engl. J. Med. 331, 771–776.

Rudmann, D.G., Cohen, I.R., Robbins, M.R., Coutant, D.E., Henck, J.W., 2005. Androgen dependent mammary gland virilism in rats given the selective estrogen receptor modulator LY2066948 hydrochloride. Toxicol. Pathol. 33, 711–719.

Rutqvist, L.E., Mattsson, A., 1993. Cardiac and thromboembolic morbidity among postmenopausal women with early-stage breast cancer in a randomized trial of adjuvant tamoxifen: The Stockholm Breast Cancer Study Group. J. Natl. Cancer Inst. 85, 1398–1406.

Saitta, A., Altavilla, D., Cucinotta, D., Morabito, N., Frisina, N., Corrado, F., D'Anna, R., Lasco, A., Squadrito, G., Caudia, A., Cancellieri, F., Arcoraci, V., Squadrito, F., 2001. Randomized, double-blind, placebo-controlled study on effects of raloxifene and hormone replacement therapy on plasma NO concentrations, endothelin-1 levels, and endothelium-dependent vasodilation in postmenopausal women. Arterioscler. Thromb. Vasc. Biol. 21, 1512–1519.

Sato, M., Glasebrook, A.L., Bryant, H.U., 1995. Raloxifene: a selective estrogen receptor modulator. J. Bone Miner. Res. 12 (Suppl. 2), S9–S20.

Sato, M., Bryant, H.U., Iversen, P., Helterbrand, J., Smietana, F., Bemis, K., Higgs, R., Turner, C., Owan, I., Takano, Y., Burr, D.B., 1996a. Advantages of raloxifene over alendronate or estrogen on non-reproductive and reproductive tissues in the long-term dosing of ovariectomized rats. J. Pharmacol. Exp. Ther. 279, 298–305.

Sato, M., Rippy, M.K., Bryant, H.U., 1996b. Raloxifene, tamoxifen, nafoxidine and estrogen effects on reproductive and nonreproductive tissues in ovariectomized rats. FASEB J. 10, 905–912.

Sato, M., Turner, C.H., Wang, T., Adrian, M.D., Rowley, E., Bryant, H.U., 1998. LY353381.HCl: a novel raloxifene analog with improved SERM potency and efficacy in vivo. J. Pharmacol. Exp. Ther. 287, 1–7.

Saunders, P.T., Maguire, S.M., Gaughan, J., Millar, M.R., 1997. Expression of oestrogen receptor beta (ER beta) in multiple rat tissues visualised by immunohistochemistry. J. Endocrinol. 154, R13–R16.

Savolainen-Peltonone, H., Luoto, N.-M., Kangas, L., Hayry, P., 2004. Selective estrogen receptor modulators prevent neointima formation after vascular injury. Mol. Cell. Endocrinol. 227, 9–20.

Seeman, E., 2001. Raloxifene. J. Bone Miner. Res. 19, 65–75.

Sgarabotto, M., Baldini, M., Dei Cas, A., Manotti, C., Barilli, A.L., Rinaldi, M., Benassi, L., Modena, A.B., 2006. Effects of raloxifene and continuous combined hormone therapy on haemostatis variables: a multicenter, randomized, double-blind study. Thromb. Res. 119, 85–91.

Shang, Y., Brown, M., 2002. Molecular determinants for the tissue specificity of SERMs. Science 295, 2465–2468.

Shita, A., Igarashi, T., Kurose, T., Ohno, M., Hando, T., 2002. Reciprocal effects of tamoxifen on hormonal cytology in postmenopausal women. Acta Cytol. 46, 499–506.

Short, L.L., Glasebrook, A.L., Adrian, M.D., Cole, H., Shetler, P., Rowley, E.R., Magee, D.E., Pell, T., Zeng, G., Sato, M., Bryant, H.U., 1996. Distinct effects of selective estrogen receptor modulators on estrogen dependent and estrogen independent human breast cancer cell proliferation. J. Bone Miner. Res. 11 (Suppl. 1), S482.

Shugrue, P.J., Merchenthaler, I., 2001. Distribution of estrogen receptor immunoreactivity in the central nervous system. J. Comp. Neurol. 43, 64–81.

Shumaker, S.A., Legault, C., Rapp, S.R., Thai, L., Wallace, R.B., Ockene, J.K., Hendrix, S.L., Jones, B.N., Assaf, A.R., Jackson, R.D., Kotchen, J.M., Wassertheil-Smoller, S., Wactawski-Wende, J., 2003. Estrogen plus progestin and the incidence of dementia and mild cognitive impairment in postmenopausal women: a randomized controlled trial. J. Am. Med. Assoc. 289, 2651–2662.

Shumaker, S.A., Legault, C., Kuller, L., Rapp, S.R., Thai, L., Lane, D.S., Fillet, H., Stefanick, M.L., Hendrix, S.L., Lewis, C.E., Masaki, K., Coker, L.H., 2004. Conjugated equine estrogens and incidence of probable dementia and mild cognitive impairment in postmenopausal women: Women's health initiative memory study. J. Am. Med. Assoc. 291, 2947–2958.

Shushan, A., Peretz, T., Uziely, B., Lewin, A., Mor-Yosef, S., 1996. Ovarian cysts in premenopausal and postmenopausal tamoxifen-treated women with breast cancer. Am. J. Obstet. Gynecol. 175 (Pt 1), 752–753.

Siefer, D.B., Roa-Pena, L., Keefe, D.L., Zhang, H., Goodman, S., Jones, E.E., Naftolin, F., 1994. Increasing hypothalamic arcuate nucleus glial peroxidase activity in aging female rats is reduced by an antiestrogen and a gonadotropin-releasing hormone agonist. Menopause 1, 83–90.

Silfen, S.L., Ciaccia, A.V., Bryant, H.U., 1999. Selective estrogen receptor modulators: tissue specificity and differential uterine effects. Climacteric 2, 268–283.

Silverman, S.L., Christiansen, K., Genant, H.K., Zanchetta, J.R., Valter, L., de Villiers, T.J., Constantine, G., Chines, A.A., 2007. Efficacy of bazedoxifene in reducing new vertebral fracture risk in postmenopausal women with osteoporosis from a 3–year randomized, placebo- and active-controlled trial. J. Bone Miner. Res. 22 (Suppl. 1), S58.

Simard, J., Labrie, C., Belanger, A., Ganther, S., Singh, S.M., Merand, Y., Labrie, F., 1997. Characterization of the effects of the novel non-steroidal antiestrogen EM-800 on basal and estrogen-induced proliferation. Int. J. Cancer 73, 104–112.

Simpkins, J.W., Rajakumar, G., Zhang, Y.Q., Simpkins, C.E., Greenwald, D., Yu, C.J., Bodor, N., Day, A.L., 1997. Estrogens may reduce mortality and ischemic damage caused by middle cerebral artery occlusion in the female rat. J. Neurosurg. 87, 724–730.

Smith, M.R., 2006. Treatment related osteoporosis in men with prostate cancer. Clin. Cancer Res. 12, 6315S–6319S.

Smith, L.J., Henderson, J.A., Abell, C.W., Bethea, C.L., 2004. Effects of ovarian steroids and raloxifene on proteins that synthesize, transport and degrade serotonin in the raphe region of macaques. Neuropsychopharmacology 29, 2035–2045.

Snyder, K.R., Sparano, N., Malinowksi, J.M., 2000. Raloxifene hydrochloride. Am. J. Health Syst. Pharm. 57, 1669–1678.

Spencer, C.P., Godsland, I.F., Stevenson, J.C., 1997. Is there a postmenopausal metabolic syndrome? Gynecol. Endocrinol. 11, 341–355.

Stamatelopoulos, K.S., Lekakis, J.P., Poulakaki, N.A., Papamichael, C.M., Venetsanou, K., Aznaouridis, K., Protogerou, A.D., Papaioannou, T.G., Kumar, S., Stamatelopoulos, S.F., 2004. Tamoxifen improves endothelial function and reduces carotid intima-media thickness in postmenopausal women. Am. Heart J. 147, 1093–1099.

Stampfer, M.J., Colditz, G.A., 1991. Estrogen replacement therapy and coronary disease: a quantitative assessment of the epidemiological evidence. Prev. Med. 20, 47–63.

Stefanick, M.L., Anderson, G.L., Margolis, K.L., Hendriz, S.L., Rodabough, R.J., Paskett, E.D., Lane, D.S., Hubbell, F.A., Assaf, A.R., Sarto, G.E., Schenken, R.S., Yasmeen, S., Lessin, L., Shlebowski, R.T., 2006. Effects of conjugated equine estrogens on breast cancer and mammography screening in postmenopausal women with hysterectomy. J. Am. Med. Assoc. 295, 1647–1657.

Stovall, D.W., Utian, W.H., Gass, M.L.S., Qu, Y., Muram, D., Wong, M., Plouffe, L., 2007. The effects of combined raloxifene and oral estrogen on vasomotor symptoms and endometrial safety. Menopause 14, 510–517.

Suh, N., Glasebrook, A.G., Palkowitz, A.D., Bryant, H.U., Burris, L.L., Starling, J.J., Pearce, H.L., Williams, C., Peer, C., Wang, Y., Sporn, M.B., 2001. Arzoxifene, a new selective estrogen receptor modulator for chemoprevention of experimental breast cancer. Cancer Res. 61, 8412–8415.

Sumner, B.E.H., Grant, K.E., Rosie, R., Hegele-Hartung, C., Fritzemeier, K.H., Fink, G., 1999. Effects of tamoxifen on serotonin transporter and 5-hydroxytryptamine 2 A receptor binding sites and mRNA levels in the brain of ovariectomized rats with or without acute estradiol replacement. Mol. Brain Res. 73, 119–128.

Sun, J., Meyers, M.J., Fink, B., Rajendran, R., Katzenellenbogen, J.A., Katzenellenbogen, B.S., 1999. Novel ligands that function as selective estrogens or antiestrogens for estrogen receptor-alpha or estrogen receptor-beta. Endocrinology 140, 800–804.

Swisher, D.K., Tague, R.M., Seyler, D.E., 1995. Effect of the selective estrogen receptor modulator raloxifene on explanted uterine growth in rats. Drug Dev. Res. 36, 43–45.

Thigpen, T., Brady, M.F., Homesley, H.D., Soper, J.T., Bell, J., 2001. Tamoxifen in the treatment of advanced or recurrent endometrial carcinoma: a gynecologic oncology group study. J. Clin. Oncol. 19, 364–367.

Tiitinen, A., Nikander, E., Hietanen, P., Metsa-Heikkila, M., Ylikorkala, O., 2004. Changes in bone mineral density during and after 3 years use of tamoxifen or toremifene. Maturitas 48, 321–327.

Tsang, S.Y., Yao, X., Essin, K., Wone, C.M., Chan, F.L., Gollasch, M., Juang, Y., 2004. Raloxifene relaxes rat cerebral arteries in vitro and inhibits L-type voltage-sensitive Ca11channels. Stroke 35, 1709–1714.

Turner, C.H., Sato, M., Bryant, H.U., 1994. Raloxifene preserves bone strength and bone mass in ovariectomized rats. Endocrinology 135, 2001–2005.

Turner, R.T., Evans, G.L., Sluka, J.P., Adrian, M.D., Bryant, H.U., Turner, C.H., Sato, M., 1998. Differential responses of estrogen target tissues in rats including bone to clomiphene, enclomiphene, and zuclomiphene. Endocrinology 139, 3712–3720.

Uusi-Rasi, K., Beck, T.J., Semanick, L.M., Daphtary, M.M., Crans, G.G., Desaiah, D., Harper, K.D., 2006. Structural effects of raloxifene on the proximal femur: results from the multiple outcomes of raloxifene evaluation trial. Osteoporos. Int. 17, 575–586.

Vanacker, J., Pettersson, K., Gustafsson, J.A., Ladet, V., 1999. Transcriptional targets shared by ERRs and ER alpha but not ER beta. EMBO J. 18, 4270–4279.

Viereck, V., Grundker, C., Blaschke, S., Niederkleine, B., Siggelkow, H., Frosck, K.-H., Raddatz, D., Emons, G., Hofbauer, L.C., 2003. Raloxifene concurrently stimulates osteoprotogerin and inhibits interleukin-6 production by human trabecular osteoblasts. J. Clin. Endocrinol. Metab. 88, 4206–4213.

Viscoli, C.M., Brass, L.M., Kernan, W.N., Sarrel, P.M., Suissa, S., Horwitz, R.I., 2001. A clinical trial of estrogen-replacement therapy after ischemic stroke. N. Engl. J. Med. 345, 1243–1249.

Vogel, V.G., Costantino, J.P., Wickerham, D.L., Cronin, W.M., Cecchini, R.S., Atkins, J.N., Bevers, T.B., Fehrenbacher, L., Pajon, E.R., Wade, J.L., Robidoux, A., Margolese, R.G., James, J., Lippman, S.M., Runowicz, C.D., Ganz, P.A., Reis, S.E., McCaskill-Stevens, W., Ford, L.G., Jordan, V.C., Wolmark, N., 2006. Effects of tamoxifen vs raloxifene on the risk of developing invasive breast cancer and other disease outcomes: the NSABP study of tamoxifen and raloxifene (STAR) P-2 trial. J. Am. Med. Assoc. 295, 2727–2741.

Wakeling, A.E., Valcaccia, B., 1987. Antiestrogenic and antitumor activities of a series of non-steroidal antiestrogens. J. Endocrinol. 99, 455–464.

Walsh, B.W., Kuller, L.H., Wild, R.A., Paul, S., Farmer, M., Lawrence, J.B., Shah, A.S., Anderson, P.W., 1998. Effects of raloxifene on serum lipids and coagulation factors in healthy postmenopausal women. J. Am. Med. Assoc. 279, 1445–1451.

Walsh, B.W., Paul, S., Wild, R.A., Dean, R.A., Tracy, R.P., Cox, D.A., Anderson, P.W., 2000. The effects of hormone replacement therapy and raloxifene on C-reactive protein and homocysteine in healthy postmenopausal women: a randomized-controlled trial. J. Clin. Endocrinol. Metab. 85, 214–218.

Wang, X.N., Simmons, H.A., Salatto, C.T., Cosgrove, P.G., Thompson, D.D., 2006. Lasofoxifene enhances vaginal mucus formation without causing hypertrophy and increases estrogen receptor beta and androgen receptor in rats. Menopause 13, 609–620.

Ward, A., Bates, P., Fisher, R., Richardson, L., Graham, C.F., 1994. Disproportionate growth in mice with IGF-2 transgenes. Proc. Natl. Acad. Sci. U.S.A. 91, 10365–10369.

Wiernicki, T., Glasebrook, A.L., Phillips, D.L., Singh, J.P., 1996. Estrogen and a novel tissue selective estrogen receptor modulator raloxifene directly modulate vascular smooth muscle cell functions: Implications in the cardioprotective mechanism of estrogen. Circulation 94 (8 Suppl. I), I278.

Writing Group for Women's Health Initiative Investigators, 2002. Risks and benefits of estrogen plus progestin in healthy postmenopausal women. J. Am. Med. Assoc. 288, 321–333.

Wu, X., Glinn, M.A., Ostrowski, N.L., Su, Y., Ni, B., Cole, H.W., Bryant, H.U., Paul, S.M., 1999. Raloxifene and estradiol benzoate both fully restore hippocampal choline acetyltransferase activity in ovariectomized rats. Brain Res. 847, 98–104.

Yaffe, K., Sawaya, G., Liebergurg, I., Grady, D., 1998. Estrogen therapy in postmenopausal women: effects on cognitive function and dementia. J. Am. Med. Assoc. 279, 688–695.

Yaffe, K., Krueger, K., Sarkar, S., Grady, D., Barrett-Connor, E., Cox, D.A., Nickelsen, T., 2001. Cognitive function in postmenopausal women treated with raloxifene. N. Engl. J. Med. 344, 1207–1213.

Yaffe, K., Krueger, K., Cummings, S.R., Blackwell, T., Henderson, V.W., Sarkar, S., Ensrud, K., Grady, D., 2005. Effect of raloxifene on prevention of dementia and cognitive impairment in older women: The Multiple Outcomes of Raloxifene Evaluation (MORE) randomized trial. Am. J. Psychiatry 162, 683–690.

Zhang, J.J., Jacob, T.J.C., Valverde, M.A., Hardy, S.P., Mintenig, G.M., Sepulveda, F.V., Gill, D.R., Hyde, S.C., Trezise, A.E.O., Higgins, C.F., 1994. Tamoxifen blocks chloride channels: a possible mechanism for cataract formation. J. Clin. Investig. 94, 1690–1697.

Zuckerman, S.H., Bryan, N., 1996. Inhibition of LDL oxidation and myeloperoxidase dependent tyrosyl radical formation by the selective estrogen receptor modulator raloxifene. Atherosclerosis 126, 65–75.

Chapter 38

Thyroid hormone and bone

Peter A. Lakatos[1,a], Bence Bakos[1,a], Istvan Takacs[1] and Paula H. Stern[2]

[1]1st Department of Medicine, Semmelweis University Medical School, Budapest, Hungary; [2]Department of Pharmacology, Northwestern University Feinberg School of Medicine, Chicago, IL, United States

Chapter outline

Introduction

Thyroid hormone is essential for skeletal development and also affects mature bone. Depending on the hormone concentration and stage of life, the effects of thyroid hormone can be either beneficial or deleterious to the skeleton. This chapter focuses on the intracellular and cellular effects of thyroid hormone on bone cells as well as its relationship to the observed effects of the hormone on the skeleton in vivo in both experimental animals and humans. Studies published since the previous edition provide information on thyroid hormone effects on additional genes of interest in osteoblasts and further assessment of the skeletal risks of excess thyroid hormone.

New data regarding nuclear and nongenomic actions of thyroid hormone are discussed. These aspects of hormone effects are accompanied by an expansion of the section on in vivo responses of the skeleton to thyroid function alterations including subclinical conditions.

Intracellular mechanism of thyroid hormone action

Nuclear actions of thyroid hormones

Thyroid hormone receptors (TRs) are members of the nuclear receptor (NR) superfamily (Germain et al., 2006). All of these receptors share a common modular structure with a centrally located DNA-binding domain composed of two zinc fingers, an amino-terminal A/B domain involved in transcription modulation, and a carboxy-terminal ligand-binding domain that is also involved in receptor dimerization and interactions with coactivators and corepressors. TRs are

[a]participated equally in the work.

Principles of Bone Biology. https://doi.org/10.1016/B978-0-12-814841-9.00038-5

nuclear proteins capable of binding to cognate DNA elements in the absence of their ligands. Binding of the ligand to the receptor alters the receptor conformation and subsequently enables the activation or repression of specific genes.

Thyroid hormone response elements (TREs) in the promoters of T3 target genes share a common hexanucleotide "half-site" sequence of (A/G)GGT(C/A/G)A. Pairs of this structure may occur as direct, everted, or inverted repeat. Promoters of certain genes have clusters of TREs with differing structures (Yen, 2001).

Activated TRs bind to TREs in the target genes' promoter either as monomer, homodimer, or as heterodimer formed with other members of the NR superfamily. These latter include the vitamin D receptor, retinoid X receptor, and retinoic acid receptors. Heterodimerization is an important modulatory mechanism of TR function and also a means of cross talk with other signaling pathways. In bone (Williams et al., 1994, 1995), as in other tissues (Glass, 1994; Brent et al., 1991), DNA binding and transcriptional activation are enhanced when the thyroid hormone receptor isoforms are present as heterodimers with retinoid or vitamin D receptors. In osteoblast cell lines, interactions among the retinoid, vitamin D, and thyroid hormone ligands appeared to mediate specific responses (Williams et al., 1994, 1995). Studies on the effects of treatment combinations on the expression of osteoblast phenotypic genes in the cell lines revealed complex responses that indicated the importance of dose, treatment duration, and degree of confluence in dictating the magnitude of response (Williams et al., 1995). In primary rat osteoblastic cells, alteration of the ligand combinations did not influence the responses (Bland et al., 1997).

In addition to differences between TREs of specific genes, variations of TR dimerization patterns and tissue-specific and developmental stage-dependent expression of different TR isoforms (discussed later), as well as cellular response to thyroid hormones, are also altered by a number of different nuclear coregulator proteins.

Coactivator proteins that bind to the liganded TR are members of the SRC/p160 family (McKenna et al., 1999; McKenna and O'Malley, 2002) or the TR-associated protein (TRAP) complex (Sharma and Fondell, 2002; Burakov et al., 2002). Besides enhancing transcriptional activity, SRC/p160 proteins such as steroid hormone receptor CoA are characterized by histone acetyltransferase activity.

Thyroid hormone receptors have a dual functionality and may act as repressors on the TRE in the absence of T3. This process is mediated by the interaction of the TR with corepressor proteins including nuclear receptor corepressor, silencing mediator of retinoid and thyroid hormone receptor, Sin3, and histone deacetylases (Torchia et al., 1998; Yen et al., 2006). This results in the condensation of chromatin structure and repression of transcription through decreased access of transcription factors (Koenig, 1998; Wu and Koenig, 2000).

TRs are products of two genes located on two different chromosomes. The TRα gene found on chromosome 17 encodes one isoform (TRα1) with T3 binding capacity, and two C-terminal splice variants (TRα2, TRα3) lacking it (Izumo and Mahdavi, 1988; Chassande et al., 1997). Truncated variants of the TRα1 isoform (TRΔα1, TRΔα2), retaining T3 binding capacity but missing the A/B domain, also exist (Plateroti et al., 2001).

Three T3 binding isoforms (TRβ1, TRβ2, TRβ3) varying only in the A/B domain are encoded by the TRβ gene situated on chromosome 3 (Williams, 2000). TRΔβ3 has T3 binding activity but lacks both the A/B and DNA binding domains.

TR isoforms are expressed in a complex, tissue, and developmental stage-dependent manner, suggesting functional differences between subtypes. TRα1 is constitutionally expressed during embryonic development and is subsequently the dominant TR isoform in the brain, heart, and bone (Vella and Hollenberg, 2017). TRβ is identified as the major isoform in the liver, kidneys, ears, retinas, the hypothalamus, pituitary, and thyroid. Differences in function between TR subtypes are confirmed by studies of thyroid hormone resistance in humans and genetically engineered mice models.

In skeletal tissues, mRNAs for TRα1, TRα2, and TRβ are found in MG63, ROS 17/2.8, and UMR-106 cell lines (Williams et al., 1994; Allain et al., 1996). TRβ2 mRNA has been found in osteoblasts (Abu et al., 2000). mRNA for TRα1 was 12 times higher than TRβ1 mRNA in tibia and femur of 7-week-old male mice (O'Shea et al., 2003). TRα1, TRα2, TRβ1, and TRβ2 mRNAs were expressed in chondrocytes at all stages of differentiation. TRα1, TRα2, and TRβ1 mRNAs were highly expressed in osteoblasts at bone-remodeling sites; and mRNAs for all isoforms were present and highly expressed in multinucleated osteoclastic cells from an osteoclastoma (Abu et al., 1997). TRα1, TRα2, and TRβ1 mRNA have also been detected in rat femurs and vertebrae (Milne et al., 1999). Immunohistochemical staining with antibodies recognizing a TRα epitope or specific TRα2 and TRβ revealed the presence of receptor protein in osteoblast cell lines and in osteoclasts in tissue smears from a human osteoclastoma (Allain et al., 1996). In contrast to mRNA expression, TRα1 protein expression was not seen in the osteoclastoma cells and was limited to osteoblasts at sites of remodeling and undifferentiated chondrocytes (Abu et al., 2000).

The syndrome of resistance to thyroid hormones (RTH) caused by dominant-negative mutations of the TRβ gene was recognized as early as 1967. Over 3000 cases have occurred, and since the identification of the first causal genetic abnormality in 1989, over 120 different mutations have been documented. In contrast, similar mutations in the TRα gene, and corresponding conditions, have only been recognized since 2012 (Bochukova et al., 2012; van Mullem et al., 2012; Moran et al., 2013).

RTHβ is characterized by an autosomal dominant inheritance, elevated thyroid hormone, and unsuppressible TSH levels. Symptoms manifest with variable expressivity and include short stature, decreased weight, goiter, cognitive impairment, tachycardia, and hypacusis. All reported cases except one are genetically heterozygous. The mutations are clustered and largely located within domains in the carboxy-terminal region. They are mainly nucleotide substitutions that result in single amino acid changes (Refetoff et al., 1993). The mutant alleles act by a dominant-negative mechanism to inhibit the ability of the normal allele to elicit normal receptor function (Chatterjee et al., 1991; Sakurai et al., 1990). The dominant-negative action appears to be at the level of DNA binding (Kopp et al., 1996).

Skeletal alterations include retarded bone age and stippled epiphyses, similar to characteristics of hypothyroidism, with a resulting short stature. In other patients there is accelerated bone age, accelerated chondrocyte maturation, and early epiphyseal closure, again resulting in short stature (Behr et al., 1997). The target sites at which resistance occurs (pituitary or peripheral) may determine the phenotype.

Patients with RTHα present with normal levels of TSH accompanied by low/normal T4 and high/normal T3 concentrations and a decreased FT4/FT3 ratio. While cognitive and motor abnormalities often vary, skeletal development is markedly delayed. Disproportionate growth retardation, delayed bone age, patent skull sutures, macrocephaly, flattened nasal bridge, short stature, epiphyseal dysgenesis, and defective bone mineralization are reported (Tylki-Szymańńska et al., 2015). Radiographic features are suggestive of hypothyroidism. Phenotype is largely dependent on the severity of the underlying genetic abnormality, the resulting hormone binding potential, and dominant-negative activity of the TRα1 receptor. Consequently, the response to T4 treatment also varies between patients. A recent report detailed the case of a patient with a mutation affecting both TRα1 and TRα2 leading to a severe, atypical skeletal phenotype with intrauterine growth retardation, macrocephaly, hypertelorism, micrognathia, short and broad nose, clavicular and 12th rib agenesis, elongated thorax, ovoid vertebrae, scoliosis, congenital hip dislocation, short limbs, humeroradial synostosis, and syndactyly (Espiard et al., 2015).

A syndrome resulting in advanced bone age was associated with a mutation in the MCT8 thyroid hormone transporter gene (Herzovich et al., 2007). A single nucleotide change (Q261X) in exon 3 on the X chromosome resulted in low serum T4 and free T4, elevated serum T3 and free T3, slightly elevated TSH. The child had severe neurological abnormalities and normal growth, which had been previously noted in other patients with mutations in this gene (Dumitrescu et al., 2004).

Knockin mice models of RTH have helped shed more light on the roles of different TR isoforms in bone and other tissues (Kaneshige et al., 2001; O'Shea et al., 2006). Carrying a C-terminal frame-shift mutation derived from a patient with severe RTH, the TRβPV mouse has TRβ receptors that are dominant-negative antagonists incapable of transactivation and T3 binding. The resulting phenotype is consistent with human RTHβ, showing serum lipid abnormalities, growth retardation, hearing loss, neurological dysfunctions, and markedly elevated TSH and thyroid hormone levels.

The bone phenotype in these mice is reminiscent of skeletal thyrotoxicosis, with advanced endochondral and intramembranous ossification, premature closure of the growth plates, and shortened body length along with increased mineralization and craniosynostosis. The narrower growth plate appears to be a consequence of faster transition through the proliferative zone. Trabecular bone mass is also decreased with more resorption and a greater number of TRAP-positive cells. Expression of fibroblast growth factor receptor-1 (FGFR1), a skeletal T3-target gene, is increased.

Mice carrying PV and other types of dominant-negative mutations in the TRα1 gene were also created (Kaneshige et al., 2001; O'Shea et al., 2006; Quignodon et al., 2007; Bassett et al., 2014). With the TRα1PV protein being a dominant-negative antagonist of both TRα1 and TRβ, the mutation was lethal in homozygotes. Heterozygotes showed mild elevation in TSH levels, accompanied with normal FT3 and FT4. Bone phenotype was hypothyroid with growth retardation, wider growth plates, delayed intramembranous and endochondral ossification, transiently decreased bone calcification, decreased resorption, and TRAP-positive cells. FGFR1 expression and adult bone remodeling were also reduced.

These findings support TRβ being the predominant regulator of the negative feedback loop of the HPT axis. Changes in the skeleton of RTH patients and PV mice models suggest TRα1 to be the dominant TR isoform in bone.

Studies done with knockout mice also illustrate the complex roles of different TR isoforms. Hormone levels in TRα1−/− mice show mild central hypothyroidism with no gross impairments of skeletal development (Wikstrom et al., 1998; Gauthier et al., 1999; Gothe et al., 1999; Gloss et at., 2001). TRα2−/− animals have mild thyroid dysfunction with decreased peripheral hormone levels accompanied by normal TSH. Growth was not impaired, but adult bone density was decreased (Saltó et al., 2001).

TRα−/−, TRα1−/− TRβ−/−, and TRα−/− TRβ−/− animals exhibit different degrees of similarly impaired bone development with growth retardation, disorganized bone plates, and delayed endochondral ossification (Fraichard et al., 1997; Gauthier et al., 1999; Göthe et al., 1999). TRα−/− mice are hormonally hypothyroid while double-knockout mice lacking TRβ have increased TSH, T3, and T4 levels. TRα0/0 mice missing not just TRα1 and TRα2 but also TRΔα1 and

TRΔα2 transcripts are hormonally euthyroid. Similarly to TRα−/− mice, they exhibit growth retardation and delayed endochondral ossification but have increased adult BMD due to defective remodeling (Bassett et al., 2007).

TRβ−/− animals exhibit elevated TSH and thyroid hormone levels, and signs of skeletal thyrotoxicosis not unlike those seen with TRβPV mice. Accelerated endochondral and intramembranous ossification, advanced bone age, increased mineral deposition, persistent short stature, and later on progressive osteoporosis, are reported (Bassett et al., 2007).

Mice lacking DIO2, the activating deiodinase catalyzing the intracellular synthesis of T3 from T4, show pituitary resistance to T4 resulting in increased TSH, slightly elevated T4, and normal T3 levels. Though postnatal skeletal development and linear growth are normal in DIO2−/− mice, osteoblast function and bone formation in adulthood were shown to be severely impaired (Bassett et al., 2010).

Differential expression and only partial overlap in functions of TR isoforms allow for the development of thyroid hormone analogs that have tissue specificity owing to their preferential interaction with one receptor isoform. As previously outlined, TRβ1 is the predominant isoform in the liver and most peripheral tissues, while heart rate and bone metabolism are influenced mostly via TRα1. Potential benefits of selective TRβ1 agonists would be lowering of body weight, serum lipid, and cholesterol levels without deleterious cardiac or skeletal side effects. Selective and partial TRα1 agonists are hoped to produce positive inotropic cardiac effects while lowering peripheral resistance in heart failure patients. Though no selective TR agonist is in clinical use at the time of writing, several compounds are under different stages of development and investigation. Selective TRβ1 agonists of interest include kb-141 (Grover et al., 2003), GC1 (Chiellini et al., 2002), eprotirome (Ladenson et al., 2010), and tiratricol (Sherman et al., 1997). DITPA is a thyroid hormone analogue tested in the treatment of chronic heart failure (Goldman et al., 2009).

Nongenomic actions of thyroid hormones

Although high-affinity binding sites for thyroid hormones on the plasma membrane were identified as early as the 1980s, specific receptors on the cell membrane, in the cytoplasm, and in mitochondria have been established and their modes of action increasingly elucidated in recent years (see reviews by Davis et al., 2008, 2011, 2013, 2016). The effects are mediated through rapid activation of signaling pathways, leading in various tissues to increased nitric oxide (NO) synthase (Hiroi et al.), mitogen-activated protein kinase (MAPK) (Davis et al., 2000; Lei et al., 2008), and the Akt activator phosphatidylinositol-3-kinase (Hiroi et al., 2006; Moeller et al., 2006). Subsequent cellular responses can result from activation of nuclear transactivator proteins or the direct effects of signaling intermediates on the plasma membrane (Davis et al., 2016). The integrin $\alpha_v\beta_3$ acts as a low-affinity membrane receptor for thyroid hormone (Bergh et al., 2005), mediating angiogenic actions and effects on platelets and neurons as well as on bone cells (Davis et al., 2011). In human osteoblastic MG63 and SaOS2 cells, an $\alpha_v\beta_3$-blocking antibody inhibited thyroid hormone stimulation of the MAPK pathway and thymidine incorporation (Scarlett et al., 2008), suggesting a role of the pathway in bone formation. The resorptive effects of thyroid hormone may also involve $\alpha_v\beta_3$, based on the finding that a vitronectin receptor antagonist inhibited thyroxin-induced bone resorption (Hoffman et al., 2002). A novel high-affinity plasma membrane TRα associated with caveolin domains in human primary osteoblasts mediated the rapid effects of T3 on NO, cyclic guanosine monophosphate (cGMP), Src phosphorylation, and activation of MAPK and Akt, leading to cell proliferation and survival (Kalyanaraman et al., 2014). Hypothyroid mice exhibited cGMP deficiency with osteocyte apoptosis and impaired bone formation (Kalyanaraman et al., 2014). Treatment with T3 rapidly decreased Src Y416 autophosphorylation, thereby stimulating osteocalcin expression in primary calvarial osteoblasts from neonatal mice (Asai et al., 2009).

Rapid (within 30 s) increases in inositol mono-, bis-, and triphosphates were elicited by treatment of fetal rat limb bones with 100 nM and 1 μM T3 (Lakatos and Stern, 1991). The inactive analogs diiodothyronine and rT3 did not increase inositol phosphates. This effect of T3 was inhibited by indomethacin and could represent an initiation pathway for the prostaglandin-dependent effects of thyroid hormones on bone resorption, discussed later. Thyroid hormones at high doses inhibit cyclic AMP phosphodiesterase (Marcus, 1975). T3 at 0.1 and 1 nM increased ornithine decarboxylase and potentiated the responses of this enzyme to parathyroid hormone (PTH) (Schmid et al., 1986).

Thyrotropin as an independent agent of bone metabolism

In the past 10−15 years, thyrotropin (TSH) has been implicated as playing a direct regulatory role in many extrathyroidal tissues. TSH receptor (TSHR) expression has been established in the brain, the pituitary, orbital preadipocytes and fibroblasts, the kidney, ovary and testis, skin and hair follicles, heart, adipose tissue, hematopoietic and immune cells, and bone. In vitro and in vivo studies of TSH action suggest multifaceted regulatory functions as well as a role in disease states such as endocrine ophthalmopathy.

TSHR is expressed on chondrocytes, osteoblasts, and osteoclasts (Abe et al., 2003; Endo and Kobayashi, 2013). Besides systemic TSH, other potential local ligands have been implied for these receptors, such as Tshb, a splice variant expressed by bone marrow derived macrophages (Vincent et al., 2009), and thyrostimulin, a glycoprotein TSH-activating hormone expressed by both osteoblasts and osteoclasts (Bassett et al., 2015).

The physiologic role of TSHR in bone cells, the pathway downstream from the receptor, and the potential effects of TSH in bone metabolism are still contradictory. In certain studies, osteoblastogenesis, type I collagen-, bone sialoprotein-, and osteocalcin expression were inhibited in osteoblasts treated with TSH, presumably via the Wnt signal pathway (Abe et al., 2003). Others found a stimulatory effect on osteoblast differentiation and function on various cell lines and animal models (Sampath et al., 2007; Baliram et al., 2011; Boutin et al., 2014). In other studies the presence and physiologic function of TSHR on osteoblasts were proposed to be insignificant (Tsai et al., 2004; Bassett and Williams, 2008). Most findings point toward a potential inhibitory role of TSH on osteoclast function, an effect mediated primarily via TNFα (Hase et al., 2006; Ma et al., 2011; Sun et al., 2013; Zhang et al., 2014).

Intermittent low-dose TSH treatment of ovariectomized rats resulted in a decrease in resorption markers, an increase in formation markers, and an improvement in BMD and overall bone strength (Sampath et al., 2007; Sun et al., 2008; Dumic-Cule et al., 2014).

Genetically modified mice models investigating the roles of TSH on bone metabolism also reported somewhat conflicting results. TSHR knockout mice that have severe congenital hypothyroidism with extremely elevated TSH levels show growth retardation and BMD reduction with histomorphometric signs of increased bone turnover; though when supplemented with thyroid extract, these animals regain normal weight following a "catch-up" growth, while bone density and calvarial thickness remain reduced. Compared with the wild genotype, a 3-week treatment with supraphysiologic thyroxine resulted in increased bone loss in TSHR knockout animals. Furthermore, while Tshr ± mice are hormonally euthyroid, have normal formation and resorption marker levels, and normal calvarial thickness, BMD was still found to be slightly reduced at sites. These findings suggest that TSH has an inhibitory effect on bone remodeling (Abe et al., 2003; Baliram et al., 2012). Comparison of the skeletal phenotype of Pax8−/− and hyt/hyt mice, however, implies that TSH has no or a minimal effect on bone metabolism. The former have impaired thyroid development due to the lack of a critical transcription factor with resulting hypothyroidism, accompanied by a 2000-fold elevation in TSH levels but an intact TSHR (Mansouri et al., 1998). Hyt/hyt mice are characterized by a loss of function mutation of TSHR also resulting in hypothyroidism and extreme elevation of TSH levels (Beamer et al., 1981). Despite the fundamental difference in TSHR function, both mice models have similar defects of skeletal metabolism typical of severe hypothyroidism. Chondrocyte, osteoblast, and osteoclast activities are decreased while impaired linear growth, delayed endochondral ossification, reduced cortical bone mass, defective trabecular bone remodeling, and reduced bone mineralization are evident (Bassett and Williams, 2008).

Thyrostimulin deficient Gpb5−/− mice show an increase in infantile bone production that is resolved by adulthood (Bassett et al., 2015). However, somewhat contrary to this finding, in vitro treatment of osteoblasts thyrostimulin resulted in no notable change in differentiation or function.

Cellular effects of thyroid hormones on the bone

Thyroid hormones exert a complex, developmental stage, and dose-dependent influence on bone formation, growth, and remodeling, affecting several critical constituents of skeletal metabolism. As we have previously discussed, the dominant TR isoform in the bone is TRα1. While compared with TRβ it is present in bone cells at 10-fold higher levels (O'Shea et al., 2003), recent studies also suggest a role for the latter (Monfoulet et al., 2011). Thyroid receptors are most notably present on reserve zone and proliferating chondrocytes (Ballock et al., 1999; Robson et al., 2000; Stevens et al., 2000), osteoblasts, and osteoblastic bone marrow stromal cells (Rizzoli et al., 1986; Allain et al., 1996; Milne et al., 1999; Siddiqi et al., 2002). Their presence and role on osteocytes and osteoclasts are still unclear (Bassett and Williams, 2003). Differentiated chondrocytes have no TR expression.

The activating deiodinase DIO2, a catalyzing intracellular formation of T3 from T4, is expressed primarily in osteoblasts (Bassett et al., 2010), and in animal models has been demonstrated to be present from early embryonal stages of skeletal development (Gouveia et al., 2005; Capelo et al., 2008). The inactivating DIO3 deiodinase has been found in all skeletal cell lines, with the highest activity in growth plate chondrocytes.

The presence of several thyroid hormone transport proteins such as MCT8, MCT10, LAT1, and LAT2 also has been demonstrated in growth plate chondrocytes, osteoblasts, and osteoclasts (Williams et al., 2008; Capelo et al., 2009; Abe et al., 2012).

Wide concentration ranges of thyroid hormones have been used in experimental studies, especially in vitro, and often markedly different dosages are required to obtain the same response in a different cell line, model system, or laboratory. The differentiation state and the production of modulating factors are potential variables that can affect the response in a given system. In addition, the presence of thyroid hormone in the added sera or the presence of binding sites in stripped sera can dramatically influence the free hormone available to the cells or tissue. Several studies have estimated the amount of free hormone available under the experimental conditions used (Sato et al., 1987; Allain et al., 1992). In one study, an equilibrium dialysis method was used to determine free T4 and T3 after treating fetal calf serum with AG1-X8 resin (Sato et al., 1987). T4 and T3 concentrations in the fetal calf serum prior to extraction were 11.1 μg/dL and 157 ng/dL, respectively. It was determined that the addition of 10 nM T4 to the stripped serum provided 80 p.m. free T4, and that addition of 1 nM T3 provided 40 p.m. free T3. In the other study, in which 10% neonatal calf serum was used, the free T3 was measured by radioimmunoassay (Allain et al., 1992). It was determined that the addition of 10 p.m. T3 yielded a free T3 concentration of 2.1 p.m., that 0.1 nM yielded 4 p.m., that 1 nM yielded 2.1 p.m., and that 10 nM yielded 0.39 p.m. (Allain et al., 1992). Although the type and percentage of serum would influence the final values, these measurements and calculations are of value in comparing studies and in relating in vitro concentrations to the concentrations of thyroid hormones in normal serum.

Osteoblasts

T3 may produce varying responses in osteoblasts in vitro depending on species, anatomical origin of cells, stage of differentiation, passage number, cell confluence, dose of T3, and duration of treatment (Rizzoli et al., 1986; Williams et al., 1994; Cray et al., 2013). Most results suggest a stimulating role of T3 on osteoblast proliferation (Ernst and Froesch, 1987; LeBron et al., 1989; Luegmayr et al., 1996), differentiation (Ohishi et al., 1994; Klaushofer et al., 1995), and function (Fratzl-Zelman et al., 1997).

T3 can increase proliferation of rodent and human osteoblastic cells (Ernst and Froesch, 1987; Kassem et al., 1993). In the rodent cell cultures, 0.01 and 1 nM were stimulatory, and 10 nM was inhibitory in longer term cultures (Ernst and Froesch, 1987). Cell number was decreased after 8 days of incubation with T4 in MC3T3-E1 cells; inhibition was observed with 10 nM T3 and was maximal at 1 μM (Kasono et al., 1988). In other investigations, T3 did not significantly affect the growth of ROS 25/1, UMR-106, and ROS 17/2.8 cells (Sato et al., 1987; LeBron et al., 1989; Williams et al., 1994).

In response to T3 treatment, an increase is seen in the expression of osteoblastic phenotypic markers, such as osteocalcin (Gouveia et al., 2001; Varga et al., 2003), osteoprotegerin (Varga et al., 2004), osteopontin, type I collagen (Kawaguchi et al., 1994a; Varga et al., 2010), and alkaline phosphatase (Sato et al., 1987; Kasono et al., 1988; Banovac and Koren, 2000). Effects are seen at concentrations in the physiologic range; however, the dose-dependence of the response is quite variable and may be dependent on cell type and culture conditions. Levels of IL-6, IL -8, MMP9, MMP13 (Varga et al., 2009), and tissue inhibitor of metalloproteinase-1 are also elevated, as are IGF-1, IGFBP-2, -3, and -4, and FGFR1, which are thought to be major secondary mediators of T3-mediated osteoblast activation (Schmid et al., 1992; Varga et al., 1994; Glantschnig et al., 1996; Huang et al., 2000; Stevens et al., 2003). IGF-I has significant anabolic effects on bone, increasing cell replication and both collagen and noncollagen protein synthesis (Canalis, 1980; Hock et al., 1986; McCarthy et al., 1989; Centrella et al., 1990; Pirskanen et al., 1993). T3 increased IGF-I expression more markedly in cells from vertebral marrow than in cells from femoral marrow (Milne et al., 1998). Interference with IGF-I action by decreasing expression or function of the IGF-I receptor by the use of antisense oligonucleotides, antibodies, and antagonist peptide decreased the anabolic effects of T3 on MC3T3-E1 cells and primary mouse calvarial osteoblasts, including effects on alkaline phosphatase, osteocalcin, and collagen synthesis (Huang et al., 2000). The effects of thyroid hormones on IGFs may be modulated by changes in IGF-binding proteins (IGFBPs). The physiological role of IGFBPs is not fully understood; however, they can influence the cellular uptake and turnover of IGF-I.

Treatment of osteoblasts with T3 stimulated expression of FGFR1 mRNA and protein (Stevens et al., 2003). PTH and PTHrp receptors are also upregulated in response to T3 treatment in osteoblastic cell lines (Schmid et al., 1986; Gu et al., 2001). Osteoblastic cell morphology, cytoskeleton formation, and cell adhesion molecules also respond to T3 stimulus in vitro (Luegmayr et al., 1996, 2000; Fratzl-Zelman et al., 1997).

Osteoclasts

T3 stimulates resorption in bone organ cultures. Fetal rat limb bones (Mundy et al., 1976; Hoffmann et al., 1986; Lakatos and Stern, 1992) and neonatal mouse calvaria (Krieger et al., 1988; Klaushofer et al., 1989; Kawaguchi et al., 1994) are the models that have been studied most extensively. Compared with the effects of PTH, T3 responses are slower to develop,

with the dose–response curves being generally shallow (Mundy et al., 1976; Krieger et al., 1988; Klaushofer et al., 1989; Kawaguchi et al., 1994b), and maximal effects are lower. Further evidence for the differing actions of T3 and PTH is supplied by the contrast in their interaction with TGFβ (Lakatos and Stern, 1992). TGFβ enhanced the early responses to PTH and inhibited later effects, whereas interaction with T3 displayed a somewhat reversed time course.

It is still unclear whether the increased osteoclastogenesis and bone resorption seen in vitro in response to T3 and in vivo in thyrotoxicosis is mediated by a direct effect of T3 on osteoclasts or is exclusively secondary to changes in the function of osteoblast, stromal osteocytes, or other bone marrow cells (Mundy et al., 1976; Klaushofer et al., 1989). T3 failed to activate isolated osteoclasts; however, when mixed bone cells were added to the cultures, a significant response was observed with 1 μM T3, although not with lower concentrations (Allain et al., 1992).

Various osteoblast-derived secondary mediators, growth factors, and cytokines have been implicated. In neonatal mouse calvaria, resorption was inhibited by indomethacin, suggesting a prostaglandin-dependent pathway (Krieger et al., 1988; Klaushofer et al., 1989; Kawaguchi et al., 1994b). Other studies have shown prostaglandin-independent effects (Conaway et al., 1998) involving other mediators, such as the RANKL/OPG pathway (Varga et al., 2004), IGF-1 (Stracke et al., 1986; Lakatos et al., 1993),TGFβ (Lakatos and Stern, 1992; Klaushofer et al., 1995), interleukins (Tarjan et al., 1995; Siddiqi et al., 1998; Schiller et al., 1998), and interferon-γ.

Remodeling

Most in vitro studies have focused on either anabolic or catabolic effects of thyroid hormone under conditions designed to optimize the study of the particular response. However, because there are dose-dependent biphasic effects on formation parameters and delayed (Klaushofer et al., 1989) and submaximal (Mundy et al., 1976; Krieger et al., 1988; Lakatos and Stern, 1992) effects on resorption, it may be that neither effect can be studied to the exclusion of the other, and the net effects on bone remodeling may be accessible to in vitro investigation. A model system designed to study growth, mineralization, and resorption in radii and ulnae of 16-day fetal mice (Soskolne et al., 1990) revealed interesting differences between effects of T3 and PTH. Effects of T3 were studied over a 0.1nM–10μM dose range. T3 concentrations in the 10nM–0.3 μM range resulted in increases in diaphyseal length, increased calcium, phosphate, and hydroxyproline content, and decreased 45Ca release. At higher concentrations (1 and 10 μM), T3 stimulated 45Ca release. In contrast, when PTH was studied over a 1pM–0.1 μM range, only resorptive effects were observed, these being at concentrations of 1 nM and higher.

Chondrocytes

Thyroid hormones exert a complex regulatory effect on chondrocyte function including proliferation, matrix synthesis, mineralization, chondrocyte maturation, endochondral ossification, and linear bone growth. In different cultures, T3 is mostly shown to inhibit chondrocyte proliferation, induce hypertrophic differentiation, and help sustain the structure and ossification of epiphyseal cartilage (Burch et al., 1982a, 1982b; Böhme et al., 1992; Quarto et al., 1992; Ballock et al., 1994; Alini et al., 1996; Ishikawa et al., 1998; Rosenthal et al., 1999; Miura et al., 2002). T3 was approximately 50 times more potent than T4 in promoting expression of the hypertrophic markers in prehypertrophic chondrocytes in cells cultured with insulin/transferrin/selenium (Alini et al., 1996). There was a biphasic dose-dependency of the effects of T3 and T4 to stimulate the synthesis of type II collagen and chondroitin sulfate-rich proteoglycans in cultured rabbit articular chondrocytes (Glade et al., 1994). The shift toward hypertrophic phenotype is mainly mediated via the upregulation of cyclin-dependent kinase inhibitors (Ballock et al., 2000). T3 also stimulates the synthesis of extracellular matrix proteins and enzymes involved in mineralization and matrix degradation including collagen X, matrix proteoglycans, ALP, MMP13, and aggrecanase-2.

In vivo responses of the skeleton to thyroid hormones: animal studies

Hypothyroidism

Animal models of hypothyroidism include the use of the antithyroid agents propylthiouracil and methimazole to block the synthesis of thyroid hormones. Treatment of young rats with methimazole for 7 weeks resulted in a marked increase in trabecular bone volume of the subchondral spongiosa of the mandibular condyles and a decrease in cartilage cellularity (Lewinson et al., 1994). IGF-I was present in the condyles of control rats but lacking in hypothyroid rats. Replacement of T4 during the last 2 weeks of treatment restored the parameters to normal (Lewinson et al., 1994). Histomorphometric

studies in iliac crest biopsies of young rats made hypothyroid by a 12-week treatment with propylthiouracil showed that both osteoid surfaces and eroded surfaces were reduced, and cancellous bone volume was increased (Allain et al., 1995). In a study in which 21-day rats were made hypothyroid by administration of methimazole, T4 given daily at doses of 2−64 μg/kg/day for 21 days elicited biphasic effects on epiphyseal growth plate width and longitudinal growth rate (Ren et al., 1990). The dose−response curve paralleled that of serum IGF-I concentrations, which were postulated to contribute to the growth responses (Ren et al., 1990). An interesting animal model for hypothyroidism utilizes transgenic mice (line TG66-19) in which the bovine thyroglobulin promoter drives the expression of the herpes simplex type I virus thymidine kinase gene in thyrocytes. This enzyme converts ganciclovir to ganciclovir-59-phosphate, which inhibits DNA replication, resulting in loss of thyrocytes, loss of follicles, and undetectable T3 and T4; levels of PTH and CT are unaffected (Wallace et al., 1991, 1995). In this transgenic mouse model, administration of 15 or 50 μg of ganciclovir to mouse dams during days 14−18 of gestation resulted in growth delay in pups carrying the transgene (Wallace et al., 1995). The authors point out that the reason their effects were more dramatic than those obtained with the hyt/hyt mouse, a strain that has an inactivating mutation in the TSH receptor, is that in the latter model, circulating T4 is still 10%−20% of normal (Adams et al., 1989). Effects of mutations in thyroid hormone receptors in mouse models were discussed earlier.

Hyperthyroidism

A range of T4 regimens has been used to elicit hyperthyroidism in animal models. The duration of treatment is generally at least 3 weeks and dosages range from 200 μg to 1 g per day. Lower concentrations have been used in animals previously made hypothyroid with antithyroid drugs (Lewinson et al., 1994). When thyroid hormones are administered to young rats, bone growth is enhanced (Glasscock and Nicoll, 1981). This response is not seen in older rats, suggesting that the stage of cellular differentiation or the environment in terms of other hormones and local factors can influence the manifestation of thyroid hormone responses. T3 treatment of neonatal rats elicited a narrowing of the sagittal suture and increased mineral apposition rates at the osseous edges of the sutures (Akita et al., 1994). Histomorphometric analysis was consistent with the conclusion that T3 is critical for bone remodeling (Allain et al., 1995). When the animals were rendered hyperthyroid by treatment with T4 (200 μg/day for 12 weeks), the mineral apposition and formation rates were increased markedly, with a smaller increase in eroded surfaces (Allain et al., 1995). A greater sensitivity of cortical bone (femur) than trabecular bone (spine) to thyroid hormone-induced bone loss has been noted in animal models of hyperthyroidism (Ongphiphadhanakul et al., 1993; Suwanwalaikorn et al., 1996, 1997; Gouveia et al., 1997; Zeni et al., 2000). Tooth movement was greater in T3-treated rats undergoing orthodontic procedures than in control untreated animals, probably reflecting greater root resorption (Shirazi et al., 1999). Rats at 10 days old, treated with 100 μg/kg/day for up to 60 days, displayed altered parameters of cranial width, narrowing of the suture gap of the sagittal suture, and intense immunohistochemical staining for IGF-I along the suture margins, consistent with the possibility that local IGF-I is involved in the effect of thyroid hormone to cause premature suture closure (Akita et al., 1996). Ovariectomized rats treated with a low dose of T4 (30 μg/kg/day for 12 weeks) showed increased bone turnover and decreased bone density compared with controls; however, in the presence of 17β-estradiol, their bone mass and mineral apposition rate were greater than those of controls (Yamaura et al., 1994). T4 (250 μg/kg/day for 5 weeks) increased serum osteocalcin and urinary pyridinoline and produced a greater loss of bone mineral compared with either ovariectomy or T4 alone (Zeni et al., 2000). In contrast to the effects of these high doses of T4, administration of a more physiological concentration (10 μg/kg/day) to ovariectomized rats resulted in a generalized increase in bone mineral density at both lumbar and vertebral sites (Gouveia et al., 1997). Estradiol prevented T3-stimulated decreases in bone mineral density in ovariectomized thyroidectomized rats, but had no effect in animals that were not treated with T3 (DiPippo et al., 1995). These results raise the possibility of cross talk at the level of binding of estradiol and T3 receptors to DNA target sites.

Pathophysiological effects of altered thyroid hormone status in humans

Hypothyroidism

With an incidence of 1:1800, hypothyroidism is the most common congenital endocrine disorder, while primary hypothyroidism caused mostly by chronic autoimmune thyroiditis is the leading cause of hypothyroidism in childhood and adolescence. Approximately 2% of US adolescents have elevated TSH. Bone turnover is decreased in hypothyroidism (Mosekilde and Melsen, 1978), which in juvenile cases leads to abnormal endochondral ossification, delayed skeletal maturation and bone age, epiphyseal dysgenesis and short stature. Due to screening efforts in the Western world, the skeletal changes of untreated congenital hypothyroidism are rarely seen today. These might include complete cessation of

bone maturation, growth arrest and skeletal dysplasia with a broad face, broad flat nasal bridge, hypertelorism, persistently patent sutures, scoliosis, vertebral immaturity and absence of ossification centers, and congenital hip dislocation. In a study of children with congenital hypothyroidism treated with T4, the bone age at 1.5 years was correlated positively with the dose of T4 administered during the first year and with the concentrations of serum T4 (Heyerdahl et al., 1994).

Adult-onset hypothyroidism leads to reduced remodeling rates with both the activity of osteoblasts and osteoclasts decreased. To present date, there are only a few studies reporting on changes of bone turnover markers in adult hypothyroidism. Urinary pyridinium cross-links (Nakamura et al., 1996) and serum IGF-I (Lakatos et al., 2000) were shown to be reduced in these patients. Changes in bone volume and density are hard to assess, as no patient remains untreated for a significant enough time. Most data come from patients with restored euthyroidism. Nevertheless, low turnover seems to result only in no change or even a slight increase in bone volume and density (Paul et al., 1988; Stamato et al., 2000; Vestergaard et al., 2002; González-Rodríguez et al., 2013).

Consistent with the lack of significant changes in bone density, the few studies that are available suggest that hypothyroidism or elevated TSH does not increase fracture risk in itself. However, as detailed below, larger doses of T4 supplementation or frank overtreatment of hypothyroidism is shown to be an independent risk factor for fracture (Cummings et al., 1995; Melton et al., 2000; Van Den Eeden et al., 2003; Ahmed et al., 2006; Flynn et al., 2010).

Subclinical hypothyroidism

Subclinical hypothyroidism—that is, elevated TSH accompanied with thyroid hormone concentrations in the normal range—is extremely prevalent, especially among the elderly. While some degree of decline in bone turnover is demonstrable in these patients (Meier et al., 2004), no association was shown with changes in BMD or fracture risk (Waring et al., 2013; Garin et al., 2014; Blum et al., 2015). Current treatment recommendations do not include skeletal considerations.

Hyperthyroidism

With Graves' disease being the leading cause, thyrotoxicosis is much less common in infants and adolescents than hypothyroidism. It results in accelerated growth and skeletal development. Advanced bone age due to the increase in chondrocyte differentiation in the epiphyseal growth plates leads to early cessation of growth and persistent short stature (Schlesinger and Fisher, 1951; Saggese et al., 1990). In severe early onset cases, craniosynostosis might occur.

In adults, hyperthyroidism shortens the bone turnover cycle, leading to high turnover rates. Histomorphometric analyses show increased osteoclast numbers and resorbing surfaces, with loss of trabecular bone volume (Mosekilde and Melsen, 1978). Histomorphometric data yield a kinetic model demonstrating accelerated bone remodeling, with a disproportionately greater increase in resorption and a net loss of bone with each cycle of remodeling (Eriksen, 1986). Since the initial description of bone loss and the "worm eaten" appearance of long bones in thyrotoxicosis by von Recklinghausen (1891) more than a century ago, substantial additional evidence has shown that excessive thyroid hormone production can lead to bone loss. In patients with hyperthyroidism, markers of bone turnover are increased in correlation with disease severity. Pyridinoline and hydroxypyridinoline cross-link excretion are elevated (Harvey et al., 1991; Garnero et al., 1994; Nagasaka et al., 1997; Engler et al., 1999), as are urinary N-terminal telopeptide of type I collagen (Mora et al., 1999; Pantazi et al., 2000) and serum carboxyterminal-1-telopeptide (Loviselli et al., 1997; Miyakawa et al., 1996; Nagasaka et al., 1997). Evidence of activation of osteoblasts in hyperthyroidism is the elevation of alkaline phosphatase (Mosekilde and Christesen, 1977; Cooper et al., 1979; Martinez et al., 1986; Nagasaka et al., 1997; Pantazi et al., 2000), osteocalcin (Martinez et al., 1986; Lee et al., 1990; Mosekilde et al., 1990; Nagasaka et al., 1997; Loviselli et al., 1997; Pantazi et al., 2000), and carboxyterminal propeptide of type I procollagen (Nagasaka et al., 1997). Consistent with the molecular studies (Varga et al., 2004) showing that T3 increases OPG in osteoblastic cells, elevated OPG has been reported in patients with Graves' disease (Amato et al., 2004; Mochizuki et al., 2006). Greater increases in the resorption markers than the formation markers verify the imbalance between resorption and formation, leading to bone loss (Garnero et al., 1994; Miyakawa et al., 1996).

Decreases in bone mineral content are established by several studies (Fraser et al., 1971; Krolner et al., 1983; Toh et al., 1985; Guo et al., 1997; Udayakumar et al., 2006; Majima et al., 2006), and a concomitant increase in fracture risk (Fraser et al., 1971; Wejda et al., 1995; Bauer et al., 2001; Vestergaard et al., 2000, 2005; Vestergaard and Mosekilde, 2003 and mortality (Franklyn et al., 1998; Patel et al., 2014) is also well documented. These latter changes are suggested by some to be only partly a result of thyrotoxicosis induced bone loss and partly a result of other aspects of the disease (Cummings et al., 1995). The skeletal effects of hyperthyroidism seem to be especially pronounced in postmenopausal women.

Recovery of bone loss in hyperthyroid patients following antithyroid treatment has been inconsistent (Fraser et al., 1971; Toh et al., 1985; Saggese et al., 1990; Diamond et al., 1994; Mudde et al., 1994; Olkawa et al., 1999; Kumeda et al., 2000; Barsal et al., 2004) but may be achieved more readily in younger individuals (Fraser et al., 1971; Saggese et al., 1990). Studies have documented protective effects of methimazole (Langdahl et al., 1996a; Nagasaka et al., 1997; Mora et al., 1999). Surgery and radioactive iodine also prevented bone loss in hyperthyroid patients (Langdahl et al., 1996b; Arata et al., 1997; Karunakaran et al., 2016) but were less protective than methimazole (Vestergaard et al., 2000a). Calcium supplementation with or without calcitonin (Kung and Yeung, 1996), estrogen (Lakatos et al., 1989), and bisphosphonates (Ongphiphadhanakul et al., 1993; Rosen et al., 1993a; Yamamoto et al., 1993; Rosen et al., 1993b; Kung and Ng., 1994; Lupoli et al., 1996) were also investigated and shown to be protective against ongoing bone loss in hyperthyroidism.

Additional to the treatment of the underlying condition, the therapy for hyperthyroidism-related osteoporosis does not differ from that of other secondary causes. Where data are available, novel antiporotic medications also seem to retain their efficacy in this clinical setting (Mirza and Canalis, 2015; Mana et al., 2017).

Subclinical hyperthyroidism

Subclinical hyperthyroidism is suggested to increase bone turnover rates. However data on whether this is actually the case and if so, whether this translates to an actual loss of bone mass and an increase in fracture risk is still controversial.

Data is derived from multiple sources including patients with endogenous subclinical hyperthyroidism and patients treated with suppressive thyroxine doses primarily for thyroid cancer and in rarer cases for euthyroid goiter. The question whether endogenous subclinical hyperthyroidism or larger amounts of exogenously administered thyroid hormones increase the risk of bone loss, especially among individuals already at risk for osteoporotic fractures, is of particular interest.

Bone turnover markers are shown to be elevated in certain studies while remaining physiologic in others (Nystrom et al., 1989; Karner et al., 2005; Reverter et al., 2005; El Hadidy et al., 2011; Lee et al., 2014). The situation regarding BMD and fracture risk is quite similar. A number of heterogeneous studies conducted in different age, gender, and disease groups show disparate degrees of TSH suppression. Densitometry was performed at varying anatomical locations using different methodologies. There are also large differences in the duration of follow-up. Effects of subclinical hyperthyroidism are thus reported to range from insignificant (Franklyn et al., 1992; Lee et al., 2014; Waring et al., 2013; Garin et al., 2014) to major (Kung and Yeung, 1996, Jódar et al., 1998; Tauchmanovà et al., 2004; Sugitani and Fujimoto, 2011; Kim et al., 2015). Where fracture risk was shown to be increased at all (Bauer et al., 2001; Turner et al., 2011; Abrahamsen et al., 2014, 2015), values of relative risk were reported between 1.25 (Vadiveloo et al., 2011) and 5 (Lee et al., 2010).

While many papers report on some degree of bone loss and increase in fracture risk, the dose of thyroxine treatment, the degree and duration of TSH suppression, sex, and postmenopausal status in women seem to be major determinants. The protective effect of adequate calcium intake was also suggested in one paper (Kung and Yeung, 1996). Meta-analyses seem to confirm these differences (Faber et al., 1994; Uzzan et al., 1996; Quan et al., 2002; Heemstra et al., 2006; Wirth et al., 2014; Blum et al., 2015). The available evidence regarding decreased BMD and increased fracture risk in subclinical hyperthyroidism of both endogenous and exogenous origin is most robust in postmenopausal women.

A few studies have also been conducted on the potential skeletal effects of variations in thyroid markers within the physiologic range. With lower TSH levels and thyroid function at the upper end of the normal range, osteoporosis and fracture risk were found to be increased again, primarily in postmenopausal women (Kim et al., 2006; Morris et al., 2007; Murphy et al., 2010; Lin et al., 2011; van Rijn et al., 2014; Noh et al., 2015; Hwangbo et al., 2016). In the case of premenopausal women and men, changes in bone metabolism related to subclinical hyperthyroidism or normal variations in TSH are much less convincing. For further assessment, possibly more prospective studies are needed.

Overview and future directions

Thyroid hormones play a major role in skeletal physiology and pathology both during development and in adult bone maintenance. Their lack results in cessation of bone maturation, growth, and remodeling, while their excess is associated with accelerated bone maturation and accelerated bone loss in adulthood. Thyrotoxicosis is a prevalent cause of secondary osteoporosis, while subclinical hyperthyroidism, suppressive doses of thyroxine treatment, and possibly higher thyroid activity within the normal range are all associated with increased bone loss and fracture risk, especially in postmenopausal women.

Osteoblasts and chondrocytes are the primary target cells of thyroid hormones, while secondary paracrine mediators are implied in the effects of T3 on osteoclasts. Different isoforms of thyroid hormone receptors, mediating their genomic

action, are well characterized, with TRα1 being the main isoform in bone. RTHα, a condition presenting with marked skeletal changes, is caused by the dominant negative mutations of the TRα gene. The disease has only been recognized in the past few years, and additional studies might bring further insights into the role of thyroid hormones on skeletal physiology. Selective thyroid receptor analogues may present a therapeutic option for metabolic syndrome or chronic heart failure in the future.

Nongenomic actions of thyroid hormones mediated via membrane and cytoplasmic receptors are increasingly recognized and pose an interesting subject for further research. The presence of a pituitary−bone axis and the potential role of TSH as a quasi-independent regulator of bone development and remodeling have also recently been posited. Though still contradictory, results are promising in this challenging topic.

References

Abe, E., Marians, R.C., Yu, W., Wu, X.B., Ando, T., Li, Y., Iqbal, J., Eldeiry, L., Rajendren, G., Blair, H.C., Davies, T.F., Zaidi, M., 2003. TSH is a negative regulator of skeletal remodeling. Cell 115 (2), 151−162.

Abe, S., Namba, N., Abe, M., Fujiwara, M., Aikawa, T., Kogo, M., Ozono, K., 2012. Monocarboxylate transporter 10 functions as a thyroid hormone transporter in chondrocytes. Endocrinology 153 (8), 4049−4058.

Abrahamsen, B., Jørgensen, H.L., Laulund, A.S., Nybo, M., Bauer, D.C., Brix, T.H., Hegedüs, L., 2015. The excess risk of major osteoporotic fractures in hypothyroidism is driven by cumulative hyperthyroid as opposed to hypothyroid time: an observational register-based time-resolved cohort analysis. J. Bone Miner. Res. 30 (5), 898−905.

Abrahamsen, B., Jørgensen, H.L., Laulund, A.S., Nybo, M., Brix, T.H., Hegedüs, L., 2014. Low serum thyrotropin level and duration of suppression as a predictor of major osteoporotic fractures-the OPENTHYRO register cohort. J. Bone Miner. Res. 29 (9), 2040−2050.

Abu, E.O., Bord, S., Horner, A., Chatterjee, V.K., Compston, J.E., 1997. The expression of thyroid hormone receptors in human bone. Bone 21 (2), 137−142.

Abu, E.O., Horner, A., Teti, A., Chatterjee, V.K., Compston, J.E., 2000. The localization of thyroid hormone receptor mRNAs in human bone. Thyroid 10 (4), 287−293.

Adams, P.M., Stein, S.A., Palnitkar, M., Anthony, A., Gerrity, L., Shanklin, D.R., 1989. Evaluation and characterization of the hypothyroid hyt/hyt mouse. I: somatic and behavioral studies. Neuroendocrinology 49 (2), 138−143.

Ahmed, L.A., Schirmer, H., Berntsen, G.K., Fønnebø, V., Joakimsen, R.M., 2006. Self-reported diseases and the risk of non-vertebral fractures: the Tromsø study. Osteoporos. Int. 17 (1), 46−53.

Akita, S., Hirano, A., Fujii, T., 1996. Identification of IGF-I in the calvarial suture of young rats: histochemical analysis of the cranial sagittal sutures in a hyperthyroid rat model. Plast. Reconstr. Surg. 97 (1), 1−12.

Akita, S., Nakamura, T., Hirano, A., Fujii, T., Yamashita, S., 1994. Thyroid hormone action on rat calvarial sutures. Thyroid 4 (1), 99−106.

Alini, M., Kofsky, Y., Wu, W., Pidoux, I., Poole, A.R., 1996. In serum-free culture thyroid hormones can induce full expression of chondrocyte hypertrophy leading to matrix calcification. J. Bone Miner. Res. 11 (1), 105−113.

Allain, T.J., Chambers, T.J., Flanagan, A.M., McGregor, A.M., 1992. Tri-iodothyronine stimulates rat osteoclastic bone resorption by an indirect effect. J. Endocrinol. 133 (3), 327−331.

Allain, T.J., Thomas, M.R., McGregor, A.M., Salisbury, J.R., 1995. A histomorphometric study of bone changes in thyroid dysfunction in rats. Bone 16 (5), 505−509.

Allain, T.J., Yen, P.M., Flanagan, A.M., McGregor, A.M., 1996. The isoform-specific expression of the tri-iodothyronine receptor in osteoblasts and osteoclasts. Eur. J. Clin. Investig. 26 (5), 418−425.

Amato, G., Mazziotti, G., Sorvillo, F., Piscopo, M., Lalli, E., Biondi, B., Iorio, S., Molinari, A., Giustina, A., Carella, C., 2004. High serum osteoprotegerin levels in patients with hyperthyroidism: effect of medical treatment. Bone 35 (3), 785−791.

Arata, N., Momotani, N., Maruyama, H., Saruta, T., Tsukatani, K., Kubo, A., Ikemoto, K., Ito, K., 1997. Bone mineral density after surgical treatment for Graves' disease. Thyroid 7 (4), 547−554.

Asai, S., Cao, X., Yamauchi, M., Funahashi, K., Ishiguro, N., Kambe, F., 2009. Thyroid hormone non-genomically suppresses Src thereby stimulating osteocalcin expression in primary mouse calvarial osteoblasts. Biochem. Biophys. Res. Commun. 387 (1), 92−96.

Baliram, R., Latif, R., Berkowitz, J., Frid, S., Colaianni, G., Sun, L., Zaidi, M., Davies, T.F., 2011. Thyroid-stimulating hormone induces a Wnt-dependent, feed-forward loop for osteoblastogenesis in embryonic stem cell cultures. Proc. Natl. Acad. Sci. U. S. A. 108 (39), 16277−16282.

Baliram, R., Sun, L., Cao, J., Li, J., Latif, R., Huber, A.K., Yuen, T., Blair, H.C., Zaidi, M., Davies, T.F., 2012. Hyperthyroid-associated osteoporosis is exacerbated by the loss of TSH signaling. J. Clin. Investig. 122 (10), 3737−3741.

Ballock, R., Mita, B.C., Zhou, X., Chen, D.H., Mink, L.M., 1999. Expression of thyroid hormone receptor isoforms in rat growth plate cartilage in vivo. J. Bone Miner. Res. 14 (9), 1550−1556.

Ballock, R.T., Reddi, A.H., 1994. Thyroxine is the serum factor that regulates morphogenesis of columnar cartilage from isolated chondrocytes in chemically defined medium. J. Cell Biol. 126 (5), 1311−1318.

Ballock, R.T., Zhou, X., Mink, L.M., Chen, D.H., Mita, B.C., Stewart, M.C., 2000. Expression of cyclin-dependent kinase inhibitors in epiphyseal chondrocytes induced to terminally differentiate with thyroid hormone. Endocrinology 141 (12), 4552−4557.

Banovac, K., Koren, E., 2000. Triiodothyronine stimulates the release of membrane-bound alkaline phosphatase in osteoblastic cells. Calcif. Tissue Int. 67 (6), 460–465.

Barsal, G., Taneli, F., Atay, A., Hekimsoy, Z., Erciyas, F., 2004. Serum osteocalcin levels in hyperthyroidism before and after antithyroid therapy. Tohoku J. Exp. Med. 203 (3), 183–188.

Bassett, J.H., Boyde, A., Howell, P.G., Bassett, R.H., Galliford, T.M., Archanco, M., Evans, H., Lawson, M.A., Croucher, P., St Germain, D.L., Galton, V.A., Williams, G.R., 2010. Optimal bone strength and mineralization requires the type 2 iodothyronine deiodinase in osteoblasts. Proc. Natl. Acad. Sci. U. S. A. 107 (16), 7604–7609.

Bassett, J.H., Boyde, A., Zikmund, T., Evans, H., Croucher, P.I., Zhu, X., Park, J.W., Cheng, S.Y., Williams, G.R., 2014. Thyroid hormone receptor α mutation causes a severe and thyroxine-resistant skeletal dysplasia in female mice. Endocrinology 155 (9), 3699–3712.

Bassett, J.H., Nordström, K., Boyde, A., Howell, P.G., Kelly, S., Vennström, B., Williams, G.R., 2007a. Thyroid status during skeletal development determines adult bone structure and mineralization. Mol. Endocrinol. 21 (8), 1893–1904.

Bassett, J.H., O'Shea, P.J., Sriskantharajah, S., Rabier, B., Boyde, A., Howell, P.G., Weiss, R.E., Roux, J.P., Malaval, L., Clement-Lacroix, P., Samarut, J., Chassande, O., Williams, G.R., 2007b. Thyroid hormone excess rather than thyrotropin deficiency induces osteoporosis in hyperthyroidism. Mol. Endocrinol. 21 (5), 1095–1107.

Bassett, J.H., van der Spek, A., Logan, J.G., Gogakos, A., Bagchi-Chakraborty, J., Murphy, E., van Zeijl, C., Down, J., Croucher, P.I., Boyde, A., Boelen, A., Williams, G.R., 2015. Thyrostimulin regulates osteoblastic bone formation during early skeletal development. Endocrinology 156 (9), 3098–3113.

Bassett, J.H., Williams, G.R., 2003. The molecular actions of thyroid hormone in bone. Trends Endocrinol. Metabol. 14 (8), 356–364.

Bassett, J.H., Williams, G.R., 2008. Critical role of the hypothalamic-pituitary-thyroid axis in bone. Bone 43 (3), 418–426.

Bauer, D.C., Ettinger, B., Nevitt, M.C., Stone, K.L., Study of Osteoporotic Fractures Research Group, 2001. Risk for fracture in women with low serum levels of thyroid-stimulating hormone. Ann. Intern. Med. 134 (7), 561–568.

Beamer, W.J., Eicher, E.M., Maltais, L.J., Southard, J.L., 1981. Inherited primary hypothyroidism in mice. Science 212 (4490), 61–63.

Behr, M., Ramsden, D.B., Loos, U., 1997. Deoxyribonucleic acid binding and transcriptional silencing by a truncated c-erbA beta 1 thyroid hormone receptor identified in a severely retarded patient with resistance to thyroid hormone. J. Clin. Endocrinol. Metab. 82 (4), 1081–1087.

Bergh, J.J., Lin, H.Y., Lansing, L., Mohamed, S.N., Davis, F.B., Mousa, S., Davis, P.J., 2005. Integrin alphaVbeta3 contains a cell surface receptor site for thyroid hormone that is linked to activation of mitogen-activated protein kinase and induction of angiogenesis. Endocrinology 146 (7), 2864–2871.

Bland, R., Sammons, R.L., Sheppard, M.C., Williams, G.R., 1997. Thyroid hormone, vitamin D and retinoid receptor expression and signalling in primary cultures of rat osteoblastic and immortalised osteosarcoma cells. J. Endocrinol. 154 (1), 63–74.

Blum, M.R., Bauer, D.C., Collet, T.H., Fink, H.A., Cappola, A.R., da Costa, B.R., Wirth, C.D., Peeters, R.P., Åsvold, B.O., den Elzen, W.P., Luben, R.N., Imaizumi, M., Bremner, A.P., Gogakos, A., Eastell, R., Kearney, P.M., Strotmeyer, E.S., Wallace, E.R., Hoff, M., Ceresini, G., Rivadeneira, F., Uitterlinden, A.G., Stott, D.J., Westendorp, R.G., Khaw, K.T., Langhammer, A., Ferrucci, L., Gussekloo, J., Williams, G.R., Walsh, J.P., Jüni, P., Aujesky, D., Rodondi, N., Collaboration, T.S., 2015. Subclinical thyroid dysfunction and fracture risk: a meta-analysis. J. Am. Med. Assoc. 313 (20), 2055–2065.

Bochukova, E., Schoenmakers, N., Agostini, M., Schoenmakers, E., Rajanayagam, O., Keogh, J.M., Henning, E., Reinemund, J., Gevers, E., Sarri, M., Downes, K., Offiah, A., Albanese, A., Halsall, D., Schwabe, J.W., Bain, M., Lindley, K., Muntoni, F., Vargha-Khadem, F., Khadem, F.V., Dattani, M., Farooqi, I.S., Gurnell, M., Chatterjee, K., 2012. A mutation in the thyroid hormone receptor alpha gene. N. Engl. J. Med. 366 (3), 243–249.

Boutin, A., Eliseeva, E., Gershengorn, M.C., Neumann, S., 2014. β-Arrestin-1 mediates thyrotropin-enhanced osteoblast differentiation. FASEB J. 28 (8), 3446–3455.

Brent, G.A., Moore, D.D., Larsen, P.R., 1991. Thyroid hormone regulation of gene expression. Annu. Rev. Physiol. 53, 17–35.

Burakov, D., Crofts, L.A., Chang, C.P., Freedman, L.P., 2002. Reciprocal recruitment of DRIP/mediator and p160 coactivator complexes in vivo by estrogen receptor. J. Biol. Chem. 277 (17), 14359–14362.

Burch, W.M., Lebovitz, H.E., 1982a. Triiodothyronine stimulates maturation of porcine growth-plate cartilage in vitro. J. Clin. Investig. 70 (3), 496–504.

Burch, W.M., Lebovitz, H.E., 1982b. Triiodothyronine stimulation of in vitro growth and maturation of embryonic chick cartilage. Endocrinology 111 (2), 462–468.

Böhme, K., Conscience-Egli, M., Tschan, T., Winterhalter, K.H., Bruckner, P., 1992. Induction of proliferation or hypertrophy of chondrocytes in serum-free culture: the role of insulin-like growth factor-I, insulin, or thyroxine. J. Cell Biol. 116 (4), 1035–1042.

Canalis, E., 1980. Effect of insulinlike growth factor I on DNA and protein synthesis in cultured rat calvaria. J. Clin. Investig. 66 (4), 709–719.

Capelo, L.P., Beber, E.H., Fonseca, T.L., Gouveia, C.H., 2009. The monocarboxylate transporter 8 and L-type amino acid transporters 1 and 2 are expressed in mouse skeletons and in osteoblastic MC3T3-E1 cells. Thyroid 19 (2), 171–180.

Capelo, L.P., Beber, E.H., Huang, S.A., Zorn, T.M., Bianco, A.C., Gouveia, C.H., 2008. Deiodinase-mediated thyroid hormone inactivation minimizes thyroid hormone signaling in the early development of fetal skeleton. Bone 43 (5), 921–930.

Centrella, M., McCarthy, T.L., Canalis, E., 1990. Receptors for insulin-like growth factors-I and -II in osteoblast-enriched cultures from fetal rat bone. Endocrinology 126 (1), 39–44.

Chassande, O., Fraichard, A., Gauthier, K., Flamant, F., Legrand, C., Savatier, P., Laudet, V., Samarut, J., 1997. Identification of transcripts initiated from an internal promoter in the c-erbA alpha locus that encode inhibitors of retinoic acid receptor-alpha and triiodothyronine receptor activities. Mol. Endocrinol. 11 (9), 1278–1290.

Chatterjee, V.K., Nagaya, T., Madison, L.D., Datta, S., Rentoumis, A., Jameson, J.L., 1991. Thyroid hormone resistance syndrome. Inhibition of normal receptor function by mutant thyroid hormone receptors. J. Clin. Investig. 87 (6), 1977–1984.

Chiellini, G., Nguyen, N.H., Apriletti, J.W., Baxter, J.D., Scanlan, T.S., 2002. Synthesis and biological activity of novel thyroid hormone analogues: 5'-aryl substituted GC-1 derivatives. Bioorg. Med. Chem. 10 (2), 333–346.

Conaway, H.H., Ransjö, M., Lerner, U.H., 1998. Prostaglandin-independent stimulation of bone resorption in mouse calvariae and in isolated rat osteoclasts by thyroid hormones (T4, and T3). Proc. Soc. Exp. Biol. Med. 217 (2), 153–161.

Cooper, D.S., Kaplan, M.M., Ridgway, E.C., Maloof, F., Daniels, G.H., 1979. Alkaline phosphatase isoenzyme patterns in hyperthyroidism. Ann. Intern. Med. 90 (2), 164–168.

Cray, J.J., Khaksarfard, K., Weinberg, S.M., Elsalanty, M., Yu, J.C., 2013. Effects of thyroxine exposure on osteogenesis in mouse calvarial preosteoblasts. PLoS One 8 (7), e69067.

Cummings, S.R., Nevitt, M.C., Browner, W.S., Stone, K., Fox, K.M., Ensrud, K.E., Cauley, J., Black, D., Vogt, T.M., 1995. Risk factors for hip fracture in white women. Study of Osteoporotic Fractures Research Group. N. Engl. J. Med. 332 (12), 767–773.

Davis, P.J., Davis, F.B., Mousa, S.A., Luidens, M.K., Lin, H.Y., 2011. Membrane receptor for thyroid hormone: physiologic and pharmacologic implications. Annu. Rev. Pharmacol. Toxicol. 51, 99–115.

Davis, P.J., Goglia, F., Leonard, J.L., 2016. Nongenomic actions of thyroid hormone. Nat. Rev. Endocrinol. 12 (2), 111–121.

Davis, P.J., Leonard, J.L., Davis, F.B., 2008. Mechanisms of nongenomic actions of thyroid hormone. Front. Neuroendocrinol. 29 (2), 211–218.

Davis, P.J., Lin, H.Y., Tang, H.Y., Davis, F.B., Mousa, S.A., 2013. Adjunctive input to the nuclear thyroid hormone receptor from the cell surface receptor for the hormone. Thyroid 23 (12), 1503–1509.

Davis, P.J., Shih, A., Lin, H.Y., Martino, L.J., Davis, F.B., 2000. Thyroxine promotes association of mitogen-activated protein kinase and nuclear thyroid hormone receptor (TR) and causes serine phosphorylation of TR. J. Biol. Chem. 275 (48), 38032–38039.

Diamond, T., Vine, J., Smart, R., Butler, P., 1994. Thyrotoxic bone disease in women: a potentially reversible disorder. Ann. Intern. Med. 120 (1), 8–11.

DiPippo, V.A., Lindsay, R., Powers, C.A., 1995. Estradiol and tamoxifen interactions with thyroid hormone in the ovariectomized-thyroidectomized rat. Endocrinology 136 (3), 1020–1033.

Dumic-Cule, I., Draca, N., Luetic, A.T., Jezek, D., Rogic, D., Grgurevic, L., Vukicevic, S., 2014. TSH prevents bone resorption and with calcitriol synergistically stimulates bone formation in rats with low levels of calciotropic hormones. Horm. Metab. Res. 46 (5), 305–312.

Dumitrescu, A.M., Liao, X.H., Best, T.B., Brockmann, K., Refetoff, S., 2004. A novel syndrome combining thyroid and neurological abnormalities is associated with mutations in a monocarboxylate transporter gene. Am. J. Hum. Genet. 74 (1), 168–175.

El Hadidy, e. H., Ghonaim, M., El Gawad, S. S. h., El Atta, M.A., 2011. Impact of severity, duration, and etiology of hyperthyroidism on bone turnover markers and bone mineral density in men. BMC Endocr. Disord. 11, 15.

Endo, T., Kobayashi, T., 2013. Excess TSH causes abnormal skeletal development in young mice with hypothyroidism via suppressive effects on the growth plate. Am. J. Physiol. Endocrinol. Metab. 305 (5), E660–E666.

Engler, H., Oettli, R.E., Riesen, W.F., 1999. Biochemical markers of bone turnover in patients with thyroid dysfunctions and in euthyroid controls: a cross-sectional study. Clin. Chim. Acta 289 (1–2), 159–172.

Eriksen, E.F., 1986. Normal and pathological remodeling of human trabecular bone: three dimensional reconstruction of the remodeling sequence in normals and in metabolic bone disease. Endocr. Rev. 7 (4), 379–408.

Ernst, M., Froesch, E.R., 1987. Triiodothyronine stimulates proliferation of osteoblast-like cells in serum-free culture. FEBS Lett. 220 (1), 163–166.

Espiard, S., Savagner, F., Flamant, F., Vlaeminck-Guillem, V., Guyot, R., Munier, M., d'Herbomez, M., Bourguet, W., Pinto, G., Rose, C., Rodien, P., Wémeau, J.L., 2015. A novel mutation in THRA gene associated with an atypical phenotype of resistance to thyroid hormone. J. Clin. Endocrinol. Metab. 100 (8), 2841–2848.

Faber, J., Galløe, A.M., 1994. Changes in bone mass during prolonged subclinical hyperthyroidism due to L-thyroxine treatment: a meta-analysis. Eur. J. Endocrinol. 130 (4), 350–356.

Flynn, R.W., Bonellie, S.R., Jung, R.T., MacDonald, T.M., Morris, A.D., Leese, G.P., 2010. Serum thyroid-stimulating hormone concentration and morbidity from cardiovascular disease and fractures in patients on long-term thyroxine therapy. J. Clin. Endocrinol. Metab. 95 (1), 186–193.

Fraichard, A., Chassande, O., Plateroti, M., Roux, J.P., Trouillas, J., Dehay, C., Legrand, C., Gauthier, K., Kedinger, M., Malaval, L., Rousset, B., Samarut, J., 1997. The T3R alpha gene encoding a thyroid hormone receptor is essential for post-natal development and thyroid hormone production. EMBO J. 16 (14), 4412–4420.

Franklyn, J.A., Betteridge, J., Daykin, J., Holder, R., Oates, G.D., Parle, J.V., Lilley, J., Heath, D.A., Sheppard, M.C., 1992. Long-term thyroxine treatment and bone mineral density. Lancet 340 (8810), 9–13.

Franklyn, J.A., Maisonneuve, P., Sheppard, M.C., Betteridge, J., Boyle, P., 1998. Mortality after the treatment of hyperthyroidism with radioactive iodine. N. Engl. J. Med. 338 (11), 712–718.

Fraser, S.A., Wilson, G.M., 1971. Plasma-calcitonin in disorders of thyroid function. Lancet 1 (7702), 725–726.

Fratzl-Zelman, N., Hörandner, H., Luegmayr, E., Varga, F., Ellinger, A., Erlee, M.P., Klaushofer, K., 1997. Effects of triiodothyronine on the morphology of cells and matrix, the localization of alkaline phosphatase, and the frequency of apoptosis in long-term cultures of MC3T3-E1 cells. Bone 20 (3), 225–236.

Garin, M.C., Arnold, A.M., Lee, J.S., Robbins, J., Cappola, A.R., 2014. Subclinical thyroid dysfunction and hip fracture and bone mineral density in older adults: the cardiovascular health study. J. Clin. Endocrinol. Metab. 99 (8), 2657–2664.

Garnero, P., Vassy, V., Bertholin, A., Riou, J.P., Delmas, P.D., 1994. Markers of bone turnover in hyperthyroidism and the effects of treatment. J. Clin. Endocrinol. Metab. 78 (4), 955–959.

Gauthier, K., Chassande, O., Plateroti, M., Roux, J.P., Legrand, C., Pain, B., Rousset, B., Weiss, R., Trouillas, J., Samarut, J., 1999. Different functions for the thyroid hormone receptors TRalpha and TRbeta in the control of thyroid hormone production and post-natal development. EMBO J. 18 (3), 623–631.

Germain, P., Staels, B., Dacquet, C., Spedding, M., Laudet, V., 2006. Overview of nomenclature of nuclear receptors. Pharmacol. Rev. 58 (4), 685–704.

Glade, M.J., Kanwar, Y.S., Stern, P.H., 1994. Insulin and thyroid hormones stimulate matrix metabolism in primary cultures of articular chondrocytes from young rabbits independently and in combination. Connect. Tissue Res. 31 (1), 37–44.

Glantschnig, H., Varga, F., Klaushofer, K., 1996. Thyroid hormone and retinoic acid induce the synthesis of insulin-like growth factor-binding protein-4 in mouse osteoblastic cells. Endocrinology 137 (1), 281–286.

Glass, C.K., 1994. Differential recognition of target genes by nuclear receptor monomers, dimers, and heterodimers. Endocr. Rev. 15 (3), 391–407.

Glasscock, G.F., Nicoll, C.S., 1981. Hormonal control of growth in the infant rat. Endocrinology 109 (1), 176–184.

Gloss, B., Trost, S., Bluhm, W., Swanson, E., Clark, R., Winkfein, R., Janzen, K., Giles, W., Chassande, O., Samarut, J., Dillmann, W., 2001. Cardiac ion channel expression and contractile function in mice with deletion of thyroid hormone receptor alpha or beta. Endocrinology 142 (2), 544–550.

Goldman, S., McCarren, M., Morkin, E., Ladenson, P.W., Edson, R., Warren, S., Ohm, J., Thai, H., Churby, L., Barnhill, J., O'Brien, T., Anand, I., Warner, A., Hattler, B., Dunlap, M., Erikson, J., Shih, M.C., Lavori, P., 2009. DITPA (3,5-Diiodothyropropionic Acid), a thyroid hormone analog to treat heart failure: phase II trial veterans affairs cooperative study. Circulation 119 (24), 3093–3100.

González-Rodríguez, L.A., Felici-Giovanini, M.E., Haddock, L., 2013. Thyroid dysfunction in an adult female population: a population-based study of Latin American Vertebral Osteoporosis Study (LAVOS) – Puerto Rico site. Puert. Rico Health Sci. J. 32 (2), 57–62.

Gorka, J., Taylor-Gjevre, R.M., Arnason, T., 2013. Metabolic and clinical consequences of hyperthyroidism on bone density. Int. J. Endocrinol. 2013, 638–727.

Gouveia, C.H., Christoffolete, M.A., Zaitune, C.R., Dora, J.M., Harney, J.W., Maia, A.L., Bianco, A.C., 2005. Type 2 iodothyronine selenodeiodinase is expressed throughout the mouse skeleton and in the MC3T3-E1 mouse osteoblastic cell line during differentiation. Endocrinology 146 (1), 195–200.

Gouveia, C.H., Jorgetti, V., Bianco, A.C., 1997. Effects of thyroid hormone administration and estrogen deficiency on bone mass of female rats. J. Bone Miner. Res. 12 (12), 2098–2107.

Gouveia, C.H., Schultz, J.J., Bianco, A.C., Brent, G.A., 2001. Thyroid hormone stimulation of osteocalcin gene expression in ROS 17/2.8 cells is mediated by transcriptional and post-transcriptional mechanisms. J. Endocrinol. 170 (3), 667–675.

Grover, G.J., Mellström, K., Ye, L., Malm, J., Li, Y.L., Bladh, L.G., Sleph, P.G., Smith, M.A., George, R., Vennström, B., Mookhtiar, K., Horvath, R., Speelman, J., Egan, D., Baxter, J.D., 2003. Selective thyroid hormone receptor-beta activation: a strategy for reduction of weight, cholesterol, and lipoprotein (a) with reduced cardiovascular liability. Proc. Natl. Acad. Sci. U. S. A. 100 (17), 10067–10072.

Gu, W.X., Stern, P.H., Madison, L.D., Du, G.G., 2001. Mutual up-regulation of thyroid hormone and parathyroid hormone receptors in rat osteoblastic osteosarcoma 17/2.8 cells. Endocrinology 142 (1), 157–164.

Guo, C.Y., Weetman, A.P., Eastell, R., 1997. Longitudinal changes of bone mineral density and bone turnover in postmenopausal women on thyroxine. Clin. Endocrinol. 46 (3), 301–307.

Göthe, S., Wang, Z., Ng, L., Kindblom, J.M., Barros, A.C., Ohlsson, C., Vennström, B., Forrest, D., 1999. Mice devoid of all known thyroid hormone receptors are viable but exhibit disorders of the pituitary-thyroid axis, growth, and bone maturation. Genes Dev. 13 (10), 1329–1341.

Harvey, R.D., McHardy, K.C., Reid, I.W., Paterson, F., Bewsher, P.D., Duncan, A., Robins, S.P., 1991. Measurement of bone collagen degradation in hyperthyroidism and during thyroxine replacement therapy using pyridinium cross-links as specific urinary markers. J. Clin. Endocrinol. Metab. 72 (6), 1189–1194.

Hase, H., Ando, T., Eldeiry, L., Brebene, A., Peng, Y., Liu, L., Amano, H., Davies, T.F., Sun, L., Zaidi, M., Abe, E., 2006. TNFalpha mediates the skeletal effects of thyroid-stimulating hormone. Proc. Natl. Acad. Sci. U. S. A. 103 (34), 12849–12854.

Heemstra, K.A., Hamdy, N.A., Romijn, J.A., Smit, J.W., 2006. The effects of thyrotropin-suppressive therapy on bone metabolism in patients with well-differentiated thyroid carcinoma. Thyroid 16 (6), 583–591.

Herzovich, V., Vaiani, E., Marino, R., Dratler, G., Lazzati, J.M., Tilitzky, S., Ramirez, P., Iorcansky, S., Rivarola, M.A., Belgorosky, A., 2007. Unexpected peripheral markers of thyroid function in a patient with a novel mutation of the MCT8 thyroid hormone transporter gene. Horm. Res. 67 (1), 1–6.

Heyerdahl, S., Kase, B.F., Stake, G., 1994. Skeletal maturation during thyroxine treatment in children with congenital hypothyroidism. Acta Paediatr. 83 (6), 618–622.

Hiroi, Y., Kim, H.H., Ying, H., Furuya, F., Huang, Z., Simoncini, T., Noma, K., Ueki, K., Nguyen, N.H., Scanlan, T.S., Moskowitz, M.A., Cheng, S.Y., Liao, J.K., 2006. Rapid nongenomic actions of thyroid hormone. Proc. Natl. Acad. Sci. U. S. A. 103 (38), 14104–14109.

Hock, J.M., Gunness-Hey, M., Poser, J., Olson, H., Bell, N.H., Raisz, L.G., 1986. Stimulation of undermineralized matrix formation by 1,25 dihydroxyvitamin D3 in long bones of rats. Calcif. Tissue Int. 38 (2), 79–86.

Hoffman, S.J., Vasko-Moser, J., Miller, W.H., Lark, M.W., Gowen, M., Stroup, G., 2002. Rapid inhibition of thyroxine-induced bone resorption in the rat by an orally active vitronectin receptor antagonist. J. Pharmacol. Exp. Ther. 302 (1), 205–211.

Hoffmann, O., Klaushofer, K., Koller, K., Peterlik, M., Mavreas, T., Stern, P.H., 1986. Indomethacin inhibits thrombin-but not thyroxin-stimulated resorption of fetal rat limb bones. Prostaglandins 31 (4), 601–608.

Huang, B.K., Golden, L.A., Tarjan, G., Madison, L.D., Stern, P.H., 2000. Insulin-like growth factor I production is essential for anabolic effects of thyroid hormone in osteoblasts. J. Bone Miner. Res. 15 (2), 188–197.

Hwangbo, Y., Kim, J.H., Kim, S.W., Park, Y.J., Park, D.J., Kim, S.Y., Shin, C.S., Cho, N.H., 2016. High-normal free thyroxine levels are associated with low trabecular bone scores in euthyroid postmenopausal women. Osteoporos. Int. 27 (2), 457–462.

Ishikawa, Y., Genge, B.R., Wuthier, R.E., Wu, L.N., 1998. Thyroid hormone inhibits growth and stimulates terminal differentiation of epiphyseal growth plate chondrocytes. J. Bone Miner. Res. 13 (9), 1398–1411.

Izumo, S., Mahdavi, V., 1988. Thyroid hormone receptor alpha isoforms generated by alternative splicing differentially activate myosin HC gene transcription. Nature 334 (6182), 539–542.

Jódar, E., Begoña López, M., García, L., Rigopoulou, D., Martínez, G., Hawkins, F., 1998. Bone changes in pre- and postmenopausal women with thyroid cancer on levothyroxine therapy: evolution of axial and appendicular bone mass. Osteoporos. Int. 8 (4), 311–316.

Kalyanaraman, H., Schwappacher, R., Joshua, J., Zhuang, S., Scott, B.T., Klos, M., Casteel, D.E., Frangos, J.A., Dillmann, W., Boss, G.R., Pilz, R.B., 2014. Nongenomic thyroid hormone signaling occurs through a plasma membrane-localized receptor. Sci. Signal. 7 (326), ra48.

Kaneshige, M., Suzuki, H., Kaneshige, K., Cheng, J., Wimbrow, H., Barlow, C., Willingham, M.C., Cheng, S., 2001. A targeted dominant negative mutation of the thyroid hormone alpha 1 receptor causes increased mortality, infertility, and dwarfism in mice. Proc. Natl. Acad. Sci. U. S. A. 98 (26), 15095–15100.

Karner, I., Hrgović, Z., Sijanović, S., Buković, D., Klobucar, A., Usadel, K.H., Fassbender, W.J., 2005. Bone mineral density changes and bone turnover in thyroid carcinoma patients treated with supraphysiologic doses of thyroxine. Eur. J. Med. Res. 10 (11), 480–488.

Karunakaran, P., Maharajan, C., Mohamed, K.N., Rachamadugu, S.V., 2016. Rapid restoration of bone mass after surgical management of hyperthyroidism: a prospective case control study in Southern India. Surgery 159 (3), 771–776.

Kasono, K., Sato, K., Han, D.C., Fujii, Y., Tsushima, T., Shizume, K., 1988. Stimulation of alkaline phosphatase activity by thyroid hormone in mouse osteoblast-like cells (MC3T3-E1): a possible mechanism of hyperalkaline phosphatasia in hyperthyroidism. Bone Miner. 4 (4), 355–363.

Kassem, M., Mosekilde, L., Eriksen, E.F., 1993. Effects of triiodothyronine on DNA synthesis and differentiation markers of normal human osteoblast-like cells in vitro. Biochem. Mol. Biol. Int. 30 (4), 779–788.

Kawaguchi, H., Pilbeam, C.C., Raisz, L.G., 1994a. Anabolic effects of 3,3',5-triiodothyronine and triiodothyroacetic acid in cultured neonatal mouse parietal bones. Endocrinology 135 (3), 971–976.

Kawaguchi, H., Pilbeam, C.C., Woodiel, F.N., Raisz, L.G., 1994b. Comparison of the effects of 3,5,3'-triiodothyroacetic acid and triiodothyronine on bone resorption in cultured fetal rat long bones and neonatal mouse calvariae. J. Bone Miner. Res. 9 (2), 247–253.

Kim, C.W., Hong, S., Oh, S.H., Lee, J.J., Han, J.Y., Kim, S.H., Nam, M., Kim, Y.S., 2015. Change of bone mineral density and biochemical markers of bone turnover in patients on suppressive levothyroxine therapy for differentiated thyroid carcinoma. J. Bone Metab. 22 (3), 135–141.

Kim, D.J., Khang, Y.H., Koh, J.M., Shong, Y.K., Kim, G.S., 2006. Low normal TSH levels are associated with low bone mineral density in healthy postmenopausal women. Clin. Endocrinol. 64 (1), 86–90.

Klaushofer, K., Hoffmann, O., Gleispach, H., Leis, H.J., Czerwenka, E., Koller, K., Peterlik, M., 1989. Bone-resorbing activity of thyroid hormones is related to prostaglandin production in cultured neonatal mouse calvaria. J. Bone Miner. Res. 4 (3), 305–312.

Klaushofer, K., Varga, F., Glantschnig, H., Fratzl-Zelman, N., Czerwenka, E., Leis, H.J., Koller, K., Peterlik, M., 1995. The regulatory role of thyroid hormones in bone cell growth and differentiation. J. Nutr. 125 (7 Suppl. l), 1996S–2003S.

Koenig, R.J., 1998. Thyroid hormone receptor coactivators and corepressors. Thyroid 8 (8), 703–713.

Kopp, P., Kitajima, K., Jameson, J.L., 1996. Syndrome of resistance to thyroid hormone: insights into thyroid hormone action. Proc. Soc. Exp. Biol. Med. 211 (1), 49–61.

Krieger, N.S., Stappenbeck, T.S., Stern, P.H., 1988. Characterization of specific thyroid hormone receptors in bone. J. Bone Miner. Res. 3 (4), 473–478.

Krølner, B., Jørgensen, J.V., Nielsen, S.P., 1983. Spinal bone mineral content in myxoedema and thyrotoxicosis. Effects of thyroid hormone(s) and antithyroid treatment. Clin. Endocrinol. 18 (5), 439–446.

Kumeda, Y., Inaba, M., Tahara, H., Kurioka, Y., Ishikawa, T., Morii, H., Nishizawa, Y., 2000. Persistent increase in bone turnover in Graves' patients with subclinical hyperthyroidism. J. Clin. Endocrinol. Metab. 85 (11), 4157–4161.

Kung, A.W., Ng, F., 1994. A rat model of thyroid hormone-induced bone loss: effect of antiresorptive agents on regional bone density and osteocalcin gene expression. Thyroid 4 (1), 93–98.

Kung, A.W., Yeung, S.S., 1996. Prevention of bone loss induced by thyroxine suppressive therapy in postmenopausal women: the effect of calcium and calcitonin. J. Clin. Endocrinol. Metab. 81 (3), 1232–1236.

Ladenson, P.W., Kristensen, J.D., Ridgway, E.C., Olsson, A.G., Carlsson, B., Klein, I., Baxter, J.D., Angelin, B., 2010. Use of the thyroid hormone analogue eprotirome in statin-treated dyslipidemia. N. Engl. J. Med. 362 (10), 906–916.

Lakatos, P., Caplice, M.D., Khanna, V., Stern, P.H., 1993. Thyroid hormones increase insulin-like growth factor I content in the medium of rat bone tissue. J. Bone Miner. Res. 8 (12), 1475–1481.

Lakatos, P., Foldes, J., Nagy, Z., Takacs, I., Speer, G., Horvath, C., Mohan, S., Baylink, D.J., Stern, P.H., 2000. Serum insulin-like growth factor-I, insulin-like growth factor binding proteins, and bone mineral content in hyperthyroidism. Thyroid 10 (5), 417–423.

Lakatos, P., Stern, P.H., 1991. Evidence for direct non-genomic effects of triiodothyronine on bone rudiments in rats: stimulation of the inositol phosphate second messenger system. Acta Endocrinol. 125 (5), 603–608.

Lakatos, P., Stern, P.H., 1992. Effects of cyclosporins and transforming growth factor beta 1 on thyroid hormone action in cultured fetal rat limb bones. Calcif. Tissue Int. 50 (2), 123–128.

Lakatos, P., Tarján, G., Mérei, J., Földes, J., Holló, I., 1989. Androgens and bone mineral content in patients with subtotal thyroidectomy for benign nodular disease. Acta Med. Hung. 46 (4), 297–305.

Langdahl, B.L., Loft, A.G., Eriksen, E.F., Mosekilde, L., Charles, P., 1996a. Bone mass, bone turnover, body composition, and calcium homeostasis in former hyperthyroid patients treated by combined medical therapy. Thyroid 6 (3), 161–168.

Langdahl, B.L., Loft, A.G., Eriksen, E.F., Mosekilde, L., Charles, P., 1996b. Bone mass, bone turnover, calcium homeostasis, and body composition in surgically and radioiodine-treated former hyperthyroid patients. Thyroid 6 (3), 169–175.

LeBron, B.A., Pekary, A.E., Mirell, C., Hahn, T.J., Hershman, J.M., 1989. Thyroid hormone 5'-deiodinase activity, nuclear binding, and effects on mitogenesis in UMR-106 osteoblastic osteosarcoma cells. J. Bone Miner. Res. 4 (2), 173–178.

Lee, J.S., Buzková, P., Fink, H.A., Vu, J., Carbone, L., Chen, Z., Cauley, J., Bauer, D.C., Cappola, A.R., Robbins, J., 2010. Subclinical thyroid dysfunction and incident hip fracture in older adults. Arch. Intern. Med. 170 (21), 1876–1883.

Lee, M.S., Kim, S.Y., Lee, M.C., Cho, B.Y., Lee, H.K., Koh, C.S., Min, H.K., 1990. Negative correlation between the change in bone mineral density and serum osteocalcin in patients with hyperthyroidism. J. Clin. Endocrinol. Metab. 70 (3), 766–770.

Lee, M.Y., Park, J.H., Bae, K.S., Jee, Y.G., Ko, A.N., Han, Y.J., Shin, J.Y., Lim, J.S., Chung, C.H., Kang, S.J., 2014. Bone mineral density and bone turnover markers in patients on long-term suppressive levothyroxine therapy for differentiated thyroid cancer. Ann. Surg. Treat. Res. 86 (2), 55–60.

Lei, J., Mariash, C.N., Bhargava, M., Wattenberg, E.V., Ingbar, D.H., 2008. T3 increases Na-K-ATPase activity via a MAPK/ERK1/2-dependent pathway in rat adult alveolar epithelial cells. Am. J. Physiol. Lung Cell Mol. Physiol. 294 (4), L749–L754.

Lewinson, D., Bialik, G.M., Hochberg, Z., 1994. Differential effects of hypothyroidism on the cartilage and the osteogenic process in the mandibular condyle: recovery by growth hormone and thyroxine. Endocrinology 135 (4), 1504–1510.

Lin, J.D., Pei, D., Hsia, T.L., Wu, C.Z., Wang, K., Chang, Y.L., Hsu, C.H., Chen, Y.L., Chen, K.W., Tang, S.H., 2011. The relationship between thyroid function and bone mineral density in euthyroid healthy subjects in Taiwan. Endocr. Res. 36 (1), 1–8.

Loviselli, A., Mastinu, R., Rizzolo, E., Massa, G.M., Velluzzi, F., Sammartano, L., Mela, Q., Mariotti, S., 1997. Circulating telopeptide type I is a peripheral marker of thyroid hormone action in hyperthyroidism and during levothyroxine suppressive therapy. Thyroid 7 (4), 561–566.

Luegmayr, E., Glantschnig, H., Varga, F., Klaushofer, K., 2000. The organization of adherens junctions in mouse osteoblast-like cells (MC3T3-E1) and their modulation by triiodothyronine and 1,25-dihydroxyvitamin D3. Histochem. Cell Biol. 113 (6), 467–478.

Luegmayr, E., Varga, F., Frank, T., Roschger, P., Klaushofer, K., 1996. Effects of triiodothyronine on morphology, growth behavior, and the actin cytoskeleton in mouse osteoblastic cells (MC3T3-E1). Bone 18 (6), 591–599.

Lupoli, G., Nuzzo, V., Di Carlo, C., Affinito, P., Vollery, M., Vitale, G., Cascone, E., Arlotta, F., Nappi, C., 1996. Effects of alendronate on bone loss in pre- and postmenopausal hyperthyroid women treated with methimazole. Gynecol. Endocrinol. 10 (5), 343–348.

Ma, R., Morshed, S., Latif, R., Zaidi, M., Davies, T.F., 2011. The influence of thyroid-stimulating hormone and thyroid-stimulating hormone receptor antibodies on osteoclastogenesis. Thyroid 21 (8), 897–906.

Majima, T., Komatsu, Y., Doi, K., Takagi, C., Shigemoto, M., Fukao, A., Morimoto, T., Corners, J., Nakao, K., 2006. Negative correlation between bone mineral density and TSH receptor antibodies in male patients with untreated Graves' disease. Osteoporos. Int. 17 (7), 1103–1110.

Mana, D.L., Zanchetta, M.B., Zanchetta, J.R., 2017. Retreatment with teriparatide: our experience in three patients with severe secondary osteoporosis. Osteoporos. Int. 28 (4), 1491–1494.

Mansouri, A., Chowdhury, K., Gruss, P., 1998. Follicular cells of the thyroid gland require Pax8 gene function. Nat. Genet. 19 (1), 87–90.

Marcus, R., 1975. Cyclic nucleotide phosphodiesterase from bone: characterization of the enzyme and studies of inhibition by thyroid hormones. Endocrinology 96 (2), 400–408.

Martinez, M.E., Herranz, L., de Pedro, C., Pallardo, L.F., 1986. Osteocalcin levels in patients with hyper- and hypothyroidism. Horm. Metab. Res. 18 (3), 212–214.

McCarthy, T.L., Centrella, M., Canalis, E., 1989. Regulatory effects of insulin-like growth factors I and II on bone collagen synthesis in rat calvarial cultures. Endocrinology 124 (1), 301–309.

McKenna, N.J., O'Malley, B.W., 2002. Combinatorial control of gene expression by nuclear receptors and coregulators. Cell 108 (4), 465–474.

McKenna, N.J., Xu, J., Nawaz, Z., Tsai, S.Y., Tsai, M.J., O'Malley, B.W., 1999. Nuclear receptor coactivators: multiple enzymes, multiple complexes, multiple functions. J. Steroid Biochem. Mol. Biol. 69 (1–6), 3–12.

Meier, C., Beat, M., Guglielmetti, M., Christ-Crain, M., Staub, J.J., Kraenzlin, M., 2004. Restoration of euthyroidism accelerates bone turnover in patients with subclinical hypothyroidism: a randomized controlled trial. Osteoporos. Int. 15 (3), 209–216.

Melton, L.J., Ardila, E., Crowson, C.S., O'Fallon, W.M., Khosla, S., 2000. Fractures following thyroidectomy in women: a population-based cohort study. Bone 27 (5), 695–700.

Milne, M., Kang, M.I., Cardona, G., Quail, J.M., Braverman, L.E., Chin, W.W., Baran, D.T., 1999. Expression of multiple thyroid hormone receptor isoforms in rat femoral and vertebral bone and in bone marrow osteogenic cultures. J. Cell. Biochem. 74 (4), 684–693.

Milne, M., Kang, M.I., Quail, J.M., Baran, D.T., 1998. Thyroid hormone excess increases insulin-like growth factor I transcripts in bone marrow cell cultures: divergent effects on vertebral and femoral cell cultures. Endocrinology 139 (5), 2527–2534.

Mirza, F., Canalis, E., 2015. Management of endocrine disease: secondary osteoporosis: pathophysiology and management. Eur. J. Endocrinol. 173 (3), R131–R151.

Miura, M., Tanaka, K., Komatsu, Y., Suda, M., Yasoda, A., Sakuma, Y., Ozasa, A., Nakao, K., 2002. Thyroid hormones promote chondrocyte differentiation in mouse ATDC5 cells and stimulate endochondral ossification in fetal mouse tibias through iodothyronine deiodinases in the growth plate. J. Bone Miner. Res. 17 (3), 443–454.

Miyakawa, M., Tsushima, T., Demura, H., 1996. Carboxy-terminal propeptide of type 1 procollagen (P1CP) and carboxy-terminal telopeptide of type 1 collagen (1CTP) as sensitive markers of bone metabolism in thyroid disease. Endocr. J. 43 (6), 701–708.

Mochizuki, Y., Banba, N., Hattori, Y., Monden, T., 2006. Correlation between serum osteoprotegerin and biomarkers of bone metabolism during antithyroid treatment in patients with Graves' disease. Horm. Res. 66 (5), 236–239.

Moeller, L.C., Cao, X., Dumitrescu, A.M., Seo, H., Refetoff, S., 2006. Thyroid hormone mediated changes in gene expression can be initiated by cytosolic action of the thyroid hormone receptor beta through the phosphatidylinositol 3-kinase pathway. Nucl. Recept. Signal. 4, e020.

Monfoulet, L.E., Rabier, B., Dacquin, R., Anginot, A., Photsavang, J., Jurdic, P., Vico, L., Malaval, L., Chassande, O., 2011. Thyroid hormone receptor β mediates thyroid hormone effects on bone remodeling and bone mass. J. Bone Miner. Res. 26 (9), 2036–2044.

Mora, S., Weber, G., Marenzi, K., Signorini, E., Rovelli, R., Proverbio, M.C., Chiumello, G., 1999. Longitudinal changes of bone density and bone resorption in hyperthyroid girls during treatment. J. Bone Miner. Res. 14 (11), 1971–1977.

Moran, C., Schoenmakers, N., Agostini, M., Schoenmakers, E., Offiah, A., Kydd, A., Kahaly, G., Mohr-Kahaly, S., Rajanayagam, O., Lyons, G., Wareham, N., Halsall, D., Dattani, M., Hughes, S., Gurnell, M., Park, S.M., Chatterjee, K., 2013. An adult female with resistance to thyroid hormone mediated by defective thyroid hormone receptor α. J. Clin. Endocrinol. Metab. 98 (11), 4254–4261.

Morris, M.S., 2007. The association between serum thyroid-stimulating hormone in its reference range and bone status in postmenopausal American women. Bone 40 (4), 1128–1134.

Mosekilde, L., Christensen, M.S., 1977. Decreased parathyroid function in hyperthyroidism: interrelationships between serum parathyroid hormone, calcium-phosphorus metabolism and thyroid function. Acta Endocrinol. 84 (3), 566–575.

Mosekilde, L., Eriksen, E.F., Charles, P., 1990. Effects of thyroid hormones on bone and mineral metabolism. Endocrinol Metab. Clin. N. Am. 19 (1), 35–63.

Mosekilde, L., Melsen, F., 1978. Morphometric and dynamic studies of bone changes in hypothyroidism. Acta Pathol. Microbiol. Scand. 86 (1), 56–62.

Mudde, A.H., Houben, A.J., Nieuwenhuijzen Kruseman, A.C., 1994. Bone metabolism during anti-thyroid drug treatment of endogenous subclinical hyperthyroidism. Clin. Endocrinol. 41 (4), 421–424.

Mundy, G.R., Shapiro, J.L., Bandelin, J.G., Canalis, E.M., Raisz, L.G., 1976. Direct stimulation of bone resorption by thyroid hormones. J. Clin. Investig. 58 (3), 529–534.

Murphy, E., Glüer, C.C., Reid, D.M., Felsenberg, D., Roux, C., Eastell, R., Williams, G.R., 2010. Thyroid function within the upper normal range is associated with reduced bone mineral density and an increased risk of nonvertebral fractures in healthy euthyroid postmenopausal women. J. Clin. Endocrinol. Metab. 95 (7), 3173–3181.

Nagasaka, S., Sugimoto, H., Nakamura, T., Kusaka, I., Fujisawa, G., Sakuma, N., Tsuboi, Y., Fukuda, S., Honda, K., Okada, K., Ishikawa, S., Saito, T., 1997. Antithyroid therapy improves bony manifestations and bone metabolic markers in patients with Graves' thyrotoxicosis. Clin. Endocrinol. 47 (2), 215–221.

Nakamura, H., Mori, T., Genma, R., Suzuki, Y., Natsume, H., Andoh, S., Kitahara, R., Nagasawa, S., Nishiyama, K., Yoshimi, T., 1996. Urinary excretion of pyridinoline and deoxypyridinoline measured by immunoassay in hypothyroidism. Clin. Endocrinol. 44 (4), 447–451.

Noh, H.M., Park, Y.S., Lee, J., Lee, W., 2015. A cross-sectional study to examine the correlation between serum TSH levels and the osteoporosis of the lumbar spine in healthy women with normal thyroid function. Osteoporos. Int. 26 (3), 997–1003.

Nyström, E., Lundberg, P.A., Petersen, K., Bengtsson, C., Lindstedt, G., 1989. Evidence for a slow tissue adaptation to circulating thyroxine in patients with chronic L-thyroxine treatment. Clin. Endocrinol. 31 (2), 143–150.

O'Shea, P.J., Bassett, J.H., Cheng, S.Y., Williams, G.R., 2006. Characterization of skeletal phenotypes of TRalpha1 and TRbeta mutant mice: implications for tissue thyroid status and T3 target gene expression. Nucl. Recept. Signal. 4, e011.

O'Shea, P.J., Harvey, C.B., Suzuki, H., Kaneshige, M., Kaneshige, K., Cheng, S.Y., Williams, G.R., 2003. A thyrotoxic skeletal phenotype of advanced bone formation in mice with resistance to thyroid hormone. Mol. Endocrinol. 17 (7), 1410–1424.

Ohishi, K., Ishida, H., Nagata, T., Yamauchi, N., Tsurumi, C., Nishikawa, S., Wakano, Y., 1994. Thyroid hormone suppresses the differentiation of osteoprogenitor cells to osteoblasts, but enhances functional activities of mature osteoblasts in cultured rat calvaria cells. J. Cell. Physiol. 161 (3), 544–552.

Olkawa, M., Kushida, K., Takahashi, M., Ohishi, T., Hoshino, H., Suzuki, M., Ogihara, H., Ishigaki, J., Inoue, T., 1999. Bone turnover and cortical bone mineral density in the distal radius in patients with hyperthyroidism being treated with antithyroid drugs for various periods of time. Clin. Endocrinol. 50 (2), 171–176.

Ongphiphadhanakul, B., Jenis, L.G., Braverman, L.E., Alex, S., Stein, G.S., Lian, J.B., Baran, D.T., 1993. Etidronate inhibits the thyroid hormone-induced bone loss in rats assessed by bone mineral density and messenger ribonucleic acid markers of osteoblast and osteoclast function. Endocrinology 133 (6), 2502–2507.

Pantazi, H., Papapetrou, P.D., 2000. Changes in parameters of bone and mineral metabolism during therapy for hyperthyroidism. J. Clin. Endocrinol. Metab. 85 (3), 1099–1106.

Patel, K.V., Brennan, K.L., Brennan, M.L., Jupiter, D.C., Shar, A., Davis, M.L., 2014. Association of a modified frailty index with mortality after femoral neck fracture in patients aged 60 years and older. Clin. Orthop. Relat. Res. 472 (3), 1010–1017.

Paul, T.L., Kerrigan, J., Kelly, A.M., Braverman, L.E., Baran, D.T., 1988. Long-term L-thyroxine therapy is associated with decreased hip bone density in premenopausal women. J. Am. Med. Assoc. 259 (21), 3137–3141.

Pirskanen, A., Jääskeläinen, T., Mäenpää, P.H., 1993. Insulin-like growth factor-1 modulates steroid hormone effects on osteocalcin synthesis in human MG-63 osteosarcoma cells. Eur. J. Biochem. 218 (3), 883–891.

Plateroti, M., Gauthier, K., Domon-Dell, C., Freund, J.N., Samarut, J., Chassande, O., 2001. Functional interference between thyroid hormone receptor alpha (TRalpha) and natural truncated TRDeltaalpha isoforms in the control of intestine development. Mol. Cell Biol. 21 (14), 4761–4772.

Quan, M.L., Pasieka, J.L., Rorstad, O., 2002. Bone mineral density in well-differentiated thyroid cancer patients treated with suppressive thyroxine: a systematic overview of the literature. J. Surg. Oncol. 79 (1), 62–69 discussion 69-70.

Quarto, R., Campanile, G., Cancedda, R., Dozin, B., 1992. Thyroid hormone, insulin, and glucocorticoids are sufficient to support chondrocyte differentiation to hypertrophy: a serum-free analysis. J. Cell Biol. 119 (4), 989–995.

Quignodon, L., Vincent, S., Winter, H., Samarut, J., Flamant, F., 2007. A point mutation in the activation function 2 domain of thyroid hormone receptor alpha1 expressed after CRE-mediated recombination partially recapitulates hypothyroidism. Mol. Endocrinol. 21 (10), 2350–2360.

Refetoff, S., Weiss, R.E., Usala, S.J., 1993. The syndromes of resistance to thyroid hormone. Endocr. Rev. 14 (3), 348–399.

Ren, S.G., Huang, Z., Sweet, D.E., Malozowski, S., Cassorla, F., 1990. Biphasic response of rat tibial growth to thyroxine administration. Acta Endocrinol. 122 (3), 336–340.

Reverter, J.L., Holgado, S., Alonso, N., Salinas, I., Granada, M.L., Sanmartí, A., 2005. Lack of deleterious effect on bone mineral density of long-term thyroxine suppressive therapy for differentiated thyroid carcinoma. Endocr. Relat. Cancer 12 (4), 973–981.

Rizzoli, R., Poser, J., Bürgi, U., 1986. Nuclear thyroid hormone receptors in cultured bone cells. Metabolism 35 (1), 71–74.

Robson, H., Siebler, T., Stevens, D.A., Shalet, S.M., Williams, G.R., 2000. Thyroid hormone acts directly on growth plate chondrocytes to promote hypertrophic differentiation and inhibit clonal expansion and cell proliferation. Endocrinology 141 (10), 3887–3897.

Rosen, H.N., Moses, A.C., Gundberg, C., Kung, V.T., Seyedin, S.M., Chen, T., Holick, M., Greenspan, S.L., 1993a. Therapy with parenteral pamidronate prevents thyroid hormone-induced bone turnover in humans. J. Clin. Endocrinol. Metab. 77 (3), 664–669.

Rosen, H.N., Sullivan, E.K., Middlebrooks, V.L., Zeind, A.J., Gundberg, C., Dresner-Pollak, R., Maitland, L.A., Hock, J.M., Moses, A.C., Greenspan, S.L., 1993b. Parenteral pamidronate prevents thyroid hormone-induced bone loss in rats. J. Bone Miner. Res. 8 (10), 1255–1261.

Rosenthal, A.K., Henry, L.A., 1999. Thyroid hormones induce features of the hypertrophic phenotype and stimulate correlates of CPPD crystal formation in articular chondrocytes. J. Rheumatol. 26 (2), 395–401.

Saggese, G., Bertelloni, S., Baroncelli, G.I., 1990. Bone mineralization and calciotropic hormones in children with hyperthyroidism. Effects of methimazole therapy. J. Endocrinol. Investig. 13 (7), 587–592.

Sakurai, A., Miyamoto, T., Refetoff, S., DeGroot, L.J., 1990. Dominant negative transcriptional regulation by a mutant thyroid hormone receptor-beta in a family with generalized resistance to thyroid hormone. Mol. Endocrinol. 4 (12), 1988–1994.

Saltó, C., Kindblom, J.M., Johansson, C., Wang, Z., Gullberg, H., Nordström, K., Mansén, A., Ohlsson, C., Thorén, P., Forrest, D., Vennström, B., 2001. Ablation of TRalpha2 and a concomitant overexpression of alpha1 yields a mixed hypo- and hyperthyroid phenotype in mice. Mol. Endocrinol. 15 (12), 2115–2128.

Sampath, T.K., Simic, P., Sendak, R., Draca, N., Bowe, A.E., O'Brien, S., Schiavi, S.C., McPherson, J.M., Vukicevic, S., 2007. Thyroid-stimulating hormone restores bone volume, microarchitecture, and strength in aged ovariectomized rats. J. Bone Miner. Res. 22 (6), 849–859.

Sato, K., Han, D.C., Fujii, Y., Tsushima, T., Shizume, K., 1987. Thyroid hormone stimulates alkaline phosphatase activity in cultured rat osteoblastic cells (ROS 17/2.8) through 3,5,3'-triiodo-L-thyronine nuclear receptors. Endocrinology 120 (5), 1873–1881.

Scarlett, A., Parsons, M.P., Hanson, P.L., Sidhu, K.K., Milligan, T.P., Burrin, J.M., 2008. Thyroid hormone stimulation of extracellular signal-regulated kinase and cell proliferationin human osteoblast-like cells is initiated at integrin alphaVbeta3. J. Endocrinol. 196 (3), 509–517.

Schiller, C., Gruber, R., Ho, G.M., Redlich, K., Gober, H.J., Katzgraber, F., Willheim, M., Hoffmann, O., Pietschmann, P., Peterlik, M., 1998. Interaction of triiodothyronine with 1alpha,25-dihydroxyvitamin D3 on interleukin-6-dependent osteoclast-like cell formation in mouse bone marrow cell cultures. Bone 22 (4), 341–346.

Schlesinger, B., Fisher, O.D., 1951. Accelerated skeletal development from thyrotoxicosis and thyroid overdosage in childhood. Lancet 2 (6677), 289–290.

Schmid, C., Schläpfer, I., Futo, E., Waldvogel, M., Schwander, J., Zapf, J., Froesch, E.R., 1992. Triiodothyronine (T3) stimulates insulin-like growth factor (IGF)-1 and IGF binding protein (IGFBP)-2 production by rat osteoblasts in vitro. Acta Endocrinol. 126 (5), 467–473.

Schmid, C., Steiner, T., Froesch, E.R., 1986. Triiodothyronine increases responsiveness of cultured rat bone cells to parathyroid hormone. Acta Endocrinol. 111 (2), 213–216.

Sharma, D., Fondell, J.D., 2002. Ordered recruitment of histone acetyltransferases and the TRAP/Mediator complex to thyroid hormone-responsive promoters in vivo. Proc. Natl. Acad. Sci. U. S. A. 99 (12), 7934–7939.

Sherman, S.I., Ringel, M.D., Smith, M.J., Kopelen, H.A., Zoghbi, W.A., Ladenson, P.W., 1997. Augmented hepatic and skeletal thyromimetic effects of tiratricol in comparison with levothyroxine. J. Clin. Endocrinol. Metab. 82 (7), 2153–2158.

Shirazi, M., Dehpour, A.R., Jafari, F., 1999. The effect of thyroid hormone on orthodontic tooth movement in rats. J. Clin. Pediatr. Dent. 23 (3), 259–264.

Siddiqi, A., Burrin, J.M., Wood, D.F., Monson, J.P., 1998. Tri-iodothyronine regulates the production of interleukin-6 and interleukin-8 in human bone marrow stromal and osteoblast-like cells. J. Endocrinol. 157 (3), 453–461.

Siddiqi, A., Parsons, M.P., Lewis, J.L., Monson, J.P., Williams, G.R., Burrin, J.M., 2002. TR expression and function in human bone marrow stromal and osteoblast-like cells. J. Clin. Endocrinol. Metab. 87 (2), 906–914.

Soskolne, W.A., Schwartz, Z., Goldstein, M., Ornoy, A., 1990. The biphasic effect of triiodothyronine compared to bone resorbing effect of PTH on bone modelling of mouse long bone in vitro. Bone 11 (5), 301–307.

Stamato, F.J., Amarante, E.C., Furlanetto, R.P., 2000. Effect of combined treatment with calcitonin on bone densitometry of patients with treated hypothyroidism. Rev. Assoc. Med. Bras. 46 (2), 177–181.

Stevens, D.A., Harvey, C.B., Scott, A.J., O'Shea, P.J., Barnard, J.C., Williams, A.J., Brady, G., Samarut, J., Chassande, O., Williams, G.R., 2003. Thyroid hormone activates fibroblast growth factor receptor-1 in bone. Mol. Endocrinol. 17 (9), 1751–1766.

Stevens, D.A., Hasserjian, R.P., Robson, H., Siebler, T., Shalet, S.M., Williams, G.R., 2000. Thyroid hormones regulate hypertrophic chondrocyte differentiation and expression of parathyroid hormone-related peptide and its receptor during endochondral bone formation. J. Bone Miner. Res. 15 (12), 2431–2442.

Stracke, H., Rossol, S., Schatz, H., 1986. Alkaline phosphatase and insulin-like growth factor in fetal rat bone under the influence of thyroid hormones. Horm. Metab. Res. 18 (11), 794.

Sugitani, I., Fujimoto, Y., 2011. Effect of postoperative thyrotropin suppressive therapy on bone mineral density in patients with papillary thyroid carcinoma: a prospective controlled study. Surgery 150 (6), 1250–1257.

Sun, L., Vukicevic, S., Baliram, R., Yang, G., Sendak, R., McPherson, J., Zhu, L.L., Iqbal, J., Latif, R., Natrajan, A., Arabi, A., Yamoah, K., Moonga, B.S., Gabet, Y., Davies, T.F., Bab, I., Abe, E., Sampath, K., Zaidi, M., 2008. Intermittent recombinant TSH injections prevent ovariectomy-induced bone loss. Proc. Natl. Acad. Sci. U. S. A. 105 (11), 4289–4294.

Sun, L., Zhu, L.L., Lu, P., Yuen, T., Li, J., Ma, R., Baliram, R., Moonga, S.S., Liu, P., Zallone, A., New, M.I., Davies, T.F., Zaidi, M., 2013. Genetic confirmation for a central role for TNFα in the direct action of thyroid stimulating hormone on the skeleton. Proc. Natl. Acad. Sci. U. S. A. 110 (24), 9891–9896.

Suwanwalaikorn, S., Ongphiphadhanakul, B., Braverman, L.E., Baran, D.T., 1996. Differential responses of femoral and vertebral bones to long-term excessive L-thyroxine administration in adult rats. Eur. J. Endocrinol. 134 (5), 655–659.

Suwanwalaikorn, S., Van Auken, M., Kang, M.I., Alex, S., Braverman, L.E., Baran, D.T., 1997. Site selectivity of osteoblast gene expression response to thyroid hormone localized by in situ hybridization. Am. J. Physiol. 272 (2 Pt 1), E212–E217.

Tarjan, G., Stern, P.H., 1995. Triiodothyronine potentiates the stimulatory effects of interleukin-1 beta on bone resorption and medium interleukin-6 content in fetal rat limb bone cultures. J. Bone Miner. Res. 10 (9), 1321–1326.

Tauchmanovà, L., Nuzzo, V., Del Puente, A., Fonderico, F., Esposito-Del Puente, A., Padulla, S., Rossi, A., Bifulco, G., Lupoli, G., Lombardi, G., 2004. Reduced bone mass detected by bone quantitative ultrasonometry and DEXA in pre- and postmenopausal women with endogenous subclinical hyperthyroidism. Maturitas 48 (3), 299–306.

Toh, S.H., Claunch, B.C., Brown, P.H., 1985. Effect of hyperthyroidism and its treatment on bone mineral content. Arch. Intern. Med. 145 (5), 883–886.

Torchia, J., Glass, C., Rosenfeld, M.G., 1998. Co-activators and co-repressors in the integration of transcriptional responses. Curr. Opin. Cell Biol. 10 (3), 373–383.

Tsai, J.A., Janson, A., Bucht, E., Kindmark, H., Marcus, C., Stark, A., Zemack, H.R., Torring, O., 2004. Weak evidence of thyrotropin receptors in primary cultures of human osteoblast-like cells. Calcif. Tissue Int. 74 (5), 486–491.

Turner, M.R., Camacho, X., Fischer, H.D., Austin, P.C., Anderson, G.M., Rochon, P.A., Lipscombe, L.L., 2011. Levothyroxine dose and risk of fractures in older adults: nested case-control study. BMJ 342, d2238.

Tylki-Szymańska, A., Acuna-Hidalgo, R., Krajewska-Walasek, M., Lecka-Ambroziak, A., Steehouwer, M., Gilissen, C., Brunner, H.G., Jurecka, A., Różdżyńska-Świątkowska, A., Hoischen, A., Chrzanowska, K.H., 2015. Thyroid hormone resistance syndrome due to mutations in the thyroid hormone receptor α gene (THRA). J. Med. Genet. 52 (5), 312–316.

Udayakumar, N., Chandrasekaran, M., Rasheed, M.H., Suresh, R.V., Sivaprakash, S., 2006. Evaluation of bone mineral density in thyrotoxicosis. Singap. Med. J. 47 (11), 947–950.

Uzzan, B., Campos, J., Cucherat, M., Nony, P., Boissel, J.P., Perret, G.Y., 1996. Effects on bone mass of long term treatment with thyroid hormones: a meta-analysis. J. Clin. Endocrinol. Metab. 81 (12), 4278–4289.

Vadiveloo, T., Donnan, P.T., Cochrane, L., Leese, G.P., 2011. The Thyroid Epidemiology, Audit, and Research Study (TEARS): morbidity in patients with endogenous subclinical hyperthyroidism. J. Clin. Endocrinol. Metab. 96 (5), 1344–1351.

Van Den Eeden, S.K., Barzilay, J.I., Ettinger, B., Minkoff, J., 2003. Thyroid hormone use and the risk of hip fracture in women > or = 65 years: a case-control study. J. Womens Health 12 (1), 27–31.

van Mullem, A., van Heerebeek, R., Chrysis, D., Visser, E., Medici, M., Andrikoula, M., Tsatsoulis, A., Peeters, R., Visser, T.J., 2012. Clinical phenotype and mutant TRα1. N. Engl. J. Med. 366 (15), 1451–1453.

van Rijn, L.E., Pop, V.J., Williams, G.R., 2014. Low bone mineral density is related to high physiological levels of free thyroxine in peri-menopausal women. Eur. J. Endocrinol. 170 (3), 461–468.

Varga, F., Rumpler, M., Klaushofer, K., 1994. Thyroid hormones increase insulin-like growth factor mRNA levels in the clonal osteoblastic cell line MC3T3-E1. FEBS Lett. 345 (1), 67–70.

Varga, F., Rumpler, M., Spitzer, S., Karlic, H., Klaushofer, K., 2009. Osteocalcin attenuates T3- and increases vitamin D3-induced expression of MMP-13 in mouse osteoblasts. Endocr. J. 56 (3), 441–450.

Varga, F., Rumpler, M., Zoehrer, R., Turecek, C., Spitzer, S., Thaler, R., Paschalis, E.P., Klaushofer, K., 2010. T3 affects expression of collagen I and collagen cross-linking in bone cell cultures. Biochem. Biophys. Res. Commun. 402 (2), 180–185.

Varga, F., Spitzer, S., Klaushofer, K., 2004. Triiodothyronine (T3) and 1,25-dihydroxyvitamin D3 (1,25D3) inversely regulate OPG gene expression in dependence of the osteoblastic phenotype. Calcif. Tissue Int. 74 (4), 382–387.

Varga, F., Spitzer, S., Rumpler, M., Klaushofer, K., 2003. 1,25-Dihydroxyvitamin D3 inhibits thyroid hormone-induced osteocalcin expression in mouse osteoblast-like cells via a thyroid hormone response element. J. Mol. Endocrinol. 30 (1), 49–57.

Vella, K.R., Hollenberg, A.N., 2017. The actions of thyroid hormone signaling in the nucleus. Mol. Cell. Endocrinol. https://doi.org/10.1016/j.mce.2017.03.001 pii: S0303-7207(17)30169-7. [Epub ahead of print].

Vestergaard, P., Mosekilde, L., 2002. Fractures in patients with hyperthyroidism and hypothyroidism: a nationwide follow-up study in 16,249 patients. Thyroid 12 (5), 411–419.

Vestergaard, P., Mosekilde, L., 2003. Hyperthyroidism, bone mineral, and fracture risk–a meta-analysis. Thyroid 13 (6), 585–593.

Vestergaard, P., Rejnmark, L., Mosekilde, L., 2005. Influence of hyper- and hypothyroidism, and the effects of treatment with antithyroid drugs and levothyroxine on fracture risk. Calcif. Tissue Int. 77 (3), 139–144.

Vestergaard, P., Rejnmark, L., Weeke, J., Mosekilde, L., 2000. Fracture risk in patients treated for hyperthyroidism. Thyroid 10 (4), 341–348.

Vincent, B.H., Montufar-Solis, D., Teng, B.B., Amendt, B.A., Schaefer, J., Klein, J.R., 2009. Bone marrow cells produce a novel TSHbeta splice variant that is upregulated in the thyroid following systemic virus infection. Genes Immun. 10 (1), 18–26.

Wallace, H., Ledent, C., Vassart, G., Bishop, J.O., al-Shawi, R., 1991. Specific ablation of thyroid follicle cells in adult transgenic mice. Endocrinology 129 (6), 3217–3226.

Wallace, H., Pate, A., Bishop, J.O., 1995. Effects of perinatal thyroid hormone deprivation on the growth and behaviour of newborn mice. J. Endocrinol. 145 (2), 251–262.

Waring, A.C., Harrison, S., Fink, H.A., Samuels, M.H., Cawthon, P.M., Zmuda, J.M., Orwoll, E.S., Bauer, D.C., Osteoporotic Fractures in Men (MrOS) Study, 2013. A prospective study of thyroid function, bone loss, and fractures in older men: the MrOS study. J. Bone Miner. Res. 28 (3), 472–479.

Wejda, B., Hintze, G., Katschinski, B., Olbricht, T., Benker, G., 1995. Hip fractures and the thyroid: a case-control study. J. Intern. Med. 237 (3), 241–247.

Wikström, L., Johansson, C., Saltó, C., Barlow, C., Campos Barros, A., Baas, F., Forrest, D., Thorén, P., Vennström, B., 1998. Abnormal heart rate and body temperature in mice lacking thyroid hormone receptor alpha 1. EMBO J. 17 (2), 455–461.

Williams, A.J., Robson, H., Kester, M.H., van Leeuwen, J.P., Shalet, S.M., Visser, T.J., Williams, G.R., 2008. Iodothyronine deiodinase enzyme activities in bone. Bone 43 (1), 126–134.

Williams, G.R., 2000. Cloning and characterization of two novel thyroid hormone receptor beta isoforms. Mol. Cell Biol. 20 (22), 8329–8342.

Williams, G.R., Bland, R., Sheppard, M.C., 1994. Characterization of thyroid hormone (T3) receptors in three osteosarcoma cell lines of distinct osteoblast phenotype: interactions among T3, vitamin D3, and retinoid signaling. Endocrinology 135 (6), 2375–2385.

Williams, G.R., Bland, R., Sheppard, M.C., 1995. Retinoids modify regulation of endogenous gene expression by vitamin D3 and thyroid hormone in three osteosarcoma cell lines. Endocrinology 136 (10), 4304–4314.

Wirth, C.D., Blum, M.R., da Costa, B.R., Baumgartner, C., Collet, T.H., Medici, M., Peeters, R.P., Aujesky, D., Bauer, D.C., Rodondi, N., 2014. Subclinical thyroid dysfunction and the risk for fractures: a systematic review and meta-analysis. Ann. Intern. Med. 161 (3), 189–199.

Wu, Y., Koenig, R.J., 2000. Gene regulation by thyroid hormone. Trends Endocrinol. Metabol. 11 (6), 207–211.

Yamamoto, M., Markatos, A., Seedor, J.G., Masarachia, P., Gentile, M., Rodan, G.A., Balena, R., 1993. The effects of the aminobisphosphonate alendronate on thyroid hormone-induced osteopenia in rats. Calcif. Tissue Int. 53 (4), 278–282.

Yamaura, M., Nakamura, T., Kanou, A., Miura, T., Ohara, H., Suzuki, K., 1994. The effect of 17 beta-estradiol treatment on the mass and the turnover of bone in ovariectomized rats taking a mild dose of thyroxin. Bone Miner. 24 (1), 33–42.

Yen, C.C., Huang, Y.H., Liao, C.Y., Liao, C.J., Cheng, W.L., Chen, W.J., Lin, K.H., 2006. Mediation of the inhibitory effect of thyroid hormone on proliferation of hepatoma cells by transforming growth factor-beta. J. Mol. Endocrinol. 36 (1), 9–21.

Yen, P.M., 2001. Physiological and molecular basis of thyroid hormone action. Physiol. Rev. 81 (3), 1097–1142.

Zeni, S., Gomez-Acotto, C., Di Gregorio, S., Mautalen, C., 2000. Differences in bone turnover and skeletal response to thyroid hormone treatment between estrogen-depleted and repleted rats. Calcif. Tissue Int. 67 (2), 173–177.

Zhang, W., Zhang, Y., Liu, Y., Wang, J., Gao, L., Yu, C., Yan, H., Zhao, J., Xu, J., 2014. Thyroid-stimulating hormone maintains bone mass and strength by suppressing osteoclast differentiation. J. Biomech. 47 (6), 1307–1314.

Chapter 39

Basic and clinical aspects of glucocorticoid action in bone

Hong Zhou[1], Mark S. Cooper[2] and Markus J. Seibel[2]

[1]The University of Sydney, ANZAC Research Institute, Sydney, NSW, Australia; [2]The University of Sydney, ANZAC Research Institute and Department of Endocrinology & Metabolism, Concord Hospital, Sydney, NSW, Australia

Chapter outline

Introduction

More than 80 years ago, Harvey Cushing described 12 patients presenting with either pituitary or adrenal adenomas. Most of these patients were found to have severe osteoporosis and Cushing noted that their "bones were easily cut with a knife" during postmortem examination (Cushing, 1932). The cause of the skeletal pathology of what is known today as "Cushing's disease" or "Cushing's syndrome" was later discovered to be the adrenal steroid hormone, 11β,17α,21-trihydroxypregn-4-ene-3,20-dione, or cortisol. In 1949, Hench and colleagues published on the use of cortisone, a glucocorticoid closely related to cortisol, in patients with rheumatoid arthritis, a report which revolutionized clinical medicine through the discovery of the potent and even today unrivaled antiinflammatory and immunosuppressive properties of glucocorticoids (Hench et al., 1949). Since then, these naturally occurring hormones as well as their pharmaceutical derivatives have been used with great benefit in the treatment of countless conditions including arthritis, inflammatory bowel disease, allergy and hypersensitivity disorders, chronic obstructive pulmonary disease, cancer, and transplant rejection.

While the clinical benefits of glucocorticoid therapy can hardly be overestimated, the use of these drugs is unfortunately associated with numerous unwanted effects such as bone loss and osteoporosis (Reid et al., 2009), insulin resistance and diabetes (Gonzalez- Gonzalez et al., 2013; Niewoehner et al., 1999), proximal myopathy, cataract, skin atrophy, delayed

Principles of Bone Biology. https://doi.org/10.1016/B978-0-12-814841-9.00039-7

wound healing, and increased risk of infection, to name only a few (Kanda et al., 2001; Natsui et al., 2006). These unwanted outcomes create a significant dilemma for clinicians, as improvements in the primary condition often seem to be achievable only by accepting significant adverse effects that are often hard to prevent or treat.

In this chapter, we will review our current understanding of the mechanisms underlying the physiology and pathophysiology of glucocorticoid action on the skeleton and discuss present and future treatments for glucocorticoid-induced osteoporosis (GIO). As a general note, it is important to realize that the actions of glucocorticoids on bone and mineral metabolism are strongly dose and time dependent. Thus, at physiological concentrations, glucocorticoids are key regulators of mesenchymal cell differentiation and therefore bone development, with additional regulatory roles in renal and intestinal calcium handling. However, at supraphysiological—i.e., therapeutic—concentrations, glucocorticoids affect the very same systems in different and often unfavorable ways. Thus, glucocorticoids can act on the skeleton in both anabolic and catabolic ways.

The physiological role of glucocorticoids in bone

Glucocorticoid signaling and prereceptor metabolism

Endogenous glucocorticoids are essential to life, as they control electrolyte and fluid homeostasis, fuel metabolism, and immune and stress responses. These actions are primarily mediated through the glucocorticoid receptor (GR) within target tissues. As such, both GR expression levels and ligand binding affinity influence glucocorticoid actions at the tissue level. The GR resides predominantly in the cytoplasm, complexed with heat-shock protein 90 (Hsp90) and several immunophilins such as FKBP51 (Zhou and Cidlowski, 2005). Upon ligand binding, the GR dissociates from this complex and undergoes a number of conformational changes that result in receptor dimerization and subsequent nuclear translocation (Lu and Cidlowski, 2006). Within the nucleus, the dimerized ligand-receptor complex binds directly to highly conserved glucocorticoid response elements (GREs) in the promoter region of target genes. This process is known as "transactivation" and usually facilitates gene transcription. The ligand-bound homodimer can also bind to negative GREs, thereby inhibiting gene transcription, an effect known as transrepression. On the other hand, the monomeric ligand-receptor complex binds to DNA-bound transcription factors such as STAT5, which enhances gene expression in a process known as tethered transactivation. The monomer can also bind to proinflammatory signaling molecules in the cytosol, preventing interaction with effector transcription factors such as AP-1 or NF-κB. This process is known as indirect or tethered transrepression (Moutsatsou et al., 2012) (Fig. 39.1). The traditional view of glucocorticoid action was that the antiinflammatory effects of glucocorticoids are caused by transrepression, whereas adverse outcomes largely arise from its transactivation capacities (Newton and Holden, 2007). However, it is now clear that this model was oversimplistic, with some antiinflammatory responses being due to transactivation—e.g., transaction induces the expression of the antiinflammatory protein dual specificity phosphatase 1 (DUSP1)—and some adverse outcomes due to transrepression—e.g., glucocorticoid inhibition of bone formation (Cooper et al., 2012; Rauch et al., 2010). Further adding to the diversity of glucocorticoid signaling mechanisms, many of the actions of the glucocorticoid receptors at the level of DNA may in fact by due to monomeric complexes (Meijsing et al., 2009). There is additionally evidence for nongenomic actions of glucocorticoids which typically happen more rapid than traditional genomic responses. These nongenomic mechanisms may involve non-GR-mediated interactions of glucocorticoids with cell membranes, nongenomic effects mediated by cytosolic GRs, or interactions of glucocorticoids with membrane-bound glucocorticoid receptors (Stahn and Buttgereit, 2008).

Endogenous glucocorticoid levels are systemically regulated via the hypothalamic−pituitary−adrenal axis. However, glucocorticoid action depends not only on plasma and interstitial fluid hormone concentrations, but also on cellular glucocorticoid levels. Within specific tissues, the 11β-hydroxysteroid dehydrogenase (11βHSD) enzymes metabolize glucocorticoids at the prereceptor level and control intracellular hormone availability via interconversion of biologically active and inactive ligands (Stewart and Krozowski, 1999). Thus, 11β-HSD type 1 (11βHSD1) predominantly catalyzes formation of active cortisol (in humans) and corticosterone (in rodents) from inactive cortisone and 11-dehydrocorticosterone, respectively, leading to increased intracellular glucocorticoid concentrations. This enzyme also converts inactive prednisone to active prednisolone—individuals who lack this activity are unresponsive to prednisone treatment but remain sensitive to prednisolone. In contrast, 11β-HSD type 2 (11βHSD2) unidirectionally catalyzes conversion of active glucocorticoids to their inactive metabolites (Fig. 39.1). The latter enzyme is primarily expressed in mineralocorticoid target tissues such as the kidney, where it protects the mineralocorticoid receptor from illicit activation by cortisol (Stewart and Krozowski, 1999). Of note, cytokines, growth factors, and certain other enzymes are able to modulate glucocorticoid metabolism via changing 11β-HSD enzyme activities on a predominantly local level (Cooper et al., 2001).

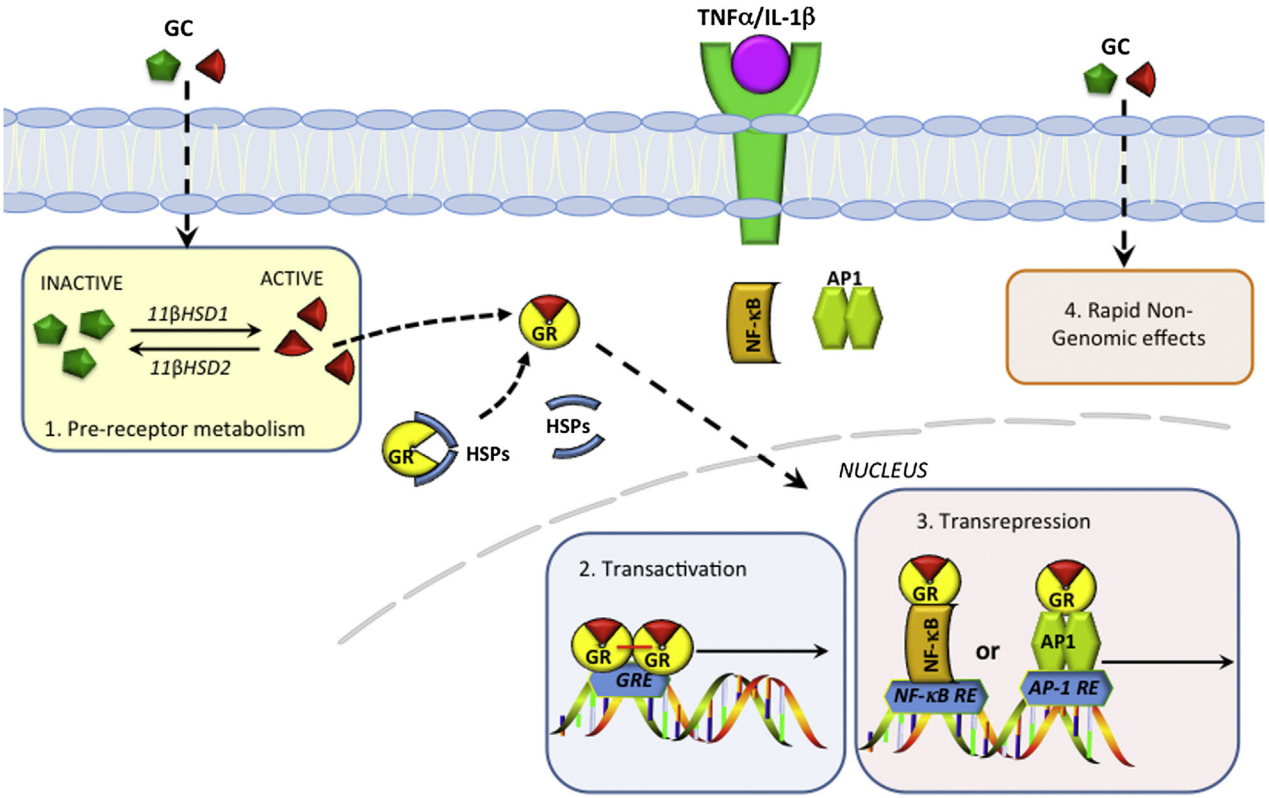

FIGURE 39.1 Glucocorticoid signaling. Glucocorticoids are lipophilic and cross the cell membrane freely. In many tissues, glucocorticoids undergo prereceptor metabolism by the cytosolic 11β-HSD enzymes. Thus, 11β-HSD type 1 converts inactive glucocorticoids (cortisone in humans, dehydrocorticosterone in rodents) to the active form (cortisol and corticosterone, respectively). Conversely, 11β-HSD type 2 converts cortisol and corticosterone into their inactive pendants. Active glucocorticoids bind to the cytoplasmic glucocorticoid receptor to form a complex that is able to translocate to the nucleus, where it either binds to its specific response element or to other transcription factors such as AP-1 (fos and jun) or NF-κβ, resulting in transactivation or transrepression of gene expression. Rapid nongenomic effects have also been described.

Local glucocorticoid metabolism in bone

As discussed above, local metabolism of glucocorticoids impacts their actions within bone. Expression of the 11βHSD1 enzyme has been extensively characterized in bone (Cooper et al., 2000; Weinstein et al., 2010b). Human bone tissue has the ability to interconvert cortisone and cortisol, but the kinetics of the reaction indicate the presence of the 11βHSD1 enzyme rather than 11βHSD2 (Cooper et al., 2000). This is supported by immunohistochemistry and in situ hybridization studies that localize the expression of 11βHSD1 primarily to osteoblasts. In ex vivo studies, the activity of 11βHSD1 in primary human osteoblasts is dependent on donor age, with expression low in young donors but high in osteoblasts isolated from older donors (Cooper et al., 2002). An age-related change in expression is paralleled in mice in vivo (Weinstein et al., 2010b). Mice with global deletion of 11βHSD1 have no overt abnormality in bone structure (Justesen et al., 2004); however, the bone phenotype of aged 11βHSD1 knockout animals has not been examined. In elderly humans, a negative correlation between plasma cortisone levels and osteocalcin has been observed, a relationship independent of plasma cortisol (Cooper et al., 2005). This study suggests that 11βHSD1 activity has functional consequences on osteoblasts in vivo. A similar negative association between cortisone and spine bone density was also seen in this study. Genetic association studies have linked the presence of allelic variants of *HSD11B1* (the gene for 11βHSD1) that predict low activity of 11βHSD1 with an increase in bone density and a reduction in vertebral fracture risk (Hwang et al., 2009). These data suggest that some of the adverse age-related changes in bone could be glucocorticoid mediated, but with exposure restricted to the osteoblast through local production by the 11βHSD1 enzyme. An analogous role for 11βHSD1 and endogenous glucocorticoids in skin aging has recently been demonstrated (Tiganescu et al., 2013).

Novel insights from targeted disruption of glucocorticoid signaling in bone

Investigating the effects of endogenous glucocorticoids on tissue function has been difficult, as global deletion of the GR in mice leads to early postnatal lethality (Cole et al., 1995). Over the past 2 decades, advances in cell-specific disruption of glucocorticoid signaling in mouse models have greatly improved our understanding of the physiological role of glucocorticoids in bone development and structure. Osteoblast-targeted deletion of the GR ($GR^{Runx2Cre}$) in mice results in an overall reduction in bone volume (Rauch et al., 2010). Correspondingly, calvarial osteoblast cultures derived from $GR^{Runx2Cre}$ mice demonstrate a reduction in osteoblast differentiation and the ability to form mineralized nodules (Rauch et al., 2010). Although not expressed naturally in postnatal bone cells, the 11βHSD2 enzyme has been used as a tool to examine the effects of endogenous glucocorticoids on the skeleton by targeted transgenic expression of 11βHSD2 within bone cells. This has the added advantage over GR deletion models that other possible signaling pathways in osteoblasts such as the mineralocorticoid receptor are also targeted. Transgenic mice in which 11βHSD2 expression is driven by a 2.3 kb collagen type I (Col2.3) promoter are characterized by targeted disruption of glucocorticoid signaling exclusively in mature osteoblasts and osteocytes (Sher et al., 2004, 2006). These mice (usually referred to as "Col2.3-11βHSD2 transgenic" mice) exhibit a phenotype of delayed calvarial bone development. Thus, embryonic and neonatal Col2.3-11βHSD2 transgenic mice display calvarial bone hypoplasia, osteopenia, increased suture patency, ectopic differentiation of cartilage in the sagittal suture, and a defect in the postnatal removal of parietal cartilage (Zhou et al., 2009). Similar to $GR^{Runx2Cre}$ mice, Col2.3-11βHSD2 transgenic adult mice of both sexes have reduced bone volume, lower trabecular number, and lower cortical bone mass (Kalak et al., 2009; Sher et al., 2004).

In a different model, the 11βHSD2 transgene is driven by the 3.6 kb collagen type I promoter ("Col3.6-11βHSD2 transgenic mice"). These animals exhibit a phenotype similar to that of Col2.3-11βHSD2 transgenic mice, including defects in calvarial bone development (Yang et al., 2010). Together, these findings strongly support the notion that endogenous glucocorticoids play a critical role in mesenchymal and osteoblast differentiation, accrual of bone mass, and the development of a healthy skeletal structure (Kalak et al., 2009; Rauch et al., 2010; Sher et al., 2004, 2006).

Endogenous glucocorticoids promote osteoblastogenesis

It has long been known from osteoblast cultures that the addition of glucocorticoids to the culture medium is crucial for the formation of mineralized nodules (Bellows et al., 1987), suggesting that these hormones are essential for differentiation of mesenchymal cells into mature osteoblasts (Haynesworth et al., 1992; Herbertson and Aubin, 1995). Evidence obtained from Col2.3-11βHSD2 transgenic mice indicates that this action of glucocorticoids is not through direct effects on mesenchymal progenitor cells but rather mediated indirectly through mature osteoblasts (Sher et al., 2006). Thus, calvarial cell cultures derived from Col2.3-11βHSD2 transgenic mice exhibit greatly reduced osteoblastogenesis and increased adipogenesis compared with cultures from animals with intact osteoblastic glucocorticoid signaling (i.e., wild-type mice). This phenotypic shift in mesenchymal progenitor cell commitment is accompanied by a reduction in Wnt7b and Wnt10b mRNA expression and β-catenin protein levels in transgenic compared with wild-type cultures. In addition, in the calvarial cell culture system, mature osteoblasts appear to be the dominant source of Wnt proteins, in particular Wnt7b, Wnt10b and Wnt9a, which are important stimulators of osteoblastogenesis. Thus, at physiological concentrations, glucocorticoids directly stimulate osteoblasts to produce and release Wnt proteins, which then act in a paracrine manner to activate the canonical Wnt signaling cascade in mesenchymal stem cells (MSCs). This results in the accumulation of β-catenin and the expression of the master regulator of osteoblast differentiation, runt-related transcription factor 2 (RUNX2) in MSCs, which drives the differentiation of these pluripotent cells toward the osteoblastic lineage. The Wnt signaling cascade in MSCs is further enhanced by the glucocorticoid-induced downregulation of potent Wnt suppressors such as sFRP1 (secreted frizzled-related protein 1) (Fig. 39.2) (Mak et al., 2009; Zhou et al., 2008). These pathways act synergistically to direct MSCs away from the adipogenic and toward the osteoblastic lineage. This mechanism is proven to be of importance in cranial bone development in vivo.

The skeletal changes in these mice are due to a lack of paracrine Wnt signaling by Col2.3-11βHSD2 transgenic osteoblasts. In addition to controlling lineage commitment, the glucocorticoid-induced increase in osteoblastic paracrine Wnt signaling affects the surrounding chondrocytes by inducing the expression of matrix metalloproteinase 14 (Mmp14). Mmp14 is central to the breakdown of extracellular matrix during development and tissue remodeling, and vital for cartilage removal during the process of ossification (Zhou et al., 2009). These concurrent and tightly interconnected pathways establish a novel role for both glucocorticoids and osteoblasts in the intricate process of intramembranous bone development.

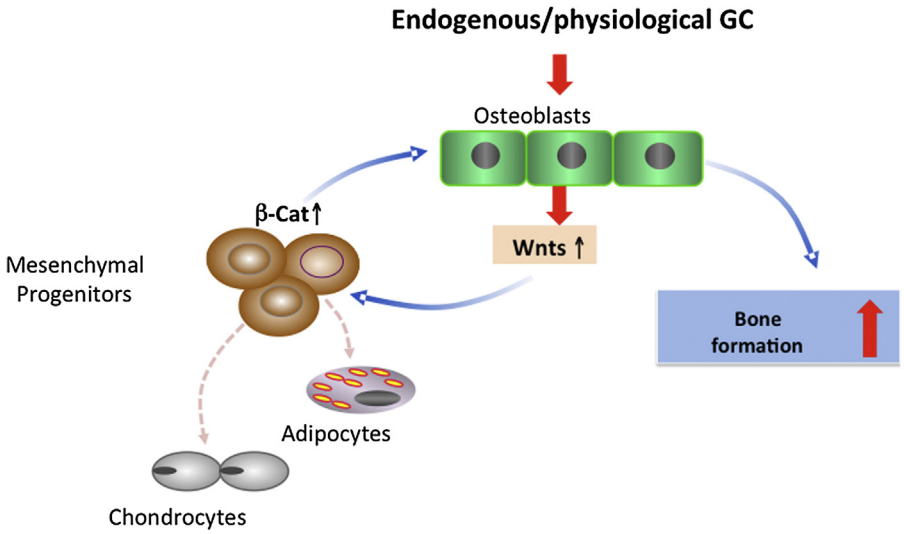

FIGURE 39.2 Schematic illustration of the effects of endogenous glucocorticoids on bone. At physiological concentrations, glucocorticoids stimulate mature osteoblasts to produce canonical Wnt proteins, which activate the β-catenin signaling cascade in mesenchymal progenitor cells. This in turn promotes differentiation of these immature cells toward the osteoblastic cell linage, with negative effects on chondro- and adipocytogenesis. Endogenous glucocorticoid signaling in osteoblasts therefore favors bone formation.

In summary, it is now clear that endogenous glucocorticoids control osteoblast differentiation, skeletal development during normal intramembranous bone formation, and trabecular and cortical bone mass accrual in mice.

Glucocorticoid excess and the skeleton

Nearly 65 years after their introduction into clinical practice by Hench and colleagues (Hench et al., 1949), glucocorticoids are still the most widely and frequently used class of antiinflammatory drugs. Survey data from 1996 estimated that in the UK, 0.5% of the population, 1.75% of women aged over 55 years, and up to 68% of patients with rheumatoid arthritis are on continuous treatment with oral glucocorticoids (Walsh et al., 1996). Later studies, also from the UK, found that up to 2.5% of people aged between 70 and 79 years receive oral glucocorticoids on an ongoing basis (van Staa et al., 2000a). A more recent multinational population-based study indicated that globally, up to 4.6% of postmenopausal women are taking oral glucocorticoids (Diez-Perez et al., 2011). In the US, data from several NHANES survey cycles demonstrate that the prevalence of glucocorticoid use remains above 1% of the general population (Overman et al., 2013) (Fig. 39.3). The major reason for the widespread use of therapeutic glucocorticoids is their unsurpassed antiinflammatory and immunomodulatory efficacy (reviewed in Buttgereit et al., 2011).

Therapeutic glucocorticoids, particularly when used over extended periods, cause significant off-target effects that are similar to the clinical signs and symptoms of endogenous hypercortisolism (Cushing's disease/syndrome). These include but are not limited to musculoskeletal conditions such as osteoporosis, osteonecrosis, myopathy, and sarcopenia, as well as metabolic effects resulting in glucose intolerance or diabetes mellitus, dyslipidemia, and excessive and abnormal fat accrual (Pereira and Freire de Carvalho, 2011; Schakman et al., 2008). Other adverse effects of prolonged glucocorticoid therapy include skin atrophy, hypertension, adrenal suppression, glaucoma, cataract, delayed wound healing, increased risk of infection, and in children, growth retardation.

Recognized as the most common form of secondary osteoporosis, GIO represents an iatrogenic problem of major clinical relevance across numerous specialties. Thus, one in five patients treated with oral glucocorticoids suffers an osteoporotic fracture within the first 12 months of therapy (Adachi et al., 1997; Cohen et al., 1999). This number increases to 50% after 5−10 years (Walsh et al., 1999, 2002), with most fractures occurring in the spine, proximal femur, and ribs. The relative risk of fracture increases as a function of glucocorticoid dose and duration of therapy, while absolute fracture risk is determined by a range of additional clinical risk factors such as age, gender, and comorbidities. Fracture risk is highest during the first few months following commencement of treatment (van Staa et al., 2000b, 2002) and decreases when therapy is ceased. Of note, even daily doses as low as 2.5 mg of prednisolone equivalent have been associated with increased fracture rates (van Staa et al., 2000b) (Fig. 39.4). Long-term inhaled glucocorticoid therapy in children and adults is also associated with significant bone loss (Wong et al., 2000). Despite the clear evidence for the detrimental effects of

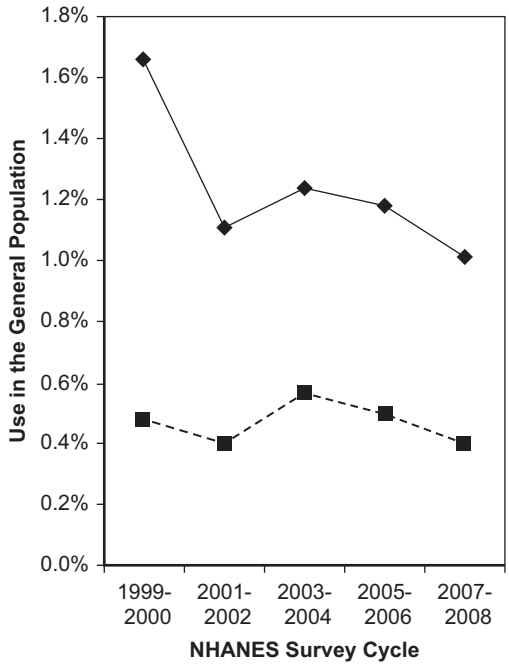

FIGURE 39.3 Prevalence of glucocorticoid use and antiosteoporosis therapy. Data were extracted from five National Health and Nutrition Examination Surveys. Diamonds represent glucocorticoid use. Squares represent concomitant antiosteoporosis therapy (Overman et al., 2013).

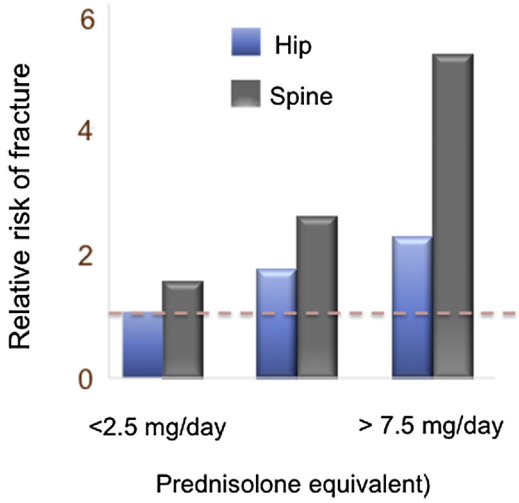

FIGURE 39.4 Relative risk of vertebral and hip fracture according to daily glucocorticoid dose. Note that even glucocorticoid doses considered by most clinicians as "low" (i.e., less than 2.5 mg prednisolone equivalent per day) are associated with a significant increase in fracture risk over time. *Adapted from van Staa, T.P., Leufkens, H.G., Abenhaim, L., Zhang, B., Cooper, C., 2000b. Oral corticosteroids and fracture risk: relationship to daily and cumulative doses. Rheumatology (Oxford) 39, 1383–1389.*

glucocorticoids on bone health, only a small proportion of patients receiving these medications are being treated to prevent bone loss and fractures (Overman et al., 2013) (Fig. 39.3).

Pathogenesis of glucocorticoid-induced osteoporosis

The main mechanisms underlying GIO are the direct action of glucocorticoids on bone cells, in particular on osteoblasts and osteocytes. Other effects are related to mineral metabolism such as decreased intestinal calcium absorption and increased renal calcium clearance (Canalis et al., 2007; Kuroki et al., 2008) as well as decreased growth hormone secretion (Mazziotti and Giustina, 2013) and alteration in sex steroid metabolism (Manolagas, 2013) (Table 39.1).

TABLE 39.1 Extraskeletal pathways contributing to glucocorticoid-induced osteoporosis.

Signaling pathway	Effect	References
Altered calcium balance	Glucocorticoid-induced decrease in calcium resorption and increase in calcium secretion may interfere with bone metabolism	Canalis et al. (2007)
Increased proteolysis in skeletal muscle	May contribute to a higher frequency of falls and fractures	Canalis et al. (2007), Pereira and Freire de Carvalho (2011), Schakman et al. (2008)
Growth hormone (GH) deficiency	Glucocorticoid-induced suppression of GH may contribute to the severity of GIO	Mazziotti and Giustina (2013)
Altered sex hormones	Glucocorticoid-induced suppression of testosterone and/or estrogen may contribute to GIO	Canalis et al. (2007), van Staa (2006)
Altered PTH pulsatility	Glucocorticoids may alter PTH pulsatility, which may contribute to bone loss	Bonadonna et al. (2005), Canalis et al. (2007)

In bone, glucocorticoid excess affects osteoblasts, osteocytes, and osteoclasts. Earlier, mostly histomorphometric studies indicated that the predominant feature of GIO is a suppression of osteoblast activity and hence of bone formation while osteoclast numbers are either unchanged or slightly increased (Weinstein et al., 1998). These data were sufficient to understand that the pathogenesis of GIO was fundamentally different from that of postmenopausal osteoporosis. The mechanisms by which glucocorticoids exert their actions on bone remained elusive, however. With the advent of more sophisticated technologies, we now have a more detailed (although still incomplete) understanding of the cellular and molecular actions of glucocorticoids in bone.

Although the individual effects of glucocorticoid excess on osteoblasts, osteocytes, and osteoclasts have been well characterized in vitro, the high degree of reciprocal interconnectivity between bone cells has made it difficult to dissect the skeletal actions of glucocorticoids in vivo. In this context, the development of genetically modified mouse models in which only one specific subset of bone cells has been shielded from the effects of exogenous glucocorticoids has provided useful information on the main target cells and molecular mechanisms involved in the pathogenesis of GIO. Thus, recent studies in rodents have demonstrated that protecting the *osteoclast* from excessive glucocorticoid signaling partly prevents the increase in osteoclast lifespan and bone resorption normally seen with glucocorticoid treatment (see also below) (Jia et al., 2006; Kim et al., 2006). However, as a consequence of the ongoing suppression of osteoblast and osteocyte function, bone formation remains compromised in most of these models (Jia et al., 2006; Rauch et al., 2010), inevitably leading to reduced bone strength over a prolonged period. Thus, in the long-term, the direct effects of glucocorticoids on osteoclasts appear to contribute little to the loss of bone mass and strength seen in GIO.

Conversely, protecting the osteoblast (and with that the osteocyte) from excessive glucocorticoid exposure and signaling not only prevents osteoblast and osteocyte apoptosis, but in fact preserves osteoblast function and bone formation (O'Brien et al., 2004). Furthermore, in these animal models, bone strength and quality are maintained despite the presence of supraphysiological plasma glucocorticoid levels (Henneicke et al., 2011; O'Brien et al., 2004; Rauch et al., 2010). Abrogating glucocorticoid signaling in osteoblasts/osteocytes also prevents the increase in osteoclast number and activity in addition to changes in bone vascularity and the lacunar–canalicular system normally seen with glucocorticoid excess (Henneicke et al., 2011; Weinstein et al., 2010b). Therefore, some of the effects of exogenous glucocorticoids on the osteoclast are preventable when the osteoblast/osteocyte system is shielded from excessive glucocorticoid signaling, pointing to the cells of the osteoblast lineage as the main target of exogenous glucocorticoids within the skeleton.

Glucocorticoid excess and its effects on osteoblast differentiation

It has been well established that glucocorticoid excess inhibits both osteoblast differentiation and function, while at the same time inducing osteoblast apoptosis, resulting in a rapid (within hours) and profound suppression of bone formation (Kauh et al., 2012; Weinstein et al., 1998). In recent years, a number of molecular targets and mechanisms underlying these osteoblast-specific glucocorticoid actions have been identified. For example, exposure to supraphysiological glucocorticoid concentrations suppresses the very pathways that at physiological levels promote osteoblastogenesis, namely Wnt and bone morphogenetic protein 2 (BMP-2) signaling: At high concentrations, glucocorticoids inhibit the synthesis and release of

Wnt-related transcription factors by mature osteoblasts (Mak et al., 2009). Downregulation of Wnt signaling leads to impaired osteoblast differentiation via a reduction in molecular downstream signals such as β-catenin and RUNX2 transcription factors (see above). Additionally, high intracellular levels of glucocorticoids enhance β-catenin degradation via increased glycogen synthase kinase 3 beta expression, a protein, which drives β-catenin ubiquitinylation and proteasomal degradation (Wang et al., 2009) and promotes the osteoblastic expression of Wnt inhibitors (Hayashi et al., 2009; Kato et al., 2018; Mak et al., 2009). These glucocorticoid-inducible soluble antagonists act on MSCs, inhibiting Wnt/β-catenin signaling and thereby reducing osteoblast differentiation (Yao et al., 2008; Zhou et al., 2008). Moreover, glucocorticoid excess concurrently increases expression of transcription factors critical for adipocyte differentiation such as peroxisome proliferator-activated receptor γ (Yao et al., 2008), suggesting that the commitment of MSC to the adipocyte lineage limits the pool of cells available to differentiate into osteoblasts. However, this hypothesis requires further investigation.

Another key regulator of osteoblast differentiation, BMP-2, is profoundly inhibited in mice receiving glucocorticoids at therapeutic concentrations (Yao et al., 2008). In addition, dexamethasone treatment of osteoblast cultures has been reported to substantially increase the expression of follistatin and Dan, two BMP-2 antagonists (Hayashi et al., 2009), thus exacerbating the inhibition of BMP-2 signaling in osteoblasts. Recent studies have demonstrated that the monomeric glucocorticoid-GR complex is sufficient to significantly impair osteoblast differentiation (Rauch et al., 2010), most likely due to interference with the proinflammatory transcription factor AP-1 and suppression of IL-11 (Rauch et al., 2011). The latter cytokine has previously been shown to promote bone formation (Takeuchi et al., 2002). Indeed, the addition of IL-11 to glucocorticoid-treated osteoblast cultures protects these cells from glucocorticoid-induced reduction in differentiation potential. IL-11 has also been shown to promote BMP-2 signaling (Takeuchi et al., 2002) and more recently demonstrated to suppress the production of Wnt antagonists (Matsumoto et al., 2012). Thus, a reduction in IL-11 activity appears to attenuate two critically important signaling pathways that control differentiation in osteoblasts. Analyzing bone specimens from patients with GIO and prednisolone-treated mice, a recent study (Liu et al., 2017a) documented increased levels of casein kinase-2 interacting protein-1 (CKIP-1), a ubiquitination-related protein facilitating Smurf1-mediated Smad1/5 ubiquitination (Lu et al., 2008). Interestingly, mice with osteoblast-specific CKIP-1 deletion maintained normal BMP signaling and were protected from glucocorticoid-induced bone loss (Liu et al., 2017a).

In recent years, microRNAs (miRs) have been discovered to play an important role in osteoblast differentiation. Excess glucocorticoids modulate the expression pattern of microRNAs, impairing osteoblastogenesis. Thus, miR-29a expression in bone has been demonstrated to decrease with glucocorticoid exposure. Overexpression of miR-29a in transgenic mice mitigates glucocorticoid-induced bone loss by protecting against impaired osteogenic differentiation (Ko et al., 2015). Glucocorticoids promote HDAC4 signaling, subsequently accelerating RUNX2 and β-catenin ubiquitination.

Overexpressing miR-29a significantly attenuates glucocorticoid-mediated RUNX2 deacetylation and β-catenin ubiquitination via inhibiting HDAC4 action (Ko et al., 2013, 2015). Dexamethasone treatment upregulates miR-199a-5p expression, inhibiting osteoblast proliferation through reducing FZD4 and Wnt2 expression. Deletion of miR-199a-5p attenuates dexamethasone-induced inhibition of osteoblast proliferation (Shi et al., 2015). More recently, it has been reported that silencing miR-106b expression provides protection from glucocorticoid-induced bone loss through restoring BMP2 expression, which consequently maintains osteoblast differentiation and bone formation (Liu et al., 2017b). In contrast to these catabolic microRNAs, miR-34a-5p promotes osteoblast differentiation through suppression of Notch signaling. Glucocorticoids reduce the expression of miR-34a-5p, thereby inhibiting osteogenic differentiation (Kang et al., 2016).

The simultaneous reduction in both Wnt/β-catenin and BMP-2 signaling during glucocorticoid excess leads to a significant shift in MSC differentiation, a reduction in osteoblastogenesis, and consequently a loss of osteoblast-generated proteins such as collagen and osteocalcin (Moutsatsou et al., 2012; Yao et al., 2008).

Glucocorticoids prevent osteoblast cell cycle progression

Exposure of osteoblasts to high concentrations of glucocorticoids in vitro has been shown to disrupt physiological cell cycle progression (Chang et al., 2009). A marked decrease in cyclin D2 and an increase in cyclin-dependent kinase inhibitor 1B ($p27^{kip1}$) following dexamethasone treatment of human osteoblasts has been observed, consistent with cell cycle arrest at the G0 and G1 phase (Chang et al., 2009). Dexamethasone has also been reported to increase the expression of DUSP1 in cultured osteoblasts, with a corresponding decrease in the phosphorylation status of mitogen-activated protein kinase 1 (MAPK1). The dephosphorylation of MAPK1 impairs osteoblast response to mitogenic signaling, inhibiting cell proliferation (Horsch et al., 2007). Furthermore, dexamethasone suppresses the osteoblastic expression of cyclin A, a protein crucial for the transition from G1 to S phase during or after commitment to the osteoblast lineage (Gabet et al.,

2011). Cell cycle progression via the canonical Wnt signaling pathway requires the association of β-catenin with LEF/TCF transcription factors, both of which are inhibited by high glucocorticoid levels. In the face of reduced Wnt and β-catenin signaling, the reduction in LEF/TCF further inhibits the G1 to S phase transition (Jia et al., 2006).

Glucocorticoids induce osteoblast apoptosis

Pharmacological doses of glucocorticoids induce osteoblast apoptosis both in vitro and in vivo through a number of proapoptotic pathways. Administration of dexamethasone to osteoblast cultures dose-dependently increases proapoptotic factors of the Bcl-2 family such as Bim (Espina et al., 2008). Correspondingly, knockdown of Bim in osteoblasts significantly reduces glucocorticoid-induced apoptosis (Espina et al., 2008). Furthermore, silencing E4BP4, a basic leucine zipper transcription factor, attenuates glucocorticoid-induced Bim expression and blocks osteoblast apoptosis induced by dexamethasone treatment (Chen et al., 2014). In addition, glucocorticoid-induced increases in Bak, another proapoptotic member of the Bcl-2 family, as well as a decrease in Bcl-XL expression, a prosurvival Bcl-2 protein, further drive osteoblasts toward cell death (Chang et al., 2009). Exposure of osteoblasts to dexamethasone in vitro also results in upregulation of the tumor suppressor and apoptosis regulator, p53, and subsequent Bcl-2 mediated cell apoptosis (Li et al., 2012). Glucocorticoids have also been found to induce osteoblast apoptosis via a reduction in β1-integrin expression, which leads to a loss of cell-matrix adhesion (Naves et al., 2011). High-dose glucocorticoids may induce osteoblast apoptosis through activation of $p66^{shc}$ and an increase in reactive oxygen species (ROS), which in turn leads to constitutive activation of the JNK pathway (Almeida et al., 2011) or induces endoplasmic reticulum (ER) stress (Sato et al., 2015). Opposing ER stress by inhibiting eIF2α dephosphorylation prevents osteoblast and osteocyte apoptosis and attenuates osteoblast dysfunction induced by glucocorticoids in vitro and in vivo (Sato et al., 2015).

In summary, glucocorticoids at supraphysiological or pharmacological concentrations are detrimental to the skeleton through potent suppression of osteoblastogenesis, induction of osteoblast dysfunction, diversion of MSC to the adipocyte lineage, as well as promotion of osteoblastic cell cycle arrest and apoptosis (Fig. 39.5). Overall, exposure to high dose glucocorticoids not only compromises the skeleton's ability to form new bone, but also profoundly disturbs the regulatory balance between bone formation and resorption, which eventually leads to a reduction in bone mass and an increase in fracture risk.

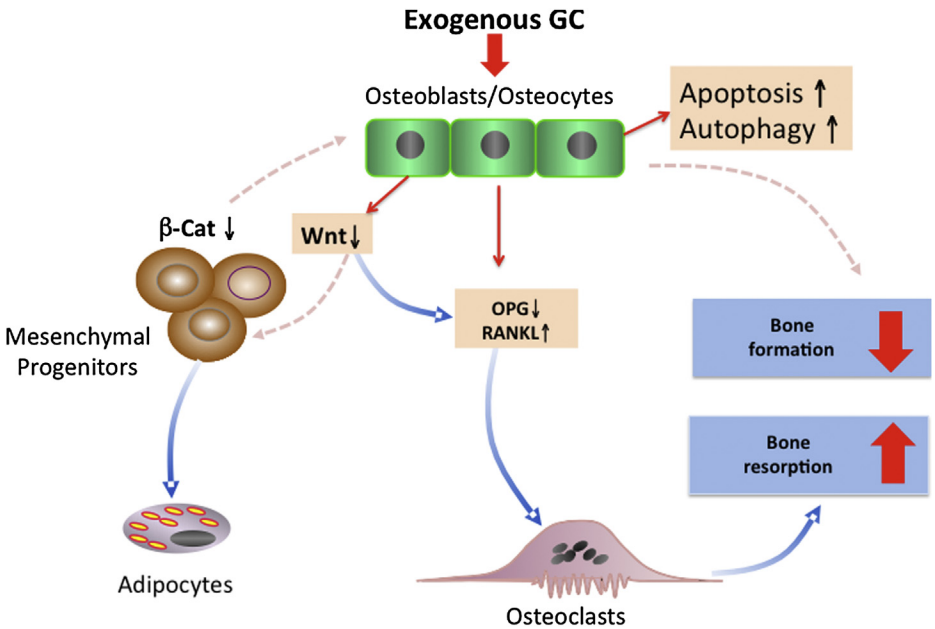

FIGURE 39.5 Schematic illustration of the effects of exogenous glucocorticoid on bone. High-dose glucocorticoids negatively impact osteoblast and osteocyte function through (1) inhibition of Wnt protein expression in mature osteoblasts (which results in mesenchymal progenitor cells differentiating preferentially toward adipocytes and away from osteoblasts); (2) stimulation of RANKL and inhibition of OPG expression (resulting in an increase in the RANKL/OPG ratio which favors bone resorption); and (3) induction of osteoblast and osteocyte apoptosis (which reduces bone formation).

Glucocorticoid excess and the osteocyte

The osteocyte is the most abundant cell type in the skeleton, representing 90%–95% of the entire cell mass (Crockett et al., 2011). The complex osteocyte network functions as a mechanosensor, which maintains bone integrity through the recruitment of osteoblasts and osteoclasts to the sites of active bone remodeling (Temiyasathit and Jacobs, 2010). Furthermore, this system as well as its fluid content has been shown to lend the skeleton a high degree of stiffness (Weinstein et al., 2010b). High glucocorticoid concentrations not only lead to a substantial loss of intraosseous vasculature, but also to a decrease in the solute transport from the circulation to the lacunar–canalicular system (Weinstein et al., 2010a, 2010b). The reduction in overall intraskeletal fluid content is strongly associated with the glucocorticoid-induced decrease in bone strength but not necessarily bone mass (Weinstein et al., 2010a).

Treatment with pharmacological doses of glucocorticoids has been shown to cause intracellular damage and induce osteocyte autophagy both in vitro and in vivo (Jia et al., 2011; Xia et al., 2010). With prolonged exposure to glucocorticoids, pathological buildup of autophagosomes occurs, and as the osteocyte is embedded in the bone matrix, the degraded materials expelled from the autophagosomes create an environment toxic to the cell, leading to cellular demise (Jia et al., 2011). Glucocorticoid-induced autophagy subsequently results in connexin43 degradation, thereby impairing osteocyte cell-cell connectivity (Gao et al., 2016). Additionally, higher rates of osteocyte apoptosis have been linked to activation of proapoptotic kinases, Pyk2 and JNK, in osteocytes (Bellido, 2010). While activation of JNK leads to an increase in ROS and eventually programmed cell death, activation of the protein tyrosine kinase Pyk2 results in the reorganization of the cytoskeleton, cell detachment, and ultimately apoptosis (Bellido, 2010).

In summary, recent evidence has highlighted both the osteocyte and the lacunar–canalicular network as important targets of glucocorticoid-induced damage to bone. The reduction in skeletal fluid content in conjunction with decreased osteocyte viability represents an important novel mechanism by which excessive levels of glucocorticoids may compromise bone stability without affecting actual bone mass.

Glucocorticoid excess and the osteoclast

During the initial stage of glucocorticoid therapy, there is a rapid but transient increase in bone resorption due to an increase in osteoclast number and activity (Dovio et al., 2004; Henneicke et al., 2011; Jia et al., 2006). In humans, biochemical markers of bone resorption increase within 24 h of exposure to therapeutic levels of glucocorticoids (Dovio et al., 2004). Experimental studies have established that glucocorticoids directly extend the lifespan of mature osteoclasts by delaying apoptotic signaling, which over time leads to a significant increase in osteoclast numbers (Jia et al., 2006; Kim et al., 2006). Osteoclast formation is further amplified indirectly through glucocorticoid-induced changes in osteoblast gene expression. For example, high levels of glucocorticoids stimulate the production of RANKL by cells of the osteoblast lineage while simultaneously reducing the expression of the RANKL decoy receptor, OPG (Hofbauer et al., 1999; Sivagurunathan et al., 2005). This imbalance in the RANKL-OPG ratio leads to a profound increase in osteoclast activity and bone resorption.

Furthermore, the effect of glucocorticoids on osteoblastic RANKL expression appears to be mediated by miR-17/20a (Shi et al., 2014).

Under physiological conditions, the major source of RANKL and hence the primary driver of osteoclastogenesis is the osteocyte rather than the osteoblast (Nakashima et al., 2011; Xiong et al., 2011). In vitro studies show that the osteocyte presents membrane-bound RANKL to osteoclast precursors at the extremities of their dendritic processes rather than secreting soluble RANKL (Honma et al., 2013). Whether this process is affected by glucocorticoids is yet to be determined. Apoptosis of osteocytes leads, seemingly paradoxically, to an increase in RANKL concentrations, possibly due to signaling of dying cells to surrounding healthy osteocytes, which then in turn express RANKL (Kennedy et al., 2012). However, another study reported that osteocyte apoptotic bodies strongly induce osteoclastogenesis in vitro, although this occurred independently of RANKL expression (Kogianni et al., 2008). As glucocorticoids are known to induce osteocyte apoptosis, the subsequent induction of RANKL or other signaling pathways may contribute to the increase in osteoclastogenesis observed following glucocorticoid exposure.

Apart from its function as a potent inhibitor of osteoblast function, sclerostin may also have a role as a potential inductor of osteoclast activity and bone resorption (Li et al., 2008). Recent studies provide in vivo evidence that sclerostin-induced bone resorption may be an important contributor to bone loss under conditions of glucocorticoid excess (Henneicke et al., 2017; Sato et al., 2016). When exposed to high concentrations of glucocorticoids, sclerostin-deficient mice are protected from increased bone resorption and bone loss. However, sclerostin deficiency does not prevent glucocorticoid-induced osteoblast/osteocyte apoptosis and impaired bone formation (Sato et al., 2016). A similar

mechanism may play a role in relaying the effects of chronic stress on bone resorption. Chronic stress exposure leads to elevated levels of circulating glucocorticoids, resulting in bone loss, increased bone resorption, and enhanced Sost/sclerostin expression in wild-type mice but not in mice where glucocorticoid signaling has been disrupted in osteoblasts and osteocytes (Henneicke et al., 2017). These results indicate that stress-related bone loss is mediated via the effects of glucocorticoids on osteoblasts/osteocytes and subsequent activation of osteoclasts through amplified expression of Sost/sclerostin (Henneicke et al., 2017).

Despite an initial increase in bone resorption, prolonged glucocorticoid excess appears to suppress osteoclast number and function, directly blocking the induction of cytoskeletal changes in the osteoclast required for bone resorption (Kim et al., 2007). There is also evidence that glucocorticoids suppress the proliferation of osteoclast precursors, or more specifically, uncommitted bone marrow macrophages (Kim et al., 2006, 2007).

Overall, exposure to exogenous glucocorticoids causes an initial rise in bone resorption, which contributes to the early and rapid loss of bone mineral density. During long-term therapy, however, the disruptive effects of glucocorticoids on the cytoskeleton and suppression of osteoclastogenesis appear to be the predominant feature as far as the osteoclast is concerned (Fig. 39.5).

Glucocorticoid excess and local glucocorticoid metabolism

Local steroid metabolism through expression of the 11βHSD1 enzyme is also likely to influence glucocorticoid impacts on bone. Prednisone and prednisolone, the main oral glucocorticoids used clinically, are metabolized by this enzyme in a similar fashion to cortisone and cortisol (Cooper et al., 2002). Systemic measures of 11βHSD1 obtained in healthy control subjects strongly predict the extent to which oral glucocorticoids have an impact on bone formation markers such as osteocalcin (Cooper et al., 2003). However, 11βHSD1 expression in osteoblasts is regulated by a range of factors that are likely to be of relevance to people treated with glucocorticoids. Both proinflammatory cytokines and glucocorticoids increase expression and activity of 11βHSD1 (Cooper et al., 2001, 2002; Kaur et al., 2010), potentially increasing the sensitivity of bone to glucocorticoids during inflammatory illness. However, 11βHSD1 expression is also increased in a range of tissues during inflammation (Kaur et al., 2010). Global deletion of 11βHSD1 in mice increases the severity of a range of models of experimental inflammation (Coutinho et al., 2012). It is therefore possible that any increased sensitivity of bone to glucocorticoids through an increase in 11βHSD1 will be matched by increased sensitivity of the underlying disease being treated. No association of systemic 11βHSD1 activity and bone loss was seen in a trial of patients with inflammatory bowel disease treated with high-dose oral prednisolone (Cooper et al., 2011).

Indirect mechanisms for glucocorticoid-induced osteoporosis

The mechanisms described so far concern the direct consequences of glucocorticoid action on bone cells and their molecular signaling. However, particularly when given at higher doses, glucocorticoids have further systemic effects (Table 39.1), not all of which have been clearly delineated. Changes in renal and intestinal calcium handling, as well as sex and growth hormone action, have been well documented. Thus, glucocorticoids reduce intestinal calcium absorption while inhibiting calcium reabsorption in the kidney (Ritz et al., 1984). This leads to a negative net calcium balance, which may adversely affect bone mineralization. It was previously thought that glucocorticoid-mediated alteration of (and in particular increased) PTH secretion was also a common feature to account for bone loss (Fucik et al., 1975). However, many studies have subsequently failed to find direct links to between glucocorticoids and increased PTH signaling, and it is now considered that changes in PTH secretion or action do not play a central role in GIO (Rubin and Bilezikian, 2002). Clearly, however, increased PTH secretion can be a secondary and appropriate response in the context of a prolonged negative net calcium balance induced by glucocorticoids.

When given at higher doses, glucocorticoids can induce hypogonadism through suppression of the HP axis, which in turn may contribute to bone loss and increased fracture risk (Chrousos et al., 1998). Other hormones have also been implicated in indirect effects of glucocorticoids on bone. In particular, glucocorticoids cause a reduction in IGF1, a powerful stimulator of osteoblast function, and thus any reduction in its levels might result in a reduced anabolic action on bone. However, studies involving calvarial bones from mice with deletion of the IGF1 receptor demonstrated that glucocorticoids still have a major negative effect on collagen synthesis, suggesting that changes in IGF1 signaling are not a major part of the actions of glucocorticoids on osteoblasts (Woitge and Kream, 2000). Although a small observational study in children with arthritis treated with glucocorticoids suggested a protective effect of growth hormone (GH) treatment on bone density GH/IGF1, treatment has not been evaluated in the context of a randomized controlled trial in patients taking glucocorticoids.

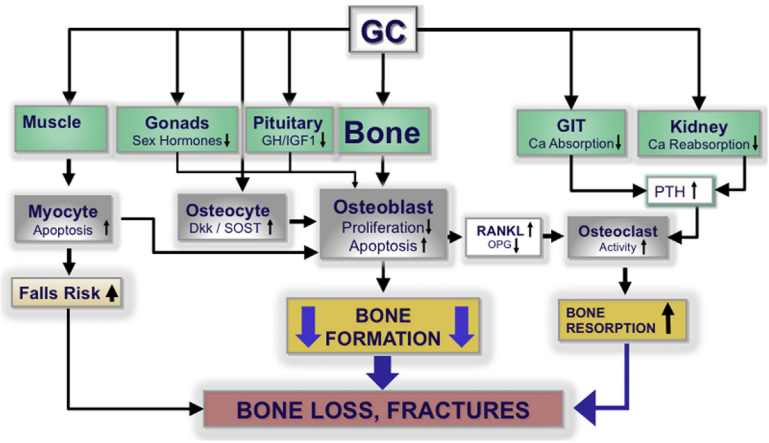

FIGURE 39.6 Schematic summary of the detrimental effects of therapeutic or excess glucocorticoids on skeletal and nonskeletal organ systems. While the skeletal adverse outcomes are mediated mainly through effects on osteoblasts, many other systems contribute to the increase in fracture risk in patients on long-term glucocorticoid therapy.

Proximal myopathy is a well-recognized feature of glucocorticoid excess (Pereira and Freire de Carvalho, 2011) and is thought to affect bone health directly (through its effects on bone strength) and indirectly (through an increase in falls risk) (Fig. 39.6).

Glucocorticoid excess and systemic fuel metabolism

Insulin resistance, dyslipidemia, and abnormal body fat accrual and distribution belong to the most common and problematic adverse effects of glucocorticoid therapy (reviewed in Rafacho et al., 2014). Short-term treatment with glucocorticoids is associated with impaired release of insulin from the pancreas. However, this mode of action does not feature prominently during long-term glucocorticoid use (Beard et al., 1984; Hazlehurst et al., 2013; Nicod et al., 2003; Petersons et al., 2013). Thus, patients with rheumatoid arthritis treated chronically with prednisolone tend to develop insulin resistance (Petersons et al., 2013). For most individuals, blood glucose levels remain in the nondiabetic range, but this is only achieved through a rise in plasma insulin levels. However, a significant proportion of glucocorticoid-treated individuals will develop glucose intolerance or overt diabetes mellitus. These patients tend to be those that already have a degree of insulin resistance due to their age, genetic or ethnic background, or other comorbidities (van Raalte et al., 2009). Many patients exposed to high doses of therapeutic glucocorticoids for prolonged periods also develop changes in body fat accrual and distribution. The basis for the changes in fat redistribution is unclear, but differences in response to glucocorticoids of subcutaneous and visceral adipose tissue have been proposed (Fernandez-Rodriguez et al., 2009).

Until recently, these metabolic changes were thought to be due to the direct effects of glucocorticoids on liver, pancreas, and adipose tissue. However, recent research has raised the possibility that the adverse effects of glucocorticoids on fuel metabolism are mediated, at least in part, through their action on bone. As mentioned above, glucocorticoids suppress osteoblast function and inhibit synthesis of osteocalcin, an osteoblast-derived peptide previously reported to be involved in normal glucose metabolism (Lee et al., 2007). Using transgenic and gene therapy approaches, experimental studies in mice found that the suppression of osteoblast function and associated reduction in osteocalcin signaling may be central to the pathogenesis of glucocorticoid-induced dysmetabolism (Brennan-Speranza et al., 2012). Thus, mice in which glucocorticoid signaling has been disrupted in osteoblasts and osteocytes (Col2.3-11βHSD2 transgenic mice) are not only protected from the bone-wasting effects of glucocorticoid excess but maintain normal insulin sensitivity, glucose tolerance, and body weight despite high-dose glucocorticoid treatment (Brennan-Speranza et al., 2012). Very similar effects were achieved by replacing osteocalcin in the circulation via gene therapy in glucocorticoid-treated animals.

The above studies point toward bone, and specifically the osteoblast and its product, osteocalcin, being significant regulators of energy metabolism in the context of glucocorticoid treatment. This may have clinical implications, since the metabolic adverse effects of glucocorticoids are difficult to counteract clinically. There is only a limited amount of clinical data relating to the relationship between glucocorticoids, osteocalcin, and changes in energy metabolism. The situation is particularly complicated, since most people treated with glucocorticoids will have an underlying disease that itself could influence systemic energy balance and glucose homeostasis (van Staa et al., 2000c). This is compounded by the lack of

availability of clinical approaches to selectively raise serum osteocalcin levels. One recent study has overcome some of these limitations by examining patients treated with bisphosphonates, teriparatide (PTH1-34), or calcium/vitamin D alone for GIO (Stockbrugger et al., 2002). Teriparatide is known to stimulate osteocalcin synthesis whereas bisphosphonates achieve the opposite effect. Over 12 months of therapy, bisphosphonates or calcium/vitamin D had no effect on glycemic control, whereas in teriparatide-treated patients, a small but statistically significant improvement in HbA1c was observed. This finding suggests that a treatment that stimulates osteocalcin has the potential to improve glycemic control in the setting of chronic glucocorticoid treatment.

In summary, there is now good evidence that the effects of glucocorticoid excess on fuel metabolism are at least in part mediated through the skeleton. While animal data suggest a relatively strong relationship, clinical studies that fully address this link in humans are lacking. Additionally, the detailed molecular mechanisms by which osteocalcin exerts its action, including the exact receptor(s) and tissues of action, remain uncertain. Although certainly a matter of future research, it is conceivable that the mechanisms related to the actions of osteocalcin and related osteoblast-derived proteins on fuel metabolism may become the basis of future therapies for the prevention and treatment of glucocorticoid-induced dysmetabolism (Ferris and Kahn, 2012).

Treatment of glucocorticoid-induced osteoporosis

While the negative effects of glucocorticoids on bone health have been known to clinicians for many years, GIO remains underdiagnosed and undertreated. Despite increasing awareness of the various forms of osteoporosis among patients and health care providers, recognition of the potentially devastating consequences of glucocorticoid therapy on the skeleton, and the knowledge of how to prevent or treat these outcomes, are still inadequate (Curtis et al., 2005; Feldstein et al., 2005; Overman et al., 2013) (Fig. 39.3). In part, this deficit may be due to the "osteoporosis care gap"—i.e., a lack of adequate medical care that worldwide leaves 70%–80% of patients with osteoporotic fractures undiagnosed and untreated (Eisman et al., 2012). In addition, the complex actions of glucocorticoids in bone and elsewhere, and the uncertainties regarding intervention thresholds for the prevention and treatment of the disease, may contribute to current inadequacies in the recognition and management of patients with GIO.

Assessment of the patient with glucocorticoid-induced osteoporosis

Oral or parental glucocorticoids are almost always used to treat systemic inflammatory conditions, which through increased inflammatory cytokine output affect bone health independent of medication-induced adverse effects (Hardy and Cooper, 2009). This is best demonstrated in rheumatoid arthritis, where inflammatory disease activity can have a substantial negative impact on bone health through the stimulation of osteoclastogenesis and bone erosions and suppression of bone formation (Bultink et al., 2005; Gough et al., 1994; Matzelle et al., 2012). Low-dose glucocorticoid therapy has been reported to suppress inflammation in patients with early arthritis, and despite the possible negative effects of glucocorticoids on bone, results in better bone status. As such, the impact of the underlying disease on bone needs to be balanced against potentially beneficial effects of glucocorticoid therapy that may result in overall beneficial effects on skeletal health if it reduces the inflammatory activity of the underlying inflammatory disease (and hence circulating cytokine levels) (Guler-Yuksel et al., 2008; Landewe et al., 2002; van der Goes et al., 2013). These partly conflicting factors need to be considered when making the clinical decision to intervene. Nevertheless, the use of therapeutic glucocorticoids—particularly at high doses—is associated with a substantial increase in fracture risk (Fig. 39.4) (van Staa et al., 2000b, 2005).

In contrast to postmenopausal osteoporosis, measurement of bone mineral density has limited value in determining fracture risk in the context of glucocorticoid therapy (Van Staa et al., 2003). As a rule, the "fracture threshold" seems to be lower in patients on glucocorticoid therapy—i.e., fractures occur at higher bone mineral density than what has been established for women with postmenopausal osteoporosis. Although new imaging techniques such as high-resolution computed tomography and volumetric quantitative computed tomography have been found to reasonably predict fracture risk even in the context of GIO, their use outside clinical studies currently remains limited (Kalpakcioglu et al., 2011).

A comprehensive review of potential risk factors for bone loss and fracture therefore remains essential to the clinical work-up of patients with GIO. Some guidelines also recommend the use of fracture risk calculators (Grossman et al., 2010; Lekamwasam et al., 2012), although these recommendations are not without controversy. For example, instead of individual or cumulative doses, FRAX uses a fixed ("average") glucocorticoid dose to calculate fracture risk, while the Garvan fracture risk calculator does not account for glucocorticoid treatment at all. It is therefore likely that both algorithms underestimate fracture risk in patients receiving glucocorticoids at therapeutic doses.

While standard diagnostic measures such as bone mineral density testing and laboratory parameters are of limited value in the work-up of the patient with GIO, they can be useful in monitoring treatment efficacy or disease progression. Since bone loss in GIO can vary considerably between individuals, monitoring changes in bone mineral density may be helpful in identifying patients particularly susceptible to the skeletal effects of glucocorticoids. Evaluation of hepatic and renal function as well as determination of serum vitamin D, calcium, phosphate, and parathyroid hormone levels are usually recommended before commencement of treatment (Grossman et al., 2010; Lekamwasam et al., 2012).

Management of glucocorticoid-induced osteoporosis

One of the core principles of treating patients with GIO is to minimize glucocorticoid use. This is easier said than done, as more often than not reductions in glucocorticoid dosing are followed by a flare-up of the underlying condition. In these cases, concomitant treatment with a bone-sparing agent is necessary. Dose, timing, and duration of such "adjuvant therapies" are a matter of ongoing debate and vary across studies and guidelines (Grossman et al., 2010; Hansen et al., 2011; Lekamwasam et al., 2012), but there is some consensus that in patients with low bone mineral density or genuinely increased fracture risk, treatment with a bisphosphonate or teriparatide should coincide with the initiation of glucocorticoid therapy (Table 39.2). In addition, supplementation with calcium and vitamin D as required is recommended (Grossman et al., 2010; Lekamwasam et al., 2012). Thus, the 2017 American College of Rheumatology Guidelines for the Prevention and Treatment of Glucocorticoid-Induced Osteoporosis (Buckley et al., 2017), while noting the "limited evidence regarding the benefits and harms of interventions" in patients treated with glucocorticoids, recommends "treating only with calcium and vitamin D in adults at low fracture risk, treating with calcium and vitamin D plus an additional osteoporosis medication (oral bisphosphonate preferred) in adults at moderate-to-high fracture risk, continuing calcium plus vitamin D but switching from an oral bisphosphonate to another anti-fracture medication in adults in whom oral bisphosphonate treatment is not appropriate, and continuing oral bisphosphonate treatment or switching to another anti-fracture medication in adults who complete a planned oral bisphosphonate regimen but continue to receive glucocorticoid treatment" (Buckley et al., 2017).

TABLE 39.2 Recommended pharmacological interventions for the prevention and treatment of glucocorticoid-induced osteoporosis.

Intervention	Dose	Evidence grade		References[b]
		(BMD)	(Fracture)[a]	
Calcium	Oral: 1000–1500 mg daily	A[c]	–	Amin et al. (1999), Buckley et al. (1996), Sambrook et al. (1993)
Vitamin D	Oral: 800–1000 IU daily	A[d]	–	Amin et al. (1999), Buckley et al. (1996), Sambrook et al. (1993)
Alendronate	Oral: 70 mg once/week	A	B	Adachi et al. (2001), Stoch et al. (2009), Yilmaz et al. (2001)
Risedronate	Oral: 35 mg once/week	A	A	Cohen et al. (1999), Eastell et al. (2000), Reid et al. (2000), (2001), Wallach et al. (2000)
Zoledronic acid	Intravenous: 5 mg once/year	A	–	Kauh et al. (2012), Sambrook et al. (2012)
Teriparatide	Subcutaneous: 20 mg once/day	A	A	Gluer et al. (2013), Karras et al. (2012), Saag et al. (2007), (2009)
Etidronate	Oral: 400 mg daily for 2 weeks every 3 months	A	A	Adachi et al. (1997), Cortet et al. (1999), Roux et al. (1998), Struys et al. (1995)

A, several RCT or meta-analysis; B, one RCT or nonrandomized studies.
[a]*Not a primary end point and vertebral fractures only.*
[b]*Reviewed in Grossman et al. (2010), Lekamwasam et al. (2012), and Rizzoli et al. (2012).*
[c]*In combination with Vitamin D.*
[d]*In combination with calcium.*

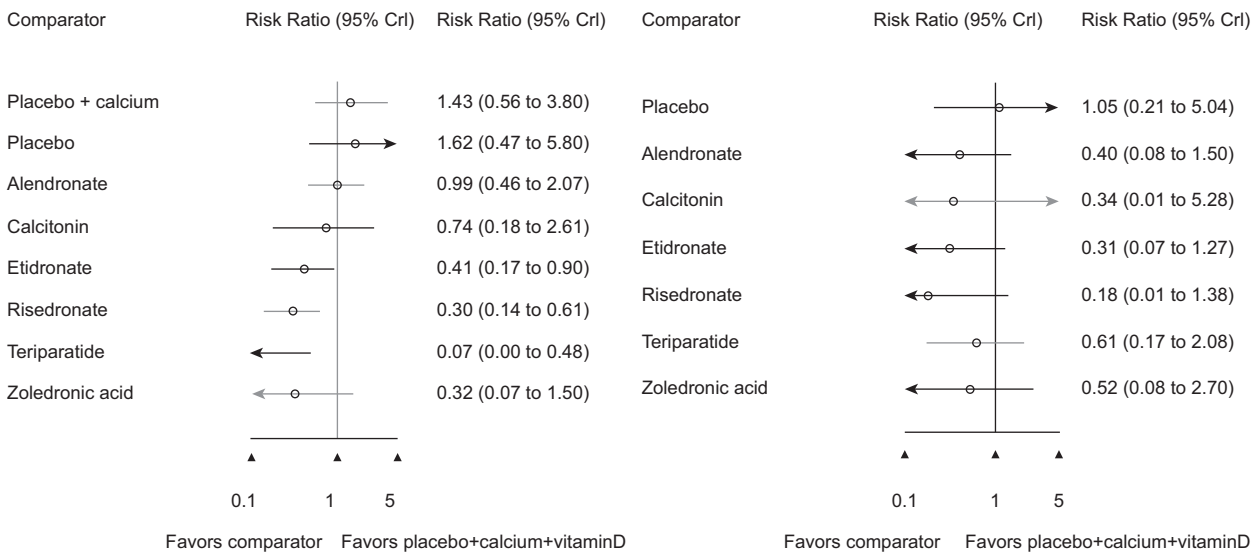

FIGURE 39.7 Efficacy of osteoporosis pharmacotherapies in preventing fracture among oral glucocorticoid users. Forest plots showing risk ratios for fracture for patients on "active" treatment versus placebo. Upper panel: Vertebral fracture. Lower panel: Nonvertebral fracture (Amiche et al., 2016).

Bisphosphonates

Bisphosphonates are the current standard in the prevention and therapy of GIO (Grossman et al., 2010; Lekamwasam et al., 2012). A recent Cochrane review concludes that "there was high-certainty evidence that bisphosphonates are beneficial in reducing the risk of vertebral fractures with data extending to 24 months of use. There was low certainty evidence that bisphosphonates may make little or no difference in preventing non-vertebral fractures" (Allen et al., 2016).

Given orally or intravenously, bisphosphonates generally act by inducing osteoclast apoptosis, thereby reducing the rate of bone resorption. While bisphosphonates prevent rapid loss of bone mineral density during the initial phase of glucocorticoid therapy, their longer-term effect on fracture risk is less well documented (de Nijs et al., 2006; Grossman et al., 2010; Saag et al., 1998). Some reports show significant reductions in vertebral or hip fracture risk (Amiche et al., 2018; Axelsson et al., 2017) but the effect on nonhip, nonvertebral fracture risk is either weak or unknown (Fig. 39.7). Most studies investigating the use of bisphosphonates in the context of GIO are underpowered to detect significant differences in fracture rates and therefore use changes in bone mineral density or other surrogates as the primary outcome measure (Lekamwasam et al., 2012). The absence of reliable fracture data is particularly problematic since glucocorticoids not only affect bone remodeling but also compromise bone strength through a number of different mechanisms that are not targeted by bisphosphonates. As outlined above, glucocorticoid-induced activation of osteoclasts and subsequent loss of bone mineral density is only one of several causal factors in the pathogenesis of GIO. Rodent models suggest that bone strength is closely linked to osteoblast and osteocyte viability, which is readily compromised under conditions of glucocorticoid excess (Weinstein et al., 2010b). Even though bisphosphonates have been shown in animal models to partially prevent glucocorticoid-induced cell apoptosis (Plotkin et al., 1999, 2005), their effects on osteoclast function always leads to a significant reduction in osteoblast activity (Saag et al., 1998). The resulting decline in bone formation comes on top of the glucocorticoid-induced suppression of osteoblast function, which poses a conundrum in regards to the use of bisphosphonates in the setting of GIO.

Denosumab

Denosumab is a potent RANKL inhibitor, and like all antiresorptive agents, acts by inhibiting osteoclast function and bone resorption. Denosumab effectively reduces fracture risk in postmenopausal osteoporosis (Brown et al., 2009), but its use in GIO has thus far not been fully assessed. A subgroup analysis of glucocorticoid-treated patients with rheumatoid arthritis demonstrated a significant increase in lumbar spine and hip bone mineral density after 12 months of treatment with denosumab (60 mg s.c. every 6 months) (Dore et al., 2010).

A recent study of 29 patients on chronic glucocorticoid therapy for a variety of systemic inflammatory conditions found that denosumab was effective in preventing bone resorption and bone loss, with increases in bone density at both the lumbar spine and hip (Sawamura et al., 2017).

In a 12-month study of patients receiving an oral bisphosphonate for chronic glucocorticoid therapy, switching to denosumab resulted in greater gains of lumbar spine bone mineral density and more pronounced suppression of bone turnover markers. The study was not powered for fracture as an end point (Mok et al., 2015). Similar findings were reported in another small study from Japan (Ishiguro et al., 2017). Since denosumab not only reduces osteoclast function but also osteoclast recruitment, activation, and survival together with a significant reduction in osteoblastic bone formation, its use in GIO may compromise bone quality over time. Additional long-term studies of GIO are therefore of paramount importance.

Raloxifene

The selective estrogen receptor modulator raloxifene has been shown to reduce fracture risk in women with postmenopausal osteoporosis (Ettinger et al., 1999). In a recent randomized double-blind placebo-controlled trial, 12 months of raloxifene (60 mg daily) significantly increased spinal and hip bone mineral density in women receiving longer-term glucocorticoids for a number of various conditions. The study was underpowered to measure the effect of raloxifene on fracture risk (Mok et al., 2011).

Teriparatide

Osteoanabolic treatments may have greater beneficial potential in GIO, particularly in patients undergoing long-term treatment. In a mouse model of GIO, intermittent treatment with parathyroid hormone (PTH) not only averted the adverse effects of glucocorticoids on bone turnover but also preserved osteocyte viability (Weinstein et al., 2010a). While the anabolic effects of PTH on bone-forming cells and their molecular pathways are not fully understood, PTH has been shown to induce several molecular pathways that are suppressed by glucocorticoid excess. For example, PTH directly induces canonical Wnt signaling in osteoblasts, a signal profoundly inhibited by supraphysiological levels of glucocorticoids (Keller and Kneissel, 2005; Weinstein et al., 2010a). This anabolic PTH signal is further amplified by the suppression of the Wnt antagonist sclerostin in osteocytes (Anastasilakis et al., 2010; Gatti et al., 2011). Intermittent administration of PTH also induces the expression of Cyclin D1 in osteoblasts and preosteoblasts (Datta et al., 2007) as well as the expression of RUNX2 (Hisa et al., 2011). As mentioned above, both of these factors are key regulators of osteoblast proliferation and differentiation and are suppressed by glucocorticoids at pharmacological doses. Overall, PTH treatment has been shown to induce differentiation of osteoblast precursors and prolong osteoblast and osteocyte survival, thereby increasing osteoblast/osteocyte numbers and overall activity.

On a structural level, PTH treatment increases the amount of trabecular bone (e.g., at the spine), while its anabolic impact is much less pronounced at cortical sites (Dempster et al., 2001; Gluer et al., 2013; Orwoll et al., 2003). This pattern is distinctively different from that of bisphosphonates, which cause smaller increases in bone mineral density across both trabecular and cortical sites (Gluer et al., 2013; Saag et al., 2007, 2009). Clinical studies indicate that the risk of vertebral fractures rises substantially with ongoing glucocorticoid therapy, whereas that of nonvertebral fracture increases only moderately (van Staa et al., 2000c). Given that PTH has its anabolic effects predominantly in trabecular bone (such as the spine), PTH may have greater therapeutic benefits in preventing vertebral fractures than bisphosphonates do. Indeed, an 18-month randomized controlled trial of alendronate versus teriparatide (recombinant human PTH[1−34]) in patients with GIO found teriparatide to be associated with increased markers of bone formation and a greater increase in areal bone mineral density at both the spine and the hip (Saag et al., 2007) (Fig. 39.8). Of note, even though the study was not adequately powered to detect differences in fracture incidence, three incident vertebral fractures occurred among the 173 patients in the teriparatide group and 13 incident vertebral fractures among the 169 patients receiving alendronate (Saag et al., 2007). Similar differences were seen at the 36-month follow-up (Saag et al., 2009). In a recent 18-month RCT of men with GIO, Gluer and colleagues compared the effect of teriparatide versus risedronate on lumbar spine bone mineral density (Gluer et al., 2013). The authors found greater increases in lumbar spine areal density with teriparatide. Interestingly, a subanalysis utilizing high-resolution quantitative CT of the T12 vertebra at 18 months of treatment revealed a greater increase in trabecular bone mineral density for teriparatide compared with risedronate (14.5% vs. 2.0%), while cortical density changed similarly in both groups (8.0% vs. 6.1%). In addition, there was a substantially greater increase in vertebral strength in the teriparatide group compared with the bisphosphonate group (Gluer et al., 2013). These results seem to confirm some predictions from rodent models regarding the effectiveness of osteoanabolic treatments versus bisphosphonates. Specifically, these data and a recent meta-analysis (Amiche et al., 2016) (Fig. 39.7) support the notion that teriparatide has greater efficacy in preserving or even increasing spinal bone strength, and reducing fracture risk in the setting of glucocorticoid treatment.

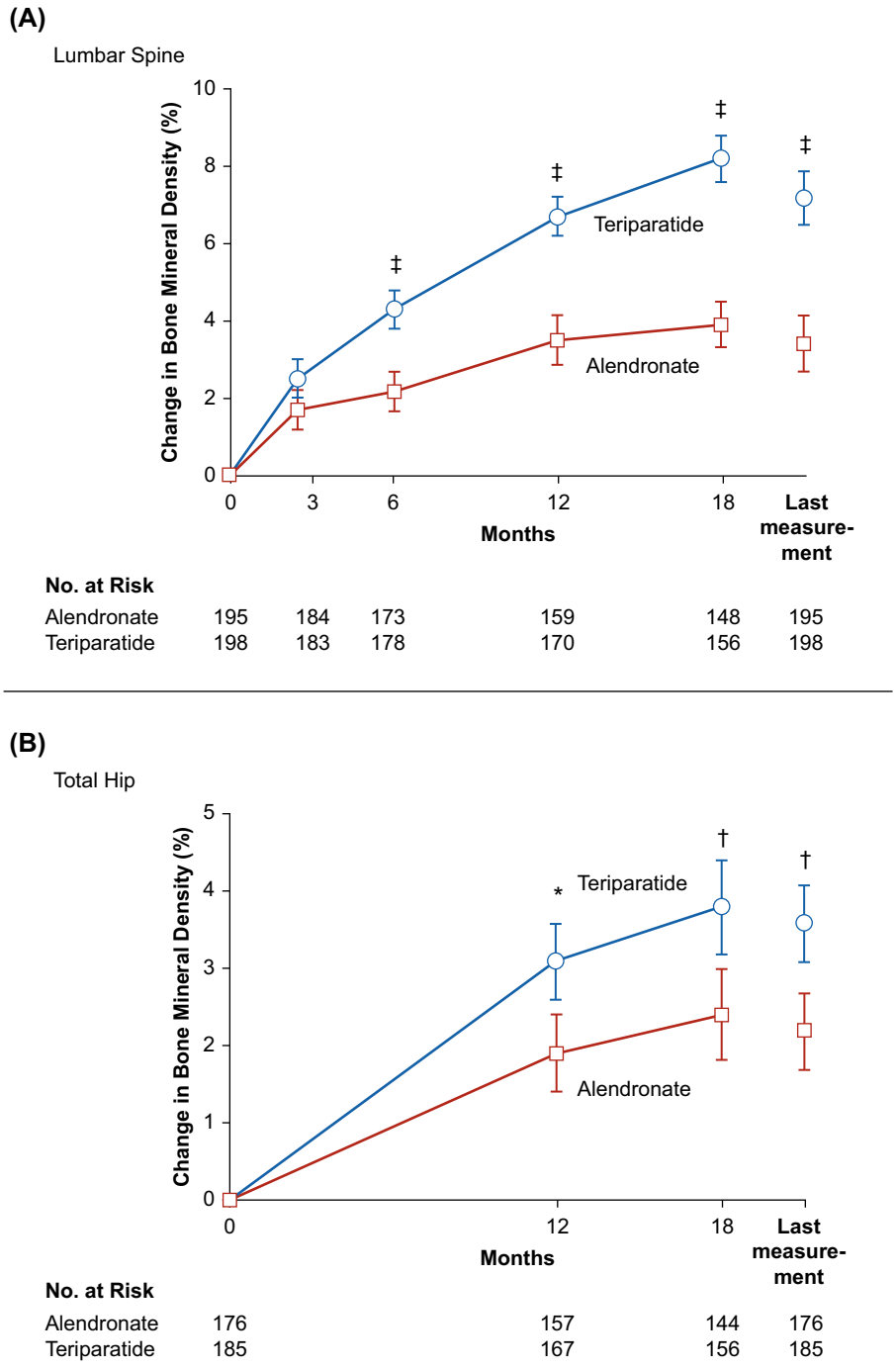

FIGURE 39.8 Effect of teriparatide or alendronate treatment on bone mineral density in patients with glucocorticoid-induced osteoporosis. The graphs show the percent change in mean bone mineral density from baseline to 18 months or last measurement. *P*-values are *< 0.05, † < 0.01, ‡< 0.001. Bars are standard error.

While these results are certainly promising, further clinical studies are required to confirm the effectiveness of osteoanabolic treatments in the management of GIO. In particular, long-term studies large enough to assess fracture rates—not bone mineral density—as a primary outcome are now required. Combinations of antiresorptive agents (such as bisphosphonates) with osteoanabolic agents (such as teriparatide) have recently been studied, with some success in the context of postmenopausal osteoporosis (Cosman et al., 2011). Whether such combination therapies yield beneficial results in GIO remains to be seen.

Sex hormone replacement

Hypogonadism is a known adverse outcome of high-dose, long-term glucocorticoid therapy (Chrousos et al., 1998; Pearce et al., 1998). Many but not all guidelines recommend sex hormone replacement in glucocorticoid-treated patients diagnosed with proven sex hormone deficiency. However, the evidence base for these recommendations is weak, as hormone replacement therapy has been studied in only a few small short-term studies. After due consideration of risks and benefits, hormone replacement might be used as either adjuvant therapy or second-line treatment in patients who cannot be treated with bisphosphonates or teriparatide.

Timing and monitoring of therapy

There is wide agreement that patients should remain on bone-protective treatments for as long as they require therapy with glucocorticoids. Drug holidays, sometimes considered in patients with postmenopausal osteoporosis, are usually not an option in GIO (Grossman et al., 2010; Nawata et al., 2005; Soen, 2011). As adherence with oral bisphosphonates is usually low, continuous surveillance and encouragement of the patient is a necessity. The introduction of intravenous bisphosphonates offers a viable and effective alternative in nonadherent patients.

There is limited data concerning the monitoring of patients with GIO. In patients whose fracture risk is deemed low, baseline and serial measurements of bone mineral density are usually recommended, although there is no clear evidence at what intervals these scans should be performed and what degree of glucocorticoid-induced bone loss should trigger an intervention. Many guidelines do, however, recommend intervening when the T-score at any site is −1.5 or lower. Patients should be carefully monitored for incident minimal trauma fractures, as these are a clear indication for the commencement of therapy. Despite the limitations of bone mineral density as a tool to monitor treatment efficacy, most guidelines recommend that patients on current bone-protective therapy have yearly bone mineral density scans. Serial determinations of bone turnover are usually not recommended.

New and emerging therapies

Despite their limitations, current treatments for GIO have proven to provide a significant degree of protection against bone loss and fracture. New therapies in this area would need to be more efficacious than existing medications, have fewer adverse effects, or have additional nonskeletal benefits.

Selective glucocorticoid receptor activators

In an attempt to develop agents with superior glucocorticoid-like properties but fewer off-target effects, a number of pharmaceutical companies have invested in the development of so-called selective glucocorticoid receptor activators (SEGRAs) (Oakley and Cidlowski, 2013; Schacke et al., 2007; Sundahl et al., 2015). This was on the basis that beneficial antiinflammatory effects of glucocorticoids could be "dissociated" from the adverse effects on bone and carbohydrate metabolism. Unfortunately, few agents able to dissociate these actions have been identified so far. The concept of GR transactivation as the cause of most adverse effects, and transrepression as the basis of most antiinflammatory effects, of glucocorticoids may be overly simplistic. Thus, some important antiinflammatory genes such as DUSP1 are clearly transactivated, and some of the adverse effects, such as the effect of glucocorticoids on bone, are primarily caused by transrepression (Rauch et al., 2010; Tchen et al., 2010). Despite this, there are clearly some agents, such as Compound A, that have useful differential effects on various GR-mediated responses (Lesovaya et al., 2015; Thiele et al., 2012). In a mouse model of GIO, mice were treated with equivalent antiinflammatory doses of prednisolone and Compound A. Prednisolone, as expected, caused a reduction in bone formation and an increased RANKL/OPG ratio (Thiele et al., 2012). These effects were not seen, however, with Compound A, indicating that it has some "bone-sparing" properties. Unfortunately, the therapeutic index for Compound A appears too narrow for use in humans. The attraction of pursuing the development of SEGRAs is their potential to reduce adverse effects on a range of tissues rather than just bone.

Antisclerostin/DKK1

As discussed above, the canonical Wnt signaling pathway is critical to bone formation. Glucocorticoid treatment causes increases in DKK1 and sclerostin, both powerful inhibitors of the Wnt pathway. Antibodies capable of neutralizing these targets are now being evaluated clinically in postmenopausal and cancer-induced bone loss. In contrast to DKK1, sclerostin

expression and action appears exclusive to osteoblasts and osteocytes. The antisclerostin antibody romosozumab has been studied in women with postmenopausal osteoporosis, where 12 months of treatment led to remarkable increases in bone mineral density and significant reductions in fracture risk (Cosman et al., 2016; Langdahl et al., 2017; Saag et al., 2017). However, so far no RCT data on the efficacy of romosozumab are available in patients with GIO.

Conclusions and future perspectives

Our understanding of the pleiotropic effects of glucocorticoids on bone cells and their signaling behavior has greatly improved over the past 2 decades, resulting in a clearer and more complete picture of the mechanism behind the developmental anabolic, and the detrimental catabolic, actions of glucocorticoids on the skeleton.

It is now evident that endogenous glucocorticoids at physiological levels are vital for the commitment and differentiation of osteoblasts and play a pivotal role in the control of skeletal development and maintenance of healthy bone. At supraphysiological levels, however, glucocorticoids become largely detrimental to bone and cause bone loss and skeletal fragility. While high levels of glucocorticoids affect all bone cells, rodent models and human studies reliably demonstrate that their key targets in the skeleton are osteoblasts and osteocytes. Newer research indicates that the adverse effects of glucocorticoids on fuel metabolism and body fat accrual are at least in part mediated through their skeletal actions on osteoblasts and osteocytes. These cells are now at the core of new and promising interventional strategies uniquely suited to offset the detrimental effects of glucocorticoids on molecular as well as structural levels.

Although the study was not powered for fracture outcomes, there was a significant difference for vertebral fractures between the alendronate (6.1%) and teriparatide (0.6%) arms ($P < .01$) (Saag et al., 2007). Similar differences were seen at the 36 months follow-up (7.7% vs. 1.7%, $P < .01$) (Saag et al., 2009).

Acknowledgments

The authors thank the National Health and Medical Research Council (NHMRC), Australia, for ongoing research support through project grants #402462, #570946, #612838, #612839, #1086100, #1087271, and #1101879.

References

Adachi, J.D., Bensen, W.G., Brown, J., Hanley, D., Hodsman, A., Josse, R., et al., 1997. Intermittent etidronate therapy to prevent corticosteroid-induced osteoporosis. N. Engl. J. Med. 337, 382–387.

Adachi, J.D., Saag, K.G., Delmas, P.D., Liberman, U.A., Emkey, R.D., Seeman, E., et al., 2001. Two-year effects of alendronate on bone mineral density and vertebral fracture in patients receiving glucocorticoids: a randomized, double-blind, placebo-controlled extension trial. Arthritis Rheum. 44, 202–211.

Allen, C.S., Yeung, J.H., Vandermeer, B., Homik, J., 2016. Bisphosphonates for steroid induced osteoporosis. Cochrane Database Syst. Rev. 10, CD001347.

Almeida, M., Han, L., Ambrogini, E., Weinstein, R.S., Manolagas, S.C., 2011. Glucocorticoids and tumor necrosis factor alpha increase oxidative stress and suppress Wnt protein signaling in osteoblasts. J. Biol. Chem. 286, 44326–44335.

Amiche, M.A., Albaum, J.M., Tadrous, M., Pechlivanoglou, P., Levesque, L.E., Adachi, J.D., Cadarette, S.M., 2016. Efficacy of osteoporosis pharmacotherapies in preventing fracture among oral glucocorticoid users: a network meta-analysis. Osteoporos. Int. 27, 1989–1998.

Amiche, M.A., Levesque, L.E., Gomes, T., Adachi, J.D., Cadarette, S.M., March, 2018. Effectiveness of oral bisphosphonates in reducing fracture risk among oral glucocorticoid users: three matched cohort analyses. J. Bone Miner. Res. 33 (3), 419–429. https://doi.org/10.1002/jbmr.3318.

Amin, S., LaValley, M.P., Simms, R.W., Felson, D.T., 1999. The role of vitamin D in corticosteroid-induced osteoporosis: a meta-analytic approach. Arthritis Rheum. 42, 1740–1751.

Anastasilakis, A.D., Polyzos, S.A., Avramidis, A., Toulis, K.A., Papatheodorou, A., Terpos, E., 2010. The effect of teriparatide on serum Dickkopf-1 levels in postmenopausal women with established osteoporosis. Clin. Endocrinol. 72, 752–757.

Axelsson, K.F., Nilsson, A.G., Wedel, H., Lundh, D., Lorentzon, M., 2017. Association between alendronate use and hip fracture risk in older patients using oral prednisolone. J. Am. Med. Assoc. 318, 146–155.

Beard, J.C., Halter, J.B., Best, J.D., Pfeifer, M.A., Porte Jr., D., 1984. Dexamethasone-induced insulin resistance enhances B cell responsiveness to glucose level in normal men. Am. J. Physiol. 247, E592–E596.

Bellido, T., 2010. Antagonistic interplay between mechanical forces and glucocorticoids in bone: a tale of kinases. J. Cell. Biochem. 111, 1–6.

Bellows, C.G., Aubin, J.E., Heersche, J.N., 1987. Physiological concentrations of glucocorticoids stimulate formation of bone nodules from isolated rat calvaria cells in vitro. Endocrinology 121, 1985–1992.

Bonadonna, S., Burattin, A., Nuzzo, M., Bugari, G., Rosei, E.A., Valle, D., et al., 2005. Chronic glucocorticoid treatment alters spontaneous pulsatile parathyroid hormone secretory dynamics in human subjects. Eur. J. Endocrinol. 152, 199–205.

Brennan-Speranza, T.C., Henneicke, H., Gasparini, S.J., Blankenstein, K.I., Heinevetter, U., Cogger, V.C., et al., 2012. Osteoblasts mediate the adverse effects of glucocorticoids on fuel metabolism. J. Clin. Investig. 122, 4172–4189.

Brown, J.P., Prince, R.L., Deal, C., Recker, R.R., Kiel, D.P., de Gregorio, L.H., et al., 2009. Comparison of the effect of denosumab and alendronate on BMD and biochemical markers of bone turnover in postmenopausal women with low bone mass: a randomized, blinded, phase 3 trial. J. Bone Miner. Res. 24, 153–161.

Buckley, L., Guyatt, G., Fink, H.A., Cannon, M., Grossman, J., Hansen, K.E., et al., 2017. 2017 American College of Rheumatology guideline for the prevention and treatment of glucocorticoid-induced osteoporosis. Arthritis Care Res. 69, 1095–1110.

Buckley, L.M., Leib, E.S., Cartularo, K.S., Vacek, P.M., Cooper, S.M., 1996. Calcium and vitamin D3 supplementation prevents bone loss in the spine secondary to low-dose corticosteroids in patients with rheumatoid arthritis. A randomized, double-blind, placebo-controlled trial. Ann. Intern. Med. 125, 961–968.

Bultink, I.E., Lems, W.F., Kostense, P.J., Dijkmans, B.A., Voskuyl, A.E., 2005. Prevalence of and risk factors for low bone mineral density and vertebral fractures in patients with systemic lupus erythematosus. Arthritis Rheum. 52, 2044–2050.

Buttgereit, F., Burmester, G.R., Straub, R.H., Seibel, M.J., Zhou, H., 2011. Exogenous and endogenous glucocorticoids in rheumatic diseases. Arthritis Rheum. 63, 1–9.

Canalis, E., Mazziotti, G., Giustina, A., Bilezikian, J.P., 2007. Glucocorticoid-induced osteoporosis: pathophysiology and therapy. Osteoporos. Int. 18, 1319–1328.

Chang, J.K., Li, C.J., Liao, H.J., Wang, C.K., Wang, G.J., Ho, M.L., 2009. Anti-inflammatory drugs suppress proliferation and induce apoptosis through altering expressions of cell cycle regulators and pro-apoptotic factors in cultured human osteoblasts. Toxicology 258, 148–156.

Chen, F., Zhang, L., OuYang, Y., Guan, H., Liu, Q., Ni, B., 2014. Glucocorticoid induced osteoblast apoptosis by increasing E4BP4 expression via up-regulation of Bim. Calcif. Tissue Int. 94, 640–647.

Chrousos, G.P., Torpy, D.J., Gold, P.W., 1998. Interactions between the hypothalamicpituitary- adrenal axis and the female reproductive system: clinical implications. Ann. Intern. Med. 129, 229–240.

Cohen, S., Levy, R.M., Keller, M., Boling, E., Emkey, R.D., Greenwald, M., et al., 1999. Risedronate therapy prevents corticosteroid-induced bone loss: a twelvemonth, multicenter, randomized, double-blind, placebo-controlled, parallel-group study. Arthritis Rheum. 42, 2309–2318.

Cole, T.J., Blendy, J.A., Monaghan, A.P., Krieglstein, K., Schmid, W., Aguzzi, A., et al., 1995. Targeted disruption of the glucocorticoid receptor gene blocks adrenergic chromaffin cell development and severely retards lung maturation. Genes Dev. 9, 1608–1621.

Cooper, M.S., Blumsohn, A., Goddard, P.E., Bartlett, W.A., Shackleton, C.H., Eastell, R., et al., 2003. 11beta-hydroxysteroid dehydrogenase type 1 activity predicts the effects of glucocorticoids on bone. J. Clin. Endocrinol. Metab. 88, 3874–3877.

Cooper, M.S., Bujalska, I., Rabbitt, E., Walker, E.A., Bland, R., Sheppard, M.C., et al., 2001. Modulation of 11beta-hydroxysteroid dehydrogenase isozymes by proinflammatory cytokines in osteoblasts: an autocrine switch from glucocorticoid inactivation to activation. J. Bone Miner. Res. 16, 1037–1044.

Cooper, M.S., Kriel, H., Sayers, A., Fraser, W.D., Williams, A.M., Stewart, P.M., et al., 2011. Can 11beta-hydroxysteroid dehydrogenase activity predict the sensitivity of bone to therapeutic glucocorticoids in inflammatory bowel disease? Calcif. Tissue Int. 89, 246–251.

Cooper, M.S., Rabbitt, E.H., Goddard, P.E., Bartlett, W.A., Hewison, M., Stewart, P.M., 2002. Osteoblastic 11beta-hydroxysteroid dehydrogenase type 1 activity increases with age and glucocorticoid exposure. J. Bone Miner. Res. 17, 979–986.

Cooper, M.S., Syddall, H.E., Fall, C.H., Wood, P.J., Stewart, P.M., Cooper, C., Dennison, E.M., 2005. Circulating cortisone levels are associated with biochemical markers of bone formation and lumbar spine BMD: the Hertfordshire Cohort Study. Clin. Endocrinol. 62, 692–697.

Cooper, M.S., Walker, E.A., Bland, R., Fraser, W.D., Hewison, M., Stewart, P.M., 2000. Expression and functional consequences of 11beta-hydroxysteroid dehydrogenase activity in human bone. Bone 27, 375–381.

Cooper, M.S., Zhou, H., Seibel, M.J., 2012. Selective glucocorticoid receptor agonists: glucocorticoid therapy with no regrets? J. Bone Miner. Res. 27, 2238–2241.

Cortet, B., Hachulla, E., Barton, I., Bonvoisin, B., Roux, C., 1999. Evaluation of the efficacy of etidronate therapy in preventing glucocorticoid-induced bone loss in patients with inflammatory rheumatic diseases. A randomized study. Rev. Rhum. Engl. Ed. 66, 214–219.

Cosman, F., Crittenden, D.B., Adachi, J.D., Binkley, N., Czerwinski, E., Ferrari, S., et al., 2016. Romosozumab treatment in postmenopausal women with osteoporosis. N. Engl. J. Med. 375, 1532–1543.

Cosman, F., Eriksen, E.F., Recknor, C., Miller, P.D., Guanabens, N., Kasperk, C., et al., 2011. Effects of intravenous zoledronic acid plus subcutaneous teriparatide [rhPTH(1-34)] in postmenopausal osteoporosis. J. Bone Miner. Res. 26, 503–511.

Coutinho, A.E., Gray, M., Brownstein, D.G., Salter, D.M., Sawatzky, D.A., Clay, S., et al., 2012. 11beta-Hydroxysteroid dehydrogenase type 1, but not type 2, deficiency worsens acute inflammation and experimental arthritis in mice. Endocrinology 153, 234–240.

Crockett, J.C., Rogers, M.J., Coxon, F.P., Hocking, L.J., Helfrich, M.H., 2011. Bone remodelling at a glance. J. Cell Sci. 124, 991–998.

Curtis, J.R., Westfall, A.O., Allison, J.J., Becker, A., Casebeer, L., Freeman, A., et al., 2005. Longitudinal patterns in the prevention of osteoporosis in glucocorticoid-treated patients. Arthritis Rheum. 52, 2485–2494.

Cushing, H., 1932. The basophil adenomas of the pituitary body and their clinical manifestations (pituitary basophilism). Bull. Johns Hopkins Hosp. 50, 137–195.

Datta, N.S., Pettway, G.J., Chen, C., Koh, A.J., McCauley, L.K., 2007. Cyclin D1 as a target for the proliferative effects of PTH and PTHrP in early osteoblastic cells. J. Bone Miner. Res. 22, 951–964.

de Nijs, R.N., Jacobs, J.W., Lems, W.F., Laan, R.F., Algra, A., Huisman, A.M., et al., 2006. Alendronate or alfacalcidol in glucocorticoid-induced osteoporosis. N. Engl. J. Med. 355, 675–684.

Dempster, D.W., Cosman, F., Kurland, E.S., Zhou, H., Nieves, J., Woelfert, L., et al., 2001. Effects of daily treatment with parathyroid hormone on bone microarchitecture and turnover in patients with osteoporosis: a paired biopsy study. J. Bone Miner. Res. 16, 1846–1853.

Diez-Perez, A., Hooven, F.H., Adachi, J.D., Adami, S., Anderson, F.A., Boonen, S., et al., 2011. Regional differences in treatment for osteoporosis. The global longitudinal study of osteoporosis in women (GLOW). Bone 49, 493–498.

Dore, R.K., Cohen, S.B., Lane, N.E., Palmer, W., Shergy, W., Zhou, L., et al., 2010. Effects of denosumab on bone mineral density and bone turnover in patients with rheumatoid arthritis receiving concurrent glucocorticoids or bisphosphonates. Ann. Rheum. Dis. 69, 872–875.

Dovio, A., Perazzolo, L., Osella, G., Ventura, M., Termine, A., Milano, E., et al., 2004. Immediate fall of bone formation and transient increase of bone resorption in the course of high-dose, short-term glucocorticoid therapy in young patients with multiple sclerosis. J. Clin. Endocrinol. Metab. 89, 4923–4928.

Eastell, R., Devogelaer, J.P., Peel, N.F., Chines, A.A., Bax, D.E., Sacco-Gibson, N., et al., 2000. Prevention of bone loss with risedronate in glucocorticoid-treated rheumatoid arthritis patients. Osteoporos. Int. 11, 331–337.

Eisman, J.A., Bogoch, E.R., Dell, R., Harrington, J.T., McKinney Jr., R.E., McLellan, A., et al., 2012. Making the first fracture the last fracture: ASBMR task force report on secondary fracture prevention. J. Bone Miner. Res. 27, 2039–2046.

Espina, B., Liang, M., Russell, R.G., Hulley, P.A., 2008. Regulation of bim in glucocorticoid-mediated osteoblast apoptosis. J. Cell. Physiol. 215, 488–496.

Ettinger, B., Black, D.M., Mitlak, B.H., Knickerbocker, R.K., Nickelsen, T., Genant, H.K., et al., 1999. Reduction of vertebral fracture risk in post-menopausal women with osteoporosis treated with raloxifene: results from a 3-year randomized clinical trial. Multiple Outcomes of Raloxifene Evaluation (MORE) Investigators. J. Am. Med. Assoc. 282, 637–645.

Feldstein, A.C., Elmer, P.J., Nichols, G.A., Herson, M., 2005. Practice patterns in patients at risk for glucocorticoid-induced osteoporosis. Osteoporos. Int. 16, 2168–2174.

Fernandez-Rodriguez, E., Stewart, P.M., Cooper, M.S., 2009. The pituitary-adrenal axis and body composition. Pituitary 12, 105–115.

Ferris, H.A., Kahn, C.R., 2012. New mechanisms of glucocorticoid-induced insulin resistance: make no bones about it. J. Clin. Investig. 122, 3854–3857.

Fucik, R.F., Kukreja, S.C., Hargis, G.K., Bowser, E.N., Henderson, W.J., Williams, G.A., 1975. Effect of glucocorticoids on function of the parathyroid glands in man. J. Clin. Endocrinol. Metab. 40, 152–155.

Gabet, Y., Noh, T., Lee, C., Frenkel, B., 2011. Developmentally regulated inhibition of cell cycle progression by glucocorticoids through repression of cyclin A transcription in primary osteoblast cultures. J. Cell. Physiol. 226, 991–998.

Gao, J., Cheng, T.S., Qin, A., Pavlos, N.J., Wang, T., Song, K., et al., 2016. Glucocorticoid impairs cell-cell communication by autophagy-mediated degradation of connexin 43 in osteocytes. Oncotarget 7, 26966–26978.

Gatti, D., Viapiana, O., Idolazzi, L., Fracassi, E., Rossini, M., Adami, S., 2011. The waning of teriparatide effect on bone formation markers in post-menopausal osteoporosis is associated with increasing serum levels of DKK1. J. Clin. Endocrinol. Metab. 96, 1555–1559.

Gluer, C.C., Marin, F., Ringe, J.D., Hawkins, F., Moricke, R., Papaioannu, N., et al., 2013. Comparative effects of teriparatide and risedronate in glucocorticoid-induced osteoporosis in men: 18-month results of the EuroGIOPs trial. J. Bone Miner. Res. 28, 1355–1368.

Gonzalez-Gonzalez, J.G., Mireles-Zavala, L.G., Rodriguez-Gutierrez, R., Gomez-Almaguer, D., Lavalle-Gonzalez, F.J., Tamez-Perez, H.E., et al., 2013. Hyperglycemia related to high-dose glucocorticoid use in noncritically ill patients. Diabetol. Metab. Syndrome 5, 18.

Gough, A.K., Lilley, J., Eyre, S., Holder, R.L., Emery, P., 1994. Generalised bone loss in patients with early rheumatoid arthritis. Lancet 344, 23–27.

Grossman, J.M., Gordon, R., Ranganath, V.K., Deal, C., Caplan, L., Chen, W., et al., 2010. American College of Rheumatology 2010 recommendations for the prevention and treatment of glucocorticoid-induced osteoporosis. Arthritis Care Res. 62, 1515–1526.

Guler-Yuksel, M., Bijsterbosch, J., Goekoop-Ruiterman, Y.P., de Vries-Bouwstra, J.K., Hulsmans, H.M., de Beus, W.M., et al., 2008. Changes in bone mineral density in patients with recent onset, active rheumatoid arthritis. Ann. Rheu. Dis. 67, 823–828.

Hansen, K.E., Wilson, H.A., Zapalowski, C., Fink, H.A., Minisola, S., Adler, R.A., 2011. Uncertainties in the prevention and treatment of glucocorticoid-induced osteoporosis. J. Bone Miner. Res. 26, 1989–1996.

Hardy, R., Cooper, M.S., 2009. Bone loss in inflammatory disorders. J. Endocrinol. 201, 309–320.

Hayashi, K., Yamaguchi, T., Yano, S., Kanazawa, I., Yamauchi, M., Yamamoto, M., Sugimoto, T., 2009. BMP/Wnt antagonists are upregulated by dexamethasone in osteoblasts and reversed by alendronate and PTH: potential therapeutic targets for glucocorticoid-induced osteoporosis. Biochem. Biophys. Res. Commun. 379, 261–266.

Haynesworth, S.E., Goshima, J., Goldberg, V.M., Caplan, A.I., 1992. Characterization of cells with osteogenic potential from human marrow. Bone 13, 81–88.

Hazlehurst, J.M., Gathercole, L.L., Nasiri, M., Armstrong, M.J., Borrows, S., Yu, J., et al., 2013. Glucocorticoids fail to cause insulin resistance in human subcutaneous adipose tissue in vivo. J. Clin. Endocrinol. Metab. 98, 1631–1640.

Hench, P.S., Kendall, E.C., et al., 1949. The effect of a hormone of the adrenal cortex (17- hydroxy-11-dehydrocorticosterone; compound E) and of pituitary adrenocorticotropic hormone on rheumatoid arthritis. Proc. Staff Meet. Mayo Clin. 24, 181–197.

Henneicke, H., Herrmann, M., Kalak, R., Brennan-Speranza, T.C., Heinevetter, U., Bertollo, N., et al., 2011. Corticosterone selectively targets endocortical surfaces by an osteoblast-dependent mechanism. Bone 49, 733–742.

Henneicke, H., Li, J., Kim, S., Gasparini, S.J., Seibel, M.J., Zhou, H., 2017. Chronic mild stress causes bone loss via an osteoblast-specific glucocorticoid-dependent mechanism. Endocrinology 158, 1939–1950.

Herbertson, A., Aubin, J.E., 1995. Dexamethasone alters the subpopulation make-up of rat bone marrow stromal cell cultures. J. Bone Miner. Res. 10, 285–294.

Hisa, I., Inoue, Y., Hendy, G.N., Canaff, L., Kitazawa, R., Kitazawa, S., et al., 2011. Parathyroid hormone-responsive Smad3-related factor, Tmem119, promotes osteoblast differentiation and interacts with the bone morphogenetic protein- Runx2 pathway. J. Biol. Chem. 286, 9787–9796.

Hofbauer, L.C., Gori, F., Riggs, B.L., Lacey, D.L., Dunstan, C.R., Spelsberg, T.C., Khosla, S., 1999. Stimulation of osteoprotegerin ligand and inhibition of osteoprotegerin production by glucocorticoids in human osteoblastic lineage cells: potential paracrine mechanisms of glucocorticoid-induced osteoporosis. Endocrinology 140, 4382–4389.

Honma, M., Ikebuchi, Y., Kariya, Y., Hayashi, M., Hayashi, N., Aoki, S., Suzuki, H., 2013. RANKL subcellular trafficking and regulatory mechanisms in osteocytes. J. Bone Miner. Res. 28, 1936–1949.

Horsch, K., de Wet, H., Schuurmans, M.M., Allie-Reid, F., Cato, A.C., Cunningham, J., et al., 2007. Mitogen-activated protein kinase phosphatase 1/dual specificity phosphatase 1 mediates glucocorticoid inhibition of osteoblast proliferation. Mol. Endocrinol. 21, 2929–2940.

Hwang, J.Y., Lee, S.H., Kim, G.S., Koh, J.M., Go, M.J., Kim, Y.J., et al., 2009. HSD11B1 polymorphisms predicted bone mineral density and fracture risk in postmenopausal women without a clinically apparent hypercortisolemia. Bone 45, 1098–1103.

Ishiguro, S., Ito, K., Nakagawa, S., Hataji, O., Sudo, A., 2017. The clinical benefits of denosumab for prophylaxis of steroid-induced osteoporosis in patients with pulmonary disease. Arch. Osteoporos. 12, 44.

Jia, D., O'Brien, C.A., Stewart, S.A., Manolagas, S.C., Weinstein, R.S., 2006. Glucocorticoids act directly on osteoclasts to increase their life span and reduce bone density. Endocrinology 147, 5592–5599.

Jia, J., Yao, W., Guan, M., Dai, W., Shahnazari, M., Kar, R., et al., 2011. Glucocorticoid dose determines osteocyte cell fate. FASEB J. 25, 3366–3376.

Justesen, J., Mosekilde, L., Holmes, M., Stenderup, K., Gasser, J., Mullins, J.J., et al., 2004. Mice deficient in 11beta-hydroxysteroid dehydrogenase type 1 lack bone marrow adipocytes, but maintain normal bone formation. Endocrinology 145, 1916–1925.

Kalak, R., Zhou, H., Street, J., Day, R.E., Modzelewski, J.R., Spies, C.M., et al., 2009. Endogenous glucocorticoid signalling in osteoblasts is necessary to maintain normal bone structure in mice. Bone 45, 61–67.

Kalpakcioglu, B.B., Engelke, K., Genant, H.K., 2011. Advanced imaging assessment of bone fragility in glucocorticoid-induced osteoporosis. Bone 48, 1221–1231.

Kanda, F., Okuda, S., Matsushita, T., Takatani, K., Kimura, K.I., Chihara, K., 2001. Steroid myopathy: pathogenesis and effects of growth hormone and insulin-like growth factor-I administration. Horm. Res. 56 (Suppl. 1), 24–28.

Kang, H., Chen, H., Huang, P., Qi, J., Qian, N., Deng, L., Guo, L., 2016. Glucocorticoids impair bone formation of bone marrow stromal stem cells by reciprocally regulating microRNA-34a-5p. Osteoporos. Int. 27, 1493–1505.

Karras, D., Stoykov, I., Lems, W.F., Langdahl, B.L., Ljunggren, O., Barrett, A., et al., 2012. Effectiveness of teriparatide in postmenopausal women with osteoporosis and glucocorticoid use: 3-year results from the EFOS study. J. Rheumatol. 39, 600–609.

Kato, T., Khanh, V.C., Sato, K., Kimura, K., Yamashita, T., Sugaya, H., et al., 2018. Elevated expression of Dkk-1 by glucocorticoid treatment impairs bone regenerative capacity of adipose tissue-derived mesenchymal stem cells. Stem Cell. Dev. 27, 85–99.

Kauh, E., Mixson, L., Malice, M.P., Mesens, S., Ramael, S., Burke, J., et al., 2012. Prednisone affects inflammation, glucose tolerance, and bone turnover within hours of treatment in healthy individuals. Eur. J. Endocrinol. 166, 459–467.

Kaur, K., Hardy, R., Ahasan, M.M., Eijken, M., van Leeuwen, J.P., Filer, A., et al., 2010. Synergistic induction of local glucocorticoid generation by inflammatory cytokines and glucocorticoids: implications for inflammation associated bone loss. Ann. Rheum. Dis. 69, 1185–1190.

Keller, H., Kneissel, M., 2005. SOST is a target gene for PTH in bone. Bone 37, 148–158.

Kennedy, O.D., Herman, B.C., Laudier, D.M., Majeska, R.J., Sun, H.B., Schaffler, M.B., 2012. Activation of resorption in fatigue-loaded bone involves both apoptosis and active pro-osteoclastogenic signaling by distinct osteocyte populations. Bone 50, 1115–1122.

Kim, H.J., Zhao, H., Kitaura, H., Bhattacharyya, S., Brewer, J.A., Muglia, L.J., et al., 2007. Glucocorticoids and the osteoclast. Ann. N. Y. Acad. Sci. 1116, 335–339.

Kim, H.J., Zhao, H., Kitaura, H., Bhattacharyya, S., Brewer, J.A., Muglia, L.J., et al., 2006. Glucocorticoids suppress bone formation via the osteoclast. J. Clin. Investig. 116, 2152–2160.

Ko, J.Y., Chuang, P.C., Chen, M.W., Ke, H.C., Wu, S.L., Chang, Y.H., et al., 2013. MicroRNA-29a ameliorates glucocorticoid-induced suppression of osteoblast differentiation by regulating beta-catenin acetylation. Bone 57, 468–475.

Ko, J.Y., Chuang, P.C., Ke, H.J., Chen, Y.S., Sun, Y.C., Wang, F.S., 2015. MicroRNA-29a mitigates glucocorticoid induction of bone loss and fatty marrow by rescuing Runx2 acetylation. Bone 81, 80–88.

Kogianni, G., Mann, V., Noble, B.S., 2008. Apoptotic bodies convey activity capable of initiating osteoclastogenesis and localized bone destruction. J. Bone Miner. Res. 23, 915–927.

Kuroki, Y., Kaji, H., Kawano, S., Kanda, F., Takai, Y., Kajikawa, M., Sugimoto, T., 2008. Short-term effects of glucocorticoid therapy on biochemical markers of bone metabolism in Japanese patients: a prospective study. J. Bone Miner. Metab. 26, 271–278.

Landewe, R.B., Boers, M., Verhoeven, A.C., Westhovens, R., van de Laar, M.A., Markusse, H.M., et al., 2002. COBRA combination therapy in patients with early rheumatoid arthritis: long-term structural benefits of a brief intervention. Arthritis Rheum. 46, 347–356.

Langdahl, B.L., Libanati, C., Crittenden, D.B., Bolognese, M.A., Brown, J.P., Daizadeh, N.S., et al., 2017. Romosozumab (sclerostin monoclonal antibody) versus teriparatide in postmenopausal women with osteoporosis transitioning from oral bisphosphonate therapy: a randomised, open-label, phase 3 trial. Lancet 390, 1585–1594.

Lee, N.K., Sowa, H., Hinoi, E., Ferron, M., Ahn, J.D., Confavreux, C., et al., 2007. Endocrine regulation of energy metabolism by the skeleton. Cell 130, 456–469.

Lekamwasam, S., Adachi, J.D., Agnusdei, D., Bilezikian, J., Boonen, S., Borgstrom, F., et al., 2012. A framework for the development of guidelines for the management of glucocorticoid-induced osteoporosis. Osteoporos. Int. 23, 2257–2276.

Lesovaya, E., Yemelyanov, A., Swart, A.C., Swart, P., Haegeman, G., Budunova, I., 2015. Discovery of Compound A–a selective activator of the glucocorticoid receptor with anti-inflammatory and anti-cancer activity. Oncotarget 6, 30730−30744.

Li, H., Qian, W., Weng, X., Wu, Z., Li, H., Zhuang, Q., et al., 2012. Glucocorticoid receptor and sequential P53 activation by dexamethasone mediates apoptosis and cell cycle arrest of osteoblastic MC3T3-E1 cells. PLoS One 7, e37030.

Li, X., Ominsky, M.S., Niu, Q.T., Sun, N., Daugherty, B., D'Agostin, D., et al., 2008. Targeted deletion of the sclerostin gene in mice results in increased bone formation and bone strength. J. Bone Miner. Res. 23, 860−869.

Liu, J., Lu, C., Wu, X., Zhang, Z., Li, J., Guo, B., et al., 2017a. Targeting osteoblastic casein kinase-2 interacting protein-1 to enhance Smad-dependent BMP signaling and reverse bone formation reduction in glucocorticoid-induced osteoporosis. Sci. Rep. 7, 41295.

Liu, K., Jing, Y., Zhang, W., Fu, X., Zhao, H., Zhou, X., et al., 2017b. Silencing miR- 106b accelerates osteogenesis of mesenchymal stem cells and rescues against glucocorticoid-induced osteoporosis by targeting BMP2. Bone 97, 130−138.

Lu, K., Yin, X., Weng, T., Xi, S., Li, L., Xing, G., et al., 2008. Targeting WW domains linker of HECT-type ubiquitin ligase Smurf1 for activation by CKIP-1. Nat. Cell Biol. 10, 994−1002.

Lu, N.Z., Cidlowski, J.A., 2006. Glucocorticoid receptor isoforms generate transcription specificity. Trends Cell Biol. 16, 301−307.

Mak, W., Shao, X., Dunstan, C.R., Seibel, M.J., Zhou, H., 2009. Biphasic glucocorticoid-dependent regulation of Wnt expression and its inhibitors in mature osteoblastic cells. Calcif. Tissue Int. 85, 538−545.

Manolagas, S.C., 2013. Steroids and osteoporosis: the quest for mechanisms. J. Clin. Investig. 123, 1919−1921.

Matsumoto, T., Kuriwaka-Kido, R., Kondo, T., Endo, I., Kido, S., 2012. Regulation of osteoblast differentiation by interleukin-11 via AP-1 and Smad signaling. Endocr. J. 59, 91−101.

Matzelle, M.M., Gallant, M.A., Condon, K.W., Walsh, N.C., Manning, C.A., Stein, G.S., et al., 2012. Resolution of inflammation induces osteoblast function and regulates the Wnt signaling pathway. Arthritis Rheum. 64, 1540−1550.

Mazziotti, G., Giustina, A., 2013. Glucocorticoids and the regulation of growth hormone secretion. Nat. Rev. Endocrinol. 9, 265−276.

Meijsing, S.H., Pufall, M.A., So, A.Y., Bates, D.L., Chen, L., Yamamoto, K.R., 2009. DNA binding site sequence directs glucocorticoid receptor structure and activity. Science 324, 407−410.

Mok, C.C., Ho, L.Y., Ma, K.M., 2015. Switching of oral bisphosphonates to denosumab in chronic glucocorticoid users: a 12-month randomized controlled trial. Bone 75, 222−228.

Mok, C.C., Ying, K.Y., To, C.H., Ho, L.Y., Yu, K.L., Lee, H.K., Ma, K.M., 2011. Raloxifene for prevention of glucocorticoid-induced bone loss: a 12-month randomised double-blinded placebo-controlled trial. Ann. Rheu. Dis. 70, 778−784.

Moutsatsou, P., Kassi, E., Papavassiliou, A.G., 2012. Glucocorticoid receptor signaling in bone cells. Trends Mol. Med. 18, 348−359.

Nakashima, T., Hayashi, M., Fukunaga, T., Kurata, K., Oh-Hora, M., Feng, J.Q., et al., 2011. Evidence for osteocyte regulation of bone homeostasis through RANKL expression. Nat. Med. 17, 1231−1234.

Natsui, K., Tanaka, K., Suda, M., Yasoda, A., Sakuma, Y., Ozasa, A., et al., 2006. High-dose glucocorticoid treatment induces rapid loss of trabecular bone mineral density and lean body mass. Osteoporos. Int. 17, 105−108.

Naves, M.A., Pereira, R.M., Comodo, A.N., de Alvarenga, E.L., Caparbo, V.F., Teixeira, V.P., 2011. Effect of dexamethasone on human osteoblasts in culture: involvement of beta1 integrin and integrin-linked kinase. Cell Biol. Int. 35, 1147−1151.

Nawata, H., Soen, S., Takayanagi, R., Tanaka, I., Takaoka, K., Fukunaga, M., et al., 2005. Guidelines on the management and treatment of glucocorticoid-induced osteoporosis of the Japanese society for bone and mineral research (2004). J. Bone Miner. Metab. 23, 105−109.

Newton, R., Holden, N.S., 2007. Separating transrepression and transactivation: a distressing divorce for the glucocorticoid receptor? Mol. Pharmacol. 72, 799−809.

Nicod, N., Giusti, V., Besse, C., Tappy, L., 2003. Metabolic adaptations to dexamethasone-induced insulin resistance in healthy volunteers. Obes. Res. 11, 625−631.

Niewoehner, D.E., Erbland, M.L., Deupree, R.H., Collins, D., Gross, N.J., Light, R.W., et al., 1999. Effect of systemic glucocorticoids on exacerbations of chronic obstructive pulmonary disease. Department of Veterans Affairs Cooperative Study Group. N. Engl. J. Med. 340, 1941−1947.

O'Brien, C.A., Jia, D., Plotkin, L.I., Bellido, T., Powers, C.C., Stewart, S.A., et al., 2004. Glucocorticoids act directly on osteoblasts and osteocytes to induce their apoptosis and reduce bone formation and strength. Endocrinology 145, 1835−1841.

Oakley, R.H., Cidlowski, J.A., 2013. The biology of the glucocorticoid receptor: new signaling mechanisms in health and disease. J. Allergy Clin. Immunol. 132, 1033−1044.

Orwoll, E.S., Scheele, W.H., Paul, S., Adami, S., Syversen, U., Diez-Perez, A., et al., 2003. The effect of teriparatide [human parathyroid hormone (1-34)] therapy on bone density in men with osteoporosis. J. Bone Miner. Res. 18, 9−17.

Overman, R.A., Yeh, J.Y., Deal, C.L., 2013. Prevalence of oral glucocorticoid usage in the United States: a general population perspective. Arthritis Care Res. 65, 294−298.

Pearce, G., Tabensky, D.A., Delmas, P.D., Baker, H.W., Seeman, E., 1998. Corticosteroid-induced bone loss in men. J. Clin. Endocrinol. Metab. 83, 801−806.

Pereira, R.M., Freire de Carvalho, J., 2011. Glucocorticoid-induced myopathy. Joint Bone Spine 78, 41−44.

Petersons, C.J., Mangelsdorf, B.L., Jenkins, A.B., Poljak, A., Smith, M.D., Greenfield, J.R., et al., 2013. Effects of low-dose prednisolone on hepatic and peripheral insulin sensitivity, insulin secretion, and abdominal adiposity in patients with inflammatory rheumatologic disease. Diabetes Care 36, 2822−2829.

Plotkin, L.I., Aguirre, J.I., Kousteni, S., Manolagas, S.C., Bellido, T., 2005. Bisphosphonates and estrogens inhibit osteocyte apoptosis via distinct molecular mechanisms downstream of extracellular signal-regulated kinase activation. J. Biol. Chem. 280, 7317−7325.

Plotkin, L.I., Weinstein, R.S., Parfitt, A.M., Roberson, P.K., Manolagas, S.C., Bellido, T., 1999. Prevention of osteocyte and osteoblast apoptosis by bisphosphonates and calcitonin. J. Clin. Investig. 104, 1363–1374.

Rafacho, A., Ortsater, H., Nadal, A., Quesada, I., 2014. Glucocorticoid treatment and endocrine pancreas function: implications for glucose homeostasis, insulin resistance and diabetes. J. Endocrinol. 223, R49–R62.

Rauch, A., Gossye, V., Bracke, D., Gevaert, E., Jacques, P., Van Beneden, K., et al., 2011. An anti-inflammatory selective glucocorticoid receptor modulator preserves osteoblast differentiation. FASEB J. 25, 1323–1332.

Rauch, A., Seitz, S., Baschant, U., Schilling, A.F., Illing, A., Stride, B., et al., 2010. Glucocorticoids suppress bone formation by attenuating osteoblast differentiation via the monomeric glucocorticoid receptor. Cell Metabol. 11, 517–531.

Reid, D.M., Adami, S., Devogelaer, J.P., Chines, A.A., 2001. Risedronate increases bone density and reduces vertebral fracture risk within one year in men on corticosteroid therapy. Calcif. Tissue Int. 69, 242–247.

Reid, D.M., Devogelaer, J.P., Saag, K., Roux, C., Lau, C.S., Reginster, J.Y., et al., 2009. Zoledronic acid and risedronate in the prevention and treatment of glucocorticoid-induced osteoporosis (HORIZON): a multicentre, double-blind, double-dummy, randomised controlled trial. Lancet 373, 1253–1263.

Reid, D.M., Hughes, R.A., Laan, R.F., Sacco-Gibson, N.A., Wenderoth, D.H., Adami, S., et al., 2000. Efficacy and safety of daily risedronate in the treatment of corticosteroid-induced osteoporosis in men and women: a randomized trial. European Corticosteroid-Induced Osteoporosis Treatment Study. J. Bone Miner. Res. 15, 1006–1013.

Ritz, E., Kreusser, W., Rambausek, M., 1984. Effects of glucocorticoids on calcium and phosphate excretion. Adv. Exp. Med. Biol. 171, 381–397.

Rizzoli, R., Adachi, J.D., Cooper, C., Dere, W., Devogelaer, J.P., Diez-Perez, A., et al., 2012. Management of glucocorticoid-induced osteoporosis. Calcif. Tissue Int. 91, 225–243.

Roux, C., Oriente, P., Laan, R., Hughes, R.A., Ittner, J., Goemaere, S., et al., 1998. Randomized trial of effect of cyclical etidronate in the prevention of corticosteroid-induced bone loss. Ciblos Study Group. J. Clin. Endocrinol. Metab. 83, 1128–1133.

Rubin, M.R., Bilezikian, J.P., 2002. Clinical review 151: the role of parathyroid hormone in the pathogenesis of glucocorticoid-induced osteoporosis: a re-examination of the evidence. J. Clin. Endocrinol. Metab. 87, 4033–4041.

Saag, K.G., Emkey, R., Schnitzer, T.J., Brown, J.P., Hawkins, F., Goemaere, S., et al., 1998. Alendronate for the prevention and treatment of glucocorticoid-induced osteoporosis. Glucocorticoid-induced osteoporosis intervention study group. N. Engl. J. Med. 339, 292–299.

Saag, K.G., Petersen, J., Brandi, M.L., Karaplis, A.C., Lorentzon, M., Thomas, T., et al., 2017. Romosozumab or alendronate for fracture prevention in women with osteoporosis. N. Engl. J. Med. 377, 1417–1427.

Saag, K.G., Shane, E., Boonen, S., Marin, F., Donley, D.W., Taylor, K.A., et al., 2007. Teriparatide or alendronate in glucocorticoid-induced osteoporosis. N. Engl. J. Med. 357, 2028–2039.

Saag, K.G., Zanchetta, J.R., Devogelaer, J.P., Adler, R.A., Eastell, R., See, K., et al., 2009. Effects of teriparatide versus alendronate for treating glucocorticoid-induced osteoporosis: thirty-six-month results of a randomized, double-blind, controlled trial. Arthritis Rheum. 60, 3346–3355.

Sambrook, P., Birmingham, J., Kelly, P., Kempler, S., Nguyen, T., Pocock, N., Eisman, J., 1993. Prevention of corticosteroid osteoporosis. A comparison of calcium, calcitriol, and calcitonin. N. Engl. J. Med. 328, 1747–1752.

Sambrook, P.N., Roux, C., Devogelaer, J.P., Saag, K., Lau, C.S., Reginster, J.Y., et al., 2012. Bisphosphonates and glucocorticoid osteoporosis in men: results of a randomized controlled trial comparing zoledronic acid with risedronate. Bone 50, 289–295.

Sato, A.Y., Cregor, M., Delgado-Calle, J., Condon, K.W., Allen, M.R., Peacock, M., et al., 2016. Protection from glucocorticoid-induced osteoporosis by anti- catabolic signaling in the absence of sost/sclerostin. J. Bone Miner. Res. 31, 1791–1802.

Sato, A.Y., Tu, X., McAndrews, K.A., Plotkin, L.I., Bellido, T., 2015. Prevention of glucocorticoid induced-apoptosis of osteoblasts and osteocytes by protecting against endoplasmic reticulum (ER) stress in vitro and in vivo in female mice. Bone 73, 60–68.

Sawamura, M., Komatsuda, A., Togashi, M., Wakui, H., Takahashi, N., 2017. Effects of denosumab on bone metabolic markers and bone mineral density in patients treated with glucocorticoids. Intern. Med. 56, 631–636.

Schacke, H., Berger, M., Rehwinkel, H., Asadullah, K., 2007. Selective glucocorticoid receptor agonists (SEGRAs): novel ligands with an improved therapeutic index. Mol. Cell. Endocrinol. 275, 109–117.

Schakman, O., Gilson, H., Thissen, J.P., 2008. Mechanisms of glucocorticoid-induced myopathy. J. Endocrinol. 197, 1–10.

Sher, L.B., Harrison, J.R., Adams, D.J., Kream, B.E., 2006. Impaired cortical bone acquisition and osteoblast differentiation in mice with osteoblast-targeted disruption of glucocorticoid signaling. Calcif. Tissue Int. 79, 118–125.

Sher, L.B., Woitge, H.W., Adams, D.J., Gronowicz, G.A., Krozowski, Z., Harrison, J.R., Kream, B.E., 2004. Transgenic expression of 11beta-hydroxysteroid dehydrogenase type 2 in osteoblasts reveals an anabolic role for endogenous glucocorticoids in bone. Endocrinology 145, 922–929.

Shi, C., Huang, P., Kang, H., Hu, B., Qi, J., Jiang, M., et al., 2015. Glucocorticoid inhibits cell proliferation in differentiating osteoblasts by microRNA-199a targeting of WNT signaling. J. Mol. Endocrinol. 54, 325–337.

Shi, C., Qi, J., Huang, P., Jiang, M., Zhou, Q., Zhou, H., et al., 2014. MicroRNA- 17/20a inhibits glucocorticoid-induced osteoclast differentiation and function through targeting RANKL expression in osteoblast cells. Bone 68, 67–75.

Sivagurunathan, S., Muir, M.M., Brennan, T.C., Seale, J.P., Mason, R.S., 2005. Influence of glucocorticoids on human osteoclast generation and activity. J. Bone Miner. Res. 20, 390–398.

Soen, S., 2011. Guidelines on the management and treatment of glucocorticoid-induced osteoporosis. Nihon Rinsho. Jpn. J. Clin. Med. 69, 1310–1314.

Stahn, C., Buttgereit, F., 2008. Genomic and nongenomic effects of glucocorticoids. Nat. Clin. Pract. Rheumatol. 4, 525–533.

Stewart, P.M., Krozowski, Z.S., 1999. 11 beta-Hydroxysteroid dehydrogenase. Vitam. Horm. 57, 249–324.

Stoch, S.A., Saag, K.G., Greenwald, M., Sebba, A.I., Cohen, S., Verbruggen, N., et al., 2009. Once-weekly oral alendronate 70 mg in patients with glucocorticoid-induced bone loss: a 12-month randomized, placebo-controlled clinical trial. J. Rheumatol. 36, 1705–1714.

Stockbrugger, R.W., Schoon, E.J., Bollani, S., Mills, P.R., Israeli, E., Landgraf, L., et al., 2002. Discordance between the degree of osteopenia and the prevalence of spontaneous vertebral fractures in Crohn's disease. Aliment Pharmacol. Ther. 16, 1519–1527.

Struys, A., Snelder, A.A., Mulder, H., 1995. Cyclical etidronate reverses bone loss of the spine and proximal femur in patients with established corticosteroid-induced osteoporosis. Am. J. Med. 99, 235–242.

Sundahl, N., Bridelance, J., Libert, C., De Bosscher, K., Beck, I.M., 2015. Selective glucocorticoid receptor modulation: new directions with non-steroidal scaffolds. Pharmacol. Ther. 152, 28–41.

Takeuchi, Y., Watanabe, S., Ishii, G., Takeda, S., Nakayama, K., Fukumoto, S., et al., 2002. Interleukin-11 as a stimulatory factor for bone formation prevents bone loss with advancing age in mice. J. Biol. Chem. 277, 49011–49018.

Tchen, C.R., Martins, J.R., Paktiawal, N., Perelli, R., Saklatvala, J., Clark, A.R., 2010. Glucocorticoid regulation of mouse and human dual specificity phosphatase 1 (DUSP1) genes: unusual cis-acting elements and unexpected evolutionary divergence. J. Biol. Chem. 285, 2642–2652.

Temiyasathit, S., Jacobs, C.R., 2010. Osteocyte primary cilium and its role in bone mechanotransduction. Ann. N. Y. Acad. Sci. 1192, 422–428.

Thiele, S., Ziegler, N., Tsourdi, E., De Bosscher, K., Tuckermann, J.P., Hofbauer, L.C., Rauner, M., 2012. Selective glucocorticoid receptor modulation maintains bone mineral density in mice. J. Bone Miner. Res. 27, 2242–2250.

Tiganescu, A., Tahrani, A.A., Morgan, S.A., Otranto, M., Desmouliere, A., Abrahams, L., et al., July, 2013. 11beta-hydroxysteroid dehydrogenase blockade prevents age-induced skin structure and function defects. J. Clin. Investig. 123 (7), 3051–3060. https://doi.org/10.1172/JCI64162.

van der Goes, M.C., Jacobs, J.W., Jurgens, M.S., Bakker, M.F., van der Veen, M.J., van der Werf, J.H., et al., 2013. Are changes in bone mineral density different between groups of early rheumatoid arthritis patients treated according to a tight control strategy with or without prednisone if osteoporosis prophylaxis is applied? Osteoporos. Int. 24, 1429–1436.

van Raalte, D.H., Ouwens, D.M., Diamant, M., 2009. Novel insights into glucocorticoid-mediated diabetogenic effects: towards expansion of therapeutic options? Eur. J. Clin. Investig. 39, 81–93.

van Staa, T.P., 2006. The pathogenesis, epidemiology and management of glucocorticoid-induced osteoporosis. Calcif. Tissue Int. 79, 129–137.

van Staa, T.P., Geusens, P., Pols, H.A., de Laet, C., Leufkens, H.G., Cooper, C., 2005. A simple score for estimating the long-term risk of fracture in patients using oral glucocorticoids. QJM 98, 191–198.

Van Staa, T.P., Laan, R.F., Barton, I.P., Cohen, S., Reid, D.M., Cooper, C., 2003. Bone density threshold and other predictors of vertebral fracture in patients receiving oral glucocorticoid therapy. Arthritis Rheum. 48, 3224–3229.

van Staa, T.P., Leufkens, H.G., Abenhaim, L., Begaud, B., Zhang, B., Cooper, C., 2000a. Use of oral corticosteroids in the United Kingdom. QJM 93, 105–111.

van Staa, T.P., Leufkens, H.G., Abenhaim, L., Zhang, B., Cooper, C., 2000b. Oral corticosteroids and fracture risk: relationship to daily and cumulative doses. Rheumatology 39, 1383–1389.

van Staa, T.P., Leufkens, H.G., Abenhaim, L., Zhang, B., Cooper, C., 2000c. Use of oral corticosteroids and risk of fractures. J. Bone Miner. Res. 15, 993–1000.

van Staa, T.P., Leufkens, H.G., Cooper, C., 2002. The epidemiology of corticosteroid-induced osteoporosis: a meta-analysis. Osteoporos. Int. 13, 777–787.

Wallach, S., Cohen, S., Reid, D.M., Hughes, R.A., Hosking, D.J., Laan, R.F., et al., 2000. Effects of risedronate treatment on bone density and vertebral fracture in patients on corticosteroid therapy. Calcif. Tissue Int. 67, 277–285.

Walsh, L.J., Lewis, S.A., Wong, C.A., Cooper, S., Oborne, J., Cawte, S.A., et al., 2002. The impact of oral corticosteroid use on bone mineral density and vertebral fracture. Am. J. Respir. Crit. Care Med. 166, 691–695.

Walsh, L.J., Wong, C.A., Cooper, S., Guhan, A.R., Pringle, M., Tattersfield, A.E., 1999. Morbidity from asthma in relation to regular treatment: a community based study. Thorax 54, 296–300.

Walsh, L.J., Wong, C.A., Pringle, M., Tattersfield, A.E., 1996. Use of oral corticosteroids in the community and the prevention of secondary osteoporosis: a cross sectional study. BMJ 313, 344–346.

Wang, F.S., Ko, J.Y., Weng, L.H., Yeh, D.W., Ke, H.J., Wu, S.L., 2009. Inhibition of glycogen synthase kinase-3beta attenuates glucocorticoid-induced bone loss. Life Sci. 85, 685–692.

Weinstein, R.S., Jilka, R.L., Almeida, M., Roberson, P.K., Manolagas, S.C., 2010a. Intermittent parathyroid hormone administration counteracts the adverse effects of glucocorticoids on osteoblast and osteocyte viability, bone formation, and strength in mice. Endocrinology 151, 2641–2649.

Weinstein, R.S., Jilka, R.L., Parfitt, A.M., Manolagas, S.C., 1998. Inhibition of osteoblastogenesis and promotion of apoptosis of osteoblasts and osteocytes by glucocorticoids. Potential mechanisms of their deleterious effects on bone. J. Clin. Investig. 102, 274–282.

Weinstein, R.S., Wan, C., Liu, Q., Wang, Y., Almeida, M., O'Brien, C.A., et al., 2010b. Endogenous glucocorticoids decrease skeletal angiogenesis, vascularity, hydration, and strength in aged mice. Aging Cell 9, 147–161.

Woitge, H.W., Kream, B.E., 2000. Calvariae from fetal mice with a disrupted Igf1 gene have reduced rates of collagen synthesis but maintain responsiveness to glucocorticoids. J. Bone Miner. Res. 15, 1956–1964.

Wong, C.A., Walsh, L.J., Smith, C.J., Wisniewski, A.F., Lewis, S.A., Hubbard, R., et al., 2000. Inhaled corticosteroid use and bone-mineral density in patients with asthma. Lancet 355, 1399–1403.

Xia, X., Kar, R., Gluhak-Heinrich, J., Yao, W., Lane, N.E., Bonewald, L.F., et al., 2010. Glucocorticoid-induced autophagy in osteocytes. J. Bone Miner. Res. 25, 2479–2488.

Xiong, J., Onal, M., Jilka, R.L., Weinstein, R.S., Manolagas, S.C., O'Brien, C.A., 2011. Matrix-embedded cells control osteoclast formation. Nat. Med. 17, 1235−1241.

Yang, M., Trettel, L.B., Adams, D.J., Harrison, J.R., Canalis, E., Kream, B.E., 2010. Col3.6- HSD2 transgenic mice: a glucocorticoid loss-of-function model spanning early and late osteoblast differentiation. Bone 47, 573−582.

Yao, W., Cheng, Z., Busse, C., Pham, A., Nakamura, M.C., Lane, N.E., 2008. Glucocorticoid excess in mice results in early activation of osteoclastogenesis and adipogenesis and prolonged suppression of osteogenesis: a longitudinal study of gene expression in bone tissue from glucocorticoid-treated mice. Arthritis Rheum. 58, 1674−1686.

Yilmaz, L., Ozoran, K., Gunduz, O.H., Ucan, H., Yucel, M., 2001. Alendronate in rheumatoid arthritis patients treated with methotrexate and glucocorticoids. Rheumatol. Int. 20, 65−69.

Zhou, H., Mak, W., Kalak, R., Street, J., Fong-Yee, C., Zheng, Y., et al., 2009. Glucocorticoid-dependent Wnt signaling by mature osteoblasts is a key regulator of cranial skeletal development in mice. Development 136, 427−436.

Zhou, H., Mak, W., Zheng, Y., Dunstan, C.R., Seibel, M.J., 2008. Osteoblasts directly control lineage commitment of mesenchymal progenitor cells through Wnt signaling. J. Biol. Chem. 283, 1936−1945.

Zhou, J., Cidlowski, J.A., 2005. The human glucocorticoid receptor: one gene, multiple proteins and diverse responses. Steroids 70, 407−417.

Chapter 40

Diabetes and bone

Caterina Conte[1,2], **Roger Bouillon**[3] and **Nicola Napoli**[4,5]

[1]Vita-Salute San Raffaele University, Milan, Italy; [2]Division of Immunology, Transplantation and Infectious Diseases, IRCCS San Raffaele Scientific Institute, Milan, Italy; [3]Laboratory of Clinical and Experimental Endocrinology, Department of Chronic Diseases, Metabolism and Aging, KU Leuven, Belgium; [4]Unit of Endocrinology and Diabetes, University Campus Bio-Medico, Rome, Italy; [5]Division of Bone and Mineral Diseases, Washington University in St Louis, St Louis, MO, United States

Chapter outline

Introduction

The term "diabetic bone disease" is used to describe the changes in bone growth, remodeling, and density as well as fracture risk imparted by the presence of type 1 diabetes mellitus (T1DM) or type 2 diabetes mellitus (T2DM). T1DM is caused by pancreatic β-cell destruction, usually leading to an absolute insulin deficiency; northern Europeans are among the populations with the highest prevalence of T1DM. However, T2DM is currently by far the most prevalent form of diabetes on all continents. Its pathophysiology is heterogeneous, ranging from predominantly insulin resistance—i.e., at any of the classical insulin-sensitive tissues, liver, skeletal muscles, and adipose tissue—with relative insulin deficiency to a predominantly insulin secretory defect with variable insulin resistance. Hence, insulin levels in T2DM vary widely, anywhere between hyper- and hypoinsulinemia. The majority of patients with T2DM are obese, and obesity itself aggravates insulin resistance. Body weight is, therefore, an important confounding factor when examining the pathophysiology of bone in T2DM individuals.

Principles of Bone Biology. https://doi.org/10.1016/B978-0-12-814841-9.00040-3

Effects of diabetes and insulin on endochondral bone growth

Effects of insulin on growth plate cartilage in nondiabetic animal models and in vitro

The classic experiments of Salter and Best (Salter and Best, 1953) demonstrated that insulin administration increased growth plate width in hypophysectomized rats. This could be a local effect, because insulin injection into the proximal tibial growth plate (Heinze et al., 1989) or insulin infusion into one hindlimb (Alarid et al., 1992) produced widening of the treated growth plates only. Such local effect might be mediated by in situ production of insulin-like growth factor 1 (IGF-1), because the trophic effect of insulin was nullified by coinfusion of an IGF-1 antiserum (Alarid et al., 1992). Mice with absent expression of insulin receptors (IRs) in bone showed normal bone length (Irwin et al., 2006). However, they overexpressed the IGF-1 receptor, which could represent a compensatory response.

In vitro studies have documented the presence of IRs in a chondrosarcoma cell line (Foley et al., 1982). Chondrocyte proliferation and $^{35}SO_4$ incorporation were stimulated by insulin in several tissue and cell culture systems (Foley et al., 1982; Heinze et al., 1989; Maor et al., 1993). These effects were obtained at physiological levels of insulin, as low as 1 nM, but equimolar IGF-1 was more potent than insulin.

Collectively, the available data suggest that growth hormone (GH) and IGF-1 are more important than insulin for chondrocyte proliferation and maturation (Yakar and Isaksson, 2016).

Skeletal growth in T1DM

Animal models

The most frequently used animal models are rats or mice with T1DM induced by β-cell-destroying drugs, alloxan or—in the large majority of studies—streptozotocin (STZ), and BB (Bio-Breeding) rats with spontaneous immune-mediated diabetes. Although T1DM can be drug induced at any age, BB rats develop diabetes past the peak growth rate (7 weeks). In both rodent models, insulin levels are very low or undetectable. The growth plate width as well as the endochondral bone growth—assessed by double fluorochrome labeling of the calcifying cartilage—at the proximal tibia was consistently lower in untreated, severely hyperglycemic STZ-induced or spontaneously diabetic BB rats, and was remedied by systemic insulin treatment (Bain et al., 1997; Epstein et al., 1994; Scheiwiller et al., 1986; Verhaeghe et al., 1992). The femur was shorter after 28 days of STZ diabetes (Lucas, 1987).

The effect of insulin on bone growth might be direct and/or indirect, for example, by restoring the depressed hepatic release of IGF-1. Although it was reported that systemic administration of IGF-1 in T1DM rats partly normalized growth plate width (Scheiwiller et al., 1986), this finding was not corroborated in a subsequent study (Verhaeghe et al., 1992). The low $^{35}SO_4$ uptake by rib cartilage explants from T1DM rats was also unresponsive to exogenous IGF-1 (Kelley et al., 1993). These data suggest that diabetic cartilage is, at least in part, resistant to the actions of IGF-1. Blunted stimulatory actions of IGF-1 on osteoblasts due to high concentrations of advanced glycation end products (AGEs) and hyperglycemia may also contribute (McCarthy et al., 2001; Terada et al., 1998).

Children

At the onset of T1DM, there is no difference in height compared with nondiabetic children. In fact, most studies have documented that children are slightly taller at the onset of diabetes compared with reference values (Bonfig et al., 2012; Holl et al., 1998). Increased growth velocity has even been associated with risk of islet autoimmunity in children at risk for T1DM (Beyerlein et al., 2014; Lamb et al., 2009; Yassouridis et al., 2017).

However, growth is affected from the clinical onset onward. In the preinsulin era, prepubertal growth virtually stopped, and stunted growth (Mauriac syndrome) was frequently observed in later decades of irregular insulin treatment. In addition, there was a delay in pubertal development and growth. Retarded growth and pubertal development remain common to this day among African children with T1DM (Elamin et al., 2006). In Western countries, the majority of recent studies have documented a mild reduction in growth from height-for-age (z) charts. This deficit was more pronounced in children with a prepubertal compared with a pubertal onset of T1DM (Holl et al., 1998). Poor glycemic control predicts growth retardation: indeed, glycated hemoglobin A1c (HbA1c) levels (a reflection of glycemic control in the previous 2−3 months) correlated inversely with height velocity (Danne et al., 1997; Holl et al., 1998), and patients with good glycemic control (HbA1c $< 7\%$) had normal near-adult height (Bonfig et al., 2012). In the larger analysis conducted so far, mean near-adult height was reduced by 0.16 SD scores in patients with onset of diabetes before age 10 years (Bonfig et al., 2012).

Considering that mean height at onset of diabetes was +0.25 SD scores (i.e., at diagnosis, children with diabetes were taller than average), 0.41 SD scores were lost since diabetes onset to near-adult age.

At diagnosis, bone maturation—determined by radiographs of hand and wrist—was not different compared with nondiabetic children (Danne et al., 1997; Holl et al., 1998). However, there was a small but significant retardation of bone maturation with increasing T1DM duration (i.e., a 1-year difference between chronological and bone age after 11 years of diabetes) (Danne et al., 1997; Holl et al., 1998). Dysregulation of the GH−IGF-1 axis, which promotes chondrocyte proliferation, differentiation, and hypertrophy, may play a role in the pathogenesis of impaired skeletal growth in T1DM (Raisingani et al., 2017).

Effects of T1DM on bone

T1DM and fracture risk

The available epidemiologic studies concur that the risk of fractures is substantially increased in individuals with T1DM, more than could be explained by the mild bone mineral density (BMD) deficit; in effect, a 1-SD reduction in areal BMD (aBMD) would translate into a twofold increased risk of hip fracture (Johnell et al., 2005). A caveat is that many studies contained few incident fractures in the diabetic group ($n = 1-18$).

In a large meta-analysis that included 7,185,572 participants from 16 prospective and 9 retrospective cohort studies, patients with T1DM had 1.5 times greater risk of total fractures, 4.4 times greater risk of hip fractures, 1.8 times greater risk of upper arm fractures, and 2 times greater risk of ankle fractures compared with nondiabetic individuals (Wang et al., 2019). Compared with T2DM, T1DM was associated with a greater risk of total, hip, and ankle fracture. There was no increase in the risk of forearm or vertebral fractures. Previous meta-analyses reported relative risks ranging from 3.2 to 6.3 for any fracture (Janghorbani et al., 2007; Shah et al., 2015), 3.8 to 6.9 for hip fracture (Fan et al., 2016; Shah et al., 2015; Vestergaard, 2007), and 2.9 for spine fracture (Shah et al., 2015). A meta-analysis that specifically addressed fracture risk in patients with T1DM ages 18−50 years ($n = 35{,}925$) compared with nondiabetic controls ($n = 2{,}455{,}016$) found that T1DM was associated with a nearly twofold increase in the risk of any fracture and a more than fourfold increase in the risk of hip fracture, this increase being greater in women than in men (Thong et al., 2018). Overall, these findings indicate that younger age does not protect against the increase in fracture risk associated with T1DM.

In T1DM, the possible association between BMD and HbA1c is still a matter of debate. One possible explanation of the discordant findings is that the relation between BMD and glycemic control, is, in fact, multifactorial, and therefore may be hardly detectable by traditional statistics. Eller-Vainicher and colleagues (Eller-Vainicher et al., 2011) adopted a special mathematic approach, the artificial neural networks (ANNs), to study 175 eugonadal T1DM patients and 151 age- and body mass index (BMI)-matched controls. The authors found that T1DM subjects had lower spine and femur BMD. Interestingly, spine BMD was independently associated with BMI and daily insulin dose (DID), whereas femur BMD was associated with BMI and creatinine clearance (CrCl). The authors found that a BMI below 23.5 kg/m^2, a DID > 0.67 units/kg, and a CrCl <88.8 mL/min were associated with low BMD. Data were also analyzed using the supervised ANNs and a semantic connectivity map that showed that low BMD at both sites was indirectly connected with HbA1c through the link with chronic diabetes complications. A 2019 large nested case−control analysis corroborated these observations, showing that T1DM patients with poor glycemic control (HbA1c $>8\%$) were 1.4 times more likely to have an incident nonvertebral low-trauma fracture than those with good glycemic control (HbA1c $\leq 7\%$) (Vavanikunnel et al., 2019). Furthermore, fracture risk was associated with comorbidities related to micro- and macrovascular complications, such as diabetic retinopathy and ischemic heart disease.

Few studies have investigated the prevalence of asymptomatic vertebral fractures in T1DM. In a study by Zhukouskaya and coauthors, patients with T1DM had a lower BMD at both spine and femur than controls and a higher prevalence of vertebral fractures (24.4% vs. 6.1%) (Zhukouskaya et al., 2013). Age, diabetes duration, age at diabetes onset, HbA1c, BMD, and the prevalence of chronic complications were similar in patients with and without fractures. Interestingly, the elevated prevalence of asymptomatic vertebral fractures was associated with the presence of T1DM independent of BMD, suggesting that impaired bone quality may contribute the increased fracture risk in T1DM.

T1DM and bone turnover

Animal models of T1DM

Several animal models have been used for T1DM (mainly alloxan- or STZ-induced diabetic rats and mice, spontaneously diabetic BB rats, and nonobese diabetic [NOD] mice). Untreated severe T1DM (hyperglycemia >300 mg/dL) was

associated with low bone formation as shown by biochemical markers, in particular osteocalcin (OC) concentrations. Plasma OC dropped exponentially after onset of T1DM in BB rats to 25% of nondiabetic levels after 5 weeks (Verhaeghe et al., 1997). Plasma OC gradually returned to the control range with increasing insulin dosage in BB rats (Verhaeghe et al., 1997) and was normalized by pancreas transplantation in STZ-diabetic rats (Ishida et al., 1992).

Histomorphometry consistently showed low bone formation on all bone surfaces (trabecular—endosteal, endocortical, and periosteal) in STZ-diabetic and BB rats. Static morphometry demonstrated a marked decline in osteoblast and osteoid surface or volume, and dynamic morphometry a decrease in both mineralizing surface and mineral apposition rate. These changes were (partly) reversed by insulin (Bain et al., 1997; Epstein et al., 1994; Glajchen et al., 1988; Shires et al., 1981; Verhaeghe et al., 1992). Electron microscopy of the endocortical surface confirmed that active, cuboidal osteoblasts are virtually absent in STZ-diabetic rats and are replaced by inactive bone-lining cells with flattened nuclei and little or no endoplasmic reticulum (Sasaki et al., 1991). Thus, most of the bone surface is in a quiescent state in severely hyperglycemic animals.

OC but not Runx2 or alkaline phosphatase mRNA levels were reduced in tibias from STZ-diabetic mice (Botolin et al., 2005), reinforcing the conclusion that loss of mature osteoblasts is a key finding in T1DM.

Regarding bone resorption, T1DM rats displayed diminished total and creatinine-corrected deoxypyridinoline excretion (Horcajada-Molteni et al., 2001; Verhaeghe et al., 2000). Most but not all histomorphometric data confirmed that the osteoclast surface/number is decreased moderately to severely in T1DM murine models and this is reversed by insulin treatment (Glajchen et al., 1988; Peng et al., 2016; Shires et al., 1981; Verhaeghe et al., 1992). Electron microscopy showed that most osteoclasts in T1DM rats lack a ruffled border—clear zone complex and that acid phosphatase activity is rarely detected (Kaneko et al., 1990). Bacterial inoculation of the scalp in *db/db* mice also generated fewer osteoclasts (He et al., 2004).

Greater marrow adiposity has been a consistent finding in animal models of T1DM compared with nondiabetic controls. Interestingly, bone marrow adiposity was increased in STZ-diabetic mice and NOD mice, with upregulation of adipogenic genes such as peroxisome proliferator-activated receptor γ_2 (PPARγ_2), adipocyte fatty acid—binding protein 2, and resistin (Botolin et al., 2005). STZ-diabetic mice and NOD mice had significant trabecular bone loss, and tended to have cortical bone loss. Despite similar earlier markers of osteoblast differentiation compared with controls, OC mRNA, a marker of mature osteoblasts, was significantly reduced (Botolin and McCabe, 2007). Bone marrow adiposity, but not bone loss, was prevented by treatment with leptin or with a PPARγ antagonist (Botolin and McCabe, 2006; Motyl and McCabe, 2009), indicating that these two manifestations of diabetic bone disease result, at least in part, from different mechanisms.

Clinical data

Only few data on bone histomorphometry are available, and the measurement of biochemical markers of bone formation/mineralization produced variable results. A case—control study of 18 patients with T1DM with varying degrees of glycemic control and a wide range of disease duration showed no significant differences between diabetics and controls in histomorphometric parameters (Armas et al., 2012). However, in the T1DM group, patients with a history of fracture tended to have histomorphometric parameters suggestive of lower bone remodeling compared with nonfractured patients.

No definitive data have been produced regarding biochemical markers of bone resorption in T1DM. In some studies, resorption markers were unchanged, or even slightly increased. A systematic review and meta-analysis of studies that assessed bone turnover markers in diabetes found no difference in procollagen type 1 N-terminal propeptide (P1NP), bone-specific alkaline phosphatase, tartrate-resistant acid phosphatase (TRAP), osteoprotegerin, and N-terminal telopeptide (NTX) (Hygum et al., 2017). Sclerostin, a potent inhibitor of bone formation, was significantly higher, and C-terminal telopeptide of type I collagen (CTX) and OC significantly lower, in patients with T1DM compared with controls. OC levels were affected by plasma glucose levels, whereas HbA1c was a significant effect modifier for sclerostin.

It has also been reported that time-related changes in circulating bone turnover markers in patients with T1DM are not different from those in the general population, with no relevant changes in women and a decrease in the bone formation markers OC and P1NP and a trend toward a decrease in the bone resorption marker CTX (Hamilton et al., 2018).

Although the evidence supports the notion that T1DM is characterized by low bone turnover, what bone turnover markers reflect in T1DM and whether they predict fracture risk have not been fully understood. As an example, an inverse association between sclerostin levels and fracture risk in T1DM has been reported (Starup-Linde et al., 2016a).

In contrast to animal models, most human studies of T1DM did not show a significant increase in bone marrow adiposity, possibly due to the relatively small number of subjects included (Abdalrahaman et al., 2015; Slade et al., 2012).

T1DM, bone density, and bone structure

Animal models of T1DM

Experimental T1DM had a negative effect on bone size (wet and dry weight, diaphyseal width) that was related to at least three factors: earlier age at which diabetes was induced or occurred spontaneously, longer diabetes duration, and more severe hyperglycemia (Dixit and Ekstrom, 1980; Einhorn et al., 1988; Locatto et al., 1993; Lucas, 1987). Thus, the impact on bone size was modest in T1DM models with onset of diabetes past the peak growth rate (Verhaeghe et al., 1994, 2000).

T1DM negatively affects both cortical bone and trabecular bone. The reduction in trabecular bone volume was the result of thinner trabeculae, while the number and separation of trabeculae remained the same (Botolin et al., 2005; Epstein et al., 1994; Suzuki et al., 2003; Thrailkill et al., 2005a). In locations with dense trabecular bone (e.g., femur, mandible), the effect of hyperglycemia was less than that in areas without dense trabecular bone such as the tibial region (Hua et al., 2018).

Clinical data

Reduced trabecular bone density and cortical thickness have been reported in children and adolescents with T1DM (Maratova et al., 2018). Similarly, lower cortical and trabecular volumetric BMD (vBMD) as well as deterioration in bone microarchitecture has been reported in adult patients with T1DM compared with nondiabetic controls (Shanbhogue et al., 2015; Verroken et al., 2017), these reductions being more evident in patients with microvascular disease (Shanbhogue et al., 2015).

Reductions in bone size and bone strength have been reported in prepubertal children with T1DM (Bechtold et al., 2006, 2007; Franceschi et al., 2018). Some (Bechtold et al., 2006, 2007) but not all (Roggen et al., 2013) studies suggest that normalization of bone size occurs after puberty.

Women with long-standing T1DM had higher BMD at the lumbar spine and lower BMD at the femoral neck and higher rates of fragility fractures compared with age- and sex-matched controls, suggesting that factors other than BMD influence fracture risk in long-standing T1DM (Alhuzaim et al., 2019). No difference in BMD was evident between men with long-standing T1DM and age-matched nondiabetic men (Alhuzaim et al., 2019; Maddaloni et al., 2017). Thus, most but not all available data indicate that there is an early but mild BMD deficit in T1DM individuals that does not appear to deteriorate over time (Hamilton et al., 2018; Krakauer et al., 1995; Moyer-Mileur et al., 2004; Shah et al., 2017). Furthermore, BMD in women with T1DM remains similar to that expected for age, BMI, and postmenopausal status (Hamilton et al., 2018). Whether long-term glycemic control is a determinant of the BMD deficit in T1DM remains a matter of controversy (Hough et al., 2016). Inhibition of the bone-anabolic Wnt pathway, as suggested by an increase in circulating sclerostin and dickkopf-1 in T1DM children, may play a role (Faienza et al., 2017; Tsentidis et al., 2017), although not all studies point toward this direction (Tsentidis et al., 2016). The aBMD deficit is more pronounced among T1DM adults with microvascular complications (Campos Pastor et al., 2000; Clausen et al., 1997; Eller-Vainicher et al., 2011; Munoz-Torres et al., 1996; Rozadilla et al., 2000; Strotmeyer et al., 2006).

T1DM and bone strength

Animal models of T1DM

The breaking strength of the femoral or tibial midshaft was assessed in several T1DM models (STZ-diabetic and BB rats, NOD mice) by various methods (perpendicular pressure, torsion, three-point bending) (Dixit and Ekstrom, 1980; Einhorn et al., 1988; Horcajada-Molteni et al., 2001; Silva et al., 2009; Thrailkill et al., 2005a; Verhaeghe et al., 1990, 1994, 2000). Most, though not all, of these studies concluded that strength parameters were reduced after a critical period of diabetes (e.g., 8 weeks in rats), even when correcting for their smaller bone size.

Diabetic bone brittleness may be related to alterations of collagen quality (collagen glycation, integrity, and secondary structure) rather than changes in the mineral component of the bone matrix (Mieczkowska et al., 2015) and appears to increase with increasing duration of T1DM (Nyman et al., 2011). In WBN/Kob rats, a model of spontaneous T1DM occurring at an advanced age (i.e., from 12 months), enzymatic collagen cross-links in femoral bone were reduced from the prediabetic stage (8 months), while nonenzymatic (glycosylated) cross-links increased from 12 months. Interestingly, the collagen cross-link parameters in prediabetic/diabetic WBN bones strongly correlated with biomechanical properties (Saito et al., 2006). Similarly, STZ-induced young diabetic rats had markedly reduced trabecular bone, a relative deficit in cortical bone, and significant deficits in whole bone stiffness and strength (i.e., structural mechanical properties) (Silva et al., 2009). These changes were associated with a significant increase in nonenzymatic cross-links.

Of note, daily subcutaneous injections of insulin nearly restored the diabetes-related loss in peak force endured by the femur midshaft during three-point bending (Rao Sirasanagandla et al., 2014) and peak bending stress of the tibia midshaft (Bortolin et al., 2017) in STZ-induced diabetic rats.

Clinical data

No studies have directly measured bone strength in T1DM. However, bone strength can be estimated using quantitative computed tomography (QCT), which allows three-dimensional noninvasive assessment of bone macro- and micro-architecture (e.g., cortical porosity and trabecular connectivity). In a study that used central QCT to estimate vBMD and strength in femoral bone subfractions of 17 male T1DM patients and 18 sex-matched nondiabetic controls ages 18–49 years, cross-sectional moment of inertia, section modulus (a geometric index of bending stress), and buckling ratio (BR; an index of cortical instability) in the femoral neck and femoral shaft were similar in the two groups (Ishikawa et al., 2015). However, BR in the intertrochanteric region was higher in patients with T1DM. This associated with lower vBMD, cortical cross-sectional area, and cortical thickness in the intertrochanteric region, possibly indicating increased susceptibility to intertrochanteric fractures in young and middle-aged men with T1DM. Another study used high-resolution peripheral QCT (HR-pQCT) to assess peripheral bone microarchitecture and bone strength in T1DM patients, with or without microvascular disease, compared with nondiabetic controls (Shanbhogue et al., 2015). Patients with T1DM and microvascular disease had significant deficits in both cortical and trabecular bone microarchitectural parameters and estimated bone strength at the distal radius and tibia compared with matched nondiabetic control subjects, suggesting a role for microvascular disease in the pathogenesis of diabetic bone disease.

Effects of T2DM and insulin on bone

T2DM and fractures

Fracture risk is elevated in individuals with T2DM, but much less so than in T1DM. Large cohorts—the Study of Osteoporotic Fractures (Schwartz et al., 2001) and, in particular, the Women's Health Initiative Observational Study (Bonds et al., 2006)—confirmed a mildly increased risk (between one- and twofold). The latter study documented an elevated age-adjusted risk of fracture at all skeletal sites except the forearm/wrist/hand. A meta-analysis of cohort studies confirmed that fracture risk in patients with T2DM is 1.24 times greater than in nondiabetic individuals (Ni and Fan, 2017).

However, comprehensive meta-analyses have confirmed a nearly doubled risk of hip fracture in T2DM (Janghorbani et al., 2007; Wang et al., 2019). An association between T2DM and risk for upper arm and ankle fractures has also been reported (Wang et al., 2019), whereas the risk of spine fractures appears to be similar to that in nondiabetic subjects (Napoli et al., 2018b; Wang et al., 2019). Several mechanisms contribute to bone loss and increased fracture risk in T2DM (Fig. 40.1), as will be detailed in the following paragraphs.

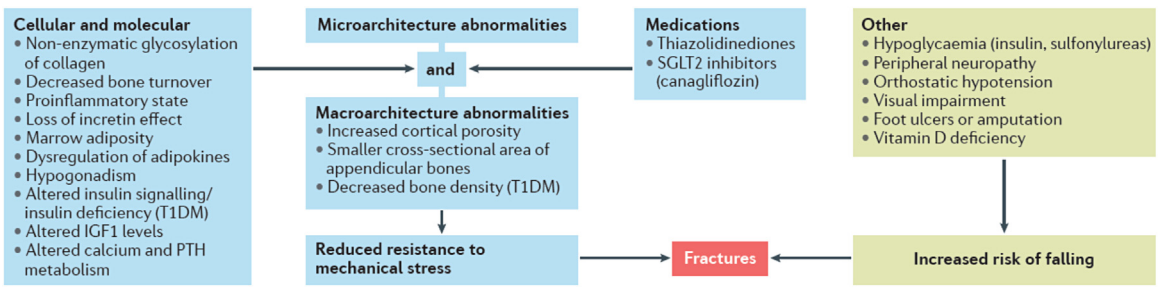

FIGURE 40.1 Mechanisms underlying bone loss and fractures in type 2 diabetes mellitus. Multiple mechanisms can contribute to the increased fracture risk observed in diabetes mellitus. Nonenzymatic glycosylation of collagen, decreased bone turnover, a proinflammatory state, and microvascular disease determine both micro– and macro–bone architecture abnormalities that cause reduced resistance to mechanical stress. Several studies have shown a different trend in terms of bone mineral density, which is generally decreased in type 1 diabetes mellitus (*T1DM*) and normal or increased in type 2 diabetes mellitus (T2DM). Alterations in bone structure in T2DM include increased cortical porosity and reduced cortical density. Insulin treatment is an additional risk factor for falls and fractures, probably because of the increased rate of hypoglycemic episodes in patients treated with insulin. The negative effect of thiazolidinediones on bone health is well known. In patients with T2DM, evidence suggests a potential negative effect also for some sodium/glucose cotransporter-2 (*SGLT2*) inhibitors. In this clinical scenario characterized by increased bone fragility, typical diabetic complications such as poor balance, diabetic retinopathy, impaired renal function, and neuropathy have been associated with an increased risk of falls and fractures. All these complications have even a greater effect in patients with T1DM. *IGF1*, insulin-like growth factor 1; *PTH*, parathyroid hormone. *Source: Napoli N et al. 2017.* Nat Rev Endocrinol. *13, 208–219.*

Limited evidence indicates that diabetes (T1DM or T2DM) delays the healing of clinical fractures, taking about twice as long (Loder, 1988; Marin et al., 2018). Furthermore, T2DM patients have a 30% increased postfracture mortality compared with nondiabetics, and a significant excess in absolute mortality risk (Martinez-Laguna et al., 2017).

T2DM and bone turnover

Animal models of T2DM

Several rodent models have been used for the study of skeletal fragility in T2DM. These models encompass various T2DM etiologies (spontaneous or diet-induced, single gene or polygenic), body types (obese or lean), and timings of T2DM onset (before or after skeletal maturity). However, current animal models are limited in their ability to mirror key metabolic features of adult-onset, obesity-related T2DM and their impact on bone metabolism, bone mass, and strength (Fajardo et al., 2014). In contrast to observations in humans, in which decreased bone formation and normal or reduced bone resorption are reported, rodent models of T2DM exhibit decreased or normal bone formation and high bone resorption, often resulting in low BMD (Devlin et al., 2014; Ducy et al., 2000; Reinwald et al., 2009; Tanaka et al., 2018; Turner et al., 2013; Zhang et al., 2009). Furthermore, the onset of diabetes is often before skeletal maturation, and inconsistent findings have been reported in some models of T2DM with respect to bone turnover. As an example, both reduced and normal levels of bone formation markers were reported for ZDF rats (Hamann et al., 2011; Liu et al., 2007; Mathey et al., 2002). Similarly, contrasting findings have been reported for bone resorption markers in this model (Hamann et al., 2011, 2013; Mathey et al., 2002).

Clinical data

Like T1DM, T2DM is accompanied by low bone formation and remodeling. In a small but interesting series of eight diabetic subjects (ages 37−67, diabetic for 2−36 years, six with T2DM), a transiliac bone biopsy was performed because of a low BMD; histomorphometry showed a significant decrease in osteoid thickness, mineralizing surface, and mineral apposition rate (Krakauer et al., 1995). Data from Dr. Rubin's group at Columbia University have proved that T2DM patients present significant reductions in mineralizing surface, bone formation rate, and osteoblast surface ($n = 9$) (Manavalan et al., 2012). Moreover, lower RUNX2 expression and an inverse association between glucose levels and mineral apposition rate in T2DM versus nondiabetics was detected (Manavalan et al., 2012).

Biochemical bone remodeling markers are also lower than in nondiabetics.

Most studies showed that the bone formation markers P1NP and OC, as well as the bone resorption marker CTX, are decreased in patients with T2DM compared with nondiabetic controls (Starup-Linde, 2013; Starup-Linde and Vestergaard, 2016). The reduction in markers of bone formation appears to be greater in T2DM than in T1DM (Starup-Linde et al., 2016b). Moreover, Starup-Linde and colleagues demonstrated an inverse relationship between glycemic control (HbA1c) and OC levels, and a similar trend for CTX and P1NP (Starup-Linde et al., 2016b). Interestingly, there appears to be a J- or U-shaped relationship between bone remodeling and fracture risk (Heaney, 2003). It has been postulated that diabetes impairs the healing of microdamage in load-bearing bones because of suppressed bone formation and that accumulated microdamage may predispose diabetic individuals to overt fractures (Krakauer et al., 1995).

Circulating levels of sclerostin are increased in T2DM, possibly accounting for the reduced bone turnover in patients with diabetes (Gaudio et al., 2012; van Lierop et al., 2012). Furthermore, sclerostin levels have been associated with fracture risk in some reports (Heilmeier et al., 2015; Yamamoto et al., 2013). Osteoprotegerin, NTX, and bone-specific alkaline phosphatase are not significantly different between T2DM patients and controls (Hygum et al., 2017).

Impaired fasting glucose was associated with lower OC (Mitchell et al., 2018), CTX, and P1NP (Holloway-Kew et al., 2019; Jiajue et al., 2014) in women, and lower β-CTX and P1NP in men (Holloway-Kew et al., 2019), suggesting that prediabetes is also associated with reduced bone turnover (Starup-Linde et al., 2016b).

T2DM, bone density, and bone structure

Hyperinsulinemia, insulin resistance, and bone density

Hyperinsulinemia is the compensatory answer to peripheral insulin resistance; when inadequate, impaired fasting glucose and/or postload hyperglycemia (impaired glucose tolerance) ensues. Several population studies have demonstrated a correlation between, on one hand, fasting insulin, the homeostatic model of insulin resistance (HOMA-IR), and/or postchallenge glucose and insulin concentrations and, on the other hand, the aBMD at the hip and/or the spine (Conte et al., 2018). The data suggest that aBMD progressively increases with worsening glucose metabolism, i.e., from normal fasting glucose to overt T2DM (Mitchell et al., 2018). Yet adjusting for BMI or fat mass often attenuates or abolishes the

correlation between aBMD and glucose metabolism parameters. Higher insulin resistance, as estimated with HOMA-IR, was associated with greater vBMD and generally favorable bone microarchitecture at both non-weight-bearing and weight-bearing skeletal sites, independent of body weight, in postmenopausal nondiabetic women (Shanbhogue et al., 2016). On the other hand, an inverse association between insulin resistance and indices of bone strength has been reported (Ahn et al., 2016; Srikanthan et al., 2014). In older nondiabetic adults participating in the Health ABC Study ($n = 2398$), increasing insulin resistance was associated with lower risk of fracture in unadjusted models (Napoli et al., 2019). However, after adjusting for BMI and BMD this relationship was lost, suggesting that higher BMD and BMI associated with insulin resistance accounted for the inverse association.

Animal models of T2DM

In contrast to T1DM, bone size was increased in T2DM models such as the Goto-Kakizaki rat, particularly at the diaphysis. Whereas cortical BMD, measured by QCT, was only mildly affected, trabecular BMD was markedly (33%−53%) decreased in these rats (Ahmad et al., 2003). T2DM may well have complex effects on bone with divergent responses generated by obesity and hyperglycemia. Disruption of leptin or leptin signaling in mice creates massive obesity with T2DM and increases bone mass via central nervous system pathways, some of which still need to be uncovered (Idelevich and Baron, 2018). As mentioned, however, concerns exist regarding the correlation between human obesity/T2DM and rodent models to study skeletal changes in obesity/T2DM (Lai et al., 2014; Rendina-Ruedy and Smith, 2016), particularly with regard to BMD, which is generally low in rodent models (Devlin et al., 2014; Ducy et al., 2000; Reinwald et al., 2009; Tanaka et al., 2018; Turner et al., 2013; Zhang et al., 2009).

Clinical data

The seminal report by Meema and Meema (Meema and Meema, 1967) that the cortical thickness at the radius was higher in aged (65−101 years) white women with T2DM than in nondiabetics was followed by numerous studies using dual-energy X-ray absorptiometry. The majority of these studies showed that aBMD is significantly increased in T2DM subjects and correlates positively with BMI and insulin levels (Ma et al., 2012). For example, in the Study of Osteoporotic Fractures, T2DM ($n < 500$) was associated with a 4.8% increase in aBMD at the radius and a 3.4% increase in aBMD at the femoral neck in multivariate analyses (Bauer et al., 1993; Orwoll et al., 1996). In the Rotterdam Study, lumbar spine and the femoral neck aBMD were also 3%−4% higher in T2DM individuals ($n = 578$) (van Daele et al., 1995). Similarly, in the Health ABC Study, total hip aBMD was 4%−5% higher in black and white men and women with T2DM ($n = 566$) after adjusting for their altered body composition (i.e., higher fat and lean mass) (Strotmeyer et al., 2004). However, total hip aBMD was inversely related to T2DM duration (Strotmeyer et al., 2004), and white women with T2DM showed increased aBMD loss compared with their nondiabetic counterparts (Schwartz et al., 2005).

Data from diabetic men enrolled in the Osteoporotic Fractures in Men (MrOS) Study have shown significantly higher aBMD (Napoli et al., 2014) and spine vBMD in T2DM subjects compared with nondiabetic ones (Napoli et al., 2018b). Importantly, higher trabecular vBMD was more strongly associated with incident vertebral fractures in nondiabetic men (odds ratio [OR] 0.33; 95% CI 0.24 to 0.45), compared with men with diabetes (OR 0.64; 95% CI 0.36 to 1.13).

Samelson and colleagues investigated the association between T2DM and cortical and trabecular bone microarchitecture and density (HR-pQCT), as well as total bone density and bone area in 1069 male and female members of the Framingham Offspring Cohort (Samelson et al., 2018). After adjustment for age, sex, weight, and height, T2DM subjects had significantly lower cortical vBMD, higher cortical porosity, and smaller cross-sectional area at the tibia, but not the radius. Furthermore, decreased cortical density and increased cortical porosity at the tibia differentiated between T2DM with prior fracture and non-T2DM with prior fracture. Trabecular indices did not differ or were more favorable in patients with T2DM than in nondiabetic subjects.

T2DM and bone strength

Animal models

In general, bone mechanical properties are reduced in murine models of T2DM. In young and adult C57BL/6 mice with high-fat diet (HFD)-induced obesity and hyperglycemia, femoral strength, stiffness, and toughness were dramatically lower than in control mice, possibly due to reduced structural quality (inferior lamellar and osteocyte alignment) (Ionova-Martin et al., 2011). HFD-fed mice demonstrated normal whole-body aBMD and femoral aBMD, but reduced spine aBMD. In Zucker diabetic fatty (ZDF) rats, shear stress testing of the femoral neck demonstrated significantly decreased maximum load and stiffness compared with nondiabetic rats, probably due to lower bone volume (Hamann et al., 2013).

An impairment in bone biomechanical properties is supported by the finding of larger indentation distances in cortical bone of murine models of T2DM (Acevedo et al., 2018; Gallant et al., 2013), possibly due to an increase in AGE content (Acevedo et al., 2018; Devlin et al., 2014).

Humans

Most studies have used HR-pQCT to assess bone microarchitecture and strength indices in humans. In a cross-sectional study of 19 elderly women with T2DM, trabecular microarchitecture was preserved but cortical porosity was higher in the radius and tibia compared with nondiabetic controls (Burghardt et al., 2010). In the radius, compressive bone strength, estimated using finite element analysis (FEA), was significantly lower. In older men with T2DM participating in the MrOS study, total bone cross-sectional area in the radius and tibia was lower in those with diabetes compared with nondiabetics, and bending strength relative to body weight was decreased in cortical regions (Petit et al., 2010). In trabecular regions, bone strength was similar between T2DM and non-T2DM older men. Fractured postmenopausal women with T2DM had significantly greater cortical porosity and lower bone strength parameters (stiffness, failure load, and cortical load fraction) compared with those without fracture (Heilmeier et al., 2016). These indices did not differ between nondiabetic women with or without fracture.

Bone microindentation allows direct assessment of the mechanical characteristics of cortical bone in humans by measuring the distance that a metal probe can enter the tibia for a given applied force (Diez-Perez et al., 2010, 2016; Nilsson et al., 2017). The bone material strength index (BMSi), assessed by bone microindentation, reflects the ability of bone to resist microcrack generation and propagation. Postmenopausal women with T2DM had lower BMSi compared with nondiabetic controls despite similar BMD (Farr et al., 2014; Furst et al., 2016; Nilsson et al., 2017), suggesting a deficit in diabetic bone material properties. In older women (75−80 years) with T2DM, BMSi by reference point indentation was lower than in nondiabetic controls despite generally better measures of trabecular and cortical bone microarchitecture and bone strength estimated by FEA (Nilsson et al., 2017). Furthermore, BMSi was inversely correlated with HbA1c levels over the prior 10 years (Farr et al., 2014) and with duration of diabetes (Furst et al., 2016).

Clinical risk factors for fractures in T1DM and T2DM

Regarding T1DM, a Swedish study (Miao et al., 2005) reported that the age-adjusted risk of hip fracture increased with longer diabetes duration. Poor glycemic control has also been associated with increased fracture risk in T1DM (Vavanikunnel et al., 2019). Longer diabetes duration and poorer glycemic control mean a greater likelihood of micro- and macrovascular complications; indeed, the risk of fracture was particularly high among T1DM patients with eye, nephropathic, neurologic, or cardiovascular complications (Miao et al., 2005; Vavanikunnel et al., 2019).

For T2DM, the elevated risk of fractures was observed in both white and black US women (Bonds et al., 2006). BMI is not a critical factor, because the risk was comparably elevated in nonobese and obese T2DM women, and controlling for BMI did not meaningfully alter the risk ratio (Janghorbani et al., 2006; Nicodemus et al., 2001; Schwartz et al., 2001). In some studies, the risk appeared to be higher among insulin-treated versus non-insulin-treated T2DM individuals (Janghorbani et al., 2006; Napoli et al., 2014; Ottenbacher et al., 2002). This may reflect the association between longer duration of T2DM and fracture: in individuals with >12 years of T2DM, the risk was increased more than twofold (Janghorbani et al., 2006; Nicodemus et al., 2001; Schwartz et al., 2001). Indeed, insulin-treated T2DM individuals showed a fourfold increased risk of falls (Schwartz et al., 2002), and repeated falls in diabetic individuals with a foot ulcer predisposed to fractures (Wallace et al., 2002). Moreover, these patients also have a longer clinical history of other complications like retinopathy or neuropathy. In the Australian Blue Mountains Eye Study, which examined 216 subjects (ages 49−97) with T1DM or T2DM, cortical cataract and especially retinopathy increased the risk of fractures (Ivers et al., 2001). Neuropathy with or without foot ulcers was another important predisposing factor for fractures in general (Strotmeyer et al., 2005), and foot fractures in particular (Cavanagh et al., 1994).

In contrast, studies performed in the Joslin "medalists," long-standing T1DM survivors (at least 50 years) with low cardiovascular risk, showed a very low prevalence of osteoporosis and fractures (Maddaloni et al., 2017). Another possible risk factor is glycemic control, tested in different studies with single measurements of HBA1c. Although limited by the short exposure (3 months), in general there is a progressive increase in risk of fractures in patients with higher HBA1c, mostly in those with levels >9% (Li et al., 2015). However, in a 2019 nested case−control analysis that used the mean of HbA1c values over 3 years to estimate glycemic control, there was no association between poor glycemic control (HbA1c >8%) and risk of nonvertebral low trauma fractures in patients with T2DM (Vavanikunnel et al., 2019). Diabetic individuals with eye, neuropathic, and vascular complications—and poor physical health in general—are more likely to fall.

It is likely, therefore, that falls mediate a significant part of the diabetes-associated risk of fractures. As a corollary, effective fall prevention strategies should be developed to prevent fractures in individuals with long-standing diabetes or diabetes complications. According to guidelines released by the American Diabetes Association/European Association for the Study of Diabetes and by the American College of Physicians (American Diabetes Association, 2019; Qaseem et al., 2018), a less stringent target in glucose control should be achieved in diabetic patients, mostly if affected by diabetes-related complications. This approach will limit the risk of hypoglycemic events, which are a main risk factor for cardiovascular mortality but also for fractures.

Effect of diabetes treatments on bone

Weight loss is recommended for overweight/obese patients with diabetes (American Diabetes Association, 2019). Due to mechanical unloading of the skeleton, weight loss might have a negative impact on bone health. An intensive lifestyle intervention resulting in long-term weight loss was not associated with an increased risk of incident total or hip fracture in overweight/obese adults with T2DM, but the risk of frailty fracture increased following weight loss (Johnson et al., 2017). Body weight loss of $\geq$ 20% from maximum weight is a significant risk factor for fragility fractures in patients with T2DM (Komorita et al., 2018). Bariatric–metabolic surgery has been recognized as an effective approach for the treatment of T2DM in obese patients (Rubino et al., 2016). Patients with T2DM undergoing bariatric surgery (roux-en-Y gastric bypass) exhibit higher bone turnover, lower aBMD, and impaired HR-pQCT-derived measurements of bone mass, structure, and strength, and more than double the likelihood of having osteopenia or osteoporosis despite adequate calcium and vitamin D supplementation compared with nonoperated patients (Madsen et al., 2019). These observations suggest that strict monitoring of bone health should be implemented for patients expected to lose large amounts of weight.

Metformin, unless contraindicated, is recommended as the first-line treatment for patients with T2DM. Most studies reported that metformin has a neutral or even favorable effect of fracture risk. In preclinical studies, metformin was shown to enhance bone-anabolic pathways, stimulating osteoblast differentiation and bone formation (Palermo et al., 2015). Treatment with metformin was associated with a 19% reduction in the risk of any fracture, although no effect on the risk of forearm, spine, or hip fracture was observed in patients with T2DM (Vestergaard et al., 2005). In the same case–control study, diabetic individuals who used sulfonylureas had a lower risk of hip fracture than diabetic individuals in general (Vestergaard et al., 2005). Another study found that treatment with a sulfonylurea was associated with reduced risk of vertebral fracture (Kanazawa et al., 2010). Data from the MrOS cohort indicate that metformin has a neutral effect on fracture risk, whereas there was an increased risk of hip fractures in patients treated with sulfonylureas (Napoli et al., 2014). However, it is likely that sulfonylureas do not exert a direct negative effect on bone but rather are associated with increased risk of hypoglycemia (Monami et al., 2014), which in turn is associated with increased fracture risk (Johnston et al., 2012). Thiazolidinediones (TZDs) or PPARγ agonists (e.g., pioglitazone, rosiglitazone) worsen diabetic bone disease. Indeed, aBMD loss at the spine and the whole body was higher among women—but not men—with T2DM who used a TZD (Schwartz et al., 2006). In line with these data, in the ADOPT trial, which compared metformin, glyburide, and rosiglitazone for 4 years in 4360 T2DM patients, the number of fractures (any site) was higher among women—but not men—treated with the TZD compared with the other two drugs (Kahn et al., 2006). Finally, a meta-analysis of randomized controlled trials of at least 12 months' duration found that TZDs were associated with a 45% increase in fracture, although the increase was significant only in women (Loke et al., 2009). In mice, TZD treatment enhanced bone marrow adiposity and caused trabecular bone loss by uncoupling resorption (activated) and formation (suppressed) (Li et al., 2006), the latter perhaps as a result of osteoblast/osteocyte apoptosis (Sorocéanu et al., 2004). Incretin-based treatments, namely, inhibitors of dipeptidyl peptidase-4 (DPP-4), an enzyme that rapidly inactivates gastric inhibitory polypeptide (GIP) and glucagon-like peptide 1 (GLP1), and GLP1 receptor agonists (GLP1RA), appear to have a neutral effect on bone, although limited data are available. Data on animals indicate that GLP1RAs may improve bone mass and architecture (Lu et al., 2015; Pereira et al., 2015). However, meta-analyses of both randomized clinical trials and population-based real-world data showed no effect of GLP1RAs on fracture risk (Driessen et al., 2017; Mabilleau et al., 2014). Conflicting data exist on DPP-4 inhibitors, which were reported to either reduce (Monami et al., 2011) or have no effect on (Driessen et al., 2017) fracture risk. Sodium/glucose cotransporter-2 (SGLT-2) inhibitors decrease plasma glucose levels by inhibiting glucose reuptake by SGLT-2 in the proximal tubule of the kidney. These drugs may affect calcium and phosphate homeostasis and potentially increase fracture risk (Meier et al., 2016). The SGLT-2 inhibitor canagliflozin was associated with a significant increase in both all fractures and low-trauma fractures in patients with T2DM (Watts et al., 2016). However, no increased risk of fracture was evident in four meta-analyses of placebo-controlled randomized controlled trials of dapagliflozin, canagliflozin, and empagliflozin (Kohler et al., 2018; Ruanpeng et al., 2017; Tang et al., 2016; Wu et al., 2016). In a nested case–control study, the use of SGLT-2 inhibitors was not associated with an increased risk of fractures of the upper or

lower limbs compared with use of DPP-4 inhibitors in patients with T2DM (Schmedt et al., 2019). Although these data are reassuring, further evidence is needed to confirm the bone safety of SGLT-2 inhibitors.

Insulin has anabolic effects of bone. Intensive insulin treatment in patients with T1DM was associated with stabilization of BMD over 7 years and a marked decrease in bone resorption, as assessed by circulating bone turnover markers (Campos Pastor et al., 2000). In contrast, a large body of evidence indicates that insulin treatment is associated with increased fracture risk in T2DM (Gilbert and Pratley, 2015). A 2018 population-based study including more than 12,000 patients with T2DM found that insulin monotherapy was associated with a 63% increase in fracture risk compared with metformin monotherapy (Losada et al., 2018). The increased fracture risk associated with insulin treatment in T2DM might be due to more advanced disease, with increased vascular complications, in insulin-treated T2DM patients.

Statins are another frequently used class of drugs in diabetic patients. In the general population, statin use was associated with reduced risk of osteoporosis (Lin et al., 2018), although the effect on fracture risk is uncertain (Toh and Hernandez-Diaz, 2007). A small study suggested that statins increase bone density at the hip in T2DM patients (Chung et al., 2000), and an inverse association of fracture risk with statin use has been reported (Martinez-Laguna et al., 2018).

Bone repair in T1DM and T2DM

Fracture healing in patients with diabetes is delayed by nearly 90%, and the risk of complications such as delayed union, nonunion, re-dislocation, or pseudoarthrosis is more than threefold compared with nondiabetic individuals (Jiao et al., 2015). Several experimental models have demonstrated an impaired bone repair in T1DM with less new bone formed, as assessed by radiographic, micro-computed tomographic, and histomorphometric analyses (Follak et al., 2004; Funk et al., 2000; Gandhi et al., 2006; Kawaguchi et al., 1994; Kayal et al., 2007; Santana et al., 2003; Thrailkill et al., 2005a). Overall, bone formation was approximately 7% lower ($P < .001$) in T1DM models compared with controls (Camargo et al., 2017). Both endochondral and periosteal postfracture repair mechanisms were defective. Both increased cartilage resorption, due to greater osteoclast number (Kayal et al., 2007), and impaired cartilage resorption, due to decreased osteoclast function (Kasahara et al., 2010), have been reported in STZ-diabetic rats. However, some local treatments also (partially) reversed the defective fracture repair, e.g., local administration of insulin (Gandhi et al., 2005; Paglia et al., 2013).

In models of T2DM, bone regeneration was significantly decreased due to impairments in angiogenesis and osteogenesis that could be reversed by local application of fibroblast growth factor 9 and, to a lesser degree, vascular endothelial growth factor (VEGF) A (Wallner et al., 2015). Increased callus adiposity due to the shift of mesenchymal stem cells toward the adipogenic lineage (Brown et al., 2014), delayed periosteal mesenchymal osteogenesis, premature apoptosis of cartilage callus, impaired microvascularization (Roszer et al., 2014), and impairment in osteoblast differentiation (Hamann et al., 2011) may also be responsible for delayed fracture healing in T2DM. Animal studies suggest that DPP-4 inhibitors may enhance fracture healing by altering stem cell lineage allocation (Ambrosi et al., 2017).

Bone and systemic metabolism: a two-way interaction?

Metabolic control of glucose and insulin in bone

Both osteoblasts (Ferron et al., 2010) and osteoclasts (Thomas et al., 1998) express the IR on their surface, insulin signaling through the IR being essential for normal bone acquisition (Fulzele et al., 2010; Thrailkill et al., 2014). In fact, insulin increases osteoblast proliferation and enhances osteoblast differentiation, collagen synthesis, alkaline phosphatase production, and glucose uptake, and inhibits osteoclast activity, leading to increased bone formation (Cornish et al., 1996; Pramojanee et al., 2013; Pun et al., 1989; Thomas et al., 1998; Thrailkill et al., 2005b; Yang et al., 2010). Osteoblasts also express the IGF-1 receptor on their surface (Fulzele et al., 2007). IGF-1 binds both the IGF-1 receptor and, with lower binding affinity, the IR, thus triggering the insulin signaling pathway. Studies investigating the effects of insulin on osteocytes are lacking, as expression of the IR on the osteocyte surface is minimal or absent.

Supraphysiological glucose concentrations and/or AGEs were shown to reduce the expression of proosteogenic markers in human osteoblasts (Ehnert et al., 2015; Miranda et al., 2016), suppress mineralization (Ogawa et al., 2007), and inhibit the Wnt signaling pathway, which is critical for osteogenic differentiation (Lopez-Herradon et al., 2013; Picke et al., 2016). Furthermore, exposure to AGEs induced osteoblast and mesenchymal stem cell apoptosis (Alikhani et al., 2007; Kume et al., 2005). Hyperglycemia inhibits osteoclastogenesis (Wittrant et al., 2008) and impairs osteoclast differentiation and activity, as measured by TRAP in embryonic stem cells (Dienelt and zur Nieden, 2011). Osteocytes exposed to high glucose concentrations increase expression of sclerostin, which inhibits bone formation by antagonizing the Wnt/β-catenin

canonical signaling pathway (Tanaka et al., 2015). Osteocyte exposure to AGEs increases sclerostin and decreases expression of receptor activator of nuclear factor κB ligand (RANKL), a member of the tumor necrosis factor (TNF) superfamily that is necessary for osteoclast formation, differentiation, activation, and survival (Tanaka et al., 2015). In addition, hyperglycemia impairs osteocyte response to mechanical stimulation, a mechanism essential for their function (Seref-Ferlengez et al., 2016; Villasenor et al., 2019).

Bone hormones control systemic metabolism

Evidence indicates a reciprocal regulation of glucose and bone metabolism (Conte et al., 2018). The osteoblast-derived bone matrix protein OC acts as a hormone, stimulating β-cell proliferation and insulin secretion. Consistently, OC-knockout mice displayed decreased β-cell proliferation, glucose intolerance, and insulin resistance (Wei et al., 2014a). In vitro, insulin secretion increased when pancreatic β cells were cocultured with osteoblasts or in the presence of supernatants from cultured osteoblasts, suggesting that an osteoblast-derived factor stimulates insulin secretion by β cells (Ferron et al., 2008; Lee et al., 2007) acting upon GPRC6A receptors (Ferron et al., 2008; Wei et al., 2014b). Administration of OC significantly decreased plasma glucose and increased insulin secretion in C57BL/6J wild-type mice (Ferron et al., 2008). In addition to stimulating insulin secretion, OC indirectly improved insulin sensitivity by stimulating the secretion of adiponectin, a white adipocyte-derived insulin-sensitizing adipokine.

Evidence from preclinical studies indicates that only undercarboxylated OC (ucOC) exerts endocrine actions (Lee et al., 2007). OC decarboxylation is a pH-dependent mechanism that occurs during bone resorption, when bone matrix is acidified by osteoclasts. However, treatment with bisphosphonates, which inhibit bone resorption and therefore pH-dependent decarboxylation of OC, is not associated with worsening glucose metabolism (Schwartz et al., 2013a). Treatment with denosumab, a fully human monoclonal antibody that inhibits bone resorption by binding to RANKL, has been associated with reductions in fasting plasma glucose in diabetic subjects (Napoli et al., 2018a). Blockade of nuclear factor κB, a proinflammatory master switch that controls the production of inflammatory markers and mediators, has been postulated as the mechanism responsible for this observation. A number of human studies have explored the relationship between OC and glucose homeostasis. OC levels have been reported to be lower in T2DM compared with healthy subjects (Oz et al., 2006), inversely related to BMI, fat mass, and plasma glucose (Kanazawa et al., 2009, 2011b; Kindblom et al., 2009; Zhou et al., 2009), but also to atherosclerosis and inflammatory parameters such as high sensitive C-reactive protein and interleukin-6 (IL-6) (Pittas et al., 2009). However, OC-stimulated IL-6 release has been postulated as a mechanism to support muscle function during exercise, through enhanced glucose and fatty acid uptake into myofibers (Mera et al., 2016a, 2016b; Tsuka et al., 2015).

Studies investigating the effects of medications or conditions that may affect OC levels yielded conflicting results, questioning the OC−glucose relationship in humans. For example, alendronate therapy, which decreases OC levels, was associated with reduced diabetes risk (Vestergaard, 2011); treatment with vitamin K, which reduces the ucOC/OC ratio, improved insulin resistance (Beulens et al., 2010; Choi et al., 2011; Yoshida et al., 2008); chronic hyperparathyroidism, which is characterized by increased OC release, was associated with increased insulin resistance and impaired glucose regulation (Taylor and Khaleeli, 2001). Less evidence is available for T1DM. No association between OC and β-cell function was found in subjects with new-onset T1DM (Napoli et al., 2013). However, in T1DM, total OC was inversely correlated with BMI and HbA1c, and ucOC was inversely correlated with HbA1c in T1DM patients with mean disease duration of 21 years (Neumann et al., 2016). Despite relevant clinical and preclinical data supporting a positive feedback between osteoblasts and β cells, it is possible that, in a condition of continuous autoimmune damage against β cells such as in T1DM, the ability of OC to modulate β-cell function is lost. On the other hand, Thrailkill et al. reported a positive effect of OC on endogenous insulin production (assessed as C-peptide/glucose ratio) (Thrailkill et al., 2012) in subjects with long-standing disease. The relationship between OC and glucose metabolism requires further investigation.

What causes diabetic bone disease?

The diabetic hormonal milieu

Lower circulating insulin-like growth factor 1

Lower circulating IGF-1 is probably a crucial factor. Downregulation of hepatic IGF-1 release resulted in a 73% drop in serum IGF-1 levels in children with new-onset T1DM (Bereket et al., 1995); circulating IGF-1 remained below control levels in T1DM adolescents and adults receiving insulin treatment (Bouillon et al., 1995; Leger et al., 2006). IGF-1 had

powerful effects on osteoblast proliferation and bone matrix formation in vitro (Hock et al., 1988). Also, disruption of the IGF-1 gene resulted in 25%−40% smaller bones in prepubertal mice and prevented periosteal expansion and BMD gain during puberty; serum OC levels in IGF-1-knockout mice were reduced by 24%−54% (Mohan et al., 2003). Depletion of circulating IGF-1 (while skeletal expression of IGF-1 remained normal) equally resulted in decreased growth and periosteal expansion, which was restored by exogenous IGF-1 (Yakar et al., 2002). Insulin and IGF-1 initiate cellular responses by binding to and activating the insulin and IGF-1 (tyrosine kinase) receptors, and phosphorylation of IR substrate (IRS)-1. As would be predicted, IRS-1-knockout mice showed smaller bones with thinner growth plates, lower trabecular and cortical bone volume, thin trabeculae, and low bone formation and resorption (Ogata et al., 2000). These mice also were hyperinsulinemic. Studies in T1DM animals showed a strong correlation between plasma IGF-1 and OC levels (Verhaeghe et al., 1997). Similarly, IGF-1 concentrations were correlated with biochemical bone formation markers in T1DM individuals (Bouillon et al., 1995). In addition, serum IGF-1 was an independent predictor of total body bone mineral content in children and adolescents with T1DM (Leger et al., 2006). Upregulation of the hepatic expression of IGF-binding protein-1 (IGFBP1) by insulin deficiency caused a sevenfold increment in circulating IGFBP1 in children with new-onset T1DM (Bereket et al., 1995). Through the accrued formation of binary IGF-1:IGFBP1 complexes (Frystyk et al., 2002), the decrement in circulating free (bioavailable) IGF-1 in T1DM is more pronounced than that of total IGF-1. It is not surprising, therefore, that IGFBP1 inhibited the osteoblastic effects of IGF-1 (Campbell and Novak, 1991). Elevated IGFBP1 levels might also explain, in part, why bone growth and remodeling in T1DM rats were resistant to the anabolic effects of exogenous IGF-1 (Verhaeghe et al., 1992).

Using the Cre-loxP technique to disrupt IGF-1R in osteoblasts in vitro, Fulzele and colleagues were able to examine insulin signaling in primary osteoblasts exclusively through its cognate receptor (Fulzele et al., 2007). In osteoblasts engineered for conditional disruption of the IGF-1R, insulin signaling was markedly increased and insulin treatment rescued the defective differentiation and mineralization, suggesting that IR signaling can compensate, at least in part, for loss of IGF-1R signaling.

Several in vivo studies have shown that the stimulatory actions of IGF-1 on osteoblasts are blunted by high concentrations of AGEs and that high glucose concentrations or AGEs might induce osteoblast resistance to the actions of IGF-1 (McCarthy et al., 2001; Terada et al., 1998). Serum levels of IGF-1 were found to be inversely associated with the presence of vertebral fractures in postmenopausal women with T2DM independent of age, glycemic control, renal function, insulin secretion, or lumbar spine BMD, and with the number of prevalent vertebral fractures in these women independent of lumbar spine BMD (Kanazawa et al., 2011a).

In 2018, a Japanese group studying a cohort of about 1000 T2DM subjects found that an IGF-1 cutoff value of 127 ng/mL was associated with higher risk of vertebral fracture (Kanazawa et al., 2018). In particular, lower IGF-1 and lower T scores were associated with significantly increased risk of vertebral fractures compared with higher IGF-1 and higher T scores, both in postmenopausal women and in men. Further evidence is needed to validate the predictive value of IGF-1 on fracture risk in individuals with diabetes.

Hypercortisolism

Several studies suggest that T2DM patients with chronic complications have an increased cortisol secretion even though within the normal range (Chiodini et al., 2006, 2007). In a case−control study on 99 T2DM postmenopausal women with good glycemic control without hypercortisolism and 107 matched nondiabetic controls, vertebral fractures were associated with cortisol secretion and sensitivity, as mirrored by the sensitizing polymorphism glucocorticoid receptor gene (Zhukouskaya et al., 2015). Thus, it is possible to hypothesize that in the presence of T2DM complications a slightly enhanced cortisol secretion may contribute to bone damage (Eller-Vainicher et al., 2017). The same authors found that trabecular bone score (TBS) was not different between T2DM postmenopausal women with good glycemic control and matched nondiabetic controls. However, TBS was reduced in T2DM patients with vertebral fractures compared with nonfractured T2DM patients. Interestingly, the presence of a TBS $\leq$ 1.130 or BMD Z score at the femoral neck below −1.0 had the best diagnostic accuracy for detecting T2DM fractured patients with a sensitivity and negative predictive value above 80% (Zhukouskaya et al., 2016).

Calciotropic hormones

There is a great deal of controversy regarding the effects of T1DM on circulating parathyroid hormone (PTH) and 1,25-dihydroxyvitamin D_3 ($1,25(OH)_2D_3$). Intermittent administration of human PTH(1−34) to T1DM rats improved trabecular bone formation, volume, and strength (Suzuki et al., 2003); however, intermittent PTH is a powerful anabolic agent for

trabecular bone in various osteopenic conditions not necessarily associated with hypoparathyroidism (e.g., postmenopausal or glucocorticoid-induced osteopenia). Although T1DM rats displayed a higher metabolic clearance rate of $1,25(OH)_2D_3$ and lower (i.e., total but not free) circulating $1,25(OH)_2D_3$, $1,25(OH)_2D_3$ infusion did not affect the osteoblast and osteoid surface on histomorphometry and barely raised serum OC (Verhaeghe et al., 1993).

Clinical data have shown that high blood glucose may increase urinary calcium excretion and PTH levels (Hofbauer et al., 2007; McNair et al., 1979; Raskin et al., 1978). Conversely, improvement of blood glucose control may reduce calcium and phosphate urinary excretion and $1,25(OH)_2D_3$ levels (Okazaki et al., 1997). Numerous studies have shown that both patients with T1DM and those with T2DM have low vitamin D levels (Scragg et al., 1995). Obesity itself is also associated with low vitamin D levels, although the pathophysiology of this is unclear. One mechanism may be related to the deposition of vitamin D in adipocytes (Wortsman et al., 2000), although altered 25-hydroxylation in the liver of obese individuals is another possibility. It is a matter of debate if vitamin D levels may predict risk of diabetes (Ebeling et al., 2018). Indeed, although higher levels of 25(OH)D have been associated with reduced risk of diabetes, other studies have not found an association between baseline vitamin D and incident diabetes (Napoli et al., 2016; Schafer et al., 2014). Vitamin D supplementation aimed at raising 25(OH)D levels above 30 ng/mL had no effect on insulin secretion, insulin sensitivity, or the development of diabetes compared with placebo (Davidson et al., 2013). Importantly, patients with new-onset T1DM have reduced levels of $1,25(OH)_2D$ and 25(OH)D compared with healthy controls (Pozzilli et al., 2005). A causative role of vitamin D deficiency in diabetes has been suggested although vitamin D supplementation in early diagnosed patients with T1DM has not improved measures of glucose control nor insulin need nor bone turnover markers (Bizzarri et al., 2010; Maddaloni et al., 2018; Napoli et al., 2013).

Low amylin

Amylin is a peptide cosecreted with insulin by pancreatic β cells in response to nutrient stimuli. Amylin treatment of STZ-diabetic rats resulted in some improvement of the diabetic syndrome, and prevented the low-formation osteopenia observed in untreated rats (Horcajada-Molteni et al., 2001). The role of amylin must be clarified in future research.

Impaired vascularization of diabetic bones

It has been postulated by some that diabetic bone disease is another manifestation of microangiopathy, but evidence supporting this hypothesis is lacking. More research on the vascularization of diabetic bones (including the growth plate), and the factors that regulate vascularization (e.g., VEGFs), is sorely needed.

Altered collagenous bone matrix

Increased collagen glycosylation

Nonenzymatic protein glycosylation and oxidation results in the gradual accumulation of AGEs in serum and various tissues. Proteins with a long half-life such as collagen are particularly susceptible to glycosylation. AGE accumulation in bone occurs with normal aging but is much accelerated in diabetes (Katayama et al., 1996). Accumulation of AGEs in aging bone was associated with increased brittleness (Wang et al., 2002), and may also be a determinant of diabetic bone brittleness. Moreover, AGE accumulation in diabetic bones affected bone cell function through inhibition of osteoblastic cell differentiation and function (Katayama et al., 1996) and stimulation of osteoblast apoptosis (Alikhani et al., 2007). RAGE, one of the receptors for AGEs, was overexpressed in healing bone tissue of STZ-diabetic mice, and local delivery of a RAGE ligand delayed bone healing in nondiabetic mice (Santana et al., 2003). These data would indicate that accumulation of AGEs explains in part the impaired fracture repair in diabetes. In a 2018 study, proximal femur specimens from T2DM ($n = 20$) and nondiabetic ($n = 33$) subjects undergoing total hip replacement surgery were imaged by micro-computed tomography, tested by cyclic reference point indentation, and quantified for AGE content (Karim et al., 2018). Bone specimens from patients with T2DM had similar cortical porosity but altered cortical bone biomechanical properties (greater creep indentation distance and indentation distance increase) and tended to have greater AGE content in cortices compared with nondiabetic bones. Conversely, biomechanical properties and AGE content of trabecular bone were similar between T2DM and nondiabetic subjects. The normal trabecular bone and modest cortical bone alterations suggest that other factors than altered bone microstructure could contribute to increased fracture risk in T2DM. A 2019 study by the Donnelly group investigated differences in material properties, microarchitecture, and mechanical performance of trabecular bone in men with and without T2DM undergoing total hip arthroplasty (Hunt et al., 2019).

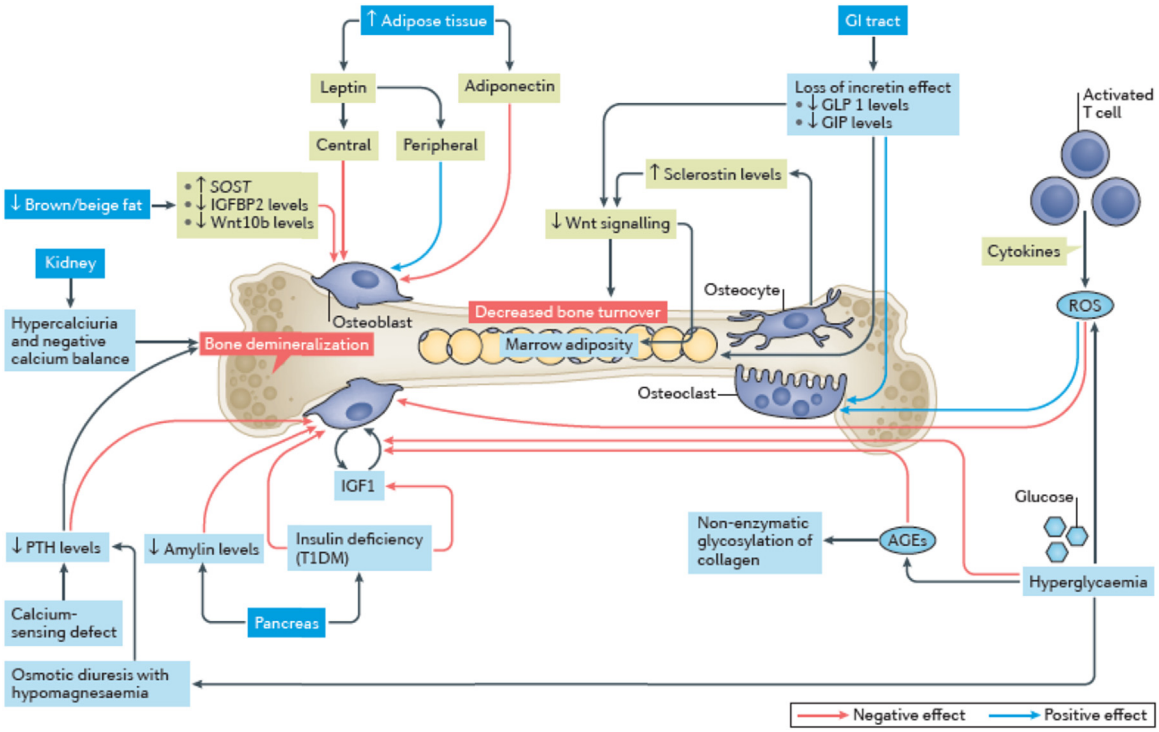

FIGURE 40.2 Cellular and molecular mechanisms of bone diseases in diabetes mellitus. Although several reports consistently indicate an increased risk of fractures in patients with diabetes mellitus, the underlying mechanisms are unclear and there is not enough evidence for a conclusive model of bone fragility in diabetes mellitus; however, some factors should be highly considered. With the decline of β-cell function, chronic hyperglycemia causes oxidative stress, inflammation, and the production of reactive oxygen species (*ROS*) and advanced glycation end products (*AGEs*), causing organ damage and reduced bone strength. In particular, accumulation of AGEs in diabetic bone collagen determines reduced material properties and increased susceptibility to fracture. AGEs and hyperglycemia also directly inhibit bone formation via suppression of osteoblast function. Low bone formation is also caused by disturbances to the Wnt signaling pathway, with increased sclerostin (*SOST*) expression, higher sclerostin levels, and decreased levels of insulin-like growth factor-binding protein 2 (*IGFBP2*) and protein *Wnt10b*. In type 1 diabetes mellitus (*T1DM*) and in the late stages of T2DM, bone formation is also decreased by insulin deficiency through an inhibitory effect on osteoblasts, either directly or through alterations in insulin-like growth factor 1 (*IGF1*) levels. Other factors typically linked to T2DM and obesity interfere with bone health. Dysregulation of adipokines like adiponectin and leptin has a negative effect through complex central and peripheral mechanisms. New evidence also indicates a negative effect on bone health by loss of the incretin effect, with reduced bone formation and increased osteoclastogenesis. Finally, alterations of the calcium−parathyroid hormone (*PTH*) axis result in a negative calcium balance, thereby contributing to bone demineralization in diabetes mellitus. *GI*, gastrointestinal; *GIP*, gastric inhibitory polypeptide; *GLP1*, glucagon-like peptide 1. *Source: Napoli N et al. 2017.* Nat Rev Endocrinol. *13, 208−219.*

Bone specimens from men with T2DM had significantly greater content of the AGE pentosidine (+36%) and sugars bound to the collagen matrix (+42%) compared with specimens from nondiabetic men. Mineral content was significantly higher (+7%) and, consistent with previous reports of increased BMD at the femoral neck and hip in T2DM, bone volume fraction (BV/TV) tended to be greater (+24%) in specimens from diabetic men. These effects favorably influenced bone strength. However, the greater values of pentosidine in T2DM men decreased post-yield strain and toughness. Overall, these findings indicate a beneficial effect of T2DM on trabecular microarchitecture, but an impairment of collagen matrix. High concentrations of AGEs can offset the favorable effect of greater mineral content, thus increasing bone fragility (Fig. 40.2).

Reduced enzymatic collagen cross-linking

Spontaneously diabetic WBN/Kob rats showed reduced serum vitamin B_6 (pyridoxal and pyridoxamine) and immature enzymatic collagen cross-links in femoral bone from the prediabetic stage onward; however, mature cross-links (pyridinoline and deoxypyridinoline) remained normal, while nonenzymatic cross-links increased from the diabetic stage. As mentioned earlier, the altered collagenous matrix composition was correlated with reduced bone strength parameters (Saito et al., 2006).

Increased bone marrow adiposity

In recent years, bone marrow fat (BMF) has received increasing attention as a determinant of bone health that is also involved in whole-body energy regulation, hematopoiesis, and possibly further functions (Veldhuis-Vlug and Rosen, 2017). A positive association between osteocyte-derived sclerostin and BMF has been described in men (Ma et al., 2014), indicating that osteocytes may influence marrow adipogenesis via inhibition of the Wnt signaling pathway, thus favoring adipogenesis at the expense of osteogenesis.

In a cross-sectional analysis of men participating in the MrOS study, a large epidemiological study of nearly 6000 men, those with diabetes ($n = 38$) had significantly higher spine BMF (59% vs. 55%), spine BMD, and total hip than nondiabetic men, despite similar body weight, BMI, and waist circumference (Sheu et al., 2017). BMF was inversely correlated with BMD in diabetic men, but not in controls. Schwartz and colleagues investigated the relationships between vertebral BMF, BMD by QCT, and fracture in 257 older adults (mean age 79 years) (Schwartz et al., 2013b). Mean BMF was 54% in men and 55% in women. Those with prevalent vertebral fracture (21 men, 32 women) had significantly higher mean BMF (57% vs. 54%) after adjustment for age, gender, and trabecular spine vBMD. When men and women were analyzed separately, gender-related differences emerged. The difference in BMF between those with or without a prevalent fracture remained statistically significant only in men. BMF was associated with lower trabecular vBMD at the spine (−10.5% difference for each 1 SD increase in BMF), total hip, and femoral neck, but not with cortical vBMD, in women. In men, BMF was marginally but significantly associated with trabecular spine vBMD (−6.1%). Total hip and spine aBMD were negatively correlated with BMF in women only.

Patients with T1DM appear to have similar marrow adiposity compared with nondiabetics. No differences in BMF were identified between male patients with T1DM and healthy controls (Armas et al., 2012; Carvalho et al., 2018), and neither duration of disease nor glycemic control was related to bone marrow adiposity. This lack of association between BMF and T1DM was confirmed in young women with T1DM compared with healthy controls (Abdalrahaman et al., 2017). Irrespective of the presence of diabetes, in young women BMF was inversely associated with BMD (Abdalrahaman et al., 2017). Carvalho and colleagues showed that BMF quantity and lipid composition (saturated and unsaturated lipids) were similar between T1DM subjects and controls (Carvalho et al., 2018). There was, however, a significant inverse correlation between BMF saturated lipids and BMD.

Inflammation and oxidative stress

Chronic low-grade inflammation underlies several metabolic diseases, including T1DM, T2DM, and associated micro- and macrovascular complications (Clark et al., 2017; Lontchi-Yimagou et al., 2013). Chronic low-grade inflammation could also have a role in diabetic bone disease. Elevated cytokine levels can activate osteoclastogenesis and suppress osteoblast differentiation (Gilbert et al., 2000; Glajchen et al., 1988). Several proinflammatory cytokines that are elevated in both T1DM and T2DM may have detrimental effects on bone health. TNF has been shown to stimulate osteoclastogenesis (Glantschnig et al., 2003) and inhibit osteoblastogenesis (Gilbert et al., 2000). Local production of inflammatory cytokines in bone tissue has been described in murine models of STZ-induced T1DM (Coe et al., 2011; Motyl et al., 2009). Furthermore, systemic exposure to proinflammatory cytokines such as IL-1, IL-6, and TNF results in increased oxidative stress, which affects differentiation and survival of osteoclasts, osteoblasts, and osteocytes (Manolagas, 2010). Mesenchymal stem cells may also be affected, as hyperglycemia-induced oxidative stress was shown to influence mesenchymal stem cell differentiation, with adipogenesis being favored over bone formation (Aguiari et al., 2008). Although these studies point toward a detrimental effect of chronic inflammation and oxidative stress on bone, further studies are needed to better define their contribution to diabetic bone disease.

Loss of incretin effect

Incretins, namely GIP and GLP1, are gut-secreted hormones that are responsible for the "incretin effect," i.e., the greater insulin response to oral versus intravenous glucose administration. Patients with T2DM have a reduced incretin effect, with impaired GLP1 production after a meal (Knop et al., 2007). GLP1 promotes proliferation of mesenchymal stem cells and prevents their differentiation into adipocytes (Sanz et al., 2010). GLP1 receptor knockout mice showed increased osteoclast numbers, bone resorption rate, and bone fragility and low calcitonin levels (Yamada et al., 2008). Increasing doses of exendin-4, a GLP1 mimetic, resulted in proportional increases in BMD, bone strength, and bone formation in rats (Ma et al., 2013). Whether loss of incretin effect contributes to bone fragility in T2DM in humans has not been established. Two

categories of incretin-based therapies are available for the treatment of T2DM: inhibitors of DPP-4, and GLP1RA. Observational studies indicate that incretin mimetics have a neutral effect on bone health in humans (Driessen et al., 2017; Mabilleau et al., 2014; Monami et al., 2011), and interventional trials are lacking.

Sclerostin

Osteocytes are the most abundant bone cell type and play a central role in bone modeling and remodeling, regulating the bone biomechanical response to loading and the capacity to repair microcracks (i.e., fracture initiators). The role of osteocytes in diabetic bone disease is often overlooked, and yet to be fully clarified. Bone expression of sclerostin (encoded by *SOST*) and dickkopf-related protein 1, two major inhibitors of bone formation via inhibition of Wnt−β-catenin signaling, were increased in rat models of T1DM and T2DM (Hie et al., 2011; Kim et al., 2013; Nuche-Berenguer et al., 2010). Sclerostin levels were also found to be higher in patients with diabetes, either type 1 or type 2, than in healthy individuals (Gennari et al., 2012; Neumann et al., 2014). In T2DM, this increase was associated with a decrease in markers of bone formation (Gaudio et al., 2012), further suggesting that sclerostin inhibits bone turnover in diabetic states.

While increased circulating levels of sclerostin were associated with vertebral fractures in postmenopausal women with T2DM (Yamamoto et al., 2013), suggesting that sclerostin could be a useful clinical tool for fracture risk assessment in patients with T2DM, T1DM patients with the highest sclerostin levels had an 81% decreased risk of fracture compared with those with the lowest levels (Starup-Linde et al., 2016a).

Treatment of bone fragility in diabetes

Anti-osteoporosis drugs appear to be as effective in diabetic as in nondiabetic individuals, although the number of studies is limited. In a post hoc analysis of the Fracture Intervention Trial, alendronate 5−10 mg for 3 years increased aBMD at the spine and hip and reduced bone remodeling indices comparably in diabetic and nondiabetic postmenopausal women (Keegan et al., 2004). A population-based study that assessed the efficacy of antiresorptive drugs for fracture prevention found no difference in the anti-fracture efficacy between patients with diabetes and nondiabetic controls or between patients with T1DM and those with T2DM (Vestergaard et al., 2011). Efficacy in reducing nonvertebral fractures, increasing BMD, and decreasing back pain was reported with the osteoanabolic agent teriparatide independent of diabetes status in the Direct Assessment of Nonvertebral Fractures in Community Experience (DANCE) observational study (Schwartz et al., 2016). Data from pooled observational studies indicate that treatment with teriparatide for more than 6 months significantly reduces risk of clinical fractures. Interestingly, the efficacy of the medication on fracture risk was superior in diabetics compared with nondiabetics (Langdahl et al., 2018).

General conclusions

- Both T1DM and T2DM are associated with higher incidence of fractures, although the risk is far greater for T1DM. The increased fracture incidence in T1DM is more pronounced than could be explained by the relatively small BMD deficit.
- T2DM is characterized by higher risk of nonvertebral fracture and normal or higher areal and volumetric BMD. The role of cortical porosity, which appears to be increased in T2DM patients, is still controversial. Insulin deficiency may explain, at least in part, bone fragility in T1DM and in the last stages of T2DM. Insulin stimulates growth and bone formation in vitro and in vivo through its receptors on the bone cells. However, absence of IR expression in bone does not cause diabetic bone disease, indicating that the effect of insulin deficiency on bone is largely if not completely indirect.
- Fracture risk increases with diabetes duration and is higher among individuals with diabetes complications and limited physical capabilities; the higher incidence of falls in diabetic individuals is probably an important mediator.
- Glucotoxicity, increased oxidative stress, and inflammation are common findings in diabetics, but their impact on bone fragility is not known.
- Bone strength is clearly impaired in T1DM and T2DM. Diabetes-induced changes in the collagenous matrix are related to its biomechanical properties. These include reduced enzymatic collagen cross-links but increased glycosylated collagen (AGEs).
- Data from histology and bone markers indicate that diabetes is accompanied by low bone remodeling (both formation and resorption), a condition that may affect bone quality. Strong evidence indicates elevated sclerostin levels in T2DM, indicating a possible dysfunction of the Wnt osteoanabolic pathway in T2DM.

- Antidiabetic medications should be used wisely in diabetic patients, avoiding those that may affect bone strength (TZDs) or increase the risk of hypoglycemic events (sulfonylureas). Target HbA1c should not be too stringent, according to the most recent guidelines.
- Antiosteoporotic medications have been proved equally effective and safe in diabetics.

Key points

- Patients with type 1 diabetes mellitus or type 2 diabetes mellitus (T2DM) have an increased risk of fractures; bone mineral density underestimates this risk in individuals with T2DM, making risk assessment challenging.
- Patients with diabetes mellitus with long-term disease, poor glycemic control, β-cell failure and who receive insulin treatment are at the highest risk of fractures.
- Low bone turnover, accumulation of advanced glycation end products, micro- and macroarchitecture alterations, and tissue material damage lead to abnormal biomechanical properties and impair bone strength.
- Other determinants of bone fragility include inflammation, oxidative stress, adipokine alterations, Wnt dysregulation, and increased marrow fat.
- Complications of diabetes mellitus, such as neuropathy, poor balance, sarcopenia, vision impairment, and frequent hypoglycemic events, increase the risk of falls and risk of fracture; preventive measures are advised, especially in patients taking insulin.
- Use of thiazolidinediones, or some SGLT-2 inhibitors might contribute to increased fracture risk; antidiabetic medications with good bone safety profiles such as metformin, glucagon-like peptide 1 analogs, or dipeptidyl peptidase-4 inhibitors are preferred.

Acknowledgments

Portions of the text were reproduced by permission of the Journal of Endocrinology Ltd.

References

Abdalrahaman, N., McComb, C., Foster, J.E., Lindsay, R.S., Drummond, R., McKay, G.A., Perry, C.G., Ahmed, S.F., 2017. The relationship between adiposity, bone density and microarchitecture is maintained in young women irrespective of diabetes status. Clin. Endocrinol. 87, 327.

Abdalrahaman, N., McComb, C., Foster, J.E., McLean, J., Lindsay, R.S., McClure, J., McMillan, M., Drummond, R., Gordon, D., McKay, G.A., Shaikh, M.G., Perry, C.G., Ahmed, S.F., 2015. Deficits in trabecular bone microarchitecture in young women with type 1 diabetes mellitus. J. Bone Miner. Res. 30, 1386.

Acevedo, C., Sylvia, M., Schaible, E., Graham, J.L., Stanhope, K.L., Metz, L.N., Gludovatz, B., Schwartz, A.V., Ritchie, R.O., Alliston, T.N., Havel, P.J., Fields, A.J., 2018. Contributions of material properties and structure to increased bone fragility for a given bone mass in the UCD-T2DM rat model of type 2 diabetes. J. Bone Miner. Res. 33, 1066.

Aguiari, P., Leo, S., Zavan, B., Vindigni, V., Rimessi, A., Bianchi, K., Franzin, C., Cortivo, R., Rossato, M., Vettor, R., Abatangelo, G., Pozzan, T., Pinton, P., Rizzuto, R., 2008. High glucose induces adipogenic differentiation of muscle-derived stem cells. Proc. Natl. Acad. Sci. U. S. A. 105, 1226.

Ahmad, T., Ohlsson, C., Saaf, M., Ostenson, C.G., Kreicbergs, A., 2003. Skeletal changes in type-2 diabetic Goto-Kakizaki rats. J. Endocrinol. 178, 111.

Ahn, S.H., Kim, H., Kim, B.J., Lee, S.H., Koh, J.M., 2016. Insulin resistance and composite indices of femoral neck strength in Asians: the fourth Korea national health and nutrition examination survey (KNHANES IV). Clin. Endocrinol. 84 (2), 185−193.

Alarid, E.T., Schlechter, N.L., Russell, S.M., Nicoll, C.S., 1992. Evidence suggesting that insulin-like growth factor-I is necessary for the trophic effects of insulin on cartilage growth in vivo. Endocrinology 130, 2305.

Alhuzaim, O.N., Lewis, E.J.H., Lovblom, L.E., Cardinez, M., Scarr, D., NBoulet, G., Weisman, A., Lovshin, J.A., Lytvyn, Y., Keenan, H.A., Brent, M.H., Paul, N., Bril, V., Cherney, D.Z.I., Perkins, B.A., 2019. Bone mineral density in patients with longstanding type 1 diabetes: results from the Canadian study of longevity in type 1 diabetes. J. Diabet. Complicat. In press.

Alikhani, M., Alikhani, Z., Boyd, C., MacLellan, C.M., Raptis, M., Liu, R., Pischon, N., Trackman, P.C., Gerstenfeld, L., Graves, D.T., 2007. Advanced glycation end products stimulate osteoblast apoptosis via the MAP kinase and cytosolic apoptotic pathways. Bone 40, 345.

Ambrosi, T.H., Scialdone, A., Graja, A., Gohlke, S., Jank, A.-M., Bocian, C., Woelk, L., Fan, H., Logan, D.W., Schürmann, A., Saraiva, L.R., Schulz, T.J., 2017. Adipocyte accumulation in the bone marrow during obesity and aging impairs stem cell-based hematopoietic and bone regeneration. Cell Stem Cell 20, 771.

American Diabetes Association, 2019. Standards of medical care in diabetes − 2019. Diabetes Care 42 (S1). Available at: http://care.diabetesjournals.org/content/42/Supplement_1.

Armas, L.A.G., Akhter, M.P., Drincic, A., Recker, R.R., 2012. Trabecular bone histomorphometry in humans with type 1 diabetes mellitus. Bone 50, 91.

Bain, S., Ramamurthy, N.S., Impeduglia, T., Scolman, S., Golub, L.M., Rubin, C., 1997. Tetracycline prevents cancellous bone loss and maintains near-normal rates of bone formation in streptozotocin diabetic rats. Bone 21, 147.

Bauer, D.C., Browner, W.S., Cauley, J.A., Orwoll, E.S., Scott, J.C., Black, D.M., Tao, J.L., Cummings, S.R., 1993. Factors associated with appendicular bone mass in older women. The Study of Osteoporotic Fractures Research Group. Ann. Intern. Med. 118, 657.

Bechtold, S., Dirlenbach, I., Raile, K., Noelle, V., Bonfig, W., Schwarz, H.P., 2006. Early manifestation of type 1 diabetes in children is a risk factor for changed bone geometry: data using peripheral quantitative computed tomography. Pediatrics 118, e627.

Bechtold, S., Putzker, S., Bonfig, W., Fuchs, O., Dirlenbach, I., Schwarz, H.P., 2007. Bone size normalizes with age in children and adolescents with type 1 diabetes. Diabetes Care 30, 2046.

Bereket, A., Lang, C.H., Blethen, S.L., Gelato, M.C., Fan, J., Frost, R.A., Wilson, T.A., 1995. Effect of insulin on the insulin-like growth factor system in children with new-onset insulin-dependent diabetes mellitus. J. Clin. Endocrinol. Metab. 80, 1312.

Beulens, J.W., van der, A.D., Grobbee, D.E., Sluijs, I., Spijkerman, A.M., van der Schouw, Y.T., 2010. Dietary phylloquinone and menaquinones intakes and risk of type 2 diabetes. Diabetes Care 33, 1699.

Beyerlein, A., Thiering, E., Pflueger, M., Bidlingmaier, M., Stock, J., Knopff, A., Winkler, C., Heinrich, J., Ziegler, A.G., 2014. Early infant growth is associated with the risk of islet autoimmunity in genetically susceptible children. Pediatr. Diabetes 15, 534.

Bizzarri, C., Pitocco, D., Napoli, N., Di Stasio, E., Maggi, D., Manfrini, S., Suraci, C., Cavallo, M.G., Cappa, M., Ghirlanda, G., Pozzilli, P., Group, I., 2010. No protective effect of calcitriol on beta-cell function in recent-onset type 1 diabetes: the IMDIAB XIII trial. Diabetes Care 33, 1962.

Bonds, D.E., Larson, J.C., Schwartz, A.V., Strotmeyer, E.S., Robbins, J., Rodriguez, B.L., Johnson, K.C., Margolis, K.L., 2006. Risk of fracture in women with type 2 diabetes: the women's health initiative observational study. J. Clin. Endocrinol. Metab. 91, 3404.

Bonfig, W., Kapellen, T., Dost, A., Fritsch, M., Rohrer, T., Wolf, J., Holl, R.W., Diabetes Patienten Verlaufsdokumentationssystem Initiative of the German Working Group for Pediatric, D., the German Bundesministerium fur Bildung und Forschung Competence Net for Diabetes, M, 2012. Growth in children and adolescents with type 1 diabetes. J. Pediatr. 160, 900.

Bortolin, R.H., Freire Neto, F.P., Arcaro, C.A., Bezerra, J.F., da Silva, F.S., Ururahy, M.A., Souza, K.S., Lima, V.M., Luchessi, A.D., Lima, F.P., Lia Fook, M.V., da Silva, B.J., Almeida, M.D., Abreu, B.J., de Rezende, L.A., de Rezende, A.A., 2017. Anabolic effect of insulin therapy on the bone: osteoprotegerin and osteocalcin up-regulation in streptozotocin-induced diabetic rats. Basic Clin. Pharmacol. Toxicol. 120, 227.

Botolin, S., Faugere, M.-C., Malluche, H., Orth, M., Meyer, R., McCabe, L.R., 2005. Increased bone adiposity and peroxisomal proliferator-activated receptor-gamma2 expression in type I diabetic mice. Endocrinology 146, 3622.

Botolin, S., McCabe, L.R., 2006. Inhibition of PPARgamma prevents type I diabetic bone marrow adiposity but not bone loss. J. Cell. Physiol. 209, 967.

Botolin, S., McCabe, L.R., 2007. Bone loss and increased bone adiposity in spontaneous and pharmacologically induced diabetic mice. Endocrinology 148, 198.

Bouillon, R., Bex, M., Van Herck, E., Laureys, J., Dooms, L., Lesaffre, E., Ravussin, E., 1995. Influence of age, sex, and insulin on osteoblast function: osteoblast dysfunction in diabetes mellitus. J. Clin. Endocrinol. Metab. 80, 1194.

Brown, M.L., Yukata, K., Farnsworth, C.W., Chen, D.G., Awad, H., Hilton, M.J., O'Keefe, R.J., Xing, L., Mooney, R.A., Zuscik, M.J., 2014. Delayed fracture healing and increased callus adiposity in a C57BL/6J murine model of obesity-associated type 2 diabetes mellitus. PLoS One 9, e99656.

Burghardt, A.J., Issever, A.S., Schwartz, A.V., Davis, K.A., Masharani, U., Majumdar, S., Link, T.M., 2010. High-resolution peripheral quantitative computed tomographic imaging of cortical and trabecular bone microarchitecture in patients with type 2 diabetes mellitus. J. Clin. Endocrinol. Metab. 95, 5045.

Camargo, W.A., de Vries, R., van Luijk, J., Hoekstra, J.W., Bronkhorst, E.M., Jansen, J.A., van den Beucken, J., 2017. Diabetes mellitus and bone regeneration: a systematic review and meta-analysis of animal studies. Tissue Eng. B Rev. 23, 471.

Campbell, P.G., Novak, J.F., 1991. Insulin-like growth factor binding protein (IGFBP) inhibits IGF action on human osteosarcoma cells. J. Cell. Physiol. 149, 293.

Campos Pastor, M.M., Lopez-Ibarra, P.J., Escobar-Jimenez, F., Serrano Pardo, M.D., Garcia-Cervigon, A.G., 2000. Intensive insulin therapy and bone mineral density in type 1 diabetes mellitus: a prospective study. Osteoporos. Int. 11, 455.

Carvalho, A.L., Massaro, B., Silva, L., Salmon, C.E.G., Fukada, S.Y., Nogueira-Barbosa, M.H., Elias Jr., J., Freitas, M.C.F., Couri, C.E.B., Oliveira, M.C., Simoes, B.P., Rosen, C.J., de Paula, F.J.A., 2018. Emerging aspects of the body composition, bone marrow adipose tissue and skeletal phenotypes in type 1 diabetes mellitus. J. Clin. Densitom. https://doi.org/10.1016/j.jocd.2018.06.007 (In press).

Cavanagh, P.R., Young, M.J., Adams, J.E., Vickers, K.L., Boulton, A.J., 1994. Radiographic abnormalities in the feet of patients with diabetic neuropathy. Diabetes Care 17, 201.

Chiodini, I., Adda, G., Scillitani, A., Coletti, F., Morelli, V., Di Lembo, S., Epaminonda, P., Masserini, B., Beck-Peccoz, P., Orsi, E., Ambrosi, B., Arosio, M., 2007. Cortisol secretion in patients with type 2 diabetes: relationship with chronic complications. Diabetes Care 30, 83.

Chiodini, I., Di Lembo, S., Morelli, V., Epaminonda, P., Coletti, F., Masserini, B., Scillitani, A., Arosio, M., Adda, G., 2006. Hypothalamic-pituitary-adrenal activity in type 2 diabetes mellitus: role of autonomic imbalance. Metabolism 55, 1135.

Choi, H.J., Yu, J., Choi, H., An, J.H., Kim, S.W., Park, K.S., Jang, H.C., Kim, S.Y., Shin, C.S., 2011. Vitamin K2 supplementation improves insulin sensitivity via osteocalcin metabolism: a placebo-controlled trial. Diabetes Care 34, e147.

Chung, Y.S., Lee, M.D., Lee, S.K., Kim, H.M., Fitzpatrick, L.A., 2000. HMG-CoA reductase inhibitors increase BMD in type 2 diabetes mellitus patients. J. Clin. Endocrinol. Metab. 85, 1137.

Clark, M., Kroger, C.J., Tisch, R.M., 2017. Type 1 diabetes: a chronic anti-self-inflammatory response. Front. Immunol. 8, 1898.

Clausen, P., Feldt-Rasmussen, B., Jacobsen, P., Rossing, K., Parving, H.H., Nielsen, P.K., Feldt-Rasmussen, U., Olgaard, K., 1997. Microalbuminuria as an early indicator of osteopenia in male insulin-dependent diabetic patients. Diabet. Med. 14, 1038.

Coe, L.M., Irwin, R., Lippner, D., McCabe, L.R., 2011. The bone marrow microenvironment contributes to type I diabetes induced osteoblast death. J. Cell. Physiol. 226, 477.

Conte, C., Epstein, S., Napoli, N., 2018. Insulin resistance and bone: a biological partnership. Acta Diabetol. 55, 305.

Cornish, J., Callon, K.E., Reid, I.R., 1996. Insulin increases histomorphometric indices of bone formation in vivo. Calcif. Tissue Int. 59, 492.

Danne, T., Kordonouri, O., Enders, I., Weber, B., 1997. Factors influencing height and weight development in children with diabetes. Results of the Berlin Retinopathy Study. Diabetes Care 20, 281.

Davidson, M.B., Duran, P., Lee, M.L., Friedman, T.C., 2013. High-dose vitamin D supplementation in people with prediabetes and hypovitaminosis D. Diabetes Care 36, 260.

Devlin, M.J., Van Vliet, M., Motyl, K., Karim, L., Brooks, D.J., Louis, L., Conlon, C., Rosen, C.J., Bouxsein, M.L., 2014. Early-onset type 2 diabetes impairs skeletal acquisition in the male TALLYHO/JngJ mouse. Endocrinology 155, 3806.

Dienelt, A., zur Nieden, N.I., 2011. Hyperglycemia impairs skeletogenesis from embryonic stem cells by affecting osteoblast and osteoclast differentiation. Stem Cell. Dev. 20, 465.

Diez-Perez, A., Bouxsein, M.L., Eriksen, E.F., Khosla, S., Nyman, J.S., Papapoulos, S., Tang, S.Y., 2016. Technical note: recommendations for a standard procedure to assess cortical bone at the tissue-level in vivo using impact microindentation. Bone Rep. 5, 181.

Diez-Perez, A., Guerri, R., Nogues, X., Caceres, E., Pena, M.J., Mellibovsky, L., Randall, C., Bridges, D., Weaver, J.C., Proctor, A., Brimer, D., Koester, K.J., Ritchie, R.O., Hansma, P.K., 2010. Microindentation for in vivo measurement of bone tissue mechanical properties in humans. J. Bone Miner. Res. 25, 1877.

Dixit, P.K., Ekstrom, R.A., 1980. Decreased breaking strength of diabetic rat bone and its improvement by insulin treatment. Calcif. Tissue Int. 32, 195.

Driessen, J.H.M., de Vries, F., van Onzenoort, H., Harvey, N.C., Neef, C., van den Bergh, J.P.W., Vestergaard, P., Henry, R.M.A., 2017. The use of incretins and fractures − a meta-analysis on population-based real life data. Br. J. Clin. Pharmacol. 83, 923.

Ducy, P., Amling, M., Takeda, S., Priemel, M., Schilling, A.F., Beil, F.T., Shen, J., Vinson, C., Rueger, J.M., Karsenty, G., 2000. Leptin inhibits bone formation through a hypothalamic relay: a central control of bone mass. Cell 100, 197.

Ebeling, P.R., Adler, R.A., Jones, G., Liberman, U.A., Mazziotti, G., Minisola, S., Munns, C.F., Napoli, N., Pittas, A.G., Giustina, A., Bilezikian, J.P., Rizzoli, R., 2018. Management of endocrine disease: Therapeutics of vitamin D. Eur. J. Endocrinol. 179, R239.

Ehnert, S., Freude, T., Ihle, C., Mayer, L., Braun, B., Graeser, J., Flesch, I., Stockle, U., Nussler, A.K., Pscherer, S., 2015. Factors circulating in the blood of type 2 diabetes mellitus patients affect osteoblast maturation − description of a novel in vitro model. Exp. Cell Res. 332, 247.

Einhorn, T.A., Boskey, A.L., Gundberg, C.M., Vigorita, V.J., Devlin, V.J., Beyer, M.M., 1988. The mineral and mechanical properties of bone in chronic experimental diabetes. J. Orthop. Res. 6, 317.

Elamin, A., Hussein, O., Tuvemo, T., 2006. Growth, puberty, and final height in children with Type 1 diabetes. J. Diabet. Complicat. 20, 252.

Eller-Vainicher, C., Scillitani, A., Chiodini, I., 2017. Is the hypothalamic-pituitary-adrenal axis disrupted in type 2 diabetes mellitus and is this relevant for bone health? Endocrine 58, 201.

Eller-Vainicher, C., Zhukouskaya, V.V., Tolkachev, Y.V., Koritko, S.S., Cairoli, E., Grossi, E., Beck-Peccoz, P., Chiodini, I., Shepelkevich, A.P., 2011. Low bone mineral density and its predictors in type 1 diabetic patients evaluated by the classic statistics and artificial neural network analysis. Diabetes Care 34, 2186.

Epstein, S., Takizawa, M., Stein, B., Katz, I.A., Joffe II, Romero, D.F., Liang, X.G., Li, M., Ke, H.Z., Jee, W.S., et al., 1994. Effect of cyclosporin A on bone mineral metabolism in experimental diabetes mellitus in the rat. J. Bone Miner. Res. 9, 557.

Faienza, M.F., Ventura, A., Delvecchio, M., Fusillo, A., Piacente, L., Aceto, G., Colaianni, G., Colucci, S., Cavallo, L., Grano, M., Brunetti, G., 2017. High sclerostin and dickkopf-1 (DKK-1) serum levels in children and adolescents with type 1 diabetes mellitus. J. Clin. Endocrinol. Metab. 102, 1174.

Fajardo, R.J., Karim, L., Calley, V.I., Bouxsein, M.L., 2014. A review of rodent models of type 2 diabetic skeletal fragility. J. Bone Miner. Res. 29, 1025.

Fan, Y., Wei, F., Lang, Y., Liu, Y., 2016. Diabetes mellitus and risk of hip fractures: a meta-analysis. Osteoporos. Int. 27, 219.

Farr, J.N., Drake, M.T., Amin, S., Melton, L.J., McCready, L.K., Khosla, S., 2014. In vivo assessment of bone quality in postmenopausal women with type 2 diabetes. J. Bone Miner. Res. 29, 787.

Ferron, M., Hinoi, E., Karsenty, G., Ducy, P., 2008. Osteocalcin differentially regulates beta cell and adipocyte gene expression and affects the development of metabolic diseases in wild-type mice. Proc. Natl. Acad. Sci. U.S.A. 105, 5266.

Ferron, M., Wei, J., Yoshizawa, T., Del Fattore, A., DePinho, R.A., Teti, A., Ducy, P., Karsenty, G., 2010. Insulin signaling in osteoblasts integrates bone remodeling and energy metabolism. Cell 142, 296.

Foley Jr., T.P., Nissley, S.P., Stevens, R.L., King, G.L., Hascall, V.C., Humbel, R.E., Short, P.A., Rechler, M.M., 1982. Demonstration of receptors for insulin and insulin-like growth factors on Swarm rat chondrosarcoma chondrocytes. Evidence that insulin stimulates proteoglycan synthesis through the insulin receptor. J. Biol. Chem. 257, 663.

Follak, N., Kloting, I., Wolf, E., Merk, H., 2004. Histomorphometric evaluation of the influence of the diabetic metabolic state on bone defect healing depending on the defect size in spontaneously diabetic BB/OK rats. Bone 35, 144.

Franceschi, R., Longhi, S., Cauvin, V., Fassio, A., Gallo, G., Lupi, F., Reinstadler, P., Fanolla, A., Gatti, D., Radetti, G., 2018. Bone geometry, quality, and bone markers in children with type 1 diabetes mellitus. Calcif. Tissue Int. 102, 657.

Frystyk, J., Hojlund, K., Rasmussen, K.N., Jorgensen, S.P., Wildner-Christensen, M., Orskov, H., 2002. Development and clinical evaluation of a novel immunoassay for the binary complex of IGF-I and IGF-binding protein-1 in human serum. J. Clin. Endocrinol. Metab. 87, 260.

Fulzele, K., DiGirolamo, D.J., Liu, Z., Xu, J., Messina, J.L., Clemens, T.L., 2007. Disruption of the insulin-like growth factor type 1 receptor in osteoblasts enhances insulin signaling and action. J. Biol. Chem. 282, 25649.

Fulzele, K., Riddle, R.C., DiGirolamo, D.J., Cao, X., Wan, C., Chen, D., Faugere, M.C., Aja, S., Hussain, M.A., Bruning, J.C., Clemens, T.L., 2010. Insulin receptor signaling in osteoblasts regulates postnatal bone acquisition and body composition. Cell 142, 309.

Funk, J.R., Hale, J.E., Carmines, D., Gooch, H.L., Hurwitz, S.R., 2000. Biomechanical evaluation of early fracture healing in normal and diabetic rats. J. Orthop. Res. 18, 126.

Furst, J.R., Bandeira, L.C., Fan, W.W., Agarwal, S., Nishiyama, K.K., McMahon, D.J., Dworakowski, E., Jiang, H., Silverberg, S.J., Rubin, M.R., 2016. Advanced glycation endproducts and bone material strength in type 2 diabetes. J. Clin. Endocrinol. Metab. 101, 2502.

Gallant, M.A., Brown, D.M., Organ, J.M., Allen, M.R., Burr, D.B., 2013. Reference-point indentation correlates with bone toughness assessed using whole-bone traditional mechanical testing. Bone 53, 301.

Gandhi, A., Beam, H.A., O'Connor, J.P., Parsons, J.R., Lin, S.S., 2005. The effects of local insulin delivery on diabetic fracture healing. Bone 37, 482.

Gandhi, A., Doumas, C., O'Connor, J.P., Parsons, J.R., Lin, S.S., 2006. The effects of local platelet rich plasma delivery on diabetic fracture healing. Bone 38, 540.

Gaudio, A., Privitera, F., Battaglia, K., Torrisi, V., Sidoti, M.H., Pulvirenti, I., Canzonieri, E., Tringali, G., Fiore, C.E., 2012. Sclerostin levels associated with inhibition of the Wnt/β-catenin signaling and reduced bone turnover in type 2 diabetes mellitus. J. Clin. Endocrinol. Metab. 97, 3744.

Gennari, L., Merlotti, D., Valenti, R., Ceccarelli, E., Ruvio, M., Pietrini, M.G., Capodarca, C., Franci, M.B., Campagna, M.S., Calabrò, A., Cataldo, D., Stolakis, K., Dotta, F., Nuti, R., 2012. Circulating sclerostin levels and bone turnover in type 1 and type 2 diabetes. J. Clin. Endocrinol. Metab. 97, 1737.

Gilbert, L., He, X., Farmer, P., Boden, S., Kozlowski, M., Rubin, J., Nanes, M.S., 2000. Inhibition of osteoblast differentiation by tumor necrosis factor-alpha. Endocrinology 141, 3956.

Gilbert, M.P., Pratley, R.E., 2015. The impact of diabetes and diabetes medications on bone health. Endocr. Rev. 36, 194.

Glajchen, N., Epstein, S., Ismail, F., Thomas, S., Fallon, M., Chakrabarti, S., 1988. Bone mineral metabolism in experimental diabetes mellitus: osteocalcin as a measure of bone remodeling. Endocrinology 123, 290.

Glantschnig, H., Fisher, J.E., Wesolowski, G., Rodan, G.A., Reszka, A.A., 2003. M-CSF, TNFalpha and RANK ligand promote osteoclast survival by signaling through mTOR/S6 kinase. Cell Death Differ. 10, 1165.

Hamann, C., Goettsch, C., Mettelsiefen, J., Henkenjohann, V., Rauner, M., Hempel, U., Bernhardt, R., Fratzl-Zelman, N., Roschger, P., Rammelt, S., Günther, K.-P., Hofbauer, L.C., 2011. Delayed bone regeneration and low bone mass in a rat model of insulin-resistant type 2 diabetes mellitus is due to impaired osteoblast function. Am. J. Physiol. Endocrinol. Metabol. 301, E1220.

Hamann, C., Rauner, M., Höhna, Y., Bernhardt, R., Mettelsiefen, J., Goettsch, C., Günther, K.-P., Stolina, M., Han, C.-Y., Asuncion, F.J., Ominsky, M.S., Hofbauer, L.C., 2013. Sclerostin antibody treatment improves bone mass, bone strength, and bone defect regeneration in rats with type 2 diabetes mellitus. J. Bone Miner. Res. 28, 627.

Hamilton, E.J., Drinkwater, J.J., Chubb, S.A.P., Rakic, V., Kamber, N., Zhu, K., Prince, R.L., Davis, W.A., Davis, T.M.E., 2018. A 10-year prospective study of bone mineral density and bone turnover in males and females with type 1 diabetes. J. Clin. Endocrinol. Metab. 103, 3531.

He, H., Liu, R., Desta, T., Leone, C., Gerstenfeld, L.C., Graves, D.T., 2004. Diabetes causes decreased osteoclastogenesis, reduced bone formation, and enhanced apoptosis of osteoblastic cells in bacteria stimulated bone loss. Endocrinology 145, 447.

Heaney, R.P., 2003. Is the paradigm shifting? Bone 33, 457.

Heilmeier, U., Carpenter, D.R., Patsch, J.M., Harnish, R., Joseph, G.B., Burghardt, A.J., Baum, T., Schwartz, A.V., Lang, T.F., Link, T.M., 2015. Volumetric femoral BMD, bone geometry, and serum sclerostin levels differ between type 2 diabetic postmenopausal women with and without fragility fractures. Osteoporos. Int. 26, 1283.

Heilmeier, U., Cheng, K., Pasco, C., Parrish, R., Nirody, J., Patsch, J.M., Zhang, C.A., Joseph, G.B., Burghardt, A.J., Schwartz, A.V., Link, T.M., Kazakia, G., 2016. Cortical bone laminar analysis reveals increased midcortical and periosteal porosity in type 2 diabetic postmenopausal women with history of fragility fractures compared to fracture-free diabetics. Osteoporos. Int. 27, 2791.

Heinze, E., Vetter, U., Voigt, K.H., 1989. Insulin stimulates skeletal growth in vivo and in vitro–comparison with growth hormone in rats. Diabetologia 32, 198.

Hie, M., Iitsuka, N., Otsuka, T., Tsukamoto, I., 2011. Insulin-dependent diabetes mellitus decreases osteoblastogenesis associated with the inhibition of Wnt signaling through increased expression of Sost and Dkk1 and inhibition of Akt activation. Int. J. Mol. Med. 28, 455.

Hock, J.M., Centrella, M., Canalis, E., 1988. Insulin-like growth factor I has independent effects on bone matrix formation and cell replication. Endocrinology 122, 254.

Hofbauer, L.C., Brueck, C.C., Singh, S.K., Dobnig, H., 2007. Osteoporosis in patients with diabetes mellitus. J. Bone Miner. Res. 22, 1317.

Holl, R.W., Grabert, M., Heinze, E., Sorgo, W., Debatin, K.M., 1998. Age at onset and long-term metabolic control affect height in type-1 diabetes mellitus. Eur. J. Pediatr. 157, 972.

Holloway-Kew, K.L., De Abreu, L.L.F., Kotowicz, M.A., Sajjad, M.A., Pasco, J.A., 2019. Bone turnover markers in men and women with impaired fasting glucose and diabetes. Calcif. Tissue Int. https://doi.org/10.1007/s00223-019-00527-y (In press).

Horcajada-Molteni, M.N., Chanteranne, B., Lebecque, P., Davicco, M.J., Coxam, V., Young, A., Barlet, J.P., 2001. Amylin and bone metabolism in streptozotocin-induced diabetic rats. J. Bone Miner. Res. 16, 958.

Hough, F.S., Pierroz, D.D., Cooper, C., Ferrari, S.L., Bone, I.C., Diabetes Working, G., 2016. Mechanisms in endocrinology: mechanisms and evaluation of bone fragility in type 1 diabetes mellitus. Eur. J. Endocrinol. 174, R127.

Hua, Y., Bi, R., Zhang, Y., Xu, L., Guo, J., Li, Y., 2018. Different bone sites-specific response to diabetes rat models: bone density, histology and microarchitecture. PLoS One 13, e0205503.

Hunt, H., Torres, A., Palomino, P., Marty, E., Saiyed, R., Cohn, M., Jo, J., Warner, S., Sroga, G., King, K., Lane, J., Vashishth, D., Hernandez, C., Donnelly, E., 2019. Altered tissue composition, microarchitecture, and mechanical performance in cancellous bone from men with type 2 diabetes mellitus. J. Bone Miner. Res. https://doi.org/10.1002/jbmr.3711 (In press).

Hygum, K., Starup-Linde, J., Harslof, T., Vestergaard, P., Langdahl, B.L., 2017. Mechanisms in endocrinology: diabetes mellitus, a state of low bone turnover − a systematic review and meta-analysis. Eur. J. Endocrinol. 176, R137.

Idelevich, A., Baron, R., 2018. Brain to bone: what is the contribution of the brain to skeletal homeostasis? Bone 115, 31.

Ionova-Martin, S.S., Wade, J.M., Tang, S., Shahnazari, M., Ager 3rd, J.W., Lane, N.E., Yao, W., Alliston, T., Vaisse, C., Ritchie, R.O., 2011. Changes in cortical bone response to high-fat diet from adolescence to adulthood in mice. Osteoporos. Int. 22, 2283.

Irwin, R., Lin, H.V., Motyl, K.J., McCabe, L.R., 2006. Normal bone density obtained in the absence of insulin receptor expression in bone. Endocrinology 147, 5760.

Ishida, H., Seino, Y., Takeshita, N., Kurose, T., Tsuji, K., Okamoto, Y., Someya, Y., Hara, K., Akiyama, Y., Imura, H., et al., 1992. Effect of pancreas transplantation on decreased levels of circulating bone gamma-carboxyglutamic acid-containing protein and osteopenia in rats with streptozotocin-induced diabetes. Acta Endocrinol. 127, 81.

Ishikawa, K., Fukui, T., Nagai, T., Kuroda, T., Hara, N., Yamamoto, T., Inagaki, K., Hirano, T., 2015. Type 1 diabetes patients have lower strength in femoral bone determined by quantitative computed tomography: a cross-sectional study. J Diabetes Investig 6, 726.

Ivers, R.Q., Cumming, R.G., Mitchell, P., Peduto, A.J., Blue Mountains Eye, S., 2001. Diabetes and risk of fracture: the Blue Mountains eye study. Diabetes Care 24, 1198.

Janghorbani, M., Feskanich, D., Willett, W.C., Hu, F., 2006. Prospective study of diabetes and risk of hip fracture: the Nurses' Health Study. Diabetes Care 29, 1573.

Janghorbani, M., Van Dam, R.M., Willett, W.C., Hu, F.B., 2007. Systematic review of type 1 and type 2 diabetes mellitus and risk of fracture. Am. J. Epidemiol. 166, 495.

Jiajue, R., Jiang, Y., Wang, O., Li, M., Xing, X., Cui, L., Yin, J., Xu, L., Xia, W., 2014. Suppressed bone turnover was associated with increased osteoporotic fracture risks in non-obese postmenopausal Chinese women with type 2 diabetes mellitus. Osteoporos. Int. 25, 1999.

Jiao, H., Xiao, E., Graves, D.T., 2015. Diabetes and its effect on bone and fracture healing. Curr. Osteoporos. Rep. 13, 327.

Johnell, O., Kanis, J.A., Oden, A., Johansson, H., De Laet, C., Delmas, P., Eisman, J.A., Fujiwara, S., Kroger, H., Mellstrom, D., Meunier, P.J., Melton 3rd, L.J., O'Neill, T., Pols, H., Reeve, J., Silman, A., Tenenhouse, A., 2005. Predictive value of BMD for hip and other fractures. J. Bone Miner. Res. 20, 1185.

Johnson, K.C., Bray, G.A., Cheskin, L.J., Clark, J.M., Egan, C.M., Foreyt, J.P., Garcia, K.R., Glasser, S., Greenway, F.L., Gregg, E.W., Hazuda, H.P., Hergenroeder, A., Hill, J.O., Horton, E.S., Jakicic, J.M., Jeffery, R.W., Kahn, S.E., Knowler, W.C., Lewis, C.E., Miller, M., Montez, M.G., Nathan, D.M., Patricio, J.L., Peters, A.L., Pi-Sunyer, X., Pownall, H.J., Reboussin, D., Redmon, J.B., Steinberg, H., Wadden, T.A., Wagenknecht, L.E., Wing, R.R., Womack, C.R., Yanovski, S.Z., Zhang, P., Schwartz, A.V., Look, A.S.G., 2017. The effect of intentional weight loss on fracture risk in persons with diabetes: results from the look AHEAD randomized clinical trial. J. Bone Miner. Res. 32, 2278.

Johnston, S.S., Conner, C., Aagren, M., Ruiz, K., Bouchard, J., 2012. Association between hypoglycaemic events and fall-related fractures in Medicare-covered patients with type 2 diabetes. Diabetes Obes. Metab. 14, 634.

Kahn, S.E., Haffner, S.M., Heise, M.A., Herman, W.H., Holman, R.R., Jones, N.P., Kravitz, B.G., Lachin, J.M., O'Neill, M.C., Zinman, B., Viberti, G., Group, A.S., 2006. Glycemic durability of rosiglitazone, metformin, or glyburide monotherapy. N. Engl. J. Med. 355, 2427.

Kanazawa, I., Notsu, M., Miyake, H., Tanaka, K., Sugimoto, T., 2018. Assessment using serum insulin-like growth factor-I and bone mineral density is useful for detecting prevalent vertebral fractures in patients with type 2 diabetes mellitus. Osteoporos. Int. 29, 2527.

Kanazawa, I., Yamaguchi, T., Sugimoto, T., 2011a. Serum insulin-like growth factor-I is a marker for assessing the severity of vertebral fractures in postmenopausal women with type 2 diabetes mellitus. Osteoporos. Int. 22, 1191.

Kanazawa, I., Yamaguchi, T., Yamamoto, M., Sugimoto, T., 2010. Relationship between treatments with insulin and oral hypoglycemic agents versus the presence of vertebral fractures in type 2 diabetes mellitus. J. Bone Miner. Metab. 28, 554.

Kanazawa, I., Yamaguchi, T., Yamamoto, M., Yamauchi, M., Kurioka, S., Yano, S., Sugimoto, T., 2009. Serum osteocalcin level is associated with glucose metabolism and atherosclerosis parameters in type 2 diabetes mellitus. J. Clin. Endocrinol. Metab. 94, 45.

Kanazawa, I., Yamaguchi, T., Yamauchi, M., Yamamoto, M., Kurioka, S., Yano, S., Sugimoto, T., 2011b. Serum undercarboxylated osteocalcin was inversely associated with plasma glucose level and fat mass in type 2 diabetes mellitus. Osteoporos. Int. 22, 187.

Kaneko, H., Sasaki, T., Ramamurthy, N.S., Golub, L.M., 1990. Tetracycline administration normalizes the structure and acid phosphatase activity of osteoclasts in streptozotocin-induced diabetic rats. Anat. Rec. 227, 427.

Karim, L., Moulton, J., Van Vliet, M., Velie, K., Robbins, A., Malekipour, F., Abdeen, A., Ayres, D., Bouxsein, M.L., 2018. Bone microarchitecture, biomechanical properties, and advanced glycation end-products in the proximal femur of adults with type 2 diabetes. Bone 114, 32.

Kasahara, T., Imai, S., Kojima, H., Katagi, M., Kimura, H., Chan, L., Matsusue, Y., 2010. Malfunction of bone marrow-derived osteoclasts and the delay of bone fracture healing in diabetic mice. Bone 47, 617.

Katayama, Y., Akatsu, T., Yamamoto, M., Kugai, N., Nagata, N., 1996. Role of nonenzymatic glycosylation of type I collagen in diabetic osteopenia. J. Bone Miner. Res. 11, 931.

Kawaguchi, H., Kurokawa, T., Hanada, K., Hiyama, Y., Tamura, M., Ogata, E., Matsumoto, T., 1994. Stimulation of fracture repair by recombinant human basic fibroblast growth factor in normal and streptozotocin-diabetic rats. Endocrinology 135, 774.

Kayal, R.A., Tsatsas, D., Bauer, M.A., Allen, B., Al-Sebaei, M.O., Kakar, S., Leone, C.W., Morgan, E.F., Gerstenfeld, L.C., Einhorn, T.A., Graves, D.T., 2007. Diminished bone formation during diabetic fracture healing is related to the premature resorption of cartilage associated with increased osteoclast activity. J. Bone Miner. Res. 22, 560.

Keegan, T.H.M., Schwartz, A.V., Bauer, D.C., Sellmeyer, D.E., Kelsey, J.L., fracture intervention, t., 2004. Effect of alendronate on bone mineral density and biochemical markers of bone turnover in type 2 diabetic women: the fracture intervention trial. Diabetes Care 27, 1547.

Kelley, K.M., Russell, S.M., Matteucci, M.L., Nicoll, C.S., 1993. An insulin-like growth factor I-resistant state in cartilage of diabetic rats is ameliorated by hypophysectomy. Possible role of metabolism. Diabetes 42, 463.

Kim, J.Y., Lee, S.K., Jo, K.J., Song, D.Y., Lim, D.M., Park, K.Y., Bonewald, L.F., Kim, B.J., 2013. Exendin-4 increases bone mineral density in type 2 diabetic OLETF rats potentially through the down-regulation of SOST/sclerostin in osteocytes. Life Sci. 92, 533.

Kindblom, J.M., Ohlsson, C., Ljunggren, O., Karlsson, M.K., Tivesten, A., Smith, U., Mellstrom, D., 2009. Plasma osteocalcin is inversely related to fat mass and plasma glucose in elderly Swedish men. J. Bone Miner. Res. 24, 785.

Knop, F.K., Vilsboll, T., Hojberg, P.V., Larsen, S., Madsbad, S., Volund, A., Holst, J.J., Krarup, T., 2007. Reduced incretin effect in type 2 diabetes: cause or consequence of the diabetic state? Diabetes 56, 1951.

Kohler, S., Kaspers, S., Salsali, A., Zeller, C., Woerle, H.J., 2018. Analysis of fractures in patients with type 2 diabetes treated with empagliflozin in pooled data from placebo-controlled trials and a head-to-head study versus glimepiride. Diabetes Care 41, 1809.

Komorita, Y., Iwase, M., Fujii, H., Ohkuma, T., Ide, H., Jodai-Kitamura, T., Sumi, A., Yoshinari, M., Nakamura, U., Kang, D., Kitazono, T., 2018. Impact of body weight loss from maximum weight on fragility bone fractures in Japanese patients with type 2 diabetes: the Fukuoka diabetes registry. Diabetes Care 41, 1061.

Krakauer, J.C., McKenna, M.J., Buderer, N.F., Rao, D.S., Whitehouse, F.W., Parfitt, A.M., 1995. Bone loss and bone turnover in diabetes. Diabetes 44, 775.

Kume, S., Kato, S., Yamagishi, S., Inagaki, Y., Ueda, S., Arima, N., Okawa, T., Kojiro, M., Nagata, K., 2005. Advanced glycation end-products attenuate human mesenchymal stem cells and prevent cognate differentiation into adipose tissue, cartilage, and bone. J. Bone Miner. Res. 20, 1647.

Lai, M., Chandrasekera, P.C., Barnard, N.D., 2014. You are what you eat, or are you? The challenges of translating high-fat-fed rodents to human obesity and diabetes. Nutr. Diabetes 4, e135.

Lamb, M.M., Yin, X., Zerbe, G.O., Klingensmith, G.J., Dabelea, D., Fingerlin, T.E., Rewers, M., Norris, J.M., 2009. Height growth velocity, islet autoimmunity and type 1 diabetes development: the Diabetes Autoimmunity Study in the Young. Diabetologia 52, 2064.

Langdahl, B.L., Silverman, S., Fujiwara, S., Saag, K., Napoli, N., Soen, S., Enomoto, H., Melby, T.E., Disch, D.P., Marin, F., Krege, J.H., 2018. Real-world effectiveness of teriparatide on fracture reduction in patients with osteoporosis and comorbidities or risk factors for fractures: integrated analysis of 4 prospective observational studies. Bone 116, 58.

Lee, N.K., Sowa, H., Hinoi, E., Ferron, M., Ahn, J.D., Confavreux, C., Dacquin, R., Mee, P.J., McKee, M.D., Jung, D.Y., Zhang, Z., Kim, J.K., Mauvais-Jarvis, F., Ducy, P., Karsenty, G., 2007. Endocrine regulation of energy metabolism by the skeleton. Cell 130, 456.

Leger, J., Marinovic, D., Alberti, C., Dorgeret, S., Chevenne, D., Marchal, C.L., Tubiana-Rufi, N., Sebag, G., Czernichow, P., 2006. Lower bone mineral content in children with type 1 diabetes mellitus is linked to female sex, low insulin-like growth factor type I levels, and high insulin requirement. J. Clin. Endocrinol. Metab. 91, 3947.

Li, C.I., Liu, C.S., Lin, W.Y., Meng, N.H., Chen, C.C., Yang, S.Y., Chen, H.J., Lin, C.C., Li, T.C., 2015. Glycated hemoglobin level and risk of hip fracture in older people with type 2 diabetes: a competing risk analysis of Taiwan diabetes cohort study. J. Bone Miner. Res. 30, 1338.

Li, M., Pan, L.C., Simmons, H.A., Li, Y., Healy, D.R., Robinson, B.S., Ke, H.Z., Brown, T.A., 2006. Surface-specific effects of a PPARgamma agonist, darglitazone, on bone in mice. Bone 39, 796.

Lin, T.K., Chou, P., Lin, C.H., Hung, Y.J., Jong, G.P., 2018. Long-term effect of statins on the risk of new-onset osteoporosis: a nationwide population-based cohort study. PLoS One 13, e0196713.

Liu, Z., Aronson, J., Wahl, E.C., Liu, L., Perrien, D.S., Kern, P.A., Fowlkes, J.L., Thrailkill, K.M., Bunn, R.C., Cockrell, G.E., Skinner, R.A., Lumpkin Jr., C.K., 2007. A novel rat model for the study of deficits in bone formation in type-2 diabetes. Acta Orthop. 78, 46.

Locatto, M.E., Abranzon, H., Caferra, D., Fernandez, M.C., Alloatti, R., Puche, R.C., 1993. Growth and development of bone mass in untreated alloxan diabetic rats. Effects of collagen glycosylation and parathyroid activity on bone turnover. Bone Miner. 23, 129.

Loder, R.T., 1988. The influence of diabetes mellitus on the healing of closed fractures. Clin. Orthop. Relat. Res. 210.

Loke, Y.K., Singh, S., Furberg, C.D., 2009. Long-term use of thiazolidinediones and fractures in type 2 diabetes: a meta-analysis. Can. Med. Assoc. J. 180, 32.

Lontchi-Yimagou, E., Sobngwi, E., Matsha, T.E., Kengne, A.P., 2013. Diabetes mellitus and inflammation. Curr. Diabetes Rep. 13, 435.

Lopez-Herradon, A., Portal-Nunez, S., Garcia-Martin, A., Lozano, D., Perez-Martinez, F.C., Cena, V., Esbrit, P., 2013. Inhibition of the canonical Wnt pathway by high glucose can be reversed by parathyroid hormone-related protein in osteoblastic cells. J. Cell. Biochem. 114, 1908.

Losada, E., Soldevila, B., Ali, M.S., Martinez-Laguna, D., Nogues, X., Puig-Domingo, M., Diez-Perez, A., Mauricio, D., Prieto-Alhambra, D., 2018. Real-world antidiabetic drug use and fracture risk in 12,277 patients with type 2 diabetes mellitus: a nested case-control study. Osteoporos. Int. 29, 2079.

Lu, N., Sun, H., Yu, J., Wang, X., Liu, D., Zhao, L., Sun, L., Zhao, H., Tao, B., Liu, J., 2015. Glucagon-like peptide-1 receptor agonist Liraglutide has anabolic bone effects in ovariectomized rats without diabetes. PLoS One 10, e0132744.

Lucas, P.D., 1987. Reversible reduction in bone blood flow in streptozotocin-diabetic rats. Experientia 43, 894.

Ma, L., Oei, L., Jiang, L., Estrada, K., Chen, H., Wang, Z., Yu, Q., Zillikens, M.C., Gao, X., Rivadeneira, F., 2012. Association between bone mineral density and type 2 diabetes mellitus: a meta-analysis of observational studies. Eur. J. Epidemiol. 27, 319.

Ma, X., Meng, J., Jia, M., Bi, L., Zhou, Y., Wang, Y., Hu, J., He, G., Luo, X., 2013. Exendin-4, a glucagon-like peptide-1 receptor agonist, prevents osteopenia by promoting bone formation and suppressing bone resorption in aged ovariectomized rats. J. Bone Miner. Res. 28, 1641.

Ma, Y.H., Schwartz, A.V., Sigurdsson, S., Hue, T.F., Lang, T.F., Harris, T.B., Rosen, C.J., Vittinghoff, E., Eiriksdottir, G., Hauksdottir, A.M., Siggeirsdottir, K., Sigurdsson, G., Oskarsdottir, D., Napoli, N., Palermo, L., Gudnason, V., Li, X., 2014. Circulating sclerostin associated with vertebral bone marrow fat in older men but not women. J. Clin. Endocrinol. Metab. 99, E2584.

Mabilleau, G., Mieczkowska, A., Chappard, D., 2014. Use of glucagon-like peptide-1 receptor agonists and bone fractures: a meta-analysis of randomized clinical trials. J. Diabetes 6, 260.

Maddaloni, E., Cavallari, I., Napoli, N., Conte, C., 2018. Vitamin D and diabetes mellitus. Front. Horm. Res. 50, 161.

Maddaloni, E., D'Eon, S., Hastings, S., Tinsley, L.J., Napoli, N., Khamaisi, M., Bouxsein, M.L., Fouda, S.M.R., Keenan, H.A., 2017. Bone health in subjects with type 1 diabetes for more than 50 years. Acta Diabetol. 54, 479.

Madsen, L.R., Espersen, R., Ornstrup, M.J., Jorgensen, N.R., Langdahl, B.L., Richelsen, B., 2019. Bone health in patients with type 2 diabetes treated by roux-en-Y gastric bypass and the role of diabetes remission. Obes. Surg. https://doi.org/10.1007/s11695-019-03753-3 (In press).

Manavalan, J.S., Cremers, S., Dempster, D.W., Zhou, H., Dworakowski, E., Kode, A., Kousteni, S., Rubin, M.R., 2012. Circulating osteogenic precursor cells in type 2 diabetes mellitus. J. Clin. Endocrinol. Metab. 97, 3240.

Manolagas, S.C., 2010. From estrogen-centric to aging and oxidative stress: a revised perspective of the pathogenesis of osteoporosis. Endocr. Rev. 31, 266.

Maor, G., Silbermann, M., von der Mark, K., Heingard, D., Laron, Z., 1993. Insulin enhances the growth of cartilage in organ and tissue cultures of mouse neonatal mandibular condyle. Calcif. Tissue Int. 52, 291.

Maratova, K., Soucek, O., Matyskova, J., Hlavka, Z., Petruzelkova, L., Obermannova, B., Pruhova, S., Kolouskova, S., Sumnik, Z., 2018. Muscle functions and bone strength are impaired in adolescents with type 1 diabetes. Bone 106, 22.

Marin, C., Luyten, F.P., Van der Schueren, B., Kerckhofs, G., Vandamme, K., 2018. The impact of type 2 diabetes on bone fracture healing. Front. Endocrinol. 9, 6.

Martinez-Laguna, D., Nogues, X., Abrahamsen, B., Reyes, C., Carbonell-Abella, C., Diez-Perez, A., Prieto-Alhambra, D., 2017. Excess of all-cause mortality after a fracture in type 2 diabetic patients: a population-based cohort study. Osteoporos. Int. 28, 2573.

Martinez-Laguna, D., Tebe, C., Nogues, X., Kassim Javaid, M., Cooper, C., Moreno, V., Diez-Perez, A., Collins, G.S., Prieto-Alhambra, D., 2018. Fracture risk in type 2 diabetic patients: a clinical prediction tool based on a large population-based cohort. PLoS One 13, e0203533.

Mathey, J., Horcajada-Molteni, M.N., Chanteranne, B., Picherit, C., Puel, C., Lebecque, P., Cubizoles, C., Davicco, M.J., Coxam, V., Barlet, J.P., 2002. Bone mass in obese diabetic Zucker rats: influence of treadmill running. Calcif. Tissue Int. 70, 305.

McCarthy, A.D., Etcheverry, S.B., Cortizo, A.M., 2001. Effect of advanced glycation endproducts on the secretion of insulin-like growth factor-I and its binding proteins: role in osteoblast development. Acta Diabetol. 38, 113.

McNair, P., Madsbad, S., Christensen, M.S., Christiansen, C., Faber, O.K., Binder, C., Transbol, I., 1979. Bone mineral loss in insulin-treated diabetes mellitus: studies on pathogenesis. Acta Endocrinol. 90, 463.

Meema, H.E., Meema, S., 1967. The relationship of diabetes mellitus and body weight to osteoporosis in elderly females. Can. Med. Assoc. J. 96, 132.

Meier, C., Schwartz, A.V., Egger, A., Lecka-Czernik, B., 2016. Effects of diabetes drugs on the skeleton. Bone 82, 93.

Mera, P., Laue, K., Ferron, M., Confavreux, C., Wei, J., Galan-Diez, M., Lacampagne, A., Mitchell, S.J., Mattison, J.A., Chen, Y., Bacchetta, J., Szulc, P., Kitsis, R.N., de Cabo, R., Friedman, R.A., Torsitano, C., McGraw, T.E., Puchowicz, M., Kurland, I., Karsenty, G., 2016a. Osteocalcin signaling in myofibers is necessary and sufficient for optimum adaptation to exercise. Cell Metabol. 23, 1078.

Mera, P., Laue, K., Wei, J., Berger, J.M., Karsenty, G., 2016b. Osteocalcin is necessary and sufficient to maintain muscle mass in older mice. Mol Metab 5, 1042.

Miao, J., Brismar, K., Nyren, O., Ugarph-Morawski, A., Ye, W., 2005. Elevated hip fracture risk in type 1 diabetic patients: a population-based cohort study in Sweden. Diabetes Care 28, 2850.

Mieczkowska, A., Mansur, S.A., Irwin, N., Flatt, P.R., Chappard, D., Mabilleau, G., 2015. Alteration of the bone tissue material properties in type 1 diabetes mellitus: a Fourier transform infrared microspectroscopy study. Bone 76, 31.

Miranda, C., Giner, M., Montoya, M.J., Vazquez, M.A., Miranda, M.J., Perez-Cano, R., 2016. Influence of high glucose and advanced glycation end-products (ages) levels in human osteoblast-like cells gene expression. BMC Muscoskelet. Disord. 17, 377.

Mitchell, A., Fall, T., Melhus, H., Wolk, A., Michaëlsson, K., Byberg, L., 2018. Type 2 diabetes in relation to hip bone density, area, and bone turnover in Swedish men and women: a cross-sectional study. Calcif. Tissue Int. 103, 501.

Mohan, S., Richman, C., Guo, R., Amaar, Y., Donahue, L.R., Wergedal, J., Baylink, D.J., 2003. Insulin-like growth factor regulates peak bone mineral density in mice by both growth hormone-dependent and -independent mechanisms. Endocrinology 144, 929.

Monami, M., Dicembrini, I., Antenore, A., Mannucci, E., 2011. Dipeptidyl peptidase-4 inhibitors and bone fractures: a meta-analysis of randomized clinical trials. Diabetes Care 34, 2474.

Monami, M., Dicembrini, I., Kundisova, L., Zannoni, S., Nreu, B., Mannucci, E., 2014. A meta-analysis of the hypoglycaemic risk in randomized controlled trials with sulphonylureas in patients with type 2 diabetes. Diabetes Obes. Metab. 16, 833.

Motyl, K.J., Botolin, S., Irwin, R., Appledorn, D.M., Kadakia, T., Amalfitano, A., Schwartz, R.C., McCabe, L.R., 2009. Bone inflammation and altered gene expression with type I diabetes early onset. J. Cell. Physiol. 218, 575.

Motyl, K.J., McCabe, L.R., 2009. Leptin treatment prevents type I diabetic marrow adiposity but not bone loss in mice. J. Cell. Physiol. 218, 376.

Moyer-Mileur, L.J., Dixon, S.B., Quick, J.L., Askew, E.W., Murray, M.A., 2004. Bone mineral acquisition in adolescents with type 1 diabetes. J. Pediatr. 145, 662.

Munoz-Torres, M., Jodar, E., Escobar-Jimenez, F., Lopez-Ibarra, P.J., Luna, J.D., 1996. Bone mineral density measured by dual X-ray absorptiometry in Spanish patients with insulin-dependent diabetes mellitus. Calcif. Tissue Int. 58, 316.

Napoli, N., Conte, C., Pedone, C., Strotmeyer, E.S., Barbour, K.E., Black, D.M., Samelson, E.J., Schwartz, A.V., 2019. Effect of insulin resistance on BMD and fracture risk in older adults. J. Clin. Endocrinol. Metab. https://doi.org/10.1210/jc.2018-02539 (In press).

Napoli, N., Pannacciulli, N., Vittinghoff, E., Crittenden, D., Yun, J., Wang, A., Wagman, R., Schwartz, A.V., 2018a. Effect of denosumab on fasting glucose in women with diabetes or prediabetes from the freedom trial. Diabetes Metab Res Rev 34, e2991.

Napoli, N., Schafer, A.L., Lui, L.Y., Cauley, J.A., Strotmeyer, E.S., Le Blanc, E.S., Hoffman, A.R., Lee, C.G., Black, D.M., Schwartz, A.V., 2016. Serum 25-hydroxyvitamin D level and incident type 2 diabetes in older men, the Osteoporotic Fractures in Men (MrOS) study. Bone 90, 181.

Napoli, N., Schwartz, A.V., Schafer, A.L., Vittinghoff, E., Cawthon, P.M., Parimi, N., Orwoll, E., Strotmeyer, E.S., Hoffman, A.R., Barrett-Connor, E., Black, D.M., Osteoporotic Fractures in Men Study Research, G., 2018b. Vertebral fracture risk in diabetic elderly men: the MrOS study. J. Bone Miner. Res. 33, 63.

Napoli, N., Strollo, R., Pitocco, D., Bizzarri, C., Maddaloni, E., Maggi, D., Manfrini, S., Schwartz, A., Pozzilli, P., Group, I., 2013. Effect of calcitriol on bone turnover and osteocalcin in recent-onset type 1 diabetes. PLoS One 8, e56488.

Napoli, N., Strotmeyer, E.S., Ensrud, K.E., Sellmeyer, D.E., Bauer, D.C., Hoffman, A.R., Dam, T.-T.L., Barrett-Connor, E., Palermo, L., Orwoll, E.S., Cummings, S.R., Black, D.M., Schwartz, A.V., 2014. Fracture risk in diabetic elderly men: the MrOS study. Diabetologia 57, 2057.

Neumann, T., Lodes, S., Kastner, B., Franke, S., Kiehntopf, M., Lehmann, T., Muller, U.A., Wolf, G., Samann, A., 2014. High serum pentosidine but not esRAGE is associated with prevalent fractures in type 1 diabetes independent of bone mineral density and glycaemic control. Osteoporos. Int. 25, 1527.

Neumann, T., Lodes, S., Kastner, B., Franke, S., Kiehntopf, M., Lehmann, T., Muller, U.A., Wolf, G., Samann, A., 2016. Osteocalcin, adipokines and their associations with glucose metabolism in type 1 diabetes. Bone 82, 50.

Ni, Y., Fan, D., 2017. Diabetes mellitus is a risk factor for low bone mass-related fractures: a meta-analysis of cohort studies. Medicine (Baltim.) 96, e8811.

Nicodemus, K.K., Folsom, A.R., Iowa Women's Health, S., 2001. Type 1 and type 2 diabetes and incident hip fractures in postmenopausal women. Diabetes Care 24, 1192.

Nilsson, A.G., Sundh, D., Johansson, L., Nilsson, M., Mellstrom, D., Rudang, R., Zoulakis, M., Wallander, M., Darelid, A., Lorentzon, M., 2017. Type 2 diabetes mellitus is associated with better bone microarchitecture but lower bone material strength and poorer physical function in elderly women: a population-based study. J. Bone Miner. Res. 32, 1062.

Nuche-Berenguer, B., Moreno, P., Portal-Nunez, S., Dapia, S., Esbrit, P., Villanueva-Penacarrillo, M.L., 2010. Exendin-4 exerts osteogenic actions in insulin-resistant and type 2 diabetic states. Regul. Pept. 159, 61.

Nyman, J.S., Even, J.L., Jo, C.H., Herbert, E.G., Murry, M.R., Cockrell, G.E., Wahl, E.C., Bunn, R.C., Lumpkin Jr., C.K., Fowlkes, J.L., Thrailkill, K.M., 2011. Increasing duration of type 1 diabetes perturbs the strength-structure relationship and increases brittleness of bone. Bone 48, 733.

Ogata, N., Chikazu, D., Kubota, N., Terauchi, Y., Tobe, K., Azuma, Y., Ohta, T., Kadowaki, T., Nakamura, K., Kawaguchi, H., 2000. Insulin receptor substrate-1 in osteoblast is indispensable for maintaining bone turnover. J. Clin. Investig. 105, 935.

Ogawa, N., Yamaguchi, T., Yano, S., Yamauchi, M., Yamamoto, M., Sugimoto, T., 2007. The combination of high glucose and advanced glycation end-products (AGEs) inhibits the mineralization of osteoblastic MC3T3-E1 cells through glucose-induced increase in the receptor for AGEs. Horm. Metab. Res. 39, 871.

Okazaki, R., Totsuka, Y., Hamano, K., Ajima, M., Miura, M., Hirota, Y., Hata, K., Fukumoto, S., Matsumoto, T., 1997. Metabolic improvement of poorly controlled noninsulin-dependent diabetes mellitus decreases bone turnover. J. Clin. Endocrinol. Metab. 82, 2915.

Orwoll, E.S., Bauer, D.C., Vogt, T.M., Fox, K.M., 1996. Axial bone mass in older women. Study of osteoporotic fractures research group. Ann. Intern. Med. 124, 187.

Ottenbacher, K.J., Ostir, G.V., Peek, M.K., Goodwin, J.S., Markides, K.S., 2002. Diabetes mellitus as a risk factor for hip fracture in mexican american older adults. J Gerontol A Biol Sci Med Sci 57, M648.

Oz, S.G., Guven, G.S., Kilicarslan, A., Calik, N., Beyazit, Y., Sozen, T., 2006. Evaluation of bone metabolism and bone mass in patients with type-2 diabetes mellitus. J. Natl. Med. Assoc. 98, 1598.

Paglia, D.N., Wey, A., Breitbart, E.A., Faiwiszewski, J., Mehta, S.K., Al-Zube, L., Vaidya, S., Cottrell, J.A., Graves, D., Benevenia, J., O'Connor, J.P., Lin, S.S., 2013. Effects of local insulin delivery on subperiosteal angiogenesis and mineralized tissue formation during fracture healing. J. Orthop. Res. 31, 783.

Palermo, A., D'Onofrio, L., Eastell, R., Schwartz, A.V., Pozzilli, P., Napoli, N., 2015. Oral anti-diabetic drugs and fracture risk, cut to the bone: safe or dangerous? A narrative review. Osteoporos. Int. 26, 2073.

Peng, J., Hui, K., Hao, C., Peng, Z., Gao, Q.X., Jin, Q., Lei, G., Min, J., Qi, Z., Bo, C., Dong, Q.N., Bing, Z.H., Jia, X.Y., Fu, D.L., 2016. Low bone turnover and reduced angiogenesis in streptozotocin-induced osteoporotic mice. Connect. Tissue Res. 57, 277.

Pereira, M., Jeyabalan, J., Jorgensen, C.S., Hopkinson, M., Al-Jazzar, A., Roux, J.P., Chavassieux, P., Orriss, I.R., Cleasby, M.E., Chenu, C., 2015. Chronic administration of Glucagon-like peptide-1 receptor agonists improves trabecular bone mass and architecture in ovariectomised mice. Bone 81, 459.

Petit, M.A., Paudel, M.L., Taylor, B.C., Hughes, J.M., Strotmeyer, E.S., Schwartz, A.V., Cauley, J.A., Zmuda, J.M., Hoffman, A.R., Ensrud, K.E., Osteoporotic Fractures in Men Study, G., 2010. Bone mass and strength in older men with type 2 diabetes: the Osteoporotic Fractures in Men Study. J. Bone Miner. Res. 25, 285.

Picke, A.K., Salbach-Hirsch, J., Hintze, V., Rother, S., Rauner, M., Kascholke, C., Moller, S., Bernhardt, R., Rammelt, S., Pisabarro, M.T., Ruiz-Gomez, G., Schnabelrauch, M., Schulz-Siegmund, M., Hacker, M.C., Scharnweber, D., Hofbauer, C., Hofbauer, L.C., 2016. Sulfated hyaluronan improves bone regeneration of diabetic rats by binding sclerostin and enhancing osteoblast function. Biomaterials 96, 11.

Pittas, A.G., Harris, S.S., Eliades, M., Stark, P., Dawson-Hughes, B., 2009. Association between serum osteocalcin and markers of metabolic phenotype. J. Clin. Endocrinol. Metab. 94, 827.

Pozzilli, P., Manfrini, S., Crino, A., Picardi, A., Leomanni, C., Cherubini, V., Valente, L., Khazrai, M., Visalli, N., group, I., 2005. Low levels of 25-hydroxyvitamin D3 and 1,25-dihydroxyvitamin D3 in patients with newly diagnosed type 1 diabetes. Horm. Metab. Res. 37, 680.

Pramojanee, S.N., Phimphilai, M., Kumphune, S., Chattipakorn, N., Chattipakorn, S.C., 2013. Decreased jaw bone density and osteoblastic insulin signaling in a model of obesity. J. Dent. Res. 92, 560.

Pun, K.K., Lau, P., Ho, P.W., 1989. The characterization, regulation, and function of insulin receptors on osteoblast-like clonal osteosarcoma cell line. J. Bone Miner. Res. 4, 853.

Qaseem, A., Wilt, T.J., Kansagara, D., Horwitch, C., Barry, M.J., Forciea, M.A., Clinical Guidelines Committee of the American College of, P., 2018. Hemoglobin A1c targets for glycemic control with pharmacologic therapy for nonpregnant adults with type 2 diabetes mellitus: a guidance statement update from the American College of Physicians. Ann. Intern. Med. 168, 569.

Raisingani, M., Preneet, B., Kohn, B., Yakar, S., 2017. Skeletal growth and bone mineral acquisition in type 1 diabetic children; abnormalities of the GH/IGF-1 axis. Growth Hormone IGF Res. 34, 13.

Rao Sirasanagandla, S., Ranganath Pai Karkala, S., Potu, B.K., Bhat, K.M., 2014. Beneficial effect of cissus quadrangularis linn. On osteopenia associated with streptozotocin-induced type 1 diabetes mellitus in male wistar rats. Adv Pharmacol Sci 2014, 483051.

Raskin, P., Stevenson, M.R., Barilla, D.E., Pak, C.Y., 1978. The hypercalciuria of diabetes mellitus: its amelioration with insulin. Clin. Endocrinol. 9, 329.

Reinwald, S., Peterson, R.G., Allen, M.R., Burr, D.B., 2009. Skeletal changes associated with the onset of type 2 diabetes in the ZDF and ZDSD rodent models. Am. J. Physiol. Endocrinol. Metab. 296, E765.

Rendina-Ruedy, E., Smith, B.J., 2016. Methodological considerations when studying the skeletal response to glucose intolerance using the diet-induced obesity model. Bone Rep. 5, 845.

Roggen, I., Gies, I., Vanbesien, J., Louis, O., De Schepper, J., 2013. Trabecular bone mineral density and bone geometry of the distal radius at completion of pubertal growth in childhood type 1 diabetes. Horm. Res. Paediatr 79, 68.

Roszer, T., Jozsa, T., Kiss-Toth, E.D., De Clerck, N., Balogh, L., 2014. Leptin receptor deficient diabetic (db/db) mice are compromised in postnatal bone regeneration. Cell Tissue Res. 356, 195.

Rozadilla, A., Nolla, J.M., Montana, E., Fiter, J., Gomez-Vaquero, C., Soler, J., Roig-Escofet, D., 2000. Bone mineral density in patients with type 1 diabetes mellitus. Joint Bone Spine 67, 215.

Ruanpeng, D., Ungprasert, P., Sangtian, J., Harindhanavudhi, T., 2017. Sodium-glucose cotransporter 2 (SGLT2) inhibitors and fracture risk in patients with type 2 diabetes mellitus: a meta-analysis. Diabetes Metab. Res. Rev. 33.

Rubino, F., Nathan, D.M., Eckel, R.H., Schauer, P.R., Alberti, K.G., Zimmet, P.Z., Del Prato, S., Ji, L., Sadikot, S.M., Herman, W.H., Amiel, S.A., Kaplan, L.M., Taroncher-Oldenburg, G., Cummings, D.E., Delegates of the 2nd Diabetes Surgery, S., 2016. Metabolic surgery in the treatment algorithm for type 2 diabetes: a joint statement by international diabetes organizations. Diabetes Care 39, 861.

Saito, M., Fujii, K., Mori, Y., Marumo, K., 2006. Role of collagen enzymatic and glycation induced cross-links as a determinant of bone quality in spontaneously diabetic WBN/Kob rats. Osteoporos. Int. 17, 1514.

Salter, J., Best, C.H., 1953. Insulin as a growth hormone. Br. Med. J. 2, 353.

Samelson, E.J., Demissie, S., Cupples, L.A., Zhang, X., Xu, H., Liu, C.T., Boyd, S.K., McLean, R.R., Broe, K.E., Kiel, D.P., Bouxsein, M.L., 2018. Diabetes and deficits in cortical bone density, microarchitecture, and bone size: Framingham HR-pQCT study. J. Bone Miner. Res. 33, 54.

Santana, R.B., Xu, L., Chase, H.B., Amar, S., Graves, D.T., Trackman, P.C., 2003. A role for advanced glycation end products in diminished bone healing in type 1 diabetes. Diabetes 52, 1502.

Sanz, C., Vazquez, P., Blazquez, C., Barrio, P.A., Alvarez Mdel, M., Blazquez, E., 2010. Signaling and biological effects of glucagon-like peptide 1 on the differentiation of mesenchymal stem cells from human bone marrow. Am. J. Physiol. Endocrinol. Metab. 298, E634.

Sasaki, T., Kaneko, H., Ramamurthy, N.S., Golub, L.M., 1991. Tetracycline administration restores osteoblast structure and function during experimental diabetes. Anat. Rec. 231, 25.

Schafer, A.L., Napoli, N., Lui, L., Schwartz, A.V., Black, D.M., Study of Osteoporotic, F., 2014. Serum 25-hydroxyvitamin D concentration does not independently predict incident diabetes in older women. Diabet. Med. 31, 564.

Scheiwiller, E., Guler, H.P., Merryweather, J., Scandella, C., Maerki, W., Zapf, J., Froesch, E.R., 1986. Growth restoration of insulin-deficient diabetic rats by recombinant human insulin-like growth factor I. Nature 323, 169.

Schmedt, N., Andersohn, F., Walker, J., Garbe, E., 2019. Sodium-glucose co-transporter-2 inhibitors and the risk of fractures of the upper or lower limbs in patients with type 2 diabetes: a nested case-control study. Diabetes Obes. Metab. 21, 52.

Schwartz, A.V., Hillier, T.A., Sellmeyer, D.E., Resnick, H.E., Gregg, E., Ensrud, K.E., Schreiner, P.J., Margolis, K.L., Cauley, J.A., Nevitt, M.C., Black, D.M., Cummings, S.R., 2002. Older women with diabetes have a higher risk of falls: a prospective study. Diabetes Care 25, 1749.

Schwartz, A.V., Pavo, I., Alam, J., Disch, D.P., Schuster, D., Harris, J.M., Krege, J.H., 2016. Teriparatide in patients with osteoporosis and type 2 diabetes. Bone 91, 152.

Schwartz, A.V., Schafer, A.L., Grey, A., Vittinghoff, E., Palermo, L., Lui, L.Y., Wallace, R.B., Cummings, S.R., Black, D.M., Bauer, D.C., Reid, I.R., 2013a. Effects of antiresorptive therapies on glucose metabolism: results from the FIT, HORIZON-PFT, and FREEDOM trials. J. Bone Miner. Res. 28, 1348.

Schwartz, A.V., Sellmeyer, D.E., Ensrud, K.E., Cauley, J.A., Tabor, H.K., Schreiner, P.J., Jamal, S.A., Black, D.M., Cummings, S.R., Study of Osteoporotic Features Research, G., 2001. Older women with diabetes have an increased risk of fracture: a prospective study. J. Clin. Endocrinol. Metab. 86, 32.

Schwartz, A.V., Sellmeyer, D.E., Strotmeyer, E.S., Tylavsky, F.A., Feingold, K.R., Resnick, H.E., Shorr, R.I., Nevitt, M.C., Black, D.M., Cauley, J.A., Cummings, S.R., Harris, T.B., Health, A.B.C.S., 2005. Diabetes and bone loss at the hip in older black and white adults. J. Bone Miner. Res. 20, 596.

Schwartz, A.V., Sellmeyer, D.E., Vittinghoff, E., Palermo, L., Lecka-Czernik, B., Feingold, K.R., Strotmeyer, E.S., Resnick, H.E., Carbone, L., Beamer, B.A., Park, S.W., Lane, N.E., Harris, T.B., Cummings, S.R., 2006. Thiazolidinedione use and bone loss in older diabetic adults. J. Clin. Endocrinol. Metab. 91, 3349.

Schwartz, A.V., Sigurdsson, S., Hue, T.F., Lang, T.F., Harris, T.B., Rosen, C.J., Vittinghoff, E., Siggeirsdottir, K., Sigurdsson, G., Oskarsdottir, D., Shet, K., Palermo, L., Gudnason, V., Li, X., 2013b. Vertebral bone marrow fat associated with lower trabecular BMD and prevalent vertebral fracture in older adults. J. Clin. Endocrinol. Metab. 98, 2294.

Scragg, R., Holdaway, I., Singh, V., Metcalf, P., Baker, J., Dryson, E., 1995. Serum 25-hydroxyvitamin D3 levels decreased in impaired glucose tolerance and diabetes mellitus. Diabetes Res. Clin. Pract. 27, 181.

Seref-Ferlengez, Z., Maung, S., Schaffler, M.B., Spray, D.C., Suadicani, S.O., Thi, M.M., 2016. P2X7R-Panx1 complex impairs bone mechanosignaling under high glucose levels associated with type-1 diabetes. PLoS One 11, e0155107.

Shah, V.N., Harrall, K.K., Shah, C.S., Gallo, T.L., Joshee, P., Snell-Bergeon, J.K., Kohrt, W.M., 2017. Bone mineral density at femoral neck and lumbar spine in adults with type 1 diabetes: a meta-analysis and review of the literature. Osteoporos. Int. 28, 2601.

Shah, V.N., Shah, C.S., Snell-Bergeon, J.K., 2015. Type 1 diabetes and risk of fracture: meta-analysis and review of the literature. Diabet. Med. 32, 1134.

Shanbhogue, V.V., Finkelstein, J.S., Bouxsein, M.L., Yu, E.W., 2016. Association between insulin resistance and bone structure in nondiabetic postmenopausal women. J. Clin. Endocrinol. Metab. 101, 3114.

Shanbhogue, V.V., Hansen, S., Frost, M., Jørgensen, N.R., Hermann, A.P., Henriksen, J.E., Brixen, K., 2015. Bone geometry, volumetric density, microarchitecture, and estimated bone strength assessed by HR-pQCT in adult patients with type 1 diabetes mellitus. J. Bone Miner. Res. 30, 2188.

Sheu, Y., Amati, F., Schwartz, A.V., Danielson, M.E., Li, X., Boudreau, R., Cauley, J.A., Osteoporotic Fractures in Men Research, G., 2017. Vertebral bone marrow fat, bone mineral density and diabetes: the Osteoporotic Fractures in Men (MrOS) study. Bone 97, 299.

Shires, R., Teitelbaum, S.L., Bergfeld, M.A., Fallon, M.D., Slatopolsky, E., Avioli, L.V., 1981. The effect of streptozotocin-induced chronic diabetes mellitus on bone and mineral homeostasis in the rat. J. Lab. Clin. Med. 97, 231.

Silva, M.J., Brodt, M.D., Lynch, M.A., McKenzie, J.A., Tanouye, K.M., Nyman, J.S., Wang, X., 2009. Type 1 diabetes in young rats leads to progressive trabecular bone loss, cessation of cortical bone growth, and diminished whole bone strength and fatigue life. J. Bone Miner. Res. 24, 1618.

Slade, J.M., Coe, L.M., Meyer, R.A., McCabe, L.R., 2012. Human bone marrow adiposity is linked with serum lipid levels not T1-diabetes. J. Diabetes Complicat. 26, 1.

Sorocéanu, M.A., Miao, D., Bai, X.-Y., Su, H., Goltzman, D., Karaplis, A.C., 2004. Rosiglitazone impacts negatively on bone by promoting osteoblast/osteocyte apoptosis. J. Endocrinol. 183, 203.

Srikanthan, P., Crandall, C.J., Miller-Martinez, D., Seeman, T.E., Greendale, G.A., Binkley, N., Karlamangla, A.S., 2014. Insulin resistance and bone strength: findings from the study of midlife in the United States. J. Bone Miner. Res. 29, 796.

Starup-Linde, J., 2013. Diabetes, biochemical markers of bone turnover, diabetes control, and bone. Front. Endocrinol. 4.

Starup-Linde, J., Lykkeboe, S., Gregersen, S., Hauge, E.-M., Langdahl, B.L., Handberg, A., Vestergaard, P., 2016a. Bone structure and predictors of fracture in type 1 and type 2 diabetes. J. Clin. Endocrinol. Metab. 101, 928.

Starup-Linde, J., Lykkeboe, S., Gregersen, S., Hauge, E.-M., Langdahl, B.L., Handberg, A., Vestergaard, P., 2016b. Differences in biochemical bone markers by diabetes type and the impact of glucose. Bone 83, 149.

Starup-Linde, J., Vestergaard, P., 2016. Biochemical bone turnover markers in diabetes mellitus - a systematic review. Bone 82, 69.

Strotmeyer, E.S., Cauley, J.A., Orchard, T.J., Steenkiste, A.R., Dorman, J.S., 2006. Middle-aged premenopausal women with type 1 diabetes have lower bone mineral density and calcaneal quantitative ultrasound than nondiabetic women. Diabetes Care 29, 306.

Strotmeyer, E.S., Cauley, J.A., Schwartz, A.V., Nevitt, M.C., Resnick, H.E., Bauer, D.C., Tylavsky, F.A., de Rekeneire, N., Harris, T.B., Newman, A.B., 2005. Nontraumatic fracture risk with diabetes mellitus and impaired fasting glucose in older white and black adults: the health, aging, and body composition study. Arch. Intern. Med. 165, 1612.

Strotmeyer, E.S., Cauley, J.A., Schwartz, A.V., Nevitt, M.C., Resnick, H.E., Zmuda, J.M., Bauer, D.C., Tylavsky, F.A., de Rekeneire, N., Harris, T.B., Newman, A.B., Health, A.B.C.S., 2004. Diabetes is associated independently of body composition with BMD and bone volume in older white and black men and women: the Health, Aging, and Body Composition Study. J. Bone Miner. Res. 19, 1084.

Suzuki, K., Miyakoshi, N., Tsuchida, T., Kasukawa, Y., Sato, K., Itoi, E., 2003. Effects of combined treatment of insulin and human parathyroid hormone(1-34) on cancellous bone mass and structure in streptozotocin-induced diabetic rats. Bone 33, 108.

Tanaka, H., Yamashita, T., Yoneda, M., Takagi, S., Miura, T., 2018. Characteristics of bone strength and metabolism in type 2 diabetic model Tsumura, Suzuki, obese diabetes mice. BoneKEy Rep. 9, 74.

Tanaka, K., Yamaguchi, T., Kanazawa, I., Sugimoto, T., 2015. Effects of high glucose and advanced glycation end products on the expressions of sclerostin and RANKL as well as apoptosis in osteocyte-like MLO-Y4-A2 cells. Biochem. Biophys. Res. Commun. 461, 193.

Tang, H.L., Li, D.D., Zhang, J.J., Hsu, Y.H., Wang, T.S., Zhai, S.D., Song, Y.Q., 2016. Lack of evidence for a harmful effect of sodium-glucose co-transporter 2 (SGLT2) inhibitors on fracture risk among type 2 diabetes patients: a network and cumulative meta-analysis of randomized controlled trials. Diabetes Obes. Metab. 18, 1199.

Taylor, W.H., Khaleeli, A.A., 2001. Coincident diabetes mellitus and primary hyperparathyroidism. Diabetes Metab Res Rev 17, 175.

Terada, M., Inaba, M., Yano, Y., Hasuma, T., Nishizawa, Y., Morii, H., Otani, S., 1998. Growth-inhibitory effect of a high glucose concentration on osteoblast-like cells. Bone 22, 17.

Thomas, D.M., Udagawa, N., Hards, D.K., Quinn, J.M., Moseley, J.M., Findlay, D.M., Best, J.D., 1998. Insulin receptor expression in primary and cultured osteoclast-like cells. Bone 23, 181.

Thong, E.P., Herath, M., Weber, D.R., Ranasinha, S., Ebeling, P.R., Milat, F., Teede, H., 2018. Fracture risk in young and middle-aged adults with type 1 diabetes mellitus: a systematic review and meta-analysis. Clin. Endocrinol. 89, 314.

Thrailkill, K., Bunn, R.C., Lumpkin, C., Wahl, E., Cockrell, G., Morris, L., Kahn, C.R., Fowlkes, J., Nyman, J.S., 2014. Loss of insulin receptor in osteoprogenitor cells impairs structural strength of bone. J. Diab. Res. 2014, 703589.

Thrailkill, K.M., Jo, C.H., Cockrell, G.E., Moreau, C.S., Lumpkin, C.K., Fowlkes, J.L., 2012. Determinants of undercarboxylated and carboxylated osteocalcin concentrations in type 1 diabetes. Osteoporos. Int. 23, 1799.

Thrailkill, K.M., Liu, L., Wahl, E.C., Bunn, R.C., Perrien, D.S., Cockrell, G.E., Skinner, R.A., Hogue, W.R., Carver, A.A., Fowlkes, J.L., Aronson, J., Lumpkin, C.K., 2005a. Bone formation is impaired in a model of type 1 diabetes. Diabetes 54, 2875.

Thrailkill, K.M., Lumpkin, C.K., Bunn, R.C., Kemp, S.F., Fowlkes, J.L., 2005b. Is insulin an anabolic agent in bone? Dissecting the diabetic bone for clues. Am. J. Physiol. Endocrinol. Metab. 289, E735.

Toh, S., Hernandez-Diaz, S., 2007. Statins and fracture risk. A systematic review. Pharmacoepidemiol. Drug Saf. 16, 627.

Tsentidis, C., Gourgiotis, D., Kossiva, L., Marmarinos, A., Doulgeraki, A., Karavanaki, K., 2016. Sclerostin distribution in children and adolescents with type 1 diabetes mellitus and correlation with bone metabolism and bone mineral density. Pediatr. Diabetes 17, 289.

Tsentidis, C., Gourgiotis, D., Kossiva, L., Marmarinos, A., Doulgeraki, A., Karavanaki, K., 2017. Increased levels of Dickkopf-1 are indicative of Wnt/beta-catenin downregulation and lower osteoblast signaling in children and adolescents with type 1 diabetes mellitus, contributing to lower bone mineral density. Osteoporos. Int. 28, 945.

Tsuka, S., Aonuma, F., Higashi, S., Ohsumi, T., Nagano, K., Mizokami, A., Kawakubo-Yasukochi, T., Masaki, C., Hosokawa, R., Hirata, M., Takeuchi, H., 2015. Promotion of insulin-induced glucose uptake in C2C12 myotubes by osteocalcin. Biochem. Biophys. Res. Commun. 459, 437.

Turner, R.T., Kalra, S.P., Wong, C.P., Philbrick, K.A., Lindenmaier, L.B., Boghossian, S., Iwaniec, U.T., 2013. Peripheral leptin regulates bone formation. J. Bone Miner. Res. 28, 22.

van Daele, P.L., Stolk, R.P., Burger, H., Algra, D., Grobbee, D.E., Hofman, A., Birkenhager, J.C., Pols, H.A., 1995. Bone density in non-insulin-dependent diabetes mellitus. The Rotterdam Study. Ann. Intern. Med. 122, 409.

van Lierop, A.H., Hamdy, N. a. T., van der Meer, R.W., Jonker, J.T., Lamb, H.J., Rijzewijk, L.J., Diamant, M., Romijn, J.A., Smit, J.W.A., Papapoulos, S.E., 2012. Distinct effects of pioglitazone and metformin on circulating sclerostin and biochemical markers of bone turnover in men with type 2 diabetes mellitus. Eur. J. Endocrinol. 166, 711.

Vavanikunnel, J., Charlier, S., Becker, C., Schneider, C., Jick, S.S., Meier, C.R., Meier, C., 2019. Association between glycemic control and risk of fracture in diabetic patients: a nested case-control study. J. Clin. Endocrinol. Metab. 104, 1645.

Veldhuis-Vlug, A.G., Rosen, C.J., 2017. Mechanisms of marrow adiposity and its implications for skeletal health. Metabolism 67, 106.

Verhaeghe, J., Suiker, A.M., Einhorn, T.A., Geusens, P., Visser, W.J., Van Herck, E., Van Bree, R., Magitsky, S., Bouillon, R., 1994. Brittle bones in spontaneously diabetic female rats cannot be predicted by bone mineral measurements: studies in diabetic and ovariectomized rats. J. Bone Miner. Res. 9, 1657.

Verhaeghe, J., Suiker, A.M., Van Bree, R., Van Herck, E., Jans, I., Visser, W.J., Thomasset, M., Allewaert, K., Bouillon, R., 1993. Increased clearance of 1,25(OH)2D3 and tissue-specific responsiveness to 1,25(OH)2D3 in diabetic rats. Am. J. Physiol. 265, E215.

Verhaeghe, J., Suiker, A.M., Visser, W.J., Van Herck, E., Van Bree, R., Bouillon, R., 1992. The effects of systemic insulin, insulin-like growth factor-I and growth hormone on bone growth and turnover in spontaneously diabetic BB rats. J. Endocrinol. 134, 485.

Verhaeghe, J., Thomsen, J.S., van Bree, R., van Herck, E., Bouillon, R., Mosekilde, L., 2000. Effects of exercise and disuse on bone remodeling, bone mass, and biomechanical competence in spontaneously diabetic female rats. Bone 27, 249.

Verhaeghe, J., Van Herck, E., van Bree, R., Moermans, K., Bouillon, R., 1997. Decreased osteoblast activity in spontaneously diabetic rats. In vivo studies on the pathogenesis. Endocrine 7, 165.

Verhaeghe, J., van Herck, E., Visser, W.J., Suiker, A.M., Thomasset, M., Einhorn, T.A., Faierman, E., Bouillon, R., 1990. Bone and mineral metabolism in BB rats with long-term diabetes. Decreased bone turnover and osteoporosis. Diabetes 39, 477.

Verroken, C., Pieters, W., Beddeleem, L., Goemaere, S., Zmierczak, H.G., Shadid, S., Kaufman, J.M., Lapauw, B., 2017. Cortical bone size deficit in adult patients with type 1 diabetes mellitus. J. Clin. Endocrinol. Metab. 102, 2887.

Vestergaard, P., 2007. Discrepancies in bone mineral density and fracture risk in patients with type 1 and type 2 diabetes–a meta-analysis. Osteoporos. Int. 18, 427.

Vestergaard, P., 2011. Risk of newly diagnosed type 2 diabetes is reduced in users of alendronate. Calcif. Tissue Int. 89, 265.

Vestergaard, P., Rejnmark, L., Mosekilde, L., 2005. Relative fracture risk in patients with diabetes mellitus, and the impact of insulin and oral antidiabetic medication on relative fracture risk. Diabetologia 48, 1292.

Vestergaard, P., Rejnmark, L., Mosekilde, L., 2011. Are antiresorptive drugs effective against fractures in patients with diabetes? Calcif. Tissue Int. 88, 209.

Villasenor, A., Aedo-Martin, D., Obeso, D., Erjavec, I., Rodriguez-Coira, J., Buendia, I., Ardura, J.A., Barbas, C., Gortazar, A.R., 2019. Metabolomics reveals citric acid secretion in mechanically-stimulated osteocytes is inhibited by high glucose. Sci. Rep. 9, 2295.

Wallace, C., Reiber, G.E., LeMaster, J., Smith, D.G., Sullivan, K., Hayes, S., Vath, C., 2002. Incidence of falls, risk factors for falls, and fall-related fractures in individuals with diabetes and a prior foot ulcer. Diabetes Care 25, 1983.

Wallner, C., Schira, J., Wagner, J.M., Schulte, M., Fischer, S., Hirsch, T., Richter, W., Abraham, S., Kneser, U., Lehnhardt, M., Behr, B., 2015. Application of VEGFA and FGF-9 enhances angiogenesis, osteogenesis and bone remodeling in type 2 diabetic long bone regeneration. PLoS One 10, e0118823.

Wang, H., Ba, Y., Xing, Q., Du, J.L., 2019. Diabetes mellitus and the risk of fractures at specific sites: a meta-analysis. BMJ Open 9, e024067.

Wang, X., Shen, X., Li, X., Agrawal, C.M., 2002. Age-related changes in the collagen network and toughness of bone. Bone 31, 1.

Watts, N.B., Bilezikian, J.P., Usiskin, K., Edwards, R., Desai, M., Law, G., Meininger, G., 2016. Effects of canagliflozin on fracture risk in patients with type 2 diabetes mellitus. J. Clin. Endocrinol. Metab. 101, 157.

Wei, J., Ferron, M., Clarke, C.J., Hannun, Y.A., Jiang, H., Blaner, W.S., Karsenty, G., 2014a. Bone-specific insulin resistance disrupts whole-body glucose homeostasis via decreased osteocalcin activation. J. Clin. Investig. 124, 1.

Wei, J., Hanna, T., Suda, N., Karsenty, G., Ducy, P., 2014b. Osteocalcin promotes beta-cell proliferation during development and adulthood through Gprc6a. Diabetes 63, 1021.

Wittrant, Y., Gorin, Y., Woodruff, K., Horn, D., Abboud, H.E., Mohan, S., Abboud-Werner, S.L., 2008. High d(+)glucose concentration inhibits RANKL-induced osteoclastogenesis. Bone 42, 1122.

Wortsman, J., Matsuoka, L.Y., Chen, T.C., Lu, Z., Holick, M.F., 2000. Decreased bioavailability of vitamin D in obesity. Am. J. Clin. Nutr. 72, 690.

Wu, J.H., Foote, C., Blomster, J., Toyama, T., Perkovic, V., Sundstrom, J., Neal, B., 2016. Effects of sodium-glucose cotransporter-2 inhibitors on cardiovascular events, death, and major safety outcomes in adults with type 2 diabetes: a systematic review and meta-analysis. Lancet Diabetes Endocrinol 4, 411.

Yakar, S., Isaksson, O., 2016. Regulation of skeletal growth and mineral acquisition by the GH/IGF-1 axis: lessons from mouse models. Growth Hormone IGF Res. 28, 26.

Yakar, S., Rosen, C.J., Beamer, W.G., Ackert-Bicknell, C.L., Wu, Y., Liu, J.-L., Ooi, G.T., Setser, J., Frystyk, J., Boisclair, Y.R., LeRoith, D., 2002. Circulating levels of IGF-1 directly regulate bone growth and density. J. Clin. Investig. 110, 771.

Yamada, C., Yamada, Y., Tsukiyama, K., Yamada, K., Udagawa, N., Takahashi, N., Tanaka, K., Drucker, D.J., Seino, Y., Inagaki, N., 2008. The murine glucagon-like peptide-1 receptor is essential for control of bone resorption. Endocrinology 149, 574.

Yamamoto, M., Yamauchi, M., Sugimoto, T., 2013. Elevated sclerostin levels are associated with vertebral fractures in patients with type 2 diabetes mellitus. J. Clin. Endocrinol. Metab. 98, 4030.

Yang, J., Zhang, X., Wang, W., Liu, J., 2010. Insulin stimulates osteoblast proliferation and differentiation through ERK and PI3K in MG-63 cells. Cell Biochem. Funct. 28, 334.

Yassouridis, C., Leisch, F., Winkler, C., Ziegler, A.G., Beyerlein, A., 2017. Associations of growth patterns and islet autoimmunity in children with increased risk for type 1 diabetes: a functional analysis approach. Pediatr. Diabetes 18, 103.

Yoshida, M., Jacques, P.F., Meigs, J.B., Saltzman, E., Shea, M.K., Gundberg, C., Dawson-Hughes, B., Dallal, G., Booth, S.L., 2008. Effect of vitamin K supplementation on insulin resistance in older men and women. Diabetes Care 31, 2092.

Zhang, L., Liu, Y., Wang, D., Zhao, X., Qiu, Z., Ji, H., Rong, H., 2009. Bone biomechanical and histomorphometrical investment in type 2 diabetic Goto-Kakizaki rats. Acta Diabetol. 46, 119.

Zhou, M., Ma, X., Li, H., Pan, X., Tang, J., Gao, Y., Hou, X., Lu, H., Bao, Y., Jia, W., 2009. Serum osteocalcin concentrations in relation to glucose and lipid metabolism in Chinese individuals. Eur. J. Endocrinol. 161, 723.

Zhukouskaya, V.V., Eller-Vainicher, C., Gaudio, A., Cairoli, E., Ulivieri, F.M., Palmieri, S., Morelli, V., Orsi, E., Masserini, B., Barbieri, A.M., Polledri, E., Fustinoni, S., Spada, A., Fiore, C.E., Chiodini, I., 2015. In postmenopausal female subjects with type 2 diabetes mellitus, vertebral fractures are independently associated with cortisol secretion and sensitivity. J. Clin. Endocrinol. Metab. 100, 1417.

Zhukouskaya, V.V., Eller-Vainicher, C., Gaudio, A., Privitera, F., Cairoli, E., Ulivieri, F.M., Palmieri, S., Morelli, V., Grancini, V., Orsi, E., Masserini, B., Spada, A.M., Fiore, C.E., Chiodini, I., 2016. The utility of lumbar spine trabecular bone score and femoral neck bone mineral density for identifying asymptomatic vertebral fractures in well-compensated type 2 diabetic patients. Osteoporos. Int. 27, 49.

Zhukouskaya, V.V., Eller-Vainicher, C., Vadzianava, V.V., Shepelkevich, A.P., Zhurava, I.V., Korolenko, G.G., Salko, O.B., Cairoli, E., Beck-Peccoz, P., Chiodini, I., 2013. Prevalence of morphometric vertebral fractures in patients with type 1 diabetes. Diabetes Care 36, 1635.

Chapter 41

Androgen receptor expression and steroid action in bone

Venkatesh Krishnan

Lilly Research Laboratories, Eli Lilly & Company, Lilly Corporate Center, Indianapolis, United States

Chapter outline

Introduction

Androgens and estrogens belong to the steroid hormone superfamily that binds to nuclear receptors that mediate their canonical actions in specific reproductive and endocrine tissues (Tsai and O'Malley, 1994). Estrogen mediates its action through two cognate receptors termed estrogen receptor alpha (ESR1) and estrogen receptor beta (ESR2)—also known as NR3A1: ERalpha and NR3A2: ERbeta (Nilsson et al., 2001). Androgen signals through the only known cognate receptor, termed androgen receptor (AR, also referred to as NR3C4) (Simental et al., 1991). Previous studies have shown that loss of estrogen following surgical removal of ovaries or an aging-related decrease in estrogen production (defined earlier as menopause) can lead to bone loss in women ((see Fig. 41.2) Albright, 1940). In a prospective study among prostate cancer patients seeking androgen-deprivation therapy (ADT) compared with age-matched patients not seeking ADT, it was shown that the absence of circulating androgens results in an increased rate of bone turnover and a loss in bone mineral density (BMD) over 2 years (Prostate Cancer, 2002). The ADT regimen included an LHRH agonist leuprolide along with concomitant administration of flutamide or bicalutamide, which are specific antagonists of AR. Therefore, both estrogen and androgen deprivation can lead to bone loss in women and men, respectively. Furthermore, surgical gonadectomy of sexually mature men resulted in bone loss as evidenced by a rapid decline in BMD and an increase in bone turnover markers (Stepan et al., 1989). Therefore, this provided a simple model that suggested a prominent role for androgen in maintaining healthy bone mass in men. However, in a landmark mechanistic study conducted by Khosla et al. in 1998, it was shown that estrogen (but not androgen) supplementation was both necessary and sufficient to recover the bone loss initiated by ADT. These results have challenged the dogma that androgens and other AR agonists are exclusive in imparting favorable skeletal effects in men. A subsequent study has corroborated this finding by exploring (Finkelstein et al., 2016) a different study design involving pharmacological induction of hypogonadism in men followed by graded doses of testosterone replacement with or without an aromatase inhibitor. Similar to the earlier study described by Khosla et al., changes in bone resorption and formation markers were predominantly regulated by estrogen and not androgen in these men. Moreover, testosterone, in the absence of aromatization to estrogen (aromatase inhibitor arm), was unable to

Principles of Bone Biology. https://doi.org/10.1016/B978-0-12-814841-9.00041-5

prevent decreases in BMD at multiple sites. Collectively, these two and additional interventional studies (Khosla et al., 2015), using variations of the approaches used in the studies just described, now provide compelling evidence in humans that in both women and men, estrogen is the dominant sex steroid regulating bone metabolism. While these mechanistic studies have employed the use of testosterone and its aromatase enzyme catalyzed conversion to estrogen, in the presence/absence of aromatase inhibitors, they do not address the direct consequences of androgen ligands in bone. These can be primarily achieved by the use of nonaromatizable androgens that may be represented by a wide array of selective androgen–receptor modulators (SARMs) (Narayanan et al., 2018). Unfortunately, most clinical development deploying these SARMs carries unknown long-term risks that have yet to warrant their use as therapeutic options in long-term disease contexts (treatment duration >2 years) other than exigent diseases such as cancer. Therefore, the field lacks access to published data describing carefully designed long-term efficacy studies with SARMs that could allow one to measure the effects of such specific AR ligands in the context of human bone health. In contrast, there is ample evidence that antiandrogens, by way of their use in prostate cancer and other benign prostate diseases, do result in loss of bone health that predisposes patients to a higher risk of fractures (Cheung et al., 2013).

The subsequent sections of the review will now explore the role of AR in affecting male bone health. It will contrast both loss-in-function and gain-in-function paradigms to help ascribe a holistic view on this topic. It is now evident that rodent models that reflect loss of function (LoF), either by way of a whole body knockout of these genes from early development or by way of tissue-specific knockout mice using tissue-specific promoters that drive *Cre* recombinase, provide useful ways to assess the importance of AR in rodent bone health. This review will capture our current understanding of these genetically modified animal models and help reconcile it with the LoF observations in man that may or may not align with these rodent observations. In addition, this article will summarize the numerous gain-in-function paradigms ranging from the use of steroidal testosterone replacement to the emerging discovery and development of SARMs as they impact bone health.

Loss-of-function evidence from rare human variants

The importance of ESR1 in male human skeleton was exemplified by a rare LoF homozygous deletion of ER-alpha in a male individual that rendered him with osteopenia and a spine BMD more than two standard deviations below the age-matched normal for 15-year-old boys (Smith et al., 1994). However, when carefully evaluating the iliac crest biopsy obtained from this rare ER-alpha-null male, it was reported to reflect reduced cancellous bone volume and cortical width at this site. It is conceivable that this is due to the absence of the direct beneficial effect of ER-alpha on strain-dependent bone formation indices, as suggested by Lanyon et al. (Lee et al., 2003). Aligned with this report were two reports of loss of hormone that was realized through a homozygous deletion of the aromatase gene that is crucial for converting circulating testosterone to estrogen, the ligand that targets the receptors ESR1 and ESR2. In both these individuals who lacked adequate circulating estrogen levels, the skeletal phenotype was near identical to that described earlier for the ER-alpha-null human (Carani et al., 1997; Bilezekian et al., 1998). Collectively, these findings, albeit rare, provide a prominent role for estrogens and ESR1 in affecting the peak bone mass in young adolescent males.

The enzyme 5-alpha reductase (type 1 and type 2) catalyzes the reduction of testosterone to the nonaromatizable and potent AR ligand dihydrotestosterone (DHT) (see Fig. 41.1), which can bind AR with greater affinity than testosterone and mediate the biological effects of testosterone as an active metabolite. Patients with mutations of 5-alpha reductase type 2 have been reported to have normal BMD (Sobel et al., 2006). These individuals have low circulating levels of DHT. Treatment of adult men with the 5-alpha reductase inhibitor finasteride does not affect BMD (Matsumoto et al., 2002). However, finasteride is a weak inhibitor of the type 2 isoform of 5-alpha reductase and does not affect the constitutively active prevalent type 1 isoform. Thus, although DHT levels are lower in finasteride-treated men than in healthy untreated controls, they are still in the low normal range in many treated men. More recent studies in dutasteride-treated patients, which is a potent inhibitor of both type 1 and type 2 isoforms of 5-alpha reductase, also have failed to elicit a significant reduction in BMD in men (Amory et al., 2008). These observations of normal bone health in light of reduced conversion of testosterone to its potent metabolite DHT further guide our conclusion for the relative importance of ESR versus AR ligands in maintaining bone mass in males.

The 3-beta hydroxysteroid dehydrogenase 2 (HSD3B2) gene is located on chromosome 1q13.1, and encodes for the human type II (3b-HSD2) isoenzyme, which is only expressed in the adrenal cortex and in steroidogenic cells within the gonads. It is an essential enzyme for the synthesis of testosterone along with cortisol and aldosterone (see Fig. 41.1). An individual who presented at birth with a salt-wasting syndrome as a result of this rare insufficiency variant, which represented an LoF for this enzyme, was rescued with cortisol treatments. This male achieved normal puberty and had the expected developmental defects in his sexual organs associated with androgen insufficiency. However, in spite of low

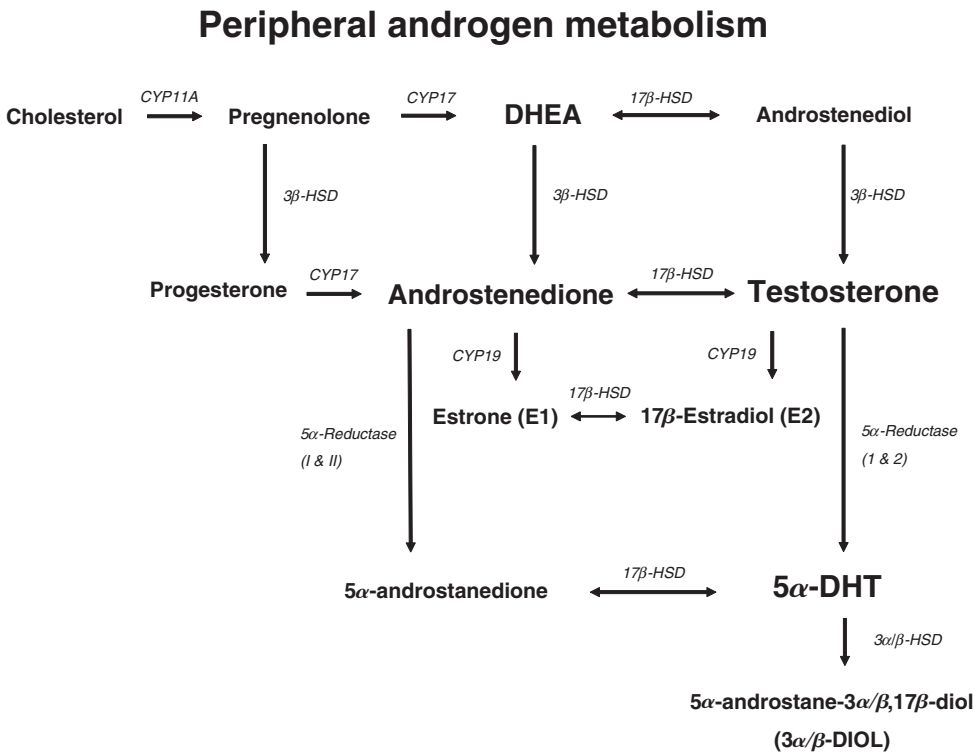

FIGURE 41.1 An outline of the steroidal synthesis of androgen and its metabolism has been provided. Of importance are the roles played by 5alpha-Reductase in converting Testosterone to 5alpha-Dihydrotestosterone, and the conversion of androstenedione to testosterone by 17 Beta HSD.

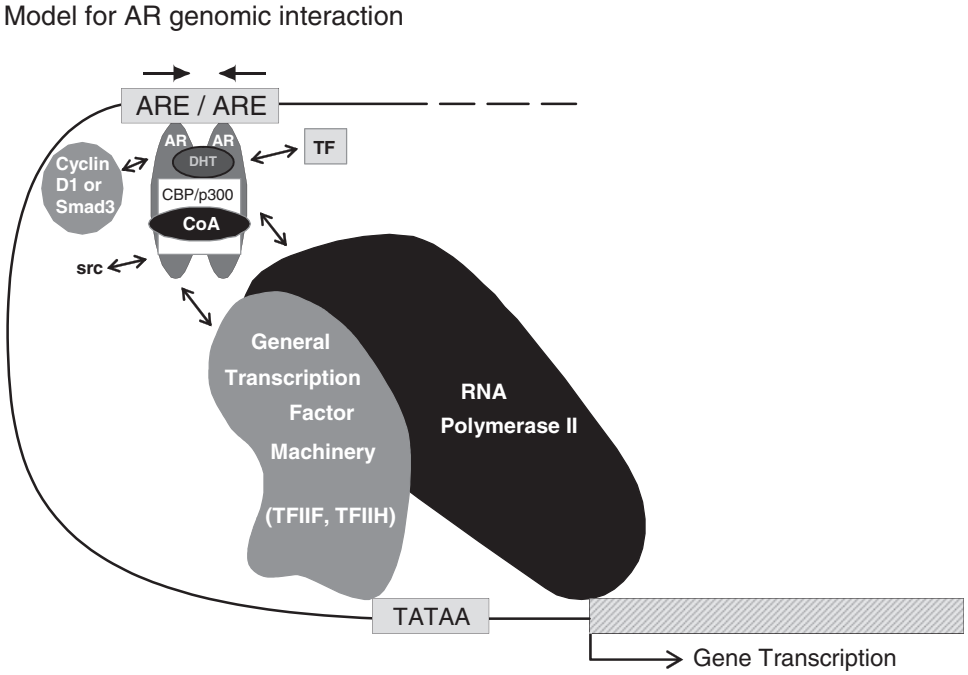

FIGURE 41.2 The molecular action of transcriptional activation by the AR homodimer acting on cis-regulatory elements identified on androgen-regulated genes is shown along with the coactivators that may influence tissue specific androgen-induced gene expression.

circulating testosterone levels (~13.8 nmol/L compared with normal range if 20−40 nmol/L), which is an expected consequence of this rare LoF variant, the patient showed a normal BMD. His bone density measured at approximately 19 years of age was normal with a femoral T-score of (+2.8 s.d.) and vertebral T-score of (+1.9 s.d.), suggestive of an absence of an obvious deleterious effect on BMD in spite of insufficient androgen levels (Bruno et al., 2018). Collectively, the rare occurrences of human LoF variants point to a prominent role for estrogen/ESR1 in maintaining male skeletal health and less so for the hormone testosterone and related androgens such as dihydrotestosterone. However, the absence of well-annotated AR LoF individuals makes it challenging to offer a comparative assessment of androgens (vs. estrogens) and their role in human bone health relying on this approach of rare LoF genetic variants.

Gain-of-function evidence from human trials

Placebo-controlled studies using various approved formulations of testosterone have been limited and often report conflicting results (Snyder et al., 1999; Kenny et al., 2001; Tenover, 1992). Some component of this discrepancy could be attributed to the study design within these trials. In the study conducted by Snyder et al., 108 men over 65 years of age were randomized to receive a testosterone or placebo patch for 36 months (Snyder et al., 1999). The majority of these subjects were neither osteoporotic by current WHO criteria, nor were they hypogonadal (mean testosterone level >350 ng/dL). The primary end point was the measure of vBMD as measured using dual-absorption X-ray absorptiometry (DEXA) measured at 6-month intervals over the 3-year period. The testosterone patch did not show significant improvement in the primary end point of *v*BMD compared with the placebo group, except for the final measure of spine BMD by DEXA at 36 months. In a posthoc analysis using secondary linear regression, it was reported that by stratifying subjects based on their pretreatment serum testosterone concentration, one could clearly show favorable effects of the testosterone patch arm compared with placebo arm on lumbar spine bone density in overtly hypogonadal patients. In contrast to the previous study of nonosteoporotic, eugonadal men, Amory et al. studied hypogonadal men ($T \leq 300$ ng/dL) over age 65, randomly assigned to placebo or testosterone, bimonthly 200 mg intramuscular injections ± finasteride, for 3 years (Amory et al., 2004). Their inclusion criteria for these elderly men used baseline mean T-scores ranging from −0.3 to −0.53, and therefore these hypogonadal men were not deemed osteoporotic. Their peak serum total testosterone levels were at the high normal serum range for the testosterone-only group, with a mean peak value for the group being 35.9 ± 12.1 nmol/L (mean ± sd). In contrast to the Snyder et al. study described above, BMD at a variety of sites including lumbar spine, total hip, and trochanter (femur site) were all increased with the testosterone ± finasteride arms at 12 months and remained significantly increased for the 3-year period compared with the results for placebo injections. It is noteworthy that the magnitude of the increases in lumbar spine BMD seen with intramuscular testosterone at 12 months were comparable to those observed in men with osteoporosis using daily injections of teriparatide, a strong well-known bone anabolic agent (Orwoll et al., 2003). However, this study could not account for these effects as being specific to the increase in serum testosterone, as testosterone could have been aromatized to estrogen in specific tissues. Consistent with this caveat, the authors measured an increase in serum estradiol throughout this 3-year period. Notably, these gains in lumbar BMD over 36 months were positively correlated with the magnitude of increase in serum total testosterone (r^2 0.44; $P \leq .001$), bioavailable testosterone (r^2 0.45 and $P \leq .009$), and serum estradiol (r^2 0.45; $P \leq .0006$). Therefore, in spite of encouraging changes in lumbar BMD comparable to those seen with anabolic agents such as teriparatide, one needs to cautiously ascribe direct beneficial effects in improving BMD for male subjects with androgens. It is important to note, however, that selective modulators of ESR1 and ESR2 ligands such as raloxifene do not provide such a robust change in lumbar spine BMD as seen with intramuscular testosterone after 12 months in patients receiving gonadotropin-releasing hormone (GnRH) agonists for prostate cancer. The mean (BMD ± SE) BMD of the posterior−anterior lumbar spine increased by 1.0 ± 0.9% in the men treated with raloxifene plus GnRH agonist and decreased by 1.0 ± 0.6% in the men who did not receive raloxifene but were taking GnRH agonist ($P = .07$) (Smith et al., 2004). It is not clear if the full complement of ESR1- and ESR2-related bone changes ascribed to estrogen-mediated action can be recapitulated by a selective ligand like raloxifene in the context of a GnRH agonist.

The use of intramuscular testosterone enanthate or cypionate, 100 mg/week, in patients with acquired hypogonadism as reported by Katznelson et al. had the most definitive gain seen in vertebral BMD (14% after 18 months) but is confounded by the fact that these were younger adults (average age 53) with lower vertebral BMD as a result of diminished peak bone mass caused by their central hypogonadism, which could have included changes in the growth hormone/IGF-1 axis. Most recently, Snyder et al. published the most extensive 1-year study in elderly (>65 years of age) hypogonadal men (serum $T < 275$ ng/dL), when approximately 790 men were randomized to placebo or a testosterone gel. However, the authors did not measure BMD or biomarkers of turnover such as CTX or P1NP (Snyder et al., 2016). In summary, while a few gain-of-function (GoF) studies have been conducted in elderly hypogonadal men, which included approximately 90 men

for a 1-year treatment duration and provided a 90% power to reliably detect vBMD changes based on the average 9% gain in vertebral BMD at 1 year as measured by Katznelson et al. (1996) using individuals with acquired hypogonadism, these results do not provide a compelling reason to ascribe this benefit in men. The primary reason to maintain a cautious position is that while all these studies provide a vignette or two of benefit in increasing BMD, in order to balance any perceived target-related risk, such as prostate and cardiovascular health, one needs larger, well-controlled, and longer-duration studies (>2 years) to provide a balanced view of the benefit−risk profile of androgen replacement to address issues with male skeletal health. In lieu of the robust efficacy of non-AR binding pharmaceuticals such as antiresorptives and anabolic agents in male patients, this data set will be challenging to seek from such well-controlled studies (Snyder et al., 2014).

Can we reliably measure androgen gain of function in bone health using end points such as bone mineral density?

It is now well established that bone quality is a measure that encompasses BMD plus aspects of bone strength that are difficult to measure using objective preestablished criteria such as bone geometry, microarchitecture, and bone tissue properties (Fonseca et al., 2014). The limitations for exclusive reliance on BMD are highlighted by the significant differences in trabecular connectivity with unit areas from subjects matched for bone volume (Recker, 1993). Also, in numerous interventional studies with antiresorptives, significant and clinically relevant reductions in fracture risk are associated with modest changes in BMD (Sarkar et al., 2002; Delmas and Seeman, 2004). Therefore, it is conceivable that clinical end points related to bone microarchitecture and other structural parameters as assessed by high-resolution computer tomography, magnetic resonance imaging, bone mineral strength by microindentation, etc. may provide valuable insight into bone quality that could supplement our experience with BMD to arrive at a holistic view of the benefits of androgen-related effects on bone quality. These alternate end points reflecting the changes in microarchitecture of bone in response to androgens are proposed due to the well-known observations related to striking changes seen in the mass, structure, and geometry of the male versus female skeleton (Bruzek, 2002).

Gender-specific differences in bone geometry and architecture

Higher peak bone mass in males compared with females would posit higher fracture risk for males (compared with females) as they progressively lose bone mass due to aging for a given BMD, because these males have a greater absolute reduction from their peak density. Yet, studies have shown that for a given DXA BMD score, the fracture risk between genders is indistinguishable (Selby et al., 2000). Characteristic differences in bone architecture between males (larger bone area) and females (smaller bone area) perhaps offer a potential advantage to males that may explain their reduced susceptibility to fracture (Seeman, 1993). Therefore, the higher peak bone mass in males compared with age-matched females offers them a distinct advantage (Lambert et al., 2011). It is also well known that the cross-sectional diameters of vertebrae and femoral necks are larger in males and that this is associated with greater bone strength than that of age-matched females (Mosekilde et al., 1990) Decreased axial width along with reduced cross-sectional area, seen in elderly men (MINOS study) with a higher risk of fragility fractures, further underscores the importance of bone geometry as an independent determinant of fracture risk in addition to BMD (Szulc et al., 2006). It is also believed that through aging, women show greater reductions in periosteal thickness compared with men (Christiansen et al., 2011) Interestingly, the type of trabecular changes that occur with aging also differ between the sexes, as males tend to have trabecular thinning and females tend to lose trabecular connectivity (Lambert et al., 2011). Therefore, despite the fact that males will have a larger reduction for any given DXA BMD value, this does not seem to translate into an increased fracture risk, and is perhaps related to the protective benefit of their peak bone characteristics and different types of bone architectural properties compared with females. Consistent with these findings, the prevalence of osteoporosis is significantly greater for women than men when stratified across age groups through deciles (Kanis, 2007). This observation is also substantiated in male rats deficient in androgen and exposed to aromatase inhibitors, which fail to convert testosterone to estrogen and show specific decrement in certain geometric features of the proximal femur, suggesting that androgens may control peak bone mass in the male rat by relying on non-BMD measures (Vanderschueren et al., 1997). The mechanistic underpinnings for the sexually dimorphic nature of skeletal geometry were described recently by Sims et al. Recent studies implicate the regulation of corticalization by SOCS-3. They used a DMP-1−driven Cre to generate an osteocyte-specific knockout of SOCS-3 that allowed them to create a sexually divergent phenotype of corticalization. The nonaromatizable androgen (i.e., DHT) can inhibit the activity of delayed corticalization in Dmp-1−specific SOCS-3-null mice by targeting IL-6 (Cho et al., 2017). This provides us with a mechanistic basis for the increased corticalization seen in the male skeleton,

which may effectively contribute to reduced fracture risk. Therefore, androgen ligands that enhance cortical bone parameters may favorably affect fracture risk. However, if these androgens resulted in changes in bone architecture or geometry such as increased cross-sectional area as a result of increased cortical area, even in the context of increasing bone mineral content, it would only reflect as a minimal change in BMD. Therefore, when it comes to androgen-mediated impact on male bone health, it may be more prudent to look beyond BMD.

Gain-of-function studies with testosterone treatment and change in bone architecture

In a small clinical study (32 hypogonadal men) exploring the use of testosterone treatment in hypogonadal men (primary hypogonadism), Leifke et al. showed that intramuscular injection of testosterone enanthate (250 mg every 2 weeks over 3 years) resulted in a 30% gain in trabecular BMD and a 9% increase in cortical BMD at the lumbar spine as measured by quantitative computer tomography (Leifke et al., 1998). These improvements were seen in all patients independent of their leading cause for primary hypogonadism. In contrast to this smaller study, Khosla et al. have shown in 269 men that there is no correlation between microstructural parameters at the wrist bone as measured by high-resolution three-dimensional quantitative computer tomography and those of bioavailable testosterone. Therefore, it is important to recognize that there may be a threshold effect of testosterone on structural properties of bone that may only be evident in men with severe hypogonadism and is less evident in the broad eugonadal population. Also, the anatomical site (wrist vs. spine) may offer distinct responses to androgens. In another very limited study (10 hypogonadal men) explored by Benito et al., it was shown that magnetic resonance microimaging-based end points highlight the integrity of the trabecular network, which is compromised in hypogonadal men and improved with testosterone replacement. These patients showed an increase in the surface-to-curve ratio (+11% vs. baseline), defined earlier (Gomberg et al., 2000), which is the topologic representation of the ratio of trabecular plates to rods and suggests that testosterone replacement partially restored trabecular connectivity. These studies show that testosterone treatment results in improvements typically seen with anabolic agents on trabecular connectivity.

Loss of function using genetically modified mice

The effects of estrogen on bone are mediated by two related but distinct receptors, ESR1 (ER-alpha) and ESR2 (ER-beta) (Nilsson et al., 2001; Almeida et al., 2017). Sims et al. published the global knockout of ESR1, and as a result of alteration in the hypothalamic−pituitary−gonadal axis, these animals had supraphysiological levels of circulating estrogen and androgen levels in females and male knockout mice. Loss of ESR1 from birth resulted in a decrease in bone turnover and an increase in cancellous bone mass accompanied by a decrease in cortical thickness (Sims et al., 2002). A follow-up study reported by Callewaert et al. pursued a strategy of creating both single- and double-knockouts of ESR1 and AR in male mice by crossing these compound heterozygotes. Removal of ESR1 resulted in an unusual gain in trabecular bone volume; in contrast, removal of AR resulted in an opposite and dramatic reduction in trabecular bone volume when assessed using computer tomography of the distal femur. These results would imply that in the absence of hypothalamic−pituitary−gonadal axis-related suppression of circulating hormones mediated by ESR1, systemic increases in serum androgens may result in this surprising increase in bone volume in ESR1-null mice. In contrast, when both ESR1 and AR were knocked out, they observed complete loss of this gain in trabecular bone volume in the single-ESR1-null mice comparable to that of the single-AR-null mice (Callewaert et al., 2009). In addition, cortical area at the femoral site was reduced with the single-ESR1-null mice, which was further reduced with the single-AR-null mice, followed by the greatest reduction in cortical area in the double-null mice. Collectively, AR may be required for male mice to accrue peak trabecular bone mass and peak cortical area. These interpretations from global ESR1 knockout mice are confounded by significant alterations in circulating sex steroid levels. To avoid these dramatic changes in circulating sex steroids that may inadvertently reflect GoF for other steroid hormone receptors that function through these circulating hormones, the field has resorted to a tissue-specific expression of Cre recombinase that allows targeted deletion of ESRs and AR in specific tissues that retain activity off these targeted promoters.

Deletion of ESR1 and AR in osteoprogenitor cells, osteocytes, and osteoclasts (Ucer et al., 2016) reported by Ucer et al. provides the most thorough assessment of the roles of these steroid hormone receptors in developing mice. In these reports, the authors were careful in not realizing systemic supraphysiological increases in circulating hormones by deleting these receptors in specific cell types. They utilized a Prx-Cre mouse to target the osteoprogenitor cells throughout development. Analysis of these mice using computer tomography showed a decrease in cancellous BV/TV and trabecular number, and an increase in trabecular separation, compared with C57BL6 mice that retain AR expression in these cells. The effect of orchidectomy on cancellous bone in the wild-type mice was similar to the effects of AR deletion from Prx-Cre-driven

mesenchymal progenitors in androgen-sufficient mice. Therefore, the targeted AR deletion in mesenchymal progenitors is similar to that observed with orchidectomy-induced loss in circulating androgens. Surprisingly, the authors noted an absence of cortical bone changes in these Prx-Cre-driven osteoprogenitor AR-null mice. Furthermore, removal of AR from osteoclast precursors that are reflected in the LysM Cre mice show that AR function in mouse bone is not dependent on osteoclast expression of AR. The LysM gene is specifically expressed in cells of the monocyte/macrophage lineage and their descendants as well as in neutrophils (Clausen et al., 1999).

Role of estrogen receptor alpha in bone using genetically modified mice is equivocal

ESR1 may arguably contribute to changes in both cancellous and cortical bone as described by the use of ESR1-floxed mice crossed to Dmp1-Cre, and ESR1-floxed mice crossed to OCN-Cre mice, both of which result in measurable decreases in cancellous bone (Maatta et al., 2013; Kondoh et al., 2014). In contrast to these reports, others have shown that removal of ESR1 from osteoprogenitor cells or osteocytes does not affect cancellous bone mass. These studies have crossed ESR1-floxed mice to osteoprogenitor-specific Prx1-Cre (Ucer et al., 2016) or osteoblast-expressed Col1-Cre mice (Almeida et al., 2013), and finally osteocyte-specific Dmp1-Cre mice (Windahl et al., 2013). In all these reports, the impact on regulating cancellous bone mass is not very evident for ESR1. However, cortical bone parameters are modestly dependent on ESR1, as reported in findings made by Almeida et al. (2013).

Factors that may contribute to these equivocal observations may be (1) the use of distinct Cre promoters that may vary in tissue specificity that has yet to be determined, (2) the limitations of using the Cre-Lox system, which may yield variable levels of gene deletion (Manolagas et al., 2014), and (3) phenotypes that are quite modest, so that subtle variations over time during development may affect how these results are interpreted. Collectively, one could suggest that ESR1 deletion in osteoblast lineage cells may result in reductions in both cancellous and cortical bone mass in female mice and only cancellous bone mass in male mice. However, an important caveat to all of these studies is that the receptor deletion, although cell-specific, has been present since conception. Therefore, the skeletal findings largely reflect developmental effects of these receptors rather than their exclusive role in the adult skeleton.

Gain-of-function studies using selective androgen receptor modulators in sexually mature animal models

LoF of AR in osteoprogenitor cells (Ucer et al., 2016) or since conception globally (Callewaert et al., 2009) leads to decreases in trabecular bone mass, connectivity, and cortical area as reported earlier. However, the most compelling data set explores GoF paradigms using nonsteroidal, nonaromatizable SARMs and offers the best approach to fully understand the effects of AR ligands in the mature skeleton.

Earlier reports included suggestions of robust activity in male orchidectomized rat models offered by perspective summaries described earlier (Rosen et al., 2002) but these did not provide an opportunity for detailed analysis of the preclinical datasets. However, the most compelling preclinical evidence was offered by Kearbey et al., who showed a dose-dependent gain in trabecular bone mass in female ovariectomized mature rats that were treated with a distinct aryl propionamide SARM (S-4) (Gao et al., 2005a). They showed protection from ovariectomy-induced trabecular bone loss using the S-4 SARM as measured by lumbar spine BMD. This benefit offered by the SARM was dependent on AR signaling, as observed by the reversal of this protection of spine BMD in the arm that combined the S-4 SARM along with the AR antagonist bicalutamide. In addition, they observed enhancements in cortical bone parameters, including cortical width, cortical density, and periosteal circumference at peak doses of 1.0−3.0 mg/kg-day. Collectively, this report provided compelling evidence of the osteoprotective effects of a nonsteroidal SARM that functions as an AR agonist in bone when used immediately after ovariectomy in female SD rats (Kearbey et al., 2007). To further evaluate the potential for an anabolic response, the same group reported deployment of the S-4 SARM in a delayed rat male orchidectomy model. In this model, the orchidectomy induced an expected loss in total whole-body bone mineral content and BMD over the 12-week wasting period. This change in whole-body BMC and BMD was completely recovered after 8 weeks of treatment with S-4 SARM given daily at 10 mg/kg-day. However, there were some modest reductions in osteocalcin levels, which may point to a decrease in bone turnover in these animals (Gao et al., 2005b). It was not clear whether the authors measured favorable changes in markers such as P1NP, which reflect de novo bone formation as reflected by changes in the N-terminus-modified epitopes presented in serum with the synthesis of new collagen molecules placed onto bone (Eastell et al., 2006). Therefore, while these results are encouraging, it is not definitive whether the gains in total bone mineral content and BMD are due to SARM-mediated gains in bone formation. The most compelling report that showcases the direct anabolic action of SARMs was reported by Hanada et al., who utilized a −tetrahydroquinoline derivative to generate

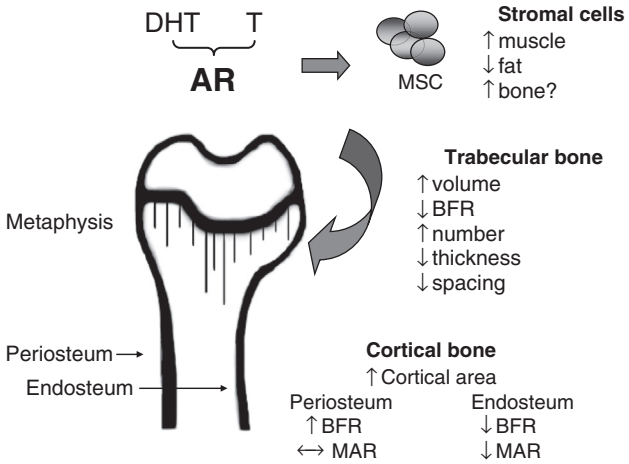

FIGURE 41.3 A summary of the expected changes in response to androgen action, at the various geometric sites associated with appendicular skeletal sites is shown.

an SARM, termed as S-40503 (Hanada et al., 2003). This molecule was shown to be very selective for AR and did not bind ESR1, ESR2, or other nuclear hormone receptors. In this report, they utilized a bilateral orchidectomized male rat that was treated with the S-40503 SARM for 4 weeks 1-day postgonadectomy. They showed increases in femoral BMD that were dose-dependent after the 4-week treatment period. To address direct anabolic action by SARM S-40503, they utilized an ovariectomized female rat model, wherein animals were allowed to lose bone mass for 4 weeks followed by 4 weeks of daily subcutaneous injections with SARM S-40503 (30 mg/kg-day), estrogen (20 μg/kg-day), or DHT (10 mg/kg-day). They measured distal femur cancellous BMD, which was most improved with estrogen followed by SARM S-40503 and DHT to a similar but qualitatively lesser extent. In contrast, they observed a robust increase in cortical BMD that was greater than intact nonovariectomized age-matched animals for both SARM S-40503 and DHT. This gain in cortical bone BMD was not apparent for the estrogen-only arm. Furthermore, they used calcein double-labeling to show direct evidence of an increased mineral apposition rate (MAR μm/day) in response to nonaromatizable DHT and SARM S-40503, which was in contrast to minimal apposition observed with estrogen (no change). Notably, the MAR observed for S-40503-treated animals was higher than for the intact nonovariectomized control, again suggesting direct anabolic action in response to this GoF paradigm using both a nonaromatizable androgen (i.e., DHT) and a nonsteroidal selective SARM, S-40503. Collectively, the use of structurally distinct nonsteroidal SARMs in preclinical models suggests a potential to directly and favorable impact bone mass in animals undergoing gonadectomy-induced bone loss (see Fig. 41.3). However, these preclinical findings have yet to translate to changes in improvements in bone mass or bone biomarkers in clinical studies exploring SARMs. This may be due to the positioning of these SARMs in diseases such as cancer cachexia and sarcopenia, which may require long-term use to determine such bone-related end points.

The muscle–bone interface and its potential impact on bone strength

Androgens in general are well known to be muscle anabolic and form the basis of numerous clinical reports on their ability to increase skeletal muscle mass (Bhasin et al., 1997). Changes in bone and muscle go hand-in-hand to affect the skeletal features of both men and women. Therefore, it is logical to expect the muscle–bone interface to provide favorable strain- or load-induced bone formation cues at these interfaces. The role played by the tendon that presents the collagen-enriched structural bridge between the muscle and bone interface is perhaps less understood for fully appreciating the impact of muscle and mobility on bone formation. The collagen fibrils, considered the fundamental force-transmitting unit of the tendon, are densely arranged within the extracellular matrix of specialized cells called tenocytes and are oriented parallel to the bone–muscle axis (Nourissat et al., 2015). Such an orientation provides a seamless transmission of the mechanical forces transduced by skeletal muscle contractions, which impinge on the enthesis within the bone–tendon interface. Evidence for such an impact was offered by Hamrick et al., who showed that gdf-8 knockout mice that had a dramatic increase in muscle weight and volume exhibited significant changes in cross-sectional area and bone mineral content in the proximal humerus and deltoid crest. These were consistent with areas closely representing sites of attachment of the muscle to the bone and further underscore the impact of muscle volume or mass on bone geometry (Hamrick et al., 2002).

Therefore, the muscle–bone relationship, expressed as the "bone–muscle unit," can be viewed as single coordinate structure that is strongly influenced by mobility-induced mechanical loading. Such differential strains imposed by increases or decreases in mechanical loading, as a result of disability or aging, can affect overall bone geometry and bone strength (Lang, 2011) (see Fig. 41.3). The close coupling between muscle and bone, and the gender differences in the relationship, are often viewed in the context of the mechanostat theory first elaborated by Frost (2000). The independent risk conferred by skeletal muscle was underscored in the Frost mechanostat review that highlighted falls as the largest "risk factor" for traumatic osteoporosis fractures, because without falls, the fractures caused by them would not occur regardless of whether some microscopic fatigue damage in bone increases the bone fragility associated with all osteopenias (Frost, 2003). However, fall risk accumulates as a result of multiple intrinsic and extrinsic risk factors such as changes in balance induced by medications or alcohol, loss in lower limb skeletal power with aging, poor vision, and a variety of environmental conditions. The independent risk factor of lower limb skeletal muscle strength and/or power was addressed by Becker et al. in the first-of-its-kind intervention on elderly weak fallers using an antimyostatin antibody (Becker et al., 2015). Results from this trial emphasized the importance of muscle power a feature of muscle strength over a fixed time period which is essential to how our body reacts to a displacement such as a fall. The intervention provided preliminary evidence that treatment with a muscle mass enhancing antibody that targets gdf-8 might improve functional measures of muscle power in elderly individuals prone to falls. Similar results have been published by Srinivas-Shankar et al., using transdermal testosterone gels for 6 months in elderly frail men with borderline low serum T levels. In this randomized controlled trial, they found that testosterone supplementation showed marked improvements in the primary outcome measure of isometric knee extension peak torque and isokinetic knee extension peak torque. Unfortunately, the study failed to measure markers of bone turnover to help inform the changes that could be affecting the muscle–bone unit. The study also did not measure the impact of testosterone gels to reduce the incidence of falls. In a separate study conducted by Bronwyn et al. in chronic glucocorticoid-treated patients, injectable testosterone esters given intramuscularly every 2 weeks for 12 months showed marked improvement in lumbar spine BMD ($+4.7\% \pm 1.1$) along with improvements in muscle strength as determined by knee flexion and extension using isokinetic dynamometry (Bronwyn et al., 2003).

Collectively, the impact of androgens on various functional parameters of skeletal muscle that impacts mobility may confer added benefit to measures of bone strength and/or geometry through the muscle–bone interface.

Future prospects for androgens and male skeletal health

The seminal findings made by Khosla et al. (1998) have provided some clarity on the importance of the ESR1–estrogen axis-mediated benefit conferred upon the male skeleton in the course of normal physiology. However, clinical interventions that address ESR1- and/or ESR2-mediated pathways to enhance skeletal health are relatively less prominent. The emergence of novel mechanisms of resistance to antagonists or inhibitors of the AR–testosterone axis as it pertains to prostate cancer (Watson et al., 2015) will naturally require better medicines that balance the benefit to the risk profiles of such agents. This will require us to be vigilant about the deleterious effects of androgen ablation as they become more prevalent and mainstream in their targeting of less severe patients suffering from PCa to help prevent the occurrence, or to add as maintenance regimens in patients undergoing remission to prevent the relapse of tumor burden. Recent advances in this approach have been seen with the development of such agents targeting distinct actions of estrogen and androgen action in breast cancer (Yu et al., 2017). Our ability to provide therapeutic options to balance cancer risk while maintaining skeletal health in these individuals would warrant more nuanced classes of agents in the future (Figs. 41.1–41.3).

SARMs offer a variety of chemical scaffolds that allow us to better design the benefit and risk profile of such interventions. However, as noted by recent reviews, the field has progressed slowly in large randomized controlled trials, querying bone-related end points as these novel agents posit risk in terms of their cardiovascular outcomes (Narayanan et al., 2018; Nique et al., 2012; Krishnan et al., 2018; Saeed et al., 2015). It is conceivable, as these agents receive prominence as they begin to discharge such risk in the clinic, that trials exploring their benefit on the muscle–bone interface will become more available for assessing the GoF paradigm with such agents. However, until such time, the use of AR ligands to better define such benefits shall remain elusive to the medical community.

References

Albright, F., 1940. Trans. Assoc. Am. Phys. 55, 298–305.
Almeida, M., et al., 2013. J. Clin. Investig. 123, 394–404.
Almeida, M., et al., 2017. Physiol. Rev. 97, 135–187.
Amory, J.K., et al., 2004. J. Clin. Endocrinol. Metab. 89 (2), 503–510.

Amory, J.K., et al., 2008. J. Urol. 179 (6), 2333–2338.
Becker, C., et al., 2015. Lancet Diabetes Endocrinol. 3, 948–957.
Bhasin, S., et al., 1997. J. Clin. Endocrinol. Metab. 82 (1), 3–8.
Bilezekian, J.P., et al., 1998. N. Engl. J. Med. 339, 599–603.
Bronwyn, A.L.C., et al., 2003. J. Clin. Endocrinol. Metab. 88 (7), 3167–3176.
Bruno, D., et al., 2018. Endocrine Connections 7, 395–402.
Bruzek, J.A., 2002. J. Phys. Anthropol. 117, 157–168.
Callewaert, F., et al., 2009. FASEB J. 23, 232–240.
Carani, C., et al., 1997. N. Engl. J. Med. 337, 91–95.
Cheung, A.S., et al., 2013. Andrology 1, 583–589.
Cho, D.-C., et al., 2017. Nat. Commun. 8 (806), 1–13.
Christiansen, B.A., et al., 2011. J. Bone Miner. Res. 26 (5), 974–983.
Clausen, B.E., et al., 1999. Transgenic Res. 8, 265–277.
Delmas, P.D., Seeman, E., 2004. Bone 34 (4), 599–604.
Eastell, R., et al., 2006. Curr. Med. Res. Opin. 22 (1), 61–66.
Finkelstein, J.S., et al., 2016. J. Clin. Investig. 126, 1114–1125.
Fonseca, H., et al., 2014. Sports Med. 4, 37–53.
Frost, H.M., 2000. Med. Sci. Sports Exerc. 32 (5), 911–917.
Frost, H., 2003. Anat. Rec. A 275A, 1081–1101.
Gao, W., et al., 2005a. Chem. Rev. 105, 3352–3370.
Gao, W., et al., 2005b. Endocrinology 146 (11), 4887–4897.
Gomberg, B.R., et al., 2000. IEEE Trans. Med. Imaging 19, 166.
Hamrick, M.W., et al., 2002. Calcif. Tissue Int. 71, 63–68.
Hanada, K., et al., 2003. Biol. Pharm. Bull. 26 (11), 1563–1569.
Kanis, J.A., 2007. Assessment of Osteoporosis at the Primary Health-Care Level. WHO Collaborating Centre, University of Sheffield, Sheffield, UK.
Katznelson, L., et al., 1996. J. Clin. Endocrinol. Metab. 81, 4358–4365.
Kearbey, J.D., et al., 2007. Pharm. Res. (N. Y.) 24 (2), 328–335.
Kenny, A.,M., et al., 2001. J. Gerontol. A Biol. Sci. Med. Sci. 56 (5), 266–272.
Khosla, S., et al., 1998. J. Clin. Endocrinol. Metab. 83, 2266–2274.
Khosla, S., et al., 2015. J. Bone Miner. Res. 30, 1134–1137.
Kondoh, S., et al., 2014. Bone 60, 68–77.
Krishnan, V., et al., March 2018. Andrology (12).
Lambert, J.K., et al., 2011. Curr. Osteoporos. Rep. 9 (4), 229–236.
Lang, T.F., 2011. J. Osteoporos. 2011, 702735. https://doi.org/10.4061/2011/702735.
Lee, K., et al., 2003. Nature 424, 389.
Leifke, E., et al., 1998. Eur. J. Endocrinol. 138, 51–58.
Maatta, J.A., et al., 2013. FASEB J. 27, 478–488.
Manolagas, S.C., et al., 2014. J. Bone Miner. Res. 29, 2131–2140.
Matsumoto, A.M., et al., 2002. J. Urol. 167 (5), 2105–2108.
Mosekilde, L., et al., 1990. Bone 11 (2), 67–73.
Narayanan, R., et al., 2018. Mol. Cell. Endocrinol. 465, 134–140.
Nilsson, S., et al., 2001. Physiol. Rev. 81, 1535–1565.
Nique, F., et al., 2012. J. Med. Chem. 55, 8225–8235.
Nourissat, G., et al., 2015. Nat. Rev. Rheumatol. 11, 223–233.
Orwoll, E.S., et al., 2003. J. Bone Miner. Res. 18 (1), 9–17.
Prostate Cancer Prostatic Dis. 5, 2002, 304–310.
Recker, R.R., 1993. Calcif. Tissue Int. 53 (1), 139–142.
Rosen, J., et al., 2002. J. Musculoskelet. Neuronal Interact. 2 (3), 222–224.
Saeed, A., et al., December 2015. J. Med. Chem. 59 (2).
Sarkar, S., et al., 2002. J. Bone Miner. Res. 17 (1), 1–10.
Seeman, E., 1993. Am. J. Med. 95 (5), 22–28.
Selby, P.L., et al., 2000. Osteoporos. Int. 11 (2), 153–157.
Simental, J.A., et al., 1991. J. Biol. Chem. 266 (1), 510–518.
Sims, N.A., et al., 2002. Bone 30, 18–25.
Smith, E.P., et al., 1994. N. Engl. J. Med. 331, 1056–1061.
Smith, M.R., et al., 2004. J. Clin. Endocrinol. Metab. 89 (8), 3841–3846.
Snyder, P.J., et al., 1999. J. Clin. Endocrinol. Metab. 84 (6), 1966–1972.
Snyder, P.J., et al., 2014. Clin. Trials 11, 362–375.

Snyder, P.J., et al., 2016. N. Engl. J. Med. 374, 611–624.
Sobel, V., et al., 2006. J. Clin. Endocrinol. Metab. 91 (8), 3017–3023.
Stepan, J.J., et al., 1989. J. Clin. Endocrinol. Metab. 69, 523–527.
Szulc, P., et al., 2006. Bone 38 (4), 595–602.
Tenover, J.S., 1992. J. Clin. Endocrinol. Metab. 75 (4), 1092–1098.
Tsai, M., O'Malley, B.W., 1994. Annu. Rev. Biochem. 63 (1), 451–486.
Ucer, S., et al., 2016. J. Bone Miner. Res. 32, 560–574.
Vanderschueren, D., et al., 1997. Endocrinology 138, 2301–2307.
Watson, P.A., et al., 2015. Nat. Rev. Canc. 15 (12), 701–711.
Windahl, S.H., et al., 2013. Proc. Natl. Acad. Sci. U.S.A. 110, 2294–2299.
Yu, Z., et al., 2017. Clin. Cancer Res. 23 (24), 7608–7620.

Chapter 42

Growth hormone, insulin-like growth factors, and IGF binding proteins

Clifford J. Rosen[1] **and Shoshana Yakar**[2]

[1]Maine Medical Center Research Institute, Scarborough, ME, United States; [2]David B. Kriser Dental Center, Department of Basic Science and Craniofacial Biology, New York University College of Dentistry New York, New York, NY, United States

Chapter outline

Introduction

I has been 60 years since Salmon and Daughaday first reported the presence of a soluble factor induced by growth hormone (GH) that had insulin-like properties and mediated somatic growth. The subsequent identification of insulin-like growth factors (IGFs) has led to remarkable discoveries and therapeutic advances, particularly in relation to the skeleton. IGFs are 7 kDa peptides that are ubiquitous in nature and regulate cellular proliferation, differentiation, and death (Daughaday et al., 1972). The liver is the main source of circulating IGF-I; fat contributes about 10% and muscle about 5%. Although bone is a very minor contributor to circulating IGFs, it is one of the richest IGF tissues relative to the composition of other peptides

Principles of Bone Biology. https://doi.org/10.1016/B978-0-12-814841-9.00042-7

and growth factors (Finkelman et al., 1990). "Local"/bone tissue IGF pools play a predominant role in skeletal modeling and acquisition. IGFs are also highly conserved across species; hence, the physiology of these peptides can be studied in numerous animal models. Although GH has been recognized as the major determinant of liver-derived IGF-I, the balance between skeletal and serum IGF-I has also been clarified, particularly with the relatively recent introduction of targeted genomic engineering.

The importance of the GH/IGF system in aging has undergone intense scrutiny in the last 3 decades. Biological aging is a normal physiological process, part of the continuum from growth to death. Like other organ systems, skeletal homeostasis is maximized during the second and third decades of life, and IGFs are essential for that process. However, trabecular bone loss also begins by the third decade even though the mechanism is not clear. The hypothalamic–pituitary axis is profoundly affected by aging. GH secretion is reduced, resulting in lower levels of circulating IGF-I and IGF-II but higher levels of IGF binding proteins (IGFBPs) 1, 2, and 4 (Kelijman, 1991; Rudman et al., 1981). Early attempts to link age-related bone loss to a suppressed GH-IGF-I axis, or enhanced IGFBP expression, spawned considerable interest in GH and/or IGF-I as therapeutic tools for osteoporosis and sarcopenia. The advent of recombinant gene technology propelled synthetic growth factors into an ever-expanding therapeutic domain, particularly in regard to short stature. Another therapeutic venue for GH has been in its potential utility for the frail elderly. The paradigm that a "somatopause," or GH deficiency state with aging, produces discrete musculoskeletal changes, has never been firmly defined, nor has it been determined whether these changes can be reversed with GH. On the other hand, GH is indicated for individuals with pituitary insufficiency, and long-term studies suggest a major benefit for GH treatment in respect to bone mineral density (BMD) and quality of life. Regardless, more attention has focused on understanding the IGF regulatory system (i.e., IGFs, IGFBPs, Type I and II IGFRs, and proteases that cleave IGFBPs) in relation to bone acquisition and maintenance (Rudman et al., 1990). In this chapter, we will review the cellular and systemic actions of IGFs in order to more fully understand the functional integration of IGF regulatory components with other skeletal and systemic factors. As such, a thorough overview of the physiology of the IGF system, from GH to receptor signaling, is warranted.

Physiology of the GH/IGF/IGFBP system

Growth hormone releasing hormone

In order to appreciate the complexity and redundancy inherent in the IGF regulatory system in bone, an overview of the physiologic aspects of IGF-I regulation is required. Although IGF-I is regulated by genetic, nutritional, hormonal (insulin and thyroxine), and environmental factors, GH is the major regulator of IGF-I expression in tissues and dominates IGF-I

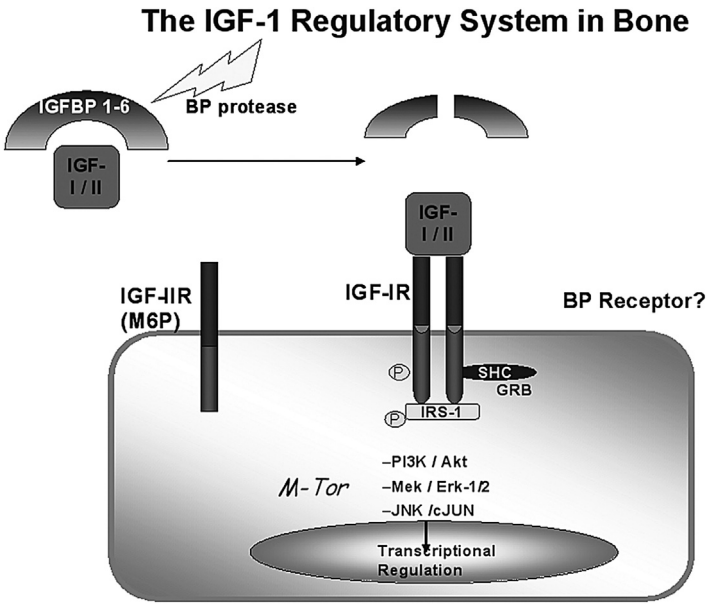

FIGURE 42.1 IGF-I is an endocrine and paracrine/autocrine growth factor. It is regulated by GH via hypothalamic GHRH. The primary source of circulating IGF-I is liver, although bone is a very rich source of IGF-I and IGF-II. Target tissues for IGF endocrine action include fat, muscle, and bone. IGF binding proteins (IGFBPs) circulate in excess of IGFs, but there is a ternary circulating IGF complex that includes the acid labile subunit (ALS) and IGFBP-3. GHBP is a growth hormone binding protein, a circulating GH receptor. The balance between circulating and skeletal IGF-I during growth and maintenance determines the overall effect of this peptide on bone.

levels in the circulation (Fig. 42.1). That process begins in the hypothalamus and ends at the tissue level. The regulation of GH secretion from the pituitary is complex and involves elaboration of discrete neurosecretory peptides from the hypothalamus. Growth hormone releasing hormone (GHRH) is a hypothalamic hormone essential for normal expansion of the somatotrope lineage during pituitary development (Frohman and Kineman, 2002). GHRH, via binding to GHRH receptor (GHRHR), acts on somatotropes to increase GH biosynthesis and secretion and is thought to cause somatotroph proliferation (Petersenn and Schulte, 2000). Release of GHRH is episodic, which accounts for the pulsatile release of GH from the pituitary. A decrease in GHRH is associated with somatotrope hypoplasia, whereas an increase in GHRH is associated with somatotrope hyperplasia (Frohman et al., 2000). Indeed, overexpression of human GHRH (hGHRH) (Mayo et al., 1998) in mice caused increased body size and skeletal gigantism. Excess in hGHRH led to systemic stimulation of endogenous GH and IGF-I, which in turn caused initial increase in bone mass (Tseng and Goldstein, 1998). However, with age, excess GH levels were associated with increases in bone resorption, thinning of the bone cortexes, and compromised mechanical properties. In contrast, a mutation in the mouse GHRH gene (lit/lit) resulted in growth retardation, where mice reached ~50%–60% of normal adult body size (Kasukawa et al., 2000). The blunted GHRH secretion inhibited GH release and IGF-I production in liver and other tissues, leading to significant decreases in BMD and reduced radial bone growth (periosteal circumference) (Kasukawa et al., 2000).

Growth hormone releasing hormone receptor

GHRHR is a G-protein-coupled receptor with seven hydrophobic transmembrane domains. The human GHRHR gene spans 15 kb and comprises 13 exons. The open reading frame was shown to extend 1269 bp and encode a protein of 423 amino acids with a predicted molecular weight of 47-kDa. After release from the hypothalamus, GHRH binds to the GHRHR predominantly located on the pituitary somatotrope (Lin-Su and Wajnrajch, 2002). GHRHR activation leads to the opening of a sodium channel in the somatotrope, which causes its depolarization. The resultant change in the intracellular voltage in turn opens a voltage-gated calcium channel, allowing for calcium influx, which directly causes the release of premade GH stored in secretory granules (Petersenn et al., 2000). The cAMP elevation stimulates protein kinase A, which phosphorylates and activates the transcription factor cAMP response element binding protein, which then stimulates de novo GH production (Petersenn et al., 2000; Muller et al., 1999; Mayo et al., 1995). Autosomal recessive mutations in the GHRHR can result in near total absence of GH and lead to short stature in humans as well as the little phenotype in mice with very low bone mass and reduced fat (Rosen and Donahue, 1998).

Somatostatin

Somatostatin (SMS) is a small (14-amino-acid) but ubiquitous polypeptide that inhibits GH synthesis and release. In concert with GHRH, SMS regulates GH secretion through a dual control system—one stimulatory, the other inhibitory. Several molecular forms of somatostatin, distinct from the native 14-amino-acid peptide, have been isolated. In addition to inhibition of GH release, SMS also inhibits secretion of thyrotropin as well as several pancreatic hormones, including glucagon and insulin. The SMS receptor has been localized to various cell types, especially those of neuroendocrine origin. Localization of this receptor suggests that SMS acts as an endocrine and a paracrine regulator in diverse tissues. A highly potent synthetic analog of SMS, octreotide, has been used therapeutically in acromegaly and diagnostically (in a radiolabeled form) for scintigraphic visualization of neuroendocrine tumors.

Growth hormone

Mechanism of growth hormone secretion

GH and its receptor belong to the cytokine superfamily of receptors and ligands. GH is an anabolic polypeptide hormone produced by the somatotropes of the anterior pituitary gland. GH is secreted under the influence of three hypothalamic hormones: (1) GHRH, which acts via the GHRHR; (2) GHS (also known as Ghrelin), which acts through the GHS receptor; and (3) somatostatin, SMS, which acts on the pituitary to suppress basal and stimulated GH secretion but is not believed to affect GH synthesis (Petersen et al., 2000; Lin-Su et al., 2002). GH secretion is pulsatile (due to the episodic release of GHRH) and circadian with the highest pulse amplitude occurring between 02:00 and 06:00 (Ho and Weissberger, 1990). Puberty has a dramatic effect on the amplitude of GH pulses due to changes in the hypothalamic milieu as a result of rising sex steroid concentrations (Jansson et al., 1985). Through binding directly to growth hormone receptor (GHR), GH has profound effects not only on somatic and bone growth but also on carbohydrate and lipid

homeostasis. GH antagonizes insulin action in muscle and fat. It activates lipase in adipose tissue and leads to mobilization of fatty acids from the adipose tissue (Liu et al., 2004; Heffernan et al., 2001). In liver, GH inhibits de novo lipid synthesis (Liu et al., 2016a,b,c).

Deletion of the GHR gene in mice (GHRKO) results in a 50%−60% reduction in body size associated with low serum and tissue IGF-I levels (Liu et al., 2004). Linear skeletal growth of GHRKO mice is severely inhibited and associated with premature growth plate contraction and reduced chondrocyte proliferation. Long bones of GHRKO mice show reductions in trabecular bone volume and all cortical bone traits (Sjogren et al., 2000). Likewise, bone turnover in the GHRKO mice severely reduced and periosteal bone apposition prematurely ceased. Gene inactivation of the GHR mediator, STAT5ab, in mice resulted in a 50% decrease in serum IGF-I levels, reduced linear growth due to abnormalities in the growth plate, and decreased cortical bone area and width.

Effects of gonadal status on the GH−IGF-I axis

Not surprisingly, the pattern of GH secretion in animals and humans depends highly on age and sex (Ho and Weissberger, 1990; Jansson et al., 1985). Both factors strongly influence the frequency and amplitude of GH pulses, which in turn determines GH basal secretory rates, and the levels of serum IGF-I. Characteristic changes during puberty in rats parallel pubertal changes in humans (Jansson et al., 1985). GH secretion in male and female rats is identical after birth but at puberty, a sexually differentiated pattern of secretion appears with male rats displaying high-amplitude, low-frequency pulses, and with female rats displaying pulses of high frequency but low amplitude (Jansson et al., 1985). In humans, sexual differences in GH secretion during puberty are less pronounced, even though administration of gonadal steroids to prepubertal children increases GH pulses and mimics the pubertal milieu of the hypothalamus. Various sampling techniques (profiles vs. stimulatory tests) and assays with different sensitivities have produced disparate findings. However, spontaneous and stimulated GH peaks in humans are enhanced during puberty. Matched for age and body mass index, young girls were found to have higher integrated GH concentrations than boys (Ho and Weissberger, 1990). Other secretory characteristics, including pulse amplitude, frequency, and the fraction of GH secreted as pulses were similar in both sexes of the same age. In one study, black adolescents (males and females) had higher GH secretory rates than age-matched white adolescents (Wright et al., 1995). Higher GH secretion rates in adolescent blacks could lead to a greater acquisition of bone mass.

Clinical and animal studies have shown that sex steroids can modulate GH secretion at the level of the pituitary, as well as GH's action in target tissues such as liver and bone (Meinhardt et al., 2006). GH levels correlate positively with estrogen and estrogen replacement therapy in postmenopausal women independent of serum IGF-I levels (Norman et al., 2013). Mean pulse amplitudes of GH are lower in older women than in premenopausal women. GH secretory indices in postmenopausal women correlate with serum estradiol but not with total serum androgen levels. During menopause, GH secretion is reduced (Ho and Weissberger, 1990). However, oral administration of estradiol (or conjugated equine estrogens) increases GH secretion as a result of reduced hepatic generation of IGF-I (Ho and Weissberger, 1990; Dawson-Hughes et al., 1986). On the other hand, transdermal administration of 17− estradiol increases serum IGF-I concentration, suggesting that suppression of IGF-I by oral estrogens is due to a "first-pass" hepatic effect. Impaired IGF-I generation in the liver removes a key component of negative feedback on the hypothalamus, resulting in increased GH release.

Effects of the GH/IGF-I/IGFBP system on the aging skeleton

GH exerts a multitude of biological effects on various tissues through the GHR. Regulation of GH bioactivity occurs at several pre- and postreceptor levels. Growth hormone binding protein (GHBP) is a plasma binding protein identical to the extracellular domain of the tissue GHR. GHBP binds exclusively to GH, and most if not all serum GH is bound to this carrier protein. Measurements of GHBP in serum are relatively stable and reflect the endogenous status of the GHR in responsive tissues (Baumann et al., 1989). With advanced age, GHBP concentrations increase substantially.

The GH-IGF-I axis undergoes changes over a life span so that elders have lower spontaneous GH secretion rates and serum IGF-I levels than in younger people (Kelijman, 1991; Rudman et al., 1981; Donahue et al., 1990). Most of these age-related differences are a function of an altered hypothalamic−pituitary set point due in part to changes in lifestyle and nutrition. The GH secretory responses to common stimuli, such as GHRH, clonidine, L-dopa, physostigmine, pyridostigmine, hypoglycemia, and met-enkephalin, but not arginine, reduced with aging. Somatotrope responsiveness to GHRH and arginine does not vary with age, implying that the maximal secretory capacity of somatotropic cells is preserved in elderly people (Corpas et al., 1993).

Age-dependent declines in GH/IGF-I signals have been causally linked to frailty in respect to musculoskeletal function. However, large cross-sectional studies have demonstrated only a weak association between diminished serum IGF-I and age-related bone loss, or between serum IGF-I and BMD (Rudman et al., 1981; Nicolas et al., 1994; Donahue et al., 1990; Corpas et al., 1993; Langlois et al., 1998). In one large cohort study, the lowest serum IGF-I quartile was associated with a significantly greater risk of hip fractures (Garnero et al., 2000). On the other hand, skeletal concentrations of IGF-I, IGF-II, and IGFBP-5 in femoral cortical and trabecular bone decline significantly with age, and these have been associated with low BMD (Rudman et al., 1981; Nicolas et al., 1994; Donahue et al., 1990; Corpas et al., 1993; Langlois et al., 1998). In contrast to the multitude of studies linking serum IGF-I to age-related frailty and muscle performance, differences in GH secretion are difficult to determine due to its normal pulsatility. There is one study in older postmenopausal women relating changes in 24-hour GH levels with BMD (Dennison et al., 2003), and a recent large and prospective study showed that GH replacement therapy in postmenopausal women had positive dose-dependent effects on BMD and sustained effects on reducing patient fracture risk, even 7 years after the GH treatment ceased (Krantz et al., 2015). Lastly, a clinical trial performed in which GH treatment was given to elderly patients with hip fractures and resulted in some positive outcomes (Yeo et al., 2003). Overall, clinical data suggest distinct and overlapping effects of the GH/IGF-I axis on the aging skeleton.

The IGF regulatory system and its relationship to the skeleton

IGF-I, IGF−II, IGFBPs, and IGF receptors

The IGFs are single-chain polypeptides. IGF-I consists of 70 amino-acid residues, and IGF-II has 67 amino acids (Fig. 42.2). They have B, C, and A domains similar to proinsulin as well as a D domain that is not found in proinsulin. This D domain may sterically hinder the interaction of IGFs with the insulin receptor (IR), leading to only weak ligand binding of IGFs to the IR. A number of posttranscriptional and posttranslational variants of IGFs have also been described (Slootweg et al., 1990). These IGFs have variable affinities for IGFBPs and IGF receptors (IGFRs). In vitro, these growth factors may have significantly greater activity than that of native IGF-I or IGF-II, especially those that exhibit weak binding to IGFBPs.

IGF-I and IGF-II differ in their abilities to promote tissue growth due in part to the presence of two distinct IGFRs, IGF-IR and IGF-IIR (Le Roith et al., 1997) (see Fig. 42.1). IGF-IR is a tetramer consisting of two identical extracellular

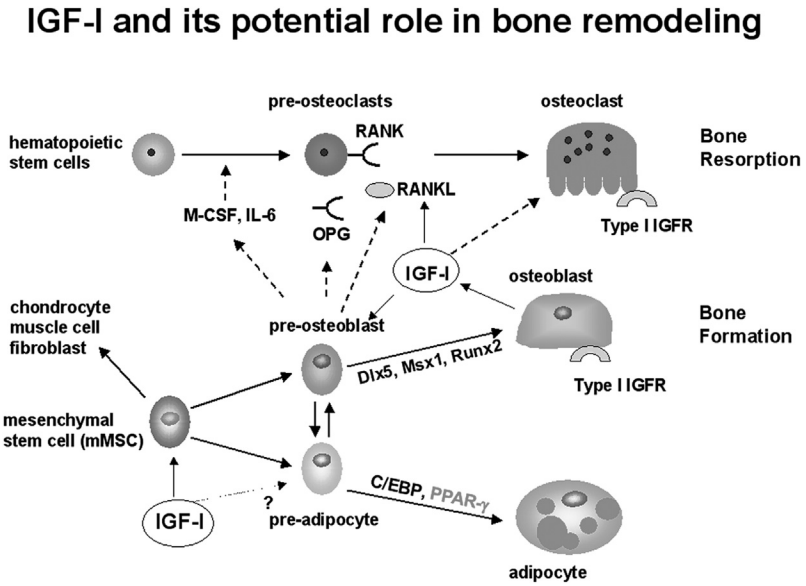

FIGURE 42.2 The IGF regulatory system contributes to bone formation through activation of the IGF type I receptor on osteoblasts. Downstream signaling is via three pathways: 1—PI3 kinase/Akt/mTor, 2—MAP kinase/ERK, and 3—JNK/Jun. PI3K/mTor regulates cell differentiation, while MAP/ERK and JNK/Jun impact cell growth. IGFBPs carry IGFs to the receptor; several proteases can cleave IGFs for binding to the type I receptor. The type II IGF receptor can bind IGF-II and generally is a clearance mechanism for IGF-II; it serves also as a mannose 6 phosphate binding site. Finally, IGFBP receptors have been theorized as possible IGF-independent signaling factors, but none have been proven. However, it is likely that IGFBPs could bind to other receptors (e.g., EGF) and affect cell growth and differentiation.

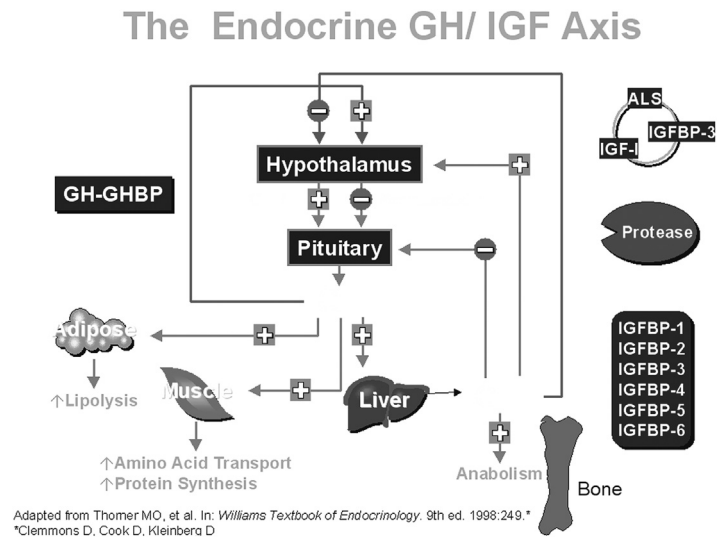

FIGURE 42.3 IGF-I serves as both a mitogen, albeit weak, and a differentiation factor for marrow stromal cells as they enter the osteoblast lineage. In addition, IGF-I can enhance osteoclast differentiation by stimulating RANKL production from stromal cells. There may be a direct effect of IGF-I on osteoclasts, because these cells express the type IGF-1 receptor and signal through IRS-2. IGF-I can also enhance adipocyte differentiation, and its role in promoting marrow adipogenesis is an area of recent investigations. Overall, IGF-I represents a coupling factor for bone remodeling.

αsubunits (conferring ligand-binding specificity) and two identical transmembrane β-subunits (possessing tyrosine kinase activity). IGF-IR resembles the IR and shares amino acid sequence homology (Zeslawski et al., 2001). IGF-II and insulin also bind to IGF-IR but with 2-fold or 15-fold to 1000-fold lower affinities, respectively (D'Ercole, 1996). It has an intrinsic tyrosine kinase activity critical for specific second message generation and indeed, ligand binding to the extracellular domain of IGF-IR results in autophosphorylation and tyrosine phosphorylation of IGF-IR substrates (Fig. 42.2). Tyrosine-phosphorylated insulin-receptor substrate-1 (IRS-1) and SHC bind different effector proteins involved in interconnecting pathways, including Ras/Raf-1/mitogen-activated protein kinase (MAPK, also known as extracellular signal-regulated kinase, or ERK) and phosphatidylinositol 3-kinase (PI3K)/phosphoinositide-dependent kinase-1 (PDK-1)/Akt (Maroni et al., 2004). Activation of the Ras/Raf-1/MAPK pathway is considered critical for cell proliferation, whereas the PI3K/PDK-1/Akt pathway is considered important for cell survival. The protein encoded by the phosphatase and tensin homologue gene deleted on chromosome 10 (PTEN) is a lipid phosphatase that decreases the activation of Akt by dephosphorylating phosphatidylinositol-3,4,5-triphosphate and phosphatidylinositol-3,4-biphosphate. Therefore, PTEN acts as an "off" switch for the PI3K/PDK-1/Akt pathway as well being a tumor suppressor. This tumor-suppressor gene is deleted or mutated in various types of human cancers (Zhao et al., 2004; Sansal and Sellers, 2004). On the other hand, the monomeric IGF type II receptor (IGF-IIR) does not bind insulin but does bind IGF-II, with a 500-fold increased affinity compared with IGF-I (Khandwala et al., 2000).

IGF-IIR exhibits no intrinsic kinase activity but is structurally very similar to the mannose 6-phosphate receptor, which is involved in targeting lysosomal enzymes intracellularly (Le Roith et al., 1997; Sell et al., 1995). Interestingly, it is now clear that in most tissues, except the hepatocytes in the liver, there are hybrid IGF-IR/IR receptors leading to significant cross-utilization between two rather distinct peptides. Hybrid receptors may also explain the growth-promoting activity of insulin, even in skeletal tissue, as well as the hypoglycemic effects of recombinant human IGF-I (rhIGF-I) when administered parenterally. However, there are little data on expression of hybrid receptors in bone.

IGFs stimulate cell proliferation and in some cases late differentiation. However, adequate nutrition is required for the full expression of IGF biologic activity in most tissues, particularly for linear growth. For example, during states of malnutrition, GH production increases but hepatic IGF-I generation is severely impaired. Resistance at the hepatic GHR reduces serum IGF-I and impairs GH bioactivity. The mechanism surrounding these nutrient-sensitive changes has not been clarified, although message stability is clearly reduced by undernutrition. For malnourished children, the result is cessation of linear growth. GH resistance, to lesser degrees, occurs in other conditions such as diabetes mellitus, acute catabolic stresses, and renal insufficiency.

IGFs are produced in virtually every tissue (Rosen et al., 1994). However, with new methods for conditional deletions of IGF-I in various tissues, it is clear that the main source of circulating IGF-I (>75%) is the liver. Other sources include

muscle and adipose tissue (Rosen et al., 1994; Mohan and Baylink, 1990). Together these three sites contribute more than 95% to the circulating IGF-I pool. With acute or chronic hepatic insufficiency, both serum IGF-I and IGF-II levels are decreased, and particularly in hepatic osteodystrophy bone formation, and cortical bone mass is impaired due to the low levels of circulating IGF-I (Liu et al., 2017).

In the circulation, IGFs are bound to six identified IGFBPs with a relatively small but detectable amount of "free" IGF-I, which also circulates but has a very short half-life. GH treatment increases total and free IGF-I levels in a dose-dependent manner. However, rhIGF-I increases "free" IGF-I considerably more than rhGH, likely due to inhibition of GH secretion and the GH-dependent production of the acid labile subunit (ALS) and IGFBP-3, the main carriers of IGF-I in serum. The clinical significance of increases in "free" IGF-I versus that bound to IGFBPs is still not clear. IGF-II also circulates in large concentrations bound to IGFBPs, and a small proportion is free. It generally is produced in much greater amounts during prenatal periods. Absence of IGF-II from genetic deletion in the embryo leads to transient but reversible growth retardation in the first 3 weeks of life that is restored by the secondary increases in endogenous IGF-I (Uchimura et al., 2017). In humans in contrast to mice, there is more circulating IGF-II than IGF-I, and this is true for the skeletal composition of IGFs.

The distribution of IGFs in the serum pool is determined by the relative saturation of IGFBPs. This may explain why treatment with IGF-I may have different tissue effects than treatment with GH. Infusions of IGF-I produce a transient rise in free IGF-I and the suppression of IGF-II, insulin, and endogenous GH (Ebeling et al., 1993). During the course of an IGF-I infusion, however, IGF-I is partitioned into several pools. This is due to the unsaturated nature of the lower molecular weight IGFBPs, and the presence of a large (150-kDa) circulating ternary IGF-binding complex. This complex, composed of IGF-I (or II), IGFBP-3 (or IGFBP-5), and an ALS, is the major circulatory reservoir for both IGFs. Normally, the majority of circulating IGF is bound to this saturated intravascular complex. However, with rapid IGF-I infusions, some IGF-I goes into the lower (50-kDa) unsaturated IGFBP fractions where transport into the extravascular space is possible. Partitioning of IGFs into various binding pools is critical to the biologic activity of GH and IGF-I.

Insulin-like growth factor binding proteins

In the circulation and in all tissues, there are six IGFBPs. IGFBPs 1−6 belong to the same gene family, and several features distinguish these known IGFBPs from one other (Rajaram et al., 1997) (Fig. 42.1). Just as IGFBPs serve important regulatory functions within the circulation, their role at the tissue level is also critical for the full biologic expression of IGFs. Binding of IGFBPs to IGFs normally blocks the interaction between IGFs and IGF-IR and consequently suppresses IGF actions (Kelley et al., 1996; Collett-Solberg and Cohen, 1996). Nevertheless, binding of IGFBPs to IGFs can also protect IGFs from proteolytic degradation and consequently enhances IGF actions by augmenting their bioavailability in local tissues (Kelley et al., 1996; Collett-Solberg and Cohen, 1996). Therefore, most IGFBPs function in a bipotential manner, and their impacts on IGFs depend to a large extent on the posttranslational modification of IGFBPs by phosphorylation and proteolysis (Kelley et al., 1996; Collett-Solberg and Cohen, 1996; Coverley and Baxter, 1997; Claussen et al., 1997). Some IGFBPs (IGFBP-3 and IGFBP-5) exhibit IGF-independent or partially independent effects (Kelley et al., 1996; Mohan et al., 1996, Xi et al., 2016).

The predominant binding protein in serum (and bone) is IGFBP-3, a 43-kDa glycosylated peptide. It is present in large concentrations in the serum and is easily measurable by radioimmunoassay (RIA). As noted earlier, IGFBP-3 is part of a larger saturated ternary complex including IGF-I (or II) and an 80-kDa ALS. The association of these three proteins requires the presence of either IGF-I or IGF-II. In turn, this complex prolongs the half-life of IGFs and provides a unique storage site. The levels of circulating IGFBP-3 are principally controlled by GH (Martin and Baxter, 1988). However, IGFBP-3 synthesis outside the liver is regulated by other endocrine and paracrine factors. At a cellular level, IGFBP-3 has stimulatory and inhibitory effects on IGF-I depending on the cell type and the physiologic milieu. IGFBP-3 action at the cell is characterized by its interaction with IGF-I or −II. In vitro, coincubation of IGFBP-3 with IGF-I can block IGF access to IGF-IR (Rosen et al., 1994; Conover, 1991). Conversely, preincubation of IGFBP-3 in certain cell systems facilitates receptor binding of the ligand by attaching to the cell membrane at a site remote from the receptor. In addition, IGFBP-3 may have IGF-independent actions on cell action. Although a putative IGFBP-3 receptor has not been cloned, IGFBP-3 has been shown to downregulate cell proliferation in certain cell lines and to enhance p53 production. Further regulation of IGF-I by IGFBP-3 can occur in the extracellular space if IGFBP-3 undergoes proteolysis. Enzymatic degradation of IGFBP-3 produces low-molecular-weight IGFBP-3 fragments that differ in their affinities for IGFs (Cohen et al., 1992; Mohan, 1993). There are numerous nonspecific IGFBP-3 proteases, which are produced by various cell types, that can be found in the intra- and extravascular space and are regulated by endocrine and paracrine factors. Prostate-

specific antigen (PSA) is a serine protease that cleaves IGFBP-3 and may be important in defining skeletal metastases with prostate cancer (Nunn et al., 1997).

IGFBPs 1−6 are also found in the circulation and may play both systemic and local roles in the regulation of IGF bioactivity at the tissue level. In contrast to IGFBP-3, these IGFBPs are not fully saturated, and they easily translocate from the circulation into the extracellular space. IGFBP-1 is a 30-kDa peptide produced primarily in the liver. Serum IGFBP-1 levels correlate inversely with circulating insulin, and in poorly controlled insulin-dependent diabetes mellitus (IDDM), serum IGFBP-1 levels are quite high (Brismar et al., 1988). Hepatic IGFBP-1 production is tightly regulated by insulin and substrate availability. However, unsaturated IGFBP-1 could also serve as a reservoir of binding activity for unbound IGF or as the initial binding site for cell-secreted IGF prior to transfer to the more stable GH-dependent 150-kDa complex. Shifts in the levels of IGFBP-1 may alter the distribution of IGFs among other IGFBPs and thus affect the relative distribution of IGFs between the intra- and extravascular space. This mechanism could be critical in controlling metabolic and mitogenic activities of IGFs (Arany et al., 1994). Indeed, mice overexpressing the hIGFBP-1 in hepatocytes (under the a1 antitrypsin promoter) show severe growth retardation (decreased linear growth) with mineralization defects and reduced BMD effects (Ben Lagha et al., 2006) that were likely mediated by sequestering IGF-I. Similarly, in vitro studies have shown that IGFBP-1 is synthesized by osteoblast and could inhibit IGF actions in bone during states of high IGFBP-1 production, such as starvation, and IDDM. In addition, Wang et al. have demonstrated that endocrine IGFBP-1 from the liver can regulate osteoclastogenesis and mediate the bone resorbing actions of fibroblast growth factor-21 (Wang et al., 2015).

Human IGFBP-2 is a 31-kDa protein that preferentially binds to IGF-II (Christiansen et al., 1991). It is found in high concentrations prenatally, and it is the major IGFBP in cerebrospinal fluid. IGFBP-2 is produced by most cells, but based on tissue-specific conditional genetic deletions, most circulating IGFBP-2 arises from the liver (DeMambro—personal communication). Insulin and dexamethasone have been shown to decrease the production of IGFBP-2 in rat osteoblasts (Schmid et al., 1992). Excess rhIGFBP-2 inhibits IGF-I−stimulated bone cell proliferation, bone collagen synthesis, and bone formation. Skeletal concentrations of IGFBP-2 are not nearly as high as the levels of IGFBPs 3−5. Interestingly, IGFBP-2 concentrations increase in puberty, with GH deficiency (GHD), and with malnutrition, as well as during aging. These changes are likely associated with circulating levels of GH and also IGF-I. Khosla et al. (1998) reported that pro-IGF-II coupled to IGFBP-2 is present in the circulation of patients with osteosclerosis due to hepatitis C infections, suggesting that IGFBP-2 may have a permissive role in enhancing skeletal turnover and in binding, through its heparin-binding domain, to extracellular matrices. In addition, animal studies using IGF-II and IGFBP-2 in a complex have demonstrated that this combination can prevent disuse- and ovariectomy-induced bone loss (Conover et al., 2002). Further support for that tenet comes from studies in the IGFBP-2-null mouse that have shown very low bone mass, particularly in males (Demambro, 2010). Importantly, Clemmons and colleagues reported that in appropriate concentrations, IGFBP-2 synergizes with IGF-I by binding to its own extracellular receptor RPTPb that inhibits PTEN activity and thereby enhances AKT-signaling from IGF-I (Xi et al., 2016). A small recombinant IGFBP-2 peptide fragment (HBD1) has also been shown to stimulate bone formation when pegylated and administered intermittently (Kawai et al., 2011).

IGFBP-4 is a glycosylated 24-kDa-binding protein. It is one IGFBP that is consistently inhibitory for IGFs in numerous cell systems. It was originally isolated from skeletal tissue and was found to inhibit IGF-mediated bone cell proliferation (Mohan et al., 1989b; Scharla et al., 1993). IGFBP-4 may serve as a reservoir for IGF-I and IGF-II in bone, and the relative proportions of IGF-I and IGFBP-4 are critical to define its function. Targeted overexpression of IGFBP-4 in osteoblasts under the osteocalcin promoter results in impaired overall postnatal skeletal growth, and reduced bone formation indices, likely via sequestration of IGF-I by IGFBP-4 and consequent impairment of IGF-I action in skeletal tissue (Zhang et al., 2003). The expression of IGFBP-4 in bone cells is regulated by cyclic adenosine monophosphate (AMP), parathyroid hormone (PTH), and 1,25-dihydroxyvitamin D. In addition, IGF-I stimulates IGFBP-4 proteolysis through the target enzyme, pregnancy-associated plasma protein-A (PAPP-A), thereby providing an autocrine/paracrine loop between the ligand and its binding protein (Durham et al., 1994). PAPP-A−deficient mice show growth retardation phenotype with reduced body size and low bone mass, suggesting a complex role for this autocrine−paracrine loop, particularly in the skeleton. Earlier studies showed that circulating IGFBP-4 was linked to hip fracture risk, although later studies have not validated this binding protein as a risk marker (Rosen et al. (1992). It is clear that there is an age-related increase in this binding protein, and in one case, a relatively strong correlation between PTH and IGFBP-4 (Honda et al., 1996)(Karasik et al., 2003).

More recently, it has been shown that global deletion of *Igfbp4* in mice resulted in sex-specific body composition and bone density phenotypes that have led to a reevaluation of the role of IGFBP-4 in peak bone acquisition. Maridas demonstrated that loss of *Igfbp4* affected mesenchymal stromal cell differentiation, regulated osteoclastogenesis, and influenced skeletal development and adult bone maintenance (Maridas et al., 2017a,b). Female *Igfbp4*-null mice had low trabecular and cortical bone mass, while male *Igfbp4* −/− were protected from changes in bone mass. In addition, fat mass

was reduced in both sexes, and IGFBP-4 was found to be essential for adipogenic differentiation and important for depot-specific changes (Maridas et al., 2017a,b).

IGFBP-5 is a nonglycosylated 31-kDa IGFBP produced by osteoblasts and numerous other cell types. It is found in relatively high concentrations in both bone and serum and can be measured by RIA (Nicolas et al., 1994). IGFBP-5 synthesis increased by PTH and other cyclic AMP analogs (Conover et al., 1993). IGFBP-5 is the only IGFBP shown to consistently stimulate osteoblast cell proliferation in vitro, thus increasing the number of osteoblasts. Recent studies suggest that the mitogenic effects of IGFBP-5 may in part be independent of IGFs and mediated through rhIGFBP-5's own signal transduction pathway (Mohan et al., 1995; Andress and Birnbaum, 1991; Schmid et al., 1996; Slootweg et al., 1996; Richman et al., 1999). IGFBP-5 is the most abundant IGFBP stored in the bone, where it is bound to hydroxyapatite and extracellular matrix proteins (Nicolas et al., 1995; Mohan et al., 1995). Intact IGFBP-5's major role in the skeleton may be as a storage component for IGFs, because both IGF-I and IGF-II have very low binding affinity for hydroxyapatite but bind avidly to IGFBP-5 (Rosen et al., 1994). During remodeling, resorption enhances proteolytic cleavage of IGFBP-5. In addition, during formation and mineralization, synthesis and release of IGFBP-5 by bone cells facilitates attachment of IGFs to the newly mineralized matrix (Koutsilieris and Polychronakos, 1992). Intact IGFBP-5 can also be found circulating in the extracellular space. In the circulation, IGFBP-5 can also bind ALS and IGF-I/IGF-II, providing an alternative ternary complex to the main complex ALS−IGFBP-3−IGF-I. In vitro, IGFBP-5 enhances IGF bioactivity, especially in bone. Yet, in vivo, IGFBP-5 action can be either inhibitory or stimulatory depending on the relative concentration of IGF-I and its mode of administration (Salih et al., 2005). Overexpression of IGFBP-5 ubiquitously in mice (under the CMV promoter) associates with reduced BMD in a gender- and an age-dependent manner, with males affected more severely (Salih et al., 2005). Expression of IGFBP-5 in osteoblasts (under the osteocalcin promoter) results in decreases in trabecular bone volume, impaired osteoblastic function, and osteopenia.

IGFBP-6 has been less well studied and slightly differs structurally from the other IGFBPs. Generally, IGFBPs are composed of three domains of approximately equal sizes (Baxter, 2000). The amino- and carboxyl-terminal domains are each internally disulfide-linked and share a high degree of sequence homology across the family (Neumann and Bach, 1999). However, little homology is exhibited among their central L-domains. The disulfide linkages of the amino-domain of IGFBP-6 differ from those of other IGFBPs, whereas the carboxyl-domain disulfides are the same for all IGFBPs so far studied (Neumann and Bach, 1999; Forbes et al., 1998; Chelius et al., 2001). IGFBP-6 differs functionally from other IGFBPs in binding IGF-II, with 20- to 100-fold higher affinity than IGF-I, whereas IGFBPs 1−5 do not have a marked IGF binding preference (Headey et al., 2004). Therefore, IGFBP-6 constitutes a relatively specific IGF-II inhibitor (Bach, 1999).

It is important to note that no mutations have been identified for any IGFBPs in humans. The importance of the ALS in keeping the IGF-I reservoir in serum was not appreciated for many years, until the generation of ALS-null mice (ALSKO) (Uekl et al., 2000) and the identification of several subjects with mutations in the *igfals* gene (Domene et al., 2004). The ALS plays fundamental roles in stabilizing two binary complexes of IGF-I with IGFBPs 3 and 5. Subjects with mutations in the *igfals* gene present with low levels of serum IGF-I, short stature, and reduced BMD (Domene et al., 2010). Similarly, ALSKO mice show ∼60% reductions in serum IGF-I levels; they are born at normal weight but show decreases in body size during early postnatal growth (3 weeks) and remain ∼20% smaller than controls throughout life (Courtland et al., 2010). Detailed morphology of the femurs by microCT revealed reduced total cross-sectional area, cortical bone area, polar moment of inertia, and reduced mechanical properties (by four-point bending assay).

Insulin-like growth factor binding protein proteases

IGF bioactivity is transcriptionally regulated by hormones and paracrine factors but also by their liberation from their respective binding proteins. Tissue-specific proteases provide another level of regulation of IGFs. Binding-protein-targeted proteases have been identified in serum and in various tissues including bone. These proteases alter the binding capacity of IGFs for IGFBPs, thereby freeing IGFs to bind to their respective IGFRs (Rosen et al., 1994). PSA and PAPP-A represent two of the most important circulating serine proteases that liberate IGFs from their IGFBPs, although these two enzymes are not specific for these binding proteins. Bone is a rich source of binding protein proteases. Proteases that cleave IGFBP play a pivotal role in determining the regulatory effects of IGFBPs on IGF actions. Three categories of known proteases proteolyze IGFBPs: (1) kallikreins; (2) neutral and acid-activated cathepsins; and (3) matrix metalloproteinases (MMPs) (Cohen et al., 1992, 1994; Conover et al., 1995; Fowlkes et al., 1994a). PSA is the first serine kallikrein IGFBP protease found to proteolyze both IGFBP-3 and IGFBP-5 into several lower molecular weight fragments and is regulated at least to some extent by testosterone and other androgens (Collett-Solberg and Cohen, 1996; Cohen et al., 1992; Koutsilieris et al., 1992). Its role in mediating the enhanced bone formation found in the lumbar spine of metastatic prostate cancer patients

remains to be determined. However, it is likely one of several mechanisms whereby IGFs stimulate the mitogenic activity of cancer and bone cells.

The concept of "soil and seed" implies that the inherent bioactivity of IGFs, whether bound or free, could stimulate growth of neoplastic tissue after homing of cancer cells to bone. A kallikrein-like IGFBP protease, 7S subunit nerve growth factor, is found to cleave both IGFBP 4 and 6. Cathepsin D is an acid-activated lysosomal protease that can cleave all six IGFBPs. MMPs are able to proteolyze a spectrum of IGFBPs including IGFBPs 2−5 (Collett-Solberg and Cohen, 1996; Fowlkes et al., 1994b; Rajah et al., 1996; Claussen et al., 1997; Marinaro et al., 1999; Braulke et al., 1995; Manes et al., 1999). PAPP-A, which is not specific for IGFBP-4, is activated by IGFs and found within skeletal tissue as well as other organs. Particularly for PAPP-A, it is clear that IGFs can regulate tissue-specific proteases, thereby establishing a complex regulatory loop in which the ligand (i.e., IGF) controls its own bioavailability through transcriptional and nontranscriptional means (Arany et al., 1994). Global deletions of PAPP-A result in smaller mice with reduced bone mass, while targeted transgenic overexpression of PAPP-A in muscle causes hypertrophy and increased body weight (BW). A human inactivating mutation in PAPA-2, a key protease of IGFBP-3 and IGFBP-5 protease, was reported in three subjects. These subjects presented with elevated serum IGF-I levels, elevated levels of IGFBPs 3 and 5, and increased levels of ALS, and showed growth failure and reduced BMD that were attributed to the inability to liberate IGF-I from its major binding proteins (IGFBPs 3 and 5) in the serum and the bone matrix (Dauber, 2016). IGF-I and IGF-II can regulate PAPP-A, but GH does not regulate PAPP-A or other proteases (Angelloz-Nicoud and Binoux, 1995; Skjaerbaek et al., 1998). Insulin and estrogen may also affect IGFBP protease activities (Bereket et al., 1995; Bang et al., 1998; Kudo et al., 1996).

Growth hormone/IGF actions on the intact skeleton

GH−IGF-I systemic effects on body size and longitudinal growth

Liu et al. (1993) were the first to report that newborn mice homozygous for a targeted disruption of Igf1 exhibit a growth deficiency of similar severity to that previously observed in viable Igf2-null mutants (i.e., 60% of normal birth weight). Depending on the genetic background, Liu found that some of the Igf1(−/−) dwarfs died shortly after birth, whereas others survived and reached adulthood (Liu et al., 1993). Conversely, null mutants for the Igf1R gene invariably die at birth of respiratory failure and exhibit a more severe growth deficiency (45% of normal size) compared with wild-type animals. In addition to generalized organ hypoplasia in IgfR(−/−) embryos, including the muscles and developmental delays in ossification, deviations from normalcy were found in the central nervous system and the epidermis. Igf1 −/−/Igf1R(−/−) double mutants did not differ in phenotype from Igf1R (−/−) single mutants, while in Igf 2(−)/Igf1R(−/−) and Igf1(−/−)/Igf 2(−) double mutants, which are phenotypically identical, dwarfism was further exacerbated (i.e., 30% of normal size).

To investigate the role of IGF-I in normal development, Powell-Braxton et al. generated mice with an inactive Igf1 gene. Heterozygous Igf1(±) mice are healthy and fertile; however, they are 10%−20% smaller than wild-type littermates and have lower levels of IGF-I (Powell-Braxton et al., 1993). The size reduction is attributable to a decrease in organ size and bone mass. This was also confirmed by the Kream laboratory, further describing a defect in osteoblast function as the major mechanism for reduced bone mass and size (He et al., 2006).

As previously noted, at birth homozygous mutant Igf1 (−/−) mice are less than 60% the BW of wild-type, and greater than 80% of the pups die perinatally. The survivors are sometimes compromised in terms of homeostatic processes, but the compensatory mechanisms in survivors are interesting. For example, Bikle et al. (2001) analyzed the structural properties of bone from mice rendered IGF-I deficient by homologous recombination. The knockout mice were 24% the size of their wild-type littermates at the time of study (4 months). The knockout tibias were 28%, and L1 vertebrae were 26% the size of wild-type bones. Bone formation rates (BFRs) of knockout tibias were 27% that of wild-type littermates (Bikle et al., 2001). The bones of mutant mice responded normally to GH (1.7-fold increase) and supranormally to IGF-I (5.2-fold increase) with respect to BFR. Cortical thickness of the proximal tibia was reduced 17% in the knockout mouse. However, trabecular bone volume (bone volume/total volume [BV/TV]) in knockout mice compared with wild-type controls was increased 23% in male mice and 88% in female mice as a result of increased connectivity, increased number, and decreased spacing of the trabeculae. Thus, absence of IGF-I causes a smaller bone that may be more compact, almost certainly due to reduced osteoclastic activity as noted earlier. The structural consequences of these bones in respect to fracture have not been studied.

As indicated previously, IGF-I acts in an endocrine (serum) and autocrine/paracrine fashion. Yakar et al. (1999) used the Cre/loxP recombination system whereby mice with loxP-flanked Igf1 gene were mated with albumin-Cre transgenic mice expressing the Cre recombinase exclusively in the liver. Liver-specific Igf1 gene-deletion (LID) mice were

macroscopically normal, suggesting that autocrine/paracrine IGF-I could support normal postnatal growth and development (Yakar et al., 1999). Nevertheless, more extensive developmental phenotyping of the LID mouse revealed a marked reduction in bone volume, periosteal circumference, and medial lateral width consistent with the hypothesis that circulating (endocrine) IGF-I had an important role in bone modeling (Yakar et al., 2002). Moreover, recent studies from Yakar et al. have shown that ALSKO mice also have reduced cortical thickness and enhanced trabecular bone, consistent with an endocrine effect of the circulating IGF complex on skeletal acquisition (Yakar et al., 2006). Finally, double-ALS and IGF-I knockout mice have a major growth phenotype as well as markedly reduced BMD despite normal expression of skeletal IGF-I (Yakar et al., 2006). Thus, it seems likely that both local and circulating IGF-I concentrations are essential for peak bone acquisition and maintenance.

GH has distinct IGF-I–independent effects on the skeleton in terms of linear growth and bone remodeling. However, due to the intimate relationship between these two hormones and their feedback loop regulatory system, it has been extremely difficult to ascertain their independent roles. Double-GH/IGF-I knockout mice exhibit significant growth retardation, suggesting that each of these two growth factors contributes distinctly to longitudinal growth (Lupu et al., 2001). Interestingly, in those studies only 17% of the growth in these mice could be attributed to non-GH and non-IGF-I determinants (Lupu et al., 2001). GH may have its own effect on linear growth independent of IGF-I. For example, GH stimulates longitudinal bone growth in normal rats, but rhIGF-I does not (Schmid and Ernst, 1991). Similarly, transgenic mice that overexpress GH grow to twice their normal size, even though administration of IGF-I to normal mice does not provoke a similar growth response. The presence of both GHR and IGFRs on bone cells complicates the interpretation of GH's action.

Longitudinal growth results from the activity of GH on the cartilaginous growth plate. In human bone, proliferating chondrocytes express IGF-IRs and are responsive to paracrine IGFs secreted by differentiated cartilage cells (Isaksson et al., 1987). The target for GH in the growth plate is the differentiated chondrocyte that synthesizes IGF-I in response to GH. Proliferating chondrocytes respond to locally produced IGF-I by differentiation, which in turn leads to cartilage expansion and linear growth. Thus, GH's stimulatory properties on the endochondral growth plate are mediated largely by induction of IGF-I. A detailed analysis of the growth plate of IGF-I–null mice showed that chondrocyte cell number and proliferation were preserved in IGF-I nulls despite significant (~35%) reductions in longitudinal growth, findings attributed to the high levels of GH in those mice (Wang et al., 1999). Further defects were found in chondrocyte hypertrophy, metabolism, and matrix production, suggesting that IGF-I plays a role in chondrocyte hypertrophy. In a separate study, the direct cellular targets for GH in the growth plate were mapped in normal, GH-deficient, and fasting mice and rats (Gevers, 2009). The authors confirmed that GH stimulated prechondrocytes and early chondrocytes but had no effect on hypertrophic chondrocytes. Chondrocyte-specific IGF-IR gene deletion using the type II collagen I (Col2a1)-driven Cre resulted in a more severe phenotype with shorter bones, disorganized chondrocyte columns, delayed ossification, and undermineralized skeletons (Wang et al., 2011). However, chondrocyte-specific IGF-I gene deletion using the same promoter (Col2a1) resulted in decreased body length, areal BMD, and bone mineral content, likely due to the compensatory effects of circulating IGF-I. Collectively, mouse studies strengthen the "dual effector hypothesis," which suggests that GH affects the resting cells of the growth plate, the perichondrium, and the groove of Ranvier to drive prechondrocytes at this region to proliferate, while locally produced IGF-I drives chondrocyte proliferation (clonal expansion at the proliferating zone) and possibly chondrocyte hypertrophy (Green et al., 1985).

Growth hormone and IGF-I effects on modeling and remodeling

Skeletal modeling during growth, and remodeling during maturation and aging, are the sum of several distinct events beginning with activation of lining cells, differentiation of osteoblast and osteocyte formation, and recruitment of osteoclasts. These processes engage multiple signaling pathways. Besides the large quantities of IGFs, there are other growth factors such as transforming growth factor-beta and fibroblast growth factors that are released during active resorption, ensuring that bone formation will be coupled to bone resorption (Mohan et al., 1991). IGFs also stimulate the differentiation and activation of osteoclasts, possibly in concert with cytokines such as receptor activator of nuclear factor Kappa β ligand (RANKL) and macrophage colony-stimulating factor (Slootweg et al., 1992; Mochizuki et al., 1992). Administration of IGF-I enhances bone formation and bone resorption to a similar degree (Ebeling et al., 1993). The acidic pH within the microenvironment of the osteoclast during active resorption permits activation of several proteases, including PAPP-A (Conover et al., 1994), that liberate IGFs from IGFBPs and allow for further recruitment of osteoblasts and osteoclasts to the remodeling site.

In vitro, GH, IGF-I, and IGF-II all have modest mitogenic effects on bone cell growth (Canalis et al., 1989; Mohan et al., 1988). This suggests that GH could act through IGFs to activate skeletal remodeling. Indeed, GH-induced cell

proliferation can be blocked by simultaneous addition of a specific monoclonal antibody to IGF-I (Mohan et al., 1991). IGF-II, on the other hand, stimulates mitogenesis independent of GH, and even if high doses of IGF-I are coadministered. This implies that IGF-II could regulate osteoblastic proliferation via IGF-IIR (Mohan et al., 1989a). In vitro, both IGF-I and IGF-II are mitogenic to rodent preosteoblasts, and both rapidly increase mRNA expression of the protooncogene, c-fos, 20- to 40-fold in less than 30 min (Merriman et al., 1990). IGFs also stimulate type I collagen synthesis, alkaline phosphatase activity, and osteocalcin in more differentiated human osteoblast-like cells (Mohan et al., 1989; Schmid et al., 1984). Taken together, IGFs are important for osteoblast activity, particularly in response to intermittent parathyroid hormone, but the effects are dose and time dependent.

Insulin-like growth factors, other transcription factors, and osteoblasts

The exact roles of IGFs in osteoblast and osteoclast differentiation are complex. In part this relates to the developmentally sensitive and finely orchestrated process that drives mesenchymal stromal cells (MSCs) into the osteogenic lineage. Not unexpectedly, this pathway involves multiple transcription factors and cytokines as well as IGFs. Hence, IGFs act directly on MSCs to drive cell growth and differentiation and also synergize with other growth factors (e.g., Wnts) and their signaling pathways (Akt, MAPK, p38, etc.) to promote osteogenesis.

Two critical transcription factors that control osteoblast fate are runt-related transcription factor 2 (Runx2) and osterix (Osx). Runx2, core binding factor 1/polyoma enhancer binding protein 2a, a transcription factor that belongs to the Runx family, is the subunit of a heterodimeric transcription factor, PEBP2/CBF, which is composed of α and β subunits (Ito, 1999). Runx2 is involved in osteoblast differentiation and bone formation. In particular, Runx2 is required for early commitment of mesenchymal stem cells into osteoprogenitors and also functions later in osteoblast differentiation to regulate the formation of the extracellular matrix (Ducy et al., 1999). IGF-I influences Runx2 expression through activation of PI3K, Pak1, and ERK (Xiao et al., 2000; Qiao et al., 2004).

Schnurri-3 (Shn3), a large zinc finger protein that functions as an adapter protein in the immune system (Oukka et al., 2002), has been shown to control the posttranslational protein expression level of Runx2 through promoting Runx2 degradation by recruitment of the WW domain containing E3 ubiquitin ligase1 to Runx2. Mice lacking Shn3 display adult-onset osteosclerosis with increased bone mass due to an augmented osteoblast activity (Jones et al., 2006). Glucose itself may also regulate Runx2 post translationally via Smurf1 that is regulated by AMP-activated protein kinase (AMPK) (Wei et al., 2015).

Osx (Sp7) is a master zinc-finger-containing transcription factor of osteoblast lineage progression that is highly specific to osteoblasts in vivo and acts downstream of bone morphogenetic protein (BMP)-2 Smad signaling (Xiao et al., 2000; Qiao et al., 2004; Nakashima et al., 2002). The Osx amino acid sequence predicts three C2H2-type zinc fingers with a high degree of identity to similar DNA-binding domains in the transcription factors Sp1, Sp3, and Sp4. The expression of Osx is more specific to osteoblasts than Runx2 (Nakashima and de Crombrugghe, 2003). Because no Osx transcripts are detected in the skeletal elements of Runx2-null mice, Osx must be downstream of Runx2 in the pathway of osteoblast differentiation (Nakashima et al., 2002). Both IGF-I and BMP-2 are shown to upregulate Osx expression during early osteoblast differentiation (Celil et al., 2005). In mesenchymal stem cells, it appears that both MAPK and PKD signaling pathways serve as points of convergence for mediating the IGF-I- and BMP-2-induced effects on Osx expression (Celil et al., 2005). IGF-I-mediated Osx expression required all three MAPK components (Erk, p38, and JNK), whereas BMP-2 required p38 and JNK signaling, and the synergistic interactions of BMP-2 and IGF-I were also disrupted by PKD inhibition (Celil et al., 2005).

It should be noted that Runx2-independent pathways of ossification also exist, including (1) the Wnt signaling pathway; (2) the Msx2-dependent vascular ossification pathway; and (3) Osx induction via Dlx5, a homeobox transcription factor, which acts downstream of BMP-2 (Kato et al., 2002; Cheng et al., 2003; Lee et al., 2003). These studies suggest additional pathways may act in parallel to, or independent of, Runx2 to regulate Osx expression during osteogenic lineage progression. Indeed, in the canonical Wnt signaling pathway, there is cross talk with the IGF pathway. For example, β-catenin binds to IRS-1 as well as other factors to enhance its transport from the cytoplasm into the nucleus where it can affect a whole series of downstream target genes.

In sum, IGFs enhance differentiation of mesenchymal stem cells. Targeted ablation of IGF-I in osteoblasts resulted in severe growth retardation and impaired bone mineralization. Reduced bone formation in Col1a2-IGF-IKO mice is attributed to decreased osteoblast function (Kesavan et al., 2011). Conditional deletion of IGF-IR in osteoblasts using the osteocalcin promoter-driven Cre recombinase led to low bone mass (Zhang et al., 2002; Wang et al., 2007). Histomorphometric indices demonstrated sufficient osteoblasts but reduced bone formation and mineralization rates, thereby implying that IGF-I must be important in late differentiation and mineralization (*See IGF actions on the skeleton*).

Moreover, IGF-I is essential for adipogenic differentiation and likely is downstream of peroxisome proliferator-activated receptor gamma (PPARγ) activation. Because mesenchymal stromal cells can enter several distinct lineages, the precise timing of IGF-I action and other factors, active in the marrow niche, some of them undefined, ultimately determine cell fate (Fig. 42.2).

Insulin-like growth factors and osteoclasts

In addition to regulating osteoblast function, several groups have shown that skeletal IGF-I can stimulate osteoclast recruitment and differentiation either directly through IGF-IR or via RANKL expression (Mochizuki et al., 1992; Rubin et al., 2002). This would place IGF-I in the category of a "coupler" for bone remodeling. Indeed, IGF-I-null mice are growth retarded, and most die after birth. Those that survive are very small and have developmental defects in brain, muscle, bone, and lung, and are infertile. However, their skeletal phenotype is particularly striking and is characterized by very little cortical bone but an increased trabecular bone volume fraction (Bikle et al., 2001, 2006). Recently, it has been demonstrated in vivo and in vitro that the absence of IGF-I impairs osteoclast recruitment and activity, although the exact mechanism is unknown (Wang et al., 2006).

Insulin-like growth factors and osteocytes

Osteocytes are terminally differentiated osteoblasts buried in the mineralized matrix and are the most abundant cells in bone. Osteocytes play fundamental roles in bone remodeling and bone response to mechanical loading. These cells are the first responders to crack or fracture and are responsible for sending signals to recruit osteoclasts to resorb and remodel the damaged site. The roles of GH or IGF-I in osteocytes function were partially elucidated recently. Using the DMP-1 promoter-driven cre, the GHR, IGF-IR, or IGF-I genes were inactivated in osteocytes. Ablation of GHR in osteocytes did not affect body weight, body length, body composition, or organ weights but led to slender bones with reduced total cross-sectional area and cortical bone area in both sexes. Likewise, Dmp-1-mediated *Igf-1 receptor (Igf-1r)* gene−deleted mice (DMP-IGF-IRKO) showed normal body and organ weights but exhibited significant reduction in cortical bone area and a reduced cortical bone thickness in both sexes. Notably, cortical bone area decreased by ∼20% while marrow area increased by 40%−50% compared with controls, suggesting that endosteal resorption increased following IGF-IR ablation in osteocytes. A similar approach was used to knock down IGF-I in bone (DMP-IGF-IKO mice) (Sheng et al., 2013). Skeletal characterization showed slender bones with reduced total cross-sectional area and reduced cortical bone area in both sexes of DMP-IGF-IKO mice. Collectively, inactivation of the GH/IGF-I axis in osteocytes leads to significant decreases in cortical bone with minimal (∼5%) effects on linear bone growth, suggesting that this axis regulates not only longitudinal growth but also radial bone growth via its actions on osteocytes.

As indicated above, osteocytes are the bone mechanosensors that initiate the anabolic response to loading or trigger the resorption process when damage occurs. In vitro and in vivo models of mechanical loading suggest that IGF-I mediates these processes. *Igf1* gene expression increases following mechanical stimulation (Lau, 2006; Reijnders et al., 2007). Mice with *Igf1* gene deletion in osteocytes showed blunted bone response to four-point bending, which was associated with significant decreases in the expression levels of cox2, c-fos, and *igf-1* (the early mechanosensitive genes) in bone and reduced Wnt signaling (Lau, 2013). Skeletal unloading, on the other hand, induced bone loss that was also shown to be dependent on IGF-I. Hind limb suspension in rats inhibited activation of IGF-IR signaling pathways and was associated with a reduced number of osteoblast progenitors, their differentiation, and reduced bone formation (Sakata et al., 2004).

Energy utilization by skeletal cells and the role of IGF-I

Both modeling and remodeling are energy requiring processes. Hence, understanding substrate utilization and ATP production, particularly by osteoblasts, is critical to defining the processes inherent in peak bone mass and maintenance. Glucose has long been known as a major nutrient for osteoblasts and other cells, and IGF-I can modulate glycolysis. Recent work with radiolabeled glucose analogs has confirmed a significant uptake of glucose by bone in the mouse (Wei, 2015; Zoch, 2016). The Glut transporters appear to be mainly responsible for glucose uptake in osteoblast lineage cells. Expression studies detected Glut1 and Glut3 in osteoblastic cell lines (Thomas et al., 1996; Zoidis et al., 2011). More recently, Glut1 was shown to be a major transporter in primary osteoblast cultures and modulates the post-translational modification of Runx2 by suppressing AMPK and blocking ubiquitination of Runx2 (Wei, 2015); selective deletion of Glut1 in osteoblast precursors suppressed osteoblast differentiation in vitro and in vivo. However, others have reported that Glut4 increases in neonatal calvarial osteoblast cultures in response to beta-glycerophosphate

and ascorbate, or insulin, even though genetic deletion of Glut4 does not cause an obvious skeletal phenotype (Li et al., 2016).

Recent work has linked the bone anabolic function of Wnts and IGFs with increased aerobic glycolysis in osteoblast-lineage cells (Esen et al., 2013; Lee et al., 2017). Both share common regulatory pathways, the former activating mTORC2 (mammalian target of rapamycin complex 2) and Akt that in turn acutely increase the protein abundance of a number of key glycolytic enzymes (e.g., Hk2, Pfk1, Pfkfb3 [6-phosphofructo-2-kinase/fructose-2,6-bisphosphatase 3], and Ldha), the latter acting through IRS-1 and AKT. But IGF-I is also a major target of PTH's anabolic actions on osteoblasts. PTH has been shown by several investigators to increase glycolysis, and that is presumed to be the source of ATP for enhanced collagen synthesis and bone formation (Zoidis et al., 2011). Studies in MC3T3-E1 cells have uncovered that PTH stimulates aerobic glycolysis via activation of IGF signaling, which in turn activates the PI3K-mTORC2 cascade and upregulates metabolic enzymes such as Hk2, Ldha, and Pdk1 in a manner analogous to the Wnts. Importantly, genetic studies have demonstrated that deletion of either *Igf1* or *Igf1r* in osteoblasts essentially abolishes the bone anabolic effect of PTH in mice (Bikle et al., 2002; Wang et al., 2007). And blocking glycolysis with 2DG or other inhibitors completely prevents osteoblast differentiation. Hence, the mechanisms that allow IGFs to drive osteoblast function are multiple and include several fuel pathways. Undoubtedly, the major driver for osteoblast differentiation is glucose, but fatty acids and glutamine contribute in a temporal-specific manner (Lee et al., 2017).

Pathogenic role of GH/IGF/IGFBPs in osteoporosis

Effects of growth hormone deficiency on bone metabolism

GHD in childhood is associated with growth failure and short stature. However, the effects of GHD on BMD in prepubertal children have been more difficult to quantify, in part because of the mixed hypopituitary syndromes that often accompany GHD. Thus, there is a paucity of studies examining BMD status in GH-deficient children. By single-photon absorptiometry of the wrist, children with GHD have been found to have low BMD (Wuster et al., 1992). Serum concentrations of osteocalcin are also reduced in children with GHD, but the response of osteocalcin to GH administration does not correlate with linear growth (Delmas et al., 1986). In several cross-sectional studies of adults with GHD, lumbar spine BMD was reduced compared with that of age-matched controls (Wuster et al., 1991; Johansson et al., 1992; Hyer et al., 1992; Rosen et al., 1993; Bing-You et al., 1993; DeBoer et al., 1994). In one group of adult GHD patients, the lowest spinal BMD was found in people who were previously treated with rhGH during childhood (Wuster et al., 1991, 1993). This degree of osteopenia was not due to cortisone or thyroxine substitution, because the BMDs of patients on hormonal substitution did not differ from those without hormone replacement (Wuster et al., 1993). In that same study, Wuster et al. (1991) showed an increased prevalence of vertebral osteoporotic fractures among GH-deficient adults. Kaufman et al. (1992) confirmed low BMD in GHD adults with or without hormonal deficiencies. However, Kann et al. (1993) found no difference in the apparent phalangeal ultrasound transmission velocity of GHD patients compared with age- and sex-matched controls. De Boer et al. (1994) noted that low BMD was partly explained by reduced body height, but with correction for body mass index, BMD was still significantly reduced compared with age- and sex-matched controls (Wuster et al., 1992).

The cause of low BMD in adult GHD has been thought to be due to insufficient bone acquisition during the adolescent years (DeBoer et al., 1994). This hypothesis is supported by bone histomorphometry. In 36 men with GHD (primarily of juvenile onset), there were increased eroded surfaces, increased osteoid thickness and increased mineralization lag time, all indicative of delayed mineralization that was probably due to changes in the timing of puberty (DeBoer et al., 1994; Bravenboer et al., 1994). In support of those histomorphometric changes, low serum levels of osteocalcin have been detected in some adult GHD patients (Delmas et al., 1986). This is in sharp contrast to patients with normal GH secretion but multiple pituitary hormone deficiencies, where serum osteocalcin levels are normal but there is markedly increased urinary pyridinoline excretion (de la Piedra et al., 1988). Fracture rates are higher in individuals with GHD, and it is established that chronic GH treatment in GHD prevents further fractures, although interestingly it does not affect quality of life (Krantz, 2015).

Effects of growth hormone excess on bone mass and bone turnover

Chronic GH excess in adults (i.e., acromegaly) has been a surrogate model for studying the effects of GH on the skeleton. Acromegaly is a multisystem progressive disorder caused by uncontrolled secretion of GH, most commonly by a pituitary adenoma (Capatina et al., 2015). A major biochemical characteristic of acromegaly is the increased production of liver-derived IGF-I. In fact, most systemic complications associated with acromegaly can be attributed to the effects of

IGF-I, which mediates the somatic and some of the metabolic effects of GH (Capatina et al., 2015). Subsequently, the objectives of treatment are twofold—inhibition of tumor growth and controlling the secretion of IGF-I.

The effects of excess GH on the skeleton in acromegaly are complicated by GH-mediated changes in vitamin D metabolism in the kidney, secondary effects of GH on PTH production, and gonadotropin secretion (Ezzat et al., 1993; Bouillon, 1991). Increased bone turnover has been reported in acromegaly by biochemical markers and histomorphometric studies (de la Piedra et al., 1988; Ezzat et al., 1993). Studies reporting BMD in patients with acromegaly used different morphometric modalities, and the findings are inconsistent. However, several cross-sectional studies suggested that acromegaly associated with increased skeletal fragility, particularly increased vertebral fracture risk (Wassenaar et al., 2011; Mazziotti et al., 2008; Ueland et al., 2002; Kayath et al., 1997) that does not always correlate with decreased BMD. In one study, computed tomography (CT) measurements of the lumbar spine revealed that trabecular BMD was elevated in only 1 of 14 patients with active acromegaly (Ezzat et al., 1993). This may have been due to hypogonadism in the acromegalics. Wuster et al. (1993) recently studied five patients with active acromegaly treated with octreotide for 5 years. All had achieved normal IGF-I levels during therapy. Spinal BMD was initially decreased in all five patients but normalized in three of them with octreotide. All patients remained eugonadal throughout follow-up.

As noted earlier, biochemical markers of bone turnover are altered in acromegaly. Many of these changes can be related to alterations in gonadal status during disease and its treatment. However, changes in bone turnover with acromegaly reflect persistent coupling of the remodeling cycle with increased resorption and formation. Serum osteocalcin and skeletal alkaline phosphatase are increased in acromegaly, as are urinary calcium and hydroxyproline excretion (de la Piedra et al., 1988; Ezzat et al., 1993). Although serum calcium, total alkaline phosphatase, and phosphorus are usually normal, there may also be increased synthesis of 1,25-dihydroxyvitamin D. This results from significant intracellular phosphate shifts due in part to an increased circulating IGF-I.

Changes in the GH−IGF-I axis in patients with osteoporosis

For several years, attempts have been made to link GH secretory status with low BMD and osteoporosis. As noted previously, efforts to find a relationship between GH secretion and age-related bone loss have been conflicted at best. However, other investigators have examined the relationship of GH to BMD in the immediate menopausal period. These efforts gained prominence in the 1980s when it was reported that GH secretion in patients with osteoporosis was reduced even after stimulation with L-arginine. Low serum IGF-I, IGF-II, and IGFBP-3 levels (by RIA) were noted in 98 females with postmenopausal osteoporosis compared with 59 normal controls and 91 patients with osteoarthritis or degenerative bone disease (Wuster et al., 1993). In a cross-sectional study of a large cohort of older postmenopausal women from Framingham, Langlois et al. (1998) reported very strong correlations between the lowest quintile of IGF-I and BMD at the spine hip and radius. Bauer et al. reported that in the Study of Osteoporotic Fractures, women in the lowest quartile for serum IGF-I had a 60% greater likelihood of hip or spine fractures, even when controlling for BMD (Bauer et al., 1997). Gamero et al. (2000) noted that low serum levels of IGF-I were associated with a significantly greater risk of hip fractures among a large cohort of older postmenopausal women in France. In a study of 61 community-dwelling men over the age of 27, who were randomly selected from the Calgary cohort of 1000 subjects in the Canadian Multicentre Osteoporosis Study, IGF-I was found to be a significant predictor of BMD at the total hip, femoral neck, and femoral trochanter neck (p # 0.001). Szulc et al. (2004) evaluated the correlation of BMD with serum IGF-I in a large cohort of 721 men aged 19−85, considering age, BW, 17 b-estradiol, free testosterone, and PTH. Serum IGF-I decreased with age (r 5 20.44, p 5 0.0001). IGF-I correlated positively with BMD at the whole body and at the third lumbar vertebra. BMD of the total hip was 6% higher in men in the highest quartile of IGF-I than in men in the lowest quartile. However, others have not found a relationship between serum IGF-I and BMD in patients with fractures, in postmenopausal osteoporosis, or in otherwise healthy subjects (Kassem et al., 1994; Lloyd et al., 1996; Rudman and Mattson, 1994).

In male osteoporotic patients, serum IGF-I and IGFBP-3 concentrations are low and correlated with lumbar BMD (Ljunghall et al., 1992; Nakamura et al., 1992). Johannsen et al. (1994a,b) noted that among healthy males, IGFBP-3 was the best predictor of femoral BMD. (Kurland et al., 1997) reported that younger males with idiopathic osteoporosis had low serum levels of IGF-I in relation to age-matched controls. Similar results were noted in premenopausal women (Rubin et al., 2005). Moreover, those men also had low rates of bone turnover by histomorphometry but normal GH dynamics (Kurland et al., 1998), similar to women with idiopathic osteoporosis (Shane). Of potential pathophysiological importance is the observation that patients with osteoarthritis have higher concentrations of IGF-II than those of normal controls (Wuster et al., 1993; Mohan et al., 1991). Other studies have related serum IGFBP-4 and IGFBP-5 due to aging and low bone mass, although causality was not established (Karasik et al., 2002). Also, Dennison and colleagues reported that low

24-hour GH profiles were associated with low BMD of the lumbar spine in older British women (Dennison et al., 2003). Further longitudinal studies will be required to determine the precise relationship among IGFs, GH, and osteoporosis.

GH and IGF-I as treatments for skeletal disorders

Anabolic agents can directly stimulate bone formation and therefore might have great potential to decrease fractures. Therefore, there is an emerging interest in developing anabolic agents including PTH, PTHrp, GH, and IGF-I to treat osteoporosis (Rubin et al., 2002).

Growth hormone treatment for skeletal disorders

GH has direct and indirect effects on bone depending on age and skeletal maturity. Indirectly, GH can enhance bone mass through its effects on muscle mass and calcium transport in the gut through IGF-I—mediated increases in 1 alpha hydroxylase that generates active 1,25 vitamin D, as well as by suppressing adipocyte differentiation in different fat depots including bone marrow (Fleet et al., 1994; Bianda et al., 1998; Menagh et al., 2010). In addition, GH can directly stimulate bone remodeling and increase endochondral growth through its actions on the osteoblast. Overall, GH is considered essential for the growth and maintenance of skeletal mass. Moreover, it is established that for virtually all cohorts of GHD subjects, whether onset is in childhood or adulthood, male or female, there is reduced areal BMD. In some but not all studies, volumetric BMD, measured either by CT or areal-adjusted algorithms, was reduced in children with GHD (Baroncelli et al., 1998). In the largest observational trial of GHD subjects to date—i.e., KIMS—GHD was associated with a marked increase in fracture risk, particularly when compared with age-matched normal controls (Rosen et al., 1997; Wuster et al., 2001). Hence, there is a strong rationale to treat GHD in children.

Substantial differences between the direct and indirect (i.e., via IGF-I) effects of GH on the osteoblast, the marrow stromal cell precursor, and the osteocyte may partially explain changes in skeletal responsiveness to GH and IGF-I. For example, exogenous GH stimulates longitudinal growth in normal rats, but rhIGF-I does not (Schmid et al., 1991). Similarly, transgenic mice who overexpress GH grow to twice their normal size, whereas exogenous administration of IGF-I is far less efficient in stimulating long bone growth. Thus, despite the fact that GH induces IGF-I production in the skeleton and elsewhere, treatments with GH and with IGF-I are not equivalent. In general, skeletal responsiveness to GH and IGF-I depend on the species, GH status of the animal, and mode of administration. Systemic side effects of rhGH and rhIGF-I therapy may differ substantially.

Growth hormone treatment for children with insufficient GH secretion

Intermittent (daily or three times weekly) injections of rhGH to children with GHD resulted in a prolonged and sustained GH profile with resultant catch-up growth evident during the first year of treatment (Rappaport and Czernichow, 1993). This increase in skeletal growth was accompanied by a rise in serum levels of type I procollagen peptide. Although dosage schemes varied between the United States and Europe (0.1 mg/kg/tiw [USA] to 0.7 U/kg/week[Europe]), there was a strong dose-related growth response to rhGH (de Muinck Keizer-Schrama et al., 1992). Indeed, most studies of preadolescent GHD children have shown significant improvements in areal BMD with GH replacement. However, the skeletal response to GH depends on several factors including (1) GH secretory status; 2) pretreatment IGF-I levels; (3) pretreatment height velocity; and (4) GH dosage (de Muinck Keizer-Schrama et al., 1992). The rate of change in serum IGF-I (rather than the absolute level of IGF-I attained by GH treatment) is a relatively nonspecific predictor of growth, as are procollagen-I and osteocalcin concentrations (Delmas et al., 1986; de Muinck Keizer-Schrama et al., 1992). Serum procollagen III levels correlate with growth rates during GH treatment (Delmas et al., 1986).

Linear growth is a measurable response to exogenous GH, but changes in BMD in children are more difficult to quantify. In some studies, bone mineral content (BMC) is increased during GH treatment to a greater extent than expected for change in bone size (Inzucchi and Robbins, 1994). In one of the longest intervention trials to date, 26 GHD children were given rhGH (0.6 IU/kg per week) for 12 months (Saggese et al., 1993). Baseline radial BMC z scores (corrected for their chronological, statural, and bone ages) were significantly reduced, as were serum osteocalcin and procollagen peptide levels. Treatment with rhGH six times per week increased BMC and normalized the z scores of the radius in nearly 50% of the subjects. Serum levels of procollagen peptide during the first week of treatment were positively related to growth velocity at 6 and 12 months and radial BMC at 12 months. In another nonrandomized trial, 32 children with GHD aged 7—16 were treated for nearly 1 year with rhGH and found to have significant improvements in areal BMD and final adult

height (Saggese et al., 1996). In adolescent GHD subjects, GH replacement had more variable effects on peak bone acquisition. Even with higher rhGH doses, significant changes in volumetric BMD have not been found, nor has acceleration in skeletal maturation (Baroncelli et al., 2004; Mauras et al., 2000; Kamp et al., 2002). Controversy continues as to whether GH treatment impacts BMD in children with idiopathic short stature or children born small for gestational age (SGA). Arends et al. (2003) demonstrated that prepubertal SGA children given 33 ug/kg/d of rhGH for 3 years had significant increases in height, areal BMD, and areal adjusted spine BMD. However, rhGH administered to children with idiopathic short stature who had low volumetric BMD did not result in further increases in BMD despite significant changes in lean body mass and bone turnover indices (Hogler et al., 2005). In cerebral palsy children (aged 4−15 years), 18 months of rhGH (50 mg/day) in a randomized placebo-controlled trial RPCT, areal BMD increased significantly, as did height, IGF-I, IGFBP-3, and osteocalcin (Ali et al., 2007). In sum, rhGH improves adult height, and areal BMD in prepubertal GHD children treated for at least 1 year. These changes are accompanied by favorable effects on body composition, muscle strength, and overall quality of life. It is still uncertain, however, how beneficial these GH-induced effects are in late adolescent GHD subjects in non-GHD states, or whether true volumetric BMD is significantly improved by long-term GH therapy.

Growth hormone administration for healthy adults

Although there were striking differences between longitudinal growth in children and remodeling in adults, criteria that determine rhGH responsiveness in children still may be relevant for older individuals. It has already been established that biochemical and histomorphometric responses to rhGH in children may differ according to their GH secretory status. The same principle probably holds for adults treated with GH. Three adult populations have been studied before and after GH treatment in order to examine predictors of skeletal responsiveness: (1) healthy adults, 2) GHD adults, and (3) elderly men and women with/without osteoporosis.

Initial studies with rhGH in adults focused primarily on changes in body composition. Short-term treatment with rhGH leads to a decrease in adiposity and an increase in lean body mass (Crist et al., 1988). There is also a marked shift in extracellular water (Holloway et al., 1994). Detailed analysis of skeletal biomarkers during GH treatment (1990) was reported in 20 male volunteers (ages 22−31) given a relatively large dose (0.1 IU/kg) of rhGH twice daily for 7 days. Serum osteocalcin increased after 2 days of treatment and remained elevated for 6 months. Bone alkaline phosphatase decreased initially (during the 7 days of GH treatment) but then increased slightly over 6 months (Brixen et al., 1990). Serum calcium and phosphate increased but only during the 7-day treatment phase. Like bone formation indices, urinary markers of bone resorption (urinary Ca/Cr and hydroxyproline/creatinine) rose during treatment and remained elevated for up to 4 weeks after the discontinuation of therapy.

Treatment with rhGH stimulates bone remodeling. More importantly, the anabolic effect on bone may persist well beyond discontinuation of GH. Early (2-day) and late (2-week) osteocalcin responses imply that GH can stimulate existing osteoblasts and enhance recruitment of new osteoblasts. Still, it is uncertain whether those effects are mediated through IGF-I. For example, Brixen et al. (1990) were unable to find a significant correlation between the rise in serum IGF-I and an increase in osteocalcin or bone alkaline phosphatase. The absence of a significant correlation between bone formation markers and serum IGF-I, however, may be due to the relatively small changes in of serum IGF-I.

Growth hormone treatment for adult-onset GH deficiency

GHD can be diagnosed by insufficient GH secretion in serial measurements in response to provocative stimuli (GHRH, insulin, glucagon) and serial GH measurements. The majority of adult patients treated with rhGH have either idiopathic GHD or a history of previous central nervous system/pituitary-hypothalamic tumors. Early trials with rhGH replacement therapy examined changes in muscle mass, muscle strength, and body fat. Daily administration of subcutaneous rhGH to GHD patients produced a marked rise in serum IGF-I and an increase in muscle mass and basal metabolic rate (Jorgensen et al., 1991). Some of those anabolic changes were noted soon after the initiation of rhGH. For example, mean nitrogen retention during the first 15 days of rhGH treatment was as much as 2.8 g per day (approximately 20 g of muscle mass) (Valk et al., 1994). GH treatment can also increase the total cross-sectional area of thigh muscles and quadriceps as well as improve hip flexors and limb girdle strength (Jorgensen et al., 1991; Valk et al., 1994). At least one group has suggested that rhGH can increase the number of type II muscle fibers. Total fat mass, however, consistently decreases during rhGH treatment (Jorgensen et al., 1989, 1991).

Several biochemical parameters reflect the pharmacologic action of GH on the skeleton. Serum calcium, osteocalcin, and urinary hydroxyproline all increase, while PTH declines slightly during rhGH treatment. Newer and more sensitive

markers of bone turnover also reflect changes during rhGH treatment. Urinary deoxypyridinoline increases threefold, and the amino-terminal propeptide of type III procollagen doubles, during 4 months of daily rhGH (Christiansen et al., 1991; Johansen et al., 1990). After cessation of rhGH treatment, deoxypyridinoline excretion decreases, but type III procollagen levels remain higher than controls for several months (Johansen et al., 1990). Serum osteocalcin and procollagen 1 N-terminal propeptide markers of bone formation also increase significantly with rhGH therapy in adults, similar to the change noted in children.

If prolonged GHD in adults results in profound changes in the musculoskeletal system, then GH replacement would be expected to enhance muscle performance and subsequently BMD. When 0.25 IU/kg/week of rhGH was administered to 12 GHD adults for 1 year, there was a marked increase in trabecular BMD (measured by single- and dual-energy QCT of the spine) at 6 and 12 months. At 12 months proximal and distal forearm BMC increased, midthigh muscle area was greater, and fat cross-sectional area decreased. Because the rise in spine BMD was noted with both single- and dual-energy CT measurements of the spine, it is possible that the enhancement in BMD was significant and not related to a reduction in marrow fat.

Several groups have performed longer nonrandomized trials with rhGH in the GHD syndrome. Changes in BMD were not significant at 12 months; however by 24 and 36 months BMD has been reported to increase by as much as 5%−8% in the spine (Janssen et al., 1998; Baum et al., 1996; Papadakis et al., 1996). Krantz et al., in a randomized double-blinded control trial, demonstrated that 10 years of GH could reduce fractures (Krantz et al., 2015). In addition, other investigators have reported a concomitant increase in muscle strength after 2 years of rhGH treatment. It appears from those studies that individuals with earlier onset of GHD, as well as those with the lowest BMD, had the greatest likelihood of showing significant changes in BMD with rhGH. More recently, four randomized placebo-controlled trials have been conducted in adult GHD subjects treated with rhGH for at least 18 months. In one study of men only, BMD increased in the lumbar spine by 5.1% and the femoral neck by 2.4% (Baum et al., 1996). In another study of both men and women, there were no significant differences in BMD after 18 months between the group treated with rhGH and those taking placebo (Sneppen et al., 2002). In the third trial, men but not women showed increases in spine BMD after 24 months of rhGH compared with untreated controls. The most definitive and most recent study was a true randomized placebo-controlled trial using physiologic rather than pharmacologic doses of rhGH in GHD patients. In contrast to the three previous studies, changes in serum IGF-I were titrated within the normal range rather than to the supraphysiologic levels achieved with higher doses of rhGH. Interestingly, in that study of 67 men and women, spine BMD increased after 18 months by nearly 4% in men, which was statistically different from the placebo control but increased much less in women, and those changes were not statistically different from placebo (Snyder et al., 2007). Neither gender showed a significant change in hip BMD in response to rhGH in doses up to 12 ug/kg/day. In sum, there are clear sex- and dose-dependent effects of rhGH on BMD in GHD subjects treated for at least 18 months.

Growth hormone administration to elderly men and women

As previously noted, elderly people have lower GH secretory amplitudes and reduced serum levels of IGF-I and IGFBP-3 compared with younger adults (Kelijman, 1991; Rudman et al., 1981; Donahue et al., 1990). Moreover, the pulse frequency for GH is reduced in the elderly population. Based on these data, it was assumed that skeletal responsiveness to GH in elders would be identical to that seen in GHD patients. In elderly men, one group reported a blunted serum IGF-I response to 0.1 mg/kg GH (36% lower) compared with that in younger men or adults with GHD (Lieberman et al., 1994). However, Rosen et al. (1999) and others have noted that the generation of IGF-I after various doses of rhGH to frail elders was not associated with significant GH resistance. GH replacement for adult GHD or for pharmacologic treatment results in similar IGF-I responses independent of age. Side effects such as fluid retention, gynecomastia, and carpal tunnel appear to be more common in the elderly who are given rhGH compared with young adults who have GHD.

Rudman gave 21 men over age 65 0.03 mg/kg of rhGH three times per week (as a subcutaneous injection), or placebo, in a randomized controlled trial. Twelve men received rhGH while nine men served as observational controls. The men were selected on the basis of a low serum IGF-I concentration (Rudman et al., 1990). The rhGH produced a threefold rise in circulating IGF-I, an increase in lean body mass (as measured by 40K analysis), and a decline in total adipose mass. BMD of the lumbar vertebrae (L1−L4) as measured by dual-energy X-ray absorptiometry (DXA) increased 1.6% after 6 months in the treatment group, while no change was noted in controls. Biochemical markers of bone turnover were not examined, and no changes in BMD were detected in the mid or distal radius or three areas of the hip. Furthermore, the spinal BMD changes at 6 months were not sustained at 1 year.

Marcus et al. studied the effects of rhGH in 16 men and women over age 60 (Marcus et al., 1990). Daily doses of rhGH (0.03, 0.06, or 0.12 mg/kg BW/day) were randomly assigned to each subject and administered once daily for 7 days. Serum IGF-I, osteocalcin, PTH, and calcitriol concentrations all increased during treatment. In this short-term study, there was also a significant rise in urinary hydroxyproline and urinary calcium excretion with a concomitant decline in urinary sodium excretion.

Holloway et al. conducted a longer double-blind RPCT of daily rhGH for 1 year in 27 healthy elderly women, 8 of whom took a stable dose of estrogen throughout the study (Holloway et al., 1994). Thirteen women completed 6 months of treatment, and fourteen women completed 6 months in the placebo group. Side effects prompted a 50% reduction in the original dose of rhGH (from 0.043 mg/kg BW or approximately 0.3 mg rhGH/kg/week to 0.02 mg/kg/day) and led to several dropouts in the treatment group. Fat mass and percentage body fat declined in the treatment group, but there were no changes in BMD at the spine or hip at 6 or 12 months in other groups (Holloway et al., 1994). Although BMD did not change, there were changes in some biochemical parameters. In particular, urinary markers of bone resorption (e.g., hydroxyproline and pyridinoline) increased after 6 months of rhGH treatment. The response of bone formation markers was more variable. Osteocalcin increased, but type I procollagen peptide levels did not change. For women taking estrogen replacement therapy, indices of bone turnover (both formation and resorption) were blunted.

Rosen et al. (1999) reported that there was a dose-dependent decrease in total body BMD after 1 year of rhGH in frail elderly men and women. This occurred despite striking increases in osteocalcin and serum IGF-I with the highest doses of rhGH (0.01 mg/kg/day). In part, the absence of a GH effect on BMD is not surprising, because resorption is coupled to formation and GH activates the entire remodeling sequence. Moreover, the skeletal response was only measured after 1 year of treatment; this was probably inadequate to determine the true effect of rhGH on BMD as noted from earlier studies in GHD. Not surprisingly, in the same trial of 132 frail elderly subjects by Rosen and colleagues, urinary N-telopeptide and osteocalcin rose to the same extent, suggesting that total bone turnover, not just bone formation, was increased by rhGH therapy. The relatively high incidence of acute side effects (weight gain, carpal tunnel syndrome, edema, and glucose intolerance) in GH trials, especially in the frail elderly, has remained particularly troublesome even with titrating doses. Moreover, high serum IGF-I levels for long periods may predispose individuals to certain malignancies. Thus, there is limited enthusiasm for rhGH or rhGHRH treatments in the frail elderly.

Growth hormone treatment for osteoporotic patients

Short nonrandomized clinical trials with GH in osteoporosis were attempted well before GH replacement therapy was approved in pituitary insufficiency. As early as 1975, two patients with osteogenesis imperfecta and one patient with involutional osteoporosis were treated with GH. Histomorphometric parameters of increased bone formation and resorption were noted. Subsequent studies employed GH with and without antiresorptive agents. Aloia et al. (1987) administered between 2 and 6 U/day of GH for 12 months to patients with postmenopausal osteoporosis (the first 6 months of treatment featured low-dose GH; the last 6 months consisted of high-dose GH (6 U/day). Radial BMC dropped slightly, and histomorphometric parameters did not change during treatment. However, severity of back pain decreased considerably in several people. Daily GH injections (4 U/day) combined with alternating doses of calcitonin produced an increase in total body calcium (measured by neutron activation analysis) but a decline in radial bone mass after 16 months. In a separate trial, 14 postmenopausal women were given 2 months of GH, then 3 months of calcitonin, in a modified form of coherence therapy. Total body calcium increased 2.3%/year with few side effects, but there were no changes in BMD or histomorphometric indices. One study administered 16 U of rhGH every other day along with daily sodium fluoride to six women with postmenopausal osteoporosis. On histomorphometric analysis, there was a significant increase in the number of osteoblasts and osteoclasts, but BMD was unchanged.

Johansson et al. (1994) conducted a crossover double-blinded RPCT of rhGH and idiopathic osteoporosis. In this 7-day trial with rhGH 2 IU/m2, procollagen peptide and osteocalcin levels increased after treatment as did urinary markers of bone resorption. The changes in osteocalcin were relatively small and were not sustained after discontinuation of GH treatment. Thus, GH stimulates bone remodeling activity, thereby leaving open the possibility that GH can be coupled to antiresorptive agents. This thesis was tested in a 2-year randomized trial by Holloway and colleagues (Holloway et al., 1997). In that study, rhGH and nasal calcitonin increased spine BMD by approximately 2%. This, however, was not much different than the use of CT alone, and certainly less than what has been seen in very large randomized trials with antiresorptive agents. Once again, there were several side effects that produced limited enthusiasm for rhGH as a primary treatment for osteoporosis. In another combination trial that was larger and longer, 80 osteoporotic postmenopausal women on hormone replacement therapy (HRT) (estrogen with or without progestin) were administered rhGH 10 2.5 U/day or placebo for 18 months, and then open-label rhGH for another 18 months. These women were then followed for an

additional 24 months. Women given GH and HRT had a marked increase in total body and spine BMD compared with placebo, which was maintained to year 3 but disappeared by year 5 (Landin-Wilhelmsen et al., 2003). This trial suggested that combination therapy of an anabolic and an antiresorptive could be used in postmenopausal osteoporosis. A similar result was noted in a 7-year follow-up of 30 men and women who received rhGH for 4 years and then were treated with alendronate for an additional 3 years. BMD increased significantly versus a control group after 3 years, especially in the males, and the addition of alendronate further enhanced spine BMD at year 7 (Biermasz et al., 2004). Therefore, it is likely that GH may induce small changes in BMD that over an extended period could translate into fewer spine fractures as noted by Krantz et al.

Insulin-like growth factor I for the treatment of osteoporosis

Overview

In the late 1980s, clinical trials with rhIGF-I for diabetes mellitus were begun. The availability of this recombinant peptide and the absence of other treatments to stimulate bone formation accelerated animal and human studies of rhIGF-I in metabolic bone diseases. Theoretically, there are potential benefits for rhIGF-I compared with rhGH. These include (1) more direct stimulation of bone formation; (2) bypass of skeletal GH resistance; and (3) reduction in GH-induced side effects such as carpal tunnel and diabetes mellitus. There are, however, considerably fewer animal and human studies using rhIGF-I than those using rhGH. Therefore, these advantages have either yet to be fully realized or have not been validated.

IGF-I is not a potent mitogen in most tissues, and bone is no exception (see Chapter 8 by Canalis). There are high-affinity receptors for IGF-I expressed on osteoblasts, and IGF-I can stimulate preosteoblast replication and provoke resting cells to proceed through their growth cycles. IGF-I maintains the differentiated osteoblast phenotype, stimulates collagen synthesis, and prevents collagen degradation. Theoretically, therefore, despite its relatively weak mitogenic properties, IGF-I could potentially have significant anabolic activity on the skeleton.

Murine studies

In hypophysectomized rats, growth can be fully restored by administration of either GH or IGF-I but not IGF-II (Schoenle et al., 1985). A similar growth response occurs after rhIGF-I in streptozotocin-diabetic rats but not in sex-linked dwarf-mutant chickens (Schoenle et al., 1985; Tixier-Boichard et al., 1992). In normal rats, rhIGF-I administrated either systemically or locally (hind limb infusions) does not stimulate longitudinal bone growth. In the spontaneously diabetic BioBreeding (BB) rat, rhIGF-I treatment did not result in changes in epiphyseal width, osteoblast surfaces, or osteocalcin concentration (Verhaeghe et al., 1992).

The skeletal response to rhIGF-I is determined by the GH/IGF-I status of the animal. For example, IGF-I does not increase bone formation in normal rats, whereas it stimulates bone growth and normalizes type I procollagen mRNA levels in hypophysectomized rats (Schmid et al., 1989; Spencer et al., 1991; Tobias et al., 1992). Similarly, in the spontaneous mouse mutant (lit/lit), GHR absence results in very low levels of IGF-I and skeletal dwarfism. IGF-I treatment restores growth and increases total body water but does not enhance BMD in these mice (Donahue et al., 1993). These findings are somewhat similar to the effects of GH on the skeleton in GHD animals. However, rhIGF-I and rhGH differ in their actions on the circulatory IGF regulatory system. GH stimulates hepatic production of IGF-I, IGFBP-3, and ALS, while rhIGF-I administration increases the total circulating pool of IGF-I but suppresses hepatic production of IGFBP-3, primarily through feedback inhibition of GH secretion. It is conceivable that variations in IGF-I biological activity (between direct IGF-I administration and endogenously produced IGF-I as a result of GH treatment) may be due to the relative proportion of free versus bound IGF-I to IGFBP-3.

Several experimental paradigms have been employed to study the effects of IGF-I on bone turnover in animals. These include (1) oophorectomy, (2) diabetes mellitus (spontaneous or induced), and (3) immobilization. In oophorectomized rats, administration of rhIGF-I has variable effects on bone remodeling, BMD, and bone strength. In older oophorectomized rats, rhIGF-I increased midshaft tibial BMD and enhanced periosteal bone apposition (Ammann et al., 1996). Six weeks of rhIGF-I (delivery by mini-osmotic pump) to older rats caused a dose-dependent increase in BMD in the lumbar spine and proximal femur, although bone strength and stiffness did not change. Muller reported that subcutaneous administration of rhIGF-I to adult oophorectomized rats stimulated bone formation as evidenced by increased osteoid surfaces, osteoblast surfaces, and mineral apposition rates. At high doses of rhIGF-I, osteoclast surface and osteoclast number also increased. In contrast, Tobias et al. (1992) found that rhIGF-I (200 mg/kg) administered for 17 days to 15-week-old rats increased longitudinal and periosteal growth of the femur but suppressed trabecular bone formation in

oophorectomized and control rats. Bone resorption was also slightly suppressed during rhIGF-I treatment, although not to the extent that bone formation was inhibited.

T1DM (Type I diabetes mellitus) is associated with decreased cortical BMD. Although the pathophysiology of diabetic osteopenia remains unknown, it appears that the duration of diabetes, the extent of diabetic control, and the timing of disease onset are each associated with higher risks of low BMD (McNair, 1988). Numerous clinical studies report abnormalities in the GH/IGF-I axis in TIDM (Rasingani, 2017) including reductions in serum IGF-I due to portal insulinopenia and elevations in GH secretion (Hourd, 1991). Diminished insulin action in TIDM is associated with increased serum IGFBP-1 levels, which can sequester IGF-I, affect its bioavailability to the skeleton, and contribute to impaired bone acquisition. The cellular mechanism leading to low BMD in TIDM relates mainly to defects in osteoblastic function, as serum levels of osteocalcin, a marker of bone formation, are reduced in TIDM (Verhaeghe et al., 1992). Serum markers of bone formation are reduced in type I diabetics, suggesting a possible defect in osteoblastic activity (Verhaeghe et al., 1992). Serum IGF-I levels are either normal or low in IDDM but often are reduced in patients with poor diabetic control. In these same people, serum IGFBP-1 levels are quite high. This has led investigators to believe that changes in the IGF regulatory system during poor metabolic control contribute to impaired growth.

Spontaneously diabetic BB rats exhibit osteopenia and therefore provide a useful model for studying the effects of IGF-I on bone remodeling. Even though bone formation is lower in BB than in control rats (as measured by serum markers), administration of rhIGF-I does not increase bone epiphyseal width, osteoblast surfaces, or serum osteocalcin (Verhaeghe et al., 1992). Thus, despite evidence that circulating levels of IGF-I are reduced in some patients with type I IDDM, preliminary animal studies have failed to show that IGF-I administration can correct any inherent defect in bone formation. However, those studies did not include insulin treatment, so it is unclear whether IGF-I could have anabolic properties on bone in the presence of adequate insulin levels.

Alternate ways of exploiting the anabolic properties of IGF-I in bone have been proposed. IGF-I has been administered by intraarterial infusion or coupled to IGFBP-3. Infusion of rhIGF-I continuously into the arterial supply of the right hind limb of ambulatory rats for 14 days led to a 22% increase in cortical and trabecular bone formation in the infused limb (Spencer et al., 1991). By histomorphometry the number of osteoblasts, but not osteoclasts, was increased. Using an alternative model, Bagi et al. (1994) administered rhIGF-I or a complex of IGF-I-IGFBP-3 to 16-week-old oophorectomized rats. The IGF-I—IGFBP-3 complex (7.5 mg/kg/day) led to greater increases in bone formation than IGF-I alone, though both treatments increased longitudinal bone growth. The highest doses of rhIGF-I and rhIGF-I-GFBP-3 enhanced trabecular thickness in the lumbar vertebrae and femoral epiphyses, and increased bone resorption, but only in the femoral metaphysis. A similar study contrasting IGF-I with IGF-I-GFBP-3 was performed in 22-week-old oophorectomized rats (Brommage et al., 1993). BMD increased in both groups, but fewer than 10% of the rats treated with IGF-I—IGFBP-3 complex developed hypoglycemia, compared with nearly 50% of those treated with rhIGF-I alone.

Human studies of insulin-like growth factor I and bone mineral density

There is one published study of bone markers that employed rhIGF-I to healthy young postmenopausal women. Doses of rhIGF-I from 30 to 180 mg/kg/day were administered daily by subcutaneous injection for 6 days to older postmenopausal women without fractures and with normal BMD (Ebeling, 1993). Very significant dose-dependent increases in serum PICP, osteocalcin, and urinary deoxypyridinoline were reported. Although the rise in PICP was greater than the increase in collagen breakdown (measured by deoxypyridinoline), it is uncertain whether this meant that formation was stimulated more than resorption. For the two highest doses of rhIGF-I (120 and 180 mg/kg/day), orthostasis, weight gain, edema, tachycardia, and parotid discomfort were noted. At lower doses (30 and 60 mg/kg/day), fewer side effects were reported, but less discrete changes in PICP were noted.

One indication for rhIGF-I treatment, which has been approved in the United States, Sweden, and other countries, is the GH-resistant short stature syndrome (Laron dwarf), in which patients lack functional GHRs and thus do not respond to GH. Laron dwarfs show very low levels of IGF-I in serum with high levels of GH (due to a lack of negative feedback on GH by IGF-I) and are growth retarded (Bondy et al., 1994). Underwood treated one such boy (age 9) with 2 weeks of continuous intravenous rhIGF-I (Bondy et al., 1994). Urinary calcium excretion increased while urinary phosphate and sodium decreased. After a 2-week continuous infusion of rhIGF-I, the patient was treated with twice-daily SC rhIGF-I (120 mg/kg) for 2 years. Growth occurred at a rate of 10 cm/year, compared with 5 cm for the 3 years prior to treatment. Subsequently, Underwood and colleagues have treated eight patients in this manner without hypoglycemia, while Laron and his group have treated five children (Bondy et al., 1994; Laron et al., 1992). More recently, a child with an IGF-I deletion mutation in exon 5 has been reported. This patient had very short stature, mental retardation, and other abnormalities along with very low levels of circulating IGF-I (Woods et al., 1996). The rhIGF-I treatment led to a marked increase in linear growth and a

huge increase in spinal bone mass. However, when corrected for changes in size of the bone, the incremental changes in volumetric bone mass were much less impressive (Camacho-Hubner et al., 1999). Hypoglycemia was avoided in these cases by having children eat 3 to 4 hours after their IGF-I injection, although several children had selective growth of adenoidal tissue.

Two unique aspects of these IGF-I data challenge previous concepts about the role of GH in skeletal homeostasis. First, IGF-I can act as a classical endocrine hormone stimulating longitudinal growth independent of GH, although not to the same extent as GH; second, GH may not be absolutely essential for statural growth; i.e., the stimulatory effect of GH on chondrocytes that permits skeletal responsiveness to IGF-I may not be as critical as once perceived. In fact, crossing Laron dwarf mice (GHR-null mice, GHRKO) with mice expressing hepatic IGF-I transgene (HIT) restored IGF-I levels in serum (GHRKO-HIT mice) and was able to promote skeletal linear growth and BMD (Wu et al., 2013). However, despite restoration of serum IGF-I in the GHRKO-HIT mice, growth was not normalized due to compromised delivery of IGF-I to the tissues, the inability of endocrine IGF-I to restore bone tissue IGF-I levels, and IGF-I-independent effects of GH on linear and radial bone growth. Caution must be undertaken in examining the effects of rhIGF-I on BMD in children, because most changes in the skeleton relate to linear growth and periosteal enhancement, both of which can contribute to two-dimensional changes in BMD as measured by DXA, but the changes are less when corrected for size (Bachrach et al., 1998).

Idiopathic osteoporosis in men is an ill-defined syndrome of low bone mass and spinal fractures without associated hypogonadism. By histomorphometry, these men often have low bone turnover, suggesting a possible defect in bone formation. Several groups of investigators have suggested that this syndrome is related to low serum IGF-I levels (Ljunghall et al., 1992; Kurland et al., 1997, 1998, Rubin and Bilezikian, 2002). Because the therapeutic options in males with osteoporosis are somewhat limited, and treatment for low bone turnover states is generally frustrating, the therapeutic potential for anabolic agents like IGF-I in this condition should be quite high. In one male with idiopathic osteoporosis and low serum IGF-I, Johansson et al. (1994) administered rhIGF-I (160 mg/kg/day SC) for 7 days. Bone alkaline phosphatase, osteocalcin, and PICP all increased more than 40% over baseline. However, urinary calcium/creatinine and hydroxyproline excretion rose during treatment. In a recent trial of rhIGF-I (at a dose of 80 mg/kg/day) and rhGH (2 IU/m2/day) in 12 men, serum osteocalcin, serum procollagen peptide, and urinary deoxypyridinoline excretion all increased following 7 days of rhIGF-I treatment (Holloway et al., 1997). Although there were slight differences in the response of certain biochemical markers to IGF-I and GH, both forms of therapy produced significant increases in bone resorption.

Anorexia nervosa is a condition characterized by amenorrhea and profoundly low BMD (due to either low peak bone mass or rapid bone loss) as well as reduced body weight, low circulating IGF-I, resistance to GH, and a marked propensity for fractures. Hence, rhIGF-I might be considered an ideal therapeutic option for this group of adolescents and young adults with severe bone disease, particularly because oral contraceptive pills (OCPs) have virtually no effect on BMD in these patients. Grinspoon et al. (2003) studied 60 anorexic women with low BMD in an RPCT of 9-month duration using rhIGF-I 30 ug/kg/d with and without OCPs (Grinspoon, 1993). The group of women receiving rhIGF-I and OCPs had the greatest increase in spine BMD (11.8%); rhIGF-I alone also increased BMD (11.1%), while bone loss occurred in the group receiving placebo or OCPs alone. Interestingly, there were virtually no side effects in the anorexic women, and serum IGFBP-2 was inversely correlated with changes in hip BMD. Although the increase in BMD was relatively modest, considering the lack of other available therapies, these changes are encouraging and suggest that further studies are needed.

Clinical trials provide evidence that IGF-I acts by increasing the generation of new osteons, thereby promoting bone resorption and formation. This action might be ideal for older individuals, because one characteristic of age-related osteoporosis is suppressed bone formation. However, concerns about dosing and side effects have limited enthusiasm for this approach. Yet it is conceivable that low doses of rhIGF-I (,30 mg/kg/day) could differentially stimulate bone formation. In one trial, 16 healthy elderly women were given 60 ug/kg/day (high dose) and 15 mg/kg/day (low dose) of rhIGF-I and tested for 28 days. The high-dose rhIGF-I increased the markers of bone resorption and formation. However, low doses of rhIGF-I caused increases in serum osteocalcin and PICP but had no effect on total pyridinoline excretion (Ghiron et al., 1995). These data would support the thesis that low doses of rhIGF-I may directly increase osteoblastic function with only a minimal increase in bone resorption. However, further studies will be needed to assess the future therapeutic role of low doses of rhIGF-I in osteoporosis.

One strategy is to administer a bone-specific agent that stimulates bone mass, such as PTH. Intermittent hPTH increases trabecular bone by stimulating osteoblasts to synthesize IGF-I and other growth factors (Rosen and Donahue, 1998). Another strategy is to administer IGF-I along with an IGFBP. Bagi et al. (1994) previously reported that the IGF-I/IGFBP-3 complex could enhance bone mass in the metaphysis and epiphysis of rats. One small randomized placebo-controlled trial utilized subcutaneous infusions of IGF-I/IGFBP-3 in 24 older women with hip fractures. Bone loss in the contralateral hip was reduced considerably after 6 months (i.e., from 6% to 1.5%) in those subjects who were given complex

IGF-I/IGFBP-3 versus those receiving saline (Geusens et al., 1998; Boonen et al., 2002). Accompanying that change in BMD was also an increase in grip strength in those that received the active agent, with no significant side effects reported.

Limitations to the clinical use of recombinant human insulin-like growth factor I

IGF-I treatment has its limitations (Zofkova, 2003). The impacts of serious sequelae of long-term administration of IGF-I remain to be evaluated. During IGF-I treatment, undesirable metabolic manifestations may develop hypoglycemia (in particular after large intravenous doses) and hypophosphatemia with subsequent hypotension (Zofkova, 2003). A more frequent incidence of gynecomastia was also observed. The use of IGF-I/IGFBP-3 complex seems to be very useful and safe in women who are older and who have a recent hip fracture (Agnusdei and Gentilella, 2005). Furthermore, the combination of an anabolic agent with an antiresorptive drug (such as calcitonin or alendronate) could be more potent than either agent alone. However, the therapeutic effects of such a combined approach on BMD at different skeletal sites have been controversial (Agnusdei et al., 2005).

Summary

Several lines of evidence point to the importance of local IGF-I in skeletal turnover. Systemic IGF-I, regulated by GH, IGFBPs, and several proteases as well as IGFRs, also must be important for full linear growth and peak skeletal acquisition. Recent work suggests that recombinant growth factors may be anabolic for the skeletal remodeling unit. First, both GH and IGF-I stimulate osteoblastic differentiation. In vivo models using targeted deletion or overexpression of IGFs or IGF-IR support a critical role for this regulatory circuit in peak bone acquisition. In respect to growth hormone, rhGH treatment increases bone mass but must continue for several years, and outcomes should be measured for several years thereafter (as the skeletal response cannot be detected shortly after treatment). Skeletal response to rhGH is greater in men than in women, and the potential long-term risks of elevated IGF-I, as well as the availability of other less expensive therapies (such as bisphosphonates, teriparatide and abaloparatide), precludes more vigorous development of these peptides. Third, in GHD children, both rhGH and rhIGF-I can enhance trabecular and cortical BMD, and certainly recombinant GH is part of current recommendations for this condition. Therefore, unless more favorable responses in properly controlled clinical trials are seen with rhGH or rhIGF-I, these drugs are not recommended for the treatment of postmenopausal osteoporosis.

Acknowledgments

This work was funded through PHS Grants from NIDDK 92790 and NIAMS AR 45433.

References

Agnusdei, D., Gentilella, R., 2005. GH and IGF-I as therapeutic agents for osteoporosis. J. Endocrinol. Investig. 28 (8 Suppl. l), 32–36.

Ali, O., et al., 2007. Growth hormone therapy improves bone mineral density in children with cerebral palsy: a preliminary pilot study. J. Clin. Endocrinol. Metab. 92 (3), 932–937.

Aloia, J.F., Vaswani, A., Meunier, P.J., Edouard, C.M., Arlot, M.E., Yeh, J.K., Cohn, S.H., 1987. Coherence treatment of postmenopausal osteoporosis with growth hormone and calcitonin. Calcif. Tissue Int. 40 (5), 253–259.

Ammann, P., et al., 1996. Bone density and shape as determinants of bone strength in IGF-I and/or pamidronate-treated ovariectomized rats. Osteoporos. Int. 6 (3), 219–227.

Andress, D.L., Birnbaum, R.S., 1991. A novel human insulin-like growth factor binding protein secreted by osteoblast-like cells. Biochem. Biophys. Res. Commun. 176 (1), 213–218.

Angelloz-Nicoud, P., Binoux, M., 1995. Autocrine regulation of cell proliferation by the insulin-like growth factor (IGF) and IGF binding protein-3 protease system in a human prostate carcinoma cell line (PC-3). Endocrinology 136 (12), 5485–5492.

Arany, E., et al., 1994. Differential cellular synthesis of insulin-like growth factor binding protein-1 (IGFBP-1) and IGFBP-30020sxyeiwithin human liver. J. Clin. Endocrinol. Metab. 79 (6), 1871–1876.

Arends, N.J., et al., 2003. GH treatment and its effect on bone mineral density, bone maturation and growth in short children born small for gestational age: 3-year results of a randomized, controlled GH trial. Clin. Endocrinol. 59 (6), 779–787.

Bach, L.A., 1999. Insulin-like growth factor binding protein-6: the "forgotten" binding protein? Horm. Metab. Res. 31 (2–3), 226–234.

Bachrach, L.K., et al., 1998. Bone mineral, histomorphometry, and body composition in adults with growth hormone receptor deficiency. J. Bone Miner. Res. 13 (3), 415–421.

Bagi, C.M., et al., 1994. Benefit of systemically administered rhIGF-I and rhIGF-I/IGFBP-3 on cancellous bone in ovariectomized rats. J. Bone Miner. Res. 9 (8), 1301–1312.

Bang, P., et al., 1998. Postoperative induction of insulin-like growth factor binding protein-3 proteolytic activity: relation to insulin and insulin sensitivity. J. Clin. Endocrinol. Metab. 83 (7), 2509–2515.

Baroncelli, G.I., et al., 1998. Measurement of volumetric bone mineral density accurately determines degree of lumbar undermineralization in children with growth hormone deficiency. J. Clin. Endocrinol. Metab. 83 (9), 3150–3154.

Baroncelli, G.I., et al., 2004. Longitudinal changes of lumbar bone mineral density (BMD) in patients with GH deficiency after discontinuation of treatment at final height; timing and peak values for lumbar BMD. Clin. Endocrinol. 60 (2), 175–184.

Bauer, D.C., et al., 1998. Low serum IGF-I but not IGFBP-3 predicts hip and spine fracture. The study of osteoporotic fracture. Bone 23, 561.

Baum, H.B., et al., 1996. Effects of physiologic growth hormone therapy on bone density and body composition in patients with adult-onset growth hormone deficiency. A randomized, placebo-controlled trial. Ann. Intern. Med. 125 (11), 883–890.

Baumann, G., et al., 1989. Regulation of plasma growth hormone-binding proteins in health and disease. Metabolism 38 (7), 683–689.

Baxter, R.C., 2000. Insulin-like growth factor (IGF)-binding proteins: interactions with IGFs and intrinsic bioactivities. Am. J. Physiol. Endocrinol. Metab. 278 (6), E967–E976.

Ben Lagha, N., et al., 2006. IGFBP-1 involvement in intrauterine growth retardation. Endocrinology 147, 4730–4737.

Bereket, A., et al., 1995. Insulin-like growth factor binding protein-3 proteolysis in children with insulin-dependent diabetes mellitus: a possible role for insulin in the regulation of IGFBP-3 protease activity. J. Clin. Endocrinol. Metab. 80 (8), 2282–2288.

Biermasz, N.R., et al., 2004. Long-term skeletal effects of recombinant human growth hormone (rhGH) alone and rhGH combined with alendronate in GH-deficient adults: a seven-year follow-up study. Clin. Endocrinol. 60 (5), 568–575.

Bikle, D.D., et al., 2001. The skeletal structure of insulin-like growth factor I-deficient mice. J. Bone Miner. Res. 16 (12), 2320–2329.

Bikle, D.D., et al., 2006. Development and progression of alopecia in the vitamin D receptor null mouse. J. Cell. Physiol. 207 (2), 340–353.

Bikle, D.D., et al., 2002. Insulin-like growth factor I is required for the anabolic actions of parathyroid hormone on mouse bone. J. Bone Miner. Res. 17, 1570–1578.

Bing-You, R.G., et al., 1993. Low bone mineral density in adults with previous hypothalamic-pituitary tumors: correlations with serum growth hormone responses to GH-releasing hormone, insulin-like growth factor I, and IGF binding protein 3. Calcif. Tissue Int. 52 (3), 183–187.

Bianda, T., et al., 1998. Effects of short term IGF-I or GH treatment on bone metabolism and production of 1,25 vitamin D in GH deficient patients. J. Clin. Endocrinol. Metab. 83, 61–67.

Bondy, C.A., et al., 1994. Clinical uses of insulin-like growth factor I. Ann. Intern. Med. 120 (7), 593–601.

Boonen, S., et al., 2002. Musculoskeletal effects of the recombinant human IGF-I/IGF binding protein-3 complex in osteoporotic patients with proximal femoral fracture: a double-blind, placebo-controlled pilot study. J. Clin. Endocrinol. Metab. 87 (4), 1593–1599.

Bouillon, R., 1991. Growth hormone and bone. Horm. Res. 36 (Suppl. 1), 49–55.

Braulke, T., et al., 1995. Proteolysis of IGFBPs by cathepsin D in vitro and in cathepsin D-deficient mice. Prog. Growth Factor Res. 6 (2–4), 265–271.

Bravenboer, N., et al., 1994. The effect of GH on bone mass and bone turnover of GHD men. J. Bone Miner. Res. 9 (S1), B253.

Brismar, K., et al., 1988. Insulin regulates the 35 kDa IGF binding protein in patients with diabetes mellitus. J. Endocrinol. Investig. 11 (8), 599–602.

Brixen, K., et al., 1990. A short course of recombinant human growth hormone treatment stimulates osteoblasts and activates bone remodeling in normal human volunteers. J. Bone Miner. Res. 5 (6), 609–618.

Brommage, R., et al., 1993. Treatment with the rhIGF-I/IGFBP-3 complex increases cortical bone and lean body mass in oophorectomized rats. J. Bone Miner. Res. 9 (Suppl. 1), 1.

Camacho-Hubner, C., et al., 1999. Effects of recombinant human insulin-like growth factor I (IGF-I) therapy on the growth hormone-IGF system of a patient with a partial IGF-I gene deletion. J. Clin. Endocrinol. Metab. 84 (5), 1611–1616.

Canalis, E., et al., 1989. Insulin-like growth factor I mediates selective anabolic effects of parathyroid hormone in bone cultures. J. Clin. Investig. 83 (1), 60–65.

Capatina, C., et al., 2015. Sixty years of neuroendocrinology: Acromegaly. J. Endocrinol. 226, T141–T160.

Celil, A.B., et al., 2005. Osx transcriptional regulation is mediated by additional pathways to BMP2/Smad signaling. J. Cell. Biochem. 95 (3), 518–528.

Chelius, D., et al., 2001. Expression, purification, and characterization of the structure and disulfide linkages of insulin-like growth factor binding protein-4. J. Endocrinol. 168 (2), 283–296.

Cheng, S.L., et al., 2003. MSX2 promotes osteogenesis and suppresses adipogenic differentiation of multipotent mesenchymal progenitors. J. Biol. Chem. 278 (46), 45969–45977.

Christiansen, J.S., et al., 1991. GH-replacement therapy in adults. Horm. Res. 36 (Suppl. 1), 66–72.

Claussen, M., et al., 1997. Proteolysis of insulin-like growth factors (IGF) and IGF binding proteins by cathepsin D. Endocrinology 138 (9), 3797–3803.

Cohen, P., et al., 1992. Prostate-specific antigen (PSA) is an insulin-like growth factor binding protein-3 protease found in seminal plasma. J. Clin. Endocrinol. Metab. 75 (4), 1046–1053.

Cohen, P., et al., 1994. Biological effects of prostate specific antigen as an insulin-like growth factor binding protein-3 protease. J. Endocrinol. 142 (3), 407–415.

Collett-Solberg, P.F., Cohen, P., 1996. The role of the insulin-like growth factor binding proteins and the IGFBP proteases in modulating IGF action. Endocrinol Metab. Clin. N. Am. 25 (3), 591–614.

Conover, C.A., 1991. Glycosylation of insulin-like growth factor binding protein-3 (IGFBP-3) is not required for potentiation of IGF-I action: evidence for processing of cell-bound IGFBP-3. Endocrinology 129 (6), 3259–3268.

Conover, C.A., et al., 1993. Regulation of insulin-like growth factor binding protein-5 messenger ribonucleic acid expression and protein availability in rat osteoblast-like cells. Endocrinology 132 (6), 2525–2530.

Conover, C.A., et al., 1994. Insulin-like growth factor-II enhancement of human fibroblast growth via a nonreceptor-mediated mechanism. Endocrinology 135 (1), 76–82.

Conover, C.A., et al., 1995. Endogenous cathepsin D-mediated hydrolysis of insulin-like growth factor-binding proteins in cultured human prostatic carcinoma cells. J. Clin. Endocrinol. Metab. 80 (3), 987–993.

Conover, C.A., et al., 2002. Subcutaneous administration of insulin-like growth factor (IGF)-II/IGF binding protein-2 complex stimulates bone formation and prevents loss of bone mineral density in a rat model of disuse osteoporosis. Growth Hormone IGF Res. 12 (3), 178–183.

Corpas, E., et al., 1993. Human growth hormone and human aging. Endocr. Rev. 14 (1), 20–39.

Courtland, H.W., et al., 2010. Sex specific regulation of body size by the acid labile subunit. J. Bone Miner. Res. 25, 2059–2068.

Coverley, J.A., Baxter, R.C., 1997. Phosphorylation of insulin-like growth factor binding proteins. Mol. Cell. Endocrinol. 128 (1–2), 1–5.

Crist, D.M., et al., 1988. Body composition response to exogenous GH during training in highly conditioned adults. J. Appl. Physiol. 65 (2), 579–584.

D'Ercole, A.J., 1996. Insulin-like growth factors and their receptors in growth. Endocrinol Metab. Clin. N. Am. 25 (3), 573–590.

Dabuer, A., 2016. Mutations in PAPPA2 causes short stature due to low IGF-1 availability. EMBO Mol. Med. 8, 363–374.

Daughaday, W.H., et al., 1972. Somatomedin: proposed designation for sulphation factor. Nature 235 (5333), 107.

Dawson-Hughes, B., et al., 1986. Regulation of growth hormone and somatomedin-C secretion in postmenopausal women: effect of physiological estrogen replacement. J. Clin. Endocrinol. Metab. 63 (2), 424–432.

de Muinck Keizer-Schrama, S.M., et al., 1992. Dose-response study of biosynthetic human growth hormone (GH) in GH-deficient children: effects on auxological and biochemical parameters. Dutch Growth Hormone Working Group. J. Clin. Endocrinol. Metab. 74 (4), 898–905.

de la Piedra, P.C., et al., 1988. Correlation among plasma osteocalcin, growth hormone, and somatomedin C in acromegaly. Calcif. Tissue Int. 43 (1), 44–45.

DeBoer, H., et al., 1994. Consequences of childhood-onset growth hormone deficiency for adult bone mass. J. Bone Miner. Res. 9, 1319–1326.

Delmas, P.D., et al., 1986. Serum bone GLA-protein in growth hormone deficient children. J. Bone Miner. Res. 1 (4), 333–338.

DeMambro, V.E., Kawai, M., Clemens, T.L., Fulzele, K., Maynard, J.A., de Evsikova, C.M., Johnson, K.R., Canalis, E., Beamer, W.G., Rosen, C.J., Donahue, L.R., 2010. A Novel Spontaneous Mutation of *Irs1* in Mice Results in Hyperinsulinemia, Reduced Growth, Low Bone Mass and Impaired Adipogenesis. J. Endocrinol. 204 (3), 241–253.

Dennison, E.M., et al., 2003. Growth hormone predicts bone density in elderly women. Bone 32 (4), 434–440.

Domene, H.M., et al., 2004. Deficiency of the circulating insulin-like growth factor system associated with inactivation of the acid-labile subunit gene. N. Engl. J. Med. 350, 570–577.

Domene, H.M., et al., 2010. Deficiency of ALS in children with short stature. Pediatr. Endocrinol. Rev. 7 (4), 339–346.

Donahue, L.R., et al., 1990. Age-related changes in serum insulin-like growth factor-binding proteins in women. J. Clin. Endocrinol. Metab. 71 (3), 575–579.

Donahue, L.R., et al., 1993. Regulation of metabolic water and protein compartments by insulin-like growth factor-I and testosterone in growth hormone-deficient lit/lit mice. J. Endocrinol. 139 (3), 431–439.

Ducy, P., et al., 1999. A Cbfa1-dependent genetic pathway controls bone formation beyond embryonic development. Genes Dev. 13 (8), 1025–1036.

Durham, S.K., et al., 1994. The insulin-like growth factor-binding protein-4 (IGFBP-4)-IGFBP-4 protease system in normal human osteoblast-like cells: regulation by transforming growth factor-beta. J. Clin. Endocrinol. Metab. 79 (6), 1752–1758.

Ebeling, P.R., et al., 1993. Short-term effects of recombinant human insulin-like growth factor I on bone turnover in normal women. J. Clin. Endocrinol. Metab. 77 (5), 1384–1387.

Esen, E., et al., 2013. WNT-LRP5 signaling induces Warburg effect through mTORC2 activation during osteoblast differentiation. Cell Metabol. 17, 745–755.

Ezzat, S., et al., 1993. Biochemical assessment of bone formation and resorption in acromegaly. J. Clin. Endocrinol. Metab. 76 (6), 1452–1457.

Finkelman, R.D., Mohan, S., Jennings, J.C., Taylor, A.K., Jepsen, S., Baylink, D.J., 1990. Quantitation of growth factors IGF-I, SGF/IGF-II, and TGF-beta in human dentin. J. Bone Miner. Res. 5 (7), 717–723.

Fleet, J.C., et al., 1994. Growth hormone and parathyroid hormone stimulate intestinal calcium absorption in aged female rats. Endocrinology 134 (4), 1755–1760.

Forbes, B.E., et al., 1998. Localization of an insulin-like growth factor (IGF) binding site of bovine IGF binding protein-2 using disulfide mapping and deletion mutation analysis of the C-terminal domain. J. Biol. Chem. 273 (8), 4647–4652.

Fowlkes, J.L., et al., 1994a. Matrix metalloproteinases degrade insulin-like growth factor-binding protein-3 in dermal fibroblast cultures. J. Biol. Chem. 269 (41), 25742–25746.

Fowlkes, J.L., et al., 1994b. Proteolysis of insulin-like growth factor binding protein-3 during rat pregnancy: a role for matrix metalloproteinases. Endocrinology 135 (6), 2810–2813.

Frohman, L.A., Kineman, R.D., 2002. Growth hormone-releasing hormone and pituitary somatotrope proliferation. Minerva Endocrinol. 27 (4), 277–285.

Frohman, L.A., et al., 2000. Secretagogues and the somatotrope: signaling and proliferation. Recent Prog. Horm. Res. 55, 269–290.

Garnero, P., et al., 2000. Biochemical markers of bone turnover, endogenous hormones, and the risk of fractures in postmenopausal women: the OFELY study. J. Bone Miner. Res. 15 (8), 1526–1536.

Gamero, P., et al., 2000. Low serum IGF-1 and occurrence of osteoporotic fractures in postmenopausal women. Lancet 355 (9207), 898–899.

Geusens, P., et al., 1998. Musculoskeletal effects of rhIGF-I/IGFBP-3 in hip fracture patients: results from double-blind, placebo-controlled phase II study. Bone 23 (Suppl. 1), 157.

Gevers, E.F., 2009. Regulation of rapid signal transducer and activator of transcription 5 phosphorylation in the resting cells of the growth plate. Endocrinology 150, 3627–3636.

Ghiron, L.J., et al., 1995. Effects of recombinant insulin-like growth factor-I and growth hormone on bone turnover in elderly women. J. Bone Miner. Res. 10 (12), 1844–1852.

Green, H., et al., 1985. A dual effector theory of growth hormone action. Differentiation 29, 195–208.

Grinspoon, S., et al., 2003. Effects of recombinant human insulin-like growth factor (IGF)-I and estrogen administration on IGF-I, IGF binding protein (IGFBP)-2, and IGFBP-3 in anorexia nervosa: a randomized-controlled study. J. Clin. Endocrinol. Metab. 88 (3), 1142–1149.

He, J., et al., 2006. Postnatal growth and bone mass in mice with IGF-I haploinsufficiency. Bone 38 (6), 826–835.

Headey, S.J., et al., 2004. C-terminal domain of insulin-like growth factor (IGF) binding protein-6: structure and interaction with IGF-II. Mol. Endocrinol. 18 (11), 2740–2750.

Heffernan, M., et al., 2001. The effects of human GH and its lipolytic fragment (AOD9604) on lipid metabolism following chronic treatment in obese mice and beta(3)-AR knockout mice. Endocrinology 142 (12), 5182–5189.

Ho, K.Y., Weissberger, A.J., 1990. Secretory patterns of growth hormone according to sex and age. Horm. Res. 33 (Suppl. 4), 7–11.

Hogler, W., et al., 2005. Effect of growth hormone therapy and puberty on bone and body composition in children with idiopathic short stature and growth hormone deficiency. Bone 37 (5), 642–650.

Holloway, L., et al., 1994. Effects of recombinant human growth hormone on metabolic indices, body composition, and bone turnover in healthy elderly women. J. Clin. Endocrinol. Metab. 79 (2), 470–479.

Holloway, L., et al., 1997. Skeletal effects of cyclic recombinant human growth hormone and salmon calcitonin in osteopenic postmenopausal women. J. Clin. Endocrinol. Metab. 82 (4), 1111–1117.

Honda, Y., et al., 1996. Recombinant synthesis of insulin-like growth factor-binding protein-4 (IGFBP-4): development, validation, and application of a radioimmunoassay for IGFBP-4 in human serum and other biological fluids. J. Clin. Endocrinol. Metab. 81 (4), 1389–1396.

Hourd, P., et al., 1991. Urinary growth excretion during puberty in type 1 diabetes mellitus. Diabet. Med. 8, 237–242.

Hyer, S.L., et al., 1992. Growth hormone deficiency during puberty reduces adult bone mineral density. Arch. Dis. Child. 67 (12), 1472–1474.

Inzucchi, S.E., Robbins, R.J., 1994. Clinical review 61: effects of growth hormone on human bone biology. J. Clin. Endocrinol. Metab. 79 (3), 691–694.

Isaksson, O.G., et al., 1987. Mechanism of the stimulatory effect of growth hormone on longitudinal bone growth. Endocr. Rev. 8 (4), 426–438.

Ito, Y., 1999. Molecular basis of tissue-specific gene expression mediated by the runt domain transcription factor PEBP2/CBF. Genes Cells 4 (12), 685–696.

Jansson, J.O., et al., 1985. Sexual dimorphism in the control of growth hormone secretion. Endocr. Rev. 6 (2), 128–150.

Janssen, Y.J., et al., 1998. Skeletal effects of two years of treatment with low physiological doses of recombinant human growth hormone (GH) in patients with adult-onset GH deficiency. J. Clin. Endocrinol. Metab. 83 (6), 2143–2148.

Johansen, J.S., et al., 1990. Effects of growth hormone (GH) on plasma bone Gla protein in GH-deficient adults. J. Clin. Endocrinol. Metab. 70 (4), 916–919.

Johansson, A.G., et al., 1992. The bone mineral density in acquired growth hormone deficiency correlates with circulating levels of insulin-like growth factor I. J. Intern. Med. 232 (5), 447–452.

Johansson, A.G., et al., 1994. Effects of short-term treatment with IGF-I and GH on markers of bone metabolism in idiopathic osteoporosis. J. Bone Miner. Res. 9 (Suppl. 1), 328.

Johansson, A.G., et al., 1994. Growth hormone-dependent insulin-like growth factor binding protein is a major determinant of bone mineral density in healthy men. J. Bone Miner. Res. 9 (6), 915–921.

Jones, D.C., et al., 2006. Regulation of adult bone mass by the zinc finger adapter protein Schnurri-3. Science 312 (5777), 1223–1227.

Jorgensen, J.O., et al., 1989. Beneficial effects of growth hormone treatment in GH-deficient adults. Lancet 1 (8649), 1221–1225.

Jorgensen, J.O., et al., 1991. Long-term growth hormone treatment in growth hormone deficient adults. Acta Endocrinol. 125 (5), 449–453.

Kamp, G.A., et al., 2002. High dose growth hormone treatment induces acceleration of skeletal maturation and an earlier onset of puberty in children with idiopathic short stature. Arch. Dis. Child. 87 (3), 215–220.

Kann, P., et al., 1993. Bone quality in growth hormone deficient adults. Acta Endocrinol. 128 (Suppl. 2), 60.

Karasik, D., et al., 2002. Insulin-like growth factor binding proteins 4 and 5 and bone mineral density in elderly men and women. Calcif. Tissue Int. 71 (4), 323–328.

Karasik, D., et al., 2003. Age, gender, and body mass effects on quantitative trait loci for bone mineral density: the Framingham Study. Bone 33 (3), 308–316.

Kassem, M., et al., 1994. No evidence for reduced spontaneous or growth-hormone-stimulated serum levels of insulin-like growth factor (IGF)-I, IGF-II or IGF binding protein 3 in women with spinal osteoporosis. Eur. J. Endocrinol. 131 (2), 150–155.

Kato, M., et al., 2002. Cbfa1-independent decrease in osteoblast proliferation, osteopenia, and persistent embryonic eye vascularization in mice deficient in Lrp5, a Wnt coreceptor. J. Cell Biol. 157 (2), 303–314.

Kaufman, J.M., et al., 1992. Bone mineral status in growth hormone-deficient males with isolated and multiple pituitary deficiencies of childhood onset. J. Clin. Endocrinol. Metab. 74 (1), 118–123.

Kawai, M., et al., 2011. The heparin binding domain of IGFBP-2 has IGF binding independent biologic activity on the growing skeleton. J. Biol. Chem. 286, 14670–14680.

Kayath, M.J., et al., 1997. Osteopenia is present in the minority of patients with acromegaly and is predominant in the spine. Osteoporos. Int. 7, 226–230.
Kelijman, M., 1991. Age-related alterations of the growth hormone/insulin-like-growth-factor I axis. J. Am. Geriatr. Soc. 39 (3), 295–307.
Kelley, K.M., et al., 1996. Insulin-like growth factor-binding proteins (IGFBPs) and their regulatory dynamics. Int. J. Biochem. Cell Biol. 28 (6), 619–637.
Kesavan, C., et al., 2011. Conditional disruption of IGF-I in type I collagen expressing cells shows an essential role of IGF-I in skeletal anabolic response to lading. Am J Physiol Endocrinol 301, E1191–E1197.
Khandwala, H.M., et al., 2000. The effects of insulin-like growth factors on tumorigenesis and neoplastic growth. Endocr. Rev. 21 (3), 215–244.
Khosla, S., et al., 1998. Insulin-like growth factor system abnormalities in hepatitis C-associated osteosclerosis. Potential insights into increasing bone mass in adults. J. Clin. Investig. 101 (10), 2165–2173.
Koutsilieris, M., Polychronakos, C., 1992. Proteinolytic activity against IGF-binding proteins involved in the paracrine interactions between prostate adenocarcinoma cells and osteoblasts. Anticancer Res. 12 (3), 905–910.
Kudo, Y., et al., 1996. Regulation of insulin-like growth factor-binding protein-4 protease activity by estrogen and parathyroid hormone in SaOS-2 cells: implications for the pathogenesis of postmenopausal osteoporosis. J. Endocrinol. 150 (2), 223–229.
Krantz, E., et al., 2015. Effects of GH treatment on fractures and quality of life in postmenopausal women. J. Clin. Endocrinol. Metab. 100, 3251–3259.
Kurland, E.S., et al., 1997. Insulin-like growth factor-I in men with idiopathic osteoporosis. J. Clin. Endocrinol. Metab. 82 (9), 2799–2805.
Kurland, E.S., et al., 1998. Normal growth hormone secretory reserve in men with idiopathic osteoporosis and reduced circulating levels of insulin-like growth factor-I. J. Clin. Endocrinol. Metab. 83 (7), 2576–2579.
Landin-Wilhelmsen, K., et al., 2003. Growth hormone increases bone mineral content in postmenopausal osteoporosis: a randomized placebo-controlled trial. J. Bone Miner. Res. 18 (3), 393–405.
Langlois, J.A., et al., 1998. Association between insulin-like growth factor I and bone mineral density in older women and men: the Framingham Heart Study. J. Clin. Endocrinol. Metab. 83 (12), 4257–4262.
Laron, Z., et al., 1992. Effects of insulin-like growth factor on linear growth, head circumference, and body fat in patients with Laron-type dwarfism. Lancet 339 (8804), 1258–1261.
Lau, K.H., et al., 2006. Upregulation of the Wnt, Estrogen receptor, IGF-I and BMP pathways in C57bl6 mice as opposed to C3H/HeJ mice in part contributes to the differential anabolic response to fluid shear. J. Biol. Chem. 281, 94768–94788.
Lau, K.H., et al., 2013. Osteocyte derived IGF-I is essential for determining bone mechanosensitivity. Am. J. Physiol. Endocrinol. Metab. 305, E271–E281.
Le Roith, D., et al., 1997. The insulin-like growth factor-I receptor and apoptosis. Implications for the aging progress. Endocrine 7 (1), 103–105.
Lee, W.C., et al., 2017. Energy metabolism of the osteoblast:implications for osteoporosis. Endocr. Rev. 38, 255–266.
Lee, M.H., et al., 2003. BMP-2-induced Osterix expression is mediated by Dlx5 but is independent of Runx2. Biochem. Biophys. Res. Commun. 309 (3), 689–694.
Lieberman, S.A., et al., 1994. The insulin-like growth factor I generation test: resistance to growth hormone with aging and estrogen replacement therapy. Horm. Metab. Res. 26 (5), 229–233.
Li, Z., et al., 2016. Glucose transporter-4 facilitates insulin-stimulated glucose uptake in osteoblasts. Endocrinology 157 (11), 4094–4103. Epub 2016 Sep 3.
Lin-Su, K., Wajnrajch, M.P., 2002. Growth hormone releasing hormone (GHRH) and the GHRH receptor. Rev. Endocr. Metab. Disord. 3 (4), 313–323.
Liu, J.L., et al., 2004. Disruption of growth hormone receptor gene causes diminished pancreatic islet size and increased insulin sensitivity in mice. Am. J. Physiol. Endocrinol. Metab. 287 (3), E405–E413.
Liu, J.P., et al., 1993. Mice carrying null mutations of the genes encoding insulin-like growth factor I (Igf-1) and type 1 IGF receptor (Igf1r). Cell 75 (1), 59–72.
Liu, Z., et al., 2016a. GH control of hepatic lipid metabolism. Diabetes 65, 3598–3609.
Liu, Z., et al., 2016b. DMP-1-mediated Ghr gene recombination compromises skeletal development and impairs skeletal response to intermittent PTH. FASEB J. 30, 635–652.
Liu, Z., et al., 2016c. Does the GH/IGF axis contribute to skeletal dimorphism. Growth Hormone IGF Res. 27, 7–17.
Liu, Z., et al., 2017. Reduced serum IGF-I associated with hepatic osteodystrophy is a main determinant of cortical but not trabecular bone mass. J. Bone Miner. Res. Epub ahead of print Sept 2017.
Ljunghall, S., et al., 1992. Low plasma levels of insulin-like growth factor 1 (IGF-1) in male patients with idiopathic osteoporosis. J. Intern. Med. 232 (1), 59–64.
Lloyd, M.E., et al., 1996. Relation between insulin-like growth factor-I concentrations, osteoarthritis, bone density, and fractures in the general population: the Chingford study. Ann. Rheum. Dis. 55 (12), 870–874.
Lupu, F., et al., 2001. Roles of growth hormone and insulin-like growth factor 1 in mouse postnatal growth. Dev. Biol. 229 (1), 141–162.
McNair, P., 1988. Bone mineral metabolism in human type 1 (insulin dependent) diabetes mellitus. Dan. Med. Bull. 35 (2), 109–121.
Manes, S., et al., 1999. The matrix metalloproteinase-9 regulates the insulin-like growth factor-triggered autocrine response in DU-145 carcinoma cells. J. Biol. Chem. 274 (11), 6935–6945.
Marcus, R., et al., 1990. Effects of short-term administration of recombinant human growth hormone to elderly people. J. Clin. Endocrinol. Metab. 70 (2), 519–527.
Maridas, D.E., et al., 2017a. IGFBP-4 regulates skeletal growth in a sex specific manner. J. Endocrinol. 233, 131–144.
Maridas, D.E., et al., 2017b. IGFBP-4 is required for adipogenesis. Endocrinology 158, 3488–3500.

Marinaro, J.A., et al., 1999. HaCaT human keratinocytes express IGF-II, IGFBP-6, and an acid-activated protease with activity against IGFBP-6. Am. J. Physiol. 276 (3 Pt 1), E536–E542.

Maroni, P.D., et al., 2004. Mitogen activated protein kinase signal transduction pathways in the prostate. Cell Commun. Signal. 2 (1), 5.

Martin, J.L., Baxter, R.C., 1988. Insulin-like growth factor-binding proteins (IGF-BPs) produced by human skin fibroblasts: immunological relationship to other human IGF-BPs. Endocrinology 123 (4), 1907–1915.

Mauras, N., et al., 2000. High-dose recombinant human growth hormone (GH) treatment of GH-deficient patients in puberty increases near-final height: a randomized, multicenter trial. Genentech, Inc., Cooperative Study Group. J. Clin. Endocrinol. Metab. 85 (10), 3653–3660.

Mayo, K.E., et al., 1988. Dramatic pituitary hyperplasia in transgenc mice expressing a GH releasing peptide. Mol. Endocrinol. 7, 606–612.

Mayo, K.E., et al., 1995. Growth hormone-releasing hormone: synthesis and signaling. Recent Prog. Horm. Res. 50, 35–73.

Mazziotti, G., et al., 2008. Prevalence of osteoporosis in men with acromegaly. J. Clin. Endocrinol. Metab. 93, 4649–4654.

Meinhardt, U.J., et al., 2006. Modulation of GH secretion by sex steroids. Clin. Endocrinol. 65, 413–422.

Menagh, P.J., et al., 2010. Growth Hormone regulates the balance between bone formation and bone marrow adiposity. J. Bone Miner. Res. 25, 757–768.

Merriman, H.L., et al., 1990. Insulin-like growth factor-I and insulin-like growth factor-II induce c-fos in mouse osteoblastic cells. Calcif. Tissue Int. 46 (4), 258–262.

Mochizuki, H., et al., 1992. Insulin-like growth factor-I supports formation and activation of osteoclasts. Endocrinology 131 (3), 1075–1080.

Mohan, S., 1993. Insulin-like growth factor binding proteins in bone cell regulation. Growth Regul. 3 (1), 67–70.

Mohan, S., Baylink, D.J., 1990. Autocrine-paracrine aspects of bone metabolism. Growth Genet. Horm. 6, 1–9.

Mohan, S., et al., 1988. Primary structure of human skeletal growth factor: homology with human insulin-like growth factor-II. Biochim. Biophys. Acta 966 (1), 44–55.

Mohan, S., et al., 1989a. Characterization of the receptor for insulin-like growth factor II in bone cells. J. Cell. Physiol. 140 (1), 169–176.

Mohan, S., et al., 1989b. Isolation of an inhibitory insulin-like growth factor (IGF) binding protein from bone cell-conditioned medium: a potential local regulator of IGF action. Proc. Natl. Acad. Sci. U. S. A 86 (21), 8338–8342.

Mohan, S., et al., 1991. Increased IGF-I and IGF-II in bone from patients with osteoarthritis. J. Bone Miner. Res. 1 (Suppl. 1), 131.

Mohan, S., et al., 1995. Age-related changes in IGFBP-4 and IGFBP-5 levels in human serum and bone: implications for bone loss with aging. Prog. Growth Factor Res. 6 (2–4), 465–473.

Mohan, S., et al., 1996. Insulin-like growth factor (IGF)-binding proteins in serum–do they have additional roles besides modulating the endocrine IGF actions? J. Clin. Endocrinol. Metab. 81 (11), 3817–3820.

Muller, E.E., et al., 1999. Neuroendocrine control of growth hormone secretion. Physiol. Rev. 79 (2), 511–607.

Nakamura, T., et al., 1992. Clinical significance of serum levels of insulin like growth factors as bone metabolic markers in postmenopausal women. Bone Miner. 17 (Suppl. 1), 170.

Nakashima, K., de Crombrugghe, B., 2003. Transcriptional mechanisms in osteoblast differentiation and bone formation. Trends Genet. 19 (8), 458–466.

Nakashima, K., et al., 2002. The novel zinc finger-containing transcription factor osterix is required for osteoblast differentiation and bone formation. Cell 108 (1), 17–29.

Neumann, G.M., Bach, L.A., 1999. The N-terminal disulfide linkages of human insulin-like growth factor-binding protein-6 (hIGFBP-6) and hIGFBP-1 are different as determined by mass spectrometry. J. Biol. Chem. 274 (21), 14587–14594.

Norman, C., et al., 2013. Estradiol regulates GH releasing peptide interaction with GHRH and somatostain. Eur. J. Endocrinol. 170, 121–129, 2013.

Nicolas, V., et al., 1994. Age-related decreases in insulin-like growth factor-I and transforming growth factor-beta in femoral cortical bone from both men and women: implications for bone loss with aging. J. Clin. Endocrinol. Metab. 78 (5), 1011–1016.

Nicolas, V., et al., 1995. An age-related decrease in the concentration of insulin-like growth factor binding protein-5 in human cortical bone. Calcif. Tissue Int. 57 (3), 206–212.

Nunn, S.E., et al., 1997. Regulation of prostate cell growth by the insulin-like growth factor binding proteins and their proteases. Endocrine 7 (1), 115–118.

Oukka, M., et al., 2002. A mammalian homolog of Drosophila schnurri, KRC, regulates TNF receptor-driven responses and interacts with TRAF2. Mol. Cell 9 (1), 121–131.

Papadakis, M.A., et al., 1996. Growth hormone replacement in healthy older men improves body composition but not functional ability. Ann. Intern. Med. 124 (8), 708–716.

Petersenn, S., Schulte, H.M., 2000. Structure and function of the growth-hormone-releasing hormone receptor. Vitam. Horm. 59, 35–69.

Powell-Braxton, L., et al., 1993. IGF-I is required for normal embryonic growth in mice. Genes Dev. 7 (12B), 2609–2617.

Qiao, M., et al., 2004. Insulin-like growth factor-1 regulates endogenous RUNX2 activity in endothelial cells through a phosphatidylinositol 3-kinase/ERK-dependent and Akt-independent signaling pathway. J. Biol. Chem. 279 (41), 42709–42718.

Raisingani, M., et al., 2017. Skeletal growth and mineral acquisition in Type I diabetic children: abnormalities of the GH/IGF axis. Growth Horm and IGF Res. 34, 13–21.

Rajah, R., et al., 1996. 7S nerve growth factor is an insulin-like growth factor-binding protein protease. Endocrinology 137 (7), 2676–2682.

Rajaram, S., et al., 1997. Insulin-like growth factor-binding proteins in serum and other biological fluids: regulation and functions. Endocr. Rev. 18 (6), 801–831.

Rappaport, R., Czernichow, P., 1993. Disorders of GH and prolactin secretion. In: Bertrand, J., et al. (Eds.), Pediatric Endocrinology. Williams and Wilkins, Baltimore, pp. 220–241.

Reijnders, C.M., et al., 2007. Effect of mechanical loading on IGF-I gene expression in rat tibia. J. Endocrinol. 192, 131–140.

Richman, C., et al., 1999. Recombinant human insulin-like growth factor- binding protein-5 stimulates bone formation parameters in vitro and in vivo. Endocrinology 140 (10), 4699–4705.

Rosen, C.J., et al., 1992. The 24/25-kDa serum insulin-like growth factor- binding protein is increased in elderly women with hip and spine fractures. J. Clin. Endocrinol. Metab. 74 (1), 24–27.

Rosen, C.J., et al., 1994. Insulin-like growth factors and bone: the osteoporosis connection. Proc. Soc. Exp. Biol. Med. 206 (2), 83–102.

Rosen, C.J., Donahue, L.R., 1998. Insulin-like growth factors and bone: the osteoporosis connection revisited. Proc. Soc. Exp. Biol. Med. 219 (1), 1–7.

Rosen, C.J., et al., 1999. The RIGHT Study: a randomized placebo-controlled trial of recombinant human growth hormone in frail elderly: dose response effects on bone mass and bone turnover. J. Bone Miner. Res. 14 (Suppl. 1), 208.

Rosen, T., et al., 1993. Reduced bone mineral content in adult patients with growth hormone deficiency. Acta Endocrinol. 129 (3), 201–206.

Rosen, T., et al., 1997. Increased fracture frequency in adult patients with hypopituitarism and GH deficiency. Eur. J. Endocrinol. 137 (3), 240–245.

Rubin, J., et al., 2002. IGF-I regulates osteoprotegerin (OPG) and receptor activator of nuclear factor-kappaB ligand in vitro and OPG in vivo. J. Clin. Endocrinol. Metab. 87 (9), 4273–4279.

Rubin, M.R., Bilezikian, J.P., 2002. New anabolic therapies in osteoporosis. Curr. Opin. Rheumatol. 14 (4), 433–440.

Rudman, D., Mattson, D.E., 1994. Serum insulin-like growth factor I in healthy older men in relation to physical activity. J. Am. Geriatr. Soc. 42 (1), 71–76.

Rudman, D., et al., 1981. Impaired growth hormone secretion in the adult population: relation to age and adiposity. J. Clin. Investig. 67 (5), 1361–1369.

Rudman, D., et al., 1990. Effects of human growth hormone in men over 60 years old. N. Engl. J. Med. 323 (1), 1–6.

Rubin, M.R., et al., 2005. Idiopathic osteoporosis in premenopausal women. Osteoporos. Int. 16, 526–533.

Saggese, G., et al., 1993. Effects of long-term treatment with growth hormone on bone and mineral metabolism in children with growth hormone deficiency. J. Pediatr. 122 (1), 37–45.

Saggese, G., et al., 1996. The effect of long-term growth hormone (GH) treatment on bone mineral density in children with GH deficiency. Role of GH in the attainment of peak bone mass. J. Clin. Endocrinol. Metab. 81 (8), 3077–3083.

Sakata, T., et al., 2004. Skeletal unloading induces resistance to IGF-I by inhibiting activation of the IGF signaling pathways. J. Bone Miner. Res. 19, 436–446.

Salih, D.A., et al., 2005a. Insulin-like growth factor-binding protein-5 induces a gender-related decrease in bone mineral density in transgenic mice. Endocrinology 146 (2), 931–940.

Sansal, I., Sellers, W.R., 2004. The biology and clinical relevance of the PTEN tumor suppressor pathway. J. Clin. Oncol. 22 (14), 2954–2963.

Scharla, S.H., et al., 1993. 1,25-Dihydroxyvitamin D3 increases secretion of insulin-like growth factor binding protein-4 (IGFBP-4) by human osteoblast-like cells in vitro and elevates IGFBP-4 serum levels in vivo. J. Clin. Endocrinol. Metab. 77 (5), 1190–1197.

Schmid, C., Ernst, M., 1991. IGF, in cytokines and bone metabolism. In: Gowen, M. (Ed.), IGFs. CRC Press, Boca Raton, pp. 229–259.

Schmid, C., et al., 1984. Insulin-like growth factor I supports differentiation of cultured osteoblast-like cells. FEBS Lett. 173 (1), 48–52.

Schmid, C., et al., 1989. Insulin-like growth factor I regulates type I procollagen messenger ribonucleic acid steady state levels in bone of rats. Endocrinology 125 (3), 1575–1580.

Schmid, C., et al., 1992. Differential regulation of insulin-like growth factor binding protein (IGFBP)-2 mRNA in liver and bone cells by insulin and retinoic acid in vitro. FEBS Lett. 303 (2–3), 205–209.

Schmid, C., et al., 1996. Effects and fate of human IGF-binding protein-5 in rat osteoblast cultures. Am. J. Physiol. 271 (6 Pt 1), E1029–E1035.

Schoenle, E., et al., 1985. Comparison of in vivo effects of insulin-like growth factors I and II and of growth hormone in hypophysectomized rats. Acta Endocrinol. 108 (2), 167–174.

Sell, C., et al., 1995. Insulin-like growth factor I (IGF-I) and the IGF-I receptor prevent etoposide-induced apoptosis. Cancer Res. 55 (2), 303–306.

Sheng, M.H., et al., 2013. Disruption of the IGF-1 gene in osteocytes impairs developmental bone growth in mice. Bone 52, 133–144.

Sjogren, K., et al., 2000. Disproportionate skeletal growth and markedly diminished bone mineral content in GH receptor null mice. Biochem. Biophys. Res. Commun. 267, 603–608.

Skjaerbaek, C., et al., 1998. No effect of growth hormone on serum insulin-like growth factor binding protein-3 proteolysis. J. Clin. Endocrinol. Metab. 83 (4), 1206–1210.

Slootweg, M.C., et al., 1990. The presence of classical insulin-like growth factor (IGF) type-I and -II receptors on mouse osteoblasts: autocrine/paracrine growth effect of IGFs? J. Endocrinol. 125 (2), 271–277.

Slootweg, M.C., et al., 1992. Osteoclast formation together with interleukin-6 production in mouse long bones is increased by insulin-like growth factor-I. J. Endocrinol. 132 (3), 433–438.

Slootweg, M.C., et al., 1996. Growth hormone receptor activity is stimulated by insulin-like growth factor binding protein 5 in rat osteosarcoma cells. Growth Regul. 6 (4), 238–246.

Sneppen, S.B., et al., 2002. Bone mineral content and bone metabolism during physiological GH treatment in GH-deficient adults–an 18-month randomized, placebo-controlled, double-blinded trial. Eur. J. Endocrinol. 146 (2), 187–195.

Snyder, P.J., et al., 2007. Effect of growth hormone replacement on bone mineral density in adult-onset growth hormone deficiency. J. Bone Miner. Res. 22 (5), 762–770.

Spencer, E.M., et al., 1991. In vivo actions of insulin-like growth factor-I (IGF-I) on bone formation and resorption in rats. Bone 12 (1), 21–26.

Szulc, P., et al., 2004. Insulin-like growth factor I is a determinant of hip bone mineral density in men less than 60 years of age: MINOS study. Calcif. Tissue Int. 74 (4), 322–329.

Tixier-Boichard, M., et al., 1992. Effects of insulin-like growth factor-I (IGF-I) infusion and dietary tri-iodothyronine (T3) supplementation on growth, body composition, and plasma hormone levels in sex-linked dwarf mutant and normal chickens. J. Endocrinol. 133 (1), 101–110.

Tobias, J.H., et al., 1992. Opposite effects of insulin-like growth factor-I on the formation of trabecular and cortical bone in adult female rats. Endocrinology 131 (5), 2387–2392.

Thomas, D.M., et al., 1996. Dexamethasone modulates insulin receptor expression and subcellular distribution of the glucose transporter GLUT 1 in UMR 106-01, a clonal osteogenic sarcoma cell line. J. Mol. Endocrinol. 17, 7–17, 1996.

Tseng, K.F., Goldstein, S.A., 1998. Systemic over secretion of growth hormone in transgenic mice. J. Bone Miner. Res. 13, 706–715.

Uchimura, T., et al., 2017. An essential role for IGFII in cartilage development and glucose metabolism during postnatal long bone growth. Development 19, 3533–3546.

Uekl, I., et al., 2000. Inactivation of the Acid labile subunit in mice results in mild retardation of growth despite profound disruptions in the IGF regulatory system. Proc. Natl. Acad. Sci. Unit. States Am. 97, 6868–6873.

Ueland, T., et al., 2002. Decreased trabecular bone content, IGFBP-5, apparent density, IGF-II content in acromegaly. Eur. J. Clin. Investig. 32, 122–128.

Valk, N.K., et al., 1994. The effects of human growth hormone (GH) administration in GH-deficient adults: a 20-day metabolic ward study. J. Clin. Endocrinol. Metab. 79 (4), 1070–1076.

Verhaeghe, J., et al., 1992. The effects of systemic insulin, insulin-like growth factor-I, and growth hormone on bone growth and turnover in spontaneously diabetic BB rats. J. Endocrinol. 134 (3), 485–492.

Wang, Y., et al., 2007. IGF-I receptor is essential for the anabolic actions of PTH on bone. J. Bone Miner Res. 22, 1329–1337.

Wang, Y., et al., 2011. IGF-1R signaling in chondrocytes modulates growth plate development by interacting with PTHrp/Ihh. J. Bone Miner. Res. 26, 1437–1446.

Wang, J., et al., 1999. Igf1 promoters long bone growth by IGF augmenting chondrocyte hypertrophy. FASEB J. 13, 1985–1990.

Wang, Y., et al., 2006. Role of IGF-I signaling in regulating osteoclastogenesis. J. Bone Miner. Res. 21 (9), 1350–1358.

Wang, X., et al., 2015. A liver bone Endocrine relay by IGFBP-1 promotes osteoclastogenesis and mediates FGF-21 induced bone resorption, 22, 811–824.

Wassenaar, M.J., et al., 2011. High prevalence of vertebral fractures despite normal bone density in patients with long term controlled acromegaly. Eur. J. Endocrinol. 164, 475–483.

Wei, J., et al., 2015. Glucose uptake and Runx2 synergize to orchestrate osteoblast differentiation. Cell 161, 1576–1591.

Woods, K.A., et al., 1996. Intrauterine growth retardation and postnatal growth failure associated with deletion of the insulin-like growth factor I gene. N. Engl. J. Med. 335 (18), 1363–1367.

Wright, N.M., et al., 1995. Greater secretion of growth hormone in black than in white men: possible factor in greater bone mineral density–a clinical research center study. J. Clin. Endocrinol. Metab. 80 (8), 2291–2297.

Wu, Y., et al., 2013. Serum IGF-I is insufficient to restore skeletal size in total absence of the growth hormone receptor. J. Bone Miner. Res. 28, 1575–1586.

Wuster, C., et al., 1991. Increased prevalence of osteoporosis and arteriosclerosis in conventionally substituted anterior pituitary insufficiency: need for additional growth hormone substitution? German. Klin. Wochenschr. 69 (16), 769–773.

Wuster, C., et al., 1992. Bone mass of spine and forearm in osteoporosis and in German normals: influences of sex, age and anthropometric parameters. Eur. J. Clin. Investig. 22 (5), 336–370.

Wuster, C., et al., 1993. Decreased serum levels of insulin-like growth factors and IGF binding protein 3 in osteoporosis. J. Intern. Med. 234 (3), 249–255.

Wuster, C., et al., 2001. The influence of growth hormone deficiency, growth hormone replacement therapy, and other aspects of hypopituitarism on fracture rate and bone mineral density. J. Bone Miner. Res. 16 (2), 398–405.

Xi, G., et al., 2016. IRS-1 functions as a molecular scaffold to coordinate IGF-I/IGFBP-2 signaling during osteoblast differentiation. J. Bone Miner. Res. 31, 1300–1314.

Xiao, G., et al., 2000. MAPK pathways activate and phosphorylate the osteoblast-specific transcription factor. Cbfa1. J. Biol. Chem. 275 (6), 4453–4459.

Yakar, S., et al., 1999. Normal growth and development in the absence of hepatic insulin-like growth factor I. Proc. Natl. Acad. Sci. U. S. A 96 (13), 7324–7329.

Yakar, S., et al., 2002. Circulating levels of IGF-1 directly regulate bone growth and density. J. Clin. Investig. 110 (6), 771–781.

Yakar, S., et al., 2006. The ternary IGF complex influences postnatal bone acquisition and the skeletal response to intermittent parathyroid hormone. J. Endocrinol. 189 (2), 289–299.

Yeo, A.L., et al., 2003. Frailty and the biochemical effects of recombinant GH in women after surgery for hip fracture. Growth Hormone IGF Res. 13, 361–370.

Zeslawski, W., et al., 2001. The interaction of insulin-like growth factor-I with the N-terminal domain of IGFBP-5. EMBO J. 20 (14), 3638–3644.

Zhang, M., et al., 2002. Osteoblast-specific knockout of the insulin-like growth factor (IGF) receptor gene reveals an essential role of IGF signaling in bone matrix mineralization. J. Biol. Chem. 277 (46), 44005–44012.

Zhang, M., et al., 2003. Paracrine over expression of IGFBP-4 in osteoblasts decreases bone turnover and global growth retardation. J. Bone Miner. Res. 18, 836–843.

Zhao, H., et al., 2004. PTEN inhibits cell proliferation and induces apoptosis by downregulating cell surface IGF-IR expression in prostate cancer cells. Oncogene 23 (3), 786–794.
Zoch, M.L., et al., 2016. In vivo radiometric analysis of glucose uptake and distribution in mouse bone. Bone Res 4, 16004, 2016.
Zofkova, I., 2003. Pathophysiological and clinical importance of insulin-like growth factor-I with respect to bone metabolism. Physiol. Res. 52 (6), 657–679.
Zoidis, E., et al., 2011. Stimulation of glucose transport in osteoblastic cells by parathyroid hormone and insulin-like growth factor I. Mol. Cell. Biochem. 348, 33–42.

Further reading

Andreassen, T.T., Oxlund, H., 2001. The effects of growth hormone on cortical and cancellous bone. J. Musculoskelet. Neuronal Interact. 2 (1), 49–58.
Bikle, D.D., et al., 1994. Skeletal unloading induces resistance to insulin-like growth factor I. J. Bone Miner. Res. 9 (11), 1789–1796.
Canalis, E., Lian, J.B., 1989. Effects of bone associated growth factors on DNA, collagen, and osteocalcin synthesis in cultured fetal rat calvariae. Bone 9 (4), 243–246.
Celil, A.B., Campbell, P.G., 2005. BMP-2 and insulin-like growth factor-I mediate Osterix (Osx) expression in human mesenchymal stem cells via the MAPK and protein kinase D signaling pathways. J. Biol. Chem. 280 (36), 31353–31359.
Daughaday, W.H., 1989. A personal history of the origin of the somatomedin hypothesis and recent challenges to its validity. Perspect. Biol. Med. 32 (2), 194–211.
Diamond, T., et al., 1989. Spinal and peripheral bone mineral densities in acromegaly: the effects of excess growth hormone and hypogonadism. Ann. Intern. Med. 111 (7), 567–573.
Ernst, M., Rodan, G.A., 1990. Increased activity of insulin-like growth factor (IGF) in osteoblastic cells in the presence of growth hormone (GH): positive correlation with the presence of the GH-induced IGF-binding protein BP-3. Endocrinology 127 (2), 807–814.
Heaney, R.P., 1962. Radiocalcium metabolism in disuse osteoporosis in man. Am. J. Med. 33, 188–200.
Kassem, M., et al., 1993. Growth hormone stimulates proliferation and differentiation of normal human osteoblast-like cells in vitro. Calcif. Tissue Int. 52 (3), 222–226.
Kasukawa, et al., 2003. Evidence that sensitivity to GH is growth period and tissue time dependent. Endocrinology 144, 3950–3957.
Madeira, M., et al., 2013. Vertebral fracture assessment in acromegaly. J. Clin. Densitom. 16, 238–243.
Machwate, M., et al., 1994. Insulin-like growth factor-I increases trabecular bone formation and osteoblastic cell proliferation in unloaded rats. Endocrinology 134 (3), 1031–1038.
Maor, G., et al., 1989. Human growth hormone enhances chondrogenesis and osteogenesis in a tissue culture system of chondroprogenitor cells. Endocrinology 125 (3), 1239–1245.
Mathews, L.S., et al., 1988. Expression of insulin-like growth factor I in transgenic mice with elevated levels of growth hormone is correlated with growth. Endocrinology 123 (1), 433–437.
Mohan, S., Baylink, D.J., 1991. Bone growth factors. Clin. Orthop. Relat. Res. 263, 30–48.
Rosen, C.J., 2004. Insulin-like growth factor I and bone mineral density: experience from animal models and human observational studies. Best Pract. Res. Clin. Endocrinol. Metabol. 18 https://doi.org/10.1016/j.beem.2004.02.007.
Salih, D.A., et al., 2005b. IGFBP-5 induces a gender related decrease in bone mineral density in transgenic mice. Endocrinology 146, 931–940.
Seeman, E., et al., 1982. Differential effects of endocrine dysfunction on the axial and the appendicular skeleton. J. Clin. Investig. 69 (6), 1302–1309.
Whitehead, H.M., et al., 1992. Growth hormone treatment of adults with growth hormone deficiency: results of a 13-month placebo controlled cross-over study. Clin. Endocrinol. 36 (1), 45–52.

Chapter 43

The periodontium

Stephen E. Harris[1], Audrey Rakian[3,4], Brian L. Foster[2], Yong-Hee Patricia Chun[1] and Rubie Rakian[3,4]

[1]Department of Periodontics, University of Texas Health Science Center at San Antonio, San Antonio, TX, United States; [2]Biosciences Division at College of Dentistry at Ohio State University, Columbus, OH, United States; [3]Department of Applied Oral Sciences, The Forsyth Institute, Cambridge, MA, United States; [4]Department of Oral Medicine, Infection, Immunity, Harvard School of Dental Medicine, Boston, MA, United States

Chapter outline

Introduction

Periodontal bone and subsequent tooth loss are a major health problem affecting over 60% of the United States population over 60 years of age. The regenerating of periodontal ligaments (PDL) has shown some limited success using PDL cells, with accomplishments in cell homing techniques and in vivo growth factors such as GDF5 and BMPs (Dangaria et al., 2011; Kim et al., 2010; Emerton et al., 2011). Understanding the complex differentiation process of periodontal stem/progenitor cells (PSCs) with these three tissues, alveolar bone, PDL, and the associated attachments to bone and tooth root surface by formation of cementum is beginning to show progress, with a combination of lineage studies in mice, new genetic mouse models, and in vitro mechanistic studies.

Periodontal stem/progenitor cells

A variety of studies over the years have identified ectomesenchyme-derived progenitor cells from the dental follicle (DF) and periodontium region of shed teeth that exhibit many properties of progenitor and stem cells with high CD146 and STRO-1 expression (Seo et al., 2004; Xu et al., 2009; Ivanovski et al., 2006). DF progenitors are fairly heterogeneous in their capacity to differentiate toward components of the periodontium and may involve mechanisms of Hertwig's epithelial root sheath during periodontium formation (Luan et al., 2006; Jung et al., 2011). In vivo αSMA+ cells, surrounding capillaries (pericytes) in the periodontium and a classical marker of the DF stem/progenitor cell population, are good candidates for a major class of stemlike cells that form alveolar bone, PDL fibroblast−PDL, and cellular cementum within the periodontium (San Miguel et al., 2010). Using lineage tracing techniques, the PSCs for alveolar bone, cellular cementum, and PDL have been identified as a αSMA+ cell population within the cervical and apical regions of the periodontium (Roguljic et al., 2013). The PDL cells were identified by scleraxis-GFP transgene, a marker of periodontal fibroblasts overlaid with the αSMA-CreERt2-dependent tdTomato signal (see chapter on lineage tracing; Kalajzic et al.). The mineralizing cementum and alveolar bone cells were identified by overlay of Col1a1-GFP signals (osteoblasts) with αSMA-CreERt2-dependent tdTomato signal. αSMA+ cells in the bone marrow are, also by lineage tracing, capable of

Principles of Bone Biology. https://doi.org/10.1016/B978-0-12-814841-9.00043-9

differentiating into osteoblasts and osteocytes (Grcevic et al., 2012). These αSMA+ cells are the progenitor/stem cells for fracture healing tissue (both chondrocytes and osteoblasts) as well as after damage to the PDL (Roguljic et al., 2013; Matthews et al., 2014). Recent studies have also shown that αSMA+ cells in the tendons are progenitors for mature mid-substance tenocytes and are the main progenitors recruited from the paratendon during a tendon injury repair model (Dyment et al., 2014). In the periodontium, αSMA+ cells are the progenitors of PDL fibroblasts, which have many properties of gene regulation similar to tendon and ligaments.

An excellent marker for mesoderm-derived progenitor cells of the periodontium (excluding the gingiva-epithelium) is the Osterix+ cells. By lineage tracing, Osterix+ cells are expressed slightly later than αSMA+ cells, and these cells have major effects on tooth root formation and cementogenesis (Cao et al., 2012). αSMA+ cells are minimally expressed in the tooth pulp, but do play a role in reparative dentinogenesis (Vidovic et al., 2017). By lineage tracing studies in long bones, Osterix+ cells overlap with αSMA+ cells as well as progress to mature osteoblasts (Chan et al., 2018). Recently, data also show that Osterix+ cells surrounding the small capillaries in the bone marrow contribute to the link of angiogenesis to osteogenesis (Kusumbe et al., 2014; Mizoguchi et al., 2014). In fact, Osterix has been shown to directly bind to the VegfA gene promoter and regulate VegfA expression (Tang et al., 2012). Osterix expression is dependent on Bmp2 signaling in long bones and in the alveolar bone and the tooth pulp (Yang et al., 2012; Yang et al., 2013; Rakian et al. 2013).

Other candidate periodontal stem/progenitor cells

Recent data demonstrate that cathepsin-K-CD200+ cells are a major population of periosteal stem cells that can self-renew and selectively form intramembranous bone (Debnath et al., 2018). The CD200+ marker alone in the context of the DF stem cell population of the periodontium marks both early cells and highly differentiated matrix-producing osteoblasts (Takahashi et al., 2018). In the mature skeleton of 4-month-old mice, leptin receptor−expressing cells have all the properties of self-renewing skeletal stem cells (Zhou et al., 2014). Leptin receptor+ cells also are a major contributor to myelofibrosis in bone marrow (Decker et al., 2017). However, in the case of the periodontium that develops early in mouse postnatal development, leptin receptor+ cells may be of less importance. Likewise, αSMA+ cells may be less important as a stem/progenitor cell population under normal homeostatic conditions at these later stages except under fracture repair or in the case of reparative regeneration as in the pulp and after PDL damage (Roguljic et al., 2013; Vidovic et al., 2017).

A new set of markers has been suggested for skeletal stem cells and bone and cartilage progenitors that in some degree overlaps with previous studies, as in CD146 and other pericyte markers such as NG2 (Cspg4) (Chan et al., 2018). One proposed marker for skeletal stem cells in this study (Chan et al., 2018) is podoplanin Pdpn, aka E11 or GP38), a general marker found in osteocytes and almost any cell with long filopodia or dendritic processes, such as osteocytes and many neural cells and lung fibroblasts (Zhang et al., 2006). The authors discuss a collection of other markers that define these skeletal stem cells, such as PDPN+, CD73, and CD164. CD164 expression is very high in PSCs, as is αSMA and Sca1. All three markers decrease expression as PSCs differentiate into mineralizing tissue (Harris SE, unpublished).

Hedgehog signaling in bone and periodontium

Another class of osteoprogenitors have been identified with a Gli1-CreERt2 model by lineage tracing and are also involved in fracture repair (Guo et al., 2018). These Gli1+ stem cells highly expressed CD146, αSMA, and leptin receptor but expressed low levels of Sca1 and NG2. In addition, the conditional removal of the smoothened receptor with Gli1-CreERt2, the key signaling receptor for hedgehog signaling (hh), decreased trabecular bone formation. Also, deletion of β-catenin with this Gli1-CreERt2 model decreased bone formation, indicating that this pool of stem cells is regulated by Wnt signaling. As related to the periodontium, Zhao et al. demonstrated that sonic hedgehog from the neurovascular bundle niche supports mesenchymal stem cell (MSC) differentiation in and around the mouse incisor (Zhao et al., 2014). Recently, these Gli+ cells have also been shown to be the key driver of bone marrow fibrosis in various pathological, hematological, and nonhematological conditions, similar to leptin receptor+ cells (Kramann et al., 2015).

In the periodontium, a critical target associated with periodontitis is the loss of attachment of PDLs to the cementum on the tooth surface and alveolar bone. This enthesis region of the periodontium has many of the same properties as the tendon/ligament attachment to bone and its biology. As discussed above, GDF5 treatment in a primate model has been shown to regenerate not only the bone but also healthy PDLs (Emerton et al., 2011). Gdf5-positive progenitors in the tendon−bone interface give rise to fibrocartilage that mineralizes by hh signaling to form the enthesis (Dyment et al., 2015). Similar mechanisms with hh are suggested to play a key role in enthesis formation in the periodontium. Analysis of the enthesis region in the periodontium has shown selective enrichment of CD31 endothelial cells with attached CD146 stem cells. As the CD146 cells migrate from the vascular niche, they increase the expression of the pericyte NG2 marker

near the bone−PDL enthesis region. GDF5 is likely to play a key role in this process as in tendon−bone enthesis biology (Lee et al., 2015).

A key role is played by hh in fracture repair and most likely in periodontium healing. During stress fracture healing, mice were given a selective hh pathway inhibitor, vismodegib. A reduction in both woven bone and later-stage lamellar bone formation and vascularization, with a major decrease in Ibsp and other osteoblast markers during healing, was observed (Kazmers et al., 2015). Follow-up studies demonstrate that activation of the hh pathway by systemic agonist, Hh-Ag1.5, during fracture healing in 18-month old female mice, accelerated the fracture repair process (McKenzie et al., 2018). Little is known about hh in the periodontium, except for its role in incisor stem cell biology. However, Ibsp, a key downstream gene, is critical for cementum-enthesis formation, likely regulated by hh, and worth further investigation (Foster et al., 2013a). Previous in vitro cell experiments suggest that hh signaling and Gli2 transcription factors play a role in regulating Bmp2 gene transcription in response to hh signaling (Zhao and el al., 2006). Whether this mechanism plays a role in vivo is unknown.

Parathyroid hormone/parathyroid hormone−related protein role in long bones and periodontium

Parathyroid hormone (PTH) is produced by the parathyroid gland, regulates calcium homeostasis, and has anabolic and catabolic effects on bone (Poole and Reeve, 2005). PTH1 receptor is expressed in osteocytes, early skeletal stem cells, and Osterix+ cells in long bones and many cell types in the periodontium including DFs that contain the stem cells for much of root, cementum, and PDL formation (Takahashi et al., 2018; Ono et al., 2016). As well, PTH1 receptor expression in the periodontium is maintained in later mature cells of the periodontium and suggests that PTH signaling plays a role in homeostatic maintenance later in life (Ono et al., 2016).

A strong anabolic effect of PTH is seen at low intermittent doses in which the activation of osteoclastogenesis and bone resorption is linked to a stronger anabolic bone-formation effect. PTH results in enhanced recruitment, proliferation, and differentiation, as well as decreased apoptosis of osteoblasts (Ishizuya et al., 1997; Jilka et al., 1999). PTH and PTH-related protein (PTHrP) (selectively expressed in early chondrocytes and highly expressed locally in DF cells of the developing periodontium) create their effects through interactions with many different cellular pathways and mechanisms. PTH/PTHrP increases the commitment of MSC precursors to an osteoblast cell fate (Baron and Hesse, 2012). PTH/PTHrP binds to PTH1 receptor, a G-protein-coupled receptor that stimulates phospholipase C, cAMP-dependent protein kinase A, and protein kinase C. The overall effect is an increase in bone formation. The PTH1 receptor is able to activate the Wnt pathway in the absence of Wnt by forming a complex with LRP5/6 after PTH binding (Wan et al., 2008). This allows for the phosphorylation and stabilization of β-catenin, permitting the Wnt signaling pathway to proceed (Guo et al., 2010). The PTH1 receptor is highly expressed on osteocytes. PTH indirectly activates the Wnt pathway in osteoblast progenitor cells by inhibiting secretion from osteocytes of SOST and Dkk1 (Prideaux et al., 2015). This interaction of the Sost gene product, Sclerostin, and PTH signaling previously demonstrated that bone formation induced by PTH is decreased in mice that overexpress Sclerostin (Kramer et al., 2010). Additionally, mice deficient in the PTH1 receptor in osteocytes show an osteogenic phenotype with increased Sclerostin expression and decreased Wnt signaling (Powell et al., 2011). Therapeutic use of PTH analogs has focused on teriparatide and related analogs. Teriparatide and related analogs have been in use for many years for the anabolic treatment of osteoporosis (Neer et al., 2001; Papapoulos, 2015).

As related to the periodontium, mechanistic and mouse models have clarified that PTH/PTHrP are critical signaling molecules in determining the fate and lineage progression of various stem/progenitor cells in the developing periodontium after birth. Osterix, a key Bmp signaling dependent-and-induced transcription factor, plays a major role in PDL and cementum formation as discussed previously (Cao et al., 2012). Osterix is highly expressed in the DF, containing stem/progenitor cells that also express PTHrP and PTH1 receptor. Osterix is also expressed in dental papilla cells that form odontoblasts and develop the dentin of the crown and roots of the tooth. Deletion of the PTH1 receptor in these Osterix+ cells leads to major failure of tooth root formation, PDL formation and redirection of acellular cementoblasts to cellular cementocytes on the root surface, and failure in primary tooth eruption (Ono et al., 2016). Many DF cells and cells on the tooth root surface express PTHrP and are likely a local autocrine-paracrine signaling mechanism. Markers of the PDL, such as periostin, are also decreased, and PDL almost disappears in these PTH1 receptor−conditional KO mice. After deletion of the PTH1 receptor, major defects in the capacity of DF cells to proliferate was demonstrated using EdU-labeling methods with overlap of a red tdTomato signal from the initial Osterix-Cre event. Histone deacetylase 4 (HDAC4), a downstream target of PTH/PTHrP signaling, is thought to play a contributing factor, and deletion of HDAC4 in Osterix+ cells leads to a major root phenotype.

Further studies enlighten our mechanistic understanding of PTH/PTHrP signaling in DF and DP stem/progenitor cells (Takahashi et al., 2018). As stated earlier, PTHrP is produced locally in the DF, DP, and other cells of the periodontium. Using a PTHrP promoter-driving mCherry reporter, these cells were isolated from the mandible and subjected to single-cell transcriptome analysis. A large fraction of these cells coexpress PTHrP and PTH1 receptor. Of eight clusters, DF cells were identified by high levels of αSMA+ cells and with Spon1 and Mkx expression (Takahashi et al., 2018). Other clusters of PTHrP cells were epithelial, DP, fibroblast-like (potential PDL), and cycling and transition cells between epithelial and mesenchymal. By lineage tracing with tdTomato and the use of a PTHrP-creERt2 model, these PTHrP+ cells differentiate into alveolar osteoblasts, PDL fibroblasts, and coronal cementoblasts. Deletion of the PTH1 receptor in PTHrP+ cells at day 3 resulted in excessive formation of cellular cementum at the expense of reduced acellular cementum by day 11−22. Proliferation by day 11 was decreased, suggesting an exhaustion of the progenitor cell pool in the absence of the PTH1 receptor. PDL formation massively decreased in this model as demonstrated by the reduction of periostin expression. As well, the molars were significantly unerupted, similar to the human condition with PTH1 receptor mutations in which there is a primary failure in tooth eruption. RNA-seq analysis of Het and cKO cells suggests the Mef2c transcription factor, a target of HDAC4, as a key node in the DF differentiation program.

The use of PTH signaling, using teriparatide in modulating periodontal disease and other bone loss in the oral cavity, has started to yield promising results. Several animal studies indicate promise with respect to the use of teriparatide in treating alveolar bone loss and the attachment loss of PDL associated with periodontitis. Periodontal defects around dental implants in dogs were treated with guided bone regeneration that included teriparatide bound to a synthetic matrix, and this demonstrated accelerated and increased osseointegration (Valderrama et al., 2010). Using a fenestration defect model created in the buccal plate in rats demonstrated enhanced new bone formation, reduced defect size, and increased newly formed cementum-like tissue after intermittent treatment with teriparatide (Vasconcelos et al., 2014). A clinical trial evaluated the effect of teriparatide on patients with severe chronic periodontitis. After periodontal surgery, patients received teriparatide injections daily for 6 weeks. Significant improvements were observed in measured periodontal parameters, with gains in linear bone around the teeth, gains in attachment, and reduction in probing depth (measure of PDL attachment to the tooth) in the teriparatide-treated group compared with controls (Bashutski et al., 2010). An overall assessment of the use of tripeptide and other agents, such as FGF2, suggests that these approaches need further evaluation; however, they show promise for periodontal regeneration (Rios et al., 2015). Since this report, mechanisms of PTH signaling in the periodontium have greatly improved, as discussed earlier, and hopefully will lead to better clinical approaches.

Wnt signaling in the periodontium and the role of the sost gene

The canonical Wnt pathway plays a fundamental role in PSC specification and differentiation (Lim et al., 2014). Axin2 (a negative regulator of Wnt signaling but a readout of cells experiencing Wnt activation-like ptch1 for hh and noggin for Bmp signaling) lacZ mice were used with a conditional KO, osteocalcin-Cre, of the Wnt-less gene (which controls processing and presentation to Frizzled receptors and blocks Wnt signaling). The mice had reduced alveolar bone and a major disruption of PDL formation. Using an Lrp5 high-bone-mass mutation mouse, in which Wnt signaling is constitutively active, a large increase in alveolar bone around the teeth and a narrow PDL space were demonstrated (Lim et al., 2015). These early studies suggest that Wnt signaling in early stem/progenitor cells in the periodontium can be "jump-started" and activated to regenerate components of the periodontium including the teeth (Yin et al., 2015).

Studies now support the view that in osteoporotic conditions, the jaw bone and surrounding tissues are a target for canonical Wnt signaling. In this study of an ovariectomized mouse, major atrophy of the PDL was shown with a reduction of the number of stem/progenitor cells in the PDL that differentiate into the alveolar bone and cementum (Arioka et al., 2019). Some implant procedures may remove the tooth and immediately place an implant into the socket. Recently, studies in mice show that if PDL cells are left on one side of the socket and PDL is removed on the other, the side with the PDL cells remaining shows accelerated bone formation, reduced osteocyte death, an increase in osteogenic gene expression, and accelerated osseointegration (Yuan et al., 2018). This demonstrates that a liposomal L-Wnt3a mixture applied to both the buccal (with PDL cells) and palatal (without PDL cells) socket side results in expanded new Wnt3a-responsive cells on the PDL buccal side, decreased bone resorption signals (tartrate-resistant acid phosphatase), and much better bone−implant contact. Even on the palatal side with few PDL cells, better bone−implant contact is observed. In the case of human patients with severe periodontal PDL and bone loss, the inflammatory aspects would need to be controlled and have some level of PDL regeneration that might make this Wnt3a approach viable for the clinic.

The PDL and its attachment to the bone and cementum is an enthesis. The normally quiescent PDL can be activated by tooth movement, as in orthodontic treatment, and the PDL is mechanically responsive to mastication. In mice, eating a soft

or liquid diet leads to major changes in collagen fiber−PDL orientation and integration into the cementum and a decrease in PDL proliferative cells (Huang et al., 2016). In the case of tooth movement, massive reorientation and integration into the cementum occurs, with increases in Runx2 and Osterix expression. Mastication has been shown to lead to a burst of Wnt-responsive cell proliferation, and if a mouse is fed a soft diet from weaning, this burst in load-mastication phenomena is reduced (Zhang et al., 2019). The alveolar bone and PDL undergo atrophy on this unloaded soft diet protocol.

A secreted and negative regulator of Wnt signaling, the Sost gene product sclerostin protein, is produced primarily by osteocytes and cementocytes (Jager et al., 2010). Sclerostin selectively binds to LRP5/6 receptors and blocks canonical Wnt signaling (Li et al., 2005). Deletion of the Sost gene in mice and in Van Buchem syndrome (human mutation in Sost leading to sclerosis) has major effects on bone composition and periodontium homeostasis (Kuchler et al., 2014; Hassler et al., 2014). In the periodontium, alveolar bone formation is accelerated and cementogenesis increases in the periodontium (Kuchler et al., 2014). Bone composition is also altered in Sost knockout gene homozygote (SostKO) mice and humans with Sost mutations, with an increased ratio of proteoglycans to calcium matrix (Hassler et al., 2014).

Expression of sclerostin is also influenced by mechanical loading. Increased mechanical loading in vivo has been shown to downregulate the SOST gene, resulting in increased bone deposition (Robling et al., 2008). In the presence of decreased load, the SOST gene is upregulated, causing bone resorption (Morse et al., 2018). Also, data now show that even in the SostKO mouse model, mechanical loading can further increase bone formation, especially in young mice (Spatz et al., 2015).

Two published studies have demonstrated alveolar bone regeneration in experimental periodontitis when the sclerostin antibody (Scl-Ab) was administerd (Taut et al., 2013; Chen et al., 2015). In ligature-induced periodontitis in ovariectomized rats, systemically administered Scl-Ab treated rats had a greater increase in regeneration of the alveolar bone around the teeth. Bone formation markers including PINP and osteocalcin in the Scl-Ab group were similar to those of the periodontal healthy group at 6 weeks (Chen et al., 2015). Dickoff1 (Dkk1) is also a potent inhibitor of Wnt signaling by binding the LRP5/6 signaling complex. New studies using a single and combination treatment with antibody to sclerostin and/or Dkk1 in a rat ovariectomized mouse model of chronic maxillary molar extraction show preserved and augmented alveolar bone volume and architecture (Liu et al., 2018). Of interest, the mandibular molar tooth across from the extracted maxilla molar tooth experiences no occlusal loading. These mandibles with unloaded teeth show massive loss of alveolar bone. This loss was prevented in the unloaded mandibles by treatment with either Scl-Ab or the combination of Scl and Dkk1 antibodies.

Periostin is a key protein expressed by primarily PDL cells in the periodontium; deletion of periostin leads to a variety of phenotypes including severe loss of PDL, cementum, and alveolar bone (Tsuji et al., 2006). Crossing periostin KO mice with SostKO mice or treating the mice with sclerostin antibody rescues these defects in the periodontium (Ren et al., 2015). Osteocyte number and connectivity in the alveolar bone of the periostin KO are greatly disrupted; however, treatment of these mice with the sclerostin antibody brings back normal and highly connected osteocyte dendritic structure. This disruption in osteocyte connectivity and orientation is correlated to poor quality of bone architecture, but the mechanisms are poorly understood. Fig. 43.1 shows how the alveolar ridge increases, bone porosity decreases, and normal osteocyte morphology is restored in periostin KO mice treated with sclerostin antibody or crossed with the SostKO mouse.

Bmp2 gene function in the periodontium

Early studies of Bmp2 (bone morphogenetic protein 2) regulation in primary and other cell models demonstrated that of all the Bmps, Bmp2 mRNA expression was sensitive to a variety of signaling molecules, such as TGFβ and Bmp itself. Bmp2 showed dynamic changes in expression in osteoblasts at different times and states of differentiation. The first conditional knockout of the Bmp2 gene, with Prx-Cre in middle stages of embryonic development, showed dramatic changes in postnatal long bones that were very narrow as well as dramatic changes in chondrogenesis. These mice developed extensive bone fractures that would not heal (Tsuji et al., 2006). Bone graft materials and techniques are critical for the periodontist to treat periodontitis and the loss of bone around the teeth. If bone graft material was from a Bmp2 cKO mouse, the bone grafts failed to incorporate into the healing process, indicating that at least one key material in bone graft material is the Bmp2 protein (Chappuis et al., 2012). Further studies of conditional KO of Bmp2 and Bmp4 demonstrate that the Bmp2 gene is critical for chondrogenesis (Shu et al., 2011). However, earlier studies of conditional Bmp4 KO with the Col1a1-3.6-Cre model indicate that Bmp4 plays a key role in development of the tooth root and periodontium and potentially an indirect role in amelogenesis (Gluhak-Heinrich et al., 2010). In these studies, deletion of the Bmp4 gene led to a dramatic decrease in Bmp2 expression. Therefore, the interacting roles of Bmp2 and Bmp4 in the periodontium, as well as in long bones needs further investigation.

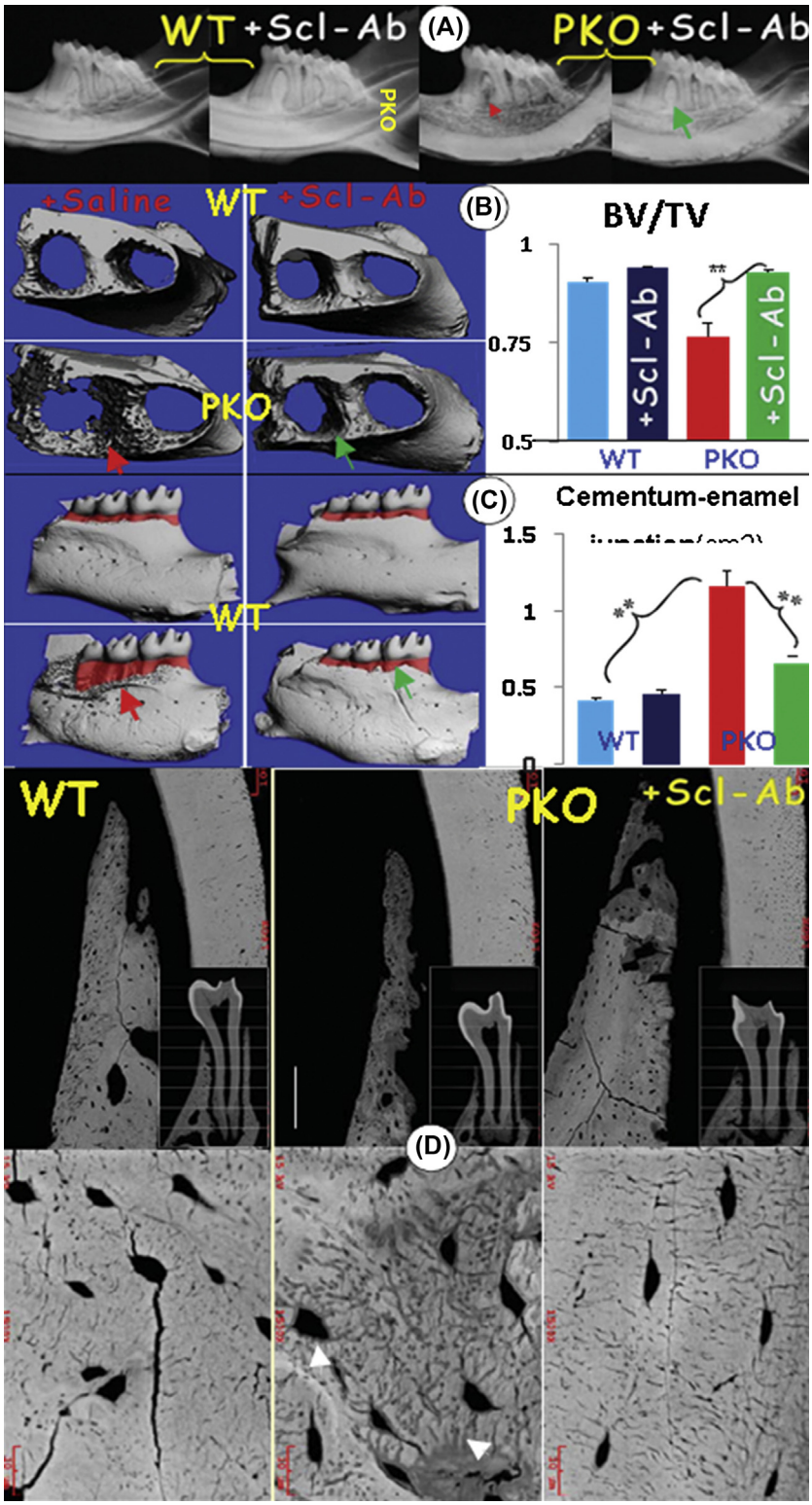

FIGURE 43.1 Restoration of bone loss, defective CEJ area (cementum-enamel junction), and defective osteocyte morphology (5 months, after 2-month Scl-Ab treatment, 25 ug/gm 2x per week) in the periostin KO (PKO) mouse model. (A) X-ray showing correction of alveolar bone loss with Scl-Ab treatment in PKO (periostin knockout) mice (3−5 month treatment, 2x per week). (B) uCT showing loss of alveolar bone in PKO mice and correction with Scl-Ab treatment. (C) uCT analysis around the CEJ region (buccal), and loss of alveolar bone ridge and correction with Scl-Ab treatment as above. Note large quanitative increase bone ridge around teeth with Scl-Ab treatment (marked cememtum). (D) Backscatter SEM shows loss of Ca++ signal in alveolar bone matrix in PKO (bone quality) and regain of bright white signal in PKO mice treated with Scl-Ab. Note the more elliptical osteocytes in control and Scl-Ab treated Periostin KO mice, and the disorganized dendritic processes in the Periostin KO, generally a reflection of poor quality of the bone matrix. Scl-Ab treatment of the Periostin KO rescues this disordered dendritic osteocyte structure. (From Ren et al, 2015, with permission from FASEB J)

The deletion of the Bmp2 gene in Osterix+ cells, with the use of an Osterix-GFP-Cre mouse model, resulted in a dramatic phenotype in the development of tooth roots as well as in major defects in cellular cementogenesis, PDL formation, and alveolar bone formation around the teeth (Rakian et al. 2013). In these mice, there were decreases in periostin, a marker for PDL; Nfic, a critical transcription factor for root and PDL formation; and VegfA, a critical factor for vascular formation produced by periodontal fibroblast, osteoblast, and odontoblast. There were also reduced CD31+ endothelial cells on capillaries and associated CD146+ and αSMA+ pericytes. This again shows the link of Bmp2-regulated VegfA production and the creation of the vascular niche for stem/progenitor cells. Also, this is demonstrated in long bones with Bmp2 cKO with the Col1a1-Cre model (Yang et al., 2013). Vascular endothelial cells make very little Bmp2, but the associated pericytes can be activated to begin production of Bmp2 in a paracrine manner from the more mature cells that produce high levels of endogenous Bmp2 protein.

Because Osterix+ cells are in both the PDL region and pulp, and deletion of Bmp2 affects both structures, separating the indirect effects on root, PDL, and cementum formation has been difficult. The αSMA-CreERt2 model was used to address these separate issues because αSMA+ cells are very low in dental pulp but highly expressed in the PDL region where these stem/progenitor cells reside. As stated earlier, αSMA+ cells, by lineage tracing, have been shown in vivo to be stem/progenitor cells in both long bones and the periodontium, at least during the first couple months of life (Roguljic et al., 2013; Grcevic et al., 2012). Lineage tracing studies with αSMA-CreERt2 with td Tomato as a marker follows the fate of these αSMA+ stem/progenitor cells. In the presence of Bmp2 cKO, with the aSMA-CreERt2 model (TAM at 6 days) in these cells, demonstrate that the Bmp2 gene is required for their lineage progression to mature PDL, as marked by colocalization of the red td Tomato+ cells and the antibody periostin. This is shown in Fig. 43.2.

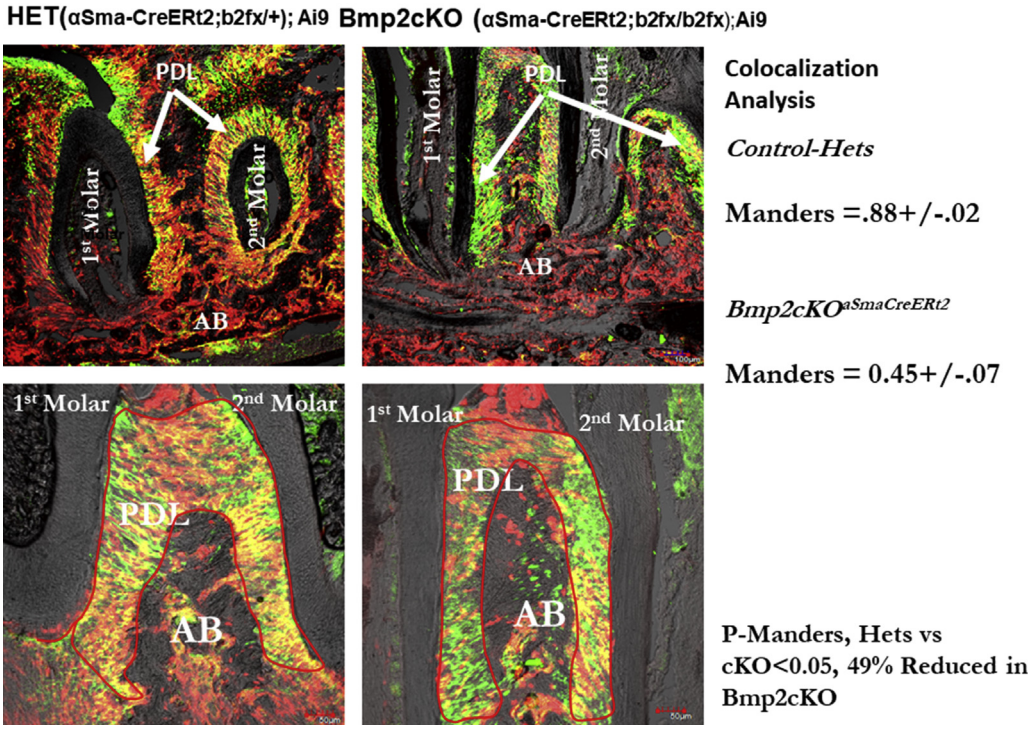

FIGURE 43.2 Deletion of the Bmp2 gene in αSMA+ cells decreases the capacity of these stem/progenitor cells to differentiate into periostin+ periodontal ligament fibroblasts. (A) Section through first and second molar (10× confocal) of heterozygous mice with αSMA-CreERt2- Bmp2 fx/+ and Rosa26-stop-tdTomato allele (Ai9). Note the high concentration of red and green colocalized in the PDL region (*yellow cells or white to light gray in the printed version*). (B) Section through the first and second molar of Bmp2 conditional knockout, αSMA-CreERt2-Bmp2fx/fx, and Rosa26-stop-tdTomato allele. Note the reduced colocalization of red and green pixels in the PDL fibroblasts. (C) Higher magnification (20×) of A. HET, with the red line defining the area quantified by the Coloc 2 program. (D) Higher magnification (20×) of B. (Bmp2 cKO), with the red outline region used for quantification. Mice were 1 month old, and the 50% reduction of periostin-tdTomato signal in the Bmp2 cKO was quantified using the Fiji ImageJ Coloc 2 program. The Manders coefficient shown on the right is a measure of threshold red and green pixel overlap. Note in A and B, the reduced tdTomato+ cells in the alveolar basal bone in the Bmp2cKO compared with the heterozygote, and no green periostin signal, reflecting the relative periodontal specificity of the periostin marker for PDL. The Manders coefficient is a quantitative measure of the true overlap of the green and red signal, thresholded using the coloc2 program in Fiji.

Lineage tracing with other markers, such as Dmp1 and Ibsp (Bsp), demonstrate that the Bmp2 gene is required for differentiation to both acellular and cellular cementoblasts and cementocytes and alveolar bone osteocytes (Rakian et al., 2019).

Since the Bmp2 gene and its endogenous expression appear to be a critical node downstream of a variety of signaling pathways, understanding how this gene is regulated at various levels has been of interest for the past 25 years. For example, statins were identified as positive regulators of Bmp2 transcription, Bmp2 protein production, and increasing bone mass in various in vivo models (Mundy et al., 1999). However, statin side effects on muscle in some individuals have limited the use of statins as an anabolic bone agent in humans. Other methods that appear promising to activate the endogenous Bmp2 gene include Wnt signaling molecules. For example, in vivo activation of the Wnt pathway with Axin2 cKO in chondrogenic models increases both Bmp2 and Bmp4 expression (Yan et al., 2009). Studies now show that Bmp2 transcription and mRNA expression are dependent on Wnt3a and B-catenin activity (Zhang et al., 2013). Blocking Wnt activity with Dkk1, sFRP4 or β-TrCP, ICAT, or delta TCF4 decreases transcription of the Bmp2 promoter-enhancer 5′ region. Site-directed mutagenesis of a Wnt/TCF response region in this Bmp2 promoter-enhancer region blocked Wnt3a activity on the Bmp2 gene. Using an immortalized mouse limb bud cell model in which the endogenous Bmp2 gene is inhibited by siRNA, studies demonstrated that the key transcription factors Osterix and alkaline phosphatase were dramatically inhibited at the basal level. Bone marrow stromal cells (BMSCs) were prepared from Bmp2fx/fx mice, and the endogenous Bmp2 gene was deleted with Ad-CMV-Cre. Recombinant Bmp2 can still stimulate Osterix expression in these in vitro Bmp2-deleted cells, but Wnt3a has now lost the ability to stimulate Osterix, alkaline phosphatase, and Col1a1. Wnt3a-stimulated mineral matrix is greatly reduced in Bmp2 KO cells. Thus, the transition to a Runx2/Osterix+ cell requires the Bmp2 gene and cannot be compensated for by canonical Wnt signaling (Salazar et al., 2016). These data support the hypothesis that the endogenous Bmp2 gene is a critical downstream node of canonical Wnt signaling in bone biology. In support of this hypothesis, the coumarin-like compound from Chinese herbs, osthole, stimulates bone formation in ovariectomized mice and calvarial assays by stimulating both β-catenin signaling and Bmp2 expression (Tang et al., 2010). Deletion of the Bmp2 gene in vitro blocks osthole-induced osteoblast differentiation through the β-catenin pathway. Osthole also decreases inflammation profiles, suppresses bone resorption, and increases osteogenic differentiation in periodontal stem cells by epigenetically increasing the positive H3K9ac states associated with increased β-catenin. This suggests that osthole can be used to treat periodontitis (Sun et al., 2017). Recent studies also show that in the presence of the SostKO model, increased canonical Wnt signaling in vivo cannot rescue the loss of bone and defective periodontium defects seen in the Bmp2 cKO with either the αSMA-CreERt2 model or the Osterix-CreERt2 model. Fig. 43.3 shows X-rays that demonstrate that in the presence of SostKO and increased canonical Wnt signaling, bone loss in both long bones and periodontium due to the absence of Bmp2 gene in these stem/progenitor cell populations cannot be rescued in the presumed presence of elevated Wnt signaling, as can be rescued in the periostin KO model.

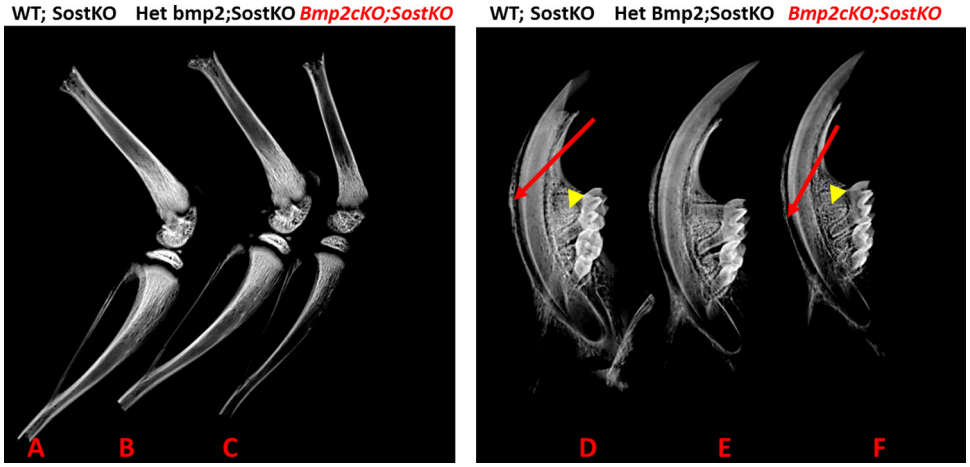

FIGURE 43.3 Decreased trabecular and cortical bone in long bones and decreased alveolar bone in the mandibles of Bmp2 cKO with the αSMA-CreERt2 model cannot be rescued by Sost knockout gene homozygotes (SostKOs). Compare A and B with C for long bones and D and E with F for mandibles. A. Wild-type for Bmp2 and SostKO. B. Heterozygote for Bmp2 gene and SostKO. C. Bmp2 cKO with SostKO—long bones. D. Wild-type for Bmp2 and SostKO. E. Heterozygote for Bmp2 gene and SostKO. F. Bmp2 cKO with SostKO—mandibles, 1-month animal at sacrifice. Tamoxifen at 100 ug/gm given at days 4, 12, and 21. In D and E, note the thinner and less radiopacity in the alveolar bone (*arrowheads*) and basal bone surrounding the incisor (*arrows*).

Also, excess Wnt signaling using a constitutively active β-catenin driven by the Dmp1 promoter causes major destruction of the PDL's fibrous nature (enthesis), excess cellular cementum formation, and ankylosis and fusion of the bone to the root of the teeth (Wu et al., 2018). Most likely, excess activation of the Bmp2 gene and other unknown genes contributes to activated mineralization programs, alveolar bone, and cellular cementum. In the clinic, the use of rBmp2 in periodontal regeneration results in the destruction of the PDL and ankylosis of teeth to the bone. This reminds us that many of these pathways, having so many feed-forward and feedback loops, are constantly searching for the optimal signal levels at a given time, what is referred to as the "goldilocks effect," or having just the right amount of a given signal for a given cell at a given time interval.

The words are heard so often at the end of various studies and presentation: "and target gene expression." What this means is that for the future, the set of target genes, and how they integrate into the biology of what is being studied, will give a better and deeper understanding of that biology. Using the new tools of epigenomics, transcriptomics of single cells, and CrispR-Cas9-selective modulations of the genome, will provide a greater depth of knowledge of these complex biological processes, especially for bone and periodontium biology. For example, the complete list of all Runx2 binding sites used during the MC3T3 osteoblast model has been defined (Meyer et al., 2014; Tai et al., 2017). These resources can be utilized for various select studies in which a deeper understanding of over 5000 Runx2 sites and interactions with other transcription factors, such as members of the C/EBP family and Sp7 (Osterix), can be investigated in the context of other individual studies. Epigenomic changes, active enhancer maps with H3K27ac, repressor maps with H3K27 and 9me3, and promoters with H3K4me3 chip-seq studies have been carried out at various stages of αSMA+ progenitor cell differentiation up to a highly mineralizing state (Wu et al., 2017). Work on defining the Osterix binding sites on a genome-wide basis, in collaboration with Dlx5 and the genes that Osterix-Dlx5 regulates during MC3T3 osteoblast differentiation and in primary calvarial osteoblasts, is a powerful resource for studying and developing gene network models for osteoblast differentiation and comparing with periodontium biology (Hojo et al., 2016).

The gene, epigenomic, and transcription network of PSCs that differentiate into three major components of the periodontium has great promise to develop specific methods and therapeutics for regeneration of the complete periodontium including alveolar bone and crest height and healthy PDLs with good attachment to both bone and cementum. The transcriptome at four different stages of differentiation of αSMA+ PSC, with and without the endogenous Bmp2 gene, has been determined on a genome-wide basis (Rakian et al., 2019). Deletion of the endogenous Bmp2 gene in this in vitro system demonstrates that the endogenous gene is critical for differentiation of PSCs to the three major cell types of the periodontium. Osterix is decreased over fivefold without the endogenous Bmp2 gene. Of the 576 genes reduced in expression, over 51 histone genes and other growth-related genes were reduced 2- to 50-fold. These studies reinforce the concept that the endogenous gene is critical not only for differentiation but also for fundamental growth and expansion of these stem/progenitor cells from their niche, in many cases the capillaries. These in vitro observations were validated in vivo using EdU-labeled animals and demonstrated that αSMA+ cells have reduced capacity to proliferate and expand in the absence of the endogenous Bmp2 gene in these PSCs (Rakian et al., 2019).

The growth-promoting activity of the Bmp2 gene may depend on the Bmp2 ligand and select receptor patterns on the cell at a given stage or time (Chapter 48, by Vicki Rosen et al, titled Bone morphogenetic proteins). Over 2500 genes change expression between the undifferentiated and mineralizing state, with many gene ontologies supporting this differentiation gene set. The major gene expression changes occur during differentiation without the addition of rBmp2. However, many of these differentiation-associated gene expression changes do not occur when endogenous Bmp2 is deleted and can only be partially rescued by the addition of rBmp2. The extent of rescue is dependent on the added rBmp2 ligand levels.

For many years, small regions of the Bmp2 gene have been studied to determine how the gene is regulated and if methods could be discovered to increase its transcription, leading to increased endogenous Bmp2 production and possible new bone formation. As discussed, there are Wnt response regions in the 3 kb enhancer-promoter region of the Bmp2 gene and Bmp2 mRNA and protein that are a critical node downstream of canonical Wnt activity. Estrogen response elements in the Bmp2 regulatory regions have also been found in vitro in osteoblast cell line studies (Zhou et al., 2003). Estrogens including tamoxifen and genistein can directly activate Bmp2 transcription through an ERE or estrogen DNA response element. A variety of studies have shown that various phytoestrogens have positive in vivo roles as traditional suppressors of osteoclastogenesis and anabolic bone-formation agents. Studies of these phytoestrogens and their mechanism of action with in vitro cell models have demonstrated that many osteogenic genes are activated including the Bmp2 gene. Quercetin stimulates matrix mineralization and the proliferation of primary osteoblasts and increases Bmp2 expression twofold through the estrogen receptor−mediated pathway (Pang et al., 2018). Another example is Icariin phytoestrogen, which stimulates osteoblast differentiation and inhibits adipocyte differentiation through an estrogen-mediated pathway (Li et al., 2018). Estrogens play an important role in bone formation and resorption in both men and women, and have been

extensively reviewed (Khosla and Monroe, 2018). Further studies on the role and action of estrogen in the presence and absence of the Bmp2 gene on both the periodontium and long bones will be of interest.

The decapentaplegic gene (dpp) in fruit flies is equivalent to the Bmp2/4 genes in mammals. Studies of the regulation of this gene in leg and wing formation found that many of the regulatory elements in the genome are 3′ and hundreds of thousands of base-pairs away from the dpp promoter region (Blackman et al., 1991). Likewise, the Bmp2 gene lies in a "genomic desert" with no other major coding gene within one million base pairs of the promoter. The part of the Bmp2 gene that has been studied for so long is like the "tip of an iceberg." If one looks at the enhancers in the Bmp2 gene in a variety of in vivo and many in vitro cell models using simple tools in NCBI, it becomes apparent that the 5′ 2-3 Kb region upstream of the transcription start side is loaded with enhancer marks, such as the H3K27ac site and open chromatin domains. However, downstream of the gene body are massive candidate-enhancer regions that are to some extent cell or tissue specific. Also, much data is available on the "connectome" of the Bmp2 gene region, distal regions of the Bmp2 gene region up to 1 Mb away that connect—loop in 3-D genomic space—with the Bmp2 promoter-enhancer region. Therefore, to understand transcription regulation and upstream pathways, this larger region of the Bmp2 gene area needs investigation. Using various epigenomic tools, enhancers in the Bmp2 area up to 1 Mb from the gene body have been studied in αSMA+ osteoblast differentiation (Wu et al., 2017), and one can now overlay with enhancer maps at various stages of αSMA+ PSCs differentiation (Rakian et al., 2019). Also, open chromatin domains activated during differentiation of PSCs have been defined, with over 30,000 ATAC-seq peaks induced 2- to 30-fold over the undifferentiated state. Motif analysis found over 5000 new Runx2 sites and 10,000 AP-1/Atf3-4 sites. Specifically in the 1 Mb region 3′ from the 10 KB Bmp2 gene body, 25 new open chromatin domains were increased on differentiation, and motif analysis again found enrichment of Runx2 sites, candidate Sp7 sites, and AP-1 sites (Rakian et al., 2019). Fig. 43.4 shows an example of this analysis for the Bmp2 gene at several stages of PSC differentiation in over the 1 Mb 3′ region with the 25 or so enhancers marked with H3K27ac peaks and overlaid with the open chromatin domains defined by ATAC-seq analysis.

Much of the genome is organized into topological-associated domains (TADs). These 3-D structures define sets of genes insulated from the regulatory regions of genes in adjacent cis regions or across chromosomes in trans within the genome. The Bmp2 gene body and 3′ 1 Mb region lie in a unique TAD as marked by the red line. Some RNA-seq data with many long-coding RNAs are associated with enhancers and likely play an enhancer RNA role. Overlaid are also maps of enhancer regions in αSMA+ BMSCs at three stages, and demonstrate that many of these enhancer regions are used in both long bone osteoblasts and the periodontal PSC differentiation program. Future studies of the interacting role of these osteoblast and PSC enhancers will lead to a deeper appreciation of the complexity of gene regulation the Bmp2 gene and hopefully new approaches to activate endogenous Bmp2 production.

Key regulators of mineral metabolism and the periodontium

Many markers we use to study BMP2- and Wnt-regulated genes control enthesis formation and mineralization and play key roles in periodontal biology. Loss-of-function mutations in the gene *ALPL* in the inherited disease hypophosphatasia (HPP; OMIM# 241500, 241510, 146300) cause reduced tissue-nonspecific alkaline phosphate (TNAP) activity and increased levels of inorganic pyrophosphate (PP_i), a potent inhibitor of mineralization (Bowden and Foster, 2018; Millan and Whyte, 2016). While severe skeletal defects, including rickets, can accompany the most severe cases of HPP, premature primary tooth loss is nearly universal among affected individuals across the disease spectrum. The cause of premature tooth loss is the reduction, absence, or hypomineralization of acellular cementum resulting in weakened or absent periodontal attachment (Fig. 43.5A) (Bruckner et al., 1962; Foster et al., 2014), Bruckner et al., 1962; Foster et al., 2014). HPP is also associated with mineralization defects in enamel, dentin, and alveolar bone, with periodontal disease demonstrated in some case reports and in global and conditional *Alpl* knockout mouse models of HPP (Fig. 43.5B) (Foster et al., 2017; Foster et al., 2013b; Hu et al., 2000; Luder, 2015; Reibel et al., 2009; van den Bos et al., 2005; Yadav et al., 2012).

While TNAP activity reduces PP_i levels, additional factors work in opposition. Ectonucleotide pyrophosphatase phosphodiesterase 1 (ENPP1) and progressive ankylosis protein (ANKH in humans/ANK in mice) both increase extracellular PP_i, and are thought to prevent ectopic calcification at distinct sites throughout the body. Loss of function of either ANK or ENPP1 in mice causes dramatically increased acellular cementum growth, while not substantially affecting enamel or dentin and only modestly affecting cellular cementum and alveolar bone (Fig. 43.5C, D) (Ao et al., 2017; Foster et al., 2012; Thumbigere-Math et al., 2018). While the effects of *ANKH* mutations on cementum in humans have yet to be demonstrated, loss of function of *ENPP1* has a similarly dramatic effect on human acellular cementum in a GACI subject (Fig. 43.5E, F) (Thumbigere-Math et al., 2018). Based on evidence from humans and mice, "tuning" of cementogenesis by PP_i appears to be a powerful evolutionarily conserved mechanism.

FIGURE 43.4 Example of transcriptome and epigenomic analysis of the Bmp2 gene region of 1.44 million base pairs. Note the turquoise regions that mark the 10 kb transcription gene body and over one million base pairs away on the 3′ side, the Hao1 gene body in turquoise. This area including the Bmp2 5′ promoter-enhancer region to almost the Hao1 gene body is of key interest because of all the regulatory regions discovered and modulated during PSC differentiation as well as long bone osteoblast BMSC differentiation. The CM6 clonal cell model is used to study the process of stem cell to cementoblast and cementocytes in the cellular cementum, and the SW3 clonal cell model is used to study the process of osteoblastogenesis, all the way to osteocytes. In all cell models, Cd1 is control at day 1—one day past confluency, Bd1-d22 are rBmp2 treated (50 ng/mL) at days 1, 5, 10, 14, 16, and 22 as indicated. In PSCs and BMSC primary cells, by day 14 a complex mineralizing culture has formed with early expression of Dmp1, osteocalcin, and Ibsp (Bsp). The double-lined box defines the Bmp2 transcription unit (turquoise) and local surrounding region, with strong overlap of ATAC peaks (open chromatin domains) with active enhancer H3K27ac chip-seq peaks in primary PSCs and BMSCs in published data on αSMA+ Bmsc (Wu et al., 2017), with a twofold to fivefold increase of both enhancer-promoter and open chromatin regions. Red boxes at the CTCF insulator marks (indirect repeats) show about a 3′ 1 Mb region that defines a TAD for the Bmp2 gene region in mouse and humans in many cell and tissues, forming a large chromatin 3-D structural loop. Light blue boxes (RNA-seq data-lower part of figure), show Bmp2 expression that increases 20-fold to 70-fold in the various models, with differentiation—i.e., Cd1 to Bd5 in the PSC, by Bd14 in long bone osteoblast BMSCs, by Bd10 in CM6 cells, and by Bd22 in SW3 cells. Light green boxes A, B, and C show overlap of ATAC-seq open chromatin domain, overlaps with enhancer regions, increased changes associated with differentiation, and associated Sp7 (Osterix), Dlx5, and Runx2 chip-seq peaks from published data in αSMA+ osteoblast models. These regions are about A. 350,000; B. 800,000; and C. 900,000 bp from the Bmp2 5′ promoter-enhancer region studied for so many years. Orange boxes in this 1 Mb 3′ region of the Bmp2 gene show areas of increased expression of long-noncoding RNAs during differentiation in these enhancer areas, overlap in the different cell models, and a subset that intersects with ATAC and H3K27ac peaks. BMSC d0 and d21 for H3K27ac and CTCF are from GEO GSE76074 (Wu et al., 2017); Sp7 and Dlx5 are from GEO GSE76187 (Hojo et al., 2016); and Runx2 are from GSE41920 (Meyer et al., 2014). Orange arrow, near the Bmp2 transcription unit, defines a Wnt/b-catenin-TCF response region.

Disorders of inorganic phosphate (P_i) metabolism can strongly affect periodontal mineralization. These include acquired conditions such as vitamin D deficiency and inherited disorders such as X-linked hypophosphatemia (XLH; OMIM# 307800; mutations in the *PHEX* gene) and autosomal recessive hypophosphatemic rickets (ARHR1; OMIM# 241520; mutations in the *DMP1* gene) (Foster et al., 2014; Biosse Duplan et al., 2016; Coyac et al., 2017; Fong et al., 2009; Ye et al., 2008). Defects in cementum and alveolar bone, and enamel and dentin, may arise from the direct effects of insufficient phosphate for mineralization as well as from disturbances in vitamin D signaling, FGF23 signaling, and local levels of ECM proteins.

Cementum and alveolar bone have significant overlap in their ECM constituents including BSP and OPN, members of the small integrin-binding ligand N-linked glycoprotein (SIBLING) family and two of the most commonly used markers for osteoblasts and cementoblasts (MacNeil et al., 1995a; MacNeil et al., 1995b; McKee et al., 1996). In vitro and in silico studies suggest that BSP promotes hydroxyapatite crystal growth (Harris et al., 2000). Genetic ablation of the *Ibsp* gene (Bsp protein) in mice results in a decrease or an absence of acellular cementum, causing periodontal detachment and breakdown (Fig. 43.5G) (Foster et al., 2013a; Soenjaya et al., 2015). Lack of BSP also causes delayed mineralization of

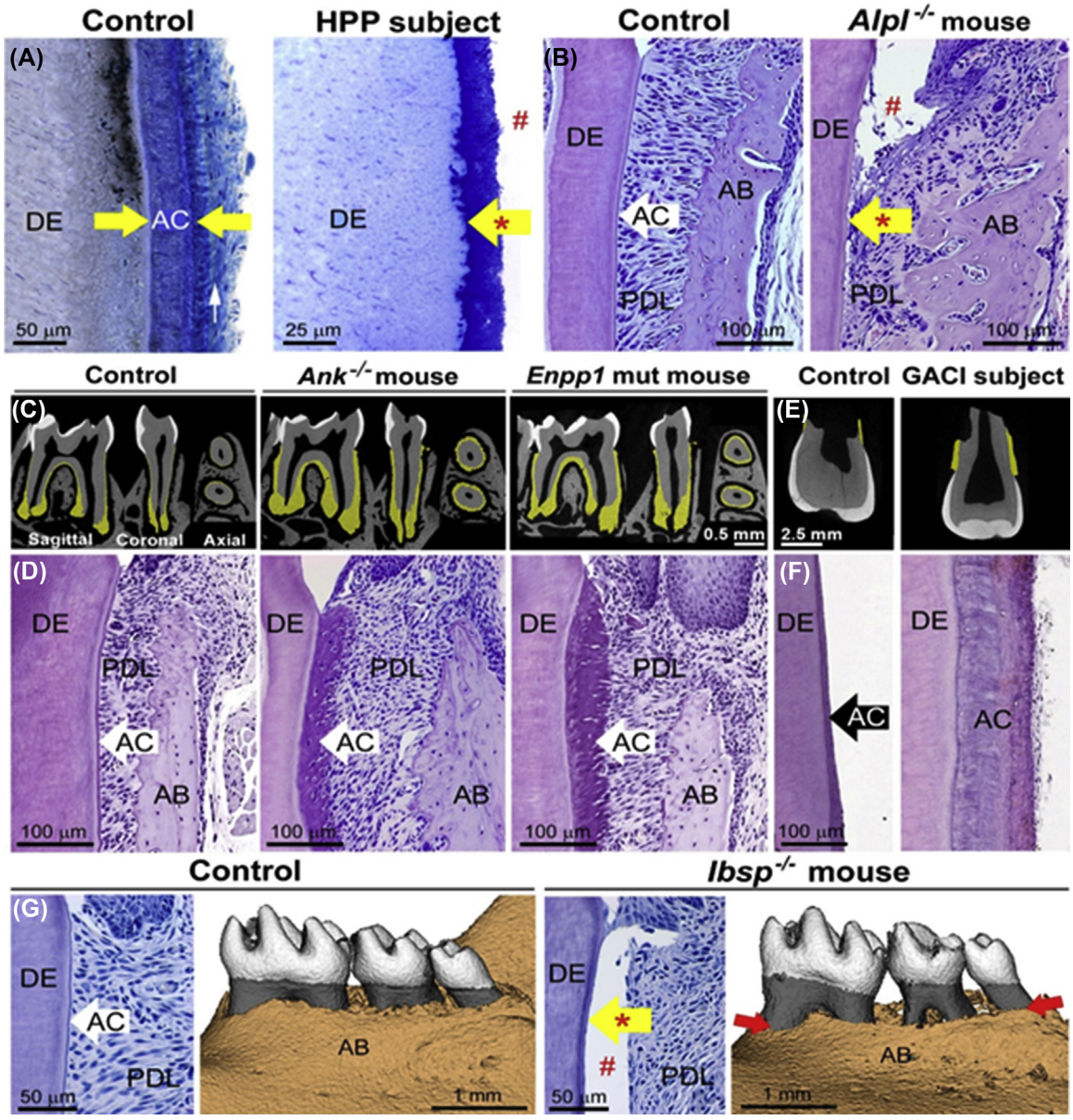

FIGURE 43.5 Key regulators of mineral metabolism and the periodontium. (A) Compared with the well-developed acellular cementum (AC) on the root dentin (DE) surface in a healthy control tooth, HPP (hypophosphatemia) inhibits AC formation, allowing bacterial invasion and formation of dental plaque (P). (B) Compared with the functional periodontium in control mice, molars from *Alpl*$^{-/-}$ mice exhibit deficient AC (*red**) (light grey in print versions), periodontal ligament (PDL) detachment (#), and accumulation of osteoid at the alveolar bone (AB) surface. (C) Compared with normal control mice, microcomputed tomography reveals that molars from *Ank*$^{-/-}$ and *Enpp1* mutant mice feature dramatically increased AC (*highlighted yellow*) (white arrowhead in print versions). (D) Histology images of H&E stained sections show increased AC in *Ank*$^{-/-}$ and *Enpp1* mutant mice compared with controls. (E) Compared with an exfoliated primary incisor from a healthy control subject, microcomputed tomography reveals that the primary incisor from an individual with GACI (loss-of-function mutations in *ENPP1*) exhibits increased AC (*highlighted yellow*). (F) H&E stained histology sections from a control and GACI subject reveal the dramatically expanded AC from loss of ENPP1 function. (G) Compared with H&E stained sections of control mouse molars, *Ibsp*$^{-/-}$ mice feature reduced or absent AC (*red* *) and PDL detachment (#). Microcomputed tomography scans of mandibles show reduced AB (*red arrows*) around roots of *Ibsp*$^{-/-}$ mouse molars. *Panel A images adapted from Luder,* Front Physiol *6:307, 2015, and reproduced with permission under the terms of the Creative Commons Attribution License (CC BY). Panel B images adapted from Bowden and Foster,* Drug Des Devel Ther *12:3147–3161, 2018. Images in panels C–G adapted from Ao et al.,* Bone *105:134–147, 2017, and reproduced by permission; and from Thumbigere-Math et al.,* J Dent Res *97(4):432–441, 2017, and used in accordance with STM permissions guidelines.*

cellular cementum and alveolar bone, with no substantial effects in dentin or enamel. By contrast, the closely related protein OPN (osteopontin or Spp1) regulates or inhibits mineralization (Boskey et al., 2002). Genetic ablation of *Spp1* did not substantially affect cementogenesis; however, there was increased volume and mineralization of alveolar bone and dentin (Foster et al., 2018). BSP, OPN, and other SIBLINGs have been increasingly linked to P_i/PP_i metabolism. OPN expression is tied to expression of *Alpl*, *Ank*, and *Enpp1*, and these work in concert to direct the P_i/PP_i ratio and mineralization milieu (Harmey et al., 2004; Harmey et al., 2006). Genetic ablation of the *Ibsp* gene resulted in perturbation of some P_i/PP_i regulators, and ablation of ANK in the absence of BSP (lowering PP_i levels) reestablished acellular cementum formation and periodontal function (Ao et al., 2017). However, genetically decreasing PP_i levels did not completely overcome the absence of BSP, confirming that BSP does not function solely through P_i/PP_i-related mechanisms and is likely exerting effects through one or more of its functional domains.

Temporal expression of Ibsp, Spp1, TNAP, ANK, and Enpp1 genes is dynamic during differentiation of osteoblasts or periodontal stem cell differentiation, and most are regulated by BMP signaling at some level as shown in Bmp2 conditional knockout studies in bone and periodontium. BMP2 gene expression and action is in part downstream of Wnt-PTH/PTHrP and hh pathways, as discussed. These observations in humans and mouse studies demonstrate the importance of Ibsp, Spp1, TNAP, and Enpp1 genes in regulating extracellular and highly organized mineralized matrix formation in both bone and the periodontium, where tight regulation of these processes is necessary for maintaining a healthy, tendon-like enthesis between the alveolar bone and cementum as well as controlled rates of spatially determined mineralization.

Periodontal stem/progenitor regeneration and methods to control inflammation in periodontal disease

As stated, PDL tissues are derived from the DF (Woodfin et al., 2011) region, which originates from the cranial neural crest during tooth development (Miletich and Sharpe, 2004; Chai et al., 2000). The DF is a condensation of the ectomesenchymal tissue (Grant and Bernick, 1972). PSCs isolated from the PDL have been shown to have MSC characteristics including in vitro trilineage differentiation potential (Gay et al., 2007). Numerous studies have reported PSCs expressing pericyte markers including CD146 and STRO-1 (Xu et al., 2009; Iwasaki et al., 2013; Nagatoma et al., 2006), which is consistent with Bruno Péault's group suggesting that MSCs originate from the perivasculature (Crisan et al., 2008; Corselli et al., 2010). PSCs isolated from the PDL using colony selection and STRO-1/CD146 developed into cementoblast-like cells and adipocytes in vitro. In vivo transplantation showed that in vitro expanded PSCs generate a cementum/PDL-like complex characterized by a layer of aligned cementum-like tissues and clearly associated PDL-like tissues. They also showed the capacity to form collagen fibers, similar to Sharpey's fibers, connecting to the cementum-like tissue (Seo et al., 2004). This study demonstrates that a large fraction of PSCs are derived from a population of perivascular cells and may be an effective target for periodontal regenerative therapy. αSMA+ cells on the capillaries are classified as pericytes (Alarcon-Martinez et al., 2018). In an in vitro study, PSCs possessed the capacity to adhere to endothelial cell capillary networks in coculture experiments, mimicking pericyte-like localization in vitro, and expressed pericyte markers NG2+ and CD146+ on the cell surface, also suggesting that these cultured PSCs originated from perivascular cells and function as pericytes (Iwasaki et al., 2013). Chen et al. also showed that STRO-1/CD146 were expressed around blood vessels in the PDL (Chen et al., 2006) Lin et al. demonstrated that regenerating periodontal tissue obtained from guided tissue regeneration procedures contained cells that express the MSC-associated markers STRO-1, CD146, and CD44 and had the capacity to form mineral deposits and fat cells in vitro (Lin et al., 2008). In another study, PSCs expressed the perivascular cell markers NG2, α-SMA, PDGFR-β, and CD146 and formed vessel-like structures in vivo (Bae et al., 2017).

Periodontitis is a chronic osteolytic inflammatory disease of bacterial etiology. The sustained microbial challenge and dysbiosis is due to a failure of endogenous resolution of inflammation pathways that results in host-mediated destruction of the hard and soft tissues of the periodontium (Taubman et al., 2007; Graves et al., 2008; Fredman et al., 2011; McCauley and Nohutcu, 2002; Van Dyke, 2011). Resolution of inflammation is an active and highly coordinated response modulated by specialized proresolving lipid mediators (SPMs) (Hasturk et al., 2007; Serhan et al., 2007) that include lipoxins (LXs), resolvins (Rvs), protectins, and maresins. SPMs are physiologic mediators and pharmacologic agonists that stimulate the resolution of inflammation and infection (Serhan, 2017). SPMs exhibit multipronged actions that improve the outcome of inflammation-related pathologies in experimental models and clinical trials (Serhan, 2007; Colas RA et al., 2014; Van Dyke et al., 2015; Cianci et al., 2016).

In periodontitis, SPMs have been shown to directly improve bone healing and regeneration (Hasturk et al., 2006, 2007). Resolvin E1 (RvE1) downregulates inflammation in vivo in periodontitis at molecular and histological levels (Hasturk et al., 2006; Bannenberg et al., 2005) and stimulates the resolution of inflammation and bone formation by directly

modulating both osteoclast and osteoblast functions (Zhu et al., 2013). RvE1 exhibits receptor-mediated control of osteoclasts and inhibits mature osteoclast formation and bone resorption in vitro (Zhu et al., 2013; Herrera et al., 2008; Gao et al., 2013). RvE1 specifically targets and downregulates the pivotal fusion protein DC-STAMP in osteoclasts and decreases DNA binding activity of the transcription factor NFATc1, leading to decreased cell fusion and attenuated bone resorption (Zhu et al., 2013). In osteoblasts, RvE1 increases the OPG/RANKL secretion ratio, favoring bone formation through a pathway that includes phosphorylation of AKT, rS6, and mTOR. In osteoclasts, RvE1 inhibits AKT pathways with activation of caspase 9 and increases apoptosis, reducing osteoclast numbers and proliferation (El Kholy et al., 2018; Papathanasiou et al., 2016).

PSCs hold great promise in periodontal tissue regeneration. Human PSCs have been able to produce cementum and PDL Sharpey's fibers (Seo et al., 2004; Trubiani et al., 2008), and participate in the process of periodontal tissue repair in immune-compromised rats (Seo et al., 2004). Human PSCs release SPMs including LXs and D-series Rvs to regulate immunomodulatory and prohealing properties (Cianci et al., 2016). Human PSCs also express the ALX/FPR2 receptor that recognizes lipoxin A_4 (LXA_4), RvE1, and annexin-A1, all of which have antiinflammatory and proresolution functions (Krishnamoorthy et al., 2010). Activation of ALX/FPR2 by LXA_4 significantly enhances the proliferation, migration, and wound-healing capacity of human PSCs in vitro (Cianci et al., 2016) through an LXA_4-driven, receptor-mediated mechanism. In an experimental periodontitis miniature pig model, the use of autologous periodontal ligament stem cells regenerated periodontal tissues including alveolar bone, cementum, and PDLs (Liu et al., 2008). In addition, the use of nanoproresolving medicines containing a novel LX analog (benzo-LXA_4, or $bLXA_4$) promoted the regeneration of hard and soft tissues that had been irreversibly lost to periodontitis in the miniature pig (Van Dyke et al., 2015). Therefore, periodontal tissue regeneration mediated by human PSCs may have potential as a stem cell–based strategy for human oral and craniofacial tissue regeneration. Treatments that activate the creation of new vascular-associated pericytes/PSCs have the potential to regenerate a healthy periodontium.

Role and mechanism of the junctional epithelium in periodontium function

Most of this chapter has focused on a few pathways that have some in vivo mouse studies and in vitro cell models of regulation of PSC differentiation to the mesenchymal components of the periodontium. However, in the oral cavity around the teeth are several key epithelial tissues that play roles in protecting the teeth and surrounding the PDL and alveolar bone from the constant onslaught of bacteria present in the oral cavity. Over 700 different species of bacteria reside close to and on the gingiva and tooth surface (Aas et al., 2005). This population of bacteria can change with increases in gram-negative species that have potent LPS antigens and can lead to severe periodontitis (Tanner et al., 1979). Because of this, it is important to understand the role, for example, of the junctional epithelium (JE) and how the JE serves as a primary barrier and protection against bacteria and mechanical insult for the progression of gingival inflammation into the underlying periodontal tissues. Thereby, epithelial integrity facilitates gingival and periodontal health. When epithelial integrity is overruled, inflammation expands into connective tissue attachment and PDL, manifesting in periodontitis.

Periodontal tissues attach to the tooth via epithelial and connective tissues. Insults to these structures can lead to inflammation, detachment, and destruction of periodontium and finally tooth loss. The epithelial tissue forming a seal on the tooth is the JE and is directly exposed to the oral cavity by virtue of its close location to the base of the gingival sulcus. Oral microbiota organized in a biofilm and their metabolic products can initiate inflammation in the gingiva, with the JE being exposed at the base of the gingival sulcus. Therefore, the JE is the first barrier for gingival inflammation. It consists of a squamous, nonkeratinizing epithelium of 3–20 cell layers. Developmentally, the JE is formed at tooth eruption upon contact between reduced enamel epithelium and oral epithelium.

The JE forms two basal laminae: the internal basal lamina facilitates the attachment to the tooth surface, while the external basal lamina is anchored to the connective tissue (Listgarten, 1966; Loe and Karring, 1969). The internal basal lamina consists of two components, the lamina lucida facing the JE and the lamina densa facing the tooth. The JE forms hemidesmosomes interacting with the lamina lucida. Lamina lucida, lamina densa, and hemidesmosome are connected by fine filaments conceived as a functional unit and containing glycoproteins (Kobayashi et al., 1976, 1977). The integrity of the seal between the enamel surface and the JE is maintained by hemidesmosomes and a basal lamina. Hemidesmosomes establish adhesion by connecting keratin intermediate filaments with the extracellular matrix. Their function is to maintain integrity and homeostasis in the JE. They contain bullous pemphigoid antigen (BPAG1) isoform e (= BP230, *DST* gene), BPAG2 (= BP180, collagen XVII, *COL17A1*), and plectin (= HD1, *PLEC* gene), consistent with type I hemidesmosomes (Hormia et al., 2001). Integrins are transmembrane receptors of hemidesmosomes consisting of alpha and beta subunits encoded by separate genes. As heterodimers, integrin α6β4 interacts together with CD151 and laminin-332 in the extracellular matrix. Integrin alpha6 interacts with BPAG2, and integrin β4 interacts with BPAG1e and plectin and

connects to keratins of the cytoskeleton (Walko et al., 2015). Kindlin1 binds to beta integrin cytoplasmic tails to facilitate binding to the extracellular matrix and cytoskeleton organization (Larjava et al., 2014). Laminin 332 is found in the internal and external basal laminae of the JE; collagen type IV is found in the external basal lamina but is lacking from the internal basal lamina (Sawada et al., 1990). Further, collagen type VII, perlecan, and laminin-111 are absent from the internal basal lamina (Hormia et al., 2001).

Mutations in genes contributing to the hemidesmosome cause epidermolysis bullosa, with blister formation within the skin or epithelium, and periodontal disease (Albandar et al., 2018; Wright, 2010). In families with mutations in the hemidesmosome-related genes *CD151* and *KIND1* (Kindler syndrome) (OMIM #173650), severe periodontal disease with tooth exfoliation has been reported (Vahidnezhad et al., 2018; Wiebe et al., 1996).

Recently, additional extracellular matrix molecules were localized to the internal basal lamina, namely amelotin, odontogenic ameloblast-associated protein (ODAM, also termed APin), and SCPP-proline/glutamine-rich-1 (Iwasaki et al., 2005; Moffatt et al., 2008, 2014; Kawasaki, 2009). The integrity of the attachment of JE is compromised in the absence of

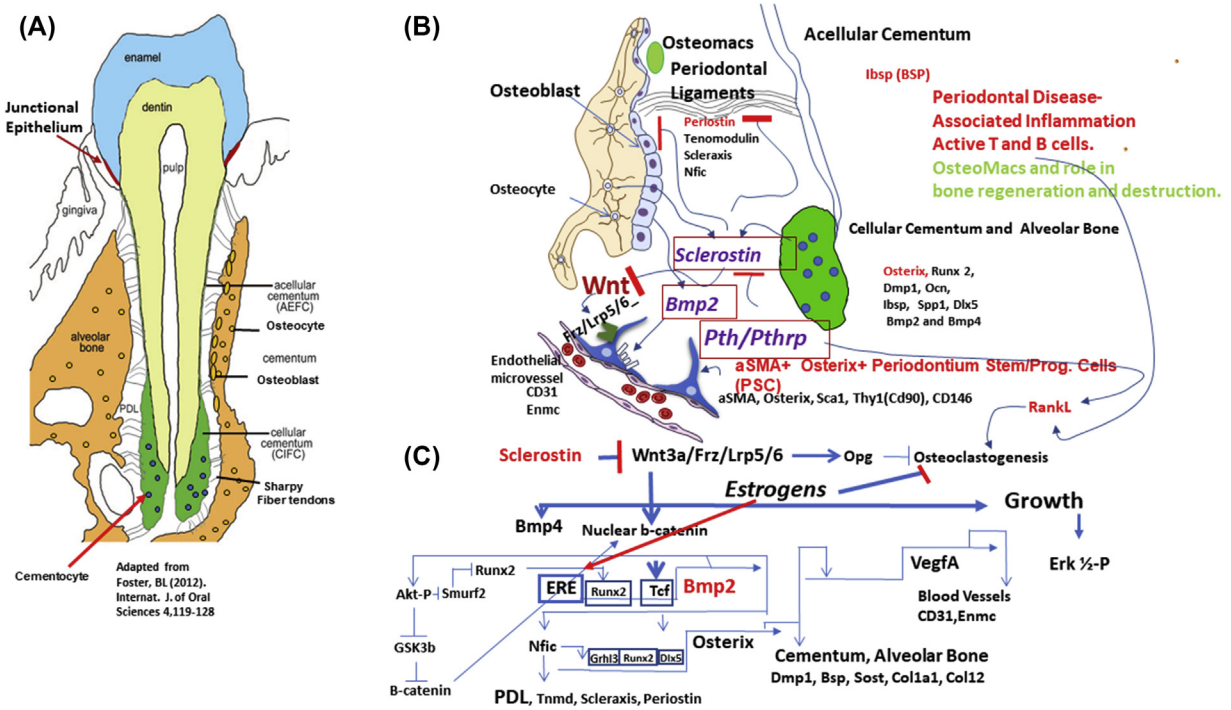

FIGURE 43.6 Overall model of the interactions of the PTH/PTHrP, Wnt, hedgehog, and Bmp2 pathways in periodontal biology. (A) Diagrammatic view of the periodontium with enamel in *blue* (grey in print versions), dentin in *light brown* (dark grey in print versions), alveolar bone in orange with marked osteoblasts and osteocytes, cellular cementum in green with cementocytes, acellular cementum along the root surface in light brown (dark grey in print versions), and junctional epithelium in maroon opposing the tooth crown. (B) Diagram of alveolar bone, periodontal ligament, and acellular and cellular cementums with markers used to study these components of the periodontium—i.e., Ibsp for acellular cementum; Runx2, Osterix, Bmp2 and Bmp4, and osteocalcin for cellular cementum; and alveolar bone, scleraxis, tenomodulin, and periostin for PDL fibroblasts. Osteomacs and T and B cells play a major role in the inflammatory process in periodontal disease but were not discussed in this chapter. The main summary in B is the interaction of PTH/PTHrP contribution to not only RankL production and bone resorption, in many cases stimulated by activated T and B cells, but the pronounced effect of PTH/PTHrP on the suppression of Sost expression from osteocytes that then leads to activated Wnt signaling. In turn, Wnt activates Opg to suppress bone resorption and activate bone formation by increasing Bmp2 expression. The emphasis is on Wnt signaling of stem progenitor cells (CD146, αSMA, Sca1, Thy1) on the small capillaries in the PDL region and alveolar bone marrow region. Wnt signaling stimulates these stem cells to begin differentiation to PDL, alveolar bone, and cementum. (C) Potential pathways for Wnt/Bmp2 signaling and downstream genes in the context of the periodontium. Canonical Wnt signaling activates both the Bmp4 and the Bmp2 genes in several systems but has not been rigorously tested in the context of the periodontium. We do know or hypothesize that without the Bmp2 gene, Wnt signaling is severely compromised in osteoblast models. Bmp2 transcription is also modulated by a variety of estrogens through at least one ERE in the promoter-enhancer region. Other EREs have been found in 3′ open chromatin domains but not characterized. Bmp2 and other Bmps are potent activators of Osterix expression in a Dlx5-Runx2-dependent manner, and the Bmp2 gene is required in the periodontium for the activation of Nfic, for PDL fibroblast differentiation, and for root formation. Bmp2-induced Osterix is a key regulator of VegfA production and links the Bmp2−Osterix−VegfA axis that connects alveolar bone formation to the creation of a new vascular−capillary stem/progenitor cells niche. Bmp signaling can also increase Akt and GSKB phosphorylation, releasing more active b-catenin in a simple feed-forward loop. Degradation of Runx2 is modulated by Smurf2 ubiquitin ligase. How Bmp2 controls growth in long bone and the periodontium is not known.

ODAM (Wazen et al., 2015). Amelotin-null mice did not have apparent defects in the JE and periodontium (Nakayama et al., 2015). In gingival inflammation, the expression of amelotin and ODAM may be altered and spread from the JE to adjacent gingiva.

In addition to its structural barrier functions, JE allows the presence and passage of antimicrobial peptides and neutrophils originating from adjacent tissues through enlarged intercellular spaces to the gingival sulcus (Hashimoto et al., 1986; Greer et al., 2013). The antimicrobial peptides in the JE belong to the family of defensins (alpha-, beta-) and cathelicidins (LL-37). Their mechanism of action is to exert pore formation on microbial membranes (Otto, 2009) and kill gram-negative bacteria associated with periodontal disease (Miyasaki et al., 1990). In addition to antimicrobial activity at homeostasis, the expression of antimicrobial molecules increases in response to periodontal disease (Gorr, 2012; Vardar-Sengul et al., 2007; Puklo et al., 2008). The JE itself does not express antimicrobial peptides but instead recruits neutrophils containing alpha-defensins and LL-37 to release them upon degranulation. Beta-defensin is produced by cells of the spinous layer of the gingiva and sulcular epithelium (Dale and Fredericks, 2005). En route to the oral cavity via intercellular spaces of the JE and gingival, the antimicrobial peptides join the gingival crevicular fluid and are exposed to periodontal microbiota.

The attachment of the JE presents a seal for mechanical insults and microbiota of the oral cavity to penetrate along the root into underlying connective tissues and PDLs via an internal basal lamina and hemidesmosomes. At the same time, the JE is permeable for neutrophils, antimicrobial peptides, and gingival crevicular fluid to assist in tissue homeostasis. When these defense mechanisms of the epithelial attachment are overwhelmed, the periodontal connective attachment apparatus succumbs to breakdown, with a clinical diagnosis of periodontal disease.

Conclusion

We have tried to integrate and connect many of the pathways that regulate the complex differentiation of PSCs to alveolar bone, PDLs, and the cellular and acellular cementum of the enthesis. Understanding the ways to regenerate this PDL and maintain a healthy JE are prime efforts in the clinic. In Fig. 43.6, we have brought together the data supporting the interacting roles of PTH, Sost, canonical Wnt signaling, and the Bmp2 and Bmp4 genes. Many of the "target" genes for these pathways are indicated, such as *Bsp, Ank, Spp1, Enpp1, and Alpl or TNAP*. We have discussed the role of the JE in the periodontium as a key initial barrier to infection in the health of the periodontium and oral cavity in general.

In particular, we have also brought together evidence that elements of estrogen action, part Sost-cWnt function, part PTH/PTHrP action, in terms of the anabolic bone formation axis, are upstream of Bmp2 action and signaling. Future studies will focus on Bmp2 and Bmp4 enhancer and repressor functions in a single-cell analysis pipeline, and complex gene network (i.e., all the genes regulated by Osterix, Runx2, AP-1, etc.) transcription factors, and how they are linked together and change over time. New approaches of single-cell sequencing and single-cell ATAC-seq will hopefully be a beginning of this effort to integrate gene networks that will predict the most effective nodes to modulate and regenerate new tissue and conserve bone mass and periodontium function as we age.

References

Aas, J.A., Paster, B.J., Stokes, L.N., Olsen, I., Dewhirst, F.E., 2005. Defining the normal bacterial flora of the oral cavity. J. Clin. Microbiol. 43, 5721−5732.

Alarcon-Martinez, L., Yilmaz-Ozcan, S., Yemisci, M., Schallek, J., Kilic, K., Can, A., Di Polo, A., Dalkara, T., 2018. Capillary pericytes express alpha-smooth muscle actin, which requires revention of filamentous-actin depolymerization for detection. Elife 7. PMC 5862523.

Albandar, J.M., Susin, C., Hughes, F.J., 2018. Manifestations of systemic diseases and conditions that affect the periodontal attachment apparatus: case definitions and diagnostic considerations. J. Periodontol. 89, S183−S203.

Ao, M., Chavez, M.B., Chu, E.Y., Hemstreet, K.C., Yin, Y., Yadav, M.C., Millan, J.L., Fisher, L.W., Goldberg, H.A., Somerman, M.J., et al., 2017. Overlapping functions of bone sialoprotein and pyrophosphate regulators in directing cementogenesis. Bone 105, 134−147.

Arioka, M., et al., 2019. Osteoporotic changes in the periodontium impair alveolar bone healing, 22034518818456 J. Dent. Res. 9. https://doi.org/10.1177/0022034518818456 [Epub ahead of print].

Bae, Y.K., Kim, G.H., Lee, J.C., Seo, B.M., Joo, K.M., Lee, G., Nam, H., 2017. The significance of sdf-1alpha-cxcr4 axis in in vivo angiogenic ability of human periodontal ligament stem cells. Mol. Cell 40 (6), 386−392.

Bannenberg, G.L., Chiang, N., Ariel, A., Arita, M., Tjonahen, E., Gotlinger, K.H., Hong, S., Serhan, C.N., 2005. Molecular circuits of resolution: formation and actions of resolvins and protectins. J. Immunol. 174 (7), 4345−4355.

Baron, R., Hesse, E., 2012. Update on bone anabolics in osteoporosis treatment: rationale, current status, and perspectives. J. Clin. Endocrinol. Metab. 97, 311−325.

Bashutski, J.D., et al., 2010. Teriparatide and osseous regeneration in the oral cavity. N. Engl. J. Med. 363, 2396−2405.

Biosse Duplan, M., Coyac, B.R., Bardet, C., Zadikian, C., Rothenbuhler, A., Kamenicky, P., Briot, K., Linglart, A., Chaussain, C., 2016. Phosphate and vitamin d prevent periodontitis in x-linked hypophosphatemia. J. Dent. Res. 96 (4), 388–395. https://doi.org/10.1177/0022034516677528. Epub 2016 Nov 13.

Blackman, R.K., et al., 1991 March. An extensive 3' cis-regulatory region directs the imaginal disk expression of decapentaplegic, a member of the TGF-beta family in Drosophila. Development 111 (3), 657–666.

Bowden, S.A., Foster, B.L., 2018. Profile of asfotase alfa in the treatment of hypophosphatasia: design, development, and place in therapy. Drug Des. Dev. Ther. 12, 3147–3161.

Bruckner, R., Rickles, N., Porter, D., 1962. Hypophosphatasia with premature shedding of teeth and aplasia of cementum. Oral Surg. Oral Med. Oral Pathol. 15, 1351–1369.

Cao, Z., et al., 2012. Genetic evidence for the vital function of Osterix in cementogenesis. J. Bone Miner. Res. 27, 1080–1092.

Chai, Y., Jiang, X., Ito, Y., Bringas Jr., P., Han, J., Rowitch, D.H., Soriano, P., McMahon, A.P., Sucov, H.M., 2000. Fate of the mammalian cranial neural crest during tooth and mandibular morphogenesis. Development 127 (8), 1671–1679.

Chan, C.K.F., et al., 2018 September 20. Identification of the human skeletal stem cell. Cell 175 (1), 43–56 e21. https://doi.org/10.1016/j.cell.2018.07.029.

Chappuis, V., et al., 2012 October. Periosteal BMP2 activity drives bone graft healing. Bone 51 (4), 800–809. https://doi.org/10.1016/j.bone.2012.07.017. Epub 2012 Jul 28.

Chen, S.C., Marino, V., Gronthos, S., Bartold, P.M., 2006. Location of putative stem cells in human periodontal ligament. Periodontal Res. 41 (6), 547–553.

Chen, H., et al., 2015. Sclerostin antibody treatment causes greater alveolar crest height and bone mass in an ovariectomized rat model of localized periodontitis. Bone 76, 141–148.

Cianci, E., Recchiuti, A., Trubiani, O., Diomede, F., Marchisio, M., Miscia, S., Colas, R.A., Dalli, J., Serhan, C.N., Romano, M., 2016. Human periodontal stem cells release specialized proresolving mediators and carry immunomodulatory and prohealing properties regulated by lipoxins. Stem Cells Transl. Med. 5 (1), 20–32. PMC4704879.

Colas, R.A., Shinohara, M., Dalli, J., Chiang, N., Serhan, C.N., 2014. Identification and signature profiles for pro-resolving and inflammatory lipid mediators in human tissue. Am. J. Physiol. Cell. Physiol.

Corselli, M., Chen, C.W., Crisan, M., Lazzari, L., Peault, B., 2010. Perivascular ancestors of adult multipotent stem cells. Arterioscler. Thromb. Vasc. Biol. 30 (6), 1104–1109.

Coyac, B.R., Falgayrac, G., Baroukh, B., Slimani, L., Sadoine, J., Penel, G., Biosse-Duplan, M., Schinke, T., Linglart, A., McKee, M.D., et al., 2017. Tissue-specific mineralization defects in the periodontium of the hyp mouse model of x-linked hypophosphatemia. Bone 103, 334–346.

Crisan, M., Deasy, B., Gavina, M., Zheng, B., Huard, J., Lazzari, L., Peault, B., 2008. Purification and long-term culture of multipotent progenitor cells affiliated with the walls of human blood vessels: myoendothelial cells and pericytes. Methods Cell Biol. 86, 295–309.

Dale, B.A., Fredericks, L.P., 2005. Antimicrobial peptides in the oral environment: expression and function in health and disease. Curr. Issues Mol. Biol. 7, 119–133.

Dangaria, S.J., et al., 2011. Successful periodontal ligament regeneration by periodontal progenitor proceeding on natural tooth root surfaces. Stem Cell. Dev. 20 (10), 1659–1668.

Debnath, S., et al., 2018. Discovery of a periosteal stem cell mediating intramembranous bone formation. Nature 562, 133–139.

Decker, M., et al., 2017 June. Leptin receptor expressing bone marrow stromal cells are myofibroblast in primary myelofibrosis. Nat. Cell Biol. 19 (6), 677–688. https://doi.org/10.1038/ncb3530. Epub 2017 May 8.

Dyment, N.A., et al., 2014. Lineage tracing of resident tendon progenitor cells during growth and natural healing. PLoS One 9 (4), e96113.

Dyment, N.A., et al., 2015 September 1. Gdf5 progenitors give rise to fibrocartilage cells that mineralize via hedgehog signaling to form the zonal enthesis. Dev. Biol. 405 (1), 96–107. https://doi.org/10.1016/j.ydbio.2015.06.020. Epub 2015 Jun 30.

El Kholy, K., Freire, M., Chen, T., Van Dyke, T.E., 2018. Resolvin e1 promotes bone preservation under inflammatory conditions. Front. Immunol. 9, 1300.

Emerton, K.B., et al., 2011. Regeneration of periodontal tissues in non-human primates with rhGDF-5 and beta-tricalcium phosphate. J. Dent. Res. 90 (12), 1416–1421.

Fong, H., Chu, E.Y., Tompkins, K.A., Foster, B.L., Sitara, D., Lanske, B., Somerman, M.J., 2009. Aberrant cementum phenotype associated with the hypophosphatemic hyp mouse. J. Periodontol. 80 (8), 1348–1354.

Foster, B.L., Nagatomo, K.J., Nociti Jr., F.H., Fong, H., Dunn, D., Tran, A.B., Wang, W., Narisawa, S., Millan, J.L., Somerman, M.J., 2012. Central role of pyrophosphate in acellular cementum formation. PLoS One 7 (6), e38393.

Foster, B.L., et al., 2013. Deficiency in acellular cementum and periodontal attachment in bsp null mice. J. Dent. Res. 92 (2), 166–172.

Foster, B.L., Nagatomo, K.J., Tso, H.W., Tran, A.B., Nociti, F.H., Narisawa, S., Yadav, M.C., McKee, M.D., Millán, J.L., Somerman, M.J., February 2013. Tooth root dentin mineralization defects in a mouse model of hypophosphatasia. J. Bone Miner. Res. 28 (2), 271–282. https://doi.org/10.1002/jbmr.1767.

Foster, B.L., Nociti Jr., F.H., Somerman, M.J., 2014. The rachitic tooth. Endocr. Rev. 35 (1), 1–34.

Foster, B.L., Kuss, P., Yadav, M.C., Kolli, T.N., Narisawa, S., Lukashova, L., Cory, E., Sah, R.L., Somerman, M.J., Millan, J.L., 2017. Conditional alpl ablation phenocopies dental defects of hypophosphatasia. J. Dent. Res. 96 (1), 81–91.

Foster, B.L., Ao, M., Salmon, C.R., Chavez, M.B., Kolli, T.N., Tran, A.B., Chu, E.Y., Kantovitz, K.R., Yadav, M., Narisawa, S., et al., 2018. Osteopontin regulates dentin and alveolar bone development and mineralization. Bone 107, 196–207.

Fredman, G., Oh, S.F., Ayilavarapu, S., Hasturk, H., Serhan, C.N., Van Dyke, T.E., 2011. Impaired phagocytosis in localized aggressive periodontitis: rescue by resolvin e1. PLoS One 6 (9), e24422.

Gao, L., Faibish, D., Fredman, G., Herrera, B.S., Chiang, N., Serhan, C.N., Van Dyke, T.E., Gyurko, R., 2013. Resolvin e1 and chemokine-like receptor 1 mediate bone preservation. J. Immunol. 190 (2), 689–694.

Gay, I.C., Chen, S., MacDougall, M., 2007. Isolation and characterization of multipotent human periodontal ligament stem cells. Orthod. Craniofac. Res. 10 (3), 149–160.

Gluhak-Heinrich, J., et al., 2010. New roles and mechanism of action of Bmp4 in postnatal tooth cytodifferentiation. Bone 46, 1533–1545.

Gorr, S.U., 2012. Antimicrobial peptides in periodontal innate defense. Front. Oral Biol. 15, 84–98.

Grant, D., Bernick, S., 1972. Formation of the periodontal ligament. J. Periodontol. 43 (1), 17–25.

Graves, D.T., Fine, D., Teng, Y.T., Van Dyke, T.E., Hajishengallis, G., 2008. The use of rodent models to investigate host-bacteria interactions related to periodontal diseases. J. Clin. Periodontol. 35 (2), 89–105.

Grcevic, D., et al., 2012. In vivo Fate mapping identifies Mesenchymal progenitor cells. Stem Cell. 3 (2), 187–196.

Greer, A., Zenobia, C., Darveau, R.P., 2013. Defensins and LL-37: a review of function in the gingival epithelium. Periodontol. 2000 63, 67–79.

Guo, J., et al., 2010. Suppression of Wnt signaling by Dkk1 attenuates PTH-mediated stromal cell response and new bone formation. Cell Metabol. 11, 161–171.

Guo, Y., et al., 2018. October 17. BMP-IHH-mediated interplay between mesenchymal stem cells and osteoclasts supports calvarial bone homeostasis and repair. Bone Res 6, 30. https://doi.org/10.1038/s41413-018-0031-x.

Harmey, D., Hessle, L., Narisawa, S., Johnson, K.A., Terkeltaub, R., Millan, J.L., 2004. Concerted regulation of inorganic pyrophosphate and osteopontin by akp2, enpp1, and ank: an integrated model of the pathogenesis of mineralization disorders. Am. J. Pathol. 164 (4), 1199–1209.

Harmey, D., Johnson, K.A., Zelken, J., Camacho, N.P., Hoylaerts, M.F., Noda, M., Terkeltaub, R., Millan, J.L., 2006. Elevated skeletal osteopontin levels contribute to the hypophosphatasia phenotype in akp2(-/-) mice. J. Bone Miner. Res. 21 (9), 1377–1386.

Harris, N., Rattray, K., Tye, C., Underhill, T., Somerman, M., D'Errico, J., Chambers, A., Hunter, G., Goldberg, H., 2000. Functional analysis of bone sialoprotein: identification of the hydroxyapatite-nucleating and cell-binding domains by recombinant peptide expression and site-directed mutagenesis. Bone 27 (6), 795–802.

Hashimoto, S., Yamaura, T., Shimono, M., 1986. Morphometric analysis of the intercellular space and desmosomes of rat junctional epithelium. J. Periodontol. Res. 21, 510–520.

Hassler, N., et al., 2014 October. Sclerostin deficiency is linked to altered bone composition. J. Bone Miner. Res. 29 (10), 2144–2151. https://doi.org/10.1002/jbmr.2259.

Hasturk, H., Kantarci, A., Ohira, T., Arita, M., Ebrahimi, N., Chiang, N., Petasis, N.A., Levy, B.D., Serhan, C.N., Van Dyke, T.E., 2006. Rve1 protects from local inflammation and osteoclast- mediated bone destruction in periodontitis. FASEB J. 20 (2), 401–403.

Hasturk, H., Kantarci, A., Goguet-Surmenian, E., Blackwood, A., Andry, C., Serhan, C.N., Van Dyke, T.E., 2007. Resolvin e1 regulates inflammation at the cellular and tissue level and restores tissue homeostasis in vivo. J. Immunol. 179 (10), 7021–7029.

Herrera, B.S., Ohira, T., Gao, L., Omori, K., Yang, R., Zhu, M., Muscara, M.N., Serhan, C.N., Van Dyke, T.E., Gyurko, R., 2008. An endogenous regulator of inflammation, resolvin e1, modulates osteoclast differentiation and bone resorption. Br. J. Pharmacol. 155 (8), 1214–1223.

Hojo, H., et al., 2016 May 9. Sp7/Osterix is restricted to bone-forming vertebrates where it acts as a Dlx Co-factor in osteoblast specification, 5 Dev. Cell 37 (3), 238. https://doi.org/10.1016/j.devcel.2016.04.002. Epub 2016. Apr 28.

Hormia, M., Owaribe, K., Vitanen, I., 2001. The dento-epithelial junction: cell adhesion by type I hemidesmosomes in the absence of a true basal lamina. J. Periodontol. 72, 788–797.

Hu, J., Plaetke, R., Mornet, E., Zhang, C., Sun, X., Thomas, H., Simmer, J., 2000. Characterization of a family with dominant hypophosphatasia. Eur. J. Oral Sci. 108 (3), 189–194.

Huang, L., et al., 2016. Mechanoresponsive properties of the periodontal ligament. J. Dent. Res. 95 (4), 467–475. https://doi.org/10.1177/0022034515626102. Epub 2016 Jan 14.

Ishizuya, T., et al., 1997. Parathyroid hormone exerts disparate effects on osteoblast differentiation depending on exposure time in rat osteoblastic cells. J. Clin. Investig. 99, 2961–2970.

Ivanovski, S., et al., 2006. Stem cells in the periodontal ligament. Oral Dis. 12 (4), 358–363.

Iwasaki, K., Bajenova, E., Somogyi-Ganss, E., Miller, M., Nguyen, V., Nourkeyhani, H., Gao, Y., Wendel, M., Ganss, B., 2005. Amelotin –a novel secreted, ameloblast-specific protein. J. Dent. Res. 84, 1127–1132.

Iwasaki, K., Komaki, M., Yokoyama, N., Tanaka, Y., Taki, A., Kimura, Y., Takeda, M., Oda, S., Izumi, Y., Morita, I., 2013. Periodontal ligament stem cells possess the characteristics of pericytes. J. Periodontol. 84 (10), 1425–1433.

Jager, A., et al., 2010. Localization of SOST/Sclerostin in cementocytes in vivo and in mineralizing periodontal ligament cells in vitro. J. Periodontal. Res. 45, 246–254.

Jilka, R.L., et al., 1999. Increased bone formation by prevention of osteoblast apoptosis with parathyroid hormone. J. Clin. Investig. 104, 439–446.

Jung, H.S., et al., 2011. Directing the differentiation of human follicle cells into cementoblasts and/or osteoblasts by a combination of HERS and pulp cells. J. Mol. Histol. 42, 227–235.

Kawasaki, K., 2009. The SCPP gene repertoire in bony, vertebrates and graded differences in mineralized tissues. Dev. Gene. Evol. 219, 147–157.

Kazmers, N.H., et al., 2015 December. Hedgehog signaling mediates woven bone formation and vascularization during stress fracture healing. Bone 81, 524–532. https://doi.org/10.1016/j.bone.2015.09.002. Epub 2015 Sep. 6.

Khosla, S., Monroe, D.G., 2018 January 2. Regulation of bone metabolism by sex steroids. pii: a031211 Cold Spring Harb Perspect Med 8 (1). https://doi.org/10.1101/cshperspect.a031211. Review.

Kim, K., et al., 2010. Anatomically shaped tooth and periodontal regeneration by cell homing. J. Dent. Res. 89 (8), 842–847.

Kobayashi, K., Rose, G.G., Mahan, C.J., 1976. Ultrastructure of the dento-epithelial junction. J. Periodontal. Res. 11, 313–330.

Kobayashi, K., Rose, G.G., Mahan, C.J., 1977. Ultrastructural histochemistry of the dento-epithelial junction. J. Periodontal. Res. 12, 351–367.

Kramann, R., et al., 2015. Perivascular Gli1+ progenitors are key contributors to injury-induced organ fibrosis. Cell stem cell 16, 51–66 [PMC free article] [PubMed].

Kramer, I., et al., 2010. Parathyroid hormone (PTH)-induced bone gain is blunted in SOST overexpressing and deficient mice. J. Bone Miner. Res. 2, 178–189.

Krishnamoorthy, S., Recchiuti, A., Chiang, N., Yacoubian, S., Lee, C.H., Yang, R., Petasis, N.A., Serhan, C.N., 2010. Resolvin d1 binds human phagocytes with evidence for proresolving receptors. Proc. Natl. Acad. Sci. U. S. A. 107 (4), 1660–1665.

Kuchler, U., et al., 2014. Dental and periodontal phenotype in sclerostin knockout mice. Int. J. Oral Sci. 6, 70–76.

Kusumbe, A.P., Ramasamy, S.K., Adams, R.H., 2014. Coupling of angiogenesis and osteogenesis by a specific vessel subtype in bone. Nature 507 (7492), 323–328. https://doi.org/10.1038/nature13145.

Larjava, H., Koivisto, L., Heino, J., Hakkinen, L., 2014. Integrin in periodontal disease. Exp. Cell Res. 325, 104–110.

Lee, J.H., et al., 2015. Differentiating zones at periodontal ligament–bone and periodontal ligament–cementum entheses. J. Periodontal. Res. 50, 870–880. https://doi.org/10.1111/jre.12281 [PMC free article] [PubMed] [CrossRef].

Li, X., et al., 2005. 20. Sclerostin binds to LRP5/6 and antagonizes canonical Wnt signaling. J. Biol. Chem. 280 (20), 19883–19887. Epub 2005 Mar 18.

Li, X., et al., 2018. Sep. Icariin stimulates osteogenic differentiation and suppresses adipogenic differentiation of rBMSCs via estrogen receptor signaling. Mol. Med. Rep. 18 (3), 3483–3489. https://doi.org/10.3892/mmr.2018.9325. Epub 2018 Jul 26.

Lim, W.H., et al., 2014. Wnt signaling regulates homeostasis of the periodontal ligament. J. Periodontal. Res. 49, 751–759.

Lim, W.H., et al., 2015. Alveolar bone turnover and periodontal ligament width are controlled by Wnt. J. Periodontol. 86 (2), 319–326. https://doi.org/10.1902/jop.2014.140286. Epub 2014 Oct 27.

Lin, N.H., Menicanin, D., Mrozik, K., Gronthos, S., Bartold, P.M., 2008. Putative stem cells in regenerating human periodontium. J. Periodontal. Res. 43 (5), 514–523.

Listgarten, M.A., 1966. Electron microscopic study of the gingivodental junction of man. Am. J. Anat. 119, 147.

Liu, Y., Zheng, Y., Ding, G., Fang, D., Zhang, C., Bartold, P.M., Gronthos, S., Shi, S., Wang, S., 2008. Periodontal ligament stem cell-mediated treatment for periodontitis in miniature swine. Stem Cell. 26 (4), 1065–1073.

Liu, M., et al., 2018. Sclerostin and DKK1 inhibition preserves and augments alveolar bone volume and architecture in rats with alveolar bone loss. J. Dent. Res. 97 (9), 1031–1038. https://doi.org/10.1177/0022034518766874. Epub 2018 Apr 4.

Loe, H., Karring, T., 1969. A quantitative analysis of the epithelium –connective tissue interface in relation to assessments of the mitotic index. J. Dent. Res. 48, 634.

Luan, X., et al., 2006. Dental follicle progenitor cell heterogeneity in the developing mouse periodontium. Stem Cell. Dev. 15 (4), 595–608.

Luder, H.U., 2015. Malformations of the tooth root in humans. Front. Physiol. 6, 307.

MacNeil, R., Berry, J., D'Errico, J., Strayhorn, C., Piotrowski, B., Somerman, M., 1995a. Role of two mineral-associated adhesion molecules, osteopontin and bone sialoprotein, during cementogenesis. Connect. Tissue Res. 33 (1–3), 1–7.

MacNeil, R., Berry, J., D'Errico, J., Strayhorn, C., Somerman, M., 1995b. Localization and expression of osteopontin in mineralized and nonmineralized tissues of the periodontium. Ann. N. Y. Acad. Sci. 760, 166–176.

Matthews, B.G., et al., 2014. Analysis of αSMA-labeled progenitor cell commitment identifies notch signaling as an important pathway in fracture healing. J. Bone Miner. Res. 29 (5), 1283–1294.

McCauley, L.K., Nohutcu, R.M., 2002. Mediators of periodontal osseous destruction and remodeling: Principles and implications for diagnosis and therapy. J. Periodontol. 73 (11), 1377–1391.

McKee, M., Zalzal, S., Nanci, A., 1996. Extracellular matrix in tooth cementum and mantle dentin: localization of osteopontin and other noncollagenous proteins, plasma proteins, and glycoconjugates by electron microscopy. Anat. Rec. 245 (2), 293–312.

McKenzie, J.A., et al., 2018 April 16. Activation of hedgehog signaling by systemic agonist improves fracture healing in aged mice. J. Orthop. Res. https://doi.org/10.1002/jor.24017 [Epub ahead of print].

Meyer, M.B., et al., 2014 June 6. The RUNX2 cistrome in osteoblasts: characterization, down-regulation following differentiation, and relationship to gene expression. J. Biol. Chem. 289 (23), 16016–16031. https://doi.org/10.1074/jbc.M114.552216. Epub 2014 Apr 24.

Miletich, I., Sharpe, P.T., 2004. Neural crest contribution to mammalian tooth formation. Birth Defects Res C Embryo Today 72 (2), 200–212.

Millan, J.L., Whyte, M.P., 2016. Alkaline phosphatase and hypophosphatasia. Calcif. Tissue Int. 98 (4), 398–416.

Miyasaki, K.T., Bodeau, A.L., Ganz, T., Selsted, M.E., Lehrer, R.I., 1990. In vitro sensitivity of oral, gram-negative, facultative bacteria to the bactericidal activity of human neutrophil defensin. Infect. Immun. 58, 3934–3940.

Mizoguchi, T., et al., 2014. Osterix marks distinct waves of primitive and definitive stromal progenitors during bone marrow development. Dev. Cell 29, 340–349.

Moffatt, P., Smith, C.E., St Arnaud, R., Nanci, A., 2008. Characterization of Apin, a secreted protein highly expressed in tooth-associated epithelia. J. Cell. Biochem. 103, 941–956.

Moffatt, P., Wazen, R.M., Dos Santos Neves, J., Nanci, A., 2014. Characterisation of secretory calcium-binding phosphoprotein-proline-glutamine-rich 1: a novel basal lamina component expressed at cell-tooth interfaces. Cell Tissue Res. 358, 843–855.

Morse, A., et al., 2018 March. Sclerostin antibody augments the anabolic bone formation response in a mouse model of mechanical tibial loading. J. Bone Miner. Res. 33 (3), 486–498. https://doi.org/10.1002/jbmr.3330. Epub 2017 Nov 29.

Mundy, G., et al., 1999 December 3. Stimulation of bone formation in vitro and in rodents by statins. Science 286 (5446), 1946–1949.

Nagatomo, K., Komaki, M., Sekiya, I., Sakaguchi, Y., Noguchi, K., Oda, S., Muneta, T., Ishikawa, I., 2006. Stem cell properties of human periodontal ligament cells. J. Periodontal. Res. 41 (4), 303–310.

Nakayama, Y., Holcroft, J., Ganss, B., 2015. Enamel hypomineralization and structural defects in amelotin deficient mice. J. Dent. Res. 94, 697−705.
Neer, R.M., et al., 2001. Effect of parathyroid hormone (1-34) on fractures and bone mineral density in postmenopausal women with osteoporosis. N. Engl. J. Med. 344, 1434−1441.
Ono, W., et al., 2016 April 12. Parathyroid hormone receptor signalling in osterix-expressing mesenchymal progenitors is essential for tooth root formation. Nat. Commun. 7, 11277. https://doi.org/10.1038/ncomms11277.
Otto, M., 2009. Bacterial sensing of antimicrobial peptides. Contrib. Microbiol. 16, 136−149.
Pang, X.G., et al., 2018 March 15. Quercetin stimulates bone marrow mesenchymal stem cell differentiation through an estrogen receptor-mediated pathway. BioMed Res. Int. 2018, 4178021. https://doi.org/10.1155/2018/4178021. eCollection 2018.
Papapoulos, S.E., 2015. Anabolic bone therapies in 2014: new boneforming treatments for osteoporosis. Nat. Rev. Endocrinol. 11, 69−70.
Papathanasiou, E., Kantarci, A., Konstantinidis, A., Gao, H., Van Dyke, T.E., 2016. Socs-3 regulates alveolar bone loss in experimental periodontitis. J. Dent. Res. 95 (9), 1018−1025.
Poole, K.E., Reeve, J., 2005. Parathyroid hormone - a bone anabolic and catabolic agent. Curr. Opin. Pharmacol. 5, 612−617.
Powell Jr., W.F., et al., 2011. Targeted ablation of the PTH/PTHrP receptor in osteocytes impairs bone structure and homeostatic calcemic responses. J. Endocrinol. 209, 21−32.
Prideaux, M., et al., 2015. Parathyroid hormone induces bone cell motility and loss of mature osteocyte phenotype through L-calcium channel dependent and independent mechanisms. PLoS One 10, e0125731.
Puklo, M., Guentsch, A., Hiemstra, P.S., Eick, S., Potempa, J., 2008. Analysis of neutrophil-derived antimicrobial peptides in gingival crevicular fluid suggests importance of cathelicidin LL-37 in the innate immune response against periodontopathogenic bacteria. Oral Microbiol. Immunol. 23, 328−335.
Rakian, A., Yang, W.C., Gluhak-Heinrich, J., Cui, Y., Harris, M.A., Villarreal, D., Feng, J.Q., Macdougall, M., Harris, S.E., 2013. Role and mechanism of Bmp2 gene in tooth root formation and supporting periodontium. Int. J. oral Sci. 5, 75−84 (Cover Article).
Rakian A., et al., Bone Morphogenetic Protein2 Gene is essential for formation and lineage commitment of periodontal stem cells to alveolar bone, periodontal ligament, and both cellular and acellular cementum, manuscript in preparation. 2019.
Reibel, A., Maniere, M.C., Clauss, F., Droz, D., Alembik, Y., Mornet, E., Bloch-Zupan, A., 2009. Orodental phenotype and genotype findings in all subtypes of hypophosphatasia. Orphanet J. Rare Dis. 4, 6.
Ren, Y., Han, X., Ho, S.P., Harris, S.E., Cao, Z., Economides, A.N., Qin, C., Ke, H., Liu, M., Feng, J.Q., 2015. Removal of the Sost or blocking its product sclerostin rescues the defects in the periodontitis mous model. FASEB J. 29 (7), 2702−2711.
Rios, H.F., et al., 2015. Emerging regenerative approaches for periodontal reconstruction: practical applications from the AAP regeneration workshop. Clin Adv Periodontics 5 (1), 40−46.
Robling, A.G., et al., 2008. Mechanical stimulation of bone in vivo reduces osteocyte expression of sost/sclerostin. J. Biol. Chem. 283, 5866−5875.
Roguljic, H., et al., 2013. In vivo identification of periodontal progenitor cells. J. Dent. Res. 92, 709−715.
Salazar, V.S., et al., 2016. Specification of osteoblast cell fate by canonical Wnt signaling requires Bmp2. Development 143 (23), 4352−4367.
San Miguel, S.M., et al., 2010. Defining a visual marker of osteoprogenitor cells within the periodontium. J. Periodontal. Res. 45 (1), 60−70.
Sawada, T., Yamamoto, T., Yanagisawa, T., Takuma, S., Hasegawa, H., Watanabe, K., 1990. Electron-immunocytochemistry of laminin and type-IV collagen in the junctional epithelium of rat molar gingiva. J. Periodontal. Res. 25, 372−376.
Seo, B.-M., Miura, M., Gronthos, S., Mark Bartold, P., Batouli, S., Brahim, J., Young, M., Gehron Robey, P., Wang, C.Y., Shi, S., 2004. Investigation of multipotent postnatal stem cells from human periodontal ligament. Lancet 364 (9429), 149−155.
Serhan, C.N., 2017. Treating inflammation and infection in the 21st century: new hints from decoding resolution mediators and mechanisms. FASEB J. 31 (4), 1273−1288.
Serhan, C.N., Brain, S.D., Buckley, C.D., Gilroy, D.W., Haslett, C., O'Neill, L.A., Perretti, M., Rossi, A.G., Wallace, J.L., 2007. Resolution of inflammation: state of the art, definitions and terms. FASEB J. 21 (2), 325−332.
Shu, B., et al., 2011 October 15. BMP2, but not BMP4, is crucial for chondrocyte proliferation and maturation during endochondral bone development. J. Cell Sci. 124 (Pt 20), 3428−3440. https://doi.org/10.1242/jcs.083659. Epub 2011 Oct 7.
Soenjaya, Y., Foster, B.L., Nociti Jr., F.H., Ao, M., Holdsworth, D.W., Hunter, G.K., Somerman, M.J., Goldberg, H.A., 2015. Mechanical forces exacerbate periodontal defects in bsp-null mice. J. Dent. Res. 94 (9), 1276−1285.
Spatz, J.M., et al., 2015. The Wnt inhibitor sclerostin is up-regulated by mechanical unloading in osteocytes in vitro. J. Biol. Chem. 290 (27), 16744−16758. https://doi.org/10.1074/jbc.M114.628313. Epub 2015 May 7.
Sun, J., et al., 2017 July 12. Osthole improves function of periodontitis periodontal ligament stem cells via epigenetic modification in cell sheets engineering. Sci. Rep. 7 (1), 5254. https://doi.org/10.1038/s41598-017-05762-7.
Tai, P.W.L., et al., 2017 November 27. Genome-wide DNase hypersensitivity, and occupancy of RUNX2 and CTCF reveal a highly dynamic gene regulome during MC3T3 pre-osteoblast differentiation. PLoS One 12 (11), e0188056. https://doi.org/10.1371/journal.pone.0188056. eCollection.
Takahashi, A., et al., 2018. 8. Autocrine regulation of mesenchymal stem progenitor cell fate during tooth eruption. Proc. Natl. Acad. Sci. U. S. A. 116 (2), 575−580. https://doi.org/10.1073/pnas.1810200115. Epub.
Tang, D.Z., et al., 2010. June. Osthole stimulates osteoblast differentiation and bone formation by activation of beta-catenin-BMP signaling. J. Bone Miner. Res. 25 (6), 1234−1245. https://doi.org/10.1002/jbmr.21.
Tang, W., et al., 2012. Transcriptional regulation of vascular endothelial growth factor (VEGF) by osteoblast-specific transcription factor osterix (Osx) in osteoblasts. J. Biol. Chem. 287, 1671−1678 [PMC free article] [PubMed].
Tanner, A.C., Haffer, C., Bratthall, G.T., Visconti, R.A., Socransky, S.S., 1979. A study of the bacteria associated with advancing periodontitis in man. J. Clin. Periodontol. 6, 278−307.

Taubman, M.A., Kawai, T., Han, X., 2007. The new concept of periodontal disease pathogenesis requires new and novel therapeutic strategies. J. Clin. Periodontol. 34 (5), 367–369.

Taut, A.D., et al., 2013. Sclerostin antibody stimulates bone regeneration after experimental periodontitis. J. Bone Miner. Res. 28, 2347–2356.

Thumbigere-Math, V., Alqadi, A., Chalmers, N.I., Chavez, M.B., Chu, E.Y., Collins, M.T., Ferreira, C.R., FitzGerald, K., Gafni, R.I., Gahl, W.A., et al., 2018. Hypercementosis associated with enpp1 mutations and gaci. J. Dent. Res. 97 (4), 432–441.

Trubiani, O., Orsini, G., Zini, N., Di Iorio, D., Piccirilli, M., Piattelli, A., Caputi, S., 2008. Regenerative potential of human periodontal ligament derived stem cells on three-dimensional biomaterials: a morphological report. J. Biomed. Mater. Res. A 87 (4), 986–993.

Tsuji, K., et al., 2006. BMP2 activity, although dispensable for bone formation, is required for the initiation of fracture healing. Nat. Genet. 38 (12), 1424–1429. Epub 2006 Nov 12.

Vahidnezhad, H., Youssefian, L., Saedian, A.H., Mahmoudi, H., Touati, A., Abiri, M., Kajbafzadeh, A.M., Aristodemou, S., Liu, L., McGrath, J.A., Ertel, A., Londin, E., Kariminejad, A., Zeinali, S., Fortina, P., Uitto, J., 2018. Recessive mutation in tetraspanin CD151 causes Kindler syndrome-like epidermolysis bullosa with multi-systemic manifestations including nephropathy. Matrix Biol. 66, 22–33.

Valderrama, P., et al., 2010. Evaluation of parathyroid hormone bound to a synthetic matrix for guided bone regeneration around dental implants: a histomorphometric study in dogs. J. Periodontol. 81, 737–747.

van den Bos, T., Handoko, G., Niehof, A., Ryan, L.M., Coburn, S.P., Whyte, M.P., Beertsen, W., 2005. Cementum and dentin in hypophosphatasia. J. Dent. Res. 84 (11), 1021–1025.

Van Dyke, T.E., 2011. Proresolving lipid mediators: potential for prevention and treatment of periodontitis. J. Clin. Periodontol. 38 (Suppl. 11), 119–125.

Van Dyke, T.E., Hasturk, H., Kantarci, A., Freire, M.O., Nguyen, D., Dalli, J., Serhan, C.N., 2015. Proresolving nanomedicines activate bone regeneration in periodontitis. J. Dent. Res. 94 (1), 148–156, 4270812.

Vardar-Sengul, S., Demirci, T., Sen, B.H., Erkizan, V., Kurulgan, E., Baylas, H., 2007. Human β-defensin-1 and -2 expression in the gingiva of patients with specific periodontal diseases. J Periodontol Res 42, 429–437.

Vasconcelos, D.F., et al., 2014. Intermittent parathyroid hormone administration improves periodontal healing in rats. J. Periodontol. 85, 721–728.

Vidovic, I., et al., 2017. αSMA-expressing perivascular cells represent dental pulp progenitors in vivo. J. Dent. Res. 96 (3), 323–330.

Walko, G., Castanon, M.J., Wiche, G., 2015. Molecular architecture and function of the hemidesmosome. Cell Tissue Res. 360, 529–544.

Wan, M., et al., 2008. Parathyroid hormone signaling through low-density lipoprotein related protein 6. Genes Dev. 22, 2968–2979.

Wazen, R.M., Moffat, P., Ponce, K.J., Kuroda, S., Nishio, C., Nanci, A., 2015. Eur. Cells Mater. 30, 187–199.

Wiebe, C.B., Silver, J.G., Larjava, H.S., 1996. Early-onset periodontitis associated with Weary-Kindler syndrome: a case report. J. Periodontal. 67, 1004–1010.

Woodfin, A., Voisin, M.B., Beyrau, M., Colom, B., Caille, D., Diapouli, F.M., Nash, G.B., Chavakis, T., Albelda, S.M., Rainger, G.E., et al., 2011. The junctional adhesion molecule jam-c regulates polarized transendothelial migration of neutrophils in vivo. Nat. Immunol. 12 (8), 761–769.

Wright, J.T., 2010. Oral manifestations in the epidermolysis bullosa spectrum. Dermatol. Clin. 28, 159–164.

Wu, H., et al., 2017 April. Chromatin dynamics regulate mesenchymal stem cell lineage specification and differentiation to osteogenesis. Biochim Biophys Acta Gene Regul Mech 1860 (4), 438–449. https://doi.org/10.1016/j.bbagrm.2017.01.003.

Wu, Y., Yuan, X., Perez, K.C., Hyman, S., Wang, L., Pellegrini, G., Salmon, B., Bellido, T., Helms, J.A., October 25, 2018. Aberrantly elevated Wnt signaling is responsible for cementum overgrowth and dental ankylosis. pii: S8756-3282 Bone (18), 30403–30404. https://doi.org/10.1016/j.bone.2018.10.023 [Epub ahead of print].

Xu, J., et al., 2009. Multiple differentiation capacity of STRO-1+/CD146+ PDL mesenchymal progenitor cells. Stem Cell. Dev. 18 (3), 487–496.

Yadav, M.C., de Oliveira, R.C., Foster, B.L., Fong, H., Cory, E., Narisawa, S., Sah, R.L., Somerman, M., Whyte, M.P., Millan, J.L., 2012. Enzyme replacement prevents enamel defects in hypophosphatasia mice. J. Bone Miner. Res. 27 (8), 1722–1734.

Yan, Y., et al., 2009. Axin2 controls bone remodeling through the beta-catenin-BMP signaling pathway in adult mice. J. Cell Sci. 122 (Pt 19), 3566–3578. https://doi.org/10.1242/jcs.051904. Epub 2009 Sep. 8.

Yang, W., et al., 2012. Bmp2 is required for odontoblast differentiation and pulp vasculogenesis. J. Dent. Res. 91, 58–64.

Yang, W., et al., 2013. Bmp2 gene controls bone quantity and quality through regulating osteoblast development and vascular-skeletal stem cell niche. J. Cell Sci. 126, 4085–4098 and Supplementary Data.

Ye, L., Zhang, S., Ke, H., Bonewald, L.F., Feng, J.Q., 2008. Periodontal breakdown in the dmp1 null mouse model of hypophosphatemic rickets. J. Dent. Res. 87 (7), 624–629.

Yin, X., et al., 2015. Wnt signaling and its contribution to craniofacial tissue homeostasis. J. Dent. Res. 94 (11), 1487–1494. https://doi.org/10.1177/0022034515599772. Epub 2015 Aug 18. Review.

Yu, J., et al., 2009. Multiple differentiation capacity of stro-1+/cd146+ pdl mesenchymal progenitor cells. Stem Cells Dev. 18, 487–496.

Yuan, X., et al., 2018. Biomechanics of immediate postextraction implant osseointegration. J. Dent. Res. 97 (9), 987–994. https://doi.org/10.1177/0022034518765757. Epub 2018 Apr 2.

Zhang, K., et al., 2006 June. E11/gp38 selective expression in osteocytes: regulation by mechanical strain and role in dendrite elongation. Mol. Cell Biol. 26 (12), 4539–4552.

Zhang, R., et al., 2013 January. Wnt/β-catenin signaling activates bone morphogenetic protein 2 expression in osteoblasts. Bone 52 (1), 145–156. https://doi.org/10.1016/j.bone.2012.09.029. Epub 2012 Sep. 29.

Zhang, X., et al., 2019. Molecular basis for periodontal ligament adaptation to in vivo loading, 22034518817305 J. Dent. Res. 5. https://doi.org/10.1177/0022034518817305 [Epub ahead of print].

Zhao, M., et al., August 2006. The zinc finger transcription factor Gli2 mediates bone morphogenetic protein 2 expression in osteoblasts in response to hedgehog signaling. Mol. Cell Biol. 26 (16), 6197–6208.

Zhao, H., et al., 2014. Secretion of Shh by a neurovascular bundle niche supports mesenchymal stem cell homeostasis in the adult mouse incisor. Cell Stem Cell 14 (2), 160–173.

Zhou, S., et al., 2003 January. Estrogens activate bone morphogenetic protein-2 gene transcription in mouse mesenchymal stem cells. Mol. Endocrinol. 17 (1), 56–66.

Zhou, B.O., et al., 2014. Leptin-receptor-expressing mesenchymal stromal cells represent the main source of bone formed by adult bone marrow. Cell stem cell 15, 154–168 [PMC free article] [PubMed].

Zhu, M., Van Dyke, T.E., Gyurko, R., 2013. Resolvin e1 regulates osteoclast fusion via dc-stamp and nfatc1. FASEB J. 27 (8), 3344–3353.

Chapter 44

Notch and its ligands

Stefano Zanotti and Ernesto Canalis

Departments of Orthopaedic Surgery and Medicine, and the UConn Musculoskeletal Institute, UConn Health, Farmington, CT, United States

Chapter outline

Introduction

The Notch signaling pathway is a mechanism of communication between neighboring cells that has important functions in the development of metazoans, and was first identified by genetic analysis in *Drosophila melanogaster* (Morgan and Bridges, 1916). Whereas *Drosophila* expresses one Notch receptor and two ligands, termed Serrate and Delta, mice and humans express four Notch receptors, two Serrate homologues termed Jagged (JAG) 1 and 2, and three Delta homologues named Delta-like (DLL) 1, 3, and 4 (Lindsell et al., 1996). Interactions of receptors expressed by a signal-receiving cell with ligands from adjacent cells lead to a series of proteolytic cleavages that result in the release of the Notch intracellular domain (NICD) from the cellular membrane (Schroeter et al., 1998). The NICD translocates to the nucleus, where it forms an active transcriptional complex with the DNA-associated protein recombination signal-binding protein for immunoglobulin of kappa J region (RBPJ) to regulate the transcription of target genes (Kovall, 2008). The NICD does not bind to DNA directly but interacts with various nuclear proteins to form a transcriptional complex that is essential for cellular response to the activation of Notch receptors. Although these signal transduction events are shared by the four receptors, each paralog has distinct functions (Groot et al., 2014).

Principles of Bone Biology. https://doi.org/10.1016/B978-0-12-814841-9.00044-0

Notch signaling from all receptors is governed by multiple mechanisms, such as posttranslational modifications and endocytosis, that determine the function of the receptor, ligands, and the several nuclear proteins that mediate the transcriptional effects of Notch (Kovall et al., 2017; Kopan and Ilagan, 2009). The importance of these regulatory mechanisms is attested by the remarkable number of diseases associated with genetic defects that cause gain- or loss-of-function of the core and ancillary components of the Notch signaling pathway (Zanotti and Canalis, 2016). The role played by Notch receptors and cognate ligands in the skeleton was established by work in genetically engineered mice and by the characterization of congenital human diseases. These studies revealed that Notch signaling regulates chondrocytic, osteoblastic, and osteoclastic differentiation and function, demonstrating that Notch receptors and ligands are critical for skeletal development, bone remodeling, and fracture healing. Efforts to reproduce disease-associated Notch mutations in mice have provided new insight into the pathogenesis of rare diseases affecting the skeleton and reaffirmed the importance of Notch receptors in skeletal biology.

Notch receptors

Structure

Notch are four single-pass transmembrane receptors characterized by a variable number of extracellular epidermal growth factor (EGF)-like tandem repeats: 36 in NOTCH1 and NOTCH2, 34 in NOTCH3, and 29 in NOTCH4 (Kovall et al., 2017; Kopan and Ilagan, 2009). Binding of calcium ions to selected EGF-like repeats determines the structure of the extracellular region and affinity of receptors for individual ligands (Weisshuhn et al., 2015a, 2015b, 2016). The EGF-like repeats forming the interface between NOTCH1 and JAG1 are distinct from those responsible for binding to DLL4. In addition, the contact area between NOTCH1 and JAG1 is larger than that between NOTCH1 and DLL4, possibly explaining the higher affinity of NOTCH1 for JAG1 than for DLL4 (Luca et al., 2015, 2017).

Notch receptors are translated as monomeric precursors that are cleaved by furin-like proprotein convertases in the Golgi compartment, and this process results in the creation of extracellular and transmembrane monomers that form a heterodimeric receptor. The C-terminus of the extracellular peptide interacts with the N-terminus of the transmembrane peptide via noncovalent bonds that occur within the heterodimerization domain (HD). The C-terminus of the extracellular monomer contains three Lin12/Notch repeats that together with the HD form the negative regulatory region (NRR), which prevents Notch activation in the absence of ligands (Sanchez-Irizarry et al., 2004; Gordon et al., 2007). The importance of the NRR is exemplified by the fact that point mutations in the HD of *NOTCH1* activate the receptor in the absence of ligands and lead to NOTCH1 gain-of-function, which is associated with over 50% of cases of T-cell acute lymphoblastic leukemias (Malecki et al., 2006). Analogous mutations in *NOTCH2* are not as common and are found in a small percentage of marginal zone B-cell lymphomas (Kiel et al., 2012). The NRR of NOTCH3 may be a less effective inhibitor of ligand-independent activation than the NRR of NOTCH1 and NOTCH2, since NOTCH3 exhibits a higher degree of basal activation than NOTCH1 and NOTCH2 (Xu et al., 2015). Limited information is available about the NRR of NOTCH4, and its three-dimensional structure has not been described. The transmembrane domain is located immediately downstream of the HD and contains three cleavage sites recognized by disintegrin and metalloprotease domain (ADAM) proteases as well as the γ-secretase complex. These sites are critical for signal activation and are not accessible to proteases in the absence of ligands because of the structural conformation of the NRR in the unbound receptors (Gordon et al., 2007).

The intracellular domain of NOTCH1, NOTCH2, and NOTCH3 consists of an RBPJ-association module (RAM) domain, a nuclear localization sequence (NLS), seven ankyrin repeats, and two additional NLS in close association. The NICD of NOTCH4 has a distinct organization and lacks the tandem NLS. A transactivation domain located downstream of this region is the most variable among the four Notch paralogs; it displays a defined spatial organization in NOTCH1 and NOTCH2 but does not appear to form an organized structure in NOTCH3 and NOTCH4. A proline (P)-, glutamic acid (E)-, serine (S)-, threonine (T)-rich motif (PEST) domain is present at the C-terminus of all Notch receptors and is recognized by ubiquitin ligases that target Notch for proteasomal degradation (Fig. 44.1A) (Kovall et al., 2017; Kopan and Ilagan, 2009).

Function

Despite their structural similarities, the functions of NOTCH1 and NOTCH2 are not redundant; the deletion of *Notch1* is developmentally lethal due to vascular malformations, whereas mice harboring a hypomorphic *Notch2* allele die perinatally because of renal and vascular defects (Swiatek et al., 1994; McCright et al., 2001). These differences may be related to the specific temporal and cellular expression patterns of the individual receptors and to variations in NOTCH1 and NOTCH2

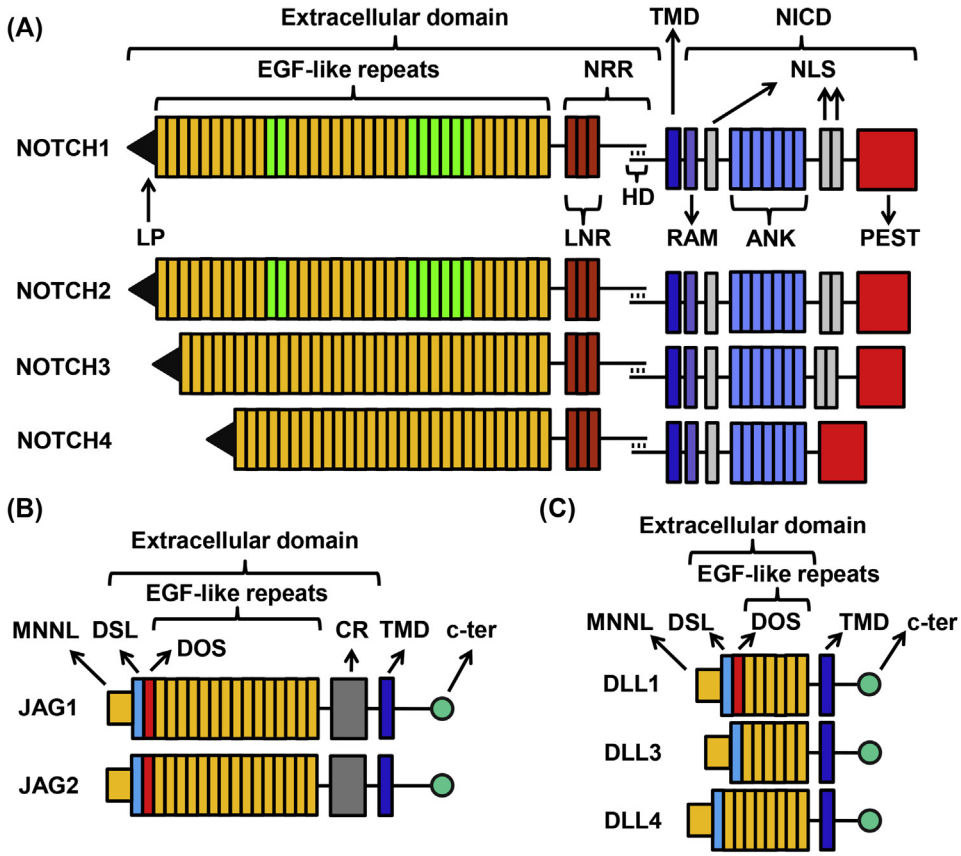

FIGURE 44.1 Domains of Notch receptors and cognate ligands. (A) Notch receptors. Extracellular domain containing a leader peptide, multiple epidermal growth factor (EGF)-like tandem repeats (36 in NOTCH1 and NOTCH2; 34 in NOTCH3 and 29 in NOTCH4), Lin12-Notch repeats (LNR) and the heterodimerization domain (HD). Negative regulatory region (NRR) formed by the LNR and HD, followed by a transmembrane domain (TMD). Intracellular domain (NICD) containing an RBPJ-association module (RAM), nuclear localization sequences (NLS; three in NOTCH1, NOTCH2, and NOTCH3, one in NOTCH4), ankyrin repeats and a proline (P)-, glutamic acid (E)-, serine (S)-, threonine (T)-rich (PEST) domain. EGF-like repeats in green are required for binding of NOTCH1 and NOTCH2 to cognate Jagged and Delta ligands. (B) Jagged ligands. Extracellular domain containing the modulus at the N-terminus of Notch ligands (MNNL), Delta/Serrate/Lag2 (DSL) and Delta and OSM11-like (DOS) domains, 15 EGF-like tandem repeats and a cysteine-rich domain, followed by the TMD and intracellular conserved c-terminus (c-ter). (C) Delta ligands. Extracellular domain containing the MNNL, DSL, DOS (only in DLL1), and EGF-like tandem repeats (six in DLL1 and DLL3, eight in DLL4), followed by a TMD and intracellular conserved c-ter. *Adapted from Zanotti, S., Canalis, E., 2016. Notch signaling and the skeleton. Endocr. Rev. 37 (3), 223–253, with permission.*

affinity for their cognate ligands. Paralog-specific functions of the NICDs may also contribute to the distinct phenotypes of *Notch1* and *Notch2*-null mice, even though their NICDs appear to have equivalent functions in various cellular contexts (Liu et al., 2013, 2015a; Yuan et al., 2012). The structure and activation mechanics of NOTCH3 diverge from those of NOTCH1 and NOTCH2, as NOTCH3 possesses fewer EGF-like repeats, displays a higher level of basal activity in the absence of ligands, and has a shorter intracellular domain (Kovall et al., 2017; Kopan and Ilagan, 2009; Xu et al., 2015). The deletion of *Notch3* causes vascular abnormalities, and *NOTCH3* mutations are found in individuals afflicted by cerebral autosomal-dominant arteriopathy with subcortical infarcts and leukoencephalopathy syndrome (Domenga et al., 2004; Joutel, 2011; Krebs et al., 2003). NOTCH4, like NOTCH3, is dispensable for embryonic development, although some of its functions overlap with those of NOTCH1 (Krebs et al., 2000). Mice that overexpress the NOTCH4 NICD in endothelial cells display brain arteriovenous malformations, attesting to the importance of signaling from all Notch receptors for the development of the vascular system (Murphy et al., 2008, 2014).

Regulatory mechanisms

The expression of individual Notch receptors is cell-specific, restricting receptor activation to selected cell types and providing initial levels of signal regulation (Wu and Bresnick, 2007). More complex regulatory mechanisms are mediated by posttranslational modifications of the extracellular and intracellular regions of Notch. The EGF-like repeats are

subjected to fucosylation and glycosylation events that regulate the specificity and binding affinity for cognate ligands. The *O*-fucosyltransferase POFUT1 is responsible for the addition of the fucosyl residues that are the site of initiation of glycosaminoglycan chains (Rampal et al., 2005). Fucosylation also facilitates folding of the nascent Notch receptors and is required for their trafficking to the cellular membrane (Stahl et al., 2008). The importance of this posttranslational modification is demonstrated by the observation that *Pofut1*-null mice die in utero and phenocopy the individual deletion of *Notch1* and *Notch2* (Shi and Stanley, 2003; Schuster-Gossler et al., 2009). In mice and humans, the *O*-fucose residues in the Notch EGF-like repeats provide the substrate for the β-1,3-*N*-acetylglucosaminyltransferases lunatic fringe (LFNG), manic fringe (MFNG), and radical fringe (RFNG). These enzymes elongate glycosaminoglycan chains of selected EGF-like repeats, promoting interaction of Notch receptors with DLL1 while hindering interactions with JAG1 (Visan et al., 2006; Stanley, 2007). The functions of the three fringe enzymes are not redundant, and the EGF-like repeats targeted by MFNG and LFNG are different from those recognized by RFNG (Kakuda and Haltiwanger, 2017).

Glycosylation of Notch receptors is carried out by protein *O*-glucosyltransferase (POGLUT)1 and is necessary for the activation of NOTCH1 and NOTCH2, since *Poglut1*-null mice die during embryonic development with a phenotype that overlaps with that of the individual deletions of *Notch1* or *Notch2* (Fernandez-Valdivia et al., 2011). A hypomorphic *POGLUT1* mutation that attenuates Notch signaling was identified in a family afflicted by muscular dystrophy, attesting to the importance of the posttranslational regulation of Notch receptor activity (Servian-Morilla et al., 2016). Selected *O*-glucose residues may be extended by GXYLT1/2 and XXYLT1, which are type II-membrane proteins with xylosyltransferase activity (Sethi et al., 2010a). In contrast to the general effects of acetylglucosamine modification, studies in *Drosophila* indicate that the addition of the xylose residues may inhibit Notch-ligand interactions, but the function of xylosylation remains to be determined (Lee et al., 2017).

The levels of Notch receptors at the cell surface are tightly regulated by posttranslational mechanisms such as endocytosis and lysosomal degradation (Nichols et al., 2007; Le et al., 2005). NOTCH1, in its unbound state, is ubiquitinated and targeted for lysosomal degradation by the sequential activities of the really interesting new gene (Ring)-finger E3 ubiquitin ligase CBL and of the itchy E3 ubiquitin protein ligase (ITCH) (Jehn et al., 2002; Chastagner et al., 2008). *Itch*-null mice exhibit enhanced NOTCH1 activity and proliferation of hematopoietic stem cells (Rathinam et al., 2011). The activity of another ring-finger protein termed deltex E3 ubiquitin ligase (DTX)1, which in itself is encoded by a Notch target gene, may direct the receptors to the recycling endosome and allow their reexposure at the cell surface (Mukherjee et al., 2005). However, the mechanisms that determine the fate of ubiquitinated Notch receptors are poorly defined (Fig. 44.2).

Notch cognate ligands

Structure and function

Notch are four single-pass transmembrane proteins that interact with Notch receptors. The interaction occurs at a conserved extracellular region containing the modulus at the N-terminus of Notch ligands domain and a Delta/Serrate/Lag2 (DSL) motif as well as the DLL and OSM11-like protein domains, which are two specialized tandem EGF-like repeats (D'Souza et al., 2010). The C-terminal domain of each ligand consistently mediates interactions with the cytoskeleton (Fig. 44.1B and C) (Pintar et al., 2007). Mice null for *Jag1, Jag2, Dll1,* or *Dll4* exhibit developmental defects and die in utero (Jiang et al., 1998; Xue et al., 1999; Hrabe de et al., 1997; Gale et al., 2004). Global *Jag1, Jag2, Dll1*-null mutants display a less severe phenotype that may be explained by the potential role of DLL3 as a mild inhibitor of Notch receptors (Kusumi et al., 1998; Ladi et al., 2005). Additional mechanisms that do not require Notch−ligand interactions, such as shear stress generated by blood flow at the surface of endothelial cells, may be capable of activating the receptors in the absence of protein ligands (Theodoris et al., 2015).

Other proteins are known to act as ligands of Notch receptors and to modulate signaling, although the nature of these interactions is not clearly defined. Delta/Notch-like EGF-related receptor (DNER) and Delta-like homolog (DLK)1, also termed PREF1, are related to Dll ligands although they lack a DSL domain. DNER induces DTX1 in the developing nervous system and mirrors Dll/Notch interactions, whereas DLK1 inhibits Notch signaling (Baladron et al., 2005; Eiraku et al., 2005). F3 and NB3 are glycosyl phosphatidylinositol-tethered proteins capable of inducing Notch signaling through DTX1-dependent mechanisms that are similar to those utilized by DNER (Hu et al., 2003; Cui et al., 2004). At least three soluble proteins have been reported as potential Notch ligands, namely microfibril-associated glycoproteins (MAGP) 1 and 2 and nephroblastoma overexpressed (NOV). The cellular context determines the effects of these ligands on Notch signaling, and both stimulatory and inhibitory effects of Notch activation have been reported for MAGP1, MAGP2, and NOV (Miyamoto et al., 2006; Albig et al., 2008; Sakamoto et al., 2002; Rydziel et al., 2007; Minamizato et al., 2007).

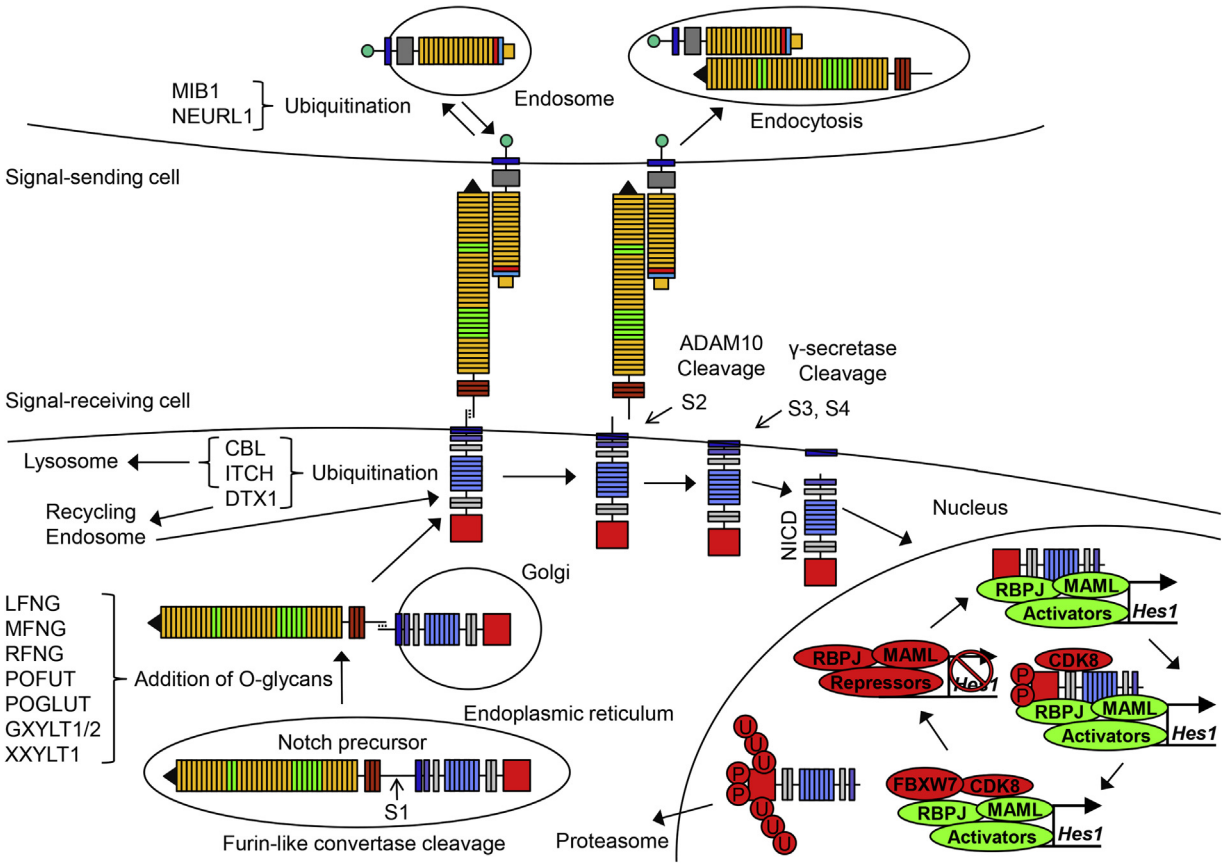

FIGURE 44.2 Regulation of Notch signaling. From the lower left corner, clockwise. The Notch precursor synthesized by the signal receiving cell is cleaved at the S1 site by a furin-like convertase in the endoplasmic reticulum, generating a mature heterodimeric receptor. O-Glycans are added by the actions of selected glycosyl-, fucosyl- and xylosyl-transferases as Notch transits through the Golgi. The receptor in its unbound state may be ubiquitinated by CBL, ITCH, and DTX1 and either directed to the lysosome for degradation or to the recycling endosome for reexpression at the cell membrane. A cognate ligand (Jag protein in diagram) expressed by a signal-sending cell must be ubiquitinated by MIB1 or NEURL1 and processed into the endosome prior to engaging a Notch receptor at the surface of the signal-receiving cell. The ligand bound to the extracellular domain of Notch is internalized by the signal-sending cell, allowing cleavage of the S2 site by ADAM10 and of the intramembranous S3 and S4 sites by the γ-secretase complex. The Notch intracellular domain (NICD) is released into the cytoplasm and translocates into the nucleus where it forms a ternary complex with RBPJ and MAML proteins. Transcriptional repressors associated with RBPJ in the absence of NICD are displaced by transcriptional activators that induce the expression of Notch target genes, such as *Hes1*. CDK8 associates with MAML and phosphorylates the PEST domain of the NICD, leading to ubiquitination by FBXW7 and targeting of the NICD for proteasomal degradation. The ternary complex is disassembled and transcriptional repression of Notch target genes is reinstituted.

Regulatory mechanisms of notch ligands

Cellular trafficking regulates the function of Notch receptors and the ability of ligand proteins to induce signaling. Ubiquitination of the intracellular portion of ligand proteins leads to endocytosis and recycling to the cellular membrane, and these processes are required for the ligands to develop sufficient affinity for Notch receptors (D'Souza et al., 2008; Heuss et al., 2008). In mammals, JAG1 and DLL1 are substrates of the ring family E3 ubiquitin ligases mind bomb (MIB)1 and neuralized E3 ubiquitin protein ligase (NEURL)1, whereas the ubiquitin ligases that act on the remaining ligand paralogs have not been identified (Fig. 44.2) (Koo et al., 2005; Koutelou et al., 2008). The deletion of *Mib1* leads to developmental defects similar to those observed in *Notch1* and *Notch2*-null mutants, whereas the deletion of *Neurl1* is compatible with life, indicating that MIB1 is necessary for signaling from NOTCH1 and NOTCH2 and might compensate for the loss of NEURL1 (Koo et al., 2005; Ruan et al., 2001). Hypomorphic *MIB1* mutations in humans are associated with suppressed Notch signaling and cardiomyopathy, documenting the importance of posttranslational modifications of Notch ligands (Luxan et al., 2013).

Mechanisms of Notch activation

Generation of the Notch intracellular domain

Proteolysis is a critical mechanism of Notch maturation and activation. Notch receptors are subjected to four cleavage events occurring at specific sites within the HD and transmembrane domains; these are sequentially termed S1 to S4 (Kovall et al., 2017; Kopan and Ilagan, 2009). Initially, the monomeric Notch precursor is cleaved in the Golgi compartment by furin-like proprotein convertases that act on the S1 site, leading to the formation of a heterodimeric receptor (Blaumueller et al., 1997). Interactions of mature receptors with ligands generate pulling forces in the order of piconewton that cause dissociation of the heterodimer and a subsequent internalization of the ligand bound to the extracellular monomer of Notch by the ligand-expressing cell (Gordon et al., 2015). This process, termed *trans-endocytosis*, unravels the NRR and exposes the S2 site to the action of ADAM10 (Kovall et al., 2017). Cleavage of the S2 site generates an unstable peptide consisting of the transmembrane and intracellular regions of Notch, and it is a substrate of the transmembrane proteases presenilin (PSEN) 1 and 2 that are the catalytic units of the γ-secretase complex and cleave the S3 and S4 sites of Notch (Sato et al., 2007). Several accessory proteins, such as nicastrin, presenilin enhancer 2, and anterior pharynx defective 1 associate with PSENs to form the γ-secretase complex (Duggan and McCarthy, 2016). PSEN1, but not PSEN2, is necessary for Notch activation, as *Psen1*-null mice die during embryonic development due to severe abnormalities of the skeleton and central nervous system, whereas *Psen2* inactivation does not lead to an appreciable phenotype (Herreman et al., 1999; Shen et al., 1997). Cleavage of the S3 and S4 sites is the final event in the generation of the NICD (Song et al., 1999).

Formation of an active transcriptional complex

The NICD translocates to the nucleus where it forms a ternary complex with the DNA binding protein RBPJ and mastermind-like (MAML). Formation of this complex results in the recruitment of transcriptional coactivators that displace transcriptional repressors associated with RBPJ, leading to the expression of Notch target genes (Kovall, 2007). RBPJ is constitutively bound to DNA to repress transcription, although increased occupancy of *Rbpj* consensus sequences by RBPJ following activation of Notch signaling was reported (Hass et al., 2015; Wang et al., 2014). RBPJ consists of N-terminal and β-trefoil domains that bind to the DNA and a C-terminal region that, in conjunction with the β-trefoil domain, interacts with the RAM domain of the NICD and with the N-terminus of MAML proteins (Kovall and Hendrickson, 2004; Nam et al., 2006). The intracellular domains of NOTCH1 (N1ICD) and NOTCH2 (N2ICD) regulate transcription by interacting with distinct regions of RBPJ. Paralog-specific NICD interactions with RBPJ and the structure of the target gene promoter may lead to differences between the transcriptional output of distinct receptors (Yuan et al., 2012). In addition, the orientation and distribution of *Rbpj* consensus sequences appears to influence the cellular response to Notch induction (Kovall et al., 2017). Humans and mice harbor a single copy of *Rbpj*, and its deletion in mice is lethal during early embryonic development due to vascular abnormalities that phenocopy the inactivation of *Notch1* and *Notch2* (Krebs et al., 2004). Although the deletion of *Rbpj* precludes the ability of NICD to induce a transcriptional response, it also relieves the transcriptional repression of DNA regulatory elements that harbor *Rbpj* consensus sequences. In addition, RBPJ has Notch-independent functions during pancreatic development (Nakhai et al., 2008; Fujikura et al., 2006, 2007).

Maml is a family of nuclear proteins consisting of an N-terminal region, which mediates binding to RBPJ and NICD, and a C-terminal region that interacts with CBP/p300, a histone acetylase that creates the necessary conditions for the core transcriptional machinery to access the targeted gene/enhancer (Wu et al., 2000; Nam et al., 2003; Fryer et al., 2002). Humans and mice harbor three homologous *Maml* genes that display a certain level of functional redundancy. *Maml1*, like *Notch2*, is required for selected aspects of lymphocyte development, as its deletion prevents the formation of the B-cell marginal zone in the spleen (Witt et al., 2003; Oyama et al., 2007). The deletion of *Maml3* has no appreciable phenotype, whereas the consequences of global *Maml2* inactivation have not been reported. Dual *Maml1*/*Maml3* deletion phenocopies the systemic loss of Notch signaling and demonstrates that both paralogs are necessary for the formation of the NICD/RBPJMAML/ complex (Oyama et al., 2011). MAML proteins also determine the duration of transcriptional response by recruiting cyclin dependent kinases (CDKs), such as CDK8, that phosphorylate the PEST domain of the NICD and lead to

the disassembly of the ternary complex (Fryer et al., 2004). The phosphorylated NICD is subsequently ubiquitinated by ubiquitin ligases, such as E3 ubiquitin-ligase F-box and WD repeat domain-containing (FBXW)7, and targeted for proteasomal degradation (Fig. 44.2) (Thompson et al., 2007).

Notch target genes

Some of the better characterized Notch transcriptional targets are the genes encoding for the hairy and enhancer of split (HES) and Hes-related with YRPW motif (HEY) transcription factors (Ohtsuka et al., 1999; Iso et al., 2001). Mice and humans express seven HES proteins, termed HES1 through HES7, and three HEY paralogs named HEY1, HEY2, and HEYL; all but HES2 and HES3 are induced by RBPJ-mediated Notch signaling (Iso et al., 2003). HES and HEY are characterized by the presence of a basic helix-loop-helix (bHLH) domain and display a high level of structural homology. The bHLH domain allows homo- or heterodimerization with other proteins containing bHLH domains (Leimeister et al., 2000). The formation of homo- or heterodimers defines the binding specificity of the transcription factor to DNA and provides an additional level of regulation of the cellular response to Notch activation (Fischer and Gessler, 2007). HES paralogs can be distinguished from HEY proteins by the presence of a proline instead of a glycine at a conserved site within the bHLH domain and by the presence of a WRPW instead of a YRPW C-terminal tetrapeptide motif (Iso et al., 2001). The bHLH domain confers HES and HEY proteins the ability to suppress transcription by allowing the recruitment of histone deacetylases to target gene promoters and by mediating interactions with other bHLH-containing nuclear factors and the core transcriptional machinery (Fischer and Gessler, 2007). The WRPW motif is required for interactions of HES1 with transducin-like enhancer of split factors and for the consequent formation of a transcriptional repressor complex (Grbavec and Stifani, 1996). Although HES and HEY are fundamentally inhibitors of gene transcription, HES paralogs may activate transcription under certain conditions (Ju et al., 2004).

HES and HEY mediate functions of Notch signaling during development and at the early stages of cell differentiation programs in tissues with high cellular turnover. HES1, HES3, and HES5 are necessary to preserve the undifferentiated state of precursor cells throughout life (Kageyama et al., 2007). HES7 governs somite segmentation and acts in part by regulating the expression of *Lfng* (Bessho et al., 2001). HES6 suppresses HES1 function and contributes to the development of the central nervous system (Bae et al., 2000). In agreement with the role of Notch in the development of the cardiovascular system, mice harboring a systemic *Hey2* deletion or a dual *Hey1*/*HeyL* inactivation display impaired vascular development, whereas dual *Hey1*/*Hey2*-null mice recapitulate the vascular phenotype of the *Notch1* global deletion (Fischer and Gessler, 2007; Xin et al., 2007; Fischer et al., 2004, 2007; Kokubo et al., 2005).

Notch receptors and ligands in chondrocytes

Role of Notch signaling in endochondral bone formation

Early investigations in mouse embryos demonstrated that NOTCH1 is expressed by chondrocytes in the proliferative zone of the growth plate, and studies addressing the function of DLL1 in embryonic chicken limbs suggested a potential inhibitory role of Notch signaling in chondrogenesis (Crowe et al., 1999; Watanabe et al., 2003). Subsequent work in mice where the N1ICD was expressed under the control of the *Prx1* or *Col2a1* promoter to induce Notch signaling in the limb bud or in chondrocytes, respectively, revealed that NOTCH1 activation suppresses endochondral bone formation (Tables 44.1 and 44.2). N1ICD expression in the limb bud impairs the development of the cartilaginous precursors of appendicular bones, whereas its induction in chondrocytes disorganizes the growth plate, with both phenotypes leading to embryonic death (Dong et al., 2010; Mead and Yutzey, 2009). Accordingly, conditional *Psen1* deletion in *Prx1*-expressing cells in a null *Psen2* genetic composition, or dual *Notch1*/*Notch2* inactivation in the limb bud, causes an accumulation of hypertrophic chondrocytes and subsequent postnatal elongation of the cancellous bone compartment. This phenotype is recapitulated by the conditional deletion of *Notch2* but not of *Notch1* (Hilton et al., 2008). Consistent with this observation, linear femoral growth is delayed in mice harboring a systemic *Notch2* gain-of-function, indicating that among Notch receptors, NOTCH2 is the predominant regulator of bone growth (Canalis et al., 2016; Zanotti et al., 2017). Elongation of the trabecular bone compartment is noted also in tibiae of skeletally mature mice harboring a *Jag1* deletion in *Prx1*-expressing cells, possibly identifying JAG1 as the ligand responsible for the activation of Notch signaling in cells of the limb bud (Lawal et al., 2017).

TABLE 44.1 Mouse models used to study Notch signaling in the skeleton. Mouse symbol in accordance to the Mouse Genome Informatics (MGI) nomenclature is included.

Mouse strain	MGI symbol	Genetic modification	Function	References
1) *Notch1* conditional-null	*Notch1*^{tm1Agt}	*LoxP* sites flanking the putative promoter and the exon encoding the signaling peptide of *Notch1*	Conditional deletion of *Notch1*	Radtke et al. (1999)
2) *Rosa*^{Notch}	*Gt(ROSA)26 Sor*$^{tm1(Notch1)Dam}$	*LoxP*-flanked neomycin selection STOP cassette and N1ICD coding sequence cloned into the *Rosa26* locus	Expression of the N1ICD under the control of the ubiquitous *Rosa26* promoter	Murtaugh et al. (2003)
3) *Col3.6-N1ICD*	N/A	Transgene consisting of a 3.6 kb fragment of the *Col1a1* promoter upstream of the N1ICD coding sequence	Expression of the N1ICD in immature osteoblasts	Zanotti et al. (2008)
4) *Notch2* conditional-null	*Notch2*^{tm3Grid}	*LoxP* sites flanking exon 3 of *Notch2*	Conditional deletion of *Notch2*	McCright et al. (2006)
5) *Notch2 HCS*	*Notch2*$^{tm1.1Ecan}$	Point mutation in exon 34 of *Notch2* upstream of the PEST domain	Systemic expression of a *Notch2* mutant lacking the PEST domain	Canalis et al. (2016)
6) *Notch2 HCS*	N/A	Point mutation in exon 34 of *Notch2* upstream of the transactivation and PEST domains	Systemic expression of a *Notch2* mutant lacking the transactivation and PEST domains	Vollersen et al. (2017)
7) *Notch2*^{COIN}	N/A	Conditional by inversion module in exon 34 of *Notch2* upstream of the PEST domain	Conditional expression of a *Notch2* mutant lacking the PEST domain	Zanotti et al. (2017)
8) *Notch3*-null	*Notch3*^{tm1Grid}	Neomycin selection cassette replacing sequences coding for EGF-like repeats 8–12 of *Notch3*	Systemic deletion of *Notch3*	Krebs et al. (2003)
9) *Psen1* conditional	*Psen1*$^{tm2.1Shn}$	*LoxP* sites flanking exons 2 and 3 of *Psen1*	Conditional deletion of *Psen1*	Yu et al. (2001)
10) *Psen2*-null	*Psen2*^{tm1Bdes}	Hygromycin selection cassette replacing exon 5 and neighboring intronic sequences of *Psen2*	Systemic deletion of *Psen2*	Herreman et al. (1999)
11) *Rbpj* conditional-null	*Rbpj*^{tm1Hon}	*LoxP* sites flanking sequences coding for the DNA binding domain of RBPJ	Conditional deletion of *Rbpj*	Han et al. (2002)
12) *Jag1* conditional-null	*Jag1*^{tm1Frad}	*LoxP* sites flanking exons 1 and 2 of *Jag1*	Conditional deletion of *Jag1*	Mancini et al. (2005)
13) *Jag1* conditional-null	*Jag1*$^{tm1.1Loo}$	*LoxP* sites flanking exons 4 and 5 of *Jag1*	Conditional deletion of *Jag1*	Loomes et al. (2007)
14) *Dll1* conditional-null	*Dll1*^{tm1Mjo}	*LoxP* sites flanking exons 3 and 4 of *Dll1*	Conditional deletion of *Dll1*	Hozumi et al. (2004)
15) *Col2.3-Dll1*	N/A	Transgene consisting of a 2.3 kb fragment of the *Col1a1* promoter upstream of the *Dll1* coding sequence	Expression of *Dll1* in mature osteoblasts	Muguruma et al. (2017)
16) *Hes1* conditional-null	*Hes1*^{tm1Kag}	*LoxP* sites flanking exons 3 and 4 of *Hes1*	Conditional deletion of *Hes1*	Imayoshi et al. (2008)
17) *Col3.6-Hes1*	N/A	Transgene consisting of a 3.6 kb fragment of the *Col1a1* promoter upstream of the HES1 coding sequence	Expression of Hes1 in immature osteoblasts	Zanotti et al. (2011)

Continued

TABLE 44.1 Mouse models used to study Notch signaling in the skeleton. Mouse symbol in accordance to the Mouse Genome Informatics (MGI) nomenclature is included.—cont'd

Mouse strain	MGI symbol	Genetic modification	Function	References
18) *Hes3*-null	*Hes3*^{tm1Kag}	Replacement of all exons of *Hes3* with a neomycin selection cassette	Systemic deletion of *Hes3*	Hirata et al. (2001)
19) *Hes5*-null	*Hes5*^{tm1Fgu}	Replacement of sequences coding for Met1 to Ala76 of HES5 with a neomycin selection cassette	Systemic deletion of *Hes5*	Cau et al. (2000)
20) *Hey1* conditional-null	*Hey1*^{tm2Gess}	*LoxP* sites flanking exons 2 to 4 of *Hey1*	Conditional deletion of *Hey1*	Fischer et al. (2005)
21) *Hey1* overexpressor	N/A	HEY1 coding sequence cloned into the *Actb* locus	Systemic overexpression of HEY1	Salie et al. (2008)
22) *Hey2* conditional-null	*Hey2*^{tm1Eno}	*LoxP* sites flanking exons 2 and 3 of *Hey2*	Conditional deletion of *Hey2*	Xin et al. (2007)
23) *Col3.6-Hey2*	N/A	Transgene consisting of a 3.6 kb fragment of the *Col1a1* promoter upstream of the HEY2 coding sequence	Expression of HEY2 in immature osteoblasts	Zanotti et al. (2013)
24) *HeyL*-null	*Heyl*^{tm1Gess}	Replacement of exons 2 to 4 of *HeyL* with a neomycin selection cassette	Systemic deletion of *HeyL*	Fischer et al. (2007)
25) dominant negative *Maml1*	*Gt(ROSA)26 Sor*$^{tm1(MAML1) Wsp}$	*LoxP*-flanked neomycin selection STOP cassette and sequences coding for amino acids 13—74 of MAML1 in the *Rosa26* locus	Inhibition of NICD/RBPJ interactions following Cre recombination	Tu et al. (2005)

Adapted from Zanotti, S., Canalis, E., 2016. Notch signaling and the skeleton. Endocr. Rev. 37 (3), 223—253, with permission.

TABLE 44.2 Cre drivers used to study the skeletal functions of Notch signaling. Mouse symbol in accordance to the MGI nomenclature is included.

Mouse strain	MGI symbol	Genetic modification	Cell population expressing Cre	References
1) *Prx1-Cre*	*Tg(Prrx1-cre)1Cjt*	Transgene consisting of the 2.3 kb *Prx1* enhancer upstream of the Cre coding sequence	Mesenchymal cells of the limb bud - osteoblast precursors	Logan et al. (2002)
2) *Wnt1-Cre*	*Tg(Wnt1-cre)11Rth*	Transgene consisting of the *Wnt1* enhancer upstream of the Cre coding sequence	Neural crest	Danielian et al. (1998)
3) *Acan-CreER*^{T2}	*Acan*$^{tm1(cre/ERT2)Crm}$	Insertion of the Cre recombinase/estrogen receptor fusion protein (CreER^{T2}) coding Sequence in the 3′-UTR of the *Acan* locus	Chondrocytes	Henry et al. (2009)
4) *Col2a1-Cre*	*Tg(Col2a1-cre) 1Bhr*	Transgene consisting of a 3 kb fragment of the *Col2a1* promoter and 3 kb fragment of *Col2a1* intron 1 upstream of the Cre coding sequence	Chondrocytes	Ovchinnikov et al. (2000)
5) *Sp7-Cre*	*Tg(Sp7-tTA,tetO-EGFP/cre)1Amc*	Transgene consisting of a bacterial artificial chromosome (BAC) where the Cre coding sequence is cloned into the *Sp7* locus, Tet-off system	Osteoblast precursors in the absence of tetracycline	Rodda & McMahon (2006)
6) *Runx2-Cre*	*Tg(Runx2-icre) 1Jtuc*	Transgene consisting of a BAC containing where the Cre coding sequence is cloned into the *Runx2* locus	Osteoblasts	Rauch et al. (2010)

Continued

TABLE 44.2 Cre drivers used to study the skeletal functions of Notch signaling. Mouse symbol in accordance to the MGI nomenclature is included.—cont'd

Mouse strain	MGI symbol	Genetic modification	Cell population expressing Cre	References
7) *BGLAP-Cre*	*Tg(BGLAP-cre) 1Clem*	Transgene consisting of a 4 kb fragment of the *BGLAP* promoter upstream of the Cre coding sequence	Osteoblasts	Zhang et al. (2002)
8) *Col2.3-Cre*	*Tg(Col1a1-cre) 1Kry*	Transgene consisting of a 2.3 kb fragment of the *Col1a1* promoter upstream of the Cre coding sequence	Mature osteoblasts	Dacquin et al. (2002)
9) *Col2.3-CreER^{T}*	*Tg(Col1a1-cre/ERT) #Hmk*	Transgene consisting of a 3.2 kb fragment of the *Col1a1* promoter upstream of the CreERT2 coding sequence	Mature osteoblasts, Cre activated by tamoxifen administration	Maes et al. (2010)
10) *Dmp1-Cre*	*Tg(Dmp1-cre)1Jqfe*	Transgene consisting of a 9.6 kb fragment of the *Dmp1* promoter upstream of the Cre coding sequence	Preferentially in osteocytes, lining cells and mature osteoblasts to a lesser extent	Lu et al. (2007)
11) *Lyz2-Cre*	*Lyz2$^{tm1(cre)Ifo}$*	Insertion of the Cre coding sequences into the *Lyz2* locus	Myeloid cells—osteoclasts	Clausen et al. (1999)

Mechanisms of notch action in endochondral bone formation

The effects of Notch signaling during skeletal development are mediated by RBPJ-dependent mechanisms, since the deletion of *Rbpj* precludes the actions of the N1ICD in the limb bud and chondrocytes (Dong et al., 2010; Kohn et al., 2012; Chen et al., 2013). Accordingly, downregulation of *Hes1* in *Prx1*-expressing cells in the context of the individual *Hes5* or the dual *Hes3*/*Hes5* global inactivation accelerates chondrogenesis and increases femoral length, whereas the overexpression of HES1 in the limb bud has opposite effects (Rutkowski et al., 2016; Zanotti et al., 2011a). Dual *Hey1*/*HeyL* global deletion has no impact on endochondral bone formation, suggesting that HES1, HES3, and HES5, but not HEY1 or HEYL, act downstream of RBPJ to mediate the effects of Notch signaling in this developmental context (Rutkowski et al., 2016). The conditional inactivation of *Hes1* in *Col2a1*-expressing cells, either in the presence or absence of *Hes5*, has no skeletal effects (Karlsson et al., 2010; Sugita et al., 2015). This indicates that other HES paralogs can compensate for the loss of *Hes1* and *Hes5* in mature chondrocytes, or that both genes are required for early chondrogenesis but dispensable in differentiated chondrocytes.

In vitro studies reveal that Notch activation inhibits chondrogenesis by suppressing the expression of *Sox9*, *Col2a1,* and *Acan* genes encoding for factors that are critical for chondrocyte differentiation and function (Olsen et al., 2000; Zanotti and Canalis, 2013b,c). Potential mechanisms for the inhibitory effect on *Sox9* are a direct suppression of promoter activity by NICD/RBPJ interactions or an indirect transcriptional action mediated by HES5 but not HES1 (Chen et al., 2013; Rutkowski et al., 2016). Although suppression of *Sox9* in the context of Notch activation might be fully accountable for the inhibition of *Col2a1*, HES1 may contribute to this effect by binding to N-boxes found in proximity of *Sox9* consensus sequences in the *Col2a1* promoter (Grogan et al., 2008). It is of interest that downregulation of *Acan* is mediated by IL6, a molecule associated with inflammatory response. However, it is not clear whether this mechanism is operational during skeletal development or active only in articular chondrocytes in the context of degenerative joint diseases (Zanotti and Canalis, 2013b; Liu et al., 2015b).

Notch receptors and ligands in osteoblasts

Role of notch signaling in osteoblasts

Initial studies in osteoblasts revealed a potential role of Notch signaling in osteoblastogenesis. Constitutive activation of Notch receptors suppressed the capacity for osteoblastic differentiation of multiple cell lines, although the transient induction of Notch signaling had the opposite effect (Nofziger et al., 1999; Deregowski et al., 2006; Sciaudone et al., 2003; Tezuka et al., 2002; Nobta et al., 2005; Ugarte et al., 2009). These results suggested that the length of exposure to activated

Notch receptors and the cellular context determine the consequences of the signaling event on osteoblastic differentiation and function. The availability of genetically modified mice made it possible to establish the cellular response to Notch signaling in cells of the osteoblast lineage at various stages of maturation (Tables 44.1 and 44.2). Early studies in transgenic mice expressing the N1ICD under the direction of a 3.6 kb fragment of the *Col1a1* promoter revealed that NOTCH1 activation in immature osteoblasts reduces osteoblast number and activity, thereby causing osteopenia (Zanotti et al., 2008). Accordingly, mice where the N1ICD is induced in *Sp7*-or *BGLAP*-expressing osteoblasts display defective bone formation and severe osteopenia, confirming that NOTCH1 inhibits osteoblastic function (Canalis et al., 2013b). Cortical bone in these mice has an embryonic appearance characterized by the absence of a compact shell, suggesting that NOTCH1 activation in osteoblasts delays cortical bone development (Sharir et al., 2011). It is of interest that work using a tamoxifen-inducible model concluded that NOTCH1 is potentially anabolic in skeletally mature mice, although an independent effect of tamoxifen on bone remodeling was not excluded and could have caused the increased bone mass ascribed to NOTCH1 activation (Liu et al., 2016; Shevde et al., 2000).

Studies of *Notch2* misexpression in mice demonstrated that NOTCH2 shares with NOTCH1 the ability to suppress osteoblast function. Mice harboring systemic or osteoblast-specific *Notch2* gain-of-function mutations are osteopenic because of enhanced bone resorption that does not trigger a bone-forming response, indicating reduced osteoblast function (Canalis et al., 2016; Zanotti et al., 2017). Accordingly, the inactivation of *Notch2* in *Runx2*-expressing cells increases cancellous bone volume by increasing osteoblast number and bone formation (Yorgan et al., 2016). In agreement with results from individual NOTCH1 or NOTCH2 gain-of-function models, dual *Notch1*/*Notch2* deletion in immature *Prx1*-or *Sp7*-expressing osteoblasts increases cancellous bone volume, providing further evidence of the inhibitory functions of both receptors on bone formation (Hilton et al., 2008; Zanotti and Canalis, 2014).

The role of NOTCH1 evolves as osteoblast differentiation progresses, and NOTCH1 induction in mature osteoblasts expressing the 2.3 kb fragment of the *Col1a1* promoter causes osteosclerosis secondary to an accumulation of dysfunctional cells that fail to deposit a mineralized matrix (Engin et al., 2008). Transgenic overexpression of DLL1 in mature osteoblasts leads to an osteosclerotic phenotype similar to the one reported for the activation of NOTCH1 in osteocytes (Muguruma et al., 2017). The conditional inactivation of *Jag1* governed by the 2.3 kb fragment of the *Col1a1* promoter causes marginal changes in bone microarchitecture, indicating that the expression of JAG1 in mature osteoblasts is dispensable for bone homeostasis (Youngstrom et al., 2016).

Mechanisms of notch action in osteoblasts

The inactivation of *Rbpj* in *Prx1*-expressing cells enhances bone formation, and its deletion in osteoblasts prevents the effects of N1ICD, suggesting that genes under the control of RBPJ, such as *Hes* and *Hey*, are accountable for the osteoblastic response to Notch signaling (Tao et al., 2010; Tu et al., 2012). The N1ICD also interacts with RUNX2 and suppresses its transcriptional activity, suggesting the existence of RBPJ-independent effects (Engin et al., 2008). Studies of osteoblast-specific gene misexpression reveal that HES1 and HEY2 suppress osteoblast function and reduce bone mass (Zanotti et al., 2011a; Zanotti and Canalis, 2013a). In contrast, the global misexpression of HEY1 has a modest effect on osteoblastic function, and HEYL is dispensable for bone homeostasis (Tu et al., 2012; Salie et al., 2010; Canalis and Zanotti, 2017). Importantly, findings from studies of systemic HEY1 misexpression must be interpreted with caution due to the potential nonskeletal effects of the genetic alterations. Collectively, the reported results suggest that HES1, HEY2, and possibly HEY1 contribute to the inhibitory actions of Notch signaling on osteoblast function. HES1 and HEY1 reduce the expression of osteoblastic gene markers by inhibiting transactivation of RUNX2 (McLarren et al., 2000; Shen and Christakos, 2005; Suh et al., 2008; Zhang et al., 2009; Zamurovic et al., 2004). The skeletal phenotypes associated with inactivation of *Hes* and *Hey* in osteoblasts are milder than those observed in the context of *Notch1* and *Notch2* deletion in the same cells, suggesting that additional factors contribute to the effects of Notch receptors in osteoblasts (Fig. 44.3 and 44.4).

Activation of Notch signaling inhibits the differentiation of immature osteoblasts by suppressing cytosolic β-catenin levels and favoring proliferation of dysfunctional osteoblasts by upregulating the expression of cyclins and KI67 (Zanotti et al., 2008; Engin et al., 2008; Muguruma et al., 2017). Notch also regulates the expression of nuclear factor of activated T-cells (NFATc), and NFATc1 and NFATc2 compete with RBPJ for binding to DNA and prevent RBPJ-mediated transcriptional responses (Zanotti et al., 2011b, 2013). These observations indicate that Notch receptors are part of a signaling network that regulates osteoblastogenesis. Notch signaling is subjected to endocrine regulation, and PTH induces JAG1 but suppresses NOTCH1 and NOTCH2 activity by altering RBPJ/DNA interactions (Zanotti and Canalis, 2017; Calvi et al., 2003). These observations indicate that suppression of Notch signaling may contribute to the stimulatory effects of PTH on osteoblast function and bone formation.

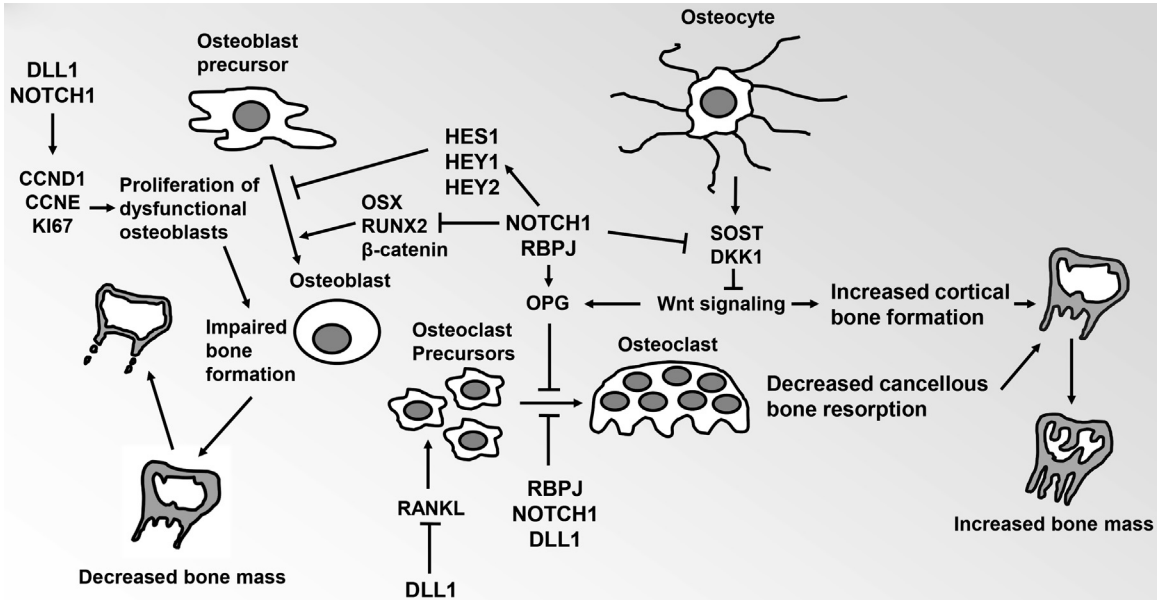

FIGURE 44.3 Regulation of bone remodeling by NOTCH1 and DLL1. NOTCH1 and DLL1 induce CCND1, CCNE, and KI67 leading to proliferation of dysfunctional osteoblasts and impaired bone formation. Activation of NOTCH1 in osteoblast precursors inhibits the function of SP7 and RUNX2 and the levels of cytosolic β-catenin by RBPJ-dependent mechanisms, thereby suppressing bone formation. Parallel induction of HES1, HEY1, and HEY2 contributes to inhibition of osteoblast function. Collectively, these events lead to a decrease in bone mass (left). NOTCH1 activation in osteocytes suppresses SOST as well as DKK1, thereby enhancing Wnt signaling and increasing cortical bone formation. In osteoblastic cells, NOTCH1 induces OPG, whereas DLL1 suppresses RANKL, and direct actions of NOTCH1 and DLL1 in osteoclast precursors inhibit osteoclastogenesis and bone resorption. The effects of NOTCH1 are mediated by RBPJ. Enhanced cortical bone formation and the inhibition of bone resorption lead to an increase in bone mass (right). *Adapted from Zanotti, S., Canalis, E., 2016. Notch signaling and the skeleton. Endocr. Rev. 37 (3), 223–253, with permission.*

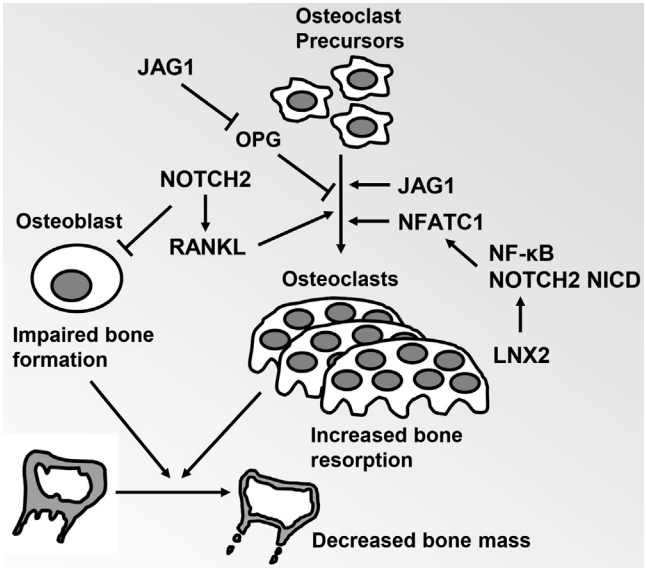

FIGURE 44.4 Regulation of bone remodeling by NOTCH2 and JAG1. Activation of NOTCH2 in osteoblasts suppresses bone formation and induces RANKL expression, thereby enhancing bone resorption. NOTCH2 activation in osteoclasts and exposure of osteoclast precursors to JAG1 enhances osteoclastogenesis and bone resorption. Interactions of nuclear factor-κB (NF-κB) with the NOTCH2 intracellular domain (N2ICD) in osteoclast precursors that lead to the induction of NFATC1 contribute to the stimulatory effects of NOTCH2 in osteoclasts. LNX2 enhances the stability of the N2ICD, thereby stimulating osteoclastogenesis. Suppressed osteoblastic function and increased bone resorption lead to a decrease in bone mass (right). *Adapted from Zanotti, S., Canalis, E., 2016. Notch signaling and the skeleton. Endocr. Rev. 37 (3), 223–253, with permission.*

Notch receptors and ligands in osteocytes

Role of Notch signaling in osteocytes

The function of Notch signaling in osteocytes was investigated in transgenic mice, where Cre expression is governed by a 9.6 kb fragment of the dentin matrix protein (*Dmp)1* promoter. *Dmp1* is expressed selectively in osteocytes but also in mature osteoblasts and in endosteal lining cells (Tables 44.1 and 44.2) (Lu et al., 2007; Xiong et al., 2015). NOTCH1 induction in *Dmp1*-expressing cells causes osteopetrosis by inducing osteoprotegerin and suppressing cancellous bone resorption. Activation of Notch in osteocytes increases cortical bone formation, although the cortex is porous and has the appearance of trabecular bone (Canalis et al., 2013a,b). The induction of N1ICD in *Sp7*-expressing cells causes a phenotype that evolves with age to resemble the effects of NOTCH1 activation in osteocytes, and this is consistent with lineage tracing studies demonstrating that *Sp7*-expressing cells have the potential to differentiate into osteocytes (Canalis et al., 2013b; Maes et al., 2010). The dual *Notch1*/*Notch2* deletion in osteocytes has minimal impact on cortical and cancellous bone remodeling and structure (Canalis et al., 2013a, 2017). The mild phenotype of the dual *Notch1*/*Notch2* deletion may be due to compensatory actions of *Notch3*, and this is consistent with the observation that *Notch3* is preferentially expressed in osteocytes (Zanotti and Canalis, 2017).

Mechanisms of Notch action in osteocytes

The conditional deletion of *Rbpj* prevents the effects of NOTCH1 activation in osteocytes, as it does in osteoblasts, supporting the notion that RBPJ carries out the functions of Notch signaling in the osteoblastic lineage (Canalis et al., 2015). In contrast to its effects in osteoblasts, activation of NOTCH1 in osteocytes suppresses the Wnt antagonists *Dkk1* and *Sost,* and as a consequence it enhances Wnt/β-catenin signaling (Canalis et al., 2013, 2015). Activation of β-catenin governed by the *Dmp1* promoter induces the expression of Notch receptors, adding a layer of complexity to the interactions of Notch and Wnt signaling in osteocytes (Tu et al., 2015). Based on this evidence, one can speculate the existence of a positive-feedback loop where Wnt enhances Notch activation, thereby leading to downregulation of *Sost* and a consequent increase in Wnt activity that sustains signaling from Notch receptors in osteocytes. Analogous mechanisms are not operational in osteoblasts, possibly because expression of *Sost* is negligible in these cells, and further downregulation by Notch would have no appreciable effect on the levels of cytosolic β-catenin (Nioi et al., 2015). It is not known whether the N1ICD/RBPJ complex inhibits *Dkk1* and *Sost* directly or whether the effect is secondary to transcriptional repressor activity of HES and HEY. JAG1 is the only Notch cognate ligand expressed in osteocytes, although it is not clear whether JAG1/Notch interactions are possible in this cellular context (Zanotti and Canalis, 2017). This is because osteocytes communicate within the confines of a canalicular network that restricts the membrane surface available for Notch receptor-ligand interactions between neighboring cells. Mechanical forces may be responsible for the induction of Notch in osteocytes (Fig. 44.3 and 44.4) (Robling et al., 2008).

Notch receptors and ligands in osteoclasts

The functions of Notch receptors in osteoclast progenitors were investigated in cultures of osteoclast precursors and conditional mouse models of gene misexpression in cells of the myeloid lineage (Clausen et al., 1999). The activation of NOTCH1 in osteoclast precursors suppresses osteoclastogenesis in vitro, and the induction of N1ICD in *Lyz2*-expressing cells inhibits bone resorption in mice exposed to tumor necrosis factor (Tables 44.1 and 44.2) (Bai et al., 2008; Zhao et al., 2012). Accordingly, myeloid-specific conditional *Notch1*/*Notch2* deletion in a *Notch3*-null genetic composition enhances osteoclastogenesis and the stimulatory effects of receptor activator of NF-kb-ligand (RANKL) on bone resorption (Bai et al., 2008). The inactivation of *Rbpj* in cultures of myeloid cells enhances osteoclastogenesis, suggesting that NOTCH1 suppresses osteoclastic differentiation with an RBPJ-dependent mechanism (Swarnkar et al., 2015). In contrast to NOTCH1, activation of NOTCH2 in osteoclast precursors induces osteoclastogenesis in vitro (Canalis et al., 2016; Fukushima et al., 2008; Jin et al., 2016; Zhou et al., 2015). However, neither the activation nor deletion of NOTCH2 in *Lyz2*-expressing cells affects osteoclastogenesis (Zanotti et al., 2017; Yorgan et al., 2016).

The identity of the ligand responsible for Notch activation in osteoclasts may influence the response to Notch signaling. Bone marrow mononuclear precursors cultured in the presence of JAG1 display enhanced Notch signaling and a capacity for osteoclastic differentiation in response to RANKL, whereas exposure to DLL1 suppresses osteoclastogenesis in vitro (Muguruma et al., 2017; Ashley et al., 2015; Nakao et al., 2009; Yamada et al., 2003). Direct stimulation of osteoclastogenesis by JAG1 was verified in vivo, since JAG1 expressed by metastatic breast cancer cells engages Notch receptors

in osteoclast precursors and contributes to the formation of lytic bone lesions (Sethi et al., 2011). However, the ligands responsible for activation of Notch receptors in osteoclasts under conditions of physiological bone remodeling remain to be determined.

Notch signaling also governs osteoclastogenesis via indirect effects on osteoblasts that lead to the regulation of *Tnfrsf11b*, the gene encoding for OPG, and *Tnfsf11*, which encodes for RANKL (Lacey et al., 1998). By downregulating *Tnfsf11*, transgenic DLL1 expression in osteoblasts inhibits osteoclastogenesis and leads to a high bone mass phenotype (Muguruma et al., 2017). In contrast to the inhibitory effects of NOTCH1 and DLL1 on osteoclast differentiation, activation of NOTCH2 in osteoblasts enhances osteoclastogenesis and bone resorption by inducing RANKL (Canalis et al., 2016; Zanotti et al., 2017). The deletion of *Jag1* in osteoblast precursors inhibits bone resorption RANKL (Lawal et al., 2017). Although JAG1 and NOTCH2 promote osteoclast differentiation through the regulation of osteoblast-derived signals, it is not clear whether JAG1 is the ligand responsible for NOTCH2 activation in this context. These observations demonstrate that NOTCH1 and DLL1 are inhibitors, whereas NOTCH2 and JAG1 are enhancers, of osteoclastogenesis, confirming that the identity of Notch receptors and cognate ligands determines the response to Notch signaling (Fig. 44.3 and 44.4).

Fracture repair and Notch signaling

Bone has a remarkable ability to regenerate following a fracture. The repair process involves complex interactions between cells of different lineages and is characterized by an initial inflammatory response and by neovascularization. Subsequently, bone tissue is regenerated either by intramembranous or endochondral ossification processes, depending on whether the fractured bone is stable or unstable (Thompson et al., 2002). Work attempting to characterize Notch expression during fracture repair has reported both upregulation and downregulation of Notch receptors and ligands, and the contradictory results may be related to experimental differences (Matthews et al., 2014; Dishowitz et al., 2012). Studies in genetically modified mice reveal that Notch signaling plays a critical role during fracture repair. Induction of a dominant negative MAML1 mutant in *Mx1*-expressing cells, and consequent inhibition of Notch signaling, prolongs the inflammatory response during fracture and delays the endochondral bone formation process (Dishowitz et al., 2013). The *Mx1* promoter is active in immune and vascular cells, so that these findings are consistent with the roles of Notch in the inflammatory response and vascularization of long bones (Ramasamy et al., 2014; Gridley, 2010; Benedito and Hellstrom, 2013). The requirement of Notch signaling for fracture healing was demonstrated by findings revealing that the *Rbpj* deletion in *Prx1*-expressing cells results in nonunion fractures. Conversely, the deletion of *Rbpj* in *Acan*-expressing cells or osteoblasts does not alter the repair process, indicating that Notch signaling is required during the early phases of cell differentiation since *Prx1* is expressed in chondroprogenitors, whereas *Acan* is expressed in mature chondrocytes (Wang et al., 2016). These findings are not congruent with the inhibitory effects of Notch on the differentiation of mesenchymal precursors, chondrocytes, and osteoblasts, and indicate that the endochondral ossification events that drive fracture repair are distinct from those that determine skeletal development (Dong et al., 2010; Mead and Yutzey, 2009; Kohn et al., 2012). Studies where *Rbpj* is conditionally deleted should be interpreted with caution, as this approach may affect the expression of genes not directly regulated by Notch signaling. It is of interest that the administration of a γ-secretase inhibitor accelerates healing in a murine model of tibial midshaft fracture (Wang et al., 2015). However, it is possible that the reported effect is secondary to downregulation of other signaling pathways affected by the broad actions of γ-secretase inhibitors (Duggan and McCarthy, 2016).

Congenital skeletal diseases caused by Notch loss of function

Alagille syndrome

Alagille syndrome is a multiorgan disease characterized by cardiovascular defects including tetralogy of Fallot, cholestatic liver disease due to bile duct atresia, and kidney anomalies that can result in renal failure (Alagille et al., 1987). Alagille syndrome is associated with mutations in either *JAG1,* or rarely, *NOTCH2*. Affected subjects present with craniofacial developmental abnormalities including craniosynostosis and distinctive facial features such as broad nasal bridge, deep set eyes, pointed chin, prominent forehead, and triangular facies. Skeletal defects extend to the spine, where vertebrae fail to fuse ventrally during development and assume a characteristic "butterfly" appearance in radiographic images. Short stature, digit abnormalities, and osteoporosis are common symptoms, although the latter is considered secondary to liver failure and subsequent malnutrition (Emerick et al., 1999). Alagille syndrome is associated with inherited loss-of-function mutations of *JAG1* such as total gene ablation, insertions that lead to protein truncations, short deletions, and nonsense mutations (Bauer et al., 2010; Crosnier et al., 1999; Morrissette et al., 2001; Boyer-Di Ponio et al., 2007). Defects are

distributed across the length of the gene and interfere with the processing of JAG1, leading to accumulation of the protein, and as a consequence, impaired Notch signaling (Morrissette et al., 2001). De novo and inherited mutations have been reported, and the disease is transmitted with an autosomal dominant pattern, suggesting that *JAG1* is haploinsufficient (Boyer-Di Ponio et al., 2007). Sporadically, patients with Alagille syndrome harbor *NOTCH2* loss-of-function mutations, either in isolation or associated with *JAG1* mutations. These subjects present with hypoplastic kidneys and renal insufficiency, which is consistent with the role of NOTCH2 in renal development (Kamath et al., 2012; McDaniell et al., 2006). Mice heterozygous for both a *Jag1*-null and a hypomorphic *Notch2* allele recapitulate selected features of Alagille syndrome, while the conditional deletion of *Jag1* in cells of the neural crest phenocopies the craniofacial abnormalities associated with the disease (McCright et al., 2002; Humphreys et al., 2012). These findings suggest that Alagille syndrome is caused by mutations in *JAG1* and *NOTCH2* resulting in loss of function.

Spondylocostal and spondylothoracic dysostosis

Spondylocostal and spondylothoracic dysostosis are diseases of defective somitogenesis that cause abnormalities in vertebral segmentation and rib structure (Turnpenny et al., 2003). These disorders are associated with dominant or recessive mutations in genes encoding components of the Notch signaling pathway, namely *DLL3*, *LFNG*, *HES7,* and mutant mesoderm posterior bHLH transcription factor (*MESP*)*2*. The mutations can occur de novo or be inherited (Zanotti and Canalis, 2012). The most frequent mutations associated with spondylocostal dysostosis, found in 20%−25% of affected individuals, occur within the coding region of *DLL3* and lead to the translation of a truncated or misfolded protein (Kusumi et al., 1998; Dunwoodie et al., 2002). Accordingly, the systemic deletion of *Dll3* in mice phenocopies the manifestations of spondylocostal dysostosis, although it remains to be determined whether these genetic defects lead to suppressed Notch signaling (Kusumi et al., 1998; Ladi et al., 2005). Homozygous missense loss-of-function mutations in *LFNG* and *HES7* are found in individuals affected by spondylocostal dysostosis, albeit with less frequency than *DLL3* mutations, and inactivation of *Lfng* or *Hes7* in mice impairs the development of the spine and rib cage (Bessho et al., 2001; Okubo et al., 2012; Sparrow et al., 2006, 2008, 2010). Spondylothoracic dysostosis is observed primarily in people of Puerto Rican descent and is associated with *MESP2* mutations, although sporadic cases in subjects homozygous for *MESP2* nonsense mutations have been reported (Cornier et al., 2008; Whittock et al., 2004). *MESP2* is a Notch transcriptional target that encodes for a bHLH transcription factor similar to HES1, as well as HEY1, and vertebral development is impaired in *Mesp2*-null mice, reaffirming the role of Notch signaling and bHLH proteins in the development of the axial skeleton (Saga, 2012; Saga et al., 1997).

Adams Oliver syndrome

Adams Oliver syndrome (AOS), a disease characterized by aplasia cutis congenita and limb defects, is associated with mutations in *NOTCH1*, *RBPJ*, *DLL4*, and *EOGT*, which encodes for EGF-domain-specific O-linked *N*-acetylglucosamine transferase (O-GlcNAc). Subjects with AOS exhibit significant phenotypic variations, with distal limb abnormalities including transverse amputations, oligodactyly, syndactyly, and hypoplastic nails (Snape et al., 2009; Adams and Oliver, 1945). AOS also presents with ventricular septal defects, tetralogy of Fallot, and anomalies of arteries and cardiac valves consistent with the role of Notch signaling in the cardiovascular system. Symptoms of peripheral vessel dysfunction, such as retinal hypovascularization and cutis marmorata telangiectatica congenita, are observed.

The mutations of *NOTCH1* associated with AOS are distributed across the length of the receptor but are more prevalent in EGF-like repeats and lead to structural changes that result in loss-of-NOTCH1 function (Stittrich et al., 2014). These mutations are associated with a higher incidence of transverse limb defects, which may be caused by developmental small vessel abnormalities and thrombosis leading to vascular obstruction rather than direct effects on mesenchymal cell differentiation (Stittrich et al., 2014; Southgate et al., 2015; Hoyme et al., 1982; Swartz et al., 1999). Two families with AOS were found to harbor heterozygous loss-of-function mutations that impair binding of RBPJ to regulatory regions of Notch target genes without interfering with RBPJ/NICD interactions (Hassed et al., 2012). Only a few AOS subjects that carry *DLL4* mutations present with cardiovascular defects, despite the fact that DLL4 is expressed in arteries and is necessary for vascular development (Gridley, 2007). Mutations of *DLL4* occur throughout the coding sequence, disrupt the structure of all known domains of DLL4, and are predicted to cause loss of function (Meester et al., 2015). Recessive mutations in *EOGT* impair O-GlcNAc activity and possibly cause defects in the glycosylation of the EGF-like domain of NOTCH1, disrupting its interactions with cognate ligands and leading to loss of function (Shaheen et al., 2013; Cohen et al., 2014; Ogawa et al., 2015).

Congenital skeletal diseases caused by Notch gain of function

Hajdu Cheney syndrome

Hajdu Cheney syndrome (HCS) is a rare disorder characterized by prominent skeletal features and phenotypical manifestations that evolve with age (Brennan and Pauli, 2001; Cheney, 1965; Currarino, 2009; Descartes et al., 2014; Gray et al., 2012; Hajdu and Kauntze, 1948; Silverman et al., 1974). Platybasia and basilar invagination are observed frequently and can result in severe neurological complications, such as hydrocephalus and central respiratory arrest with sudden death. Some subjects present with renal cysts, polycystic kidneys, or cardiovascular defects, including septal and valve abnormalities (Kaler et al., 1990; Sargin et al., 2013). The facial appearance is distinctive, with micrognathia, flattening of the midface, and abnormal dental eruptions as well as premature tooth decay and loss. Kyphosis, scoliosis, and long bone deformities, including serpentine fibula, have been reported, indicating involvement of both the axial and appendicular skeleton (Currarino, 2009; Gray et al., 2012). Focal lysis of the distal phalanxes leads to short and broad digits; histopathology is characterized by neovascularization or inflammation, and fibrosis can present with pain and swelling (Elias et al., 1978; Nunziata et al., 1990; Udell et al., 1986). Generalized osteoporosis affects most subjects, and increased bone resorption was documented in iliac crest biopsies of selected cases (Sakka et al., 2017). A recent report of an HCS patient with increased RANKL serum levels suggests that enhanced osteoclastogenesis and bone resorption are a possible mechanism for the bone loss (Adami et al., 2016).

HCS cases are frequently sporadic, although familial transmission via an autosomal dominant mechanism is possible. HCS is associated with point mutations or small deletions/insertions in exon 34 of *NOTCH2* that lead to the creation of a premature stop codon upstream of sequences coding for the PEST domain and downstream of the domains required for N2ICD/RBPJ interactions (Isidor et al., 2011; Majewski et al., 2011; Simpson et al., 2011; Zhao et al., 2013). Mutant transcripts are predicted to translate a truncated and stable NOTCH2, since the PEST domain is necessary for proteasomal degradation. This may lead to gain of function, as the sequences required to induce a transcriptional response are preserved. Pedigree analysis in affected families indicates that penetrance of the mutation is complete, whereas its expressivity is variable, as clinical manifestations of HCS can differ significantly between affected individuals. It is of interest that analogous somatic *NOTCH2* mutations increasing Notch activity are found in splenic marginal zone B-cell lymphoma (Kiel et al., 2012; Lee et al., 2009; Rossi et al., 2012; Zhang et al., 2014). Although splenomegaly has been reported in one case, there is no apparent increase in the incidence of B-cell lymphoma in HCS subjects (Adami et al., 2016).

Work in mutant mice harboring a truncating *Notch2* mutation that replicates the one found in an HCS subject demonstrates that NOTCH2 gain-of-function is the mechanism responsible for the bone loss (Canalis et al., 2016). The mutant (MGI symbol *Notch2*$^{tm1.1Ecan}$) exhibits osteopenia secondary to increased bone resorption associated with increased RANKL expression. There is no corresponding enhancement of bone formation, indicative of an inhibitory effect of the mutation on osteoblastic function. Further work in a conditional model of HCS demonstrated that deletion of the NOTCH2 PEST domain in osteoblasts, but not in myeloid cells, reproduced the osteopenic phenotype of *Notch2*$^{tm1.1Ecan}$ mutants; the mechanism was increased RANKL in *Bglap*-expressing cells (Zanotti et al., 2017). These initial reports were corroborated by another model of HCS, termed here *Notch2HCS*$^{(Yorgan)}$, that displays generalized bone loss and increased RANKL expression (Vollersen et al., 2017). This particular *NOTCH2* mutant triggers a bone-forming response and enhanced bone remodeling, indicating variations in the skeletal phenotype of the HCS mutation in mice.

Lateral meningocele syndrome

Lateral meningocele syndrome (LMS), also known as Lehman syndrome, is a rare disorder characterized by hypotonia and meningocele associated with neurological dysfunction (Lehman et al., 1977). Clinical features include empty sella and craniofacial abnormalities that lead to distinctive facies with hypertelorism, high arched eyebrows, ptosis and low set eyes, a cleft, high and narrow palate, and mandibular hypoplasia. LMS subjects have developmental delay, intellectual disability, hypotonia, decreased muscle mass, and syringomyelia as well as cardiac valve defects. There are prominent skeletal manifestations, such as short stature, scoliosis, pectus excavatum, thick calvariae, wormian bones, and high density of the base of the skull (Gripp et al., 1997). A generalized increase in bone remodeling and osteopenia are present.

Whole-exome sequencing in affected families demonstrated that LMS is associated with point mutations or deletions of up to 80 bases in exon 33 of *NOTCH3*, upstream of the PEST domain but downstream of sequences required for N3ICD/RBPJ interactions (Gripp et al., 2015; Ejaz et al., 2016). The resulting mutant NOTCH3 is truncated and presumably stable due to the absence of the PEST domain, possibly leading to enhanced Notch signaling. The etiology is analogous to the one proposed for HCS, and there is a certain degree of overlap in the clinical manifestations of both conditions (Gripp, 2011).

However, acroosteolysis, a defining feature of HCS, is not reported in LMS. Most documented cases of LMS are associated with de novo heterozygous truncating mutations in exon 33 of *NOTCH3,* and the mode of inheritance is not established, although a dominant mechanism is suspected (Gripp et al., 1997).

Brachydactyly

Brachydactylies are a group of diverse congenital disorders often associated with dysregulated bone morphogenetic protein and hedgehog signaling pathways. Genetic analysis in a Jordanian family afflicted by symmetric bilateral preaxial brachydactyly, short stature, micrognathia, and learning disabilities identified a recessive nonsense mutation in chondroitin sulfate synthase (*CHSY)1* as the potentially causative genetic defect (Tian et al., 2010). In zebrafish, downregulation of *Chsy1* results in enhanced Notch signaling and impairs skeletal development; moreover, cultured fibroblasts from individuals affected by brachydactyly exhibit upregulation of *JAG1* and enhanced Notch activity (Tian et al., 2010). Although these observations suggest that gain-of-Notch function drives the disease, the *Chsy1* inactivation in mice does not affect the expression of genes coding for components of the Notch signaling pathway, suggesting that murine CHSY1 does not regulate Notch activity. *Chsy1*-null mice display skeletal defects compatible with brachydactyly and osteopenia that are ascribed to reduced chondroitin sulfation, a shift in cellular orientation, and induction of growth differentiation factor 5, a member of the bone morphogenetic family of proteins (Wilson et al., 2012). A recent study in humans identified several distinct *CHSY1* loss-of-function mutations in brachydactyly but no abnormalities in parameters of Notch activity, questioning whether brachydactyly is a disease of enhanced Notch signaling (Li et al., 2010).

Notch and skeletal malignancies

Osteosarcoma

Osteosarcoma is the most common primary malignancy affecting bone tissue. The tumor is of osteoblastic origin, and the molecular events that determine the onset of the cancerous lesion and drive the evolution of the disease remain poorly understood. Enhanced Notch signaling was demonstrated in human and canine osteosarcoma (Tanaka et al., 2009; Dailey et al., 2013). Analysis of gene expression in biopsies from subjects with osteosarcoma has demonstrated frequent upregulation of *NOTCH1*, *NOTCH2,* and *JAG1* as well as sporadic enhanced expression of *DLL1* (Dailey et al., 2013; Engin et al., 2009). In addition, induction of *HEY1* and *HEY2* was reported, verifying increased RBPJ-mediated Notch signaling in osteosarcoma, and this may be responsible for the proliferation of tumor cells (Tanaka et al., 2009). Notch signaling promotes tumor invasiveness, and *NOTCH1*, *NOTCH2*, *DLL1,* and *HES1* are highly expressed in osteosarcoma cell lines with the ability to metastasize (Hughes, 2009). These observations are corroborated by a study where the induction of the N1ICD in murine osteoblasts leads to the development of osteosarcoma in vivo (Tao et al., 2014). The mechanism of Notch action is *Rbpj*-dependent, as its inactivation prevents the effects of N1ICD overexpression, and the process is accelerated by loss of p53. Collectively, findings in humans, dogs, and mice suggest that somatic gain-of-function mutations affecting the Notch signaling pathway play a role in the initiation and invasive potential of osteosarcoma.

Multiple myeloma

Multiple myeloma is a primary tumor affecting the bone marrow and characterized by the expansion of monoclonal plasma cells. This malignancy is associated frequently with lytic bone lesions caused by interactions of tumor cells with osteoblasts and osteocytes that induce RANKL expression. Cocultures of multiple myeloma cells and osteocytes induce Notch signaling in both cell types. Cell contact is required for this effect, suggesting that bidirectional Notch induction occurs between multiple myeloma cells and osteocytes. NOTCH3 appears to mediate these interactions, as osteocytes induce Notch target genes only in multiple myeloma cells with high *NOTCH3* expression irrespective of *NOTCH1* and *NOTCH2* transcript levels (Delgado-Calle et al., 2016). Osteocytes in contact with myeloma cells exhibit increased expression of *Sost*, and this effect contributes to the establishment of the lytic lesions in mice (Delgado-Calle et al., 2017). It is not clear whether *Sost* induction is mediated by engagement of osteocytic Notch receptors by myeloma cells, as under physiological conditions Notch inhibits *Sost* expression in osteocytes (Canalis et al., 2013a, 2015).

Metastatic carcinoma of the breast and prostate

Carcinoma of the breast frequently metastasizes to bone, and Notch signaling appears to mediate interactions between osteoblasts and carcinoma cells. Human osteoblasts residing in bone marrow are capable of inducing *NOTCH3* and *JAG1* and

to promote the formation of colonies by human breast carcinoma cell lines. Cardiac inoculation or direct injection of carcinoma cells into the bone marrow of athymic mice causes osteolytic bone metastases, while downregulation of *NOTCH3* in tumor cells reduced their metastatic potential, suggesting that NOTCH3 contributes to the invasiveness of breast cancer (Zhang et al., 2010). Accordingly, *JAG1* expression in mammary cancer cells correlates with tumor load and metastatic potential of breast cancer in mice (Sethi et al., 2011). JAG1 expressed by the tumor engages osteoblastic Notch receptors, leading to induction of IL6, enhanced osteoclastogenesis, and ultimately formation of osteolytic metastases. As bone is resorbed, transforming growth factor β is released from the matrix, upregulates *JAG1*, and induces Notch activation, establishing a positive-feedback loop that contributes to the metastatic potential of the tumor. Downregulation of *JAG1* by RNA interference or administration of γ-secretase inhibitors decreases the formation of osteolytic metastasis, confirming that Notch activity is important for the localization of tumor cells to bone in a murine model of breast carcinoma.

Bone metastases are a serious complication of prostate carcinoma and characterized by excessive production of osteoblastic woven bone associated with variable levels of osteoclastic bone resorption (Koutsilieris, 1993). Expression of *NOTCH1* and *JAG1* in carcinoma of the prostate is associated with metastatic potential and tumor recurrence, suggesting that dysregulated Notch activity may be accountable for the progression of metastatic prostate carcinoma (Zayzafoon et al., 2004; Santagata et al., 2004). This is consistent with the observation that downregulation of *NOTCH1* by RNA interference in human prostate cancer cells decreased tumor invasiveness by suppressing the expression of matrix metalloprotease 9 and of urokinase plasminogen activator receptor (Bin Hafeez et al., 2009). Expression of *NOTCH1* and of molecular markers of the epithelial−mesenchymal transition (EMT), a cellular event that occurs during cancer progression and tumor invasiveness, can be observed in metastatic carcinoma of the prostate by immunohistochemical analysis (Emadi Baygi et al., 2010; Sethi et al., 2010b). Thus, Notch may contribute to tumor aggressiveness by favoring the EMT and the metastatic potential of prostate cancer.

Conclusions

Over the past decade, work in genetically modified mice demonstrated that Notch signaling in mesenchymal precursors and in the chondrocytic, osteoblastic, and osteoclastic lineages must be tightly regulated to preserve bone homeostasis. The effects of Notch are determined by the cellular context, and distinct skeletal outcomes are observed when Notch activity is perturbed in immature or mature chondrocytes and osteoblasts. NOTCH1 and NOTCH2 in immature and differentiated osteoblasts act as inhibitors of bone formation, whereas Notch activation in more mature osteoblasts or in osteocytes leads to osteosclerosis. Notch signaling is integrated with the signaling network that governs the osteoblast differentiation program, and Notch receptors engage in complex interactions with local regulators of cell function. Investigations on the individual effects of NOTCH1, NOTCH2, JAG1, and DLL1 misexpression in osteoblasts and osteoclasts demonstrate that different Notch receptors and cognate ligands have distinct skeletal functions. Because of this, studies addressing the role of individual Notch receptors, cognate ligands and associated proteins should lead to a more accurate understanding of the role of Notch signaling in skeletal remodeling. The importance of Notch signaling in skeletal health is underscored by the fact that Notch activity is necessary for fracture healing. Clinical studies have established a strong association between gain- and loss-of-Notch-function mutations and congenital diseases with severe skeletal manifestations. Somatic mutations in Notch receptors as well as Jag ligands are a common occurrence in osteosarcoma and may enhance the metastatic potential of breast and prostate carcinoma.

In conclusion, Notch receptors and ligands play critical roles in skeletal development, in the regulation of bone remodeling, and during fracture repair; the genetic defects affecting the various components of Notch signaling have serious consequences on skeletal development.

Abbreviations

ADAM A disintegrin and metalloprotease domain
AOS Adams Oliver syndrome
ANK Ankyrin repeat
bHLH Basic helix-loop-helix
BAC Bacterial artificial chromosome
c-ter c-terminus
CADASIL Cerebral autosomal dominant arteriopathy with subcortical infarcts and leukoencephalopathy
CHSY Chondroitin sulfate synthase
CreER^{T2} Cre recombinase/estrogen receptor fusion protein
CDK Cyclin dependent kinases

CR Cysteine-rich
DLL Delta-like
DLK Delta-like homolog
DNER Delta/Notch-like EGF related receptor
DOS Delta and OSM11-like
DSL Delta/Serrate/Lag2
DMP Dentin matrix protein
DTX Deltex E3 ubiquitin ligase
EGF Epidermal growth factor
EMT Epithelial mesenchymal transition
FBXW7 F-box and WD repeat domain-containing
HCS Hajdu Cheney syndrome
HES Hairy and enhancer of split
HEY Hes-related with YRPW motif
HD Heterodimerization
ITCH Itchy E3 ubiquitin protein ligase
JAG Jagged
LMS Lateral meningocele syndrome
LP Leader peptide
LNR Lin12-Notch repeats
LFNG Lunatic fringe
MFNG Manic fringe
MAML Mastermind-like
MESP Mesoderm posterior bHLH transcription factor
MAGP Microfibril-associated glycoproteins
MGI Mouse Genome Informatics
MIB Mind bomb
MNNL Modulus at the N-terminus of Notch ligands
NRR Negative regulatory region
NOV Nephroblastoma overexpression
NEURL Neuralized E3 ubiquitin protein ligase
NICD Notch intracellular domain
N1ICD NOTCH1 intracellular domain
N2ICD NOTCH2 notch intracellular domain
Nf Nuclear factor
NFAT Nuclear factor of activated T cells
NLS Nuclear localization sequences
O-GlcNAc O-linked *N*-acetylglucosamine transferase
PSEN Presenilin
PEST Proline (P)-, glutamic acid (E)-, serine (S)-, threonine (T)-rich motif
POGLUT Protein *O*-glucosyltransferase
RFNG Radical fringe
RANKL Receptor activation of NF-kb-ligand
RBPJ Recombination signal-binding protein for immunoglobulin of kappa region
RAM RBPJ-association module
Ring Really interesting new gene
TMD Transmembrane domain.

References

Adams, F., Oliver, C., 1945. Hereditary deformities in man: due to arrested development. J. Hered. 36, 3−7.

Adami, G., Rossini, M., Gatti, D., Orsolini, G., Idolazzi, L., Viapiana, O., Scarpa, A., Canalis, E., 2016. Hajdu cheney syndrome; report of a novel notch2 mutation and treatment with denosumab. Bone 92, 150−156.

Alagille, D., Estrada, A., Hadchouel, M., Gautier, M., Odievre, M., Dommergues, J.P., 1987. Syndromic paucity of interlobular bile ducts (alagille syndrome or arteriohepatic dysplasia): review of 80 cases. J. Pediatircs 110 (2), 195−200.

Albig, A.R., Becenti, D.J., Roy, T.G., Schiemann, W.P., 2008. Microfibril-associate glycoprotein-2 (magp-2) promotes angiogenic cell sprouting by blocking notch signaling in endothelial cells. Microvasc. Res. 76 (1), 7−14.

Ashley, J.W., Ahn, J., Hankenson, K.D., 2015. Notch signaling promotes osteoclast maturation and resorptive activity. J. Cell. Biochem. 116 (11), 2598–2609.

Bae, S., Bessho, Y., Hojo, M., Kageyama, R., 2000. The bhlh gene hes6, an inhibitor of hes1, promotes neuronal differentiation. Development 127 (13), 2933–2943.

Bai, S., Kopan, R., Zou, W., Hilton, M.J., Ong, C.T., Long, F., Ross, F.P., Teitelbaum, S.L., 2008. Notch1 regulates osteoclastogenesis directly in osteoclast precursors and indirectly via osteoblast lineage cells. J. Biol. Chem. 283 (10), 6509–6518.

Baladron, V., Ruiz-Hidalgo, M.J., Nueda, M.L., az-Guerra, M.J., Garcia-Ramirez, J.J., Bonvini, E., Gubina, E., Laborda, J., 2005. Dlk acts as a negative regulator of notch1 activation through interactions with specific egf-like repeats. Exp. Cell Res. 303 (2), 343–359.

Bauer, R.C., Laney, A.O., Smith, R., Gerfen, J., Morrissette, J.J., Woyciechowski, S., Garbarini, J., Loomes, K.M., Krantz, I.D., Urban, Z., Gelb, B.D., Goldmuntz, E., Spinner, N.B., 2010. Jagged1 (jag1) mutations in patients with tetralogy of fallot or pulmonic stenosis. Hum. Mutat. 31 (5), 594–601.

Benedito, R., Hellstrom, M., 2013. Notch as a hub for signaling in angiogenesis. Exp. Cell Res. 319 (9), 1281–1288.

Bessho, Y., Sakata, R., Komatsu, S., Shiota, K., Yamada, S., Kageyama, R., 2001. Dynamic expression and essential functions of hes7 in somite segmentation. Genes Dev. 15 (20), 2642–2647.

Bin Hafeez, B., Adhami, V.M., Asim, M., Siddiqui, I.A., Bhat, K.M., Zhong, W., Saleem, M., Din, M., Setaluri, V., Mukhtar, H., 2009. Targeted knockdown of notch1 inhibits invasion of human prostate cancer cells concomitant with inhibition of matrix metalloproteinase-9 and urokinase plasminogen activator. Clin. Cancer Res. 15 (2), 452–459.

Blaumueller, C.M., Qi, H., Zagouras, P., rtavanis-Tsakonas, S., 1997. Intracellular cleavage of notch leads to a heterodimeric receptor on the plasma membrane. Cell 90 (2), 281–291.

Boyer-Di Ponio, J., Wright-Crosnier, C., Groyer-Picard, M.T., Driancourt, C., Beau, I., Hadchouel, M., Meunier-Rotival, M., 2007. Biological function of mutant forms of jagged1 proteins in alagille syndrome: inhibitory effect on notch signaling. Hum. Mol. Genet. 16 (22), 2683–2692.

Brennan, A.M., Pauli, R.M., 2001. Hajdu–cheney syndrome: evolution of phenotype and clinical problems. Am. J. Med. Genet. 100 (4), 292–310.

Calvi, L.M., Adams, G.B., Weibrecht, K.W., Weber, J.M., Olson, D.P., Knight, M.C., Martin, R.P., Schipani, E., Divieti, P., Bringhurst, F.R., Milner, L.A., Kronenberg, H.M., Scadden, D.T., 2003. Osteoblastic cells regulate the haematopoietic stem cell niche. Nature 425 (6960), 841–846.

Canalis, E., Zanotti, S., 2017. Hairy and enhancer of split-related with yrpw motif-like (heyl) is dispensable for bone remodeling in mice. J. Cell. Biochem. 118 (7), 1819–1826.

Canalis, E., Adams, D.J., Boskey, A., Parker, K., Kranz, L., Zanotti, S., 2013a. Notch signaling in osteocytes differentially regulates cancellous and cortical bone remodeling. J. Biol. Chem. 288 (35), 25614–25625.

Canalis, E., Parker, K., Feng, J.Q., Zanotti, S., 2013b. Osteoblast lineage-specific effects of notch activation in the skeleton. Endocrinology 154 (2), 623–634.

Canalis, E., Bridgewater, D., Schilling, L., Zanotti, S., 2015. Canonical notch activation in osteocytes causes osteopetrosis. Am. J. Physiol. Endocrinol. Metab. 310 (2), E171–E182.

Canalis, E., Schilling, L., Yee, S.P., Lee, S.K., Zanotti, S., 2016. Hajdu cheney mouse mutants exhibit osteopenia, increased osteoclastogenesis and bone resorption. J. Biol. Chem. 291, 1538–1551.

Canalis, E., Schilling, L., Zanotti, S., 2017. Effects of sex and notch signaling on the osteocyte cell pool. J. Cell. Physiol. 232 (2), 363–370.

Cau, E., Gradwohl, G., Casarosa, S., Kageyama, R., Guillemot, F., 2000. Hes genes regulate sequential stages of neurogenesis in the olfactory epithelium. Development 127 (11), 2323–2332.

Chastagner, P., Israel, A., Brou, C., 2008. Aip4/itch regulates notch receptor degradation in the absence of ligand. PLoS One 3 (7), e2735.

Chen, S., Tao, J., Bae, Y., Jiang, M.M., Bertin, T., Chen, Y., Yang, T., Lee, B., 2013. Notch gain of function inhibits chondrocyte differentiation via rbpj-dependent suppression of sox9. J. Bone Miner. Res. 28 (3), 649–659.

Cheney, W.D., 1965. Acro-osteolysis. Am. J. Roentgenol. Radium Ther. Nucl. Med. 94, 595–607.

Clausen, B.E., Burkhardt, C., Reith, W., Renkawitz, R., Forster, I., 1999. Conditional gene targeting in macrophages and granulocytes using lysmcre mice. Transgenic Res. 8 (4), 265–277.

Cohen, I., Silberstein, E., Perez, Y., Landau, D., Elbedour, K., Langer, Y., Kadir, R., Volodarsky, M., Sivan, S., Narkis, G., Birk, O.S., 2014. Autosomal recessive adams-oliver syndrome caused by homozygous mutation in eogt, encoding an egf domain-specific o-glcnac transferase. Eur. J. Hum. Genet. 22 (3), 374–378.

Cornier, A.S., Staehling-Hampton, K., Delventhal, K.M., Saga, Y., Caubet, J.F., Sasaki, N., Ellard, S., Young, E., Ramirez, N., Carlo, S.E., Torres, J., Emans, J.B., Turnpenny, P.D., Pourquie, O., 2008. Mutations in the mesp2 gene cause spondylothoracic dysostosis/jarcho-levin syndrome. Am. J. Hum. Genet. 82 (6), 1334–1341.

Crosnier, C., Driancourt, C., Raynaud, N., Dhorne-Pollet, S., Pollet, N., Bernard, O., Hadchouel, M., Meunier-Rotival, M., 1999. Mutations in jagged1 gene are predominantly sporadic in alagille syndrome. Gastroenterology 116 (5), 1141–1148.

Crowe, R., Zikherman, J., Niswander, L., 1999. Delta-1 negatively regulates the transition from prehypertrophic to hypertrophic chondrocytes during cartilage formation. Development 126 (5), 987–998.

Cui, X.Y., Hu, Q.D., Tekaya, M., Shimoda, Y., Ang, B.T., Nie, D.Y., Sun, L., Hu, W.P., Karsak, M., Duka, T., Takeda, Y., Ou, L.Y., Dawe, G.S., Yu, F.G., Ahmed, S., Jin, L.H., Schachner, M., Watanabe, K., Arsenijevic, Y., Xiao, Z.C., 2004. Nb-3/notch1 pathway via deltex1 promotes neural progenitor cell differentiation into oligodendrocytes. J. Biol. Chem. 279 (24), 25858–25865.

Currarino, G., 2009. Hajdu-cheney syndrome associated with serpentine fibulae and polycystic kidney disease. Pediatr. Radiol. 39 (1), 47–52.

D'Souza, B., Miyamoto, A., Weinmaster, G., 2008. The many facets of notch ligands. Oncogene 27 (38), 5148–5167.

D'Souza, B., Meloty-Kapella, L., Weinmaster, G., 2010. Canonical and non-canonical notch ligands. Curr. Top. Dev. Biol. 92, 73–129.

Dacquin, R., Starbuck, M., Schinke, T., Karsenty, G., 2002. Mouse alpha1(i)-collagen promoter is the best known promoter to drive efficient cre recombinase expression in osteoblast. Dev. Dynam. 224 (2), 245–251.

Dailey, D.D., Anfinsen, K.P., Pfaff, L.E., Ehrhart, E.J., Charles, J.B., Bonsdorff, T.B., Thamm, D.H., Powers, B.E., Jonasdottir, T.J., Duval, D.L., 2013. Hes1, a target of notch signaling, is elevated in canine osteosarcoma, but reduced in the most aggressive tumors. BMC Vet. Res. 9, 130.

Danielian, P.S., Muccino, D., Rowitch, D.H., Michael, S.K., McMahon, A.P., 1998. Modification of gene activity in mouse embryos in utero by a tamoxifen-inducible form of cre recombinase. Curr. Biol. 8 (24), 1323–1326.

Delgado-Calle, J., Anderson, J., Cregor, M.D., Hiasa, M., Chirgwin, J.M., Carlesso, N., Yoneda, T., Mohammad, K.S., Plotkin, L.I., Roodman, G.D., Bellido, T., 2016. Bidirectional notch signaling and osteocyte-derived factors in the bone marrow microenvironment promote tumor cell proliferation and bone destruction in multiple myeloma. Cancer Res. 76 (5), 1089–1100.

Delgado-Calle, J., Anderson, J., Cregor, M.D., Condon, K.W., Kuhstoss, S.A., Plotkin, L.I., Bellido, T., Roodman, G.D., 2017. Genetic deletion of sost or pharmacological inhibition of sclerostin prevent multiple myeloma-induced bone disease without affecting tumor growth. Leukemia 31, 2686–2694.

Deregowski, V., Gazzerro, E., Priest, L., Rydziel, S., Canalis, E., 2006. Notch 1 overexpression inhibits osteoblastogenesis by suppressing wnt/beta-catenin but not bone morphogenetic protein signaling. J. Biol. Chem. 281 (10), 6203–6210.

Descartes, M., Rojnueangnit, K., Cole, L., Sutton, A., Morgan, S.L., Patry, L., Samuels, M.E., 2014. Hajdu-cheney syndrome: phenotypical progression with de-novo notch2 mutation. Clin. Dysmorphol. 23 (3), 88–94.

Dishowitz, M.I., Terkhorn, S.P., Bostic, S.A., Hankenson, K.D., 2012. Notch signaling components are upregulated during both endochondral and intramembranous bone regeneration. J. Orthop. Res. 30 (2), 296–303.

Dishowitz, M.I., Mutyaba, P.L., Takacs, J.D., Barr, A.M., Engiles, J.B., Ahn, J., Hankenson, K.D., 2013. Systemic inhibition of canonical notch signaling results in sustained callus inflammation and alters multiple phases of fracture healing. PLoS One 8 (7), e68726.

Domenga, V., Fardoux, P., Lacombe, P., Monet, M., Maciazek, J., Krebs, L.T., Klonjkowski, B., Berrou, E., Mericskay, M., Li, Z., Tournier-Lasserve, E., Gridley, T., Joutel, A., 2004. Notch3 is required for arterial identity and maturation of vascular smooth muscle cells. Genes Dev. 18 (22), 2730–2735.

Dong, Y., Jesse, A.M., Kohn, A., Gunnell, L.M., Honjo, T., Zuscik, M.J., O'Keefe, R.J., Hilton, M.J., 2010. Rbpjkappa-dependent notch signaling regulates mesenchymal progenitor cell proliferation and differentiation during skeletal development. Development 137 (9), 1461–1471.

Duggan, S.P., McCarthy, J.V., 2016. Beyond gamma-secretase activity: the multifunctional nature of presenilins in cell signalling pathways. Cell. Signal. 28 (1), 1–11.

Dunwoodie, S.L., Clements, M., Sparrow, D.B., Sa, X., Conlon, R.A., Beddington, R.S., 2002. Axial skeletal defects caused by mutation in the spondylocostal dysplasia/pudgy gene dll3 are associated with disruption of the segmentation clock within the presomitic mesoderm. Development 129 (7), 1795–1806.

Eiraku, M., Tohgo, A., Ono, K., Kaneko, M., Fujishima, K., Hirano, T., Kengaku, M., 2005. Dner acts as a neuron-specific notch ligand during bergmann glial development. Nat. Neurosci. 8 (7), 873–880.

Ejaz, R., Qin, W., Huang, L., Blaser, S., Tetreault, M., Hartley, T., Boycott, K.M., Carter, M.T., C. Care4Rare Canada, 2016. Lateral meningocele (lehman) syndrome: a child with a novel notch3 mutation. Am. J. Med. Genet. 170A (4), 1070–1075.

Elias, A.N., Pinals, R.S., Anderson, H.C., Gould, L.V., Streeten, D.H., 1978. Hereditary osteodysplasia with acro-osteolysis. (the hajdu-cheney syndrome). Am. J. Med. 65 (4), 627–636.

Emadi Baygi, M., Soheili, Z.S., Schmitz, I., Sameie, S., Schulz, W.A., 2010. Snail regulates cell survival and inhibits cellular senescence in human metastatic prostate cancer cell lines. Cell Biol. Toxicol. 26 (6), 553–567.

Emerick, K.M., Rand, E.B., Goldmuntz, E., Krantz, I.D., Spinner, N.B., Piccoli, D.A., 1999. Features of alagille syndrome in 92 patients: frequency and relation to prognosis. Hepatology 29 (3), 822–829.

Engin, F., Yao, Z., Yang, T., Zhou, G., Bertin, T., Jiang, M.M., Chen, Y., Wang, L., Zheng, H., Sutton, R.E., Boyce, B.F., Lee, B., 2008. Dimorphic effects of notch signaling in bone homeostasis. Nat. Med. 14 (3), 299–305.

Engin, F., Bertin, T., Ma, O., Jiang, M.M., Wang, L., Sutton, R.E., Donehower, L.A., Lee, B., 2009. Notch signaling contributes to the pathogenesis of human osteosarcomas. Hum. Mol. Genet. 18 (8), 1464–1470.

Fernandez-Valdivia, R., Takeuchi, H., Samarghandi, A., Lopez, M., Leonardi, J., Haltiwanger, R.S., Jafar-Nejad, H., 2011. Regulation of mammalian notch signaling and embryonic development by the protein o-glucosyltransferase rumi. Development 138 (10), 1925–1934.

Fischer, A., Gessler, M., 2007. Delta-notch–and then? Protein interactions and proposed modes of repression by hes and hey bhlh factors. Nucleic Acids Res. 35 (14), 4583–4596.

Fischer, A., Schumacher, N., Maier, M., Sendtner, M., Gessler, M., 2004. The notch target genes hey1 and hey2 are required for embryonic vascular development. Genes Dev. 18 (8), 901–911.

Fischer, A., Klattig, J., Kneitz, B., Diez, H., Maier, M., Holtmann, B., Englert, C., Gessler, M., 2005. Hey basic helix-loop-helix transcription factors are repressors of gata4 and gata6 and restrict expression of the gata target gene anf in fetal hearts. Mol. Cell Biol. 25 (20), 8960–8970.

Fischer, A., Steidl, C., Wagner, T.U., Lang, E., Jakob, P.M., Friedl, P., Knobeloch, K.P., Gessler, M., 2007. Combined loss of hey1 and heyl causes congenital heart defects because of impaired epithelial to mesenchymal transition. Circ. Res. 100 (6), 856–863.

Fryer, C.J., Lamar, E., Turbachova, I., Kintner, C., Jones, K.A., 2002. Mastermind mediates chromatin-specific transcription and turnover of the notch enhancer complex. Genes Dev. 16 (11), 1397–1411.

Fryer, C.J., White, J.B., Jones, K.A., 2004. Mastermind recruits cycc:Cdk8 to phosphorylate the notch icd and coordinate activation with turnover. Mol. Cell 16 (4), 509–520.

Fujikura, J., Hosoda, K., Iwakura, H., Tomita, T., Noguchi, M., Masuzaki, H., Tanigaki, K., Yabe, D., Honjo, T., Nakao, K., 2006. Notch/rbp-j signaling prevents premature endocrine and ductal cell differentiation in the pancreas. Cell Metabol. 3 (1), 59–65.

Fujikura, J., Hosoda, K., Kawaguchi, Y., Noguchi, M., Iwakura, H., Odori, S., Mori, E., Tomita, T., Hirata, M., Ebihara, K., Masuzaki, H., Fukuda, A., Furuyama, K., Tanigaki, K., Yabe, D., Nakao, K., 2007. Rbp-j regulates expansion of pancreatic epithelial cells and their differentiation into exocrine cells during mouse development. Dev. Dynam. 236 (10), 2779–2791.

Fukushima, H., Nakao, A., Okamoto, F., Shin, M., Kajiya, H., Sakano, S., Bigas, A., Jimi, E., Okabe, K., 2008. The association of notch2 and nf-kappab accelerates rankl-induced osteoclastogenesis. Mol. Cell Biol. 28 (20), 6402–6412.

Gale, N.W., Dominguez, M.G., Noguera, I., Pan, L., Hughes, V., Valenzuela, D.M., Murphy, A.J., Adams, N.C., Lin, H.C., Holash, J., Thurston, G., Yancopoulos, G.D., 2004. Haploinsufficiency of delta-like 4 ligand results in embryonic lethality due to major defects in arterial and vascular development. Proc. Natl. Acad. Sci. U.S.A. 101 (45), 15949–15954.

Gordon, W.R., Vardar-Ulu, D., Histen, G., Sanchez-Irizarry, C., Aster, J.C., Blacklow, S.C., 2007. Structural basis for autoinhibition of notch. Nat. Struct. Mol. Biol. 14 (4), 295–300.

Gordon, W.R., Zimmerman, B., He, L., Miles, L.J., Huang, J., Tiyanont, K., McArthur, D.G., Aster, J.C., Perrimon, N., Loparo, J.J., Blacklow, S.C., 2015. Mechanical allostery: evidence for a force requirement in the proteolytic activation of notch. Dev. Cell 33 (6), 729–736.

Gray, M.J., Kim, C.A., Bertola, D.R., Arantes, P.R., Stewart, H., Simpson, M.A., Irving, M.D., Robertson, S.P., 2012. Serpentine fibula polycystic kidney syndrome is part of the phenotypic spectrum of hajdu-cheney syndrome. Eur. J. Hum. Genet. 20 (1), 122–124.

Grbavec, D., Stifani, S., 1996. Molecular interaction between tle1 and the carboxyl-terminal domain of hes-1 containing the wrpw motif. Biochem. Biophys. Res. Commun. 223 (3), 701–705.

Gridley, T., 2007. Notch signaling in vascular development and physiology. Development 134 (15), 2709–2718.

Gridley, T., 2010. Notch signaling in the vasculature. Curr. Top. Dev. Biol. 92, 277–309.

Gripp, K.W., 2011. Lateral meningocele syndrome and hajdu-cheney syndrome: different disorders with overlapping phenotypes. Am. J. Med. Genet. 155A (7), 1773–1774 author reply 1775.

Gripp, K.W., Scott Jr., C.I., Hughes, H.E., Wallerstein, R., Nicholson, L., States, L., Bason, L.D., Kaplan, P., Zderic, S.A., Duhaime, A.C., Miller, F., Magnusson, M.R., Zackai, E.H., 1997. Lateral meningocele syndrome: three new patients and review of the literature. Am. J. Med. Genet. 70 (3), 229–239.

Gripp, K.W., Robbins, K.M., Sobreira, N.L., Witmer, P.D., Bird, L.M., Avela, K., Makitie, O., Alves, D., Hogue, J.S., Zackai, E.H., Doheny, K.F., Stabley, D.L., Sol-Church, K., 2015. Truncating mutations in the last exon of notch3 cause lateral meningocele syndrome. Am. J. Med. Genet. 167A (2), 271–281.

Grogan, S.P., Olee, T., Hiraoka, K., Lotz, M.K., 2008. Repression of chondrogenesis through binding of notch signaling proteins hes-1 and hey-1 to n-box domains in the col2a1 enhancer site. Arthritis Rheum. 58 (9), 2754–2763.

Groot, A.J., Habets, R., Yahyanejad, S., Hodin, C.M., Reiss, K., Saftig, P., Theys, J., Vooijs, M., 2014. Regulated proteolysis of notch2 and notch3 receptors by adam10 and presenilins. Mol. Cell Biol. 34 (15), 2822–2832.

Hajdu, N., Kauntze, R., 1948. Cranio-skeletal dysplasia. Br. J. Radiol. 21 (241), 42–48.

Han, H., Tanigaki, K., Yamamoto, N., Kuroda, K., Yoshimoto, M., Nakahata, T., Ikuta, K., Honjo, T., 2002. Inducible gene knockout of transcription factor recombination signal binding protein-j reveals its essential role in t versus b lineage decision. Int. Immunol. 14 (6), 637–645.

Hass, M.R., Liow, H.H., Chen, X., Sharma, A., Inoue, Y.U., Inoue, T., Reeb, A., Martens, A., Fulbright, M., Raju, S., Stevens, M., Boyle, S., Park, J.S., Weirauch, M.T., Brent, M.R., Kopan, R., 2015. Spdamid: marking DNA bound by protein complexes identifies notch-dimer responsive enhancers. Mol. Cell 59 (4), 685–697.

Hassed, S.J., Wiley, G.B., Wang, S., Lee, J.Y., Li, S., Xu, W., Zhao, Z.J., Mulvihill, J.J., Robertson, J., Warner, J., Gaffney, P.M., 2012. Rbpj mutations identified in two families affected by adams-oliver syndrome. Am. J. Hum. Genet. 91 (2), 391–395.

Henry, S.P., Jang, C.W., Deng, J.M., Zhang, Z., Behringer, R.R., de Crombrugghe, B., 2009. Generation of aggrecan-creert2 knockin mice for inducible cre activity in adult cartilage. Genesis 47 (12), 805–814.

Herreman, A., Hartmann, D., Annaert, W., Saftig, P., Craessaerts, K., Serneels, L., Umans, L., Schrijvers, V., Checler, F., Vanderstichele, H., Baekelandt, V., Dressel, R., Cupers, P., Huylebroeck, D., Zwijsen, A., Van, L.F., De, S.B., 1999. Presenilin 2 deficiency causes a mild pulmonary phenotype and no changes in amyloid precursor protein processing but enhances the embryonic lethal phenotype of presenilin 1 deficiency. Proc. Natl. Acad. Sci. U.S.A. 96 (21), 11872–11877.

Heuss, S.F., Ndiaye-Lobry, D., Six, E.M., Israel, A., Logeat, F., 2008. The intracellular region of notch ligands dll1 and dll3 regulates their trafficking and signaling activity. Proc. Natl. Acad. Sci. U.S.A. 105 (32), 11212–11217.

Hilton, M.J., Tu, X., Wu, X., Bai, S., Zhao, H., Kobayashi, T., Kronenberg, H.M., Teitelbaum, S.L., Ross, F.P., Kopan, R., Long, F., 2008. Notch signaling maintains bone marrow mesenchymal progenitors by suppressing osteoblast differentiation. Nat. Med. 14 (3), 306–314.

Hirata, H., Tomita, K., Bessho, Y., Kageyama, R., 2001. Hes1 and hes3 regulate maintenance of the isthmic organizer and development of the mid/hindbrain. EMBO J. 20 (16), 4454–4466.

Hoyme, H.E., Jones, K.L., Van Allen, M.I., Saunders, B.S., Benirschke, K., 1982. Vascular pathogenesis of transverse limb reduction defects. Journal of Pediatircs 101 (5), 839–843.

Hozumi, K., Negishi, N., Suzuki, D., Abe, N., Sotomaru, Y., Tamaoki, N., Mailhos, C., Ish-Horowicz, D., Habu, S., Owen, M.J., 2004. Delta-like 1 is necessary for the generation of marginal zone b cells but not t cells in vivo. Nat. Immunol. 5 (6), 638–644.

Hrabe de, A.M., McIntyre, J., Gossler, A., 1997. Maintenance of somite borders in mice requires the delta homologue dii1. Nature 386 (6626), 717–721.

Hu, Q.D., Ang, B.T., Karsak, M., Hu, W.P., Cui, X.Y., Duka, T., Takeda, Y., Chia, W., Sankar, N., Ng, Y.K., Ling, E.A., Maciag, T., Small, D., Trifonova, R., Kopan, R., Okano, H., Nakafuku, M., Chiba, S., Hirai, H., Aster, J.C., Schachner, M., Pallen, C.J., Watanabe, K., Xiao, Z.C., 2003. F3/contactin acts as a functional ligand for notch during oligodendrocyte maturation. Cell 115 (2), 163–175.

Hughes, D.P., 2009. How the notch pathway contributes to the ability of osteosarcoma cells to metastasize. Cancer Treat Res. 152, 479–496.

Humphreys, R., Zheng, W., Prince, L.S., Qu, X., Brown, C., Loomes, K., Huppert, S.S., Baldwin, S., Goudy, S., 2012. Cranial neural crest ablation of jagged1 recapitulates the craniofacial phenotype of alagille syndrome patients. Hum. Mol. Genet. 21 (6), 1374–1383.

Imayoshi, I., Shimogori, T., Ohtsuka, T., Kageyama, R., 2008. Hes genes and neurogenin regulate non-neural versus neural fate specification in the dorsal telencephalic midline. Development 135 (15), 2531–2541.

Isidor, B., Lindenbaum, P., Pichon, O., Bezieau, S., Dina, C., Jacquemont, S., Martin-Coignard, D., Thauvin-Robinet, C., Le, M.M., Mandel, J.L., David, A., Faivre, L., Cormier-Daire, V., Redon, R., Le, C.C., 2011. Truncating mutations in the last exon of notch2 cause a rare skeletal disorder with osteoporosis. Nat. Genet. 43 (4), 306–308.

Iso, T., Sartorelli, V., Poizat, C., Iezzi, S., Wu, H.Y., Chung, G., Kedes, L., Hamamori, Y., 2001. Herp, a novel heterodimer partner of hes/e(spl) in notch signaling. Mol. Cell Biol. 21 (17), 6080–6089.

Iso, T., Kedes, L., Hamamori, Y., 2003. Hes and herp families: multiple effectors of the notch signaling pathway. J. Cell. Physiol. 194 (3), 237–255.

Jehn, B.M., Dittert, I., Beyer, S., von der, M.K., Bielke, W., 2002. C-cbl binding and ubiquitin-dependent lysosomal degradation of membrane-associated notch1. J. Biol. Chem. 277 (10), 8033–8040.

Jiang, R., Lan, Y., Chapman, H.D., Shawber, C., Norton, C.R., Serreze, D.V., Weinmaster, G., Gridley, T., 1998. Defects in limb, craniofacial, and thymic development in jagged2 mutant mice. Genes Dev. 12 (7), 1046–1057.

Jin, W.J., Kim, B., Kim, J.W., Kim, H.H., Ha, H., Lee, Z.H., 2016. Notch2 signaling promotes osteoclast resorption via activation of pyk2. Cell. Signal. 28 (5), 357–365.

Joutel, A., 2011. Pathogenesis of cadasil: transgenic and knock-out mice to probe function and dysfunction of the mutated gene, notch3, in the cerebrovasculature. Bioessays 33 (1), 73–80.

Ju, B.G., Solum, D., Song, E.J., Lee, K.J., Rose, D.W., Glass, C.K., Rosenfeld, M.G., 2004. Activating the parp-1 sensor component of the groucho/tle1 corepressor complex mediates a camkinase iidelta-dependent neurogenic gene activation pathway. Cell 119 (6), 815–829.

Kageyama, R., Ohtsuka, T., Kobayashi, T., 2007. The hes gene family: repressors and oscillators that orchestrate embryogenesis. Development 134 (7), 1243–1251.

Kakuda, S., Haltiwanger, R.S., 2017. Deciphering the fringe-mediated notch code: identification of activating and inhibiting sites allowing discrimination between ligands. Dev. Cell 40 (2), 193–201.

Kaler, S.G., Geggel, R.L., Sadeghi-Nejad, A., 1990. Hajdu-cheney syndrome associated with severe cardiac valvular and conduction disease. Dysmorph. Clin. Genet. 4, 43–47.

Kamath, B.M., Bauer, R.C., Loomes, K.M., Chao, G., Gerfen, J., Hutchinson, A., Hardikar, W., Hirschfield, G., Jara, P., Krantz, I.D., Lapunzina, P., Leonard, L., Ling, S., Ng, V.L., Hoang, P.L., Piccoli, D.A., Spinner, N.B., 2012. Notch2 mutations in alagille syndrome. J. Med. Genet. 49 (2), 138–144.

Karlsson, C., Brantsing, C., Kageyama, R., Lindahl, A., 2010. Hes1 and hes5 are dispensable for cartilage and endochondral bone formation. Cells Tissues Organs 192 (1), 17–27.

Kiel, M.J., Velusamy, T., Betz, B.L., Zhao, L., Weigelin, H.G., Chiang, M.Y., Huebner-Chan, D.R., Bailey, N.G., Yang, D.T., Bhagat, G., Miranda, R.N., Bahler, D.W., Medeiros, L.J., Lim, M.S., Elenitoba-Johnson, K.S., 2012. Whole-genome sequencing identifies recurrent somatic notch2 mutations in splenic marginal zone lymphoma. J. Exp. Med. 209 (9), 1553–1565.

Kohn, A., Dong, Y., Mirando, A.J., Jesse, A.M., Honjo, T., Zuscik, M.J., O'Keefe, R.J., Hilton, M.J., 2012. Cartilage-specific rbpjkappa-dependent and -independent notch signals regulate cartilage and bone development. Development 139 (6), 1198–1212.

Kokubo, H., Miyagawa-Tomita, S., Nakazawa, M., Saga, Y., Johnson, R.L., 2005. Mouse hesr1 and hesr2 genes are redundantly required to mediate notch signaling in the developing cardiovascular system. Dev. Biol. 278 (2), 301–309.

Koo, B.K., Lim, H.S., Song, R., Yoon, M.J., Yoon, K.J., Moon, J.S., Kim, Y.W., Kwon, M.C., Yoo, K.W., Kong, M.P., Lee, J., Chitnis, A.B., Kim, C.H., Kong, Y.Y., 2005. Mind bomb 1 is essential for generating functional notch ligands to activate notch. Development 132 (15), 3459–3470.

Kopan, R., Ilagan, M.X., 2009. The canonical notch signaling pathway: unfolding the activation mechanism. Cell 137 (2), 216–233.

Koutelou, E., Sato, S., Tomomori-Sato, C., Florens, L., Swanson, S.K., Washburn, M.P., Kokkinaki, M., Conaway, R.C., Conaway, J.W., Moschonas, N.K., 2008. Neuralized-like 1 (neurl1) targeted to the plasma membrane by n-myristoylation regulates the notch ligand jagged1. J. Biol. Chem. 283 (7), 3846–3853.

Koutsilieris, M., 1993. Osteoblastic metastasis in advanced prostate cancer. Anticancer Res. 13 (2), 443–449.

Kovall, R.A., 2007. Structures of csl, notch and mastermind proteins: piecing together an active transcription complex. Curr. Opin. Struct. Biol. 17 (1), 117–127.

Kovall, R.A., 2008. More complicated than it looks: assembly of notch pathway transcription complexes. Oncogene 27 (38), 5099–5109.

Kovall, R.A., Hendrickson, W.A., 2004. Crystal structure of the nuclear effector of notch signaling, csl, bound to DNA. EMBO J. 23 (17), 3441–3451.

Kovall, R.A., Gebelein, B., Sprinzak, D., Kopan, R., 2017. The canonical notch signaling pathway: structural and biochemical insights into shape, sugar, and force. Dev. Cell 41 (3), 228–241.

Krebs, L.T., Xue, Y., Norton, C.R., Shutter, J.R., Maguire, M., Sundberg, J.P., Gallahan, D., Closson, V., Kitajewski, J., Callahan, R., Smith, G.H., Stark, K.L., Gridley, T., 2000. Notch signaling is essential for vascular morphogenesis in mice. Genes Dev. 14 (11), 1343–1352.

Krebs, L.T., Xue, Y., Norton, C.R., Sundberg, J.P., Beatus, P., Lendahl, U., Joutel, A., Gridley, T., 2003. Characterization of notch3-deficient mice: normal embryonic development and absence of genetic interactions with a notch1 mutation. Genesis 37 (3), 139–143.

Krebs, L.T., Shutter, J.R., Tanigaki, K., Honjo, T., Stark, K.L., Gridley, T., 2004. Haploinsufficient lethality and formation of arteriovenous malformations in notch pathway mutants. Genes Dev. 18 (20), 2469–2473.

Kusumi, K., Sun, E.S., Kerrebrock, A.W., Bronson, R.T., Chi, D.C., Bulotsky, M.S., Spencer, J.B., Birren, B.W., Frankel, W.N., Lander, E.S., 1998. The mouse pudgy mutation disrupts delta homologue dll3 and initiation of early somite boundaries. Nat. Genet. 19 (3), 274–278.

Lacey, D.L., Timms, E., Tan, H.L., Kelley, M.J., Dunstan, C.R., Burgess, T., Elliott, R., Colombero, A., Elliott, G., Scully, S., Hsu, H., Sullivan, J., Hawkins, N., Davy, E., Capparelli, C., Eli, A., Qian, Y.X., Kaufman, S., Sarosi, I., Shalhoub, V., Senaldi, G., Guo, J., Delaney, J., Boyle, W.J., 1998. Osteoprotegerin ligand is a cytokine that regulates osteoclast differentiation and activation. Cell 93 (2), 165–176.

Ladi, E., Nichols, J.T., Ge, W., Miyamoto, A., Yao, C., Yang, L.T., Boulter, J., Sun, Y.E., Kintner, C., Weinmaster, G., 2005. The divergent dsl ligand dll3 does not activate notch signaling but cell autonomously attenuates signaling induced by other dsl ligands. J. Cell Biol. 170 (6), 983–992.

Lawal, R.A., Zhou, X., Batey, K., Hoffman, C.M., Georger, M.A., Radtke, F., Hilton, M.J., Xing, L., Frisch, B.J., Calvi, L.M., 2017. The notch ligand jagged1 regulates the osteoblastic lineage by maintaining the osteoprogenitor pool. J. Bone Miner. Res. 32, 1320–1331.

Le, B.R., Bardin, A., Schweisguth, F., 2005. The roles of receptor and ligand endocytosis in regulating notch signaling. Development 132 (8), 1751–1762.

Lee, S.Y., Kumano, K., Nakazaki, K., Sanada, M., Matsumoto, A., Yamamoto, G., Nannya, Y., Suzuki, R., Ota, S., Ota, Y., Izutsu, K., Sakata-Yanagimoto, M., Hangaishi, A., Yagita, H., Fukayama, M., Seto, M., Kurokawa, M., Ogawa, S., Chiba, S., 2009. Gain-of-function mutations and copy number increases of notch2 in diffuse large b-cell lymphoma. Cancer Sci. 100 (5), 920–926.

Lee, T.V., Pandey, A., Jafar-Nejad, H., 2017. Xylosylation of the notch receptor preserves the balance between its activation by trans-delta and inhibition by cis-ligands in drosophila. PLoS Genet. 13 (4), e1006723.

Lehman, R.A., Stears, J.C., Wesenberg, R.L., Nusbaum, E.D., 1977. Familial osteosclerosis with abnormalities of the nervous system and meninges. J. Pediatir. 90 (1), 49–54.

Leimeister, C., Dale, K., Fischer, A., Klamt, B., Hrabe de, A.M., Radtke, F., McGrew, M.J., Pourquie, O., Gessler, M., 2000. Oscillating expression of c-hey2 in the presomitic mesoderm suggests that the segmentation clock may use combinatorial signaling through multiple interacting bhlh factors. Dev. Biol. 227 (1), 91–103.

Li, Y., Laue, K., Temtamy, S., Aglan, M., Kotan, L.D., Yigit, G., Canan, H., Pawlik, B., Nurnberg, G., Wakeling, E.L., Quarrell, O.W., Baessmann, I., Lanktree, M.B., Yilmaz, M., Hegele, R.A., Amr, K., May, K.W., Nurnberg, P., Topaloglu, A.K., Hammerschmidt, M., Wollnik, B., 2010. Temtamy preaxial brachydactyly syndrome is caused by loss-of-function mutations in chondroitin synthase 1, a potential target of bmp signaling. Am. J. Hum. Genet. 87 (6), 757–767.

Lindsell, C.E., Boulter, J., diSibio, G., Gossler, A., Weinmaster, G., 1996. Expression patterns of jagged, delta1, notch1, notch2, and notch3 genes identify ligand-receptor pairs that may function in neural development. Mol. Cell. Neurosci. 8 (1), 14–27.

Liu, Z., Chen, S., Boyle, S., Zhu, Y., Zhang, A., Piwnica-Worms, D.R., Ilagan, M.X., Kopan, R., 2013. The extracellular domain of notch2 increases its cell-surface abundance and ligand responsiveness during kidney development. Dev. Cell 25 (6), 585–598.

Liu, Z., Brunskill, E., Varnum-Finney, B., Zhang, C., Zhang, A., Jay, P.Y., Bernstein, I., Morimoto, M., Kopan, R., 2015a. The intracellular domains of notch1 and notch2 are functionally equivalent during development and carcinogenesis. Development 142 (14), 2452–2463.

Liu, Z., Chen, J., Mirando, A.J., Wang, C., Zuscik, M.J., O'Keefe, R.J., Hilton, M.J., 2015b. A dual role for notch signaling in joint cartilage maintenance and osteoarthritis. Sci. Signal. 8 (386), ra71.

Liu, P., Ping, Y., Ma, M., Zhang, D., Liu, C., Zaidi, S., Gao, S., Ji, Y., Lou, F., Yu, F., Lu, P., Stachnik, A., Bai, M., Wei, C., Zhang, L., Wang, K., Chen, R., New, M.I., Rowe, D.W., Yuen, T., Sun, L., Zaidi, M., 2016. Anabolic actions of notch on mature bone. Proc. Natl. Acad. Sci. U.S.A. 113 (15), E2152–E2161.

Logan, M., Martin, J.F., Nagy, A., Lobe, C., Olson, E.N., Tabin, C.J., 2002. Expression of cre recombinase in the developing mouse limb bud driven by a prxl enhancer. Genesis 33 (2), 77–80.

Loomes, K.M., Russo, P., Ryan, M., Nelson, A., Underkoffler, L., Glover, C., Fu, H., Gridley, T., Kaestner, K.H., Oakey, R.J., 2007. Bile duct proliferation in liver-specific jag1 conditional knockout mice: effects of gene dosage. Hepatology 45 (2), 323–330.

Lu, Y., Xie, Y., Zhang, S., Dusevich, V., Bonewald, L.F., Feng, J.Q., 2007. Dmp1-targeted cre expression in odontoblasts and osteocytes. J. Dent. Res. 86 (4), 320–325.

Luca, V.C., Jude, K.M., Pierce, N.W., Nachury, M.V., Fischer, S., Garcia, K.C., 2015. Structural biology. Structural basis for notch1 engagement of delta-like 4. Science 347 (6224), 847–853.

Luca, V.C., Kim, B.C., Ge, C., Kakuda, S., Wu, D., Roein-Peikar, M., Haltiwanger, R.S., Zhu, C., Ha, T., Garcia, K.C., 2017. Notch-jagged complex structure implicates a catch bond in tuning ligand sensitivity. Science 355 (6331), 1320–1324.

Luxan, G., Casanova, J.C., Martinez-Poveda, B., Prados, B., D'Amato, G., MacGrogan, D., Gonzalez-Rajal, A., Dobarro, D., Torroja, C., Martinez, F., Izquierdo-Garcia, J.L., Fernandez-Friera, L., Sabater-Molina, M., Kong, Y.Y., Pizarro, G., Ibanez, B., Medrano, C., Garcia-Pavia, P., Gimeno, J.R., Monserrat, L., Jimenez-Borreguero, L.J., de la Pompa, J.L., 2013. Mutations in the notch pathway regulator mib1 cause left ventricular noncompaction cardiomyopathy. Nat. Med. 19 (2), 193–201.

Maes, C., Kobayashi, T., Selig, M.K., Torrekens, S., Roth, S.I., Mackem, S., Carmeliet, G., Kronenberg, H.M., 2010. Osteoblast precursors, but not mature osteoblasts, move into developing and fractured bones along with invading blood vessels. Dev. Cell 19 (2), 329–344.

Majewski, J., Schwartzentruber, J.A., Caqueret, A., Patry, L., Marcadier, J., Fryns, J.P., Boycott, K.M., Ste-Marie, L.G., McKiernan, F.E., Marik, I., Van, E.H., Michaud, J.L., Samuels, M.E., 2011. Mutations in notch2 in families with hajdu-cheney syndrome. Hum. Mutat. 32 (10), 1114–1117.

Malecki, M.J., Sanchez-Irizarry, C., Mitchell, J.L., Histen, G., Xu, M.L., Aster, J.C., Blacklow, S.C., 2006. Leukemia-associated mutations within the notch1 heterodimerization domain fall into at least two distinct mechanistic classes. Mol. Cell Biol. 26 (12), 4642–4651.

Mancini, S.J., Mantei, N., Dumortier, A., Suter, U., MacDonald, H.R., Radtke, F., 2005. Jagged1-dependent notch signaling is dispensable for hematopoietic stem cell self-renewal and differentiation. Blood 105 (6), 2340–2342.

Matthews, B.G., Grcevic, D., Wang, L., Hagiwara, Y., Roguljic, H., Joshi, P., Shin, D.G., Adams, D.J., Kalajzic, I., 2014. Analysis of alphasma-labeled progenitor cell commitment identifies notch signaling as an important pathway in fracture healing. J. Bone Miner. Res. 29 (5), 1283–1294.

McCright, B., Gao, X., Shen, L., Lozier, J., Lan, Y., Maguire, M., Herzlinger, D., Weinmaster, G., Jiang, R., Gridley, T., 2001. Defects in development of the kidney, heart and eye vasculature in mice homozygous for a hypomorphic notch2 mutation. Development 128 (4), 491–502.

McCright, B., Lozier, J., Gridley, T., 2002. A mouse model of alagille syndrome: notch2 as a genetic modifier of jag1 haploinsufficiency. Development 129 (4), 1075–1082.

McCright, B., Lozier, J., Gridley, T., 2006. Generation of new notch2 mutant alleles. Genesis 44 (1), 29–33.

McDaniell, R., Warthen, D.M., Sanchez-Lara, P.A., Pai, A., Krantz, I.D., Piccoli, D.A., Spinner, N.B., 2006. Notch2 mutations cause alagille syndrome, a heterogeneous disorder of the notch signaling pathway. Am. J. Hum. Genet. 79 (1), 169–173.

McLarren, K.W., Lo, R., Grbavec, D., Thirunavukkarasu, K., Karsenty, G., Stifani, S., 2000. The mammalian basic helix loop helix protein hes-1 binds to and modulates the transactivating function of the runt-related factor cbfa1. J. Cell. Biochem. 275 (1), 530–538.

Mead, T.J., Yutzey, K.E., 2009. Notch pathway regulation of chondrocyte differentiation and proliferation during appendicular and axial skeleton development. Proc. Natl. Acad. Sci. U.S.A. 106 (34), 14420–14425.

Meester, J.A., Southgate, L., Stittrich, A.B., Venselaar, H., Beekmans, S.J., den Hollander, N., Bijlsma, E.K., Helderman-van den Enden, A., Verheij, J.B., Glusman, G., Roach, J.C., Lehman, A., Patel, M.S., de Vries, B.B., Ruivenkamp, C., Itin, P., Prescott, K., Clarke, S., Trembath, R., Zenker, M., Sukalo, M., Van Laer, L., Loeys, B., Wuyts, W., 2015. Heterozygous loss-of-function mutations in dll4 cause adams-oliver syndrome. Am. J. Hum. Genet. 97 (3), 475–482.

Minamizato, T., Sakamoto, K., Liu, T., Kokubo, H., Katsube, K., Perbal, B., Nakamura, S., Yamaguchi, A., 2007. Ccn3/nov inhibits bmp-2-induced osteoblast differentiation by interacting with bmp and notch signaling pathways. Biochem. Biophys. Res. Commun. 354 (2), 567–573.

Miyamoto, A., Lau, R., Hein, P.W., Shipley, J.M., Weinmaster, G., 2006. Microfibrillar proteins magp-1 and magp-2 induce notch1 extracellular domain dissociation and receptor activation. J. Cell. Biochem. 281 (15), 10089–10097.

Morgan, T.H., Bridges, C.B., 1916. Sex-linked Inheritance in drosophila, vol. 237. Carnegie Institute of Washington Publication, pp. 1–88.

Morrissette, J.D., Colliton, R.P., Spinner, N.B., 2001. Defective intracellular transport and processing of jag1 missense mutations in alagille syndrome. Hum. Mol. Genet. 10 (4), 405–413.

Muguruma, Y., Hozumi, K., Warita, H., Yahata, T., Uno, T., Ito, M., Ando, K., 2017. Maintenance of bone homeostasis by dll1-mediated notch signaling. J. Cell. Physiol. 232 (9), 2569–2580.

Mukherjee, A., Veraksa, A., Bauer, A., Rosse, C., Camonis, J., rtavanis-Tsakonas, S., 2005. Regulation of notch signalling by non-visual beta-arrestin. Nat. Cell Biol. 7 (12), 1191–1201.

Murphy, P.A., Lam, M.T., Wu, X., Kim, T.N., Vartanian, S.M., Bollen, A.W., Carlson, T.R., Wang, R.A., 2008. Endothelial notch4 signaling induces hallmarks of brain arteriovenous malformations in mice. Proc. Natl. Acad. Sci. U.S.A. 105 (31), 10901–10906.

Murphy, P.A., Kim, T.N., Huang, L., Nielsen, C.M., Lawton, M.T., Adams, R.H., Schaffer, C.B., Wang, R.A., 2014. Constitutively active notch4 receptor elicits brain arteriovenous malformations through enlargement of capillary-like vessels. Proc. Natl. Acad. Sci. U.S.A. 111 (50), 18007–18012.

Murtaugh, L.C., Stanger, B.Z., Kwan, K.M., Melton, D.A., 2003. Notch signaling controls multiple steps of pancreatic differentiation. Proc. Natl. Acad. Sci. U.S.A. 100 (25), 14920–14925.

Nakao, A., Kajiya, H., Fukushima, H., Fukushima, A., Anan, H., Ozeki, S., Okabe, K., 2009. Pthrp induces notch signaling in periodontal ligament cells. J. Dent. Res. 88 (6), 551–556.

Nakhai, H., Siveke, J.T., Klein, B., Mendoza-Torres, L., Mazur, P.K., Algul, H., Radtke, F., Strobl, L., Zimber-Strobl, U., Schmid, R.M., 2008. Conditional ablation of notch signaling in pancreatic development. Development 135 (16), 2757–2765.

Nam, Y., Weng, A.P., Aster, J.C., Blacklow, S.C., 2003. Structural requirements for assembly of the csl.Intracellular notch1.Mastermind-like 1 transcriptional activation complex. J. Cell. Biochem. 278 (23), 21232–21239.

Nam, Y., Sliz, P., Song, L., Aster, J.C., Blacklow, S.C., 2006. Structural basis for cooperativity in recruitment of maml coactivators to notch transcription complexes. Cell 124 (5), 973–983.

Nichols, J.T., Miyamoto, A., Weinmaster, G., 2007. Notch signaling–constantly on the move. Traffic 8 (8), 959–969.

Nioi, P., Taylor, S., Hu, R., Pacheco, E., He, Y.D., Hamadeh, H., Paszty, C., Pyrah, I., Ominsky, M.S., Boyce, R.W., 2015. Transcriptional profiling of laser capture microdissected subpopulations of the osteoblast lineage provides insight into the early response to sclerostin antibody in rats. J. Bone Miner. Res. 30 (8), 1457–1467.

Nobta, M., Tsukazaki, T., Shibata, Y., Xin, C., Moriishi, T., Sakano, S., Shindo, H., Yamaguchi, A., 2005. Critical regulation of bone morphogenetic protein-induced osteoblastic differentiation by delta1/jagged1-activated notch1 signaling. J. Cell. Biochem. 280 (16), 15842–15848.

Nofziger, D., Miyamoto, A., Lyons, K.M., Weinmaster, G., 1999. Notch signaling imposes two distinct blocks in the differentiation of c2c12 myoblasts. Development 126 (8), 1689–1702.

Nunziata, V., di, G.G., Ballanti, P., Bonucci, E., 1990. High turnover osteoporosis in acro-osteolysis (hajdu-cheney syndrome). J. Endocrinol. Investig. 13 (3), 251–255.

Ogawa, M., Sawaguchi, S., Kawai, T., Nadano, D., Matsuda, T., Yagi, H., Kato, K., Furukawa, K., Okajima, T., 2015. Impaired o-linked n-acetylglucosaminylation in the endoplasmic reticulum by mutated epidermal growth factor (egf) domain-specific o-linked n-acetylglucosamine transferase found in adams-oliver syndrome. J. Biol. Chem. 290 (4), 2137–2149.

Ohtsuka, T., Ishibashi, M., Gradwohl, G., Nakanishi, S., Guillemot, F., Kageyama, R., 1999. Hes1 and hes5 as notch effectors in mammalian neuronal differentiation. EMBO J. 18 (8), 2196–2207.

Okubo, Y., Sugawara, T., Abe-Koduka, N., Kanno, J., Kimura, A., Saga, Y., 2012. Lfng regulates the synchronized oscillation of the mouse segmentation clock via trans-repression of notch signalling. Nat. Commun. 3, 1141.

Olsen, B.R., Reginato, A.M., Wang, W., 2000. Bone development. Annu. Rev. Cell Dev. Biol. 16, 191–220.

Ovchinnikov, D.A., Deng, J.M., Ogunrinu, G., Behringer, R.R., 2000. Col2a1-directed expression of cre recombinase in differentiating chondrocytes in transgenic mice. Genesis 26 (2), 145–146.

Oyama, T., Harigaya, K., Muradil, A., Hozumi, K., Habu, S., Oguro, H., Iwama, A., Matsuno, K., Sakamoto, R., Sato, M., Yoshida, N., Kitagawa, M., 2007. Mastermind-1 is required for notch signal-dependent steps in lymphocyte development in vivo. Proc. Natl. Acad. Sci. U.S.A. 104 (23), 9764–9769.

Oyama, T., Harigaya, K., Sasaki, N., Okamura, Y., Kokubo, H., Saga, Y., Hozumi, K., Suganami, A., Tamura, Y., Nagase, T., Koga, H., Nishimura, M., Sakamoto, R., Sato, M., Yoshida, N., Kitagawa, M., 2011. Mastermind-like 1 (maml1) and mastermind-like 3 (maml3) are essential for notch signaling in vivo. Development 138 (23), 5235–5246.

Pintar, A., De, B.A., Popovic, M., Ivanova, N., Pongor, S., 2007. The intracellular region of notch ligands: does the tail make the difference? Biol. Direct 2, 19.

Radtke, F., Wilson, A., Stark, G., Bauer, M., van, M.J., MacDonald, H.R., Aguet, M., 1999. Deficient t cell fate specification in mice with an induced inactivation of notch1. Immunity 10 (5), 547–558.

Ramasamy, S.K., Kusumbe, A.P., Wang, L., Adams, R.H., 2014. Endothelial notch activity promotes angiogenesis and osteogenesis in bone. Nature 507 (7492), 376–380.

Rampal, R., rboleda-Velasquez, J.F., Nita-Lazar, A., Kosik, K.S., Haltiwanger, R.S., 2005. Highly conserved o-fucose sites have distinct effects on notch1 function. J. Biol. Chem. 280 (37), 32133–32140.

Rathinam, C., Matesic, L.E., Flavell, R.A., 2011. The e3 ligase itch is a negative regulator of the homeostasis and function of hematopoietic stem cells. Nat. Immunol. 12 (5), 399–407.

Rauch, A., Seitz, S., Baschant, U., Schilling, A.F., Illing, A., Stride, B., Kirilov, M., Mandic, V., Takacz, A., Schmidt-Ullrich, R., Ostermay, S., Schinke, T., Spanbroek, R., Zaiss, M.M., Angel, P.E., Lerner, U.H., David, J.P., Reichardt, H.M., Amling, M., Schutz, G., Tuckermann, J.P., 2010. Glucocorticoids suppress bone formation by attenuating osteoblast differentiation via the monomeric glucocorticoid receptor. Cell Metabol. 11 (6), 517–531.

Robling, A.G., Niziolek, P.J., Baldridge, L.A., Condon, K.W., Allen, M.R., Alam, I., Mantila, S.M., Gluhak-Heinrich, J., Bellido, T.M., Harris, S.E., Turner, C.H., 2008. Mechanical stimulation of bone in vivo reduces osteocyte expression of sost/sclerostin. J. Biol. Chem. 283 (9), 5866–5875.

Rodda, S.J., McMahon, A.P., 2006. Distinct roles for hedgehog and canonical wnt signaling in specification, differentiation and maintenance of osteoblast progenitors. Development 133 (16), 3231–3244.

Rossi, D., Trifonov, V., Fangazio, M., Bruscaggin, A., Rasi, S., Spina, V., Monti, S., Vaisitti, T., Arruga, F., Fama, R., Ciardullo, C., Greco, M., Cresta, S., Piranda, D., Holmes, A., Fabbri, G., Messina, M., Rinaldi, A., Wang, J., Agostinelli, C., Piccaluga, P.P., Lucioni, M., Tabbo, F., Serra, R., Franceschetti, S., Deambrogi, C., Daniele, G., Gattei, V., Marasca, R., Facchetti, F., Arcaini, L., Inghirami, G., Bertoni, F., Pileri, S.A., Deaglio, S., Foa, R., Dalla-Favera, R., Pasqualucci, L., Rabadan, R., Gaidano, G., 2012. The coding genome of splenic marginal zone lymphoma: activation of notch2 and other pathways regulating marginal zone development. J. Exp. Med. 209 (9), 1537–1551.

Ruan, Y., Tecott, L., Jiang, M.M., Jan, L.Y., Jan, Y.N., 2001. Ethanol hypersensitivity and olfactory discrimination defect in mice lacking a homolog of drosophila neuralized. Proc. Natl. Acad. Sci. U.S.A. 98 (17), 9907–9912.

Rutkowski, T.P., Kohn, A., Sharma, D., Ren, Y., Mirando, A.J., Hilton, M.J., 2016. Hes factors regulate specific aspects of chondrogenesis and chondrocyte hypertrophy during cartilage development. J. Cell Sci. 129 (11), 2145–2155.

Rydziel, S., Stadmeyer, L., Zanotti, S., Durant, D., Smerdel-Ramoya, A., Canalis, E., 2007. Nephroblastoma overexpressed (nov) inhibits osteoblastogenesis and causes osteopenia. J. Biol. Chem. 282 (27), 19762–19772.

Saga, Y., 2012. The mechanism of somite formation in mice. Curr. Opin. Genet. Dev. 22 (4), 331–338.

Saga, Y., Hata, N., Koseki, H., Taketo, M.M., 1997. Mesp2: a novel mouse gene expressed in the presegmented mesoderm and essential for segmentation initiation. Genes Dev. 11 (14), 1827–1839.

Sakamoto, K., Yamaguchi, S., Ando, R., Miyawaki, A., Kabasawa, Y., Takagi, M., Li, C.L., Perbal, B., Katsube, K., 2002. The nephroblastoma overexpressed gene (nov/ccn3) protein associates with notch1 extracellular domain and inhibits myoblast differentiation via notch signaling pathway. J. Biol. Chem. 277 (33), 29399–29405.

Sakka, S., Gafni, R.I., Davies, J.H., Clarke, B., Tebben, P., Samuels, M., Saraff, V., Klaushofer, K., Fratzl-Zelman, N., Roschger, P., Rauch, F., Högler, W., 2017. Bone structural characteristics and response to bisphosphonate treatment in children with hajdu-cheney syndrome. J. Clin. Endocrinol. Metab. 102, 4163–4172.

Salie, R., Kneissel, M., Vukcevic, M., Serbanovic, J., Zamurovic, N., Kramer, I., Evans, G., Gerwin, N., Mueller, M., Kinzel, B., Susa, M., 2008. Hey1 regulates bone mass and cartilage hypertrophy by linking bmp signaling with the pth receptor. Calcif. Tissue Int. 82 (Suppl. 1), S119.

Salie, R., Kneissel, M., Vukevic, M., Zamurovic, N., Kramer, I., Evans, G., Gerwin, N., Mueller, M., Kinzel, B., Susa, M., 2010. Ubiquitous overexpression of hey1 transcription factor leads to osteopenia and chondrocyte hypertrophy in bone. Bone 46 (3), 680–694.

Sanchez-Irizarry, C., Carpenter, A.C., Weng, A.P., Pear, W.S., Aster, J.C., Blacklow, S.C., 2004. Notch subunit heterodimerization and prevention of ligand-independent proteolytic activation depend, respectively, on a novel domain and the lnr repeats. Mol. Cell Biol. 24 (21), 9265–9273.

Santagata, S., Demichelis, F., Riva, A., Varambally, S., Hofer, M.D., Kutok, J.L., Kim, R., Tang, J., Montie, J.E., Chinnaiyan, A.M., Rubin, M.A., Aster, J.C., 2004. Jagged1 expression is associated with prostate cancer metastasis and recurrence. Cancer Res. 64 (19), 6854–6857.

Sargin, G., Cildag, S., Senturk, T., 2013. Hajdu-cheney syndrome with ventricular septal defect. Kaohsiung J. Med. Sci. 29 (6), 343–344.

Sato, T., Diehl, T.S., Narayanan, S., Funamoto, S., Ihara, Y., De, S.B., Steiner, H., Haass, C., Wolfe, M.S., 2007. Active gamma-secretase complexes contain only one of each component. J. Biol. Chem. 282 (47), 33985–33993.

Schroeter, E.H., Kisslinger, J.A., Kopan, R., 1998. Notch-1 signalling requires ligand-induced proteolytic release of intracellular domain. Nature 393 (6683), 382–386.

Schuster-Gossler, K., Harris, B., Johnson, K.R., Serth, J., Gossler, A., 2009. Notch signalling in the paraxial mesoderm is most sensitive to reduced pofut1 levels during early mouse development. BMC Dev. Biol. 9, 6.

Sciaudone, M., Gazzerro, E., Priest, L., Delany, A.M., Canalis, E., 2003. Notch 1 impairs osteoblastic cell differentiation. Endocrinology 144 (12), 5631–5639.

Servian-Morilla, E., Takeuchi, H., Lee, T.V., Clarimon, J., Mavillard, F., Area-Gomez, E., Rivas, E., Nieto-Gonzalez, J.L., Rivero, M.C., Cabrera-Serrano, M., Gomez-Sanchez, L., Martinez-Lopez, J.A., Estrada, B., Marquez, C., Morgado, Y., Suarez-Calvet, X., Pita, G., Bigot, A., Gallardo, E., Fernandez-Chacon, R., Hirano, M., Haltiwanger, R.S., Jafar-Nejad, H., Paradas, C., 2016. A poglut1 mutation causes a muscular dystrophy with reduced notch signaling and satellite cell loss. EMBO Mol. Med. 8 (11), 1289–1309.

Sethi, M.K., Buettner, F.F., Krylov, V.B., Takeuchi, H., Nifantiev, N.E., Haltiwanger, R.S., Gerardy-Schahn, R., Bakker, H., 2010a. Identification of glycosyltransferase 8 family members as xylosyltransferases acting on o-glucosylated notch epidermal growth factor repeats. J. Biol. Chem. 285 (3), 1582–1586.

Sethi, S., Macoska, J., Chen, W., Sarkar, F.H., 2010b. Molecular signature of epithelial-mesenchymal transition (emt) in human prostate cancer bone metastasis. Am J Transl Res 3 (1), 90–99.

Sethi, N., Dai, X., Winter, C.G., Kang, Y., 2011. Tumor-derived jagged1 promotes osteolytic bone metastasis of breast cancer by engaging notch signaling in bone cells. Cancer Cell 19 (2), 192–205.

Shaheen, R., Aglan, M., Keppler-Noreuil, K., Faqeih, E., Ansari, S., Horton, K., Ashour, A., Zaki, M.S., Al-Zahrani, F., Cueto-Gonzalez, A.M., Abdel-Salam, G., Temtamy, S., Alkuraya, F.S., 2013. Mutations in eogt confirm the genetic heterogeneity of autosomal-recessive adams-oliver syndrome. Am. J. Hum. Genet. 92 (4), 598–604.

Sharir, A., Stern, T., Rot, C., Shahar, R., Zelzer, E., 2011. Muscle force regulates bone shaping for optimal load-bearing capacity during embryogenesis. Development 138 (15), 3247–3259.

Shen, Q., Christakos, S., 2005. The vitamin d receptor, runx2, and the notch signaling pathway cooperate in the transcriptional regulation of osteopontin. J. Biol. Chem. 280 (49), 40589–40598.

Shen, J., Bronson, R.T., Chen, D.F., Xia, W., Selkoe, D.J., Tonegawa, S., 1997. Skeletal and cns defects in presenilin-1-deficient mice. Cell 89 (4), 629–639.

Shevde, N.K., Bendixen, A.C., Dienger, K.M., Pike, J.W., 2000. Estrogens suppress rank ligand-induced osteoclast differentiation via a stromal cell independent mechanism involving c-jun repression. Proc. Natl. Acad. Sci. U.S.A. 97 (14), 7829–7834.

Shi, S., Stanley, P., 2003. Protein o-fucosyltransferase 1 is an essential component of notch signaling pathways. Proc. Natl. Acad. Sci. U.S.A. 100 (9), 5234–5239.

Silverman, F.N., Dorst, J.P., Hajdu, N., 1974. Acroosteolysis (hajdu-cheney syndrome), birth defects orig. Artic. Ser. 10 (12), 106–123.

Simpson, M.A., Irving, M.D., Asilmaz, E., Gray, M.J., Dafou, D., Elmslie, F.V., Mansour, S., Holder, S.E., Brain, C.E., Burton, B.K., Kim, K.H., Pauli, R.M., Aftimos, S., Stewart, H., Kim, C.A., Holder-Espinasse, M., Robertson, S.P., Drake, W.M., Trembath, R.C., 2011. Mutations in notch2 cause hajdu-cheney syndrome, a disorder of severe and progressive bone loss. Nat. Genet. 43 (4), 303–305.

Snape, K.M., Ruddy, D., Zenker, M., Wuyts, W., Whiteford, M., Johnson, D., Lam, W., Trembath, R.C., 2009. The spectra of clinical phenotypes in aplasia cutis congenita and terminal transverse limb defects. Am. J. Med. Genet. 149A (8), 1860–1881.

Song, W., Nadeau, P., Yuan, M., Yang, X., Shen, J., Yankner, B.A., 1999. Proteolytic release and nuclear translocation of notch-1 are induced by presenilin-1 and impaired by pathogenic presenilin-1 mutations. Proc. Natl. Acad. Sci. U.S.A. 96 (12), 6959–6963.

Southgate, L., Sukalo, M., Karountzos, A.S., Taylor, E.J., Collinson, C.S., Ruddy, D., Snape, K.M., Dallapiccola, B., Tolmie, J.L., Joss, S., Brancati, F., Digilio, M.C., Graul-Neumann, L.M., Salviati, L., Coerdt, W., Jacquemin, E., Wuyts, W., Zenker, M., Machado, R.D., Trembath, R.C., 2015. Haploinsufficiency of the notch1 receptor as a cause of adams-oliver syndrome with variable cardiac anomalies. Circ Cardiovasc Genet 8 (4), 572–581.

Sparrow, D.B., Chapman, G., Wouters, M.A., Whittock, N.V., Ellard, S., Fatkin, D., Turnpenny, P.D., Kusumi, K., Sillence, D., Dunwoodie, S.L., 2006. Mutation of the lunatic fringe gene in humans causes spondylocostal dysostosis with a severe vertebral phenotype. Am. J. Hum. Genet. 78 (1), 28–37.

Sparrow, D.B., Guillen-Navarro, E., Fatkin, D., Dunwoodie, S.L., 2008. Mutation of hairy-and-enhancer-of-split-7 in humans causes spondylocostal dysostosis. Hum. Mol. Genet. 17 (23), 3761–3766.

Sparrow, D.B., Sillence, D., Wouters, M.A., Turnpenny, P.D., Dunwoodie, S.L., 2010. Two novel missense mutations in hairy-and-enhancer-of-split-7 in a family with spondylocostal dysostosis. Eur. J. Hum. Genet. 18 (6), 674–679.

Stahl, M., Uemura, K., Ge, C., Shi, S., Tashima, Y., Stanley, P., 2008. Roles of pofut1 and o-fucose in mammalian notch signaling. J. Biol. Chem. 283 (20), 13638–13651.

Stanley, P., 2007. Regulation of notch signaling by glycosylation. Curr. Opin. Struct. Biol. 17 (5), 530–535.

Stittrich, A.B., Lehman, A., Bodian, D.L., Ashworth, J., Zong, Z., Li, H., Lam, P., Khromykh, A., Iyer, R.K., Vockley, J.G., Baveja, R., Silva, E.S., Dixon, J., Leon, E.L., Solomon, B.D., Glusman, G., Niederhuber, J.E., Roach, J.C., Patel, M.S., 2014. Mutations in notch1 cause adams-oliver syndrome. Am. J. Hum. Genet. 95 (3), 275–284.

Sugita, S., Hosaka, Y., Okada, K., Mori, D., Yano, F., Kobayashi, H., Taniguchi, Y., Mori, Y., Okuma, T., Chang, S.H., Kawata, M., Taketomi, S., Chikuda, H., Akiyama, H., Kageyama, R., Chung, U.I., Tanaka, S., Kawaguchi, H., Ohba, S., Saito, T., 2015. Transcription factor hes1 modulates osteoarthritis development in cooperation with calcium/calmodulin-dependent protein kinase 2. Proc. Natl. Acad. Sci. U.S.A. 112 (10), 3080–3085.

Suh, J.H., Lee, H.W., Lee, J.W., Kim, J.B., 2008. Hes1 stimulates transcriptional activity of runx2 by increasing protein stabilization during osteoblast differentiation. Biochem. Biophys. Res. Commun. 367 (1), 97–102.

Swarnkar, G., Karuppaiah, K., Mbalaviele, G., Chen, T.H., Abu-Amer, Y., 2015. Osteopetrosis in tak1-deficient mice owing to defective nf-kappab and notch signaling. Proc. Natl. Acad. Sci. U.S.A. 112 (1), 154–159.

Swartz, E.N., Sanatani, S., Sandor, G.G., Schreiber, R.A., 1999. Vascular abnormalities in adams-oliver syndrome: cause or effect? Am. J. Med. Genet. 82 (1), 49–52.

Swiatek, P.J., Lindsell, C.E., del Amo, F.F., Weinmaster, G., Gridley, T., 1994. Notch1 is essential for postimplantation development in mice. Genes Dev. 8 (6), 707–719.

Tanaka, M., Setoguchi, T., Hirotsu, M., Gao, H., Sasaki, H., Matsunoshita, Y., Komiya, S., 2009. Inhibition of notch pathway prevents osteosarcoma growth by cell cycle regulation. Br. J. Canc. 100 (12), 1957–1965.

Tao, J., Chen, S., Yang, T., Dawson, B., Munivez, E., Bertin, T., Lee, B., 2010. Osteosclerosis owing to notch gain of function is solely rbpj-dependent. J. Bone Miner. Res. 25 (10), 2175–2183.

Tao, J., Jiang, M.M., Jiang, L., Salvo, J.S., Zeng, H.C., Dawson, B., Bertin, T.K., Rao, P.H., Chen, R., Donehower, L.A., Gannon, F., Lee, B.H., 2014. Notch activation as a driver of osteogenic sarcoma. Cancer Cell 26 (3), 390–401.

Tezuka, K., Yasuda, M., Watanabe, N., Morimura, N., Kuroda, K., Miyatani, S., Hozumi, N., 2002. Stimulation of osteoblastic cell differentiation by notch. J. Bone Miner. Res. 17 (2), 231–239.

Theodoris, C.V., Li, M., White, M.P., Liu, L., He, D., Pollard, K.S., Bruneau, B.G., Srivastava, D., 2015. Human disease modeling reveals integrated transcriptional and epigenetic mechanisms of notch1 haploinsufficiency. Cell 160 (6), 1072–1086.

Thompson, Z., Miclau, T., Hu, D., Helms, J.A., 2002. A model for intramembranous ossification during fracture healing. J. Orthop. Res. 20 (5), 1091–1098.

Thompson, B.J., Buonamici, S., Sulis, M.L., Palomero, T., Vilimas, T., Basso, G., Ferrando, A., Aifantis, I., 2007. The scffbw7 ubiquitin ligase complex as a tumor suppressor in t cell leukemia. J. Exp. Med. 204 (8), 1825–1835.

Tian, J., Ling, L., Shboul, M., Lee, H., O'Connor, B., Merriman, B., Nelson, S.F., Cool, S., Ababneh, O.H., Al-Hadidy, A., Masri, A., Hamamy, H., Reversade, B., 2010. Loss of chsy1, a secreted fringe enzyme, causes syndromic brachydactyly in humans via increased notch signaling. Am. J. Hum. Genet. 87 (6), 768–778.

Tu, L., Fang, T.C., Artis, D., Shestova, O., Pross, S.E., Maillard, I., Pear, W.S., 2005. Notch signaling is an important regulator of type 2 immunity. J. Exp. Med. 202 (8), 1037–1042.

Tu, X., Chen, J., Lim, J., Karner, C.M., Lee, S.Y., Heisig, J., Wiese, C., Surendran, K., Kopan, R., Gessler, M., Long, F., 2012. Physiological notch signaling maintains bone homeostasis via rbpjk and hey upstream of nfatc1. PLoS Genet. 8 (3), e1002577.

Tu, X., Delgado-Calle, J., Condon, K.W., Maycas, M., Zhang, H., Carlesso, N., Taketo, M.M., Burr, D.B., Plotkin, L.I., Bellido, T., 2015. Osteocytes mediate the anabolic actions of canonical wnt/beta-catenin signaling in bone. Proc. Natl. Acad. Sci. U.S.A. 112 (5), E478–E486.

Turnpenny, P.D., Whittock, N., Duncan, J., Dunwoodie, S., Kusumi, K., Ellard, S., 2003. Novel mutations in dll3, a somitogenesis gene encoding a ligand for the notch signalling pathway, cause a consistent pattern of abnormal vertebral segmentation in spondylocostal dysostosis. J. Med. Genet. 40 (5), 333–339.

Udell, J., Schumacher Jr., H.R., Kaplan, F., Fallon, M.D., 1986. Idiopathic familial acroosteolysis: histomorphometric study of bone and literature review of the hajdu-cheney syndrome. Arthritis Rheum. 29 (8), 1032–1038.

Ugarte, F., Ryser, M., Thieme, S., Fierro, F.A., Navratiel, K., Bornhauser, M., Brenner, S., 2009. Notch signaling enhances osteogenic differentiation while inhibiting adipogenesis in primary human bone marrow stromal cells. Exp. Hematol. 37 (7), 867–875.

Visan, I., Tan, J.B., Yuan, J.S., Harper, J.A., Koch, U., Guidos, C.J., 2006. Regulation of t lymphopoiesis by notch1 and lunatic fringe-mediated competition for intrathymic niches. Nat. Immunol. 7 (6), 634–643.

Vollersen, N., Hermans-Borgmeyer, I., Cornils, K., Fehse, B., Rolvien, T., Triviai, I., Jeschke, A., Oheim, R., Amling, M., Schinke, T., Yorgan, T.A., 2017. High bone turnover in mice carrying a pathogenic notch2-mutation causing hajdu-cheney syndrome. J. Bone Miner. Res.

Wang, H., Zang, C., Taing, L., Arnett, K.L., Wong, Y.J., Pear, W.S., Blacklow, S.C., Liu, X.S., Aster, J.C., 2014. Notch1-rbpj complexes drive target gene expression through dynamic interactions with superenhancers. Proc. Natl. Acad. Sci. U.S.A. 111 (2), 705–710.

Wang, C., Shen, J., Yukata, K., Inzana, J.A., O'Keefe, R.J., Awad, H.A., Hilton, M.J., 2015. Transient gamma-secretase inhibition accelerates and enhances fracture repair likely via notch signaling modulation. Bone 73, 77–89.

Wang, C., Inzana, J.A., Mirando, A.J., Ren, Y., Liu, Z., Shen, J., O'Keefe, R.J., Awad, H.A., Hilton, M.J., 2016. Notch signaling in skeletal progenitors is critical for fracture repair. J. Clin. Investig. 126 (4), 1471–1481.

Watanabe, N., Tezuka, Y., Matsuno, K., Miyatani, S., Morimura, N., Yasuda, M., Fujimaki, R., Kuroda, K., Hiraki, Y., Hozumi, N., Tezuka, K., 2003. Suppression of differentiation and proliferation of early chondrogenic cells by notch. J. Bone Miner. Metab. 21 (6), 344–352.

Weisshuhn, P.C., Handford, P.A., Redfield, C., 2015a. (1)h, (13)c and (15)n assignments of egf domains 4 to 7 of human notch-1. Biomol NMR Assign 9 (2), 275–279.

Weisshuhn, P.C., Handford, P.A., Redfield, C., 2015b. (1)h, (13)c and (15)n assignments of egf domains 8-11 of human notch-1. Biomol NMR Assign 9 (2), 375–379.

Weisshuhn, P.C., Sheppard, D., Taylor, P., Whiteman, P., Lea, S.M., Handford, P.A., Redfield, C., 2016. Non-linear and flexible regions of the human notch1 extracellular domain revealed by high-resolution structural studies. Structure 24 (4), 555–566.

Whittock, N.V., Sparrow, D.B., Wouters, M.A., Sillence, D., Ellard, S., Dunwoodie, S.L., Turnpenny, P.D., 2004. Mutated mesp2 causes spondylocostal dysostosis in humans. Am. J. Hum. Genet. 74 (6), 1249–1254.

Wilson, D.G., Phamluong, K., Lin, W.Y., Barck, K., Carano, R.A., Diehl, L., Peterson, A.S., Martin, F., Solloway, M.J., 2012. Chondroitin sulfate synthase 1 (chsy1) is required for bone development and digit patterning. Dev. Biol. 363 (2), 413–425.

Witt, C.M., Won, W.J., Hurez, V., Klug, C.A., 2003. Notch2 haploinsufficiency results in diminished b1 b cells and a severe reduction in marginal zone b cells. J. Immunol. 171 (6), 2783–2788.

Wu, J., Bresnick, E.H., 2007. Bare rudiments of notch signaling: how receptor levels are regulated. Trends Biochem. Sci. 32 (10), 477–485.

Wu, L., Aster, J.C., Blacklow, S.C., Lake, R., rtavanis-Tsakonas, S., Griffin, J.D., 2000. Maml1, a human homologue of drosophila mastermind, is a transcriptional co-activator for notch receptors. Nat. Genet. 26 (4), 484–489.

Xin, M., Small, E.M., van, R.E., Qi, X., Richardson, J.A., Srivastava, D., Nakagawa, O., Olson, E.N., 2007. Essential roles of the bhlh transcription factor hrt2 in repression of atrial gene expression and maintenance of postnatal cardiac function. Proc. Natl. Acad. Sci. U.S.A. 104 (19), 7975–7980.

Xiong, J., Piemontese, M., Onal, M., Campbell, J., Goellner, J.J., Dusevich, V., Bonewald, L., Manolagas, S.C., O'Brien, C.A., 2015. Osteocytes, not osteoblasts or lining cells, are the main source of the rankl required for osteoclast formation in remodeling bone. PLoS One 10 (9), e0138189.

Xu, X., Choi, S.H., Hu, T., Tiyanont, K., Habets, R., Groot, A.J., Vooijs, M., Aster, J.C., Chopra, R., Fryer, C., Blacklow, S.C., 2015. Insights into autoregulation of notch3 from structural and functional studies of its negative regulatory region. Structure 23 (7), 1227–1235.

Xue, Y., Gao, X., Lindsell, C.E., Norton, C.R., Chang, B., Hicks, C., Gendron-Maguire, M., Rand, E.B., Weinmaster, G., Gridley, T., 1999. Embryonic lethality and vascular defects in mice lacking the notch ligand jagged1. Hum. Mol. Genet. 8 (5), 723–730.

Yamada, T., Yamazaki, H., Yamane, T., Yoshino, M., Okuyama, H., Tsuneto, M., Kurino, T., Hayashi, S., Sakano, S., 2003. Regulation of osteoclast development by notch signaling directed to osteoclast precursors and through stromal cells. Blood 101 (6), 2227–2234.

Yorgan, T., Vollersen, N., Riedel, C., Jeschke, A., Peters, S., Busse, B., Amling, M., Schinke, T., 2016. Osteoblast-specific notch2 inactivation causes increased trabecular bone mass at specific sites of the appendicular skeleton. Bone 87, 136–146.

Youngstrom, D.W., Dishowitz, M.I., Bales, C.B., Carr, E., Mutyaba, P.L., Kozloff, K.M., Shitaye, H., Hankenson, K.D., Loomes, K.M., 2016. Jagged1 expression by osteoblast-lineage cells regulates trabecular bone mass and periosteal expansion in mice. Bone 91, 64–74.

Yu, H., Saura, C.A., Choi, S.Y., Sun, L.D., Yang, X., Handler, M., Kawarabayashi, T., Younkin, L., Fedeles, B., Wilson, M.A., Younkin, S., Kandel, E.R., Kirkwood, A., Shen, J., 2001. App processing and synaptic plasticity in presenilin-1 conditional knockout mice. Neuron 31 (5), 713–726.

Yuan, Z., Friedmann, D.R., Vanderwielen, B.D., Collins, K.J., Kovall, R.A., 2012. Characterization of csl (cbf-1, su(h), lag-1) mutants reveals differences in signaling mediated by notch1 and notch2. J. Biol. Chem. 287 (42), 34904–34916.

Zamurovic, N., Cappellen, D., Rohner, D., Susa, M., 2004. Coordinated activation of notch, wnt, and transforming growth factor-beta signaling pathways in bone morphogenic protein 2-induced osteogenesis. Notch target gene hey1 inhibits mineralization and runx2 transcriptional activity. J. Biol. Chem. 279 (36), 37704–37715.

Zanotti, S., Canalis, E., 2012. Notch regulation of bone development and remodeling and related skeletal disorders. Calcif. Tissue Int. 90 (2), 69–75.

Zanotti, S., Canalis, E., 2013a. Hairy and enhancer of split-related with yrpw motif (hey)2 regulates bone remodeling in mice. J. Biol. Chem. 288 (30), 21547–21557.

Zanotti, S., Canalis, E., 2013b. Interleukin 6 mediates select effects of notch in chondrocytes. Osteoarthritis Cartilage 21 (11), 1766–1773.

Zanotti, S., Canalis, E., 2013c. Notch suppresses nuclear factor of activated t cells (nfat) transactivation and nfatc1 expression in chondrocytes. Endocrinology 154 (2), 762–772.

Zanotti, S., Canalis, E., 2014. Notch1 and notch2 expression in osteoblast precursors regulates femoral microarchitecture. Bone 62, 22–28.

Zanotti, S., Canalis, E., 2016. Notch signaling and the skeleton. Endocr. Rev. 37 (3), 223–253.

Zanotti, S., Canalis, E., 2017. Parathyroid hormone inhibits notch signaling in osteoblasts and osteocytes. Bone 103, 159–167.

Zanotti, S., Smerdel-Ramoya, A., Stadmeyer, L., Durant, D., Radtke, F., Canalis, E., 2008. Notch inhibits osteoblast differentiation and causes osteopenia. Endocrinology 149 (8), 3890–3899.

Zanotti, S., Smerdel-Ramoya, A., Canalis, E., 2011a. Hairy and enhancer of split (hes)1 is a determinant of bone mass. J. Biol. Chem. 286 (4), 2648–2657.

Zanotti, S., Smerdel-Ramoya, A., Canalis, E., 2011b. Reciprocal regulation of notch and nuclear factor of activated t-cells (nfat) c1 transactivation in osteoblasts. J. Biol. Chem. 286 (6), 4576–4588.

Zanotti, S., Smerdel-Ramoya, A., Canalis, E., 2013. Nuclear factor of activated t-cells (nfat)c2 inhibits notch signaling in osteoblasts. J. Biol. Chem. 288 (1), 624–632.

Zanotti, S., Yu, J., Sanjay, A., Schilling, L., Schoenherr, C., Economides, A.N., Canalis, E., 2017. Sustained notch2 signaling in osteoblasts, but not in osteoclasts, is linked to osteopenia in a mouse model of hajdu-cheney syndrome. J. Biol. Chem. 292 (29), 12232–12244.

Zayzafoon, M., Abdulkadir, S.A., McDonald, J.M., 2004. Notch signaling and erk activation are important for the osteomimetic properties of prostate cancer bone metastatic cell lines. J. Biol. Chem. 279 (5), 3662–3670.

Zhang, M., Xuan, S., Bouxsein, M.L., von Stechow, D., Akeno, N., Faugere, M.C., Malluche, H., Zhao, G., Rosen, C.J., Efstratiadis, A., Clemens, T.L., 2002. Osteoblast-specific knockout of the insulin-like growth factor (igf) receptor gene reveals an essential role of igf signaling in bone matrix mineralization. J. Biol. Chem. 277 (46), 44005−44012.

Zhang, Y., Lian, J.B., Stein, J.L., van Wijnen, A.J., Stein, G.S., 2009. The notch-responsive transcription factor hes-1 attenuates osteocalcin promoter activity in osteoblastic cells. J. Cell. Biochem. 108 (3), 651−659.

Zhang, Z., Wang, H., Ikeda, S., Fahey, F., Bielenberg, D., Smits, P., Hauschka, P.V., 2010. Notch3 in human breast cancer cell lines regulates osteoblast-cancer cell interactions and osteolytic bone metastasis. Am. J. Pathol. 177 (3), 1459−1469.

Zhang, X., Shi, Y., Weng, Y., Lai, Q., Luo, T., Zhao, J., Ren, G., Li, W., Pan, H., Ke, Y., Zhang, W., He, Q., Wang, Q., Zhou, R., 2014. The truncate mutation of notch2 enhances cell proliferation through activating the nf-kappab signal pathway in the diffuse large b-cell lymphomas. PLoS One 9 (10), e108747.

Zhao, B., Grimes, S.N., Li, S., Hu, X., Ivashkiv, L.B., 2012. Tnf-induced osteoclastogenesis and inflammatory bone resorption are inhibited by transcription factor rbp-j. J. Exp. Med. 209 (2), 319−334.

Zhao, W., Petit, E., Gafni, R.I., Collins, M.T., Robey, P.G., Seton, M., Miller, K.K., Mannstadt, M., 2013. Mutations in notch2 in patients with hajdu-cheney syndrome. Osteoporos. Int. 24 (8), 2275−2281.

Zhou, J., Fujiwara, T., Ye, S., Li, X., Zhao, H., 2015. Ubiquitin e3 ligase lnx2 is critical for osteoclastogenesis in vitro by regulating m-csf/rankl signaling and notch2. Calcif. Tissue Int. 96 (5), 465−475.

Chapter 45

Fibroblast growth factor (FGF) and FGF receptor families in bone

Pierre J. Marie[1], Marja Hurley[2] and David M. Ornitz[3]

[1]*UMR-1132 Inserm (Institut national de la Santé et de la Recherche Médicale) and University Paris Diderot, Sorbonne Paris Cité, Paris, France;* [2]*Department of Medicine, University of Connecticut School of Medicine, UConn Health, Farmington, CT, United States;* [3]*Department of Developmental Biology, Washington University School of Medicine, St. Louis, MO, United States*

Chapter outline

Fibroblast growth factor production and regulation in bone

Fibroblast growth factors (FGFs) are a family of polypeptides found in metazoan organisms ranging from nematodes to humans (Gospadorowicz et al., 1974; Itoh et al., 2007; Fon Tacer et al., 2010). There are 22 members of the human/rodent FGF gene family (FGFs 1−23), of which FGF15 is the mouse ortholog of human FGF19. Based on sequence homology and phylogeny, the mouse and human FGF families are divided into seven subfamilies: FGFs 1 and 2 are members of the FGF1 subfamily; FGFs 4, 5, and 6 belong to the FGF4 subfamily; FGFs 3, 7, 10, and 22 are comprised in the FGF7 subfamily; the FGF8 subfamily consists of FGFs 8, 17, and 18; the FGF9 subfamily includes FGFs 9, 16, and 20; the FGF11 subfamily consists of FGFs 11−14; and the endocrine/hormonal FGF15/19 subfamily consists of FGFs 15/19, 21, and 23 (Itoh and Ornitz, 2004, 2008; Ornitz and Marie, 2015; Ornitz and Itoh, 2015). Members of the FGF family of ligands have important roles in the regulation of osteogenesis, osteoclastogenesis, and bone and mineral homeostasis, and there is evidence of the mRNA expression of some but not all FGF ligands in bones. Among the *Fgf* mRNAs expressed in rodent bones are *Fgf1, Fgf2, Fgf6, Fgf7, Fgf18,* and *Fgf23* (Fon Taser et al., 2010). Expression profiling of *Fgf* gene expression during rat calvarial osteoblast differentiation demonstrated low levels of expression of *Fgf2, Fgf4, Fgf7, Fgf18*,

Principles of Bone Biology. https://doi.org/10.1016/B978-0-12-814841-9.00045-2

and *Fgf20* throughout the culture period, although there was a progressive increase in Fgf9 and Fgf23 during the late differentiation stages (Takei et al., 2015).

FGF1, also known as acidic FGF, is a 155-amino-acid-long nonglycosylated polypeptide produced by bone (Hauechka et al., 1986). FGF1 is not released from cells under normal physiological conditions, but is secreted in response to stress conditions such as heat shock, hypoxia (Carreira et al., 2001; Jackson et al., 1992), serum starvation (Shin et al., 1996), and exposure to low-density lipoproteins (Ananyeva et al., 1997). FGF2, like FGF1, is stored in the bone matrix (Hauschka et al., 1986), with FGF2 levels being 10-fold higher than than those of FGF1 (Seyedin et al., 1985). FGF2 is produced by osteoblasts (Globus et al., 1989). In cultures of mouse osteoblastic MC3T3-E1 cells, exogenous FGF2 increases its own mRNA (Hurley et al., 1994). Transforming growth factor beta (TGF-β) also increases Fgf2 mRNA and protein in MC3T3-E1 cells (Hurley et al., 1994). However, there was no measurable FGF2 in the conditioned medium. The significance of TGF-β regulation of FGF2 in osteoblasts is not clear. Amplification of the responses to both FGF and TGF-β could occur from an increase in endogenous FGF2. Other regulators of FGF2 expression include parathyroid hormone (PTH) (Hurley et al., 1999) and prostaglandins (Sabbieti et al., 1999) that increase *Fgf2* mRNA and protein levels in osteoblasts, suggesting that anabolic factors for bone may act in part by stimulating endogenous FGF2 in osteoblasts. Interestingly, FGF2 is an immediate-early gene induced by mechanical stress in osteoblasts, an effect that results in activation of the protein kinase A (PKA) and MAP kinases ERK1/2 pathways, suggesting that FGF2 may mediate some osteogenic effects induced by mechanical forces (Li and Hughes-Fulford, 2016). FGF8 is expressed in chondrocytes, perichondrium and calvarial osteoblasts, and the growth plate of developing bones. FGF8 also regulates osteoblast and chondrocyte differentiation (Xu et al., 1999; Ornitz and Marie, 2002, 2015). *Fgf8* knockout in mice resulted in embryonic lethality; therefore, there are limited data on its role in bone homeostasis (Sun et al., 1999). FGF9 has an important role in skeletal development and repair. It is expressed in multiple tissues including the perichondrium/periosteum, chondrocytes, and primary spongiosa (Garafolo et al., 1999; Colvin et al., 1999; Hung et al., 2007). *Fgf9* knockout in mice resulted in lethality at the neonatal stage (Colvin et al., 2001). *Fgf9* knockout mice also have shortening of the proximal skeletal elements (Hung et al., 2007). In addition, knockout of *Fgf9* results in osteoclast deficiency (Hung et al., 2007). These data imply that FGF9 positively regulates osteogenesis and osteoclastogenesis. FGF18 is expressed in osteoprogenitor cells, differentiated osteoblasts, perichondrium, joints, and growth plates of long bones (Lazarus et al., 2007; Liu et al., 2007; Obayashi et al., 2002). Mice with global *Fgf18* knockout die perinatally and display expansion of proliferating chondrocyte (PC) and hypertrophic chondrocyte (HC) zones consistent with a negative regulatory role of FGF18 on chondrogenesis. FGF18 also contributes to bone development by its effects to induce vascularization of bone and recruitment of osteoclast progenitors during bone development (Liu et al., 2007). In vitro, *Fgf18* expression is upregulated by Wnt signaling in chondrocytes (Kapadia et al., 2005) and by Runx2 in cooperation with Wnt signaling (Reinhold and Naski, 2007), suggesting a link between Wnt signaling and FGF signaling during endochondral bone development. To date, there are no data on regulators of FGF18 expression in bone in vivo.

FGF23 functions as an endocrine hormone that interacts with FGF tyrosine kinase receptors and FGF alpha-Klotho coreceptor to regulate phosphate homeostasis and vitamin D metabolism (Quarles et al., 2012). Although FGF23 is expressed in many tissues (Yamashita et al., 2000), it is mainly secreted by differentiated osteoblasts and osteocytes (Liu et al., 2003, 2006; Yoshiko et al., 2007) and may locally control the differentiation of bone marrow stromal cells (Li et al., 2013). In addition to osteoblasts and osteocytes, mesenchymal tumors (Shimada et al., 2001) and osteogenic cells in fibrous dysplastic lesions (Riminucci et al., 2003) also increases FGF23 production. The regulation of FGF23 expression is quite complex. Studies have demonstrated that systemic factors including ions such as calcium, phosphate, and iron, as well as hormones such as PTH and 1,25-dihydroxyvitamin D, in combination with local factors such as FGFs, highly regulate bone FGF23 production, intracellular processing, and function (Quarles 2012; Larsson et al., 2003; Stubbs et al., 2012; Clinkenbeard and White., 2016). Reduced serum iron is associated with increased serum FGF23 in autosomal dominant hypophosphatemic rickets (ADHR) subjects (Imel et al., 2011), and C-terminal FGF23 is negatively correlated with ferritin (Durham et al., 2007; Clinkenbeard et al., 2014; Farrow et al., 2011). Iron chelation in vitro results in significantly increased Fgf23 mRNA via increased MAPK signaling (Farrow et al., 2011). The expression of FGF23 in osteoblasts and osteocytes is in part controlled by signaling from fibroblast growth factor receptor (FGFR) 1 (Martin et al., 2011). Conditional deletion of *Fgfr1* in osteocytes of Hyp mice, a mouse model of ADHR, reduced FGF23 production and partially rescued the abnormal phenotype in these mice (Xiao et al., 2014). Moreover, pharmacological FGFR inhibition ameliorates FGF23-mediated ADHR (Wohrle et al., 2013) whereas pharmacological activation of FGFR1 in osteoblasts leads to increased FGF23 secretion and hypophosphatemia in adult mice (Wu et al., 2013).

Novel studies have demonstrated FGF2 isoform−mediated regulation of FGF23 production in bone (Xiao et al., 2010a). The low-molecular-weight isoform of FGF2 (LMW 18kD) signals via cell-surface FGFRs, but high-molecular-weight isoforms (HMWFGF2) interact with intranuclear FGFR1 to activate integrative nuclear FGFR1 signaling

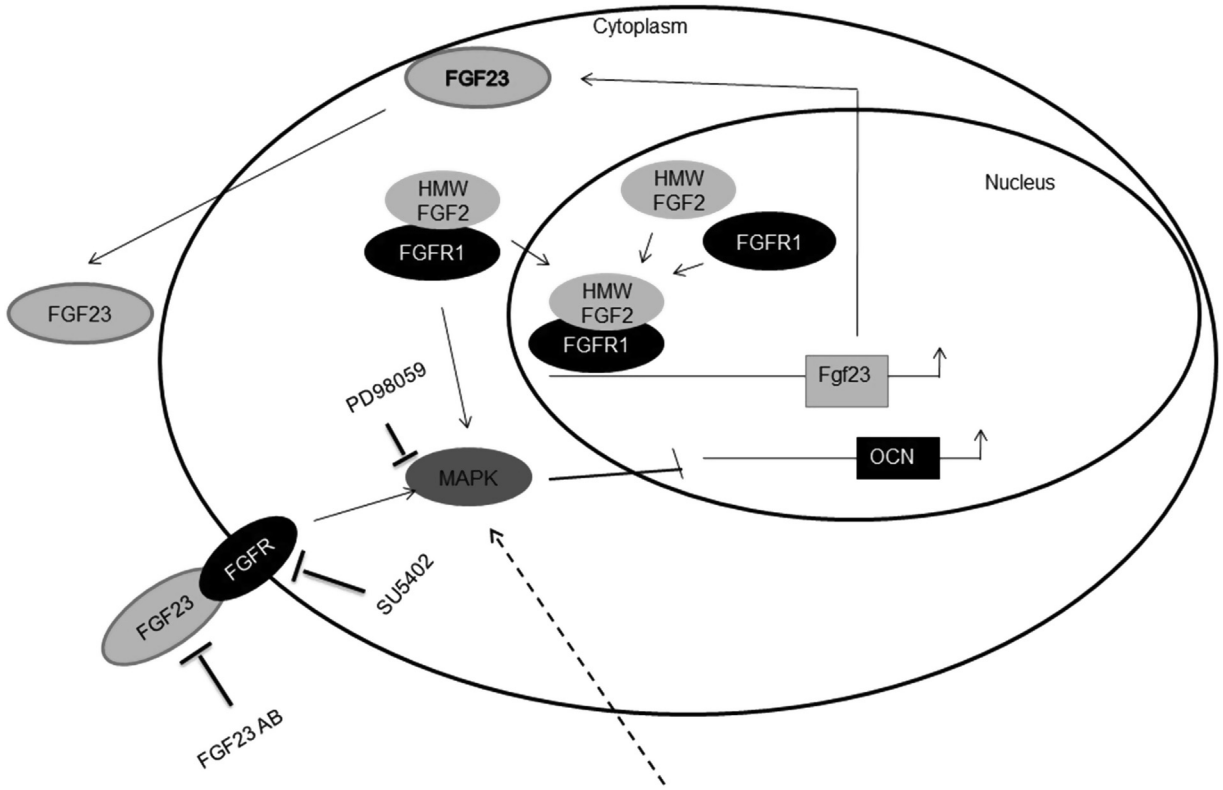

FIGURE 45.1 A schematic model depicting how high-molecular-weight (HMW) isoforms regulate bone formation. HMW isoforms, which have nuclear targeting sequences, translocate to the nucleus to upregulate FGF23 expression. FGF23 is secreted into the media and activates the tyrosine kinase domain of FGFR on the cell surface, triggering the downstream ERK signaling pathway. *Reprinted from Xiao L, Esliger A, Hurley MM., 2013. Nuclear fibroblast growth factor 2 (FGF2) isoforms inhibit bone marrow stromal cell mineralization through FGF23/FGFR/MAPK in vitro. J. Bone Miner. Res. 28, 35–45, with permission.*

(Clinkenbeard and White, 2016). Importantly, overexpression of nuclear HMWFGF2 in osteoblast lineage cells increased FGF23 production and induced an ADHR phenotype in mice (Xiao et al., 2010a). FGF23 production was increased by bone marrow stromal cell cultures from HMWFGF2 transgenic mice, and an intrinsic defect in mineralization was rescued by an FGF23-neutralizing antibody, an MAPK inhibitor, and an FGFR tyrosine kinase inhibitor (Xiao et al., 2013). In contrast, ablation of HMWFGF2 resulted in mice with high BMD versus wild-type littermates with increased osteoblastic activity (Homer-Bouthiette et al., 2014) associated with reduced *Fgf23* mRNA in the HMWFGF2-KO mice. These data suggest that HMWFGF2 isoforms may affect bone homeostasis through regulation of FGF23 production (Fig. 45.1). Conditional knockout of HMWFGF2 should clarify their role in FGF23 production and phosphate homeostasis.

Fibroblast growth factor receptor expression in bone

The FGF family comprises 18 secreted proteins that bind to 4 receptor tyrosine kinase FGFRs (Ornitz and Itoh, 2015). FGFRs 1, 2, and 3 undergo alternative splicing to produce variants that have distinct ligand-binding specificities and are differentially expressed. FGFRb splice variants bind FGF7 and FGF10 in mesenchymal tissues. FGFRc splice variants in mesenchymal tissues bind FGF ligands in epithelial and mesenchymal tissues. During skeletal development, *Fgfs* and *Fgfrs* are expressed in a time- and space-dependent manner in the condensing mesenchyme and intramembranous bone (Ornitz and Marie, 2002). In the distal limb bud mesenchyme, *Fgfr1* and *Fgfr2*, but not *Fgfr3* and *Fgfr4*, are expressed at the precondensation stage (Sheeba et al., 2010). At a later stage in the condensing mesenchyme, *Fgfr2* expression increases (Eswarakumar et al., 2002; Sheeba et al., 2010). Conditional inactivation of *Fgfr1* and *Fgfr2* in limb bud mesenchyme (using *Prx1-Cre)* or inactivation of *Fgfr1* in all mesenchyme (using *T(brachyury)-Cre)* causes severe skeletal hypoplasia (Verheyden et al., 2005; Yu and Ornitz, 2008), whereas inactivation of *Fgfr1* or *Fgfr2* in distal limb bud mesenchyme (using *AP2-Cre*) causes only a mild skeletal phenotype (Coumoul et al., 2005; Li et al., 2005), suggesting redundancy between FGFRs 1 and 2 in distal limb mesenchyme. During early stages of intramembranous bone formation, *Fgfs 2, 4, 9,*

and *18* and *Fgfrs 1, 2,* and *3* are coexpressed (Rice et al., 2000; Britto et al., 2001; Liu et al., 2002; Ohbayashi et al., 2002; Quarto et al., 2009; Marie et al., 2010). The FGFR2c splice variant expressed in early mesenchymal condensations and in sites of intramembranous ossification interacts with FGF18 (Eswarakumar et al., 2002). At later stages of cranial bone development, *Fgf18* is expressed in mesenchymal cells and differentiating osteoblasts (Ohbayashi et al., 2002; Reinhold and Naski, 2007), whereas *Fgf9* is expressed during mid to late stages of development in calvarial mesenchyme (Kim et al., 1998). Mice lacking both *Fgf9* and *Fgf18* have severely deficient cranial bone formation (Hung et al., 2016), as these FGFs interact with *Fgfr1* and *Fgfr2* expressed in preosteoblasts and osteoblasts in the developing membranous bone (Rice et al., 2003). *Fgfr1* and *Fgfr2* are also expressed in the periphery of mesenchyme condensations that will form the perichondrium and periosteum (Eswarakumar et al., 2002). At later stages in the perichondrium and trabecular bone, FGFR1 is expressed in mesenchymal progenitors, and FGFR2 in differentiating osteoblasts (Ohbayashi et al., 2002; Jacob et al., 2006; Coutu et al., 2011). *Fgfr3* expression occurs when condensed mesenchyme differentiates into chondrocytes, while *Fgfr2* expression decreases (Purcell et al., 2009). *Fgfr3* expression decreases when central chondrocytes begin to hypertrophy, while *Fgfr1* expression is increased (Jacob et al., 2006; Karolak et al., 2015). Thereafter, FGFR1 and FGFR3 are both expressed in mouse and human articular chondrocytes (Yan et al., 2011; Weng et al., 2012).

Fibroblast growth factor and FGF receptor signaling

Binding of FGF ligands to FGFRs induces dimerization and juxtaposition of the tyrosine kinase domains, leading to transphosphorylation of six tyrosine residues (Furdui et al., 2006; Goetz and Mohammadi, 2013), followed by phosphorylation of FGFR substrate 2α (FRS2α), a docked adaptor protein, and binding of other adaptor proteins including phospholipase Cγ (PLCγ) and signal transducer and activator of transcriptions (STATs) 1, 3, and 5 (Ornitz and Itoh, 2015). The phosphorylation of FRS2α leads to the recruitment of another adaptor protein, GRB2, which activates MAPKs through SOS and the PI3K−AKT pathway through GAB1 (Kouhara et al., 1997; Lamothe et al., 2004). FGF binding to FGFR1/2 can activate several MAP kinases including ERK1/2, JNK, and p38 (Tsang and Dawid, 2004; House et al., 2005; Liao et al., 2007; Kanazawa et al., 2010). FGFR intracellular signaling is downregulated by GRB2, which blocks PLCγ binding to FGFRs, and Sprouty (Spry), which interacts with GRB2 to block MAPK and PI3K signaling (Hanafusa et al., 2002; Timsah et al., 2014). Downstream of these events, SEF (similar expression to FGF) antagonizes the MAPK pathway by interacting with MEK (Torii et al., 2004) and DUSP6 (dual-specificity phosphatase 6), which reduces MAPK signaling through ERK1/2 dephosphorylation (Camps et al., 1998). Furthermore, GRB14, an adaptor protein, binds to FGFR phosphotyrosine 766 and interferes with phosphorylation and activation of PLCγ (Browaeys-Poly et al., 2010). Extracellularly, the biological activity of FGFs is tightly regulated by sulfated polysaccharides (Shimokawa et al., 2011; Ornitz and Itoh, 2015). Notably, heparan sulfate proteoglycans (HSPGs) such as syndecans bind to diffusible FGFs and thereby control the affinity of FGF to FGFR and receptor activation (Belov and Mohammadi, 2013; Xu and Esko, 2014; Ornitz and Itoh, 2015).

Fibroblast growth factor and FGF receptor signaling in chondrogenesis

Initiation of chondrogenesis

The differentiation of cells in the mesenchymal condensation to chondrocytes is regulated in part by FGF signaling (Kumar and Lassar, 2014; Mariani et al., 2008; Murakami et al., 2000; Ten Berge et al., 2008; Yu and Ornitz, 2008). In cooperation with Wnt signals, FGF signaling maintains mesenchymal progenitor cells in an undifferentiated and proliferative state, in part through the inhibition of Sox9 expression (Ten Berge et al., 2008). In the absence of Wnt signaling, FGF signaling increases Sox9 expression in mesenchymal progenitor cells and chondrocytes (Kumar and Lassar, 2014; Murakami et al., 2000; Shung et al., 2012; Ten Berge et al., 2008). Once cells are committed to the chondrogenic lineage, Sox9 directly increases expression of the *Fgfr3* gene, and FGFR3 signaling promotes Sox9 expression, forming a potential feed-forward loop (Murakami et al., 2000; Oh et al., 2014). These cells downregulate expression of FGFR2; however, the mechanisms regulating this are not known. This is consistent with the lack of an effect of FGFR2 on growth plate function and chondrocyte proliferation (Yu et al., 2003). In the definitive growth plate, *Fgfr3* is maintained at high levels in PC- and prehypertrophic chondrocytes (PHCs)-zone chondrocytes, and *Fgfr1* is expressed in HCs (Delezoide et al., 1998; Eswarakumar et al., 2002; Hamada et al., 1999; Jacob et al., 2006; Karolak et al., 2015; Karuppaiah et al., 2016; Lazarus et al., 2007; Ornitz and Marie, 2002; Peters et al., 1993; Yu et al., 2003). FGFR3 is a key regulator of chondrogenesis. In early embryonic stages of skeletal development during establishment of the growth plate, FGFR3 promotes chondrocyte proliferation and is most likely activated by FGF9 and FGF18 signals that arise from adjacent mesenchyme in the

perichondrium (Havens et al., 2008; Hung et al., 2007; Iwata et al. 2000, 2001; Liu et al. 2002, 2007; Ohbayashi et al., 2002). However, in the mature growth plate (after formation of the secondary ossification center), FGFR3 signaling potently inhibits chondrogenesis, primarily acting on PCs and their differentiation into PHCs and HCs (Colvin et al., 1996; Deng et al., 1996). The mechanisms that regulate this change in the response of chondrocytes to FGFR3 during development are not known. Recent data indicate that FGF signaling regulates autophagy during bone growth (Cinque et al., 2015). Postnatal induction of chondrocyte autophagy is mediated by FGF18 through FGFR4 and is suppressed in growth plates from *Fgf18−/−* embryos, indicating that FGF signaling acts as a crucial regulator of autophagy in chondrocytes.

Regulation of fibroblast growth factor receptor 3 expression

Several signaling pathways regulate growth plate chondrocytes, in part through the regulation of FGFR3 expression. Thyroid hormone inhibits chondrocyte proliferation and promotes chondrocyte hypertrophy, similar to signaling through FGFR3. In cultured chondrocytes, thyroid hormone increased *Fgfr3* expression, and mice lacking thyroid hormone receptor have low levels of *Fgfr3* in growth plate chondrocytes (Barnard et al., 2005). Signaling through the PTH receptor PTH1R directly suppressed *Fgfr3* expression through a cAMP- and PKA-dependent regulatory element in the *Fgfr3* promoter (McEwen et al., 1999). Treatment of mice with PTH suppressed *Fgfr3* expression and partially rescued dwarfism phenotypes in a mouse model for thanatophoric dysplasia, where *Fgfr3* has an activating mutation, and in other mouse models in which *Fgfr3* is overexpressed (Karuppaiah et al., 2016; Xie et al., 2012). Interestingly, in bladder cancer cells, *Fgfr3* expression was induced by hypoxia in an HIF-1α−dependent manner (Blick et al., 2013). Because growth plate chondrocytes are avascular and functionally hypoxic, it will be interesting to determine whether *Fgfr3* expression in chondrocytes is also regulated by hypoxia.

Fibroblast growth factor receptor 3 signaling in growth plate chondrocytes

In the mature growth plate, FGFR3 suppresses chondrocyte proliferation and differentiation through the activation of several downstream signaling pathways (Fig. 45.2). These include activation of STAT1, ERK1/2, and p38, decreased AKT phosphorylation, increased protein phosphatase 2a (PP2a), dephosphorylation (activation) of p107 and p130, and increased expression of the cell cycle inhibitor $p21^{Waf1/Cip1}$ (Aikawa et al., 2001; Chapman et al., 2017; Cobrinik et al., 1996; Dailey

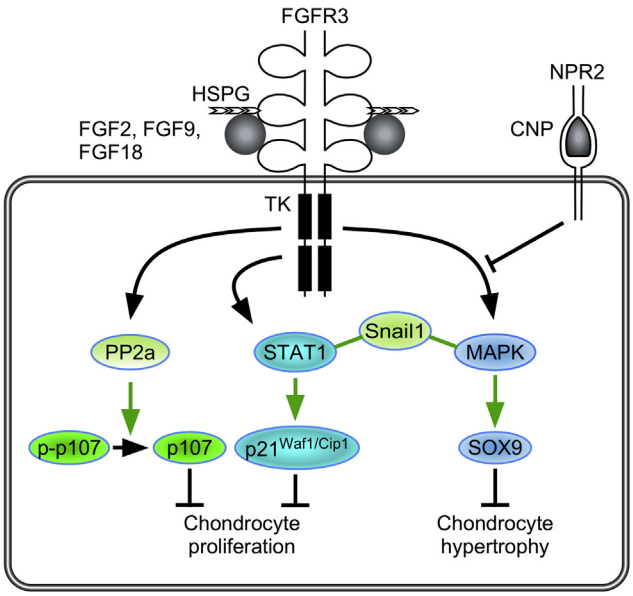

FIGURE 45.2 FGF/FGFR signaling in growth plate chondrocytes. FGF9 and FGF18 bind to heparan sulfate proteoglycans (HSPGs) and FGFR3 to activate the FGFR3 tyrosine kinase (TK) domain. This leads to activation of downstream signals, PP2a and STAT1, activating p107 and $p21^{Waf1/Cip1}$, respectively, which function to suppress chondrocyte proliferation. Activation of the MAPKs, ERK1 and ERK2, regulate Sox9 expression, which functions to suppress chondrocyte terminal differentiation and endochondral ossification. C-natriuretic peptide (CNP) signals through natriuretic peptide receptor 2 (NPR2) and inhibits the MAPK signaling pathway downstream of FGFR3, resulting in increased chondrocyte hypertrophy and increased longitudinal bone growth.

et al., 2003; de Frutos et al., 2007; Kolupaeva et al. 2008, 2013; Kurimchak et al., 2013; Laplantine et al., 2002; Legeai-Mallet et al., 2004; Priore et al., 2006; Raucci et al., 2004; Su et al., 1997). In a recent phosphoproteomic analysis of FGF signaling in chondrocytes, FGF activation of GSK3β (and degradation of β-catenin) was necessary for the inhibition of chondrocyte proliferation, identifying a potential role for Wnt/β-catenin signaling in regulating chondrogenesis (Chapman et al., 2017).

Regulation of chondrogenesis by FGFR3 may involve *Snail1,* a transcriptional repressor that is expressed in PHCs and induced in thanatophoric dysplasia bone tissue and mouse models that activate FGFR3 (see later) (de Frutos et al., 2007; Karuppaiah et al., 2016; Seki et al., 2003). At late embryonic stages, ectopic activation of SNAIL1 resulted in an achondroplasia-like phenotype in mice, with decreased chondrocyte proliferation and decreased longitudinal bone growth (de Frutos et al., 2007). This phenotype required activation of STAT1 (which increases $p21^{Waf1/Cip1}$ expression) and MAPK downstream of FGFR3 (de Frutos et al., 2007). Interestingly, conditional inactivation of both *Snail1* and *Snail2* in limb bud mesenchyme also resulted in increased $p21^{Waf1/Cip1}$ and decreased chondrocyte proliferation in embryonic bone (Chen and Gridley, 2013). Mechanistically, SNAIL1 may regulate the nuclear localization of p-ERK, and ERK2 activation directly phosphorylates SNAIL1, leading to nuclear accumulation and increased protein stability (Smith et al., 2014; Zhang et al., 2013). In cancer cells, GSK3β binds and phosphorylates Snail, leading to its degradation (Zhou et al., 2004). Future studies will be required to determine the relationship between FGFR3, GSK3β, and Snail in chondrocytes.

Requirements for STAT1 regulation of chondrocyte proliferation comes from in vivo experiments in which inactivation of *Stat1* partially rescues chondrocyte proliferation in mice with activating mutations in FGFR3 (Murakami et al., 2004). However, inactivation of *Stat1* did not rescue the defect in chondrocyte hypertrophy in these mice, which is under the control of MAPK signaling (Murakami et al., 2004). Mechanistically, activated FGFR3 signaling and increased p-ERK may stabilize SOX9 in PHCs and suppress hypertrophic differentiation (Murakami et al., 2000; Shung et al., 2012; Zhou et al., 2015).

Further support for a role for STAT1 suppression of chondrocyte proliferation, and MAPK regulation of chondrocyte differentiation, comes from interactions between FGFR3 and the c-natriuretic peptide (CNP) signaling pathways. The CNP signaling pathway increases bone growth through increased extracellular matrix production as well as hypertrophic differentiation in chondrocytes through the inhibition of MAPK signaling (Yasoda et al., 2004) (Fig. 45.2). The CNP signaling pathway did not affect STAT1 activity or chondrocyte proliferation (Yasoda et al., 2004). CNP analogues are currently in clinical trials for achondroplasia (Legeai-Mallet, 2016; Lorget et al., 2012; Ornitz and Legeai-Mallet, 2017).

FGFR3 also regulates chondrogenesis through interactions with BMP, Wnt, IHH, and PTHLH/PTH1R signaling pathways. In chondrocyte cultures, FGF signaling activates Wnt/β-catenin signaling through phosphorylation of LRP6 and suppression of hypertrophic differentiation (Buchtova et al., 2015; Krejci et al., 2012). FGFR3 signaling suppresses the expression of *Bmp4, BMPR1a, Ihh*, and *Pth1r* in the postnatal growth plate (Chen et al., 2001; Naski et al., 1998; Qi et al., 2014). Additionally, in a chondrocyte cell line, overexpression of FGFR3 suppresses the expression of both *Pthlh* and its receptor, *Pth1r* (Li et al., 2010).

Fibroblast growth factor receptor 1 signaling in hypertrophic chondrocytes

Fgfr1 is expressed in PHCs, HCs, and surrounding perichondrial and periosteal tissue. Although FGFR1 signaling appears to have only small effects on chondrogenesis, it has been difficult to distinguish direct effects on HCs from indirect effects resulting from gene inactivation in surrounding tissue. Inactivation of *Fgfr1* in limb bud mesenchyme using *Dermo1(Twist2)-Cre* impairs chondrocyte hypertrophy (Hung et al., 2007). In contrast, inactivation of *Fgfr1* at later stages of development with *Col2a1-Cre* or *Osx-Cre* results in an expanded HC zone (Jacob et al., 2006; Karuppaiah et al., 2016). Both *Dermo1-Cre* and *Col2a1-Cre* efficiently target chondrocytes, but they also target the osteoblast lineage (Ford-Hutchinson et al., 2007; Jacob et al., 2006; Ono et al., 2014; Wang et al., 2011; Yu et al., 2003). In contrast, Osx-Cre is more specific for osteoblasts (Karuppaiah et al., 2016). These studies suggest that FGFR1 signaling in osteoblast development could indirectly affect chondrogenesis (Jacob et al., 2006; Karolak et al., 2015; Karuppaiah et al., 2016). A definitive assessment of FGFR1 function in HCs will require more precise gene targeting.

Fibroblast growth factor receptors and chondrodysplasia syndromes

Genetic mapping studies identified a missense mutation in *Fgfr3* that accounts for almost all cases of achondroplasia, the most common form of dwarfism in humans (Shiang et al., 1994; Shiang et al., 1994). Subsequent to this initial discovery, additional mutations have been identified in FGFRs 1, 2, and 3 that cause skeletal dwarfism, craniosynostosis, and skeletal overgrowth. The clinical and genetic features of these diseases have been extensively reviewed (Vajo et al., 2000; Ornitz

and Marie, 2002; Chen and Deng, 2005; Ornitz, 2005; Melville et al., 2010; Johnson and Wilkie, 2011; Foldynova-Trantirkova et al., 2012; Krejci, 2014; Xie et al., 2014; Yeung Tsang et al., 2014; Narayana and Horton, 2015; Ornitz and Itoh, 2015; Ornitz and Legeai-Mallet, 2017; Pauli, 2019; Rosello-Diez and Joyner, 2015).

Mutations in fibroblast growth factor receptor 3 and fibroblast growth factor 9

The *FGFR3* G380R autosomal dominant missense mutation accounts for over 97% of cases of achondroplasia (Rousseau et al., 1994; Shiang et al., 1994; Vajo et al., 2000; Wilkin et al., 1998). Related autosomal dominant chondrodysplasia syndromes include thanatophoric dysplasia types I and II, which are caused by mutations in K650E or R248C mutations in *FGFR,* and hypochondroplasia, which is caused by an N540K or K650N mutation in *FGFR3* (Bellus et al. 1995, 2000; Bonaventure et al., 1996; Tavormina et al., 1995). SADDAN syndrome (severe achondroplasia with developmental delay and acanthosis nigricans) (Bellus et al., 1999; Tavormina et al., 1999) and platyspondylic lethal skeletal dysplasia, San Diego type (Brodie et al., 1999), are both caused by a K650M mutation in *FGFR3*. These mutations in FGFR3 cause disproportional (rhizomelic) short stature.

Mutations in FGFR3 associated with dwarfism activate the receptor in proportion to disease severity (Krejci et al., 2008; Naski et al., 1996). Hypochondroplasia is associated with a weak gain-of-function mutation, whereas achondroplasia and thanatophoric dysplasia result from progressively stronger activating mutations. Activation of FGFR3 in growth plate chondrocytes results in decreased chondrocyte proliferation, impaired hypertrophic differentiation, and increased apoptosis (Legeai-Mallet et al. 1998, 2004; Naski et al., 1998; Wang et al. 1999, 2001; Krejci et al., 2008; Pannier et al., 2009; Xie et al., 2014; Yeung Tsang et al., 2014; Narayana and Horton, 2015; Rosello-Diez and Joyner, 2015; Ornitz and Legeai-Mallet, 2017). A dominant mutation (M528I) in *FGFR3* had been identified that causes proportionate short stature (Kant et al., 2015). Functional studies suggest that this mutation also activates FGFR3 signaling; however, the mechanisms that determine proportionate versus rhizomelic limb shortening are not known.

Mutations in *FGF9* have also been identified in mice and humans and are generally associated with defects in joint development. Elbow knee synostosis in mice is caused by an N143T mutation in *Fgf9,* and multiple synostosis syndrome is cause by *S99N, S99D*, or *R62G* mutations in *FGF9* in humans (Harada et al., 2009; Wu et al., 2009; Rodriguez-Zabala et al., 2017; Tang et al., 2017). Mechanistically, *Fgf9* N143T and R62G mutations reduce homodimerization and the affinity of FGF9 for heparin and FGFR3, and increase FGF9 diffusion through developing joint tissue (Harada et al., 2009; Rodriguez-Zabala et al., 2017). In contrast, the *S99N* mutation increases the affinity of FGF9 for heparin and decreases its affinity for FGFR3c (Tang et al., 2017).

Skeletal overgrowth and CATSHL syndrome

Inactivation of FGFR3 in mice results in skeletal overgrowth (Colvin et al., 1996; Deng et al., 1996; Eswarakumar and Schlessinger, 2007). In mice lacking *Fgfr3*, bones of the appendicular and axial skeleton were disproportionally long, resulting in an abnormal gait and scoliosis. *Mi*ce lacking *Fgfr3* also have defects in inner ear development that result in deafness (Colvin et al., 1996). These phenotypes suggested that loss-of-function mutations in *FGFR3* in humans could also result in skeletal overgrowth and hearing loss and lead to the identification of humans with dominantly inherited camptodactyly, tall stature, and hearing loss (CATSHL) with missense mutations (R621H, T546K) in *FGFR3* (Toydemir et al., 2006; Makrythanasis et al., 2014; Escobar et al., 2016). A recessive mutation in FGFR3 (V700E) in sheep results in spider lamb syndrome, with phenotypes similar to those of CATSHL patients (Beever et al., 2006; Smith et al., 2006).

Fibroblast growth factor and FGF receptor signaling in bone formation and repair

Fibroblast growth factor and FGF receptor signaling in osteoblasts

The signaling mechanisms induced by FGF/FGFR in osteogenic cells are complex (Marie, 2003, 2012). After FGFR activation by FGF ligands, several signaling pathways are activated depending on the stage of osteogenic cell differentiation (Dailey et al., 2005; Marie et al., 2005), resulting in a fine modulation of osteogenic cell proliferation and differentiation (Fig. 45.3). At an early stage, activation of FGFR1/FGFR2 by FGF2 in osteoblast precursors leads to increased ERK1/2 MAPK, causing increased cell proliferation (Xiao et al., 2002; Kim et al., 2003; Shimoaka et al., 2002; Choi et al., 2008; Miraoui et al., 2009). FGF2 or FGR2 activation may also activate PKC signaling in osteogenic cells, which is involved in growth response (Hurley et al., 1996), increased fibronectin expression (Hurley et al., 1996; Tang et al., 2007), and differentiation marker expression in osteoblasts (Debiais et al., 2001, Lemonnier et al., 2001a)(. At later stages,

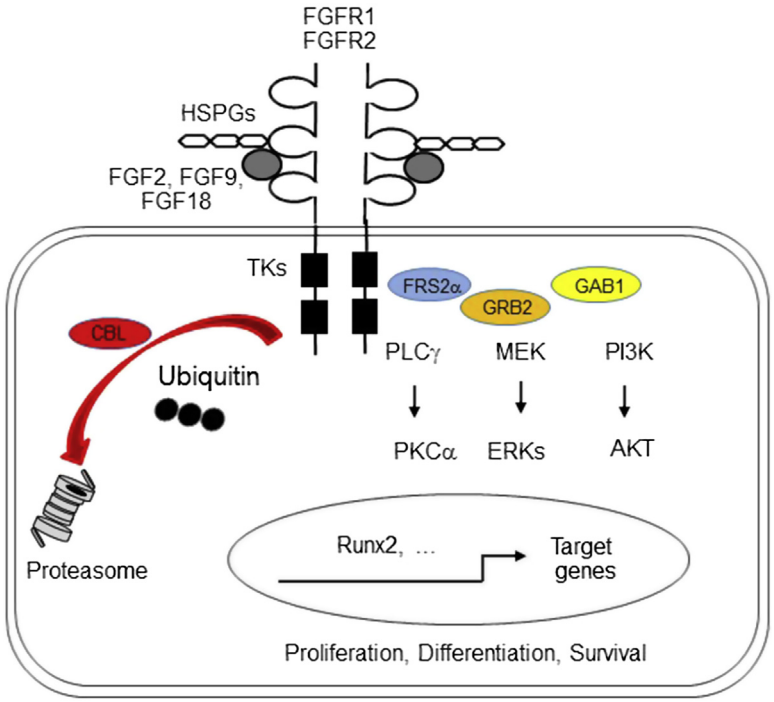

FIGURE 45.3 FGF/FGFR signaling in osteogenic cells. FGF2, FGF9, and FGF18 bind to heparan sulfate proteoglycans (HSPGs) and FGFR1 or FGFR2 to activate tyrosine kinases (TKs). This leads to the recruitment of substrates and activation of various kinases, such as PLCγ, PKCα, ERK MAPKs, and PI3K/AKT, which results in the expression of transcription factors controlling cell proliferation, differentiation, or survival. FGFR activation also leads to c-CBL recruitment, resulting in FGFR ubiquitination and downregulation by proteasome degradation.

ERK1/2 activation by FGF2 induces RUNX2 acetylation and stabilization (Xiao et al., 2002; Park et al., 2010; Yoon et al., 2014). FGFR1/FGFR2 activation by FGF18 also leads to ERK1/2-mediated increased *Runx2* expression in osteoblast precursor cells, resulting in osteoblast differentiation (Hamidouche et al., 2010). *Runx*2 expression is also increased by PKC activation induced by FGF/FGFR (Kim et al., 2003; Niger et al., 2013). In cells of the perichondrium, a positive loop involves RUNX2-mediated increased expression of *Fgfr2*, *Fgf18*, and proteoglycans, which in turn control FGF signaling (Hinoi et al., 2006; Reinhold and Naski, 2007; Teplyuk et al., 2009). At a later stage of differentiation, FGF2-mediated ERK1/2 activation in an osteocyte cell line increases the expression of *Dmp1*, a marker of osteocytes, indicating that FGF/ERK/1/2 signaling also regulates osteocyte differentiation (Kyono et al., 2012).

Several positive interactions between FGF signaling and other pathways have been described. FGF1 and FGF2 increase the production of TGF-β in vitro and in vivo (Noda and Vogel, 1989), and TGF-β and FGF1 or FGF2 interact to modulate their mitogenic effects (Globus et al., 1989). In human calvaria osteoblasts, FGF2 decreases TGF-β2 production in immature cells but increases TGF-β2 synthesis by more differentiated cells (Debiais et al., 1998). In addition, FGF2 increases vascular endothelial cell growth factor (VEGF) (Saadeh et al., 2000) and hepatocyte growth factor expression in cultured osteoblasts (Takai et al., 2007; Blanquaert et al., 1999). FGF18 also promotes VEGF expression and subsequent neovascularization (Liu et al., 2007) that may mediate part of the effects of FGF on osteogenesis. On the other hand, FGF2 enhances canonical BMP2 signaling in osteoblastic cells by promoting phospho-SMAD1/5/8 and RUNX2 transactivation (Agas et al., 2013). Functionally, FGF2 isoforms directly modulate BMP2 function (Sabbieti et al., 2013), whereas FGF2, FGF9, and FGF18 positively control BMP function through inhibition of the BMP antagonist noggin (Warren et al., 2003; Reinhold et al., 2004; Fakhry et al., 2005). In vivo, FGF2 stimulates *Bmp2* expression in osteoblasts during cranial bone ossification (Choi et al., 2005; Fakhry et al., 2005), and BMP2 expression is reduced in bones of *Fgf2*-null mice (Naganawa et al., 2008), further indicating that FGF and BMP signaling cooperates to modulate osteogenesis (Nakamura et al., 2005; Kuhn et al., 2013).

FGF signaling interacts negatively or positively with Wnt/β-catenin signaling, depending on the stage of cell differentiation (Dailey et al., 2005; Miraoui and Marie, 2010). In early osteoprogenitors, FGF2 antagonizes WNT/β-catenin signaling (Mansukhani et al., 2005; Ambrosetti et al., 2008). However, *Fgf2−/−* mice show decreased Wnt genes expression in osteoblasts, and FGF2 promoted canonical Wnt/β-catenin signaling and rescued osteoblast differentiation in

Fgf2−/− mice, indicating that FGF signaling positively cooperates with Wnt/β-catenin signaling to promote osteoblast differentiation in vivo (Fei et al., 2011). Conversely, FGF18 is positively regulated by canonical Wnt signaling in osteogenic cells (Kapadia et al., 2005; Reinhold and Naski, 2007). PTH also cooperates with FGF signaling by increasing *Fgf2*, *Fgfr1*, and *Fgfr2* expression in osteoblastic cells (Hurley et al., 1999). In vitro, FGF2 is required for the positive PTH effects on osteoblast proliferation and differentiation. In vivo, the anabolic effect of intermittent PTH is impaired in *Fgf2*-null and heterozygous mice (Hurley et al., 1999), indicating that FGF signaling is part of the anabolic PTH effect on osteogenesis (Sabbieti et al., 2009).

After activation, FGFR signaling is downregulated by several negative feedback mechanisms. Spry2 acts as a negative regulator of FGFR signaling. Consistently, a dominant-negative mutant of Spry2 (Y55A-Spry2) promotes FGF2-induced ERK activation in murine osteoblastic cells, resulting in increased *Runx2* expression and osteoblastogenesis (Sanui et al., 2015). In addition, activated FGFR interacts with the ubiquitin ligase c-CBL, leading to FGFR ubiquitination and its subsequent degradation by the proteasome (Lemmon and Schlessinger, 2010; Sévère et al., 2013). In osteoblasts, FGFR2 ubiquitination by c-CBL leads to FGFR2 downregulation and results in decreased osteogenic differentiation (Kaabeche, 2004). Consistently, inhibition of c-CBL interaction with FGFR2 promotes osteoblast differentiation and survival through increased ERK1/2 and PI3K signaling (Sévère et al., 2011). FGFR2 activation also leads to increased c-CBL interaction with PI3K in osteoblasts, leading to PI3K ubiquitination and degradation and decreased osteoblast survival (Dufour et al., 2008). Overall, these data illustrate the complexity of the regulation of FGF/FGFR signaling in positively or negatively controlling osteogenic cells (Fig. 45.3).

Fibroblast growth factor regulation of bone formation

The regulation of bone formation by FGF/FGFR signaling depends on the stage of osteoblast lineage differentiation, FGF/FGFR expression, and low-affinity coreceptors in the bone microenvironment. In osteoprogenitor cells, FGFR1/2 inhibit cell senescence and thereby maintain mesenchymal cell stemness (Coutu et al., 2011; Di Maggio et al., 2012). In immature osteoblasts, FGF2 signaling increases cell proliferation (Debiais et al., 1998; Shimoaka et al., 2002; Ignelzi et al., 2003; Fakhry et al., 2005), although the mitogenic effect of FGF2 on rat calvaria cells decreases with age (Tanaka et al., 1999). FGF18 also stimulates the proliferation of cultured osteoblasts through activation of ERK signaling (Shimoaka et al., 2002). These effects lead to expand the pool of osteoblast precursor cells (Fakhry et al., 2005), and consistently blocking FGF2 biological activity reduces osteogenesis in vivo (Moore et al., 2002). In cultured osteoblastic cells, FGF2 inhibits collagen synthesis transcriptionally (Hurley et al., 1994) but stimulates fibronectin expression through PLCγ, PKCα, c-Src, NF-κB, and p300 pathways (Tang et al., 2007), as well as affecting osteocalcin transcription in mouse calvaria cells (Boudreaux et al., 1996; Newberry et al., 1996). The effect of FGF/FGFR signaling on osteoblast apoptosis also depends on the stage of cell maturation. In osteoblast precursor cells, FGF2 reduces apoptosis through activated PI3K/AKT signaling (Debiais et al., 1998), and FGFR1 increases the Bcl2/Bax ratio (Agas et al., 2008), which contributes to enhance the pool of osteoprogenitors. In more mature osteoblasts, FGF treatment or overexpression of FGF2 in transgenic mice induces osteoblast apoptosis (Mansukhani et al., 2000; Ignelzi et al., 2003), which contributes to reduce the pool of more mature cells. The control of osteogenesis by FGF/FGFR signaling also depends on the type and level of FGFs expressed. Mice lacking *Fgf2* show decreased bone formation due to altered osteoblast differentiation (Montero et al., 2000; Xiao et al., 2010b). *Fgf18*-deficient mice display reduced osteogenic mesenchymal cell proliferation, decreased osteoblast differentiation, and delayed ossification (Liu et al., 2002; Ohbayashi et al., 2002). Consistently, FGF18 is an autocrine-positive regulator of osteogenic differentiation (Jeon et al., 2012) through FGFR1/FGFR2-mediated activation of ERK1/2 and PI3K signaling (Hamidouche et al., 2010).

In addition to FGFs, FGFR expression controls osteoblastogenesis in a complex manner. Elevated *Fgfr1/Fgfr2* expression is associated with a high FGF2-mediated proliferative response (Cowan et al., 2003; Haupt et al., 2009). In contrast, decreased expression of *Fgfr1* and increased expression of *Fgfrs 2, 3,* and *4* in more mature osteoblasts is associated with reduced FGF2 responsiveness (Haupt et al., 2009). Inactivation of *Fgfr1* in differentiated osteoblasts accelerates differentiation, possibly through increased expression of FGFR3 (Jacob et al., 2006). In older mice inactivation of Fgfr1 results in increased bone formation and osteocyte death (McKenzie et al., 2019). In mice conditionally lacking *Fgfr2* or harboring a mutation in *Fgfr2c*, *Runx2* expression and bone mineral density are decreased due to defective proliferation of osteoprogenitor cells and function of mature osteoblasts, suggesting that *Fgfr2* positively regulates osteoblast maturation (Eswarakumar et al., 2002; Yu et al., 2003). Consistently, constitutive *Fgfr2* activation enhances ERK1/2 and PKCα signaling and *Runx2* expression, resulting in increased osteoblast differentiation (Miraoui et al. 2009, 2010b). FGFR3 may also play a role in postnatal bone formation, since young adult *Fgfr3*-null mice show decreased osteoblast maturation and trabecular bone mineralization (Valverde-Franco et al., 2004).

The effects of FGF/FGFR on osteogenesis are also tightly controlled by the local expression of HSPGs (Eswarakumar et al., 2005; Ornitz and Itoh, 2015). This includes both cell surface and secreted HSPGs, such as syndecans, which serve as coreceptors for FGFs and can promote FGF/FGFR signaling in osteogenic cells (Jackson et al., 2007). During development, syndecan-1 is expressed in limb bud and affects bone cell differentiation (Dhodapkar et al., 1998). Syndecan-2 is expressed in the perichondrium and periosteum at the onset of osteogenesis (Molténi et al., 1999a), whereas syndecan-3 is expressed in mesenchymal cells during limb bud formation (Gould et al., 1992). Syndecan-4 is expressed in calvaria osteoblasts (Molténi et al., 1999a) and is upregulated by FGF2 (Song et al., 2007). Rat calvaria osteoblasts coexpress syndecans 1, 2, and 4 with FGFR1 and FGFR2, indicating that syndecans locally interact at the cell surface with FGFRs to control FGF actions during osteogenesis (Molténi et al., 1999a, 1999b; Jackson et al., 2007). Notably, syndecan-2, whose expression increases during osteoblast differentiation, enhances the osteoblast response to FGF2 during in vitro osteogenesis (Molténi et al., 1999a; Mansouri et al., 2015). The expression of both FGFRs and syndecans is positively controlled by *Runx2* in osteoblasts, suggesting a positive mechanism controlling osteoblastogenesis (Fromigué et al., 2004; Teplyuk et al., 2009). Another HSPG, glypican-3, is essential for *Runx2* expression and osteoblast differentiation in vitro (Haupt et al., 2009).

Fibroblast growth factor and FGF receptor signaling in bone repair

FGF/FGFR signaling plays important roles during fracture repair (Marie, 2000; Du et al., 2012; Fei et al., 2013; Charoenlaro et al., 2017). During fracture repair in mice, *Fgfs 2, 5, 6,* and *9*, as well as *Fgfrs,* are upregulated distinctly depending on the stage of healing (Schmid and Ornitz, 2009). There is evidence that the exogenous application of FGFs can accelerate bone healing (Charoenlarp et al., 2017). In various models of bone defects, the local delivery of FGF2 or LMWFGF2 can promote bone healing (Kodama et al., 2009; Kawaguchi et al., 2010; Kwan et al., 2011; Hurley et al., 2016), although the effects depend on the dose and duration of treatment (Du et al., 2012; Fei et al., 2013; Charoenlarp et al., 2017). The positive effect on bone healing by FGF2 results in part from expansion of the osteoblast precursor cell pool which subsequently differentiates into osteoblasts (Nakamura et al., 1998; Nakajima et al., 2007). In addition, FGF2 and FGF9 can promote bone repair through activation of angiogenesis via increased *Vegf* expression by osteoblasts (Takai et al., 2007; Behr et al., 2010). Mice overexpressing the LMW isoform of FGF2 in mature osteoblasts show accelerated fracture healing associated with increased expression of factors involved in osteoblast differentiation and vascular invasion (Hurley et al., 2016). A functional link between FGF9 and VEGF is provided by the finding that $Fgf9^{-/+}$ mice show delayed cortical bone repair, reduced *Vegf* expression, and impaired neovascularization associated with decreased osteoblast proliferation and differentiation, a phenotype which can be rescued by exogenous FGF9 (Behr et al., 2010). VEGF by itself can promote bone healing by enhancing mesenchymal stem cell differentiation into osteoblasts (Liu and Olsen, 2014), and consistently, both angiogenesis and osteogenesis are promoted by VEGF alone (Behr et al., 2012). Although $Fgf18^{-/+}$ mice show reduced cortical bone healing, this is due only to decreased osteoblast differentiation, indicating that FGF18 is not required for angiogenesis during bone repair (Behr et al., 2011). When injected locally, FGF18 increased peri-implant bone formation in $Fgfr3^{+/+}$ and $Fgfr3^{-/-}$ mice, indicating that FGF18 promotes bone repair through activation of FGFR1 and/or FGFR2 (Carli et al., 2012). The cross talk between osteoblasts and endothelial cells during bone fracture repair is in part mediated by DJ-1, which stimulates human mesenchymal cell differentiation to osteoblasts and induces angiogenesis through FGFR1 activation, resulting in enhanced bone regeneration (Kim et al., 2012). Overall, current data indicate that FGF/FGFR signaling plays an important role in bone repair through activation of angiogenesis and osteogenesis, which may have therapeutic implications for promoting bone regeneration.

Fibroblast growth factor and FGF receptor signaling in bone resorption

Several studies have demonstrated a role for FGFR/FGF ligand signaling in the regulation of osteoclast production and bone resorption. Of the four FGF tyrosine kinase receptors, only *Fgfr1* was produced by osteoclasts (Chikazu et al., 2000). FGFR1 was shown to regulate the differentiation and activation of osteoclasts via the ERK1/2 pathway. In addition, conditional deletion of *Fgfr1* in osteoclasts leads to reduced osteoclast formation and activity (Lu et al., 2009). Further analysis showed that osteoclasts with *Fgfr1* deficiency exhibited downregulated expression of genes related to osteoclastic activity including tartrate-resistant acid phosphatase (TRAP) and matrix metalloproteinase-9. The phosphorylation of ERK1/2 MAP kinase was also decreased. These results suggest that FGFR1 is indispensable for complete differentiation and activation of osteoclasts in mice (Lu et al., 2009).

Among FGF ligands, FGF2 has previously been shown to induce osteoclast formation in murine bone marrow cultures (Hurley et al., 1998) and to stimulate resorption of mature osteoclasts through activation of ERK1/2 MAP kinase

(Chikazu et al., 2000). The importance of endogenous FGF2 in osteoclast formation and bone resorption is demonstrated by reduced osteoclast formation in *Fgf2* KO mice and impaired osteoclast formation in response to PTH, interleukin 11, and receptor activator of NF−B ligand (RANKL) (Okada et al., 2003). Modulation of suppressors of cytokine signaling (SOCS) may also be important in FGF2 regulation of RANKL. Interestingly, *Fgf2* expression was shown to be increased in Paget's disease of bone and human Pagetic mononuclear cells, and FGF2 modulated SOCS signaling to induce RANKL expression in PDB. Furthermore, siRNA inhibition of *Stat-1* suppresses FGF2-increased *Socs-1/3* expression in Pagetic osteoclasts (Sundaram et al., 2009).

FGF6 has also been shown to enhance osteoclast formation and promote absorption (Bosetti et al., 2010). To study FGF6 activity on osteoclast differentiation, human bone marrow cells were used, and TRAP-positive multinucleated cells together with actin filaments arrangements were quantified. Human primary mature osteoclasts were used to evaluate the effect of FGF6 on osteoclast reabsorbing activity by reabsorbed pit measurements. FGF6 increased the formation of TRAP-positive multinucleated cells in a dose-dependent manner, and a greater percentage of TRAP-positive cells formed typical osteoclast sealing zones. Mature osteoclasts cultured on dentine slice increased the area of reabsorption with a dose-dependent maximal effect of FGF6.

A role for FGF8 in osteoclastogenesis has also been reported. Studies by Lin et al. (2009) examined the isoforms of FGF8 on osteoclast formation. FGF8a, unlike FGF8b, inhibited osteoclastogenesis in mouse bone marrow cultures in an RANKL/osteoprotegerin (OPG)-independent manner. However, FGF8a did not affect osteoclastogenesis in RAW 264.7 cells (a macrophage cell line devoid of stromal cells) exogenously stimulated by RANKL, nor did it affect mature osteoclast function as assessed in rat calvarial organ cultures and isolated mature osteoclasts.

FGF11, also known as FGF homologous factor 3, belongs to the family of intracellular nonsecreted FGFs that resides in the nucleus and does not bind either the classical FGFR or HSPGs and are thought to bind target proteins distinct from those of the classical FGFs (Olsen et al., 2003). Intriguingly, studies by Knowles (2017) investigated the effects of FGF11 on osteoclast function. FGF11 was induced by both hypoxia and inhibition of the HIF-regulating prolyl hydroxylase enzyme in osteoclasts. Isoform-specific siRNA demonstrated that the induction of *Fgf11* mRNA expression by hypoxia is HIF-1α−dependent. Hypoxic stimulation of bone resorption was inhibited in osteoclasts treated with siRNA targeting *Fgf11*. This was at least partially due to reduced secretion of an unidentified proresorptive factor downstream of FGF11. FGF11 expression within hypoxic, resorbing osteoclasts was colocalized with microtubule-associated alpha-tubulin. *Fgf11* was also abundantly expressed in osteoclasts within the rheumatoid synovium and in giant cell tumor of bone. There is a gap in knowledge about whether other intranuclear FGFs, specifically FGF12, FGF13, and FGF14, also modulate osteoclastogenesis.

FGF18 is important in bone development and has been shown to be necessary in recruitment and formation of osteoclasts in developing long bone (Liu et al., 2007). In addition, Shimoaka et al., (2002) studied the action of FGF18 on bone resorption. FGF18 induced osteoclast formation through RANKL and cyclooxygenase-2 and also stimulated osteoclast function to form resorbed pits on a dentine slice in the mouse coculture system.

FGF21's role in osteoclastogenesis is controversial. FGF21 was reported to stimulate osteoclastogenesis and bone resorption by activation of PPARγ and to change of the ratio of RANKL/OPG (Wei et al., 2012). Furthermore, studies by Wang et al. (2015) proposed that a liver−bone endocrine relay by IGFBP1 promotes osteoclastogenesis and mediates FGF21-induced bone resorption. Mechanistically, IGFBP1 functioned via its RGD domain to bind to its receptor integrin β1 on osteoclast precursors, thereby potentiating RANKL-stimulated ERK phosphorylation and NFATc1 activation. Consequently, osteoclastic integrin β1 deletion conferred resistance to the resorption-enhancing effects of both IGFBP1 and FGF21. In contrast to these reports, recent studies in which mice with high-fat-diet-induced obesity were administered vehicle or recombinant human FGF21 failed to demonstrate a role for FGF21 in bone turnover (Li et al., 2017). There was no evidence of bone loss or changes in bone resorption markers, histologic bone resorption indices, or *Rankl/Opg* mRNA expression. Furthermore, in contrast to the studies of Wei et al. (2012), FGF21 knockout mice did not show a high bone mass phenotype (Li et al., 2017). Further studies are warranted to clarify the role of FGF21 in bone homeostasis.

There are limited studies on the direct effect of FGF23 on osteoclast biology, and studies from mouse models of ADHR with increased FGF23 have reported decreased osteoclast number in the Hyp mouse (Hayashibara et al., 2007) and in a transgenic murine model overexpressing FGF23, and while there were no significant modifications of the osteoclast number as compared with WT mice, there was a trend toward a decreased ratio of osteoclast volume to bone volume on histomorphometric values (Holberg et al., 2008). In studies of the direct effect of FGF23 on osteoclast formation and function, Allard et al. (2015) used human monocytes differentiated by MCSF and RANKL to demonstrate a biphasic effect of FGF23 on human osteoclast metabolism, with an inhibition of osteoclast differentiation at the early stages and a moderate albeit significant stimulation of osteoclast activity. This effect of FGF23 appears to be mediated by FGFR/AKT/

ERK signaling independent of Klotho. FGF23 also upregulated the mRNA expression of osteoclastogenic factors (e.g., *Mcsf, Mcp-1, Il-6*, and *Tnf-α*), and bone-resorption regulators (*Rankl* and *Opg*) in UMR-106 cells (Teerapornpuntakit et al., 2016).

Fibroblast growth factor receptors and craniosynostosis

Skeletal phenotype

Several mutations in *FGFRs 1* to *3* cause cranial dysplasias, called craniosynostosis, in Apert, Crouzon, and other syndromes, characterized by premature fusion of one or more cranial sutures (Ornitz and Marie, 2002; Johnson and Wilkie, 2011). Mutations in *FGFR2* may also induce bent bone dysplasia, a dysmorphology of the appendicular skeleton (Merrill et al., 2012). The molecular mechanisms involved in these syndromes induced by *FGFR* mutations include ligand-independent or ligand-dependent FGFR activation, loss of function, and altered FGFR trafficking (Yu et al., 2000; Ibrahimi et al., 2001; Yu and Ornitz, 2001; Neben et al., 2014). The skeletal abnormalities induced by gain-of-function *FGFR* mutations have been extensively studied (Hajihosseini, 2008; Marie et al., 2008; Senarath-Yapa et al., 2012). The phenotype induced by FGFR mutations in mice and humans is variable due to distinct environmental factors or genetic background, although the resulting effect is premature suture fusion induced by increased osteogenesis (Marie et al., 2005; Wilkie, 2005). In Apert syndrome, *FGFR2* mutations induce abnormal mesodermal progenitor cell proliferation, differentiation, and cell fate in cranial sutures. Conditional expression of the Apert *FGFR2* (S252W) mutation in cells derived from mesoderm is sufficient to cause coronal craniosynostosis (Heuze et al., 2014). However, the cellular abnormalities caused by this mutation are variable, depending on the affected suture and the stage of cell differentiation (Wang et al., 2005; Holmes et al., 2009; Heuze et al., 2014; Motch Perrine et al., 2014). In mice, osteoprogenitor cell proliferation is unchanged (Chen et al., 2003) or is transiently and slightly increased by activating Apert and Crouzon *FGFR2* mutations in cranial sutures at an early stage of development (Mansukhani et al., 2000, 2005), whereas at a later stage, osteoblast maturation is increased (Eswarakumar et al., 2004; Yang et al., 2008; Yin et al., 2008; Holmes et al., 2009; Yeh et al., 2012; Liu et al., 2013a, 2013b; Morita et al., 2014). In mice, gain-of-function mutations in *FGFR1*, *FGFR2,* or *FGFR2c* cause increased expression of *Runx2* (Zhou et al., 2000; Baroni et al., 2005; Eswarakumar et al., 2004). In humans, Apert and Crouzon *FGFR2* mutations promote *Runx2* expression and osteoblast maturation and function in postnatal suture development (Lomri et al., 1998; Lemonnier et al., 2001b; Tanimoto et al., 2004; Baroni et al., 2005; Guénou et al., 2005). In mice, disruption of *FGFR2IIIc*, the mesenchymal splice variant of *FGFR2*, decreases *Runx2* transcription and thereby retards ossification (Eswarakumar et al., 2002). *FGFR2*-activating mutations also increase *Sox2* expression in murine osteoblasts and reduce Wnt target genes (Mansukhani et al., 2005), although the role of these genes in craniosynostosis remains unclear. In bent bone dysplasia syndrome, *FGFR2* mutations (M391R or Y381D) reduce ligand-dependent receptor activation, which leads to increased nucleolar activity of the mutant FGFR2, resulting in increased proliferation and decreased differentiation of osteoprogenitor cells (Merrill et al., 2012; Neben et al. 2014, 2017). In humans and mice, *FGFR2* mutations are associated with increased osteoblast apoptosis in fused sutures (Lemonnier et al., 2001a; Lomri et al., 2001; Kaabeche et al., 2005; Mansukhani et al., 2005; Chen et al., 2014), which may in part be mediated by increased IL-1 expression (Lomri et al., 2001) and may occur as a consequence of the premature osteoblast maturation (Holmes et al., 2009) (Fig. 45.3). Activating *FGFR3* mutations was also found to cause partial premature fusion of the coronal sutures in mice (Twigg et al., 2009; Di Rocco et al., 2014). In the growth plate, chondrocyte-specific activation of *Fgfr3* was reported to induce premature suture closure indirectly through activation of MAPK and BMP signaling, leading to increased osteoblast differentiation (Matsushita et al., 2009b). In long bones, activating *FGFR3* mutations in chondrocytes led to increased osteoclast recruitment and decreased trabecular bone mass (Su et al., 2010; Mugniery et al., 2012). In contrast, conditional knockout of *Fgfr3* in chondrocytes indirectly leads to increased bone mass due to reduced osteoclast number and increased osteoblast number and bone formation by upregulating the expression of *Ihh*, *Bmp2*, *Bmp4*, *Bmp7*, *Wnt4*, and *Tgf-β1* (Wen et al., 2016).

Fibroblast growth factor receptor signaling in craniosynostosis

The premature suture fusion induced by *FGFR* mutations occurs subsequently to the activation of several signaling pathways (Miraoui and Marie, 2010; Su et al., 2014; Marie, 2015). In mice, gain-of-function *FGFR2* mutations activate ERK1/2 and p38 MAPKs, AKT and PLCγ, in osteogenic cells (Chen et al., 2003; Kim et al., 2003; Shukla et al., 2007; Yin et al., 2008; Wang et al., 2010; Suzuki et al., 2012; Pfaff et al., 2016). Reduced expression of ERF, an inhibitory ETS transcription factor directly bound by ERK1/2, causes craniosynostosis in humans and mice, indicating a role of ERF and

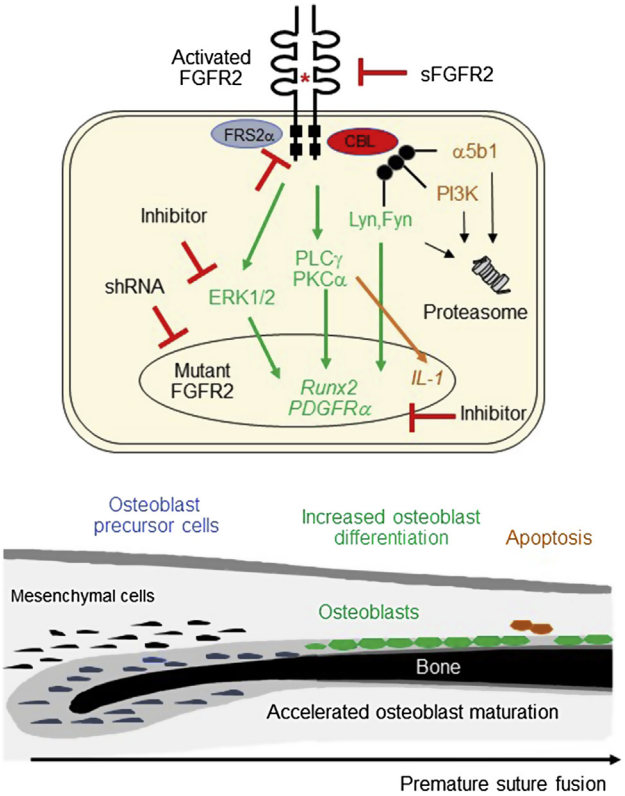

FIGURE 45.4 FGFR signaling in craniosynostosis. Gain-of-function *FGFR2* mutations induce constitutive activation of FGFR2, resulting in activation of PKCα, downregulation of the SRC proteins LYN and FYN, and increased PDGFRα expression, all leading to increased *Runx2* expression and premature osteoblast maturation and suture fusion. FGFR2 activation also leads to increased *IL-1* expression and α5β1 integrin proteasome degradation, resulting in increased apoptosis of more mature osteoblasts. Potential therapeutic strategies to attenuate the aberrant FGFR2 signaling in craniosynostosis include uncoupling of FRS2α with the mutant FGFR2c (1), targeting the mutant FGFR2 with a small hairpin RNA (2), inhibition of ERK1/2 MAPK (3) or PDGFRα (4), or the use of a soluble mutant form of FGFR2 (4).

ERK signaling in cranial suture ossification (Twigg et al., 2013). In human cranial osteoblasts, Apert *FGFR2* (S252W) mutation induces PLCɣ and PKCα activation (Lemonnier et al., 2001b), resulting in increased *Runx2* expression. This effect leads to increased osteoblast gene expression and premature fusion of cranial sutures in both mice and humans (Zhou et al., 2000; Eswarakumar et al., 2002; Tanimoto et al., 2004; Baroni et al., 2005; Guénou et al., 2005). In human cranial sutures, Apert *FGFR2* (S252W) mutation increases the expression of platelet-derived growth factor receptor α (*PDGFRα*) and epidermal growth factor receptor via activation of PKCα-mediated AP-1 transcription, which contributes to the premature suture ossification (Miraoui et al., 2010a). Consistently, conditional expression of activated *PDGFRα* in neural crest cells causes premature cranial fusion at early postnatal stages in mice (Moenning et al., 2009). Downregulation of regulatory molecules induced by activated *FGFR2* mutations may also contribute to craniosynostosis. In both mice and humans, the Apert *FGFR2* (S252W) mutation induces c-CBL–mediated ubiquitination and degradation of FGFR2 (Kaabeche et al., 2004; Holmes et al., 2009). In addition, activated FGFR2 leads to c-CBL–mediated ubiquitination of the SRC family members LYN and FYN (Kaabeche et al., 2004), α5β1 integrin (Kaabeche et al., 2005), and PI3K (Dufour et al., 2008), and the attenuation of these signals contributes to enhance osteoblast differentiation and apoptosis in human mutant osteoblasts. Increased binding of activated FGFR2 to the adaptor protein FRS2α also contributes to the negative feedback mechanism induced by FGFR activation in murine Crouzon-like craniosynostosis (Eswarakumar et al., 2006). These data emphasize the complexity of the aberrant signaling pathways induced by gain-of-function *FGFR* mutations in cells of the osteoblast lineage (Fig. 45.4).

Potential therapeutic approaches

Several potential therapeutic strategies targeting the aberrant cellular signaling induced by *FGFR* mutations have been proposed (Wilkie, 2007; Melville et al., 2010). In vitro, Apert and Crouzon FGFR2 signaling can be attenuated using either

specific glycosaminoglycans (McDowell et al., 2006), inhibitors of FGFR or tyrosine kinase (Perlyn et al., 2006), or a dominant negative FGFR2 (Tanimoto et al., 2004). In mice, activated FGFR2c signaling can be attenuated by selective uncoupling of the docking protein FRS2α and the mutant FGFR2c (Eswarakumar et al., 2006). Other therapeutic strategies include treatments with a small hairpin RNA targeting the Apert *FGFR2 (*S252W*)* mutation, an ERK1/2 MAPK inhibitor (Shukla et al., 2007), or a soluble mutant form of FGFR2 (Morita et al., 2014; Yokota et al., 2014). Since activated FGFR2 cooperates with other signaling pathways, such as PDGFRα (Moenning et al., 2009; Miraoui et al., 2010a), targeting these pathways may attenuate the aberrant signals induced by *FGFR* mutations in osteogenic cells (Miraoui and Marie, 2010). Furthers studies are needed to determine whether these strategies may correct the abnormal osteoblast phenotype and premature suture fusion in craniosynostosis.

Conclusion

During the last decade, novel cellular, molecular, and genetic studies have led to a better understanding of the role of FGF/FGFR signaling in chondrogenesis, bone formation and resorption, bone remodeling, and repair. The pathways and mechanisms induced by FGF/FGFR signaling that regulate chondrogenesis and osteogenesis are now better understood. The role of FGFs in the regulation of bone and other tissues has also been clarified. The analysis of human skeletal dysplasias and the use of genetic mouse models has improved our knowledge of the pathogenesis of chondrodysplasias and craniosynostosis induced by *FGFR* mutations. Genetic and functional studies have also allowed for the identification of some key pathways altered by *FGFR* mutations, which may in turn be targeted to reduce their impact on skeletal development and remodeling. Further genetic studies in mice are needed to identify more precisely the role of the various FGFs and FGFRs in skeletal cells at specific stages of development in order to generate safe and efficient targeted therapeutic interventions in skeletal dysplasias associated with *FGFR* mutations.

Acknowledgments

The authors thank all collaborators who contributed to the work reviewed in this chapter. This work was supported by the Agence Nationale de la Recherche and the European Commission FP6 and FP7 programs (PJM), by NIH grant AR072985-05 (MH), and by NIH grant HD049808 and the Department of Developmental Biology at Washington University (DMO).

References

Agas, D., Sabbieti, M.G., Marchetti, L., et al., 2013. FGF-2 enhances Runx-2/Smads nuclear localization in BMP-2 canonical signaling in osteoblasts. J. Cell. Physiol. 228, 2149–2158.

Agas, D., Marchetti, L., Menghi, G., et al., 2008. Anti-apoptotic Bcl-2 enhancing requires FGF-2/FGF receptor 1 binding in mouse osteoblasts. J. Cell. Physiol. 214, 145–152.

Aikawa, T., Segre, G.V., Lee, K., 2001. Fibroblast growth factor inhibits chondrocytic growth through induction of p21 and subsequent inactivation of cyclin E-Cdk2. J. Biol. Chem. 276, 29347–29352.

Allard, L., Demoncheaux, N., Machuca-Gayet, I., et al., 2015. Biphasic Effects of vitamin D and FGF23 on human osteoclast biology. Calcif. Tissue Int. 97, 69–79.

Ambrosetti, D., Holmes, G., Mansukhani, A., et al., 2008. Fibroblast growth factor signaling uses multiple mechanisms to inhibit Wnt-induced transcription in osteoblasts. Mol. Cell Biol. 28, 4759–4771.

Ananyeva, N.M., Tjurmin, A., Berliner, J.A., et al., 1997. Oxidized LDL mediates the release of fibroblast growth factor-1. Arterioscler. Thromb. Vasc. Biol. 17, 445–453.

Barnard, J.C., Williams, A.J., Rabier, B., et al., 2005. Thyroid hormones regulate fibroblast growth factor receptor signaling during chondrogenesis. Endocrinology 146, 5568–5580.

Baroni, T., Carinci, P., Lilli, C., et al., 2005. P253R fibroblast growth factor receptor-2 mutation induces RUNX2 transcript variants and calvarial osteoblast differentiation. J. Cell. Physiol. 202, 524–535.

Beever, J.E., Smit, M.A., Meyers, et al., 2006. A single-base change in the tyrosine kinase II domain of ovine FGFR3 causes hereditary chondrodysplasia in sheep. Anim. Genet. 37, 66–71.

Behr, B., Leucht, P., Longaker, M.T., et al., 2010. Fgf-9 is required for angiogenesis and osteogenesis in long bone repair. Proc. Natl. Acad. Sci. U.S.A. 107, 11853–11858.

Behr, B., Sorkin, M., Lehnhardt, M., et al., 2012. A comparative analysis of the osteogenic effects of BMP-2, FGF-2, and VEGFA in a calvarial defect model. Tissue Eng. 18, 1079–1086.

Behr, B., Sorkin, M., Manu, A., et al., 2011. Fgf-18 is required for osteogenesis but not angiogenesis during long bone repair. Tissue Eng. 17, 2061–2069.

Bellus, G.A., McIntosh, I., Smith, E.A., et al., 1995. A recurrent mutation in the tyrosine kinase domain of fibroblast growth factor receptor 3 causes hypochondroplasia. Nat. Genet. 10, 357–359.

Bellus, G.A., Bamshad, M.J., Przylepa, K.A., et al., 1999. Severe achondroplasia with developmental delay and acanthosis nigricans (SADDAN): phenotypic analysis of a new skeletal dysplasia caused by a Lys650Met mutation in fibroblast growth factor receptor 3. Am. J. Med. Genet. 85, 53–65.

Bellus, G.A., Spector, E.B., Speiser, et al., 2000. Distinct missense mutations of the FGFR3 lys650 codon modulate receptor kinase activation and the severity of the skeletal dysplasia phenotype. Am. J. Hum. Genet. 67, 1411–1421.

Belov, A.A., Mohammadi, M., 2013. Molecular mechanisms of fibroblast growth factor signaling in physiology and pathology. Cold Spring Harb Perspect Biol. 5, 1–24.

Blanquaert, F., Delany, A.M., Canalis, E., 1999. Fibroblast growth factor-2 induces hepatocyte growth factor/scatter factor expression in osteoblasts. Endocrinology 140, 1069–1074.

Blick, C., Ramachandran, A., Wigfield, S., et al., 2013. Hypoxia regulates FGFR3 expression via HIF-1alpha and miR-100 and contributes to cell survival in non-muscle invasive bladder cancer. Br. J. Canc. 109, 50–59.

Bonaventure, J., Rousseau, F., Legeai-Mallet, L., et al., 1996. Common mutations in the fibroblast growth factor receptor 3 (FGFR 3) gene account for achondroplasia, hypochondroplasia, and thanatophoric dwarfism. Am. J. Med. Genet. 63, 148–154.

Bosetti, M., Leigheb, M., Brooks, R.A., et al., 2010. Regulation of osteoblast and osteoclast functions by FGF-6. J. Cell. Physiol. 225, 466–471.

Boudreaux, J.M., Towler, D.A., 1996. Synergistic induction of osteocalcin gene expression: identification of a bipartite element conferring fibroblast growth factor 2 and cyclic AMP responsiveness in the rat osteocalcin promoter. J. Biol. Chem. 271, 7508–7515.

Britto, J.A., Evans, R.D., Hayward, R.D., et al., 2001. From genotype to phenotype: the differential expression of FGF, FGFR, and TGFbeta genes characterizes human cranioskeletal development and reflects clinical presentation in FGFR syndromes. Plast. Reconstr. Surg. 108, 2026–2039 discussion 2040-2026.

Brodie, S.G., Kitoh, H., Lachman, R.S., et al., 1999. Platyspondylic lethal skeletal dysplasia, San Diego type, is caused by FGFR3 mutations. Am. J. Med. Genet. 84, 476–480.

Browaeys-Poly, E., Blanquart, C., Perdereau, D., et al., 2010. Grb14 inhibits FGF receptor signaling through the regulation of PLCgamma recruitment and activation. FEBS Lett. 584, 4383–4388.

Buchtova, M., Oralova, V., Aklian, A., et al., 2015. Fibroblast growth factor and canonical WNT/beta-catenin signaling cooperate in suppression of chondrocyte differentiation in experimental models of FGFR signaling in cartilage. Biochim. Biophys. Acta 1852, 839–850.

Camps, M., Nichols, A., Gillieron, C., et al., 1998. Catalytic activation of the phosphatase MKP-3 by ERK2 mitogen-activated protein kinase. Science 280, 1262–1265.

Carli, A., Gao, C., Khayyat-Kholghi, M., et al., 2012. FGF18 augments osseointegration of intra-medullary implants in osteopenic FGFR3(-/-) mice. Eur. Cells Mater. 24, 107–116 discussion 116-107.

Carreira, C.M., Landriscina, M., Bellum, S., et al., 2001. The comparative release of FGF1 by hypoxia and temperature stress. Growth Factors 18, 277–285.

Chaorenlarp, P., Kumar Rajendran, A., Iseki, S., 2017. Role of fibroblast growth factors in bone regeneration. Inflamm. Regen. 37, 10.

Chapman, J.R., Katsara, O., Ruoff, R., et al., 2017. Phosphoproteomics of FGF1 signaling in chondrocytes: identifying the signature of inhibitory response. Mol. Cell. Proteomics 16, 1126–1137.

Chen, L., Li, C., Qiao, W., et al., 2001. A Ser(365)–>Cys mutation of fibroblast growth factor receptor 3 in mouse downregulates Ihh/PTHrP signals and causes severe achondroplasia. Hum. Mol. Genet. 10, 457–465.

Chen, L., Li, D., Li, C., et al., 2003. A Ser252Trp [corrected] substitution in mouse fibroblast growth factor receptor 2 (Fgfr2) results in craniosynostosis. Bone 33, 169–178.

Chen, L., Deng, C.X., 2005. Roles of FGF signaling in skeletal development and human genetic diseases. Front. Biosci. 10, 1961–1976.

Chen, Y., Gridley, T., 2013. Compensatory regulation of the Snai1 and Snai2 genes during chondrogenesis. J. Bone Miner. Res. 28, 1412–1421.

Chen, P., Zhang, L., Weng, T., et al., 2014. A Ser252Trp mutation in fibroblast growth factor receptor 2 (FGFR2) mimicking human Apert syndrome reveals an essential role for FGF signaling in the regulation of endochondral bone formation. PLoS One 9, e87311.

Chikazu, D., Hakeda, Y., Ogata, N., et al., 2000. Fibroblast growth factor (FGF)-2 directly stimulates mature osteoclast function through activation of FGF receptor 1 and p42/p44 MAP kinase. J. Biol. Chem. 275, 31444–31450.

Choi, K.Y., Kim, H.J., Lee, M.H., et al., 2005. Runx2 regulates FGF2-induced Bmp2 expression during cranial bone development. Dev. Dynam. 233, 115–121.

Choi, S.C., Kim, S.J., Choi, J.H., et al., 2008. Fibroblast growth factor-2 and -4 promote the proliferation of bone marrow mesenchymal stem cells by the activation of the PI3K-Akt and ERK1/2 signaling pathways. Stem Cell. Dev. 17, 725–736.

Cinque, L., Forrester, A., Bartolomeo, R., et al., 2015. FGF signalling regulates bone growth through autophagy. Nature 528, 272–275.

Clinkenbeard, E.L., Farrow, E.G., Summers, L.J., et al., 2014. Neonatal iron deficiency causes abnormal phosphate metabolism by elevating FGF23 in normal and ADHR mice. J. Bone Miner. Res. 29, 361–369.

Clinkenbeard, E.L., White, K.E., 2016. Systemic control of bone homeostasis by FGF23 signaling. Curr. Mol. Biol. Rep. 2, 62–71.

Cobrinik, D., Lee, M.H., Hannon, G., et al., 1996. Shared role of the pRB-related p130 and p107 proteins in limb development. Genes Dev. 10, 1633–1644.

Colvin, J.S., Bohne, B.A., Harding, G.W., et al., 1996. Skeletal overgrowth and deafness in mice lacking fibroblast growth factor receptor 3. Nat. Genet. 12, 390–397.

Colvin, J.S., Feldman, B., Nadeau, et al., 1999. Genomic organization and embryonic expression of the mouse fibroblast growth factor 9 gene. Dev. Dynam. 216, 72–88.

Colvin, J.S., White, A.C., Pratt, S.J., et al., 2001. Lung hypoplasia and neonatal death in Fgf9-null mice identify this gene as an essential regulator of lung mesenchyme. Development 128, 2095–2106.

Coumoul, X., Shukla, V., Li, C., et al., 2005. Conditional knockdown of Fgfr2 in mice using Cre-LoxP induced RNA interference. Nucleic Acids Res. 33, e102.

Coutu, D.L., Francois, M., Galipeau, J., 2011. Inhibition of cellular senescence by developmentally regulated FGF receptors in mesenchymal stem cells. Blood 117, 6801–6812.

Cowan, C.M., Quarto, N., Warren, S.M., et al., 2003. Age-related changes in the biomolecular mechanisms of calvarial osteoblast biology affect fibroblast growth factor-2 signaling and osteogenesis. J. Biol. Chem. 278, 32005–32013.

Dailey, L., Laplantine, E., Priore, R., et al., 2003. A network of transcriptional and signaling events is activated by FGF to induce chondrocyte growth arrest and differentiation. J. Cell Biol. 161, 1053–1066.

Dailey, L., Ambrosetti, D., Mansukhani, A., et al., 2005. Mechanisms underlying differential responses to FGF signaling. Cytokine Growth Factor Rev. 16, 233–247.

De Frutos, C.A., Vega, S., Manzanares, M., et al., 2007. Snail1 is a transcriptional effector of FGFR3 signaling during chondrogenesis and achondroplasias. Dev. Cell 13, 872–883.

Debiais, F., Hott, M., Graulet, A.M., et al., 1998. The effects of fibroblast growth factor-2 on human neonatal calvaria osteoblastic cells are differentiation stage specific. J. Bone Miner. Res. 13, 645–654.

Debiais, F., Lemonnier, J., Hay, E., Delannoy, P., Caverzasio, J., Marie, P.J., 2001. Fibroblast growth factor-2 (FGF-2) increases N-cadherin expression through protein kinase C and Src-kinase pathways in human calvaria osteoblasts. J. Cell. Biochem. 81 (1), 68–81.

Delezoide, A.L., Benoist-Lasselin, C., Legeai-Mallet, L., et al., 1998. Spatio-temporal expression of FGFR 1, 2 and 3 genes during human embryo-fetal ossification. Mech. Dev. 77, 19–30.

Deng, C., Wynshaw-Boris, A., Zhou, F., et al., 1996. Fibroblast growth factor receptor 3 is a negative regulator of bone growth. Cell 84, 911–921.

Dhodapkar, M.V., Abe, E., Theus, A., Lacy, M., Langford, J.K., Barlogie, B., Sanderson, R.D., 1998. Syndecan-1 is a multifunctional regulator of myeloma pathobiology: control of tumor cell survival, growth, and bone cell differentiation. Blood 91, 2679–2688.

Di Maggio, N., Mehrkens, A., Papadimitropoulos, A., et al., 2012. Fibroblast growth factor-2 maintains a niche-dependent population of self-renewing highly potent non-adherent mesenchymal progenitors through FGFR2c. Stem Cell. 30, 1455–1464.

Di Rocco, F., Biosse Duplan, M., et al., 2014. FGFR3 mutation causes abnormal membranous ossification in achondroplasia. Hum. Mol. Genet. 23, 2914–2925.

Du, X., Xie, Y., Xian, C.J., et al., 2012. Role of FGFs/FGFRs in skeletal development and bone regeneration. J. Cell. Physiol. 227, 3731–3743.

Dufour, C., Guénou, H., Kaabeche, K., et al., 2008. FGFR2-Cbl interaction in lipid rafts triggers attenuation of PI3K/Akt signaling and osteoblast survival. Bone 42, 1032–1039.

Durham, B.H., Joseph, F., Bailey, L.M., et al., 2007. The association of circulating ferritin with serum concentrations of fibroblast growthfactor-23 measured by three commercial assays. Ann. Clin. Biochem. 44, 463–466.

Escobar, L.F., Tucker, M., Bamshad, M., 2016. A second family with CATSHL syndrome: confirmatory report of another unique FGFR3 syndrome. Am. J. Med. Genet. A. 170, 1908–1911.

Eswarakumar, V.P., Monsonego-Ornan, E., Pines, M., et al., 2002. The IIIc alternative of Fgfr2 is a positive regulator of bone formation. Development 129, 3783–3793.

Eswarakumar, V.P., Horowitz, M.C., Locklin, R., et al., 2004. A gain-of-function mutation of Fgfr2c demonstrates the roles of this receptor variant in osteogenesis. Proc. Natl. Acad. Sci. U.S.A. 101, 12555–12560.

Eswarakumar, V.P., Lax, I., Schlessinger, J., 2005. Cellular signaling by fibroblast growth factor receptors. Cytokine Growth Factor Rev. 16, 139–149.

Eswarakumar, V.P., Ozcan, F., Lew, E.D., et al., 2006. Attenuation of signaling pathways stimulated by pathologically activated FGF-receptor 2 mutants prevents craniosynostosis. Proc. Natl. Acad. Sci. U.S.A. 103, 18603–18608.

Eswarakumar, V.P., Schlessinger, J., 2007. Skeletal overgrowth is mediated by deficiency in a specific isoform of fibroblast growth factor receptor 3. Proc. Natl. Acad. Sci. U.S.A. 104, 3937–3942.

Fakhry, A., Ratisoontorn, C., Vedhachalam, C., et al., 2005. Effects of FGF-2/-9 in calvarial bone cell cultures: differentiation stage-dependent mitogenic effect, inverse regulation of BMP-2 and noggin, and enhancement of osteogenic potential. Bone 36, 254–266.

Farrow, E.G., Yu, X., Summers, L.J., et al., 2011. Iron deficiency drives an autosomal dominant hypophosphatemic rickets (ADHR) phenotype in fibroblast growth factor-23 (Fgf23) knock-in mice. Proc. Natl. Acad. Sci. U.S.A. 108, E1146–E1155.

Fei, Y., Xiao, L., Doetschman, T., et al., 2011. Fibroblast growth factor 2 stimulation of osteoblast differentiation and bone formation is mediated by modulation of the Wnt signaling pathway. J. Biol. Chem. 286, 40575–40583.

Fei, Y., Gronowicz, G., Hurley, M.M., 2013. Fibroblast growth factor-2, bone homeostasis and fracture repair. Curr. Pharmaceut. Des. 19, 3354–3363.

Foldynova-Trantirkova, S., Wilcox, W.R., Krejci, P., 2012. Sixteen years and counting: the current understanding of fibroblast growth factor receptor 3 (FGFR3) signaling in skeletal dysplasias. Hum. Mutat. 33, 29–41.

Fon Tacer, K., Bookout, A.L., Ding, X., et al., 2010. Research resource: comprehensive expression atlas of the fibroblast growth factor system in adult mouse. Mol. Endocrinol. 24, 2050–2064.

Ford-Hutchinson, A.F., Ali, Z., Lines, S.E., et al., 2007. Inactivation of Pten in osteo-chondroprogenitor cells leads to epiphyseal growth plate abnormalities and skeletal overgrowth. J. Bone Miner. Res. 22, 1245–1259.

Fromigué, O., Modrowski, D., Marie, P.J., 2004. Growth factors and bone formation in osteoporosis: roles for fibroblast growth factor and transforming growth factor beta. Curr. Pharmaceut. Des. 10, 2593–2603.

Furdui, C.M., Lew, E.D., Schlessinger, J., et al., 2006. Autophosphorylation of FGFR1 kinase is mediated by a sequential and precisely ordered reaction. Mol. Cell 21, 711–717.

Garofalo, S., Kliger-Spatz, M., Cooke, J.L., et al., 1999. Skeletal dysplasia and defective chondrocyte differentiation by targeted overexpression of fibroblast growth factor 9 in transgenic mice. J. Bone Miner. Res. 14, 1909–1915.

Globus, R.K., Plouet, J., Gospodarowicz, D., 1989. Cultured bovine bone cells synthesize basic fibroblast growth factor and store it in their extracellular matrix. Endocrinology 124, 1539–1547.

Goetz, R., Mohammadi, M., 2013. Exploring mechanisms of FGF signalling through the lens of structural biology. Nat. Rev. Mol. Cell Biol. 14, 166–180.

Gospodarowicz, D., 1974. Localization of a fibroblast growth factor and its effect alone and with hydrocortisone on 3T3 cell growth. Nature 249, 123–127.

Gould, S.E., Upholt, W.B., Kosher, R.A., 1992. Syndecan 3: a member of the syndecan family of membrane-intercalated proteoglycans that is expressed in high amounts at the onset of chicken limb cartilage differentiation. Proc. Natl. Acad. Sci. U.S.A. 89, 3271–3275.

Guénou, H., Kaabeche, K., Mee, S.L., et al., 2005. A role for fibroblast growth factor receptor-2 in the altered osteoblast phenotype induced by Twist haploinsufficiency in the Saethre-Chotzen syndrome. Hum. Mol. Genet. 14, 1429–1439.

Hajihosseini, M.K., 2008. Fibroblast growth factor signaling in cranial suture development and pathogenesis. Front Oral Biol 12, 160–177.

Haupt, L.M., Murali, S., Mun, F.K., et al., 2009. The heparan sulfate proteoglycan (HSPG) glypican-3 mediates commitment of MC3T3-E1 cells toward osteogenesis. J. Cell. Physiol. 220, 780–791.

Heuze, Y., Singh, N., Basilico, C., et al., 2014. Morphological comparison of the craniofacial phenotypes of mouse models expressing the Apert FGFR2 S252W mutation in neural crest- or mesoderm-derived tissues. Bone 63, 101–109.

Holmes, G., Rothschild, G., Roy, U.B., et al., 2009. Early onset of craniosynostosis in an Apert mouse model reveals critical features of this pathology. Dev. Biol. 328, 273–284.

Hamada, T., Suda, N., Kuroda, T., 1999. Immunohistochemical localization of fibroblast growth factor receptors in the rat mandibular condylar cartilage and tibial cartilage. J. Bone Miner. Metab. 17 (4), 274–282.

Hamidouche, Z., Fromigue, O., Nuber, U., et al., 2010. Autocrine fibroblast growth factor 18 mediates dexamethasone-induced osteogenic differentiation of murine mesenchymal stem cells. J. Cell. Physiol. 224, 509–515.

Hanafusa, H., Torii, S., Yasunaga, T., et al., 2002. Sprouty1 and Sprouty2 provide a control mechanism for the Ras/MAPK signalling pathway. Nat. Cell Biol. 4, 850–858.

Harada, M., Murakami, H., Okawa, A., et al., 2009. FGF9 monomer/dimer equilibrium regulates extracellular matrix affinity and tissue diffusion. Nat. Genet. 41, 289–298.

Hauschka, P.V., Mavrakos, A.E., Iafrati, M.D., et al., 1986. Growth factors in bone matrix. J. Biol. Chem. 261, 12665–12674.

Havens, B.A., Velonis, D., Kronenberg, M.S., et al., 2008. Roles of FGFR3 during morphogenesis of Meckel's cartilage and mandibular bones. Dev. Biol. 316, 336–349.

Hayashibara, T., Hiraga, T., Sugita, A., et al., 2007. Regulation of osteoclast differentiation and function by phosphate: potential role of osteoclasts in the skeletal abnormalities in hypophosphatemic conditions. J. Bone Miner. Res. 22, 1743–1751.

Hinoi, E., Bialek, P., Chen, et al., 2006. Runx2 inhibits chondrocyte proliferation and hypertrophy through its expression in the perichondrium. Genes Dev. 20, 2937–2942.

Hollberg, K., Marsell, R., Norgard, M., et al., 2008. Osteoclast polarization is not required for degradation of bone matrix in rachitic FGF23 transgenic mice. Bone 42, 1111–1121.

Homer-Bouthiette, C., Doetschman, T., Xiao, L., et al., 2014. Knockout of nuclear high molecular weight FGF2 isoforms in mice modulates bone and phosphate homeostasis. J. Biol. Chem. 289, 36303–36314.

House, S.L., Branch, K., Newman, G., et al., 2005. Cardioprotection induced by cardiac-specific overexpression of fibroblast growth factor-2 is mediated by the MAPK cascade. Am. J. Physiol. Heart Circ. Physiol. 289, H2167–H2175.

Hung, I.H., Yu, K., Lavine, K.J., et al., 2007. FGF9 regulates early hypertrophic chondrocyte differentiation and skeletal vascularization in the developing stylopod. Dev. Biol. 307, 300–313.

Hung, I.H., Schoenwolf, G.C., Lewandoski, M., et al., 2016. A combined series of Fgf9 and Fgf18 mutant alleles identifies unique and redundant roles in skeletal development. Dev. Biol. 411, 72–84.

Hurley, M.M., Abreu, C., Gronowicz, G., et al., 1994. Expression and regulation of basic fibroblast growth factor mRNA levels in mouse osteoblastic MC3T3-E1 cells. J. Biol. Chem. 269, 9392–9396.

Hurley, M.M., Marcello, K., Abreu, C., Kessler, M., 1996 Sep. Signal transduction by basic fibroblast growth factor in rat osteoblastic Py1a cells. J. Bone Miner. Res. 11 (9), 1256–1263.

Hurley, M.M., Lee, S.K., Raisz, L.G., et al., 1998. Basic fibroblast growth factor induces osteoclast formation in murine bone marrow cultures. Bone 22, 309–316.

Hurley, M.M., Tetradis, S., Huang, Y.F., et al., 1999. Parathyroid hormone regulates the expression of fibroblast growth factor-2 mRNA and fibroblast growth factor receptor mRNA in osteoblastic cells. J. Bone Miner. Res. 14, 776–783.

Hurley, M.M., Adams, D.J., Wang, L., et al., 2016. Accelerated fracture healing in transgenic mice overexpressing an anabolic isoform of fibroblast growth factor 2. J. Cell. Biochem. 117, 599–611.

Ibrahimi, O.A., Eliseenkova, A.V., Plotnikov, A.N., et al., 2001. Structural basis for fibroblast growth factor receptor 2 activation in Apert syndrome. Proc. Natl. Acad. Sci. U.S.A. 98, 7182–7187.

Ignelzi Jr., M.A., Wang, W., Young, A.T., 2003. Fibroblast growth factors lead to increased Msx2 expression and fusion in calvarial sutures. J. Bone Miner. Res. 18, 751−759.

Imel, E.A., Peacock, M., Gray, A.K., et al., 2011. Iron modifies plasma FGF23 differently in autosomal dominant hypophosphatemic rickets and healthy humans. J. Clin. Endocrinol. Metab. 96, 3541−3549.

Itoh, N., Ornitz, D.M., 2004. Evolution of the Fgf and Fgfr gene families. Trends Genet. 20, 563−569.

Itoh, N., 2007. The Fgf families in humans, mice, and zebrafish: their evolutional processes and roles in development, metabolism, and disease. Biol. Pharm. Bull. 30, 1819−1825.

Itoh, N., Ornitz, D.M., 2008. Functional evolutionary history of the mouse Fgf gene family. Dev. Dynam. 237, 18−27.

Iwata, T., Chen, L., Li, C., et al., 2000. A neonatal lethal mutation in FGFR3 uncouples proliferation and differentiation of growth plate chondrocytes in embryos. Hum. Mol. Genet. 9, 1603−1613.

Iwata, T., Li, C.L., Deng, C.X., et al., 2001. Highly activated Fgfr3 with the K644M mutation causes prolonged survival in severe dwarf mice. Hum. Mol. Genet. 10, 1255−1264.

Jackson, A., Friedman, S., Zhan, X., et al., 1992. Heat shock induces the release of fibroblast growth factor 1 from NIH 3T3 cells. Proc. Natl. Acad. Sci. U.S.A. 89, 10691−10695.

Jackson, R.A., Murali, S., van Wijnen, A.J., et al., 2007. Heparan sulfate regulates the anabolic activity of MC3T3-E1 preosteoblast cells by induction of Runx2. J. Cell. Physiol. 210, 38−50.

Jacob, A.L., Smith, C., Partanen, J., et al., 2006. Fibroblast growth factor receptor 1 signaling in the osteo-chondrogenic cell lineage regulates sequential steps of osteoblast maturation. Dev. Biol. 296, 315−328.

Jeon, E., Yun, Y.R., Kang, W., et al., 2012. Investigating the role of FGF18 in the cultivation and osteogenic differentiation of mesenchymal stem cells. PLoS One 7, e43982.

Johnson, D., Wilkie, A.O., 2011. Craniosynostosis. Eur. J. Hum. Genet. 19, 369−376.

Kaabeche, K., Lemonnier, J., Le Mee, S., et al., 2004. Cbl-mediated degradation of Lyn and Fyn induced by constitutive fibroblast growth factor receptor-2 activation supports osteoblast differentiation. J. Biol. Chem. 279, 36259−36267.

Kaabeche, K., Guénou, H., Bouvard, D., et al., 2005. Cbl-mediated ubiquitination of alpha5 integrin subunit mediates fibronectin-dependent osteoblast detachment and apoptosis induced by FGFR2 activation. J. Cell Sci. 118, 1223−1232.

Kanazawa, S., Fujiwara, T., Matsuzaki, et al., 2010. bFGF regulates PI3-kinase Rac1-JNK pathway and promotes fibroblast migration in wound healing. PLoS One 5, e12228.

Kant, S.G., Cervenkova, I., Balek, L., et al., 2015. A novel variant of FGFR3 causes proportionate short stature. Eur. J. Endocrinol. 172, 763−770.

Kapadia, R.M., Guntur, A.R., Reinhold, M.I., et al., 2005. Glycogen synthase kinase 3 controls endochondral bone development: contribution of fibroblast growth factor 18. Dev. Biol. 285, 496−507.

Karolak, M.R., Yang, X., Elefteriou, F., 2015. FGFR1 signaling in hypertrophic chondrocytes is attenuated by the Ras-GAP neurofibromin during endochondral bone formation. Hum. Mol. Genet. 24, 2552−2564.

Karuppaiah, K., Yu, K., Lim, J., et al., 2016. FGF signaling in the osteoprogenitor lineage non-autonomously regulates postnatal chondrocyte proliferation and skeletal growth. Development 143, 1811−1822.

Kawaguchi, H., Oka, H., Jingushi, S., et al., 2010. A local application of recombinant human fibroblast growth factor-2 for tibial shaft fractures: a randomized, placebo-controlled trial. J. Bone Miner. Res. 25, 2735−2743.

Kim, H.J., Rice, D.P., Kettunen, P.J., et al., 1998. FGF-, BMP- and Shh-mediated signalling pathways in the regulation of cranial suture morphogenesis and calvarial bone development. Development 125, 1241−1251.

Kim, H.J., Kim, J.H., Bae, et al., 2003. The protein kinase C pathway plays a central role in the fibroblast growth factor-stimulated expression and transactivation activity of Runx2. J. Biol. Chem. 278, 319−326.

Kim, J.M., Shin, H.I., Cha, S.S., et al., 2012. DJ-1 promotes angiogenesis and osteogenesis by activating FGF receptor-1 signaling. Nat. Commun. 3, 1296.

Knowles, H., 2017. Hypoxia-induced fibroblast growth factor 11 stimulates osteoclast-mediated resorption of bone. Calcif. Tissue Int. 100, 382−391.

Kodama, N., Nagata, M., Tabata, Y., et al., 2009. A local bone anabolic effect of rhFGF2-impregnated gelatin hydrogel by promoting cell proliferation and coordinating osteoblastic differentiation. Bone 44, 699−707.

Kolupaeva, V., Laplantine, E., Basilico, C., 2008. PP2A-mediated dephosphorylation of p107 plays a critical role in chondrocyte cell cycle arrest by FGF. PLoS One 3, e3447.

Kolupaeva, V., Daempfling, L., Basilico, C., 2013. The B55alpha regulatory subunit of protein phosphatase 2A mediates fibroblast growth factor-induced p107 dephosphorylation and growth arrest in chondrocytes. Mol. Cell Biol. 33, 2865−2878.

Kouhara, H., Hadari, Y.R., Spivak-Kroizman, T., et al., 1997. A lipid-anchored Grb2-binding protein that links FGF-receptor activation to the Ras/MAPK signaling pathway. Cell 89, 693−702.

Krejci, P., Salazar, L., Goodridge, H.S., et al., 2008a. STAT1 and STAT3 do not participate in FGF-mediated growth arrest in chondrocytes. J. Cell Sci. 121, 272−281.

Krejci, P., Salazar, L., Kashiwada, T.A., et al., 2008b. Analysis of STAT1 activation by six FGFR3 mutants associated with skeletal dysplasia undermines dominant role of STAT1 in FGFR3 signaling in cartilage. PLoS One 3, e3961.

Krejci, P., Aklian, A., Kaucka, M., et al., 2012. Receptor tyrosine kinases activate canonical WNT/beta-catenin signaling via MAP kinase/LRP6 pathway and direct beta-catenin phosphorylation. PLoS One 7, e35826.

Krejci, P., 2014. The paradox of FGFR3 signaling in skeletal dysplasia: why chondrocytes growth arrest while other cells over proliferate. Mutat. Res. Rev. Mutat. Res. 759, 40–48.

Kuhn, L.T., Ou, G., Charles, L., et al., 2013. Fibroblast growth factor-2 and bone morphogenetic protein-2 have a synergistic stimulatory effect on bone formation in cell cultures from elderly mouse and human bone. J. Gerontol. A Biol. Sci. Med. Sci. 68, 1170–1180.

Kumar, D., Lassar, A.B., 2014. Fibroblast growth factor maintains chondrogenic potential of limb bud mesenchymal cells by modulating DNMT3A recruitment. Cell Rep. 8, 1419–1431.

Kurimchak, A., Haines, D.S., Garriga, J., et al., 2013. Activation of p107 by fibroblast growth factor, which is essential for chondrocyte cell cycle exit, is mediated by the protein phosphatase 2A/B55alpha holoenzyme. Mol. Cell Biol. 33, 3330–3342.

Kwan, M.D., Sellmyer, M.A., Quarto, N., et al., 2011. Chemical control of FGF-2 release for promoting calvarial healing with adipose stem cells. J. Biol. Chem. 286, 11307–11313.

Kyono, A., Avishai, N., Ouyang, Z., et al., 2012. FGF and ERK signaling coordinately regulate mineralization-related genes and play essential roles in osteocyte differentiation. J. Bone Miner. Metab. 30, 19–30.

Lamothe, B., Yamada, M., Schaeper, U., et al., 2004. The docking protein Gab1 is an essential component of an indirect mechanism for fibroblast growth factor stimulation of the phosphatidylinositol 3-kinase/Akt antiapoptotic pathway. Mol. Cell Biol. 24, 5657–5666.

Laplantine, E., Rossi, F., Sahni, M., et al., 2002. FGF signaling targets the pRb-related p107 and p130 proteins to induce chondrocyte growth arrest. J. Cell Biol. 158, 741–750.

Larsson, T., Nisbeth, U., Ljunggren, O., et al., 2003. Circulating concentration of FGF-23 increases as renal function declines in patients with chronic kidney disease, but does not change in response to variation in phosphate intake in healthy volunteers. Kidney Int. 64, 2272–2279.

Lazarus, J.E., Hegde, A., Andrade, A.C., et al., 2007. Fibroblast growth factor expression in the postnatal growth plate. Bone 40, 577–586.

Legeai-Mallet, L., Benoist-Lasselin, C., Delezoide, A.L., et al., 1998. Fibroblast growth factor receptor 3 mutations promote apoptosis but do not alter chondrocyte proliferation in thanatophoric dysplasia. J. Biol. Chem. 273, 13007–13014.

Legeai-Mallet, L., Benoist-Lasselin, C., Munnich, A., et al., 2004. Overexpression of FGFR3, Stat1, Stat5 and p21Cip1 correlates with phenotypic severity and defective chondrocyte differentiation in FGFR3-related chondrodysplasias. Bone 34, 26–36.

Legeai-Mallet, L., 2016. C-Type natriuretic peptide analog as therapy for Achondroplasia. Endocr. Dev. 30, 98–105.

Lemmon, M.A., Schlessinger, J., 2010. Cell signaling by receptor tyrosine kinases. Cell 141, 1117–1134.

Lemonnier, J., Haÿ, E., Delannoy, P., et al., 2001a. Increased osteoblast apoptosis in apert craniosynostosis: role of protein kinase C and interleukin-1. Am. J. Pathol. 158, 1833–1842.

Lemonnier, J., Haÿ, E., Delannoy, P., et al., 2001b. Role of N-cadherin and protein kinase C in osteoblast gene activation induced by the S252W fibroblast growth factor receptor 2 mutation in Apert craniosynostosis. J. Bone Miner. Res. 16, 832–845.

Li, C., Xu, X., Nelson, D.K., Williams, T., et al., 2005. FGFR1 function at the earliest stages of mouse limb development plays an indispensable role in subsequent autopod morphogenesis. Development 132, 4755–4764.

Li, C.F., Hughes-Fulford, M., 2006. Fibroblast growth factor-2 is an immediate-early gene induced by mechanical stress in osteogenic cells. J. Bone Miner. Res. 21, 946–955.

Li, M., Seki, Y., Freitas, P.H., et al., 2010. FGFR3 down-regulates PTH/PTHrP receptor gene expression by mediating JAK/STAT signaling in chondrocytic cell line. J. Electron. Microsc. 59, 227–236.

Li, Y., He, X., Olauson, H., et al., 2013. FGF23 affects the lineage fate determination of mesenchymal stem cells. Calcif. Tissue Int. 93, 556–564.

Li, X., Stanislaus, S., Asuncion, F., et al., 2017. FGF21 is not a major mediator for bone homeostasis or metabolic actions of PPARα and PPARγ Agonists. J. Bone Miner. Res. 32, 834–845.

Liao, S., Porter, D., Scott, A., et al., 2007. The cardioprotective effect of the low molecular weight isoform of fibroblast growth factor-2: the role of JNK signaling. J. Mol. Cell. Cardiol. 42, 106–120.

Lin, J.M., Callon, K.E., Lin, J.S., et al., 2009. Actions of fibroblast growth factor-8 in bone cells in vitro. Am. J. Physiol. Endocrinol. Metab. 297, E142–E150.

Liu, Z., Xu, J., Colvin, J.S., et al., 2002. Coordination of chondrogenesis and osteogenesis by fibroblast growth factor 18. Genes Dev. 16, 859–869.

Liu, S., Guo, R., Simpson, L.G., et al., 2003. Regulation of fibroblastic growth factor 23 expression but not degradation by PHEX. J. Biol. Chem. 278, 37419–37426.

Liu, S., Zhou, J., Tang, W., et al., 2006. Pathogenic role of Fgf23 in Hyp mice. Am. J. Physiol. Endocrinol. Metab. 291, E38–E49.

Liu, Z., Lavine, K.J., Hung, I.H., et al., 2007. FGF18 is required for early chondrocyte proliferation, hypertrophy and vascular invasion of the growth plate. Dev. Biol. 302, 80–91.

Liu, J., Kwon, T.G., Nam, H.K., et al., 2013a. Craniosynostosis-associated Fgfr2(C342Y) mutant bone marrow stromal cells exhibit cell autonomous abnormalities in osteoblast differentiation and bone formation. BioMed Res. Int. 2013, 292506.

Liu, J., Nam, H.K., Wang, E., et al., 2013b. Further analysis of the Crouzon mouse: effects of the FGFR2(C342Y) mutation are cranial bone-dependent. Calcif. Tissue Int. 92, 451–466.

Liu, Y., Olsen, B.R., 2014. Distinct VEGF functions during bone development and homeostasis. Arch. Immunol. Ther. Exp. 62, 363–368.

Lomri, A., Lemonnier, J., Hott, M., et al., 1998. Increased calvaria cell differentiation and bone matrix formation induced by fibroblast growth factor receptor 2 mutations in Apert syndrome. J. Clin. Investig. 101, 1310–1317.

Lomri, A., Lemonnier, J., Delannoy, P., et al., 2001. Increased expression of protein kinase C alpha, interleukin-1 alpha, and RhoA guanosine 5'-triphosphatase in osteoblasts expressing the Ser252Trp fibroblast growth factor 2 Apert mutation: identification by analysis of complementary DNA microarray. J. Bone Miner. Res. 16, 705–712.

Lorget, F., Kaci, N., Peng, J., et al., 2012. Evaluation of the therapeutic potential of a CNP analog in a Fgfr3 mouse model recapitulating achondroplasia. Am. J. Hum. Genet. 91, 1108–1114.

Lu, X., Su, N., Yang, J., et al., 2009. Fibroblast growth factor receptor 1 regulates the differentiation and activation of osteoclasts through Erk1/2 pathway. Biochem. Biophys. Res. Commun. 390, 494–499.

Makrythanasis, P., Temtamy, S., Aglan, M.S., et al., 2014. A novel homozygous mutation in FGFR3 causes tall stature, severe lateral tibial deviation, scoliosis, hearing impairment, camptodactyly, and arachnodactyly. Hum. Mutat. 35, 959–963.

Mansouri, R., Haÿ, E., Marie, P.J., Modrowski, D., 2015. Role of syndecan-2 in osteoblast biology and pathology. Bonekey Rep. 4, 666.

Mansukhani, A., Ambrosetti, D., Holmes, G., et al., 2005. Sox2 induction by FGF and FGFR2 activating mutations inhibits Wnt signaling and osteoblast differentiation. J. Cell Biol. 168, 1065–1076.

Mansukhani, A., Bellosta, P., Sahni, M., et al., 2000. Signaling by fibroblast growth factors (FGF) and fibroblast growth factor receptor 2 (FGFR2)-activating mutations blocks mineralization and induces apoptosis in osteoblasts. J. Cell Biol. 149, 1297–1308.

Mariani, F.V., Ahn, C.P., Martin, G.R., 2008. Genetic evidence that FGFs have an instructive role in limb proximal-distal patterning. Nature 453, 401–405.

Marie, P., 2000. Significance of growth factors in bone repair: growth factors and bone tissue. Rev. Chir. Orthop. Reparatrice Appar. Mot. 86 (Suppl. 1), 150–151.

Marie, P.J., 2003. Fibroblast growth factor signaling controlling osteoblast differentiation. Gene 316, 23–32.

Marie, P.J., Coffin, J.D., Hurley, M.M., 2005. FGF and FGFR signaling in chondrodysplasias and craniosynostosis. J. Cell. Biochem. 96, 888–896.

Marie, P.J., Kaabeche, K., Guénou, H., 2008. Roles of FGFR2 and twist in human craniosynostosis: insights from genetic mutations in cranial osteoblasts. Front Oral Biol. 12, 144–159.

Marie, P.J., 2010. FGF/FGFR signalling in skeletal dysplasias. In: Bronner, F., Farach-Carson, M.C., Roach, H.I. (Eds.), Bone and Development, Topics in Bone Biology Series, vol. 6, pp. 93–106.

Marie, P.J., 2012. Fibroblast growth factor signaling controlling bone formation: an update. Gene 498, 1–4.

Marie, P.J., 2015. Osteoblast dysfunctions in bone diseases: from cellular and molecular mechanisms to therapeutic strategies. Cell. Mol. Life Sci. 72, 1347–1361.

Melville, H., Wang, Y., Taub, P.J., et al., 2010. Genetic basis of potential therapeutic strategies for craniosynostosis. Am. J. Med. Genet. A. 152A, 3007–3015.

Moore, R., Ferretti, P., Copp, A., et al., 2002. Blocking endogenous FGF-2 activity prevents cranial osteogenesis. Dev. Biol. 243, 99–114.

Murakami, S., Balmes, G., McKinney, S., et al., 2004. Constitutive activation of MEK1 in chondrocytes causes Stat1-independent achondroplasia-like dwarfism and rescues the Fgfr3-deficient mouse phenotype. Genes Dev. 18, 290–305.

Martin, A., Liu, S., David, V., et al., 2011. Bone proteins PHEX and DMP1 regulate fibroblastic growth factor Fgf23 expression in osteocytes through a common pathway involving FGF receptor (FGFR) signaling. FASEB J. 25, 2551–2562.

Matsushita, T., Wilcox, W.R., Chan, Y.Y., et al., 2009b. FGFR3 promotes synchondrosis closure and fusion of ossification centers through the MAPK pathway. Hum. Mol. Genet. 18, 227–240.

McDowell, L.M., Frazier, B.A., Studelska, D.R., et al., 2006. Inhibition or activation of Apert syndrome FGFR2 (S252W) signaling by specific glycosaminoglycans. J. Biol. Chem. 281, 6924–6930.

McEwen, D.G., Green, R.P., Naski, M.C., et al., 1999. Fibroblast growth factor receptor 3 gene transcription is suppressed by cyclic Adenosine 3',5'-monophosphate: identification of a chondrocytic regulatory element. J. Biol. Chem. 274, 30934–30942.

McKenzie, J., Smith, C., Karuppaiah, K., Langberg, J., Silva, M.J., Ornitz, D.M., 2019. Osteocyte death and bone overgrowth in mice lacking Fibroblast Growth Factor Receptors 1 and 2 in mature osteoblasts and osteocytes. JBMR in press.

Merrill, A.E., Sarukhanov, A., Krejci, P., et al., 2012. Bent bone dysplasia-FGFR2 type, a distinct skeletal disorder, has deficient canonical FGF signaling. Am. J. Hum. Genet. 90, 550–557.

Miraoui, H., Oudina, K., Petite, H., et al., 2009. Fibroblast growth factor receptor 2 promotes osteogenic differentiation in mesenchymal cells via ERK1/2 and protein kinase C signaling. J. Biol. Chem. 284, 4897–4904.

Miraoui, H., Marie, P.J., 2010. Fibroblast growth factor receptor signaling crosstalk in skeletogenesis. Sci. Signal. 3, re9.

Miraoui, H., Ringe, J., Haupl, T., et al., 2010a. Increased EFG- and PDGFalpha-receptor signaling by mutant FGF-receptor 2 contributes to osteoblast dysfunction in Apert craniosynostosis. Hum. Mol. Genet. 19, 1678–1689.

Miraoui, H., Sévère, N., Vaudin, P., et al., 2010b. Molecular silencing of Twist1 enhances osteogenic differentiation of murine mesenchymal stem cells: implication of FGFR2 signaling. J. Cell. Biochem. 110, 1147–1154.

Moenning, A., Jager, R., Egert, A., et al., 2009. Sustained platelet-derived growth factor receptor alpha signaling in osteoblasts results in craniosynostosis by overactivating the phospholipase C-gamma pathway. Mol. Cell Biol. 29, 881–891.

Molteni, A., Modrowski, D., Hott, M., et al., 1999a. Alterations of matrix- and cell-associated proteoglycans inhibit osteogenesis and growth response to fibroblast growth factor-2 in cultured rat mandibular condyle and calvaria. Cell Tissue Res. 295, 523–536.

Molteni, A., Modrowski, D., Hott, M., et al., 1999b. Differential expression of fibroblast growth factor receptor-1, -2, and -3 and syndecan-1, -2, and -4 in neonatal rat mandibular condyle and calvaria during osteogenic differentiation in vitro. Bone 24, 337–347.

Montero, A., Okada, Y., Tomita, M., et al., 2000. Disruption of the fibroblast growth factor-2 gene results in decreased bone mass and bone formation. J. Clin. Investig. 105, 1085–1093.

Morita, J., Nakamura, M., Kobayashi, Y., et al., 2014. Soluble form of FGFR2 with S252W partially prevents craniosynostosis of the apert mouse model. Dev. Dynam. 243, 560–567.

Motch Perrine, S.M., Cole 3rd, T.M., Martinez-Abadias, N., et al., 2014. Craniofacial divergence by distinct prenatal growth patterns in Fgfr2 mutant mice. BMC Dev. Biol. 14, 8.

Mugniery, E., Dacquin, R., Marty, C., et al., 2012. An activating Fgfr3 mutation affects trabecular bone formation via a paracrine mechanism during growth. Hum. Mol. Genet. 21, 2503−2513.

Murakami, S., Kan, M., McKeehan, W.L., et al., 2000a. Up-regulation of the chondrogenic Sox9 gene by fibroblast growth factors is mediated by the mitogen-activated protein kinase pathway. Proc. Natl. Acad. Sci. U.S.A. 97, 1113−1118.

Murakami, S., Kan, M., McKeehan, W.L., et al., 2000b. Up-regulation of the chondrogenic Sox9 gene by fibroblast growth factors is mediated by the mitogen-activated protein kinase pathway. Proc. Natl. Acad. Sci. U.S.A. 97, 1113−1118.

Naganawa, T., Xiao, L., Coffin, J.D., et al., 2008. Reduced expression and function of bone morphogenetic protein-2 in bones of Fgf2 null mice. J. Cell. Biochem. 103, 1975−1988.

Nakajima, F., Nakajima, A., Ogasawara, A., et al., 2007. Effects of a single percutaneous injection of basic fibroblast growth factor on the healing of a closed femoral shaft fracture in the rat. Calcif. Tissue Int. 81, 132−138.

Nakamura, T., Hara, Y., Tagawa, M., et al., 1998. Recombinant human basic fibroblast growth factor accelerates fracture healing by enhancing callus remodeling in experimental dog tibial fracture. J. Bone Miner. Res. 13, 942−949.

Nakamura, Y., Tensho, K., Nakaya, H., et al., 2005. Low dose fibroblast growth factor-2 (FGF-2) enhances bone morphogenetic protein-2 (BMP-2)-induced ectopic bone formation in mice. Bone 36, 399−407.

Narayana, J., Horton, W.A., 2015. FGFR3 biology and skeletal disease. Connect. Tissue Res. 1−18.

Naski, M.C., Wang, Q., Xu, J., et al., 1996. Graded activation of fibroblast growth factor receptor 3 by mutations causing achondroplasia and thanatophoric dysplasia. Nat. Genet. 13, 233−237.

Naski, M.C., Colvin, J.S., Coffin, J.D., et al., 1998. Repression of hedgehog signaling and BMP4 expression in growth plate cartilage by fibroblast growth factor receptor 3. Development 125, 4977−4988.

Neben, C.L., Idoni, B., Salva, J.E., et al., 2014. Bent bone dysplasia syndrome reveals nucleolar activity for FGFR2 in ribosomal DNA transcription. Hum. Mol. Genet. 23, 5659−5671.

Neben, C.L., Tuzon, C.T., Mao, X., et al., 2017. FGFR2 mutations in bent bone dysplasia syndrome activate nucleolar stress and perturb cell fate determination. Hum. Mol. Genet. 26, 3253−3270.

Newberry, E.P., Boudreaux, J.M., Towler, D.A., 1996. The rat osteocalcin fibroblast growth factor (FGF)-responsive element: an okadaic acid-sensitive, FGF-selective transcriptional response motif. Mol. Endocrinol. 10, 1029−1040.

Niger, C., Luciotti, M.A., Buo, A.M., et al., 2013. The regulation of runt-related transcription factor 2 by fibroblast growth factor-2 and connexin43 requires the inositol polyphosphate/protein kinase Cdelta cascade. J. Bone Miner. Res. 28, 1468−1477.

Noda, M., Vogel, R., 1989. Fibroblast growth factor enhances type beta 1 transforming growth factor gene expression in osteoblast-like cells. J. Cell Biol. 109, 2529−2535.

Oh, C.D., Lu, Y., Liang, S., et al., 2014. SOX9 regulates multiple genes in chondrocytes, including genes encoding ECM proteins, ECM modification enzymes, receptors, and transporters. PLoS One 9, e107577.

Ohbayashi, N., Shibayama, M., Kurotaki, Y., et al., 2002. FGF18 is required for normal cell proliferation and differentiation during osteogenesis and chondrogenesis. Genes Dev. 16, 870−879.

Okada, Y., Montero, A., Zhang, X., et al., 2003. Impaired osteoclast formation in bone marrow cultures of Fgf2 null mice in response to parathyroid hormone. J. Biol. Chem. 278, 21258−21266.

Olsen, S.K., Garbi, M., Zampieri, N., et al., 2003. Fibroblast growth factor (FGF) homologous factors share structural but not functional homology with FGFs. J. Biol. Chem. 278, 34226−34236.

Ono, N., Ono, W., Nagasawa, T., et al., 2014. A subset of chondrogenic cells provides early mesenchymal progenitors in growing bones. Nat. Cell Biol. 16, 1157−1167.

Ornitz, D.M., 2005. FGF signaling in the developing endochondral skeleton. Cytokine Growth Factor Rev. 16, 205−213.

Ornitz, D.M., Marie, P.J., 2002. FGF signaling pathways in endochondral and intramembranous bone development and human genetic disease. Genes Dev. 16, 1446−1465.

Ornitz, D.M., Itoh, N., 2015. The fibroblast growth factor signaling pathway. Wiley Interdiscip Rev. Dev. Biol. 4, 215−266.

Ornitz, D.M., Marie, P.J., 2015. Fibroblast growth factor signaling in skeletal development and disease. Genes Dev. 29, 1463−1486.

Ornitz, D.M., Legeai-Mallet, L., 2017. Achondroplasia: development, pathogenesis, and therapy. Dev. Dynam. 246, 291−309.

Pannier, S., Couloigner, V., Messaddeq, N., et al., 2009. Activating Fgfr3 Y367C mutation causes hearing loss and inner ear defect in a mouse model of chondrodysplasia. Biochim. Biophys. Acta 1792, 140−147.

Pauli, R.M., 2019. Achondroplasia: a comprehensive clinical review. Orphanet J Rare Dis 14 (1), 1 PubMed: PMID30606190.

Park, O.J., Kim, H.J., Woo, K.M., et al., 2010. GF2-activated ERK mitogen-activated protein kinase enhances Runx2 acetylation and stabilization. J. Biol. Chem. 285, 3568−3574.

Perlyn, C.A., Morriss-Kay, G., Darvann, T., et al., 2006. A model for the pharmacological treatment of crouzon syndrome. Neurosurgery 59, 210−215 discussion 210-215.

Peters, K., Ornitz, D., Werner, S., et al., 1993. Unique expression pattern of the FGF receptor 3 gene during mouse organogenesis. Dev. Biol. 155, 423−430.

Pfaff, M.J., Xue, K., Li, L., et al., 2016. FGFR2c-mediated ERK-MAPK activity regulates coronal suture development. Dev. Biol. 415, 242−250.

Priore, R., Dailey, L., Basilico, C., 2006. Downregulation of Akt activity contributes to the growth arrest induced by FGF in chondrocytes. J. Cell. Physiol. 207, 800–808.

Purcell, P., Joo, B.W., Hu, J.K., et al., 2009. Temporomandibular joint formation requires two distinct hedgehog-dependent steps. Proc. Natl. Acad. Sci. U.S.A. 106, 18297–18302.

Qi, H., Jin, M., Duan, Y., et al., 2014. FGFR3 induces degradation of BMP type I receptor to regulate skeletal development. Biochim. Biophys. Acta 1843, 1237–1247.

Quarles, L.D., 2012. Skeletal secretion of FGF-23 regulates phosphate and vitamin D metabolism. Nat. Rev. Endocrinol. 8, 276–286.

Quarto, N., Behr, B., Li, S., et al., 2009. Differential FGF ligands and FGF receptors expression pattern in frontal and parietal calvarial bones. Cells Tissues Organs. 190, 158–169.

Raucci, A., Laplantine, E., Mansukhani, A., et al., 2004. Activation of the ERK1/2 and p38 mitogen-activated protein kinase pathways mediates fibroblast growth factor-induced growth arrest of chondrocytes. J. Biol. Chem. 279, 1747–1756.

Reinhold, M.I., Abe, M., Kapadia, R.M., et al., 2004. FGF18 represses noggin expression and is induced by calcineurin. J. Biol. Chem. 279, 38209–38219.

Reinhold, M.I., Naski, M.C., 2007. Direct interactions of Runx2 and canonical Wnt signaling induce FGF18. J. Biol. Chem. 282, 3653–3663.

Rice, D.P., Aberg, T., Chan, Y., et al., 2000. Integration of FGF and TWIST in calvarial bone and suture development. Development 127, 1845–1855.

Rice, D.P., Rice, R., Thesleff, I., 2003. Fgfr mRNA isoforms in craniofacial bone development. Bone 33, 14–27.

Riminucci, M., Collins, M.T., Fedarko, N.S., et al., 2003. FGF-23 in fibrous dysplasia of bone and its relationship to renal phosphate wasting. J. Clin. Investig. 112, 683–692.

Rodriguez-Zabala, M., Aza-Carmona, M., Rivera-Pedroza, C.I., et al., 2017. FGF9 mutation causes craniosynostosis along with multiple synostoses. Hum. Mutat. 38, 1471–1476.

Rosello-Diez, A., Joyner, A.L., 2015. Regulation of long bone growth in vertebrates; it is time to catch up. Endocr. Rev. 36, 646–680.

Rousseau, F., Bonaventure, J., Legeai-Mallet, L., Pelet, A., Rozet, J.M., Maroteaux, P., Le Merrer, M., Munnich, A., 1994. Mutations in the gene encoding fibroblast growth factor receptor-3 in achondroplasia. Nature 371 (6494), 252–254. PubMed: PMID8078586.

Saadeh, P.B., Mehrara, B.J., Steinbrech, D.S., et al., 2000. Mechanisms of fibroblast growth factor-2 modulation of vascular endothelial growth factor expression by osteoblastic cells. Endocrinology 141, 2075–2083.

Sabbieti, M.G., Marchetti, L., Abreu, C., et al., 1999. Prostaglandins regulate the expression of fibroblast growth factor-2 in bone. Endocrinology 140, 434–444.

Sabbieti, M.G., Agas, D., Xiao, L., et al., 2009. Endogenous FGF-2 is critically important in PTH anabolic effects on bone. J. Cell. Physiol. 219, 143–151.

Sabbieti, M.G., Agas, D., Marchetti, L., et al., 2013. BMP-2 differentially modulates FGF-2 isoform effects in osteoblasts from newborn transgenic mice. Endocrinology 154, 2723–2733.

Sanui, T., Tanaka, U., Fukuda, T., Toyoda, K., Taketomi, T., Atomura, R., Yamamichi, K., Nishimura, F., 2015. Mutation of Spry2 induces proliferation and differentiation of osteoblasts but inhibits proliferation of gingival epithelial cells. J. Cell. Biochem. 116, 628–639.

Schmid, G.J., Kobayashi, C., Sandell, L.J., et al., 2009. Fibroblast growth factor expression during skeletal fracture healing in mice. Dev. Dynam. 238, 766–774.

Seki, K., Fujimori, T., Savagner, P., et al., 2003. Mouse Snail family transcription repressors regulate chondrocyte, extracellular matrix, type II collagen, and aggrecan. J. Biol. Chem. 278, 41862–41870.

Senarath-Yapa, K., Chung, M.T., McArdle, A., et al., 2012. Craniosynostosis: molecular pathways and future pharmacologic therapy. Organogenesis 8, 103–113.

Sévère, N., Miraoui, H., Marie, P.J., 2011 Jul 8. The Casitas B lineage lymphoma (Cbl) mutant G306E enhances osteogenic differentiation in human mesenchymal stromal cells in part by decreased Cbl-mediated platelet-derived growth factor receptor alpha and fibroblast growth factor receptor 2 ubiquitination. J. Biol. Chem. 286 (27), 24443–24450.

Sévère, N., Dieudonne, F.X., Marie, P.J., 2013. E3 ubiquitin ligase-mediated regulation of bone formation and tumorigenesis. Cell Death Dis. 4, e463.

Seyedin, S.M., Thomas, T.C., Thompson, A.Y., et al., 1985. Purification and characterization of two cartilage inducing factors from bovine demineralized bone. Proc. Natl. Acad. Sci. U.S.A. 82, 2267–2271.

Sheeba, C.J., Andrade, R.P., Duprez, D., et al., 2010. Comprehensive analysis of fibroblast growth factor receptor expression patterns during chick forelimb development. Int. J. Dev. Biol. 54, 1517–1526.

Shiang, R., Thompson, L.M., Zhu, Y.Z., et al., 1994. Mutations in the transmembrane domain of FGFR3 cause the most common genetic form of dwarfism, achondroplasia. Cell 78, 335–342.

Shimada, T., Mizutani, S., Muto, T., et al., 2001. Cloning and characterization of FGF23 as a causative factor of tumor-induced osteomalacia. Proc. Natl. Acad. Sci. U.S.A. 98, 6500–6505.

Shimoaka, T., Ogasawara, T., Yonamine, A., et al., 2002. Regulation of osteoblast, chondrocyte, and osteoclast functions by fibroblast growth factor (FGF)-18 in comparison with FGF-2 and FGF-10. J. Biol. Chem. 277, 7493–7500.

Shimokawa, K., Kimura-Yoshida, C., Nagai, N., et al., 2011. Cell surface heparan sulfate chains regulate local reception of FGF signaling in the mouse embryo. Dev. Cell 21, 257–272.

Shin, J.T., Opalenik, S.R., Wehby, J.N., et al., 1996. Serum-starvation induces the extracellular appearance of FGF-1. Biochim. Biophys. Acta Mol. Cell Res. 1312, 27–38.

Shukla, V., Coumoul, X., Wang, R.H., et al., 2007. RNA interference and inhibition of MEK-ERK signaling prevent abnormal skeletal phenotypes in a mouse model of craniosynostosis. Nat. Genet. 39, 1145−1150.

Shung, C.Y., Ota, S., Zhou, Z.Q., et al., 2012. Disruption of a Sox9-beta-catenin circuit by mutant Fgfr3 in thanatophoric dysplasia type II. Hum. Mol. Genet. 21, 4628−4644.

Smith, L.B., Dally, M.R., Sainz, R.D., et al., 2006. Enhanced skeletal growth of sheep heterozygous for an inactivated fibroblast growth factor receptor 3. J. Anim. Sci. 84, 2942−2949.

Smith, B.N., Burton, L.J., Henderson, V., et al., 2014. Snail promotes epithelial mesenchymal transition in breast cancer cells in part via activation of nuclear ERK2. PLoS One 9, e104987.

Song, S.J., Cool, S.M., Nurcombe, V., 2007. Regulated expression of syndecan-4 in rat calvaria osteoblasts induced by fibroblast growth factor-2. J. Cell. Biochem. 100 (2), 402−411.

Stubbs, J.R., He, N., Idiculla, A., et al., 2012. Longitudinal evaluation of FGF23 changes and mineral metabolism abnormalities in a mouse model of chronic kidney disease. J. Bone Miner. Res. 27, 38−46.

Su, W.C., Kitagawa, M., Xue, N., et al., 1997. Activation of Stat1 by mutant fibroblast growth-factor receptor in thanatophoric dysplasia type II dwarfism. Nature 386, 288−292.

Su, N., Sun, Q., Li, C., et al., 2010. Gain-of-function mutation in FGFR3 in mice leads to decreased bone mass by affecting both osteoblastogenesis and osteoclastogenesis. Hum. Mol. Genet. 19, 1199−1210.

Su, N., Jin, M., Chen, L., 2014. Role of FGF/FGFR signaling in skeletal development and homeostasis: learning from mouse models. Bone Res 2, 14003.

Sun, X., Meyers, E.N., Lewandoski, M., et al., 1999. Targeted disruption of Fgf8 causes failure of cell migration in the gastrulating mouse embryo. Genes Dev. 13, 1834−1846.

Sundaram, K., Senn, J., Reddy, S.V., 2009. SOCS-1/3 participation in FGF-2 signaling to modulate RANK ligand expression in Paget's disease of bone. J. Cell. Biochem. 114, 2032−2038.

Suzuki, H., Suda, N., Shiga, M., et al., 2012. Apert syndrome mutant FGFR2 and its soluble form reciprocally alter osteogenesis of primary calvarial osteoblasts. J. Cell. Physiol. 227, 3267−3277.

Takai, S., Tokuda, H., Hanai, Y., et al., 2007. Negative regulation by p70 S6 kinase of FGF-2-stimulated VEGF release through stress-activated protein kinase/c-Jun N-terminal kinase in osteoblasts. J. Bone Miner. Res. 22, 337−346.

Takei, Y., Minamizaki, T., Yoshiko, Y., 2015. Functional diversity of fibroblast growth factors in bone formation. Internet J. Endocrinol. 2015, 729352.

Tanaka, H., Ogasa, H., Barnes, J., et al., 1999. Actions of bFGF on mitogenic activity and lineage expression in rat osteoprogenitor cells: effect of age. Mol. Cell. Endocrinol. 150, 1−10.

Tang, C.H., Yang, R.S., Chen, Y.F., Fu, W.M., 2007 Apr. Basic fibroblast growth factor stimulates fibronectin expression through phospholipase C gamma, protein kinase C alpha, c-Src, NF-kappaB, and p300 pathway in osteoblasts. J. Cell. Physiol. 211 (1), 45−55.

Tang, L., Wu, X., Zhang, H., et al., 2017. A point mutation in Fgf9 impedes joint interzone formation leading to multiple synostoses syndrome. Hum. Mol. Genet. 26, 1280−1293.

Tanimoto, Y., Yokozeki, M., Hiura, K., et al., 2004. A soluble form of fibroblast growth factor receptor 2 (FGFR2) with S252W mutation acts as an efficient inhibitor for the enhanced osteoblastic differentiation caused by FGFR2 activation in Apert syndrome. J. Biol. Chem. 279, 45926−45934.

Tavormina, P.L., Shiang, R., Thompson, L.M., et al., 1995. Thanatophoric dysplasia (types I and II) caused by distinct mutations in fibroblast growth factor receptor 3. Nat. Genet. 9, 321−328.

Tavormina, P.L., Bellus, G.A., Webster, M.K., et al., 1999. A novel skeletal dysplasia with developmental delay and acanthosis nigricans is caused by a Lys650Met mutation in the fibroblast growth factor receptor 3 gene. Am. J. Hum. Genet. 64, 722−731.

Teerapornpuntakit, J., Wongdee, K., Krishnamra, N., et al., 2016. Expression of osteoclastogenic factor transcripts in osteoblast-like UMR-106 cells after exposure to FGF-23 or FGF-23 combined with parathyroid hormone. Cell Biol. Int. 40, 329−340.

Ten Berge, D., Brugmann, S.A., Helms, J.A., et al., 2008. Wnt and FGF signals interact to coordinate growth with cell fate specification during limb development. Development 135, 3247−3257.

Teplyuk, N.M., Haupt, L.M., Ling, L., et al., 2009. The osteogenic transcription factor Runx2 regulates components of the fibroblast growth factor/proteoglycan signaling axis in osteoblasts. J. Cell. Biochem. 107, 144−154.

Timsah, Z., Ahmed, Z., Lin, C.C., et al., 2014. Competition between Grb2 and Plcgamma1 for FGFR2 regulates basal phospholipase activity and invasion. Nat. Struct. Mol. Biol. 21, 180−188.

Torii, S., Kusakabe, M., Yamamoto, T., et al., 2004. Sef is a spatial regulator for Ras/MAP kinase signaling. Dev. Cell 7, 33−44.

Toydemir, R.M., Brassington, A.E., Bayrak-Toydemir, P., et al., 2006. A novel mutation in FGFR3 causes camptodactyly, tall stature, and hearing loss (CATSHL) syndrome. Am. J. Hum. Genet. 79, 935−941.

Tsang, M., Dawid, I.B., 2004. Promotion and attenuation of FGF signaling through the Ras-MAPK pathway. Sci. STKE. 2004, pe17.

Twigg, S.R., Healy, C., Babbs, C., et al., 2009. Skeletal analysis of the Fgfr3(P244R) mouse, a genetic model for the Muenke craniosynostosis syndrome. Dev. Dynam. 238, 331−342.

Twigg, S.R., Vorgia, E., McGowan, S.J., et al., 2013. Reduced dosage of ERF causes complex craniosynostosis in humans and mice and links ERK1/2 signaling to regulation of osteogenesis. Nat. Genet. 45, 308−313.

Vajo, Z., Francomano, C.A., Wilkin, D.J., 2000. The molecular and genetic basis of fibroblast growth factor receptor 3 disorders: the achondroplasia family of skeletal dysplasias, Muenke craniosynostosis, and Crouzon syndrome with acanthosis nigricans. Endocr. Rev. 21, 23−39.

Valverde-Franco, G., Liu, H., Davidson, D., et al., 2004. Defective bone mineralization and osteopenia in young adult FGFR3-/- mice. Hum. Mol. Genet. 13, 271−284.

Verheyden, J.M., Lewandoski, M., Deng, C., et al., 2005. Conditional inactivation of Fgfr1 in mouse defines its role in limb bud establishment, outgrowth and digit patterning. Development 132, 4235–4245.

Wang, Y., Spatz, M.K., Kannan, K., et al., 1999. A mouse model for achondroplasia produced by targeting fibroblast growth factor receptor 3. Proc. Natl. Acad. Sci. U.S.A. 96, 4455–4460.

Wang, Q., Green, R.P., Zhao, G., et al., 2001. Differential regulation of endochondral bone growth and joint development by FGFR1 and FGFR3 tyrosine kinase domains. Development 128, 3867–3876.

Wang, Y., Xiao, R., Yang, F., et al., 2005. Abnormalities in cartilage and bone development in the Apert syndrome FGFR2(+/S252W) mouse. Development 132, 3537–3548.

Wang, Y., Sun, M., Uhlhorn, V.L., et al., 2010. Activation of p38 MAPK pathway in the skull abnormalities of Apert syndrome Fgfr2(+P253R) mice. BMC Dev. Biol. 10, 22.

Wang, W., Nyman, J.S., Ono, K., et al., 2011. Mice lacking Nf1 in osteochondroprogenitor cells display skeletal dysplasia similar to patients with neurofibromatosis type I. Hum. Mol. Genet. 20, 3910–3924.

Wang, X., Wei, W., Krzeszinski, J.Y., et al., 2015. A liver-bone endocrine relay by igfbp1 promotes osteoclastogenesis and mediates FGF21-induced bone resorption. Cell Metabol. 22, 811–824.

Warren, S.M., Brunet, L.J., Harland, R.M., et al., 2003. The BMP antagonist noggin regulates cranial suture fusion. Nature 422, 625–629.

Wei, W., Dutchak, P.A., Wang, X., et al., 2012. Fibroblast growth factor 21 promotes bone loss by potentiating the effects of peroxisome proliferator-activated receptor gamma. Proc. Natl. Acad. Sci. U.S.A. 109, 3143–3148.

Wen, X., Li, X., Tang, Y., et al., 2016. Chondrocyte FGFR3 regulates bone mass by inhibiting osteogenesis. J. Biol. Chem. 291, 24912–24921.

Weng, T., Yi, L., Huang, J., et al., 2012. Genetic inhibition of FGFR1 in cartilage attenuates articular cartilage degeneration in adult mice. Arthritis Rheum. 64, 3982–3992.

Wilkie, A.O., 2005 Apr. Bad bones, absent smell, selfish testes: the pleiotropic consequences of human FGF receptor mutations. Cytokine Growth Factor Rev 16 (2), 187–203.

Wilkie, A.O., 2007. Cancer drugs to treat birth defects. Nat. Genet. 39, 1057–1059.

Wilkin, D.J., Szabo, J.K., Cameron, R., et al., 1998. Mutations in fibroblast growth-factor receptor 3 in sporadic cases of achondroplasia occur exclusively on the paternally derived chromosome. Am. J. Hum. Genet. 63, 711–716.

Wohrle, S., Henninger, C., Bonny, O., et al., 2013. Pharmacological inhibition of fibroblast growth factor (FGF) receptor signaling ameliorates FGF23-mediated hypophosphatemic rickets. J. Bone Miner. Res. 28, 899–911.

Wu, X.L., Gu, M.M., Huang, L., et al., 2009. Multiple synostoses syndrome is due to a missense mutation in exon 2 of FGF9 gene. Am. J. Hum. Genet. 85, 53–63.

Wu, A.L., Feng, B., Chen, M.Z., et al., 2013. Antibody-mediated activation of FGFR1 induces FGF23 production and hypophosphatemia. PLoS One 8, e57322.

Xiao, G., Jiang, D., Gopalakrishnan, R., et al., 2002. Fibroblast growth factor 2 induction of the osteocalcin gene requires MAPK activity and phosphorylation of the osteoblast transcription factor, Cbfa1/Runx2. J. Biol. Chem. 277, 36181–36187.

Xiao, L., Naganawa, T., Lorenzo, J., et al., 2010a. Nuclear isoforms of fibroblast growth factor 2 are novel inducers of hypophosphatemia via modulation of FGF23 and KLOTHO. J. Biol. Chem. 285, 2834–2846.

Xiao, L., Sobue, T., Esliger, A., et al., 2010b. Disruption of the Fgf2 gene activates the adipogenic and suppresses the osteogenic program in mesenchymal marrow stromal stem cells. Bone 47, 360–370.

Xiao, L., Esliger, A., Hurley, M.M., 2013. Nuclear fibroblast growth factor 2 (FGF2) isoforms inhibit bone marrow stromal cell mineralization through FGF23/FGFR/MAPK in vitro. J. Bone Miner. Res. 28, 35–45.

Xiao, Z., Huang, J., Cao, L., et al., 2014. Osteocyte-specific deletion of Fgfr1 suppresses FGF23. PLoS One 9, e104154.

Xie, Y., Su, N., Jin, M., et al., 2012. Intermittent PTH (1-34) injection rescues the retarded skeletal development and postnatal lethality of mice mimicking human achondroplasia and thanatophoric dysplasia. Hum. Mol. Genet. 21, 3941–3955.

Xie, Y., Zhou, S., Chen, H., et al., 2014. Recent research on the growth plate: advances in fibroblast growth factor signaling in growth plate development and disorders. J. Mol. Endocrinol. 53, T11–T34.

Xu, J., Lawshe, A., MacArthur, C.A., et al., 1999. Genomic structure, mapping, activity and expression of fibroblast growth factor 17. Mech. Dev. 83, 165–178.

Xu, D., Esko, J.D., 2014. Demystifying heparan sulfate-protein interactions. Annu. Rev. Biochem. 83, 129–157.

Yamashita, T., Yoshioka, M., Itoh, N., 2000. Identification of a novel fibroblast growth factor, FGF-23, preferentially expressed in the ventrolateral thalamic nucleus of the brain. Biochem. Biophys. Res. Commun. 277, 494–498.

Yan, D., Chen, D., Cool, S.M., et al., 2011. Fibroblast growth factor receptor 1 is principally responsible for fibroblast growth factor 2-induced catabolic activities in human articular chondrocytes. Arthritis Res. Ther. 13, R130.

Yang, F., Wang, Y., Zhang, Z., et al., 2008. The study of abnormal bone development in the Apert syndrome Fgfr2+/S252W mouse using a 3D hydrogel culture model. Bone 43, 55–63.

Yasoda, A., Komatsu, Y., Chusho, H., et al., 2004. Overexpression of CNP in chondrocytes rescues achondroplasia through a MAPK-dependent pathway. Nat. Med. 10, 80–86.

Yeh, E., Atique, R., Ishiy, F.A., et al., 2012. FGFR2 mutation confers a less drastic gain of function in mesenchymal stem cells than in fibroblasts. Stem Cell Rev. 8, 685–695.

Yeung Tsang, K., Wa Tsang, S., Chan, D., et al., 2014. The chondrocytic journey in endochondral bone growth and skeletal dysplasia. Birth Defects Res. C Embryo Today 102, 52–73.

Yin, L., Du, X., Li, C., et al., 2008. A Pro253Arg mutation in fibroblast growth factor receptor 2 (Fgfr2) causes skeleton malformation mimicking human Apert syndrome by affecting both chondrogenesis and osteogenesis. Bone 42, 631–643.

Yokota, M., Kobayashi, Y., Morita, J., et al., 2014. Therapeutic effect of nanogel-based delivery of soluble FGFR2 with S252W mutation on cranio-synostosis. PLoS One 9, e101693.

Yoon, W.J., Cho, Y.D., Kim, W.J., et al., 2014. Prolyl isomerase Pin1-mediated conformational change and subnuclear focal accumulation of Runx2 are crucial for fibroblast growth factor 2 (FGF2)-induced osteoblast differentiation. J. Biol. Chem. 289, 8828–8838.

Yoshiko, Y., Wang, H., Minamizaki, T., et al., 2007. Mineralized tissue cells are a principal source of FGF23. Bone 40, 1565–1573.

Yu, K., Herr, A.B., Waksman, G., et al., 2000. Loss of fibroblast growth factor receptor 2 ligand-binding specificity in Apert syndrome. Proc. Natl. Acad. Sci. U.S.A. 97, 14536–14541.

Yu, K., Ornitz, D.M., 2001. Uncoupling fibroblast growth factor receptor 2 ligand binding specificity leads to Apert syndrome-like phenotypes. Proc. Natl. Acad. Sci. U.S.A. 98, 3641–3643.

Yu, K., Xu, J., Liu, Z., et al., 2003. Conditional inactivation of FGF receptor 2 reveals an essential role for FGF signaling in the regulation of osteoblast function and bone growth. Development 130, 3063–3074.

Yu, K., Ornitz, D.M., 2008. FGF signaling regulates mesenchymal differentiation and skeletal patterning along the limb bud proximodistal axis. Development 135, 483–491.

Zhang, K., Corsa, C.A., Ponik, S.M., et al., 2013. The collagen receptor discoidin domain receptor 2 stabilizes SNAIL1 to facilitate breast cancer metastasis. Nat. Cell Biol. 15, 677–687.

Zhou, Y.X., Xu, X., Chen, L., et al., 2000. A Pro250Arg substitution in mouse Fgfr1 causes increased expression of Cbfa1 and premature fusion of calvarial sutures. Hum. Mol. Genet. 9, 2001–2008.

Zhou, B.P., Deng, J., Xia, W., et al., 2004. Dual regulation of Snail by GSK-3beta-mediated phosphorylation in control of epithelial-mesenchymal transition. Nat. Cell Biol. 6, 931–940.

Zhou, Z.Q., Ota, S., Deng, C., et al., 2015. Mutant activated FGFR3 impairs endochondral bone growth by preventing SOX9 downregulation in differentiating chondrocytes. Hum. Mol. Genet. 24, 1764–1773.

Further reading

Abad, V., Meyers, J.L., Weise, M., et al., 2002. The role of the resting zone in growth plate chondrogenesis. Endocrinology 143, 1851–1857.

Agoston, H., Khan, S., James, C.G., et al., 2007. C-type natriuretic peptide regulates endochondral bone growth through p38 MAP kinase-dependent and -independent pathways. BMC Dev. Biol. 7, 18.

Ahmad, I., Iwata, T., Leung, H.Y., 2010. Mechanisms of FGFR-mediated carcinogenesis. Biochim. Biophys. Acta 1823, 850–860.

Akiyama, H., Chaboissier, M.C., Martin, J.F., et al., 2002. The transcription factor Sox9 has essential roles in successive steps of the chondrocyte differentiation pathway and is required for expression of Sox5 and Sox6. Genes Dev. 16, 2813–2828.

Bi, W., Deng, J.M., Zhang, Z., et al., 1999. Sox9 is required for cartilage formation. Nat. Genet. 22, 85–89.

Bocciardi, R., Giorda, R., Buttgereit, J., et al., 2007. Overexpression of the C-type natriuretic peptide (CNP) is associated with overgrowth and bone anomalies in an individual with balanced t(2;7) translocation. Hum. Mutat. 28, 724–731.

Chen, W.J., Jingushi, S., Aoyama, I., et al., 2004. Effects of FGF-2 on metaphyseal fracture repair in rabbit tibiae. J. Bone Miner. Metab. 22, 303–309.

Chikazu, D., Katagiri, M., Ogasawara, T., et al., 2001. Regulation of osteoclast differentiation by fibroblast growth factor 2: stimulation of receptor activator of nuclear factor kappaB ligand/osteoclast differentiation factor expression in osteoblasts and inhibition of macrophage colony-stimulating factor function in osteoclast precursors. J. Bone Miner. Res. 16, 2074–2081.

Dakouane Giudicelli, M., Serazin, V., et al., 2008. Increased achondroplasia mutation frequency with advanced age and evidence for G1138A mosaicism in human testis biopsies. Fertil. Steril. 89, 1651–1656.

Dirckx, N., Van Hul, M., Maes, C., 2013. Osteoblast recruitment to sites of bone formation in skeletal development, homeostasis, and regeneration. Birth Defects Res C Embryo Today 99, 170–191.

Dy, P., Wang, W., Bhattaram, P., et al., 2012. Sox9 directs hypertrophic maturation and blocks osteoblast differentiation of growth plate chondrocytes. Dev. Cell 22, 597–609.

Feng, J.Q., Clinkenbeard, E.L., Yuan, B., et al., 2013. Osteocyte regulation of phosphate homeostasis and bone mineralization underlies the patho-physiology of the heritable disorders of rickets and osteomalacia. Bone 54, 213–221.

Feng, S., Zhou, L., Nice, E.C., et al., 2015. Fibroblast growth factor receptors: multifactorial-contributors to tumor initiation and progression. Histol. Histopathol. 30, 13–31.

Fernanda Amary, M., Ye, H., Berisha, F., et al., 2014. Fibroblastic growth factor receptor 1 amplification in osteosarcoma is associated with poor response to neo-adjuvant chemotherapy. Cancer Med. 3, 980–987.

Garcia, S., Dirat, B., Tognacci, T., et al., 2013. Postnatal soluble FGFR3 therapy rescues achondroplasia symptoms and restores bone growth in mice. Sci. Transl. Med. 5, 203ra124.

Girnita, L., Girnita, A., Wang, M., et al., 2000. A link between basic fibroblast growth factor (bFGF) and EWS/FLI-1 in Ewing's sarcoma cells. Oncogene 19, 4298–4301.

Gonzalez, A.M., Hill, D.J., Logan, A., et al., 1996. Distribution of fibroblast growth factor (FGF)-2 and FGF receptor-1 messenger RNA expression and protein presence in the mid-trimester human fetus. Pediatr. Res. 39, 375–385.

Gordon, J.A., Montecino, M.A., Aqeilan, R.I., et al., 2014. Epigenetic pathways regulating bone homeostasis: potential targeting for intervention of skeletal disorders. Curr. Osteoporos. Rep. 12, 496–506.

Goriely, A., McVean, G.A., Rojmyr, M., et al., 2003. Evidence for selective advantage of pathogenic FGFR2 mutations in the male germ line. Science 301, 643–646.

Goriely, A., McVean, G.A., van Pelt, A.M., et al., 2005. Gain-of-function amino acid substitutions drive positive selection of FGFR2 mutations in human spermatogonia. Proc. Natl. Acad. Sci. U.S.A. 102, 6051–6056.

Goriely, A., Wilkie, A.O., 2012. Paternal age effect mutations and selfish spermatogonial selection: causes and consequences for human disease. Am. J. Hum. Genet. 90, 175–200.

Guagnano, V., Kauffmann, A., Wohrle, S., et al., 2012. FGFR genetic alterations predict for sensitivity to NVP-BGJ398, a selective pan-FGFR inhibitor. Cancer Discov. 2, 1118–1133.

Hadari, Y., Schlessinger, J., 1999. FGFR3-targeted mAb therapy for bladder cancer and multiple myeloma. J. Clin. Investig. 119, 1077–1079.

Han, X., Xiao, Z., Quarles, L.D., 2015. Membrane and integrative nuclear fibroblastic growth factor receptor (FGFR) regulation of FGF-23. J. Biol. Chem. 290, 10447–10459.

Hannema, S.E., van Duyvenvoorde, H.A., Premsler, T., et al., 2013. An activating mutation in the kinase homology domain of the natriuretic peptide receptor-2 causes extremely tall stature without skeletal deformities. J. Clin. Endocrinol. Metab. 98, E1988–E1998.

Hatch, N.E., Hudson, M., Seto, M.L., et al., 2006. Intracellular retention, degradation, and signaling of glycosylation-deficient FGFR2 and craniosynostosis syndrome-associated FGFR2C278F. J. Biol. Chem. 281, 27292–27305.

Hamada, T., Suda, N., Kuroda, T., 2009. Immunohistochemical localization of fibroblast growth factor receptors in the rat mandibular condylar cartilage and tibial cartilage. J. Bone Miner. Metab. 17, 274–282.

Horton, W.A., Hall, J.G., Hecht, J.T., 2007. Achondroplasia. Lancet 370, 162–172.

Hunziker, E.B., Schenk, R.K., Cruz-Orive, L.M., 1987. Quantitation of chondrocyte performance in growth-plate cartilage during longitudinal bone growth. J. Bone Joint Surg. Am. 69, 162–173.

Hunziker, E.B., Schenk, R.K., 1989. Physiological mechanisms adopted by chondrocytes in regulating longitudinal bone growth in rats. J. Physiol. 414, 55–71.

Hutchison, M.R., 2012. BDNF alters ERK/p38 MAPK activity ratios to promote differentiation in growth plate chondrocytes. Mol. Endocrinol. 26, 1406–1416.

Ikegami, D., Akiyama, H., Suzuki, A., et al., 2011. Sox9 sustains chondrocyte survival and hypertrophy in part through Pik3ca-Akt pathways. Development 138, 1507–1519.

Kalinina, J., Byron, S.A., Makarenkova, H.P., et al., 2009. Homodimerization controls the fibroblast growth factor 9 subfamily's receptor binding and heparan sulfate-dependent diffusion in the extracellular matrix. Mol. Cell Biol. 29, 4663–4678.

Kamura, S., Matsumoto, Y., Fukushi, J.I., et al., 2010. Br. J. Canc. 103, 370–381.

Kanazawa, H., Tanaka, H., Inoue, M., et al., 2003. Efficacy of growth hormone therapy for patients with skeletal dysplasia. J. Bone Miner. Metab. 21, 307–310.

Karlsson, C., Thornemo, M., Henriksson, H.B., et al., 2009. Identification of a stem cell niche in the zone of Ranvier within the knee joint. J. Anat. 215, 355–363.

Katoh, M., 2009. FGFR2 abnormalities underlie a spectrum of bone, skin, and cancer pathologies. J. Investig. Dermatol. 129, 1861–1867.

Katoh, M., 2010. Genetic alterations of FGF receptors: an emerging field in clinical cancer diagnostics and therapeutics. Expert Rev. Anticancer Ther. 10, 1375–1379.

Kawaguchi, H., Pilbeam, C.C., Gronowicz, G., et al., 1995. Transcriptional induction of prostaglandin G/H synthase-2 by basic fibroblast growth factor. J. Clin. Investig. 96, 923–930.

Kawaguchi, H., Chikazu, D., Nakamura, K., et al., 2000. Direct and indirect actions of fibroblast growth factor 2 on osteoclastic bone resorption in cultures. J. Bone Miner. Res. 15, 466–473.

Komaki, H., Tanaka, T., Chazono, M., et al., 2006. Repair of segmental bone defects in rabbit tibiae using a complex of beta-tricalcium phosphate, type I collagen, and fibroblast growth factor-2. Biomaterials 27, 5118–5126.

Kosher, R.A., Kulyk, W.M., Gay, S.W., 1986. Collagen gene expression during limb cartilage differentiation. J. Cell Biol. 102, 1151–1156.

Kozhemyakina, E., Lassar, A.B., Zelzer, E., 2015. A pathway to bone: signaling molecules and transcription factors involved in chondrocyte development and maturation. Development 142, 817–831.

Kuro-o, M., 2008. Endocrine FGFs and Klothos: emerging concepts. Trends Endocrinol. Metabol. 19, 239–245.

Kurosu, H., Ogawa, Y., Miyoshi, M., et al., 2006. Regulation of fibroblast growth factor-23 signaling by klotho. J. Biol. Chem. 281, 6120–6123.

Laederich, M.B., Horton, W.A., 2012. FGFR3 targeting strategies for achondroplasia. Expert Rev. Mol. Med. 14, e11.

Li, Y., Ahrens, M.J., Wu, A., et al., 2011. Calcium/calmodulin-dependent protein kinase II activity regulates the proliferative potential of growth plate chondrocytes. Development 138, 359–370.

Lian, J.B., Stein, G.S., Javed, A., et al., 2006. Networks and hubs for the transcriptional control of osteoblastogenesis. Rev. Endocr. Metab. Disord. 7, 1–16.

Liang, G., Chen, G., Wei, X., et al., 2013. Small molecule inhibition of fibroblast growth factor receptors in cancer. Cytokine Growth Factor Rev. 24, 467–475.

Lim, J., Tu, X., Choi, K., et al., 2015. BMP-Smad4 signaling is required for precartilaginous mesenchymal condensation independent of Sox9 in the mouse. Dev. Biol. 400, 132−138.

Long, F., 2012. Building strong bones: molecular regulation of the osteoblast lineage. Nat. Rev. Mol. Cell Biol. 13, 27−38.

Long, F., Ornitz, D.M., 2013. Development of the endochondral skeleton. Cold Spring Harb. Perspect. Biol. 5, 1−20.

Maes, C., Kobayashi, T., Selig, M.K., et al., 2010. Osteoblast precursors, but not mature osteoblasts, move into developing and fractured bones along with invading blood vessels. Dev. Cell 19, 329−344.

Martinez-Torrecuadrada, J., Cifuentes, G., Lopez-Serra, P., et al., 2005. Targeting the extracellular domain of fibroblast growth factor receptor 3 with human single-chain Fv antibodies inhibits bladder carcinoma cell line proliferation. Clin. Cancer Res. 11, 6280−6290.

Maruyama, T., Mirando, A.J., Deng, C.X., et al., 2010. The balance of WNT and FGF signaling influences mesenchymal stem cell fate during skeletal development. Sci. Signal. 3, ra40.

Matsushita, T., Chan, Y.Y., Kawanami, A., et al., 2009a. Extracellular signal-regulated kinase 1 (ERK1) and ERK2 play essential roles in osteoblast differentiation and in supporting osteoclastogenesis. Mol. Cell Biol. 29, 5843−5857.

Matsushita, M., Kitoh, H., Ohkawara, B., et al., 2013. Meclozine facilitates proliferation and differentiation of chondrocytes by attenuating abnormally activated FGFR3 signaling in achondroplasia. PLoS One 8, e81569.

Matsushita, M., Hasegawa, S., Kitoh, H., et al., 2015. Meclozine promotes longitudinal skeletal growth in transgenic mice with achondroplasia carrying a gain-of-function mutation in the FGFR3 gene. Endocrinology 156, 548−554.

Moon, A.M., Guris, D.L., Seo, J.H., et al., 2006. Crkl deficiency disrupts Fgf8 signaling in a mouse model of 22q11 deletion syndromes. Dev. Cell 10, 71−80.

Nah, H.D., Rodgers, B.J., Kulyk, W.M., et al., 1998. In situ hybridization analysis of the expression of the type II collagen gene in the developing chicken limb bud. Collagen Relat. Res. 8, 277−294.

Nakao, K., Osawa, K., Yasoda, A., et al., 2015. The Local CNP/GC-B system in growth plate is responsible for physiological endochondral bone growth. Sci. Rep. 5, 10554.

Namlos, H.M., Meza-Zepeda, L.A., Baroy, T., et al., 2012. Modulation of the osteosarcoma expression phenotype by microRNAs. PLoS One 7, e48086.

Noonan, K.J., Hunziker, E.B., Nessler, J., et al., 1998. Changes in cell, matrix compartment, and fibrillar collagen volumes between growth-plate zones. J. Orthop. Res. 16, 500−508.

Olney, R.C., Prickett, T.C., Espiner, E.A., et al., 2015. C-type natriuretic peptide plasma levels are elevated in subjects with achondroplasia, hypochondroplasia, and thanatophoric dysplasia. J. Clin. Endocrinol. Metab. 100, E355−E359.

Ornitz, D.M., 2000. FGFs, heparan sulfate and FGFRs: complex interactions essential for development. Bioessays 22, 108−112.

Orr-Urtreger, A., Givol, D., Yayon, A., et al., 1991. Developmental expression of two murine fibroblast growth factor receptors, flg and bek. Development 113, 1419−1434.

Ozasa, A., Komatsu, Y., Yasoda, A., et al., 2005. Complementary antagonistic actions between C-type natriuretic peptide and the MAPK pathway through FGFR-3 in ATDC5 cells. Bone 36, 1056−1064.

Peake, N.J., Hobbs, A.J., Pingguan-Murphy, B., et al., 2014. Role of C-type natriuretic peptide signalling in maintaining cartilage and bone function. Osteoarthritis Cartilage 22, 1800−1807.

Peschard, P., Park, M., 2003. Escape from Cbl-mediated downregulation: a recurrent theme for oncogenic deregulation of receptor tyrosine kinases. Cancer Cell 3, 519−523.

Peters, K.G., Werner, S., Chen, G., et al., 1992. Two FGF receptor genes are differentially expressed in epithelial and mesenchymal tissues during limb formation and organogenesis in the mouse. Development 114, 233−243.

Qing, J., Du, X., Chen, Y., et al., 2009. Antibody-based targeting of FGFR3 in bladder carcinoma and t(4;14)-positive multiple myeloma in mice. J. Clin. Investig. 119, 1216−1229.

Rapraeger, A.C., Krufka, A., Olwin, B., 1991. Requirement of heparan sulfate for bFGF-mediated fibroblast growth and myoblast differentiation. Science 252, 1705−1708.

Robinson, D., Hasharoni, A., Cohen, N., et al., 1999. Fibroblast growth factor receptor-3 as a marker for precartilaginous stem cells. Clin. Orthop. Relat. Res. S163−S175.

Sahni, M., Ambrosetti, D.C., Mansukhani, A., et al., 1999. FGF signaling inhibits chondrocyte proliferation and regulates bone development through the STAT-1 pathway. Genes Dev. 13, 1361−1366.

Saran, U., Gemini Piperni, S., Chatterjee, S., 2014. Role of angiogenesis in bone repair. Arch. Biochem. Biophys. 561, 109−117.

Schlessinger, J., 2000. Cell signaling by receptor tyrosine kinases. Cell 103, 211−225.

Schlessinger, J., 2003. Signal transduction. Autoinhibition control. Science 300, 750−752.

Schmidt, M.H., Dikic, I., 2005. The Cbl interactome and its functions. Nat. Rev. Mol. Cell Biol. 6, 907−918.

Sebastian, A., Matsushita, T., Kawanami, A., et al., 2011. Genetic inactivation of ERK1 and ERK2 in chondrocytes promotes bone growth and enlarges the spinal canal. J. Orthop. Res. 29, 375−379.

Shinde, D.N., Elmer, D.P., Calabrese, P., et al., 2013. New evidence for positive selection helps explain the paternal age effect observed in achondroplasia. Hum. Mol. Genet. 22, 4117−4126.

Sun, X.H., Geng, X.L., Zhang, J., et al., 2015. miRNA-646 suppresses osteosarcoma cell metastasis by downregulating fibroblast growth factor 2 (FGF2). Tumour Biol. 36, 2127−2134.

Szebenyi, G., Savage, M.P., Olwin, B.B., et al., 1995. Changes in the expression of fibroblast growth factor receptors mark distinct stages of chondrogenesis in vitro and during chick limb skeletal patterning. Dev. Dynam. 204, 446−456.

Tan, Y., Rouse, J., Zhang, A., et al., 1996. FGF and stress regulate CREB and ATF-1 via a pathway involving p38 MAP kinase and MAPKAP kinase-2. EMBO J. 15, 4629–4642.

Tsuji, T., Kunieda, T., 2005. A loss-of-function mutation in natriuretic peptide receptor 2 (Npr2) gene is responsible for disproportionate dwarfism in cn/cn mouse. J. Biol. Chem. 280, 14288–14292.

Turner, N., Grose, R., 2010. Fibroblast growth factor signalling: from development to cancer. Nat. Rev. Canc. 10, 116–129.

Urakawa, I., Yamazaki, Y., Shimada, T., et al., 2006. Klotho converts canonical FGF receptor into a specific receptor for FGF23. Nature 444, 770–774.

Wendt, D.J., Dvorak-Ewell, M., Bullens, S., et al., 2015. Neutral endopeptidase-resistant C-type natriuretic peptide variant represents a new therapeutic approach for treatment of fibroblast growth factor receptor 3-related dwarfism. J. Pharmacol. Exp. Ther. 353, 132–149.

White, K.E., Cabral, J.M., Davis, S.I., et al., 2005. Mutations that cause osteoglophonic dysplasia define novel roles for FGFR1 in bone elongation. Am. J. Hum. Genet. 76, 361–367.

Wiedemann, M., Trueb, B., 2000. Characterization of a novel protein (FGFRL1) from human cartilage related to FGF receptors. Genomics 69, 275–279.

Wong, A., Lamothe, B., Lee, A., et al., 2002. FRS2 alpha attenuates FGF receptor signaling by Grb2-mediated recruitment of the ubiquitin ligase Cbl. Proc. Natl. Acad. Sci. U.S.A. 99, 6684–6689.

Wu, Z.L., Zhang, L., Yabe, T., et al., 2003. The involvement of heparan sulfate (HS) in FGF1/HS/FGFR1 signaling complex. J. Biol. Chem. 278, 17121–17129.

Xiao, L., Naganawa, T., Obugunde, E., et al., 2004. Stat1 controls postnatal bone formation by regulating fibroblast growth factor signaling in osteoblasts. J. Biol. Chem. 279, 27743–27752.

Xiao, L., Liu, P., Li, X., et al., 2009. Exported 18-kDa isoform of fibroblast growth factor-2 is a critical determinant of bone mass in mice. J. Biol. Chem. 284, 3170–3182.

Yamashita, A., Morioka, M., Kishi, H., et al., 2014. Statin treatment rescues FGFR3 skeletal dysplasia phenotypes. Nature 513, 507–511.

Yang, L., Tsang, K.Y., Tang, H.C., et al., 2014. Hypertrophic chondrocytes can become osteoblasts and osteocytes in endochondral bone formation. Proc. Natl. Acad. Sci. U.S.A. 111, 12097–12102.

Yayon, A., Klagsbrun, M., Esko, J.D., et al., 1991. Cell surface, heparin-like molecules are required for binding of basic fibroblast growth factor to its high affinity receptor. Cell 64, 841–848.

Yoon, B.S., Ovchinnikov, D.A., Yoshii, I., et al., 2005. Bmpr1a and Bmpr1b have overlapping functions and are essential for chondrogenesis in vivo. Proc. Natl. Acad. Sci. U.S.A. 102, 5062–5067.

Yoshida, C.A., Yamamoto, H., Fujita, T., et al., 2004. Runx2 and Runx3 are essential for chondrocyte maturation, and Runx2 regulates limb growth through induction of Indian hedgehog. Genes Dev. 18, 952–963.

Zeller, R., Lopez-Rios, J., Zuniga, A., 2009. Vertebrate limb bud development: moving towards integrative analysis of organogenesis. Nat. Rev. Genet. 10, 845–858.

Zhou, X., von der Mark, K., Henry, S., et al., 2014. Chondrocytes transdifferentiate into osteoblasts in endochondral bone during development, postnatal growth and fracture healing in mice. PLoS Genet. 10, e1004820.

Chapter 46

Vascular endothelial growth factor and bone–vascular interactions

Steve Stegen[1,2] and Geert Carmeliet[1,2]

[1]*Laboratory of Clinical and Experimental Endocrinology, Department of Chronic Diseases, Metabolism and Ageing, KU Leuven, Leuven, Belgium;*
[2]*Prometheus, Division of Skeletal Tissue Engineering, KU Leuven, Leuven, Belgium*

Chapter outline

Introduction

It has been long established that a functional vascular system is crucial for skeletal development and homeostasis (Trueta and Morgan, 1960; Trueta and Amato, 1960). Skeletal blood vessels not only supply oxygen and nutrients to ensure proper functioning of bone-forming and bone-resorbing cells but also deliver calcium and phosphate to sites of active bone mineralization, together with hormones and growth factors that regulate the function of skeletal cells (Marenzana and Arnett, 2013). Moreover, the bone marrow vasculature provides a niche for skeletal stem and progenitor cells next to blood-forming hematopoietic stem cells (HSCs) (Gomez-Gaviro et al., 2012). Particular to the skeleton is that in contrast to the highly vascularized bone tissue, the cartilaginous part is avascular. The intimate connection of the vascular system with bone cells occurs not only during development (Stegen and Carmeliet, 2018) but also during bone repair (Trueta, 1974; Stegen et al., 2015), indicating that a better understanding of the mechanisms that couple bone and blood vessels may provide new therapeutic options for skeletal pathologies.

Recent work using transgenic mouse models and technical advances in bone imaging have substantially improved our knowledge about the role, molecular regulation, and cellular interplay of skeletal vascularization processes during bone development, homeostasis, and repair. In this edition, we first discuss the current understanding of the vascular organization and structure in bone and the interplay of blood vessels and skeletal cells. We specifically focus on the coupling of angiogenesis and osteogenesis by vascular endothelial growth factor (VEGF), the prime angiogenic mediator. Only a brief overview will be given on VEGF molecular biology, and the reader is referred to earlier editions of this volume and excellent recent reviews (Bilzikian et al., 2002; Simons et al., 2016; Chung and Ferrara, 2011; Potente et al., 2011; Towler, 2008). In the final part, we will briefly discuss the therapeutic potential of VEGF modulation during fracture healing.

Principles of Bone Biology. https://doi.org/10.1016/B978-0-12-814841-9.00046-4

Bone development and the skeletal vascular system

Bone is formed through either intramembranous or endochondral ossification (Harada and Rodan, 2003; Long, 2011). During intramembranous bone formation, mesenchymal cells condense at the site of the future bone and differentiate directly into bone-forming osteoblasts. These osteoblasts synthesize a collagenous bone matrix, which later becomes mineralized. Intramembranous ossification primarily forms the flat craniofacial bones and part of the clavicle. Endochondral bone formation, on the other hand, regulates especially the development of the long bones of the axial and appendicular skeleton. Typical for this bone formation process is the conversion of cartilage into bone, which mainly happens at three different stages. The first time is when the primary ossification center (POC) is formed. This process encompasses several consecutive steps including condensation of mesenchymal cells, followed by differentiation of the centrally localized cells into chondrocytes to form a cartilage template, and finally replacement of this anlage by bone tissue through the coordinated action of invading blood vessels, osteoprogenitors, and osteoclasts. The second site is the chondro−osseous junction between growth plate and bone metaphysis, where hypertrophic chondrocytes and cartilage matrix are continuously being replaced by trabecular bone. This process is crucial for bone lengthening. The third stage is the conversion of the epiphyseal cartilage into the secondary ossification center (SOC); this process is comparable, but not identical, to the formation of the POC.

Both intramembranous and endochondral bone formation are closely associated with angiogenesis, ultimately giving rise to bone tissue that is highly vascularized. The blood supply of long bones is partially provided by nutrient arteries that enter the diaphyseal cortex, link to capillaries in the bone marrow and then connect to the venous tree, characterized by a central sinus, which finally exits the bone (Marenzana and Arnett, 2013). Recent evidence shows, however, that most of the blood circulation enters and leaves the bone by hundreds of transcortical vessels expressing arterial or venous markers (Grüneboom et al., 2019). How these vessels connect with the blood vessels in the bone marrow is still unknown.

Skeletal blood vessels in the bone marrow of long bones are thus highly heterogeneous and functionally specialized. Typical for the bone vascular system is that the connection between arterial and venous systems is formed by a serial organization of two capillary systems, each of which displays specific morphological and physiological features, and together they form the majority of medullary vessels (Stegen and Carmeliet, 2018). Blood from the arteries first flows to capillaries at the endosteum and chondro−osseous junction. These highly organized capillary vessels, especially in the metaphysis, display a columnar structure, are interconnected by distal loops or arches (Ramasamy et al., 2016), and are called type H vessels because of their high expression of the endothelial cell markers CD31 and endomucin (Kusumbe et al., 2014). Type H vessels then connect to the dense, highly branched capillary network in the bone marrow cavity of the diaphysis, which corresponds to the sinusoidal vasculature described previously. These vessels express lower levels of CD31 and endomucin, and are therefore called type L vessels (Kusumbe et al., 2014). Thus, blood from arteries first flows into type H vessels and subsequently enters the type L sinusoidal network and finally drains into the large central vein (Kusumbe et al., 2014). An important feature of type H capillaries is the close association with Osterix (Osx)-expressing osteoprogenitor cells that are involved in the maintenance of trabecular bone mass. Indeed, endothelial cells from type H vessels express relatively high levels of proosteogenic factors, which may explain the coupling of angiogenesis and osteogenesis at the molecular level (Kusumbe et al., 2014; Ramasamy et al., 2014). In contrast, type L vessels lack perivascular Osx-positive cells and are instead surrounded by cells from the hematopoietic system. The distinct structural and functional properties of type H and L endothelium likely also affect the local microenvironment and the function of associated cells. For example, the bone marrow diaphysis is suggested to be more hypoxic than the metaphyseal and endosteal regions (Kusumbe et al., 2014; Spencer et al., 2014), which may be related to the serial organization of the two capillary systems and the potential reduced delivery of oxygen by the type L vessels or sinusoids to the diaphysis. Moreover, the relatively higher blood flow and shear rate in arteriolar capillaries, compared with sinusoids, are suggested to be involved in the regulation of osteoprogenitor function (Ramasamy et al., 2016). On the other hand, HSCs mainly reside near endosteal capillaries, which display a tight endothelial blood−bone marrow barrier, whereas highly permeable sinusoids serve as a site for cell trafficking (Itkin et al., 2016).

Taken together, despite recent advances, the mechanisms that govern the establishment, growth, and maintenance of the bone vascular system are not yet fully understood and require further investigation. However, several studies have provided more insight on the molecular regulation of skeletal angiogenesis by VEGF, which will be further discussed below. We will primarily focus on findings evidenced by in vivo experiments and less on those only supported by in vitro analyses.

Vascular endothelial growth factor, a crucial angiogenic factor

In recent years, several molecular factors that control bone vascularization have been identified. Some of these stimulate angiogenesis directly by inducing neoangiogenesis and include factors such as VEGF, placental growth factor (PlGF),

fibroblast growth factor (FGF), and members of the transforming growth factor β (TGF-β) family. Others primarily regulate the production of angiogenic molecules; examples are bone morphogenetic proteins (BMPs), angiopoietin, platelet-derived growth factor, and insulin-like growth factor family members.

The most extensively studied group of angiogenic growth factors in bone is the VEGF family, which includes VEGF-A, VEGF-B, VEGF-C, VEGF-D, VEGF-E, and PlGF (Ferrara et al., 2003; Tjwa et al., 2003). Skeletal cells, including chondrocytes, osteoblasts, osteocytes, and osteoclasts, mainly express VEGF-A, although additional roles for PlGF, VEGF-C, and VEGF-D have been recently proposed in osteolineage cells (Hominick et al., 2018; Deckers et al., 2000; Orlandini et al., 2006; Maes et al., 2006; Coenegrachts et al., 2010). VEGF-A, hereafter referred to as VEGF, controls angiogenesis and vascular function at multiple levels. First, as a mitogen for endothelial cells derived from arteries, veins, and lymphatics, VEGF induces sprouting angiogenesis and new blood vessel formation. Second, it functions as a survival factor for endothelial cells. Third, VEGF controls hemodynamics by inducing vasodilatation and enhancing vascular permeability (Potente et al., 2011; Stegen and Carmeliet, 2018). The requirement for VEGF signaling in early vasculogenesis is underscored by the phenotypic lethality of mice lacking even a single VEGF allele (Carmeliet et al., 1996; Ferrara et al., 1996). Moreover, pharmacological inactivation of VEGF signaling in neonatal mice results in stunted growth and increased apoptosis of endothelial cells (Gerber et al., 1999).

The human *VEGF* gene, encoded on chromosome 6, is organized as eight exons separated by seven introns. Alternative splicing results in several protein isoforms, including VEGF121, VEGF165, VEGF189, and VEGF206 as the most predominantly expressed, with different matrix-binding affinities (Ferrara et al., 2003). VEGF121 freely diffuses throughout the extracellular matrix (ECM) because it lacks heparin-binding properties, whereas VEGF198 and VEGF206 are almost completely sequestered in the ECM. VEGF165 has intermediary properties—it is secreted, but a significant fraction remains bound to the cell surface and ECM (Fig. 46.1A). Only three isoforms have been identified in mice (VEGF120, VEGF164, and VEGF188), with similar heparin-binding affinities as their respective human isoforms (Ferrara et al., 2003; Tjwa et al., 2003). In murine bone, VEGF164 is the most expressed isoform, followed by VEGF120 and VEGF188 (Maes et al., 2002).

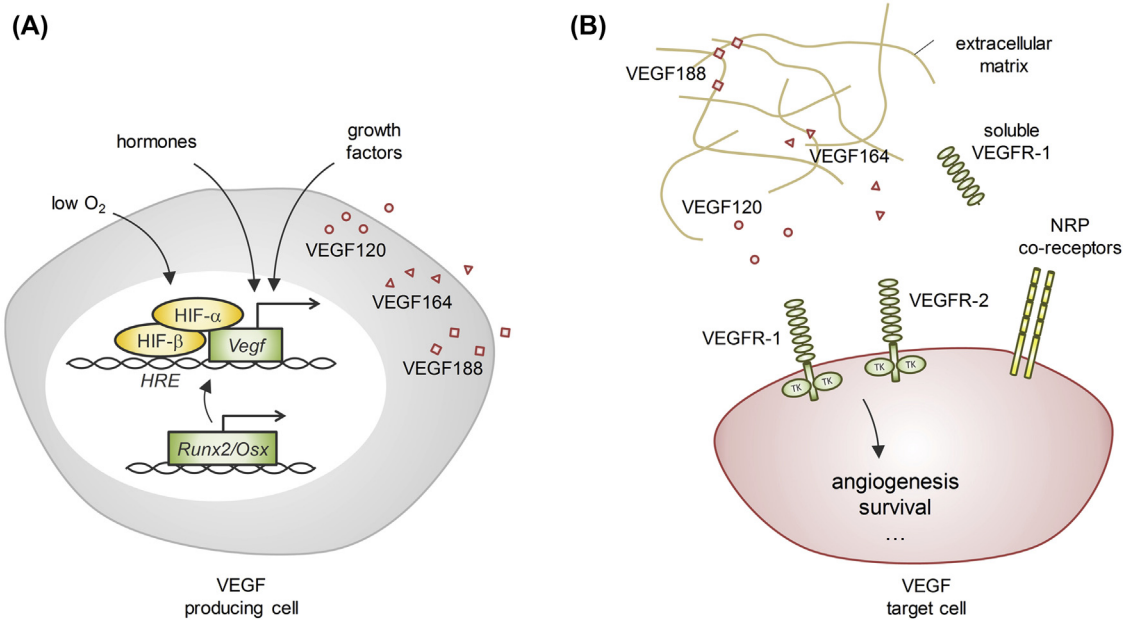

FIGURE 46.1 Regulation and signaling of VEGF in skeletal cells. (A) During bone development, vascular endothelial growth factor (VEGF) is mainly expressed by osteochondroprogenitors and hypertrophic chondrocytes. Bone-specific transcription factors like Runx2 and Osterix (Osx) regulate VEGF expression, which is further controlled by hormones and growth factors. At several stages, skeletal cells become hypoxic because of blood vessel scarcity. In response to the resulting decrease in oxygen tension, the hypoxia-inducible factor HIF-α is stabilized, forms a heterodimer with HIF-β and induces VEGF expression through binding to the hypoxia response element (HRE). The combined secretion of three VEGF isoforms (VEGF120, VEGF164 and VEGF188) results in a VEGF gradient that controls guided angiogenesis. (B) The VEGF isoforms differ in matrix-binding properties, with VEGF120 being the most diffusible isoform and VEGF188 the isoform that is most sequestered in the extracellular matrix. VEGF binds to VEGFR2, which is the main angiogenic receptor. Neuropilin (NRP) co-receptors of VEGFR2 increase VEGF signaling. VEGFR1, and certainly soluble VEGFR1, may act as a sink by sequestering VEGF. *TK*, tyrosine kinase.

To exert its proangiogenic function, VEGF binds to and activates two tyrosine kinase receptors, VEGF receptor 1 (VEGFR-1, also known as fms-like tyrosine kinase/Flt-1) and VEGFR-2 (also known as kinase domain region/KDR or Flk-1) (Fig. 46.1B). Both receptors consist of seven extracellular immunoglobulin-like domains, a transmembrane region, and an intracellular consensus tyrosine kinase domain interrupted by a kinase-insert domain. VEGFR-1 also exists as a soluble form (sVEGFR-1), resulting from alternative splicing, that lacks the transmembrane domain and cytoplasmic regions but retains the ability to bind its ligands. Additionally, neuropilin (NRP) coreceptors augment VEGF signaling in a ligand-specific, VEGFR-specific, and cell-type-dependent manner (Tjwa et al., 2003; Simons et al., 2016). Indeed, whereas all VEGF isoforms can bind VEGFR-1 and VEGFR2, only VEGF164, but not VEGF120, contains the domains that mediate binding to NRP coreceptors. Besides being known as a receptor for the semaphorin family involved in neuronal guidance, NRP1 also modulates the activation of VEGFR-2-mediated signal transduction. When coexpressed with VEGFR-2, NRP1 enhances the binding of VEGF164 to VEGFR-2 and increases VEGF164-mediated chemotaxis (Simons et al., 2016). Although VEGF has a higher affinity for VEGFR-1 than for VEGFR-2, the latter receptor is generally considered to primarily mediate endothelial cell mitogenesis and vascular permeability. In contrast, the role of VEGFR-1 is more complex and context dependent. Indeed, VEGFR-1 promotes the secretion of proteases and growth factors by endothelial cells and the migration of monocytes, whereas sVEGFR-1 negatively regulates VEGFR-2 signaling via VEGF sequestration (Shibuya, 2006). Activation of VEGFR-2 signaling in endothelial cells results in sprouting angiogenesis. During this process, a few endothelial cells with high VEGFR-2 signaling become invading tip cells that lead angiogenic sprouts toward the proangiogenic signal and thereby induce migration and vessel branching. Molecularly, VEGF induces the expression of delta-like ligand 4 (DLL-4) in tip cells. DLL-4 binds to its receptors, Notch 1 and Notch 4, on adjacent stalk endothelial cells to downregulate VEGFR-2 expression in these cells, thus functioning as a dampening mechanism that prevents excess angiogenesis and promotes the orderly development of new vessels. In a final step, proliferating stalk cells eventually form a lumen and thus establish a perfused new vessel, which is stabilized by the recruitment of perivascular cells and ECM deposition. These quiescent endothelial cells then depend on (autocrine) VEGF signaling for survival (Potente et al., 2011; Blanco and Gerhardt, 2013).

Taken together, extensive research has led to the discovery of a plethora of angiogenesis-stimulating growth factors produced by bone cells, of which VEGF is the most important driver of blood vessel growth.

Vascular endothelial growth factor and endochondral ossification

In general, the process of vascular invasion of cartilage and its conversion into bone is a coordinated interaction between several cell types. The best-characterized stage is the formation of the POC, where in response to the proangiogenic factor VEGF, activated endothelial cells in the perichondrium invade and migrate into the cartilage matrix, likely by local protease production (Shibuya, 2006). At the same moment, most of the terminally differentiated hypertrophic chondrocytes will undergo apoptosis. The growing blood vessels are accompanied by osteoclasts and chondroclasts, cells that are well equipped to resorb the cartilaginous matrix. Together with the invading vessels, Osx-positive osteoprogenitors migrate alongside and deposit a typical bone matrix on the remaining cartilage matrix that serves as scaffold (Maes et al., 2010b) (Fig. 46.2A).

The skeletal vasculature appears to be formed predominantly by angiogenesis (i.e., the formation of new blood vessels from preexisting ones) (Stegen and Carmeliet, 2018). The process of sprouting angiogenesis is likely active at the formation of the POC (Langen et al., 2017). However, a rather bone-specific angiogenic mechanism regulates vascular growth at the chondro−osseous junction. Here, no real tip cells are detected, although endothelial cells form filopodia. Vessel growth is rather characterized by bud-shaped protrusions developing from the distal arches that later form anastomoses between each other (Ramasamy et al., 2016). Little is known, however, about the type of angiogenesis during SOC formation, although recent evidence indicates that VEGF-expressing periarticular mesenchymal progenitors migrate ahead of endothelial cells and thereby promote vasculogenesis of the SOC (Tong et al., 2019).

The main angiogenic factor at these different stages of cartilage-to-bone transition is VEGF, as evidenced by different transgenic mouse models. Moreover, the different VEGF isoforms contribute in specific ways to each stage. The general concept is that local concentrations of VEGF are critical to attract and guide endothelial cells, and that a well-balanced combination of diffusible and matrix-binding VEGF isoforms results in a VEGF gradient that controls guided angiogenesis. Because VEGF164 combines both properties, mice that express only VEGF164 display normal bone development with appropriate conversion of cartilage into bone at the three different sites (Maes et al., 2004). On the other hand, mice that selectively express VEGF120 or VEGF188 show delayed vascular invasion at two of the three sites of endochondral ossification (Maes et al. 2002, 2004).

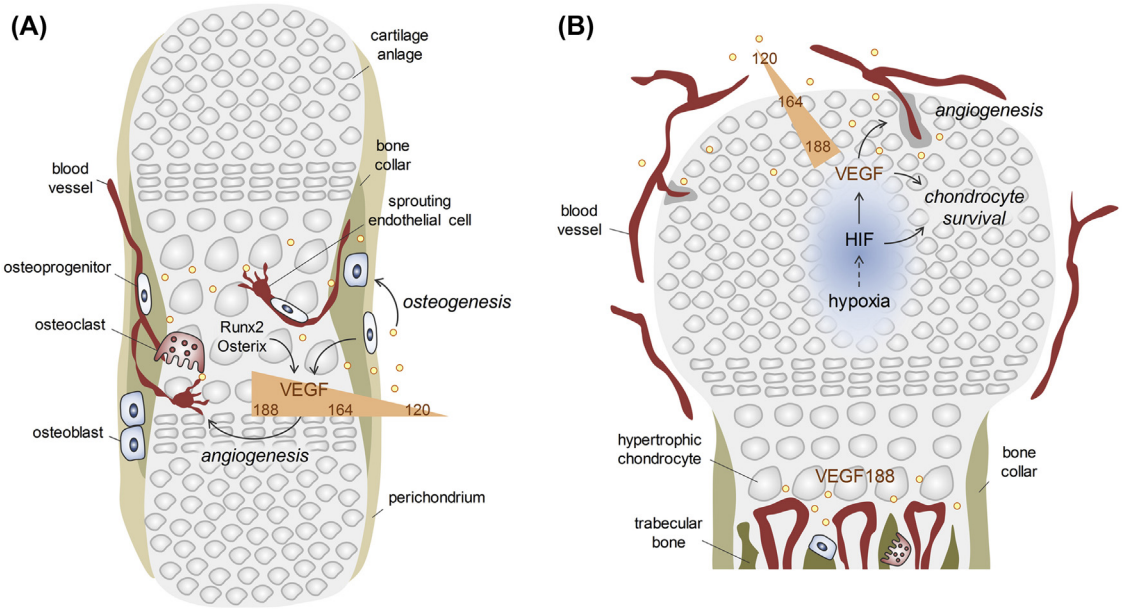

FIGURE 46.2 Angiogenic-osteogenic coupling during bone development. (A) After formation and growth of the cartilage anlage, perichondrial osteochondroprogenitors and hypertrophic chondrocytes start to secrete VEGF in a process mainly regulated by the transcription factors Runx2 and Osterix. An appropriate combination of three VEGF isoforms (VEGF120, VEGF164 and VEGF188) induces blood vessel invasion from the perichondrium, which is directed towards the cartilage template. This angiogenic response is accompanied by osteoclastic cartilage resorption and osteoprogenitors that move into the nascent primary ossification center. (B) During longitudinal bone growth, hypertrophic chondrocytes at the chondro-osseous interface secrete VEGF to attract the metaphyseal H-type blood vessels by a bone-specific angiogenic mechanism. Matrix-binding VEGF isoforms are needed to correctly orient blood vessel growth. In the avascular epiphyseal growth plate, the centrally localized chondrocytes become hypoxic, resulting in HIF stabilization and chondrocytic VEGF expression. The VEGF120 and VEGF164 isoforms are critical to diffuse to the outer layers of the epiphysis to stimulate ingrowth of the surrounding epiphyseal vessels. HIF is also essential for chondrocyte survival, possibly by mediating a metabolic switch.

First, the formation of the POC is delayed when only VEGF120 or VEGF188 is expressed (Maes et al. 2002, 2004), characterized by slower blood vessel invasion of the cartilage template and its removal by osteoclasts, similar to the phenotype observed in mice with deletion of *Vegf* in collagen type II (COL2)-expressing cells (Haigh et al., 2000; Zelzer et al., 2001). Together, these findings suggest that the diffusible VEGF120 isoform is required to attract blood vessels present in the perichondrium, whereas the matrix-binding VEGF188 likely provides directional cues upon the resorption of the cartilage matrix. A balanced secretion of all VEGF isoforms by hypertrophic chondrocytes in the center of the cartilage anlage is thus required for an adequate angiogenic response and timely formation of the POC (Fig. 46.2A).

Second, matrix-binding VEGF isoforms are required for the cartilage-to-bone conversion at the metaphyseal region. Here, VEGF is mainly secreted by the hypertrophic chondrocytes. Mice that only express the VEGF120 isoform display a decreased number of blood vessels near the growth plate, and these vessels are disorganized, lacking a longitudinal orientation (Maes et al., 2002). Consequently, the conversion of cartilage into bone is impaired, evidenced by lower trabecular bone mass together with an enlarged hypertrophic zone of the growth plate. When only VEGF164 or VEGF188 is present, the cartilage-to-bone transition in the metaphysis is normal, showing that matrix-binding VEGF isoforms need to be present to achieve normal endochondral ossification. Likely, these matrix-bound VEGF isoforms are released from the cartilage matrix by invading osteoclasts and orient the blood vessels longitudinally between the cartilage remnants. Indeed, mice with inactivation of matrix metalloproteinase 9 show decreased metaphyseal vascularization, and this phenotype was largely rescued by treating the mice with VEGF (Vu et al., 1998; Ortega et al., 2010). A comparable phenotype, showing an enlarged zone of hypertrophic chondrocytes in the growth plate, is also observed in mice in which VEGF action is inhibited by injection of a sFlt-1 chimeric protein (Gerber et al., 1999) or in mice with deletion of a single *Vegf* allele in COL2-expressing cells (Haigh et al., 2000).

The third site of angiogenesis coupled to cartilage-to-bone transition is the formation of the SOC at the ends of the long bones. When the epiphyseal growth plate enlarges during bone growth, the chondrocytes in the center of the avascular growth plate become hypoxic because they depend on the vascular network overlying the epiphysis for their oxygen and nutrient supply. Activation of the hypoxia signaling pathway (see below) stimulates VEGF expression to induce vascular

invasion (Pugh and Ratcliffe, 2003). This angiogenic response is certainly important, as VEGF deletion in chondrocytes results in cell death of the centrally localized chondrocytes (Zelzer et al., 2004). However, VEGF expression in the epiphyseal growth plate is not sufficient to prevent centrally localized chondrocytes from becoming hypoxic (Maes et al., 2012a) (see below). In addition, when only VEGF188 is produced, the number of chondrocytes in the center of the growth plate that become hypoxic is increased, resulting in enhanced cell death, and consequently reduced longitudinal bone growth (Maes et al., 2004). No changes in epiphyseal vascularization are observed when only VEGF120 or VEGF164 is expressed. These data indicate that diffusible VEGF isoforms need to be present for timely formation of the SOC. Likely, only diffusible VEGF molecules can reach the outer layers of the epiphysis to instruct endothelial cells to proliferate and invade the avascular epiphyseal growth plate.

A special type of cartilage is Meckel's cartilage in the mandible, where the chondrocytes derive from cranial neural crest cells (NCCs). These NCCs are an important source of VEGF during jaw morphogenesis. Deletion of *Vegf* from WNT1-positive NCCs results in reduced jaw vascularization (Wiszniak et al., 2015). Likely, the attracted blood vessels secrete factors that stimulate chondrocyte proliferation and thereby the extension of the mandible.

Taken together, not only appropriate VEGF levels but also the correct combination of VEGF isoforms is essential to allow timely and normal endochondral ossification at each of the three stages.

Vascular endothelial growth factor during intramembranous bone formation

In addition to their involvement in endochondral bone formation, blood vessels are also implicated during intramembranous ossification and are likely regulated through similar mechanisms (Percival and Richtsmeier, 2013). Intramembranous ossification is important for craniofacial development, where NCCs differentiate to osteoblasts, and for cortical bone formation, where osteoprogenitors in the perichondrium/periosteum directly differentiate into osteoblasts.

During craniofacial development, VEGF is expressed by NCCs. Mice with conditional deletion of *Vegf* in WNT1-positive NCCs show craniofacial defects including cleft palate, unfused cranial sutures, and shorter jaws (Hill et al., 2015). This bone phenotype results from reduced vascularization and decreased BMP2 expression, which is required for normal ossification. Mice expressing only VEGF120 show similar calvarial and mandibular malformations (Stalmans et al., 2003). Furthermore, inactivation of *Vegf* in Osx-positive osteoprogenitors of the cranial bones reduces the ossification of calvarial and mandibular bones (Duan et al., 2016). However, this effect was not due to changes in vascularization but likely to decreased BMP-mediated proliferation of cells in the jaw mesenchyme.

With respect to cortical bone formation of the long bones, mice with deletion of *Vegf* in Osx-positive osteolineage cells show decreased numbers of blood vessels in the perichondrium and impaired differentiation of osteogenic precursors into osteoblasts at these sites (Duan et al., 2015). Mechanistically, VEGF derived from perichondrial osteolineage cells controls osteoblast differentiation in a VEGFR2-dependent manner, likely involving Indian hedgehog, β-catenin, and Notch2-mediated pathways.

Taken together, adequate VEGF expression is required for the development of the craniofacial bones and the cortical part of the long bones by angiogenic and non-endothelial-specific effects.

Nonendothelial effects of vascular endothelial growth factor

Although the principal function of VEGF is to induce new blood vessel formation, its actions are not exclusive to endothelial cells and may influence skeletal cell behavior directly. Indeed, chondrocytes, skeletal progenitor cells, osteoblasts, and osteoclasts all express VEGF receptors. In vitro data show that these cell types respond to VEGF by enhanced recruitment, differentiation, activity, and/or survival, although not all findings are yet confirmed by observations in vivo (Dai and Rabie, 2007). Moreover, although VEGF primarily functions in a paracrine manner, it also controls the survival of HSCs and endothelial cells via autocrine or intracrine mechanisms (Gerber et al., 2002; Lee et al., 2007; Liu et al., 2012). Analogously, young mice with conditional deletion of *Vegfr1* or *Vegfr2* in osteoblastic cells show decreased bone mass (Liu et al., 2012), and their bone marrow contains reduced numbers of osteoprogenitors. Mechanistically, VEGF stimulates the formation of osteoblasts and suppresses adipogenesis through intracrine signaling in osteoprogenitors (Liu et al., 2012). These findings suggest that both VEGFR1 and VEGFR2 are positive regulators of skeletal development, and that VEGF regulates lineage specification of osteoprogenitors via intracrine mechanisms.

Although VEGF is a critical determinant of bone development, its expression levels need to be tightly controlled. Indeed, overexpression of VEGF in osteochondroprogenitors resulted in increased bone mass with abnormal vascularization and signs of myelofibrosis in the bone marrow (Maes et al., 2010a). Mechanistically, VEGF induces stabilization of β-catenin in endothelial and osteogenic cells by binding to VEGFR2.

Finally, VEGF can contribute to osteoclast formation. The differentiation and activation of osteoclasts are predominantly regulated by RANK ligand and macrophage colony-stimulating factor (M-CSF). However, VEGF can substitute for M-CSF to promote osteoclast differentiation and bone resorption (Niida et al., 1999).

Vascular endothelial growth factor homologues

PlGF is a homologue of VEGF and specifically binds to VEGR1. Deletion of *Plgf* does not affect angiogenesis during development, but in vivo observations indicate that PlGF becomes important during pathological processes. PlGF may then induce inflammation and angiogenesis and synergize with VEGF (Carmeliet et al., 2001; Luttun et al., 2002). Related to bone biology, mice with *Plgf* inactivation show normal bone development and homeostasis, but healing of a semistabilized fracture is impaired (Maes et al., 2006). PlGF regulates several phases during fracture repair, as PLGF (1) initiates the inflammatory and angiogenic response shortly after bone trauma, (2) stimulates the proliferation of osteolineage cells in the periosteum, (3) decreases the differentiation of periosteal cells into chondrocytes, and (4) promotes the conversion of cartilage callus into bone callus, likely by attracting osteoclasts.

VEGF-C is the major lymphangiogenic factor interacting with VEGFR2 and VEGFR3. Lymphatic vessels are present in most soft tissues but not in bone. However, inducible expression of VEGF-C in Osx-positive osteogenic cells induces the formation of lymphatic vessels in cortical bone, trabecular bone, and the bone marrow cavity. This increase in lymphatic vessels stimulates the formation of osteoclasts, resulting in increased cortical porosity, and mimics the bone pathology observed in patients with Gorham–Stout disease (Hominick et al., 2018).

Regulation of vascular endothelial growth factor expression by oxygen levels

Physiological VEGF levels in the bone are tightly regulated, since overactivation of osteoblastic VEGF signaling results in excessively ossified bones with bone marrow fibrosis, abnormal blood vessel morphology, and extramedullary hematopoiesis (Maes et al., 2010a). The precise mechanisms of the regulation of skeletal VEGF expression are not yet completely understood and may vary depending on the developmental state and specific cell type. Yet some regulators have been proposed, predominantly in vitro, including osteogenic transcription factors (Runx2, Osx), hormones (parathyroid hormone, 1,25-dihydroxyvitamin D_3), and growth factors (BMPs, FGFs, TGF-β) (Dai and Rabie, 2007; Zelzer et al., 2001; Tang et al., 2012) (Fig. 46.1A).

However, one of the most prominent regulatory factors of VEGF expression in skeletal tissues is the hypoxia-inducible transcription factor (HIF) (Pugh and Ratcliffe, 2003) (Fig. 46.1A). This family of transcription factors enables cells to survive and function in low-oxygen (i.e., hypoxic) conditions, among others, by stimulating angiogenesis to correct oxygen supply. HIF-1, HIF-2, and HIF-3 are heterodimeric proteins consisting of an oxygen-sensitive HIF-α subunit and a constitutively expressed HIF-β subunit (Ke and Costa, 2006; Weidemann and Johnson, 2008; Aragones et al., 2009). In well-oxygenated tissues, the half-life of HIF-α is less than 5 min, and this rapid turnover is facilitated by HIF prolyl hydroxylase (PHD)-mediated hydroxylation of specific proline residues within a central oxygen-dependent degradation domain. Hydroxylation prompts polyubiquitination of HIF-α and is essential for interaction with the von Hippel–Lindau tumor-suppressor protein (pVHL), which is the recognition component of an E3 ubiquitin ligase complex that will target HIF-α for proteolytic degradation (Ke and Costa, 2006; Weidemann and Johnson, 2008; Aragones et al., 2009). When physiological or pathological hypoxia occurs, as caused by absence, destruction, or malfunctioning of blood vessels, PHDs become inactive, resulting in reduced hydroxylation and thus stabilization of HIF-α. When stable, HIF-α translocates to the nucleus, dimerizes with HIF-β, and after recruitment of transcriptional coactivators such as Cbp/p300, binds to hypoxia response elements (HREs) of HIF-responsive genes (Ke and Costa, 2006; Weidemann and Johnson, 2008). Hypoxic induction of VEGF expression is regulated by active HIF signaling at multiple levels. First, *VEGF* transcription is directly controlled by binding of HIF heterodimers to an HRE located at base pairs −947 to −939 relative to the transcription start site (Forsythe et al., 1996). Second, the biological activity of secreted VEGF is further determined by hypoxia/HIF-induced expression of the Flt-1 receptor and posttranslational regulation of the Flk-1 receptor (Gerber et al., 1997; Waltenberger et al., 1996), possibly in an attempt to avoid uncontrolled vascular sprouting.

In recent years, several studies have linked HIF signaling and angiogenesis to skeletal cell function during bone development, homeostasis, and pathology (Maes et al., 2012b). During endochondral ossification, HIF-1α is necessary for the survival and function of epiphyseal growth plate chondrocytes (Schipani et al., 2001; Maes et al., 2012a) (Fig. 46.2B). Indeed, the centrally localized chondrocytes become hypoxic when the avascular growth plate expands, and deletion of HIF-1α in these cells results in massive apoptosis of the hypoxic chondrocytes (Schipani et al., 2001). Restoring VEGF expression in these HIF-1α-null chondrocytes diminishes, but does not prevent, chondrocyte cell death,

indicating that cell-intrinsic mechanisms, like metabolic adaptations, contribute to an appropriate hypoxic response (Maes et al., 2012a).

In addition to its prosurvival role in chondrocytes, activation of HIF signaling in bone-forming osteoblasts has been implicated in the stimulation of angiogenesis and the coupling of osteogenic and angiogenic processes. Conditional deletion of *Hif1α* in osteoprogenitors or mature osteoblasts decreases bone volume and blood vessel number, the latter being caused by downregulation of local VEGF production (Wang et al., 2007; Shomento et al., 2010; Rankin et al., 2012). Conversely, genetic ablation of *pVhl* or *Phd* isoforms stabilizes endogenous HIF, resulting in a high bone mass phenotype (Wang et al., 2007; Rankin et al., 2012; Stegen et al. 2016, 2018; Rauner et al., 2016). Although changes in vascular density have been proposed as the key mechanism for HIF-mediated effects on cartilage and bone, recent evidence indicates that HIF also controls skeletal cell function in an angiogenesis-independent manner. Indeed, HIF-induced cell-intrinsic adaptations in metabolism are likely necessary to support the bone anabolic response and maintain cell survival (Regan et al., 2014; Maes et al., 2012a; Stegen et al., 2016), whereas increased osteoprotegerin expression and enhanced WNT signaling affect bone turnover (Wu et al., 2015; Stegen et al., 2018). Recently, the role of HIF signaling specifically in skeletal blood vessels was investigated, adding another layer of complexity to the regulation of angiogenic−osteogenic coupling. H-type vessels express high HIF-1α levels, and consequently, postnatal inactivation of *Hif1α* in endothelial cells severely reduces metaphyseal and endosteal type H endothelium without affecting L-type vessels. This vascular defect is associated with a reduced number of perivascular Runx2 and Osx-positive osteoprogenitors. Conversely, activation of HIF signaling in bone endothelium through pVHL deletion results in the opposite phenotype, with increased osteoprogenitor numbers, bone formation, and consequently a higher trabecular bone volume (Kusumbe et al., 2014). The precise mechanisms that mediate this angiogenic−osteogenic coupling are not fully understood, but VEGF may be a coupling factor. Together, HIF signaling influences skeletal cell function during bone development and homeostasis at least in part through VEGF signaling and the resulting changes in vascularization.

Therapeutic potential of vascular endothelial growth factor for bone repair

VEGF is thus a critical factor that links angiogenesis and skeletal cell function during bone development and homeostasis. This interplay also exists in the context of bone repair, which critically depends on optimal proangiogenic signaling to induce sufficient and timely blood vessel ingrowth (Stegen et al., 2015).

As one of the few tissues in the human body, bone has the remarkable ability to heal without the formation of scar tissue. When bone fractures, disruption of the local vascular system results in blood clotting and hematoma formation (Gerstenfeld et al., 2003). The hematoma holds strong proangiogenic potential, likely caused by the high concentrations of angiogenic growth factors, and is thus indispensable for proper bone healing (Street et al., 2000). Indeed, removal of the hematoma attenuates fracture repair, whereas its transplantation stimulates new bone formation (Street et al., 2000). Although several proangiogenic growth factors are involved in the bone repair cascade, VEGF is the most extensively studied. VEGF levels are strongly increased locally in the early fracture hematoma, but also systemically in injured patients (Street et al., 2000; Beamer et al., 2010). The reestablishment of a vascular network is crucial to the success of the repair process, as blocking VEGF activity using VEGF antagonists or soluble VEGFR results in an impaired vascular response and consequently compromised bone healing (Street et al., 2002). On the other hand, administration of recombinant VEGF accelerates blood vessel ingrowth and bone formation in preclinical models of endochondral and intramembranous bone repair (Street et al., 2002). Since VEGF expression within the fracture callus is spatially and temporally tightly controlled, changes in the local microenvironment are likely to be involved in the regulation of the proangiogenic response. Indeed, as a consequence of the vascular damage, the fracture site becomes hypoxic, and to withstand hypoxia-induced apoptosis, cells activate a survival mechanism controlled by HIF (Maes et al., 2012b). Activation of HIF signaling by cells within the fracture callus is critical for adequate bone healing, since genetic inactivation of HIF-1α in mature osteoblasts impairs blood vessel ingrowth at the fracture site and consequently bone healing, whereas HIF-1α overexpression improves angiogenesis and bone repair (Wan et al., 2008; Shen et al., 2009). Whether other cell types of the fracture callus, including chondrocytes, also activate a vascular response via HIFs, or whether HIF signaling controls other angiogenesis-independent steps during bone healing, however, remains unknown.

The stimulatory effects of VEGF on angiogenesis and osteogenesis have prompted the exploration of these growth factors as therapeutic agents for bone repair. Administration of recombinant VEGF, alone or in combination with osteogenic growth factors, induces vascularization of the bone defect and in turn accelerates fracture healing in several preclinical models (Stegen et al., 2015). However, translation into the clinic is still limited, as administration of recombinant VEGF may have some limitations due to protein instability in vivo and undesirable side effects as mentioned earlier. Moreover, uncontrolled VEGF diffusion to surrounding tissues may increase the risk of developing adverse vascular

effects including malignancy. Current strategies are therefore focused on more localized, controlled release of these growth factors. Another approach to avoid the potential side effects of VEGF administration is to stimulate angiogenesis in a more physiological way. Activation of HIF signaling induces vascular ingrowth and accelerates bone repair, but therapeutic targeting of the HIF transcription factors is challenging (Stiers et al., 2016). PHD oxygen sensors, which act upstream of HIFs, are therefore increasingly being considered as druggable targets. Indeed, several studies in preclinical animal models have shown that blocking PHD activity improves bone repair, which is at least in part mediated by a VEGF-dependent increase in vascularization (Stegen et al., 2015; Stiers et al., 2016).

Thus, although stimulation of VEGF-dependent angiogenesis is an appealing strategy to enhance fracture repair, future studies are required to accelerate the development of novel therapies for patients with impaired bone healing.

Acknowledgments

This work was supported by grants from the Fund for Scientific Research Flanders (FWO; G.0A72.13, G.0964.14 and G.0A42.16) and the KU Leuven (BOF-KU Leuven). SS is a postdoctoral fellow of the Research Foundation – Flanders (FWO; 12H5917N). This work is part of Prometheus, the KU Leuven R&D division for skeletal tissue engineering, http://www.kuleuven.be/prometheus.

Disclaimer: The authors declare no conflict of interest.

References

Aragones, J., Fraisl, P., Baes, M., Carmeliet, P., 2009. Oxygen sensors at the crossroad of metabolism. Cell Metabol. 9, 11–22.

Beamer, B., Hettrich, C., Lane, J., 2010. Vascular endothelial growth factor: an essential component of angiogenesis and fracture healing. HSS J. 6, 85–94.

Bilzikian, J.P., Raisz, L.G., Rodan, G.A., 2002. Principles of Bone Biology. Academic Press, San Diego, Calif.

Blanco, R., Gerhardt, H., 2013. VEGF and Notch in tip and stalk cell selection. Cold Spring Harb. Perspect Med. 3, a006569.

Carmeliet, P., Ferreira, V., Breier, G., Pollefeyt, S., Kieckens, L., Gertsenstein, M., Fahrig, M., Vandenhoeck, A., Harpal, K., Eberhardt, C., Declercq, C., Pawling, J., Moons, L., Collen, D., Risau, W., Nagy, A., 1996. Abnormal blood vessel development and lethality in embryos lacking a single VEGF allele. Nature 380, 435–439.

Carmeliet, P., Moons, L., Luttun, A., Vincenti, V., Compernolle, V., De Mol, M., Wu, Y., Bono, F., Devy, L., Beck, H., Scholz, D., Acker, T., DiPalma, T., Dewerchin, M., Noel, A., Stalmans, I., Barra, A., Blacher, S., VandenDriessche, T., Ponten, A., Eriksson, U., Plate, K.H., Foidart, J.M., Schaper, W., Charnock-Jones, D.S., Hicklin, D.J., Herbert, J.M., Collen, D., Persico, M.G., 2001. Synergism between vascular endothelial growth factor and placental growth factor contributes to angiogenesis and plasma extravasation in pathological conditions. Nat. Med. 7, 575–583.

Chung, A.S., Ferrara, N., 2011. Developmental and pathological angiogenesis. Annu. Rev. Cell Dev. Biol. 27, 563–584.

Coenegrachts, L., Maes, C., Torrekens, S., Van Looveren, R., Mazzone, M., Guise, T.A., Bouillon, R., Stassen, J.M., Carmeliet, P., Carmeliet, G., 2010. Anti-placental growth factor reduces bone metastasis by blocking tumor cell engraftment and osteoclast differentiation. Cancer Res. 70, 6537–6547.

Dai, J., Rabie, A.B., 2007. VEGF: an essential mediator of both angiogenesis and endochondral ossification. J. Dent. Res. 86, 937–950.

Deckers, M.M., Karperien, M., van der Bent, C., Yamashita, T., Papapoulos, S.E., Lowik, C.W., 2000. Expression of vascular endothelial growth factors and their receptors during osteoblast differentiation. Endocrinology 141, 1667–1674.

Duan, X., Bradbury, S.R., Olsen, B.R., Berendsen, A.D., 2016. VEGF stimulates intramembranous bone formation during craniofacial skeletal development. Matrix Biol. 52–54, 127–140.

Duan, X., Murata, Y., Liu, Y., Nicolae, C., Olsen, B.R., Berendsen, A.D., 2015. Vegfa regulates perichondrial vascularity and osteoblast differentiation in bone development. Development 142, 1984–1991.

Ferrara, N., Carver-Moore, K., Chen, H., Dowd, M., Lu, L., O'Shea, K.S., Powell-Braxton, L., Hillan, K.J., Moore, M.W., 1996. Heterozygous embryonic lethality induced by targeted inactivation of the VEGF gene. Nature 380, 439–442.

Ferrara, N., Gerber, H.P., LeCouter, J., 2003. The biology of VEGF and its receptors. Nat. Med. 9, 669–676.

Forsythe, J.A., Jiang, B.H., Iyer, N.V., Agani, F., Leung, S.W., Koos, R.D., Semenza, G.L., 1996. Activation of vascular endothelial growth factor gene transcription by hypoxia-inducible factor 1. Mol. Cell Biol. 16, 4604–4613.

Gerber, H.P., Condorelli, F., Park, J., Ferrara, N., 1997. Differential transcriptional regulation of the two vascular endothelial growth factor receptor genes. Flt-1, but not Flk-1/KDR, is up-regulated by hypoxia. J. Biol. Chem. 272, 23659–23667.

Gerber, H.P., Malik, A.K., Solar, G.P., Sherman, D., Liang, X.H., Meng, G., Hong, K., Marsters, J.C., Ferrara, N., 2002. VEGF regulates haematopoietic stem cell survival by an internal autocrine loop mechanism. Nature 417, 954–958.

Gerber, H.P., Vu, T.H., Ryan, A.M., Kowalski, J., Werb, Z., Ferrara, N., 1999. VEGF couples hypertrophic cartilage remodeling, ossification and angiogenesis during endochondral bone formation. Nat. Med. 5, 623–628.

Gerstenfeld, L.C., Cullinane, D.M., Barnes, G.L., Graves, D.T., Einhorn, T.A., 2003. Fracture healing as a post-natal developmental process: molecular, spatial, and temporal aspects of its regulation. J. Cell. Biochem. 88, 873–884.

Gomez-Gaviro, M.V., Lovell-Badge, R., Fernandez-Aviles, F., Lara-Pezzi, E., 2012. The vascular stem cell niche. J. Cardiovasc. Transl. Res. 5, 618–630.

Grüneboom, A., Hawwari, I., Weidner, D., Culemann, S., Müller, S., Henneberg, S., Brenzel, A., Merz, S., Bornemann, L., Zec, K., Wuelling, M., Kling, L., Hasenberg, M., Voortmann, S., Lang, S., Baum, W., Ohs, A., Oliver, K., Quick, H.H., Marcus, J., Landgraeber, S., Dudda, M., Danuser, R., Stein, J.V., Rohde, M., Gelse, K., Garbe, A.I., Alexandra Adamczyk, Westendorf, A.M., Hoffmann, D., Christiansen, S., Engel, D.R., Vortkamp, A., Krönke, G., Herrmann, M., Kamradt, T., Schett, G., Hasenberg, A., Gunzer, M., 2019. A network of trans-cortical capillaries as mainstay for blood circulation in long bones. Nat. Metabol. 1, 236−250.

Haigh, J.J., Gerber, H.P., Ferrara, N., Wagner, E.F., 2000. Conditional inactivation of VEGF-A in areas of collagen2a1 expression results in embryonic lethality in the heterozygous state. Development 127, 1445−1453.

Harada, S., Rodan, G.A., 2003. Control of osteoblast function and regulation of bone mass. Nature 423, 349−355.

Hill, C., Jacobs, B., Kennedy, L., Rohde, S., Zhou, B., Baldwin, S., Goudy, S., 2015. Cranial neural crest deletion of VEGFa causes cleft palate with aberrant vascular and bone development. Cell Tissue Res. 361, 711−722.

Hominick, D., Silva, A., Khurana, N., Liu, Y., Dechow, P.C., Feng, J.Q., Pytowski, B., Rutkowski, J.M., Alitalo, K., Dellinger, M.T., 2018. VEGF-C promotes the development of lymphatics in bone and bone loss. Elife 7.

Itkin, T., Gur-Cohen, S., Spencer, J.A., Schajnovitz, A., Ramasamy, S.K., Kusumbe, A.P., Ledergor, G., Jung, Y., Milo, I., Poulos, M.G., Kalinkovich, A., Ludin, A., Kollet, O., Shakhar, G., Butler, J.M., Rafii, S., Adams, R.H., Scadden, D.T., Lin, C.P., Lapidot, T., 2016. Distinct bone marrow blood vessels differentially regulate haematopoiesis. Nature 532, 323−328.

Ke, Q., Costa, M., 2006. Hypoxia-inducible factor-1 (HIF-1). Mol. Pharmacol. 70, 1469−1480.

Kusumbe, A.P., Ramasamy, S.K., Adams, R.H., 2014. Coupling of angiogenesis and osteogenesis by a specific vessel subtype in bone. Nature 507, 323−328.

Langen, U.H., Pitulescu, M.E., Kim, J.M., Enriquez-Gasca, R., Sivaraj, K.K., Kusumbe, A.P., Singh, A., Di Russo, J., Bixel, M.G., Zhou, B., Sorokin, L., Vaquerizas, J.M., Adams, R.H., 2017. Cell-matrix signals specify bone endothelial cells during developmental osteogenesis. Nat. Cell Biol. 19, 189−201.

Lee, S., Chen, T.T., Barber, C.L., Jordan, M.C., Murdock, J., Desai, S., Ferrara, N., Nagy, A., Roos, K.P., Iruela-Arispe, M.L., 2007. Autocrine VEGF signaling is required for vascular homeostasis. Cell 130, 691−703.

Liu, Y., Berendsen, A.D., Jia, S., Lotinun, S., Baron, R., Ferrara, N., Olsen, B.R., 2012. Intracellular VEGF regulates the balance between osteoblast and adipocyte differentiation. J. Clin. Investig. 122, 3101−3113.

Long, F., 2011. Building strong bones: molecular regulation of the osteoblast lineage. Nat. Rev. Mol. Cell Biol. 13, 27−38.

Luttun, A., Brusselmans, K., Fukao, H., Tjwa, M., Ueshima, S., Herbert, J.M., Matsuo, O., Collen, D., Carmeliet, P., Moons, L., 2002. Loss of placental growth factor protects mice against vascular permeability in pathological conditions. Biochem. Biophys. Res. Commun. 295, 428−434.

Maes, C., Araldi, E., Haigh, K., Khatri, R., Van Looveren, R., Giaccia, A.J., Haigh, J.J., Carmeliet, G., Schipani, E., 2012a. VEGF-independent cell-autonomous functions of HIF-1alpha regulating oxygen consumption in fetal cartilage are critical for chondrocyte survival. J. Bone Miner. Res. 27, 596−609.

Maes, C., Carmeliet, G., Schipani, E., 2012b. Hypoxia-driven pathways in bone development, regeneration and disease. Nat. Rev. Rheumatol. 8, 358−366.

Maes, C., Carmeliet, P., Moermans, K., Stockmans, I., Smets, N., Collen, D., Bouillon, R., Carmeliet, G., 2002. Impaired angiogenesis and endochondral bone formation in mice lacking the vascular endothelial growth factor isoforms VEGF164 and VEGF188. Mech. Dev. 111, 61−73.

Maes, C., Coenegrachts, L., Stockmans, I., Daci, E., Luttun, A., Petryk, A., Gopalakrishnan, R., Moermans, K., Smets, N., Verfaillie, C.M., Carmeliet, P., Bouillon, R., Carmeliet, G., 2006. Placental growth factor mediates mesenchymal cell development, cartilage turnover, and bone remodeling during fracture repair. J. Clin. Investig. 116, 1230−1242.

Maes, C., Goossens, S., Bartunkova, S., Drogat, B., Coenegrachts, L., Stockmans, I., Moermans, K., Nyabi, O., Haigh, K., Naessens, M., Haenebalcke, L., Tuckermann, J.P., Tjwa, M., Carmeliet, P., Mandic, V., David, J.P., Behrens, A., Nagy, A., Carmeliet, G., Haigh, J.J., 2010a. Increased skeletal VEGF enhances beta-catenin activity and results in excessively ossified bones. EMBO J. 29, 424−441.

Maes, C., Kobayashi, T., Selig, M.K., Torrekens, S., Roth, S.I., Mackem, S., Carmeliet, G., Kronenberg, H.M., 2010b. Osteoblast precursors, but not mature osteoblasts, move into developing and fractured bones along with invading blood vessels. Dev. Cell 19, 329−344.

Maes, C., Stockmans, I., Moermans, K., Van Looveren, R., Smets, N., Carmeliet, P., Bouillon, R., Carmeliet, G., 2004. Soluble VEGF isoforms are essential for establishing epiphyseal vascularization and regulating chondrocyte development and survival. J. Clin. Investig. 113, 188−199.

Marenzana, M., Arnett, T.R., 2013. The key role of the blood supply to bone. Bone Res. 1, 203−215.

Niida, S., Kaku, M., Amano, H., Yoshida, H., Kataoka, H., Nishikawa, S., Tanne, K., Maeda, N., Nishikawa, S., Kodama, H., 1999. Vascular endothelial growth factor can substitute for macrophage colony-stimulating factor in the support of osteoclastic bone resorption. J. Exp. Med. 190, 293−298.

Orlandini, M., Spreafico, A., Bardelli, M., Rocchigiani, M., Salameh, A., Nucciotti, S., Capperucci, C., Frediani, B., Oliviero, S., 2006. Vascular endothelial growth factor-D activates VEGFR-3 expressed in osteoblasts inducing their differentiation. J. Biol. Chem. 281, 17961−17967.

Ortega, N., Wang, K., Ferrara, N., Werb, Z., Vu, T.H., 2010. Complementary interplay between matrix metalloproteinase-9, vascular endothelial growth factor and osteoclast function drives endochondral bone formation. Dis. Model Mech. 3, 224−235.

Percival, C.J., Richtsmeier, J.T., 2013. Angiogenesis and intramembranous osteogenesis. Dev. Dynam. 242, 909−922.

Potente, M., Gerhardt, H., Carmeliet, P., 2011. Basic and therapeutic aspects of angiogenesis. Cell 146, 873−887.

Pugh, C.W., Ratcliffe, P.J., 2003. Regulation of angiogenesis by hypoxia: role of the HIF system. Nat. Med. 9, 677−684.

Ramasamy, S.K., Kusumbe, A.P., Schiller, M., Zeuschner, D., Bixel, M.G., Milia, C., Gamrekelashvili, J., Limbourg, A., Medvinsky, A., Santoro, M.M., Limbourg, F.P., Adams, R.H., 2016. Blood flow controls bone vascular function and osteogenesis. Nat. Commun. 7, 13601.

Ramasamy, S.K., Kusumbe, A.P., Wang, L., Adams, R.H., 2014. Endothelial Notch activity promotes angiogenesis and osteogenesis in bone. Nature 507, 376−380.

Rankin, E.B., Wu, C., Khatri, R., Wilson, T.L., Andersen, R., Araldi, E., Rankin, A.L., Yuan, J., Kuo, C.J., Schipani, E., Giaccia, A.J., 2012. The HIF signaling pathway in osteoblasts directly modulates erythropoiesis through the production of EPO. Cell 149, 63–74.

Rauner, M., Franke, K., Murray, M., Singh, R.P., Hiram-Bab, S., Platzbecker, U., Gassmann, M., Socolovsky, M., Neumann, D., Gabet, Y., Chavakis, T., Hofbauer, L.C., Wielockx, B., 2016. Increased EPO levels are associated with bone loss in mice lacking PHD2 in EPO-producing cells. J. Bone Miner. Res. 31, 1877–1887.

Regan, J.N., Lim, J., Shi, Y., Joeng, K.S., Arbeit, J.M., Shohet, R.V., Long, F., 2014. Up-regulation of glycolytic metabolism is required for HIF1alpha-driven bone formation. Proc. Natl. Acad. Sci. U. S. A. 111, 8673–8678.

Schipani, E., Ryan, H.E., Didrickson, S., Kobayashi, T., Knight, M., Johnson, R.S., 2001. Hypoxia in cartilage: HIF-1alpha is essential for chondrocyte growth arrest and survival. Genes Dev. 15, 2865–2876.

Shen, X., Wan, C., Ramaswamy, G., Mavalli, M., Wang, Y., Duvall, C.L., Deng, L.F., Guldberg, R.E., Eberhart, A., Clemens, T.L., Gilbert, S.R., 2009. Prolyl hydroxylase inhibitors increase neoangiogenesis and callus formation following femur fracture in mice. J. Orthop. Res. 27, 1298–1305.

Shibuya, M., 2006. Vascular endothelial growth factor receptor-1 (VEGFR-1/Flt-1): a dual regulator for angiogenesis. Angiogenesis 9, 225–230 discussion 31.

Shomento, S.H., Wan, C., Cao, X., Faugere, M.C., Bouxsein, M.L., Clemens, T.L., Riddle, R.C., 2010. Hypoxia-inducible factors 1alpha and 2alpha exert both distinct and overlapping functions in long bone development. J. Cell. Biochem. 109, 196–204.

Simons, M., Gordon, E., Claesson-Welsh, L., 2016. Mechanisms and regulation of endothelial VEGF receptor signalling. Nat. Rev. Mol. Cell Biol. 17, 611–625.

Spencer, J.A., Ferraro, F., Roussakis, E., Klein, A., Wu, J., Runnels, J.M., Zaher, W., Mortensen, L.J., Alt, C., Turcotte, R., Yusuf, R., Cote, D., Vinogradov, S.A., Scadden, D.T., Lin, C.P., 2014. Direct measurement of local oxygen concentration in the bone marrow of live animals. Nature 508, 269–273.

Stalmans, I., Lambrechts, D., De Smet, F., Jansen, S., Wang, J., Maity, S., Kneer, P., von der Ohe, M., Swillen, A., Maes, C., Gewillig, M., Molin, D.G., Hellings, P., Boetel, T., Haardt, M., Compernolle, V., Dewerchin, M., Plaisance, S., Vlietinck, R., Emanuel, B., Gittenberger-de Groot, A.C., Scambler, P., Morrow, B., Driscol, D.A., Moons, L., Esguerra, C.V., Carmeliet, G., Behn-Krappa, A., Devriendt, K., Collen, D., Conway, S.J., Carmeliet, P., 2003. VEGF: a modifier of the del22q11 (DiGeorge) syndrome? Nat. Med. 9, 173–182.

Stegen, S., Carmeliet, G., 2018. The skeletal vascular system - breathing life into bone tissue. Bone 115, 50–58.

Stegen, S., Stockmans, I., Moermans, K., Thienpont, B., Maxwell, P.H., Carmeliet, P., Carmeliet, G., 2018. Osteocytic oxygen sensing controls bone mass through epigenetic regulation of sclerostin. Nat. Commun. 9, 2557.

Stegen, S., van Gastel, N., Carmeliet, G., 2015. Bringing new life to damaged bone: the importance of angiogenesis in bone repair and regeneration. Bone 70, 19–27.

Stegen, S., van Gastel, N., Eelen, G., Ghesquiere, B., D'Anna, F., Thienpont, B., Goveia, J., Torrekens, S., Van Looveren, R., Luyten, F.P., Maxwell, P.H., Wielockx, B., Lambrechts, D., Fendt, S.M., Carmeliet, P., Carmeliet, G., 2016. HIF-1alpha promotes glutamine-mediated redox homeostasis and glycogen-dependent bioenergetics to support postimplantation bone cell survival. Cell Metabol. 23, 265–279.

Stiers, P.J., van Gastel, N., Carmeliet, G., 2016. Targeting the hypoxic response in bone tissue engineering: a balance between supply and consumption to improve bone regeneration. Mol. Cell. Endocrinol. 432, 96–105.

Street, J., Bao, M., deGuzman, L., Bunting, S., Peale Jr., F.V., Ferrara, N., Steinmetz, H., Hoeffel, J., Cleland, J.L., Daugherty, A., van Bruggen, N., Redmond, H.P., Carano, R.A., Filvaroff, E.H., 2002. Vascular endothelial growth factor stimulates bone repair by promoting angiogenesis and bone turnover. Proc. Natl. Acad. Sci. U. S. A. 99, 9656–9661.

Street, J., Winter, D., Wang, J.H., Wakai, A., McGuinness, A., Redmond, H.P., 2000. Is human fracture hematoma inherently angiogenic? Clin. Orthop. Relat. Res. 224–237.

Tang, W., Yang, F., Li, Y., de Crombrugghe, B., Jiao, H., Xiao, G., Zhang, C., 2012. Transcriptional regulation of vascular endothelial growth factor (VEGF) by osteoblast-specific transcription factor Osterix (Osx) in osteoblasts. J. Biol. Chem. 287, 1671–1678.

Tjwa, M., Luttun, A., Autiero, M., Carmeliet, P., 2003. VEGF and PlGF: two pleiotropic growth factors with distinct roles in development and homeostasis. Cell Tissue Res. 314, 5–14.

Tong, W., Tower, R.J., Chen, C., Wang, L., Zhong, L., Wei, Y., Sun, H., Cao, G., Jia, H., Pacifici, M., Koyama, E., Enomoto-Iwamoto, M., Qin, L., 2019. Periarticular mesenchymal progenitors initiate and contribute to secondary ossification center formation during mouse long bone development. Stem Cells E-pub ahead of print.

Towler, D.A., 2008. Vascular Endothelial Growth Factor and Osteogenic-Angiogenic Coupling. Academic Press, San Diego, Calif.

Trueta, J., 1974. Blood supply and the rate of healing of tibial fractures. Clin. Orthop. Relat. Res. 11–26.

Trueta, J., Amato, V.P., 1960. The vascular contribution to osteogenesis. III. Changes in the growth cartilage caused by experimentally induced ischaemia. J. Bone Joint Surg. Br. 42-B, 571–587.

Trueta, J., Morgan, J.D., 1960. The vascular contribution to osteogenesis. I. Studies by the injection method. J. Bone Joint Surg. Br. 42-B, 97–109.

Vu, T.H., Shipley, J.M., Bergers, G., Berger, J.E., Helms, J.A., Hanahan, D., Shapiro, S.D., Senior, R.M., Werb, Z., 1998. MMP-9/gelatinase B is a key regulator of growth plate angiogenesis and apoptosis of hypertrophic chondrocytes. Cell 93, 411–422.

Waltenberger, J., Mayr, U., Pentz, S., Hombach, V., 1996. Functional upregulation of the vascular endothelial growth factor receptor KDR by hypoxia. Circulation 94, 1647–1654.

Wan, C., Gilbert, S.R., Wang, Y., Cao, X., Shen, X., Ramaswamy, G., Jacobsen, K.A., Alaql, Z.S., Eberhardt, A.W., Gerstenfeld, L.C., Einhorn, T.A., Deng, L., Clemens, T.L., 2008. Activation of the hypoxia-inducible factor-1alpha pathway accelerates bone regeneration. Proc. Natl. Acad. Sci. U. S. A. 105, 686–691.

Wang, Y., Wan, C., Deng, L., Liu, X., Cao, X., Gilbert, S.R., Bouxsein, M.L., Faugere, M.C., Guldberg, R.E., Gerstenfeld, L.C., Haase, V.H., Johnson, R.S., Schipani, E., Clemens, T.L., 2007. The hypoxia-inducible factor alpha pathway couples angiogenesis to osteogenesis during skeletal development. J. Clin. Investig. 117, 1616−1626.

Weidemann, A., Johnson, R.S., 2008. Biology of HIF-1alpha. Cell Death Differ. 15, 621−627.

Wiszniak, S., Mackenzie, F.E., Anderson, P., Kabbara, S., Ruhrberg, C., Schwarz, Q., 2015. Neural crest cell-derived VEGF promotes embryonic jaw extension. Proc. Natl. Acad. Sci. U. S. A. 112, 6086−6091.

Wu, C., Rankin, E.B., Castellini, L., Alcudia, J.F., LaGory, E.L., Andersen, R., Rhodes, S.D., Wilson, T.L., Mohammad, K.S., Castillo, A.B., Guise, T.A., Schipani, E., Giaccia, A.J., 2015. Oxygen-sensing PHDs regulate bone homeostasis through the modulation of osteoprotegerin. Genes Dev. 29, 817−831.

Zelzer, E., Glotzer, D.J., Hartmann, C., Thomas, D., Fukai, N., Soker, S., Olsen, B.R., 2001. Tissue specific regulation of VEGF expression during bone development requires Cbfa1/Runx2. Mech. Dev. 106, 97−106.

Zelzer, E., Mamluk, R., Ferrara, N., Johnson, R.S., Schipani, E., Olsen, B.R., 2004. VEGFA is necessary for chondrocyte survival during bone development. Development 131, 2161−2171.

Chapter 47

Transforming growth factor-β and skeletal homeostasis[1]

Xin Xu[1] and Xu Cao[2]

[1]State Key Laboratory of Oral Diseases & National Clinical Research Center for Oral Diseases, Department of Cariology and Endodontics, West China Hospital of Stomatology, Sichuan University, Chengdu, PR China; [2]Department of Orthopedic Surgery, Johns Hopkins University School of Medicine, Baltimore, MD, United States

Chapter outline

Transforming growth factor-βs as the molecular sensor in the extracellular matrix

Transforming growth factor (TGF)-β proteins belong to the TGF-β superfamily, which consists of TGF-β1−3, activins/inhibins/Müllerian-inhibiting substances, bone morphogenetic proteins (BMPs), nodal, growth/differentiation factors (GDFs), and the distantly related glial cell line–derived neurotrophic factors family (Chang et al., 2002; Javelaud and Mauviel, 2004; Kingsley, 1994). TGF-β1−3 are present only in mammals. They are pleiotropic; regulate cell proliferation, migration, and differentiation during embryonic development; and play an essential role in maintaining tissue homeostasis in adults. In mammals, distinct genes encode TGF-β 1-3 isoforms that are expressed in unique, occasionally overlapping patterns and can perform a variety of distinct functions in vivo (Letterio and Roberts, 1996; Proetzel et al., 1995; Sanford et al., 1997). Initially cloned from human term placenta mRNA, TGF-β1 is the most abundant and ubiquitously expressed isoform (Derynck et al., 1985). TGF-β1 has been identified in cartilage as well as endochondral and intramembranous bone

1. Portions of this chapter were adapted from Xu, X, Zheng, L, Yuan, Q, Zhen, G, Crane, JL, Zhou, X, Cao, X. Transforming growth factor-β in stem cells and tissue homeostasis. Bone Res. 2018, 6, 2.

Principles of Bone Biology. https://doi.org/10.1016/B978-0-12-814841-9.00047-6

and skin during mouse development, thereby indicating its involvement in the development of these tissues/organs (Dickinson et al., 1990). TGF-β2, also known as glioblastoma-derived T cell suppressor factor, was first discovered in human glioblastoma cells. During embryonic development, TGF-β2 is expressed by neurons and astroglial cells (Flanders et al., 1991), while pathologically it is also involved in tumorigenesis by enhancing cell proliferation and reducing host immune surveillance against tumor development (de Martin et al., 1987). TGF-β3 was first identified from the cDNA library of a human rhabdomyosarcoma cell line. It plays an essential role in the development of the palate and lungs, mainly through the regulation of epithelial−mesenchymal interactions during embryonic, fetal, and neonatal development (Kaartinen et al., 1995; Proetzel et al., 1995). TGF-β3 is also possibly involved in the wound healing process, orchestrating an orderly migration of dermal and epidermal cells in injured skin (Bandyopadhyay et al., 2006b).

Unlike most growth factors, which are ready to function upon secretion, TGF-β is unique in that it is secreted as part of a latent complex stored in the extracellular matrix (ECM). Thereby, the magnitude and duration of TGF-β signaling is carefully controlled at multiple levels, including the synthesis and activation of latent TGF-β isoforms, receptor activation and stability, and the activation and stability of intracellular Smad molecules and other downstream signaling molecules. Plenty of molecules have been identified as "TGF-β activators" whose mutation will lead to aberrant activation of TGF-β and ultimately pathological phenotypes. Although distal effects from circulating factors have been reported, TGF-β-mediated effects are usually restricted at the sites where the active ligand is released. Therefore, the temporal and spatial activation of this growth factor is critical for its context-dependent physiological effects in vivo. Considering the close relationship of TGF-β and ECM homeostasis, increasing evidence has indicated that TGF-β complex is more like a molecular sensor that responds instantly to ECM perturbations through the release of an active ligand that exerts physiological effects at a cellular level, thus ensuring normal tissue homeostasis (Annes et al., 2003).

Latent transforming growth factor-βs in the extracellular matrix

TGF-β family members are typically secreted and deposited in ECM such as bone matrix in their latent form, and their biological effects can only be delivered upon ligand activation. TGF-βs contain a characteristic cysteine knot formed from multiple intrachain disulfide bonds (Chang et al., 2002; Javelaud and Mauviel, 2004; Kingsley, 1994). The precursor of TGF-β1 peptide contains 390 amino acid (aa), including a signal peptide and a TGF-β1 proprotein. This proprotein (361 aa) is processed intracellularly by a furin-like convertase to generate an N-terminal latency-associated peptide (LAP, 249 aa) and a C-terminal mature TGF-β1 (Clark and Coker, 1998; Derynck et al., 1986; Dubois et al., 1995; Kondaiah et al., 1988; Manning et al., 1995; Qian et al., 1990). Both LAP and mature TGF-β1 form homodimers via disulfide bonds. After secretion, the LAP and TGF-β1 homodimers are further noncovalently associated as the small latent TGF-β1 complex (SLC). LAP-growth factor association is both necessary and sufficient to confer latency of TGF-β1-3, BMP-10, and GDF-8/myostatin. However, for BMPs 4, 5, and 7, although LAP and the mature growth factor are also noncovalently associated, the complex is still active (Sengle et al., 2011).

In most cases, LAP of the SLC is further covalently associated with a latent TGF-β binding protein (LTBP) in the ECM, thus creating the large latent complex (LLC) that functions as an ECM reservoir of TGF-β. The LAP−LTBP association mainly functions to anchor the complex to ECM components such as fibrillin (Annes et al., 2003). LTBP is also involved in the proper folding and secretion of the SLC (Brunner et al., 1989; Gray and Mason, 1990; Mangasser-Stephan and Gressner, 1999; Mittl et al., 1996; Oklu and Hesketh, 2000; Saharinen et al., 1996). To date, four LTBPs (LTBP1−4) have been identified, among which LTBPs 1, 3, 4 are able to bind the SLC of all TGF-β isoforms (Koli et al., 2001). Therefore, although TGF-βs are abundant in the ECM (Bismar et al., 1999; Roberts et al., 1983; Seyedin et al., 1985), they are secreted and deposited in the latent form and not able to induce downstream signaling to elicit biological effects (Pedrozo et al., 1999; Pfeilschifter et al., 1990).

Activation of transforming growth factor-βs

Although TGF-β ligands and receptors are ubiquitous in many types of cells, their biological effects are usually restricted at sites where the ligand is activated. Storage of inactive TGF-β in the matrix enables temporal and spatial regulation of TGF-β activation during tissue homeostasis. Precise activation of latent TGF-β is a prerequisite for it to function in the right locations within a specific time frame. In general, the activation of TGF-β requires the release of the LLC from the ECM and further proteolysis/deformation of LAP to release active TGF-β (Jenkins, 2008). TGF-β1 can be activated by plasmin, matrix metalloproteinases (MMPs), thrombospondin-1 (TSP-1), lower pH, and reactive oxygen species (ROS) (Annes et al., 2003). More importantly, TGF-β can also be activated by specific integrins that bind the Arg−Gly−Asp (RGD) sequence of LAPs. The integrin−RGD association results in a contractile force-dependent conformational change

of the latent complex, which releases TGF-β in its active form (Munger et al., 1999; Shi et al., 2011). In addition, a plethora of soluble extracellular agonists and antagonists coexist at the site where active TGF-β is released and further complicate the temporal and spatial access of ligands to receptors (Derynck and Miyazono, 2008).

Proteolytic activation

Many proteases including plasmin and matrix metalloproteinases (e.g., MMP-2 and MMP-9) have been identified in vitro as TGF-β activators (Sato and Rifkin, 1989; Yu and Stamenkovic, 2000). Plasmin and MMP-2/9 are the primary enzymes involved in ECM degradation (Werb, 1997). Proteases can cleave the covalent bond between LAP and TGF-β peptide in the proLLC, thereby rendering the LLC activation competent. Proteases can also target the protease-sensitive hinge region of LTBP to liberate the LLC, which can then be further processed for activation (Taipale et al., 1994). Proteases may directly cleave LAP to release TGF-β in its active form (Lyons et al., 1988). The aforementioned enzymatic activation couples matrix turnover with the generation of active TGF-β to maintain matrix homeostasis (Ignotz and Massague, 1986; Verrecchia et al., 2001). More notably, plasminogen-null animals fail to replicate the pathology of TGF-β1-null animals, and the multisystem pathology of plasminogen-null animals can be alleviated by removal of fibrinogen (Bugge et al., 1996). These observations suggest that plasmin is not solely responsible for the majority of the activation of TGF-β1 in vivo.

Activation by thrombospondin-1

TSP-1 is a complex multifunctional glycoprotein that mediates cell-to-cell and cell-to-matrix interactions during multiple cellular events in a temporally regulated manner (Agah et al., 2002; DiPietro et al., 1996; Murphy-Ullrich and Mosher, 1985; Raugi et al., 1987; Reed et al., 1993). TSP-1 plays an important role in the wound healing process, regulating hemostasis, cell adhesion/migration/proliferation, ECM remodeling, and growth factor (e.g., TGF-β) activation (Adams and Lawler, 2004). In addition to tissue repair, TSP-1 is involved in tissue fibrosis, possibly by activating TGF-β. Either the blockage of TSP-1 activity or deletion of TSP-1 expression can attenuate pathological tissue fibrogenesis (Daniel et al., 2007; Hugo, 2003; Poczatek et al., 2000).

The primary role of TSP-1 in modulating TGF-β activation is observed during injury, under stress, or in other pathologies involved with ECM perturbations. This phenomenon further supports the concept that the latent TGF-β complex embedded in the ECM functions as a sensor to environmental stimuli. TSP-1 will mobilize the necessary molecular machineries to release TGF-β in its active form to meet the needs of tissue repair/remodeling, whereas an excessive response to ECM perturbation may superactivate TGF-β and exacerbate adversary effects such as fibrogenesis. Mechanistically, TSP-1 activates TGF-β by binding to specific sequences of the latent complex and inducing a conformational change to release active TGF-β (Murphy-Ullrich and Poczatek, 2000; Schultz-Cherry and Murphy-Ullrich, 1993). In the latent TGF-β complex, the RKPK sequence in the receptor-binding region of mature TGF-β binds to the LSKL sequence at the amino terminus of LAP, thus enabling ligand latency (Shi et al., 2011; Walton et al., 2010; Young and Murphy-Ullrich, 2004). TSP-1 activates TGF-β through the specific association of its type 1 repeats (TSRs) with LAP and the mature ligand. When the tryptophan-rich motifs present in each of the three TSRs of TSP-1 bind to the VLAL sequence in both LAP and the mature TGF-β ligand, it deforms the LAP—TGF-β complex by "inserting" a TSP-1 molecule. Additionally, the KRFK sequence in the second TSR of TSP-1 can competitively bind to the LSKL sequence in the LAP and present to the receptor the mature TGF-β domain (Sweetwyne and Murphy-Ullrich, 2012). In vivo evidence for the role of TSP-1 in TGF-β activation is shown by the fact that both TSP-1- and TGF-β1-null animals developed strikingly similar pathologies in multiple organs, particularly in the lungs and pancreas. During the perinatal period, administration of the KRFK peptide partially resolved the abnormal TSP-1 depletion phenotypes, specifically airway epithelial hyperplasia and pancreatic islet hyperplasia/acinar hypoplasia. In addition, wild-type mice treated with the LSKL blocking peptide in the perinatal period showed features similar to those of the TSP-1 knockout phenotype in both the airways and pancreas (Crawford et al., 1998). Double knockout of β6 integrin and TSP-1 led to a phenotype different from either single knockout, characterized by cardiac degeneration, severe inflammation, and epithelial hyperplasia, which suggests a potential synergy between β6 integrin and TSP-1 in regulating latent TGF-β activation (Ludlow et al., 2005).

TSP-1-mediated TGF-β activation is observed in multiorgan fibrosis. Moreover, the expression of TSP-1 is induced by factors such as ROS, high glucose, and angiotensin II that are closely associated with systemic diseases that have fibrotic end-organ involvement (Wang et al. 2002, 2004; Yevdokimova et al., 2001; Zhou et al., 2006). Studies using TSP-1 antagonist peptides and diabetic TSP-1 knockout mice have demonstrated that TSP-1 is a major factor inducing fibrotic end-organ complications in diabetes (Belmadani et al., 2007; Daniel et al., 2007; Lu et al., 2011). Treatment of diabetic mice with intraperitoneal injections of LSKL improved left ventricular function and reduced Smad phosphorylation

and cardiac fibrosis (Belmadani et al., 2007). Similarly, treatment with LSKL suppressed urinary TGF-β activity and improved markers of tubulointerstitial injury and podocyte function in diabetic mice (Lu et al., 2011). Moreover, TSP-1 can activate alveolar macrophage-dependent TGF-β in bleomycin-induced pulmonary fibrosis animal models, and either CD36 antagonist peptides or TSP-1 can reduce TGF-β activity and ameliorate pulmonary fibrosis (Chen et al., 2009; Yehualaeshet et al., 2000).

TSP-1-mediated TGF-β activation is also involved in the dermal wound healing process. The phenotype of excisional wound healing in the TSP-1-null mouse is consistent with a decrease in local TGF-β activation (Agah et al., 2002), a delay in macrophage recruitment and capillary angiogenesis, and a persistence of inflammation, granulation tissue, and neovascularization (Nor et al., 2005). The TSP-1-null wound phenotype can be largely rescued by topical treatment with the KRFK-activating peptide (Nor et al., 2005). KRFK treatment increased the TGF-β levels in these wounds, and its effects were blocked by a pan-specific anti-TGF-β antibody. These data suggest that TSP-1 is essential for the local activation of TGF-β during injury and may affect the wound healing process. In addition, subcutaneous implantation of TSP-1-soaked sponges increased the levels of active TGF-β and induced fibroblast migration (Sakai et al., 2003). Overexpression of TSP-1 in scleroderma and keloids induces increased TGF-β activity (Chen et al., 2011; Chipev et al., 2000; Mimura et al., 2005). All these data validate the involvement of TSP-1-induced TGF-β activation in dermal wound healing and sclerosis. However, how to modulate TSP-1 activity to avoid either defective or excessive wound repair processes in vivo remains to be determined.

Activation by integrins

Integrins are dimeric cell surface receptors composed of α and β subunits (van der Flier and Sonnenberg, 2001). They recently have been shown to play a central role in TGF-β activation (Nishimura, 2009). Current data show that at least two mechanisms are involved in the activation of latent TGF-β by integrins (Fig. 47.1). The first proposed mechanism is MMP-dependent. Specifically, integrins are suggested to spatially arrange MMPs, latent TGF-β, and the TGF-β receptor in close proximity, which promotes further activation of latent TGF-β by proteolytic cleavage. The second mechanism is proteolytic action-independent but more closely associated with cell traction forces directly transmitted to the LLC via integrin binding. The cellular contractile force can lead to conformational change of the latent complex, thus liberating TGF-β in its active form and/or presenting it to its receptor. It should be noted that both mechanisms are not mutually exclusive, and it is conceivable that cells can use either or both mechanisms at the same time depending on the specific organs or conditions (Wipff and Hinz, 2008).

$\alpha_v\beta_6$ was the first integrin identified as a TGF-β activator (Munger et al., 1999). The mechanism of activation depends on a direct interaction between $\alpha_v\beta_6$ and the RGD amino acid sequence of the prodomains (LAPs). The prodomains of TGF-β1 and TGF-β3 contain an RGD motif recognized by α_v integrins. Mice with the integrin-binding RGD motif mutation show similar phenotypes to TGF-β1-null mice, such as multiorgan inflammation and defects in vasculogenesis, confirming the essential role of integrins in TGF-β activation (Yang et al., 2007).

$\alpha_v\beta_6$ is normally expressed in epithelial cells at low levels (Breuss et al., 1993). Inflammation or injury can increase the expression of αvβ6 (Breuss et al., 1995; Miller et al., 2001). Therefore, upregulation of αvβ6 and subsequent TGF-β activation in epithelial cells are believed to be a cellular response to suppress perturbations such as inflammation. Consistent with the ability of β_6 integrin to activate latent TGF-β and the profibrotic effects of TGF-β (Border and Ruoslahti, 1992), in the mouse model of pulmonary fibrosis induced by bleomycin, wild-type mice develop pulmonary inflammation with subsequent fibrosis, while integrin $\beta_6^{-/-}$ mice show a minor fibrotic response in response to bleomycin (Munger et al., 1999). Moreover, TGF-β-targeted genes in the lungs of integrin $\beta6^{-/-}$mice are not significantly induced by bleomycin compared with wild-type mice. These data indicate that the inflammatory stimulus upregulates the expression of αvβ6 and consequently induces excessive activation of TGF-β that results in fibrosis. Since TGF-β dramatically upregulates expression of αvβ6 by primary airway epithelial cells in vitro (Wang et al., 1996), it is likely that bleomycin triggers a feed-forward mechanism for coordinately upregulating integrin expression and TGF-β generation. We suggest that fibrosis is the result of a failure to interrupt this feed-forward loop that is perpetuated by persistent ECM perturbation after injury or inflammation.

Accumulating evidence has suggested the important role of force-resistant ECM in contractile-force-dependent TGF-β activation. Activation by $\alpha_v\beta_6$ integrin requires LTBP-mediated incorporation of TGF-β into the ECM and the association of the β6 cytoplasmic domain with the actin cytoskeleton (Annes et al., 2004; Munger et al., 1999; Yoshinaga et al., 2008). Furthermore, contractile force is necessary for TGF-β activation by myofibroblasts (Wipff and Hinz, 2008). Thus, tensile force exerted by integrins across the LTBP—prodomain—TGF-β complex is necessary to change the conformation of the prodomain and free active TGF-β for receptor binding (Annes et al., 2004; Wipff and Hinz, 2008). A recent study by

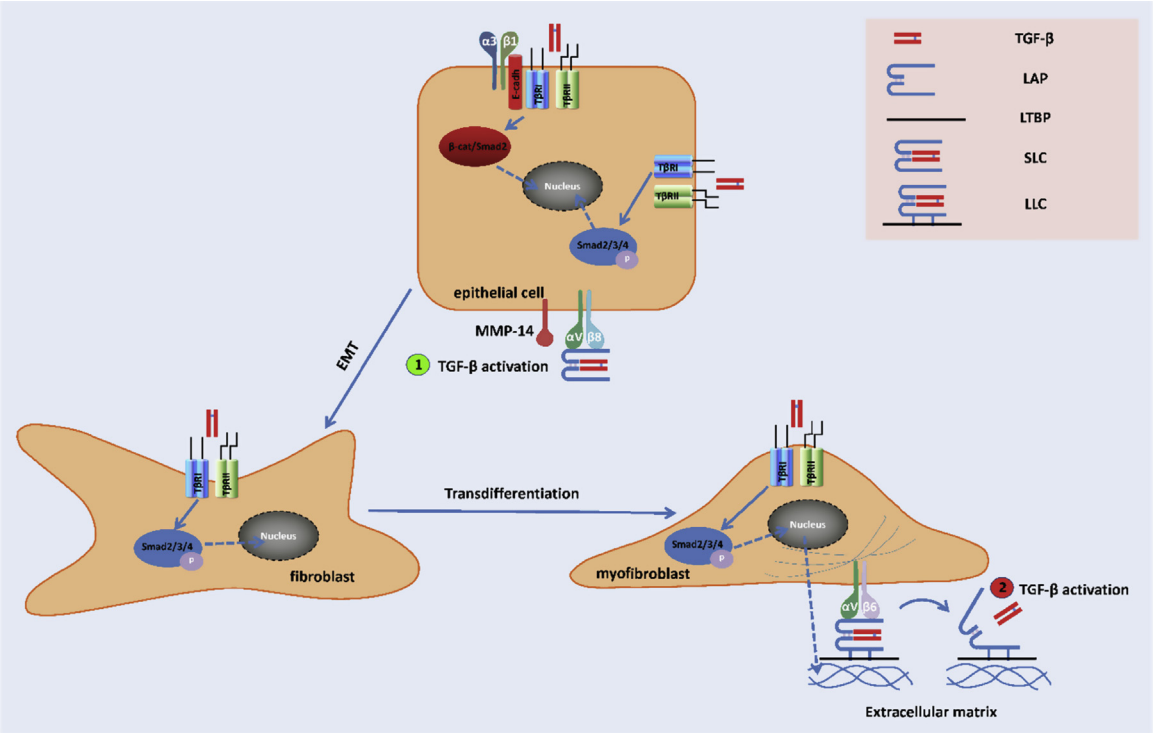

FIGURE 47.1 A model of integrin-mediated TGF-β activation during tissue/organ fibrosis. Epithelial cells activate TGF-β by enriching the latent complex through αvβ8-RGD association and recruiting membrane-bound matrix metalloproteinases (e.g., MMP-14) in proximity for further proteolytic cleavage ①. Active TGF-β can act on resident fibroblasts, inducing its transdifferentiation into myofibroblasts, which are the major contributor to excessive ECM (e.g., collagen) deposition and fibrosis. The myofibroblasts can further activate TGF-β in a contractile force-dependent manner through the αvβ6-RGD association ②. The active TGF-β can in turn act on epithelial cells, fibroblasts and myofibroblasts in a paracrine/autocrine manner, and thus form a feed-forward loop for a sustained TGF-β activation and fibrogenesis. Of note, sustained activation of TGF-β can also induce the epithelial–mesenchymal transition (EMT) of epithelial cells with the assistance of integrin α3β1, which forms a complex with TGF-β type I and II receptors (TβRI/II) and E-cadherin, facilitating β-catenin/Smad2 complex formation and nuclear translocation. LAP: latency-associated peptide; LTBP: latent TGF-β binding protein; SLC: small latent complex; LLC: large latent complex. *Figure is reused with authors' permission Xu, X, Zheng, L, Yuan, Q, Zhen, G, Crane, JL, Zhou, X, Cao, X. Transforming growth factor-β in stem cells and tissue homeostasis. Bone Res. 2018, 6, 2.*

Shi et al. has solved the structure of latent TGF-β and provided mechanistic insights into latency and force-dependent activation by integrins. By using multi- and single-wavelength anomalous diffraction, they found that the two prodomains (LAPs) form a ringlike structure with arms forming a "straitjacket" that fastens each TGF-β monomer. The RGD motifs of LAPs locate to each shoulder, binding to the α_v integrins. Upon applied tensile force, TGF-β1 is freed by the opening of the straitjacket and subsequently released from the prodomain and activated for receptor binding (Shi et al., 2011). At least four conditions need to be fulfilled to enable the cell traction-dependent integrin-mediated TGF-β1 activation: (1) the presence of the actin cytoskeleton to generate force and/or to provide mechanical resistance, (2) specific integrins that transmit this force on the LLC, (3) incorporation of latent TGF-β1 into the ECM as LLC, and (4) a second anchor point—i.e., an ECM that mechanically resists the cellular traction forces exerted on the LLC. Therefore, the activation of latent TGF-β1 is confined to cells expressing the appropriate integrin in a specific physiological/pathological context. Similar to contractile force-directed activation, a recent study from Coller's group revealed that intravascular shear force was also able to activate latent TGF-β1 released from platelets (Ahamed et al., 2008). Since TGF-β1 released from platelets during trauma or surgery might also contribute to the transient increase in plasma levels of plasminogen activator inhibitor-1 by activating endothelial cells (Aoki et al., 2001; Christ et al., 2005; Gando, 2001; Kluft et al., 1985; Pretorius et al., 2007; Rahr et al., 1995; Seeber et al., 1992), shear force–induced TGF-β1 activation likely coordinates the process of platelet activation to arrest hemorrhage and transient inhibition of fibrinolysis to allow an unopposed deposition of fibrin at the early stage of hemostasis. The shear force–activation model makes TGF-β1 a potential shear sensor as well as an effector. Hence, TGF-β1 may contribute to the vascular remodeling that occurs in response to changes in shear forces and maintain intravascular arterial shear within a limited range (Malek et al., 1999).

In addition to force-directed activation, integrins can also activate latent TGF-β1 with the assistance of protease. $\alpha_v\beta_8$ is believed to be able to recruit membrane-bound MT1-MMP to the latent complex. This close proximity promotes activation

of latent TGF-β1 by further proteolytic cleavage (Mu et al., 2002). Similarly, integrin $\alpha_v\beta_3$ has been proposed to act as a docking point for MMP-9 in metastatic breast cancer cells (Rolli et al., 2003) and for MMP-2 in melanoma cells (Brooks et al., 1996). Additionally, integrins can cluster with TGF-β-RII, thereby improving its availability to locally activate TGF-β1. Direct interaction with TGF-β-RII has been demonstrated for $\alpha_v\beta_3$ integrin upon stimulation with active TGF-β1 using a bioluminescence resonance energy transfer approach (Scaffidi et al., 2004) and immunoprecipitation. Interestingly, a similar interaction between different classes of latent TGF-β activator has also previously been suggested (Yehualaeshet et al., 1999)—the cell surface–associated proteins (CD36 and TSP-1) concentrate latent TGF-β on the membrane where it is subsequently activated by plasmin. This cell surface–enrichment theory might also explain why mice with null mutations in the genes encoding known protease activators thus far do not demonstrate any phenotype consistent with TGF-β deficiency. It is conceivable that protease activity is intricately modulated by its activators and inhibitors in vivo as well as the surface concentration of proteases, and a proper spatial arrangement of latent TGF-β1, proteases, and TGF-β receptor is a prerequisite for in vivo activation of TGF-β1 through proteolytic pathways.

The two sets of activation mechanisms by integrins may help explain some "contradictory" data about integrin-mediated TGF-β activation in different tissues/organs or disease models. The involvement of β integrins in the activation of TGF-β is equivocal, mainly because the deletion of β integrins usually presents contradictory phenotypes in different disease models. Deletion of β6 integrin has been reported to protect mice from bile duct ligation-induced hepatic fibrosis (Wang et al., 2007), while global deletion of β3, β5, or β6 integrins or the conditional deletion of β8 integrins in hepatic stellate cells cannot protect mice from carbon tetrachloride–induced hepatic fibrosis (Henderson et al., 2013). Because TGF-β activation in a bile duct ligation model is more likely to be contractile force-dependent, β6 anchorage to cytoskeleton is likely essential to ligand activation in the disease model, thereby conveying that β6 deletion is protective. Conversely, in carbon tetrachloride-induced hepatic fibrosis, excessive proteases are released due to extensive cytotoxic damage. In this case, integrin-mediated surface enrichment of proteases may be the major contributor to TGF-β activation, and hence single deletion of β subunits is not sufficient to disrupt superactivation of TGF-β. A similar theory can also explain the observation that integrin $\beta6^{-/-}$ mice have only minor lung fibrosis in response to bleomycin induction (105). Because the lungs are a highly contractile organ and its compliance is closely associated with the force-directed activation of TGF-β, β6 deletion directly disrupts intracellular anchorage and thus may significantly retard the activation of TGF-β and lung fibrosis.

Activation by osteoclasts

Latent TGF-β present in conditioned medium can be activated by mild acid treatment (pH = 4.5) (Lyons et al., 1988), which probably denatures LAP and thus dissociates TGF-β. In vivo, osteoclasts generate a similar pH during bone resorption when an integrin-dependent sealing zone is generated between the bone and the cell (Teitelbaum, 2000). Since the bone matrix deposited by osteoblasts contains abundant TGF-β in its latent form (approximately 200 μg/kg) (Hering et al., 2001; Seyedin et al., 1985), the acidic environment created by osteoclasts offers an ideal condition for TGF-β activation (Oreffo et al., 1989; Oursler, 1994). Bone-conditioned medium harvested from bone cultures during bone resorption usually contains an increased level of active TGF-β, and the isolated osteoclasts are able to activate bone-latent TGF-β in vitro (Pfeilschifter and Mundy, 1987; Tang et al., 2009). All this evidence indicates that latent TGF-β from surrounding bone tissue or stored in bone matrix becomes activated and released at this site during the bone resorption process. Alternatively, osteoclasts may activate latent TGF-β by secretion of proteases in the absence of a low-pH environment. Protease action at a pH higher than the optimum for lysosomal enzyme activity may sufficiently retard enzyme activity to prevent degradation of TGF-β. It is therefore possible that osteoclast-mediated activation of latent TGF-β occurs outside the low-pH resorption lacuna, resulting in the presence of active TGF-β within the immediate environment of the bone resorption site (Oursler, 1994). Since active TGF-β released during osteoclastic bone resorption is able to induce migration of osteogenic bone marrow mesenchymal stem cells (MSCs) to the bone resorption sites (Tang et al., 2009), osteoclast-mediated activation of TGF-β may represent one of the mechanisms that couples bone resorption to new bone formation. Indeed, our recent study has shown that osteoclast-mediated release of active TGF-β1 is essential for the recruitment of MSCs to the bone resorption site during the PTH-induced bone remodeling process. By inhibiting osteoclast bone resorption with alendronate, osteoblast recruitment is uncoupled from PTH-induced bone resorption (Wu et al., 2010).

Activation by reactive oxygen species

Another potential mechanism for in vivo activation of TGF-β involves ROS (Barcellos-Hoff et al., 1994; Barcellos-Hoff and Dix, 1996). Barcellos-Hoff and her coworkers have shown that ionizing radiation increases the level of active TGF-β in exposed tissues, and that a ROS-generating metal ion-catalyzed ascorbate system is also able to activate recombinant

latent TGF-β in vitro (Barcellos-Hoff et al., 1994; Barcellos-Hoff and Dix, 1996). ROS can stimulate the expression and secretion of TGF-β in a positive feedback loop in many types of cells, including hepatic stellate cells and hepatocytes (Boudreau et al., 2009; Proell et al., 2007). In addition, low-level photodynamic therapy (10 J/cm^2), which releases free radicals by light activation, has been shown to increase active TGF-β when applied to cultured smooth muscle cells (Statius van Eps and LaMuraglia, 1997). It is currently believed that site-specific oxidation of LAP elicits a conformational change in the latent complex releasing free active TGF-β (Barcellos-Hoff et al., 1994). ROS may also indirectly activate TGF-β through MMP activation (Wang et al., 2005). The activation of TGF-β in response to oxidative stress may reflect a need for the human body to produce TGF-β to maintain tissue homeostasis after perturbation such as inflammation. Indeed, the LAP/TGF-β1 complex has been proposed to function as an oxidative stress sensor (Jobling et al., 2006).

Transforming growth factor-β signaling

Active TGF-β ligands signal by binding and bringing together two transmembrane serine-threonine kinases, known as receptor types I and II (Derynck, 1994). In vertebrates, seven type I receptors, known as activin receptor-like kinases (ALKs) 1−7, and five type II receptors have been identified so far (Schmierer and Hill, 2007). TGF-β superfamily ligands bind to and signal through specific type I and type II receptor complexes. Accessory receptors, including the type III receptor TGF-βR III (also known as betaglycan), and endoglin, have also been identified (Chai et al., 2003; de Caestecker, 2004; Derynck and Feng, 1997; Javelaud and Mauviel, 2004; ten Dijke et al., 1996). Nevertheless, neither betaglycan nor endoglin is directly involved in intracellular TGF-β signaling due to the deficiency of a kinase domain. Instead, they affect the access of the TGF-β ligand to its receptors and consequently modulate intracellular signaling (Esparza-Lopez et al., 2001; Lopez-Casillas et al., 1993). Betaglycan binds all three isoforms of TGF-β, with a particularly higher affinity for TGF-β2. However, endoglin binds TGF-β1 and TGF-β3 with identical affinity, and it has weak affinity for TGF-β2 (Cheifetz et al., 1992; Yamashita et al., 1994).

Canonical signaling pathways (smad-mediated signaling)

In most contexts, active TGF-β signals through a canonical (Smad-mediated) pathway. Upon ligand activation, a type II receptor phosphorylates its type I receptor partner, which then transmits the signal by phosphorylation of intracellular downstream substrates—i.e., Smads. Eight Smads (Smad1 to Smad8) have been identified in vertebrates (Massague et al., 2005). They have conserved Mad homology 1 (MH1) and 2 (MH2) domains connected by a linker region. The N-terminal MH1 domain has a β-hairpin loop that can bind to DNA, and the C-terminal MH2 domain mediates interaction with other molecules (e.g., receptors and other Smad isoforms) (Moustakas and Heldin, 2009). The linker region is subject to posttranslational modifications that affect the interactions and stability of Smad molecules. Upon ligand stimulation and subsequent activation by type II receptors, type I receptors transmit intracellular signaling through phosphorylation of downstream effector Smads (Derynck and Zhang, 2003; Feng and Derynck, 2005; Massague et al., 2005). Specifically, Smad1/5/8 are activated by BMP receptors, whereas Smad2/3 are activated by TGF-β/activin/nodal receptors. These receptor-activated Smads (R-Smads) form heterotrimers with a common Smad (Smad4) shared by the TGF-β/activin/nodal and BMP signaling pathways, and translocate into the nucleus. The R-Smads, except Smad2, which has two extra sequences inserted in the MH1 domain perturbing its DNA binding affinity, can bind to preferred DNA sequences. The DNA sequence specificities of R-Smads add further diversity to the transcriptional responses of TGF-β signaling. Complexes of phosphorylated Smad2/3 and Smad4 bind to AGAC or its complement GTCT, known as a Smad-binding element (Dennler et al., 1998; Zawel et al., 1998). However, Smad4-pSmad1/5/8 complexes preferentially bind to GGCGCC or GGAGCC, known as the BMP-response element (BRE) (Katagiri et al., 2002; Korchynskyi and ten Dijke, 2002; Morikawa et al., 2011). Although most TGF-β signaling pathways go through phosphorylated R-Smads, not all transcriptional responses have Smad4 involvement. For example, in cultured epidermal keratinocytes, IκB kinase of the classical nuclear factor κB pathway recruits pSmad2/3 to a specific promoter region that drives cell differentiation (Descargues et al., 2008). R-Smads can regulate miRNA processing in a Smad4-independent and RNA-sequence-specific manner by associating with the p68/Drosha/DGCR8 miRNA processing complex (Davis et al. 2008, 2010).

Since TGF-β superfamily signaling requires the interaction of type I and type II receptors, the interplay between the canonical BMP and canonical TGF-β/activin signaling pathways has been noted (Hinck, 2012). The type 1 BMP receptors (ALK2/3/6) + BMPR2 specifically transduce BMP signals; the type 1 activin receptors (ALK4/7) specifically transduce signals from activin/activin-like ligands. In contrast, the type 2 receptors ACVR2A/B are shared between the BMP and activin pathways and elicit activation of Smad1/5/8 or Smad2/3 in response to BMP or activin-like ligands, respectively. TGF-β ligands elicit activation of Smad2/3 but do not share any receptors with BMPs or activin/activin-like ligands.

In addition, TGF-βs and BMPs bind and assemble their receptors in a distinct manner. TGF-β binds TβR-II first and then cross-links to TβR-I. This pattern was also adopted by activin (Attisano et al., 1996), suggesting that TGF-βs/activins assemble their receptors in an ordered manner (Massague, 1998). Conversely, BMPs and GDFs exhibit a much more heterogeneous pattern of cross-linking, with some binding to their receptors in a stepwise manner, while others exhibit weak affinity to a single receptor and instead cross-link to TβR-I and TβR-II simultaneously (Koenig et al., 1994; Liu et al., 1995; Nishitoh et al., 1996; Nohno et al., 1995; Penton et al., 1994; Yamashita et al., 1995). These findings indicate that TGF-β superfamily members might differ in how they bind and assemble their receptors into signaling complexes.

Notably, although TGF-β does not share or compete for receptors with BMPs, both strongly induce phosphorylation of Smad1/5/8 in many different cell types, including fibroblasts, endothelial cells, epithelial cells, and epithelium-derived cancer cells (Bharathy et al., 2008; Daly et al., 2008; Goumans et al., 2002; Liu et al., 2009; Wrighton et al., 2009b). Despite this common phosphorylation event, TGF-β cannot induce BMP-like transcriptional responses. Grönroos et al. found that although TGF-β is able to stimulate the phosphorylation of Smad1/5/8 in parallel with the classical induction of Smad2/3 phosphorylation, pSmad1/5 and pSmad3 can form complexes readily binding to BMP-responsive elements and mediate TGF-β-induced transcriptional repression on BMP responses (Gronroos et al., 2012). Therefore, Smad3 plays an important role in restricting TGF-β signaling to canonical transcriptional output and effectively prevents TGF-β from eliciting BMP-like "off-target" responses.

The DNA binding affinity of Smad complexes is not strong. Hence, they need to interact and cooperate with other DNA sequence-specific transcription factors to target specific downstream genes (Massague and Wotton, 2000). The requirement of DNA-binding cofactors either activates or represses transcription results in a context-dependent and cell type-specific response (Massague et al., 2005; Wrana and Attisano, 2000). The forkhead-box family member FoxH1 (previously known as Fast1) was the first identified transcription factor that facilitates Smad-mediated transcription. The Foxh1—Smad2/3—Smad4 complex binds to a composite site known as the "activin response element" on target differentiation genes in embryonic cells (Silvestri et al., 2008). Accredited to the advancement from ChIP-seq, various families of DNA-binding transcription factors that interact with Smads have been identified. These transcription factors cooperate with Smad complexes, targeting a specific subset of TGF-β-responsive genes for coordinated regulation of cellular activities (Massague and Gomis, 2006). Among the many factors utilizing Smad complexes as transcriptional cofactors, FOXH1 (Labbe et al., 1998), EOMES (Teo et al., 2011), OCT4 (Mullen et al., 2011), and NANOG (Suzuki et al., 2006; Vallier et al., 2009) are particularly involved in stem cells, while MYOD1 and PU.1 are more relevant to muscle cells and pro-B cells, respectively. These findings support the notion that the availability of cell type-specific cofactors determines the cellular response to TGF-β signaling by providing context and directing the transcriptional activity of Smad proteins. Smad-mediated assembly of basal transcription machinery is also dependent on chromatin conformation, and thus Smads interact with and recruit various chromatin-modifying enzymes to DNA (Ross and Hill, 2008; van Grunsven et al., 2005). Smad2/3 can interact with the histone acetyltransferases CBP/p300 and recruit basal transcription machinery, thus initiating transcription from the associated promoter (Feng et al., 1998; Janknecht et al., 1998). Alternatively, depending on the context, the Smad complex can recruit histone deacetylases (HDAC1/3/4/5/6) to remove acetyl residues on histone tails, and it thus condenses chromatin and represses transcription (Beyer et al., 2013).

In the unstimulated state, Smad proteins interact with components of the Ran GTPase export/import system (Watanabe et al., 2000) and the nuclear pore complex (Xu et al., 2002), resulting in the formation of a highly dynamic equilibrium in which unphosphorylated Smad proteins constantly shuttle between the nucleus and the cytoplasm (Hill, 2009). Upon phosphorylation of R-Smads and the formation of the heteromeric complex with co-Smad in the cytoplasm, the increased import rate and decreased export rate of the trimer lead to its accumulation in the nucleus. This increased nuclear retention is mediated by transcriptional cofactors such as TAZ and YAP, which are the downstream effectors of the Hippo pathway. This cross talk links the TGF-β and Hippo pathways and the sensing of cell density and cell polarity (Varelas et al. 2008, 2010). Protein phosphatases (e.g., PPMA1 or SCPs) can dephosphorylate R-Smads, leading to the disruption of the trimer and eventually turning off Smad signaling (Lin et al., 2006; Wrighton et al., 2009a).

Surface receptors are regulated by endocytosis and degraded by SMURF2 and other HECT E3 ligases (Di Guglielmo et al., 2003). Inhibitory Smads (I-Smads) such as Smad6 and Smad7 are transcriptional targets of TGF-β superfamily signaling and bind to activated receptors competing with R-Smad binding and recruiting the SMURF ubiquitin ligases, thus establishing a classical negative feedback loop (Hayashi et al., 1997; Nakao et al., 1997). Activated R-Smad proteins could also be degraded via the proteasome by ubiquitination through HECT E3 ligases such as SMURF1,2, NEDD4L, and WWP2 (Gao et al., 2009; Soond and Chantry, 2011; Zhu et al., 1999). R-Smad proteins contain multiple PY motifs in the linker region (Gao et al., 2009). The serine/threonine and proline residues of these PY motifs can be phosphorylated by ERK, GSK3 (Fuentealba et al., 2007), and CDKs 8 and 9 (Alarcon et al., 2009), thereby interacting with the WW domains

of HECT E3. R-Smads are subsequently degraded by the proteasome, and transcriptional activity is terminated. This provides a platform in which the duration of TGF-β family signaling integrates with other pathways such as insulin-like growth factor (IGF), fibroblast growth factor (FGF), and WNT.

TGF-β signaling can also be fine-tuned by association with other factors. Our recent study has shown that parathyroid hormone (PTH), which regulates calcium homeostasis and bone metabolism by binding to and activating a G-protein-coupled receptor, can induce the recruitment and colocalization of TβRII with β-arrestin, an adaptor protein involved in PTH receptor endocytosis, thus mediating the internalization of TβRII−PTH type 1 receptor (PTH1R) as a complex in osteoblasts (Qiu et al., 2010). The interaction of PTH and TGF-β signaling at the membrane receptor level may have significant physiological importance in maintaining tissue homeostasis, especially in coupling bone resorption to bone formation. We have demonstrated that the anabolic action of PTH on bone is dependent on active TGF-β1 released by PTH-mediated osteoclastic bone resorption (Wu et al., 2010). However, overproduction of active TGF-β ligand in the local microenvironment may blunt the migration of MSCs to the bone resorption sites for coupled bone formation (Tang et al., 2009). Through the endocytosis of the TβRII−PTH1R complex, PTH provides surveillance of the overactivation of TGF-β signaling so as to ensure proper MSC migration mediated by the local gradient of TGF-β.

Smad-independent signaling pathways

The Smad-independent signaling pathways of TGF-β are generally considered important effector pathways for tyrosine kinase receptors (Derynck and Zhang, 2003; Moustakas and Heldin, 2005; Zhang, 2009). TGF-β activates these non-Smad pathways through interactions of signaling mediators with type I/II receptors, either directly or through adaptor proteins. The Smad-mediated downstream gene expression may also activate non-Smad pathways. TGF-β can directly activate the Ras−Raf−MEK−ERK/MAPK pathway through the interaction of ShcA and the TGF-β receptor complex. In response to TGF-β, TGF-β type I receptor mediates tyrosine phosphorylation of ShcA, which then recruits Grb2 and Sos to form a complex, initiating Ras activation and consequently the ERK/MAPK signaling cascade (Lee et al., 2007). TGF-β can also activate TAK1 through TRAF6, a ubiquitin ligase that interacts with the TGF-β receptor complex, leading to induction of p38 and JNK MAPK signaling (Sorrentino et al., 2008; Yamashita et al., 2008). TGF-β also modulates the activities of the small GTPase proteins Rho, Rac, and Cdc42, which regulate cytoskeletal organization and gene expression (Bhowmick et al., 2001; Edlund et al., 2002; Ozdamar et al., 2005); however, the exact mechanism still remains to be explored. TGF-β-activated RhoA can activate its downstream targets ROCK and LIM kinase (Vardouli et al., 2005). TGF-β activates Akt through PI3K (Bakin et al., 2000; Shin et al., 2001) and consequently initiates signaling pathways—e.g., through mTOR—that play roles in cell survival, growth, migration, and invasion (Lamouille et al., 2012; Lamouille and Derynck, 2007). The roles of TGF-β-induced Smad-independent signaling in stem cells are still unclear and remain to be elucidated.

TGF-β can also cross talk with several other signaling pathways at the level of ligands, receptors, agonists, and antagonists, and thus elicits a context-dependent biological effect to meet specific needs during development or tissue repair (Ikushima and Miyazono, 2012).

Wnt is implicated in the stimulation of cell proliferation during embryonal development and tumorigenesis. Key molecules in the Wnt signaling pathway are the transcription factors β-catenin, T cell factor, and lymphoid enhancer factor (LEF). Smads form complexes with both LEF1 (Vincent et al., 2009) and β-catenin (Kim et al., 2009; Zhou et al., 2012) that enhance the induction of epithelial−mesenchymal transition (EMT). In addition, Smad7 forms a complex with β-catenin that is important for TGF-β-induced apoptosis (Edlund et al., 2005). Cross talk between the TGF-β superfamily and Wnt signaling pathways plays an essential role in dictating stem cell homeostasis in concert with combinatorial activities of other signaling pathways. A typical example of how cross talk between nodal/activin/Smad2/3, ERK/MAPK, and Wnt/GSK3β/β-catenin pathways affects the balance of self-renewal and the differentiation status of ESCs has recently been described by Singh et al. (Singh et al., 2012). Specifically, activation of PI3K/Akt signaling establishes conditions where activin A/Smad2/3 performs a pro-self-renewal function by activating target genes, such as Nanog. In the absence of PI3K signaling, Wnt effectors are activated by ERK targeting GSK3β and function in conjunction with Smad2/3 to promote differentiation. This signaling paradigm with convergence on Smad2/3 is believed to have far-reaching implications for cell fate decisions during early embryonic development.

PTH regulates calcium homeostasis and bone metabolism by binding to and activating a G-protein-coupled receptor. TβRII forms a complex with and phosphorylates the PTH receptor that modulates the internalization of the receptor complex. Specifically, PTH induces the recruitment of TβRII as an endocytic activator that phosphorylates the cytoplasmic domain of PTH1R and facilitates PTH-induced endocytosis of the PTH1R−TβRII complex and consequently results in downregulation of TGF-β signaling (Qiu et al., 2010).

The Notch pathway specifies cell fate determination during development. TGF-β induces several Notch receptor ligands including Jagged1 (Niimi et al., 2007; Zavadil et al., 2004), and Notch signaling induces TGF-β (Aoyagi-Ikeda et al., 2011). The cooperation between TGF-β and Notch signaling enhances EMT. However, there are reports that in certain cell types (e.g., esophageal epithelial cells), Notch signaling counteracts EMT by the induction of miR200 that targets ZEB and TGF-β (Ohashi et al., 2011).

The Hippo pathway senses cell density and controls cell growth via the transcriptional regulators TAZ and YAP. TAZ/YAP binds Smad complexes and sequesters them in the cytoplasm in high-density cell cultures, thereby attenuating TGF-β signaling (Varelas et al., 2008). Moreover, the Crumbs polarity complex interacts with TAZ/YAP and promotes their phosphorylation and cytoplasmic retention; disruption of the Crumbs complex enhances TGF-β signaling and promotes EMT (Varelas et al., 2010).

Transforming growth factor-β signaling and cell reprogramming

Adult somatic cells can be forced to reprogram into induced pluripotent stem cells (iPSCs) by ectopically expressing certain transcription factors. The classical iPSC techniques were pioneered by forced expression of the four "Yamanaka factors" *Oct4*, *Sox2*, *Klf4,* and *c-Myc* in mouse embryonic fibroblasts and thus reset the differentiation clock of these cells back to the pluripotent state equivalent to a blastocyst (Takahashi and Yamanaka, 2006). Many other reprogramming techniques and conditions were developed afterward, mainly aimed at decreasing the risk of genomic insertions of exogenous reprogramming factors or to increase the efficiency of the reprogramming process. Because the four "Yamanaka" factors orchestrate to inhibit the TGF-β signaling pathway that induces EMT through Snails, factors that antagonize TGF-β signaling are believed to enhance reprogramming. Indeed, small molecules that can selectively inhibit TGF-β type I receptor kinases enhance iPSC induction and can replace the requirement of Sox2 for iPSC induction. Inhibition of TGF-β signaling in partially reprogrammed iPSCs even induces Nanog expression and ultimately promotes full reprogramming (Ichida et al., 2009; Lin et al., 2009; Maherali and Hochedlinger, 2009). Like small molecules, Smad7, one of the I-Smad proteins, can also replace *Sox2* to enhance the reprogramming process (Li et al., 2010). Conversely, either treating reprogramming iPSCs with TGF-β or introducing an activated TGF-β type I receptor decreases reprogramming efficiency (Li et al., 2011; Maherali and Hochedlinger, 2009). Furthermore, miRNA expression that inhibits TGF-β signaling and EMT enhances iPSC reprogramming (Li et al., 2011; Miyoshi et al., 2011; Subramanyam et al., 2011). Therefore, TGF-β signaling suppresses somatic cell reprogramming, possibly by induction of EMT, although it is important for ESC self-renewal. Conversely, BMP signaling can induce the mesenchymal−epithelial transition (MET) process, a reversal process to EMT, and thus counteracts TGF-β stimulation in some contexts and promotes reprogramming into iPSCs (Li et al., 2010; Samavarchi-Tehrani et al., 2010).

Transforming growth factor-β signaling in mesenchymal stem cells

The differentiation potential of MSCs depends on the niche where they locate. The proliferation of human MSCs can be stimulated by Wnt or TGF-β signaling (Baksh et al., 2007; Boland et al., 2004; Jian et al., 2006). TGF-β1 induces Smad3-dependent nuclear accumulation of β-catenin, thereby stimulating MSC proliferation. On the other hand, BMP2 antagonizes Wnt3a signaling and inhibits the proliferation of MSCs through interaction of Smad1/5 with Dishevelled-1(Liu et al., 2006). In addition to proliferation, TGF-β signaling directs the differentiation fate of MSCs (Roelen and Dijke, 2003). BMPs can induce differentiation of MSCs into chondroblasts or osteoblasts in vitro. TGF-β and activin also promote chondroblast differentiation at early stages, whereas TGF-β inhibits osteoblast maturation at late stages in differentiation (Roelen and Dijke, 2003). Hence, inhibition of TGF-β/activin signaling strongly enhances osteoblast maturation (Maeda et al., 2004). These inhibitory effects of TGF-β/activin signaling on MSC differentiation are possibly mediated by the induction of expression of inhibitory Smads, such as Smad6, that in turn repress BMP signaling (Lin et al., 2003). In addition, BMP7 has been shown to induce the generation of brown fat from MSCs in the absence of the normally required hormonal induction (Tseng et al., 2008). TGF-β is also involved in cardiomyocyte lineage differentiation of MSCs. In human MSCs, TGF-β treatment induces the expression of cardiomyocyte markers including α-smooth muscle actin, myocardin, and calponin 1 along with the Notch ligand, Jagged 1. Increased expression of these genes is Smad3- and Rho kinase-dependent. Prevention of Jagged 1 expression blocks the expression of cardiomyocyte genes, suggesting that Jagged 1 plays an important role in the TGF-β-induced expression of cardiomyocyte marker genes (Kurpinski et al., 2010). These studies implicate that the microenvironment is critical for the induction of MSC differentiation into different lineages. Considering the complexity of the bone marrow niche and the involvement of multiple cell-secreted or bone-matrix-derived factors in the determination of cell fate, it is more likely that TGF-β functions as a pleiotropic growth

factor that reactivates quiescent stem cells into transient amplification in response to environmental cues (e.g., ECM perturbation). In the meantime, TGF-β acts as a promigratory factor recruiting MSCs to the sites where the cell fate is ultimately determined, in consultation with other niche-specific factors, to meet the tissue need.

Normal adult bone undergoes continual remodeling by precisely coordinating the activities of osteoblasts and osteoclasts. Osteoblasts derived from bone marrow MSCs deposit calcified bone matrix, while osteoclasts, which are multinucleated cells derived from macrophages/monocytes in the hematopoietic stem cell (HSC) lineage, resorb bone (Bianco et al., 2013; Zaidi, 2007). Factors released from bone matrix during osteoclastic bone resorption orchestrate the migration of MSCs to the resorptive surfaces of the bone. Particularly, osteoclastic bone resorption releases and activates TGF-β1 previously stored in the bone matrix, which recruits bone MSCs to active bone remodeling sites through the canonical pSmad2/3 signaling pathway. TGF-β recruits MSCs in a gradient-dependent manner—i.e., osteoclastic bone resorption induces the activation of TGF-β1, which diffuses from the bone resorption site and acts as a chemoattractant for bone marrow stromal cells (BMSCs). Osteoblastic progenitors sense the TGF-β1 gradient and subsequently migrate to the bone resorption site, where they are induced to differentiate into osteoblasts in response to other environmental factors such as bone matrix-derived IGF 1 (IGF-1) (Xian et al., 2012). Interestingly, either overactivation or inhibition of TGF-β signaling that distorts the local TGF-β gradient may impede the migration of MSCs to the normal bone remodeling surfaces. With this hypothesis, we have delineated the pathogenesis of Camurati−Engelmann disease (CED), in which mutations in LAP cause conformational dissociation (Janssens et al., 2005), resulting in increased release of activated TGF-β1 and distortion of resorption-induced TGF-β1 gradients. Due to inadequate recruitment of BMSCs to sites of resorption, poor-quality bone is formed with unfilled resorbed areas and haphazard sclerotic areas (Tang et al., 2009). This theory has also been expanded to explain the pathogenesis of osteoarthritis (OA), in which enhanced osteoclastic bone resorption caused by joint instability results in the release of excessive TGF-β1. The pathologically high level of TGF-β1 ligand in the tibial subchondral bone distorts the physiological TGF-β1 gradients, leading to osteoblastic progenitor aggregation in the bone marrow with compromised bone formation capability ("osteoid islet"). Aberrant bone formation in the subchondral bone in turn causes uneven distribution of stress on the articular cartilage, and in a feed-forward manner leads to cartilage degeneration (Zhen et al., 2013). In addition, we have demonstrated in vivo that the anabolic action of PTH on bone is dependent on the active TGF-β1 released during osteoclastic bone resorption. By inhibition of osteoclastic bone resorption with alendronate, the depleted active TGF-β1 released from bone matrix is insufficient to recruit MSCs to the proper resorptive sites, thus impairing the anabolic action of PTH on bone (Wu et al., 2010).

Active TGF-β also controls the mobilization and recruitment of MSCs to participate in tissue repair. A recent study of ours has shown that TGF-βs were activated in the vascular matrix in both rat and mouse models of mechanical injury of arteries. The active TGF-β released from injured vessels induced the migration of MSCs and the cascade expression of monocyte chemotactic protein-1 (MCP-1), which amplified the signal for migration. Specifically, sustained activation of TGF-β was observed in peripheral blood, and $Sca1^{+}CD29^{+}CD11b^{-}CD45^{-}$ MSCs, of which 91% were also $nestin^{+}$, were mobilized to peripheral blood and migrated to the remodeling arteries. The MSCs were noted to differentiate into endothelial cells for reendothelialization and myofibroblastic cells to form thick neointima. Intravenous injection of recombinant active TGF-β1 in uninjured mice was also sufficient to rapidly mobilize MSCs into circulation. Blockade of TGF-β signaling with TGF-β type I receptor kinase inhibitor significantly attenuated the mobilization and recruitment of MSCs to the injured arteries (Wan et al., 2012). These findings strongly indicate that TGF-β is an injury-activated messenger essential for the mobilization and recruitment of MSCs to participate in tissue repair/remodeling.

Consistently, our study on the pathogenesis of asthma demonstrates the involvement of TGF-β1 in MSC migration. By using a cockroach allergen-induced asthma mouse model, we found increased MSCs, TGF-β1 activation, and downstream signaling in the lungs of CRE (cockroach extract)-treated mice. Further, in vitro transwell assay confirmed that TGF-β1 released from allergen-activated epithelium functions as the primary chemoattractant that induces MSC migration. Consistently, by either intravenous injection of GFP^{+} MSCs (sorted from the bone marrow of Nestin-GFP mice) to CRE-treated mice, or directly immunizing Nestin-GFP mice with CRE, we observed significantly increased accumulation of GFP^{+} MSCs in asthma airways. Importantly, the airway accumulation of MSCs was significantly attenuated by systemic administration of a TGF-β1 neutralization antibody. Taken together, we believe that TGF-β1 is a primary promigratory factor released into the circulation from the injured vessels of the CRE-challenged lung tissue. It mediates the mobilization of MSCs to the circulation and further recruits these cells to the perturbed airways in asthma, likely to participate in tissue repair (Gao et al., 2014).

Interestingly, one study from Mao's group has also demonstrated the cell-homing capacity of TGF-β3 in the functional regeneration of the articular surface of the rabbit synovial joint (Lee et al., 2010). By replacing the excised proximal humeral condyles of skeletally mature rabbits with cell-free bioscaffolds spatially infused with TGF-β3-adsorbed hydrogel, weight-bearing and locomotion of the rabbits were resumed 3−4 weeks after surgery. Histological and mechanical analysis

of the joint revealed that the TGF-β3-infused bioscaffolds had recruited more cells than did spontaneous cell migration without TGF-β3. As a result, TGF-β3-infused bioscaffolds were fully covered with avascular hyaline cartilage and integrated with regenerated subchondral bone that had well-defined blood vessels 4 months after surgery. On the contrary, TGF-β3-free bioscaffolds had only scattered cartilage formation with compromised compressive and shear properties. It should be noted the that the lineage of the recruited endogenous cells was not delineated. However, this study further underscores the importance of TGF-β-mediated cell homing in tissue regeneration.

In addition to the mobilization and recruitment of MSCs to meet tissue needs, TGF-β mediates the homing of bone marrow-derived human MSCs to glioma stem cells (GSCs) (Shinojima et al., 2013). By using glioma models, Shinojima et al. found that TGF-β attracts BM-hMSCs via TGF-β receptors (TGFβRs). Intravascularly administered BM-hMSCs home to GSC-xenografts that express TGF-β. BM-hMSCs carrying the oncolytic adenovirus Delta-24-RGD prolonged the survival of TGF-β-secreting GSC xenografts, and this effect was abrogated by the inhibition of TGFβR on BM-hMSCs. These data show that the TGF-β/TGFβR axis can mediate the tropism of BM-hMSCs for GSCs, and TGF-β may serve as a predictor for patients in whom BM-hMSC delivery could be effective (Shinojima et al., 2013).

Transforming growth factor-β signaling and bone remodeling

The musculoskeletal system is dynamic in that it undergoes continual adaptations during vertebrate life to attain and preserve skeletal size, shape, and microstructure as well as regulate mineral homeostasis. In addition, its matrix is a major reservoir of growth factors whose bioavailability and temporal and spatial activation modulate the balance between normal physiology and pathology of tissue/organs involved. Skeletal homeostasis is maintained by intricate regulation of the bone remodeling process. A typical bone remodeling cycle consists of three distinct phases: (1) initiation phase, during which osteoclasts are formed and resorb damaged bone; (2) reversal phase, the transition of osteoclast to osteoblast activity; and (3) formation phase, when osteoblasts rebuild an equivalent amount of bone to that resorbed (Crane and Cao, 2014). Termination of osteoclast bone resorption and recruitment/differentiation of MSCs are generally recognized as essential steps in the reversal phase.

Transforming growth factor-β as the coupler of bone resorption and formation

Osteoblasts are derived from bone marrow MSCs (Bianco et al., 2013). Ex vivo mouse MSCs can be identified based on the absence of hematopoietic and endothelial markers and the presence of PDGFRa (Morikawa et al., 2009; Omatsu et al., 2010; Park et al., 2012). PDGFRa^{+} Sca-1^{-}CD45^{-}Ter119^{-} cells also express high levels of HSC niche factors *Cxcl12* and Stem cell factor (*Scf*) (Morikawa et al., 2009; Omatsu et al., 2010); hence they not only contribute to osteoblast and adipocyte lineage (Omatsu et al., 2010) but also constitute the cellular component of the HSC niche. Cells that express the Nestin-GFP transgene (Nes-GFP) contain all of the mesenchymal progenitor activity (fibroblastic colony-forming units; CFU-Fs) in mouse bone marrow (Kunisaki et al., 2013; Mendez-Ferrer et al., 2010). These Nes-GFP^{+} cells segregate with distinct vessels in vivo. The Nes-GFP bright cells, which exclusively locate along arterioles, are much rarer than the reticular Nes-GFP dim cells largely associated with sinusoids. Nes-GFP bright cells are quiescent, contain the most CFU-Fs, and closely associate with HSC quiescence and maintenance in bone marrow (Kunisaki et al., 2013). Notably, a recent study reported that the number of both Nes-GFP bright and Nes-GFP dim cells significantly decreased in adult endochondral bone, and only a small number of Nes-GFP dim cells were detectable in adult bone marrow (Ono et al., 2014). These data indicate that Nestin^{+} MSCs may be more relevant to endochondral ossification during development than the skeletal remodeling process in adulthood, or the expression of Nestin is transient in MSCs. The Morrison group has demonstrated that leptin receptor (LepR) is a marker that highly enriches bone marrow MSCs, accounting for 94% of adult bone marrow CFU-Fs (Zheng and Geiger, 2014). LepR^{+} cells are Scf-GFP^{+}, Cxcl12^{-}DsRed^{high}, and Nes-GFP dim. They emerge postnatally and give rise to most bone and adipocytes formed in adult bone marrow. LepR^{+} cells are normally quiescent, but they transiently proliferate to participate in bone regeneration after irradiation or fracture (Zheng and Geiger, 2014). Therefore, LepR^{+} cells may represent the major cellular source of bone and adipocytes in adult bone marrow and possibly account for the largest proportion of MSCs that participate in the bone remodeling process and maintain HSCs in adult bone marrow (Ding et al., 2012).

To overcome the challenge during evolution of vertebrate animals transitioning from ocean to land, cytokines and growth factors were likely selected to deposit in the bone matrix during bone formation. A large reservoir of factors in the bone matrix becomes available during osteoclastic bone resorption to induce recruitment and differentiation of MSCs and limit further osteoclastic resorption, thereby coupling bone resorption and formation. A critical step of coupled bone remodeling is to recruit MSCs to bone resorption sites. Vertebrate TGF-βs 1-3, which appear to have no counterparts in

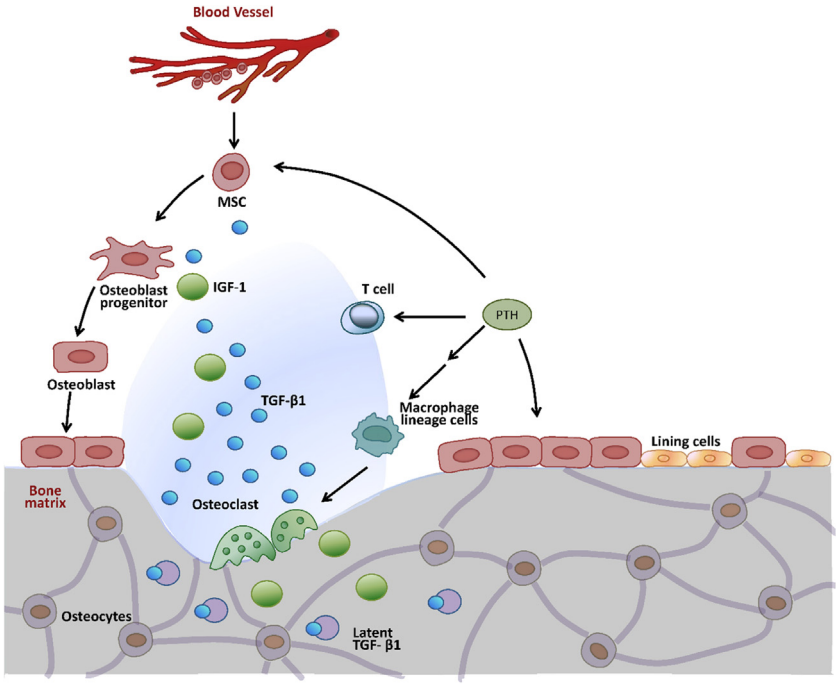

FIGURE 47.2 Activation of TGF-β recruits mesenchymal stem cells (MSCs) during bone remodeling. TGF-β1 is released from the bone matrix and activated during osteoclast-mediated bone resorption, creating a gradient. TGF-β1 induces migration of MSCs to the bone remodeling sites to couple bone resorption and formation. The bone-resorptive microenvironment also provides signals (e.g., IGF-1) that direct the lineage-specific differentiation of MSCs. In addition, PTH orchestrates signaling of local factors and thus regulates cellular activities, including those of MSCs, T cells, and other PTH-responsive cells in the bone marrow to coordinate bone remodeling. *Figure is reused with authors' permission Xu, X, Zheng, L, Yuan, Q, Zhen, G, Crane, JL, Zhou, X, Cao, X. Transforming growth factor-β in stem cells and tissue homeostasis. Bone Res. 2018, 6, 2.*

nematodes (*Caenorhabditis elegans*) or insects (*Drosophila*) (Lapraz et al., 2006), may have evolved to serve as the major coupling factor that coordinates the dynamic bone remodeling process of vertebrate mammals after they transitioned from ocean to land (Fig. 47.2). A more complex mechanical loading to terrestrial vertebrates may promote the release of active TGF-β from the bone matrix (Neidlinger-Wilke et al., 1995) for a coupled bone remodeling. In addition, osteoclastic bone resorption evolved by terrestrial vertebrates plays an essential role in activating TGF-β during bone remodeling. Osteoclasts can form an integrin-dependent sealing zone between bone and cell (Teitelbaum, 2000), generating an acidic environment ideal for the activation of latent TGF-β richly deposited in the bone matrix (Hering et al., 2001; Oreffo et al., 1989; Oursler, 1994; Seyedin et al., 1985). Osteoclasts can also activate latent TGF-β by secretion of proteases in the absence of a low-pH environment (Oursler, 1994), leading to proteolytic cleavage of LTBP1 (Dallas et al., 2002) and enrichment of active TGF-β within the immediate environment of the bone resorption site. More importantly, our recent work has clearly demonstrated that TGF-β1, as one of the most abundant bone matrix cytokines (Engler et al., 2006), is activated during osteoclastic bone resorption and induces the migration of MSCs to bone remodeling sites via Smad-dependent signaling (Tang et al., 2009). TGF-β can also promote the migration of MSCs via the JNK pathway and induced expression of MCP-1, although these findings have only been reported in an artery injury model (Wan et al., 2012). In parallel, other growth factors released from bone matrix during resorption, such as IGF-1, promote osteoblast differentiation of MSCs (Xian et al., 2012). Studies of the effects of TGF-β1 on osteoclast activity show that high concentrations and prolonged exposure to active TGF-β1 inhibit migration of osteoclast precursors (macrophages/monocytes) (Kim et al., 2006). Hence, the gradient of TGF-β1 generated at the resorptive site inhibits further recruitment of osteoclast precursors and avoids excessive bone resorption. This is particularly important for coupled bone remodeling since continuously elevated osteoclastic activity reduces the quality of bone and results in pathologic conditions.

Interestingly, osteoblast bone formation still exists in vertebrates that have defective osteoclast function to release sufficient bone matrix-derived growth factors, indicating that osteoclasts per se may also be able to produce coupling factor(s) (Martin and Sims, 2005). These potential coupling factors released by osteoclast include Sphingosine 1-phosphate, platelet-derived growth factor-bb (PDGF-bb), and the EphB4.ephrin-B2 bidirectional signaling complex. Sphingosine 1-phosphate is secreted by osteoclasts and functions to recruit osteoblasts and promote the survival of mature osteoblasts (Pederson et al., 2008). Osteoclasts can also secrete PDGF-bb, which not only induces the migration and

osteogenic differentiation of MSCs (Kreja et al., 2010) but also controls osteoblast chemotaxis via PDGF-bb/PDGFR-beta signaling (Sanchez-Fernandez et al., 2008). More importantly, our recent findings have shown that PDGF-bb secreted by preosteoclasts is able to induce the formation of CD31(hi)Emcn(hi) vessel, a specific vessel subtype that functions to couple angiogenesis and osteogenesis during bone modeling and remodeling (Xie et al., 2014). EphB4 receptors are expressed on osteoblasts, whereas the ligand ephrin-B2 is expressed by osteoclasts. Signaling through EphB4 receptors induces osteoblastic differentiation, whereas signaling through ephrin-B2 inhibits osteoclastogenesis (Zhao et al., 2006). The bidirectional signaling complex of EphB4−ephrin-B2 functions to activate osteoblastic bone formation and inhibit osteoclastic bone resorption simultaneously, and this is particularly critical at the transition point of bone remodeling. Notably, direct cell contact between osteoblasts and osteoclasts within the BMU is not always possible, and osteoblastic bone formation could sustain long after osteoclasts vacate the resorption site. This fact suggests that both contact-dependent and contact-independent signals are involved in a coupled bone remodeling process.

In addition, elasticity of the bone matrix plays an important role, with a stiffer matrix directing differentiation of MSCs into osteoblasts (Engler et al., 2006). At fresh bone resorption sites, the bone mineral matrix without lining cells is exposed, providing a stiff elastic microenvironment in favor of osteoblastic differentiation. Blood vessels are in close proximity to bone remodeling, and a complex interrelationship between angiogenesis and osteogenesis has been reported (Chim et al., 2013). Basic fibroblast growth factor (FGF2) is a potent mitogenic factor that can promote angiogenesis by inducing endothelial cell proliferation, migration, and the expression of necessary angiogenic factors including proteases, growth factors, and integrins (Beck and D'Amore, 1997; Klein et al., 1996; Klein et al., 1993; Seghezzi et al., 1998). TGF-β has been shown to enhance FGF2 production in osteoblasts (Sabbieti et al. 1999, 2005; Sobue et al., 2002). In aortic endothelial cells, TGF-β stimulation of an ALK5/TβRII-Smad2 complex enhances expression of vascular endothelial growth factor (VEGF) (Shao et al., 2009), which is a strong proangiogenic factor. Whether a similar mechanism of action exists in cells in the bone remodeling site remains to be investigated. HSCs are present in the same niche as MSCs (Morrison and Scadden, 2014). While MSCs and osteoblast precursors can influence the fate of HSCs by producing several key maintenance factors including CXC chemokine ligand 12, angiopoietin 1, KIT ligand, and vascular cell adhesion molecule 1 (Calvi et al., 2003; Hsu and Fuchs, 2012; Mendez-Ferrer et al., 2010; Morrison and Scadden, 2014), the opposite remains unknown.

Parathyroid hormone as an endocrine regulator of skeletal transforming growth factor-β signaling

The parathyroid gland evolved in amphibians (Okabe and Graham, 2004) and represents the transition of aquatic to terrestrial life. PTH is the major endocrine hormone produced by the parathyroid gland, which regulates calcium homeostasis. Interestingly, permanent emergence of osteoclasts and bone resorption is also observed as vertebrates transitioned to land (Glowacki et al., 1986; Moss, 1965; Weiss and Watabe, 1979; Witten and Huysseune, 2009) and favors survival by a lightening of skeletal weight and a ready source of calcium. In addition to the critical role of PTH mobilizing calcium in times of need, it has also been shown to orchestrate the signaling of local bone factors including TGF-β, Wnts, BMP, and IGF-1, integrating systemic control of bone remodeling (Bikle et al., 2002; Canalis et al., 1989; Lombardi et al., 2010; Miyakoshi et al., 2001; Pfeilschifter et al., 1995; Qiu et al., 2010; Wan et al., 2008; Watson et al., 1995; Yu et al., 2012) (Fig. 47.2).

PTH orchestrates the signaling of many local factors that determine the fate of MSCs. Endocytosis of growth factors and G-protein-coupled receptors is known to integrate different signaling pathways (Polo and Di Fiore, 2006). PTH can induce the recruitment of TβRII as an endocytic activator (Qiu et al., 2010). TβRII directly phosphorylates the cytoplasmic domain of PTH1R and facilitates PTH-induced endocytosis of a PTH1R−TβRII complex, resulting in downregulation of TGF-β effects, likely limiting further MSC recruitment. Concomitantly, PTH stimulates the commitment of MSCs to the osteoblast lineage by enhancing BMP and Wnt signaling. Low-density lipoprotein-related protein 6 (LRP6) serves as a coreceptor in the canonical Wnt pathway (He et al., 2004) and interacts with BMP signaling (Itasaki and Hoppler, 2010). PTH has been shown to recruit LRP6 as a coreceptor, which recruits axin from the cytoplasm to stabilize β-catenin (Wan et al., 2008). PTH binding to PTH1R can also induce endocytosis of a PTH1R/LRP6 complex, resulting in enhanced BMP-pSmad1 downstream signaling, and ultimately promotes osteoblastic differentiation of MSCs (Yu et al., 2012). Deleting LRP6 in mature osteoblasts in mice results in a loss of anabolic response to PTH (Li et al., 2013). PTH can expand Nestin-positive MSC populations (Calvi et al., 2003; Jiang et al., 2002; Mendez-Ferrer et al., 2010), although the precise mechanism of action remains unclear. PTH enhancement of MSC transient amplification, differentiation, and function is a part of the integration of the signaling networks of local factors for the spatial-temporal regulation of bone remodeling.

PTH can modify other cells in the bone marrow microenvironment. Intermittent PTH treatment increases the number of osteoblasts by converting lining cells to active osteoblasts (Kim et al., 2012). PTH stimulates bone marrow $CD8^+$ T cells to produce large amounts of Wnt10b, which activates Wnt signaling in MSCs and osteoblast precursors, thus increasing osteoblast proliferation and differentiation (Terauchi et al., 2009). PTH has also been shown to improve the bone marrow microenvironment by spatially relocating small blood vessels in proximity to sites of new bone formation, possibly via upregulation of VEGF-A and neuropilins 1 and 2 (Prisby et al., 2011). The consequent proximity of blood vessels allows more efficient delivery of nutrients to support new bone formation.

Taken together, TGF-β is a critical factor in the temporal and spatial coupling of bone remodeling. PTH, the hormone with evolutionary significance, may act as the major endocrine regulator of bone remodeling by orchestrating the signaling of many pathways and directing the fate of MSC.

Musculoskeletal pathologies associated with aberrant transforming growth factor-β signaling

Temporal and spatial regulation of TGF-β activation is essential for maintenance of musculoskeletal tissue homeostasis and regeneration of damaged tissue by recruiting stem/progenitor cells to the right place at the right time, whereas sustained abnormal activation of TGF-β may lead to pathological conditions due to excessive recruitment of stem/progenitor cells and their subsequent differentiation.

Osteoarthritis associated with aberrant activation of transforming growth factor-β signaling in the subchondral bone

OA is a degenerative joint disease characterized by progressive articular cartilage degradation, subchondral bone sclerosis, reduced mobility, and debilitating joint pain. Although it is still under debate whether OA starts in cartilage or bone (Goldring and Goldring, 2010), subchondral bone sclerosis has now been recognized as a major contributor to cartilage degeneration by generating unevenly distributed stress on the articular cartilage, leading to its gradual deterioration (Newberry et al., 1997; Radin and Rose, 1986). Recent evidence has demonstrated that the onset of OA is associated with increased bone remodeling in the early stage (Intema et al., 2010; Sniekers et al., 2008), subsequent slow turnover/densification of the subchondral plate, and complete loss of cartilage (Burr and Gallant, 2012; Grynpas et al., 1991; Karsdal et al., 2008). Notably, subchondral sclerosis without a precedent stage of increased bone remodeling does not lead to progressive OA in experimental models (Burr and Gallant, 2012; Huebner et al., 2002). Therefore, both early-stage increased bone loss and late-stage subchondral densification are important for the pathogenesis of cartilage degeneration in OA. Importantly, our recent findings have shown that this spatial and temporal separation of subchondral bone phenotype is likely initiated by the abnormal activation of TGF-β (Zhen et al., 2013).

Bone is constantly remodeled or modeled in response to changes in mechanical loading, particularly when joint stability is decreased such as occurs during aging or with ligament injury or obesity. As osteocytes are the principal mechanosensors, aberrant mechanical loading may result in alterations in the release of signaling molecules such as OPG, RANKL, and sclerostin to increase osteoclast activity and turnover rate in OA subchondral bone. In the postsurgery of anterior cruciate ligament transection (ACLT) OA mice, osteoclastic bone resorption in the subchondral bone was significantly increased as early as 7 days. The excessive release of active TGF-β1 to the bone marrow caused by osteoclastic bone resorption recruits $nestin^+$ MSCs to form marrow osteoid islets. Notably, osteoclastic bone resorption was temporally and spatially separated from TGF-β1-induced recruitment of MSCs in the marrow, resulting in aberrant bone formation. The uncoupled bone remodeling process in subchondral bone alters its microarchitecture and eventually compromises the functional integrity of the "subchondral bone-articular cartilage complex" (Burr and Radin, 2003). This notion was further supported by the development of OA-like changes in the CED mouse model with aberrant activation of TGF-β1 (Zhen et al., 2013).

Biomechanical factors play an essential role in the degenerative process of articular cartilage, which is maintained in a mechanically active environment. Subchondral bone volume and subchondral bone plate (SBP) thickness fluctuate substantially in ACLT rodent models. In human OA joints, SBP is markedly thicker relative to those of healthy subjects (Burr and Gallant, 2012). Computerized stimulation models of human knee OA suggest that expansion of 1%−2% subchondral bone significantly changes the distribution of articular cartilage stress. In addition, the formation of osteoid islets and aberrant bone formation induced by TGF-β1 changes the microarchitecture of subchondral bone (Zhen et al., 2013). Although intermittent articular loading seems necessary for normal cartilage metabolism, abnormal loading patterns

mediated by TGF-β1 may irregularly induce progressive cartilage degeneration (Ni et al., 2011). Cell death, water content, and fibronectin content in cartilage explants were increased in a load-duration and magnitude-dependent manner (Farquhar et al., 1996). Chondrocytes in the superficial zone are more vulnerable to repetitive mechanical loading than those in the deeper layer of articular cartilage (Chen et al., 2003; Clements et al., 2001). Vigorous cyclic loading also leads to cartilage matrix damage such as breakage of collagen fiber and proteoglycan depletion, possibly due to increased MMP-3 (Lin et al., 2004). Therefore, fluctuation of the mechanical property of subchondral bone inevitably affects its capacity to dissipate mechanical stimuli from the joint surface and consequently leads to cartilage degeneration in OA. The loss of cartilage integrity will in turn increase the overload of the joint, leading to subchondral bone sclerosis as the joint attempts to adapt to the increased loads. Ultimately, this positive feedback loop causes progressive deterioration of articular cartilage in clinically evident OA (Burr and Gallant, 2012).

In addition to induction of aberrant bone formation in the subchondral bone of OA, excessive activation of TGF-β can affect multiple joint tissues. TGF-β signaling is crucial in normal cartilage development and the maintenance of articular chondrocyte homeostasis in synovial joints (Serra et al., 1997; Yang et al., 2001). However, recent findings by van der Kraan et al. have shown that the aging process may switch TGF-β signaling in chondrocytes from the canonical anabolic ALK5-Smad2/3 pathway to the catabolic ALK1-Smad1/5/8 pathway (van der Kraan et al., 2012), suggesting that excessive activation of TGF-β in aged individuals might actually exacerbate cartilage deterioration. Excessive TGF-β also induces synovial fibrosis and osteophyte formation (Scharstuhl et al., 2003; van Beuningen et al., 1994), which are common features of OA and also closely associated with its progression.

Intriguingly, our recent study on rheumatoid arthritis (RA) also showed an aberrant activation of TGF-β in the subchondral bone marrow of RA-afflicted knee joints. Either systemic or local blockade of TGF-β activity in the subchondral bone attenuated articular cartilage degeneration in RA. Moreover, conditional deletion of TGF-β receptor II (Tgfbr2) in nestin^{+} cells effectively halted progression of RA joint destruction (Xu et al., 2015). Our data indicate that the pathogenesis of cartilage degeneration in RA and OA may converge on the aberrant activation of TGF-β in the subchondral bone, although they are recognized as two different arthritic diseases with distinct etiologies and clinical manifestations. Inhibition of TGF-β activity in the subchondral bone could help quell cartilage degeneration and joint damage and offers an additional therapeutic drug target to improve outcomes in both OA and RA.

Musculoskeletal disorders associated with genetic mutations in transforming growth factor-β signaling components

TGF-β and its family members are multifunctional growth factors that play critical roles in the development and maintenance of the skeleton. Various pathological skeletal phenotypes are consequent to mutations in genes encoding ligands, receptors, and signaling molecules of the TGF-β family. TGF-β-related diseases form an important subgroup of skeletal dysplasia (Warman et al., 2011), which covers both monogenic and polygenic diseases involving the skeletal system. Monogenic skeletal disease is caused by a single gene mutation and belongs to relatively simple and traceable Mendelian disease. In contrast, polygenic skeletal disease is multifactorial (e.g., osteoporosis). Its phenotype is determined by combined and concerted effects of a group of genes (susceptibility genes) and the environment. Hence, its inheritance is complex and less predictable. These diseases give us clues to delineate the roles of TGF-β in the skeleton in vivo as well as the physiological mechanisms controlling the skeletal system. Here we discuss representative monogenic and polygenic bone disorders associated with TGF-β mutations with a focus on their significance for understanding mechanisms regulating the skeletal system.

In general, most if not all monogenic TGF-β-related skeletal disorders share a common pathogenesis. A specific gene mutation leads to excessive and sustained production or activation of TGF-β ligand (Fig. 47.3) that distorts the normal bone remodeling process. The temporally and spatially regulated physiological TGF-β gradient may be disrupted and lead to excessive recruitment of MSCs or altered downstream targeted effects. Skeletal phenotypes with uncoupled bone remodeling appearing as sclerosis result in addition to other specific end-organ effects.

CED is characterized by a fusiform thickening of the diaphysis of the long bones and skull. CED is caused by mutations in the TGF-β1 gene, resulting in premature activation of TGF-β1 (Janssens et al. 2000, 2003; Kinoshita et al., 2000; Saito et al., 2001). Approximately 11 different TGF-β1 mutations have been identified from CED-afflicted families (Janssens et al., 2006; Whyte et al., 2011). All mutations are in the region encoding LAP and either destabilize the disulfide bridging of LAP or affect secretion of the protein, leading to enhanced TGF-β1 signaling. Patients with CED show a typical uncoupled bone remodeling phenotype characterized by decreased trabecular connectivity despite normal osteoblast and osteoclast numbers (Bondestam et al., 2007; Whyte et al., 2011). The conditioned medium collected from cells expressing CED mutant TGF-β1 shows a significantly increased ratio of active/total TGF-β1, and it hyperactively induces the

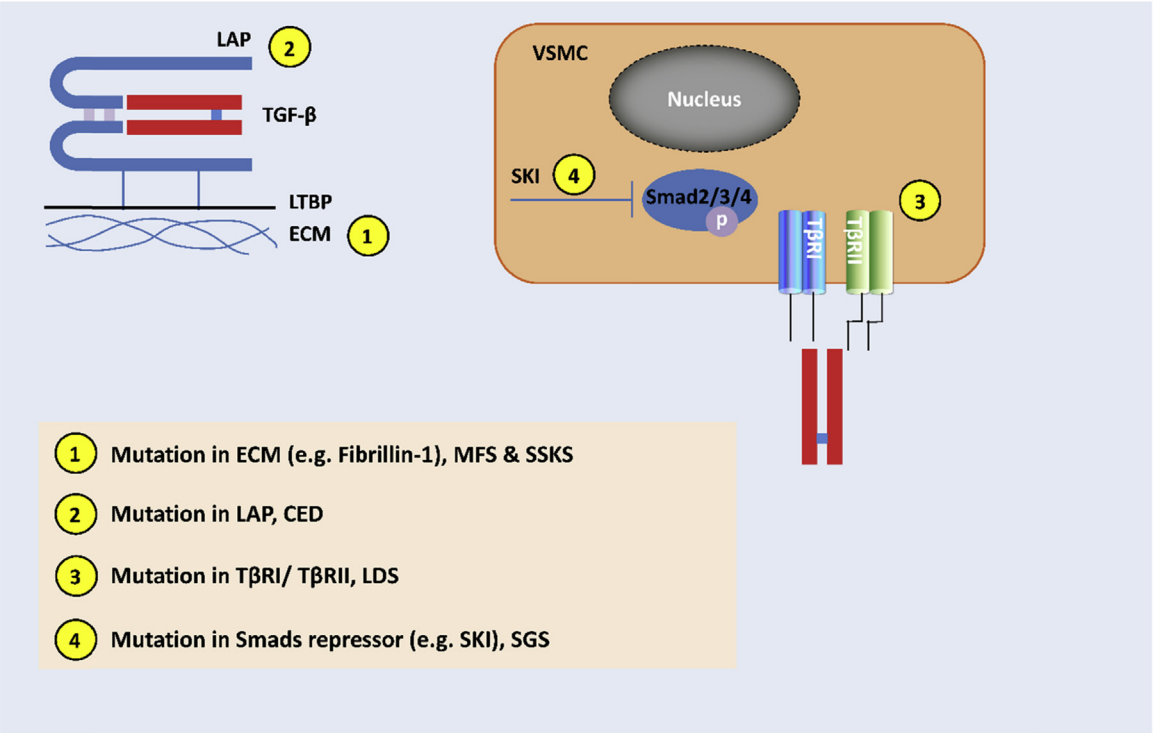

FIGURE 47.3 Common genetic disorders with aberrant TGF-β activity. ① Mutations in genes involved in the synthesis/assembly of extracellular matrix (ECM), e.g., Fibrillin-1, cause compromised matrix sequestration of the large latent complex of TGF-β and excessive TGF signaling, ultimately resulting in genetic disorders such as Marfan syndrome (MFS) and stiff skin syndrome (SSKS). ②Mutations in the region encoding latency-associated peptide (LAP) increase the release of active TGF-β, and cause Camurati−Engelmann disease (CED). ③ Mutations in genes encoding TGF-β type I and II receptors (TβRI/II) lead to compensatory synthesis of TGF-β ligand, and cause Loeys−Dietz syndrome (LDS). ④ Mutations in Smad repressors, such as SKI, superactivate TGF-β signaling and cause Shprintzen−Goldberg syndrome (SGS) phenotypes. VSMC: vascular smooth muscle cell. *Figure is reused with authors' permission Xu, X, Zheng, L, Yuan, Q, Zhen, G, Crane, JL, Zhou, X, Cao, X. Transforming growth factor-β in stem cells and tissue homeostasis. Bone Res. 2018, 6, 2.*

migration of MSCs (Tang et al., 2009). However, targeted recruitment of MSCs to the bone remodeling site is likely disrupted due to loss of the TGF-β gradient.

In addition to CED, several other genetic disorders with skeletal manifestations including Marfan syndrome (MFS), Loeys−Dietz syndrome (LDS), Shprintzen−Goldberg syndrome (SGS), and neurofibromatosis type 1 (NF1) also involve aberrant TGF-β signaling. MFS is caused by mutations in the fibrillin-1 encoding gene and often results in aortic dilatation, myopia, bone overgrowth, and joint laxity (Dietz et al. 1991a, 1991b, 2005; Kainulainen et al., 1994). Fibrillin-1 is deposited in the ECM and interacts directly with latent TGF-β-binding proteins (LTBPs), keeping TGF-β sequestered and unable to exert its biological activity. In MFS, secondary to mutated structural fibrillin-1, excessive activation of TGF-β in the lungs, heart valves, and aorta causes pathological features (Dietz et al., 2005; Neptune et al., 2003). LDS is caused by inactivating mutations in genes encoding TβRI and TβRII (Loeys et al., 2005). Physical manifestations of LDS include arterial aneurysms, hypertelorism, bifid uvula/cleft palate, and bone overgrowth resulting in arachnodactyly, joint laxity, and scoliosis. Although the exact mechanism is still unclear, TGF-β signaling is elevated in the affected tissues of LDS despite the inactivating mutation (Loeys et al., 2005). A recent study by Dietz et al. suggests that vascular smooth muscle cells (VSMCs) that carry the LDS mutation may compensate for their signaling deficiency by upregulating the expression of TGF-β ligands (Gallo et al., 2014). Indeed, tissue from LDS patients and mice shows increased expression of TGF-β1 regardless of etiology (Lindsay et al., 2012; van de Laar et al., 2011). Upregulated TGF-β1 production by specific cell types (e.g., VSMCs) could lead to paracrine overdrive of TGF-β signaling in neighboring cells despite the presence of mutant receptors. Infiltrating $CD45^{+}$ cells in the aortic root adventitia as the disease progresses might also contribute to excessive TGF-β1 production (Gallo et al., 2014). SGS is caused by mutations in the Sloan-Kettering Institute proto-oncoprotein (SKI) (Carmignac et al., 2012; Doyle et al., 2012) and results in physical features similar to those of MFS plus craniosynostosis. SKI negatively regulates Smad-dependent TGF-β signaling by impeding Smad2 and Smad3 activation, preventing nuclear translocation of the SMAD4 complex, and inhibiting TGF-β target gene output by

competing with p300/CBP for SMAD binding and recruiting transcriptional repressor proteins, such as mSin3A and HDACs (Nomura et al., 1999; Prunier et al., 2003; Reed et al., 2001). The neurocutaneous syndrome NF1 has skeletal features including kyphoscoliosis, osteoporosis, and tibial pseudoarthrosis. The $Nf1^{flox/};Col2.3^{Cre+}$ mouse model that closely recapitulates the skeletal abnormalities found in human NF1 disease has hyperactive TGF-β1 signaling (Rhodes et al., 2013). The exact mechanisms underlying mutant neurofibromin-associated hyperactivation of TGF-β signaling remain unknown, particularly in relation to osseous defects.

Osteoporosis is the pathological decrease of bone tissue leading to an increased risk of fracture, mainly in the spine (vertebral body), distal radius, and femoral neck. It has been estimated that osteoporosis results in more than 1.3 million osteoporotic fractures per year in the US, and more than 40% of postmenopausal women are reported to have sustained a fracture (Cummings et al., 1985; Ray et al., 1997). Osteoporosis is classified as primary and secondary osteoporosis based on its etiology. Primary osteoporosis consists of postmenopausal and senile osteoporosis. Postmenopausal osteoporosis is the most common bone and joint disease in women after menopause. Secondary osteoporosis results from various diseases relating to bone metabolism or prolonged use of medications such as glucocorticoids. The underlying mechanism in all cases of osteoporosis is an imbalance between bone resorption and bone formation. Three main mechanisms interplay and underlie the development of bone fragility, including inadequate peak bone mass, excessive bone resorption, and inadequate bone formation during remodeling (Raisz, 2005). Polymorphisms in several genes associated with bone mass or osteoporotic fracture have been identified by population-based and case-controlled studies. Candidate genes include TGF-β, vitamin D receptor, estrogen receptor, and type I collagen (Xu et al., 2010). Specific TGF-β gene polymorphisms associated with BMD and/or osteoporotic fractures have been identified (Langdahl et al., 1997; Yamada et al., 2001). A C/T polymorphism that causes a proline−leucine substitution at amino acid 10 in the TGF-β1 encoding region has been identified. The C allele is associated with increased BMD and reduced osteoporotic fracture risk in postmenopausal Japanese women. In addition, the C allele is associated with circulating levels of TGF-β1, suggesting that the C allele may influence protein secretion or stability (Yamada et al., 1998). However, the underlying molecular mechanisms are still unclear. Of note, subsequent large-scale association studies in Japanese (Kou et al., 2011) and other ethnic populations (Hubacek et al., 2006; Tural et al., 2013) have not been able to replicate the association.

Skeletal metastases of cancer associated with bone matrix−derived transforming growth factor-β

Cancer diagnosed at an early stage can usually be effectively treated with some combination of surgery, radiation, hormonal therapy, and chemotherapy. However, treatment options for metastatic or recurrent cancer with acceptable outcomes are still limited. Bones are a common place for metastasis. Skeletal metastasis of cancer is a complex process, including cancer cells escaping the primary site, circulating to distant sites, evading the host immune response, and proliferating into the metastatic site (Gupta and Massague, 2006). Tumor cells could generate adhesive molecules that mediate binding to BMSCs and bone matrix. The interactions between tumor cells and bone promote the production of angiogenic and bone-resorbing factors by tumor and further enhance tumor growth in bone (van der Pluijm et al., 2001). Of note, the bone microenvironment houses abundant growth factors including TGF-β, IGF1/2, FGFs, PDGFs, and BMPs (Mohan and Baylink, 1991). During tumor-induced osteoclastic bone resorption, these factors are released and enriched in the bone microenvironment. These bone matrix-derived factors, particularly TGF-β, can act back upon the tumor to facilitate further tumor expansion and enhance cytokine production and upon osteoblasts to suppress bone formation, further promoting tumor growth and metastasis in bone (Juarez and Guise, 2011).

In cancer, TGF-β can be either a tumor suppressor or a tumor promoter depending on the temporal stage of the disease (Siegel and Massague, 2003). In the early stage of tumor initiation, TGF-β limits the growth of tumor cells through its antiproliferative and proapoptotic actions (Derynck et al., 2001). Conversely, during tumor progression, TGF-β acts as a tumor promoter by inducing proliferation, angiogenesis, and immunosuppression, and thus promotes the invasion and metastasis of cancer (Massague, 2008). The loss of function of TGF-β signaling also contributes to certain tumor types. Mutations in TβRII are frequently detected in colon cancer, gastric tumors, and gliomas. These mutations may result in DNA repair defects and cancer predisposition, likely due to cellular escape from TGF-β-mediated growth surveillance (Izumoto et al., 1997; Markowitz and Roberts, 1996; Ohue et al., 1996; Park et al., 1994). Loss-of-function mutations in TβRI have been observed in ovarian cancers, metastatic breast cancers, pancreatic carcinomas, and T cell lymphomas (Chen et al. 1998, 2001; Goggins et al., 1998; Schiemann et al., 1999). In addition, mutations in the TGF-β signaling components, such as Smad protein mutations, have been detected in several carcinomas. Smad2 mutations have been identified in human colorectal cancer and lung cancers (Eppert et al., 1996; Takagi et al., 1998). Smad4 mutations have been detected in pancreatic carcinomas and familial juvenile polyposis (Howe et al., 1998; Schutte et al., 1996), and Smad2

and Smad4 double mutations have been detected in hepatocellular carcinoma (Yakicier et al., 1999). Moreover, Smad3 is frequently downregulated in cancer, and inactivating mutations have also been reported (Daly et al., 2010; Jones et al., 2008; Leary et al., 2008). TGF-β can antagonize BMP-like responses by the formation of a pSmad1/5-pSmad3 complex specifically binding to BRE and suppressing the transcription of downstream genes (Gronroos et al., 2012). Inactivation of Smad3 in cancer alleviates the antagonism of TGF-β on BMP responses and enables TGF-β to induce BRE downstream ID genes (Gronroos et al., 2012) that are potent tumor promoters normally suppressed by canonical TGF-β signaling (Massague, 2008). The induction of ID genes thus deregulates tumor cell proliferation and confers invasiveness, angiogenesis, and metastasis (Iavarone and Lasorella, 2006).

In advanced cancer, cells lose TGF-β suppressive effects, resulting in compensatory overproduction of TGF-β. Elevated levels of TGF-β in serum are often observed in the later stages of cancer and are associated with increased invasiveness and a poor clinical outcome of cancer (Gold, 1999). TGF-β signaling can act on multiple cells in the local microenvironment of bone and consequently enhance tumor growth and invasiveness (Padua and Massague, 2009; Siegel and Massague, 2003). Specifically, TGF-β could induce the expression, secretion, and activation of MMPs that mediate the migration of endothelial cells, thus promoting tumor angiogenesis (Hagedorn et al., 2001; Padua and Massague, 2009). TGF-β could also indirectly induce the expression of proangiogenic factors such as VEGF and connective tissue growth factor (CTGF) in fibroblastic and epithelial cells (Kang et al., 2003; Pertovaara et al., 1994) and thus further contribute to the angiogenesis and invasiveness of tumor (de Jong et al., 1998; Hasegawa et al., 2001). Inhibition of TGF-β signaling with TGF-β-neutralizing antibodies can suppress angiogenesis in human breast and prostate cancers (Tuxhorn et al., 2002), further validating the critical role of TGF-β as a proangiogenic factor during tumor. Furthermore, excessive production of tumor-derived TGF-β could suppress T lymphocytes and natural killer cells, leading to cellular escape of cancer cells from cytotoxic T lymphocyte clearance (Thomas and Massague, 2005). Target blockade of TGF-β signaling in T cells results in eradication of tumors in mice challenged with live tumor cells (Gorelik and Flavell, 2001), indicating the suppressive action of TGF-β signaling on T cell−mediated antitumor immunity.

TGF-β is also involved in the EMT of cancer (Lopez-Novoa and Nieto, 2009; Xu et al., 2009), which is essential for increasing tumor cell mobility and invasiveness closely related to metastasis. TGF-β interacts with other oncogenic pathways to maintain the mesenchymal phenotype of tumor cells by downregulating E-cadherin and upregulating mesenchymal genes (Zavadil and Bottinger, 2005). Smads, Ras, Rho, ERK MAPK, p38 MAPK, and Wnt signaling pathways have been implicated in TGF-β-induced EMT (Xu et al., 2009). TGF-β activates transcriptional factors such as Snail and Slug to regulate EMT (Batlle et al., 2000; Cano et al., 2000). Particularly, Snail could repress E-cadherin and activate the transcription of mesenchymal genes, such as vimentin and αSMA. In addition, Snail could promote collagen I synthesis/deposition and upregulate proinflammatory interleukins (ILs) such as IL-1, IL-6, and IL-8 (Boutet et al., 2006; Lyons et al., 2008), thus enhancing the invasiveness of tumor.

Based on the aforementioned oncogenic activity of TGF-β, a feed-forward loop has been proposed to describe skeletal metastasis. Tumor cells in bone secrete osteolytic factors, such as PTHrP and IL-11, leading to osteolytic bone resorption. Active TGF-β is released from bone matrix by osteoclastic resorption and further induces tumor production of osteolytic and prometastatic factors including PTHrP and IL-11. Of note, PTHrP is a central mediator of TGF-β-induced osteolytic metastases. Increased expression of PTHrP has been observed in human breast cancer with bone metastases, compared with that of primary breast cancers (Henderson et al., 2006). PTHrP can stimulate RANKL and inhibit OPG expression in osteoblasts to favor osteoclastogenesis (Thomas et al., 1999). TGF-β induces PTHrP secretion from MDA-MB-231 cells via Smad and p38 MAP kinase pathways (Kakonen et al., 2002). Stable inactivation of TβRII in the breast cancer cell line MDA-MB-231 inhibited TGF-β-induced PTHrP secretion and suppressed bone metastases in a mouse model (Yin et al., 1999). Direct neutralization of PTHrP with PTHrP-neutralizing antibodies inhibits the development and progression of breast cancer bone metastases in mouse models (Guise et al., 1996). TGF-β released during bone resorption can also directly act on bone cells. Within a given range of concentrations, TGF-β stimulates osteoclastic bone resorption while inhibiting osteoblastic differentiation. Transcriptional profiling of human breast cancer cells with an aggressive bone metastatic phenotype has identified the upregulation of several genes, such as IL-11, CTGF, CXCR4, and MMP1, associated with bone metastases. These genes act cooperatively to cause skeletal metastasis by promoting homing to bone, angiogenesis, and invasion of tumor. Notably, these genes are all regulated by TGF-β via the canonical TGF-β/Smad pathway in metastatic cells (Dunn et al., 2009; Kang and Massague, 2004; Kang et al., 2003). Inhibition of either TGF-β signaling with small-molecule inhibitors or bone resorption with bisphosphonate is effective in decreasing TGF-β signaling activity in bone metastases (Korpal et al., 2009). This indicates that TGF-β released by osteoclastic bone resorption is the major source of TGF-β acting on tumor cells in bone. Inhibition of either the TGF-β pathway or osteoclastic bone resorption may represent a novel therapeutic for the treatment of skeletal metastasis.

Several preclinical studies have shown that the TGF-β signaling pathway is a potential target for the inhibition of bone metastases. Knockdown of Smad4 expression in breast cancer cells reduces growth of bone metastases (Deckers et al., 2006; Kang et al., 2005), while overexpression of Smad7 reduces bone metastases of melanoma (Javelaud et al., 2007). Small-molecule inhibitors of the TβRI kinase have been used to reduce bone metastasis through blockage of TGF-β signaling. Systemic administration of small molecule [3-(pyridine-2yl)-4-(4-quinonyl)]-1H pyrazole], which is able to inhibit TβRI kinase activity, has been shown to effectively reduce the number and size of lung metastases and the incidence of skeletal metastases in an experimental mice model of bone and lung metastasis (Bandyopadhyay et al., 2006a). Systemic administration of Ki26894 (a TβRI kinase inhibitor) decreased skeletal metastasis and prolonged survival of a nude mouse model with bone metastasis (Ehata et al., 2007). Consistently, preventive treatment with TβRI the kinase inhibitor LY2109761 led to a reduction in the number of bone lesions and skeletal tumor burden in a bone metastatic mice model. Although LY2109761 was less effective in the treatment of established bone metastases (Korpal et al., 2009), SD-208, a more potent TβRI kinase inhibitor, was effective in the treatment of mice with established bone metastases (Dunn et al., 2009). The use of TGF-β-neutralizing antibodies is another possible modality for the treatment of bone metastases (Biswas et al., 2007). Treatment with a neutralizing pan-TGF-β antibody (1D11, Genzyme) has been shown to decrease metastases to the lungs in a transplantable 4T1 mice model of metastatic breast cancer (Nam et al., 2008) and reduce skeletal tumor burden in mice while also increasing bone volume (Biswas et al., 2011).

The combination of anti-TGF-β therapies with other therapeutics is promising for the treatment of patients with bone metastases. Bone is a hypoxic microenvironment, and hypoxia-inducible factor 1α (HIF-1α) has been implicated in enhancing tumor growth and metastasis (Dunn et al., 2009; Hiraga et al., 2007). Hypoxia also stimulates the expression of CXCR4 and DUSP1 (Lu et al., 2010), whose upregulation is associated with bone metastatic (Kang et al., 2003). TGF-β stabilizes HIF-1α by inhibiting its degradation (McMahon et al., 2006). TGF-β and hypoxia signaling pathways in breast cancer cells are additive to induce VEGF and CXCR4 (Dunn et al., 2009; McMahon et al., 2006). Inhibition of both TGF-β and hypoxia signaling pathways decreased bone metastases more than inhibition of either alone, resulting in enhanced osteoblastic activity and suppressed osteoclastic bone resorption as well as reduced tumor growth (Dunn et al., 2009). Other possible therapies include halofuginone, a natural product derivative that inhibits TGF-β signaling possibly via induction of Smad7. Halofuginone treatment can significantly suppress osteolysis and skeletal tumor burden in mice with established bone metastases (Juarez et al., 2012).

In conclusion, bone is the most common site of cancer metastases. Active TGF-β released from bone matrix is the major component of the bone microenvironment, functioning to drive a feed-forward cycle of tumor growth and osteolysis in bone. Modulation of TGF-β signaling in cancer cells has been proven effective in decreasing bone metastases in in vitro and animal models. Development of anti-TGF-β therapies, administered alone or supplementing other therapies, for bone metastasis of cancer is promising. Since TGF-β can be either tumor-suppressive or prometastatic, a long-term global blockade of this signaling pathway may result in off-target effects. Hence, delicate modulation of TGF-β signaling during tumor onset and progression is necessary for the development of the most effective antineoplastic therapy with minimal toxicity but potent efficacy.

Transforming growth factor-β modulation as a promising approach to the management of osteoarthritis

Excessive activation of TGF-β in subchondral bone has been reported at the onset of OA in animal models (Zhen et al., 2013). Active TGF-β1 concentrations are also high in the subchondral bone of people affected by OA. All these data suggest that modulation of TGF-β signaling may provide a promising disease-modifying approach for OA. In ACLT rodent models, systemic inhibition of TGF-β signaling with intraperitoneal administration of TβRI inhibitor or specific blockade of active TGF-β ligand in the tibial subchondral bone with TGF-β-neutralizing antibody at the time of injury was sufficient to attenuate the degeneration of articular cartilage (Zhen et al., 2013). Furthermore, TGF-β signaling activated in the subchondral bone through osteoclast bone resorption in these animal OA models suggests that inhibition of osteoclast bone resorption may also delay the progression of OA. Several clinical trials and preclinical studies support this hypothesis. In addition to many animal studies that reveal the positive effect of bisphosphonates for delaying OA progression (Hayami et al., 2004; Panahifar et al., 2012; Shirai et al., 2011; Zhang et al., 2011; Zhu et al., 2013), in the most recent prospective 2-year trial, alendronate treatment successfully improved the Western Ontario and McMaster Universities Osteoarthritis (WOMAC) pain scores and decreased biochemical markers in hip OA patients (Nishii et al., 2013). In a cross-sectional study, elderly women who were being treated with alendronate were found to have significantly decreased the prevalence of knee OA as assessed by WOMAC pain scales, and subchondral bone lesions by MR imaging, compared

with elderly women not taking alendronate (Carbone et al., 2004). Randomized controlled trials are needed to assess the efficacy of bisphosphonates as a potential OA treatment. The detailed mechanisms also still need to be further elucidated, anticipating that at least part of the effect is through the inhibition of osteoclast activity and subsequent reduction in TGF-β levels. As many musculoskeletal disorders also involve excessive TGF-β signaling, attenuating the TGF-β signaling pathway could also benefit the management of these diseases.

High levels of active TGF-β also alter the microenvironment of subchondral bone, leading to aggregation of osteoprogenitors and increased angiogenesis in bone marrow. PTH is FDA-approved as an anabolic therapy for osteoporosis. Daily injection of PTH increases bone formation with normal microarchitecture (Bikle et al., 2002; Canalis et al., 1989; Lombardi et al., 2010; Miyakoshi et al., 2001; Pfeilschifter et al., 1995; Qiu et al., 2010; Wan et al., 2008; Watson et al., 1995; Yu et al., 2012). PTH can improve the bone marrow microenvironment by orchestrating the signaling of local factors for bone remodeling, reducing ROS, and stimulating Wnt signaling in bone of senescent mice (Bikle et al., 2002; Canalis et al., 1989; Jilka et al., 2010; Khosla et al., 2008; Lombardi et al., 2010; Miyakoshi et al., 2001; Pfeilschifter et al., 1995; Qiu et al., 2010; Raggatt and Partridge, 2010; Wan et al., 2008; Watson et al., 1995; Yu et al., 2012). In addition, PTH has demonstrated potent chondroprotective and chondroregenerative effects by inducing cartilage matrix synthesis and suppressing chondrocyte hypertrophy and matrix metalloproteinase 13 expression in different OA animal models (Orth et al., 2013; Sampson et al., 2011). The dual beneficiary effects of PTH on both cartilage and subchondral bone make PTH another promising candidate for the treatment of OA. A recent study using a rabbit model of OA preceded by osteoporosis has demonstrated that PTH treatment in the early stage of OA is able to improve the microstructure and quality of subchondral bone and thus attenuate subsequent cartilage damage (Bellido et al., 2011). This data supports the relevance of the role of subchondral bone osteopenia in the pathogenesis of OA and indicates the potential application of anabolic agents (such as PTH) to treatment in the early stages of OA associated with osteoporosis. The osteogenic microenvironment created by PTH has also been shown to expand HSPC niches (Calvi et al., 2003; Mendez-Ferrer et al., 2010) and could also potentially be translated into therapies for hematologic diseases such as cytopenias, myelodysplastic syndromes, and myeloproliferative disorders (Smith and Calvi, 2013).

Articular cartilage and subchondral bone constantly interact as a functional unit. TGF-β plays a critical role in maintaining bone and articular cartilage homeostasis. Joint instability causes increased subchondral bone remodeling, which releases excessive active TGF-β1 through osteoclastic bone resorption. The pathologically high level of TGF-β1 in subchondral bone leads to aberrant bone remodeling and the formation of marrow osteoid islets. The abnormal subchondral bone microstructure in turn likely alters the stress distribution on the articular cartilage, eventually resulting in cartilage degeneration. The concept of holism is essential for exploring therapeutic strategies for OA. Improving the mechanical properties of subchondral bone and its physiological function are at least equally important as directly targeting articular cartilage. Therapies that can normalize TGF-β signaling, either directly by neutralizing TGF-β overactivation or indirectly by PTH-mediated modulation of the bone marrow microenvironment, may serve as a potential approach to the management of joint disorders.

Summary

TGF-β, as a dual functional growth factor, has been attracting major research efforts ever since its discovery. Unlike most growth factors that are ready to function upon secretion, TGF-β is unique because it is secreted as part of a latent complex stored in the ECM for activation and action at a later time point. Precise temporal and spatial activation of TGF-β signaling is necessary to counter tissue perturbations, either by suppressing excessive adversary cellular responses such as inflammation or by recruiting adult stem cells to participate in the tissue repair/remodeling process. The bone remodeling process clearly underscores the importance of proper activation of TGF-β in the maintenance of tissue homeostasis. The physiological gradient of active TGF-β formed by normal bone remodeling functions as a coupling factor that directs MSCs/osteoprogenitors to bone-resorbing sites for coupled bone formation, whereas sustained activation of TGF-β by either genetic mutations or pathologically elevated osteoclastic activity recruits excessive MSCs/osteoprogenitors for aberrant bone remodeling. The same theory can be applied to other pathologies with TGF-β involvement, where the normal functions of this growth factor are switched to an off-target activity that disrupts tissue homeostasis. Therefore, a comprehensive understanding of the mechanisms that underlie the physiological and pathological effects of TGF-β, and full interpretation of how cells integrate these signals into coherent responses in a context-dependent way, can lead to promising therapeutics for TGF-β-involved pathologies. Novel strategies that intricately tune TGF-β signaling to properly respond to specific contexts are being developed with anticipated clinical implications.

References

Adams, J.C., Lawler, J., 2004. The thrombospondins. Int. J. Biochem. Cell Biol. 36 (6), 961–968.

Agah, A., Kyriakides, T.R., Lawler, J., Bornstein, P., 2002. The lack of thrombospondin-1 (tsp1) dictates the course of wound healing in double-tsp1/tsp2-null mice. Am. J. Pathol. 161 (3), 831–839.

Ahamed, J., Burg, N., Yoshinaga, K., Janczak, C.A., Rifkin, D.B., Coller, B.S., 2008. In vitro and in vivo evidence for shear-induced activation of latent transforming growth factor-beta1. Blood 112 (9), 3650–3660.

Alarcon, C., Zaromytidou, A.I., Xi, Q., Gao, S., Yu, J., Fujisawa, S., Barlas, A., Miller, A.N., Manova-Todorova, K., Macias, M.J., et al., 2009. Nuclear cdks drive smad transcriptional activation and turnover in bmp and tgf-beta pathways. Cell 139 (4), 757–769.

Annes, J.P., Chen, Y., Munger, J.S., Rifkin, D.B., 2004. Integrin alphavbeta6-mediated activation of latent tgf-beta requires the latent tgf-beta binding protein-1. J. Cell Biol. 165 (5), 723–734.

Annes, J.P., Munger, J.S., Rifkin, D.B., 2003. Making sense of latent tgfbeta activation. J. Cell Sci. 116 (Pt 2), 217–224.

Aoki, K., Aikawa, N., Sekine, K., Yamazaki, M., Mimura, T., Urano, T., Takada, A., 2001. Elevation of plasma free pai-1 levels as an integrated endothelial response to severe burns. Burns 27 (6), 569–575.

Aoyagi-Ikeda, K., Maeno, T., Matsui, H., Ueno, M., Hara, K., Aoki, Y., Aoki, F., Shimizu, T., Doi, H., Kawai-Kowase, K., et al., 2011. Notch induces myofibroblast differentiation of alveolar epithelial cells via transforming growth factor-{beta}-smad3 pathway. Am. J. Respir. Cell Mol. Biol. 45 (1), 136–144.

Attisano, L., Wrana, J.L., Montalvo, E., Massague, J., 1996. Activation of signalling by the activin receptor complex. Mol. Cell Biol. 16 (3), 1066–1073.

Bakin, A.V., Tomlinson, A.K., Bhowmick, N.A., Moses, H.L., Arteaga, C.L., 2000. Phosphatidylinositol 3-kinase function is required for transforming growth factor beta-mediated epithelial to mesenchymal transition and cell migration. J. Biol. Chem. 275 (47), 36803–36810.

Baksh, D., Boland, G.M., Tuan, R.S., 2007. Cross-talk between wnt signaling pathways in human mesenchymal stem cells leads to functional antagonism during osteogenic differentiation. J. Cell. Biochem. 101 (5), 1109–1124.

Bandyopadhyay, A., Agyin, J.K., Wang, L., Tang, Y., Lei, X., Story, B.M., Cornell, J.E., Pollock, B.H., Mundy, G.R., Sun, L.Z., 2006a. Inhibition of pulmonary and skeletal metastasis by a transforming growth factor-beta type i receptor kinase inhibitor. Cancer Res. 66 (13), 6714–6721.

Bandyopadhyay, B., Fan, J., Guan, S., Li, Y., Chen, M., Woodley, D.T., Li, W., 2006b. A "traffic control" role for tgfbeta3: orchestrating dermal and epidermal cell motility during wound healing. J. Cell Biol. 172 (7), 1093–1105.

Barcellos-Hoff, M.H., Derynck, R., Tsang, M.L., Weatherbee, J.A., 1994. Transforming growth factor-beta activation in irradiated murine mammary gland. J. Clin. Investig. 93 (2), 892–899.

Barcellos-Hoff, M.H., Dix, T.A., 1996. Redox-mediated activation of latent transforming growth factor-beta 1. Mol. Endocrinol. 10 (9), 1077–1083.

Batlle, E., Sancho, E., Franci, C., Dominguez, D., Monfar, M., Baulida, J., Garcia De Herreros, A., 2000. The transcription factor snail is a repressor of e-cadherin gene expression in epithelial tumour cells. Nat. Cell Biol. 2 (2), 84–89.

Beck Jr., L., D'Amore, P.A., 1997. Vascular development: cellular and molecular regulation. FASEB J. 11 (5), 365–373.

Bellido, M., Lugo, L., Roman-Blas, J.A., Castaneda, S., Calvo, E., Largo, R., Herrero-Beaumont, G., 2011. Improving subchondral bone integrity reduces progression of cartilage damage in experimental osteoarthritis preceded by osteoporosis. Osteoarthritis Cartilage 19 (10), 1228–1236.

Belmadani, S., Bernal, J., Wei, C.C., Pallero, M.A., Dell'italia, L., Murphy-Ullrich, J.E., Berecek, K.H., 2007. A thrombospondin-1 antagonist of transforming growth factor-beta activation blocks cardiomyopathy in rats with diabetes and elevated angiotensin ii. Am. J. Pathol. 171 (3), 777–789.

Beyer, T.A., Narimatsu, M., Weiss, A., David, L., Wrana, J.L., 2013. The tgfbeta superfamily in stem cell biology and early mammalian embryonic development. Biochim. Biophys. Acta 1830 (2), 2268–2279.

Bharathy, S., Xie, W., Yingling, J.M., Reiss, M., 2008. Cancer-associated transforming growth factor beta type ii receptor gene mutant causes activation of bone morphogenic protein-smads and invasive phenotype. Cancer Res. 68 (6), 1656–1666.

Bhowmick, N.A., Ghiassi, M., Bakin, A., Aakre, M., Lundquist, C.A., Engel, M.E., Arteaga, C.L., Moses, H.L., 2001. Transforming growth factor-beta1 mediates epithelial to mesenchymal transdifferentiation through a rhoa-dependent mechanism. Mol. Biol. Cell 12 (1), 27–36.

Bianco, P., Cao, X., Frenette, P.S., Mao, J.J., Robey, P.G., Simmons, P.J., Wang, C.Y., 2013. The meaning, the sense and the significance: translating the science of mesenchymal stem cells into medicine. Nat. Med. 19 (1), 35–42.

Bikle, D.D., Sakata, T., Leary, C., Elalieh, H., Ginzinger, D., Rosen, C.J., Beamer, W., Majumdar, S., Halloran, B.P., 2002. Insulin-like growth factor i is required for the anabolic actions of parathyroid hormone on mouse bone. J. Bone Miner. Res. 17 (9), 1570–1578.

Bismar, H., Kloppinger, T., Schuster, E.M., Balbach, S., Diel, I., Ziegler, R., Pfeilschifter, J., 1999. Transforming growth factor beta (tgf-beta) levels in the conditioned media of human bone cells: relationship to donor age, bone volume, and concentration of tgf-beta in human bone matrix in vivo. Bone 24 (6), 565–569.

Biswas, S., Guix, M., Rinehart, C., Dugger, T.C., Chytil, A., Moses, H.L., Freeman, M.L., Arteaga, C.L., 2007. Inhibition of tgf-beta with neutralizing antibodies prevents radiation-induced acceleration of metastatic cancer progression. J. Clin. Investig. 117 (5), 1305–1313.

Biswas, S., Nyman, J.S., Alvarez, J., Chakrabarti, A., Ayres, A., Sterling, J., Edwards, J., Rana, T., Johnson, R., Perrien, D.S., et al., 2011. Anti-transforming growth factor ss antibody treatment rescues bone loss and prevents breast cancer metastasis to bone. PLoS One 6 (11), e27090.

Boland, G.M., Perkins, G., Hall, D.J., Tuan, R.S., 2004. Wnt 3a promotes proliferation and suppresses osteogenic differentiation of adult human mesenchymal stem cells. J. Cell. Biochem. 93 (6), 1210–1230.

Bondestam, J., Mayranpaa, M.K., Ikegawa, S., Marttinen, E., Kroger, H., Makitie, O., 2007. Bone biopsy and densitometry findings in a child with camurati-engelmann disease. Clin. Rheumatol. 26 (10), 1773–1777.

Border, W.A., Ruoslahti, E., 1992. Transforming growth factor-beta in disease: the dark side of tissue repair. J. Clin. Investig. 90 (1), 1–7.

Boudreau, H.E., Emerson, S.U., Korzeniowska, A., Jendrysik, M.A., Leto, T.L., 2009. Hepatitis c virus (hcv) proteins induce nadph oxidase 4 expression in a transforming growth factor beta-dependent manner: a new contributor to hcv-induced oxidative stress. J. Virol. 83 (24), 12934–12946.

Boutet, A., De Frutos, C.A., Maxwell, P.H., Mayol, M.J., Romero, J., Nieto, M.A., 2006. Snail activation disrupts tissue homeostasis and induces fibrosis in the adult kidney. EMBO J. 25 (23), 5603–5613.

Breuss, J.M., Gallo, J., DeLisser, H.M., Klimanskaya, I.V., Folkesson, H.G., Pittet, J.F., Nishimura, S.L., Aldape, K., Landers, D.V., Carpenter, W., et al., 1995. Expression of the beta 6 integrin subunit in development, neoplasia and tissue repair suggests a role in epithelial remodeling. J. Cell Sci. 108 (Pt 6), 2241–2251.

Breuss, J.M., Gillett, N., Lu, L., Sheppard, D., Pytela, R., 1993. Restricted distribution of integrin beta 6 mrna in primate epithelial tissues. J. Histochem. Cytochem. 41 (10), 1521–1527.

Brooks, P.C., Stromblad, S., Sanders, L.C., von Schalscha, T.L., Aimes, R.T., Stetler-Stevenson, W.G., Quigley, J.P., Cheresh, D.A., 1996. Localization of matrix metalloproteinase mmp-2 to the surface of invasive cells by interaction with integrin alpha v beta 3. Cell 85 (5), 683–693.

Brunner, A.M., Marquardt, H., Malacko, A.R., Lioubin, M.N., Purchio, A.F., 1989. Site-directed mutagenesis of cysteine residues in the pro region of the transforming growth factor beta 1 precursor. Expression and characterization of mutant proteins. J. Biol. Chem. 264 (23), 13660–13664.

Bugge, T.H., Kombrinck, K.W., Flick, M.J., Daugherty, C.C., Danton, M.J., Degen, J.L., 1996. Loss of fibrinogen rescues mice from the pleiotropic effects of plasminogen deficiency. Cell 87 (4), 709–719.

Burr, D.B., Gallant, M.A., 2012. Bone remodelling in osteoarthritis. Nat. Rev. Rheumatol. 8 (11), 665–673.

Burr, D.B., Radin, E.L., 2003. Microfractures and microcracks in subchondral bone: are they relevant to osteoarthrosis? Rheum. Dis. Clin. N. Am. 29 (4), 675–685.

Calvi, L.M., Adams, G.B., Weibrecht, K.W., Weber, J.M., Olson, D.P., Knight, M.C., Martin, R.P., Schipani, E., Divieti, P., Bringhurst, F.R., et al., 2003. Osteoblastic cells regulate the haematopoietic stem cell niche. Nature 425 (6960), 841–846.

Canalis, E., Centrella, M., Burch, W., McCarthy, T.L., 1989. Insulin-like growth factor i mediates selective anabolic effects of parathyroid hormone in bone cultures. J. Clin. Investig. 83 (1), 60–65.

Cano, A., Perez-Moreno, M.A., Rodrigo, I., Locascio, A., Blanco, M.J., del Barrio, M.G., Portillo, F., Nieto, M.A., 2000. The transcription factor snail controls epithelial-mesenchymal transitions by repressing e-cadherin expression. Nat. Cell Biol. 2 (2), 76–83.

Carbone, L.D., Nevitt, M.C., Wildy, K., Barrow, K.D., Harris, F., Felson, D., Peterfy, C., Visser, M., Harris, T.B., Wang, B.W., et al., 2004. The relationship of antiresorptive drug use to structural findings and symptoms of knee osteoarthritis. Arthritis Rheum. 50 (11), 3516–3525.

Carmignac, V., Thevenon, J., Ades, L., Callewaert, B., Julia, S., Thauvin-Robinet, C., Gueneau, L., Courcet, J.B., Lopez, E., Holman, K., et al., 2012. In-frame mutations in exon 1 of ski cause dominant shprintzen-goldberg syndrome. Am. J. Hum. Genet. 91 (5), 950–957.

Chai, Y., Ito, Y., Han, J., 2003. Tgf-beta signaling and its functional significance in regulating the fate of cranial neural crest cells. Crit. Rev. Oral Biol. Med. 14 (2), 78–88.

Chang, H., Brown, C.W., Matzuk, M.M., 2002. Genetic analysis of the mammalian transforming growth factor-beta superfamily. Endocr. Rev. 23 (6), 787–823.

Cheifetz, S., Bellon, T., Cales, C., Vera, S., Bernabeu, C., Massague, J., Letarte, M., 1992. Endoglin is a component of the transforming growth factor-beta receptor system in human endothelial cells. J. Biol. Chem. 267 (27), 19027–19030.

Chen, C.T., Bhargava, M., Lin, P.M., Torzilli, P.A., 2003. Time, stress, and location dependent chondrocyte death and collagen damage in cyclically loaded articular cartilage. J. Orthop. Res. 21 (5), 888–898.

Chen, T., Carter, D., Garrigue-Antar, L., Reiss, M., 1998. Transforming growth factor beta type i receptor kinase mutant associated with metastatic breast cancer. Cancer Res. 58 (21), 4805–4810.

Chen, T., Triplett, J., Dehner, B., Hurst, B., Colligan, B., Pemberton, J., Graff, J.R., Carter, J.H., 2001. Transforming growth factor-beta receptor type i gene is frequently mutated in ovarian carcinomas. Cancer Res. 61 (12), 4679–4682.

Chen, Y., Leask, A., Abraham, D.J., Kennedy, L., Shi-Wen, X., Denton, C.P., Black, C.M., Verjee, L.S., Eastwood, M., 2011. Thrombospondin 1 is a key mediator of transforming growth factor beta-mediated cell contractility in systemic sclerosis via a mitogen-activated protein kinase kinase (mek)/extracellular signal-regulated kinase (erk)-dependent mechanism. Fibrogenesis Tissue Repair 4 (1), 9.

Chen, Y., Wang, X., Weng, D., Tian, L., Lv, L., Tao, S., Chen, J., 2009. A tsp-1 synthetic peptide inhibits bleomycin-induced lung fibrosis in mice. Exp. Toxicol. Pathol. 61 (1), 59–65.

Chim, S.M., Tickner, J., Chow, S.T., Kuek, V., Guo, B., Zhang, G., Rosen, V., Erber, W., Xu, J., 2013. Angiogenic factors in bone local environment. Cytokine Growth Factor Rev. 24 (3), 297–310.

Chipev, C.C., Simman, R., Hatch, G., Katz, A.E., Siegel, D.M., Simon, M., 2000. Myofibroblast phenotype and apoptosis in keloid and palmar fibroblasts in vitro. Cell Death Different. 7 (2), 166–176.

Christ, G., Nikfardjam, M., Huber-Beckmann, R., Gottsauner-Wolf, M., Glogar, D., Binder, B.R., Wojta, J., Huber, K., 2005. Predictive value of plasma plasminogen activator inhibitor-1 for coronary restenosis: dependence on stent implantation and antithrombotic medication. J. Thromb. Haemost. 3 (2), 233–239.

Clark, D.A., Coker, R., 1998. Transforming growth factor-beta (tgf-beta). Int. J. Biochem. Cell Biol. 30 (3), 293–298.

Clements, K.M., Bee, Z.C., Crossingham, G.V., Adams, M.A., Sharif, M., 2001. How severe must repetitive loading be to kill chondrocytes in articular cartilage? Osteoarthritis Cartilage 9 (5), 499–507.

Crane, J.L., Cao, X., 2014. Bone marrow mesenchymal stem cells and tgf-beta signaling in bone remodeling. J. Clin. Investig. 124 (2), 466–472.

Crawford, S.E., Stellmach, V., Murphy-Ullrich, J.E., Ribeiro, S.M., Lawler, J., Hynes, R.O., Boivin, G.P., Bouck, N., 1998. Thrombospondin-1 is a major activator of tgf-beta1 in vivo. Cell 93 (7), 1159–1170.

Cummings, S.R., Kelsey, J.L., Nevitt, M.C., O'Dowd, K.J., 1985. Epidemiology of osteoporosis and osteoporotic fractures. Epidemiol. Rev. 7, 178–208.
Dallas, S.L., Rosser, J.L., Mundy, G.R., Bonewald, L.F., 2002. Proteolysis of latent transforming growth factor-beta (tgf-beta)-binding protein-1 by osteoclasts. A cellular mechanism for release of tgf-beta from bone matrix. J. Biol. Chem. 277 (24), 21352–21360.
Daly, A.C., Randall, R.A., Hill, C.S., 2008. Transforming growth factor beta-induced smad1/5 phosphorylation in epithelial cells is mediated by novel receptor complexes and is essential for anchorage-independent growth. Mol. Cell Biol. 28 (22), 6889–6902.
Daly, A.C., Vizan, P., Hill, C.S., 2010. Smad3 protein levels are modulated by ras activity and during the cell cycle to dictate transforming growth factor-beta responses. J. Biol. Chem. 285 (9), 6489–6497.
Daniel, C., Schaub, K., Amann, K., Lawler, J., Hugo, C., 2007. Thrombospondin-1 is an endogenous activator of tgf-beta in experimental diabetic nephropathy in vivo. Diabetes 56 (12), 2982–2989.
Davis, B.N., Hilyard, A.C., Lagna, G., Hata, A., 2008. Smad proteins control drosha-mediated microrna maturation. Nature 454 (7200), 56–61.
Davis, B.N., Hilyard, A.C., Nguyen, P.H., Lagna, G., Hata, A., 2010. Smad proteins bind a conserved rna sequence to promote microrna maturation by drosha. Mol. Cell 39 (3), 373–384.
de Caestecker, M., 2004. The transforming growth factor-beta superfamily of receptors. Cytokine Growth Factor Rev. 15 (1), 1–11.
de Jong, J.S., van Diest, P.J., van der Valk, P., Baak, J.P., 1998. Expression of growth factors, growth-inhibiting factors, and their receptors in invasive breast cancer. II: correlations with proliferation and angiogenesis. J. Pathol. 184 (1), 53–57.
de Martin, R., Haendler, B., Hofer-Warbinek, R., Gaugitsch, H., Wrann, M., Schlusener, H., Seifert, J.M., Bodmer, S., Fontana, A., Hofer, E., 1987. Complementary DNA for human glioblastoma-derived t cell suppressor factor, a novel member of the transforming growth factor-beta gene family. EMBO J. 6 (12), 3673–3677.
Deckers, M., van Dinther, M., Buijs, J., Que, I., Lowik, C., van der Pluijm, G., ten Dijke, P., 2006. The tumor suppressor smad4 is required for transforming growth factor beta-induced epithelial to mesenchymal transition and bone metastasis of breast cancer cells. Cancer Res. 66 (4), 2202–2209.
Dennler, S., Itoh, S., Vivien, D., ten Dijke, P., Huet, S., Gauthier, J.M., 1998. Direct binding of smad3 and smad4 to critical tgf beta-inducible elements in the promoter of human plasminogen activator inhibitor-type 1 gene. EMBO J. 17 (11), 3091–3100.
Derynck, R., 1994. Tgf-beta-receptor-mediated signaling. Trends Biochem. Sci. 19 (12), 548–553.
Derynck, R., Akhurst, R.J., Balmain, A., 2001. Tgf-beta signaling in tumor suppression and cancer progression. Nat. Genet. 29 (2), 117–129.
Derynck, R., Feng, X.H., 1997. Tgf-beta receptor signaling. Biochim. Biophys. Acta 1333 (2), F105–F150.
Derynck, R., Jarrett, J.A., Chen, E.Y., Eaton, D.H., Bell, J.R., Assoian, R.K., Roberts, A.B., Sporn, M.B., Goeddel, D.V., 1985. Human transforming growth factor-beta complementary DNA sequence and expression in normal and transformed cells. Nature 316 (6030), 701–705.
Derynck, R., Jarrett, J.A., Chen, E.Y., Goeddel, D.V., 1986. The murine transforming growth factor-beta precursor. J. Biol. Chem. 261 (10), 4377–4379.
Derynck, R., Miyazono, K., 2008. The tgf-[beta] Family Cold Spring Harbor. Cold Spring Harbor Laboratory Press, NY.
Derynck, R., Zhang, Y.E., 2003. Smad-dependent and smad-independent pathways in tgf-beta family signalling. Nature 425 (6958), 577–584.
Descargues, P., Sil, A.K., Sano, Y., Korchynskyi, O., Han, G., Owens, P., Wang, X.J., Karin, M., 2008. Ikkalpha is a critical coregulator of a smad4-independent tgfbeta-smad2/3 signaling pathway that controls keratinocyte differentiation. Proc. Natl. Acad. Sci. U. S. A 105 (7), 2487–2492.
Di Guglielmo, G.M., Le Roy, C., Goodfellow, A.F., Wrana, J.L., 2003. Distinct endocytic pathways regulate tgf-beta receptor signalling and turnover. Nat. Cell Biol. 5 (5), 410–421.
Dickinson, M.E., Kobrin, M.S., Silan, C.M., Kingsley, D.M., Justice, M.J., Miller, D.A., Ceci, J.D., Lock, L.F., Lee, A., Buchberg, A.M., et al., 1990. Chromosomal localization of seven members of the murine tgf-beta superfamily suggests close linkage to several morphogenetic mutant loci. Genomics 6 (3), 505–520.
Dietz, H.C., Cutting, G.R., Pyeritz, R.E., Maslen, C.L., Sakai, L.Y., Corson, G.M., Puffenberger, E.G., Hamosh, A., Nanthakumar, E.J., Curristin, S.M., et al., 1991a. Marfan syndrome caused by a recurrent de novo missense mutation in the fibrillin gene. Nature 352 (6333), 337–339.
Dietz, H.C., Loeys, B., Carta, L., Ramirez, F., 2005. Recent progress towards a molecular understanding of marfan syndrome. Am. J. Med. Genet. Part C Seminars Med. Gen. 139C (1), 4–9.
Dietz, H.C., Pyeritz, R.E., Hall, B.D., Cadle, R.G., Hamosh, A., Schwartz, J., Meyers, D.A., Francomano, C.A., 1991b. The marfan syndrome locus: confirmation of assignment to chromosome 15 and identification of tightly linked markers at 15q15-q21.3. Genomics 9 (2), 355–361.
Ding, L., Saunders, T.L., Enikolopov, G., Morrison, S.J., 2012. Endothelial and perivascular cells maintain haematopoietic stem cells. Nature 481 (7382), 457–462.
DiPietro, L.A., Nissen, N.N., Gamelli, R.L., Koch, A.E., Pyle, J.M., Polverini, P.J., 1996. Thrombospondin 1 synthesis and function in wound repair. Am. J. Pathol. 148 (6), 1851–1860.
Doyle, A.J., Doyle, J.J., Bessling, S.L., Maragh, S., Lindsay, M.E., Schepers, D., Gillis, E., Mortier, G., Homfray, T., Sauls, K., et al., 2012. Mutations in the tgf-beta repressor ski cause shprintzen-goldberg syndrome with aortic aneurysm. Nat. Genet. 44 (11), 1249–1254.
Dubois, C.M., Laprise, M.H., Blanchette, F., Gentry, L.E., Leduc, R., 1995. Processing of transforming growth factor beta 1 precursor by human furin convertase. J. Biol. Chem. 270 (18), 10618–10624.
Dunn, L.K., Mohammad, K.S., Fournier, P.G., McKenna, C.R., Davis, H.W., Niewolna, M., Peng, X.H., Chirgwin, J.M., Guise, T.A., 2009. Hypoxia and tgf-beta drive breast cancer bone metastases through parallel signaling pathways in tumor cells and the bone microenvironment. PLoS One 4 (9), e6896.
Edlund, S., Landstrom, M., Heldin, C.H., Aspenstrom, P., 2002. Transforming growth factor-beta-induced mobilization of actin cytoskeleton requires signaling by small gtpases cdc42 and rhoa. Mol. Biol. Cell 13 (3), 902–914.

Edlund, S., Lee, S.Y., Grimsby, S., Zhang, S., Aspenstrom, P., Heldin, C.H., Landstrom, M., 2005. Interaction between smad7 and beta-catenin: importance for transforming growth factor beta-induced apoptosis. Mol. Cell Biol. 25 (4), 1475–1488.

Ehata, S., Hanyu, A., Fujime, M., Katsuno, Y., Fukunaga, E., Goto, K., Ishikawa, Y., Nomura, K., Yokoo, H., Shimizu, T., et al., 2007. Ki26894, a novel transforming growth factor-beta type i receptor kinase inhibitor, inhibits in vitro invasion and in vivo bone metastasis of a human breast cancer cell line. Cancer Sci. 98 (1), 127–133.

Engler, A.J., Sen, S., Sweeney, H.L., Discher, D.E., 2006. Matrix elasticity directs stem cell lineage specification. Cell 126 (4), 677–689.

Eppert, K., Scherer, S.W., Ozcelik, H., Pirone, R., Hoodless, P., Kim, H., Tsui, L.C., Bapat, B., Gallinger, S., Andrulis, I.L., et al., 1996. Madr2 maps to 18q21 and encodes a tgfbeta-regulated mad-related protein that is functionally mutated in colorectal carcinoma. Cell 86 (4), 543–552.

Esparza-Lopez, J., Montiel, J.L., Vilchis-Landeros, M.M., Okadome, T., Miyazono, K., Lopez-Casillas, F., 2001. Ligand binding and functional properties of betaglycan, a co-receptor of the transforming growth factor-beta superfamily. Specialized binding regions for transforming growth factor-beta and inhibin a. J. Biol. Chem. 276 (18), 14588–14596.

Farquhar, T., Xia, Y., Mann, K., Bertram, J., Burton-Wurster, N., Jelinski, L., Lust, G., 1996. Swelling and fibronectin accumulation in articular cartilage explants after cyclical impact. J. Orthop. Res. 14 (3), 417–423.

Feng, X.H., Derynck, R., 2005. Specificity and versatility in tgf-beta signaling through smads. Annu. Rev. Cell Dev. Biol. 21, 659–693.

Feng, X.H., Zhang, Y., Wu, R.Y., Derynck, R., 1998. The tumor suppressor smad4/dpc4 and transcriptional adaptor cbp/p300 are coactivators for smad3 in tgf-beta-induced transcriptional activation. Genes Dev. 12 (14), 2153–2163.

Flanders, K.C., Ludecke, G., Engels, S., Cissel, D.S., Roberts, A.B., Kondaiah, P., Lafyatis, R., Sporn, M.B., Unsicker, K., 1991. Localization and actions of transforming growth factor-beta s in the embryonic nervous system. Development 113 (1), 183–191.

Fuentealba, L.C., Eivers, E., Ikeda, A., Hurtado, C., Kuroda, H., Pera, E.M., De Robertis, E.M., 2007. Integrating patterning signals: wnt/gsk3 regulates the duration of the bmp/smad1 signal. Cell 131 (5), 980–993.

Gallo, E.M., Loch, D.C., Habashi, J.P., Calderon, J.F., Chen, Y., Bedja, D., van Erp, C., Gerber, E.E., Parker, S.J., Sauls, K., et al., 2014. Angiotensin ii-dependent tgf-beta signaling contributes to loeys-dietz syndrome vascular pathogenesis. J. Clin. Investig. 124 (1), 448–460.

Gando, S., 2001. Disseminated intravascular coagulation in trauma patients. Semin. Thromb. Hemost. 27 (6), 585–592.

Gao, P., Zhou, Y., Xian, L., Li, C., Xu, T., Plunkett, B., Huang, S.K., Wan, M., Cao, X., 2014. Functional effects of tgf-beta1 on mesenchymal stem cell mobilization in cockroach allergen-induced asthma. J. Immunol. 192 (10), 4560–4570.

Gao, S., Alarcon, C., Sapkota, G., Rahman, S., Chen, P.Y., Goerner, N., Macias, M.J., Erdjument-Bromage, H., Tempst, P., Massague, J., 2009. Ubiquitin ligase nedd4l targets activated smad2/3 to limit tgf-beta signaling. Mol. Cell 36 (3), 457–468.

Glowacki, J., Cox, K.A., O'Sullivan, J., Wilkie, D., Deftos, L.J., 1986. Osteoclasts can be induced in fish having an acellular bony skeleton. Proc. Natl. Acad. Sci. U. S. A 83 (11), 4104–4107.

Goggins, M., Shekher, M., Turnacioglu, K., Yeo, C.J., Hruban, R.H., Kern, S.E., 1998. Genetic alterations of the transforming growth factor beta receptor genes in pancreatic and biliary adenocarcinomas. Cancer Res. 58 (23), 5329–5332.

Gold, L.I., 1999. The role for transforming growth factor-beta (tgf-beta) in human cancer. Crit. Rev. Oncog. 10 (4), 303–360.

Goldring, M.B., Goldring, S.R., 2010. Articular cartilage and subchondral bone in the pathogenesis of osteoarthritis. Ann. N. Y. Acad. Sci. 1192, 230–237.

Gorelik, L., Flavell, R.A., 2001. Immune-mediated eradication of tumors through the blockade of transforming growth factor-beta signaling in t cells. Nat. Med. 7 (10), 1118–1122.

Goumans, M.J., Valdimarsdottir, G., Itoh, S., Rosendahl, A., Sideras, P., ten Dijke, P., 2002. Balancing the activation state of the endothelium via two distinct tgf-beta type i receptors. EMBO J. 21 (7), 1743–1753.

Gray, A.M., Mason, A.J., 1990. Requirement for activin a and transforming growth factor–beta 1 pro-regions in homodimer assembly. Science 247 (4948), 1328–1330.

Gronroos, E., Kingston, I.J., Ramachandran, A., Randall, R.A., Vizan, P., Hill, C.S., 2012. Transforming growth factor beta inhibits bone morphogenetic protein-induced transcription through novel phosphorylated smad1/5-smad3 complexes. Mol. Cell Biol. 32 (14), 2904–2916.

Grynpas, M.D., Alpert, B., Katz, I., Lieberman, I., Pritzker, K.P., 1991. Subchondral bone in osteoarthritis. Calcif. Tissue Int. 49 (1), 20–26.

Guise, T.A., Yin, J.J., Taylor, S.D., Kumagai, Y., Dallas, M., Boyce, B.F., Yoneda, T., Mundy, G.R., 1996. Evidence for a causal role of parathyroid hormone-related protein in the pathogenesis of human breast cancer-mediated osteolysis. J. Clin. Investig. 98 (7), 1544–1549.

Gupta, G.P., Massague, J., 2006. Cancer metastasis: building a framework. Cell 127 (4), 679–695.

Hagedorn, H.G., Bachmeier, B.E., Nerlich, A.G., 2001. Synthesis and degradation of basement membranes and extracellular matrix and their regulation by tgf-beta in invasive carcinomas (review). Int. J. Oncol. 18 (4), 669–681.

Hasegawa, Y., Takanashi, S., Kanehira, Y., Tsushima, T., Imai, T., Okumura, K., 2001. Transforming growth factor-beta1 level correlates with angiogenesis, tumor progression, and prognosis in patients with nonsmall cell lung carcinoma. Cancer 91 (5), 964–971.

Hayami, T., Pickarski, M., Wesolowski, G.A., McLane, J., Bone, A., Destefano, J., Rodan, G.A., Duong, le T., 2004. The role of subchondral bone remodeling in osteoarthritis: reduction of cartilage degeneration and prevention of osteophyte formation by alendronate in the rat anterior cruciate ligament transection model. Arthritis Rheum. 50 (4), 1193–1206.

Hayashi, H., Abdollah, S., Qiu, Y., Cai, J., Xu, Y.Y., Grinnell, B.W., Richardson, M.A., Topper, J.N., Gimbrone Jr., M.A., Wrana, J.L., et al., 1997. The mad-related protein smad7 associates with the tgfbeta receptor and functions as an antagonist of tgfbeta signaling. Cell 89 (7), 1165–1173.

He, X., Semenov, M., Tamai, K., Zeng, X., 2004. Ldl receptor-related proteins 5 and 6 in wnt/beta-catenin signaling: arrows point the way. Development 131 (8), 1663–1677.

Henderson, M.A., Danks, J.A., Slavin, J.L., Byrnes, G.B., Choong, P.F., Spillane, J.B., Hopper, J.L., Martin, T.J., 2006. Parathyroid hormone-related protein localization in breast cancers predict improved prognosis. Cancer Res. 66 (4), 2250–2256.

Henderson, N.C., Arnold, T.D., Katamura, Y., Giacomini, M.M., Rodriguez, J.D., McCarty, J.H., Pellicoro, A., Raschperger, E., Betsholtz, C., Ruminski, P.G., et al., 2013. Targeting of alphav integrin identifies a core molecular pathway that regulates fibrosis in several organs. Nat. Med. 19 (12), 1617–1624.

Hering, S., Isken, E., Knabbe, C., Janott, J., Jost, C., Pommer, A., Muhr, G., Schatz, H., Pfeiffer, A.F., 2001. Tgfbeta1 and tgfbeta2 mrna and protein expression in human bone samples. Exp. Clin. Endocrinol. Diabet. 109 (4), 217–226.

Hill, C.S., 2009. Nucleocytoplasmic shuttling of smad proteins. Cell Res. 19 (1), 36–46.

Hinck, A.P., 2012. Structural studies of the tgf-betas and their receptors - insights into evolution of the tgf-beta superfamily. FEBS Lett. 586 (14), 1860–1870.

Hiraga, T., Kizaka-Kondoh, S., Hirota, K., Hiraoka, M., Yoneda, T., 2007. Hypoxia and hypoxia-inducible factor-1 expression enhance osteolytic bone metastases of breast cancer. Cancer Res. 67 (9), 4157–4163.

Howe, J.R., Roth, S., Ringold, J.C., Summers, R.W., Jarvinen, H.J., Sistonen, P., Tomlinson, I.P., Houlston, R.S., Bevan, S., Mitros, F.A., et al., 1998. Mutations in the smad4/dpc4 gene in juvenile polyposis. Science 280 (5366), 1086–1088.

Hsu, Y.C., Fuchs, E., 2012. A family business: stem cell progeny join the niche to regulate homeostasis. Nat. Rev. Mol. Cell Biol. 13 (2), 103–114.

Hubacek, J.A., Weichetova, M., Bohuslavova, R., Skodova, Z., Stepan, J.J., Adamkova, V., 2006. No associations between genetic polymorphisms of tgf-beta, pai-1, and col1a1, and bone mineral density in caucasian females. Endocr. Regul. 40 (4), 107–112.

Huebner, J.L., Hanes, M.A., Beekman, B., TeKoppele, J.M., Kraus, V.B., 2002. A comparative analysis of bone and cartilage metabolism in two strains of Guinea-pig with varying degrees of naturally occurring osteoarthritis. Osteoarthritis Cartilage 10 (10), 758–767.

Hugo, C., 2003. The thrombospondin 1-tgf-beta axis in fibrotic renal disease. Nephrol. Dial. Transplant. 18 (7), 1241–1245.

Iavarone, A., Lasorella, A., 2006. Id proteins as targets in cancer and tools in neurobiology. Trends Mol. Med. 12 (12), 588–594.

Ichida, J.K., Blanchard, J., Lam, K., Son, E.Y., Chung, J.E., Egli, D., Loh, K.M., Carter, A.C., Di Giorgio, F.P., Koszka, K., et al., 2009. A small-molecule inhibitor of tgf-beta signaling replaces sox2 in reprogramming by inducing nanog. Cell Stem Cell 5 (5), 491–503.

Ignotz, R.A., Massague, J., 1986. Transforming growth factor-beta stimulates the expression of fibronectin and collagen and their incorporation into the extracellular matrix. J. Biol. Chem. 261 (9), 4337–4345.

Ikushima, H., Miyazono, K., 2012. Tgf-beta signal transduction spreading to a wider field: a broad variety of mechanisms for context-dependent effects of tgf-beta. Cell Tissue Res. 347 (1), 37–49.

Intema, F., Sniekers, Y.H., Weinans, H., Vianen, M.E., Yocum, S.A., Zuurmond, A.M., DeGroot, J., Lafeber, F.P., Mastbergen, S.C., 2010. Similarities and discrepancies in subchondral bone structure in two differently induced canine models of osteoarthritis. J. Bone Miner. Res. 25 (7), 1650–1657.

Itasaki, N., Hoppler, S., 2010. Crosstalk between wnt and bone morphogenic protein signaling: a turbulent relationship. Dev. Dynam. 239 (1), 16–33.

Izumoto, S., Arita, N., Ohnishi, T., Hiraga, S., Taki, T., Tomita, N., Ohue, M., Hayakawa, T., 1997. Microsatellite instability and mutated type ii transforming growth factor-beta receptor gene in gliomas. Cancer Lett. 112 (2), 251–256.

Janknecht, R., Wells, N.J., Hunter, T., 1998. Tgf-beta-stimulated cooperation of smad proteins with the coactivators cbp/p300. Genes Dev. 12 (14), 2114–2119.

Janssens, K., Gershoni-Baruch, R., Guanabens, N., Migone, N., Ralston, S., Bonduelle, M., Lissens, W., Van Maldergem, L., Vanhoenacker, F., Verbruggen, L., et al., 2000. Mutations in the gene encoding the latency-associated peptide of tgf-beta 1 cause camurati-engelmann disease. Nat. Genet. 26 (3), 273–275.

Janssens, K., ten Dijke, P., Janssens, S., Van Hul, W., 2005. Transforming growth factor-beta1 to the bone. Endocr. Rev. 26 (6), 743–774.

Janssens, K., ten Dijke, P., Ralston, S.H., Bergmann, C., Van Hul, W., 2003. Transforming growth factor-beta 1 mutations in camurati-engelmann disease lead to increased signaling by altering either activation or secretion of the mutant protein. J. Biol. Chem. 278 (9), 7718–7724.

Janssens, K., Vanhoenacker, F., Bonduelle, M., Verbruggen, L., Van Maldergem, L., Ralston, S., Guanabens, N., Migone, N., Wientroub, S., Divizia, M.T., et al., 2006. Camurati-engelmann disease: review of the clinical, radiological, and molecular data of 24 families and implications for diagnosis and treatment. J. Med. Genet. 43 (1), 1–11.

Javelaud, D., Mauviel, A., 2004. Mammalian transforming growth factor-betas: smad signaling and physio-pathological roles. Int. J. Biochem. Cell Biol. 36 (7), 1161–1165.

Javelaud, D., Mohammad, K.S., McKenna, C.R., Fournier, P., Luciani, F., Niewolna, M., Andre, J., Delmas, V., Larue, L., Guise, T.A., et al., 2007. Stable overexpression of smad7 in human melanoma cells impairs bone metastasis. Cancer Res. 67 (5), 2317–2324.

Jenkins, G., 2008. The role of proteases in transforming growth factor-beta activation. Int. J. Biochem. Cell Biol. 40 (6–7), 1068–1078.

Jian, H., Shen, X., Liu, I., Semenov, M., He, X., Wang, X.F., 2006. Smad3-dependent nuclear translocation of beta-catenin is required for tgf-beta1-induced proliferation of bone marrow-derived adult human mesenchymal stem cells. Genes Dev. 20 (6), 666–674.

Jiang, Y., Jahagirdar, B.N., Reinhardt, R.L., Schwartz, R.E., Keene, C.D., Ortiz-Gonzalez, X.R., Reyes, M., Lenvik, T., Lund, T., Blackstad, M., et al., 2002. Pluripotency of mesenchymal stem cells derived from adult marrow. Nature 418 (6893), 41–49.

Jilka, R.L., Almeida, M., Ambrogini, E., Han, L., Roberson, P.K., Weinstein, R.S., Manolagas, S.C., 2010. Decreased oxidative stress and greater bone anabolism in the aged, when compared to the young, murine skeleton with parathyroid hormone administration. Aging Cell 9 (5), 851–867.

Jobling, M.F., Mott, J.D., Finnegan, M.T., Jurukovski, V., Erickson, A.C., Walian, P.J., Taylor, S.E., Ledbetter, S., Lawrence, C.M., Rifkin, D.B., et al., 2006. Isoform-specific activation of latent transforming growth factor beta (ltgf-beta) by reactive oxygen species. Radiat. Res. 166 (6), 839–848.

Jones, S., Zhang, X., Parsons, D.W., Lin, J.C., Leary, R.J., Angenendt, P., Mankoo, P., Carter, H., Kamiyama, H., Jimeno, A., et al., 2008. Core signaling pathways in human pancreatic cancers revealed by global genomic analyses. Science 321 (5897), 1801–1806.

Juarez, P., Guise, T.A., 2011. Tgf-beta in cancer and bone: implications for treatment of bone metastases. Bone 48 (1), 23–29.

Juarez, P., Mohammad, K.S., Yin, J.J., Fournier, P.G., McKenna, R.C., Davis, H.W., Peng, X.H., Niewolna, M., Javelaud, D., Chirgwin, J.M., et al., 2012. Halofuginone inhibits the establishment and progression of melanoma bone metastases. Cancer Res. 72 (23), 6247–6256.

Kaartinen, V., Voncken, J.W., Shuler, C., Warburton, D., Bu, D., Heisterkamp, N., Groffen, J., 1995. Abnormal lung development and cleft palate in mice lacking tgf-beta 3 indicates defects of epithelial-mesenchymal interaction. Nat. Genet. 11 (4), 415–421.

Kainulainen, K., Karttunen, L., Puhakka, L., Sakai, L., Peltonen, L., 1994. Mutations in the fibrillin gene responsible for dominant ectopia lentis and neonatal marfan syndrome. Nat. Genet. 6 (1), 64–69.

Kakonen, S.M., Selander, K.S., Chirgwin, J.M., Yin, J.J., Burns, S., Rankin, W.A., Grubbs, B.G., Dallas, M., Cui, Y., Guise, T.A., 2002. Transforming growth factor-beta stimulates parathyroid hormone-related protein and osteolytic metastases via smad and mitogen-activated protein kinase signaling pathways. J. Biol. Chem. 277 (27), 24571–24578.

Kang, Y., He, W., Tulley, S., Gupta, G.P., Serganova, I., Chen, C.R., Manova-Todorova, K., Blasberg, R., Gerald, W.L., Massague, J., 2005. Breast cancer bone metastasis mediated by the smad tumor suppressor pathway. Proc. Natl. Acad. Sci. U. S. A 102 (39), 13909–13914.

Kang, Y., Massague, J., 2004. Epithelial-mesenchymal transitions: twist in development and metastasis. Cell 118 (3), 277–279.

Kang, Y., Siegel, P.M., Shu, W., Drobnjak, M., Kakonen, S.M., Cordon-Cardo, C., Guise, T.A., Massague, J., 2003. A multigenic program mediating breast cancer metastasis to bone. Cancer Cell 3 (6), 537–549.

Karsdal, M.A., Leeming, D.J., Dam, E.B., Henriksen, K., Alexandersen, P., Pastoureau, P., Altman, R.D., Christiansen, C., 2008. Should subchondral bone turnover be targeted when treating osteoarthritis? Osteoarthritis Cartilage 16 (6), 638–646.

Katagiri, T., Imada, M., Yanai, T., Suda, T., Takahashi, N., Kamijo, R., 2002. Identification of a bmp-responsive element in id1, the gene for inhibition of myogenesis. Genes Cells 7 (9), 949–960.

Khosla, S., Westendorf, J.J., Oursler, M.J., 2008. Building bone to reverse osteoporosis and repair fractures. J. Clin. Investig. 118 (2), 421–428.

Kim, J.S., Kim, J.G., Moon, M.Y., Jeon, C.Y., Won, H.Y., Kim, H.J., Jeon, Y.J., Seo, J.Y., Kim, J.I., Kim, J., et al., 2006. Transforming growth factor-beta1 regulates macrophage migration via rhoa. Blood 108 (6), 1821–1829.

Kim, K.K., Wei, Y., Szekeres, C., Kugler, M.C., Wolters, P.J., Hill, M.L., Frank, J.A., Brumwell, A.N., Wheeler, S.E., Kreidberg, J.A., et al., 2009. Epithelial cell alpha3beta1 integrin links beta-catenin and smad signaling to promote myofibroblast formation and pulmonary fibrosis. J. Clin. Investig. 119 (1), 213–224.

Kim, S.W., Pajevic, P.D., Selig, M., Barry, K.J., Yang, J.Y., Shin, C.S., Baek, W.Y., Kim, J.E., Kronenberg, H.M., 2012. Intermittent parathyroid hormone administration converts quiescent lining cells to active osteoblasts. J. Bone Miner. Res. 27 (10), 2075–2084.

Kingsley, D.M., 1994. The tgf-beta superfamily: new members, new receptors, and new genetic tests of function in different organisms. Genes Dev. 8 (2), 133–146.

Kinoshita, A., Saito, T., Tomita, H., Makita, Y., Yoshida, K., Ghadami, M., Yamada, K., Kondo, S., Ikegawa, S., Nishimura, G., et al., 2000. Domain-specific mutations in tgfb1 result in camurati-engelmann disease. Nat. Genet. 26 (1), 19–20.

Klein, S., Bikfalvi, A., Birkenmeier, T.M., Giancotti, F.G., Rifkin, D.B., 1996. Integrin regulation by endogenous expression of 18-kda fibroblast growth factor-2. J. Biol. Chem. 271 (37), 22583–22590.

Klein, S., Giancotti, F.G., Presta, M., Albelda, S.M., Buck, C.A., Rifkin, D.B., 1993. Basic fibroblast growth factor modulates integrin expression in microvascular endothelial cells. Mol. Biol. Cell 4 (10), 973–982.

Kluft, C., Verheijen, J.H., Jie, A.F., Rijken, D.C., Preston, F.E., Sue-Ling, H.M., Jespersen, J., Aasen, A.O., 1985. The postoperative fibrinolytic shutdown: a rapidly reverting acute phase pattern for the fast-acting inhibitor of tissue-type plasminogen activator after trauma. Scand. J. Clin. Lab. Investig. 45 (7), 605–610.

Koenig, B.B., Cook, J.S., Wolsing, D.H., Ting, J., Tiesman, J.P., Correa, P.E., Olson, C.A., Pecquet, A.L., Ventura, F., Grant, R.A., et al., 1994. Characterization and cloning of a receptor for bmp-2 and bmp-4 from nih 3t3 cells. Mol. Cell Biol. 14 (9), 5961–5974.

Koli, K., Saharinen, J., Karkkainen, M., Keski-Oja, J., 2001. Novel non-tgf-beta-binding splice variant of ltbp-4 in human cells and tissues provides means to decrease tgf-beta deposition. J. Cell Sci. 114 (Pt 15), 2869–2878.

Kondaiah, P., Van Obberghen-Schilling, E., Ludwig, R.L., Dhar, R., Sporn, M.B., Roberts, A.B., 1988. Cdna cloning of porcine transforming growth factor-beta 1 mrnas. Evidence for alternate splicing and polyadenylation. J. Biol. Chem. 263 (34), 18313–18317.

Korchynskyi, O., ten Dijke, P., 2002. Identification and functional characterization of distinct critically important bone morphogenetic protein-specific response elements in the id1 promoter. J. Biol. Chem. 277 (7), 4883–4891.

Korpal, M., Yan, J., Lu, X., Xu, S., Lerit, D.A., Kang, Y., 2009. Imaging transforming growth factor-beta signaling dynamics and therapeutic response in breast cancer bone metastasis. Nat. Med. 15 (8), 960–966.

Kou, I., Takahashi, A., Urano, T., Fukui, N., Ito, H., Ozaki, K., Tanaka, T., Hosoi, T., Shiraki, M., Inoue, S., et al., 2011. Common variants in a novel gene, fong on chromosome 2q33.1 confer risk of osteoporosis in Japanese. PLoS One 6 (5), e19641.

Kreja, L., Brenner, R.E., Tautzenberger, A., Liedert, A., Friemert, B., Ehrnthaller, C., Huber-Lang, M., Ignatius, A., 2010. Non-resorbing osteoclasts induce migration and osteogenic differentiation of mesenchymal stem cells. J. Cell. Biochem. 109 (2), 347–355.

Kunisaki, Y., Bruns, I., Scheiermann, C., Ahmed, J., Pinho, S., Zhang, D., Mizoguchi, T., Wei, Q., Lucas, D., Ito, K., et al., 2013. Arteriolar niches maintain haematopoietic stem cell quiescence. Nature 502 (7473), 637–643.

Kurpinski, K., Lam, H., Chu, J., Wang, A., Kim, A., Tsay, E., Agrawal, S., Schaffer, D.V., Li, S., 2010. Transforming growth factor-beta and notch signaling mediate stem cell differentiation into smooth muscle cells. Stem Cell. 28 (4), 734–742.

Labbe, E., Silvestri, C., Hoodless, P.A., Wrana, J.L., Attisano, L., 1998. Smad2 and smad3 positively and negatively regulate tgf beta-dependent transcription through the forkhead DNA-binding protein fast2. Mol. Cell 2 (1), 109–120.

Lamouille, S., Connolly, E., Smyth, J.W., Akhurst, R.J., Derynck, R., 2012. Tgf-beta-induced activation of mtor complex 2 drives epithelial-mesenchymal transition and cell invasion. J. Cell Sci. 125 (Pt 5), 1259–1273.

Lamouille, S., Derynck, R., 2007. Cell size and invasion in tgf-beta-induced epithelial to mesenchymal transition is regulated by activation of the mtor pathway. J. Cell Biol. 178 (3), 437–451.

Langdahl, B.L., Knudsen, J.Y., Jensen, H.K., Gregersen, N., Eriksen, E.F., 1997. A sequence variation: 713-8delc in the transforming growth factor-beta 1 gene has higher prevalence in osteoporotic women than in normal women and is associated with very low bone mass in osteoporotic women and increased bone turnover in both osteoporotic and normal women. Bone 20 (3), 289–294.

Lapraz, F., Rottinger, E., Duboc, V., Range, R., Duloquin, L., Walton, K., Wu, S.Y., Bradham, C., Loza, M.A., Hibino, T., et al., 2006. Rtk and tgf-beta signaling pathways genes in the sea urchin genome. Dev. Biol. 300 (1), 132–152.

Leary, R.J., Lin, J.C., Cummins, J., Boca, S., Wood, L.D., Parsons, D.W., Jones, S., Sjoblom, T., Park, B.H., Parsons, R., et al., 2008. Integrated analysis of homozygous deletions, focal amplifications, and sequence alterations in breast and colorectal cancers. Proc. Natl. Acad. Sci. U. S. A 105 (42), 16224–16229.

Lee, C.H., Cook, J.L., Mendelson, A., Moioli, E.K., Yao, H., Mao, J.J., 2010. Regeneration of the articular surface of the rabbit synovial joint by cell homing: a proof of concept study. Lancet 376 (9739), 440–448.

Lee, M.K., Pardoux, C., Hall, M.C., Lee, P.S., Warburton, D., Qing, J., Smith, S.M., Derynck, R., 2007. Tgf-beta activates erk map kinase signalling through direct phosphorylation of shca. EMBO J. 26 (17), 3957–3967.

Letterio, J.J., Roberts, A.B., 1996. Transforming growth factor-beta1-deficient mice: identification of isoform-specific activities in vivo. J. Leukoc. Biol. 59 (6), 769–774.

Li, C., Xing, Q., Yu, B., Xie, H., Wang, W., Shi, C., Crane, J.L., Cao, X., Wan, M., 2013. Disruption of lrp6 in osteoblasts blunts the bone anabolic activity of pth. J. Bone Miner. Res. 28 (10), 2094–2108.

Li, R., Liang, J., Ni, S., Zhou, T., Qing, X., Li, H., He, W., Chen, J., Li, F., Zhuang, Q., et al., 2010. A mesenchymal-to-epithelial transition initiates and is required for the nuclear reprogramming of mouse fibroblasts. Cell Stem Cell 7 (1), 51–63.

Li, Z., Yang, C.S., Nakashima, K., Rana, T.M., 2011. Small rna-mediated regulation of ips cell generation. EMBO J. 30 (5), 823–834.

Lin, P.M., Chen, C.T., Torzilli, P.A., 2004. Increased stromelysin-1 (mmp-3), proteoglycan degradation (3b3- and 7d4) and collagen damage in cyclically load-injured articular cartilage. Osteoarthritis Cartilage 12 (6), 485–496.

Lin, T., Ambasudhan, R., Yuan, X., Li, W., Hilcove, S., Abujarour, R., Lin, X., Hahm, H.S., Hao, E., Hayek, A., et al., 2009. A chemical platform for improved induction of human ipscs. Nat. Methods 6 (11), 805–808.

Lin, X., Duan, X., Liang, Y.Y., Su, Y., Wrighton, K.H., Long, J., Hu, M., Davis, C.M., Wang, J., Brunicardi, F.C., et al., 2006. Ppm1a functions as a smad phosphatase to terminate tgfbeta signaling. Cell 125 (5), 915–928.

Lin, X., Liang, Y.Y., Sun, B., Liang, M., Shi, Y., Brunicardi, F.C., Feng, X.H., 2003. Smad6 recruits transcription corepressor ctbp to repress bone morphogenetic protein-induced transcription. Mol. Cell Biol. 23 (24), 9081–9093.

Lindsay, M.E., Schepers, D., Bolar, N.A., Doyle, J.J., Gallo, E., Fert-Bober, J., Kempers, M.J., Fishman, E.K., Chen, Y., Myers, L., et al., 2012. Loss-of-function mutations in tgfb2 cause a syndromic presentation of thoracic aortic aneurysm. Nat. Genet. 44 (8), 922–927.

Liu, F., Ventura, F., Doody, J., Massague, J., 1995. Human type ii receptor for bone morphogenic proteins (bmps): extension of the two-kinase receptor model to the bmps. Mol. Cell Biol. 15 (7), 3479–3486.

Liu, I.M., Schilling, S.H., Knouse, K.A., Choy, L., Derynck, R., Wang, X.F., 2009. Tgfbeta-stimulated smad1/5 phosphorylation requires the alk5 l45 loop and mediates the pro-migratory tgfbeta switch. EMBO J. 28 (2), 88–98.

Liu, Z., Tang, Y., Qiu, T., Cao, X., Clemens, T.L., 2006. A dishevelled-1/smad1 interaction couples wnt and bone morphogenetic protein signaling pathways in uncommitted bone marrow stromal cells. J. Biol. Chem. 281 (25), 17156–17163.

Loeys, B.L., Chen, J., Neptune, E.R., Judge, D.P., Podowski, M., Holm, T., Meyers, J., Leitch, C.C., Katsanis, N., Sharifi, N., et al., 2005. A syndrome of altered cardiovascular, craniofacial, neurocognitive and skeletal development caused by mutations in tgfbr1 or tgfbr2. Nat. Genet. 37 (3), 275–281.

Lombardi, G., Di Somma, C., Vuolo, L., Guerra, E., Scarano, E., Colao, A., 2010. Role of igf-i on pth effects on bone. J. Endocrinol. Investig. 33 (7 Suppl. l), 22–26.

Lopez-Casillas, F., Wrana, J.L., Massague, J., 1993. Betaglycan presents ligand to the tgf beta signaling receptor. Cell 73 (7), 1435–1444.

Lopez-Novoa, J.M., Nieto, M.A., 2009. Inflammation and emt: an alliance towards organ fibrosis and cancer progression. EMBO Mol. Med. 1 (6–7), 303–314.

Lu, A., Miao, M., Schoeb, T.R., Agarwal, A., Murphy-Ullrich, J.E., 2011. Blockade of tsp1-dependent tgf-beta activity reduces renal injury and proteinuria in a murine model of diabetic nephropathy. Am. J. Pathol. 178 (6), 2573–2586.

Lu, X., Yan, C.H., Yuan, M., Wei, Y., Hu, G., Kang, Y., 2010. In vivo dynamics and distinct functions of hypoxia in primary tumor growth and organotropic metastasis of breast cancer. Cancer Res. 70 (10), 3905–3914.

Ludlow, A., Yee, K.O., Lipman, R., Bronson, R., Weinreb, P., Huang, X., Sheppard, D., Lawler, J., 2005. Characterization of integrin beta6 and thrombospondin-1 double-null mice. J. Cell Mol. Med. 9 (2), 421–437.

Lyons, J.G., Patel, V., Roue, N.C., Fok, S.Y., Soon, L.L., Halliday, G.M., Gutkind, J.S., 2008. Snail up-regulates proinflammatory mediators and inhibits differentiation in oral keratinocytes. Cancer Res. 68 (12), 4525–4530.

Lyons, R.M., Keski-Oja, J., Moses, H.L., 1988. Proteolytic activation of latent transforming growth factor-beta from fibroblast-conditioned medium. J. Cell Biol. 106 (5), 1659–1665.

Maeda, S., Hayashi, M., Komiya, S., Imamura, T., Miyazono, K., 2004. Endogenous tgf-beta signaling suppresses maturation of osteoblastic mesenchymal cells. EMBO J. 23 (3), 552–563.

Maherali, N., Hochedlinger, K., 2009. Tgfbeta signal inhibition cooperates in the induction of ipscs and replaces sox2 and cmyc. Curr. Biol. 19 (20), 1718–1723.

Malek, A.M., Alper, S.L., Izumo, S., 1999. Hemodynamic shear stress and its role in atherosclerosis. J. Am. Med. Assoc. 282 (21), 2035–2042.

Mangasser-Stephan, K., Gressner, A.M., 1999. Molecular and functional aspects of latent transforming growth factor-beta binding protein: just a masking protein? Cell Tissue Res. 297 (3), 363–370.

Manning, A.M., Auchampach, J.A., Drong, R.F., Slightom, J.L., 1995. Cloning of a canine cdna homologous to the human transforming growth factor-beta 1-encoding gene. Gene 155 (2), 307–308.

Markowitz, S.D., Roberts, A.B., 1996. Tumor suppressor activity of the tgf-beta pathway in human cancers. Cytokine Growth Factor Rev. 7 (1), 93–102.

Martin, T.J., Sims, N.A., 2005. Osteoclast-derived activity in the coupling of bone formation to resorption. Trends Mol. Med. 11 (2), 76–81.

Massague, J., 1998. Tgf-beta signal transduction. Annu. Rev. Biochem. 67, 753–791.

Massague, J., 2008. Tgfbeta in cancer. Cell 134 (2), 215–230.

Massague, J., Gomis, R.R., 2006. The logic of tgfbeta signaling. FEBS Lett. 580 (12), 2811–2820.

Massague, J., Seoane, J., Wotton, D., 2005. Smad transcription factors. Genes Dev. 19 (23), 2783–2810.

Massague, J., Wotton, D., 2000. Transcriptional control by the tgf-beta/smad signaling system. EMBO J. 19 (8), 1745–1754.

McMahon, S., Charbonneau, M., Grandmont, S., Richard, D.E., Dubois, C.M., 2006. Transforming growth factor beta1 induces hypoxia-inducible factor-1 stabilization through selective inhibition of phd2 expression. J. Biol. Chem. 281 (34), 24171–24181.

Mendez-Ferrer, S., Michurina, T.V., Ferraro, F., Mazloom, A.R., Macarthur, B.D., Lira, S.A., Scadden, D.T., Ma'ayan, A., Enikolopov, G.N., Frenette, P.S., 2010. Mesenchymal and haematopoietic stem cells form a unique bone marrow niche. Nature 466 (7308), 829–834.

Miller, L.A., Barnett, N.L., Sheppard, D., Hyde, D.M., 2001. Expression of the beta6 integrin subunit is associated with sites of neutrophil influx in lung epithelium. J. Histochem. Cytochem. 49 (1), 41–48.

Mimura, Y., Ihn, H., Jinnin, M., Asano, Y., Yamane, K., Tamaki, K., 2005. Constitutive thrombospondin-1 overexpression contributes to autocrine transforming growth factor-beta signaling in cultured scleroderma fibroblasts. Am. J. Pathol. 166 (5), 1451–1463.

Mittl, P.R., Priestle, J.P., Cox, D.A., McMaster, G., Cerletti, N., Grutter, M.G., 1996. The crystal structure of tgf-beta 3 and comparison to tgf-beta 2: implications for receptor binding. Protein Sci. 5 (7), 1261–1271.

Miyakoshi, N., Kasukawa, Y., Linkhart, T.A., Baylink, D.J., Mohan, S., 2001. Evidence that anabolic effects of pth on bone require igf-i in growing mice. Endocrinology 142 (10), 4349–4356.

Miyoshi, N., Ishii, H., Nagano, H., Haraguchi, N., Dewi, D.L., Kano, Y., Nishikawa, S., Tanemura, M., Mimori, K., Tanaka, F., et al., 2011. Reprogramming of mouse and human cells to pluripotency using mature micrornas. Cell Stem Cell 8 (6), 633–638.

Mohan, S., Baylink, D.J., 1991. Bone growth factors. Clin. Orthop. Relat. Res. 263, 30–48.

Morikawa, M., Koinuma, D., Tsutsumi, S., Vasilaki, E., Kanki, Y., Heldin, C.H., Aburatani, H., Miyazono, K., 2011. Chip-seq reveals cell type-specific binding patterns of bmp-specific smads and a novel binding motif. Nucleic Acids Res. 39 (20), 8712–8727.

Morikawa, S., Mabuchi, Y., Kubota, Y., Nagai, Y., Niibe, K., Hiratsu, E., Suzuki, S., Miyauchi-Hara, C., Nagoshi, N., Sunabori, T., et al., 2009. Prospective identification, isolation, and systemic transplantation of multipotent mesenchymal stem cells in murine bone marrow. J. Exp. Med. 206 (11), 2483–2496.

Morrison, S.J., Scadden, D.T., 2014. The bone marrow niche for haematopoietic stem cells. Nature 505 (7483), 327–334.

Moss, M.L., 1965. Studies of the acellular bone of teleost fish. V. Histology and mineral homeostasis of fresh-water species. Acta Anatomica 60, 262–276.

Moustakas, A., Heldin, C.H., 2005. Non-smad tgf-beta signals. J. Cell Sci. 118 (Pt 16), 3573–3584.

Moustakas, A., Heldin, C.H., 2009. The regulation of tgfbeta signal transduction. Development 136 (22), 3699–3714.

Mu, D., Cambier, S., Fjellbirkeland, L., Baron, J.L., Munger, J.S., Kawakatsu, H., Sheppard, D., Broaddus, V.C., Nishimura, S.L., 2002. The integrin alpha(v)beta8 mediates epithelial homeostasis through mt1-mmp-dependent activation of tgf-beta1. J. Cell Biol. 157 (3), 493–507.

Mullen, A.C., Orlando, D.A., Newman, J.J., Loven, J., Kumar, R.M., Bilodeau, S., Reddy, J., Guenther, M.G., DeKoter, R.P., Young, R.A., 2011. Master transcription factors determine cell-type-specific responses to tgf-beta signaling. Cell 147 (3), 565–576.

Munger, J.S., Huang, X., Kawakatsu, H., Griffiths, M.J., Dalton, S.L., Wu, J., Pittet, J.F., Kaminski, N., Garat, C., Matthay, M.A., et al., 1999. The integrin alpha v beta 6 binds and activates latent tgf beta 1: a mechanism for regulating pulmonary inflammation and fibrosis. Cell 96 (3), 319–328.

Murphy-Ullrich, J.E., Mosher, D.F., 1985. Localization of thrombospondin in clots formed in situ. Blood 66 (5), 1098–1104.

Murphy-Ullrich, J.E., Poczatek, M., 2000. Activation of latent tgf-beta by thrombospondin-1: mechanisms and physiology. Cytokine Growth Factor Rev. 11 (1–2), 59–69.

Nakao, A., Afrakhte, M., Moren, A., Nakayama, T., Christian, J.L., Heuchel, R., Itoh, S., Kawabata, M., Heldin, N.E., Heldin, C.H., et al., 1997. Identification of smad7, a tgfbeta-inducible antagonist of tgf-beta signalling. Nature 389 (6651), 631–635.

Nam, J.S., Terabe, M., Mamura, M., Kang, M.J., Chae, H., Stuelten, C., Kohn, E., Tang, B., Sabzevari, H., Anver, M.R., et al., 2008. An anti-transforming growth factor beta antibody suppresses metastasis via cooperative effects on multiple cell compartments. Cancer Res. 68 (10), 3835–3843.

Neidlinger-Wilke, C., Stalla, I., Claes, L., Brand, R., Hoellen, I., Rubenacker, S., Arand, M., Kinzl, L., 1995. Human osteoblasts from younger normal and osteoporotic donors show differences in proliferation and tgf beta-release in response to cyclic strain. J. Biomech. 28 (12), 1411–1418.

Neptune, E.R., Frischmeyer, P.A., Arking, D.E., Myers, L., Bunton, T.E., Gayraud, B., Ramirez, F., Sakai, L.Y., Dietz, H.C., 2003. Dysregulation of tgf-beta activation contributes to pathogenesis in marfan syndrome. Nat. Genet. 33 (3), 407–411.

Newberry, W.N., Zukosky, D.K., Haut, R.C., 1997. Subfracture insult to a knee joint causes alterations in the bone and in the functional stiffness of overlying cartilage. J. Orthop. Res. 15 (3), 450–455.

Ni, G.X., Zhan, L.Q., Gao, M.Q., Lei, L., Zhou, Y.Z., Pan, Y.X., 2011. Matrix metalloproteinase-3 inhibitor retards treadmill running-induced cartilage degradation in rats. Arthritis Res. Ther. 13 (6), R192.

Niimi, H., Pardali, K., Vanlandewijck, M., Heldin, C.H., Moustakas, A., 2007. Notch signaling is necessary for epithelial growth arrest by tgf-beta. J. Cell Biol. 176 (5), 695−707.

Nishii, T., Tamura, S., Shiomi, T., Yoshikawa, H., Sugano, N., 2013. Alendronate treatment for hip osteoarthritis: prospective randomized 2-year trial. Clin. Rheumatol. 32 (12), 1759−1766.

Nishimura, S.L., 2009. Integrin-mediated transforming growth factor-beta activation, a potential therapeutic target in fibrogenic disorders. Am. J. Pathol. 175 (4), 1362−1370.

Nishitoh, H., Ichijo, H., Kimura, M., Matsumoto, T., Makishima, F., Yamaguchi, A., Yamashita, H., Enomoto, S., Miyazono, K., 1996. Identification of type i and type ii serine/threonine kinase receptors for growth/differentiation factor-5. J. Biol. Chem. 271 (35), 21345−21352.

Nohno, T., Ishikawa, T., Saito, T., Hosokawa, K., Noji, S., Wolsing, D.H., Rosenbaum, J.S., 1995. Identification of a human type ii receptor for bone morphogenetic protein-4 that forms differential heteromeric complexes with bone morphogenetic protein type i receptors. J. Biol. Chem. 270 (38), 22522−22526.

Nomura, T., Khan, M.M., Kaul, S.C., Dong, H.D., Wadhwa, R., Colmenares, C., Kohno, I., Ishii, S., 1999. Ski is a component of the histone deacetylase complex required for transcriptional repression by mad and thyroid hormone receptor. Genes Dev. 13 (4), 412−423.

Nor, J.E., Dipietro, L., Murphy-Ullrich, J.E., Hynes, R.O., Lawler, J., Polverini, P.J., 2005. Activation of latent tgf-beta1 by thrombospondin-1 is a major component of wound repair. Oral Biosci. Med. 2 (2), 153−161.

Ohashi, S., Natsuizaka, M., Naganuma, S., Kagawa, S., Kimura, S., Itoh, H., Kalman, R.A., Nakagawa, M., Darling, D.S., Basu, D., et al., 2011. A notch3-mediated squamous cell differentiation program limits expansion of emt-competent cells that express the zeb transcription factors. Cancer Res. 71 (21), 6836−6847.

Ohue, M., Tomita, N., Monden, T., Miyoshi, Y., Ohnishi, T., Izawa, H., Kawabata, Y., Sasaki, M., Sekimoto, M., Nishisho, I., et al., 1996. Mutations of the transforming growth factor beta type ii receptor gene and microsatellite instability in gastric cancer. Int. J. Cancer 68 (2), 203−206.

Okabe, M., Graham, A., 2004. The origin of the parathyroid gland. Proc. Natl. Acad. Sci. U. S. A 101 (51), 17716−17719.

Oklu, R., Hesketh, R., 2000. The latent transforming growth factor beta binding protein (ltbp) family. Biochem. J. 352 (Pt 3), 601−610.

Omatsu, Y., Sugiyama, T., Kohara, H., Kondoh, G., Fujii, N., Kohno, K., Nagasawa, T., 2010. The essential functions of adipo-osteogenic progenitors as the hematopoietic stem and progenitor cell niche. Immunity 33 (3), 387−399.

Ono, N., Ono, W., Mizoguchi, T., Nagasawa, T., Frenette, P.S., Kronenberg, H.M., 2014. Vasculature-associated cells expressing nestin in developing bones encompass early cells in the osteoblast and endothelial lineage. Dev. Cell 29 (3), 330−339.

Oreffo, R.O., Mundy, G.R., Seyedin, S.M., Bonewald, L.F., 1989. Activation of the bone-derived latent tgf beta complex by isolated osteoclasts. Biochem. Biophys. Res. Commun. 158 (3), 817−823.

Orth, P., Cucchiarini, M., Zurakowski, D., Menger, M.D., Kohn, D.M., Madry, H., 2013. Parathyroid hormone [1-34] improves articular cartilage surface architecture and integration and subchondral bone reconstitution in osteochondral defects in vivo. Osteoarthritis Cartilage 21 (4), 614−624.

Oursler, M.J., 1994. Osteoclast synthesis and secretion and activation of latent transforming growth factor beta. J. Bone Miner. Res. 9 (4), 443−452.

Ozdamar, B., Bose, R., Barrios-Rodiles, M., Wang, H.R., Zhang, Y., Wrana, J.L., 2005. Regulation of the polarity protein par6 by tgfbeta receptors controls epithelial cell plasticity. Science 307 (5715), 1603−1609.

Padua, D., Massague, J., 2009. Roles of tgfbeta in metastasis. Cell Res. 19 (1), 89−102.

Panahifar, A., Maksymowych, W.P., Doschak, M.R., 2012. Potential mechanism of alendronate inhibition of osteophyte formation in the rat model of post-traumatic osteoarthritis: evaluation of elemental strontium as a molecular tracer of bone formation. Osteoarthritis Cartilage 20 (7), 694−702.

Park, D., Spencer, J.A., Koh, B.I., Kobayashi, T., Fujisaki, J., Clemens, T.L., Lin, C.P., Kronenberg, H.M., Scadden, D.T., 2012. Endogenous bone marrow mscs are dynamic, fate-restricted participants in bone maintenance and regeneration. Cell Stem Cell 10 (3), 259−272.

Park, K., Kim, S.J., Bang, Y.J., Park, J.G., Kim, N.K., Roberts, A.B., Sporn, M.B., 1994. Genetic changes in the transforming growth factor beta (tgf-beta) type ii receptor gene in human gastric cancer cells: correlation with sensitivity to growth inhibition by tgf-beta. Proc. Natl. Acad. Sci. U. S. A 91 (19), 8772−8776.

Pederson, L., Ruan, M., Westendorf, J.J., Khosla, S., Oursler, M.J., 2008. Regulation of bone formation by osteoclasts involves wnt/bmp signaling and the chemokine sphingosine-1-phosphate. Proc. Natl. Acad. Sci. U. S. A 105 (52), 20764−20769.

Pedrozo, H.A., Schwartz, Z., Robinson, M., Gomes, R., Dean, D.D., Bonewald, L.F., Boyan, B.D., 1999. Potential mechanisms for the plasmin-mediated release and activation of latent transforming growth factor-beta1 from the extracellular matrix of growth plate chondrocytes. Endocrinology 140 (12), 5806−5816.

Penton, A., Chen, Y., Staehling-Hampton, K., Wrana, J.L., Attisano, L., Szidonya, J., Cassill, J.A., Massague, J., Hoffmann, F.M., 1994. Identification of two bone morphogenetic protein type i receptors in drosophila and evidence that brk25d is a decapentaplegic receptor. Cell 78 (2), 239−250.

Pertovaara, L., Kaipainen, A., Mustonen, T., Orpana, A., Ferrara, N., Saksela, O., Alitalo, K., 1994. Vascular endothelial growth factor is induced in response to transforming growth factor-beta in fibroblastic and epithelial cells. J. Biol. Chem. 269 (9), 6271−6274.

Pfeilschifter, J., Bonewald, L., Mundy, G.R., 1990. Characterization of the latent transforming growth factor beta complex in bone. J. Bone Miner. Res. 5 (1), 49−58.

Pfeilschifter, J., Laukhuf, F., Muller-Beckmann, B., Blum, W.F., Pfister, T., Ziegler, R., 1995. Parathyroid hormone increases the concentration of insulin-like growth factor-i and transforming growth factor beta 1 in rat bone. J. Clin. Investig. 96 (2), 767−774.

Pfeilschifter, J., Mundy, G.R., 1987. Modulation of type beta transforming growth factor activity in bone cultures by osteotropic hormones. Proc. Natl. Acad. Sci. U. S. A 84 (7), 2024−2028.

Poczatek, M.H., Hugo, C., Darley-Usmar, V., Murphy-Ullrich, J.E., 2000. Glucose stimulation of transforming growth factor-beta bioactivity in mesangial cells is mediated by thrombospondin-1. Am. J. Pathol. 157 (4), 1353–1363.

Polo, S., Di Fiore, P.P., 2006. Endocytosis conducts the cell signaling orchestra. Cell 124 (5), 897–900.

Pretorius, M., Donahue, B.S., Yu, C., Greelish, J.P., Roden, D.M., Brown, N.J., 2007. Plasminogen activator inhibitor-1 as a predictor of postoperative atrial fibrillation after cardiopulmonary bypass. Circulation 116 (11 Suppl. l), I1–I7.

Prisby, R., Guignandon, A., Vanden-Bossche, A., Mac-Way, F., Linossier, M.T., Thomas, M., Laroche, N., Malaval, L., Langer, M., Peter, Z.A., et al., 2011. Intermittent pth(1-84) is osteoanabolic but not osteoangiogenic and relocates bone marrow blood vessels closer to bone-forming sites. J. Bone Miner. Res. 26 (11), 2583–2596.

Proell, V., Carmona-Cuenca, I., Murillo, M.M., Huber, H., Fabregat, I., Mikulits, W., 2007. Tgf-beta dependent regulation of oxygen radicals during transdifferentiation of activated hepatic stellate cells to myofibroblastoid cells. Comp. Hepatol. 6, 1.

Proetzel, G., Pawlowski, S.A., Wiles, M.V., Yin, M., Boivin, G.P., Howles, P.N., Ding, J., Ferguson, M.W., Doetschman, T., 1995. Transforming growth factor-beta 3 is required for secondary palate fusion. Nat. Genet. 11 (4), 409–414.

Prunier, C., Pessah, M., Ferrand, N., Seo, S.R., Howe, P., Atfi, A., 2003. The oncoprotein ski acts as an antagonist of transforming growth factor-beta signaling by suppressing smad2 phosphorylation. J. Biol. Chem. 278 (28), 26249–26257.

Qian, S.W., Kondaiah, P., Roberts, A.B., Sporn, M.B., 1990. Cdna cloning by pcr of rat transforming growth factor beta-1. Nucleic Acids Res. 18 (10), 3059.

Qiu, T., Wu, X., Zhang, F., Clemens, T.L., Wan, M., Cao, X., 2010. Tgf-beta type ii receptor phosphorylates pth receptor to integrate bone remodelling signalling. Nat. Cell Biol. 12 (3), 224–234.

Radin, E.L., Rose, R.M., 1986. Role of subchondral bone in the initiation and progression of cartilage damage. Clin. Orthop. Relat. Res. (213), 34–40.

Raggatt, L.J., Partridge, N.C., 2010. Cellular and molecular mechanisms of bone remodeling. J. Biol. Chem. 285 (33), 25103–25108.

Rahr, H.B., Sorensen, J.V., Larsen, J.F., Jensen, F.S., Bredahl, C., 1995. Plasminogen activators and plasminogen activator inhibitor before and after surgery in patients with and without gastric malignancy. Haemostasis 25 (5), 248–256.

Raisz, L.G., 2005. Pathogenesis of osteoporosis: concepts, conflicts, and prospects. J. Clin. Investig. 115 (12), 3318–3325.

Raugi, G.J., Olerud, J.E., Gown, A.M., 1987. Thrombospondin in early human wound tissue. J. Investig. Dermatol. 89 (6), 551–554.

Ray, N.F., Chan, J.K., Thamer, M., Melton 3rd, L.J., 1997. Medical expenditures for the treatment of osteoporotic fractures in the United States in 1995: report from the national osteoporosis foundation. J. Bone Miner. Res. 12 (1), 24–35.

Reed, J.A., Bales, E., Xu, W., Okan, N.A., Bandyopadhyay, D., Medrano, E.E., 2001. Cytoplasmic localization of the oncogenic protein ski in human cutaneous melanomas in vivo: functional implications for transforming growth factor beta signaling. Cancer Res. 61 (22), 8074–8078.

Reed, M.J., Puolakkainen, P., Lane, T.F., Dickerson, D., Bornstein, P., Sage, E.H., 1993. Differential expression of sparc and thrombospondin 1 in wound repair: immunolocalization and in situ hybridization. J. Histochem. Cytochem. 41 (10), 1467–1477.

Rhodes, S.D., Wu, X., He, Y., Chen, S., Yang, H., Staser, K.W., Wang, J., Zhang, P., Jiang, C., Yokota, H., et al., 2013. Hyperactive transforming growth factor-beta1 signaling potentiates skeletal defects in a neurofibromatosis type 1 mouse model. J. Bone Miner. Res. 28 (12), 2476–2489.

Roberts, A.B., Frolik, C.A., Anzano, M.A., Sporn, M.B., 1983. Transforming growth factors from neoplastic and nonneoplastic tissues. Fed. Proc. 42 (9), 2621–2626.

Roelen, B.A., Dijke, P., 2003. Controlling mesenchymal stem cell differentiation by tgfbeta family members. J. Orthop. Sci. 8 (5), 740–748.

Rolli, M., Fransvea, E., Pilch, J., Saven, A., Felding-Habermann, B., 2003. Activated integrin alphavbeta3 cooperates with metalloproteinase mmp-9 in regulating migration of metastatic breast cancer cells. Proc. Natl. Acad. Sci. U. S. A 100 (16), 9482–9487.

Ross, S., Hill, C.S., 2008. How the smads regulate transcription. Int. J. Biochem. Cell Biol. 40 (3), 383–408.

Sabbieti, M.G., Marchetti, L., Abreu, C., Montero, A., Hand, A.R., Raisz, L.G., Hurley, M.M., 1999. Prostaglandins regulate the expression of fibroblast growth factor-2 in bone. Endocrinology 140 (1), 434–444.

Sabbieti, M.G., Marchetti, L., Gabrielli, M.G., Menghi, M., Materazzi, S., Menghi, G., Raisz, L.G., Hurley, M.M., 2005. Prostaglandins differently regulate fgf-2 and fgf receptor expression and induce nuclear translocation in osteoblasts via mapk kinase. Cell Tissue Res. 319 (2), 267–278.

Saharinen, J., Taipale, J., Keski-Oja, J., 1996. Association of the small latent transforming growth factor-beta with an eight cysteine repeat of its binding protein ltbp-1. EMBO J. 15 (2), 245–253.

Saito, T., Kinoshita, A., Yoshiura, K., Makita, Y., Wakui, K., Honke, K., Niikawa, N., Taniguchi, N., 2001. Domain-specific mutations of a transforming growth factor (tgf)-beta 1 latency-associated peptide cause camurati-engelmann disease because of the formation of a constitutively active form of tgf-beta 1. J. Biol. Chem. 276 (15), 11469–11472.

Sakai, K., Sumi, Y., Muramatsu, H., Hata, K., Muramatsu, T., Ueda, M., 2003. Thrombospondin-1 promotes fibroblast-mediated collagen gel contraction caused by activation of latent transforming growth factor beta-1. J. Dermatol. Sci. 31 (2), 99–109.

Samavarchi-Tehrani, P., Golipour, A., David, L., Sung, H.K., Beyer, T.A., Datti, A., Woltjen, K., Nagy, A., Wrana, J.L., 2010. Functional genomics reveals a bmp-driven mesenchymal-to-epithelial transition in the initiation of somatic cell reprogramming. Cell Stem Cell 7 (1), 64–77.

Sampson, E.R., Hilton, M.J., Tian, Y., Chen, D., Schwarz, E.M., Mooney, R.A., Bukata, S.V., O'Keefe, R.J., Awad, H., Puzas, J.E., et al., 2011. Teriparatide as a chondroregenerative therapy for injury-induced osteoarthritis. Sci. Transl. Med. 3 (101), 101–193.

Sanchez-Fernandez, M.A., Gallois, A., Riedl, T., Jurdic, P., Hoflack, B., 2008. Osteoclasts control osteoblast chemotaxis via pdgf-bb/pdgf receptor beta signaling. PLoS One 3 (10), e3537.

Sanford, L.P., Ormsby, I., Gittenberger-de Groot, A.C., Sariola, H., Friedman, R., Boivin, G.P., Cardell, E.L., Doetschman, T., 1997. Tgfbeta2 knockout mice have multiple developmental defects that are non-overlapping with other tgfbeta knockout phenotypes. Development 124 (13), 2659–2670.

Sato, Y., Rifkin, D.B., 1989. Inhibition of endothelial cell movement by pericytes and smooth muscle cells: activation of a latent transforming growth factor-beta 1-like molecule by plasmin during co-culture. J. Cell Biol. 109 (1), 309–315.

Scaffidi, A.K., Petrovic, N., Moodley, Y.P., Fogel-Petrovic, M., Kroeger, K.M., Seeber, R.M., Eidne, K.A., Thompson, P.J., Knight, D.A., 2004. Alpha(v) beta(3) integrin interacts with the transforming growth factor beta (tgfbeta) type ii receptor to potentiate the proliferative effects of tgfbeta1 in living human lung fibroblasts. J. Biol. Chem. 279 (36), 37726–37733.

Scharstuhl, A., Vitters, E.L., van der Kraan, P.M., van den Berg, W.B., 2003. Reduction of osteophyte formation and synovial thickening by adenoviral overexpression of transforming growth factor beta/bone morphogenetic protein inhibitors during experimental osteoarthritis. Arthritis Rheum. 48 (12), 3442–3451.

Schiemann, W.P., Pfeifer, W.M., Levi, E., Kadin, M.E., Lodish, H.F., 1999. A deletion in the gene for transforming growth factor beta type i receptor abolishes growth regulation by transforming growth factor beta in a cutaneous t-cell lymphoma. Blood 94 (8), 2854–2861.

Schmierer, B., Hill, C.S., 2007. Tgfbeta-smad signal transduction: molecular specificity and functional flexibility. Nat. Rev. Mol. Cell Biol. 8 (12), 970–982.

Schultz-Cherry, S., Murphy-Ullrich, J.E., 1993. Thrombospondin causes activation of latent transforming growth factor-beta secreted by endothelial cells by a novel mechanism. J. Cell Biol. 122 (4), 923–932.

Schutte, M., Hruban, R.H., Hedrick, L., Cho, K.R., Nadasdy, G.M., Weinstein, C.L., Bova, G.S., Isaacs, W.B., Cairns, P., Nawroz, H., et al., 1996. Dpc4 gene in various tumor types. Cancer Res. 56 (11), 2527–2530.

Seeber, C., Hiller, E., Holler, E., Kolb, H.J., 1992. Increased levels of tissue plasminogen activator (t-pa) and tissue plasminogen activator inhibitor (pai) correlate with tumor necrosis factor alpha (tnf alpha)-release in patients suffering from microangiopathy following allogeneic bone marrow transplantation (bmt). Thromb. Res. 66 (4), 373–383.

Seghezzi, G., Patel, S., Ren, C.J., Gualandris, A., Pintucci, G., Robbins, E.S., Shapiro, R.L., Galloway, A.C., Rifkin, D.B., Mignatti, P., 1998. Fibroblast growth factor-2 (fgf-2) induces vascular endothelial growth factor (vegf) expression in the endothelial cells of forming capillaries: an autocrine mechanism contributing to angiogenesis. J. Cell Biol. 141 (7), 1659–1673.

Sengle, G., Ono, R.N., Sasaki, T., Sakai, L.Y., 2011. Prodomains of transforming growth factor beta (tgfbeta) superfamily members specify different functions: extracellular matrix interactions and growth factor bioavailability. J. Biol. Chem. 286 (7), 5087–5099.

Serra, R., Johnson, M., Filvaroff, E.H., LaBorde, J., Sheehan, D.M., Derynck, R., Moses, H.L., 1997. Expression of a truncated, kinase-defective tgf-beta type ii receptor in mouse skeletal tissue promotes terminal chondrocyte differentiation and osteoarthritis. J. Cell Biol. 139 (2), 541–552.

Seyedin, S.M., Thomas, T.C., Thompson, A.Y., Rosen, D.M., Piez, K.A., 1985. Purification and characterization of two cartilage-inducing factors from bovine demineralized bone. Proc. Natl. Acad. Sci. U. S. A 82 (8), 2267–2271.

Shao, E.S., Lin, L., Yao, Y., Bostrom, K.I., 2009. Expression of vascular endothelial growth factor is coordinately regulated by the activin-like kinase receptors 1 and 5 in endothelial cells. Blood 114 (10), 2197–2206.

Shi, M., Zhu, J., Wang, R., Chen, X., Mi, L., Walz, T., Springer, T.A., 2011. Latent tgf-beta structure and activation. Nature 474 (7351), 343–349.

Shin, I., Bakin, A.V., Rodeck, U., Brunet, A., Arteaga, C.L., 2001. Transforming growth factor beta enhances epithelial cell survival via akt-dependent regulation of fkhrl1. Mol. Biol. Cell 12 (11), 3328–3339.

Shinojima, N., Hossain, A., Takezaki, T., Fueyo, J., Gumin, J., Gao, F., Nwajei, F., Marini, F.C., Andreeff, M., Kuratsu, J., et al., 2013. Tgf-beta mediates homing of bone marrow-derived human mesenchymal stem cells to glioma stem cells. Cancer Res. 73 (7), 2333–2344.

Shirai, T., Kobayashi, M., Nishitani, K., Satake, T., Kuroki, H., Nakagawa, Y., Nakamura, T., 2011. Chondroprotective effect of alendronate in a rabbit model of osteoarthritis. J. Orthop. Res. 29 (10), 1572–1577.

Siegel, P.M., Massague, J., 2003. Cytostatic and apoptotic actions of tgf-beta in homeostasis and cancer. Nat. Rev. Canc. 3 (11), 807–821.

Silvestri, C., Narimatsu, M., von Both, I., Liu, Y., Tan, N.B., Izzi, L., McCaffery, P., Wrana, J.L., Attisano, L., 2008. Genome-wide identification of smad/foxh1 targets reveals a role for foxh1 in retinoic acid regulation and forebrain development. Dev. Cell 14 (3), 411–423.

Singh, A.M., Reynolds, D., Cliff, T., Ohtsuka, S., Mattheyses, A.L., Sun, Y., Menendez, L., Kulik, M., Dalton, S., 2012. Signaling network crosstalk in human pluripotent cells: a smad2/3-regulated switch that controls the balance between self-renewal and differentiation. Cell Stem Cell 10 (3), 312–326.

Smith, J.N., Calvi, L.M., 2013. Concise review: current concepts in bone marrow microenvironmental regulation of hematopoietic stem and progenitor cells. Stem Cell. 31 (6), 1044–1050.

Sniekers, Y.H., Intema, F., Lafeber, F.P., van Osch, G.J., van Leeuwen, J.P., Weinans, H., Mastbergen, S.C., 2008. A role for subchondral bone changes in the process of osteoarthritis; a micro-ct study of two canine models. BMC Musculoskeletal Disorders 9, 20.

Sobue, T., Gravely, T., Hand, A., Min, Y.K., Pilbeam, C., Raisz, L.G., Zhang, X., Larocca, D., Florkiewicz, R., Hurley, M.M., 2002. Regulation of fibroblast growth factor 2 and fibroblast growth factor receptors by transforming growth factor beta in human osteoblastic mg-63 cells. J. Bone Miner. Res. 17 (3), 502–512.

Soond, S.M., Chantry, A., 2011. Selective targeting of activating and inhibitory smads by distinct wwp2 ubiquitin ligase isoforms differentially modulates tgfbeta signalling and emt. Oncogene 30 (21), 2451–2462.

Sorrentino, A., Thakur, N., Grimsby, S., Marcusson, A., von Bulow, V., Schuster, N., Zhang, S., Heldin, C.H., Landstrom, M., 2008. The type i tgf-beta receptor engages traf6 to activate tak1 in a receptor kinase-independent manner. Nat. Cell Biol. 10 (10), 1199–1207.

Statius van Eps, R.G., LaMuraglia, G.M., 1997. Photodynamic therapy inhibits transforming growth factor beta activity associated with vascular smooth muscle cell injury. J. Vasc. Surg. 25 (6), 1044–1052 discussion 1052–1043.

Subramanyam, D., Lamouille, S., Judson, R.L., Liu, J.Y., Bucay, N., Derynck, R., Blelloch, R., 2011. Multiple targets of mir-302 and mir-372 promote reprogramming of human fibroblasts to induced pluripotent stem cells. Nat. Biotechnol. 29 (5), 443–448.

Suzuki, A., Raya, A., Kawakami, Y., Morita, M., Matsui, T., Nakashima, K., Gage, F.H., Rodriguez-Esteban, C., Izpisua Belmonte, J.C., 2006. Nanog binds to smad1 and blocks bone morphogenetic protein-induced differentiation of embryonic stem cells. Proc. Natl. Acad. Sci. U. S. A 103 (27), 10294–10299.

Sweetwyne, M.T., Murphy-Ullrich, J.E., 2012. Thrombospondin1 in tissue repair and fibrosis: tgf-beta-dependent and independent mechanisms. Matrix Biol. 31 (3), 178–186.

Taipale, J., Miyazono, K., Heldin, C.H., Keski-Oja, J., 1994. Latent transforming growth factor-beta 1 associates to fibroblast extracellular matrix via latent tgf-beta binding protein. J. Cell Biol. 124 (1–2), 171–181.

Takagi, Y., Koumura, H., Futamura, M., Aoki, S., Ymaguchi, K., Kida, H., Tanemura, H., Shimokawa, K., Saji, S., 1998. Somatic alterations of the smad-2 gene in human colorectal cancers. Br. J. Canc. 78 (9), 1152–1155.

Takahashi, K., Yamanaka, S., 2006. Induction of pluripotent stem cells from mouse embryonic and adult fibroblast cultures by defined factors. Cell 126 (4), 663–676.

Tang, Y., Wu, X., Lei, W., Pang, L., Wan, C., Shi, Z., Zhao, L., Nagy, T.R., Peng, X., Hu, J., et al., 2009. Tgf-beta1-induced migration of bone mesenchymal stem cells couples bone resorption with formation. Nat. Med. 15 (7), 757–765.

Teitelbaum, S.L., 2000. Bone resorption by osteoclasts. Science 289 (5484), 1504–1508.

ten Dijke, P., Miyazono, K., Heldin, C.H., 1996. Signaling via hetero-oligomeric complexes of type i and type ii serine/threonine kinase receptors. Curr. Opin. Cell Biol. 8 (2), 139–145.

Teo, A.K., Arnold, S.J., Trotter, M.W., Brown, S., Ang, L.T., Chng, Z., Robertson, E.J., Dunn, N.R., Vallier, L., 2011. Pluripotency factors regulate definitive endoderm specification through eomesodermin. Genes Dev. 25 (3), 238–250.

Terauchi, M., Li, J.Y., Bedi, B., Baek, K.H., Tawfeek, H., Galley, S., Gilbert, L., Nanes, M.S., Zayzafoon, M., Guldberg, R., et al., 2009. T lymphocytes amplify the anabolic activity of parathyroid hormone through wnt10b signaling. Cell Metabol. 10 (3), 229–240.

Thomas, D.A., Massague, J., 2005. Tgf-beta directly targets cytotoxic t cell functions during tumor evasion of immune surveillance. Cancer Cell 8 (5), 369–380.

Thomas, R.J., Guise, T.A., Yin, J.J., Elliott, J., Horwood, N.J., Martin, T.J., Gillespie, M.T., 1999. Breast cancer cells interact with osteoblasts to support osteoclast formation. Endocrinology 140 (10), 4451–4458.

Tseng, Y.H., Kokkotou, E., Schulz, T.J., Huang, T.L., Winnay, J.N., Taniguchi, C.M., Tran, T.T., Suzuki, R., Espinoza, D.O., Yamamoto, Y., et al., 2008. New role of bone morphogenetic protein 7 in brown adipogenesis and energy expenditure. Nature 454 (7207), 1000–1004.

Tural, S., Alayli, G., Kara, N., Tander, B., Bilgici, A., Kuru, O., 2013. Association between osteoporosis and polymorphisms of the il-10 and tgf-beta genes in Turkish postmenopausal women. Hum. Immunol. 74 (9), 1179–1183.

Tuxhorn, J.A., McAlhany, S.J., Yang, F., Dang, T.D., Rowley, D.R., 2002. Inhibition of transforming growth factor-beta activity decreases angiogenesis in a human prostate cancer-reactive stroma xenograft model. Cancer Res. 62 (21), 6021–6025.

Vallier, L., Mendjan, S., Brown, S., Chng, Z., Teo, A., Smithers, L.E., Trotter, M.W., Cho, C.H., Martinez, A., Rugg-Gunn, P., et al., 2009. Activin/nodal signalling maintains pluripotency by controlling nanog expression. Development 136 (8), 1339–1349.

van Beuningen, H.M., van der Kraan, P.M., Arntz, O.J., van den Berg, W.B., 1994. Transforming growth factor-beta 1 stimulates articular chondrocyte proteoglycan synthesis and induces osteophyte formation in the murine knee joint. Lab. Investig. 71 (2), 279–290.

van de Laar, I.M., Oldenburg, R.A., Pals, G., Roos-Hesselink, J.W., de Graaf, B.M., Verhagen, J.M., Hoedemaekers, Y.M., Willemsen, R., Severijnen, L.A., Venselaar, H., et al., 2011. Mutations in smad3 cause a syndromic form of aortic aneurysms and dissections with early-onset osteoarthritis. Nat. Genet. 43 (2), 121–126.

van der Flier, A., Sonnenberg, A., 2001. Function and interactions of integrins. Cell Tissue Res. 305 (3), 285–298.

van der Kraan, P.M., Goumans, M.J., Blaney Davidson, E., ten Dijke, P., 2012. Age-dependent alteration of tgf-beta signalling in osteoarthritis. Cell Tissue Res. 347 (1), 257–265.

van der Pluijm, G., Sijmons, B., Vloedgraven, H., Deckers, M., Papapoulos, S., Lowik, C., 2001. Monitoring metastatic behavior of human tumor cells in mice with species-specific polymerase chain reaction: elevated expression of angiogenesis and bone resorption stimulators by breast cancer in bone metastases. J. Bone Miner. Res. 16 (6), 1077–1091.

van Grunsven, L.A., Verstappen, G., Huylebroeck, D., Verschueren, K., 2005. Smads and chromatin modulation. Cytokine Growth Factor Rev. 16 (4–5), 495–512.

Vardouli, L., Moustakas, A., Stournaras, C., 2005. Lim-kinase 2 and cofilin phosphorylation mediate actin cytoskeleton reorganization induced by transforming growth factor-beta. J. Biol. Chem. 280 (12), 11448–11457.

Varelas, X., Sakuma, R., Samavarchi-Tehrani, P., Peerani, R., Rao, B.M., Dembowy, J., Yaffe, M.B., Zandstra, P.W., Wrana, J.L., 2008. Taz controls smad nucleocytoplasmic shuttling and regulates human embryonic stem-cell self-renewal. Nat. Cell Biol. 10 (7), 837–848.

Varelas, X., Samavarchi-Tehrani, P., Narimatsu, M., Weiss, A., Cockburn, K., Larsen, B.G., Rossant, J., Wrana, J.L., 2010. The crumbs complex couples cell density sensing to hippo-dependent control of the tgf-beta-smad pathway. Dev. Cell 19 (6), 831–844.

Verrecchia, F., Chu, M.L., Mauviel, A., 2001. Identification of novel tgf-beta/smad gene targets in dermal fibroblasts using a combined cdna microarray/promoter transactivation approach. J. Biol. Chem. 276 (20), 17058–17062.

Vincent, T., Neve, E.P., Johnson, J.R., Kukalev, A., Rojo, F., Albanell, J., Pietras, K., Virtanen, I., Philipson, L., Leopold, P.L., et al., 2009. A snail1-smad3/4 transcriptional repressor complex promotes tgf-beta mediated epithelial-mesenchymal transition. Nat. Cell Biol. 11 (8), 943–950.

Walton, K.L., Makanji, Y., Chen, J., Wilce, M.C., Chan, K.L., Robertson, D.M., Harrison, C.A., 2010. Two distinct regions of latency-associated peptide coordinate stability of the latent transforming growth factor-beta1 complex. J. Biol. Chem. 285 (22), 17029–17037.

Wan, M., Li, C., Zhen, G., Jiao, K., He, W., Jia, X., Wang, W., Shi, C., Xing, Q., Chen, Y.F., et al., 2012. Injury-activated transforming growth factor beta controls mobilization of mesenchymal stem cells for tissue remodeling. Stem Cell. 30 (11), 2498−2511.

Wan, M., Yang, C., Li, J., Wu, X., Yuan, H., Ma, H., He, X., Nie, S., Chang, C., Cao, X., 2008. Parathyroid hormone signaling through low-density lipoprotein-related protein 6. Genes Dev. 22 (21), 2968−2979.

Wang, A., Yokosaki, Y., Ferrando, R., Balmes, J., Sheppard, D., 1996. Differential regulation of airway epithelial integrins by growth factors. Am. J. Respir. Cell Mol. Biol. 15 (5), 664−672.

Wang, B., Dolinski, B.M., Kikuchi, N., Leone, D.R., Peters, M.G., Weinreb, P.H., Violette, S.M., Bissell, D.M., 2007. Role of alphavbeta6 integrin in acute biliary fibrosis. Hepatology 46 (5), 1404−1412.

Wang, L., Clutter, S., Benincosa, J., Fortney, J., Gibson, L.F., 2005. Activation of transforming growth factor-beta1/p38/smad3 signaling in stromal cells requires reactive oxygen species-mediated mmp-2 activity during bone marrow damage. Stem Cell. 23 (8), 1122−1134.

Wang, S., Shiva, S., Poczatek, M.H., Darley-Usmar, V., Murphy-Ullrich, J.E., 2002. Nitric oxide and cgmp-dependent protein kinase regulation of glucose-mediated thrombospondin 1-dependent transforming growth factor-beta activation in mesangial cells. J. Biol. Chem. 277 (12), 9880−9888.

Wang, S., Skorczewski, J., Feng, X., Mei, L., Murphy-Ullrich, J.E., 2004. Glucose up-regulates thrombospondin 1 gene transcription and transforming growth factor-beta activity through antagonism of cgmp-dependent protein kinase repression via upstream stimulatory factor 2. J. Biol. Chem. 279 (33), 34311−34322.

Warman, M.L., Cormier-Daire, V., Hall, C., Krakow, D., Lachman, R., LeMerrer, M., Mortier, G., Mundlos, S., Nishimura, G., Rimoin, D.L., et al., 2011. Nosology and classification of genetic skeletal disorders: 2010 revision. Am. J. Med. Genet. 155A (5), 943−968.

Watanabe, M., Masuyama, N., Fukuda, M., Nishida, E., 2000. Regulation of intracellular dynamics of smad4 by its leucine-rich nuclear export signal. EMBO Reports 1 (2), 176−182.

Watson, P., Lazowski, D., Han, V., Fraher, L., Steer, B., Hodsman, A., 1995. Parathyroid hormone restores bone mass and enhances osteoblast insulin-like growth factor i gene expression in ovariectomized rats. Bone 16 (3), 357−365.

Weiss, R.E., Watabe, N., 1979. Studies on the biology of fish bone. III. Ultrastructure of osteogenesis and resorption in osteocytic (cellular) and anosteocytic (acellular) bones. Calcif. Tissue Int. 28 (1), 43−56.

Werb, Z., 1997. Ecm and cell surface proteolysis: regulating cellular ecology. Cell 91 (4), 439−442.

Whyte, M.P., Totty, W.G., Novack, D.V., Zhang, X., Wenkert, D., Mumm, S., 2011. Camurati-engelmann disease: unique variant featuring a novel mutation in tgfbeta1 encoding transforming growth factor beta 1 and a missense change in tnfsf11 encoding rank ligand. J. Bone Miner. Res. 26 (5), 920−933.

Wipff, P.J., Hinz, B., 2008. Integrins and the activation of latent transforming growth factor beta1-an intimate relationship. Eur. J. Cell Biol. 87 (8−9), 601−615.

Witten, P.E., Huysseune, A., 2009. A comparative view on mechanisms and functions of skeletal remodelling in teleost fish, with special emphasis on osteoclasts and their function. Biol. Rev. Camb. Philos. Soc. 84 (2), 315−346.

Wrana, J.L., Attisano, L., 2000. The smad pathway. Cytokine Growth Factor Rev. 11 (1−2), 5−13.

Wrighton, K.H., Lin, X., Feng, X.H., 2009a. Phospho-control of tgf-beta superfamily signaling. Cell Res. 19 (1), 8−20.

Wrighton, K.H., Lin, X., Yu, P.B., Feng, X.H., 2009b. Transforming growth factor {beta} can stimulate smad1 phosphorylation independently of bone morphogenic protein receptors. J. Biol. Chem. 284 (15), 9755−9763.

Wu, X., Pang, L., Lei, W., Lu, W., Li, J., Li, Z., Frassica, F.J., Chen, X., Wan, M., Cao, X., 2010. Inhibition of sca-1-positive skeletal stem cell recruitment by alendronate blunts the anabolic effects of parathyroid hormone on bone remodeling. Cell Stem Cell 7 (5), 571−580.

Xian, L., Wu, X., Pang, L., Lou, M., Rosen, C.J., Qiu, T., Crane, J., Frassica, F., Zhang, L., Rodriguez, J.P., et al., 2012. Matrix igf-1 maintains bone mass by activation of mtor in mesenchymal stem cells. Nat. Med. 18 (7), 1095−1101.

Xie, H., Cui, Z., Wang, L., Xia, Z., Hu, Y., Xian, L., Li, C., Xie, L., Crane, J., Wan, M., et al., 2014. Pdgf-bb secreted by preosteoclasts induces angiogenesis during coupling with osteogenesis. Nat. Med. 20 (11), 1270−1278.

Xu, J., Lamouille, S., Derynck, R., 2009. Tgf-beta-induced epithelial to mesenchymal transition. Cell Res. 19 (2), 156−172.

Xu, L., Kang, Y., Col, S., Massague, J., 2002. Smad2 nucleocytoplasmic shuttling by nucleoporins can/nup214 and nup153 feeds tgfbeta signaling complexes in the cytoplasm and nucleus. Mol. Cell 10 (2), 271−282.

Xu, X., Zheng, L., Bian, Q., Xie, L., Liu, W., Zhen, G., Crane, J.L., Zhou, X., Cao, X., 2015. Aberrant activation of tgf-beta in subchondral bone at the onset of rheumatoid arthritis joint destruction. J. Bone Miner. Res. 30 (11), 2033−2043.

Xu, X.H., Dong, S.S., Guo, Y., Yang, T.L., Lei, S.F., Papasian, C.J., Zhao, M., Deng, H.W., 2010. Molecular genetic studies of gene identification for osteoporosis: the 2009 update. Endocr. Rev. 31 (4), 447−505.

Yakicier, M.C., Irmak, M.B., Romano, A., Kew, M., Ozturk, M., 1999. Smad2 and smad4 gene mutations in hepatocellular carcinoma. Oncogene 18 (34), 4879−4883.

Yamada, Y., Miyauchi, A., Goto, J., Takagi, Y., Okuizumi, H., Kanematsu, M., Hase, M., Takai, H., Harada, A., Ikeda, K., 1998. Association of a polymorphism of the transforming growth factor-beta1 gene with genetic susceptibility to osteoporosis in postmenopausal Japanese women. J. Bone Miner. Res. 13 (10), 1569−1576.

Yamada, Y., Miyauchi, A., Takagi, Y., Tanaka, M., Mizuno, M., Harada, A., 2001. Association of the c-509–>t polymorphism, alone of in combination with the t869–>c polymorphism, of the transforming growth factor-beta1 gene with bone mineral density and genetic susceptibility to osteoporosis in Japanese women. J. Mol. Med. (Berl.) 79 (2−3), 149−156.

Yamashita, H., Ichijo, H., Grimsby, S., Moren, A., ten Dijke, P., Miyazono, K., 1994. Endoglin forms a heteromeric complex with the signaling receptors for transforming growth factor-beta. J. Biol. Chem. 269 (3), 1995−2001.

Yamashita, H., ten Dijke, P., Huylebroeck, D., Sampath, T.K., Andries, M., Smith, J.C., Heldin, C.H., Miyazono, K., 1995. Osteogenic protein-1 binds to activin type ii receptors and induces certain activin-like effects. J. Cell Biol. 130 (1), 217–226.

Yamashita, M., Fatyol, K., Jin, C., Wang, X., Liu, Z., Zhang, Y.E., 2008. Traf6 mediates smad-independent activation of jnk and p38 by tgf-beta. Mol. Cell 31 (6), 918–924.

Yang, X., Chen, L., Xu, X., Li, C., Huang, C., Deng, C.X., 2001. Tgf-beta/smad3 signals repress chondrocyte hypertrophic differentiation and are required for maintaining articular cartilage. J. Cell Biol. 153 (1), 35–46.

Yang, Z., Mu, Z., Dabovic, B., Jurukovski, V., Yu, D., Sung, J., Xiong, X., Munger, J.S., 2007. Absence of integrin-mediated tgfbeta1 activation in vivo recapitulates the phenotype of tgfbeta1-null mice. J. Cell Biol. 176 (6), 787–793.

Yehualaeshet, T., O'Connor, R., Begleiter, A., Murphy-Ullrich, J.E., Silverstein, R., Khalil, N., 2000. A cd36 synthetic peptide inhibits bleomycin-induced pulmonary inflammation and connective tissue synthesis in the rat. Am. J. Respir. Cell Mol. Biol. 23 (2), 204–212.

Yehualaeshet, T., O'Connor, R., Green-Johnson, J., Mai, S., Silverstein, R., Murphy-Ullrich, J.E., Khalil, N., 1999. Activation of rat alveolar macrophage-derived latent transforming growth factor beta-1 by plasmin requires interaction with thrombospondin-1 and its cell surface receptor, cd36. Am. J. Pathol. 155 (3), 841–851.

Yevdokimova, N., Wahab, N.A., Mason, R.M., 2001. Thrombospondin-1 is the key activator of tgf-beta1 in human mesangial cells exposed to high glucose. J. Am. Soc. Nephrol. 12 (4), 703–712.

Yin, J.J., Selander, K., Chirgwin, J.M., Dallas, M., Grubbs, B.G., Wieser, R., Massague, J., Mundy, G.R., Guise, T.A., 1999. Tgf-beta signaling blockade inhibits pthrp secretion by breast cancer cells and bone metastases development. J. Clin. Investig. 103 (2), 197–206.

Yoshinaga, K., Obata, H., Jurukovski, V., Mazzieri, R., Chen, Y., Zilberberg, L., Huso, D., Melamed, J., Prijatelj, P., Todorovic, V., et al., 2008. Perturbation of transforming growth factor (tgf)-beta1 association with latent tgf-beta binding protein yields inflammation and tumors. Proc. Natl. Acad. Sci. U. S. A 105 (48), 18758–18763.

Young, G.D., Murphy-Ullrich, J.E., 2004. Molecular interactions that confer latency to transforming growth factor-beta. J. Biol. Chem. 279 (36), 38032–38039.

Yu, B., Zhao, X., Yang, C., Crane, J., Xian, L., Lu, W., Wan, M., Cao, X., 2012. Parathyroid hormone induces differentiation of mesenchymal stromal/stem cells by enhancing bone morphogenetic protein signaling. J. Bone Miner. Res. 27 (9), 2001–2014.

Yu, Q., Stamenkovic, I., 2000. Cell surface-localized matrix metalloproteinase-9 proteolytically activates tgf-beta and promotes tumor invasion and angiogenesis. Genes Dev. 14 (2), 163–176.

Zaidi, M., 2007. Skeletal remodeling in health and disease. Nat. Med. 13 (7), 791–801.

Zavadil, J., Bottinger, E.P., 2005. Tgf-beta and epithelial-to-mesenchymal transitions. Oncogene 24 (37), 5764–5774.

Zavadil, J., Cermak, L., Soto-Nieves, N., Bottinger, E.P., 2004. Integration of tgf-beta/smad and jagged1/notch signalling in epithelial-to-mesenchymal transition. EMBO J. 23 (5), 1155–1165.

Zawel, L., Dai, J.L., Buckhaults, P., Zhou, S., Kinzler, K.W., Vogelstein, B., Kern, S.E., 1998. Human smad3 and smad4 are sequence-specific transcription activators. Mol. Cell 1 (4), 611–617.

Zhang, L., Hu, H., Tian, F., Song, H., Zhang, Y., 2011. Enhancement of subchondral bone quality by alendronate administration for the reduction of cartilage degeneration in the early phase of experimental osteoarthritis. Clin. Exp. Med. 11 (4), 235–243.

Zhang, Y.E., 2009. Non-smad pathways in tgf-beta signaling. Cell Res. 19 (1), 128–139.

Zhao, C., Irie, N., Takada, Y., Shimoda, K., Miyamoto, T., Nishiwaki, T., Suda, T., Matsuo, K., 2006. Bidirectional ephrinb2-ephb4 signaling controls bone homeostasis. Cell Metabol. 4 (2), 111–121.

Zhen, G., Wen, C., Jia, X., Li, Y., Crane, J.L., Mears, S.C., Askin, F.B., Frassica, F.J., Chang, W., Yao, J., et al., 2013. Inhibition of tgf-beta signaling in mesenchymal stem cells of subchondral bone attenuates osteoarthritis. Nat. Med. 19 (6), 704–712.

Zheng, Y., Geiger, H., 2014. Hspcs get their motors running for asymmetric fate choice. Cell Stem Cell 14 (1), 1–2.

Zhou, B., Liu, Y., Kahn, M., Ann, D.K., Han, A., Wang, H., Nguyen, C., Flodby, P., Zhong, Q., Krishnaveni, M.S., et al., 2012. Interactions between beta-catenin and transforming growth factor-beta signaling pathways mediate epithelial-mesenchymal transition and are dependent on the transcriptional co-activator camp-response element-binding protein (creb)-binding protein (cbp). J. Biol. Chem. 287 (10), 7026–7038.

Zhou, Y., Poczatek, M.H., Berecek, K.H., Murphy-Ullrich, J.E., 2006. Thrombospondin 1 mediates angiotensin ii induction of tgf-beta activation by cardiac and renal cells under both high and low glucose conditions. Biochem. Biophys. Res. Commun. 339 (2), 633–641.

Zhu, H., Kavsak, P., Abdollah, S., Wrana, J.L., Thomsen, G.H., 1999. A smad ubiquitin ligase targets the bmp pathway and affects embryonic pattern formation. Nature 400 (6745), 687–693.

Zhu, S., Chen, K., Lan, Y., Zhang, N., Jiang, R., Hu, J., 2013. Alendronate protects against articular cartilage erosion by inhibiting subchondral bone loss in ovariectomized rats. Bone 53 (2), 340–349.

Chapter 48

Bone morphogenetic proteins

David E. Maridas[1], Marina Feigenson[1], Nora E. Renthal[2], Shek Man Chim[3], Laura W. Gamer[1] and Vicki Rosen[1]

[1]*Department of Developmental Biology, Harvard School of Dental Medicine, Boston, MA, United States;* [2]*Division of Endocrinology, Children's Hospital Boston, Boston, MA, United States;* [3]*Regeneron Pharmaceuticals, Inc. Tarrytown, NY, United States*

Chapter outline

Introduction

Bone morphogenetic proteins (BMPs) regulate endochondral ossification and postnatal skeletal growth, bone homeostasis, and fracture repair. Without BMP signaling, limb skeletogenesis cannot occur—ablation of BMP signaling by deletion of type I BMP receptors or *Smad4* results in failure of mesenchyme condensation prior endochondral ossification (Lim et al., 2015), while conditional deletion of *Smad4* in chondrocytes or osteoblasts is sufficient to cause severe skeletal growth retardation or decreased bone mass in mice (Zhang et al., 2005; Tan et al., 2007). Clinical studies have demonstrated that exogenously supplied BMPs are safe and efficient bone-inducing agents for use in specific orthopedic and dental surgery procedures. Yet comparatively little is known about the roles of endogenous BMPs in skeletal tissue throughout development, adulthood, and aging, which is information required to expand their therapeutic utility. Over the last decade, research has begun to shed light on the complexity of BMP signaling mechanisms. With more evidence for the fine-tuning of BMPs and BMP signaling in spatial and temporal contexts, we have come closer to appreciating the importance of their intricate biology. This chapter aims to review our current understanding of BMP signaling and its importance during skeletal development and maintenance.

Canonical bone morphogenetic protein signaling

The intracellular signaling pathway triggered by BMP involves a cascade of phosphorylation. Upon binding a BMP ligand, a Type II and a Type I receptor form an active complex. The Type II receptor kinase phosphorylates the Type I receptor, which in turn activates a subset of intracellular mediators, SMAD1/5/8. Activated SMAD1/5/8 recruits SMAD4 to form complexes (Salazar et al., 2016). SMAD1/5/8 proteins are the direct mediators of BMP signaling and have distinct roles during endochondral ossification. SMADs 1 and 5 are required for limb formation, whereas SMAD8 is not essential for skeletal development, as evidenced by SMAD8 knockout mice, which are viable and do not exhibit any skeletal phenotype (Retting et al., 2009). When activated, SMAD complexes translocate to the nucleus to regulate gene expression (Fig. 48.1). Osteo-associated genes specifically induced by BMP signaling include *Runx2*, Distal-Less Homeobox 5 (*Dlx5*), and Osterix (*Sp7*).

Principles of Bone Biology. https://doi.org/10.1016/B978-0-12-814841-9.00048-8

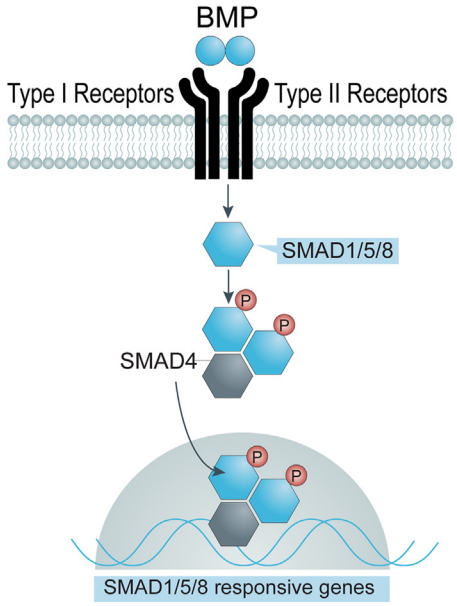

FIGURE 48.1 Canonical BMP signaling. Binding of BMP to its receptor results in the phosphorylation of SMAD1/5/8, which then recruits SMAD4 to form a complex capable of translocating to the nucleus to activate or inhibit the transcription of specific genes.

In addition to canonical BMP signaling, some studies suggest that other BMP pathways (noncanonical) play a role in bone formation. One such noncanonical BMP pathway is initiated by TGF-β activated kinase 1 (TAK1). The deletion of TAK1 results in fusion of joints, highlighting an important regulatory role in bone development (Greenblatt et al., 2010; Gunnell et al., 2010). While the canonical pathway remains the cornerstone of BMP signaling in the skeleton, the discovery of a myriad of ligands and multiple receptors suggested that this seemingly simple BMP signaling mechanism is actually much more complex than originally appreciated.

Diversity of the ligand and receptor environment

BMP signaling is mediated by the binding of ligand dimers to heteromeric receptor complexes. This simple system in theory is made complex by the diversity of BMP ligands and receptor components. To date, over 15 BMPs have been identified in humans and rodents. In the skeleton, multiple BMP ligands are synthesized and secreted by osteoblasts, chondrocytes, and their progenitors. Invading macrophages and vascular endothelial cells are also known to secrete BMPs during fracture repair (Rosen V and J.M. Wozney, 2002; Sipe et al., 2004; Csiszar et al., 2005). Not only is the ligand environment heterogeneous, its diversity is regulated and modified throughout life. For example, while BMPs 2, 4, and 7, as well as GDF5, are all expressed in early stages of skeletogenesis, embryonic deletions of each result in early diverse skeletal phenotypes. Deletion of *Bmp4* within the limb bud mesenchyme with *Prx1-Cre* causes a delayed formation of the apical ectodermal ridge and polydactyly affecting hind limbs more severely than forelimbs (Selever et al., 2004). Mice lacking GDF5 have defects in early mesenchymal condensation required for chondrogenesis, which leads to shorter limbs, with distal elements more affected than proximal elements, and missing or altered joints at some sites within appendages (Mikic, 2004). BMPs 6 and 7, and GDF6, are present in later stages of skeletal development. Global deletion of the *Bmp6* gene results in a mild skeletal phenotype with delayed ossification of the sternum (Solloway et al., 1998), while *Gdf6*-null mice show fusion between some bones in the wrists and ankles and variable alterations of cartilage and ligaments (Settle et al., 2003). No skeletal phenotypes were reported in mice with deletions of *Bmp8* or *Bmp10* (Zhao et al., 1998; Chen et al., 2004). Taken together, these findings suggest that specific BMPs need to be present during specific times, at a specific place, in order for bone formation to occur normally.

With the availability of floxed alleles, studies using CRE drivers have shed light on the complexity of BMP activity in the skeleton. For instance, deletion of *Bmp2* with *Prx1-Cre* results in mice with limbs that appear indistinguishable from wild-type littermates at birth, but who then suffer from multiple spontaneous fractures that do not heal, a phenotype thought to be caused by a failure of mesenchymal stem cells to undergo the chondrogenesis necessary for bone

repair (Tsuji et al., 2006). Furthermore, when *Bmp2* was removed specifically in early osteoblasts using the *3.6Col1a1-Cre* driver, mice also had increased bone fragility and decreased osteoblast function with altered vasculature of the long bones (Yang et al., 2013). However, experiments using *Osx-Cre* revealed that only the bones were altered by deletion of *Bmp2* in osteoblasts without affecting the vasculature (McBride et al., 2014). This demonstrates that BMP2 needs to be expressed at specific times and stages in osteogenic lineage cells in order to orchestrate bone development, homeostasis, and repair.

The importance of the spatiotemporal regulation of BMP ligands may be in part due to the ability of these signaling molecules to act in both an autocrine and a paracrine manner. When BMPs are secreted from cells, they may either act locally via BMP receptors on the surface of target cells or interact with extracellular matrix proteins that anchor BMPs to the matrix. Matrix interactions can then either augment or sequester BMP activity by modulating BMP availability for target cell interactions (Arteaga-Solis et al., 2001; Ohkawara et al., 2002; Larrain et al., 2001). Storage within the bone matrix allows BMPs to participate in osteoblast- and osteoclast-directed bone modeling and remodeling. Thus, the availability of BMP to bind its receptor is governed by its expression, cellular localization, and storage in extracellular matrix for later use.

Multiple receptors on bone cells

The BMP receptor environment on skeletal cells is also diverse. There are three Type I receptors (ACVR1, BMPR1A, and BMPR1B) and three Type II receptors (BMPR2, ACVR2A, and ACVR2B) expressed by bone cells. Each has specific and often overlapping patterns of expression in the skeleton. Additionally, while Type 1 BMP receptors only bind BMP ligands, ACVR2A and ACVR2B are multifunctional and capable of binding BMPs and related BMP family members including activin, Gdf8, and Gdf11. Hence, the loss of any individual receptor in mice causes unpredictable phenotypes. For example, removing *Bmpr2* in *Prx1*$^{+}$ cells results in high bone mass due to increased osteoblastic activity, which is thought to be due to altered competition between ligands for the remaining type II receptors (Lowery et al., 2015). Deletion of *Bmpr1a* in *Prx1*$^{+}$ progenitors results in shorter limbs and the loss of autopod skeletal elements, while deletions of the same receptor in osteoblasts and osteocytes result in high bone mass in both instances (Ovchinnikov et al., 2006; Kamiya et al, 2008b, 2016). Thus, the presence of multiple receptors in bone allows for binding by multiple BMPs, which creates a complex environment of competition and collaboration between BMPs to direct specific outcomes for the skeleton (Fig. 48.2).

Combinatorial signals

At the molecular level, the distinct receptor affinities and activities of individual BMPs create a system by which skeletal target cells respond to the distribution of available ligands in their environment. For example, a BMP ligand with higher affinity and weaker activity could antagonize a higher activity but weaker affinity BMP ligand by competing for shared receptors, resulting in functional antagonism via weak agonism. Recently, this mechanism was demonstrated using a cell-based reporter system, which established that cells perceive combinations of BMP ligands. Investigators demonstrated that BMP signaling by 15 different ligands was attenuated by increasing concentrations of either BMP3 or GDF5, whereas BMP signaling was increased universally by the addition of BMP2 to the ligand environment. Most interestingly, it was found that some BMPs, for example BMPs 7 and 4, exhibited a mixture of antagonistic and synergistic interactions with

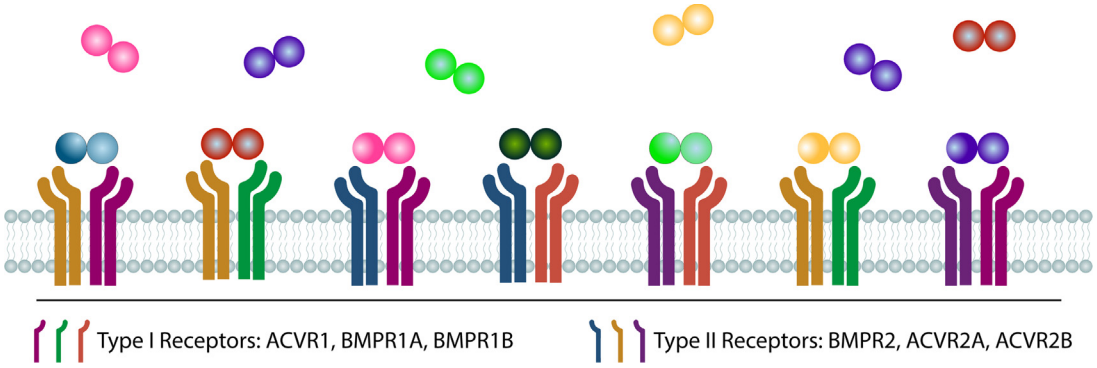

FIGURE 48.2 Multiple BMPs and receptors expressed in bone. In the bone microenvironment, BMPs are present as dimers forming a multitude of possible complexes. These complexes then interact with several type I and type II receptors.

other ligands (Antebi et al., 2017). This concept of combinatorial signals helps to explain the phenotypes observed in mice carrying multiple BMP deletions such as mice lacking both *Bmp5* and *Bmp7*, which die after embryonic day 10, with more severe phenotypes than seen in either *Bmp5* and *Bmp7* single-knockout mutants (Solloway and Robertson, 1999). Similarly, mice carrying both *Gdf5* and *Gdf6* deletions manifest an accentuated phenotype as compared with the single knockout with many reduced or absent bones. Double-mutant mice also have vertebral defects not seen in *Gdf5* and *Gdf6* single knockouts (Settle et al., 2003). Thus, mixtures of BMP dimers in the ligand environment are capable of altering signaling output in a nonlinear fashion, with the cell perceiving more than simple antagonism or agonism.

Antagonizing bone morphogenetic protein signaling

Another layer of regulation of BMP signaling in the skeleton is orchestrated by the presence of endogenous BMP antagonists including gremlin and noggin. Noggin and gremlin bind to distinct subsets of BMPs, GDFs, and/or activins to titrate active ligands out of the extracellular environment (Balemans and Van Hul, 2002). Gremlin is expressed in the posterior limb bud mesenchyme and is required for normal skeletal development. Mice lacking *Grem1* have abnormal forelimbs and hind limbs, with fewer digits (Khokha et al., 2003; Canalis et al., 2012). Noggin is expressed early in the notochord and dorsal neural tube and is required for chondrocyte condensation and joint formation but not for early limb patterning. Noggin-deficient mice lack joints and manifest fused digits and bones (Brunet et al., 1998). In addition, conditional deletion of noggin in osteoblasts results in decreased bone mass in adult mice (Canalis et al., 2012). In both gremlin and noggin deficiency, the skeletal phenotype results from unabated BMP signaling, demonstrating the importance of precise titration of the BMP pathway in skeletal development and homeostasis.

Activins display another mechanism of antagonizing BMP signaling in the skeleton. Activins inhibit BMP signaling by binding to ACVR2A and ACVR2B, receptors that are also utilized on skeletal cells by BMPs. By binding to ACVR2A or ACVR2B, activins prevent BMPs from activating SMAD1/5/8. Furthermore, they activate SMAD2/3, which serves to dampen endogenous BMP signaling (Olsen et al., 2015). Another form of BMP signaling antagonism occurs when BMP3 is present in the skeletal environment. While noggin and gremlin associate with BMPs to prevent BMP binding to receptors, BMP3 directly binds ACVR2B, inhibiting the interaction of this receptor with other BMPs. Mice overexpressing *Bmp3* under the *Col1* promoter have normal skeletal patterning but develop multiple spontaneous rib fractures around E17 due to defects in chondrogenesis that occur when BMP signaling is suppressed (Gamer et al., 2009). Whether direct or indirect, multiple types of BMP antagonism allow skeletal target cells to precisely balance the amount of BMP available to activate signaling, such that neither too much nor too little BMP signaling occurs (Fig. 48.3).

Pathway cross talk in bone

BMP signaling can regulate the expression of proteins involved in other signaling pathways important in skeletal homeostasis, creating a complex mechanism of cross talk (Fig. 48.4). For example, BMP signaling can induce expression

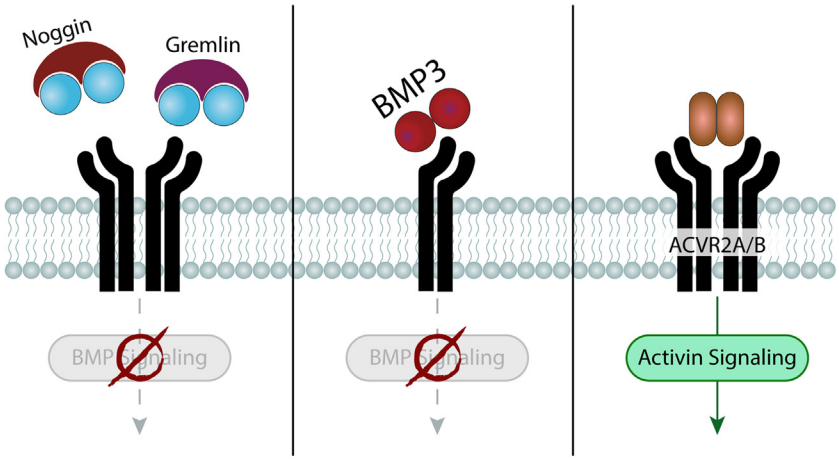

FIGURE 48.3 Antagonism of BMP signaling by endogenous factors. BMPs can be sequestered by noggin and gremlin and no longer capable of binding to their receptors. BMP3 is a particular BMP that binds to the ACVR2B receptor but does not recruit a type I receptor and therefore does not produce a signal acting as an inhibitor by competition. Activins compete with BMPs for their shared receptors ACVR2A and ACVR2B.

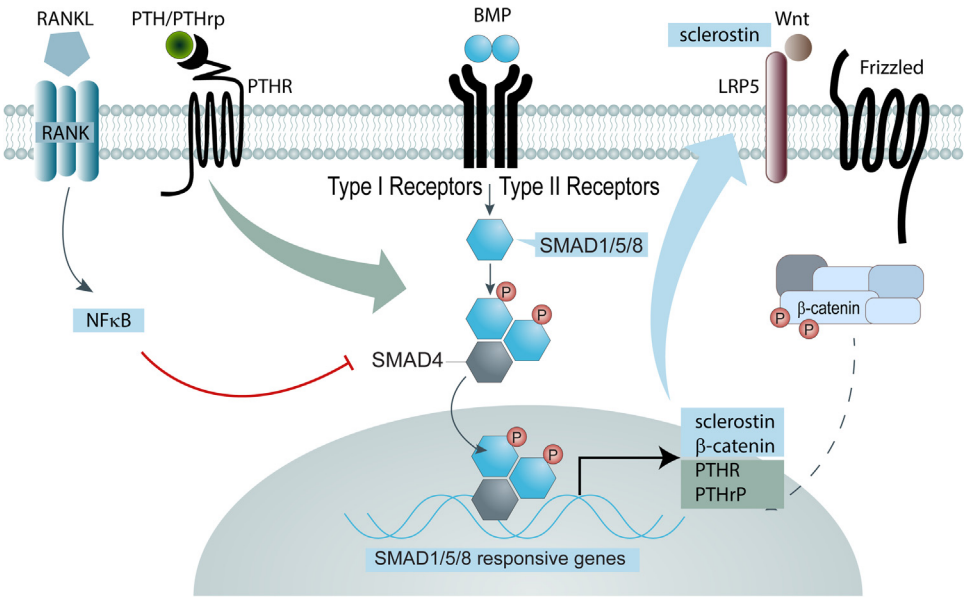

FIGURE 48.4 Intersection with other pathways in bone. BMP signaling can regulate the expression of factors involved in other pathways important in bone such as Wnt, PTH/PTHrp, and NFkB. Reciprocally, those other pathways can also modulate the downstream targets of canonical BMP signaling.

of sclerostin through BMPR1A activation (Kamiya et al, 2008a). Sclerostin acts as an inhibitor of Wnt activity to prevent bone formation by osteoblasts, thus establishing a regulatory intersection between BMP and Wnt signaling pathways. In addition, in vitro experiments have revealed that SMAD4 can regulate β-catenin expression, and in turn β-catenin can directly interact with SMAD4 (Freeman et al., 2012; Salazar et al., 2013), therefore forming a link between BMP signaling and the downstream target of Wnt signaling. Interestingly, Wnt and BMP signaling can be synergistic or antagonistic depending on the genes targeted (Itasaki and Hoppler, 2010), as it has been reported that BMP2 could synergize with Wnt in multipotent murine cell lines containing a constitutively active β-catenin signal (Mbalaviele et al., 2005).

Parathyroid hormone (PTH) and PTHrp analogs are also crucial regulators of bone homeostasis, and the PTH signaling pathway appears to intersect with BMP signaling. PTH is capable of inducing SMAD1/5/8 phosphorylation and activating the BMP signaling pathway in periosteal cells to induce osteoblast differentiation (Ogita et al., 2008). One in vitro model using C2C12 cells showed that BMP2 could decrease the expression of *Pthrp* while increasing the expression of its receptor (Susperregui et al., 2008). However, another study indicates that BMP signaling does not regulate *Pthrp* directly, but rather acts indirectly through IHH to orchestrate chondrogenesis (Susperregui et al., 2008). These data suggest intersections between BMP and PTH/PTHrp signaling pathways that are crucial for both chondrocyte and osteoblast differentiation. However, more research is required to clarify the times and places in which PTH and BMP cross talk occurs.

There is also evidence that BMP and NFκB signaling intersect. In MC3T3 cells, which are an osteoblast precursor cell line derived from mouse calvaria, NFκB activation by TNFα diminishes the binding of Runx2 on the *Bglap* promoter induced by BMP2 (Tarapore et al., 2016). An earlier article suggested that NFκB is able to bind directly or indirectly to SMAD1 and SMAD4 and interfere with their subsequent binding to DNA targets (Yamazaki et al., 2009). Since NFκB is known to induce osteoclastogenesis (Boyce et al., 2015), this could be a biological mechanism by which NFκB can reduce osteoblastic function while inducing osteoclastogenesis.

Much remains to be uncovered regarding the intersection of BMP and other signaling pathways, and this lack of knowledge has reduced our ability to use BMPs as therapeutics since one must consider the ligand/receptor environment, the target cell, the timing, and the integration with other signaling pathways in order to engineer a precise and efficient drug.

Therapeutics and bone diseases

Therapeutic applications for BMPs are wide-ranging, from bone grafting in orthopedic and dental applications to the enhancement of fracture healing. Recombinant human BMPs (rhBMPs) were first approved by the US Food and Drug Administration for clinical use in 2002. Today, two BMPs are available in clinical care: rhBMP2 and rhBMP7.

Officially, BMP2 is approved in adult patients for anterior lumbar interbody fusion, for augmentation of tibial fracture repair, and to aid in bone regeneration in the oral cavity. BMP7 received a humanitarian use device approval in 2003 for treatment of recalcitrant tibial nonunions. In these clinical settings, BMPs are typically applied with a matrix that serves as a carrier for the recombinant protein and also aids in defining the shape and volume of the new bone produced. Improvements in BMP delivery are an area of active investigation, with novel developments including BMP sequestering extracellular matrix mimetic hydrogels (Yan et al., 2018) and immune-modulated gelatin microspheres for spatiotemporal control of BMP release (Annamalai et al., 2018). More recently, genetically modified BMPs have been synthesized with properties that enhance their binding to their carrier matrix. Specifically, modified BMP2 has been generated that contains a collagen-binding domain, allowing for more efficient binding to a collagen carrier matrix and thus enhanced biological performance (Chen et al, 2007a,b; Zhao et al., 2009). Studies in animal models suggest that collagen-based BMP2 targeting improved bone formation when compared with unmodified recombinant BMP2; however, genetically modified BMPs have not yet undergone clinical trials in humans.

Fracture repair and periosteum

Studies examining the expression pattern of BMP ligands, receptors, and antagonists demonstrate that BMP signaling is an essential component of the fracture repair process. Mice lacking *Bmp2* are unable to initiate fracture healing, but this deficit can be rescued by the addition of exogenous BMPs (Tsuji et al., 2006; Meyer et al., 2004). The BMP antagonists BMP3 and noggin exhibit enhanced expression in the inflammatory stage of the fracture repair process as well as in the soft-callus stage. Their expression is reduced at the hard callus stage of repair consistent with the idea that BMP signaling is required for initiation of fracture healing but then needs to be tightly regulated (Morgan et al., 2016; Ehnert et al., 2016). Interestingly, BMP signaling is barely detectable in the process of intramembranous fracture repair (Yu et al, 2010b).

Periosteal cells have a crucial role during fracture repair, as the periosteum contains skeletal progenitors that participate in the healing response. Recent studies have demonstrated that BMP2 is produced by periosteal skeletal progenitors at the site of the fracture and promotes callus formation to stimulate fracture healing (Yu et al, 2010a). This effect starts at the early stages of repair during inflammation and continues to the last stage of remodeling (Yu et al, 2010a). In addition, mice lacking *Bmp2* cannot support bone graft healing despite having periosteal progenitors, indicating that *Bmp2* is required for skeletal progenitor cell activation to initiate repair but not for maintenance of the skeletal progenitor cell niche within the periosteum (Chappuis et al., 2012), consistent with the ability of BMP2 to induce endochondral ossification of the periosteum in a model of middle phalanx regeneration (Dawson et al., 2017). With regard to human periosteal progenitors, a combination of BMP2 and BMP6 was shown to promote chondrogenesis and matrix deposition that was sustained for 4 weeks after human cells underwent implantation in mice (Mendes et al., 2016).

Osteoporosis

BMP expression levels are decreased in aged bone in parallel with declining anabolic function of skeletal progenitors (Bessho and Iizuka, 1993; Fleet et al., 1996). In addition, in mouse models of bone loss, decreased expression of BMP family members has been associated with the development of osteoporosis. *Bmp2* expression is decreased in both steroid-induced osteopenic mice and ovariectomized mice (Lee et al., 2015). In vitro studies revealed that osteoprogenitors from older mice exhibit reduced differentiation potential when stimulated with rhBMP2 (Tang et al., 2008; Pountos et al., 2010). Local administration of rhBMP7 improves bone microarchitecture and strength in an osteoporotic sheep model (Phillips et al., 2006). Moreover, ovariectomized rats were shown to have accelerated fracture repair upon systemic administration of BMP7 (Mathavan et al., 2017; Blokhuis et al., 2012). These data suggest that BMP signaling is fundamental to bone homeostasis throughout life.

Osteoarthritis and articular cartilage maintenance

BMP signaling is also important for maintaining healthy articular cartilage. BMP2 and BMP6 are highly expressed in the superficial zone, while the BMP antagonists, gremlin and noggin, are highly expressed in the middle and deeper zones consistent with reduced levels of pSMAD1/5/8 in these zones of articular cartilage (Garrison et al., 2017). This BMP signaling gradient may maintain the function of normal articular cartilage (Garrison et al., 2017; Lui et al., 2015) and may be disrupted upon development of osteoarthritis (OA). Data in support of this hypothesis come from the observation that loss of BMP signaling results in degeneration of articular cartilage and early onset of OA in mice (Tsuji et al., 2006; Rountree et al., 2004). However, the roles of individual BMPs in joint homeostasis, independent of joint formation, remain

largely unexplored. BMP7 appears to be of particular importance for the maintenance of articular cartilage (Abula et al., 2015; Hurtig et al., 2009; Sekiya et al., 2009), but further studies are needed to separate out developmental effects from those specific to adult articular cartilage maintenance. GDF5 appears to have a fundamental role in determining joint shape, which has an important role in the development of OA (Pregizer et al., 2018; Baker-LePain & Lane, 2010). Concordantly, single-nucleotide polymorphisms (SNPs) in GDF5 have been associated with development of OA; some variants are associated with increased susceptibility, while others are associated with a lower risk of developing OA (Yin and Wang, 2017). These discrepancies highlight the complicated role that GDF5 plays in synovial joints. Since the regulation of *Gdf5* expression is complex (Chen et al., 2016; Capellini et al., 2017), it is possible that SNPs in different regions of *Gdf5* have unique effects on gene expression. A clear consensus is also lacking for the true role of BMP signaling in OA—evidence consistent with a deleterious effect is counterbalanced by data suggesting a positive therapeutic role. The ability to specifically activate or extinguish BMP signaling in adult joint tissues should begin to resolve this dilemma (Tardif et al., 2009; Leijten et al., 2013; Yu et al., 2017).

Conclusions

BMPs are involved in almost every aspect of skeletal biology. BMPs exert their effects on skeletal cells through signaling cascades that are increasingly appreciated to be tightly regulated and highly dependent on cell-type, timing, and the receptor-ligand environment. Several important questions about the role of BMP signaling in the skeleton remain to be addressed, including the ways in which BMP signaling is integrated with other signals to maintain skeletal homeostasis, and the composition of BMP ligand and receptor partners in osteoprogenitors and differentiated bone cells. With a more comprehensive understanding of BMP biology in bone, the potential for BMPs as therapeutics could be greatly maximized.

References

Annamalai, R.T., et al., 2018. Harnessing macrophage-mediated degradation of gelatin microspheres for spatiotemporal control of BMP2 release. Biomaterials 161, 216–227.

Abula, K., et al., 2015. Elimination of BMP7 from the developing limb mesenchyme leads to articular cartilage degeneration and synovial inflammation with increased age. FEBS Lett. 589 (11), 1240–1248.

Antebi, Y.E., et al., 2017. Combinatorial signal perception in the BMP pathway. Cell 170 (6), 1184–1196 e24.

Arteaga-Solis, E., et al., 2001. Regulation of limb patterning by extracellular microfibrils. J. Cell Biol. 154 (2), 275–281.

Baker-LePain, J.C., Lane, N.E., 2010. Relationship between joint shape and the development of osteoarthritis. Curr. Opin. Rheumatol. 22 (5), 538–543.

Balemans, W., Van Hul, W., 2002. Extracellular regulation of BMP signaling in vertebrates: a cocktail of modulators. Dev. Biol. 250 (2), 231–250.

Bessho, K., Iizuka, T., 1993. Changes in bone inducing activity of bone morphogenetic protein with aging. Ann. Chir. Gynaecol. Suppl. 207, 49–53.

Blokhuis, T.J., et al., 2012. BMP-7 stimulates early diaphyseal fracture healing in estrogen deficient rats. J. Orthop. Res. 30 (5), 720–725.

Boyce, B.F., et al., 2015. NF-kappaB-Mediated regulation of osteoclastogenesis. Endocrinol. Metab. (Seoul) 30 (1), 35–44.

Brunet, L.J., et al., 1998. Noggin, cartilage morphogenesis, and joint formation in the mammalian skeleton. Science 280 (5368), 1455–1457.

Canalis, E., et al., 2012. Conditional inactivation of noggin in the postnatal skeleton causes osteopenia. Endocrinology 153 (4), 1616–1626.

Canalis, E., Parker, K., Zanotti, S., 2012. Gremlin1 is required for skeletal development and postnatal skeletal homeostasis. J. Cell. Physiol. 227 (1), 269–277.

Capellini, T.D., et al., 2017. Ancient selection for derived alleles at a GDF5 enhancer influencing human growth and osteoarthritis risk. Nat. Genet. 49 (8), 1202–1210.

Chappuis, V., et al., 2012. Periosteal BMP2 activity drives bone graft healing. Bone 51 (4), 800–809.

Chen, H., et al., 2004. BMP10 is essential for maintaining cardiac growth during murine cardiogenesis. Development 131 (9), 2219–2231.

Chen, B., et al., 2007a. Activation of demineralized bone matrix by genetically engineered human bone morphogenetic protein-2 with a collagen binding domain derived from von Willebrand factor propolypeptide. J. Biomed. Mater. Res. A 80 (2), 428–434.

Chen, B., et al., 2007b. Homogeneous osteogenesis and bone regeneration by demineralized bone matrix loading with collagen-targeting bone morphogenetic protein-2. Biomaterials 28 (6), 1027–1035.

Chen, H., et al., 2016. Heads, shoulders, elbows, knees, and toes: modular Gdf5 enhancers control different joints in the vertebrate skeleton. PLoS Genet. 12 (11), e1006454.

Csiszar, A., et al., 2005. Regulation of bone morphogenetic protein-2 expression in endothelial cells: role of nuclear factor-kappaB activation by tumor necrosis factor-alpha, H2O2, and high intravascular pressure. Circulation 111 (18), 2364–2372.

Dawson, L.A., et al., 2017. The periosteal requirement and temporal dynamics of BMP2-induced middle phalanx regeneration in the adult mouse. Regeneration (Oxf) 4 (3), 140–150.

Ehnert, S., et al., 2016. Distinct gene expression patterns defining human osteoblasts' response to BMP2 treatment: is the therapeutic success all a matter of timing? Eur. Surg. Res. 57 (3–4), 197–210.

Fleet, J.C., et al., 1996. The effects of aging on the bone inductive activity of recombinant human bone morphogenetic protein-2. Endocrinology 137 (11), 4605–4610.

Freeman, T.J., et al., 2012. Smad4-mediated signaling inhibits intestinal neoplasia by inhibiting expression of beta-catenin. Gastroenterology 142 (3), 562–571 e2.

Gamer, L.W., et al., 2009. Overexpression of BMP3 in the developing skeleton alters endochondral bone formation resulting in spontaneous rib fractures. Dev. Dynam. 238 (9), 2374–2381.

Garrison, P., et al., 2017. Spatial regulation of bone morphogenetic proteins (BMPs) in postnatal articular and growth plate cartilage. PLoS One 12 (5), e0176752.

Greenblatt, M.B., Shim, J.H., Glimcher, L.H., 2010. TAK1 mediates BMP signaling in cartilage. Ann. N. Y. Acad. Sci. 1192, 385–390.

Gunnell, L.M., et al., 2010. TAK1 regulates cartilage and joint development via the MAPK and BMP signaling pathways. J. Bone Miner. Res. 25 (8), 1784–1797.

Hurtig, M., et al., 2009. BMP-7 protects against progression of cartilage degeneration after impact injury. J. Orthop. Res. 27 (5), 602–611.

Itasaki, N., Hoppler, S., 2010. Crosstalk between Wnt and bone morphogenic protein signaling: a turbulent relationship. Dev. Dynam. 239 (1), 16–33.

Kamiya, N., et al., 2008a. BMP signaling negatively regulates bone mass through sclerostin by inhibiting the canonical Wnt pathway. Development 135 (22), 3801–3811.

Kamiya, N., et al., 2008b. Disruption of BMP signaling in osteoblasts through type IA receptor (BMPRIA) increases bone mass. J. Bone Miner. Res. 23 (12), 2007–2017.

Kamiya, N., et al., 2016. Targeted disruption of BMP signaling through type IA receptor (BMPR1A) in osteocyte suppresses SOST and RANKL, leading to dramatic increase in bone mass, bone mineral density and mechanical strength. Bone 91, 53–63.

Khokha, M.K., et al., 2003. Gremlin is the BMP antagonist required for maintenance of Shh and Fgf signals during limb patterning. Nat. Genet. 34 (3), 303–307.

Larrain, J., et al., 2001. Proteolytic cleavage of Chordin as a switch for the dual activities of Twisted gastrulation in BMP signaling. Development 128 (22), 4439–4447.

Lee, J.H., et al., 2015. Effects of ovariectomy and corticosteroid-induced osteoporosis on the osteoinductivity of rhBMP-2 in a segmental long-bone defect model. Tissue Eng. 21 (15–16), 2262–2271.

Leijten, J.C., et al., 2013. GREM1, FRZB and DKK1 mRNA levels correlate with osteoarthritis and are regulated by osteoarthritis-associated factors. Arthritis Res. Ther. 15 (5), R126.

Lim, J., et al., 2015. BMP-Smad4 signaling is required for precartilaginous mesenchymal condensation independent of Sox9 in the mouse. Dev. Biol. 400 (1), 132–138.

Lowery, J.W., et al., 2015. Loss of BMPR2 leads to high bone mass due to increased osteoblast activity. J. Cell Sci. 128 (7), 1308–1315.

Lui, J.C., et al., 2015. Spatial regulation of gene expression during growth of articular cartilage in juvenile mice. Pediatr. Res. 77 (3), 406–415.

Mathavan, N., Tagil, M., Isaksson, H., 2017. Do osteoporotic fractures constitute a greater recalcitrant challenge for skeletal regeneration? Investigating the efficacy of BMP-7 and zoledronate treatment of diaphyseal fractures in an open fracture osteoporotic rat model. Osteoporos. Int. 28 (2), 697–707.

Mbalaviele, G., et al., 2005. Beta-catenin and BMP-2 synergize to promote osteoblast differentiation and new bone formation. J. Cell. Biochem. 94 (2), 403–418.

McBride, S.H., et al., 2014. Long bone structure and strength depend on BMP2 from osteoblasts and osteocytes, but not vascular endothelial cells. PLoS One 9 (5), e96862.

Mendes, L.F., et al., 2016. Combinatorial analysis of growth factors reveals the contribution of bone morphogenetic proteins to chondrogenic differentiation of human periosteal cells. Tissue Eng. C Methods 22 (5), 473–486.

Meyer, M.H., Etienne, W., Meyer Jr., R.A., 2004. Altered mRNA expression of genes related to nerve cell activity in the fracture callus of older rats: a randomized, controlled, microarray study. BMC Muscoskelet. Disord. 5, 24.

Mikic, B., 2004. Multiple effects of GDF-5 deficiency on skeletal tissues: implications for therapeutic bioengineering. Ann. Biomed. Eng. 32 (3), 466–476.

Morgan, E.F., et al., 2016. BMPR1A antagonist differentially affects cartilage and bone formation during fracture healing. J. Orthop. Res. 34 (12), 2096–2105.

Ogita, M., et al., 2008. Differentiation and proliferation of periosteal osteoblast progenitors are differentially regulated by estrogens and intermittent parathyroid hormone administration. Endocrinology 149 (11), 5713–5723.

Ohkawara, B., et al., 2002. Action range of BMP is defined by its N-terminal basic amino acid core. Curr. Biol. 12 (3), 205–209.

Olsen, O.E., et al., 2015. Activin A inhibits BMP-signaling by binding ACVR2A and ACVR2B. Cell Commun. Signal. 13, 27.

Ovchinnikov, D.A., et al., 2006. BMP receptor type IA in limb bud mesenchyme regulates distal outgrowth and patterning. Dev. Biol. 295 (1), 103–115.

Phillips, F.M., et al., 2006. In vivo BMP-7 (OP-1) enhancement of osteoporotic vertebral bodies in an ovine model. Spine J. 6 (5), 500–506.

Pountos, I., et al., 2010. The effect of bone morphogenetic protein-2, bone morphogenetic protein-7, parathyroid hormone, and platelet-derived growth factor on the proliferation and osteogenic differentiation of mesenchymal stem cells derived from osteoporotic bone. J. Orthop. Trauma 24 (9), 552–556.

Pregizer, S.K., et al., 2018. Impact of broad regulatory regions on Gdf5 expression and function in knee development and susceptibility to osteoarthritis. Ann. Rheum. Dis. 77 (3), 450.

Retting, K.N., et al., 2009. BMP canonical Smad signaling through Smad1 and Smad5 is required for endochondral bone formation. Development 136 (7), 1093–1104.

Rosen, V., Wozney, J.M., 2002. Bone morphogenetic proteins. In: Bilezikian, J.P., Raisz, L.G., Rodan, G.A. (Eds.), Principles of Bone Biology. Academic Press, San Diego, CA, pp. 919–929.

Rountree, R.B., et al., 2004. BMP receptor signaling is required for postnatal maintenance of articular cartilage. PLoS Biol. 2 (11), e355.

Salazar, V.S., et al., 2013. Postnatal ablation of osteoblast Smad4 enhances proliferative responses to canonical Wnt signaling through interactions with beta-catenin. J. Cell Sci. 126 (Pt 24), 5598–5609.

Salazar, V.S., Gamer, L.W., Rosen, V., 2016. BMP signalling in skeletal development, disease and repair. Nat. Rev. Endocrinol. 12 (4), 203–221.

Sekiya, I., et al., 2009. Periodic knee injections of BMP-7 delay cartilage degeneration induced by excessive running in rats. J. Orthop. Res. 27 (8), 1088–1092.

Selever, J., et al., 2004. Bmp4 in limb bud mesoderm regulates digit pattern by controlling AER development. Dev. Biol. 276 (2), 268–279.

Settle Jr., S.H., et al., 2003. Multiple joint and skeletal patterning defects caused by single and double mutations in the mouse Gdf6 and Gdf5 genes. Dev. Biol. 254 (1), 116–130.

Sipe, J.B., et al., 2004. Localization of bone morphogenetic proteins (BMPs)-2, -4, and -6 within megakaryocytes and platelets. Bone 35 (6), 1316–1322.

Solloway, M.J., Robertson, E.J., 1999. Early embryonic lethality in Bmp5;Bmp7 double mutant mice suggests functional redundancy within the 60A subgroup. Development 126 (8), 1753–1768.

Solloway, M.J., et al., 1998. Mice lacking Bmp6 function. Dev. Genet. 22 (4), 321–339.

Susperregui, A.R., et al., 2008. BMP-2 regulation of PTHrP and osteoclastogenic factors during osteoblast differentiation of C2C12 cells. J. Cell. Physiol. 216 (1), 144–152.

Tan, X., et al., 2007. Smad4 is required for maintaining normal murine postnatal bone homeostasis. J. Cell Sci. 120 (Pt 13), 2162–2170.

Tang, Y., et al., 2008. Combination of bone tissue engineering and BMP-2 gene transfection promotes bone healing in osteoporotic rats. Cell Biol. Int. 32 (9), 1150–1157.

Tarapore, R.S., et al., 2016. NF-kappaB has a direct role in inhibiting Bmp- and Wnt-induced matrix protein expression. J. Bone Miner. Res. 31 (1), 52–64.

Tardif, G., et al., 2009. The BMP antagonists follistatin and gremlin in normal and early osteoarthritic cartilage: an immunohistochemical study. Osteoarthritis Cartilage 17 (2), 263–270.

Tsuji, K., et al., 2006. BMP2 activity, although dispensable for bone formation, is required for the initiation of fracture healing. Nat. Genet. 38 (12), 1424–1429.

Yamazaki, M., et al., 2009. Tumor necrosis factor alpha represses bone morphogenetic protein (BMP) signaling by interfering with the DNA binding of Smads through the activation of NF-kappaB. J. Biol. Chem. 284 (51), 35987–35995.

Yan, H.J., et al., 2018. Synthetic design of growth factor sequestering extracellular matrix mimetic hydrogel for promoting in vivo bone formation. Biomaterials 161, 190–202.

Yang, W., et al., 2013. Bmp2 in osteoblasts of periosteum and trabecular bone links bone formation to vascularization and mesenchymal stem cells. J. Cell Sci. 126 (Pt 18), 4085–4098.

Yin, Y., Wang, Y., 2017. Association of BMP-14 rs143383 ploymorphism with its susceptibility to osteoarthritis: a meta-analysis and systematic review according to PRISMA guideline. Medicine (Baltim.) 96 (42), e7447.

Yu, Y.Y., et al., 2010a. Bone morphogenetic protein 2 stimulates endochondral ossification by regulating periosteal cell fate during bone repair. Bone 47 (1), 65–73.

Yu, Y.Y., et al., 2010b. Immunolocalization of BMPs, BMP antagonists, receptors, and effectors during fracture repair. Bone 46 (3), 841–851.

Yu, X., et al., 2017. Expression of Noggin and Gremlin1 and its implications in fine-tuning BMP activities in mouse cartilage tissues. J. Orthop. Res. 35 (8), 1671–1682.

Zhang, J., et al., 2005. Smad4 is required for the normal organization of the cartilage growth plate. Dev. Biol. 284 (2), 311–322.

Zhao, G.Q., Liaw, L., Hogan, B.L., 1998. Bone morphogenetic protein 8A plays a role in the maintenance of spermatogenesis and the integrity of the epididymis. Development 125 (6), 1103–1112.

Zhao, Y., et al., 2009. The bone-derived collagen containing mineralized matrix for the loading of collagen-binding bone morphogenetic protein-2. J. Biomed. Mater. Res. A 88 (3), 725–734.

Chapter 49

Extraskeletal effects of RANK ligand

Andy Göbel[1,2], Tilman D. Rachner[1,2,3] and Lorenz C. Hofbauer[1,3,4]

[1]*Department of Medicine III, Technische Universität Dresden, Dresden, Germany;* [2]*German Cancer Consortium (DKTK), Partner site Dresden and German Cancer Research Center (DKFZ), Heidelberg, Germany;* [3]*Center for Healthy Aging and Division of Endocrinology, Diabetes, and Bone Diseases, Technische Universität Dresden, Dresden, Germany;* [4]*Center for Regenerative Therapies Dresden, Dresden, Germany*

Chapter outline

The role of RANKL in mammary gland development and tumorigenesis

RANKL in the lactating mammary gland

One of the first studies to demonstrate the potential extraskeletal effects of receptor activator of nuclear factor-κB ligand (RANKL) was on its expression in several murine tissues, such as the brain, heart, kidney, muscle, skin, and spleen (Kartsogiannis et al., 1999). Studies using RANKL-deficient mice were key to establishing its role in bone, but importantly also pointed to a role in mammary gland physiology (Fig. 49.1).

The development of a lactating mammary gland during pregnancy is essential for the nutrition, passive immunity, and survival of the newborn. The mammary ductal and alveolar epithelium undergoes expansion and proliferation to increase ductal side branching and to form lobuloalveolar structures. This process of cellular development arrests in pregnant *RANKL*$^{-/-}$ mice before the final differentiation of lobuloalveolar mammary structures (Fata et al., 2000). In line with this finding, mouse mammary glands overexpressing RANK display increased proliferation and decreased apoptosis (Gonzalez-Suarez et al., 2007). In addition, newborn *RANKL*$^{-/-}$ pups die due to an incomplete composition of milk lacking milk proteins such as β-casein. These detrimental effects can be rescued by administration of recombinant RANKL. Mechanistically, progesterone, prolactin, and parathyroid hormone−related peptide, which are upregulated during pregnancy and important for lactation, induce RANKL expression in mammary epithelial cells (Fata et al., 2000). The induction of proliferation by progesterone is mediated both directly in progesterone receptor−positive epithelial cells and indirectly by a paracrine mechanism involving RANKL in those cells that lack this receptor (Beleut et al., 2010). Progesterone also mediates the expansion of mammary stem cells during the reproductive cycle, at least partially by RANKL serving as a paracrine effector (Joshi et al., 2010). The concerted regulation of the RANKL/progesterone axis on mammary tissue architecture has been confirmed for human breast using an ex vivo system with mammoplasty specimens (Tanos et al., 2013).

RANKL in breast cancer development and metastasis

Mammary gland epithelium is the predominant site for the development of breast cancer (Hinck and Näthke, 2014). As RANKL supports mammary gland differentiation during pregnancy and is controlled by sex hormones, subsequent studies focused on hormone-driven mammary tumor models. The RANKL receptor, RANK, was found to be expressed on

Principles of Bone Biology. https://doi.org/10.1016/B978-0-12-814841-9.00049-X

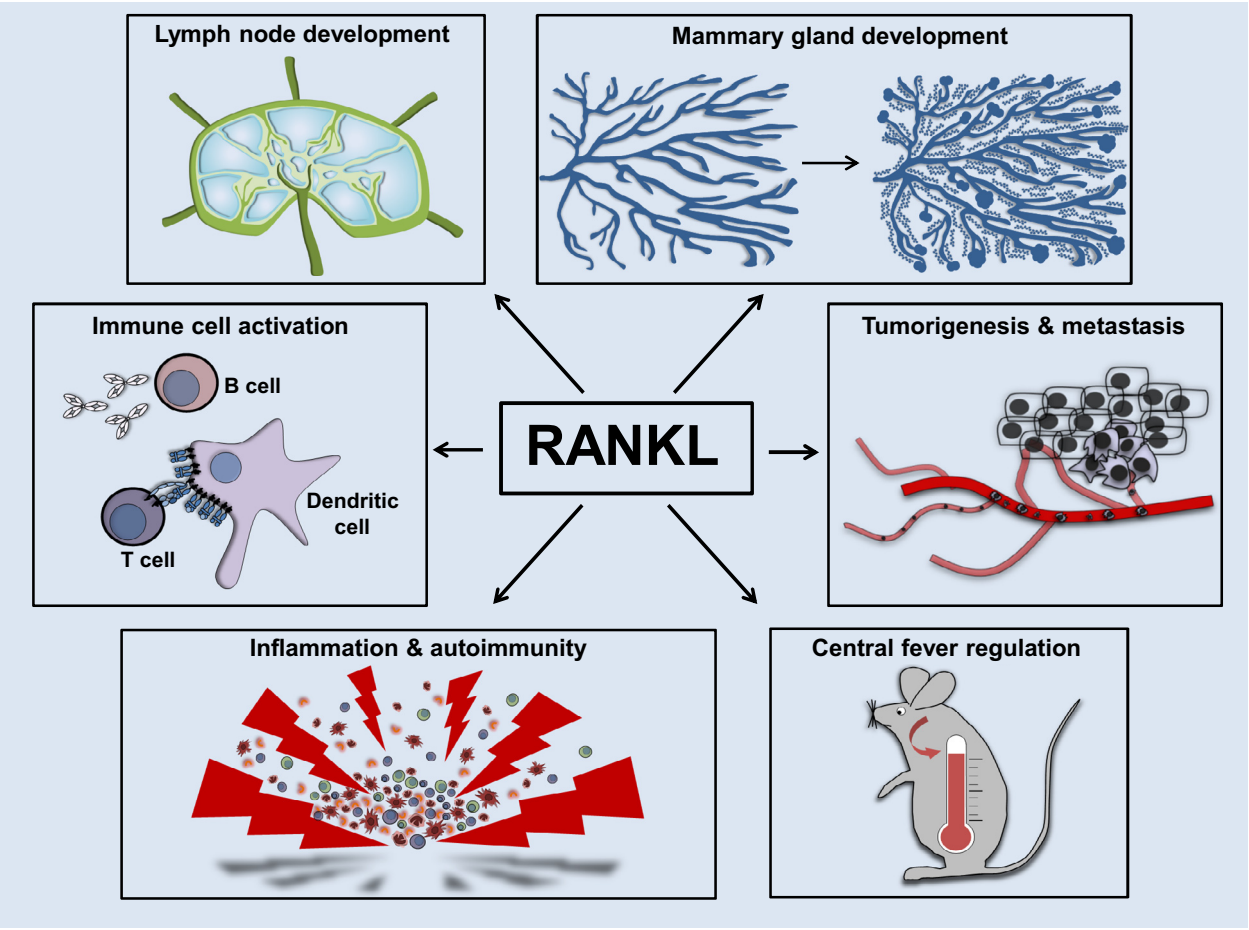

FIGURE 49.1 Nonskeletal effects of receptor activator of nuclear factor-κB ligand (*RANKL*). Despite its central role in bone physiology, RANKL has pleiotropic nonskeletal effects in mammary gland and lymph node development, tumorigenesis and metastasis, and central fever regulation as well as in inflammation and autoimmunity.

primary breast cancer cells, and treatment with recombinant RANKL enhanced migration of both normal and malignant mammary epithelial cells (Jones et al., 2006). The synthetic progesterone medroxyprogesterone acetate was shown to massively induce RANKL expression in mammary epithelial cells and to trigger carcinogenesis when combined with tumorigenic agents, such as the DNA-damaging agent 7,12-dimethylbenz[*a*]anthracene. The development of tumors was significantly suppressed in mice in which RANK was genetically inactivated in mammary epithelial cells (Schramek et al., 2010). The contribution of RANKL to mammary tumorigenesis was conclusively established by similar work in which RANKL signaling was inhibited by the pharmacological inhibitor RANK-Fc. These studies highlighted RANKL's role in promoting initial steps in breast cancer development (Gonzalez-Suarez et al., 2010) and led to further studies in humans.

In line with the findings of Schramek et al. and Gonzalez-Suarez et al., postmenopausal women with high serum progesterone and RANKL are at increased risk of developing breast cancer (Kiechl et al., 2017). Remarkably, RANK expression in primary human breast cancer is associated with an increased sensitivity to chemotherapy, but RANK is also a predictor of relapse and poor survival (Pfitzner et al., 2014). In addition, RANK expression in primary human breast tumors is a predictive marker for the occurrence of bone metastases and skeletal disease-free survival (Santini et al., 2011). Data indicate that the contribution of RANKL signaling to mammary tumorigenesis is not limited to hormone-dependent cancer cells. Triple-negative breast cancers (TNBCs) have a high propensity to relapse, to metastasize, and to resist multimodal therapies. The dual expression of RANK and RANKL in these patients has been shown to be associated with a poorer recurrence-free and overall survival compared with patients with RANK-positive RANKL-negative TNBCs (Reyes et al., 2017).

Further investigations were conducted in hereditary forms of breast cancer: women carrying *BRCA1/2* mutations have an increased risk of developing breast cancer (Robson and Offit, 2007). Mechanistic studies have shown that the progesterone receptor in mammary epithelial cells that lack a functional BRCA1 is stabilized, and progesterone serves as a

mitogen in these cells (Poole et al., 2006). The dysregulation of osteoprotegerin (OPG), the natural decoy receptor of RANKL, might mediate the relationship between progesterone and the breast cancer risk in *BRCA1* mutation carriers. Here, the presence of progesterone was associated with low serum OPG levels, which in turn showed an inverse correlation with breast cancer risk. Reduced OPG was hypothesized to increase the net RANKL signaling in the mammary tissue (Widschwendter et al., 2015; Rachner and Rauner, 2015).

The contribution of RANKL to mammary tumorigenesis appears to be even more complex, as tumor-infiltrating regulatory T cells (Tregs) support pulmonary metastasis by producing RANKL in mammary carcinoma cells overexpressing the protooncogene *Erbb2* (Tan et al., 2011). In addition, novel RANK isoforms have been identified through alternative splicing, one of which was shown to impair cell survival and migration of invasive breast cancer cells (Papanastasiou et al., 2012).

In summary, these results confirm a role for the RANKL system in breast cancer (Fig. 49.1) and make it a chemotherapeutic target (Infante et al., 2019).

The role of RANKL in other malignancies

The central function of RANKL in bone homeostasis and bone-metastatic malignancies (summarized in Chapter 73) has led to investigations using other osteotropic cancer models. RANKL supports the migration of clear cell renal cell carcinomas, and elevated RANKL serum levels are an independent predictor for recurrence and poor prognosis (Mikami et al., 2009). In prostate cancer, RANKL is associated with enhanced epithelial−mesenchymal transition (EMT), a process that favors the migratory and metastatic potential of tumor cells, thereby potentially serving as a link between primary tumor and the formation of bone metastases (Odero-Marah et al., 2008). A supportive role of RANKL has also been confirmed for hepatocellular carcinoma. Here, RANKL is increased in patient-derived tumor specimens and favors EMT, migration, and invasion involving an NF-κB-dependent mechanism (Song et al., 2014).

The RANKL/RANK system has been studied in other human cancer subtypes, including bladder, colon, and cervical cancer; lymphoma; myeloma; and thyroid cancer. These studies revealed a wide distribution of either RANK or RANKL, or both, within tumor tissue and confirmed the principle of RANKL-induced cancer cell migration (reviewed in Renema et al., 2016). In addition to migration, RANKL promotes angiogenesis in cooperation with vascular endothelial growth factor, which increases RANK in endothelial cells. RANKL enhances their survival and the production of inflammatory cell adhesion molecules as well as in vitro and in vivo angiogenesis (Min et al., 2007).

Functions of RANKL in immune and thermal regulation

A number of studies in the last 10 years have contributed to an enhanced understanding of the functions of RANKL beyond its key role in bone homeostasis. The identification of cross talk between bone and other organ systems led to the emergence of new concepts and research fields such as osteoimmunology and osteohematology in which the RANKL/RANK/OPG system links bone with the immune system and hematopoiesis (Takayanagi, 2007; Bulycheva et al., 2015).

Immune system development and thermoregulation

RANKL-deficient mice lack lymph nodes and have an impaired early differentiation of B and T lymphocytes (Fig. 49.1) (Kong et al., 1999). These mice also show a marked decrease of microfold cells (M cells) and cryptopatches. M cells are specialized epithelial cells situated over Peyer patches, which are important for the sampling of potential antigens (e.g., bacteria) from the intestinal lumen (Knoop et al., 2009). Cryptopatches are an organized lymphoid system in the intestine, which contains RANKL-expressing stromal cells. RANKL-deficient mice show no B cell development in these cryptopatches of the small intestine (Knoop et al., 2011). In addition, RANKL is implicated in the development of medullary thymic epithelial cells, which are important for central tolerance and protecting the body from self-reactive T cells. Consequently, central tolerance limits the generation of tumor-specific T cells. The blockade of RANKL was able to rescue melanoma-specific T cells from thymic selection and to enhance antitumor immunity (Khan et al., 2014). Furthermore, RANKL supports the survival of dendritic cells, their interaction with T cells (Wong et al., 1997), and their potential to stimulate T cell proliferation (Anderson et al., 1997).

In humans, mutations of the RANK gene *TNFRSF11A* lead to an impairment of immunoglobulin production by B cells (Guerrini et al., 2008). However, in patients exposed to RANKL-blocking antibodies, no specific immune disturbances have been described, including no effects on normal B-cell physiology (Nagy and Penninger, 2015), lack of opportunistic infections (Watts et al., 2017), and normal response to influenza infection (Miller et al., 2007).

Apart from the immune system, RANKL and RANK are both expressed in the brain (Kartsogiannis et al., 1999), where they play an essential role in the regulation of central fever. Intracerebroventricular injections of RANKL induce a strong fever response in mice and rats (Fig. 49.1), which is reversible by OPG. RANKL specifically stimulates thermoregulatory brain regions and induces fever by activation of prostaglandins. By contrast, intraperitoneal injections of RANKL have no impact on body temperature. Hence, the fever response requires only central RANKL/RANK signaling. In line with this, patients suffering from a severe form of autosomal-recessive osteopetrosis due to RANK mutations fail to develop fever during pneumonia (Hanada et al., 2009). Hence, the RANKL/RANK axis is an important thermoregulatory system. Apart from this very rare disease, it is important to note that RANKL blockade has not been linked to altered thermoregulation in humans.

Inflammation, autoimmunity, and antitumor effects

A disturbance of the RANKL/RANK/OPG system is a common characteristic of inflammatory diseases. Inflammation is a tightly controlled defense strategy to protect the host from pathogens. The failure to resolve this inflammatory process leads to a chronic setting associated with tissue damage and an increased risk of developing secondary complications (Schett and Neurath, 2018). RANKL exerts pleiotropic effects in normal and pathological inflammatory conditions. In inflammatory bowel disease, such as Crohn's disease and ulcerative colitis, the RANKL/OPG system is activated and seems to contribute to bone loss in affected patients (Moschen et al., 2005). Furthermore, patients suffering from systemic lupus erythematosus (SLE) display an increased ratio of soluble RANKL/OPG levels, which may contribute to the lower bone mineral density in these patients. SLE is a complex disease, characterized by systemic chronic inflammation and multiple tissue damage (Carmona-Fernandes et al., 2011). In chronic obstructive pulmonary disease (COPD), osteoporosis is a common co-morbidity. In COPD patients with lower bone mineral density, RANKL and RANKL/OPG ratios are increased, a potential link between inflammation and bone loss. During intestinal inflammation, mediated by autoreactive T cells, dendritic cell survival is enhanced by RANKL, and its neutralization by recombinant OPG decreases inflammation and associated bone abnormalities (Ashcroft et al., 2003). In addition, in rheumatoid arthritis, T cells in arthritic joints express RANKL and promote RANKL production in osteoblasts by the release of inflammatory cytokines as a self-amplifying effect, thereby promoting bone destruction (Holstead Jones et al., 2002).

Whereas the former studies present disease-promoting effects of RANKL, other investigations report that RANKL protects from autoimmunity and excessive inflammation. Using a cytotoxic T cell−mediated model of type 1 diabetes, RANKL signaling has been demonstrated to be essential for the generation and activation of Tregs, which prevent β-cell destruction in Langerhans islets (Green et al., 2002). During skin inflammation, RANKL is expressed in keratinocytes and alters the function of epidermal dendritic cells as well as increasing Tregs, thereby mediating immunosuppression and reduction of contact hypersensitivity responses (Loser et al., 2006). The same group demonstrated that RANK/RANKL signaling in the skin is involved in inducing and sustaining a cytotoxic T cell−mediated immune response against herpes simplex virus by supporting antigen transport to lymph nodes, improving dendritic cell function and preventing their apoptosis (Klenner et al., 2015). Furthermore, RANKL signaling supports the function of Tregs in limiting the excess of mucosal inflammation during colitis (Totsuka et al., 2009). Whether an increased incidence of skin eczema and cellulitis after treatment with RANKL antibodies in humans (Cummings et al., 2009) is linked to these mechanisms is unclear. Of note, the induction of Tregs is considered a limiting factor in the effectiveness of antitumor therapies, as they are used by tumors as an immune escape mechanism. Data demonstrated that the combination of immunotherapy (e.g., checkpoint inhibitors such as anti-CTLA-4) can be potentiated by the blockade of RANKL (van Dam et al., 2019). In a clinical case of metastatic melanoma, the concomitant administration of denosumab and the anti-CTLA-4 antibody ipilimumab led to a dramatic partial response including pain resolution (Smyth et al., 2016).

These results emphasize a regulatory role of the RANKL/RANK system in human immunity (Fig. 49.1) and should pave the way to clinical studies investigating the potential of its therapeutic modification in inflammatory and autoimmune diseases as well as a strategy to improve the immunotherapy of a variety of disorders.

References

Anderson, D.M., Maraskovsky, E., Billingsley, W.L., Dougall, W.C., Tometsko, M.E., Roux, E.R., et al., 1997. A homologue of the TNF receptor and its ligand enhance T-cell growth and dendritic-cell function. Nature 390, 175−179.

Ashcroft, A., Cruickshank, S., Croucher, P., Perry, M., Rollinson, S., Lippitt, J.M., et al., December 2003. Colonic dendritic cells, intestinal inflammation, and T cell-mediated bone destruction are modulated by recombinant osteoprotegerin. Immunity 19, 849−861.

Beleut, M., Devi, R., Caikovski, M., Ayyanan, A., Germano, D., 2010. Two distinct mechanisms underlie progesterone- induced proliferation in the mammary gland. Proc. Natl. Acad. Sci. Unit. States Am. 107, 2989−2994.

Bulycheva, E., Rauner, M., Medyouf, H., Theurl, I., Bornhäuser, M., Hofbauer, L.C., et al., 2015. Myelodysplasia is in the niche : novel concepts and emerging therapies. Leukemia 29, 259−268.

Carmona-Fernandes, D., Santos, M.J., Perpétuo, I.P., Fonseca, J.E., Canhão, H., 2011. Soluble receptor activator of nuclear factor κB ligand/osteoprotegerin ratio is increased in systemic lupus erythematosus patients. Arthritis Res. Ther. 13, R175.

Cummings, S.R., San Martin, J., McClung, M.R., Siris, E.S., Eastell, R., Reid, I.R., et al., August 2009. Denosumab for prevention of fractures in postmenopausal women with osteoporosis. N. Engl. J. Med. 361 (8), 756−765.

Fata, J.E., Kong, Y.Y., Li, J., Sasaki, T., Irie-Sasaki, J., Moorehead, R.A., et al., 2000. The osteoclast differentiation factor osteoprotegerin-ligand is essential for mammary gland development. Cell 103, 41−50.

Gonzalez-Suarez, E., Branstetter, D., Armstrong, A., Dinh, H., Blumberg, H., Dougall, W.C., 2007. RANK overexpression in transgenic mice with mouse mammary tumor virus promoter-controlled RANK increases proliferation and impairs alveolar differentiation in the mammary epithelia and disrupts lumen formation in cultured epithelial acini. Mol. Cell Biol. 27, 1442−1454.

Gonzalez-Suarez, E., Jacob, A.P., Jones, J., Miller, R., Roudier-meyer, M.P., Erwert, R., et al., 2010. RANK ligand mediates progestin-induced mammary epithelial proliferation and carcinogenesis. Nature 468, 103−107.

Green, E.A., Choi, Y., Flavell, R.A., Haven, N., 2002. Pancreatic lymph node-derived $CD4^+$ $CD25^+$ treg Cells : highly potent regulators of diabetes that require TRANCE-RANK signals. Immunity 16, 183−191.

Guerrini, M.M., Sobacchi, C., Cassani, B., Abinun, M., Kilic, S.S., Pangrazio, A., et al., 2008. Human osteoclast-poor osteopetrosis with hypogammaglobulinemia due to TNFRSF11A (RANK) mutations. Am. J. Hum. Genet. 83, 64−76.

Hanada, R., Leibbrandt, A., Hanada, T., Kitaoka, S., Furuyashiki, T., Fujihara, H., et al., 2009. Central control of fever and female body temperature by RANKL/RANK. Nature 462, 505−509.

Hinck, L., Näthke, I., 2014. Changes in cell and tissue organization in cancer of the breast and colon. Curr. Opin. Cell Biol. 0, 87−95.

Holstead Jones, D., Kong, Y., Penninger, J.M., 2002. Role of RANKL and RANK in bone loss and arthritis. Ann. Rheum. Dis. 61, 32−39.

Infante, M., Fabi, A., Cognetti, F., Gorini, S., Caprio, M., Fabbri, A., 2019. RANKL/RANK/OPG system beyond bone remodeling : involvement in breast cancer and clinical perspectives. J. Exp. Clin. Cancer Res. 2, 1−18.

Jones, D.H., Nakashima, T., Sanchez, O.H., Kozieradzki, I., Komarova, S.V., Sarosi, I., et al., 2006. Regulation of cancer cell migration and bone metastasis by RANKL. Nature 440, 692−696.

Joshi, P.A., Jackson, H.W., Beristain, A.G., Di Grappa, M.A., Mote, P.A., Clarke, C.L., et al., 2010. Progesterone induces adult mammary stem cell expansion. Nature 465, 803−807.

Kartsogiannis, V., Zhou, H., Horwood, N.J., Thomas, R.J., Hards, D.K., Quinn, J.M., et al., 1999. Localization of RANKL (receptor activator of NF kappa B ligand) mRNA and protein in skeletal and extraskeletal tissues. Bone 25, 525−534.

Khan, I.S., Mouchess, M.L., Zhu, M., Conley, B., Fasano, K.J., Hou, Y., et al., 2014. Enhancement of an anti-tumor immune response by transient blockade of central T cell tolerance. J. Exp. Med. 211, 761−768.

Kiechl, S., Schramek, D., Widschwendter, M., Zaikin, A., Jones, A., Jaeger, B., et al., 2017. Aberrant regulation of RANKL/OPG in women at high risk of developing breast cancer. Oncotarget 8, 3811−3825.

Klenner, L., Hafezi, W., Clausen, B.E., Lorentzen, E.U., Luger, T.A., Beissert, S., et al., 2015. Cutaneous RANK − RANKL signaling upregulates CD8-mediated antiviral immunity during Herpes simplex virus infection by preventing virus-induced Langerhans cell apoptosis. J. Investig. Dermatol. 135, 2676−2687.

Knoop, K.A., Kumar, N., Butler, B.R., Sakthivel, S.K., Taylor, R.T., Akiba, H., et al., 2009. RANKL is necessary and sufficient to initiate development of Antigen-Sampling M Cells in the Intestinal Epithelium 1. J. Immunol. 183, 5738−5747.

Knoop, K.A., Butler, B.R., Kumar, N., Newberry, R.D., Williams, I.R., 2011. Distinct developmental requirements for isolated lymphoid follicle formation in the small and large intestine RANKL is essential only in the small intestine. AJPA 179, 1861−1871.

Kong, Y.Y., Yoshida, H., Sarosi, I., Tan, H.L., Timms, E., Capparelli, C., et al., January 1999. OPGL is a key regulator of osteoclastogenesis, lymphocyte development and lymph-node organogenesis. Nature 397, 315−323.

Loser, K., Mehling, A., Loeser, S., Apelt, J., Kuhn, A., Grabbe, S., et al., 2006. Epidermal RANKL controls regulatory T-cell numbers via activation of dendritic cells. Nat. Med. 12, 1372−1379.

Mikami, S., Katsube, K., Oya, M., Ishida, M., Kosaka, T., Mizuno, R., et al., 2009. Increased RANKL expression is related to tumour migration and metastasis of renal cell carcinomas. J. Pathol. 218, 530−539.

Miller, R.E., Branstetter, D., Armstrong, A., Kennedy, B., Jones, J., Cowan, L., et al., 2007. Receptor activator of NF-κ B ligand inhibition suppresses bone resorption and hypercalcemia but does not affect host immune responses to influenza infection. J. Immunol. 179, 266−274.

Min, J., Cho, Y., Choi, J., Kim, Y., Kim, J.H., Yu, Y.S., et al., 2007. Receptor activator of nuclear factor (NF)−kappaB ligand (RANKL) increases vascular permeability : impaired permeability and angiogenesis in eNOS-deficient mice. Blood 109, 1495−1503.

Moschen, A., Kaser, A., Enrich, B., Ludwiczek, O., Gabriel, M., Obrist, P., et al., 2005. The RANKL/OPG system is activated in inflammatory bowel disease and relates to the state of bone loss. Gut 54, 479−487.

Nagy, V., Penninger, J.M., 2015. The RANKL-RANK story. Gerontology 61, 534−542.

Odero-Marah, V.A., Wang, R., Chu, G., Zayzafoon, M., Xu, J., Shi, C., et al., 2008. Receptor activator of NF-κB Ligand (RANKL) expression is associated with epithelial to mesenchymal transition in human prostate cancer cells. Cell Res. 18, 858−870.

Papanastasiou, A.D., Sirinian, C., Kalofonos, H.P., 2012. Identification of novel human receptor activator of nuclear factor-kB isoforms generated through alternative splicing : implications in breast cancer cell survival and migration. Breast Cancer Res. 14, 1−16.

Pfitzner, B.M., Branstetter, D., Loibl, S., Denkert, C., Lederer, B., Schmitt, W.D., et al., 2014. RANK expression as a prognostic and predictive marker in breast cancer. Breast Canc. Res. Treat. 145, 307−315.

Poole, A.J., Li, Y., Kim, Y., Lin, S.J., Lee, W., 2006. Prevention of Brca1 -mediated mammary tumorigenesis in mice by a progesterone antagonist. Science 66, 1467−1471.

Rachner, T.D., Rauner, M., 2015. RANKL/OPG in breast cancer — extending its territory to BRCA mutation carriers. EBIOM 2, 1270−1271.

Renema, N., Navet, B., Heymann, D., 2016. RANK − RANKL signalling in cancer. Biosci. Rep. 36, 1−17.

Reyes, M.E., Fujii, T., Branstetter, D., Krishnamurthy, S., Reuben, J.M., 2017. Poor prognosis of patients with triple-negative breast cancer can be stratified by RANK and RANKL dual expression. Breast Canc. Res. Treat. 164, 57−67.

Robson, M., Offit, K., 2007. Management of an inherited predisposition to breast cancer. N. Engl. J. Med. 375, 154−162.

Santini, D., Schiavon, G., Vincenzi, B., Gaeta, L., Pantano, F., Russo, A., et al., 2011. Receptor activator of NF-kB (RANK) expression in primary tumors associates with bone metastasis occurrence in breast cancer patients. PLoS One 6, e19234.

Schett, G., Neurath, M.F., 2018. Resolution of chronic inflammatory disease: universal and tissue-specific concepts. Nat. Commun. 9, 1−8.

Schramek, D., Leibbrandt, A., Sigl, V., Kenner, L., Pospisilik, J.A., Lee, H.J., et al., 2010. Osteoclast differentiation factor RANKL controls development of progestin-driven mammary cancer. Nature 468, 98−102.

Smyth, M.J., Yagita, H., McArthur, G.A., 2016. Combination anti-CTLA-4 and anti-RANKL in metastatic melanoma. J. Clin. Oncol. 34, 104−106.

Song, F., Duan, M., Liu, L., Wang, Z., Shi, J., Yang, L., et al., 2014. RANKL promotes migration and invasion of hepatocellular carcinoma cells via NF- k B-mediated epithelial-mesenchymal transition. PLoS One 9, 1−7.

Takayanagi, H., 2007. Osteoimmunology : shared mechanisms and crosstalk between the immune and bone systems. Nat. Rev. Immunol. 7, 292−304.

Tan, W., Zhang, W., Strasner, A., Grivennikov, S., Cheng, J.Q., Hoffman, R.M., et al., 2011. Tumour-infiltrating regulatory T cells stimulate mammary cancer metastasis through RANKL−RANK signalling. Nature 470, 548−553.

Tanos, T., Sflomos, G., Echeverria, P.C., Ayyanan, A., Gutierrez, M., Delaloye, J., et al., 2013. Progesterone/RANKL is a major regulatory Axis in the human breast. Sci. Transl. Med. 182, 1−10.

Totsuka, T., Kanai, T., Nemoto, Y., Okamoto, R., Tsuchiya, K., Sakamoto, N., et al., 2009. RANK-RANKL signaling pathway is critically involved in the function of CD4+ CD25+ regulatory T cells in chronic colitis. J. Immunol. 182, 6079−6087.

van Dam, P.A., Verhoeven, Y., Trinh, X.B., Wouters, A., Lardon, F., Prenen, H., et al., 2019. RANK/RANKL signaling inhibition may improve the effectiveness of checkpoint blockade in cancer treatment. Crit. Rev. Oncol.Hematol. 133, 85−91.

Watts, N.B., Brown, J.P., Papapoulos, S., Lewiecki, E.M., Kendler, D.L., Dakin, P., et al., 2017. Safety observations with 3 years of denosumab Exposure : comparison between subjects who received denosumab during the randomized FREEDOM trial and subjects who crossed over to denosumab during the FREEDOM extension. J. Bone Miner. Res. 32, 1481−1485.

Widschwendter, M., Burnell, M., Fraser, L., Rosenthal, A.N., Philpott, S., Reisel, D., et al., 2015. Osteoprotegerin (OPG), the endogenous inhibitor of receptor activator of NF- κ B ligand (RANKL), is dysregulated in BRCA mutation carriers. EBIOM 2, 1331−1339.

Wong, B.B.R., Josien, R., Lee, S.Y., Sauter, B., Li, H., Steinman, R.M., et al., 1997. Activation-induced cytokine, a new TNF family member cell − specific survival factor. J. Exp. Med. 186, 2075−2080.

Chapter 50

Local regulators of bone

Interleukin-1, tumor necrosis factor, interferons, the IL-6 family, and additional cytokines

Natalie A. Sims[1] **and Joseph A. Lorenzo**[2]

[1]*St. Vincent's Institute of Medical Research, Melbourne, Australia; Department of Medicine at St. Vincent's Hospital, The University of Melbourne, Melbourne, Australia;* [2]*The Departments of Medicine and Orthopaedics, UConn Health, Farmington, CT, United States*

Chapter outline

Introduction

Bone development, bone growth, and the bone remodeling cycle are regulated by a variety of factors (e.g., hormones, cytokines, growth factors, and physical force). These are produced both locally and systemically and act in concert to direct local rates of bone resorption and formation. Many studies of the mechanisms regulating bone resorption and formation have concentrated on the role of cytokines because these factors appear to have crucial roles in both normal and pathological bone cell function. A variety of cytokines originally identified by their ability to regulate immune and hematopoietic cells are produced in the bone microenvironment either spontaneously or in response to specific stimuli. It has become apparent that during both health and disease, the production of cytokines by cells in the bone microenvironment and the responses of bone cells to these cytokines are regulated in a highly ordered manner. It is

Principles of Bone Biology. https://doi.org/10.1016/B978-0-12-814841-9.00050-6

hypothesized that the spectrum of cytokines that are produced in bone defines the responses of bone cells to a particular state and predicts the subsequent development of normal and pathological bone. Diseases of bone where cytokines are believed to play an important role include osteoporosis, Paget's disease, periodontal disease, inflammatory arthritis, and the effects of malignancy on bone. Studies of the production of cytokines in bone and the responses of bone cells to these cytokines provide insights into not only normal physiological mechanisms, but also mechanisms that regulate the development of these diseases and could lead to new therapies for these conditions. The following is a broad overview of the actions of a number of cytokines on bone and the mechanisms by which bone cells respond to these cytokines.

Interleukin-1

Interleukin-1 (IL-1) is a cytokine with a wide variety of activities. It comprises two gene products, IL-1α and IL-1β, with identical activities (Dinarello, 1991). IL-1 is a potent stimulator of in vitro bone resorption (Lorenzo et al., 1987) and has powerful in vivo actions (Sabatini et al., 1988). Its effects on resorption appear to be both direct on osteoclasts (Jimi et al., 1999) and indirect through its ability to stimulate RANKL production (Hofbauer et al., 1999). In addition, both RANKL- and 1,25-dihydroxyvitamin D_3-stimulated osteoclast formation in vitro were found to be mediated in part by IL-1 production (Lee et al., 2002a, 2005a; Nakamura and Jimi, 2006). IL-1 also increases prostaglandin synthesis in bone (Lorenzo et al., 1987; Sato et al., 1986), which may enhance its resorptive activity because prostaglandins are potent resorption stimuli (Klein and Raisz, 1970). Importantly, the rate at which IL-1 enhances RANKL-induced osteoclastogenesis is partially dependent on the type of osteoclast precursor examined (Cao et al., 2016).

In mouse models, IL-1 appears to be involved in normal growth plate development (Simsa-Maziel et al., 2013) and bone remodeling (Lee et al., 2010). It also may be essential for the systemic bone loss seen in some inflammatory conditions due to high tumor necrosis factor (TNF) production (Polzer et al., 2010). In addition, it mediates some effects of estrogen withdrawal on bone loss in mice (Lorenzo et al., 1998) and humans (Charatcharoenwitthaya et al., 2007), potentially through effects on p38α MAPK (Thouverey and Caverzasio, 2015). In humans, serum IL-1 levels have been linked to measurements of bone mass (Ivanova et al., 2012; Zupan et al., 2012) and bone turnover (Al-Daghri et al., 2017).

IL-1 is produced in bone (Lorenzo et al., 1990), and its activity is present in bone marrow serum (Kawaguchi et al., 1995; Miyaura et al., 1995). One source of bone cell-derived IL-1 is osteoclast precursor cells, which produce IL-1 when they interact with bone matrix (Yao et al., 2008). A natural inhibitor of IL-1, IL-1 receptor antagonist, is an analogue of IL-1 that binds but does not activate the biologically important type I IL-1 receptors (Arend et al., 1990; Eisenberg et al., 1990; Hannum et al., 1990).

There are two receptors for IL-1, type I and type II (Dinarello, 1993). All known biologic responses to IL-1 are mediated exclusively through the type I receptor (Sims et al., 1993). IL-1 receptor type I requires interaction with a second protein, IL-1 receptor accessory protein, to generate postreceptor signals (Huang et al., 1997; Korherr et al., 1997; Wesche et al., 1997). Signaling through type I receptors involves activation of specific TRAFs and NF-κB (Eder, 1997; Martin and Falk, 1997). IL-1 receptor type II is a decoy receptor that prevents activation of type I receptors (Colotta et al., 1993). One report found a decrease in the bone mass of mice deficient in the bioactive type I IL-1 receptor (Bajayo et al., 2005). However, this has not been our experience (Vargas et al., 1996).

Expression of myeloid differentiation factor 88 (MyD88), but not Toll/IL-1 receptor domain-containing adaptor inducing interferon-beta, was necessary for IL-1 to stimulate RANKL production in osteoblasts and prolong the survival of osteoclasts (Sato et al., 2004). Survival of osteoclasts by treatment with IL-1 appears to require PI3-kinase/AKT and ERK (Lee et al., 2002c).

The effects of IL-1 on bone in inflammatory states, such as rheumatoid arthritis, are multiple and mediated by both direct and indirect mechanisms. IL-1 stimulates bone resorption and inhibits bone formation through, respectively, its effects on osteoclasts and osteoblasts (Boyce et al., 1989; Canalis, 1986; Tsuboi et al., 1999). In addition, it stimulates the production of a variety of secondary factors in the bone microenvironment including prostaglandins and GM-CSF, which have complex effects of their own on bone cells (Niki et al., 2007). IL-1 has been reported both to inhibit and stimulate production of osteoprotegerin (OPG) in various osteoblastic cell models in vitro (Tanabe et al., 2005; Lambert et al., 2007). Its stimulatory effect was dependent on p38 and ERK MAP kinases (Lambert et al., 2007). The ability of IL-1 to enhance osteoclastogenesis is in contrast to the inhibitory effects of toll-like receptors (TLRs). Why these responses differ is a matter of some investigation because both signaling pathways overlap through MyD88 adaptor protein. One possible reason is their divergent effects on B lymphocyte—induced maturation protein-1 (Blimp1), a transcriptional repressor of antiosteoclastogenic genes—IL-1 enhances RANKL-induced Blimp1 gene expression while TLR inhibits Blimp1 (Chen et al., 2015).

IL-1 induces the differentiation of mesenchymal stem cells toward osteoblasts via the noncanonical Wnt-5a/Ror2 pathway (Sonomoto et al., 2012) and inhibits osteoblast migration (Hengartner et al., 2013). Osteocytes regulate osteoclastogenesis by producing a variety of factors including RANKL (Nakashima et al., 2011; Xiong et al., 2011). Treatment of the MLO-Y4 osteocyte-like cell line with IL-1 enhanced RANKL and decreased OPG production, which was reversed by mechanically loading the cells (Kulkarni et al., 2012).

Tumor necrosis factor

Like IL-1, TNF represents a family of two related polypeptides (α and β) that are the products of separate genes (Beutler and Cerami, 1986, 1987; Old, 1985; Oliff, 1988; Paul and Ruddle, 1988). TNFα and TNFβ have similar biologic activities and are both potent stimulators of bone resorption (Bertolini et al., 1986; Lorenzo et al., 1987; Tashjian et al., 1987).

In vivo administration of TNFα to mice was shown to increase their serum calcium (Tashjian et al., 1987) and stimulate new osteoclast formation and bone resorption (Stashenko et al., 1987b). Like IL-1, TNF also enhances the formation of osteoclast-like cells in bone marrow culture (Tashjian et al., 1987) through its ability to increase RANKL production and the RANKL/OPG ratio (Hofbauer et al., 1999). In mixed cultures of osteoblast and osteoclast precursors, TNF was most effective at stimulating osteoclastogenesis when osteoblasts were derived from calvaria rather than long bones (Wan et al., 2016). It also has direct effects on RANKL-induced osteoclastogenesis that vary depending on the type of osteoclast precursor examined and timing of TNF exposure relative to RANKL (Cao et al., 2017; Zhao et al., 2015) and can be dependent on the degradation of TRAF3 (Yao et al., 2009, 2017).

In addition to RANKL, TNF stimulates a variety of additional cytokines in the bone microenvironment, and many of these enhance the response to RANKL (Boyce et al., 2005). For example, TNF stimulates osteoclast formation in mixed stromal cell/osteoclast precursor cell cultures by a mechanism that was partially dependent on the production of IL-1 (Wei et al., 2005; Zwerina et al., 2007; Polzer et al., 2009). In addition, TNF-induced osteolysis was found to be dependent on CSF-1 production (Kitaura et al., 2005).

TNF can also directly stimulate osteoclast formation in vitro, independent of RANK, because it occurred in cells from RANK-deficient mice (Azuma et al., 2000; Kim et al., 2005; Kobayashi et al., 2000). However, the significance of this in vitro finding is questionable because in vivo administration of TNF to RANK-deficient mice caused only an occasional osteoclast to form (Li et al., 2000). In addition, RANK-deficient mice that overexpressed TNF had severe osteopetrosis and no osteoclasts (Li et al., 2004a). It was also demonstrated that TNF can stimulate osteoclastogenesis in the absence of RANKL in mice that are deficient in the p100 precursor protein of NF-κB, which is a critical signaling molecule in RANKL-mediated stimulation of osteoclastogenesis and bone resorption (Yao et al., 2009). TNF also stimulated production of Blimp1, an inhibitor of multiple antiosteoclastogenic genes (Wu et al., 2017). These results demonstrate that although both TNF and RANKL are members of the same cytokine superfamily and share multiple overlapping signaling pathways, there are crucial differences between RANKL- and TNF-induced signaling pathways in osteoclast precursor cells.

As with IL-1, TNF binds to two cell surface receptors, TNF receptor 1, or p55, and TNF receptor 2, or p75 (Fiers and Sim, 1993). In contrast to IL-1, both receptors transmit biologic responses. However, the principal effects on bone cells appear to be mediated through TNF receptor 1 (Zhang et al., 2001; Abbas et al., 2003). Mice deficient in both TNF receptor 1 and TNF receptor 2 appear healthy and are not reported to have an abnormal bone phenotype (Erickson et al., 1994; Pfeffer et al., 1993; Rothe et al., 1993).

TNF can stimulate expression of colony-stimulating factor 1 receptor in osteoclast precursor cells (Yao et al., 2006a), and through this mechanism increase the abundance of these cells (Yao et al., 2006b). It also enhances RANK signaling, which activates osteoclasts and their precursor cells (Lam et al., 2000), and increases the expression of the costimulatory molecule, paired Ig-like receptor A, which augments NFATc1 activation (Ochi et al., 2007). Mice that overexpress TNF have an increased number of $CD11b^{high}$ osteoclast precursor cells in their spleen and blood (Li et al., 2004b).

TNF has biphasic effects on bone formation and osteoblast function, which may be dose- and time-dependent (Osta et al., 2014; Daniele et al., 2017). At lower doses, it is stimulatory for the differentiation of mesenchymal precursor cells into osteoblasts (Osta et al., 2014; Daniele et al., 2017), while at higher concentrations it inhibits osteoblast function and bone formation (Bertolini et al., 1986; Canalis, 1987; Stashenko et al., 1987a; Nanes et al., 1989). It was reported to promote fracture repair by enhancing the recruitment of precursor cells to the osteoblastic lineage (Glass et al., 2011). The inhibitory effects of TNF on osteoblasts appear to be direct and mediated by downregulation of the critical transcription factors RUNX2 and osterix (Gilbert et al., 2002, 2004) as well as type 1 collagen (Mori et al., 1996) and osteocalcin (Gowen et al., 1988; Nanes et al., 1991), which are essential for differentiated osteoblast function. It also stimulates

osteoblast apoptosis (Kitajima et al., 1996; Hock et al., 2001) and suppresses production of insulin-like growth factor-1 in osteoblasts (Scharla et al., 1994).

TNF mediates many effects of inflammatory arthritis on periarticular bone, and some of these responses may be selectively mediated by its interactions with TNFR1 (Espirito Santo et al., 2015). Most recently, patients with inflammatory diseases who were treated with anti-TNF therapy were found to have increased bone mineral density (Nigil Haroon et al., 2014; Durnez et al., 2013). These results suggest that circulating TNF, which is produced by localized inflammatory pathology, has systemic effects on bone mass. TNF may also be involved in the development of osteoporosis because mice in which the activity of this cytokine was blocked or are deficient in TNF fail to lose bone after ovariectomy (Kimble et al., 1997; Roggia et al., 2001). In addition, men with relatively high serum TNF levels have an increased risk of hip and vertebral fractures (Cauley et al., 2016).

Additional tumor necrosis factor superfamily members

Fas-ligand

Fas-ligand (FasL) binds its receptor, Fas, on responsive cells, and regulates apoptosis and other cellular processes in multiple cell types (Wesche et al., 2005). In osteoblasts, FasL inhibits differentiation through a caspase 8-mediated mechanism (Kovacic et al., 2007). Osteoclast precursors and mature osteoclasts express Fas and FasL (Park et al., 2005), and this pathway has been shown to mediate apoptosis in mature osteoclasts (Wang et al., 2015) and in osteoclast precursor cells (Liu et al., 2015). However, at high concentrations RANKL inhibited the ability of FasL to induce apoptosis in osteoclasts (Wu et al., 2005). The effect that FasL deficiency has on bone mass is controversial. One group has found bone mass to be decreased in FasL-deficient mice (Wu et al., 2003) while another found it to be increased (Katavic et al., 2003). However, the significance of studying bone mass in Fas- or FasL-deficient mice is difficult to interpret because these models have a generalized lymphoproliferative disorder that activates a wide variety of immune responses that can affect bone.

It appears the Fas signaling is involved in the effects of estrogen on bone, although there is controversy about its role. One group found that stimulation of estrogen receptor α in osteoclasts in mice enhanced FasL production, which in turn reduced rates of bone loss by increasing osteoclast apoptosis (Nakamura et al., 2007). In contrast, a second group failed to detect expression of FasL in osteoclasts (Krum et al., 2008). Rather, they found that estrogen enhanced FasL production in osteoblasts. They speculated that the estrogen-induced increase in FasL production by osteoblasts regulates osteoclast apoptosis through a paracrine mechanism (Krum et al., 2008). More recently, Fas receptor was shown to be required for estrogen deficiency-induced bone loss (Kovacic et al., 2010) and that estrogens interacting through ERα regulate metalloproteinase 3 expression on osteoblasts, which in turn induces FasL cleavage from osteoblasts and osteoclast apoptosis (Garcia et al., 2012). Fas/FasL interactions may also mediate some effects of interferon γ on bone (Kohara et al., 2011). Production of receptor-interacting protein 140 by a Fas/FasL pathway has been implicated in the effects of estrogen on bone (Piao et al., 2017).

Tumor necrosis factor–related apoptosis-inducing ligand

TNF-related apoptosis-inducing ligand (TRAIL) is another TNF-superfamily member that has a wide variety of activities. Its effects on osteoclast function and bone are also controversial. Some groups have found that treatment of osteoclasts with TRAIL induced apoptosis (Roux et al., 2005) through effects that were mediated by the receptor TRAIL-R2, also known as "death receptor 5" (DR5) (Zauli et al., 2010; Colucci et al., 2007). Others have found that TRAIL stimulated osteoclast differentiation through a TRAF-6-dependent mechanism (Yen et al., 2012). In vivo, injection of TRAIL for 8 days into 4-week-old mice induced an increase in bone mass. In vitro, this effect was associated with an increase in the cyclin-dependent kinase inhibitor $p27^{Kip1}$ through effects of TRAIL on the ubiquitin–proteasome pathway (Zauli et al., 2008). TRAIL may also be a factor in the effects of myeloma on osteoblasts (Tinhofer et al., 2006), the effects of microgravity on bone (Sambandam et al., 2016), and the bone disease associated with chronic obstructive pulmonary disease (Kochetkova et al., 2016). Significantly, one group failed to find either in vitro or in vivo effects of recombinant TRAIL on osteoclasts or in vivo effects on bone mass (Labrinidis et al., 2008).

In cultured human osteoblasts, the ability of TRAIL to induce apoptosis was dependent on their differentiation state, with early cells being more responsive than more mature cells (Brunetti et al., 2013). This effect was regulated by differential expression of the active DR5 and decoy DcR2 TRAIL receptors during osteoblast differentiation.

Cluster of differentiation 40 ligand

Cluster of differentiation 40 ligand (CD40L) is involved in the differentiation of naïve T lymphocytes into T_H1 effector cells (Loskog and Totterman, 2007). In humans, deficiency of CD40L causes X-linked hyper IgM (XHIM) syndrome. Bones of XHIM patients develop spontaneous fractures and are osteopenic (Lopez-Granados et al., 2007). Activated T lymphocytes from XHIM patients have normal amounts of RANKL but deficient INFγ production, which may contribute to the decreased bone mass in these individuals (Lopez-Granados et al., 2007). In addition, expression of CD40L in rheumatoid arthritis synovial cells induced RANKL expression in these cells and enhanced their ability to stimulate osteoclastogenesis. This suggests that this mechanism is involved in the destructive effects of rheumatoid arthritis on bone (Lee et al., 2006a). CD40L was also found to accelerate the osteoclastogenesis induced by RANKL and lipopolysaccharide (LPS) (Yokoyama et al., 2011). The ability of parathyroid hormone (PTH) to stimulate osteoclastogenesis involves induction of CD40L on T lymphocytes and the subsequent induction of responses in stromal cells expressing the CD40 receptor (Gao et al., 2008). T cell CD40L also potentiates the bone anabolic activity of intermittent PTH treatment (Robinson et al., 2015). CD40L has been implicated in the bone loss that occurs after ovariectomy in mice (Li et al., 2011), and T lymphocyte−derived CD40L mediates the ability of osteoclasts to suppress T lymphocyte activation (Li et al., 2014). A polymorphism in CD40 has also been correlated with bone mass (Panach et al., 2016).

Interferons

Type I interferons (IFNα and IFNβ) are typically produced in response to invading pathogens (Takayanagi, 2005). Mice deficient in IFNα/β have reduced trabecular bone mass and an increased number of osteoclasts (Takayanagi et al., 2002). RANKL induces IFNβ in osteoclasts, and IFNβ in turn inhibits RANKL-mediated osteoclastogenesis by decreasing c-fos expression (Takayanagi et al., 2002) and inducing the production of micro-RNA 155 (Zhang et al., 2012). Osteocytes are also a source of IFNβ (Hayashida et al., 2014). IFNα has also been shown to inhibit bone resorption although its mechanism of action is not as well studied as that of IFNγ and β (Jilka and Hamilton, 1984). In vivo, IFNα had no effect on bone turnover (Goodman et al., 1999). The ability of titanium wear debris to induce osteoclastogenesis and aseptic artificial joint loosening may be mediated by downregulation of IFNβ production (Wang et al., 2017).

Interferon γ (IFNγ) is a type II interferon with a wide variety of biologic activities. In vitro, IFNγ has generally been found to have inhibitory actions on bone resorption (Gowen and Mundy, 1986; Peterlik et al., 1985). These appear to be direct and are mediated by its effects on osteoclast progenitor cells. IFNγ inhibits the ability of 1,25-dihydroxyvitamin D_3, PTH, and IL-1 to stimulate the formation of osteoclast-like cells in cultures of human bone marrow (Takahashi et al., 1986). IFNγ also inhibits RANK signaling by accelerating the degradation of TRAF6 through activation of the ubiquitin/proteasome system (Takayanagi et al., 2000), by inhibiting NFATc1 expression, and by activating the NF-κB and JNK pathways (Cheng et al., 2012). Curiously, it is reported to not inhibit resorption in mature osteoclasts (Hattersley et al., 1988). IFNγ is also reported to have stimulatory effects on resorption through its ability to increase RANKL and TNFα production in T lymphocytes (Gao et al., 2007) and through its ability to enhance the fusion of preosteoclasts (Kim et al., 2012). It appears to mediate the ability of γδ T lymphocytes, CD8 regulatory T lymphocytes, IL-27, and M1 macrophages to inhibit osteoclastogenesis and resorptive activity (Pappalardo and Thompson, 2013; Park et al., 2012; Shashkova et al., 2016; Yamaguchi et al., 2016). T cell−derived IFNγ has been shown to induce osteoclasts to secrete factors that feed back to T cells to limit their proliferation (Li et al., 2014).

In osteoblasts, IFNγ is an inhibitor of proliferation (Cornish et al., 2003; Gowen et al., 1988; Nanes et al., 1989) and has variable effects on differentiation (Gowen et al., 1988; Shen et al., 1988; Smith et al., 1987).

The effects of IFNγ on bone in vivo are also variable, as both inhibitory and stimulatory effects have been reported. In mice with collagen-induced arthritis, loss of the IFNγ receptor (IFNγR) leads to increased bone destruction (Manoury-Schwartz et al., 1997; Vermeire et al., 1997). Similarly, in mice that are injected over their calvaria with bacterial endotoxin, which activates TLRs, loss of IFNγR resulted in an enhanced resorptive response (Takayanagi et al., 2000). This result is consistent with findings demonstrating that the inhibitory effects of IFNγ on osteoclastogenesis are enhanced by activation of TLRs (Ji et al., 2009). Finally, in mice that underwent ovariectomy to induce estrogen withdrawal, administration of IFNγ prevented the development of the bone loss otherwise seen in this condition (Duque et al., 2011).

In contrast, intraperitoneal injection of IFNγ for 8 days in rats induced osteopenia (Mann et al., 1994). In patients who have osteopetrosis, because they produce defective osteoclasts, administration of IFNγ stimulated bone resorption and appeared to partially reverse the disease. The latter effects are possibly due to the ability of IFNγ to stimulate osteoclast superoxide synthesis (Key et al., 1992, 1995), osteoclast formation in vivo (Vignery et al., 1990), or a generalized immune response (Schoenborn and Wilson, 2007).

Interleukin-7

Interleukin-7 (IL-7) is a cytokine that has diverse effects on the hematopoietic and immunologic systems (Namen et al., 1988). It is best known for its nonredundant role in supporting B- and T lymphopoiesis. Studies have demonstrated that IL-7 also plays an important role in the regulation of bone homeostasis (Miyaura et al., 1997; Weitzmann et al., 2002). However, the precise nature of how IL-7 affects osteoclasts and osteoblasts is controversial because it has a variety of actions in different target cells. Systemic administration of IL-7 upregulated osteoclast formation in human peripheral blood cells by increasing osteoclastogenic cytokine production in T lymphocytes (Weitzmann et al., 2000). Furthermore, mice with global overexpression of IL-7 had a phenotype of decreased bone mass with increased osteoclasts and no change in osteoblasts (Salopek et al., 2008). Significantly, IL-7 did not induce bone resorption and bone loss in T cell−deficient nude mice (Toraldo et al., 2003). In addition, treatment of mice with a neutralizing anti-IL-7 antibody inhibited ovariectomy-induced proliferation of early T cell precursors in the thymus, demonstrating that ovariectomy upregulates T-cell development through IL-7. This latter effect may be a mechanism by which IL-7 regulates ovariectomy-induced bone loss (Ryan et al., 2005). However, the interpretation of results from in vivo IL-7 treatment studies is complicated by secondary effects of IL-7, which result from the production of bone-resorbing cytokines by T cells in response to activation by this cytokine (Toraldo et al., 2003; Weitzmann et al., 2000; Gendron et al., 2008).

In contrast with previously reported studies (Miyaura et al., 1997; Toraldo et al., 2003; Weitzmann et al., 2000), we found differential effects of IL-7 on osteoclastogenesis (Lee et al., 2003). IL-7 inhibited osteoclast formation in murine bone marrow cells cultured for 5 days with CSF-1 and RANKL (Lee et al., 2003). Furthermore, IL-7-deficient mice had markedly increased osteoclast number and decreased trabecular bone mass compared with wild-type controls (Lee et al., 2006b). In addition, we found that trabecular bone loss after ovariectomy was similar in wild-type and IL-7-deficient mice (Lee et al., 2006b). Curiously, IL-7 mRNA levels in bone increase with ovariectomy, and this effect may be linked to alterations in osteoblast function with estrogen withdrawal (Sato et al., 2007; Weitzmann et al., 2002). Treatment of newborn murine calvaria organ cultures with IL-7 inhibited bone formation, as did injection of IL-7 above the calvaria of mice in vivo (Weitzmann et al., 2002). When IL-7 was overexpressed locally by osteoblasts, trabecular bone mass was increased compared with wild-type mice (Lee et al., 2004). Furthermore, targeted overexpression of IL-7 rescued the osteoporotic bone phenotype of IL-7-deficient mice (Lee et al., 2005b). These studies indicated that the actions of IL-7 on bone cells are dependent on whether IL-7 is delivered systemically or locally. Production of IL-7 by osteoblasts appears critical for normal B lymphopoiesis (Wu et al., 2008). This effect may be mediated by the response of osteoblasts to PTH (Panaroni et al., 2015) because induction of this cytokine in osteoblasts is mediated by $G_s\alpha$-dependent signaling. Osteoclast-mediated bone resorption can also influence B lymphopoiesis through effects on local IL-7 production in the bone marrow (Mansour et al., 2011).

Interleukin-10

Interleukin-10 (IL-10), the product of activated T and B lymphocytes (Moore et al., 2001), is a direct inhibitor of osteoclastogenesis (Owens et al., 1996; Xu et al., 1995) and osteoblastogenesis (Van Vlasselaer et al., 1993). These effects are associated with increased tyrosine phosphorylation of multiple proteins in osteoclast precursor cells (Hong et al., 2000). The direct effects of IL-10 on RANKL-stimulated osteoclastogenesis include decreases in NFATc1 expression, its reduced translocation into the nucleus (Evans and Fox, 2007), and suppressed c-Fos and c-Jun expression (Mohamed et al., 2007). Administration of IL-10 may have utility as a mechanism to control wear-induced osteolysis (Carmody et al., 2002) and the alveolar bone loss of periodontal disease (Zhang et al., 2014). In dental follicle cells, which function to regulate tooth eruption, in vitro treatment with IL-10 inhibited RANKL production and enhanced OPG (Liu et al., 2006). Hence, there also appears to be an indirect effect of IL-10 on osteoclastogenesis that is mediated by its ability to regulate RANKL and OPG production.

Treatment of bone marrow cell cultures with IL-10 suppressed the production of osteoblastic proteins and prevented the onset of mineralization (Van Vlasselaer et al., 1993). IL-10 also inhibited osteoclast formation in bone marrow cultures without affecting macrophage formation or the resorptive activity of mature osteoclasts (Owens and Chambers, 1995). This effect appears to involve the production of novel phosphotyrosine proteins in osteoclast precursor cells (Hong et al., 2000). IL-10 also stimulates a novel inducible nitric oxide synthase (Sunyer et al., 1996), and it regulates macrophage-mediated clearance of apoptotic cells (efferocytosis) (Michalski et al., 2016). IL-10-deficient mice have decreased alveolar bone and indices of osteoblast differentiation (Claudino et al., 2010). Most recently, polymorphisms of the IL-10 gene in humans have been associated with an increased risk of osteoporosis (Kotrych et al., 2016; Tural et al., 2013).

The inducible T cell costimulatory molecule 4-1BB interacts with the 4-1BB ligand. In vitro treatment of RANKL-stimulated osteoclast precursor cells with 4-1BB ligand enhanced IL-10 production. In addition, expression of IL-10 was greater in RANKL-stimulated wild-type osteoclast precursor cell cultures than in cultured cells from 4-1BB-deficient mice (Shin et al., 2006). These results imply that some effects of IL-10 on osteoclasts are mediated through interactions of 4-1BB and 4-1BB ligand.

Interleukin-12

Interleukin-12 (IL-12) is a cytokine produced by myeloid and other cell types. It induces T_H1 differentiation in T lymphocytes and the subsequent expression of IFNγ (Hsieh et al., 1993). IL-12 has an inhibitory effect on osteoclastogenesis (Horwood et al., 2001). However, the mechanisms by which this effect occurs in vitro are controversial. Some authors have demonstrated direct inhibitory effects of IL-12 on RANKL-stimulated osteoclastogenesis in purified primary osteoclast precursors and RAW 264.7 cells (Amcheslavsky and Bar-Shavit, 2006), which was associated with the inhibition of NFATc1 expression in the osteoclast precursor cells. Interestingly, the inhibitory effects of IL-12 on osteoclastogenesis were absent in cells pretreated with RANKL (Amcheslavsky and Bar-Shavit, 2006). In contrast, others have found that the inhibitory effects of IL-12 on osteoclastogenesis are indirect. One group demonstrated that the inhibitory effects of IL-12 are mediated by T lymphocytes and do not involve production of IFNγ (Horwood et al., 2001). A second group disputes this result and found inhibition of osteoclastogenesis by IL-12 in cells from T lymphocyte−depleted cultures and cells from T lymphocyte−deficient nude mice (Nagata et al., 2003). The latter authors also demonstrated that antibody neutralization of IFNγ blocked some of the inhibitory effect of IL-12 on RANKL-stimulated osteoclast formation. Production of IL-12 by M1 inflammatory macrophages was shown to be a mechanism by which these cells downregulated RANKL-induced osteoclastogenesis (Yamaguchi et al., 2016). Unexpectedly, one group found that IL-12 enhanced RANKL production in human periodontal ligament cells (Issaranggun Na Ayuthaya et al., 2017).

The effects of IL-12 on TNFα- and LPS-induced osteoclastogenesis have been examined in vivo (Yoshimatsu et al., 2009, 2015). It was found that osteoclastogenesis stimulated by the injection of TNFα or LPS over the calvariae of mice decreased when the mice were also treated with IL-12. In addition, the Fas/FasL system seems to be involved in these responses (Kitaura et al., 2002; Yoshimatsu et al., 2015).

Interleukin-15

Interleukin-15 (IL-15), like IL-7, is a member of the interleukin-2 (IL-2) superfamily and shares many activities with IL-2 including the ability to stimulate lymphocytes. It has been shown to enhance osteoclast progenitor cell number in culture (Ogata et al., 1999). Production of IL-15 by T lymphocytes has been linked to the increased osteoclastogenesis and bone destruction seen in the bone lesions of rheumatoid arthritis (Miranda-Carus et al., 2006). In animal models of inflammatory bowel disease and *Staphylococcus aureus* sepsis, lack of IL-15 or treatment with an IL-15 inhibitor reduced the severity of the disease and bone loss (Brounais-Le Royer et al., 2013; Henningsson et al., 2012). Mice with deficient IL-15 receptor α were found to have a low rate of bone formation (Loro et al., 2017). In vitro, IL-15 treatment of mixed murine bone marrow and osteoblast cocultures demonstrated a role of natural killer (NK) cells in the ability of IL-15 to induce apoptosis in osteoblasts (Takeda et al., 2014; Feng et al., 2015). IL-15 was also shown to enhance RANKL-mediated stimulation of osteoclastogenesis in vitro through an ERK-mediated mechanism (Okabe et al., 2017). Polymorphisms of the IL-15 gene have also been linked to variations in bone mineral density in women (Koh et al., 2009). In rheumatoid arthritis, IL-15 is reported to promote osteoclastogenesis via a pathway dependent on phospholipase D1 (Park et al., 2011).

Interleukin-17

Interleukin-17 (IL-17) is a family of related cytokines that are unique and contain at least six members (A−F) (Weaver et al., 2007). IL-17E is also called interleukin-25 (Fort et al., 2001). These cytokines are central for the development of the adaptive immune response and the products of a subset of CD4 T lymphocytes with a unique cytokine expression profile, termed T_H17. This is in contrast to the more traditional T lymphocyte cytokine-expressing subsets T_H1 and T_H2.

IL-17A was initially shown to be a stimulator of osteoclastogenesis in mixed cultures of mouse hematopoietic cells and osteoblasts (Kotake et al., 1999). This enhanced resorptive activity was mediated through increased production of prostaglandin and RANKL. The direct effects of IL-17A on the differentiation of osteoclast precursor cells is controversial, with some investigators finding stimulatory (Yago et al., 2009) and others finding inhibitory effects (Kitami et al., 2010).

These conflicting results may be due to variations in the response to IL-17A of different osteoclast precursor subtypes (Sprangers et al., 2016). In another report, IL-17 stimulated rheumatoid synoviocytes (Zhao et al., 2016) to produce RANKL only with 1,25 dihydroxy-vitamin D_3 and PGE_2 (Ota et al., 2015). Production of IL-17A in rheumatoid arthritis appears to be involved in the production of activated osteoclasts and bone destruction in involved joints (Kotake et al., 1999; Lubberts et al., 2000, 2003). Effects of IL-17 on osteoclastogenesis and bone resorption are enhanced by TNFα, which is also produced in the inflamed joints of patients with rheumatoid arthritis (Van Bezooijen et al., 1999) and inhibited by shear stress (Liao et al., 2017). Inhibition of IL-17A in an antigen-induced arthritis model reduced the joint and bone destruction typically seen and decreased the production of RANKL, IL-1β, and TNFα in the involved lesions (Koenders et al., 2005). Multiple reports have now implicated IL-17 as a critical mediator of the bone loss that occurs in animal models after estrogen withdrawal (Tyagi et al., 2012, 2014; DeSelm et al., 2012). In addition, patients with osteoporosis have higher serum levels of IL-17A than osteopenic and normal subjects (Zhang et al., 2015; Zhao et al., 2016). This effect may be related to estrogen levels, as postmenopausal women have higher serum IL-17 levels than premenopausal women (Molnar et al., 2014). In addition, a polymorphism of the IL-17 gene was associated with decreased bone mineral density in humans (Boron et al., 2014).

The effects of IL-17 on bone formation are complex. It stimulates mesenchymal cell proliferation (Huang et al., 2009). However, it inhibits mature osteoblast differentiation in vitro and the reparative response to a calvaria critical size defect in vivo (Kim et al., 2014). In an inflammatory arthritis model and a skin inflammation model, deletion or inhibition of IL-17A enhanced bone formation through a mechanism dependent on Wnt signaling (Shaw et al., 2016; Uluckan et al., 2016). In contrast, it was found that IL-17A-producing γδ and T_H17 T cells can enhance bone formation (Ono et al., 2016; Croes et al., 2016).

Interleukin-23

Interleukin-23 (IL-23) is an IL-12-related cytokine composed of one subunit of p40, which it shares with IL-12, and one subunit of p19, which is unique (Kastelein et al., 2007). It is critical for the differentiation of the T_H17 subset of T lymphocytes along with TGFβ and IL-6 (Bettelli et al., 2006). IL-23 appears most important for expanding the population of T_H17 T lymphocytes. This subset of T lymphocytes, which produces RANKL, has a high osteoclastogenic potential that is mediated by their production of IL-17 (Sato et al., 2006). In an LPS-induced model of inflammatory bone destruction, it was found that there was markedly less bone loss in mice deficient in either IL-17 or IL-23 (Sato et al., 2006). Hence, production of both is involved in the bone loss in this model. IL-23 induces RANKL expression in CD4 T lymphocytes (Ju et al., 2008) and RANK expression in osteoclast precursor cells (Chen et al., 2008). However, the actions of IL-23 on bone in vivo are controversial. IL-23-deficient mice have decreased bone mass in one report (Quinn et al., 2008) but increased bone mass in another (Adamopoulos et al., 2011). In some studies, IL-23 inhibited osteoclastogenesis through actions mediated by CD4 T lymphocytes (Quinn et al., 2008; Kamiya et al., 2007). In contrast, in another study it stimulated osteoclastogenesis in mixed osteoblast-osteoclast precursor cultures (Kang and Zhang, 2014). Shin et al. reported that IL-23 promoted osteoclastogenesis through a DNAX-activating protein of 12 kDa-dependent pathways (DAP12)−mediated mechanism (Shin et al., 2015).

Interleukin-18 and interleukin-33

Interleukin-18 (IL-18) is similar to IL-1 in its structure and a member of the IL-1 superfamily (Orozco et al., 2007). IL-18 synergizes with IL-12 to induce INFγ production (Okamura et al., 1995), and its levels are increased at sites of inflammation in rheumatoid arthritis (Yamamura et al., 2001). Osteoblastic cells express IL-18, and its production is induced by treatment with endothelin-1 (Zhong et al., 2014). IL-18 inhibits osteoclast formation through a variety of mechanisms. These include its ability to stimulate GM-CSF (100), which is produced by T cells in response to IL-18 treatment (Horwood et al., 1998b). It also stimulates INFγ production in vivo in bone (Kawase et al., 2003), and its inhibitory effects on osteoclastogenesis and bone resorption are enhanced by cotreatment with IL-12 (Yamada et al., 2002). IL-18 has been shown to indirectly stimulate osteoclastogenesis through its effects on T lymphocytes (Dai et al., 2004). Finally, IL-18 is reported to increase the production of OPG (Makiishi-Shimobayashi et al., 2001). In IL-18-overexpressing transgenic mice, osteoclasts were decreased, although curiously, so was bone mass. These results indicate that IL-18 may also have effects on bone formation (Kawase et al., 2003). In confirmation of this hypothesis, it was demonstrated that PTH treatment of osteoblasts stimulated IL-18 production. In addition, the anabolic effects of intermittent PTH treatment on trabecular bone mass in IL-18-deficient mice were reduced (Raggatt et al., 2008). IL-18 is also a mitogen for osteoblastic cells in vitro (Cornish et al., 2003).

An antagonist of IL-18, named IL-18 binding protein (IL-18BP), was shown to prevent some bone loss associated with ovariectomy in mice, and it was found that osteoporotic postmenopausal women had lower levels of IL-18BP compared to controls (Mansoori Sci Rep, 2016).

Interleukin-33 (IL-33) is another member of the IL-1 family that has primarily been studied for its effects on T lymphocytes (Villarreal and Weiner, 2014). Its specific receptor is the orphan IL-1 receptor ST2 (also called IL-1R-like-1) (Villarreal and Weiner, 2014). IL-33 is expressed by osteoblasts (Schulze et al., 2011; Saleh et al., 2011), and production in these cells is stimulated by PTH and oncostatin M (Saleh et al., 2011). Its effects on bone cells are varied. One report found it to stimulate osteoclastogenesis (Mun et al., 2010), while multiple others have found it to be inhibitory (Zaiss et al., 2011; Schulze et al., 2011; Saleh et al., 2011; Kang et al., 2017). In addition, there is a report that it had no effect on bone remodeling (Saidi et al., 2011), although these same authors suggested that it may be involved in the development of osteonecrosis of the femoral head (Saidi and Magne, 2011). These conflicting results may reflect differences in the response to IL-33 by different types of osteoclast progenitors (Eeles et al., 2015). IL-33-deficient mice had a higher bone mass phenotype only in the lumber vertebrae and distal femur of female mice with no change in cortical bone parameters through 8 months of age (Okragly et al., 2016). ST2-deficient mice demonstrated increased bone resorption with mechanical loading compared with controls (Lima et al., 2015). In transgenic mice that overexpress IL-33 in osteoblasts, osteoclastogenesis was decreased (Keller et al., 2012). In osteoblasts, hypoxia-inducible factor-1α activation facilitates IL-33 expression (Kang et al., 2017).

Interleukin-4, interleukin-13, and interleukin-32

IL-4 and IL-13 are members of a group of locally acting factors that have been termed "inhibitory cytokines." The effects of IL-4 and IL-13 seem related and appear to affect both osteoblasts and osteoclasts. Transgenic mice that overexpress IL-4 had an osteoporotic phenotype (Lewis et al., 1993). This effect may result from an inhibition of both osteoclast formation and activity (Nakano et al., 1994; Shioi et al., 1991) and an inhibition of bone formation (Okada et al., 1998). IL-13 and IL-4 inhibited IL-1-stimulated bone resorption by decreasing the production of prostaglandins and the activity of cyclooxygenase-2 (Onoe et al., 1996). The direct inhibitory effects of IL-4 on osteoclast precursor cell maturation are more potent than that of IL-13 and involve effects on signal transducer and activator of transcription (STAT) 6 (or STAT6), NF-κB, peroxisome proliferator-activated receptor γ1, mitogen-activated protein kinase signaling, Ca^{++} signaling, NFATc1, c-Fos, and enhanced apoptosis (Bendixen et al., 2001; Kamel Mohamed et al., 2005; Mangashetti et al., 2005; Moreno et al., 2003; Wei et al., 2001; Yamada et al., 2007; Wu et al., 2016). IL-4 induces myeloid cell differentiation toward the dendritic cell lineage and M2 macrophage activation away from the osteoclast lineage (Hiasa et al., 2009; Freire et al., 2016).

IL-13 and IL-4 induce cell migration (chemotaxis) in osteoblastic cells, and they regulate the ability of osteoblasts and vascular endothelial cells to control OPG and RANKL production (Palmqvist et al., 2006; Yamada et al., 2007; Stein et al., 2008; Fujii et al., 2012). IL-13 also inhibits Cyp27b1 in human CD14-expressing myeloid cells (Ding et al., 2017). This is the enzyme that hydroxylates 25 OH vitamin D at the 1-α position to activate it.

IL-32 is a cytokine involved in innate and adoptive immunity. It is produced by T lymphocytes, NK cells, and epithelial cells (Felaco et al., 2009). IL-32 stimulates the formation of multinuclear cells that were TRAP- and vitronectin receptor-positive but did not resorb. In addition, it inhibited resorption that was stimulated by RANKL (Mabilleau and Sabokbar, 2009). IL-32γ was also shown to enhance osteoblast differentiation (Lee et al., 2015), and mice that overexpress IL-32γ were found to have increasing bone mass with age and increased bone formation (Lee et al., 2017).

Macrophage migration inhibitory factor

Macrophage migration inhibitory factor (MIF) was initially identified as an activity in conditioned medium from activated T lymphocytes that inhibited macrophage migration in capillary tube assays (Baugh and Bucala, 2002). Once purified and cloned (Weiser et al., 1989), it became available for functional studies and was shown to have a variety of activities. In addition to T lymphocytes, it is produced by pituitary cells and activated macrophages. MIF is a direct inhibitor of osteoclastogenesis in vitro (Jacquin et al., 2009; Gu et al., 2015) through its ability to activate Lyn tyrosine kinase (Mun et al., 2014) and a variety of RANKL-mediated pathways (Gu et al., 2015). MIF also stimulates the homing of osteoclast precursor cells to sites of osteolysis (Movila et al., 2016).

In vivo, its effects are complex. Mice that overexpress MIF globally have high turnover osteopenia (Onodera et al., 2006), while mice deficient in MIF have low turnover osteopenia with decreased serum indices of bone resorption and bone formation (Jacquin et al., 2009). MIF-deficient mice are also reported to neither lose bone mass nor increase

osteoblast or osteoclast number in bone with ovariectomy (Oshima et al., 2006). Hence, MIF may be another mediator of the effects of estrogen withdrawal on bone. Consistent with this hypothesis, estrogen downregulates MIF expression in activated macrophages (Ashcroft et al., 2003). A similar response may occur in bone or bone marrow and mediate some effects that ovariectomy has on bone mass. It was recently shown that an MIF polymorphism is more frequent in women with osteoporosis (Ozsoy et al., 2018), and there is an inverse correlation between plasma MIF levels and bone mineral density (Kim et al., 2016).

MIF is made by osteoblasts (Onodera et al., 1996), and its production in these cells was upregulated by a variety of growth factors including TGF-β, FGF-2, IGF-II, and fetal calf serum (Onodera et al., 1999). In vitro, MIF increased MMP9 and MMP13 expression in osteoblasts (Onodera et al., 2002) and inhibited RANKL-stimulated osteoclastogenesis by decreasing the fusion of precursors, possibly through its ability to inhibit the migration of these cells (Jacquin et al., 2009).

Deletion of CD74, a putative MIF receptor, in mice produced a phenotype of enhanced osteoclastogenesis and decreased bone mass (Mun et al., 2013).

The interleukin-6 cytokine family

The interleukin-6 (IL-6) family is a large group of cytokines that all use the glycoprotein 130 (gp130) co-receptor, a ubiquitously expressed transmembrane receptor subunit with intracellular signaling capacity. Each family member generates specific intracellular Janus kinase (JAK)/STAT or Erk signaling cascades by forming specific receptor:ligand complexes, each with distinct components (Fig. 50.1). When IL-6 family cytokines form a receptor:ligand complex, gp130 (Haan et al., 1999), oncostatin M receptor (OSMR) (Hermanns, 2015) and/or leukemia inhibitory factor receptor (LIFR) (Stahl et al., 1995) are phosphorylated, providing docking sites for STAT1, STAT3, and STAT5 proteins (Fig. 50.2). Subsequent STAT phosphorylation by JAK allows their homo- or heterodimerization and nuclear translocation to modify transcription. Negative feedback is provided by suppressors of cytokine signaling including suppressor-of-cytokine-signaling (SOCS) proteins SOCS1 and SOCS3, and cytokine-inducible SH2-containing protein (CISH) (Croker et al., 2003; Alexander et al., 1999b; Matsumoto et al., 1997).

IL-6 family cytokines are expressed in all bone cells (Table 50.1); and while early work focused on their levels in the circulation, these cytokines are generally detected at high levels only in pathological states. Studies in knockout mice and human mutations (Table 50.2), outlined below, indicate that IL-6 family cytokines play important paracrine roles to regulate bone formation and resorption during normal bone development, growth, and remodeling.

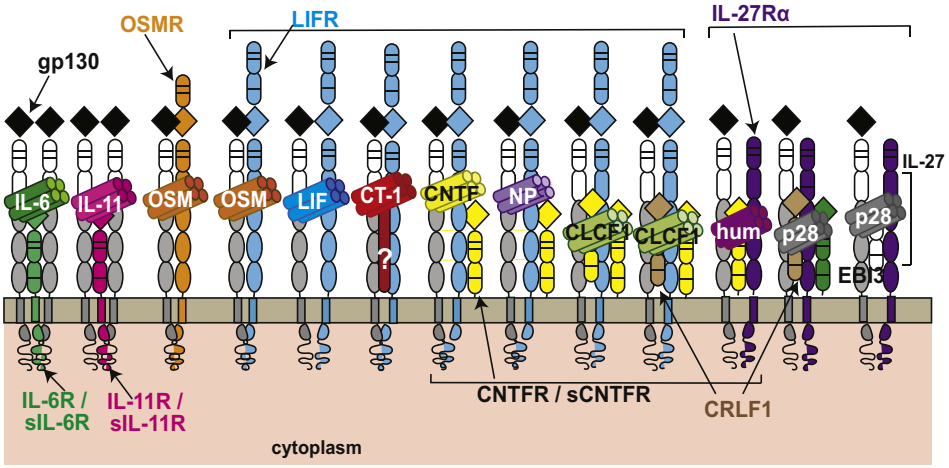

FIGURE 50.1 Cytokine receptor complexes formed by IL-6 family cytokines: Complexes are shown, left to right, in the order in which they are discussed in this chapter. gp130 is shown in gray on the left of each complex. IL-6 and IL-11 bind to ligand-specific β-receptor subunits (IL-6R and IL-11R, or their soluble counterparts, sIL-6R and sIL-11R, respectively) and complex with gp130 homodimers. The Oncostatin M (OSM) receptor (OSMR) is used by OSM, which then recruits gp130 to form a heterodimer. OSM also uses Leukemia inhibitory factor receptor (LIFR). LIFR is also used by LIF in a heterodimer with gp130. Cardiotrophin 1 (CT-1) also signals through LIFR and gp130 as well as, potentially, a CT-1-specific receptor subunit that remains undefined. Ciliary neurotrophic factor (CNTF) and neuropoietin (NP) signal through a complex containing LIFR, gp130 and either the membrane bound or soluble CNTF receptor (CNTFR or sCNTFR). Cardiotrophin-like cytokine factor 1 (CLCF1) acts as a compound cytokine either bound to sCNTFR or cytokine receptor-like factor (CRLF), both of which bind to a gp130:LIFR:CNTFR multimer. Finally, three signaling complexes are shown that contain a heterodimer of gp130 and IL-27Rα: humanin, which requires CNTFR, and p28, which can signal either as a gp130:IL-27Rα complex containing CRLF1 and the IL-6 receptor, or as IL-27, in complex with gp130:IL-27Rα and EBI3. For simplicity, soluble receptors are not pictured.

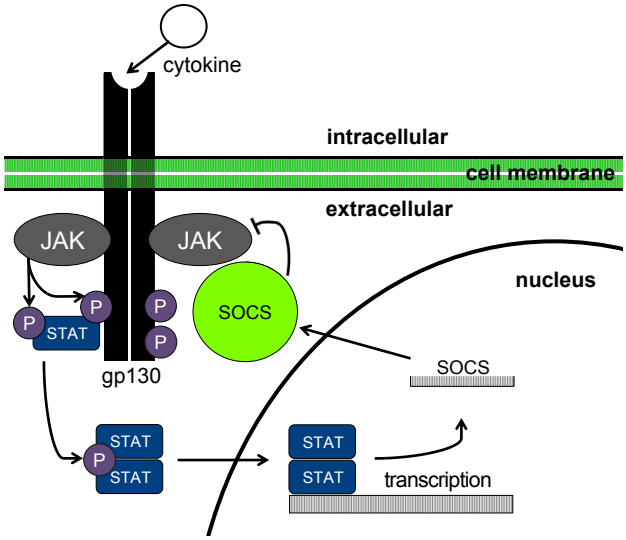

FIGURE 50.2 Basic concept of intracellular signaling by IL-6 family cytokines: Upon formation of a transmembrane signaling complex (as shown in Fig. 50.1), Janus kinases (JAK) phosphorylate the receptor complex, providing docking sites for STAT proteins. Their subsequent phosphorylation, dimerization (either as homo or heterodimers) and translocation to the nucleus initiates transcription of STAT target genes, which includes the transcription of SOCS proteins. SOCS proteins are exported to the cytoplasm where they provide negative feedback to the receptor complex to stop continued phosphorylation and signaling.

We will describe each family member's influences on the mineralized skeleton in turn, beginning with the prototypical ligand, IL-6, and ending with gp130's negative feedback pathways. Although elevated IL-6 family signaling contributes to focal and systemic bone loss in pathologies such as colitis (Mitsuyama et al., 1995), inflammatory arthritis (Kotake et al., 1996; Wong et al., 2006b), multiple myeloma (Kyrtsonis et al., 1996), Gorham−Stout disease (Devlin et al., 1996), breast cancer metastasis to bone (Johnson et al., 2016), and heterotopic ossifications (Torossian et al., 2017), this chapter will focus on their essential physiological functions.

Interleukin-6

A role for interleukin-6 (IL-6) family cytokines in the skeleton was first discovered by the finding that IL-6 robustly stimulates osteoclast formation in culture (Tamura et al., 1993). This did not result from direct action on osteoclasts or their precursors, even though they express transmembrane IL-6 receptor (IL-6R) (Gao et al., 1998). Instead, IL-6 stimulated bone resorption indirectly by promoting the expression of RANKL, the essential osteoclastogenic factor, in osteoblast precursors (Tamura et al., 1993; Palmqvist et al., 2002). This local IL-6 action occurs because it is produced by many cell types in the bone microenvironment, including osteoblasts and osteoclasts (Liang et al., 1999; Ishimi et al., 1990) and other cells such as macrophages, T cells (Briso et al., 2008), and neutrophils (Modur et al., 1997). IL-6 also promotes RANKL expression by pathogenic cells, such as synovial fibroblasts in rheumatoid arthritis (Wong et al., 2006b).

Although IL-6 stimulates osteoclastogenesis, and transgenic mice overexpressing IL-6 exhibit low trabecular bone mass due to elevated osteoclast numbers (De Benedetti et al., 2006), IL-6 knockout mice exhibit no defect in physiological osteoclastogenesis or trabecular bone mass (Table 50.2) (Poli et al., 1994). Instead, IL-6 appears to play a significant role only in pathological conditions in which osteoclast numbers are elevated; IL-6-null mice showed blunted ovariectomy-induced bone loss (Poli et al., 1994) and reduced osteoclast formation in experimental inflammatory arthritis (Wong et al., 2006b).

IL-6 exerts its biological activity via two pathways (Scheller et al., 2014). Classic IL-6 signaling (*cis*) occurs in cells expressing membrane-bound IL-6R. When this pathway is used, IL-6 binds the transmembrane IL-6R and recruits a gp130 homodimer through which it signals (see Fig. 50.1). In contrast, when the alternative *trans*-signaling pathway is used, although IL-6 recruits and signals through a gp130 homodimer, it binds first to soluble IL-6R (sIL-6R); this pathway allows IL-6 to act in cells lacking transmembrane IL-6R and amplifies IL-6 effects in IL-6R-expressing cells. For IL-6 to promote osteoclast formation in culture, sIL-6R must be added (Tamura et al., 1993); therefore, IL-6 promotes osteoclastogenesis only through IL-6 *trans*-signaling.

TABLE 50.1 Expression of IL-6 family cytokines and receptors in the cells of bone and cartilage.

	Osteoclast	Osteoblast	Osteocyte	Chondrocyte
Receptors				
gp130	+ (Gao et al., 1998)	+ (Romas et al., 1996)	+ (Walker et al., 2010)	+ (Rowan et al., 2001)
IL-6R	+ (Gao et al., 1998)	+ (Udagawa et al., 1995)	+ (Dame and Juul, 2000)	+ (Legendre et al., 2003)
IL-11R	+ (Romas et al., 1996)	+ (Romas et al., 1996)	Implied (Walker et al., 2010)	Not reported
LIFR	− (Allan et al., 1990)	+ (Allan et al., 1990)	+ (Walker et al., 2010)	− (Rowan et al., 2001)
CNTFR	Low (McGregor et al., 2010)	+ (Bellido et al., 1996)	+ (Walker et al., 2012)	Not reported
OSMR	− (Walker et al., 2010)	+ (Walker et al., 2010)	+ (Walker et al., 2010)	+ (Rowan et al., 2001)
WSX-1	Low (Kamiya et al., 2007)	+ (Kamiya et al., 2007)	Not reported	Not reported
CRLF1	Not reported	+ (Walker et al., 2012)	Not reported	+ (Tsuritani et al., 2010)
Sortilin	+ (Boggild et al., 2016)	+ (Maeda et al., 2002)	Not reported	+ (Boggild et al., 2016)
Ligands				
IL-6	Some (Liang et al., 1999)	+ (Ishimi et al., 1990)	Some (Liang et al., 1999)	+ (Guerne et al., 1990)
IL-11	− (Maier et al., 1993)	+ (Romas et al., 1996)	Not reported	+ (Maier et al., 1993)
LIF	Not reported	+ (Ishimi et al., 1992)	Not reported	+ (Grimaud et al., 2002)
OSM	− (Walker et al., 2010)	+ (Walker et al., 2010)	+ (Walker et al., 2010)	Not reported
CT-1	+ (Walker et al., 2008)	− (Walker et al., 2008)	- (Walker et al., 2008)	+ (Sheng et al., 1996)
CNTF	+ (McGregor et al., 2010)	+ (Liu et al., 2002)	+ (McGregor et al., 2010)	+ (McGregor et al., 2010)
IL-27	Not reported	Not reported	Not reported	Not reported
CLCF1	Low (McGregor et al., 2010)	+ (McGregor et al., 2010)	Not reported	Not reported
Humanin	Not reported	Not reported	Not reported	Not reported
Neuropoietin*	− (McGregor et al., 2010)	− (McGregor et al., 2010)	Not reported	Not reported

*, neuropoietin is a pseudogene in humans; −, reported as absent at the protein level; +, reported at the protein level; *Implied*, a functional response has been observed, but the receptor has not been detected; *mRNA*, reported at the mRNA level, but not (yet) at the protein level.

TABLE 50.2 Functional characterizations in mice and humans with genetic alterations in IL-6 family receptors and ligands.

	Knockout (murine)	Overexpression/activation (murine)	Human mutation phenotype (only skeletal effects are noted)
Receptors			
gp130	Neonate lethal, low bone mass, many large osteoclasts (Shin et al., 2004; Kawasaki et al., 1997) *Osx1Cre* and *Dmp1Cre* gp130 knockouts: Low trabecular bone mass, increased periosteal diameter, low bone formation, normal osteoclasts (Johnson et al., 2014a). *CtskCre* gp130 knockout: Low bone formation, reduced periosteal diameter (Johnson et al., 2015).	Gp130-STAT3 hyperactivation: Low bone mass, excessive osteoclasts (rescued by IL-6 deletion or STAT3 suppression) (Sims et al., 2004; Walker et al., 2016). gp130-STAT3 deletion: Dwarfism (Sims et al., 2004); *Dmp1CreSocs3* deletion (gp130 hyperactivation): Sex-specific delayed corticalisation (Cho et al., 2017).	Missense mutation with loss of IL-6, IL-11, IL-27, and OSM signaling but intact LIF response: Craniosynostosis, dental abnormalities, progressive scoliosis (Schwerd et al., 2017);
IL-6R	–	–	–
IL-11R	High trabecular bone mass, low bone formation, low resorption (Sims et al., 2005), disturbed cranial growth (Nieminen et al., 2011)	–	Loss of function: Craniosynostosis, dental abnormalities (Nieminen et al., 2011; Keupp et al., 2013)
LIFR	Neonate lethal, low bone mass, many large osteoclasts (Ware et al., 1995)	–	Loss of function: Stüve–Wiedemann syndrome, variable phenotype with bowing of long bones, cortical thickening, flared metaphyses with coarse trabeculae, camptodactyly (Dagoneau et al., 2004; Jung et al., 2010)
OSMR	High trabecular bone mass, low bone formation, low resorption (Walker et al., 2010)	–	Loss of function: No bone defect noted, cutaneous amyloidosis (Arita et al., 2008).
CNTFR	– (Neonate lethal) (DeChiara et al., 1995)	–	–
CRLF1	– (Neonate lethal) (Alexander et al., 1999a)	–	Loss of function: Crisponi/cold-induced sweating syndrome 1, kyphoscoliosis, palatal and frontonasal malformations (Hahn et al., 2006; Piras et al., 2014)
Ligands			
IL-6	Normal trabecular bone mass, reduced periosteal growth (Sims et al., 2005; Johnson et al., 2015; Poli et al., 1994)	Transgenic: Osteopenia, few osteoblasts, many osteoclasts, growth retardation (De Benedetti et al., 2006)	Variants linked with osteoporosis and osteopenia (Ota et al., 1999, 2001).
IL-11	–	Transgenic: Increased bone formation and cortical thickness (Takeuchi et al., 2002)	–
LIF	Dwarfism, region-specific effects on osteoclasts and osteoblasts (Poulton et al., 2012)	Engraftment: High bone mass (Metcalf and Gearing, 1989)	–
OSM	–	Transgenic: High bone mass (Juan et al., 2009)	–
CT-1	High trabecular bone mass, poorly-resorbing osteoclasts, low bone formation (Walker et al., 2008)	–	–
CNTF	High trabecular bone mass, high bone formation in females, low cortical width in males (McGregor et al., 2010)	–	Loss of function in 2.3% of Japanese population; no data on skeletal effect (Takahashi et al., 1994).
CLCF1	– (Neonatal lethal) (Zou et al., 2009)	–	Cold-induced sweating syndrome 2; palatal and frontonasal malformations, kyphoscoliosis (Hahn et al., 2006; Piras et al., 2014).

"–" indicates unknown phenotype or absence of an appropriate model. IL-27R, Sortilin, humanin, IL-27, and neuropoietin are not included due to lack of information on skeletal phenotypes associated with mutations in those genes.

The requirement of IL-6 *trans*-signaling for osteoclastogenesis and elevated circulating sIL-6R levels in pathological bone loss such as rheumatoid arthritis (Kotake et al., 1996) in ovariectomized women (Girasole et al., 1999) and colitis (Mitsuyama et al., 1995) provide a strong case that IL-6 stimulates pathological osteoclastogenesis through *trans*-signaling. Earlier studies assessing IL-6 in estrogen deficiency bone loss used an antibody directed to full-length IL-6 ligand, likely blocking both *cis*- and *trans*-signaling. This led to some conflicting results, with some authors reporting that IL-6 neutralizing antibody treatment blunted the high osteoclast numbers associated with ovariectomy (Jilka et al., 1992) and others showing no effect (Kitazawa et al., 1994). We recently reported, by using *trans*-signaling-specific antibodies, that IL-6 has compartment-specific actions in ovariectomy-induced bone loss. The trabecular bone loss and increased trabecular osteoclast numbers associated with ovariectomy require IL-6 *trans*-signaling (Lazzaro et al., 2018). In contrast, the cortical bone loss associated with ovariectomy was not IL-6-dependent (Lazzaro et al., 2018). This may explain the earlier controversy over antibody-based studies because they did not distinguish between cortical and trabecular bone loss or osteoclastogenesis.

Although IL-6 is best known for stimulating osteoclastogenesis, there is some evidence that IL-6 might also stimulate bone formation, at least in cortical appositional growth. Early in vitro studies showed IL-6 can act directly on osteoblasts. Cultured osteoblast-like UAMS-32 and MG-63 cells expressed IL-6R (Bellido et al., 1996) and responded to IL-6 with STAT dimerization and increased alkaline phosphatase activity (Bellido et al., 1997). This was observed without adding the soluble receptor but was amplified when sIL-6R was provided, indicating that early-stage osteoblasts respond to both *cis*- and *trans*-signaling. Since osteoblasts mount a STAT3 phosphorylation response to IL-6 without requiring sIL-6R addition, it is not clear why they do not support osteoclastogenesis in culture without it; perhaps a higher STAT3 phosphorylation level is required for RANKL production to occur. IL-6 has recently been reported also to stimulate bone formation in vivo through *trans*-signaling (McGregor et al., 2019). The impaired periosteal bone formation (Sims et al., 2005; Johnson et al., 2015) and thin cortices (Poli et al., 1994; Johnson et al., 2015) in IL-6-null mice suggest that IL-6 is required for bone formation on the periosteum.

The impairment in periosteal bone formation and radial growth in IL-6-null mice was also observed in mice lacking gp130 in osteoclasts (*Ctsk.gp130$^{f/f}$* mice) (Johnson et al., 2015). Since the periosteal site at which bone formation was measured in both models lacks osteoclasts, we suggested that osteoclasts on the endocortical surface may respond to IL-6 by releasing signals that are transmitted through the cortical bone to periosteal osteoblasts, either by passing through the lacuno-canalicular network or by acting on osteocytes within the cortical bone. To distinguish this activity from trabecular "coupling factors," the term "osteotransmitter" was coined to emphasize that these factors, released from osteoclasts in response to IL-6, are unlikely to signal directly from the osteoclast to the distant osteoblast on the periosteal surface. Instead, the message is transmitted through other cells (e.g., the cortical osteocyte network) to influence osteoblasts at the appropriate location.

In humans, variants in the IL-6 gene are linked with osteoporosis and osteopenia (Ota et al., 1999, 2001); whether this is due to increased inflammation and elevated osteoclast formation, differences in bone resorption or impaired cortical growth is not known. Treatment with the IL-6 inhibitory antibody tocilizumab in arthritic patients reduces inflammation and leads to reduced biochemical markers of resorption but also elevated bone formation markers (Karsdal et al., 2012; Terpos et al., 2011). Such opposing influences of IL-6 inhibition on bone formation and resorption are consistent with earlier evidence for an IL-6-dependent pathway that couples trabecular bone formation to increased resorption caused by elevated STAT3 signaling (Sims et al., 2004).

Evidence has been accumulating that IL-6 is produced and regulated in osteocytes. The proportion of osteocytes staining for IL-6 by immunohistochemistry was dramatically elevated in models of stress fracture (Wu et al., 2014) and inflammatory bowel disease (Metzger et al., 2017), and IL-6 mRNA levels were elevated when an osteocyte-like cell line was subjected to fluid flow (an in vitro model for mechanical loading) (Bakker et al., 2014). Our recent evidence that the sex-specific differences in cortical bone development requires osteocyte-specific negative feedback and testosterone action through IL-6 in male mice (Cho et al., 2017) implies that local IL-6 regulation in osteocytes may drive the formation of strong, mature cortical bone (see later). Whether IL-6 produced by osteocytes stimulates bone formation or resorption, and whether this is mediated by *cis*- or *trans*-signaling, remains to be established. Our very recent work indicates that osteocytes are responding both to IL-6 *cis*- and *trans*-signaling with STAT3 phosphorylation, and although they produce elevated RANKL in response to *trans*-signaling, this is insufficient to fully support osteoclast formation (McGregor et al, 2019).

Interleukin-11

Like IL-6, interleukin-11 (IL-11) signals by binding to a ligand-specific receptor (in this case, IL-11 receptor [IL-11R]) and then to a gp130 homodimer (Fig. 50.1). Like IL-6, IL-11 also stimulates osteoclastogenesis in coculture (Tamura et al.,

1993) by stimulating RANKL production in osteoblast lineage cells (Horwood et al., 1998a). Although IL-11 can use a soluble receptor (sIL-11R) for *trans*-signaling (Lokau et al., 2016), soluble receptor addition is not required for IL-11 to stimulate osteoclastogenesis (Tamura et al., 1993).

IL-11 stimulates osteoblast differentiation (Sims et al., 2005; Suga et al., 2001) in vitro. It has been suggested that this, rather than its proosteoclastogenic action, is IL-11's dominant effect because mice overexpressing IL-11 exhibit elevated bone formation and cortical thickening but no change in osteoclastogenesis (Takeuchi et al., 2002). There are at least two mechanisms by which this occurs. Osteoblasts are derived from pluripotent progenitors capable also of adipocytic differentiation (Sabatakos et al., 2000), and IL-11 promotes their commitment toward the osteoblast lineage while suppressing adipogenesis (Sims et al., 2005). A second mechanism is that IL-11 suppresses the expression of sclerostin (Walker et al., 2010), an osteocyte-derived inhibitor of bone formation.

Mice null for the IL-11R exhibit features consistent with all three reported effects of IL-11: reduced osteoclastogenesis, impaired bone formation, and increased marrow adiposity (Sims et al., 2005). This indicates IL-11 signaling is essential for these processes, at least in the adult skeleton. IL-11R-null mice, like IL-6-null mice, also exhibit impaired periosteal bone formation, indicating that the effect on osteoblast differentiation is not restricted to the trabecular bone environment (Sims et al., 2005; Sims and Vrahnas, 2014).

IL-11 may also promote bone formation in response to mechanical loading. Early evidence was that IL-11 suppressed expression of the mechanically sensitive osteocyte gene sclerostin (Walker et al., 2010), and IL-11R-null and transgenic mice demonstrated opposing cortical phenotypes (Sims et al., 2005; Takeuchi et al., 2002). IL-11 mRNA levels are elevated in bone after loading (Mantila Roosa et al., 2011), and ΔFosB, an AP-1 family member that promotes osteoblast differentiation (Sabatakos et al., 2000; Sims et al., 2002) and is rapidly upregulated with mechanical load (Kido et al., 2009), promotes IL-11 transcription in osteoblasts (Kido et al., 2009, 2010). Similar mechanisms might promote IL-11 expression in osteocytes during mechanical loading.

After these studies in cell culture and genetically modified mice, IL-11R's importance in human skeletal biology was confirmed when inactivating mutations in the human IL-11R gene were identified (Nieminen et al., 2011; Keupp et al., 2013) (Table 50.2). Individuals lacking IL-11R signaling exhibited multiple symptoms including premature cranial bone fusion (craniosynostosis), dental abnormalities, and digit malformations (Nieminen et al., 2011). The craniosynostosis was mimicked in IL-11R-null mice, and IL-11R expression was shown to be lowest in mature calvarial suture regions (Nieminen et al., 2011). This suggests IL-11 may suppress calvarial suture fusion in addition to its functions listed previously.

Oncostatin M

Oncostatin M (OSM) is a pleiotropic cytokine first identified as a secreted macrophage product (Zarling et al., 1986). Within the skeletal microenvironment, besides macrophages, it is also expressed at all stages in the osteoblast lineage (Table 50.1), including bone-lining cells, matrix-producing osteoblasts, osteocytes in murine bone (Walker et al., 2010), and bone marrow stromal cells (MSCs) and osteoblasts in human bone (Lisignoli et al., 2000); their gp130 and OSMR expression is strongly stimulated by PTH and PTH-related protein (PTHrP) (Walker et al., 2012). Osteoblast lineage cells express all three receptor subunits that can be utilized by OSM (gp130, OSMR, and LIFR) (Walker et al., 2010), but osteoclasts do not (Walker et al., 2010); and in whole bones subjected to mechanical loading, OSM and OSMR are significantly upregulated (Mantila Roosa et al., 2011).

Like IL-11 and IL-6, OSM promotes osteoclast differentiation in vitro (Tamura et al., 1993). Again, this occurs indirectly; OSM promotes RANKL transcription by stromal cells (Palmqvist et al., 2002). OSM also promotes osteoblast differentiation in vitro (Bellido et al., 1997; Walker et al., 2010; Song et al., 2007) and stimulates bone formation when provided in vivo either by injecting recombinant peptide (Walker et al., 2010) or by transgenic overexpression (Juan et al., 2009). OSM's actions to promote bone formation are mediated by promoting stromal cell commitment to osteoblast differentiation rather than adipogenesis (Walker et al., 2010; Gimble et al., 1994; Song et al., 2007), and by suppressing osteocytic expression of the Wnt antagonist sclerostin (Walker et al., 2010; Johnson et al., 2014a). Although OSM stimulates osteoblast commitment in early precursors, OSM promotes bone formation in vivo through osteocytes, as indicated when mice lacking gp130 in osteocytes failed to increase bone formation in response to OSM (Johnson et al., 2014a).

OSM is unusual in the IL-6 family because it can act through two distinct heterodimeric receptor complexes (Fig. 50.1). OSM binds first to gp130, which then heterodimerizes with OSMR or LIFR. OSM has different actions in bone through these receptors; this was uncovered by studying mice lacking OSMR (Walker et al., 2010).

Mice with global OSMR deletion demonstrated low osteoclast numbers, low osteoblast numbers, impaired bone formation on trabecular surfaces, and increased marrow adiposity (Walker et al., 2010), consistent with all effects of

OSM noted previously. In culture, osteoclast differentiation was supported poorly by osteoblasts lacking OSMR, whether OSM or 1,25-dihydroxyvitamin-D_3 was used as the stimulus, and OSM did not stimulate RANKL expression by these cells (Walker et al., 2010). When mice lacking OSMR were treated with OSM, we were surprised to find that bone formation was increased, and that OSM suppressed sclerostin expression in cultured OSMR-null osteocytes to the same level as wild-type osteocytes (Walker et al., 2010). This indicated the presence of an OSMR-independent pathway by which OSM promotes bone formation. Use of an LIFR-antagonist revealed that OSM suppressed sclerostin through the LIFR (Walker et al., 2010). We concluded that OSM stimulated RANKL and osteoclastogenesis through an OSMR:gp130 heterodimer but suppressed sclerostin and stimulated bone formation through an LIFR:gp130 heterodimer. This was surprising because although human OSM recruits OSMR and LIFR with equal affinity (Mosley et al., 1996), murine OSM binds LIFR with only very low affinity and was presumed to act in mice entirely through OSMR (Ichihara et al., 1997).

Initially, sclerostin was the only factor we could find that was regulated through the LIFR:gp130 heterodimer by OSM. A microarray study was used to define the other targets of this interaction that might promote bone formation. This revealed that murine OSM acts through LIFR to stimulate a STAT3-responsive gene signature with little effect on STAT1-responsive genes (Walker et al., 2016). Western blotting analysis revealed that murine OSM induces STAT3, but not STAT1, phosphorylation in OSMR-null cells through LIFR (Walker et al., 2016), suggesting that intracellular action favoring STAT3 over STAT1 signaling may be anabolic for bone. To test this, STAT1-null mice were crossed with an osteopenic mouse model caused by gp130-STAT1/3 hyperactivation ($gp130^{Y757F/Y757F}$, see later). Prevention of that osteopenia by reducing STAT1 availability (Walker et al., 2016) suggests that such an approach could be exploited in skeletal pathologies where gp130 signaling is elevated, such as inflammatory or metastatic bone loss.

In contrast to OSM, LIF action through LIFR (see later section) results in STAT1 and STAT3 phosphorylation in osteoblasts (Walker et al., 2016), stimulates RANKL (Palmqvist et al., 2002), and suppresses sclerostin (Walker et al., 2010). How can murine OSM act through gp130:LIFR to regulate only some gene targets of murine LIF when it binds to the same receptor complex? Such a question is common to all receptors with multiple ligands producing different biological effects within a single cell type. In the case of OSM, our data suggest that impaired gp130 and LIFR phosphorylation may be responsible for the bias toward STAT3 signaling (Walker et al., 2016), but how this is controlled remains unknown. It may relate to altered binding conformation, affinity, or stability that could be better understood by structural studies.

Macrophages support bone formation, and this has been reported to require their OSM production by three groups independently (Fernandes et al., 2013; Nicolaidou et al., 2012; Guihard et al., 2012). The studies differ in their conclusions as to whether OSM production by macrophages requires M1 activation (Guihard et al., 2012), contact with MSCs (Nicolaidou et al., 2012), or M2 polarization (Fernandes et al., 2013). Nevertheless, they provide a mechanism by which resident tissue macrophages may stimulate bone formation both in normal physiology (Chang et al., 2008) and in fracture healing (Alexander et al., 2010).

One recent finding has provided information on a pathological situation that may depend on OSM emanating from resident tissue macrophages. Formation of heterotopic ossifications in muscle resulting from trauma, such as spinal cord injury, has been shown to depend on macrophages (Genet et al., 2015). These ossifications are reduced in OSMR-null mice, suggesting OSMR targeting could provide therapeutic benefit for patients affected by this condition (Torossian et al., 2017). Genetically driven heterotopic ossifications also depend on macrophage activation (Convente et al., 2018) and may also depend on OSMR (Levesque et al., 2018).

Other leukemia inhibitory factor receptor–binding cytokines

Despite its name, the LIF receptor is used by multiple cytokines for intracellular signaling (Fig. 50.1). Leukemia inhibitory factor (LIF) itself, OSM (as described above) and cardiotrophin-1 (CT-1) each signal through a gp130:LIFR heterodimer (Fig. 50.1). In addition, some cytokines utilize a complex containing gp130:LIFR and the ciliary neurotrophic factor (CNTF) receptor (CNTFR). Consistent with LIFR's pleiotropic role, LIF and LIFR knockout mice are not identical. Most strikingly, the LIFR KO exhibits early neonatal lethality (Ware et al., 1995), while LIF knockout mice survive to early adulthood (Poulton et al., 2012).

Osteoblast lineage cells have been shown to express LIF receptor by autoradiography in cultured rat preosteoblasts (Rodan et al., 1990), murine osteoblasts (Allan et al., 1990), and labeled LIF administration in vivo (Hilton et al., 1991). In contrast, osteoclasts did not bind LIF (Allan et al., 1990). LIFR expression in osteoblasts and osteocytes has been confirmed by immunohistochemistry (Walker et al., 2010). Active LIFR signaling in cultured osteoblasts was indicated by LIFR phosphorylation in response to LIF treatment (Lowe et al., 1995; Bellido et al., 1996).

LIFR-null mice are neonatal lethal, indicating that LIFR-binding cytokines are required for early life (Ware et al., 1995). These mice had many enlarged osteoclasts at their growth plates, suggesting LIFR-binding cytokines are essential inhibitors of osteoclast formation (Ware et al., 1995). This finding is opposite to that expected, given that LIFR-binding cytokines stimulate osteoclastogenesis in vitro (Tamura et al., 1993; Richards et al., 2000). This will be discussed in more detail in Leukemia inhibitory factor and Cardiotrophin 1. LIFR-binding cytokines also modify the adult skeleton since systemic treatment with an LIFR antagonist inhibited osteoblast and osteoclast formation and increased bone mass in adult mice (Menkhorst et al., 2011).

In humans, mutations in LIFR are associated with Stüve–Wiedemann syndrome (STWS). This is a rare but severe autosomal recessive condition, often lethal during infancy due to respiratory distress and sporadic hyperthermia (Dagoneau et al., 2004). Patients exhibit dwarfism, bowing of the lower limbs, wide metaphyses, and in contrast to LIFR-null mice, high trabecular bone mass (Cormier-Daire et al., 1998; Jung et al., 2010). Although LIFR is used by many cytokines, the STWS phenotype has many similarities with the LIF-null mice (Poulton et al., 2012), consistent with defective LIF binding reported in fibroblasts from one patient with the disorder (Dagoneau et al., 2004). The mutations leading to this syndrome are diverse, and symptom severity may relate to the LIFR region affected and to which LIFR-binding cytokines have reduced affinity for the receptor. This will be discussed in more detail below.

Leukemia inhibitory factor

LIF is produced in bone by osteoblast precursors, osteoblasts (Shiina-Ishimi et al., 1986; Allan et al., 1990), hypertrophic and prehypertrophic chondrocytes, and mesenchymal cells in the invading vascular sprout during endochondral ossification (Grimaud et al., 2002). Factors that stimulate osteoblast differentiation and osteoclast formation, such as IL-1, TNFα, LPS, TGF-β, PTH, PTHrP, and retinoic acid increase LIF mRNA and protein levels in osteoblast cultures (Allan et al., 1990; Ishimi et al., 1992). In contrast, LIFR mRNA levels are inhibited by PTH treatment in osteoblasts (Walker et al., 2012). Other cells in close proximity to bone secrete LIF, such as exercised myocytes (Broholm and Pedersen, 2010), synovial fibroblasts (Le Goff et al., 2014), and breast cancer cells in the bone microenvironment (Johnson et al., 2016). Neither LIF activity nor expression has been detected in osteoclasts (Allan et al., 1990).

Like IL-6, IL-11, and OSM (Interleukin-6, Interleukin-11, and Oncostatin M sections previously), LIF is a potent stimulus of RANKL in osteoblast lineage cells (Walker et al., 2010). Despite this, and although LIF consistently increased bone resorption in organ culture (Ishimi et al., 1992), LIF concentrations must be 1000-fold greater than other osteoclastogenic factors to stimulate osteoclast formation in coculture with osteoblasts, and even then only a very mild effect is achieved (Tamura et al., 1993).

Like IL-11 and OSM, LIF stimulates bone formation in vivo, either when recombinant LIF is injected (Cornish et al., 1993) or when overexpressing cells are transplanted (Metcalf and Gearing, 1989). LIF effects on osteoblast differentiation in vitro vary between culture models used (Noda et al., 1990; Hakeda et al., 1991; Malaval et al., 1995) (for detailed discussion, see Sims and Johnson, 2012). The mechanisms by which LIF stimulates bone formation reflect many actions noted previously for IL-11 and OSM (Interleukin-11 and Oncostatin M sections). LIF alters stromal cell lineage commitment toward osteoblastogenesis rather than adipogenesis by downregulating peroxisome proliferator-activated receptor gamma (PPARγ) (Poulton et al., 2012), consistent with early effects showing that LIF inhibits adipocyte differentiation when administered early in adipocyte differentiation (Gimble et al., 1994) (for detailed discussion, see Sims and Johnson, 2012). And like IL-11 and OSM, LIF also inhibits sclerostin expression (Walker et al., 2010).

Since LIF promotes osteoclast formation and bone formation in organ culture or in vivo while having mild effects on cultured cells, LIF's osteoclastogenic action may require additional factors and cell types present in vivo but not in vitro. In line with such a hypothesis, the LIF-null mouse showed region-specific phenotypes.

The most obvious change in LIF-null mice was a 20% reduction in bone length that occurred after the immediate postnatal period (Poulton et al., 2012). Since no other gp130 ligand or ligand-specific receptor knockout displayed such a growth defect (McGregor et al., 2010; Walker et al., 2008; Poli et al., 1994; Sims et al., 2005), this suggests LIF is the main gp130-signaling cytokine regulating longitudinal bone growth. The impairment in growth was related to activities at the chondro-osseous junction, not to any change in chondrocyte proliferation.

In normal skeletal development, endochondral ossification begins when chondrocytes in the central region undergo hypertrophy due to hypoxia, followed by vascular invasion and formation of chondroclasts (osteoclasts resorbing cartilage). In LIF-null mice, chondrocyte differentiation, vascular invasion and chondroclast-mediated destruction of the cartilage anlagen followed normal chronology. However, early work noted enlarged, hyperactive osteoclasts at the chondro-osseous junction in LIF, LIFR, and gp130 neonates (Bozec et al., 2008; Ware et al., 1995; Shin et al., 2004). These enlarged osteoclasts were also observed in adult LIF-null mice but only at the chondro-osseous junction (i.e. in

chondro-clasts) and not in remodeling bone (Poulton et al., 2012). This region-specific defect in osteoclast/chondroclast formation was associated with increased VEGFA expression by hypertrophic chondrocytes and enhanced vascularization specific to the chondro-osseous junction (Poulton et al., 2012). The increased vascularization may provide more precursors, thereby allowing larger chondroclasts to form. The enlarged chondroclasts in LIF-null mice might also result from a difference in the cartilage matrix produced by LIF-deficient chondrocytes. The importance of this local influence was indicated by normal osteoclast morphology when LIF-null osteoclasts were formed in vitro. While chondroclast morphology and number depend on LIF, osteoclasts generated on LIF-null trabecular bone surfaces were normal, indicating that osteoclast formation (on bone) is not LIF-dependent.

In LIF-null mice, immediately below the growth plate, newly formed clumps of woven bone formed despite resorption of the calcified cartilage template by the enlarged chondroclasts (Poulton et al., 2012). This was again region-specific because it was not observed in the secondary spongiosa. Increased vessel formation at the transition zone from the growth plate to trabecular bone may also be the stimulus for increased bone formation and bone mass in this region. The sudden end to the growth plate in LIF-null mice and areas of woven bone immediately below it are strikingly similar to STWS histology (Cormier-Daire et al., 1998). The reduced bone length and low trabecular bone mass in remodeling bone are consistent with the growth retardation and osteoporosis in STWS patients that survive beyond 1 year (Jung et al., 2010). This indicates that although there are many cytokines that act through the LIFR, it is most likely that the main defect leading to the STWS skeletal phenotype is defective LIF binding to the LIFR (Dagoneau et al., 2004).

A third region-specific phenotype was observed in LIF-null mice. In the bone remodeling trabeculae in adult mice, blood vessel morphology was normal but trabecular bone mass was low due to suppressed bone formation (Poulton et al., 2012). These mice also exhibited high marrow adiposity (Poulton et al., 2012) consistent with the LIF actions on sclerostin expression and osteoblast and adipocyte differentiation noted in vitro.

Cardiotrophin 1

CT-1 signals through a gp130:LIFR heterodimer in a complex that may include a CT-1-specific receptor (Pennica et al., 1995). Like IL-11, OSM, and LIF, CT-1 acts in vitro to stimulate osteoclast formation in coculture by inducing RANKL in osteoblast lineage cells (Richards et al., 2000). CT-1 also stimulates bone formation in vivo and promotes osteoblast differentiation rather than adipogenesis in vitro (Walker et al., 2008). Like IL-11R and OSMR-null mice, CT-1-null mice exhibit low bone formation and bone resorption in adulthood with elevated marrow adiposity (Walker et al., 2008). The mechanisms by which CT-1 stimulates bone formation appears to relate to three key activities that are again shared by other family members: (1) promoting osteoblast commitment by stimulating C/EBPδ and C/EBPβ transcription (Walker et al., 2008), (2) suppressing adipocyte differentiation by reducing *Zfp467* transcription (Quach et al., 2011), and (3) stimulating Wnt signaling by suppressing sclerostin production in osteocytes (Walker et al., 2010). Even though IL-11, OSM, LIF and CT-1 share all these actions, it is striking that the IL-11R-, OSMR-, LIF-, and CT-1-null phenotypes are all significant, revealing critical roles for each cytokine and their inability to compensate for one another.

CT-1 has two unique functions. The first is its role as a coupling factor. CT-1 expression has not been found in the osteoblast lineage, but it is expressed specifically by osteoclasts in the bone microenvironment (Walker et al., 2008). This suggests it acts as an osteoclast-derived "coupling factor" that stimulates bone formation to follow bone resorption during remodeling (Walker et al., 2008).

CT-1's other unique function was revealed by the enlarged osteoclasts throughout the skeleton of CT-1-null mice (Walker et al., 2008). This was intrinsic to the hematopoietic lineage because CT-1-null osteoclasts were also enlarged when formed in vitro from CT-1-null osteoclast precursors (Walker et al., 2008). CT-1-null osteoclasts also had defective resorption activity and resorbed cartilage with greater than usual efficiency but had poor resorptive action on bone. Consequently, the mice exhibited a mild osteopetrosis with substantial cartilage remnants within the bone matrix in adult mice (Walker et al., 2008). It is not known whether CT-1-deficient osteoclasts are large due to their defective function on bone as observed in other mice with defects in osteoclast attachment or function (Gil-Henn et al., 2007; Neutzsky-Wulff et al., 2010). The mechanisms by which CT-1 controls osteoclast formation, morphology and activity remain unresolved.

Cytokines that complex with ciliary neurotrophic factor receptor

Some LIFR-binding cytokines also complex with the CNTFR (Fig. 50.1). These include CNTF itself, which acts through a gp130:LIFR:CNTFR heteromer, and some less clearly described cytokines: neuropoietin (sometimes known by its gene name *Ctf2/CTF2*) and cardiotrophin-like cytokine factor 1 (CLCF1). The latter has also been known as cardiotrophin-like cytokine and was earlier known as new neurotrophin-1 or B-cell stimulatory factor-3. CLCF1 acts as two possible

"compound cytokines": either bound to the soluble ciliary neurotrophic factor receptor (sCNTFR) or to cytokine receptor-like factor 1 (CRLF1). CRLF1 is also known as cytokine like factor 1 and NR6. These compound cytokines will be referred to as CLCF1/CRLF1 and CLCF1/sCNTFR.

CLCF1, neuropoietin (NP), and CNTF contain a highly conserved tryptophan hot spot that enables them all to bind at the same location on CNTFR (Rousseau et al., 2008). The resulting complex then recruits gp130 and LIFR (Elson et al., 2000; Derouet et al., 2004; Rousseau et al., 2008). Since CNTFR exists as either a membrane-anchored form or a soluble form (sCNTFR) (Davis et al., 1993), these cytokines can also influence cells that do not express the membrane-bound receptor through *trans*-signaling if sCNTFR is made available to them. NP and CLCF1 signaling are reportedly enhanced by sortilin, which binds directly to LIFR and promotes gp130:LIFR heterodimer assembly (Larsen et al., 2010).

CNTFR-binding cytokines differ markedly in their actions to all IL-6 cytokines listed above and have been less intensely studied in the skeleton. Each will now be discussed in turn.

Ciliary neurotrophic factor

CNTF, unlike all the previously described cytokines, does not stimulate osteoclast formation in culture (McGregor et al., 2010), does not suppress sclerostin expression or promote osteoblast mineralization (McGregor et al., 2010), and does not suppress adipogenesis (McGregor et al., 2010; White et al., 2008).

CNTF was detected by immunohistochemistry in osteoclasts, osteoblasts, and osteocytes (McGregor et al., 2010). CNTF is also expressed at very high levels in skeletal muscle, where its mRNA levels were >10-fold higher than all other IL-6 family cytokines (Johnson et al., 2014b). This suggested CNTF is a bone-active myokine, a factor released by muscle either locally or into the circulation. Other IL-6 family members known to modify bone structure have also been postulated to be circulating myokines, including IL-6 and LIF (Whitham et al., 2012; Broholm et al., 2011; Hamrick, 2011). When recombinant CNTF was applied to cultured osteoblasts without adding soluble receptor, it mildly inhibited osteoblast differentiation, reducing their ability to form mineralized nodules, and transiently suppressed osteoblast transcription factor, osterix (McGregor et al., 2010). Adding the soluble receptor amplified this effect but did not modify RANKL expression (Johnson et al., 2014b).

Global CNTF deletion resulted in mice with a mild reduction in bone length (McGregor et al., 2010), indicating a minor role in bone growth. Apart from this, the CNTF-null phenotype was sex-specific—female CNTF-null mice had high trabecular bone volume caused by increased bone formation rate compared with controls, while male CNTF nulls had normal trabecular bone mass but impaired periosteal growth. This suggests that CNTF plays different roles in trabecular and periosteal bone formation. This sex and region specificity may result from a difference in muscle development, which is also sex-specific (Park et al., 1999), and CNTF's myokine action (Johnson et al., 2014b).

Both sex-specific bone CNTF-null phenotypes (high trabecular number in females and slim cortical bone in males) were recapitulated by bone marrow transfer from CNTF-null mice to wild-type recipients (Askmyr et al., 2015). The trabecular phenotype is difficult to interpret due to a 10-fold reduction in trabecular bone mass caused by marrow transfer alone. However, the change in periosteal perimeter induced by marrow transplantation suggests CNTF may influence cortical mass from within the internal bone marrow compartment. This is similar to IL-6's action as an osteotransmitter (Johnson et al., 2015) (see IL-6 section, previous) and suggests that CNTF may also have an osteotransmitter function.

Cardiotrophin-like cytokine factor 1 and cytokine receptor-like factor 1

Although CLCF1 contains a signal sequence (Senaldi et al., 1999), its secretion is inefficient unless coexpressed with its chaperone CRLF1 (Elson et al., 2000; Alexander et al., 1999a). Forced CLCF/sCNTFR coexpression allows sCNTFR to act as a substitute chaperone (Plun-Favreau et al., 2001), but whether this compound cytokine exists physiologically is not known. CLCF1 therefore acts as two possible "compound cytokines": CLCF1/CRLF1 and CLCF1/sCNTFR. Their actions in multiple organs are discussed in a recent review (Sims, 2015).

CRLF1 and CLCF1 human gene mutations both lead to syndromes that include "cold-induced sweating" (CISS—profuse sweating after exposure to cold), suckling problems during infancy and feeding difficulties in adult life, as well as skeletal abnormalities including spinal kyphoscoliosis, and palatal and frontonasal malformations (Knappskog et al., 2003; Rousseau et al., 2006). Since human mutations in CNTF are common, but are not associated with any notable health problems (Takahashi et al., 1994), and neuropoietin is a pseudogene in humans (Derouet et al., 2004), CLCF1 and CRLF1 are the most biologically important ligands for CNTFR in human development. Similarly in mice,

CLCF1 (Zou et al., 2009), CRLF1 (Alexander et al., 1999a) and CNTFR-null (DeChiara et al., 1995) mice all die in the perinatal period due to a suckling defect.

Skeletal symptoms of human *CRLF1* and *CLCF1* mutations are less severe than those observed with *LIFR* mutations, which is not surprising given that many other cytokines use LIFR. The mechanisms by which CLCF1 composite cytokines support skeletal functions have not been examined in either humans or mice deficient in these cytokines or receptors, due to the early lethality. It is unknown whether defects in the skeleton are caused by a lack of direct CLCF1 effect on the skeleton or result from the motor neuron dysfunction and subsequent muscle atrophy.

CLCF1 and CRLF1 are expressed within the developing murine skeleton, both in limb buds (Alexander et al., 1999a; Elson et al., 1998) and in embryonic muscle and cartilage (Forger et al., 2003). CRLF1 was also detected by in situ hybridization in osteoblasts and osteocytes in a mouse model of ectopic bone formation (Clancy et al., 2003). CLCF1 and CRLF1 are detected in cultured murine primary osteoblasts, and are stimulated by PTH (McGregor et al., 2010; Walker et al., 2012). In contrast, CLCF1 and CRLF mRNA levels are lowered in bones subjected to mechanical loading (Zhang et al., 2009). Like CNTF, CLCF1 administration mildly inhibited late osteoblast differentiation and suppressed osterix expression (McGregor et al., 2010), suggesting CLCF1 composite cytokines suppress bone formation by direct action on osteoblasts.

Neuropoietin

NP also forms a receptor complex with CNTFR, LIFR and gp130 (Fig. 50.1). It was identified by an IL-6 structural profile-based computational genetic screen and purified from embryonic mouse brain (Derouet et al., 2004). While the earliest analysis could identify no NP transcripts in adult murine tissues (Derouet et al., 2004), NP mRNA has been detected in bone marrow macrophages isolated from adult mice (McGregor et al., 2010). NP has been reported to inhibit adipogenesis by 3T3-L1 cells in vitro (White et al., 2008), but did not increase osteoblast differentiation or suppress adipogenesis in bipotential mesenchymal cells (McGregor et al., 2010), suggesting this may be an effect on late adipocyte differentiation. While the NP gene has orthologues in rat, chimpanzee and human, the human gene lacks the third exon and NP protein is not expressed (Derouet et al., 2004). This suggests NP exists only as a pseudogene in humans and has no function in human biology or pathology. Since it acts through receptors that are present in the human, further research may reveal roles useful for therapeutic approaches.

IL-27Rα-binding cytokines

Other cytokines that act through gp130-containing complexes utilize a gp130 heterodimer with the interleukin-27 receptor (IL-27Rα/WSX-1) (Fig. 50.1). These include the heterodimeric protein IL-27 (p28:EBI3) and the mitochondrial gene product humanin. Humanin has no known action in bone.

IL-27R is expressed in osteoclast precursors (Kalliolias et al., 2010) and osteoblasts (Kamiya et al., 2011). Although IL-27 does not appear to influence osteoblast differentiation, it suppresses osteoclastogenesis, both by direct action on osteoclast precursors (Kalliolias et al., 2010; Kamiya et al., 2011) and through indirect actions on T cells (Adamopoulos and Pflanz, 2013). IL-27-Fc treatment suppressed both inflammation and osteoclastogenesis in an animal model of rheumatoid arthritis (Park et al., 2012). Although IL-27Rα-null mice have heightened responses to inflammatory stimuli (Batten et al., 2006; Holscher et al., 2005), no bone phenotype has been described for mice or humans null in either IL-27 subunit (p28 or EBI3).

Effects of global, cell-specific, and pathway-specific gp130 modulation

The above work indicates that IL-6 family members have many roles that regulate bone metabolism and that CRLF1/CLCF1 actions through CNTFR and LIFR are necessary for life, as indicated by neonatal lethality in global knockouts for these genes (Ware et al., 1995; Alexander et al., 1999a; Zou et al., 2009; DeChiara et al., 1995). It is not surprising then that global null mice for gp130 itself also exhibited neonatal lethality due to myocardial, skeletal, respiratory and hematological defects (Yoshida et al., 1996). Skeletal analysis showed many large, active osteoclasts (Kawasaki et al., 1997; Shin et al., 2004). Due to the early lethality, gp130-null mice could not provide information on gp130's roles in the adult skeleton, on relative contributions of gp130 signaling in specific cell types, the importance of gp130's specific intracellular downstream signaling pathways, or the requirements for negative feedback mechanisms. The next sections will discuss these aspects.

Insights from mice and a patient with gp130 signaling mutations

A recent publication has identified a human gp130 missense mutation with loss of IL-6, IL-11, IL-27 and OSM signaling, but intact LIF response (Schwerd et al., 2017). This patient exhibited multiple symptoms, including emphysema, immunological defects and skeletal phenotypes including craniosynostosis, dental abnormalities and progressive scoliosis. These are consistent with murine and human deficiencies in IL-6, IL-11, IL-27 and OSM described previously. The authors noted that the phenotype that was similar to the Hyper-IgE syndrome described in patients with dominant negative STAT3 mutations (Minegishi et al., 2007; Holland et al., 2007), consistent with STAT3 as the key signal transducer for IL-6 family cytokines. The parallel syndromes suggest it is the loss of IL-6 family cytokines that cause the phenotypes, even though other cytokines, such as leptin, erythropoietin, and granulocyte colony stimulating factor (G-CSF), signal through STAT3. The human gp130 missense condition has some similarities with a previously described phenotype in mice with a knock-in gp130 mutation lacking STAT3 signaling (Ernst et al., 2001). These mice had immune deficiency and reduced lifespan due to gastrointestinal ulceration (Ernst et al., 2001). They also exhibited reduced femoral length due to early growth plate closure (Sims et al., 2004) and severe inflammatory joint disease (Ernst et al., 2001). Surprisingly, although many IL-6 family cytokines act through STAT3 to induce osteoclast formation and bone formation (O'Brien et al., 1999; Bellido et al., 1997; Walker et al., 2016), the mice showed no alteration in osteoclast or osteoblast numbers, nor any change in trabecular bone mass when corrected for their reduced size (Sims et al., 2004).

In contrast, a second mouse model with a gp130 knock-in mutation targeting the tyrosine that initiates SHP2/Ras/MAPK activation (*gp130*$^{Y575F/Y757F}$ mice) showed normal bone size, but significant osteopenia (Sims et al., 2004). Although both bone resorption and bone formation are elevated, the resorption outstrips formation, resulting in osteopenia. The primary defect in osteoclastogenesis in these mice led to a coupling-induced increase in bone formation that was rescued by deleting IL-6, providing early indication that coupling signals from the osteoclast to the osteoblast may be IL-6-dependent (see Chapter 10) (Sims et al., 2004). While that early work suggested the phenotype resulted from SHP2/Ras/MAPK pathway deletion (Sims et al., 2004), these mice also exhibited elevated hyperactive STAT1 and STAT3 signaling (Jenkins et al., 2005). We recently noted the *gp130*$^{Y575F/Y757F}$ phenotype could be rescued by blocking STAT1 signaling but not by reducing STAT3 activation (Walker et al., 2016). This indicates that increasing the ratio of STAT3:STAT1 signaling downstream of gp130 may provide therapeutic benefit in patients with bone loss related to elevated IL-6 family cytokines, such as colitis or rheumatoid arthritis.

Contributions of gp130 in the osteoblast lineage to bone structure and parathyroid hormone anabolic action

With the advent of mice that express Cre-recombinase in a cell-lineage restricted manner, it became possible to test the contributions of gp130 signaling within the osteoblast lineage to bone formation and resorption. Although most IL-6 family cytokines promote osteoclast formation by promoting RANKL expression in the osteoblast lineage (see previous), when gp130 deletion was directed to the entire osteoblast lineage (*Osx1Cre.gp130*$^{f/f}$) or to late stage osteoblasts and osteocytes (using *Dmp1Cre.gp130*$^{f/f}$), there was no change in osteoclast numbers in vivo (Johnson et al., 2014a). This supported earlier conclusions that RANKL production by osteoblasts in response to IL-6 family cytokines may be restricted to pathological states including inflammatory arthritis, periodontal disease and inflammatory bowel disease (see previous). Although many IL-6 family cytokines shift bipotential osteoblast precursors toward osteoblast differentiation rather than adipogenesis, no change in marrow adiposity was observed in *Osx1Cre.gp130*$^{f/f}$ or *Dmp1Cre.gp130*$^{f/f}$ mice, consistent with these effects occurring earlier in the lineage. Instead, gp130 deletion in committed osteoblasts or osteocytes reduced trabecular bone formation, resulting in low trabecular bone mass (Johnson et al., 2014a). This established that the main role for gp130 in the osteoblast lineage in trabecular bone physiology is not to support osteoclastogenesis, or to suppress adipogenesis, but to promote bone formation. The phenotype was identical in both models, indicating that IL-6 family cytokines promote bone formation through gp130 signaling in osteocytes, consistent with IL-11, OSM, LIF and CT-1 suppressing sclerostin expression (Walker et al., 2010).

In contrast to their low trabecular bone mass, *Osx1Cre.gp130*$^{f/f}$ and *Dmp1Cre.gp130*$^{f/f}$ mice exhibited greater cortical bone diameter than controls (Johnson et al., 2014a). This was in direct opposition to the slimmer cortices observed in global knockouts for IL-6, IL-11R, CT-1 and OSMR (Sims et al., 2005; Walker et al., 2008, 2010), and may occur as compensation for poor cortical bone material properties and low collagen production when osteocytes lack gp130 (Johnson et al., 2014a). IL-6 family cytokines' ability to regulate intrinsic bone matrix strength is consistent with earlier work

showing that IL-6-null cortical bone has a lower mineral-to-matrix ratio than controls (Yang et al., 2007). The mechanisms by which IL-6 family cytokines regulate collagen deposition and mineral accumulation in newly formed bone remain largely unexplored.

Intermittent PTH administration robustly stimulates bone formation, which is why it is used as a bone-building therapy for osteoporosis (Lindsay et al., 1997). Mice with osteocyte-targeted gp130 deletion showed no anabolic response to PTH in trabecular or cortical bone (Standal et al., 2014). This is consistent with PTH actions to rapidly stimulate IL-6 (Greenfield et al., 1996; Lowik et al., 1989), IL-11, OSMR, LIF, CRLF1 (Walker et al., 2012), and gp130 (Romas et al., 1996) expression in osteoblasts. The suppressed PTH effect was explained, at least in part, by impaired osteoblast differentiation and reduced PTH receptor expression in bones lacking gp130 in osteocytes (Standal et al., 2014). PTH anabolic action also requires suppression of the Wnt signaling inhibitors sclerostin and Dickkopf 1 (Dkk1) (Kulkarni et al., 2005; Kramer et al., 2010). In mice lacking osteocytic gp130, although PTH still stimulated RANKL expression, indicating an intact PTH response, it did not suppress sclerostin or Dkk1 transcription (Standal et al., 2014). This suggests PTH anabolic action in bone is mediated by gp130-dependent cytokines acting in osteocytes to suppress sclerostin and Dkk1.

The gp130-binding cytokine mediating PTH anabolic action in osteocytes is not yet known. It may be OSM, LIF, IL-11 or CT-1, or a combination of these because they all suppress sclerostin (Walker et al., 2010). It is unlikely to be mediated by OSMR, because OSMR deletion did not ablate PTH anabolic effect but converted it to a catabolic (bone destroying) action. When OSMR-deficient osteoblasts were stimulated with PTH in vitro, osteoclast formation was much greater than in wild-type osteoblasts (Walker et al., 2012). This was also observed in vivo, where OSMR-null mice treated with PTH converted an anabolic treatment protocol to a catabolic effect (Walker et al., 2012). Anabolic intermittent PTH treatment is normally associated with only a short and transient induction of RANKL (Ma et al., 2001), while persistently high circulating PTH levels are catabolic (Frolik et al., 2003) due to a persistently high RANKL level (Ma et al., 2001). In OSMR-null osteoblasts, RANKL was persistently high after PTH injection; this could explain how a normally PTH anabolic treatment was converted to a catabolic response (Walker et al., 2012). In addition, OSM stimulates Wnt16 production (Moverare-Skrtic et al., 2014) through OSMR (Walker et al., 2016). This is an osteoblast-derived stimulus of OPG production; OSMR may restrain osteoclast formation through this pathway within the osteoblast lineage.

Contribution of gp130 in osteoclasts to bone physiology

Mature osteoclasts have the capacity to respond to IL-6 and IL-11 because IL-6R, IL-11R and gp130 itself have been identified in mature osteoclasts (Table 50.1) (Gao et al., 1998; Romas et al., 1996). OSMR and LIFR have not been detected in osteoclasts or their precursors (Allan et al., 1990; Walker et al., 2010) precluding OSM, CT-1, LIF or CNTFR-associated cytokines from acting on these cells. The direct action of IL-6 on osteoclasts has been controversial. Some studies detected no effect of IL-6 on osteoclastic resorption in vitro (Axmann et al., 2009; Hattersley et al., 1988), others report increased resorption and differentiation (Gao et al., 1998). Others report IL-6 can directly stimulate osteoclast precursors to form osteoclasts (Kudo et al., 2003) and partially facilitate RANKL or TNF-induced osteoclastogenesis (Axmann et al., 2009). However, most published work indicates IL-6 family cytokines require RANKL-producing cells such as osteoblasts (Tamura et al., 1993), or (in the context of arthritis) T lymphocytes (Horwood et al., 1999) to be present to promote osteoclast formation.

When gp130 was deleted from osteoclasts in the *Ctsk.gp130$^{f/f}$* mouse, there was no change in osteoclast numbers, nor any change in bone resorption. In contrast, bone formation was reduced on both trabecular and periosteal surfaces. Although osteoclasts are defined by their ability to resorb bone, they also stimulate bone forming osteoblasts by releasing "coupling factors" (Martin and Sims, 2005), such as CT-1 (described previously and Chapter 10). The phenotype of the *Ctsk.gp130$^{f/f}$* mouse suggests that gp130's main physiological role in osteoclasts is to promote coupling factor release or activity. This was consistent with earlier work showing that coupling factor release in mice with a high osteoclast activity due to enhanced STAT3 signaling requires IL-6 (Sims et al., 2004). While IL-6 stimulated STAT3 phosphorylation in cultured osteoclasts, previously described coupling factors were not regulated by IL-6 at the mRNA level. Since the periosteal site at which bone formation was measured in both models lacks osteoclasts, we suggested that the IL-6 dependent factor/s emanating from the osteoclast to maintain periosteal bone formation is an "osteotransmitter" action. This emphasizes that these factors are unlikely to signal directly from the osteoclast to the distant periosteal surface, but are transmitted through other cells (e.g., the cortical osteocyte network).

The contributions of intracellular negative feedback through suppressor-of-cytokine-signaling proteins

JAK/STAT signaling depends on intracellular negative feedback from SOCS proteins to switch off STAT phosphorylation once target gene transcription is initiated (Croker et al., 2008) (Fig. 50.2). Three SOCS proteins limit IL-6 family cytokines: SOCS1, which provides negative feedback for STAT1; SOCS3, which provides negative feedback for STAT3; and CISH, which provides negative feedback for STAT5. These proteins are not specific for the IL-6 family, because they also provide this feedback to other cytokines and factors that utilize STAT1, STAT3 or STAT5, such as granulocyte-colony stimulating factor (G-CSF), leptin, growth hormone and type I interferons, which all have actions on the skeleton (Winkler et al., 2010; Sims et al., 2000; Takayanagi et al., 2002; Lee et al., 2002b).

Mice with global SOCS1 deletion do not survive beyond weaning (Starr et al., 1998), but exhibit small size and some evidence of low osteoblast activity (Abe et al., 2006). This is consistent with the proposal (Walker et al., 2016) that favoring STAT3 intracellular signaling over STAT1 would suppress osteoblast differentiation. CISH-null mice survive to adulthood (Yang et al., 2013), and our preliminary observations detected increased periosteal growth (Alister Ward, Saeed Mahmoudi Meimand, Natalie A Sims, personal communication) consistent with hyperactive growth hormone signaling. Whether these phenotypes are directly related to hyperactivation of IL-6 family signaling is not known.

SOCS3-null mice are neonatal lethal (Marine et al., 1999), but a requirement for SOCS3 negative feedback in bone has been reported in chondrocytes (Liu et al., 2014), in the hematopoietic lineage (Wong et al., 2006a), and in osteocytes (Cho et al., 2017). Mice lacking SOCS3 in chondrocytes and in the hematopoietic lineage exhibited increased susceptibility to joint disease, including increased osteoclastic bone destruction (Wong et al., 2006a; Liu et al., 2014). In the mice null for SOCS3 in the hematopoietic lineage, increased osteoclast and osteoblast numbers, and low trabecular bone mass were observed (Wong et al., 2006a). This was not reproduced in mice with SOCS3 deletion restricted to the macrophage/osteoclast lineage (Wong et al., 2006a), suggesting it occurs indirectly.

We recently reported that SOCS3 negative feedback in osteocytes is required for the process by which cortical bone forms during growth (corticalization) (Cho et al., 2017). Mice with SOCS3 deletion targeted to osteocytes (*Dmp1Cre.Socs3*$^{f/f}$ mice) showed a unique and dramatic phenotype of delayed corticalization in the metaphysis. In young *Dmp1Cre.Socs3*$^{f/f}$ mice, the same delay in corticalization, associated with high bone formation was seen in both males and females. This phenotype persisted in females, resulting in a profound high trabecular bone mass phenotype in their adult skeleton. In male mice, the phenotype resolved after puberty (Cho et al., 2017). This indicates that SOCS3 in osteocytes restrains bone formation throughout life by providing negative feedback to those cytokines previously shown to promote bone formation, such as OSM, CT-1 and LIF (Poulton et al., 2012; Walker et al., 2008, 2010). The male *Dmp1Cre.Socs3*$^{f/f}$ mice recovered from the phenotype by an increase in resorption to match the high bone formation. This suggests that when osteoblast numbers decrease with maturity, which occurs earlier in male mice than in females, SOCS3 restrains both bone formation and resorption. This is probably achieved by providing negative feedback to cytokines (such as OSM, CT-1, IL-6 and IL-11) that act on the osteoblast lineage to stimulate RANKL production (Tamura et al., 1993; Udagawa et al., 1995; Romas et al., 1996).

Differences in skeletal structure are well-described in male and female mammals. In humans, this difference arises because boys have a longer growth period, during which the periosteum continues to expand, while girls form bone on the endocortical metaphysis via endocortical apposition (Seeman, 1997; Schoenau et al., 2001). The extended delay in corticalization in female *Dmp1Cre.Socs3*$^{f/f}$ mice compared with males suggested that androgen stimulates corticalization through SOCS3 negative feedback in osteocytes. This was confirmed by sex hormone treatment studies (Cho et al., 2017). Since many cytokines that require SOCS3 for negative feedback act in osteocytes, including IL-6 family members (see previously and Table 50.1), G-CSF (Winkler et al., 2010) and leptin (Lee et al., 2002b), the delay in corticalization could be explained by hyperactivity in osteocytes of many cytokines. The specific hyperactive cytokine/s that must be suppressed by SOCS3 for corticalization to occur has not been identified. However, the sex-specificity of the phenotype was partially ablated by genetic deletion of IL-6 (Cho et al., 2017). This is consistent with feminization of cortical bone in male IL-6-null mice, which exhibit narrow cortices equivalent to their female wildtype counterparts (Sims et al., 2005) and indicates that androgen-receptor-mediated regulation of IL-6 in osteocytes promotes male-specific pattern of corticalization.

References

Abbas, S., Zhang, Y.H., Clohisy, J.C., Abu-Amer, Y., 2003. Tumor necrosis factor-alpha inhibits pre-osteoblast differentiation through its type-1 receptor. Cytokine 22, 33–41.

Abe, T., Nomura, S., Nakagawa, R., Fujimoto, M., Kawase, I., Naka, T., 2006. Osteoblast differentiation is impaired in SOCS-1-deficient mice. J. Bone Miner. Metab. 24, 283–290.

Adamopoulos, I.E., Pflanz, S., 2013. The emerging role of Interleukin 27 in inflammatory arthritis and bone destruction. Cytokine Growth Factor Rev. 24, 115–121.

Adamopoulos, I.E., Tessmer, M., Chao, C.C., Adda, S., Gorman, D., Petro, M., Chou, C.C., Pierce, R.H., Yao, W., Lane, N.E., Laface, D., Bowman, E.P., 2011. IL-23 is critical for induction of arthritis, osteoclast formation, and maintenance of bone mass. J. Immunol. 13, 13.

Al-Daghri, N.M., Aziz, I., Yakout, S., Aljohani, N.J., Al-Saleh, Y., Amer, O.E., Sheshah, E., Younis, G.Z., Al-Badr, F.B., 2017. Inflammation as a contributing factor among postmenopausal Saudi women with osteoporosis. Medicine (Baltim.) 96, e5780.

Alexander, K.A., Chang, M.K., Maylin, E.R., Kohler, T., Muller, R., Wu, A.C., van Rooijen, N., Sweet, M.J., Hume, D.A., Raggatt, L.J., Pettit, A.R., 2010. Osteal macrophages promote in vivo intramembranous bone healing in a mouse tibial injury model. J. Bone Miner. Res. 26, 1517–1532.

Alexander, W.S., Rakar, S., Robb, L., Farley, A., Willson, T.A., Zhang, J.G., Hartley, L., Kikuchi, Y., Kojima, T., Nomura, H., Hasegawa, M., Maeda, M., Fabri, L., Jachno, K., Nash, A., Metcalf, D., Nicola, N.A., Hilton, D.J., 1999a. Suckling defect in mice lacking the soluble hemopoietin receptor NR6. Curr. Biol. 9, 605–608.

Alexander, W.S., Starr, R., Fenner, J.E., Scott, C.L., Handman, E., Sprigg, N.S., Corbin, J.E., Cornish, A.L., Darwiche, R., Owczarek, C.M., Kay, T.W.H., Nicola, N.A., Hertzog, P.J., Metcalf, D., Hilton, D.J., 1999b. SOCS1 is a critical inhibitor of interferon γ signaling and prevents the potentially fatal neonatal actions of this cytokine. Cell 98, 597–608.

Allan, E.H., Hilton, D.J., Brown, M.A., Evely, R.S., Yumita, S., Metcalf, D., Gough, N.M., Ng, K.W., Nicola, N.A., Martin, T.J., 1990. Osteoblasts display receptors for and responses to leukemia-inhibitory factor. J. Cell. Physiol. 145, 110–119.

Amcheslavsky, A., Bar-Shavit, Z., 2006. Interleukin (IL)-12 mediates the anti-osteoclastogenic activity of CpG-oligodeoxynucleotides. J. Cell. Physiol. 207, 244–250.

Arend, W.P., Welgus, H.G., Thompson, C., Eisenberg, S.P., 1990. Biological properties of recombinant human monocyte-derived interleukin 1 receptor antagonist. J. Clin. Investig. 85, 1694–1697.

Arita, K., South, A.P., Hans-Filho, G., Sakuma, T.H., Lai-Cheong, J., Clements, S., Odashiro, M., Odashiro, D.N., Hans-Neto, G., Hans, N.R., Holder, M.V., Bhogal, B.S., Hartshorne, S.T., Akiyama, M., Shimizu, H., Mcgrath, J.A., 2008. Oncostatin M receptor-beta mutations underlie familial primary localized cutaneous amyloidosis. Am. J. Hum. Genet. 82, 73–80.

Ashcroft, G.S., Mills, S.J., Lei, K., Gibbons, L., Jeong, M.J., Taniguchi, M., Burow, M., Horan, M.A., Wahl, S.M., Nakayama, T., 2003. Estrogen modulates cutaneous wound healing by downregulating macrophage migration inhibitory factor. J. Clin. Investig. 111, 1309–1318.

Askmyr, M., White, K.E., Jovic, T., King, H.A., Quach, J.M., Maluenda, A.C., Baker, E.K., Smeets, M.F., Walkley, C.R., Purton, L.E., 2015. Ciliary neurotrophic factor has intrinsic and extrinsic roles in regulating B cell differentiation and bone structure. Sci. Rep. 5, 15529.

Axmann, R., Bohm, C., Kronke, G., Zwerina, J., Smolen, J., Schett, G., 2009. Inhibition of interleukin-6 receptor directly blocks osteoclast formation in vitro and in vivo. Arthritis Rheum. 60, 2747–2756.

Azuma, Y., Kaji, K., Katogi, R., Takeshita, S., Kudo, A., 2000. Tumor necrosis factor-alpha induces differentiation of and bone resorption by osteoclasts. J. Biol. Chem. 275, 4858–4864.

Bajayo, A., Goshen, I., Feldman, S., Csernus, V., Iverfeldt, K., Shohami, E., Yirmiya, R., Bab, I., 2005. Central IL-1 receptor signaling regulates bone growth and mass. Proc. Natl. Acad. Sci. U. S. A. 102, 12956–12961.

Bakker, A.D., Kulkarni, R.N., Klein-Nulend, J., Lems, W.F., 2014. IL-6 alters osteocyte signaling toward osteoblasts but not osteoclasts. J. Dent. Res. 93, 394–399.

Batten, M., Li, J., Yi, S., Kljavin, N.M., Danilenko, D.M., Lucas, S., Lee, J., de Sauvage, F.J., Ghilardi, N., 2006. Interleukin 27 limits autoimmune encephalomyelitis by suppressing the development of interleukin 17–producing T cells. Nat. Immunol. 7, 929.

Baugh, J.A., Bucala, R., 2002. Macrophage migration inhibitory factor. Crit. Care Med. 30, S27–S35.

Bellido, T., Borba, V.Z., Roberson, P., Manolagas, S.C., 1997. Activation of the Janus kinase/STAT (signal transducer and activator of transcription) signal transduction pathway by interleukin-6-type cytokines promotes osteoblast differentiation. Endocrinology 138, 3666–3676.

Bellido, T., Stahl, N., Farruggella, T.J., Borba, V., Yancopoulos, G.D., Manolagas, S.C., 1996. Detection of receptors for interleukin-6, interleukin-11, leukemia inhibitory factor, oncostatin M, and ciliary neurotrophic factor in bone marrow stromal/osteoblastic cells. J. Clin. Investig. 97, 431–437.

Bendixen, A.C., Shevde, N.K., Dienger, K.M., Willson, T.M., Funk, C.D., Pike, J.W., 2001. IL-4 inhibits osteoclast formation through a direct action on osteoclast precursors via peroxisome proliferator-activated receptor gamma 1. Proc. Natl. Acad. Sci. U. S. A. 98, 2443–2448.

Bertolini, D.R., Nedwin, G.E., Bringman, T.S., Smith, D.D., Mundy, G.R., 1986. Stimulation of bone resorption and inhibition of bone formation in vitro by human tumour necrosis factors. Nature 319, 516–518.

Bettelli, E., Carrier, Y., Gao, W., Korn, T., Strom, T.B., Oukka, M., Weiner, H.L., Kuchroo, V.K., 2006. Reciprocal developmental pathways for the generation of pathogenic effector TH17 and regulatory T cells. Nature 441, 235–238.

Beutler, B., Cerami, A., 1986. Cachectin and tumour necrosis factor as two sides of the same biological coin. Nature 320, 584–588.

Beutler, B., Cerami, A., 1987. Cachectin: more than a tumor necrosis factor. N. Engl. J. Med. 316, 379–385.

Boggild, S., Molgaard, S., Glerup, S., Nyengaard, J.R., 2016. Spatiotemporal patterns of sortilin and SorCS2 localization during organ development. BMC Cell Biol. 17, 8.

Boron, D., Agnieszka, S.M., Daniel, K., Anna, B., Adam, K., 2014. Polymorphism of interleukin-17 and its relation to mineral density of bones in perimenopausal women. Eur. J. Med. Res. 19, 69.

Boyce, B.F., Aufdemorte, T.B., Garrett, R., Yates, A.J.P., Mundy, G.R., 1989. Effects of interleukin-1 on bone turnover in normal mice. Endocrinology 125, 1142.

Boyce, B.F., Li, P., Yao, Z., Zhang, Q., Badell, I.R., Schwarz, E.M., O'keefe, R.J., Xing, L., 2005. TNFa and pathologic bone resorption. Keio J. Med. 54, 127–131.

Bozec, A., Bakiri, L., Hoebertz, A., Eferl, R., Schilling, A.F., Komnenovic, V., Scheuch, H., Priemel, M., Stewart, C.L., Amling, M., Wagner, E.F., 2008. Osteoclast size is controlled by Fra-2 through LIF/LIF-receptor signalling and hypoxia. Nature 454, 221–225.

Briso, E.M., Dienz, O., Rincon, M., 2008. Cutting edge: soluble IL-6R is produced by IL-6R ectodomain shedding in activated CD4 T cells. J. Immunol. 180, 7102–7106.

Broholm, C., Laye, M.J., Brandt, C., Vadalasetty, R., Pilegaard, H., Pedersen, B.K., Scheele, C., 2011. LIF is a contraction-induced myokine stimulating human myocyte proliferation. J. Appl. Physiol. 111, 251–259.

Broholm, C., Pedersen, B.K., 2010. Leukaemia inhibitory factor–an exercise-induced myokine. Exerc. Immunol. Rev. 16, 77–85.

Brounais-Le Royer, B., Pierroz, D.D., Velin, D., Frossard, C., Zheng, X.X., Lehr, H.A., Ferrari-Lacraz, S., Ferrari, S.L., 2013. Effects of an interleukin-15 antagonist on systemic and skeletal alterations in mice with DSS-induced colitis. Am. J. Pathol. 182, 2155–2167.

Brunetti, G., Oranger, A., Carbone, C., Mori, G., Sardone, F.R., Mori, C., Celi, M., Faienza, M.F., Tarantino, U., Zallone, A., Grano, M., Colucci, S., 2013. Osteoblasts display different responsiveness to TRAIL-induced apoptosis during their differentiation process. Cell Biochem. Biophys. 67, 1127–1136.

Canalis, E., 1986. Interleukin-1 has independent effects on deoxyribonucleic acid and collagen synthesis in cultures of rat calvariae. Endocrinology 118, 74–81.

Canalis, E., 1987. Effects of tumor necrosis factor on bone formation in vitro. Endocrinology 121, 1596–1604.

Cao, Y., Jansen, I.D., Sprangers, S., Stap, J., Leenen, P.J., Everts, V., de Vries, T.J., 2016. IL-1beta differently stimulates proliferation and multinucleation of distinct mouse bone marrow osteoclast precursor subsets. J. Leukoc. Biol. 100, 513–523.

Cao, Y., Jansen, I.D.C., Sprangers, S., de Vries, T.J., Everts, V., 2017. TNF-alpha has both stimulatory and inhibitory effects on mouse monocyte-derived osteoclastogenesis. J. Cell. Physiol. 232, 3273–3285.

Carmody, E.E., Schwarz, E.M., Puzas, J.E., Rosier, R.N., O'keefe, R.J., 2002. Viral interleukin-10 gene inhibition of inflammation, osteoclastogenesis, and bone resorption in response to titanium particles. Arthritis Rheum. 46, 1298–1308.

Cauley, J.A., Barbour, K.E., Harrison, S.L., Cloonan, Y.K., Danielson, M.E., Ensrud, K.E., Fink, H.A., Orwoll, E.S., Boudreau, R., 2016. Inflammatory markers and the risk of hip and vertebral fractures in men: the osteoporotic fractures in men (MrOS). J. Bone Miner. Res. 31, 2129–2138.

Chang, M.K., Raggatt, L.J., Alexander, K.A., Kuliwaba, J.S., Fazzalari, N.L., Schroder, K., Maylin, E.R., Ripoll, V.M., Hume, D.A., Pettit, A.R., 2008. Osteal tissue macrophages are intercalated throughout human and mouse bone lining tissues and regulate osteoblast function in vitro and in vivo. J. Immunol. 181, 1232–1244.

Charatcharoenwitthaya, N., Khosla, S., Atkinson, E.J., Mccready, L.K., Riggs, B.L., 2007. Effect of blockade of TNF-alpha and interleukin-1 action on bone resorption in early postmenopausal women. J. Bone Miner. Res. 22, 724–729.

Chen, L., Wei, X.Q., Evans, B., Jiang, W., Aeschlimann, D., 2008. IL-23 promotes osteoclast formation by up-regulation of receptor activator of NF-kappaB (RANK) expression in myeloid precursor cells. Eur. J. Immunol. 38, 2845–2854.

Chen, Z., Su, L., Xu, Q., Katz, J., Michalek, S.M., Fan, M., Feng, X., Zhang, P., 2015. IL-1R/TLR2 through MyD88 divergently modulates osteoclastogenesis through regulation of nuclear factor of activated T cells c1 (NFATc1) and B lymphocyte-induced maturation protein-1 (Blimp1). J. Biol. Chem. 290, 30163–30174.

Cheng, J., Liu, J., Shi, Z., Jules, J., Xu, D., Luo, S., Wei, S., Feng, X., 2012. Molecular mechanisms of the biphasic effects of interferon-gamma on osteoclastogenesis. J. Interferon Cytokine Res. 32, 34–45.

Cho, D.C., Brennan, H.J., Johnson, R.W., Poulton, I.J., Gooi, J.H., Tonkin, B.A., Mcgregor, N.E., Walker, E.C., Handelsman, D.J., Martin, T.J., Sims, N.A., 2017. Bone corticalization requires local SOCS3 activity and is promoted by androgen action via interleukin-6. Nat. Commun. 8, 806.

Clancy, B.M., Johnson, J.D., Lambert, A.J., Rezvankhah, S., Wong, A., Resmini, C., Feldman, J.L., Leppanen, S., Pittman, D.D., 2003. A gene expression profile for endochondral bone formation: oligonucleotide microarrays establish novel connections between known genes and BMP-2-induced bone formation in mouse quadriceps. Bone 33, 46–63.

Claudino, M., Garlet, T.P., Cardoso, C.R., de Assis, G.F., Taga, R., Cunha, F.Q., Silva, J.S., Garlet, G.P., 2010. Down-regulation of expression of osteoblast and osteocyte markers in periodontal tissues associated with the spontaneous alveolar bone loss of interleukin-10 knockout mice. Eur. J. Oral Sci. 118, 19–28.

Colotta, F., Re, F., Muzio, M., Bertini, R., Polentarutti, N., Sironi, M., Giri, J.G., Dower, S.K., Sims, J.E., Mantovani, A., 1993. Interleukin-1 type II receptor: a decoy target for IL-1 that is regulated by IL-4. Science 261, 472–475.

Colucci, S., Brunetti, G., Cantatore, F.P., Oranger, A., Mori, G., Pignataro, P., Tamma, R., Grassi, F.R., Zallone, A., Grano, M., 2007. The death receptor DR5 is involved in TRAIL-mediated human osteoclast apoptosis. Apoptosis 12, 1623–1632.

Convente, M.R., Chakkalakal, S.A., Yang, E., Caron, R.J., Zhang, D., Kambayashi, T., Kaplan, F.S., Shore, E.M., 2018. Depletion of mast cells and macrophages impairs heterotopic ossification in an Acvr1(R206H) mouse model of fibrodysplasia ossificans progressiva. J. Bone Miner. Res. 33 (2), 269–282.

Cormier-Daire, V., Munnich, A., Lyonnet, S., Rustin, P., Delezoide, A.L., Maroteaux, P., Le Merrer, M., 1998. Presentation of six cases of Stuve-Wiedemann syndrome. Pediatr. Radiol. 28, 776–780.

Cornish, J., Callon, K., King, A., Edgar, S., Reid, I.R., 1993. The effect of leukemia inhibitory factor on bone in vivo. Endocrinology 132, 1359–1366.

Cornish, J., Gillespie, M.T., Callon, K.E., Horwood, N.J., Moseley, J.M., Reid, I.R., 2003. Interleukin-18 is a novel mitogen of osteogenic and chondrogenic cells. Endocrinology 144, 1194–1201.

Croes, M., Oner, F.C., van Neerven, D., Sabir, E., Kruyt, M.C., Blokhuis, T.J., Dhert, W.J., Alblas, J., 2016. Proinflammatory T cells and IL-17 stimulate osteoblast differentiation. Bone 84, 262–270.

Croker, B.A., Kiu, H., Nicholson, S.E., 2008. SOCS regulation of the JAK/STAT signalling pathway. Semin. Cell Dev. Biol. 19, 414–422.

Croker, B.A., Krebs, D.L., Zhang, J.G., Wormald, S., Willson, T.A., Stanley, E.G., Robb, L., Greenhalgh, C.J., Forster, I., Clausen, B.E., Nicola, N.A., Metcalf, D., Hilton, D.J., Roberts, A.W., Alexander, W.S., 2003. SOCS3 negatively regulates IL-6 signaling in vivo. Nat. Immunol. 4, 540–545.

Dagoneau, N., Scheffer, D., Huber, C., Al-Gazali, L.I., di Rocco, M., Godard, A., Martinovic, J., Raas-Rothschild, A., Sigaudy, S., Unger, S., Nicole, S., Fontaine, B., Taupin, J.L., Moreau, J.F., Superti-Furga, A., Le Merrer, M., Bonaventure, J., Munnich, A., Legeai-Mallet, L., Cormier-Daire, V., 2004. Null leukemia inhibitory factor receptor (LIFR) mutations in Stuve-Wiedemann/Schwartz-Jampel type 2 syndrome. Am. J. Hum. Genet. 74, 298–305.

Dai, S.M., Nishioka, K., Yudoh, K., 2004. Interleukin (IL) 18 stimulates osteoclast formation through synovial T cells in rheumatoid arthritis: comparison with IL1 beta and tumour necrosis factor alpha. Ann. Rheum. Dis. 63, 1379–1386.

Dame, J.B., Juul, S.E., 2000. The distribution of receptors for the pro-inflammatory cytokines interleukin (IL)-6 and IL-8 in the developing human fetus. Early Hum. Dev. 58, 25–39.

Daniele, S., Natali, L., Giacomelli, C., Campiglia, P., Novellino, E., Martini, C., Trincavelli, M.L., 2017. Osteogenesis is improved by low tumor necrosis factor alpha concentration through the modulation of Gs-coupled receptor signals. Mol. Cell Biol. 37.

Davis, S., Aldrich, T.H., Ip, N.Y., Stahl, N., Scherer, S., Farruggella, T., Distefano, P.S., Curtis, R., Panayotatos, N., Gascan, H., et al., 1993. Released form of CNTF receptor alpha component as a soluble mediator of CNTF responses. Science 259, 1736–1739.

De Benedetti, F., Rucci, N., del Fattore, A., Peruzzi, B., Paro, R., Longo, M., Vivarelli, M., Muratori, F., Berni, S., Ballanti, P., Ferrari, S., Teti, A., 2006. Impaired skeletal development in interleukin-6-transgenic mice: a model for the impact of chronic inflammation on the growing skeletal system. Arthritis Rheum. 54, 3551–3563.

DeChiara, T.M., Vejsada, R., Poueymirou, W.T., Acheson, A., Suri, C., Conover, J.C., Friedman, B., Mcclain, J., Pan, L., Stahl, N., Ip, N.Y., Yancopoulos, G.D., 1995. Mice lacking the CNTF receptor, unlike mice lacking CNTF, exhibit profound motor neuron deficits at birth. Cell 83, 313–322.

Derouet, D., Rousseau, F., Alfonsi, F., Froger, J., Hermann, J., Barbier, F., Perret, D., Diveu, C., Guillet, C., Preisser, L., Dumont, A., Barbado, M., Morel, A., Delapeyriere, O., Gascan, H., Chevalier, S., 2004. Neuropoietin, a new IL-6-related cytokine signaling through the ciliary neurotrophic factor receptor. Proc. Natl. Acad. Sci. U. S. A. 101, 4827–4832.

DeSelm, C.J., Takahata, Y., Warren, J., Chappel, J.C., Khan, T., Li, X., Liu, C., Choi, Y., Kim, Y.F., Zou, W., Teitelbaum, S.L., 2012. IL-17 mediates estrogen-deficient osteoporosis in an Act1-dependent manner. J. Cell. Biochem. 113, 2895–2902.

Devlin, R.D., Bone 3rd, H.G., Roodman, G.D., 1996. Interleukin-6: a potential mediator of the massive osteolysis in patients with Gorham-Stout disease. J. Clin. Endocrinol. Metab. 81, 1893–1897.

Dinarello, C.A., 1991. Interleukin-1 and interleukin-1 antagonism. Blood 77, 1627–1652.

Dinarello, C.A., 1993. Blocking interleukin-1 in disease. Blood Purif. 11, 118–127.

Ding, Q., Zhou, H., Yun, B., Zhou, L., Zhang, N., Yin, G., Fan, J., 2017. Interleukin-13 inhibits expression of cyp27b1 in peripheral CD14+ cells that is correlated with vertebral bone mineral density of patients with ulcerative colitis. J. Cell. Biochem. 118, 376–381.

Duque, G., Huang, D.C., Dion, N., Macoritto, M., Rivas, D., Li, W., Yang, X.F., Li, J., Liang, J., Marino, F.T., Barralet, J., Lascau, V., Deschenes, C., Ste-Marie, L.G., Kremer, R., 2011. Interferon gamma plays a role in bone formation in vivo and rescues osteoporosis in ovariectomized mice. J. Bone Miner. Res. 3, 350.

Durnez, A., Paternotte, S., Fechtenbaum, J., Landewe, R.B., Dougados, M., Roux, C., Briot, K., 2013. Increase in bone density in patients with spondyloarthritis during anti-tumor necrosis factor therapy: 6-year followup study. J. Rheumatol. 40, 1712–1718.

Eder, J., 1997. Tumour necrosis factor alpha and interleukin 1 signalling: do MAPKK kinases connect it all? Trends Pharmacol. Sci. 18, 319–322.

Eeles, D.G., Hodge, J.M., Singh, P.P., Schuijers, J.A., Grills, B.L., Gillespie, M.T., Myers, D.E., Quinn, J.M., 2015. Osteoclast formation elicited by interleukin-33 stimulation is dependent upon the type of osteoclast progenitor. Mol. Cell. Endocrinol. 399, 259–266.

Eisenberg, S.P., Evans, R.J., Arend, W.P., Verderber, E., Brewer, M.T., Hannum, C.H., Thompson, R.C., 1990. Primary structure and functional expression from complementary DNA of a human inteìeukin-1 receptor antagonist. Nature 343, 341–346.

Elson, G.C., Graber, P., Losberger, C., Herren, S., Gretener, D., Menoud, L.N., Wells, T.N., Kosco-Vilbois, M.H., Gauchat, J.F., 1998. Cytokine-like factor-1, a novel soluble protein, shares homology with members of the cytokine type I receptor family. J. Immunol. 161, 1371–1379.

Elson, G.C., Lelievre, E., Guillet, C., Chevalier, S., Plun-Favreau, H., Froger, J., Suard, I., de Coignac, A.B., Delneste, Y., Bonnefoy, J.Y., Gauchat, J.F., Gascan, H., 2000. CLF associates with CLC to form a functional heteromeric ligand for the CNTF receptor complex. Nat. Neurosci. 3, 867–872.

Erickson, S.L., De, S.F.J., Kikly, K., Carver-Moore, K., Pitts-Meek, S., Gillett, N., Sheehan, K.C., Schreiber, R.D., Goeddel, D.V., Moore, M.W., 1994. Decreased sensitivity to tumour-necrosis factor but normal T-cell development in TNF receptor-2-deficient mice. Nature 372, 560–563.

Ernst, M., Inglese, M., Waring, P., Campbell, I.K., Bao, S., Clay, F.J., Alexander, W.S., Wicks, I.P., Tarlinton, D.M., Novak, U., Heath, J.K., Dunn, A.R., 2001. Defective gp130-mediated signal transducer and activator of transcription (STAT) signaling results in degenerative joint disease, gastrointestinal ulceration, and failure of uterine implantation. J. Exp. Med. 194, 189–203.

Espirito Santo, A.I., Ersek, A., Freidin, A., Feldmann, M., Stoop, A.A., Horwood, N.J., 2015. Selective inhibition of TNFR1 reduces osteoclast numbers and is differentiated from anti-TNF in a LPS-driven model of inflammatory bone loss. Biochem. Biophys. Res. Commun. 464, 1145–1150.

Evans, K.E., Fox, S.W., 2007. Interleukin-10 inhibits osteoclastogenesis by reducing NFATc1 expression and preventing its translocation to the nucleus. BMC Cell Biol. 19, 4.

Felaco, P., Castellani, M.L., de Lutiis, M.A., Felaco, M., Pandolfi, F., Salini, V., de Amicis, D., Vecchiet, J., Tete, S., Ciampoli, C., Conti, F., Cerulli, G., Caraffa, A., Antinolfi, P., Cuccurullo, C., Perrella, A., Theoharides, T.C., Conti, P., Toniato, E., Kempuraj, D., Shaik, Y.B., 2009. IL-32: a newly-discovered proinflammatory cytokine. J. Biol. Regul. Homeost. Agents 23, 141–147.

Feng, S., Madsen, S.H., Viller, N.N., Neutzsky-Wulff, A.V., Geisler, C., Karlsson, L., Soderstrom, K., 2015. Interleukin-15-activated natural killer cells kill autologous osteoclasts via LFA-1, DNAM-1 and TRAIL, and inhibit osteoclast-mediated bone erosion in vitro. Immunology 145, 367–379.

Fernandes, T.J., Hodge, J.M., Singh, P.P., Eeles, D.G., Collier, F.M., Holten, I., Ebeling, P.R., Nicholson, G.C., Quinn, J.M., 2013. Cord blood-derived macrophage-lineage cells rapidly stimulate osteoblastic maturation in mesenchymal stem cells in a glycoprotein-130 dependent manner. PLoS One 8, e73266.

Fiers, W., Sim, E., 1993. Tumor Necrosis Factor. The Natural Immune System: Humoral Factors. IRL Press at Oxford University Press, Oxford.

Forger, N.G., Prevette, D., Delapeyriere, O., de Bovis, B., Wang, S., Bartlett, P., Oppenheim, R.W., 2003. Cardiotrophin-like cytokine/cytokine-like factor 1 is an essential trophic factor for lumbar and facial motoneurons in vivo. J. Neurosci. 23, 8854–8858.

Fort, M.M., Cheung, J., Yen, D., Li, J., Zurawski, S.M., Lo, S., Menon, S., Clifford, T., Hunte, B., Lesley, R., Muchamuel, T., Hurst, S.D., Zurawski, G., Leach, M.W., Gorman, D.M., Rennick, D.M., 2001. IL-25 induces IL-4, IL-5, and IL-13 and Th2-associated pathologies in vivo. Immunity 15, 985–995.

Freire, M.S., Cantuaria, A.P.C., Lima, S.M.F., Almeida, J.A., Murad, A.M., Franco, O.L., Rezende, T.M.B., 2016. NanoUPLC-MS(E) proteomic analysis of osteoclastogenesis downregulation by IL-4. J Proteomic. 131, 8–16.

Frolik, C.A., Black, E.C., Cain, R.L., Satterwhite, J.H., Brown-Augsburger, P.L., Sato, M., Hock, J.M., 2003. Anabolic and catabolic bone effects of human parathyroid hormone (1-34) are predicted by duration of hormone exposure. Bone 33, 372–379.

Fujii, T., Kitaura, H., Kimura, K., Hakami, Z.W., Takano-Yamamoto, T., 2012. IL-4 inhibits TNF-alpha-mediated osteoclast formation by inhibition of RANKL expression in TNF-alpha-activated stromal cells and direct inhibition of TNF-alpha-activated osteoclast precursors via a T-cell-independent mechanism in vivo. Bone 51, 771–780.

Gao, Y., Grassi, F., Ryan, M.R., Terauchi, M., Page, K., Yang, X., Weitzmann, M.N., Pacifici, R., 2007. IFN-gamma stimulates osteoclast formation and bone loss in vivo via antigen-driven T cell activation. J. Clin. Investig. 117, 122–132.

Gao, Y., Morita, I., Maruo, N., Kubota, T., Murota, S., Aso, T., 1998. Expression of IL-6 receptor and GP130 in mouse bone marrow cells during osteoclast differentiation. Bone 22, 487–493.

Gao, Y., Wu, X., Terauchi, M., Li, J.Y., Grassi, F., Galley, S., Yang, X., Weitzmann, M.N., Pacifici, R., 2008. T cells potentiate PTH-induced cortical bone loss through CD40L signaling. Cell Metabol. 8, 132–145.

Garcia, A.J., Tom, C., Guemes, M., Polanco, G., Mayorga, M.E., Wend, K., Miranda-Carboni, G.A., Krum, S.A., 2012. ERalpha signaling regulates MMP3 expression to induce FasL cleavage and osteoclast apoptosis. J. Bone Miner. Res. 28 (2), 283–290.

Gendron, S., Boisvert, M., Chetoui, N., Aoudjit, F., 2008. Alpha1beta1 integrin and interleukin-7 receptor up-regulate the expression of RANKL in human T cells and enhance their osteoclastogenic function. Immunology 125, 359–369.

Genet, F., Kulina, I., Vaquette, C., Torossian, F., Millard, S., Pettit, A.R., Sims, N.A., Anginot, A., Guerton, B., Winkler, I.G., Barbier, V., Lataillade, J.J., Le Bousse-Kerdiles, M.C., Hutmacher, D.W., Levesque, J.P., 2015. Neurological heterotopic ossification following spinal cord injury is triggered by macrophage-mediated inflammation in muscle. J. Pathol. 236, 229–240.

Gil-Henn, H., Destaing, O., Sims, N.A., Aoki, K., Alles, N., Neff, L., Sanjay, A., Bruzzaniti, A., de Camilli, P., Baron, R., Schlessinger, J., 2007. Defective microtubule-dependent podosome organization in osteoclasts leads to increased bone density in Pyk2(-/-) mice. J. Cell Biol. 178, 1053–1064.

Gilbert, L., He, X., Farmer, P., Rubin, J., Drissi, H., van Wijnen, A.J., Lian, J.B., Stein, G.B., Nanes, M.S., 2002. Expression of the osteoblast differentiation factor RUNX2 (Cbfa1/AML3/Pebp2alphaA)is inhibited by tumor necrosis factor-alpha. J. Biol. Chem. 277.

Gilbert, L.C., Rubin, J., Nanes, M.S., 2004. The p55 TNF receptor mediates TNF inhibition of osteoblast differentiation independent of apoptosis. Am. J. Physiol. Endocrinol. Metab. 288 (5), E1011–E1018.

Gimble, J.M., Wanker, F., Wang, C.S., Bass, H., Wu, X., Kelly, K., Yancopoulos, G.D., Hill, M.R., 1994. Regulation of bone marrow stromal cell differentiation by cytokines whose receptors share the gp130 protein. J. Cell. Biochem. 54, 122–133.

Girasole, G., Giuliani, N., Modena, A.B., Passeri, G., Pedrazzoni, M., 1999. Oestrogens prevent the increase of human serum soluble interleukin-6 receptor induced by ovariectomy in vivo and decrease its release in human osteoblastic cells in vitro. Clin. Endocrinol. 51, 801–807.

Glass, G.E., Chan, J.K., Freidin, A., Feldmann, M., Horwood, N.J., Nanchahal, J., 2011. TNF-alpha promotes fracture repair by augmenting the recruitment and differentiation of muscle-derived stromal cells. Proc. Natl. Acad. Sci. U. S. A. 108, 1585–1590.

Goodman, G.R., Dissanayake, I.R., Gorodetsky, E., Zhou, H., Ma, Y.F., Jee, W.S., Epstein, S., 1999. Interferon-alpha, unlike interferon-gamma, does not cause bone loss in the rat. Bone 25, 459–463.

Gowen, M., Macdonald, B.R., Russell, G.G., 1988. Actions of recombinant human gamma-interferon and tumor necrosis factor alpha on the proliferation and osteoblastic characteristics of human trabecular bone cells in vitro. Arthritis Rheum. 31, 1500–1507.

Gowen, M., Mundy, G.R., 1986. Actions of recombinant interleukin 1, interleukin 2, and interferon-gamma on bone resorption in vitro. J. Immunol. 136, 2478–2482.

Greenfield, E.M., Horowitz, M.C., Lavish, S.A., 1996. Stimulation by parathyroid hormone of interleukin-6 and leukemia inhibitory factor expression in osteoblasts is an immediate-early gene response induced by cAMP signal transduction. J. Biol. Chem. 271, 10984–10989.

Grimaud, E., Blanchard, F., Charrier, C., Gouin, F., Redini, F., Heymann, D., 2002. Leukaemia inhibitory factor (lif) is expressed in hypertrophic chondrocytes and vascular sprouts during osteogenesis. Cytokine 20, 224–230.

Gu, R., Santos, L.L., Ngo, D., Fan, H., Singh, P.P., Fingerle-Rowson, G., Bucala, R., Xu, J., Quinn, J.M., Morand, E.F., 2015. Macrophage migration inhibitory factor is essential for osteoclastogenic mechanisms in vitro and in vivo mouse model of arthritis. Cytokine 72, 135–145.

Guerne, P.A., Carson, D.A., Lotz, M., 1990. IL-6 production by human articular chondrocytes. Modulation of its synthesis by cytokines, growth factors, and hormones in vitro. J. Immunol. 144, 499–505.

Guihard, P., Danger, Y., Brounais, B., David, E., Brion, R., Delecrin, J., Richards, C.D., Chevalier, S., Redini, F., Heymann, D., Gascan, H., Blanchard, F., 2012. Induction of osteogenesis in mesenchymal stem cells by activated monocytes/macrophages depends on oncostatin M signaling. Stem Cell. 30, 762–772.

Haan, S., Hemmann, U., Hassiepen, U., Schaper, F., Schneider-Mergener, J., Wollmer, A., Heinrich, P.C., Grotzinger, J., 1999. Characterization and binding specificity of the monomeric STAT3-SH2 domain. J. Biol. Chem. 274, 1342–1348.

Hahn, A.F., Jones, D.L., Knappskog, P.M., Boman, H., Mcleod, J.G., 2006. Cold-induced sweating syndrome A report of two cases and demonstration of genetic heterogeneity. J. Neurol. Sci. 250, 62–70.

Hakeda, Y., Sudo, T., Ishizuka, S., Tanaka, K., Higashino, K., Kusuda, M., Kodama, H., Kumegawa, M., 1991. Murine recombinant leukemia inhibitory factor modulates inhibitory effect of 1,25 dihydroxyvitamin D3 on alkaline phosphatase activity in MC3T3-E1 cells. Biochem. Biophys. Res. Commun. 175, 577–582.

Hamrick, M.W., 2011. A role for myokines in muscle-bone interactions. Exerc. Sport Sci. Rev. 39, 43–47.

Hannum, C.H., Wilcox, C.J., Arend, W.P., Joslin, F.G., Dripps, D.J., Heimdal, P.L., Armes, L.G., Sommer, A., Eisenberg, S.P., Thompson, R.C., 1990. Interleukin-1 receptor antagonist activity of a human interleukin- 1 inhibitor. Nature 343, 336–340.

Hattersley, G., Dorey, E., Horton, M.A., Chambers, T.J., 1988. Human macrophage colony-stimulating factor inhibits bone resorption by osteoclasts disaggregated from rat bone. J. Cell. Physiol. 137, 199–203.

Hayashida, C., Ito, J., Nakayachi, M., Okayasu, M., Ohyama, Y., Hakeda, Y., Sato, T., 2014. Osteocytes produce interferon-beta as a negative regulator of osteoclastogenesis. J. Biol. Chem. 289, 11545–11555.

Hengartner, N.E., Fiedler, J., Ignatius, A., Brenner, R.E., 2013. IL-1beta inhibits human osteoblast migration. Mol. Med. 19, 36–42.

Henningsson, L., Jirholt, P., Bogestal, Y.R., Eneljung, T., Adiels, M., Lindholm, C., Mcinnes, I., Bulfone-Paus, S., Lerner, U.H., Gjertsson, I., 2012. Interleukin 15 mediates joint destruction in *Staphylococcus aureus* arthritis. J. Infect. Dis. 206, 687–696.

Hermanns, H.M., 2015. Oncostatin M and interleukin-31: cytokines, receptors, signal transduction and physiology. Cytokine Growth Factor Rev. 26, 545–558.

Hiasa, M., Abe, M., Nakano, A., Oda, A., Amou, H., Kido, S., Takeuchi, K., Kagawa, K., Yata, K., Hashimoto, T., Ozaki, S., Asaoka, K., Tanaka, E., Moriyama, K., Matsumoto, T., 2009. GM-CSF and IL-4 induce dendritic cell differentiation and disrupt osteoclastogenesis through M-CSF receptor shedding by up-regulation of TNF-{alpha} converting enzyme (TACE). Blood 17, 17.

Hilton, D.J., Nicola, N.A., Waring, P.M., Metcalf, D., 1991. Clearance and fate of leukemia-inhibitory factor (LIF) after injection into mice. J. Cell. Physiol. 148, 430–439.

Hock, J.M., Krishnan, V., Onyia, J.E., Bidwell, J.P., Milas, J., Stanislaus, D., 2001. Osteoblast apoptosis and bone turnover. J. Bone Miner. Res. 16, 975–984.

Hofbauer, L.C., Lacey, D.L., Dunstan, C.R., Spelsberg, T.C., Riggs, B.L., Khosla, S., 1999. Interleukin-1beta and tumor necrosis factor-alpha, but not interleukin-6, stimulate osteoprotegerin ligand gene expression in human osteoblastic cells. Bone 25, 255–259.

Holland, S.M., Deleo, F.R., Elloumi, H.Z., Hsu, A.P., Uzel, G., Brodsky, N., Freeman, A.F., Demidowich, A., Davis, J., Turner, M.L., Anderson, V.L., Darnell, D.N., Welch, P.A., Kuhns, D.B., Frucht, D.M., Malech, H.L., Gallin, J.I., Kobayashi, S.D., Whitney, A.R., Voyich, J.M., Musser, J.M., Woellner, C., Schaffer, A.A., Puck, J.M., Grimbacher, B., 2007. STAT3 mutations in the hyper-IgE syndrome. N. Engl. J. Med. 357, 1608–1619.

Holscher, C., Holscher, A., Ruckerl, D., Yoshimoto, T., Yoshida, H., Mak, T., Saris, C., Ehlers, S., 2005. The IL-27 receptor chain WSX-1 differentially regulates antibacterial immunity and survival during experimental tuberculosis. J. Immunol. 174, 3534–3544.

Hong, M.H., Williams, H., Jin, C.H., Pike, J.W., 2000. The inhibitory effect of interleukin-10 on mouse osteoclast formation involves novel tyrosine-phosphorylated proteins. J. Bone Miner. Res. 15, 911–918.

Horwood, N.J., Elliott, J., Martin, T.J., Gillespie, M.T., 1998a. Osteotropic agents regulate the expression of osteoclast differentiation factor and osteoprotegerin in osteoblastic stromal cells. Endocrinology 139, 4743–4746.

Horwood, N.J., Elliott, J., Martin, T.J., Gillespie, M.T., 2001. IL-12 alone and in synergy with IL-18 inhibits osteoclast formation in vitro. J. Immunol. 166, 4915–4921.

Horwood, N.J., Kartsogiannis, V., Quinn, J.M., Romas, E., Martin, T.J., Gillespie, M.T., 1999. Activated T lymphocytes support osteoclast formation in vitro. Biochem. Biophys. Res. Commun. 265, 144–150.

Horwood, N.J., Udagawa, N., Elliott, J., Grail, D., Okamura, H., Kurimoto, M., Dunn, A.R., Martin, T., Gillespie, M.T., 1998b. Interleukin 18 inhibits osteoclast formation via T cell production of granulocyte macrophage colony-stimulating factor. J. Clin. Investig. 101, 595–603.

Hsieh, C.S., Macatonia, S.E., Tripp, C.S., Wolf, S.F., O'garra, A., Murphy, K.M., 1993. Development of TH1 CD4+ T cells through IL-12 produced by Listeria-induced macrophages. Science 260, 547–549.

Huang, H., Kim, H.J., Chang, E.J., Lee, Z.H., Hwang, S.J., Kim, H.M., Lee, Y., Kim, H.H., 2009. IL-17 stimulates the proliferation and differentiation of human mesenchymal stem cells: implications for bone remodeling. Cell Death Differ. 16 (10), 1332–1343.

Huang, J., Gao, X., Li, S., Cao, Z., 1997. Recruitment of IRAK to the interleukin 1 receptor complex requires interleukin 1 receptor accessory protein. Proc. Natl. Acad. Sci. U. S. A. 94, 12829–12832.

Ichihara, M., Hara, T., Kim, H., Murate, T., Miyajima, A., 1997. Oncostatin M and leukemia inhibitory factor do not use the same functional receptor in mice. Blood 90, 165–173.

Ishimi, Y., Abe, E., Jin, C.H., Miyaura, C., Hong, M.H., Oshida, M., Kurosawa, H., Yamaguchi, Y., Tomida, M., Hozumi, M., Suda, T., 1992. Leukemia inhibitory factor/differentiation-stimulating factor (LIF/D-factor): regulation of its production and possible roles in bone metabolism. J. Cell. Physiol. 152, 71–78.

Ishimi, Y., Miyaura, C., Jin, C.H., Akatsu, T., Abe, E., Nakamura, Y., Yamaguchi, A., Yoshiki, S., Matsuda, T., Hirano, T., Kishimoto, T., Suda, T., 1990. IL-6 is produced by osteoblasts and induces bone resorption. J. Immunol. 145, 3297–3303.

Issaranggun Na Ayuthaya, B., Everts, V., Pavasant, P., 2017. Interleukin-12 induces receptor activator of nuclear factor-kappa B ligand expression by human periodontal ligament cells. J. Periodontol. 88, e109–e119.

Ivanova, J.T., Boyanov, M.A., Toshev, A.K., 2012. Polymorphisms of the human IL-1 receptor antagonist gene and forearm bone mineral density in postmenopausal women. Indian J. Endocrinol. Metab. 16, 580–584.

Jacquin, C., Koczon-Jaremko, B., Aguila, H.L., Leng, L., Bucala, R., Kuchel, G.A., Lee, S.K., 2009. Macrophage migration inhibitory factor inhibits osteoclastogenesis. Bone 45, 640–649.

Jenkins, B.J., Grail, D., Nheu, T., Najdovska, M., Wang, B., Waring, P., Inglese, M., Mcloughlin, R.M., Jones, S.A., Topley, N., Baumann, H., Judd, L.M., Giraud, A.S., Boussioutas, A., Zhu, H.J., Ernst, M., 2005. Hyperactivation of Stat3 in gp130 mutant mice promotes gastric hyperproliferation and desensitizes TGF-beta signaling. Nat. Med. 11, 845–852.

Ji, J.D., Park-Min, K.H., Shen, Z., Fajardo, R.J., Goldring, S.R., Mchugh, K.P., Ivashkiv, L.B., 2009. Inhibition of RANK expression and osteoclastogenesis by TLRs and IFN-{gamma} in human osteoclast precursors. J. Immunol. 4, 4.

Jilka, R.L., Hamilton, J.W., 1984. Inhibition of parathormone-stimulated bone resorption by Type 1 interferon. Biochem. Biophys. Res. Commun. 120, 553–558.

Jilka, R.L., Hangoc, G., Girasole, G., Passeri, G., Williams, D.C., Abrams, J.S., Boyce, B., Broxmeyer, H., Manolagas, S.C., 1992. Increased osteoclast development after estrogen loss: mediation by interleukin-6. Science 257, 88–91.

Jimi, E., Nakamura, I., Duong, L.T., Ikebe, T., Takahashi, N., Rodan, G.A., Suda, T., 1999. Interleukin 1 induces multinucleation and bone-resorbing activity of osteoclasts in the absence of Osteoblasts/Stromal cells. Exp. Cell Res. 247, 84–93.

Johnson, R.W., Brennan, H.J., Vrahnas, C., Poulton, I.J., Mcgregor, N.E., Standal, T., Walker, E.C., Koh, T.T., Nguyen, H., Walsh, N.C., Forwood, M.R., Martin, T.J., Sims, N.A., 2014a. The primary function of gp130 signaling in osteoblasts is to maintain bone formation and strength, rather than promote osteoclast formation. J. Bone Miner. Res. 29, 1492–1505.

Johnson, R.W., Finger, E.C., Olcina, M.M., Vilalta, M., Aguilera, T., Miao, Y., Merkel, A.R., Johnson, J.R., Sterling, J.A., Wu, J.Y., Giaccia, A.J., 2016. Induction of LIFR confers a dormancy phenotype in breast cancer cells disseminated to the bone marrow. Nat. Cell Biol. 18, 1078–1089.

Johnson, R.W., Mcgregor, N.E., Brennan, H.J., Crimeen-Irwin, B., Poulton, I.J., Martin, T.J., Sims, N.A., 2015. Glycoprotein130 (Gp130)/interleukin-6 (IL-6) signalling in osteoclasts promotes bone formation in periosteal and trabecular bone. Bone 81, 343–351.

Johnson, R.W., White, J.D., Walker, E.C., Martin, T.J., Sims, N.A., 2014b. Myokines (muscle-derived cytokines and chemokines) including ciliary neurotrophic factor (CNTF) inhibit osteoblast differentiation. Bone 64, 47–56.

Ju, J.H., Cho, M.L., Moon, Y.M., Oh, H.J., Park, J.S., Jhun, J.Y., Min, S.Y., Cho, Y.G., Park, K.S., Yoon, C.H., Min, J.K., Park, S.H., Sung, Y.C., Kim, H.Y., 2008. IL-23 induces receptor activator of NF-kappaB ligand expression on CD4+ T cells and promotes osteoclastogenesis in an autoimmune arthritis model. J. Immunol. 181, 1507–1518.

Juan, T.S.-C., Bolon, B., Lindberg, R.A., Sun, Y., Van, G., Fletcher, F.A., 2009. Mice overexpressing murine oncostatin M (OSM) exhibit changes in hematopoietic and other organs that are distinct from those of mice overexpressing human OSM or bovine OSM. Veterin. Pathol. 46, 124–137.

Jung, C., Dagoneau, N., Baujat, G., Le Merrer, M., David, A., di Rocco, M., Hamel, B., Megarbane, A., Superti-Furga, A., Unger, S., Munnich, A., Cormier-Daire, V., 2010. Stuve-Wiedemann syndrome: long-term follow-up and genetic heterogeneity. Clin. Genet. 77, 266–272.

Kalliolias, G.D., Zhao, B., Triantafyllopoulou, A., Park-Min, K.H., Ivashkiv, L.B., 2010. Interleukin-27 inhibits human osteoclastogenesis by abrogating RANKL-mediated induction of nuclear factor of activated T cells c1 and suppressing proximal RANK signaling. Arthritis Rheum. 62, 402–413.

Kamel Mohamed, S.G., Sugiyama, E., Shinoda, K., Hounoki, H., Taki, H., Maruyama, M., Miyahara, T., Kobayashi, M., 2005. Interleukin-4 inhibits RANKL-induced expression of NFATc1 and c-Fos: a possible mechanism for downregulation of osteoclastogenesis. Biochem. Biophys. Res. Commun. 329, 839–845.

Kamiya, S., Nakamura, C., Fukawa, T., Ono, K., Ohwaki, T., Yoshimoto, T., Wada, S., 2007. Effects of IL-23 and IL-27 on osteoblasts and osteoclasts: inhibitory effects on osteoclast differentiation. J. Bone Miner. Metab. 25, 277–285.

Kamiya, S., Okumura, M., Chiba, Y., Fukawa, T., Nakamura, C., Nimura, N., Mizuguchi, J., Wada, S., Yoshimoto, T., 2011. IL-27 suppresses RANKL expression in CD4+ T cells in part through STAT3. Immunol. Lett. 138, 47–53.

Kang, H., Yang, K., Xiao, L., Guo, L., Guo, C., Yan, Y., Qi, J., Wang, F., Ryffel, B., Li, C., Deng, L., 2017. Osteoblast hypoxia-inducible factor-1alpha pathway activation restrains osteoclastogenesis via the interleukin-33-microRNA-34a-notch1 pathway. Front. Immunol. 8, 1312.

Kang, Y.K., Zhang, M.C., 2014. IL-23 promotes osteoclastogenesis in osteoblast-osteoclast co-culture system. Genet. Mol. Res. 13, 4673–4679.

Karsdal, M.A., Schett, G., Emery, P., Harari, O., Byrjalsen, I., Kenwright, A., Bay-Jensen, A.C., Platt, A., 2012. IL-6 receptor inhibition positively modulates bone balance in rheumatoid arthritis patients with an inadequate response to anti-tumor necrosis factor therapy: biochemical marker analysis of bone metabolism in the tocilizumab RADIATE study (NCT00106522). Semin. Arthritis Rheum. 42, 131–139.

Kastelein, R.A., Hunter, C.A., Cua, D.J., 2007. Discovery and biology of IL-23 and IL-27: related but functionally distinct regulators of inflammation. Annu. Rev. Immunol. 25, 221–242.

Katavic, V., Lukic, I.K., Kovacic, N., Grcevic, D., Lorenzo, J.A., Marusic, A., 2003. Increased bone mass is a part of the generalized lymphoproliferative disorder phenotype in the mouse. J. Immunol. 170, 1540–1547.

Kawaguchi, H., Pilbeam, C.C., Vargas, S.J., Morse, E.E., Lorenzo, J.A., Raisz, L.G., 1995. Ovariectomy enhances and estrogen replacement inhibits the activity of bone marrow factors that stimulate prostaglandin production in cultured mouse calvaria. Ovariectomy enhances and estrogen replacement inhibits the activity of bone marrow factors that stimulate prostaglandin production in cultured mouse calvariae. J. Clin. Investig. 96, 539–548.

Kawasaki, K., Gao, Y.H., Yokose, S., Kaji, Y., Nakamura, T., Suda, T., Yoshida, K., Taga, T., Kishimoto, T., Kataoka, H., Yuasa, T., Norimatsu, H., Yamaguchi, A., 1997. Osteoclasts are present in gp130-deficient mice. Endocrinology 138, 4959–4965.

Kawase, Y., Hoshino, T., Yokota, K., Kuzuhara, A., Nakamura, M., Maeda, Y., Nishiwaki, E., Zenmyo, M., Hiraoka, K., Aizawa, H., Yoshino, K., 2003. Bone malformations in interleukin-18 transgenic mice. J. Bone Miner. Res. 18, 975–983.

Keller, J., Catala-Lehnen, P., Wintges, K., Schulze, J., Bickert, T., Ito, W., Horst, A.K., Amling, M., Schinke, T., 2012. Transgenic over-expression of interleukin-33 in osteoblasts results in decreased osteoclastogenesis. Biochem. Biophys. Res. Commun. 417 (1), 217–222.

Keupp, K., Li, Y., Vargel, I., Hoischen, A., Richardson, R., Neveling, K., Alanay, Y., Uz, E., Elcioglu, N., Rachwalski, M., Kamaci, S., Tuncbilek, G., Akin, B., Grotzinger, J., Konas, E., Mavili, E., Muller-Newen, G., Collmann, H., Roscioli, T., Buckley, M.F., Yigit, G., Gilissen, C., Kress, W., Veltman, J., Hammerschmidt, M., Akarsu, N.A., Wollnik, B., 2013. Mutations in the interleukin receptor IL11RA cause autosomal recessive Crouzon-like craniosynostosis. Mol. Genet. Genom. Med. 1, 223–237.

Key Jr., L.L., Ries, W.L., Rodriguiz, R.M., Hatcher, H.C., 1992. Recombinant human interferon gamma therapy for osteopetrosis. J. Pediatr. 121, 119–124.

Key Jr., L.L., Rodriguiz, R.M., Willi, S.M., Wright, N.M., Hatcher, H.C., Eyre, D.R., Cure, J.K., Griffin, P.P., Ries, W.L., 1995. Long-term treatment of osteopetrosis with recombinant human interferon gamma. N. Engl. J. Med. 332–9, 1594.

Kido, S., Kuriwaka-Kido, R., Imamura, T., Ito, Y., Inoue, D., Matsumoto, T., 2009. Mechanical stress induces Interleukin-11 expression to stimulate osteoblast differentiation. Bone 45, 1125–1132.

Kido, S., Kuriwaka-Kido, R., Umino-Miyatani, Y., Endo, I., Inoue, D., Taniguchi, H., Inoue, Y., Imamura, T., Matsumoto, T., 2010. Mechanical stress activates Smad pathway through PKCdelta to enhance interleukin-11 gene transcription in osteoblasts. PLoS One 5.

Kim, H., Ahn, S.H., Shin, C., Lee, S.H., Kim, B.J., Koh, J.M., 2016. The association of higher plasma macrophage migration inhibitory factor levels with lower bone mineral density and higher bone turnover rate in postmenopausal women. Endocrinol. Metab. 31, 454–461.

Kim, J.W., Lee, M.S., Lee, C.H., Kim, H.Y., Chae, S.U., Kwak, H.B., Oh, J., 2012. Effect of interferon-gamma on the fusion of mononuclear osteoclasts into bone-resorbing osteoclasts. BMB Rep. 45, 281–286.

Kim, N., Kadono, Y., Takami, M., Lee, J., Lee, S.H., Okada, F., Kim, J.H., Kobayashi, T., Odgren, P.R., Nakano, H., Yeh, W.C., Lee, S.K., Lorenzo, J.A., Choi, Y., 2005. Osteoclast differentiation independent of the TRANCE-RANK-TRAF6 axis. J. Exp. Med. 202, 589–595.

Kim, Y.G., Park, J.W., Lee, J.M., Suh, J.Y., Lee, J.K., Chang, B.S., Um, H.S., Kim, J.Y., Lee, Y., 2014. IL-17 inhibits osteoblast differentiation and bone regeneration in rat. Arch. Oral Biol. 59, 897–905.

Kimble, R.B., Bain, S., Pacifici, R., 1997. The functional block of TNF but not of IL-6 prevents bone loss in ovariectomized mice. J. Bone Miner. Res. 12, 935–941.

Kitajima, I., Soejima, Y., Takasaki, I., Beppu, H., Tokioka, T., Maruyama, I., 1996. Ceramide-induced nuclear translocation of NF-kappaB is a potential mediator of the apoptotic response to TNF-à in murine clonal osteoblasts. Bone 19, 263–270.

Kitami, S., Tanaka, H., Kawato, T., Tanabe, N., Katono-Tani, T., Zhang, F., Suzuki, N., Yonehara, Y., Maeno, M., 2010. IL-17A suppresses the expression of bone resorption-related proteinases and osteoclast differentiation via IL-17RA or IL-17RC receptors in RAW264.7 cells. Biochimie 2, 2.

Kitaura, H., Nagata, N., Fujimura, Y., Hotokezaka, H., Yoshida, N., Nakayama, K., 2002. Effect of IL-12 on TNF-alpha-mediated osteoclast formation in bone marrow cells: apoptosis mediated by Fas/Fas ligand interaction. J. Immunol. 169, 4732–4738.

Kitaura, H., Zhou, P., Kim, H.J., Novack, D.V., Ross, F.P., Teitelbaum, S.L., 2005. M-CSF mediates TNF-induced inflammatory osteolysis. J. Clin. Investig. 115, 3418–3427.

Kitazawa, R., Kimble, R.B., Vannice, J.L., Kung, V.T., Pacifici, R., 1994. Interleukin-1 receptor antagonist and tumor necrosis factor binding protein decrease osteoclast formation and bone resorption in ovariectomized mice. J. Clin. Investig. 94, 2397–2406.

Klein, D.C., Raisz, L.G., 1970. Prostaglandins: stimulation of bone resorption in tissue culture. Endocrinology 86, 1436–1440.

Knappskog, P.M., Majewski, J., Livneh, A., Nilsen, P.T., Bringsli, J.S., Ott, J., Boman, H., 2003. Cold-induced sweating syndrome is caused by mutations in the CRLF1 gene. Am. J. Hum. Genet. 72, 375–383.

Kobayashi, K., Takahashi, N., Jimi, E., Udagawa, N., Takami, M., Kotake, S., Nakagawa, N., Kinosaki, M., Yamaguchi, K., Shima, N., Yasuda, H., Morinaga, T., Higashio, K., Martin, T.J., Suda, T., 2000. Tumor necrosis factor alpha stimulates osteoclast differentiation by a mechanism independent of the ODF/RANKL-RANK interaction. J. Exp. Med. 191, 275–286.

Kochetkova, E.A., Nevzorova, V.A., Ugai, L.G., Maistrovskaia, Y.V., Massard, G., 2016. The role of tumor necrosis factor Alpha and TNF superfamily members in bone damage in patients with end-stage chronic obstructive lung disease prior to lung transplantation. Calcif. Tissue Int. 99, 578–587.

Koenders, M.I., Lubberts, E., Oppers-Walgreen, B., van Den, B.L., Helsen, M.M., di Padova, F.E., Boots, A.M., Gram, H., Joosten, L.A., van den Berg, W.B., 2005. Blocking of interleukin-17 during reactivation of experimental arthritis prevents joint inflammation and bone erosion by decreasing RANKL and interleukin-1. Am. J. Pathol. 167, 141–149.

Koh, J.M., Oh, B., Ha, M.H., Cho, K.W., Lee, J.Y., Park, B.L., Shin, H.D., Bae, M.A., Kim, H.J., Hong, J.M., Kim, T.H., Shin, H.I., Lee, S.H., Kim, G.S., Kim, S.Y., Park, E.K., 2009. Association of IL-15 polymorphisms with bone mineral density in postmenopausal Korean women. Calcif. Tissue Int. 11, 11.

Kohara, H., Kitaura, H., Fujimura, Y., Yoshimatsu, M., Morita, Y., Eguchi, T., Masuyama, R., Yoshida, N., 2011. IFN-gamma directly inhibits TNF-alpha-induced osteoclastogenesis in vitro and in vivo and induces apoptosis mediated by Fas/Fas ligand interactions. Immunol. Lett. 18, 18.

Korherr, C., Hofmeister, R., Wesche, H., Falk, W., 1997. A critical role for interleukin-1 receptor accessory protein in interleukin-1 signaling. Eur. J. Immunol. 27, 262–267.

Kotake, S., Sato, K., Kim, K.J., Takahashi, N., Udagawa, N., Nakamura, I., Yamaguchi, A., Kishimoto, T., Suda, T., Kashiwazaki, S., 1996. Interleukin-6 and soluble interleukin-6 receptors in the synovial fluids from rheumatoid arthritis patients are responsible for osteoclast-like cell formation. J. Bone Miner. Res. 11, 88–95.

Kotake, S., Udagawa, N., Takahashi, N., Matsuzaki, K., Itoh, K., Ishiyama, S., Saito, S., Inoue, K., Kamatani, N., Gillespie, M.T., Martin, T.J., Suda, T., 1999. IL-17 in synovial fluids from patients with rheumatoid arthritis is a potent stimulator of osteoclastogenesis. J. Clin. Investig. 103, 1345–1352.

Kotrych, D., Dziedziejko, V., Safranow, K., Sroczynski, T., Staniszewska, M., Juzyszyn, Z., Pawlik, A., 2016. TNF-alpha and IL10 gene polymorphisms in women with postmenopausal osteoporosis. Eur. J. Obstet. Gynecol. Reprod. Biol. 199, 92–95.

Kovacic, N., Grcevic, D., Katavic, V., Lukic, I.K., Grubisic, V., Mihovilovic, K., Cvija, H., Croucher, P.I., Marusic, A., 2010. Fas receptor is required for estrogen deficiency-induced bone loss in mice. Lab. Invest. 18, 18.

Kovacic, N., Lukic, I.K., Grcevic, D., Katavic, V., Croucher, P., Marusic, A., 2007. The Fas/Fas ligand system inhibits differentiation of murine osteoblasts but has a limited role in osteoblast and osteoclast apoptosis. J. Immunol. 178, 3379–3389.

Kramer, I., Loots, G.G., Studer, A., Keller, H., Kneissel, M., 2010. Parathyroid hormone (PTH)-induced bone gain is blunted in SOST overexpressing and deficient mice. J. Bone Miner. Res. 25, 178–189.

Krum, S.A., Miranda-Carboni, G.A., Hauschka, P.V., Carroll, J.S., Lane, T.F., Freedman, L.P., Brown, M., 2008. Estrogen protects bone by inducing Fas ligand in osteoblasts to regulate osteoclast survival. EMBO J. 27, 535–545.

Kudo, O., Sabokbar, A., Pocock, A., Itonaga, I., Fujikawa, Y., Athanasou, N.A., 2003. Interleukin-6 and interleukin-11 support human osteoclast formation by a RANKL-independent mechanism. Bone 32, 1–7.

Kulkarni, N.H., Halladay, D.L., Miles, R.R., Gilbert, L.M., Frolik, C.A., Galvin, R.J., Martin, T.J., Gillespie, M.T., Onyia, J.E., 2005. Effects of parathyroid hormone on Wnt signaling pathway in bone. J. Cell. Biochem. 95, 1178–1190.

Kulkarni, R.N., Bakker, A.D., Everts, V., Klein-Nulend, J., 2012. Mechanical loading prevents the stimulating effect of IL-1beta on osteocyte-modulated osteoclastogenesis. Biochem. Biophys. Res. Commun. 420, 11–16.

Kyrtsonis, M.C., Dedoussis, G., Zervas, C., Perifanis, V., Baxevanis, C., Stamatelou, M., Maniatis, A., 1996. Soluble interleukin-6 receptor (sIL-6R), a new prognostic factor in multiple myeloma. Br. J. Haematol. 93, 398–400.

Labrinidis, A., Liapis, V., Thai Le, M., Atkins, G.J., Vincent, C., Hay, S., Sims, N.A., Zannettino, A.C., Findlay, D.M., Evdokiou, A., 2008. Does Apo2L/TRAIL play any physiologic role in osteoclastogenesis? Blood 111, 5411–5412 autor reply 5413.

Lam, J., Takeshita, S., Barker, J.E., Kanagawa, O., Ross, F.P., Teitelbaum, S.L., 2000. TNF-alpha induces osteoclastogenesis by direct stimulation of macrophages exposed to permissive levels of RANK ligand. J. Clin. Investig. 106, 1481–1488.

Lambert, C., Oury, C., Dejardin, E., Chariot, A., Piette, J., Malaise, M., Merville, M.P., Franchimont, N., 2007. Further insights in the mechanisms of interleukin-1beta stimulation of osteoprotegerin in osteoblast-like cells. J. Bone Miner. Res. 22, 1350–1361.

Larsen, J.V., Hansen, M., Moller, B., Madsen, P., Scheller, J., Nielsen, M., Petersen, C.M., 2010. Sortilin facilitates signaling of ciliary neurotrophic factor and related helical type 1 cytokines targeting the gp130/leukemia inhibitory factor receptor beta heterodimer. Mol. Cell Biol. 30, 4175–4187.

Lazzaro, L., Tonkin, B.A., Poulton, I.J., Mcgregor, N.E., Ferlin, W., Sims, N.A., 2018. IL-6 trans-signalling mediates trabecular (but not cortical) bone loss after ovariectomy. Bone 112, 120–127 (in review).

Le Goff, B., Singbrant, S., Tonkin, B.A., Martin, T.J., Romas, E., Sims, N.A., Walsh, N.C., 2014. Oncostatin M acting via OSMR, augments the actions of IL-1 and TNF in synovial fibroblasts. Cytokine 68, 101–109.

Lee, E.J., Kim, S.M., Choi, B., Kim, E.Y., Chung, Y.H., Lee, E.J., Yoo, B., Lee, C.K., Hong, S., Kim, B.J., Koh, J.M., Kim, S.H., Kim, Y.G., Chang, E.J., 2017. Interleukin-32 gamma stimulates bone formation by increasing miR-29a in osteoblastic cells and prevents the development of osteoporosis. Sci. Rep. 7, 40240.

Lee, E.J., Lee, E.J., Chung, Y.H., Song, D.H., Hong, S., Lee, C.K., Yoo, B., Kim, T.H., Park, Y.S., Kim, S.H., Chang, E.J., Kim, Y.G., 2015. High level of interleukin-32 gamma in the joint of ankylosing spondylitis is associated with osteoblast differentiation. Arthritis Res. Ther. 17, 350.

Lee, H.Y., Jeon, H.S., Song, E.K., Han, M.K., Park, S.I., Lee, S.I., Yun, H.J., Kim, J.R., Kim, J.S., Lee, Y.C., Kim, S.I., Kim, H.R., Choi, J.Y., Kang, I., Kim, H.Y., Yoo, W.H., 2006a. CD40 ligation of rheumatoid synovial fibroblasts regulates RANKL-medicated osteoclastogenesis: evidence of NF-kappaB-dependent, CD40-mediated bone destruction in rheumatoid arthritis. Arthritis Rheum. 54, 1747–1758.

Lee, S., Kalinowski, J., Adams, D.J., Aguila, H.L., Lorenzo, J.A., 2005b. Osteoblast specific overexpression of human interlukin-7 rescues the bone phenotype of interleukin-7 deficient female mice. J. Bone Miner. Res. 20, S48.

Lee, S., Kalinowski, J.F., Adams, D.J., Aguila, H.L., Lorenzo, J.A., 2004. Osteoblast specific overexpression of human interleukin-7 increases femoral trabecular bone mass in female mice and inhibits in vitro osteoclastogenesis. J. Bone Miner. Res. 19, S410.

Lee, S.K., Gardner, A.E., Kalinowski, J.F., Jastrzebski, S.L., Lorenzo, J.A., 2005a. RANKL-stimulated osteoclast-like cell formation in vitro is partially dependent on endogenous interleukin-1 production. Bone 38, 678–685.

Lee, S.K., Kalinowski, J., Jastrzebski, S., Lorenzo, J.A., 2002a. 1,25 (OH)(2) vitamin D(3)-stimulated osteoclast formation in spleen-osteoblast cocultures is mediated in part by enhanced IL-1alpha and receptor activator of NF-kappaB ligand production in osteoblasts. J. Immunol. 169, 2374–2380.

Lee, S.K., Kalinowski, J.F., Jacquin, C., Adams, D.J., Gronowicz, G., Lorenzo, J.A., 2006b. Interleukin-7 influences osteoclast function in vivo but is not a critical factor in ovariectomy-induced bone loss. J. Bone Miner. Res. 21, 695–702.

Lee, S.K., Kalinowski, J.F., Jastrzebski, S.L., Puddington, L., Lorenzo, J.A., 2003. Interleukin-7 is a direct inhibitor of in vitro osteoclastogenesis. Endocrinology 144, 3524–3531.

Lee, Y.-J., Park, J.-H., Ju, S.-K., You, K.-H., Ko, J.S., Kim, H.-M., 2002b. Leptin receptor isoform expression in rat osteoblasts and their functional analysis. FEBS (Fed. Eur. Biochem. Soc.) Lett. 528, 43–47.

Lee, Y.M., Fujikado, N., Manaka, H., Yasuda, H., Iwakura, Y., 2010. IL-1 plays an important role in the bone metabolism under physiological conditions. Int. Immunol. 22, 805–816.

Lee, Z.H., Lee, S.E., Kim, C.W., Lee, S.H., Kim, S.W., Kwack, K., Walsh, K., Kim, H.H., 2002c. IL-1alpha stimulation of osteoclast survival through the PI 3-kinase/Akt and ERK pathways. J. Biochem. 131, 161–166.

Legendre, F., Dudhia, J., Pujol, J.P., Bogdanowicz, P., 2003. JAK/STAT but not ERK1/ERK2 pathway mediates interleukin (IL)-6/soluble IL-6R down-regulation of Type II collagen, aggrecan core, and link protein transcription in articular chondrocytes. Association with a down-regulation of SOX9 expression. J. Biol. Chem. 278, 2903–2912.

Levesque, J.P., Sims, N.A., Pettit, A.R., Alexander, K.A., Tseng, H.W., Torossian, F., Genet, F., Lataillade, J.J., Bousse-Kerdiles, M.L., 2018. Macrophages driving heterotopic ossification: convergence of genetically-driven and trauma-driven mechanisms. J. Bone Miner. Res. 33 (2), 365–366.

Lewis, D.B., Liggitt, H.D., Effmann, E.L., Motley, S.T., Teitelbaum, S.L., Jepsen, K.J., Goldstein, S.A., Bonadio, J., Carpenter, J., Perlmutter, R.M., 1993. Osteoporosis induced in mice by overproduction of interleukin 4. Proc. Natl. Acad. Sci. U. S. A. 90, 11618–11622.

Li, H., Lu, Y., Qian, J., Zheng, Y., Zhang, M., Bi, E., He, J., Liu, Z., Xu, J., Gao, J.Y., Yi, Q., 2014. Human osteoclasts are inducible immunosuppressive cells in response to T cell-derived IFN-gamma and CD40 ligand in vitro. J. Bone Miner. Res. 29 (12), 2666–2675.

Li, J., Sarosi, I., Yan, X.Q., Morony, S., Capparelli, C., Tan, H.L., Mccabe, S., Elliott, R., Scully, S., Van, G., Kaufman, S., Juan, S.C., Sun, Y., Tarpley, J., Martin, L., Christensen, K., Mccabe, J., Kostenuik, P., Hsu, H., Fletcher, F., Dunstan, C.R., Lacey, D.L., Boyle, W.J., 2000. RANK is the intrinsic hematopoietic cell surface receptor that controls osteoclastogenesis and regulation of bone mass and calcium metabolism. Proc. Natl. Acad. Sci. U. S. A. 97, 1566–1571.

Li, J.Y., Tawfeek, H., Bedi, B., Yang, X., Adams, J., Gao, K.Y., Zayzafoon, M., Weitzmann, M.N., Pacifici, R., 2011. Ovariectomy disregulates osteoblast and osteoclast formation through the T-cell receptor CD40 ligand. Proc. Natl. Acad. Sci. U. S. A. 108, 768–773.

Li, P., Schwarz, E.M., O'Keefe, R.J., Ma, L., Boyce, B.F., Xing, L., 2004a. RANK signaling is not required for TNFalpha-mediated increase in CD11(hi) osteoclast precursors but is essential for mature osteoclast formation in TNFalpha-mediated inflammatory arthritis. J. Bone Miner. Res. 19, 207–213.

Li, P., Schwarz, E.M., O'keefe, R.J., Ma, L., Looney, R.J., Ritchlin, C.T., Boyce, B.F., Xing, L., 2004b. Systemic tumor necrosis factor alpha mediates an increase in peripheral CD11bhigh osteoclast precursors in tumor necrosis factor alpha-transgenic mice. Arthritis Rheum. 50, 265–276.

Liang, J.D., Hock, J.M., Sandusky, G.E., Santerre, R.F., Onyia, J.E., 1999. Immunohistochemical localization of selected early response genes expressed in trabecular bone of young rats given hPTH 1-34. Calcif. Tissue Int. 65, 369–373.

Liao, C., Cheng, T., Wang, S., Zhang, C., Jin, L., Yang, Y., 2017. Shear stress inhibits IL-17A-mediated induction of osteoclastogenesis via osteocyte pathways. Bone 101, 10–20.

Lima, I.L., Macari, S., Madeira, M.F., Rodrigues, L.F., Colavite, P.M., Garlet, G.P., Soriani, F.M., Teixeira, M.M., Fukada, S.Y., Silva, T.A., 2015. Osteoprotective effects of IL-33/ST2 link to osteoclast apoptosis. Am. J. Pathol. 185, 3338–3348.

Lindsay, R., Nieves, J., Formica, C., Henneman, E., Woelfert, L., Shen, V., Dempster, D., Cosman, F., 1997. Randomised controlled study of effect of parathyroid hormone on vertebral-bone mass and fracture incidence among postmenopausal women on oestrogen with osteoporosis. Lancet 350, 550–555.

Lisignoli, G., Piacentini, A., Toneguzzi, S., Grassi, F., Cocchini, B., Ferruzzi, A., Gualtieri, G., Facchini, A., 2000. Osteoblasts and stromal cells isolated from femora in rheumatoid arthritis (RA) and osteoarthritis (OA) patients express IL-11, leukaemia inhibitory factor and oncostatin M. Clin. Exp. Immunol. 119, 346–353.

Liu, D., Yao, S., Wise, G.E., 2006. Effect of interleukin-10 on gene expression of osteoclastogenic regulatory molecules in the rat dental follicle. Eur. J. Oral Sci. 114, 42–49.

Liu, F., Aubin, J.E., Malaval, L., 2002. Expression of leukemia inhibitory factor (LIF)/interleukin-6 family cytokines and receptors during in vitro osteogenesis: differential regulation by dexamethasone and LIF. Bone 31, 212–219.

Liu, W., Xu, C., Zhao, H., Xia, P., Song, R., Gu, J., Liu, X., Bian, J., Yuan, Y., Liu, Z., 2015. Osteoprotegerin induces apoptosis of osteoclasts and osteoclast precursor cells via the fas/fas ligand pathway. PLoS One 10, e0142519.

Liu, X., Croker, B.A., Campbell, I.K., Gauci, S.J., Alexander, W.S., Tonkin, B.A., Walsh, N.C., Linossi, E.M., Nicholson, S.E., Lawlor, K.E., Wicks, I.P., 2014. Key role of suppressor of cytokine signaling 3 in regulating gp130 cytokine-induced signaling and limiting chondrocyte responses during murine inflammatory arthritis. Arthritis Rheum. 66, 2391–2402.

Lokau, J., Nitz, R., Agthe, M., Monhasery, N., Aparicio-Siegmund, S., Schumacher, N., Wolf, J., Moller-Hackbarth, K., Waetzig, G.H., Grotzinger, J., Muller-Newen, G., Rose-John, S., Scheller, J., Garbers, C., 2016. Proteolytic cleavage Governs interleukin-11 trans-signaling. Cell Rep. 14, 1761–1773.

Lopez-Granados, E., Temmerman, S.T., Wu, L., Reynolds, J.C., Follmann, D., Liu, S., Nelson, D.L., Rauch, F., Jain, A., 2007. Osteopenia in X-linked hyper-IgM syndrome reveals a regulatory role for CD40 ligand in osteoclastogenesis. Proc. Natl. Acad. Sci. U. S. A. 104, 5056–5061.

Lorenzo, J.A., Naprta, A., Rao, Y., Alander, C., Glaccum, M., Widmer, M., Gronowicz, G., Kalinowski, J., Pilbeam, C.C., 1998. Mice lacking the type I interleukin-1 receptor do not lose bone mass after ovariectomy. Endocrinology 139, 3022–3025.

Lorenzo, J.A., Sousa, S., Alander, C., Raisz, L.G., Dinarello, C.A., 1987. Comparison of the bone-resorbing activity in the supernatants from phytohemagglutinin-stimulated human peripheral blood mononuclear cells with that of cytokines through the use of an antiserum to interleukin 1. Endocrinology 121, 1164–1170.

Lorenzo, J.A., Sousa, S.L., van den Brink-Webb, S.E., Korn, J.H., 1990. Production of both interleukin-1 à and á by newborn mouse calvaria cultures. J. Bone Miner. Res. 5, 77–83.

Loro, E., Ramaswamy, G., Chandra, A., Tseng, W.J., Mishra, M.K., Shore, E.M., Khurana, T.S., 2017. IL15RA is required for osteoblast function and bone mineralization. Bone 103, 20–30.

Loskog, A., Totterman, T.H., 2007. CD40L - a multipotent molecule for tumor therapy. Endocr. Metab. Immune Disord. - Drug Targets 7, 23–28.

Lowe, C., Gillespie, G.A., Pike, J.W., 1995. Leukemia inhibitory factor as a mediator of JAK/STAT activation in murine osteoblasts. J. Bone Miner. Res. 10, 1644–1650.

Lowik, C.W., van der Pluijm, G., Bloys, H., Hoekman, K., Bijvoet, O.L., Aarden, L.A., Papapoulos, S.E., 1989. Parathyroid hormone (PTH) and PTH-like protein (PLP) stimulate interleukin-6 production by osteogenic cells: a possible role of interleukin-6 in osteoclastogenesis. Biochem. Biophys. Res. Commun. 162, 1546–1552.

Lubberts, E., Joosten, L.A.B., Chabaud, M., van den Bersselaar, L., Oppers, B., Coenen-de Roo, C.J.J., Richards, C.D., Miossec, P., van den Berg, W.B., 2000. IL-4 gene therapy for collagen arthritis suppresses synovial IL-17 and osteoprotegerin ligand and prevents bone erosion. J. Clin. Investig. 105, 1697–1710.

Lubberts, E., van den, B.L., Oppers-Walgreen, B., Schwarzenberger, P., Coenen-de Roo, C.J., Kolls, J.K., Joosten, L.A., van den Berg, W.B., 2003. IL-17 promotes bone erosion in murine collagen-induced arthritis through loss of the receptor activator of NF-kappaB ligand/osteoprotegerin balance. J. Immunol. 170, 2655–2662.

Ma, Y.L., Cain, R.L., Halladay, D.L., Yang, X., Zeng, Q., Miles, R.R., Chandrasekhar, S., Martin, T.J., Onyia, J.E., 2001. Catabolic effects of continuous human PTH (1–38) in vivo is associated with sustained stimulation of RANKL and inhibition of osteoprotegerin and gene-associated bone formation. Endocrinology 142, 4047–4054.

Mabilleau, G., Sabokbar, A., 2009. Interleukin-32 promotes osteoclast differentiation but not osteoclast activation. PLoS One 4, e4173.

Maeda, S., Nobukuni, T., Shimo-Onoda, K., Hayashi, K., Yone, K., Komiya, S., Inoue, I., 2002. Sortilin is upregulated during osteoblastic differentiation of mesenchymal stem cells and promotes extracellular matrix mineralization. J. Cell. Physiol. 193, 73–79.

Maier, R., Ganu, V., Lotz, M., 1993. Interleukin-11, an inducible cytokine in human articular chondrocytes and synoviocytes, stimulates the production of the tissue inhibitor of metalloproteinases. J. Biol. Chem. 268, 21527–21532.

Makiishi-Shimobayashi, C., Tsujimura, T., Iwasaki, T., Yamada, N., Sugihara, A., Okamura, H., Hayashi, S.S., Terada, N., 2001. Interleukin-18 up-regulates osteoprotegerin expression in stromal/osteoblastic cells. Biochem. Biophys. Res. Commun. 281, 361–366.

Malaval, L., Gupta, A.K., Aubin, J.E., 1995. Leukemia inhibitory factor inhibits osteogenic differentiation in rat calvaria cell cultures. Endocrinology 136, 1411–1418.

Mangashetti, L.S., Khapli, S.M., Wani, M.R., 2005. IL-4 inhibits bone-resorbing activity of mature osteoclasts by affecting NF-kappa B and Ca2+ signaling. J. Immunol. 175, 917–925.

Mann, G.N., Jacobs, T.W., Buchinsky, F.J., Armstrong, E.C., Li, M., Ke, H.Z., Ma, Y.F., Jee, W.S.S., Epstein, S., 1994. Interferon-gamma causes loss of bone volume in vivo and fails to ameliorate cyclosporin A-induced osteopenia. Endocrinology 135, 1077–1083.

Manoury-Schwartz, B., Chiocchia, G., Bessis, N., Abehsira-Amar, O., Batteux, F., Muller, S., Huang, S., Boissier, M.C., Fournier, C., 1997. High susceptibility to collagen-induced arthritis in mice lacking IFN-gamma receptors. J. Immunol. 158, 5501–5506.

Mansoori, M.N., Shukla, P., Kakaji, M., Tyagi, A.M., Srivastava, K., Shukla, M., Dixit, M., Kureel, J., Gupta, S., Singh, D., 2016. IL-18BP is decreased in osteoporotic women: Prevents Inflammasome mediated IL-18 activation and reduces Th17 differentiation. Sci. Rep. 6:33680.

Mansour, A., Anginot, A., Mancini, S.J., Schiff, C., Carle, G.F., Wakkach, A., Blin-Wakkach, C., 2011. Osteoclast activity modulates B-cell development in the bone marrow. Cell Res. 15, 15.

Mantila Roosa, S.M., Liu, Y., Turner, C.H., 2011. Gene expression patterns in bone following mechanical loading. J. Bone Miner. Res. 26, 100–112.

Marine, J.C., Mckay, C., Wang, D., Topham, D.J., Parganas, E., Nakajima, H., Pendeville, H., Yasukawa, H., Sasaki, A., Yoshimura, A., Ihle, J.N., 1999. SOCS3 is essential in the regulation of fetal liver erythropoiesis. Cell 98, 617–627.

Martin, M.U., Falk, W., 1997. The interleukin-1 receptor complex and interleukin-1 signal transduction. Eur. Cytokine Netw. 8, 5–17.

Martin, T.J., Sims, N.A., 2005. Osteoclast-derived activity in the coupling of bone formation to resorption. Trends Mol. Med. 11, 76–81.

Matsumoto, A., Masuhara, M., Mitsui, K., Yokouchi, M., Ohtsubo, M., Misawa, H., Miyajima, A., Yoshimura, A., 1997. CIS, a cytokine inducible SH2 protein, is a target of the JAK-STAT5 pathway and modulates STAT5 activation. Blood 89, 3148–3154.

McGregor, N.E., Murat, M., Elango, J., Poulton, I.J., Walker, E.C., Crimeen-Irwin, B., Ho, P.W.M., Gooi, J.H., Martin, T.J., Sims, N.A., 2019. Il-6 exhibits both cis and trans signaling in osteocytes and osteoblasts, but only trans signaling promotes bone formation and osteoclastogenesis. J. Biol. Chem. (In Press).

McGregor, N.E., Poulton, I.J., Walker, E.C., Pompolo, S., Quinn, J.M., Martin, T.J., Sims, N.A., 2010. Ciliary neurotrophic factor inhibits bone formation and plays a sex-specific role in bone growth and remodeling. Calcif. Tissue Int. 86, 261–270.

Menkhorst, E., Zhang, J.G., Sims, N.A., Morgan, P.O., Soo, P., Poulton, I.J., Metcalf, D., Alexandrou, E., Gresle, M., Salamonsen, L.A., Butzkueven, H., Nicola, N.A., Dimitriadis, E., 2011. Vaginally administered PEGylated LIF antagonist blocked embryo implantation and eliminated non-target effects on bone in mice. PLoS One 6, e19665.

Metcalf, D., Gearing, D.P., 1989. Fatal syndrome in mice engrafted with cells producing high levels of the leukemia inhibitory factor. Proc. Natl. Acad. Sci. U. S. A. 86, 5948–5952.

Metzger, C.E., Narayanan, A., Zawieja, D.C., Bloomfield, S.A., 2017. Inflammatory bowel disease in a Rodent model alters osteocyte protein levels controlling bone turnover. J. Bone Miner. Res. 32, 802–813.

Michalski, M.N., Koh, A.J., Weidner, S., Roca, H., Mccauley, L.K., 2016. Modulation of osteoblastic cell efferocytosis by bone marrow macrophages. J. Cell. Biochem. 117, 2697–2706.

Minegishi, Y., Saito, M., Tsuchiya, S., Tsuge, I., Takada, H., Hara, T., Kawamura, N., Ariga, T., Pasic, S., Stojkovic, O., Metin, A., Karasuyama, H., 2007. Dominant-negative mutations in the DNA-binding domain of STAT3 cause hyper-IgE syndrome. Nature 448, 1058−1062.

Miranda-Carus, M.E., Ito-Miguel, M., Balsa, A., Cobo-Ibanez, T., Perez De, A.C., Pascual-Salcedo, D., Martin-Mola, E., 2006. Peripheral blood T lymphocytes from patients with early rheumatoid arthritis express RANKL and interleukin-15 on the cell surface and promote osteoclastogenesis in autologous monocytes. Arthritis Rheum. 54, 1151−1164.

Mitsuyama, K., Toyonaga, A., Sasaki, E., Ishida, O., Ikeda, H., Tsuruta, O., Harada, K., Tateishi, H., Nishiyama, T., Tanikawa, K., 1995. Soluble interleukin-6 receptors in inflammatory bowel disease: relation to circulating interleukin-6. Gut 36, 45−49.

Miyaura, C., Kusano, K., Masuzawa, T., Chaki, O., Onoe, Y., Aoyagi, M., Sasaki, T., Tamura, T., Koishihara, Y., Ohsugi, Y., Suda, T., 1995. Endogenous bone-resorbing factors in estrogen deficiency: cooperative effects of IL-1 and IL-6. J. Bone Miner. Res. 10, 1365−1463.

Miyaura, C., Onoe, Y., Inada, M., Maki, K., Ikuta, K., Ito, M., Suda, T., 1997. Increased B-lymphopoiesis by interleukin 7 induces bone loss in mice with intact ovarian function: similarity to estrogen deficiency. Proc. Natl. Acad. Sci. U. S. A. 94, 9360−9365.

Modur, V., Li, Y., Zimmerman, G.A., Prescott, S.M., Mcintyre, T.M., 1997. Retrograde inflammatory signaling from neutrophils to endothelial cells by soluble interleukin-6 receptor alpha. J. Clin. Investig. 100, 2752−2756.

Mohamed, S.G., Sugiyama, E., Shinoda, K., Taki, H., Hounoki, H., Bdel-Aziz, H.O., Maruyama, M., Kobayashi, M., Ogawa, H., Miyahara, T., 2007. Interleukin-10 inhibits RANKL-mediated expression of NFATc1 in part via suppression of c-Fos and c-Jun in RAW264.7 cells and mouse bone marrow cells. Bone 41 (4), 592−602.

Molnar, I., Bohaty, I., Somogyine-Vari, E., 2014. High prevalence of increased interleukin-17A serum levels in postmenopausal estrogen deficiency. Menopause 21, 749−752.

Moore, K.W., de Waal, M.R., Coffman, R.L., O'garra, A., 2001. Interleukin-10 and the interleukin-10 receptor. Annu. Rev. Immunol. 19, 683−765.

Moreno, J.L., Kaczmareck, M., Keegan, A.D., Tondravi, M., 2003. IL-4 suppresses both osteoclast development and mature osteoclast function by a STAT6-dependent mechanism: irreversible inhibition of the differentiation program activated by RANKL. Blood 102, 1078−1086.

Mori, L., Iselin, S., de Libero, G., Lesslauer, W., 1996. Attenuation of collagen-induced arthritis in 55-kDa TNF receptor type 1 (TNFR1)-IgG1-treated and TNFR1-deficient mice. J. Immunol. 157, 3178−3182.

Mosley, B., de Imus, C., Friend, D., Boiani, N., Thoma, B., Park, L.S., Cosman, D., 1996. Dual oncostatin M (OSM) receptors. Cloning and characterization of an alternative signaling subunit conferring OSM-specific receptor activation. J. Biol. Chem. 271, 32635−32643.

Moverare-Skrtic, S., Henning, P., Liu, X., Nagano, K., Saito, H., Borjesson, A.E., Sjogren, K., Windahl, S.H., Farman, H., Kindlund, B., Engdahl, C., Koskela, A., Zhang, F.P., Eriksson, E.E., Zaman, F., Hammarstedt, A., Isaksson, H., Bally, M., Kassem, A., Lindholm, C., Sandberg, O., Aspenberg, P., Savendahl, L., Feng, J.Q., Tuckermann, J., Tuukkanen, J., Poutanen, M., Baron, R., Lerner, U.H., Gori, F., Ohlsson, C., 2014. Osteoblast-derived WNT16 represses osteoclastogenesis and prevents cortical bone fragility fractures. Nat. Med. 20 (11), 1279−1288.

Movila, A., Ishii, T., Albassam, A., Wisitrasameewong, W., Howait, M., Yamaguchi, T., Ruiz-Torruella, M., Bahammam, L., Nishimura, K., van Dyke, T., Kawai, T., 2016. Macrophage migration inhibitory factor (MIF) supports homing of osteoclast precursors to peripheral osteolytic lesions. J. Bone Miner. Res. 31 (9), 1688−1700.

Mun, S.H., Ko, N.Y., Kim, H.S., Kim, J.W., Kim, D.K., Kim, A.R., Lee, S.H., Kim, Y.G., Lee, C.K., Kim, B.K., Beaven, M.A., Kim, Y.M., Choi, W.S., 2010. Interleukin-33 stimulates formation of functional osteoclasts from human CD14(+) monocytes. Cell. Mol. Life Sci. 67 (22), 3883−3892.

Mun, S.H., Oh, D., Lee, S.K., 2014. Macrophage migration inhibitory factor down-regulates the RANKL-RANK signaling pathway by activating Lyn tyrosine kinase. Arthritis Rheum.

Mun, S.H., Won, H.Y., Hernandez, P., Aguila, H.L., Lee, S.K., 2013. Deletion of CD74, a putative MIF receptor, in mice enhances osteoclastogenesis and decreases bone mass. J. Bone Miner. Res. 28, 948−959.

Nagata, N., Kitaura, H., Yoshida, N., Nakayama, K., 2003. Inhibition of RANKL-induced osteoclast formation in mouse bone marrow cells by IL-12: involvement of IFN-gamma possibly induced from non-T cell population. Bone 33, 721−732.

Nakamura, I., Jimi, E., 2006. Regulation of osteoclast differentiation and function by interleukin-1. Vitam. Horm. 74, 357−370.

Nakamura, T., Imai, Y., Matsumoto, T., Sato, S., Takeuchi, K., Igarashi, K., Harada, Y., Azuma, Y., Krust, A., Yamamoto, Y., Nishina, H., Takeda, S., Takayanagi, H., Metzger, D., Kanno, J., Takaoka, K., Martin, T.J., Chambon, P., Kato, S., 2007. Estrogen prevents bone loss via estrogen receptor alpha and induction of fas ligand in osteoclasts. Cell 130, 811−823.

Nakano, Y., Watanabe, K., Morimoto, I., Okada, Y., Ura, K., Sato, K., Kasono, K., Nakamura, T., Eto, S., 1994. Interleukin-4 inhibits spontaneous and parathyroid hormone- related protein-stimulated osteoclast formation in mice. J. Bone Miner. Res. 9, 1533−1539.

Nakashima, T., Hayashi, M., Fukunaga, T., Kurata, K., Oh-Hora, M., Feng, J.Q., Bonewald, L.F., Kodama, T., Wutz, A., Wagner, E.F., Penninger, J.M., Takayanagi, H., 2011. Evidence for osteocyte regulation of bone homeostasis through RANKL expression. Nat. Med. 17, 1231−1234.

Namen, A.E., Lupton, S., Hjerrild, K., Wignall, J., Mochizuki, D.Y., Schmierer, A., Mosley, B., March, C.J., Urdal, D., Gillis, S., Cosman, D., Goodwin, R.G., 1988. Stimulation of B-cell progenitors by cloned murine interleukin-7. Nature 333, 571−573.

Nanes, M.S., Mckoy, W.M., Marx, S.J., 1989. Inhibitory effects of tumor necrosis factor-alpha and interferon-gamma on deoxyribonucleic acid and collagen synthesis by rat osteosarcoma cells (ROS 17/2.8). Endocrinology 124, 339−345.

Nanes, M.S., Rubin, J., Titus, L., Hendy, G.N., Catherwood, B., 1991. Tumor necrosis factor-à inhibits 1,25-dihydroxyvitamin D 3 - stimulated bone Gla protein synthesis in rat osteosarcoma cells (ROS 17/2.8) by a pretranslational mechanism. Endocrinology 128, 2577−2582.

Neutzsky-Wulff, A.V., Sims, N.A., Supanchart, C., Kornak, U., Felsenberg, D., Poulton, I.J., Martin, T.J., Karsdal, M.A., Henriksen, K., 2010. Severe developmental bone phenotype in ClC-7 deficient mice. Dev. Biol. 344, 1001−1010.

Nicolaidou, V., Wong, M.M., Redpath, A.N., Ersek, A., Baban, D.F., Williams, L.M., Cope, A.P., Horwood, N.J., 2012. Monocytes induce STAT3 activation in human mesenchymal stem cells to promote osteoblast formation. PLoS One 7, e39871.

Nieminen, P., Morgan, N.V., Fenwick, A.L., Parmanen, S., Veistinen, L., Mikkola, M.L., van der Spek, P.J., Giraud, A., Judd, L., Arte, S., Brueton, L.A., Wall, S.A., Mathijssen, I.M., Maher, E.R., Wilkie, A.O., Kreiborg, S., Thesleff, I., 2011. Inactivation of IL11 signaling causes craniosynostosis, delayed tooth eruption, and supernumerary teeth. Am. J. Hum. Genet. 89, 67–81.

Nigil Haroon, N., Sriganthan, J., Al Ghanim, N., Inman, R.D., Cheung, A.M., 2014. Effect of TNF-alpha inhibitor treatment on bone mineral density in patients with ankylosing spondylitis: a systematic review and meta-analysis. Semin. Arthritis Rheum. 44 (2), 155–161.

Niki, Y., Takaishi, H., Takito, J., Miyamoto, T., Kosaki, N., Matsumoto, H., Toyama, Y., Tada, N., 2007. Administration of cyclooxygenase-2 inhibitor reduces joint inflammation but exacerbates osteopenia in IL-1 alpha transgenic mice due to GM-CSF overproduction. J. Immunol. 179, 639–646.

Noda, M., Vogel, R.L., Hasson, D.M., Rodan, G.A., 1990. Leukemia inhibitory factor suppresses proliferation, alkaline phosphatase activity, and type I collagen messenger ribonucleic acid level and enhances osteopontin mRNA level in murine osteoblast-like (MC3T3E1) cells. Endocrinology 127, 185–190.

O'Brien, C.A., Gubrij, I., Lin, S.C., Saylors, R.L., Manolagas, S.C., 1999. STAT3 activation in stromal/osteoblastic cells is required for induction of the receptor activator of NF-kappaB ligand and stimulation of osteoclastogenesis by gp130-utilizing cytokines or interleukin-1 but not 1,25-dihydroxyvitamin D3 or parathyroid hormone. J. Biol. Chem. 274, 19301–19308.

Ochi, S., Shinohara, M., Sato, K., Gober, H.J., Koga, T., Kodama, T., Takai, T., Miyasaka, N., Takayanagi, H., 2007. Pathological role of osteoclast costimulation in arthritis-induced bone loss. Proc. Natl. Acad. Sci. U. S. A. 104, 11394–11399.

Ogata, Y., Kukita, A., Kukita, T., Komine, M., Miyahara, A., Miyazaki, S., Kohashi, O., 1999. A novel role of IL-15 in the development of osteoclasts: inability to replace its activity with IL-2. J. Immunol. 162, 2754–2760.

Okabe, I., Kikuchi, T., Mogi, M., Takeda, H., Aino, M., Kamiya, Y., Fujimura, T., Goto, H., Okada, K., Hasegawa, Y., Noguchi, T., Mitani, A., 2017. IL-15 and RANKL play a synergistically important role in osteoclastogenesis. J. Cell. Biochem. 118, 739–747.

Okada, Y., Morimoto, I., Ura, K., Nakano, Y., Tanaka, Y., Nishida, S., Nakamura, T., Eto, S., 1998. Short-term treatment of recombinant murine interleukin-4 rapidly inhibits bone formation in normal and ovariectomized mice. Bone 22, 361–365.

Okamura, H., Tsutsui, H., Komatsu, T., Yutsudo, M., Hakura, A., Tanimoto, T., Torigoe, K., Okura, T., Nukada, Y., Hattori, K., Akita, K., Namba, M., Tanabe, F., Konishi, K., Fukuda, S., Kurimoto, M., 1995. Cloning of a new cytokine that induces IFN-gamma production by T cells. Nature 378, 88–91.

Okragly, A.J., Hamang, M.J., Pena, E.A., Baker, H.E., Bullock, H.A., Lucchesi, J., Martin, A.P., Ma, Y.L., Benschop, R.J., 2016. Elevated levels of Interleukin (IL)-33 induce bone pathology but absence of IL-33 does not negatively impact normal bone homeostasis. Cytokine 79, 66–73.

Old, L.J., 1985. Tumor necrosis factor (TNF). Science 230, 630–632.

Oliff, A., 1988. The role of tumor necrosis factor (cachectin) in cachexia. Cell 54, 141–142.

Ono, T., Okamoto, K., Nakashima, T., Nitta, T., Hori, S., Iwakura, Y., Takayanagi, H., 2016. IL-17-producing gammadelta T cells enhance bone regeneration. Nat. Commun. 7, 10928.

Onodera, S., Nishihira, J., Iwabuchi, K., Koyama, Y., Yoshida, K., Tanaka, S., Minami, A., 2002. Macrophage migration inhibitory factor up-regulates matrix metalloproteinase-9 and -13 in rat osteoblasts. Relevance to intracellular signaling pathways. J. Biol. Chem. 277, 7865–7874.

Onodera, S., Sasaki, S., Ohshima, S., Amizuka, N., Li, M., Udagawa, N., Irie, K., Nishihira, J., Koyama, Y., Shiraishi, A., Tohyama, H., Yasuda, K., 2006. Transgenic mice overexpressing macrophage migration inhibitory factor (MIF) exhibit high-turnover osteoporosis. J. Bone Miner. Res. 21, 876–885.

Onodera, S., Suzuki, K., Kaneda, K., Fujinaga, M., Nishihira, J., 1999. Growth factor-induced expression of macrophage migration inhibitory factor in osteoblasts: relevance to the plasminogen activator system. Semin. Thromb. Hemost. 25, 563–568.

Onodera, S., Suzuki, K., Matsuno, T., Kaneda, K., Kuriyama, T., Nishihira, J., 1996. Identification of macrophage migration inhibitory factor in murine neonatal calvariae and osteoblasts. Immunology 89, 430–435.

Onoe, Y., Miyaura, C., Kaminakayashiki, T., Nagai, Y., Noguchi, K., Chen, Q.R., Seo, H., Ohta, H., Nozawa, S., Kudo, I., Suda, T., 1996. IL-13 and IL-4 inhibit bone resorption by suppressing cyclooxygenase- 2-dependent prostaglandin synthesis in osteoblasts. J. Immunol. 156, 758–764.

Orozco, A., Gemmell, E., Bickel, M., Seymour, G.J., 2007. Interleukin 18 and periodontal disease. J. Dent. Res. 86, 586–593.

Oshima, S., Onodera, S., Amizuka, N., Li, M., Irie, K., Watanabe, S., Koyama, Y., Nishihira, J., Yasuda, K., Minami, A., 2006. Macrophage migration inhibitory factor-deficient mice are resistant to ovariectomy-induced bone loss. FEBS Lett. 580, 1251–1256.

Osta, B., Benedetti, G., Miossec, P., 2014. Classical and paradoxical effects of TNF-alpha on bone homeostasis. Front. Immunol. 5, 48.

Ota, M., Yanagisawa, M., Tachibana, H., Yokota, K., Araki, Y., Sato, K., Mimura, T., 2015. A significant induction of neutrophilic chemoattractants but not RANKL in synoviocytes stimulated with interleukin 17. J. Bone Miner. Metab. 33 (1), 40–47.

Ota, N., Hunt, S.C., Nakajima, T., Suzuki, T., Hosoi, T., Orimo, H., Shirai, Y., Emi, M., 1999. Linkage of interleukin 6 locus to human osteopenia by sibling pair analysis. Hum. Genet. 105, 253–257.

Ota, N., Nakajima, T., Nakazawa, I., Suzuki, T., Hosoi, T., Orimo, H., Inoue, S., Shirai, Y., Emi, M., 2001. A nucleotide variant in the promoter region of the interleukin-6 gene associated with decreased bone mineral density. J. Hum. Genet. 46, 267–272.

Owens, J., Chambers, T.J., 1995. Differential regulation of osteoclast formation: interleukin 10 (cytokine synthesis inhibitory factor) suppresses formation of osteoclasts but not macrophages in murine bone marrow cultures. J. Bone Miner. Res. 10, S220.

Owens, J.M., Gallagher, A.C., Chambers, T.J., 1996. IL-1O modulates formation of osteoclasts in murine hemopoietic cultures. J. Immunol. 157, 936–940.

Ozsoy, A.Z., Karakus, N., Tural, S., Yigit, S., Kara, N., Alayli, G., Tumer, M.K., Kuru, O., 2018. Influence of the MIF polymorphism -173G > C on Turkish postmenopausal women with osteoporosis. Z. Rheumatol. 77 (7), 629–632.

Palmqvist, P., Lundberg, P., Persson, E., Johansson, A., Lundgren, I., Lie, A., Conaway, H.H., Lerner, U.H., 2006. Inhibition of hormone and cytokine-stimulated osteoclastogenesis and bone resorption by interleukin-4 and interleukin-13 is associated with increased osteoprotegerin and decreased RANKL and RANK in a STAT6-dependent pathway. J. Biol. Chem. 281, 2414–2429.

Palmqvist, P., Persson, E., Conaway, H.H., Lerner, U.H., 2002. IL-6, leukemia inhibitory factor, and oncostatin M stimulate bone resorption and regulate the expression of receptor activator of NF-kappa B ligand, osteoprotegerin, and receptor activator of NF-kappa B in mouse calvariae. J. Immunol. 169, 3353–3362.

Panach, L., Pineda, B., Mifsut, D., Tarin, J.J., Cano, A., Garcia-Perez, M.A., 2016. The role of CD40 and CD40L in bone mineral density and in osteoporosis risk: a genetic and functional study. Bone 83, 94–103.

Panaroni, C., Fulzele, K., Saini, V., Chubb, R., Pajevic, P.D., Wu, J.Y., 2015. PTH signaling in osteoprogenitors is essential for B-lymphocyte differentiation and mobilization. J. Bone Miner. Res. 30, 2273–2286.

Pappalardo, A., Thompson, K., 2013. Activated gammadelta T cells inhibit osteoclast differentiation and resorptive activity in vitro. Clin. Exp. Immunol. 174, 281–291.

Park, H., Jung, Y.K., Park, O.J., Lee, Y.J., Choi, J.Y., Choi, Y., 2005. Interaction of fas ligand and fas expressed on osteoclast precursors increases osteoclastogenesis. J. Immunol. 175, 7193–7201.

Park, J.J., Howell, M., Winseck, A., Forger, N.G., 1999. Effects of testosterone on the development of a sexually dimorphic neuromuscular system in ciliary neurotrophic factor receptor knockout mice. J. Neurobiol. 41, 317–325.

Park, J.S., Jung, Y.O., Oh, H.J., Park, S.J., Heo, Y.J., Kang, C.M., Kwok, S.K., Ju, J.H., Park, K.S., Cho, M.L., Sung, Y.C., Park, S.H., Kim, H.Y., 2012. Interleukin-27 suppresses osteoclastogenesis via induction of interferon-gamma. Immunology 137, 326–335.

Park, M.K., Her, Y.M., Cho, M.L., Oh, H.J., Park, E.M., Kwok, S.K., Ju, J.H., Park, K.S., Min, D.S., Kim, H.Y., Park, S.H., 2011. IL-15 promotes osteoclastogenesis via the PLD pathway in rheumatoid arthritis. Immunol. Lett. 139, 42–51.

Paul, N.L., Ruddle, N.H., 1988. Lymphotoxin. Annu. Rev. Immunol. 6, 407–438.

Pennica, D., Shaw, K.J., Swanson, T.A., Moore, M.W., Shelton, D.L., Zioncheck, K.A., Rosenthal, A., Taga, T., Paoni, N.F., Wood, W.I., 1995. Cardiotrophin-1. Biological activities and binding to the leukemia inhibitory factor receptor/gp130 signaling complex. J. Biol. Chem. 270, 10915–10922.

Peterlik, M., Hoffmann, O., Swetly, P., Klaushofer, K., Koller, K., 1985. Recombinant gamma-interferon inhibits prostaglandin-mediated and parathyroid hormone-induced bone resorption in cultured neonatal mouse calvaria. FEBS Lett. 185, 287–290.

Pfeffer, K., Matsuyama, T., Kündig, T.M., Wakeham, A., Kishihara, K., Shahinian, A., Wiegmann, K., Ohashi, P.S., Kronke, M., Mak, T.W., 1993. Mice deficient for the 55 kd tumor necrosis factor receptor are resistant to endotoxic shock, yet succumb to L. monocytogenes infection. Cell 73, 457–467.

Piao, H., Chu, X., Lv, W., Zhao, Y., 2017. Involvement of receptor-interacting protein 140 in estrogen-mediated osteoclasts differentiation, apoptosis, and bone resorption. J. Physiol. Sci. 67, 141–150.

Piras, R., Chiappe, F., Torraca, I.L., Buers, I., Usala, G., Angius, A., Akin, M.A., Basel-Vanagaite, L., Benedicenti, F., Chiodin, E., El Assy, O., Feingold-Zadok, M., Guibert, J., Kamien, B., Kasapkara, Ç.S., Kiliç, E., Boduroğlu, K., Kurtoglu, S., Manzur, A.Y., Onal, E.E., Paderi, E., Roche, C.H., Tümer, L., Unal, S., Utine, G.E., Zanda, G., Zankl, A., Zampino, G., Crisponi, G., Crisponi, L., Rutsch, F., 2014. Expanding the mutational spectrum of CRLF1 in crisponi/CISS1 syndrome. Hum. Mutat. 35, 424–433.

Plun-Favreau, H., Elson, G., Chabbert, M., Froger, J., Delapeyriere, O., Lelievre, E., Guillet, C., Hermann, J., Gauchat, J.F., Gascan, H., Chevalier, S., 2001. The ciliary neurotrophic factor receptor alpha component induces the secretion of and is required for functional responses to cardiotrophin-like cytokine. EMBO J. 20, 1692–1703.

Poli, V., Balena, R., Fattori, E., Markatos, A., Yamamoto, M., Tanaka, H., Ciliberto, G., Rodan, G.A., Costantini, F., 1994. Interleukin-6 deficient mice are protected from bone loss caused by estrogen depletion. EMBO J. 13, 1189–1196.

Polzer, K., Joosten, L., Gasser, J., Distler, J.H., Ruiz, G., Baum, W., Redlich, K., Bobacz, K., Smolen, J.S., van den Berg, W., Schett, G., Zwerina, J., 2010. Interleukin-1 is essential for systemic inflammatory bone loss. Ann. Rheum. Dis. 69, 284–290.

Polzer, K., Joosten, L., Gasser, J., Distler, J.H., Ruiz, G., Baum, W., Redlich, K., Bobacz, K., Smolen, J.S., van den Berg, W., Schett, G., Zwerina, J., Kronke, G., Distler, J., Hess, A., Pundt, N., Pap, T., Hoffmann, O., Scheinecker, C., 2009. IL-1 is essential for systemic inflammatory bone loss TNF-induced structural joint damage is mediated by IL-1. Ann. Rheum. Dis. 5, 5.

Poulton, I.J., Mcgregor, N.E., Pompolo, S., Walker, E.C., Sims, N.A., 2012. Contrasting roles of leukemia inhibitory factor in murine bone development and remodeling involve region-specific changes in vascularization. J. Bone Miner. Res. 27, 586–595.

Quach, J.M., Walker, E.C., Allan, E., Solano, M., Yokoyama, A., Kato, S., Sims, N.A., Gillespie, M.T., Martin, T.J., 2011. Zinc finger protein 467 is a novel regulator of osteoblast and adipocyte commitment. J. Biol. Chem. 286, 4186–4198.

Quinn, J.M., Sims, N.A., Saleh, H., Mirosa, D., Thompson, K., Bouralexis, S., Walker, E.C., Martin, T.J., Gillespie, M.T., 2008. IL-23 inhibits osteoclastogenesis indirectly through lymphocytes and is required for the maintenance of bone mass in mice. J. Immunol. 181, 5720–5729.

Raggatt, L.J., Qin, L., Tamasi, J., Jefcoat Jr., S.C., Shimizu, E., Selvamurugan, N., Liew, F.Y., Bevelock, L., Feyen, J.H., Partridge, N.C., 2008. Interleukin-18 is regulated by parathyroid hormone and is required for its bone anabolic actions. J. Biol. Chem. 283, 6790–6798.

Richards, C.D., Langdon, C., Deschamps, P., Pennica, D., Shaughnessy, S.G., 2000. Stimulation of osteoclast differentiation in vitro by mouse oncostatin M, leukaemia inhibitory factor, cardiotrophin-1 and interleukin 6: synergy with dexamethasone. Cytokine 12, 613–621.

Robinson, J.W., Li, J.Y., Walker, L.D., Tyagi, A.M., Reott, M.A., Yu, M., Adams, J., Weitzmann, M.N., Pacifici, R., 2015. T cell-expressed CD40L potentiates the bone anabolic activity of intermittent PTH treatment. J. Bone Miner. Res. 30, 695–705.

Rodan, S.B., Wesolowski, G., Hilton, D.J., Nicola, N.A., Rodan, G.A., 1990. Leukemia inhibitory factor binds with high affinity to preosteoblastic RCT-1 cells and potentiates the retinoic acid induction of alkaline phosphatase. Endocrinology 127, 1602–1608.

Roggia, C., Gao, Y., Cenci, S., Weitzmann, M.N., Toraldo, G., Isaia, G., Pacifici, R., 2001. Up-regulation of TNF-producing T cells in the bone marrow: a key mechanism by which estrogen deficiency induces bone loss in vivo. Proc. Natl. Acad. Sci. U. S. A 98, 13960–13965.

Romas, E., Udagawa, N., Zhou, H., Tamura, T., Saito, M., Taga, T., Hilton, D.J., Suda, T., Ng, K.W., Martin, T.J., 1996. The role of gp130-mediated signals in osteoclast development: regulation of interleukin 11 production by osteoblasts and distribution of its receptor in bone marrow cultures. J. Exp. Med. 183, 2581–2591.

Rothe, J., Lesslauer, W., Lotscher, H., Lang, Y., Koebel, P., Kontgen, F., Althage, A., Zinkernagel, R., Steinmetz, M., Bluethmann, H., 1993. Mice lacking the tumour necrosis factor receptor 1 are resistant to TNF-mediated toxicity but highly susceptible to infection by Listeria monocytogenes. Nature 364, 798–802.

Rousseau, F., Chevalier, S., Guillet, C., Ravon, E., Diveu, C., Froger, J., Barbier, F., Grimaud, L., Gascan, H., 2008. Ciliary neurotrophic factor, cardiotrophin-like cytokine, and neuropoietin share a conserved binding site on the ciliary neurotrophic factor receptor α chain. J. Biol. Chem. 283, 30341–30350.

Rousseau, F., Gauchat, J.F., Mcleod, J.G., Chevalier, S., Guillet, C., Guilhot, F., Cognet, I., Froger, J., Hahn, A.F., Knappskog, P.M., Gascan, H., Boman, H., 2006. Inactivation of cardiotrophin-like cytokine, a second ligand for ciliary neurotrophic factor receptor, leads to cold-induced sweating syndrome in a patient. Proc. Natl. Acad. Sci. U. S. A. 103, 10068–10073.

Roux, S., Lambert-Comeau, P., Saint-Pierre, C., Lepine, M., Sawan, B., Parent, J.L., 2005. Death receptors, Fas and TRAIL receptors, are involved in human osteoclast apoptosis. Biochem. Biophys. Res. Commun. 333, 42–50.

Rowan, A.D., Koshy, P.J., Shingleton, W.D., Degnan, B.A., Heath, J.K., Vernallis, A.B., Spaull, J.R., Life, P.F., Hudson, K., Cawston, T.E., 2001. Synergistic effects of glycoprotein 130 binding cytokines in combination with interleukin-1 on cartilage collagen breakdown. Arthritis Rheum. 44, 1620–1632.

Ryan, M.R., Shepherd, R., Leavey, J.K., Gao, Y.H., Grassi, F., Schnell, F.J., Qian, W.P., Kersh, G.J., Weitzmann, M.N., Pacifici, R., 2005. An IL-7-dependent rebound in thymic T cell output contributes to the bone loss induced by estrogen deficiency. Proc. Natl. Acad. Sci. U. S. A. 102, 16735–16740.

Sabatakos, G., Sims, N.A., Chen, J., Aoki, K., Kelz, M.B., Amling, M., Bouali, Y., Mukhopadhyay, K., Ford, K., Nestler, E.J., Baron, R., 2000. Overexpression of DeltaFosB transcription factor(s) increases bone formation and inhibits adipogenesis. Nat. Med. 6, 985–990.

Sabatini, M., Boyce, B., Aufdemorte, T., Bonewald, L., Mundy, G.R., 1988. Infusions of recombinant human interleukins 1 alpha and 1 beta cause hypercalcemia in normal mice. Proc. Natl. Acad. Sci. U.S.A. 85, 5235–5239.

Saidi, S., Bouri, F., Lencel, P., Duplomb, L., Baud'huin, M., Delplace, S., Leterme, D., Miellot, F., Heymann, D., Hardouin, P., Palmer, G., Magne, D., 2011. IL-33 is expressed in human osteoblasts, but has no direct effect on bone remodeling. Cytokine 53, 347–354.

Saidi, S., Magne, D., 2011. Interleukin-33: a novel player in osteonecrosis of the femoral head? Joint Bone Spine 78, 550–554.

Saleh, H., Eeles, D., Hodge, J.M., Nicholson, G.C., Gu, R., Pompolo, S., Gillespie, M.T., Quinn, J.M., 2011. Interleukin-33, a target of parathyroid hormone and oncostatin M, increases osteoblastic matrix mineral deposition and inhibits osteoclast formation in vitro. Endocrinology 1, 1.

Salopek, D., Grcevic, D., Katavic, V., Kovacic, N., Lukic, I.K., Marusic, A., 2008. Increased bone resorption and osteopenia are a part of the lymphoproliferative phenotype of mice with systemic over-expression of interleukin-7 gene driven by MHC class II promoter. Immunol. Lett. 121, 134–139.

Sambandam, Y., Baird, K.L., Stroebel, M., Kowal, E., Balasubramanian, S., Reddy, S.V., 2016. Microgravity induction of TRAIL expression in pre-osteoclast cells enhances osteoclast differentiation. Sci. Rep. 6, 25143.

Sato, K., Fujii, Y., Asano, S., Ohtsuki, T., Kawakami, M., Kasono, K., Tsushima, T., Shizume, K., 1986. Recombinant human interleukin 1 alpha and beta stimulate mouse osteoblast-like cells (MC3T3-E1) to produce macrophage-colony stimulating activity and prostaglandin E2. Biochem. Biophys. Res. Commun. 141, 285–291.

Sato, K., Suematsu, A., Okamoto, K., Yamaguchi, A., Morishita, Y., Kadono, Y., Tanaka, S., Kodama, T., Akira, S., Iwakura, Y., Cua, D.J., Takayanagi, H., 2006. Th17 functions as an osteoclastogenic helper T cell subset that links T cell activation and bone destruction. J. Exp. Med. 203, 2673–2682.

Sato, N., Takahashi, N., Suda, K., Nakamura, M., Yamaki, M., Ninomiya, T., Kobayashi, Y., Takada, H., Shibata, K., Yamamoto, M., Takeda, K., Akira, S., Noguchi, T., Udagawa, N., 2004. MyD88 but not TRIF is essential for osteoclastogenesis induced by lipopolysaccharide, diacyl lipopeptide, and IL-1alpha. J. Exp. Med. 200, 601–611.

Sato, T., Watanabe, K., Masuhara, M., Hada, N., Hakeda, Y., 2007. Production of IL-7 is increased in ovariectomized mice, but not RANKL mRNA expression by osteoblasts/stromal cells in bone, and IL-7 enhances generation of osteoclast precursors in vitro. J. Bone Miner. Res. 25, 19–27.

Scharla, S.H., Strong, D.D., Mohan, S., Chevalley, T., Linkhart, T.A., 1994. Effect of tumor necrosis factor-alpha on the expression of insulin-like growth factor I and insulin-like growth factor binding protein 4 in mouse osteoblasts. Eur. J. Endocrinol. 131, 293–301.

Scheller, J., Garbers, C., Rose-John, S., 2014. Interleukin-6: from basic biology to selective blockade of pro-inflammatory activities. Semin. Immunol. 26 (1), 2–12.

Schoenau, E., Neu, C.M., Rauch, F., Manz, F., 2001. The development of bone strength at the proximal radius during childhood and adolescence. J. Clin. Endocrinol. Metab. 86, 613–618.

Schoenborn, J.R., Wilson, C.B., 2007. Regulation of interferon-gamma during innate and adaptive immune responses. Adv. Immunol. 96, 41–101.

Schulze, J., Bickert, T., Beil, F.T., Zaiss, M.M., Albers, J., Wintges, K., Streichert, T., Klaetschke, K., Keller, J., Hissnauer, T.N., Spiro, A.S., Gessner, A., Schett, G., Amling, M., Mckenzie, A.N., Horst, A.K., Schinke, T., 2011. Interleukin-33 is expressed in differentiated osteoblasts and blocks osteoclast formation from bone marrow precursor cells. J. Bone Miner. Res. 26, 704–717.

Schwerd, T., Twigg, S.R.F., Aschenbrenner, D., Manrique, S., Miller, K.A., Taylor, I.B., Capitani, M., Mcgowan, S.J., Sweeney, E., Weber, A., Chen, L., Bowness, P., Riordan, A., Cant, A., Freeman, A.F., Milner, J.D., Holland, S.M., Frede, N., Muller, M., Schmidt-Arras, D., Grimbacher, B., Wall, S.A., Jones, E.Y., Wilkie, A.O.M., Uhlig, H.H., 2017. A biallelic mutation in IL6ST encoding the GP130 co-receptor causes immunodeficiency and craniosynostosis. J. Exp. Med. 214, 2547−2562.

Seeman, E., 1997. From density to structure: growing up and growing old on the surfaces of bone. J. Bone Miner. Res. 12, 509−521.

Senaldi, G., Varnum, B.C., Sarmiento, U., Starnes, C., Lile, J., Scully, S., Guo, J., Elliott, G., Mcninch, J., Shaklee, C.L., Freeman, D., Manu, F., Simonet, W.S., Boone, T., Chang, M.S., 1999. Novel neurotrophin-1/B cell-stimulating factor-3: a cytokine of the IL-6 family. Proc. Natl. Acad. Sci. U. S. A. 96, 11458−11463.

Shashkova, E.V., Trivedi, J., Cline-Smith, A.B., Ferris, C., Buchwald, Z.S., Gibbs, J., Novack, D., Aurora, R., 2016. Osteoclast-primed Foxp3+ CD8 T cells induce T-bet, eomesodermin, and IFN-gamma to regulate bone resorption. J. Immunol. 197, 726−735.

Shaw, A.T., Maeda, Y., Gravallese, E.M., 2016. IL-17A deficiency promotes periosteal bone formation in a model of inflammatory arthritis. Arthritis Res. Ther. 18, 104.

Shen, V., Kohler, G., Jeffrey, J.J., Peck, W.A., 1988. Bone-resorbing agents promote and interferon-gamma inhibits bone cell collagenase production. J. Bone Miner. Res. 3, 657−666.

Sheng, Z., Pennica, D., Wood, W.I., Chien, K.R., 1996. Cardiotrophin-1 displays early expression in the murine heart tube and promotes cardiac myocyte survival. Development 122, 419−428.

Shiina-Ishimi, Y., Abe, E., Tanaka, H., Suda, T., 1986. Synthesis of colony-stimulating factor (CSF) and differentiation-inducing factor (D-factor) by osteoblastic cells, clone MC3T3-E1. Biochem. Biophys. Res. Commun. 134, 400−406.

Shin, H.H., Lee, J.E., Lee, E.A., Kwon, B.S., Choi, H.S., 2006. Enhanced osteoclastogenesis in 4-1BB-deficient mice caused by reduced interleukin-10. J. Bone Miner. Res. 21, 1907−1912.

Shin, H.I., Divieti, P., Sims, N.A., Kobayashi, T., Miao, D., Karaplis, A.C., Baron, R., Bringhurst, R., Kronenberg, H.M., 2004. Gp130-mediated signaling is necessary for normal osteoblastic function in vivo and in vitro. Endocrinology 145, 1376−1385.

Shin, H.S., Sarin, R., Dixit, N., Wu, J., Gershwin, E., Bowman, E.P., Adamopoulos, I.E., 2015. Crosstalk among IL-23 and DNAX activating protein of 12 kDa-dependent pathways promotes osteoclastogenesis. J. Immunol. 194, 316−324.

Shioi, A., Teitelbaum, S.L., Ross, F.P., Welgus, H.G., Suzuki, H., Ohara, J., Lacey, D.L., 1991. Interleukin 4 inhibits murine osteoclast formation in vitro. J. Cell. Biochem. 47, 272−277.

Sims, J.E., Gayle, M.A., Slack, J.L., Alderson, M.R., Bird, T.A., Giri, J.G., Colotta, F., Re, F., Mantovani, A., Shanebeck, K., Grabstein, K.H., Dower, S.K., 1993. Interleukin 1 signaling occurs exclusively via the type I receptor. Proc. Natl. Acad. Sci. U. S. A. 90, 6155−6159.

Sims, N.A., 2015. Cardiotrophin-like cytokine factor 1 (CLCF1) and neuropoietin (NP) signalling and their roles in development, adulthood, cancer and degenerative disorders. Cytokine Growth Factor Rev. 26, 517−522.

Sims, N.A., Clement-Lacroix, P., da Ponte, F., Bouali, Y., Binart, N., Moriggl, R., Goffin, V., Coschigano, K., Gaillard-Kelly, M., Kopchick, J., Baron, R., Kelly, P.A., 2000. Bone homeostasis in growth hormone receptor-null mice is restored by IGF-I but independent of Stat5. J. Clin. Investig. 106, 1095−1103.

Sims, N.A., Jenkins, B.J., Nakamura, A., Quinn, J.M., Li, R., Gillespie, M.T., Ernst, M., Robb, L., Martin, T.J., 2005. Interleukin-11 receptor signaling is required for normal bone remodeling. J. Bone Miner. Res. 20, 1093−1102.

Sims, N.A., Jenkins, B.J., Quinn, J.M., Nakamura, A., Glatt, M., Gillespie, M.T., Ernst, M., Martin, T.J., 2004. Glycoprotein 130 regulates bone turnover and bone size by distinct downstream signaling pathways. J. Clin. Investig. 113, 379−389.

Sims, N.A., Johnson, R.W., 2012. Leukemia inhibitory factor: a paracrine mediator of bone metabolism. Growth Factors 30, 76−87.

Sims, N.A., Sabatakos, G., Chen, J.S., Kelz, M.B., Nestler, E.J., Baron, R., 2002. Regulating DeltaFosB expression in adult tet-off-DeltaFosB transgenic mice alters bone formation and bone mass. Bone 30, 32−39.

Sims, N.A., Vrahnas, C., 2014. Regulation of cortical and trabecular bone mass by communication between osteoblasts, osteocytes and osteoclasts. Arch. Biochem. Biophys. 561, 22−28.

Simsa-Maziel, S., Zaretsky, J., Reich, A., Koren, Y., Shahar, R., Monsonego-Ornan, E., 2013. IL-1RI participates in normal growth plate development and bone modeling. Am. J. Physiol. Endocrinol. Metab. 305, E15−E21.

Smith, D.D., Gowen, M., Mundy, G.R., 1987. Effects of interferon-gamma and other cytokines on collagen synthesis in fetal rat bone cultures. Endocrinology 120, 2494−2499.

Song, H.Y., Jeon, E.S., Kim, J.I., Jung, J.S., Kim, J.H., 2007. Oncostatin M promotes osteogenesis and suppresses adipogenic differentiation of human adipose tissue-derived mesenchymal stem cells. J. Cell. Biochem. 101, 1238−1251.

Sonomoto, K., Yamaoka, K., Oshita, K., Fukuyo, S., Zhang, X., Nakano, K., Okada, Y., Tanaka, Y., 2012. Interleukin-1beta induces differentiation of human mesenchymal stem cells into osteoblasts via the Wnt-5a/receptor tyrosine kinase-like orphan receptor 2 pathway. Arthritis Rheum. 64, 3355−3363.

Sprangers, S., Schoenmaker, T., Cao, Y., Everts, V., de Vries, T.J., 2016. Different blood-borne human osteoclast precursors respond in distinct ways to IL-17A. J. Cell. Physiol. 231, 1249−1260.

Stahl, N., Farruggella, T.J., Boulton, T.G., Zhong, Z., Darnell Jr., J.E., Yancopoulos, G.D., 1995. Choice of STATs and other substrates specified by modular tyrosine-based motifs in cytokine receptors. Science 267, 1349−1353.

Standal, T., Johnson, R.W., Mcgregor, N.E., Poulton, I.J., Ho, P.W., Martin, T.J., Sims, N.A., 2014. gp130 in late osteoblasts and osteocytes is required for PTH-induced osteoblast differentiation. J. Endocrinol. 223, 181−190.

Starr, R., Metcalf, D., Elefanty, A.G., Brysha, M., Willson, T.A., Nicola, N.A., Hilton, D.J., Alexander, W.S., 1998. Liver degeneration and lymphoid deficiencies in mice lacking suppressor of cytokine signaling-1. Proc. Natl. Acad. Sci. U. S. A. 95, 14395−14399.

Stashenko, P., Dewhirst, F.E., Peros, W.J., Kent, R.L., Ago, J.M., 1987a. Synergistic interactions between interleukin 1, tumor necrosis factor, and lymphotoxin in bone resorption. J. Immunol. 138, 1464–1468.

Stashenko, P., Dewhirst, F.E., Peros, W.J., Kent, R.L., Ago, J.M., 1987b. Synergistic interactions between interleukin 1, tumor necrosis factor, and lymphotoxin in bone resorption. J. Immunol. 138, 1464–1468.

Stein, N.C., Kreutzmann, C., Zimmermann, S.P., Niebergall, U., Hellmeyer, L., Goettsch, C., Schoppet, M., Hofbauer, L.C., 2008. Interleukin-4 and interleukin-13 stimulate the osteoclast inhibitor osteoprotegerin by human endothelial cells through the STAT6 pathway. J. Bone Miner. Res. 23, 750–758.

Suga, K., Saitoh, M., Fukushima, S., Takahashi, K., Nara, H., Yasuda, S., Miyata, K., 2001. Interleukin-11 induces osteoblast differentiation and acts synergistically with bone morphogenetic protein-2 in c3h10t1/2 cells. J. Interferon Cytokine Res. 21, 695–707.

Sunyer, T., Rothe, L., Jiang, X.S., Osdoby, P., Collin-Osdoby, P., 1996. Proinflammatory agents, IL-8 and IL-10, upregulate inducible nitric oxide synthase expression and nitric oxide production in avian osteoclast-like cells. J. Cell. Biochem. 60, 469–483.

Takahashi, N., Mundy, G.R., Roodman, G.D., 1986. Recombinant human interferon-gamma inhibits formation of human osteoclast-like cells. J. Immunol. 137, 3544–3549.

Takahashi, R., Yokoji, H., Misawa, H., Hayashi, M., Hu, J., Deguchi, T., 1994. A null mutation in the human CNTF gene is not causally related to neurological diseases. Nat. Genet. 7, 79–84.

Takayanagi, H., 2005. Inflammatory bone destruction and osteoimmunology. J. Periodontal. Res. 40, 287–293.

Takayanagi, H., Kim, S., Matsuo, K., Suzuki, H., Suzuki, T., Sato, K., Yokochi, T., Oda, H., Nakamura, K., Ida, N., Wagner, E.F., Taniguchi, T., 2002. RANKL maintains bone homeostasis through c-Fos-dependent induction of interferon-beta. Nature 416, 744–749.

Takayanagi, H., Ogasawara, K., Hida, S., Chiba, T., Murata, S., Sato, K., Takaoka, A., Yokochi, T., Oda, H., Tanaka, K., Nakamura, K., Taniguchi, T., 2000. T-cell-mediated regulation of osteoclastogenesis by signalling cross-talk between RANKL and IFN-gamma. Nature 408, 600–605.

Takeda, H., Kikuchi, T., Soboku, K., Okabe, I., Mizutani, H., Mitani, A., Ishihara, Y., Noguchi, T., 2014. Effect of IL-15 and natural killer cells on osteoclasts and osteoblasts in a mouse coculture. Inflammation 37, 657–669.

Takeuchi, Y., Watanabe, S., Ishii, G., Takeda, S., Nakayama, K., Fukumoto, S., Kaneta, Y., Inoue, D., Matsumoto, T., Harigaya, K., Fujita, T., 2002. Interleukin-11 as a stimulatory factor for bone formation prevents bone loss with advancing age in mice. J. Biol. Chem. 277, 49011–49018.

Tamura, T., Udagawa, N., Takahashi, N., Miyaura, C., Tanaka, S., Yamada, Y., Koishihara, Y., Ohsugi, Y., Kumaki, K., Taga, T., Kishimoto, T., Suda, T., 1993. Soluble interleukin-6 receptor triggers osteoclast formation by interleukin 6. Proc. Natl. Acad. Sci. U. S. A. 90, 11924–11928.

Tanabe, N., Maeno, M., Suzuki, N., Fujisaki, K., Tanaka, H., Ogiso, B., Ito, K., 2005. IL-1 alpha stimulates the formation of osteoclast-like cells by increasing M-CSF and PGE2 production and decreasing OPG production by osteoblasts. Life Sci. 77, 615–626.

Tashjian Jr., A.H., Voelkel, E.F., Lazzaro, M., Goad, D., Bosma, T., Levine, L., 1987. Tumor necrosis factor-alpha (Cachectin) stimulates bone resorption in mouse calvaria via a prostaglandin-mediated mechanism. Endocrinology 120, 2029–2036.

Terpos, E., Fragiadaki, K., Konsta, M., Bratengeier, C., Papatheodorou, A., Sfikakis, P.P., 2011. Early effects of IL-6 receptor inhibition on bone homeostasis: a pilot study in women with rheumatoid arthritis. Clin. Exp. Rheumatol. 29, 921–925.

Thouverey, C., Caverzasio, J., 2015. Ablation of p38alpha MAPK signaling in osteoblast lineage cells protects mice from bone loss induced by estrogen deficiency. Endocrinology 156, 4377–4387.

Tinhofer, I., Biedermann, R., Krismer, M., Crazzolara, R., Greil, R., 2006. A role of TRAIL in killing osteoblasts by myeloma cells. FASEB J. 20, 759–761.

Toraldo, G., Roggia, C., Qian, W.P., Pacifici, R., Weitzmann, M.N., 2003. IL-7 induces bone loss in vivo by induction of receptor activator of nuclear factor kappa B ligand and tumor necrosis factor alpha from T cells. Proc. Natl. Acad. Sci. U. S. A. 100, 125–130.

Torossian, F., Guerton, B., Anginot, A., Alexander, K.A., Desterke, C., Soave, S., Tseng, H.W., Arouche, N., Boutin, L., Kulina, I., Salga, M., Jose, B., Pettit, A.R., Clay, D., Rochet, N., Vlachos, E., Genet, G., Debaud, C., Denormandie, P., Genet, F., Sims, N.A., Banzet, S., Levesque, J.P., Lataillade, J.J., Le Bousse-Kerdiles, M.C., 2017. Macrophage-derived oncostatin M contributes to human and mouse neurogenic heterotopic ossifications. JCI Insight 2.

Tsuboi, M., Kawakami, A., Nakashima, T., Matsuoka, N., Urayama, S., Kawabe, Y., Fujiyama, K., Kiriyama, T., Aoyagi, T., Maeda, K., Eguchi, K., 1999. Tumor necrosis factor-alpha and interleukin-1beta increase the Fas-mediated apoptosis of human osteoblasts. J. Lab. Clin. Med. 134, 222–231.

Tsuritani, K., Takeda, J., Sakagami, J., Ishii, A., Eriksson, T., Hara, T., Ishibashi, H., Koshihara, Y., Yamada, K., Yoneda, Y., 2010. Cytokine receptor-like factor 1 is highly expressed in damaged human knee osteoarthritic cartilage and involved in osteoarthritis downstream of TGF-beta. Calcif. Tissue Int. 86, 47–57.

Tural, S., Alayli, G., Kara, N., Tander, B., Bilgici, A., Kuru, O., 2013. Association between osteoporosis and polymorphisms of the IL-10 and TGF-beta genes in Turkish postmenopausal women. Hum. Immunol. 74, 1179–1183.

Tyagi, A.M., Mansoori, M.N., Srivastava, K., Khan, M.P., Kureel, J., Dixit, M., Shukla, P., Trivedi, R., Chattopadhyay, N., Singh, D., 2014. Enhanced immunoprotective effects by anti-IL-17 antibody translates to improved skeletal parameters under estrogen deficiency compared with anti-RANKL and anti-TNF-alpha antibodies. J. Bone Miner. Res. 29, 1981–1992.

Tyagi, A.M., Srivastava, K., Mansoori, M.N., Trivedi, R., Chattopadhyay, N., Singh, D., 2012. Estrogen deficiency induces the differentiation of IL-17 secreting Th17 cells: a new candidate in the pathogenesis of osteoporosis. PLoS One 7, e44552.

Udagawa, N., Takahashi, N., Katagiri, T., Tamura, T., Wada, S., Findlay, D.M., Martin, T.J., Hirota, H., Taga, T., Kishimoto, T., Suda, T., 1995. Interleukin (IL)-6 induction of osteoclast differentiation depends on IL-6 receptors expressed on osteoblastic cells but not on osteoclast progenitors. J. Exp. Med. 182, 1461–1468.

Uluckan, O., Jimenez, M., Karbach, S., Jeschke, A., Grana, O., Keller, J., Busse, B., Croxford, A.L., Finzel, S., Koenders, M., van den Berg, W., Schinke, T., Amling, M., Waisman, A., Schett, G., Wagner, E.F., 2016. Chronic skin inflammation leads to bone loss by IL-17-mediated inhibition of Wnt signaling in osteoblasts. Sci. Transl. Med. 8, 330ra37.

van Bezooijen, R.L., Farih-Sips, H.C., Papapoulos, S.E., Lowik, C.W., 1999. Interleukin-17: a new bone acting cytokine in vitro. J. Bone Miner. Res. 14, 1513−1521.

Van Vlasselaer, P., Borremans, B., van der Heuvel, R., van Gorp, U., de Waal Malefyt, R., 1993. Interleukin-10 inhibits the osteogenic activity of mouse bone marrow. Blood 82, 2361−2370.

Vargas, S.J., Naprta, A., Glaccum, M., Lee, S.K., Kalinowski, J., Lorenzo, J.A., 1996. Interleukin-6 expression and histomorphometry of bones from mice deficient for receptors for interleukin-1 or tumor necrosis factor. J. Bone Miner. Res. 11, 1736−1740.

Vermeire, K., Heremans, H., Vandeputte, M., Huang, S., Billiau, A., Matthys, P., 1997. Accelerated collagen-induced arthritis in IFN-gamma receptor-deficient mice. J. Immunol. 158, 5507−5513.

Vignery, A., Niven-Fairchild, T., Shepard, M.H., 1990. Recombinant murine interferon-gamma inhibits the fusion of mouse alveolar macrophages in vitro but stimulates the formation of osteoclast-like cells on implanted syngenic bone particles in mice in vivo. J. Bone Miner. Res. 5, 637−644.

Villarreal, D.O., Weiner, D.B., 2014. Interleukin 33: a switch-hitting cytokine. Curr. Opin. Immunol. 28, 102−106.

Walker, E.C., Johnson, R.W., Hu, Y., Brennan, H.J., Poulton, I.J., Zhang, J.G., Jenkins, B.J., Smyth, G.K., Nicola, N.A., Sims, N.A., 2016. Murine oncostatin M acts via leukemia inhibitory factor receptor to phosphorylate signal transducer and activator of transcription 3 (STAT3) but not STAT1, an effect that protects bone mass. J. Biol. Chem. 291, 21703−21716.

Walker, E.C., Mcgregor, N.E., Poulton, I.J., Pompolo, S., Allan, E.H., Quinn, J.M., Gillespie, M.T., Martin, T.J., Sims, N.A., 2008. Cardiotrophin-1 is an osteoclast-derived stimulus of bone formation required for normal bone remodeling. J. Bone Miner. Res. 23, 2025−2032.

Walker, E.C., Mcgregor, N.E., Poulton, I.J., Solano, M., Pompolo, S., Fernandes, T.J., Constable, M.J., Nicholson, G.C., Zhang, J.G., Nicola, N.A., Gillespie, M.T., Martin, T.J., Sims, N.A., 2010. Oncostatin M promotes bone formation independently of resorption when signaling through leukemia inhibitory factor receptor in mice. J. Clin. Investig. 120, 582−592.

Walker, E.C., Poulton, I.J., Mcgregor, N.E., Ho, P.W., Allan, E.H., Quach, J.M., Martin, T.J., Sims, N.A., 2012. Sustained RANKL response to parathyroid hormone in oncostatin M receptor-deficient osteoblasts converts anabolic treatment to a catabolic effect in vivo. J. Bone Miner. Res. 27, 902−912.

Wan, Q., Schoenmaker, T., Jansen, I.D., Bian, Z., de Vries, T.J., Everts, V., 2016. Osteoblasts of calvaria induce higher numbers of osteoclasts than osteoblasts from long bone. Bone 86, 10−21.

Wang, L., Liu, S., Zhao, Y., Liu, D., Liu, Y., Chen, C., Karray, S., Shi, S., Jin, Y., 2015. Osteoblast-induced osteoclast apoptosis by fas ligand/FAS pathway is required for maintenance of bone mass. Cell Death Differ. 22, 1654−1664.

Wang, Z., Deng, Z., Gan, J., Zhou, G., Shi, T., Wang, Z., Huang, Z., Qian, H., Bao, N., Guo, T., Chen, J., Zhang, J., Liu, F., Dong, L., Zhao, J., 2017. TiAl6V4 particles promote osteoclast formation via autophagy-mediated downregulation of interferon-beta in osteocytes. Acta Biomater. 48, 489−498.

Ware, C.B., Horowitz, M.C., Renshaw, B.R., Hunt, J.S., Liggitt, D., Koblar, S.A., Gliniak, B.C., Mckenna, H.J., Papayannopoulou, T., Thoma, B., Cheng, L., Donovan, P.J., Peschon, J.J., Bartlett, P.F., Willis, C.R., Wright, B.D., Carpenter, M.K., Davison, B.L., Gearing, D.P., 1995. Targeted disruption of the low-affinity leukemia inhibitory factor receptor gene causes placental, skeletal, neural and metabolic defects and results in perinatal death. Development 121, 1283−1299.

Weaver, C.T., Hatton, R.D., Mangan, P.R., Harrington, L.E., 2007. IL-17 family cytokines and the expanding diversity of effector T cell lineages. Annu. Rev. Immunol. 25, 821−852.

Wei, S., Kitaura, H., Zhou, P., Ross, F.P., Teitelbaum, S.L., 2005. IL-1 mediates TNF-induced osteoclastogenesis. J. Clin. Investig. 115, 282−290.

Wei, S., Wang, M.W., Teitelbaum, S.L., Ross, F.P., 2001. Interleukin-4 reversibly inhibits osteoclastogenesis via inhibition of NF-{kappa}B and MAP kinase signaling. J. Biol. Chem. 277, 6622−6630.

Weiser, W.Y., Temple, P.A., Witek-Giannotti, J.S., Remold, H.G., Clark, S.C., David, J.R., 1989. Molecular cloning of a cDNA encoding a human macrophage migration inhibitory factor. Proc. Natl. Acad. Sci. U. S. A. 86, 7522−7526.

Weitzmann, M.N., Cenci, S., Rifas, L., Brown, C., Pacifici, R., 2000. Interleukin-7 stimulates osteoclast formation by up-regulating the T- cell production of soluble osteoclastogenic cytokines. Blood 96, 1873−1878.

Weitzmann, M.N., Roggia, C., Toraldo, G., Weitzmann, L., Pacifici, R., 2002. Increased production of IL-7 uncouples bone formation from bone resorption during estrogen deficiency. J. Clin. Investig. 110, 1643−1650.

Wesche, D.E., Lomas-Neira, J.L., Perl, M., Chung, C.S., Ayala, A., 2005. Leukocyte apoptosis and its significance in sepsis and shock. J. Leukoc. Biol. 78, 325−337.

Wesche, H., Korherr, C., Kracht, M., Falk, W., Resch, K., Martin, M.U., 1997. The interleukin-1 receptor accessory protein (IL-1RAcP) is essential for IL-1-induced activation of interleukin-1 receptor-associated kinase (IRAK) and stress-activated protein kinases (SAP kinases). J. Biol. Chem. 272, 7727−7731.

White, U.A., Stewart, W.C., Mynatt, R.L., Stephens, J.M., 2008. Neuropoietin attenuates adipogenesis and induces insulin resistance in adipocytes. J. Biol. Chem. 283 (33), 22505−22512.

Whitham, M., Chan, M.H., Pal, M., Matthews, V.B., Prelovsek, O., Lunke, S., El-Osta, A., Broenneke, H., Alber, J., Bruning, J.C., Wunderlich, F.T., Lancaster, G.I., Febbraio, M.A., 2012. Contraction-induced interleukin-6 gene transcription in skeletal muscle is regulated by c-Jun terminal kinase/activator protein-1. J. Biol. Chem. 287, 10771−10779.

Winkler, I.G., Sims, N.A., Pettit, A.R., Barbier, V., Nowlan, B., Helwani, F., Poulton, I.J., van Rooijen, N., Alexander, K.A., Raggatt, L.J., Levesque, J.P., 2010. Bone marrow macrophages maintain hematopoietic stem cell (HSC) niches and their depletion mobilizes HSCs. Blood 116, 4815−4828.

Wong, P.K., Egan, P.J., Croker, B.A., O'donnell, K., Sims, N.A., Drake, S., Kiu, H., Mcmanus, E.J., Alexander, W.S., Roberts, A.W., Wicks, I.P., 2006a. SOCS-3 negatively regulates innate and adaptive immune mechanisms in acute IL-1-dependent inflammatory arthritis. J. Clin. Investig. 116, 1571–1581.

Wong, P.K., Quinn, J.M., Sims, N.A., van Nieuwenhuijze, A., Campbell, I.K., Wicks, I.P., 2006b. Interleukin-6 modulates production of T lymphocyte-derived cytokines in antigen-induced arthritis and drives inflammation-induced osteoclastogenesis. Arthritis Rheum. 54, 158–168.

Wu, A.C., Kidd, L.J., Cowling, N.R., Kelly, W.L., Forwood, M.R., 2014. Osteocyte expression of caspase-3, COX-2, IL-6 and sclerostin are spatially and temporally associated following stress fracture initiation. BoneKEy Rep. 3, 571.

Wu, J.Y., Purton, L.E., Rodda, S.J., Chen, M., Weinstein, L.S., Mcmahon, A.P., Scadden, D.T., Kronenberg, H.M., 2008. Osteoblastic regulation of B lymphopoiesis is mediated by Gs{alpha}-dependent signaling pathways. Proc. Natl. Acad. Sci. U. S. A 105, 16976–16981.

Wu, L., Guo, Q., Yang, J., Ni, B., 2017. Tumor necrosis factor Alpha promotes osteoclast formation via PI3K/Akt pathway-mediated Blimp1 expression upregulation. J. Cell. Biochem. 118, 1308–1315.

Wu, X., Feng, X., He, Y., Gao, Y., Yang, S., Shao, Z., Yang, C., Wang, H., Ye, Z., 2016. IL-4 administration exerts preventive effects via suppression of underlying inflammation and TNF-alpha-induced apoptosis in steroid-induced osteonecrosis. Osteoporos. Int. 27, 1827–1837.

Wu, X., Mckenna, M.A., Feng, X., Nagy, T.R., Mcdonald, J.M., 2003. Osteoclast apoptosis: the role of fas in vivo and in vitro. Endocrinology 144, 5545–5555.

Wu, X., Pan, G., Mckenna, M.A., Zayzafoon, M., Xiong, W.C., Mcdonald, J.M., 2005. RANKL regulates Fas expression and Fas-mediated apoptosis in osteoclasts. J. Bone Miner. Res. 20, 107–116.

Xiong, J., Onal, M., Jilka, R.L., Weinstein, R.S., Manolagas, S.C., O'brien, C.A., 2011. Matrix-embedded cells control osteoclast formation. Nat. Med. 17, 1235–1241.

Xu, L.X., Kukita, T., Kukita, A., Otsuka, T., Niho, Y., Iijima, T., 1995. Interleukin-10 selectively inhibits osteoclastogenesis by inhibiting differentiation of osteoclast progenitors into preosteoclast-like cells in rat bone marrow culture system. J. Cell. Physiol. 165, 624–629.

Yago, T., Nanke, Y., Ichikawa, N., Kobashigawa, T., Mogi, M., Kamatani, N., Kotake, S., 2009. IL-17 induces osteoclastogenesis from human monocytes alone in the absence of osteoblasts, which is potently inhibited by anti-TNF-alpha antibody: a novel mechanism of osteoclastogenesis by IL-17. J. Cell. Biochem. 2, 2.

Yamada, A., Takami, M., Kawawa, T., Yasuhara, R., Zhao, B., Mochizuki, A., Miyamoto, Y., Eto, T., Yasuda, H., Nakamichi, Y., Kim, N., Katagiri, T., Suda, T., Kamijo, R., 2007. Interleukin-4 inhibition of osteoclast differentiation is stronger than that of interleukin-13 and they are equivalent for induction of osteoprotegerin production from osteoblasts. Immunology 120, 573–579.

Yamada, N., Niwa, S., Tsujimura, T., Iwasaki, T., Sugihara, A., Futani, H., Hayashi, S., Okamura, H., Akedo, H., Terada, N., 2002. Interleukin-18 and interleukin-12 synergistically inhibit osteoclastic bone-resorbing activity. Bone 30, 901–908.

Yamaguchi, T., Movila, A., Kataoka, S., Wisitrasameewong, W., Ruiz Torruella, M., Murakoshi, M., Murakami, S., Kawai, T., 2016. Proinflammatory M1 macrophages inhibit RANKL-induced osteoclastogenesis. Infect. Immun. 84, 2802–2812.

Yamamura, M., Kawashima, M., Taniai, M., Yamauchi, H., Tanimoto, T., Kurimoto, M., Morita, Y., Ohmoto, Y., Makino, H., 2001. Interferon-gamma-inducing activity of interleukin-18 in the joint with rheumatoid arthritis. Arthritis Rheum. 44, 275–285.

Yang, X., Ricciardi, B.F., Hernandez-Soria, A., Shi, Y., Camacho, N.P., Bostrom, M.P.G., 2007. Callus mineralization and maturation are delayed during fracture healing in interleukin-6 knockout mice. Bone 41, 928–936.

Yang, X.O., Zhang, H., Kim, B.S., Niu, X., Peng, J., Chen, Y., Kerketta, R., Lee, Y.H., Chang, S.H., Corry, D.B., Wang, D., Watowich, S.S., Dong, C., 2013. The signaling suppressor CIS controls proallergic T cell development and allergic airway inflammation. Nat. Immunol. 14, 732–740.

Yao, Z., Lei, W., Duan, R., Li, Y., Luo, L., Boyce, B.F., 2017. RANKL cytokine enhances TNF-induced osteoclastogenesis independently of TNF receptor associated factor (TRAF) 6 by degrading TRAF3 in osteoclast precursors. J. Biol. Chem. 292, 10169–10179.

Yao, Z., Li, P., Zhang, Q., Schwarz, E.M., Keng, P., Arbini, A., Boyce, B.F., Xing, L., 2006a. Tnf increases circulating osteoclast precursor numbers by promoting their proliferation and differentiation in the bone marrow through up-regulation of c-fms expression. J. Biol. Chem. 281, 11846–11855.

Yao, Z., Li, P., Zhang, Q., Schwarz, E.M., Keng, P., Arbini, A., Boyce, B.F., Xing, L., 2006b. Tumor necrosis factor-alpha increases circulating osteoclast precursor numbers by promoting their proliferation and differentiation in the bone marrow through up-regulation of c-Fms expression. J. Biol. Chem. 281, 11846–11855.

Yao, Z., Xing, L., Boyce, B.F., 2009. NF-kappaB p100 limits TNF-induced bone resorption in mice by a TRAF3-dependent mechanism. J. Clin. Investig. 21.

Yao, Z., Xing, L., Qin, C., Schwarz, E.M., Boyce, B.F., 2008. Osteoclast precursor interaction with bone matrix induces osteoclast formation directly by an interleukin-1-mediated autocrine mechanism. J. Biol. Chem. 283, 9917–9924.

Yen, M.L., Hsu, P.N., Liao, H.J., Lee, B.H., Tsai, H.F., 2012. TRAF-6 dependent signaling pathway is essential for TNF-related apoptosis-inducing ligand (TRAIL) induces osteoclast differentiation. PLoS One 7, e38048.

Yokoyama, M., Ukai, T., Ayon Haro, E.R., Kishimoto, T., Yoshinaga, Y., Hara, Y., 2011. Membrane-bound CD40 ligand on T cells from mice injected with lipopolysaccharide accelerates lipopolysaccharide-induced osteoclastogenesis. J. Periodontal. Res. 46 (4), 464–474.

Yoshida, K., Taga, T., Saito, M., Suematsu, S., Kumanogoh, A., Tanaka, T., Fujiwara, H., Hirata, M., Yamagami, T., Nakahata, T., Hirabayashi, T., Yoneda, Y., Tanaka, K., Wang, W.Z., Mori, C., Shiota, K., Yoshida, N., Kishimoto, T., 1996. Targeted disruption of gp130, a common signal transducer for the interleukin 6 family of cytokines, leads to myocardial and hematological disorders. Proc. Natl. Acad. Sci. U. S. A. 93, 407–411.

Yoshimatsu, M., Kitaura, H., Fujimura, Y., Eguchi, T., Kohara, H., Morita, Y., Yoshida, N., 2009. IL-12 inhibits TNF-alpha induced osteoclastogenesis via a T cell-independent mechanism in vivo. Bone.

Yoshimatsu, M., Kitaura, H., Fujimura, Y., Kohara, H., Morita, Y., Yoshida, N., 2015. IL-12 inhibits lipopolysaccharide stimulated osteoclastogenesis in mice. J. Immunol. Res. 2015, 214878.

Zaiss, M.M., Kurowska-Stolarska, M., Bohm, C., Gary, R., Scholtysek, C., Stolarski, B., Reilly, J., Kerr, S., Millar, N.L., Kamradt, T., Mcinnes, I.B., Fallon, P.G., David, J.P., Liew, F.Y., Schett, G., 2011. IL-33 shifts the balance from osteoclast to alternatively activated macrophage differentiation and protects from TNF-{alpha}-Mediated bone loss. J. Immunol. 22, 22.

Zarling, J.M., Shoyab, M., Marquardt, H., Hanson, M.B., Lioubin, M.N., Todaro, G.J., 1986. Oncostatin M: a growth regulator produced by differentiated histiocytic lymphoma cells. Proc. Natl. Acad. Sci. U. S. A. 83, 9739–9743.

Zauli, G., Rimondi, E., Celeghini, C., Milani, D., Secchiero, P., 2010. Dexamethasone counteracts the anti-osteoclastic, but not the anti-leukemic, activity of TNF-related apoptosis inducing ligand (TRAIL). J. Cell. Physiol. 222, 357–364.

Zauli, G., Rimondi, E., Stea, S., Baruffaldi, F., Stebel, M., Zerbinati, C., Corallini, F., Secchiero, P., 2008. TRAIL inhibits osteoclastic differentiation by counteracting RANKL-dependent p27(Kip1) accumulation in pre-osteoclast precursors. J. Cell. Physiol. 214 (1), 117–125.

Zhang, J., Fu, Q., Ren, Z., Wang, Y., Wang, C., Shen, T., Wang, G., Wu, L., 2015. Changes of serum cytokines-related Th1/Th2/Th17 concentration in patients with postmenopausal osteoporosis. Gynecol. Endocrinol. 31, 183–190.

Zhang, J., Zhao, H., Chen, J., Xia, B., Jin, Y., Wei, W., Shen, J., Huang, Y., 2012. Interferon-beta-induced miR-155 inhibits osteoclast differentiation by targeting SOCS1 and MITF. FEBS Lett. 586, 3255–3262.

Zhang, P., Turner, C.H., Yokota, H., 2009. Joint loading-driven bone formation and signaling pathways predicted from genome-wide expression profiles. Bone 44, 989–998.

Zhang, Q., Chen, B., Yan, F., Guo, J., Zhu, X., Ma, S., Yang, W., 2014. Interleukin-10 inhibits bone resorption: a potential therapeutic strategy in periodontitis and other bone loss diseases. BioMed Res. Int. 2014, 284836.

Zhang, Y.H., Heulsmann, A., Tondravi, M.M., Mukherjee, A., Abu-Amer, Y., 2001. Tumor necrosis factor-alpha (TNF) stimulates RANKL-induced osteoclastogenesis via coupling of TNF type 1 receptor and RANK signaling pathways. J. Biol. Chem. 276, 563–568.

Zhao, R., Wang, X., Feng, F., 2016. Upregulated cellular expression of IL-17 by CD4+ T-cells in osteoporotic postmenopausal women. Ann. Nutr. Metab. 68, 113–118.

Zhao, Z., Hou, X., Yin, X., Li, Y., Duan, R., Boyce, B.F., Yao, Z., 2015. TNF induction of NF-kappaB RelB enhances RANKL-induced osteoclastogenesis by promoting inflammatory macrophage differentiation but also limits it through suppression of NFATc1 expression. PLoS One 10, e0135728.

Zhong, X., Wang, H., Huang, S., 2014. Endothelin-1 induces interleukin-18 expression in human osteoblasts. Arch. Oral Biol. 59, 289–296.

Zou, X., Bolon, B., Pretorius, J.K., Kurahara, C., Mccabe, J., Christiansen, K.A., Sun, N., Duryea, D., Foreman, O., Senaldi, G., Itano, A.A., Siu, G., 2009. Neonatal death in mice lacking cardiotrophin-like cytokine is associated with multifocal neuronal hypoplasia. Vet. Pathol. 46, 514–519.

Zupan, J., Pristovsek, N., Mencej-Bedrac, S., Komadina, R., Prezelj, J., Marc, J., 2012. Interleukin-1alpha gene variants influence bone mineral density and the risk of osteoporotic hip fractures in elderly Slovenian people. Clin. Chem. Lab. Med. 50, 1379–1385.

Zwerina, J., Redlich, K., Polzer, K., Joosten, L., Kronke, G., Distler, J., Hess, A., Pundt, N., Pap, T., Hoffmann, O., Gasser, J., Scheinecker, C., Smolen, J.S., van den Berg, W., Schett, G., 2007. TNF-induced structural joint damage is mediated by IL-1. Proc. Natl. Acad. Sci. U. S. A. 104, 11742–11747.

Chapter 51

Prostaglandins and bone metabolism

Shilpa Choudhary and Carol Pilbeam

Department of Medicine and Musculoskeletal Institute, UConn Health, Farmington, CT, United States

Chapter outline

Introduction

Prostaglandins (PGs) are autocrine–paracrine fatty acids, commonly called local factors. The lipid soluble acid originally identified in seminal fluid as an activity causing muscle contraction was named "prostaglandin" because it was thought to originate from the prostate gland (von Euler, 1936). We now know that PGs are produced in most cells. They are not stored but are synthesized and released as needed and rapidly metabolized. Since prostaglandin E_2 (PGE_2) was first shown to stimulate cyclic AMP production and resorption in bone organ cultures (Klein and Raisz, 1970), bone cells have been shown to produce abundant PGs, especially PGE_2. PGs in bone cells are largely the result of the inducible cyclooxygenase enzyme (COX-2), which can be induced by multiple systemic hormones and local factors involved in bone metabolism. PGE_2 can stimulate bone resorption and formation and mediate the effects of COX-2 agonists. A major function of PGE_2, however, may be to integrate, amplify, or as we have recently shown for PTH, block the responses to these agonists at the cellular level.

Prostaglandin production

Eicosanoids

Eicosanoids are bioactive lipids derived via oxygenation from arachidonic acid (AA) and other 20-carbon polyunsaturated (i.e., containing double bonds) fatty acids (PUFAs). AA is the PUFA precursor for major groups of eicosanoids (Buczynski et al., 2009). AA is metabolized by (1) cyclooxygenases (COXs) to PGs and thromboxanes (TXAs); (2) lipoxygenases 5, 12, and 15 to leukotrienes, lipoxins, and hydroxyeicosatetraenoic acids (HETEs); (3) cytochrome P450 to HETEs; and

Principles of Bone Biology. https://doi.org/10.1016/B978-0-12-814841-9.00051-8

(4) nonenzymatic pathways to isoprostanes and HETEs. The term "prostanoid" refers to products of the COX pathway: PGEs, PGDs, PGFs, prostacyclins (PGIs), and TXAs (Smith et al., 2011). PGs are 20-carbon fatty acids with a cyclopentane ring. Although TXAs have an oxane ring, they are generally discussed under the "PG" heading. The subscript for prostanoids denotes the number of double bonds (e.g., PGE_1, PGE_2, and PGE_3).

PUFAs are metabolized from linoleic acid and α-linolenic acid, essential fatty acids that must be obtained from the diet (Wilson, 2004; Edwards and O'Flaherty, 2008). (The shorthand for fatty acids, X:YωZ, refers to X carbon atoms and Y double bonds, while Z is the position of the first double bond counting from the terminal methyl [CH_3] group.) The Western diet is high in an omega 6 fatty acid, linoleic acid (18:2ω6), that is metabolized to dihomo-γ-linolenic acid (20:3ω6). Dihomo-γ-linolenic acid is the substrate for 1-series (1 double bond) PGs (e.g., PGE_1) and gives rise to AA (20:4 ω6), the substrate for the 2 series (e.g., PGE_2). An omega 3 fatty acid, α-linolenic acid (18:3ω3), is metabolized to eicosatetraenoic acid (20:4ω3) and then to eicosapentaenoic acid (EPA, 20:5ω3), which is the substrate of the 3 series (e.g., PGE_3).

The 2-series prostanoids are the most abundant and most characterized. The roles of the 1-series and 3-series PGs in normal physiology are unclear. However, PGE_1 and synthetic analogues have been used to treat many conditions, including patent ductus arteriosus in neonates, arterial occlusive disease, erectile dysfunction, contrast-induced nephropathy, chronic idiopathic constipation, and ARDS (Creutzig et al., 2004; Ivey and Srivastava, 2006; Fuller et al., 2015; Berkseth et al., 2016; Li et al., 2016; Ye et al., 2016). In contrast to 2-series prostanoids, especially PGE_2, which is positively associated with inflammation and tumorigenesis, the 3-series prostanoids, along with the 5-series leukotrienes, derived from EPA and the resolvins derived from the metabolite of EPA, docosahexaenoic acid (22:6ω3), are thought to have some antiinflammatory and antitumorigenic properties (Wiktorowska-Owczarek et al., 2015; Araki et al., 2017).

There are three steps in the production of 2-series prostanoids (Fig. 51.1). The first is the mobilization of AA from membranes by phospholipases. The second step is catalyzed by a bifunctional enzyme that converts free AA to prostaglandin G_2 (PGG_2) in a COX reaction followed by the reduction of PGG_2 to prostaglandin H_2 (PGH_2) in a peroxidase (POX) reaction. The first step or COX reaction is inhibited by nonsteroidal antiinflammatory drugs (NSAIDs). The bifunctional enzyme is formally named prostaglandin endoperoxide H synthase or prostaglandin G/H synthase (PGHS), and the gene name is *Ptgs*. (There are two PGHSs, which will be discussed in more detail later.) PGH_2 is then converted by terminal synthases to PGE_2, PGD_2, $PGF_{2\alpha}$, PGI_2, and TXA_2 (Smith et al., 2011). PGI_2 and TXA_2 are rapidly hydrolyzed to 6-keto $PGF_{1\alpha}$ and TXB_2, respectively. All three enzymatic steps are subject to transient activation, and any of the three steps may be limiting under some circumstances.

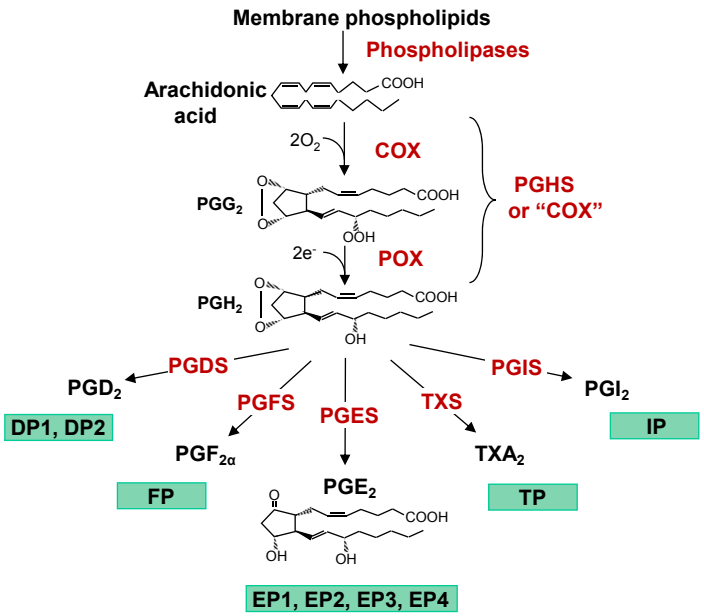

FIGURE 51.1 Major prostanoids generated from arachidonic acid (AA) and their receptors. Free AA, released from membrane phospholipids by phospholipases, is converted by the bifunctional PGHS enzyme (or cyclooxygenase, COX) to prostaglandin G_2 (PGG_2) in a COX reaction followed by the reduction of PGG_2 to prostaglandin H_2 (PGH_2) in a peroxidase (POX) reaction. PGH_2 is then converted to specific prostanoids by the terminal synthases PGDS, PGFS, PGDS, TXS, and PGIS. The respective receptors are shown below the prostanoids.

Mobilization of arachidonic acid

Phospholipase A_2 (PLA_2) enzymes catalyze the hydrolysis of membrane phospholipids from the *sn*-2 position of membrane glycerophospholipids, releasing free fatty acids such as AA. The PLA_2 superfamily is currently divided into 16 groups (GI−GXVI) and many subgroups (Dennis et al., 2011; Murakami et al., 2011, 2015; Vasquez et al., 2017). There is tremendous diversity among these enzymes, with some having actions independent of their phospholipase activity. The most important PLAs for PG production are Ca^{2+}-independent PLA_2s (iPLA_2s), Ca^{2+}-dependent cytosolic PLA_2s (cPLA_2s), and secreted PLA_2s (sPLA_2s). In general, iPLA_2 is thought to be the primary PLA_2 in cells, producing the low levels of free fatty acids, some of which may be AA, needed for daily cellular functions; cPLA_2 is the major inducible enzyme hydrolyzing AA-containing phospholipids during infection or inflammation; and sPLA_2 is also inducible and augments cPLA_2 function (Dennis and Norris, 2015).

Group VI (GVI) enzymes are cytosolic proteins with calcium-independent phospholipase A_2 activity (Dennis et al., 2011). There are six members of the group, but GVIA is the enzyme commonly called calcium-independent PLA_2 or iPLA_2. This group does not show AA specificity in the *sn*-2 position. The activities of this group are diverse, involving many organelles including mitochondria and associated with membrane homeostasis and remodeling and with basic cellular functions of proliferation and apoptosis.

Group IV (GIV) cPLA_2s are large cytosolic proteins dependent on Ca^{2+} activation (Dennis et al., 2011; Vasquez et al., 2017; Murakami et al., 2011). GIVA cPLA_2 (85 kDa) is the most studied of six subgroups and likely the most important cPLA_2 for PG production. GIVA cPLA_2 is highly selective for AA at the *sn*-2 position of membrane lipids. It is constitutively expressed in most cells but can also be regulated. PGs themselves can enhance both COX-2 and cPLA_2 expression (Murakami et al., 1997), and IL-4 can inhibit both COX-2 and cPLA_2 expression (Kawaguchi et al., 1996). Activation of cPLA_2 requires that it be sequestered at a phospholipid interface. The first step is the Ca^{2+} (submicromolar concentration)-dependent translocation of GIV cPLA_2 from the cytosol to nuclear/endoplasmic reticulum (ER) membranes, which is also where the COX enzymes reside. Binding to membranes can be enhanced by several mechanisms including phosphorylation of the enzyme. Since GIV cPLA_2 is the major enzyme for releasing AA substrate for COX activity, its biological functions as determined from knockout (KO) mice are largely those expected from COX or eicosanoid deficiency. For example, KO mice have decreased inflammatory responses and associated diseases, such as collagen-induced arthritis, and less induced tumors than those of wild-type (WT) controls (Dennis et al., 2011). There are multiple inhibitors of GIV cPLA_2, but the therapeutic use of these inhibitors is likely to be hindered by the same side effects as those of NSAIDs.

sPLA_2s are low-molecular-weight secreted proteins that require millimolar Ca^{2+} concentrations for activation. There are 10 isoforms in mammals; 9 are expressed in humans and 10 in mice (Dennis et al., 2011; Vasquez et al., 2017). They have many functions, some independent of their hydrolytic activity. They have antibacterial and antiviral function and are thought to contribute significantly to atherosclerosis, perhaps by increasing fatty acids in plaques. sPLA_2 expression is stimulated by proinflammatory agents, and sPLA_2s play roles in innate immunity and inflammation-associated diseases, such as rheumatoid arthritis (Dennis et al., 2011; Murakami et al., 2015). sPLA_2s do not have a distinct preference for the *sn*-2 position of phospholipid substrates but can release AA. sPLA_2s can hydrolyze phospholipids in the outer plasma membrane of the cell of origin and neighboring cells or can be internalized and release AA from ER/perinuclear membranes.

One of the sPLA_2s, group IIA (GIIA) sPLA_2, deserves special attention. GIIA and the group V sPLA_2s are thought to be the main sPLA_2s for releasing AA for eicosanoid production and are associated with all the functions discussed for sPLA_2s above. However, the mice used for most KO and transgenic studies, C57Bl/6 and 129Sv, are naturally missing the gene for GIIA sPLA_2 (Kennedy et al., 1995) and may have increased resistance to colorectal tumorigenesis (MacPhee et al., 1995). Many KOs of PLA_2s and other enzymes in the eicosanoid pathway are in a C57Bl/6 or 129Sv background, and they are really double KOs. It should also be noted that the MC3T3-E1 osteoblastic cell line, commonly used to study osteoblastic function and differentiation in vitro, was derived from C57Bl/6 mice and should therefore lack GIIA PLA_2.

Two isoforms for prostaglandin G/H synthase (cyclooxygenase)

During the development of drugs specific for inhibiting the COX reaction of PGHS, it became popular to call the bifunctional enzyme "cyclooxygenase" or "COX" in reference to its first function. We will use the colloquial name COX from here on, but it should be noted that much of past literature and some current experts in the field still use the formal name.

The two enzymes for COX, COX-1 and COX-2, are encoded by separate genes. In humans, the gene for COX-1, *PTGS1*, is located on chromosome 9, and *PTGS2* is located on chromosome 1 (Herschman, 1994; Smith et al., 2000). The gene for COX-2 was initially cloned as an inducible gene from murine 3T3 cells (Kujubu et al., 1991), chicken fibroblasts (Xie et al., 1991), and human umbilical vein endothelial cells (Hla and Neilson, 1992). There is 60%−65% amino acid sequence identity between COX-1 and COX-2 isoforms within a species and 85%−90% identity between individual isoforms between mammalian species (Smith et al., 2011). COX-1 is expressed at relatively stable levels in most tissues and is considered "constitutive," while COX-2 is generally expressed at low levels in most tissues but can be induced to high levels by multiple factors. Both COX-1 and COX-2 are N-glycosylated dimeric proteins inserted into the luminal face of the ER and the contiguous inner membrane of the nuclear envelope (Smith et al., 2011).

COXs are said to be sequence homodimers but conformational heterodimers (Dong et al., 2011, 2016; Mitchener et al., 2015; Smith et al., 2011). The primary structure of each monomer is the same, but one monomer functions as a regulatory allosteric subunit and the other as a catalytic subunit. The catalytic subunit binds heme with higher affinity than the allosteric subunit, and maximal activity occurs with one heme bound. Various fatty acids, both substrates and nonsubstrates for COX as well as NSAIDs, can bind to the allosteric site and regulate activity of the catalytic site. Hence, activity and inhibition of the active COX site may be modulated by the fatty acid milieu or "tone" as determined by diet, drugs, and other environmental factors.

COX-1 and COX-2 have similar catalytic mechanisms (Kulmacz et al., 2003; Smith et al., 2011). COX and POX active sites are in physically separated regions of the proteins. The initiation of COX activity is dependent on heme oxidation in the POX site by peroxidase. Heme oxidation leads to oxidation of a critical tyrosine in the COX active site. The tyrosyl radical in the COX site converts AA to an arachidonoyl radical, the arachidonoyl radical reacts with two molecules of oxygen to produce PGG_2, and then PGG_2 diffuses to the POX site where it is reduced to PGH_2.

Despite having similar catalytic mechanisms, COX-1 and COX-2 are independently functioning pathways (Simmons et al., 2004; Smith and Langenbach, 2001). This is due in part to the differential regulation of their expression. The COX-1 promoter has relatively few identified functional regulatory elements, and COX-1 mRNA is constitutively expressed in most tissues. The COX-2 promoter has multiple potential transcriptional regulatory elements typical of early response genes, and COX-2 mRNA is rapidly and transiently inducible in many tissues (Kang et al., 2007). The half-life of COX-2 protein has been reported as 2−7 h in various tissues, whereas the half-life of COX-1 protein is much longer (Kang et al., 2007; Mbonye et al., 2006). The differential responses of COX-1 and COX-2 mRNA are exemplified by their responses to serum in osteoblastic MC3T3-E1 cells (Pilbeam et al., 1993). With the advent of PCR as the routine method for measuring gene expression, it became evident that COX-2 was expressed "constitutively" at low levels in many tissues and cells. A recent study examined the signaling pathways underlying constitutive expression of COX-2 in kidney, gastrointestinal tract, and brain, but it is still unclear how much this expression contributes to PG production (Kirkby et al., 2016).

There are other differences between COX-1 and COX-2 in addition to their patterns of regulation. The active site of COX-2 is larger than that of COX-1, allowing COX-2 to oxygenate bulkier amide and ester analogs of AA that are poor COX-1 substrates, including the endocannabinoids 2-arachidonoylglycerol and arachidonoylethanolamide (Rouzer and Marnett, 2011). This difference has led to the ability to make NSAIDs selective for COX-2. Another difference is that COX-2 is much more efficient at using low AA concentrations (below 5 μM) than is COX-1 (Swinney et al., 1997). This difference is exemplified in studies showing that osteoblasts from COX-2 KO mice make little PG in culture despite the constitutive expression of COX-1 (Chikazu et al., 2005; Choudhary et al., 2003; Okada et al., 2000a; Xu et al., 2007). However, these cells make large amounts of PG when exogenous AA is added. An explanation for this difference may lie in the greater cellular peroxide level required for COX-1 activation compared with COX-2 (Kulmacz et al., 2003). Finally, allosteric regulators can have different effects on COX-1 and COX-2 activities (Smith et al., 2011).

Insertion of *Ptgs1* under the regulatory sequences that drive *Ptgs2* expression in mice or vice versa indicated that in many tissues, each COX isoform could compensate for the other to some degree (Yu et al., 2007; Li et al., 2018a, 2018b). In macrophages, COX-1 was shown to compensate for PG synthesis at high concentrations of substrate, whereas elevated lipopolysaccharide (LPS)-induced PG production was only observed for cells expressing endogenous COX-2. Inflammatory signaling pathways showed reduced activation when endogenous COX-2 was not expressed, indicating that COX-1 could be replaced by COX-2 in the inflammatory milieu but not vice versa. Clearly there is compensation by one COX for the other in some tissues, because double COX-1/COX-2-deficient mice die from failure of ductus arteriosus closure shortly after birth (Loftin et al., 2001). One caveat with regard to these studies is that they were done in C57Bl/6 or mixed C57Bl/6 and 129 background mice, which naturally lack the GIIA $sPLA_2$ as previously discussed, and this could affect the ability of one or both COXs to make PGs.

Because of the differential responses of COX-1 and COX-2, it was initially hypothesized that COX-2 was predominantly responsible for acute pathological PG responses, such as those associated with inflammation and pain, while COX-1

produced those prostanoids needed for ongoing "housekeeping" functions, including maintenance of renal blood flow, platelet aggregation, and gastric cytoprotection. This hypothesis led to the development of highly selective inhibitors of COX-2 activity for the treatment of pain and inflammation associated with diseases such as arthritis and periodontitis. Studies using these inhibitors led to the realization that COX-2 has physiologic functions in many tissues, as well as pathologic functions. COX-2 selective NSAIDs, or coxibs, turned out to have serious adverse side effects, especially on the cardiovascular system, that would limit their use (Grosser et al., 2017a, 2017b).

Prostaglandin E_2 synthases

PGH_2 is converted to each PG species by species-specific PG terminal synthases (Fig. 51.1). The individual synthases influence PG production by determining the predominant type of prostanoid synthesized in a particular tissue. Prostaglandin E synthase (PGES), which converts PGH_2 to PGE_2, occurs in multiple forms (Hara et al., 2010; Hara, 2017). Membrane-bound glutathione-dependent PGES (mPGES-1) is inducible, located in ER and perinuclear membranes, and the predominant PGES metabolizing PGH_2 produced by COX-2. Because mPGES-1 is coordinately regulated by factors that regulate COX-2, mPGES-1 is said to be coupled to COX-2. It has been recently reported that COX-2 and mPGES-1 are also located in the Golgi apparatus (Yuan and Smith, 2015). (COX-1, unlike COX-2, does not have an ER-to-Golgi trafficking signal.) Because $cPLA_2$ preferentially binds to Golgi membranes, the Golgi apparatus may be a site for dedicated COX-2-dependent PGE_2 synthesis (Leslie, 2015).

A second membrane-bound form, mPGES-2, is synthesized in the Golgi membrane and then released into the cytosol after proteolytic removal of an N-terminal hydrophobic domain (Watanabe et al., 1997). mPGES-2 is constitutively expressed and functionally coupled with both COX-1 and COX-2. A third form, cytosolic PGES (cPGES), is preferentially coupled to COX-1 and thought to maintain PGE_2 production for cellular homeostasis (Tanioka et al., 2000).

KO mice for synthases are reviewed in existing research (Hara et al., 2010; Hara, 2017). Mice deficient for mPGES-1 develop normally but have reduced inflammatory and pain responses as well as decreased tumorigenesis. LPS-induced bone resorption and bone loss are reduced in mice deficient for mPGES-1 (Inada et al., 2006), and collagen-induced arthritis is suppressed (Trebino et al., 2003). Mice deficient for mPGES-2 have no specific phenotype, and mice deficient for cPGES are perinatal lethal.

Because inducible mPGES-1 is considered largely responsible for excessive PGE_2 synthesis during inflammation, it is considered a promising drug target, and a number of potential inhibitory drugs have been developed (Psarra et al., 2017). It is possible that an inhibitor of mPGES-1 may have less adverse side effects than traditional NSAIDs but be just as effective. However, because mPGES1-derived PGE_2 is responsible for some homeostatic processes, blockade of mPGES-1 could shunt PGH_2 into the production of other PGs that might not be desirable (Hara, 2017).

Prostaglandin E_2 receptors

There are nine G-protein-coupled receptors (GPCRs) mediating prostanoid actions (Fig. 51.1). A detailed discussion of these receptors, their signaling pathways, and their potential functions is available (Woodward et al., 2011). The GPCRs for $PGF_{2\alpha}$, PGI_2, PGD_2, and TXA are called FP, IP, DP1, and TP, respectively. PGD_2 also acts via DP2, which belongs to the chemoattractant receptor family (Kostenis and Ulven, 2006). $PGF_{2\alpha}$ and TP couple to $G\alpha_q$ and initiate the phospholipase C (PLC) pathway, raising intracellular Ca^{2+} and activating protein kinase C (PKC). DP1 is $G\alpha_s$-coupled and stimulates cAMP formation. The IP receptor is both $G\alpha_s$- and $G\alpha_q$-coupled, resulting in increased cAMP formation, PLC pathway activation, and Ca^{2+} signaling.

PGE_2 effects are associated with four classes of GPCRs, called EP1, EP2, EP3, and EP4. Much of the complexity of PGE_2 effects on skeletal tissues may be attributable to the multiple GPCRs for PGE_2, and these receptors may heterodimerize with other receptors or transactivate the epidermal growth factor receptor (EGFR) signaling pathway (Woodward et al., 2011). The EP1 receptor is known to increase Ca^{2+} and may couple to $G\alpha_q$, because studies have reported the involvement of the PLC/PKC pathway (Tang et al., 2005). The major signaling pathway for EP3 receptors is $G\alpha_i$-induced adenylate cyclase inhibition. However, multiple alternative transcripts of this receptor may act through other signal transduction pathways (An et al., 1994).

EP2 and EP4 are the receptors that have been most extensively studied in bone. Mice deficient in each EP receptor subtype have been generated, and highly selective agonists for the receptors have been developed (Sugimoto and Narumiya, 2007; Woodward et al., 2011). Despite their importance in bone, much of what is known about EP2 and EP4 receptor signaling pathways comes from studies to elucidate the role of PGE_2 in promoting inflammation or tumorigenesis in nonbone tissues (Buchanan and DuBois, 2006; Castellone et al., 2006; Dorsam and Gutkind, 2007; Eisinger et al., 2007;

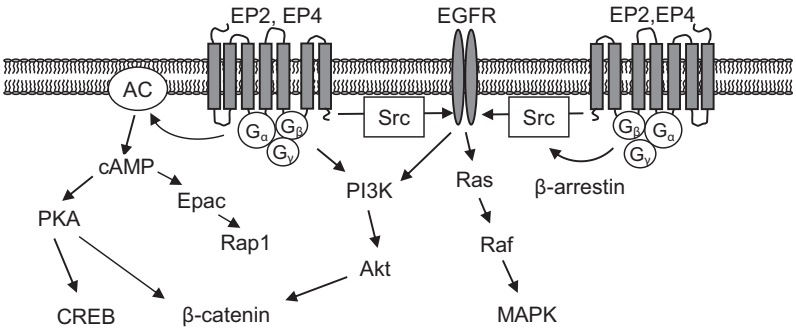

FIGURE 51.2 Signaling pathways activated by PGE_2 acting via the EP2 and EP4 receptors. Both EP2 and EP4 can activate $G\alpha_s$ and activate adenylyl cyclase (AC), leading to an increase in cAMP and activation of protein kinase A (PKA). The increased cAMP can potentially act independently of PKA to activate exchange protein directly activated by cAMP (Epac). The PKA pathway can cross talk with other pathways to activate β-catenin signaling. β-catenin activation may also occur via the phosphatidylinositol 3-kinase (PI3K)-Akt pathway. EP receptors may activate c-Src, which then transactivates epidermal growth factor receptor (EGFR), leading to multiple signaling pathways including PI3K/Akt/β-catenin and Ras/Raf/MAPK. The recruitment of β-arrestin by EP receptors may also activate c-Src, resulting in EGFR transactivation (O'Callaghan and Houston, 2015).

Ganesh, 2014; Jiang and Dingledine, 2013; O'Callaghan and Houston, 2015; Yokoyama et al., 2013). Some potential signaling pathways by which PGE_2 may act via EP2 and EP4 are shown in Fig. 51.2.

Both EP2 and EP4 stimulate $G\alpha_s$ to activate ACs and produce cAMP, which can then activate protein kinase A (PKA) or a PKA-independent pathway mediated by the guanine exchange factor Epac. The PKA pathway is able to cross talk with several other pathways that regulate cell growth, motility, migration, and apoptosis, including the Wnt/β-catenin signaling pathway (Buchanan and DuBois, 2006; Castellone et al., 2005, 2006; Estus et al., 2016; Hino et al., 2005; Shao et al., 2005). Studies in human embryonic kidney-293 cells stably transfected with EP receptors suggested that the activation of β-catenin signaling occurred primarily through a PKA-dependent pathway for EP2 and through a PI3K-dependent pathway for EP4 (Fujino et al., 2002). PGE_2 can also transactivate the EGFR signaling pathway by various mechanisms (Buchanan et al., 2003; Pai et al., 2002; Shao et al., 2003). Recent studies have shown that signaling from both receptors can be modulated by β-arrestin. In brain microglia, IL-10 production was inhibited by PGE_2 via an EP2-β-arrestin signaling pathway (Chu et al., 2015). In gastric mucosal cells, PGE_2 stimulated cell proliferation via activation of a β-arrestin/Src/EGFR/Akt pathway downstream of EP4 (Tan et al., 2017).

Prostaglandin E_2: role in bone formation and resorption

Production in bone and osteoblastic cultures

Early studies showed that complement-sufficient antisera, which contain antibodies to rodent cell surface antigens, could increase resorption of fetal rat long bones by stimulating endogenous PG production (Raisz et al., 1974). Subsequently, many regulators of bone metabolism were found to stimulate PG production in bone, although it was not always clear what cells were responsible. In the early 1990s, inducible COX-2 was identified (O'Banion et al., 1991; Kujubu et al., 1991; Xie et al., 1991). Subsequently, the induction of COX-2 was shown to be responsible for most acutely stimulated PG responses in osteoblastic cells. Multiple agonists were shown to induce COX-2 in osteoblastic cells, including cytokines IL-1 (Harrison et al., 1994; Kawaguchi et al., 1994; Min et al., 1998), TNF-α (Kawaguchi et al., 1996), and IL-6 (Tai et al., 1997); growth factors TGFα (Harrison et al., 1994), TGFβ (Pilbeam et al., 1997a), basic fibroblast growth factor (FGF-2) (Kawaguchi et al., 1995), and bone morphogenetic protein (BMP-2) (Chikazu et al., 2005); systemic hormones PTH (Kawaguchi et al., 1994; Tetradis et al., 1996, 1997) and $1,25(OH)_2$ vitamin D_3 (Okada et al., 2000a); calcium (Choudhary et al., 2003) and strontium (Choudhary et al., 2007); and fluid shear stress (FSS) and mechanical loading (Klein-Nulend et al., 1997; Mehrotra et al., 2006; Pavalko et al., 1998; Wadhwa et al., 2002a).

Serum is also a potent stimulator of COX-2 expression and PG production in cultured osteoblasts (Pilbeam et al., 1993). Endogenous PGs produced by the addition of serum can increase the differentiation of cultured osteoblasts (Choudhary et al., 2013). In the absence of serum, some osteoblastic cell cultures produce little PGE_2 despite the presence of COX-2 expression unless AA is added, suggesting that serum may facilitate substrate in some cultures (Pilbeam et al., 1994). Perhaps the varying ability of serum to induce COX-2/PG production or release AA may contribute to the observation that some batches of serum are "better" for studying osteoblastic differentiation than others.

Some osteoblastic cell lines do not express COX-2. In our studies, the rat osteosarcoma cell line, ROS 17/2.8, expressed only COX-1 mRNA (Pilbeam et al., 1997b). Because of the difficulty of obtaining freshly isolated osteoblasts from humans, osteosarcoma cell lines are often used to study human osteoblastic function. Expression of COX-2 mRNA can be highly variable among and within these osteosarcoma cell lines. Expression of COX-2 mRNA in U2OS, TE85, and Saos-2 osteosarcoma cell lines, measured by reverse transcriptase-PCR, ranged from easily detectable constitutive and inducible expression to no detectable constitutive or inducible expression (Xu et al., 2006). Similar variability was seen in three lines of Saos-2 cells (called strains) derived originally from the same tumor but carried for years by different labs. COX-1 was constitutively expressed in all three Saos-2 strains, but PGE_2 production depended on COX-2 expression. It is unclear which, if any, of these strains reflect the expression of COX-2 in the original tumor.

PGE_2 can amplify its own production by stimulating COX-2 and $cPLA_2$ expression (Kawaguchi et al., 1994; Murakami et al., 1997; Pilbeam et al., 1993, 1994). Agonists acting via IP, TP, FP, and DP receptors have also been shown to stimulate COX-2 expression (Sakuma et al., 2004), and PGE_2 may be the major PG produced in response. For example, $PGF_{2\alpha}$, which is a poor stimulator of resorption, increases PGE_2 production in organ culture that enhances resorptive effects (Raisz et al., 1990). This amplifying mechanism could be important in prolonging the effects of short periods of impact loading on the skeleton or the effects of cytokines in inflammatory diseases. PG autoamplification is likely to involve different signaling pathways than the initial cytokine or other agonist induction of COX-2 and may complicate interpretation if unrecognized.

Glucocorticoids (GCs) are potent inhibitors of stimulated PG production, and their antiinflammatory actions are thought to be due in part to this inhibition. Prior to the identification of COX-2, GCs were thought to work predominantly through interference with the release of AA. Although GCs can inhibit agonist-stimulated release of AA (Sampey et al., 2000), their major inhibitory effect is on inducible COX-2 mRNA and protein expression (Kawaguchi et al., 1994; Pilbeam et al., 1993). GCs can also inhibit mPGES-1(Korotkova et al., 2005). The GC inhibition of COX-2 occurs by both transcriptional and posttranscriptional mechanisms (DeWitt and Meade, 1993; Lasa et al., 2001; Newton et al., 1998). The use of GCs to promote differentiation in osteoblastic cultures may actually decrease osteoblastic differentiation by reducing COX-2 produced PGE_2. This was observed for strontium ranelate−induced osteoblastic differentiation in murine bone marrow stromal cells (Choudhary et al., 2007).

NSAIDs inhibit PG production by binding to the cyclooxygenase catalytic site. Since PGs themselves can induce COX-2 expression, NSAIDs can also decrease COX-2 expression by reducing PG-mediated autoamplification. NSAIDs are widely used to study the effects of endogenous PGs. NS-398 is the selective NSAID most widely available for in vitro and animal studies. In rodent osteoblastic cells, NS-398 at a concentration of 0.01 μM was selective for the inhibition of COX-2 activity; however, at concentrations of 0.1 and 1 μM, NS-398 also inhibited COX-1 activity by 60% and 85%, respectively (Pilbeam et al., 1997b). In addition, NSAIDs can have multiple effects independent of COX activity, especially at high doses (Grosch et al., 2006; Paik et al., 2000). Hence, in using NSAIDs to study PGE_2 effects, the lowest dose that inhibits PGE_2 production should be used.

Prostaglandin E_2 and bone formation

Many studies have shown that PGE_2 stimulates osteoblastic differentiation in murine and rat bone marrow stromal cell and primary osteoblast/calvarial cell cultures (Choudhary et al., 2013; Flanagan and Chambers, 1992; Kaneki et al., 1999; Nagata et al., 1994; Scutt and Bertram, 1995). In addition, PGE_2 given to rats in vivo stimulated osteoblastic differentiation in ex vivo cultured bone marrow (Keila et al., 1994; Weinreb et al., 1997). For some osteogenic factors, such as serum, BMP-2, and strontium ranelate, their ability to stimulate osteoblast differentiation in vitro is due largely to their induction of COX-2 produced PGs (Pilbeam et al., 1993; Chikazu et al., 2005; Choudhary et al., 2007). In cultured marrow stromal cells or primary osteoblasts from mice with deletion of *Ptgs2* or treated with NSAIDs to inhibit COX-2 activity, osteoblastic differentiation is decreased (Choudhary et al., 2007, 2013; Okada et al., 2000b; Xu et al., 2004; Zhang et al., 2002b). An example of osteoblastic differentiation in bone marrow stromal cell cultures from COX-2 WT and KO mice is shown in Fig. 51.3.

Systemic injections of PGE_2 can increase both periosteal and endosteal bone formation in the rat and produce substantial increases in bone mass similar to the effects of PTH (Jee and Ma, 1997; Lin et al., 1994; Suponitzky and Weinreb, 1998). Systemic administration of PGE_2 or PGE_1 in humans (Faye-Petersen et al., 1996; Ueda et al., 1980) and dogs (Norrdin and Shih, 1988) has also been shown to increase cortical and cancellous bone mass. Local infusion of PGE_2 has been shown to increase bone in mice (Yoshida et al., 2002). However, systemic injection of PGE_2 in mice following the

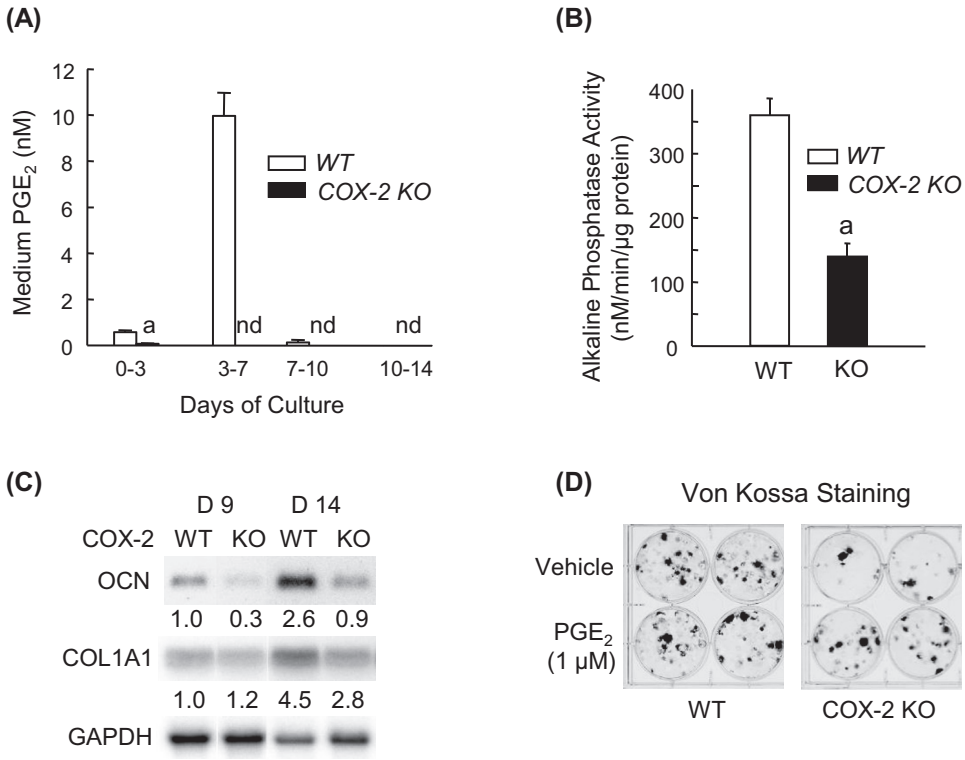

FIGURE 51.3 Osteoblastic differentiation in bone marrow stromal cell cultures from COX-2 knockout (KO) mice compared with cultures from wild-type (WT) mice (Pilbeam, C., unpublished data). Whole bone marrow from long bone was cultured in α-MEM, 10% fetal calf serum, and 50 μg/mL phosphoascorbate. β-glycerophosphate (10 mM) was added for the last 2 weeks of culture. All measures of osteoblast differentiation including alkaline phosphatase (ALP) staining, osteocalcin (OCN) mRNA expression, and Von Kossa staining for mineralization were decreased in COX-2 KO cells compared with WT cells. (A) Medium PGE_2 production peaked between days 3–7 of culture in WT cultures but was undetectable at all times in KO cultures. (B) ALP activity normalized to total protein at day 14. (C) Northern analysis for type 1 collagen and OCN mRNA. Ratio of mRNA level to housekeeping gene GAPDH is shown below the bands. (D) Von Kossa staining of mineralized nodules at day 21. Bars are means ± SEM for $n = 3$ wells. a, Significantly different from WT, $P < .01$.

protocols established for rats was found to increase turnover, with resorption increasing more than formation and resulting in bone loss, or resorption and formation increasing similarly and resulting in no bone loss or a gain (Gao et al., 2009a). Despite using different doses and injection regimens, we were never able to achieve the sort of anabolic effects with systemic PGE_2 in mice that can be seen with intermittent PTH (i.e., increased formation greater than increased resorption) (Raisz and Pilbeam, unpublished data).

Prostaglandin E_2 receptors and bone formation

A review of EP receptor actions in bone is available (Woodward et al., 2011). Both EP2 and EP4 have been implicated in the osteogenic and anabolic effects of PGE_2 (Alander and Raisz, 2006; Choudhary et al., 2008; Li et al., 2007). Bone mechanical properties were reduced in both EP2 and EP4 KO mice (Akhter et al., 2001, 2006). Reduced bone mass and impaired fracture healing were found in aged EP4 receptor KO mice compared with WT mice (Li et al., 2005). However, we did not find any differences in bone formation between aged WT and EP4 KO mice (Gao et al., 2009b). EP4 KO mice are difficult to breed in a pure C57Bl/6 background because neonates die shortly after birth due to patent ductus arteriosus (Segi et al., 1998). To combat this problem, mice for the two latter studies were bred in multiple mixed backgrounds. Hence, the difference in EP4 KO phenotypes might be due to variability in backgrounds.

The EP1 receptor may be a negative regulator of bone formation. EP1 KO mice have been shown to have enhanced fracture healing, stronger cortical bones, higher trabecular bone volume, increased bone formation, and accelerated osteoblastic differentiation compared with WT mice (Zhang et al., 2011, 2015a). The effects of EP1 deletion on osteoblastic differentiation may occur via regulation of energy metabolism (Feigenson et al., 2017).

Prostaglandin E_2 and bone resorption

Early work on the effects of PGs in organ culture showed that exogenous PGs of the E series were potent activators of resorption (Klein and Raisz, 1970). PGE_1 and PGE_2 were shown to stimulate osteoclast formation in marrow cultures (Collins and Chambers, 1991). Subsequently, multiple resorption agonists were shown to stimulate PG-dependent osteoclast formation in marrow cultures including cytokines IL-1 (Akatsu et al., 1991; Lader and Flanagan, 1998; Sato et al., 1996), IL-6 (Tai et al., 1997), IL-11 (Girasole et al., 1994; Morinaga et al., 1998), IL-17 (Kotake et al., 1999), and TNF-α (Lader and Flanagan, 1998); hormones PTH (Inoue et al., 1995; Okada et al., 2000a; Sato et al., 1997) and $1,25(OH)_2D_3$ (Collins and Chambers, 1992; Okada et al., 2000a); and growth factors FGF-2 (Hurley et al., 1998) and BMP-2 at high doses (Chikazu et al., 2005). TGFβ enhanced osteoclastogenesis at low concentrations by a PG-dependent mechanism but inhibited osteoclastogenesis at higher concentrations (Shinar and Rodan, 1990).

The major role for PGE_2 in increasing bone resorption is thought to be indirect via the upregulation of receptor activator of NFκB ligand (RANKL) expression and the inhibition of osteoprotegerin expression in osteoblastic lineage cells (Li et al., 2000; Suda et al., 2004; Suzawa et al., 2000; Tsukii et al., 1998). In models used to study the direct effects of PGE_2 on hematopoietic lineage cells, in which RANKL must be added to stimulate osteoclast formation, the results have been contradictory. For example, exogenous PGE_2 increased RANKL-stimulated osteoclast differentiation in RAW264.7 cells (Kobayashi et al., 2005) and inhibited RANKL-stimulated differentiation in cultured human peripheral blood mononuclear cells (Take et al., 2005). In spleen cells, exogenous PGE_2 had biphasic effects on RANKL-stimulated osteoclast formation, with an initial inhibitory effect and a later stimulatory effect (Ono et al., 2005). COX-2 is also expressed in cells of the hematopoietic lineage (Hackett et al., 2006; North et al., 2007). In bone marrow macrophages cultured with M-CSF, we see the RANKL induction of COX-2/PGE_2 within minutes after addition, but we have been unable to demonstrate any consistent regulation by COX-2 of osteoclast differentiation in these cultures (data not shown). Some inconsistencies between studies may be due to different timing of measurements. The peak in osteoclast number in these culture models generally occurs rapidly and transiently over 24 h. If only a single time point is measured, the results can be misleading if potential shifting of the peak with regard to time is not recognized (Blackwell et al., 2010).

As a further complication, early studies found that PGE_2 added to isolated osteoclasts in vitro transiently inhibited bone resorption (Fuller and Chambers, 1989). A similar transient inhibition of bone resorption in mouse calvarial bone was observed (Lerner et al., 1987). The transient decrease in serum calcium that occurred after systemic injection of IL-1 in mice was PG-mediated and might be related to this early inhibitory effect of PGE_2 (Boyce et al., 1989b).

The effects of PGs in vivo often fail to be predicted by in vitro studies. For example, in vivo injection of IL-1 above the calvaria in mice for 3 days was shown to stimulate PG-independent resorption when mice were sacrificed 24 h after the last injection. However, resorption continued for 3−4 weeks after the IL-1 injections were stopped, and this resorption was PG-dependent (Boyce et al., 1989a).

Prostaglandin E_2 receptors and bone resorption

Studies in bone marrow cultures and cocultures of osteoblasts and spleen cells have shown PGE_2-stimulated osteoclast formation to be impaired when cells from either EP2 or EP4 KO animals are used (Li et al., 2000; Sakuma et al., 2000). A selective antagonist for EP4 partially inhibited osteoclastogenesis in murine marrow cultures not only in response to PGE_2 but also in response to $1,25(OH)_2D_3$ and PTH (Tomita et al., 2002), confirming earlier results using selective EP agonists and antagonists (Ono et al., 1998). However, administration of an EP4 selective agonist to rats subjected to protocols causing bone loss, such as immobilization, did not increase osteoclasts relative to control animals (Yoshida et al., 2002). Neonatal murine calvarial cultures express all PGE_2 receptor subtypes, but PGE_2-stimulated resorption is largely mediated via EP4 with only a minor contribution from EP2 (Suzawa et al., 2000). There was a marked decrease in resorptive response to PGE_2 in cultured calvariae from EP4 KO animals and an impaired response to PGE_2 even in calvariae from mice with only one EP4 allele disrupted (Miyaura et al., 2000; Zhan et al., 2005). In fetal rat long bone cultures treated with agonists selective for EP2 and EP4, only the EP4 agonist was effective in stimulating resorption (Raisz and Woodiel, 2003). Interestingly, aged EP4 KO mice are reported to have significantly increased osteoclast numbers on trabecular surfaces and increased eroded surface on the endocortical surface compared with WT mice (Li et al., 2005).

Thus, the majority of data indicates that EP4 is the more important EP receptor for resorption. It is not clear, however, how the results of PGE_2 experiments in vitro translate to the endogenous effects of PGE_2 in vivo, or why EP4 should be the major receptor involved, when both EP2 and EP4 have so much potential overlap in signaling. It would be helpful to compare resorption in EP2 and EP4 receptor KO mice in response to exogenous PGE_2 and in response to agonists that induce PGE_2, such as PTH and IL-1.

Inducible cyclooxygenase knockout mice

Basal skeletal phenotype

Initial studies by the investigators who generated mice with disruption of COX-1 or COX-2 showed that COX-2 deficiency had more profound effects than deficiency of COX-1 (Dinchuk et al., 1995; Langenbach et al., 1995, 1999; Morham et al., 1995). COX-1 KO mice were healthy, survived normally, and have subsequently been little studied. COX-2 KO mice, on the other hand, had increased mortality. One study reported that 35% of COX-2 KO mice died with a patent ductus arteriosus within 48 h of birth (Loftin et al., 2001). Other studies found shortened life span in COX-2 KO mice secondary to renal dysplasia (Morham et al., 1995). Renal development in COX-2 KO mice appeared normal until postnatal day 10, after which there was progressive renal architectural disruption and functional deterioration, with about 20% of COX-2 KO mice dying from renal failure between 7 and 23 weeks of age (Norwood et al., 2000). COX-2-deficient females were infertile, with multiple failures in female reproductive processes, including ovulation, fertilization, and implantation (Lim et al., 1997). Mice for these initial studies were in a C57Bl/6129 genetic background.

A study of 4.5-month-old female in the C57Bl/6129 background found reduced femoral BMD by DXA, reduced cortical thickness, and reduced mechanical properties, but increased distal femoral trabecular bone volume, in COX-2 KO mice compared with WT (Alam et al., 2005). In this same study, only 60% of KO mice survived to weaning, and 28% died after weaning before they could be studied. In contrast, in another study of 4-month-old mice, COX-2 KO females were normal, but males had decreased femoral trabecular bone volume fraction and cortical bone mineral density compared with WT mice (Robertson et al., 2006).

We found that COX-2 KO mice in the C57Bl/6129 background died four times faster after weaning than was the case for WT mice, with about 40% dying between 2 and 10 months of age, while mice heterozygous for COX-2 gene disruption had normal mortality (Xu et al., 2005). In a cohort of 10-month-old WT and COX-2 KO mice with normal serum creatinine, KO mice had significantly increased levels of PTH (114% in females, 150% in males) and $1,25(OH)_2D_3$ (180% for both genders) compared with WT mice, suggesting that older, apparently healthy COX-2 KO mice might have primary hyperparathyroidism (HPTH). The skeletal phenotype of the COX-2 male and female mice was very difficult to interpret in any consistent manner and was attributed in part to HPTH.

Improved survival was seen in COX-2 KO mice in the DBA1 or DBA1,C57Bl/6 background (Chen et al., 2003; Myers et al., 2006). The bones from COX-2 KO mice in these studies also had inferior mechanical properties compared with those of WT mice. Elevated PTH levels were also found in apparently healthy 3-month-old female COX-2 KO mice in a DBA1 background (Myers et al., 2006).

As discussed above, C57Bl/6 and 129Sv mice are naturally missing the gene for GIIA $sPLA_2$ (Kennedy et al., 1995). It is possible that the absence of type GIIA secretory PLA_2 in mice with C57Bl/6 and 129 genetic backgrounds might result in a more severe phenotype in the absence of COX-2 (Kennedy et al., 1995). We crossed C57Bl/6129 COX-2 KO mice into an outbred CD-1 background. In this background, COX-2 KO mice had no increased mortality after weaning and no renal dysfunction (Xu et al., 2010). In addition, CD-1 COX-2 KO females were fertile, as also observed by others (Wang et al., 2004). The generation of healthy and fertile COX-2 KO mice has made it possible for us to do multiple studies with these mice. Despite being healthy, 5-month-old male COX-2 KO mice in the CD-1 background also had twofold elevated PTH compared with that of WT mice. COX-2 KO mice had increased serum markers of bone turnover, decreased femoral BMD and cortical bone thickness, but no differences in trabecular bone volume by μCT or dynamic histomorphometry. We concluded that this bone phenotype could be due to HPTH, COX-2 deficiency, or both.

Several studies that compared COX-1 mRNA expression in WT and COX-2 KO mice have suggested that COX-1 mRNA was elevated in COX-2-deficient mice (Alam et al., 2005; Wang et al., 2004; Zhang et al., 2002a). However, we have never found increased COX-1 mRNA expression in freshly isolated bone or cultured osteoblastic cells from COX-2 KO mice in the C56Bl/6129 or CD-1 background under basal or stimulated conditions (Pilbeam, unpublished observations). It is possible that other aspects of the PG production pathway may be upregulated in COX-2 KO mice.

Inducible cyclooxygenase modulation of the effects of parathyroid hormone

Inducible cyclooxygenase knockout mice and parathyroid hormone

PTH induces COX-2 in bone rapidly and transiently (Xu et al., 2010). We examined the effects of intermittent PTH for 3 weeks on skeletal responses in WT and COX-2 KO mice (Xu et al., 2010). PTH increased serum markers of bone formation and resorption more in KO than in WT mice, but there was no significant effect of genotype on resorption. We were surprised to find that intermittent PTH increased femoral BMD and cortical bone area more in KO mice than in WT

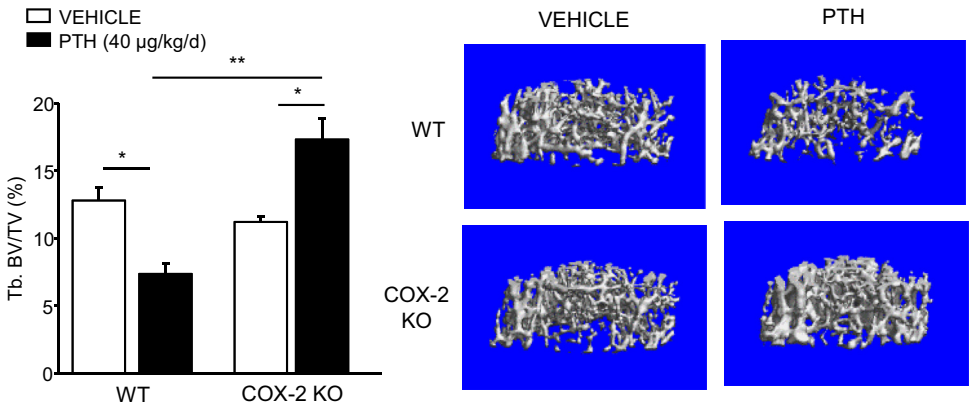

FIGURE 51.4 Continuous PTH infusion caused trabecular bone loss in WT mice but increased trabecular bone in COX-2 KO mice (Choudhary and Pilbeam, unpublished data). Three-month-old WT and COX-2 KO male mice were infused with vehicle or PTH (hPTH 1−34, 40 µg/kg/day) for 12 days using ALZET microosmotic pumps. Left panel: Trabecular bone volume fraction (Tb. BV/TV) in the distal femur as determined by micro-CT. Right panel: representative trabecular bone images. Bars are means ± SEM for $n = 3$ mice per genotype and treatment group. Data were analyzed by two-way ANOVA and post hoc Bonferroni pairwise multiple comparisons. $^{*}P < .05$, $^{**}P < .01$.

mice and that there was a trend for the PTH-stimulated increase in trabecular bone to be greater in KO mice than in WT mice. The ratio of osteoblastic surface to osteoclastic surface was increased only in KO mice. In addition, PTH increased the femoral mineral apposition rates and bone formation rates more in KO mice than it did in WT mice.

We subsequently infused WT and COX-2 KO mice with vehicle and continuous PTH, which generally results in bone loss (Choudhary et al., 2015). Continuous PTH infusion increased COX-2 expression continuously. As seen previously, continuous PTH infusion was catabolic in WT mice. In COX-2 KO mice, however, PTH infusion was anabolic, increasing trabecular bone mass and bone formation. An example of the anabolic effects of continuous PTH infusion in COX-2 KO mice is shown in Fig. 51.4. In contrast to the inhibitory effects of COX-2 expression on PTH-stimulated bone formation, PTH-stimulated bone resorption was the same in both WT and COX-2 KO mice. These data suggested that the bone loss associated with continuously infused PTH was due largely to suppression of bone formation and that this suppression was mediated by COX-2.

An inducible cyclooxygenase–dependent inhibitor of the anabolic effects of continuous parathyroid hormone

Because COX-2 inhibited the anabolic effects of PTH in vivo, we examined its modulation of PTH effects in bone marrow stromal cell cultures (Choudhary et al., 2013). It had been known for a long time that it was difficult to find an in vitro model for the anabolic effects of PTH seen in vivo. Likewise, we found that continuous PTH (added at each media change) inhibited or had no effect on osteoblastic differentiation in WT cultures. However, in COX-2 KO cultures, PTH dramatically and consistently stimulated osteoblastic differentiation. The COX-2-dependent inhibition of the osteogenic effects of PTH were shown to be due to a secreted factor. This factor was secreted by hematopoietic lineage cells in the cultures in response to a combination of RANKL from osteoblastic lineage cells and PGE_2 produced by osteoblastic or hematopoietic lineage cells acting via the EP4 receptor (Choudhary et al., 2013).

We identified the COX-2-dependent secreted inhibitor in vitro as serum amyloid A3 (Choudhary et al., 2016). Serum amyloid A (SAA) is a family of four highly conserved apolipoproteins, some of which can increase 1000-fold in the circulation during episodes of inflammation (De Buck et al., 2016; Sun and Ye, 2016; Uhlar and Whitehead, 1999; Ye and Sun, 2015). Serum amyloid A3 (SAA3) is the major inducible SAA in mice. We also showed that SAA3 was secreted by the preosteoclast population of myeloid cells in response to RANKL (as long as COX-2-produced PGE_2 was present) and inhibited PTH-stimulated cAMP signaling in osteoblastic cells by stimulating Gαi signaling, likely via formyl peptide receptor 2 (Choudhary et al., 2016). Recently, we examined the effects of continuous PTH infusion in SAA3 KO mice, which have a normal COX-2 response to PTH, and confirmed the role of SAA3 in mediating COX-2 suppression of the anabolic effects of continuous PTH infusion on trabecular bone (Choudhary et al., 2018). This study also confirmed that SAA3 had no effect on resorption stimulated by continuous PTH. Thus, COX-2-dependent SAA3 appears to suppress the

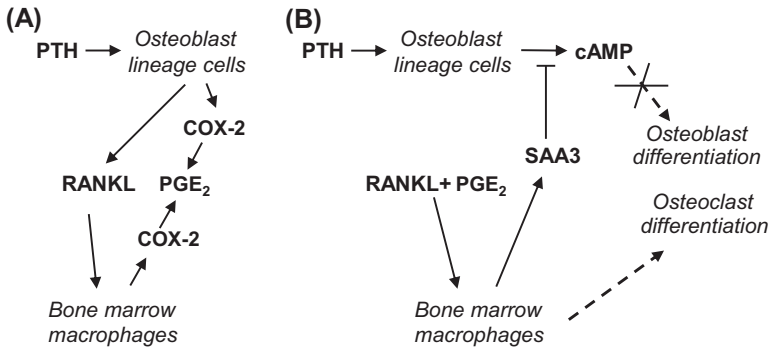

FIGURE 51.5 Role of SAA3 in blocking the osteoblastic response to continuous PTH. Panel (A): PTH induces RANKL and COX-2/PGE_2 in osteoblastic lineage cells. RANKL also induces COX-2/PGE_2 in bone marrow macrophages (BMMs). Panel (B): RANKL initiates the differentiation of BMMs to become osteoclasts at the same time that RANKL in combination with PGE_2 induces the expression of SAA3 in BMMs. SAA3 is secreted and acts on osteoblastic lineage cells to block the PTH stimulation of cAMP production and subsequently PTH stimulation of osteoblast differentiation.

anabolic effects of continuous PTH by inhibiting PTH-stimulated cAMP but has no effect on the resorption stimulated by continuous PTH. A summary of the proposed production and actions of SAA3 in response to PTH is shown in Fig. 51.5.

Prostaglandin E_2 and bone physiology

As discussed above, PGE_2, similar to PTH, can regulate both bone resorption and formation in experimental models. Whether either role is important in bone physiology has been difficult to determine. Here we discuss some proposed roles for PGE_2 in bone physiology.

Mechanical loading of bone

Bone is a dynamic tissue that adapts to mechanical loading with changes in structure to achieve a better balance between stresses and load-bearing capacity.

Early studies showed that mechanical loading of bone cells increased PG production and that inhibition of PG production by NSAIDs could inhibit new bone formation in response to applied loading in vivo (Cheng et al., 1997; Chow and Chambers, 1994; Lanyon, 1992; Li et al., 2006; Pead and Lanyon, 1989; Rawlinson et al., 1991). Orthodontic tooth movement was also shown to stimulate PG production, and it was proposed that PGs enhanced the orthodontic movement of teeth as a result of PG-stimulated bone resorption (Giunta et al., 1995; Kehoe et al., 1996; Sandy et al., 1993).

Osteocytes are thought to be the major strain-sensing cells in bone and coupled to mechanical loading at least in part via interstitial fluid flow in the lacunar–canalicular network in bone, where large stresses on cells can be generated by fluid flow in narrow channels (Burger and Klein-Nulend, 1999; Han et al., 2004; Hillsley and Frangos, 1994; Knothe et al., 1998; Srinivasan and Gross, 2000; Turner et al., 1994; Weinbaum et al., 1994). In vitro studies examining the effects of FSS on osteoblastic cells showed rapid induction of COX-2 mRNA and PG production (Klein-Nulend et al., 1997; Norvell et al., 2004; Pavalko et al., 1998; Wadhwa et al., 2002b). FSS-induced PGE_2 may also mediate intracellular osteocyte communication through gap junctions via the prostaglandin EP2 receptor (Cherian et al., 2003). A role for COX-2-produced PGE_2 in triggering the anabolic Wnt/β-catenin signaling pathway in osteocytes in response to loading has also been proposed (Bonewald and Johnson, 2008; Kitase et al., 2010). PGE_2 is known to inhibit sclerostin, a Wnt antagonist (Genetos et al., 2011), and several studies suggest that this is one way that PGE_2 increases Wnt signaling and bone formation in response to mechanical loading (Galea et al., 2011, 2017; Lara-Castillo et al., 2015; Tu et al., 2012).

However, a study examining ulnar loading in COX-2 WT and KO mice reported that a functional *Ptgs2* gene was not required for anabolic response in the periosteum to loading, suggesting that COX-1 might compensate for absent COX-2 (Alam et al., 2005). It is also possible that HPTH reported in COX-2 KO mice, discussed previously, may have compensated in part for COX-2 deficiency. However, in a more recent study of female mice, NS-398 did not reduce trabecular or cortical bone response to repeated loading (Sugiyama et al., 2013). Until an in vivo loading experiment elucidates a clear role for COX-2/PG in mediating bone formation response to loading, it seems prudent to conclude that COX-2/PG is one of many early responses to strain, all of which interact to regulate the adaptation of bone to loading (Price et al., 2011).

Fracture and wound healing

In the early years following the development of COX-2-selective NSAIDs, many studies in animals suggested that NSAIDs could impair fracture healing, although results were variable (Altman et al., 1995; Bergenstock et al., 2005; Brown et al., 2004; Einhorn, 2003; Endo et al., 2005; Murnaghan et al., 2006; Simon and O'Connor, 2007). Other studies indicated that NSAID impairment of fracture healing was dose- and duration-dependent, and reversible after discontinuation of brief treatment (Gerstenfeld et al., 2007). Mice with absent COX-2 were also shown to have impaired fracture healing and allograft incorporation (O'Keefe et al., 2006; Xie et al., 2009; Zhang et al., 2002b). Several reviews of animal studies concluded that the loss of COX-2 activity primarily affected fracture healing via callus chondrogenesis or endochondral ossification (Geusens et al., 2013; O'Connor et al., 2014), and a recent study in rabbits showed that a selective COX-2 inhibitor (celecoxib) impaired the chondrogenic phase of endochondral ossification (Janssen et al., 2017).

A number of reviews of human data have concluded that there is no compelling evidence that short-term use of NSAIDs impairs fracture healing (Kurmis et al., 2012; Marquez-Lara et al., 2016; Pountos et al., 2012), cruciate ligament repair (Soreide et al., 2016), or spinal fusion surgery (Sivaganesan et al., 2017). In contrast, 6 weeks of indomethacin was reported to increase the risk of nonunion after acetabular fracture surgery (Sagi et al., 2014), and chronic use of NSAIDs was found to increase the risk of a second hip fracture after hip fracture surgery (Huang et al., 2015). Hence, the consensus at this time would be to use NSAIDs cautiously in situations of bone repair, at a low dose and for a short duration.

Agonists of EP2 and EP4 can increase healing in animals. Local application of an EP2 agonist and local and systemic application of EP4 agonists have been shown to accelerate bone repair (Li et al., 2003; Paralkar et al., 2003; Tanaka et al., 2004; Yoshida et al., 2002). Clinical studies have not been done with these agonists, perhaps because increased PG can have adverse effects, and their pharmacological relevance in enhancing human bone repair is still unknown (Markovic et al., 2017).

PGs may also be important for wound healing in unmineralized tissues. The first step in the degradation of PGE_2 is mediated by the enzyme 15-dehydroxyprostaglandin dehydrogenase (15-PGDH), which generates 15-keto-PGE_2, and this intermediate metabolite is further catabolized to 13,14-dihydro-15-keto-PGE_2 by 15-oxoprostaglandin-Δ^{13}-reductase (Tai et al., 2006). These metabolites are orders of magnitude less potent at the EP2 and EP4 receptors than PGE_2 itself (Nishigaki et al., 1996). Inhibition of 15-PGDH increases PGE_2, potentiating recovery in mouse models of marrow transplant and accelerating tissue generation in mouse models of colon and liver injury (Antczak et al., 2017; Desai et al., 2018; Zhang et al., 2015b). Although the known associations of elevated PGE_2 with increased inflammation and tumorigenesis might be thought to limit the usefulness of inhibiting 15-PGDH, initial studies suggest that a small molecule inhibitor can promote transplant recovery without any limiting side effects in animal models (Desai et al., 2018).

Skeletal response to nonsteroidal antiinflammatory drugs

Several studies in older men and women with regular NSAID use suggested some increase in BMD but found no increase in markers of bone formation (Carbone et al., 2003; Cauley et al., 2005; Bauer et al., 1996; Lane et al., 1997). Selective COX-2 inhibitors may affect BMD differently in men and women. In a study of men and women age 65 and older, daily COX-2 inhibitor use in men was associated with 2.4%−5.3% lower hip and spine BMD compared with those of nonusers (Richards et al., 2006). In postmenopausal women not on estrogen replacement therapy, it was associated with 0.9%−5.7% higher BMD. COX-2 inhibitor had no effect in women on estrogen replacement. The authors speculated that the beneficial effects of mechanical loading might be reduced by COX-2 inhibition in men, while the proinflammatory state and increased bone turnover associated with estrogen withdrawal might be suppressed by COX-2 inhibition in postmenopausal women. A recent review of the literature on controlled randomized clinical trials with bone remodeling outcomes concluded that there was some evidence of increased BMD, no evidence for increased bone formation, and some evidence of a decreased resorption rate in NSAID users (Konstantinidis et al., 2013). However, the data were too limited for firm conclusions.

Observational studies of the effect of NSAIDs on bone mass may be misleading because the regular use of NSAIDs is likely to be associated with other characteristics that can affect bone, such as a decreased level of physical activity or the presence of inflammatory conditions. There is also considerable variability at an individual level in the degree of COX-2 inhibition and the selectivity attained by selective COX-2 inhibitors (Fries et al., 2006). Approximately one-third of the variability was attributable to differences between individuals, suggesting the contribution of genetic sources of variance.

A driving factor in producing selective COX-2 NSAIDs was to prevent gastric bleeding, but the adverse cardiovascular side effects of selective NSAIDs have become the current limiting factor. It is a very complex problem, complicated by the variable response to NSAIDs, the interference of selective NSAIDs with the beneficial effect of aspirin (mainly an inhibitor

of COX-1), and an unclear risk−benefit for treating pain (Grosser et al., 2017a, 2017b; Li et al., 2014; Ricciotti et al., 2013). However, given the need to treat inflammation and musculoskeletal pain and the emerging interest in the role of COX-2/PGs in cancer, it is likely that NSAIDs will continue to be widely used.

Summary

PGs are abundant in bone and are potent regulators of bone cell function. Cells of both osteoblastic and osteoclastic lineage produce PGs, and this production is highly regulated by local and systemic factors. Stimulated production of PGs requires the availability of arachidonic acid substrate, the induction of COX-2 expression, and the presence of terminal synthases. PGE_2, which may be the most important local eicosanoid in skeletal regulation, can stimulate both bone resorption and formation. In vitro, PGE_2 can stimulate the differentiation of osteoblast differentiation, and indirectly via the stimulation of RANKL in osteoblastic cells, the differentiation of osteoclasts. The net balance of these two effects under physiologic and pathologic conditions in vivo is not yet clear. Some of the complexity of PG actions on bone can be explained by the multiplicity of receptors for PGs. There are at least four distinct receptors for PGE_2 with differential signaling pathways that have not yet been fully elucidated. Further studies are needed to clarify the specific pathways of PG actions in bone. Once this is accomplished, it may be possible to identify therapeutic applications of manipulating PGs in skeletal disorders.

Acknowledgments

This effort was supported by a National Institute of Health Grants NIAMS award AR060286 (CP). We dedicate the chapter to Larry Raisz, who loved prostaglandins and who was an editor of this book as well as an author of this chapter for the first three editions and whose words still linger on in this one.

References

Akatsu, T., Takahashi, N., Udagawa, N., Imamura, K., Yamaguchi, A., Sato, K., Nagata, N., Suda, T., 1991. Role of prostaglandins in interleukin-1-induced bone resorption in mice in vitro. J. Bone Miner. Res. 6, 183−189.

Akhter, M.P., Cullen, D.M., Gong, G., Recker, R.R., 2001. Bone biomechanical properties in prostaglandin EP1 and EP2 knockout mice. Bone 29, 121−125.

Akhter, M.P., Cullen, D.M., Pan, L.C., 2006. Bone biomechanical properties in EP4 knockout mice. Calcif. Tissue Int. 78, 357−362.

Alam, I., Warden, S.J., Robling, A.G., Turner, C.H., 2005. Mechanotransduction in bone does not require a functional cyclooxygenase-2 (COX-2) gene. J. Bone Miner. Res. 20, 438−446.

Alander, C.B., Raisz, L.G., 2006. Effects of selective prostaglandins E2 receptor agonists on cultured calvarial murine osteoblastic cells. Prostag. Other Lipid Mediat. 81, 178−183.

Altman, R.D., Latta, L.L., Keer, R., Renfree, K., Hornicek, F.J., Banovac, K., 1995. Effect of nonsteroidal antiinflammatory drugs on fracture healing: a laboratory study in rats. J. Orthop. Trauma 9, 392−400.

An, S., Yang, J., So, S.W., Zeng, L., Goetzl, E.J., 1994. Isoforms of the EP3 subtype of human prostaglandin E2 receptor transduce both intracellular calcium and cAMP signals. Biochemistry 33, 14496−14502.

Antczak, M.I., Zhang, Y., Wang, C., Doran, J., Naidoo, J., Voruganti, S., Williams, N.S., Markowitz, S.D., Ready, J.M., 2017. Inhibitors of 15-prostaglandin dehydrogenase to potentiate tissue repair. J. Med. Chem. 60, 3979−4001.

Araki, Y., Suganami, A., Endo, S., Masuda, Y., Fukushima, K., Regan, J.W., Murayama, T., Tamura, Y., Fujino, H., 2017. PGE1 and E3 show lower efficacies than E2 to beta-catenin-mediated activity as biased ligands of EP4 prostanoid receptors. FEBS Lett. 591, 3771−3780.

Bauer, D.C., Orwoll, E.S., Fox, K.M., Vogt, T.M., Lane, N.E., Hochberg, M.C., Stone, K., Nevitt, M.C., 1996. Aspirin and NSAID use in older women: effect on bone mineral density and fracture risk. Study of Osteoporotic Fractures Research Group. J. Bone Miner. Res. 11, 29−35.

Bergenstock, M., Min, W., Simon, A.M., Sabatino, C., O'Connor, J.P., 2005. A comparison between the effects of acetaminophen and celecoxib on bone fracture healing in rats. J. Orthop. Trauma 19, 717−723.

Berkseth, K.E., Thirumalai, A., Amory, J.K., 2016. Pharmacologic therapy in men's Health: hypogonadism, erectile dysfunction, and benign prostatic hyperplasia. Med. Clin. 100, 791−805.

Blackwell, K.A., Raisz, L.G., Pilbeam, C.C., 2010. Prostaglandins in bone: bad cop, good cop? Trends Endocrinol. Metabol. 21, 294−301.

Bonewald, L.F., Johnson, M.L., 2008. Osteocytes, mechanosensing and Wnt signaling. Bone 42, 606−615.

Boyce, B.F., Aufdemorte, T.B., Garrett, I.R., Yates, A.J., Mundy, G.R., 1989a. Effects of interleukin-1 on bone turnover in normal mice. Endocrinology 125, 1142−1150.

Boyce, B.F., Yates, A.J., Mundy, G.R., 1989b. Bolus injections of recombinant human interleukin-1 cause transient hypocalcemia in normal mice. Endocrinology 125, 2780−2783.

Brown, K.M., Saunders, M.M., Kirsch, T., Donahue, H.J., Reid, J.S., 2004. Effect of COX-2-specific inhibition on fracture-healing in the rat femur. J Bone Joint Surg. Am 86-A, 116−123.

Buchanan, F.G., DuBois, R.N., 2006. Connecting COX-2 and Wnt in cancer. Cancer Cell 9, 6–8.
Buchanan, F.G., Wang, D., Bargiacchi, F., DuBois, R.N., 2003. Prostaglandin E2 regulates cell migration via the intracellular activation of the epidermal growth factor receptor. J. Biol. Chem. 278, 35451–35457.
Buczynski, M.W., Dumlao, D.S., Dennis, E.A., 2009. Thematic Review Series: proteomics. An integrated omics analysis of eicosanoid biology. J. Lipid Res. 50, 1015–1038.
Burger, E.H., Klein-Nulend, J., 1999. Mechanotransduction in bone–role of the lacuno-canalicular network. FASEB J. 13 (Suppl. S101–12), S101–S112.
Carbone, L.D., Tylavsky, F.A., Cauley, J.A., Harris, T.B., Lang, T.F., Bauer, D.C., Barrow, K.D., Kritchevsky, S.B., 2003. Association between bone mineral density and the use of nonsteroidal anti-inflammatory drugs and aspirin: impact of cyclooxygenase selectivity. J. Bone Miner. Res. 18, 1795–1802.
Castellone, M.D., Teramoto, H., Gutkind, J.S., 2006. Cyclooxygenase-2 and colorectal cancer chemoprevention: the beta-catenin connection. Cancer Res. 66, 11085–11088.
Castellone, M.D., Teramoto, H., Williams, B.O., Druey, K.M., Gutkind, J.S., 2005. Prostaglandin E2 promotes colon cancer cell growth through a Gs-axin-beta-catenin signaling axis. Science 310, 1504–1510.
Cauley, J.A., Fullman, R.L., Stone, K.L., Zmuda, J.M., Bauer, D.C., Barrett-Connor, E., Ensrud, K., Lau, E.M., Orwoll, E.S., 2005. Factors associated with the lumbar spine and proximal femur bone mineral density in older men. Osteoporos. Int. 16, 1525–1537.
Chen, Q., Rho, J.Y., Fan, Z., Laulederkind, S.J., Raghow, R., 2003. Congenital lack of COX-2 affects mechanical and geometric properties of bone in mice. Calcif. Tissue Int. 73, 387–392.
Cheng, M.Z., Zaman, G., Rawlinson, S.C., Pitsillides, A.A., Suswillo, R.F., Lanyon, L.E., 1997. Enhancement by sex hormones of the osteoregulatory effects of mechanical loading and prostaglandins in explants of rat ulnae. J. Bone Miner. Res. 12, 1424–1430.
Cherian, P.P., Cheng, B., Gu, S., Sprague, E., Bonewald, L.F., Jiang, J.X., 2003. Effects of mechanical strain on the function of Gap junctions in osteocytes are mediated through the prostaglandin EP2 receptor. J. Biol. Chem. 278, 43146–43156.
Chikazu, D., Li, X., Kawaguchi, H., Sakuma, Y., Voznesensky, O.S., Adams, D.J., Xu, M., Hoshi, K., Katavic, V., Herschman, H.R., Raisz, L.G., Pilbeam, C.C., 2005. Bone morphogenetic protein 2 induces cyclo-oxygenase 2 in osteoblasts via a Cbfa1 binding site: role in effects of bone morphogenetic protein 2 in vitro and in vivo. J. Bone Miner. Res. 20, 1888–1898.
Choudhary, S., Alander, C., Zhan, P., Gao, Q., Pilbeam, C., Raisz, L., 2008. Effect of deletion of the prostaglandin EP2 receptor on the anabolic response to prostaglandin E2 and a selective EP2 receptor agonist. Prostag. Other Lipid Mediat. 86, 35–40.
Choudhary, S., Blackwell, K., Voznesensky, O., Deb, R.A., Pilbeam, C., 2013. Prostaglandin E2 acts via bone marrow macrophages to block PTH-stimulated osteoblast differentiation in vitro. Bone 56, 31–41.
Choudhary, S., Canalis, E., Estus, T., Adams, D., Pilbeam, C., 2015. Cyclooxygenase-2 suppresses the anabolic response to PTH infusion in mice. PLoS One 10, e0120164.
Choudhary, S., Goetjen, A., Estus, T., Jacome-Galarza, C.E., Aguila, H.L., Lorenzo, J., Pilbeam, C., 2016. Serum amyloid A3 secreted by preosteoclasts inhibits parathyroid hormone-stimulated cAMP signaling in murine osteoblasts. J. Biol. Chem. 19 (291), 3882–3894.
Choudhary, S., Halbout, P., Alander, C., Raisz, L., Pilbeam, C., 2007. Strontium ranelate promotes osteoblastic differentiation and mineralization of murine bone marrow stromal cells: involvement of prostaglandins. J. Bone Miner. Res. 22, 1002–1010.
Choudhary, S., Santone, E., Yee, S.-P., Lorenzo, J., Adams, D.J., Goetjen, A., McCarthy, M.B., Mazzocca, A., Pilbeam, C., 2018. Continuous PTH in Mice Causes Bone Loss Because it Induces Serum Amyloid A (SAA) Endocrinology (in press).
Choudhary, S., Wadhwa, S., Raisz, L.G., Alander, C., Pilbeam, C.C., 2003. Extracellular calcium is a potent inducer of cyclo-oxygenase-2 in murine osteoblasts through an ERK signaling pathway. J. Bone Miner. Res. 18, 1813–1824.
Chow, J.W., Chambers, T.J., 1994. Indomethacin has distinct early and late actions on bone formation induced by mechanical stimulation. Am. J. Physiol. 267, E287–E292.
Chu, C.H., Chen, S.H., Wang, Q., Langenbach, R., Li, H., Zeldin, D., Chen, S.L., Wang, S., Gao, H., Lu, R.B., Hong, J.S., 2015. PGE2 inhibits IL-10 production via EP2-mediated beta-arrestin signaling in neuroinflammatory condition. Mol. Neurobiol. 52, 587–600. https://doi.org/10.1007/s12035-014-8889-0. Epub 2014 Sep. 14.
Collins, D.A., Chambers, T.J., 1991. Effect of prostaglandins E1, E2, and F2 alpha on osteoclast formation in mouse bone marrow cultures. J. Bone Miner. Res. 6, 157–164.
Collins, D.A., Chambers, T.J., 1992. Prostaglandin E2 promotes osteoclast formation in murine hematopoietic cultures through an action on hematopoietic cells. J. Bone Miner. Res. 7, 555–561.
Creutzig, A., Lehmacher, W., Elze, M., 2004. Meta-analysis of randomised controlled prostaglandin E1 studies in peripheral arterial occlusive disease stages III and IV. Vasa 33, 137–144.
De Buck, M., Gouwy, M., Wang, J.M., Van, S.J., Proost, P., Struyf, S., Van, D.J., 2016. The cytokine-serum amyloid A-chemokine network. Cytokine Growth Factor Rev. 30, 55–69. https://doi.org/10.1016/j.cytogfr.2015.12.010.
Dennis, E.A., Cao, J., Hsu, Y.H., Magrioti, V., Kokotos, G., 2011. Phospholipase A2 enzymes: physical structure, biological function, disease implication, chemical inhibition, and therapeutic intervention. Chem. Rev. 111, 6130–6185.
Dennis, E.A., Norris, P.C., 2015. Eicosanoid storm in infection and inflammation. Nat. Rev. Immunol. 15, 511–523.
Desai, A., Zhang, Y., Park, Y., Dawson, D.M., Larusch, G.A., Kasturi, L., Wald, D., Ready, J.M., Gerson, S.L., Markowitz, S.D., 2018. A second-generation 15-PGDH inhibitor promotes bone marrow transplant recovery independent of age, transplant dose, and G-CSF support. Haematol. 103, 1054–1064. https://doi.org/10.3324/haematol.2017.178376. Epub 2018 Feb 22. PMID: 29472361.

DeWitt, D.L., Meade, E.A., 1993. Serum and glucocorticoid regulation of gene transcription and expression of the Prostaglandin H Synthase-1 and Prostaglandin H Synthase-2 isozymes. Arch. Biochem. Biophys. 306, 94–102.

Dinchuk, J.E., Car, B.D., Focht, R.J., Johnston, J.J., Jaffee, B.D., Covington, M.B., Contel, N.R., Eng, V.M., Collins, R.J., Czerniak, P.M., 1995. Renal abnormalities and an altered inflammatory response in mice lacking cyclooxygenase II. Nature 378, 406–409.

Dong, L., Vecchio, A.J., Sharma, N.P., Jurban, B.J., Malkowski, M.G., Smith, W.L., 2011. Human cyclooxygenase-2 is a sequence homodimer that functions as a conformational heterodimer. J. Biol. Chem. 286, 19035–19046.

Dong, L., Zou, H., Yuan, C., Hong, Y.H., Uhlson, C.L., Murphy, R.C., Smith, W.L., 2016. Interactions of 2-O-arachidonylglycerol ether and ibuprofen with the allosteric and catalytic subunits of human COX-2. J. Lipid Res. 57, 1043–1050.

Dorsam, R.T., Gutkind, J.S., 2007. G-protein-coupled receptors and cancer. Nat. Rev. Canc. 7, 79–94.

Edwards, I.J., O'Flaherty, J.T., 2008. Omega-3 fatty acids and PPARgamma in cancer. PPAR Res. 2008, 358052. https://doi.org/10.1155/2008/358052.

Einhorn, T.A., 2003. Cox-2: where are we in 2003? - the role of cyclooxygenase-2 in bone repair. Arthritis Res. Ther. 5, 5–7.

Eisinger, A.L., Prescott, S.M., Jones, D.A., Stafforini, D.M., 2007. The role of cyclooxygenase-2 and prostaglandins in colon cancer. Prostag. Other Lipid Mediat. 82, 147–154.

Endo, K., Sairyo, K., Komatsubara, S., Sasa, T., Egawa, H., Ogawa, T., Yonekura, D., Murakami, R., Yasui, N., 2005. Cyclooxygenase-2 inhibitor delays fracture healing in rats. Acta Orthop. 76, 470–474.

Estus, T.L., Choudhary, S., Pilbeam, C.C., 2016. Prostaglandin-mediated inhibition of PTH-stimulated beta-catenin signaling in osteoblasts by bone marrow macrophages. Bone 85, 123–130. https://doi.org/10.1016/j.bone.2016.01.023.

Faye-Petersen, O.M., Johnson Jr., W.H., Carlo, W.A., Hedlund, G.L., Pacifico, A.D., Blair, H.C., 1996. Prostaglandin E1-induced hyperostosis: clinicopathologic correlations and possible pathogenetic mechanisms. Pediatr. Pathol. Lab. Med. 16, 489–507.

Feigenson, M., Eliseev, R.A., Jonason, J.H., Mills, B.N., O'Keefe, R.J., 2017. PGE2 receptor subtype 1 (EP1) regulates mesenchymal stromal cell osteogenic differentiation by modulating cellular energy metabolism. J. Cell. Biochem. 118, 4383–4393. https://doi.org/10.1002/jcb.26092.

Flanagan, A.M., Chambers, T.J., 1992. Stimulation of bone nodule formation in vitro by prostaglandins E1 and E2. Endocrinology 130, 443–448.

Fries, S., Grosser, T., Price, T.S., Lawson, J.A., Kapoor, S., DeMarco, S., Pletcher, M.T., Wiltshire, T., Fitzgerald, G.A., 2006. Marked interindividual variability in the response to selective inhibitors of cyclooxygenase-2. Gastroenterology 130, 55–64.

Fujino, H., West, K.A., Regan, J.W., 2002. Phosphorylation of glycogen synthase kinase-3 and stimulation of T-cell factor signaling following activation of EP2 and EP4 prostanoid receptors by prostaglandin E2. J. Biol. Chem. 277, 2614–2619.

Fuller, B.M., Mohr, N.M., Skrupky, L., Fowler, S., Kollef, M.H., Carpenter, C.R., 2015. The use of inhaled prostaglandins in patients with ARDS: a systematic review and meta-analysis. Chest 147, 1510–1522.

Fuller, K., Chambers, T.J., 1989. Effect of arachidonic acid metabolites on bone resorption by isolated rat osteoclasts. J. Bone Miner. Res. 4, 209–215.

Galea, G.L., Lanyon, L.E., Price, J.S., 2017. Sclerostin's role in bone's adaptive response to mechanical loading. Bone 96, 38–44. https://doi.org/10.1016/j.bone.2016.10.008. Epub 2016 Oct 12.

Galea, G.L., Sunters, A., Meakin, L.B., Zaman, G., Sugiyama, T., Lanyon, L.E., Price, J.S., 2011. Sost down-regulation by mechanical strain in human osteoblastic cells involves PGE2 signaling via EP4. FEBS Lett. 585, 2450–2454. https://doi.org/10.1016/j.febslet.2011.06.019. Epub 2011 Jun 28.

Ganesh, T., 2014. Prostanoid receptor EP2 as a therapeutic target. J. Med. Chem. 57, 4454–4465. https://doi.org/10.1021/jm401431x. Epub 2013 Dec 4.

Gao, Q., Xu, M., Alander, C.B., Choudhary, S., Pilbeam, C.C., Raisz, L.G., 2009a. Effects of prostaglandin E2 on bone in mice in vivo. Prostag. Other Lipid Mediat. 89, 20–25. https://doi.org/10.1016/j.prostaglandins.2009.03.003. Epub 2009 Mar 25.

Gao, Q., Zhan, P., Alander, C.B., Kream, B.E., Hao, C., Breyer, M.D., Pilbeam, C.C., Raisz, L.G., 2009b. Effects of global or targeted deletion of the EP4 receptor on the response of osteoblasts to prostaglandin in vitro and on bone histomorphometry in aged mice. Bone 45, 98–103.

Genetos, D.C., Yellowley, C.E., Loots, G.G., 2011. Prostaglandin E2 signals through PTGER2 to regulate sclerostin expression. PLoS One 6, e17772. https://doi.org/10.1371/journal.pone.0017772.

Gerstenfeld, L.C., Al-Ghawas, M., Alkhiary, Y.M., Cullinane, D.M., Krall, E.A., Fitch, J.L., Webb, E.G., Thiede, M.A., Einhorn, T.A., 2007. Selective and nonselective cyclooxygenase-2 inhibitors and experimental fracture-healing. Reversibility of effects after short-term treatment. J Bone Joint Surg. Am 89, 114–125.

Geusens, P., Emans, P.J., de Jong, J.J., van den Bergh, J., 2013. NSAIDs and fracture healing. Curr. Opin. Rheumatol. 25, 524–531. https://doi.org/10.1097/BOR.0b013e32836200b8.

Girasole, G., Passeri, G., Jilka, R.L., Manolagas, S.C., 1994. Interleukin-11: a new cytokine critical for osteoclast development. J. Clin. Investig. 93, 1516–1524.

Giunta, D., Keller, J., Nielsen, F.F., Melsen, B., 1995. Influence of indomethacin on bone turnover related to orthodontic tooth movement in miniature pigs. Am. J. Orthod. Dentofacial Orthop. 108, 361–366.

Grosch, S., Maier, T.J., Schiffmann, S., Geisslinger, G., 2006. Cyclooxygenase-2 (COX-2)-independent anticarcinogenic effects of selective COX-2 inhibitors. J. Natl. Cancer Inst. 98, 736–747.

Grosser, T., Ricciotti, E., FitzGerald, G.A., 2017a. The cardiovascular pharmacology of nonsteroidal anti-inflammatory drugs. Trends Pharmacol. Sci. 38, 733–748. https://doi.org/10.1016/j.tips.2017.05.008. Epub 2017 Jun 23.

Grosser, T., Theken, K.N., FitzGerald, G.A., 2017b. Cyclooxygenase inhibition: pain, inflammation, and the cardiovascular system. Clin. Pharmacol. Ther. 102, 611–622. https://doi.org/10.1002/cpt.794. Epub 2017 Aug 17.

Hackett, J.A., lard-Chamard, H., Sarrazin, P., de Fatima, L.M., Gallant, M.A., Fortier, I., Nader, M., Parent, J.L., Bkaily, G., de Brum-Fernandes, A.J., 2006. Prostaglandin production by human osteoclasts in culture. J. Rheumatol. 33, 1320–1328.

Han, Y., Cowin, S.C., Schaffler, M.B., Weinbaum, S., 2004. Mechanotransduction and strain amplification in osteocyte cell processes. Proc. Natl. Acad. Sci. U. S. A 101, 16689–16694.

Hara, S., 2017. Prostaglandin terminal synthases as novel therapeutic targets. Proc. Jpn. Acad. Ser. B Phys. Biol. Sci. 93, 703–723. https://doi.org/10.2183/pjab.93.044.

Hara, S., Kamei, D., Sasaki, Y., Tanemoto, A., Nakatani, Y., Murakami, M., 2010. Prostaglandin E synthases: understanding their pathophysiological roles through mouse genetic models. Biochimie 92, 651–659. https://doi.org/10.1016/j.biochi.2010.02.007. Epub 2010 Feb 14.

Harrison, J.R., Lorenzo, J.A., Kawaguchi, H., Raisz, L.G., Pilbeam, C.C., 1994. Stimulation of prostaglandin E_2 production by interleukin-1 and transforming growth factor-α in osteoblastic MC3T3-E1 cells. J. Bone Miner. Res. 9, 817–823.

Herschman, H.R., 1994. Regulation of prostaglandin synthase-1 and prostaglandin synthase-2. Cancer Metastasis Rev. 13, 241–256.

Hillsley, M.V., Frangos, J.A., 1994. Bone tissue engineering: the role of interstitial fluid flow. Biotechnol. Bioeng. 43, 573–581.

Hino, S., Tanji, C., Nakayama, K.I., Kikuchi, A., 2005. Phosphorylation of beta-catenin by cyclic AMP-dependent protein kinase stabilizes beta-catenin through inhibition of its ubiquitination. Mol. Cell Biol. 25, 9063–9072.

Hla, T., Neilson, K., 1992. Human cyclooxygenase-2 cDNA. Proc. Natl. Acad. Sci. U. S. A 89, 7384–7388.

Hurley, M.M., Lee, S.K., Raisz, L.G., Bernecker, P., Lorenzo, J., 1998. Basic fibroblast growth factor induces osteoclast formation in murine bone marrow cultures. Bone 22, 309–316.

Huang, K.C., Huang, T.W., Yang, T.Y., Lee, M.S., 2015. Chronic NSAIDs use increases the risk of a second hip fracture in patients after hip fracture surgery: evidence from a STROBE-compliant population-based study. Medicine (Baltimore) 94, e1566. https://doi.org/10.1097/MD.0000000000001566.

Inada, M., Matsumoto, C., Uematsu, S., Akira, S., Miyaura, C., 2006. Membrane-bound prostaglandin E synthase-1-mediated prostaglandin E2 production by osteoblast plays a critical role in lipopolysaccharide-induced bone loss associated with inflammation. J. Immunol. 177, 1879–1885.

Inoue, H., Tanaka, N., Uchiyama, C., 1995. Parathyroid hormone increases the number of tartrate-resistant acid phosphatase-positive cells through prostaglandin E2 synthesis in adherent cell culture of neonatal rat bones. Endocrinology 136, 3648–3656.

Ivey, K.N., Srivastava, D., 2006. The paradoxical patent ductus arteriosus. J. Clin. Investig. 116, 2863–2865.

Janssen, M.P., Caron, M.M., van Rietbergen, B., Surtel, D.A., van Rhijn, L.W., Welting, T.J., Emans, P.J., 2017. Impairment of the chondrogenic phase of endochondral ossification in vivo by inhibition of cyclooxygenase-2. Eur. Cells Mater. 34, 202–216. https://doi.org/10.22203/eCM.v034a13.

Jee, W.S., Ma, Y.F., 1997. The in vivo anabolic actions of prostaglandins in bone. Bone 21, 297–304.

Jiang, J., Dingledine, R., 2013. Prostaglandin receptor EP2 in the crosshairs of anti-inflammation, anti-cancer, and neuroprotection. Trends Pharmacol. Sci. 34, 413–423. https://doi.org/10.1016/j.tips.2013.05.003. Epub 2013 Jun 21.

Kaneki, H., Takasugi, I., Fujieda, M., Kiriu, M., Mizuochi, S., Ide, H., 1999. Prostaglandin E2 stimulates the formation of mineralized bone nodules by a cAMP-independent mechanism in the culture of adult rat calvarial osteoblasts. J. Cell. Biochem. 73, 36–48.

Kang, Y.J., Mbonye, U.R., Delong, C.J., Wada, M., Smith, W.L., 2007. Regulation of intracellular cyclooxygenase levels by gene transcription and protein degradation. Prog. Lipid Res. 46, 108–125.

Kawaguchi, H., Nemoto, K., Raisz, L.G., Harrison, J.R., Voznesensky, O.S., Alander, C.B., Pilbeam, C.C., 1996. Interleukin-4 inhibits prostaglandin G/H synthase-2 and cytosolic phospholipase A2 induction in neonatal mouse parietal bone cultures. J. Bone Miner. Res. 11, 358–366.

Kawaguchi, H., Pilbeam, C.C., Gronowicz, G., Abreu, C., Fletcher, B.S., Herschman, H.R., Raisz, L.G., Hurley, M.M., 1995. Transcriptional induction of prostaglandin G/H synthase-2 by basic fibroblast growth factor. J. Clin. Investig. 96, 923–930.

Kawaguchi, H., Raisz, L.G., Voznesensky, O.S., Alander, C.B., Hakeda, Y., Pilbeam, C.C., 1994. Regulation of the two prostaglandin G/H synthases by parathyroid hormone, interleukin-1, cortisol and prostaglandin E_2 in cultured neonatal mouse calvariae. Endocrinology 135, 1157–1164.

Kehoe, M.J., Cohen, S.M., Zarrinnia, K., Cowan, A., 1996. The effect of acetaminophen, ibuprofen, and misoprostol on prostaglandin E2 synthesis and the degree and rate of orthodontic tooth movement. Angle Orthod. 66, 339–349.

Keila, S., Pitaru, S., Grosskopf, A., Weinreb, M., 1994. Bone marrow from mechanically unloaded rat bones expresses reduced osteogenic capacity in vitro. J. Bone Miner. Res. 9, 321–327.

Kennedy, B.P., Payette, P., Mudgett, J., Vadas, P., Pruzanski, W., Kwan, M., Tang, C., Rancourt, D.E., Cromlish, W.A., 1995. A natural disruption of the secretory group II phospholipase A2 gene in inbred mouse strains. J. Biol. Chem. 270, 22378–22385.

Kirkby, N.S., Chan, M.V., Zaiss, A.K., Garcia-Vaz, E., Jiao, J., Berglund, L.M., Verdu, E.F., Ahmetaj-Shala, B., Wallace, J.L., Herschman, H.R., Gomez, M.F., Mitchell, J.A., 2016. Systematic study of constitutive cyclooxygenase-2 expression: role of NF-kappaB and NFAT transcriptional pathways. Proc. Natl. Acad. Sci. U. S. A 113, 434–439.

Kitase, Y., Barragan, L., Qing, H., Kondoh, S., Jiang, J.X., Johnson, M.L., Bonewald, L.F., 2010. Mechanical induction of PGE2 in osteocytes blocks glucocorticoid-induced apoptosis through both the beta-catenin and PKA pathways. J. Bone Miner. Res. 25, 2657–2668. https://doi.org/10.1002/jbmr.168. Epub 2010 Jun 24.

Klein-Nulend, J., Burger, E.H., Semeins, C.M., Raisz, L.G., Pilbeam, C.C., 1997. Pulsating fluid flow stimulates prostaglandin release and inducible prostaglandin G/H synthase mRNA expression in primary mouse bone cells. J. Bone Miner. Res. 12, 45–51.

Klein, D.C., Raisz, L.G., 1970. Prostaglandins: stimulation of bone resorption in tissue culture. Endocrinology 86, 1436–1440.

Knothe, T.M., Knothe, U., Niederer, P., 1998. Experimental elucidation of mechanical load-induced fluid flow and its potential role in bone metabolism and functional adaptation. Am. J. Med. Sci. 316, 189–195.

Kobayashi, Y., Mizoguchi, T., Take, I., Kurihara, S., Udagawa, N., Takahashi, N., 2005. Prostaglandin E2 enhances osteoclastic differentiation of precursor cells through protein kinase A-dependent phosphorylation of TAK1. J. Biol. Chem. 280, 11395–11403.

Konstantinidis, I., Papageorgiou, S.N., Kyrgidis, A., Tzellos, T.G., Kouvelas, D., 2013. Effect of non-steroidal anti-inflammatory drugs on bone turnover: an evidence-based review. Rev. Recent Clin. Trials 8, 48–60.

Korotkova, M., Westman, M., Gheorghe, K.R., af, K.E., Trollmo, C., Ulfgren, A.K., Klareskog, L., Jakobsson, P.J., 2005. Effects of antirheumatic treatments on the prostaglandin E2 biosynthetic pathway. Arthritis Rheum. 52, 3439–3447.

Kostenis, E., Ulven, T., 2006. Emerging roles of DP and CRTH2 in allergic inflammation. Trends Mol. Med. 12, 148–158.

Kotake, S., Udagawa, N., Takahashi, N., Matsuzaki, K., Itoh, K., Ishiyama, S., Saito, S., Inoue, K., Kamatani, N., Gillespie, M.T., Martin, T.J., Suda, T., 1999. IL-17 in synovial fluids from patients with rheumatoid arthritis is a potent stimulator of osteoclastogenesis. J. Clin. Investig. 103, 1345–1352.

Kujubu, D.A., Fletcher, B.S., Varnum, B.C., Lim, R.W., Herschman, H.R., 1991. TIS10, a phorbol ester tumor promoter-inducible mRNA from Swiss 3T3 cells, encodes a novel prostaglandin synthase/cyclooxygenase homologue. J. Biol. Chem. 266, 12866–12872.

Kulmacz, R.J., van der Donk, W.A., Tsai, A.L., 2003. Comparison of the properties of prostaglandin H synthase-1 and -2. Prog. Lipid Res. 42, 377–404.

Kurmis, A.P., Kurmis, T.P., O'Brien, J.X., Dalen, T., 2012. The effect of nonsteroidal anti-inflammatory drug administration on acute phase fracture-healing: a review. J. Bone Joint Surg. Am. 94, 815–823. https://doi.org/10.2106/JBJS.J.01743.

Lader, C.S., Flanagan, A.M., 1998. Prostaglandin E2, interleukin 1alpha, and tumor necrosis factor-alpha increase human osteoclast formation and bone resorption in vitro. Endocrinology 139, 3157–3164.

Lane, N.E., Bauer, D.C., Nevitt, M.C., Pressman, A.R., Cummings, S.R., 1997. Aspirin and nonsteroidal antiinflammatory drug use in elderly women: effects on a marker of bone resorption. The Study of Osteoporotic Fractures Research Group. J. Rheumatol. 24, 1132–1136.

Langenbach, R., Loftin, C., Lee, C., Tiano, H., 1999. Cyclooxygenase knockout mice: models for elucidating isoform-specific functions. Biochem. Pharmacol. 58, 1237–1246.

Langenbach, R., Morham, S.G., Tiano, H.F., Loftin, C.D., Ghanayem, B.I., Chulada, P.C., Mahler, J.F., Lee, C.A., Goulding, E.H., Kluckman, K.D., 1995. Prostaglandin synthase 1 gene disruption in mice reduces arachidonic acid-induced inflammation and indomethacin-induced gastric ulceration. Cell 83, 483–492.

Lanyon, L.E., 1992. Control of bone architecture by functional load bearing. J. Bone Miner. Res. 7, S369–S375.

Lara-Castillo, N., Kim-Weroha, N.A., Kamel, M.A., Javaheri, B., Ellies, D.L., Krumlauf, R.E., Thiagarajan, G., Johnson, M.L., 2015. In vivo mechanical loading rapidly activates beta-catenin signaling in osteocytes through a prostaglandin mediated mechanism. Bone 76, 58–66. https://doi.org/10.1016/j.bone.2015.03.019. Epub 2015 Mar 30.

Lasa, M., Brook, M., Saklatvala, J., Clark, A.R., 2001. Dexamethasone destabilizes cyclooxygenase 2 mRNA by inhibiting mitogen-activated protein kinase p38. Mol. Cell Biol. 21, 771–780.

Lerner, U.H., Ransjo, M., Ljunggren, O., 1987. Prostaglandin E2 causes a transient inhibition of mineral mobilization, matrix degradation, and lysosomal enzyme release from mouse calvarial bones in vitro. Calcif. Tissue Int. 40, 323–331.

Leslie, C.C., 2015. Cytosolic phospholipase A(2): physiological function and role in disease. J. Lipid Res. 56, 1386–1402.

Li, F., Fu, T., Tong, W.D., Liu, B.H., Li, C.X., Gao, Y., Wu, J.S., Wang, X.F., Zhang, A.P., 2016. Lubiprostone is effective in the treatment of chronic idiopathic constipation and irritable bowel syndrome: a systematic review and meta-analysis of randomized controlled trials. Mayo Clin. Proc. 91, 456–468.

Li, L., Pettit, A.R., Gregory, L.S., Forwood, M.R., 2006. Regulation of bone biology by prostaglandin endoperoxide H synthases (PGHS): a rose by any other name. Cytokine Growth Factor Rev. 17, 203–216.

Li, M., Healy, D.R., Li, Y., Simmons, H.A., Crawford, D.T., Ke, H.Z., Pan, L.C., Brown, T.A., Thompson, D.D., 2005. Osteopenia and impaired fracture healing in aged EP4 receptor knockout mice. Bone 37, 46–54.

Li, M., Thompson, D.D., Paralkar, V.M., 2007. Prostaglandin E(2) receptors in bone formation. Int. Orthop. 31, 767–772.

Li, M., Ke, H.Z., Qi, H., Healy, D.R., Li, Y., Crawford, D.T., Paralkar, V.M., Owen, T.A., Cameron, K.O., Lefker, B.A., Brown, T.A., Thompson, D.D., 2003. A novel, non-prostanoid EP2 receptor-selective prostaglandin E2 agonist stimulates local bone formation and enhances fracture healing. J. Bone Miner. Res. 18, 2033–2042.

Li, X., Fries, S., Li, R., Lawson, J.A., Propert, K.J., Diamond, S.L., Blair, I.A., FitzGerald, G.A., Grosser, T., 2014. Differential impairment of aspirin-dependent platelet cyclooxygenase acetylation by nonsteroidal antiinflammatory drugs. Proc. Natl. Acad. Sci. U. S. A. 111, 16830–16835. https://doi.org/10.1073/pnas.1406997111. Epub 2014 Nov 10.

Li, X., Mazaleuskaya, L.L., Ballantyne, L.L., Meng, H., FitzGerald, G.A., Funk, C.D., 2018a. Genomic and lipidomic analyses differentiate the compensatory roles of two COX isoforms during systemic inflammation in mice. J. Lipid Res. 59, 102–112. https://doi.org/10.1194/jlr.M080028. Epub 2017 Nov 27.

Li, X., Mazaleuskaya, L.L., Yuan, C., Ballantyne, L.L., Meng, H., Smith, W.L., Fitzgerald, G.A., Funk, C.D., 2018b. Flipping the cyclooxygenase (Ptgs) genes reveals isoform-specific compensatory functions. J. Lipid Res. 59, 89–101.

Li, X., Okada, Y., Pilbeam, C.C., Lorenzo, J.A., Kennedy, C.R., Breyer, R.M., Raisz, L.G., 2000. Knockout of the murine prostaglandin EP2 receptor impairs osteoclastogenesis in vitro. Endocrinology 141, 2054–2061.

Lim, H., Paria, B.C., Das, S.K., Dinchuk, J.E., Langenbach, R., Trzaskos, J.M., Dey, S.K., 1997. Multiple female reproductive failures in cyclooxygenase 2-deficient mice. Cell 91, 197–208.

Lin, B.Y., Jee, W.S.S., Ma, Y.F., Ke, H.Z., Kimmel, D.B., Li, X.J., 1994. Effects of prostaglandin E2 and risedronate administration on cancellous bone in older female rats. Bone 15, 489–496.

Loftin, C.D., Trivedi, D.B., Tiano, H.F., Clark, J.A., Lee, C.A., Epstein, J.A., Morham, S.G., Breyer, M.D., Nguyen, M., Hawkins, B.M., Goulet, J.L., Smithies, O., Koller, B.H., Langenbach, R., 2001. Failure of ductus arteriosus closure and remodeling in neonatal mice deficient in cyclooxygenase-1 and cyclooxygenase-2. Proc. Natl. Acad. Sci. U. S. A 98, 1059–1064.

MacPhee, M., Chepenik, K.P., Liddell, R.A., Nelson, K.K., Siracusa, L.D., Buchberg, A.M., 1995. The secretory phospholipase A2 gene is a candidate for the Mom1 locus, a major modifier of ApcMin-induced intestinal neoplasia. Cell 81, 957–966.

Markovic, T., Jakopin, Z., Dolenc, M.S., Mlinaric-Rascan, I., 2017. Structural features of subtype-selective EP receptor modulators. Drug Discov. Today 22, 57–71. https://doi.org/10.1016/j.drudis.2016.08.003. Epub 2016 Aug 6.

Marquez-Lara, A., Hutchinson, I.D., Nunez Jr., F., Smith, T.L., Miller, A.N., 2016. Nonsteroidal anti-inflammatory drugs and bone-healing: a systematic review of research quality. JBJS Rev. 4 (3) https://doi.org/10.2106/JBJS.RVW.O.00055, 01874474-201603000-00005.

Mbonye, U.R., Wada, M., Rieke, C.J., Tang, H.Y., DeWitt, D.L., Smith, W.L., 2006. The 19-amino acid cassette of cyclooxygenase-2 mediates entry of the protein into the endoplasmic reticulum-associated degradation system. J. Biol. Chem. 281, 35770–35778.

Mehrotra, M., Saegusa, M., Voznesensky, O., Pilbeam, C., 2006. Role of Cbfa1/Runx2 in the fluid shear stress induction of COX-2 in osteoblasts. Biochem. Biophys. Res. Commun. 341, 1225–1230.

Min, Y.K., Rao, Y., Okada, Y., Raisz, L.G., Pilbeam, C.C., 1998. Regulation of prostaglandin G/H synthase-2 expression by interleukin-1 in human osteoblast-like cells. J. Bone Miner. Res. 13, 1066–1075.

Mitchener, M.M., Hermanson, D.J., Shockley, E.M., Brown, H.A., Lindsley, C.W., Reese, J., Rouzer, C.A., Lopez, C.F., Marnett, L.J., 2015. Competition and allostery govern substrate selectivity of cyclooxygenase-2. Proc. Natl. Acad. Sci. U. S. A. 112, 12366–12371. https://doi.org/10.1073/pnas.1507307112. Epub 2015 Sep. 21.

Miyaura, C., Inada, M., Suzawa, T., Sugimoto, Y., Ushikubi, F., Ichikawa, A., Narumiya, S., Suda, T., 2000. Impaired bone resorption to prostaglandin E2 in prostaglandin E receptor EP4-knockout mice. J. Biol. Chem. 275, 19819–19823.

Morham, S.G., Langenbach, R., Loftin, C.D., Tiano, H.F., Vouloumanos, N., Jennette, J.C., Mahler, J.F., Kluckman, K.D., Ledford, A., Lee, C.A., 1995. Prostaglandin synthase 2 gene disruption causes severe renal pathology in the mouse. Cell 83, 473–482.

Morinaga, Y., Fujita, N., Ohishi, K., Zhang, Y., Tsuruo, T., 1998. Suppression of interleukin-11-mediated bone resorption by cyclooxygenases inhibitors. J. Cell. Physiol. 175, 247–254.

Murakami, M., Kuwata, H., Amakasu, Y., Shimbara, S., Nakatani, Y., Atsumi, G., Kudo, I., 1997. Prostaglandin E2 amplifies cytosolic phospholipase A2- and cyclooxygenase-2-dependent delayed prostaglandin E2 generation in mouse osteoblastic cells. Enhancement by secretory phospholipase A2. J. Biol. Chem. 272, 19891–19897.

Murakami, M., Sato, H., Miki, Y., Yamamoto, K., Taketomi, Y., 2015. A new era of secreted phospholipase A(2). J. Lipid Res. 56, 1248–1261.

Murakami, M., Taketomi, Y., Miki, Y., Sato, H., Hirabayashi, T., Yamamoto, K., 2011. Recent progress in phospholipase A(2) research: from cells to animals to humans. Prog. Lipid Res. 50, 152–192.

Murnaghan, M., Li, G., Marsh, D.R., 2006. Nonsteroidal anti-inflammatory drug-induced fracture nonunion: an inhibition of angiogenesis? J Bone Joint Surg. Am 88 (Suppl. 3), 140–147.

Myers, L.K., Bhattacharya, S.D., Herring, P.A., Xing, Z., Goorha, S., Smith, R.A., Bhattacharya, S.K., Carbone, L., Faccio, R., Kang, A.H., Ballou, L.R., 2006. The isozyme-specific effects of cyclooxygenase-deficiency on bone in mice. Bone 39, 1048–1052.

Nagata, T., Kaho, K., Nishikawa, S., Shinohara, H., Wakano, Y., Ishida, H., 1994. Effect of prostaglandin E_2 on mineralization of bone nodules formed by fetal rat calvarial cells. Calcif. Tissue Int. 55, 451–457.

Newton, R., Seybold, J., Kuitert, L.M., Bergmann, M., Barnes, P.J., 1998. Repression of cyclooxygenase-2 and prostaglandin E2 release by dexamethasone occurs by transcriptional and post-transcriptional mechanisms involving loss of polyadenylated mRNA. J. Biol. Chem. 273, 32312–32321.

Nishigaki, N., Negishi, M., Ichikawa, A., 1996. Two Gs-coupled prostaglandin E receptor subtypes, EP2 and EP4, differ in desensitization and sensitivity to the metabolic inactivation of the agonist. Mol. Pharmacol. 50, 1031–1037.

Norrdin, R.W., Shih, M.S., 1988. Systemic effects of prostaglandin E2 on vertebral trabecular remodeling in beagles used in a healing study. Calcif. Tissue Int. 42, 363–368.

North, T.E., Goessling, W., Walkley, C.R., Lengerke, C., Kopani, K.R., Lord, A.M., Weber, G.J., Bowman, T.V., Jang, I.H., Grosser, T., Fitzgerald, G.A., Daley, G.Q., Orkin, S.H., Zon, L.I., 2007. Prostaglandin E2 regulates vertebrate haematopoietic stem cell homeostasis. Nature 447, 1007–1011.

Norvell, S.M., Ponik, S.M., Bowen, D.K., Gerard, R., Pavalko, F.M., 2004. Fluid shear stress induction of COX-2 protein and prostaglandin release in cultured MC3T3-E1 osteoblasts does not require intact microfilaments or microtubules. J. Appl. Physiol. 96, 957–966.

Norwood, V.F., Morham, S.G., Smithies, O., 2000. Postnatal development and progression of renal dysplasia in cyclooxygenase-2 null mice. Kidney Int. 58, 2291–2300.

O'Banion, M.K., Sadowski, H.B., Winn, V., Young, D.A., 1991. A serum- and glucorticoid-regulated 4-kilobase mRNA encodes a cyclooxygenase-related protein. J. Biol. Chem. 266, 23261–23267.

O'Callaghan, G., Houston, A., 2015. Prostaglandin E2 and the EP receptors in malignancy: possible therapeutic targets? Br. J. Pharmacol. 172, 5239–5250. https://doi.org/10.1111/bph.13331. Epub 2015 Oct 26.

O'Connor, J.P., Manigrasso, M.B., Kim, B.D., Subramanian, S., 2014. Fracture healing and lipid mediators. BoneKEy Rep. 3, 517. https://doi.org/10.1038/bonekey.2014.12 eCollection 2014.

O'Keefe, R.J., Tiyapatanaputi, P., Xie, C., Li, T.F., Clark, C., Zuscik, M.J., Chen, D., Drissi, H., Schwarz, E., Zhang, X., 2006. COX-2 has a critical role during incorporation of structural bone allografts. Ann. N. Y. Acad. Sci. 1068, 532–542.

Okada, Y., Lorenzo, J.A., Freeman, A.M., Tomita, M., Morham, S.G., Raisz, L.G., Pilbeam, C.C., 2000a. Prostaglandin G/H synthase-2 is required for maximal formation of osteoclast-like cells in culture. J. Clin. Investig. 105, 823–832.

Okada, Y., Tomita, M., Gronowicz, G., Kawaguchi, H., Sohn, J., Tanaka, Y., Morimoto, I., Nakamura, T., Raisz, L., Pilbeam, C., 2000b. Effects of cyclooxygenase-2 gene disruption on osteoblastic function. J. Bone Miner. Res. 15, S217.

Ono, K., Akatsu, T., Murakami, T., Nishikawa, M., Yamamoto, M., Kugai, N., Motoyoshi, K., Nagata, N., 1998. Important role of EP4, a subtype of prostaglandin (PG) E receptor, in osteoclast-like cell formation from mouse bone marrow cells induced by PGE2 [published erratum appears in J Endocrinol 1998 Dec; 159(3):527] J. Endocrinol. 158, R1−R5.

Ono, K., Kaneko, H., Choudhary, S., Pilbeam, C.C., Lorenzo, J.A., Akatsu, T., Kugai, N., Raisz, L.G., 2005. Biphasic effect of prostaglandin E2 on osteoclast formation in spleen cell cultures: role of the EP2 receptor. J. Bone Miner. Res. 20, 23−29.

Pai, R., Soreghan, B., Szabo, I.L., Pavelka, M., Baatar, D., Tarnawski, A.S., 2002. Prostaglandin E2 transactivates EGF receptor: a novel mechanism for promoting colon cancer growth and gastrointestinal hypertrophy. Nat. Med. 8, 289−293.

Paik, J.H., Ju, J.H., Lee, J.Y., Boudreau, M.D., Hwang, D.H., 2000. Two opposing effects of non-steroidal anti-inflammatory drugs on the expression of the inducible cyclooxygenase. Mediation through different signaling pathways. J. Biol. Chem. 275, 28173−28179.

Paralkar, V.M., Borovecki, F., Ke, H.Z., Cameron, K.O., Lefker, B., Grasser, W.A., Owen, T.A., Li, M., DaSilva-Jardine, P., Zhou, M., Dunn, R.L., Dumont, F., Korsmeyer, R., Krasney, P., Brown, T.A., Plowchalk, D., Vukicevic, S., Thompson, D.D., 2003. An EP2 receptor-selective prostaglandin E2 agonist induces bone healing. Proc. Natl. Acad. Sci. U. S. A 100, 6736−6740.

Pavalko, F.M., Chen, N.X., Turner, C.H., Burr, D.B., Atkinson, S., Hsieh, Y.F., Qiu, J., Duncan, R.L., 1998. Fluid shear-induced mechanical signaling in MC3T3-E1 osteoblasts requires cytoskeleton-integrin interactions. Am. J. Physiol. 275, C1591−C1601.

Pead, M.J., Lanyon, L.E., 1989. Indomethacin modulation of load-related stimulation of new bone formation in vivo. Calcif. Tissue Int. 45, 34−40.

Pilbeam, C., Rao, Y., Voznesensky, O., Kawaguchi, H., Alander, C., Raisz, L.G., Herschman, H., 1997a. Transforming growth factor-β1 regulation of prostaglandin G/H syntase-2 expression in osteoblastic MC3T3-E1 cells. Endocrinology 138, 4672−4682.

Pilbeam, C.C., Fall, P.M., Alander, C.B., Raisz, L.G., 1997b. Differential effects of nonsteroidal anti-inflammatory drugs on constitutive and inducible prostaglandin G/H synthase in cultured bone cells. J. Bone Miner. Res. 12, 1198−1203.

Pilbeam, C.C., Kawaguchi, H., Hakeda, Y., Voznesensky, O., Alander, C.B., Raisz, L.G., 1993. Differential regulation of inducible and constitutive prostaglandin endoperoxide synthase in osteoblastic MC3T3-E1 cells. J. Biol. Chem. 268, 25643−25649.

Pilbeam, C.C., Raisz, L.G., Voznesensky, O., Alander, C.B., Delman, B.N., Kawaguchi, K., 1994. Autoregulation of inducible prostaglandin G/H synthase in osteoblastic cells by prostaglandins. J. Bone Miner. Res. 10, 406−414.

Pountos, I., Georgouli, T., Calori, G.M., Giannoudis, P.V., 2012. Do nonsteroidal anti-inflammatory drugs affect bone healing? A critical analysis. ScientificWorldJournal 2012, 606404. https://doi.org/10.1100/2012/606404. Epub 2012 Jan 4.

Price, J.S., Sugiyama, T., Galea, G.L., Meakin, L.B., Sunters, A., Lanyon, L.E., 2011. Role of endocrine and paracrine factors in the adaptation of bone to mechanical loading. Curr. Osteoporos. Rep. 9, 76−82. https://doi.org/10.1007/s11914-011-0050-7.

Psarra, A., Nikolaou, A., Kokotou, M.G., Limnios, D., Kokotos, G., 2017. Microsomal prostaglandin E2 synthase-1 inhibitors: a patent review. Expert Opin. Ther. Pat. 27, 1047−1059. https://doi.org/10.1080/13543776.2017.1344218. Epub 2017 Jun 26.

Raisz, L.G., Alander, C.B., Fall, P.M., Simmons, H.A., 1990. Effects of prostaglandin $F_{2\alpha}$ on bone formation and resorption in cultured neonatal mouse calvariae: role of prostaglandin E_2 production. Endocrinology 126, 1076−1079.

Raisz, L.G., Sandberg, A.L., Goodson, J.M., Simmons, H.A., Mergenhagen, S.E., 1974. Complement-dependent stimulation of prostaglandin synthesis and bone resorption. Science 185, 789−791.

Raisz, L.G., Woodiel, F.N., 2003. Effects of selective prostaglandin EP2 and EP4 receptor agonists on bone resorption and formation in fetal rat organ cultures. Prostag. Other Lipid Mediat. 71, 287−292.

Rawlinson, S.C.F., El-Haj, A.J., Minter, S.L., Tavares, I.A., Bennett, A., Lanyon, L.E., 1991. Loading-related increases in prostaglandin production in cores of adult canine cancellous bone in vitro: a role for prostacyclin in adaptive bone remodeling? J. Bone Miner. Res. 6, 1345−1352.

Ricciotti, E., Yu, Y., Grosser, T., Fitzgerald, G.A., 2013. COX-2, the dominant source of prostacyclin. Proc. Natl. Acad. Sci. U. S. A. 110, E183. https://doi.org/10.1073/pnas.1219073110. Epub 2013 Jan 4.

Richards, J.B., Joseph, L., Schwartzman, K., Kreiger, N., Tenenhouse, A., Goltzman, D., 2006. The effect of cyclooxygenase-2 inhibitors on bone mineral density: results from the Canadian Multicentre Osteoporosis Study. Osteoporos. Int. 17, 1410−1419.

Robertson, G., Xie, C., Chen, D., Awad, H., Schwarz, E.M., O'Keefe, R.J., Guldberg, R.E., Zhang, X., 2006. Alteration of femoral bone morphology and density in COX-2-/- mice. Bone 39, 767−772.

Rouzer, C.A., Marnett, L.J., 2011. Endocannabinoid oxygenation by cyclooxygenases, lipoxygenases, and cytochromes P450: cross-talk between the eicosanoid and endocannabinoid signaling pathways. Chem. Rev. 111, 5899−5921. https://doi.org/10.1021/cr2002799. Epub 2011 Sep. 19.

Sagi, H.C., Jordan, C.J., Barei, D.P., Serrano-Riera, R., Steverson, B., 2014. Indomethacin prophylaxis for heterotopic ossification after acetabular fracture surgery increases the risk for nonunion of the posterior wall. J. Orthop. Trauma 28, 377−383. https://doi.org/10.1097/BOT.0000000000000049.

Sakuma, Y., Li, Z., Pilbeam, C.C., Alander, C.B., Chikazu, D., Kawaguchi, H., Raisz, L.G., 2004. Stimulation of cAMP production and cyclooxygenase-2 by prostaglandin E(2) and selective prostaglandin receptor agonists in murine osteoblastic cells. Bone 34, 827−834.

Sakuma, Y., Tanaka, K., Suda, M., Komatsu, Y., Yasoda, A., Miura, M., Ozasa, A., Narumiya, S., Sugimoto, Y., Ichikawa, A., Ushikubi, F., Nakao, K., 2000. Impaired bone resorption by lipopolysaccharide in vivo in mice deficient in the prostaglandin E receptor EP4 subtype. Infect. Immun. 68, 6819−6825.

Sampey, A.V., Hutchinson, P., Morand, E.F., 2000. Annexin I and dexamethasone effects on phospholipase and cyclooxygenase activity in human synoviocytes. Mediat. Inflamm. 9, 125−132.

Sandy, J.R., Farndale, R.W., Meikle, M.C., 1993. Recent advances in understanding mechanically induced bone remodeling and their relevance to orthodontic theory and practice. Am. J. Orthod. Dentofacial Orthop. 103, 212−222.

Sato, T., Morita, I., Murota, S., 1997. Prostaglandin E2 mediates parathyroid hormone induced osteoclast formation by cyclic AMP independent mechanism. Adv. Exp. Med. Biol. 407 (383−6), 383−386.

Sato, T., Morita, I., Sakaguchi, K., Nakahama, K.I., Smith, W.L., DeWitt, D.L., Murota, S.I., 1996. Involvement of prostaglandin endoperoxide H synthase-2 in osteoclast-like cell formation induced by interleukin-1 beta. J. Bone Miner. Res. 11, 392–400.

Scutt, A., Bertram, P., 1995. Bone marrow cells are targets for the anabolic actions of prostaglandin E_2 on bone: induction of a transition from nonadherent to adherent osteoblast precursors. J. Bone Miner. Res. 10, 474–487.

Segi, E., Sugimoto, Y., Yamasaki, A., Aze, Y., Oida, H., Nishimura, T., Murata, T., Matsuoka, T., Ushikubi, F., Hirose, M., Tanaka, T., Yoshida, N., Narumiya, S., Ichikawa, A., 1998. Patent ductus arteriosus and neonatal death in prostaglandin receptor EP4-deficient mice. Biochem. Biophys. Res. Commun. 246, 7–12.

Shao, J., Jung, C., Liu, C., Sheng, H., 2005. Prostaglandin E2 Stimulates the beta-catenin/T cell factor-dependent transcription in colon cancer. J. Biol. Chem. 280, 26565–26572.

Shao, J., Lee, S.B., Guo, H., Evers, B.M., Sheng, H., 2003. Prostaglandin E2 stimulates the growth of colon cancer cells via induction of amphiregulin. Cancer Res. 63, 5218–5223.

Shinar, D., Rodan, G.A., 1990. Biphasic effects of transforming growth factor-beta on the production of osteoclast-like cells in mouse bone marrow cultures: the role of prostaglandins in the generation of these cells. Endocrinology 126, 3153–3158.

Simmons, D.L., Botting, R.M., Hla, T., 2004. Cyclooxygenase isozymes: the biology of prostaglandin synthesis and inhibition. Pharmacol. Rev. 56, 387–437.

Simon, A.M., O'Connor, J.P., 2007. Dose and time-dependent effects of cyclooxygenase-2 inhibition on fracture-healing. J Bone Joint Surg. Am 89, 500–511.

Sivaganesan, A., Chotai, S., White-Dzuro, G., McGirt, M.J., Devin, C.J., 2017. The effect of NSAIDs on spinal fusion: a cross-disciplinary review of biochemical, animal, and human studies. Eur. Spine J. 26, 2719–2728. https://doi.org/10.1007/s00586-017-5021-y. Epub 2017 Mar 10.

Smith, W.L., DeWitt, D.L., Garavito, R.M., 2000. Cyclooxygenases: structural, cellular, and molecular biology. Annu. Rev. Biochem. 69, 145–182.

Smith, W.L., Langenbach, R., 2001. Why there are two cyclooxygenase isozymes. J. Clin. Investig. 107, 1491–1495.

Smith, W.L., Urade, Y., Jakobsson, P.J., 2011. Enzymes of the cyclooxygenase pathways of prostanoid biosynthesis. Chem. Rev. 111, 5821–5865.

Soreide, E., Granan, L.P., Hjorthaug, G.A., Espehaug, B., Dimmen, S., Nordsletten, L., 2016. The effect of limited perioperative nonsteroidal anti-inflammatory drugs on patients undergoing anterior cruciate ligament reconstruction. Am. J. Sports Med. 44, 3111–3118. https://doi.org/10.1177/0363546516657539. Epub 2016 Aug 5.

Srinivasan, S., Gross, T.S., 2000. Canalicular fluid flow induced by bending of a long bone. Med. Eng. Phys. 22, 127–133.

Suda, K., Udagawa, N., Sato, N., Takami, M., Itoh, K., Woo, J.T., Takahashi, N., Nagai, K., 2004. Suppression of osteoprotegerin expression by prostaglandin E2 is crucially involved in lipopolysaccharide-induced osteoclast formation. J. Immunol. 172, 2504–2510.

Sugimoto, Y., Narumiya, S., 2007. Prostaglandin E receptors. J. Biol. Chem. 282, 11613–11617.

Sugiyama, T., Meakin, L.B., Galea, G.L., Lanyon, L.E., Price, J.S., 2013. The cyclooxygenase-2 selective inhibitor NS-398 does not influence trabecular or cortical bone gain resulting from repeated mechanical loading in female mice. Osteoporos. Int. 24, 383–388. https://doi.org/10.1007/s00198-012-1922-0. Epub 2012 Feb 14.

Sun, L., Ye, R.D., 2016. Serum amyloid A1: structure, function and gene polymorphism. Gene 583, 48–57.

Suponitzky, I., Weinreb, M., 1998. Differential effects of systemic prostaglandin E2 on bone mass in rat long bones and calvariae. J. Endocrinol. 156, 51–57.

Suzawa, T., Miyaura, C., Inada, M., Maruyama, T., Sugimoto, Y., Ushikubi, F., Ichikawa, A., Narumiya, S., Suda, T., 2000. The role of prostaglandin E receptor subtypes (EP1, EP2, EP3, and EP4) in bone resorption: an analysis using specific agonists for the respective EPs. Endocrinology 141, 1554–1559.

Swinney, D.C., Mak, A.Y., Barnett, J., Ramesha, C.S., 1997. Differential allosteric regulation of prostaglandin H synthase 1 and 2 by arachidonic acid. J. Biol. Chem. 272, 12393–12398.

Tai, H., Miyaura, C., Pilbeam, C.C., Tamura, T., Ohsugi, Y., Koishihara, Y., Kubodera, N., Kawaguchi, H., Raisz, L.G., Suda, T., 1997. Transcriptional induction of cyclooxygenase-2 in osteoblasts is involved in interleukin-6-induced osteoclast formation. Endocrinology 138, 2372–2379.

Tai, H.H., Cho, H., Tong, M., Ding, Y., 2006. NAD+-linked 15-hydroxyprostaglandin dehydrogenase: structure and biological functions. Curr. Pharmaceut. Des. 12, 955–962.

Take, I., Kobayashi, Y., Yamamoto, Y., Tsuboi, H., Ochi, T., Uematsu, S., Okafuji, N., Kurihara, S., Udagawa, N., Takahashi, N., 2005. Prostaglandin E2 strongly inhibits human osteoclast formation. Endocrinology 146, 5204–5214.

Tan, S., Chen, X., Xu, M., Huang, X., Liu, H., Jiang, J., Lu, Y., Peng, X., Wu, B., 2017. PGE2/EP4 receptor attenuated mucosal injury via beta-arrestin1/Src/EGFR-mediated proliferation in portal hypertensive gastropathy. Br. J. Pharmacol. 174, 848–866. https://doi.org/10.1111/bph.13752. Epub 2017 Mar 25.

Tang, C.H., Yang, R.S., Fu, W.M., 2005. Prostaglandin E2 stimulates fibronectin expression through EP1 receptor, phospholipase C, protein kinase Calpha, and c-Src pathway in primary cultured rat osteoblasts. J. Biol. Chem. 280, 22907–22916.

Tanaka, M., Sakai, A., Uchida, S., Tanaka, S., Nagashima, M., Katayama, T., Yamaguchi, K., Nakamura, T., 2004. Prostaglandin E2 receptor (EP4) selective agonist (ONO-4819.CD) accelerates bone repair of femoral cortex after drill-hole injury associated with local upregulation of bone turnover in mature rats. Bone 34, 940–948.

Tanioka, T., Nakatani, Y., Semmyo, N., Murakami, M., Kudo, I., 2000. Molecular identification of cytosolic prostaglandin E_2 synthase that is functionally coupled with cyclooxygenase-1 in immediate prostaglandin E_2 biosynthesis. J. Biol. Chem. 275, 32775–82.

Tetradis, S., Pilbeam, C.C., Liu, Y., Herschman, H.R., Kream, B.E., 1997. Parathyroid hormone increases prostaglandin G/H synthase-2 transcription by a cyclic adenosine 3',5'-month nophosphate-mediated pathway in murine osteoblastic MC3T3-E1 cells. Endocrinology 138, 3594–3600.

Tetradis, S., Pilbeam, C.C., Liu, Y., Kream, B.E., 1996. Parathyroid hormone induces prostaglandin G/H synthase-2 expression by a cyclic adenosine 3',5'-monophosphate-mediated pathway in the murine osteoblastic cell line MC3T3-E1. Endocrinology 137, 5435–5440.

Tomita, M., Li, X., Okada, Y., Woodiel, F.N., Young, R.N., Pilbeam, C.C., Raisz, L.G., 2002. Effects of selective prostaglandin EP4 receptor antagonist on osteoclast formation and bone resorption in vitro. Bone 30, 159–163.

Trebino, C.E., Stock, J.L., Gibbons, C.P., Naiman, B.M., Wachtmann, T.S., Umland, J.P., Pandher, K., Lapointe, J.M., Saha, S., Roach, M.L., Carter, D., Thomas, N.A., Durtschi, B.A., McNeish, J.D., Hambor, J.E., Jakobsson, P.J., Carty, T.J., Perez, J.R., Audoly, L.P., 2003. Impaired inflammatory and pain responses in mice lacking an inducible prostaglandin E synthase. Proc. Natl. Acad. Sci. U. S. A 100, 9044–9049.

Tsukii, K., Shima, N., Mochizuki, S., Yamaguchi, K., Kinosaki, M., Yano, K., Shibata, O., Udagawa, N., Yasuda, H., Suda, T., Higashio, K., 1998. Osteoclast differentiation factor mediates an essential signal for bone resorption induced by 1 alpha,25-dihydroxyvitamin D3, prostaglandin E2, or parathyroid hormone in the microenvironment of bone. Biochem. Biophys. Res. Commun. 246, 337–341 [In Process Citation].

Tu, X., Rhee, Y., Condon, K.W., Bivi, N., Allen, M.R., Dwyer, D., Stolina, M., Turner, C.H., Robling, A.G., Plotkin, L.I., Bellido, T., 2012. Sost downregulation and local Wnt signaling are required for the osteogenic response to mechanical loading. Bone 50, 209–217. https://doi.org/10.1016/j.bone.2011.10.025. Epub 2011 Oct 30.

Turner, C.H., Forwood, M.R., Otter, M.W., 1994. Mechanotransduction in bone: do bone cells act as sensors of fluid flow? FASEB J. 8, 875–878.

Ueda, K., Saito, A., Nakano, H., Aoshima, M., Yokota, M., Muraoka, R., Iwaya, T., 1980. Cortical hyperostosis following long-term administration of prostaglandin E1 in infants with cyanotic congenital heart disease. J. Pediatr. 97, 834–836.

Uhlar, C.M., Whitehead, A.S., 1999. Serum amyloid A, the major vertebrate acute-phase reactant. Eur. J. Biochem. 265, 501–523.

Vasquez, A.M., Mouchlis, V.D., Dennis, E.A., 2017. Review of four major distinct types of human phospholipase A2. Adv. Biol. Regul. 10.

von Euler, U., 1936. On specific vasodilating and plain muscle stimulating substances from accessory genital glands in man and certain animals (prostaglandin and vesiglandin). J. Physiol. 88, 213–234.

Wadhwa, S., Choudhary, S., Voznesensky, M., Epstein, M., Raisz, L., Pilbeam, C., 2002a. Fluid flow induces COX-2 expression in MC3T3-E1 osteoblasts via a PKA signaling pathway. Biochem. Biophys. Res. Commun. 297, 46–51.

Wadhwa, S., Godwin, S.L., Peterson, D.R., Epstein, M.A., Raisz, L.G., Pilbeam, C.C., 2002b. Fluid flow induction of cyclo-oxygenase 2 gene expression in osteoblasts is dependent on an extracellular signal-regulated kinase signaling pathway. J. Bone Miner. Res. 17, 266–274.

Wang, H., Ma, W.G., Tejada, L., Zhang, H., Morrow, J.D., Das, S.K., Dey, S.K., 2004. Rescue of female infertility from the loss of cyclooxygenase-2 by compensatory up-regulation of cyclooxygenase-1 is a function of genetic makeup. J. Biol. Chem. 279, 10649–10658.

Watanabe, K., Kurihara, K., Tokunaga, Y., Hayaishi, O., 1997. Two types of microsomal prostaglandin E synthase: glutathione-dependent and -independent prostaglandin E synthases. Biochem. Biophys. Res. Commun. 235, 148–152.

Weinbaum, S., Cowin, S.C., Zeng, Y., 1994. A model for the excitation of osteocytes by mechanical loading- induced bone fluid shear stresses. J. Biomech. 27, 339–360.

Weinreb, M., Suponitzky, I., Keila, S., 1997. Systemic administration of an anabolic dose of PGE2 in young rats increases the osteogenic capacity of bone marrow. Bone 20, 521–526.

Wiktorowska-Owczarek, A., Berezinska, M., Nowak, J.Z., 2015. PUFAs: structures, metabolism and functions. Adv. Clin. Exp. Med. 24, 931–941.

Wilson, N.H., 2004. Synthetic eicosanoids. In: Curtis-Prior, P. (Ed.), The Eicosanoids. John Wiley & Sons, Ltd, West Sussex, England.

Woodward, D.F., Jones, R.L., Narumiya, S., 2011. International Union of Basic and Clinical Pharmacology. LXXXIII: classification of prostanoid receptors, updating 15 years of progress. Pharmacol. Rev. 63, 471–538. https://doi.org/10.1124/pr.110.003517. Epub 2011 Jul 13.

Xie, C., Liang, B., Xue, M., Lin, A.S., Loiselle, A., Schwarz, E.M., Guldberg, R.E., O'Keefe, R.J., Zhang, X., 2009. Rescue of impaired fracture healing in COX-2-/- mice via activation of prostaglandin E2 receptor subtype 4. Am. J. Pathol. 175, 772–785. https://doi.org/10.2353/ajpath.2009.081099. Epub 2009 Jul 23.

Xie, W.L., Chipman, J.G., Robertson, D.L., Erikson, R.L., Simmons, D.L., 1991. Expression of a mitogen-responsive gene encoding prostaglandin synthase is regulated by mRNA splicing. Proc. Natl. Acad. Sci. U. S. A 88, 2692–2696.

Xu, M., Choudhary, S., Goltzman, D., Ledgard, F., Adams, D., Gronowicz, G., Koczon-Jaremko, B., Raisz, L., Pilbeam, C., 2005. Do cyclooxygenase knockout mice have primary hyperparathyroidism? Endocrinology 146, 1843–1853.

Xu, M., Choudhary, S., Voznesensky, O., Gao, Q., Adams, D., Diaz-Doran, V., Wu, Q., Goltzman, D., Raisz, L.G., Pilbeam, C.C., 2010. Basal bone phenotype and increased anabolic responses to intermittent parathyroid hormone in healthy male COX-2 knockout mice. Bone 47, 341–352.

Xu, Z., Choudhary, S., Alander, C.B., Raisz, L.G., Pilbeam, C.C., 2004. Effects of cyclooxygenase-2 gene disruption on osteoblastic cell growth. J. Bone Miner. Res. 17, S340.

Xu, Z., Choudhary, S., Okada, Y., Voznesensky, O., Alander, C., Raisz, L., Pilbeam, C., 2007. Cyclooxygenase-2 gene disruption promotes proliferation of murine calvarial osteoblasts in vitro. Bone 41, 68–76.

Xu, Z., Choudhary, S., Voznesensky, O., Mehrotra, M., Woodard, M., Hansen, M., Herschman, H., Pilbeam, C., 2006. Overexpression of COX-2 in human osteosarcoma cells decreases proliferation and increases apoptosis. Cancer Res. 66, 6657–6664.

Ye, R.D., Sun, L., 2015. Emerging functions of serum amyloid A in inflammation. J. Leukoc. Biol. 98, 923–929.

Ye, Z., Lu, H., Guo, W., Dai, W., Li, H., Yang, H., Li, L., 2016. The effect of alprostadil on preventing contrast-induced nephropathy for percutaneous coronary intervention in diabetic patients: a systematic review and meta-analysis. Medicine (Baltim.) 95, e5306.

Yokoyama, U., Iwatsubo, K., Umemura, M., Fujita, T., Ishikawa, Y., 2013. The prostanoid EP4 receptor and its signaling pathway. Pharmacol. Rev. 65, 1010–1052. https://doi.org/10.1124/pr.112.007195. Print 2013 Jul.

Yoshida, K., Oida, H., Kobayashi, T., Maruyama, T., Tanaka, M., Katayama, T., Yamaguchi, K., Segi, E., Tsuboyama, T., Matsushita, M., Ito, K., Ito, Y., Sugimoto, Y., Ushikubi, F., Ohuchida, S., Kondo, K., Nakamura, T., Narumiya, S., 2002. Stimulation of bone formation and prevention of bone loss by prostaglandin E EP4 receptor activation. Proc. Natl. Acad. Sci. U. S. A 99, 4580–4585.

Yu, Y., Fan, J., Hui, Y., Rouzer, C.A., Marnett, L.J., Klein-Szanto, A.J., Fitzgerald, G.A., Funk, C.D., 2007. Targeted cyclooxygenase gene (ptgs) exchange reveals discriminant isoform functionality. J. Biol. Chem. 282, 1498–1506.

Yuan, C., Smith, W.L., 2015. A cyclooxygenase-2-dependent prostaglandin E2 biosynthetic system in the Golgi apparatus. J. Biol. Chem. 290, 5606–5620.

Zhan, P., Alander, C., Kaneko, H., Pilbeam, C.C., Guan, Y., Zhang, Y., Breyer, M.D., Raisz, L.G., 2005. Effect of deletion of the prostaglandin EP4 receptor on stimulation of calcium release from cultured mouse calvariae: impaired responsiveness in heterozygotes. Prostag. Other Lipid Mediat. 78, 19–26.

Zhang, J., Goorha, S., Raghow, R., Ballou, L.R., 2002a. The tissue-specific, compensatory expression of cyclooxygenase-1 and -2 in transgenic mice. Prostag. Other Lipid Mediat. 67, 121–135.

Zhang, M., Feigenson, M., Sheu, T.J., Awad, H.A., Schwarz, E.M., Jonason, J.H., Loiselle, A.E., O'Keefe, R.J., 2015a. Loss of the PGE2 receptor EP1 enhances bone acquisition, which protects against age and ovariectomy-induced impairments in bone strength. Bone 72, 92–100. https://doi.org/10.1016/j.bone.2014.11.018. Epub 2014 Nov 29.

Zhang, M., Ho, H.C., Sheu, T.J., Breyer, M.D., Flick, L.M., Jonason, J.H., Awad, H.A., Schwarz, E.M., O'Keefe, R.J., 2011. EP1(-/-) mice have enhanced osteoblast differentiation and accelerated fracture repair. J. Bone Miner. Res. 26, 792–802.

Zhang, X., Schwarz, E.M., Young, D.A., Puzas, J.E., Rosier, R.N., O'Keefe, R.J., 2002b. Cyclooxygenase-2 regulates mesenchymal cell differentiation into the osteoblast lineage and is critically involved in bone repair. J. Clin. Investig. 109, 1405–1415.

Zhang, Y., Desai, A., Yang, S.Y., Bae, K.B., Antczak, M.I., Fink, S.P., Tiwari, S., Willis, J.E., Williams, N.S., Dawson, D.M., Wald, D., Chen, W.D., Wang, Z., Kasturi, L., Larusch, G.A., He, L., Cominelli, F., Di, M.L., Djuric, Z., Milne, G.L., Chance, M., Sanabria, J., Dealwis, C., Mikkola, D., Naidoo, J., Wei, S., Tai, H.H., Gerson, S.L., Ready, J.M., Posner, B., Willson, J.K., Markowitz, S.D., 2015b. Tissue Regeneration. Inhibition of the prostaglandin-degrading enzyme 15-PGDH potentiates tissue regeneration. Science 348, aaa2340.

Chapter 52

The molecular actions of parathyroid hormone/parathyroid hormone–related protein receptor type 1 and their implications

Michael Mannstadt and Marc N. Wein

Endocrine Unit, Massachusetts General Hospital, Harvard Medical School, Boston, MA, United States

Chapter outline

Introduction

The primary effects of parathyroid hormone (PTH) are to regulate calcium and phosphate homeostasis through signaling in kidney and bone. The parathyroid hormone–related protein (PTHrP) exerts multiple roles during bone, skin, and breast development. PTH and PTHrP trigger downstream signaling in cells through a common shared G-protein-coupled receptor, PTH/PTHrP receptor type 1 (PTH1R) (Gardella and Juppner, 2000). Beyond the crucial roles of PTH and PTHrP in mineral ion homeostasis and development, both hormones play central roles in diseases including osteoporosis, chronic kidney disease, bone metastases, and cancer-related hypercalcemia and cachexia. The PTH/PTHrP analogs teriparatide and abaloparatide are the only FDA-approved osteoporosis medications that stimulate new bone formation (Rubin and Bilizekian, 2003).

Given the immense importance of this signaling system in physiology and disease, it is not surprising that considerable progress has been made in understanding the molecular events immediately downstream of PTH1R signaling (Cheloha et al., 2015). Here we will review recent progress in our understanding of these signaling events. With this information in hand, we will discuss illustrative mechanisms used by PTH/PTHrP to influence the behavior of target cells in kidney and

Principles of Bone Biology. https://doi.org/10.1016/B978-0-12-814841-9.00052-X

bone in vivo. Notably, the vast majority of our current knowledge in this area derives from studies in which cells or mice have been treated with high doses of N-terminal PTH or PTHrP peptide fragments. These studies have been extremely important in defining the pharmacologic actions of these hormones. However, phenomena ascribed to pharmacologic PTH/PTHrP treatment may not perfectly reflect the normal physiology of this signaling system. Individuals with hypoparathyroidism reflect an ideal opportunity to define the physiologic actions of parathyroid hormone. Whenever possible, we will highlight potential differences between pharmacologic and physiologic actions of PTH1R in the mechanisms described below.

Parathyroid hormone/parathyroid hormone−related protein receptor type 1 and its ligands

PTH1R is a glucagon-like family B G-protein-coupled receptor (GPCR) (Juppner et al., 1991). Family B GPCR members bind over a dozen different peptide hormones including secretin, glucagon, calcitonin, and growth hormone-releasing hormone (Hollenstein et al., 2014). Among GPCRs, PTH1R is unique, as it transmits extracellular stimuli from two distinct naturally occurring peptide ligands, PTH and PTHrP (Vilardaga et al., 2011). These two ligands have very different physiologic functions. PTH, secreted by the parathyroid glands, is a circulating hormone that acts on target cells in bone and kidney to regulate levels of calcium and phosphate in the blood and enhance bone remodeling, as evidenced by slow bone turnover in individuals with hypoparathyroidism (Potts, 2005). PTHrP, in contrast, is produced in many tissues, acts locally, and has broad roles in cell differentiation and proliferation—for example, in skin cells, breast cells, and the differentiation of chondrocytes in the growth plate (Wysolmerski, 2012).

How does the same receptor carry out the diverse functions of two distinct ligands? The difference in tissue distribution and local concentration of ligand could be major determinants, but another intriguing possibility is that the two ligands activate different intracellular responses from PTH1R. The concept of biased signaling through GPCRs appeals to researchers because ligands that elicit different signaling pathways for a given receptor could be a powerful tool in drug development (Smith et al., 2018).

Indeed, the development of novel PTH1R agonists may be informed by an understanding of the so-called temporal bias, a particular kind of biased signaling of PTH and PTHrP on PTH1R. Intermittent administration of PTH leads to a net increase in bone mass, while persistent exposure to PTH, as in primary hyperparathyroidism, leads to a net bone loss. Work over many years by different laboratories has uncovered mechanisms responsible for the temporal bias of PTH1R activation. Short-acting agonists, such as PTHrP, prefer to bind to the G-protein-bound (R^G) conformation of PTH1R and signal as ligand−receptor complexes from the cell surface; long-acting agonists, such as PTH, show stronger binding to the G-protein-unbound (R^0) state of the receptor (Dean et al., 2006; Ferrandon et al., 2008). These R^0-agonist complexes are internalized but appear to continue to signal from endosomes (Ferrandon et al., 2009). This concept of temporal bias (differences in response duration) has immediate applications for drug development. Short-acting R^G analogs (such as PTHrP) may be ideal candidates for osteoporosis drugs, while long-acting R^0 analogs (such as PTH) are predicted to be better suited for the treatment of hypoparathyroidism (Cheloha et al., 2015). Indeed, the osteoporosis drug abaloparatide is an R^G analog, and long-acting PTH, a drug undergoing evaluation as a treatment for hypoparathyroidism, is an R^0 analog (Hattersley et al., 2016). Nonetheless, here it is important to highlight that differences in R^0- versus R^G-based receptor engagement have yet to be determined in vivo. Therefore, the cellular consequences of these proposed differences in pharmacologic effects of PTH versus abaloparatide remain to be determined.

Native PTH comprises 84 amino acids, and PTHrP has isoforms of 139, 141, and 173 amino acids (Potts, 2005; Wysolmerski, 2012). PTH and PTHrP share high homologies in the amino-terminus; 8 of the first 13 amino acids are identical. The short synthetic amino-terminal peptides PTH(1−34) and PTHrP(1−36) are both fully functional for binding to and activation of PTH1R and have been used for the majority of in vitro experiments to decipher the molecular actions of the receptor (Cheloha et al., 2015). Multiple carboxy-terminal fragments of PTH are present in circulation in humans; in sum, these are more abundant than circulating intact PTH (D'Amour, 2012). It is not known whether these fragments are merely inert degradation products of the intact molecule or if they have specific functions. Although carboxy-terminal fragments of PTH do not activate PTH1R, binding assays using PTH1R knockout cells in culture showed that carboxy-terminal fragments do bind to cells (Divieti et al., 2001; Murray et al., 2005). These observations provide evidence for a specific carboxy-terminal PTH receptor. However, very little is known about its potential function. In rat osteosarcoma ROS17/2.8 cells, PTH(53−84) increased alkaline phosphatase activity, while PTH(1−34) and PTH(1−84) inhibited it (Murray et al., 1989; Rao and Muzaffar, 1991). The proposed carboxy-terminal receptor of PTH has yet to be identified.

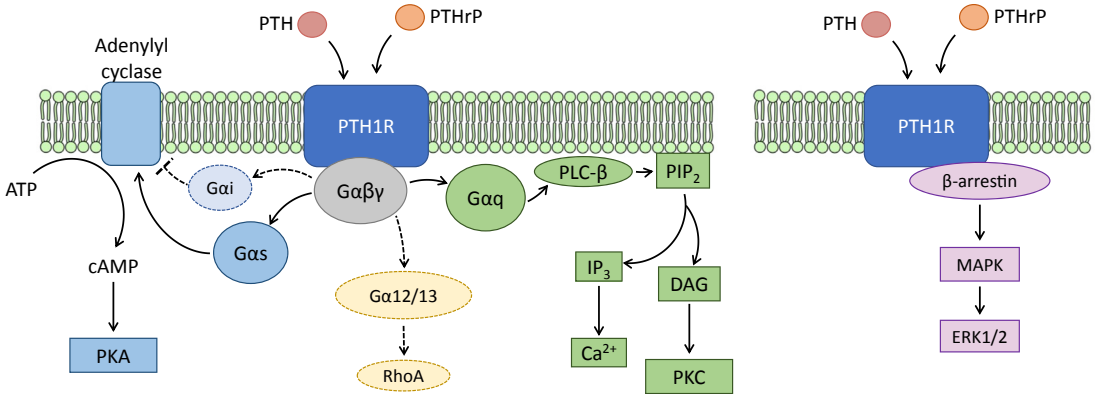

FIGURE 52.1 Overview of known membrane-proximal signaling pathways downstream of the PTH/PTHrP receptor (PTH1R). On activation by PTH or PTHrP, G-protein α subunits exchange GDP for GTP, dissociate from the other G-protein subunits, and regulate activation of downstream enzymes. The Gαs/cAMP/PKA and Gαq/11/PLC/PKC pathways are the principal signaling mechanisms of PTH1R in kidney and bone. β-arrestins play an important role in both G-protein-independent signaling via β-arrestin/MAPK/ERK1/2 and in prolonged signaling from endosomes.

A detailed structure–activity analysis of PTH revealed that the PTH(15–34) fragment contains the major receptor binding domain and that the amino-terminus (PTH(1–14)) comprises the major signaling domain (Cheloha et al., 2015). Activation of PTH1R leads to the activation of two main trimeric G-proteins, Gαs and Gαq/11, which activate the 3′,5′ cyclic AMP (cAMP)/protein kinase A (PKA) and phospholipase C (PLC)/Ca^{2+}/protein kinase C (PKC) pathways, respectively (Cheloha et al., 2015). PTH1R also signals through other G-proteins and G-protein-independent pathways (summarized in Fig. 52.1). These pathways are discussed in more detail in the sections that follow.

Gαs/adenylyl cyclase/protein kinase A signaling

The primary signaling pathway of PTH1R is through the G-protein Gαs (Juppner et al., 1991). Ligand-bound PTH1R couples to and activates Gαs, leading to the activation of adenylyl cyclase (AC), which catalyzes the conversion of adenosine triphosphate (ATP) to cAMP. A classic second messenger, cAMP regulates a wide range of biologic functions. During PTH/PTHrP signaling, it activates PKA by binding to and triggering dissociation of its regulatory subunits (Sassone-Corsi, 2012). Once activated, PKA can phosphorylate other kinases to yield diverse effects. For example, PKA-driven phosphorylation inhibits glycogen synthase kinase 3 β and enhances Wnt signaling in bone (Fang et al., 2000; Kulkarni et al., 2005). Recent studies have revealed that PKA-dependent inactivation of salt-inducible kinases (SIKs) drives expression of genes related to bone turnover in response to PTH (Wein et al., 2016). PKA also activates the transcription factor cAMP-response element-binding protein (CREB), which regulates the expression of other genes necessary for PTH1R-driven cellular processes (Bastepe et al., 2017).

Gαs-cAMP-PKA signaling is activated by the amino terminal residues of PTH or PTHrP. The first nine amino acids are sufficient for cAMP activation; this minimum peptide length was identified using a recombinant tethered ligand-receptor approach in which PTH was tethered to the amino-terminus of PTH1R (Carter and Gardella, 2000). Fragments that lack the amino-terminal residues, such as PTH(3–34), PTH(7–34), and PTHrP(7–36), bind to PTH1R but do not elicit a significant cAMP response.

Ligands designed to be PKA-selective, such as Trp1-M-PTH(1–28) (see later), retain their ability to acutely downregulate expression of the sodium-dependent phosphate cotransporter 2a (Npt2a) in OK cells, indicating that the Gαs pathway is involved in Npt2a regulation (Nagai et al., 2011). PKA-selective analogs have also been shown to mediate the bone anabolic effects of PTH (Yang et al., 2007). Expression of a mutant form of PTH1R, called DSEL, that lacks Gq/11/PLC signaling has been shown to slow the growth and differentiation of hypertrophic chondrocytes in mice (Guo et al., 2002, 2010).

In addition, the critical importance of the Gαs-associated signaling pathway for some functions of PTH1R is demonstrated by the rare disease pseudohypoparathyroidism (PHP), a condition of PTH resistance. Genetic or epigenetic inactivating mutations of the maternal allele of GNAS, the gene encoding Gαs, cause classic PHP types 1a and 1b (Bastepe and Juppner, 2005). In certain tissues, including the thyroid gland, gonads, and pituitary gland as well as in cells such as the proximal renal tubule, GNAS is imprinted to express only from the maternal allele. These mutations result in a loss of Gαs function in these tissues and lead to hypocalcemia, hyperphosphatemia, and relatively low levels of 1,25-$(OH)_2$-vitamin D despite the compensatory elevated PTH levels. Therefore, Gαs signaling is necessary for the calcemic action of PTH, the phosphaturic effect of PTH, and the conversion of 25-(OH)-vitamin D to 1,25-$(OH)_2$-vitamin D.

Gq/11/phospholipase C/protein kinase C signaling

PTH1R also couples to G-proteins of the Gq/11 class. Gq/11-GTP stimulates the membrane-associated PLCβ, which signals through the inositol phospholipid-signaling pathway (Taylor et al., 1991). PLCβ hydrolyzes phosphatidylinositol-4,5-bisphosphate and releases inositol-1,4,5-trisphosphate (IP_3) and diacylglycerol (DAG) (Neves et al., 2002). Membrane-bound DAG activates PKC, which in turn phosphorylates substrates such as enzymes that drive diverse cellular responses. Cytoplasmic IP_3 binds to and activates an intracellular receptor on the endoplasmic reticulum to release calcium into the cytoplasm, where it plays a similarly vital role in signaling pathways.

At least two regions in PTH determine PKC signaling. One is the first amino acid, which is serine in PTH and alanine in PTHrP. Deletion of this first amino acid or replacement with a bulkier residue selectively impairs PLC-dependent PKC signaling (Takasu et al., 1999). The modified PTH analogs Gly1-PTH(1−34) and Gly1, Arg19-PTH(1−28), as well as truncated peptide PTH(3−34), were all found to be selectively defective in PLCβ activation. A long-acting PTH analog, M-PTH(1−28), when modified at position 1 to produce Trp1-M-PTH(1−28), is PLC-deficient but retains potent cAMP responses (Nagai et al., 2011; Gesty-Palmer et al., 2006). Similarly, substituting Ala1 in PTHrP(1−36) with Bpa (p-benzoyl-L-phenylalanine) or Trp specifically reduces PLC signaling (Behar et al., 2000). These selectively defective analogs have been useful in differentiating the effects of Gαs versus Gαq/11 signaling of PTH1R. The findings are consistent with a predominant role of Gαs/cAMP/PKA in mediating both the bone anabolic response and the phosphaturic response to PTH (Nagai et al., 2011; Yang et al., 2007).

Unlike Gαs-specific signaling, which is also determined by position 1 of PTH and PTHrP, Gq/11 signaling involves additional residues beyond the first nine; PTH(29−32) can activate PKC in a PLC-independent fashion (Jouishomme et al., 1994; Yang et al., 2006). In this case, other phospholipases are likely involved—for example, phospholipase D, which is active in the distal tubular cells in the kidney and involved in the PTH-mediated renal reabsorption of extracellular calcium (Bastepe et al., 2017).

Coupling to other G-proteins

Gα12/13-phospholipase-transforming protein RhoA pathway

Activation of PTH1R by PTH also leads to the stimulation of Gα12/13 proteins and activation of phospholipase D (PLD) through a RhoA-dependent mechanism in UMR-106 osteoblastic cells (Singh et al., 2005). A role for PLD signaling in PTH1R trafficking was proposed and supported by studies in Chinese hamster ovary cells and rat osteosarcoma 17.28 cells (Garrido et al., 2009).

Gαi/o pathway

PTH1R was also shown to couple to the pertussis-toxin-sensitive inhibitory Gαi/o class of G-proteins (Schwindinger et al., 1998; Tanaka et al., 1995). The physiologic role of PTH1R coupling to Gαi is unclear.

Extracellular signal-related 1/2−mitogen-activated protein kinase pathway

PTH activates the extracellular signal-related 1/2 (ERK1/2)−mitogen-activated protein kinase (MAPK) cascade through PKA and PKC in a G-protein-dependent manner (Verheijen and Defize, 1997; Cole, 1999; Lederer et al., 2000). ERK1/2 can also be activated through a G-protein-independent, β-arrestin-associated second mechanism (Gesty-Palmer et al., 2006). When HEK293 cells that transiently express human PTH1R are treated with PTH(1−34), an early (2−5 min) and rapid activation of ERK1/2 phosphorylation is observed that is prevented by inhibitors of PKA or PKC. In contrast, a sustained ERK1/2 activation (lasting 30−60 min) has been shown to be PKA- and PKC-independent. This long-term activation was shown to be dependent on β-arrestins 1 and 2, as knockdown of β-arrestin 1 or 2 specifically decreases the sustained phase of ERK1/2 activation (Gesty-Palmer et al., 2006). PTH-stimulated ERK1/2 activation has been shown to increase DNA synthesis and proliferation in bone cells (Swarthout et al., 2001).

Like most GPCRs, PTH1R is a target for the intracellular G-protein-coupled receptor kinases (GRKs), which phosphorylate the activated receptor and help terminate signaling (Vilardaga et al., 2001). A cluster of seven serine residues in the proximal carboxy-terminal tail of PTH1R are phosphorylated upon agonist activation (Tawfeek et al., 2002). In the canonical model of the activation cycle of PTH1R, receptor phosphorylation leads to the recruitment of β-arrestins followed by clathrin-based endocytosis and rapid desensitization of the receptor (Ferrari and Bisello, 2001; Bisello et al., 2002; Chauvin et al., 2002; Tawfeek and Abou-Samra, 2004; Rey et al., 2006; Sneddon and Friedman, 2007).

β-arrestins function as adapters for other effector molecules and allow ERK1/2-MAPK signaling (DeWire et al., 2007). These mechanisms have been further explored by using signal-selective PTH ligands. The analog D-Trp^{12}bPTH(7–34), which elicits no or minimal cAMP response, is able to induce ERK1/2 phosphorylation and can therefore be regarded as a biased agonist for the β-arrestin pathway (DeWire et al., 2007; Gesty-Palmer et al., 2009). Mice treated with daily injections of bPTH(7–34) show an increase in bone formation and expansion of the osteoblast pool (Gesty-Palmer et al., 2009). Importantly, mice lacking β-arrestin 2 did not show these bone anabolic effects. In addition, transcriptome analysis and in vitro assays demonstrated effects of the β-arrestin-biased analog on cell cycle regulation, cell survival, and migration (Gesty-Palmer et al., 2013). However, not all studies have been successful in replicating these results (Cupp and Thomsen, 2013; van der Lee et al., 2013). These conflicting studies, which were performed in HEK293 or Chinese hamster ovary cells rather than in mice, indicate a probable role for cellular context in driving PTH1R signaling. Although more work remains to be done to establish the efficacy of biased agonists to drive the β-arrestin/ERK1/2 endosomal pathway, evidence suggests specific beneficial effects in vitro and in vivo and reveals opportunities for drug development (Luttrell et al., 2018).

More recently, a different role of β-arrestin recruitment on activated PTH1R has been elucidated. While β-arrestins are involved in the process that leads to signal termination, they are also necessary components for the prolonged signaling of R^0-biased ligands, which are internalized as a ligand-receptor-β-arrestin complex but continue to signal from within endosomes (Vilardaga et al., 2012). The capacity of β-arrestins to recruit signaling proteins and stimulate MAPK has been suggested as the mechanism by which they contribute to prolonged endosomal signaling (Sorkin and von Zastrow, 2009; Feinstein et al., 2011). While it has long been believed that GPCR/β-arrestin interaction requires GRK-mediated GPCR tail phosphorylation, recently a distinct GRK-independent mechanism of β-arrestin recruitment has been described. In this model, GPCR engagement triggers a conformational change in the receptor itself that then recruits β-arrestin (Eichel et al., 2018).

Sodium/hydrogen exchanger regulatory factors

The carboxy-terminus of PTH1R provides likely docking sites for signaling proteins. One group of potential PTH1R-interacting proteins are the sodium/hydrogen exchanger regulatory factors (NHERFs), which interact with the PTH1R carboxy-terminus via a PDZ domain and influence signaling and targeting of the receptor to the plasma membrane. Specifically, NHERFs 1 and 2 can bind the amino acid sequence ETVM located at the extreme carboxy-terminus of PTH1R (Donowitz et al., 2002; Cole et al., 2003; Sneddon et al., 2003). PTH signaling promotes the phosphorylation of NHERF-1, which triggers dissociation from Npt2a and is therefore instrumental for the phosphaturic effect of PTH in the proximal renal tubule.

Parathyroid hormone actions in kidney

Having reviewed the intracellular signaling mechanisms that can be used by PTH1R, next we will discuss current knowledge of how these mechanisms contribute to the physiologic functions of this receptor's action, focusing on kidney and bone. In the kidney, PTH exerts effects on mineral metabolism in vivo via PTH1R, which is expressed at high levels by epithelial cells in the proximal and distal tubules. In the proximal tubule, PTH signaling leads to two actions with respect to mineral metabolism (Gardella and Juppner, 2000): increased synthesis of 1,25-$(OH)_2$-vitamin D and decreased phosphate reabsorption. In the distal nephron, a key net effect of PTH is to stimulate calcium reabsorption (Rubin and Bilizekian, 2003). These physiologic renal actions of PTH are reviewed elsewhere in this textbook. Here we will review current understanding of the intracellular signaling mechanisms used by PTH to cause these effects.

Control of 1,25-$(OH)_2$-vitamin D synthesis by CYP27B1 expression

The ability of pharmacologically administered PTH to control 1,25-$(OH)_2$-vitamin D synthesis was first described in experimental animals over 4 decades ago. In these seminal studies, parathyroidectomized rats were unable to convert 25-(OH)-vitamin D to 1,25-$(OH)_2$-vitamin D, while treatment with purified parathyroid extract restored 1,25-$(OH)_2$-vitamin D production (Garabedian et al., 1972). Subsequent in vitro studies on cultured proximal tubule cells demonstrated that this activity of PTH requires new RNA synthesis (Korkor et al., 1987). As discussed above, signaling downstream of the PTH1R activates multiple second messenger pathways including the Gαs-linked cAMP/PKA pathway and the Gq/11-linked PLC/PKC pathway (Gensure et al., 2005; Bringhurst et al., 1993). Inhibitor-based studies have suggested that PKC activity participates in PTH-induced 1,25-$(OH)_2$-vitamin D synthesis (Janulis et al., 1992); however, multiple laboratories have described the involvement of a cAMP/PKA pathway in cultured proximal tubule cells (Korkor et al., 1987; Henry, 1985). Experiments using mice expressing a PTH receptor that activates AC but cannot activate PLC/PKC

(Guo et al., 2002) showed that PTH-dependent increases in 1,25-$(OH)_2$-vitamin D levels in vivo do not require PKC signaling (Venter et al., 2001).

CYP27B1 encodes the 1α-hydroxylase responsible for conversion of 25(OH)-vitamin D into 1,25-$(OH)_2$-vitamin D. Cloning of the CYP27B1 gene facilitated analysis of its proximal promoter (Shinki et al., 1997; Takeyama et al., 1997; St-Arnaud et al., 1997). In kidney cell lines, PTH increases the activity of the murine and human Cyp27B1 proximal promoters (Brenza et al., 1998; Murayama et al., 1998). This same promoter region linked to a reporter gene in transgenic mice is activated in vivo by secondary hyperparathyroidism due to vitamin D or dietary calcium deficiencies (Hendrix et al., 2005). While a complete understanding of the transcription factors mediating PTH-dependent CYP27B1 promoter activation is lacking, overexpression and mutagenesis studies have suggested stimulatory roles for NR4A2 (Nurr1, whose expression itself is induced by PTH), Sp1, and NF−Y, and an inhibitory role for C/EBPβ (Zierold et al., 2007; Gao et al., 2002).

More recently, studies have identified key hormone-sensitive CYP27B1 regulatory regions beyond the gene's proximal promoter (Meyer et al., 2017). By examining global patterns of phosphorylated CREB binding in mouse kidney after acute administration of 1,25-$(OH)_2$-vitamin D or PTH, a putative "M1" CYP27B1 enhancer region was identified ∼5 kB upstream of the transcription start site of the CYP27B1 gene. This enhancer is located within an intronic sequence of the adjacent gene METTL1. Specific deletion of this evolutionarily conserved noncoding sequence leads to significant mineral metabolism and skeletal consequences. Specifically, "M1" knockout mice show hypocalcemia, secondary hyperparathyroidism, osteopenia, and increased cortical porosity. These phenotypes are remarkably similar to those observed with the deletion of CYP27B1 itself. Indeed, "M1" knockout mice show reduced basal CYP27B1 renal gene expression. Attesting to the importance of this enhancer element in PTH-regulated CYP27B1 expression, "M1"-deficient mice fail to upregulate renal CYP27B1 expression in response to acute PTH administration in vivo (Meyer et al., 2017). Taken together, this work identifies the M1 enhancer as a key element required for PTH to regulate CYP27B1 expression. Future studies are needed to characterize the transcription factors that activate this CYP27B1 M1 element and to understand how their activity is regulated by PTH signaling in renal proximal tubule cells. Moreover, although extrarenal CYP27B1 expression is well documented (Anderson et al., 2008), we currently do not understand the molecular determinants of tissue-specific expression. It is interesting that the expression of this gene in some tissue types is not regulated by PTH or other cAMP-inducing agents (Young et al., 2004).

Parathyroid hormone-mediated control of proximal tubule phosphate handling

The second distinct physiologic action of PTH in the proximal tubule is to increase urinary phosphate excretion. This action of PTH synergizes with that of fibroblast growth factor-23 (FGF-23), the other known circulating phosphatonin (Bergwitz and Juppner, 2010). Phosphate reabsorption in the proximal tubule is controlled by the number of type II sodium/phosphate cotransporters (Npt2a and Npt2c) found on the apical brush border membrane (Biber et al., 1996). Both PTH and FGF-23 acutely inhibit renal phosphate reabsorption in the proximal tubule by reducing the surface levels and activity of these cotransporters (Pfister et al., 1998). In addition, chronic hyperparathyroidism leads to reductions in Npt2a gene expression (Gattineni and Friedman, 2015).

The signaling pathways from the PTH receptor to Npt2a downregulation have been the subject of intense investigation over the past 20 years (Weinman and Lederer, 2012). A major advance came in 2002 when NHERF-1 was identified as a key regulator of apical membrane Npt2a (Hernando et al., 2002; Shenolikar et al., 2002). Mice lacking NHERF-1 have renal phosphate wasting and ineffective membrane targeting of Npt2a (Shenolikar et al., 2002). Furthermore, mutations in NHERF-1 have been described in humans with low tubular phosphate reabsorption, nephrolithiasis, and bone demineralization (Karim et al., 2008).

Proximal tubule cells from mice lacking NHERF-1 show resistance to the inhibitory effects of PTH on phosphate transport (Cunningham et al., 2006). While Npt2a itself is not directly regulated by PTH, NHERF-1 is phosphorylated at serine 77 downstream of PTH receptor signaling in a PKA-dependent manner. Phosphorylation at this site decreases NHERF-1/Npt2a interaction and leads to Npt2a internalization (Weinman et al., 2007). NHERF-1 and NHERF-2 constitutively bind to the PTH receptor and may dictate downstream coupling to a PKA versus PKC pathway (Donowitz et al., 2002). More recently, the cytoskeleton-associated protein ezrin has been implicated in dynamic regulation of NHERF-1/Npt2a interactions by PTH (Wang et al., 2012; Guo et al., 2012).

The relative contribution to PTH-mediated PKA versus PKC activation with respect to Npt2a-mediated phosphate reabsorption has been tested in vivo using two complementary experimental systems. First, PTH analogs defective in PKC activation were competent to cause acute phosphaturia (Nagai et al., 2011). Second, phosphaturic responses to PTH were investigated in mice expressing PTH receptors that cannot activate PKC. Interestingly, while acute hypophosphatemia due to PTH infusion was comparable in control and PTH receptor mutant mice, prolonged hypophosphatemia required PTH

receptors that can activate PKC (Venter et al., 2001). Future studies will be required to completely delineate the mechanism whereby PKC signaling stimulated by PTH1R is required for prolonged (but not acute) PTH-mediated phosphaturia. In addition, an area ripe for future investigation is the interplay between the effects of PTH and FGF-23 on phosphate handling in the proximal tubule (Sneddon et al., 2016).

Parathyroid hormone-mediated control of distal tubule calcium reabsorption

PTH promotes calcium reabsorption in the distal convoluted tubule (DCT) (Lau and Bourdeau, 1995). Conversely, hypoparathyroidism is associated with hypercalciuria and nephrolithiasis (Mitchell et al., 2012). Studies in isolated rabbit kidney tubules demonstrated that PTH (as well as cAMP) increases cytosolic intracellular calcium concentrations, but only when calcium is present in luminal fluid (Bourdeau and Lau, 1989). Pharmacologic inhibitor studies indicate that cAMP-dependent PKA activation is required for this effect (Lau and Bourdeau, 1989). PTH regulates transcellular calcium fluxes in the DCT through apical calcium channel transient receptor potential vanilloid 5 (TRPV5) (Hoenderop et al., 2003). Once calcium enters the cell via the TRPV5 channel, it is chaperoned across the cell via association with carrier proteins (calbindin D28 and calmodulin) and ultimately extruded into the bloodstream via the Na^+/Ca^{2+} exchanger (NCX1) and the plasma membrane Ca^{2+}-ATPase (PMCA1b) (Hoenderop et al., 2002).

Three lines of evidence demonstrate that TRPV5-mediated transcellular calcium transport is regulated by PTH. First, PTH controls expression levels of TRPV5, as evidenced by reduced TRPV5 mRNA after parathyroidectomy (van Abel et al., 2005). Second, PTH increases cell surface TRPV5 levels by reducing TRPV5 endocytosis through an incompletely described mechanism that may be sensitive to PKC inhibitors (Cha et al., 2008). Third, the TRPV5 channel itself is a direct PKA substrate at threonine 709 (de Groot et al., 2009). This phosphorylation event increases the probability of the TRPV5 channel opening. TRPV5 channel activity is negatively modulated by calmodulin binding to its intracellular domain. Calmodulin/TRVP5 binding is diminished by PKA-dependent threonine 709 phosphorylation (de Groot et al., 2009, 2011). At this point, the relative contributions of PKA versus PKC signaling with respect to PTH-mediated transcellular calcium reabsorption in the DCT in vivo have not been reported. In addition, the precise function of TRPV5 threonine 709 phosphorylation in vivo remains to be established.

In addition to PTH-mediated regulation of TRPV5 activity by the mechanisms outlined previously, parathyroidectomy in rodents reduces the expression of calbindin D28, NCX1, and PMCA1b in the DCT (van Abel et al., 2005). However, PTH-dependent expression of these calcium handling factors in the DCT may be regulated in an indirect manner via 1,25-$(OH)_2$-vitamin D. Nonetheless, it is likely that PTH coordinates a program of gene expression in DCT cells that is necessary for optimal transcellular calcium reabsorption. Recently, this model was explored by deleting PTH1R selectively in the DCT (Sato et al., 2017). As predicted, these mice showed hypocalcemia, hypercalciuria, and secondary hyperparathyroidism. Surprisingly, the aforementioned proteins involved in transcellular calcium reabsorption were not affected by DCT PTH1R deletion. However, expression of claudin-14 (CLDN14), a tight junction protein that inhibits paracellular calcium reabsorption, was significantly upregulated (Sato et al., 2017). Therefore, PTH signaling in the DCT might control both transcellular (through TRPV5) and paracellular (through CLDN14) calcium reabsorption. Future studies are needed to clarify the mechanisms through which PTH1R signaling regulates CLDN14 expression and activity and to delineate the relative importance of PTH1R-regulated transcellular and paracellular calcium reabsorption in the distal tubule.

Skeletal parathyroid hormone actions: Focusing on osteocytes

PTH exerts its skeletal effects through multiple cellular mechanisms. The evolved function of this hormone is to maintain normocalcemia; therefore, increasing osteoclastic bone resorption to liberate skeletal calcium stores is a major physiologic action of PTH on bone. However, it has long been appreciated that pharmacologically administered PTH also stimulates bone formation (Lindsay et al., 1997). Consistent with this, individuals with hypoparathyroidism show reduced bone formation (Cusano et al., 2016; Rubin et al., 2008), pointing toward a physiologic role of circulating PTH in controlling osteoblast activity. While the teleology behind this phenomenon remains unknown, perhaps the ability of PTH to stimulate bone formation evolved to protect from excessive bone loss during times of dietary calcium deficiency. Both continuous and intermittent (pharmacologic) hyperparathyroidism increase bone resorption and formation. However, for reasons that remain incompletely understood, continuous hyperparathyroidism causes net bone loss while intermittent hyperparathyroidism boosts bone mass.

Since intermittent PTH is the only FDA-approved osteoporosis treatment strategy that stimulates new bone formation, the mechanisms underlying this therapeutic effect have been a major research focus over the past 30+ years. Multiple complementary cellular mechanisms have been proposed to explain how intermittent PTH treatment increases

bone formation. Intermittent pharmacologic PTH administration reduces osteoblast apoptosis (Jilka et al., 1999) and inhibits adipocyte differentiation of skeletal stem cells (Fan et al., 2017). Direct effects of PTH on early cells in the osteoblast lineage have been suggested from in vitro studies using cultured bone marrow−derived stromal cells (for example, Nishida et al., 1994), and more recently, in vivo lineage tracing studies (Balani et al., 2017; Yang et al., 2017). Rapid increases in osteoblast numbers seen after intermittent PTH treatment can be due to direct conversion of quiescent bone-lining cells into active osteoblasts (Kim et al., 2012). Non-cell-autonomous effects of PTH on osteoblast activity also occur. For example, PTH-induced bone resorption may liberate growth factors from bone matrix that in turn stimulate osteoblast progenitors (Wu et al., 2010; Linkhart et al., 1988). T lymphocytes in the bone marrow microenvironment respond to intermittent PTH by producing cytokines that stimulate osteoblast differentiation on cancellous bone surfaces (Pacifici, 2013).

Osteocytes represent a key additional cell type in bone that responds to PTH and PTHrP through PTH1R. The most abundant cell type in bone (Bonewald, 2011), osteocytes are former osteoblasts ensconced within mineralized bone matrix. Osteocytes relay hormonal and mechanical signals to osteoblasts and osteoclasts on bone surfaces. In the past 10 years, work has demonstrated that osteocytes are central to understanding skeletal responses to PTH and PTHrP (Bellido et al., 2013). Here we will focus on PTH1R signaling in osteocytes, highlighting existing knowledge of the signaling pathways involved and pointing out important and unresolved questions. First, osteocytic mechanisms of PTH-induced bone resorption will be reviewed. Then, mechanisms through which PTH and PTHrP stimulate bone formation through effects in osteocytes will be discussed.

Signaling mechanisms controlling parathyroid hormone-induced nuclear factor kappa-B ligand expression

One major mechanism through which PTH induces osteoclastic bone resorption is via upregulation of receptor activator of nuclear factor kappa-B ligand (RANKL) (Xiong and O'Brien, 2012), the key osteoclastogenic cytokine. Two lines of evidence point to osteocytes as a major source of RANKL during normal bone remodeling. First, osteoblast depletion largely preserves osteoclasts and bone RANKL levels (Corral et al., 1998; Galli et al., 2009). Second, conditional deletion of RANKL using the best-available osteocytic Cre deleter strains leads to reduced osteoclasts and high bone mass (Nakashima et al., 2011; Xiong et al., 2011, 2015). Future studies are needed to determine whether soluble or membrane-bound RANKL (Honma et al., 2013, 2014) participates in osteocyte regulation of remodeling on bone surfaces. An added layer of complexity might emerge from the observation that sclerostin (discussed later) has been suggested to promote RANKL expression by osteocytes (Wijenayaka et al., 2011).

Multiple signals increase skeletal RANKL expression, including PTH, 1,25-$(OH)_2$-vitamin D, and proinflammatory cytokines such as IL-6 and TNFα (Fu et al., 2002; Kondo et al., 2002a). Significant progress has been made toward understanding RANKL transcriptional regulation. Importantly, the majority of these mechanistic studies have been performed in osteoblast-like cell lines. It is possible that some of the lessons learned from immortalized osteoblastic lines may not apply to osteocytes. Cyclic AMP signaling downstream of PTH1R induces RANKL expression via a distinct "D5" enhancer located ~75 kB upstream of the gene's transcription start site (Fu and O'Brien, 2006; Kim et al., 2007; Kim et al., 2006). Deletion of this enhancer reduces basal- and PTH-induced RANKL expression in bone, leading to hypoparathyroidism-like skeletal changes (Galli et al., 2008). Deletion of this enhancer is sufficient to blunt skeletal RANKL upregulation stimulated by dietary calcium deficiency and lactation but does not block bone loss associated with these conditions (Onal et al., 2012). Therefore, additional mechanisms can compensate to promote skeletal calcium liberation when RANKL upregulation cannot occur. Multiple possibilities may explain this apparent paradox. RANKL expression by other cell types might substitute for skeletal sources of RANKL to promote bone loss when this particular enhancer is deleted. PTH-dependent RANKL-independent mechanisms that drive osteocytic perilacunar remodeling (see later) might compensate when RANKL cannot be upregulated due to enhancer deletion. Third, secondary hyperparathyroidism massively increases circulating levels of 1,25-$(OH)_2$-vitamin-D. It is possible that vitamin D also might have direct effects on osteocytes that promote RANKL-independent liberation of calcium stores.

In addition to the −75kB "D5" RANKL enhancer, additional upstream regulatory regions have been identified that contribute to cell-type-specific RANKL expression (Onal et al., 2015). For example, while the D5 enhancer appears to be most important in bone lineage cells, a distinct regulatory region located ~200 kB upstream of the human RANKL gene is involved in T cell RANKL expression (Bishop et al., 2015). GWAS studies have identified several variants near RANKL (TNFSF11) that are linked to bone density variation and fracture risk (Rivadeneira et al., 2009). Several bone mineral density−associated variants map to T cell enhancer regions (Rivadeneira et al., 2009). Corresponding murine enhancer regions are required for T cell RANKL expression during inflammatory conditions in vivo (Onal et al., 2016). Finally, recent studies have identified a second "D2" RANKL enhancer ~23 kB upstream of the gene's start site, the

deletion of which leads to a phenotype similar to mice lacking the −75kB D5 enhancer (Onal et al., 2015). Future studies are needed to define the relationship between the D2 and D5 enhancers in basal and PTH-stimulated osteocytic RANKL regulation.

PTH-induced RANKL upregulation requires cAMP/PKA signaling (Kondo et al., 2002a, 2002b); however, the nature of the downstream signaling steps has remained somewhat mysterious. The transcription factor CREB is a well-known PKA substrate at serine 133 (Shaywitz and Greenberg, 1999), and phospho-CREB RANKL enhancer association is observed in response to PTH and other cAMP-inducing signals (Kim et al., 2007). However, CREB deletion in osteoblast/osteocyte lineage cells does not reduce osteoclast numbers or RANKL expression in vivo (Kajimura et al., 2011). Provocatively, activating transcription factor 4 (ATF4), a related bZIP family transcription factor, is required for RANKL upregulation in osteoblastic cells in response to β2-adrenergic (but not PTH) signaling in osteoblasts. ATF4 binds to the proximal RANKL promoter to mediate RANKL induction downstream of catecholamine signaling (Takeda et al., 2002). Therefore, distinct bZIP family transcription factors likely participate in different ligand-induced RANKL upregulation pathways. Future studies will be needed to understand how two ligands (PTH and isoproterenol) that signal through Gαs-linked GPCRs regulate RANKL through distinct downstream mechanisms.

Cyclic AMP-regulated transcriptional coactivators (CRTCs) (Altarejos and Montminy, 2011) provide an additional layer of regulation in PTH-induced RANKL induction. CRTC proteins are coactivators of CREB (and other bZIP family transcription factors) that shuttle from the cytoplasm to the nucleus in response to upstream signals. In osteocytes, CRTC2 is tonically phosphorylated by SIK2 (see further for additional details) and therefore sequestered in the cytoplasm. Upon PKA-mediated SIK2 phosphorylation and inactivation, CRTC2 phosphorylation levels decrease, and this protein translocates from the cytoplasm to the nucleus. In the nucleus, PTH-regulated CRTC2 associates with the aforementioned D2 and D5 RANKL enhancer regions and is required for PTH-induced RANKL upregulation in vitro in Ocy454 cells (Wein et al., 2016). Whether CRTC2 functions with CREB or with other bZIP factors remains unknown, as does the role of CRTC2 in osteocyte function in vivo.

Sclerostin: a parathyroid hormone-suppressed osteocyte-derived osteoblast inhibitor

A crucial observation for the osteocyte biology field was provided by human genetics. Individuals with sclerosteosis display very high bone mass and fracture resistance. This rare Mendelian skeletal dyscrasia is caused by mutations in SOST, which encodes the protein sclerostin, an osteocyte-specific secreted Wnt inhibitor (Brunkow et al., 2001). Sclerostin inhibits osteoblastic bone formation (Baron and Kneissel, 2013); therefore, reducing SOST expression is a common mechanism through which bone anabolic signals may trigger new osteoblast activity. Indeed, both skeletal loading (Robling et al., 2008) and PTH (Keller and Kneissel, 2005; Bellido et al., 2005) rapidly reduce SOST expression. These simple observations moved osteocytes to the forefront in our thinking about how bone responds to PTH. In addition to SOST, osteocytes also are a major source of RANKL (Nakashima et al., 2011; Xiong et al., 2011). Osteocytic RANKL is upregulated by PTH and plays a key role in how PTH stimulates bone resorption (see previous) (Xiong et al., 2014; Ben-awadh et al., 2014). Therefore, transcriptional regulation of paracrine mediators such as SOST and RANKL is a mechanism through which PTH signaling in osteocytes influences bone remodeling.

Studies in genetically modified mice have highlighted the importance of PTH1R signaling in osteocytes. First, increasing PTH1R signaling in osteocytes (achieved via transgenic expression of a constitutively active PTH1R cDNA under the control of 8 kB osteocyte-enriched DMP1 promoter, DMP1-caPTHR1, in mice) leads to increased trabecular bone mass and high bone turnover (O'Brien et al., 2008; Rhee et al., 2011). In these animals, constitutively active PTH receptor signaling leads to reduced SOST expression and increased Wnt activity in osteocytes and osteoblasts. Accordingly, blocking Wnt signaling (via transgenic SOST overexpression or lipoprotein receptor-related protein 5 deletion) abrogates the bone phenotype in DMP1-caPTHR1 animals.

Since sclerostin, a Wnt inhibitor, is downregulated by PTH, and intact Wnt signaling is required for bone anabolism in response to PTH (Kedlaya et al., 2016), it has been of interest to determine if PTH-induced SOST downregulation is required for PTH-induced bone anabolism. When a human SOST bacterial artificial chromosome (BAC) is used to overexpress sclerostin in bone, PTH responses are blunted (Kramer et al., 2010). In contrast, when similar experiments are performed using an SOST transgene driven by the osteocytic DMP1 promoter, pharmacologic PTH administration normally boosts bone mass (Delgado-Calle et al., 2016). It is likely that differences between these two transgenic models account for these discordant results. For example, the human SOST BAC is probably expressed at higher levels at baseline than the DMP1-SOST transgene. However, the fact that SOST-deficient mice still boost bone mass in response to PTH (Kramer et al., 2010) provides further credence to the notion that sclerostin downregulation is just one of many molecular and cellular mechanisms used by PTH to stimulate Wnt signaling and bone formation. For example, T lymphocytes

produce WNT10B in response to intermittent PTH treatment, and this is needed for gains in trabecular bone mass (Terauchi et al., 2009). T cell−derived WNT10B and SOST downregulation work together for pharmacologic PTH treatment to increase bone mass (Li et al., 2014).

Recent progress has been made toward understanding the molecular mechanisms within osteocytes through which PTH regulates gene expression. Again, insights from human genetics have proved vital. Individuals with van Buchem disease have high bone mass, resistance to fractures, and high sclerostin levels. This monogenic disorder is caused by an intergenic deletion near the SOST gene that includes a key enhancer element (Balemans et al., 2002). Pioneering work toward understanding the function of this downstream enhancer-containing region (Loots et al., 2005) ultimately identified a key binding site for the transcription factor myocyte-specific enhancer factor 2C (MEF2C) (Leupin et al., 2007). Deleting MEF2C in osteocytes (Kramer et al., 2012) or the MEF2 binding enhancer element in osteoblasts and osteocytes (Collette et al., 2012) leads to low SOST expression and high bone mass.

Having identified that MEF2C is a key transcription factor for osteocytes to express SOST, an obvious question that emerges is whether PTH regulates SOST by blocking MEF2C activity. Studies in heterologous reporter systems suggested that cAMP signaling might regulate MEF2C activity in the setting of the +45 kB SOST enhancer (Leupin et al., 2007; St John et al., 2015a). In other cell types, upstream signals regulate MEF2 transcriptional activity via nucleocytoplasmic shuttling of class IIa HDAC proteins that, when present in the nucleus, potently inhibit MEF2 activity (Haberland et al., 2009). PTHrP blocks MEF2C-driven chondrocyte hypertrophy (Arnold et al., 2007) by driving HDAC4 from the cytoplasm to the nucleus (Kozhemyakina et al., 2009). In UMR106 osteocytic cells, PTH-induced SOST suppression is associated with nuclear accumulation of HDAC5 (Baertschi et al., 2014).

Loss-of-function studies in conditionally immortalized Ocy454 cells (a PTH-responsive murine osteocyte-like cell line [Spatz et al., 2015; Wein et al., 2015]) and mice reveal that deletion of both HDAC4 and HDAC5 is required to block PTH-dependent SOST downregulation (Wein et al., 2016). Detailed studies into the signaling mechanisms upstream of PTH-induced HDAC4/5 nuclear translocation have identified SIK2 as a crucial mediator of PTH signaling in osteocytes. SIK2 is a PKA-regulated phosphoprotein; PKA-mediated SIK2 phosphorylation reduces SIK2 cellular activity (Henriksson et al., 2012). In the absence of PKA phosphorylation, SIK2 tonically phosphorylates class IIa HDACs and promotes their cytoplasmic sequestration. As predicted by this model, small-molecule SIK inhibitors (Clark et al., 2012; Sundberg et al., 2014, 2016) such as YKL-05-099 reduce HDAC4/5 phosphorylation, promote their nuclear translocation, and reduce SOST expression in vitro and in vivo without increasing intracellular cAMP levels (Wein et al., 2016).

Small-molecule SIK inhibitors mimic transcriptional effects of PTH beyond SOST regulation. By reducing CRTC2 phosphorylation, these agents induce RANKL expression (see previous). At the transcriptomic level, approximately 32% of PTH-regulated genes are coregulated by SIK inhibitors. While HDAC4/5 deficient mice show normal bone anabolic responses to intermittent PTH, YKL-05-099 treatment boosts bone formation and bone mass in vivo (Wein et al., 2016). These studies highlight the importance of SIK2-regulated phosphoproteins (such as HDAC4/5 and CRTC2) in mediating the intracellular effects of PTH in osteocytes and identify SIK inhibitors as promising agents to mimic skeletal effects of PTH (Fig. 52.2). Many questions remain regarding the role of SIKs downstream of PTH receptor signaling. First, it is not known whether these kinases participate in PTH responses in other PTH target cells. Second, we do not know if PTH-regulated SIK2 substrates in osteocytes exist beyond class IIa HDACs and CRTC proteins. Third, genetic evidence that SIK deletion leads to a skeletal phenotype similar to constitutively active PTH receptor overexpression remains to be determined. Fourth, PKA-mediated inhibition of SIK activity appears to be a conserved feature downstream of multiple Gαs-linked hormonal signaling modules (Henriksson et al., 2012; Screaton et al., 2004; Patel et al., 2014; Wang et al., 2011). Therefore, future studies are needed to understand how unique transcriptional outputs are achieved downstream of PTH/SIK pathway engagement in osteocytes. Finally, additional studies are needed to further explore the utility of small-molecule SIK inhibitors (like YKL-05-099) as potential therapeutic agents for osteoporosis treatment.

Additional parathyroid hormone/parathyroid hormone−related protein receptor type 1 actions in osteocytes

Many PTH-regulated genes in osteocytes are regulated in an SIK-independent manner. Therefore, important additional intracellular signaling mechanisms downstream of the PTH receptor must exist. Nascent polypeptide-associated complex and coregulator alpha (αNAC) is another phosphoprotein that translocates from the cytoplasm to the nucleus upon PKA-dependent phosphorylation (Pellicelli et al., 2014). In the nucleus, αNAC associates with bZIP family transcription factors and enhances their activity (Akhouayri et al., 2005). Low-density lipoprotein receptor-related protein 6 (LRP6) represents one important PTH-induced αNAC target gene (Hariri et al., 2017). As a Wnt coreceptor, LRP6 is needed for intermittent

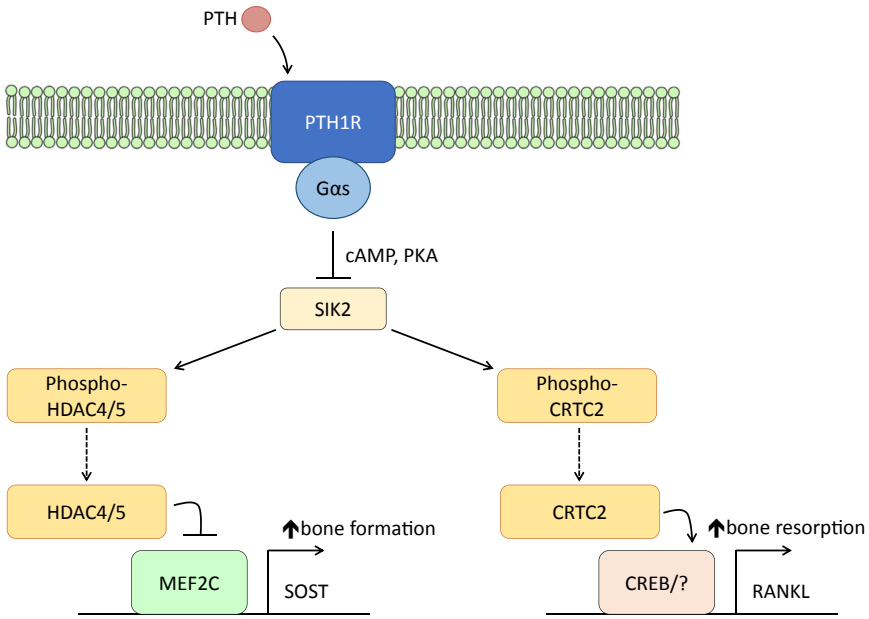

FIGURE 52.2 Model demonstrating the role of salt-inducible kinase 2 (SIK2) in osteocytic PTH1R action. Downstream of Gαs signaling, PKA-mediated SIK2 phosphorylation on S358 (among other sites) blocks SIK2 cellular activity. This leads to reduced phosphorylation of the SIK2 substrates HDAC4/5 and CRTC2. When dephosphorylated (by an unknown phosphatase), these proteins translocate into the nucleus, where they regulate gene expression. Class IIa HDACs block MEF2C-driven SOST expression, while CRTC2 activates RANKL expression through CREB (and perhaps other related transcription factors). Since PTH signaling blocks cellular SIK2 activity, small-molecule SIK inhibitors, such as YKL-05-099, mimic the effects of PTH in osteocytes.

PTH-induced bone anabolism (Li et al., 2013, 2015). Therefore, PTH employs complementary intra- and intercellular mechanisms to stimulate Wnt signaling.

Beyond studies on candidate signaling proteins, several groups have recently performed unbiased approaches to define PTH-regulated genes in osteocytes. Like Ocy454 cells, IDG-SW3 cells are a conditionally immortalized murine osteocyte-like cell line (Woo et al., 2011). RNA-seq profiling of these cells during differentiation and in response to PTH has been reported (St John et al., 2014, 2015b). PTH treatment of IDG-SW3 cells leads to reversion to a less mature, more osteoblastic phenotype. When mature IDG-SW3 cells are treated with PTH, morphologic changes are observed, including fewer dendritic extensions and increased motility (Prideaux et al., 2015). While the mechanistic basis for these phenomena remains incompletely understood, effects on calcium channel gene expression may play a role. PTH increases the expression of L-type (osteoblastic) calcium channels and reduces expression of T-type (osteocytic) channels. L-type calcium channels are partially responsible for PTH-induced changes in osteocyte morphology, as evidenced by pharmacologic experiments with diltiazem (Prideaux et al., 2015).

The physiologic significance of these PTH-dependent changes in osteocyte morphology remains to be determined. Recently, it has been reported that cross talk between PTH and insulin-like growth factor 1 (IGF-1) receptor signaling leads to tyrosine phosphorylation, which localizes the PTH1R to barbed ends of actin filaments. Furthermore, deletion of either the IGF1 receptor or PTH1R in osteoblast lineage cells reduces osteocyte dendritic projections in vivo (Qiu et al., 2018). Therefore, noncanonical PTH1R signaling in preosteocytes may be important for the establishment of the osteocyte lacunar-canalicular network in normal physiologic conditions. The role of PTH1R in establishing an optimal network of osteocyte projections may provide one explanation for the recent observation that mice lacking PTH1R in osteocytes fail to exhibit normal skeletal responses to loading (Delgado-Calle et al., 2016). That being said, it is also known that osteocyte-derived autocrine/paracrine PTHrP promotes bone formation during normal physiologic conditions (Ansari et al., 2018). Therefore, PTH1R signaling in osteocytes can influence bone remodeling through multiple mechanisms. Integrating these findings must be a focus of future studies.

Changes in osteocyte morphology may provide an important mechanistic clue into how PTH and PTHrP rapidly liberate skeletal calcium stores during the normal physiologic stresses of calcium deficiency and lactation (Qing et al., 2012). Osteocytes can remove bone matrix during lactation by reversible remodeling of the perilacunar/canalicular network. Notably, during lactation, osteocytes express "osteoclast specific" genes such as cathepsin K and TRAP.

Pharmacologic infusion of PTHrP, whose levels are normally high during lactation (Kovacs and Kronenberg, 1997), mimics these changes. Mice lacking mammary gland PTHrP fail to lose bone during lactation (VanHouten et al., 2003), highlighting the importance of breast-derived PTHrP as a physiologic signal for lactation-induced bone remodeling. Furthermore, PTH1R-deficient osteocytes fail to undergo perilacunar remodeling during lactation (Qing et al., 2012). Beyond upregulating cathepsin K and TRAP, PTHrP promotes osteocytic expression of ATP6V0D2, the vacuolar ATPase associated with osteoclastic bone resorption. Lactating calcium-deficient mice show reduced perilacunar pH, as assessed using a novel GFP-based reporter system (Jahn et al., 2017). PTH/PTHrP-dependent regulation of perilacunar pH may represent a rapid mechanism for osteocytes to liberate readily accessible pools of calcium. A major unanswered question is the relative contribution of osteocytic osteolysis versus osteoclastic bone resorption in lactation-induced skeletal calcium liberation.

Recent clinical data have suggested potential beneficial effects of the PTHrP analog abaloparatide at predominantly cortical sites (Miller et al., 2016). Therefore, future studies are needed to understand differences between PTH and PTHrP in inducing osteocytic gene expression and perilacunar remodeling. At present, little is known about mechanistic differences between these two PTH1R ligands. In overexpressed receptors in heterologous systems, it appears that PTH preferentially binds to the R^0 PTH1R conformation, while abaloparatide favors the transient R^G configuration (Hattersley et al., 2016). This difference in receptor engagement could lead to biologic differences in signaling outputs, although this appealing hypothesis remains to be tested in bone cells expressing PTH1R at endogenous/physiologic levels.

Summary

Here we have reviewed the cellular and molecular actions of PTH1R in kidney and bone. Starting with a detailed knowledge of the membrane proximal signaling pathways engaged by this class B GPCR, it is now possible to understand some of the major physiologic actions of this hormone in detail. However, major unanswered questions remain. For example, the relative contributions of canonical versus noncanonical PTH1R signaling in distinct physiologic actions of hormone action are still incompletely understood. In addition, whether the signaling pathways described herein also participate in PTH/PTHrP action in cell types and organs outside of bone and kidney remains unknown. Although some differences have been described between PTH and PTHrP with respect to receptor engagement, a complete mechanistic understanding of the differences between these two hormones and their distinct biologic actions remains to be determined. Finally, the paradox of the differential effects on bone mass between continuous and intermittent hyperparathyroidism remains to be solved.

References

Akhouayri, O., Quelo, I., St-Arnaud, R., 2005. Sequence-specific DNA binding by the alphaNAC coactivator is required for potentiation of c-Jun-dependent transcription of the osteocalcin gene. Mol. Cell Biol. 25 (9), 3452−3460.

Altarejos, J.Y., Montminy, M., 2011. CREB and the CRTC co-activators: sensors for hormonal and metabolic signals. Nat. Rev. Mol. Cell Biol. 12 (3), 141−151.

Anderson, P.H., Hendrix, I., Sawyer, R.K., Zarrinkalam, R., Manavis, J., Sarvestani, G.T., et al., 2008. Co-expression of CYP27B1 enzyme with the 1.5kb CYP27B1 promoter-luciferase transgene in the mouse. Mol. Cell. Endocrinol. 285 (1−2), 1−9.

Ansari, N., Ho, P.W., Crimeen-Irwin, B., Poulton, I.J., Brunt, A.R., Forwood, M.R., et al., 2018. Autocrine and paracrine regulation of the murine skeleton by osteocyte-derived parathyroid hormone-related protein. J. Bone Miner. Res. 33 (1), 137−153.

Arnold, M.A., Kim, Y., Czubryt, M.P., Phan, D., McAnally, J., Qi, X., et al., 2007. MEF2C transcription factor controls chondrocyte hypertrophy and bone development. Dev. Cell 12 (3), 377−389.

Baertschi, S., Baur, N., Lueders-Lefevre, V., Voshol, J., Keller, H., 2014. Class I and IIa histone deacetylases have opposite effects on sclerostin gene regulation. J. Biol. Chem. 289 (36), 24995−25009.

Balani, D.H., Ono, N., Kronenberg, H.M., 2017. Parathyroid hormone regulates fates of murine osteoblast precursors in vivo. J. Clin. Investig. 127 (9), 3327−3338.

Balemans, W., Patel, N., Ebeling, M., Van Hul, E., Wuyts, W., Lacza, C., et al., 2002. Identification of a 52 kb deletion downstream of the SOST gene in patients with van Buchem disease. J. Med. Genet. 39 (2), 91−97.

Baron, R., Kneissel, M., 2013. WNT signaling in bone homeostasis and disease: from human mutations to treatments. Nat. Med. 19 (2), 179−192.

Bastepe, M., Juppner, H., 2005. GNAS locus and pseudohypoparathyroidism. Horm. Res. 63 (2), 65−74.

Bastepe, M., Turan, S., He, Q., 2017. Heterotrimeric G proteins in the control of parathyroid hormone actions. J. Mol. Endocrinol. 58 (4), R203−R224.

Behar, V., Bisello, A., Bitan, G., Rosenblatt, M., Chorev, M., 2000. Photoaffinity cross-linking identifies differences in the interactions of an agonist and an antagonist with the parathyroid hormone/parathyroid hormone-related protein receptor. J. Biol. Chem. 275 (1), 9−17.

Bellido, T., Ali, A.A., Gubrij, I., Plotkin, L.I., Fu, Q., O'Brien, C.A., et al., 2005. Chronic elevation of parathyroid hormone in mice reduces expression of sclerostin by osteocytes: a novel mechanism for hormonal control of osteoblastogenesis. Endocrinology 146 (11), 4577−4583.

Bellido, T., Saini, V., Pajevic, P.D., 2013. Effects of PTH on osteocyte function. Bone 54 (2), 250–257.

Ben-awadh, A.N., Delgado-Calle, J., Tu, X., Kuhlenschmidt, K., Allen, M.R., Plotkin, L.I., et al., 2014. Parathyroid hormone receptor signaling induces bone resorption in the adult skeleton by directly regulating the RANKL gene in osteocytes. Endocrinology 155 (8), 2797–2809.

Bergwitz, C., Juppner, H., 2010. Regulation of phosphate homeostasis by PTH, vitamin D, and FGF23. Annu. Rev. Med. 61, 91–104.

Biber, J., Custer, M., Magagnin, S., Hayes, G., Werner, A., Lotscher, M., et al., 1996. Renal Na/Pi-cotransporters. Kidney Int. 49 (4), 981–985.

Bisello, A., Chorev, M., Rosenblatt, M., Monticelli, L., Mierke, D.F., Ferrari, S.L., 2002. Selective ligand-induced stabilization of active and desensitized parathyroid hormone type 1 receptor conformations. J. Biol. Chem. 277 (41), 38524–38530.

Bishop, K.A., Wang, X., Coy, H.M., Meyer, M.B., Gumperz, J.E., Pike, J.W., 2015. Transcriptional regulation of the human TNFSF11 gene in T cells via a cell type-selective set of distal enhancers. J. Cell. Biochem. 116 (2), 320–330.

Bonewald, L.F., 2011. The amazing osteocyte. J. Bone Miner. Res. 26 (2), 229–238.

Bourdeau, J.E., Lau, K., 1989. Effects of parathyroid hormone on cytosolic free calcium concentration in individual rabbit connecting tubules. J. Clin. Investig. 83, 373–379.

Brenza, H.L., Kimmel-Jehan, C., Jehan, F., Shinki, T., Wakino, S., Anazawa, H., et al., 1998. Parathyroid hormone activation of the 25-hydroxyvitamin D3-1alpha-hydroxylase gene promoter. Proc. Natl. Acad. Sci. U.S.A. 95 (4), 1387–1391.

Bringhurst, F.R., Jüppner, H., Guo, J., Urena, P., Potts Jr., J.T., Kronenberg, H.M., et al., 1993. Cloned, stably expressed parathyroid hormone (PTH)/PTH-related peptide receptors activate multiple messenger signals and biological responses in LLC-PK1 kidney cells. Endocrinology 132 (5), 2090–2098.

Brunkow, M.E., Gardner, J.C., Van Ness, J., Paeper, B.W., Kovacevich, B.R., Proll, S., et al., 2001. Bone dysplasia sclerosteosis results from loss of the SOST gene product, a novel cystine knot-containing protein. Am. J. Hum. Genet. 68 (3), 577–589.

Shimizu, M., Carter, P.H., Gardella, T.J., 2000. Autoactivation of type-1 parathyroid hormone receptors containing a tethered ligand. J. Biol. Chem. 275 (26), 19456–19460.

Cha, S.K., Wu, T., Huang, C.L., 2008. Protein kinase C inhibits caveolae-mediated endocytosis of TRPV5. Am. J. Physiol. Renal. Physiol. 294 (5), F1212–F1221.

Chauvin, S., Bencsik, M., Bambino, T., Nissenson, R.A., 2002. Parathyroid hormone receptor recycling: role of receptor dephosphorylation and beta-arrestin. Mol. Endocrinol. 16 (12), 2720–2732.

Cheloha, R.W., Gellman, S.H., Vilardaga, J.P., Gardella, T.J., 2015. PTH receptor-1 signalling-mechanistic insights and therapeutic prospects. Nat. Rev. Endocrinol. 11 (12), 712–724.

Clark, K., MacKenzie, K.F., Petkevicius, K., Kristariyanto, Y., Zhang, J., Choi, H.G., et al., 2012. Phosphorylation of CRTC3 by the salt-inducible kinases controls the interconversion of classically activated and regulatory macrophages. Proc. Natl. Acad. Sci. U.S.A. 109 (42), 16986–16991.

Cole, J.A., 1999. Parathyroid hormone activates mitogen-activated protein kinase in opossum kidney cells. Endocrinology 140 (12), 5771–5779.

Mahon, M.J., Cole, J.A., Lederer, E.D., Segre, G.V., 2003. Na^+/H^+ exchanger-regulatory factor 1 mediates inhibition of phosphate transport by parathyroid hormone and second messengers by acting at multiple sites in opossum kidney cells. Mol. Endocrinol. 17 (11), 2355–2364.

Collette, N.M., Genetos, D.C., Economides, A.N., Xie, L., Shahnazari, M., Yao, W., et al., 2012. Targeted deletion of Sost distal enhancer increases bone formation and bone mass. Proc. Natl. Acad. Sci. U.S.A. 109 (35), 14092–14097.

Corral, D., Amling, M., Prienel, M., Loyer, E., Fuchs, S., Ducy, P., et al., 1998. Dissociation between bone resorption and bone formation in osteopenic transgenic mice. Proc. Natl. Acad. Sci. U.S.A. 95, 13835–13840.

Cunningham, R., Steplock, D., E X, Biswas, R.S., Wang, F., Shenolikar, S., et al., 2006. Adenoviral expression of NHERF-1 in NHERF-1 null mouse renal proximal tubule cells restores Npt2a regulation by low phosphate media and parathyroid hormone. Am. J. Physiol. Renal. Physiol. 291 (4), F896–F901.

Cupp, M.E., Nayak, S.K., Adem, A.S., Thomsen, W.J., 2013. Parathyroid hormone (PTH) and PTH-related peptide domains contributing to activation of different PTH receptor-mediated signaling pathways. J. Pharmacol. Exp. Ther. 345 (3), 404–418.

Cusano, N.E., Nishiyama, K.K., Zhang, C., Rubin, M.R., Boutroy, S., McMahon, D.J., et al., 2016. Noninvasive assessment of skeletal microstructure and estimated bone strength in hypoparathyroidism. J. Bone Miner. Res. 31 (2), 308–316.

D'Amour, P., 2012. Acute and chronic regulation of circulating PTH: significance in health and in disease. Clin. Biochem. 45 (12), 964–969.

Dean, T., Linglart, A., Mahon, M.J., Bastepe, M., Juppner, H., Potts Jr., J.T., et al., 2006. Mechanisms of ligand binding to the parathyroid hormone (PTH)/PTH-related protein receptor: selectivity of a modified PTH(1-15) radioligand for GalphaS-coupled receptor conformations. Mol. Endocrinol. 20 (4), 931–943.

Delgado-Calle, J., Tu, X., Pacheco-Costa, R., McAndrews, K., Edwards, R., Pellegrini, G., et al., 2016. Control of bone anabolism in response to mechanical loading and PTH by distinct mechanisms downstream of the PTH receptor. J. Bone Miner. Res. 32 (3), 522–535.

DeWire, S.M., Ahn, S., Lefkowitz, R.J., Shenoy, S.K., 2007. Beta-arrestins and cell signaling. Annu. Rev. Physiol. 69, 483–510.

Divieti, P., Inomata, N., Chapin, K., Singh, R., Juppner, H., Bringhurst, F.R., 2001. Receptors for the carboxyl-terminal region of pth(1-84) are highly expressed in osteocytic cells. Endocrinology 142 (2), 916–925.

Mahon, M.J., Donowitz, M., Yun, C.C., Segre, G.V., 2002. Na(+)/H(+) exchanger regulatory factor 2 directs parathyroid hormone 1 receptor signalling. Nature 417 (6891), 858–861.

Eichel, K., Jullie, D., Barsi-Rhyne, B., Latorraca, N.R., Masureel, M., Sibarita, J.B., et al., 2018. Catalytic activation of beta-arrestin by GPCRs. Nature 557 (7705), 381–386.

Fan, Y., Hanai, J.I., Le, P.T., Bi, R., Maridas, D., DeMambro, V., et al., 2017. Parathyroid hormone directs bone marrow mesenchymal cell fate. Cell Metabol. 25 (3), 661–672.

Fang, X., Yu, S.X., Lu, Y., Bast Jr., R.C., Woodgett, J.R., Mills, G.B., 2000. Phosphorylation and inactivation of glycogen synthase kinase 3 by protein kinase A. Proc. Natl. Acad. Sci. U.S.A. 97 (22), 11960–11965.

Feinstein, T.N., Wehbi, V.L., Ardura, J.A., Wheeler, D.S., Ferrandon, S., Gardella, T.J., et al., 2011. Retromer terminates the generation of cAMP by internalized PTH receptors. Nat. Chem. Biol. 7 (5), 278–284.

Okazaki, M., Ferrandon, S., Vilardaga, J.P., Bouxsein, M.L., Potts Jr., J.T., Gardella, T.J., 2008. Prolonged signaling at the parathyroid hormone receptor by peptide ligands targeted to a specific receptor conformation. Proc. Natl. Acad. Sci. U.S.A. 105 (43), 16525–16530.

Ferrandon, S., Feinstein, T.N., Castro, M., Wang, B., Bouley, R., Potts, J.T., et al., 2009. Sustained cyclic AMP production by parathyroid hormone receptor endocytosis. Nat. Chem. Biol. 5 (10), 734–742.

Ferrari, S.L., Bisello, A., 2001. Cellular distribution of constitutively active mutant parathyroid hormone (PTH)/PTH-related protein receptors and regulation of cyclic adenosine 3',5'-monophosphate signaling by beta-arrestin2. Mol. Endocrinol. 15 (1), 149–163.

Fu, Q., Manolagas, S.C., O'Brien, C.A., 2006. Parathyroid hormone controls receptor activator of NF-kappaB ligand gene expression via a distant transcriptional enhancer. Mol. Cell Biol. 26 (17), 6453–6468.

Fu, Q., Jilka, R.L., Manolagas, S.C., O'Brien, C.A., 2002. Parathyroid hormone stimulates receptor activator of NFkappa B ligand and inhibits osteoprotegerin expression via protein kinase A activation of cAMP-response element-binding protein. J. Biol. Chem. 277 (50), 48868–48875.

Galli, C., Zella, L.A., Fretz, J.A., Fu, Q., Pike, J.W., Weinstein, R.S., et al., 2008. Targeted deletion of a distant transcriptional enhancer of the receptor activator of nuclear factor-kappaB ligand gene reduces bone remodeling and increases bone mass. Endocrinology 149 (1), 146–153.

Galli, C., Fu, Q., Wang, W., Olsen, B.R., Manolagas, S.C., Jilka, R.L., et al., 2009. Commitment to the osteoblast lineage is not required for RANKL gene expression. J. Biol. Chem. 284 (19), 12654–12662.

Gao, X.H., Dwivedi, P.P., Choe, S., Alba, F., Morris, H.A., Omdahl, J.L., et al., 2002. Basal and parathyroid hormone induced expression of the human 25-hydroxyvitamin D 1alpha-hydroxylase gene promoter in kidney AOK-B50 cells: role of Sp1, Ets and CCAAT box protein binding sites. Int. J. Biochem. Cell Biol. 34 (8), 921–930.

Garabedian, M., Holick, M.F., DeLuca, H.F., Boyle, I.T., 1972. Control of 25-hydroxycholecalciferol metabolism by parathyroid glands. Proc. Natl. Acad. Sci. U.S.A. 69, 1673–1676.

Gardella, T.J., Juppner, H., 2000. Interaction of PTH and PTHrP with their receptors. Rev. Endocr. Metab. Disord. 1 (4), 317–329.

Garrido, J.L., Wheeler, D., Vega, L.L., Friedman, P.A., Romero, G., 2009. Role of phospholipase D in parathyroid hormone type 1 receptor signaling and trafficking. Mol. Endocrinol. 23 (12), 2048–2059.

Gattineni, J., Friedman, P.A., 2015. Regulation of hormone-sensitive renal phosphate transport. Vitam. Horm. 98, 249–306.

Gensure, R.C., Gardella, T.J., Juppner, H., 2005. Parathyroid hormone and parathyroid hormone-related peptide, and their receptors. Biochem. Biophys. Res. Commun. 328 (3), 666–678.

Gesty-Palmer, D., Chen, M., Reiter, E., Ahn, S., Nelson, C.D., Wang, S., et al., 2006. Distinct beta-arrestin- and G protein-dependent pathways for parathyroid hormone receptor-stimulated ERK1/2 activation. J. Biol. Chem. 281 (16), 10856–10864.

Gesty-Palmer, D., Flannery, P., Yuan, L., Corsino, L., Spurney, R., Lefkowitz, R.J., et al., 2009. A beta-arrestin-biased agonist of the parathyroid hormone receptor (PTH1R) promotes bone formation independent of G protein activation. Sci. Transl. Med. 1 (1), 1ra.

Gesty-Palmer, D., Yuan, L., Martin, B., Wood 3rd, W.H., Lee, M.H., Janech, M.G., et al., 2013. beta-arrestin-selective G protein-coupled receptor agonists engender unique biological efficacy in vivo. Mol. Endocrinol. 27 (2), 296–314.

de Groot, T., Lee, K., Langeslag, M., Xi, Q., Jalink, K., Bindels, R.J., et al., 2009. Parathyroid hormone activates TRPV5 via PKA-dependent phosphorylation. J. Am. Soc. Nephrol. 20 (8), 1693–1704.

de Groot, T., Kovalevskaya, N.V., Verkaart, S., Schilderink, N., Felici, M., van der Hagen, E.A., et al., 2011. Molecular mechanisms of calmodulin action on TRPV5 and modulation by parathyroid hormone. Mol. Cell Biol. 31 (14), 2845–2853.

Guo, J., Chung, U.I., Kondo, H., Bringhurst, F.R., Kronenberg, H.M., 2002. The PTH/PTHrP receptor can delay chondrocyte hypertrophy in vivo without activating phospholipase C. Dev. Cell 3 (2), 183–194.

Guo, J., Liu, M., Yang, D., Bouxsein, M.L., Thomas, C.C., Schipani, E., et al., 2010. Phospholipase C signaling via the parathyroid hormone (PTH)/PTH-related peptide receptor is essential for normal bone responses to PTH. Endocrinology 151 (8), 3502–3513.

Guo, J., Song, L., Liu, M., Mahon, M.J., 2012. Fluorescent ligand-directed co-localization of the parathyroid hormone 1 receptor with the brush-border scaffold complex of the proximal tubule reveals hormone-dependent changes in ezrin immunoreactivity consistent with inactivation. Biochim. Biophys. Acta 1823 (12), 2243–2253.

Haberland, M., Montgomery, R.L., Olson, E.N., 2009. The many roles of histone deacetylases in development and physiology: implications for disease and therapy. Nat. Rev. Genet. 10 (1), 32–42.

Hariri, H.P., Pellicelli, M., St-Arnaud, R., 2017. New PTH signals mediating bone anabolism. Curr Mol Biol Rep 3, 133–141.

Hattersley, G., Dean, T., Corbin, B.A., Bahar, H., Gardella, T.J., 2016. Binding selectivity of abaloparatide for PTH-type-1-receptor conformations and effects on downstream signaling. Endocrinology 157 (1), 141–149.

Hendrix, I., Anderson, P.H., Omdahl, J.L., May, B.K., Morris, H.A., 2005. Response of the 5'-flanking region of the human 25-hydroxyvitamin D 1alpha-hydroxylase gene to physiological stimuli using a transgenic mouse model. J. Mol. Endocrinol. 34 (1), 237–245.

Henriksson, E., Jones, H.A., Patel, K., Peggie, M., Morrice, N., Sakamoto, K., et al., 2012. The AMPK-related kinase SIK2 is regulated by cAMP via phosphorylation at Ser358 in adipocytes. Biochem. J. 444 (3), 503–514.

Henry, H.L., 1985. Parathyroid hormone modulation of 25-hydroxyvitamin D3 metabolism by cultured chick kidney cells is mimicked and enhanced by forskolin. Endocrinology 116 (2), 503–510.

Hernando, N., Deliot, N., Gisler, S.M., Lederer, E., Weinman, E.J., Biber, J., et al., 2002. PDZ-domain interactions and apical expression of type IIa Na/P(i) cotransporters. Proc. Natl. Acad. Sci. U.S.A. 99 (18), 11957–11962.

Hoenderop, J.G., Nilius, B., Bindels, R.J., 2002. Molecular mechanism of active Ca^{2+} reabsorption in the distal nephron. Annu. Rev. Physiol. 64, 529–549.

Hoenderop, J.G., van Leeuwen, J.P., van der Eerden, B.C., Kersten, F.F., van der Kemp, A.W., Merillat, A.M., et al., 2003. Renal Ca^{2+} wasting, hyperabsorption, and reduced bone thickness in mice lacking TRPV5. J. Clin. Investig. 112 (12), 1906–1914.

Hollenstein, K., de Graaf, C., Bortolato, A., Wang, M.W., Marshall, F.H., Stevens, R.C., 2014. Insights into the structure of class B GPCRs. Trends Pharmacol. Sci. 35 (1), 12–22.

Honma, M., Ikebuchi, Y., Kariya, Y., Hayashi, M., Hayashi, N., Aoki, S., et al., 2013. RANKL subcellular trafficking and regulatory mechanisms in osteocytes. J. Bone Miner. Res. 28 (9), 1936–1949.

Honma, M., Ikebuchi, Y., Kariya, Y., Suzuki, H., 2014. Regulatory mechanisms of RANKL presentation to osteoclast precursors. Curr. Osteoporos. Rep. 12 (1), 115–120.

Jahn, K., Kelkar, S., Zhao, H., Xie, Y., Tiede-Lewis, L.M., Dusevich, V., et al., 2017. Osteocytes acidify their microenvironment in response to PTHrP in vitro and in lactating mice in vivo. J. Bone Miner. Res. 32 (8), 1761–1772.

Janulis, M., Tembe, V., Favus, M.J., 1992. Role of protein kinase C in parathyroid hormone stimulation of renal 1,25-dihydroxyvitamin D3 secretion. J. Clin. Investig. 90 (6), 2278–2283.

Jilka, R.L., Weinstein, R.S., Bellido, T., Roberson, P., Parfitt, A.M., Manolagas, S.C., 1999. Increased bone formation by prevention of osteoblast apoptosis with parathyroid hormone. J. Clin. Investig. 104 (4), 439–446.

Jouishomme, H., Whitfield, J.F., Gagnon, L., Maclean, S., Isaacs, R., Chakravarthy, B., et al., 1994. Further definition of the protein kinase C activation domain of the parathyroid hormone. J. Bone Miner. Res. 9 (6), 943–949.

Juppner, H., Abou-Samra, A.B., Freeman, M., Kong, X.F., Schipani, E., Richards, J., et al., 1991. A G protein-linked receptor for parathyroid hormone and parathyroid hormone-related peptide. Science 254 (5034), 1024–1026.

Kajimura, D., Hinoi, E., Ferron, M., Kode, A., Riley, K.J., Zhou, B., et al., 2011. Genetic determination of the cellular basis of the sympathetic regulation of bone mass accrual. J. Exp. Med. 208 (4), 841–851.

Karim, Z., Gerard, B., Bakouh, N., Alili, R., Leroy, C., Beck, L., et al., 2008. NHERF1 mutations and responsiveness of renal parathyroid hormone. N. Engl. J. Med. 359 (11), 1128–1135.

Kedlaya, R., Kang, K.S., Hong, J.M., Bettagere, V., Lim, K.E., Horan, D., et al., 2016. Adult-onset deletion of beta-catenin in (10kb)Dmp1-expressing cells prevents intermittent PTH-induced bone gain. Endocrinology 157 (8), 3047–3057.

Keller, H., Kneissel, M., 2005. SOST is a target gene for PTH in bone. Bone 37 (2), 148–158.

Kim, S., Yamazaki, M., Zella, L.A., Shevde, N.K., Pike, J.W., 2006. Activation of receptor activator of NF-kappaB ligand gene expression by 1,25-dihydroxyvitamin D3 is mediated through multiple long-range enhancers. Mol. Cell Biol. 26 (17), 6469–6486.

Kim, S., Yamazaki, M., Shevde, N.K., Pike, J.W., 2007. Transcriptional control of receptor activator of nuclear factor-kappaB ligand by the protein kinase A activator forskolin and the transmembrane glycoprotein 130-activating cytokine, oncostatin M, is exerted through multiple distal enhancers. Mol. Endocrinol. 21 (1), 197–214.

Kim, S.W., Pajevic, P.D., Selig, M., Barry, K.J., Yang, J.Y., Shin, C.S., et al., 2012. Intermittent parathyroid hormone administration converts quiescent lining cells to active osteoblasts. J. Bone Miner. Res. 27 (10), 2075–2084.

Kondo, H., Guo, J., Bringhurst, F.R., 2002. Cyclic adenosine monophosphate/protein kinase A mediates parathyroid hormone/parathyroid hormone-related protein receptor regulation of osteoclastogenesis and expression of RANKL and osteoprotegerin mRNAs by marrow stromal cells. J. Bone Miner. Res. 17 (9), 1667–1679.

Kondo, H., Guo, J., Chung, U.-I., Kasugai, S., Kronenberg, H.M., Bringhurst, F.R., 2002. Effects of PTH/PTHrP receptor-generated signals on RANKL/RANK-Induced osteoclastogenesis : analyses in vitro, in vivo, and ex vivo. J. Bone Miner. Res. 17 (Suppl. 1) (xxxx).

Korkor, A.B., Gray, R.W., Henry, H.L., Kleinman, J.G., Blumenthal, S.S., Garancis, J.C., 1987. Evidence that stimulation of 1,25(OH)2D3 production in primary cultures of mouse kidney cells by cyclic AMP requires new protein synthesis. J. Bone Miner. Res. 2 (6), 517–524.

Kovacs, C.S., Kronenberg, H.M., 1997. Maternal-fetal calcium and bone metabolism during pregnancy, puerperium, and lactation. Endocr. Rev. 18 (6), 832–872.

Kozhemyakina, E., Cohen, T., Yao, T.P., Lassar, A.B., 2009. Parathyroid hormone-related peptide represses chondrocyte hypertrophy through a protein phosphatase 2A/histone deacetylase 4/MEF2 pathway. Mol. Cell Biol. 29 (21), 5751–5762.

Kramer, I., Loots, G.G., Studer, A., Keller, H., Kneissel, M., 2010. Parathyroid hormone (PTH)-induced bone gain is blunted in SOST overexpressing and deficient mice. J. Bone Miner. Res. 25 (2), 178–189.

Kramer, I., Baertschi, S., Halleux, C., Keller, H., Kneissel, M., 2012. Mef2c deletion in osteocytes results in increased bone mass. J. Bone Miner. Res. 27 (2), 360–373.

Kulkarni, N.H., Halladay, D.L., Miles, R.R., Gilbert, L.M., Frolik, C.A., Galvin, R.J., et al., 2005. Effects of parathyroid hormone on Wnt signaling pathway in bone. J. Cell. Biochem. 95 (6), 1178–1190.

Lau, K., Bourdeau, J.E., 1989. Evidence for cAMP-dependent protein kinase in mediating the parathyroid hormone-stimulated rise in cytosolic free calcium in rabbit connecting tubules. J. Biol. Chem. 264 (7), 4028–4032.

Lau, K., Bourdeau, J.E., 1995. Parathyroid hormone action in calcium transport in the distal nephron. Curr. Opin. Nephrol. Hypertens. 4 (1), 55–63.

Lederer, E.D., Sohi, S.S., McLeish, K.R., 2000. Parathyroid hormone stimulates extracellular signal-regulated kinase (ERK) activity through two independent signal transduction pathways: role of ERK in sodium-phosphate cotransport. J. Am. Soc. Nephrol. 11 (2), 222–231.

Leupin, O., Kramer, I., Collette, N.M., Loots, G.G., Natt, F., Kneissel, M., et al., 2007. Control of the SOST bone enhancer by PTH using MEF2 transcription factors. J. Bone Miner. Res. 22 (12), 1957–1967.

Li, C., Xing, Q., Yu, B., Xie, H., Wang, W., Shi, C., et al., 2013. Disruption of LRP6 in osteoblasts blunts the bone anabolic activity of PTH. J. Bone Miner. Res. 28 (10), 2094–2108.

Li, J.Y., Walker, L.D., Tyagi, A.M., Adams, J., Weitzmann, M.N., Pacifici, R., 2014. The sclerostin-independent bone anabolic activity of intermittent PTH treatment is mediated by T-cell-produced Wnt10b. J. Bone Miner. Res. 29 (1), 43–54.

Li, C., Wang, W., Xie, L., Luo, X., Cao, X., Wan, M., 2015. Lipoprotein receptor-related protein 6 is required for parathyroid hormone-induced Sost suppression. Ann. N.Y. Acad. Sci. 1364, 62–73.

Lindsay, R., Nieves, J., Formica, C., Henneman, E., Woelfert, L., Shen, V., et al., 1997. Randomised controlled study of effect of parathyroid hormone on vertebral-bone mass and fracture incidence among postmenopausal women on oestrogen with osteoporosis. Lancet 350 (9077), 550–555.

Linkhart, T.A., Mohan, S., Baylink, D.J., 1988. Bone repletion in vitro: evidence for a locally regulated bone repair response to PTH treatment. Bone 9 (6), 371–379.

Loots, G.G., Kneissel, M., Keller, H., Baptist, M., Chang, J., Collette, N.M., et al., 2005. Genomic deletion of a long-range bone enhancer misregulates sclerostin in Van Buchem disease. Genome Res. 15 (7), 928–935.

Luttrell, L.M., Maudsley, S., Gesty-Palmer, D., 2018. Translating in vitro ligand bias into in vivo efficacy. Cell. Signal. 41, 46–55.

Meyer, M.B., Benkusky, N.A., Kaufmann, M., Lee, S.M., Onal, M., Jones, G., et al., 2017. A kidney-specific genetic control module in mice governs endocrine regulation of the cytochrome P450 gene Cyp27b1 essential for vitamin D3 activation. J. Biol. Chem. 292 (42), 17541–17558.

Miller, P.D., Hattersley, G., Riis, B.J., Williams, G.C., Lau, E., Russo, L.A., et al., 2016. Effect of abaloparatide vs placebo on new vertebral fractures in postmenopausal women with osteoporosis: a randomized clinical trial. J. Am. Med. Assoc. 316 (7), 722–733.

Mitchell, D.M., Regan, S., Cooley, M.R., Lauter, K.B., Vrla, M.C., Becker, C.B., et al., 2012. Long-term follow-up of patients with hypoparathyroidism. J. Clin. Endocrinol. Metab. 97 (12), 4507–4514.

Murayama, A., Takeyama, K., Kitanaka, S., Kodera, Y., Hosoya, T., Kato, S., 1998. The promoter of the human 25-hydroxyvitamin D3 1 alpha-hydroxylase gene confers positive and negative responsiveness to PTH, calcitonin, and 1 alpha,25(OH)2D3. Biochem. Biophys. Res. Commun. 249 (1), 11–16.

Murray, T.M., Rao, L.G., Muzaffar, S.A., Ly, H., 1989. Human parathyroid hormone carboxyterminal peptide (53-84) stimulates alkaline phosphatase activity in dexamethasone-treated rat osteosarcoma cells in vitro. Endocrinology 124 (2), 1097–1099.

Murray, T.M., Rao, L.G., Muzaffar, S.A., 1991. Dexamethasone-treated ROS 17/2.8 rat osteosarcoma cells are responsive to human carboxyl terminal parathyroid hormone peptide hPTH (53-84): stimulation of alkaline phosphatase. Calcif. Tissue Int. 49 (2), 120–123.

Murray, T.M., Rao, L.G., Divieti, P., Bringhurst, F.R., 2005. Parathyroid hormone secretion and action: evidence for discrete receptors for the carboxyl-terminal region and related biological actions of carboxyl- terminal ligands. Endocr. Rev. 26 (1), 78–113.

Nagai, S., Okazaki, M., Segawa, H., Bergwitz, C., Dean, T., Potts Jr., J.T., et al., 2011. Acute down-regulation of sodium-dependent phosphate transporter NPT2a involves predominantly the cAMP/PKA pathway as revealed by signaling-selective parathyroid hormone analogs. J. Biol. Chem. 286 (2), 1618–1626.

Nakashima, T., Hayashi, M., Fukunaga, T., Kurata, K., Oh-Hora, M., Feng, J.Q., et al., 2011. Evidence for osteocyte regulation of bone homeostasis through RANKL expression. Nat. Med. 17 (10), 1231–1234.

Neves, S.R., Ram, P.T., Iyengar, R., 2002. G protein pathways. Science 296 (5573), 1636–1639.

Nishida, S., Yamaguchi, A., Tanizawa, T., Endo, N., Mashiba, T., Uchiyama, Y., et al., 1994. Increased bone formation by intermittent parathyroid hormone administration is due to the stimulation of proliferation and differentiation of osteoprogenitor cells in bone marrow. Bone 15 (6), 717–723.

O'Brien, C.A., Plotkin, L.I., Galli, C., Goellner, J.J., Gortazar, A.R., Allen, M.R., et al., 2008. Control of bone mass and remodeling by PTH receptor signaling in osteocytes. PLoS One 3 (8), e2942.

Onal, M., Galli, C., Fu, Q., Xiong, J., Weinstein, R.S., Manolagas, S.C., et al., 2012. The RANKL distal control region is required for the increase in RANKL expression, but not the bone loss, associated with hyperparathyroidism or lactation in adult mice. Mol. Endocrinol. 26 (2), 341–348.

Onal, M., St John, H.C., Danielson, A.L., Pike, J.W., 2015. Deletion of the distal Tnfsf11 RL-D2 enhancer that contributes to PTH-mediated RANKL expression in osteoblast lineage cells results in a high bone mass phenotype in mice. J. Bone Miner. Res. 31 (2), 416–429.

Onal, M., St John, H.C., Danielson, A.L., Markert, J.W., Riley, E.M., Pike, J.W., 2016. Unique distal enhancers linked to the mouse Tnfsf11 gene direct tissue-specific and inflammation-induced expression of RANKL. Endocrinology 157 (2), 482–496.

Pacifici, R., 2013. Role of T cells in the modulation of PTH action: physiological and clinical significance. Endocrine 44 (3), 576–582.

Patel, K., Foretz, M., Marion, A., Campbell, D.G., Gourlay, R., Boudaba, N., et al., 2014. The LKB1-salt-inducible kinase pathway functions as a key gluconeogenic suppressor in the liver. Nat. Commun. 5, 4535.

Pellicelli, M., Miller, J.A., Arabian, A., Gauthier, C., Akhouayri, O., Wu, J.Y., et al., 2014. The PTH-Galphas-protein kinase A cascade controls alphaNAC localization to regulate bone mass. Mol. Cell Biol. 34 (9), 1622–1633.

Pfister, M.F., Ruf, I., Stange, G., Ziegler, U., Lederer, E., Biber, J., et al., 1998. Parathyroid hormone leads to the lysosomal degradation of the renal type II Na/Pi cotransporter. Proc. Natl. Acad. Sci. U.S.A. 95 (4), 1909–1914.

Potts, J.T., 2005. Parathyroid hormone: past and present. J. Endocrinol. 187 (3), 311–325.

Prideaux, M., Dallas, S.L., Zhao, N., Johnsrud, E.D., Veno, P.A., Guo, D., et al., 2015. Parathyroid hormone induces bone cell motility and loss of mature osteocyte phenotype through L-calcium channel dependent and independent mechanisms. PLoS One 10 (5), e0125731.

Qing, H., Ardeshirpour, L., Pajevic, P.D., Dusevich, V., Jahn, K., Kato, S., et al., 2012. Demonstration of osteocytic perilacunar/canalicular remodeling in mice during lactation. J. Bone Miner. Res. 27 (5), 1018–1029.

Qiu, T., Crane, J.L., Xie, L., Xian, L., Xie, H., Cao, X., 2018. IGF-I induced phosphorylation of PTH receptor enhances osteoblast to osteocyte transition. Bone Res 6, 5.

Rey, A., Manen, D., Rizzoli, R., Caverzasio, J., Ferrari, S.L., 2006. Proline-rich motifs in the parathyroid hormone (PTH)/PTH-related protein receptor C terminus mediate scaffolding of c-Src with beta-arrestin2 for ERK1/2 activation. J. Biol. Chem. 281 (50), 38181–38188.

Rhee, Y., Allen, M.R., Condon, K., Lezcano, V., Ronda, A.C., Galli, C., et al., 2011. PTH receptor signaling in osteocytes governs periosteal bone formation and intracortical remodeling. J. Bone Miner. Res. 26 (5), 1035–1046.

Rivadeneira, F., Styrkarsdottir, U., Estrada, K., Halldorsson, B.V., Hsu, Y.H., Richards, J.B., et al., 2009. Twenty bone-mineral-density loci identified by large-scale meta-analysis of genome-wide association studies. Nat. Genet. 41 (11), 1199–1206.

Robling, A.G., Niziolek, P.J., Baldridge, L.A., Condon, K.W., Allen, M.R., Alam, I., et al., 2008. Mechanical stimulation of bone in vivo reduces osteocyte expression of Sost/sclerostin. J. Biol. Chem. 283 (9), 5866–5875.

Rubin, M., Bilizekian, J., 2003. New anabolic therapies in osteoporosis. Endocrinol Metab. Clin. North Am. 32, 285–307.

Rubin, M.R., Dempster, D.W., Zhou, H., Shane, E., Nickolas, T., Sliney Jr., J., et al., 2008. Dynamic and structural properties of the skeleton in hypoparathyroidism. J. Bone Miner. Res. 23 (12), 2018–2024.

Sassone-Corsi, P., 2012. The cyclic AMP pathway. Cold Spring Harb Perspect Biol 4 (12).

Sato, T., Courbebaisse, M., Ide, N., Fan, Y., Hanai, J.I., Kaludjerovic, J., et al., 2017. Parathyroid hormone controls paracellular Ca(2+) transport in the thick ascending limb by regulating the tight-junction protein Claudin14. Proc. Natl. Acad. Sci. U.S.A. 114 (16), E3344–E3353.

Schwindinger, W.F., Fredericks, J., Watkins, L., Robinson, H., Bathon, J.M., Pines, M., et al., 1998. Coupling of the PTH/PTHrP receptor to multiple G-proteins. Direct demonstration of receptor activation of Gs, Gq/11, and Gi(1) by [alpha-32P]GTP-gamma-azidoanilide photoaffinity labeling. Endocrine 8 (2), 201–209.

Screaton, R.A., Conkright, M.D., Katoh, Y., Best, J.L., Canettieri, G., Jeffries, S., et al., 2004. The CREB coactivator TORC2 functions as a calcium- and cAMP-sensitive coincidence detector. Cell 119 (1), 61–74.

Shaywitz, A.J., Greenberg, M.E., 1999. CREB: a stimulus-induced transcription factor activated by a diverse array of extracellular signals. Annu. Rev. Biochem. 68, 821–861.

Shenolikar, S., Voltz, J.W., Minkoff, C.M., Wade, J.B., Weinman, E.J., 2002. Targeted disruption of the mouse NHERF-1 gene promotes internalization of proximal tubule sodium-phosphate cotransporter type IIa and renal phosphate wasting. Proc. Natl. Acad. Sci. U.S.A. 99 (17), 11470–11475.

Shinki, T., Shimada, H., Wakino, S., Anazawa, H., Hayashi, M., Saruta, T., et al., 1997. Cloning and expression of rat 25-hydroxyvitamin D3-1alpha-hydroxylase cDNA. Proc. Natl. Acad. Sci. U.S.A. 94 (24), 12920–12925.

Singh, A.T., Gilchrist, A., Voyno-Yasenetskaya, T., Radeff-Huang, J.M., Stern, P.H., 2005. G alpha12/G alpha13 subunits of heterotrimeric G proteins mediate parathyroid hormone activation of phospholipase D in UMR-106 osteoblastic cells. Endocrinology 146 (5), 2171–2175.

Smith, J.S., Lefkowitz, R.J., Rajagopal, S., 2018. Biased signalling: from simple switches to allosteric microprocessors. Nat. Rev. Drug Discov. 17 (4), 243–260.

Sneddon, W.B., Friedman, P.A., 2007. Beta-arrestin-dependent parathyroid hormone-stimulated extracellular signal-regulated kinase activation and parathyroid hormone type 1 receptor internalization. Endocrinology 148 (8), 4073–4079.

Sneddon, W.B., Syme, C.A., Bisello, A., Magyar, C.E., Rochdi, M.D., Parent, J.L., et al., 2003. Activation-independent parathyroid hormone receptor internalization is regulated by NHERF1 (EBP50). J. Biol. Chem. 278 (44), 43787–43796.

Sneddon, W.B., Ruiz, G.W., Gallo, L.I., Xiao, K., Zhang, Q., Rbaibi, Y., et al., 2016. Convergent signaling pathways regulate parathyroid hormone and fibroblast growth factor-23 action on NPT2A-mediated phosphate transport. J. Biol. Chem. 291 (36), 18632–18642.

Sorkin, A., von Zastrow, M., 2009. Endocytosis and signalling: intertwining molecular networks. Nat. Rev. Mol. Cell Biol. 10 (9), 609–622.

Spatz, J.M., Wein, M.N., Gooi, J.H., Qu, Y., Garr, J.L., Liu, S., et al., 2015. The Wnt inhibitor sclerostin is up-regulated by mechanical unloading in osteocytes in vitro. J. Biol. Chem. 290 (27), 16744–16758.

St John, H.C., Bishop, K.A., Meyer, M.B., Benkusky, N.A., Leng, N., Kendziorski, C., et al., 2014. The osteoblast to osteocyte transition: epigenetic changes and response to the vitamin D3 hormone. Mol. Endocrinol. 28 (7), 1150–1165.

St John, H.C., Hansen, S.J., Pike, J.W., 2015. Analysis of SOST expression using large minigenes reveals the MEF2C binding site in the evolutionarily conserved region (ECR5) enhancer mediates forskolin, but not 1,25-dihydroxyvitamin D or TGFbeta responsiveness. J. Steroid Biochem. Mol. Biol. 164, 277–280.

St John, H.C., Meyer, M.B., Benkusky, N.A., Carlson, A.H., Prideaux, M., Bonewald, L.F., et al., 2015. The parathyroid hormone-regulated transcriptome in osteocytes: parallel actions with 1,25-dihydroxyvitamin D3 to oppose gene expression changes during differentiation and to promote mature cell function. Bone 72, 81–91.

St-Arnaud, R., Messerlian, S., Moir, J.M., Omdahl, J.L., Glorieux, F.H., 1997. The 25-hydroxyvitamin D 1-alpha-hydroxylase gene maps to the pseudovitamin D-deficiency rickets (PDDR) disease locus. J. Bone Miner. Res. 12 (10), 1552–1559.

Sundberg, T.B., Choi, H.G., Song, J.H., Russell, C.N., Hussain, M.M., Graham, D.B., et al., 2014. Small-molecule screening identifies inhibition of salt-inducible kinases as a therapeutic strategy to enhance immunoregulatory functions of dendritic cells. Proc. Natl. Acad. Sci. U.S.A. 111 (34), 12468–12473.

Sundberg, T.B., Liang, Y., Wu, H., Choi, H.G., Kim, N.D., Sim, T., et al., 2016. Development of chemical probes for investigation of salt-inducible kinase function in vivo. ACS Chem. Biol. 11 (8), 2105–2111.

Swarthout, J.T., Doggett, T.A., Lemker, J.L., Partridge, N.C., 2001. Stimulation of extracellular signal-regulated kinases and proliferation in rat osteoblastic cells by parathyroid hormone is protein kinase C-dependent. J. Biol. Chem. 276 (10), 7586–7592.

Takasu, H., Gardella, T.J., Luck, M.D., Potts Jr., J.T., Bringhurst, F.R., 1999. Amino-terminal modifications of human parathyroid hormone (PTH) selectively alter phospholipase C signaling via the type 1 PTH receptor: implications for design of signal-specific PTH ligands. Biochemistry 38 (41), 13453−13460.

Takeda, S., Elefteriou, F., Levasseur, R., Liu, X., Zhao, L., Parker, K.L., et al., 2002. Leptin regulates bone formation via the sympathetic nervous system. Cell 111 (3), 305−317.

Takeyama, K., Kitanaka, S., Sato, T., Kobori, M., Yanagisawa, J., Kato, S., 1997. 25-Hydroxyvitamin D3 1alpha-hydroxylase and vitamin D synthesis. Science 277 (5333), 1827−1830.

Tanaka, H., Smogorzewski, M., Koss, M., Massry, S.G., 1995. Pathways involved in PTH-induced rise in cytosolic Ca2+ concentration of rat renal proximal tubule. Am. J. Physiol. 268 (2 Pt 2), F330−F337.

Tawfeek, H.A., Abou-Samra, A.B., 2004. Important role for the V-type H(+)-ATPase and the Golgi apparatus in the recycling of PTH/PTHrP receptor. Am. J. Physiol. Endocrinol. Metab. 286 (5), E704−E710.

Tawfeek, H.A., Qian, F., Abou-Samra, A.B., 2002. Phosphorylation of the receptor for PTH and PTHrP is required for internalization and regulates receptor signaling. Mol. Endocrinol. 16 (1), 1−13.

Taylor, S.J., Chae, H.Z., Rhee, S.G., Exton, J.H., 1991. Activation of the beta 1 isozyme of phospholipase C by alpha subunits of the Gq class of G proteins. Nature 350 (6318), 516−518.

Terauchi, M., Li, J.Y., Bedi, B., Baek, K.H., Tawfeek, H., Galley, S., et al., 2009. T lymphocytes amplify the anabolic activity of parathyroid hormone through Wnt10b signaling. Cell Metabol. 10 (3), 229−240.

van Abel, M., Hoenderop, J.G., van der Kemp, A.W., Friedlaender, M.M., van Leeuwen, J.P., Bindels, R.J., 2005. Coordinated control of renal Ca(2+) transport proteins by parathyroid hormone. Kidney Int. 68 (4), 1708−1721.

van der Lee, M.M., Verkaar, F., Wat, J.W., van Offenbeek, J., Timmerman, M., Voorneveld, L., et al., 2013. beta-Arrestin-biased signaling of PTH analogs of the type 1 parathyroid hormone receptor. Cell. Signal. 25 (2), 527−538.

VanHouten, J.N., Dann, P., Stewart, A.F., Watson, C.J., Pollak, M., Karaplis, A.C., et al., 2003. Mammary-specific deletion of parathyroid hormone-related protein preserves bone mass during lactation. J. Clin. Investig. 112 (9), 1429−1436.

Venter, J.C., Adams, M.D., Myers, E.W., Li, P.W., Mural, R.J., Sutton, G.G., et al., 2001. The sequence of the human genome. Science 291 (5507), 1304−1351.

Verheijen, M.H., Defize, L.H., 1997. Parathyroid hormone activates mitogen-activated protein kinase via a cAMP-mediated pathway independent of Ras. J. Biol. Chem. 272 (6), 3423−3429.

Vilardaga, J.P., Frank, M., Krasel, C., Dees, C., Nissenson, R.A., Lohse, M.J., 2001. Differential conformational requirements for activation of G proteins and the regulatory proteins arrestin and G protein-coupled receptor kinase in the G protein-coupled receptor for parathyroid hormone (PTH)/PTH-related protein. J. Biol. Chem. 276 (36), 33435−33443.

Vilardaga, J.P., Romero, G., Friedman, P.A., Gardella, T.J., 2011. Molecular basis of parathyroid hormone receptor signaling and trafficking: a family B GPCR paradigm. Cell. Mol. Life Sci. 68 (1), 1−13.

Vilardaga, J.P., Gardella, T.J., Wehbi, V.L., Feinstein, T.N., 2012. Non-canonical signaling of the PTH receptor. Trends Pharmacol. Sci. 33 (8), 423−431.

Wang, B., Moya, N., Niessen, S., Hoover, H., Mihaylova, M.M., Shaw, R.J., et al., 2011. A hormone-dependent module regulating energy balance. Cell 145 (4), 596−606.

Wang, B., Means, C.K., Yang, Y., Mamonova, T., Bisello, A., Altschuler, D.L., et al., 2012. Ezrin-anchored protein kinase A coordinates phosphorylation-dependent disassembly of a NHERF1 ternary complex to regulate hormone-sensitive phosphate transport. J. Biol. Chem. 287 (29), 24148−24163.

Wein, M.N., Spatz, J., Nishimori, S., Doench, J., Root, D., Babij, P., et al., 2015. HDAC5 controls MEF2C-driven sclerostin expression in osteocytes. J. Bone Miner. Res. 30 (3), 400−411.

Wein, M.N., Liang, Y., Goransson, O., Sundberg, T.B., Wang, J., Williams, E.A., et al., 2016. SIKs control osteocyte responses to parathyroid hormone. Nat. Commun. 7, 13176.

Weinman, E.J., Lederer, E.D., 2012. PTH-mediated inhibition of the renal transport of phosphate. Exp. Cell Res. 318 (9), 1027−1032.

Weinman, E.J., Biswas, R.S., Peng, G., Shen, L., Turner, C.L., E X, et al., 2007. Parathyroid hormone inhibits renal phosphate transport by phosphorylation of serine 77 of sodium-hydrogen exchanger regulatory factor-1. J. Clin. Investig. 117 (11), 3412−3420.

Wijenayaka, A.R., Kogawa, M., Lim, H.P., Bonewald, L.F., Findlay, D.M., Atkins, G.J., 2011. Sclerostin stimulates osteocyte support of osteoclast activity by a RANKL-dependent pathway. PLoS One 6 (10), e25900.

Woo, S.M., Rosser, J., Dusevich, V., Kalajzic, I., Bonewald, L.F., 2011. Cell line IDG-SW3 replicates osteoblast-to-late-osteocyte differentiation in vitro and accelerates bone formation in vivo. J. Bone Miner. Res. 26 (11), 2634−2646.

Wu, X., Pang, L., Lei, W., Lu, W., Li, J., Li, Z., et al., 2010. Inhibition of Sca-1-positive skeletal stem cell recruitment by alendronate blunts the anabolic effects of parathyroid hormone on bone remodeling. Cell Stem Cell 7 (5), 571−580.

Wysolmerski, J.J., 2012. Parathyroid hormone-related protein: an update. J. Clin. Endocrinol. Metab. 97 (9), 2947−2956.

Xiong, J., O'Brien, C.A., 2012. Osteocyte RANKL: new insights into the control of bone remodeling. J. Bone Miner. Res. 27 (3), 499−505.

Xiong, J., Onal, M., Jilka, R.L., Weinstein, R.S., Manolagas, S.C., O'Brien, C.A., 2011. Matrix-embedded cells control osteoclast formation. Nat. Med. 17 (10), 1235−1241.

Xiong, J., Piemontese, M., Thostenson, J.D., Weinstein, R.S., Manolagas, S.C., O'Brien, C.A., 2014. Osteocyte-derived RANKL is a critical mediator of the increased bone resorption caused by dietary calcium deficiency. Bone 66, 146−154.

Xiong, J., Piemontese, M., Onal, M., Campbell, J., Goellner, J.J., Dusevich, V., et al., 2015. Osteocytes, not osteoblasts or lining cells, are the main source of the RANKL required for osteoclast formation in remodeling bone. PLoS One 10 (9), e0138189.

Yang, D., Guo, J., Divieti, P., Bringhurst, F.R., 2006. Parathyroid hormone activates PKC-delta and regulates osteoblastic differentiation via a PLC-independent pathway. Bone 38 (4), 485–496.

Yang, D., Singh, R., Divieti, P., Guo, J., Bouxsein, M.L., Bringhurst, F.R., 2007. Contributions of parathyroid hormone (PTH)/PTH-related peptide receptor signaling pathways to the anabolic effect of PTH on bone. Bone 40 (6), 1453–1461.

Yang, M., Arai, A., Udagawa, N., Hiraga, T., Lijuan, Z., Ito, S., et al., 2017. Osteogenic factor Runx2 marks a subset of leptin receptor-positive cells that sit atop the bone marrow stromal cell hierarchy. Sci. Rep. 7 (1), 4928.

Young, M.V., Schwartz, G.G., Wang, L., Jamieson, D.P., Whitlatch, L.W., Flanagan, J.N., et al., 2004. The prostate 25-hydroxyvitamin D-1 alpha-hydroxylase is not influenced by parathyroid hormone and calcium: implications for prostate cancer chemoprevention by vitamin D. Carcinogenesis 25 (6), 967–971.

Zierold, C., Nehring, J.A., DeLuca, H.F., 2007. Nuclear receptor 4A2 and C/EBPbeta regulate the parathyroid hormone-mediated transcriptional regulation of the 25-hydroxyvitamin D3-1alpha-hydroxylase. Arch. Biochem. Biophys. 460 (2), 233–239.

Chapter 53

Multiple endocrine neoplasia type 1

Francesca Giusti, Francesca Marini, Francesco Tonelli and Maria Luisa Brandi
Department of Experimental and Clinical Biomedical Sciences, University of Florence, Florence, Italy

Chapter outline

Introduction

Multiple endocrine neoplasia type 1 (MEN1) is a rare inherited syndrome caused by inactivating heterozygote mutations of the *MEN1* tumor-suppressor gene. It is inherited as an autosomal dominant trait, with complete penetrance by the age of 50 and different clinical phenotypes even in the presence of the same *MEN1* mutation and between identical twins.

MEN1 has a prevalence of approximately 1 in 30,000 births with equal gender distribution. Clinical diagnosis of MEN1 usually includes the presence of at least two neuroendocrine tumors affecting the parathyroid glands, gastroenteropancreatic tract, and anterior pituitary gland or by the occurrence of one of these three main tumors plus one first-degree relative clinically affected by the syndrome.

Principal clinical manifestations of the MEN1 syndrome are primary hyperparathyroidism (PHPT), gastroenteropancreatic neuroendocrine tumors (GEP-NETs), and tumors of the anterior pituitary (Table 53.1).

PHPT is characterized by multiple hyperplasia/adenomas of parathyroid glands (all the glands are usually affected during a lifetime). It can remain asymptomatic and normocalcemic for years and incidentally discovered during blood tests following the development of an increased serum value of parathyroid hormone (PTH).

GEP-NETs usually occur as multiple functioning and/or nonfunctioning (NF) tumors in the stomach, pancreatic islets, and duodenum (Fig. 53.1).

Pituitary tumors are the third most common manifestation of the disease, principally including prolactinoma (PRLoma), and less frequently somatotropinoma, adrenocorticotropina, and NF adenomas.

Other less frequent tumors/lesions affect MEN1 patients: neuroendocrine tumors (NETs) of the thoracic tract (thymus and bronchi), adrenocortical tumors, lipomas, visceral leiomyomas, truncal and facial collagenomas, facial angiofibromas (Fig. 53.2), and breast carcinoma. The presence of these tumors, in particular skin lesions (which often manifest even before main MEN1 tumors), can help the differential and early clinical diagnosis of index cases (Thakker et al., 2012).

Primary hyperparathyroidism

PHPT is generally the first endocrine manifestation in MEN1 patients, affecting more than 95% of cases by the age of 50. Age of onset is between 20 and 25 years, more than 2 decades before sporadic PHPT and with equal distribution between

Principles of Bone Biology. https://doi.org/10.1016/B978-0-12-814841-9.00053-1

TABLE 53.1 Main characteristics and frequency of NETs in MEN1.

Syndrome	Prevalence	Gene	Main clinical features	pNETs Type and frequency (%)	Other NET types and frequencies (%)
MEN1	1/30,000	*MEN1*	Multiple adenomas of parathyroid glands (PHPT), adenomas of anterior pituitary, neuroendocrine tumors of the gastroentero-pancreatic (GEP-NETs) and thoracic tracts	Duodenal gastrinoma >50% Pancreatic gastrinoma <10% Insulinoma 15%–30% NFTs and PPoma (60%–80%) Glucagonoma (<3%) VIPoma (<1%) Somatostatinoma (<1%)	Adrenal cortical tumors (40%) PHEOs (<1%) Gastric NETs (10%) Bronchopulmonary NETs (2%) Thymic NETs (2%)

GEP-NETs, gastroenteropancreatic neuroendocrine tumors; *NETs,* Neuroendocrine tumors; *NFTs,* Nonfunctioning tumors, *PHEOs,* Pheochromocytomas; *PHPT,* primary hyperparathyroidism; *pNETs,* pancreatic neuroendocrine tumors; *PPoma,* neuroendocrine tumor secreting pancreatic polypeptide.

males and females. PHPT is generally caused by parathyroid hyperplasia and/or multiple adenomas of the glands; all four parathyroid glands are usually affected during a lifetime. Ectopic or supernumerary parathyroid glands are a frequent occurrence.

PHPT in MEN1 is usually recognized by elevated PTH serum level in association with hypercalcemia, or in some cases with normocalcemia. PHPT can remain asymptomatic for years; symptomatic PHPT causes nephrolithiasis and is responsible for a reduction in bone mass by the age of 35 years. Biochemical screening includes dosage of intact serum PTH, calcemia, and calciuria; they must be measured yearly in all MEN1 patients and all MEN1 mutation carriers. Neck ultrasound and Tc99m-sestamibi parathyroid scintigraphy are of limited benefit as all parathyroid glands may be affected, but can show ectopic parathyroid glands. Ultrasound of the urinary tract (to prevent nephrolithiasis) and bone mineral density evaluation by dual-energy X-ray absorptiometry should be performed regularly (Thakker et al., 2012).

Surgery is the treatment of choice for PHPT. The timing and type of operation for parathyroid surgery in MEN1 patients are still controversial. Three surgical approaches are available: (1) partial parathyroidectomy with ablation of only the enlarged glands (up to three glands); (2) subtotal parathyroidectomy: removal of greater than three glands, leaving a normal parathyroid gland or a viable remnant (approximately 50 mg) from the most normal-appearing gland; and (3) total parathyroidectomy—ablation of all parathyroid glands (including ectopic and supernumerary glands) with the heterotopic autotransplantation of fresh or cryopreserved normal parathyroid tissue into the brachioradialis muscle of the nondominant forearm (Norton et al., 2015). An intraoperative dosage of PTH is suggested to minimize the risk of postintervention persistence of PHPT, allowing the correct ablation of all adenomatous and/or hyperplastic parathyroid glands to be

FIGURE 53.1 Numerous scattered islet cell adenomas (numbered 1 − 6) of various size and architecture in a transverse section of the pancreas of a patient with MEN1 syndrome and ZES (H&E, 4). *Reprinted with permission from Pilato et al. (1988).*

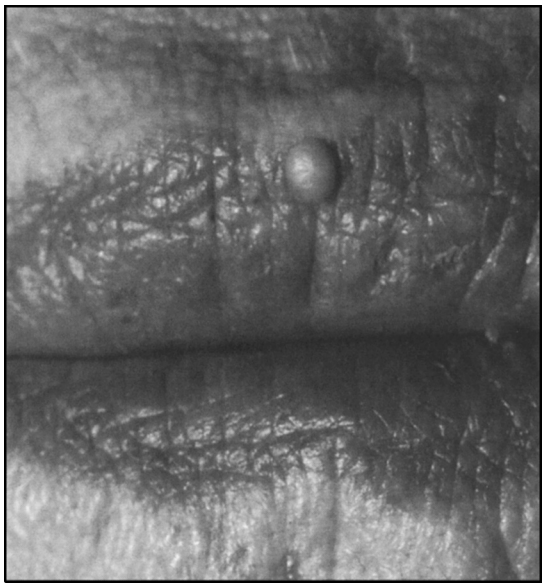

FIGURE 53.2 MEN1-associated angiofibroma.

monitored (Nilubol et al., 2013). Both partial and subtotal parathyroidectomy have a higher probability of persistence and recurrence (i.e., 40%−60% of MEN1 patients within 10−12 years after surgery) than does total parathyroidectomy; total parathyroidectomy, even with reimplantation, presents a higher incidence of permanent hypoparathyroidism but a lower incidence of recurrence than other procedures. Transcervical thymectomy at the time of neck surgery is strongly suggested to remove ectopic parathyroid glands and to avoid thymic NETs. Minimizing the persistence and recurrence of hyperparathyroidism by surgery seems to be an important tool. A recent study shows that persistent hypercalcemia is associated with higher levels of anxiety, depression, and fatigue, as well as decreased social functioning, in MEN1 patients. Interestingly, a similar reduction in the quality of life is not observed in patients affected by hypoparathyroidism after surgery (Goswami et al., 2017).

PHPT can also be pharmacologically controlled by calcimimetics (i.e., cinacalcet) as an alternative to parathyroid surgery in patients who do not meet the criteria for parathyroidectomy, for those who failed a previous intervention, and for those presenting recurrence who refuse to undergo any further surgical interventions. Calcimimetics are a class of calcium-sensing receptor agonists that have been demonstrated to normalize serum calcium level, reduce PTH release by parathyroid cells, and reduce parathyroid cell growth. Cinacalcet has been demonstrated to be well tolerated and safe in MEN1 patients and to restore normal calcium homeostasis (Moyes et al., 2010; Giusti et al., 2016).

Gastroenteropancreatic neuroendocrine tumors

GEP-NETs affect 30%−80% of MEN1 patients and are classified in functioning GEP-NETs and nonfunctioning GEP-NETs (NF GEP-NETs).

NF GEP-NETs are the most frequent pancreatic NETs (pNETs) in MEN1. They are usually multiple, asymptomatic, and characterized by later onset. They are discovered incidentally either by imaging exams or by assessing the increase of the pancreatic polypeptide (PP), which is secreted by approximately half of them.

Functioning GEP-NETs are characterized by excessive hormone production and usually associated with a typical hormone excess clinical syndrome: gastrinoma in over 50% of MEN1 patients (gastrin), insulinoma in 15%−30% of MEN1 patients (insulin), glucagonoma in <3% of MEN1 patients (glucagon), VIPoma in <1% of MEN1 patients (vasoactive intestinal polypeptide; VIP), and somatostatinomas in <1% of MEN1 patients (somatostatin).

Management of functioning GEP-NETs includes:

1. Confirm the diagnosis based on the clinical presentation by dosage of the basal levels of the specific hormones and/or their modifications after provocative test.

2. Assess whether the GEP-NETs belong to the MEN1 syndrome, researching other endocrinopathies either in the patients or in family members and searching for mutations of the *MEN1* gene.
3. Control the life-threatening metabolic consequences (hypoglycemia, hypokalemia, dehydration, etc) and hormonal excess by supportive medical treatment.
4. Localize the site of the primary tumor.
5. Stage the tumor, evaluating the eventual invasion of surrounding structures and/or diffusion into the periduodenal and peripancreatic lymph nodes, liver, and other viscera.
6. Evaluate the possibility of radical surgical resection of the primary functioning NET and/or of the possible metastases.
7. Consider cytoreductive surgery and/or alternative medical therapies for unresectable tumors.
8. Set up an appropriate follow-up for recurrence of NETs or appearance of other MEN1-related endocrine tumors.

Gastrinoma

The most common MEN1 GEP-NET is gastrinoma, occurring principally in the duodenal mucosa or submucosa (more than 90% of cases); less than 10% of MEN1 gastrinomas are located in the pancreas, contrary to its sporadic counterpart.

MEN1 gastrinomas usually manifest as multiple microadenomas (<0.5 cm) with a low grade of growth (Ki67 < 2%) (Fig. 53.3). They are diagnosed by the age of 40, and at the time of diagnosis in 34%−85% of cases present lymph node metastases (Yates et al., 2015); fast growth and liver metastases are rare, but they are principal causes of MEN1-related death. Ectopic gastrinomas, arising in the gallbladder or in the biliary tree, are very rare, but they can be the cause of hypergastrinemia persistence or recurrence after surgical resection of duodenal gastrinoma (Tonelli et al., 2013).

Clinically, gastrinomas induce the Zollinger−Ellison syndrome (ZES), a hypersecretion of gastric acid that causes diarrhea, multiple peptic ulcers, reflux, and esophagitis. The presence of hypercalcemia due to PHPT worsens the symptoms of ZES, as it increases the gastric acid secretion; normalization of calcemia improves gastroenteric symptomatology, and parathyroidectomy is strongly indicated in hypercalcemic patients with gastrinomas.

The diagnosis of gastrinomas is made by elevated basal serum gastrin levels accompanied by the presence of hyperchloryhydria or pH < 2; stimulation tests with secretin, or more rarely calcium, can be performed. Imaging screening is useful in localizing the tumor; these consist of endoscopic ultrasonography (EUS), multislice computed tomography (CT), magnetic resonance imaging (MRI), selective abdominal angiography, and somatostatin-receptor scintigraphy (Thakker et al., 2012). The multiplicity of MEN1 gastrinomas, their very small size, and common localization in the duodenal wall make these tumors very difficult to localize before surgery. Liver MRI is used to detect liver metastases and possible extrahepatic biliary tree ectopic gastrinomas. Neither the diagnostic efficacy of gallium-68 DOTATOC PET/CT nor the prognostic role of Ki67 tumor grading by EUS-guided tissue biopsy has been correctly evaluated in MEN1 patients yet.

The main objective of medical therapy is to reduce and control gastric acid hypersecretion. Medical therapy is the same as sporadic ZES with the administration, alone or in combination, of histamine-2 receptor antagonists (cimetidine, ranitidine, and famotidine), proton pump inhibitors (PPIs: omeprazole, lansoprazole, and pantoprazole), and somatostatin analogues (SSAs: octreotide and lanreotide). All these molecules have demonstrated long-term effectiveness in controlling

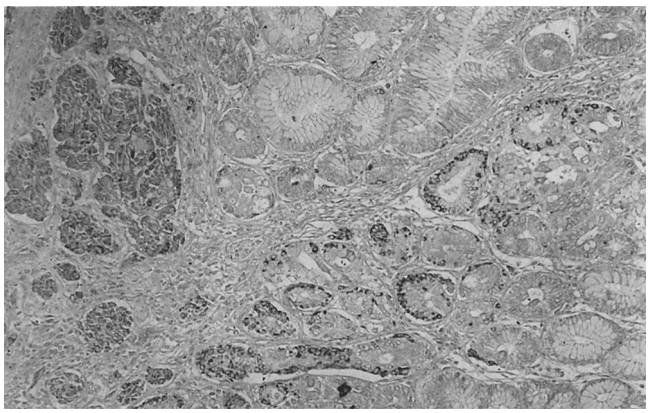

FIGURE 53.3 Immunostaining for basic FGF in the gastric endocrine cells of a patient with MEN1 syndrome and ZES. The peptide is expressed by both intraglandular cells showing hyperplastic pre- tumoral lesions (on the right) and carcinoid tumor (on the left) (immunoperoxidase, 100).

clinical symptoms and an absence of important adverse events. SSAs are synthetic molecules that retain binding affinity for somatostatin receptors (SSTRs), at least with high affinity for SSTR2 and moderate affinity for SSTR5, that are able to inhibit both pancreatic and gastrointestinal hormone secretion (i.e., insulin, glucagon, gastrin, secretin, and VIP) and control the growth of GEP-NETs (Rinke and Krug, 2016; Wolin, 2012).

Surgery is proposed to avoid neoplastic progression and to restore normal gastrinemia, preventing the development of gastric carcinoids. However, timing and type of surgery are still controversial. Some situations pose an absolute indication for surgery: fast-growing gastrinomas, diagnosis of pancreatic gastrinoma, and the presence of severe hypergastrinemia. However, overall growth of concomitant pNETs is what moves to operate in order to avoid the development of a neuroendocrine carcinoma (Falconi et al., 2016). The choice of surgery depends on where the pNETS are prevalently located. When pNETs are predominant in the right pancreas, pancreatoduodenectomy (PD) or pylorus-preserving PD represent a surgical option with a high probability (around 80%) of being curative for hypergastrinemia, because all of the duodenum, where most gastrinomas arise, is removed. When pancreatic NETs are predominant in the left pancreas, Thompson's procedure can be chosen. This procedure consists of a longitudinal duodenotomy with mucosal enucleation or resection by full-thickness duodenal wall excision (if the gastrinoma is > 0.5 cm) of the discovered duodenal gastrinomas and a peripancreatic lymph-node resection associated to distal pancreatic resection (DPR) (Thompson, 1998). Enucleation of tumors in the residual pancreas is necessary, both for PD and DPR, for adenoma greater than 1 cm in diameter. Another surgical option for the cure of ZES is pancreas-preserving total duodenectomy. It consists of the resection of the entire duodenum and gastric antrum, the ligation of the accessory pancreatic duct, the sphincterotomy of the major papilla after removing its mucosal lining, and the anastomosis of the Vater papilla on a Roux-en-Y jejunal loop (Imamura). Surgery carries the risk of mortality and morbidity. The main cause of a compromised quality of life can be the occurrence of insulin-dependent diabetes. However, data on the prevalence of diabetes in MEN1 patients that have undergone pancreatic resection are limited. Currently, the benefit of surgery compared with medical treatment with PPIs and/or SSAs has not been tested with clinical trials. Failure to correct hypergastrinemia can favor the occurrence of gastric carcinoids (type 2 gastric NETs) in MEN1 patients. These tumors arise from ECL cells and grow in the mucosa or submucosa of the stomach. They are multiple and just a few millimeters in size, remaining stable for a long time. Risk of malignant progression is less than 10%. Therefore, endoscopic surveillance with excision of the biggest tumors is currently the most followed therapeutic choice. SSAs and cholecystokinin B receptor antagonists have also been employed for the treatment of type 2 gastric NETs with a significant reduction in gastrin levels and tumor dimension (Norton 2015).

Insulinoma

Insulinoma can represent the first clinical manifestation of the MEN1 syndrome in at least 15% of affected patients (Sakurai et al., 2012; Goncales et al., 2014; Thakker et al., 2012), occurring prevalently in females (Levi-Bohbot 2004; O'Riordain et al., 1994; Sakurai et al., 2012). Mean age at diagnosis for insulinoma varies from 24 to 36 years, but it can manifest as early as 5 years, with an age of onset younger than that of other MEN one associated GEP-NETs (Sakurai et al., 2012). Neuroglycopenic symptoms, due to the oversecretion of insulin, can be the first manifestation of MEN1 syndrome in some patients; the occurrence of insulinomas during childhood or adolescence should suggest the presence of MEN1. MEN1 insulinomas represents 5% of all diagnosed cases in adults, but 15%−20% in childhood (Goncales et al., 2014). MEN1 insulinomas are characterized by (1) localization exclusively pancreatic, (2) scattered through all the pancreas, (3) dimension variable from 2 mm to >3 cm, and (4) multiple insulinomas found in 30%−60% of patients (Giudici et al., 2012; Anlauf et al., 2009). Some authors suggest that a dominant lesion (at least 1 cm in diameter) is responsible for hypoglycemia, also in presence of multiple insulinomas (Bartsch et al., 2013; Jensen et al., 2012), but it is still not clear. It is probable that microinsulinomas (less than 5 mm in diameter) could be clinically silent, since persistence of hypoglycemia after enucleation of a single insulinoma manifests at a lower rate than in the case of multiple insulinomas.

Unlike for sporadic insulinoma, whose localization can be done intraoperatively by inspection, palpation of the pancreas, and ultrasound, in MEN1 multiple insulinomas the challenge is to detect which of several tumors is responsible for the neuroglycopenic syndrome, which is impossible via conventional imaging techniques. Other methods, which are more difficult and invasive, allow the insulinoma to be preoperatively localized:

1. EUS (or CT)-guided fine-needle aspiration collects samples for immunohistochemistry or for insulin dosage (Fig. 53.4). This technique is difficult or impossible to apply if several pancreatic lesions are present or if the nodules are small, and it has rarely been employed in MEN1 patients (Goncales et al., 2014; Tonelli 2014; Lee et al., 2013).
2. Transhepatic portal venous sampling has been widely used in the past, even if rarely used for MEN1 pancreatic lesions, and eventually was abandoned due to the low accuracy of the examination, its invasiveness, and its difficulty.

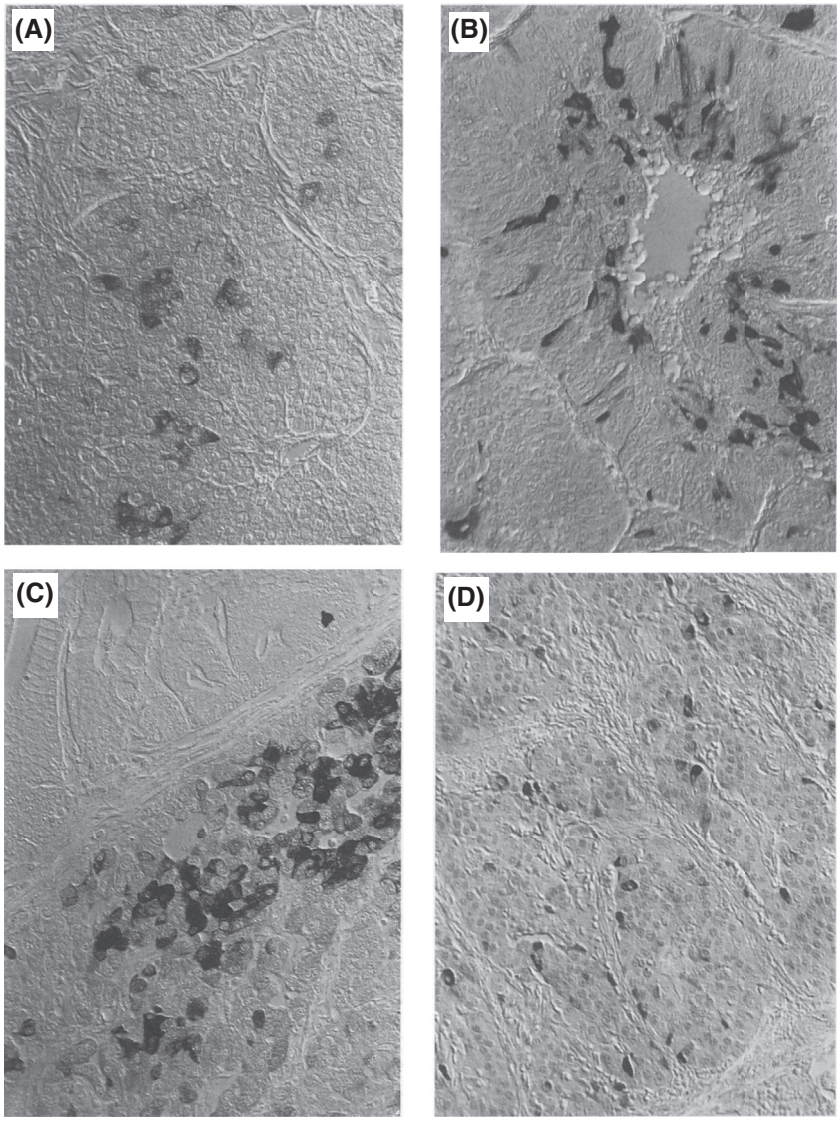

FIGURE 53.4 Immunohistochemical expression of -subunit of glycoprotein hormones in different types of tumors in MEN1 patients: parathyroid (A); lung carcinoid (B); gastric carcinoid (C); duodenal gastrinoma (D); (immunoperoxidase, 170).

3. Selective intraarterial calcium injection (SACI) of the major pancreatic arteries with hepatic venous sampling for insulin assay was developed by Doppman et al., in 1991 (Doppman et al., 1991). The proper hepatic, gastroduodenal, superior mesenteric, and splenic arteries are selectively catheterized and subsequently injected with calcium gluconate (0.025 mEq calcium/kg body weight). Blood samples for insulin determination are obtained from a major hepatic vein prior to and 30, 60, and 120 s after calcium infusion. The detection of insulinomas with this method is based on the production of insulin (or proinsulin and C-peptide) from the insulinomas. Insulinomas with a diameter of less than 1 mm can also be diagnosed by this method (Hayashi et al., 2001). However, the insulinoma cannot be visualized directly but only localized in a part of the pancreas (usually the right or left pancreatic region) on the basis of the insulin dosage in the hepatic venous blood samples. A twofold increase in the insulin concentration from baseline localizes the insulinoma within the anatomic region perfused by the injected artery. SACI requires specific expertise that may be available only in dedicated centers. The experience performed up until now has been done prevalently in sporadic insulinoma, being anecdotal in MEN1 insulinomas (Bartsch et al., 2013; Guettier et al., 2009). Only 14 cases of MEN1 insulinomas can be found in the literature of the last 20 years, and in two of these the examination was not informative. False negatives due to technical flaws and anatomical variants of pancreatic vascularization, or false positives with regionalization of the insulinoma in a wrong pancreatic region, are possible. Therefore, it is not clear whether small

insulinomas are also eventually detected on histological examination of the resected pancreas as evidenced by the SACI test, and how it can be possible to localize more than one insulinoma scattered in different parts of the pancreas.

In conclusion, since these methods are rarely employed, it is currently difficult to establish their accuracy for localizing insulinoma in the MEN1 setting. In a great majority of patients, surgery is carried out without knowing the site, dimension, and number of insulinomas.

Surgery is mandatory to cure severe hypoglycemia in patients with hyperinsulinism and to avoid brain damage from neuroglycopenic attacks. The absence of controlled studies makes the choice of surgery controversial. Data about the modality and result of surgical treatment of MEN1 insulinomas can be retrieved from 10 retrospective case series (O'Riordain et al., 1994; Giudici et al., 2012; Anlauf et al., 2009; Bartsch et al., 2013; Thompson 1998; Demeure et al., 1991; Lo et al., 1998; Jordan 1999). Two surgical modalities are most frequently employed: enucleation of the greatest pancreatic lesions or DPR preserving splenic vessels and spleen. PD rather than DPR should be adopted for MEN1 insulinomas when large and deep tumors are found within the pancreatic head. This is especially important if the insulinomas are situated close to the Wirsung duct, if there is a risk of lymph nodes surrounding the pancreatic head being metastatic, or concomitant ZES syndrome is present (Tonelli et al., 2017).

Glucagonoma

Glucagonomas occur in fewer than 3% of patients with MEN1, usually before 40 years of age. They can manifest with hyperglycemia, anorexia, glossitis, anemia, diarrhea, venous thrombosis, and skin rash. The characteristic sign (necrolytic migratory erythema) can be absent, and the diagnosis is made by hyperglucagonemia (levels >1000 pg/mL). The presence of clinical manifestations and malignancy are related to the size of the tumor. A tumor less than 2 cm in diameter has a low incidence of malignancy, but when the tumor size is more than 5 cm in diameter, two-thirds of glucagonomas are malignant (Economopoulos et al., 2001). The liver is the most common site for distal metastases.

VIPoma

VIPoma is diagnosed in less than 3% of MEN1 patients. Watery diarrhea, hypokalemia, and achlorhydria (WDHA syndrome) are often present. The electrolytic imbalance must be corrected before surgery. The majority of VIPomas are greater than 3 cm in diameter, malignant, and associated with synchronous or metachronous liver metastases.

Somatostatinoma

Somatostatinoma is particularly rare, manifesting in less than 1% of MEN1 patients. Usually, the somatostatin syndrome is absent or incomplete, and diagnosis is based on high levels of somatostatin in the plasma or somatostatin-immunoreactive cells within the tumors (>80%−100%) (Garbrecht et al., 2008). A majority of somatostatinomas are diagnosed in the fifth decade of life. Either pancreas or duodenum and first jejunal loop can be the site of the tumor. Most of the time, somatostatinomas localized in the duodenum or jejunum have a small dimension (around 0.5−1 mm), are multiple, and represent an incidental finding in MEN1 patients suffering from ZES due to duodenal gastrinomas. Metastases in the peripancreatic lymph nodes are found, but they are usually positive for gastrin and not for somatostatin (Garbrecht et al., 2008). Pancreatic somatostatinomas have a large dimension (3−5 cm), are frequently multiple, and can metastasize to peripancreatic lymph nodes and liver (Lévy-Bohbot et al., 2004; Economopoulos et al., 2001).

Nonfunctioning neuroendocrine tumors of the gastroenteropancreatic tract

NF GEP-NETs are the most frequently observed GEP-NETs in MEN1 patients and are characterized by later onset. The number is variable from few to more than 50 tumors. A majority of NF GEP-NETs in MEN1 are microscopic, well differentiated, and have a low (<5%) ki67 index. Their diagnosis is difficult because they are usually asymptomatic and discovered incidentally either by imaging exams or by assessing the increase of PP. NF GEP-NETs are the most common cause of death in MEN1 patients due to their malignant progression and metastases (Thakker et al., 2012). Tumor size is usually correlated with metastases (Triponez et al., 2017). The treatment of choice is surgery. Timing of operation is suggested when the dimension of NF pNETs is approximately 2 cm in diameter or when imaging exams during follow-up show a significant growth of lesions (Table 53.2) (Triponez et al., 2006; Triponez et al., 2017).

The most used surgical procedure is DPR, with or without enucleation of macroadenomas in the pancreatic head. PD is rarely performed. This probably reflects the fear that this more complex operation can be affected by major postoperative

complications more often than DPR. However, overall morbidity, and especially the rate and severity of pancreatic fistulas, are similar when both procedures are compared. Furthermore, morbidity and mortality after PD have been dramatically reduced in current surgical practice, particularly in the experience of dedicated centers.

All surgical procedures on the pancreas are at risk for pancreatitis or pancreatic fistula. Enucleation cannot avoid these postoperative complications. In particular, the rate of pancreatic fistula (grades A, B, and C) observed in recent reviews of large institutional experiences concerning surgery for endocrine pancreatic tumors is often higher than in surgery for pancreatic adenocarcinoma (Fendrich et al., 2011). Furthermore, it is surprising that the rate of fistula is higher for enucleation procedures than for resection of the left or right pancreas (Pitt et al., 2009). In the presence of MEN1 pNETs, postoperative fistulas frequently approach 100% for enucleation and 84% for hemipancreatectomy and have been observed significantly more often than in sporadic pNETs (Inchauste et al., 2012). The MEN1 pancreas harbors all the factors responsible for the occurrence of the fistula: the softness of the pancreatic parenchyma, the small diameter of the Wirsung duct, and the macro- and microscopic pancreatic alterations due to the presence of multiple NETs. The remnant pancreatic volume after the surgical procedure is another risk factor, and the volume is higher after enucleation than after resection.

In case of unresectable tumors or advanced metastatic cancer, some medical therapies, such as SSAs, peptide receptor radionuclide therapy (PRRT), cytotoxic chemotherapy (i.e., streptozocin and 5-fluorouracil, doxorubicin, temozolomide with capecitabine), inhibitors of tyrosine kinase receptors (i.e., sunitinib), and inhibitors of mammalian target of rapamycin (mTOR; i.e., everolimus) have been demonstrated to increase the median progression-free survival in sporadic pNETs. No specific trials have been performed in MEN1 patients (Fine et al., 2013; Bodei et al., 2015; Yao et al., 2011; Raymond et al., 2011).

Anterior pituitary tumors

The incidence of anterior pituitary tumors in MEN1 syndrome varies from 15% to 55% in different series with a mean age of onset in the fourth decade of life, with early cases described by the age of 5. Prolactin-secreting adenoma (PRLoma) is the most common pituitary tumor (60%), followed by growth hormone (GH)-secreting adenoma (somatotropinoma or GHoma; 25%), adrenocorticotropic hormone-secreting adenoma (adrenocorticotropina or ACTHoma; 5%), and NF tumors (10%) (Thakker et al., 2012).

The signs and symptoms of patients with pituitary adenomas are caused by "mass effects" of macroadenomas (mostly NF adenomas) or secondary to excessive pituitary hormone production by functioning adenomas:

1. PRLomas manifest as oligomenorrhea/amenorrhea and galactorrhea in females, and sexual dysfunction and (more rarely) gynecomastia in males.
2. GHomas are tumors that occur with the signs and symptoms of acromegaly.
3. Growth hormone/prolactin-secreting anterior pituitary adenomas manifest as signs/symptoms of acromegaly, as oligomenorrhea/amenorrhea and galactorrhea in females, and as sexual dysfunction and (more rarely) gynecomastia in males.
4. ACTHomas are mostly associated with Cushing's syndrome.
5. Thyroid-stimulating hormone−secreting anterior pituitary tumors occur with the signs/symptoms of hyperthyroidism;
6. Nonsecreting pituitary tumors usually manifest as silent macroadenoma compressing adjacent structures, such as optic chiasm with subsequent severe headaches, visual field defects, and/or hypopituitarism.

Anterior pituitary tumors are relatively benign; however, macroadenomas can be aggressive, invasive, inoperable, therapy-resistant tumors causing significant morbidity even when they are not metastatic (they tend to be larger in size than their sporadic counterparts) (Thakker et al., 2012). Vergès et al., (2002) reported that 32% of pituitary macroadenomas were invasive.

TABLE 53.2 Management in MEN1 nonfunctioning pancreatic NETs.

Tumor size	Follow up	Management
<2 cm	EUS−MRI	Follow-up
>2 cm	EUS−MRI gallium-68 DOTATOC PET/CT	Surgery

EUS, endoscopic ultrasound; *MEN1,* multiple endocrine neoplasia type 1; *MRI,* magnetic resonance imaging; *NETs,* neuroendocrine tumors.

A metastatic gonadotropic pituitary carcinoma in a woman with MEN1 (Benito et al., 2005) and a metastatic prolactinoma that presented as a cervical spinal cord tumor (Gordon et al., 2007) have been described. No increased prevalence of pituitary carcinoma is observed in individuals with MEN1 with respect to sporadic counterpart and general population (Thakker et al., 2012).

Pituitary adenomas can be classified by their size, extent of invasion through the cavernous sinus, and clinical function or ability to produce hormones; in 2017, the revised WHO classification recognized the role of transcription factors in tumor differentiation according to cellular lineage, regulation of specific pituitary hormones production, and possible adenoma tumorigenesis (Lloyd et al., 2017).

MRI is the diagnostic imaging of choice, and timing of screening is controversial (Livshits et al., 2016).

The therapy of MEN1 anterior pituitary tumor adenoma is the same as for sporadic counterparts. Medical therapies of PRLoma with dopamine agonists (bromocriptine and cabergoline) is the gold standard; transsphenoidal surgery and radiotherapy are reserved for drug-resistant tumors and macroadenomas that compress adjacent structures and generate neuro-ophthalmologic complications that cannot be managed through pharmacologic therapy.

Transsphenoidal surgery is the treatment of choice for growing hormone-secreting pituitary adenomas. Pharmacological treatment includes SSAs (octreotide, lanreotide, and pasireotide), dopamine agonist (cabergoline), and GH receptor antagonist (pegvisomant).

In ACTH-secreting pituitary tumors, the treatment is excision of adenoma.

In drug-resistant tumors, macroadenoma radiation therapy can be used as an alternative to surgery or in patients who have failed other modalities. The use of modern stereotaxic radiosurgery can minimize the problem of hypopituitarism often seen after conventional radiation therapy (Lim and Korbonitis, 2018).

Thymic and bronchial neuroendocrine tumors

A percentage of MEN1 patients manifest NETs (previously referred to as carcinoids) in the thoracic tract, affecting thymus and bronchi.

NETs of the thymus occur in 3%−8% of MEN1 patients and are diagnosed at a mean age of 39. They arise almost exclusively in men (male/female ratio = 20:1) with a significantly higher percentage in smokers. However, some authors have recently reported a largely different sex ratio (male/female ratio = 2:1) (Christakis et al., 2016). The great majority of thymic NETs are discovered incidentally or only when they have already invaded adjacent tissues and/or metastasized to the lung, liver, and bones. They represent the second cause of death in MEN1 patients after NF GEP-NETs. This unfavorable outcome indicates the need for accurate screening. MRI or CT has been proposed every 3−5 years, but the cost of the examinations and exposure to radiation limit its use. Preventive total thymectomy is suggested at the time of parathyroid surgery, but its effectiveness in preventing thymic carcinoids is questioned, as cases of thymic carcinoids have been reported in patients who have undergone thymectomy at the time of parathyroidectomy. This phenomenon probably depends on an incomplete thymectomy that leaves a part of the thymus in the mediastinum. Radical surgical removal of thymic carcinoids is possible, especially with early intervention. Frequently, it can require resection of surrounding involved structures, such as pleura, pericardium, lung, and major vessels. Radical surgery may have a solely palliative purpose when the tumor grossly invades mediastinal organs; however, it does serve to limit the effects of local compression. Radiotherapy and chemotherapy (temozolomide/5-fluorouracil/oxaliplatin) can be administered either as adjuvant therapy or as a palliative therapy for advanced cases. SSAs, mTor inhibitors (everolimus), and PRRT have also been employed (Sadowski et al., 2017). The prognosis is poor, with a 10-year survival of around 30%.

Bronchial carcinoids are diagnosed in 4%−6% of MEN1 patients when lesions discovered in the lung are biopsied and studied by immunophenotyping for chromogranin A and/or synaptophysin, but the frequency increases to 31% if only imaging findings are considered (Sadowski et al., 2017). These tumors are discovered at the age of 50 years as a mean, without a predominance of one of the sexes but with a major frequency in smokers and in families with other patients affected by this tumor. The discovery of bronchial carcinoid is usually incidental. A majority of bronchial NETs have an indolent progression, remaining stable for years, and the progression toward more aggressive forms (large-cell neuroendocrine carcinomas or small-cell neuroendocrine carcinomas) is rare. Tumor doubling time in males was 2.5 years versus 5.5 years in females (de Laat et al., 2014). Screening every 2−3 years starting from the age of 20 years is recommended using a low-dosage CT scan (Thakker et al., 2012; de Laat et al., 2014). Future trials will determine if other modalities of screening, such as MRI, can be a valid alternative to CT, thereby eliminating the risk of radiation. Surgery is the therapy of choice and should be as lung-sparing as possible, considering the low malignancy of bronchial NETs.

Genetics and molecular biology of multiple endocrine neoplasia type 1

MEN1 is caused by inactivating mutations of the tumor-suppressor gene *MEN1*, encoding a 610 amino acid nuclear protein named menin. The identification of the causative gene in 1997 gave us the possibility of genetic testing and presymptomatic diagnosis of the disease in mutated pedigrees. Over 1500 different MEN1 loss-of-function mutations (1341 germinal and 203 somatic variants) had been described up to September 2015 (Lemos and Thakker 2008; Concolino et al., 2016), affecting the coding region (exons 2−10) and splicing sites or deleting large intragenic regions (Fig. 53.5). A great majority of mutations account for a truncated protein that is unable to reach the nucleus and exert its biological functions. About 10% of patients have de novo mutations developed at the embryonic level and thus lack a family history; 90% of *MEN1* mutations are inherited from one parent in an autosomal-dominant manner and equal sex distribution. Twelve exon polymorphisms have been reported (Lemos and Thakker 2008), ten synonymous and two nonsynonymous, and need to be distinguished from mutations during genetic screening. Two clinical and functional studies have investigated the two nonsynonymous polymorphic variants, Arg171Gln in exon 3 and Ala541Thr in exon 10, for their potential roles in MEN1 tumorigenesis (De Carlo et al., 2008; Nozières et al., 2014), suggesting that both might be regarded as point mutations with the low-penetrance MEN1 phenotype.

Genetic testing is recommended for index cases with two or more MEN1-associated endocrine tumors (for the confirmation of clinical diagnosis), for first-degree relatives and family members of known *MEN1* mutation carriers, and for patients with a suspicious MEN1 phenotype. First-degree relatives of a mutated individual should undergo the genetic screening as early as possible before the age of 5, since MEN1 tumors have been described in some children at 5−8 years. A positive MEN1 genetic test is an indication for annual biochemical and imaging screenings for MEN1-associated tumor detection, according to international MEN1 guidelines (Table 53.3) (Thakker et al., 2012). Early surveillance in mutation carriers grants the detection of MEN1 tumors about 10 years before clinical manifestation. A negative test in relatives indicates they have the same risk of developing MEN1 as the general population, and it allows them to avoid further nonuseful diagnostic screenings. No direct genotype−phenotype correlation has been reported, and thus the individual

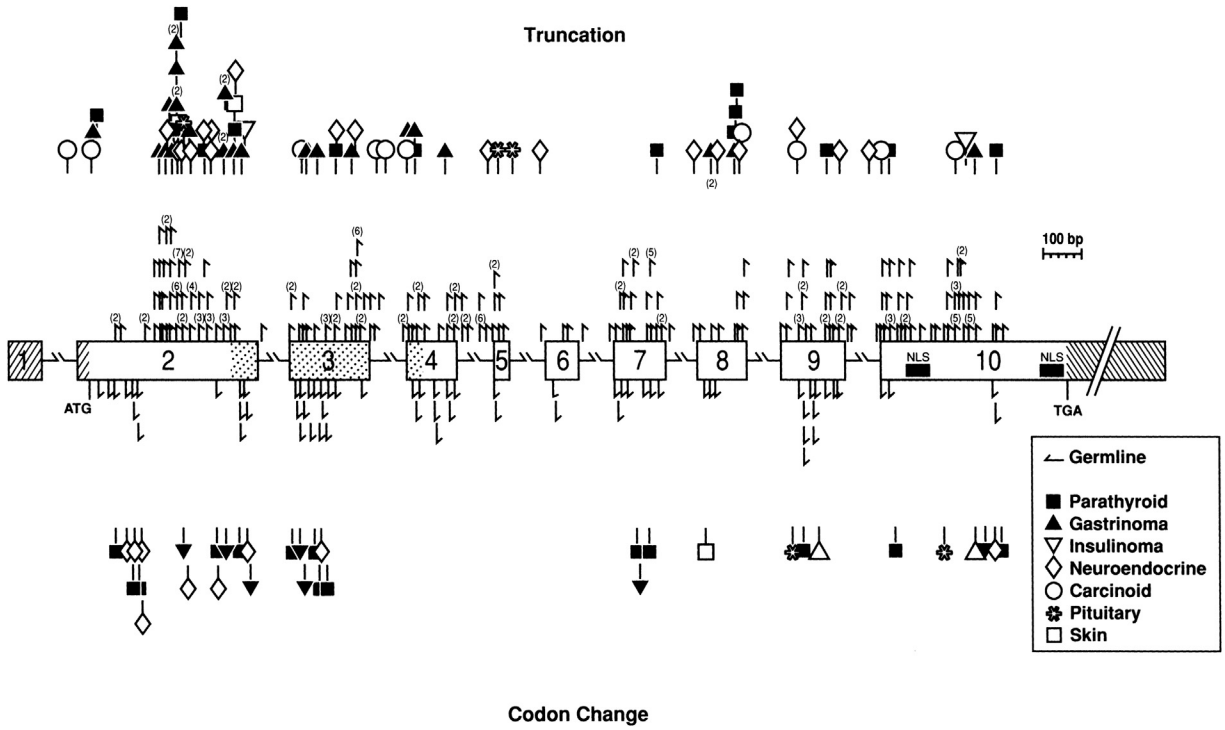

FIGURE 53.5 Genomic organization of the *MEN1* gene and of *MEN1* germline and somatic mutations, published as of June 2000. The gene con- tains 10 exons (with the first exon untranslated) and extends across 9 kb. Mutations shown above the exons cause menin truncation, and those shown below the exons cause a codon change. All unique mutations are represented; numbers in parenthesis designate multiple reports of the same mutation in presumed unrelated persons. The hatched areas indicate the untranslated regions. The location of the two nuclear localization signals (NLS), at codons 479−497 and 588−608, are indicated. Missense mutations in a region of menin (aa 139−242) (identified by stippling) prevented interaction with the AP1 transcription factor JunD.

TABLE 53.3 Diagnosis and clinical surveillance of NETs in MEN1.

	Biochemical test		Imaging test	
Syndrome	Type	Surveillance starting age (years) and periodical frequency	Type	Surveillance starting age (years) and periodical frequency
MEN1				
Parathyroid adenoma	Morning fast serum calcium, PTH, and serum ionized calcium1	8 annually	None	–
Anterior pituitary tumors	Morning fast serum PRL, GH, IGF-1, ACTH, cortisol, FSH, LH, TSH	5 annual	Head noncontrast MRI	5 every 3–5 years
Gastrinoma	Fasting serum gastrin (±gastric pH; diagnostic values < 2),	20 annually	None	–
Insulinoma	Fasting plasma insulin and glucose	5 annually	None	–
Other pancreatic NET (glucagonoma, VIPoma, NFTs)	Plasma glucagon, VIP, PP, CgA	10 annually	MRI or EUS or (CT scan)	10 annually
Carcinoids: (Foregut/stomach, lung/bronchi, thymus)	None (they are typically nonsecretory tumors)	–	EUS of the stomach Low dose CT scan and MRI of neck and chest	15 Annually Every 1–2 years
Adrenal lesions	Plasma renin, aldosterone, low-dose dexamethasone suppression test, urinary catecholamines and/or metanephrines	<10	Abdominal imaging by MRI or CT scan	Annually with pancreatic imaging

ACTH, adrenocorticotropic hormone (corticotropin); *CgA*, chromogranin A; *CT*, computed tomography; *EUS*, endoscopic ultrasounds; *FSH*, follicle-stimulating hormone; *GEP-NETs*, gastroenteropancreatic neuroendocrine tumors; *GH*, growth hormone; *IGF-1*, insulin-like growth factor-1; *LH*, luteinizing hormone; *MRI*, magnetic resonance imaging; *PP*, pancreatic polypeptide; *PRL*, prolactin; *PTH*, parathyroid hormone; *TSH*, thyroid-stimulating hormone; *VIP*, vasoactive intestinal peptide.

gene variation cannot lead to a personal diagnostic and therapeutic program; all MEN1 patients and mutation carriers undergo the same diagnostic tumor screenings.

Sequencing analysis fails in identifying mutations in about 10%–30% of clinical MEN1 cases (Agarwal 2017). Multiplex ligation probe amplification can detect large intragenic deletions, which are estimated to represent about 1%–3% of *MEN1* mutations. Current genetic testing does not investigate noncoding and regulatory regions; identification of MEN1 regulatory regions and the application of next-generation sequencing techniques may improve genetic diagnosis and early disease prediction. Clinical phenocopies, presumably caused by mutations in genes encoding menin-interacting proteins (i.e., *CDKN* genes) or in genes regulating *MEN1* expression might account for up to 5% of clinical cases of MEN1 without a *MEN1* mutation.

The protein product of MEN1, menin, is a ubiquitously expressed tumor suppressor showing no homology with any known human protein and having a high sequence homology with other animal species. Menin has been shown to directly interact with more than 50 different proteins involved in the regulation of chromatin modification, DNA repair, cell cycle control, transcription regulation, cell adhesion and mobility, cell signaling, cytoskeletal structure, apoptosis, etc. Also, direct DNA binding property and direct protranscriptional activity of menin have been reported. It is prevalently a nuclear protein that possesses three nuclear localization sites (NLSs) in the C-terminal region; loss of one or more of these NLSs, caused by truncating mutations, makes menin unable to reach the nucleus and become active as a tumor suppressor.

Studies on mouse models knocked out for the *Men1* gene have shown that the germline homozygote loss of *Men1* leads to uterine death, while germline heterozygote loss of *Men1* manifests a clinical phenotype similar to human MEN1

patients, confirming the central role of *MEN1* mutations in MEN1 tumorigenesis. The second wild-type copy of the gene is lost at the somatic level in tumors, as also happens in human MEN1 tumors, according to the "two hits" mechanism of action for tumor-suppressor genes. Somatic *Men1* homozygote knockout in specific endocrine tissues confirmed the development of MEN1 typical tumors, suggesting that menin tumor-suppressor action is tissue-specific (Agarwal 2017). In addition to somatic *MEN1* loss of heterozygosity, epigenetic gene expression regulation by microRNAs (miRNAs) appears to be involved in *MEN1* regulation and MEN1 tumorigenesis. Some miRNAs (i.e., miR-24, miR-17, mir-762, and miR-802) have been shown to directly target MEN1 miRNA (Luzi et al., 2012; Lu et al., 2015; Hou et al., 2017; Wang et al., 2014); particularly, overexpression of miR-24 was described in parathyroid adenomas (Luzi et al., 2012), GEP-NETs (Vijayaraghavan J et al., 2014) and pituitary tumors (Campanini ML et al., 2010), leading to downregulation of menin expression and subsequently enhancing cell proliferation. On the other hand, acting as a transcription factor, menin has been demonstrated to be involved in the biogenesis of let-7 (Gurung et al., 2014a) and miR-155 (Gurung et al., 2014b); let-7 negatively targets proproliferative genes and genes involved in insulin-mediated signals (i.e., *IRS2*) in pancreas beta cells, and thus reduced biogenesis of let-7 due to *MEN1* mutations could be suspected as the molecular mechanism responsible for beta cell uncontrolled growth and insulinoma development (Gurung et al., 2014b).

References

Anlauf, M., Bauersfeld, J., Raffel, A., Koch, C.A., Henopp, T., Alkatout, I., Schmitt, A., Weber, A., Kruse, M.L., Braunstein, S., Kaserer, K., Brauckhoff, M., Dralle, H., Moch, H., Heitz, P.U., Komminoth, P., Knoefel, W.T., Perren, A., Klöppel, G., 2009. Insulinomatosis: a multicentric insulinoma disease that frequently causes early recurrent hyperinsulinemic hypoglycemia. Am. J. Surg. Pathol. 33, 339−346.

Agarwal, S.K., 2017. The Future: genetics advances in mEN1 therapeutic approached and management strategies. Endrocr. Relat. Cancer 24, T119−T134.

Bartsch, D.K., Albers, M., Knoop, R., Kann, P.H., Fendrich, V., Waldmann, J., 2013. Enucleation and limited pancreatic resection provide long-term cure for insulinoma in multiple endocrine neoplasia type 1. Neuroendocrinology 98, 290−298.

Benito, M., Asa, S.L., Livolsi, V.A., West, V.A., Snyder, P.J., 2005. Gonadotroph tumor associated with multiple endocrine neoplasia type 1. J. Clin. Endocrinol. Metab. 90, 570−574.

Bodei, L., Kidd, M., Paganelli, G., et al., 2015. Long-term tolerability of PRRT in 807 patients with neuroendocrine tumours: the value and limitations of clinical factors. Eur. J. Nucl. Med. Mol. Imaging 42, 5−19.

Campanini, M.L., Colli, L.M., Paixao, B.M., Cabral, T.P., Amaral, F.C., Machado, H.R., Neder, L.S., Saggioro, F., Moreira, A.C., Antonini, S.R., de Castro, M., 2010. CTNNB1 gene mutations, pituitary transcription factors, and MicroRNA expression involvement in the pathogenesis of adamantinomatous craniopharyngiomas. Horm Cancer 1 (4), 187−196.

Christakis, I., Qiu, W., Silva Figueroa, A.M., Hyde, S., Cote, G.J., Busaidy, N.L., Williams, M., Grubbs, E., Lee, J.E., Perrier, N.D., 2016. Clinical features, treatments, and outcomes of patients with thymic carcinoids and multiple endocrine neoplasia type 1 syndrome at MD anderson cancer center. Horm. Cancer 7 (4), 279−287.

Concolino, P., Costella, A., Capoluongo, E., 2016. Multiple endcorine neoplasia type 1 (MEN1): an update of 208 new germline variants reported in the last nine years. Cancer Genetics 209, 36−41.

De Carlo, E., Pilon, C., Zatelli, M.C., degli Uberti, E.C., Fallo, F., 2008. Isolated R171Q amino acid change in MEN1 gene: polymorphism or mutation? Clin. Endocrinol. 69 (3), 511.

de Laat, J.M., Pieterman, C.R., van den Broek, M.F., Twisk, J.W., Hermus, A.R., Dekkers, O.M., de Herder, W.W., van der Horst-Schrivers, A.N., Drent, M.L., Bisschop, P.H., Havekes, B., Vriens, M.R., Valk, G.D., 2014. Natural course and survival of neuroendocrine tumors of thymus and lung in MEN1 patients. J. Clin. Endocrinol. Metab. 99 (9), 3325−3333.

Demeure, M.J.1, Klonoff, D.C., Karam, J.H., Duh, Q.Y., Clark, O.H., 1991. Insulinomas associated with multiple endocrine neoplasia type 1: the need for a different surgical approach. Surgery 110, 998−1005.

Doppman, J.L., Miller, D.L., Chang, R., Shawker, T.H., Gorden, P., Norton, J.A., 1991. Insulinomas: localization with selective intrarterial injection of calcium. Radiology 178, 237−241.

Economopoulos, P., Christopoulos, C., Glucagonoma, 2001. Ann. Gastroenterol. 14, 99−108.

Falconi, M., Eriksson, B., Kaltsas, G., Bartsch, D.K., Capdevila, J., Caplin, M., Kos-Kudla, B., Kwekkeboom, D., Rindi, G., Klöppel, G., Reed, N., Kianmanesh, R., Jensen, R.T., Vienna Consensus Conference participants, 2016. Vienna consensus conference participants 2016 ENETS consensus guidelines update for the management of patients with functional pancreatic neuroendocrine tumors and non-functional pancreatic neuroendocrine tumors. Neuroendocrinology 103, 153−171.

Fendrich, V., Merz, M.K., Waldmann, J., Langer, P., Heverhagen, A.E., Dietzel, K., Bartsch, D.K., 2011. Neuroendocrine pancreatic tumors are risk factors for pancreatic fistula after pancreatic surgery. Dig. Surg. 28, 263−269.

Fine, R.L., Gulati, A.P., Krantz, B.A., et al., 2013. Capecitabine and temozolomide (CAPTEM) for metastatic, well-differentiated neuroendocrine cancers: the Pancreas Center at Columbia University experience. Cancer Chemother. Pharmacol. 71 (3), 663−670.

Garbrecht, N., Anlauf, M., Schmitt, A., Henopp, T., Sipos, B., Raffel, A., Eisenberger, C.F., Knoefel, W.T., Pavel, M., Fottner, C., Musholt, T.J., Rinke, A., Arnold, R., Berndt, U., Plöckinger, U., Wiedenmann, B., Moch, H., Heitz, P.U., Komminoth, P., Perren, A., Klöppel, G., 2008. Somatostatin-producing neuroendocrine tumors of the duodenum and pancreas.: incidence, types, biological behaviour, association with inherited syndromes, and functional activity. Endocr. Relat. Cancer 15, 229−241.

Giudici, F., Nesi, G., Brandi, M.L., Tonelli, F., 2012. Surgical management of insulinomas in multiple endocrine neoplasia type 1. Pancreas 41, 547–553.

Giusti, F., Cianferotti, L., Gronchi, G., Cioppi, F., Masi, L., Faggiano, A., Colao, A., Ferolla, P., Brandi, M.L., 2016. Cinacalcet therapy in patients affected by primary hyperparathyroidism associated to Multiple Endocrine Neoplasia Syndrome type 1 (MEN1). Endocrine 52, 495–506.

Gonçalves, T.D., Toledo, R.A., Sekiya, T., Matuguma, S.E., Maluf Filho, F., Rocha, M.S., Siqueira, S.A., Glezer, A., Bronstein, M.D., Pereira, M.A., Jureidini, R., Bacchella, T., Machado, M.C., Toledo, S.P., Lourenço Jr., D.M., 2014. Penetrance of functioning and nonfunctioning pancreatic neuroendocrine tumors in multiple endocrine neoplasia type 1 in the second decade of life. J. Clin. Endocrinol. Metab. 99, E89–E96.

Gordon, M.V., Varma, D., McLean, C.A., Bittar, R.G., Burgess, J.R., Topliss, D.J., 2007. Metastatic prolactinoma presenting as a cervical spinal cord tumour in multiple endocrine neoplasia type one (MEN-1). Clin. Endocrinol. 66, 150–152.

Goswami, S., Peipert, B.J., Helenowski, I., Yount, S.E., Sturgeon, C., 2017. Disease and treatment factors associated with lower quality of life scores in adults with multiple endocrine neoplasia type I. Surgery 162 (6), 1270–1277.

Guettier, J.M., Kam, A., Chang, R., Skarulis, M.C., Cochran, C., Alexander, H.R., Libutti, S.K., Pingpank, J.F., Gorden, P., 2009. Localization of insulinomas to regions of the pancreas by intraarterial calcium stimulation: the NIH experience. J. Clin. Endocrinol. Metab. 94, 1074–1080.

Gurung, B., Katona, B.W., Hua, X., 2014b. Menin-mediated regulation of miRNA biogenesis uncovers the IRS2 pathway as a target for regulating pancreatic beta cells. Oncoscience 1 (9), 562–566.

Gurung, B., Muhammad, A.B., Hua, X., 2014a. Menin is required for optimal processing of the microRNA let-7a. J. Biol. Chem. 289 (14), 9902–9908.

Hayashi, Y., Masuda, H., Eizawa, T., Yamanaka, T., Naka, M., 2001. Usefulness of the combination of pre- and intraoperative selective intraarterial calcium injection to detect residual insulinomas. Intern. Med. 40, 48–51.

Hou, R., Yang, Z., Wang, S., Chu, D., Liu, Q., Liu, J., Jiang, L., 2017. miR-762 can negatively regulate menin in ovarian cancer. OncoTargets Ther. 10, 2127–2137.

Inchauste, S.M., Lanier, B.J., Libutti, S.K., Phan, G.Q., Nilubol, N., Steinberg, S.M., Kebebew, E., Hughes, M.S., 2012. Rate of clinically significant postoperative pancreatic fistula in pancreatic neuroendocrine tumors. World J. Surg. 36, 1517–1526.

Jensen, R.T., Cadiot, G., Brandi, M.L., de Herder, W.W., Kaltsas, G., Komminoth, P., Scoazec, J.Y., Salazar, R., Sauvanet, A., Kianmanesh, R., Barcelona Consensus Conference participants, 2012. ENETS Consensus Guidelines for the management of patients with digestive neuroendocrine neoplasms: functional pancreatic endocrine tumor syndromes. Neuroendocrinology 95, 98–119.

Jordan, P.H., 1999. A personal experience with pancreatic and duodenal neuroendocrine tumors. J. Am. Coll. Surg. 189, 470–482.

Lee, M.J., Jung, C.H., Jang, J.E., Hwang, J.Y., Park, D.H., Park, T.S., Lee, W.J., 2013. Successful endoscopic ultrasound-guided ethanol ablation of multiple insulinoma accompanied with multiple endocrine neoplasia type 1. Int. Med. J. 948–950.

Lemos, M.C., Thakker, R.V., 2008. Multiple endocrine neoplasia type 1 (MEN1): analysis of 1336 mutations reported in the first decade following identification of the gene. Hum. Mutat. 29, 22–32.

Lévy-Bohbot, N., Merle, C., Goudet, P., Delemer, B., Calender, A., Jolly, D., Thiéfin, G., Cadiot, G., Groupe des Tumeurs Endocrines, 2004. Prevalence, characteristic and prognosis of MEN 1-associated glucagonomas, VIPomas, and somatostatinomas. Study from the GTE. Gastroenterol. Clin. Biol. 28, 1075–1081.

Livshits, A., Kravarusic, J., Chuang, E., Molitch, M.E., 2016. Pituitary tumors in MEN1: do not be misled by borderline elevated prolactin levels. Pituitary 19, 601–604.

Lim, C.T., Korbonits, M., 2018. Update on the clinicopathology of pituitary adenomas. Endocr. Pract. 24 (5), 473–488.

Lo, C., Lam, K., Fan, S., 1998. Surgical strategy for insulinomas in multiple endocrine neoplasia type 1. Am. J. Surg. 175, 305–307.

Lloyd, R., Osamura, R., Klöppel, G., Rosai, J., 2017. WHO Classification of Tumours of Endocrine Organs, fourth ed. IARC Publication, p. 10.

Lu, Y., Fei, X.Q., Yang, S.F., Xu, B.K., Li, Y.Y., 2015. Glucose-induced microRNA-17 promotes pancreatic beta cell proliferation through down-regulation of Menin. Eur. Rev. Med. Pharmacol. Sci. 19 (4), 624–629.

Luzi, E., Marini, F., Giusti, F., Galli, G., Cavalli, L., Brandi, M.L., 2012. The negative feedback-loop between the oncomir Mir-24-1 and menin modulates the Men1 tumorigenesis by mimicking the "Knudson's second hit". PLoS One 7 (6), e39767.

Moyes, V.J., Monson, J.P., Chew, S.L., Akker, S.A., 2010. Clinical use of cinacalcet in MEN1 hyperparathyroidism. Internet J. Endocrinol. 2010, 906163.

Nilubol, N., Weisbrod, A.B., Weinstein, L.S., Simonds, W.F., Jensen, R.T., Phan, G.Q., Hughes, M.S., Libutti, S.K., Marx, S., Kebebew, E., 2013. Utility of intraoperative parathyroid hormone monitoring in patients with multiple endocrine neoplasia type 1-associated primary hyperparathyroidism undergoing initial parathyroidectomy. World J. Surg. 37, 1966–1972.

Norton, J.A., Krampitz, G., Zemek, A., Longacre, T., Jensen, R.T., 2015. Better survival but changing causes of death in patients with multiple endocrine neoplasia type 1. Ann. Surg. 261, e147–e148.

Nozières, C., Zhang, C.X., Buffet, A., Dupasquier, S., Vargas-Poussou, R., Guillaud-Bataille, M., Cordier-Bussat, M., Ruszniewski, P., Christin-Maitre, S., Murat, A., Groussin, L., Vezzosi, D., Cardot-Bauters, C., Hervieu, V., Joly, M.O., Giraud, S., Odou, M.F., Gimenez-Roqueplo, A.P., Goudet, P., Borson-Chazot, F., Calender, A., Groupe français des tumeurs endocrines (GTE), 2014. p.Ala541Thr variant of MEN1 gene: a non deleterious polymorphism or a pathogenic mutation? Ann. Endocrinol. 75 (3), 133–140.

O'Riordain, D.S., O'Brien, T., van Heerden, J.A., Service, F.J., Grant, C.S., 1994. Surgical management of insulinoma associated with multiple endocrine neoplasia type 1. World J. Surg. 18, 488–493.

Pilato, F.P., D'Adda, T., Banchini, E., Bordi, C., 1988. Nonrandom expression of polypeptide hormones in pancreatic endocrine tumors. An immunohistochemical study in a case of multiple islet cell neoplasia. Cancer 61 (9), 1815–1820.

Pitt, S.C., Pitt, H.A., Baker, M.S., Christians, K., Touzios, J.G., Kiely, J.M., Weber, S.M., Wilson, S.D., Howard, T.J., Talamonti, M.S., Rikkers, L.F., 2009. Small pancreatic and periampullary neuroendocrine tumors: resect or enucleate? J. Gastrointest. Surg. 13, 1692–1698.

Raymond, E., Dahan, L., Raoul, J.L., et al., 2011. Sunitinib malate for the treatment of pancreatic neuroendocrine tumours. N. Engl. J. Med. 364, 501−513.

Rinke, A., Krug, S., 2016. Neuroendocrine tumours - medical therapy: biological. Best Pract. Res. Clin. Endocrinol. Metabol. 30, 79−91.

Sadowski, S.M., Cadiot, G., Dansin, E., Goudet, P., Triponez, F., 2017. The future: surgical advances in MEN1 therapeutic approaches and management strategies. Endocr Relat Cancer 24 (10), T243−T260.

Sakurai, A., Yamazaki, M., Suzuki, S., Fukushima, T., Imai, T., Kikumori, T., Okamoto, T., Horiuchi, K., Uchino, S., Kosugi, S., Yamada, M., Komoto, I., Hanazaki, K., Itoh, M., Kondo, T., Mihara, M., Imamura, M., 2012. Clinical features of insulinoma in patients with multiple endocrine neoplasia type 1: analysis of the database of the MEN Consortium of Japan. Endocr. J. 59, 859−866.

Thakker, R.V., Newey, P.J., Walls, G.V., Bilezikian, J., Dralle, H., Ebeling, P.R., Melmed, S., Sakurai, A., Tonelli, F., Brandi, M.L., Endocrine Society, 2012. Clinical practice guidelines for multiple endocrine neoplasia type 1 (MEN1). J. Clin. Endocrinol. Metab. 97, 2990−3011.

Thompson, N.W., 1998. Current concepts in the surgical management of multiple endocrine neoplasia type 1pancreatic-duodenal disease. Results in the treatment of 40 patients with Zollinger-Ellison syndrome, hypoglycaemia or both. J. Intern. Med. 243, 495−500.

Tonelli, F., Giudici, F., Nesi, G., Batignani, G., Brandi, M.L., 2013. Biliary tree gastrinomas in multiple endocrine neoplasia type 1 syndrome. World J. Gastroenterol. 19 (45), 8312−8320.

Tonelli, F., 2014. How to follow and when to operate asymptomatic neuroendocrine pancreatic tumors in multiple endocrine neoplasia type 1? J. Clin. Gastroenterol. 48, 387−389.

Tonelli, F., Giudici, F., Nesi, G., Batignani, G., Brandi, M.L., 2017. Operation for insulinomas in multiple endocrine neoplasia type 1: when pancreatoduodenectomy is appropriate. Surgery 161 (3), 727−734.

Triponez, F., Goudet, P., Dosseh, D., Cougard, P., Bauters, C., Murat, A., Cadiot, G., Niccoli-Sire, P., Calender, A., Proye, C.A., French Endocrine Tumor Study Group, 2006. French Endocrine Tumor Study Group. Is surgery beneficial for MEN1 patients with small (< or = 2 cm), nonfunctioning pancreaticoduodenal endocrine tumor? An analysis of 65 patients from the GTE. World J. Surg. 30, 654−662 discussion 663-664.

Triponez, F.1, Sadowski, S.M., Pattou, F., Cardot-Bauters, C., Mirallié, E., Le Bras, M., Sebag, F., Niccoli, P., Deguelte, S., Cadiot, G., Poncet, G., Lifante, J.C., Borson-Chazot, F., Chaffanjon, P., Chabre, O., Menegaux, F., Baudin, E., Ruszniewski, P., Du Boullay, H., Goudet, P., 2018. Long-term Follow-up of MEN1 Patients Who Do Not Have Initial Surgery for Small ≤2 cm Nonfunctioning Pancreatic Neuroendocrine Tumors, an AFCE and GTE Study: association Francophone de Chirurgie Endocrinienne & Groupe d'Etude des Tumeurs Endocrines. Ann. Surg. 268 (1), 158−164.

Vergès, B., Boureille, F., Goudet, P., Murat, A., Beckers, A., Sassolas, G., Cougard, P., Chambe, B., Montvernay, C., Calender, A., 2002. Pituitary disease in MEN type 1 (MEN1): data from the France-Belgium MEN1 multicenter study. J. Clin. Endocrinol. Metab. 87, 457−465.

Vijayaraghavan, J., Maggi, E.C., Crabtree, J.S., 2014. miR-24 regulates menin in the endocrine pancreas. Am. J. Physiol. Endocrinol. Metab. 307 (1), E84−E92.

Wang, L.Q., Chen, G., Liu, X.Y., Liu, F.Y., Jiang, S.Y., Wang, Z., 2014. microRNA-802 promotes lung carcinoma proliferation by targeting the tumor suppressor menin. Mol. Med. Rep. 10 (3), 1537−1542.

Wolin, E.M., 2012. The expanding role of somatostatin analogs in the management of neuroendocrine tumors. Gastrointest Cancer Res 5, 161−168.

Yao, J.C., Shah, M.H., Ito, T., et al., 2011. Everolimus for advanced pancreatic neuroendocrine tumours. N. Engl. J. Med. 364, 514−523.

Yates, C.J., Newey, P.J., Thakker, R.V., 2015. Challenges and controversies in management of pancreatic neuroendocrine tumours in patients with MEN1. Lancet Diabetes Endocrinol. 3, 895−905.

Chapter 54

Parathyroid hormone-related peptide and other mediators of skeletal manifestations of malignancy

Richard Kremer and David Goltzman

Calcium Research Laboratories and Department of Medicine, McGill University and McGill University Health Centre, Montreal, QC, Canada

Chapter outline

Introduction

Hypercalcemia is one of the most frequent paraneoplastic syndromes and often occurs in advanced stages of the disease. The median survival rate usually varies between 6 and 10 weeks following the onset of hypercalcemia (Body, 2000); however, breast cancer patients experience a somewhat longer median survival of 3–4.5 months (De Wit and Cleton, 1994).

The association between elevated blood calcium and neoplastic disease was first noted in the 1920s (Zondek et al., 1923), when it was postulated that release of calcium from bone by the direct osteolytic action of malignant cells was responsible for hypercalcemia associated with malignancy. However, hypercalcemia was often accompanied by hypophosphatemia, the hallmark of hyperparathyroidism (HPT), and also occurred in the absence of skeletal metastases. In 1941 it was hypothesized that a malignant tumor might release a systemically active factor resulting in hypercalcemia (Albright, 1941). This hypothesis was raised when a patient with a renal carcinoma, metastatic to bone, presented with

Principles of Bone Biology. https://doi.org/10.1016/B978-0-12-814841-9.00054-3

hypercalcemia and hypophosphatemia in the absence of any obvious parathyroid dysfunction. The patient's biochemical abnormalities were temporarily normalized following tumor reduction but became apparent again as the tumor resumed its growth. It was reasoned that since hyperphosphatemia did not accompany hypercalcemia despite evidence of osteolysis, perhaps the tumor was secreting a phosphaturic substance like parathyroid hormone (PTH). Although no bioassayable hormone was detected in the tumor, the important observation had been made that malignancy-associated hypercalcemia (MAH) could have a humoral basis and the factor might be related to PTH. The search for a novel protein with PTH-like bioactivity intensified using several bioassays that had been developed for PTH (Goltzman et al., 1981; Nissenson et al., 1981; Rodan et al., 1983). Using both in vivo and in vitro approaches, PTH-like bioactivity was identified in the blood and in tumor extracts from patients with MAH. These same bioassays were used in various combinations during the purification of a novel protein, initially named parathyroid-hormone-like peptide, from tumor tissue (Burtis et al., 1987; Moseley et al., 1987; Strewler et al., 1987). When the gene was cloned and demonstrated to be structurally homologous to PTH, the protein was renamed parathyroid-hormone-related protein, or PTHrP (Mangin et al., 1989; Suva et al., 1987).

The term humoral hypercalcemia of malignancy (HHM) was later coined to distinguish the syndrome caused by a circulating factor, now known to be PTHrP, from hypercalcemia caused by the direct lytic action of tumor cells in bone. The demonstration that neutralizing antibodies to PTHrP could reduce or eliminate the hypercalcemia in animal models of HHM (Kukreja et al., 1988; Henderson et al., 1990a,b) provided strong evidence that this was indeed the causal factor of this syndrome. HHM was associated primarily with renal cell carcinomas and squamous cell cancers originating in a variety of primary sites, whereas hypercalcemia due to local osteolysis was commonly associated with metastatic breast disease and hematologic malignancies. Nevertheless, it is now clear that the "direct" lytic action of tumor cells is also mediated in part by PTHrP, and that PTHrP released by these tumors may also act on a systemic basis.

Characterization of hypercalcemia in malignancy

Despite the striking similarities between the biochemical manifestations of HPT and MAH that precipitated Albright's hypothesis, it subsequently became apparent that there were also a number of important differences between these syndromes.

Early attempts at the differential diagnosis of these hypercalcemic disorders identified not only subnormal concentrations of immunoreactive PTH (Powell et al., 1973) and no detectable PTH mRNA in the tumors (Simpson et al., 1983) but also a mild hypokalemic alkalosis in patients with MAH. In contrast, elevated PTH and mild metabolic acidosis were associated with HPT (Lafferty, 1966). In addition, circulating levels of 1,25D were reported low in PTHrP-associated hypercalcemia in contrast to patients with HPT, where 1,25D is often elevated (Stewart et al., 1980). Potential explanations for this apparent discrepancy were the very high calcium levels often seen in MAH that are known to inhibit 1alpha-hydroxylase in vitro and in vivo (Bikle, 2014) or possibly unknown inhibitors of 1alpha hydroxylase released by tumor cells. Nevertheless, the occurrence of low 1,25-dihydroxyvitamin D(1,25(OH)2D levels in MAH is not widely accepted and low, normal, or even high levels of 1.25(OH)2D were later reported in this syndrome (Schweitzer et al., 1994; Ralston et al., 1984). Indeed, in a large series of hypercalcemic patients with various malignancies and elevated PTHrP levels, the mean circulating levels of 1,25(OH)2D were normal (Donovan et al., 2015). Another important difference between MAH and HPT has been the histomorphometric changes observed in bone biopsy specimens and a report by Stewart et al. (1982) of uncoupling between resorption and formation in hypercalcemic cancer patients. These findings in cancer patients are also in sharp contrast with studies in animal models of MAH, in which circulating 1,25D levels are high and bone turnover appeared to be coupled (Sica et al., 1983; Strewler et al., 1986). Similar results were obtained in tumor-bearing rats producing PTHrP prior to the development of hypercalcemia (Yamamoto et al., 1995). Furthermore, administration of an N-terminal fragment of PTHrP to human volunteers suggests that PTHrP has similar bioactivity to that of PTH (Fraher et al., 1992).

Molecular and cellular biology of PTH-related protein

Purification and cloning of PTH-related protein

Despite many unsuccessful attempts to identify the PTH-like factor(s) in the blood of hypercalcemic patients using immunoassays directed at PTH (Powell et al., 1973), and later the lack of expression of PTH mRNA in tumors of hypercalcemic cancer patients (Simpson et al., 1983), the search for this elusive factor continued. Using several bioassays, PTH-like bioactivity was identified in the blood (Goltzman et al., 1981) and in tumor extracts from patients with MAH (Nissenson et al., 1981; Rodan et al., 1983). Using similar bioassays, a fragment of the PTH-like protein was purified (Moseley et al., 1987; Strewler et al., 1987), and soon after complementary DNA (cDNA) clones encoding PTHrP were isolated (Strewler et al., 1987; Suva et al., 1987; Mangin et al., 1988).

Characteristics of the gene encoding PTH-related protein

The *PTH* and *PTHLH* genes respectively encoding PTH and PTHrP have been localized to the short arms of the respective human chromosomes 11 and 12, placing them among syntenic groups of functionally related genes and suggesting a common ancestral origin (Goltzman et al., 1989). Similarities in their structural organization and the functional properties of their amino termini provide further support for the hypothesis that *PTH* and *PTHLH* are members of a single gene family. The human *PTHLH* gene is a complex unit with at least seven exons driven by several promoters at the 5′ end that span more than 15 kb of DNA (Goltzman et al., 1989; Mangin et al., 1989). Its mRNA is transcribed from at least three promoters and undergoes differential splicing, giving rise to heterogenous mRNA species. The cDNA encodes a prototypical secretory protein with predicted mature isoforms of 139, 141, and 173 amino acids that exhibit a high degree of homology within the first 13 amino acids to the N-terminus of PTH; this facilitates its cross-reactivity with a G-protein coupled PTH receptor, the type 1 PTH/PTHrP receptor (PTH1R) (Jüppner et al., 1991) (Fig. 54.1). The sequence beyond amino acid 141 is unique to the human species and nonhuman primates. Interestingly, the three isoforms were shown to be expressed and secreted by both normal and tumor tissues in humans (Campos et al., 2006), but PTHrP 1−139 and 1−141 were considerably more abundant than PTHrP 1−173 in nonneoplastic tissues, whereas an increase in PTHrP 1−173 was observed in a large proportion of neoplastic tissues. The rat *PTHLH* gene is driven by a single promoter and encodes a protein of 141 amino acids with marked sequence homology to human PTHrP up to residue 111, which suggests conserved functionality (Yasuda et al., 1989). Indeed, species conservation of PTHrP is evident with high homology across a variety of mammalian species (Burtis, 1992). The gene structure of *PTHLH* was also elucidated in several other species (Mangin et al., 1989; Yasuda et al., 1989; Suva et al., 1989; Karaplis et al., 1990) also revealing similarities with the PTH gene structure organization, suggesting that the two genes probably arose from a common ancestor through gene duplication.

Eutopic PTH-related protein overproduction in malignancy

PTHrP is widely distributed in embryonic and adult tissues and has essential functions in development and growth. In view of its broad distribution pattern in many cell types, overproduction of PTHrP by malignant cells most likely results from deregulated expression of an endogenous protein during the process of malignant transformation; that is, "eutopic" rather than "ectopic" production.

Transcriptional and posttranscriptional regulation

A number of potential mechanisms have been invoked to explain overexpression of PTHrP in malignant cells, including gene amplification (Sidler et al., 1996) and alterations in the methylation status of critical regulatory regions of the gene during neoplastic transformation (Broadus and Stewart, 1994; Ganderton and Briggs, 1997). Furthermore, the complex

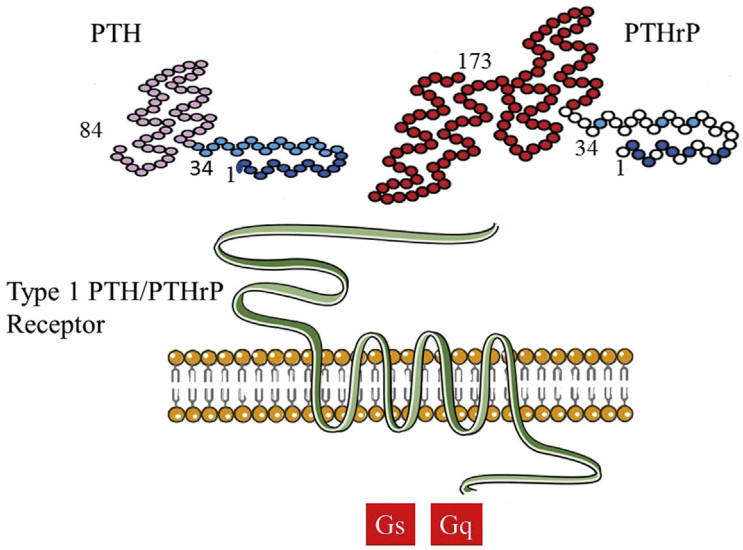

FIGURE 54.1 Interaction of PTH and of PTHrP with the type 1 PTH/PTHrP receptor. PTH(1−84) and PTHrP, which can occur as isoforms of 139, 141, and 173 amino acids, share limited amino acid sequence homology within the 1−34 domain. As a result, they can interact with a G-protein-coupled receptor, the type1 PTH/PTHrP receptor, which is linked to Gs and Gq.

organization of the human PTHrP gene suggests that changes in tissue-specific promoter usage or splice variants might also contribute to overproduction of PTHrP during the process of malignant transformation. One extensive clinical study examined a variety of tumors, including 13 breast malignancies, with exon-specific probes to identify transcripts arising from all three promoters and from the different 3′ splice variants (Southby et al., 1995). Although the authors failed to identify tissue-specific or tumor-specific transcripts, they did show that PTHrP was transcribed from multiple promoters in tumor samples, compared with a single promoter in normal tissue harvested from the same individual. The resulting overall increase in transcription could then lead to cumulative overexpression of the protein in neoplastic tissue. Others, however, have reported the presence of specific transcripts related to the stage of cancer progression. Thus Bouizar et al. (1999) investigated the differential expression of PTHrP isoforms in different stages of breast cancer progression as a result of differential use of a downstream TATA promoter. The amount of mRNA encoding the 1−139 isoform was much higher in the tumors of patients who later developed metastases than in those of patients who developed no metastases. The mRNA encoding this isoform was also more abundant in breast tumors from patients who developed bone metastases than in those of patients who developed metastases in soft tissues. In contrast, the amounts of mRNA encoding the 1−141 isoform were similar in these different groups.

Transcriptional regulators of PTH-related protein

Viral proteins

Viral proteins, notably Tax, have been implicated in transcriptional stimulation of PTHrP production in malignant states. TAX is a 40-kDa nuclear phosphoprotein that transactivates its own promoter as well as those of a number of host genes. It interacts with a variety of transcription complexes that bind to DNA consensus elements in the *PTHrP* promoter including the cAMP response element, Ets-1, serum response element, and the AP-1 binding site (Dittmer et al., 1993; Ejima et al., 1993). PTHrP mRNA has been identified in samples harvested from asymptomatic human T-cell leukemia virus type I (HTLV-I) carriers as well as from leukemic cells of ATL patients (Motokura et al., 1989), and elevated circulating levels of PTHrP were detected in most hypercalcemic individuals in the acute phase of the disease (Ikeda et al., 1993). In view of the documented role of HTLV-I infection in the pathogenesis of adult T-cell leukemia-lymphoma and the high incidence of PTHrP overexpression in these patients, it was proposed that the TAX might stimulate PTHrP gene transcription. The MT-2 cell line, in which TAX is overexpressed, was used to determine that PTHrP gene transcription was indeed enhanced and that maximal stimulation of *PTHrP* involved activation of protein kinase A (PKA) and protein kinase C (PKC) (Motokura et al., 1989).

Growth factors and hormone regulation of PTH-related protein production

Growth factors and cytokines. A variety of growth factors are potent stimulators of *PTHrP* gene transcription: epidermal growth factor (EGF), insulin-like growth factor (IGF)-1 (Kremer et al., 1991; Sebag et al., 1994), and transforming growth factor beta (in both normal and cancer cells).

Whereas mitogenic stimuli induce PTHrP expression in primary rat aortic smooth cells (Hongo et al., 1991), in nonmalignant established cell lines from normal human keratinocytes (Henderson et al., 1991) and normal human cervical epithelial cells (Kremer et al., 1996a,b,c), transforming growth factor (TGF) beta has antagonistic effects to EGF in normal mammary epithelial cells (Feffari et al., 1994). TGF beta enhances the production of PTHrP in cancer cells in vitro (Zakalik et al., 1992; Kiriyama et al., 1993), and cooperating with PTHrP, enhances osteolytic bone metastases in vivo (Yin et al., 1999).

Several studies indicate that PTHrP expression increases in parallel to tumor progression. PTHrP is overexpressed in normal human keratinocytes (Henderson et al., 1991) and normal human prostate cells (Kremer et al., 1997) following activation by the ras oncogene. PTHrP is also overexpressed in the human melanoma A375 cell line compared with normal human melanocytes (El Abdaimi et al., 2000a,b). In the pYMT model of breast tumor progression (Guy et al., 1992; Li et al., 2011), PTHrP expression progressively increases with tumor stage from hyperplasia to carcinoma.

The mechanism(s) of overexpression is still poorly understood. One of the hallmarks of cancer, however, is the growth of cells independently of mitogenic stimuli (Hanahan and Weinberg, 2011). In contrast to normal or established keratinocytes, PTHrP is expressed constitutively in ras-transformed keratinocytes (Henderson et al., 1991).

Signaling by growth factors through receptor tyrosine kinases (RTKs) appears to be an important mechanism for regulating PTHrP gene expression and for oncogenic transformation by the Ras component of the RTK signal transduction pathway in many malignant cells. Transfection of Tpr-Met, a constitutively active derivative of the hepatocyte growth factor receptor, into PTHrP-producing cells resulted in a substantial increase in the expression and release of

PTHrP (Aklilu et al., 1996). Introduction of a point mutation into Tpr-Met, which prevented its association with the Ras signaling pathway, led to a significant reduction in PTHrP expression and release. Similar reductions were observed in cells treated with agents that inhibit Ras function by preventing it from anchoring to the cell membrane and transducing a signal (Ras farnesylation inhibitors) (Aklilu et al., 1997). These studies demonstrated an important role for Ras in enhancing PTHrP production in transformed cells.

Steroid hormones. Several steroid hormones have been reported to influence the production of PTHrP. Thus estradiol has been reported to inhibit PTHrP gene promoter activity in breast cancer cell models in vitro and to diminish PTHrP production in vivo (Rabbani et al., 2005). Similarly androgens (dihydrotestosterone) have also been shown to inhibit PTHrP production in models of prostate cancer both in vitro and in vivo at least in part via a transcriptional mechanism (Pizzi et al., 2003). Glucocorticoids have also been shown to inhibit PTHrP production (Sebag et al., 1994; Tenta et al., 2005; Glatz et al., 1994).

The secosteroid 1,25 dihydroxyvitaminD and its analogs 1,25 dihydroxyvitamin D ($1,25(OH)_2D$) have been shown to inhibit PTHrP gene transcription (Kremer et al., 1991; Sebag et al., 1992). A $1,25(OH)_2D$ responsive repressor sequence was identified between bases −1121 to −1075 upstream of the single promoter in the rat *PTHrP* gene (Kremer et al., 1996a,b,c), and the PTHrP repressor site binds a vitamin D receptor (VDR)-retinoid X receptor (RXR) heterodimer in normal keratinocytes. The VDR−RXR complex was also identified in extracts of nuclei from immortalized keratinocytes but VDR−RXR interaction was disrupted in Ras transformed cells that had previously shown resistance to $1,25(OH)_2D_3$-induced inhibition of PTHrP expression (Solomon et al., 1998). Expression of wild-type RXRα in the transformed cells resulted in reconstitution of the VDR−RXR heterodimer. Subsequent work determined that disruption of the VDR−RXR complex in Ras-transformed keratinocytes resulted from mitogen-activated protein kinase (MAPK)-stimulated phosphorylation of RXRα by the activated Ras/Raf/MAPK pathway (Solomon et al., 1999).

Based on observations that $1,25(OH)_2D$ is a strong inhibitor of PTHrP expression and production in cancer cells, we hypothesized that this mechanism could be used advantageously in MAH. Our strategy was to use $1,25(OH)_2D$ analogs with low calcemic activity that would efficiently inhibit PTHrP expression and production in vivo. One such analog, EB1089, was then used in two animal models of MAH and shown to both prevent and reverse the development of hypercalcemia by inhibiting PTHrP expression in the primary tumor and subsequent release of PTHrP in the circulation (Haq et al., 1993; El Abdaimi et al., 1999).

Regulation by calcium. Early studies in the keratinocyte model of tumor progression showed that an increase in extracellular calcium stimulated the expression and production of PTHrP (Henderson et al., 1991). Following the cloning of the calcium-sensing receptor (CaSR) (Brown et al., 1993) various well-established cancer cell lines have been found to express both CaSR mRNA and protein (Cattopadhyay, 2006). These include cell lines derived from breast cancer [MCF-7, MDA-MB-231] (Sanders et al., 2000) and prostate cancer [PC-3, LnCaP] (Sanders et al., 2001). Both pharmacological and molecular evidence indicates that elevated Ca^{2+} upregulates PTHrP synthesis and release via CasR activation in these cell lines. Stimulation of PTHrP release due to CasR activation involves de novo synthesis of PTHrP mRNA, in view of the fact that the pan-RNA polymerase inhibitor actinomycin D inhibits the effect of Ca^{2+} on the expression of PTHrP mRNA and protein release. Consequently, elevated calcium induced by circulating PTHrP may have a stimulatory effect on further PTHrP release by the tumor. Furthermore, the majority of calcium in the body is stored in bone, and bone-derived calcium is released during bone resorption, resulting in an increase in extracellular calcium (Ca^{2+}) in the bony microenvironment to levels in the vicinity of resorbing osteoclasts that are manyfold higher (ranging from 8 to 40 mM) than the level of systemic Ca^{2+} (Silver et al., 1988). Evidence is accumulating that these large local changes in Ca^{2+} may be "sensed" by cancer cells metastatic to bone and could enhance further PTHrP release from tumor cells metastatic to bone. Additionally, more recent evidence indicates that disruption of upregulation of PTHrP by the CaSR through conditional ablation of the CaR in mammary epithelial cells inhibits tumor growth in the PyMT model of breast cancer progression (Kim et al., 2016).

Overall, therefore, these studies indicate that increased PTHrP production can result from alterations in the interaction between stimulatory and inhibitory signaling pathways in malignant cells.

Processing and degradation of PTH-related protein

Like PTH, PTHrP is synthesized as a prohormone with an amino-terminal extension. The biological potency of pro-PTHrP is considerably less than that of PTHrP-(1−34) (Liu et al., 1995). A furin recognition sequence is found between the propeptide and the mature protein, and studies (Liu et al., 1995) have shown that pro-PTHrP was indeed a substrate for the prohormone convertase furin.

Examination of the amino acid sequences of the three major isoforms of PTHrP revealed the presence of several proteolytic sites, amidation consensus sites, and sites of 0-glycosylation (Philbrick et al., 1996; Orloff et al., 1989;

Wu et al., 1991; Sowers et al., 1996; VanHouten et al., 2003). PTHrP appears to undergo endoproteolytic cleavage in the secretory pathway, resulting in the release of multiple fragments. PTHrP is secreted by normal and cancer cells as short N-terminal fragments of approximately 36 amino acids, as well as longer N-terminal fragments. In vitro studies in human renal carcinoma cell lines and rat insulinoma cell lines (Soifer et al., 1992) transfected with a cDNA encoding PTHrP1-141 demonstrated the presence of several immunoreactive moieties including PTHrP1-36, PTHrP38-94, PTHrP1-74, and a midregion fragment of 7 kDa likely PTHrP38-101 (Wu et al., 1996). Processing of endogenous, internally labeled PTHrP in rat leydig cells revealed the presence of three bioactive moieties, PTHrP1-141, PTHrP1-86, and PTHrP1-36. PTHrP1-141 represented only 7% of newly synthesized material, suggesting rapid degradation of the secreted intact molecule (Rabbani et al., 1993).

Mechanisms of action of PTH-related protein

Interaction of amino-terminal PTH-related protein with cell surface receptors

Sequence homology between PTH and PTHrP is restricted to only 8 of the first 13 residues; however, this domain is known to be required for activation of signal transduction cascades. Additional conformational similarities in the 14−34 region, a domain that appears critical for peptide binding to the receptor, permit amino-terminal fragments of the proteins to act as equivalent agonists for their common receptor, PTH1R (Fig. 54.1). PTH1R is a seven-transmembrane G-protein linked receptor with the "signature" G protein-coupled receptor (GPCR) topology, a seven-membrane-spanning, "serpentine" domain, as well as a large extracellular ligand-binding domain and an intracellular COOH-terminal domain. The receptor couples to Gs and Gq leading to activation of the PKA and PKC pathways (Mannstadt et al., 1999), and like other GPCRs, undergoes cyclical receptor activation, desensitization, and internalization (Weinman et al., 2006) (Fig. 54.1). After ligand binding and endocytosis, the PTH1R is either recycled to the cell membrane or targeted for degradation. Arrestins contribute to the desensitization of both Gs- and Gq-mediated PTH1R signaling. PTH1R activation and internalization can be selectively dissociated (Sneddon et al., 2004). PTH1R signaling can be modified by scaffolding proteins such as the Na^+/H^+ exchanger regulatory factors 1 and 2 through PDZ1 and PDZ2 domains (Mahon et al., 2002; Sneddon et al., 2003).

PTH1R signaling via the cAMP pathway, leading to PKA activation and phosphorylation of the cyclic AMP response element binding protein (CREB), has been extensively documented. CREB binds to the cyclic AMP response element in the promoter region of many genes and transcriptionally modulates their expression.

Although PTHR1 signals primarily by coupling with PKA, it can also signal through PKC (Abou-Samra et al., 1992), RhoA pathway (Singh et al., 2005), and the β-arrestin−extracellular signal-regulated kinase 1/2 (ERK1/2) pathway (Syme et al., 2005; Gesty-Palmer et al., 2006). The PTH and PTHrP 1−34 amino-terminal regions are presumed to contain all the structural elements for downstream signaling through PTH1R.

PTH1R, as with PTHrP, is expressed in a wide variety of embryonic and adult tissues, including cartilage and bone, and therefore mediates the autocrine/paracrine actions of locally produced and secreted PTHrP.

Although PTH is expressed almost exclusively in parathyroid cells, PTHrP is broadly expressed in many fetal and adult tissues (Goltzman et al., 1989), consistent with its physiologic functions as a modulator of cell growth, differentiation, and programmed cell death (see chapter by Martin et al.: "Paracrine PTHrp actions"). Many critical effects of PTHrP are mediated via the interaction of the amino-terminal domain of PTHrP with PTH1R. These include roles in the normal development of the cartilaginous growth plate (Goltzman et al., 1989), in bone anabolism (Miao et al., 2005), in mammary gland development including the development of mammary ducts and nipple formation (Foley et al., 2001) in calcium transport across the placenta (Kovacs et al., 1996), in smooth muscle relaxation, in vasodilatation (Schordan et al., 2004), and in tooth eruption (Philbrick et al., 1998). The most striking developmental effects of PTHrP have been demonstrated in the skeleton of mice with targeted deletion of PTHrP ($PTHrP^{-/-}$ mice), where PTHrP has been shown to be essential for normal development of the cartilaginous growth plate and endochondral bone formation. Thus in the absence of full-length PTHrP, chondrocyte proliferation is reduced and accelerated chondrocyte differentiation and apoptosis occurs in the growth plate; the overall effect is a severely deformed skeleton and early lethality (Karaplis et al., 1994; Amizuka et al., 1994) (see chapter by Martin: "Paracrine actions of PTHrp in bone").

In humans, an inactivating mutation of PTH1R produces a similar lethal chondro-osseous dysplasia, termed Blomstrand syndrome (Zhang et al., 1998). Mice heterozygous for PTHrP ablation appear normal at birth but develop reduced trabecular bone as they age, demonstrating an osseous phenotype due to haploinsufficiency (Amizuka et al., 1996). In humans, variants of the *PTHLH* gene have been associated, in genome wide association studies, with reduced bone mineral density (Estrada et al., 2012).

With respect to ion homeostasis, in the fetus PTHrP appears necessary for normal calcium homeostasis (Kovacs et al., 1996), but in the adult, PTH rather than PTHrP assumes the major role in calcium and phosphorus homeostasis, with serum PTHrP concentrations being either very low or undetectable in normal adults. In contrast, when neoplasms hypersecrete PTHrP, the effects of PTH are mimicked on bone and kidney, and the hypercalcemia that results suppresses endogenous PTH secretion.

Functions of carboxyl and midregion circulating fragments of PTH-related protein

Several investigators have reported a variety of functions for fragments of PTHrP that share no homology with PTH. These include the pentapeptide PTHrP-(107−111), which was named osteostatin for its potential to inhibit osteoclastic bone resorption in culture (Fenton et al., 1991). Other studies using carboxy-terminal fragments of PTHrP have shown that such fragments inhibit production of the early osteoblast marker osteopontin (Seitz et al., 1995) in isolated osteoblasts and are almost as effective as PTHrP-(1−34) in stimulating functional osteoclast formation from progenitor cells (Kaji et al., 1995). These studies support in vivo observations demonstrating decreased osteoblastic and increased osteoclastic activity in association with elevated circulating levels of carboxy-terminal fragments of PTHrP in patients with HHM (Burtis et al., 1994).

In contrast to the well-known mechanism of action of the N-terminal moiety of PTHrP, the mechanism of action of the C-terminal moieties with unique biological functions is poorly understood. It is possible that the distinct biological actions of PTHrP occur through as-yet-unidentified receptors or binding proteins.

In the brain, it has been reported that N-terminal and C-terminal sequences of PTHrP act through distinct signaling mechanism activating cAMP/PKA and changes in intracellular calcium, respectively (Fukayama et al., 1995), suggesting that the C-terminal domain of PTHrP acts through a distinct receptor. Others have reported the presence of cell surface binding proteins for carboxyl terminal fragments of PTHrP on skeletal cells (Orloff and Stewart, 1995); however, to date the molecular nature of these receptors and binding proteins remain unclear.

PTHrP has also been reported to be a key regulator of fetal calcium, in view of the fact that deletion of its gene in murine fetuses of mice with ablation of the PTHrP gene (i.e., in $PTHrP^{-/-}$ mice) results in hypocalcemia and hyperphosphatemia (Kovacs, 2015). Much of the PTHrP in fetal circulation may arise from the placenta. Studies in lambs and rodents have shown that PTHrP stimulates active placental calcium transport. Although there have been no direct measurements of placental mineral transport in human babies, in vitro study of intact placentas as well as isolated trophoblast membranes has provided some supportive evidence for the roles of PTHrP in stimulating placental calcium transport and gene expression. The bioactivity of PTHrP for placental calcium transport is specified by a midmolecular region, PTHrP-(67−86), that does not use PTH1R (Kovacs et al., 1996); however, the receptor for this region has not been identified.

Intracellular mechanism of PTH-related protein action

Although most cellular actions of PTHrP have been attributed to the interaction of its amino-terminus with the cell surface PTH1R, there are also reports that PTHrP may have a direct, intracellular mode of action(Fig. 54.2). There is evidence in the literature for three potential mechanisms for the translocation of PTHrP, a prototypical secretory protein, into the cytoplastic compartment of target cells. One involves the alternative initiation of PTHrP translation to exclude the “pre” or leader sequence, which is necessary for entry of the molecule into the endoplasmic reticulum and secretory pathway (Nguyen et al., 2001). A second involves retrograde transport of nascent PTHrP from the endoplasmic reticulum (Meerovitch et al., 1998) into the cytoplasm. Finally, a third involves internalization of secreted PTHrP via a PTH1R-independent cell-surface-binding protein for PTHrP (Aarts et al., 1999).

The intracrine action of PTHrP appears to be mediated at least in part through residues 87−107 in the midregion of the protein. This region shares sequence homology with a lysine-rich bipartite nuclear localization sequence (NLS) in nucleolin (Schmidt-Zachmann et al., 1993) and with an arginine-rich NLS in the retroviral regulatory protein TAT (Dang et al., 1989). The PTHrP NLS is both necessary and sufficient to direct the passage of PTHrP to the nuclear compartment of transfected cells and to localize endogenously expressed PTHrP to nucleoli in chondrocytes and osteoblasts in vitro and in vivo (Henderson et al., 1995). Endogenous PTHrP has been identified in the coarse fibrillar component of nucleoli by immunoelectron microscopy. This compartment is occupied by complexes of newly transcribed 45s ribosomal RNA and protein that are destined for assembly into ribosomes, and PTHrP has been shown to bind to GC-rich homopolymeric RNA and total cellular RNA with specificity and high affinity (Aarts et al., 1999), compatible with a role in ribosomal biogenesis. The biological impact of nucleolar PTHrP on cell function was demonstrated in vitro when chondrocytes

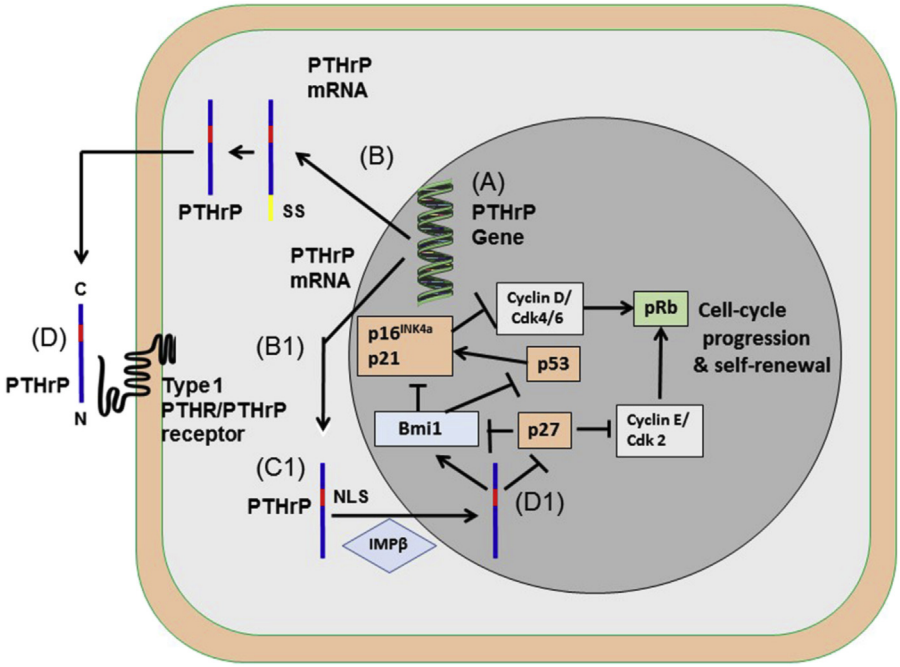

FIGURE 54.2 Model of dual action of PTHrP. PTHrP is transcribed from a single gene, but the translation product may enter the secretory pathway (B) and be secreted from the synthesizing cell to act as an endocrine/paracrine/autocrine factor by interacting with the cell membrane type 1 PTH/PTHrP receptor. Alternatively, PTHrP may be retained within the cytoplasm (B1) and PTHrP may bind with high affinity to importin β1 and the GDP-bound protein, Ran (C). PTHrP, transported into the nucleus(D1), acts as an intracrine factor by increasing the polycomb ring finger oncogene, Bmi1, leading to inhibition of the action of the cyclin-dependent kinase inhibitors p16INK4a and p21 and therefore facilitating increased activity of cyclin-dependent kinase D/Cdk4/6. Bmi1 may also inhibit p53 preventing its stimulation of p16INK4a and p21. Intranuclear PTHrP may also inhibit the cyclin-dependent kinase inhibitor p27, allowing increased cyclin E/Cdk2 activity. The net result is increased phosphorylation and inactivation of the retinoblastoma gene, resulting in increased cell cycle progression and self-renewal.

expressing wild-type PTHrP were protected from apoptosis induced by serum deprivation, whereas cells expressing the protein without NLS were not. Subsequently, the nuclear localization of PTHrP was also found to be protective in studies in vitro for prostate cancer cell apoptosis (Dougherty et al., 1999) and breast cancer (Sepulveda et al., 2002).

Nuclear localization of PTHrP occurs in a cell cycle-dependent manner, with higher expression in the G2 and M phases of the cycle (Okano et al., 1995; Lam et al., 1997). The cell cycle-dependent localization of PTHrP is regulated by the activity of the cyclin-dependent kinases (cdks) cdc2 and cdk2, which phosphorylate PTHrP at threonine 85 within a consensus cdc2/cdk2 site (Lam et al., 2000). Phosphorylation increases as cells progress from G1 to G2 and M of the cell cycle and leads to decreased nuclear entry, perhaps by enhancing binding to a cytoplasmic retention factor. PTHrP appears to bind with high affinity to importin β1 and the GDP-bound protein, Ran (Lam et al., 1999). PTHrP nuclear import seems dependent on microtubular integrity implicating a role for the cytoskeleton in transport to the nucleus (Lam et al., 2002). After translocation across the nuclear envelope, GTP-bound Ran may release PTHrP into the nucleus where it apparently can act, at least in part, in the nucleolus to bind RNA, thereby regulating mRNA processing or mRNA transport. Functionally, intranuclear PTHrP seems to delay apoptosis (Henderson et al., 1995) and increase cell proliferation. Indeed, a series of studies (Zhang et al., 2010; Jiang et al., 2015), using knockin mice that express PTHrP(1−86) but not NLS (nor the carboxy terminal region) have shown that intranuclear PTHrP may increase the polycomb ring finger oncogene, Bmi1, leading to inhibition of the action of the cyclin-dependent kinase inhibitors $p16^{INK4a}$, and p21, and therefore facilitate increased activity of cyclin-dependent kinase D/Cdk4/6. Intranuclear PTHrP may also inhibit the cyclin-dependent kinase inhibitor 1B, $p27^{Kip1}$, allowing increased cyclin E/Cdk2 activity. The net result is increased phosphorylation and inactivation of the retinoblastoma gene, resulting in increased cell cycle progression and self-renewal (Fig. 54.2). This may provide a molecular basis for the phenotypic changes in the knockin mice. Whether this intracrine action of PTHrP promotes tumor progression in tumors in which PTHrP is expressed remains to be determined.

Deletion of the NLS and the C-terminus sequence of PTHrP was engineered in PTHrP "knockin" mice that still expressed PTHrP(1−86). Deletion of these sequences in vivo resulted in growth failure, premature osteoporosis, reduced hematopoiesis, altered energy metabolism, and ultimately premature death (Miao et al., 2008; Toribio et al., 2010).

The abnormality in growth of PTHrP knockin mice expressing PTHrP(1−84) was characterized by a markedly abnormal epiphyseal growth plate, but in contrast to the deletion of the full-length sequence of PTHrP, the abnormality in the knockin mice consisted of a reduced proliferative zone but normal hypertrophic zone architecture, suggesting that secreted PTHrP acting via PTHR1 and intracellular PTHrP may act synergistically to regulate the growth plate. PTHrP knockin mice also develop reductions in osteoblastic activity, again suggesting synergy between the paracrine and intracrine actions of PTHrP (Miao et al., 2005).

PTH-related protein actions to produce the manifestations of humoral hypercalcemia of malignancy

Actions in kidney

An elevation in the circulating level of PTHrP in patients with HHM initially results in phosphate wasting and calcium retention by the kidney in association with an increase in the nephrogenous component of excreted cAMP (Fig. 54.3) (see also chapter by Friedman: "PTH and PTHrp actions on kidney"). This is analogous to the endocrine effects of excess circulating PTH in HPT and results from the interaction of PTHrP with PTH1R. Thus in the proximal tubule, stimulation of adenylate cyclase causes internalization of the type II Na^+/Pi^- (inorganic phosphate) cotransporter, leading to reduced apical Na^+/Pi^- cotransport, decreased phosphate reabsorption, and phosphaturia (Keusch et al., 1998). About 20% of filtered calcium is reabsorbed in the cortical thick ascending limb of the loop of Henle (CTAL) and 15% in the distal convoluted tubule (DCT), and it is here that PTHrP also binds to the PTH1R, and again by a cyclic AMP-mediated mechanism enhances calcium reabsorption. In the CTAL, at least, this appears to occur by increasing the activity of the Na/K/2Cl cotransporter that drives NaCl reabsorption and stimulates paracellular calcium and magnesium reabsorption. PTHrP can also influence transcellular calcium transport in the DCT. This is a multistep process involving transfer of luminal Ca^{2+} into the renal tubule cell via the transient receptor potential channel, translocation of Ca^{2+} across the cell from apical to basolateral surface (a process involving proteins such as calbindin-D28K), and finally active extrusion of Ca^{2+} from the cell into the blood via a Na^+/Ca^{2+} exchanger, designated NCX1. PTHrP most likely stimulates Ca^{2+} reabsorption in the DCT primarily by augmenting NCX1 activity via a cyclic AMP-mediated mechanism. In the proximal tubule, PTH can, after binding to PTH1R, also stimulate the 25-hydroxyvitamin D 1α hydroxylase [1a(OH)ase], leading to increased synthesis of $1,25(OH)_2D$. Consequently, increased circulating levels of $1,25(OH)_2D$ are often observed in HPT. In contrast, circulating $1,25(OH)_2D$ levels may be low in patients with HHM (Stewart et al., 1980). These apparent discrepancies were not resolved by early animal models of HHM, in which circulating $1,25(OH)_2D_3$ levels were high (Sica et al., 1983; Strewler et al., 1986). Neither was the problem solved by in vivo and in vitro studies performed with synthetic amino terminal fragments of PTHrP, which suggested that the peptides had identical bioactivity (Chorev et al., 1994; Fraher et al., 1992; Rabbani et al., 1988). However, continuous infusion of PTH(1−34) and of PTHrP(1−36) into

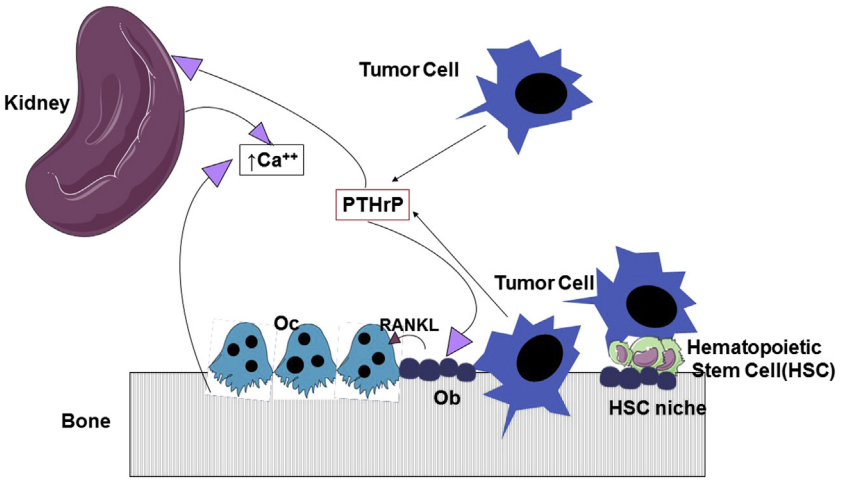

FIGURE 54.3 Interaction of PTHrP with bone and kidney to produce hypercalcemia [$\uparrow Ca^{++}$]. Tumor cells outside of bone can release PTHrP that acts on the renal tubule to enhance calcium reabsorption. PTHrP can also bind to osteoblasts and increase the osteoclastogenic cytokine, RANKL. RANKL can stimulate osteoclasts to resorb bone and mobilize calcium from bone, contributing to hypercalcemia. Tumor cells may also metastasize to bone, and initially bind to cells of the hematopoietic stem cell niche (HSC niche). Tumor cells in bone may also produce PTHrP that can increase bone resorption.

healthy young adults for 2−4 days demonstrated that renal $1,25(OH)_2D$ synthesis was stimulated effectively by PTH but poorly by PTHrP (Horwitz et al., 2005), supporting the apparent discrepancies between the circulating concentrations of $1,25(OH)_2D$ in HPT and HHM.

Actions in bone

In bone, PTH1R is localized on cells of the osteoblast phenotype that are of mesenchymal origin (Rouleau et al., 1990). Nevertheless, both PTH and PTHrP enhance osteoclastic bone resorption (Fig. 54.3). This effect of PTH on increasing osteoclast stimulation is indirect, with PTH binding to the PTH1R on preosteoblastic stromal cells (Rouleau et al., 1990) and enhancing the production of the cytokine RANKL [receptor activator of nuclear factor (NF) kappaB ligand], a member of the tumor necrosis factor (TNF) family. Simultaneously, levels of a soluble decoy receptor for RANKL, termed osteoprotegerin, are diminished, facilitating the capacity for increased stromal cell-bound RANKL to interact with its cognate receptor, RANK, on cells of the osteoclast series. Under the influence of RANKL stimulation, multinucleated osteoclasts, are derived from hematogenous precursors committed to the monocyte/macrophage lineage and then proliferate and differentiate as mononuclear precursors, eventually fusing to form multinucleated osteoclasts. These can then be activated to form bone-resorbing osteoclasts (Fig. 54.3). RANKL can drive all of these proliferation/differentiation/fusion/activation steps although other cytokines, notably monocyte-colony-stimulating factor, may also participate in this process (see Chapter by Martin et al. PTHrp paracrine actions in bone).

As indicated earlier in comparing HPT and HHM, histomorphometric evaluation of bone biopsies revealed that whereas catabolic activity was significantly increased in both disorders, discrepancies in bone formation were noted with decreases in HHM but increases in parathyroid disease (Stewart et al., 1982). Interestingly, in more recent infusion studies in humans, both PTH and PTHrP appeared to produce inhibition of formation and stimulation of resorption when administered continuously (Horwitz et al., 2005), which could explain these earlier findings on uncoupling between resorption and formation on the basis of sustained versus intermittent production of PTH and PTHrP depending on the clinical context. At least part of the osteoblast-stimulating activity of PTH, and therefore likely of PTHrP, occurs via inhibition of sclerostin, an antagonist of the osteoblast growth factor wingless-type (Wnt) (Bellido et al., 2013). Whether this inhibition occurs differently when PTHrP is administered intermittently versus continuously remains to be determined.

Effect of PTH-related protein on tumor progression and survival

PTHrP appears to be a prognostic indicator in patients with MAH (174; 175), with a very significant increase in mortality in patients with elevated circulating PTHrP. This relationship persists in a multivariate model independent of serum calcium elevation (Truong et al., 2003).

PTH1R and PTHrP are frequently coexpressed in tumors (Downey et al., 1997), and PTHrP has been reported to stimulate cell proliferation in MCF-7 breast cancer cells (Hoey et al., 2003), SV-40 immortalized breast epithelial cells (Hoey et al., 2003), renal carcinoma cells (Massfelder et al., 2004), and colon cancer cells (Shen and Falzon, 2005). The amino-terminal domain of PTHrP via PTH1R has also been reported to inhibit apoptosis (Hastings et al., 2003) and to enhance cancer cell adhesion to bone matrix components (Shen and Falzon, 2003). In tumors that secrete it, PTHrP has also been shown to promote growth and survival by the NLS via an intracrine mechanism (Sepulveda et al., 2002). PTHrP could therefore offer a selective advantage to tumor cells by contributing to tumor cell survival and growth.

Several animal cancer models associated with PTHrP production without concomitant hypercalcemia have been reported in the context of skeletal metastases and breast cancer (Guise et al., 1996; Mundy, 2002). PTHrP was described as a predominant mediator of the bone metastatic process. The developmental transcription factor Gli2 was identified as a positive regulator of PTHrP and osteolysis in metastatic human breast cancer cells (Sterling et al., 2006), and necessary for TGF beta activation of PTHrP (Johnson et al., 2011). Similarly, PTHrP overproduction was reported in the A375 metastatic melanoma model (El Abdaimi et al., 2000a,b). Using a PTHrP knockout approach and intracardiac transplantation of cancer cells, Huang et al. (Huang et al., 2014) indicated that PTHrP plays a predominant role in the metastatic process within and outside the skeleton. Furthermore, it would appear that PTHrP regulates cell invasion in vivo through alteration of the actin cytoskeleton. Using the pYMT model of breast tumor progression characterized by rapid progression to metastases in less than 11 weeks, Li et al. (Li et al., 2011) demonstrated that PTHrP is critical for tumor initiation and growth as well as lung metastases. Also, it upregulates tumor cell expression of CXCR4,

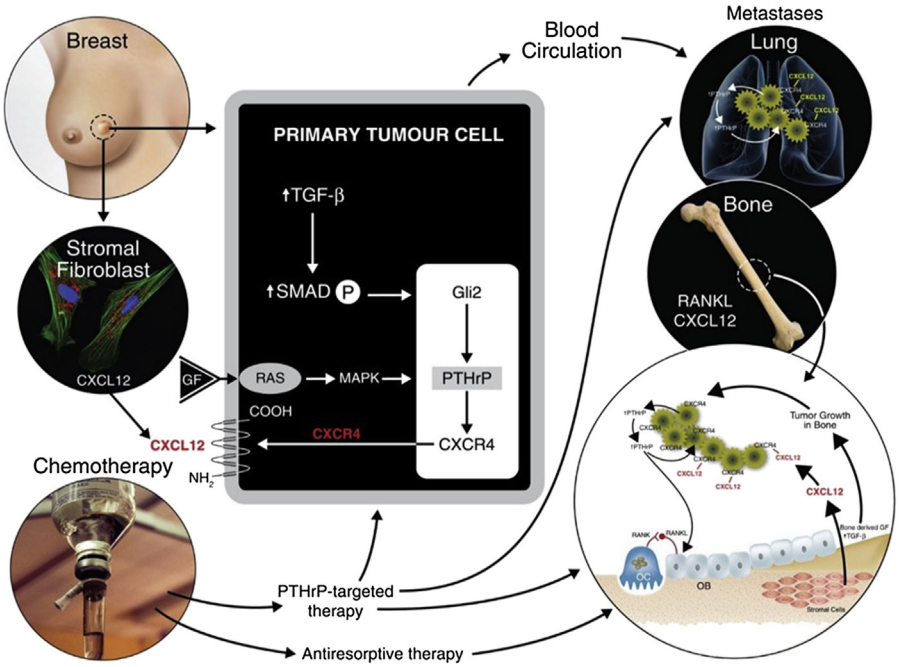

FIGURE 54.4 Figure Y: PTHrP regulation, signaling, and therapeutic targeting. In the breast, PTHrP is overexpressed by tumor cells as compared with the normal mammary epithelium. PTHrP expression is controlled by a variety of growth factors (GFs) that act via the Ras pathway to stimulate MAPK and increase PTHrP gene transcription. After transcription and translation, preproPTHrP is converted to proPTHrP that must then be processed to the active form of PTHrP before it is secreted. PTHrP production is also stimulated by Gli signaling molecules, members of the developmental Hedgehog pathway under the control of TGFβ. In bone, PTHrP-induced osteolysis results from upregulation of RANKL expression by osteoblasts. In addition, the abundance of TGFβ in bone is a major source of activation of PTHrP-induced osteolysis. PTHrP also promotes tumor initiation, growth, and invasion through its regulation of the CXCR4/CXCL12 axis. CXCL12, the natural ligand of CXCR4, is produced by stromal cells surrounding the primary tumor to enhance the metastatic ability of primary tumor cells. In metastatic sites such as bone, lungs, and liver, CXCL12 is also very abundant and acts as a chemoattractant of circulating tumor cells to facilitate seeding of tumor cells. Consequently, PTHrP-targeted therapy may provide a multiprong strategy by preventing tumor expansion and recurrence locally and tumor progression to skeletal and extraskeletal sites. Its combination with antiresorptive agents may prove extremely valuable by targeting both the "seed and the soil" and thus breaking the vicious cycle created by the release of PTHrP and GFs into the bone microenvironment.

a critical mediator of skeletal, liver, and lung metastases, where its ligand CXCL12 is produced in large quantities (Hirbe et al., 2010). This PTHrP CXCR4CXCL12 axis may therefore be critical in the homing of tumor cells in bone (Fig. 54.4). Also, CXCR4 is known to activate the AKT cell survival pathway (Zhang et al., 2009), which is under control of PTHrP (Li et al., 2011), thus supporting the importance of this novel PTHrP-CXCR4-CXCL12 axis. Furthermore, a monoclonal antibody raised against PTHrP1-33 administered to nude mice transplanted with the human breast cancer cell line MDAMB435 into the mammary fat pad, significantly reduced tumor growth and the occurrence of lung metastases (Li et al., 2011). A recent large genome-wide association study, identified PTHrP as one of three critical breast cancer susceptibility genes (Ghoussaini et al., 2012), which supports this novel role of PTHrP in tumor initiation and progression.

Cachexia is yet another syndrome invariably associated with human cancer progression. Its mechanism is complex (Tisdale, 2009). Earlier studies in animal models of lung cancer and skeletal metastases (Iguchi et al., 2001; Hashimoto et al., 2007) indicate that tumor-produced PTHrP is involved in cachexia and accumulation of orixogenic peptides such as neuropeptide Y in the hypothalamus. Administration of monoclonal antibodies against PTHrP ameliorates the condition with a concomitant reduction in expression of the hypothalamic orixogenic peptides. In a rapidly progressing model of human melanoma associated with rapid weight loss, ablation of PTHrP or administration of monoclonal antibodies against PTHrP had a profound effect on weight loss and improved survival (Huang et al., 2014). In a more recent study using a Lewis lung carcinoma model of cancer cachexia, tumour-derived PTHrP drove the expression of genes involved in thermogenesis in adipose tissues, and administration of neutralizating antibodies against PTHrP blocked adipose tissue browning and increased muscle mass and strength, partially reversing cancer cachexia (Kir et al., 2014).

Detection of PTH-related protein produced by tumors

Circulating levels of PTH-related protein

Shortly after the discovery and characterization of PTHrP, assays were developed to detect this factor in the circulation. With the development of immunoassays against specific regions of PTHrP, it was revealed that serum of patients with MAH contained both N and C-terminal reactive fragments (Burtis et al., 1990), including N-terminal moieties of at least 74 amino acids and C-terminal moieties of at least 29 amino acids beyond amino acid 109. Using an immunoassay recognizing both the N-Terminal (1−36) and C-Terminal (109−136) regions (Burtis et al., 1990), little or no immunoreactivity was detected, which suggests that the full length molecule PTHrP1-141 was rapidly metabolized. This latter study also reported the presence of fragments larger than the intact molecule, but their identity has not yet been determined. Discrepancies in results among these assays may depend at least in part on the variable molecular nature of PTHrP forms that circulate, either due to variable tumor production or clearance, especially in the presence of altered hepatic and/or renal function in cancer patients. PTHrP is cleared by the kidney (Imamura et al., 1991) and patients with renal insufficiency have elevated levels of PTHrP C-terminal fragments (Burtis et al., 1990) without elevation of N-terminal fragments. To date the production, circulating nature and clearance of heterogeneous PTHrP forms has not been nearly as well characterized as has the production, circulating nature and clearance of heterogeneous PTH forms. Such heterogeneous PTHrP moieties may be differently detected by individual assays and therefore yield different results. Nevertheless certain consistent themes have emerged from the use of PTHrP assays.

The first generalized finding is that circulating PTHrP levels are increased in virtually all patients with HHM as reported by Burtis et al. (1990). Using a two-site immunoassay, also called sandwich assay, they were able to characterize PTHrP in a variety of cancer conditions. This immunoradiometric assay used two polyclonal antibodies, a capture antibody raised against PTHrP 37−74 and a signal antibody raised against PTHrP1-36. Therefore, the specificity of this two-site assay was for a moiety that contained at least the first 74 amino acids of the molecule. The assay sensitivity was 1.0 pmol/L and did not cross-react with PTH1-84 or C-terminal fragments of PTHrP. Burtis et al. also developed a C-terminal radioimmunoassay using a polyclonal antibody raised against PTHrP 109−138. Although all normal volunteers had undetectable levels, this assay detected high levels of PTHrP in the circulation of renal failure patients, with a mean similar to patients with MAH (29.6 ± 14.1 pmol/L).

The second important observation is that although renal and squamous cell carcinomas have most frequently been associated with HHM, assays capable of directly measuring PTHrP demonstrated a much broader spectrum of tumors associated with excess PTHrP production than was previously considered, including breast, colon, and hematologic cancers (Henderson et al., 1990a,b). Thus, PTHrP overproduction is commonly associated with squamous cell tumors arising in most sites including lung, esophagus, cervix, vulva, skin and head and neck. Bladder and ovarian carcinomas are also commonly associated with the syndrome. On the other hand, patients with colon, gastric, thyroid, and nonsquamous cell lung cancers manifest hypercalcemia less commonly. Several studies have indicated that elevated PTHrP correlates better with hypercalcemia than does the presence or absence of skeletal metastases (Ejima et al., 1993). This appears particularly relevant to certain neoplasms such as breast cancer, which are commonly associated with hypercalcemia but are even more commonly associated with osteolytic skeletal metastases. Furthermore, cases of prostate cancer (Burtis et al., 1990) and melanoma (Kageshita et al., 1999), not typically believed to be part of the HHM spectrum, have been reported in association with high circulating PTHrP levels. Thus, circulating PTHrP levels have been reported as elevated in 50%−90% of hypercalcemic cancer patients with solid tumors (Henderson et al., 1990a,b; Budayr et al., 1989; Ratcliffe et al., 1992; Ralston et al., 1990; Burtis et al., 1990; Kao et al., 1990; Rankin et al., 1997) and in 25%−60% of such patients with hematologic malignancies (Kremer et al., 1996a,b,c; Firkin et al., 1996; Donovan et al., 2015). In support of the clinical usefulness of these two-site immunoassays, reduction in tumor burden following chemotherapy is associated with a reduction in circulating levels of PTHrP and correction of hypercalcemia (Henderson et al., 1990a,b), but to date PTHrP has not been widely utilized to monitor disease status.

The third observation is that circulating PTHrP concentrations have frequently been reported as elevated in hypercalcemic patients having skeletal metastases. Thus, hypercalcemia with breast cancer has been classically associated with osteolytic lesions but assays have generally detected elevated PTHrP in breast cancer, regardless of whether skeletal metastases were present (Grill et al., 1991). These studies therefore suggested that PTHrP as a systemic factor may contribute to the hypercalcemia of tumors that have spread to bone as well as to the hypercalcemia of those that have not.

To date, measurement of serum PTHrP has not, however, been a useful method for early tumor detection, possibly because of assay limitations related to the molecular heterogeneity of PTHrP released into the circulation and the low sensitivity of commercial assays unable to measure normal levels of PTHrP. Almost invariably current assays only detect

PTHrP in advanced cancer stages when hypercalcemia is present (Kremer et al., 1996a,b,c; Rankin et al., 1997). Furthermore, the finding of hypercalcemia in association with suppressed PTH using highly sensitive and specific assays to measure intact PTH has often been taken as presumptive evidence of elevated circulating PTHrP as the cause of the hypercalcemia, in lieu of direct measurement of PTHrP.

PTHrP may have value in prognostic evaluation. Thus, PTHrP assays have generally shown that there is a positive correlation between circulating PTHrP levels and more advanced stages of cancer (Kremer et al., 1996a,b,c; Rankin et al., 1997; Firkin et al., 1996), and several studies have reported that elevation of serum PTHrP levels was associated with a worse prognosis (Truong et al., 2003; Pecherstorfer et al., 1994; Hiraki et al., 2002). One study, which did not find that serum concentrations of PTHrP was associated with a poor prognostic factor, did not correct for confounding factors (Lee et al., 1997).

An ultrasensitive multiplex two-site immunoassay capable of simultaneously measuring several circulating forms of PTHrP with a sensitivity of 150 a.m. (approximately 1000-fold lower than current immunoradiometric assays) (Otieno et al., 2016) has been reported. This assay accurately measures normal levels of PTHrP in healthy volunteers and elevated levels in hypercalcemic cancer patients. Prospective measurements are underway in early-stage cancer patients and normocalcemic cancer patients at more advanced stages to determine its usefulness as a prognostic biomarker and to monitor tumor recurrence.

Overall, the clinical significance of PTHrP assays in diagnosis and disease monitoring requires more extensive evaluation in well-established populations.

PTH-related protein in tumor tissue

PTHrP is frequently expressed in a wide variety of tumor tissues including breast (Southby et al., 1990; Kohno et al., 1994), lung (Brandt et al., 1991), and renal cell cancer (Iwamura et al., 1999). The prognostic value of PTHrP expression in breast cancer tissue is uncertain because PTHrP immunostaining is reported to be either positively or negatively associated with prognosis. The presence of PTHrP in tissue samples from the primary tumor obtained from breast cancer patients has been associated with a more favorable outcome by one group (Henderson et al., 2001), but not by two others (Liapis et al., 1993; Yoshida et al., 2000). The study of Henderson et al. excluded patients with the more aggressive types of breast cancer who were receiving neoadjuvant therapy because tissue was not procured during surgery. The discrepancies in these findings may be due to differences in patient populations or the choice of PTHrP antibodies for immunohistochemical analysis.

PTHrP expression examined in the context of skeletal metastasis was found to be significantly overexpressed in bone metastatic lesions as compared with the primary tumor (Southby et al., 1990; Powell et al., 1991). PTHrP expression examined in prostate cancer tissues in patients without hypercalcemia was found to correlate with tumor stage (Defto, 2000).

Increased PTHrP expression in tumors colocalizes with the PTH/PTHrP receptor (Kunisada et al., 2002), and correlates with tumor grade. Also, a monoclonal antibody against PTHrP was effective in vitro in promoting cell death of chondrosarcoma cells (Bovee et al., 2000; Miyaji et al., 2003) Finally, PTHrP expression in tumor samples appears to be correlated in some reports with poor prognosis in lung cancer (Hidaka et al., 1998), renal carcinoma (Iwamura et al., 1999), and colorectal tumors (Nishihara et al., 1999).

Relationship of PTH-related protein-producing tumors with the bone microenvironment

Up to two-thirds of patients with MAH have bone metastases, and as indicated above, elevated circulating levels of PTHrP have been detected in association with hypercalcemic tumors that have spread to bone (Henderson et al., 1990a,b). Thus, certain malignancies, notably breast, lung, and renal carcinomas, which are frequently associated with hypercalcemia, have as well a strong propensity to spread to bone. PTHrP is thus expressed by not only tissues of tumors associated with hypercalcemia that have not metastasized to bone but also those that have colonized the skeleton (Powell et al., 1991; Southby et al., 1990; Vargas et al., 1992).

Following homing to bone, osteotropic tumor cells adapt to the bone marrow space by producing factors that allow development and progression in their new microenvironment, in part by inducing osteolysis (Waning and Guise, 2014). For example, secreted connective tissue growth factor stimulates osteoblast proliferation, and interleukin (IL)-11 and matrix metalloproteinase 1 (MMP-1) increase osteoblastic RANKL production, thus enhancing bone resorption. Additionally, MMP-1 and a disintegrin and metalloproteinase with thrombospondin motifs suppress osteoprotegerin (OPG) expression in osteoblasts, increasing the ratio of RANKL to OPG and thus further enhance increased osteolysis.

Tumor cells may also produce prostaglandins, and the interleukins Il-1, IL-6, and IL-8, leading to bone resorption. In addition to secreted factors, tumor cells express transcription factors that support growth in bone. These include the transcription factors, GLI2, part of the Hedgehog signaling network, which induces PTHrP expression; runt related transcription factor 2, which regulates matrix metalloproteinase-9 transcription that can degrade the extracellular matrix; hypoxia-induced growth factor 1 α (HIF1α), which promotes osteolysis and inhibits osteoblast differentiation; and Jagged1 (Jag1), which activates the Notch pathway to activate osteoclast differentiation. The result is the facilitation of the growth of the metastases and the mobilization of calcium from resorbed bone that may lead to hypercalcemia.

PTHrP may therefore act as a mediator of focal osteolysis induced by skeletal metastases while acting in a paracrine mode (El Abdaimi et al., 2000a,b; Guise et al., 1996; Rabbani et al., 1999). Tumor cells can thus release PTHrP, which acts at both the systemic (primary tumor) and local (skeletal metastases) levels to stimulate osteoclastic bone resorption, at least in part, through the receptor activator of NF-kappaB ligand (RANKL)/RANK/osteoprotegerin (OPG) system (Fig. 54.3).

Bone provides a fertile environment for the growth of tumors that are metastatic to the skeleton, with a well-developed blood supply (in hematopoietic marrow) as a source of nutrients and numerous growth factors that can provide a growth advantage. Thus, bone matrix is a unique storage site of immobilized growth factors such as TGF-β, IGFs I and II, fibroblast growth factors 1 and 2, and platelet-derived growth factors. Tumor-derived PTHrP that produces osteolysis results in the release of such active growth factors from the matrix, that facilitates the growth of tumor cells. In turn, growth factors such as TGF-β (Kakonen et al., 2002; Yin et al., 1999) as well as calcium per se, following their local release during osteoclastic resorption, may not only enhance the growth of tumor cells but also further stimulate PTHrP production. This enhancement of PTHrP production by tumors in the bone microenvironment may explain the observation that breast cancer tissue from skeletal metastases may be more frequently positive for PTHrP expression than from other sites (Powell et al., 1991), and that patients with PTHrP negative primary breast cancers may have PTHrP positive metastatic lesions (Henderson et al., 2006). PTHrP from skeletal metastases may also have direct effects of PTHrP on tumor growth, survival, and possibly adhesion to bone matrix (Shen et al., 2003).

It seems unlikely that local osteolysis per se will produce sustained hypercalcemia in the absence of a reduction of the renal clearance of calcium caused either by kidney damage or by the calcium-reabsorptive action of a humoral agent such as PTHrP. Therefore, PTHrP as an endocrine factor is an important contributor to the pathophysiology of the hypercalcemia, not only of those tumors that have not metastasized to bone but also for those that have already colonized bone.

Resistance to antiresorptive agents in malignancy-associated hypercalcemia caused by PTH-related protein

From a clinical standpoint, one needs to stress the importance of the biological actions of PTHrP on bone and kidney in the therapeutic approach to patients with MAH. The mainstay of treatment of patients presenting with severe hypercalcemia is a combination of rehydration and antiresorptive agents including bisphosphonates and monoclonal antibodies against RANKL (denosumab). Bisphosphonates work by inhibiting the skeletal component of hypercalcemia and are often less effective in hypercalcemic cancer patients with elevated PTHrP levels. Such patients require a higher dosage of bisphosphonate at shorter intervals, and the proportion of recurrence following calcium normalization is higher than in patients with MAH and normal levels of PTHrP (Grill et al., 1992; Wimalawansa, 1993; Gurney et al., 1993; Walls et al., 1994) despite almost complete suppression of bone turnover markers. Interestingly, a recent report showed that denosumab, a monoclonal antibody to RANKL that inhibits its activity, may be effective in refractory hypercalcemia due to PTHrP (Hu et al., 2014). A possible explanation for this unexpected superior efficacy may be related to a possible direct effect of denosumab on cancer cells. Earlier studies showed that RANK is often overexpressed on the surface of cancer cells and that RANK signaling drives mammary tumorigenesis (Gonzalez-Suarez et al., 2010; Schramek et al., 2010). Importantly, pharmacological treatment with RANK-Fc, which binds to RANKL and subsequently blocks RANK−RANKL signaling, reduces mammary tumorigenesis. In a large cohort of breast cancer patients, RANK overexpression was preferentially associated with triple-negative breast cancer (Pfitzner et al., 2014) a treatment-resistant breast cancer often associated with high PTHrP expression (Camirand et al., 2013). All in all, these studies suggest that denosumab could potentially target cancer cells and bone turnover simultaneously through PTHrP suppression—directly, indirectly, or by both methods. In any event eliminating or diminishing PTHrP production through alternate approaches would be of significant benefit for these patients using novel targeted therapies directed at PTHrP.

Experimental approaches to controlling overproduction or overactivity of PTH-related protein in malignancy-associated hypercalcemia

Although effective antitumor treatment is still the best means to obtain long-term normalization of serum calcium in MAH, a marked reduction of tumor burden often is not attainable because hypercalcemia generally complicates advanced and refractory cancer. Consequently, volume repletion and bisphosphonates, which inhibit osteoclastic bone resorption, have become the standard of therapy for MAH (Body et al., 1998). Newer antiresorptive agents are being developed (Capparelli et al., 2000). Bisphosphonates normalize serum Ca levels in more than 90% of patients with MAH, but they appear to be less efficient when hypercalcemia recurs in association with high circulating levels of PTHrP, possibly due to the renal calcium reabsorbing effects of PTHrP (Rizzoli et al., 1999; Onuma et al., 2005). As indicated earlier, denosumab appears to normalize calcium levels in a significant proportion of patients resistant to bisphosphonate therapy (Hu et al., 2014). The central role of PTHrP in MAH has, however, stimulated the exploration of preventive and therapeutic measures by targeting PTHrP.

Anti-PTHrP neutralizing antibodies have been shown to be effective in reducing skeletal metastasis, bone lesions, and hypercalcemia (Iguchi et al., 1996; Guise et al., 2002), and humanized anti-PTHrP antibody has been engineered for therapeutic purposes (Saito et al., 2005). Administration of $1,25(OH)_2D_3$, which may inhibit PTHrP production, is counterproductive in cases of MAH due to its intrinsic hypercalcemic effects. A concentrated effort has therefore focused on the development of low-calcemic analogs of $1,25(OH)_2D_3$ that will effectively suppress PTHrP production without stimulating calcium absorption by the gut, calcium reabsorption by the kidney, and most importantly, bone resorption. EB1089 and MC903, two $1,25(OH)_2D_3$ analogs with conservative side-chain modifications, have been used to inhibit PTHrP production in vitro, with varying degrees of success, to prevent the hypercalcemic syndrome in models of MAH (El Abdaimi et al., 2000a,b; Haq et al., 1993; Yu et al., 1995; El Abdaimi et al., 1999; Nakagawa et al., 2005). These studies suggest that low-calcemic vitamin D analogs and nonsteroidal activators of VDR that selectively fail to augment intestinal calcium absorption may prove useful in the management of MAH associated with excess PTHrP production.

Growth factors acting via RTKs have been shown to be potent stimuli of PTHrP gene transcription. One of the best characterized signal transduction pathways downstream of RTKs is the Ras/Raf/Mek pathway. Activation of this pathway by growth factors or activated Ras was shown to increase PTHrP expression and release from a variety of cells in culture. Conversely, inhibition of the pathway through pharmacologic intervention—e.g., by small molecules that act as a competitive inhibitor of Ras farnesylation, one of the metabolic conversions required for Ras to be anchored to the inner aspect of the cell membrane and transmit a signal downstream (Aklilu et al., 1997) or by using dominant negative forms of Ras and Raf (Aklilu et al., 2000) successfully reduced PTHrP production. This suggests that specific inhibitors of components of the Ras signaling pathway could be used for therapeutic intervention to prevent the hypercalcemic syndrome associated with PTHrP overproduction in vivo.

An alternative approach for diminishing PTHrP overproduction in malignancy employed antisense technology to inhibit endogenous PTHrP expression and diminish hypercalcemia. The use of antisense PTHrP (Rabbani et al., 1995) and the use of antisense furin (Liu et al., 1995) to reduce bioactive PTHrP in MAH models in vivo led to diminished hypercalcemia, decreased tumor cell proliferation, and the prolonged survival of host animals. To date, neither approach has been shown successful in clinical trials in humans, nor has either been approved by regulatory agencies. Newer techniques using small interfering RNA may prove useful in the future in furthering these initial approaches.

Treatment of local osteolysis

PTHrP may be a valid target in cancer therapy. Targeting PTHrP in skeletal metastases is supported by carefully conducted preclinical studies in animal models of breast, prostate, and lung metastases to bone (Rabbani et al., 1999; Guise et al., 1996; Miki et al., 2004), the three most common human malignancies. The majority of patients suffering from these conditions will develop metastatic spread to the skeleton. Despite the enhanced clinical efficacy of the newest generation of amino-bisphosphonates and the highly potent monoclonal antibody against RANKL denosumab (Coleman et al., 2012), skeletal metastases remain a major public health challenge with few therapeutic options. Emerging evidence in preclinical models of breast and lung cancer support the principle that combination therapies targeting both PTHrP with monoclonal antibodies and the bone microenvironment with the potent bisphosphonate zoledronic acid are superior to either agent administered separately (Luco et al., 2013; Yamada et al., 2009; Powell et al., 1991). Additional support for this approach comes from clinical studies indicating that cancer patients overexpress PTHrP at the bone metastatic site (Powell et al., 1991), a feature that is likely to exacerbate the vicious cycle occurring in bone once cancer cells invade the skeleton.

Another interesting clinical observation is the apparent resistance to bisphosphonate therapy in terminal cancer patients with hypercalcemia and the elevation of circulating levels of PTHrP (Walls et al., 1994). The majority of these patients, particularly breast cancer patients, have both skeletal and extraskeletal tumor spread. A possible explanation of this resistance is the lack of effect of bisphosphonates on the local production of PTHrP by metastatic sites. Although the renal component of MAH through the systemic effect of PTHrP on tubular reabsorption of calcium may play a role in maintaining hypercalcemia (Onuma et al., 2005), it is likely that local production of PTHrP diminishes the efficacy of bisphosphonates on bone. PTHrP has a direct effect on RANKL production by osteoblasts (Roodman, 2004a,b) as well as direct effects on tumor cell proliferation (Maioli et al., 2004; Li et al., 2011). A recent study indicates that the blockade of PTHrP with monoclonal antibodies in PTHrP producing human breast cancer cell lines (Camirand et al., 2013) has a strong antiproliferative effect in vitro. Furthermore, this study shows that zoledronic acid also inhibits breast tumor cell proliferation and that the combination has an additive effect, which suggests that concomitant administration of zoledronic acid and monoclonal antibodies against PTHrP in vivo could target the "seed" and the "soil" in a very powerful way. Indeed, recent studies in animal models of breast cancer suggest that zoledronic acid has a direct effect on tumor cell proliferation in vivo (Ottewell et al., 2008). An alternate approach has been attempted that blocks PTHrP by using small molecule inhibitors of PTHrP transcription in tumor cells (Gallwitz et al., 2002). This approach may also inhibit the intracrine actions of PTHrP and needs further study.

Although skeletal metastases are associated with skeletal related events such as pain, nerve compression and fractures that severely affect the patients' quality of life (Sullivan, 1996), rapid disease progression usually involves extraskeletal sites resulting in metastatic spread to vital organs that is resistant to most therapeutic regimen. This is particularly true for breast cancer expressing the triple-negative phenotype. In a recent study of a model of breast tumor progression, PTHrP was critical for tumor initiation, growth, and metastases to lungs (Li et al., 2011). Targeting PTHrP was proposed as a potential new therapy for breast and other types of cancer. Indeed, administration of monoclonal antibodies against PTHrP reduced breast tumor growth and lung metastases in breast cancer (Li et al., 2011) and reduced disease spread at multiple sites including liver, lungs, and bones in a human melanoma model (Huang et al., 2014). Similarly, in a model of renal cancer, anti-PTHrP antibodies slowed tumor progression and its metastatic spread (Massfelder et al., 2004). Numerous in vitro studies support the role of PTHrP in growth and invasion in breast, colon, prostate, and giant tumor cells of bone cancers, among others (Li et al., 2011; Mula et al., 2010; Downs et al., 2011; Mak et al., 2011). Interestingly, anti-PTHrP monoclonal antibodies have recently been shown to be potent growth inhibitors of triple-negative breast cancer, potentiating the effect of doxorubicin and taxol (Camirand et al., 2013). Taken together, these studies support the rationale of targeting PTHrP as a novel approach to cancer treatment, possibly in the most refractory types such as triple-negative breast cancer.

Overall, these studies suggest that knowledge of the regulation of PTHrP production, processing, and action may identify targets that could prove useful for the development of agents to reduce circulating concentrations of bioactive PTHrP in vivo and diminish hypercalcemia. Furthermore, such agents could prove beneficial in inhibiting the production of PTHrP by tumors, which might diminish the establishment and growth of metastatic lesions and potentially of primary tumors.

Hypercalcemia caused by other systemic and local factors produced by neoplastic cells

Cytokines and humoral hypercalcemia of malignancy

Circulating proinflammatory cytokines most probably contribute to a number of systemic manifestations of malignancy such as anorexia, dehydration, and cachexia (Ogata, 2000). Mounting evidence also suggests that cytokines released into the systemic circulation by a variety of solid tumors, which often coexpress PTHrP, contribute to the bone destruction associated with MAH. In this respect, it is interesting to note that circulating concentrations of IL-6 correlate in a positive manner with tumor burden in patients with squamous and renal cell carcinoma, the two prototypical malignancies associated with hypercalcemia and elevated circulating levels of PTHrP (Costes et al., 1997; Nagai et al., 1998).

Many other factors, including vascular endothelial growth factor, granulocyte colony-stimulating factor, and cytokines such as interleukins 8 and 11, and soluble RANKL (Nagai et al., 2000), have been implicated in promoting HHM (Horwitz et al., 2003). The relative contributions of systemically active PTHrP and cytokines to MAH have been examined in immune-compromised rodents carrying human tumors that overexpress both factors (Nagai et al., 1998). Nude rats transplanted with a human squamous carcinoma of the oral cavity (OCC), which was shown to overproduce both PTHrP and IL-6, rapidly developed severe hypercalcemia in association with high circulating levels of PTHrP and IL-6. Hypercalcemic animals immunized with anti-IL-6 monoclonal antibody demonstrated a complete reversal in the

biochemical abnormalities associated with elevated circulating IL-6 but only a small reduction in serum calcium. As measured by quantitative histomorphometry, there was a significant decrease in indices of bone resorption as well as an increase in the mineral apposition rate in rats that received the neutralizing antibody. These results suggest that although IL-6 contributed to the skeletal abnormalities seen in OCC tumor-bearing rats, its contribution to the hypercalcemic syndrome was minor compared with that of PTHrP.

Using an alternate model, others demonstrated that mice carrying a human esophageal tumor that coexpresses PTHrP and IL-1 develop a modest elevation in blood calcium (Sato et al., 1989). A comparable level of hypercalcemia was observed in normal mice receiving a continuous infusion of IL-1. However, a significant increase in blood calcium was noted in mice that received a minimal daily dose of PTHrP in addition to the IL-1 infusion, suggesting a synergistic effect of PTHrP and IL-1 on bone resorption in this model. This hypothesis was supported by experiments in which the addition of a small amount of synthetic PTHrP to the culture medium greatly enhanced ^{45}Ca release from prelabeled mouse bones in response to recombinant IL-1.

This work using animal models of human disease predicts that PTHrP may be the principal mediator of MAH. The hypothesis is further supported by clinical studies in which elevated circulating levels of PTHrP correlate strongly with hypercalcemia in patients with tumors of widely diverse histological origin (Ogata, 2000). No such correlation has been demonstrated for hypercalcemia and elevated circulating levels of cytokines such as IL-6 or IL-1. However, it has been proposed that a systemic increase in PTHrP not only promotes hypercalcemia but also stimulates normal cells to produce factors such as TNF-α, IL-1, IL-5, IL-6, and IL-8 in patients presenting with end-stage malignancy. The observation that infusion of anti-PTHrP antibody into mice with high circulating levels of PTHrP and IL-6 resulted in a prolonged decrease in the concentration of both factors in the bloodstream lends some support to this hypothesis.

Cytokines and local osteolysis

Multiple myeloma is a B cell malignancy characterized by clonal expansion of terminally differentiated, immunoglobulin-producing, transformed plasma cells in the bone marrow (Roodman, 2004b). Osteolytic bone disease is a central feature of multiple myeloma and is caused by factors produced by tumor cells and the bone microenvironment that stimulate osteoclasts and inhibit osteoblasts (Terpos et al., 2017; Galson et al., 2012). Adhesion of multiple myeloma cells to bone marrow stromal cells in the bone marrow microenvironment stimulates RANKL expression and OPG inhibition by osteoblasts, leading to osteolysis (Pearse et al., 2001). Multiple myeloma, bone marrow stromal, and bone cells also secrete a variety of inflammatory cytokines including IL-6, TNFα, IL-1, IL-3, macrophage inflammatory protein-1α (MIP-1α) MIP-1β, decoy receptor 3, and activin, which activate osteoclasts and inhibit osteoblasts. Wnt signaling inhibitors, including sclerostin and dickkopf-1 (Tian et al., 2003), as well as the growth factor independence-1, are considered among the most important factors for osteoblast inhibition in multiple myeloma (Terpos et al., 2017; Breslau et al., 1984). Such unbalanced bone resorption results in osteolytic bone disease and ultimately in hypercalcemia.

1,25-Dihydroxyvitamin D (1,25(OH)$_2$D) and humoral hypercalcemia of malignancy

The site of conversion of 25 hydroxyvitamin D [25(OH)D] to its active metabolite, 1,25(OH)$_2$D, by the 25(OH)D 1α-hydroxylase enzyme, is known not to be restricted to the kidney. Although the kidney is still recognized as the primary site of circulating 1,25(OH)$_2$D production in vivo, several extrarenal sites of 1 α-hydroxylase activity have been identified. These include cells of the hematopoietic and immune systems as well as cells in many other tissues that give may give rise to solid tumors associated with MAH. In contrast to the systemic role played by kidney-derived 1,25(OH)$_2$D$_3$ in calcium homeostasis, locally produced hormone is thought to regulate cell proliferation and differentiation in normal cells (Holick, 1999) and could modulate the development of neoplastic transformation within these cells.

Elevated serum concentrations of 1,25(OH)$_2$D$_3$ have been reported in some cases of non-Hodgkin's (Breslau et al., 1984) and Hodgkin's lymphoma (Jacobson et al., 1988), in contrast to the low circulating levels seen in the majority of hypercalcemic cancer patients. This increase in circulating 1,25(OH)$_2$D$_3$ was often seen in the presence of renal impairment, suggesting an extrarenal source of the hormone. Occasionally solid tumors such as the human small cell lung cancer cell line NCI H82 have been reported to synthesize a vitamin D metabolite with similar biochemical properties and bioactivity to authentic 1,25(OH)$_2$D$_3$ (Mawer et al., 1994). The systemic increase in 1,25(OH)$_2$D$_3$ may be accompanied by the elease of lymphoid cytokines and PTHrP, which are also known mediators of MAH and may therefore contribute to the hypercalcemia.

Parathyroid hormone and humoral hypercalcemia of malignancy

Although PTH is normally only secreted by the parathyroid glands, authentic ectopic secretion of PTH (ectopic hyperparathyroidism) has been well documented in a variety of histological types of tumors including lung, ovary, thyroid, and thymus and has been associated with hypercalcemia (Nussbaum et al., 1990; Yoshimoto et al., 1989; Strewler et al., 1993; Rizzoli et al., 1994). Although this syndrome is well documented, it appears to represent an exceedingly rare event.

References

Aarts, M.M., Rix, A., Guo, J., Bringhurst, R., Henderson, J.E., 1999. The nucleolar targeting signal (NTS) of parathyroid hormone related protein mediates endocytosis and nucleolar translocation. J. Bone Miner. Res. 14 (9), 1493–1503.

Abou-Samra, A.B., Jüppner, H., Force, T., Freeman, M.W., Kong, X.F., Schipani, E., Urena, P., Richards, J., Bonventre, J.V., Potts Jr., J.T., et al., 1992. Expression cloning of a common receptor for parathyroid hormone and parathyroid hormone-related peptide from rat osteoblast-like cells: a single receptor stimulates intracellular accumulation of both cAMP and inositol trisphosphates and increases intracellular free calcium. Proc. Natl. Acad. Sci. U.S.A. 89, 2732–2736.

Aklilu, F., Gladu, J., Goltzman, D., Rabbani, S.A., 2000. Role of mitogen-activated protein kinases in the induction of parathyroid hormone related peptide. Cancer Res. 60, 1753–1760.

Aklilu, F., Park, M., Goltzman, D., Rabbani, S.A., 1996. Increased PTHrP production by a tyrosine kinase oncogene Tpr-Met: role of the Ras signalling pathway. Am. J. Physiol. 271, E277–E283.

Aklilu, F., Park, M., Goltzman, D., Rabbani, S.A., 1997. Induction of parathyroid hormone related peptide by the Ras oncogene: role of Ras farnesylation inhibitors as potential therapeutic agents for hypercalcemia of malignancy. Cancer Res. 57, 4517–4522.

Albright, F., 1941. Case records of the Massachusetts general hospital (case 27461). N. Engl. J. Med. 225, 789–791.

Amizuka, N., Warshawsky, H., Henderson, J.E., Goltzman, D., Karaplis, A.C., 1994. Parathyroid hormone-related peptide-depleted mice show abnormal epiphyseal cartilage development and altered endochondral bone formation. J. Cell Biol. 126 (6), 1611–1623.

Amizuka, N., Karaplis, A.C., Henderson, J.E., Warshawsky, H., Lipman, M.L., Matsuki, Y., Ejiri, S., Tanaka, M., Izumi, N., Ozawa, H., Goltzman, D., 1996. Haploinsufficiency of parathyroid hormone-related peptide (PTHrP) results in abnormal postnatal bone development. Dev. Biol. 175 (1), 166–176.

Bellido, T., Saini, V., Pajevic, P.D., 2013. Effects of PTH on osteocyte function. Bone 54 (2), 250–257.

Bikle, D.D., 2014. Vitamin D metabolism, mechanism of action, and clinical applications. Chem. Biol. 21, 319–329.

Body, J.J., 2000. Current and future directions in medical therapy: hypercalcemia. Cancer 88 (Suppl. l), 3054–3058.

Body, J.J., Bartl, R., Burckhardt, P., Delmas, P.D., Diel, I.J., Fleisch, H., Kanis, J.A., Kyle, R.A., Mundy, G.R., Paterson, A.H., Rubens, R.D., 1998. Current use of bisphosphonates in oncology. International bone and cancer study group. J. Clin. Oncol. 16, 3890–3899.

Bouizar, Z., Spyratos, F., De Vernejoul, M.C., 1999. The parathyroid hormone-related protein (PTHrP) gene: use of downstream TATA promotor and PTHrP 1–139 coding pathways in primary breast cancers vary with the occurrence of bone metastasis. J. Bone Miner. Res. 14, 406–414.

Bovee, J.V., van den Broek, L.J., Cleton-Jansen, A.M., Hogendoorn, P.C., 2000. Up-regulation of PTHrP and Bcl-2 expression characterizes the progression of osteochondroma towards peripheral chondrosarcoma and is a late event in central chondrosarcoma. Lab. Invest. 80, 1925–1934.

Brandt, D.W., Burton, D.W., Gazdar, A.F., Oie, H.E., Deftos, L.J., 1991. All major lung cancer cell types produce parathyroid hormone-like protein: heterogeneity assessed by high performance liquid chromatography. Endocrinology 129, 2466–2470.

Breslau, N.A., McGuire, J.L., Zerwech, J.E., Frenkel, E.P., Pak, C.Y.C., 1984. Hypercalcemia associated with increased calcitriol levels in three patients with lymphoma. Ann. Intern. Med. 100, 1–7.

Broadus, A.E., Stewart, A.F., 1994. Parathyroid hormone-related protein: structure, processing and physiological actions. In: Bilezekian, J.P., Levine, M.A., Markus, R. (Eds.), The Parathyroids. Raven Press, New York, pp. 259–294.

Brown, E.M., Gamba, G., Riccardi, D., Lombardi, M., Butters, R., Kifor, O., Sun, A., Hediger, M.A., Lytton, J., Hebert, S.C., 1993. Cloning and characterization of an extracellular Ca(2+)-sensing receptor from bovine parathyroid. Nature 366, 575–580.

Budayr, A.A., Nissenson, R.A., Klein, R.F., Pun, K.K., Clark, O.H., Diep, D., Arnaud, C.D., Strewler, G.J., 1989. Increased serum levels of a parathyroid hormone-like protein in malignancy-associated hypercalcemia. Ann. Intern. Med. 111, 807–812.

Burtis, W.J., Brady, T.G., Orloff, J.J., Ersbak, J.B., Warrell, R.P., Olson, B.R., Wu, T.L., Mitnick, M.E., Broadus, A.E., Stewart, A.F., 1990. Immunochemical characterization of circulating parathyroid hormone-related protein in patients with humoral hypercalcemia of cancer. N. Engl. J. Med. 322, 1106–1112.

Burtis, W.J., 1992. Parathyroid hormone-related protein: structure, function, and measurement. Clin. Chem. 38, 2171–2183.

Burtis, W.J., Dann, P., Gaich, G.A., Soifer, N.E., 1994. A high abundance midregion species of parathyroid hormone-related protein: immunological and chromatographic characterization in plasma. J. Clin. Endocrinol. Metab. 78, 317–322.

Burtis, W.J., Wu, T., Bunch, C., Wysolmerski, J.J., Insogna, K.L., Weir, E.C., Broadus, A.E., Stewart, A.F., 1987. Identification of a novel 17000 dalton parathyroid hormone-like adenylate cyclase stimulating protein from a tumor associated with humoral hypercalcemia of malignancy. J. Biol. Chem. 262, 7151–7156.

Camirand, A., Fadhil, I., Luco, A.L., Ochietti, B., Kremer, R.B., 2013. Enhancement of taxol, doxorubicin and zoledronate anti-proliferation action on triple-negative breast cancer cells by a PTHrP blocking monoclonal antibody. Am J Cancer Res 3, 500–508.

Campos, R.V., Zhang, L., Drucker, D.J., 2006. Differential expression of RNA transcripts. Mol. Endocrinol. 8, 1656–1666.

Capparelli, C., Kostenuik, P.J., Morony, S., Starnes, C., Weimann, B., Van, G., Scully, S., Qi, M., Lacey, D.L., Dunstan, C.R., 2000. Osteoprotegerin prevents and reverses hypercalcemia in a murine model of humoral hypercalcemia of malignancy. Cancer Res. 60, 783−787.

Cattopadhyay, N., 2006. Effects of calcium-sensing receptor on the secretion of parathyroid hormone-related peptide and its impact on humoral hypercalcemia of malignancy. Am. J. Physiol. Endocrinol. Metab. 290, E761−E770.

Chorev, M., Rosenblatt, M., 1994. Structure-function analysis of parathyroid hormone and parathyroid hormone-related protein. In: Bilezikian, J.P., Marcus, R., Levine, M.A. (Eds.), The Parathyroids: Basic and Clinical Aspects. Raven Press, New York, pp. 139−156.

Coleman, R., Gnant, M., Morgan, G., Clezardin, P., 2012. Effects of bone-targeted agents on cancer progression and mortality. J. Natl. Cancer Inst. 104, 1059−1067.

Costes, V., Liautard, J., Picot, M.C., Robert, M., Lequeux, N., Brochier, J., Baldet, P., Rossi, J.F., 1997. Expression of interleukin-6 receptor in primary renal cell carcinoma. J. Clin. Pathol. 50, 835−840.

Dang, C.V., Lee, W.M.F., 1989. Nuclear and nucleolar targeting sequences of c-erb, c-myb, N-myc, p53, HSP70, and HIV tat proteins. J. Biol. Chem. 264, 18019−18023.

De Wit, S., Cleton, F., 1994. Hypercalcemia in patients with breast cancer: a survival study. J. Cancer Res. Clin. Oncol. 120, 610−614.

Deftos, L.J., 2000. Prostate carcinoma: production of bioactive factors. Cancer 88, 3002−3008.

Dittmer, J., Gitlin, S.D., Reid, R.L., Brady, J.N., 1993. Transactivation of the P2 promoter of parathyroid hormone-related protein by human T-cell lymphotropic virus type I tax I: evidence for the involvement of transcription factor Ets *I*. J. Virol. 67, 6087−6095.

Donovan, P.J., Achong, N., Griffin, K., Galligan, J., Pretorius, C.J., McLeod, D.S., 2015. PTHrP-mediated hypercalcemia: causes and survival in 138 patients. J. Clin. Endocrinol. Metab. 100, 2024−2029.

Dougherty, K.M., Blomme, E.A., Koh, A.J., Henderson, J.E., Pienta, K.J., Rosol, T.J., McCauley, L.K., 1999. Parathyroid hormone-related protein as a growth regulator of prostate carcinoma. Cancer Res. 59, 6015−6022.

Downey, S.E., Hoyland, J., Freemont, A.J., Knox, F., Walls, J., Bundred, N.J., 1997. Expression of the receptor for parathyroid hormone-related protein in normal and malignant breast tissue. J. Pathol. 183, 212−217.

Downs, T.M., Burton, D.W., Araiza, F.L., Hastings, R.H., Deftos, L.J., 2011. PTHrP stimulates prostate cancer cell growth and upregulates aldo-keto reductase 1C3. Cancer Lett. 306, 52−59.

Ejima, E., Rosenblatt, J.D., Massari, M., Quan, E., Stephens, D., Rosen, C., Prager, D., 1993. Cell-type-specific trans-activation of the parathyroid hormone-related protein gene promoter by the human T-cell leukemia virus type I (HTLV-I) tax and HTLV-II tax protein. Blood 81, 1017−1024.

El Abdaimi, K.E., Dion, N., Papavasiliou, V., Cardinal, P.-E., Binderup, L., Goltzman, D., Ste-Marie, L.-G., Kremer, R., 2000. The vitamin D analogue EB 1089 prevents skeletal metastasis and prolongs survival time in nude mice transplanted with human breast cancer cells. Cancer Res. 60, 4412−4418.

El Abdaimi, K.E., Papavasiliou, V., Rabbani, S.A., Rhim, J.S., Goltzman, D., Kremer, R., 1999. Reversal of hypercalcemia with the vitamin D analog EB1089 in a model of human squamous cancer. Cancer Res. 59, 3325−3328.

El Abdaimi, K.E., Papavasilious, V., Goltzman, D., Kremer, R., 2000. Expression and regulation of parathyroid hormone-related peptide in normal and malignant melanocytes. Am. J. Physiol. Cell Physiol. 279, C1230−C1238.

Estrada, K., Styrkarsdottir, U., Evangelou, E., Hsu, Y.H., Duncan, E.L., Ntzani, E.E., Oei, L., Albagha, O.M., Amin, N., Kemp, J.P., Koller, D.L., Li, G., Liu, C.T., Minster, R.L., Moayyeri, A., Vandenput, L., Willner, D., Xiao, S.M., Yerges-Armstrong, L.M., Zheng, H.F., Alonso, N., Eriksson, J., Kammerer, C.M., Kaptoge, S.K., Leo, P.J., Thorleifsson, G., Wilson, S.G., Wilson, J.F., Aalto, V., Alen, M., Aragaki, A.K., Aspelund, T., Center, J.R., Dailiana, Z., Duggan, D.J., Garcia, M., Garcia-Giralt, N., Giroux, S., Hallmans, G., Hocking, L.J., Husted, L.B., Jameson, K.A., Khusainova, R., Kim, G.S., Kooperberg, C., Koromila, T., Kruk, M., Laaksonen, M., Lacroix, A.Z., Lee, S.H., Leung, P.C., Lewis, J.R., Masi, L., Mencej-Bedrac, S., Nguyen, T.V., Nogues, X., Patel, M.S., Prezelj, J., Rose, L.M., Scollen, S., Siggeirsdottir, K., Smith, A.V., Svensson, O., Trompet, S., Trummer, O., van Schoor, N.M., Woo, J., Zhu, K., Balcells, S., Brandi, M.L., Buckley, B.M., Cheng, S., Christiansen, C., Cooper, C., Dedoussis, G., Ford, I., Frost, M., Goltzman, D., González-Macías, J., Kähönen, M., Karlsson, M., Khusnutdinova, E., Koh, J.M., Kollia, P., Langdahl, B.L., Leslie, W.D., Lips, P., Ljunggren, Ö., Lorenc, R.S., Marc, J., Mellström, D., Obermayer-Pietsch, B., Olmos, J.M., Pettersson-Kymmer, U., Reid, D.M., Riancho, J.A., Ridker, P.M., Rousseau, F., Slagboom, P.E., Tang, N.L., Urreizti, R., Van Hul, W., Viikari, J., Zarrabeitia, M.T., Aulchenko, Y.S., Castano-Betancourt, M., Grundberg, E., Herrera, L., Ingvarsson, T., Johannsdottir, H., Kwan, T., Li, R., Luben, R., Medina-Gómez, C., Palsson, S.T., Reppe, S., Rotter, J.I., Sigurdsson, G., van Meurs, J.B., Verlaan, D., Williams, F.M., Wood, A.R., Zhou, Y., Gautvik, K.M., Pastinen, T., Raychaudhuri, S., Cauley, J.A., Chasman, D.I., Clark, G.R., Cummings, S.R., Danoy, P., Dennison, E.M., Eastell, R., Eisman, J.A., Gudnason, V., Hofman, A., Jackson, R.D., Jones, G., Jukema, J.W., Khaw, K.T., Lehtimäki, T., Liu, Y., Lorentzon, M., McCloskey, E., Mitchell, B.D., Nandakumar, K., Nicholson, G.C., Oostra, B.A., Peacock, M., Pols, H.A., Prince, R.L., Raitakari, O., Reid, I.R., Robbins, J., Sambrook, P.N., Sham, P.C., Shuldiner, A.R., Tylavsky, F.A., van Duijn, C.M., Wareham, N.J., Cupples, L.A., Econs, M.J., Evans, D.M., Harris, T.B., Kung, A.W., Psaty, B.M., Reeve, J., Spector, T.D., Streeten, E.A., Zillikens, M.C., Thorsteinsdottir, U., Ohlsson, C., Karasik, D., Richards, J.B., Brown, M.A., Stefansson, K., Uitterlinden, A.G., Ralston, S.H., Ioannidis, J.P., Kiel, D.P., Rivadeneira, F., 2012. Genome-wide meta-analysis identifies 56 bone mineral density loci and reveals 14 loci associated with risk of fracture. Nat. Genet. 44 (5), 491−501.

Feffari, S.L., Rizzoli, R., Bonjour, J.P., 1994. Effect of EGF on parathyroid hormone related protein (PTHRP) production by mammary epithelial cells. J. Bone Miner. Res. 9, 639−644.

Fenton, A.J., Kemp, B.E., Hammonds, R.G., Mitchellhill, K., Moseley, S.M., Martin, T.S., Nicholson, G.C., 1991. A potent inhibitor of osteoclastic bone resorption within a highly conserved pentapeptide region of PTHrP: PTHrP[107−111]. Endocrinology 129, 3424−3426.

Firkin, F., Seymour, J.F., Watson, A.M., Grill, V., Martin, T.J., 1996. Parathyroid hormone-related protein in hypercalcaemia associated with haematological malignancy. Br. J. Haematol. 94, 486−492.

Foley, J., Dann, P., Hong, J., Cosgrove, J., Dreyer, B., Rimm, D., Dunbar, M., Philbrick, W., Wysolmerski, J., 2001. Parathyroid hormone-related protein maintains mammary epithelial fate and triggers nipple skin differentiation during embryonic breast development. Development 128, 513–525.

Fraher, L.J., Hodsman, A.B., Jonas, K., Saunders, D., Rose, C.I., Henderson, J.E., Hendy, G.N., Goltzman, D., 1992. A comparison of the in vivo biochemical responses to exogenous parathyroid hormone (1-34) and parathyroid hormone-related peptide (1-34) in man. J. Clin. Endocrinol. Metab. 75, 417–423.

Fukayama, S., Tashjian Jr., A.H., Davis, J.N., Chisholm, J.C., 1995. Signaling by N- and C-terminal sequences of parathyroid hormone-related protein in hippocampal neurons. Proc. Natl. Acad. Sci. U.S.A. 92, 10182–10186.

Gallwitz, W.E., Guise, T.A., Mundy, G.R., 2002. Guanosine nucleotides inhibit different syndromes of PTHrP excess caused by human cancers in vivo. J. Clin. Investig. 110, 1559–1572.

Galson, D.L., Silbermann, R., Roodman, G.D., 2012. Mechanisms of multiple myeloma bone disease. Bonekey Rep. 1, 135.

Ganderton, R.H., Briggs, R.S., 1997. CpG island methylation and promoter usage in the parathyroid hormone-related protein gene of cultured lung cells. Biochem. Biophys. Acta 1352, 303–310.

Gesty-Palmer, D., Chen, M., Reiter, E., Ahn, S., Nelson, C.D., Wang, S., Eckhardt, A.E., Cowan, C.L., Spurney, R.F., Luttrell, L.M., Lefkowitz, R.J., 2006. Distinct β-arrestin- and G protein-dependent pathways for parathyroid hormone receptor-stimulated ERK1/2 activation. J. Biol. Chem. 281, 10856–10864.

Ghoussaini, M., Fletcher, O., Netherlands Collaborative Group on Hereditary Breast and Ovarian Cancer (HEBON), Michailidou, K., Turnbull, C., 2012. Genome-wide association analysis identifies three new breast cancer susceptibility loci. Nat. Genet. 44, 312–318.

Glatz, J.A., Heath, J.K., Southby, J., O'Keeffe, L.M., Kiriyama, T., Moseley, J.M., Martin, T.J., Gillespie, M.T., 1994. Dexamethasone regulation of parathyroid hormone-related protein (PTHrP) expression in a squamous cancer cell line. Mol. Cell. Endocrinol. 101, 295–306.

Goltzman, D., Hendy, G.N., Banville, D., 1989. Parathyroid hormone-like peptide: molecular characterization and biological properties. Trends Endocrinol. Metabol. 1, 39–44.

Goltzman, D., Stewart, A.F., Broadus, A.E., 1981. Malignancy associated hypercalcemia: evaluation with cytochemical bioassay for parathyroid hormone. J. Clin. Endocrinol. Metab. 53, 899–904.

Gonzalez-Suarez, E., Jacob, A.P., Jones, J., Miller, R., Roudier-Meyer, M.P., Erwert, R., Pinkas, J., Branstetter, D., Dougall, W.C., 2010. RANK ligand mediates progestin-induced mammary epithelial proliferation and carcinogenesis. Nature 468, 103–107.

Grill, V., Ho, P., Body, J.J., Johanson, N., Lee, S.C., Kukreja, S.C., Moseley, J.M., Martin, T.J., 1991. Parathyroid hormone-related protein: elevated levels in both humoral hypercalcemia of malignancy and hypercalcemia complicating metastatic breast cancer. J. Clin. Endocrinol. Metab. 73, 1309–1315.

Grill, V., Murray, R.M., Ho, P.W., Santamaria, J.D., Pitt, P., Potts, C., Jerums, G., Martin, T.J., 1992. Circulating PTH and PTHrP levels before and after treatment of tumor induced hypercalcemia with Pamidronate Disodium (APD). J. Clin. Endocrinol. Metab. 74, 1468–1470.

Guise, T.A., Yin, J.J., Taylor, S.D., Kumagai, Y., Dallas, M., Boyce, B.F., Yoneda, T., Mundy, G.R., 1996. Evidence for a causal role of parathyroid hormone-related protein in the pathogenesis of human breast cancer-mediated osteolysis. J. Clin. Investig. 98, 1544–1549.

Guise, T.A., Yin, J.J., Thomas, R.J., Dallas, M., Cui, Y., Gillespie, M.T., 2002. Parathyroid hormone-related protein (PTHrP)-(1–139) isoform is efficiently secreted in vitro and enhances breast cancer metastasis to bone in vivo. Bone 30, 670–676.

Gurney, H., Grill, V., Martin, T.J., 1993. Parathyroid hormone-related protein and response to pamidronate in tumor induced hypercalcemia. Lancet 341, 1611–1613.

Guy, C.T., Cardiff, R.D., Muller, W.J., 1992. Induction of mammary tumors by expression of polyomavirus middle T oncogene: a transgenic mouse model for metastatic disease. Mol. Cell Biol. 12, 954–961.

Hastings, R.H., Araiza, F., Burton, D.W., Zhang, L., Bedley, M., Deftos, L.J., 2003. Parathyroid hormone-related protein ameliorates death receptor-mediated apoptosis in lung cancer cells. Am. J. Physiol. Cell Physiol. 285, C1429–C1436.

Haq, M., Kremer, R., Goltzman, D., Rabbani, S.A., 1993. A vitamin D analogue (EB1089) inhibits parathyroid hormone-related peptide production and prevents the development of malignancy-associated hypercalcemia in vivo. J. Clin. Investig. 91, 2416–2422.

Hanahan, D., Weinberg, R.A., 2011. Hallmarks of cancer: the next generation. Cell 144, 646–674.

Hashimoto, H., Azuma, Y., Kawasaki, M., Fujihara, H., Onuma, E., Yamada-Okabe, H., Takuwa, Y., Ogata, E., Ueta, Y., 2007. Parathyroid hormone-related protein induces cachectic syndromes without directly modulating the expression of hypothalamic feeding-regulating peptides. Clin. Cancer Res. 13, 292–298.

Henderson, J.E., Amizuka, N., Warshawsky, H., Biasotto, D., Lanske, B.M.K., Goltzman, D., Karaplis, A.C., 1995. Nucleolar targeting of PTHrP enhances survival of chondrocytes under conditions that promote cell death by apoptosis. Mol. Cell Biol. 15, 4064–4075.

Henderson, J.E., Bernier, S., D'Amour, P., Goltzman, D., 1990a. Effects of passive immunization against parathyroid hormone (PTH)-like peptide and PTH in hypercalcemic tumor-bearing rats and normocalcemic controls. Endocrinology 127, 1310–1318.

Henderson, J.E., Sebag, M., Rhim, J., Goltzman, D., Kremer, R., 1991. Dysregulation of parathyroid hormone-like peptide expression and secretion in a keratinocyte model of tumor-progression. Cancer Res. 51, 6521–6528.

Henderson, J.E., Shustik, C., Kremer, R., Rabbani, S.A., Hendy, G.N., Goltzman, D., 1990b. Circulating concentrations of parathyroid hormone-like peptide in malignancy and hyperparathyroidism. J. Bone Miner. Res. 5, 105–113.

Henderson, M., Danks, J., Moseley, J., Slavin, J., Harris, T., McKinlay, M., Hopper, J., Martin, T., 2001. Parathyroid hormone-related protein production by breast cancers, improved survival, and reduced bone metastases. J. Natl. Cancer Inst. 93, 234–237.

Henderson, M.A., Danks, J.A., Slavin, J.L., Byrnes, G.B., Choong, P.F., Spillane, J.B., Hopper, J.L., Martin, T.J., 2006. Parathyroid hormone related protein localization in breast cancers predict improved prognosis. Cancer Res. 66, 2250–2256.

Hidaka, N., Nishimura, M., Nagao, K., 1998. Establishment of two human small cell lung cancer cell lines: the evidence of accelerated production of parathyroid hormone-related protein with tumor progression. Cancer Lett. 125, 149–155.

Hiraki, A., Ueoka, H., Bessho, A., Segawa, Y., Takigawa, N., Kiura, K., Eguchi, K., Yoneda, T., Tanimoto, M., Harada, M., 2002. Parathyroid hormone-related protein measured at the time of first visit is an indicator of bone metastases and survival in lung carcinoma patients with hypercalcemia. Cancer 95, 1706–1713.

Hirbe, A.C., Morgan, E.A., Weilbaecher, K.N., 2010. The CXCR4/SDF-1 chemokine axis: a potential therapeutic target for bone metastases? Curr. Pharmaceut. Des. 16, 1284–1290.

Hoey, R.P., Sanderson, C., Iddon, J., Brady, G., Bundred, N.J., Anderson, N.G., 2003. The parathyroid hormone-related protein receptor is expressed in breast cancer bone metastases and promotes autocrine proliferation in breast carcinoma cells. Br. J. Canc. 88, 567–573.

Holick, M.F., 1999. Vitamin D: photobiology, metabolism, mechanism of action and clinical applications. In: Favus, M.J. (Ed.), Primer on the Metabolic Bone Diseases and Disorders of Mineral Metabolism. Lippincott Williams and Wilkins, Baltimore, pp. 92–98.

Hongo, T., Kupfer, J., Enomoto, H., Sharifi, B., Giannella-Neto, D., Forrester, J.S., Singer, F.R., Goltzman, D., Hendy, G.N., Pirola, C., Fagin, J.A., Clemens, T.L., 1991. Abundant expression of parathyroid hormone-related protein in primary rat aortic smooth muscle cells accompanies serum induced proliferation. J. Clin. Investig. 88, 1841–1847.

Horwitz, M.J., Stewart, A.F., 2003. Humoral hypercalcemia of malignancy. In: Favus, M.J. (Ed.), Primer on the Metabolic Bone Diseases and Disorders of Mineral Metabolism, fifth ed. Lippincott Williams & Wilkins, Philadelphia, PA, pp. 246–250.

Horwitz, M.J., Tedesco, M.B., Sereika, S.M., Syed, M.A., Garcia-Ocana, A., Bisello, A., Hollis, B.W., Rosen, C.J., Wysolmerski, J.J., Dann, P., Gundberg, C., Stewart, A.F., 2005. Continuous PTH and PTHrP infusion causes suppression of bone formation and discordant effects on 1,25(OH)2 vitamin D. J. Bone Miner. Res. 20, 1792–1803.

Hu, M.I., Glezerman, I.G., Leboulleux, S., Insogna, K., Gucalp, R., Misiorowski, W., Yu, B., Zorsky, P., Tosi, D., Bessudo, A., Jaccard, A., Tonini, G., Ying, W., Braun, A., Jain, R.K., 2014. Denosumab for treatment of hypercalcemia of malignancy. J. Clin. Endocrinol. Metab. 99, 3144–3152.

Huang, D., Yang, X.F., Ochietti, B., Fadhil, I., Camirand, A., Kremer, R., 2014. Parathyroid hormone-related protein: potential therapeutic target for melanoma invasion and metastasis. Endocrinology 155, 3739–3749.

Iguchi, H., Tanaka, S., Ozawa, Y., Kashiwakuma, T., Kimura, T., Hiraga, T., Ozawa, H., Kono, A., 1996. An experimental model of bone metastasis by human lung cancer cells: the role of parathyroid hormone-related protein in bone metastasis. Cancer Res. 56, 4040–4043.

Iguchi, H., Onuma, E., Sato, K., Sato, K., Ogata, E., 2001. Involvement of parathyroid hormone-related protein in experimental cachexia induced by a human lung cancer-derived cell line established from a bone metastasis specimen. Int. J. Cancer 94, 24–27.

Ikeda, K., Okazaki, R., Inoue, D., Ohno, H., Ogata, E., Matsumoto, T., 1993. Interleukin-2 increases production and secretion of parathyroid hormone-related peptide by human T cell leukemia virus type I-infected T cells: possible role in hypercalcemia associated with adult T cell leukemia. Endocrinology 132, 2551–2556.

Imamura, H., Sato, K., Shizume, K., Satoh, T., Kasono, K., Ozawa, M., Ohmura, E., Tsushima, T., Demura, H., 1991. Urinary excretion of parathyroid hormone-related protein fragments in patients with humoral hypercalcemia of malignancy and hypercalcemic tumor-bearing nude mice. J. Bone Miner. Res. 6, 77–84.

Iwamura, M., Wu, W., Muramoto, M., Ohori, M., Egawa, S., Uchida, T., Baba, S., 1999. Parathyroid hormone-related protein is an independent prognostic factor for renal cell carcinoma. Cancer 86, 1028–1034.

Jacobson, J.O., Bringhurst, F.R., Harris, N.L., Weitzman, S.A., Aisenberg, A.C., 1988. Humoral hypercalcemia in Hodgkin's disease. Clin. Lab. Eval. Cancer 163, 917–923.

Jiang, M., Chen, G., Lu, N., Zhang, Y., Jin, S., Karaplis, A., Goltzman, D., Miao, D., 2015. Deficiency of the parathyroid hormone-related peptide nuclear localization and carboxyl terminal sequences leads to premature skin ageing partially mediated by the upregulation of p27. Exp. Dermatol. 24 (11), 847–852.

Johnson, R.W., Nguyen, M.P., Padalecki, S.S., Grubbs, B.G., Merkel, A.R., Oyajobi, B.O., Matrisian, L.M., Mundy, G.R., Sterling, J.A., 2011. TGF-beta promotion of Gli2-induced expression of parathyroid hormone-related protein, an important osteolytic factor in bone metastasis, is independent of canonical Hedgehog signaling. Cancer Res. 71, 822–823.

Jüppner, H., Abou-Samra, A.B., Freemanm, M., Kong, X.F., Schipani, E., Richards, J., Kolakowskim Jr., L.F., Hock, J., Potts Jr., J.T., Kronenberg, H.M., Segre, G.V., 1991. A G protein-linked receptor for parathyroid hormone and parathyroid hormone-related peptide. Science 254, 1024–1026.

Kageshita, T., Matsui, T., Hirai, S., Fukuda, Y., Ono, T., 1999. Hypercalcaemia in melanoma patients associated with increased levels of parathyroid hormone-related protein. Melanoma Res. 9, 69–73.

Kaji, H., Sugimoto, T., Kanatani, M., Fukase, M., Chihara, K., 1995. Carboxyl-terminal peptides from parathyroid hormone-related protein stimulate osteoclast-like cell formation. Endocrinology 136, 842–848.

Kakonen, S.M., Selander, K.S., Chirgwin, J.M., Yin, J.J., Burns, S., Rankin, W.A., Grubbs, B.G., Dallas, M., Cui, Y., Guise, T.A., 2002. Transforming growth factor-beta stimulates parathyroid hormone-related protein and osteolytic metastases via Smad and mitogen-activated protein kinase signaling pathways. J. Biol. Chem. 277, 24571–24578.

Kao, P.C., Klee, G.G., Taylor, R.L., Heath 3rd, H., 1990. Parathyroid hormone-related peptide in plasma of patients with hypercalcemia and malignant lesions. Mayo Clin. Proc. 65, 1399–1407.

Karaplis, A.C., Yasuda, T., Hendy, G.N., Goltzman, D., Banville, D., 1990. Gene-encoding parathyroid hormone-like peptide: nucleotide sequence of the rat gene and comparison with the human homologue. Mol. Endocrinol. 4, 441–446.

Karaplis, A.C., Luz, A., Glowacki, J., Bronson, R.T., Tybulewicz, V.L., Kronenberg, H.M., Mulligan, R.C., 1994. Lethal skeletal dysplasia from targeted disruption of the parathyroid hormone-related peptide gene. Genes Dev. 8 (3), 277–289.

Kim, W., Takyar, F.M., Swan, K., Jeong, J., VanHouten, J., Sullivan, C., Dann, P., Yu, H., Fiaschi-Taesch, N., Chang, W., Wysolmerski, J., 2016. Calcium-sensing receptor promotes breast cancer by stimulating intracrine actions of parathyroid hormone-related protein. Cancer Res. 76, 5348−5360.

Kohno, N., Kitazawa, S., Fukase, M., Sakoda, Y., Kanbara, Y., Furuya, Y., Ohashi, O., Ishikawa, Y., Saitoh, T., 1994. The expression of parathyroid hormone-related protein in human breast cancer with skeletal metastases. Surg. Today 24, 215−220.

Keusch, I., Traebert, M., Lotscher, M., Kaissling, G., Murer, H., Biber, J., 1998. Parathyroid hormone and dietary phosphate provoke a lysosomal routing of the proximal tubular Na/Pi-cotransporter type II. Kidney Int. 54, 1224−1232.

Kir, S., White, J.P., Kleiner, S., Kazak, L., Cohen, P., Baracos, V.E., Spiegelman, B.M., 2014. Tumour-derived PTH-related protein triggers adipose tissue browning and cancer cachexia. Nature 513, 100−104.

Kiriyama, T., Gillespie, M.T., Glatz, J.A., Fukumoto, S., Moseley, J.M., Martin, T.J., 1993. Transforming growth factor beta stimulation of parathyroid hormone-related protein (PTHrP): a paracrine regulator? Mol. Cell. Endocrinol. 92, 55−62.

Kovacs, C.S., Lanske, B., Hunzelman, J.L., Guo, J., Karaplis, A.C., Kronenberg, H.M., 1996. Parathyroid hormone-related peptide (PTHrP) regulates fetal-placental calcium transport through a receptor distinct from the PTH/PTHrP receptor. Proc. Natl. Acad. Sci. U.S.A. 93, 15233−15238.

Kovacs, C.S., 2015. Calcium, phosphorus, and bone metabolism in the fetus and newborn. Early Hum. Dev. 91 (11), 623−628.

Kremer, R., Karaplis, A.C., Henderson, J.E., Gulliver, W., Banville, D., Hendy, G.N., Goltzman, D., 1991. Regulation of parathyroid hormone-like peptide in cultured normal human keratinocytes. J. Clin. Investig. 87, 884−893.

Kremer, R., Sebag, M., Champigny, C., Meerovitch, K., Hendy, G.N., White, J., Goltzman, D., 1996a. Identification and characterization of 1,25-dihydroxyvitamin D3-responsive repressor sequences in the rat parathyroid hormone-related peptide gene. J. Biol. Chem. 271, 16310−16316.

Kremer, R., Shustik, C., Tabak, T., Papavasiliou, V., Goltzman, D., 1996b. Parathyroid hormone-related peptide (PTHrP) in hematological malignancies. Am. J. Med. 100, 406−411.

Kremer, R., Woodworth, C.D., Goltzman, D., 1996c. Expression and action of parathyroid hormone related peptide in human cervical epithelial cells. Am. J. Physiol. 271, C164−C171.

Kremer, R., Goltzman, D., Amizuka, N., Webber, M.M., Rhim, J.S., 1997. Ras Activation of human prostate epithelial cells induces overexpression of parathyroid hormone-related peptide. Clin. Cancer Res. 3, 855−859.

Kukreja, S.C., Shevrin, D.H., Wimbiscus, S.A., Ebeling, P.R., Danks, J.A., Rodda, C.P., Wood, W.I., Martin, T.J., 1988. Antibodies to parathyroid hormone-related protein lower serum calcium in athymic mouse models of malignancy-associated hypercalcemia due to human tumors. J. Clin. Investig. 82, 1798−1802.

Kunisada, T., Moseley, J.M., Slavin, J.L., Martin, T.J., Choong, P.F., 2002. Co-expression of parathyroid hormone-related protein (PTHrP) and PTH/PTHrP receptor in cartilaginous tumours: a marker for malignancy? Pathology 34, 133−137.

Lafferty, F.W., 1966. Pseudohyperparathyroidism. Medicine 45, 247−260.

Lam, M.H., Olsen, S.L., Rankin, W.A., Ho, P.W., Martin, T.J., Gillespie, M.T., Moseley, J.M., 1997. PTHrP and cell division: expression and localization of PTHrP in a keratinocyte cell line (HaCaT) during the cell cycle. J. Cell. Physiol. 173, 433−446.

Lam, M.H.C., House, C.M., Tiganis, T., Mitchelhill, K.I., Sarcevic, B., Cures, A., Ramsay, R., Kemp, B.E., Martin, T.J., Gillespie, M.T., 1999. Phosphorylation at the cyclin-dependent kinase site (Thr85) of parathyroid hormone related protein negatively regulates its nuclear localization. J. Biol. Chem. 274, 18559−18566.

Lam, M.H., Thomas, R.J., Martin, T.J., Gillespie, M.T., Jans, D.A., 2000. Nuclear and nucleolar localization of parathyroid hormone-related protein. Immunol. Cell Biol. 78, 395−402.

Lam, M.H., Thomas, R.J., Loveland, K.L., Schilders, S., Gu, M., Martin, T.J., Gillespie, M.T., Jans, D.A., 2002. Nuclear transport of parathyroid hormone (PTH)-related protein is dependent on microtubules. Mol. Endocrinol. 16, 390−401.

Lee, J.K., Chuang, M.J., Lu, C.C., Hao, L.J., Yang, C.Y., Han, T.M., Lam, H.C., 1997. Parathyroid hormone and parathyroid hormone related protein assays in the investigation of hypercalcemic patients in hospital in a Chinese population. J. Endocrinol. Investig. 20, 404−409.

Li, J., Karaplis, A.C., Huang, D.C., Siegel, P.M., Camirand, A., Yang, X.F., Muller, W.J., Kremer, R., 2011. PTHrP drives breast tumor initiation, progression, and metastasis in mice and is a potential therapy target. J. Clin. Investig. 121, 4655−4669.

Liapis, H., Crouch, E.C., Grosso, L.E., Kitazawa, S., Wick, M.R., 1993. Expression of parathyroid like protein in normal, proliferative, and neoplastic human breast tissues. Am. J. Pathol. 143, 1169−1178.

Liu, B., Goltzman, D., Rabbani, S.A., 1995. Processing of pro-PTHRP by the prohormone convertase, furin: effect on biological activity. Am. J. Physiol. 268, E832−838.

Luco, A., Li, J., Ochietti, B., Camirand, A., Karaplis, A., Kremer, R., 2013. Parathyroid hormone-related peptide (PTHrP) blockade inhibits the development of bone metastasis and potentiates the effect of zoledronic acid in vitro and in vivo in a mouse model of breast tumor progression. J. Bone Miner. Res. 28 (Suppl. 1). Available at: http://www.asbmr.org/education/AbstractDetail?aid=b11119c7-2d2c-49d2-9e63-d14f978732cc.

Mahon, M.J., Donowitz, M., Yun, C.C., Segre, G.V., 2002. Na(+)/H(+) exchanger regulatory factor 2 directs parathyroid hormone 1 receptor signalling. Nature 417, 858−861.

Maioli, E., Fortino, V., 2004. The complexity of parathyroid hormone-related protein signalling. Cell. Mol. Life Sci. 61, 257−262.

Mak, I.W., Cowan, R.W., Turcotte, R.E., Singh, G., Ghert, M., 2011. PTHrP induces autocrine/paracrine proliferation of bone tumor cells through inhibition of apoptosis. PLoS One. 6 (5), e19975.

Mangin, M., Webb, A.C., Dreyer, B.E., Posillico, J.T., Ikeda, K., Weir, E.C., Stewart, A.F., Bander, N.H., Milstone, L., Barton, D.E., Francke, U.T.A., Broadus, A.E., 1988. Identification of a cDNA encoding a parathyroid hormone-like peptide from a human tumor associated with humoral hypercalcemia of malignancy. Proc. Natl. Acad. Sci. U.S.A. 85, 597−601.

Mangin, M., Ikeda, K., Dreyer, B.E., Broadus, A.E., 1989. Isolation and characterization of the human parathyroid hormone-like peptide gene. Proc. Natl. Acad. Sci. U.S.A. 86, 2408–2412.

Mannstadt, M., Juppner, H., Gardella, T.J., 1999. Receptors for PTH and PTHrP: their biological importance and functional properties. Am. J. Physiol. 277, F665–F675.

Massfelder, T., Lang, H., Schordan, E., Lindner, V., Rothhut, S., Welsch, S., Simon-Assman, P., Barthelmebs, M., Jacqmin, D., Helwig, J.J., 2004. Parathyroid hormone-related protein is an essential growth factor for human clear cell renal carcinoma and a target for the von Hippel–Lindau tumor suppressor gene. Cancer Res. 64, 180–188.

Mawer, E.B., Hayes, M.E., Heys, S.E., Davies, M., White, A., Stewart, M.F., Smith, G.N., 1994. Constitutive syhthesis of 1,25(OH)2D3 by a human small cell lung cancer cell line. J. Clin. Endocrinol. Metab. 79, 554–560.

Meerovitch, K., Wing, S., Goltzman, D., 1998. Proparathyroid hormone-related protein is associated with the chaperone protein BiP and undergoes proteasome-mediated degradation. J. Biol. Chem. 273, 21025–21030.

Miao, D., He, B., Jiang, Y., Kobayashi, T., Soroceanu, M.A., Zhao, J., Su, H., Tong, X., Amizuka, N., Gupta, A., Genant, H.K., Kronenberg, H.M., Goltzman, D., Karaplis, A.C., 2005. Osteoblast-derived PTHrP is a potent endogenous bone anabolic agent that modifies the therapeutic efficacy of administered PTH 1-34. J. Clin. Investig. 115, 2402–2411.

Miao, D., Su, H., He, B., Gao, J., Xia, Q., Zhu, M., Gu, Z., Goltzman, D., Karaplis, A.C., 2008. Severe growth retardation and early lethality in mice lacking the nuclear localization sequence and C-terminus of PTH-related protein. Proc. Natl. Acad. Sci. U.S.A. 105, 20309–20314.

Miki, T., Yano, S., Hanibuchi, M., Kanematsu, T., Muguruma, H., Sone, S., 2004. Parathyroid hormone-related protein (PTHrP) is responsible for production of bone metastasis, but not visceral metastasis, by human small cell lung cancer SBC-5 cells in natural killer cell-depleted SCID mice. Int. J. Cancer 108, 511–515.

Miyaji, T., Nakase, T., Onuma, E., Sato, K., Myoui, A., Tomita, T., Joyama, S., Ariga, K., Hashimoto, J., Ueda, T., Yoshikawa, H., 2003. Monoclonal antibody to parathyroid hormone-related protein induces differentiation and apoptosis of chondrosarcoma cells. Cancer Lett. 199, 147–155.

Moseley, J.M., Kubota, M., Diefenbach-Jagger, H., Wettenhall, R.E.H., Kemp, B.E., Suva, L.J., Rodda, C.P., Ebeling, P.R., Hudson, P.J., Zajac, J.D., Martin, T.J., 1987. Parathyroid hormone-related protein purified from a human lung cancer cell line. Proc. Natl. Acad. Sci. U.S.A. 84, 5048–5052.

Motokura, T., Fukumoto, S., Matsumoto, T., Takahashi, S., Fujita, A., Yamashita, T., Igarashi, T., Ogata, E., 1989. Parathyroid hormone-related protein in adult T-cell leukemia-lymphoma. Ann. Intern. Med. 111, 484–488.

Mula, R.V., Bhatia, V., Falzon, M., 2010. PTHrP promotes colon cancer cell migration and invasion in an integrin alpha6beta4-dependent manner through activation of Rac1. Cancer Lett. 298, 119–127.

Mundy, G.R., 2002. Metastasis to bone: causes, consequences and therapeutic opportunities. Nat. Rev. Canc. 2, 584–593.

Nakagawa, K., Sasaki, Y., Kato, S., Kubodera, N., Okano, T., 2005. 22-Oxa-1alpha,25-dihydroxyvitamin D3 inhibits metastasis and angiogenesis in lung cancer. Carcinogenesis 26, 1044–1054.

Nagai, M., Kyakumoto, S., Sato, N., 2000. Cancer cells responsible for humoral hypercalcemia express mRNA encoding a secreted form of ODF/TRANCE that induces osteoclast formation. Biochem. Biophys. Res. Commun. 269, 532–536.

Nagai, Y., Yamamoto, H., Akaogi, K., Hirose, K., Ueyama, Y., Ikeda, K., Matsumoto, T., Fujita, T., Ogata, E., 1998. Role of interleukin-6 in uncoupling of bone in vivo in a human squamous carcinoma coproducing parathyroid hormone-related peptide and interleukin-6. J. Bone Miner. Res. 13, 664–672.

Nguyen, M., He, B., Karaplis, A., 2001. Nuclear forms of parathyroid hormone-related peptide are translated from non-AUG start sites downstream from the initiator methionine. Endocrinology 142, 694–703.

Nishihara, M., Ito, M., Tomioka, T., Ohtsuru, A., Taguchi, T., Kanematsu, T., 1999. Clinicopathological implications of parathyroid hormone-related protein in human colorectal tumours. J. Pathol. 187, 217–222.

Nissenson, R.A., Abbott, S.R., Teitelbaum, A.P., Clark, O.H., Arnaud, C.D., 1981. Endogenous biologically active human parathyroid hormone measurement by a guanyl nucleotide-amplified renal adenylate cyclase assay. J. Clin. Endocrinol. Metab. 52, 840–844.

Nussbaum, S.R., Gaz, R.D., Arnold, A., 1990. Hypercalcemia and ectopic secretion of parathyroid hormone by an ovarian carcinoma with rearrangement of the gene for parathyroid hormone. N. Engl. J. Med. 323, 1324–1328.

Ogata, E., 2000. Parathyroid hormone related protein as a potential target of therapy for cancer associated morbidity. Cancer 88, 2909–2911.

Okano, K., Pirola, C.J., Wang, H.M., Forrester, J.S., Fagin, J.A., Clemens, T.L., 1995. Involvement of cell cycle and mitogen-activated pathways in induction of parathyroid hormone-related protein gene expression in rat aortic smooth muscle cells. Endocrinology 136, 1782–1789.

Onuma, E., Azuma, Y., Saito, H., Tsunenari, T., Watanabe, T., Hirabayashi, M., Sato, K., Yamada-Okabe, H., Ogata, E., 2005. Increased renal calcium reabsorption by parathyroid hormone-related protein is a causative factor in the development of humoral hypercalcemia of malignancy refractory to osteoclastic bone resorption inhibitors. Clin. Cancer Res. 11, 4198–4203.

Orloff, J.J., Stewart, A.F., 1995. Editorial: the carboxy-terminus of parathyroid hormone-inert or invaluable. Endocrinology 136, 4729–4731.

Orloff, J.J., Wu, T.L., Stewart, A.F., 1989. Parathyroid hormone-like proteins: biochemical responses and receptor interactions. Endocrinology 10, 476–495.

Otieno, B.A., Krause, C.E., Jones, A.L., Kremer, R.B., Rusling, J.F., 2016. Cancer diagnostics via ultrasensitive multiplexed detection of parathyroid hormone-related peptides with a microfluidic immunoarray. Anal. Chem. 88, 9269–9275.

Ottewell, P.D., Monkkonen, H., Jones, M., Lefley, D.V., Coleman, R.E., Holen, I., 2008. Antitumor effects of doxorubicin followed by zoledronic acid in a mouse model of breast cancer. J. Natl. Cancer Inst. 100, 1167–1178.

Pearse, R.N., Sordillo, E.M., Yaccoby, S., Wong, B.R., Liau, D.F., Colman, N., Michaeli, J., Epstein, J., Choi, Y., 2001. Multiple myeloma disrupts the TRANCE/osteoprotegerin cytokine axis to trigger bone destruction and promote tumor progression. Proc. Natl. Acad. Sci. U.S.A. 98, 11581–11586.

Pecherstorfer, M., Schilling, T., Blind, E., Zimmer-Roth, I., Baumgartner, G., Ziegler, R., Raue, F., 1994. Parathyroid hormone-related protein and life expectancy in hypercalcemic cancer patients. J. Clin. Endocrinol. Metab. 78, 1268–1270.

Pfitzner, B.M., Branstetter, D., Loibl, S., Denkert, C., Lederer, B., Schmitt, W.D., Dombrowski, F., Werner, M., Rudiger, T., Dougall, W.C., von Minckwitz, G., 2014. RANK expression as a prognostic and predictive marker in breast cancer. Breast Canc. Res. Treat. 145, 307–315.

Philbrick, W.M., Dreyer, B.E., Nakchbandi, I.A., Karaplis, A.C., 1998. PTHrP is required for tooth eruption. Proc. Natl. Acad. Sci. U.S.A. 95, 11846–11851.

Philbrick, W.M., Wysolmerski, J.J., Galbraith, S., Holt, E., Orloff, J.J., Yang, K.H., Vasavada, R.C., Weir, E.C., Broadus, A.E., Stewart, A.F., 1996. Defining the roles of parathyroid hormone-related protein in normal physiology. Physiol. Rev. 76, 127–173.

Pizzi, H., Gladu, J., Carpio, L., Miao, D., Goltzman, D., Rabbani, S.A., 2003. Androgen regulation of parathyroid hormone-related peptide production in human prostate cells. Endocrinology 144, 858–867.

Powell, D., Singer, F.R., Murray, T.M., Minkin, C., Potts, J.T., 1973. Non-parathyroid humoral hypercalcemia in patients with neoplastic diseases. N. Engl. J. Med. 289, 176–180.

Powell, G.J., Southby, J., Danks, J.A., Stilwell, R.G., Haymen, J.A., Henderson, M.A., Bennett, R.C., Martin, T.J., 1991. Localization of parathyroid hormone-related protein in breast cancer metastases: increased incidence in bone compared with other sites. Cancer Res. 51, 3059–3061.

Rabbani, S.A., Gladu, J., Harakidas, P., Jamison, B., Goltzman, D., 1999. Over production of parathyroid hormone related peptide results in increased osteolytic skeletal metastasis by prostate cancer cells in vivo. Int. J. Cancer 80, 257–264.

Rabbani, S.A., Gladu, J., Liu, B., Goltzman, D., 1995. Regulation in vivo of the growth of Leydig cell tumors by antisense RNA for parathyroid hormone-related peptide. Endocrinology 136, 5416–5422.

Rabbani, S.A., Haq, M., Goltzman, D., 1993. Biosynthesis and processing of endogenous parathyroid hormone-related peptide (PTHrP) by the rat Leydig cell tumor H-500. Biochemistry 32, 4931–4937.

Rabbani, S.A., Khalili, P., Arakelian, A., Pizzi, H., Chen, G., Goltzman, D., 2005. Regulation of parathyroid hormone related peptide by estrogen: effect on tumor growth and metastasis in vitro and in vivo. Endocrinology 146, 2885–2894.

Rabbani, S.A., Mitchell, J., Roy, D.R., Hendy, G.N., Goltzman, D., 1988. Influence of the amino-terminus on in vitro and in vivo biological activity of synthetic parathyroid hormone and parathyroid hormone-like peptides of malignancy. Endocrinology 123, 2709–2716.

Ralston, S.H., Gallacher, S.J., Patel, U., Campbell, J., Boyle, I.T., 1990. Cancer-associated hypercalcemia: morbidity and mortality. Clinical experience in 126 treated patients. Ann. Intern. Med. 112, 499–504.

Ralston, S.H., Cowan, R.A., Robertson, A.G., Gardner, M.D., Boyle, I.T., 1984. Circulating vitamin D metabolites and hypercalcaemia of malignancy. Acta Endocrinol. 106, 556–563.

Rankin, W., Grill, V., Martin, T.J., 1997. Parathyroid hormone-related protein and hypercalcemia. Cancer 80, 1564–1571.

Ratcliffe, W.A., Hutchesson, A.C., Bundred, N.J., Ratcliffe, J.G., 1992. Role of assays for parathyroid-hormone-related protein in investigation of hypercalcaemia. Lancet 339, 164–167.

Rizzoli, R., Pache, J.C., Didierjean, L., Burger, A., Bonjour, J.P., 1994. A thymoma as a cause of true ectopic hyperparathyroidism. J. Clin. Endocrinol. Metab. 79, 912–915.

Rizzoli, R., Thiebaud, D., Bundred, N., Pecherstrofer, M., Herrmann, Z., Huss, H.J., Ruckert, F., Manegold, C., Tubiana-Hulin, M., Steinhauer, E.U., Degardin, M., Thurliman, B., Clemens, M.R., Eghbali, H., Body, J.J., 1999. Serum parathyroid hormone related protein levels and response to bisphosphonate treatment in hypercalcemia of malignancy. J. Clin. Endocrinol. Metab. 84, 3545–3550.

Rodan, S.B., Insogna, K.L., Vignery, A.M.C., Stewart, A.F., Broadus, A.E., D'Souza, S.M., Bertolini, D.R., Mundy, G.R., Rodan, G.A., 1983. Factors associated with humoral hypercalcemia of malignancy stimulate adenylate cyclase in osteoblastic cells. J. Clin. Investig. 72, 1511–1515.

Roodman, G.D., 2004a. Mechanisms of bone metastasis. N. Engl. J. Med. 350, 1655–1664.

Roodman, G.D., 2004b. Pathogenesis of myeloma bone disease. Blood Cells Mol. Dis. 32 (2), 290–292.

Rouleau, M.F., Mitchell, J., Goltzman, D., 1990. Characterization of the major parathyroid hormone target cell in the endosteal metaphysis of rat long bones. J. Bone Miner. Res. 5, 1043–1053.

Saito, H., Tsunenari, T., Onuma, E., Sato, K., Ogata, E., Yamada-Okabe, H., 2005. Humanized monoclonal antibody against parathyroid hormone-related protein suppresses osteolytic bone metastasis of human breast cancer cells derived from MDA-MB-231. Anticancer Res. 25, 3817–3823.

Sanders, J.L., Chattopadhyay, N., Kifor, O., Yamaguchi, T., Butters, R.R., Brown, E.M., 2000. Extracellular calcium-sensing receptor expression and its potential role in regulating parathyroid hormone-related peptide secretion in human breast cancer cell lines. Endocrinology 141, 4357–4364.

Sanders, J.L., Chattopadhyay, N., Kifor, O., Yamaguchi, T., Brown, E.M., 2001. Ca^{2+}-sensing receptor expression and PTHrP secretion in PC-3 human prostate cancer cells. Am. J. Physiol. Endocrinol. Metab. 281, E1267–E1274.

Sato, K., Fuji, Y., Kasono, K., Imamura, H., Kondo, Y., Mano, H., Okabe, T., Asano, S., Takaku, F., 1989. Parathyroid hormone-related protein and interleukin-la stimulate bone resorption in vitro and increase the serum calcium concentration in mice in vivo. Endocrinology 124, 2172–2178.

Schmidt-Zachmann, M.S., Nigg, E.A., 1993. Protein localization to the nucleolus: a search for targeting domains in nucleolin. J. Cell Sci. 105, 799–806.

Schordan, E., Welsch, S., Rothhut, S., Lambert, A., Barthelmebs, M., Helwig, J.J., Massfelder, T., 2004. Role of parathyroid hormone-related protein in the regulation of stretch-induced renal vascular smooth muscle cell proliferation. J. Am. Soc. Nephrol. 15, 3016–3025.

Schramek, D., Leibbrandt, A., Sigl, V., Kenner, L., Pospisilik, J.A., Lee, H.J., Hanada, R., Joshi, P.A., Aliprantis, A., Glimcher, L., Pasparakis, M., Khokha, R., Ormandy, C.J., Widschwendter, M., Schett, G., Penninger, J.M., 2010. Osteoclast differentiation factor RANKL controls development of progestin-driven mammary cancer. Nature 468, 98–102.

Schweitzer, D.H., Hamdy, N.A., Frolich, M., Zwinderman, A.H., Papapoulos, S.E., 1994. Malignancy-associated hypercalcaemia: resolution of controversies over vitamin D metabolism by a pathophysiological approach to the syndrome. Clin. Endocrinol. 41, 251–256.

Sebag, M., Henderson, J.E., Goltzman, D., Kremer, R., 1994. Regulation of parathyroid hormone-related peptide production in normal human mammary epithelial cells in vitro. Am. J. Physiol. 267, C723–C730.

Sebag, M., Henderson, J.E., Rhim, J., Kremer, R., 1992. Relative resistance to 1,25-dihydroxyvitamin D3 in a keratinocyte model of tumor progression. J. Biol. Chem. 267, 12162–12167.

Seitz, P.K., Zhang, R.-W., Simmons, D.J., Cooper, C.W., 1995. Effects of C-terminal parathyroid hormone-related peptide on osteoblasts. Miner. Electrolyte Metab. 21, 180–183.

Sepulveda, T.V.A., Shen, X., Falzon, M., 2002. Intracrine PTHrP protects against serum starvation-induced apoptosis and regulates the cell cycle in MCF-7 breast cancer cells. Endocrinology 143, 596–606.

Shen, X., Falzon, M., 2003. PTH-related protein modulates PC-3 prostate cancer cell adhesion and integrin subunit profile. Mol. Cell. Endocrinol. 199, 165–177.

Shen, X., Falzon, M., 2005. PTH-related protein enhances LoVo colon cancer cell proliferation, adhesion, and integrin expression. Regul. Pept. 125, 17–27.

Sica, D.A., Martodam, R.R., Aronow, J., Mundy, G.R., 1983. The hypercalcemic rat leydig cell tumor: a model of the humoral hypercalcemia of malignancy. Calcif. Tissue Int. 35, 287–293.

Sidler, B., Alpert, L., Henderson, J.E., Deckelbaum, R., Amizuka, N., Silva, E., Goltzman, D., Karaplis, A.C., 1996. Overexpression of parathyroid hormone-related peptide (PTHrP) by gene amplification in colonic carcinoma. J. Clin. Endocrinol. Metab. 81, 2841–2847.

Silver, I.A., Murrils, R.J., Etherington, D.J., 1988. Microelectrode studies on the acid microenvironment beneath adherent macrophages and osteoclasts. Exp. Cell Res. 175, 266–276.

Simpson, E.L., Mundy, G.R., D'Souza, S.M., Ibbotson, K.J., Bockman, M.D., Jacobs, J.W., 1983. Absence of parathyroid hormone messenger RNA in non-parathyroid tumors associated with hypercalcemia. N. Engl. J. Med. 309, 325–330.

Singh, A.T., Gilchrist, A., Voyno-Yasenetskaya, T., Radeff-Huang, J.M., Stern, P.H., 2005. Gα12/Gα13 subunits of heterotrimeric G proteins mediate parathyroid hormone activation of phospholipase D in UMR-106 osteoblastic cells. Endocrinology 146, 2171–2175.

Sneddon, W.B., Magyar, C.E., Willick, G.E., Syme, C.A., Galbiati, F., Bisello, A., Friedman, P.A., 2004. Ligand-selective dissociation of activation and internalization of the parathyroid hormone (PTH) receptor: conditional efficacy of PTH peptide fragments. Endocrinology 145, 2815–2823.

Sneddon, W.B., Syme, C.A., Bisello, A., Magyar, C.E., Rochdi, M.D., Parent, J.L., Weinman, E.J., Abou-Samra, A.B., Friedman, P.A., 2003. Activation-independent parathyroid hormone receptor internalization is regulated by NHERF1 (EBP50). J. Biol. Chem. 278, 43787–43796.

Soifer, N.E., Dee, K.E., Insogna, K.L., Burtis, W.J., Matovcik, L.M., Wu, T.L., Milstone, L.M., Broadus, A.E., Philbrick, W.M., Stewart, A.F., 1992. Parathyroid hormone-related protein. Evidence for secretion of a novel mid-region fragment by three different cell types. J. Biol. Chem. 267, 18236–18243.

Solomon, C., Sebag, M., White, J.H., Rhim, J., Kremer, R., 1998. Disruption of vitamin D receptor retinoid X receptor heterodimer formation following ras transformation of human keratinocytes. J. Biol. Chem. 273, 17573–17578.

Solomon, C., White, J.H., Kremer, R., 1999. Mitogen activated protein kinase inhibits 1,25-dihydroxyvitamin D3-dependent signal transduction by phosphorylating human retinoid X receptor alpha. J. Clin. Investig. 103, 1729–1735.

Southby, J., Kissin, M.W., Danks, J.A., Hayman, J.A., Moseley, J.M., Henderson, M.A., Bennett, R.C., Martin, T.J., 1990. Immunohistochemical localization of parathyroid hormone-related protein in human breast cancer. Cancer Res. 50, 7710–7716.

Southby, J., O'Keefe, L.M., Martin, T.J., Gillespie, M.T., 1995. Alternative promoter usage and mRNA splicing pathways for parathyroid hormone-related protein in normal tissues and tumours. Br. J. Cancer 72, 702–707.

Sowers, M.F., Hollis, B.W., Shapiro, B., Randolph, J., Janney, C.A., Zhang, D., Schork, A., Crutchfield, M., Stanczyk, F., Russell-Aulet, M., 1996. Elevated parathyroid hormone-related peptide associated with lactation and bone density loss. J. Am. Med. Assoc. 276, 549–554.

Sterling, J.A., Oyajobi, B.O., Grubbs, B., Padalecki, S.S., Munoz, S.A., Gupta, A., Story, B., Zhao, M., Mundy, G.R., 2006. The hedgehog signaling molecule Gli2 induces parathyroid hormone-related peptide expression and osteolysis in metastatic human breast cancer cells. Cancer Res. 66, 7548–7553.

Stewart, A.F., Horst, R., Deftos, L.J., Cadman, E.C., Lang, R., Broadus, A.E., 1980. Biochemical evaluation of patients with cancer-associated hypercalcemia: evidence for humoral and non-humoral groups. N. Engl. J. Med. 303, 1377–1383.

Stewart, A.F., Vignery, A., Silvergate, A., Ravin, N.D., LiVolsi, V., Broadus, A.E., Baron, R., 1982. Quantitative bone histomorphometry in humoral hypercalcemia of malignancy: uncoupling of bone cell activity. J. Clin. Endocrinol. Metab. 55, 219–227.

Strewler, G.J., Budayr, A.A., Clark, O.H., Nissenson, R.A., 1993. Production of parathyroid hormone by a malignant nonparathyroid tumor in a hypercalcemic patient. J. Clin. Endocrinol. Metab. 76, 1373–1375.

Strewler, G.J., Stern, P.H., Jacobs, W.J., Eveloff, J., Klein, R.F., Leung, S.C., Rosenblatt, M., Nissenson, R.A., 1987. Parathyroid hormone-like protein from human renal carcinoma cells: structural and functional homology with parathyroid hormone. J. Clin. Investig. 80, 1803–1807.

Strewler, G.J., Wronski, T.J., Halloran, B.P., Miller, S.C., Leung, S.C., Williams, R.D., Nissenson, R.A., 1986. Pathogenesis of hypercalcemia in nude mice bearing a human renal carcinoma. Endocrinology 119, 303–310.

Sullivan, F.J., 1996. Palliative radiotherapy for lung cancer. In: Pass, H.I., Mitchell, J.B., Johnson, D.H., Turrisi, A.T. (Eds.), Lung Cancer: Principles and Practice. Lippincott-Raven, Philadelphia, pp. 775–789.

Suva, L.J., Winslow, G.A., Wettenhall, R.E.H., Hammonds, R.G., Moseley, J.M., Diefenbach-Jagger, H., Rodda, C.P., Kemp, B.E., Rodriguez, H., Chen, E.Y., Hudson, P.J., Martin, T.J., Wood, W.I., 1987. A parathyroid hormone-related protein implicated in malignant hypercalcemia: cloning and expression. Science 237, 893–896.

Suva, L.J., Mather, K.A., Gillespie, M.T., Webb, G.C., Ng, K.W., Winslow, G.A., Wood, W.I., Martin, T.J., Hudson, P.J., 1989. Structure of the 5' flanking region of the gene encoding human parathyroid-hormone-related protein (PTHrP). Gene 77, 95–105.

Syme, C.A., Friedman, P.A., Bisello, A., 2005. Parathyroid hormone receptor trafficking contributes to the activation of extracellular signal-regulated kinases but is not required for regulation of cAMP signaling. J. Biol. Chem. 280, 11281–11288.

Tenta, R., Sourla, A., Lembessis, P., Luu-The, V., Koutsilieris, M., 2005. Bone microenvironment-related growth factors, zoledronic acid and dexamethasone differentially modulate PTHrP expression in PC-3 prostate cancer cells. Horm. Metab. Res. 37, 593–601.

Terpos, E., Christoulas, D., Gavriatopoulou, M., Dimopoulos, M.A., 2017. Mechanisms of bone destruction in multiple myeloma. Eur. J. Cancer Care 26 (6). https://doi.org/10.1111/ecc.12761. Epub 2017 Sep 21. Review. PubMed PMID: 28940410.

Tian, E., Zahn, F., Walker, R., Rasmussen, E., Ma, Y., Barlogie, B., Shaughnessy Jr., J.D., 2003. The role of the Wnt-signaling antagonist DKK1 in the development of osteolytic lesions in multiple myeloma. N. Engl. J. Med. 349, 2483–2494.

Tisdale, M.J., 2009. Mechanisms of cancer cachexia. Physiol. Rev. 89, 381–410.

Toribio, R.E., Brown, H.A., Novince, C.M., Marlow, B., Hernon, K., Lanigan, L.G., Hildreth 3rd, B.E., Werbeck, J.L., Shu, S.T., Lorch, G., Carlton, M., Foley, J., Boyaka, P., McCauley, L.K., Rosol, T.J., 2010. The midregion, nuclear localization sequence, and C terminus of PTHrP regulate skeletal development, hematopoiesis, and survival in mice. FASEB J. 24, 1947–1957.

Tovar Sepulveda, VA., Shen, X., Falzon, M., 2002 Feb. Intracrine PTHrP protects against serum starvation-induced apoptosis and regulates the cell cycle in MCF-7 breast cancer cells. Endocrinology, 143 (2), 596–606.

Truong, N.U., deB Edwardes, M.D., Papavasiliou, V., Goltzman, D., Kremer, R., 2003. Parathyroid hormone-related peptide and survival of patients with cancer and hypercalcemia. Am. J. Med. 115, 115–121.

VanHouten, J.N., Dann, P., Stewart, A.F., Watson, C.J., Pollak, M., Karaplis, A.C., Wysolmerski, J.J., 2003. Mammary-specific deletion of parathyroid hormone-related protein preserves bone mass during lactation. J. Clin. Investig. 112, 1429–1436.

Vargas, S.J., Gillespie, M.T., Powell, G.J., Southby, J., Danks, J.A., Moseley, J.M., 1992. Localization of parathyroid hormone-related protein mRNA expression in breast cancer and metastatic lesions by in situ hybridization. J. Bone Miner. Res. 7, 971–979.

Walls, J., Ratcliffe, W.A., Howell, A., Bundred, N.J., 1994. Response to intravenous bisphosphonate therapy in hypercalcaemic patients with and without bone metastases: the role of parathyroid hormone-related protein. Br. J. Canc. 70, 169–172.

Waning, D.L., Guise, T.A., 2014. Molecular mechanisms of bone metastasis and associated muscle weakness. Clin. Cancer Res. 20 (12), 3071–3077.

Weinman, E.J., Hall, R.A., Friedman, P.A., Liu-Chen, L.Y., Shenolikar, S., 2006. The association of NHERF adaptor proteins with g protein-coupled receptors and receptor tyrosine kinases. Annu. Rev. Physiol. 68, 491–505.

Wimalawansa, S.J., 1993. Significance of plasma PTHrP in patients with hypercalcemia of malignancy treated with bisphosphonates. Cancer 73, 2223–2230.

Wu, T.L., Vasavada, R.C., Yang, K., Massfelder, T., Ganz, M., Abbas, S.K., Care, A.D., Stewart, A.F., 1996. Structural and physiologic characterization of the mid-region secretory species of parathyroid hormone-related protein. J. Biol. Chem. 271, 24371–24381.

Wu, T.L., Soifer, N.E., Burtis, W.J., Milstone, L.M., Stewart, A.F., 1991. Glycosylation of parathyroid hormone-related secreted by human epidermal keratinocytes. J. Clin. Endocrinol. Metab. 73, 1002–1007.

Yamada, T., Muguruma, H., Yano, S., 2009. Intensification therapy with anti-parathyroid hormone-related protein. Mol. Canc. Therapeut. 8, 119–126.

Yamamoto, H., Nagai, Y., Inoue, D., Ohnishi, Y., Ueyama, Y., Ohno, H., Matsumoto, T., Ogata, E., Ikeda, K., 1995. In vivo evidence for progressive activation of parathyroid hormone-related peptide gene transcription with tumor growth and stimulation of osteoblastic bone formation at an early stage of humoral hypercalcemia of cancer. J. Bone Miner. Res. 10, 36–44.

Yasuda, T., Banville, D., Rabbani, S.A., Hendy, G.N., Goltzman, D., 1989. Rat parathyroid hormone-like peptide: comparison with the human homologue and expression in malignant and normal tissue. Mol. Endocrinol. 3, 518–525.

Yin, J.J., Selander, K., Chirgwin, J.M., Dallas, M., Grubbs, B.G., Wieser, R., Massague, J., Mundy, G.R., Guise, T.A., 1999. TGF-β signaling blockade inhibits PTHrP secretion by breast cancer cells and bone metastases development. J. Clin. Investig. 103, 197–206.

Yoshida, A., Nakamura, Y., Shimizu, A., Harada, M., Kameda, Y., Nagano, A., Inuba, M., Asaga, T., 2000. Significance of the parathyroid hormone-related protein expression in breast carcinoma. Breast Canc. 7, 215–222.

Yoshimoto, K., Yamasaki, R., Sakai, H., Tezuka, U., Takahashi, M., Iizuka, M., Sekiya, T., Saito, S., 1989. Ectopic production of parathyroid hormone by small cell lung cancer in a patient with hypercalcemia. J. Clin. Endocrinol. Metab. 68, 976–981.

Yu, J., Papavasiliou, V., Rhim, J., Goltzman, D., Kremer, R., 1995. Vitamin D analogs: new therapeutic agents for the treatment of squamous cancer and its associated hypercalcemia. Anti Cancer Drugs 6, 101–108.

Zakalik, D., Diep, D., Hooks, M.A., Nissenson, R.A., Strewler, G.J., 1992. Transforming growth factor b increases stability of parathyroid hormone-related protein messenger RNA. J. Bone Miner. Res. 7 (104A), S118–S119.

Zhang, H.W., Ding, J., Jin, J.L., Guo, J., Liu, J.N., Karaplis, A., Goltzman, D., Miao, D., 2010. Defects in mesenchymal stem cell self-renewal and cell fate determination lead to an osteopenic phenotype in Bmi-1 null mice. J. Bone Miner. Res. 25 (3), 640–652.

Zhang, P., Jobert, A.S., Couvineau, A., Silve, C., 1998. A homozygous inactivating mutation in the parathyroid hormone/parathyroid hormone-related peptide receptor causing Blomstrandi chondrodysplasia. J. Clin. Endocrinol. Metab. 83 (9), 3365–3368.

Zhang, X.H., Wang, Q., Gerald, W., Hudis, C.A., Norton, L., Smid, M., Foekens, J.A., Massagué, J., 2009. Latent bone metastasis in breast cancer tied to Src-dependent survival signals. Cancer Cell 16, 67–78.

Zondek, H., Petrow, H., Siebert, W., 1923. Die bedeutung der calcium-bestimmung im blute Fur die diagnose der nierrenin-siffizientz. Z. Clin. Med. 99, 129–132.

Further Reading

Cataisson, C., Lieberherr, M., Cros, M., Gauville, C., Graulet, A.M., Cotton, J., Calfo, F., de Vernejoul, M.C., Foley, J., Bouizar, Z., 2000. Parathyroid hormone-related peptide stimulates proliferation of highly tumorigenic human SV40- immortalized breast epithelial cells. J. Bone Miner. Res. 15, 2129–2139.

Ikeda, K., Inoue, D., Okazaki, R., Kikuchi, T., Ogata, E., Matsumoto, T., 1995. Parathyroid hormone-related peptide in hypercalcemia associated with adult T-cell leukemia/lymphoma: molecular and cellular mechanism of parathyroid hormone-related peptide overexpression in HTLV-I infected cells. Miner. Electrolyte Metab. 21, 166–170.

Sepulveda, T.V.A., Falzon, M., 2002. Parathyroid hormone-related protein enhances PC-3 prostate cancer cell growth via both autocrine/paracrine and intracrine pathways. Regul. Pept. 105, 109–120.

Chapter 55

Localized osteolysis

Julie A. Rhoades (Sterling)[1,2,3], Rachelle W. Johnson[2] and Conor C. Lynch[4]

[1]*Department of Veterans Affairs, Nashville, TN, United States;* [2]*Vanderbilt Center for Bone Biology, Department of Medicine, Division of Clinical Pharmacology, Nashville, TN, United States;* [3]*Department of Biomedical Engineering, Nashville, TN, United States;* [4]*Department of Tumor Biology, Moffitt Cancer Center, Tampa, FL, United States*

Chapter outline

Introduction

Tumors such as those of the breast, prostate, and lung frequently metastasize to the bone where they induce changes to the bone microenvironment that can lead to bone destruction (osteolytic disease) and/or bone formation (osteoblastic disease) (Mundy, 2002). In many patients there is a mix of both; patients with primarily osteoblastic tumors may still have some phases of osteolytic disease. In both cases, patients experience an increase in skeletal fracture, pain, and morbidity (Coleman et al., 1998). Despite improvements in the early detection and treatment of primary tumors, patients still experience bone metastases and die from metastatic disease. Once a patient is diagnosed with bone metastases, frequently as a result of a skeletal-related event, they are placed on a bisphosphonate (and in some cases denosumab) to block bone resorption. While these therapies improve morbidity, they do not significantly improve mortality, and patients still die from disease (Coleman et al., 2014a, 2014b; Coleman, 2006; Saad et al., 2007).

Decades of research have described the pathways that regulate tumor metastasis to bone and tumor-induced bone disease. Much of this work has been centered on the "vicious cycle" model originally described by Gregory Mundy et al. (Guise and Mundy, 1998; Mundy, 1997; Sterling et al., 2011). This hypothesis centered on interactions between tumors and osteoblasts and osteoclasts and was one of the first examples of studies of tumor interactions with the microenvironment. In this model, the tumor cells release factors—e.g., parathyroid hormone–related protein (PTHrP), interleukin-8 (IL-8), and interleukin-11—that stimulate the osteoblasts to produce receptor activator of nuclear factor kappa-B ligand (RANKL), which in turn activates osteoclast-mediated bone destruction. RANKL, a member of the tumor necrosis factor family, is a trimeric cell surface ligand that is essential for promoting the fusion of myeloid cells into multinucleated osteoclasts (Kong et al., 1999). Osteoclasts bind to the surface of mineralized bone matrix subsequent to osteoblast retraction and demineralize the bone via the release of hydrochloric acid (Blair, 1998). Tight resorptive seals permit localized acidification under the osteoclast. Approximately 90% of the bone matrix is composed of type-I collagen, and

Principles of Bone Biology. https://doi.org/10.1016/B978-0-12-814841-9.00055-5

osteoclast secretion of cathepsin-K, an acidophilic type I collagenase, facilitates the breakdown of the collagen fibers (Saftig et al., 1998). During bone apposition phases, osteoblasts not only lay down extracellular matrix (ECM) proteins but also incorporate a number of growth factors and cytokines into bone such as transforming growth factor-beta (TGF-β) that can be released during osteoclast-mediated resorption (Bonewald and Mundy, 1990; Hock et al., 1990; Robey et al., 1987). Transcytosis of bone matrix products through the osteoclasts in vesicles results in pH buffering prior to apical secretion (Coxon et al., 2008; Salo et al., 1997). The resultant release of bioavailable growth factors in turn supports the growth of cancer cells, thereby generating a feed-forward "vicious cycle" of tumor–bone interactions (Kakonen and Mundy, 2003). Therapies that target factors driving the vicious cycle, such as bisphosphonates and denosumab, have focused on reducing osteoclast-mediated bone destruction. While these approaches have improved morbidity as previously described, they do not eliminate tumor burden. Therefore, more research is needed to develop drugs that can both reach and eliminate tumors growing in the bone. While many overlapping features between tumors can establish in the bone, we will focus the description within this chapter on the mechanisms driving osteotropism, colonization of the bone marrow, and tumor-induced bone disease (Fig. 55.1).

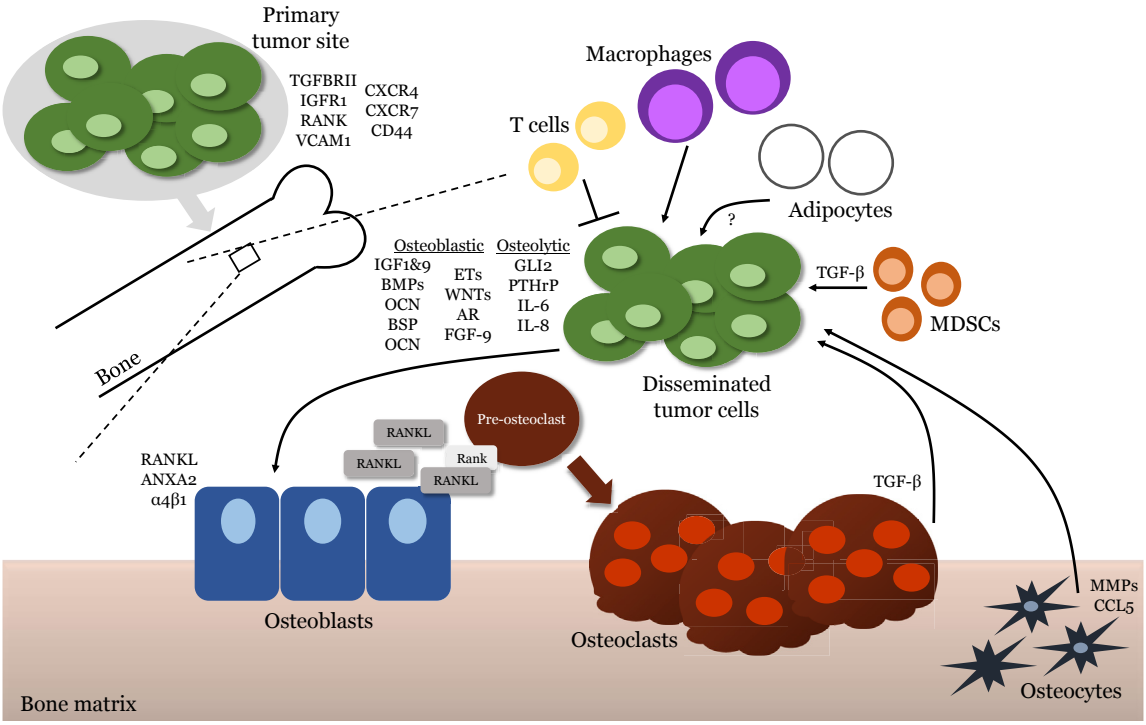

FIGURE 55.1 Key cellular and molecular mechanisms in tumor-induced bone disease. Tumor cells residing in the primary tumor site express factors that promote homing to the bone marrow. These factors interact with receptors expressed by mature osteoblasts and osteoblast precursors in the bone marrow to recruit tumor cells. Once disseminated to the bone marrow, tumor cells express and secrete a number of factors to induce osteolytic/osteoblastic bone disease. These molecules are known to act on the osteoblast lineage cells to promote bone growth or to induce osteoclastogenesis through stimulation of RANK/RANKL signaling between osteoblast lineage cells and osteoclast precursors. Localized induction of osteoclastogenesis leads to the release of factors stored in the bone matrix that promote tumor cell growth and further enhance tumor-induced bone destruction (i.e., the vicious cycle). Other cell types that we are beginning to appreciate in tumor-induced bone disease are T cells, which have been observed to limit tumor growth in bone, as well as osteocytes, macrophages, MDSCs, and adipocytes. Multiple studies suggest that these cell types promote tumor growth in the bone. Future studies will more clearly define the roles of these cell types and the mechanisms by which they limit or promote tumor colonization of the bone marrow. *ANXA2*, annexin A2; *AR*, androgen receptor; *BMP*, bone morphogenetic protein; *BSP*, bone sialoprotein; *CCL5*, C–C motif chemokine ligand 5; *CXCR4*, chemokine receptor 4; *CXCR7*, chemokine receptor 7; *ET*, endothelin; *FGF*, fibroblast growth factor; *GLI2*, GLI family zinc finger 2; *IGF*, insulin like growth factor; *IGFRI*, insulin-like growth factor receptor I; *IL-6*, interleukin-6; *IL-8*, interleukin-8; *MMP*, matrix metalloproteinase; *OCN*, osteocalcin; *OPN*, osteopontin; *PTHrP*, parathyroid 1-related protein; *RANK*, receptor activator of nuclear factor κB; *RANKL*, receptor activator of nuclear factor κB ligand; *TGFβ*, transforming growth factor-β; *TGFβRII*, transforming growth factor-β receptor type II; *VCAM1*, vascular cell adhesion molecule 1; *WNT*, wingless-type MMTV integration site family.

Osteotropism

Intravasation of cancer cells into the vasculature or lymphatics draining the primary cancer is a key event in the dissemination of tumor cells to the bone marrow (Weilbaecher et al., 2011). However, before cancer cells metastasize to the skeleton, it is hypothesized that secreted or shed factors prepare future metastatic niches for cancer cell colonization (Kaplan et al., 2006). While secreted cytokines, growth factors, and RNA molecules can regulate the behavior of these metastatic niches, cancer-derived vesicles such as exosomes, microvesicles, and oncosomes shed by cancer and host microenvironmental cells of the primary tumor are also proposed to play a part (Psaila and Lyden, 2009). These shed vesicles can be loosely categorized based on their size, although there are differences in the mechanisms regulating how they are shed. Exosomes are classified as small vesicles that range from 50 to 150 nm in size and display cell surface receptors that aid in their binding to the ECM of distant sites or their integration/uptake by cells in the evolving pre-metastatic niche. Remarkably, the exosomal cargo contains a vast array of molecules ranging from microRNAs, including microRNA processing machinery, DNA, cytokines, growth factors, and proteases. Causal roles for exosomes in metastasis have been described. For example, exosomes educate the stromal cells of the premetastatic niche and promote ECM remodeling and the recruitment of bone marrow−derived cells that in turn prepare the soil of the niche for the future arrival of metastatic prostate cancer cells (Erler et al., 2009; Shay et al., 2015). This phenomenon has also been demonstrated for the larger microvesicles and oncosomes (Di Vizio et al., 2012). In prostate cancer, the number of oncosomes (vesicles larger than exosomes that range in size from 1 to 10 μm) in patient plasma was found to correlate with Gleason scores of 7 and higher, while exosomes isolated from LNCaP, DU145, and PC3 prostate cancer cell lines have been found to enhance osteoblast differentiation (Itoh et al., 2012) and induce the differentiation of bone marrow−derived mesenchymal stem cells (MSCs) into myofibroblasts that promote tumor growth (Di Vizio et al., 2012; Webber et al., 2010). Collectively, these data suggest a role for oncosomes in cancer malignancy and potentially in the establishment of premetastatic niches in the bone microenvironment. While causal roles for these vesicles in cancer metastasis are being described, it should be noted that they are also proving to be valuable biomarkers of cancer prognosis and therapeutic response (Peinado et al., 2011).

How do prostate cancer cells that have escaped the primary cancer sense or home to prepared premetastatic niches or other niches within the bone microenvironment? Circulating tumor cells (CTCs) isolated from peripheral blood are a poor prognostic indicator for metastasis-free survival, and genetic analyses of the CTCs demonstrate/reflect the heterogeneity of the tumor at the primary site (Millner et al., 2013; Liu et al., 2009; Mader and Pantel, 2017). Not all CTCs will reach bone, but those that do are drawn to the rich milieu of growth factors and nutrients present in the skeletal tissue. Chemokine receptors have been largely implicated in cancer cell osteotropism (Weilbaecher et al., 2011). Chemokine receptors are G-protein-coupled receptors on the cell surface that sense and are chemoattracted to their cognate ligands. Chemokine receptor 4 (CXCR4) is a critical component in driving a bone metastatic program for breast cancer and is also commonly expressed by metastatic prostate cancer cells (Kang et al., 2003; Wang et al., 2006; Sun et al., 2005; Taichman et al., 2002). CXCR4 binds to chemokine ligand 12 (CXCL12) or stromal-derived factor-1 (SDF-1) to promote cell migration. CXCL12 is highly expressed in the skeletal tissue, where it plays important roles in cell−cell communication between bone-lining osteoblasts and hematopoietic progenitor cells. Studies have determined that ablation of CXCR4 on metastatic prostate cancer cells greatly diminishes bone metastasis, implying a major role for this receptor in osteotropism. CXCL12 can also bind to CXCR7 that is expressed at higher levels in aggressive disease (Wang et al., 2008). CXCR7 activation can lead to increased expression of the cell adhesion molecules CD44 and cadherin-11, which can facilitate invasion and metastasis. Other chemokines including CXCL16 have also been demonstrated to play a role in bone homing of prostate cancer cells. Using the Gleason system, the CXCL16 receptor, CXCR6, has been shown to correlate with disease aggressiveness (Lu et al., 2008). Prostate cancer cells are highly migratory toward CXCL16. Studies exploring the inhibition of CXCR6 with small-molecule inhibitors show that inhibiting this receptor can greatly mitigate prostate cancer cell invasion and metastasis *in vivo* (Hershberger et al., 2010). Like CXCL12, CXCL16 has been shown to be highly expressed in bone tissue (Ha et al., 2011).

In addition to chemokine-regulated osteotropism, several growth factors, cytokines, and bone remodeling by-products have been implicated in the process. Bone is one of the richest reservoirs of TGF-β, insulin-like growth factors (IGFs I and II), and RANKL (Cook et al., 2014). The expression of cognate receptors for these ligands on metastatic cancer cells (TGFβ receptor I and II, IGF-receptor 1, and RANK, respectively) have been described as increasing the frequency of bone metastasis given the heightened levels of these ligands in the bone microenvironment. By-products of the normal bone remodeling process, such as collagen fragments generated by osteoclast-mediated bone resorption, can also act as a potent chemoattractant for cancer cells, thus influencing the osteotropic nature of the metastases (Mundy et al., 1981).

Adhesion and invasion into bone metastatic niches

Once in the bone microenvironment, it is possible for cancer cells to bind to or interact with the ECM/cells of vascular or endosteal niches (Yu et al., 2012; Dasgupta et al., 2017). Both niches play important roles in maintaining hematopoietic stem cell (HSC) quiescence and mobilization from the bone marrow (Levesque et al., 2010). The ECM and cellular landscape of the niches and their interaction with metastatic cancer cells are critical steps during the early phases of cancer cell extravasation. Cell and matrix adhesion molecules are implicated in this process. αvβ3 integrin is expressed by metastatic cancer cells and binds to arginine−glycine−asparagine sequences in ECM proteins such as vitronectin and osteopontin, and binding to these proteins promotes reassembly of the cancer cell cytoskeleton and the activation of kinases such as focal adhesion kinases and SRC that promote cell survival (Kwakwa and Sterling, 2017; Teti et al., 2002). Lateral associations between αvβ3 other receptor tyrosine kinases such as TGF-β receptor II (TGFβRII) further promote cancer survival and growth, provided the cancer cells do not become quiescent/dormant (Galliher and Schiemann, 2006). α4β1, also known as very late antigen-4 (VLA-4), binds to CD106/vascular cell adhesion molecule-1 (VCAM-1), which is highly expressed by the bone marrow MSCs present in vascular and endosteal niches (Esposito and Kang, 2014; Ren et al., 2010). Similarly to αvβ3, α4β1 binding to VCAM-1 promotes the activation of c-Src to promote colonization of the bone microenvironment (Esposito and Kang, 2014; Hsia et al., 2005). Further, in the endosteal niche, osteoblast soluble-derived factors such as WISP-1 promote the expression of α4β1, reinforcing the interaction between metastatic VCAM-1-expressing cells and α4β1 (Tai et al., 2014). Cancer cells have also been shown to express α2β1, α5β1, and α9β1 that bind to ECM proteins in the bone microenvironment such as collagen, fibronectin, and tenascin, respectively, thereby further enhancing the ability of the metastases to invade the bone matrix (San Martin et al., 2017).

Additional classes of cell adhesion molecules such as annexin II (ANXA2) and CD44 are also implicated in bone homing and colonization. ANXA2 is commonly expressed by osteoblasts and endothelial cells and is an important regulator of HSC homing and adhesion to the endosteal and vascular niches (Jung et al., 2007). Cancer cells are known to express the ANXA2 receptor, and the interaction between the receptor and ligand facilitates colonization of HSC niches in bone (Shiozawa et al., 2008). CD44, a heavily glycosylated transmembrane protein, has long been associated with cancer cell migration and invasion and is commonly used as one of a number of markers for cancer stem cells. CD44 post-translational modifications also facilitate interaction with selectins on the endothelial cell surface that can help in the attachment of cancer cells to the sinusoidal vasculature prior to extravasation. Further, CD44 interacts with a variety of molecules present in the bone microenvironment including ECM proteins (collagens and osteopontin), hyaluronic acid, and growth factors such as TGFβ (Draffin et al., 2004) that can enhance cell adhesion, invasion, and survival in the bone marrow microenvironment.

Tumor dormancy and awakening

Prior to the initiation of osteolysis, tumor cells may enter a prolonged latency period after disseminating to the bone marrow. The mechanisms that direct these disseminated tumor cells (DTCs) to enter and exit a dormant state remain largely unknown, and it remains unclear whether this is driven by cell-autonomous mechanisms, the bone microenvironment, or a combination of both. Tumor dormancy itself remains ill-defined; during prolonged latency periods, tumor cells in the bone marrow may (1) reside as truly quiescent, nonproliferating cells, (2) slowly proliferate, or (3) proliferate and turn over at the same rate such that the undetectable micrometastasis remains below the level of clinical detection. Evidence for all three mechanisms exists (Zhang et al., 2013a), and it is possible that these mechanisms are not mutually exclusive. It is possible, if not likely, that multiple mechanisms of tumor dormancy exist even within the same patient. DTCs are protected from neoadjuvant or adjuvant therapies or immune surveillance, and the mechanisms that enable tumor cells to evade these systems are beginning to emerge.

To date, relatively few targets have been identified as dormancy-regulating genes in the bone marrow, and interestingly, the dormancy genes that have been identified appear to be highly tissue- and isoform-specific (Dasgupta et al., 2017). For example, TGFβ has three isoforms, and TGFβ2, expressed in bone marrow, has been shown to promote dormancy in breast cancer via the activation of TGFβR1 and TGFβR3 receptors. This interaction activates MAPK p38α/β, resulting in an ERK/p38 low signaling ratio (Bragado et al., 2013). Subsequent reductions in the cell cycle promoter CDK4 render the cells dormant. Interestingly, TGFβ1, which is highly sequestered in the bone matrix, promotes the awakening of dormant cells in neovascular tips (Ghajar et al., 2013), suggesting distinct roles for TGFβ isoforms in regulating the process. Mechanisms specific to prostate cancer dormancy in bone have been described in the context of the endosteal niche. The binding of annexin II receptor−expressing prostate cancer cells to osteoblasts in the endosteal niche promotes the expression and secretion of growth arrest specific 6 (GAS6), which in turn binds to the receptor Axl and results in a

suppression of prostate cancer cell growth (Yumoto et al., 2016). Bone morphogenetic proteins (BMPs) regulate osteoblast behavior, and one family member, BMP-7, is described as playing a role in dormancy. BMP-7 secretion by bone stromal cells can bind to BMP receptor II (BMPR-II) on prostate cancer cells and induce p21-mediated cell cycle arrest via activation of p38 (Kobayashi et al., 2011). Metastatic cancer cell–derived proteins such as SPARC (secreted protein acidic and rich in cysteine—osteonectin) also induce the expression of BMP-7 in bone stromal cells and osteoblasts in addition to the Wnt antagonist Dickkopf-1 (DKK-1), which in other metastatic settings has been implicated in promoting dormancy (Malladi et al., 2016; Sharma et al., 2016). Leukemia inhibitory factor (LIF) receptor (LIFR) is expressed on breast cancer cells that disseminate to the bone marrow but do not induce osteolysis. Loss of LIFR expression on breast cancer cells enables the tumor cells to aggressively colonize the bone marrow, and loss of LIFR is hypothesized to be driven in part through the low oxygen tensions of the bone marrow microenvironment (Johnson et al., 2016). It remains unclear whether the effects of LIFR are ligand-dependent, and if so, which of the IL-6 family cytokines induce dormancy, since several members of this cytokine family can complex with LIFR. Many IL-6 family cytokines are produced by osteoblasts, including LIF and oncostatin M, which suggests that the bone may provide prodormancy signals that are lost when breast cancer cells lose or downregulate LIFR. Thrombospondin 1 has been identified as a microenvironmental prodormancy factor that is produced by endothelial cells in the perivascular niche and may function to promote adhesion of tumor cells to endothelial stalks (Ghajar et al., 2013). Many of the just-illustrated mechanisms primarily relate to single-cell dormancy, but population dormancy in which the rates of cancer cell proliferation and apoptosis are balanced have been described. This steady-state phenomenon can be enforced by the microenvironment due to restricted blood supply or active immune surveillance recognizing and eliminating metastatic cancer cells (Osisami and Keller, 2013).

It is feasible that in the endosteal niche, factors involved in mobilizing HSCs can perturb DTCs occupying those niches, causing cancer cell outgrowth. Osteoclasts are essential for HSC mobilization, and recruited osteoclasts expressing MMP-9 can result in KIT-ligand cleavage. KIT-ligand is essential for maintaining HSCs in the niche, and HSCs are mobilized as a result of MMP-9 processing (Heissig et al., 2002). The recruitment of osteoclasts to the endosteal niche can also be mediated by α4β1 binding to VLA-4 on the cell surface of niche resident cancer cells (Lu et al., 2011). The resultant bone remodeling and release of cytokines such as the TGFβ1 isoform from bone can in turn override the dormancy program and result in the establishment of micrometastatic outgrowth (Bragado et al., 2012, 2013).

Cancer-induced bone disease

Breast cancer

The majority of studies investigating tumor-induced bone disease (TIBD) have focused on studying breast tumors that have metastasized to the bone. This is primarily because between 70% and 90% of breast cancer patients that die from disease will have bone metastatic disease (Johnson et al., 2015). In these cases, the women are often younger, and reducing TIBD has a high potential to improve their quality of life. While triple-negative (ER-, PR-, Her2-) breast cancer has been the focus of most breast cancer TIBD studies, in part due to the availability of preclinical models that aggressively colonize the bone and accurately mimic the late stages of disease, these patients often have widespread metastatic disease. In contrast, ER+ patients frequently experience more bone-only metastatic disease (Coleman et al., 1998; Coleman, 2006; Kennecke et al., 2010; Smid et al., 2008; Kunikullaya et al., 2017; Wu et al., 2016). Thus, these patients would likely experience the most impact from improved therapies. However, since even ER+ patients can have ER- tumor cells or metastases, and patient ER status can change (Schrijver et al., 2018), studies in both patient populations can yield promising new leads to improve therapy.

Much of the focus on studying signaling pathways in breast cancer–induced bone disease has been on the regulation of PTHrP by the TGF-β signaling pathway. Early studies by the Guise and Mundy groups demonstrated that tumor expression of TGF-βRII was required for tumors to produce PTHrP (Guise and Mundy, 1998; Kakonen and Mundy, 2003; Yin et al., 1999; Guise et al., 1996). In these and other studies, loss of TGF-β response reduces bone destruction. Other studies have shown that TGF-β inhibitors also reduce tumor burden and bone destruction. Although some groups only see a moderate (not complete) reduction in tumor burden, all groups see an improvement in bone volume (both new bone generation and smaller osteolytic lesions) (Yin et al., 1999; Biswas et al., 2011; Edwards et al., 2010; Johnson et al., 2011a; Nyman et al., 2016; Hu et al., 2012; Javelaud et al., 2011a; Kakonen et al., 2002; Mohammad et al., 2011; Waning et al., 2015). This suggests that while TGF-β is an important factor in TIBD, inhibiting it alone is not sufficient to eliminate tumor.

Other signaling pathways that have been implicated in breast cancer–induced bone disease include the Hedgehog signaling transcription factor GLI2, which is overexpressed in tumors that induce bone destruction (Sterling et al., 2006).

Work from multiple groups has demonstrated that GLI2 expression can be regulated by TGF-β to stimulate the transcription of PTHrP (Johnson et al., 2011a, 2011b; Javelaud et al., 2011a; Cannonier et al., 2016; Cannonier and Sterling, 2015; Alexaki et al., 2010). It remains unclear whether GLI2 regulates other pathways involved in TIBD beyond the regulation of TGF-β and PTHrP signaling, but other pathways are currently being investigated (Page et al., 2015a, 2015b; Johnson et al., 2014; Shimoyama et al., 2007).

Endothelins (ETs) consist of three related 21-amino-acid peptides (ET-1, ET-2, and ET-3) with ET-1 being the most abundantly expressed (Carducci and Jimeno, 2006). ETs are recognized for their role in vasoconstriction, but depending on the cell context, ET-1 can, for example, promote angiogenesis by stimulating endothelial cell proliferation and expression of vascular endothelial growth factor-A or bone formation by promoting osteoblast differentiation. While on balance, human bone metastatic breast cancers tend to be more osteolytic, some lesions can be osteoblastic or have areas of osteoblastic activity. This is reflected in cell line models of the disease. A differential analysis of factors derived from an osteolytic (MDA-MB-231) versus osteoblastic (ZR-75-1) breast cancer cell line revealed ET-1 as a major driver of breast cancer–induced bone formation (Yin et al., 2003). Normal and cancerous prostate cells express high amounts of ET that can protect cells from undergoing apoptosis (Nelson et al., 2005). ET expression is associated with advanced and bone metastatic prostate cancer, where a number of studies have described a role for ET-1 in driving the sclerotic phenotype of these lesions.

Prostate cancer

Similar to bone metastatic breast cancer cells, prostate cancer cells can secrete PTHrP, IL-6, and IL-8, which can induce RANKL expression (Liao et al., 2008; Deftos et al., 2005; Park et al., 2015; Pencik et al., 2015; Rojas et al., 2011). While bone metastatic prostate lesions contain areas of bone destruction, in contrast to other lytic metastases such those of a breast, lung, or renal origin, the lesions are typically hallmarked by areas of extensive bone formation (Keller and Brown, 2004). Metastatic prostate cancer cells are often resistant to androgen deprivation therapy (ADT) but are still dependent on androgens for survival and growth (Frieling et al., 2017). This is in large part due to mutations in the androgen receptor (AR) itself that make it highly efficient in using low levels of androgen, ligand-independent, or able to synthesize testosterone through the rewiring of metabolic pathways (Mostaghel et al., 2011; Kantoff and Mohler, 2013). AR activity in bone stromal cells such as osteoblasts enhances bone formation and mass, and therefore androgens derived from bone metastatic prostate cancer cells can have potent effects on bone formation. In addition to AR activity, Wnts, BMPs, and as discussed in breast cancer, ETs, have been noted as having roles in promoting prostate cancer induced osteogenesis.

Wnts have noted roles in cancer progression and in the regulation of bone remodeling. In prostate cancer, Wnt pathway activation (canonical and noncanonical) has been associated with poor outcomes and resistance to ADT (Thiele et al., 2016; Miyamoto et al., 2015; Wang et al., 2017). Canonical pathways involve Wnt ligand binding to receptors such as Frz, lipoprotein receptor-related proteins (Lrps), and receptor tyrosine kinase-like orphan receptors, leading to the stabilization of β-catenin and the transcription of β-catenin target genes. Noncanonical activation generally involves protein kinase A or Jun kinase activation. Evidence supports roles for Wnts 1, 2, 3a, 4, 7b, and 10b in promoting osteoblast differentiation. Studies have revealed that osteogenic prostate cancer cell lines express several of these Wnt ligands (Hall et al., 2005; Li et al., 2008a). For example, approximately 42% of prostate cancer specimen patient tissues were positive for Wnt7b compared with normal tissues. Wnt7b is a potent mediator of MSCs to osteoblast differentiation and is highly expressed by prostate cancer (Zheng et al., 2013). Endogenous natural Wnt antagonists such as members of the DKK and secreted frizzled-related proteins can block the potent effects of Wnt ligands. Paradoxically, DKK-1 has been shown to be highly produced during the early development of skeletal metastases but decreases as those metastases progress (Hall and Keller, 2006). These data suggest that in the initial phase of the vicious cycle, DKK-1 may tip the balance in favor of osteolysis prior to giving way to heightened Wnt expression and increased osteoblast activity.

Fibroblast growth factors (FGFs) play important developmental roles, are often highly expressed in the tumor microenvironment, and mediate their effects via binding to FGF receptors (FGFRs 1–4) (McKeehan et al., 1998; Powers et al., 2000; Wan et al., 2014). Analysis of human samples shows that FGFR1 is overexpressed in prostate cancers and that prostate cancer cell–derived factors induce the expression of FGFRs 1 and 2 in osteoblasts (Wan et al., 2014). Activation of the receptors by FGF ligands has effects on both the prostate cancer and bone stromal compartments (Murphy et al., 2010). For example, FGF-8 was discovered in the conditioned medium of an androgen-dependent mouse mammary tumor cell line and can promote osteoblast differentiation via three distinct transmembrane tyrosine kinase receptors (FGFR2-IIIC, FGFR3-IIIc, and FGFR-4) (Valta et al., 2006; Ellman et al., 2013). Studies have shown that over 75% of human bone metastatic prostate cancer specimens are positive for FGF-8 (Valta et al., 2008). *In vivo* studies demonstrated that FGF-8 can promote prostate cancer growth in bone and modulate bone formation (Valta et al., 2008). Several

patient-derived xenograft (PDX) models from bone metastatic prostate cancer have been generated, with some models having the ability to promote ectopic bone formation upon subcutaneous implantation. Differential analysis of PDX models that can generate ectopic bone versus those that do not revealed IGF-1 and FGF-9 as major candidates driving bone formation. Further tests of the effect of these factors on the growth of primary mouse osteoblasts revealed that FGF9, but not IGF1, induced osteoblast proliferation. Furthermore, FGF9-induced osteoblast proliferation and bone formation could be significantly blocked *in vitro* and *in vivo* via an FGF-9 neutralizing antibody, underscoring the potential importance of this ligand in mediating prostate cancer–induced bone formation (Li et al., 2008b).

Over 30 members of the BMP family exist, but to date functions with respect to modulating osteoblast function and bone formation have been best described for BMP-2 and BMP-7. BMPs mediate their action via signaling through BMP receptors (BMPR-IA, BMPR-IB, and BMPR-II). Several BMPs can be inhibited by noggin and gremlin, which bind directly to BMP and prevent receptor interaction (Chen et al., 2004). Prostate tumors have been shown to express BMPs (BMP-2, BMP-4, and BMP-7) (Yang et al., 2005) and their receptors, BMPR-IB and BMPR-II (Yang et al., 2005; Ye et al., 2007). The expression of BMPs and the BMP receptors in primary prostate cancer is intriguing and may play an important role in prostate cancer osteotropism. In this regard, the overexpression of noggin in the prostate tumor cell line PC-3 significantly reduced the size of the osteolytic lesions induced by the tumor (Feeley et al., 2006). Stromal-derived factors such as Wnt5a promote the expression of BMP-6 in prostate cancer cells, and this process is implicated in resistance to ADT (Miyamoto et al., 2015). Conversely, roles for BMPs 2, 6, and 7 have been defined in regulating osteoblast differentiation, underscoring the importance of BMP signaling in prostate cancer cell–osteoblast cross talk.

While these cancer cell–derived factors can induce osteoblast responses, studies have also revealed that prostate cancer cells can acquire an osteoblast-like phenotype that contributes to their ability to colonize and grow in the bone microenvironment (Curatolo et al., 1992). In clinical specimens, prostate cancer cells were found to express osteocalcin, bone sialoprotein (BSP), and osteopontin (OPN), ECM proteins that can facilitate attachment and invasion into the bone matrix. Further, analysis of prostate cancer cells exposed to osteoblast-derived factors revealed an increase in BMP-2, alkaline phosphatase, α-type I collagen, OPN, and osteocalcin (Koeneman et al., 1999). Runx2 has been shown to be induced in prostate cancer cells as a result of heightened TGFβ and BMP signaling in the bone. EMT program drivers such as TWIST also lead to the activation of Runx2 and the subsequent activation of downstream targets such as BSP and OPN (Yuen et al., 2008). Runx2 also regulates RANKL expression, and previous reports have shown that prostate cancer cell–derived RANKL can kick-start osteoclastogenesis, bypassing the need for osteoblast-derived RANKL (Inman and Shore, 2003; Banerjee et al., 2001; Enomoto et al., 2003; Barnes et al., 2003). Interestingly, the induction of the osteomimetic program contributes to an increase in cellular adhesion and a slowdown in proliferation of the prostate cancer cells (Chung et al., 2005). This in turn could increase the resistance of bone metastatic prostate cancers to applied ADTs and chemotherapies. Furthermore, the increased adhesion of osteomimetic prostate cells to the bone matrix may enhance their bone invasive phenotype via mechanotransductive effects. Scaffolds that mimic the rigidity of the bone matrix (3800 MPa) compared with those of soft tissue (70 MPa) enhanced the expression of factors associated with bone destruction including β3 integrin in PC3 prostate cancer cell lines. Interestingly, β3 integrin associated with the TGFβ type II receptor in rigid conditions to trigger the expression of PTHrP and GLI2, which promote osteoclast formation (Sterling et al., 2011; Ruppender et al., 2010).

Other skeletal malignancies

While much research has focused on breast and prostate cancer metastasis to bone, other tumor types that metastasize to the bone marrow include lung, multiple myeloma, osteosarcoma, invasive melanoma, and invasive head and neck tumors (Johnson et al., 2015). While each has a different primary tumor signature, they share many similarities behind the signaling pathways involved. For example, the most common primary bone tumors are osteosarcomas. While the initiating mutations are likely quite different from metastatic tumors, osteosarcoma cells often express factors that promote bone remodeling and formation such as PTHrP and RANKL. This heightened remodeling around the developing osteosarcoma can release IGFs and TGFβ that stimulate cancer survival and growth. In a retrospective study, 75% of osteosarcoma tumors ($n = 40$) that stained positive for RANKL had poorer overall survival of 17.8% (Lee et al., 2011). Transduction of osteosarcoma cells with the soluble decoy receptor osteoprotegerin (OPG) prevented osteolytic lesions and reduced tumor growth *in vivo* (Lamoureux et al., 2010). The bone marrow is a natural reservoir for MSCs, and this cell type has been explored as a therapeutic vehicle for the delivery of OPG to block bone destruction in murine models of osteosarcoma and metastatic prostate cancer with some success (Chanda et al., 2010; Qiao et al., 2015). In addition to being used to treat bone metastatic disease, denosumab, a monoclonal antibody against RANKL, is approved for the treatment of other primary

bone lesions such as giant cell tumor, where it has been shown to reduce tumor size by up to 90% (Branstetter et al., 2012) and is currently being clinically evaluated for the treatment of osteosarcoma.

Tumors that originate in the bone marrow can also alter normal bone remodeling. While leukemias and other blood tumors can induce a bone phenotype, the most studied bone marrow tumor that induces bone loss is multiple myeloma (MM). MM is the second most common adult hematologic malignancy and causes osteolytic bone disease in the axial and longitudinal skeleton (Silbermann and Roodman, 2013). However, even the most potent bisphosphonate, zoledronic acid, does not prevent fractures from eventually occurring in many patients, though it reduces the proportion of myeloma patients who experience skeletal-related events (Terpos et al., 2014, 2015). Alternatively, drugs such as the proteasome inhibitor bortezomib have been demonstrated to reduce MM tumor burden (Richardson et al., 2003). Other key pathways in MM that have been investigated include MIP1α (Oyajobi et al., 2003), DKK-1 (Fowler et al., 2012), and TGF-β (Nyman et al., 2016; Matsumoto and Abe, 2011). Important interactions between MM and the bone microenvironment include adipocytes and osteocytes. Adipocytes have been demonstrated to support MM establishment and growth in the bone (Fowler et al., 2011; McDonald et al., 2016). Osteocyte secretion of sclerostin and Wnt-signaling molecules has also been demonstrated to support MM tumor growth in the bone (Delgado-Calle et al., 2016; McDonald et al., 2017).

Other tumors that can invade the bone include melanoma, which can induce similar disease progression as metastatic tumors in bone. These tumors seem to rely on pathways similar to those of metastatic tumors including TGF-β (Mohammad et al., 2011; Javelaud et al., 2011b; Morris et al., 2014), GLI2 (Javelaud et al., 2011c), and hypoxia (Finger et al., 2015). Another common tumor is oral tumor invasion into the mandible (Zini et al., 2010). Much less is known about these tumors, but GLI2 activation and PTHrP have been demonstrated in multiple models to drive mandibular invasion (Cannonier et al., 2016; Jimi et al., 2013; Martin et al., 2011; Takayama et al., 2010; Yan et al., 2011).

Contribution of the bone microenvironment to bone lesion progression

Since osteoclast inhibitors have not significantly impacted patient survival as expected, the idea of the vicious cycle has been questioned. Despite this, the vicious cycle concept seems to accurately describe the interactions between tumor cells, osteoblasts, and osteoclasts. Where it fails to predict drug responses, it is perhaps because it is overly simplified. The bone/bone marrow microenvironment contains many cell types, each of which contributes to aspects of tumor-induced bone disease. Without understanding these interactions, it will not be possible to predict patient outcomes or drug responses. Some of these interactions include myeloid cells, other immune cells, fibroblasts, the physical microenvironment, and hypoxia.

Myeloid cells

One of the first bone marrow cell types investigated in TIBD was the myeloid-derived suppressor cells (MDSCs), due to their known role in other tumors for establishing the premetastatic niche (Yang et al., 2004, 2008a). They have since been demonstrated to expand and contribute to tumor growth and bone destruction in bone metastatic breast and prostate cancer (Park et al., 2011, 2013; Danilin et al., 2012; Capietto et al., 2013; Luo et al., 2016). In prostate cancer, tumor-derived PTHrP was shown to indirectly increase MDSC angiogenic potential, thus promoting tumor metastasis and growth in bone (Park et al., 2013). In breast cancer, Danilin et al. demonstrated that MDSCs contributed to bone destruction by activating tumor expression of GLI2 and PTHrP, thus stimulating bone destruction (Danilin et al., 2012). Two studies have also demonstrated that MDSCs from a tumor-bearing mouse have the potential to differentiate into osteoclasts; therefore, the expansion of this population leads to a larger pool of osteoclast progenitors, which may explain the ability of MDSCs to contribute to bone destruction (Danilin et al., 2012; Sawant et al., 2013). While the signaling pathways involved in the cross talk between MDSCs and tumor cells is still being investigated, the cross talk between phospholipase C gamma 2 (PLCγ2) and β-catenin has been shown to promote MDSC expansion in bone (Capietto et al., 2013).

Macrophages

Another cell type that has been demonstrated to play an important role in TIBD is the macrophage. For example, bone marrow macrophages have been shown to support prostate cancer growth in bone (Park et al., 2011; Soki et al., 2015) and to modulate osteoblasts (Michalski et al., 2016). Another group demonstrated that tumor-associated macrophages (TAMs) may take up bisphosphonates bound to calcified nodules in the primary site (Junankar et al., 2014). Whether this uptake alters the behavior of the TAMS or metastasis to the bone remains to be determined.

T cells

While T cells are known to be important for immune surveillance in tumors, studies on T cells in TIBD have been limited due to a lack of appropriate models of TIBD in immune-competent mice. However, many groups have begun to investigate T cells using syngeneic models and other approaches. As anticipated, it has been demonstrated that stimulating T cell response in mice reduces tumor burden in bone (Zhang et al., 2011), and depletion of CD8+ T cells results in accelerated growth of dormant melanoma cells disseminated to multiple organ sites including the bone marrow (Eyles et al., 2010). However, a recent study also suggests that tumor-associated T cells can induce osteolytic bone disease prior to bone colonization. In this study, they show that T cell−produced RANKL can induce osteoclastogenesis and bone destruction (Monteiro et al., 2013). These data suggest that T cells may have a dual role in bone disease in that they can reduce tumor growth but stimulate bone destruction. As immunotherapy research expands, it has become imperative to better understand these T cell responses to determine if these approaches that have been successful in specific tumor types may be beneficial to patients with TIBD.

Osteoblasts

The importance of the osteoblast in TIBD has been well described in the vicious cycle model, where tumor-produced factors stimulate osteoblasts to produce RANKL to promote osteoclast-mediated bone destruction (Mundy, 2002; Weilbaecher et al., 2011; Guise et al., 1996). More recent studies have suggested that osteoblasts can function as a prometastatic population of cells. Taichman et al. demonstrated that CXCL12/SDF-1 (expressed by osteoblasts and endothelial cells) and its receptor (CXCR4, expressed by prostate cancer cells) regulate the bone-tropism of prostate cancer cells (Taichman et al., 2002). In addition to the CXCL12/CXCR4/CXCR7 axis (Sun et al., 2010), annexin II, expressed by osteoblasts and endothelium, regulates HSC adhesion, homing, and engraftment (Jung et al., 2007). GAS6 in bone stromal cells (predominantly osteoblasts) induces metastatic tumor cell dormancy and determines site-specificity (i.e., increased localization in vertebrae and hind limb long bone compared with forelimb bones) (Jung et al., 2012). The osteoblastic niche has also been implicated as the direct target of tumor cell localization in bone (Jung et al., 2011). This work demonstrated that administration of PTH to induce osteoblast proliferation promoted skeletal localization of prostate cancer cells, while decreasing ablation of the osteoblasts reduced tumor cell localization.

Osteocytes

In addition to osteoblasts, there is an increasing appreciation for tumor−osteocyte interactions in the field. As breast cancer cells expand within the bone marrow microenvironment, they are proposed to increase intraosseous pressure and therefore promote osteocyte MMP and CCL5 signaling to further promote the outgrowth of prostate cancer cells (Sottnik et al., 2015). Multiple myeloma cells also interact with and can induce osteocyte apoptosis and osteolysis, fueling osteolytic bone disease (Delgado-Calle et al., 2016; McDonald et al., 2017).

Bone marrow fibroblasts

Bone marrow fibroblasts have been established in many tumor types to contribute to tumor growth, invasion, and establishment in secondary sites (Direkze et al., 2004; Dutsch-Wicherek and Kazmierczak, 2013; Eck et al., 2009; Luga and Wrana, 2013; Madar et al., 2013; Orimo et al., 2005; Owens et al., 2013; Togo et al., 2013). Their role is less defined in TIBD, but it has been established that they influence bone metastatic diseases (Johnson et al., 2014). When TGF-βRII was deleted in the CAFs in a prostate cancer model, tumor cell growth in bone was increased (Li et al., 2012). Furthermore, fibroblasts have been shown to promote breast and lung cancer growth in bone through Wnt signaling (Johnson et al., 2014). Joan Massague's group demonstrated that bone marrow fibroblast content in triple-negative tumors was associated with bone metastases, but not lung metastases, in patient samples (Zhang et al., 2013b).

Adipocytes

There has been a surge in interest in adipocyte−tumor cell interactions (McDonald et al., 2016; Morris and Edwards, 2016), and while many groups are currently investigating the significance of the marrow adipocyte in bone colonization and disease progression, as of yet little has been published. Bone marrow adipocytes have been shown to enhance the Warburg effect in prostate cancer cells via HIF-1α activation, and tumor cells in turn promote adipocyte lipolysis (Diedrich et al., 2016). This was tested extensively *in vitro* but has not been functionally tested *in vivo*, and thus its role in promoting

bone colonization remains unknown. In support of a role for adipocytes in disease progression, marrow adipose tissue and serum adiponectin increase during cancer therapy (Cawthorn et al., 2014), suggesting marrow adipocytes may play an endocrine role in cancer progression. There is great interest in this particular area of the field, and there is still much to be learned about these interactions.

Sympathetic and parasympathetic nerve system signaling

Interactions between nerves and the tumor—bone microenvironment have been demonstrated to enhance TIBD through osteoblasts (Elefteriou, 2016; Elefteriou et al., 2014). For example, we now know that the increased flow of the sympathetic nervous system stimulates RANKL expression on osteoblast-lineage cells and that the direct interactions of $RANKL^{osteoblast} - RANK^{tumor\ cell}$ promotes breast cancer bone colonization (Campbell et al., 2012). The bone marrow and bone tissue are richly innervated with nerve fibers that typically parallel blood vessels and have been demonstrated to control bone metabolism (Cook et al., 2014; Campbell et al., 2012; Elefteriou, 2008). Studies have shown that the autonomic nervous system contributes to primary prostate cancer growth and metastasis (Magnon et al., 2013). Nerve-derived signals such as epinephrine and norepinephrine may directly drive prostate cancer cell growth and invasion via activation of sympathetic nervous system receptors such as β2-adrenergic receptor (β2AR). In addition, β2AR agonists stimulate osteoblasts to express RANKL and IL-6 that contribute to osteoclast formation. Of note, β2AR inhibits osteoblast proliferation, and therefore these mechanisms may be important in areas of metastases where osteolysis is predominantly occurring (Campbell et al., 2012; Mulcrone et al., 2017). Conversely, parasympathetic nervous system (PSNS) (Magnon et al., 2013) signaling is thought to favor bone formation, with deletion of the muscarinic M3 receptor showing bone mass loss in mice (Shi et al., 2010). Prostate cancer cells express the muscarinic M3 receptor and ligand stimulation—for example, with acetylcholine—can enhance their invasion and growth (Guo et al., 2016). Thus, increased PSNS signaling may be involved with a more osteoblastic lesion phenotype that is commonly associated with prostate cancer.

Physical microenvironment

In addition to interactions between tumor cells and bone/bone marrow cells, several groups have demonstrated that interactions with the physical bone microenvironment also influence TIBD (Kostic et al., 2009; Provenzano et al., 2009). For example, the rigidity of bone has been shown to mediate cross talk between the integrinβ3 and TGF-β signaling pathways (Page et al., 2015b; Ruppender et al., 2010), leading to an increase in GLI2 and PTHrP expression and subsequent bone destruction. Interestingly, the rigidity of the bone not only influences gene expression within the tumor cells but also affects gene expression of fibroblasts (Johnson et al., 2014) and MSCs (Guo et al., 2015). In addition to the influence of the bone on tumor cell behavior, tumor cells and drug treatments are known to alter bone quality and structure (Biswas et al., 2011; Edwards et al., 2010; Nyman et al., 2016), suggesting that there may be a bidirectional interaction between tumor cells and the physical properties of bone.

In addition to the rigidity of the bone microenvironment, the architecture of the microenvironment is an important factor. Bone has unique architecture that varies from bone to bone. While it is unclear whether this contributes to tumor establishment, it has recently been demonstrated that the variable architecture between bones can contribute to bone resorption and formation (Vanderburgh et al., 2017). As pore size and architecture are tuned to increase mechanical forces, bone formation is increased. Since these forces would be internalized similarly to rigidity, it is likely that they would have a similar effect on tumor cell gene expression.

Hypoxia and alteration of cancer cell metabolism

The bone microenvironment is relatively hypoxic (Mohyeldin et al., 2010; Chow et al., 2001; Harrison et al., 2002; Spencer et al., 2014), but much of the data describing oxygen tensions in the bone marrow has relied on fiber optic probes in the calvarium (Spencer et al., 2014) and math modeling of oxygen gradients across the marrow and trabeculae (Zahm et al., 2010). In fact, we know very little about the actual oxygen tensions within the marrow of the long bones. Staining for pimonidazole, a marker of hypoxia that detects oxygen levels below 10 mmHg, reveals that the bone microenvironment is distinctly hypoxic, and it can therefore be assumed with high likelihood that tumor cells will encounter hypoxia in the bone metastatic site; what is less clear are the actual oxygen tensions that they encounter and the oxygen flux throughout the marrow space and across the trabecular bone.

Hypoxia in the primary breast tumor site is well established to promote tumor progression (Finger et al., 2015; Chaturvedi et al., 2013; Erler et al., 2006; Yang et al., 2008b), and staining for HIF1α is correlated with significantly worse

patient survival in breast cancer (Schindl et al., 2002); however, its role in tumor dissemination to bone and the outgrowth of tumor cells in bone is less clear. Previous studies from independent groups indicate that blockade or loss of HIF signaling in MDA-MB-231 breast cancer cells inhibits breast cancer colonization of the bone marrow (Dunn et al., 2009; Hiraga et al., 2007; Lu et al., 2010), but the mechanism by which hypoxia promotes tumor homing to bone marrow remains unclear. It is possible that the effects are through the establishment of a premetastatic niche in bone (Peinado et al., 2017) but may also be due to hypoxic signaling in the primary tumor, possibly through HIF1α induction of a glycolytic phenotype, discussed in more detail following.

Hypoxia is often associated with lower pH. Altered metabolism and the ability to survive in harsh acidic environments is a hallmark of cancer cells. Decades ago, the ability and preference of cancer cells to use glucose metabolism to support anabolic processes for growth was described and is known as the "Warburg effect" (Hanahan and Weinberg, 2011). Of note, the metabolic pathways active in cancer can vary in regards to cancer stage and their interactions with cells of the surrounding microenvironment. Primary prostate cancers have heightened β-oxidation pathway activity and can exploit fatty acids either generated via *de novo* synthesis or uptaken from the microenvironment to support growth and progression (Zadra et al., 2013; Menendez and Lupu, 2007). The bone marrow contains many adipocytes, and *in vitro* and *in vivo* models of bone marrow−adipocyte interaction and *in vivo* models of bone marrow adiposity generated by a high-fat diet have shown that adipocytes regulate the glycolytic phenotype by enhancing glycolytic enzymes, increased lactate production, and decreased mitochondrial oxidative phosphorylation in cancer cells (Diedrich et al., 2016). Heightened metabolic activity in cancer cells and glycolysis also result in further acidification of the cancer bone microenvironment (Damaghi et al., 2013). Lower pH has been demonstrated to be permissive for osteoclast formation, and the increased expression of acid transporters such as carbonic anhydrase XI allow cancer cells to buffer intracellular pH and survive in these conditions (Arnett, 2008; Ibrahim-Hashim et al., 2012).

Monoamine oxidase A (MAOA) is a mitochondrial membrane-bound enzyme that catalyzes the degradation of monoamines by oxidative deanimation (Shih et al., 1999). MAOA is associated with prostate cancer progression and is a poor prognostic indicator (True et al., 2006). MAOA can also induce the EMT program by producing excessive levels of hydrogen peroxide, a major by-product of MAOA activity, and promoting the expression of Sonic Hedgehog (Shh) (Wu et al., 2014). In the context of the bone microenvironment, prostate cancer−derived Shh can bind to the patched homolog 1 (PTCH1) receptor on osteoblasts. Activation of PTCH1 results in increased GLI1/2 transcription factor activity and the induction of target genes such as IL-6 and RANKL that in turn promote osteoclast formation. Increased osteoclast activity then completes the vicious cycle loop via the increased availability of factors such as TGFβ and BMPs (Wu et al., 2017).

Conclusion

Tumor-induced bone disease involves complex interactions between multiple cell types and physical properties that are specific to the bone and bone marrow microenvironment. While substantial research has been performed over several decades, more work is needed to fully understand these interactions. Understanding these interactions will help with beginning to predict patient outcomes and potentially developing novel therapies for patients with TIBD. The multiple and complex mechanisms governing interactions between tumors and bone have revealed a number of exciting therapeutic opportunities that have the potential to impact patient care.

References

Alexaki, V.I., Javelaud, D., Van Kempen, L.C., Mohammad, K.S., Dennler, S., Luciani, F., Hoek, K.S., Juarez, P., Goydos, J.S., Fournier, P.J., Sibon, C., Bertolotto, C., Verrecchia, F., Saule, S., Delmas, V., Ballotti, R., Larue, L., Saiag, P., Guise, T.A., Mauviel, A., 2010. GLI2-mediated melanoma invasion and metastasis. J. Natl. Cancer Inst. 102, 1148−1159.

Arnett, T.R., 2008. Extracellular pH regulates bone cell function. J. Nutr. 138, 415S−418S.

Banerjee, C., Javed, A., Choi, J.Y., Green, J., Rosen, V., van Wijnen, A.J., Stein, J.L., Lian, J.B., Stein, G.S., 2001. Differential regulation of the two principal Runx2/Cbfa1 n-terminal isoforms in response to bone morphogenetic protein-2 during development of the osteoblast phenotype. Endocrinology 142, 4026−4039.

Barnes, G.L., Javed, A., Waller, S.M., Kamal, M.H., Hebert, K.E., Hassan, M.Q., Bellahcene, A., Van Wijnen, A.J., Young, M.F., Lian, J.B., Stein, G.S., Gerstenfeld, L.C., 2003. Osteoblast-related transcription factors Runx2 (Cbfa1/AML3) and MSX2 mediate the expression of bone sialoprotein in human metastatic breast cancer cells. Cancer Res. 63, 2631−2637.

Biswas, S., Nyman, J.S., Alvarez, J., Chakrabarti, A., Ayres, A., Sterling, J., Edwards, J., Rana, T., Johnson, R., Perrien, D.S., Lonning, S., Shyr, Y., Matrisian, L.M., Mundy, G.R., 2011. Anti-transforming growth factor ss antibody treatment rescues bone loss and prevents breast cancer metastasis to bone. PLoS One 6, e27090.

Blair, H.C., 1998. How the osteoclast degrades bone. BioEssays 20, 837−846.

Bonewald, L.F., Mundy, G.R., 1990. Role of transforming growth factor-beta in bone remodeling. Clin. Orthop. Relat. Res. 261–276.

Bragado, P., Sosa, M.S., Keely, P., Condeelis, J., Aguirre-Ghiso, J.A., 2012. Microenvironments dictating tumor cell dormancy. Recent Results Canc. Res. 195, 25–39.

Bragado, P., Estrada, Y., Parikh, F., Krause, S., Capobianco, C., Farina, H.G., Schewe, D.M., Aguirre-Ghiso, J.A., 2013. TGF-beta2 dictates disseminated tumour cell fate in target organs through TGF-beta-RIII and p38alpha/beta signalling. Nat. Cell Biol. 15, 1351–1361.

Branstetter, D.G., Nelson, S.D., Manivel, J.C., Blay, J.Y., Chawla, S., Thomas, D.M., Jun, S., Jacobs, I., 2012. Denosumab induces tumor reduction and bone formation in patients with giant-cell tumor of bone. Clin. Cancer Res. 18, 4415–4424.

Campbell, J.P., Karolak, M.R., Ma, Y., Perrien, D.S., Masood-Campbell, S.K., Penner, N.L., Munoz, S.A., Zijlstra, A., Yang, X., Sterling, J.A., Elefteriou, F., 2012. Stimulation of host bone marrow stromal cells by sympathetic nerves promotes breast cancer bone metastasis in mice. PLoS Biol. 10, e1001363.

Cannonier, S.A., Sterling, J.A., 2015. The role of hedgehog signaling in tumor induced bone disease. Cancers 7, 1658–1683.

Cannonier, S.A., Gonzales, C.B., Ely, K., Guelcher, S.A., Sterling, J.A., 2016. Hedgehog and TGFbeta signaling converge on Gli2 to control bony invasion and bone destruction in oral squamous cell carcinoma. Oncotarget 7, 76062–76075.

Capietto, A.H., Kim, S., Sanford, D.E., Linehan, D.C., Hikida, M., Kumosaki, T., Novack, D.V., Faccio, R., 2013. Down-regulation of PLCgamma2-beta-catenin pathway promotes activation and expansion of myeloid-derived suppressor cells in cancer. J. Exp. Med. 210, 2257–2271.

Carducci, M.A., Jimeno, A., 2006. Targeting bone metastasis in prostate cancer with endothelin receptor antagonists. Clin. Cancer Res. 12, 6296s–6300s.

Cawthorn, W.P., Scheller, E.L., Learman, B.S., Parlee, S.D., Simon, B.R., Mori, H., Ning, X., Bree, A.J., Schell, B., Broome, D.T., Soliman, S.S., DelProposto, J.L., Lumeng, C.N., Mitra, A., Pandit, S.V., Gallagher, K.A., Miller, J.D., Krishnan, V., Hui, S.K., Bredella, M.A., Fazeli, P.K., Klibanski, A., Horowitz, M.C., Rosen, C.J., MacDougald, O.A., 2014. Bone marrow adipose tissue is an endocrine organ that contributes to increased circulating adiponectin during caloric restriction. Cell Metabol. 20, 368–375.

Chanda, D., Kumar, S., Ponnazhagan, S., 2010. Therapeutic potential of adult bone marrow-derived mesenchymal stem cells in diseases of the skeleton. J. Cell. Biochem. 111, 249–257.

Chaturvedi, P., Gilkes, D.M., Wong, C.C., Kshitiz, Luo, W., Zhang, H., Wei, H., Takano, N., Schito, L., Levchenko, A., Semenza, G.L., 2013. Hypoxia-inducible factor-dependent breast cancer-mesenchymal stem cell bidirectional signaling promotes metastasis. J. Clin. Investig. 123, 189–205.

Chen, D., Zhao, M., Mundy, G.R., 2004. Bone morphogenetic proteins 1. Growth Factors 22, 233–241.

Chow, D.C., Wenning, L.A., Miller, W.M., Papoutsakis, E.T., 2001. Modeling pO(2) distributions in the bone marrow hematopoietic compartment. I. Krogh's model. Biophys. J. 81, 675–684.

Chung, L.W., Baseman, A., Assikis, V., Zhau, H.E., 2005. Molecular insights into prostate cancer progression: the missing link of tumor microenvironment. J. Urol. 173, 10–20.

Coleman, R.E., 2006. Clinical features of metastatic bone disease and risk of skeletal morbidity. Clin. Cancer Res. 12, 6243s–6249s.

Coleman, R.E., Smith, P., Rubens, R.D., 1998. Clinical course and prognostic factors following bone recurrence from breast cancer. Br. J. Canc. 77, 336–340.

Coleman, R., Body, J.J., Aapro, M., Hadji, P., Herrstedt, J., Group EGW, 2014. Bone health in cancer patients: ESMO clinical practice guidelines. Ann. Oncol. 25 (Suppl. 3), iii124–i137.

Coleman, R., Cameron, D., Dodwell, D., Bell, R., Wilson, C., Rathbone, E., Keane, M., Gil, M., Burkinshaw, R., Grieve, R., Barrett-Lee, P., Ritchie, D., Liversedge, V., Hinsley, S., Marshall, H., investigators, A., 2014. Adjuvant zoledronic acid in patients with early breast cancer: final efficacy analysis of the AZURE (BIG 01/04) randomised open-label phase 3 trial. Lancet Oncol. 15, 997–1006.

Cook, L.M., Shay, G., Aruajo, A., Lynch, C.C., 2014. Integrating new discoveries into the "vicious cycle" paradigm of prostate to bone metastases. Cancer Metastasis Rev. 33 (2–3), 511–525.

Coxon, F.P., Thompson, K., Roelofs, A.J., Ebetino, F.H., Rogers, M.J., 2008. Visualizing mineral binding and uptake of bisphosphonate by osteoclasts and non-resorbing cells. Bone 42, 848–860.

Curatolo, C., Ludovico, G.M., Correale, M., Pagliarulo, A., Abbate, I., Cirrillo Marucco, E., Barletta, A., 1992. Advanced prostate cancer follow-up with prostate-specific antigen, prostatic acid phosphatase, osteocalcin and bone isoenzyme of alkaline phosphatase. Eur. Urol. 21 (Suppl. 1), 105–107.

Damaghi, M., Wojtkowiak, J.W., Gillies, R.J., 2013. pH sensing and regulation in cancer. Front. Physiol. 4, 370.

Danilin, S., Merkel, A.R., Johnson, J.R., Johnson, R.W., Edwards, J.R., Sterling, J.A., 2012. Myeloid-derived suppressor cells expand during breast cancer progression and promote tumor-induced bone destruction. Oncoimmunology 1, 1484–1494.

Dasgupta, A., Lim, A.R., Ghajar, C.M., 2017. Circulating and disseminated tumor cells: harbingers or initiators of metastasis? Mol Oncol 11, 40–61.

Deftos, L.J., Barken, I., Burton, D.W., Hoffman, R.M., Geller, J., 2005. Direct evidence that PTHrP expression promotes prostate cancer progression in bone. Biochem. Biophys. Res. Commun. 327, 468–472.

Delgado-Calle, J., Anderson, J., Cregor, M.D., Hiasa, M., Chirgwin, J.M., Carlesso, N., Yoneda, T., Mohammad, K.S., Plotkin, L.I., Roodman, G.D., Bellido, T., 2016. Bidirectional notch signaling and osteocyte-derived factors in the bone marrow microenvironment promote tumor cell proliferation and bone destruction in multiple myeloma. Cancer Res. 76, 1089–1100.

Di Vizio, D., Morello, M., Dudley, A.C., Schow, P.W., Adam, R.M., Morley, S., Mulholland, D., Rotinen, M., Hager, M.H., Insabato, L., Moses, M.A., Demichelis, F., Lisanti, M.P., Wu, H., Klagsbrun, M., Bhowmick, N.A., Rubin, M.A., D'Souza-Schorey, C., Freeman, M.R., 2012. Large oncosomes in human prostate cancer tissues and in the circulation of mice with metastatic disease. Am. J. Pathol. 181, 1573–1584.

Diedrich, J.D., Rajagurubandara, E., Herroon, M.K., Mahapatra, G., Huttemann, M., Podgorski, I., 2016. Bone marrow adipocytes promote the warburg phenotype in metastatic prostate tumors via HIF-1alpha activation. Oncotarget 7, 64854–64877.

Direkze, N.C., Hodivala-Dilke, K., Jeffery, R., Hunt, T., Poulsom, R., Oukrif, D., Alison, M.R., Wright, N.A., 2004. Bone marrow contribution to tumor-associated myofibroblasts and fibroblasts. Cancer Res. 64, 8492–8495.

Draffin, J.E., McFarlane, S., Hill, A., Johnston, P.G., Waugh, D.J., 2004. CD44 potentiates the adherence of metastatic prostate and breast cancer cells to bone marrow endothelial cells. Cancer Res. 64, 5702–5711.

Dunn, L.K., Mohammad, K.S., Fournier, P.G., McKenna, C.R., Davis, H.W., Niewolna, M., Peng, X.H., Chirgwin, J.M., Guise, T.A., 2009. Hypoxia and TGF-beta drive breast cancer bone metastases through parallel signaling pathways in tumor cells and the bone microenvironment. PLoS One 4, e6896.

Dutsch-Wicherek, M., Kazmierczak, W., 2013. Creation of a suppressive microenvironment by macrophages and cancer-associated fibroblasts. Front. Biosci. 18, 1003–1016.

Eck, S.M., Cote, A.L., Winkelman, W.D., Brinckerhoff, C.E., 2009. CXCR4 and matrix metalloproteinase-1 are elevated in breast carcinoma-associated fibroblasts and in normal mammary fibroblasts exposed to factors secreted by breast cancer cells. Mol. Canc. Res. 7, 1033–1044.

Edwards, J.R., Nyman, J.S., Lwin, S.T., Moore, M.M., Esparza, J., O'Quinn, E.C., Hart, A.J., Biswas, S., Patil, C.A., Lonning, S., Mahadevan-Jansen, A., Mundy, G.R., 2010. Inhibition of TGF-beta signaling by 1D11 antibody treatment increases bone mass and quality in vivo. J. Bone Miner. Res. 25, 2419–2426.

Elefteriou, F., 2008. Regulation of bone remodeling by the central and peripheral nervous system. Arch. Biochem. Biophys. 473, 231–236.

Elefteriou, F., 2016. Role of sympathetic nerves in the establishment of metastatic breast cancer cells in bone. J. Bone Oncol. 5, 132–134.

Elefteriou, F., Campbell, P., Ma, Y., 2014. Control of bone remodeling by the peripheral sympathetic nervous system. Calcif. Tissue Int. 94, 140–151.

Ellman, M.B., Yan, D., Ahmadinia, K., Chen, D., An, H.S., Im, H.J., 2013. Fibroblast growth factor control of cartilage homeostasis. J. Cell. Biochem. 114, 735–742.

Enomoto, H., Shiojiri, S., Hoshi, K., Furuichi, T., Fukuyama, R., Yoshida, C.A., Kanatani, N., Nakamura, R., Mizuno, A., Zanma, A., Yano, K., Yasuda, H., Higashio, K., Takada, K., Komori, T., 2003. Induction of osteoclast differentiation by Runx2 through receptor activator of nuclear factor-kappa B ligand (RANKL) and osteoprotegerin regulation and partial rescue of osteoclastogenesis in Runx2$^{-/-}$ mice by RANKL transgene. J. Biol. Chem. 278, 23971–23977.

Erler, J.T., Bennewith, K.L., Nicolau, M., Dornhofer, N., Kong, C., Le, Q.T., Chi, J.T., Jeffrey, S.S., Giaccia, A.J., 2006. Lysyl oxidase is essential for hypoxia-induced metastasis. Nature 440, 1222–1226.

Erler, J.T., Bennewith, K.L., Cox, T.R., Lang, G., Bird, D., Koong, A., Le, Q.T., Giaccia, A.J., 2009. Hypoxia-induced lysyl oxidase is a critical mediator of bone marrow cell recruitment to form the premetastatic niche. Cancer Cell 15, 35–44.

Esposito, M., Kang, Y., 2014. Targeting tumor-stromal interactions in bone metastasis. Pharmacol. Ther. 141, 222–233.

Eyles, J., Puaux, A.L., Wang, X., Toh, B., Prakash, C., Hong, M., Tan, T.G., Zheng, L., Ong, L.C., Jin, Y., Kato, M., Prevost-Blondel, A., Chow, P., Yang, H., Abastado, J.P., 2010. Tumor cells disseminate early, but immunosurveillance limits metastatic outgrowth, in a mouse model of melanoma. J. Clin. Investig. 120, 2030–2039.

Feeley, B.T., Liu, N.Q., Conduah, A.H., Krenek, L., Roth, K., Dougall, W.C., Huard, J., Dubinett, S., Lieberman, J.R., 2006. Mixed metastatic lung cancer lesions in bone are inhibited by noggin overexpression and Rank:Fc administration. J. Bone Miner. Res. 21, 1571–1580.

Finger, E.C., Castellini, L., Rankin, E.B., Vilalta, M., Krieg, A.J., Jiang, D., Banh, A., Zundel, W., Powell, M.B., Giaccia, A.J., 2015. Hypoxic induction of AKAP12 variant 2 shifts PKA-mediated protein phosphorylation to enhance migration and metastasis of melanoma cells. Proc. Natl. Acad. Sci. U.S.A. 112, 4441–4446.

Fowler, J.A., Lwin, S.T., Drake, M.T., Edwards, J.R., Kyle, R.A., Mundy, G.R., Edwards, C.M., 2011. Host-derived adiponectin is tumor-suppressive and a novel therapeutic target for multiple myeloma and the associated bone disease. Blood 118, 5872–5882.

Fowler, J.A., Mundy, G.R., Lwin, S.T., Edwards, C.M., 2012. Bone marrow stromal cells create a permissive microenvironment for myeloma development: a new stromal role for Wnt inhibitor Dkk1. Cancer Res. 72, 2183–2189.

Frieling, J.S., Shay, G., Izumi, V., Aherne, S.T., Saul, R.G., Budzevich, M., Koomen, J., Lynch, C.C., 2017. Matrix metalloproteinase processing of PTHrP yields a selective regulator of osteogenesis, PTHrP1-17. Oncogene 36 (31), 4498–4507.

Galliher, A.J., Schiemann, W.P., 2006. Beta3 integrin and Src facilitate transforming growth factor-beta mediated induction of epithelial-mesenchymal transition in mammary epithelial cells. Breast Cancer Res. 8, R42.

Ghajar, C.M., Peinado, H., Mori, H., Matei, I.R., Evason, K.J., Brazier, H., Almeida, D., Koller, A., Hajjar, K.A., Stainier, D.Y., Chen, E.I., Lyden, D., Bissell, M.J., 2013. The perivascular niche regulates breast tumour dormancy. Nat. Cell Biol. 15, 807–817.

Guise, T.A., Mundy, G.R., 1998. Cancer and bone. Endocr. Rev. 19, 18–54.

Guise, T.A., Yin, J.J., Taylor, S.D., Kumagai, Y., Dallas, M., Boyce, B.F., Yoneda, T., Mundy, G.R., 1996. Evidence for a causal role of parathyroid hormone-related protein in the pathogenesis of human breast cancer-mediated osteolysis. J. Clin. Investig. 98, 1544–1549.

Guo, R., Ward, C.L., Davidson, J.M., Duvall, C.L., Wenke, J.C., Guelcher, S.A., 2015. A transient cell-shielding method for viable MSC delivery within hydrophobic scaffolds polymerized in situ. Biomaterials 54, 21–33.

Guo, L., Liu, Y., Ding, Z., Sun, W., Yuan, M., 2016. Signal transduction by M3 muscarinic acetylcholine receptor in prostate cancer. Oncol Lett 11, 385–392.

Ha, H.K., Lee, W., Park, H.J., Lee, S.D., Lee, J.Z., Chung, M.K., 2011. Clinical significance of CXCL16/CXCR6 expression in patients with prostate cancer. Mol. Med. Rep. 4, 419–424.

Hall, C.L., Keller, E.T., 2006. The role of Wnts in bone metastases. Cancer Metastasis Rev. 25, 551–558.

Hall, C.L., Bafico, A., Dai, J., Aaronson, S.A., Keller, E.T., 2005. Prostate cancer cells promote osteoblastic bone metastases through Wnts. Cancer Res. 65, 7554–7560.

Hanahan, D., Weinberg, R.A., 2011. Hallmarks of cancer: the next generation. Cell 144, 646–674.

Harrison, J.S., Rameshwar, P., Chang, V., Bandari, P., 2002. Oxygen saturation in the bone marrow of healthy volunteers. Blood 99, 394.

Heissig, B., Hattori, K., Dias, S., Friedrich, M., Ferris, B., Hackett, N.R., Crystal, R.G., Besmer, P., Lyden, D., Moore, M.A., Werb, Z., Rafii, S., 2002. Recruitment of stem and progenitor cells from the bone marrow niche requires mmp-9 mediated release of kit-ligand. Cell 109, 625–637.

Hershberger, P.M., Peddibhotla, S., Sugarman, E., Maloney, P., Key, D., Suyama, E., Nguyen, K., Vasile, S., Kraft, M., Stonich, D., Mangravita-Novo, A., Vicchiarelli, M., Gosalia, P., Milewski, M., Li, L., Hedrick, M., Sun, Q., Sergienko, E., Cheltsov, A., Salanawil, S., Diwan, J., Smith, L.H., Taichman, R.S., Chung, T.D.Y., Pinkerton, A.B., Malany, S., Roth, G.P., 2010. Probing the CXCR6/CXCL16 Axis: targeting prevention of prostate cancer metastasis. In: Probe Reports from the NIH Molecular Libraries Program. Bethesda, MD.

Hiraga, T., Kizaka-Kondoh, S., Hirota, K., Hiraoka, M., Yoneda, T., 2007. Hypoxia and hypoxia-inducible factor-1 expression enhance osteolytic bone metastases of breast cancer. Cancer Res. 67, 4157–4163.

Hock, J.M., Canalis, E., Centrella, M., 1990. Transforming growth factor-beta stimulates bone matrix apposition and bone cell replication in cultured fetal rat calvariae. Endocrinology 126, 421–426.

Hsia, D.A., Lim, S.T., Bernard-Trifilo, J.A., Mitra, S.K., Tanaka, S., den Hertog, J., Streblow, D.N., Ilic, D., Ginsberg, M.H., Schlaepfer, D.D., 2005. Integrin alpha4beta1 promotes focal adhesion kinase-independent cell motility via alpha4 cytoplasmic domain-specific activation of c-Src. Mol. Cell Biol. 25, 9700–9712.

Hu, Z., Gupta, J., Zhang, Z., Gerseny, H., Berg, A., Chen, Y.J., Zhang, Z., Du, H., Brendler, C.B., Xiao, X., Pienta, K.J., Guise, T., Lee, C., Stern, P.H., Stock, S., Seth, P., 2012. Systemic delivery of oncolytic adenoviruses targeting transforming growth factor-beta inhibits established bone metastasis in a prostate cancer mouse model. Hum. Gene Ther. 23, 871–882.

Ibrahim-Hashim, A., Cornnell, H.H., Abrahams, D., Lloyd, M., Bui, M., Gillies, R.J., Gatenby, R.A., 2012. Systemic buffers inhibit carcinogenesis in TRAMP mice. J. Urol. 188, 624–631.

Inman, C.K., Shore, P., 2003. The osteoblast transcription factor Runx2 is expressed in mammary epithelial cells and mediates osteopontin expression. J. Biol. Chem. 278, 48684–48689.

Itoh, T., Ito, Y., Ohtsuki, Y., Ando, M., Tsukamasa, Y., Yamada, N., Naoe, T., Akao, Y., 2012. Microvesicles released from hormone-refractory prostate cancer cells facilitate mouse pre-osteoblast differentiation. J. Mol. Histol. 43, 509–515.

Javelaud, D., Alexaki, V.I., Dennler, S., Mohammad, K.S., Guise, T.A., Mauviel, A., 2011. TGF-beta/SMAD/GLI2 signaling axis in cancer progression and metastasis. Cancer Res. 71, 5606–5610.

Javelaud, D., van Kempen, L., Alexaki, V.I., Le Scolan, E., Luo, K., Mauviel, A., 2011. Efficient TGF-beta/SMAD signaling in human melanoma cells associated with high c-SKI/SnoN expression. Mol. Canc. 10, 2.

Javelaud, D., Alexaki, V.I., Pierrat, M.J., Hoek, K.S., Dennler, S., Van Kempen, L., Bertolotto, C., Ballotti, R., Saule, S., Delmas, V., Mauviel, A., 2011. GLI2 and M-MITF transcription factors control exclusive gene expression programs and inversely regulate invasion in human melanoma cells. Pigment Cell Melanoma Res. 24, 932–943.

Jimi, E., Shin, M., Furuta, H., Tada, Y., Kusukawa, J., 2013. The RANKL/RANK system as a therapeutic target for bone invasion by oral squamous cell carcinoma (review). Int. J. Oncol. 42, 803–809.

Johnson, R.W., Nguyen, M.P., Padalecki, S.S., Grubbs, B.G., Merkel, A.R., Oyajobi, B.O., Matrisian, L.M., Mundy, G.R., Sterling, J.A., 2011. TGF-beta promotion of Gli2-induced expression of parathyroid hormone-related protein, an important osteolytic factor in bone metastasis, is independent of canonical Hedgehog signaling. Cancer Res. 71, 822–831.

Johnson, R.W., Merkel, A.R., Danilin, S., Nguyen, M.P., Mundy, G.R., Sterling, J.A., 2011. 6-Thioguanine inhibition of parathyroid hormone-related protein expression is mediated by GLI2. Anticancer Res. 31, 2705–2712.

Johnson, R.W., Merkel, A.R., Page, J.M., Ruppender, N.S., Guelcher, S.A., Sterling, J.A., 2014. Wnt signaling induces gene expression of factors associated with bone destruction in lung and breast cancer. Clin. Exp. Metastasis 31 (8), 945–959.

Johnson, R.W., Schipani, E., Giaccia, A.J., 2015. HIF targets in bone remodeling and metastatic disease. Pharmacol. Ther. 150, 169–177.

Johnson, R.W., Finger, E.C., Olcina, M.M., Vilalta, M., Aguilera, T., Miao, Y., Merkel, A.R., Johnson, J.R., Sterling, J.A., Wu, J.Y., Giaccia, A.J., 2016. Induction of LIFR confers a dormancy phenotype in breast cancer cells disseminated to the bone marrow. Nat. Cell Biol. 18 (10), 1078–1089.

Junankar, S., Shay, G., Jurczyluk, J., Ali, N., Down, J., Pocock, N., Parker, P., Nguyen, A., Sun, S., Kashemirov, B., McKenna, C.E., Croucher, P.I., Swarbrick, A., Weilbaecher, K., Phan, T.G., Rogers, M.J., 2015. Real-time intravital imaging establishes tumour-associated macrophages as the extraskeletal target of bisphosphonate action in cancer. Cancer Discov. 5 (1), 35–42.

Jung, Y., Wang, J., Song, J., Shiozawa, Y., Wang, J., Havens, A., Wang, Z., Sun, Y.X., Emerson, S.G., Krebsbach, P.H., Taichman, R.S., 2007. Annexin II expressed by osteoblasts and endothelial cells regulates stem cell adhesion, homing, and engraftment following transplantation. Blood 110, 82–90.

Jung, Y., Shiozawa, Y., Wang, J., Patel, L.R., Havens, A.M., Song, J., Krebsbach, P.H., Roodman, G.D., Taichman, R.S., 2011. Annexin-2 is a regulator of stromal cell-derived factor-1/CXCL12 function in the hematopoietic stem cell endosteal niche. Exp. Hematol. 39, 151–166 e1.

Jung, Y., Shiozawa, Y., Wang, J., McGregor, N., Dai, J., Park, S.I., Berry, J.E., Havens, A.M., Joseph, J., Kim, J.K., Patel, L., Carmeliet, P., Daignault, S., Keller, E.T., McCauley, L.K., Pienta, K.J., Taichman, R.S., 2012. Prevalence of prostate cancer metastases after intravenous inoculation provides clues into the molecular basis of dormancy in the bone marrow microenvironment. Neoplasia 14, 429–439.

Kakonen, S.M., Mundy, G.R., 2003. Mechanisms of osteolytic bone metastases in breast carcinoma. Cancer 97, 834–839.

Kakonen, S.M., Selander, K.S., Chirgwin, J.M., Yin, J.J., Burns, S., Rankin, W.A., Grubbs, B.G., Dallas, M., Cui, Y., Guise, T.A., 2002. Transforming growth factor-beta stimulates parathyroid hormone-related protein and osteolytic metastases via Smad and mitogen-activated protein kinase signaling pathways. J. Biol. Chem. 277, 24571–24578.

Kang, Y., Siegel, P.M., Shu, W., Drobnjak, M., Kakonen, S.M., Cordon-Cardo, C., Guise, T.A., Massague, J., 2003. A multigenic program mediating breast cancer metastasis to bone. Cancer Cell 3, 537–549.

Kantoff, P.W., Mohler, J.L., 2013. New developments in the management of prostate cancer. J. Natl. Compr. Cancer Netw. 11, 653–657.
Kaplan, R.N., Rafii, S., Lyden, D., 2006. Preparing the "soil": the premetastatic niche. Cancer Res. 66, 11089–11093.
Keller, E.T., Brown, J., 2004. Prostate cancer bone metastases promote both osteolytic and osteoblastic activity. J. Cell. Biochem. 91, 718–729.
Kennecke, H., Yerushalmi, R., Woods, R., Cheang, M.C., Voduc, D., Speers, C.H., Nielsen, T.O., Gelmon, K., 2010. Metastatic behavior of breast cancer subtypes. J. Clin. Oncol. 28, 3271–3277.
Kobayashi, A., Okuda, H., Xing, F., Pandey, P.R., Watabe, M., Hirota, S., Pai, S.K., Liu, W., Fukuda, K., Chambers, C., Wilber, A., Watabe, K., 2011. Bone morphogenetic protein 7 in dormancy and metastasis of prostate cancer stem-like cells in bone. J. Exp. Med. 208, 2641–2655.
Koeneman, K.S., Yeung, F., Chung, L.W., 1999. Osteomimetic properties of prostate cancer cells: a hypothesis supporting the predilection of prostate cancer metastasis and growth in the bone environment. Prostate 39, 246–261.
Kong, Y.Y., Yoshida, H., Sarosi, I., Tan, H.L., Timms, E., Capparelli, C., Morony, S., Oliveira-dos-Santos, A.J., Van, G., Itie, A., Khoo, W., Wakeham, A., Dunstan, C.R., Lacey, D.L., Mak, T.W., Boyle, W.J., Penninger, J.M., 1999. OPGL is a key regulator of osteoclastogenesis, lymphocyte development and lymph-node organogenesis. Nature 397, 315–323.
Kostic, A., Lynch, C.D., Sheetz, M.P., 2009. Differential matrix rigidity response in breast cancer cell lines correlates with the tissue tropism. PLoS One 4, e6361.
Kunikullaya, S.U., Poddar, J., Sharma, A.D., Patel, S., 2017. Pattern of distant metastasis in molecular subtypes of carcinoma breast: an institutional study. Indian J. Cancer 54, 327–332.
Kwakwa, K.A., Sterling, J.A., 2017. Integrin alphavbeta3 signaling in tumor-induced bone disease. Cancers 9.
Lamoureux, F., Moriceau, G., Picarda, G., Rousseau, J., Trichet, V., Redini, F., 2010. Regulation of osteoprotegerin pro- or anti-tumoral activity by bone tumor microenvironment. Biochim. Biophys. Acta 1805, 17–24.
Lee, J.A., Jung, J.S., Kim, D.H., Lim, J.S., Kim, M.S., Kong, C.B., Song, W.S., Cho, W.H., Jeon, D.G., Lee, S.Y., Koh, J.S., 2011. RANKL expression is related to treatment outcome of patients with localized, high-grade osteosarcoma. Pediatr. Blood Canc. 56, 738–743.
Levesque, J.P., Helwani, F.M., Winkler, I.G., 2010. The endosteal 'osteoblastic' niche and its role in hematopoietic stem cell homing and mobilization. Leukemia 24, 1979–1992.
Li, Z.G., Yang, J., Vazquez, E.S., Rose, D., Vakar-Lopez, F., Mathew, P., Lopez, A., Logothetis, C.J., Lin, S.H., Navone, N.M., 2008. Low-density lipoprotein receptor-related protein 5 (LRP5) mediates the prostate cancer-induced formation of new bone. Oncogene 27, 596–603.
Li, Z.G., Mathew, P., Yang, J., Starbuck, M.W., Zurita, A.J., Liu, J., Sikes, C., Multani, A.S., Efstathiou, E., Lopez, A., Wang, J., Fanning, T.V., Prieto, V.G., Kundra, V., Vazquez, E.S., Troncoso, P., Raymond, A.K., Logothetis, C.J., Lin, S.H., Maity, S., Navone, N.M., 2008. Androgen receptor-negative human prostate cancer cells induce osteogenesis in mice through FGF9-mediated mechanisms. J. Clin. Investig. 118, 2697–2710.
Li, X., Sterling, J.A., Fan, K.H., Vessella, R.L., Shyr, Y., Hayward, S.W., Matrisian, L.M., Bhowmick, N.A., 2012. Loss of TGF-beta responsiveness in prostate stromal cells alters chemokine levels and facilitates the development of mixed osteoblastic/osteolytic bone lesions. Mol. Canc. Res. 10, 494–503.
Liao, J., Li, X., Koh, A.J., Berry, J.E., Thudi, N., Rosol, T.J., Pienta, K.J., McCauley, L.K., 2008. Tumor expressed PTHrP facilitates prostate cancer-induced osteoblastic lesions. Int. J. Cancer 123, 2267–2278.
Liu, M.C., Shields, P.G., Warren, R.D., Cohen, P., Wilkinson, M., Ottaviano, Y.L., Rao, S.B., Eng-Wong, J., Seillier-Moiseiwitsch, F., Noone, A.M., Isaacs, C., 2009. Circulating tumor cells: a useful predictor of treatment efficacy in metastatic breast cancer. J. Clin. Oncol. 27, 5153–5159.
Lu, Y., Wang, J., Xu, Y., Koch, A.E., Cai, Z., Chen, X., Galson, D.L., Taichman, R.S., Zhang, J., 2008. CXCL16 functions as a novel chemotactic factor for prostate cancer cells in vitro. Mol. Canc. Res. 6, 546–554.
Lu, X., Yan, C.H., Yuan, M., Wei, Y., Hu, G., Kang, Y., 2010. In vivo dynamics and distinct functions of hypoxia in primary tumor growth and organotropic metastasis of breast cancer. Cancer Res. 70, 3905–3914.
Lu, X., Mu, E., Wei, Y., Riethdorf, S., Yang, Q., Yuan, M., Yan, J., Hua, Y., Tiede, B.J., Haffty, B.G., Pantel, K., Massague, J., Kang, Y., 2011. VCAM-1 promotes osteolytic expansion of indolent bone micrometastasis of breast cancer by engaging alpha4beta1-positive osteoclast progenitors. Cancer Cell 20, 701–714.
Luga, V., Wrana, J.L., 2013. Tumor-stroma interaction: revealing fibroblast-secreted exosomes as potent regulators of Wnt-planar cell polarity signaling in cancer metastasis. Cancer Res. 73, 6843–6847.
Luo, X., Fu, Y., Loza, A.J., Murali, B., Leahy, K.M., Ruhland, M.K., Gang, M., Su, X., Zamani, A., Shi, Y., Lavine, K.J., Ornitz, D.M., Weilbaecher, K.N., Long, F., Novack, D.V., Faccio, R., Longmore, G.D., Stewart, S.A., 2016. Stromal-initiated changes in the bone promote metastatic niche development. Cell Rep. 14, 82–92.
Madar, S., Goldstein, I., Rotter, V., 2013. 'Cancer associated fibroblasts' – more than meets the eye. Trends Mol. Med. 19, 447–453.
Mader, S., Pantel, K., 2017. Liquid biopsy: current status and future perspectives. Oncol. Res. Treat. 40, 404–408.
Magnon, C., Hall, S.J., Lin, J., Xue, X., Gerber, L., Freedland, S.J., Frenette, P.S., 2013. Autonomic nerve development contributes to prostate cancer progression. Science 341, 1236361.
Malladi, S., Macalinao, D.G., Jin, X., He, L., Basnet, H., Zou, Y., de Stanchina, E., Massague, J., 2016. Metastatic latency and immune evasion through autocrine inhibition of WNT. Cell 165, 45–60.
Martin, C.K., Tannehill-Gregg, S.H., Wolfe, T.D., Rosol, T.J., 2011. Bone-invasive oral squamous cell carcinoma in cats: pathology and expression of parathyroid hormone-related protein. Vet. Pathol. 48, 302–312.
Matsumoto, T., Abe, M., 2011. TGF-beta-related mechanisms of bone destruction in multiple myeloma. Bone 48, 129–134.
McDonald, M.M., Fairfield, H., Falank, C., Reagan, M.R., 2016. Adipose, bone, and myeloma: contributions from the microenvironment. Calcif. Tissue Int. 100 (5), 433–448.

McDonald, M.M., Reagan, M.R., Youlten, S.E., Mohanty, S.T., Seckinger, A., Terry, R.L., Pettitt, J.A., Simic, M.K., Cheng, T.L., Morse, A., Le, L.M.T., Abi-Hanna, D., Kramer, I., Falank, C., Fairfield, H., Ghobrial, I.M., Baldock, P.A., Little, D.G., Kneissel, M., Vanderkerken, K., Bassett, J.H.D., Williams, G.R., Oyajobi, B.O., Hose, D., Phan, T.G., Croucher, P.I., 2017. Inhibiting the osteocyte-specific protein sclerostin increases bone mass and fracture resistance in multiple myeloma. Blood 129, 3452−3464.

McKeehan, W.L., Wang, F., Kan, M., 1998. The heparan sulfate-fibroblast growth factor family: diversity of structure and function. Prog. Nucleic Acid Res. Mol. Biol. 59, 135−176.

Menendez, J.A., Lupu, R., 2007. Fatty acid synthase and the lipogenic phenotype in cancer pathogenesis. Nat. Rev. Canc. 7, 763−777.

Michalski, M.N., Koh, A.J., Weidner, S., Roca, H., McCauley, L.K., 2016. Modulation of osteoblastic cell efferocytosis by bone marrow macrophages. J. Cell. Biochem. 117 (12), 2697−2706.

Millner, L.M., Linder, M.W., Valdes Jr., R., 2013. Circulating tumor cells: a review of present methods and the need to identify heterogeneous phenotypes. Ann. Clin. Lab. Sci. 43, 295−304.

Miyamoto, D.T., Zheng, Y., Wittner, B.S., Lee, R.J., Zhu, H., Broderick, K.T., Desai, R., Fox, D.B., Brannigan, B.W., Trautwein, J., Arora, K.S., Desai, N., Dahl, D.M., Sequist, L.V., Smith, M.R., Kapur, R., Wu, C.L., Shioda, T., Ramaswamy, S., Ting, D.T., Toner, M., Maheswaran, S., Haber, D.A., 2015. RNA-Seq of single prostate CTCs implicates noncanonical Wnt signaling in antiandrogen resistance. Science 349, 1351−1356.

Mohammad, K.S., Javelaud, D., Fournier, P.G., Niewolna, M., McKenna, C.R., Peng, X.H., Duong, V., Dunn, L.K., Mauviel, A., Guise, T.A., 2011. TGF-beta-RI kinase inhibitor SD-208 reduces the development and progression of melanoma bone metastases. Cancer Res. 71, 175−184.

Mohyeldin, A., Garzon-Muvdi, T., Quinones-Hinojosa, A., 2010. Oxygen in stem cell biology: a critical component of the stem cell niche. Cell Stem Cell 7, 150−161.

Monteiro, A.C., Leal, A.C., Goncalves-Silva, T., Mercadante, A.C., Kestelman, F., Chaves, S.B., Azevedo, R.B., Monteiro, J.P., Bonomo, A., 2013. T cells induce pre-metastatic osteolytic disease and help bone metastases establishment in a mouse model of metastatic breast cancer. PLoS One 8, e68171.

Morris, E.V., Edwards, C.M., 2016. Bone marrow adipose tissue: a new player in cancer metastasis to bone. Front. Endocrinol. 7, 90.

Morris, J.C., Tan, A.R., Olencki, T.E., Shapiro, G.I., Dezube, B.J., Reiss, M., Hsu, F.J., Berzofsky, J.A., Lawrence, D.P., 2014. Phase I study of GC1008 (fresolimumab): a human anti-transforming growth factor-beta (TGFbeta) monoclonal antibody in patients with advanced malignant melanoma or renal cell carcinoma. PLoS One 9, e90353.

Mostaghel, E.A., Marck, B.T., Plymate, S.R., Vessella, R.L., Balk, S., Matsumoto, A.M., Nelson, P.S., Montgomery, R.B., 2011. Resistance to CYP17A1 inhibition with abiraterone in castration-resistant prostate cancer: induction of steroidogenesis and androgen receptor splice variants. Clin. Cancer Res. 17, 5913−5925.

Mulcrone, P.L., Campbell, J.P., Clement-Demange, L., Anbinder, A.L., Merkel, A.R., Brekken, R.A., Sterling, J.A., Elefteriou, F., 2017. Skeletal colonization by breast cancer cells is stimulated by an osteoblast and beta2AR-dependent neo-angiogenic switch. J. Bone Miner. Res. 32, 1442−1454.

Mundy, G.R., 1997. Mechanisms of bone metastasis. Cancer 80, 1546−1556.

Mundy, G.R., 2002. Metastasis to bone: causes, consequences and therapeutic opportunities. Nat. Rev. Canc. 2, 584−593.

Mundy, G.R., DeMartino, S., Rowe, D.W., 1981. Collagen and collagen-derived fragments are chemotactic for tumor cells. J. Clin. Investig. 68, 1102−1105.

Murphy, T., Darby, S., Mathers, M.E., Gnanapragasam, V.J., 2010. Evidence for distinct alterations in the FGF axis in prostate cancer progression to an aggressive clinical phenotype. J. Pathol. 220, 452−460.

Nelson, J.B., Udan, M.S., Guruli, G., Pflug, B.R., 2005. Endothelin-1 inhibits apoptosis in prostate cancer. Neoplasia 7, 631−637.

Nyman, J.S., Merkel, A.R., Uppuganti, S., Nayak, B., Rowland, B., Makowski, A.J., Oyajobi, B.O., Sterling, J.A., 2016. Combined treatment with a transforming growth factor beta inhibitor (1D11) and bortezomib improves bone architecture in a mouse model of myeloma-induced bone disease. Bone 91, 81−91.

Orimo, A., Gupta, P.B., Sgroi, D.C., Arenzana-Seisdedos, F., Delaunay, T., Naeem, R., Carey, V.J., Richardson, A.L., Weinberg, R.A., 2005. Stromal fibroblasts present in invasive human breast carcinomas promote tumor growth and angiogenesis through elevated SDF-1/CXCL12 secretion. Cell 121, 335−348.

Osisami, M., Keller, E.T., 2013. Mechanisms of metastatic tumor dormancy. J. Clin. Med. 2, 136−150.

Owens, P., Polikowsky, H., Pickup, M.W., Gorska, A.E., Jovanovic, B., Shaw, A.K., Novitskiy, S.V., Hong, C.C., Moses, H.L., 2013. Bone Morphogenetic Proteins stimulate mammary fibroblasts to promote mammary carcinoma cell invasion. PLoS One 8, e67533.

Oyajobi, B.O., Franchin, G., Williams, P.J., Pulkrabek, D., Gupta, A., Munoz, S., Grubbs, B., Zhao, M., Chen, D., Sherry, B., Mundy, G.R., 2003. Dual effects of macrophage inflammatory protein-1alpha on osteolysis and tumor burden in the murine 5TGM1 model of myeloma bone disease. Blood 102, 311−319.

Page, J.M., Merkel, A.R., Ruppender, N.S., Guo, R., Dadwal, U.C., Cannonier, S., Basu, S., Guelcher, S.A., Sterling, J.A., 2015. Altering adsorbed proteins or cellular gene expression in bone-metastatic cancer cells affects PTHrP and Gli2 without altering cell growth. Data Brief 4, 440−446.

Page, J.M., Merkel, A.R., Ruppender, N.S., Guo, R., Dadwal, U.C., Cannonier, S.A., Basu, S., Guelcher, S.A., Sterling, J.A., 2015. Matrix rigidity regulates the transition of tumor cells to a bone-destructive phenotype through integrin beta3 and TGF-beta receptor type II. Biomaterials 64, 33−44.

Park, S.I., Soki, F.N., McCauley, L.K., 2011. Roles of bone marrow cells in skeletal metastases: no longer bystanders. Cancer Microenviron. 4, 237−246.

Park, S.I., Lee, C., Sadler, W.D., Koh, A.J., Jones, J., Seo, J.W., Soki, F.N., Cho, S.W., Daignault, S.D., McCauley, L.K., 2013. Parathyroid hormone-related protein drives a $CD11b^{+}Gr1^{+}$ cell-mediated positive feedback loop to support prostate cancer growth. Cancer Res. 73 (22), 6574−6583.

Park, H.J., Baek, K., Baek, J.H., Kim, H.R., 2015. The cooperation of CREB and NFAT is required for PTHrP-induced RANKL expression in mouse osteoblastic cells. J. Cell. Physiol. 230, 667−679.

Peinado, H., Lavotshkin, S., Lyden, D., 2011. The secreted factors responsible for pre-metastatic niche formation: old sayings and new thoughts. Semin. Canc. Biol. 21, 139–146.

Peinado, H., Zhang, H., Matei, I.R., Costa-Silva, B., Hoshino, A., Rodrigues, G., Psaila, B., Kaplan, R.N., Bromberg, J.F., Kang, Y., Bissell, M.J., Cox, T.R., Giaccia, A.J., Erler, J.T., Hiratsuka, S., Ghajar, C.M., Lyden, D., 2017. Pre-metastatic niches: organ-specific homes for metastases. Nat. Rev. Canc. 17, 302–317.

Pencik, J., Schlederer, M., Gruber, W., Unger, C., Walker, S.M., Chalaris, A., Marie, I.J., Hassler, M.R., Javaheri, T., Aksoy, O., Blayney, J.K., Prutsch, N., Skucha, A., Herac, M., Kramer, O.H., Mazal, P., Grebien, F., Egger, G., Poli, V., Mikulits, W., Eferl, R., Esterbauer, H., Kennedy, R., Fend, F., Scharpf, M., Braun, M., Perner, S., Levy, D.E., Malcolm, T., Turner, S.D., Haitel, A., Susani, M., Moazzami, A., Rose-John, S., Aberger, F., Merkel, O., Moriggl, R., Culig, Z., Dolznig, H., Kenner, L., 2015. STAT3 regulated ARF expression suppresses prostate cancer metastasis. Nat. Commun. 6, 7736.

Powers, C.J., McLeskey, S.W., Wellstein, A., 2000. Fibroblast growth factors, their receptors and signaling. Endocr. Relat. Cancer 7, 165–197.

Provenzano, P.P., Inman, D.R., Eliceiri, K.W., Keely, P.J., 2009. Matrix density-induced mechanoregulation of breast cell phenotype, signaling, and gene expression through a FAK-ERK linkage. Oncogene 28, 4326–4343.

Psaila, B., Lyden, D., 2009. The metastatic niche: adapting the foreign soil. Nat. Rev. Canc. 9, 285–293.

Qiao, B., Shui, W., Cai, L., Guo, S., Jiang, D., 2015. Human mesenchymal stem cells as delivery of osteoprotegerin gene: homing and therapeutic effect for osteosarcoma. Drug Des. Dev. Ther. 9, 969–976.

Ren, G., Zhao, X., Zhang, L., Zhang, J., L'Huillier, A., Ling, W., Roberts, A.I., Le, A.D., Shi, S., Shao, C., Shi, Y., 2010. Inflammatory cytokine-induced intercellular adhesion molecule-1 and vascular cell adhesion molecule-1 in mesenchymal stem cells are critical for immunosuppression. J. Immunol. 184, 2321–2328.

Richardson, P.G., Hideshima, T., Anderson, K.C., 2003. Bortezomib (PS-341): a novel, first-in-class proteasome inhibitor for the treatment of multiple myeloma and other cancers. Cancer Control 10, 361–369.

Robey, P.G., Young, M.F., Flanders, K.C., Roche, N.S., Kondaiah, P., Reddi, A.H., Termine, J.D., Sporn, M.B., Roberts, A.B., 1987. Osteoblasts synthesize and respond to transforming growth factor-type beta (TGF-beta) in vitro. J. Cell Biol. 105, 457–463.

Rojas, A., Liu, G., Coleman, I., Nelson, P.S., Zhang, M., Dash, R., Fisher, P.B., Plymate, S.R., Wu, J.D., 2011. IL-6 promotes prostate tumorigenesis and progression through autocrine cross-activation of IGF-IR. Oncogene 30, 2345–2355.

Ruppender, N.S., Merkel, A.R., Martin, T.J., Mundy, G.R., Sterling, J.A., Guelcher, S.A., 2010. Matrix rigidity induces osteolytic gene expression of metastatic breast cancer cells. PLoS One 5, e15451.

Saad, F., Lipton, A., Cook, R., Chen, Y.M., Smith, M., Coleman, R., 2007. Pathologic fractures correlate with reduced survival in patients with malignant bone disease. Cancer 110, 1860–1867.

Saftig, P., Hunziker, E., Wehmeyer, O., Jones, S., Boyde, A., Rommerskirch, W., Moritz, J.D., Schu, P., von Figura, K., 1998. Impaired osteoclastic bone resorption leads to osteopetrosis in cathepsin-K-deficient mice. Proc. Natl. Acad. Sci. U.S.A. 95, 13453–13458.

Salo, J., Lehenkari, P., Mulari, M., Metsikko, K., Vaananen, H.K., 1997. Removal of osteoclast bone resorption products by transcytosis. Science 276, 270–273.

San Martin, R., Pathak, R., Jain, A., Jung, S.Y., Hilsenbeck, S.G., Pina-Barba, M.C., Sikora, A.G., Pienta, K.J., Rowley, D.R., 2017. Tenascin-C and integrin alpha9 mediate interactions of prostate cancer with the bone microenvironment. Cancer Res. 77, 5977–5988.

Sawant, A., Deshane, J., Jules, J., Lee, C.M., Harris, B.A., Feng, X., Ponnazhagan, S., 2013. Myeloid-derived suppressor cells function as novel osteoclast progenitors enhancing bone loss in breast cancer. Cancer Res. 73, 672–682.

Schindl, M., Schoppmann, S.F., Samonigg, H., Hausmaninger, H., Kwasny, W., Gnant, M., Jakesz, R., Kubista, E., Birner, P., Oberhuber, G., Austrian, B., Colorectal Cancer Study, G., 2002. Overexpression of hypoxia-inducible factor 1alpha is associated with an unfavorable prognosis in lymph node-positive breast cancer. Clin. Cancer Res. 8, 1831–1837.

Schrijver, W., Suijkerbuijk, K.P.M., van Gils, C.H., van der Wall, E., Moelans, C.B., van Diest, P.J., 2018. Receptor conversion in distant breast cancer metastases: a systematic review and meta-analysis. J. Natl. Cancer Inst. 110 (6), 568–580.

Sharma, S., Xing, F., Liu, Y., Wu, K., Said, N., Pochampally, R., Shiozawa, Y., Lin, H.K., Balaji, K.C., Watabe, K., 2016. Secreted protein acidic and rich in cysteine (SPARC) mediates metastatic dormancy of prostate cancer in bone. J. Biol. Chem. 291, 19351–19363.

Shay, G., Lynch, C.C., Fingleton, B., 2015. Moving targets: emerging roles for MMPs in cancer progression and metastasis. Matrix Biol. 44–46, 200–206.

Shi, Y., Oury, F., Yadav, V.K., Wess, J., Liu, X.S., Guo, X.E., Murshed, M., Karsenty, G., 2010. Signaling through the M(3) muscarinic receptor favors bone mass accrual by decreasing sympathetic activity. Cell Metabol. 11, 231–238.

Shih, J.C., Chen, K., Ridd, M.J., 1999. Monoamine oxidase: from genes to behavior. Annu. Rev. Neurosci. 22, 197–217.

Shimoyama, A., Wada, M., Ikeda, F., Hata, K., Matsubara, T., Nifuji, A., Noda, M., Amano, K., Yamaguchi, A., Nishimura, R., Yoneda, T., 2007. Ihh/Gli2 signaling promotes osteoblast differentiation by regulating Runx2 expression and function. Mol. Biol. Cell 18, 2411–2418.

Shiozawa, Y., Havens, A.M., Jung, Y., Ziegler, A.M., Pedersen, E.A., Wang, J., Wang, J., Lu, G., Roodman, G.D., Loberg, R.D., Pienta, K.J., Taichman, R.S., 2008. Annexin II/annexin II receptor axis regulates adhesion, migration, homing, and growth of prostate cancer. J. Cell. Biochem. 105, 370–380.

Silbermann, R., Roodman, G.D., 2013. Myeloma bone disease: pathophysiology and management. J Bone Oncol 2, 59–69.

Smid, M., Wang, Y., Zhang, Y., Sieuwerts, A.M., Yu, J., Klijn, J.G., Foekens, J.A., Martens, J.W., 2008. Subtypes of breast cancer show preferential site of relapse. Cancer Res. 68, 3108–3114.

Soki, F.N., Cho, S.W., Kim, Y.W., Jones, J.D., Park, S.I., Koh, A.J., Entezami, P., Daignault-Newton, S., Pienta, K.J., Roca, H., McCauley, L.K., 2015. Bone marrow macrophages support prostate cancer growth in bone. Oncotarget 6, 35782–35796.

Sottnik, J.L., Dai, J., Zhang, H., Campbell, B., Keller, E.T., 2015. Tumor-induced pressure in the bone microenvironment causes osteocytes to promote the growth of prostate cancer bone metastases. Cancer Res. 75, 2151–2158.

Spencer, J.A., Ferraro, F., Roussakis, E., Klein, A., Wu, J., Runnels, J.M., Zaher, W., Mortensen, L.J., Alt, C., Turcotte, R., Yusuf, R., Cote, D., Vinogradov, S.A., Scadden, D.T., Lin, C.P., 2014. Direct measurement of local oxygen concentration in the bone marrow of live animals. Nature 508, 269–273.

Sterling, J.A., Oyajobi, B.O., Grubbs, B., Padalecki, S.S., Munoz, S.A., Gupta, A., Story, B., Zhao, M., Mundy, G.R., 2006. The hedgehog signaling molecule Gli2 induces parathyroid hormone-related peptide expression and osteolysis in metastatic human breast cancer cells. Cancer Res. 66, 7548–7553.

Sterling, J.A., Edwards, J.R., Martin, T.J., Mundy, G.R., 2011. Advances in the biology of bone metastasis: how the skeleton affects tumor behavior. Bone 48, 6–15.

Sun, Y.X., Schneider, A., Jung, Y., Wang, J., Dai, J., Cook, K., Osman, N.I., Koh-Paige, A.J., Shim, H., Pienta, K.J., Keller, E.T., McCauley, L.K., Taichman, R.S., 2005. Skeletal localization and neutralization of the SDF-1(CXCL12)/CXCR4 axis blocks prostate cancer metastasis and growth in osseous sites in vivo. J. Bone Miner. Res. 20, 318–329.

Sun, X., Cheng, G., Hao, M., Zheng, J., Zhou, X., Zhang, J., Taichman, R.S., Pienta, K.J., Wang, J., 2010. CXCL12/CXCR4/CXCR7 chemokine axis and cancer progression. Cancer Metastasis Rev. 29, 709–722.

Tai, H.C., Chang, A.C., Yu, H.J., Huang, C.Y., Tsai, Y.C., Lai, Y.W., Sun, H.L., Tang, C.H., Wang, S.W., 2014. Osteoblast-derived WNT-induced secreted protein 1 increases VCAM-1 expression and enhances prostate cancer metastasis by down-regulating miR-126. Oncotarget 5, 7589–7598.

Taichman, R.S., Cooper, C., Keller, E.T., Pienta, K.J., Taichman, N.S., McCauley, L.K., 2002. Use of the stromal cell-derived factor-1/CXCR4 pathway in prostate cancer metastasis to bone. Cancer Res. 62, 1832–1837.

Takayama, Y., Mori, T., Nomura, T., Shibahara, T., Sakamoto, M., 2010. Parathyroid-related protein plays a critical role in bone invasion by oral squamous cell carcinoma. Int. J. Oncol. 36, 1387–1394.

Terpos, E., Berenson, J., Raje, N., Roodman, G.D., 2014. Management of bone disease in multiple myeloma. Expert Rev. Hematol. 7, 113–125.

Terpos, E., Confavreux, C.B., Clezardin, P., 2015. Bone antiresorptive agents in the treatment of bone metastases associated with solid tumours or multiple myeloma. Bonekey Rep. 4, 744.

Teti, A., Migliaccio, S., Baron, R., 2002. The role of the alphaVbeta3 integrin in the development of osteolytic bone metastases: a pharmacological target for alternative therapy? Calcif. Tissue Int. 71, 293–299.

Thiele, S., Rachner, T.D., Rauner, M., Hofbauer, L.C., 2016. WNT5A and its receptors in the bone-cancer dialogue. J. Bone Miner. Res. 31, 1488–1496.

Togo, S., Polanska, U.M., Horimoto, Y., Orimo, A., 2013. Carcinoma-associated fibroblasts are a promising therapeutic target. Cancers 5, 149–169.

True, L., Coleman, I., Hawley, S., Huang, C.Y., Gifford, D., Coleman, R., Beer, T.M., Gelmann, E., Datta, M., Mostaghel, E., Knudsen, B., Lange, P., Vessella, R., Lin, D., Hood, L., Nelson, P.S., 2006. A molecular correlate to the Gleason grading system for prostate adenocarcinoma. Proc. Natl. Acad. Sci. U.S.A. 103, 10991–10996.

Valta, M.P., Hentunen, T., Qu, Q., Valve, E.M., Harjula, A., Seppanen, J.A., Vaananen, H.K., Harkonen, P.L., 2006. Regulation of osteoblast differentiation: a novel function for fibroblast growth factor 8. Endocrinology 147, 2171–2182.

Valta, M.P., Tuomela, J., Bjartell, A., Valve, E., Vaananen, H.K., Harkonen, P., 2008. FGF-8 is involved in bone metastasis of prostate cancer. Int. J. Cancer 123, 22–31.

Vanderburgh, J.P., Fernando, S.J., Merkel, A.R., Sterling, J.A., Guelcher, S.A., 2017. Fabrication of trabecular bone-templated tissue-engineered constructs by 3D inkjet printing. Adv. Healthc. Mater. 6 (22).

Wan, X., Corn, P.G., Yang, J., Palanisamy, N., Starbuck, M.W., Efstathiou, E., Li Ning Tapia, E.M., Zurita, A.J., Aparicio, A., Ravoori, M.K., Vazquez, E.S., Robinson, D.R., Wu, Y.M., Cao, X., Iyer, M.K., McKeehan, W., Kundra, V., Wang, F., Troncoso, P., Chinnaiyan, A.M., Logothetis, C.J., Navone, N.M., 2014. Prostate cancer cell-stromal cell crosstalk via FGFR1 mediates antitumor activity of dovitinib in bone metastases. Sci. Transl. Med. 6, 252ra122.

Wang, J., Loberg, R., Taichman, R.S., 2006. The pivotal role of CXCL12 (SDF-1)/CXCR4 axis in bone metastasis. Cancer Metastasis Rev. 25, 573–587.

Wang, J., Shiozawa, Y., Wang, J., Wang, Y., Jung, Y., Pienta, K.J., Mehra, R., Loberg, R., Taichman, R.S., 2008. The role of CXCR7/RDC1 as a chemokine receptor for CXCL12/SDF-1 in prostate cancer. J. Biol. Chem. 283, 4283–4294.

Wang, L., Dehm, S.M., Hillman, D.W., Sicotte, H., Tan, W., Gormley, M., Bhargava, V., Jimenez, R., Xie, F., Yin, P., Qin, S., Quevedo, F., Costello, B.A., Pitot, H.C., Ho, T., Bryce, A.H., Ye, Z., Li, Y., Eiken, P., Vedell, P.T., Barman, P., McMenomy, B.P., Atwell, T.D., Carlson, R.E., Ellingson, M., Eckloff, B., Qin, R., Ou, F., Hart, S.N., Huang, H., Jen, J., Wieben, E.D., Kalari, K.R., Weinshilboum, R.M., Wang, L., Kohli, M., 2017. A prospective genome-wide study of prostate cancer metastases reveals association of Wnt pathway activation and increased cell cycle proliferation with primary resistance to abiraterone acetate-prednisone. Ann. Oncol. 29 (2), 352–360.

Waning, D.L., Mohammad, K.S., Reiken, S., Xie, W., Andersson, D.C., John, S., Chiechi, A., Wright, L.E., Umanskaya, A., Niewolna, M., Trivedi, T., Charkhzarrin, S., Khatiwada, P., Wronska, A., Haynes, A., Benassi, M.S., Witzmann, F.A., Zhen, G., Wang, X., Cao, X., Roodman, G.D., Marks, A.R., Guise, T.A., 2015. Excess TGF-beta mediates muscle weakness associated with bone metastases in mice. Nat. Med. 21, 1262–1271.

Webber, J., Steadman, R., Mason, M.D., Tabi, Z., Clayton, A., 2010. Cancer exosomes trigger fibroblast to myofibroblast differentiation. Cancer Res. 70, 9621–9630.

Weilbaecher, K.N., Guise, T.A., McCauley, L.K., 2011. Cancer to bone: a fatal attraction. Nat. Rev. Canc. 11, 411–425.

Wu, J.B., Shao, C., Li, X., Li, Q., Hu, P., Shi, C., Li, Y., Chen, Y.T., Yin, F., Liao, C.P., Stiles, B.L., Zhau, H.E., Shih, J.C., Chung, L.W., 2014. Monoamine oxidase A mediates prostate tumorigenesis and cancer metastasis. J. Clin. Investig. 124, 2891–2908.

Wu, X., Baig, A., Kasymjanova, G., Kafi, K., Holcroft, C., Mekouar, H., Carbonneau, A., Bahoric, B., Sultanem, K., Muanza, T., 2016. Pattern of local recurrence and distant metastasis in breast cancer by molecular subtype. Cureus 8, e924.

Wu, J.B., Yin, L., Shi, C., Li, Q., Duan, P., Huang, J.M., Liu, C., Wang, F., Lewis, M., Wang, Y., Lin, T.P., Pan, C.C., Posadas, E.M., Zhau, H.E., Chung, L.W., 2017. MAOA-dependent activation of shh-IL6-RANKL signaling network promotes prostate cancer metastasis by engaging tumor-stromal cell interactions. Cancer Cell 31, 368–382.

Yan, M., Wang, L., Zuo, H., Zhang, Z., Chen, W., Mao, L., Zhang, P., 2011. HH/GLI signalling as a new therapeutic target for patients with oral squamous cell carcinoma. Oral Oncol. 47, 504–509.

Yang, L., DeBusk, L.M., Fukuda, K., Fingleton, B., Green-Jarvis, B., Shyr, Y., Matrisian, L.M., Carbone, D.P., Lin, P.C., 2004. Expansion of myeloid immune suppressor Gr+CD11b+ cells in tumor-bearing host directly promotes tumor angiogenesis. Cancer Cell 6, 409–421.

Yang, S., Zhong, C., Frenkel, B., Reddi, A.H., Roy-Burman, P., 2005. Diverse biological effect and Smad signaling of bone morphogenetic protein 7 in prostate tumor cells. Cancer Res. 65, 5769–5777.

Yang, L., Huang, J., Ren, X., Gorska, A.E., Chytil, A., Aakre, M., Carbone, D.P., Matrisian, L.M., Richmond, A., Lin, P.C., Moses, H.L., 2008. Abrogation of TGF beta signaling in mammary carcinomas recruits Gr-1^{+}CD11b^{+} myeloid cells that promote metastasis. Cancer Cell 13, 23–35.

Yang, M.H., Wu, M.Z., Chiou, S.H., Chen, P.M., Chang, S.Y., Liu, C.J., Teng, S.C., Wu, K.J., 2008. Direct regulation of TWIST by HIF-1alpha promotes metastasis. Nat. Cell Biol. 10, 295–305.

Ye, L., Lewis-Russell, J.M., Davies, G., Sanders, A.J., Kynaston, H., Jiang, W.G., 2007. Hepatocyte growth factor up-regulates the expression of the bone morphogenetic protein (BMP) receptors, BMPR-IB and BMPR-II, in human prostate cancer cells. Int. J. Oncol. 30, 521–529.

Yin, J.J., Selander, K., Chirgwin, J.M., Dallas, M., Grubbs, B.G., Wieser, R., Massague, J., Mundy, G.R., Guise, T.A., 1999. TGF-beta signaling blockade inhibits PTHrP secretion by breast cancer cells and bone metastases development. J. Clin. Investig. 103, 197–206.

Yin, J.J., Mohammad, K.S., Kakonen, S.M., Harris, S., Wu-Wong, J.R., Wessale, J.L., Padley, R.J., Garrett, I.R., Chirgwin, J.M., Guise, T.A., 2003. A causal role for endothelin-1 in the pathogenesis of osteoblastic bone metastases. Proc. Natl. Acad. Sci. U.S.A. 100, 10954–10959.

Yu, C., Shiozawa, Y., Taichman, R.S., McCauley, L.K., Pienta, K., Keller, E., 2012. Prostate cancer and parasitism of the bone hematopoietic stem cell niche. Crit. Rev. Eukaryot. Gene Expr. 22, 131–148.

Yuen, H.F., Kwok, W.K., Chan, K.K., Chua, C.W., Chan, Y.P., Chu, Y.Y., Wong, Y.C., Wang, X., Chan, K.W., 2008. TWIST modulates prostate cancer cell-mediated bone cell activity and is upregulated by osteogenic induction. Carcinogenesis 29, 1509–1518.

Yumoto, K., Eber, M.R., Wang, J., Cackowski, F.C., Decker, A.M., Lee, E., Nobre, A.R., Aguirre-Ghiso, J.A., Jung, Y., Taichman, R.S., 2016. Axl is required for TGF-beta2-induced dormancy of prostate cancer cells in the bone marrow. Sci. Rep. 6, 36520.

Zadra, G., Photopoulos, C., Loda, M., 2013. The fat side of prostate cancer. Biochim. Biophys. Acta 1831, 1518–1532.

Zahm, A.M., Bucaro, M.A., Ayyaswamy, P.S., Srinivas, V., Shapiro, I.M., Adams, C.S., Mukundakrishnan, K., 2010. Numerical modeling of oxygen distributions in cortical and cancellous bone: oxygen availability governs osteonal and trabecular dimensions. Am. J. Physiol. Cell Physiol. 299, C922–C929.

Zhang, K., Kim, S., Cremasco, V., Hirbe, A.C., Collins, L., Piwnica-Worms, D., Novack, D.V., Weilbaecher, K., Faccio, R., 2011. CD8^{+} T cells regulate bone tumor burden independent of osteoclast resorption. Cancer Res. 71, 4799–4808.

Zhang, X.H., Giuliano, M., Trivedi, M.V., Schiff, R., Osborne, C.K., 2013. Metastasis dormancy in estrogen receptor-positive breast cancer. Clin. Cancer Res. 19, 6389–6397.

Zhang, X.H., Jin, X., Malladi, S., Zou, Y., Wen, Y.H., Brogi, E., Smid, M., Foekens, J.A., Massague, J., 2013. Selection of bone metastasis seeds by mesenchymal signals in the primary tumor stroma. Cell 154, 1060–1073.

Zheng, D., Decker, K.F., Zhou, T., Chen, J., Qi, Z., Jacobs, K., Weilbaecher, K.N., Corey, E., Long, F., Jia, L., 2013. Role of WNT7B-induced non-canonical pathway in advanced prostate cancer. Mol. Canc. Res. 11, 482–493.

Zini, A., Czerninski, R., Sgan-Cohen, H.D., 2010. Oral cancer over four decades: epidemiology, trends, histology, and survival by anatomical sites. J. Oral Pathol. Med. 39, 299–305.

Chapter 56

Genetic regulation of parathyroid gland development

Fadil M. Hannan[1,2] **and Rajesh V. Thakker**[2]

[1]Department of Musculoskeletal Biology, Institute of Ageing and Chronic Disease, Faculty of Health & Life Sciences, University of Liverpool, Liverpool, United Kingdom; [2]Academic Endocrine Unit, Radcliffe Department of Medicine, University of Oxford, Oxford Centre for Diabetes, Endocrinology and Metabolism (OCDEM), Churchill Hospital, Oxford, United Kingdom

Chapter outline

Congenital anomalies of parathyroid gland development, which lead to hypoparathyroidism, are common and occur in more than 1 in 4000 births. The four human parathyroid glands develop from transient bilateral outpocketings of the pharyngeal endoderm, which are referred to as the pharyngeal pouches. There are four pairs of pharyngeal pouches; the superior parathyroid glands develop from the fourth pharyngeal pouches, which are the most caudal, while the inferior parathyroid glands together with the thymus develop from the third pharyngeal pouches. The pharyngeal pouches together with the branchial arches and grooves form the branchial apparatus that gives rise to a number of structures that include the face, jaws, oral cavity, neck, pharynx, larynx, ear, aortic arch, tonsils, thyroid, parathyroids, thymus, ultimobranchial body that results in calcitonin-producing cells, carotid glomus, and the epibranchial placodes that contribute to the facial, glossopharyngeal, and vagus nerves (Grigorieva and Thakker, 2011). Thus, developmental abnormalities of the branchial apparatus and pharyngeal pouches may lead to hypoparathyroidism that may be part of a complex congenital defect, as for example in the DiGeorge syndrome or a solitary endocrinopathy which is called *isolated* or *idiopathic* hypoparathyroidism. In addition, hypoparathyroidism may occur in association with other developmental anomalies involving dysmorphic features, sensorineural deafness, lymphoedema, nephropathy, and growth retardation (Table 56.1). The molecular genetic basis for such forms of hypoparathyroidism has been investigated and this has helped to elucidate further the mechanisms involved in the genetic regulation of parathyroid gland development. This chapter will focus on those forms of hypoparathyroidism that often present in early life, as these are likely to be associated with parathyroid gland agenesis or

Principles of Bone Biology. https://doi.org/10.1016/B978-0-12-814841-9.00056-7

TABLE 56.1 Inherited forms of hypoparathyroidism and their chromosomal locations.

Disease	Inheritance	Gene	Chromosomal location
Isolated hypoparathyroidism			
Autosomal dominant hypoparathyroidism	Autosomal dominant	GCM2, PTH	6p24.2, 11p15
Autosomal recessive hypoparathyroidism	Autosomal recessive	GCM2, PTH, AIRE	6p24.2, 11p15, 21q22.3
X-linked recessive hypoparathyroidism	X-linked recessive	SOX3[a], FHL1[a]	Xq26-27, Xq26.3
Autosomal dominant hypocalcemia			
Autosomal dominant hypocalcemia type 1	Autosomal dominant	CASR	3q21.1
Autosomal dominant hypocalcemia type 2	Autosomal dominant	GNA11	19p13.3
DiGeorge syndromes			
DiGeorge syndrome type 1	Autosomal dominant	TBX1	22q11.2
DiGeorge syndrome type 2	Autosomal dominant	NEBL[a]	10p13–14
CHARGE syndrome	Autosomal dominant	CHD7	8q12.1
Syndromes associated with deafness and/or renal anomalies			
HDR	Autosomal dominant	GATA3	10p15
Barakat syndrome	Autosomal recessive[a]	Unknown	Unknown
Nephropathy, nerve deafness	Autosomal dominant[a]	Unknown	Unknown
Nerve deafness without renal dysplasia	Autosomal dominant	Unknown	Unknown
Lymphedema, hypoparathyroidism, nephropathy, mitral valve prolapse, and brachytelephalangy	Autosomal recessive[a]	Unknown	Unknown
Autoimmune polyglandular syndrome type 1	Autosomal recessive	AIRE	21q22.3
Mitochondrial syndromes			
Kearns-Sayre syndrome	Maternal	Mitochondrial genome	-
MELAS	Maternal	Mitochondrial genome	-
MTP deficiency	Autosomal recessive	HADHB	2p23
Syndromes associated with growth failure/dwarfism			
Kenny–Caffey syndrome type 1	Autosomal recessive	TBCE	1q42.3
Sanjad–Sakati syndrome	Autosomal recessive	TBCE	1q42.3
Kenny–Caffey syndrome type 2	Autosomal dominant	FAM111A	11q12.1
Dubowitz syndrome	Autosomal recessive[a]	Unknown	Unknown

HDR, Hypoparathyroidism, deafness, and renal anomalies; MELAS, Mitochondrial encephalopathy, stroke like episodes and lactic acidosis; MTP, Mitochondrial trifunctional protein.
[a]*Most likely gene (or inheritance) shown.*

hypoplasia, congenital deficiency of parathyroid hormone (PTH), or early destruction of the parathyroids (Table 56.1). The hypoparathyroidism in these forms is characterized by hypocalcemia and hyperphosphatemia due to a deficiency in PTH secretion (Mannstadt et al., 2017).

Complex syndromes associated with hypoparathyroidism

Hypoparathyroidism may occur as part of a complex syndrome that may be associated with either a congenital developmental anomaly or an autoimmune syndrome (Mannstadt et al., 2017). The congenital developmental anomalies associated with hypoparathyroidism include the DiGeorge, HDR (hypoparathyroidism, deafness, and renal anomalies), Kenny−Caffey, and Barakat syndromes as well as syndromes associated with either lymphoedema or dysmorphic features and growth failure (Table 56.1).

DiGeorge syndrome

Clinical features and genetic abnormalities

Patients with DiGeorge syndrome (DGS) typically suffer from hypoparathyroidism, immunodeficiency, cardiac outflow tract malformations, facial dysmorphia, and palatal dysfunction (Kobrynski and Sullivan, 2007). DGS has been reported in up to 60% of children with familial or idiopathic forms of hypoparathyroidism (Kim et al., 2015) and has a wide spectrum of severity. Most commonly, hypoparathyroidism associated with DGS presents in the neonatal period with marked hypocalcemia, which may cause laryngospasm or seizures (Hieronimus et al., 2006). However, the hypoparathyroidism may be transient and characterized by serum calcium concentrations that normalize during infancy and early childhood. Some individuals with DGS may only develop hypocalcemic symptoms in adolescence or adulthood (Hieronimus et al., 2006; Nakada et al., 2013). The disorder arises from a congenital failure in the development of the derivatives of the third and fourth pharyngeal pouches with resulting absence or hypoplasia of the parathyroids and thymus. Most cases of DGS are sporadic, but an autosomal dominant inheritance of DGS has been observed in up to 28% of cases (Kobrynski and Sullivan, 2007), and an association between the syndrome and an unbalanced translocation and deletions involving 22q11.2 have also been reported (Scambler et al., 1991), and this is referred to as DGS type 1 (DGS1). Mapping studies of the DGS1 deleted region on chromosome 22q11.2 defined a 250−3000 kb critical region (Gong et al., 1996; Scambler, 2000) that contained approximately 30 genes. Studies of DGS1 patients reported deletions of several genes (e.g., rnex40, nex2.2−nex 3, *UDF1L,* and *TBX1*) from the critical region (Augusseau et al., 1986; Budarf et al., 1995; Scambler et al., 1991; Yamagishi et al., 1999), and studies of transgenic mice deleted for such genes (e.g., *Udf1l*, *Hira,* and *Tbx1*) revealed developmental abnormalities of the pharyngeal arches (Jerome and Papaioannou, 2001; Lindsay et al., 2001). However, point mutations in DGS1 patients have only been detected in the *TBX1* gene (Yagi et al., 2003), and *TBX1* is now considered to be the gene causing DGS1 (Baldini, 2003). *TBX1* encodes a DNA binding transcriptional factor of the T-box family that regulates histone modification (Fulcoli et al., 2016) and is known to have an important role in vertebrate and invertebrate organogenesis and pattern formation. The *TBX1* gene is deleted in ∼96% of all DGS1 patients. Moreover, DNA sequence analysis of unrelated DGS1 patients who did not have deletions of chromosome 22q11.2, has revealed the occurrence of three heterozygous point mutations (Yagi et al., 2003). One of these mutations resulted in a frameshift with a premature truncation, while the other two were missense mutations (p.Phe148Tyr and p.Gly310Ser). All of these patients had the complete pharyngeal phenotype but did not have mental retardation or learning difficulties. These disease-causing mutations may have paradoxical effects on TBX1 function. Thus, while a DGS-associated truncating (c.1223delC) *TBX1* mutation has been shown to impair transcriptional activation in vitro consistent with a loss of function, disease-causing missense *TBX1* mutations may in contrast increase transcriptional activation, suggestive of a gain of function (Zweier et al., 2007). Interestingly, mice with deletion of *Tbx1* have a phenotype similar to that of DGS1 patients (Jerome and Papaioannou, 2001). Thus, *Tbx1*-null mutant-mice ($Tbx1^{-/-}$) had all the developmental anomalies of DGS1 (i.e., thymic and parathyroid hypoplasia; abnormal facial structures and cleft palate; skeletal defects; and cardiac outflow tract abnormalities), while Tbx1 haploinsufficiency in mutant mice ($Tbx1^{+/-}$) was associated only with defects of the fourth branchial pouch (i.e., cardiac outflow tract abnormalities). The basis of the phenotypic differences between DGS1 patients, who are heterozygous, and the $Tbx1^{+/-}$ mice remains to be elucidated. It is plausible that Tbx1 dosage together with the downstream genes that are regulated by Tbx1 could provide an explanation, but the roles of these putative genes in DGS1 remains to be elucidated. In some patients, deletions of another locus on chromosome 10p has been observed in association with DGS (Monaco et al., 1991), and this is referred to as DGS type 2 (DGS2). Patients with DGS2 may have a more severe phenotype than DGS1, and present with marked cognitive impairment in addition to cardiac abnormalities and

immune deficiency (Lindstrand et al., 2010; Van Esch et al., 1999). The nebulette, or *NEBL*, gene has been reported to be heterozygous deleted in cell lines from two female DGS2 patients and thus may be the responsible gene (Villanueva et al., 2002). Moreover, some patients presenting with the clinical manifestations of DGS, such as thymic aplasia and hypoparathyroidism, may additionally have features of the CHARGE syndrome, which is characterized by the combined occurrence of coloboma, heart abnormalities, choanal atresia, retardation of growth and/or development, and genitourinary and/or ear anomalies (Inoue et al., 2010). Such patients with overlapping features of DGS and the CHARGE syndrome have been revealed to harbor heterozygous mutations in the *CHD7* gene on chromosome 8q12.1, which encodes the chromodomain helicase DNA binding protein 7 (Inoue et al., 2010). The *CHD7* gene is expressed within the pharyngeal ectoderm, and *Chd7*-haploinsufficient mice have been noted to have thymic aplasia (Randall et al., 2009). These findings highlight a role for CHD7 in pharyngeal region development during embryogenesis.

Mouse models developing features of DiGeorge syndrome reveal roles of Hox and Pax genes in parathyroid and thymus development

In the mouse, the parathyroids develop with the thymus from common primordia that arise from the third pharyngeal pouch endoderm (Grigorieva and Thakker, 2011). The molecular mechanisms that regulate parathyroid/thymus organogenesis from the pharyngeal pouch endoderm have been investigated using knockout models, and the roles of transcription regulators e.g., Hoxa3, Pax1, Pax9, Eyal, Six1 and Six4 defined (Manley and Capecchi, 1998; Xu et al., 2002; Zou et al., 2006). The roles of *Hoxa3* and *Pax* genes will be briefly reviewed as they form a genetic pathway with glial cells missing homolog 2 (*Gcm2*) (see below) that regulates parathyroid organogenesis (Fig. 56.1).

Homeobox (Hox) genes. The *Hox* genes are a group of evolutionarily conserved genes that contain a 180 bp motif, which encodes a 60 amino acid DNA-binding domain called the homeodomain (Quinonez and Innis, 2014). These genes are involved in early embryogenesis and determine the body plans of invertebrates such as *Drosophila* by specifying the identity of cells within each parasegment along the main anterior–posterior body axis (Deschamps, 2007). The role of the *Hox* genes in mammals remains to be fully elucidated, and recent studies indicate that these genes may not regulate the overall layout of the vertebrate body plan, but instead mediate region-specific patterning and development such as with limb morphogenesis (Mallo, 2018). In mammals, *Hox* genes are distributed in the genome in four separate clusters (Hox A, B, C, and D), which may have arisen during chordate evolution as the result of two duplications of chromosomal segments (Kappen et al., 1989; Manley and Capecchi, 1998). Each *Hox* cluster contains up to 13 genes, which are numbered 1–13 based on their position in the cluster as well as their homology with genes in other *Hox* clusters (Mallo, 2018). In order to determine the genetic function of some *Hox* genes, mouse knockout models have been generated. Disruption of *Hoxa3* resulted in an abnormal phenotype with similarities to DGS (Chisaka and Capecchi, 1991; Manley and Capecchi, 1995). Null mutant mice ($Hoxa3^{-/-}$) died in the neonatal period and were found to be lacking the thymus and parathyroids because of a failure to initiate the formation of the parathyroid–thymus primordia. These $Hoxa3^{-/-}$ mice also had defects

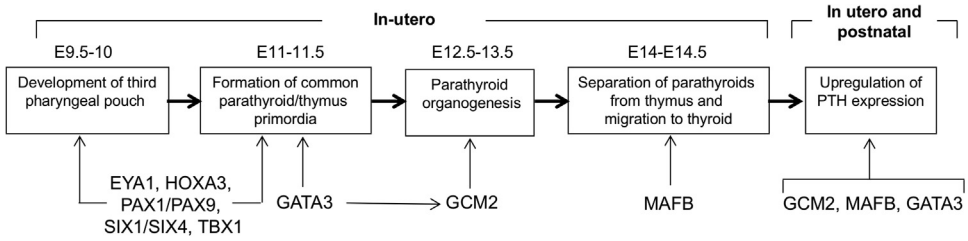

FIGURE 56.1 Transcription factors involved in parathyroid gland development and function. Mouse model studies have shown that a network of transcription factors such as the EYA1, HOXA3, TBX1, PAX1/PAX9, SIX1/SIX4, and GATA3 proteins mediate patterning of the third pharyngeal pouch and formation of the common parathyroid-thymus primordia (Grigorieva and Thakker, 2011; Kamitani-Kawamoto et al., 2011). These transcription factors act in a spatiotemporal manner; for example, TBX1 is expressed in the pharyngeal endoderm and required for the development of the third pharyngeal pouch (Jerome and Papaioannou, 2001); whereas GATA3 is expressed in the common parathyroid-thymus primordia and mediates the differentiation and survival of parathyroid and thymus progenitor cells (Grigorieva et al., 2010; Grigorieva and Thakker, 2011). Moreover, GATA3 regulates the expression of GCM2, which is expressed in the parathyroid domain of the common primordia and mediates the initial stages of parathyroid organogenesis (Grigorieva et al., 2010; Grigorieva and Thakker, 2011). MAFB is also expressed in the parathyroid domain and facilitates the separation of the parathyroid glands from the thymus, and also the migration of the parathyroids toward the thyroid (Kamitani-Kawamoto et al., 2011). GATA3, GCM2 and MAFB also act synergistically to upregulate PTH expression (Han et al., 2015). As the expression of GATA3, GCM2, and MAFB persists into adulthood, it is likely that these transcription factors are required for the postnatal expression of PTH (Han et al., 2015). E = embryonic day. *Adapted from Mannstadt et al.* Nat Rev Dis Primer, *3, 17055.*

of the heart and arteries, craniofacial abnormalities, and a reduction in the mass of the thyroid and submaxillary tissues. The *Hoxa3*$^{+/-}$ mice were phenotypically normal. Thus, although the *Hoxa3*$^{-/-}$ mice clearly indicated an important role for the *Hoxa3* gene in parathyroid and thymus organogenesis, there were nevertheless important differences between this mouse, having an autosomal recessive syndrome, and DGS, which is an autosomal dominant trait. Studies involving mice with an endoderm-specific and/or neural crest cell-specific ablation of *Hoxa3* have shown that *Hoxa3* deletion inhibited parathyroid gland development by impairing the expression of the parathyroid-specific *Gcm2* transcription factor (Chojnowski et al., 2014), which in turn leads to apoptosis of the embryonic parathyroid domain (Liu et al., 2007).

Paired box (Pax) genes. The paired box (*Pax*) genes comprise an evolutionarily conserved family of transcriptional factors that contain a highly conserved 128 amino acid DNA-binding domain, called the paired box (Relaix, 2015). Mammals have nine *Pax* genes, and these are expressed in a spatially and temporally restricted manner during embryonic development and play a key role in the patterning of the nervous system (Relaix, 2015). The Pax1, Pax3, Pax7, and Pax9 transcription factors have been shown to regulate multiple neural crest cell lineages. In particular, Pax1 and Pax9 are expressed in the endoderm-derived epithelium of the third and fourth pharyngeal pouches and play a role in the development of the thymus, parathyroid glands, and ultimobranchial bodies (Monsoro-Burq, 2015). Indeed, mice deficient in either Pax1 or Pax9 (i.e., *Pax1* $^{-/-}$ or *Pax9* $^{-/-}$) have congenital parathyroid and thymic defects (Peters et al., 1998; Su et al., 2001). Studies of double-knockout mice indicated that there is a genetic pathway that involves Hoxa3, Pax1 and Gcm2 (see below) in parathyroid development (Su et al., 2001). Thus, Gcm2 expression is absent in *Hoxa3*$^{-/-}$ mouse embryos that are 10.5 days postcoitum (dpc), reduced in *Pax1* $^{-/-}$ mouse embryos that are 11.5 dpc, and absent in *Hoxa3*$^{+/-}$*/Pax1* $^{-/-}$ mice at 11.5 dpc (Su et al., 2001). These studies have revealed that Hoxa3 is required for initiation of parathyroid organogenesis and for initial Gcm2 expression and that both Hoxa3 and Pax1 are required for Gcm2 expression. Failure of Gcm2 expression results in a lack of parathyroids; this is due to programmed cell death (apoptosis) of the parathyroid primordia at 12 dpc in mouse embryos (Liu et al., 2007; Su et al., 2001). Thus, there is an important transcription cascade involving Hoxa3, Pax1, and Gcm2 in the embryonic development of parathyroids.

Hypoparathyroidism, deafness, and renal anomalies syndrome

Clinical features and role of GATA3 mutations

The combined inheritance of HDR as an autosomal dominant trait was reported in one family in 1992 (Bilous et al., 1992). Patients had asymptomatic hypocalcemia with undetectable or inappropriately normal serum concentrations of PTH and normal brisk increases in serum cAMP in response to the infusion of PTH. The patients also had bilateral and symmetrical sensorineural deafness involving all frequencies. The renal abnormalities consisted mainly of bilateral cysts that compressed the glomeruli and tubules and led to renal impairment in some patients. Cytogenetic abnormalities were not detected, and abnormalities of the PTH gene were excluded (Bilous et al., 1992). However, cytogenetic abnormalities involving chromosome 10p14−10pter were identified in two unrelated patients with features consistent with HDR. These two patients suffered from hypoparathyroidism, deafness, and growth and mental retardation; one patient also had a solitary dysplastic kidney with vesicoureteral reflux and a uterus bicornis unicollis (Fryns et al., 1981), and the other patient, who had a complex reciprocal insertional translocation of chromosomes 10p and 8q, had cartilaginous exostoses (Van Esch et al., 1999). Neither of these patients had immunodeficiency or heart defects, which are key features of DGS2 (see previous), and further studies defined two nonoverlapping regions; thus, the DGS2 region was located on 10p13−p14 and HDR on 10p14−10pter. Deletion mapping studies in two other HDR patients further defined a critical 200-kb region that contained the *GATA3* gene (Van Esch et al., 2000). GATA3 belongs to a family of dual zinc-finger transcription factors involved in vertebrate embryonic development. DNA sequence analysis in other HDR patients identified mutations that resulted in a haploinsufficiency and loss of GATA3 function (Ali et al., 2007; Nesbit et al., 2004; Van Esch et al., 2000). To date, $>$ 50 different heterozygous germline *GATA3* abnormalities, which comprise point-mutations and whole gene deletions, have been reported (Adachi et al., 2006; Ali et al., 2007; Fukami et al., 2011; Gaynor et al., 2009; Mino et al., 2005; Muroya et al., 2001; Nesbit et al., 2004; Van Esch et al., 2000; Zahirieh et al., 2005). The majority ($>$ 75%) of these HDR-associated mutations are predicted to result in truncated forms of the GATA3 protein. Each proband and family will generally have its own unique mutation, and there appears to be no correlation with the underlying genetic defect and the phenotypic variation—e.g., the presence or absence of renal dysplasia. Over 90% of patients with two or three of the major clinical features of HDR syndrome—i.e., hypoparathyroidism, deafness, or renal abnormalities—have a *GATA3* mutation (Ali et al., 2007). The remaining 10% of HDR of patients who do not have a mutation of the *GATA3* coding region may harbor mutations in the regulatory sequences flanking the *GATA3* gene, or they may represent heterogeneity. The phenotypes of HDR patients with *GATA3* mutations appear to be similar to those without *GATA3* mutations (Ali et al., 2007).

The HDR-associated *GATA3* mutations are predicted to disrupt either one or both of the zinc finger domains (Nesbit et al., 2004). The C-terminal finger (ZnF2) of GATA proteins binds DNA, whereas the N-terminal finger (ZnF1) stabilizes this DNA binding and interacts with other zinc-finger proteins, such as friends of GATA (FOGs) (Svensson et al., 1999; Tevosian et al., 1999; Tsang et al., 1997). The functional consequences of these HDR-associated *GATA3* mutations have been assessed by electrophoretic mobility shift assays to detect alterations in DNA binding and by yeast two-hybrid assays to detect alterations in protein−protein interactions (Ali et al., 2007; Nesbit et al., 2004). These studies have revealed that HDR-associated mutations involving the GATA3 ZnF2 or the adjacent basic amino acids result in a loss of DNA binding to the consensus motif, GATA, that would be associated with the promoter of the gene being regulated by GATA3 (Ali et al., 2007; Nesbit et al., 2004; Van Esch et al., 2000). However, those HDR-associated mutations involving ZnF1 led to either a loss of interaction with FOG2 ZnFs or altered DNA-binding affinity (Ali et al., 2007; Nesbit et al., 2004). These findings are consistent with the proposed three-dimensional model of GATA3 ZnF1, which has separate DNA and protein-binding surfaces (Ali et al., 2007; Nesbit et al., 2004). Thus, HDR-associated *GATA3* mutations can be subdivided into two broad classes depending on whether they disrupt ZnF1 or ZnF2 and their subsequent effects on interactions with FOG2 and altered DNA binding, respectively.

Phenotype of the GATA3 knockout mouse model

The HDR phenotype is consistent with the expression pattern of GATA3 during human and mouse embryogenesis in the developing kidney, otic vesicle, and parathyroids. However, GATA3 is also expressed in the developing central nervous system (CNS) and the hematopoietic organs, and this suggests that GATA3 may have a more complex role. Indeed, studies of *Gata3*$^{+/-}$ and *Gata3*$^{-/-}$ mice have revealed important roles for *Gata3* in the development of the brain, spinal cord, peripheral auditory system, T cells, fetal liver hematopoiesis, and urogenital system (Pandolfi et al., 1995). *Gata3*$^{-/-}$ mice die between E11.5 and E12.5 (Pandolfi et al., 1995), but *Gata3*$^{+/-}$ mice are viable, appear to be normal with a normal life span, and are fertile (Pandolfi et al., 1995). However, *Gata3*$^{+/-}$ mice have hearing loss that commences in the early postnatal period, is progressive through adulthood, and is associated with cochlear abnormalities, which consist of a significant progressive morphological degeneration that starts with the outer hair cells at the apex and eventually involves all the inner hair cells, pillar cells, and nerve fibers (van der Wees et al., 2004; van Looij et al., 2006). *Gata3* loss also resulted in parathyroid abnormalities. Thus, *Gata3*$^{-/-}$ and *Gata3*$^{+/-}$ embryos lacked or had smaller parathyroid−thymus primordia, respectively, and the parathyroids of adult *Gata3*$^{+/-}$ mice did not enlarge or have an increased proliferation rate in response to hypocalcemia induced by a low-calcium/vitamin D diet (Grigorieva et al., 2010). Moreover, the adult *Gata3*$^{+/-}$ mice had an inadequate increase in plasma PTH in response to the induced hypocalcemia (Grigorieva et al., 2010). These findings in the *Gata3*$^{+/-}$ mice are consistent with the observed hypocalcemia that occurs in association with inappropriately normal or low plasma PTH concentrations in patients who have the HDR syndrome due to *GATA3* haploinsufficiency (Bilous et al., 1992; Van Esch et al., 2000).

Examination of *Gata3*$^{-/-}$ embryos has revealed a variety of abnormalities that include massive internal bleeding resulting in anemia, marked growth retardation, severe deformities of the brain and spinal cord, a hypopigmented retina, gross aberrations in fetal liver hematopoiesis, impaired T cell differentiation, and a retarded or missing lower jaw area (Grote et al., 2006, 2008; Lim et al., 2000; Pandolfi et al., 1995). These *Gata3*$^{-/-}$ mice had an anatomically normal sympathetic nervous system, yet the sympathetic ganglia lacked tyrosine hydroxylase and dopamine beta-hydroxylase, which are key enzymes that convert tyrosine to L-DOPA, and dopamine to noradrenaline, respectively, in the catecholamine synthesis pathway. Thus, the *Gata3*$^{-/-}$ mice lacked noradrenaline in the sympathetic neurons, and this contributed to early embryonic lethality (Lim et al., 2000). Feeding of catecholamine intermediates to pregnant dams helped to partially rescue the *Gata3*$^{-/-}$ embryos from E12.5 to E16.5 (Lim et al., 2000). These older, pharmacologically rescued *Gata3*$^{-/-}$ embryos showed abnormalities that could not be detected in the untreated mice (Lim et al., 2000). These late embryonic defects included thymic hypoplasia, a thin-walled ventricular septum, a poorly developed mandible, other developmental defects in structures derived from the cephalic neural crest cells, renal hypoplasia, a failure to form the metanephros, and an aberrant elongation of the nephric duct along the anteroposterior axis of the embryo (Grote et al., 2006, 2008; Lim et al., 2000). The defect of the nephric duct, which consisted of an abnormal morphogenesis and guidance in the developing kidney, was characterized by the loss of *Ret* expression that is an essential component of the glial-derived-nerve-factor signaling pathway involved in ureteric bud formation and nephric duct guidance (Grote et al., 2006). Thus, *Gata3* has a role in the differentiation of multiple cell lineages during embryogenesis as well as being a key regulator of nephric duct morphogenesis and guidance of the nephric duct in its caudal extension in the pro/mesonephric kidney (Grote et al., 2006; Lim et al., 2000).

Role of GATA3 in developmental pathogenesis

The mechanisms whereby GATA3 haploinsufficiency leads to the phenotypic features of the HDR syndrome remain to be elucidated. Important clues have been obtained from in vitro and in vivo studies of knockout mice. Indeed, the smaller size or absence of the parathyroids in the *Gata3*$^{+/-}$ and *Gata3*$^{-/-}$ embryos, respectively, was found to be associated with a markedly reduced number of *Gcm2*-expressing cells in the third pharyngeal pouch (Grigorieva et al., 2010), thereby indicating that GATA3 is likely to be critical for maintaining differentiation and subsequent survival of parathyroid and thymus progenitor cells. Furthermore, in vitro studies showed that GCM2 is transcriptionally regulated by GATA3 (Grigorieva et al., 2010) and that GATA3 acts synergistically with GCM2 and also the parathyroid MafB transcription factor, most likely by forming a transcriptional complex, to upregulate PTH gene expression (Fig. 56.1) (Grigorieva et al., 2010; Han et al., 2015). GATA3 also plays an essential role in determining T cell lineage during thymopoiesis (Hosoya et al., 2010). However, it is important to note that GATA3 haploinsufficiency in the HDR patients is not associated with immunodeficiency (Lichtner et al., 2000; Van Esch et al., 2000), indicating that either reduced amounts of GATA3 are sufficient for T cell development or that GATA1 and GATA2 may be able to compensate for the loss of GATA3. The urogenital defects of HDR patients and knockout mice have highlighted a role for GATA3 in the development of the kidney and nephric duct. In support of this, mouse embryos with conditional inactivation of Gata3 in the urogenital system have been shown to develop ectopic ureter budding that leads to renal dysplasia, duplex systems, and hydroureter (Grote et al., 2008). These studies have additionally demonstrated that renally expressed Gata3 acts downstream of beta-catenin but upstream of Ret to prevent ectopic uretic budding and premature differentiation of nephric duct cells (Grote et al., 2008). However, it is important to note that the altered renal morphogenesis is observed only in *Gata3*$^{-/-}$ mice and not in *Gata3*$^{+/-}$ mice, which unlike HDR patients who are also heterozygous for the GATA3 mutation, have normal kidneys (Pandolfi et al., 1995). Thus, there are important phenotypic differences between *Gata3*$^{+/-}$ mice and HDR patients, who are heterozygous for GATA3 mutations, and the mechanisms underlying these interspecies differences and the tissue-specific differences that confer susceptibility to GATA3 haploinsufficiency remain to be elucidated. In contrast to these renal differences between HDR patients and *Gata3*$^{+/-}$ mice, there are marked similarities in hearing loss (Bilous et al., 1992; Lichtner et al., 2000; van der Wees et al., 2004; van Looij et al., 2005). It has not been possible to perform detailed functional and histological studies on the auditory system of HDR patients, but such studies in *Gata3*$^{+/-}$ mice have revealed that the hearing loss is due to degeneration and loss of the outer hair cells that progressively involve the other types of hair cells and nerve fibers in the cochlea (van der Wees et al., 2004; van Looij et al., 2005). Moreover, studies involving mice with a conditional knockout of Gata3 specifically in the developing inner ear have shown that this transcription factor specifies the prosensory domain in the cochlea and enhances the survival of spiral ganglion neurons (Luo et al., 2013). However, the genes under transcriptional regulation of GATA3 in the cochlea remain to be identified. The morphological changes and genetic pathways involved in the parathyroids of HDR patients and Gata3 knockout mice also remain to be fully elucidated. Thus, although the HDR phenotype is consistent with the expression pattern of GATA3 during human and mouse embryogenesis in the developing kidney (ureteric bud, collecting duct system, and mesangial cells), otic vesicle, and parathyroids, much remains unknown regarding the underlying transcription pathways and the basis of the interspecies differences between *Gata3*$^{+/-}$ mice and HDR patients.

Kenny–Caffey and Sanjad–Sakati syndromes

Hypoparathyroidism has been reported to occur in over 50% of patients with Kenny–Caffey syndrome (KCS), which is associated with short stature, osteosclerosis and cortical thickening of the long bones, delayed closure of the anterior fontanel, basal ganglia calcification, nanophthalmos, and hyperopia (Bergada et al., 1988; Fanconi et al., 1986; Franceschini et al., 1992). KCS may be inherited as an autosomal recessive (KCS type 1, KCS1) or autosomal dominant (KCS type 2, KCS2) disorder (Mannstadt et al., 2017). Parathyroid tissue could not be found in a detailed postmortem examination of one KCS patient (Boynton et al., 1979), and this suggests that hypoparathyroidism may be due to an embryological defect of parathyroid development. In Sanjad–Sakati syndrome, hypoparathyroidism is associated with severe growth failure and dysmorphic features, and this has been reported in 12 patients from Saudi Arabia (Sanjad et al., 1991). Consanguinity was noted in 11 of the 12 patients' families, the majority of which originated from the Western province of Saudi Arabia. Sanjad–Sakati syndrome, which is inherited as an autosomal recessive disorder, has also been identified in families of Bedouin origin and homozygosity, and linkage disequilibrium studies have mapped this gene to chromosome 1q42-q43 (Parvari et al., 1998). Molecular genetic investigations have identified that mutations of the tubulin-specific chaperone (*TBCE*) are associated with KCS1 and Sanjad–Sakati syndromes (Parvari et al., 2002). *TBCE* encodes one of several chaperone proteins required for the proper folding of α-tubulin subunits and the formation of α-β tubulin

heterodimers (Parvari et al., 2002). Whole-exome sequencing has demonstrated KCS2 to be caused by heterozygous missense mutations of the family with sequence similarity 111 member A (*FAM111A*) gene, which encodes a protein with homology to trypsin-like peptidases (Isojima et al., 2014; Unger et al., 2013). The FAM111A protein has been revealed to modulate DNA replication and chromatin maturation, and may play a role in embryonic development (Alabert et al., 2014; Unger et al., 2013).

Additional familial syndromes

Single familial syndromes in which hypoparathyroidism is a component have been reported (Table 56.1). The inheritance of the disorder in some instances has been established, and molecular genetic analysis of the PTH gene has revealed no abnormalities. Thus, an association of hypoparathyroidism, renal insufficiency, and developmental delay has been reported in one Asian family in whom autosomal recessive inheritance of the disorder was established (Parkinson et al., 1993). An analysis of the PTH gene in this family revealed no abnormalities (Parkinson et al., 1993). The occurrence of hypoparathyroidism, nerve deafness, and a steroid-resistant nephrosis leading to renal failure, which has been referred to as the *Barakat syndrome* (Barakat et al., 1977), has been reported in four brothers from one family, and an association of hypoparathyroidism with congenital lymphoedema, nephropathy, mitral valve prolapse, and brachytelephalangy has been observed in two brothers from another family (Dahlberg et al., 1983). Molecular genetic studies have not been reported from these two families. Hypoparathyroidism has also been reported in association with Dubowitz syndrome, which is characterized by multiple congenital anomalies that include microcephaly and growth retardation (Lerman-Sagie et al., 1990).

Mitochondrial disorders associated with hypoparathyroidism

Hypoparathyroidism has been reported to occur in three disorders associated with mitochondrial dysfunction: the Kearns−Sayre syndrome (KSS), MELAS syndrome, and a mitochondrial trifunctional protein (MTP) deficiency syndrome. KSS is characterized by progressive external ophthalmoplegia and pigmentary retinopathy before the age of 20 years and is often associated with heart block or cardiomyopathy. MELAS syndrome consists of a childhood onset of mitochondrial encephalopathy, lactic acidosis, and stroke-like episodes. In addition, varying degrees of proximal myopathy can be seen in both conditions. Both the KSS and MELAS syndromes have been reported to occur with insulin-dependent diabetes mellitus and hypoparathyroidism (Moraes et al., 1989; Morten et al., 1993). A point mutation in the mitochondrial gene tRNA leucine has been reported in one patient with MELAS syndrome who also suffered from hypoparathyroidism and diabetes mellitus (Morten et al., 1993). Large deletions, consisting of 6741 and 6903 bp and involving $> 38\%$ of the mitochondrial genome, have been reported in other patients who suffered from KSS, hypoparathyroidism, and sensorineural deafness (Isotani et al., 1996). Rearrangements and duplication of mitochondrial DNA have also been reported in KSS (Abramowicz et al., 1996; Wilichowski et al., 1997). Mitochondrial trifunctional protein deficiency is a disorder of fatty-acid oxidation associated with peripheral neuropathy, pigmentary retinopathy, and acute fatty liver degeneration in pregnant women who carry an affected fetus. Hypoparathyroidism has been reported in three cases of MTP deficiency and presents in the infantile period in association with rhabdomyolysis and polyneuropathy (Naiki et al., 2014). Hypoparathyroidism caused by MTP deficiency has been associated with homozygous mutations of the *HADHB* gene, which encodes the β-subunit of the MTP protein, in two cases (Naiki et al., 2014). The role of mutations affecting the mitochondrial genome or *HADHB* gene in the etiology of hypoparathyroidism remains to be further elucidated, and as yet mouse models have not been generated to facilitate in vivo studies.

Pluriglandular autoimmune hypoparathyroidism

Hypoparathyroidism may occur in association with candidiasis and autoimmune Addison's disease, and the disorder has been referred to as either autoimmune polyendocrinopathy-candidiasis-ectodermal dystrophy (APECED) syndrome or autoimmune polyglandular syndrome type 1 (Husebye et al., 2018). This disorder has a high incidence in Finland (Perheentupa, 2002), and a genetic analysis of Finnish families indicated autosomal recessive inheritance of the disorder. In addition, the disorder has been reported to have a high incidence among Iranian Jews, although the occurrence of candidiasis was less common in this population (Zlotogora and Shapiro, 1992). Linkage studies of Finnish families mapped the APECED gene to chromosome 21q22.3 (Aaltonen et al., 1994). Further positional cloning approaches led to the isolation of a novel gene from chromosome 21q22.3. This gene, referred to as *AIRE* (autoimmune regulator), encodes a 545 amino acid protein that contains motifs suggestive of a transcriptional factor and includes two zinc-finger motifs, a

proline-rich region, and three LXXLL motifs (Finnish-German APECED Consortium, 1997; Nagamine et al., 1997). Greater than 100 APECED-causing *AIRE* mutations have been reported to date (Husebye et al., 2018), and four *AIRE* mutations have been shown to commonly occur in APECED families: p.Arg257Stop in Finnish, German, Swiss, British, Norwegian, and Northern Italian families; p.Arg139Stop in Sardinian families; p.Tyr85Cys in Iranian Jewish families; and a 13 bp deletion in exon 8 in British, Dutch, German, Norwegian, and Finnish families (Heino et al., 1999; Nagamine et al., 1997; Pearce et al., 1998; Wolff et al., 2007). Occasionally, biallelic *AIRE* mutations have been reported in patients with isolated hypoparathyroidism (Li et al., 2017; Sahoo et al., 2016). AIRE has been shown to regulate the elimination of organ-specific T cells in the thymus, and thus APECED is likely to be caused by a failure of this specialized mechanism for deleting forbidden T cells and establishing immunologic tolerance (Liston et al., 2003). AIRE also promotes the thymic development of regulatory T cells (Tregs) that express the Foxp3 transcription factor (Husebye et al., 2018; Malchow et al., 2013). These Foxp3+ Treg cells suppress autoreactive T cells and are considered to play a key role in the prevention of autoimmunity (Husebye et al., 2018; Leonard et al., 2017). Furthermore, the T cell−mediated loss of immune tolerance that occurs in APECED is associated with the presence of autoantibodies that target organ-specific antigens such as NACHT leucine-rich-repeat-protein 5, which is mainly expressed in the parathyroid glands (Alimohammadi et al., 2008). Greater than 95% of APECED patients also develop autoantibodies against cytokines such as type 1 interferons, and the detection of autoantibodies against type 1 interferons has been shown to have clinical utility for the diagnosis of APECED (Husebye et al., 2018; Orlova et al., 2017).

Isolated hypoparathyroidism

Isolated hypoparathyroidism may be inherited either as an autosomal dominant, autosomal recessive, or X-linked recessive disorder (Table 56.1) (Mannstadt et al., 2017). Some autosomal forms of hypoparathyroidism have been shown to be due to abnormalities of the *PTH* and *GCM2* genes.

Parathyroid hormone gene abnormalities

Parathyroid hormone gene structure and function

The *PTH* gene is located on chromosome 11p15 and consists of three exons, which are separated by two introns (Naylor et al., 1983). Exon 1 of the *PTH* gene is 85 bp in length and is untranslated (Fig. 56.2), whereas exons 2 and 3 encode the 115-amino-acid pre-pro-PTH peptide. Exon 2 is 90 bp in length and encodes the initiation codon (ATG), the prehormone sequence, and part of the prohormone sequence. Exon 3 is 612 bp in size and encodes the remainder of the prohormone sequence, the mature PTH peptide, and the 3′ untranslated region (Vasicek et al., 1983). The 5′ regulatory sequence of the human *PTH* gene contains a vitamin D response element 125 bp upstream of the transcription start site, which down-regulates PTH mRNA transcription in response to vitamin D receptor binding (Demay et al., 1992; Okazaki et al., 1988). *PTH* gene transcription (as well as PTH peptide secretion) is also dependent upon extracellular calcium and phosphate concentrations (Almaden et al., 1996; Naveh-Many et al., 1995; Slatopolsky et al., 1996), and this effect may potentially be mediated by the parathyroid-expressed calcium-sensing receptor (CaSR), as recent crystallographic studies have shown that the extracellular domain of the CaSR possesses binding sites for calcium and phosphate (Geng et al., 2016). The mature PTH peptide is secreted from the parathyroid chief cell as an 84-amino-acid peptide and this is regulated by the CaSR, which is also expressed in renal tubules. However, when the PTH mRNA is first translated, it is as a pre-pro-PTH peptide. The "pre" sequence consists of a 25-amino-acid signal peptide (leader sequence) responsible for directing the nascent peptide into the endoplasmic reticulum to be packaged for secretion from the cell (Kemper et al., 1974). The "pro" sequence is six amino acids in length, and although its function is less well defined than that of the "pre" sequence, it is also essential for correct PTH processing and secretion (Kemper et al., 1974). After the 84-amino-acid mature PTH peptide is secreted from the parathyroid cell, it is cleared from the circulation with a short half-life of about 2 min via nonsaturable hepatic uptake and renal excretion. PTH shares a receptor with PTH-related peptide (PTHrP, also known as PTHrH or PTH-related hormone) (Juppner et al., 1991), and this receptor is a member of a subgroup of G-protein-coupled receptors (GPCRs). The PTH/PTHrP receptor gene is located on chromosome 3p21−p24 (Gelbert et al., 1994) and is highly expressed in kidney and bone, where PTH is its predominant agonist (Abou-Samra et al., 1992). However, the most abundant expression of the PTH/PTHrP receptor occurs in chondrocytes of the metaphyseal growth plate, where it mediates predominantly the autocrine/paracrine actions of PTHrP (Segre, 1996). Five polymorphisms of the PTH gene have been reported; two of these are associated with restriction fragment length polymorphisms (RFLPs) (Schmidtke et al., 1984), another two are the result of single base changes not associated with RFLPs (Miric and Levine, 1992), and one is

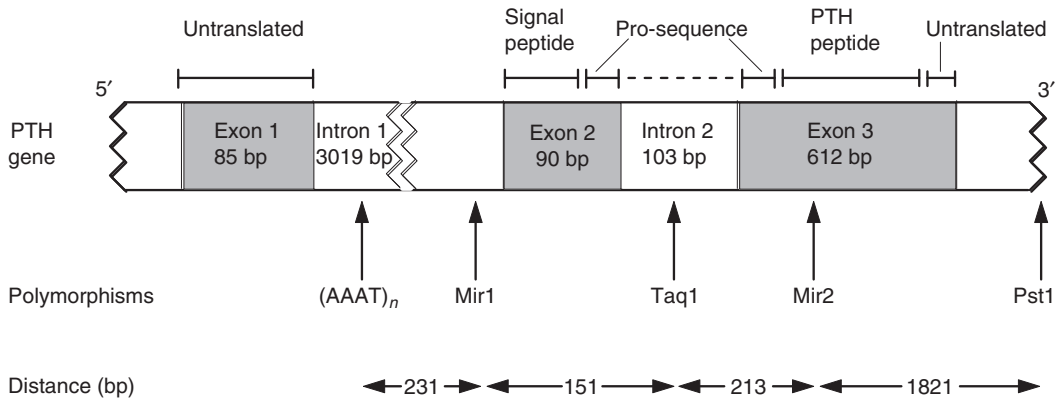

FIGURE 56.2 Schematic representation of the PTH gene. The PTH gene consists of three exons and two introns; the peptide is encoded by exons 2 and 3. The PTH peptide is synthesized as a precursor which contains a pre- and a prosequence. The mature PTH peptide, which contains 84 amino acids, and larger carboxy-terminal PTH fragments are secreted from the parathyroid cell. The polymorphic sites associated with the PTH gene are indicated. Two restriction fragment length polymorphisms (RFLPs) are associated with the PTH gene, and the *Taq*I polymorphic site is within intron 2 and the *PstI* polymorphic site is 1.7 kbp downstream in the 3′ direction of the gene (Schmidtke et al., 1984). Two other polymorphisms (Miric and Levine, 1992) of the PTH gene designated Mir1 and Mir2 are located in intron 1 and exon 3, respectively, and the tetranucleotide $(AAAT)_n$ polymorphism is in intron 1 (Parkinson et al., 1993). The distance between the $(AAAT)_n$ polymorphism and the Mir1 polymorphism is 231 base pairs (bp), that between the Mir1 polymorphism and the *Taq*1 RFLP is 152 bp, that between the *Taq*I RFLP site and the Mir2 polymorphism is 212 bp, and that between the Mir2 polymorphism and the *Pst*I RFLP is 1821 bp. Linkage disequilibrium between the $(AAAT)_n$, *Taq*I, and *Pst*I polymorphic sites has been established (Parkinson et al., 1993). *Adapted from Parkinson, D. B. & Thakker, R. V. 1992. A donor splice site mutation in the parathyroid hormone gene is associated with autosomal recessive hypoparathyroidism. Nat. Genet., 1, 149–152.*

due to a variation in the length of a microsatellite repetitive sequence in intron 1 (Parkinson et al., 1993). These polymorphisms are inherited in a Mendelian manner and are thus useful as genetic markers in family studies. Mutations involving the PTH gene affect the regulation of calcium homeostasis and are associated with hypoparathyroidism (Table 56.1).

Autosomal dominant hypoparathyroidism

DNA sequence analysis of the *PTH* gene (Fig. 56.2) from one patient with autosomal dominant isolated hypoparathyroidism has revealed a heterozygous single base substitution (T→C) in codon 18 of exon 2 (Arnold et al., 1990), which resulted in the substitution of arginine for the normal cysteine (p.Cys18Arg) in the signal peptide. The presence of this charged amino acid in the midst of the hydrophobic core of the signal peptide impeded the processing of the mutant pre-pro-PTH, as demonstrated by in vitro studies. These revealed that the mutation impaired the interaction with the nascent protein and translocation machinery, and that cleavage of the mutant signal sequence by solubilized signal peptidase was ineffective (Arnold et al., 1990; Karaplis et al., 1995). Ineffective cleavage of the pre-pro-PTH sequence results in a molecule that does not proceed successfully through the subsequent intracellular steps required for ultimate delivery of PTH to secretory granules. The parathyroid cell, therefore, cannot respond to hypocalcemia with the secretion of native, biologically active PTH. However, it should be noted that in vitro studies have shown that secretion of the mutant pre-pro-PTH peptide harboring the p.Cys18Arg missense substitution can be enhanced by the addition of 4-phenylbutyric acid, which is a pharmacological chaperone (Datta et al., 2007). Recently, a heterozygous single base substitution (T→A) in codon 14 of exon 2 of the *PTH* gene, which resulted in methionine to lysine substitution (p.Met14Lys) in the signal peptide, has been reported in a family with autosomal dominant hypoparathyroidism (Cinque et al., 2017). This mutation was predicted to impair cleavage of pre-pro-PTH, and studies in HEK293 cells showed intracellular retention of the mutant pre-pro-PTH peptide, which could be partially rescued by the addition of 4-phenylbutyric acid (Cinque et al., 2017).

Autosomal recessive hypoparathyroidism

Autosomal recessive hypoparathyroidism has usually arisen in families with consanguineous marriages (Parkinson et al., 1993; Parkinson and Thakker, 1992). Abnormalities in the *PTH* gene have been sought (Parkinson et al., 1993), and homozygous mutations that lead to impaired processing of the PTH peptide have been identified in three unrelated families (Ertl et al., 2012; Parkinson and Thakker, 1992; Sunthornthepvarakul et al., 1999). In one such family, a donor splice site at

the exon 2−intron 2 boundary has been identified (Parkinson and Thakker, 1992). This mutation involved a single base transition (**g→c**) at position one of intron 2, and the effects of this alteration in the invariant **gt** dinucleotide of the 5′ donor splice site consensus on mRNA processing were assessed by an analysis of the non-tissue-specific transcription of normal and mutant *PTH* genes. This non-tissue-specific expression of genes has been estimated to be at the rate of one molecule of correctly spliced mRNA per 1000 cells (Chelly et al., 1989; von Heijne, 1983). Although the physiological relevance of this low level of non-tissue-specific or illegitimate transcription is not known, it is of clinical importance. Easily accessible peripheral blood lymphocytes can be used to detect abnormalities in mRNA processing, thereby avoiding the requirement for tissue that may only be obtainable by biopsy. Use of these methods revealed that the donor splice site mutation resulted in exon skipping, in which exon 2 of the *PTH* gene was lost, and exon 1 was spliced to exon 3. The lack of exon 2 would lead to a loss of the ATG and signal peptide sequence required, respectively, for the commencement of PTH mRNA translation and translocation of the PTH peptide. Thus, the patients' parathyroid cells would not contain any translated PTH products.

Mutations involving codon 23, which encodes a serine (Ser), have been reported in two unrelated families with autosomal recessive hypoparathyroidism (Ertl et al., 2012; Sunthornthepvarakul et al., 1999). In one family, a homozygous single base substitution (**T→C**) involving codon 23 of exon 2 was detected. This resulted in the substitution of proline for normal serine in the signal peptide (Sunthornthepvarakul et al., 1999). This missense mutation (p.Ser23Pro) alters the −3 position of the pre-pro-PTH protein cleavage site (von Heijne, 1983). Indeed, amino acid residues at the −3 and −1 positions of the signal peptidase recognition site have to conform to certain criteria for correct processing through the rough endoplasmic reticulum (RER), and one of these is an absence of proline in the region −3 and +1 of the site (von Heijne, 1983). Thus, the presence of a proline, which is a strong helix-breaking residue, at the −3 position is likely to disrupt cleavage of the mutant pre-pro-PTH that would be subsequently degraded in the RER, and PTH would not be available (Sunthornthepvarakul et al., 1999). In the other unrelated family, a homozygous single base substitution (**C→A**) involving codon 23 was detected in a proband with isolated hypoparathyroidism (Ertl et al., 2012). This mutation is predicted to result in a stop codon (p.Ser23Stop) being introduced at the pre-pro-PTH protein cleavage site and would lead to a truncated and inactive PTH peptide (Ertl et al., 2012).

Recently, a homozygous arginine-to-cysteine mutation was identified at codon 25, p.Arg25Cys, of the mature PTH (1−84) peptide in a family with hypocalcemia and hyperphosphatemia (Lee et al., 2015). The plasma PTH levels of affected family members varied from low-normal to markedly elevated depending on the type of PTH assay used (Lee et al., 2015). Administration of recombinant PTH (1−34) increased urinary cAMP excretion in affected family members, thus indicating they did not have pseudohypoparathyroidism (Lee et al., 2015). In contrast to previously reported *PTH* gene mutations that affect the secretion of PTH, the p.Arg25Cys missense substitution was shown to diminish the binding of the mutant PTH peptide with the PTH/PTHrP receptor (Lee et al., 2015). Moreover, the *PTH* p.Arg25Cys mutation interfered with PTH immunoassays that utilized antibodies affinity-purified using PTH 1−34 and 13−34 fragments, thereby explaining why some assays were unable to detect the mutant PTH peptide (Lee et al., 2015).

Glial cells missing homolog 2 gene abnormalities

Glial cells missing homolog 2 (GCM2), which is the human homolog of the Drosophila gene, *Gcm*, and of the mouse *Gcm2* gene, is expressed exclusively in the parathyroid glands, suggesting that it may be a specific regulator of parathyroid gland development (Gunther et al., 2000; Kim et al., 1998). In order to investigate this, mice deleted for *Gcm2* were generated by the method of homologous recombination using embryonic stem cells. Mice that were heterozygous ($Gcm2^{+/-}$) for the deletion were normal, whereas mice that were homozygous ($Gcm2^{-/-}$) for the deletion lacked parathyroid glands and developed the hypocalcemia and hyperphosphatemia observed in hypoparathyroidism (Gunther et al., 2000). However, despite their lack of parathyroid glands, $Gcm2^{-/-}$ mice did not have undetectable serum PTH levels but instead had PTH levels identical to those of normal ($Gcm2^{+/+}$, wild-type) mice. This endogenous level of PTH in $Gcm2^{-/-}$ mice was too low to correct the hypocalcemia, but exogenous continuous PTH infusion could correct the hypocalcemia (Gunther et al., 2000). Interestingly, there were no compensatory increases in PTHrP or 1,25$(OH)_2$ vitamin D_3. These findings indicate that $Gcm2^{-/-}$ mice have a normal response (and not resistance) to PTH and that the PTH in the serum of $Gcm2^{-/-}$ mice was biologically active. The auxillary source of PTH was determined by combined expression and ablation studies (Gunther et al., 2000). These revealed a cluster of PTH-expressing cells under the thymic capsule in both $Gcm2^{-/-}$ and wild-type mice. These thymic PTH-producing cells also expressed the CaSR, and long-term treatment of $Gcm2^{-/-}$ mice with 1,25$(OH)_2$ vitamin D_3 restored the serum calcium concentrations to normal and reduced the serum PTH levels, thereby indicating that thymic production of PTH can be downregulated (Gunther et al., 2000). However, it appears that this thymic production of PTH cannot be upregulated, as serum PTH levels are not high despite the hypocalcemia in the

Gcm2$^{-/-}$ mice. This absence of upregulation would be consistent with the very small size of the thymic PTH-producing cell cluster when compared with the size of normal parathyroid glands. The development of the thymic PTH-producing cells likely involves Gcm1, which is the other mouse homolog of Drosophila, Gcm (Kim et al., 1998). Gcm1 expression, which could not be detected in parathyroid glands, colocalized with PTH expression in the thymus (Gunther et al., 2000).

The specific role of Gcm2 in the development of the parathyroids from the third pharyngeal pouch has been further investigated by studying the expression of the Hoxa3-Pax1/9-Eya1 transcription factor and sonic hedgehog−bone morphogenetic protein 4 (Shh-Bmp4) signaling networks (Liu et al., 2007). These studies have revealed that *Gcm2*$^{-/-}$ embryos that are 12 d.p.c. have a parathyroid-specific domain, but that this parathyroid domain undergoes coordinated programmed cell death (apoptosis) by 12.5 d.p.c. in *Gcm2*$^{-/-}$ mouse embryos (Liu et al., 2007). Moreover, the expression of the transcription factors Hoxa3 (see above), Pax 1, Pax 9, Eya1, and Tbx1, as well as Shh and Bmp4, was normal in the third pharyngeal pouch of these *Gcm2*$^{-/-}$ mouse embryos. These findings indicate that the Hoxa3-Pax1/9-Eya transcription factor cascade, the transcription factor Tbx1 (Fig. 56.1), and the Shh−Bmp4 signaling network all act upstream of Gcm2 (Liu et al., 2007). Moreover, these studies have revealed that Gcm2 has a role in promoting differentiation and survival of parathyroid cells in the developing embryo (Liu et al., 2007). The downstream targets of GCM2 within the parathyroid cell have begun to be elucidated, and GCM2 has been shown to upregulate CaSR expression by directly binding to its promoter region (Canaff et al., 2009). Moreover, GCM2 acts together with the GATA3 and MafB transcription factors to upregulate PTH expression (Fig. 56.1) by binding to a conserved region within the *PTH* promoter (Han et al., 2015; Kamitani-Kawamoto et al., 2011). In addition to its in utero role in parathyroid organogenesis, GCM2 is also expressed in the parathyroid glands postnatally, where it may play an ongoing role in upregulating CaSR and PTH expression (Mizobuchi et al., 2009).

Homozygous *GCM2* mutations have been identified in patients with autosomal recessive hypoparathyroidism (Ding et al., 2001), while in another family a homozygous missense mutation (p.Arg47Leu) of the DNA binding domain was identified (Baumber et al., 2005). Functional analysis, using electrophoretic mobility shift assays, of this p.Arg47Leu *GCM2* mutation revealed that it resulted in a loss of DNA binding to the *GCM2* DNA binding site (Baumber et al., 2005). Heterozygous *GCM2* mutations, which consist of single nucleotide deletions (c.1389deT and c.1399delC) that introduce frameshifts and premature truncations, and a missense mutation, p.Asn502His, have also been identified in three unrelated families with autosomal dominant hypoparathyroidism (Mannstadt et al., 2008; Mirczuk et al., 2010). These mutations were shown using a *GCM2*-associated luciferase reporter to inhibit the action of the wild-type transcription factor, thereby indicating that these *GCM2* mutants have dominant-negative properties (Mannstadt et al., 2008; Mirczuk et al., 2010). More recently, activating *GCM2* mutations have been identified in kindreds with familial isolated hyperparathyroidism (Guan et al., 2016), thereby revealing that *GCM2* abnormalities have roles in the etiology of hypo- and hyperparathyroidism.

X-linked recessive hypoparathyroidism

Hypoparathyroidism with an X-linked recessive transmission pattern was initially reported in two multigenerational kindreds (Peden, 1960; Whyte and Weldon, 1981). Only males were affected, and they suffered from infantile epilepsy and hypocalcemia. The hypoparathyroidism is due to a defect in parathyroid gland development (Whyte et al., 1986). Linkage studies utilizing X-linked RFLPs in these two families assigned the mutant gene to chromosome Xq26−q27 (Thakker et al., 1990). An approach utilizing mitochondrial DNA analysis established a common ancestry in these two X-linked hypoparathyroid kindreds (Mumm et al., 1997). A common ancestry for these two kindreds from eastern Missouri had been suspected, but it could not be established despite five generations of extensive genealogical records (Whyte and Weldon, 1981). The mitochondrial genes are transmitted through the maternal line exclusively. If relatedness among the two kindreds involved the maternal lines, analysis of mitochondrial genetic markers would reveal common features. The DNA sequence of the mitochondrial (mt) D-loop was compared among individuals in both kindreds. The mt DNA sequence was identical among affected males and their maternal lineage for individuals in both kindreds, but differed at 3 to 6 positions when compared with the mitochondrial DNA of the fathers. These results demonstrated that the two kindreds with X-linked recessive hypoparathyroidism are indeed related and that an identical gene defect is likely to be responsible for the disease. Additional studies refined the location of this gene to be between the locus for diffuse B cell lymphoma and DXS984, a 906 kb region in Xq27.1 (Andrew Nesbit et al., 2004; Trump et al., 1998). Furthermore, DNA sequence analyses of the coding regions of the three genes—adenosine triphosphatase 11C (*ATP11C*), U7snRNA homolog, and Sry-box3 (*SOX3*)— contained within this 906 kb interval did not reveal any abnormalities (Andrew Nesbit et al., 2004). These findings together with the reported absence of hypocalcemia in a boy with hemophilia B and mental retardation who had a

chromosomal deletion that encompassed the entire 906 kb interval containing *ATP11C*, U7snRNA, and *SOX3* genes (Stevanovic et al., 1993) suggested that other genomic abnormalities such as molecular duplications for translocations, which could cause altered gene function, may underlie the etiology of X-linked recessive hyperparathyroidism (Bowl et al., 2005). Indeed, this proved to be the case, and a complex interstitial deletion-insertion involving chromosomes 2p25.3 and Xq27.1, near *SOX3*, was shown to cosegregate with X-linked recessive hypoparathyroidism (Bowl et al., 2005). This deletion-insertion was located approximately 67 kb downstream of *SOX3*, and hence it was likely to exert a position effect on SOX3 expression. Moreover, *SOX*3 was shown to be expressed in the developing parathyroids of mouse embryos, and this indicates a likely role for *SOX3* in the embryonic development of the parathyroid glands (Bowl et al., 2005). More recently, another unrelated family with X-linked hypoparathyroidism was identified, and whole-genome sequence analysis revealed an interstitial deletion-insertion that cosegregated with the hypoparathyroidism (Taylor et al., 2015). This deletion-insertion involves an approximately 50 kb region of chromosome 2p25.3 that has been duplicated and inserted into the X chromosome, resulting in a 1.4 kb deletion located 81.5 kb downstream of *SOX3* (Taylor et al., 2015). Thus, these findings support a role for *SOX3* in the embryonic development of the parathyroid glands (Taylor et al., 2015).

SOX3 belongs to a family of genes encoding high-mobility group box transcription factors and is related to *SRY*, the sex-determining gene on the Y chromosome. The mouse homolog is expressed in the prestreak embryo and subsequently in the developing CNS, which includes the region of the ventral diencephalon that induces development of the anterior pituitary and gives rise to the hypothalamus and olfactory placodes (Collignon et al., 1996; Rizzoti et al., 2004; Solomon et al., 2002). Patients with X-linked hypopituitarism have been reported to have duplications involving a 686 kb−13 Mb region that contains SOX3 (Solomon et al., 2002, 2004; Woods et al., 2005), and overexpression of SOX3 has been reported to inhibit Wnt signaling, which has an important role in pituitary development (Zorn et al., 1999). Furthermore, increased levels of SOX3 have been shown to cause developmental hypoplasia of tissues, such as the lens and otic placodes in fish embryos (Koster et al., 2000). Reduced levels of SOX3 expression also result in hypopituitarism. Thus, *Sox3* null mice have abnormal pituitary development associated with hypopituitarism, craniofacial abnormalities, and midline CNS defects (Rizzoti et al., 2004). These phenotypic features are similar to those observed in patients with X-linked hypopituitarism as well as with X-linked mental retardation and growth hormone deficiency, who have in-frame duplications of 21bp or 33bp encoding for 7 or 11 alanines, respectively, in a polyalanine tract of the *SOX3* gene (Laumonnier et al., 2002; Woods et al., 2005). The polyalanine tract expansion resulted in a reduction of SOX3 transcriptional activity that was associated with an impaired nuclear localization of the mutant protein (Woods et al., 2005). These findings demonstrate that pituitary development is sensitive to *SOX3* dosage and that both loss- and gain-of-function mutations can result in X-linked hypopituitarism (Rizzoti et al., 2004; Solomon et al., 2002, 2004; Laumonnier et al., 2002; Schlosser and Ahrens, 2004).

Patients with X-linked hypopituitarism have not been reported to suffer from hypoparathyroidism (Solomon et al., 2002, 2004; Laumonnier et al., 2002; Woods et al., 2005) and conversely the patients affected with X-linked recessive hypoparathyroidism do not suffer from hypopituitarism (Peden, 1960; Trump et al., 1998; Whyte and Weldon, 1981). These clinical differences may be due to differences in the temporal expression patterns of SOX3 in the pituitary and parathyroids or to interactions with different tissue-specific enhancers or repressors. Alternatively, they may be due to differences in the locations of the associated *SOX3* genomic abnormalities, and it is important to note that X-linked hypopituitarism is associated with either duplications of the entire *SOX3* coding region or with an intragenic expansion of a polyalanine tract (Solomon et al., 2002, 2004; Laumonnier et al., 2002; Woods et al., 2005), whereas X-linked recessive hypoparathyroidism is associated with deletions that are ∼67 kb and 81.5 kb downstream from the *SOX3* coding region (Bowl et al., 2005; Taylor et al., 2015). This situation may be analogous to that reported to occur in disorders associated with abnormalities of the sonic hedgehog (*SHH*) gene (Kleinjan and van Heyningen, 2005). SHH is a secreted protein that provides key inductive signals for patterning of the ventral neural tube, anterior posterior limb axis, and ventral somites. *SHH* gene abnormalities lead to holoprosencephaly type 3 (HPE3) and preaxial polydactyly (PPD) in man. HPE3 is caused by deletions or point mutations that involve the coding region and result in haploinsufficiency of *SHH*, while PPD is caused by breakpoints or point mutations within a limb regulatory element that is 1 Mb upstream of *SHH* (Kleinjan and van Heyningen, 2005). These findings illustrate that phenotypes caused by mutations in regulatory elements can be very different from those caused by mutations of coding regions, and that point mutations in regulatory elements at a distance as far as 1 Mb from the gene promoter can have a detrimental affect on embryonic development (Kleinjan and van Heyningen, 2005). Thus, it seems likely that the differences between X-linked recessive hypoparathyroidism and hypopituitarism occur because the hypoparathyroidism deletion-insertions, which are ∼67 kb and 81.5 kb downstream of *SOX3*, involve disruption of regulatory elements, whereas the abnormalities resulting in hypopituitarism involve alterations of the *SOX3* coding region. It is also important to note that the disruption in the regulatory region could also lead to upregulation or misregulation of the gene, thereby resulting in phenotypes due to gain-of-function (i.e., hypermorphic or neomorphic).

The location of the deletion-insertions ~67 kb and 81.5 kb downstream of *SOX3* in X-linked recessive hypoparathyroid patients are likely to result in altered SOX3 expression, as SOX3 expression has been reported to be sensitive to position-effects caused by X chromosome abnormalities (Kleinjan and van Heyningen, 2005). Indeed, reporter-construct studies of the mouse *Sox3* gene have demonstrated the presence of both 5′ and 3′ regulatory elements (Brunelli et al., 2003), and thus it is possible that the deletion-insertions in X-linked recessive hypoparathyroid patients may have a position-effect on SOX3 expression and parathyroid development from the pharyngeal pouches. Indeed, such position effects on *SOX* genes, which may be exerted over large distances, have been reported. For example, the very closely related *Sox2* gene has been shown to have regulatory regions spread over a long distance, both 5′ and 3′ to the coding region (Uchikawa et al., 2003), and disruption of sequences at some distance 3′ have been reported to lead to loss of expression in the developing inner ear and absence of sensory cells, whereas expression in other sites is unaffected (Kiernan et al., 2005). Similarly for the *SRY* gene, which probably originated from *SOX3* (Stevanovic et al., 1993), both 5′ and 3′ deletions result in abnormalities of sexual development, and translocation breakpoints over 1 Mb upstream of the *SOX9* gene have been reported to result in campomelic dysplasia due to removal of elements that regulate *SOX9* expression (Kleinjan and van Heyningen, 2005). The molecular deletion-insertions identified in X-linked recessive hypoparathyroidism may similarly cause position-effects on SOX3 expression, and this points to a potential role for the *SOX3* gene in the embryological development of the parathyroid glands from the pharyngeal pouches.

A recent report has also highlighted that the four-and-a-half LIM domains 1 (*FHL1*) gene, which is located on chromosome Xq26.3, may also represent an additional gene for X-linked hypoparathyroidism (Pillar et al., 2017), as an *FHL1* missense variant (p.Arg95Trp) was detected in a 4-year-old male with isolated severe hypoparathyroidism (Pillar et al., 2017). Functional studies have shown that knockdown of the FHL1 paralog in zebrafish increased plasma calcium concentrations, and that introduction of wild-type FHL1 into HEK293 cells transfected with a luciferase reporter gene that is under the control of the human PTH promoter resulted in increased PTH promoter activity (Pillar et al., 2017). However, FHL1 is predicted to have a low level of expression in human parathyroids (Pillar et al., 2017), and thus the role of this protein in calcium homeostasis remains to be established. The possible deleterious effects on mammalian parathyroid gland activity of this p.Arg95Trp missense variant of FHL1 also remain to be established.

Autosomal dominant hypocalcemia

Autosomal dominant hypocalcemia (ADH) is characterized by hypocalcemia in association with inappropriately normal or low PTH concentrations, and comprises two genetically distinct disorders, designated as ADH types 1 and 2, which are caused by germline gain-of-function mutations of the CaSR and G-protein subunit α_{11} ($G\alpha_{11}$) proteins, respectively (Table 56.1) (Hannan et al., 2016).

Calcium-sensing receptor and $G\alpha_{11}$

The human CaSR is a 1078 amino acid dimeric cell-surface protein that belongs to class C of the GPCR superfamily and is encoded by the *CASR* gene on human chromosome 3q21.1 (Hannan et al., 2016). The CaSR is most highly expressed in the parathyroid glands and kidneys, and has a large (612 amino acid) extracellular domain, which is predicted to adopt a venus flytrap (VFT) conformation that binds calcium at multiple sites (Fig. 56.3) (Geng et al., 2016). Activation of the CaSR leads to signaling via intracellular pathways that includes $G\alpha_{11}$-dependent stimulation of phospholipase C, which causes an accumulation of inositol 1,4,5-triphosphate together with the rapid mobilization of intracellular calcium ($Ca^{2+}{}_i$), and also activates the mitogen-activated protein kinase pathway (Fig. 56.3) (Hannan et al., 2016). These intracellular events mediate a reduction in PTH secretion and decrease in renal tubular calcium reabsorption (Fig. 56.3). CaSR cell-surface expression is regulated by agonist-driven insertional signaling, which promotes anterograde trafficking of newly synthesized CaSRs to the plasma membrane (Grant et al., 2011), and also by retrograde trafficking of cell-surface CaSRs, which is mediated by adaptor-related protein complex 2 (Fig. 56.3) (Gorvin et al., 2018).

Autosomal dominant hypocalcemia type 1

Autosomal dominant hypocalcemia type 1 (ADH1), which is due to gain-of-function CaSR mutations, is characterized by mild-to-moderate hypocalcemia in association with mild hypomagnesemia; hyperphosphatemia; and serum PTH concentrations that are often detectable and within the lower half of the reference range (Nesbit et al., 2013). Patients with ADH have significantly increased urinary calcium excretion compared with hypoparathyroid patients (Yamamoto et al., 2000), and ~10% of ADH1 patients have an absolute hypercalciuria (Nesbit et al., 2013). It has been reported that the urinary calcium-to-creatinine (Ca/Cr) ratio may be used to distinguish ADH1 from hypoparathyroidism, with untreated

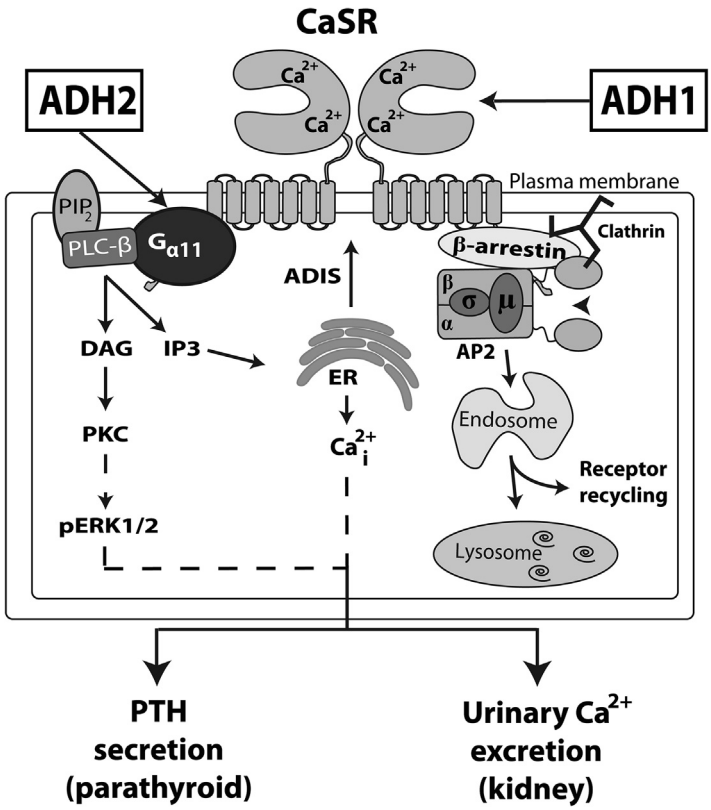

FIGURE 56.3 Overview of calcium-sensing receptor signaling and trafficking. The binding of calcium (Ca^{2+}) to the calcium-sensing receptor (CaSR) extracellular domain leads to $G\alpha_{11}$-dependent activation of phospholipase C-β (PLC-β) and the production of diacylglycerol (DAG) and inositol 1,4,5-trisphosphate (IP_3) from membrane-bound phosphatidylinositol 4,5-bisphosphate (PIP_2). The increase in intracellular IP_3 levels facilitates the release of Ca^{2+} from intracellular stores such as the endoplasmic reticulum (ER). DAG activates protein kinase C (PKC) and the mitogen-activated protein kinase pathway. These signaling events lead to a decrease in parathyroid hormone (PTH) secretion and reduction in renal tubular Ca^{2+} reabsorption. CaSR cell-surface expression is regulated by agonist-driven insertional signaling (ADIS) (Grant et al., 2011) and also by an endocytic complex comprising clathrin, β-arrestin, and adaptor-related protein complex 2 (AP2) (Gorvin et al., 2018), which may traffic this G-protein-coupled receptor to the endosomal–lysosomal degradation pathway or recycle the CaSR back to the cell surface. Gain-of-function mutations of the CaSR lead to autosomal dominant hypocalcemia type 1 (ADH1), and gain-of function mutations of the $G\alpha_{11}$ subunit cause autosomal dominant hypocalcemia type 2 (ADH2). *Adapted from Hannan et al.* Br J Pharmacol *2017 https://doi.org/10.1111/bph.14086. [Epub ahead of print].*

ADH1 patients having a mean Ca/Cr ratio of >3.0 mmol/mmol creatinine, which was similar to the urinary Ca/Cr ratio of unaffected normocalcemic subjects, whereas untreated hypoparathyroid patients had a significantly lower mean Ca/Cr ratio of <0.1 mmol/mmol creatinine (Yamamoto et al., 2000). Some patients with ADH1 may have ectopic calcifications affecting the basal ganglia and/or elevations in bone mineral density (BMD) (Pearce et al., 1996), and some patients with severe gain-of-function CaSR mutations may also develop a Bartter syndrome (referred to as Bartter syndrome type V), which is characterized by renal salt wasting leading to volume depletion, hyperreninemic hyperaldosteronism and hypokalemic alkalosis (Watanabe et al., 2002). Over 70 different CaSR mutations have been identified in ADH1 patients and families (Hannan et al., 2016; Hannan and Thakker, 2013), and structure–function analysis have shown that ADH1-causing gain-of-function mutations cluster within the second peptide loop of the extracellular VFT domain (residues 116–136), which contributes to the dimeric CaSR interface (Geng et al., 2016). A second hotspot for ADH1 mutations is located in a region that encompasses transmembrane helices 6 and 7, and the intervening third extracellular loop of the CaSR (residues 819–837) (Hannan et al., 2016). This transmembrane region may play a role in locking the ligand-unbound receptor in an inactive conformation by forming a network of interactions with other transmembrane helices (Dore et al., 2014).

Autosomal dominant hypocalcemia type 2

Mutations of the *CASR* gene are not detected in ~30% of ADH patients, and heterozygous germline mutations of $G\alpha_{11}$, which is encoded by the *GNA11* gene, have been reported in seven such ADH patients and families (Li et al., 2014;

Mannstadt et al., 2013; Nesbit et al., 2013; Piret et al., 2016; Tenhola et al., 2016). In vitro functional studies of these $G\alpha_{11}$ mutations, which all comprise missense substitutions, have shown cells expressing the mutant $G\alpha_{11}$ proteins to have enhanced CaSR-mediated signaling responses, consistent with a gain-of-function (Li et al., 2014; Nesbit et al., 2013; Piret et al., 2016). These individuals and families with gain-of-function $G\alpha_{11}$ mutations, who were designated as having ADH type 2 (ADH2), generally had mild-to-moderate hypocalcemia, which is in keeping with the serum biochemical phenotype of ADH1 (Hannan et al., 2016). However, ADH2 is associated with a milder urinary phenotype, with significantly reduced urinary calcium excretion compared with ADH1 (Li et al., 2014). Moreover, short stature caused by postnatal growth insufficiency has been reported in two ADH2 kindreds (Li et al., 2014; Tenhola et al., 2016). Structural and functional studies of ADH2-causing gain-of-function $G\alpha_{11}$ mutations have revealed residues critical for Gα-subunit function. The $G\alpha_{11}$-subunit consists of a Ras-like GTPase domain that binds GDP and GTP, and a smaller helical domain that acts as a clasp to secure these bound guanine-nucleotides (Hannan et al., 2016). The ADH2-causing mutations have been shown to cluster at the interface between these two domains (Piret et al., 2016), and may enhance the exchange of GDP and GTP, thereby leading to G-protein activation. ADH2 mutations also affect the C-terminal portion of the $G\alpha_{11}$ protein, which facilitates G-protein-GPCR coupling (Piret et al., 2016). Thus, these ADH2-causing mutations have provided insights into Gα-subunit structure−function relationships, which may aid the design of targeted therapeutic agents for the treatment of ADH, for which there is currently a lack of adequate drugs (Hannan et al., 2015).

Mouse models for autosomal dominant hypocalcemia types 1 and 2

Mouse models with gain-of-function germline *Casr* or *Gna11* mutations have been generated by chemical mutagenesis and knockin strategies (Dong et al., 2015; Hough et al., 2004; Roszko et al., 2017). One ADH1 mouse model, termed "Nuclear flecks" or "*Nuf*" due to the presence of opaque flecks within the lens nucleus, was generated using the alkylating agent isopropyl methane sulfonate (iPMS) (Hough et al., 2004). The *Nuf* gene locus was mapped to mouse chromosome 16 and a germline leucine-to-glutamine missense substitution identified at codon 723 of the *Casr*. The mutant p.Leu723Gln Casr protein was shown to cause a gain-of-function when expressed in HEK293 cells (Hough et al., 2004). *Nuf* mice have a phenotype consisting of hypocalcemia, hyperphosphatemia, low circulating PTH concentrations and widespread ectopic calcifications (Hough et al., 2004). Homozygote (*Nuf/Nuf*) mice are viable but have a more severe phenotype than heterozygote (*Nuf/+*) mice (Hough et al., 2004). Two *Casr* knockin mouse models, which harbor mutations (p.Cys129Ser and p.Ala843Glu) causing ADH1 in humans, have also been generated. Both knockin mouse models had a more marked phenotype than *Nuf* mice. Thus, the knockin mice with germline homozygous *Casr* mutations had embryonic or perinatal lethality (Dong et al., 2015), and the heterozygous *Casr* knockin mice had a phenotype resembling ADH1, which was characterized by hypocalcemia, hyperphosphatemia, low plasma PTH, and hypercalciuria (Dong et al., 2015). These ADH1 models have been utilized to evaluate calcilytic compounds, which are negative allosteric CaSR modulators that represent a potential targeted therapy for ADH (Hannan et al., 2017). Indeed, single dose administration of a calcilytic compound known as NPS-2143 has been shown in vivo to rectify the hypocalcemia of *Nuf* mice (Hannan et al., 2015), while, longer-term administration of the JTT-305/MK-5442 calcilytic compound in the two knockin *Casr* mouse models, has been shown to lead to sustained increases in serum calcium concentrations and significant reductions in urinary calcium excretion (Dong et al., 2015).

To establish a mouse model for ADH2, studies were undertaken to characterize the calcitropic phenotype of a previously reported mouse mutant known as *dark skin seven* or, "*Dsk7*", which has increased dermal pigmentation in association with a germline hypermorphic *Gna11* mutation, p.Ile62Val (Van Raamsdonk et al., 2004). These findings revealed *Dsk7* mice to have hypocalcemia and reduced PTH concentrations, and in vitro analysis of the mutant p.Ile62Val $G\alpha_{11}$ protein showed this to enhance CaSR-mediated signaling, consistent with a gain-of-function (Gorvin et al., 2017). Another mouse model for ADH2 was generated by the knockin of an ADH2-causing *Gna11* mutation, p.Arg60Cys, and this was found to have a similar phenotype to *Dsk7* mice with hypocalcemia, reduced PTH concentrations and increased skin pigmentation (Roszko et al., 2017). NPS-2143 was shown to rectify the gain-of-function caused by p.Ile62Val and p.Arg60Cys *Gna11* mutations in vitro, and single dose administration of NPS-2143 ameliorated the hypocalcemia of the two ADH2 mouse models in vivo (Gorvin et al., 2017; Roszko et al., 2017). Thus, these in vivo studies have demonstrated that calcilytics have potential as a treatment for ADH2.

Conclusions

Application of the methods of molecular genetics to the study of hypoparathyroid disorders has resulted in considerable advances that have identified some genes and their encoded proteins involved in the embryological development of the

parathyroids and mediating its actions in different target issues. In addition, the identification of mutations has helped to provide molecular explanations and insights into a variety of familial and sporadic forms of hypoparathyroidism. Moreover, investigation of mouse models has helped to increase our understanding of the molecular regulation of pharyngeal pouch development. However, many challenges remain in this complex field, in particular resolving the issues of phenotypic variance and interspecies differences as well as further elucidating the interplay between the genes involved in mediating parathyroid gland development.

Acknowledgments

R.V.T. is supported by the Medical Research Council (UK), Wellcome Trust and National Institute for Health Research. F.M.H. and R.V.T. are supported by the Horizon 2020 program of the European Union.

References

Aaltonen, J., Bjorses, P., Sandkuijl, L., Perheentupa, J., Peltonen, L., 1994. An autosomal locus causing autoimmune disease: autoimmune polyglandular disease type I assigned to chromosome 21. Nat. Genet. 8, 83–87.

Abou-Samra, A.B., Juppner, H., Force, T., Freeman, M.W., Kong, X.F., Schipani, E., Urena, P., Richards, J., Bonventre, J.V., Potts JR., J.T., et al., 1992. Expression cloning of a common receptor for parathyroid hormone and parathyroid hormone-related peptide from rat osteoblast-like cells: a single receptor stimulates intracellular accumulation of both cAMP and inositol trisphosphates and increases intracellular free calcium. Proc. Natl. Acad. Sci. U. S. A. 89, 2732–2736.

Abramowicz, M.J., Cochaux, P., Cohen, L.H., Vamos, E., 1996. Pernicious anaemia and hypoparathyroidism in a patient with Kearns-Sayre syndrome with mitochondrial DNA duplication. J. Inherit. Metab. Dis. 19, 109–111.

Adachi, M., Tachibana, K., Asakura, Y., Tsuchiya, T., 2006. A novel mutation in the GATA3 gene in a family with HDR syndrome (Hypoparathyroidism, sensorineural Deafness and Renal anomaly syndrome). J. Pediatr. Endocrinol. Metab. 19, 87–92.

Alabert, C., Bukowski-Wills, J.C., Lee, S.B., Kustatscher, G., Nakamura, K., De Lima Alves, F., Menard, P., Mejlvang, J., Rappsilber, J., Groth, A., 2014. Nascent chromatin capture proteomics determines chromatin dynamics during DNA replication and identifies unknown fork components. Nat. Cell Biol. 16, 281–293.

Ali, A., Christie, P.T., Grigorieva, I.V., Harding, B., Van Esch, H., Ahmed, S.F., Bitner-Glindzicz, M., Blind, E., Bloch, C., Christin, P., Clayton, P., Gecz, J., Gilbert-Dussardier, B., Guillen-Navarro, E., Hackett, A., Halac, I., Hendy, G.N., Lalloo, F., Mache, C.J., Mughal, Z., Ong, A.C., Rinat, C., Shaw, N., Smithson, S.F., Tolmie, J., Weill, J., Nesbit, M.A., Thakker, R.V., 2007. Functional characterization of GATA3 mutations causing the hypoparathyroidism-deafness-renal (HDR) dysplasia syndrome: insight into mechanisms of DNA binding by the GATA3 transcription factor. Hum. Mol. Genet. 16, 265–275.

Alimohammadi, M., Bjorklund, P., Hallgren, A., Pontynen, N., Szinnai, G., Shikama, N., Keller, M.P., Ekwall, O., Kinkel, S.A., Husebye, E.S., Gustafsson, J., Rorsman, F., Peltonen, L., Betterle, C., Perheentupa, J., Akerstrom, G., Westin, G., Scott, H.S., Hollander, G.A., Kampe, O., 2008. Autoimmune polyendocrine syndrome type 1 and NALP5, a parathyroid autoantigen. N. Engl. J. Med. 358, 1018–1028.

Almaden, Y., Canalejo, A., Hernandez, A., Ballesteros, E., Garcia-Navarro, S., Torres, A., Rodriguez, M., 1996. Direct effect of phosphorus on PTH secretion from whole rat parathyroid glands in vitro. J. Bone Miner. Res. 11, 970–976.

Andrew Nesbit, M., Bowl, M.R., Harding, B., Schlessinger, D., Whyte, M.P., Thakker, R.V., 2004. X-linked hypoparathyroidism region on Xq27 is evolutionarily conserved with regions on 3q26 and 13q34 and contains a novel P-type ATPase. Genomics 84, 1060–1070.

Arnold, A., Horst, S.A., Gardella, T.J., Baba, H., Levine, M.A., Kronenberg, H.M., 1990. Mutation of the signal peptide-encoding region of the preproparathyroid hormone gene in familial isolated hypoparathyroidism. J. Clin. Invest. 86, 1084–1087.

Augusseau, S., Jouk, S., Jalbert, P., Prieur, M., 1986. DiGeorge syndrome and 22q11 rearrangements. Hum. Genet. 74, 206.

Baldini, A., 2003. DiGeorge's syndrome: a gene at last. Lancet 362, 1342–1343.

Barakat, A.Y., D'albora, J.B., Martin, M.M., Jose, P.A., 1977. Familial nephrosis, nerve deafness, and hypoparathyroidism. J. Pediatr. 91, 61–64.

Baumber, L., Tufarelli, C., Patel, S., King, P., Johnson, C.A., Maher, E.R., Trembath, R.C., 2005. Identification of a novel mutation disrupting the DNA binding activity of GCM2 in autosomal recessive familial isolated hypoparathyroidism. J. Med. Genet. 42, 443–448.

Bergada, I., Schiffrin, A., ABU Srair, H., Kaplan, P., Dornan, J., Goltzman, D., Hendy, G.N., 1988. Kenny syndrome: description of additional abnormalities and molecular studies. Hum. Genet. 80, 39–42.

Bilous, R.W., Murty, G., Parkinson, D.B., Thakker, R.V., Coulthard, M.G., Burn, J., Mathias, D., Kendall-Taylor, P., 1992. Brief report: autosomal dominant familial hypoparathyroidism, sensorineural deafness, and renal dysplasia. N. Engl. J. Med. 327, 1069–1074.

Bowl, M.R., Nesbit, M.A., Harding, B., Levy, E., Jefferson, A., Volpi, E., Rizzoti, K., Lovell-Badge, R., Schlessinger, D., Whyte, M.P., Thakker, R.V., 2005. An interstitial deletion-insertion involving chromosomes 2p25.3 and Xq27.1, near SOX3, causes X-linked recessive hypoparathyroidism. J. Clin. Invest. 115, 2822–2831.

Boynton, J.R., Pheasant, T.R., Johnson, B.L., Levin, D.B., Streeten, B.W., 1979. Ocular findings in Kenny's syndrome. Arch. Ophthalmol. 97, 896–900.

Brunelli, S., Silva Casey, E., Bell, D., Harland, R., Lovell-Badge, R., 2003. Expression of Sox3 throughout the developing central nervous system is dependent on the combined action of discrete, evolutionarily conserved regulatory elements. Genesis 36, 12–24.

Budarf, M.L., Collins, J., Gong, W., Roe, B., Wang, Z., Bailey, L.C., Sellinger, B., Michaud, D., Driscoll, D.A., Emanuel, B.S., 1995. Cloning a balanced translocation associated with DiGeorge syndrome and identification of a disrupted candidate gene. Nat. Genet. 10, 269–278.

Canaff, L., Zhou, X., Mosesova, I., Cole, D.E., Hendy, G.N., 2009. Glial cells missing-2 (GCM2) transactivates the calcium-sensing receptor gene: effect of a dominant-negative GCM2 mutant associated with autosomal dominant hypoparathyroidism. Hum. Mutat. 30, 85–92.

Chelly, J., Concordet, J.P., Kaplan, J.C., Kahn, A., 1989. Illegitimate transcription: transcription of any gene in any cell type. Proc. Natl. Acad. Sci. U. S. A. 86, 2617–2621.

Chisaka, O., Capecchi, M.R., 1991. Regionally restricted developmental defects resulting from targeted disruption of the mouse homeobox gene hox-1.5. Nature 350, 473–479.

Chojnowski, J.L., Masuda, K., Trau, H.A., Thomas, K., Capecchi, M., Manley, N.R., 2014. Multiple roles for HOXA3 in regulating thymus and parathyroid differentiation and morphogenesis in mouse. Development 141, 3697–3708.

Cinque, L., Sparaneo, A., Penta, L., Mencarelli, A., Rogaia, D., Esposito, S., Fabrizio, F.P., Baorda, F., Verrotti, A., Falorni, A., Stangoni, G., Hendy, G.N., Guarnieri, V., Prontera, P., 2017. Autosomal dominant PTH gene signal sequence mutation in a family with familial isolated hypoparathyroidism. J. Clin. Endocrinol. Metab. 102, 3961–3969.

Collignon, J., Sockanathan, S., Hacker, A., COHEN-Tannoudji, M., Norris, D., Rastan, S., Stevanovic, M., Goodfellow, P.N., Lovell-Badge, R., 1996. A comparison of the properties of Sox-3 with Sry and two related genes, Sox-1 and Sox-2. Development 122, 509–520.

Dahlberg, P.J., Borer, W.Z., Newcomer, K.L., Yutuc, W.R., 1983. Autosomal or X-linked recessive syndrome of congenital lymphedema, hypoparathyroidism, nephropathy, prolapsing mitral valve, and brachytelephalangy. Am. J. Med. Genet. 16, 99–104.

Datta, R., Waheed, A., Shah, G.N., Sly, W.S., 2007. Signal sequence mutation in autosomal dominant form of hypoparathyroidism induces apoptosis that is corrected by a chemical chaperone. Proc. Natl. Acad. Sci. U. S. A. 104, 19989–19994.

Demay, M.B., Kiernan, M.S., Deluca, H.F., Kronenberg, H.M., 1992. Sequences in the human parathyroid hormone gene that bind the 1,25-dihydroxyvitamin D3 receptor and mediate transcriptional repression in response to 1,25-dihydroxyvitamin D3. Proc. Natl. Acad. Sci. U. S. A. 89, 8097–8101.

Deschamps, J., 2007. Ancestral and recently recruited global control of the Hox genes in development. Curr. Opin. Genet. Dev. 17, 422–427.

Ding, C., Buckingham, B., Levine, M.A., 2001. Familial isolated hypoparathyroidism caused by a mutation in the gene for the transcription factor GCMB. J. Clin. Invest. 108, 1215–1220.

Dong, B., Endo, I., Ohnishi, Y., Kondo, T., Hasegawa, T., Amizuka, N., Kiyonari, H., Shioi, G., Abe, M., Fukumoto, S., Matsumoto, T., 2015. Calcilytic ameliorates abnormalities of mutant calcium-sensing receptor (CaSR) knock-in mice mimicking autosomal dominant hypocalcemia (ADH). J. Bone Miner. Res. 30, 1980–1993.

Dore, A.S., Okrasa, K., Patel, J.C., Serrano-Vega, M., Bennett, K., Cooke, R.M., Errey, J.C., Jazayeri, A., Khan, S., Tehan, B., Weir, M., Wiggin, G.R., Marshall, F.H., 2014. Structure of class C GPCR metabotropic glutamate receptor 5 transmembrane domain. Nature 511, 557–562.

Ertl, D.A., Stary, S., Streubel, B., Raimann, A., Haeusler, G., 2012. A novel homozygous mutation in the parathyroid hormone gene (PTH) in a girl with isolated hypoparathyroidism. Bone 51, 629–632.

Fanconi, S., Fischer, J.A., Wieland, P., Atares, M., Fanconi, A., Giedion, A., Prader, A., 1986. Kenny syndrome: evidence for idiopathic hypoparathyroidism in two patients and for abnormal parathyroid hormone in one. J. Pediatr. 109, 469–475.

Franceschini, P., Testa, A., Bogetti, G., Girardo, E., Guala, A., Lopez-Bell, G., Buzio, G., Ferrario, E., Piccato, E., 1992. Kenny-Caffey syndrome in two sibs born to consanguineous parents: evidence for an autosomal recessive variant. Am. J. Med. Genet. 42, 112–116.

Fryns, J.P., DE Muelenaere, A., van den Berghe, H., 1981. Distal 10p deletion syndrome. Ann. Genet. 24, 189–190.

Fukami, M., Muroya, K., Miyake, T., Iso, M., Kato, F., Yokoi, H., Suzuki, Y., Tsubouchi, K., Nakagomi, Y., Kikuchi, N., Horikawa, R., Ogata, T., 2011. GATA3 abnormalities in six patients with HDR syndrome. Endocr. J. 58, 117–121.

Fulcoli, F.G., Franzese, M., Liu, X.Y., Zhang, Z., Angelini, C., Baldini, A., 2016. Rebalancing gene haploinsufficiency in vivo by targeting chromatin. Nat. Commun. 7.

Gaynor, K.U., Grigorieva, I.V., Nesbit, M.A., Cranston, T., Gomes, T., Gortner, L., Thakker, R.V., 2009. A missense GATA3 mutation, Thr272Ile, causes the hypoparathyroidism, deafness, and renal dysplasia syndrome. J. Clin. Endocrinol. Metab. 94, 3897–3904.

Gelbert, L., Schipani, E., Juppner, H., Abou-Samra, A.B., Segre, G.V., Naylor, S., Drabkin, H., Heath 3rd, H., 1994. Chromosomal localization of the parathyroid hormone/parathyroid hormone-related protein receptor gene to human chromosome 3p21.1-p24.2. J. Clin. Endocrinol. Metab. 79, 1046–1048.

Geng, Y., Mosyak, L., Kurinov, I., Zuo, H., Sturchler, E., Cheng, T.C., Subramanyam, P., Brown, A.P., Brennan, S.C., Mun, H.C., Bush, M., Chen, Y., Nguyen, T.X., Cao, B., Chang, D.D., Quick, M., Conigrave, A.D., Colecraft, H.M., Mcdonald, P., Fan, Q.R., 2016. Structural mechanism of ligand activation in human calcium-sensing receptor. Elife 5.

Gong, W., Emanuel, B.S., Collins, J., Kim, D.H., Wang, Z., Chen, F., Zhang, G., Roe, B., Budarf, M.L., 1996. A transcription map of the DiGeorge and velo-cardio-facial syndrome minimal critical region on 22q11. Hum. Mol. Genet. 5, 789–800.

Gorvin, C.M., Hannan, F.M., Howles, S.A., Babinsky, V.N., Piret, S.E., Rogers, A., Freidin, A.J., Stewart, M., Paudyal, A., Hough, T.A., Nesbit, M.A., Wells, S., Vincent, T.L., Brown, S.D., Cox, R.D., Thakker, R.V., 2017. Galpha11 mutation in mice causes hypocalcemia rectifiable by calcilytic therapy. JCI Insight 2, e91103.

Gorvin, C.M., Rogers, A., Hastoy, B., Tarasov, A.I., Frost, M., Sposini, S., Inoue, A., Whyte, M.P., Rorsman, P., Hanyaloglu, A.C., Breitwieser, G.E., Thakker, R.V., 2018. AP2? Mutations impair calcium-sensing receptor trafficking and signaling, and show an endosomal pathway to spatially direct G-protein selectivity. Cell Rep. 22, 1054–1066.

Grant, M.P., Stepanchick, A., Cavanaugh, A., Breitwieser, G.E., 2011. Agonist-driven maturation and plasma membrane insertion of calcium-sensing receptors dynamically control signal amplitude. Sci. Signal. 4, ra78.

Grigorieva, I.V., Mirczuk, S., Gaynor, K.U., Nesbit, M.A., Grigorieva, E.F., Wei, Q., Ali, A., Fairclough, R.J., Stacey, J.M., Stechman, M.J., Mihai, R., Kurek, D., Fraser, W.D., Hough, T., Condie, B.G., Manley, N., Grosveld, F., Thakker, R.V., 2010. Gata3-deficient mice develop parathyroid abnormalities due to dysregulation of the parathyroid-specific transcription factor Gcm2. J. Clin. Invest. 120, 2144–2155.

Grigorieva, I.V., Thakker, R.V., 2011. Transcription factors in parathyroid development: lessons from hypoparathyroid disorders. Ann. N. Y. Acad. Sci. 1237, 24–38.

Grote, D., Boualia, S.K., Souabni, A., Merkel, C., Chi, X., Costantini, F., Carroll, T., Bouchard, M., 2008. Gata3 acts downstream of beta-catenin signaling to prevent ectopic metanephric kidney induction. PLoS Genet. 4, e1000316.

Grote, D., Souabni, A., Busslinger, M., Bouchard, M., 2006. Pax 2/8-regulated Gata 3 expression is necessary for morphogenesis and guidance of the nephric duct in the developing kidney. Development 133, 53–61.

Guan, B., Welch, J.M., Sapp, J.C., Ling, H., Li, Y., Johnston, J.J., Kebebew, E., Biesecker, L.G., Simonds, W.F., Marx, S.J., Agarwal, S.K., 2016. GCM2-Activating mutations in familial isolated hyperparathyroidism. Am. J. Hum. Genet. 99, 1034–1044.

Gunther, T., Chen, Z.F., Kim, J., Priemel, M., Rueger, J.M., Amling, M., Moseley, J.M., Martin, T.J., Anderson, D.J., Karsenty, G., 2000. Genetic ablation of parathyroid glands reveals another source of parathyroid hormone. Nature 406, 199–203.

Han, S.I., Tsunekage, Y., Kataoka, K., 2015. Gata3 cooperates with Gcm2 and MafB to activate parathyroid hormone gene expression by interacting with SP1. Mol. Cell. Endocrinol. 411, 113–120.

Hannan, F.M., Babinsky, V.N., Thakker, R.V., 2016. Disorders of the calcium-sensing receptor and partner proteins: insights into the molecular basis of calcium homeostasis. J. Mol. Endocrinol. 57, R127–R142.

Hannan, F.M., Olesen, M.K., Thakker, R.V., 2017. Calcimimetic and calcilytic therapies for inherited disorders of the calcium-sensing receptor signalling pathway. Br. J. Pharmacol. https://doi.org/10.1111/bph.14086.

Hannan, F.M., Thakker, R.V., 2013. Calcium-sensing receptor (CaSR) mutations and disorders of calcium, electrolyte and water metabolism. Best Pract. Res. Clin. Endocrinol. Metabol. 27, 359–371.

Hannan, F.M., Walls, G.V., Babinsky, V.N., Nesbit, M.A., Kallay, E., Hough, T.A., Fraser, W.D., Cox, R.D., Hu, J., Spiegel, A.M., Thakker, R.V., 2015. The calcilytic agent NPS 2143 rectifies hypocalcemia in a mouse model with an activating calcium-sensing receptor (CaSR) mutation: relevance to autosomal dominant hypocalcemia type 1 (ADH1). Endocrinology 156, 3114–3121.

Heino, M., Peterson, P., Kudoh, J., Nagamine, K., Lagerstedt, A., Ovod, V., Ranki, A., Rantala, I., Nieminen, M., Tuukkanen, J., Scott, H.S., Antonarakis, S.E., Shimizu, N., Krohn, K., 1999. Autoimmune regulator is expressed in the cells regulating immune tolerance in thymus medulla. Biochem. Biophys. Res. Commun. 257, 821–825.

Hieronimus, S., Bec-Roche, M., Pedeutour, F., Lambert, J.C., Wagner-Malher, K., Mas, J.C., Sadoul, J.L., Fenichel, P., 2006. The spectrum of parathyroid gland dysfunction associated with the microdeletion 22q11. Eur. J. Endocrinol. 155, 47–52.

Hosoya, T., Maillard, I., Engel, J.D., 2010. From the cradle to the grave: activities of GATA-3 throughout T-cell development and differentiation. Immunol. Rev. 238, 110–125.

Hough, T.A., Bogani, D., Cheeseman, M.T., Favor, J., Nesbit, M.A., Thakker, R.V., Lyon, M.F., 2004. Activating calcium-sensing receptor mutation in the mouse is associated with cataracts and ectopic calcification. Proc. Natl. Acad. Sci. U. S. A. 101, 13566–13571.

Husebye, E.S., Anderson, M.S., Kampe, O., 2018. Autoimmune polyendocrine syndromes. N. Engl. J. Med. 378, 1132–1141.

Inoue, H., Takada, H., Kusuda, T., Goto, T., Ochiai, M., Kinjo, T., Muneuchi, J., Takahata, Y., Takahashi, N., Morio, T., Kosaki, K., Hara, T., 2010. Successful cord blood transplantation for a CHARGE syndrome with CHD7 mutation showing DiGeorge sequence including hypoparathyroidism. Eur. J. Pediatr. 169, 839–844.

Isojima, T., Doi, K., Mitsui, J., Oda, Y., Tokuhiro, E., Yasoda, A., Yorifuji, T., Horikawa, R., Yoshimura, J., Ishiura, H., Morishita, S., Tsuji, S., Kitanaka, S., 2014. A recurrent de novo FAM111A mutation causes Kenny-Caffey syndrome type 2. J. Bone Miner. Res. 29, 992–998.

Isotani, H., Fukumoto, Y., Kawamura, H., Furukawa, K., Ohsawa, N., Goto, Y., Nishino, I., Nonaka, I., 1996. Hypoparathyroidism and insulin-dependent diabetes mellitus in a patient with Kearns-Sayre syndrome harbouring a mitochondrial DNA deletion. Clin. Endocrinol. 45, 637–641.

Jerome, L.A., Papaioannou, V.E., 2001. DiGeorge syndrome phenotype in mice mutant for the T-box gene, Tbx1. Nat. Genet. 27, 286–291.

Juppner, H., Abou-Samra, A.B., Freeman, M., Kong, X.F., Schipani, E., Richards, J., Kolakowski JR., L.F., Hock, J., Potts JR., J.T., Kronenberg, H.M., et al., 1991. A G protein-linked receptor for parathyroid hormone and parathyroid hormone-related peptide. Science 254, 1024–1026.

Kamitani-Kawamoto, A., Hamada, M., Moriguchi, T., Miyai, M., Saji, F., Hatamura, I., Nishikawa, K., Takayanagi, H., Hitoshi, S., Ikenaka, K., Hosoya, T., Hotta, Y., Takahashi, S., Kataoka, K., 2011. MafB interacts with Gcm2 and regulates parathyroid hormone expression and parathyroid development. J. Bone Miner. Res. 26, 2463–2472.

Kappen, C., Schughart, K., Ruddle, F.H., 1989. Two steps in the evolution of Antennapedia-class vertebrate homeobox genes. Proc. Natl. Acad. Sci. U. S. A. 86, 5459–5463.

Karaplis, A.C., Lim, S.K., Baba, H., Arnold, A., Kronenberg, H.M., 1995. Inefficient membrane targeting, translocation, and proteolytic processing by signal peptidase of a mutant preproparathyroid hormone protein. J. Biol. Chem. 270, 1629–1635.

Kemper, B., Habener, J.F., Mulligan, R.C., Potts JR., J.T., Rich, A., 1974. Pre-proparathyroid hormone: a direct translation product of parathyroid messenger RNA. Proc. Natl. Acad. Sci. U. S. A. 71, 3731–3735.

Kiernan, A.E., Pelling, A.L., Leung, K.K., Tang, A.S., Bell, D.M., Tease, C., Lovell-Badge, R., Steel, K.P., Cheah, K.S., 2005. Sox2 is required for sensory organ development in the mammalian inner ear. Nature 434, 1031–1035.

Kim, J., Jones, B.W., Zock, C., Chen, Z., Wang, H., Goodman, C.S., Anderson, D.J., 1998. Isolation and characterization of mammalian homologs of the Drosophila gene glial cells missing. Proc. Natl. Acad. Sci. U. S. A. 95, 12364–12369.

Kim, J.H., Shin, Y.L., Yang, S., Cheon, C.K., Cho, J.H., Lee, B.H., Kim, G.H., Lee, J.O., Seo, E.J., Choi, J.H., Yoo, H.W., 2015. Diverse genetic aetiologies and clinical outcomes of paediatric hypoparathyroidism. Clin. Endocrinol. 83, 790–796.

Kleinjan, D.A., Van Heyningen, V., 2005. Long-range control of gene expression: emerging mechanisms and disruption in disease. Am. J. Hum. Genet. 76, 8–32.

Kobrynski, L.J., Sullivan, K.E., 2007. Velocardiofacial syndrome, DiGeorge syndrome: the chromosome 22q11.2 deletion syndromes. Lancet 370, 1443−1452.

Koster, R.W., Kuhnlein, R.P., Wittbrodt, J., 2000. Ectopic Sox3 activity elicits sensory placode formation. Mech. Dev. 95, 175−187.

Laumonnier, F., Ronce, N., Hamel, B.C., Thomas, P., Lespinasse, J., Raynaud, M., Paringaux, C., VAN Bokhoven, H., Kalscheuer, V., Fryns, J.P., Chelly, J., Moraine, C., Briault, S., 2002. Transcription factor SOX3 is involved in X-linked mental retardation with growth hormone deficiency. Am. J. Hum. Genet. 71, 1450−1455.

Lee, S., Mannstadt, M., Guo, J., Kim, S.M., Yi, H.S., Khatri, A., Dean, T., Okazaki, M., Gardella, T.J., Juppner, H., 2015. A homozygous [Cys25]PTH(1-84) mutation that impairs PTH/PTHrP receptor activation defines a novel form of hypoparathyroidism. J. Bone Miner. Res. 30, 1803−1813.

Leonard, J.D., Gilmore, D.C., Dileepan, T., Nawrocka, W.I., Chao, J.L., Schoenbach, M.H., Jenkins, M.K., Adams, E.J., Savage, P.A., 2017. Identification of natural regulatory T cell epitopes reveals convergence on a dominant autoantigen. Immunity 47, 107−117 e8.

Lerman-Sagie, T., Merlob, P., Shuper, A., Kauli, R., Kozokaro, Z., Grunebaum, M., Mimouni, M., 1990. New findings in a patient with Dubowitz syndrome: velopharyngeal insufficiency and hypoparathyroidism. Am. J. Med. Genet. 37, 241−243.

Li, D., Opas, E.E., Tuluc, F., Metzger, D.L., Hou, C., Hakonarson, H., Levine, M.A., 2014. Autosomal dominant hypoparathyroidism caused by germline mutation in GNA11: phenotypic and molecular characterization. J. Clin. Endocrinol. Metab. 99, E1774−E1783.

Li, D., Streeten, E.A., Chan, A., Lwin, W., Tian, L., Pellegrino DA Silva, R., Kim, C.E., Anderson, M.S., Hakonarson, H., Levine, M.A., 2017. Exome sequencing reveals mutations in AIRE as a cause of isolated hypoparathyroidism. J. Clin. Endocrinol. Metab. 102, 1726−1733.

Lichtner, P., Konig, R., Hasegawa, T., VAN Esch, H., Meitinger, T., Schuffenhauer, S., 2000. An HDR (hypoparathyroidism, deafness, renal dysplasia) syndrome locus maps distal to the DiGeorge syndrome region on 10p13/14. J. Med. Genet. 37, 33−37.

Lim, K.C., Lakshmanan, G., Crawford, S.E., Gu, Y., Grosveld, F., Engel, J.D., 2000. Gata3 loss leads to embryonic lethality due to noradrenaline deficiency of the sympathetic nervous system. Nat. Genet. 25, 209−212.

Lindsay, E.A., Vitelli, F., Su, H., Morishima, M., Huynh, T., Pramparo, T., Jurecic, V., Ogunrinu, G., Sutherland, H.F., Scambler, P.J., Bradley, A., Baldini, A., 2001. Tbx1 haploinsufficieny in the DiGeorge syndrome region causes aortic arch defects in mice. Nature 410, 97−101.

Lindstrand, A., Malmgren, H., Verri, A., Benetti, E., Eriksson, M., Nordgren, A., Anderlid, B.M., Golovleva, I., Schoumans, J., Blennow, E., 2010. Molecular and clinical characterization of patients with overlapping 10p deletions. Am. J. Med. Genet. 152A, 1233−1243.

Liston, A., Lesage, S., Wilson, J., Peltonen, L., Goodnow, C.C., 2003. Aire regulates negative selection of organ-specific T cells. Nat. Immunol. 4, 350−354.

Liu, Z., Yu, S., Manley, N.R., 2007. Gcm2 is required for the differentiation and survival of parathyroid precursor cells in the parathyroid/thymus primordia. Dev. Biol. 305, 333−346.

Luo, X.J., Deng, M., Xie, X., Huang, L., Wang, H., Jiang, L., Liang, G., Hu, F., Tieu, R., Chen, R., Gan, L., 2013. GATA3 controls the specification of prosensory domain and neuronal survival in the mouse cochlea. Hum. Mol. Genet. 22, 3609−3623.

Malchow, S., Leventhal, D.S., Nishi, S., Fischer, B.I., Shen, L., Paner, G.P., Amit, A.S., Kang, C., Geddes, J.E., Allison, J.P., Socci, N.D., Savage, P.A., 2013. Aire-dependent thymic development of tumor-associated regulatory T cells. Science 339, 1219−1224.

Mallo, M., 2018. Reassessing the role of hox genes during vertebrate development and evolution. Trends Genet. 34, 209−217.

Manley, N.R., Capecchi, M.R., 1995. The role of Hoxa-3 in mouse thymus and thyroid development. Development 121, 1989−2003.

Manley, N.R., Capecchi, M.R., 1998. Hox group 3 paralogs regulate the development and migration of the thymus, thyroid, and parathyroid glands. Dev. Biol. 195, 1−15.

Mannstadt, M., Bertrand, G., Muresan, M., Weryha, G., Leheup, B., Pulusani, S.R., Grandchamp, B., Juppner, H., Silve, C., 2008. Dominant-negative GCMB mutations cause an autosomal dominant form of hypoparathyroidism. J. Clin. Endocrinol. Metab. 93, 3568−3576.

Mannstadt, M., Bilezikian, J.P., Thakker, R.V., Hannan, F.M., Clarke, B.L., Rejnmark, L., Mitchell, D.M., Vokes, T.J., Winer, K.K., Shoback, D.M., 2017. Hypoparathyroidism. Nat Rev Dis Primers 3, 17055.

Mannstadt, M., Harris, M., Bravenboer, B., Chitturi, S., Dreijerink, K.M., Lambright, D.G., Lim, E.T., Daly, M.J., Gabriel, S., Juppner, H., 2013. Germline mutations affecting Galpha11 in hypoparathyroidism. N. Engl. J. Med. 368, 2532−2534.

Mino, Y., Kuwahara, T., Mannami, T., Shioji, K., Ono, K., Iwai, N., 2005. Identification of a novel insertion mutation in GATA3 with HDR syndrome. Clin. Exp. Nephrol. 9, 58−61.

Mirczuk, S.M., Bowl, M.R., Nesbit, M.A., Cranston, T., Fratter, C., Allgrove, J., Brain, C., Thakker, R.V., 2010. A missense glial cells missing homolog B (GCMB) mutation, Asn502His, causes autosomal dominant hypoparathyroidism. J. Clin. Endocrinol. Metab. 95, 3512−3516.

Miric, A., Levine, M.A., 1992. Analysis of the preproPTH gene by denaturing gradient gel electrophoresis in familial isolated hypoparathyroidism. J. Clin. Endocrinol. Metab. 74, 509−516.

Mizobuchi, M., Ritter, C.S., Krits, I., Slatopolsky, E., Sicard, G., Brown, A.J., 2009. Calcium-sensing receptor expression is regulated by glial cells missing-2 in human parathyroid cells. J. Bone Miner. Res. 24, 1173−1179.

Monaco, G., Pignata, C., Rossi, E., Mascellaro, O., Cocozza, S., Ciccimarra, F., 1991. DiGeorge anomaly associated with 10p deletion. Am. J. Med. Genet. 39, 215−216.

Monsoro-Burq, A.H., 2015. PAX transcription factors in neural crest development. Semin. Cell Dev. Biol. 44, 87−96.

Moraes, C.T., Dimauro, S., Zeviani, M., Lombes, A., Shanske, S., Miranda, A.F., Nakase, H., Bonilla, E., Werneck, L.C., Servidei, S., et al., 1989. Mitochondrial DNA deletions in progressive external ophthalmoplegia and Kearns-Sayre syndrome. N. Engl. J. Med. 320, 1293−1299.

Morten, K.J., Cooper, J.M., Brown, G.K., Lake, B.D., Pike, D., Poulton, J., 1993. A new point mutation associated with mitochondrial encephalomyopathy. Hum. Mol. Genet. 2, 2081−2087.

Mumm, S., Whyte, M.P., Thakker, R.V., Buetow, K.H., Schlessinger, D., 1997. mtDNA analysis shows common ancestry in two kindreds with X-linked recessive hypoparathyroidism and reveals a heteroplasmic silent mutation. Am. J. Hum. Genet. 60, 153–159.

Muroya, K., Hasegawa, T., Ito, Y., Nagai, T., Isotani, H., Iwata, Y., Yamamoto, K., Fujimoto, S., Seishu, S., Fukushima, Y., Hasegawa, Y., Ogata, T., 2001. GATA3 abnormalities and the phenotypic spectrum of HDR syndrome. J. Med. Genet. 38, 374–380.

Nagamine, K., Peterson, P., Scott, H.S., Kudoh, J., Minoshima, S., Heino, M., Krohn, K.J., Lalioti, M.D., Mullis, P.E., Antonarakis, S.E., Kawasaki, K., Asakawa, S., Ito, F., Shimizu, N., 1997. Positional cloning of the APECED gene. Nat. Genet. 17, 393–398.

Naiki, M., Ochi, N., Kato, Y.S., Purevsuren, J., Yamada, K., Kimura, R., Fukushi, D., Hara, S., Yamada, Y., Kumagai, T., Yamaguchi, S., Wakamatsu, N., 2014. Mutations in HADHB, which encodes the beta-subunit of mitochondrial trifunctional protein, cause infantile onset hypoparathyroidism and peripheral polyneuropathy. Am. J. Med. Genet. 164A, 1180–1187.

Nakada, Y., Terui, K., Kageyama, K., Tsushima, Y., Murakami, H., Soma, Y., Nigawara, T., Sakihara, S., 2013. An adult case of 22q11.2 deletion syndrome diagnosed in a 36-year-old woman with hypocalcemia caused by hypoparathyroidism and Hashimoto's thyroiditis. Intern. Med. 52, 1365–1368.

Naveh-Many, T., Rahamimov, R., Livni, N., Silver, J., 1995. Parathyroid cell proliferation in normal and chronic renal failure rats. The effects of calcium, phosphate, and vitamin D. J. Clin. Investig. 96, 1786–1793.

Naylor, S.L., Sakaguchi, A.Y., Szoka, P., Hendy, G.N., Kronenberg, H.M., Rich, A., Shows, T.B., 1983. Human parathyroid hormone gene (PTH) is on short arm of chromosome 11. Somat. Cell Genet. 9, 609–616.

Nesbit, M.A., Bowl, M.R., Harding, B., Ali, A., Ayala, A., Crowe, C., Dobbie, A., Hampson, G., Holdaway, I., Levine, M.A., Mcwilliams, R., Rigden, S., Sampson, J., Williams, A.J., Thakker, R.V., 2004. Characterization of GATA3 mutations in the hypoparathyroidism, deafness, and renal dysplasia (HDR) syndrome. J. Biol. Chem. 279, 22624–22634.

Nesbit, M.A., Hannan, F.M., Howles, S.A., Babinsky, V.N., Head, R.A., Cranston, T., Rust, N., Hobbs, M.R., Heath 3RD, H., Thakker, R.V., 2013. Mutations affecting G-protein subunit alpha11 in hypercalcemia and hypocalcemia. N. Engl. J. Med. 368, 2476–2486.

Okazaki, T., Igarashi, T., Kronenberg, H.M., 1988. 5'-flanking region of the parathyroid hormone gene mediates negative regulation by 1,25-(OH)2 vitamin D3. J. Biol. Chem. 263, 2203–2208.

Orlova, E.M., Sozaeva, L.S., Kareva, M.A., Oftedal, B.E., Wolff, A.S.B., Breivik, L., Zakharova, E.Y., Ivanova, O.N., Kampe, O., Dedov, I., Knappskog, P.M., Peterkova, V.A., Husebye, E.S., 2017. Expanding the phenotypic and genotypic landscape of autoimmune polyendocrine syndrome type 1. J. Clin. Endocrinol. Metab. 102, 3546–3556.

Pandolfi, P.P., Roth, M.E., Karis, A., Leonard, M.W., Dzierzak, E., Grosveld, F.G., Engel, J.D., Lindenbaum, M.H., 1995. Targeted disruption of the GATA3 gene causes severe abnormalities in the nervous system and in fetal liver haematopoiesis. Nat. Genet. 11, 40–44.

Parkinson, D.B., Shaw, N.J., Himsworth, R.L., Thakker, R.V., 1993. Parathyroid hormone gene analysis in autosomal hypoparathyroidism using an intragenic tetranucleotide (AAAT)n polymorphism. Hum. Genet. 91, 281–284.

Parkinson, D.B., Thakker, R.V., 1992. A donor splice site mutation in the parathyroid hormone gene is associated with autosomal recessive hypoparathyroidism. Nat. Genet. 1, 149–152.

Parvari, R., Hershkovitz, E., Grossman, N., Gorodischer, R., Loeys, B., Zecic, A., Mortier, G., Gregory, S., Sharony, R., Kambouris, M., Sakati, N., Meyer, B.F., AL Aqeel, A.I., AL Humaidan, A.K., AL Zanhrani, F., AL Swaid, A., AL Othman, J., Diaz, G.A., Weiner, R., Khan, K.T., Gordon, R., Gelb, B.D., Consortium, H. R. A. R. K.-C. S, 2002. Mutation of TBCE causes hypoparathyroidism-retardation-dysmorphism and autosomal recessive Kenny-Caffey syndrome. Nat. Genet. 32, 448–452.

Parvari, R., Hershkovitz, E., Kanis, A., Gorodischer, R., Shalitin, S., Sheffield, V.C., Carmi, R., 1998. Homozygosity and linkage-disequilibrium mapping of the syndrome of congenital hypoparathyroidism, growth and mental retardation, and dysmorphism to a 1-cM interval on chromosome 1q42-43. Am. J. Hum. Genet. 63, 163–169.

Pearce, S.H., Cheetham, T., Imrie, H., Vaidya, B., Barnes, N.D., Bilous, R.W., Carr, D., Meeran, K., Shaw, N.J., Smith, C.S., Toft, A.D., Williams, G., Kendall-Taylor, P., 1998. A common and recurrent 13-bp deletion in the autoimmune regulator gene in British kindreds with autoimmune polyendocrinopathy type 1. Am. J. Hum. Genet. 63, 1675–1684.

Pearce, S.H., Williamson, C., Kifor, O., Bai, M., Coulthard, M.G., Davies, M., Lewis-Barned, N., Mccredie, D., Powell, H., Kendall-Taylor, P., Brown, E.M., Thakker, R.V., 1996. A familial syndrome of hypocalcemia with hypercalciuria due to mutations in the calcium-sensing receptor. N. Engl. J. Med. 335, 1115–1122.

Peden, V.H., 1960. True idiopathic hypoparathyroidism as a sex-linked recessive trait. Am. J. Hum. Genet. 12, 323–337.

Perheentupa, J., 2002. APS-I/APECED: the clinical disease and therapy. Endocrinol Metab. Clin. N. Am. 31, 295–320 vi.

Peters, H., Neubuser, A., Kratochwil, K., Balling, R., 1998. Pax9-deficient mice lack pharyngeal pouch derivatives and teeth and exhibit craniofacial and limb abnormalities. Genes Dev. 12, 2735–2747.

Pillar, N., Pleniceanu, O., Fang, M., Ziv, L., Lahav, E., Botchan, S., Cheng, L., Dekel, B., Shomron, N., 2017. A rare variant in the FHL1 gene associated with X-linked recessive hypoparathyroidism. Hum. Genet. 136, 835–845.

Piret, S.E., Gorvin, C.M., Pagnamenta, A.T., Howles, S.A., Cranston, T., Rust, N., Nesbit, M.A., Glaser, B., Taylor, J.C., Buchs, A.E., Hannan, F.M., Thakker, R.V., 2016. Identification of a G-protein subunit-alpha11 gain-of-function mutation, Val340Met, in a family with autosomal dominant hypocalcemia type 2 (ADH2). J. Bone Miner. Res. 31, 1207–1214.

Quinonez, S.C., Innis, J.W., 2014. Human HOX gene disorders. Mol. Genet. Metabol. 111, 4–15.

Randall, V., Mccue, K., Roberts, C., Kyriakopoulou, V., Beddow, S., Barrett, A.N., Vitelli, F., Prescott, K., Shaw-Smith, C., Devriendt, K., Bosman, E., Steffes, G., Steel, K.P., Simrick, S., Basson, M.A., Illingworth, E., Scambler, P.J., 2009. Great vessel development requires biallelic expression of Chd7 and Tbx1 in pharyngeal ectoderm in mice. J. Clin. Invest. 119, 3301–3310.

Relaix, F., 2015. Pax genes: master regulators of development and tissue homeostasis. Semin. Cell Dev. Biol. 44, 62–63.

Rizzoti, K., Brunelli, S., Carmignac, D., Thomas, P.Q., Robinson, I.C., Lovell-Badge, R., 2004. SOX3 is required during the formation of the hypothalamo-pituitary axis. Nat. Genet. 36, 247–255.

Roszko, K.L., Bi, R., Gorvin, C.M., Brauner-Osborne, H., Xiong, X.F., Inoue, A., Thakker, R.V., Stromgaard, K., Gardella, T., Mannstadt, M., 2017. Knockin mouse with mutant Galpha11 mimics human inherited hypocalcemia and is rescued by pharmacologic inhibitors. JCI Insight 2, e91079.

Sahoo, S.K., Zaidi, G., Srivastava, R., Sarangi, A.N., Bharti, N., Eriksson, D., Bensing, S., Kampe, O., Aggarwal, A., Aggarwal, R., Bhatia, E., 2016. Identification of autoimmune polyendocrine syndrome type 1 in patients with isolated hypoparathyroidism. Clin. Endocrinol. 85, 544–550.

Sanjad, S.A., Sakati, N.A., Abu-Osba, Y.K., Kaddoura, R., Milner, R.D., 1991. A new syndrome of congenital hypoparathyroidism, severe growth failure, and dysmorphic features. Arch. Dis. Child. 66, 193–196.

Scambler, P.J., 2000. The 22q11 deletion syndromes. Hum. Mol. Genet. 9, 2421–2426.

Scambler, P.J., Carey, A.H., Wyse, R.K., Roach, S., Dumanski, J.P., Nordenskjold, M., Williamson, R., 1991. Microdeletions within 22q11 associated with sporadic and familial DiGeorge syndrome. Genomics 10, 201–206.

Schlosser, G., Ahrens, K., 2004. Molecular anatomy of placode development in *Xenopus laevis*. Dev. Biol. 271, 439–466.

Schmidtke, J., Pape, B., Krengel, U., Langenbeck, U., Cooper, D.N., Breyel, E., Mayer, H., 1984. Restriction fragment length polymorphisms at the human parathyroid hormone gene locus. Hum. Genet. 67, 428–431.

Segre, G.V., 1996. Receptors for parathyroid hormone and parathyroid hormone-related protein. In: Bilezikian, J.P. (Ed.), Principles in Bone Biology. Academic Press, San Diego, CA.

Slatopolsky, E., Finch, J., Denda, M., Ritter, C., Zhong, M., Dusso, A., Macdonald, P.N., Brown, A.J., 1996. Phosphorus restriction prevents parathyroid gland growth. High phosphorus directly stimulates PTH secretion in vitro. J. Clin. Invest. 97, 2534–2540.

Solomon, N.M., Nouri, S., Warne, G.L., Lagerstrom-Fermer, M., Forrest, S.M., Thomas, P.Q., 2002. Increased gene dosage at Xq26-q27 is associated with X-linked hypopituitarism. Genomics 79, 553–559.

Solomon, N.M., Ross, S.A., Morgan, T., Belsky, J.L., Hol, F.A., Karnes, P.S., Hopwood, N.J., Myers, S.E., Tan, A.S., Warne, G.L., Forrest, S.M., Thomas, P.Q., 2004. Array comparative genomic hybridisation analysis of boys with X linked hypopituitarism identifies a 3.9 Mb duplicated critical region at Xq27 containing SOX3. J. Med. Genet. 41, 669–678.

Stevanovic, M., Lovell-Badge, R., Collignon, J., Goodfellow, P.N., 1993. SOX3 is an X-linked gene related to SRY. Hum. Mol. Genet. 2, 2013–2018.

Su, D., Ellis, S., Napier, A., Lee, K., Manley, N.R., 2001. Hoxa3 and pax1 regulate epithelial cell death and proliferation during thymus and parathyroid organogenesis. Dev. Biol. 236, 316–329.

Sunthornthepvarakul, T., Churesigaew, S., Ngowngarmratana, S., 1999. A novel mutation of the signal peptide of the preproparathyroid hormone gene associated with autosomal recessive familial isolated hypoparathyroidism. J. Clin. Endocrinol. Metab. 84, 3792–3796.

Svensson, E.C., Tufts, R.L., Polk, C.E., Leiden, J.M., 1999. Molecular cloning of FOG-2: a modulator of transcription factor GATA-4 in cardiomyocytes. Proc. Natl. Acad. Sci. U. S. A. 96, 956–961.

Taylor, J.C., Martin, H.C., Lise, S., Broxholme, J., Cazier, J.B., Rimmer, A., Kanapin, A., Lunter, G., Fiddy, S., Allan, C., Aricescu, A.R., Attar, M., Babbs, C., Becq, J., Beeson, D., Bento, C., Bignell, P., Blair, E., Buckle, V.J., Bull, K., Cais, O., Cario, H., Chapel, H., Copley, R.R., Cornall, R., Craft, J., Dahan, K., Davenport, E.E., Dendrou, C., Devuyst, O., Fenwick, A.L., Flint, J., Fugger, L., Gilbert, R.D., Goriely, A., Green, A., Greger, I.H., Grocock, R., Gruszczyk, A.V., Hastings, R., Hatton, E., Higgs, D., Hill, A., Holmes, C., Howard, M., Hughes, L., Humburg, P., Johnson, D., Karpe, F., Kingsbury, Z., Kini, U., Knight, J.C., Krohn, J., Lamble, S., Langman, C., Lonie, L., Luck, J., Mccarthy, D., Mcgowan, S.J., Mcmullin, M.F., Miller, K.A., Murray, L., Nemeth, A.H., Nesbit, M.A., Nutt, D., Ormondroyd, E., Oturai, A.B., Pagnamenta, A., Patel, S.Y., Percy, M., Petousi, N., Piazza, P., Piret, S.E., Polanco-Echeverry, G., Popitsch, N., Powrie, F., Pugh, C., Quek, L., Robbins, P.A., Robson, K., Russo, A., Sahgal, N., Van Schouwenburg, P.A., Schuh, A., Silverman, E., Simmons, A., Sorensen, P.S., Sweeney, E., Taylor, J., Thakker, R.V., Tomlinson, I., Trebes, A., Twigg, S.R., Uhlig, H.H., Vyas, P., Vyse, T., Wall, S.A., Watkins, H., Whyte, M.P., Witty, L., et al., 2015. Factors influencing success of clinical genome sequencing across a broad spectrum of disorders. Nat. Genet. 47, 717–726.

Tenhola, S., Voutilainen, R., Reyes, M., Toiviainen-Salo, S., Juppner, H., Makitie, O., 2016. Impaired growth and intracranial calcifications in autosomal dominant hypocalcemia caused by a GNA11 mutation. Eur. J. Endocrinol. 175, 211–218.

Tevosian, S.G., Deconinck, A.E., Cantor, A.B., Rieff, H.I., Fujiwara, Y., Corfas, G., Orkin, S.H., 1999. FOG-2: a novel GATA-family cofactor related to multitype zinc-finger proteins Friend of GATA-1 and U-shaped. Proc. Natl. Acad. Sci. U. S. A. 96, 950–955.

Thakker, R.V., Davies, K.E., Whyte, M.P., Wooding, C., O'riordan, J.L., 1990. Mapping the gene causing X-linked recessive idiopathic hypoparathyroidism to Xq26-Xq27 by linkage studies. J. Clin. Invest. 86, 40–45.

The Finnish-German APECED Consortium, 1997. An autoimmune disease, APECED, caused by mutations in a novel gene featuring two PHD-type zinc finger domains. Nat. Genet. 17, 399–403.

Trump, D., Dixon, P.H., Mumm, S., Wooding, C., Davies, K.E., Schlessinger, D., Whyte, M.P., Thakker, R.V., 1998. Localisation of X linked recessive idiopathic hypoparathyroidism to a 1.5 Mb region on Xq26-q27. J. Med. Genet. 35, 905–909.

Tsang, A.P., Visvader, J.E., Turner, C.A., Fujiwara, Y., Yu, C., Weiss, M.J., Crossley, M., Orkin, S.H., 1997. FOG, a multitype zinc finger protein, acts as a cofactor for transcription factor GATA-1 in erythroid and megakaryocytic differentiation. Cell 90, 109–119.

Uchikawa, M., Ishida, Y., Takemoto, T., Kamachi, Y., Kondoh, H., 2003. Functional analysis of chicken Sox2 enhancers highlights an array of diverse regulatory elements that are conserved in mammals. Dev. Cell 4, 509–519.

Unger, S., Gorna, M.W., Le Bechec, A., Do Vale-Pereira, S., Bedeschi, M.F., Geiberger, S., Grigelioniene, G., Horemuzova, E., Lalatta, F., Lausch, E., Magnani, C., Nampoothiri, S., Nishimura, G., Petrella, D., Rojas-Ringeling, F., Utsunomiya, A., Zabel, B., Pradervand, S., Harshman, K.,

Campos-Xavier, B., Bonafe, L., Superti-Furga, G., Stevenson, B., Superti-Furga, A., 2013. FAM111A mutations result in hypoparathyroidism and impaired skeletal development. Am. J. Hum. Genet. 92, 990–995.

Van deR Wees, J., Van Looij, M.A., de Ruiter, M.M., Elias, H., Van der Burg, H., Liem, S.S., Kurek, D., Engel, J.D., Karis, A., Van Zanten, B.G., de Zeeuw, C.I., Grosveld, F.G., Van Doorninck, J.H., 2004. Hearing loss following Gata3 haploinsufficiency is caused by cochlear disorder. Neurobiol. Dis. 16, 169–178.

Van Esch, H., Groenen, P., Fryns, J.P., Van de Ven, W., Devriendt, K., 1999. The phenotypic spectrum of the 10p deletion syndrome versus the classical DiGeorge syndrome. Genet. Couns. 10, 59–65.

Van Esch, H., Groenen, P., Nesbit, M.A., Schuffenhauer, S., Lichtner, P., Vanderlinden, G., Harding, B., Beetz, R., Bilous, R.W., Holdaway, I., Shaw, N.J., Fryns, J.P., Van de Ven, W., Thakker, R.V., Devriendt, K., 2000. GATA3 haplo-insufficiency causes human HDR syndrome. Nature 406, 419–422.

van Looij, M.A., Meijers-Heijboer, H., Beetz, R., Thakker, R.V., Christie, P.T., Feenstra, L.W., Van Zanten, B.G., 2006. Characteristics of hearing loss in HDR (hypoparathyroidism, sensorineural deafness, renal dysplasia) syndrome. Audiol. Neuro. Otol. 11, 373–379.

van Looij, M.A., Van der Burg, H., Van der Giessen, R.S., de Ruiter, M.M., Van der Wees, J., Van Doorninck, J.H., de Zeeuw, C.I., Van Zanten, G.A., 2005. GATA3 haploinsufficiency causes a rapid deterioration of distortion product otoacoustic emissions (DPOAEs) in mice. Neurobiol. Dis. 20, 890–897.

van Raamsdonk, C.D., Fitch, K.R., Fuchs, H., de Angelis, M.H., Barsh, G.S., 2004. Effects of G-protein mutations on skin color. Nat. Genet. 36, 961–968.

Vasicek, T.J., Mcdevitt, B.E., Freeman, M.W., Fennick, B.J., Hendy, G.N., Potts JR., J.T., Rich, A., Kronenberg, H.M., 1983. Nucleotide sequence of the human parathyroid hormone gene. Proc. Natl. Acad. Sci. U. S. A. 80, 2127–2131.

Villanueva, M.P., Aiyer, A.R., Muller, S., Pletcher, M.T., Liu, X., Emanuel, B., Srivastava, D., Reeves, R.H., 2002. Genetic and comparative mapping of genes dysregulated in mouse hearts lacking the Hand2 transcription factor gene. Genomics 80, 593–600.

von Heijne, G., 1983. Patterns of amino acids near signal-sequence cleavage sites. Eur. J. Biochem. 133, 17–21.

Watanabe, S., Fukumoto, S., Chang, H., Takeuchi, Y., Hasegawa, Y., Okazaki, R., Chikatsu, N., Fujita, T., 2002. Association between activating mutations of calcium-sensing receptor and Bartter's syndrome. Lancet 360, 692–694.

Whyte, M.P., Kim, G.S., Kosanovich, M., 1986. Absence of parathyroid tissue in sex-linked recessive hypoparathyroidism. J. Pediatr. 109, 915.

Whyte, M.P., Weldon, V.V., 1981. Idiopathic hypoparathyroidism presenting with seizures during infancy: X-linked recessive inheritance in a large Missouri kindred. J. Pediatr. 99, 608–611.

Wilichowski, E., Gruters, A., Kruse, K., Rating, D., Beetz, R., Korenke, G.C., Ernst, B.P., Christen, H.J., Hanefeld, F., 1997. Hypoparathyroidism and deafness associated with pleioplasmic large scale rearrangements of the mitochondrial DNA: a clinical and molecular genetic study of four children with Kearns-Sayre syndrome. Pediatr. Res. 41, 193–200.

Wolff, A.S., Erichsen, M.M., Meager, A., Magitta, N.F., Myhre, A.G., Bollerslev, J., Fougner, K.J., Lima, K., Knappskog, P.M., Husebye, E.S., 2007. Autoimmune polyendocrine syndrome type 1 in Norway: phenotypic variation, autoantibodies, and novel mutations in the autoimmune regulator gene. J. Clin. Endocrinol. Metab. 92, 595–603.

Woods, K.S., Cundall, M., Turton, J., Rizotti, K., Mehta, A., Palmer, R., Wong, J., Chong, W.K., AL-Zyoud, M., EL-Ali, M., Otonkoski, T., Martinez-Barbera, J.P., Thomas, P.Q., Robinson, I.C., Lovell-Badge, R., Woodward, K.J., Dattani, M.T., 2005. Over- and underdosage of SOX3 is associated with infundibular hypoplasia and hypopituitarism. Am. J. Hum. Genet. 76, 833–849.

Xu, P.X., Zheng, W., Laclef, C., Maire, P., Maas, R.L., Peters, H., Xu, X., 2002. Eya1 is required for the morphogenesis of mammalian thymus, parathyroid and thyroid. Development 129, 3033–3044.

Yagi, H., Furutani, Y., Hamada, H., Sasaki, T., Asakawa, S., Minoshima, S., Ichida, F., Joo, K., Kimura, M., Imamura, S., Kamatani, N., Momma, K., Takao, A., Nakazawa, M., Shimizu, N., Matsuoka, R., 2003. Role of TBX1 in human del22q11.2 syndrome. Lancet 362, 1366–1373.

Yamagishi, H., Garg, V., Matsuoka, R., Thomas, T., Srivastava, D., 1999. A molecular pathway revealing a genetic basis for human cardiac and craniofacial defects. Science 283, 1158–1161.

Yamamoto, M., Akatsu, T., Nagase, T., Ogata, E., 2000. Comparison of hypocalcemic hypercalciuria between patients with idiopathic hypoparathyroidism and those with gain-of-function mutations in the calcium-sensing receptor: is it possible to differentiate the two disorders? J. Clin. Endocrinol. Metab. 85, 4583–4591.

Zahirieh, A., Nesbit, M.A., Ali, A., Wang, K., He, N., Stangou, M., Bamichas, G., Sombolos, K., Thakker, R.V., Pei, Y., 2005. Functional analysis of a novel GATA3 mutation in a family with the hypoparathyroidism, deafness, and renal dysplasia syndrome. J. Clin. Endocrinol. Metab. 90, 2445–2450.

Zlotogora, J., Shapiro, M.S., 1992. Polyglandular autoimmune syndrome type I among Iranian Jews. J. Med. Genet. 29, 824–826.

Zorn, A.M., Barish, G.D., Williams, B.O., Lavender, P., Klymkowsky, M.W., Varmus, H.E., 1999. Regulation of Wnt signaling by Sox proteins: XSox17 alpha/beta and XSox3 physically interact with beta-catenin. Mol. Cell 4, 487–498.

Zou, D., Silvius, D., Davenport, J., Grifone, R., Maire, P., Xu, P.X., 2006. Patterning of the third pharyngeal pouch into thymus/parathyroid by Six and Eya1. Dev. Biol. 293, 499–512.

Zweier, C., Sticht, H., Aydin-Yaylagul, I., Campbell, C.E., Rauch, A., 2007. Human TBX1 missense mutations cause gain of function resulting in the same phenotype as 22q11.2 deletions. Am. J. Hum. Genet. 80, 510–517.

Chapter 57

Genetic disorders caused by mutations in the parathyroid hormone/parathyroid hormone–related peptide receptor, its ligands, and downstream effector molecules

Caroline Silve[1,2,3] **and Harald Jüppner**[4,5]

[1]Hôpital Bicêtre, Paris, France; [2]Centre de Référence des Maladies rares du Calcium et du Phosphore and Filière de Santé Maladies Rares OSCAR, AP-HP, Paris, France; [3]Service de Biochimie et Génétique Moléculaires, Hôpital Cochin, AP-HP, Paris, France; [4]Endocrine Unit, Department of Medicine and Pediatric Nephrology, MassGeneral Hospital for Children, Massachusetts General Hospital and Harvard Medical School, Boston, MA, United States; [5]Pediatric Nephrology, MassGeneral Hospital for *Children, Massachusetts General Hospital and Harvard Medical School, Boston, MA, United States*

Chapter outline

Introduction

The PTH/PTHrP receptor (PTHR1; also referred to as type I PTH/PTHrP receptor; gene name *PTHR1*) is a G-protein-coupled receptor (GPCR) that mediates the actions of two ligands, parathyroid hormone (PTH; gene name *PTH*) and PTH-related peptide (PTHrP; also referred to as PTH-like peptide, PTHLP; gene name *PTHLH*). PTHR1 stimulates at least two distinct second-messenger pathways, cAMP/protein kinase A (PKA) and IP_3/Ca^{++}/PKC (for review see Gardella et al., 2016). It is most abundantly expressed in kidney, bone, and growth plates, as well as at lower levels in a large variety of

Principles of Bone Biology. https://doi.org/10.1016/B978-0-12-814841-9.00057-9

other tissues. The critical role of PTH in the endocrine regulation of mineral ion homeostasis had been explored for several decades through numerous studies in intact and parathyroidectomized animals (Potts and Gardella, 2007). Subsequent studies in mice with ablation of the genes encoding PTH (Miao et al., 2002) or GCM2 (Günther et al., 2000), a parathyroid-specific transcription factor, confirmed the importance of PTH for maintaining blood calcium levels within normal limits. PTHrP was first isolated from tumors that cause humeral hypercalcemia of malignancy syndrome (for review see Suva et al., 2015). Because its biological properties were largely indistinguishable from those of PTH, it was predicted that PTHrP acts through the same receptor as that of PTH, which turned out to be the case. However, through analysis of genetically manipulated mice, it became apparent that PTHrP has a particularly important role in the autocrine/paracrine regulation of chondrocyte growth and differentiation. Thus, animals "null" for *Pthlh* die in utero or shortly thereafter, and they show a profound acceleration of growth plate mineralization (Karaplis et al., 1994; Maes and Kronenberg, 2016). In contrast, mice overexpressing PTHrP under the control of a growth plate-specific promoter are viable but show a severe delay in chondrocyte maturation that leads to impaired bone growth and elongation (Weir et al., 1996). Consistent with these latter findings, homozygous ablation of PTHR1 leads to similar, albeit more severe, developmental abnormalities (Maes and Kronenberg, 2016; Lanske et al., 1996). The analysis of different genetically manipulated animals thus provided important clues regarding the phenotypic abnormalities that were to be expected in humans with mutations in PTHR1, its ligands, and some downstream signaling and effector proteins. Likewise, analysis of rare genetic disorders in humans has provided major new insights into the molecules involved in these processes.

The parathyroid hormone/parathyroid hormone–related peptide receptor system

Parathyroid hormone

Besides 1,25 dihydroxy vitamin D {1,25$(OH)_2$D}, PTH is the most important endocrine regulator of extracellular calcium homeostasis in mammals (Gardella et al., 2016; St-Arnaud & Demay, 2011). PTH is almost exclusively expressed in the parathyroid glands; lower protein and mRNA levels were identified only in the hypothalamus and thymus of glial cells missing 2 (*GCM2*)-ablated mice (Günther et al., 2000). Its synthesis and secretion by the parathyroid glands are dependent predominantly on the extracellular concentration of calcium (Silver and Kronenberg, 1996) monitored by the calcium-sensing receptor (Brown et al., 1993), and probably to a lesser extent by 1,25$(OH)_2$D, phosphate and FGF23 (Silver and Kronenberg, 1996; Almaden et al., 1996; Slatopolsky et al., 1996; Ben-Dov et al., 2007; Krajisnik et al., 2007).

PTH acts primarily on kidney and bone, where it binds to cells expressing PTHR1 and thereby initiates a series of processes that serve to maintain blood calcium and phosphate concentrations within narrow limits (Fig. 57.1). In kidney, the mRNA encoding PTHR1 is expressed primarily in the convoluted and straight proximal tubules, the cortical portion of thick ascending limb, and the distal convoluted renal tubules (Riccardi et al., 1996; Lee et al., 1996; Yang et al., 1997)—i.e., in those renal segments that respond to PTH with an increase in cAMP accumulation (Chabardes et al., 1975; Morel et al., 1981). PTHR1s appear to be expressed on the basolateral and brush border membranes, raising the possibility that PTH acts not only via blood circulation from basolateral membrane, but also, after glomerular filtration, from the luminal side (Lupp et al., 2010).

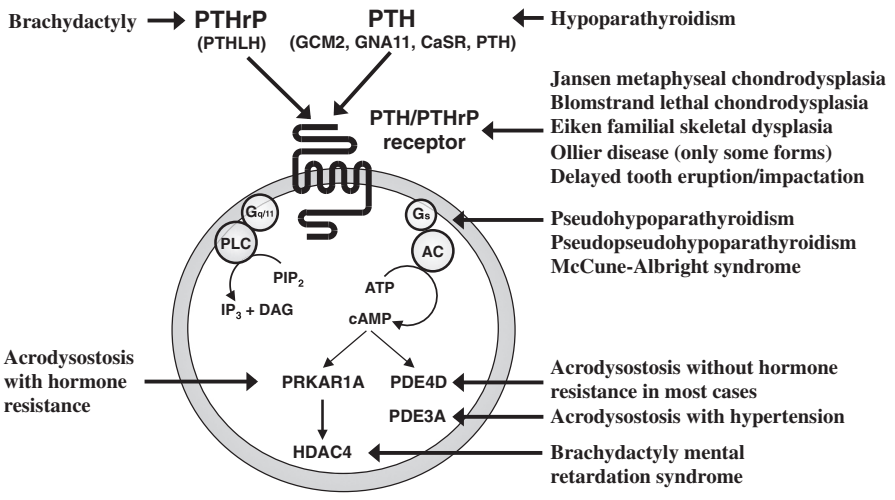

FIGURE 57.1 Human disorders and PTHR1–Gsα–cAMP–PKA signaling pathway. The PTH/PTHrP receptor (PTHR1) is abundantly expressed in kidney and bone, where it mediates the PTH-dependent regulation of calcium and phosphate homeostasis. It is also expressed in numerous other tissues, particularly growth plate chondrocytes, where it mediates, following activation by PTHrP, the regulation of cellular proliferation and differentiation during development. The activated PTHR1 stimulates two second-messenger pathways, cAMP/PKA and IP_3/Ca^{++}/PKC. Genetic diseases associated with defects in the cAMP/PKA pathway are indicated.

The most important PTH-mediated actions in the kidney affect the synthesis of $1,25(OH)_2D$ from its precursor 25(OH)D, excretion of phosphate, and reabsorption of calcium. The stimulation of 1α-hydroxylase activity, an at least partially cAMP-dependent action (Kong et al., 1999; Takeyama et al., 1997), is largely restricted to the proximal convoluted tubule. The resulting increase in $1,25(OH)_2D$ production enhances the absorption of calcium and phosphate from the intestine. PTH-dependent inhibition of renal tubular phosphate reabsorption has been extensively documented in a variety of in vivo and in vitro studies (for reviews see Bacic et al., 2004; Berndt & Kumar, 2007; Bergwitz and Jüppner, 2010; Blaine et al., 2011). To increase urinary phosphate excretion, PTH reduces the abundance of two type II sodium−phosphate cotransporters (NPT2a and NPT2c, also referred to as NaPi-IIa and NaPi-IIc) on the apical surface of proximal tubules (Bacic et al., 2004; Segawa et al., 2002). In rodents, which can be readily studied, Npt2a is expressed in segments S1−S3, while Npt2c is expressed mainly in the S1 segment (Segawa et al., 2007). Acute PTH effects appear to be mediated in vivo prominently by cAMP/PKA-dependent mechanisms (Nagai et al., 2011), which is consistent with the severely diminished PTH-stimulated phosphaturic response in patients with pseudohypoparathyroidism, a group of related disorders caused by maternally inherited mutations in *GNAS*, the gene encoding Gsα, the alpha-subunit of the stimulatory G-protein, and several different splice variants thereof (Patten et al., 1990; Weinstein et al., 1990). However, studies with genetically engineered mice expressing a mutant PTHR1 deficient in signaling through Ca^{2+}/IP_3/PKC-dependent mechanisms have shown that this latter second-messenger pathway contributes also to PTH-mediated phosphaturic response (Guo et al., 2010, 2013). The increase in urinary phosphate excretion stimulated by PTH is associated with increased internalization and subsequent lysosomal degradation of Npt2a, and similar mechanisms appear to apply to the regulation of Npt2c (Segawa et al., 2002, 2007; Biber et al., 2009).

PTHR1 protein expression has been demonstrated by immunohistochemical and immunoelectron microscopic analysis, and functional studies on both basolateral and luminal membranes in proximal tubular cells in vitro as well as in intact proximal tubules (Lupp et al., 2010; Kaufmann et al., 1994; Traebert et al., 2000). Apical receptors may be preferentially coupled to the cAMP-independent signaling pathway, while basolateral receptor activation initiates both cAMP-dependent and cAMP-independent effects (Mahon et al., 2002; Mahon and Segre, 2004). However, PTH(1−34) with a 20-kD polyethylene glycol moiety attached to the C-terminus (PEGylated PTH[1−34]), which shows much reduced glomerular filtration, increases urinary phosphate excretion equivalently to that of unmodified PTH(1−34), indicating that signaling at the basolateral membrane is sufficient for the peptide's phosphaturic response (Guo et al., 2017). On the other hand, megalin, a multifunctional clearance receptor expressed on the apical surface of proximal tubular cells, has been shown to contribute to catabolism of PTH and may antagonize PTHR1 activity (Hilpert et al., 1999). In the distal convoluted tubule, PTH stimulates, possibly through second messengers other than cAMP, the reabsorption of calcium (Friedman et al., 1996; Linglart et al., 2011), which is associated with an increased expression of the calcium channel TRPV5 (Mensenkamp et al., 2007).

Similar to its renal tubular effects, PTH-dependent actions on bone are complex and difficult to study. As outlined later in more detail, PTH can influence, either directly or indirectly, the proliferation and differentiation of several bone cell precursors. Furthermore, the effects resulting from PTH stimulation of mature osteoblasts appear to be different depending on the intensity and duration of the stimulus, type of bone (trabecular vs. cortical), and hormonal exposure of bone. As a result, the hormonal effects observed in vitro often fail to reflect the conditions in vivo. For example, PTH stimulates both bone formation and osteoclastic bone resorption; however, the continuous administration of PTH in vivo is thought to favor bone resorption over formation, whereas intermittent doses of the hormone result in net anabolic effects (Neer et al., 2001; Finkelstein et al., 2003). However, the transgenic expression of a constitutively active human PTHR1 under control of the collagen type Ia1 promoter to target expression to osteoblasts (Calvi et al., 2001), or under the control of the DMP1 promoter to target expression to osteocytes (Rhee et al., 2011), causes a dramatic increase in bone formation, suggesting that continuous low-level receptor activation leads to bone changes similar to those from intermittent treatment with PTH.

Parathyroid hormone−related peptide

PTHrP was first discovered as the major cause of humoral hypercalcemia of malignancy syndrome (for review see Suva et al., 2015). Within its amino-terminal portion, PTHrP shares partial amino acid sequence homology with PTH, and as a result of these limited structural similarities, amino-terminal fragments of both peptides have largely indistinguishable biological properties, at least when tested in different in vitro systems. PTHrP and its mRNA are also found in a large variety of fetal and adult tissues, suggesting that this peptide has an important biological role throughout life. In fact, PTHrP has a prominent role in the regulation of chondrocyte proliferation and differentiation during the process of endochondral bone formation (Maes and Kronenberg, 2016) and epithelial−mesenchymal interactions during

organogenesis of certain epithelial organs including skin, mammary gland, and teeth (Wysolmerski et al., 1996, 1998; Strewler, 2000; Hens et al., 2007).

The parathyroid hormone/parathyroid hormone–related peptide receptor and its role in endochondral bone formation

PTHR1 belongs to the class B family of heptahelical GPCRs, which also comprises the receptors for secretin, calcitonin, glucagon, and several other peptide hormones; it binds PTH and PTHrP (Gardella et al., 2016). Similar to the widely expressed PTHrP, the mRNA encoding PTHR1 is found in a large variety of fetal and adult tissues (Riccardi et al., 1996; Lee et al., 1995) and at particularly abundant concentrations in proximal tubular cells, osteoblasts, and prehypertrophic chondrocytes of metaphyseal growth plate (Maes and Kronenberg, 2016).

Mice with ablation of both *Pthlh* alleles die during the perinatal period and show striking skeletal changes that include domed skulls, short snouts and mandibles, and disproportionately short extremities, yet with no obvious developmental defects in other organs. These skeletal changes are caused by a dramatic acceleration of chondrocyte differentiation that leads to premature growth plate mineralization. Heterozygous animals lacking only one copy of the *Pthlh* gene show normal growth and development and are fertile, but develop, despite apparently normal calcium and phosphorus homeostasis, mild osteopenia later in life (Amizuka et al., 1996). Growth plate abnormalities that are in many aspects the opposite of those found in *Pthlh*-ablated mice are observed in animals that overexpress *PTHLH* under control of the collagen α1(II) promoter (Weir et al., 1996). Throughout life, these animals are smaller in size than their wild-type littermates and show a disproportionate foreshortening of limbs and tail, which is most likely due to a severe delay in chondrocyte differentiation and endochondral ossification. Thus, too little or too much PTHrP expression in the growth plate leads to short-limbed dwarfism, although through entirely different mechanisms.

From these and other studies, it is now well established that PTHrP facilitates the continuous proliferation of chondrocytes in the growth plate and postpones their programmed differentiation into hypertrophic chondrocytes (for review see Maes and Kronenberg, 2016). Consistent with this role of PTHrP in endochondral bone formation, earlier in vitro studies showed that PTH (used in these studies instead of PTHrP) affects chondrocyte maturation and activity. Subsequent studies confirmed these findings by showing that PTH and PTHrP stimulate, presumably through cAMP-dependent mechanisms, the proliferation of fetal growth plate chondrocytes, inhibit the differentiation of these cells into hypertrophic chondrocytes, and stimulate the accumulation of cartilage-specific proteoglycans thought to act as inhibitors of mineralization (Koike et al., 1990; Iwamoto et al., 1994). In the absence of these cartilage-specific PTHrP effects, growth plates of homozygous *Pthlh* gene-ablated mice have a thinner layer of proliferating chondrocytes, while the layer of hypertrophic chondrocytes is relatively normal in thickness but somewhat disorganized. Taken together, these findings suggest that a lack of PTHrP accelerates the normal differentiation process of growth plate chondrocytes—i.e., resting and proliferating chondrocytes undergo fewer cycles of cell division and differentiate prematurely into hypertrophic cells that then undergo apoptosis before being replaced by invading osteoblasts.

The phenotypic changes in mice "null" for either *Pthlh* or PTHR1 are similar, and current evidence indicates that the autocrine/paracrine actions of PTHrP within the growth plate are mediated through the PTHR1 (Maes and Kronenberg, 2016). Furthermore, mice missing either *Pthlh* or its receptor are resistant to the actions of Indian Hedgehog (Ihh), a developmentally important protein that is most abundantly expressed in growth plate chondrocytes, which are about to differentiate into hypertrophic cells. Ihh binds directly to *patched,* a membrane receptor that interacts with smoothened and thereby suppresses the constitutive activity of the latter protein (Stone et al., 1996; Marigo et al., 1996). The ectopic expression of Ihh in the chicken wing cartilage stimulates the production of PTHrP and thereby blocks the normal chondrocyte differentiation program; whether PTHrP represses the expression of Ihh as part of a feedback loop remains to be established. PTHrP and Ihh are thus critically important components of normal bone growth and elongation (Maes and Kronenberg, 2016). However, not all actions of PTHrP appear to be mediated through the PTHR1, since ablation of *Pthlh* or *Pthr1* leads to subtle but distinctly different abnormalities in early bone development (Lanske et al., 1999).

Human disorders caused by mutations in the parathyroid hormone/parathyroid hormone-related peptide signaling pathway

Parathyroid hormone, glial cells missing 2, and *GNA11* mutations

Heterozygous mutations in the calcium-sensing receptor are the most frequent cause of autosomal dominant hypocalcemia (Pollak et al., 1993, 1994; Pearce et al., 1996). Only very few *PTH* gene mutations have been identified as the cause of

isolated hypoparathyroidism (IHP) in families with an autosomal dominant or recessive transmission (Arnold et al., 1990; Parkinson and Thakker, 1992; Sunthornthepvarakul et al., 1999; Ertl et al., 2012; Tomar et al., 2010). Five of these mutations are located in the hormone's prepro-leader segment and thus impair hormone synthesis or secretion. The more recently identified mutation, a homozygous (R25C) in the mature PTH(1−84) polypeptide, reduces the bioactivity of the secreted hormone (Lee et al., 2015). Interestingly, depending on the assay used for evaluating patients carrying this mutation, plasma PTH levels were either low or elevated, thus leading to ambiguities regarding the underlying diagnosis, namely IHP or pseudohypoparathyroidism (PHP) type Ib (PHP1B). In this context, a novel homozygous mutation in PTHR1 (R186H) was hypothesized to result in impaired interaction between PTH and PTHR1, thus postulating that this genetic defect leads to a PHP1B phenotype (Guerreiro et al., 2016). However, the index case presented initially with severe hypocalcemia and hyperphosphatemia yet with normal PTH levels; she revealed no methylation changes at the *GNAS* locus. In contrast, two other family members, both the same homozygous R186H mutation in PTHR1, had laboratory findings consistent with PHP1B; however, no *GNAS* methylation studies were reported for these family members, and no in vitro studies with the mutant PTHR1 were conducted.

More frequently, there are mutations in glial cells missing 2 (*GCM2*), the human homologue of the Drosophila gene, *Gcm*a, and a specific regulator of parathyroid gland development that is expressed exclusively in the parathyroid glands (Günther et al., 2000). Studies of patients with isolated hypoparathyroidism have shown that *GCM2* mutations can be associated with autosomal recessive and dominant forms of the disease (Tomar et al., 2010; Ding et al., 2001; Baumber et al., 2005; Thomee et al., 2005; Mannstadt et al., 2008; Mirczuk et al., 2010; Yi et al., 2012). Mutations in *GNA11* (the gene encoding Gα11, one of the signaling proteins at the calcium-sensing receptor) were shown to cause an autosomal dominant form of hypoparathyroidism (Mannstadt et al., 2013; Nesbit et al., 2013; Piret et al., 2016; Tenhola et al., 2016) that can be associated with short stature (Tenhola et al., 2016; Li et al., 2014). FAM111A mutations have been identified in patients with hypoparathyroidism associated with impaired skeletal development in the context of Kenny−Caffey syndrome type 2 (Unger et al., 2013; Isojima et al., 2014).

Parathyroid hormone−like peptide mutations

Brachydactyly type E (BDE) is characterized by a general shortening of metacarpals, metatarsals, and/or phalanges (Maroteaux, 2002; Mundlos, 2009). BDE can be isolated or occurs as part of familial syndromes such as *GNAS* haploinsufficiency (Bastepe and Jüppner, 2016); furthermore, it is part of a syndrome that includes mental retardation in addition to brachydactyly (Williams et al., 2010). Within families, the phenotype is usually variable, ranging from moderate shortening of individual metacarpals to a shortening of all bones in the hands and/or feet.

Several groups have identified *PTHLH* haploinsufficiency as the cause of autosomal dominant BDE with short stature. *PTHLH* molecular defects causing BDE are heterogeneous and include (1) a balanced translocation with breakpoints upstream of *PTHLH* on chromosome 12p11.2 that introduces a novel C-ets-1/EBS binding site leading to cis-regulated downregulation of *PTHLH* expression (Maass et al., 2010); (2) a microdeletion on chromosome 12p encompassing *PTHLH* (Klopocki et al., 2010) as well as smaller deletions within the *PTHLH* (Thomas-Teinturier et al., 2016); and (3) heterozygous missense, nonstop, and nonsense mutations (Klopocki et al., 2010; Thomas-Teinturier et al., 2016; Wang et al., 2015; Jamsheer et al., 2016; Pereda et al., 2017; Reyes et al., 2019). In all studies, the mutations segregated with the disorder and were not found in control alleles. Thus, BDE with short stature can be caused by mutations that lead to haploinsufficiency of *PTHLH*.

As observed in the other rare human syndromes associated with mutations in the *PTHR1* gene, BDE caused by *PTHLH* haploinsufficiency phenocopies important aspects of PTHR1 functions, albeit with variable expressivity. Interestingly, a de novo duplication in the *PTHLH* gene was associated in one patient with symmetrical enchondromatosis (Collinson et al., 2010). These findings underscore that normal pre- and postnatal bone development and growth require quantitatively normal levels of PTHrP expression (Silve, 2010).

Parathyroid hormone/parathyroid hormone-related peptide receptor mutations

Jansen's metaphyseal chondrodysplasia

Jansen's metaphyseal chondrodysplasia (JMC), first described in 1934 (Jansen, 1934), is a rare autosomal dominant form of short-limbed dwarfism associated with laboratory abnormalities typically observed only in patients with either primary hyperparathyroidism or with humoral hypercalcemia of malignancy syndrome (reviewed in Jüppner et al., 2002; Parfitt et al., 1996). These biochemical changes, i.e., hypercalcemia, increased urinary phosphate excretion and increased urinary

cAMP excretion occur despite low or undetectable concentrations of PTH in the circulation as well as PTHrP concentrations that are not elevated. Severe hypercalcemia and hypophosphatemia had been noted in Dr. Murk Jansen's first patient (De Haas et al., 1969) and a subsequently described child with the same disorder (Cameron et al., 1954). It was not until the description of a third patient, however, that an association between the abnormalities in endochondral bone formation and mineral ion homeostasis was formally considered (Gram et al., 1959). At that time, the biochemical abnormalities could not be readily distinguished from those observed in primary hyperparathyroidism, and the surgical exploration of the patient revealed no obvious abnormalities of the parathyroid glands leading, to the conclusion that the changes in mineral metabolism were caused by an undefined metabolic defect (Gram et al., 1959). Most reported cases of JMC are sporadic, but the description of two unrelated affected females that gave birth to affected daughters (Lenz, 1969; Holthusen et al., 1975; Charrow and Poznanski, 1984) suggested an autosomal dominant mode of inheritance; this conclusion was subsequently confirmed at the molecular level for four families (Schipani et al., 1996; Bastepe et al., 2004; Nampoothiri et al., 2016; Saito et al., 2018).

At birth, some patients with JMC have dysmorphic features, which can include high skull vault, flattening of the nose and forehead, low-set ears, hypertelorism, high-arched palate, and micrognathia or retrognathia (Jüppner et al., 2002; Nampoothiri et al., 2016). Marked hypomineralization may also be observed, suggesting hypophosphatasia (Savoldi et al., 2013). Although body length is within normal limits at birth, growth becomes increasingly abnormal, eventually leading to the development of short stature. Additional signs may include kyphoscoliosis with a bell-shaped thorax and widened costochondral junctions, metaphyseal enlargement of the joints, waddling gait, prominent supraorbital ridges, and frontonasal hyperplasia. The legs are usually bowed and short, while the arms are relatively long.

Radiological studies have shown considerable age-dependent differences in the osseous manifestations of JMC. In younger patients, severe metaphyseal changes, especially of the long bones, are present (Fig. 57.2). The metaphyses are enlarged and expanded, giving a club-like appearance to the ends of the long bones with a wide zone of irregular calcifications. Patches of partially calcified cartilage that protrude into the diaphyses are also present and appear relatively radiolucent. These findings, which are characteristically observed throughout early childhood, are similar to the lesions in rickets. However, distinct from the findings in rickets, metacarpal and metatarsal bones are also involved.

Later in childhood, the changes are no longer reminiscent of rickets. Until the onset of puberty, almost all tubular bones show irregular patches of partially calcified cartilage that protrude into the diaphyses; the spine and vertebral bodies show no obvious abnormalities. After adolescence, cartilaginous tissue in the metaphyses gradually disappears and turns into bone, leading to bulbous deformities (see Fig. 57.2). The ends of most tubular bones remain expanded, deformed, and radiolucent, but a more normal trabecular pattern gradually emerges (Jüppner et al., 2002; Nampoothiri et al., 2016).

In addition, sclerosis and thickening of the base of the skull and of the calvaria are noted in most cases. The former changes are thought to be the cause of cranial auditory and optical nerve compression, which has been observed later in life in some affected individuals. Loss of the normal cortical outline, areas of subperiosteal bone resorption, and generalized osteopenia are reminiscent of the changes seen in hyperparathyroidism. Furthermore, there is an increase in trabecular bone volume and a thinning of cortical bone (Parfitt et al., 1996). The only two reports that investigated histological changes in

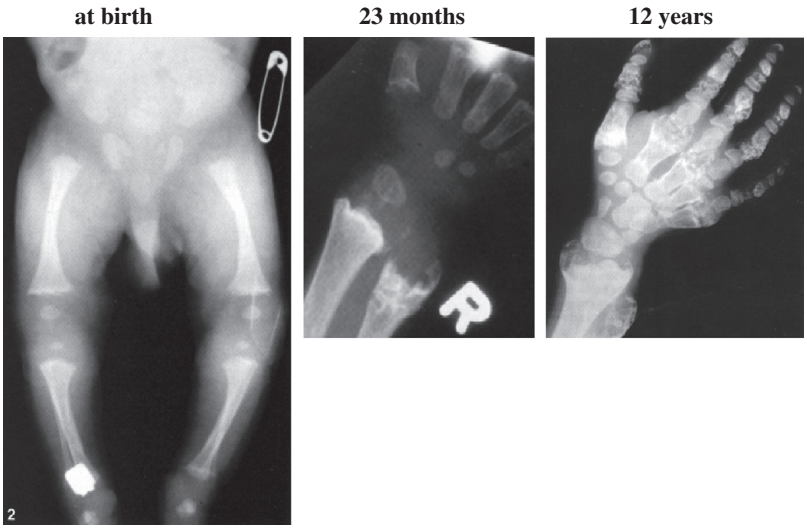

FIGURE 57.2 A patient with Jansen's disease and his radiological findings at birth, 23 months, and 12 years of age. *From Silverthorn, K.G., Houston, C.S., and Duncan, B.P. 1983. Murk Jansen's metaphyseal chondrodysplasia with long-term followup. Pediatr. Radiol. 17, 119–123, with permission.*

the growth plates described a severe delay in endochondral ossification of the metaphyses, including a lack of the regular columnar arrangement of the maturing cartilage cells, a lack of excess osteoid (which is usually indicative of active rickets or osteomalacia), little or no vascularization of cartilage, and no evidence for osteitis fibrosa (Cameron et al., 1954; Jaffe, 1972). Tooth development can be delayed, but enamel formation appears normal in patients with JMC. Intelligence appears normal in all reported cases.

Most laboratory findings of JMC are reminiscent of those observed in patients with primary hyperparathyroidism or with the syndrome of humoral hypercalcemia of malignancy. In the newborn, blood phosphorus levels are typically at the lower end of the normal range, while alkaline phosphatase activity is almost invariably elevated. Hypercalcemia is usually absent at birth but develops during the first months of life and persists throughout life, but is most pronounced during infancy and childhood (Fig. 57.3) (Saito et al., 2018). Hypercalciuria is usually present and can be associated with an increased incidence of nephrocalcinosis (Saito et al., 2018; Kessel et al., 1992; Onuchic et al., 2012). $1,25(OH)_2D$ levels have been reported as normal or at the upper end of the normal range. Serum alkaline phosphatase activity and osteocalcin concentration are elevated throughout life, indicating that osteoblast activity is increased; compatible with increased osteoclastic activity, urinary hydroxyproline excretion is elevated (Kruse and Schütz, 1993; Schipani et al., 1999).

Jansen's disease is caused by activating parathyroid hormone/parathyroid hormone-related peptide receptor mutations

Because of the findings in the various genetically manipulated mice described previously, and because of the abundant expression of PTHR1 in the three organs most obviously affected in JMC—i.e., kidney, bone, and metaphyseal growth plates—activating receptor mutations were considered as a cause of this rare disease. Indeed, in most patients with this disorder, a heterozygous nucleotide exchange, which changes a histidine at position 223 to arginine, has been identified at the border between the first intracellular loop and the second membrane-spanning domain of PTHR1 (Fig. 57.4) (Saito et al., 2018; Nampoothiri et al., 2016; Onuchic et al., 2012; Schipani et al., 1995; Minagawa et al., 1997; Brown et al., 2009). In other patients, four additional heterozygous nucleotide exchanges were identified that change either a threonine at position 410 to proline or arginine (sixth membrane-spanning domain) or isoleucine at position 458 (seventh membrane-spanning domain) to arginine (Schipani et al., 1995) or lysine (Savoldi et al., 2013) (Table 57.1). The mutated residues are predicted to be located at or close to the intracellular surface of the cell membrane and are strictly conserved in all mammalian members of this receptor family (Gardella et al., 2016), suggesting an important functional role for these three residues. With the exception of four families where parental transmission of the *PTHR1* mutation was documented (Schipani et al., 1996; Bastepe et al., 2004; Saito et al., 2018; Nampoothiri et al., 2016). This suggests that JMC is usually caused by de novo mutations.

To test in vitro the functional consequences of the identified missense mutations in JMC, each of the five different nucleotide exchanges was introduced into the cDNA encoding wild-type human PTHR1 (Saito et al., 2018; Savoldi et al., 2013; Schipani et al., 1995; Schipani et al., 1997). Different cell lines transiently expressing PTHR1s with the different H223R mutations showed a significantly higher basal accumulation of cAMP than cells expressing wild-type PTHR1.

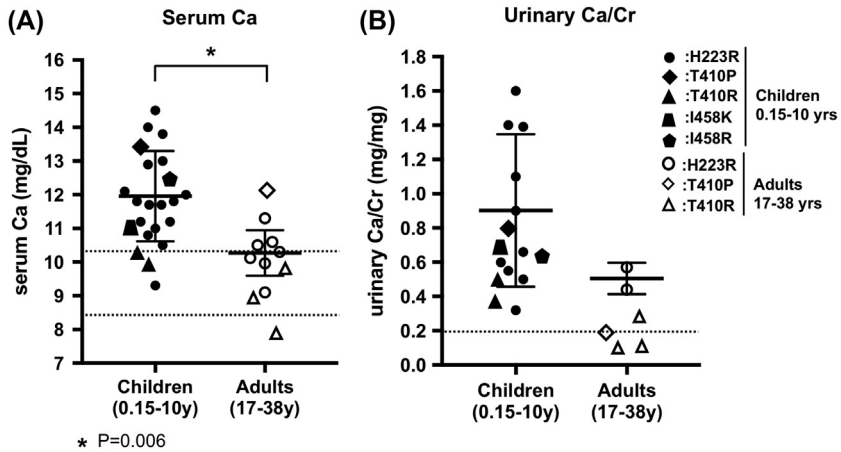

FIGURE 57.3 Serum and urinary calcium measurements for multiple children (0.15−10 years; n = 22 for serum calcium, n = 15 for urinary calcium/creatinine) and multiple adults (17−38 years; n = 11 for serum calcium; n = 8 for urinary calcium/creatinine) with Jansen's disease due to different PTHR1 mutations. Each data point represents the mean if a patient had multiple measurements during the two observation periods. **Panel A:** total calcium levels; dashed lines represent the upper/lower end of the adult normal range (8.6 −10.2 mg/dL). **Panel B:** urinary calcium-to-creatinine (Ca/Cr) ratio; all individual data points are shown. Mean ± SDs for patients with the H223R mutation. Dashed lines represent the upper end of normal for adult patients (<0.2). Children and adults showed no significant difference in the urinary Ca/Cr ratio. *From Saito, H., Noda, H., Gatault, P., Böckenhauer, D., Loke, K., Hiort, O., Silve, C., Sharwood, E., Matsunaga Martin, R., Dillon, M., et al. 2018. Progression of mineral ion abnormalities in patients with Jansen's metaphyseal chondrodysplasia. J. Clin. Endocrinol. Metab. 2018, with permission.*

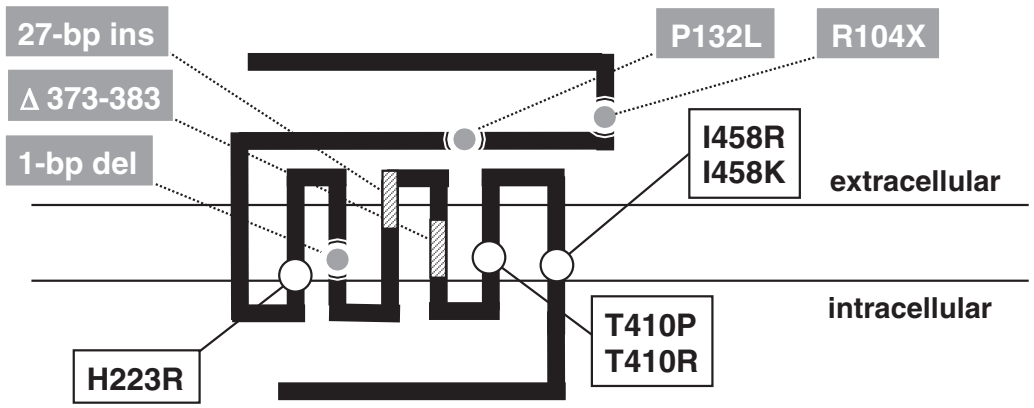

FIGURE 57.4 Schematic representation of the PTH/PTHrP receptor and approximate locations of mutations identified in patients with Jansen's or Blomstrand's disease.

Cells expressing mutant PTHR1s showed no evidence for increased basal accumulation of IP3, indicating that this signaling pathway is either not constitutively activated or that the assays evaluating this signaling pathway are not sufficiently sensitive.

The T410R mutation seems to lead to a less severe form of JMC (Bastepe et al., 2004). Patients carrying this mutation show only mild skeletal dysplasia with relatively normal stature as well as serum calcium levels within the normal range. The adult heights of patients with this mutations are much closer to the reference range (Saito et al., 2018). In fact, while the mean final adult height for patients with the H223R mutation was 127.0 ± 6.0 cm for males ($n = 4$) and 120.4 ± 10.3 cm for females ($n = 5$) (Fig. 57.5), the mean adult height of the three male patients with the T410R mutation was 157.7 ± 6.4 cm; the maximal adult height of the single patient with the T410P mutation was 96 cm. When tested in vitro, the degree of constitutive activity of the T410R mutant was significantly lower when compared with H223R, T410P, and I458R mutants, respectively (Bastepe et al., 2004; Schipani et al., 1997). This finding provided the first evidence for a correlation between severity of phenotypical features and degree of constitutive PTHR1 activity in Jansen's disease. Surprisingly, however, while H223R mutation is typically associated with profound hypercalcemia, a recently reported JMC patient with a de novo H223R mutation revealed no overt hypercalcemia, indicating that the mutation had occurred later in embryonic development (Nampoothiri et al., 2016).

Blomstrand's lethal chondrodysplasia

Blomstrand's lethal chondrodysplasia (BLC) is a recessive human disorder characterized by early lethality, advanced bone maturation, and accelerated chondrocyte differentiation, and most likely severe abnormalities in mineral ion homeostasis. The first patient was described by Blomstrand and colleagues in 1985 (Blomstrand et al., 1985); descriptions of several other patients followed (Young et al., 1993; Leroy et al., 1996; Loshkajian et al., 1997; den Hollander et al., 1997; Oostra et al., 1998; Galera et al., 1999; Karperien et al., 1999). The disorder was shown to occur in families of different ethnic backgrounds and appears to affect males and females equally. Most affected infants are born to consanguineous parents (only in one instance were unrelated parents reported to have two offspring both affected by Blomstrand's disease (Loshkajian et al., 1997), suggesting that BLC is an autosomal recessive disease. Infants with BLC are typically born prematurely and die shortly after birth. Birth weight corrected for gestational age appears to be normal but may be overestimated, because most infants are hydroptic; also, the placenta can be immature and edematous. Nasal, mandibular, and facial bones are hypoplastic; the base of the skull is short and narrow; the ears are low set; and the thoracic cage is hypoplastic and narrow with short, thick ribs and hypoplastic vertebrae. In contrast, the clavicles are relatively long and often abnormally shaped, the limbs are extremely short, and only the hands and feet are of relatively normal size and shape. Internal organs show no apparent structural or histological anomalies, but preductal aortic coarctation was observed in most published cases. The lungs are hypoplastic, and the protruding eyes typically show cataracts. Defects in mammary gland and tooth development, previously overlooked, were demonstrated in two studied fetuses with BLC. In these fetuses, nipples were absent, and no subcutaneous ductal tissue could be identified by histochemical analysis. Tooth buds were present, but developing teeth were severely impacted within the surrounding alveolar bone, leading to distortions in their architecture and orientation (Wysolmerski et al., 2001). Interestingly, heterozygous loss-of-function mutations in PTHR1 have been associated with autosomal dominant isolated primary failure of tooth eruption (PFE) (see paragraph later).

TABLE 57.1 Mutations in the parathyroid hormone/parathyroid hormone-related peptide receptor gene associated with different human disorders.

Disorder prompting search for PTHR1 mutation	Location (exon/ receptor domain)	Nucleotide change	Amino acid change	Mutation type	Category	Comment	References
Blomstrand	Ex U3 - intron 1			Deletion (10 kb)	LOF	Homozygous	Unpublished personal data
Blomstrand	Ex 3/E2	c.310C > T	p.R104[a]	Nonsense	LOF	Homozygous	Hoogendam et al. (2007)
PFE	Ex 3/E2	c.322delT	p.C108Vfs[a]82	Frame shift	LOF	Heterozygous	Roth et al. (2014)
PFE	Ex 3/E3	c.331G > T	p.E111[a]	Nonsense	LOF	Heterozygous	Roth et al. (2014); Pilz et al. (2014)
PFE	Ex 4/E3	c.356C > T	p.P119L	Missense	LOF[b]	Heterozygous	Yamaguchi et al., 2011; Roth et al., 2014
Enchondromatosis	Ex 4/E3	c.362G > A	p.G121E	Missense	Regulatory	Heterozygous	Couvineau et al. (2008)
Enchondromatosis	Ex 4/E3	c.364G > A	p.A122T	Missense	Regulatory	Heterozygous	Couvineau et al. (2008)
Blomstrand	Ex 4/E3	c.395C > T	p.P132L	Missense	LOF	Homozygous	Jobert et al., 1998; Karaplis et al., 1998; Hoogendam et al., 2007
PFE	Ex 4/E3	c.395C > T	p.P132L	Missense	LOF	Heterozygous	Yamaguchi et al. (2011)
PFE	Ex 4/E3	c.434A > G	p.Y145C	Missense	LOF[b]	Heterozygous	Roth et al. (2014)
PFE	Ex 4/E3	c.436C > T	p.R146[a]	Nonsense	LOF	Heterozygous	Roth et al. (2014); Pilz et al. (2014)
PFE	Ex 5/G	c.439C > T	p.R147C	Missense	LOF[b]	Heterozygous	Yamaguchi et al. (2011)
Enchondromatosis—growth	Ex 5/G	c.448C > T	p.R150C (rs73067029)	Missense	GOF[b]	Heterozygous	Hopyan et al., 2002; Marouli et al., 2017
PFE	Ex 5/G	c.463G > T	p.E155[a]	Missense	LOF	Heterozygous	Decker et al., 2008; Roth et al., 2014
PFE	Ex 6/M1	c.543+1G > A	p.?	Altered splicing	LOF	Heterozygous	Decker et al. (2008)
PFE	Ex 6/M1	c.544−26_544-23del	p.E182Afs[a]38	Frame shift	LOF	Heterozygous	Frazier-Bowers et al. (2010); Risom et al. (2013)
PFE	Ex 6/M1	c.543+1G > A	p.E182Vfs[a]20	Frame shift	LOF	Heterozygous	Decker et al. (2008)
PHP1B (?)	Ex 6/M1	c.557G > A	p.R186H	Missense	LOF[b]	Homozygous	Guerreiro et al. (2016)
PFE	Ex 6/M2	c.572delA	p.Y191Sfs[a]14	Frame shift	LOF	Heterozygous	Frazier-Bowers et al. (2014)
PFE	Ex 7/M2	c.590T > A	p.V197E	Missense	LOF[b]	Heterozygous	Roth et al. (2014)
PFE	Ex 7/M2	c.611T > A	p.V204E	Missense	LOF	Heterozygous	Jelani et al. (2016)

Continued

TABLE 57.1 Mutations in the parathyroid hormone/parathyroid hormone-related peptide receptor gene associated with different human disorders.—cont'd

Disorder prompting search for PTHR1 mutation	Location (exon/ receptor domain)	Nucleotide change	Amino acid change	Mutation type	Category	Comment	References
PFE	Ex 7/M2	636dupT	p.A213[a]	Frame shift	LOF	Heterozygous	Roth et al. (2014); Pilz et al. (2014)
PFE	Ex 8/M3	639-2A > C	p.?	Splice defect	LOF	Heterozygous	Roth et al. (2014); Pilz et al. (2014)
PFE	Ex 8/M3	639-2A > G	p.?	Splice defect	LOF	Heterozygous	Roth et al. (2014); Pilz et al. (2014)
Jansen	Ex 7/M2	c.668A > G	p.H223R	Missense	GOF	Heterozygous	Schipani et al., 1996; Schipani et al., 1999; Schipani et al., 1995; Minagawa et al., 1997; Nampoothiri et al., 2016; Saito et al., 2018; Brown et al., 2009
PFE	Ex 7/M2	c.695T > G	p.L232R	Missense	LOF[b]	Heterozygous	Roth et al. (2014)
PFE	Ex 7/M2	c.698G > A	p.R233H	Missense	LOF[b]	Heterozygous	Roth et al. (2014)
Enchondromatosis	Ex 7/M2	c.764G > A	p.R255H	Missense	Regulatory	Heterozygous	Couvineau et al. (2008)
PFE	Ex 8/M3	c.813dupT	p.A272Cfs[a]127	Duplication	LOF	Heterozygous	Roth et al. (2014); Pilz et al. (2014)
PFE	Ex 8/M3	c.875T > C	p.L292P	Missense	LOF[b]	Heterozygous	Roth et al. (2014)
PFE	Ex 8/M3	c.892T > G	p.W298G	Missense	LOF	Heterozygous	Risom et al. (2013)
PFE	Ex 8/M3	c.947C > A	p.S316[a]	Nonsense	LOF	Heterozygous	Risom et al. (2013)
PFE	Ex 8/M3	c.989G > T	p.G330V	Altered splicing	LOF	Heterozygous	Risom et al. (2013)
PFE	Ex 8/M3	c.996_997insC	p.A333Rfs[a]66	Frame shift	LOF	Heterozygous	Frazier-Bowers et al. (2014)
PFE	Ex 8/M3	c.1016G > A	p.W339[a]	Nonsense	LOF	Heterozygous	Roth et al. (2014); Pilz et al. (2014)

PFE	Ex 8/M3	c.1036delC	p.L346Wfs[a]9	Nonsense	LOF	Heterozygous	Roth et al. (2014)
Blomstrand	Ex 9/M4	c.1049 + 27C > T	p.G350fs[a]351	Splice donor	LOF	Homozygous	Hoogendam et al. (2007)
PFE	Ex 10/El2	c.1050-3C>G	p.C351Sfs[a]133	Frame shift	LOF	Heterozygous	Decker et al. (2008)
PFE	Ex 10/El2	c.1082G > A	p.W361[a]	Nonsense	LOF	Heterozygous	Risom et al. (2013)
Blomstrand	Ex 10/El2	c.1093delG	p.V365Cfs[a]141	Frame shift	LOF	Heterozygous	Karperien et al., 1999; Roth et al., 2014
Blomstrand	Ex 11/M5	c.1148G > A	p.L373_R383del	Novel splice acceptor	LOF	Compound Het.	Jobert et al. (1998)
PFE	Ex 11/M5	c.1148G > A	p.L373_R383del	Novel splice acceptor	LOF	Heterozygous	Yamaguchi et al. (2011)
PFE	Ex 11/M5	c.1142T > G	p.I381S	Novel splice acceptor	LOF[b]	Heterozygous	Roth et al. (2014)
PFE	Ex 11/M5	c.1148G > A	p.R383Q	Missense	LOF	Heterozygous	Yamaguchi et al. (2011); Roth et al. (2014)
Jansen	Ex 12/M6-7	c.1228A > C	p.T410P	Missense	GOF	Heterozygous	Schipani et al. (1999)
Jansen	Ex 12/M6-7	c.1229C > G	p.T410R	Missense	GOF	Heterozygous	Bastepe et al. (2004)
PFE	Ex 12/M6-7	c.1324C > G	p.H442R	Missense	LOF[b]	Heterozygous	Roth et al. (2014)
PFE	Ex 12/M6-7	c.1348_1350del	p.F450del	Deletion	LOF	Heterozygous	Risom et al. (2013)
PFE	Ex 13/M7	c.1352A > G	p.Q451R	Missense	LOF	Heterozygous	Quinque et al. (2016)
PFE	Ex 13/M7	c.1355G > A	p.G452E	Missense	LOF[b]	Heterozygous	Roth et al. (2014)
PFE	Ex 13/M7	c.1354-1G>A	p.G452_E465del	Deletion	LOF	Heterozygous	Frazier-Bowers et al. (2007)
Jansen	Ex 13/M7	c.1373T > G	p.I458R	Missense	GOF	Heterozygous	Schipani et al. (1999)
Jansen	Ex 13/M7	c.1373T > G	p.I458K	Missense	GOF	Heterozygous	Savoldi et al. (2013)
Eiken	Ex 14/T	c.1453C > T	p.R485[a]	Nonsense	Regulatory	Homozygous	Duchatelet et al. (2005)
PFE	Ex 14/T	c.1736A > C	p.E579A	Missense	LOF[b]	Heterozygous	Roth et al. (2014)

GOF, gain-of-function; *LOF*, loss-of-function.
[a]*Termination codon*
[b]*Biological significance remains undefined*

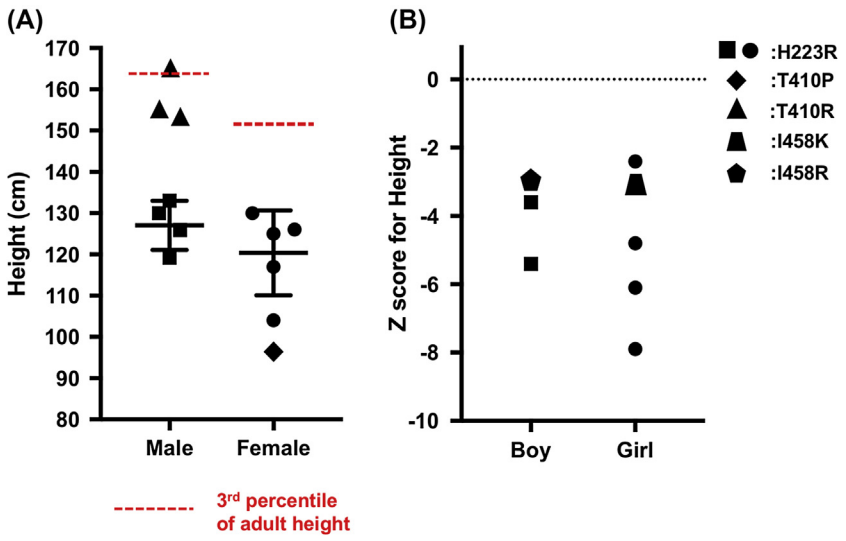

FIGURE 57.5 Height data for different patients affected by Jansen's disease due to different PTHR1 mutations. **Panel A:** individual final heights for 13 adult JMC patients. Mean ± SDs are shown for the final heights of patients with the H223R mutation; the red broken lines indicate the third percentile for normal adult heights. **Panel B:** individual height z scores for eight children. *From Saito, H., Noda, H., Gatault, P., Böckenhauer, D., Loke, K., Hiort, O., Silve, C., Sharwood, E., Matsunaga Martin, R., Dillon, M., et al. 2018. Progression of mineral ion abnormalities in patients with Jansen's metaphyseal chondrodysplasia. J. Clin. Endocrinol. Metab. 2018, with permission.*

Radiological studies of patients with BLC reveal pronounced hyperdensity of the entire skeleton and markedly advanced ossification (Fig. 57.6). As mentioned earlier, the long bones are extremely short and poorly modeled, show markedly increased density, and lack metaphyseal growth plates. Endochondral bone formation is dramatically advanced and is associated with a major reduction in epiphyseal resting cartilage preventing the development of epiphyseal ossification centers (Fig. 57.7). The zones of chondrocyte proliferation and column formation are lacking, and the zone that normally comprises the layer of hypertrophic chondrocytes is poorly defined, narrow, and irregular (Oostra et al., 2000). Cortical bone is thickened and bone trabeculae are coarse with reduced diaphyseal marrow spaces. Capillary ingrowth, bone resorption, and bone formation are reported by some authors as unaltered (Leroy et al., 1996), while others describe these bone remodeling events as deficient (Loshkajian et al., 1997).

Blomstrand's disease is caused by inactivating parathyroid hormone/parathyroid hormone-related peptide receptor mutations

Different defects in the PTHR1 gene have been described in genomic DNA from patients affected by BLC (see Table 57.1). The first reported case, a product of nonconsanguineous parents, was shown to have two distinct abnormalities in the PTHR1 gene (Jobert et al., 1998). Through a nucleotide exchange in exon M5 of the maternal PTHR1 allele, a novel splice acceptor site was introduced that led to a mutant mRNA encoding an abnormal receptor that lacks a portion of the fifth membrane-spanning domain (amino acids 373 to 383; Δ373-383). This receptor mutant fails, despite seemingly normal cell surface expression, to respond to PTH or PTHrP with an accumulation of cAMP and inositol phosphate (Jobert et al., 1998). For yet-unknown reasons, the paternal PTHR1 allele from this patient was very poorly expressed, suggesting an unidentified mutation in one of the different promoter regions or in a putative enhancer element.

A second patient with BLC, the product of a consanguineous marriage, was shown to have a nucleotide exchange that leads to a proline-to-leucine mutation at position 132 (P132L) (Zhang et al., 1998; Karaplis et al., 1998). This residue in the amino-terminal extracellular domain of PTHR1 is invariant in all mammalian members of this family of GPCRs, indicating that the identified mutation is likely to have significant functional consequences. Indeed, COS-7 cells expressing this mutant PTHR1 showed, despite apparently normal cell surface expression, dramatically impaired binding of radiolabeled PTH and PTHrP analogs, greatly reduced agonist-stimulated cAMP accumulation, and no measurable inositol phosphate response. It is important to note, however, that cells expressing the P132L mutant receptor showed some agonist-induced second-messenger response and showed little, yet detectable, specific binding of radiolabeled PTHrP. To date, the P132L mutation has been identified in two additional patients affected with BLC (Hoogendam et al., 2007). Although not definitive, haplotype analysis performed on the genomic DNA of these patients with the P132L mutation is consistent with an ancient founder effect (Hoogendam et al., 2007).

A homozygous deletion of G at position 1093 (from A of the ATG-translation initiation codon) (exon EL2) was identified in a third case of BLC (Karperien et al., 1999). This mutation led to a shift in the open reading frame, which

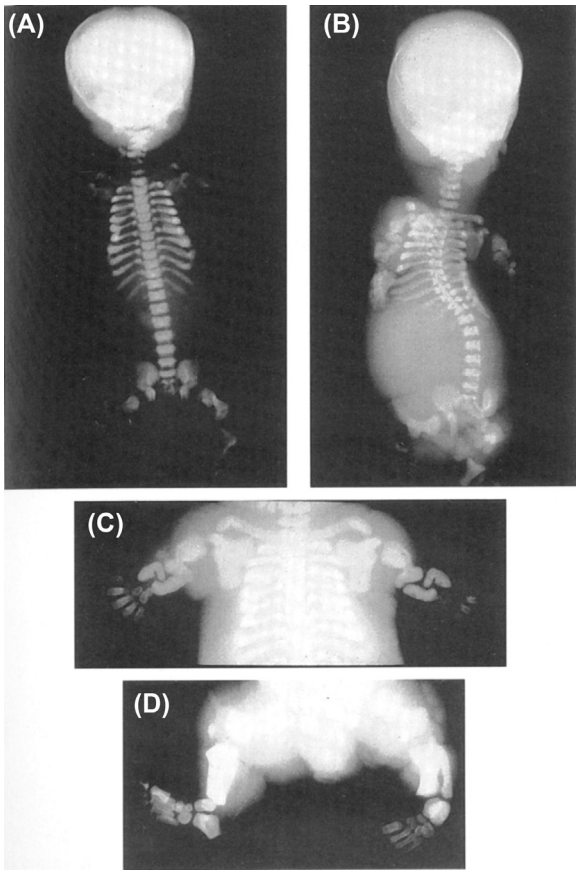

FIGURE 57.6 Radiological findings in two fetuses with Blomstrand's lethal chondrodysplasia (BLC). Anterio−posterior (A) and lateral (B) views of a male fetus at 26 weeks of gestation; upper (C) and lower (D) limbs of a female fetus with BLC at 33 weeks of gestation. Particularly striking is the dramatic acceleration of endochondral bone formation in all skeletal elements. No secondary ossification centers are seen in the long bones. The limbs are coarsely shaped and extremely short, while carpal and tarsal bones have a comparatively normal shape and size. Note also that the clavicles are relatively long but show abnormal bending. *From Loshkajian, A., Roume, J., Stanescu, V., Delezoide, A.L., Stampf, F., and Maroteaux, P. 1997. Familial Blomstrand Chondrodysplasia with advanced skeletal maturation: further delineation. Am. J. Med. Genet. 71, 283−288, with permission.*

resulted in a truncated protein that completely diverged from the wild-type receptor sequence after amino acid 364 and thus lacked transmembrane domains 5, 6, and 7, the connecting intra- and extracellular loops, and the cytoplasmic tail (Δ365-593).

As for the other cases of BLC, these findings provided a plausible explanation for the severe abnormalities in endochondral bone formation. The abnormalities in mammary gland and tooth development further supports the conclusion that

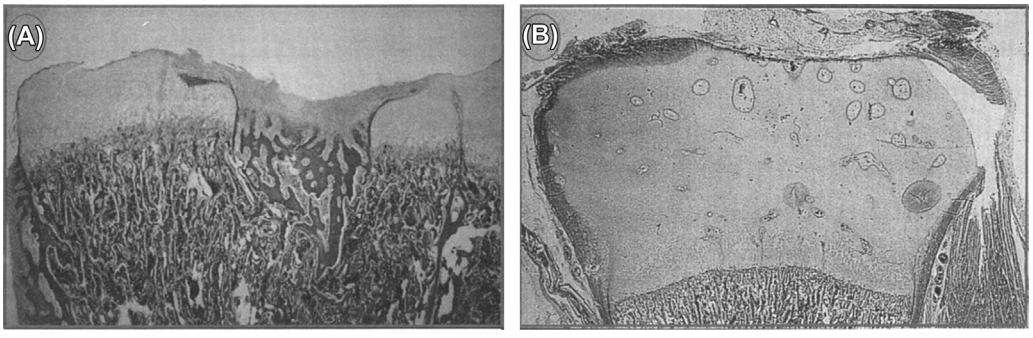

FIGURE 57.7 Section of the upper tibia end from a patient with BLC (A) and an age-matched control. Note the severely reduced size of the growth plate, the irregular boundary between the growth plate and the primary spongiosa, and the increased cortical bone thickness. *From Loshkajian, A., Roume, J., Stanescu, V., Delezoide, A.L., Stampf, F., and Maroteaux, P. 1997. Familial Blomstrand Chondrodysplasia with advanced skeletal maturation: further delineation. Am. J. Med. Genet. 71, 283−288, with permission, and Anne-Lise Delezoide, personal collection.*

PTHR1 has identical roles in humans and mice in the development of these organs. Compatible with the role of PTHR1 and PTHrP in organogenesis, both were demonstrated to be expressed in the developing breast and tooth of human control fetuses (Wysolmerski et al., 2001). It is also worth noting that the abnormalities in skeletal development in fetuses carrying the P132L mutation, which inactivates PTHR1 incompletely, are less severe than those observed in most cases, particularly with regard to the bones of the lower limbs (Young et al., 1993; Karperien et al., 1999). This led to the proposal that two forms of BLC can be distinguished clinically and on the basis of the in vitro characteristics of the mutant PTHR1s (Oostra et al., 2000).

Two additional homozygous mutations in PTHR1 have been identified in fetuses affected by BLC that further document the molecular basis for the two forms of BLC (Hoogendam et al., 2007) (see Table 57.1). A homozygous point mutation causing a premature stop codon at position 104 (R104X) and therefore resulting in a truncated completely inactive protein has been identified in a case affected with the severe (type I) form. A homozygous nucleotide change (c.1049 + 27C > T, hg19) generating a novel splice site has been identified in a case affected with the less severe form (type II). This novel splice site, which results in an aberrant transcript with a premature stop codon after codon 350, was shown to be preferentially used in dermal fibroblasts, but the wild-type transcript remained expressed, albeit at low levels. Taken together, the findings in patients with BLC suggested that this rare human disease is the equivalent of mice "null" for PTHR1 (Lanske et al., 1996).

Eiken familial skeletal dysplasia

In addition to BLC and JMC, PTHR1 gene mutations have been associated with two other diseases, Eiken familial skeletal dysplasia (Duchatelet et al., 2005) and enchondromatosis (Ollier's disease) (Hopyan et al., 2002). Eiken familial skeletal dysplasia has been described in a single consanguineous family (Eiken et al., 1984). The disease is characterized by multiple epiphyseal dysplasia with extremely retarded ossification, abnormal modeling of the bones in hands and feet, abnormal persistence of cartilage in the pelvis, and mild growth retardation. Serum calcium and phosphate levels have been normal in all examined patients; serum PTH level was measured in only one patient and was found to be slightly elevated with a normal $1,25(OH)_2D$ level. A homozygous mutation in PTHR1, R485X, that leads to the truncation of the last 108 amino acids of PTHR1, was identified in all affected patients but was not found in DNA from healthy controls (Duchatelet et al., 2005). The functional properties of mutant PTHR1 have not been characterized in vitro. However, based on the properties of a receptor mutant with deletion after amino acid 480 (Iida-Klein et al., 1995), it appears plausible that the truncated receptor has an imbalance between the different signaling pathways activated by PTH. Why the deletion of the carboxy-terminal tail of PTHR1 results in a bone phenotype but no obvious abnormality in the regulation of mineral ion homeostasis remains unclear.

Enchondromatosis (Ollier's disease)

Enchondromatosis is usually a nonfamilial disorder characterized by the presence of multiple enchondromas. It is characterized by an asymmetric distribution of the cartilaginous lesions, which can be extremely variable (in terms of size, number, location, evolution of enchondromas, age of onset and diagnosis, and requirement for surgery). Clinical problems caused by enchondromas include skeletal deformities, limb-length discrepancy, and the potential risk for malignant change to chondrosarcoma. The condition in which multiple enchondromatosis is associated with soft tissue hemangiomas is also referred to as Maffucci syndrome. The irregular distribution of the lesions in Ollier's disease strongly suggests that it is a disorder of endochondral bone formation that occurs due to a postzygotic somatic mutation that results in mosaicism. A mutant PTHR1 (R150C) was found to be expressed in the enchondromas from two of six unrelated patients with enchondromatosis (Hopyan et al., 2002). The mutation was found on one parental allele in one patient and his father, who presented with atypical mild skeletal dysplasia but not enchondromatosis; interestingly, this PTHR1 variant was furthermore found to be associated with adult height (Marouli et al., 2017). Consistent with a role of PTHR1, in some forms of Ollier's disease novel heterozygous *PTHR1* mutations (either germline or somatic mutations in tumor tissue) have been found in several additional cases; no mutations were identified in *GNAS* or *PTHLH* (Couvineau et al., 2008). As indicated earlier, a de novo duplication comprised in the *PTHLH* gene has been associated with symmetrical enchondromatosis (Collinson et al., 2010). However, neither the R150C mutation (26 tumors) nor any other mutation in the *PTHR1* gene (11 patients) could be identified in another study (Rozeman et al., 2005). In fact, most cases of Ollier's or the related Maffucci disease are now known to be caused by mutations in the isocitrate dehydrogenases IDH1 and IDH2. Somatic heterozygous mutations in IDH1, and less frequently in IDH2, were reported in 35 of 43 (81%) subjects with Ollier's disease, while 10 of 13 (77%) with Maffucci syndrome carried IDH1 (98%) or IDH2 (2%) mutations in their tumors. IDH1 and IDH2 mutations with evidence of intraneoplastic and somatic mosaicism were also identified in 87% of

enchondromas (benign cartilage tumors), 70% of spindle cell hemangiomas (benign vascular lesions), and 40% of solitary central cartilaginous tumors (Pansuriya et al., 2011). IDH1 and IDH2 catalyze the oxidative decarboxylation of isocitrate to 2-oxoglutarate, which increases d-2-hydroxyglutarate production and depletes the formation of α-ketoglutarate, a cofactor for the actions of Jumonji-domain-containing proteins involved in the demethylation of histone arginine and lysine residues. Lack of α-ketoglutarate further increases HIF-1α expression, which cause abnormal sensing of hypoxia within the growth plate cartilage, which may lead to an uncontrolled proliferation of chondrocytes. Taken together, these studies indicate heterogeneity in the molecular defects leading to enchondromatosis.

Delayed tooth eruption due to parathyroid hormone/parathyroid hormone-related peptide receptor mutations

PFE can be associated with several syndromes but is also observed as a nonsyndromic isolated autosomal dominant condition with high penetrance and variable expressivity. Heterozygous *PTHR1* mutations were first identified in individuals affected by PFE after the genetic locus had been determined through linkage analysis in four multiplex pedigrees (Decker et al., 2008). Three distinct mutations were initially identified as truncating the mature protein and are therefore expected to lead to a functionless receptor. These studies were subsequently confirmed and extended (Frazier-Bowers et al., 2007, 2010, 2014; Yamaguchi et al., 2011; Risom et al., 2013; Roth et al., 2014; Pilz et al., 2014; Jelani et al., 2016; Quinque et al., 2016) and indicate that haplo-insufficiency of PTHR1 is an underlying cause of nonsyndromic PFE. The PTHR1 mutations responsible for PFE include nonsense, missense, splice-site mutations, and insertion—deletion mutations. Several missense mutations, including P132L, were first identified in Blomstrand cases (Jobert et al., 1998). Tooth bud impaction has been described in Blomstrand's lethal osteochondrodysplasia (Wysolmerski et al., 2001), thus supporting the important role of PTHR1 in normal tooth development.

Mutations in genes downstream of the parathyroid hormone/parathyroid hormone-related peptide receptor

GNAS mutations

Shortly after Aurbach and colleagues had discovered that kidney- and bone-derived tissues increase cAMP formation in response to PTH (Chase & Aurbach, 1967, 1970; Chase et al., 1969a,b; Marcus and Aurbach, 1971), the same group revealed that patients with PHP and clinically obvious features of Albright's hereditary osteodystrophy (AHO) (now referred to as PHP1A) failed to respond to a PTH challenge with an increase in urinary cAMP excretion (Chase et al., 1969a,b). This observation linked the lack of PTH-induced phosphaturia, initially described by F. Albright and colleagues (Albright et al., 1942), to this second-messenger system. However, homogenates from the renal cortex of a PHP-Ia patient showed PTH-induced cAMP formation, leading Aurbach's group to conclude that this disorder is not caused by a mutation in PTHR1 or the effector enzyme that generates cAMP—i.e., adenylate cyclase (Marcus et al., 1971). In fact, it was the discovery that tissues from PHP1A patients show reduced G-protein activity that provided the first evidence for abnormal coupling between the PTH receptor and adenylate cyclase (Levine et al., 1980; Farfel et al., 1980), which subsequently led to the identification of heterozygous mutations in *GNAS,* the gene encoding the alpha-subunit of the heterotrimeric stimulatory G-protein (Gsα) (Patten et al., 1990; Weinstein et al., 1990). However, it remained a conundrum why heterozygous Gsα mutations should lead to PTH resistance, until Davies and Hughes revealed that PTH resistance becomes apparent only when the genetic defect is inherited maternally (Davies and Hughes, 1993).

It is now well established that Gsα, which is ubiquitously expressed, couples a large number of other GPCRs, including PTHR1, to the effector enzyme, adenylyl cyclase, required for receptor-stimulated intracellular cAMP generation and PKA activation. Gsα is derived from the *GNAS* locus, a complex imprinted genomic region located on chromosome 20q13 that encodes, in addition to Gsα, several other alternatively spliced transcripts (Bastepe and Jüppner, 2016). In some tissues such as renal proximal tubules (PTH target), thyroid, or pituitary gland, the expression of Gsα is predominantly or exclusively monoallelic. In these tissues, Gsα is derived mainly from the maternal allele, while expression from the paternal allele is silenced through as-of-yet unknown mechanisms.

Genetic and epigenetic defects in the *GNAS* complex locus cause, according to their allelic origin, heterogeneous diseases—i.e., different forms of PHP, pseudopseudohypoparathyroidism (PPHP), and progressive osseous heteroplasia—each with distinctive characteristics. The clinical and biochemical distinction between these pathologies relies mainly but not exclusively the presence or absence of AHO and the presence of hormonal resistance, in particular PTH resistance. AHO is a distinctive constellation of variable developmental and skeletal defects (rounded face, short

stocky appearance, brachydactyly type E, early-onset obesity, heterotopic ossification, and variable neurocognitive abnormalities) associated with Gsα haploinsufficiency. Obesity, initially thought to be part of the spectrum of AHO features, has now been shown to occur only upon maternal inheritance of *GNAS* mutations (Long et al., 2007). PHP is divided into type I (PHP1) and type II (PHP2). PHP1 is characterized by resistance to PTH in the proximal renal tubules, resulting in little or no urinary cAMP excretion after injection of PTH. In PHP2, PTH injection causes a normal increase in urinary cAMP excretion but no phosphaturic response. Most forms of PHP1 and PPHP appear to be linked to genetic (PHP1A, PHP1C, and PPHP) and/or epigenetic (PHP1B) abnormalities at the *GNAS* complex locus. Patients who inherit Gsα mutations from their mother express both the AHO phenotype and resistance to various hormones (PTH, TSH, calcitonin, GHRH, epinephrine, LH, and FSH) (for a review see (Bastepe and Jüppner, 2016; Levine, 2002; Linglart et al., 2013; Elli et al., 2016a,b) that stimulate the Gsα-cAMP-PKA pathway in their respective target tissues; this condition is referred to as PHP1A. PTH resistance is the most obvious endocrine deficiency that is almost always accompanied by hypocalcemia, hyperphosphatemia, and low or inappropriately normal levels of $1,25(OH)_2D$ despite elevated PTH levels (and the absence of vitamin D deficiency or chronic kidney disease). Following the injection of PTH, these patients exhibited a defect in the formation of cAMP in the renal proximal tubules and thus reduced phosphaturic response and reduced $1,25(OH)_2D$ production. These findings were consistent with the loss-of-function mutations in Gsα that are required for the formation of cAMP.

Protein kinase type 1A regulatory subunit protein mutations

Acrodysostosis refers to a group of rare skeletal dysplasias that share common characteristic clinical and radiological features, including severe brachydactyly (Fig. 57.8), facial dysostosis, and nasal hypoplasia, and in some cases resistance to multiple hormones that mediate actions through the cAMP/PKA pathway (Ablow et al., 1977; Davies and Hughes, 1992). Several forms of acrodysostosis are now recognized (ACRDYS1: OMIM 101800, ACRDYS2: OMIM 614613, hypertension and brachydactyly syndrome: OMIM 112410), which are caused, respectively, by heterozygous mutations in the genes coding for the cAMP-dependent protein kinase type 1A regulatory subunit protein (PRKAR1A) (Linglart et al., 2011), phosphodiesterase (PDE) 4D (PDE4D) (Lee et al., 2012; Michot et al., 2012; Linglart et al., 2012; Lindstrand et al., 2014), and PDE3A (Bilginturan et al., 1973; Schuster et al., 1996; Maass et al., 2015; Boda et al., 2016). Of note, heterotopic ossifications, a hallmark of AHO and Gsα haploinsufficiency, are rarely observed in acrodysostosis.

Using a candidate gene approach, a recurrent heterozygous missense mutation (c.1101C→T, p.Arg368X) was identified in three unrelated patients affected by ACRDYS1 in the gene *PRKAR1A*, which encodes the regulatory subunit of PKA (Linglart et al., 2011). Since then, 18 additional heterozygous missense *PRKAR1A* mutations have been documented in ACRDYS1 patients (Silve et al., 2012a,b; Silve et al., 2012a,b; Elli et al., 2016a,b) (Fig. 57.9). The first-described mutation, Arg368X, has been subsequently found in 10 additional patients, confirming that it is the most frequent

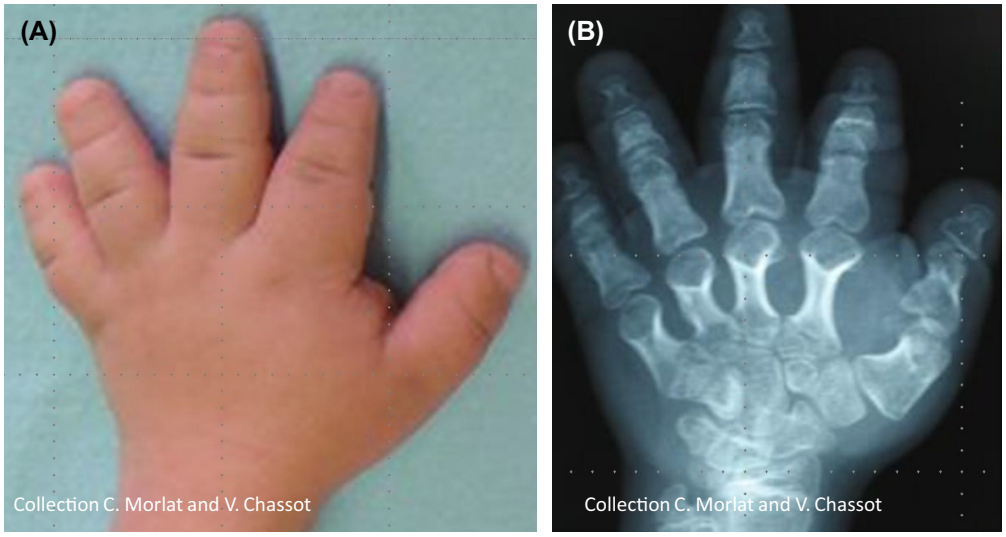

FIGURE 57.8 Picture (A) and X-ray (B) of one hand of a 13-year-old patient affected with ACRDYS1. The patient presents the shortening of metacarpals, metatarsals, and phalanges characterizing brachydactyly type E (BDE). Note the shortening of all bones and the bulky and stocky aspect of affected bones.

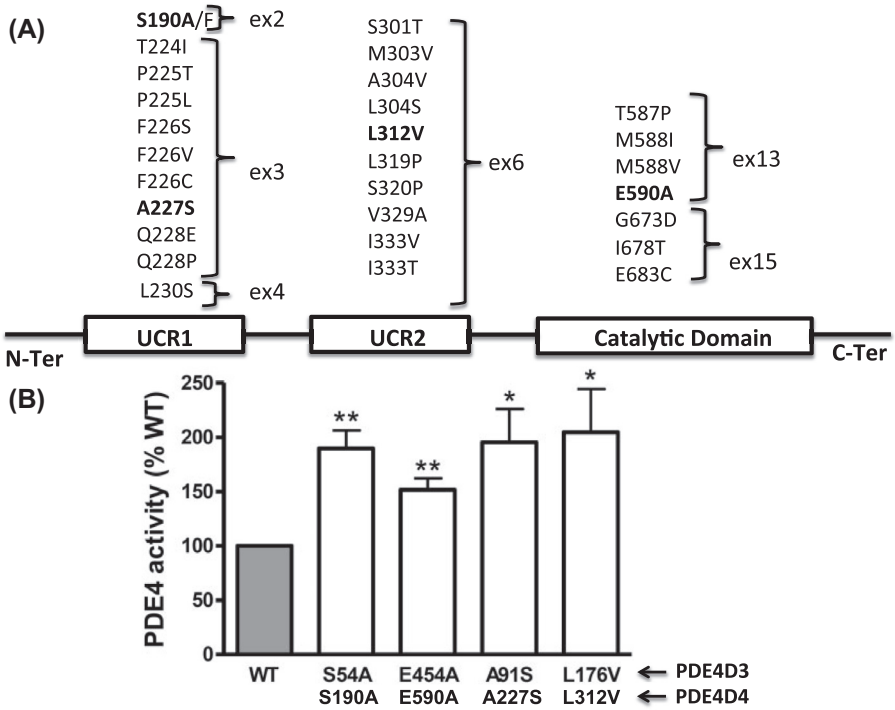

FIGURE 57.9 **Panel A.** Schematic representation of PRKAR1A indicating the functionally important domains and positions of amino acid residues mutated in patients affected with acrodysostosis (ACRDYS1). DD: dimerization domain; IS: inhibitory site; domains A and B: cAMP-binding domains A and B. PBC: phosphate binding cassette. **Panel B.** PKA transcriptional activity in cells cotransfected with plasmids encoding WT PRKAR1A, or the indicated mutants and stimulated with various concentrations of forskolin in the presence of 1 mM isobutylmethylxanthine (IBMX) as measured by the cAMP-responsive element (CRE)—luciferase reporter assay. The results are expressed as fold stimulation over basal. After stimulation with forskolin, the dose—response curves for cells expressing mutant PRKAR1A subunits are all shifted to the right compared with those observed in cells expressing the WT PRKAR1A subunit, indicating that all of the mutant regulatory subunits are less sensitive to cAMP. This results in impaired activation of PKA. *From Rhayem, Y., Le Stunff, C., Abdel Khalek, W., Auzan, C., Bertherat, J., Linglart, A., Couvineau, A., Silve, C., and Clauser, E. 2015. Functional characterization of PRKAR1A mutations reveals a unique molecular mechanism causing acrodysostosis but multiple mechanisms causing carney complex. J. Biol. Chem. 290, 27816—27828, with permission.*

recurrent *PRKAR1A* mutation in ACDRYS1. Each of the other 17 mutations was identified in a single patient, all being sporadic cases.

As indicated above, the most commonly used effector system downstream of cAMP is PKA. In the absence of cAMP, PKA exists as a tetramer in which two regulatory (R) subunits lock the two catalytic (C) subunits in an inactive state. Activation of the enzyme requires the release of the catalytic subunits, which is triggered by the sequential binding of cAMP molecules first to domain B, then to domain A of the R subunit (Tasken et al., 1997; Taylor et al., 1990, 2008). Briefly, there are four different regulatory subunit isoforms: PRKAR1A and PRKAR2A are ubiquitously expressed, whereas PRKAR1B is found only in brain and testis (R1B), and PRKAR2B is found only in adrenal and adipose tissue (R2B). These regulatory subunits associate to two different catalytic subunits, ubiquitous Ca and brain-specific Cb. The quantitatively and qualitatively predominant subunits are Ca and PRKAR1A; the Arg368X mutation results in deletion of cAMP binding site B of this regulatory subunit. This subunit constitutively represses the catalytic subunit, thereby impairing PKA response to cAMP stimulation (Linglart et al., 2011). Subsequent functional characterization of PRKAR1A mutations causing acrodysostosis revealed that all mutations lead to a cAMP binding defect as the unique molecular mechanism for resistance of PKA activation (Rhayem et al., 2015). This mechanism explains the hormonal resistance observed in ACRDYS1 patients and explains why their skeletal abnormalities resemble those observed in PHP1A/PPHP patients.

A knock-in of the recurrent R368X PRKAR1A mutation was recently developed in the mouse (Le Stunff et al., 2017). Heterozygous R368X KI mice presented the two main features of the ACRDYS1 phenotype in humans—i.e., renal proximal tubule resistance to PTH and chondrodysplasia. In addition, heterozygous R368X KI mice presented a striking and unexpected delay in endochondral ossification, raising the possibility that PRKAR1A/PKA is a molecular switch at the crossroads of pathways orchestrating chondrocyte proliferation and differentiation. A dissociation between chondrocyte

proliferation and differentiation is also observed in acromesomelic dysplasia, type Maroteaux (AMDM), a bone dysplasia characterized by severe short stature and short limbs, with no advance in bone age (in fact, a delay is observed) caused by homozygous mutations in the C-type natriuretic peptide-natriuretic peptide receptor B (Bartels et al., 2004). AMDM should be included in the differential diagnosis of acrodysostosis.

Phosphodiesterase 4D mutations

Defects in *PDE4D*, first identified by exome sequencing, cause acrodysostosis without obvious evidence for hormonal resistance (Lee et al., 2012; Michot et al., 2012; Linglart et al., 2012; Lindstrand et al., 2014). PDE4D belongs to the class IV of cAMP-specific phosphodiesterases that hydrolyze cAMP. In humans, a single *PDE4D* gene gives rise, through differential splicing that modifies the N-terminal portion of the protein, to at least nine different isoforms (Houslay and Adams, 2003). All isoforms comprise the same C-terminal catalytic domain. Six isoforms, classified as 'long' PDE4D variants, contain two conserved upstream regions (UCR1 and UCR2), while two short isoforms contain only the UCR2 region, and one 'super-short' isoform of the enzyme contains only the catalytic domain. Little is known about the tissue-specific expression, function, and regulation of each of these isoforms in human tissues. All long isoforms are activated by PKA-mediated phosphorylation of a single serine residue within a PKA consensus phosphorylation site in UCR1. To date, 32 heterozygous missense mutations in PDE4D have been identified in patients with acrodysostosis (ACRDYS2) (Lindstrand et al., 2014; Silve et al., 2012a,b; Silve et al., 2012a,b; Elli et al., 2016a,b; Kaname et al., 2014; Lynch et al., 2013) (Fig. 57.10). Interestingly, PDE4D mutations are located in all three main functional domains (UCR1, UCR2, and catalytic), indicating that defects in all isoforms (long, short, and supershort) can putatively cause ACRDYS2. The location of PDE4D mutations occurring in ACRDYS2 indicate that they could influence the regulation of PDE activity by PKA without impairing the functional activity of the activated enzyme (Cedervall et al., 2015). In agreement, recent findings indicate that PDE4D3 (one of the long PDE4D isoforms) variants carrying ACRDYS2 mutations are more readily activated over a wide range of intracellular cAMP concentrations by PKA-induced phosphorylation than wild-type PDE4D3 (Briet et al., 2017); furthermore, basal activity is enhanced in cells expressing PDE4D3 variants compared with that of cells expressing wild-type PDE4D3 (Briet et al., 2017). These studies indicate that ACRDYS2 mutations result in the increased hydrolytic activity of PDE4D. Mutations in PDE3A causing hypertension and brachydactyly syndrome have also been demonstrated to increase PKA-mediated activation of PDE3A (see later) (Maass et al., 2015). These findings may offer new perspectives into the selection of specific PDE inhibitors and possible therapeutic intervention for these patients.

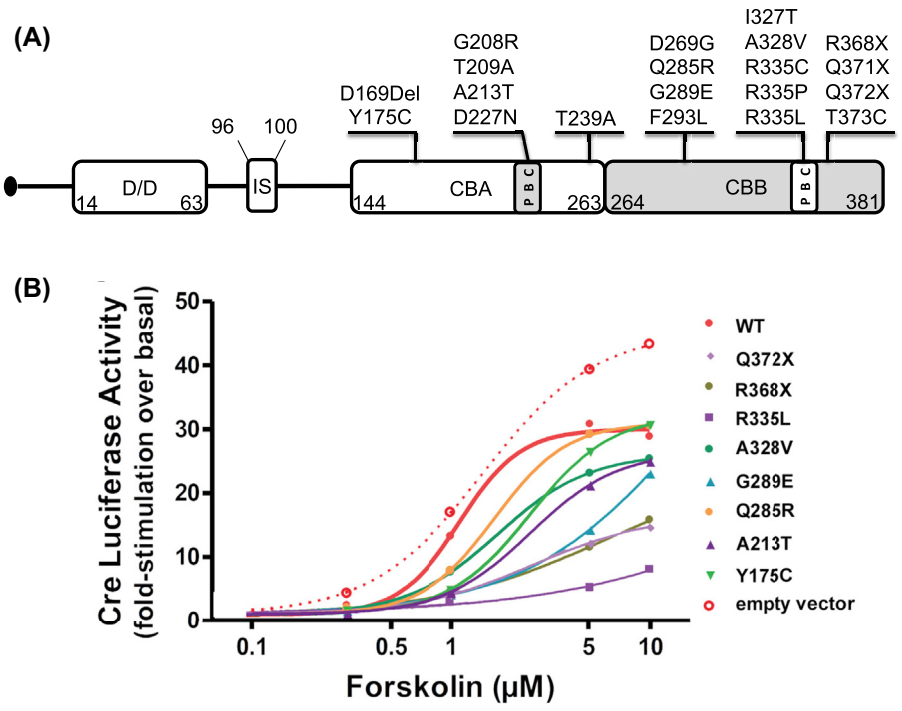

FIGURE 57.10 **Panel A.** Schematic representation of PDE4D indicating the functionally important domains and positions of amino acid residues mutated in patients affected with acrodysostosis (ACRDYS2). The positions are indicated for the PDE4D4 isoform. UCR: upstream conserved region. **Panel B.** Comparison of the phosphodiesterase activity of PDE4D3 carrying ACRDYS2 mutations and WT PDE4D3. The results are expressed as % WT activity. Increases in activity are observed, with the four different ACRDYS2 mutations occurring in the different functional domains of the protein. Mutations causing acrodysostosis-2 facilitate the activation of phosphodiesterase 4D3. *Adapted from Briet, C., Pereda, A., Le Stunff, C., Motte, E., de Dios Garcia-Diaz, J., de Nanclares, G.P., Dumaz, N., and Silve, C. 2017. Mutations causing acrodysostosis-2 facilitate activation of phosphodiesterase 4D3. Hum. Mol. Genet. 26, 3883–3894, with permission.*

Another group, however, reported that PDE4D mutations causing acrodysostosis without hormone resistance resulted in impaired enzyme activity and that the observed phenotype resulted from overcompensatory increased expression of other PDE4 isoforms (Kaname et al., 2014).

Since the first reports, some clinical and radiological findings in acrodysostosis were noted as similar to those observed in PHP1A/PPHP syndromes (Ablow et al., 1977; Davies and Hughes, 1992); however, distinct differences exist. In particular, although the different conditions present with stocky appearance and BDE, brachydactyly type E, the brachydactyly in the *GNAS*-related disorders, is variable and usually less severe than it is in both forms of acrodysostosis. The skeletal phenotype in acrodysostosis is usually quite uniform and more severe than in PHP1A/PPHP (Fig. 57.8). In contrast to severe skeletal dysplasia, resistance toward PTH and other hormones is less pronounced in ACRDYS2 (Linglart et al., 2011, 2012; Lindstrand et al., 2014; Silve et al., 2012a,b). Recent work indicates that the ability of PDE4 to modulate signaling through the GPCR−cAMP−PKA pathway depends on cell type and stimulus intensity. Thus, PDE4D mutations would be expected to impair some but not all responses, potentially explaining the presence of acrodysostosis without hormonal resistance in ACRDYS2 (Motte et al., 2017).

Phosphodiesterase 3A mutations

PDE3A is a member of a PDE family that hydrolyzes both cAMP and cGMP with high affinity. It is characterized by competitive inhibition of its cAMP hydrolytic activity by cGMP and certain positive inotropic agents. Heterozygous mutations that activate PDE3A have been identified in patients affected by BDE with hypertension syndrome (Maass et al., 2015). The mutations, which occur within a cluster located N-terminal to the PDE3A catalytic unit increase PKA-mediated activation of PDE3A, resulting in increased PDE activity (Maass et al., 2015). The increased phosphorylation of PDE3A was found to decrease the Km for cAMP without changing Vmax, whereas phosphorylation of PDE4D has been found to increase Vmax without changing the Km for cAMP (Mika and Conti, 2016).

Histone deacetylase 4-mutations

Brachydactyly mental retardation syndrome (BDMR) presents with a range of features including intellectual disabilities, developmental delays, behavioral abnormalities, sleep disturbance, and craniofacial and skeletal abnormalities comprising brachydactyly type E and autism spectrum disorder. BDMR had been associated with large deletions of 2q37. Clinical and molecular analysis of individuals with overlapping deletions involving 2q37.3 that refined this critical region led to sequencing of histone deacetylase 4 (*HDAC4*) as a candidate gene and the identification of de novo mutations including one intragenic deletion that probably disrupts normal splicing and one intragenic insertion causing a frame shift and premature stop codon in BDMR-affected patients (Williams et al., 2010). HDAC4 is a histone deacetylase that regulates genes important in bone, muscle, neurological, and cardiac development. Identification of *HDAC4* deletions and mutations in multiple subjects with BDMR and the phenotype of *Hdac4*(−/−) mice indicate that haploinsufficiency of *HDAC4* results in BDMR.

Conclusions

Mutations in the genes encoding PTH, PTHrP, or PTHR1 as well as downstream signaling and effector proteins have been identified as causes of rare inherited disorders. Identification of these mutations has provided important new insights into the regulation of bone and cartilage development as well as mineral ion homeostasis.

References

Albright, F., Burnett, C.H., Smith, P.H., Parson, W., 1942. Pseudohypoparathyroidism − an example of "Seabright-Bantam syndrome". Endocrinology 30, 922−932.

Ablow, R.C., Hsia, Y.E., Brandt, I.K., 1977. Acrodysostosis coinciding with pseudohypoparathyroidism and pseudo-pseudohypoparathyroidism. AJR Am. J. Roentgenol. 128, 95−99.

Almaden, Y., Canalejo, A., Hernandez, A., Ballesteros, E., Garcia-Navarro, S., Torres, A., Rodriguez, M., 1996. Direct effect of phosphorus on PTH secretion from whole rat parathyroid glands in vitro. J. Bone Miner. Res. 11, 970−976.

Amizuka, N., Karaplis, A.C., Henderson, J.E., Warshawsky, H., Lipman, M.L., Matsuki, Y., Ejiri, S., Tanaka, M., Izumi, N., Ozawa, H., et al., 1996. Haploinsufficiency of parathyroid hormone-related peptide (PTHrP) results in abnormal post-natal bone development. Dev. Biol. 175, 166−176.

Arnold, A., Horst, S.A., Gardella, T.J., Baba, H., Levine, M.A., Kronenberg, H.M., 1990. Mutation of the signal peptide-encoding region of the pre-proparathyroid hormone gene in familial isolated hypoparathyroidism. J. Clin. Investig. 86, 1084−1087.

Bacic, D., Wagner, C.A., Hernando, N., Kaissling, B., Biber, J., Murer, H., 2004. Novel aspects in regulated expression of the renal type IIa Na/Pi-cotransporter. Kidney Int. Suppl. S5–S12.

Bartels, C.F., Bukulmez, H., Padayatti, P., Rhee, D.K., van Ravenswaaij-Arts, C., Pauli, R.M., Mundlos, S., Chitayat, D., Shih, L.Y., Al-Gazali, L.I., et al., 2004. Mutations in the transmembrane natriuretic peptide receptor NPR-B impair skeletal growth and cause acromesomelic dysplasia, type Maroteaux. Am. J. Hum. Genet. 75, 27–34.

Bastepe, M., Jüppner, H., 2016. Pseudohypoparathyroidism, albright's hereditary osteodystrophy, and progressive osseous Heteroplasia: disorders caused by inactivating *GNAS* mutations. In: DeGroot, L.J., Jameson, J.L. (Eds.), Endocrinology. W.B. Saunders Company, Philadelphia, PA, pp. 1147–1159.

Bastepe, M., Raas-Rothschild, A., Silver, J., Weissman, I., Jüppner, H., Gillis, D., 2004. A form of Jansen's metaphyseal chondrodysplasia with limited metabolic and skeletal abnormalities is caused by a novel activating PTH/PTHrP receptor mutation. J. Clin. Endocrinol. Metab. 89, 3595–3600.

Baumber, L., Tufarelli, C., Patel, S., King, P., Johnson, C.A., Maher, E.R., Trembath, R.C., 2005. Identification of a novel mutation disrupting the DNA binding activity of GCM2 in autosomal recessive familial isolated hypoparathyroidism. J. Med. Genet. 42, 443–448.

Ben-Dov, I.Z., Galitzer, H., Lavi-Moshayoff, V., Goetz, R., Kuro-o, M., Mohammadi, M., Sirkis, R., Naveh-Many, T., Silver, J., 2007. The parathyroid is a target organ for FGF23 in rats. J. Clin. Investig. 117, 4003–4008.

Bergwitz, C., Jüppner, H., 2010. Regulation of phosphate homeostasis by PTH, vitamin D, and FGF23. Annu. Rev. Med. 61, 91–104.

Berndt, T., Kumar, R., 2007. Phosphatonins and the regulation of phosphate homeostasis. Annu. Rev. Physiol. 69, 341–359.

Biber, J., Hernando, N., Forster, I., Murer, H., 2009. Regulation of phosphate transport in proximal tubules. Pflügers Archiv 458, 39–52.

Bilginturan, N., Zileli, S., Karacadag, S., Pirnar, T., 1973. Hereditary brachydactyly associated with hypertension. J. Med. Genet. 10, 253–259.

Blaine, J., Weinman, E.J., Cunningham, R., 2011. The regulation of renal phosphate transport. Adv. Chron. Kidney Dis. 18, 77–84.

Blomstrand, S., Claësson, I., Säve-Söderbergh, J., 1985. A case of lethal congenital dwarfism with accelerated skeletal maturation. Pediatr. Radiol. 15, 141–143.

Boda, H., Uchida, H., Takaiso, N., Ouchi, Y., Fujita, N., Kuno, A., Hata, T., Nagatani, A., Funamoto, Y., Miyata, M., et al., 2016. A PDE3A mutation in familial hypertension and brachydactyly syndrome. J. Hum. Genet. 61, 701–703.

Briet, C., Pereda, A., Le Stunff, C., Motte, E., de Dios Garcia-Diaz, J., de Nanclares, G.P., Dumaz, N., Silve, C., 2017. Mutations causing acrodysostosis-2 facilitate activation of phosphodiesterase 4D3. Hum. Mol. Genet. 26, 3883–3894.

Brown, E.M., Gamba, G., Riccardi, D., Lombardi, M., Butters, R., Kifor, O., Sun, A., Hediger, M.A., Lytton, J., Hebert, S.C., 1993. Cloning and characterization of an extracellular Ca^{2+}-sensing receptor from bovine parathyroid. Nature 366, 575–580.

Brown, W.W., Jüppner, H., Langman, C.B., Price, H., Farrow, E.G., White, K.E., McCormick, K.L., 2009. Hypophosphatemia with elevations in serum fibroblast growth factor 23 in a child with Jansen's metaphyseal chondrodysplasia. J. Clin. Endocrinol. Metab. 94, 17–20.

Calvi, L., Sims, N., Hunzelman, J., Knight, M., Giovannetti, A., Saxton, J., Kronenberg, H.M., Baron, R., Schipani, E., 2001. Activation of the PTH/PTHrP receptor in osteoblastic cells has differential effects on cortical and trabecular bone. J. Clin. Investig. 107, 277–286.

Cameron, J.A.P., Young, W.B., Sissons, H.A., 1954. Metaphysial dysostosis. Report of a case. J. Bone Jt. Surg. 36B, 622–629.

Cedervall, P., Aulabaugh, A., Geoghegan, K.F., McLellan, T.J., Pandit, J., 2015. Engineered stabilization and structural analysis of the autoinhibited conformation of PDE4. Proc. Natl. Acad. Sci. U. S. A. 112, E1414–E1422.

Chabardes, D., Imbert, M., Clique, A., Montegut, M., Morel, F., 1975. PTH sensitive adenyl cyclase activity in different segments of the rabbit nephron. Pflügers Archiv. 354, 229–239.

Charrow, J., Poznanski, A.K., 1984. The Jansen type of metaphyseal chondrodysplasia: conformation of dominant inheritance and review of radiographic manifestations in the newborn and adult. J. Med. Genet. 18, 321–327.

Chase, L.R., Aurbach, G.D., 1967. Parathyroid function and the renal excretion of 3'5'-adenylic acid. Proc. Natl. Acad. Sci. U. S. A. 58, 518–525.

Chase, L.R., Aurbach, G.D., 1970. The effect of parathyroid hormone on the concentration of adenosine 3',5'-monophosphate in skeletal tissue in vitro. J. Biol. Chem. 245, 1520–1526.

Chase, L.R., Fedak, S.A., Aurbach, G.D., 1969a. Activation of skeletal adenyl cyclase by parathyroid hormone in vitro. Endocrinology 84, 761–768.

Chase, L.R., Melson, G.L., Aurbach, G.D., 1969b. Pseudohypoparathyroidism: defective excretion of 3',5'-AMP in response to parathyroid hormone. J. Clin. Investig. 48, 1832–1844.

Collinson, M., Leonard, S.J., Charlton, J., Crolla, J.A., Silve, C., Hall, C.M., Oglivie, C., James, M.A., Smithson, S.F., 2010. Symmetrical enchondromatosis is associated with duplication of 12p11.23 to 12p11.22 including PTHLH. Am. J. Med. Genet. 152A, 3124–3128.

Couvineau, A., Wouters, V., Bertrand, G., Rouyer, C., Gerard, B., Boon, L.M., Grandchamp, B., Vikkula, M., Silve, C., 2008. PTHR1 mutations associated with Ollier disease result in receptor loss of function. Hum. Mol. Genet. 17, 2766–2775.

Davies, S.J., Hughes, H.E., 1992. Familial acrodysostosis: can it be distinguished from Albright's hereditary osteodystrophy? Clin. Dysmorphol. 1, 207–215.

Davies, S.J., Hughes, H.E., 1993. Imprinting in Albright's hereditary osteodystrophy. J. Med. Genet. 30, 101–103.

De Haas, W.H.D., De Boer, W., Griffioen, F., 1969. Metaphysial dysostosis. A late follow-up of the first reported case. J. Bone Jt. Surg. 51B, 290–299.

Decker, E., Stellzig-Eisenhauer, A., Fiebig, B.S., Rau, C., Kress, W., Saar, K., Ruschendorf, F., Hubner, N., Grimm, T., Weber, B.H., 2008. PTHR1 loss-of-function mutations in familial, nonsyndromic primary failure of tooth eruption. Am. J. Hum. Genet. 83, 781–786.

den Hollander, N.S., van der Harten, H.J., Vermeij-Keers, C., Niermeijer, M.F., Wladimiroff, J.W., 1997. First-trimester diagnosis of Blomstrand lethal osteochondrodysplasia. Am. J. Med. Genet. 73, 345–350.

Ding, C., Buckingham, B., Levine, M.A., 2001. Familial isolated hypoparathyroidism caused by a mutation in the gene for the transcription factor GCMB. J. Clin. Investig. 108, 1215–1220.

Duchatelet, S., Ostergaard, E., Cortes, D., Lemainque, A., Julier, C., 2005. Recessive mutations in PTHR1 cause contrasting skeletal dysplasias in Eiken and Blomstrand syndromes. Hum. Mol. Genet. 14, 1–5.

Eiken, M., Prag, J., Petersen, K., Kaufmann, H., 1984. A new familial skeletal dysplasia with severely retarded ossification and abnormal modeling of bones especially of the epiphyses, the hands, and feet. Eur. J. Pediatr. 141, 231–235.

Elli, F.M., Linglart, A., Garin, I., de Sanctis, L., Bordogna, P., Grybek, V., Pereda, A., Giachero, F., Verrua, E., Hanna, P., et al., 2016a. The prevalence of GNAS deficiency-related diseases in a large cohort of patients characterized by the EuroPHP network. J. Clin. Endocrinol. Metab. 101, 3657–3668.

Elli, F.M., Bordogna, P., de Sanctis, L., Giachero, F., Verrua, E., Segni, M., Mazzanti, L., Boldrin, V., Toromanovic, A., Spada, A., et al., 2016b. Screening of PRKAR1A and PDE4D in a large Italian series of patients clinically diagnosed with Albright hereditary osteodystrophy and/or pseudohypoparathyroidism. J. Bone Miner. Res. 31, 1215–1224.

Ertl, D.A., Stary, S., Streubel, B., Raimann, A., Haeusler, G., 2012. A novel homozygous mutation in the parathyroid hormone gene (PTH) in a girl with isolated hypoparathyroidism. Bone 51, 629–632.

Farfel, Z., Brickman, A.S., Kaslow, H.R., Brothers, V.M., Bourne, H.R., 1980. Defect of receptor-cyclase coupling protein in pseudohypoparathyroidism. N. Engl. J. Med. 303, 237–242.

Finkelstein, J., Hayes, A., Hunzelman, J., Wyland, J., Lee, H., Neer, R., 2003. The effects of parathyroid hormone, alendronate, or both in men with osteoporosis. N. Engl. J. Med. 349, 1216–1226.

Frazier-Bowers, S.A., Koehler, K.E., Ackerman, J.L., Proffit, W.R., 2007. Primary failure of eruption: further characterization of a rare eruption disorder. Am. J. Orthod. Dentofacial Orthop. 131, 578 e571–511.

Frazier-Bowers, S.A., Simmons, D., Wright, J.T., Proffit, W.R., Ackerman, J.L., 2010. Primary failure of eruption and PTH1R: the importance of a genetic diagnosis for orthodontic treatment planning. Am. J. Orthod. Dentofacial Orthop. 137, 160 e161–167 discussion 160-161.

Frazier-Bowers, S.A., Hendricks, H.M., Wright, J.T., Lee, J., Long, K., Dibble, C.F., Bencharit, S., 2014. Novel mutations in PTH1R associated with primary failure of eruption and osteoarthritis. J. Dent. Res. 93, 134–139.

Friedman, P.A., Coutermarsh, B.A., Kennedy, S.M., Gesek, F.A., 1996. Parathyroid hormone stimulation of calcium transport is mediated by dual signaling mechanisms involving protein kinase A and protein kinase C. Endocrinology 137, 13–20.

Galera, M., de Silva Patricio, F., Lederman, H., Porciuncula, C., Lopes Monlleo, I., Brunoni, D., 1999. Blomstrand chondrodysplasia: a lethal sclerosing skeletal dysplasia. Case report and review. Pediatr. Radiol. 29, 842–845.

Gardella, T.J., Jüppner, H., Brown, E.M., Kronenberg, H.M., Potts Jr., J.T., 2016. Parathyroid hormone and parathyroid hormone receptor type 1 in the regulation of calcium and phosphate homeostasis and bone metabolism. In: DeGroot, L.J., Jameson, J.L. (Eds.), Endocrinology. W.B. Saunders Company, Philadelphia, PA, pp. 969–990.

Gram, P.B., Fleming, J.L., Frame, B., Fine, G., 1959. Metaphyseal chondrodysplasia of Jansen. J. Bone Jt. Surg. 41A, 951–959.

Guerreiro, R., Brás, J., Batista, S., Pires, P., Ribeiro, H., Almeida, R., Oliveira, C., Hardy, J., Santana, I., 2016. Pseudohypoparathyroidism Type I-b with neurological involvement is associated with a homozygous PTH1R mutation. Genes Brain Behav. 15, 669–677.

Günther, T., Chen, Z.F., Kim, J., Priemel, M., Rueger, J.M., Amling, M., Moseley, J.M., Martin, T.J., Anderson, D.J., Karsenty, G., 2000. Genetic ablation of parathyroid glands reveals another source of parathyroid hormone. Nature 406, 199–203.

Guo, J., Liu, M., Yang, D., Bouxsein, M.L., Thomas, C.C., Schipani, E., Bringhurst, F.R., Kronenberg, H.M., 2010. Phospholipase C signaling via the parathyroid hormone (PTH)/PTH-related peptide receptor is essential for normal bone responses to PTH. Endocrinology 151, 3502–3513.

Guo, J., Song, L., Liu, M., Segawa, H., Miyamoto, K., Bringhurst, F.R., Kronenberg, H.M., Jüppner, H., 2013. Activation of a non-cAMP/PKA signaling pathway downstream of the PTH/PTHrP receptor is essential for a sustained hypophosphatemic response to PTH infusion in male mice. Endocrinology 154, 1680–1689.

Guo, J., Khatri, A., Maeda, A., Potts Jr., J.T., Jüppner, H., Gardella, T.J., 2017. Prolonged pharmacokinetic and pharmacodynamic actions of a pegylated parathyroid hormone (1-34) peptide fragment. J. Bone Miner. Res. 32, 86–98.

Hens, J.R., Dann, P., Zhang, J.P., Harris, S., Robinson, G.W., Wysolmerski, J., 2007. BMP4 and PTHrP interact to stimulate ductal outgrowth during embryonic mammary development and to inhibit hair follicle induction. Development 134, 1221–1230.

Hilpert, J., Nykjaer, A., Jacobsen, C., Wallukat, G., Nielsen, R., Moestrup, S.K., Haller, H., Luft, F.C., Christensen, E.I., Willnow, T.E., 1999. Megalin antagonizes activation of the parathyroid hormone receptor. J. Biol. Chem. 274, 5620–5625.

Holthusen, W., Holt, J.F., Stoeckenius, M., 1975. The skull in metaphyseal chondrodysplasia type Jansen. Pediatr. Radiol. 3, 137–144.

Hoogendam, J., Farih-Sips, H., Wynaendts, L.C., Lowik, C.W., Wit, J.M., Karperien, M., 2007. Novel mutations in the parathyroid hormone (PTH)/PTH-related peptide receptor type 1 causing Blomstrand osteochondrodysplasia types I and II. J. Clin. Endocrinol. Metab. 92, 1088–1095.

Hopyan, S., Gokgoz, N., Poon, R., Gensure, R., Yu, C., Cole, W., Bell, R., Jüppner, H., Andrulis, I., Wunder, J., et al., 2002. A mutant type I PTH/PTHrP receptor in enchondromatosis. Nat. Genet. 30, 306–310.

Houslay, M.D., Adams, D.R., 2003. PDE4 cAMP phosphodiesterases: modular enzymes that orchestrate signalling cross-talk, desensitization and compartmentalization. Biochem. J. 370, 1–18.

Iida-Klein, A., Guo, J., Xie, L.Y., Jüppner, H., Potts Jr., J.T., Kronenberg, H.M., Bringhurst, F.R., Abou-Samra, A.B., Segre, G.V., 1995. Truncation of the carboxyl-terminal region of the parathyroid hormone (PTH)/PTH-related peptide receptor enhances PTH stimulation of adenylate cyclase but not phospholipase C. J. Biol. Chem. 270, 8458–8465.

Isojima, T., Doi, K., Mitsui, J., Oda, Y., Tokuhiro, E., Yasoda, A., Yorifuji, T., Horikawa, R., Yoshimura, J., Ishiura, H., et al., 2014. A recurrent de novo FAM111A mutation causes Kenny-Caffey syndrome type 2. J. Bone Miner. Res. 29, 992–998.

Iwamoto, M., Jikko, A., Murakami, H., Shimazu, A., Nakashima, K., Iwamoto, M., Takigawa, M., Baba, H., Suzuki, F., Kato, Y., 1994. Changes in parathyroid hormone receptors during chondrocyte cytodifferentiation. J. Biol. Chem. 269, 17245–17251.

Jaffe, H.L., 1972. Certain Other Anomalies of Skeletal Development (Chapter 9). Lea and Febiger, Philadelphia, 222-226 pp.

Jamsheer, A., Sowinska-Seidler, A., Olech, E.M., Socha, M., Kozlowski, K., Pyrkosz, A., Trzeciak, T., Materna-Kiryluk, A., Latos-Bielenska, A., 2016. Variable expressivity of the phenotype in two families with brachydactyly type E, craniofacial dysmorphism, short stature and delayed bone age caused by novel heterozygous mutations in the PTHLH gene. J. Hum. Genet. 61, 457–461.

Jansen, M., 1934. Über atypische Chondrodystrophie (Achondroplasie) und über eine noch nicht beschriebene angeborene Wachstumsstörung des Knochensystems: metaphysäre Dysostosis. Zeitschr Orthop Chir 61, 253–286.

Jelani, M., Kang, C., Mohamoud, H.S., Al-Rehaili, R., Almramhi, M.M., Serafi, R., Yang, H., Al-Aama, J.Y., Naeem, M., Alkhiary, Y.M., 2016. A novel homozygous PTH1R variant identified through whole-exome sequencing further expands the clinical spectrum of primary failure of tooth eruption in a consanguineous Saudi family. Arch. Oral Biol. 67, 28–33.

Jobert, A.S., Zhang, P., Couvineau, A., Bonaventure, J., Roume, J., LeMerrer, M., Silve, C., 1998. Absence of functional receptors parathyroid hormone and parathyroid hormone-related peptide in Blomstrand chondrodysplasia. J. Clin. Investig. 102, 34–40.

Jüppner, H., Schipani, E., Silve, C., 2002. Jansen's metaphyseal chondrodysplasia and Blomstrand's lethal chondrodysplasia: two genetic disorders caused by PTH/PTHrP receptor mutations. In: Bilezikian, J., Raisz, L., Rodan, G. (Eds.), Principles of Bone Biology. Academic Press, San Diego, CA, pp. 1117–1135.

Kaname, T., Ki, C.S., Niikawa, N., Baillie, G.S., Day, J.P., Yamamura, K., Ohta, T., Nishimura, G., Mastuura, N., Kim, O.H., et al., 2014. Heterozygous mutations in cyclic AMP phosphodiesterase-4D (PDE4D) and protein kinase A (PKA) provide new insights into the molecular pathology of acrodysostosis. Cell. Signal. 26, 2446–2459.

Karaplis, A.C., Luz, A., Glowacki, J., Bronson, R., Tybulewicz, V., Kronenberg, H.M., Mulligan, R.C., 1994. Lethal skeletal dysplasia from targeted disruption of the parathyroid hormone-related peptide gene. Genes Dev. 8, 277–289.

Karaplis, A.C., Bin He, M.T., Nguyen, A., Young, I.D., Semeraro, D., Ozawa, H., Amizuka, N., 1998. Inactivating mutation in the human parathyroid hormone receptor type 1 gene in Blomstrand chondrodysplasia. Endocrinology 139, 5255–5258.

Karperien, M.C., van der Harten, H.J., van Schooten, R., Farih-Sips, H., den Hollander, N.S., Kneppers, A.L.J., Nijweide, P., Papapoulos, S.E., Löwik, C.W.G.M., 1999. A frame-shift mutation in the type I parathyroid hormone/parathyroid hormone-related peptide receptor causing Blomstrand lethal osteochondrodysplasia. J. Clin. Endocrinol. Metab. 84, 3713–3720.

Kaufmann, M., Muff, R., Born, W., Fischer, J., 1994. Functional expression of a stably transfected parathyroid hormone/parathyroid hormone related protein receptor complementary DNA in CHO cells. Mol. Cell. Endocrinol. 104, 21–27.

Kessel, D., Hall, C.M., Shaw, D.G., 1992. Two unusual cases of nephrocalcinosis in infancy. Pediatr. Radiol. 22, 470–471.

Klopocki, E., Hennig, B.P., Dathe, K., Koll, R., de Ravel, T., Baten, E., Blom, E., Gillerot, Y., Weigel, J.F., Kruger, G., et al., 2010. Deletion and point mutations of PTHLH cause brachydactyly type E. Am. J. Hum. Genet. 86, 434–439.

Koike, T., Iwamoto, M., Shimazu, A., Nakashima, K., Suzuki, F., Kato, Y., 1990. Potent mitogenic effects of parathyroid hormone (PTH) on embryonic chick and rabbit chondrocytes. Differential effects of age on growth, proteoglycan, and cyclic AMP responses of chondrocytes to PTH. J. Clin. Investig. 85, 626–631.

Kong, X.F., Zhu, X.H., Pei, Y.L., Jackson, D.M., Holick, M.F., 1999. Molecular cloning, characterization, and promoter analysis of the human 25-hydroxyvitamin D3-1alpha-hydroxylase gene. Proc. Natl. Acad. Sci. U. S. A. 96, 6988–6993.

Krajisnik, T., Bjorklund, P., Marsell, R., Ljunggren, O., Akerstrom, G., Jonsson, K.B., Westin, G., Larsson, T.E., 2007. Fibroblast growth factor-23 regulates parathyroid hormone and 1alpha-hydroxylase expression in cultured bovine parathyroid cells. J. Endocrinol. 195, 125–131.

Kruse, K., Schütz, C., 1993. Calcium metabolism in the Jansen type of metaphyseal dysplasia. Eur. J. Pediatr. 152, 912–915.

Lanske, B., Karaplis, A.C., Lee, K., Luz, A., Vortkamp, A., Pirro, A., Karperien, M., Defize, L.H., Ho, C., Mulligan, R.C., et al., 1996. PTH/PTHrP receptor in early development and Indian hedgehog-regulated bone growth. Science 273, 663–666.

Lanske, B., Divieti, P., Kovacs, C.S., Pirro, A., Landis, W.J., Krane, S.M., Bringhurst, F.R., Kronenberg, H.M., 1999. The parathyroid hormone (PTH)/PTH-related peptide receptor mediates actions of both ligands in murine bone. Endocrinology 139, 5194–5204.

Le Stunff, C., Tilotta, F., Sadoine, J., Le Denmat, D., Briet, C., Motte, E., Clauser, E., Bougneres, P., Chaussain, C., Silve, C., 2017. Knock-in of the recurrent R368X mutation of PRKAR1A that represses cAMP-dependent protein kinase a activation: a model of type 1 acrodysostosis. J. Bone Miner. Res. 32, 333–346.

Lee, K., Deeds, J.D., Segre, G.V., 1995. Expression of parathyroid hormone-related peptide and its receptor messenger ribonucleic acid during fetal development of rats. Endocrinology 136, 453–463.

Lee, K., Brown, D., Urena, P., Ardaillou, N., Ardaillou, R., Deeds, J., Segre, G.V., 1996. Localization of parathyroid hormone/parathyroid hormone-related peptide receptor mRNA in kidney. Am. J. Physiol. 270, F186–F191.

Lee, H., Graham Jr., J.M., Rimoin, D.L., Lachman, R.S., Krejci, P., Tompson, S.W., Nelson, S.F., Krakow, D., Cohn, D.H., 2012. Exome sequencing identifies PDE4D mutations in acrodysostosis. Am. J. Hum. Genet. 90, 746–751.

Lee, S., Mannstadt, M., Guo, J., Kim, S.M., Yi, H.S., Khatri, A., Dean, T., Okazaki, M., Gardella, T.J., Jüppner, H., 2015. A homozygous [Cys25] PTH(1-84) mutation that impairs PTH/PTHrP receptor activation defines a novel form of hypoparathyroidism. J. Bone Miner. Res. 30, 1803–1813.

Lenz, W.D., 1969. Skeletal dysplasias. In: Bergsma, D. (Ed.), The First Conference on the Clinical Delineation of Birth Defects. The Johns Hopkins Hospital, Baltimore, MD, pp. 71–72. The National Foundation-March of Dimes.

Leroy, J.G., Keersmaeckers, G., Coppens, M., Dumon, J.E., Roels, H., 1996. Blomstrand lethal chondrodysplasia. Am. J. Med. Genet. 63, 84–89.

Levine, M.A., 2002. Pseudohypoparathyroidism. In: JP Bilezikian, L.R., Rodan, G.A. (Eds.), Principles of Bone Biology. Academic Press, New York, pp. 1137–1159.

Levine, M.A., Downs Jr., R.W., Singer, M., Marx, S.J., Aurbach, G.D., Spiegel, A.M., 1980. Deficient activity of guanine nucleotide regulatory protein in erythrocytes from patients with pseudohypoparathyroidism. Biochem. Biophys. Res. Commun. 94, 1319−1324.

Li, D., Opas, E.E., Tuluc, F., Metzger, D.L., Hou, C., Hakonarson, H., Levine, M.A., 2014. Autosomal dominant hypoparathyroidism caused by germline mutation in GNA11: phenotypic and molecular characterization. J. Clin. Endocrinol. Metab. 99, E1774−E1783.

Lindstrand, A., Grigelioniene, G., Nilsson, D., Pettersson, M., Hofmeister, W., Anderlid, B.M., Kant, S.G., Ruivenkamp, C.A., Gustavsson, P., Valta, H., et al., 2014. Different mutations in PDE4D associated with developmental disorders with mirror phenotypes. J. Med. Genet. 51, 45−54.

Linglart, A., Menguy, C., Couvineau, A., Auzan, C., Gunes, Y., Cancel, M., Motte, E., Pinto, G., Chanson, P., Bougneres, P., et al., 2011. Recurrent PRKAR1A mutation in acrodysostosis with hormone resistance. N. Engl. J. Med. 364, 2218−2226.

Linglart, A., Fryssira, H., Hiort, O., Holterhus, P.M., Perez de Nanclares, G., Argente, J., Heinrichs, C., Kuechler, A., Mantovani, G., Leheup, B., et al., 2012. PRKAR1A and PDE4D mutations cause acrodysostosis but two distinct syndromes with or without GPCR-signaling hormone resistance. J. Clin. Endocrinol. Metab. 97, E2328−E2338.

Linglart, A., Maupetit-Mehouas, S., Silve, C., 2013. GNAS -related loss-of-function disorders and the role of imprinting. Horm Res Paediatr 119−129.

Long, D.N., McGuire, S., Levine, M.A., Weinstein, L.S., Germain-Lee, E.L., 2007. Body mass index differences in pseudohypoparathyroidism type 1a versus pseudopseudohypoparathyroidism may implicate paternal imprinting of Galpha(s) in the development of human obesity. J. Clin. Endocrinol. Metab. 92, 1073−1079.

Loshkajian, A., Roume, J., Stanescu, V., Delezoide, A.L., Stampf, F., Maroteaux, P., 1997. Familial Blomstrand Chondrodysplasia with advanced skeletal maturation: further delineation. Am. J. Med. Genet. 71, 283−288.

Lupp, A., Klenk, C., Rocken, C., Evert, M., Mawrin, C., Schulz, S., 2010. Immunohistochemical identification of the PTHR1 parathyroid hormone receptor in normal and neoplastic human tissues. Eur. J. Endocrinol. 162, 979−986.

Lynch, D.C., Dyment, D.A., Huang, L., Nikkel, S.M., Lacombe, D., Campeau, P.M., Lee, B., Bacino, C.A., Michaud, J.L., Bernier, F.P., et al., 2013. Identification of novel mutations confirms PDE4D as a major gene causing acrodysostosis. Hum. Mutat. 34, 97−102.

Maass, P.G., Wirth, J., Aydin, A., Rump, A., Stricker, S., Tinschert, S., Otero, M., Tsuchimochi, K., Goldring, M.B., Luft, F.C., et al., 2010. A cis-regulatory site downregulates PTHLH in translocation t(8;12)(q13;p11.2) and leads to Brachydactyly Type E. Hum. Mol. Genet. 19, 848−860.

Maass, P.G., Aydin, A., Luft, F.C., Schachterle, C., Weise, A., Stricker, S., Lindschau, C., Vaegler, M., Qadri, F., Toka, H.R., et al., 2015. PDE3A mutations cause autosomal dominant hypertension with brachydactyly. Nat. Genet. 47, 647−653.

Maes, C., Kronenberg, H.M., 2016. Bone development and remodeling. In: DeGroot, L.J., Jameson, J.L. (Eds.), Endocrinology. W.B. Saunders Company, Philadelphia, PA, pp. 1038−1062.

Mahon, M., Segre, G., 2004. Stimulation by parathyroid hormone of a NHERF-1-assembled complex consisting of the parathyroid hormone I receptor, phospholipase Cbeta, and actin increases intracellular calcium in opossum kidney cells. J. Biol. Chem. 279, 23550−23558.

Mahon, M.J., Donowitz, M., Yun, C.C., Segre, G.V., 2002. Na(+)/H(+) exchanger regulatory factor 2 directs parathyroid hormone 1 receptor signalling. Nature 417, 858−861.

Mannstadt, M., Bertrand, G., Muresan, M., Weryha, G., Leheup, B., Pulusani, S.R., Grandchamp, B., Jüppner, H., Silve, C., 2008. Dominant-negative GCMB mutations cause an autosomal dominant form of hypoparathyroidism. J. Clin. Endocrinol. Metab. 93, 3568−3576.

Mannstadt, M., Harris, M., Bravenboer, B., Chitturi, S., Dreijerink, K.M., Lambright, D.G., Lim, E.T., Daly, M.J., Gabriel, S., Jüppner, H., 2013. Germline mutations affecting Galpha11 in hypoparathyroidism. N. Engl. J. Med. 368, 2532−2534.

Marcus, R., Aurbach, G.D., 1971. Adenyl cyclase from renal cortex. Biochim. Biophys. Acta 242, 410−421.

Marcus, R., Wilber, J.F., Aurbach, G.D., 1971. Parathyroid hormone-sensitive adenyl cyclase from the renal cortex of a patient with pseudohypoparathyroidism. J. Clin. Endocrinol. Metab. 33, 537−541.

Marigo, V., Davey, R.A., Zuo, Y., Cunningham, J.M., Tabin, C.J., 1996. Biochemical evidence that Patched is the Hedgehog receptor. Nature 384, 176−179.

Maroteaux, P.L.M., 2002. Les Maladies Osseuses de l'Enfant. Médecine-Sciences Flammarion, Paris, 682 pp.

Marouli, E., Graff, M., Medina-Gomez, C., Lo, K.S., Wood, A.R., Kjaer, T.R., Fine, R.S., Lu, Y., Schurmann, C., Highland, H.M., et al., 2017. Rare and low-frequency coding variants alter human adult height. Nature 542, 186−190.

Mensenkamp, A.R., Hoenderop, J.G., Bindels, R.J., 2007. TRPV5, the gateway to Ca2+ homeostasis. Handb. Exp. Pharmacol. 207−220.

Miao, D., He, B., Karaplis, A., Goltzman, D., 2002. Parathyroid hormone is essential for normal fetal bone formation. J. Clin. Investig. 109, 1173−1182.

Michot, C., Le Goff, C., Goldenberg, A., Abhyankar, A., Klein, C., Kinning, E., Guerrot, A.M., Flahaut, P., Duncombe, A., Baujat, G., et al., 2012. Exome sequencing identifies PDE4D mutations as another cause of acrodysostosis. Am. J. Hum. Genet. 90, 740−745.

Mika, D., Conti, M., 2016. PDE4D phosphorylation: a coincidence detector integrating multiple signaling pathways. Cell. Signal. 28, 719−724.

Minagawa, M., Arakawa, K., Minamitani, K., Yasuda, T., Niimi, H., 1997. Jansen-type metaphyseal chondrodysplasia: analysis of PTH/PTH-related protein receptor messenger RNA by the reverse transcription-polymerase chain method. Endocr. J. 44, 493−499.

Mirczuk, S.M., Bowl, M.R., Nesbit, M.A., Cranston, T., Fratter, C., Allgrove, J., Brain, C., Thakker, R.V., 2010. A missense glial cells missing homolog B (GCMB) mutation, Asn502His, causes autosomal dominant hypoparathyroidism. J. Clin. Endocrinol. Metab. 95, 3512−3516.

Morel, F., Imbert-Teboul, M., Chabardes, D., 1981. Distribution of hormone-dependent adenylate cyclase in the nephron and its physiological significance. Annu. Rev. Physiol. 43, 569−581.

Motte, E., Le Stunff, C., Briet, C., Dumaz, N., Silve, C., 2017. Modulation of signaling through GPCR-cAMP-PKA pathways by PDE4 depends on stimulus intensity: possible implications for the pathogenesis of acrodysostosis without hormone resistance. Mol. Cell. Endocrinol. 442, 1−11.

Mundlos, S., 2009. The brachydactylies: a molecular disease family. Clin. Genet. 76, 123−136.

Nagai, S., Okazaki, M., Segawa, H., Bergwitz, C., Dean, T., Potts Jr., J.T., Mahon, M.J., Gardella, T.J., Jüppner, H., 2011. Acute down-regulation of sodium-dependent phosphate transporter NPT2a involves predominantly the cAMP/PKA pathway as revealed by signaling-selective parathyroid hormone analogs. J. Biol. Chem. 286, 1618–1626.

Nampoothiri, S., Fernandez-Rebollo, E., Yesodharan, D., Gardella, T.J., Rush, E.T., Langman, C.B., Jüppner, H., 2016. Jansen metaphyseal chondrodysplasia due to heterozygous H223R-PTH1R mutations with or without overt hypercalcemia. J. Clin. Endocrinol. Metab. 101, 4283–4289.

Neer, R., Arnaud, C., Zanchetta, J., Prince, R., Gaich, G., Reginster, J., Hodsman, A., Eriksen, E., Ish-Shalom, S., Genant, H., et al., 2001. Effect of parathyroid hormone (1-34) on fractures and bone mineral density in postmenopausal women with osteoporosis. N. Engl. J. Med. 344, 1434–1441.

Nesbit, M.A., Hannan, F.M., Howles, S.A., Babinsky, V.N., Head, R.A., Cranston, T., Rust, N., Hobbs, M.R., Heath 3rd, H., Thakker, R.V., 2013. Mutations affecting G-protein subunit alpha11 in hypercalcemia and hypocalcemia. N. Engl. J. Med. 368, 2476–2486.

Onuchic, L., Ferraz-de-Souza, B., Mendonca, B.B., Correa, P.H., Martin, R.M., 2012. Potential effects of alendronate on fibroblast growth factor 23 levels and effective control of hypercalciuria in an adult with Jansen's metaphyseal chondrodysplasia. J. Clin. Endocrinol. Metab. 97, 1098–1103.

Oostra, R.J., Baljet, B., Dijkstra, P.F., Hennekam, R.C.M., 1998. Congenital anomalies in the teratological collection of museum Vrolik in Amsterdam, The Netherlands. II: skeletal dysplasia. Am. J. Med. Genet. 77, 116–134.

Oostra, R., van der Harten, J., Rijnders, W., Scott, R., Young, M., Trump, D., 2000. Blomstrand osteochondrodysplasia: three novel cases and histological evidence for heterogeneity. Virchows Arch. 436, 28–35.

Pansuriya, T.C., van Eijk, R., d'Adamo, P., van Ruler, M.A., Kuijjer, M.L., Oosting, J., Cleton-Jansen, A.M., van Oosterwijk, J.G., Verbeke, S.L., Meijer, D., et al., 2011. Somatic mosaic IDH1 and IDH2 mutations are associated with enchondroma and spindle cell hemangioma in Ollier disease and Maffucci syndrome. Nat. Genet. 43, 1256–1261.

Parfitt, A.M., Schipani, E., Rao, D.S., Kupin, W., Han, Z.-H., Jüppner, H., 1996. Hypercalcemia due to constitutive activity of the PTH/PTHrP receptor. Comparison with primary hyperparathyroidism. J. Clin. Endocrinol. Metab. 81, 3584–3588.

Parkinson, D., Thakker, R., 1992. A donor splice site mutation in the parathyroid hormone gene is associated with autosomal recessive hypoparathyroidism. Nat. Genet. 1, 149–153.

Patten, J.L., Johns, D.R., Valle, D., Eil, C., Gruppuso, P.A., Steele, G., Smallwood, P.M., Levine, M.A., 1990. Mutation in the gene encoding the stimulatory G protein of adenylate cyclase in Albright's hereditary osteodystrophy. N. Engl. J. Med. 322, 1412–1419.

Pearce, S.H., Williamson, C., Kifor, O., Bai, M., Coulthard, M.G., Davies, M., Lewis-Barned, N., McCredie, D., Powell, H., Kendall-Taylor, P., et al., 1996. A familial syndrome of hypocalcemia with hypercalciuria due to mutations in the calcium-sensing receptor. N. Engl. J. Med. 335, 1115–1122.

Pereda, A., Garzon-Lorenzo, L., Garin, I., Cruz-Rojo, J., Sanchez Del Pozo, J., Perez de Nanclares, G., 2017. The p.R56* mutation in PTHLH causes variable brachydactyly type E. Am. J. Med. Genet. 173, 816–819.

Pilz, P., Meyer-Marcotty, P., Eigenthaler, M., Roth, H., Weber, B.H., Stellzig-Eisenhauer, A., 2014. Differential diagnosis of primary failure of eruption (PFE) with and without evidence of pathogenic mutations in the PTHR1 gene. J. Orofac. Orthop. 75, 226–239.

Piret, S.E., Gorvin, C.M., Pagnamenta, A.T., Howles, S.A., Cranston, T., Rust, N., Nesbit, M.A., Glaser, B., Taylor, J.C., Buchs, A.E., et al., 2016. Identification of a G-protein subunit-alpha11 gain-of-function mutation, Val340Met, in a family with autosomal dominant hypocalcemia type 2 (ADH2). J. Bone Miner. Res. 31, 1207–1214.

Pollak, M.R., Brown, E.M., WuChou, Y.H., Hebert, S.C., Marx, S.J., Steinmann, B., Levi, T., Seidman, C.E., Seidman, J.G., 1993. Mutations in the human Ca^{2+}-sensing receptor gene cause familial hypocalciuric hypercalcemia and neonatal severe hyperparathyroidism. Cell 75, 1297–1303.

Pollak, M.R., Brown, E.M., Estep, H.L., McLaine, P.N., Kifor, O., Park, J., Hebert, S.C., Seidman, C.E., Seidman, J.G., 1994. Autosomal dominant hypocalcaemia caused by a Ca^{2+}-sensing receptor gene mutation. Nat. Genet. 8, 303–307.

Potts, J.T., Gardella, T.J., 2007. Progress, paradox, and potential: parathyroid hormone Research over five decades. Ann. N. Y. Acad. Sci. 1117, 196–208.

Quinque, E., Clauss, F., Siebert, T., Jung-Clauss, S., Bahi-Gross, S., 2016. Un contexte familial de défaut primaire d'éruption (DPE): identification d'une nouvelle mutation du gène PTHR-1. Cas clinique et revue de littérature. Med Buccale Chir Buccale 22, 35–42.

Reyes, M., Bravenboer, B., Jüppner, H., 2019. A Heterozygous Splice-Site Mutation in PTHLH Causes Autosomal Dominant Shortening of Metacarpals and Metatarsals. J. Bone Miner. Res. 34, 482–489.

Rhayem, Y., Le Stunff, C., Abdel Khalek, W., Auzan, C., Bertherat, J., Linglart, A., Couvineau, A., Silve, C., Clauser, E., 2015. Functional characterization of PRKAR1A mutations reveals a unique molecular mechanism causing acrodysostosis but multiple mechanisms causing carney complex. J. Biol. Chem. 290, 27816–27828.

Rhee, Y., Bivi, N., Farrow, E., Lezcano, V., Plotkin, L.I., White, K.E., Bellido, T., 2011. Parathyroid hormone receptor signaling in osteocytes increases the expression of fibroblast growth factor-23 in vitro and in vivo. Bone 49, 636–643.

Riccardi, D., Lee, W.S., Lee, K., Segre, G.V., Brown, E.M., Hebert, S.C., 1996. Localization of the extracellular Ca(2+)-sensing receptor and PTH/PTHrP receptor in rat kidney. Am. J. Physiol. 271, F951–F956.

Risom, L., Christoffersen, L., Daugaard-Jensen, J., Hove, H.D., Andersen, H.S., Andresen, B.S., Kreiborg, S., Duno, M., 2013. Identification of six novel PTH1R mutations in families with a history of primary failure of tooth eruption. PLoS One 8, e74601.

Roth, H., Fritsche, L.G., Meier, C., Pilz, P., Eigenthaler, M., Meyer-Marcotty, P., Stellzig-Eisenhauer, A., Proff, P., Kanno, C.M., Weber, B.H., 2014. Expanding the spectrum of PTH1R mutations in patients with primary failure of tooth eruption. Clin. Oral Investig. 18, 377–384.

Rozeman, L., Hameetman, L., Cleton-Jansen, A., Taminiau, A., Hogendoorn, P., Bovee, J., 2005. Absence of IHH and retention of PTHrP signalling in enchondromas and central chondrosarcomas. J. Pathol. 205, 476–482.

Saito, H., Noda, H., Gatault, P., Böckenhauer, D., Loke, K., Hiort, O., Silve, C., Sharwood, E., Matsunaga Martin, R., Dillon, M., et al., 2018. Progression of mineral ion abnormalities in patients with Jansen's metaphyseal chondrodysplasia. J. Clin. Endocrinol. Metab. in press.

Savoldi, G., Izzi, C., Signorelli, M., Bondioni, M.P., Romani, C., Lanzi, G., Moratto, D., Verdoni, L., Pinotti, M., Prefumo, F., et al., 2013. Prenatal presentation and postnatal evolution of a patient with Jansen metaphyseal dysplasia with a novel missense mutation in PTH1R. Am. J. Med. Genet. 161, 2614–2619.

Schipani, E., Kruse, K., Jüppner, H., 1995. A constitutively active mutant PTH-PTHrP receptor in Jansen-type metaphyseal chondrodysplasia. Science 268, 98–100.

Schipani, E., Langman, C.B., Parfitt, A.M., Jensen, G.S., Kikuchi, S., Kooh, S.W., Cole, W.G., Jüppner, H., 1996. Constitutively activated receptors for parathyroid hormone and parathyroid hormone-related peptide in Jansen's metaphyseal chondrodysplasia. N. Engl. J. Med. 335, 708–714.

Schipani, E., Jensen, G.S., Pincus, J., Nissenson, R.A., Gardella, T.J., Jüppner, H., 1997. Constitutive activation of the cAMP signaling pathway by parathyroid hormone (PTH)/PTH-related peptide (PTHrP) receptors mutated at the two loci for Jansen's metaphyseal chondrodysplasia. Mol. Endocrinol. 11, 851–858.

Schipani, E., Langman, C.B., Hunzelman, J., LeMerrer, M., Loke, K.Y., Dillon, M.J., Silve, C., Jüppner, H., 1999. A novel PTH/PTHrP receptor mutation in Jansen's metaphyseal chondrodysplasia. J. Clin. Endocrinol. Metab. 84, 3052–3057.

Schuster, H., Wienker, T.E., Bahring, S., Bilginturan, N., Toka, H.R., Neitzel, H., Jeschke, E., Toka, O., Gilbert, D., Lowe, A., et al., 1996. Severe autosomal dominant hypertension and brachydactyly in a unique Turkish kindred maps to human chromosome 12. Nat. Genet. 13, 98–100.

Segawa, H., Kaneko, I., Takahashi, A., Kuwahata, M., Ito, M., Ohkido, I., Tatsumi, S., Miyamoto, K., 2002. Growth-related renal type II Na/Pi cotransporter. J. Biol. Chem. 277, 19665–19672.

Segawa, H., Yamanaka, S., Onitsuka, A., Tomoe, Y., Kuwahata, M., Ito, M., Taketani, Y., Miyamoto, K., 2007. Parathyroid hormone-dependent endocytosis of renal type IIc Na-Pi cotransporter. Am. J. Physiol. Renal. Physiol. 292, F395–F403.

Silve, C., 2010. A cup half-full or half-empty? When PTHrP levels matter. IBMS BoneKEy 7 (9), 325–332.

Silve, C., Clauser, E., Linglart, A., 2012a. Acrodysostosis. Horm. Metab. Res. 44, 749–758.

Silve, C., Le-Stunff, C., Motte, E., Gunes, Y., Linglart, A., Clauser, E., 2012b. Acrodysostosis syndromes. Bone (Tarrytown) 11, 21.

Silver, J., Kronenberg, H.M., 1996. Parathyroid hormone – molecular biology and regulation. In: Bilezikian, J.P., Raisz, L.G., Rodan, G.A. (Eds.), Principles of Bone Biology. Academic Press, New York, pp. 325–346.

Silverthorn, K.G., Houston, C.S., Duncan, B.P., 1983. Murk Jansen's metaphyseal chondrodysplasia with long-term followup. Pediatr. Radiol. 17, 119–123.

Slatopolsky, E., Finch, J., Denda, M., Ritter, C., Zhong, M., Dusso, A., MacDonald, P., Brown, A., 1996. Phosphorus restriction prevents parathyroid gland growth. High phosphorus directly stimulates PTH secretion in vitro. J. Clin. Investig. 97, 2534–2540.

St-Arnaud, R., Demay, M.B., 2011. Vitamin D biology. In: Pediatric Bone: Biology and Diseases. Academic Press, San Diego, pp. 163–187.

Stone, D.M., Hynes, M., Armanini, M., Swanson, T.A., Gu, Q., Johnson, R.L., Scott, M.P., Pennica, D., Goddard, A., Phillips, H., et al., 1996. The tumour-suppressor gene *patched* encodes a candiadate receptor for Sonic hedgehog. Nature 384, 129–134.

Strewler, G.J., 2000. Mechanisms of disease: the physiology of parathyroid hormone-related protein. N. Engl. J. Med. 342, 177–185.

Sunthornthepvarakul, T., Churesigaew, S., Ngowngarmratana, S., 1999. A novel mutation of the signal peptide of the preproparathyroid hormone gene associated with autosomal recessive familial isolated hypoparathyroidism. J. Clin. Endocrinol. Metab. 84, 3792–3796.

Suva, L., Freeman, A., Martin, T., 2015. Parathyroid hormone-related peptide. In: Bilezikian, J. (Ed.), The Parathyroids: Basic and Clinical Concepts. Academic Press, San Diego, pp. 45–64.

Takeyama, K., Kitanaka, S., Sato, T., Kobori, M., Yanagisawa, J., Kato, S., 1997. 25-Hydroxyvitamin D3 1alpha-hydroxylase and vitamin D synthesis. Science 277, 1827–1830.

Tasken, K., Skalhegg, B.S., Tasken, K.A., Solberg, R., Knutsen, H.K., Levy, F.O., Sandberg, M., Orstavik, S., Larsen, T., Johansen, A.K., et al., 1997. Structure, function, and regulation of human cAMP-dependent protein kinases. Adv. Second Messenger Phosphoprotein Res. 31, 191–204.

Taylor, S.S., Buechler, J.A., Yonemoto, W., 1990. cAMP-dependent protein kinase: framework for a diverse family of regulatory enzymes. Annu. Rev. Biochem. 59, 971–1005.

Taylor, S.S., Kim, C., Cheng, C.Y., Brown, S.H., Wu, J., Kannan, N., 2008. Signaling through cAMP and cAMP-dependent protein kinase: diverse strategies for drug design. Biochim. Biophys. Acta 1784, 16–26.

Tenhola, S., Voutilainen, R., Reyes, M., Toiviainen-Salo, S., Juppner, H., Makitie, O., 2016. Impaired growth and intracranial calcifications in autosomal dominant hypocalcemia caused by a GNA11 mutation. Eur. J. Endocrinol. 175, 211–218.

Thomas-Teinturier, C., Pereda, A., Garin, I., Diez-Lopez, I., Linglart, A., Silve, C., de Nanclares, G.P., 2016. Report of two novel mutations in PTHLH associated with brachydactyly type E and literature review. Am. J. Med. Genet. 170, 734–742.

Thomee, C., Schubert, S.W., Parma, J., Le, P.Q., Hashemolhosseini, S., Wegner, M., Abramowicz, M.J., 2005. GCMB mutation in familial isolated hypoparathyroidism with residual secretion of parathyroid hormone. J. Clin. Endocrinol. Metab. 90, 2487–2492.

Tomar, N., Bora, H., Singh, R., Gupta, N., Kaur, P., Chauhan, S.S., Sharma, Y.D., Goswami, R., 2010. Presence and significance of a R110W mutation in the DNA-binding domain of GCM2 gene in patients with isolated hypoparathyroidism and their family members. Eur. J. Endocrinol. 162, 407–421.

Traebert, M., Roth, J., Biber, J., Murer, H., Kaissling, B., 2000. Internalization of proximal tubular type II Na-P_i cotransporter by PTH: immunogold electron microscopy. Am. J. Physiol. 278, F148–F154.

Unger, S., Gorna, M.W., Le Bechec, A., Do Vale-Pereira, S., Bedeschi, M.F., Geiberger, S., Grigelioniene, G., Horemuzova, E., Lalatta, F., Lausch, E., et al., 2013. FAM111A mutations result in hypoparathyroidism and impaired skeletal development. Am. J. Hum. Genet. 92, 990–995.

Wang, J., Wang, Z., An, Y., Wu, C., Xu, Y., Fu, Q., Shen, Y., Zhang, Q., 2015. Exome sequencing reveals a novel PTHLH mutation in a Chinese pedigree with brachydactyly type E and short stature. Clin. Chim. Acta 446, 9–14.

Weinstein, L.S., Gejman, P.V., Friedman, E., Kadowaki, T., Collins, R.M., Gershon, E.S., Spiegel, A.M., 1990. Mutations of the Gs α−subunit gene in Albright hereditary osteodystrophy detected by denaturing gradient gel electrophoresis. Proc. Natl. Acad. Sci. U.S.A. 87, 8287−8290.

Weir, E.C., Philbrick, W.M., Amling, M., Neff, L.A., Baron, R., Broadus, A.E., 1996. Targeted overexpression of parathyroid hormone-related peptide in chondrocytes causes skeletal dysplasia and delayed endochondral bone formation. Proc. Natl. Acad. Sci. U.S.A. 93, 10240−10245.

Williams, S.R., Aldred, M.A., Der Kaloustian, V.M., Halal, F., Gowans, G., McLeod, D.R., Zondag, S., Toriello, H.V., Magenis, R.E., Elsea, S.H., 2010. Haploinsufficiency of HDAC4 causes brachydactyly mental retardation syndrome, with brachydactyly type E, developmental delays, and behavioral problems. Am. J. Hum. Genet. 87, 219−228.

Wysolmerski, J.J., McCaughern-Carucci, J.F., Daifotis, A.G., Broadus, A.E., Philbrick, W.M., 1996. Overexpression of parathyroid hormone-related protein or parathyroid hormone in transgenic mice impairs branching morphogenesis during mammary gland development. Development 121, 3539−3547.

Wysolmerski, J., Philbrick, W., Dunbar, M., Lanske, B., Kronenberg, H., Broadus, A., 1998. Rescue of the parathyroid hormone-related protein knockout mouse demonstrates that parathyroid hormone-related protein is essential for mammary gland development. Development 125, 1285−1294.

Wysolmerski, J.J., Cormier, S., Philbrick, W., Dann, P., Zhang, J., Roume, J., Delezoide, A., Silve, C., 2001. Absence of functional type 1 PTH/PTHrP receptors in humans is associated with abnormal breast development and tooth impactation. J. Clin. Endocrinol. Metab. 86, 1788−1794.

Yamaguchi, T., Hosomichi, K., Narita, A., Shirota, T., Tomoyasu, Y., Maki, K., Inoue, I., 2011. Exome resequencing combined with linkage analysis identifies novel PTH1R variants in primary failure of tooth eruption in Japanese. J. Bone Miner. Res. 26, 1655−1661.

Yang, T., Hassan, S., Huang, Y.G., Smart, A.M., Briggs, J.P., Schnermann, J.B., 1997. Expression of PTHrP, PTH/PTHrP receptor, and Ca(2+)-sensing receptor mRNAs along the rat nephron. Am. J. Physiol. 272, F751−F758.

Yi, H.S., Eom, Y.S., Park Ie, B., Lee, S., Hong, S., Jüppner, H., Mannstadt, M., Lee, S., 2012. Identification and characterization of C106R, a novel mutation in the DNA-binding domain of GCMB, in a family with autosomal-dominant hypoparathyroidism. Clin. Endocrinol. 76, 625−633.

Young, I.D., Zuccollo, J.M., Broderick, N.J., 1993. A lethal skeletal dysplasia with generalised sclerosis and advanced skeletal maturation: Blomstrand chondrodysplasia. J. Med. Genet. 30, 155−157.

Zhang, P., Jobert, A.S., Couvineau, A., Silve, C., 1998. A homozygous inactivating mutation in the parathyroid hormone/parathyroid hormone-related peptide receptor causing Blomstrand chondrodysplasia. J. Clin. Endocrinol. Metab. 83, 3365−3368.

Chapter 58

Molecular basis of parathyroid hormone overexpression

Geoffrey N. Hendy[1,†] and Andrew Arnold[2]

[1]*Metabolic Disorders and Complications, McGill University Health Center Research Institute, and Departments of Medicine, Physiology and Human Genetics, McGill University, Montreal, QC, Canada;* [2]*Center for Molecular Oncology and Division of Endocrinology and Metabolism, University of Connecticut School of Medicine, Farmington, CT, United States*

Chapter outline

Introduction

Over the past several years, the application of powerful molecular biology techniques has provided a wealth of new information and insights into the development of tumors. The purpose of this chapter is to review this information as it relates to our understanding of parathyroid tumorigenesis. Parathyroid hyperfunction is found in several disease states including sporadic primary and secondary hyperparathyroidism (the latter is not addressed in this chapter) as well as familial disorders such as multiple endocrine neoplasia (MEN) and familial hypocalciuric hypercalcemia (FHH) syndromes.

Primary hyperparathyroidism is a common disorder classically characterized by hypercalcemia caused by excessive secretion of parathyroid hormone (PTH). This is due to both an increased parathyroid gland mass and a resetting of the control of PTH secretion from the parathyroid cell by the ambient calcium concentration. Patients with primary hyperparathyroidism have one or more enlarged parathyroid glands with a single benign adenoma occurring in almost 85% of cases; multiple hypercellular glands are present in about 15% of patients (Black and Utley, 1968; Castleman and Roth, 1978). In modern series, parathyroid carcinoma occurs in less than 1% of cases, and the ectopic secretion of PTH from nonparathyroid tumors is extremely rare.

Hyperparathyroidism may also occur as part of familial syndromes, such as MEN types 1 and 2 (MEN1, MEN2), hereditary hyperparathyroidism-jaw tumor syndrome (HPT-JT), FHH, and neonatal severe hyperparathyroidism (NSHPT).

Molecular oncology

Neoplastic cells contain genetic damage to key growth-regulating genes, thus directly contributing to the abnormal neoplastic phenotype. A cardinal feature of cancers is their clonal, or monoclonal, nature. They arise from a single

† Deceased.

Principles of Bone Biology. https://doi.org/10.1016/B978-0-12-814841-9.00058-0

precursor cell that has a selective growth advantage over normal cells and whose progeny outgrow them and ultimately make up the tumor. Typically, certain identical patterns of DNA damage are seen in each cell of such a tumor, indicating that important underlying genetic events occurred early before the major proliferation or clinically significant clonal expansion took place. The clonality of tumors also implies that the combination of such events necessary for causing neoplasia occurs only rarely in the large population of cells making up a tissue.

It is important to note the molecular heterogeneity underlying the development of neoplasia (Vogelstein and Kinzler, 2004). Generally, accumulating damage to several distinct genes within the same cell is required for the expression of the complete neoplastic phenotype. Whereas certain genes are implicated in tumors of only one or a few cell types, other genes may be involved in many different types of tumor. However, in most cases, no single gene will be both a necessary and a sufficient neoplastic agent. More commonly, the emergence of a particular tumor type may relate to disruption of specific biochemical pathways that can be achieved by different combinations of mutated genes, resulting in similar cellular and clinical consequences.

Clonal DNA damage in two groups of normal cellular genes contributes to the development of neoplasia. These are protooncogenes and tumor-suppressor genes. Protooncogenes are often involved in the physiological control of cellular growth, proliferation, and differentiation. Conversion of a protooncogene to an "oncogene" is caused by deregulation of the expression of its normal protein product or by the formation of an intrinsically abnormal product. The products of tumor-suppressor genes normally restrain cellular proliferation, and their gene inactivation contributes to neoplasia. Protooncogenes can be activated by mechanisms such as chromosome translocations or inversions, gene amplification, and intragenic point mutation. Inactivation of tumor-suppressor genes can occur via mechanisms like missense or frameshift mutation and larger-scale deletion.

Clonality of parathyroid tumors

Assessments of clonality have been crucial to our understanding of human tumors. In this context, evidence that most cells in a hypercellular mass were derived from a single progenitor cell implies a clinically important selective advantage transmittable to progeny of the cell. Even the potential presence of two to three clones in the same mass, for example, would carry similar implications and have similar relevance for tumorigenic mechanisms and vulnerability to therapeutic agents. Such monoclonality, or even oligoclonality, would stand in marked contrast to the generalized growth of an entire tissue or gland (e.g., the thyroid in Graves' disease) in which all cells are responding equally to a proliferative stimulus with no apparent selective advantage to any subpopulation. The latter types of growth/hyperplasia may be best and most intuitively labeled as "nonclonal," but have typically been termed "polyclonal" in classic literature—this unfortunately may have opened the door to potential confusion of the term with oligoclonality. Evidence for clonal (usually monoclonal but including oligoclonal) growth can be direct—i.e., the observation of acquired tumor-specific DNA/chromosomal defects—or indirect as in X chromosome inactivation assays. Interpretation of the latter carries numerous pitfalls, most of which can result in misleading nonclonal/polyclonal patterns even in a monoclonal tumor. Most notably, aberrant DNA methylation—known to be common in human tumors—is a potential source of such error. Thus, in X-inactivation assays a result of monoclonality is much more definitive than a polyclonal result (Arnold et al., 1988), and building a compelling case for polyclonality requires the additional use of more sensitive and direct methods (Corrado et al., 2015).

In the modern era of molecular genetics, the clonal status of parathyroid tumors was initially examined by use of an X chromosome inactivation method and by the direct demonstration of monoclonal DNA alterations in parathyroid adenomas (Arnold et al., 1988). It was determined that most parathyroid adenomas are monoclonal, a novel result that stood in marked contrast with a prior finding of polyclonality from older X-linked G6PD protein isoform expression methodology (Fialkow et al., 1977; Jackson et al., 1982). That many typical sporadic parathyroid adenomas are monoclonal was rapidly confirmed by direct detection of a variety of monoclonal defects including clonal loss of heterozygosity (Arnold and Kim, 1989; Friedman et al., 1989; Bystrom et al., 1990), clonal cytogenetic abnormality (Orndal et al., 1990), and fluorescence in situ hybridization (Yi et al., 2008), emphasizing that they are true neoplastic outgrowths of a single abnormal cell. It is important to understand that the percentages of adenomas shown to be monoclonal by these methods represent only a solid floor/minimum for the true percentage, given the nondefinitiveness of polyclonal patterns in X-inactivation assays and, in the more direct assays, the fact that a tumor without an identified monoclonal defect might still be revealed as monoclonal if subjected to a more sensitive/comprehensive assay. The advent of massively parallel next-generation DNA sequencing tools in recent years has provided just that sort of increased sensitivity for detecting monoclonal tumor-specific alterations. Of 24 parathyroid adenomas subjected to whole-exome sequencing in two studies (Cromer et al., 2012; Newey et al., 2012), fully 23 adenomas (96%) showed clear evidence of monoclonality—i.e., at least one tumor-specific, somatic mutation/variant, independently verified, marking a major dominant clone. Such powerful and direct evidence for clonal growth of the overwhelming majority of sporadic solitary parathyroid adenomas needs to be expanded with larger numbers (and the identical panel subjected to X-inactivation assays as well), but it does suggest that polyclonal X-inactivation

patterns found in a substantial minority (25%–35%) of solitary adenomas (Arnold et al., 1988; Shi et al., 2014) may nonetheless occur in monoclonal tumors, and this potentially misleading pattern should be interpreted with due caution. That said, an interesting and important hypothesis to consider would be whether a polyclonal X-inactivation pattern in adenomas proven to be monoclonal by direct genetic analysis might represent a marker of widespread aberrant DNA methylation in such tumors, reflecting an alternative pathway of molecular pathogenesis. The finding of predominantly clonal growth in solitary adenomas is consistent with the general experience that surgical removal of such tumors is curative of the disease. Not surprisingly, if cases are selected differently to allow the inclusion of multigland disease, the observed yield of polyclonal/nonclonal X-inactivation patterns is higher (Shi et al., 2018; Arnold et al., 1995); it will be informative to analyze such cases directly for clonal changes to help distinguish truly nonclonal hyperplastic growth from dominant clonal outgrowths on a background of nonclonal hyperplasia. As would be expected, parathyroid carcinomas are also monoclonal (Cryns et al., 1994b; Shattuck et al., 2003a,b; Howell et al., 2003; Cetani et al., 2004; Pandya et al., 2017). In addition, monoclonal and oligoclonal parathyroid tumors are seen in familial MEN1 (Friedman et al., 1989; Thakker et al., 1989; Lubensky et al., 1996), in nonfamilial, sporadic, primary parathyroid hyperplasia (Arnold et al., 1995), and in the refractory secondary or tertiary parathyroid hyperplasia of uremia (Arnold et al., 1995; Falchetti et al., 1993). Therefore, even in parathyroid hyperplasia, which begins with a stimulus for generalized, polyclonal, parathyroid cell proliferation affecting all of a patient's glands, clonal tumors can arise, at least in some glands. Such tumors may be more autonomous and exhibit a more marked dysregulation of PTH secretory control than the hyperplastic, polyclonal glands within the same patient.

An important goal is to identify the specific protooncogenes and tumor-suppressor genes that are clonally activated or inactivated, respectively, in parathyroid tumors. Notable successes in approaching this aim have already been achieved.

Genetic derangements in benign parathyroid tumors

DNA rearrangements are some of the best characterized clonal oncogenic abnormalities, and they frequently involve juxtaposition of cellular protooncogenes with regulatory sequences of other genes. This then results in overexpression or deregulated expression of the protooncogene, converting it to an oncogene. To date the only oncogene solidly established to be a driver in benign parathyroid neoplasia is *cyclin D1/PRAD1*, and the sole tumor-suppressor gene established as a major driver in sporadic parathyroid adenomas is *MEN1*.

Cyclin D1/PRAD1

A subset of parathyroid adenomas contains a tumor-specific DNA rearrangement that separates the 5′ regulatory region of the PTH gene from its protein-coding exons (Fig. 58.1). These tumor cells still possess one intact copy of the PTH gene, which accounts for the expression of PTH by the tumor. The non-PTH gene sequences adjacent to the breakpoint were originally cloned from a genomic DNA library (Arnold et al., 1989) and revealed a then-novel putative oncogene, first called PRAD1, located on chromosome band 11q13. PRAD1 is now most often called cyclin D1 or CCND1 and has been fully established as a key human oncogene. The normal chromosomal cyclin D1 gene contains five exons and four introns

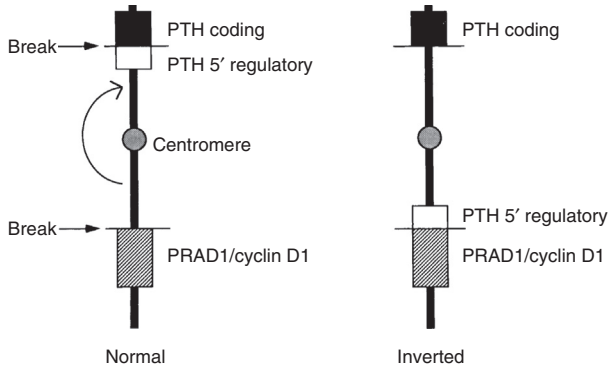

FIGURE 58.1 Schematic diagram of rearrangement of chromosome 11 in parathyroid tumors. In a subset of parathyroid adenomas, a pericentromeric inversion of chromosome 11 is the most likely cause of the observed rearrangement involving the PTH gene and the *PRAD1* gene. Each tumor has another copy of chromosome 11 that bears a normal PTH gene. *Reproduced with permission from Arnold, A. 1993. Genetic basis of endocrine disease 5: molecular genetics of parathyroid gland neoplasia. J. Clin. Endocrinol. Metab. 77, 1108–1112.*

spanning approximately 15 kb and is transcribed in a centromeric to telomeric direction (Motokura and Arnold, 1993). In the cases of PTH/cyclin D1 rearrangements characterized to date, the 11q13 breakpoints have occurred from 1 to 450 kb upstream of cyclin D1 exon 1 with the PTH gene 5′ regulatory region and noncoding exon 1 placed upstream of the breakpoint (Friedman et al., 1990; Rosenberg et al., 1991; Mallya et al., 2010) (Fig. 58.2). The overexpression of the cyclin D1 gene is likely caused by its aberrant placement in close proximity to the strong tissue-specific enhancer elements of the PTH gene (Rosenberg et al., 1993; Mallya et al., 2010).

On the order of 8% of parathyroid adenomas have been shown to contain an activated form of the cyclin D1 oncogene (Westin, 2016). However, rearrangement breakpoints on 11q13 associated with overexpression of cyclin D1 in other tumors that occur more than 15−20 kb upstream of the gene could easily have been missed in past studies, and the application of modern molecular cytogenetic approaches could increase the accuracy of this estimate. In addition, it seems plausible that cyclin D1 expression could be deregulated in some parathyroid tumors by rearrangement with genes other than the PTH gene. Thus, previous studies may not have revealed the full frequency with which cyclin D1 deregulation occurs in parathyroid neoplasia. Indeed, studies assessing the cyclin D1 protein product have revealed its overexpression in 20%−40% of parathyroid adenomas (Hsi et al., 1996; Vasef et al., 1999; Tominaga et al., 1999). This overexpression may occur more commonly by a trans-acting regulatory disturbance like that observed for cyclin D1 overexpression in a variety of human cancer cells (Hosokawa and Arnold, 1998) rather than a clonal mutation in one gene allele. However achieved by the cell, such overexpressed cyclin D1 is a potent driver of abnormal parathyroid cell proliferation (Imanishi et al., 2001; Mallya et al., 2005).

Cyclin D1 is a 295-amino acid protein homologous to various members of the cyclin family (Motokura et al., 1991). Cyclins play important roles in the regulation of cell cycle progression, and human cyclins have been grouped into several types based on sequence similarities. Each cyclin appears to regulate the cell cycle at a specific time point by binding to and activating cyclin-dependent kinases (CDKs) (Sherr, 1996; Sherr et al., 2016). Expression of these cyclins is cell cycle phase-dependent and controlled by both transcriptional and posttranscriptional mechanisms. Cyclin D1 is a key regulator of the critical G1−S phase transition in the cell cycle. In so doing, its major CDK partners are CDK4 or CDK6 depending upon the tissue type examined. Evidence indicates that cyclin D1 has other cellular functions as well, mediated through CDK-independent pathways (Bernards, 1999; Arnold and Papanikolaou, 2005; Ewen and Lamb, 2004; Fu et al., 2004; Casimiro et al., 2015).

Adding to the strong genetic evidence for cyclin D1's role as a parathyroid oncogene, animal modeling has provided direct experimental confirmation that cyclin D1 overexpression is capable of driving parathyroid tumorigenesis. A transgenic mouse model for parathyroid neoplasia was generated (Imanishi et al., 2001) in which the cyclin D1 gene is under the control of the regulatory region of the PTH gene, mimicking the rearrangement and resultant overexpression observed in human tumors. These mice develop parathyroid enlargement and increased serum calcium and PTH levels, and their study has illuminated the relationship in hyperparathyroidism between abnormal parathyroid proliferation and the biochemical phenotype (Imanishi et al., 2001; Mallya et al., 2005). Finally, cyclin D1 is being vigorously pursued as a target for antineoplastic therapy, noting its major role in human breast cancer, lymphoma, and squamous cell cancers. If

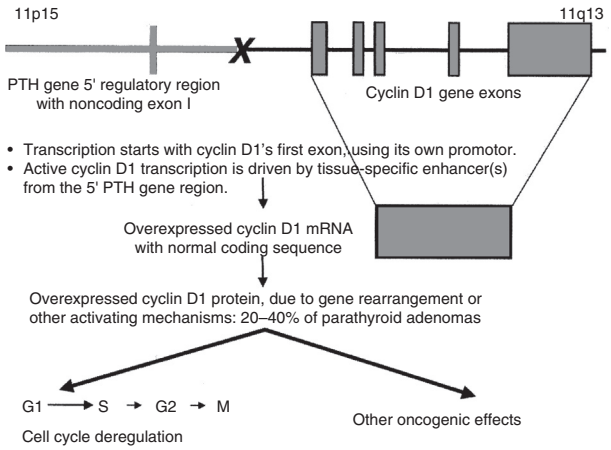

FIGURE 58.2 Diagram of directly observed molecular structure of the PTH/cyclin D1 (PRAD1) DNA rearrangement and its functional consequences. *Modified with permission from Arnold, A. 1993. Genetic basis of endocrine disease 5: molecular genetics of parathyroid gland neoplasia. J. Clin. Endocrinol. Metab. 77, 1108−1112.*

such efforts are successful, an anti−cyclin D1 agent would also be expected to have efficacy against the cyclin D1−driven subset of parathyroid tumors. In addition, therapeutic agents that inhibit CDK4 and CDK6 have improved the progression-free survival in breast cancer and been approved for clinical use (Sherr et al., 2016).

Tumor-suppressor genes: multiple endocrine neoplasia type 1 and cyclin-dependent kinase inhibitors

The MEN1 syndrome, which is inherited in an autosomal dominant fashion, is characterized classically by tumors of the parathyroids, pancreatic islets, and anterior pituitary. It was established by genetic mapping studies in families affected by MEN1 that the gene responsible is on chromosome 11q13 (Larsson et al., 1988). Early evidence that the *MEN1* gene is a tumor-suppressor gene was provided by the demonstration of somatic genetic alterations in MEN1 tumors that inactivate one allele of a gene region at 11q13 and so reveal the inherited *MEN1* mutation on the other allele (Fig. 58.3). In fact, allelic loss of polymorphic marker DNAs from this region of chromosome 11 has been found in the majority of MEN1-associated tumors including those of the parathyroid (Thakker, 2010).

The *MEN1* gene was identified by positional cloning (Chandrasekharappa et al., 1997; European Consortium on MEN1, 1997). Almost 600 independent germline mutations scattered throughout the protein-coding region have been identified (Lemos and Thakker, 2007; Concolino et al., 2015). There is no genotype and phenotype correlation. Somatic mutations are common in sporadic parathyroid adenoma (12%−35%) (Heppner et al., 1997; Carling et al., 1998; Farnebo et al., 1998a; Tanaka et al., 2002; Cromer et al., 2012; Newey et al., 2012) and also occur in gastrinoma, insulinoma, lung carcinoid, and anterior pituitary tumors. *MEN1* mutations have been found in familial isolated hyperparathyroidism (FIHP) (Concolino et al., 2015) and very rarely have been associated with parathyroid carcinoma (Cinque et al., 2017a,b). Over 70% of mutations are clearly inactivating, being nonsense or frameshift, leading to a truncated product. This would be consistent with *MEN1* acting as a tumor-suppressor gene and a lack of menin protein caused by the loss of both alleles leading to tumor development. The human gene encodes a 610-amino acid protein, although it should be noted that in addition to this originally identified protein, there is a 615-amino acid form derived from an alternatively spliced transcript. In most publications, mutations are numbered according to the 610-amino acid protein. Confusingly, however, in most

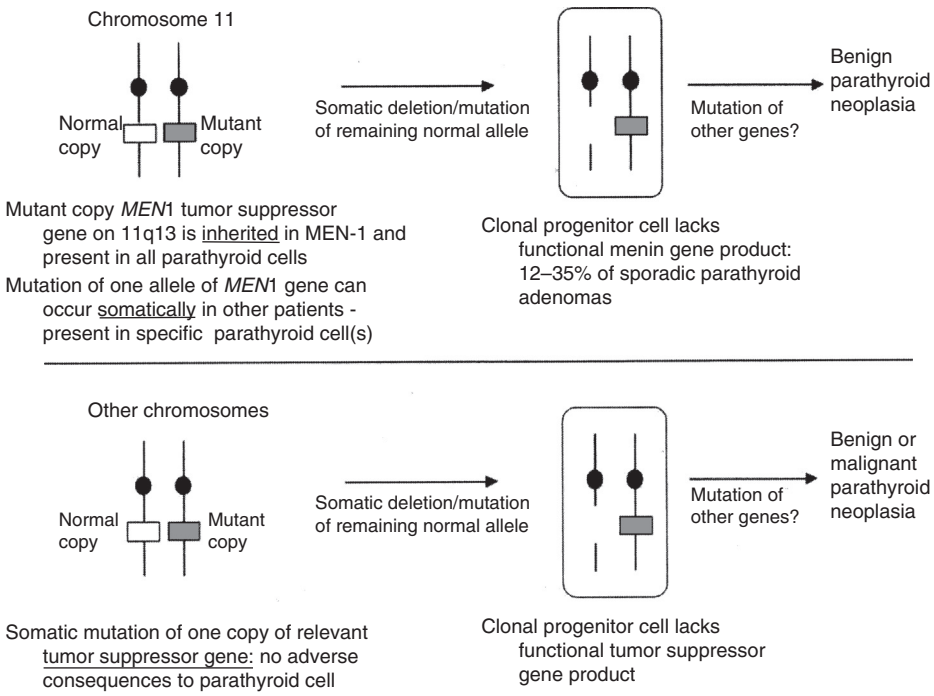

FIGURE 58.3 Schematic diagram illustrating the established (for multiple endocrine neoplasia type 1, *MEN1*) and hypothesized roles of inactivation of classic tumor-suppressor genes as contributory mechanisms in parathyroid neoplasia. A similar scheme applies to the role of the *HRPT2/CDC73* tumor-suppressor gene in the pathogenesis of parathyroid carcinoma. *Modified with permission from Arnold, A. 1993. Genetic basis of endocrine disease 5: molecular genetics of parathyroid gland neoplasia. J. Clin. Endocrinol. Metab. 77, 1108−1112.*

databases (such as ExAC and gnomAD) the numbering is according to the 615-amino acid form. The same version of menin must be used for comparative purposes after amino acid 148.

Two main nuclear localization signal sequences are present at the COOH-terminal portion of the menin protein, which is predominantly located in the nucleus (Guru et al., 1998; Kaji et al., 1999). The first protein shown to be a menin-interacting protein was the activator protein 1 factor, JunD, with resultant downregulation of JunD-activated transcription (Agarwal et al., 1999). Because JunD is antimitogenic in contrast to other Jun and Fos family members, and menin is a tumor suppressor, this appeared to be paradoxical. Further studies in vitro have suggested that the functions of JunD as a growth suppressor require interaction with menin, and that JunD is a growth promoter if menin is absent or inactive (Agarwal et al., 2003). The level of menin changes throughout the cell cycle. Pituitary cells synchronized at the G1−S-phase boundary express menin at a lower level than G0−G1-synchronized cells (Kaji et al., 1999). The expression of menin increases as the cell enters S phase, at which time JunD expression also increases. Cells synchronized at the G2−M phase express lower levels of menin.

Menin upregulates the CDK inhibitors (CDKIs), p18 and p27, important for cell cycle regulation (Karnik et al., 2005; Milne et al., 2005). Menin reexpression in *Men1*-deficient cells blocks the transition from G0/G1 to S phase of the cell cycle and increases apoptosis (Hussein et al., 2007). Mice dually deficient in p18 and p27 develop a range of endocrine tumors representing those found in MEN1 and MEN2 syndromes (Franklin et al., 2000). Mice with knockout of genes that regulate the cell cycle (Rb, p53, p18, p27, CDK2, CDK4) have been placed on the Men1+/− background (Bai et al., 2007; Loffler et al, 2007a, 2012). Overall, these studies indicate that decreased p18 and increased CDK4 may contribute further to MEN1-associated tumors upon menin loss, whereas the other cell cycle regulators are functioning in the same pathway as menin.

Mixed lineage leukemia (MLL) proteins are members of the lysine methyltransferase (KMT) family and comprise MLL1/KMT2A and MLL2/KMT2B. Menin functions as a scaffold protein and binds MLL proteins in histone methyltransferase complexes that stimulate H3K4me3, which increases p18 and p27 for cell cycle control, the *Hox* gene expression important for early development, and cell proliferation and differentiation (Hughes et al., 2004; Milne et al., 2005; Yokoyama et al., 2004; Yokoyama and Cleary, 2008). Menin may be involved in telomere biology and DNA replication and repair. Menin interacts with several transcription factors including Smads, JunD, and NF-κB and modulates their activities (see Hendy et al., 2009a; Matkar et al., 2013; Agarwal, 2017 for further details of menin functions and interacting proteins). Menin is a Smad3-interacting protein, and inactivation of menin blocks transforming factor-β (TGF-β) and activin signaling, antagonizing their growth-inhibitory properties (as well as the inhibition of prolactin expression) in anterior pituitary cells (Kaji et al., 2001; Lacerte et al., 2004). In cultured parathyroid cells, menin inactivation achieved by menin antisense oligonucleotides leads to loss of TGF-β inhibition of cell proliferation and PTH secretion (Sowa et al., 2004). Moreover, TGF-β does not affect (decrease) the proliferation and PTH production of parathyroid cells from MEN1 patients (Sowa et al., 2004; Naito et al., 2006). Loss of various TGF-β signaling pathway components by genetic or epigenetic means is common in cancer and is likely to be important in MEN1 tumorigenesis (Canaff et al., 2012a) despite the fact that thus far, no acquired clonal mutations, insertions, or microdeletions in the Smad3 gene have been detected in a series of sporadic parathyroid adenomas and enteropancreatic tumors (Shattuck et al., 2002).

The three-dimensional structure of menin is known, and this has aided its functional analysis. The crystallographic structure of the starlet sea anemone *Nematostella* menin was deciphered initially (Murai et al., 2011), and then a structure of human menin was determined by homology modeling (Canaff et al., 2012a, b) followed by the elucidation of the crystallographic structure of human menin itself (Huang et al., 2012). To facilitate the crystallization of the molecule, modified forms of menin were generated in which some unstructured parts of menin were deleted. Menin is predominantly an α-helical protein with the core comprising three tetratricopeptide motifs flanked by two α-helical bundles and covered by a β-sheet motif. A large central cavity binds the MLL proteins important for histone methyl transferase activity as well as binding the JunD transcription factor (Murai et al., 2011; Huang et al., 2012). The binding site for Smad transcription factors important for TGF-β ligand family member action is distinct from the central cavity and located on the exposed surface neighboring the β-sheet motif (Canaff et al., 2012a).

Mice heterozygous for genetic ablation of the *Men1* gene develop endocrine tumors similar to those of human MEN1 patients (Crabtree et al., 2001; Bertolino et al., 2003a; Loffler et al., 2007b; Harding et al., 2009). Parathyroid gland-specific deletion of the mouse *Men1* gene results in parathyroid neoplasia and hypercalcemic hyperparathyroidism (Libutti et al., 2003). In mice (and humans), tissue expression of menin is widespread throughout development and into adult life and occurs early in fetal life. In mice, homozygous deletion of *Men1* is embryonic lethal. The affected fetuses die at midgestation with defects in multiple organs (Bertolino et al., 2003b). This may reflect defective TGF-β/bone morphogenetic protein ligand signaling or *Hox* gene expression brought about by the epigenetic histone methyl transferase mechanisms alluded to previously.

Conditional knockouts of Men1 in tissues other than those known to be involved in the MEN1 disorder have provided insight into the physiological actions of menin as opposed to its tumor-suppressor actions revealed in MEN1. For example, evidence has been provided for the importance of menin for bone development and maintenance (Kanazawa et al., 2015; Liu et al., 2017). Furthermore, studies of the bone disease of patients with MEN1 versus those with sporadic hyperparathyroidism suggested that the bone disease of the former is more severe than that of the latter despite the fact that the levels of circulating PTH of the former are lower than in the latter group (Eller-Vainicher et al., 2009; Lourenco et al., 2010). Therefore, while menin has been considered haplosufficient with respect to tissue development and function, for tissues such as bone this might not be the case, with haploinsufficiency being suggested by decreased bone volume and trabecular number in Men1+/− mice heterozygous for menin loss (Hendy et al., 2017; Abi-Rafeh et al., 2017).

About 30% of menin mutations are missense (or have small insertions or deletions) and are found throughout the entire sequence with no clear-cut hotspots. It might have been anticipated that analysis of missense mutations would provide insight into which of many proteins that menin interacts with are actually critical for MEN1 tumorigenesis when the interaction is lost; with some exceptions, however, this promise has yet to be fulfilled. To some extent this is because most (but not all) missense menin mutants are markedly unstable, targeted to the ubiquitin−proteasome pathway, and expressed at very low levels if at all (Yaguchi et al., 2004; Shimazu et al., 2011: Canaff et al., 2012b) (see Fig. 58.4).

The frequency of *MEN1* coding region mutations in several kindreds with a variant of MEN1 in which only parathyroid and pituitary tumors develop, is very low (10%) versus typical MEN1 kindreds (75%). In one case of this MEN1 variant in which *MEN1* mutation was not detected, a germline mutation of the *CDKN1B* gene encoding p27 was identified (Pellegata et al., 2006). Heterozygous mutations have been identified in 2% of these MEN1-variant cases and classified as the MEN4 disorder (Pellegata, 2012). Also, less than 1% of MEN1-like cases carry p15, p18, or p21 heterozygous mutations (Agarwal et al., 2009; Thakker, 2014). In addition, germline mutations in *CDKN1B* and the genes encoding p15, p18, and

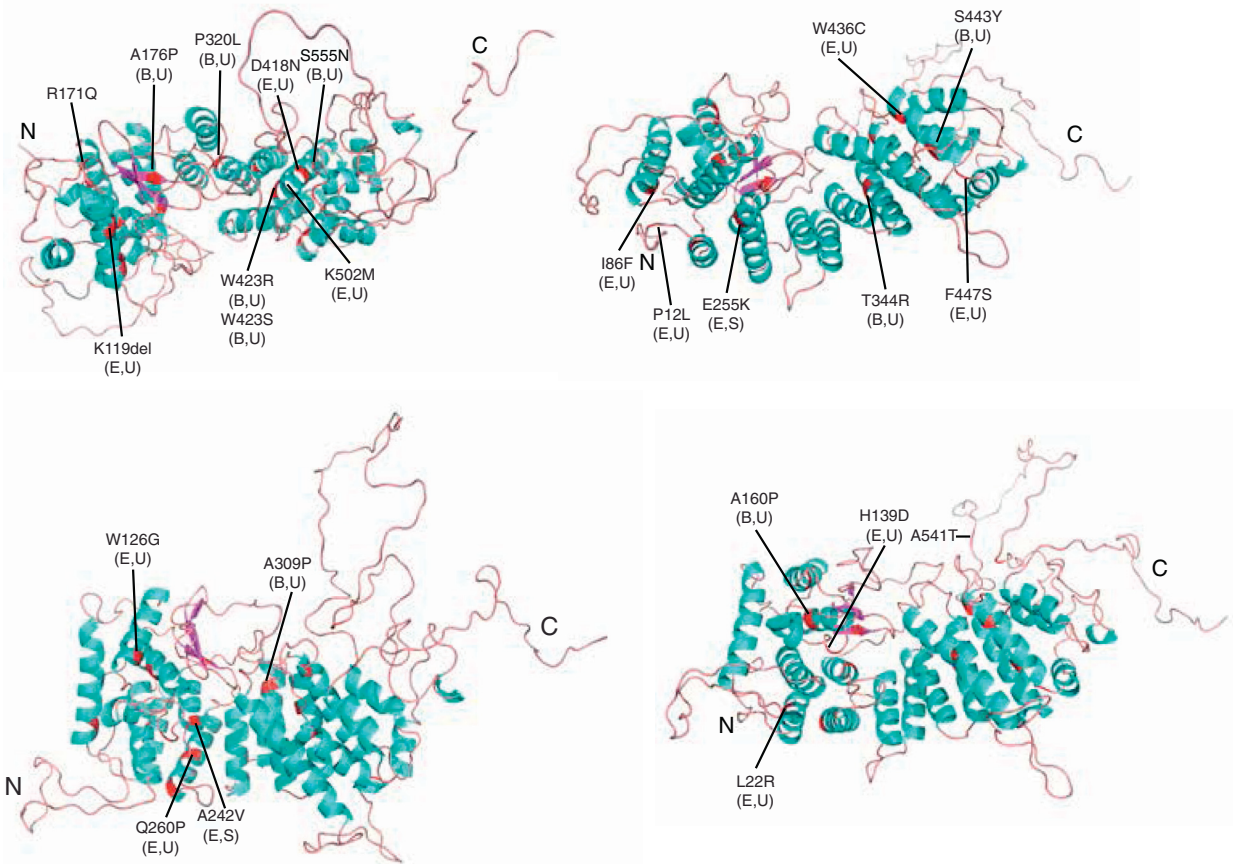

FIGURE 58.4 Positions of missense mutations on a homology model of human menin encoded by the multiple endocrine neoplasia type 1 gene. The majority of the mutants are unstable and poorly expressed but their expression and activity may be restored by siRNA against components of the chaperone machinery that directs the mutants to the proteasome (see Canaff et al., 2012b). E, exposed; B, buried; U, unstable; S, stable.

p21 may be found in sporadic primary hyperparathyroidism (Costa-Guda et al, 2011, 2013a; Borsari et al., 2017), and more frequent loss of p27 expression and cellular mislocalization is associated with MEN1 mutations in sporadic parathyroid adenomas (Borsari et al., 2017).

Candidate oncogenes and tumor-suppressor genes

Comparative genomic hybridization—a molecular cytogenetic technique in which the entire tumor genome is screened for chromosomal gains and/or losses—has identified amplified regions on several chromosomes (most consistently 7, 16, and 19). These observations suggest the presence of novel parathyroid oncogenes (Palanisamy et al., 1998; Agarwal et al., 1998; Farnebo et al., 1999; Dwight et al., 2002) in these locations that remain to be identified.

Besides loci on chromosome 11, several other regions of nonrandom clonal allelic loss have been documented in parathyroid adenomas, pointing to the location of novel tumor-suppressor genes. This finding of the involvement of multiple chromosomal regions, which include 1p (Cryns et al., 1995; Williamson et al., 1997), 1q, 6q, 9p, and 15q (Tahara et al., 1996a, b), emphasize the molecular heterogeneity of parathyroid adenomatosis.

Comparative genomic hybridization has confirmed the chromosomal losses identified by loss of heterozygosity analysis (allelotyping) (Palanisamy et al., 1998; Agarwal et al., 1998; Farnebo et al., 1999). One common defect uncovered to date involves allelic loss on chromosome 1p (Cryns et al., 1995). Interestingly, chromosome 1p loss occurs in several other neoplasms including medullary thyroid carcinomas and pheochromocytomas that occur in association with MEN2A inherited cancer syndrome, of which parathyroid tumors are also a part. Benign parathyroid tumors are found in 10%−20% of MEN2A patients. This pattern of allelic loss is consistent with the existence of a tumor-suppressor gene(s) on 1p, whose loss or inactivation is pathogenetically important. Numerous candidate genes are present in this region, but the involvement of any of them in the development of parathyroid or other types of tumors remains to be established. Some candidates on 1p, such as genes for the p18 CDKI and RAD54, have been excluded as commonly involved parathyroid tumor suppressors (Tahara et al., 1997; Carling et al., 1999a). Mutations within the 9p region of candidate genes encoding the p16 and p15 CDKIs do not appear to be frequently involved in parathyroid tumorigenesis (Tahara et al., 1996b). A major goal for future work is the identification of the entire constellation of oncogenes and tumor-suppressor genes that contribute to the development of parathyroid adenomatosis.

Further genetic aspects

Some genes that play an important role in the pathogenesis of other tumor types might have been expected to be involved in the pathogenesis of benign parathyroid adenomas. However, candidate genes such as *RAS* (Friedman et al., 1990), p53 (Yoshimoto et al., 1992; Cryns et al., 1994a; Hakim and Levine, 1994) and RB (Cryns et al., 1994b) seem rarely, or not at all, to contribute to the development of benign adenomas. The development of primary hyperparathyroidism occurs with increased frequency in individuals exposed to ionizing radiation of the neck. Thus, mutations in genes involved in DNA repair and recombination may contribute to parathyroid tumorigenesis irrespective of the actual involvement of irradiation. Such candidates include the *RAD51* and *RAD54* genes on chromosomes 15q and 1p, respectively, within regions that demonstrate allelic loss in parathyroid adenomas. However, no evidence for a role of somatic inactivation of these particular genes in parathyroid neoplasia has been found (Carling et al., 1999a, b).

In some cases, those genes responsible for the rare inherited predisposition to a particular tumor also play a role in the development of the more common sporadic type. The *MEN1* gene, as detailed earlier, has proved to be such an example. Germline gain-of-function mutations in the *RET* protooncogene cause MEN2 (Eng et al., 1996). This made the *RET* gene, which encodes a tyrosine kinase receptor, a candidate for involvement in nonfamilial hyperparathyroidism. However, although MEN2-type *RET* mutations have been implicated in the pathogenesis of some sporadic medullary thyroid carcinomas and pheochromocytomas, there is no evidence of these *RET* mutations in sporadic parathyroid adenomas (Pausova et al., 1996; Kimura et al., 1996). Thus, while RET is expressed in both MEN2A parathyroid tumors and in sporadic adenomas (Pausova et al., 1996; Kimura et al., 1996), and parathyroid disease is an integral part of the MEN2A syndrome, MEN2-type mutations in *RET* rarely if ever play a role in the pathogenesis of sporadic parathyroid tumors. Mutations within the coding region of glial cell−derived neurotrophic factor, one of the RET ligands, do not appear to play a role in the genesis of MEN2 neoplasms or in sporadic neuroendocrine tumors such as parathyroid adenomas (Marsh et al., 1997). An interesting candidate parathyroid tumor suppressor, the vitamin D receptor, encoded by the *VDR* gene, is also lacking in evidence for a direct pathogenetic driver role by specific clonal mutation (Brown et al., 2000; Samander and Arnold, 2006).

Components of the Wnt signaling pathway, implicated in other forms of tumorigenesis, are candidates for involvement in parathyroid neoplasia. In the absence of Wnt signaling, β-catenin encoded by the *CTNNB1* gene is phosphorylated and

subsequently degraded by a protein complex consisting of axin, adenomatous polyposis coli (APC), and glycogen synthase kinase-3β (GSK3β). Upon Wnt binding to its cell-surface frizzled receptor and a coreceptor such as LRP5, the resultant signaling causes the inhibitory complex to be dissociated, and unphosphorylated (active) β-catenin accumulates in the cytoplasm and the nucleus where it activates cell growth-promoting genes. Virtually all *CTNNB1* mutations identified in human tumors are located in exon 3 (the GSK3β recognition motif) and affect serine-threonine phosphorylation sites or adjacent residues. Studies of Swedish primary hyperparathyroid patients found a somatic homozygous *CTNNB1* S37A mutation in 9 of 194 adenomas studied (Bjorklund et al., 2007a, 2008). Aberrant β-catenin immunohistochemical staining was found in all tumors irrespective of mutation status. In other studies, nearly 600 additional parathyroid adenomas have been examined without the identification of any *CTNNB1* S37A mutations (Semba et al., 2000; Ikeda et al., 2002; Costa-Guda and Arnold, 2007; Juhlin et al., 2009; Cetani et al., 2010; Haglund et al., 2010). A heterozygous somatic *CTNNB1* S33C mutation was identified in distinct patients from two different cohorts (Guarnieri et al., 2012a; Starker et al., 2012). A heterozygous mutation would be more consistent (than a homozygous one) with *CTNNB1*'s direct role as an oncogene as observed in other tumor types. Overall, *CTNNB1*'s mutation frequency in parathyroid adenomas is very low ($< 2\%$), and in studies not including the initial Swedish cohorts, only 2 parathyroid adenomas of 115 examined had abnormal β-catenin immunohistochemical staining (Ikeda et al., 2002; Starker et al., 2012), more consistent with the observed mutation frequency observed in most studies. Aberrant splicing of the Wnt coreceptor LRP5 resulting in increased expression of β-catenin has been described in parathyroid adenomas (Bjorklund et al., 2007b). Lastly, loss of expression for the Wnt pathway components APC and GSK3β has been noted in parathyroid carcinoma, although altered expression of β-catenin and cyclin D1 was not found (Juhlin et al., 2009). Hence, the role of Wnt signaling pathway components in parathyroid tumorigenesis merits further study.

Calcium-sensing receptor and associated proteins

The calcium-sensing receptor (CaSR) expressed in the parathyroid and kidney tubule serves as the body's calciostat for modulating the functions of those cell types that participate in extracellular Ca^{2+} homeostasis (Brown et al., 1993; Brown, 2013; Hendy, 2019). CaSR is a member of G-protein-coupled receptor (GPCR) family C, a GPCR family that includes metabolic glutamate, γ-aminobutyric acid B, and taste and odorant receptors. The single-copy human *CASR* gene has two promoters, P1 and P2, that drive transcription from exon 1A and 1B, respectively, and the alternative transcripts splice to the common exon 2 that has the translation initiation ATG codon (Hendy et al., 2013a). Exons 2 to 7 encode the CaSR protein of 1078 amino acids. Both promoters have vitamin D response elements (Canaff & Hendy, 2002) and cis-acting elements responsive to the parathyroid-specific transcription factor, glial cells missing-2 (GCM2) (Canaff et al., 2009; Hendy and Canaff, 2016). It has been reported that more than half the parathyroid glands of patients with primary and severe uremic secondary hyperparathyroidism show reduced *CASR* expression (Kifor et al., 1996; Farnebo et al., 1997, 1998b; Gogusev et al., 1997; Chikatsu et al., 2000). The reduced levels of vitamin D receptor (VDR) observed in parathyroid tumors may contribute in part to decreased *CASR* expression (Hendy, 2018). A mutation in a gene involved in calcium set point control (Balenga et al., 2017; Mingione et al., 2017) might secondarily stimulate proliferation until the serum calcium concentration surpasses the abnormal set point (Parfitt, 1994). Data indicating that the growth rate of parathyroid tumors is generally low but must have been higher earlier in their development (Parfitt et al., 1994) are consistent with this hypothesis. Interestingly, however, calcium regulatory abnormalities found in transgenic mice with cyclin D1−driven hyperparathyroidism show that mutations in "set point" genes need not be the primary instigators in this disease (Imanishi et al., 2001; Mallya et al., 2005).

The human CaSR has a 19-amino acid signal peptide targeting it to the endoplasmic reticulum (Pidasheva et al., 2005; Hu and Spiegel, 2007), and the mature protein has a 593-amino acid extracellular domain (ECD), a 250-amino acid transmembrane domain (TMD), and a 216-amino acid cytoplasmic tail. In the endoplasmic reticulum (Pidasheva et al., 2006) the receptor dimerizes via both covalent and noncovalent interactions and undergoes immature and mature glycosylation before trafficking to the cell surface in its mature dimeric state (Breitwieser, 2013). CaSR interacts with several diverse proteins that may aid its trafficking to the cell surface, maintain its expression there, and facilitate its signaling, endocytosis, and recycling to the cell surface (Ray, 2015). The ECD of each CaSR monomer has a bilobed Venus flytrap−like structure (VFT). Immediately following the VFT is a cysteine-rich domain and then a linker sequence before the TMD. There is marked cooperativity of binding of Ca^{2+} with the receptor, and several Ca^{2+} binding sites have been proposed, most within the VFT domain.

The crystal structure of the entire ECD (the VFT and the cysteine-rich domain) of CaSR has been determined in resting and active conformations (Geng et al., 2016). Initial binding of an amino acid, in this case L-tryptophan, was essential for the fully active structure to be achieved upon subsequent cation (Ca^{2+}) binding. Multiple novel binding sites were revealed

for Ca^{2+} and PO_4^{3-} ions, with both being crucial for structural integrity of the receptor. Ca^{2+} ions stabilize the active state, and PO_4^{3-} ions reinforce the inactive conformation. In a second study, the crystal structure of the ECD VFT (without the cysteine-rich domain) of human CaSR was determined in the closed state bound with Mg^{2+} (Zhang et al., 2016). A novel high-affinity coagonist, a tryptophan derivative, bound in the hinge region between the two lobes of the VFT, was identified in the crystal. The Ca^{2+} ion is directly involved in receptor activation by stabilizing the unique homodimer interface between membrane proximal lobes 2 of the VFT and the cysteine-rich domains in the active state. Exactly how ligand-activated conformational changes alter the structure of the heptahelical TMD, initiating coupling to G proteins, remains to be elucidated.

Besides Ca^{2+} and Mg^{2+}, CaSR has many other orthosteric ligands that bind within the ECD including other polycations, charged polyamines, and certain L-amino acids that positively modulate sensitivity of CaSR to Ca^{2+} (Conigrave and Ward, 2013). The polycationic agonists have been termed type I agonists and can activate the receptor in the absence of Ca^{2+}. In contrast, type II agonists require some Ca^{2+} (or an equivalent type 1 agonist) to be present to activate CaSR. With respect to binding by anions, such as phosphate, that stabilize the inactive conformation, it can be noted that metabolic balances of Ca^{2+} and PO_4^{3-} are linked through hormones such as PTH, $1,25(OH)_2D$, and the phosphatonin, fibroblast growth factor-23, that control the homeostasis of both ions. CaSR may also regulate phosphate homeostasis independently of other factors, but further studies will be required to evaluate CaSR as a "phosphate sensor."

At the plasma membrane, CaSR can couple to the G proteins Gq/11, Gi/o, G12/13, and in rare cases, Gs (Conigrave and Ward, 2013). The respective signaling pathways activated are phospholipase C, increasing diacyl glycerol and inositol trisphosphate production, inhibition of adenylate cyclase or activating phosphodiesterase, activation of Rho kinases, and in rare cases, activation of adenylate cyclase.

Extracellular Ca^{2+} fluctuations just above or below the normal range do not alter CaSR expression in the parathyroid gland and kidney, consistent with the requirement to maintain the expression of CaSR—the calciostat—at a constant level at these extracellular Ca^{2+} concentrations. In normal rats, no evidence was found for extracellular Ca^{2+} modulation of parathyroid gland CaSR expression (Rogers et al., 1995; Brown et al., 1996). An additional element of the regulation of CaSR by extracellular Ca^{2+} relates to the reported ability of the ligand to stimulate trafficking of CaSR from intracellular stores to the plasma membrane by so-called agonist driven insertional secretion (Breitwieser, 2013). Expression at the cell surface increases, whereas overall CaSR may not necessarily be changed.

Calcimimetics are low-molecular-weight positive allosteric modulators (PAMs) of CaSR. One calcimimetic, cinacalcet (Sensipar, Mimpara), is used clinically to suppress severe secondary hyperparathyroidism in patients with end-stage renal disease on hemodialysis and in hypercalcemic patients with primary hyperparathyroidism (including parathyroid carcinoma) in whom curative parathyroidectomy is not possible or appropriate (Nemeth and Shoback, 2013). PAMs bind in the TMD of CaSR and stabilize the receptor in a more active state. Phenylalkylamine calcimimetics such as cinacalcet bind in the TMD in a cavity that overlaps a putative Ca^{2+} binding site and the extracellular loops (Leach et al., 2016). Calcilytics such as the amino alcohol NPS-2143 that are negative allosteric modulators also bind within the TMD and induce a more inactive conformation (Nemeth and Goodman, 2016). The pockets for cinacalcet and NPS-2143 overlap to an extent, with some of the receptor amino acids contacted being common and others not.

Activation of CaSR on parathyroid chief cells inhibits PTH synthesis and suppresses parathyroid secretion. CaSR-mediated change in PTH gene expression is the result of a change in PTH mRNA stability rather than in PTH gene transcription. High extracellular calcium recruits a degradation complex comprising both endo- and exoribonucleases to the 3′-untranslated region of the PTH mRNA to destabilize it (Naveh-Many, 2010). Extracellular calcium also exerts a posttranslational effect on PTH expression by promoting cleavage of intact PTH stored within secretory vesicles to yield fragments comprising the mid- and COOH-terminal regions, some of which are only truncated at the far NH_2-terminus (Kawata et al., 2005). There is evidence that the inhibition of CaSR downstream signaling is not just due to reversal or relaxation of CaSR activation, but rather that CaSR inhibition by hypocalcemia is an active process that requires the involvement of microRNAs and the proteins they control (Shilo et al., 2015).

With respect to ligand-bound CaSR inhibiting PTH secretion, activating Gq/11 is essential because mice with knockout of both these G proteins in the parathyroid gland have severe hyperparathyroidism similar to that present in mice homozygous for global knockout of *Casr* (Wettschureck et al., 2007). Confirmation that the Gq-coupled pathway may be important in part comes from the finding that transgenic mice specifically overexpressing a dominant-negative Gαq loop minigene in parathyroid chief cells had increased serum PTH as well as increased PTH mRNA and cellular proliferation (Pi et al., 2008). The abnormalities that reflected reduced sensitivity of the parathyroid gland to extracellular calcium were similar to those of heterozygous *Casr*-knockout mice (Ho et al., 1995). In humans, the parathyroid expresses predominantly *GNA11* rather than *GNAQ* (Nesbit et al., 2013a).

Downstream signaling pathways involved in extracellular calcium-regulated PTH release may include products of the 12- and 15-lipoxygenase pathways of arachidonate metabolism and/or $ERK_{1/2}$ that may be mediated by the interaction of CaSR and $G_{i/o}$ (Corbetta et al., 2002). A further downstream mechanism may involve rearrangement of the cytoskeleton to block access of PTH-containing secretory vesicles to the plasma membrane (Quinn et al., 2007).

The apparent link between parathyroid calcium-sensing and proliferative pathways as evidenced by marked parathyroid hyperplasia of mice with global knockout of *Casr* (Ho et al., 1995) suggested that somatic alterations in the *CASR* gene could be tumorigenic in sporadic parathyroid tumors. However, several studies have failed to document somatic mutation of the *CASR* gene as a significant factor in parathyroid tumorigenesis (Hosokawa et al., 1995; Thompson et al., 1995; Degenhardt et al., 1998; Cetani et al., 1999).

Familial hypocalciuric hypercalcemia

FHH is classically described as an autosomal dominant condition characterized by lifelong mild-to-moderate elevations of serum calcium concentrations in association with normal or mildly raised serum PTH concentrations and low urinary calcium excretion (Marx et al., 1981; Law et al., 1985; Marx, 2018). FHH is genetically heterogeneous and at present comprises three subtypes (FHH1−3). Two-thirds of FHH cases are the FHH1 subtype, which is due to heterozygous inactivating mutations affecting G-protein-coupled CaSR encoded by the *CASR* gene (3q13.3−21.1) (Pollak et al., 1993). FHH2 is due to heterozygous inactivating mutations of the G-protein alpha-11 subunit (Gα11) encoded by the *GNA11* gene (19p13.3) (Nesbit et al., 2013a). FHH3 is caused by mutations of the adapter-related protein complex 2 (AP2) sigma subunit (AP2σ) encoded by the *AP2S1* gene (19q13.3) (Nesbit et al., 2013b). Other FHH cases negative for *CASR*, *GNA11,* and *AP2S1* mutations have been described (Vargas-Poussou et al., 2016).

With respect to FHH1, individuals homozygous (or compound heterozygous) for *CASR* mutations present with NSHPT with marked parathyroid hypercellularity (Pollak et al., 1994), and the tumors constitute polyclonal growths rather than monoclonal neoplasms (Corrado et al., 2015). Almost 200 mutations in *CASR* have been identified in FHH1 and NSHPT patients (Hendy et al., 2009; Guarnieri et al., 2010; Hannan et al., 2012; Vargas-Poussou et al., 2016). In FHH1, lifelong hypercalcemia is accompanied by normal or elevated serum PTH levels as in mild sporadic primary hyperparathyroidism (PHPT). However, renal and skeletal manifestations of sporadic PHPT are generally absent. A family history and hypocalciuria—calcium-to-creatinine clearance ratios (< 0.01) that are low relative to the filtered load of calcium—are important in distinguishing FHH patients from those with a biochemical diagnosis of PHPT. With rare exceptions, subtotal parathyroidectomy in FHH cases does not achieve normocalcemia, and therefore surgical intervention is generally contraindicated. However, NSHPT is life-threatening and requires timely parathyroidectomy in newborns. The mutations are scattered throughout the CaSR protein sequence, although with some clustering in the extracellular domain at putative Ca^{2+}-binding sites and within parts of the TMD. Eighty-five percent of mutations are missense with some frameshift, nonsense, in-frame, and splicing mutations represented. Some mutations exert a dominant-negative effect on wild-type CaSR, and such cases may present in a more severe phenotype than loss-of-activity mutations. Calcimimetics have been used successfully in rare cases of FHH1 that present symptomatically to reduce serum calcium levels (Timmers et al., 2006). In addition, calcimimetics have provided clinical benefit in neonatal hyperparathyroid cases with heterozygous *CASR* mutations (Reh et al., 2011). However, calcimimetics are ineffective in NSHPT cases caused by biallelic deletion *CASR* mutations (Atay et al., 2014). In-depth views of the use of calcimimetics in patients harboring *CASR* mutations are available (Mayr et al., 2016; Marx, 2017).

With respect to FHH2, in 2013 Nesbit and colleagues (Nesbit et al., 2013a) reported the identification of heterozygous germline mutations in *GNA11* encoding Gα11 in affected members of a kindred with FHH2, and one unrelated FHH patient. *GNA11* was selected using a candidate gene approach because it is located at the locus of the FHH2 trait. Since that time, other FHH2 mutations have been identified (Gorvin et al., 2016, 2018), and some heterozygous activating mutations in autosomal dominant hypocalcemia type 2 (Mannstadt et al., 2013; Nesbit et al., 2013a; Li et al., 2014; Piret et al., 2016) have been identified, emphasizing the importance of Gα11 coupling for CaSR action. Somatic activating mutations of Gα11 cause uveal melanomas. Clinically, FHH2 patients present a milder phenotype than that of FHH1 patients, with a lower serum calcium concentration. In vivo administration of cinacalcet in an FHH2 patient harboring a *GNA11* inactivating mutation normalized the serum calcium concentration (Gorvin et al., 2018).

The FHH trait had also been mapped in two unrelated kindreds to a third locus distinct from that for FHH1 and FHH2. Ultimately, heterozygous germline mutations in the *AP2S1* gene were shown to underlie this subtype, FHH3 (Nesbit et al., 2013b). The *AP2S1* gene encodes the σ-subunit of the adaptor-related protein complex 2 critical for clathrin-mediated endocytosis of cell-surface proteins including GPCRs. AP2 is a heterotetramer of α-, β-. μ-, and σ-subunits and links clathrin to vesicle membranes by binding to tyrosine- and dileucine-based motifs of membrane-associated cargo proteins.

Exome capture and high-throughput sequence analysis of affected individuals of the FHH3 kindreds identified mutations of Arg15 in AP2σ. Further heterozygous alterations, all affecting Arg15 (Arg15Cys, Arg15His, and Arg15 Leu), were identified in subsets of unrelated FHH individuals (Nesbit et al., 2013b; Fujisawa et al., 2013; Hendy et al., 2014; Tenhola et al., 2015; Hannan et al., 2015; Vargas-Poussou et al., 2016). It is predicted that these FHH3-causing Arg15 mutations disrupt an interaction between the AP2 complex and the intracellular carboxyl terminus of CaSR, thereby impairing endocytosis of CaSR. Normally, CaSR coupled to G11/q proteins continues to be active, as the complex is endocytosed, and this activity is lost with the mutated AP2σ proteins that act in a dominant-negative manner (Gorvin, 2018). Administration of cinacalcet to FHH3 patients has been successful in lowering serum calcium concentration (Tenhola et al., 2015; Howles et al., 2016). This was the case for all three Arg15 mutations (Howles et al., 2016).

The few reported individuals with FHH2 appear to present with a milder phenotype than that of FHH1. More conclusive evidence of similarities and differences between FHH1 and FHH3 has been obtained by studying two relatively large FHH3 cohorts (Hannan et al., 2015; Vargas-Poussou et al., 2016). FHH3 patients present with higher mean levels of plasma calcium (and magnesium) than FHH1 patients despite having similar PTH levels and urinary calcium excretion. Mean renal tubular reabsorption levels are higher in FHH3 than in FHH1. In one study, a comparison was made with patients with mild PHPT, with the conclusion that plasma calcium levels were higher in FHH while PTH levels and urinary calcium excretion were lower (Vargas-Poussou et al., 2016). There was marked overlap between groups, emphasizing that diagnostic difficulties exist, as they do for FHH1 and for FHH3 versus non-FHH PHPT. This was also exemplified by the finding that in a separate study of five patients subsequently identified as FHH3, three had undergone unsuccessful subtotal parathyroidectomy (Hendy et al., 2014).

Hyperparathyroidism-jaw tumor syndrome

The syndrome of hereditary HPT-JT is a rare autosomal dominant disorder inherited with incomplete penetrance and characterized by early-onset recurrent parathyroid tumors (80%) and fibrous ossifying tumors of the mandibula or maxilla (30%). Less frequent renal lesions (10%) include Wilms' tumor, hamartomas, and polycystic kidney disease (Jackson et al., 1990; Chen et al., 2003). Uterine tumors include adenosarcoma, but benign adenofibromas and leiomyomas are more common (Bradley et al., 2005). While most resected parathyroid tumors in this syndrome are still benign, there is a heightened likelihood of progression to adenomas with atypical features and frank malignancy; parathyroid carcinoma occurs at increased frequency (15%−35%) in this syndrome (Mehta et al., 2014). In contrast to the multiglandular enlargement typically found at presentation in other classical forms of inherited hyperparathyroidism, a solitary, enlarged, and often cystic gland may be found in an HPT-JT patient, although multigland disease is sometimes present on initial presentation. Normocalcemia is often achieved after removal of the tumor(s); however, recurrence is well documented. In a large group of families, the HPT-JT trait was linked to 1q21-32 (Szabo et al., 1995; Hobbs et al., 2002). The responsible gene, HRPT2 at 1q31.2, was identified by positional cloning and mutation analysis and encodes parafibromin, a protein of 531 amino acids (Carpten et al., 2002). Consistent with a tumor-suppressor mechanism, many observed mutations within the gene would be predicted to cause loss of function (e.g., frameshifts, nonsense), and large gene deletions are also common (10%) in HPT-JT-affected individuals (Guarnieri et al., 2017) (Fig. 58.5). Parafibromin is expressed in a broad array of tissues, is highly conserved across species, and within the parathyroid gland it is reported in both the cytoplasmic and nuclear compartments (Woodard et al., 2005). Nuclear localization signals are present, and nucleolar location may have particular importance in its functions relevant to tumorigenesis (Panicker et al., 2010; Pazienza et al., 2013; Masi et al., 2014). Nuclear parafibromin has a proapoptotic activity (Lin et al., 2007). Transfection experiments have demonstrated the ability of parafibromin to inhibit cell proliferation and block cyclin D1 expression (Woodard et al., 2005). Experimental overexpression of wild-type parafibromin in transformed cell lines inhibits cell proliferation and induces G1-phase cell cycle arrest (Zhang et al., 2006). Parafibromin HPT-JT mutants act in a dominant-negative manner to abolish the ability of wild-type parafibromin to inhibit cell growth (Zhang et al., 2006). In mammalian cells, parafibromin is part of an RNA polymerase II−associated factor complex and has sequence homology to yeast Cdc73, a constituent of a protein multimer important for transcription initiation/elongation, histone methylation, and RNA processing (Rozenblatt-Rosen et al., 2005; Yart et al., 2005). In response, the human *HRPT2* gene was renamed *CDC73*. Parafibromin binds directly to the COOH-terminal part of β-catenin and transduces Wnt pathway signals into transcriptional initiation and elongation by RNA polymerase II (Mosimann et al., 2006). However, it is unclear how this or other proposed actions of parafibromin specifically relate to its role as a tumor suppressor. Initial studies in mouse models have tended to reinforce the key role of parafibromin loss in parathyroid neoplasia, with parathyroid-specific or conventional *Cdc73* knockout being reported to cause hypercalcemia and parathyroid proliferation (Wang et al., 2008; Walls et al., 2017).

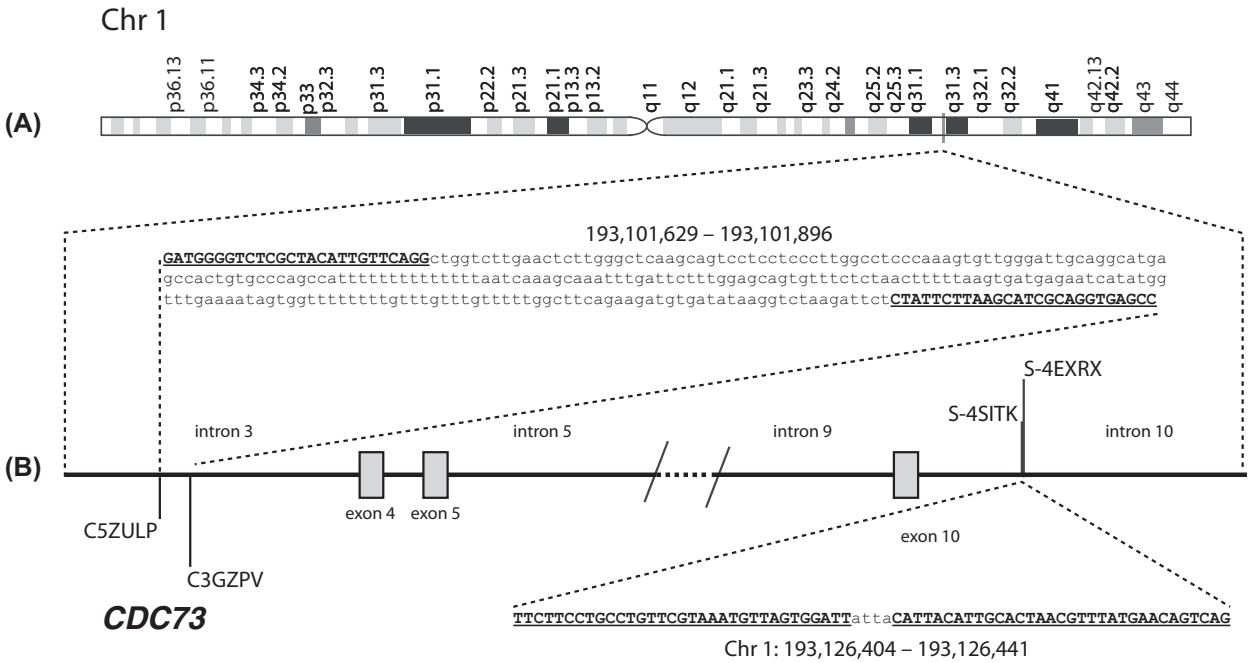

FIGURE 58.5 Intragenic deletion of *CDC73* is common in HPT-JT affected individuals, and one example is shown here. (A) SNP array analysis revealed an interstitial microdeletion of 0.25 Mb in band 1q31.2. (B) The hemizygous region was covered by 76 SNP array probes (from C-3GZPV to S−4S1TK) and encompassed part of the *CDC73* coding sequence from exons 4 to 10. The proximal (centromeric) breakpoint was located between the last present probe C-5ZULP (193,101,629 bp) and the first deleted probe C-3GZPV (193,101,895 bp), while the distal (telomeric) breakpoint was located between the last deleted probe S-4SITK (193,126,404 bp) and the first present probe S-4EXRX (193,126,441 bp) (see Guarnieri et al., 2017).

Familial isolated hyperparathyroidism

FIHP has been defined as hereditary primary hyperparathyroidism without the association of other disease or tumors. Although listed as a distinct genetic entity, some cases presenting as FIHP have been shown by gene mutation analysis to be variants of other monogenic diseases—FHH (Simonds et al., 2002; Warner et al., 2004), MEN1 (Carrasco et al., 2004; Pannett et al., 2003), and HPT-JT (Guarnieri et al., 2006; Kelly et al., 2006; Villablanca et al., 2004; Simonds et al., 2004). A personal or family history of parathyroid carcinoma in FIHP warrants strong consideration to determine germline *CDC73* (*HRPT2*) mutation status, which can lead to early detection and removal of potentially malignant parathyroid tumors (Kelly et al., 2006; Guarnieri et al., 2006). In addition, specific germline variants in the *GCM2* gene encoding the parathyroid-specific GCM2 transcription factor have been reported to be overrepresented in some autosomal dominant FIHP kindreds, especially those of Ashkenazi Jewish descent, as compared with their allelic frequencies in the general population (Guan et al., 2016, 2017). The penetrance of these variants and the contextual constraints in which they may contribute to the hyperparathyroid phenotype and thus have potential value in clinical management require further study. For most FIHP kindreds, the causative genes remain to be identified.

Molecular pathogenesis of parathyroid carcinoma

Mutation of the *CDC73* tumor-suppressor gene (formerly/also known as *HRPT2*) is a major driver in parathyroid carcinoma, whether in the context of familial or sporadic disease. Such mutations are detectable in up to 75% of unequivocally diagnosed parathyroid cancers (Shattuck et al., 2003a; Howell et al., 2003; Cetani et al., 2004; Gill, 2014; Pandya et al., 2017), with percentages varying among series probably due to relatively small sample sizes and differences in the selection of cases. Inactivating mutations in noncoding regions, and larger deletions in some series, would have escaped detection. Most such mutations in sporadic cases are somatic. In addition, about 20%−25% of patients with the clinical presentation of sporadic parathyroid carcinoma bear unsuspected germline mutations in *CDC73*/*HRPT2* (Shattuck et al., 2003). Such patients may represent de novo examples or lower penetrance variants of HPT-JT, and the opportunity for early diagnosis to prevent or cure parathyroid cancer in their family members established an important role for DNA testing in this circumstance.

Because of the impressive genetic evidence for *CDC73's* role, parafibromin immunostaining has been evaluated as a potential diagnostic test for parathyroid carcinoma (Tan et al., 2004; Gill et al., 2006; Juhlin et al., 2006). Several studies reported virtually complete loss of nuclear immunostaining in most parathyroid carcinomas in comparison with positive staining in benign parathyroid tumors. However, because of technical, case selection, and/or biological factors, not all studies yielded such uniform results (Juhlin et al., 2007), and parafibromin staining must be interpreted with caution in the clinical setting (Guarnieri et al., 2012b; Gill, 2014; Rosai et al., 2014; DeLellis et al., 2017; Lloyd et al., 2017).

Genetic evidence examining the relative frequency of clonal markers suggests that, in general, sporadic parathyroid carcinomas develop de novo as opposed to evolving from preexisting clinically apparent benign adenomas (Costa-Guda et. al., 2013b, 2014). However, parathyroid carcinomas that occur in the context of germline *CDC73* mutation may, in contrast, develop through a progression—i.e., from adenoma to atypical adenoma to carcinoma. Interestingly, adenomas and atypical adenomas in patients with germline *CDC73* mutations have been reported to be parafibromin negative and/or biallelically inactivated for *CDC73* (Kelly et al., 2006; Cetani et al., 2007), suggesting that loss of parafibromin is a crucial but not sufficient molecular genetic step in a parathyroid cell's acquisition of a frankly malignant phenotype in this context.

Additional insights have been gained using "next-generation" massively parallel sequencing technologies. Whole-exome sequencing and related methods not only confirmed the key role of *CDC73* inactivation but revealed a number of other recurrent gene alterations as putative or candidate drivers in the pathogenesis of parathyroid carcinoma (Kasaian et al., 2013; Yu et al., 2015; Pandya et al., 2017). These include mutations in well-established cancer genes not previously implicated in parathyroid carcinoma, such as *PIK3CA* and *MTOR*, and amplification of *cyclin D1* as well as novel candidate oncogenes like *ADCK1*. To the extent that some of these somatically mutated genes can be targeted by current or future cancer therapeutic agents, the findings provide a rationale for sequencing tumors from patients with surgically incurable parathyroid cancer and considering the use of such agents in appropriately selected cases.

Complementing the aforementioned finding of the extra copy number of *CCND1*, the cyclin D1 oncoprotein, overexpressed in 20%−40% of adenomas, appears to be even more frequently overexpressed in parathyroid carcinomas (Vasef et al., 1999; Hsi et al., 1996; Zhao et al., 2014). These observations strengthen the likelihood that cyclin D1 is a driver oncogene that contributes to the pathogenesis of parathyroid cancers and adenomas. As such, patients with metastatic disease and this tumor genotype might be considered for treatment with CDK4/6 inhibitors and/or eventual inclusion in clinical trials once novel anti−cyclin D1 therapies are developed. Evidence for the involvement of the Wnt signaling pathway provides additional leads toward pathogenetic mechanisms and potential therapeutic vulnerabilities (Svedlund et al., 2010; Juhlin et al., 2009; Pandya et al., 2017). *MEN1* mutations have been only rarely reported in parathyroid carcinoma and generally in series where inclusion did not require malignant clinical behavior of the tumor. Hints as to the chromosomal location of other, still unidentified, parathyroid cancer genes include the common loss of chromosome region 13q, which contains *RB* and *BRCA2* (Cryns et al., 1994b; Dotzenrath et al., 1996; Pearce et al., 1996; Kytola et al., 2000). However, the absence of detectable mutations in *RB* and *BRCA2* suggests that any major role for these genes would be indirect rather than as classical tumor suppressors (Shattuck et al., 2003b). Similarly, loss of putative tumor-suppressor genes in genomic regions including 1p, 3q, 4q, and 21q may be involved as significant factors in malignant parathyroid tumors (Cryns et al., 1995; Kytola et al., 2000; Agarwal et al., 1998). Specific chromosome regional gains, suggesting the involvement of oncogenes, have been found in parathyroid carcinomas by comparative genomic hybridization (Kytola et al., 2000; Agarwal et al., 1998), but the involved genomic locations show little consistency among the existing reports, and the results require confirmation by complementary methods. Identification of more genetic lesions that are highly specific for the malignant phenotype would be helpful in bringing molecular diagnostics to bear on this disease, which would aid in overcoming the well-known difficulties in distinguishing malignant versus benign parathyroid tumors histopathologically.

Ectopic secretion of parathyroid hormone

The ectopic secretion of PTH by nonparathyroid tumors is an extremely rare cause of hyperparathyroidism. The use of modern immunometric assays for PTH that show no cross-reactivity with PTH-related protein, the major cause of the hypercalcemia of malignancy, combined in some cases with molecular analysis using specific human *PTH* gene probes (Hendy et al., 1981; Vasicek et al., 1983), has suggested or confirmed the occurrence of this syndrome in several cases (see VanHouten et al., 2006 and references therein).

In one case of an ovarian carcinoma (Nussbaum et al., 1990), the molecular basis for the aberrant expression of PTH was determined. This involved a rearrangement (Fig. 58.6) and amplification of the PTH gene such that it was no longer under the control of upstream regulatory elements that may normally act to silence PTH gene expression in nonparathyroid tissue. This case provided strong documentation that the tumor was in fact the source of high circulating PTH levels and

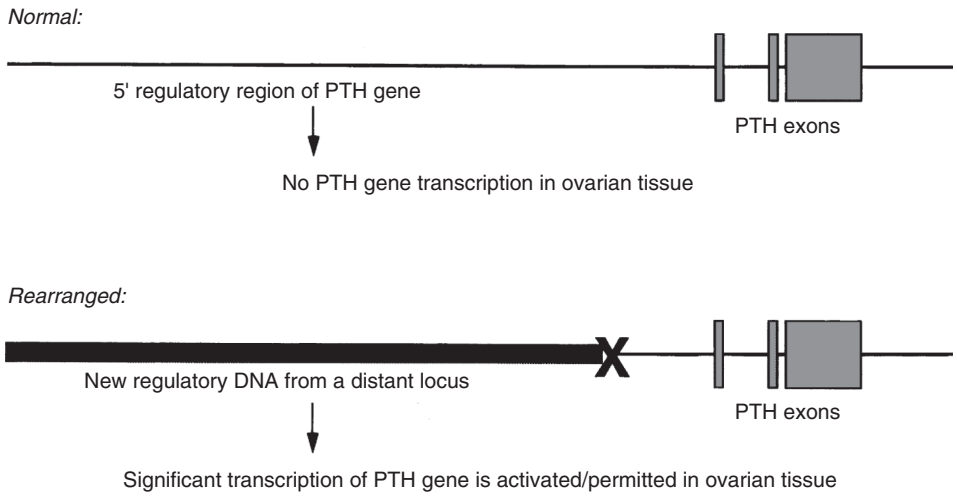

FIGURE 58.6 Molecular pathology of the ectopic production of PTH by an ovarian cancer. Schematic diagram of the normal PTH gene region (*top*) and the rearranged, amplified PTH gene region (*bottom*) in a PTH-secreting ovarian tumor. The bold **"X"** represents the breakpoint of the DNA rearrangement. *Reproduced with permission from Arnold, A. 1993. Genetic basis of endocrine disease 5: molecular genetics of parathyroid gland neoplasia. J. Clin. Endocrinol. Metab. 77, 1108–1112.*

the patient's hypercalcemia. In a case of severe hyperparathyroidism resulting from ectopic PTH production by a pancreatic malignancy, a mechanism of transactivation of the PTH gene was suggested by the finding of hypomethylation of the PTH gene promoter in tumor tissue (VanHouten et al., 2006).

References

Abi-Rafeh, J., Troka, I., Canaff, L., Faugere, M.-C., Clemens, T.L., Hendy, G.N., 2017. Deletion of menin early in the osteoblast lineage leads to increased bone resorption, and reduced bone mass and strength in adult mice. J. Bone Miner. Res. 32 (Suppl. 1), 1091.

Agarwal, S.K., 2017. The future: genetic advances in MEN1 therapeutics and management strategies. Endocr. Relat. Cancer 24, T119–T134.

Agarwal, S.K., Guru, S.C., Heppner, C., Erdos, M.R., Collins, R.M., Park, S.Y., Saggar, S., Chandrasekharappa, S.C., Collins, F.S., Spiegel, A.M., Marx, S.J., Burns, A.L., 1999. Menin interacts with the AP-1 transcription factor JunD and represses JunD-activated transcription. Cell 96, 143–152.

Agarwal, S.K., Mateo, C.M., Marx, S.J., 2009. Rare germline mutations in cyclin-dependent kinase inhibitor genes in multiple endocrine neoplasia type 1 and related states. J. Clin. Endocrinol. Metab. 94, 1826–1834.

Agarwal, S.K., Novotny, E.A., Crabtree, J.S., Weitzman, J.B., Yaniv, M., Burns, A.L., Chandrasekharappa, S.C., Collins, F.S., Spiegel, A.M., Marx, S.J., 2003. Transcription factor JunD, deprived of menin, switches from growth suppressor to growth promoter. Proc. Natl. Acad. Sci. U.S.A. 100, 10770–10775.

Agarwal, S.K., Schrock, E., Kester, M.B., Burns, A.L., Heffess, C.S., Ried, T., Marx, S.J., 1998. Comparative genomic hybridization analysis of human parathyroid tumors. Cancer Genet. Cytogenet. 106, 30–36.

Arnold, A., 1993. Genetic basis of endocrine disease 5: molecular genetics of parathyroid gland neoplasia. J. Clin. Endocrinol. Metab. 77, 1108–1112.

Arnold, A., Kim, H.G., 1989. Clonal loss of one chromosome 11 in a parathyroid adenoma. J. Clin. Endocrinol. Metab. 69, 496–499.

Arnold, A., Papanikolaou, A., 2005. Biology of neoplasia—cyclin D1 in breast cancer pathogenesis. J. Clin. Oncol. 23, 4215–4224.

Arnold, A., Staunton, C.E., Kim, H.G., Gaz, R.D., Kronenberg, H.M., 1988. Monoclonality and abnormal parathyroid hormone genes in parathyroid adenomas. N. Engl. J. Med. 318, 658–662.

Arnold, A., Kim, H.G., Gaz, R.D., Eddy, R.L., Fukushima, Y., Byers, M.G., Shows, T.B., Kronenberg, H.M., 1989. Molecular cloning and chromosomal mapping of DNA rearranged with the parathyroid hormone gene in a parathyroid adenoma. J. Clin. Investig. 83, 2034–2040.

Arnold, A., Brown, M., Urena, P., Gaz, R.D., Sarfati, E., Drueke, T., 1995. Monoclonality of parathyroid tumors in chronic renal failure and in primary parathyroid hyperplasia. J. Clin. Investig. 95, 2047–2053.

Atay, Z., Bereket, A., Haliloglu, B., Abali, S., Ozdogan, T., Altuncu, E., Canaff, L., Vilaça, T., Wong, B.Y., Cole, D.E., Hendy, G.N., Turan, S., 2014. Novel homozygous inactivating mutation of the calcium-sensing receptor gene (CASR) in neonatal severe hyperparathyroidism-lack of effect of cinacalcet. Bone 64, 102–107.

Bai, F., Pei, X.H., Nishikawa, T., Smith, M.D., Xiong, Y., 2007. p18Ink4c, but not p27Kip1, collaborates with Men1 to suppress neuroendocrine organ tumors. Mol. Cell Biol. 27, 1495–1504.

Balenga, N., Azimzadeh, P., Hogue, J.A., Staats, P.N., Shi, Y., Koh, J., Dressman, H., Olson Jr., J.A., 2017. Orphan adhesion GPCR GPR64/ADGRG2 is overexpressed in parathyroid tumors and attenuates calcium-sensing receptor-mediated signalling. J. Bone Miner. Res. 32, 654–666.

Bernards, R., 1999. CDK-independent activities of D type cyclins. Biochem. Biophys. Acta 1424, M17–M22.

Bertolino, P., Tong, W.M., Galendo, D., Wang, Z.Q., Zhang, C.X., 2003a. Heterozygous Men1 mutant mice develop a range of endocrine tumors mimicking multiple endocrine neoplasia type 1. Mol. Endocrinol. 17, 1880–1892.

Bertolino, P., Radovanovic, I., Casse, H., Aguzzi, A., Wang, Z.Q., Zhang, C.X., 2003b. Genetic ablation of the tumor suppressor menin causes lethality at mid-gestation with defects in multiple organs. Mech. Dev. 120, 549–560.

Bjorkland, P., Akerstrom, G., Westin, G., 2007. Accumulation of nonphosphorylated β-catenin and c-myc in primary and uremic secondary hyperparathyroid tumors. J. Clin. Endocrinol. Metab. 92, 338–344.

Björklund, P., Akerström, G., Westin, G., 2007. An LRP5 receptor with internal deletion in hyperparathyroid tumors with implications for deregulated WNT/beta-catenin signalling. PLoS Med. 4, e328.

Björklund, P., Lindberg, D., Akerström, G., Westin, G., 2008. Stabilizing mutation of CTNNB1/beta-catenin and protein accumulation analyzed in a large series of parathyroid tumors of Swedish patients. Mol. Canc. 7, 53.

Black III., W.C., Utley, J.R., 1968. The differential diagnosis of parathyroid adenoma and chief cell hyperplasia. Am. J. Clin. Pathol. 49, 761–775.

Borsari, S., Pardi, E., Pellegata, N.S., Lee, M., Saponaro, F., Torregrossa, L., Basolo, F., Paltrinieri, E., Zatelli, M.C., Materazzi, G., Miccoli, P., Marcocci, C., Cetani, E., 2017. Loss of p27 expression is associated with *MEN1* gene mutations sporadic parathyroid adenomas. Endocrine 55, 386–397.

Bradley, K.J., Hobbs, M.R., Buley, I.D., Carpten, J.D., Cavaco, B.M., Fares, J.E., Laidler, P., Manek, S., Robbins, C.M., Salti, I.S., Thompson, N.W., Jackson, C.E., Thakker, R.V., 2005. Uterine tumours are a phenotypic manifestation of the hyperparathyroidism-jaw tumour syndrome. J. Intern. Med. 257, 18–26.

Breitwieser, G.E., 2013. The calcium sensing receptor life cycle: trafficking, cell surface expression, and degradation. Best Pract. Res. Clin. Endocrinol. Metabol. 27, 303–313.

Brown, A.J., Zhong, M., Finch, J., Ritter, C., McCracken, R., Morrissey, J., Slatopolsky, E., 1996. Rat calcium-sensing receptor is regulated by vitamin D but not by calcium. Am. J. Physiol. 270, F454–F460.

Brown, E.M., 2013. Role of the calcium-sensing receptor in extracellular calcium homeostasis. Best Pract. Res. Clin. Endocrinol. Metabol. 27, 333–343.

Brown, E.M., Gamba, G., Riccardi, D., Lombardi, M., Butters, R., Kifor, O., Sun, A., Hediger, M.A., Lytton, J., Hebert, S.C., 1993. Cloning and characterization of an extracellular Ca(2+)-sensing receptor from bovine parathyroid. Nature 366, 575–580.

Brown, S.B., Brierley, T.T., Palanisamy, N., Salusky, I.B., Goodman, W., Brandi, M.L., Drueke, T.B., Sarfati, E., Urena, P., Chaganti, R.S.K., Pike, J.W., Arnold, A., 2000. Vitamin D receptor as a candidate tumor-suppressor gene in severe hyperparathyroidism of uremia. J. Clin. Endocrinol. Metab. 85, 868–872.

Bystrom, C., Larsson, C., Blomberg, C., Sandelin, K., Falkmer, U., Skogseid, B., Oberg, K., Werner, S., Nordenskjold, M., 1990. Localization of the MEN1 gene to a small region within chromosome 11q13 by deletion mapping in tumors. Proc. Natl. Acad. Sci. U.S.A. 87, 1968–1972.

Canaff, L., Hendy, G.N., 2002. Human calcium-sensing receptor gene: vitamin D response elements in promoters P1 and P2 confer transcriptional responsiveness to 1,25-dihydroxyvitamin D. J. Biol. Chem. 277, 30337–30350.

Canaff, L., Vanbellinghen, J.F., Kaji, H., Goltzman, D., Hendy, G.N., 2012a. Impaired transforming growth factor-β (TGF-β) transcriptional activity and cell proliferation control of a menin in-frame deletion mutant associated with multiple endocrine neoplasia type 1 (MEN1). J. Biol. Chem. 287, 8584–8597.

Canaff, L., Vanbellinghen, J.F., Kanazawa, I., Kwak, H., Garfield, N., Vautour, L., Hendy, G.N., 2012b. Menin missense mutants encoded by the MEN1 gene that are targeted to the proteasome: restoration of expression and activity by CHIP siRNA. J. Clin. Endocrinol. Metab. 97, E282–E291.

Canaff, L., Zhou, X., Mosesova, I., Cole, D.E., Hendy, G.N., 2009. Glial cells missing-2 (GCM2) transactivates the calcium-sensing receptor gene: effect of a dominant negative GCM2 mutant associated with autosomal dominant hypoparathyroidism. Hum. Mutat. 30, 85–92.

Carling, T., Correa, P., Hessman, O., Hedberg, J., Skogseid, B., Lindberg, D., Rastad, J., Westin, G., Akerström, G., 1998. Parathyroid MEN1 gene mutations in relation to clinical characteristics of nonfamilial primary hyperparathyroidism. J. Clin. Endocrinol. Metab. 83, 2960–2963.

Carling, T., Imanishi, Y., Gaz, R.D., Arnold, A., 1999a. Analysis of the RAD54 gene on chromosome 1p as a potential tumor-suppressor gene in parathyroid adenomas. Int. J. Cancer 83, 80–82.

Carling, T., Imanishi, Y., Gaz, R.D., Arnold, A., 1999b. RAD51 as a candidate parathyroid tumor suppressor gene on chromosome 15q: absence of somatic mutations. Clin. Endocrinol. 51, 403–407.

Carpten, J.D., Robbins, C.M., Villablanca, A., Forsberg, L., Presciuttini, S., Bailey-Wilson, J., Simonds, W.F., Gillanders, E.M., Kennedy, A.M., Chen, J.D., Agarwal, S.K., Sood, R., Jones, M.P., Moses, T.Y., Haven, C., Petillo, D., Leotlela, P.D., Harding, B., Cameron, D., Pannett, A.A., Hoog, A., Heath III., H., James-Newton, L.A., Robinson, B., Zarbo, R.J., Cavaco, B.M., Wassif, W., Perrier, N.D., Rosen, I.B., Kristofferson, U., Turnpenny, P.D., Farnebo, L.O., Besser, G.M., Jackson, C.E., Morreau, H., Trent, J.M., Thakker, R.V., Marx, S.J., Teh, B.T., Larsson, C., Hobbs, M.R., 2002. HRPT2, encoding parafibromin, is mutated in hyperparathyroidism-jaw tumor syndrome. Nat. Genet. 32, 676–680.

Carrasco, C.A., Gonzalez, A.A., Carvajal, C.A., Campusano, C., Oestreicher, E., Arteaga, E., Wohlik, N., Fardella, C.E., 2004. Novel intronic mutation of MEN1 gene causing familial isolated primary hyperparathyroidism. J. Clin. Endocrinol. Metab. 89, 4124–4129.

Castleman, B., Roth, S.I., 1978. Tumors of the parathyroid glands. In: Hartman, W.H. (Ed.), Atlas of Tumor Pathology, Armed Forces Institute of Pathology. Washington, DC. second series, fascicle 14.

Casimiro, M.C., Di Sante, G., Crosariol, M., Loro, E., Dampier, W., Ertel, A., Yu, Z., Saria, E.A., Papanikolaou, A., Li, Z., Wang, C., Addya, S., Lisanti, M.P., Fortina, P., Cardiff, R.D., Tozeren, A., Knudsen, E.S., Arnold, A., Pestell, R.,G., 2015. Kinase-independent role of cyclin D1 in chromosomal instability and mammary tumorigenesis. Oncotarget 6, 8525–8538.

Cetani, F., Pinchera, A., Pardi, E., Cianferotti, L., Vignali, E., Picone, E., Miccoli, P., Viacava, P., Marcocci, C., 1999. No evidence for mutations in the calcium-sensing receptor gene in sporadic parathyroid adenomas. J. Bone Miner. Res. 14, 878–882.

Cetani, F., Pardi, E., Banti, C., Collecchi, P., Viacava, P., Borsari, S., Fanelli, G., Naccarato, A.G., Saponaro, F., Berti, P., Miccoli, P., Pinchera, A., Marcocci, C., 2010. Beta-catenin activation is not involved in sporadic parathyroid carcinomas and adenomas. Endocr. Relat. Cancer 17, 1–6.

Cetani, F., Pardi, E., Borsari, S., Viacava, P., Dipollina, G., Cianferotti, L., Ambrogini, E., Gazzerro, E., Colussi, G., Berti, P., Miccoli, P., Pinchera, A., Marcocci, C., 2004. Genetic analyses of the HRPT2 gene in primary hyperparathyroidism: germline and somatic mutations in familial and sporadic parathyroid tumors. J. Clin. Endocrinol. Metab. 89, 5583–5591.

Cetani, F., Pardi, E., Ambrogini, E., Viacava, P., Borsari, S., Lemmi, M., Cianferotti, L., Miccoli, P., Pinchera, A., Arnold, A., Marcocci, C., 2007. Different somatic alterations of the *HRPT2* gene in a patient with recurrent sporadic primary hyperparathyroidism carrying an *HRPT2* germline mutation. Endocr. Relat. Cancer 14, 493–499.

Chandrasekharappa, S.C., Guru, S.C., Manickam, P., Olufemi, S.E., Collins, F.S., Emmert-Buck, M.R., Debelenko, L.V., Zhuang, Z., Lubensky, I.A., Liotta, L.A., Crabtree, J.S., Wang, Y., Roe, B.A., Weisemann, J., Boguski, M.S., Agarwal, S.K., Kester, M.B., Kim, Y.S., Heppner, C., Dong, Q., Spiegel, A.M., Burns, A.L., Marx, S.J., 1997. Positional cloning of the gene for multiple endocrine neoplasia-type 1. Science 276, 404–407.

Chen, J.D., Morrison, C., Zhang, C., Kahnoski, K., Carpten, J.D., Teh, B.T., 2003. Hyperparathyroidism-jaw tumour syndrome. J. Intern. Med. 253, 634–642.

Chikatsu, N., Fukumoto, S., Takeuchi, Y., Suzawa, M., Obara, T., Matsumoto, T., Fujita, T., 2000. Cloning and characterization of two promoters for the human calcium-sensing receptor (CaSR) and changes of CaSR expression in parathyroid adenomas. J. Biol. Chem. 275, 7553–7557.

Cinque, L., Sparaneo, A., Cetani, F., Coco, M., Clemente, C., Chetta, M., Balsamo, T., Battista, C., Sanpaolo, E., Pardi, E., D'Agruma, L., Marcocci, C., Maiello, E., Hendy, G.N., Cole, D.E.C., Scillitani, A., Guarnieri, V., 2017a. Novel association of MEN1 gene mutations with parathyroid carcinoma. Oncol Lett 14, 23–30.

Cinque, L., Sparaneo, A., Salcuni, A.S., de Martino, D., Battista, C., Logoluso, F., Palumbo, O., Cocchi, R., Maiello, E., Graziano, P., Hendy, G.N., Cole, D.E.C., Scillitani, A., Guarnieri, V., 2017b. MEN1 gene mutation with parathyroid carcinoma: first report of a familial case. Endocr Connect 6, 886–891.

Concolino, P., Costella, A., Capoluongo, E., 2015. Multiple endocrine neoplasia type 1 (MEN1): an update of 208 new germline variants reported in the last nine years. Cancer Genetics 209, 36–41.

Conigrave, A.D., Ward, D.T., 2013. Calcium-sensing receptor (CaSR): pharmacological properties and signaling pathways. Best Pract. Res. Clin. Endocrinol. Metabol. 27, 315–331.

Corbetta, S., Lania, A., Filopanti, M., Vicentini, L., Ballaré, E., Spada, A., 2002. Mitogen-activated protein kinase cascade in human normal and tumoral parathyroid cells. J. Clin. Endocrinol. Metab. 87, 2201–2205.

Corrado, K.R., Andrade, S.C., Bellizzi, J., D'Souza-Li, L., Arnold, A., 2015. Polyclonality of parathyroid tumors in neonatal severe hyperparathyroidism. J. Bone Miner. Res. 30, 1797–1802.

Costa-Guda, J., Arnold, A., 2007. Absence of stabilizing mutations of β-catenin encoded by CTNNB1 exon 3 in a large series of sporadic parathyroid adenomas. J. Clin. Endocrinol. Metab. 92, 1564–1566.

Costa-Guda, J., Arnold, A., 2014. Genetic and epigenetic changes in sporadic endocrine tumors: parathyroid tumors. Mol. Cell. Endocrinol. 386, 46–54.

Costa-Guda, J., Maroni, I., Molatore, S., Pellagata, N.S., Arnold, A., 2011. Somatic mutation and germline sequence abnormalities in CDKN1B, encoding p27Kip1, in sporadic parathyroid adenomas. J. Clin. Endocrinol. Metab. 96, E701–E706.

Costa-Guda, J., Imanishi, Y., Palanisamy, N., Kawamata, N., Koeffler, P.H., Chaganti, R.S., Arnold, A., 2013b. Allelic imbalance in sporadic parathyroid carcinoma and evidence for its de novo origins. Endocrine 44, 489–495.

Costa-Guda, J., Soong, C.P., Parekh, V.I., Agarwal, S.K., Arnold, A., 2013a. Germline and somatic mutations in cyclin-dependent kinase inhibitor genes CDKN1A, CDKN2B, and CDKN2C in sporadic parathyroid adenomas. Horm Cancer 4, 301–307.

Crabtree, J.S., Scacheri, P.C., Ward, J.M., Garrett-Beal, L., Emmert-Buck, M.R., Edgemon, K.A., Lorang, D., Libutti, S.K., Chandrasekharappa, S.C., Marx, S.J., Spiegel, A.M., Collins, F.S., 2001. A mouse model of multiple endocrine neoplasia type 1 develops multiple endocrine tumors. Proc. Natl. Acad. Sci. U.S.A. 98, 1118–1123.

Cromer, M.K., Starker, L.F., Choi, M., Udelsman, R., Nelson-Williams, C., Lifton, R.P., Carling, T., 2012. Identification of somatic mutations in parathyroid tumors using whole-exome sequencing. J. Clin. Endocrinol. Metab. 97, E1774–E1781.

Cryns, V.L., Rubio, M.P., Thor, A.D., Louis, D.N., Arnold, A., 1994a. p53 abnormalities in human parathyroid carcinoma. J. Clin. Endocrinol. Metab. 78, 1320–1324.

Cryns, V.L., Thor, A., Xu, H.J., Hu, S.X., Wierman, M.E., Vickery, A.L., Benedict, W.F., Arnold, A., 1994b. Loss of the retinoblastoma tumor suppressor gene in parathyroid carcinoma. N. Engl. J. Med. 330, 757–761.

Cryns, V.L., Yi, S.M., Tahara, H., Gaz, R.D., Arnold, A., 1995. Frequent loss of chromosome arm 1p DNA in parathyroid adenomas. Genes Chromosomes Cancer 13, 9–17.

Degenhardt, S., Toell, A., Weidmann, W., Dotzenrath, C., Spindler, K.D., 1998. Point mutations of the human parathyroid calcium receptor gene are not responsible for non-suppressible renal hyperparathyroidism. Kidney Int. 53, 556–561.

DeLellis, R.A., Arnold, A., Bilezikian, J.P., Eng, C., Larsson, C., Lloyd, R.V., Mete, O., 2017. Parathyroid carcinoma. In: Lloyd, R.V., Osamura, R.Y., Klöppel, G., Rosai, J. (Eds.), World Health Organization (WHO) Classification of Tumours of Endocrine Organs, fourth ed. IARC Press, Lyon, pp. 147–152.

Dotzenrath, C., Teh, B.T., Farnebo, F., Cupisti, K., Svensson, A., Toell, A., Goretzki, P., Larsson, C., 1996. Allelic loss of the retinoblastoma tumor suppressor gene: a marker for aggressive parathyroid tumors? J. Clin. Endocrinol. Metab. 81.

Dwight, T., Nelson, A.E., Theodosopoulos, G., Richardson, A.L., Learoyd, D.L., Philips, J., Delbridge, L., Zedenius, J., Teh, B.T., Larsson, C., Marsh, D.J., Robinson, B.G., 2002. Independent genetic events associated with the development of multiple parathyroid tumors in patients with primary hyperparathyroidism. Am. J. Pathol. 161, 1299−1306.

Eller-Vainicher, C., Chiodini, I., Battista, C., Viti, R., Mascia, M.L., Massironi, S., Peracchi, M., D'Agruma, L., Minisola, S., Corbetta, S., Cole, D.E.C., Spada, A., Scillitani, A., 2009. Sporadic and MEN1-related primary hyperparathyroidism: differences in clinical expression and severity. J. Bone Miner. Res. 24, 1404−1410.

Eng, C., Clayton, D., Schuffenecker, I., Lenoir, G., Cote, G., Gagel, R.F., van Amstel, H.K., Lips, C.J., Nishisho, I., Takai, S.I., Marsh, D.J., Robinson, B.G., Frank-Raue, K., Raue, F., Xue, F., Noll, W.W., Romei, C., Pacini, F., Fink, M., Niederle, B., Zedenius, J., Nordenskjöld, M., Komminoth, P., Hendy, G.N., Mulligan, L.M., 1996. The relationship between specific RET proto-oncogene mutations and disease phenotype in multiple neoplasia type 2. J. Am. Med. Assoc. 276, 1575−1579.

European Consortium on MEN1, 1997. Identification of the multiple endocrine neoplasia type 1 (MEN1) gene. Hum. Mol. Genet. 6, 1177−1183.

Ewen, M.E., Lamb, J., 2004. The activities of cyclin D1 that drive tumorigenesis. Trends Mol. Med. 10, 158−162.

Falchetti, A., Bale, A.E., Amorosi, A., Bordi, C., Cicchi, P., Bandini, S., Marx, S.J., Brandi, M.L., 1993. Progression of uremic hyperparathyroidism involves allelic loss on chromosome 11. J. Clin. Endocrinol. Metab. 76, 139−144.

Farnebo, F., Enberg, U., Grimelius, L., Backdahl, M., Schalling, M., Larsson, C., Farnebo, L.O., 1997. Tumor-specific decreased expression of calcium sensing receptor messenger ribonucleic acid in sporadic primary hyperparathyroidism. J. Clin. Endocrinol. Metab. 82, 3481−3486.

Farnebo, F., Teh, B.T., Kytölä, S., Svensson, A., Phelan, C., Sandelin, K., Thompson, N.W., Höög, A., Weber, G., Farnebo, L.O., Larsson, C., 1998a. Alterations of the MEN1 gene in sporadic parathyroid tumors. J. Clin. Endocrinol. Metab. 83, 2627−2630.

Farnebo, F., Hoog, A., Sandelin, K., Larsson, C., Farnebo, L.O., 1998b. Decreased expression of calcium-sensing receptor messenger ribonucleic acids in parathyroid adenomas. Surgery 124, 1094−1098.

Farnebo, F., Kytola, S., Teh, B.T., Dwight, T., Wong, F.K., Hoog, A., Elvius, M., Wassif, W.S., Thompson, N.W., Farnebo, L.O., Sandelin, K., Larsson, C., 1999. Alternative genetic pathways in parathyroid tumorigenesis. J. Clin. Endocrinol. Metab. 84, 3775−3780.

Fialkow, P.J., Jackson, C.E., Block, M.A., Greenawald, K.A., 1977. Multicellular origin of parathyroid "adenomas". N. Engl. J. Med. 297, 696−698.

Franklin, D.S., Godfrey, V.L., O' Brien, D.A., Deng, C., Xiong, Y., 2000. Functional collaboration between different cyclin-dependent kinase inhibitors suppresses tumor growth with distinct issue specificity. Mol. Cell Biol. 20, 6147−6156.

Friedman, E., Sakaguchi, K., Bale, A.E., Falchetti, A., Streeten, E., Zimering, M.B., Weinstein, L.S., McBride, W.O., Nakamura, Y., Brandi, M.-L., Norton, J.A., Aurbach, G.D., Spiegel, A.M., Marx, S.J., 1989. Clonality of parathyroid tumors in familial multiple endocrine neoplasia type 1. N. Engl. J. Med. 321, 213−218.

Friedman, E., Bale, A.E., Marx, S.J., Norton, J.A., Arnold, A., Tu, T., Aurbach, G.D., Spiegel, A.M., 1990. Genetic abnormalities in sporadic parathyroid adenomas. J. Clin. Endocrinol. Metab. 71, 293−297.

Fu, M., Wang, C., Li, Z., Sakamaki, T., Pestell, R.G., 2004. Cyclin D1: normal and abnormal functions. Endocrinology 145, 5439−5447.

Fujisawa, Y., Yamaguchi, R., Satake, E., Ohtaka, K., Nakanishi, T., Ozono, K., Ogata, T., 2013. Identification of AP2S1 mutation and effects of low calcium formula in an infant with hypercalcemia and hypercalciuria. J. Clin. Endocrinol. Metab. 98, E2022−E2027.

Geng, Y., Mosyak, L., Kurinov, I., Zuo, H., Sturchler, E., Cheng, T.C., Subramanyam, P., Brown, A.P., Brennan, S.C., Mun, H.C., Bush, M., Chen, Y., Nguyen, T.X., Cao, B., Chang, D.D., Quick, M., Conigrave, A.D., Colecraft, H.M., McDonald, P., Fan, Q.R., 2016. Structural mechanism of ligand activation in human calcium-sensing receptor. Elife 5, e13662 pii.

Gill, A.J., Clarkson, A., Gimm, O., Keil, J., Dralle, H., Howell, V.M., Marsh, D.J., 2006. Loss of nuclear expression of parafibromin distinguishes parathyroid carcinomas and hyperparathyroidism-jaw tumor (HPT-JT) syndrome-related adenomas from sporadic parathyroid adenomas and hyperplasias. Am. J. Surg. Pathol. 30, 1140−1149.

Gill, A.J., 2014. Understanding the genetic basis of parathyroid carcinoma. Endocr. Pathol. 25, 30−34.

Gogusev, J., Duchambon, P., Hory, B., Giovannini, M., Goureau, Y., Sarfati, E., Drueke, T., 1997. Depressed expression of calcium receptor in parathyroid gland tissue of patients with hyperparathyroidism. Kidney Int. 51, 328−336.

Gorvin, C.M., 2018. Insights into calcium-sensing receptor trafficking and biased signalling by studies of calcium homeostasis. J. Mol. Endocrinol. 61, R1−R12.

Gorvin, C.M., Cranston, T., Hannan, F.M., Rust, N., Qureshi, A., Nesbit, M.A., Thakker, R.V., 2016. A G-protein subunit-α11 loss-of-function mutations, Thr54Met, causes familial hypocalciuric hypercalcemia type 2 (FHH2). J. Bone Miner. Res. 31, 1200−1206.

Gorvin, C.M., Hannan, F.M., Cranston, T., Valta, H., Makitie, O., Schalin-Jantti, C., Thakker, R.V., 2018. Cianacalcet rectifies hypercalcemia in a patient with familial hypocalciuric hypercalcemia type 2 (FHH2) caused by a germline loss-of-function $G\alpha_{11}$ mutation. J. Bone Miner. Res. 33, 32−41.

Guan, B., Welch, J.M., Sapp, J.C., Ling, H., Li, Y., Johnston, J.J., Kebebew, E., Biesecker, L.G., Simonds, W.F., Marx, S.J., Agarwal, S.K., 2016. GCM2-activating mutations in familial isolated hyperparathyroidism. Am. J. Hum. Genet. 99, 1034−1044.

Guan, B., Welch, J.M., Vemulapalli, M., Li, Y., Ling, H., Kebebew, E., Simonds, W.F., Marx, S.J., Agarwal, S.K., 2017. Ethnicity of patients with germline GCM2-activating variants and primary hyperparathyroidism. J Endocr Soc 1, 488−499.

Guarnieri, V., Baorda, F., Battista, C., Bisceglia, M., Balsamo, T., Gruppioni, E., Fiorentino, M., Muscarella, L.A., Coco, M., Barbano, R., Corbetta, S., Spada, A., Cole, D.E.C., Canaff, L., Hendy, G.N., Carella, M., Scillitani, A., 2012a. A rare S33C mutation of CTNNB1 encoding β-catenin in a parathyroid adenoma found in an Italian parathyroid cohort. Endocrine 41, 152−155.

Guarnieri, V., Battista, C., Muscarella, L.A., Bisceglia, M., de Martino, D., Baorda, F., Maiello, E., D'Agruma, L., Chiodini, I., Clemente, C., Minisola, S., Romagnoli, E., Corbetta, S., Viti, R., Eller-Vainicher, C., Spada, A., Iacobellis, M., Malavolta, N., Carella, M., Canaff, L., Hendy, G.N.,

Cole, D.E.C., Scillitani, A., 2012b. *CDC73* mutations and parafibromin immunohistochemistry in parathyroid tumors: clinical correlations in a single-centre patient cohort. Cell. Oncol. 35, 411−422.

Guarnieri, V., Canaff, L., Yun, F.H.J., Scillitani, A., Battista, C., Muscarella, L.A., Wong, B.Y.L., Notarangelo, A., D'Agruma, L., Sacco, M., Cole, D.E.C., Hendy, G.N., 2010. Calcium-sensing receptor (*CASR*) mutations in hypercalcemic states: studies from a single endocrine clinic over three years. J. Clin. Endocrinol. Metab. 95, 1819−1829.

Guarnieri, V., Scillitani, A., Muscarella, L.A., Battista, C., Bonfitto, N., Bisceglia, M., Minisola, S., Mascia, M.L., D'Agruma, L., Cole, D.E.C., 2006. Diagnosis of parathyroid tumors in familial isolated hyperparathyroidism with HRPT2 mutation: implications for cancer surveillance. J. Clin. Endocrinol. Metab. 91, 2827−2832.

Guarnieri, V., Seaberg, R.M., Kelly, C., Davidson, M.J., Raphael, S., Shuen, A.Y., Baorda, F., Palumbo, O., Scillitani, A., Hendy, G.N., Cole, D.E.C., 2017. Large intragenic deletion of CDC73 (exons 4-10) in a three-generation hyperparathyroidism-jaw tumor (HPT-JT) syndrome family. BMC Med. Genet. 18, 83.

Guru, S.C., Goldsmith, P.K., Burns, A.L., Marx, S.J., Spiegel, A.M., Collins, F.C., Chandrasekharappa, S.C., 1998. Menin, the product of the MEN1 gene, is a nuclear protein. Proc. Natl. Acad. Sci. U.S.A. 95, 1630−1634.

Haglund, F., Andreasson, A., Nilsson, I.L., Hoog, A., Larsson, C., Juhlin, C.C., 2010. Lack of S37A CTNNB1/β-catenin mutations in a Swedish cohort of 98 parathyroid adenomas. Clin. Endocrinol. 73, 552−553.

Hakim, J.P., Levine, M.A., 1994. Absence of p53 point mutations in parathyroid adenoma and carcinoma. J. Clin. Endocrinol. Metab. 78, 103−106.

Hannan, F.M., Howles, S.A., Rogers, A., Cranston, T., Gorvin, C.M., Babinsky, V.N., Reed, A.A., Thakker, C.E., Bockenhauer, D., Brown, R.S., Connell, J.M., Cook, J., Darzy, K., Ehtisham, S., Graham, U., Hulse, T., Hunter, S.J., Izatt, L., Kumar, D., McKenna, M.J., McKnight, J.A., Morrison, P.J., Mughal, M.Z., O'Halloran, D., Pearce, S.H., Porteous, M.E., Rahman, M., Richardson, T., Robinson, R., Scheers, I., Siddique, H., Van't Hoff, W.G., Wang, T., Whyte, M.P., Nesbit, M.A., Thakker, R.V., 2015. Adaptor protein-2 sigma subunit mutations causing familial hypocalciuric hypercalcemia type 3 (FHH3) demonstrate genotype-phenotype correlations, codon bias and dominant-negative effects. Hum. Mol. Genet. 24, 5079−5092.

Hannan, F.M., Nesbit, M.A., Zhang, C., Cranston, T., Curley, A.J., Harding, B., Fratter, C., Rust, N., Christie, P.T., Turner, J.J., Lemos, M.C., Bowl, M.R., Bouillon, R., Brain, C., Bridges, N., Burren, C., Connell, J.M., Jung, H., Marks, E., McCredie, D., Mughal, Z., Rodda, C., Tollefsen, S., Brown, E.M., Yang, J.J., Thakker, R.V., 2012. Identification of 70 calcium-sensing receptor mutations in hyper-and hypo-calcemic patients: evidence for clustering of extracellular domain mutations at calcium-binding sites. Hum. Mol. Genet. 21, 2768−2778.

Harding, B., Lemos, M.C., Reed, A.A., Walls, G.V., Jeyabalan, J., Bowl, M.R., Tateossian, H., Sullivan, N., Hough, T., Fraser, W.D., Ansorge, O., Cheeseman, M.T., Thakker, R.V., 2009. Multiple endocrine neoplasia type 1 knockout mice develop parathyroid, pancreatic, pituitary and adrenal tumours with hypercalcaemia, hypophosphataemia and hypercorticosteronaemia. Endocr. Relat. Cancer 16, 1313−1327.

Hendy, G.N., 2019. Chapter 29. Calcium-sensing receptor. In: Bilezikian, J.P. (Ed.), Primer on the Metabolic Bone Diseases and Disorders of Mineral Metabolism, ninth ed. American Society for Bone and Mineral Research. John Wiley & Sons, Inc., pp. 221−229

Hendy, G.N., 2018. In: Feldman, D., Pike, W., Bouillon, R., Giovannucci, E., Goltzman, D., Hewison, M. (Eds.), Vitamin D, Biochemistry, Physiology and Diagnostics, fourth ed., vol. 1. Elsevier, pp. 477−495.

Hendy, G.N., Abi-Rafeh, J., Canaff, L., Troka, L., 2017. Osteoblast menin and bone mass: studies in conditional knockout mice. Osteoporos. Int. 28 (S1), P593.

Hendy, G.N., Canaff, L., 2016. Calcium-sensing receptor gene: regulation of expression. Front. Physiol. 7, 394.

Hendy, G.N., Canaff, L., Cole, D.E., 2013. The CASR gene: alternative splicing and transcriptional control, and calcium-sensing receptor (CaSR) protein: structure and ligand binding sites. Best Pract. Res. Clin. Endocrinol. Metabol. 27, 285−301.

Hendy, G.N., Canaff, L., Newfield, R.S., Tripto-Shkolnik, L., Wong, B.Y., Lee, B.S., Cole, D.E., 2014. Codon Arg15 mutations of the AP2S1 gene: common occurrence in familial hypocalciuric hypercalcemia cases negative for calcium-sensing receptor (CASR) mutations. J. Clin. Endocrinol. Metab. 99, E1311−E1315.

Hendy, G.N., Kaji, H., Canaff, L., 2009a. Cellular functions of menin. Adv. Exp. Med. Biol. 668, 37−50.

Hendy, G.N., Guarnieri, V., Canaff, L., 2009. Calcium-sensing receptor and associated diseases. Prog. Mol. Biol. Transl. Sci. 89, 31−95.

Hendy, G.N., Kronenberg, H.M., Potts Jr., J.T., Rich, A., 1981. Nucleotide sequence of cloned cDNAs encoding human pre-proparathyroid hormone. Proc. Natl. Acad. Sci. U.S.A. 78, 7365−7369.

Heppner, C., Kester, M.B., Agarwal, S.K., Debelenko, L.V., Emmert-Buck, M.R., Guru, S.C., Manickam, P., Olufemi, S.E., Skarulis, M.C., Doppman, J.L., Alexander, R.H., Kim, Y.S., Saggar, S.K., Lubensky, I.A., Zhuang, Z., Liotta, L.A., Chandrasekharappa, S.C., Collins, F.S., Spiegel, A.M., Burns, A.L., Marx, S.J., 1997. Somatic mutation of the MEN1 gene in parathyroid tumours. Nat. Genet. 16, 375−378.

Ho, C., Conner, D.A., Pollak, M.R., Ladd, D.J., Kifor, O., Warren, H.B., Brown, E.M., Seidman, J.G., Seidman, C.E., 1995. A mouse model of human familial hypocalciuric hypercalcemia and neonatal severe hyperparathyroidism. Nat. Genet. 11, 389−394.

Hobbs, M.R., Rosen, I.B., Jackson, C.E., 2002. Revised 14.7-cM locus for the hyperparathyroidism-jaw tumor syndrome gene, HRPT2. Am. J. Hum. Genet. 70, 1376−1377.

Hosokawa, Y., Arnold, A., 1998. Mechanism of cyclin D1 (CCND1, PRAD1) overexpression in human cancer cells: analysis of allele specific expression. Genes Chromosom. Cancer 22, 66−71.

Hosokawa, Y., Pollak, M.R., Brown, E.M., Arnold, A., 1995. Mutational analysis of the extracellular Ca2+-sensing receptor gene in human parathyroid tumors. J. Clin. Endocrinol. Metab. 80, 3107−3110.

Howell, V.M., Haven, C.J., Kahnoski, K., Khoo, S.K., Petillo, D., Chen, J., Fleuren, G.J., Robinson, B.G., Delbridge, L.W., Philips, J., Nelson, A.E., Krause, U., Hammje, K., Dralle, H., Hoang-Vu, C., Gimm, O., Marsh, D.J., Morreau, H., Teh, B.T., 2003. HRPT2 mutations are associated with malignancy in sporadic parathyroid tumours. J. Mol. Genet. 40, 657–663.

Howles, S.A., Hannan, F.M., Babinsky, V.N., Rogers, A., Gorvin, C.M., Rust, N., Richardson, T., McKenna, M.J., Nesbit, M.A., Thakker, R.V., 2016. Cinacalcet for symptomatic hypercalcemia caused by AP2S1 mutations. N. Engl. J. Med. 374 (14), 1396–1398.

Hsi, E., Zukerberg, L.R., Yang, W.I., Arnold, A., 1996. Cyclin D1 (PRAD1) expression in parathyroid adenomas: an immunohistochemical study. J. Clin. Endocrinol. Metab. 81, 1736–1739.

Hu, J., Spiegel, A.M., 2007. Structure and function of the human calcium-sensing receptor: insights from natural and engineered mutations and allosteric modulators. J. Cell Mol. Med. 11, 908–922.

Huang, J., Gurung, B., Wan, B., Matkar, S., Veniaminova, N.A., Wan, K., Merchant, J.L., Hua, X., Lei, M., 2012. The same pocket in menin binds both MLL and JUND but has opposite effects on transcription. Nature 482, 542–546.

Hughes, C.M., Rozenblatt-Rosen, O., Milne, T.A., Copeland, T.D., Levine, S.S., Lee, J.C., Hayes, D.N., Shanmugam, K.S., Bhattacharjee, A., Biondi, C.A., Kay, G.F., Hayward, N.K., Hess, J.L., Meyerson, M., 2004. Menin associates with a trithorax family histone methyltransferase complex and with the hoxc8 locus. Mol. Cell 13, 587–597.

Hussein, N., Casses, H., Fontaniere, S., Morera, A.M., Asensio, M.J., Bakeli, S., Lu, J.L., Coste, I., Di Clemente, N., Bertolino, P., Zhang, C.X., 2007. Reconstituted expression of menin in *Men1*-deficient mouse Leydig tumour cells induces cell cycle arrest and apoptosis. Eur. J. Cancer 43, 402–414.

Ikeda, S., Ishizaki, Y., Shimizu, Y., Fujimori, M., Ojima, Y., Okajima, M., Sugino, K., Asahara, T., 2002. Immunochemistry of cyclin D1 and β-catenin, and mutational analysis of exon 3 of β-catenin gene in parathyroid adenomas. Int. J. Oncol. 20, 463–466.

Imanishi, Y., Hosokawa, Y., Yoshimoto, K., Schipani, E., Mallya, S., Papanikolaou, A., Kifor, O., Tokura, T., Sablosky, M., Ledgard, F., Gronowicz, G., Wang, T.C., Schmidt, E.V., Hall, C., Brown, E.M., Bronson, R., Arnold, A., 2001. Primary hyperparathyroidism caused by parathyroid-targeted overexpression of cyclin D1 in transgenic mice. J. Clin. Investig. 107, 1093–1102.

Jackson, C.E., Cerny, J.C., Block, M.A., Fialkow, P.J., 1982. Probable clonal origin of aldosteronomas versus multicellular origin of parathyroid "adenomas". Surgery 92, 875–879.

Jackson, C.E., Norum, R.A., Boyd, S.B., Talpos, G.B., Wilson, S.D., Taggart, R.T., Mallette, L.E., 1990. Hereditary hyperparathyroidism and multiple ossifying jaw fibromas: a clinically and genetically distinct syndrome. Surgery 108, 1006–1012.

Juhlin, C.C., Larsson, C., Yakoleva, T., Leibiger, I., Leibiger, B., Alimov, A., Weber, G., Hoog, A., Villablanca, A., 2006. Loss of parafibromin expression in a subset of parathyroid adenomas. Endocr. Relat. Cancer 13, 509–523.

Juhlin, C.C., Villablanca, A., Sandelin, K., Haglund, F., Nordenström, J., Forsberg, L., Bränström, R., Obara, T., Arnold, A., Larsson, C., Höög, A., 2007. Parafibromin immunoreactivity – its use as an additional diagnostic marker for parathyroid tumour classification. Endocr. Relat. Cancer 14, 501–512.

Juhlin, C.C., Haglund, F., Villablanca, A., Forsberg, L., Sandelin, K., Bränström, R., Larsson, C., Höög, A., 2009. Loss of expression for the Wnt pathway components adenomatous polyposis coli and glycogen synthase kinase 3-beta in parathyroid carcinomas. Int. J. Oncol. 34, 481–492.

Kaji, H., Canaff, L., Goltzman, D., Hendy, G.N., 1999. Cell cycle regulation of menin expression. Cancer Res. 59, 5097–5101.

Kaji, H., Canaff, L., Lebrun, J.J., Goltzman, D., Hendy, G.N., 2001. Inactivation of menin, a Smad3-interacting protein, blocks transforming growth factor type β signaling. Proc. Natl. Acad. Sci. U.S.A. 98, 3837–3842.

Kanazawa, I., Canaff, L., Abi-Rafeh, J., Angrula, A., Li, J., Riddle, R.C., Boraschi- Diaz, I., Komarova, S.V., Clemens, T.L., Murshed, M., Hendy, G.N., 2015. Osteoblast menin regulates bone mass in vivo. J. Biol. Chem. 290, 3910–3924.

Karnik, S.K., Hughes, C.M., Gu, X., Rozenblatt-Rosen, O., McLean, G.W., Xiong, Y., Meyerson, M., Kim, S.K., 2005. Menin regulates pancreatic islet growth by promoting histone methylation and expression of genes encoding p27Kip1 and p18INK4c. Proc. Natl. Acad. Sci. U.S.A. 102, 14659–14664.

Kasaian, K., Wiseman, S.M., Thiessen, N., Mungall, K.L., Corbett, R.D., Qian, J.Q., Nip, K.M., He, A., Tse, K., Chuah, E., Varhol, R.J., Pandoh, P., McDonald, H., Zeng, T., Tam, A., Schein, J., Birol, I., Mungall, A.J., Moore, R.A., Zhao, Y., Hirst, M., Marra, M.A., Walker, B.A., Jones, S.J., 2013. Complete genomic landscape of a recurring sporadic parathyroid carcinoma. J. Pathol. 230, 249–260.

Kawata, T., Imanishi, Y., Kobayashi, K., Onoda, N., Takemoto, Y., Tahara, H., Okuno, S., Ishimura, E., Miki, T., Ishikawa, T., Inaba, M., Nishizawa, Y., 2005. Direct in vitro evidence of extracellular Ca2+-induced amino-terminal truncation of human parathyroid hormone (1-84) by human parathyroid cells. J. Clin. Endocrinol. Metab. 90, 5774–5778.

Kelly, T.G., Shattuck, T.M., Reyes-Mugica, M., Stewart, A.F., Simonds, W.F., Udelsman, R., Arnold, A., Carpenter, T.O., 2006. Surveillance for early detection of aggressive parathyroid disease: carcinoma and atypical adenoma in familial isolated hyperparathyroidism associated with germline HRPT2 mutation. J. Bone Miner. Metab. 21, 1666–1671.

Kifor, O., Moore, F.D., Wang, P., Goldstein, M., Vassilev, P., Kifor, I., Hebert, S., Brown, E.M., 1996. Reduced immunostaining for the extracellular Ca2+-receptor in primary and uremic secondary hyperparathyroidism. J. Clin. Endocrinol. Metab. 81, 1598–1606.

Kimura, T., Yoshimoto, K., Tanaka, C., Ohkura, T., Iwahana, H., Miyauchi, A., Sano, T., Itakura, M., 1996. Obvious mRNA and protein expression but absence of mutations of the RET proto-oncogene in parathyroid tumors. Eur. J. Endocrinol. 134, 314–319.

Kytola, S., Farnebo, F., Obara, T., Isola, J., Grimelius, L., Farnebo, L.O., Sandelin, K., Larsson, C., 2000. Patterns of chromosomal imbalances in parathyroid carcinomas. Am. J. Pathol. 157, 579–586.

Lacerte, A., Lee, E.H., Reynaud, R., Canaff, L., DeGuise, C., Devost, D., Ali, S., Hendy, G.N., Lebrun, J.J., 2004. Activin inhibits pituitary prolactin expression and cell growth through Smads, Pit-1 and Menin. Mol. Endocrinol. 18, 1558–1569.

Larsson, C., Skogseid, B., Oberg, K., Nakamura, Y., Nordenskjold, M., 1988. Multiple endocrine neoplasia type 1 gene maps to chromosome 11 and is lost in insulinoma. Nature 332, 85–87.

Law Jr., W.M., Heath III, H., 1985. Familial benign hypercalcemia (hypocalciuric hypercalcemia). Clinical and pathogenic studies in 21 families. Ann. Intern. Med. 102, 511–519.

Leach, K., Gregory, K.J., Kufareva, I., Khajehali, E., Cook, A.E., Abagyan, R., Conigrave, A.D., Sexton, P.M., Christopoulos, A., 2016. Towards a structural understanding of allosteric drugs at the human calcium-sensing receptor. Cell Res. 26, 574–592.

Lemos, M.C., Thakker, R.V., 2008. Multiple endocrine neoplasia type 1 (MEN1): analysis of 1336 mutations reported in the first decade following identification of the gene. Hum. Mutat. 29, 22–32.

Li, D., Opas, E.E., Tuluc, F., Metzger, D.L., Hou, C., Hakonarson, H., Levine, M.A., 2014. Autosomal dominant hypoparathyroidism caused by germline mutation in GNA11: phenotypic and molecular characterization. J. Clin. Endocrinol. Metab. 99, E1774–E1783.

Libutti, S.K., Crabtree, J.S., Lorang, D., Burns, A.L., Mazzanti, C., Hewitt, S.M., O'Connor, S., Ward, J.M., Emmert-Buck, M.R., Remaley, A., Miller, M., Turner, E., Alexander, H.R., Arnold, A., Marx, S.J., Collins, F.S., Spiegel, A.M., 2003. Parathyroid gland-specific deletion of the mouse Men1 gene results in parathyroid neoplasia and hypercalcemic hyperparathyroidism. Cancer Res. 63, 8022–8028.

Lin, L., Czapiga, M., Nini, L., Zhang, J.H., Simonds, W.F., 2007. Nuclear localization of the parafibromin tumor suppressor protein implicated in the hyperparathyroidism-jaw tumor syndrome enhances its proapoptotic function. Mol. Canc. Res. 5, 183–193.

Liu, P., Lee, S., Knoll, J., Rauch, A., Ostermay, S., Luther, J., Malkusch, N., Lerner, U.H., Zaiss, M.M., Neven, M., Wittig, R., Rauner, M., David, J.P., Bertolino, P., Zhang, C.X., Tuckermann, J.P., 2017. Loss of menin in osteoblast lineage affects osteocyte-osteoclast crosstalk causing osteoporosis. Cell Death Differ. 24, 672–682.

Lloyd, R.V., Arnold, A., Gill, A., Morreau, H., 2017. Hyperparathyroidism-jaw tumour syndrome. In: Lloyd, R.V., Osamura, R.Y., Klöppel, G., Rosai, J. (Eds.), World Health Organization (WHO) Classification of Tumours of Endocrine Organs, fourth ed. IARC Press, Lyon, pp. 255–256.

Loffler, K.A., Biondi, C.A., Gartside, M.G., Serewko-Auret, M.M., Duncan, R., Tonks, I.D., Mould, A.W., Waring, P., Muller, H.K., Kay, G.F., Hayward, N.K., 2007a. Lack of augmentation of tumor spectrum or severity in dual heterozygous Men1 and Rb1 knockout mice. Oncogene 26, 4009–4017.

Loffler, K.A., Biondi, C.A., Gartside, M., Waring, P., Starkm, M., Serewko-Auret, M.M., Muller, H.K., Hayward, N.K., Kay, G.F., 2007b. Broad tumor spectrum in a mouse model of multiple endocrine neoplasia type 1. Int. J. Cancer 120, 259–267.

Loffler, K.A., Mould, A.W., Waring, P.M., Hayward, N.K., Kay, G.F., 2012. Menin and p53 have non-synergistic effects on tumorigenesis in mice. BMC Canc. 12, 252.

Lourenço Jr., D.M., Coutinho, F.L., Toledo, R.A., Montenegro, F.L., Correia-Deur, J.E., Toledo, S.P., 2010. Early-onset, progressive, frequent, extensive, and severe bone mineral and renal complications in multiple endocrine neoplasia type 1-associated primary hyperparathyroidism. J. Bone Miner. Res. 25, 2382–2391.

Lubensky, I.A., Debelenko, L.V., Zhuang, Z., Emmert-Buck, M.R., Dong, Q., Chandrasekharapp, a S., Guru, S.C., Manickam, P., Olufemi, S.E., Marx, S.J., Spiegel, A.M., Collins, F.S., Liotta, L.A., 1996. Allelic deletions on chromosome 11q13 in multiple tumors from individual MEN1 patients. Cancer Res. 56, 5272–5278.

Mallya, S.M., Gallagher, J.J., Wild, Y.K., Kifor, O., Costa-Guda, J., Saucier, K., Brown, E.M., Arnold, A., 2005. Abnormal parathyroid cell proliferation precedes biochemical abnormalities in a mouse model of primary hyperparathyroidism. Mol. Endocrinol. 19, 2603–2609.

Mallya, S.M., Wu, H.I., Saria, E.A., Corrado, K.R., Arnold, A., 2010. Tissue-specific regulatory regions of the PTH gene localized by novel chromosome 11 rearrangement breakpoints in a parathyroid adenoma. J. Bone Miner. Res. 25, 2606–2612.

Mannstadt, M., Harris, M., Bravenboer, B., Chitturi, S., Dreijerink, K.M., Lambright, D.G., Lim, E.T., Daly, M.J., Gabriel, S., Jüppner, H., 2013. Germline mutations affecting Gα11 in hypoparathyroidism. N. Engl. J. Med. 368, 2532–2534.

Marsh, D.J., Zheng, Z., Arnold, A., Andrew, S.D., Learoyd, D., Frilling, A., Komminoth, P., Neumann, H.P., Ponder, B.A., Rollins, B.J., Shapiro, G.I., Robinson, B.G., Mulligan, L.M., Eng, C., 1997. Mutation analysis of glial cell line-derived neurotrophic factor, a ligand for a RET/coreceptor complex, in multiple endocrine neoplasia type 2 and sporadic neuroendocrine tumors. J. Clin. Endocrinol. Metab. 82, 3025–3028.

Marx, S.J., 2017. Calcimimetic use in familial hypocalciuric hypercalcemia-A perspective in endocrinology. J. Clin. Endocrinol. Metab. 102, 3933–3936.

Marx, S.J., 2018. Familial hypocalciuric hypercalcemia as an atypical form of primary hyperparathyroidism. J. Bone Miner. Res. 33, 27–31.

Marx, S.J., Attie, M.F., Levine, M.A., Spiegel, A.M., Downs Jr., R.W., Lasker, R.D., 1981. The hypocalciuric or benign variant of familial hypercalcemia: clinical and biochemical features in fifteen kindreds. Medicine 60, 397–412.

Masi, G., Iacobone, M., Sinigaglia, A., Mantelli, B., Pennelli, G., Castagliuolo, I., Palù, G., Barzon, L., 2014. Characterization of a new CDC73 missense mutation that impairs parafibromin expression and nucleolar localization. PLoS One 9, e97994.

Matkar, S., Thiel, A., Hua, X., 2013. Menin: a scaffold protein that controls gene expression and cell signaling. Trends Biochem. Sci. 38, 394–402.

Mayr, B., Schnabel, D., Dörr, H.G., Schöfl, C., 2016. Genetics in Endocrinology: gain and loss of function mutations of the calcium-sensing receptor and associated proteins: current treatment concepts. Eur. J. Endocrinol. 174, R189–R208.

Mehta, A., Patel, D., Rosenberg, A., Boufraqech, M., Ellis, R.J., Nilubol, N., Quezado, M.M., Marx, S.J., Simonds, W.F., Kebebew, E., 2014. Hyperparathyroidism-jaw tumor syndrome: results of operative management. Surgery 156, 1315–1324.

Milne, T.A., Hughes, C.M., Lloyd, R., Yang, Z., Rozenblatt-Rosen, O., Dou, Y., Schnepp, R.W., Krankel, C., Livolsi, V.A., Gibbs, D., Hua, X., Roeder, R.G., Meyerson, M., Hess, J.L., 2005. Menin and MLL cooperatively regulate expression of cyclin-dependent kinase inhibitors. Proc. Natl. Acad. Sci. U.S.A. 102, 749–754.

Mingione, A., Verdelli, C., Ferrero, S., Vaira, V., Guarnieri, V., Scillitani, A., Vicentini, L., Balza, G., Beretta, E., Terranegra, A., Vezzoli, G., Soldati, L., Corbetta, S., 2017. Filamin A is reduced and contributes to the CASR sensitivity in human parathyroid tumors. J. Mol. Endocrinol. 58, 91–103.

Mosimann, C., Hausmann, G., Basler, K., 2006. Parafibromin/Hydrax activates Wnt/Wg target gene transcription by direct association with β-catenin/Armadillo. Cell 125, 327–341.

Motokura, T., Arnold, A., 1993. PRAD1/cyclin D1 proto-oncogene: genomic organization, 5′ DNA sequence, and sequence of a tumor-specific rearrangement breakpoint. Genes Chromosomes Cancer 7, 89–95.

Motokura, T., Bloom, T., Kim, H.G., Juppner, H., Ruderman, J.V., Kronenberg, H.M., Arnold, A., 1991. A novel cyclin encoded by a bcll-linked candidate oncogene. Nature 350, 512–515.

Murai, M.J., Chruszcz, M., Reddy, G., Grembecka, J., Cierpicki, T., 2011. Crystal structure of menin reveals binding site for mixed lineage leukemia (MLL) protein. J. Biol. Chem. 286, 31742–31748.

Naito, J., Kaji, H., Sowa, H., Kitazawa, R., Kitazawa, S., Tsukada, T., Hendy, G.N., Sugimoto, T., Chihara, K., 2006. Expression and functional analysis of menin in a multiple endocrine neoplasia type 1 (MEN1) patient with somatic loss of heterozygosity in chromosome 11q13 and unidentified germline mutation of the MEN1 gene. Endocrine 29, 485–490.

Naveh-Many, T., 2010. Minireview: the play of proteins on the parathyroid hormone messenger ribonucleic acid regulates its expression. Endocrinology 151, 1398–1402.

Nemeth, E.F., Goodman, W.G., 2016. Calcimimetic and calcilytic drugs: feats, flops, and futures. Calcif. Tissue Int. 98, 341–358.

Nemeth, E.F., Shoback, D., 2013. Calcimimetic and calcilytic drugs for treating bone and mineral-related disorders. Best Pract. Res. Clin. Endocrinol. Metabol. 27, 373–384.

Nesbit, M.A., Hannan, F.M., Howles, S.A., Babinsky, V.N., Head, R.A., Cranston, T., Rust, N., Hobbs, M.R., Heath 3rd, H., Thakker, R.V., 2013a. Mutations affecting G-protein subunit α11 in hypercalcemia and hypocalcemia. N. Engl. J. Med. 368, 2476–2486.

Nesbit, M.A., Hannan, F.M., Howles, S.A., Reed, A.A., Cranston, T., Thakker, C.E., Gregory, L., Rimmer, A.J., Rust, N., Graham, U., Morrison, P.J., Hunter, S.J., Whyte, M.P., McVean, G., Buck, D., Thakker, R.V., 2013b. Mutations in AP2S1 cause familial hypocalciuric hypercalcemia type 3. Nat. Genet. 45, 93–97.

Newey, P.J., Nesbit, M.A., Rimmer, A.J., Attar, M., Head, R.T., Christie, P.T., Gorvin, C.M., Stechman, M., Gregory, L., Mihai, R., Sadler, G., McVean, G., Buck, D., Thakker, R.V., 2012. Whole-exome sequencing studies of nonhereditary (sporadic) parathyroid adenomas. J. Clin. Endocrinol. Metab. 97, E1995–E2005.

Nussbaum, S.R., Gaz, R.D., Arnold, A., 1990. Hypercalcemia and ectopic secretion of parathyroid hormone by an ovarian carcinoma with rearrangement of the gene for parathyroid hormone. N. Engl. J. Med. 323, 1324–1328.

Orndal, C., Johansson, M., Heim, S., Mandahl, N., Mansson, B., Alumets, J., Mitelman, F., 1990. Parathyroid adenoma with t(1:5)(p22:q32) as the sole clonal chromosomal abnormality. Cancer Genet. Cytogenet. 48, 225–228.

Palanisamy, N., Imanishi, Y., Rao, P.H., Tahara, H., Chaganti, R.S., Arnold, A., 1998. Novel chromosomal abnormalities identified by comparative genomic hybridization in parathyroid adenomas. J. Clin. Endocrinol. Metab. 83, 1766–1770.

Pandya, C., Uzilov, A.V., Bellizzi, J., Lau, C.Y., Moe, A.S., Strahl, M., Hamou, W., Newman, L.C., Fink, M.Y., Antipin, Y., Yu, W., Stevenson, M., Cavaco, B.M., The, B.T., Thakker, R.V., Morreau, H., Schadt, E.E., Sebra, R., Li, S.D., Arnold, A., Chen, R., 2017. Genomic profiling reveals mutational landscape in parathyroid carcinomas. JCI Insight 2, e92061.

Panicker, L.M., Zhang, J.H., Dagur, P.K., Gastinger, M.J., Simonds, W.F., 2010. Defective nucleolar localization and dominant interfering properties of a parafibromin L95P missense mutant causing the hyperparathyroidism-jaw tumor syndrome. Endocr. Relat. Cancer 17, 513–524.

Pannett, A.A.J., Kennedy, A.M., Turner, J.J., Forbes, S.A., Cavaco, B.M., Bassett, J.H., Cianferotti, L., Harding, B., Shine, B., Flinter, F., Maidment, C.G., Trembath, R., Thakker, R.V., 2003. Multiple endocrine neoplasia type 1 (MEN1) germline mutations in familial isolated primary hyperparathyroidism. Clin. Endocrinol. 58, 639–646.

Parfitt, A.M., 1994. Parathyroid growth, normal and abnormal. In: Bilezekian, J.P., Marcus, R., Levine, M.A. (Eds.), The Parathyroids. Raven Press, New York, pp. 373–405.

Pausova, Z., Soliman, E., Amizuka, N., Janicic, N., Konrad, E.M., Arnold, A., Goltzman, D., Hendy, G.N., 1996. Role of the RET proto-oncogene in sporadic hyperparathyroidism and in hyperparathyroidism of multiple endocrine neoplasia type 2. J. Clin. Endocrinol. Metab. 81, 2711–2718.

Pazienza, V., la Torre, A., Baorda, F., Alfarano, M., Chetta, M., Muscarella, L.A., Battista, C., Copetti, M., Kotzot, D., Kapelari, K., Al-Abdulrazzaq, D., Perlman, K., Sochett, E., Cole, D.E.C., Pellegrini, F., Canaff, L., Hendy, G.N., D'Agruma, L., Zelante, L., Carella, M., Scillitani, A., Guarnieri, V., 2013. Identification and functional characterization of three NoLS (nucleolar localization signal) mutations of the *CDC73* gene. PLoS One 8, e82292.

Pearce, S.H.S., Trump, D., Wooding, C., Sheppard, M.N., Clayton, R.N., Thakker, R.V., 1996. Loss of heterozygosity studies at the retinoblastoma and breast cancer susceptibility (BRCA2) loci in pituitary, parathyroid, pancreatic and carcinoid tumours. Clin. Endocrinol. 45, 195–200.

Pellegata, N.S., 2012. MENX and MEN4. Clinics 67 (Suppl. 1), 13–18.

Pellegata, N.S., Quintanilla-Martinez, L., Samson, E., Siggelkow, H., Bink, K., Graw, J., Hofler, H., Atkinson, M.J., 2006. Germ-line mutations in p27Kip1 cause a multiple endocrine neoplasia syndrome in rats and humans. Proc. Natl. Acad. Sci. U.S.A. 103, 15558–15563.

Pi, M., Chen, L., Huang, M., Lou, Q., Quarles, L.D., 2008. Parathyroid-specific interaction of the calcium-sensing receptor and G-alpha q. Kidney Int. 74, 1548–1556.

Pidasheva, S., Canaff, L., Simonds, W.F., Marx, S.J., Hendy, G.N., 2005. Impaired cotranslational process of the calcium-sensing receptor due to signal peptide missense mutations in familial hypocalciuric hypercalcemia. Hum. Mol. Genet. 14, 1679–1690.

Pidasheva, S., Grant, M., Canaff, L., Ercan, O., Kumar, U., Hendy, G.N., 2006. Calcium-sensing receptor dimerizes in the endoplasmic teticulum: biochemical and biophysical characterization of CASR mutants is retained intracellularly. Hum. Mol. Genet. 15, 2200–2209.

Piret, S.E., Gorvin, C.M., Pagnamenta, A.T., Howles, S.A., Cranston, T., Rust, N., Nesbit, M.A., Glaser, B., Taylor, J.C., Buchs, A.E., Hannan, F.M., Thakker, R.V., 2016. Identification of a G-protein subunit-α11 gain-of-function mutation, Val340Met, in a family with autosomal dominant hypocalcemia type 2 (ADH2). J. Bone Miner. Res. 31, 1207–1214.

Pollak, M.R., Brown, E.M., Chou, Y.H.W., Hebert, S.C., Marx, S.J., Steinmann, B., Levi, T., Seidman, C.E., Seidman, J.G., 1993. Mutations in the human Ca21-sensing receptor gene cause familial hypocalciuric hypercalcemia and neonatal severe hyperparathyroidism. Cell 75, 1297−1303.

Pollak, M.R., Chou, Y.H.W., Marx, S.J., Steinmann, B., Cole, D.E.C., Brandi, M.L., Papapoulos, S.E., Menko, F.H., Hendy, G.N., Brown, E.M., Seidman, C.E., Seidman, J.G., 1994. Familial hypocalciuric hypercalcemia and neonatal severe hyperparathyroidism. Effects of mutant gene dosage on phenotype. J. Clin. Investig. 93, 1108−1112.

Quinn, S.J., Kifor, O., Kifor, I., Butters Jr., R.R., Brown, E.M., 2007. Role of the cytoskeleton in extracellular calcium-regulated PTH release. Biochem. Biophys. Res. Commun. 354, 8−13.

Ray, K., 2015. Calcium-sensing receptor: trafficking, endocytosis, recycling, and importance of interacting proteins. Prog Mol Biol Transl Sci 132, 127−150.

Reh, C.M., Hendy, G.N., Cole, D.E., Jeandron, D.D., 2011. Neonatal hyperparathyroidism with a heterozygous calcium-sensing receptor (CASR) R185Q mutation: clinical benefit from cinacalcet. J. Clin. Endocrinol. Metab. 96, E707−E712.

Rogers, K.V., Dunn, C.K., Conklin, R.L., Hadfield, S., Petty, B.A., Brown, E.M., Hebert, S.C., Nemeth, E.F., Fox, J., 1995. Calcium receptor messenger ribonucleic acid levels in the parathyroid glands and kidney of vitamin D-deficient rats are not regulated by plasma calcium or 1,25-dihydroxyvitamin D3. Endocrinology 136, 499−504.

Rosai, J., DeLellis, R.A., Carcangiu, M.L., Frable, W.J., Tallini, G., 2014. Tumors of the Thyroid and Parathyroid Glands. AFIP Atlas of Tumor Pathology. Fourth Series, Fascicle 21. American Registry of Pathology, Silver Spring, MD, pp. 543−560.

Rosenberg, C.L., Kim, H.G., Shows, T.B., Kronenberg, H.M., Arnold, A., 1991. Rearrangement and overexpression of D11S287E, a candidate oncogene on chromosome 11q13 in benign parathyroid tumors. Oncogene 6, 449−453.

Rosenberg, C.L., Motokura, T., Kronenberg, H.M., Arnold, A., 1993. Coding sequence of the overexpressed transcript of the putative oncogene PRAD1/cyclin D1 in two primary human tumors. Oncogene 8, 519−521.

Rozenblatt-Rosen, O., Hughes, C.M., Nannepaga, S.J., Shanmugam, K.S., Copeland, T.D., Guszczynski, T., Resau, J.H., Meyerson, M., 2005. The parafibromin tumor suppressor protein is part of a human Paf1 complex. Mol. Cell Biol. 25, 612−620.

Samander, E.H., Arnold, A., 2006. Mutational analysis of the vitamin D receptor does not support its candidacy as a tumor suppressor gene in parathyroid adenomas. J. Clin. Endocrinol. Metab. 91, 5019−5021.

Semba, S., Kusumi, R., Moriya, Sasano, H., 2000. Nuclear accumulation of β-catenin in human endocrine tumors: association with Ki-67 (MIB-1) proliferative activity. Endocr. Pathol. 11, 243−250.

Shattuck, T.H., Costa, J., Bernstein, M., Jensen, R.T., Chung, D.C., Arnold, A., 2002. Mutational analysis of Smad3, a candidate tumor suppressor implicated in TGF-β and menin pathways, in parathyroid adenomas and enetropancreatic endocrine tumors. J. Clin. Endocrinol. Metab. 87, 3911−3914.

Shattuck, T.M., Valimaki, S., Obara, T., Gaz, R.D., Clark, O.H., Shoback, D., Wierman, M.E., Tojo, K., Robbins, C.M., Carpten, J.D., Farnebo, L.O., Larsson, C., Arnold, A., 2003a. Somatic and germ-line mutations of the HRPT2 gene in sporadic parathyroid carcinoma. N. Engl. J. Med. 349, 1722−1729.

Shattuck, T.M., Kim, T.S., Costa, J., Yandell, D.W., Imanishi, Y., Palanisamy, N., Gaz, R.D., Shoback, D., Clark, O.H., Monchik, J.M., Wierman, M.E., Hollenberg, A., Tojo, K., Chaganti, R.S.K., Arnold, A., 2003b. Mutational analyses of RB and BRCA2 as candidate tumour suppressor genes in parathyroid carcinoma. Clin. Endocrinol. 59, 180−189.

Sherr, C.J., 1996. Cancer cell cycles. Science 274, 1672−1677.

Sherr, C.J., Beach, D., Shapiro, G.I., 2016. Targeting CDK4 and CDK6: from discovery to therapy. Cancer Discov. 6, 353−367.

Shi, Y., Hogue, J., Dixit, D., Koh, J., Olson Jr., J.A., 2014. Functional and genetic studies of isolated cells from parathyroid tumors reveal the complex pathogenesis of parathyroid neoplasia. Proc. Natl. Acad. Sci. U. S. A. 111, 3092−3097.

Shi, Y., Azimzadeh, P., Jamingal, S., Wentworth, S., Ferlitch, J., Koh, J., Balenga, N., Olson Jr., J.A., 2018. Polyclonal origin of parathyroid tumors is common and is associated with multiple gland disease in primary hyperparathyroidism. Surgery 163, 9−14.

Shilo, V., Ben-Dov, I.Z., Nechama, M., Silver, J., Naveh-Many, T., 2015. Parathyroid-specific deletion of dicer-dependent microRNAs abrogates the response of the parathyroid to acute and chronic hypocalcemia and uremia. FASEB J. 29, 3964−3976.

Shimazu, S., Nagamura, Y., Yaguchi, H., Ohkura, N., Tsukada, T., 2011. Correlation of mutant menin stability with clinical expression of multiple endocrine neoplasia type 1 and its incomplete forms. Cancer Sci. 102, 2097−2102.

Simonds, W.F., James-Newton, L.A., Agarwal, S.K., Yang, B., Skarulis, M.C., Hendy, G.N., Marx, S.J., 2002. Familial isolated hyperparathyroidism: clinical and genetic characteristics of 36 kindreds. Medicine 81, 1−26.

Simonds, W.F., Robbins, C.M., Agarwal, S.K., Hendy, G.N., Carpten, J.D., Marx, S.J., 2004. Familial isolated hyperparathyroidism is rarely caused by germline mutation in HRPT2, the gene for the hyperparathyroidism-jaw tumor syndrome. J. Clin. Endocrinol. Metab. 89, 96−102.

Sowa, H., Kaji, H., Kitazawa, R., Kitazawa, S., Tsukamoto, T., Yano, S., Canaff, L., Hendy, G.N., Sugimoto, T., Chihara, K., 2004. Menin inactivation leads to loss of TGF-β inhibition of parathyroid cell proliferation and PTH secretion. Cancer Res. 64, 2222−2228.

Starker, L.F., Fonseca, A.L., Akerström, G., Björklund, P., Westin, G., Carling, T., 2012. Evidence of a stabilizing mutation of β-catenin encoded by CTNNB1 exon 3 in a large series of sporadic parathyroid adenomas. Endocrine 42, 612−615.

Svedlund, J., Aurén, M., Sundström, M., Dralle, H., Akerström, G., Björklund, P., Westin, G., 2010. Aberrant WNT/β-catenin signaling in parathyroid carcinoma. Mol. Canc. 9, 294.

Szabo, J., Heath, B., Hill, V.M., Jackson, C.E., Zarbo, R.J., Mallette, L.E., Chew, S.L., Besser, G.M., Thakker, R.V., Huff, V., Leppert, M.F., Heath III., H., 1995. Hereditary hyperparathyroidism-jaw syndrome: the endocrine tumor gene HRPT2 maps to chromosome 1q21-q31. Am. J. Hum. Genet. 56, 944−950.

Tahara, H., Smith, A.P., Gaz, R.D., Cryns, V.L., Arnold, A., 1996a. Genomic localization of novel candidate tumor suppressor gene loci in human parathyroid adenomas. Cancer Res. 56, 599–605.

Tahara, H., Smith, A.P., Gaz, R.D., Arnold, A., 1996b. Loss of chromosome arm 9p DNA and analysis of the p16 and p15 cyclin-dependent kinase inhibitor genes in human parathyroid adenomas. J. Clin. Endocrinol. Metab. 81, 3663–3667.

Tahara, H., Smith, A.P., Gaz, R.D., Zariwala, M., Xiong, Y., Arnold, A., 1997. Parathyroid tumor suppressor on 1p: analysis of the p18 cyclin-dependent kinase inhibitor gene as a candidate. J. Bone Miner. Res. 12, 1330–1334.

Tan, M.H., Morrison, C., Wang, P., Yang, X., Haven, C.J., Zhang, C., Zhao, P., Tretiakova, M.S., Korpi-Hvovalti, F., Burgess, J.R., Soo, K.C., Cheah, W.K., Cao, B., Resau, J., Morreau, H., Teh, B.T., 2004. Loss of parafibromin immunoreactivity is a distinguishing feature of parathyroid carcinoma. Clin. Cancer Res. 10, 6629–6637.

Tanaka, C., Uchino, S., Noguchi, S., Nishioka, T., Yamasaki, H., Hashimoto, K., Yoshimoto, K., 2002. Biallelic inactivation by somatic mutations of the MEN1 gene in sporadic parathyroid tumors. Cancer Lett. 175, 175–179.

Tenhola, S., Hendy, G.N., Valta, H., Canaff, L., Lee, B.S., Wong, B.,Y., Välimäki, M.J., Cole, D.E., Mäkitie, O., 2015. Cinacalcet treatment in an adolescent with concurrent 22q11.2 deletion syndrome and familial hypocalciuric hypercalcemia type 3 caused by AP2S1 mutation. J. Clin. Endocrinol. Metab. 100, 2515–2518.

Thakker, R.V., 2010. Multiple endocrine neoplasia type 1 (MEN1). Best Pract. Res. Clin. Endocrinol. Metabol. 24, 355–370.

Thakker, R.V., 2014. Multiple endocrine neoplasia type 1 (MEN1) and type 4 (MEN4). Mol. Cell. Endocrinol. 386, 2–15.

Thakker, R.V., Bouloux, P., Wooding, C., Chotal, K., Broad, P.M., Spurr, N.K., Besser, G.M., O'Riordan, J.L.H., 1989. Association of parathyroid tumors in multiple endocrine neoplasia type 1 with loss of alleles on chromosome 11. N. Engl. J. Med. 321, 218–224.

Thompson, D.B., Samowitz, W.S., Odelberg, S., Davis, R.K., Szabo, J., Heath III., H., 1995. Genetic abnormalities in sporadic parathyroid adenomas: loss of heterozygosity for chromosome 3q markers flanking the calcium receptor locus. J. Clin. Endocrinol. Metab. 80, 3377–3380.

Timmers, H.J., Karperien, M., Hamdy, N.A., de Boer, H., Hermus, A.R., 2006. Normalization of serum calcium by cinacalcet in a patient with hypercalcemia due to a de novo inactivating mutation of the calcium-sensing receptor. J. Intern. Med. 260, 177–182.

Tominaga, Y., Tsuzuki, T., Uchida, K., Haba, T., Otsuka, S., Ichimori, I., Yamada, K., Numano, M., Tanaka, Y., Takagi, H., 1999. Expression of PRAD1/cyclin D1, retinoblastoma gene products, and Ki67 in parathyroid hyperplasia caused by chronic renal failure versus primary adenoma. Kidney Int. 55, 1375–1383.

VanHouten, J.N., Yu, N., Rimm, D., Dotto, J., Arnold, A., Wysolmerski, J.J., Udelsman, R., 2006. Hypercalcemia of malignancy due to ectopic transactivation of the parathyroid hormone gene. J. Clin. Endocrinol. Metab. 91, 580–583.

Vargas-Poussou, R., Mansour-Hendili, L., Baron, S., Bertocchio, J.P., Travers, C., Simian, C., Treard, C., Baudouin, V., Beltran, S., Broux, F., Camard, O., Cloarec, S., Cormier, C., Debussche, X., Dubosclard, E., Eid, C., Haymann, J.P., Kiando, S.R., Kuhn, J.M., Lefort, G., Linglart, A., Lucas-Pouliquen, B., Macher, M.A., Maruani, G., Ouzounian, S., Polak, M., Requeda, E., Robier, D., Silve, C., Souberbielle, J.C., Tack, I., Vezzosi, D., Jeunemaitre, X., Houillier, P., 2016. Familial hypocalciuric hypercalcemia types 1 and 3 and primary hyperparathyroidism: similarities and differences. J. Clin. Endocrinol. Metab. 101, 2185–2195.

Vasef, M.A., Brynes, R.K., Sturm, M., Bromley, C., Robinson, R.A., 1999. Expression of cyclin D1 in parathyroid carcinomas, adenomas, and hyperplasias: a paraffin immunohistochemical study. Mol. Pathol. 12, 412–416.

Vasicek, T.J., McDevitt, B.E., Freeman, M.W., Fennick, B.J., Hendy, G.N., Potts Jr., J.T., Rich, A., Kronenberg, H.M., 1983. Nucleotide sequence of the human parathyroid hormone gene. Proc. Natl. Acad. Sci. U.S.A. 80, 2127–2131.

Villablanca, A., Calendar, A., Forsberg, L., Hoog, A., Cheng, J.-D., Petillo, D., Bauters, C., Kahnoski, K., Ebeling, T., Salmela, P., Richardson, A.-L., Delbridge, L., Meyrier, A., Proye, C., Carpten, J.D., Teh, B.T., Robinson, B.G., Larsson, C., 2004. Germline and de novo mutations in the HRPT2 tumour suppressor gene in familial isolated hyperparathyroidism. J. Med. Genet. 41, e32.

Vogelstein, B., Kinzler, K.W., 2004. Cancer genes and the pathways they control. Nat. Med. 10, 789–799.

Walls, G.V., Stevenson, M., Lines, K.E., Newey, P.J., Reed, A.A.C., Bowl, M.R., Jeyabalan, J., Harding, B., Bradley, K.J., Manek, S., Chen, J., Wang, P., Williams, B.O., Teh, B.T., Thakker, R.V., 2017. Mice deleted for cell division cycle 73 gene develop parathyroid and uterine tumours: model for the hyperparathyroidism-jaw tumour syndrome. Oncogene 36, 4025–4036.

Wang, P., Bowl, M.R., Bender, S., Peng, J., Farber, L., Chen, J., Ali, A., Zhang, Z., Alberts, A.S., Thakker, R.V., Shilatifard, A., Williams, B.O., Teh, B.T., 2008. Parafibromin, a component of the human PAF complex, regulates growth factors and is required for embryonic development and survival in adult mice. Mol. Cell Biol. 28, 2930–2940.

Warner, J., Epstein, M., Sweet, A., Singh, D., Burgess, J., Stranks, S., Hill, P., Perry-Keene, D., Learoyd, D., Robinson, B., Birdsey, P., Mackenzie, E., Teh, B.T., Prins, J.B., Cardinal, J., 2004. Genetic testing in familial hyperparathyroidism: unexpected results and their implications. J. Med. Genet. 41, 155–160.

Westin, G., 2016. Molecular genetics and epigenetics of nonfamilial (sporadic) parathyroid tumours. J. Intern. Med. 280, 551–558.

Wettschureck, N., Lee, E., Libutti, S.K., Offermanns, S., Robey, P.G., Spiegel, A.M., 2007. Parathyroid-specific double knockout of Gq and G11 alpha-subunits leads to a phenotype resembling germline knockout of the extracellular Ca2+ -sensing receptor. Mol. Endocrinol. 21, 274–280.

Williamson, C., Pannett, A.J., Pang, J.T., Wooding, C., McCarthy, M., Sheppard, M.N., Monson, J.P., Clayton, R.N., Thakker, R.V., 1997. Localization of a gene causing endocrine neoplasia to a 4 cM region on chromosome 1p35-p36. J. Med. Genet. 34, 617–619.

Woodard, G.E., Lin, L., Zhang, J.H., Agarwal, S.K., Marx, S.J., Simonds, W.F., 2005. Parafibromin, product of the hyperparathyroidism-jaw tumor syndrome gene HRPT2, regulates cyclin D1/PRAD1 expresssion. Oncogene 24, 1272–1276.

Yart, A., Gstaiger, M., Wirbelauer, C., Pecnik, M., Anastasiou, D., Hess, D., Krek, W., 2005. The HRPT2 tumor suppressor gene product parafibromin associates with human PAF1 and RNA polymerase II. Mol. Cell Biol. 25, 5052–5060.

Yaguchi, H., Ohkura, N., Takahashi, M., Nagamura, Y., Kitabayashi, I., Tsukada, T., 2004. Menin missense mutants associated with multiple endocrine neoplasia type 1 are rapidly degraded via the ubiquitin-proteasome pathway. Mol. Cell Biol. 24, 6569–6580.

Yi, Y., Nowak, N.J., Pacchia, A.L., Morrison, C., 2008. Chromosome 11 genomic changes in parathyroid adenoma and hyperplasia: array CGH, FISH, and tissue microarrays. Genes Chromosomes Cancer 47, 639–648.

Yokoyama, A., Cleary, M.L., 2008. Menin critically links MLL proteins with LEDGF on cancer-associated target genes. Cancer Cell 14, 36–46.

Yokoyama, A., Wang, Z., Wysocka, J., Sanval, M., Aufiero, D.J., Kitabayashi, I., Herr, W., Cleary, M.L., 2004. Leukemia proto-oncoprotein MLL forms a SET1-like histone methyltransferase complex with menin to regulate Hox gene expression. Mol. Cell Biol. 24, 5639–5649.

Yoshimoto, K., Iwahana, H., Fukuda, A., Sano, T., Saito, S., Itakura, M., 1992. Role of p53 mutations in endocrine tumorigenesis: mutation detection by polymerase chain reaction-single strand conformation polymorphism. Cancer Res. 52, 5061–5064.

Yu, W., McPherson, J.R., Stevenson, M., van Eijk, R., Heng, H.L., Newey, P., Gan, A., Ruano, D., Huang, D., Poon, S.L., Ong, C.K., van Wezel, T., Cavaco, B., Rozen, S.G., Tan, P., Teh, B.T., Thakker, R.V., Morreau, H., 2015. Whole-exome sequencing studies of parathyroid carcinomas reveal novel PRUNE2 mutations, distinctive mutational spectra related to APOBEC-catalyzed DNA mutagenesis and mutational enrichment in kinases associated with cell migration and invasion. J. Clin. Endocrinol. Metab. 100, E360–E364.

Zhang, C., Kong, D., Tan, M.H., Pappas Jr., D.L., Wang, P.F., Chen, J., Farber, L., Zhang, N., Koo, H.M., Weinreich, M., Williams, B.O., Teh, B.T., 2006. Parafibromin inhibits cancer cell growth and causes G1 phase arrest. Biochem. Biophys. Res. Commun. 350, 17–24.

Zhang, C., Zhang, T., Zou, J., Miller, C.L., Gorkhali, R., Yang, J.Y., Schilmiller, A., Wang, S., Huang, K., Brown, E.M., Moremen, K.W., Hu, J., Yang, J.J., 2016. Structural basis for regulation of human calcium-sensing receptor by magnesium ions and an unexpected tryptophan derivative co-agonist. Sci Adv 2, e1600241.

Zhao, L., Sun, L.H., Liu, D.M., He, X.Y., Tao, B., Ning, G., Liu, J.M.,., Zhao, H.Y., 2014. Copy number variation in CCND1 gene is implicated in the pathogenesis of sporadic parathyroid carcinoma. World J. Surg. 38, 1730–1737.

Chapter 59

Diseases resulting from defects in the G protein $G_s\alpha$

Lee S. Weinstein[1] **and Michael T. Collins**[2]

[1]Metabolic Diseases Branch, National Institute of Diabetes, Digestive, and Kidney Diseases, Bethesda, MD, United States; [2]Skeletal Disorders and Mineral Homeostasis Section, National Institute for Dental and Craniofacial Research, National Institutes of Health, Bethesda, MD, United States

Chapter outline

Overview

$G_s\alpha$ is a ubiquitously expressed heterotrimeric G protein α subunit that couples cell surface receptors for hormones and other extracellular ligands to adenylyl cyclase and mediates receptor-stimulated intracellular cyclic adenosine monophosphate (cAMP) generation. Upon ligand binding, receptors promote the release of GDP and binding of GTP to $G_s\alpha$, leading to its activation. The "turn-off" mechanism is an intrinsic GTPase activity of $G_s\alpha$ that hydrolyzes bound GTP to GDP. Genetic defects involving $G_s\alpha$ are associated with a wide variety of human disorders, which are summarized in Table 59.1. Heterozygous inactivating $G_s\alpha$ mutations in the germ line usually lead to Albright hereditary osteodystrophy (AHO) and, less often, to progressive osseous heteroplasia (POH). Paternal transmission of these mutations leads to the AHO phenotype alone (pseudopseudohypoparathyroidism, PPHP), while maternal transmission leads to AHO plus obesity and multihormone resistance (pseudohypoparathyroidism type IA, PHPIA). The clinical differences between PHPIA and PPHP result from the fact that $G_s\alpha$ is imprinted in a tissue-specific manner, being primarily expressed from the maternal allele in specific hormone target tissues. $G_s\alpha$ is encoded by a complex imprinted gene (*GNAS*), which encodes gene products other than $G_s\alpha$. Patients with isolated renal parathyroid hormone (PTH) resistance without AHO (pseudohypoparathyroidism type IB, PHPIB) have a *GNAS* imprinting defect that presumably leads to tissue-specific $G_s\alpha$ deficiency. Endocrine tumors, fibrous dysplasia of bone (FD), and the McCune–Albright syndrome (MAS) result from gain-of-function, somatic mutations in $G_s\alpha$ that lead to constitutive adenylyl cyclase activation and cAMP signaling.

Principles of Bone Biology. https://doi.org/10.1016/B978-0-12-814841-9.00059-2

TABLE 59.1 Human diseases associated with *GNAS* gene defects.

GNAS gene defect	Disease
$G_s\alpha$ null mutations (maternal)	PHPIA (AHO + multihormone resistance and obesity PHPIA + POH
$G_s\alpha$ null mutations (paternal)	PPHP (AHO alone) POH
$G_s\alpha$ A366S mutation (maternal)	PHPIA + testotoxicosis
Loss of exon 1A maternal imprinting (sporadic or associated with *STX16* or NESP55 deletion) Paternal UPD of chromosome 20q $G_s\alpha$ ΔI382 mutation (maternal)	PHPIB
$G_s\alpha$-activating mutations (somatic)	GH-secreting pituitary tumors Thyroid adenomas, carcinomas Leydig cell tumors Pheochromocytoma Parathyroid adenoma ACTH-secreting pituitary tumor McCune–Albright syndrome Fibrous dysplasia Skeletal muscle myxomas Premature thelarche Intraductal papillary mucinous neoplasms of the pancreas

ACTH, adrenocorticotropic hormone; *AHO,* Albright hereditary osteodystrophy; *GH,* growth hormone; *PHPIA,* pseudohypoparathyroidism type IA; *PHPIB,* pseudohypoparathyroidism type IB; *POH,* progressive osseous heteroplasia; *UPD,* uniparental disomy.

$G_s\alpha$ structure and function

Like all heterotrimeric G proteins, G_s is composed of a specific α subunit ($G_s\alpha$) associated with tightly but noncovalently bound βγ dimers. These heterotrimeric complexes reside in the inner leaflet of the plasma membrane as well as in intracellular membranes. $G_s\alpha$ is ubiquitously expressed and couples a wide variety of seven-transmembrane receptors, including those for glycoprotein and peptide hormones, biogenic amines, and neurotransmitters, to the stimulation of adenylyl cyclase and generation of the intracellular second messenger cAMP (Weinstein et al., 2001, 2004). cAMP mediates many of its downstream effects by activating cAMP-dependent protein kinase (protein kinase A [PKA]), a serine/threonine protein kinase that phosphorylates many substrates, including enzymes involved in intermediary metabolism and transcription factors such as the cAMP-response element binding protein CREB (Montminy, 1997). cAMP also binds to and modulates the activity of other molecules (Richards, 2001), including ion channels (Sudlow et al., 1993; Wainger et al., 2001) and guanine nucleotide exchange factors for the small guanine nucleotide binding protein Rap1 (de Rooij et al., 1998; Kawasaki et al., 1998). While in many tissues cAMP is antimitogenic, in many neuroendocrine cell types it is mitogenic through activation of Rap1, which stimulates various mitogenic pathways, including B-Raf/mitogen-activated protein kinase, p70S6 kinase, and Akt (Miller et al., 1997; Vossler et al., 1997; Cass and Meinkoth, 1998; Mei et al., 2002; Wang et al., 2006).

$G_s\alpha$ may also be activated by tyrosine kinase (growth factor) receptors through tyrosine phosphorylation (Poppleton et al., 1996; Sun et al., 1997; Krieger-Brauer et al., 2000) and may activate other effectors, including cardiac Ca^{2+} channels (Yatani et al., 1988; Mattera et al., 1989) and Src tyrosine kinases (Ma et al., 2000). In addition to its role as a signal transducer at the plasma membrane, $G_s\alpha$ may also play a role in the control of intracellular membrane and vesicle trafficking (Bomsel and Mostov, 1992; Zheng et al., 2001).

Like all G proteins, G_s undergoes activation and deactivation through a "GTPase" cycle (Fig. 59.1). In the inactive state GDP is bound to $G_s\alpha$, which is localized to the inner leaflet of the plasma membrane associated with βγ. Ligand-bound receptors promote GDP release and binding of ambient GTP, allowing $G_s\alpha$ to attain an active conformation and to dissociate from βγ. Dissociation from βγ as well as depalmitoylation results in $G_s\alpha$ being released from the plasma membrane upon activation (Wedegaertner et al., 1996; Huang et al., 1999; Yu and Rasenick, 2002; Allen et al., 2005). GTP-bound $G_s\alpha$ directly binds to and activates its effectors, including adenylyl cyclase. The turn-off mechanism is an intrinsic GTPase activity that hydrolyzes bound GTP to GDP, allowing $G_s\alpha$ to reassociate with βγ.

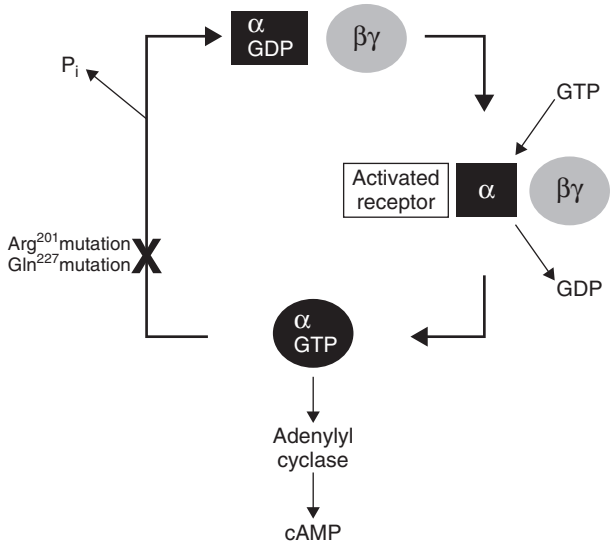

FIGURE 59.1 The G_s GTPase cycle. In the basal state $G_s\alpha$ has GDP bound to it and it associates with βγ to form a heterotrimer with GDP. Activated (ligand-bound) receptors promote the exchange of GTP for GDP on $G_s\alpha$, which allows $G_s\alpha$ to attain an active conformation and dissociate from βγ. GTP-bound $G_s\alpha$ directly activates adenylyl cyclase to generate cAMP. $G_s\alpha$ is deactivated through an intrinsic GTPase activity that hydrolyzes bound GTP to GDP, allowing $G_s\alpha$ to reassociate with βγ. Mutation of Arg^{201} or Gln^{227} leads to constitutive activation by disruption of the GTPase activity.

An RGS (regulator of G protein signaling) protein that stimulates the GTPase activity of $G_s\alpha$ has been identified (Zheng et al., 2001). Crystal structures have identified two highly conserved residues (Arg^{201} and Gln^{227} in the long form of $G_s\alpha$) that are critical for catalyzing the GTPase reaction (Graziano and Gilman, 1989; Landis et al., 1989; Coleman et al., 1994; Sondek et al., 1994), and mutation or posttranslational modifications of these residues lead to constitutive activation and human disease (see later). More recent work suggests that activating $G_s\alpha$ mutations may also activate the G protein via a mechanism other than impairment of GTPase activity (Hu and Shokat, 2018).

Like all Gα's, $G_s\alpha$ contains two structural domains, a Ras-like GTPase domain, which includes the sites for guanine nucleotide binding and effector interaction, and a helical domain (Sunahara et al., 1997; Tesmer et al., 1997). Alternative splicing leads to two long and two short forms of $G_s\alpha$ with helical domains of slightly differing length (Bray et al., 1986; Kozasa et al., 1988), which have only subtle biochemical differences between them (Jones et al., 1990; Seifert et al., 1998). Contacts between the helical and GTPase domains may be important for maintaining the binding of guanine nucleotide, which sits within a cleft between the two domains (Mixon et al., 1995; Warner et al., 1998). GTP binding leads to an active conformation by altering the positions of three regions (named switches 1, 2, and 3) within the GTPase domain (Noel et al., 1993; Lambright et al., 1994). In particular, switches 2 and 3 move toward each other and the active conformation is stabilized through mutual interactions between acidic and basic residues within these regions (Iiri et al., 1997; Li and Cerione, 1997; Warner et al., 1999). Interactions between switch 3 and helical domain residues may also be important for receptor-mediated activation (Grishina and Berlot, 1998; Marsh et al., 1998; Warner et al., 1998; Warner and Weinstein, 1999). The carboxy terminus is the major site of interaction with receptors (Sullivan et al., 1987; Simonds et al., 1989; Schwindinger et al., 1994; Conklin et al., 1996; Grishina and Berlot, 2000; Mazzoni et al., 2000).

The $G_s\alpha$ Gene *GNAS*

GNAS, the gene encoding $G_s\alpha$, is located at 20q13.2−q13.3 (Gejman et al., 1991; Levine et al., 1991; Rao et al., 1991). *GNAS* generates several gene products in addition to $G_s\alpha$ through the use of alternative promoters and first exons that splice onto a common exon (exon 2) (Fig. 59.2). In addition, *GNAS* is affected by genomic imprinting, an epigenetic phenomenon that leads to partial or complete suppression of gene expression from one parental allele (Reik and Walter, 2001). Allele-specific differences in gene expression are most likely the result of allele-specific differences in DNA methylation, which are observed in all imprinted genes. Primary imprinting centers are regions of differential methylation in which DNA methylation is erased in primordial germ cells, reestablished in either male or female gametes, and maintained in all tissues throughout development. Differential gene expression may result from differential methylation of gene promoters (with the silenced allele methylated) or may result from more indirect mechanisms.

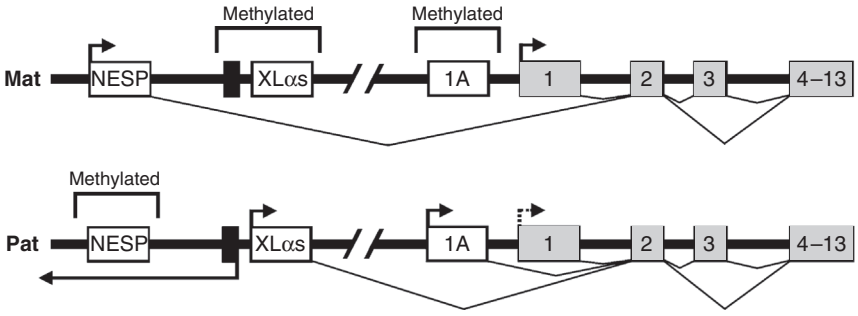

FIGURE 59.2 Organization and imprinting of *GNAS*. The maternal (*Mat*) allele is shown above and paternal (*Pat*) allele below (not to scale), indicating regions of DNA methylation, active promoters (*arrows*), and exon splicing. $G_s\alpha$ coding exons are depicted as *gray* boxes with exons 4–13 shown as a single box. Three other alternative first exons are shown as *white* boxes and the first exon of the antisense transcript is shown as a *black* box. The *dashed arrow* for the paternal $G_s\alpha$ promoter indicates that the promoter is silenced in a tissue-specific manner. Long and short forms of $G_s\alpha$ result from alternative splicing of exon 3. *NESP,* Neuroendocrine specific protein. *Reproduced from Weinstein, L.S., 2004. GNAS and McCune-Albright syndrome/fibrous dysplasia, Albright hereditary osteodystrophy/pseudohypoparathyroidism type 1A, progressive osseous heteroplasia, and pseudohypoparathyroidism type 1B. In: Epstein, C.J., Erickson, R. P. and Wynshaw-Boris, A. (Eds.), Molecular Basis of Inborn Errors of Development. Oxford University Press, San Francisco, pp. 849–866.*

$G_s\alpha$ mRNA transcripts are generated from the most downstream *GNAS* promoter and span 13 exons (Kozasa et al., 1988). Biologically active long and short forms of $G_s\alpha$ are generated by alternative splicing of exon 3, which encodes 15 amino acids within the helical domain (Bray et al., 1986; Kozasa et al., 1988). $G_s\alpha$ is imprinted in a tissue-specific manner, being primarily from the maternal allele in a few tissues (e.g., the pituitary, thyroid, and renal proximal tubules) and biallelically expressed in most tissues (Davies and Hughes, 1993; Campbell et al., 1994; Yu et al., 1998; Hayward et al., 2001; Weinstein et al., 2001; Germain-Lee et al., 2002; Mantovani et al., 2002; Liu et al., 2003). This imprinting is not associated with methylation of its promoter (Kozasa et al., 1988; Hayward et al., 1998; Peters et al., 1999; Liu et al., 2000). Rather, $G_s\alpha$ imprinting is controlled by a primary imprinting center located ~2 kb upstream of its promoter, which is methylated on the maternal allele (Liu et al., 2000, 2005; Williamson et al., 2004). This region contains a promoter and first exon (exon 1A or A/B), which splices to exon 2 to generate untranslated mRNA transcripts from the paternal allele (Fig. 59.2) (Ishikawa et al., 1990; Liu et al., 2000; Liu et al., 2000, 2000). Maternal imprinting (methylation) of the exon 1A region is absent in PHPIB patients, as discussed in greater detail later.

Alternative promoters and first exons located 46 and 35 kb upstream of the $G_s\alpha$ promoter generate transcripts that encode the chromogranin-like protein NESP55 and the alternative $G_s\alpha$ isoform XLαs, respectively (Hayward et al., 1998; Hayward et al., 1998; Kelsey et al., 1999; Peters et al., 1999) (Fig. 59.2). The NESP55 and XLαs promoter regions are oppositely imprinted: NESP55 is expressed only from the maternal allele and its promoter is methylated on the paternal allele, while XLαs is expressed only from the paternal allele and its promoter is methylated on the maternal allele. Both NESP55 and XLαs are expressed primarily in neuroendocrine tissues. NESP55 is unrelated to the Gα family and its coding sequence is restricted to its specific upstream exon. Its biological function is unknown and studies in mouse and humans suggest that loss of its expression leads to minimal phenotypic consequences (Liu et al., 2000; Plagge et al., 2005). Imprinting of NESP55 is not established until after implantation and is dependent upon a primary imprinting center located within the promoter region of a paternally expressed antisense transcript that traverses the NESP55 promoter from the opposite direction (Liu et al., 2000; Williamson et al., 2006). XLαs is a $G_s\alpha$ isoform in which the first 47 amino acids of $G_s\alpha$ are replaced with a long amino-terminal extension encoded by its specific first exon (Kehlenbach et al., 1994; Pasolli et al., 2000). XLαs is capable of signal transduction and activation of adenylyl cyclase (Klemke et al., 2000; Bastepe et al., 2002). Although XLαs is critical for postnatal feeding and metabolic regulation in mice (Plagge et al., 2004; Xie et al., 2006), its role in humans is less clear.

Albright hereditary osteodystrophy

Clinical presentation

Patients with AHO may present with one or more of the following clinical features: short stature, round face, broad body habitus, brachydactyly, subcutaneous ossifications, depressed nasal bridge, hypertelorism, low birth rate, and mental deficits or developmental delay (Fig. 59.3) (Ringel et al., 1996; Weinstein, 1998; Spiegel and Weinstein, 2001; Weinstein et al., 2001; Richard et al., 2013). None of these features are completely specific for this disorder, although subcutaneous ossifications are a fairly specific sign for AHO. The severity of the phenotype varies greatly, and some

FIGURE 59.3 Albright hereditary osteodystrophy (AHO). (Left) AHO patient with short stature, obesity, and rounded face with depressed nasal bridge. (Right) Photograph (top) and radiograph (bottom) of hand with severe brachydactyly of the first, fourth, and fifth metacarpals. *Reproduced from Weinstein, L.S., 2004. GNAS and McCune-Albright syndrome/fibrous dysplasia, Albright hereditary osteodystrophy/pseudohypoparathyroidism type 1A, progressive osseous heteroplasia, and pseudohypoparathyroidism type 1B. In: Epstein, C.J., Erickson, R. P. and Wynshaw-Boris, A. (Eds.), Molecular Basis of Inborn Errors of Development. Oxford University Press, San Francisco, pp. 849–866.*

patients who carry the genetic trait present with few or no clinical manifestations (Farfel and Friedman, 1986; Weinstein et al., 1990; Miric et al., 1993; Shore et al., 2002).

Ectopic ossifications in AHO (osteoma or calcinosis cutis) are often one of the earliest features of the disease (Gelfand et al., 2006; Poomthavorn and Zacharin, 2006) and can occur in any location. They present as punctate hard nodules or as subcutaneous calcifications on radiographs located within the dermis and subcutaneous tissue (Eyre and Reed, 1971; Prendiville et al., 1992; Goeteyn et al., 1999; Sethuraman et al., 2006) that occasionally enlarge to form more plate-like lesions but do not invade into deeper tissues. These lesions result from intramembranous, as opposed to endochondral, ossification and may be surrounded by inflammation (Riepe et al., 2005). They are caused by a primary cellular defect, rather than a defect in mineral metabolism, as they are absent in patients with primary hypoparathyroidism and are present in PPHP patients, who are normocalcemic and have no evidence for PTH resistance.

Brachydactyly refers to shortening and widening of the long bones in the hands and feet. Patients with AHO have a relatively specific pattern, which most often involves the distal thumb and third, fourth, and fifth metacarpals and is often asymmetric (Steinbach and Young, 1966; Poznanski et al., 1977; Graudal et al., 1986; Mantovani et al., 2004). Brachydactyly is generally not observed in early childhood but becomes apparent later in the first decade of life due to premature growth plate closure with coning of the epiphysis (Gelfand et al., 2006). Spinal cord compression occurs rarely, either from calcifications of longitudinal spinal ligaments (Yamamoto et al., 1997; Chen et al., 2005; Mak and Mok, 2005) or from spinal canal narrowing (Goadsby et al., 1991; Okada et al., 1994). Other musculoskeletal features that have been reported in AHO include carpal tunnel syndrome (Joseph et al., 2011), increased incidence of sleep apnea (Landreth et al., 2015), dental abnormalities (Reis et al., 2016), Madelung deformity (Rump et al., 2011; Sanchez et al., 2011), and acroscyphodysplasia (Mitsui et al., 2014).

Neurobehavioral abnormalities are also common in AHO patients, occurring in up to 50% of cases (Farfel and Friedman, 1986). There is no distinct neurocognitive syndrome associated with AHO, although psychomotor delay and mental retardation are relatively common. Some evidence suggests that these features are more prevalent in PHP1A than in PPHP (Mouallem et al., 2008). Psychiatric conditions and juvenile dementia have also been described in AHO patients (Maeda et al., 2005). In rare cases, basal ganglia calcification resulting from the hypoparathyroid biochemical state may lead to Parkinsonian symptoms.

In addition to the aforementioned physical features, AHO patients who inherit the disease from their mother (or have a de novo $G_s\alpha$ mutation on the maternal allele) also develop obesity and multihormone resistance, a condition known as PHPIA (Long et al., 1988; Davies and Hughes, 1993; Weinstein et al., 2001). In patients who inherit AHO from their father (or have a de novo mutation on the paternal allele) obesity and multihormone resistance are absent. This condition, in which patients present with only AHO, is also known as PPHP. Both PHPIA and PPHP often occur in the same kindred with the presentation of each case determined by parental inheritance. The multihormone resistance in PHPIA primarily involves PTH, thyroid-stimulating hormone (TSH), growth hormone-releasing hormone (GHRH), and the gonadotropins, all of which activate G_s pathways in their target tissues. There is no resistance, at least based upon clinical parameters, to other hormones that also activate G_s, such as glucagon (Levine et al., 1983; Brickman et al., 1986), adrenocorticotropic hormone (ACTH) (Levine et al., 1983; Faull et al., 1991), isoproterenol (Carlson and Brickman, 1983), and vasopressin (Moses et al., 1986; Faull et al., 1991).

PHPIA patients develop renal PTH resistance during early childhood but may initially present with acute symptoms of hypocalcemia (seizures, tetany, numbness) at any time of life, often during early adolescence. Generally, there is no evidence for PTH resistance at birth or even in the first year of life, but soon thereafter PTH levels rise followed by the development of hyperphosphatemia and finally hypocalcemia (Werder et al., 1978; Tsang et al., 1984; Barr et al., 1994; Yu et al., 1999; Riepe et al., 2005; Gelfand et al., 2006). Over time patients develop chronic features of biochemical hypoparathyroidism, including basal ganglia calcifications, cataracts, and calcifications at other sites, and on rare occasions may develop rickets. Some PHPIA patients have elevated PTH levels but remain eucalcemic (Balachandar et al., 1975; Drezner and Haussler, 1979; Breslau et al., 1980). The PTH signaling defect is primarily localized to the renal proximal tubule, and this results in hyperphosphatemia due to increased phosphate reabsorption and low or inappropriate normal serum 1,25-dihydroxyvitamin D ($1,25(OH)_2D$) levels (Lambert et al., 1980; Braun et al., 1981; Breslau and Weinstock, 1988; Miura et al., 1990). Because the defect is limited to the proximal tubules, the ability of the distal tubules to reabsorb calcium in response to PTH remains intact, and therefore PHP patients do not tend to develop hypercalciuria upon treatment as do patients with primary hypoparathyroidism. Consistent with the presence of a G_s defect, the acute PTH-stimulated urinary cAMP response is markedly blunted in PHPIA patients, while it is normal in PPHP patients (Chase et al., 1969; Levine et al., 1986). Although one bone sample from a PHPIA patient showed no defect in PTH−$G_s\alpha$ signaling (Ish-Shalom et al., 1996), the occurrence of secondary skeletal effects of chronically elevated PTH is lower in PHPIA than in PHPIB, perhaps due to partial $G_s\alpha$ deficiency in osteoblasts from these patients.

TSH resistance is present in virtually all PHPIA patients and is often the first observed manifestation, as TSH levels are generally elevated in neonatal screening (Levine et al., 1985; Weisman et al., 1985; Yokoro et al., 1990; Yu et al., 1999; Gelfand et al., 2006). TSH levels may normalize for several months before once again becoming elevated (Yu et al., 1999). Once TSH resistance is established, TSH levels are mildly or moderately elevated and thyroid hormone levels are normal or slightly low. As the defect is at the level of TSH signaling, which also stimulates thyroid growth, goiter is usually absent. Antithyroid antibodies are usually absent.

Female PHPIA patients often present with signs of clinical hypogonadism, including delayed or incomplete sexual maturation, oligomenorrhea, or infertility, associated with mildly low estrogen levels (Wolfsdorf et al., 1978; Shapiro et al., 1980; Levine et al., 1983; Shima et al., 1988; Namnoum et al., 1998; de Sanctis et al., 2003). Although it is assumed that these patients are resistant to gonadotropins, studies have not consistently demonstrated that they have elevated gonadotropin levels. It has been proposed that PHPIA patients may have a more subtle form of gonadotropin resistance that leads to an ovulatory defect due to a poor ovulatory response to the midcycle luteinizing hormone surge (Namnoum et al., 1998). Some PHPIA patients also have prolactin deficiency (Carlson et al., 1977; Brickman et al., 1981; Kruse et al., 1981; Levine et al., 1983; Faull et al., 1991; Schuster et al., 1993).

Many, although not all, PHPIA patients have growth hormone (GH) deficiency, presumably secondary to pituitary resistance to GHRH (Shima et al., 1988; Faull et al., 1991; Germain-Lee et al., 2003; Mantovani et al., 2003; de Sanctis et al., 2007). However, short stature in PHPIA does not correlate with GH deficiency and appears to result from a primary skeletal growth plate defect leading to premature maturation and closure. In fact, prior to puberty PHPIA patients often are tall for their biological age and have advanced bone ages. Severe early-onset obesity and primary insulin resistance (not accounted for by obesity) are also observed in PHP1A (Long et al., 2007; Muniyappa et al., 2013). Olfactory defects have also been described in PHPIA (but not PPHP) patients, although it is unclear whether this reflects a true sensory defect or a central neurological defect (Henkin, 1968; Weinstock et al., 1986; Ikeda et al., 1988; Doty et al., 1997).

Molecular genetics

AHO was initially shown to be associated with a G_s signaling defect by biochemical and cellular assays performed on membrane samples from various tissues (Farfel and Bourne, 1980; Farfel et al., 1980, 1981, 1982; Levine et al., 1980, 1986; Bourne et al., 1981; Mallet et al., 1982; Spiegel et al., 1982; Downs et al., 1983; Heinsimer et al., 1984; Ong et al., 1996). In these assays G_s signaling activity was similarly reduced by ~50% in tissues from both PHPIA and PPHP patients, suggesting that these patients have similar genetic G_s defects resulting from a genetic defect in one parental allele. Consistent with these findings, these patients were shown to have similar reductions in $G_s\alpha$ mRNA (Carter et al., 1987; Levine et al., 1988) and protein (Patten and Levine, 1990), and to have heterozygous $G_s\alpha$ loss-of-function mutations (Patten et al., 1990; Weinstein et al., 1990; Miric et al., 1993; Oude Luttikhuis et al., 1994; Shapira et al., 1996; Ahmed et al., 1998; Aldred et al., 2000; Aldred and Trembath, 2000; Ahrens et al., 2001; Spiegel and Weinstein, 2001; Linglart et al., 2002; de Sanctis et al., 2003; Rickard and Wilson, 2003; Weinstein, 2004; Thiele et al., 2007). All AHO patients within the same kindred (both those with PHPIA and those with PPHP) have identical mutations, confirming that AHO is an autosomal dominant disorder (Weinstein et al., 1990; Wilson et al., 1994; Fischer et al., 1998; Nakamoto et al., 1998; Walden et al., 1999; Yu et al., 1999; Mantovani et al., 2000). Whether an individual has PHPIA or PPHP is determined by parental inheritance, as discussed under "Pathogenesis."

$G_s\alpha$ mutations in AHO are spread throughout the coding exons and in the majority of cases are unique to each kindred, although some identical mutations or mutations affecting the same amino acid have been identified in more than one kindred (Miric et al., 1993; Iiri et al., 1994; Farfel et al., 1996; Ahmed et al., 1998; Aldred and Trembath, 2000; Ahrens et al., 2001). One 4-bp deletion in exon 7 has been identified in many families (Yu et al., 1995; Aldred and Trembath, 2000; Mantovani et al., 2000; Ahrens et al., 2001; Linglart et al., 2002; Shore et al., 2002; de Sanctis et al., 2003), as this site appears prone to de novo mutation due to pausing of DNA polymerase and slipped-strand mispairing (Yu et al., 1995). In most cases there is no genotype–phenotype correlation as the mutations completely disrupt $G_s\alpha$ mRNA expression (frameshift, nonsense, or splice junction mutations) or $G_s\alpha$ protein stability (Warner et al., 1997, 1998, 1999). Mutations in exon 1, which specifically encodes $G_s\alpha$, provide strong evidence that deficiency of $G_s\alpha$, as opposed to other *GNAS* gene products, underlies this disorder (Thiele et al., 2010). Mutation within the alternatively spliced exon 3 was associated with loss of expression of the long but not short form of $G_s\alpha$, leading to normocalcemic PHP1A with no obesity (Thiele et al., 2007).

Several missense mutations have specific effects on $G_s\alpha$ function. For example, mutations at the carboxy terminus uncouple $G_s\alpha$ from receptors (Schwindinger et al., 1994; Wu et al., 2001; Linglart et al., 2002, 2006). Mutation of either Arg^{231} within the switch 2 region or Glu^{259} within the switch 3 region leads to a receptor activation defect by destabilizing interactions between the two switch regions that are necessary to maintain the active conformation (Iiri et al., 1997; Warner et al., 1999). The Arg^{258}Trp mutation results in decreased GDP binding in the basal state as well as a receptor-activation defect due to increased GTPase activity (Warner et al., 1998; Warner and Weinstein, 1999). The Ala^{366}Ser mutation results in PHPIA plus male gonadotropin-independent precocious puberty (testotoxicosis) (Iiri et al., 1994). This mutation leads to increased GDP release in a temperature-sensitive manner. At core body temperature the mutant protein is thermolabile due to an inability to maintain GDP binding, which results in PHPIA. At the lower testicular temperature, the GDP binding defect is subtler, allowing the protein to remain stable. However, testotoxicosis results from constitutive activation of $G_s\alpha$ due to increased GDP/GTP exchange in the absence of receptor stimulation.

Diagnosis and management

Although PTH stimulation of urinary cAMP (Ellsworth–Howard test) is the classical test for confirming the presence of PTH resistance (Chase et al., 1969), the PTH analog is no longer clinically available, and with modern PTH assays the diagnosis can usually be made based on baseline hormonal measures once nutritional vitamin D deficiency and renal dysfunction are ruled out. Patients with a blunted urinary cAMP response to PTH are classified as having PHPI. PHPI is further subclassified as PHPIA or PHPIB based on the presence or absence of AHO and multihormone resistance, respectively. Rarely, patients have the PHPIA phenotype without evidence for a $G_s\alpha$ defect because the functional assay does not assess receptor–G protein coupling, and they are classified as PHPIC (Thiele et al., 2011). Patients who have a normal urinary cAMP response but a defective phosphaturic response to PTH are classified as PHP type II (Rao et al., 1985).

As many of the features of AHO (brachydactyly, obesity, neurobehavioral abnormalities) are nonspecific, the diagnosis should not be made based upon the presence of these features alone, especially in the absence of family history, multihormone resistance, or subcutaneous ossifications, which is a more specific feature of AHO. These features are also present in other known genetic syndromes (e.g., Prader–Willi, brachydactyly syndromes, Turner's syndrome, Rubinstein–Taybi syndrome) and have also been found in association with chromosomal deletion of 2q37 (Phelan et al., 1995; Wilson et al.,

1995). Therefore, to confirm the diagnosis of PHPIA or PPHP one must confirm the presence of a $G_s\alpha$ defect by biochemical or genetic studies. Acrodysostosis presents with severe generalized skeletal abnormalities, and hormone resistance is associated with mutations in the genes encoding PKA regulatory-1α subunit (Linglart et al., 2011) or phosphodiesterase 4D.

The most direct way to confirm the presence of a $G_s\alpha$ defect is by *GNAS* mutation screening, which is commercially available but has a sensitivity of only ~70%. Alternatively, one can assay for G_s signaling activity in an erythrocyte membrane sample, but this is available in only a small number of research laboratories and is more technically difficult. In at least some cases patients have been diagnosed as having PHPIC because a nonhydrolyzable GTP analog was used to stimulate G_s in the biochemical assay. As this bypasses the necessity for receptor stimulation, it will give a normal result even when the mutation produces a specific defect in receptor-stimulated signaling (Iiri et al., 1997; Linglart et al., 2002, 2006). For this reason, biochemical assays should be performed using a receptor ligand (e.g., isoproterenol) so that these $G_s\alpha$ biochemical defects are not missed.

There is no specific therapy for the physical and neurocognitive manifestations of AHO. Rarely the subcutaneous ossifications require surgical excision to relieve discomfort or disfigurement. PTH resistance in PHPIA (and PHPIB) patients should be aggressively managed with oral calcium and vitamin D (either 50−100,000 IU/day of ergocalciferol or cholecalciferol or 0.5−2 μg/day of calcitriol). The goal is to try to normalize calcium and PTH, if possible, to prevent the skeletal effects of chronically elevated PTH and the development of autonomous (tertiary) hyperparathyroidism. Treatment should be initiated when patients develop high PTH levels even if normocalcemic. If autonomous parathyroid tumors develop, surgical excision may be required to reverse hypercalcemia, but management of the underlying PTH resistance will still be required postoperatively. PHP patients generally do not develop hypercalciuria upon treatment because the PTH defect is localized to the renal proximal tubule and the distal tubules can still increase calcium reabsorption in response to circulating PTH (Mizunashi et al., 1990; Stone et al., 1993). However, patients still need to be periodically monitored for hypercalciuria while on therapy.

Levothyroxine should be prescribed to normalize TSH levels and hypogonadism can be managed with oral contraceptives in females and testosterone in males. GH testing should be performed in children with PHPIA and GH therapy may be instituted if GH deficiency is diagnosed (Germain-Lee et al., 2003; Mantovani et al., 2003; de Sanctis et al., 2007). The more general use of GH in AHO patients to maximize height is under investigation.

Pathogenesis

The first clue that *GNAS* imprinting may be important for the clinical variability of AHO (PHPIA vs. PPHP) came from the observation that maternal inheritance produces offspring with PHPIA, while paternal inheritance produces offspring with PPHP (Davies and Hughes, 1993; Wilson et al., 1994; Nakamoto et al., 1998). Molecular studies in mice and humans have confirmed that $G_s\alpha$ is imprinted in a tissue-specific manner, being expressed primarily from the maternal allele in pituitary, thyroid, gonads, and renal proximal tubules (Yu et al., 1998; Hayward et al., 2001; Germain-Lee et al., 2002; Mantovani et al., 2002; Liu et al., 2003). In these tissues mutation of the active maternal allele will result in $G_s\alpha$ deficiency and impaired hormone signaling, while mutation of the inactive paternal allele would have little effect on $G_s\alpha$ expression or hormone action (Fig. 59.4). Therefore $G_s\alpha$ imprinting in renal proximal tubules would account for the fact that PTH-stimulated urinary cAMP is markedly reduced in PHPIA but is normal in PPHP (Chase et al., 1969; Levine et al., 1986). In most other nonendocrine tissues $G_s\alpha$ is biallelically expressed (Campbell et al., 1994; Hayward et al., 1998; Hayward et al., 1998, 1998), which accounts for a similar ~50% reduction in $G_s\alpha$ expression being observed in erythrocytes and other tissues in both PHPIA and PPHP patients (Levine et al., 1986).

In renal proximal tubules PTH normally stimulates G_s/cAMP signaling pathways, which leads to decreased phosphate reabsorption and increased $1,25(OH)_2D$ production by induction of the 1α-hydroxylase gene. Therefore $G_s\alpha$ deficiency in PHPIA (and PHPIB) leads to decreased $1,25(OH)_2D$ production and hyperphosphatemia due to low urinary phosphate excretion. Hyperphosphatemia also acts to inhibit $1,25(OH)_2D$ production. Hypocalcemia results from the combined effects of hyperphosphatemia and low $1,25(OH)_2D$ levels, as the latter results in decreased intestinal calcium absorption and skeletal calcium mobilization (Drezner et al., 1976; Drezner and Haussler, 1979; Epstein et al., 1983). Hypocalcemia, hyperphosphatemia, and low $1,25(OH)_2D$ levels all contribute to secondary hyperparathyroidism. The onset of renal PTH resistance occurs in early childhood after the first year of life and may correlate to the onset of $G_s\alpha$ imprinting in the renal proximal tubule (Turan et al., 2014). Likewise, hypothyroidism, hypogonadism, and GH deficiency in PHPIA result from resistance to TSH, gonadotropins, and GHRH in their respective target tissues (thyroid, gonads, pituitary) (Mallet et al., 1982; Namnoum et al., 1998; Germain-Lee et al., 2003; Mantovani et al., 2003). $G_s\alpha$ is imprinted in all of these tissues and therefore maternal, but not paternal, $G_s\alpha$ mutation leads to $G_s\alpha$-deficiency hormone resistance.

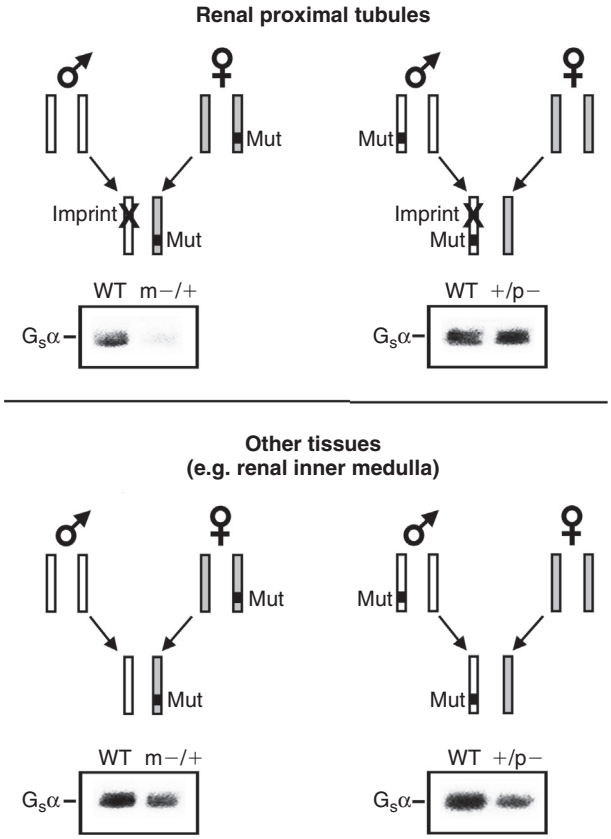

FIGURE 59.4 The role of tissue-specific $G_s\alpha$ imprinting in the pathogenesis of pseudohypoparathyroidism type IA and pseudopseudohypoparathyroidism. (Top) $G_s\alpha$ is paternally imprinted (denoted with an *X*) in renal proximal tubules and therefore mutation (*Mut*) of the active maternal allele (*gray*) results in loss of $G_s\alpha$ expression and parathyroid hormone resistance (left), while mutations in the inactive paternal allele (*white*) do not effect $G_s\alpha$ expression or hormone signaling (right), as shown below in immunoblots of renal cortical membranes from wild-type (*WT*) mice and mice with a $G_s\alpha$ mutation on the maternal or paternal allele (*m−/+* or *+/p−*, respectively) using a $G_s\alpha$-specific antibody (Yu et al., 1998). (Bottom) In other tissues $G_s\alpha$ is not imprinted and therefore maternal and paternal $G_s\alpha$ mutations both lead to ~50% loss of $G_s\alpha$ expression, as shown below in immunoblots of renal inner medullary membranes (Yu et al., 1998). *Reproduced from Weinstein, L.S., 2004. GNAS and McCune-Albright syndrome/fibrous dysplasia, Albright hereditary osteodystrophy/pseudohypoparathyroidism type 1A, progressive osseous heteroplasia, and pseudohypoparathyroidism type 1B. In: Epstein, C.J., Erickson, R. P. and Wynshaw-Boris, A. (Eds.), Molecular Basis of Inborn Errors of Development. Oxford University Press, San Francisco, pp. 849–866.*

A likely explanation for why PHPIA patients do not show clinical resistance to other hormones that also activate $G_s\alpha$ in their target tissues (e.g., ACTH or vasopressin) is that $G_s\alpha$ is not imprinted in these target tissues and therefore $G_s\alpha$ expression is reduced to only ~50% in these tissues (Weinstein et al., 2000). This partial $G_s\alpha$ deficiency may be insufficient to produce clinical hormone resistance, either because $G_s\alpha$ is not rate limiting for generating the cAMP second messenger or because the cAMP levels, while reduced, are still sufficient to elicit a normal physiological response (Carlson et al., 1985; Brickman et al., 1986; Weinstein et al., 2000). This would also explain why PTH resistance is evident in the renal proximal tubule, but not in the distal tubule or in the skeleton (Stone et al., 1993; Ish-Shalom et al., 1996).

Obesity is also a feature specific for PHPIA and therefore is also a consequence of severe $G_s\alpha$ deficiency in a tissue in which $G_s\alpha$ expression is normally affected by imprinting (Long et al., 1988). This is confirmed by mouse studies showing that germ-line disruption of $G_s\alpha$ expression on the maternal allele leads to severe obesity and insulin resistance, while disruption of the paternal allele leads to a much less severe metabolic phenotype (Chen et al., 2005). One potential mechanism for the pathogenesis of obesity in PHPIA would be $G_s\alpha$ deficiency in adipocytes, leading to decreased ability of sympathetic nervous system (SNS) activity and hormones to stimulate lipolysis in these cells, which has been documented in these patients (Kaartinen et al., 1994; Carel et al., 1999). Moreover, genetic manipulations in mice that increase or decrease cAMP or its downstream effectors can lead to a lean or obese phenotype, respectively (Cummings et al., 1996; Martinez-Botas et al., 2000; Valet et al., 2000). However, $G_s\alpha$ has been shown not to be imprinted in adipose tissue (Mantovani et al., 2004) and mice with adipose tissue-specific $G_s\alpha$ deficiency do not develop obesity (Li et al., 2016).

Genetically modified mouse models indicate that imprinting in the central nervous system underlies the obesity that is associated with $G_s\alpha$ and that these mutations impair the stimulation of SNS activity and energy expenditure by central melanocortins (Chen et al., 2009). More recently this parent-of-origin effect of $G_s\alpha$ mutations on energy expenditure was shown to be due to $G_s\alpha$ imprinting in the dorsomedial hypothalamus (Chen et al., 2017). This model is consistent with the finding of reduced serum norepinephrine levels and resting energy expenditure in PHP1A patients (Carel et al., 1999; Shoemaker et al., 2013; Roizen et al., 2016). The role of hyperphagia, if any, on the development of obesity in PHP1A requires further study. $G_s\alpha$ imprinting in brain probably explains why neurocognitive problems are more prevalent in PHP1A (Mouallem et al., 2008).

The other AHO features that are present in both PHPIA and PPHP patients are also most likely to be caused by $G_s\alpha$ deficiency rather than NESP55 or XLαs deficiency, as these gene products would be disrupted only by maternal or paternal mutations, respectively, and AHO is absent in PHPIB patients in whom NESP55 is not expressed due to biallelic methylation of its promoter (Liu et al., 2000). Brachydactyly is probably the result of $G_s\alpha$ deficiency in growth plate chondrocytes, which normally mediates the paracrine effects of PTH-related peptide (PTHrP) to inhibit hypertrophic differentiation of chondrocytes (Vortkamp et al., 1996; Kronenberg, 2003). Mice with disruption of the gene encoding PTHrP (Karaplis et al., 1994) or its receptor (Lanske et al., 1996; Jobert et al., 1998) develop severe skeletal dysplasia with stunted long bone growth resulting from accelerated chondrocyte differentiation. Other studies in mice have confirmed that $G_s\alpha$ deficiency in growth plate chondrocytes leads to a similar cellular and whole-animal phenotype (Bastepe et al., 2004; Sakamoto et al., 2005). Osteoma cutis appears to result from the fact that $G_s\alpha$ deficiency in mesenchymal cells promotes osteoblast differentiation, as discussed in more detail in the sections on POH and MAS/FD. The exact mechanisms by which some AHO patients develop mental deficits are not clear, but may also be related to $G_s\alpha$ deficiency, as cAMP and PKA are known to be important for learning and memory (Levin et al., 1992; Wu et al., 1995; Abel et al., 1997; Rotenberg et al., 2000) and for neurite outgrowth and differentiation (Vossler et al., 1997; Jessen et al., 2001).

Progressive osseous heteroplasia

Clinical features

POH is a more severe form of the ectopic ossification observed in AHO in which dermal and subcutaneous ossifications coalesce to form large plaques and invade deep connective tissues and skeletal muscle, leading to joint stiffness and bone deformity (Kaplan and Shore, 2000). Its onset is generally in early childhood, although one case of adult-onset POH has been reported in whom a $G_s\alpha$ mutation was not identified (Seror et al., 2007). POH may occur sporadically or in a familial manner. In many cases there are no other features of AHO, although POH has been reported to coexist with other features of AHO or multihormone resistance (Eddy et al., 2000; Gelfand et al., 2007). There is no specific therapy for the ossifications. A report on one case suggested that intravenous pamidronate may have slowed the progression of new lesions, although it did not affect the lesions that already had developed (Hou, 2006).

Genetics

In most cases POH is associated with heterozygous germ-line $G_s\alpha$ loss-of-function mutations that are similar, and in some cases identical, to those observed in patients with PHPIA and PPHP (Eddy et al., 2000; Yeh et al., 2000; Ahmed et al., 2002; Shore et al., 2002; Gelfand et al., 2007). Although it has been reported that POH occurs only with paternal inheritance of *GNAS* mutations (Shore et al., 2002), POH has been shown to occur upon maternal transmission of mutations in two cases, one of which also had features of PHPIA (Eddy et al., 2000; Ahmed et al., 2002). In one of these cases, the proband had POH, while his affected sister presented with PHPIA without POH (Ahmed et al., 2002). Moreover, another case showed features consistent with POH, AHO, and multihormone resistance (PHPIA) (Gelfand et al., 2007). Although neither parent had the mutation, the presence of hormone resistance in the proband strongly suggests that the mutation was on the maternal allele. In one family, paternal transmission of a $G_s\alpha$ mutation resulted in five cases of POH in one generation, while maternal transmission of the mutation resulted in AHO (PHPIA vs. PPHP not determined) in the next generation (Shore et al., 2002). Based on its often unilateral and segmental involvement, it has been suggested that POH is a segmental disorder caused by a somatic inactivating mutation of the wild-type allele at an early stage during development (Happle, 2016), and evidence for this hypothesis has been found in chick embryos with somatic disruption of *GNAS* (Cairns et al., 2013).

Pathogenesis

As in AHO, the ectopic ossifications in POH form by intramembranous ossification. Given that AHO and POH patients have similar mutations that completely disrupt $G_s\alpha$ expression, the severity of ectopic ossification in an individual patient is most likely determined by other factors, including differences in genetic background. Other genes that may modify the severity of ossification include those that may affect $G_s\alpha$ expression from the unaffected allele or those that encode other proteins involved in $G_s\alpha$ signaling or bone formation. It remains unclear why many POH patients do not also have other features of AHO. Although it has been reported that POH is associated with mutation only on the paternal allele (Shore et al., 2002), several reports have contradicted this conclusion (Eddy et al., 2000; Ahmed et al., 2002; Gelfand et al., 2007).

While activating $G_s\alpha$ mutations appear to inhibit osteoblast differentiation in FD, as discussed later, decreased $G_s\alpha$ expression promotes osteoblast differentiation in cultured cells with increased expression of the osteogenic transcription factor Cbfa1/RUNX2 and other osteoblast-specific genes (Lietman et al., 2005). The effect of reduced cAMP on cellular levels of Cbfa1/RUNX2 protein may be in part the result of reduced degradation (Tintut et al., 1999). This regulation may be bidirectional, as one study showed that Cbfa1/RUNX2 suppresses the expression of $G_s\alpha$ in a cultured osteoblastic cell line (Bertaux et al., 2006). $G_s\alpha$ deficiency in mesenchymal precursor cells may promote osteoblast differentiation, leading to ectopic ossification in AHO and POH. Consistent with this, Cbfa1/RUNX2 mRNA was shown to be expressed in dermal fibroblasts from a POH patient (Yeh et al., 2000). Work has shown that activation of Hedgehog signaling in progenitor cells with loss of $G_s\alpha$ plays a key role in ectopic ossification (Regard et al., 2013).

Pseudohypoparathyroidism type IB

Clinical features

PHPIB patients present with renal PTH resistance in much the same way as PHPIA patients, with diminished urinary cAMP response to administered PTH or its analogs, but do not exhibit the AHO phenotype or resistance to most other hormones (Levine et al., 1983). Consistent with the absence of AHO, G_s bioactivity is unaffected in erythrocyte membranes derived from PHPIB patients (Levine et al., 1983; Silve et al., 1986). About half of the patients show evidence of borderline TSH resistance, with slightly elevated TSH levels, which in some cases may be intermittent (Liu et al., 2003; Foppiani et al., 2006). PHP1B patients are born with higher than normal birth weights (Brehin et al., 2015) and rarely may develop GH deficiency (Fernandez-Rebollo et al., 2013; Sano et al., 2015).

Some PHPIB patients present with elevated serum alkaline phosphatase, cortical bone resorption, osteitis fibrosa cystica, or slipped capital femoral epiphysis, presumably due to skeletal effects of chronically elevated PTH levels (Kolb and Steinbach, 1962; Costello and Dent, 1963; Agarwal et al., 2006), and can rarely present with a rachitic picture. These complications seem to be relatively specific for PHPIB, as this is not a feature of PHPIA. Management of the PTH and TSH resistance is similar to that discussed for PHPIA, except that normalization of PTH levels may be more critical to prevent skeletal manifestations of elevated PTH levels and the development of autonomous (tertiary) hyperparathyroidism (Neary et al., 2012). Occasionally PHP1B patients (as defined by their molecular genetic defect) may have one or more AHO features, particularly brachydactyly (Mariot et al., 2008; Mantovani et al., 2010). In one kindred PHPIB was associated with increased urine uric acid excretion and hypouricemia (Laspa et al., 2004), while in another kindred the affected patients initially presented with paroxysmal dyskinesia (Mahmud et al., 2005).

Genetics

Most cases of PHPIB are sporadic, but some are familial. In familial cases the PTH resistance occurs only upon maternal transmission of the trait, similar to the inheritance pattern in PHPIA (Juppner et al., 1998). Those who inherit the trait paternally are asymptomatic carriers. Although mapping studies linked familial PHPIB to the vicinity of *GNAS* on 20q13 (Juppner et al., 1998), the presence of normal erythrocyte G_s function in PHPIB patients ruled out the possibility that the disease is due to mutations that directly disrupt the $G_s\alpha$ coding exons (Levine et al., 1983; Silve et al., 1986). Rather PHPIB is associated with a *GNAS* imprinting defect in which maternal-specific imprinting (methylation) of the exon 1A imprinting control region is absent in virtually all cases, resulting in a paternal-specific imprinting pattern (unmethylated) on both parental alleles (Liu et al., 2000, 2005; Bastepe et al., 2001a,b; Jan de Beur et al., 2003). In sporadic cases the upstream NESP55, XLαs, and antisense promoters are usually also abnormally imprinted with a maternal-specific methylation pattern on both alleles, while imprinting of these upstream regions is unaffected in most

familial cases (Liu et al., 2005). PTH resistance specifically correlates with loss of exon 1A maternal imprinting, and there is no phenotypic correlation with the imprinting status of NESP55, XLαs, or the antisense promoter (Linglart et al., 2007; Elli et al., 2014). Paternal uniparental disomy of chromosome 20 is another mechanism for the development of PHP1B as both *GNAS* alleles would have a paternal epigenotype (Bastepe et al., 2001a, 2011; Takatani et al., 2015). PHP1B with broad methylation changes across the *GNAS* locus is also rarely observed in patients with a broader imprinting abnormality affecting multiple imprinted genes (Court et al., 2013; Maupetit-Mehouas et al., 2013; Bakker et al., 2015; Rochtus et al., 2016; Sano et al., 2016).

Familial PHPIB in almost all cases is associated with a deletion within the linked *STX16* gene (Bastepe and Juppner, 2000; Linglart et al., 2005; Liu et al., 2005). Upon maternal transmission the deletion results in the loss of maternal exon 1A methylation and PHPIB, while paternal transmission has no effect on exon 1A imprinting as the region is normally unmethylated on this allele and does not produce a phenotype. Although this region is presumed to have one or more *cis*-acting elements required for the establishment or maintenance of exon 1A methylation, deletion of the orthologous region in mice did not result in the exon 1A methylation defect or PTH resistance (Frohlich et al., 2007). Less commonly familial PHP1B is associated with maternal deletions involving NESP55 (Bastepe et al., 2005; Richard et al., 2012; Rezwan et al., 2015) or NESPAS (Chillambhi et al., 2010) leading to a paternal epigenotype throughout the *GNAS* locus or with duplications within the *GNAS* upstream region (Perez-Nanclares et al., 2015). In another kindred PHPIB resulted from maternal, but not paternal, inheritance of a 3-bp deletion that removes the carboxy-terminal residue Ile^{382} in $G_s\alpha$ (Wu et al., 2001). The original report showed evidence that this mutation resulted in selective uncoupling of the G protein from the PTH/PTHrP receptor, but a subsequent study showed evidence that the mutation leads to uncoupling from other receptors as well (Linglart et al., 2006).

Pathogenesis

Loss of exon 1A imprinting in PHPIB strongly suggests that this region, which is a primary imprinting control center (Liu et al., 2000), is required for tissue-specific imprinting of $G_s\alpha$. A model has been proposed in which the exon 1A region contains one or more *cis*-acting regulatory elements that inhibit the activity of the $G_s\alpha$ promoter in a methylation-sensitive and tissue-specific manner (Weinstein et al., 2001). In the model shown in Fig. 59.5, the exon 1A region contains a silencer element that binds a *trans*-acting repressor protein that is expressed only in specific tissues such as renal proximal tubules. Normally the repressor binds to the paternal allele and inhibits the paternal $G_s\alpha$ promoter but is unable to bind to the maternal allele due to methylation, allowing the maternal $G_s\alpha$ promoter to remain active. In PHPIB both parental alleles are unmethylated and therefore the repressor can bind to and suppress $G_s\alpha$ expression from both alleles, resulting in renal PTH resistance. In most other tissues the repressor is not expressed and therefore $G_s\alpha$ is expressed from both parental alleles.

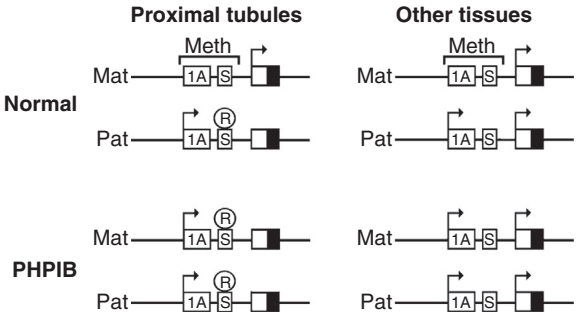

FIGURE 59.5 Model for tissue-specific $G_s\alpha$ imprinting and the pathogenesis of pseudohypoparathyroidism type IB. The model shown predicts that the exon 1A differentially methylated region has a *cis*-acting silencer element (*S*) that inhibits the paternal $G_s\alpha$ promoter (shown as *half-filled box*) in a tissue-specific manner by binding a repressor (*R*) that is expressed in a tissue-specific manner. In renal proximal tubules (left) the repressor can bind to and silence $G_s\alpha$ on the paternal (*Pat*) allele but is unable to bind to or silence $G_s\alpha$ on the maternal (*Mat*) allele as the binding site is methylated. In most other tissues (right) the repressor is not expressed and therefore $G_s\alpha$ is biallelically expressed. In pseudohypoparathyroidism type IB (*PHPIB*) methylation of the maternal allele is absent, allowing the repressor to bind to and silence $G_s\alpha$ from both alleles in renal proximal tubules, leading to $G_s\alpha$ deficiency and renal parathyroid hormone resistance. In most other tissues $G_s\alpha$ expression is unaffected because the repressor is not expressed. This would explain why PHPIB patients have normal $G_s\alpha$ expression in erythrocytes and why they do not develop Albright hereditary osteodystrophy. *Reproduced from Weinstein, L.S., 2004. GNAS and McCune-Albright syndrome/fibrous dysplasia, Albright hereditary osteodystrophy/pseudohypoparathyroidism type 1A, progressive osseous heteroplasia, and pseudohypoparathyroidism type 1B. In: Epstein, C.J., Erickson, R. P. and Wynshaw-Boris, A. (Eds.), Molecular Basis of Inborn Errors of Development. Oxford University Press, San Francisco, pp. 849–866.*

Moreover, the absence of the repressor would predict that loss of maternal exon 1A methylation in PHPIB patients would have no effect on $G_s\alpha$ expression, which is consistent with the fact that $G_s\alpha$ is unaffected in erythrocyte membranes from these patients. The absence of the AHO phenotype in PHPIB patients presumably is due to the fact that $G_s\alpha$ expression levels are unaffected in the vast majority of tissues where $G_s\alpha$ is normally expressed equally from both parental alleles. As $G_s\alpha$ is not imprinted in bone; this tissue would be expected to have normal $G_s\alpha$ levels and PTH responsiveness and therefore be prone to the adverse effects of chronically elevated PTH levels (Murray et al., 1993).

This model is supported by the observation that deletion of the exon 1A region from the paternal allele in mice leads to loss of tissue-specific $G_s\alpha$ imprinting (Williamson et al., 2004; Liu et al., 2005) and can reverse the effects of a $G_s\alpha$-null mutation on the maternal allele (Xie et al., 2008). In fact, these mice have markedly reduced circulating PTH levels presumably due to increased PTH sensitivity in renal proximal tubules due to $G_s\alpha$ overexpression. Borderline TSH resistance in PHPIB results from the fact that $G_s\alpha$ expression from the paternal allele is normally only partially suppressed (Liu et al., 2003). The occasional appearance of AHO features, particularly brachydactyly, in PHP1B patients may correlate with the extent of tissue-specific $G_s\alpha$ imprinting (Zazo et al., 2011).

Fibrous dysplasia of bone and the McCune–Albright syndrome

Clinical features

FD is a benign skeletal disorder with a broad spectrum of severity. It may involve a single bone (monostotic fibrous dysplasia, MFD), multiple bones (polyostotic fibrous dysplasia, PFD), or, in rare circumstances, the entire skeleton (panostotic fibrous dysplasia) (Lichtenstein and Jaffe, 1942; Bianco et al., 2003; Collins and Bianco, 2003; Collins, 2006; Boyce and Collins, 2015).

When FD is found in association with characteristic skin spots and hyperfunctioning endocrinopathies it is known as MAS (McCune, 1936; Albright Fuller et al., 1937). The skin lesions (café-au-lait macules) have a characteristic appearance of jagged borders (resembling the cartographic appearance of the coast of Maine), and tend to follow the developmental lines of Blaschko (Fig. 59.6). The hyperfunctioning endocrinopathies include gonadotropin-independent precocious puberty, thyroid nodules with hyperthyroidism, GH excess (acromegaly/gigantism), and/or adrenal hyperplasia with glucocorticoid excess (Cushing's syndrome). In each case the associated pituitary trophic hormones (gonadotropins, thyrotropin, ACTH) are undetectable, indicating a primary defect in each endocrine gland. Renal phosphate wasting leading to hypophosphatemia, rickets, and osteomalacia can also be present, and is usually seen in patients with extensive FD (Collins et al., 2001; Riminucci et al., 2003; Bhattacharyya et al., 2012). It is caused by the production of the phosphate- and vitamin D-regulating hormone fibroblast growth factor 23 (FGF23) by cells in FD lesions (Riminucci et al., 2003).

FD was described by Donovan McCune and Fuller Albright in association with café-au-lait spots and endocrine hyperfunction; Albright labeled the disease as osteitis fibrosa disseminata (McCune, 1936; Albright Fuller et al., 1937). This name was assigned because of the resemblance, at the histopathological level, to the bone disease of hyperparathyroidism, osteitis fibrosa cystica. In the original cases Albright described, the patients had extensive (disseminated) PFD, thus disseminata. It was Lichtenstein who labeled the disease FD (Lichtenstein, 1938), and Lichtenstein and Jaffe were the first to report extensively on the spectrum, radiographic appearance, and histopathology of

FIGURE 59.6 A typical café-au-lait spot in a patient with McCune–Albright syndrome. Note the relationship of the skin lesions to the midline, the jagged (coast of Maine) borders, and the relationship to the developmental lines of Blaschko. The linear patch at the nape of the neck is seen quite commonly, either in isolation or in association with the larger skin lesions.

FD (Lichtenstein and Jaffe, 1942). FD in the long bones usually presents in childhood as a limp, pain, or a pathologic fracture (DiCaprio and Enneking, 2005; Leet and Collins, 2007; Paul et al., 2014). FD in the skull may first appear as subtle facial asymmetry, or a "lump," and is sometimes associated with pain and dental complications (Riminucci et al., 2002; Burke et al., 2017). Fractures (especially low trauma, pathologic fractures) are more common in childhood, but can persist into adulthood (Leet et al., 2004). Pain, sometimes severe, even in the absence of fractures or trauma is a common feature of FD, particularly in adults (Kelly et al., 2008). The extent of the disease (skeletal disease burden score) can be quantified with the use of nuclear medicine bone scans (Collins et al., 2005), and the skeletal disease burden score directly correlates with fracture rate and number, but surprisingly not with the extent of pain. The skeletal disease burden score also has a direct correlation with the extent to which FD has a deleterious effect on the health-related quality of life (Kelly et al., 2005), with the predominant factor affecting quality of life being the extent to which the skeletal disease burden affects the ability to ambulate without assistance.

FD affects the spine commonly and can be associated with scoliosis (Leet et al., 2004; Berglund et al., 2018) (Fig. 59.7). The FD-associated scoliosis usually appears in childhood and can progress rapidly, even into adulthood, and can rarely be lethal. An uncommon finding in association with FD can be intramuscular myxomas, known as Mazabraud's syndrome (Mazabraud and Girard, 1957; Biazzo et al., 2017). Isolated intramuscular myxomas, in the absence of FD, are also caused by the same $G_s\alpha$ mutations (Okamoto et al., 2000). Rarely (<1% of cases), FD can undergo malignant transformation. Cancer will usually present as the rapid expansion of a preexisting FD lesion in association with pain. On imaging studies there will be a disruption of the cortex in association with a soft tissue mass. Bone cancers have been reported in 123 cases in two large case series (Schwartz and Alpert, 1964; Ruggieri et al., 1999) and in two large reviews (Yabut et al., 1988; Lopez-Ben et al., 1999), wherein it was found that approximately half of the cases of cancer arose in MFD and half in PFD. When one considers that MFD is more common, cancer is more likely to occur in PFD. The regions or bones most commonly involved are the craniofacial bones, the femur, and the tibia. In these series, the most commonly seen histological types were osteosarcoma, fibrosarcoma, and chondrosarcoma. There are reports suggesting that malignant transformation may be more common in patients with Mazabraud's syndrome (Lopez-Ben et al., 1999; Jhala et al., 2003). However, this is probably not the case, but rather represents an ascertainment bias, as the actual prevalence of intramuscular myxomas in association with FD may be more common than expected because most intramuscular myxomas are asymptomatic and go undetected.

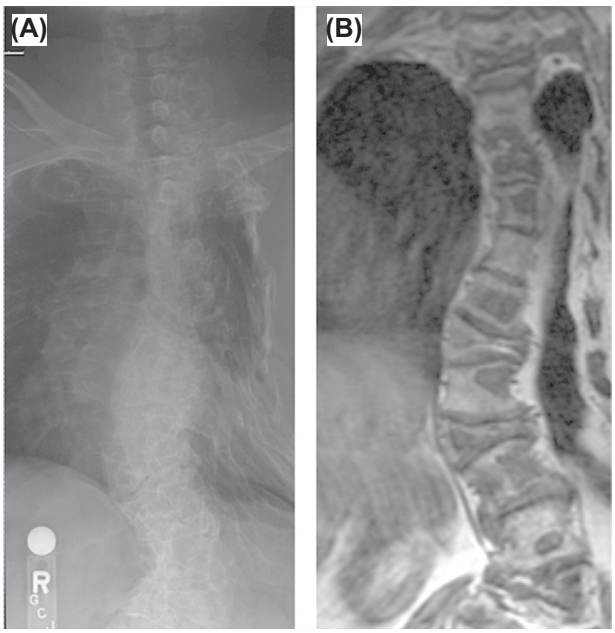

FIGURE 59.7 Scoliosis in FD. Scoliosis of the spine is demonstrated in (A) an X-ray and (B) magnetic resonance imaging (MRI) of the spine in a 54-year-old woman with FD. The extent of the involvement of the vertebral columns with FD is demonstrated in the MRI, where large parts of the vertebrae are shown to be replaced with FD. Surprisingly, and typically, the woman had neither pain nor any evidence of neurological compromise, despite extensive disease and multiple compression fractures.

Genetics

FD/MAS is the result of activating mutations in $G_s\alpha$ (Weinstein et al., 1991; Schwindinger et al., 1992). The vast majority of the mutations (>95% in our series, unpublished data, and 100% in a large published series, Lumbroso et al., 2004) occur at Arg^{201} and are divided roughly equally between either Arg^{201} to His or Arg^{201} to Cys. However, a 2007 report from a large series of patients with FD found three cases (5%) in which the patients had Gln^{227} to Leu mutations (Idowu et al., 2007). The lack of vertical transmission of FD or MAS, the fact that the skin lesions appear to roughly follow the developmental lines of Blaschko, and the fact that the skeletal lesions often tend to affect one side of the body has led to the widely held concept that FD and MAS are the manifestation of somatically acquired *GNAS* mutations and that patients are mosaics. The concept, first proposed by Happle (Happle, 1986), is that if germ-line, the *GNAS* mutations that cause FD and MAS would be lethal, and that the mutation "survives" only due to the somatic, mosaic nature of the mutation. The implication of this line of reasoning is that for a patient with MAS whose disease is manifested by, for example, café-au-lait skin spots (a tissue of ectodermal origin), FD of the long bones (a tissue of mesodermal origin), and hyperthyroidism (a tissue of endodermal origin), the mutation must have occurred very early in development at the inner cell mass stage, prior to the development of the three germ layers (Fig. 59.8). While the clinical data appear to support this model, it has yet to be proven experimentally. In fact, there is an animal model with transgenic expression of a typical $G_s\alpha$ mutation that survives and appears to model at least the FD aspect of MAS (Saggio et al., 2014). As $G_s\alpha$ is imprinted in a tissue-specific manner, the clinical presentation of individuals may also be affected by the parental allele that harbors the mutation, particularly with respect to the presence or absence of acromegaly (Mantovani et al., 2004).

Pathogenesis

FD is the result of $G_s\alpha$-activating mutations in bone marrow stromal cells, which are a subset of skeletal stem cells that gives rise to osteogenic cells, including chondrocytes, osteoblasts, and osteocytes, as well as bone marrow adipocytes and hematopoietic supportive stromal cells (Bianco and Robey, 1999, 2015). Lichtenstein was the first to speculate that FD is the result of the "perverted activity of the specific bone-forming mesenchyme" (Lichtenstein, 1938) and Bianco and colleagues were the first to prove that FD results specifically from bone marrow stromal cells harboring activating $G_s\alpha$ mutations (Riminucci et al., 1997; Bianco et al., 1998; Bianco and Robey, 1999). In addition, it has been shown that the ability of cells harboring the $G_s\alpha$ mutation to produce an FD lesion is dependent on the presence of both mutated and

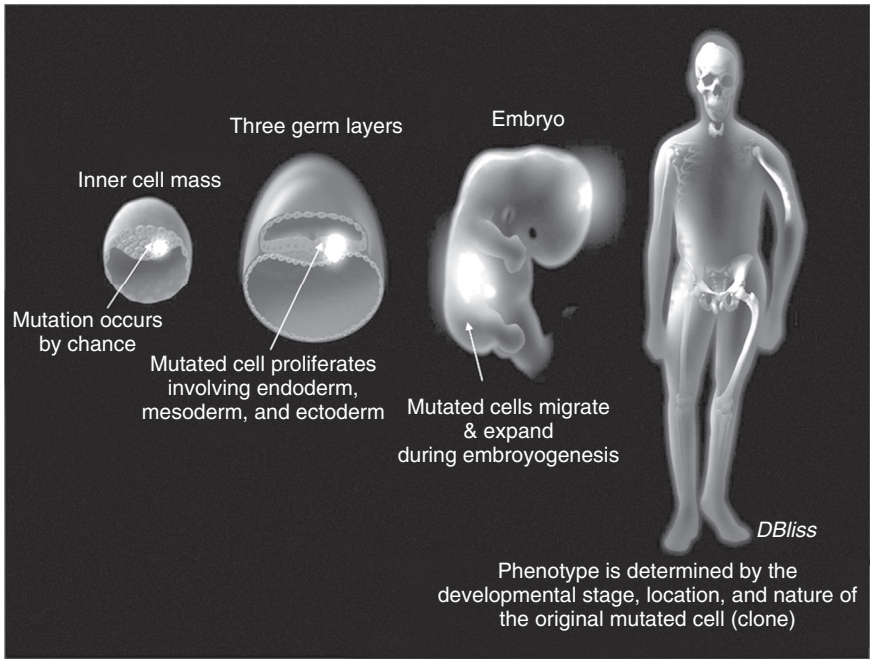

FIGURE 59.8 Developmental explanation for fibrous dysplasia of bone and McCune–Albright syndrome. For involvement of tissues that derive from all three germ layers (skin, bone, and thyroid, for example), the mutation must have occurred in the inner cell mass at the blastocyst stage. The clone in which the mutation occurs is propagated into the three germ layers and the cells migrate and proliferate, leading to the final phenotype.

nonmutated cells (Bianco et al., 1998). It is the fate of the original clone in which the mutation occurs that dictates the phenotype of an individual patient (Fig. 59.8). If the mutation occurs very early in development in a clone in the inner cell mass there will be widespread tissue involvement, perhaps involving all bones and multiple endocrine glands as well. If it occurs later in development, lateral to the midline, there may be only skeletal tissue on one side of the body involved. The "map" of affected tissue is established early in life, with the majority of FD lesions established by the age of 5 and with virtually no new lesions occurring after the age of 15 (Hart et al., 2007). Developmentally, the skeleton forms normally, in that all bones are present in the appropriate anatomical location and relative size, growth plates form normally, and the cortex of bones is intact and normal (at least initially). FD first appears in the bone marrow space of an anatomically normal bone. The fibroosseous tissue that makes up FD replaces the normal bone marrow. It can, and often does, expand within the bone marrow space, increasing the relative size of the bone marrow compartment, deforming the segment of the involved bone in an expansile fashion, and thinning the bone cortices. While entire bones, or even the entire skeleton, can be involved, the disease involves only the bone marrow compartment. Due to the fibrous nature of the tissue and the thinning of the cortex, the weight-bearing bones, especially the femurs, will often bow, giving rise to the "shepherd's crook" deformity of the proximal femur and the "windswept" deformity of the lower extremities (Fig. 59.9).

The genesis of an FD lesion, from a nascent, virtually undetectable collection of bone marrow stromal cells harboring the $G_s\alpha$ mutation and residing in the marrow of an as yet clinically unaffected young child to the full-blown, clinically significant lesion giving rise to the shepherd's crook or windswept deformity, is a complex process that involves all steps in bone development and maintenance, including modeling, bone deposition, mineralization, and remodeling (Riminucci et al., 2007). These processes give rise to a fibroosseous bone disease with a distinct and unique histopathology (Fig. 59.10). The details of the histopathology are complex and are detailed elsewhere (Riminucci et al., 1997, 1999, 2003, 2006, 2007; Bianco et al., 1998, 2000; Bianco and Robey, 1999), but the essentials include a bone marrow space that is replaced with a "fibrous" tissue that is composed of cells that express markers of osteogenic cells. The islands of bone within the fibrous tissue are abnormal in that they are immature, woven bone and have increased numbers of osteocytes. In some cases, the lesions may also include islands of chondrocytic cells. There are two hallmarks of FD histopathology: one is the presence of retracted, stellate-shaped osteoblastic cells, which is due to the effect of excess cAMP (Miller et al., 1976; Riminucci et al., 1997), and the second is the arrays of collagen bundles running perpendicular to the trabecular surface, known as Sharpey fibers (Riminucci et al., 1997), which are a normal feature at sites of tendon and ligament insertion into bone. In addition, FD, which is created by the intrinsic genetic defect in the bone marrow stromal cell, is further influenced by the abnormal extrinsic hormonal milieu that can exist as part of MAS.

It was an understanding of the signaling pathways in the involved endocrine tissues that led to the discovery of the molecular defect underlying FD. The realization that the hormonal hypersecretion was taking place in the absence of trophic hormones suggested that the defect was downstream of the cell surface receptors for these hormones and may

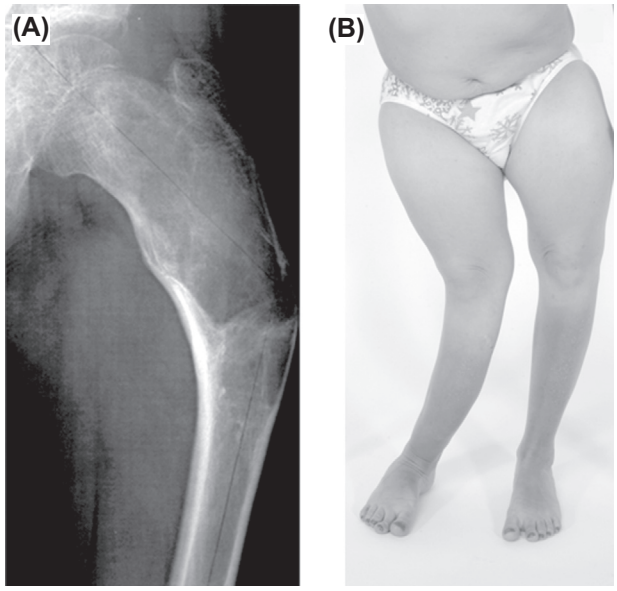

FIGURE 59.9 Classic deformities associated with fibrous dysplasia of bone. (A) The shepherd's crook deformity of the proximal femur and (B) the "windswept" deformity often seen in severe bilateral lower extremity disease are shown.

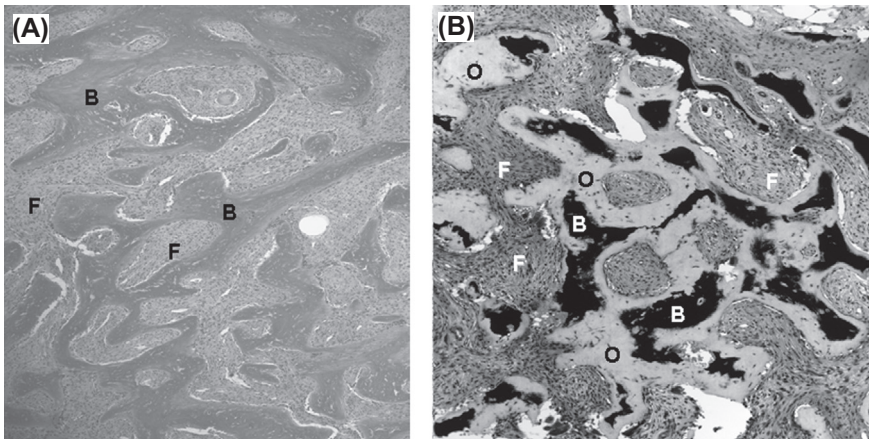

FIGURE 59.10 Histopathological appearance of fibrous dysplasia of bone. (A) Hematoxylin and eosin staining of a demineralized section of fibrous dysplasia of bone showing the classic "Chinese characters" made of trabecular bone (labeled *B*) with fibrous tissue interwoven between (labeled *F*). (B) Von Kossa stain of an un-demineralized, plastic-embedded section of bone, useful for inspecting the degree of mineralization, shows that the trabeculae of bone are composed of bone (*black*, labeled *B*) as well as osteoid (labeled *O*). The fibrous tissue is labeled (*F*). The presence of the unmineralized bone confirms the osteomalacic nature of the lesions.

involve the G proteins that are coupled to cell surface receptors in the generation of downstream signaling (Weinstein et al., 1991; Schwindinger et al., 1992). The activating mutations in $G_s\alpha$ that give rise to FD lead to ligand-independent generation of intracellular cAMP by inhibiting its intrinsic GTPase activity, leading to activation of downstream signaling pathways (Fig. 59.11) (Spiegel and Weinstein, 2004), and/or by allowing GDP-bound $G_s\alpha$ to interact with and activate adenylyl cyclase to generate cAMP (Hu and Shokat, 2018).

The endocrine organs involved, in order of prevalence, include the gonads, thyroid, pituitary (either somatotrophs or developmentally immature somatolactotrophs), and the adrenals (Danon and Crawford, 1987; Ringel et al., 1996; Collins and Shenker, 1999; Boyce and Collins, 2015). Parathyroid gland involvement has been reported to be part of the syndrome, but it is questionable if this is a feature of the disease. In the one reported case of hyperparathyroidism associated with FD/MAS in which a mutation in the hyperplastic gland was sought, it was not present. Some of the suspected cases of familial FD may represent hyperparathyroidism–jaw tumor syndrome, in which fibroosseous lesions (somewhat reminiscent of FD at the clinical, radiographic, and histopathological level) arise in the gnathic bones in association with hyperparathyroidism (Osundwa et al., 2001; Carpten et al., 2002).

Another metabolic syndrome that is commonly seen in association with FD is renal phosphate wasting (Collins et al., 2001; Bhattacharyya et al., 2012). It was originally thought that the phosphaturia and hypophosphatemia of FD were the result of activated $G_s\alpha$ in the kidney (Zung et al., 1995). However, it was subsequently demonstrated that phosphaturia is caused by oversecretion of the phosphate- and vitamin D-regulating FGF23 by FD bone cells (Riminucci et al., 2003). As such, the degree of renal phosphate wasting is directly correlated with the extent of the FD skeletal disease burden (Collins et al., 2005). Of the associated extrinsic endocrine/metabolic syndromes associated with FD, it is hypophosphatemia that probably has the most profound effect on FD. Hypophosphatemia will exacerbate the intrinsic hypomineralization that exists in FD lesions (Bianco et al., 2000; Corsi et al., 2003), and is associated with a greater degree of deformity and an increased number of fractures that occur at a younger age (Leet et al., 2004). GH excess worsens craniofacial fibrous dysplasia, leading to bone overgrowth, vision and hearing loss due to nerve compression (Cutler et al., 2006), and increased risk of malignancies (Uwaifo et al., 2001; Lee et al., 2002; Burke et al., 2017) (Fig. 59.12).

An involvement of the gastrointestinal tract with neoplasms harboring $G_s\alpha$ mutations has been found to be part of MAS. Findings range from small, asymptomatic luminal polyps to benign intraductal papillary mucinous neoplasms (IPMNs) in the pancreas, highly dysplastic luminal neoplasms, and pancreatic cancer (Gaujoux et al., 2014; Wood et al., 2017). This is not surprising, given that the same $G_s\alpha$ mutations that cause MAS have been found to be driver mutations in IPMNs (Wu et al., 2011).

Diagnosis and management

Clinically significant disease is usually diagnosed in childhood; the more significant, the earlier the presentation. The initial presentation of disease in the long bones is usually a limp, pain, or fracture through an FD lesion. Disease in the craniofacial region usually presents as a "lump." X-rays usually have a characteristic "ground glass" appearance

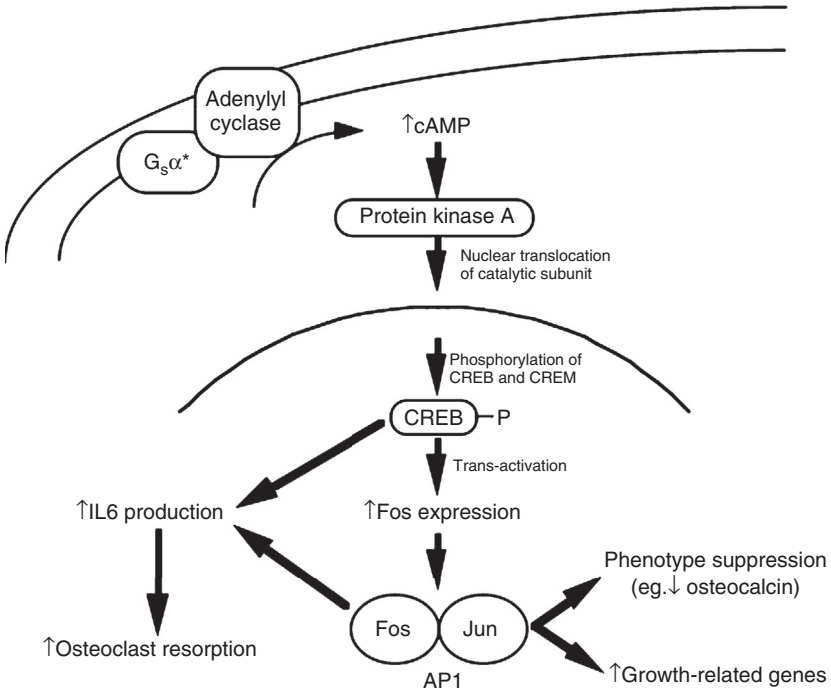

FIGURE 59.11 Possible mechanisms by which activated G_s in osteogenic cells may lead to fibrous dysplasia of bone. G_s activation increases the activity of the effector adenylyl cyclase, leading to increased intracellular cAMP levels. Binding of cAMP to the regulatory subunits of cAMP-dependent protein kinase (protein kinase A) allows release of its catalytic subunits, which translocate to the nucleus and phosphorylate proteins such as cAMP-responsive element binding protein (*CREB*) and cAMP-responsive element modulator (*CREM*). Phosphorylated CREB binds to promoters of cAMP-responsive immediate—early genes (e.g., c-*fos*) and increases their expression. Fos, the product of c-*fos*, binds with Jun to form activator protein 1 (*AP1*). AP1 is a transcription factor that increases the expression of growth-related genes and decreases the expression of osteoblast-specific genes, such as osteocalcin (phenotype suppression). Phosphorylated CREB and AP1 also stimulate the transcription of the interleukin-6 (*IL6*) gene. IL6 may be important in recruiting osteoclasts and stimulating osteoclastic bone resorption.

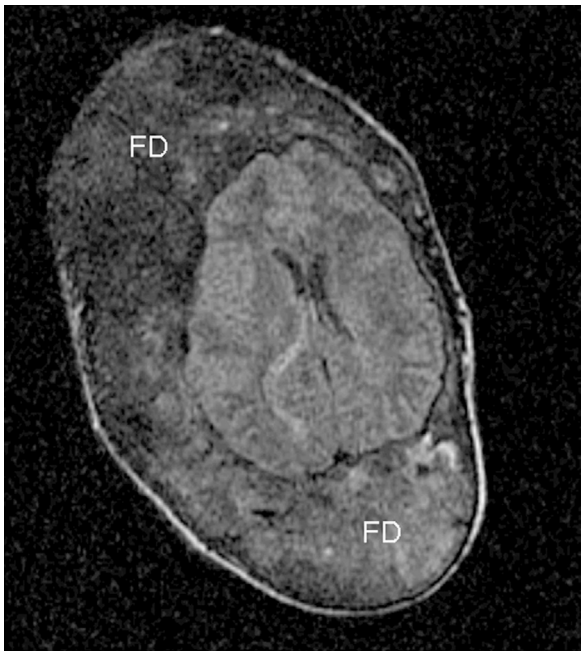

FIGURE 59.12 Craniofacial fibrous dysplasia of bone complicated by growth hormone excess. Areas of fibrous dysplasia of bone (*FD*) that have undergone massive expansion under the stimulation of excess growth hormone (GH)/insulin-like growth factor 1 in a patient with McCune—Albright syndrome are shown. The craniofacial bones are the only bones to undergo such expansion in patients with FD and GH excess.

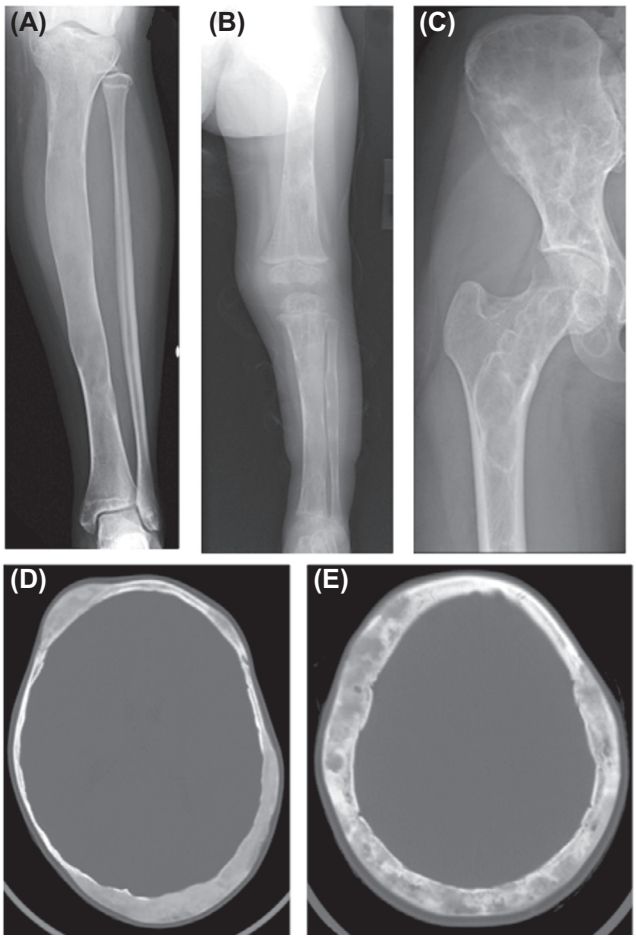

FIGURE 59.13 Radiographic appearance of fibrous dysplasia of bone. (A) The classic description of the radiographic appearance of fibrous dysplasia of bone (FD) is "ground glass," which is depicted in the tibia. (B) In very young children, there is more of a streaked appearance, and (C) in older patients with less active disease there is often a sclerotic rim around FD lesions. (D) On computed tomographic scanning in young children the appearance is, again, homogeneous and ground glass, but (E) with age, the appearance is inhomogeneous, mottled, and sometimes reported to be "cystic."

(Fig.59.13A). However, this classic ground glass appearance is age dependent. In fact, in very young children, FD is often not apparent on X-rays, and when detected has an inhomogeneous "streaked" appearance, rather than the typical ground glass appearance (Fig. 59.13B). This streaked appearance is sometimes mistaken for the "dripping candle wax" appearance of Ollier's disease. In older patients, sclerosis can appear at the edges of FD lesions, representing the reaction of the adjacent normal bone to the FD, and indicating less active disease (Fig. 59.13C). The same is true of FD in the craniofacial region. By computed tomography (CT), the modality of choice for imaging craniofacial FD, the appearance is homogeneous and ground glass in young children (Fig. 59.13D). With time, the lesions develop a mottled appearance, as they are an admixture of typical fibroosseous tissue with islands of what is essentially soft tissue (Fig. 59.13E). This appearance is often referred to as "cystic," which is a useful descriptor, but it must not be mistaken for true, fluid-filled cysts, which can also occur uncommonly in FD. Fluid-filled cysts, with pathognomonic fluid levels, which are best seen by magnetic resonance imaging, occur in $<5\%$ of cases of FD. These truly cystic lesions often behave aggressively, rapidly expanding into adjacent tissue, destroying cortex, and when they are adjacent to vital structures, especially in the skull, they can have significant morbidity (Diah et al., 2007). These lesions require immediate surgical attention. Fluid-filled cysts in the craniofacial region can be distinguished from soft tissue "cystic" lesions on CT scanning by measuring the Houndsfield units; fluid-filled lesions will be ≤ 10 HU, while cystic lesions will be > 10 HU (Collins and Bianco, 2006).

When FD lesions occur in the setting of either typical café-au-lait spots or hyperfunctioning endocrinopathies, the diagnosis is straightforward. However, if there is confusion, a biopsy demonstrating the typical histopathological changes cited earlier can aid in the diagnosis. Finally, if confusion still exists, mutation analysis on affected tissue can confirm the diagnosis if positive for a $G_s\alpha$ mutation. Another factor that can aid in the diagnosis is consideration of the bones involved

and/or the distribution of the disease. FD most commonly involves the proximal femur and skull base, and in polyostotic disease at least one of these two areas will always be involved. When multiple bones are involved, asymmetry is the rule, and the presence of bilateral, symmetric disease is suggestive of another process. In addition, measurement of skeletal disease burden by bone scan can quantify the extent of the disease and aid in prognostication in terms of potential future morbidity (Collins et al., 2005).

In evaluating and caring for patients with FD, it is important to screen for and treat associated endocrinopathies. The correlation between the extent of the skeletal disease and the extent of endocrine involvement is not high, so one cannot assume that minimal skeletal disease automatically excludes the presence of significant endocrine disease. A careful history, physical examination, evaluation of the growth chart, and focused laboratory testing are necessary. The evaluation should assess for precocious puberty, hyperthyroidism, hypophosphatemia (with a low serum $1,25(OH)_2D$ and renal phosphate wasting), and GH excess. Glucocorticoid excess can also occur, usually in the neonatal period. The altered phosphate and vitamin D metabolism is due to overproduction of the phosphaturic factor FGF23 by FD bone, so measurement of serum FGF23 can aid in the diagnosis (Collins et al., 2001; Riminucci et al., 2003). There is a direct correlation between the risk for hypophosphatemia and the FD skeletal burden, with FGF23-mediated renal phosphate wasting seen only in cases of fairly extensive FD.

Surgery remains the mainstay of treatment for FD of the appendicular skeleton. Yet, there is no consensus as of this writing as to the timing or indications and which techniques are best for which indication and at which age. There is an emerging consensus that, when their use is possible, intramedullary rods are better than side plates and screws (Ippolito et al., 2003; Stanton, 2006; Leet and Collins, 2007; Majoor et al., 2018). While bone grafting (filling FD lesions with grafting material, often bone bank, cadaveric bone) was at one time considered useful, a consensus is emerging, especially in children, that this is not the best practice (Ippolito et al., 2003; Leet et al., 2016).

The skull base, through which the optic nerves pass, is the most common site for FD involvement, and it was believed that optic nerve encasement was progressive and visual impairment the rule if untreated (Moore et al., 1985; Chen et al., 1997). For this reason, prophylactic decompression of the optic nerves was recommended. However, evidence has shown this not to be the case (Lee et al., 2002). In fact, the majority of patients with skull base FD, despite extensive disease, will have normal vision throughout their life. It has been further shown that the one group of patients who do suffer functional morbidity due to craniofacial FD (blindness and deafness) are the subgroup of patients with GH excess (Cutler et al., 2006; Amit et al., 2011; Boyce et al., 2013, 2016). This point emphasizes the importance for screening and treatment of GH excess in patients with craniofacial FD.

Another aspect of the disease that needs to be noted because of the possibility of significant morbidity, and even mortality, is that of scoliosis associated with FD of the vertebral column (Mancini et al., 2009). FD in the spine was thought to be an uncommon occurrence, probably because it is difficult to detect on plain radiographs. However, it has been shown that when the sensitive detection technique of ^{99}Tc−methylene diphosphonate bone scanning is used, FD in the spine can be seen in up to 63% of the patients, and that in 64% of the patients who had FD in the spine there was associated scoliosis (Leet et al., 2004a,b). Importantly, while scoliosis can be progressive and associated with significant morbidity and mortality, it is also amenable to surgical correction. Surgical correction is usually effective and lasting, more so than most other surgical interventions in FD.

Bisphosphonates are a useful adjuvant in the treatment of some patients with FD. Early reports contained great enthusiasm for the use of bisphosphonates having a significant effect on the natural history of the disease (Liens et al., 1994; Chapurlat et al., 1997; Zacharin and O'Sullivan, 2000; Parisi et al., 2001). However, subsequent studies and longer follow-up have not substantiated this benefit (Plotkin et al., 2003; Chan and Zacharin, 2006), including the only randomized, placebo-controlled study published as of this writing (Boyce et al., 2014). Yet, it is clear that bisphosphonates can be effective in the relief of pain associated with FD in some patients (Plotkin et al., 2003; Chapurlat, 2006; Lala et al., 2006). Pain is one of the most significant causes of disease-related loss of quality of life in FD (Kelly et al., 2005, 2008). The pain can often be debilitating and require the use of narcotic analgesics. Quite often this pain can be controlled with the use of high-dose intravenous bisphosphonates. However, it has been our experience that the pain of craniofacial FD is often less amenable to treatment with bisphosphonates. Other medical treatments have been tried, including calcitonin (Bell et al., 1970), glucocorticoids (Di Figlia, 1951), and external beam radiation (Tanner et al., 1961), but with no benefit. In fact, it has been demonstrated that external beam radiation is probably associated with an increased rate of sarcomatous transformation (Ruggieri et al., 1994).

More recently, case reports and small series suggest the anti-RANKL drug denosumab may be an effective treatment (Boyce et al., 2012; Benhamou et al., 2014; Ganda and Seibel, 2014). However, as with other high-turnover bone diseases, when denosumab is discontinued, there can be a dramatic increase in bone turnover and hypercalcemia (Boyce et al., 2012). Based on the finding of increased levels of interleukin-6 (IL-6) production by mutation-bearing FD bone cells in

preclinical in vitro models (Riminucci et al., 2003), anti-IL-6 therapy with the anti-IL-6 receptor drug tocilizumab has been undertaken with apparent benefit (Chapurlat et al., 2012).

In summary, FD is a complicated disease that results from somatic mutations in *GNAS* that occur early in embryogenesis and lead to a specific mosaic pattern of involved bones that is established early in development. The intrinsic genetic defect can be influenced by associated endocrine dysfunction that can occur as part of MAS, and highlights the need for screening and treatment of associated endocrine diseases. While a consensus on surgical treatment is lacking, progress has been made. As of this writing medical treatment appears to be palliative, with bisphosphonates offering significant benefit in terms of pain control. Denosumab and tocilizumab show promise for the future. Improvement in both medical and surgical care is needed, and given the relative rarity of the disease, will come only from multicenter, international cooperative studies.

References

Abel, T., et al., 1997. Genetic demonstration of a role for PKA in the late phase of LTP and in hippocampus-based long-term memory. Cell 88, 615–626.

Agarwal, C., et al., 2006. Pseudohypoparathyroidism: a rare cause of bilateral slipped capital femoral epiphysis. J. Pediatr. 149, 406–408.

Ahmed, S.F., et al., 2002. *GNAS1* mutations and progressive osseous heteroplasia. N. Engl. J. Med. 346, 166–1670. Letter to Editor.

Ahmed, S.F., et al., 1998. *GNAS1* mutational analysis in pseudohypoparathyroidism. Clin. Endocrinol. 49, 525–531.

Ahrens, W., et al., 2001. Analysis of the *GNAS1* gene in Albright's hereditary osteodystrophy. J. Clin. Endocrinol. Metab. 86, 4630–4634.

Albright Fuller, B.A., Hampton, A.O., Smith, P., 1937. Syndrome characterized by osteitis fibrosa disseminata, areas, of pigmentation, and endocrine dysfunction, with precocious puberty in females: report of 5 cases. N. Engl. J. Med. 216, 727–746.

Aldred, M.A., et al., 2000. Germline mosaicism for a *GNAS1* mutation and Albright hereditary osteodystrophy. J. Med. Genet. 37, E35.

Aldred, M.A., Trembath, R.C., 2000. Activating and inactivating mutations in the human *GNAS1* gene. Hum. Mutat. 16, 183–189.

Allen, J.A., et al., 2005. β-adrenergic receptor stimulation promotes Gαs internalization through lipid rafts: a study in living cells. Mol. Pharmacol. 67, 1493–1504.

Amit, M., et al., 2011. Surgery versus watchful waiting in patients with craniofacial fibrous dysplasia–a meta-analysis. PLoS One 6, e25179.

Bakker, B., et al., 2015. A girl with Beckwith-Wiedemann syndrome and pseudohypoparathyroidism type 1B due to multiple imprinting defects. J. Clin. Endocrinol. Metab. 100, 3963–3966.

Balachandar, V., et al., 1975. Pseudohypoparathyroidism with normal serum calcium level. Am. J. Dis. Child. 129, 1092–1095.

Barr, D.G.D., et al., 1994. Evolution of pseudohypoparathyroidism: an informative family study. Arch. Dis. Child. 70, 337–338.

Bastepe, M., et al., 2011. Paternal uniparental isodisomy of the entire chromosome 20 as a molecular cause of pseudohypoparathyroidism type Ib (PHP-Ib). Bone 48, 659–662.

Bastepe, M., et al., 2005. Deletion of the NESP55 differentially methylated region causes loss of maternal *GNAS* imprints and pseudohypoparathyroidism type Ib. Nat. Genet. 37, 25–27.

Bastepe, M., et al., 2002. Receptor-mediated adenylyl cyclase activation through XLαs, the extra-large variant of the stimulatory G protein α subunit. Mol. Endocrinol. 16, 1912–1919.

Bastepe, M., Juppner, H., 2000. Identification and characterization of two new, highly polymorphic loci adjacent to *GNAS1* on chromosome 20q13.3. Mol. Cell. Probes 14, 261–264.

Bastepe, M., et al., 2001a. Paternal uniparental disomy of chromosome 20q- and the resulting changes in *GNAS1* methylation- as a plausible cause of pseudohypoparathyroidism. Am. J. Hum. Genet. 68, 1283–1289.

Bastepe, M., et al., 2001b. Positional dissociation between the genetic mutation responsible for pseudohypoparathyroidism type Ib and the associated methylation defect at exon A/B: evidence for a long-range regulatory element within the imprinted *GNAS1* locus. Hum. Mol. Genet. 10, 1231–1241.

Bastepe, M., et al., 2004. Stimulatory G protein directly regulates hypertrophic differentiation of growth plate cartilage *in vivo*. Proc. Natl. Acad. Sci. U. S. A 101, 14794–14799.

Bell, N.H., et al., 1970. Effects of calcitonin in Paget's disease and polyostotic fibrous dysplasia. J. Clin. Endocrinol. Metab. 31, 283–290.

Benhamou, J., et al., 2014. Transient improvement of severe pain from fibrous dysplasia of bone with denosumab treatment. Joint Bone Spine 81, 549–550.

Berglund, J.A., et al., 2018. Scoliosis in fibrous dysplasia/McCune-Albright syndrome: factors associated with curve progression and effects of bisphosphonates. J. Bone Miner. Res. https://doi.org/10.1002/jbmr.3446. E-published.

Bertaux, K., et al., 2006. Runx2 regulates the expression of *GNAS* on SaOs-2 cells. Bone 38, 943–950.

Bhattacharyya, N., et al., 2012. Mechanism of FGF23 processing in fibrous dysplasia. J. Bone Miner. Res. 27, 1132–1141.

Bianco, P., et al., 1998. Reproduction of human fibrous dysplasia of bone in immunocompromised mice by transplanted mosaics of normal and Gsα-mutated skeletal progenitor cells. J. Clin. Investig. 101, 1737–1744.

Bianco, P., et al., 2000. Mutations of the *GNAS1* gene, stromal cell dysfunction, and osteomalacic changes in non-McCune-Albright fibrous dysplasia of bone. J. Bone Miner. Res. 15, 120–128.

Bianco, P., Robey, P., 1999. Diseases of bone and the stromal cell lineage. J. Bone Miner. Res. 14, 336–341.

Bianco, P., Robey, P.G., 2015. Skeletal stem cells. Development 142, 1023–1027.

Bianco, P., et al., 2003. In: Glorieux, F.H., Pettifor, J., Juppner, H. (Eds.), Fibrous Dysplasia. Pediatric Bone: Biology and Disease. Academic Press, Elsevier, New York, NY, pp. 509–539.

Biazzo, A., et al., 2017. Mazabraud syndrome associated with McCune-Albright syndrome: a case report and review of the literature. Acta Biomed. 88, 198–200.

Bomsel, M., Mostov, K., 1992. Role of heterotrimeric G proteins in membrane traffic. Mol. Biol. Cell 3, 1317–1328.

Bourne, H.R., et al., 1981. Fibroblast defect in pseudohypoparathyroidism, type I: reduced activity of receptor-cyclase coupling protein. J. Clin. Endocrinol. Metab. 53, 636–640.

Boyce, A.M., et al., 2016. Surgical management of polyostotic craniofacial fibrous dysplasia: long-term outcomes and predictors for postoperative regrowth. Plast. Reconstr. Surg. 137, 1833–1839.

Boyce, A.M., et al., 2012. Denosumab treatment for fibrous dysplasia. J. Bone Miner. Res. 27, 1462–1470.

Boyce, A.M., Collins, M.T., 2015. Fibrous dysplasia/McCune-Albright syndrome. In: Pagon, R.A., Adam, M.P., Ardinger, H.H., et al. (Eds.), GeneReviews. University of Washington, Seattle (WA), pp. 1993–2018.

Boyce, A.M., et al., 2013. Optic neuropathy in McCune-Albright syndrome: effects of early diagnosis and treatment of growth hormone excess. J. Clin. Endocrinol. Metab. 98, E126–E134.

Boyce, A.M., et al., 2014. A randomized, double blind, placebo-controlled trial of alendronate treatment for fibrous dysplasia of bone. J. Clin. Endocrinol. Metab. 99, 4133–4140.

Braun, J.J., et al., 1981. Lack of response of 1,25-dihydroxycholecalciferol to exogenous parathyroid hormone in a patient with treated pseudohypoparathyroidism. Clin. Endocrinol. 14, 403–407.

Bray, P., et al., 1986. Human cDNA clones for four species of $G_{\alpha s}$ signal transduction protein. Proc. Natl. Acad. Sci. U. S. A 83, 8893–8897.

Brehin, A.C., et al., 2015. Loss of methylation at *GNAS* exon A/B is associated with increased intrauterine growth. J. Clin. Endocrinol. Metab. 100, E623–E631.

Breslau, N.A., et al., 1980. Studies on the attainment of normocalcemia in patients with pseudohypoparathyroidism. Am. J. Med. 68, 856–860.

Breslau, N.A., Weinstock, R.S., 1988. Regulation of 1,25 (OH)2D synthesis in hypoparathyroidism and pseudohypoparathyroidism. Am. J. Physiol. 255, E730–E736.

Brickman, A.S., et al., 1981. Prolactin and calcitonin responses to parathyroid hormone infusion in hypoparathyroid, pseudohypoparathyroid, and normal subjects. J. Clin. Endocrinol. Metab. 53, 661–664.

Brickman, A.S., et al., 1986. Responses to glucagon infusion in pseudohypoparathyroidism. J. Clin. Endocrinol. Metab. 63, 1354–1360.

Burke, A.B., et al., 2017. Fibrous dysplasia of bone: craniofacial and dental implications. Oral Dis. 23, 697–708.

Cairns, D.M., et al., 2013. Somitic disruption of *GNAS* in chick embryos mimics progressive osseous heteroplasia. J. Clin. Investig. 123, 3624–3633.

Campbell, R., et al., 1994. Parental origin of transcription from the human *GNAS1* gene. J. Med. Genet. 31, 607–614.

Carel, J.C., et al., 1999. Resistance to the lipolytic action of epinephrine: a new feature of protein G_s deficiency. J. Clin. Endocrinol. Metab. 84, 4127–4131.

Carlson, H.E., Brickman, A.S., 1983. Blunted plasma cyclic adenosine monophosphate response to isoproterenol in pseudohypoparathyroidism. J. Clin. Endocrinol. Metab. 56, 1323–1326.

Carlson, H.E., et al., 1977. Prolactin deficiency in pseudohypoparathyroidism. N. Engl. J. Med. 296, 140–144.

Carlson, H.E., et al., 1985. Normal free fatty acid response to isoproterenol in pseudohypoparathyroidism. J. Clin. Endocrinol. Metab. 61, 382–384.

Carpten, J.D., et al., 2002. HRPT2, encoding parafibromin, is mutated in hyperparathyroidism-jaw tumor syndrome. Nat. Genet. 32, 676–680.

Carter, A., et al., 1987. Reduced expression of multiple forms of the α subunit of the stimulatory GTP-binding protein in pseudohypoparathyroidism type Ia. Proc. Natl. Acad. Sci. U. S. A 84, 7266–7269.

Cass, L.A., Meinkoth, J.L., 1998. Differential effecs of cyclic adenosine 3′,5′-monophosphate on p70 ribosomal S6 kinase. Endocrinology 139, 1991–1998.

Chan, B., Zacharin, M., 2006. Pamidronate treatment of polyostotic fibrous dysplasia: failure to prevent expansion of dysplastic lesions during childhood. J. Pediatr. Endocrinol. Metab. 19, 75–80.

Chapurlat, R.D., 2006. Medical therapy in adults with fibrous dysplasia of bone. J. Bone Miner. Res. 21 (Suppl. 2), P114–P119.

Chapurlat, R.D., et al., 1997. Long-term effects of intravenous pamidronate in fibrous dysplasia of bone. J. Bone Miner. Res. 12, 1746–1752.

Chapurlat, R.D., et al., 2012. Pathophysiology and medical treatment of pain in fibrous dysplasia of bone. Orphanet J. Rare Dis. 7 (Suppl. 1), S3.

Chase, L.R., et al., 1969. Pseudohypoparathyroidism: defective excretion of 3′,5′-AMP in response to parathyroid hormone. J. Clin. Investig. 48, 1832–1844.

Chen, H., et al., 2005a. Multiple intracranial calcifications and spinal compressions: rare complications of type la pseudohypoparathyroidism. J. Endocrinol. Investig. 28, 646–650.

Chen, M., et al., 2005b. Alternative *Gnas* gene products have opposite effects on glucose and lipid metabolism. Proc. Natl. Acad. Sci. U. S. A 102, 7386–7391.

Chen, M., et al., 2017. $G_s\alpha$ deficiency in the dorsomedial hypothalamus underlies obesity associated with $G_s\alpha$ mutations. J. Clin. Investig. 127, 500–510.

Chen, M., et al., 2009. Central nervous system imprinting of the G protein $G_s\alpha$ and its role in metabolic regulation. Cell Metabol. 9, 548–555.

Chen, Y.R., et al., 1997. Optic nerve decompression in fibrous dysplasia: indications, efficacy, and safety. Plast. Reconstr. Surg. 99, 22–30.

Chillambhi, S., et al., 2010. Deletion of the noncoding *GNAS* antisense transcript causes pseudohypoparathyroidism type Ib and biparental defects of *GNAS* methylation in *cis*. J. Clin. Endocrinol. Metab. 95, 3993–4002.

Coleman, D.E., et al., 1994. Structures of active conformations of $G_{i\alpha 1}$ and the mechanism of GTP hydrolysis. Science 265, 1405–1412.
Collins, M., Shenker, A., 1999. McCune-Albright syndrome: new insights. Curr. Opin. Endocrinol. Diabetes 6, 119–125.
Collins, M.T., 2006. Spectrum and natural history of fibrous dysplasia of bone. J. Bone Miner. Res. 21 (Suppl. 2), P99–P104.
Collins, M.T., Bianco, P., 2003. Fibrous dysplasia. In: Favus, M.J. (Ed.), Primer on the Metabolic Bone Diseases and Disorders of Mineral Metabolism. American Society for Bone and Mineral Research, Washington, D.C., pp. 466–470
Collins, M.T., Bianco, P., 2006. Fibrous dysplasia. In: Favus, M.J. (Ed.), Primer on the Metabolic Bone Diseases and Disorders of Mineral Metabolism. American Society for Bone and Mineral Research, Washington, D.C., pp. 415–418
Collins, M.T., et al., 2001. Renal phosphate wasting in fibrous dysplasia of bone is part of a generalized renal tubular dysfunction similar to that seen in tumor-induced osteomalacia. J. Bone Miner. Res. 16, 806–813.
Collins, M.T., et al., 2005. An instrument to measure skeletal burden and predict functional outcome in fibrous dysplasia of bone. J. Bone Miner. Res. 20, 219–226.
Conklin, B.R., et al., 1996. Carboxyl-terminal mutations of Gqα and Gsα that alter the fidelity of receptor activation. Mol. Pharmacol. 50, 885–890.
Corsi, A., et al., 2003. Osteomalacic and hyperparathyroid changes in fibrous dysplasia of bone: core biopsy studies and clinical correlations. J. Bone Miner. Res. 18, 1235–1246.
Costello, J.M., Dent, C.E., 1963. Hypo-hyperparathyroidism. Arch. Dis. Child. 38, 397.
Court, F., et al., 2013. Genome-wide allelic methylation analysis reveals disease-specific susceptibility to multiple methylation defects in imprinting syndromes. Hum. Mutat. 34, 595–602.
Cummings, D.E., et al., 1996. Genetically lean mice result from targeted disruption of the RIIb subunit of protein kinase A. Nature 382, 622–626.
Cutler, C.M., et al., 2006. Long-term outcome of optic nerve encasement and optic nerve decompression in patients with fibrous dysplasia: risk factors for blindness and safety of observation. Neurosurgery 59, 1011–1017.
Danon, M., Crawford, J.D., 1987. The McCune-Albright syndrome. Engeb. Inn. Med. Kinderheilkd. 55, 81–115.
Davies, S.J., Hughes, H.E., 1993. Imprinting in Albright's hereditary osteodystrophy. J. Med. Genet. 30, 101–103.
de Rooij, J., et al., 1998. Epac is a Rap1 guanine-nucleotide-exchange factor directly activated by cyclic AMP. Nature 396, 474–477.
de Sanctis, C., et al., 2003. Pubertal development in patients with McCune-Albright syndrome or pseudohypoparathyroidism. J. Pediatr. Endocrinol. Metab. 16 (Suppl. 2), 293–296.
de Sanctis, L., et al., 2007. GH secretion in a cohort of children with pseudohypoparathyroidism type Ia. J. Endocrinol. Investig. 30, 97–103.
Di Figlia, S.E., 1951. Cortisone in polyostotic fibrous dysplasia. N. Y. State J. Med. 51, 2665.
Diah, E., et al., 2007. Cyst degeneration in craniofacial fibrous dysplasia: clinical presentation and management. J. Neurosurg. 107, 504–508.
DiCaprio, M.R., Enneking, W.F., 2005. Fibrous dysplasia. Pathophysiology, evaluation, and treatment. J. Bone Joint. Surg. Am. 87, 1848–1864.
Doty, R.L., et al., 1997. Olfactory dysfunction in type I pseudohypoparathyroidism: dissociation from G_sa deficiency. J. Clin. Endocrinol. Metab. 82, 247–250.
Downs Jr., R.W., et al., 1983. Deficient adenylate cyclase regulatory protein in renal membranes from a patient with pseudohypoparathyroidism. J. Clin. Investig. 71, 231–235.
Drezner, M.K., Haussler, M.R., 1979. Normocalcemic pseudohypoparathyroidism. Association with normal vitamin D3 metabolism. Am. J. Med. 66, 503–508.
Drezner, M.K., et al., 1976. 1,25-dihydroxycholecalciferol deficiency: the probable cause of hypocalcemia and metabolic bone disease in pseudohypoparathyroidism. J. Clin. Endocrinol. Metab. 42, 621–628.
Eddy, M.C., et al., 2000. Deficiency of the α-subunit of the stimulatory G protein and severe extraskeletal ossification. J. Bone Miner. Res. 15, 2074–2083.
Elli, F.M., et al., 2014. Quantitative analysis of methylation defects and correlation with clinical characteristics in patients with pseudohypoparathyroidism type I and *GNAS* epigenetic alterations. J. Clin. Endocrinol. Metab. 99, E508–E517.
Epstein, S., et al., 1983. 1a,25-dihydroxyvitamin D3 corrects osteomalacia in hypoparathyroidism and pseudohypoparathyroidism. Acta Endocrinol. 103, 241–247.
Eyre, W.G., Reed, W.B., 1971. Albright's hereditary osteodystrophy with cutaneous bone formation. Arch. Dermatol. 104, 634–642.
Farfel, Z., et al., 1982. Deficient activity of receptor-cyclase coupling protein in transformed lymphoblasts of patients with pseudohypoparathyroidism type I. J. Clin. Endocrinol. Metab. 55, 113–117.
Farfel, Z., Bourne, H.R., 1980. Deficient activity of receptor-cyclase coupling protein in platelets of patients with pseudohypoparathyroidism. J. Clin. Endocrinol. Metab. 51, 1202–1204.
Farfel, Z., et al., 1980. Defect of receptor-cyclase coupling protein in pseudohypoparathyroidism. N. Engl. J. Med. 303, 237–242.
Farfel, Z., et al., 1981. Pseudohypoparathyroidism: inheritance of deficient receptor-cyclase coupling activity. Proc. Natl. Acad. Sci. U. S. A 78, 3098–3102.
Farfel, Z., Friedman, E., 1986. Mental deficiency in pseudohypoparathyroidism type I is associated with Ns-protein deficiency. Ann. Intern. Med. 105, 197–199.
Farfel, Z., et al., 1996. Pseudohypoparathyroidism: a novel mutation in the βγ-contact region of $G_s\alpha$ impairs receptor stimulation. J. Biol. Chem. 271, 19653–19655.
Faull, C.M., et al., 1991. Pseudohypoparathyroidism: its phenotypic variability and associated disorders in a large family. Q. J. Med. 78, 251–264.
Fernandez-Rebollo, E., et al., 2013. Endocrine profile and phenotype-(epi)genotype correlation in Spanish patients with pseudohypoparathyroidism. J. Clin. Endocrinol. Metab. 98, E996–E1006.

Fischer, J.A., et al., 1998. An inherited mutation associated with functional deficiency of the α-subunit of the guanine nucleotide-binding protein G_s in pseudo- and pseudopseudohypoparathyroidism. J. Clin. Endocrinol. Metab. 83, 935–938.

Foppiani, L., et al., 2006. Clinical heterogeneity of familial pseudohypoparathyroidism. J. Endocrinol. Investig. 29, 94–96.

Frohlich, L.F., et al., 2007. Lack of *Gnas* epigenetic changes and pseudohypoparathyroidism type Ib in mice with targeted disruption of syntaxin-16. Endocrinology 148, 2925–2935.

Ganda, K., Seibel, M.J., 2014. Rapid biochemical response to denosumab in fibrous dysplasia of bone: report of two cases. Osteoporos. Int. 25, 777–782.

Gaujoux, S., et al., 2014. Hepatobiliary and pancreatic neoplasms in patients with McCune-Albright syndrome. J. Clin. Endocrinol. Metab. 99, E97–E101.

Gejman, P.V., et al., 1991. Genetic mapping of the Gs-α subunit gene (*GNAS1*) to the distal long arm of chromosome 20 using a polymorphism detected by denaturing gradient gel electrophoresis. Genomics 9, 782–783.

Gelfand, I.M., et al., 2006. Presentation and clinical progression of pseudohypoparathyroidism with multi-hormone resistance and Albright hereditary osteodystrophy: a case series. J. Pediatr. 149, 877–880.

Gelfand, I.M., et al., 2007. Progressive osseous heteroplasia-like heterotopic ossification in a male infant with pseudohypoparathyroidism type Ia: a case report. Bone 40, 1425–1428.

Germain-Lee, E.L., et al., 2002. Paternal imprinting of Gαs in the human thyroid as the basis of TSH resistance in pseudohypoparathyroidism type 1a. Biochem. Biophys. Res. Commun. 296, 67–72.

Germain-Lee, E.L., et al., 2003. Growth hormone deficiency in pseudohypoparathyroidism type 1a: another manifestation of multihormone resistance. J. Clin. Endocrinol. Metab. 88, 4059–4069.

Goadsby, P.J., et al., 1991. Pseudopseudohypoparathyroidism and spinal cord compression. J. Neurol. Neurosurg. Psychiatry 54, 929–931.

Goeteyn, V., et al., 1999. Osteoma cutis in pseudohypoparathyroidism. Dermatology 198, 209–211.

Graudal, N., et al., 1986. Coexistent pseudohypoparathyroidism and D brachydactyly in a family. Clin. Genet. 30, 449–455.

Graziano, M.P., Gilman, A.G., 1989. Synthesis in *Escherichia coli* of GTPase-deficient mutants of Gsα. J. Biol. Chem. 264, 15475–15482.

Grishina, G., Berlot, C.H., 1998. Mutations at the interface of $G_{s\alpha}$ impair receptor-mediated activation by altering receptor and guanine nucleotide binding. J. Biol. Chem. 273, 15053–15060.

Grishina, G., Berlot, C.H., 2000. A surface-exposed region of $G_{s\alpha}$ in which substitutions decrease receptor-mediated activation and increase receptor affinity. Mol. Pharmacol. 57, 1081–1092.

Happle, R., 1986. The McCune-Albright syndrome: a lethal gene surviving by mosaicism. Clin. Genet. 29, 321–324.

Happle, R., 2016. Progressive osseous heteroplasia is not a Mendelian trait but a type 2 segmental manifestation of *GNAS* inactivation disorders: a hypothesis. Eur. J. Med. Genet. 59, 290–294.

Hart, E.S., et al., 2007. Onset, progression, and plateau of skeletal lesions in fibrous dysplasia, and the relationship to functional outcome. J. Bone Miner. Res. 22, 1468–1474.

Hayward, B.E., et al., 2001. Imprinting of the $G_s\alpha$ gene *GNAS1* in the pathogenesis of acromegaly. J. Clin. Investig. 107, R31–R36.

Hayward, B.E., et al., 1998a. The human *GNAS1* gene is imprinted and encodes distinct paternally and biallelically expressed G proteins. Proc. Natl. Acad. Sci. U. S. A 95, 10038–10043.

Hayward, B.E., et al., 1998b. Bidirectional imprinting of a single gene: *GNAS1* encodes maternally, paternally, and biallelically derived proteins. Proc. Natl. Acad. Sci. U. S. A 95, 15475–15480.

Heinsimer, J.A., et al., 1984. Impaired formation of β-adrenergic receptor-nucleotide regulatory protein complexes in pseudohypoparathyroidism. J. Clin. Investig. 73, 1335–1343.

Henkin, R.I., 1968. Impairment of olfaction and of the tastes of sour and bitter in pseudohypoparathyroidism. J. Clin. Endocrinol. Metab. 28, 624–628.

Hou, J.-W., 2006. Progressive osseous heteroplasia controlled by intravenous administration of pamidronate. Am. J. Med. Genet. 140A, 910–913.

Hu, Q., Shokat, K.M., 2018. Disease-causing mutations in the G protein Gαs subvert the roles of GDP and GTP. Cell 173, 1254–1264.

Huang, C., et al., 1999. Persistent membrane association of activated and depalmitoylated G protein α subunits. Proc. Natl. Acad. Sci. U. S. A 96, 412–417.

Idowu, B.D., et al., 2007. A sensitive mutation-specific screening technique for *GNAS1* mutations in cases of fibrous dysplasia: the first report of a codon 227 mutation in bone. Histopathology 50, 691–704.

Iiri, T., et al., 1997. Conditional activation defect of a human $G_{s\alpha}$ mutant. Proc. Natl. Acad. Sci. U. S. A 94, 5656–5661.

Iiri, T., et al., 1994. Rapid GDP release from Gsα in patients with gain and loss of endocrine function. Nature 371, 164–167.

Ikeda, K., et al., 1988. Clinical investigation of olfactory and auditory function in type I pseudohypoparathyroidism: participation of adenylate cyclase system. J. Laryngol. Otol. 102, 1111–1114.

Ippolito, E., et al., 2003. Natural history and treatment of fibrous dysplasia of bone: a multicenter clinicopathologic study promoted by the European Pediatric Orthopaedic Society. J. Pediatr. Orthop. B 12, 155–177.

Ish-Shalom, S., et al., 1996. Normal parathyroid hormone responsiveness of bone-derived cells from a patient with pseudohypoparathyroidism. J. Bone Miner. Res. 11, 8–14.

Ishikawa, Y., et al., 1990. Alternative promoter and 5′ exon generate a novel $G_s\alpha$ mRNA. J. Biol. Chem. 265, 8458–8462.

Jan de Beur, S., et al., 2003. Discordance between genetic and epigenetic defects in pseudohypoparathyroidism type 1b revealed by inconsistent loss of maternal imprinting at *GNAS1*. Am. J. Hum. Genet. 73, 314–322.

Jessen, U., et al., 2001. The transcriptional factors CREB and c-Fos play key roles in NCAM-mediated neuritogenesis in PC12-E2 cells. J. Neurochem. 79, 1149–1160.

Jhala, D.N., et al., 2003. Osteosarcoma in a patient with McCune-Albright syndrome and Mazabraud's syndrome: a case report emphasizing the cytological and cytogenetic findings. Hum. Pathol. 34, 1354–1357.

Jobert, A.S., et al., 1998. Absence of functional receptors for parathyroid hormone and parathyroid hormone-related peptide in Blomstrand chondrodysplasia. J. Clin. Investig. 102, 34–40.

Jones, D.T., et al., 1990. Biochemical characterization of three stimulatory GTP-binding proteins. The large and small forms of Gs and the olfactory-specific G-protein, Golf. J. Biol. Chem. 265, 2671–2676.

Joseph, A.W., et al., 2011. Increased prevalence of carpal tunnel syndrome in albright hereditary osteodystrophy. J. Clin. Endocrinol. Metab. 96, 2065–2073.

Juppner, H., et al., 1998. The gene responsible for pseudohypoparathyroidism type Ib is paternally imprinted and maps in four unrelated kindreds to chromosome 20q13.3. Proc. Natl. Acad. Sci. U. S. A 95, 11798–11803.

Kaartinen, J.M., et al., 1994. Defective stimulation of adipocyte adenylate cyclase, blunted lipolysis, and obesity in pseudohypoparathyroidism 1a. Pediatr. Res. 35, 594–597.

Kaplan, F.S., Shore, E.I., 2000. Progressive osseous heteroplasia. J. Bone Miner. Res. 15, 2084–2094.

Karaplis, A.C., et al., 1994. Lethal skeletal dysplasia from targeted disruption of the parathyroid hormone-related peptide gene. Genes Dev. 8, 277–289.

Kawasaki, H., et al., 1998. A family of cAMP-binding proteins that directly activate Rap1. Science 282, 2275–2279.

Kehlenbach, R.H., et al., 1994. XLαs is a new type of G protein. Nature 372, 804–809.

Kelly, M.H., et al., 2008. Pain in fibrous dysplasia of bone: age-related changes and the anatomical distribution of skeletal lesions. Osteoporos. Int. 19, 57–63.

Kelly, M.H., et al., 2005. Physical function is impaired but quality of life preserved in patients with fibrous dysplasia of bone. Bone 37, 388–394.

Kelsey, G., et al., 1999. Identification of imprinted loci by methylation-sensitive representational difference analysis: application to mouse distal chromosome 2. Genomics 62, 129–138.

Klemke, M., et al., 2000. Characterization of the extra-large G protein α-subunit XLαs. II. Signal transduction properties. J. Biol. Chem. 275, 33633–33640.

Kolb, F.O., Steinbach, H.L., 1962. Pseudohypoparathyroidism with secondary hyperparathyroidism and osteitis fibrosa. J. Clin. Endocrinol. Metab. 22, 59–70.

Kozasa, T., et al., 1988. Isolation and characterization of the human Gsα gene. Proc. Natl. Acad. Sci. U. S. A 85, 2081–2085.

Krieger-Brauer, H.I., et al., 2000. Basic fibroblast growth factor utilized both types of component subunits of G_s for dual signaling in human adipocytes. Stimulation of adenylyl cyclase vis $G\alpha_s$ and inhibition of NADPH oxidase by $G\beta\gamma_s$. J. Biol. Chem. 275, 35920–35925.

Kronenberg, H.M., 2003. Developmental regulation of the growth plate. Nature 423, 332–336.

Kruse, K., et al., 1981. Deficient prolactin response to parathyroid hormone in hypocalcemic and normocalcemic pseudohypoparathyroidism. J. Clin. Endocrinol. Metab. 52, 1099–1105.

Lala, R., et al., 2006. Bisphosphonate treatment of bone fibrous dysplasia in McCune-Albright syndrome. J. Pediatr. Endocrinol. Metab. 19 (Suppl. 2), 583–593.

Lambert, P.W., et al., 1980. Demonstration of a lack of change in serum 1α,25-dihydroxyvitamin D in response to parathyroid extract in pseudohypoparathyroidism. J. Clin. Investig. 66, 782–791.

Lambright, D.G., et al., 1994. Structural determinants for activation of the α-subunit of a heterotrimeric G protein. Nature 369, 621–628.

Landis, C.A., et al., 1989. GTPase inhibiting mutations activate the a chain of G_s and stimulate adenylyl cyclase in human pituitary tumours. Nature 340, 692–696.

Landreth, H., et al., 2015. Increased prevalence of sleep apnea in children with pseudohypoparathyroidism type 1a. Horm. Res. Paediatr. 84, 1–5.

Lanske, B., et al., 1996. PTH/PTHrP receptor in early development and Indian hedgehog-regulated bone growth. Science 273, 663–666.

Laspa, E., et al., 2004. Phenotypic and molecular genetic aspects of pseudohypoparathyroidism type Ib in a Greek kindred: evidence for enhanced uric acid excretion due to parathyroid hormone resistance. J. Clin. Endocrinol. Metab. 89, 5942–5947.

Lee, J.S., et al., 2002. Normal vision despite narrowing of the optic canal in fibrous dysplasia. N. Engl. J. Med. 347, 1670–1676.

Leet, A.I., et al., 2016. Bone-grafting in polyostotic fibrous dysplasia. J. Bone Joint Surg. Am. 98, 211–219.

Leet, A.I., et al., 2004a. Fracture incidence in polyostotic fibrous dysplasia and the McCune-Albright syndrome. J. Bone Miner. Res. 19, 571–577.

Leet, A.I., Collins, M.T., 2007. Current approach to fibrous dysplasia of bone and McCune-Albright syndrome. J. Child Orthop. 1, 3–17.

Leet, A.I., et al., 2004b. Fibrous dysplasia in the spine: prevalence of lesions and association with scoliosis. J. Bone Joint. Surg. Am. 86-A, 531–537.

Levin, L.R., et al., 1992. The Drosophila learning and memory gene *rutabaga* encodes a Ca^{2+}/calmodulin-responsive adenylyl cyclase. Cell 68, 479–489.

Levine, M.A., et al., 1988. Genetic deficiency of the α subunit of the guanine nucleotide-binding protein G_s as the molecular basis for Albright hereditary osteodystrophy. Proc. Natl. Acad. Sci. U. S. A 85, 617–621.

Levine, M.A., et al., 1983. Resistance to multiple hormones in patients with pseudohypoparathyroidism. Association with deficient activity of guanine nucleotide regulatory protein. Am. J. Med. 74, 545–556.

Levine, M.A., et al., 1980. Deficient activity of guanine nucleotide regulatory protein in erythrocytes from patients with pseudohypoparathyroidism. Biochem. Biophys. Res. Commun. 94, 1319–1324.

Levine, M.A., et al., 1985. Infantile hypothyroidism in two sibs: an unusual presentation of pseudohypoparathyroidism type Ia. J. Pediatr. 107, 919–922.

Levine, M.A., et al., 1986. Activity of the stimulatory guanine nucleotide-binding protein is reduced in erythrocytes from patients with pseudohypoparathyroidism and pseudopseudohypoparathyroidism: biochemical, endocrine, and genetic analysis of Albright's hereditary osteodystrophy in six kindreds. J. Clin. Endocrinol. Metab. 62, 497–502.

Levine, M.A., et al., 1991. Mapping of the gene encoding the a subunit of the stimulatory G protein of adenylyl cyclase (*GNAS1*) to 20q13.2-q13.3 in human by *in situ* hybridization. Genomics 11, 478–479.

Li, Q.B., Cerione, R.A., 1997. Communication between switch II and switch III of the transducin a subunit is essential for target activation. J. Biol. Chem. 272, 21673–21676.

Li, Y.Q., et al., 2016. $G_s\alpha$ deficiency in adipose tissue improves glucose metabolism and insulin sensitivity without an effect on body weight. Proc. Natl. Acad. Sci. U. S. A 113, 446–451.

Lichtenstein, L., 1938. Poloyostotic fibrous dysplasia. Arch. Surg. 36, 874–898.

Lichtenstein, L., Jaffe, H.L., 1942. Fibrous dysplasia of bone: a condition affecting one, several or many bones, graver cases of which may present abnormal pigmentation of skin, premature sexual development, hyperthyroidism or still other extraskeletal abnormalities. Arch. Pathol. 33, 777–816.

Liens, D., et al., 1994. Long-term effects of intravenous pamidronate in fibrous dysplasia of bone. Lancet 343, 953–954.

Lietman, S.A., et al., 2005. Reduction in Gsα induces osteogenic differentiation in human mesenchymal stem cells. Clin. Orthop. Relat. Res. 434, 231–238.

Linglart, A., et al., 2007. Similar clinical and laboratory findings in patients with symptomatic autosomal dominant and sporadic pseudohypoparathyroidism type Ib despite different epigenetic changes at the *GNAS* locus. Clin. Endocrinol. 67, 822–831.

Linglart, A., et al., 2002. *GNAS1* lesions in pseudohypoparathyroidism Ia and Ic: genotype phenotype relationship and evidence of the maternal transmission of the hormone resistance. J. Clin. Endocrinol. Metab. 87, 189–197.

Linglart, A., et al., 2005. A novel *STX16* deletion in autosomal dominant pseudohypoparathyroidism type Ib redefines the boundaries of a *cis*-acting imprinting control element of *GNAS*. Am. J. Hum. Genet. 76, 804–814.

Linglart, A., et al., 2006. Coding *GNAS* mutations leading to hormone resistance impair in vitro agonist- and cholera toxin-induced adenosine cyclic 3',5'-monophosphate formation mediated by human XLαs. Endocrinology 147, 2253–2262.

Linglart, A., et al., 2011. Recurrent PRKAR1A mutation in acrodysostosis with hormone resistance. N. Engl. J. Med. 364, 2218–2226.

Liu, J., et al., 2005a. Identification of the control region for tissue-specific imprinting of the stimulatory G protein α-subunit. Proc. Natl. Acad. Sci. U. S. A 102, 5513–5518.

Liu, J., et al., 2003. The stimulatory G protein α-subunit $G_s\alpha$ is imprinted in human thyroid glands: implications for thyroid function in pseudohypoparathyroidism types 1A and 1B. J. Clin. Endocrinol. Metab. 88, 4336–4341.

Liu, J., et al., 2000a. A *GNAS1* imprinting defect in pseudohypoparathyroidism type IB. J. Clin. Investig. 106, 1167–1174.

Liu, J., et al., 2005b. Distinct patterns of abnormal *GNAS* imprinting in familial and sporadic pseudohypoparathyroidism type IB. Hum. Mol. Genet. 14, 95–102.

Liu, J., et al., 2000b. Identification of a methylation imprint mark within the mouse *Gnas* locus. Mol. Cell Biol. 20, 5808–5817.

Long, A., et al., 1988. Polyostotic fibrous dysplasia with contrasting responses to calcitonin and mithramycin: aetiological and therapeutic implications. Ir. J. Med. Sci. 157, 229–234.

Long, D.N., et al., 2007. Body mass index differences in pseudohypoparathyroidism type 1a versus pseudopseudohypoparathyroidism may implicate paternal imprinting of $G\alpha_s$ in the development of human obesity. J. Clin. Endocrinol. Metab. 92, 1073–1079.

Lopez-Ben, R., et al., 1999. Osteosarcoma in a patient with McCune-Albright syndrome and Mazabraud's syndrome. Skeletal Radiol. 28, 522–526.

Lumbroso, S., et al., 2004. Activating $G_s\alpha$ mutations: analysis of 113 patients with signs of McCune-Albright syndrome-a European Collaborative Study. J. Clin. Endocrinol. Metab. 89, 2107–2113.

Ma, Y., et al., 2000. Src tyrosine kinase is a novel direct effector of G proteins. Cell 102, 635–646.

Maeda, K., et al., 2005. Case of pseudo-pseudohypoparathyroidism associated with juvenile dementia. Psychiatr. Clin. Neurosci. 59, 111.

Mahmud, F.H., et al., 2005. Molecular diagnosis of pseudohypoparathyroidism type Ib in a family with presumed paroxysmal dyskinesia. Pediatrics 115, e242–244.

Majoor, B.C.J., et al., 2018. Individualized approach to the surgical management of fibrous dysplasia of the proximal femur. Orphanet J. Rare Dis. 13, 72.

Mak, A., Mok, C.C., 2005. Diffuse skeletal hyperostosis and pseudohypoparathyroidism. Rheumatology 44, 182.

Mallet, E., et al., 1982. Coupling defect of thyrotropin receptor and adenylate cyclase in a pseudohypoparathyroid patient. J. Clin. Endocrinol. Metab. 54, 1028–1032.

Mancini, F., et al., 2009. Scoliosis and spine involvement in fibrous dysplasia of bone. Eur. Spine J. 18, 196–202.

Mantovani, G., et al., 2002. The $G_s\alpha$ gene: predominant maternal origin of transcription in human thyroid gland and gonads. J. Clin. Endocrinol. Metab. 87, 4736–4740.

Mantovani, G., et al., 2004a. Parental origin of $G_s\alpha$ mutations in McCune-Albright syndrome and in isolated endocrine tumors. J. Clin. Endocrinol. Metab. 89, 3007–3009.

Mantovani, G., et al., 2004b. Biallelic expression of the Gsα gene in human bone and adipose tissue. J. Clin. Endocrinol. Metab. 89, 6316–6319.

Mantovani, G., et al., 2010. Pseudohypoparathyroidism and *GNAS* epigenetic defects: clinical evaluation of albright hereditary osteodystrophy and molecular analysis in 40 patients. J. Clin. Endocrinol. Metab. 95, 651–658.

Mantovani, G., et al., 2003. Growth hormone-releasing hormone resistance in pseudohypoparathyroidism type 1a: new evidence for imprinting of the $G_s\alpha$ gene. J. Clin. Endocrinol. Metab. 88, 4070–4074.

Mantovani, G., et al., 2000. Mutational analysis of *GNAS1* in patients with pseudohypoparathyroidism: identification of two novel mutations. J. Clin. Endocrinol. Metab. 85, 4243–4248.

Mariot, V., et al., 2008. A maternal epimutation of *GNAS* leads to Albright osteodystrophy and parathyroid hormone resistance. J. Clin. Endocrinol. Metab. 93, 661–665.

Marsh, S.R., et al., 1998. Receptor-mediated activation of $G_{s\alpha}$: evidence for intramolecular signal transduction. Mol. Pharmacol. 53, 981–990.
Martinez-Botas, J., et al., 2000. Absence of perilipin results in leanness and reverses obesity in *Lepr* db/db mice. Nat. Genet. 26, 474–479.
Mattera, R., et al., 1989. Splice variants of the α subunit of the G protein G_s activate both adenylyl cyclase and calcium channels. Science 243, 804–807.
Maupetit-Mehouas, S., et al., 2013. Simultaneous hyper- and hypomethylation at imprinted loci in a subset of patients with *GNAS* epimutations underlies a complex and different mechanism of multilocus methylation defect in pseudohypoparathyroidism type 1b. Hum. Mutat. 34, 1172–1180.
Mazabraud, A., Girard, J., 1957. A peculiar case of fibrous dysplasia with osseous and tendinous localizations. Rev. Rhum. Mal. Osteoartic. 24, 652–659.
Mazzoni, M.R., et al., 2000. A $G\alpha_s$ carboxyl-terminal peptide prevents G_s activation by the A_{2A} adenosine receptor. Mol. Pharmacol. 58, 226–236.
McCune, D.J., 1936. Osteitis fibrosa cystica: the case of a nine-year-old girl who also exhibits precocious puberty, multiple pigmentation of the skin and hyperthyroidism. Am. J. Dis. Child. 52, 743–744.
Mei, F.C., et al., 2002. Differential signaling of cyclic AMP: opposing effects of exchange protein directly activated by cyclic AMP and cAMP-dependent protein kinase on protein kinase B activation. J. Biol. Chem. 277, 11497–11504.
Miller, M.J., et al., 1997. RalGDS functions in Ras- and cAMP-mediated growth stimulation. J. Biol. Chem. 272, 5600–5605.
Miller, S.S., et al., 1976. Bone cells in culture: morphologic transformation by hormones. Science 192, 1340–1343.
Miric, A., et al., 1993. Heterogeneous mutations in the gene encoding the α subunit of the stimulatory G protein of adenylyl cyclase in Albright hereditary osteodystrophy. J. Clin. Endocrinol. Metab. 76, 1560–1568.
Mitsui, T., et al., 2014. Acroscyphodysplasia as a phenotypic variation of pseudohypoparathyroidism and acrodysostosis type 2. Am. J. Med. Genet. 164A, 2529–2534.
Miura, R., et al., 1990. Response of plasma 1,25-dihydroxyvitamin D in the human PTH(1-34) infusion test: an improved index for the diagnosis of idiopathic hypoparathyroidism and pseudohypoparathyroidism. Calcif. Tissue Int. 46, 309–313.
Mixon, M.B., et al., 1995. Tertiary and quaternary structural changes in $G_{i\alpha 1}$. Science 270, 954–960.
Mizunashi, K., et al., 1990. Heterogeneity of pseudohypoparathyroidism type I from the aspect of urinary excretion of calcium and serum levels of parathyroid hormone. Calcif. Tissue Int. 46, 227–232.
Montminy, M., 1997. Transcriptional regulation by cyclic AMP. Annu. Rev. Biochem. 66, 807–822.
Moore, A.T., et al., 1985. Fibrous dysplasia of the orbit in childhood. Clinical features and management. Ophthalmology 92, 12–20.
Moses, A.M., et al., 1986. Evidence for normal antidiuretic responses to endogenous and exogenous arginine vasopressin in patients with guanine nucleotide-binding stimulatory protein-deficient pseudohypoparathyroidism. J. Clin. Endocrinol. Metab. 62, 221–224.
Mouallem, M., et al., 2008. Cognitive impairment is prevalent in pseudohypoparathyroidism type Ia, but not in pseudopseudohypoparathyroidism: possible cerebral imprinting of Gsα. Clin. Endocrinol. 68, 233–239.
Muniyappa, R., et al., 2013. Reduced insulin sensitivity in adults with pseudohypoparathyroidism type 1a. J. Clin. Endocrinol. Metab. 98, E1796–E1801.
Murray, T.M., et al., 1993. Pseudohypoparathyroidism with osteitis fibrosa cystica: direct demonstration of skeletal responsiveness to parathyroid hormone in cells cultured from bone. J. Bone Miner. Res. 8, 83–91.
Nakamoto, J.M., et al., 1998. Pseudohypoparathyroidism type Ia from maternal but not paternal transmission of a $G_s\alpha$ gene mutation. Am. J. Med. Genet. 77, 61–67.
Namnoum, A.B., et al., 1998. Reproductive dysfunction in women with Albright's hereditary osteodystrophy. J. Clin. Endocrinol. Metab. 83, 824–829.
Neary, N.M., et al., 2012. Development and treatment of tertiary hyperparathyroidism in patients with pseudohypoparathyroidism type 1B. J. Clin. Endocrinol. Metab. 97, 3025–3030.
Noel, J.P., et al., 1993. The 2.2 Å crystal structure of transducin-α complexed with GTPγS. Nature 366, 654–663.
Okada, K., et al., 1994. Pseudohypoparathyroidism-associated spinal stenosis. Spine 19, 1186–1189.
Okamoto, S., et al., 2000. Activating Gs_α mutation in intramuscular myxomas with and without fibrous dysplasia of bone. Virchows Arch. 437, 133–137.
Ong, O.C., et al., 1996. Real-time monitoring of reduced β-adrenergic response in fibroblasts from patients with pseudohypoparathyroidism. Anal. Biochem. 238, 76–81.
Osundwa, T.M., et al., 2001. McCune Albright syndrome: autosomal dominant trait in a family of eight. East Afr. Med. J. 78, S40–S42.
Oude Luttikhuis, M.E.M., et al., 1994. Characterization of a *de novo* 43-bp deletion of the Gsα gene (*GNAS1*) in Albright hereditary osteodystrophy. Genomics 21, 455–457.
Parisi, M.S., et al., 2001. Bone mineral density response to long-term bisphosphonate therapy in fibrous dysplasia. J. Clin. Densitom. 4, 167–172.
Pasolli, H.A., et al., 2000. Characterization of the extra-large G protein α-subunit XLαs. I. Tissue distribution and subcellular localization. J. Biol. Chem. 275, 33622–33632.
Patten, J.L., et al., 1990. Mutation in the gene encoding the stimulatory G protein of adenylate cyclase in Albright's hereditary osteodystrophy. N. Engl. J. Med. 322, 1412–1419.
Patten, J.L., Levine, M.A., 1990. Immunochemical analysis of the α-subunit of the stimulatory G-protein of adenylyl cyclase in patients with Albright's hereditary osteodystrophy. J. Clin. Endocrinol. Metab. 71, 1208–1214.
Paul, S.M., et al., 2014. Disease severity and functional factors associated with walking performance in polyostotic fibrous dysplasia. Bone 60, 41–47.
Perez-Nanclares, G., et al., 2015. Pseudohypoparathyroidism type Ib associated with novel duplications in the *GNAS* locus. PLoS One 10, e0117691.
Peters, J., et al., 1999. A cluster of oppositely imprinted transcripts at the *Gnas* locus in the distal imprinting region of mouse chromosome 2. Proc. Natl. Acad. Sci. U. S. A 96, 3830–3835.
Phelan, M.C., et al., 1995. Albright hereditary osteodystrophy and del(2)(q37.3) in four unrelated individuals. Am. J. Med. Genet. 58, 1–7.
Plagge, A., et al., 2004. The imprinted signaling protein XLαs is required for postnatal adaptation to feeding. Nat. Genet. 36, 818–826.
Plagge, A., et al., 2005. Imprinted Nesp55 influences behavioral reactivity to novel environments. Mol. Cell Biol. 25, 3019–3026.

Plotkin, H., et al., 2003. Effect of pamidronate treatment in children with polyostotic fibrous dysplasia of bone. J. Clin. Endocrinol. Metab. 88, 4569–4575.

Poomthavorn, P., Zacharin, M., 2006. Early manifestation of obesity and calcinosis cutis in infantile pseudohypoparathyroidism. J. Paediatr. Child Health 42, 821–823.

Poppleton, H., et al., 1996. Activation of $G_s\alpha$ by the epidermal growth factor receptor involves phosphorylation. J. Biol. Chem. 271, 6947–6951.

Poznanski, A.K., et al., 1977. The pattern of shortening of the bones of the hand in pseudohypoparathyroidism and pseudopseudohypoparathyroidism–a comparison with brachydactyly E, Turner syndrome, and acrodysostosis. Radiology 123, 707–718.

Prendiville, J.S., et al., 1992. Osteoma cutis as a presenting sign of pseudohypoparathyroidism. Pediatr. Dermatol. 9, 11–18.

Rao, D.S., et al., 1985. Dissociation between the effects of endogenous parathyroid hormone on adenosine 3',5'-monophosphate generation and phosphate reabsorption in hypocalcemia due to vitamin D depletion: an acquired disorder resembling pseudohypoparathyroidism type II. J. Clin. Endocrinol. Metab. 61, 285–290.

Rao, V.V., et al., 1991. G protein Gsα (*GNAS1*), the probable candidate gene for Albright hereditary osteodystrophy, is assigned to human chromosome 20q12-q13.2. Genomics 10, 257–261.

Regard, J.B., et al., 2013. Activation of Hedgehog signaling by loss of *GNAS* causes heterotopic ossification. Nat. Med. 19, 1505–1512.

Reik, W., Walter, J., 2001. Genomic imprinting: parental influence on the genome. Nat. Rev. Genet. 2, 21–32.

Reis, M.T., et al., 2016. Falue of tooth eruption and brachdactyly in pseudohypoparahypoparathyoidism are not related to plasma parathyroid hormone-related protein levels. Bone 85, 138–141.

Rezwan, F.I., et al., 2015. Very small deletions within the NESP55 gene in pseudohypoparathyroidism type 1b. Eur. J. Hum. Genet. 23, 494–499.

Richard, N., et al., 2012. A new deletion ablating NESP55 causes loss of maternal imprint of A/B GNAS and autosomal dominant pseudohypoparathyroidism type Ib. J. Clin. Endocrinol. Metab. 97, E863–E867.

Richard, N., et al., 2013. Paternal GNAS mutations lead to severe intrauterine growth retardation (IUGR) and provide evidence for a role of XLαs in fetal development. J. Clin. Endocrinol. Metab. 98, E1549–E1556.

Richards, J.S., 2001. New signaling pathways for hormones and cyclic adenosine 3′,5′-monophosphate action in endocrine cells. Mol. Endocrinol. 15, 209–218.

Rickard, S.J., Wilson, L.C., 2003. Analysis of *GNAS1* and overlapping transcripts identifies the parental origin of mutations in patients with sporadic Albright hereditary osteodystrophy and reveals a model system in which to observe the effects of splicing mutations on translated messenger RNA. Am. J. Hum. Genet. 72, 961–974.

Riepe, F.G., et al., 2005. Early manifestation of calcinosis cutis in pseudohypoparathyroidism type Ia associated with a novel mutation in the *GNAS* gene. Eur. J. Endocrinol. 152, 515–519.

Riminucci, M., et al., 2003a. FGF-23 in fibrous dysplasia of bone and its relationship to renal phosphate wasting. J. Clin. Investig. 112, 683–692.

Riminucci, M., et al., 2002. Craniofacial fibrous dysplasia. In: Lin, K.Y., Ogle, R.C., Jane, J.A. (Eds.), Craniofacial Surgery. W.B.Saunders, Philadelphia, PA, pp. 366–381.

Riminucci, M., et al., 1997. Fibrous dysplasia of bone in the McCune-Albright syndrome: abnormalities in bone formation. Am. J. Pathol. 151, 1587–1600.

Riminucci, M., et al., 2003b. Osteoclastogenesis in fibrous dysplasia of bone: in situ and in vitro analysis of IL-6 expression. Bone 33, 434–442.

Riminucci, M., et al., 1999. The histopathology of fibrous dysplasia of bone in patients with activating mutations of the Gsα gene: site-specific patterns and recurrent histological hallmarks. J. Pathol. 187, 249–258.

Riminucci, M., et al., 2007. The pathology of fibrous dysplasia and the McCune-Albright syndrome. Pediatr. Endocrinol. Rev. 4 (Suppl. 4), 401–411.

Riminucci, M., et al., 2006. Fibrous dysplasia as a stem cell disease. J. Bone Miner. Res. 21 (Suppl. 2), P125–P131.

Ringel, M.D., et al., 1996. Clinical implications of genetic defects in G proteins. The molecular basis of McCune-Albright syndrome and Albright hereditary osteodystrophy. Medicine (Baltim.) 75, 171–184.

Rochtus, A., et al., 2016. Genome-wide DNA methylation analysis of pseudohypoparathyroidism patients with GNAS imprinting defects. Clin. Epigenet. 8, 10.

Roizen, J.D., et al., 2016. Resting energy expenditure is decreased in pseudohypoparathyroidism type 1A. J. Clin. Endocrinol. Metab. 101, 880–888.

Rotenberg, A., et al., 2000. Parallel instabilities of long-term potentiation, place cells, and learning caused by decreased protein kinase A activity. J. Neurosci. 20, 8096–8102.

Ruggieri, M., et al., 1999. Unusual form of recurrent giant cell granuloma of the mandible and lower extremities in a patient with neurofibromatosis type 1. Oral Surg. Oral Med. Oral Pathol. Oral Radiol. Endod. 87, 67–72.

Ruggieri, P., et al., 1994. Malignancies in fibrous dysplasia. Cancer 73, 1411–1424.

Rump, P., et al., 2011. Madelung deformity in a girl with a novel and *de novo* mutation in the *GNAS* gene. Am. J. Med. Genet. 155A, 2566–2570.

Saggio, I., et al., 2014. Constitutive expression of Gsα (R201C) in mice produces a heritable, direct replica of human fibrous dysplasia bone pathology and demonstrates its natural history. J. Bone Miner. Res. 29, 2357–2368.

Sakamoto, A., et al., 2005. Chondrocyte-specific knockout of the G protein $G_s\alpha$ leads to epiphyseal and growth plate abnormalities and ectopic chondrocyte formation. J. Bone Miner. Res. 20, 663–671.

Sanchez, J., et al., 2011. Madelung-like deformity in pseudohypoparathyroidism type 1b. J. Clin. Endocrinol. Metab. 96, E1507–E1511.

Sano, S., et al., 2015. Growth hormone deficiency in monozygotic twins with autosomal dominant pseudohypoparathyroidism type Ib. Endocr. J. 62, 523–529.

Sano, S., et al., 2016. Beckwith-Wiedemann syndrome and pseudohypoparathyroidism type Ib in a patient with multilocus imprinting disturbance: a female-dominant phenomenon? J. Hum. Genet. 61, 765–769.

Schuster, V., et al., 1993. Endocrine and molecular biological studies in a German family with Albright hereditary osteodystrophy. Eur. J. Pediatr. 152, 185–189.

Schwartz, D.T., Alpert, M., 1964. The malignant transformation of fibrous dysplasia. Am. J. Med. Sci. 247, 1–20.

Schwindinger, W.F., et al., 1992. Identification of a mutation in the gene encoding the α subunit of the stimulatory G protein of adenylyl cyclase in McCune-Albright syndrome. Proc. Natl. Acad. Sci. U. S. A 89, 5152–5156.

Schwindinger, W.F., et al., 1994. A novel $G_s\alpha$ mutant in a patient with Albright hereditary osteodystrophy uncouples cell surface receptors from adenylyl cyclase. J. Biol. Chem. 269, 25387–25391.

Seifert, R., et al., 1998. Different effects of $G_s\alpha$ splice variants on β2-adrenoreceptor-mediated signaling. The β2-adrenoreceptor coupled to the long splice variant of $G_s\alpha$ has properties of a constitutively active receptor. J. Biol. Chem. 273, 5109–5116.

Seror, R., et al., 2007. Progressive osseous heteroplasia: a rare case of late onset. Rheumatology 46, 716–717. Letter to Editor.

Sethuraman, G., et al., 2006. Osteoma cutis in pseudohypoparathyroidism. Clin. Exp. Dermatol. 31, 225–227.

Shapira, H., et al., 1996. Pseudohypoparathyroidism type Ia: two new heterozygous frameshift mutations in exons 5 and 10 of the Gsα gene. Hum. Genet. 97, 73–75.

Shapiro, M.S., et al., 1980. Multiple abnormalities of anterior pituitary hormone secretion in association with pseudohypoparathyroidism. J. Clin. Endocrinol. Metab. 51, 483–487.

Shima, M., et al., 1988. Multiple associated endocrine abnormalities in a patient with pseudohypoparathyroidism type 1a. Eur. J. Pediatr. 147, 536–538.

Shoemaker, A.H., et al., 2013. Energy expenditure in obese children with pseudohypoparathyroidism type 1a. Int. J. Obes. 37, 1147–1153.

Shore, E.M., et al., 2002. Paternally inherited inactivating mutations of the *GNAS1* gene in progressive osseous heteroplasia. N. Engl. J. Med. 346, 99–106.

Silve, C., et al., 1986. Selective resistance to parathyroid hormone in cultured skin fibroblasts from patients with pseudohypoparathyroidism type Ib. J. Clin. Endocrinol. Metab. 62, 640–644.

Simonds, W.F., et al., 1989. Receptor and effector interactions of Gs. Functional studies with antibodies to the αs carboxyl-terminal decapeptide. FEBS Lett. 249, 189–194.

Sondek, J., et al., 1994. GTPase mechanism of G proteins from the 1.7-Å crystal structure of transducin α-GDP-AlF_4^-. Nature 372, 276–279.

Spiegel, A.M., et al., 1982. Deficiency of hormone receptor-adenylate cyclase coupling protein: basis for hormone resistance in pseudohypoparathyroidism. Am. J. Physiol. 243, E37–E42.

Spiegel, A.M., Weinstein, L.S., 2001. Pseudohypoparathyroidism. In: Scriver, C.R., Beaudet, A.L., Sly, W.S., Valle, D. (Eds.), The Metabolic and Molecular Bases of Inherited Disease. McGraw-Hill, New York, pp. 4205–4221.

Spiegel, A.M., Weinstein, L.S., 2004. Inherited diseases involving G proteins and G protein-coupled receptors. Annu. Rev. Med. 55, 27–39.

Stanton, R.P., 2006. Surgery for fibrous dysplasia. J. Bone Miner. Res. 21 (Suppl. 2), P105–P109.

Steinbach, H.L., Young, D.A., 1966. The roentgen appearance of pseudohypoparathyroidism (PH) and pseudo-pseudohypoparathyroidism (PPH). Differentiation from other syndromes associated with short metacarpals, metatarsals, and phalanges. Am. J. Roentgenol. Radium Ther. Nucl. Med. 97, 49–66.

Stone, M.D., et al., 1993. The renal response to exogenous parathyroid hormone in treated pseudohypoparathyroidism. Bone 14, 727–735.

Sudlow, L.C., et al., 1993. cAMP-activated Na^+ cuurent of molluscum neurons is resistant to kinase inhibitors and is gated by cAMP in the isolated patch. J. Neurosci. 13, 5188–5193.

Sullivan, K.A., et al., 1987. Identification of receptor contact site involved in receptor-G protein coupling. Nature 330, 758–760.

Sun, H., et al., 1997. The juxtamembrane, cytosolic region of the epidermal growth factor receptor is involved in association with a-subunit of G_s. J. Biol. Chem. 272, 5413–5420.

Sunahara, R.K., et al., 1997. Crystal structure of the adenylyl cyclase activator $G_{s\alpha}$. Science 278, 1943–1947.

Takatani, R., et al., 2015. Similar frequency of paternal uniparental disomy involving chromosome 20q (patUPD20q) in Japanese and Caucasian patients affected by sporadic pseudohypoparathyroidism type Ib (sporPHP1B). Bone 79, 15–20.

Tanner Jr., H.C., et al., 1961. Sarcoma complicating fibrous dysplasia. Probable role of radiation therapy. Oral Surg. Oral Med. Oral Pathol. 14, 837–846.

Tesmer, J.J., et al., 1997. Crystal structure of the catalytic domains of adenylyl cyclase in a complex with Gsα.GTPγS. Science 278, 1907–1916.

Thiele, S., et al., 2011. Functional characterization of *GNAS* mutations found in patients with pseudohypoparathyroidism type Ic defines a new subgroup of pseudohypoparathyroidism affecting selectively Gsα-receptor interaction. Hum. Mutat. 32, 653–660.

Thiele, S., et al., 2007. A disruptive mutation in exon 3 of the *GNAS* gene with albright hereditary osteodystrophy, normocalcemic pseudohypoparathyroidism, and selective long transcript variant Gsalpha-L deficiency. J. Clin. Endocrinol. Metab. 92, 1764–1768.

Thiele, S., et al., 2010. Selective deficiency of Gsα and the possible role of alternative gene products of *GNAS* in Albright hereditary osteodystrophy and pseudohypoparathyroidism type Ia. Exp. Clin. Endocrinol. Diabetes 118, 127–132.

Tintut, Y., et al., 1999. Inhibition of osteoblast-specific transcription factor Cbfa1 by the cAMP pathway in osteoblasts. J. Biol. Chem. 274, 28875–28879.

Tsang, R.C., et al., 1984. The development of pseudohypoparathyroidism. Involvement of progressively increasing serum parathyroid hormone concentrations, increased 1,25-dihydroxyvitamin D concentrations, and 'migratory' subcutaneous calcifications. Am. J. Dis. Child. 138, 654–658.

Turan, S., et al., 2014. Postnatal establishment of allelic Gαs silencing as a plausible explanation for delayed onset of parathyroid hormone resistance owing to heterozygous Gαs disruption. J. Bone Miner. Res. 29, 749–760.

Uwaifo, G.I., et al., 2001. Clinical picture: fuel on the fire. Lancet 357, 2011.

Valet, P., et al., 2000. Expression of human α2-adrenergic receptors in adipose tissue of β3-adrenergic receptor deficient mice promotes diet-induced obesity. J. Biol. Chem. 275, 34797–34802.

Vortkamp, A., et al., 1996. Regulation of rate of cartilage differentiation by Indian hedgehog and PTH-related protein. Science 273, 613–622.
Vossler, M.R., et al., 1997. cAMP activates MAP kinase and Elk-1 through a B-Raf- and Rap1-dependent pathway. Cell 89, 73–82.
Wainger, B.J., et al., 2001. Molecular mechanism of cAMP modulation of HCN pacemaker channels. Nature 411, 805–810.
Walden, U., et al., 1999. Stimulatory guanine nucleotide binding protein subunit 1 mutation in two siblings with pseudohypoparathyroidism type Ia and mother with pseudopseudohypoparathyroidism. Eur. J. Pediatr. 158, 200–203.
Wang, Z., et al., 2006. Rap1-mediated activation of extracellular signal-regulated kinases by cyclic AMP is dependent on the mode of Rap1 activation. Mol. Cell Biol. 26, 2130–2145.
Warner, D.R., et al., 1997. A novel mutation adjacent to the switch III domain of $G_{s\alpha}$ in a patient with pseudohypoparathyroidism. Mol. Endocrinol. 11, 1718–1727.
Warner, D.R., et al., 1999. Mutagenesis of the conserved residue Glu^{259} of $G_s\alpha$ demonstrates the importance of interactions between switches 2 and 3 for activation. J. Biol. Chem. 274, 4977–4984.
Warner, D.R., Weinstein, L.S., 1999. A mutation in the heterotrimeric stimulatory guanine nucleotide binding protein α-subunit with impaired receptor-mediated activation because of elevated GTPase activity. Proc. Natl. Acad. Sci. U. S. A 96, 4268–4272.
Warner, D.R., et al., 1998. A novel mutation in the switch 3 region of $G_s\alpha$ in a patient with Albright hereditary osteodystrophy impairs GDP binding and receptor activation. J. Biol. Chem. 273, 23976–23983.
Wedegaertner, P.B., et al., 1996. Activation-induced subcellular redistribution of Gsα. Mol. Biol. Cell 7, 1225–1233.
Weinstein, L.S., 1998. Albright hereditary osteodystrophy, pseudohypoparathyroidism and Gs deficiency. In: Spiegel, A.M. (Ed.), G Proteins, Receptors, and Disease. Humana Press, Totowa, NJ, pp. 23–56.
Weinstein, L.S., 2004. GNAS and McCune-Albright syndrome/fibrous dysplasia, Albright hereditary osteodystrophy/pseudohypoparathyroidism type 1A, progressive osseous heteroplasia, and pseudohypoparathyroidism type 1B. In: Epstein, C.J., Erickson, R.P., Wynshaw-Boris, A. (Eds.), Molecular Basis of Inborn Errors of Development. Oxford University Press, San Francisco, pp. 849–866.
Weinstein, L.S., et al., 1990. Mutations of the G_s α-subunit gene in Albright hereditary osteodystrophy detected by denaturing gradient gel electrophoresis. Proc. Natl. Acad. Sci. U. S. A 87, 8287–8290.
Weinstein, L.S., et al., 2004. Minireview: *GNAS*: normal and abnormal functions. Endocrinology 145, 5459–5464.
Weinstein, L.S., et al., 1991. Activating mutations of the stimulatory G protein in the McCune- Albright syndrome. N. Engl. J. Med. 325, 1688–1695.
Weinstein, L.S., et al., 2000. Variable imprinting of the heterotrimeric G protein G_s α-subunit within different segments of the nephron. Am. J. Physiol. 278, F507–F514.
Weinstein, L.S., et al., 2001. Endocrine manifestations of stimulatory G protein α-subunit mutations and the role of genomic imprinting. Endocr. Rev. 22, 675–705.
Weinstock, R.S., et al., 1986. Olfactory dysfunction in humans with deficient guanine nucleotide-binding protein. Nature 322, 635–636.
Weisman, Y., et al., 1985. Pseudohypoparathyroidism type Ia presenting as congenital hypothyroidism. J. Pediatr. 107, 413–415.
Werder, E.A., et al., 1978. Pseudohypoparathyroidism and idiopathic hypoparathyroidism: relationship between serum calcium and parathyroid hormone levels and urinary cyclic adenosine-3',5'-monophosphate response to parathyroid extract. J. Clin. Endocrinol. Metab. 46, 872–879.
Williamson, C.M., et al., 2004. A cis-acting control region is required exclusively for the tissue-specific imprinting of *Gnas*. Nat. Genet. 36, 894–899.
Williamson, C.M., et al., 2006. Identification of an imprinting control region affecting the expression of all transcripts in the *Gnas* cluster. Nat. Genet. 38, 350–355.
Wilson, L.C., et al., 1995. Brachydactyly and mental retardation: an Albright hereditary osteodystrophy-like syndrome localized to 2q37. Am. J. Hum. Genet. 56, 400–407.
Wilson, L.C., et al., 1994. Parental origin of Gsα gene mutations in Albright's hereditary osteodystrophy. J. Med. Genet. 31, 835–839.
Wolfsdorf, J.I., et al., 1978. Partial gonadotrophin-resistance in pseudohypoparathyroidism. Acta Endocrinol. 88, 321–328.
Wood, L.D., et al., 2017. Patients with McCune-Albright syndrome have a broad spectrum of abnormalities in the gastrointestinal tract and pancreas. Virchows Arch. 470, 391–400.
Wu, J., et al., 2011. Recurrent *GNAS* mutations define an unexpected pathway for pancreatic cyst development. Sci. Transl. Med. 3, 92ra66.
Wu, W.I., et al., 2001. Selective resistance to parathyroid hormone caused by a novel uncoupling mutation in the carboxyl terminus of $G_{\alpha s}$. A cause of pseudohypoparathyroidism type Ib. J. Biol. Chem. 276, 165–171.
Wu, Z.L., et al., 1995. Altered behavior and long-term potentiation in type I adenylyl cyclase mutant mice. Proc. Natl. Acad. Sci. U. S. A 92, 220–224.
Xie, T., et al., 2008. Severe obesity and insulin resistance due to deletion of the maternal $G_s\alpha$ allele is reversed by paternal deletion of the $G_s\alpha$ imprint control region. Endocrinology 149, 2443–2450.
Xie, T., et al., 2006. The alternative stimulatory G protein α-subunit XLαs is a critical regulator of energy and glucose metabolism and sympathetic nerve activity in adult mice. J. Biol. Chem. 281, 18989–18999.
Yabut Jr., S.M., et al., 1988. Malignant transformation of fibrous dysplasia. A case report and review of the literature. Clin. Orthop. 288, 281–289.
Yamamoto, Y., et al., 1997. Spinal cord compression by heterotopic ossification associated with pseudohypoparathyroidism. J. Int. Med. Res. 25, 364–368.
Yatani, A., et al., 1988. The stimulatory G protein of adenylyl cyclase, Gs, also stimulates dihydropyridine-sensitive Ca^{2+} channels. Evidence for direct regulation independent of phosphorylation by cAMP-dependent protein kinase or stimulation by a dihydropyridine agonist. J. Biol. Chem. 263, 9887–9895.
Yeh, G.L., et al., 2000. *GNAS1* mutation and Cbfa1 misexpression in a child with severe congenital platelike osteoma cutis. J. Bone Miner. Res. 15, 2063–2073.

Yokoro, S., et al., 1990. Hyperthyrotropinemia in a neonate with normal thyroid hormone levels: the earliest diagnostic clue for pseudohypoparathyroidism. Biol. Neonate 58, 69–72.

Yu, D., et al., 1999. Identification of two novel deletion mutations within the $G_s\alpha$ gene (*GNAS1*) in Albright hereditary osteodystrophy. J. Clin. Endocrinol. Metab. 84, 3254–3259.

Yu, J.Z., Rasenick, M.M., 2002. Real-time visualization of a fluorescent $G_{\alpha s}$: dissociation of the activated G protein from plasma membrane. Mol. Pharmacol. 61, 352–359.

Yu, S., et al., 1995. A deletion hot-spot in exon 7 of the $G_s\alpha$ gene (*GNAS1*) in patients with Albright hereditary osteodystrophy. Hum. Mol. Genet. 4, 2001–2002.

Yu, S., et al., 1998. Variable and tissue-specific hormone resistance in heterotrimeric G_s protein α-subunit ($G_s\alpha$) knockout mice is due to tissue-specific imprinting of the $G_s\alpha$ gene. Proc. Natl. Acad. Sci. U. S. A 95, 8715–8720.

Zacharin, M., O'Sullivan, M., 2000. Intravenous pamidronate treatment of polyostotic fibrous dysplasia associated with the McCune Albright syndrome. J. Pediatr. 137, 403–409.

Zazo, C., et al., 2011. Gsα activity is reduced in erythrocyte membranes of patients with psedohypoparathyroidism due to epigenetic alterations at the *GNAS* locus. J. Bone Miner. Res. 26, 1864–1870.

Zheng, B., et al., 2001. RGS-PX1, a GAP for $G\alpha_s$ and sorting nexin in vesicular trafficking. Science 294, 1939–1942.

Zung, A., et al., 1995. Urinary cyclic adenosine 3′,5′-monophosphate response in McCune-Albright syndrome: clinical evidence for altered renal adenylate cyclase activity. J. Clin. Endocrinol. Metab. 80, 3576–3581.

Chapter 60

Renal osteodystrophy and chronic kidney disease–mineral bone disorder

Sharon M. Moe[1] and Thomas L. Nickolas[2]

[1]*Division of Nephrology, Indiana University School of Medicine, Rodebush Veterans Administration Medical Center, Indianapolis, IN, United States;*
[2]*Division of Nephrology, Department of Medicine, Columbia University Medical Center, New York, NY, United States*

Chapter outline

Introduction to chronic kidney disease

Chronic kidney disease (CKD) affects over 20 million individuals in the United States, and 752 million individuals worldwide (Bikbov et al., 2018). Progressive kidney disease that leads to the need for dialysis (end-stage kidney disease or ESKD) or transplantation affects over 700,000 individuals in the United States. CKD is defined as abnormalities of kidney structure or function present for >3 months, with stratification based on estimated glomerular filtration rate (eGFR) category and the magnitude of albuminuria (Group, 2013). The Kidney Disease: Improving Global Outcomes (KDIGO) group has updated the classification of CKD and changed the term "stage" to "grade," as not all kidney disease is progressive, and noted that the presence or absence of albuminuria can greatly influence prognosis (Levin and Stevens, 2014). There is considerable overlap between individuals identified with osteoporosis and CKD (KDIGO, 2009), and at every stage/grade of kidney disease, there is increased fracture risk (Moe and Nickolas, 2016), demonstrating the important contribution of CKD to bone fragility (Fig. 60.1).

The major causes of CKD are diabetes and hypertension, but there are many other causes of kidney disease, including genetic defects, glomerular lesions, and syndromes of tubular abnormalities. All forms of kidney disease are associated with bone and mineral abnormalities, but the specific causes of the kidney damage or treatments may have additional effects on bone. For example, cystic kidney diseases can be due to genetic alterations in cilia leading to cyst growth in the kidneys and also affect osteocyte function, at least in animal models (Xiao and Quarles, 2010). Patients with glomerulonephritis are often treated with steroids that may lead to steroid-induced osteoporosis. Some kidney tubular defects such as Fanconi's syndrome or the genetic defect Dent's disease lead to proximal tubule phosphate wasting and can lead to osteomalacia. Primary gonadal dysfunction is nearly universal in patients with ESKD, leading to the equivalent of

Principles of Bone Biology. https://doi.org/10.1016/B978-0-12-814841-9.00060-9

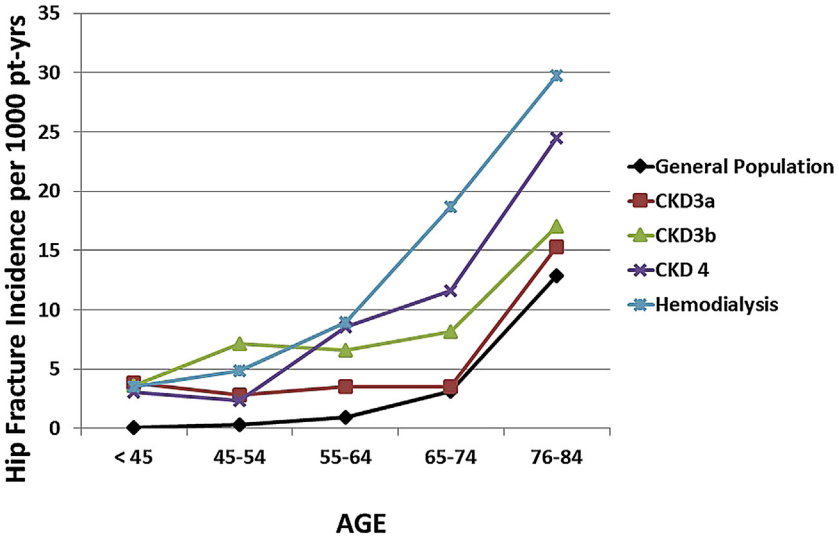

FIGURE 60.1 Hip fracture incidence increases with progressive CKD. As patients age in the general population there is a higher increased incidence of hip fracture. This incidence increases with progression of CKD. *CKD*, chronic kidney disease; *pt-yrs*, patient years. *Data from Alem et al. for dialysis patients and the general population from Olmstead, Minnesota (Alem, A.M., Sherrard, D.J., Gillen, D.L., Weiss, N.S., Beresford, S.A., Heckbert, S.R., Wong, C., Stehman-Breen, C., 2000. Increased risk of hip fracture among patients with end-stage renal disease. Kidney Int. 58, 396–399), Naylor et al. (2013) for CKD stages 3–4 (Naylor, K., Mcarthur, E., Leslie, W., Fraser, L., Jamal, S., Cadarette, S., Pouget, J., Lok, C., Hodsman, A., Adachi, J., Garg, A., 2013. 3-Year incidence of fracture in chronic kidney disease. Kidney Int.) courtesy of the Canadian Institute for Clinical Evaluative Sciences (ICES). Reprinted with permission from Moe, S.M., Nickolas, T.L., 2016. Fractures in patients with CKD: time for action. Clin. J. Am. Soc. Nephrol. 11, 1929–1931.*

postmenopausal osteoporosis or osteoporosis due to testosterone deficiency. Even with the best treatment possible for CKD, kidney transplant, the resulting kidney function is still impaired, and the prevention of transplant rejection with steroids can further increase the risk of bone abnormalities. Finally, CKD is more common in older individuals. Although there is some loss of GFR with normal aging, in patients with eGFR <60 mL/min/m^2 (grade 3–5 CKD) there is clearly loss of normal mineral homeostasis. As a result, there is considerable overlap between CKD and age-related/postmenopausal osteoporosis (Fig. 60.2). Thus, bone and mineral disorders in patients with CKD may be due to the underlying loss of kidney function, but also due to the underlying cause of the CKD and the treatments given.

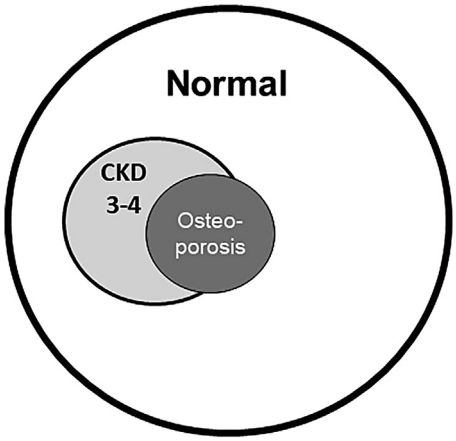

FIGURE 60.2 Overlap between osteoporosis and CKD stages 3–4. This graph shows the overlap between osteoporosis and CKD stages 3–4 in women from the United States, using data from the NHANES III survey. The kidney function was estimated using the Cockcroft–Gault equation, which results in a greater prevalence of CKD stages 3–4 than when other methods are used. *CKD*, chronic kidney disease; *NHANES III survey*, the Third National Health and Nutrition Examination Survey. *Reprinted with permission from Kidney Disease: Improving Global Outcomes, 2009. Clinical practice guidelines for the management of CKD–MBD. Kidney Int. 76, S1–S130.*

Chronic kidney disease–mineral bone disorder

Abnormalities of bone in patients with kidney disease were identified as early as the 1800s in isolated case reports (Ott, 2017). The magnitude of the problem was further illuminated with the onset of modern dialysis. The initial report of the first 16 patients on chronic hemodialysis noted that five had severe bone problems, including fractures (Pendras and Erickson, 1966). The term "renal osteodystrophy" was first used in 1942 to clearly denote that the abnormalities in bone were due to the presence of kidney disease (Liu and Chu, 1942). This term has continued to be used to describe the abnormalities of bone. However, since the beginning of the 21st century, there has been increasing research connecting abnormalities of bone and mineral metabolism to both skeletal and nonskeletal disorders, including cardiovascular disease, anemia, neuropathy, muscle weakness and impaired mobility, immune dysregulation, and altered mental status. The international organization KDIGO held a consensus conference in October 2005 to define and classify renal osteodystrophy. The conclusions of this expert panel of nearly 80 individuals from around the world was that the manifestations of mineral and bone abnormalities were so diverse, and included extraskeletal manifestations, that a new systemic disorder should be defined, called CKD–mineral and bone disorder (CKD–MBD; Table 60.1) (Moe et al., 2006). In contrast, the experts felt the term renal osteodystrophy should be reserved to define an alteration of bone morphology in patients with CKD, quantifiable by histomorphometry of bone obtained by biopsy. Renal osteodystrophy is one manifestation of abnormal bone of CKD–MBD. The goal of this new terminology is to provide consistency in the literature and raise awareness of the importance of these abnormalities in CKD.

The abnormalities that constitute CKD–MBD are interrelated. All three components of CKD–MBD are associated with increased morbidity and mortality in CKD patients and will be described in the following, with the major focus on the abnormalities of bone.

CKD–MBD: biochemical abnormalities

The four hormones parathyroid hormone (PTH), fibroblast growth factor-23 (FGF23), 1,25-dihydroxyvitamin D ($1,25(OH)_2D$), and α-klotho regulate normal calcium and phosphorus levels in a series of feedback loops. In addition to the maintenance of normal extracellular and intracellular levels of calcium and phosphorus, the long-term goal is to ensure adequate availability of these ions for bone that is growing (modeling) or remodeling and minimize extraskeletal calcification in soft tissues and vasculature. The kidney is involved in all of these homeostatic loops, and thus, it is not surprising that homeostasis is disrupted in patients with CKD.

Abnormalities begin early in the course of CKD. The expression of α-klotho in the kidney is reduced by 50% in humans (Asai et al., 2012) and rodents (Moe et al., 2011) at eGFR near 60 mL/min/1.73 m^2. Similarly, at this level of GFR, levels of $1,25(OH)_2D$ are decreased and PTH and FGF23 increased (Fig. 60.3). In patients with an eGFR of less than 60 mL/min/1.73 m^2, over 50% have an elevated FGF23 level greater than 100 RU/mL and 25% have an elevated intact PTH greater than 65 pg/mL. In patients with eGFR <30 mL/min/1.73 m^2, over 90% have FGF23 levels >100 RU/mL, and 75% have an elevated PTH greater than 65 pg/mL (Isakova et al., 2011a). It is believed that with progression of CKD, the body attempts to maintain normal serum concentrations of calcium and phosphorus via increased PTH and FGF23. However, a recent study monitored serial FGF23 levels and found that the FGF23 levels remained stable in the majority of patients, but in those patients with rising levels, there was a marked increase in mortality (Isakova et al., 2017). It is

TABLE 60.1 Kidney Disease Improving Global Outcomes classification of CKD–MBD and renal osteodystrophy.

Definition of CKD–MBD
A systemic disorder of mineral and bone metabolism due to CKD manifested by either one or a combination of the following: • abnormalities of calcium, phosphorus, PTH, or vitamin D metabolism • abnormalities in bone turnover, mineralization, volume, linear growth, or strength • vascular or other soft tissue calcification
Definition of renal osteodystrophy • Renal osteodystrophy is an alteration of bone morphology in patients with CKD. • It is one measure of the skeletal component of the systemic disorder of CKD–MBD that is quantifiable by histomorphometry of bone biopsy.

CKD–MBD, chronic kidney disease–mineral bone disorder; *PTH*, parathyroid hormone.
From Moe, S., Drueke, T., Cunningham, J., et al., 2006. Definition, evaluation, and classification of renal osteodystrophy: a position statement from Kidney Disease: Improving Global Outcomes (KDIGO). Kidney Int. 69, 1945–1953.

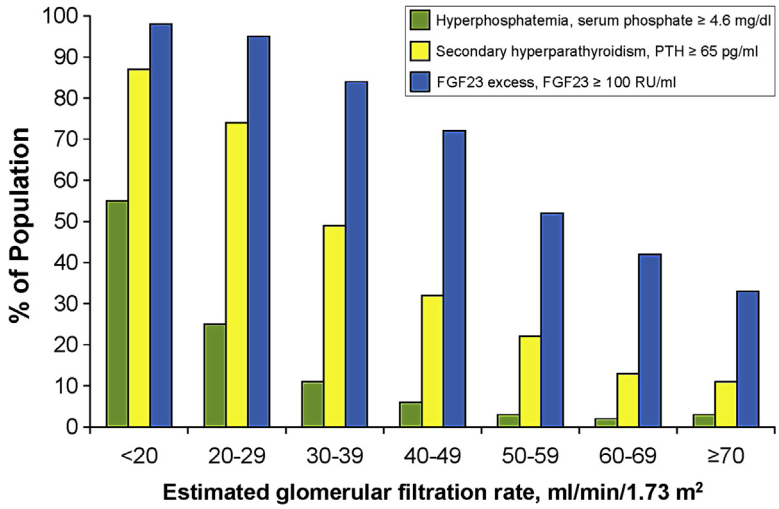

FIGURE 60.3 Prevalence of hyperphosphatemia, secondary hyperparathyroidism, and elevated FGF23 in relation to eGFR. Hyperphosphatemia was defined as serum phosphate ≥4.6 mg/dL, secondary hyperparathyroidism as parathyroid hormone (*PTH*) ≥65 pg/mL and fibroblast growth hormone-23 (*FGF23*) excess as FGF23 ≥ 100 RU/mL. *eGFR*, estimated glomerular filtration rate. *Reprinted with permission from Isakova, T., et al., 2011. Fibroblast growth factor 23 is elevated before parathyroid hormone and phosphate in chronic kidney disease. Kidney Int. 79, 1370−1378.*

presumed that the low expression of α-klotho creates an FGF23-resistant state in the kidneys, leading to increased FGF23 levels in kidney disease. The elevated FGF23 also leads to increased catabolism of both 25(OH)D and $1,25(OH)_2D$. Thus, as early as eGFR <60 mL/min/m^2, there is evidence of the biochemical abnormalities of CKD−MBD.

In contrast to the early rise in FGF23 and PTH and decrease in $1,25(OH)_2D$, serum levels of calcium and phosphorus are abnormal only when the eGFR is <30 mL/min/m^2. Thus, calcium and phosphorus levels do not reflect underlying hormonal derangements. There is decreased calcium absorption in the intestine that can be corrected with the administration of $1,25(OH)_2D$, which has been the practice for over 40 years. However, in CKD stages 3 and 4, there is also a marked reduction in urine calcium excretion. The mechanism by which this occurs is not well understood. It is possible that increased PTH leads to reabsorption; however, the urine calcium does not change in response to treatments with $1,25(OH)_2D$ or its analogs in which PTH is lowered by 30% (Coyne et al., 2006).

These decreases in calcium intestinal absorption and kidney excretion with CKD put patients at risk of positive calcium balance. Two recent calcium balance studies (Spiegel and Brady, 2012; Hill et al., 2012) have demonstrated positive calcium with oral intake from diet and supplements/binders of 800−1000 mg. The potential adverse consequences of positive calcium balance or excess calcium intake include suppression of bone remodeling rates and extraskeletal calcium deposition, at least in patients with ESKD (Barreto et al., 2008). Thus, indiscriminate use of calcium supplements in patients with CKD should be avoided.

Epidemiologic data have demonstrated that hyperphosphatemia in patients with both CKD and ESKD is associated with increased morbidity, and all-cause and cardiovascular mortality in patients with CKD (Kestenbaum et al., 2005; Isakova et al., 2009; Block et al., 2004). In patients with CKD stages 3−5 there are no data to support an increased risk of mortality or fracture with increasing serum calcium concentrations. However, similar to phosphate, there are several studies in dialysis patients demonstrating that hypercalcemia is associated with increased mortality (Block et al., 2004; Tentori et al., 2008). Similar to other biochemical measures of CKD−MBD, most observational studies have found an association of all-cause mortality with elevated levels of PTH; the mortality risk appears to increase at levels greater than 600 pg/mL (Block et al., 2004; KDIGO, 2009). In contrast, nearly all studies have identified an association with elevated FGF23 and adverse outcomes at all stages of kidney disease (Isakova et al., 2011b; Faul et al., 2011; Gutierrez et al., 2008, 2009; Isakova, 2012). Meta-analyses examining the risk of serum levels of calcium, phosphorus, PTH, and FGF23 in patients with CKD have demonstrated the strongest association with mortality with elevated phosphorus and FGF23 (Palmer et al., 2011; Krupp and Madhivanan, 2014). The reality is that none of these biochemical measures of CKD−MBD move in isolation. Thus it is not surprising that the combination of more than two abnormalities (for example, high phosphorus and high PTH) is associated with a greater risk of mortality than any single biochemical measure (Stevens et al., 2004; Tentori et al., 2008; Danese et al., 2015). Importantly, these data are all from observational studies and it is not yet clear that lowering these circulating biochemistries with interventions affects outcomes.

CKD–MBD: vascular calcification

In 1979, Ibels et al. demonstrated that both renal and internal iliac arteries of patients undergoing a renal transplant had increased atherogenic/intimal disease and increased calcification (detected by biochemical methods) compared with transplant donors. In addition, the medial layer was thicker and more calcified in uremic patients compared with the donors (Ibels et al., 1979). When coronary arteries from patients with ESKD who died from a cardiovascular event were compared with those of non-CKD patients who similarly died of a cardiovascular event, there was increased medial thickening, medial calcification, and calcification of intimal plaques in the patients with ESKD. However, the actual area of plaque was similar in the two groups (Schwarz et al., 2000). We examined the inferior epigastric artery of patients undergoing a kidney transplant, and demonstrated medial (nonatherosclerotic) calcification in 31% of patients with associated deposition of bone matrix proteins (Moe et al., 2002). We also identified upregulation of RUNX2 in areas of arteries with calcification, demonstrating that the vascular smooth muscle cells dedifferentiate to osteochondrocyte-like cells in vivo (Moe and Chen, 2008) (Fig. 60.4). These observations demonstrate that arterial calcification in arteries of patients with CKD is not just due to dystrophic (precipitation of calcium-phosphate salts) calcification, but rather to an active cell-mediated process. Hyperphosphatemia, present late in the course of CKD, can induce RUNX2 expression in vascular smooth muscle cells (Jono et al., 2000). However, the effect of uremic serum on calcification is greater than that of phosphorus alone (Moe et al., 2003), indicating that multiple uremic toxins can induce aberrant mineralization.

Coronary artery calcification can be detected with electron beam computed tomography (EBCT) or multislice CT scan. In 1996, Braun et al. first demonstrated by EBCT that coronary artery calcification increased with advancing age in patients on dialysis and that the calcification scores were 2 to 5-fold greater in dialysis patients than in age-matched individuals with normal renal function and angiographically proven coronary artery disease. The prevalence of detectable coronary disease is higher in CKD patients with diabetes than without, with an overall incidence of significant calcification of 47%–63% (Mehrotra et al., 2004). By the time patients reach the need for dialysis, significant coronary artery calcification is observed in over 80% of patients (Block et al., 2005).

There is an inverse relationship between bone mineralization and vascular calcification in patients on dialysis. London and colleagues evaluated hemodialysis patients who underwent bone biopsy with histomorphometry and assessment of vascular calcification by ultrasound with semiquantitative scoring. Those patients with lowest bone formation rates and decreased osteoblast surfaces had the greatest degree of peripheral artery calcification (London et al., 2004). Barreto found that patients on dialysis with low-turnover bone disease by biopsy, compared with high turnover, were more likely to have progression of coronary artery calcification over 1 year as assessed by serial multislice CT scan (Barreto et al., 2008). The mechanism by which turnover affects arterial calcification was studied by Kurz et al. These studies used radiolabeled calcium in CKD patients, demonstrating that in the setting of very-low-turnover bone, versus high-turnover bone, the calcium is not taken up into the bone (Kurz et al., 1994). However, as detailed later, bone disease is far more complex than just abnormal bone turnover.

CKD–MBD: bone abnormalities

The bone component of CKD–MBD consists of abnormalities in linear growth (Ingulli and Mak, 2014), fragility (increased fractures; Fig. 60.1), and abnormal pathology. The last, renal osteodystrophy, is one component of the skeletal outcomes that are associated with CKD–MBD and is defined as an alteration in bone morphology in patients with CKD; it can also be characterized as a global disorder of bone quality that encompasses abnormalities in bone turnover, collagen structure, cortical and trabecular microarchitecture, and/or mineralization (Moe et al., 2006).

Historical classification

Renal osteodystrophy was classified by bone biopsy with tetracycline double labeling and quantitative histomorphometry, and the underlying associated pathologies were categorized by the turnover or mineralization of bone (Table 60.2). This classification utilizes measures of unmineralized osteoid as a percentage of total bone area and quantified fibrosis. These two static measures in conjunction with dynamic measures of bone turnover (i.e., bone formation rate, activation frequency) were used to define the type of renal osteodystrophy.

Fig. 60.5 illustrates types of renal osteodystrophy based on the historical nomenclature. *Normal bone* is illustrated in Fig. 60.5A. *Osteitis fibrosa cystica* (i.e., high-turnover bone disease, hyperparathyroid bone disease) is illustrated in Fig. 60.5B. Sustained hyperparathyroidism results in high bone turnover, excessive numbers and activity of osteoblasts and osteoclasts, disordered collagen production (i.e., formation of woven bone), and accumulation of fibroblastic osteoprogenitors not in the osteoblastic differentiation program, resulting in peritrabecular bone marrow fibrosis. Excessive

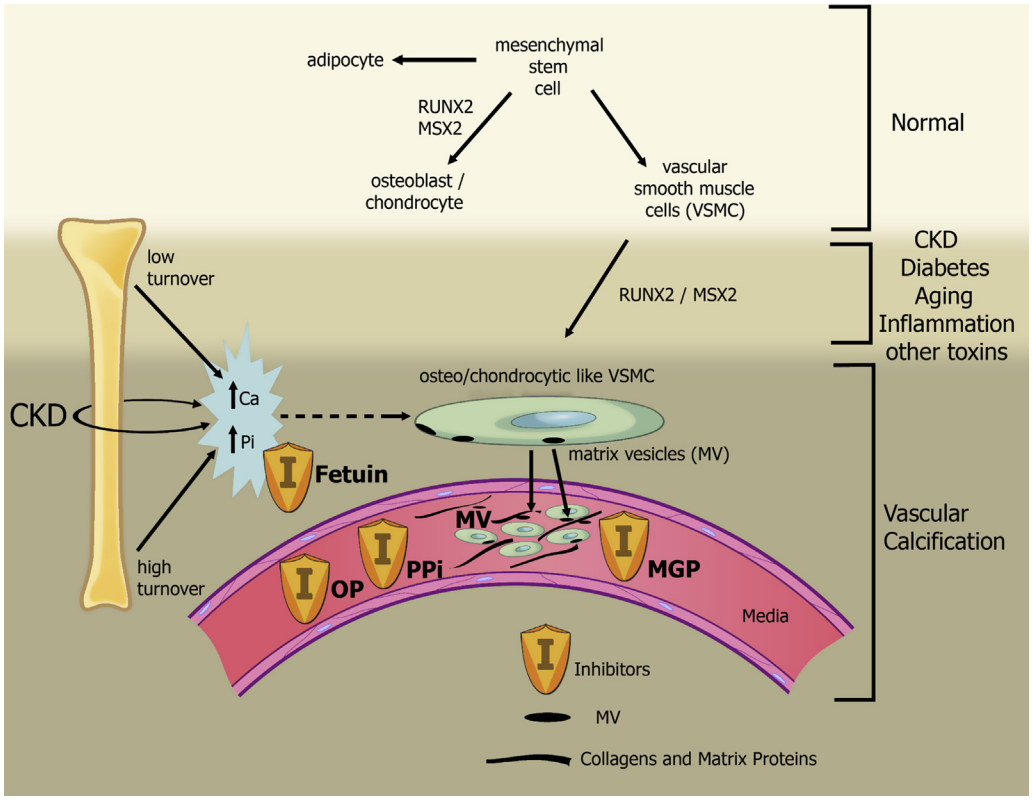

FIGURE 60.4 Overview of pathogenesis of arterial calcification in kidney disease. Normally, mesenchymal stem cells differentiate to adipocytes, osteoblasts, chondrocytes, and vascular smooth muscle cells (VSMCs). In the setting of chronic kidney disease, diabetes, aging, inflammation, and multiple other toxins, these VSMCs can dedifferentiate or transform into osteo/chondrocyte-like cells by upregulation of transcription factors such as RUNX2 and MSX2. These transcription factors are critical for normal bone development and thus their upregulation in VSMCs is indicative of a phenotypic switch. These osteo/chondrocyte-like VSMCs then become calcified in a process similar to bone formation. These cells lay down collagen and noncollagenous proteins in the intima or media and incorporate calcium and phosphorus into matrix vesicles to initiate mineralization and further mineralize into hydroxyapatite. The overall positive calcium and phosphorus balance of most dialysis patients feeds both the cellular transformation and the generation of matrix vesicles. In addition, the extremes of bone turnover in chronic kidney disease (low and high or adynamic and hyperparathyroid bone, respectively) will increase the available calcium and phosphorus by altering the bone content of these minerals. Ultimately, whether an artery calcifies or not depends on the strength of the army of inhibitors (*I*) standing by in the circulation (fetuin-A) and in the arteries (*PPI*, pyrophosphate; *MGP*, matrix Gla protein; *OP*, osteopontin, as examples). *From Moe, S.M., Chen, N.X., 2008. Mechanisms of vascular calcification in chronic kidney disease. J. Am. Soc. Nephrol. 19, 213–216, with permission.*

TABLE 60.2 Historical classification of renal osteodystrophy.

High-turnover bone disease
Osteitis fibrosa cystica
Mild hyperparathyroid bone disease (no fibrosis)
Mixed osteodystrophy
Low-turnover bone disease
Osteomalacia
Adynamic bone disease

Adapted from Sherrard, et al., 1993. The spectrum of bone disease in end-stage renal failure—an evolving disorder. Kidney Int. 43, 436–442, with permission.

osteoblast activity is characterized by unmineralized osteoid. Excessive osteoclast activity is characterized by an elevated resorption surface and tunneling into individual trabecula. *Adynamic bone disease* is illustrated in Fig. 60.5C. The hallmark of adynamic bone disease is a profound decrease in or lack of bone turnover, with an absence of osteoblast and osteoclast activity, osteoid formation, and endosteal fibrosis. In contrast to osteomalacia, in adynamic bone there is no increase in

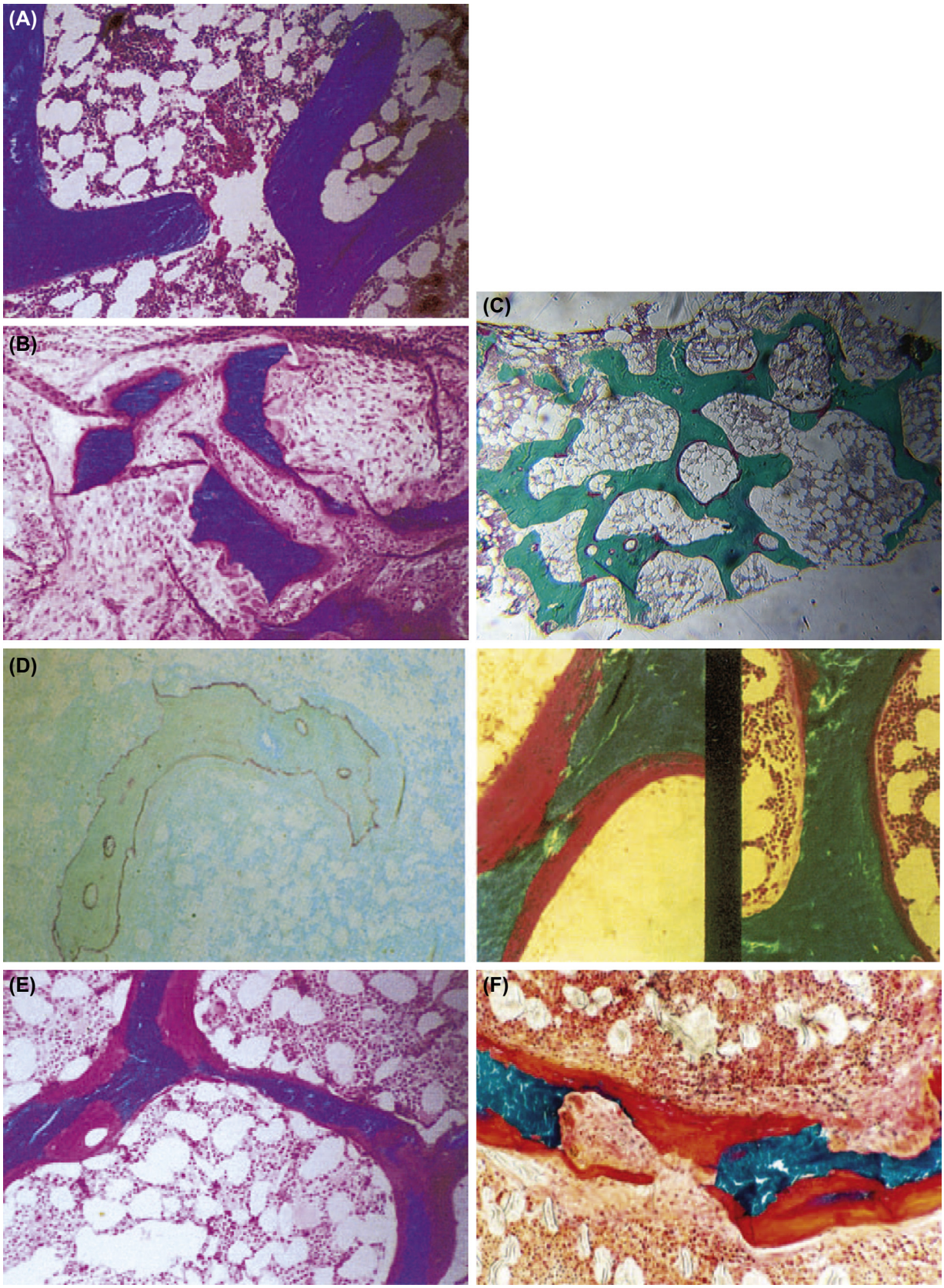

FIGURE 60.5 Bone histology categorized by historical classification system. (A) Normal bone. (B) Hyperparathyroid bone (increased osteoclast and osteoblasts and fibrosis). (C) Adynamic bone (no cellular activity and no osteoid). (D) Aluminum bone disease. (Left) Aluminum staining at mineralization front. (Right) Accumulation of osteoid (orange-red stain). (E) Osteomalacia (increased unmineralized osteoid in pink/red). (F) Mixed uremic osteodystrophy presence of increase osteoid (orange red) indicating mineralization defect, and increased osteoclast activity. ***A, B, D [right],*** *and* ***E,*** *Courtesy S.L. Teitelbaum, MD;* ***D [left],*** *Courtesy D. J. Sherrard, MD.*

osteoid. The majority of the bone surface is covered by lining cells, with few bone-forming and -resorbing cells. The bone structure is predominantly lamellar and the extent of the mineralizing surface is markedly reduced, with thin, single or no tetracycline labels present. Low-turnover bone disease was initially described as a complication of aluminum toxicity resulting from high aluminum content in dialysis water and aluminum-based phosphate binders. Aluminum bone disease (Fig. 60.5D) was histologically characterized by the presence of aluminum deposits at the mineralization front and was frequently associated with osteomalacia (Fig. 60.5E). Aluminum bone disease is now rarely reported due to monitoring of aluminum content in dialysis water and the extremely rare use of aluminum-based phosphate binders (Malluche et al., 2011). Low turnover also occurs in the absence of aluminum exposure; therefore, the etiology of adynamic/low-turnover bone disease is multifactorial. Major contributory factors include diabetes, older age, and malnutrition, along with factors that are unique to uremia (Andress, 2008) (see "Pathogenesis of abnormal bone"). *Mixed uremic osteodystrophy* is illustrated in Fig. 60.5F and describes bone that has features of both renal hyperparathyroidism and defects in mineralization. Therefore, there is excessive osteoblast and osteoclast activity, increased endosteal and peritrabecular fibrosis, and more osteoid than expected, and tetracycline labeling uncovers a mineralization defect.

TMV classification system

In 2009, the KDIGO committee proposed a new classification system, based on the three key histologic features of renal osteodystrophy, bone turnover, mineralization, and volume (TMV [turnover, mineralization, volume] system; Table 60.3), to better describe the bone abnormalities present in CKD and to assist with clinical decision-making. In this system, the histomorphometric abnormalities are reported using standard nomenclature as recommended by the American Society of Bone and Mineral Research (Parfitt et al., 1987). This shift in classification recognized that the historical definition could not accommodate advances in our understanding of the diverse and complex pathobiology of bone disease in CKD patients. For example, the historic renal osteodystrophy classification system relied on assessments of bone turnover and mineralization but was unable to appreciate the increasingly recognized and important role of bone volume as an indicator of bone disease and fracture risk in CKD (Barreto et al., 2006). The TMV classification system provides a clinically relevant description of the underlying bone pathology as assessed by histomorphometry, which in turn helps define the pathophysiology and thereby guide therapy. Fig. 60.6 compares the older classification of renal osteodystrophy based on turnover with the new TMV classification system.

Turnover reflects the rate of bone remodeling. In health, remodeling is a coupled process of bone resorption and formation and is measured on histomorphometry by dynamic measurements of osteoblast function using double tetracycline labeling. The bone formation rate and activation frequency represent parameters for assessing bone turnover. Bone turnover is influenced by hormones, cytokines, mechanical stimuli, and growth factors that influence the recruitment, differentiation, and activity of osteoclasts and osteoblasts. It is important to clarify that although bone formation rate is frequently similar to bone resorption rate, which cannot be measured directly, it is not always so. Imbalance in these processes can affect bone volume. For example, if resorption exceeds formation, negative bone balance and decreased bone volume result.

Mineralization reflects the degree and rate of calcium deposition on bone collagen. By histomorphometry, both static and dynamic parameters contribute to the assessment of mineralization. Static parameters include osteoid surface, which quantifies the percentage of cancellous surface with unmineralized osteoid, with and without osteoblasts, and osteoid thickness, which is the mean thickness of the osteoid on cancellous surfaces. Dynamic parameters, based on tetracycline double labeling, include the mineralizing surface, mineral apposition rate, and mineralization lag time. Causes of

TABLE 60.3 TMV classification system for renal osteodystrophy.

Turnover	Mineralization	Volume
Low	Normal	Low
Normal	Abnormal	Normal
High		High

From Moe, S., Drueke, T., Cunningham, J., et al., 2006. Definition, evaluation, and classification of renal osteodystrophy: a position statement from Kidney Disease: Improving Global Outcomes (KDIGO). Kidney Int. 69 (11), 1945–1953.

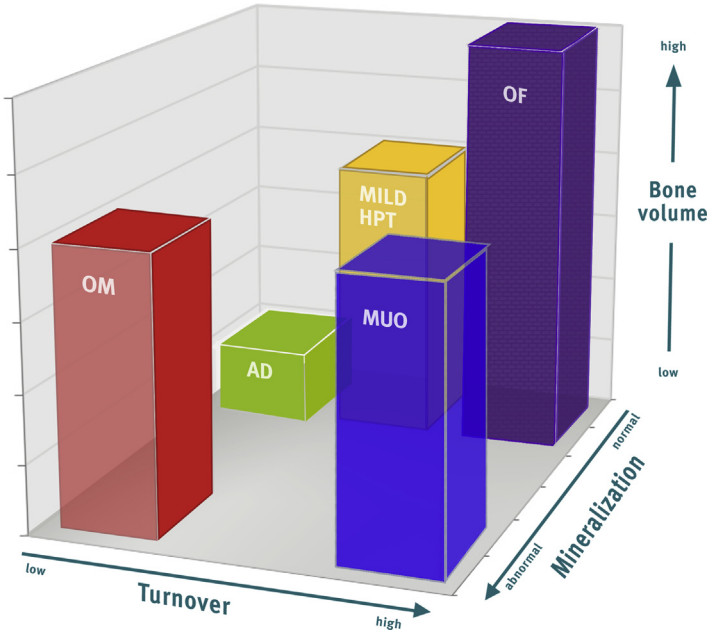

FIGURE 60.6 Comparison of older classification of renal osteodystrophy with TMV classification. The figure is a graphical example of how the TMV system provides more information than the present, commonly used classification scheme. Each axis represents one of the descriptors in the TMV classification: turnover (from low to high), mineralization (from normal to abnormal), and bone volume (from low to high). Individual patient parameters could be plotted on the graph, or means and ranges of grouped data could be shown. For example, many patients with renal osteodystrophy cluster in areas shown by the bars. The *red* bar (osteomalacia [*OM*]) is currently described as low-turnover bone with abnormal mineralization. The bone volume may be low to medium, depending on the severity and duration of the process and other factors that affect bone. The *green* bar (adynamic bone disease [*AD*]) is currently described as low-turnover bone with normal mineralization, and the bone volume in this example is at the lower end of the spectrum, but other patients with normal mineralization and low turnover will have normal bone volume. The *yellow* bar (mild hyperparathyroid [*HPT*]-related bone disease) and the *purple* bar (osteitis fibrosa [*OF*] or advanced HPT-related bone disease) are currently used distinct categories, but in actuality represent a range of abnormalities along a continuum of medium to high turnover and any bone volume depending on the duration of the disease process. Finally, the *blue* bar (mixed uremic osteodystrophy [*MUO*]) is variably defined internationally. In this graph, it is depicted as high-turnover, normal bone volume, with abnormal mineralization. In summary, the TMV classification system more precisely describes the range of pathologic abnormalities that can occur in patients with CKD. *From Moe, S., Drueke, T., Cunningham, J., et al., 2006. Definition, evaluation, and classification of renal osteodystrophy: a position statement from Kidney Disease: Improving Global Outcomes (KDIGO). Kidney Int. 69 (11), 1945–1953, with permission.*

mineralization defects in CKD include vitamin D deficiency, mineral abnormalities, metabolic acidosis, and aluminum and iron bone toxicity.

Volume reflects the amount of bone per unit volume and is the percentage total marrow area (including trabeculae) occupied by cancellous bone. Bone volume is determined by age, gender, race, genetic factors, nutrition, endocrine disorders, mechanical stimuli, toxicities, neurologic function, vascular supply, growth factors, and cytokines.

The spectrum of renal osteodystrophy in CKD

Renal osteodystrophy type may be based on the severity of kidney disease, demographic factors, genetics, exposure to medications that are toxic to the skeleton, and hormonal and metabolic abnormalities that are associated with CKD. Bone biopsy studies in CKD patients also demonstrate that renal osteodystrophy results in global abnormalities in both bone quality and strength; thus, renal osteodystrophy can be considered a form of osteoporosis as defined by the National Institutes of Health Consensus Conference on Osteoporosis.

Some data suggest that up to three-quarters of predialysis patients (CKD stages 3 and 4) have histologic evidence of renal osteodystrophy (Elder, 2002). Of 132 patients with CKD stages 3–5 (not on dialysis), Lehmann et al. (2008) reported that 68.8% patients had mild or full-blown osteitis fibrosa cystica (58.3% CKD stages 3–4; 72.8% CKD stage 5), 8.3% of patients had either adynamic bone disease or mixed uremic osteodystrophy, and 3.8% had osteomalacia (5.5% CKD stages 3–4; 3.1% CKD stage 5). Of 84 predialysis patients, Spasovski et al. (2003) reported that 23%, 38%, 9%, 15%, and 12% had adynamic bone disease, normal bone, hyperparathyroid bone disease, mixed osteodystrophy, and osteomalacia,

respectively. In a more recent analysis that reflects contemporary trends in management of CKD−MBD, Carvalho et al. (2016) compared histomorphometric findings between 16 and 15 patients who were either predialysis (CKD stages 3−5) or on dialysis, respectively, using the TMV system. The prevalence of turnover types differed by dialysis status: (1) for predialysis, 50% had normal turnover, 31% had high turnover, and 19% had low bone turnover, and (2) for dialysis, 50% had high turnover, 31% had low turnover, and 19% had normal bone turnover. Differences in mineralization based on dialysis status were not noted. However, they reported differences in cortical bone volume based on dialysis status: patients with more severe CKD had thinner and more porous cortices.

In patients undergoing dialysis, several recent studies have used the TMV classification system to describe contemporary trends in renal osteodystrophy and characterize tissue-level impairments in bone quality (Sprague et al., 2015; Malluche et al., 2011, 2012). Malluche et al. (2011) evaluated 630 bone biopsies from adult hemodialysis patients from Europe and the United States. For turnover, 58%, 25%, and 18% of patients had low, high, and normal turnover, respectively. There were clear racial differences in turnover: low bone turnover predominated in whites (62%) and normal or high turnover predominated in blacks (68%). For mineralization, defects were uncommon (3% of patients). For volume, low, normal, or high cancellous bone volume was equally distributed among whites, but high volume predominated in blacks. Furthermore, blacks had normal cortical thickness with higher porosity, but whites had an equal distribution of low or normal thickness with high or normal porosity. Trabecular microarchitecture was also examined, with trabecular thickness being low in 37% of patients, normal in 40% of patients, and high in 13% of patients. Trabecular separation was normal in most (78%) of the patients. Interestingly, both black and white patients with high bone turnover had increased porosity, and more than 80% of patients with low cancellous bone volume had thin trabeculae.

The KDIGO consortium (Sprague et al., 2015) evaluated 492 bone biopsies in adult hemodialysis patients from Brazil, Turkey, Venezuela, and Portugal. Similar to Malluche et al. (2011), the prevalence of low-turnover renal osteodystrophy predominated (59%), but only 17% compared with 25% had high turnover. In a smaller study of 35 hemodialysis patients, those with low bone turnover had more microstructural abnormalities (lower cancellous bone volume and thinner trabeculae) than those with high or normal turnover, while those with high turnover had reduced bone strength as measured by nanoindentation (Malluche et al., 2012). In this same study, mineralization defects were common. In children, defective mineralization (defined as increased in osteoid in combination with low mineralization rates) was present in as many as 29% of CKD stage 2 patients, 42% of CKD stage 3 patients, and 79% of patients with CKD stages 4 and 5 (Wesseling-Perry, 2015).

Pathogenesis of abnormal bone

The pathogenesis of abnormal bone in CKD is complex and multifactorial (Table 60.4). Clinically, the focus of treatment of renal osteodystrophy is to lower PTH with calcitriol, or its analogs, or calcimimetics. More recently, animal studies have led to an appreciation of non-PTH-mediated mechanisms.

Parathyroid hormone and decreased $1,25(OH)_2D_3$

The original "trade-off hypothesis," suggested by Bricker et al., deduced that as individual nephrons were lost, the trade-off for maintaining external solute balance for a given solute as renal disease advances would be the induction of one, or more, of the abnormalities of the uremic state (Bricker, 1972). Bricker and Slatopolsky noted from dog experiments that the compensatory response to loss of nephrons and the inability to excrete phosphorus was an increase in PTH secretion (Slatopolsky et al., 1971). The effect of phosphate and PTH increase on bone was detailed in these dogs in 1977 (Slatopolsky et al., 1977), providing the biologic rationale for treating renal osteodystrophy by suppressing PTH with phosphate restriction and $1,25(OH)_2D_3$ in animal models (Rutherford et al., 1977), and eventually in humans (Slatopolsky et al., 1984). Multiple studies demonstrated that low levels of $1,25(OH)_2D_3$ (Martinez et al., 1996) and decreased repression of the PTH gene transcription led to greater synthesis and secretion of PTH. As kidney disease progresses, the number of vitamin D receptors in the parathyroid glands decreases (Merke et al., 1987). These studies led to the primary approach to the treatment of secondary hyperparathyroidism with calcitriol or its analogs for over 40 years.

Interestingly, the data supporting the efficacy of calcitriol or its analogs on improving renal osteodystrophy in humans are limited. An initial study showed improvement in bone formation rate by bone biopsy in 11 patients on hemodialysis treated with intravenous calcitriol (Andress et al., 1989). Subsequent studies in patients with CKD not yet on dialysis demonstrated decreased bone turnover in 30%−50% of subjects treated with calcitriol or its analogs (Baker et al., 1989; Hamdy et al., 1995; Nordal and Dahl, 1988). A study in children undergoing treatment with peritoneal dialysis showed similar results (Salusky et al., 1987). Initially the increase in calcium as a result of calcitriol/analog therapy was presumed

TABLE 60.4 Contributions to the pathogenesis of renal osteodystrophy.

Decreased or aberrant hormones
Increased or decreased PTH
Decreased $1,25(OH)_2D_3$
Increased FGF23
Reduced gonadal hormones
Reduced growth hormone/IGF signaling in children
Abnormal mineralization
Hypocalcemia, or altered calcium-phosphate ratio or product
Decreased $1,25(OH)_2D_3$
Decreased mobility
Abnormal FGF23/klotho signaling in osteocytes
Abnormal cellular function
Decreased mesenchymal differentiation
Abnormal RANK/RANKL/OPG
Abnormal Wnt signaling (elevated sclerostin and Dkk-1)
Inflammation; increased cytokines
Increased TGFβ
Increased FGF23 and osteocyte dysfunction
Abnormal collagen
Increased advanced glycation end product formation
Oxidative stress
Inflammation

$1,25(OH)_2D_3$, 1,25-dihydroxyvitamin D_3; *Dkk-1*, Dickkopf-1; *FGF23*, fibroblast growth factor-23; *IGF*, insulin-like growth factor; *OPG*, osteoprotegerin; *PTH*, parathyroid hormone; *RANK*, receptor activator of NF-κB; *RANKL*, receptor activator of NF-κB ligand; *TGFβ*, transforming growth factor β.

to be favorable for bone mineralization. However, with the recognition of diffuse extraskeletal calcification and resulting cardiac morbidity and mortality, new analogs of calcitriol were developed to be "less calcemic." Unfortunately, human studies have failed to show differences in hypercalcemia (Coyne et al., 2006). Thus, therapy with calcitriol and its analogs, while efficacious in reducing PTH, does not uniformly correct bone turnover or mineralization (reviewed in Newman et al., 2016), suggesting additional non-PTH-mediated mechanisms.

The expression of the calcium-sensing receptor (CASR) is also downregulated in hypertrophied parathyroid glands in CKD (Sumida et al., 2013). Calcimimetics, allosteric activators of the CASR, are used clinically to lower PTH while lowering calcium, phosphorus, and FGF23 (Investigators et al., 2012; Parfrey et al., 2013; Moe et al., 2015c). Animal studies of the $5/6^{th}$ nephrectomy rat model showed improved volumetric cortical bone mineral density (BMD) and cortical stiffness but a nonsignificant lowering of bone formation rate (Wada et al., 1998). In a prospective, randomized controlled study, cinacalcet reduced bone formation rate and fibrosis in dialysis patients. In 77 patients treated with 6–12 months of the calcimimetic cinacalcet, there was a decrease in PTH and a reduction in bone formation rate, mineralization lag time, and osteoblast perimeter and a borderline decrease in osteoclast perimeter (Behets et al., 2015). In small studies, cinacalcet improved BMD (Lien et al., 2005; Tsuruta et al., 2013; Ishimura et al., 2011) but the effect was in general limited to cortical sites. In a study of 163 kidney transplant recipients, cinacalcet therapy (used to treat residual hyperparathyroidism) improved BMD of the hip despite lowering serum calcium levels (Cho et al., 2010). In a secondary analysis of the Evaluation of Cinacalcet HCl Therapy to Lower Cardiovascular Events (EVOLVE) trial comparing cinacalcet with placebo on top of usual care (generally calcitriol and its analogs and phosphate binders), a reduction in cortical fractures was found, although the majority of efficacy was in patients older than 65 years of age (Moe et al., 2015a).

Thus, elevated PTH may explain some of the abnormalities of renal osteodystrophy, particularly the cortical porosity and thinning. However, studies have demonstrated that the incidence of age-adjusted hip fracture has actually increased over the past decades despite an intensive use of PTH-lowering therapies (Wagner et al., 2014; Wakasugi et al., 2013). However, bone is still abnormal in the absence of elevated PTH in patients with CKD (e.g., adynamic bone disease), supporting other factors in the pathogenesis of renal osteodystrophy.

Abnormalities in the fibroblast growth factor-23–klotho pathway

Both FGF23 and klotho are expressed in osteocytes, with a complex interrelationship (Rhee et al., 2011; Kaludjerovic et al., 2017a). Expression of FGF23 in osteocytes is markedly increased in early CKD (Wesseling-Perry and Juppner, 2013; Wesseling-Perry, 2010; Graciolli et al., 2017). This may be due to elevated PTH, but there is also decreased expression of the FGF23 regulatory proteins dentin matrix protein 1 and sclerostin in CKD (Pereira et al., 2009). In biopsies from children, the greater the osteocyte expression of FGF23, the greater the mineralization defect (Wesseling-Perry, 2015). Interestingly, klotho is also expressed in osteocytes and klotho-null animals have osteoporosis (Kuro-o et al., 1997), but it is not clear if this was due to klotho changes in bone or the myriad of other systemic abnormalities in mineral metabolism seen in these animals. Concomitant deletion of PTH receptors reverses this phenotype (Yuan et al., 2012). Targeted deletion of klotho from osteocytes in normal animals led to increased bone formation and bone volume, with enhanced osteoblast activity (Komaba et al., 2017). However, when these same animals were induced to have CKD through nephrectomies, the klotho expression was markedly downregulated and there was decreased mineralization and osteoblast activity (Komaba et al., 2017). In long bones, klotho stimulates FGF23 production in animal models of CKD (Kaludjerovic et al., 2017b). Similarly, the exogenous administration of soluble klotho markedly stimulates FGF23 production from bone. Unfortunately, this led to hypophosphatemia, osteomalacia, and fractures in animals (Smith et al., 2012). These studies exemplify the importance of the FGF23–klotho pathway in mediating kidney–bone abnormalities and suggest that downregulation of klotho in osteocytes in CKD, similar to the low expression in kidney and parathyroid glands, may be a factor in the pathogenesis of renal osteodystrophy.

Disordered osteoblast function or differentiation

When PTH is suppressed in the setting of CKD, there are low bone remodeling rates and, in some cases, a paucity of cells. The latter is often called adynamic or aplastic bone disease. The paucity of cells in true adynamic bone disease differs from simple suppression of bone turnover as is seen with, for example, bisphosphonates and indicates abnormal osteoblast differentiation. Studies of mesenchymal stem cell (MSC) differentiation have demonstrated impaired osteoblast differentiation of MSCs in the presence of uremic serum (Della Bella et al., 2017), perhaps due to cytotoxic effects of uremic toxins such as asymmetric dimethylarginine (Xiao et al., 2001). In our rat model of slowly progressive CKD, we found that low PTH and low bone remodeling were associated with decreased vascular endothelial growth factor A (VEGF-A), RUNX2, and Nrf2 (nuclear factor [erythroid-derived 2]-like 2), a master regulator of oxidative stress (Chen et al., 2015). The low VEGF-A and RUNX2 signaling would preferentially lead to adipocyte differentiation of MSCs instead of osteoblasts (Liu et al., 2012b). Adipocyte content of marrow is increased in bone with aging (Justesen et al., 2001), and we also found increased bone marrow fat in patients with CKD compared with matched controls (Moorthi et al., 2015). Taken together, these data support impaired osteoblast differentiation in CKD.

Impaired Wnt signaling

Sclerostin and Dickkopf-1 (Dkk-1) are circulating inhibitors that prevent LRP5/6 activation of Wnt signaling. Such signaling is known to inhibit osteoblastic bone formation and thus may play a role in the development of abnormal bone cell differentiation in CKD where levels of both inhibitors are elevated (Cejka et al., 2011a; Ferreira et al., 2013; Fang et al., 2014; Sabbagh et al., 2012). Sabbagh et al., using the jck mouse model of progressive CKD, identified an increase in sclerostin-positive osteocytes and corresponding reduction in Wnt/β-catenin target genes, indicating impaired osteoblast differentiation. These changes were observed despite increased osteoclastic-mediated bone remodeling and before major increases in PTH (Sabbagh et al., 2012). Parallel studies of human biopsies from patients with CKD showed increased sclerostin in osteocytes, with only slight attenuation in the setting of elevated PTH (Sabbagh et al., 2012). We further examined this pathway in our Cy/+ rat model of CKD and found that anti-sclerostin antibody treatment was effective in restoring bone volume and cortical geometry only in animals with PTH suppression and low bone turnover, and not in the high-PTH animals (Moe et al., 2015b). Even with improved bone volume, there was no improvement in biomechanical testing with the anti-sclerostin antibody as was seen in normal animals (Moe et al., 2015b).

Dkk-1 was examined in the LDL receptor knockout mouse with surgically induced CKD. Early in the course of CKD (stage 2), animals were given a monoclonal antibody against Dkk-1. The treatment stimulated bone formation rates, corrected the osteodystrophy, and prevented CKD-stimulated vascular calcification. The treatment also decreased the elevated levels of sclerostin, but not FGF23 (Fang et al., 2014). Moyses and colleagues (Ferreira et al., 2013) examined these Wnt antagonists in rats subjected to both nephrectomy and parathyroidectomy and then fed either a low- or a

high-phosphate diet. The result was low-turnover bone in both groups. However, when the animals were fed a high-phosphorus diet there was a decrease in bone volume, and higher sclerostin and Dkkl-1 gene expression compared with the normal phosphate diet—treated animals, suggesting phosphate may also regulate these pathways in a PTH-independent mechanism.

Transforming growth factor β family abnormalities

Expression of transforming growth factor β (TGFβ) is increased in bone biopsies from patients with CKD (Santos et al., 2003; Duarte et al., 2002), and TGFβ is known to regulate bone remodeling by enhancing osteoblast differentiation (Filvaroff et al., 1999; Erlebacher et al., 1998). A neutralizing antibody to TGFβ increased bone volume and suppressed bone turnover, with reduction in both osteoblasts and osteoclasts (Liu et al., 2014). Hruska and colleagues have found that there is increased circulating activin A, a TGFβ superfamily member, released into the circulation in the setting of kidney injury (Hruska et al., 2017). It is believed to be derived from peritubular myofibroblasts, where it stimulates fibrosis in the kidney. Activin A binds the activin type 2A receptor to stimulate osteoclasts (Williams et al., 2018; Sugatani et al., 2003) and in the presence of CKD leads to increased bone remodeling and bone loss. Blockade of this pathway with a ligand trap reversed these abnormalities (Sugatani et al., 2017).

Abnormalities of bone collagen

In addition to cellular abnormalities in bone, the abnormal bone quality seen by imaging studies is suggestive of abnormal collagen. Bone represents the largest collection of long-lived proteins in the body, principally collagen, and thus is highly susceptible to alteration. A major mechanism of collagen changes is through accumulation of advanced glycation end products (AGEs). In patients with CKD, regardless of the presence or absence of diabetes, there are increased circulating levels of AGE proteins (pentosidine and CML) compared with age-matched controls (Thornalley and Rabbani, 2009). AGE levels increase with progression of CKD (Misselwitz et al., 2002), probably due to increased oxidative stress and chronic inflammation (Small et al., 2012), which facilitate AGE formation. In vitro (Willett et al., 2013) and in human bone biopsy studies from patients with postmenopausal osteoporosis (Ural et al., 2015; Abraham et al., 2015), AGE accumulation is associated with reduced bone mechanical properties and impaired osteoblast activity (Gangoiti et al., 2013; Weinberg et al., 2014). In vitro, bone that is nonenzymatically glycated has reduced post-yield strain, a property that can be linked to brittle bone (Willett et al., 2013). We and others have found increased skeletal AGE levels in a CKD animal model, and we have shown these levels to be independent of PTH levels and bone turnover (Aoki et al., 2013; Allen et al., 2015). These and probably other abnormalities in collagen may impair bone quality in CKD.

Diagnostic tests for abnormal bone in CKD

Bone biopsy is the gold standard for assessing bone quality and strength and can inform treatment options for renal osteodystrophy based on the formation, resorption, and mineralization characteristics of bone measured by quantitative histomorphometry. However, bone biopsy's utility in the clinic is limited by its availability at only a few centers worldwide, invasiveness, cost, degree of patient discomfort, and long duration of time needed to process and analyze bone tissue. Noninvasive approaches to assess bone quality and strength in patients with renal osteodystrophy can be implemented in the clinic and can inform treatment decisions without the need for an invasive bone biopsy procedure. Areal BMD can be measured by dual-energy X-ray absorptiometry (DXA), and trabecular microarchitecture can be assessed with the trabecular bone score (TBS). Cortical and trabecular microarchitecture and mechanical estimation of bone strength can be quantified by high-resolution peripheral quantitative CT (HR-pQCT) or micro—magnetic resonance imaging (micro-MRI) with application of micro—finite element analysis (FEA). Finally, bone turnover and mineralization can be assessed by measuring calciotropic hormones and circulating markers of bone formation and resorption. Each of these tools will be discussed.

Bone density and the fracture risk assessment tool

DXA is the clinical standard to measure areal BMD and fracture risk in the general population and is integral to the World Health Organization's (WHO) definition of osteoporosis (T score ≤ -2.5) (Kanis et al., 1994). Historically the role of DXA to assess bone health and fracture risk in CKD was controversial because in small cross-sectional studies, DXA did not discriminate prevalent fractures, and measurements of areal BMD do not predict type of renal osteodystrophy.

However, longitudinal studies in patients across the spectrum of CKD have demonstrated that low areal BMD at the hip and forearm predict incident fractures (West et al., 2015; Iimori et al., 2012; Naylor et al., 2015; Yenchek et al., 2012). Furthermore, these studies reported that the WHO T scores performed similarly in patients with and without CKD for fracture prediction. Based on these studies, the KDIGO guidelines were revised in 2017 to recommend measurement of areal BMD by DXA in CKD patients to assess fracture risk when clinically indicated.

In the general population, the sensitivity of fracture prediction by DXA is improved by the addition of clinical risk factors to measures of areal BMD. The Fracture Risk Assessment (FRAX) tool was developed to provide 10-year absolute risk of major osteoporotic and hip fracture by including 10 clinical risk factors, with or without areal BMD of the femoral neck, into a fracture risk prediction model (Kanis et al., 2008). FRAX has been studied in CKD. In a study from the Canadian Multicentre Osteoporosis Study, 320 individuals with an eGFR <60 mL/min and 1787 with an eGFR ≥60 mL/min were followed for a mean of 4.8 years (Naylor et al., 2015). FRAX performed similarly in its ability to predict major osteoporotic fractures in patients with and without kidney disease. In a cross-sectional study of 353 patients with a mean eGFR of 28 mL/min (∼30% with prevalent fractures), FRAX with femoral neck BMD discriminated those with and without fractures, but was not superior to femoral neck BMD alone (Jamal et al., 2014). FRAX alone, FRAX with BMD, and BMD alone were better discriminants of fracture than age alone. In a study of 485 Japanese hemodialysis patients FRAX did not predict increased fracture risk over a 3.3-year median follow-up (Iimori et al., 2012). It is important to note that for all these studies, the follow-up time was short (with FRAX being validated in general population cohorts to predict fractures over 10 years), and fracture event data from administrative data sets may not have ascertained all fracture types (e.g., occult vertebral fractures). These studies suggest that more research is needed to determine the usefulness of FRAX in CKD. More specifically, some of the clinical factors included in current FRAX algorithms may not be relevant in CKD patients. CKD-specific fracture assessment tools need to be developed, which should incorporate CKD-specific predictors of fracture.

Bone quality imaging: TBS, QCT, HR-pQCT, and micro-MRI

An important limitation of DXA is that it does not assess the three-dimensional microarchitecture of trabecular bone; therefore, DXA cannot assess bone quality. TBS is a novel, widely available, gray-scale textural parameter developed to assess trabecular microarchitecture from lumbar spine areal BMD measures obtained by DXA. In patients without kidney disease, TBS has been shown to predict fracture (Pothuaud et al., 2009; Boutroy et al., 2013; Iki et al., 2014). TBS has been validated against both three-dimensional trabecular microarchitecture assessed by micro-CT in human cadaver vertebrae and two-dimensional transiliac bone biopsy from patients with idiopathic osteoporosis and low trauma fractures (Hans et al., 2011; Roux et al., 2013; Muschitz et al., 2015). We recently demonstrated that TBS was significantly associated with trabecular bone volume (BV/TV), trabecular width (Tb.Wi), trabecular spacing, cortical width on bone biopsy in patients on dialysis (Ramalho et al, 2018). In studies of patients with ESKD and after kidney transplantation, TBS measures were reported to be lower than in matched controls (Yavropoulou et al., 2017; Perez-Saez et al., 2017; Naylor et al., 2016a) and to predict fracture independent of BMD and clinical risk factors for fracture (Naylor et al., 2016a, 2016b). We (Luckman et al., 2017) reported that TBS measures correlated with both cortical and trabecular microarchitecture by HR-pQCT before kidney transplantation, and that changes in TBS measurements reflected changes in trabecular microarchitecture and failure load but not cortical microarchitecture 12 months after transplantation.

QCT has a resolution of 300 μm^3 and quantifies cortical and trabecular volumetric BMD and geometry. Studies using QCT have shown that in CKD cortical deficits predominated and discriminated and predicted future fractures (Jamal et al., 2006; Leonard, 2009; Denburg et al., 2013). HR-pQCT has a higher nominal resolution (60−82 μm^3), which measures trabecular number, thickness, and separation and cortical porosity at the distal radius and tibia. Micro-FEA applied to HR-pQCT data sets has been used to determine the mechanical competence (strength) of cortical and trabecular bone (Pistoia et al., 2004; Boutroy et al., 2008), and advances in image processing methods permit measurement of cortical porosity and trabecular rod and plate structure, which have been associated with bone strength (Nishiyama et al., 2010; Liu et al., 2011, 2012a). The utility of HR-pQCT to quantify cortical and trabecular microarchitecture at the distal radius and tibia to describe microarchitectural mechanisms that account for bone loss over time and to assess fracture risk has been investigated in patients with CKD. Trombetti et al. (2012) compared cortical and trabecular microarchitecture and FEA-calculated bone strength between 33 patients with ESKD and 33 age-matched controls. Patients, compared with controls, had cortices that were thinner and less dense, with higher degree of porosity, and lower trabecular number with higher trabecular network heterogeneity; these impairments were more severe in women than in men. We used HR-pQCT to describe the microarchitectural mechanisms of bone loss in a longitudinal study of 54 patients with CKD stages 2 to 5D. Mean annualized loss of areal BMD by DXA at the forearm was 2.9% (Nickolas et al., 2013). With HR-pQCT, we

identified microstructural mechanisms of the forearm bone loss detected by DXA; there was significant loss of cortical area (−2.9%), density (−1.3%), and thickness (−2.8%) and significant increases in cortical porosity (+4.2%). HR-pQCT discriminated and predicted fractures, defined abnormalities in bone quality that adversely affected bone strength, and identified microstructural abnormalities that accounted for reduced bone density as measured by DXA (West et al., 2015; Trombetti et al., 2012; Nickolas et al., 2010, 2011, 2013; Cejka et al., 2011b). We (Nickolas et al., 2010, 2011) reported that abnormalities in cortical and trabecular bone were more severe with longer duration and severity of CKD. Cortices were thinner and less dense at the radius and tibia, and trabeculae that were less dense, fewer in number, and, with greater network heterogeneity at the radius, highly discriminated predialysis CKD patients with and without fracture (Fig. 60.7) (Nickolas et al., 2010, 2011). Similarly, in a study of 74 hemodialysis patients with and without fracture, Cejka et al. (2011b) reported that patients with fractures had lower cortical and trabecular density, thinner cortices, and fewer trabecular that were more widely spaced apart. In a longitudinal study of 211 patients with CKD stages 3–5, West et al. (2015) reported that cortical measures from HR-pQCT predicted incident fractures.

Micro-MRI also measures bone microarchitecture, but studies of micro-MRI and fracture discrimination and prediction are lacking in CKD. Micro-MRI assessment of trabecular bone microarchitecture has been validated in general population cohorts (Majumdar, 1998; Wehrli et al., 1998). Technical limitations have made cortical bone assessment more difficult, but the development of reduced-acquisition pulse sequence protocols such as ultrashort echo time has made this possible (Seifert and Wehrli, 2016). These can measure the water content of cortical bone as a surrogate marker of cortical porosity,

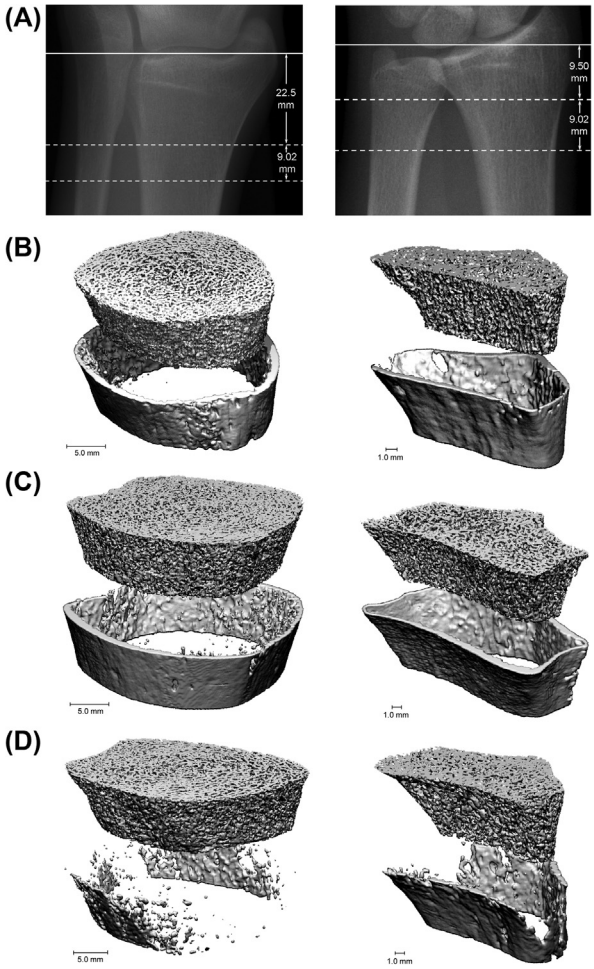

FIGURE 60.7 HR-pQCT provides detailed images of bone geometry and microarchitecture. The left represents the radius and the right the tibia. (A) Scout view represents the reference line position (solid line) and the measurement site (dotted line). (B) Images from a healthy, postmenopausal white woman. (C) Images from a predialysis female patient with CKD and without fracture. (D) Images from a predialysis female patient with CKD and with prevalent fracture. *From Nickolas, T.L., et al., 2010. Bone mass and microarchitecture in CKD patients with fracture. J. Am. Soc. Nephrol. 21, 1371–1380, with permission.*

and may provide fracture discrimination in addition to volumetric BMD (Techawiboonwong et al., 2008). In ESKD, Wehrli et al. (2004) reported that compared with age, gender, and body mass index-matched controls, ESKD patients had thinner cortices with lower cortical cross-sectional area. Furthermore, Rajapakse et al. (2012) reported that stiffness and failure load measured by micro-FEA applied to micro-MRI data sets are reduced over the first 6 months of kidney transplantation.

Calciotropic hormones and bone turnover markers

In patients with CKD, measuring calciotropic hormones and bone turnover markers provides mild to moderate accuracy in the noninvasive assessment of bone turnover and mineralization. However, the utility of measuring these markers in improving patient-related outcomes, such as fractures, remains unproven. Calciotropic hormones include PTH and 25-hydroxyvitamin D; markers of bone formation include bone-specific alkaline phosphatase (BSAP), total alkaline phosphatase (TAP), osteocalcin, and procollagen type 1 N-terminal propeptide (P1NP); and markers of bone resorption (osteoclast function) include tartrate-resistant acid phosphatase 5b (TRAP), C-terminal telopeptide of type 1 collagen (CTX), pyridinoline (PYD), and deoxypyridinoline (DPD). TAP has sometimes been used as a surrogate marker of BSAP, particularly in the absence of liver disease. However, total alkaline phosphatase has high biological variation (>20%) and a high BSAP can still result in a normal TAP level (Pagani and Panteghini, 2001; Tibi et al., 1991). Unfortunately, many of these markers are cleared by the kidney, leading to the possibility of falsely elevated values on standard assays; only alkaline phosphatase and TRAP are not cleared at all by the kidneys (Moorthi and Moe, 2013). The 2017 KDIGO guidelines recommend measuring PTH and BSAP to assess turnover type in patients with CKD and to inform treatment of the underlying bone disease when bone biopsy is not available (Ketteler et al., 2017).

PTH and BSAP are the most widely used bone turnover markers to assess bone turnover and BSAP, vitamin D, calcium, and phosphorus are the most common serologic markers to assess mineralization (Ketteler et al., 2017; Malluche et al., 2011; Sprague et al., 2015; Lehmann et al., 2008). Generally, extremes of PTH and BSAP identify bone turnover type based on gold standard bone biopsy. In a comprehensive analysis across the spectrum of CKD, Lehman et al. (Lehmann et al., 2008) studied the utility of PTH, BSAP, TAP, osteocalcin, TRAP, PYD, and DPD in 132 patients with CKD stages 3−5 (not on dialysis). For all patients, regardless of CKD stage, PTH measurements distinguished patients with low/normal versus high bone turnover with a sensitivity, positive and negative predictive value, and accuracy of 91%, 79%, 82%, and 80%, respectively. BSAP, TAP, and TRAP discriminated low/normal from high turnover in CKD stage 5; in contrast, TAP and TRAP did not discriminate in CKD stages 3 and 4.

The two largest studies as of this writing also found only a weak relationship with these biomarkers and bone histomorphometry. In 630 patients with CKD stage 5D (dialysis), Malluche et al. (2011) reported that low-turnover renal osteodystrophy was prevalent in the majority of patients (58%), while only a minority of patients (3%) had a defect in mineralization. Levels of PTH were lower in patients with low- compared with high-turnover renal osteodystrophy, but TAP did not differ between turnover types. Patients with, compared to without, defective mineralization had lower levels of calcium and higher levels of TAP and PTH. Similarly, the KDIGO consortium (Sprague et al., 2015) studied 492 patients on dialysis from four countries who had undergone bone biopsy and assessed the diagnostic accuracy of PTH, BSAP, and P1NP for turnover type. Correlations between bone biopsy−based bone formation rate/bone surface and PTH, BSAP, and P1NP were mild to moderate, ranging from ρ 0.21 for P1NP to ρ 0.52 for BSAP. Similar to Malluche et al. (2011), the prevalence of low-turnover renal osteodystrophy predominated (59%). PTH, BSAP, and P1NP all similarly discriminated low from nonlow and high from nonhigh turnover, with areas under the curve (AUCs) ranging from 0.650 for P1NP (low vs. nonlow) to 0.757 for BSAP (low vs. nonlow); combining biomarkers together did not improve their ability to discriminate turnover type. For PTH, the AUC, sensitivity, and specificity for discriminating low- versus nonlow-turnover renal osteodystrophy were 0.701%, 65%, and 67%, respectively, and for discriminating high- versus nonhigh-turnover renal osteodystrophy were 0.724%, 37%, and 86%, respectively. Combining PTH with BSAP did not improve accuracy, with AUCs of 0.718 for identifying both low- and high-turnover renal osteodystrophy (Sprague et al., 2015). Multiple other studies have evaluated bone biomarkers, reviewed in Moorthi and Moe (2013) and Evenepoel et al. (2017). Table 60.5 summarizes the associations of bone biomarkers with bone outcomes.

These data suggest that PTH and bone turnover markers may have high clinical utility in assessing bone quality and fracture risk in CKD, in particular when used in conjunction with bone imaging methods and as discussed in a recent review (Khairallah and Nickolas, 2018). For example, fracture risk can be measured by DXA. However, deciding on a treatment (vitamin D, calcimimetic, antiresorptive, anabolic) will need to consider the underlying turnover type. PTH and bone turnover markers can potentially be used to inform which pharmacologic agent is most appropriate. However, before bone turnover markers can be widely used to manage renal bone disease, several limitations need to be overcome. BSAP

TABLE 60.5 Association of bone biomarkers and bone outcomes in chronic kidney disease.

Biomarker	Cleared by the kidney	Predictor of histomorphometry for patients	Predictor of fractures	Predictor of bone loss
Marker of bone turnover				
Parathyroid hormone (PTH)	Yes	PTH levels are higher with increased bone turnover than in those with adynamic bone disease (Sprague et al., 2015; Malluche and Monier-Faugere, 2006; Barreto et al., 2008)	Inconsistent results for risk stratification between high or low PTH and fractures (KDIGO, 2009)	Predicted loss of cortical area and thickness in patients with CKD 3–5D (Nickolas et al., 2013)
		No consistent relationship between PTH and bone formation rates or bone volume (Sprague et al., 2015; Malluche and Monier-Faugere, 2006; Barreto et al., 2008)	Decreased fracture risk after parathyroidectomy (Isaksson et al., 2017)	
		Racial differences (Moore et al., 2009)		
Marker of bone formation				
Bone-specific alkaline phosphatase (BSAP)	No	BSAP levels are higher in patients with high turnover in CKD 5D (Sprague et al., 2015; Lehmann et al., 2008; de Oliveira et al., 2015; Coen et al., 1998; Urena et al., 1996)	Predicted fractures in patients on dialysis (Iimori et al., 2012)	Predicted loss of cortical area and thickness in patients with CKD 3–5D (Nickolas et al., 2013)
		Inconsistent discrimination in predialysis CKD (Bervoets et al., 2003; Salam et al., 2018)	No prospective data in patients with CKD 3–5	
Osteocalcin	Yes	Inconsistent discrimination in predialysis CKD (Bervoets et al., 2003; Lehmann et al., 2008; Salam et al., 2018)	No data in CKD	Predicted loss of cortical area and thickness in patients with CKD 3–5D (Nickolas et al., 2013)
Procollagen type 1 N-terminal propeptide (P1NP)	Yes, monomer; no, multimer	P1NP levels are higher in patients with high turnover in CKD 5D (Sprague et al., 2015)	No data in CKD	Predicted loss of cortical area and thickness in patients with CKD 3–5D
		P1NP levels discriminated low from nonlow and high from nonhigh turnover in patients with CKD 3–5D (Salam et al., 2018)		Predicted loss of total volumetric and cortical BMD in patients with CKD 5D (Malluche et al., 2014)
Markers of bone resorption				
C-telopeptide (CTX)	Yes	CTX levels discriminated low from nonlow and high from nonhigh turnover in patients with CKD 3–5D (Salam et al., 2018)	No data in CKD	Predicted loss of cortical area, density, and thickness in patients with CKD 3–5D (Nickolas et al., 2013)
Tartrate-resistant acid phosphatase 5b (TRAP5b)	No	TRAP5b levels discriminated low from nonlow and high from nonhigh turnover in patients with CKD 3–5D (Salam et al., 2018)	No data in CKD	Predicted loss of cortical area, density, and thickness in patients with CKD 3–5D (Nickolas et al., 2013)
		TRAP5b discriminated high from non-high in patients with CKD 5 (Lehmann et al., 2008)		Predicted loss of total volumetric BMD in patients with CKD 5D (Malluche et al., 2014)

Continued

TABLE 60.5 Association of bone biomarkers and bone outcomes in chronic kidney disease.—cont'd

Biomarker	Cleared by the kidney	Predictor of histomorphometry for patients	Predictor of fractures	Predictor of bone loss
Pyridinoline	Yes	Discriminated high from nonhigh in patients with CKD 3−5 (Lehmann et al., 2008)	No data in CKD	No data in CKD
Deoxypyridinoline	Yes	Discriminated high from nonhigh in patients with CKD 3−5 (Lehmann et al., 2008) and Patients on PD (de Oliveira et al., 2015)	No data in CKD	No data in CKD

BMD, bone mineral density; *CKD,* chronic kidney disease; *PD,* peritoneal dialysis. CKD 3−5 are patients with estimated glomerular filtration rate less than 60.

lacks a readily available automated assay and there are concerns of cross-reactivity with the liver isoenzyme; there are no validated reference ranges for bone turnover markers in patients with CKD; most bone turnover markers are cleared by the kidney (monomeric P1NP, osteocalcin, and CTX) and have high intra- and interassay variability and biological variability. Future research needs to address these issues and study their impact on hard clinical end points.

Conclusion

Bone disease is a major complication of CKD and is one manifestation of CKD−MBD. Renal osteodystrophy is an alteration of bone morphology in patients with CKD and is one measure of the skeletal component of the systemic disorder of CKD−MBD that is quantifiable by histomorphometry assessed on bone biopsy (Moe et al., 2006). The pathogenesis of renal osteodystrophy is complex. Traditionally, the primary focus on bone health in patients with CKD has been to control PTH with calcitriol or other vitamin D analogs and more recently with calcimimetics. Clearly secondary and tertiary hyperparathyroidism has a major role in stimulating bone remodeling, especially in inducing cortical porosity. Imaging studies are consistent with a primary cortical defect; however, overall bone microarchitecture is impaired when patients with CKD are examined by HR-pQCT. Recent data have demonstrated abnormalities in FGF23/klotho signaling in bone, mesenchymal differentiation of osteoblasts, and Wnt signaling. It is therefore no surprise that PTH alone is an insufficient biomarker for predicting bone histology, and thus future research needs to determine improved molecular signatures of various forms of renal osteodystrophy to optimize both diagnostic and treatment strategies. Such signatures, together with newer imaging modalities, should allow reduction of the ultimate adverse bone outcome: fractures.

References

Abraham, A.C., Agarwalla, A., Yadavalli, A., Mcandrew, C., Liu, J.Y., Tang, S.Y., 2015. Multiscale predictors of femoral neck in situ strength in aging women: contributions of Bmd, cortical porosity, reference point indentation, and nonenzymatic glycation. J. Bone Miner. Res. 30, 2207−2214.

Alem, A.M., Sherrard, D.J., Gillen, D.L., Weiss, N.S., Beresford, S.A., Heckbert, S.R., Wong, C., Stehman-Breen, C., 2000. Increased risk of hip fracture among patients with end-stage renal disease. Kidney Int. 58, 396−399.

Allen, M.R., Newman, C.L., Chen, N., Granke, M., Nyman, J.S., Moe, S.M., 2015. Changes in skeletal collagen cross-links and matrix hydration in high- and low-turnover chronic kidney disease. Osteoporos. Int. 26, 977−985.

Andress, D.L., 2008. Adynamic bone in patients with chronic kidney disease. Kidney Int. 73, 1345−1354.

Andress, D.L., Norris, K.C., Coburn, J.W., Slatopolsky, E.A., Sherrard, D.J., 1989. Intravenous calcitriol in the treatment of refractory osteitis fibrosa of chronic renal failure. N. Engl. J. Med. 321, 274−279.

Aoki, C., Uto, K., Honda, K., Kato, Y., Oda, H., 2013. Advanced glycation end products suppress lysyl oxidase and induce bone collagen degradation in a rat model of renal osteodystrophy. Lab. Invest. 93, 1170−1183.

Asai, O., Nakatani, K., Tanaka, T., Sakan, H., Imura, A., Yoshimoto, S., Samejima, K., Yamaguchi, Y., Matsui, M., Akai, Y., Konishi, N., Iwano, M., Nabeshima, Y., Saito, Y., 2012. Decreased renal alpha-Klotho expression in early diabetic nephropathy in humans and mice and its possible role in urinary calcium excretion. Kidney Int. 81, 539−547.

Baker, L.R., Abrams, L., Roe, C.J., Faugere, M.C., Fanti, P., Subayti, Y., Malluche, H.H., 1989. 1,25(OH)2D3 administration in moderate renal failure: a prospective double-blind trial. Kidney Int. 35, 661−669.

Barreto, D.V., Barreto Fde, C., Carvalho, A.B., Cuppari, L., Draibe, S.A., Dalboni, M.A., Moyses, R.M., Neves, K.R., Jorgetti, V., Miname, M., Santos, R.D., Canziani, M.E., 2008. Association of changes in bone remodeling and coronary calcification in hemodialysis patients: a prospective study. Am. J. Kidney Dis. 52, 1139–1150.

Barreto, F.C., Barreto, D.V., Moyses, R.M., Neves, C.L., Jorgetti, V., Draibe, S.A., Canziani, M.E., Carvalho, A.B., 2006. Osteoporosis in hemodialysis patients revisited by bone histomorphometry: a new insight into an old problem. Kidney Int. 69, 1852–1857.

Behets, G.J., Spasovski, G., Sterling, L.R., Goodman, W.G., Spiegel, D.M., DE Broe, M.E., D'haese, P.C., 2015. Bone histomorphometry before and after long-term treatment with cinacalcet in dialysis patients with secondary hyperparathyroidism. Kidney Int. 87, 846–856.

Bervoets, A.R., Spasovski, G.B., Behets, G.J., Dams, G., Polenakovic, M.H., Zafirovska, K., Van Hoof, V.O., DE Broe, M.E., D'haese, P.C., 2003. Useful biochemical markers for diagnosing renal osteodystrophy in predialysis end-stage renal failure patients. Am. J. Kidney Dis. 41, 997–1007.

Bikbov, B., Perico, N., Remuzzi, G., On Behalf of the, G. B. D. G. D. E. G., 2018. Disparities in chronic kidney disease prevalence among males and females in 195 countries: analysis of the global Burden of disease 2016 study. Nephron 139, 313–318.

Block, G.A., Klassen, P.S., Lazarus, J.M., Ofsthun, N., Lowrie, E.G., Chertow, G.M., 2004. Mineral metabolism, mortality, and morbidity in maintenance hemodialysis. J. Am. Soc. Nephrol. 15, 2208–2218.

Block, G.A., Spiegel, D.M., Ehrlich, J., Mehta, R., Lindbergh, J., Dreisbach, A., Raggi, P., 2005. Effects of sevelamer and calcium on coronary artery calcification in patients new to hemodialysis. Kidney Int. 68, 1815–1824.

Boutroy, S., Hans, D., Sornay-Rendu, E., Vilayphiou, N., Winzenrieth, R., Chapurlat, R., 2013. Trabecular bone score improves fracture risk prediction in non-osteoporotic women: the OFELY study. Osteoporos. Int. 24, 77–85.

Boutroy, S., Van Rietbergen, B., Sornay-Rendu, E., Munoz, F., Bouxsein, M.L., Delmas, P.D., 2008. Finite element analysis based on in vivo HR-pQCT images of the distal radius is associated with wrist fracture in postmenopausal women. J. Bone Miner. Res. 23, 392–399.

Braun, J., Oldendorf, M., Moshage, W., Heidler, R., Zeitler, E., Luft, F.C., 1996. Electron beam computed tomography in the evaluation of cardiac calcification in chronic dialysis patients. Am. J. Kidney Dis. 27, 394–401.

Bricker, N.S., 1972. On the pathogenesis of the uremic state. An exposition of the "trade-off hypothesis". N. Engl. J. Med. 286, 1093–1099.

Carvalho, C., Magalhaes, J., Neto, R., Pereira, L., Branco, P., Adragao, T., Frazao, J.M., 2017. Cortical bone analysis in a predialysis population: a comparison with a dialysis population. J. Bone Miner. Metabol. 35, 513–521.

Cejka, D., Herberth, J., Branscum, A.J., Fardo, D.W., Monier-Faugere, M.C., Diarra, D., Haas, M., Malluche, H.H., 2011a. Sclerostin and Dickkopf-1 in renal osteodystrophy. Clin. J. Am. Soc. Nephrol. 6, 877–882.

Cejka, D., Patsch, J.M., Weber, M., Diarra, D., Riegersperger, M., Kikic, Z., Krestan, C., Schueller-Weidekamm, C., Kainberger, F., Haas, M., 2011b. Bone microarchitecture in hemodialysis patients assessed by HR-pQCT. Clin. J. Am. Soc. Nephrol. 6, 2264–2271.

Chen, N.X., O'neill, K.D., Allen, M.R., Newman, C.L., Moe, S.M., 2015. Low bone turnover in chronic kidney disease is associated with decreased VEGF-A expression and osteoblast differentiation. Am. J. Nephrol. 41, 464–473.

Cho, M.E., Duan, Z., Chamberlain, C.E., Reynolds, J.C., Ring, M.S., Mannon, R.B., 2010. Cinacalcet improves bone density in post-kidney transplant hyperparathyroidism. Transplant. Proc. 42, 3554–3558.

Coen, G., Ballanti, P., Bonucci, E., Calabria, S., Centorrino, M., Fassino, V., Manni, M., Mantella, D., Mazzaferro, S., Napoletano, I., Sardella, D., Taggi, F., 1998. Bone markers in the diagnosis of low turnover osteodystrophy in haemodialysis patients. Nephrol. Dial. Transplant. 13, 2294–2302.

Coyne, D., Acharya, M., Qiu, P., Abboud, H., Batlle, D., Rosansky, S., Fadem, S., Levine, B., Williams, L., Andress, D.L., Sprague, S.M., 2006. Paricalcitol capsule for the treatment of secondary hyperparathyroidism in stages 3 and 4 CKD. Am. J. Kidney Dis. 47, 263–276.

Danese, M.D., Halperin, M., Lowe, K.A., Bradbury, B.D., Do, T.P., Block, G.A., 2015. Refining the definition of clinically important mineral and bone disorder in hemodialysis patients. Nephrol. Dial. Transplant. 30, 1336–1344.

De Oliveira, R.A., Barreto, F.C., Mendes, M., Dos Reis, L.M., Castro, J.H., Britto, Z.M., Marques, I.D., Carvalho, A.B., Moyses, R.M., Jorgetti, V., 2015. Peritoneal dialysis per se is a risk factor for sclerostin-associated adynamic bone disease. Kidney Int. 87, 1039–1045.

Della Bella, E., Pagani, S., Giavaresi, G., Capelli, I., Comai, G., Donadei, C., Cappuccilli, M., La Manna, G., Fini, M., 2017. Uremic serum impairs osteogenic differentiation of human bone marrow mesenchymal stromal cells. J. Cell. Physiol. 232, 2201–2209.

Denburg, M.R., Tsampalieros, A.K., De Boer, I.H., Shults, J., Kalkwarf, H.J., Zemel, B.S., Foerster, D., Stokes, D., Leonard, M.B., 2013. Mineral metabolism and cortical volumetric bone mineral density in childhood chronic kidney disease. J. Clin. Endocrinol. Metab. 98, 1930–1938.

Duarte, M.E., Carvalho, E.F., Cruz, E.A., Lucena, S.B., Andress, D.L., 2002. Cytokine accumulation in osteitis fibrosa of renal osteodystrophy. Braz. J. Med. Biol. Res. 35, 25–29.

Elder, G., 2002. Pathophysiology and recent advances in the management of renal osteodystrophy. J. Bone Miner. Res. 17, 2094–2105.

Erlebacher, A., Filvaroff, E.H., Ye, J.Q., Derynck, R., 1998. Osteoblastic responses to TGF-beta during bone remodeling. Mol. Biol. Cell 9, 1903–1918.

Evenepoel, P., Cavalier, E., D'haese, P.C., 2017. Biomarkers predicting bone turnover in the setting of CKD. Curr. Osteoporos. Rep. 15, 178–186.

Fang, Y., Ginsberg, C., Seifert, M., Agapova, O., Sugatani, T., Register, T.C., Freedman, B.I., Monier-Faugere, M.C., Malluche, H., Hruska, K.A., 2014. CKD-induced wingless/integration1 inhibitors and phosphorus cause the CKD-mineral and bone disorder. J. Am. Soc. Nephrol. 25, 1760–1773.

Faul, C., Amaral, A.P., Oskouei, B., Hu, M.C., Sloan, A., Isakova, T., Gutierrez, O.M., Aguillon-Prada, R., Lincoln, J., Hare, J.M., Mundel, P., Morales, A., Scialla, J., Fischer, M., Soliman, E.Z., Chen, J., Go, A.S., Rosas, S.E., Nessel, L., Townsend, R.R., Feldman, H.I., St John Sutton, M., Ojo, A., Gadegbeku, C., DI Marco, G.S., Reuter, S., Kentrup, D., Tiemann, K., Brand, M., Hill, J.A., Moe, O.W., Kuro, O.M., Kusek, J.W., Keane, M.G., Wolf, M., 2011. FGF23 induces left ventricular hypertrophy. J. Clin. Invest. 121, 4393–4408.

Ferreira, J.C., Ferrari, G.O., Neves, K.R., Cavallari, R.T., Dominguez, W.V., Dos Reis, L.M., Graciolli, F.G., Oliveira, E.C., Liu, S., Sabbagh, Y., Jorgetti, V., Schiavi, S., Moyses, R.M., 2013. Effects of dietary phosphate on adynamic bone disease in rats with chronic kidney disease–role of sclerostin? PLoS One 8, e79721.

Filvaroff, E., Erlebacher, A., Ye, J., Gitelman, S.E., Lotz, J., Heillman, M., Derynck, R., 1999. Inhibition of TGF-beta receptor signaling in osteoblasts leads to decreased bone remodeling and increased trabecular bone mass. Development 126, 4267–4279.

Gangoiti, M.V., Anbinder, P.S., Cortizo, A.M., Mccarthy, A.D., 2013. Morphological changes induced by advanced glycation endproducts in osteoblastic cells: effects of co-incubation with alendronate. Acta Histochem. 115, 649–657.

Graciolli, F.G., Neves, K.R., Barreto, F., Barreto, D.V., Dos Reis, L.M., Canziani, M.E., Sabbagh, Y., Carvalho, A.B., Jorgetti, V., Elias, R.M., Schiavi, S., Moyses, R.M.A., 2017. The complexity of chronic kidney disease-mineral and bone disorder across stages of chronic kidney disease. Kidney Int. 91, 1436–1446.

Group, K. D. I. G. O. K. C. W., 2013. KDIGO 2012 clinical practice guideline for the evaluation and management of chronic kidney disease. Kidney Int. Suppl. 3, 1–150.

Gutierrez, O.M., Januzzi, J.L., Isakova, T., Laliberte, K., Smith, K., Collerone, G., Sarwar, A., Hoffmann, U., Coglianese, E., Christenson, R., Wang, T.J., Defilippi, C., Wolf, M., 2009. Fibroblast growth factor 23 and left ventricular hypertrophy in chronic kidney disease. Circulation 119, 2545–2552.

Gutierrez, O.M., Mannstadt, M., Isakova, T., Rauh-Hain, J.A., Tamez, H., Shah, A., Smith, K., Lee, H., Thadhani, R., Juppner, H., Wolf, M., 2008. Fibroblast growth factor 23 and mortality among patients undergoing hemodialysis. N. Engl. J. Med. 359, 584–592.

Hamdy, N.A., Kanis, J.A., Beneton, M.N., Brown, C.B., Juttmann, J.R., Jordans, J.G., Josse, S., Meyrier, A., Lins, R.L., Fairey, I.T., 1995. Effect of alfacalcidol on natural course of renal bone disease in mild to moderate renal failure. BMJ 310, 358–363.

Hans, D., Barthe, N., Boutroy, S., Pothuaud, L., Winzenrieth, R., Krieg, M.A., 2011. Correlations between trabecular bone score, measured using anteroposterior dual-energy X-ray absorptiometry acquisition, and 3-dimensional parameters of bone microarchitecture: an experimental study on human cadaver vertebrae. J. Clin. Densitom. 14, 302–312.

Hill, K.M., Martin, B.R., Wastney, M.E., Mccabe, G.P., Moe, S.M., Weaver, C.M., Peacock, M., 2013. Oral calcium carbonate affects calcium but not phosphorus balance in stage 3–4 chronic kidney disease. Kidney Int. 83, 959–966.

Hruska, K.A., Sugatani, T., Agapova, O., Fang, Y., 2017. The chronic kidney disease - mineral bone disorder (CKD-MBD): advances in pathophysiology. Bone 100, 80–86.

Ibels, L.S., Alfrey, A.C., Huffer, W.E., Craswell, P.W., Anderson, J.T., Weil, R.D., 1979. Arterial calcification and pathology in uremic patients undergoing dialysis. Am. J. Med. 66, 790–796.

Iimori, S., Mori, Y., Akita, W., Kuyama, T., Takada, S., Asai, T., Kuwahara, M., Sasaki, S., Tsukamoto, Y., 2012. Diagnostic usefulness of bone mineral density and biochemical markers of bone turnover in predicting fracture in CKD stage 5D patients–a single-center cohort study. Nephrol. Dial. Transplant. 27, 345–351.

Iki, M., Tamaki, J., Kadowaki, E., Sato, Y., Dongmei, N., Winzenrieth, R., Kagamimori, S., Kagawa, Y., Yoneshima, H., 2014. Trabecular bone score (TBS) predicts vertebral fractures in Japanese women over 10 years independently of bone density and prevalent vertebral deformity: the Japanese Population-Based Osteoporosis (JPOS) cohort study. J. Bone Miner. Res. 29, 399–407.

Ingulli, E.G., Mak, R.H., 2014. Growth in children with chronic kidney disease: role of nutrition, growth hormone, dialysis, and steroids. Curr. Opin. Pediatr. 26, 187–192.

Investigators, E.T., Chertow, G.M., Block, G.A., Correa-Rotter, R., Drueke, T.B., Floege, J., Goodman, W.G., Herzog, C.A., Kubo, Y., London, G.M., Mahaffey, K.W., Mix, T.C., Moe, S.M., Trotman, M.L., Wheeler, D.C., Parfrey, P.S., 2012. Effect of cinacalcet on cardiovascular disease in patients undergoing dialysis. N. Engl. J. Med. 367, 2482–2494.

Isakova, T., 2012. Fibroblast growth factor 23 and adverse clinical outcomes in chronic kidney disease. Curr. Opin. Nephrol. Hypertens. 21, 334–340.

Isakova, T., Cai, X., Lee, J., Xie, D., Wang, X., Mehta, R., Allen, N.B., Scialla, J.J., Pencina, M.J., Anderson, A.H., Talierco, J., Chen, J., Fischer, M.J., Steigerwalt, S.P., Leonard, M.B., Hsu, C.Y., DE Boer, I.H., Kusek, J.W., Feldman, H.I., Wolf, M., Chronic Renal Insufficiency Cohort Study, I., 2018. Longitudinal FGF23 trajectories and mortality in patients with CKD. J. Am. Soc. Nephrol. 29, 579–590.

Isakova, T., Gutierrez, O.M., Chang, Y., Shah, A., Tamez, H., Smith, K., Thadhani, R., Wolf, M., 2009. Phosphorus binders and survival on hemodialysis. J. Am. Soc. Nephrol. 20, 388–396.

Isakova, T., Wahl, P., Vargas, G.S., Gutierrez, O.M., Scialla, J., Xie, H., Appleby, D., Nessel, L., Bellovich, K., Chen, J., Hamm, L., Gadegbeku, C., Horwitz, E., Townsend, R.R., Anderson, C.A., Lash, J.P., Hsu, C.Y., Leonard, M.B., Wolf, M., 2011a. Fibroblast growth factor 23 is elevated before parathyroid hormone and phosphate in chronic kidney disease. Kidney Int. 79, 1370–1378.

Isakova, T., Xie, H., Yang, W., Xie, D., Anderson, A.H., Scialla, J., Wahl, P., Gutierrez, O.M., Steigerwalt, S., He, J., Schwartz, S., Lo, J., Ojo, A., Sondheimer, J., Hsu, C.Y., Lash, J., Leonard, M., Kusek, J.W., Feldman, H.I., Wolf, M., 2011b. Fibroblast growth factor 23 and risks of mortality and end-stage renal disease in patients with chronic kidney disease. J. Am. Med. Assoc. 305, 2432–2439.

Isaksson, E., Ivarsson, K., Akaberi, S., Muth, A., Sterner, G., Karl-Goran, P., Clyne, N., Almquist, M., 2017. The effect of parathyroidectomy on risk of hip fracture in secondary hyperparathyroidism. World J. Surg. 41, 2304–2311.

Ishimura, E., Okuno, S., Tsuboniwa, N., Ichii, M., Yamakawa, K., Yamakawa, T., Shoji, S., Nishizawa, Y., Inaba, M., 2011. Effect of cinacalcet on bone mineral density of the radius in hemodialysis patients with secondary hyperparathyroidism. Clin. Nephrol. 76, 259–265.

Jamal, S.A., Gilbert, J., Gordon, C., Bauer, D.C., 2006. Cortical pQCT measures are associated with fractures in dialysis patients. J. Bone Miner. Res. 21, 543–548.

Jamal, S.A., West, S.L., Nickolas, T.L., 2014. The clinical utility of FRAX to discriminate fracture status in men and women with chronic kidney disease. Osteoporos. Int. 25, 71–76.

Jono, S., Mckee, M.D., Murry, C.E., Shioi, A., Nishizawa, Y., Mori, K., Morii, H., Giachelli, C.M., 2000. Phosphate regulation of vascular smooth muscle cell calcification. Circ. Res. 87, E10–E17.

Justesen, J., Stenderup, K., Ebbesen, E.N., Mosekilde, L., Steiniche, T., Kassem, M., 2001. Adipocyte tissue volume in bone marrow is increased with aging and in patients with osteoporosis. Biogerontology 2, 165–171.

Kaludjerovic, J., Komaba, H., Lanske, B., 2017a. Effects of klotho deletion from bone during chronic kidney disease. Bone 100, 50–55.

Kaludjerovic, J., Komaba, H., Sato, T., Erben, R.G., Baron, R., Olauson, H., Larsson, T.E., Lanske, B., 2017b. Klotho expression in long bones regulates FGF23 production during renal failure. FASEB J. 31, 2050–2064.

Kanis, J.A., Johnell, O., Oden, A., Johansson, H., Mccloskey, E., 2008. FRAX and the assessment of fracture probability in men and women from the UK. Osteoporos. Int. 19, 385–397.

Kanis, J.A., Melton 3rd, L.J., Christiansen, C., Johnston, C.C., Khaltaev, N., 1994. The diagnosis of osteoporosis [see comments]. J. Bone Miner. Res. 9, 1137–1141.

KDIGO, 2009. Clinical practice guidelines for the management of CKD-MBD. Kidney Int. 76, S1–S130.

Kestenbaum, B., Sampson, J.N., Rudser, K.D., Patterson, D.J., Seliger, S.L., Young, B., Sherrard, D.J., Andress, D.L., 2005. Serum phosphate levels and mortality risk among people with chronic kidney disease. J. Am. Soc. Nephrol. 16, 520–528.

Ketteler, M., Block, G.A., Evenepoel, P., Fukagawa, M., Herzog, C.A., Mccann, L., Moe, S.M., Shroff, R., Tonelli, M.A., Toussaint, N.D., Vervloet, M.G., Leonard, M.B., 2017. Executive summary of the 2017 KDIGO chronic kidney disease-mineral and bone disorder (CKD-MBD) guideline update: what's changed and why it matters. Kidney Int. 92, 26–36.

Khairallah, P., Nickolas, T.L., 2018. Management of osteoporosis in CKD. Clin. J. Am. Soc. Nephrol. 13, 962–969.

Komaba, H., Kaludjerovic, J., Hu, D.Z., Nagano, K., Amano, K., Ide, N., Sato, T., Densmore, M.J., Hanai, J.I., Olauson, H., Bellido, T., Larsson, T.E., Baron, R., Lanske, B., 2017. Klotho expression in osteocytes regulates bone metabolism and controls bone formation. Kidney Int. 92, 599–611.

Krupp, K., Madhivanan, P., 2014. FGF23 and risk of all-cause mortality and cardiovascular events: a meta-analysis of prospective cohort studies. Int. J. Cardiol. 176, 1341–1342.

Kuro-o, M., Matsumura, Y., Aizawa, H., Kawaguchi, H., Suga, T., Utsugi, T., Ohyama, Y., Kurabayashi, M., Kaname, T., Kume, E., Iwasaki, H., Iida, A., Shiraki-Iida, T., Nishikawa, S., Nagai, R., Nabeshima, Y.I., 1997. Mutation of the mouse klotho gene leads to a syndrome resembling ageing. Nature 390, 45–51.

Kurz, P., Monier-Faugere, M.C., Bognar, B., Werner, E., Roth, P., Vlachojannis, J., Malluche, H.H., 1994. Evidence for abnormal calcium homeostasis in patients with adynamic bone disease. Kidney Int. 46, 855–861.

Lehmann, G., Ott, U., Kaemmerer, D., Schuetze, J., Wolf, G., 2008. Bone histomorphometry and biochemical markers of bone turnover in patients with chronic kidney disease Stages 3 - 5. Clin. Nephrol. 70, 296–305.

Leonard, M.B., 2009. A structural approach to skeletal fragility in chronic kidney disease. Semin. Nephrol. 29, 133–143.

Levin, A., Stevens, P.E., 2014. Summary of KDIGO 2012 CKD Guideline: behind the scenes, need for guidance, and a framework for moving forward. Kidney Int. 85, 49–61.

Lien, Y.H., Silva, A.L., Whittman, D., 2005. Effects of cinacalcet on bone mineral density in patients with secondary hyperparathyroidism. Nephrol. Dial. Transplant. 20, 1232–1237.

Liu, S., Song, W., Boulanger, J.H., Tang, W., Sabbagh, Y., Kelley, B., Gotschall, R., Ryan, S., Phillips, L., Malley, K., Cao, X., Xia, T.H., Zhen, G., Cao, X., Ling, H., Dechow, P.C., Bellido, T.M., Ledbetter, S.R., Schiavi, S.C., 2014. Role of TGF-beta in a mouse model of high turnover renal osteodystrophy. J. Bone Miner. Res. 29, 1141–1157.

Liu, S.H., Chu, H.I., 1942. Treatment of renal osteodystrophy with dihydrotachysterol (A.T.10) and iron. Science 95, 388–389.

Liu, X.S., Shane, E., Mcmahon, D.J., Guo, X.E., 2011. Individual trabecula segmentation (ITS)-based morphological analysis of microscale images of human tibial trabecular bone at limited spatial resolution. J. Bone Miner. Res. 26, 2184–2193.

Liu, X.S., Stein, E.M., Zhou, B., Zhang, C.A., Nickolas, T.L., Cohen, A., Thomas, V., Mcmahon, D.J., Cosman, F., Nieves, J., Shane, E., Guo, X.E., 2012a. Individual trabecula segmentation (ITS)-based morphological analyses and microfinite element analysis of HR-pQCT images discriminate postmenopausal fragility fractures independent of DXA measurements. J. Bone Miner. Res. 27, 263–272.

Liu, Y., Berendsen, A.D., Jia, S., Lotinun, S., Baron, R., Ferrara, N., Olsen, B.R., 2012b. Intracellular VEGF regulates the balance between osteoblast and adipocyte differentiation. J. Clin. Invest. 122, 3101–3113.

London, G.M., Marty, C., Marchais, S.J., Guerin, A.P., Metivier, F., De Vernejoul, M.C., 2004. Arterial calcifications and bone histomorphometry in end-stage renal disease. J. Am. Soc. Nephrol. 15, 1943–1951.

Luckman, M., Hans, D., Cortez, N., Nishiyama, K.K., Agarawal, S., Zhang, C., Nikkel, L., Iyer, S., Fusaro, M., Guo, E.X., Mcmahon, D.J., Shane, E., Nickolas, T.L., 2017. Spine trabecular bone score as an indicator of bone microarchitecture at the peripheral skeleton in kidney transplant recipients. Clin. J. Am. Soc. Nephrol. 12, 644–652.

Majumdar, S., 1998. A review of magnetic resonance (MR) imaging of trabecular bone micro-architecture: contribution to the prediction of biomechanical properties and fracture prevalence. Technol. Health Care 6, 321–327.

Malluche, H.H., Davenport, D.L., Cantor, T., Monier-Faugere, M.C., 2014. Bone mineral density and serum biochemical predictors of bone loss in patients with CKD on dialysis. Clin. J. Am. Soc. Nephrol. 9, 1254–1262.

Malluche, H.H., Mawad, H.W., Monier-Faugere, M.C., 2011. Renal osteodystrophy in the first decade of the new millennium: analysis of 630 bone biopsies in black and white patients. J. Bone Miner. Res. 26, 1368–1376.

Malluche, H.H., Monier-Faugere, M.C., 2006. Renal osteodystrophy: what's in a name? Presentation of a clinically useful new model to interpret bone histologic findings. Clin. Nephrol. 65, 235–242.

Malluche, H.H., Porter, D.S., Monier-Faugere, M.C., Mawad, H., Pienkowski, D., 2012. Differences in bone quality in low- and high-turnover renal osteodystrophy. J. Am. Soc. Nephrol. 23, 525–532.

Martinez, I., Saracho, R., Montenegro, J., Llach, F., 1996. A deficit of calcitriol synthesis may not be the initial factor in the pathogenesis of secondary hyperparathyroidism. Nephrol. Dial. Transplant. 11 (Suppl. 3), 22–28.

Mehrotra, R., Budoff, M., Christenson, P., Ipp, E., Takasu, J., Gupta, A., Norris, K., Adler, S., 2004. Determinants of coronary artery calcification in diabetics with and without nephropathy. Kidney Int. 66, 2022–2031.

Merke, J., Hugel, U., Zlotkowski, A., Szabo, A., Bommer, J., Mall, G., Ritz, E., 1987. Diminished parathyroid 1,25(OH)2D3 receptors in experimental uremia. Kidney Int. 32, 350–353.

Misselwitz, J., Franke, S., Kauf, E., John, U., Stein, G., 2002. Advanced glycation end products in children with chronic renal failure and type 1 diabetes. Pediatr. Nephrol. 17, 316–321.

Moe, S., Drueke, T., Cunningham, J., Goodman, W., Martin, K., Olgaard, K., Ott, S., Sprague, S., Lameire, N., Eknoyan, G., Kidney Disease: Improving Global, O, 2006. Definition, evaluation, and classification of renal osteodystrophy: a position statement from Kidney Disease: improving Global Outcomes (KDIGO). Kidney Int. 69, 1945–1953.

Moe, S.M., Abdalla, S., Chertow, G.M., Parfrey, P.S., Block, G.A., Correa-Rotter, R., Floege, J., Herzog, C.A., London, G.M., Mahaffey, K.W., Wheeler, D.C., Dehmel, B., Goodman, W.G., Drueke, T.B., 2015a. Effects of cinacalcet on fracture events in patients receiving hemodialysis: the EVOLVE trial. J. Am. Soc. Nephrol. 26, 1466–1475.

Moe, S.M., Chen, N.X., 2008. Mechanisms of vascular calcification in chronic kidney disease. J. Am. Soc. Nephrol. 19, 213–216.

Moe, S.M., Chen, N.X., Newman, C.L., Organ, J.M., Kneissel, M., Kramer, I., Gattone 2nd, V.H., Allen, M.R., 2015b. Anti-sclerostin antibody treatment in a rat model of progressive renal osteodystrophy. J. Bone Miner. Res. 30, 499–509.

Moe, S.M., Chertow, G.M., Parfrey, P.S., Kubo, Y., Block, G.A., Correa-Rotter, R., Drueke, T.B., Herzog, C.A., London, G.M., Mahaffey, K.W., Wheeler, D.C., Stolina, M., Dehmel, B., Goodman, W.G., Floege, J., Evaluation of Cinacalcet, H. T. T. L. C. E. T. I., 2015c. Cinacalcet, fibroblast growth factor-23, and cardiovascular disease in hemodialysis: the evaluation of cinacalcet HCl therapy to lower cardiovascular events (EVOLVE) trial. Circulation 132, 27–39.

Moe, S.M., Duan, D., Doehle, B.P., O'neill, K.D., Chen, N.X., 2003. Uremia induces the osteoblast differentiation factor Cbfa1 in human blood vessels. Kidney Int. 63, 1003–1011.

Moe, S.M., Nickolas, T.L., 2016. Fractures in patients with CKD: time for action. Clin. J. Am. Soc. Nephrol. 11, 1929–1931.

Moe, S.M., O'neill, K.D., Duan, D., Ahmed, S., Chen, N.X., Leapman, S.B., Fineberg, N., Kopecky, K., 2002. Medial artery calcification in ESRD patients is associated with deposition of bone matrix proteins. Kidney Int. 61, 638–647.

Moe, S.M., Radcliffe, J.S., White, K.E., Gattone 2nd, V.H., Seifert, M.F., Chen, X., Aldridge, B., Chen, N.X., 2011. The pathophysiology of early-stage chronic kidney disease-mineral bone disorder (CKD-MBD) and response to phosphate binders in the rat. J. Bone Miner. Res. 26, 2672–2681.

Moore, C., Yee, J., Malluche, H., Rao, D.S., Monier-Faugere, M.C., Adams, E., Daramola-Ogunwuyi, O., Fehmi, H., Bhat, S., Osman-Malik, Y., 2009. Relationship between bone histology and markers of bone and mineral metabolism in African-American hemodialysis patients. Clin. J. Am. Soc. Nephrol. 4, 1484–1493.

Moorthi, R.N., Fadel, W., Eckert, G.J., Ponsler-Sipes, K., Moe, S.M., Lin, C., 2015. Bone marrow fat is increased in chronic kidney disease by magnetic resonance spectroscopy. Osteoporos. Int. 26, 1801–1807.

Moorthi, R.N., Moe, S.M., 2013. Recent advances in the noninvasive diagnosis of renal osteodystrophy. Kidney Int. 84, 886–894.

Muschitz, C., Kocijan, R., Haschka, J., Pahr, D., Kaider, A., Pietschmann, P., Hans, D., Muschitz, G.K., Fahrleitner-Pammer, A., Resch, H., 2015. TBS reflects trabecular microarchitecture in premenopausal women and men with idiopathic osteoporosis and low-traumatic fractures. Bone 79, 259–266.

Naylor, K., Mcarthur, E., Leslie, W., Fraser, L., Jamal, S., Cadarette, S., Pouget, J., Lok, C., Hodsman, A., Adachi, J., Garg, A., 2014. 3-Year incidence of fracture in chronic kidney disease. Kidney Int. 86, 810–818.

Naylor, K.L., Garg, A.X., Zou, G., Langsetmo, L., Leslie, W.D., Fraser, L.A., Adachi, J.D., Morin, S., Goltzman, D., Lentle, B., Jackson, S.A., Josse, R.G., Jamal, S.A., 2015. Comparison of fracture risk prediction among individuals with reduced and normal kidney function. Clin. J. Am. Soc. Nephrol. 10, 646–653.

Naylor, K.L., Lix, L.M., Hans, D., Garg, A.X., Rush, D.N., Hodsman, A.B., Leslie, W.D., 2016a. Trabecular bone score in kidney transplant recipients. Osteoporos. Int. 27, 1115–1121.

Naylor, K.L., Prior, J., Garg, A., Berger, C., Langsetmo, L., Adachi, J.D., Goltzman, D., Kovacs, C., Josse, R., Leslie, W., 2016. Trabecular bone score and incident fragility fracture risk in adults with reduced kidney function. Clin. J. Am. Soc. Nephrol. 11, 2032–2040.

Newman, C.L., Tian, N., Hammond, M.A., Wallace, J.M., Brown, D.M., Chen, N.X., Moe, S.M., Allen, M.R., 2016. Calcitriol suppression of parathyroid hormone fails to improve skeletal properties in an animal model of chronic kidney disease. Am. J. Nephrol. 43, 20–31.

Nickolas, T.L., Cremers, S., Zhang, A., Thomas, V., Stein, E., Cohen, A., Chauncey, R., Nikkel, L., Yin, M.T., Liu, X.S., Boutroy, S., Staron, R.B., Leonard, M.B., Mcmahon, D.J., Dworakowski, E., Shane, E., 2011. Discriminants of prevalent fractures in chronic kidney disease. J. Am. Soc. Nephrol. 22, 1560–1572.

Nickolas, T.L., Stein, E., Cohen, A., Thomas, V., Staron, R.B., Mcmahon, D.J., Leonard, M.B., Shane, E., 2010. Bone mass and microarchitecture in CKD patients with fracture. J. Am. Soc. Nephrol. 21, 1371–1380.

Nickolas, T.L., Stein, E.M., Dworakowski, E., Nishiyama, K.K., Komandah-Kosseh, M., Zhang, C.A., Mcmahon, D.J., Liu, X.S., Boutroy, S., Cremers, S., Shane, E., 2013. Rapid cortical bone loss in patients with chronic kidney disease. J. Bone Miner. Res. 28, 1811–1820.

Nishiyama, K.K., Macdonald, H.M., Buie, H.R., Hanley, D.A., Boyd, S.K., 2010. Postmenopausal women with osteopenia have higher cortical porosity and thinner cortices at the distal radius and tibia than women with normal aBMD: an in vivo HR-pQCT study. J. Bone Miner. Res. 25, 882–890.

Nordal, K.P., Dahl, E., 1988. Low dose calcitriol versus placebo in patients with predialysis chronic renal failure. J. Clin. Endocrinol. Metab. 67, 929–936.

Ott, S.M., 2017. Renal osteodystrophy-time for common nomenclature. Curr. Osteoporos. Rep. 15, 187–193.

Pagani, F., Panteghini, M., 2001. 5'-Nucleotidase in the detection of increased activity of the liver form of alkaline phosphatase in serum. Clin. Chem. 47, 2046–2048.

Palmer, S.C., Hayen, A., Macaskill, P., Pellegrini, F., Craig, J.C., Elder, G.J., Strippoli, G.F., 2011. Serum levels of phosphorus, parathyroid hormone, and calcium and risks of death and cardiovascular disease in individuals with chronic kidney disease: a systematic review and meta-analysis. J. Am. Med. Assoc. 305, 1119–1127.

Parfitt, A.M., Drezner, M.K., Glorieux, F.H., Kanis, J.A., Malluche, H., Meunier, P.J., Ott, S.M., Recker, R.R., 1987. Bone histomorphometry: standardization of nomenclature, symbols, and units. Report of the ASBMR Histomorphometry Nomenclature Committee. J. Bone Miner. Res. 2, 595–610.

Parfrey, P.S., Chertow, G.M., Block, G.A., Correa-Rotter, R., Drueke, T.B., Floege, J., Herzog, C.A., London, G.M., Mahaffey, K.W., Moe, S.M., Wheeler, D.C., Dehmel, B., Trotman, M.L., Modafferi, D.M., Goodman, W.G., 2013. The clinical course of treated hyperparathyroidism among patients receiving hemodialysis and the effect of cinacalcet: the EVOLVE trial. J. Clin. Endocrinol. Metab. 98, 4834–4844.

Pendras, J.P., Erickson, R.V., 1966. Hemodialysis: a successful therapy for chronic uremia. Ann. Intern. Med. 64, 293–311.

Pereira, R.C., Juppner, H., Azucena-Serrano, C.E., Yadin, O., Salusky, I.B., Wesseling-Perry, K., 2009. Patterns of FGF-23, DMP1, and MEPE expression in patients with chronic kidney disease. Bone 45, 1161–1168.

Perez-Saez, M.J., Herrera, S., Prieto-Alhambra, D., Vilaplana, L., Nogues, X., Vera, M., Redondo-Pachon, D., Mir, M., Guerri, R., Crespo, M., Diez-Perez, A., Pascual, J., 2017. Bone density, microarchitecture, and material strength in chronic kidney disease patients at the time of kidney transplantation. Osteoporos. Int. 28, 2723–2727.

Pistoia, W., Van Rietbergen, B., Lochmuller, E.M., Lill, C.A., Eckstein, F., Ruegsegger, P., 2004. Image-based micro-finite-element modeling for improved distal radius strength diagnosis: moving from bench to bedside. J. Clin. Densitom. 7, 153–160.

Pothuaud, L., Barthe, N., Krieg, M.A., Mehsen, N., Carceller, P., Hans, D., 2009. Evaluation of the potential use of trabecular bone score to complement bone mineral density in the diagnosis of osteoporosis: a preliminary spine BMD-matched, case-control study. J. Clin. Densitom. 12, 170–176.

Rajapakse, C.S., Leonard, M.B., Bhagat, Y.A., Sun, W., Magland, J.F., Wehrli, F.W., 2012. Micro-MR imaging-based computational biomechanics demonstrates reduction in cortical and trabecular bone strength after renal transplantation. Radiology 262, 912–920.

Ramalho, J., Marques, I.D.B., Hans, D., Dempster, D., Zhou, H., Patel, P., Pereira, R.M.R., Jorgetti, V., Moyses, R.M.A, Nickolas, T.L., 2018. The trabecular bone score: relationships with trabecular and cortical microarchitecture measured by HR-pQCT and histomorphometry in patients with chronic kidney disease. Bone 116, 215–220.

Rhee, Y., Bivi, N., Farrow, E., Lezcano, V., Plotkin, L.I., White, K.E., Bellido, T., 2011. Parathyroid hormone receptor signaling in osteocytes increases the expression of fibroblast growth factor-23 in vitro and in vivo. Bone 49, 636–643.

Roux, J.P., Wegrzyn, J., Boutroy, S., Bouxsein, M.L., Hans, D., Chapurlat, R., 2013. The predictive value of trabecular bone score (TBS) on whole lumbar vertebrae mechanics: an ex vivo study. Osteoporos. Int. 24, 2455–2460.

Rutherford, W.E., Bordier, P., Marie, P., Hruska, K., Harter, H., Greenwalt, A., Blondin, J., Haddad, J., Bricker, N., Slatopolsky, E., 1977. Phosphate control and 25-hydroxycholecalciferol administration in preventing experimental renal osteodystrophy in the dog. J. Clin. Invest. 60, 332–341.

Sabbagh, Y., Graciolli, F.G., O'brien, S., Tang, W., Dos Reis, L.M., Ryan, S., Phillips, L., Boulanger, J., Song, W., Bracken, C., Liu, S., Ledbetter, S., Dechow, P., Canziani, M.E., Carvalho, A.B., Jorgetti, V., Moyses, R.M., Schiavi, S.C., 2012. Repression of osteocyte Wnt/beta-catenin signaling is an early event in the progression of renal osteodystrophy. J. Bone Miner. Res. 27, 1757–1772.

Salam, S., Gallagher, O., Gossiel, F., Paggiosi, M., Khwaja, A., Eastell, R., 2018. Diagnostic accuracy of biomarkers and imaging for bone turnover in renal osteodystrophy. J. Am. Soc. Nephrol. 29, 1557–1565.

Salusky, I.B., Fine, R.N., Kangarloo, H., Gold, R., Paunier, L., Goodman, W.G., Brill, J.E., Gilli, G., Slatopolsky, E., Coburn, J.W., 1987. "High-dose" calcitriol for control of renal osteodystrophy in children on CAPD. Kidney Int. 32, 89–95.

Santos, F.R., Moyses, R.M., Montenegro, F.L., Jorgetti, V., Noronha, I.L., 2003. IL-1beta, TNF-alpha, TGF-beta, and bFGF expression in bone biopsies before and after parathyroidectomy. Kidney Int. 63, 899–907.

Schwarz, U., Buzello, M., Ritz, E., Stein, G., Raabe, G., Wiest, G., Mall, G., Amann, K., 2000. Morphology of coronary atherosclerotic lesions in patients with end-stage renal failure. Nephrol. Dial. Transplant. 15, 218–223.

Seifert, A.C., Wehrli, F.W., 2016. Solid-state quantitative (1)H and (31)P MRI of cortical bone in humans. Curr. Osteoporos. Rep. 14, 77–86.

Slatopolsky, E., Caglar, S., Pennell, J.P., Taggart, D.D., Canterbury, J.M., Reiss, E., Bricker, N.S., 1971. On the pathogenesis of hyperparathyroidism in chronic experimental renal insufficiency in the dog. J. Clin. Invest. 50, 492–499.

Slatopolsky, E., Rutherford, W.E., Martin, K., Hruska, K., 1977. The role of phosphate and other factors on the pathogenesis of renal osteodystrophy. Adv. Exp. Med. Biol. 81, 467–475.

Slatopolsky, E., Weerts, C., Thielan, J., Horst, R., Harter, H., Martin, K.J., 1984. Marked suppression of secondary hyperparathyroidism by intravenous administration of 1,25-dihydroxy-cholecalciferol in uremic patients. J. Clin. Invest. 74, 2136–2143.

Small, D.M., Coombes, J.S., Bennett, N., Johnson, D.W., Gobe, G.C., 2012. Oxidative stress, anti-oxidant therapies and chronic kidney disease. Nephrology 17, 311–321.

Smith, R.C., O'bryan, L.M., Farrow, E.G., Summers, L.J., Clinkenbeard, E.L., Roberts, J.L., Cass, T.A., Saha, J., Broderick, C., Ma, Y.L., Zeng, Q.Q., Kharitonenkov, A., Wilson, J.M., Guo, Q., Sun, H., Allen, M.R., Burr, D.B., Breyer, M.D., White, K.E., 2012. Circulating alphaKlotho influences phosphate handling by controlling FGF23 production. J. Clin. Invest. 122, 4710–4715.

Spasovski, G.B., Bervoets, A.R., Behets, G.J., Ivanovski, N., Sikole, A., Dams, G., Couttenye, M.M., DE Broe, M.E., D'haese, P.C., 2003. Spectrum of renal bone disease in end-stage renal failure patients not yet on dialysis. Nephrol. Dial. Transplant. 18, 1159–1166.

Spiegel, D.M., Brady, K., 2012. Calcium balance in normal individuals and in patients with chronic kidney disease on low- and high-calcium diets. Kidney Int. 81, 1116–1122.

Sprague, S.M., Bellorin-Font, E., Jorgetti, V., Carvalho, A.B., Malluche, H.H., Ferreira, A., D'haese, P.C., Drueke, T.B., Du, H., Manley, T., Rojas, E., Moe, S.M., 2016. Diagnostic accuracy of bone turnover markers and bone histology in patients with CKD treated by dialysis. Am. J. Kidney Dis. 67, 559–566.

Stevens, L.A., Djurdjev, O., Cardew, S., Cameron, E.C., Levin, A., 2004. Calcium, phosphate, and parathyroid hormone levels in combination and as a function of dialysis duration predict mortality: evidence for the complexity of the association between mineral metabolism and outcomes. J. Am. Soc. Nephrol. 15, 770–779.

Sugatani, T., Agapova, O.A., Fang, Y., Berman, A.G., Wallace, J.M., Malluche, H.H., Faugere, M.C., Smith, W., Sung, V., Hruska, K.A., 2017. Ligand trap of the activin receptor type IIA inhibits osteoclast stimulation of bone remodeling in diabetic mice with chronic kidney disease. Kidney Int. 91, 86–95.

Sugatani, T., Alvarez, U.M., Hruska, K.A., 2003. Activin A stimulates IkappaB-alpha/NFkappaB and RANK expression for osteoclast differentiation, but not AKT survival pathway in osteoclast precursors. J. Cell. Biochem. 90, 59–67.

Sumida, K., Nakamura, M., Ubara, Y., Marui, Y., Tanaka, K., Takaichi, K., Tomikawa, S., Inoshita, N., Ohashi, K., 2013. Cinacalcet upregulates calcium-sensing receptors of parathyroid glands in hemodialysis patients. Am. J. Nephrol. 37, 405–412.

Techawiboonwong, A., Song, H.K., Leonard, M.B., Wehrli, F.W., 2008. Cortical bone water: in vivo quantification with ultrashort echo-time MR imaging. Radiology 248, 824–833.

Tentori, F., Blayney, M.J., Albert, J.M., Gillespie, B.W., Kerr, P.G., Bommer, J., Young, E.W., Akizawa, T., Akiba, T., Pisoni, R.L., Robinson, B.M., Port, F.K., 2008. Mortality risk for dialysis patients with different levels of serum calcium, phosphorus, and PTH: the Dialysis Outcomes and Practice Patterns Study (DOPPS). Am. J. Kidney Dis. 52, 519–530.

Thornalley, P.J., Rabbani, N., 2009. Highlights and hotspots of protein glycation in end-stage renal disease. Semin. Dial. 22, 400–404.

Tibi, L., Chhabra, S.C., Sweeting, V.M., Winney, R.J., Smith, A.F., 1991. Multiple forms of alkaline phosphatase in plasma of hemodialysis patients. Clin. Chem. 37, 815–820.

Trombetti, A., Stoermann, C., Chevalley, T., Van Rietbergen, B., Herrmann, F.R., Martin, P.Y., Rizzoli, R., 2013. Alterations of bone microstructure and strength in end-stage renal failure. Osteoporos. Int. 24, 1721–1732.

Tsuruta, Y., Okano, K., Kikuchi, K., Tsuruta, Y., Akiba, T., Nitta, K., 2013. Effects of cinacalcet on bone mineral density and bone markers in hemodialysis patients with secondary hyperparathyroidism. Clin. Exp. Nephrol. 17, 120–126.

Ural, A., Janeiro, C., Karim, L., Diab, T., Vashishth, D., 2015. Association between non-enzymatic glycation, resorption, and microdamage in human tibial cortices. Osteoporos. Int. 26, 865–873.

Urena, P., Hruby, M., Ferreira, A., Ang, K.S., De Vernejoul, M.C., 1996. Plasma total versus bone alkaline phosphatase as markers of bone turnover in hemodialysis patients. J. Am. Soc. Nephrol. 7, 506–512.

Wada, M., Ishii, H., Furuya, Y., Fox, J., Nemeth, E.F., Nagano, N., 1998. NPS R-568 halts or reverses osteitis fibrosa in uremic rats. Kidney Int. 53, 448–453.

Wagner, J., Jhaveri, K.D., Rosen, L., Sunday, S., Mathew, A.T., Fishbane, S., 2014. Increased bone fractures among elderly United States hemodialysis patients. Nephrol. Dial. Transplant. 29, 146–151.

Wakasugi, M., Kazama, J.J., Taniguchi, M., Wada, A., Iseki, K., Tsubakihara, Y., Narita, I., 2013. Increased risk of hip fracture among Japanese hemodialysis patients. J. Bone Miner. Metabol. 31, 315–321.

Wehrli, F.W., Hwang, S.N., Song, H.K., 1998. New architectural parameters derived from micro-MRI for the prediction of trabecular bone strength. Technol. Health Care 6, 307–320.

Wehrli, F.W., Leonard, M.B., Saha, P.K., Gomberg, B.R., 2004. Quantitative high-resolution magnetic resonance imaging reveals structural implications of renal osteodystrophy on trabecular and cortical bone. J. Magn. Reson. Imag. 20, 83–89.

Weinberg, E., Maymon, T., Weinreb, M., 2014. AGEs induce caspase-mediated apoptosis of rat BMSCs via TNFalpha production and oxidative stress. J. Mol. Endocrinol. 52, 67–76.

Wesseling-Perry, K., 2010. FGF-23 in bone biology. Pediatr. Nephrol. 25, 603–608.

Wesseling-Perry, K., 2015. Defective skeletal mineralization in pediatric CKD. Curr. Osteoporos. Rep. 13, 98–105.

Wesseling-Perry, K., Juppner, H., 2013. The osteocyte in CKD: new concepts regarding the role of FGF23 in mineral metabolism and systemic complications. Bone 54, 222–229.

West, S.L., Lok, C.E., Langsetmo, L., Cheung, A.M., Szabo, E., Pearce, D., Fusaro, M., Wald, R., Weinstein, J., Jamal, S.A., 2015. Bone mineral density predicts fractures in chronic kidney disease. J. Bone Miner. Res. 30, 913–919.

Willett, T.L., Sutty, S., Gaspar, A., Avery, N., Grynpas, M., 2013. In vitro non-enzymatic ribation reduces post-yield strain accommodation in cortical bone. Bone 52, 611–622.

Williams, M.J., Sugatani, T., Agapova, O.A., Fang, Y., Gaut, J.P., Faugere, M.C., Malluche, H.H., Hruska, K.A., 2018. The activin receptor is stimulated in the skeleton, vasculature, heart, and kidney during chronic kidney disease. Kidney Int. 93, 147–158.

Xiao, Z.S., Quarles, L.D., 2010. Role of the polycytin-primary cilia complex in bone development and mechanosensing. Ann. N. Y. Acad. Sci. 1192, 410–421.

Xiao, Z.S., Quarles, L.D., Chen, Q.Q., Yu, Y.H., Qu, X.P., Jiang, C.H., Deng, H.W., Li, Y.J., Zhou, H.H., 2001. Effect of asymmetric dimethylarginine on osteoblastic differentiation. Kidney Int. 60, 1699–1704.

Yavropoulou, M.P., Vaios, V., Pikilidou, M., Chryssogonidis, I., Sachinidou, M., Tournis, S., Makris, K., Kotsa, K., Daniilidis, M., Haritanti, A., Liakopoulos, V., 2017. Bone quality assessment as measured by trabecular bone score in patients with end-stage renal disease on dialysis. J. Clin. Densitom. 20, 490–497.

Yenchek, R.H., Ix, J.H., Shlipak, M.G., Bauer, D.C., Rianon, N.J., Kritchevsky, S.B., Harris, T.B., Newman, A.B., Cauley, J.A., Fried, L.F., Health, A., Body Composition, S., 2012. Bone mineral density and fracture risk in older individuals with CKD. Clin. J. Am. Soc. Nephrol. 7, 1130–1136.

Yuan, Q., Sato, T., Densmore, M., Saito, H., Schuler, C., Erben, R.G., Lanske, B., 2012. Deletion of PTH rescues skeletal abnormalities and high osteopontin levels in Klotho-/- mice. PLoS Genet. 8, e1002726.

Chapter 61

Osteogenesis imperfecta

David W. Rowe

Center for Regenerative Medicine and Skeletal Development, Department of Reconstructive Sciences, Biomaterials and Skeletal Development, School of Dental Medicine, University of Connecticut Health Center, Farmington, CT, United States

Chapter outline

Introduction

There has been a remarkable expansion in the complexity of the genetic mechanisms that result in a clinical diagnosis of osteogenesis imperfecta (OI). This genetic disorder continues to be the paradigm for understanding the molecular basis of heritable connective tissues and evaluating therapeutic strategies for disorders affecting the mineralized skeleton. Some advances are a consequence of the new DNA sequencing technologies, transgenic animal models, and precise clinical observation, while others reflect the concerted efforts of parent supports and collaborating clinical centers to develop multicenter observational studies and clinical trials. This chapter will attempt to convey why this is an exciting time for physicians and scientists, who are beginning to see significant progress in appreciating the complexities of the disease and developing treatments tailored for the specific individual.

While it is still useful to characterize the clinical severity of OI as nondeforming, progressively deforming, and perinatal lethal, this does not help in appreciating the diverse genetic causes of the bone disease, and it probably oversimplifies the clinical spectrum of any specific mutation. Specifically, the heterogeneity of clinical severity is remarkable for a similar type of mutation, even with the same mutation within the same family. This variability is evident in recent reviews of the genetic subtypes of OI, in which almost all are described as variable or mild to severe. The basis for this clinical appearance is termed phenotypic variance and ascribed to both environmental factors and genetic loci that can interact with dominantly inherited mutations. A recent example is demonstrated in a Wnt1 mutation in a three-generational family with different disease severity that was attributable to a small gene duplication unrelated to the location of Wnt1 (Alhamdi et al., 2018). Similar intrafamilial variability has been observed in other genetic forms of OI (Pollitt et al., 2016; Rauch et al., 2013; Galicka et al., 2005). A more detail discussion for the basis of genetic variation affecting phenotype is found in the genetic literature (Pai et al., 2015; Burrows et al., 2016), and its implications for OI will be discussed in the last section of this chapter.

Principles of Bone Biology. https://doi.org/10.1016/B978-0-12-814841-9.00061-0

The major contribution to assessing the disease severity and natural history of OI has come from the interinstitutional collaborations that arose from the leadership of patient-support groups including the Osteogenesis Imperfecta Foundation (OIF, 2019), Children's Brittle Bone Foundation (CBBF, 2019), and the National Organization for Rare Disorders (NORD, 2019). The initial consortium, called the Linked Clinical Research Centers, demonstrated its ability to capture and analyze clinical data from 544 OI subjects. This accomplishment led to the formation of the Brittle Bone Disorders Consortium (BBDC) (BBDC, 2019) as a recognized part of the NIH-funded Rare Diseases Clinical Research Network (RDCRN, 2019). From these efforts, more comprehensive descriptions of disease severity, nonskeletal effects, and treatment outcomes are being to appear.

Clinical classification

Severe-deforming osteogenesis imperfecta

With the prenatal identification of OI using 3-D ultrasound and CT imaging (Ulla et al., 2011; Akizawa et al., 2012; Suzumori et al., 2011), infants that in the past would not have survived a vaginal delivery are now among those individuals with the most severe forms of skeletal deformity. The cranium is unusually soft and molded and may be fractured at birth. Intracranial bleeding may have occurred. The sclerae are deep blue. The limbs are deformed and short, raising the consideration of hypophosphatasia, achondrogenesis, and thanatophoric dwarfism in the diagnosis. Multiple fractures are seen on X-ray, and the extremities appear broad and crumpled. The critical problem is neonatal pulmonary insufficiency that may lead to death in the first postnatal week (Shapiro et al., 1989). Faulty thoracic musculoskeletal development also limits respiratory function in the majority of cases (LoMauro et al., 2018). Retrospective studies prior to (Shapiro, 1985) and after instituting advanced neonatal care (Folkestad, 2018) still find a higher rate of death in the first year of life than for a reference population, which persists through early childhood. The impact of drug intervention on these early disease processes is yet to be determined (Palomo et al., 2015).

Infants born with fractures and deformity who survive the perinatal period continue to experience multiple fractures with deformities and significant molding of the calvarium (Sinikumpu et al., 2015). Fractures may continue to occur during early childhood that may preclude a normal pattern of ambulation and require the assistance of a walker or wheelchair. Surgical intervention with limb straightening using expandable rods appears to improve ambulation (Franzone et al., 2017; Grossman et al., 2018; Ashby et al., 2018; Gardner et al., 2018), particularly when used in combination with antiresorptive therapy (Ruck et al., 2011, Anam, 2015). Deformity of the thoracic cage (pectus carinatum, pectus excavatum) may be present in early childhood and advance as scoliosis and vertebral compression increase (LoMauro et al., 2018). Vertebral compression, most commonly of the central or "codfish" type, begins shortly after birth and progresses relentlessly prior to puberty (Engelbert et al., 2003; Wallace et al., 2017). Although antiresorptive drugs increase vertebral bone density, they do not affect the progression of kyphoscoliosis. Surgical correction becomes necessary when lung mechanics are compromised (Liu et al., 2017; Piantoni et al., 2017; O'Donnell et al., 2017). Fortunately, the complication associated with the anesthesia needed for these orthopedic procedures is well appreciated and rarely experienced (Bojanic et al., 2011; Rothschild et al., 2018).

Young adults who reach skeletal maturity, many of whom have been treated with antiresorptives, still have short stature, usually in proportion to the severity of their skeletal deformities (Palomo et al., 2015; Germain-Lee et al., 2016; Jain et al., 2019). Dental abnormalities including malocclusion (Nguyen et al., 2017; Jabbour et al., 2018), tooth agenesis (Malmgren et al., 2017), and tooth degeneration requiring dental interventions (Thuesen et al., 2018), resulting in a low oral health-related quality of life (Najirad et al., 2018). Despite dental issues and enduring bone pain with or without an associated fracture (Zack et al., 2005; Folkestad et al., 2017; Tsimicalis et al., 2018), overall quality of life is remarkably positive (Dahan-Oliel et al., 2016; Hald et al., 2017; Tsimicalis et al., 2018; Bendixen et al., 2018). Developing better tools for assessing quality of life issues not currently appreciated by the medical community is a major focus of the BBDC (Swezey et al., 2019).

Issues that develop with increasing age for individuals with OI include cardiovascular, pulmonary, and neurological difficulties, which probably account for the modestly reduced life span of adults with the severer forms of OI (Folkestad, 2018). Beginning in childhood, evidence can be demonstrated of aortic root enlargement (Al-Senaidi et al., 2015; Rush et al., 2017) that can lead to valvular insufficiency (Migliaccio et al., 2009; Radunovic et al., 2011; Ashournia et al., 2015), heart failure (Radunovic et al., 2015; Folkestad et al., 2016), and reports of aortic dissection (Balasubramanian et al., 2019). In addition to structural deformities of the chest wall that compromise pulmonary function, primary pathology within the lung tissue, and skeletal muscle weakness, may also contribute to respiratory symptoms (Arponen et al., 2018; Tam et al., 2018). Because of molding of the base of the skull, subjects with severely compromised bone strength are at risk for developing basilar invagination (Janus et al., 2003; Khandanpour et al., 2012; Cobanoglu et al., 2018) that may

cause brain stem compression with both respiratory and neurological complications and sudden death (Janus et al., 2003; Kovero et al., 2006). Charnas reported communicating hydrocephalus in 17 out of 76 subjects with OI (Charnas et al., 1993). Brain stem compression requiring surgical decompression or reinforcement of the craniocervical junction is extremely complex, requiring mechanical support, transoral clivectomy, and decompression of the posterior fossa where respiratory center function is compromised (Cobanoglu et al., 2018).

Mild nondeforming osteogenesis imperfecta

Individuals who sustain an increased number of fractures that heal without deforming are considered to have type I OI. Despite their apparent normalcy, they are susceptible to complications that affect quality of life, particularly scoliosis and vertebral compression fractures (Ben Amor et al., 2013). A recent survey of 117 affected individuals demonstrated a smaller birth size, impaired adolescent growth spurt, and eventually lower height (Graff et al., 2017). Even during childhood and early adolescence, reduced measurements of gait strength, possibly reflecting muscle weakness (Veilleux et al., 2014; Pouliot-Laforte et al., 2015; Pavone et al., 2017) or ligamentous laxity, are evident by formal gait analysis (Garman et al., 2017). Because patients with type I OI do not benefit from antiresorptive drugs, there was little to offer this large segment of individuals with OI. However, recent studies show the promise of a significant response to anabolic agents such as PTH (Gatti et al., 2013; Orwoll et al., 2014; Leali et al., 2017) and antisclerostin (Glorieux et al., 2017; Nicol et al., 2018) that, if utilized as the skeleton is forming, might mitigate many of these complications.

Molecular classification

The previous edition of the chapter listed nine OI types, two of which were based on clinical phenotyping. In the past 2 years there have been five comprehensive review articles (Forlino et al., 2016; Kang et al., 2017; Lim et al., 2017; Marini et al., 2017; Morello, 2018) listing 18 recognized types and another 2 with OI features and a known genetic mechanism that have not joined the typing list. These review articles provide clear distinctions of the broad range of mutations that interfere with the formation of a stable type I collagen extracellular matrix, the major component of bone, skin, and tendons/ligaments. Rather than repeat the important contributions of these reviews, highlights of each type of molecular mechanism will be presented.

Primary mutations within type I collagen genes A1 and A2

By far, these mutations are the most common genetic cause of OI (Rauch et al., 2010; Zhang et al., 2012), but the location of the mutation has a large impact on clinical severity. The more severe forms (types II, III, and IV) usually result from a mutation in either gene that interferes with the formation of a stable collagen helix and its ability to interact with non-collagenous protein within the bone matrix (Marini et al., 2007). The mutations can be a single base change (usually glycine substitution) or the deletion of an internal segment of the gene. Efforts to associate disease severity with mutation location have been published (Marini et al., 2007; Bodian et al., 2009), but its utility as a predictor of individual skeletal health has not reached clinical fruition, in part due to variations in genetic background and the increasing use of drug interventions. Because these are dominant mutations, pedigrees with multiple affected individuals across generations are the rule. However, the occurrence of OI in a family without a prior history, particularly if more than one child is affected, raises the possibility of germinal mosaicism in one of the parents (Pyott et al., 2011). Thus, knowing the underlying mutation in the affected child is essential in genetic testing of the parents to distinguish germinal mosaicism from a recessive form of OI (see below). Qualified academic and commercial sites for obtaining mutation discovery are maintained on the Osteogenesis Imperfecta Foundation website (OIF-Testing, 2019).

Type I OI is clinically and molecularly distinct from types II, III, and IV. The molecular hallmark is half-normal production of a normal type I collagen molecule and an apparently normal extracellular matrix. The mutation is usually due to either single base change in the collagen type I, alpha 1 (Col1A1) gene that generates a premature stop codon or a splice site mutation that deletes an exon and places the downstream exons out of frame, bringing a stop codon in-frame. In either case, the affected Col1A1 transcript is destroyed by a cellular mechanism called nonsense-mediated decay (Lykke-Andersen et al., 2015). Although this haploid-insufficient mutation is inherited as dominant (Ben Amor et al., 2013), the phenotypic variation may omit family members that only present in later life with osteoporosis. This is another example of why knowing the mutation of affected family members is useful for detecting those who would be predisposed to early-onset osteoporosis (Arundel et al., 2015; Makitie et al., 2017) and might benefit from therapy to delay that outcome (see later).

Mutation of genes that modify the synthesis of type I collagen chains

The majority of these mutations are recessively inherited because they affect enzymes or other processing proteins that provide sufficient activity in the heterozygous state. These disorders usually appear as new disorders within families without previous skeletal abnormalities and point to the importance of mutation identification for predicting natural history and recurrence risk. A number of genes that encode the enzyme complexes that hydroxylate proline at the 3-OH (OI types VII-CRTAP, VIII-P3H1, and IX-PPIB; Barbirato et al., 2015) and 4OH positions (Cole—Carpenter syndrome, P4H1; Balasubramanian et al., 2018; Rauch et al., 2015), and lysine within the helical or telopeptide (Bruck syndrome, PLOD2; Lv et al., 2018; Leal et al., 2018), have been identified and have clinical features of the more severe forms of OI.

The hydroxylation steps occur within the Golgi system and are dependent on proper folding and transit through the system by specific chaperones (OI type X, SERPINH1— Song et al., 2018; Marshall et al., 2016 and OI type XI, FKBP10—Kelley et al., 2011). These mutations either slow transit of the assembly of normal collagen molecules through the rough ER or fail to detect and remove misfolded collagen molecules. The importance of the TMEM38B gene that encodes an ER calcium transport protein necessary for efficient processing and secretion of collagen was revealed by studying another rare recessive OI phenotype classified as OI type XIV (Volodarsky et al., 2013; Webb et al., 2017).

Mutations that control the level of differentiation of osteoblasts

The osteogenic lineage is first recognized as a migratory myofibroblast that enters the nonproliferative stage of enhanced production of extracellular matrix proteins and ends as an embedded osteocyte. Mutations of type I collagen disrupt this sequence of events, which can be recognized in primary cell culture by the low expression of genes that reflect full osteogenic differentiation. Thus, it would not be surprising that other genes controlling differentiation may result in an OI phenotype, although in these cases severity may be less because the extracellular matrix is not abnormal. The first example was the discovery of a heterozygous null mutation of Sp7/Osterix (OI type XIII; Lapunzina et al., 2010; Fiscaletti et al., 2018), a transcription factor required for progenitor cells to enter into and maintain osteogenic differentiation. Subsequently, homozygous null mutations of the Wnt 1 gene (OI type XV), which maintains the differentiated state of the osteoblast, were demonstrated to cause severe OI, while the heterozygous state presented as premature osteoporosis (Palomo et al., 2014; Panigrahi et al., 2018).

Additional mutations resulting in OI have directed attention to more complex and previously unappreciated mechanisms that impact the extent or tempo of osteogenic differentiation. OI type V is dominantly inherited and has the distinctive phenotype features of interosseous membrane calcification, hyperplastic callus formation at sites of bone fracture, and severe bimaxillary malocclusion in addition to bone fragility (Cheung et al. 2007, 2008; Retrouvey et al., 2018). The phenotype is linked to the IFITM5 gene, which encodes the BRIL protein strongly expressed in osteoblasts. The IFITM5 mutation either adds an additional five amino acids to the N-terminal of the protein or a point mutation in the body of the gene (Shapiro et al., 2013; Rauch et al., 2013; Fitzgerald et al., 2013; Brizola et al., 2015). In either case, enhanced osteogenic differentiation and excessive mineralization of the extracellular matrix in cultured cells and mouse models appears to be a consequence of this gene mutation (Rauch et al., 2018; Blouin et al., 2017). In contrast, OI type VI is recessively inherited and has the unusual history of mild to no skeletal abnormalities at birth followed by development of typical bone fractures with deformity during childhood. Histological analysis of bones revealed distorted and impaired matrix mineralization (Trejo et al., 2017). Null mutations in the SERPINf1 gene have been identified for this phenotype (Wang et al., 2017; Homan et al., 2011). This gene produces the well-characterized pigment epithelium-derived factor (PEDF) studied in other clinical settings for its antithrombotic and antivascular properties (Yamagishi et al., 2010; Michalczyk et al., 2018; Eslani et al., 2017). When a mouse model was created, a defect in osteoblast differentiation to a mature osteocyte was demonstrated. Currently, mechanisms dependent on PEDF interaction with Wnt signaling pathways that control differentiation and mineralization are being studied. Because PEDF is a circulating protein (Rauch et al., 2012), efforts to provide this factor using genetic tools are being explored in mouse models with equivocal results to date (Al-Jallad et al., 2015; Belinsky et al., 2016).

Mutation of genes that regulate the maturation of secreted procollagen into collagen fibril

Extracellular processing procollagen is required for helical domains to self-align into growing collagen fibril prior to interaction with the other noncollagenous proteins that embed the growth factors necessary for the regenerative properties of bone. The first example is loss of function of the BMP1 gene resulting in type XII OI (Xu et al., 2019; Pollitt et al., 2016;

Cho et al., 2015). The encoded protein is a metalloproteinase that not only cleaves the C-terminal propeptide of types I and III collagen but also is a protease for other proteins including prodecorin (Syx et al., 2015), lysyl oxidase, latent TGF-β1, BMP-2/4, GDF-8/11, and IGFs as well as the release of antiangiogenic fragments from parent proteins, all of which promote bone healing (Muir et al. 2014, 2016; Asharani et al., 2012; Jasuja et al., 2007; Ge et al., 2006). Another example of a collagen-interacting protein was found in homozygous base substitutions of the SPARC gene (OI type IV; Mendoza-Londono et al., 2015). Osteonectin is the encoded protein widely expressed in many connective tissues and in bone appears to influence both osteogenic differentiation and collagen cross-linking (Rosset et al., 2016).

Pathophysiology of osteogenesis imperfecta

The fundamental abnormality in OI is an inability to produce a bone matrix capable of providing the mechanical, remodeling, and regenerative properties of the axial, appendicular, and cranial skeleton. While most attention is focused on bone and dentin, other type I collagen–rich mineralizing tissues such as the enthesis, periodontal ligaments, and a fibrocartilaginous joint (the temporomandibular joint) are also likely to be affected. Two fundamental differences in the pathophysiologic mechanisms of OI influence how to conceptualize the disease process and eventually shape a therapeutic response. Type I OI and to a lesser extent types XIII (Sp7) and XV (Wnt) produce a normal collagen molecule, although of insufficient quantity to meet load requirements. In contrast, types II–XI produce an abnormal collagen molecule that has adverse effects on osteoblasts and the function of the extracellular matrix. Even though disease severity may merge between the clinical types, it is important to distinguish the cellular and regulatory differences of low production versus an abnormal collagen molecule.

Osteogenesis imperfecta secondary to production of an abnormal collagen molecule

Whether due to a primary mutation with the type I collagen gene or in genes that modify the formation of the triple helical molecule, the resulting consequences act at cellular and physiological levels (Fig. 61.1). The impaired processing of the mutant collagen through the rough ER adversely impedes the progression to full differentiation of the osteogenic lineage, possibly due to activation of ER stress responses (Scheiber et al., 2019; Mirigian et al., 2016; Lindert et al., 2015; Bateman et al., 2019). In vitro this effect can be observed as failure to achieve gene markers of full osteogenic differentiation (Fedarko et al., 1995; Kalajzic et al., 2002; Gioia et al., 2012), while in vivo there is an imbalance in the RANKL/OPG ratio indicative of a preponderance of early osteogenic linage cells (Li et al., 2010). During childhood when the need for matrix apposition and bone remodeling is the greatest, this primary abnormality of lineage progression is compounded by deposition of a defective bone matrix that sustains microfractures. Osteocytes, in response to changes in perceived load, may initiate additional sites of bone resorption/remodeling by the release of RANKL (Zimmerman et al., 2018). The combined result is high osteoclastic activity and a high bone turnover rate that cannot be compensated for by the osteoblast lineage. Clinically this high turnover state is assessed by the type I collagen cross-linking peptides (CTXs) and histologically by markers of high bone formation and bone erosion (Rauch et al., 2006). Intervention with inhibitors of osteoclast formation, either a bisphosphonate or anti-RANKL antibody, is effective in interrupting high turnover state and providing the osteogenic cells to enhance overall matrix accumulation (Palomo et al., 2015). Bone apposition does increase in spite of a suppression of osteogenic markers in growing children. However, once full somatic growth is achieved, the effect of osteoclastic suppression diminishes because bone remodeling is impacted, and the consequences of continued treatment can become evident (Nicolaou et al., 2012; Hegazy et al., 2016; Trejo et al., 2017; Andersen et al., 2019).

Anabolic therapies have generally been ineffective during the period of rapid growth, in part because the osteogenic lineage is fully taxed at this time. However, mouse model studies suggest these agents may play roles in enhancing matrix formation during somatic growth when used sequentially with an antiresorptive agent (Olvera et al., 2018). Another approach for stimulating bone anabolism is based on the known weakness of skeletal muscle in OI and the loading effect muscle has on maintaining bone mass. Because the myostatin D knockout mouse has a high skeletal muscle mass (McPherron et al., 1997), drug inhibition of this muscle mass regulator has been shown to increase bone mass in experimental mouse models (Lee et al., 2016). This logic appears to apply to OI also, as two different research groups have shown increases in bone and muscle mass in a mouse model of severe OI (DiGirolamo et al., 2015; Oestreich et al., 2016).

Left unexplained are the nonosseous features of the more severe forms of OI, which include pulmonary fibrosis and aortic root dilatation. These are features of Marfan's disease that have previously been associated with a chronic TGFβ-induced inflammatory state. A seminal paper reported that a similarly high TGFβ state exists in murine models of OI and that treatment with anti-TGFß antibodies both increased bone mass and reduced pulmonary inflammation (Grafe

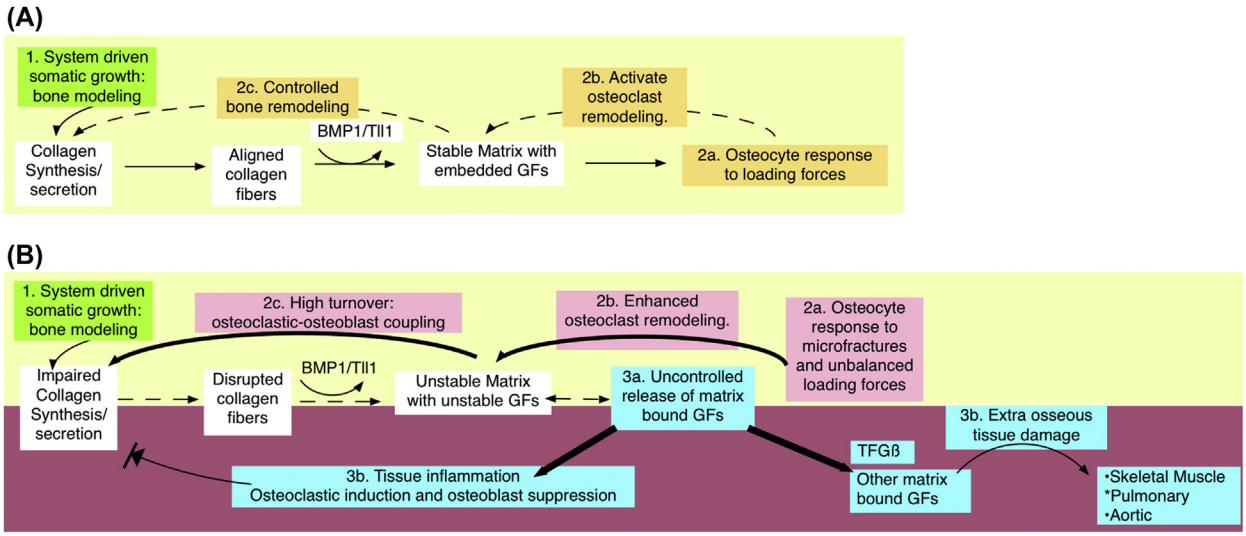

FIGURE 61.1 Pathophysiological dynamics in OI. (A) Normal physiological regulation. Osteoblasts have an exceptionally high production rate of extracellular matrix molecules including type I collagen. The secreted fibrils align into collagen fibrils, bind other matrix molecules and sequester a variety of local acting bone growth factors including TGFs, BMPs and IGFs. During somatic growth (1), systemic hormones drive osteoblasts to meet the need of the elongating bones and increasing body weight. This net accumulation of bone matrix is termed bone modeling. Additional loading forces, probably acting through osteocytes (2a), initiate the bone remodeling process in which osteoclasts resorb bone matrix and release bone growth factors (2b) that in turn activate the osteogenic lineage to proliferate and replace the resorbed bone matrix (2c). (B) Pathophysiological regulation of OI. The inherent inability of the osteogenic lineage to produce mature osteoblasts and the inefficient production/secretion of type I collagen in those cells that do achieve full differentiation reduce the amount of matrix that can be produced in a growing bone. Furthermore, the matrix formed is not normally aligned and probably does not properly bind matrix proteins and growth factors (1). Thus, during the bone modeling phase of skeletal growth, both the mechanical and regulatory function of the growing bone is compromised. (a) mechanical: The innumerable asymptomatic microfractures activate the osteocyte remodeling process (2a). Because the intensity of the osteoclastic activity (2b) drives the recruitment of the osteoblastic lineage (2c), the process is termed a high bone turnover state, but in this case the matrix produced is no better than what was removed. The unabated high remodeling state is associated with an extremely low bone mass, multiple fractures, bone pain and bone deformity. Thus, suppression of the osteoclast function breaks this cycle and allows for bone matrix accumulation particularly during somatic growth. (b) regulatory: Because the disordered matrix does not retain embedded growth factors adequately, the high turnover state releases more factors than usual (3a). The inflammatory growth factors (Fig. 61.2) can act locally by augmenting the myeloid precursor balance of macrophages to osteoclasts, while impeding the expansion of the osteoblast lineage. When these growth factors escape to the peripheral circulation, they can induce an inflammatory state in peripheral tissues. Thus, suppression of high bone turnover in children can lead to bone accumulation and possibly less peripheral inflammatory activity. However, in adults in which a moderately elevated rate of bone turnover is not a basis for osteoclast suppression, the released growth factors could lead to inflammatory tissue damage in OI target tissues. Such a mechanism argues for the use of pharamcologics that suppress the action of the released inflammatory growth factors.

et al., 2014). This systemic inflammatory state is also evident in hematopoietic tissues in mice (Matthews et al., 2017) and human subjects (Brunetti et al., 2016). What is the cause of this increase in circulating TGFβ? The mechanism in Marfan's disease is mutations in the fibrillin-1 gene that inactivate the ability of this protein to maintain TGBFβ in a latent inactive form (Ramirez et al., 2018). Perhaps the same mechanism exists in bone. Numerous growth factors including TGFβ, BMPs, and IGFs are contained with the bone matrix, and the loss of their regulated release, particularly in a high turnover state, may be another consequence of the disrupted bone matrix. Support for this circular mechanism for high bone resorption is the direct effect that TGFβ has on stimulating the macrophage-to-osteoclast lineage (Yasui et al., 2011; Omata et al., 2016) and the observation that anti-TGFß treated OI mice increased their bone mass by a suppression of osteoclast number and reduction in bone formation markers (Grafe et al., 2014). Furthermore, the increased bone mass observed in anti-myostatin D-treated mice resulted from the same combination of reduced osteoclast number and reduced markers of bone formation (DiGirolamo et al., 2015; Oestreich et al., 2016). Myostatin has additional effects on tissues other than muscle including promoting osteoclast differentiation (Dankbar et al., 2015), so the muscle-loading effect on bone may in part be attributable to suppression of the cell inflammatory process. The similarity of effect of anti-TGBß and antimyostatin/activin 2A receptor decoy therapy becomes clearer when the confluence of pathways that influence the SMAD 2/3 pathway in different types is examined (Fig. 61.2). Thus, blocking activation of this pathway using antibodies to ligands or solubilized receptor peptides may be an additional therapeutic strategy that can be tailored to specific forms of OI or stages of its natural history.

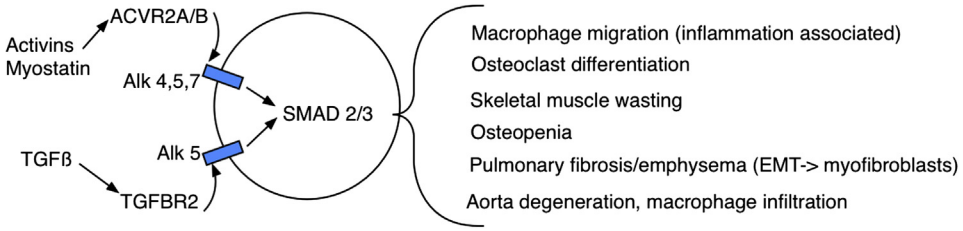

FIGURE 61.2 Inflammatory growth factors. Both activins/myostatin and TGFs can have an equivalent influence on the SMAD 2/3 pathway to activate the macrophage-driven inflammatory state as well as having primary effects on certain target tissues. The ligands bind to separate type 2 receptors (ACVR2A/B and TGBβR2) that in turn bind to different type I receptors (*blue* [gray in print version]) to activate the same SMAD pathway. The pathways can be interrupted either with antibodies to the ligands or soluble type 2 receptors that bind and inactivate the ligands.

Where these considerations may become important is with the use of therapeutics that suppress resorption or stimulate formation. Currently, CTXs are used to assess osteoclastic activity, but the use of additional blood studies that assess mediators or markers of chronic inflammation, as well as measures of bone matrix protein activity, may provide a better window into the balance of bone-intrinsic versus bone growth factor derived drivers of bone turnover (Nicol et al., 2019). Thus, states associated with bone modeling may facilitate a matrix that stabilizes the release of the bone-derived growth factors while high bone turnover in individuals who have achieved full somatic growth may favor the release of these factors. At this point it is unknown whether the suppression of osteoclastogenesis will have the effect of reducing the nonosseous complications of OI either directly, as with bisphonphonates and anti-RANKL drugs, or more systemically with drugs that act through activin−Smad2/3 pathways. Conversely, drugs that stimulate new bone formation may have different effects on nonosseous tissues depending on the balance of modeling versus remodeling achieved by their administration.

Osteogenesis imperfecta due to underproduction of a normal type I collagen molecule

The only mouse model of type I OI utilized a now disbanded genetic technique that shortened the life span of the line due to leukemia (Jacobsen et al., 2016; Jepsen et al., 1997). Thus, lacking a model that replicates this form of OI has hindered fully appreciating the pathogenesis and natural history effect of chronic underproduction of type I collagen. What is known from human fibroblast studies is that unlike the normal setting of twofold greater collagen chain production of α1(I) versus α2(I), equal production of α1(I) and α2(I) proteins results in the formation of a normal collagen heterotrimer, ($\alpha1(I)_2$ $\alpha2(I)_1$) (Rowe et al., 1985), while trimeric molecules composed of $\alpha1(I)_1$ $\alpha2(I)_2$ or $\alpha2(I)_3$ are unstable and degraded (Gauba et al., 2008; Kuznetsova et al., 2003). At this point, it is unclear whether this degradation process contributes to ER stress similar to that observed for cells exposed to a mutant collagen gene product. An additional complication for understanding the cellular environment are splice site mutations of the Col1A1 gene in which the resulting in-frame stop that normally would inactivate the transcript is alternatively skipped to create an in-frame deletion and a mutant Col1A1 chain (Bateman et al., 1999). Because the toxic effect of an abnormal collagen chain is strong, just a small proportion this product relative to total type I collagen produced in a type I OI mutation would contribute to a more severe clinical phenotype. Distinguishing the impact of low type I collagen accumulation alone versus a low product containing a small proportion of mutant molecules will be a challenge.

Inactivation mutations of the collagen type I, alpha 2 (Col1A2) gene would be expected to produce a heterotrimer of three alpha chains ($\alpha1(I)_3$) that lacks the stability of the heterotrimer and would be expected to cause a bone phenotype (Kuznetsova et al., 2003). A spontaneous mutation in the Col1A2 gene in mouse that precludes formation of a heterotrimer is one of the major murine models for studying OI pathogenesis and various therapeutic interventions. Human subjects with a similar mutation have a severe phenotype in proportion to the extent that heterotrimer formation is impeded (Pace et al., 2008). However, a human subject with an inactivating mutation of the Col1A2 gene has been identified who presented as Ehlers−Danlos and not OI (Schwarze et al., 2004). Reconciling these differences using murine models is likely to provide additional insights into cell and matrix factors that influence skeletal health.

Even less understood is the consequence of a diminished content of type I collagen−containing matrix in bone and other tissues relative the other matrix proteins that interact with this organizing molecule. Until shown otherwise, the underlying assumption is that increasing the type I collagen output should have a positive impact on skeletal health. The anabolic agents that enhance matrix production from osteoblasts and other type I collagen−producing cells needs to be explored, again using animal models prior to clinical trials. In contrast, OI-causing mutations that affect the progression of

osteogenic lineage will require a different therapeutic approach utilizing agents that enhance or block the pathways affected by the mutation. Many potential drug candidates are already available that will have to be personalized for the offending mutation. In all cases, including type I OI, initiating the intervention early in childhood when bone matrix is being accumulated will be important, and maintaining a lifestyle that is anabolic for the skeleton will have to be emphasized.

In summary, the pathophysiological basis for OI is extremely heterogeneous and cannot be anticipated by clinical presentation alone. Clearly, molecular diagnosis will provide some insight into the likely cell and matrix consequences, and improved testing for bone metabolic and inflammatory markers will further refine the underlying factors determining disease severity and nonosseous outcomes.

Therapeutic options

Although anti−bone resorptive agents have changed the natural history of the more severe forms of OI, particularly in children, the specific drugs, how they are used, and their durations of treatment are not uniformly applied in the different treatment centers in the United States and elsewhere. Thus, for the individual physician who encounters an individual with OI, it is probably wise to refer to one of the major treatment centers so that the individual can be enrolled in one of a number of multicenter trials and benefit from the best clinical experience available (Montpetit et al., 2015). The centers provide the additional health-supporting advantages of physical and occupational therapies, contact with other affected families, and the resources of the Osteogenesis Imperfecta Foundation. Agents approved or under evaluation can be divided into three classes: antiresorptive, anti-Tgfß and antiactivin, and anabolic.

Antiresorptive agents

Bisphosphonate in the form of short-acting pamidronate was the first agent successful in reducing fracture frequency in growing children. A major experience in using this drug was assembled by the Montreal treatment center (Glorieux et al., 1998; Arikoski et al., 2004) and was subsequently replicated at other centers (DiMeglio et al., 2004; Fleming et al., 2005). Most notable were a reduction in fractures, better formation vertebra, and improved linear growth. Because the drug requires intravenous administration that must be repeated 2−3 times each year, longer-acting forms such as zoledronate have received greater usage (Palomo et al., 2015; Tsimicalis et al., 2018). Oral forms such as alendronate and risedronate are also effective (Ward et al., 2011; Bishop et al., 2013) but have not become standard practice.

The introduction of the anti-RANKL drug denosumab provided an entirely different approach for inhibiting bone resorption. Unlike bisphosphonates that induce osteoclast death after full differentiation has been achieved, denosumab prevents osteoclast differentiation. It has the advantage of infrequent injections and a predictable therapeutic window, and it has proven effective in early clinical trials (Hoyer-Kuhn et al., 2016). However, it has not become the primary treatment as of 2019.

Anti-TGFß and anti-activin agents

Although there is strong data in mouse models of OI that these antibodies and soluble receptor peptides can be effective in suppressing osteoclastogenesis and potentially having other beneficial nonosseous effects (Grafe et al., 2014), a clinical trial is just being initiated through the BBDC.

Anabolic agents

The use of bone anabolic agents to overcome the severe osteopenia of OI has always been an attractive approach and was the basis of growth hormone treatment in growing children. However, the experience in humans was inconclusive (Wright, 2000), and its use is no longer recommended. Use of PTH, teriparatide, has shown promise in adults, but its expense and a lack of coverage by most insurance companies has limited its use. The recent introduction of a PthrP analog, Abaloparatide, not only is as effective as PTH in increasing bone anabolism (Makino et al., 2018), but costs significantly less. Studies from osteoporotic patients that use PthrP and an antiresorptive sequentially are particularly encouraging (Le et al., 2019; Hiligsmann et al., 2019) and are leading to similar ongoing trials in adults with OI.

Stimulating bone anabolism with antisclerostin antibodies shows significant positive effects in adults with OI. Markers of bone anabolism without an increase in bone turnover markers (Glorieux et al., 2017; Sridharan et al., 2018) suggest the modeling effect this drug is expected to deliver (Sinder et al., 2016; Sridharan et al., 2018). Although the initial application for osteoporosis was rejected by the FDA in 2017, this hurdle was cleared in 2019.

Cell and gene-therapy options

The high-profile announcements of stem cell and gene-correction possibilities for human disease have impacted potential treatment options for OI, particularly in young severely affected individuals. The rationale for either approach is the observation that parents with somatic mosaicism for a mutation that causes a severe form of OI in their child rarely have features of skeletal disfunction. The basis for this observation has not been directly tested, but it may reflect the superior competitive advantage that normal osteoblasts have for cell proliferation and matrix production relative to osteoblasts compromised by mutant collagen chains. It is possible that a degree of mosaicism sufficient to affect skeletal health could be achieved by either a cell-based or gene-therapy approach.

Initial reports of bone marrow and bone marrow mesenchymal cell transplantation were performed without solid animal studies demonstrating that osteoblast engraftment by this means would have a significant impact on disease severity (Horwitz et al. 1999, 2002, 2008). Subsequent studies using more sensitive GFP reporter-based methods in mouse models have clearly demonstrated that systemic administration of stem cells capable of osteogenic differentiation does not engraft trabecular bone (Wang et al., 2005; Boban et al., 2010; Otsuru et al., 2017). Despite this basic animal work (Featherall et al., 2018), infusion of marrow-derived stromal cells is still being performed on an experimental basis (Le Blanc et al., 2005; Westgren et al., 2015; Gotherstrom et al., 2014) without clear-cut animal data to show that it is effective for engraftment (Millard et al., 2015).

Direct introduction of mouse bone progenitor cells into the bone marrow cavity or an experimental defect space in mice leads to engraftment and integration with the host bone (Pauley et al., 2014; Gohil et al., 2016). In contrast, direct injection of whole bone marrow is not effective (Wang et al., 2005; Lee et al., 2019). Given the increasing success of drug interventions, this type of strategy would be limited as a supplement to orthopedic reconstructive procedures of the limb, vertebral, or basilar skull bones. However, this type of use will only be meaningful in the human clinical setting if the cells are isogenic with the individual subject. Claims that mesenchymal-derived cells are immune-privileged have not been validated for osteogenic engraftment (Bilic-Curcic et al., 2005). A possible solution to this problem is the use of patient-derived induced pluripotential stem cells (iPSCs). By engineering a correction of the underlying OI mutation using CRISPR/Cas9 technology, it should be possible to generate otherwise normal patient-specific progenitor cells that would generate normal bone matrix in the region of their application.

The molecular technologies to safely introduce a new gene into cells have improved to the point that they are now being applied in clinical trials for a number of hematopoietic disorders (Herrmann et al., 2018; Ahmed et al., 2018; Elsner et al., 2017). Animal studies are promising for other tissue types, particularly those that do not have a high level of cell turnover (Tabebordbar et al., 2016; Deverman et al., 2018). In the case of recessive forms of OI that result from a loss of enzymatic or chaperone function, gene replacement could be effective. The issue is the delivery method. While systemic administration is possible, the vast majority of osteogenic cells targeted would be mature cells that eventually would be replaced by nontargeted progenitors. However, it might be possible to transiently increase the progenitor cell number prior to administering the targeting vector to achieve a sufficient number of transformed cells to reach a mosaic threshold effect. While this might be an issue for children, bone-lining cells in adults may harbor the capacity for bone remodeling (Matic et al., 2016), making them an excellent target for genetic engineering.

All of these potentially attractive approaches require small animal testing, which provides exquisitely sensitive and relatively low-cost test platforms to identify the most positive candidate vectors and application strategies. Once identified, they will need to be validated in principle in larger animal models prior to a stepwise clinical safety and efficacy trial.

Use of induced pluripotential stem cells as a diagnostic tool

Given the increasing complexity of the various molecular forms of OI and the strong influence of background genes that further complicate disease pathogenesis, it is likely that animal models will never fully serve as models for specific individuals with OI. Because iPSCs express the genetic heterogeneity of their donor, they provide the opportunity for developing personalized therapeutic decisions (Kilpinen et al., 2017; DeBoever et al., 2017; Rowe et al., 2019). While obtaining primary osteoblastic cells from individual subjects is difficult, generation of iPSCs from peripheral blood provides the opportunity to direct these cells into the osteogenic lineage for detailed testing (Chen et al., 2013). Once a model for full osteogenic differentiation is achieved, protein and RNA expression studies can be initiated with best model in an in vivo setting for that specific subject (Xin et al., 2018). In this setting, not only can the effect of the mutation be assessed but also the identification of other genes whose products might interact with mutation becomes possible. To test the relative

impact of the candidate background gene to overall cellular phenotype, the CRISPR/Cas9 system can be used to revert the background gene to its wild-type form and determine whether this change improves the matrix production capability of the engineered osteoblasts (Xin, 2017, 2018). Knowing the contribution background gene may influence other combinatorial therapeutic options that are becoming available from osteoporosis/osteopenia research areas.

References

Ahmed, S.G., Waddington, S.N., Boza-Moran, M.G., Yanez-Munoz, R.J., 2018. High-efficiency transduction of spinal cord motor neurons by intrauterine delivery of integration-deficient lentiviral vectors. J. Control. Release 273, 99−107.

Akizawa, Y., Nishimura, G., Hasegawa, T., Takagi, M., Kawamichi, Y., Matsuda, Y., Matsui, H., Saito, K., 2012. Prenatal diagnosis of osteogenesis imperfecta type II by three-dimensional computed tomography: the current state of fetal computed tomography. Congenital. Anom. 52, 203−206.

Al-Jallad, H., Palomo, T., Roughley, P., Glorieux, F.H., McKee, M.D., Moffatt, P., Rauch, F., 2015. The effect of SERPINF1 in-frame mutations in osteogenesis imperfecta type VI. Bone 76, 115−120.

Al-Senaidi, K.S., Ullah, I., Javad, H., Al-Khabori, M., Al-Yaarubi, S., 2015. Echocardiographic evidence of early diastolic dysfunction in asymptomatic children with osteogenesis imperfecta. Sultan Qaboos Univ. Med. J. 15, e456−e462.

Alhamdi, S., Lee, Y.C., Chowdhury, S., Byers, P.H., Gottschalk, M., Taft, R.J., Joeng, K.S., Lee, B.H., Bird, L.M., 2018. Heterozygous WNT1 variant causing a variable bone phenotype. Am. J. Med. Genet. 176, 2419−2424.

Anam, E.A., Rauch, F., Glorieux, F.H., Fassier, F., Hamdy, R., 2015. Osteotomy healing in children With osteogenesis imperfecta receiving bisphosphonate treatment. J. Bone Miner Res 30, 1362−1368.

Andersen, J.D., Bunger, M.H., Rahbek, O., Hald, J.D., Harslof, T., Langdahl, B.L., 2019. Do femoral fractures in adult patients with osteogenesis imperfecta imitate atypical femoral fractures? A case series. Osteoporos. Int. 30, 513−517.

Arikoski, P., Silverwood, B., Tillmann, V., Bishop, N.J., 2004. Intravenous pamidronate treatment in children with moderate to severe osteogenesis imperfecta: assessment of indices of dual-energy X-ray absorptiometry and bone metabolic markers during the first year of therapy. Bone 34, 539−546.

Arponen, H., Bachour, A., Back, L., Valta, H., Makitie, A., Waltimo-Siren, J., Makitie, O., 2018. Is sleep apnea underdiagnosed in adult patients with osteogenesis imperfecta? -a single-center cross-sectional study. Orphanet J. Rare Dis. 13, 231.

Arundel, P., Bishop, N., 2015. Primary osteoporosis. Endocr. Dev. 28, 162−175.

Asharani, P.V., Keupp, K., Semler, O., Wang, W., Li, Y., Thiele, H., Yigit, G., Pohl, E., Becker, J., Frommolt, P., Sonntag, C., Altmuller, J., Zimmermann, K., Greenspan, D.S., Akarsu, N.A., Netzer, C., Schonau, E., Wirth, R., Hammerschmidt, M., Nurnberg, P., Wollnik, B., Carney, T.J., 2012. Attenuated BMP1 function compromises osteogenesis, leading to bone fragility in humans and zebrafish. Am. J. Hum. Genet. 90, 661−674.

Ashby, E., Montpetit, K., Hamdy, R.C., Fassier, F., 2018. Functional outcome of humeral rodding in children with osteogenesis imperfecta. J. Pediatr. Orthop. 38, 49−53.

Ashournia, H., Johansen, F.T., Folkestad, L., Diederichsen, A.C., Brixen, K., 2015. Heart disease in patients with osteogenesis imperfecta - a systematic review. Int. J. Cardiol. 196, 149−157.

Balasubramanian, M., Padidela, R., Pollitt, R.C., Bishop, N.J., Mughal, M.Z., Offiah, A.C., Wagner, B.E., McCaughey, J., Stephens, D.J., 2018. P4HB recurrent missense mutation causing Cole-Carpenter syndrome. J. Med. Genet. 55, 158−165.

Balasubramanian, M., Verschueren, A., Kleevens, S., Luyckx, I., Perik, M., Schirwani, S., Mortier, G., Morisaki, H., Rodrigus, I., Van Laer, L., Verstraeten, A., Loeys, B., 2019. Aortic aneurysm/dissection and osteogenesis imperfecta: four new families and review of the literature. Bone 121, 191−195.

Barbirato, C., Trancozo, M., Almeida, M.G., Almeida, L.S., Santos, T.O., Duarte, J.C., Reboucas, M.R., Sipolatti, V., Nunes, V.R., Paula, F., 2015. Mutational characterization of the P3H1/CRTAP/CypB complex in recessive osteogenesis imperfecta. Genet. Mol. Res. 14, 15848−15858.

Bateman, J.F., Freddi, S., Lamande, S.R., Byers, P., Nasioulas, S., Douglas, J., Otway, R., Kohonen-Corish, M., Edkins, E., Forrest, S., 1999. Reliable and sensitive detection of premature termination mutations using a protein truncation test designed to overcome problems of nonsense-mediated mRNA instability. Hum. Mutat. 13, 311−317.

Bateman, J.F., Sampurno, L., Maurizi, A., Lamande, S.R., Sims, N.A., Cheng, T.L., Schindeler, A., Little, D.G., 2019. Effect of rapamycin on bone mass and strength in the alpha2(I)-G610C mouse model of osteogenesis imperfecta. J. Cell Mol. Med. 23, 1735−1745.

BBDC, 2019. Brittle Bone Disease Consortium. https://www.rarediseasesnetwork.org/cms/BBD.

Belinsky, G.S., Sreekumar, B., Andrejecsk, J.W., Saltzman, W.M., Gong, J., Herzog, R.I., Lin, S., Horsley, V., Carpenter, T.O., Chung, C., 2016. Pigment epithelium-derived factor restoration increases bone mass and improves bone plasticity in a model of osteogenesis imperfecta type VI via Wnt3a blockade. FASEB J. 30, 2837−2848.

Ben Amor, I.M., Roughley, P., Glorieux, F.H., Rauch, F., 2013. Skeletal clinical characteristics of osteogenesis imperfecta caused by haploinsufficiency mutations in COL1A1. J. Bone Miner. Res. 28, 2001−2007.

Bendixen, K.H., Gjorup, H., Baad-Hansen, L., Dahl Hald, J., Harslof, T., Schmidt, M.H., Langdahl, B.L., Haubek, D., 2018. Temporomandibular disorders and psychosocial status in osteogenesis imperfecta - a cross-sectional study. BMC Oral Health 18, 35.

Bilic-Curcic, I., Kalajzic, Z., Wang, L., Rowe, D.W., 2005. Origins of endothelial and osteogenic cells in the subcutaneous collagen gel implant. Bone 37, 678−687.

Bishop, N., Adami, S., Ahmed, S.F., Anton, J., Arundel, P., Burren, C.P., Devogelaer, J.P., Hangartner, T., Hosszu, E., Lane, J.M., Lorenc, R., Makitie, O., Munns, C.F., Paredes, A., Pavlov, H., Plotkin, H., Raggio, C.L., Reyes, M.L., Schoenau, E., Semler, O., Sillence, D.O., Steiner, R.D., 2013. Risedronate in children with osteogenesis imperfecta: a randomised, double-blind, placebo-controlled trial. Lancet 382, 1424−1432.

Blouin, S., Fratzl-Zelman, N., Glorieux, F.H., Roschger, P., Klaushofer, K., Marini, J.C., Rauch, F., 2017. Hypermineralization and high osteocyte lacunar density in osteogenesis imperfecta type V bone indicate exuberant primary bone formation. J. Bone Miner. Res. 32, 1884−1892.

Boban, I., Barisic-Dujmovic, T., Clark, S.H., 2010. Parabiosis model does not show presence of circulating osteoprogenitor cells. Genesis 48, 171−182.

Bodian, D.L., Chan, T.F., Poon, A., Schwarze, U., Yang, K., Byers, P.H., Kwok, P.Y., Klein, T.E., 2009. Mutation and polymorphism spectrum in osteogenesis imperfecta type II: implications for genotype-phenotype relationships. Hum. Mol. Genet. 18, 463−471.

Bojanic, K., Kivela, J.E., Gurrieri, C., Deutsch, E., Flick, R., Sprung, J., Weingarten, T.N., 2011. Perioperative course and intraoperative temperatures in patients with osteogenesis imperfecta. Eur. J. Anaesthesiol. 28, 370−375.

Brizola, E., Mattos, E.P., Ferrari, J., Freire, P.O., Germer, R., Llerena Jr., J.C., Felix, T.M., 2015. Clinical and molecular characterization of osteogenesis imperfecta type V. Mol. Syndromol. 6, 164−172.

Brunetti, G., Papadia, F., Tummolo, A., Fischetto, R., Nicastro, F., Piacente, L., Ventura, A., Mori, G., Oranger, A., Gigante, I., Colucci, S., Ciccarelli, M., Grano, M., Cavallo, L., Delvecchio, M., Faienza, M.F., 2016. Impaired bone remodeling in children with osteogenesis imperfecta treated and untreated with bisphosphonates: the role of DKK1, RANKL, and TNF-alpha. Osteoporos. Int. 27, 2355−2365.

Burrows, C.K., Banovich, N.E., Pavlovic, B.J., Patterson, K., Gallego Romero, I., Pritchard, J.K., Gilad, Y., 2016. Genetic variation, not cell type of origin, underlies the majority of identifiable regulatory differences in iPSCs. PLoS Genet. 12, e1005793.

CBBF, 2019. Children's Brittle Bone Foundation. https://globalgenes.org/support_organization/childrens-brittle-bone-foundation/.

Charnas, L.R., Marini, J.C., 1993. Communicating hydrocephalus, basilar invagination, and other neurologic features in osteogenesis imperfecta. Neurology 43, 2603−2608.

Chen, I.P., Fukuda, K., Fusaki, N., Iida, A., Hasegawa, M., Lichtler, A., Reichenberger, E.J., 2013. Induced pluripotent stem cell reprogramming by integration-free Sendai virus vectors from peripheral blood of patients with craniometaphyseal dysplasia. Cell. Reprogr. 15, 503−513.

Cheung, M.S., Azouz, E.M., Glorieux, F.H., Rauch, F., 2008. Hyperplastic callus formation in osteogenesis imperfecta type V: follow-up of three generations over ten years. Skeletal Radiol. 37, 465−467.

Cheung, M.S., Glorieux, F.H., Rauch, F., 2007. Natural history of hyperplastic callus formation in osteogenesis imperfecta type V. J. Bone Miner. Res. 22, 1181−1186.

Cho, S.Y., Asharani, P.V., Kim, O.H., Iida, A., Miyake, N., Matsumoto, N., Nishimura, G., Ki, C.S., Hong, G., Kim, S.J., Sohn, Y.B., Park, S.W., Lee, J., Kwun, Y., Carney, T.J., Huh, R., Ikegawa, S., Jin, D.K., 2015. Identification and in vivo functional characterization of novel compound heterozygous BMP1 variants in osteogenesis imperfecta. Hum. Mutat. 36, 191−195.

Cobanoglu, M., Bauer, J.M., Campbell, J.W., Shah, S.A., 2018. Basilar impression in osteogenesis imperfecta treated with staged halo traction and posterior decompression with short-segment fusion. J. Craniovertebral Junction Spine 9, 212−215.

Dahan-Oliel, N., Oliel, S., Tsimicalis, A., Montpetit, K., Rauch, F., Dogba, M.J., 2016. Quality of life in osteogenesis imperfecta: a mixed-methods systematic review. Am. J. Med. Genet. 170A, 62−76.

Dankbar, B., Fennen, M., Brunert, D., Hayer, S., Frank, S., Wehmeyer, C., Beckmann, D., Paruzel, P., Bertrand, J., Redlich, K., Koers-Wunrau, C., Stratis, A., Korb-Pap, A., Pap, T., 2015. Myostatin is a direct regulator of osteoclast differentiation and its inhibition reduces inflammatory joint destruction in mice. Nat. Med. 21, 1085−1090.

DeBoever, C., Li, H., Jakubosky, D., Benaglio, P., Reyna, J., Olson, K.M., Huang, H., Biggs, W., Sandoval, E., D'Antonio, M., Jepsen, K., Matsui, H., Arias, A., Ren, B., Nariai, N., Smith, E.N., D'Antonio-Chronowska, A., Farley, E.K., Frazer, K.A., 2017. Large-scale profiling reveals the influence of genetic variation on gene expression in human induced pluripotent stem cells. Cell Stem Cell 20, 533−546 e7.

Deverman, B.E., Ravina, B.M., Bankiewicz, K.S., Paul, S.M., Sah, D.W.Y., 2018. Gene therapy for neurological disorders: progress and prospects. Nat. Rev. Drug Discov. 17, 641−659.

DiGirolamo, D.J., Singhal, V., Chang, X., Lee, S.J., Germain-Lee, E.L., 2015. Administration of soluble activin receptor 2B increases bone and muscle mass in a mouse model of osteogenesis imperfecta. Bone Res. 3, 14042.

DiMeglio, L.A., Ford, L., McClintock, C., Peacock, M., 2004. Intravenous pamidronate treatment of children under 36 months of age with osteogenesis imperfecta. Bone 35, 1038−1045.

Elsner, C., Bohne, J., 2017. The retroviral vector family: something for everyone. Virus Gene. 53, 714−722.

Engelbert, R.H., Uiterwaal, C.S., van der Hulst, A., Witjes, B., Helders, P.J., Pruijs, H.E., 2003. Scoliosis in children with osteogenesis imperfecta: influence of severity of disease and age of reaching motor milestones. Eur. Spine J. 12, 130−134.

Eslani, M., Putra, I., Shen, X., Hamouie, J., Afsharkhamseh, N., Besharat, S., Rosenblatt, M.I., Dana, R., Hematti, P., Djalilian, A.R., 2017. Corneal mesenchymal stromal cells are directly antiangiogenic via PEDF and sFLT-1. Investig. Ophthalmol. Vis. Sci. 58, 5507−5517.

Featherall, J., Robey, P.G., Rowe, D.W., 2018. Continuing challenges in advancing preclinical science in skeletal cell-based therapies and tissue regeneration. J. Bone Miner. Res. 33, 1721−1728.

Fedarko, N.S., D'Avis, P., Frazier, C.R., Burrill, M.J., Fergusson, V., Tayback, M., Sponseller, P.D., Shapiro, J.R., 1995. Cell proliferation of human fibroblasts and osteoblasts in osteogenesis imperfecta: influence of age. J. Bone Miner. Res. 10, 1705−1712.

Fiscaletti, M., Biggin, A., Bennetts, B., Wong, K., Briody, J., Pacey, V., Birman, C., Munns, C.F., 2018. Novel variant in Sp7/Osx associated with recessive osteogenesis imperfecta with bone fragility and hearing impairment. Bone 110, 66−75.

Fitzgerald, J., Holden, P., Wright, H., Wilmot, B., Hata, A., Steiner, R.D., Basel, D., 2013. Phenotypic variability in individuals with type V osteogenesis imperfecta with identical Ifitm5 mutations. J. Rare Disord. 1, 37−42.

Fleming, F., Woodhead, H.J., Briody, J.N., Hall, J., Cowell, C.T., Ault, J., Kozlowski, K., Sillence, D.O., 2005. Cyclic bisphosphonate therapy in osteogenesis imperfecta type V. J. Paediatr. Child Health 41, 147–151.

Folkestad, L., 2018. Mortality and morbidity in patients with osteogenesis imperfecta in Denmark. Dan. Med. J. 65.

Folkestad, L., Hald, J.D., Ersboll, A.K., Gram, J., Hermann, A.P., Langdahl, B., Abrahamsen, B., Brixen, K., 2017. Fracture rates and fracture sites in patients with osteogenesis imperfecta: a nationwide register-based cohort study. J. Bone Miner. Res. 32, 125–134.

Folkestad, L., Hald, J.D., Gram, J., Langdahl, B.L., Hermann, A.P., Diederichsen, A.C., Abrahamsen, B., Brixen, K., 2016. Cardiovascular disease in patients with osteogenesis imperfecta - a nationwide, register-based cohort study. Int. J. Cardiol. 225, 250–257.

Forlino, A., Marini, J.C., 2016. Osteogenesis imperfecta. Lancet 387, 1657–1671.

Franzone, J.M., Bober, M.B., Rogers, K.J., McGreal, C.M., Kruse, R.W., 2017. Re-alignment and intramedullary rodding of the humerus and forearm in children with osteogenesis imperfecta: revision rate and effect on fracture rate. J. Child. Orthopaed. 11, 185–190.

Galicka, A., Surazynski, A., Wolczynski, S., Palka, J., Popko, J., Gindzienski, A., 2005. Phenotype variability in a daughter and father with mild osteogenesis imperfecta correlated with collagen and prolidase levels in cultured skin fibroblasts. Ann. Clin. Biochem. 42, 80–84.

Gardner, A., Sahota, J., Dong, H., Saraff, V., Hogler, W., Shaw, N.J., 2018. The use of magnetically controlled growing rods in paediatric Osteogenesis Imperfecta with early onset, progressive scoliosis. J. Surg. Case Rep. 2018, rjy043.

Garman, C.R., Graf, A., Krzak, J., Caudill, A., Smith, P., Harris, G., 2017. Gait deviations in children with osteogenesis imperfecta type I. J. Pediatr. Orthop. https://doi.org/10.1016/B978-0-12-817454-8.00005-8. PMID 28777275.

Gatti, D., Rossini, M., Viapiana, O., Povino, M.R., Liuzza, S., Fracassi, E., Idolazzi, L., Adami, S., 2013. Teriparatide treatment in adult patients with osteogenesis imperfecta type I. Calcif. Tissue Int. 93, 448–452.

Gauba, V., Hartgerink, J.D., 2008. Synthetic collagen heterotrimers: structural mimics of wild-type and mutant collagen type I. J. Am. Chem. Soc. 130, 7509–7515.

Ge, G., Greenspan, D.S., 2006. BMP1 controls TGFbeta1 activation via cleavage of latent TGFbeta-binding protein. J. Cell Biol. 175, 111–120.

Germain-Lee, E.L., Brennen, F.S., Stern, D., Kantipuly, A., Melvin, P., Terkowitz, M.S., Shapiro, J.R., 2016. Cross-sectional and longitudinal growth patterns in osteogenesis imperfecta: implications for clinical care. Pediatr. Res. 79, 489–495.

Gioia, R., Panaroni, C., Besio, R., Palladini, G., Merlini, G., Giansanti, V., Scovassi, I.A., Villani, S., Villa, I., Villa, A., Vezzoni, P., Tenni, R., Rossi, A., Marini, J.C., Forlino, A., 2012. 'Impaired osteoblastogenesis in a murine model of dominant osteogenesis imperfecta (OI), a new target for OI pharmacological therapy. Stem Cells 30, 1465–1476.

Glorieux, F.H., Bishop, N.J., Plotkin, H., Chabot, G., Lanoue, G., Travers, R., 1998. Cyclic administration of pamidronate in children with severe osteogenesis imperfecta. N. Engl. J. Med. 339, 947–952.

Glorieux, F.H., Devogelaer, J.P., Durigova, M., Goemaere, S., Hemsley, S., Jakob, F., Junker, U., Ruckle, J., Seefried, L., Winkle, P.J., 2017. BPS804 anti-sclerostin antibody in adults with moderate osteogenesis imperfecta: results of a randomized phase 2a trial. J. Bone Miner. Res. 32, 1496–1504.

Gohil, S.V., Kuo, C.L., Adams, D.J., Maye, P., Rowe, D.W., Nair, L.S., 2016. Evaluation of the donor cell contribution in rhBMP-2 mediated bone formation with chitosan thermogels using fluorescent protein reporter mice. J. Biomed. Mater. Res. A 104, 928–941.

Gotherstrom, C., Westgren, M., Shaw, S.W., Astrom, E., Biswas, A., Byers, P.H., Mattar, C.N., Graham, G.E., Taslimi, J., Ewald, U., Fisk, N.M., Yeoh, A.E., Lin, J.L., Cheng, P.J., Choolani, M., Le Blanc, K., Chan, J.K., 2014. Pre- and postnatal transplantation of fetal mesenchymal stem cells in osteogenesis imperfecta: a two-center experience. Stem Cells Transl. Med. 3, 255–264.

Grafe, I., Yang, T., Alexander, S., Homan, E.P., Lietman, C., Jiang, M.M., Bertin, T., Munivez, E., Chen, Y., Dawson, B., Ishikawa, Y., Weis, M.A., Sampath, T.K., Ambrose, C., Eyre, D., Bachinger, H.P., Lee, B., 2014. Excessive transforming growth factor-beta signaling is a common mechanism in osteogenesis imperfecta. Nat. Med. 20, 670–675.

Graff, K., Syczewska, M., 2017. Developmental charts for children with osteogenesis imperfecta, type I (body height, body weight and BMI). Eur. J. Pediatr. 176, 311–316.

Grossman, L.S., Price, A.L., Rush, E.T., Goodwin, J.L., Wallace, M.J., Esposito, P.W., 2018. Initial experience with percutaneous IM rodding of the humeri in children with osteogenesis imperfecta. J. Pediatr. Orthop. 38, 484–489.

Hald, J.D., Folkestad, L., Harslof, T., Brixen, K., Langdahl, B., 2017. Health-related quality of life in adults with osteogenesis imperfecta. Calcif. Tissue Int. 101, 473–478.

Hegazy, A., Kenawey, M., Sochett, E., Tile, L., Cheung, A.M., Howard, A.W., 2016. Unusual femur stress fractures in children with osteogenesis imperfecta and intramedullary rods on long-term intravenous pamidronate therapy. J. Pediatr. Orthop. 36, 757–761.

Herrmann, A.K., Grimm, D., 2018. High-throughput dissection of AAV-host interactions: the fast and the curious. J. Mol. Biol. 430, 2626–2640.

Hiligsmann, M., Williams, S.A., Fitzpatrick, L.A., Silverman, S.S., Weiss, R., Reginster, J.Y., 2019. Cost-effectiveness of sequential treatment with abaloparatide vs. teriparatide for United States women at increased risk of fracture. Semin. Arthritis Rheum. https://doi.org/10.1016/j.semarthrit.2019.01.006. PMID 30737062.

Homan, E.P., Rauch, F., Grafe, I., Lietman, C., Doll, J.A., Dawson, B., Bertin, T., Napierala, D., Morello, R., Gibbs, R., White, L., Miki, R., Cohn, D.H., Crawford, S., Travers, R., Glorieux, F.H., Lee, B., 2011. Mutations in SERPINF1 cause osteogenesis imperfecta type VI. J. Bone Miner. Res. 26, 2798–2803.

Horwitz, E.M., Dominici, M., 2008. How do mesenchymal stromal cells exert their therapeutic benefit? Cytotherapy 10, 771–774.

Horwitz, E.M., Gordon, P.L., Koo, W.K., Marx, J.C., Neel, M.D., McNall, R.Y., Muul, L., Hofmann, T., 2002. Isolated allogeneic bone marrow-derived mesenchymal cells engraft and stimulate growth in children with osteogenesis imperfecta: implications for cell therapy of bone. Proc. Natl. Acad. Sci. U. S. A 99, 8932–8937.

Horwitz, E.M., Prockop, D.J., Fitzpatrick, L.A., Koo, W.W., Gordon, P.L., Neel, M., Sussman, M., Orchard, P., Marx, J.C., Pyeritz, R.E., Brenner, M.K., 1999. Transplantability and therapeutic effects of bone marrow-derived mesenchymal cells in children with osteogenesis imperfecta. Nat. Med. 5, 309−313.

Hoyer-Kuhn, H., Franklin, J., Allo, G., Kron, M., Netzer, C., Eysel, P., Hero, B., Schoenau, E., Semler, O., 2016. Safety and efficacy of denosumab in children with osteogenesis imperfect–a first prospective trial. J. Musculoskelet. Neuronal Interact. 16, 24−32.

Jabbour, Z., Al-Khateeb, A., Eimar, H., Retrouvey, J.M., Rizkallah, J., Glorieux, F.H., Rauch, F., Tamimi, F., 2018. Genotype and malocclusion in patients with osteogenesis imperfecta. Orthod. Craniofac. Res. 21, 71−77.

Jacobsen, C.M., Schwartz, M.A., Roberts, H.J., Lim, K.E., Spevak, L., Boskey, A.L., Zurakowski, D., Robling, A.G., Warman, M.L., 2016. Enhanced Wnt signaling improves bone mass and strength, but not brittleness, in the Col1a1(+/mov13) mouse model of type I Osteogenesis Imperfecta. Bone 90, 127−132.

Jain, M., Tam, A., Shapiro, J.R., Steiner, R.D., Smith, P.A., Bober, M.B., Hart, T., Cuthbertson, D., Krischer, J., Mullins, M., Bellur, S., Byers, P.H., Pepin, M., Durigova, M., Glorieux, F.H., Rauch, F., Lee, B., Sutton, V.R., Members of the Brittle Bone Disorders Consortium, Nagamani, S.C.S., 2019. Growth characteristics in individuals with osteogenesis imperfecta in North America: results from a multicenter study. Genet. Med. 21, 275−283.

Janus, G.J., Engelbert, R.H., Beek, E., Gooskens, R.H., Pruijs, J.E., 2003. Osteogenesis imperfecta in childhood: MR imaging of basilar impression. Eur. J. Radiol. 47, 19−24.

Jasuja, R., Ge, G., Voss, N.G., Lyman-Gingerich, J., Branam, A.M., Pelegri, F.J., Greenspan, D.S., 2007. Bone morphogenetic protein 1 prodomain specifically binds and regulates signaling by bone morphogenetic proteins 2 and 4. J. Biol. Chem. 282, 9053−9062.

Jepsen, K.J., Schaffler, M.B., Kuhn, J.L., Goulet, R.W., Bonadio, J., Goldstein, S.A., 1997. Type I collagen mutation alters the strength and fatigue behavior of Mov13 cortical tissue. J. Biomech. 30, 1141−1147.

Kalajzic, I., Terzic, J., Rumboldt, Z., Mack, K., Naprta, A., Ledgard, F., Gronowicz, G., Clark, S.H., Rowe, D.W., 2002. Osteoblastic response to the defective matrix in the osteogenesis imperfecta murine (oim) mouse. Endocrinology 143, 1594−1601.

Kang, H., Aryal, A.C.S., Marini, J.C., 2017. Osteogenesis imperfecta: new genes reveal novel mechanisms in bone dysplasia. Transl. Res. 181, 27−48.

Kelley, B.P., Malfait, F., Bonafe, L., Baldridge, D., Homan, E., Symoens, S., Willaert, A., Elcioglu, N., Van Maldergem, L., Verellen-Dumoulin, C., Gillerot, Y., Napierala, D., Krakow, D., Beighton, P., Superti-Furga, A., De Paepe, A., Lee, B., 2011. Mutations in FKBP10 cause recessive osteogenesis imperfecta and Bruck syndrome. J. Bone Miner. Res. 26, 666−672.

Khandanpour, N., Connolly, D.J., Raghavan, A., Griffiths, P.D., Hoggard, N., 2012. Craniospinal abnormalities and neurologic complications of osteogenesis imperfecta: imaging overview. Radiographics 32, 2101−2112.

Kilpinen, H., Goncalves, A., Leha, A., Afzal, V., Alasoo, K., Ashford, S., Bala, S., Bensaddek, D., Casale, F.P., Culley, O.J., Danecek, P., Faulconbridge, A., Harrison, P.W., Kathuria, A., McCarthy, D., McCarthy, S.A., Meleckyte, R., Memari, Y., Moens, N., Soares, F., Mann, A., Streeter, I., Agu, C.A., Alderton, A., Nelson, R., Harper, S., Patel, M., White, A., Patel, S.R., Clarke, L., Halai, R., Kirton, C.M., Kolb-Kokocinski, A., Beales, P., Birney, E., Danovi, D., Lamond, A.I., Ouwehand, W.H., Vallier, L., Watt, F.M., Durbin, R., Stegle, O., Gaffney, D.J., 2017. Common genetic variation drives molecular heterogeneity in human iPSCs. Nature 546, 370−375.

Kovero, O., Pynnonen, S., Kuurila-Svahn, K., Kaitila, I., Waltimo-Siren, J., 2006. Skull base abnormalities in osteogenesis imperfecta: a cephalometric evaluation of 54 patients and 108 control volunteers. J. Neurosurg. 105, 361−370.

Kuznetsova, N.V., McBride, D.J., Leikin, S., 2003. Changes in thermal stability and microunfolding pattern of collagen helix resulting from the loss of alpha2(I) chain in osteogenesis imperfecta murine. J. Mol. Biol. 331, 191−200.

Lapunzina, P., Aglan, M., Temtamy, S., Caparros-Martin, J.A., Valencia, M., Leton, R., Martinez-Glez, V., Elhossini, R., Amr, K., Vilaboa, N., Ruiz-Perez, V.L., 2010. Identification of a frameshift mutation in Osterix in a patient with recessive osteogenesis imperfecta. Am. J. Hum. Genet. 87, 110−114.

Le Blanc, K., Gotherstrom, C., Ringden, O., Hassan, M., McMahon, R., Horwitz, E., Anneren, G., Axelsson, O., Nunn, J., Ewald, U., Norden-Lindeberg, S., Jansson, M., Dalton, A., Astrom, E., Westgren, M., 2005. Fetal mesenchymal stem-cell engraftment in bone after in utero transplantation in a patient with severe osteogenesis imperfecta. Transplantation 79, 1607−1614.

Le, Q.A., Hay, J.W., Becker, R., Wang, Y., 2019. Cost-effectiveness analysis of sequential treatment of abaloparatide followed by alendronate versus teriparatide followed by alendronate in postmenopausal women with osteoporosis in the United States. Ann. Pharmacother. 53, 134−143.

Leal, G.F., Nishimura, G., Voss, U., Bertola, D.R., Astrom, E., Svensson, J., Yamamoto, G.L., Hammarsjo, A., Horemuzova, E., Papadiogannakis, N., Iwarsson, E., Grigelioniene, G., Tham, E., 2018. Expanding the clinical spectrum of phenotypes caused by pathogenic variants in PLOD2. J. Bone Miner. Res. 33, 753−760.

Leali, P.T., Balsano, M., Maestretti, G., Brusoni, M., Amorese, V., Ciurlia, E., Andreozzi, M., Caggiari, G., Doria, C., 2017. Efficacy of teriparatide vs neridronate in adults with osteogenesis imperfecta type I: a prospective randomized international clinical study. Clin. Cases Miner. Bone Metab. 14, 153−156.

Lee, L.R., Peacock, L., Ginn, S.L., Cantrill, L.C., Cheng, T.L., Little, D.G., Munns, C.F., Schindeler, A., 2019. Bone marrow transplantation for treatment of the col1a2(+/G610C) osteogenesis imperfecta mouse model. Calcif. Tissue Int. 104, 426−436.

Lee, Y.S., Huynh, T.V., Lee, S.J., 2016. Paracrine and endocrine modes of myostatin action. J. Appl. Physiol. 120, 592−598.

Li, H., Jiang, X., Delaney, J., Franceschetti, T., Bilic-Curcic, I., Kalinovsky, J., Lorenzo, J.A., Grcevic, D., Rowe, D.W., Kalajzic, I., 2010. Immature osteoblast lineage cells increase osteoclastogenesis in osteogenesis imperfecta murine. Am. J. Pathol. 176, 2405−2413.

Lim, J., Grafe, I., Alexander, S., Lee, B., 2017. Genetic causes and mechanisms of osteogenesis imperfecta. Bone 102, 40−49.

Lindert, U., Weis, M.A., Rai, J., Seeliger, F., Hausser, I., Leeb, T., Eyre, D., Rohrbach, M., Giunta, C., 2015. Molecular consequences of the SERPINH1/HSP47 mutation in the dachshund natural model of osteogenesis imperfecta. J. Biol. Chem. 290, 17679−17689.

Liu, G., Chen, J., Zhou, Y., Zuo, Y., Liu, S., Chen, W., Wu, Z., Wu, N., 2017. The genetic implication of scoliosis in osteogenesis imperfecta: a review. J. Spine Surg. 3, 666−678.

LoMauro, A., Fraschini, P., Pochintesta, S., Romei, M., D'Angelo, M.G., Aliverti, A., 2018. Ribcage deformity and the altered breathing pattern in children with osteogenesis imperfecta. Pediatr. Pulmonol. 53, 964−972.

Lv, F., Xu, X., Song, Y., Li, L., Asan, Wang, J., Yang, H., Wang, O., Jiang, Y., Xia, W., Xing, X., Li, M., 2018. Novel mutations in PLOD2 cause rare Bruck syndrome. Calcif. Tissue Int. 102, 296−309.

Lykke-Andersen, S., Jensen, T.H., 2015. Nonsense-mediated mRNA decay: an intricate machinery that shapes transcriptomes. Nat. Rev. Mol. Cell Biol. 16, 665−677.

Makino, A., Takagi, H., Takahashi, Y., Hase, N., Sugiyama, H., Yamana, K., Kobayashi, T., 2018. Abaloparatide exerts bone anabolic effects with less stimulation of bone resorption-related factors: a comparison with teriparatide. Calcif. Tissue Int. 103, 289−297.

Makitie, R.E., Kampe, A.J., Taylan, F., Makitie, O., 2017. Recent discoveries in monogenic disorders of childhood bone fragility. Curr. Osteoporos. Rep. 15, 303−310.

Malmgren, B., Andersson, K., Lindahl, K., Kindmark, A., Grigelioniene, G., Zachariadis, V., Dahllof, G., Astrom, E., 2017. Tooth agenesis in osteogenesis imperfecta related to mutations in the collagen type I genes. Oral Dis. 23, 42−49.

Marini, J.C., Forlino, A., Bachinger, H.P., Bishop, N.J., Byers, P.H., Paepe, A., Fassier, F., Fratzl-Zelman, N., Kozloff, K.M., Krakow, D., Montpetit, K., Semler, O., 2017. Osteogenesis imperfecta. Nat. Rev. Dis. Primers 3, 17052.

Marini, J.C., Forlino, A., Cabral, W.A., Barnes, A.M., San Antonio, J.D., Milgrom, S., Hyland, J.C., Korkko, J., Prockop, D.J., De Paepe, A., Coucke, P., Symoens, S., Glorieux, F.H., Roughley, P.J., Lund, A.M., Kuurila-Svahn, K., Hartikka, H., Cohn, D.H., Krakow, D., Mottes, M., Schwarze, U., Chen, D., Yang, K., Kuslich, C., Troendle, J., Dalgleish, R., Byers, P.H., 2007. Consortium for osteogenesis imperfecta mutations in the helical domain of type I collagen: regions rich in lethal mutations align with collagen binding sites for integrins and proteoglycans. Hum. Mutat. 28, 209−221.

Marshall, C., Lopez, J., Crookes, L., Pollitt, R.C., Balasubramanian, M., 2016. A novel homozygous variant in SERPINH1 associated with a severe, lethal presentation of osteogenesis imperfecta with hydranencephaly. Gene 595, 49−52.

Matic, I., Matthews, B.G., Wang, X., Dyment, N.A., Worthley, D.L., Rowe, D.W., Grcevic, D., Kalajzic, I., 2016. Quiescent bone lining cells are a major source of osteoblasts during adulthood. Stem Cells 34, 2930−2942.

Matthews, B.G., Roeder, E., Wang, X., Aguila, H.L., Lee, S.K., Grcevic, D., Kalajzic, I., 2017. Splenomegaly, myeloid lineage expansion and increased osteoclastogenesis in osteogenesis imperfecta murine. Bone 103, 1−11.

McPherron, A.C., Lawler, A.M., Lee, S.J., 1997. Regulation of skeletal muscle mass in mice by a new TGF-beta superfamily member. Nature 387, 83−90.

Mendoza-Londono, R., Fahiminiya, S., Majewski, J., Consortium Care4Rare Canada, Tetreault, M., Nadaf, J., Kannu, P., Sochett, E., Howard, A., Stimec, J., Dupuis, L., Roschger, P., Klaushofer, K., Palomo, T., Ouellet, J., Al-Jallad, H., Mort, J.S., Moffatt, P., Boudko, S., Bachinger, H.P., Rauch, F., 2015. Recessive osteogenesis imperfecta caused by missense mutations in SPARC. Am. J. Hum. Genet. 96, 979−985.

Michalczyk, E.R., Chen, L., Fine, D., Zhao, Y., Mascarinas, E., Grippo, P.J., DiPietro, L.A., 2018. Pigment epithelium-derived factor (PEDF) as a regulator of wound angiogenesis. Sci. Rep. 8, 11142.

Migliaccio, S., Barbaro, G., Fornari, R., Di Lorenzo, G., Celli, M., Lubrano, C., Falcone, S., Fabbrini, E., Greco, E., Zambrano, A., Brama, M., Prossomariti, G., Marzano, S., Marini, M., Conti, F., D'Eufemia, P., Spera, G., 2009. Impairment of diastolic function in adult patients affected by osteogenesis imperfecta clinically asymptomatic for cardiac disease: casuality or causality? Int. J. Cardiol. 131, 200−203.

Millard, S.M., Pettit, A.R., Ellis, R., Chan, J.K., Raggatt, L.J., Khosrotehrani, K., Fisk, N.M., 2015. Intrauterine bone marrow transplantation in osteogenesis imperfecta mice yields donor osteoclasts and osteomacs but not osteoblasts. Stem Cell Reports 5, 682−689.

Mirigian, L.S., Makareeva, E., Mertz, E.L., Omari, S., Roberts-Pilgrim, A.M., Oestreich, A.K., Phillips, C.L., Leikin, S., 2016. Osteoblast malfunction caused by cell stress response to procollagen misfolding in alpha2(I)-G610C mouse model of osteogenesis imperfecta. J. Bone Miner. Res. 31, 1608−1616.

Montpetit, K., Palomo, T., Glorieux, F.H., Fassier, F., Rauch, F., 2015. Multidisciplinary treatment of severe osteogenesis imperfecta: functional outcomes at skeletal maturity. Arch. Phys. Med. Rehabil. 96, 1834−1839.

Morello, R., 2018. Osteogenesis imperfecta and therapeutics. Matrix Biol. 71−72, 294−312.

Muir, A.M., Massoudi, D., Nguyen, N., Keene, D.R., Lee, S.J., Birk, D.E., Davidson, J.M., Marinkovich, M.P., Greenspan, D.S., 2016. BMP1-like proteinases are essential to the structure and wound healing of skin. Matrix Biol. 56, 114−131.

Muir, A.M., Ren, Y., Butz, D.H., Davis, N.A., Blank, R.D., Birk, D.E., Lee, S.J., Rowe, D., Feng, J.Q., Greenspan, D.S., 2014. Induced ablation of Bmp1 and Tll1 produces osteogenesis imperfecta in mice. Hum. Mol. Genet. 23, 3085−3101.

Najirad, M., Ma, M.S., Rauch, F., Sutton, V.R., Lee, B., Retrouvey, J.M., Members of the, B.B.D., Esfandiari, S., 2018. Oral health-related quality of life in children and adolescents with osteogenesis imperfecta: cross-sectional study. Orphanet J. Rare Dis. 13, 187.

Nguyen, M.S., Binh, H.D., Nguyen, K.M., Maasalu, K., Koks, S., Martson, A., Saag, M., Jagomagi, T., 2017. Occlusal features and need for orthodontic treatment in persons with osteogenesis imperfecta. Clin. Exp. Dent. Res. 3, 19−24.

Nicol, L., Morar, P., Wang, Y., Henriksen, K., Sun, S., Karsdal, M., Smith, R., Nagamani, S.C.S., Shapiro, J., Lee, B., Orwoll, E., 2019. Alterations in non-type I collagen biomarkers in osteogenesis imperfecta. Bone 120, 70−74.

Nicol, L., Wang, Y., Smith, R., Sloan, J., Nagamani, S.C., Shapiro, J., Lee, B., Orwoll, E., 2018. Serum sclerostin levels in adults with osteogenesis imperfecta: comparison with normal individuals and response to teriparatide therapy. J. Bone Miner. Res. 33, 307−315.

Nicolaou, N., Agrawal, Y., Padman, M., Fernandes, J.A., Bell, M.J., 2012. Changing pattern of femoral fractures in osteogenesis imperfecta with prolonged use of bisphosphonates. J. Child. Orthopaed. 6, 21−27.

NORD, 2019. National Organization for Rare Diseases. https://rarediseases.org.

O'Donnell, C., Bloch, N., Michael, N., Erickson, M., Garg, S., 2017. Management of scoliosis in children with osteogenesis imperfecta. JBJS Rev. 5, e8.

Oestreich, A.K., Carleton, S.M., Yao, X., Gentry, B.A., Raw, C.E., Brown, M., Pfeiffer, F.M., Wang, Y., Phillips, C.L., 2016. Myostatin deficiency partially rescues the bone phenotype of osteogenesis imperfecta model mice. Osteoporos. Int. 27, 161−170.

OIF, 2019. Osteogenesis Imperfecta Foundation. http://www.oif.org/site/PageServer.

OIF-Testing, 2019. Genetic Testing for OI. http://www.oif.org/site/PageServer?pagename=Testing.

Olvera, D., Stolzenfeld, R., Marini, J.C., Caird, M.S., Kozloff, K.M., 2018. Low dose of bisphosphonate enhances sclerostin antibody-induced trabecular bone mass Gains in Brtl/+ osteogenesis imperfecta mouse model. J. Bone Miner. Res. 33, 1272−1282.

Omata, Y., Nakamura, S., Koyama, T., Yasui, T., Hirose, J., Izawa, N., Matsumoto, T., Imai, Y., Seo, S., Kurokawa, M., Tsutsumi, S., Kadono, Y., Morimoto, C., Aburatani, H., Miyamoto, T., Tanaka, S., 2016. Identification of Nedd9 as a TGF-beta-Smad2/3 target gene involved in RANKL-induced osteoclastogenesis by comprehensive analysis. PLoS One 11, e0157992.

Orwoll, E.S., Shapiro, J., Veith, S., Wang, Y., Lapidus, J., Vanek, C., Reeder, J.L., Keaveny, T.M., Lee, D.C., Mullins, M.A., Nagamani, S.C., Lee, B., 2014. Evaluation of teriparatide treatment in adults with osteogenesis imperfecta. J. Clin. Investig. 124, 491−498.

Otsuru, S., Overholt, K.M., Olson, T.S., Hofmann, T.J., Guess, A.J., Velazquez, V.M., Kaito, T., Dominici, M., Horwitz, E.M., 2017. Hematopoietic derived cells do not contribute to osteogenesis as osteoblasts. Bone 94, 1−9.

Pace, J.M., Wiese, M., Drenguis, A.S., Kuznetsova, N., Leikin, S., Schwarze, U., Chen, D., Mooney, S.H., Unger, S., Byers, P.H., 2008. Defective C-propeptides of the proalpha2(I) chain of type I procollagen impede molecular assembly and result in osteogenesis imperfecta. J. Biol. Chem. 283, 16061−16067.

Pai, A.A., Pritchard, J.K., Gilad, Y., 2015. The genetic and mechanistic basis for variation in gene regulation. PLoS Genet. 11, e1004857.

Palomo, T., Al-Jallad, H., Moffatt, P., Glorieux, F.H., Lentle, B., Roschger, P., Klaushofer, K., Rauch, F., 2014. Skeletal characteristics associated with homozygous and heterozygous WNT1 mutations. Bone 67, 63−70.

Palomo, T., Fassier, F., Ouellet, J., Sato, A., Montpetit, K., Glorieux, F.H., Rauch, F., 2015. Intravenous bisphosphonate therapy of young children with osteogenesis imperfecta: skeletal findings during follow up throughout the growing years. J. Bone Miner. Res. 30, 2150−2157.

Panigrahi, I., Didel, S., Kirpal, H., Bellampalli, R., Miyanath, S., Mullapudi, N., Rao, S., 2018. Novel mutation in a family with WNT1-related osteoporosis. Eur. J. Med. Genet. 61, 369−371.

Pauley, P., Matthews, B.G., Wang, L., Dyment, N.A., Matic, I., Rowe, D.W., Kalajzic, I., 2014. Local transplantation is an effective method for cell delivery in the osteogenesis imperfecta murine model. Int. Orthop. 38, 1955−1962.

Pavone, V., Mattina, T., Pavone, P., Falsaperla, R., Testa, G., 2017. Early motor delay: an outstanding, initial Sign of osteogenesis imperfecta type 1. J. Orthop. Case Rep. 7, 63−66.

Piantoni, L., Noel, M.A., Francheri Wilson, I.A., Tello, C.A., Galaretto, E., Remondino, R.G., Bersusky, E.S., 2017. Surgical treatment with pedicle Screws of scoliosis associated with osteogenesis imperfecta in children. Spine Deform 5, 360−365.

Pollitt, R.C., Saraff, V., Dalton, A., Webb, E.A., Shaw, N.J., Sobey, G.J., Mughal, M.Z., Hobson, E., Ali, F., Bishop, N.J., Arundel, P., Hogler, W., Balasubramanian, M., 2016. Phenotypic variability in patients with osteogenesis imperfecta caused by BMP1 mutations. Am. J. Med. Genet. 170, 3150−3156.

Pouliot-Laforte, A., Veilleux, L.N., Rauch, F., Lemay, M., 2015. Physical activity in youth with osteogenesis imperfecta type I. J. Musculoskelet. Neuronal Interact. 15, 171−176.

Pyott, S.M., Pepin, M.G., Schwarze, U., Yang, K., Smith, G., Byers, P.H., 2011. Recurrence of perinatal lethal osteogenesis imperfecta in sibships: parsing the risk between parental mosaicism for dominant mutations and autosomal recessive inheritance. Genet. Med. 13, 125−130.

Radunovic, Z., Steine, K., 2015. Prevalence of cardiovascular disease and cardiac symptoms: left and right ventricular function in adults with osteogenesis imperfecta. Can. J. Cardiol. 31, 1386−1392.

Radunovic, Z., Wekre, L.L., Diep, L.M., Steine, K., 2011. Cardiovascular abnormalities in adults with osteogenesis imperfecta. Am. Heart J. 161, 523−529.

Ramirez, F., Caescu, C., Wondimu, E., Galatioto, J., 2018. Marfan syndrome; A connective tissue disease at the crossroads of mechanotransduction, TGFbeta signaling and cell stemness. Matrix Biol. 71-72, 82−89.

Rauch, F., Fahiminiya, S., Majewski, J., Carrot-Zhang, J., Boudko, S., Glorieux, F., Mort, J.S., Bachinger, H.P., Moffatt, P., 2015. Cole-Carpenter syndrome is caused by a heterozygous missense mutation in P4HB. Am. J. Hum. Genet. 96, 425−431.

Rauch, F., Geng, Y., Lamplugh, L., Hekmatnejad, B., Gaumond, M.H., Penney, J., Yamanaka, Y., Moffatt, P., 2018. Crispr-Cas9 engineered osteogenesis imperfecta type V leads to severe skeletal deformities and perinatal lethality in mice. Bone 107, 131−142.

Rauch, F., Husseini, A., Roughley, P., Glorieux, F.H., Moffatt, P., 2012. Lack of circulating pigment epithelium-derived factor is a marker of osteogenesis imperfecta type VI. J. Clin. Endocrinol. Metab. 97, E1550−E1556.

Rauch, F., Lalic, L., Roughley, P., Glorieux, F.H., 2010. Relationship between genotype and skeletal phenotype in children and adolescents with osteogenesis imperfecta. J. Bone Miner. Res. 25, 1367−1374.

Rauch, F., Moffatt, P., Cheung, M., Roughley, P., Lalic, L., Lund, A.M., Ramirez, N., Fahiminiya, S., Majewski, J., Glorieux, F.H., 2013. Osteogenesis imperfecta type V: marked phenotypic variability despite the presence of the IFITM5 c.-14C>T mutation in all patients. J. Med. Genet. 50, 21−24.

Rauch, F., Travers, R., Glorieux, F.H., 2006. Pamidronate in children with osteogenesis imperfecta: histomorphometric effects of long-term therapy. J. Clin. Endocrinol. Metab. 91, 511–516.

RDCRN, 2019. Rare Diseases Clinical Research Network. https://ncats.nih.gov/rdcrn.

Retrouvey, J.M., Taqi, D., Tamimi, F., Dagdeviren, D., Glorieux, F.H., Lee, B., Hazboun, R., Krakow, D., Sutton, V.R., Consortium Members of the, B.B.D., 2018. Oro-dental and cranio-facial characteristics of osteogenesis imperfecta type V. Eur. J. Med. Genet. https://doi.org/10.1016/j.ejmg.2018.12.011.

Rosset, E.M., Bradshaw, A.D., 2016. SPARC/osteonectin in mineralized tissue. Matrix Biol. 52–54, 78–87.

Rothschild, L., Goeller, J.K., Voronov, P., Barabanova, A., Smith, P., 2018. Anesthesia in children with osteogenesis imperfecta: retrospective chart review of 83 patients and 205 anesthetics over 7 years. Paediatr. Anaesth. 28, 1050–1058.

Rowe, D.W., Shapiro, J.R., Poirier, M., Schlesinger, S., 1985. Diminished type I collagen synthesis and reduced alpha 1(I) collagen messenger RNA in cultured fibroblasts from patients with dominantly inherited (type I) osteogenesis imperfecta. J. Clin. Investig. 76, 604–611.

Rowe, R.G., Daley, G.Q., 2019. Induced pluripotent stem cells in disease modelling and drug discovery. Nat. Rev. Genet. https://doi.org/10.1038/s41576-019-0100-z.

Ruck, J., Dahan-Oliel, N., Montpetit, K., Rauch, F., Fassier, F., 2011. Fassier-Duval femoral rodding in children with osteogenesis imperfecta receiving bisphosphonates: functional outcomes at one year. J. Child. Orthopaed. 5, 217–224.

Rush, E.T., Li, L., Goodwin, J.L., Kreikemeier, R.M., Craft, M., Danford, D.A., Kutty, S., 2017. Echocardiographic phenotype in osteogenesis imperfecta varies with disease severity. Heart 103, 443–448.

Scheiber, A.L., Guess, A.J., Kaito, T., Abzug, J.M., Enomoto-Iwamoto, M., Leikin, S., Iwamoto, M., Otsuru, S., 2019. Endoplasmic reticulum stress is induced in growth plate hypertrophic chondrocytes in G610C mouse model of osteogenesis imperfecta. Biochem. Biophys. Res. Commun. 509, 235–240.

Schwarze, U., Hata, R., McKusick, V.A., Shinkai, H., Hoyme, H.E., Pyeritz, R.E., Byers, P.H., 2004. Rare autosomal recessive cardiac valvular form of Ehlers-Danlos syndrome results from mutations in the COL1A2 gene that activate the nonsense-mediated RNA decay pathway. Am. J. Hum. Genet. 74, 917–930.

Shapiro, F., 1985. Consequences of an osteogenesis imperfecta diagnosis for survival and ambulation. J. Pediatr. Orthop. 5, 456–462.

Shapiro, J.R., Burn, V.E., Chipman, S.D., Jacobs, J.B., Schloo, B., Reid, L., Larsen, N., Louis, F., 1989. Pulmonary hypoplasia and osteogenesis imperfecta type II with defective synthesis of alpha I(1) procollagen. Bone 10, 165–171.

Shapiro, J.R., Lietman, C., Grover, M., Lu, J.T., Nagamani, S.C., Dawson, B.C., Baldridge, D.M., Bainbridge, M.N., Cohn, D.H., Blazo, M., Roberts, T.T., Brennen, F.S., Wu, Y., Gibbs, R.A., Melvin, P., Campeau, P.M., Lee, B.H., 2013. Phenotypic variability of osteogenesis imperfecta type V caused by an IFITM5 mutation. J. Bone Miner. Res. 28, 1523–1530.

Sinder, B.P., Lloyd, W.R., Salemi, J.D., Marini, J.C., Caird, M.S., Morris, M.D., Kozloff, K.M., 2016. Effect of anti-sclerostin therapy and osteogenesis imperfecta on tissue-level properties in growing and adult mice while controlling for tissue age. Bone 84, 222–229.

Sinikumpu, J.J., Ojaniemi, M., Lehenkari, P., Serlo, W., 2015. Severe osteogenesis imperfecta Type-III and its challenging treatment in newborn and preschool children. A systematic review. Injury 46, 1440–1446.

Song, Y., Zhao, D., Xu, X., Lv, F., Li, L., Jiang, Y., Wang, O., Xia, W., Xing, X., Li, M., 2018. Novel compound heterozygous mutations in SERPINH1 cause rare autosomal recessive osteogenesis imperfecta type X. Osteoporos. Int. 29, 1389–1396.

Sridharan, K., Sivaramakrishnan, G., 2018. Interventions for improving bone mineral density and reducing fracture risk in osteogenesis imperfecta: a mixed treatment comparison Network meta-analysis of randomized controlled clinical trials. Curr. Clin. Pharmacol. 13, 190–198.

Suzumori, N., Hasegawa, T., Sugiura-Ogasawara, M., 2011. Prenatal diagnosis of osteogenesis imperfecta type II by three-dimensional ultrasound and computed tomography. J. Obstet. Gynaecol. Res. 37, 664–665.

Swezey, T., Reeve, B.B., Hart, T.S., Floor, M.K., Dollar, C.M., Gillies, A.P., Tosi, L.L., 2019. Incorporating the patient perspective in the study of rare bone disease: insights from the osteogenesis imperfecta community. Osteoporos. Int. 30, 507–511.

Syx, D., Guillemyn, B., Symoens, S., Sousa, A.B., Medeira, A., Whiteford, M., Hermanns-Le, T., Coucke, P.J., De Paepe, A., Malfait, F., 2015. Defective proteolytic processing of fibrillar procollagens and prodecorin due to Biallelic BMP1 mutations results in a severe, progressive form of osteogenesis imperfecta. J. Bone Miner. Res. 30, 1445–1456.

Tabebordbar, M., Zhu, K., Cheng, J.K.W., Chew, W.L., Widrick, J.J., Yan, W.X., Maesner, C., Wu, E.Y., Xiao, R., Ran, F.A., Cong, L., Zhang, F., Vandenberghe, L.H., Church, G.M., Wagers, A.J., 2016. In vivo gene editing in dystrophic mouse muscle and muscle stem cells. Science 351, 407–411.

Tam, A., Chen, S., Schauer, E., Grafe, I., Bandi, V., Shapiro, J.R., Steiner, R.D., Smith, P.A., Bober, M.B., Hart, T., Cuthbertson, D., Krischer, J., Mullins, M., Byers, P.H., Sandhaus, R.A., Durigova, M., Glorieux, F.H., Rauch, F., Reid Sutton, V., Lee, B., Consortium Members of the Brittle Bone Disorders, Rush, E.T., Nagamani, S.C.S., 2018. A multicenter study to evaluate pulmonary function in osteogenesis imperfecta. Clin. Genet. 94, 502–511.

Thuesen, K.J., Gjorup, H., Hald, J.D., Schmidt, M., Harslof, T., Langdahl, B., Haubek, D., 2018. The dental perspective on osteogenesis imperfecta in a Danish adult population. BMC Oral Health 18, 175.

Trejo, P., Fassier, F., Glorieux, F.H., Rauch, F., 2017a. Diaphyseal femur fractures in osteogenesis imperfecta: characteristics and relationship with bisphosphonate treatment. J. Bone Miner. Res. 32, 1034–1039.

Trejo, P., Palomo, T., Montpetit, K., Fassier, F., Sato, A., Glorieux, F.H., Rauch, F., 2017b. Long-term follow-up in osteogenesis imperfecta type VI. Osteoporos. Int. 28, 2975–2983.

Tsimicalis, A., Boitor, M., Ferland, C.E., Rauch, F., Le May, S., Carrier, J.I., Ngheim, T., Bilodeau, C., 2018. Pain and quality of life of children and adolescents with osteogenesis imperfecta over a bisphosphonate treatment cycle. Eur. J. Pediatr. 177, 891–902.

Ulla, M., Aiello, H., Cobos, M.P., Orioli, I., Garcia-Monaco, R., Etchegaray, A., Igarzabal, M.L., Otano, L., 2011. Prenatal diagnosis of skeletal dysplasias: contribution of three-dimensional computed tomography. Fetal Diagn. Ther. 29, 238–247.

Veilleux, L.N., Lemay, M., Pouliot-Laforte, A., Cheung, M.S., Glorieux, F.H., Rauch, F., 2014. Muscle anatomy and dynamic muscle function in osteogenesis imperfecta type I. J. Clin. Endocrinol. Metab. 99, E356–E362.

Volodarsky, M., Markus, B., Cohen, I., Staretz-Chacham, O., Flusser, H., Landau, D., Shelef, I., Langer, Y., Birk, O.S., 2013. A deletion mutation in TMEM38B associated with autosomal recessive osteogenesis imperfecta. Hum. Mutat. 34, 582–586.

Wallace, M.J., Kruse, R.W., Shah, S.A., 2017. The spine in patients with osteogenesis imperfecta. J. Am. Acad. Orthop. Surg. 25, 100–109.

Wang, J.Y., Liu, Y., Song, L.J., Lv, F., Xu, X.J., San, A., Wang, J., Yang, H.M., Yang, Z.Y., Jiang, Y., Wang, O., Xia, W.B., Xing, X.P., Li, M., 2017. Novel mutations in SERPINF1 result in rare osteogenesis imperfecta type VI. Calcif. Tissue Int. 100, 55–66.

Wang, L., Liu, Y., Kalajzic, Z., Jiang, X., Rowe, D.W., 2005. Heterogeneity of engrafted bone-lining cells after systemic and local transplantation. Blood 106, 3650–3657.

Ward, L.M., Rauch, F., Whyte, M.P., D'Astous, J., Gates, P.E., Grogan, D., Lester, E.L., McCall, R.E., Pressly, T.A., Sanders, J.O., Smith, P.A., Steiner, R.D., Sullivan, E., Tyerman, G., Smith-Wright, D.L., Verbruggen, N., Heyden, N., Lombardi, A., Glorieux, F.H., 2011. Alendronate for the treatment of pediatric osteogenesis imperfecta: a randomized placebo-controlled study. J. Clin. Endocrinol. Metab. 96, 355–364.

Webb, E.A., Balasubramanian, M., Fratzl-Zelman, N., Cabral, W.A., Titheradge, H., Alsaedi, A., Saraff, V., Vogt, J., Cole, T., Stewart, S., Crabtree, N.J., Sargent, B.M., Gamsjaeger, S., Paschalis, E.P., Roschger, P., Klaushofer, K., Shaw, N.J., Marini, J.C., Hogler, W., 2017. Phenotypic spectrum in osteogenesis imperfecta due to mutations in TMEM38B: unraveling a complex cellular defect. J. Clin. Endocrinol. Metab. 102, 2019–2028.

Westgren, M., Gotherstrom, C., 2015. Stem cell transplantation before birth - a realistic option for treatment of osteogenesis imperfecta? Prenat. Diagn. 35, 827–832.

Wright, N.M., 2000. Just taller or more bone? The impact of growth hormone on osteogenesis imperfecta and idiopathic juvenile osteoporosis. J. Pediatr. Endocrinol. Metab. 13 (Suppl. 2), 999–1002.

Xin, X., Kronenberg, M., Chen, L., Wu, Z., Wang, L., Jiang, X., Rowe, D.W., Lichtler, A., 2017. Mutation Correction in OI iPSCs Restores Bone Formation. http://www.asbmr.org/education/AbstractDetail?aid=47690120-1c03-4151-a399-7ea0b7bab156.

Xin, X., Kronenberg, M., Lichtler, A., Rowe, D.W., 2018a. Continued development of hiPSCs as an in vivo platform for exploring heritable disorders of the human skeleton. J. Bone Miner. Res. 33.

Xin, X., Jiang, X., Lichtler, A., Kronenberg, M., Rowe, D., Pachter, J.S., 2018b. Laser-capture microdissection and RNA extraction from perfusion-fixed cartilage and bone tissue from mice implanted with human iPSC-derived MSCs in a calvarial defect model. Methods Mol. Biol. 1723, 385–396.

Xu, X.J., Lv, F., Song, Y.W., Li, L.J., Asan, Wei, X.X., Zhao, X.L., Jiang, Y., Wang, O., Xing, X.P., Xia, W.B., Li, M., 2019. Novel mutations in BMP1 induce a rare type of osteogenesis imperfecta. Clin. Chim. Acta 489, 21–28.

Yamagishi, S., Matsui, T., Nakamura, K., Takenaka, K., 2010. Pigment epithelium-derived factor (PEDF) inhibits collagen-induced platelet activation by reducing intraplatelet nitrotyrosine levels. Int. J. Cardiol. 140, 121–122.

Yasui, T., Kadono, Y., Nakamura, M., Oshima, Y., Matsumoto, T., Masuda, H., Hirose, J., Omata, Y., Yasuda, H., Imamura, T., Nakamura, K., Tanaka, S., 2011. Regulation of RANKL-induced osteoclastogenesis by TGF-beta through molecular interaction between Smad3 and Traf6. J. Bone Miner. Res. 26, 1447–1456.

Zack, P., Franck, L., Devile, C., Clark, C., 2005. Fracture and non-fracture pain in children with osteogenesis imperfecta. Acta Paediatr. 94, 1238–1242.

Zhang, Z.L., Zhang, H., Ke, Y.H., Yue, H., Xiao, W.J., Yu, J.B., Gu, J.M., Hu, W.W., Wang, C., He, J.W., Fu, W.Z., 2012. The identification of novel mutations in COL1A1, COL1A2, and LEPRE1 genes in Chinese patients with osteogenesis imperfecta. J. Bone Miner. Metab. 30, 69–77.

Zimmerman, S.M., Heard-Lipsmeyer, M.E., Dimori, M., Thostenson, J.D., Mannen, E.M., O'Brien, C.A., Morello, R., 2018. Loss of RANKL in osteocytes dramatically increases cancellous bone mass in the osteogenesis imperfecta mouse (oim). Bone Rep. 9, 61–73.

Further reading

Treatment, O.I.F., 2017. Treatment Recommendation from OIF. http://www.oif.org/site/PageServer?pagename=oif_mc_home_page.

Chapter 62

Hereditary deficiencies in vitamin D action

Uri A. Liberman

Department of Physiology and Pharmacology, Sackler Faculty of Medicine, Tel Aviv University, Tel-Aviv, Israel

Chapter outline

Introduction

Hereditary deficiencies in vitamin D action can be caused by disturbances in the synthesis or degradation of the hormonal form of the vitamin 1,25-dihydroxyvitamin D (1,25$(OH)_2$D, calcitriol) or defects in the interaction of calcitriol and its target tissues.

Vitamin D derived from endogenous production in the skin or absorbed from the gut is transformed into its active form by two successive steps: (1) hydroxylation in the liver to 25-hydroxyvitamin D [25(OH)D] and (2) 1α-hydroxylation in the renal proximal tubule to 1,25$(OH)_2$D. Some other cells exhibit 1α-hydroxylase activity: placental decidual cells, keratinocytes, macrophages of various origins, and some tumor cells. The role of the extrarenal production of 1,25$(OH)_2$D is unknown, and under normal conditions it does not significantly contribute to circulating levels of the hormone. Hydroxylation at carbon 24, to produce 24, 25-dihydroxyvitamin D [24,25$(OH)_2$D] or 1,24,25-trihydroxyvitamin D is performed in a wide range of normal tissues and is believed to be important in the removal of vitamin D metabolites. All these enzymes are mitochondrial mixed-function oxidases containing cytochrome P450 and having ferredoxin- and heme-binding domains (CYP enzyme system). Cloning of cDNA for porcine 25-hydroxylase and the mouse, rat, and human 24- and 1-hydroxylase, as well as the genes for the latter two enzymes, has been reported (Akeno et al., 1997; Fu et al., 1997a; Jehan et al., 1998; Jones et al., 1999; Monkawa et al., 1997; Murayama et al., 1999; Ohyama et al., 1993; Shinki et al., 1997; Takeyama et al., 1997). Hereditary defects along the cascade of 1,25$(OH)_2$D synthesis or degradation lead to a deficiency in the vitamin D hormonal form—i.e., low to undetectable circulating levels of calcitriol. All patients with these

Principles of Bone Biology. https://doi.org/10.1016/B978-0-12-814841-9.00062-2

defects will experience complete cure of all clinical and radiological signs and symptoms of their hypocalcemic rickets as well as biochemical aberrations on high doses of vitamin D, and for the hereditary defects in calcitriol biosynthesis it could be achieved by physiological replacement doses of calcitriol—the hormonally active form of vitamin D. Continuous treatment is necessary to keep patients in remission. As far as bone deformities are concerned, they depend on the age when treatment is initiated. In view of the foregoing, it is suggested that the name allocated to this group of hereditary deficiencies more than 50 years ago, hereditary vitamin D–dependent rickets (HVDDR), should be retained, with an additional letter to denote the functional defect—i.e., HVDDR type A (HVDDR-A) to specify a defect in the 25-hydroxyvitamin D 1-alpha hydroxylase (CYP27B1); HVDDR-B to define a defect in the vitamin D 25-hydroxylase (CYP2R1), and HVDDR-C for defects causing increased degradation of calcitriol (CYP3R1).

Regarding defects in the interaction of calcitriol with its target tissue, as detailed elsewhere in this book, calcitriol effects are mediated via a high-affinity intracellular receptor, the vitamin D receptor (VDR). VDR acts as a ligand-modulated transcription factor that belongs to the steroid, thyroid, and retinoic acid receptors gene family (Baker et al., 1988; Burmester et al., 1988; Evans, 1988; Ozur et al., 1991). Thus, hereditary defects in the interaction of calcitriol and its target tissues could evolve from defects in hormone binding to VDR, defects in the heterodimerization with retinoid X receptor (RXR), the interaction of the receptor complexes with particular regions of DNA known as vitamin D–response elements (VDREs) that regulate the activity of vitamin D–responsive genes, or defects in translational or posttranslational modulatory functions. Patients with hereditary defects in the interaction of calcitriol and its target tissues have elevated to extremely high circulating levels of $1,25(OH)_2D$ (depending on previous treatment), and the majority of patients do not respond to treatment with any dose of vitamin D or its active 1-alpha hydroxylated metabolites. Based on the foregoing, it is suggested that this group of hereditary deficiencies in vitamin D be called hereditary calcitriol-resistant rickets (HCRR). All of these isolated deficiencies are very rare and usually autosomal recessive.

Though VDRs were demonstrated in most if not all tissues, leading to increased recognition of multiple target organs and actions of the hormone, it seems that most if not all clinical signs and symptoms associated with deficient vitamin D actions are caused by perturbations in mineral metabolism.

$1,25(OH)_2D$ is the most powerful physiological agent that stimulates active transport of calcium, and to a lesser degree phosphorus and magnesium, across the small intestine (DeLuca, 1984; Mayer et al., 1984). Thus, deficiencies in vitamin D action will lead to a decrease in the net flux of mineral to the extracellular compartment, causing hypocalcemia and secondary hyperparathyroidism. Hypophosphatemia will ensue as a result of both reduced absorption of phosphorus owing to deficient calcitriol action on the gut and increased renal phosphate clearance owing to secondary hyperparathyroidism. Low concentrations of calcium and phosphorus in the extracellular fluid will lead to defective mineralization of organic bone matrix. Defective bone matrix mineralization of the newly formed bone and growth plate cartilage will produce the characteristic morphological and clinical signs and symptoms of rickets, whereas at sites of bone remodeling, it will cause osteomalacia. Deficiencies in vitamin D action may impair the differentiation of osteoblasts and thus their functional capacity to mineralize bone matrix; this may be an additional mechanism leading to rickets and osteomalacia (Owen et al., 1991; Reichel et al., 1989).

Because all hereditary deficiencies in vitamin D action will lead to the same clinical, radiological, and histological aberrations as well as most biochemical ones, those common features will be discussed first.

Clinical features of rickets and osteomalacia

Children with hereditary deficiencies in vitamin D action appear normal at birth and usually develop the characteristic features of rickets within the first 2 years of life. Defects in bone mineralization are particularly evident in regions of rapid bone growth including, during the first year of life, the cranium, wrist, and ribs. Rickets at this time will lead to widened cranial sutures, frontal bossing, posterior flattening of the skull (craniotabes), bulging of costochondral junction (rachitic rosary), indentation of the ribs at the diaphragmatic insertion (Harrison's groove), and widening of the wrists. After the first year of life with the acquisition of erect posture and rapid linear growth, the deformities are most severe in the legs. Bow legs (genu varum) or knock-knee (genu valgum) deformities of varying severity develop as well as widening of the ends of long bones. If not treated, rickets may cause severe lasting deformities, compromise adult height, and increase susceptibility to pathological fractures.

The specific radiographic features of rickets reflect the failure of cartilage calcification and endochondral ossification and therefore are best seen in the metaphysis of rapidly growing bones. The metaphyses are widened, uneven, concave, or cupped, and because of the delay in or absence of calcification, the metaphyses could become partially or totally invisible (Fig. 62.1). In more severe forms or in patients untreated for prolonged periods, rarefaction and thinning of the cortex of the entire shaft, as well as bone deformities and greenstick fractures, will become evident.

FIGURE 62.1 Radiographs of wrists and hands of a patient with hereditary vitamin D–dependent rickets. Note the signs of severe rickets and demineralization.

The clinical features of osteomalacia are subtle and could be manifested as bone pain or low-back pain of varying severity in some cases. The first clinical presentation could be an acute fracture of the long bones, pubic rami, ribs, or spine. The radiographic manifestations could be mild—e.g., generalized, nonspecific osteopenia—or more specific, such as pseudofractures commonly seen at the medial edges of long bone shafts.

In hypocalcemic rickets and/or osteomalacia, as is the case in deficiencies in vitamin D action, radiographic features of secondary hyperparathyroidism such as subperiosteal resorption and cysts of the long bones may exist.

The characteristic histological feature of rickets and osteomalacia is deficiency or lack of mineralization of the organic matrix of bone. Because in clinical practice a bone specimen can be obtained only from the iliac crest, the histological picture is osteomalacia. Osteomalacia is defined as excess osteoid (hyperosteoidosis) and quantitative dynamic proof of defective bone matrix mineralization obtained by analysis of time-spaced tetracycline labeling (Parfitt, 1983; Teitelbaum and Bollough, 1979).

The biochemical parameters characterizing deficiencies in vitamin D action can be divided into those associated with vitamin D status, the primary disturbance in mineral homeostasis and the respective compensatory mechanisms, and changes in bone metabolism. Changes in mineral and bone metabolism will be similar in all states of deficient vitamin D action, whereas serum levels of vitamin D metabolites will characterize each of the two classes delineated in the introduction (Table 62.1).

TABLE 62.1 Biochemical features of hereditary vitamin D–dependent rickets (HVDDR) types A, B, and C and hereditary calcitriol-resistant rickets (HCRR).

	Serum concentrations					
	Calcium	Phosphorus	Alkaline phosphatase	iPTH	25(OH)D	$1,25(OH)_2D$
HVDDR						
Type A	↓	↓	↑	↑	N–↑	↓
Type B	↓	↓	↑	↑	↓	↓
Type C	↓	↓	↑	↑	↓	↓
HCRR	↓	↓	↑	↑	N–↑	↑

As previously discussed, deficiencies in vitamin D action will lead to hypocalcemia and secondary hyperparathyroidism. Thus, the characteristic biochemical features are low to low-normal concentrations of serum calcium (depending on compensatory parathyroid activity), low urinary calcium excretion, hypophosphatemia, increased serum parathyroid hormone (iPTH) levels, and decreased tubular reabsorption of phosphate (the last measure reflects the biological activity of elevated iPTH). Biochemical markers associated with increased osteoid production, such as bone-specific alkaline phosphatase and osteocalcin, will be elevated in states of rickets and osteomalacia (Cole et al., 1985). However, as $1,25(OH)_2D$ stimulates osteocalcin synthesis in vivo and in vitro, serum levels of this biochemical bone marker are unreliable measures in hereditary vitamin D–deficient states.

Hereditary vitamin D–dependent rickets

Genetic defects in the biosynthesis or degradation of 1,25-dihydroxycholecalciferol cause deficiencies in the biological active hormonal form of vitamin D. All of these patients will suffer from hypocalcemic rickets with the typical clinical and radiological signs and symptoms, as well as the classical aberrations in mineral homeostasis, as discussed previously. All patients with HVDDR could be completely cured by massive doses (50,000 IU/day or higher) of vitamin D. In patients with genetic defects in calcitriol biosynthesis, complete cure could be achieved as well by physiological replacement doses (0.25–2 μg/day) of calcitriol. Remission is dependent on continuous treatment as detailed above, thus the name vitamin D–dependent rickets. These defects in the activities of enzymes belonging to the CYP family system are the end result of mutations in different genes that encode the enzymes involved in the biosynthesis and catabolism of calcitriol:

a. kidney mitochondrial CYP27B1; it is suggested that the disease associated with such a defect be called HVDDR-A
b. liver microsomal enzyme CYP2R1; it is suggested that the disease caused by such a deficiency be called HVDDR-B
c. the enzyme that controls degradation of calcitriol and 25-hydroxy vitamin D (CYP3A4) increased activity; it is suggested that the hereditary disease caused by such activity be called HVDDR-C

Hereditary vitamin D–dependent rickets type A

HVDDR-A results from hereditary deficiencies in the biosynthesis of 1,25-dihydroxy vitamin D caused by mutations in the gene encoding the renal mitochondrial enzyme 25-hydroxy vitamin D 1-alpha hydroxylase (CYP27B1). This is a rare defect but may be more common in genetically isolated populations, a result of a founder effect, as is the case in some French-Canadian communities. Prader et al. (1961) were the first to describe two young children who showed all the usual clinical features of vitamin D deficiency despite adequate intake of the vitamin, thus coining the name "pseudovitamin D deficiency." Complete remission depended on continuous therapy with high doses of vitamin D, thus the term "vitamin D–dependent rickets." However, remission of the disease could be achieved by continuous therapy with physiological (microgram) doses of calcitriol or its active 1α-hydroxylated vitamin D metabolites (Delvin et al., 1981; Fraser et al., 1973; Miller, 2017).

Family studies have revealed that HVDDR-A is an autosomal recessive disease. Linkage analysis in a subset of French-Canadian families assigned the gene responsible for the disease to chromosome 12q13 (De Brackeleer and Larochell, 1991; Labuda et al., 1990). The gene encoding the 1α-hydroxylase of mouse kidney, human keratinocyte, and peripheral mononuclear cells was localized on chromosome 12q13.1-q13.3, which maps to the disease locus of HVDDR-A (Fu et al., 1997b; Kitanaka et al., 1998; Smith et al., 1999; St. Arnaud et al., 1997, Wang et al., 1998; Yoshida et al., 1998). There are no direct measures of the renal enzyme proving defective 1α-hydroxylase activity. This is virtually impossible to obtain because of both the difficulty in obtaining tissue and the low level of expression. There are, however, several indirect observations to support this etiology. First, circulating levels of 25-hydroxyvitamin D (25(OH)D) are normal or elevated, depending on previous vitamin D treatment. Second, serum concentrations of $1,25(OH)_2D$ are very low (see Table 62.1). Third, although massive doses (100–300 times the daily recommended dose) of vitamin D or 25(OH)D are required to maintain the remission of rickets, and physiological replacement doses of calcitriol are sufficient to achieve the same effect. Fourth, it was reported that cells isolated from the placenta of two women with this disease had deficient activity of the decidual enzyme 25(OH)D-1α-hydroxylase (Glorieux et al., 1995). It is noteworthy that human decidual cells do produce $1,25(OH)_2D$ and that this enzyme was regulated by feedback mechanisms (Delvin and Arabian, 1987; Diaz et al., 2000; Weisman et al., 1979). Finally, the 1α-hydroxylase gene from more than 100 families with HVDDR-A, and some of their first-degree healthy relatives were analyzed by direct sequencing, site-directed mutagenesis, and cDNA expression in transfected cells (Fu et al., 1997; Kitanaka et al., 1998–1999; Smith et al., 1999; St. Arnaud et al., 1997; Wang et al., 1998; Yoshida et al., 1998). All patients had homozygous mutations, whereas parents and other healthy siblings were

heterozygous for the mutation. Most patients of French-Canadian origin had the same mutation causing a frameshift and a premature stop codon in the putative heme-binding domain. The same mutation was observed in additional families of diverse origins (Smith et al., 1999). All other patients had either a base-pair deletion causing premature termination codon upstream from the putative ferredoxin and heme-binding domains, or missense mutations (Fu et al., 1997b; Kitanaka et al., 1999; Smith et al., 1999; Wang et al., 1998; Yoshida et al., 1998). No 1α-hydroxylase activity was detected when the mutant enzyme was expressed in various cells. The sequence of the human 1α-hydroxylase gene from keratinocytes and peripheral blood mononuclear cells has been shown to be identical with that of the renal gene (Fu et al., 1997b; Kitanaka et al., 1999; Smith et al., 1999; Wang et al., 1998; Yoshida et al., 1998), thus supporting the use of these accessible cells as a proxy to study the renal tubular enzymatic defect. Taken together, these observations support the notion that the etiology of this hereditary disease is a defect in renal tubular 25(OH)D-1α-hydroxylase activity.

The beneficial therapeutic effect of high serum concentrations of 25(OH)D in patients treated with massive doses of vitamin D while $1,25(OH)_2D$ levels remain low may have several possible explanations. First, high levels of 25-(OH)D may activate VDR, whose affinity for this metabolite is approximately two orders of magnitude lower than for $1,25(OH)_2D$. Second, a metabolite of 25(OH)D may act directly on target tissues. Finally, high levels of 25(OH)D may drive the local production of $1,25(OH)_2D$ via a paracrine−autocrine pathway, assuming that the tissue enzyme is controlled differently than the renal and decidual enzyme.

Hereditary vitamin D−dependent rickets type B

Serum concentrations of 25-hydroxy vitamin D [25(OH)D] reflect vitamin D status because 25(OH)D is the principal circulating form of vitamin D produced in the skin and ingested in the diet. It is an intermediate metabolite that serves as a reservoir for the highly regulated kidney production of the active hormonal form of vitamin D (calcitriol, $1,25(OH)_2D$). Some human enzymes possess vitamin D-25 hydroxylase activity, but current evidence indicates that the liver microsomal cytochrome P450 enzyme CYP2R1 is the principal vitamin D 25-hydroxylase in humans. A possible genetic defect in 25-hydroxylase as a cause of hereditary rickets was first reported in 1994 in two brothers of Nigerian descent (Casella et al., 1994). Both children had rickets associated with low 25(OH)D circulating levels at baseline. Relatively high doses of vitamin D restored serum levels of 25(OH)D toward normal, but somewhat lowering vitamin D intake caused a recurrent reduction in 25(OH)D levels. The authors concluded that the children had an inherited defect in 25(OH)D synthesis from parent vitamin D. In the last few years, additional reports and studies, including DNA sequencing of children with hereditary familial hypocalcemic rickets with low serum levels of 25(OH)D and no response to physiological doses of vitamin D, were published (Al Mutair et al., 2012; Thacher et al., 2015; Thacher and Levine, 2017; Miller, 2017). Most of these children were of Nigerian origin except for one family of Saudi Arabian descent (Al Mutair et al., 2012). Genomic DNA from 39 Nigerian children with rickets was extracted, amplified, and sequenced. The subjects included children with sporadic rickets and 12 children with one or more first-degree relatives having a history compatible with rickets in the past—so-called familial rickets. Of the 12 patients with familial rickets, 2 families had missense mutations in the gene encoding CYP2R1 (the main 25-hydroxylase enzyme). One mutation caused a substitution of proline for leucine at position 99 of the encoded pattern (L99P). Leucine is a conserved amino acid in the CYP2R1 of humans, mouse, and rat. It is predicted that this mutation impairs CYP2R1 folding. The patients with rickets were homozygous for this mutation. As was previously reported in an unrelated child of Nigerian origin with rickets, heterozygous patients did not have rickets. In the second family, including three children with rickets who were heterozygous to the L99P mutation, a second missense mutation originating from the mother was revealed. In this mutation, lysine in position 242 of the enzyme was replaced by asparagine. This mutation is predicted to impair the interaction of CYP2R1 with its substrate (vitamin D). No mutation was observed in the Nigerian children with sporadic rickets. The Saudi children were found to have compound heterozygous mutations of CYP2R1. One mutation, inherited from the father, was in a highly conserved splice down sequence that controls mRNA slicing. This mutation is predicted to lead to a truncated CYP2R1 protein or unstable mRNA. The second mutation, inherited from the mother, was a thymine insertion in exon 3 that is predicted to produce a truncated CYP2R1 protein.

Various functional activities were measured in vitro in transfected cells and revealed the relationship between the mutation and biological−biochemical effects.

Hereditary vitamin D−dependent rickets type C

Two unrelated female patients from nonconsanguineous families with early-onset rickets were recently described (Roizen et al., 2018). Both patients had detectable serum vitamin D but low circulating concentrations of 25-hydroxy vitamin D and

1,25-dihydroxy vitamin D that increased only after administration of very large doses of vitamin D and declined rapidly thereafter. There was no family history of rickets and all available first-degree relatives had normal circulating vitamin D metabolites as well as serum levels of calcium, phosphorous, PTH, and alkaline phosphatase. Targeted sequencing did not reveal mutations in any gene that is involved in vitamin D biosynthesis or action. Whole-exome sequencing analysis performed in the patients and their parents revealed recurrent de novo gain-of-function missense mutation in CYP3A4, a P450 enzyme that metabolizes many xenobiotics and drugs. An identical heterozygous single-nucleotide change that results in replacement of isoleucine by threonine at codon 301 was found only in the two patients and not in any available relative who was unaffected. Isoleucine 301 is highly conserved and forms a critical position of substrate recognition site 4 that determines CYP3A4 substrate selectivity. Replacement of isoleucine by threonine in position 301 substantially increases oxidation of 25-hydroxy vitamin D and 1,25-dihydroxy vitamin D. In vitro, the mutant CYP3A4 oxidized $1,25(OH)_2D$ with 10-fold greater activity than the wild-type CYP3A4 and twofold greater activity than CYP24A1, the principal inactivator of vitamin D metabolites. The CYP3A4 mutant may have changes in activity for other substrates not connected to vitamin D.

This is a third form of HVDDR, suggested to be called HVDDR-C. Similar to the other forms, it is caused by a deficiency in the hormonal form of vitamin D ($1,25(OH)_2$ vitamin D), it could be cured by high doses of vitamin D or its active metabolites, and remission is dependent on continuous treatment. However, as distinct from HVDDR-A and HVDDR-B, in which the deficiency of the hormone is caused by defects in biosynthesis, HVDDR-C is the end result of high degradation rates of calcitriol and its precursor. These findings raise an interesting possible function of vitamin D catabolism as a regulator of vitamin D status.

Diagnosis and treatment

The differential diagnosis of the various forms of hereditary hypocalcemic rickets is based on serum concentrations of $1,25(OH)_2$ vitamin D and 25(OH) vitamin D; the changes in serum concentration of these metabolites following a bolus administration of vitamin D, and the response to treatment with vitamin D or its active metabolites. The active metabolites include calcitriol and/or a synthetic 1-alpha hydroxylated form of vitamin D that requires hepatic 25-hydroxylation (not tightly controlled) to become fully active.

Based on etiology and pathogenesis, the various forms of hereditary hypocalcemic rickets just discussed include defects in the biosynthesis of calcitriol (HVDDR-A and HVDDR-B), its degradation (HVDDR-C), and defects in the vitamin D receptor–effector system, suggested to be called hereditary calcitriol-resistant rickets, or HCRR, discussed later in this manuscript (Table 62.2).

Circulating levels of $1,25(OH)_2$ vitamin D are low to undetectable in HVDDR-A and HVDDR-C and may be low to normal in HVDDR-B. However, normal serum levels of $1,25(OH)_2D$ could be considered inappropriately low in face of the marked secondary hyperparathyroidism recorded in these patients. In all patients with HCRR, serum concentrations of

TABLE 62.2 Response to treatment of patients with hereditary vitamin D–dependent rickets (HVDDR) types A, B, and C and hereditary calcitriol-resistant rickets (HCRR).

	Vitamin D		1α-Hydroxylated active vitamin D metabolites	
	Physiological	Pharmacological	Physiological	Pharmacological
HVDDR				
Type A	2	1	1	Toxic
Type B	2	1	1	Toxic
Type C	2	1	2	1
HCRR	2	1 or 2	2	1 or 2

Note. Physiological doses are those recommended or being used as replacement therapy. Pharmacological doses are 100 times or more than physiological doses (see details in text).
1—a positive response; a "positive response" means complete remission of skeletal signs and symptoms as well as aberrations in mineral metabolism.
2—no response.

$1,25(OH)_2D$ are high to very high (the highest values one can measure in a biological system), usually when the patients are on very high doses of vitamin D and its active 1-alpha hydroxylated metabolites.

Circulating levels of 25(OH) vitamin D are low to undetectable in HVDDR-B and HVDDR-C and normal to elevated in HVDDR-A (depending on previous or concomitant therapy with vitamin D). Serum 25(OH)D levels in patients with HCRR reflect vitamin D therapy and usually are high. One has to keep in mind that in HCRR there is no defect in vitamin D metabolism, and serum levels reflect drugs administered or secondary changes in mineral homeostasis.

A vitamin D loading test is not used very often. It consists of the administration of a high bolus dose, usually 50,000 IU of vitamin D_3 or D_2, followed by measuring the serum levels of 25(OH) vitamin D from the third day. In HVDDR-B and HVDDR-C, baseline values of 25(OH) vitamin D are low and the response is blunted. In HVDDR-A and HCRR, it is supposed to be normal.

The diagnostic possibility of a form of HVDDR or HCRR must be considered in patients with the clinical and radiological signs and symptoms, and biochemical aberrations, compatible with early-onset hypocalcemic rickets with no history of vitamin D deficiency and no response to vitamin D administration in doses recommended for vitamin D–deficiency rickets.

Response to treatment is measured by changes in clinical and radiological signs and symptoms of rickets, normalization of biochemical aberrations in mineral and bone metabolism, and catch-up growth in the long run.

High to very high doses of vitamin D will completely cure all patients with HVDDR, with remission dependent on continuous treatment. Patients with HVDDR-A and HVDDR-B could be cured and maintained in remission by physiological replacement doses (0.25–2 μg/day) of the active hormonal form of vitamin D ($1,25(OH)_2$ vitamin D) or its synthetic 1-alpha hydroxylated metabolite (not available in the USA) in doses of 1–3 μg/day. Less than 50% of patients with HCRR will respond to any treatment with very high doses of vitamin D or its active 1-alpha hydroxylated metabolites. Patients with HVDDR-C (only two patients with this defect were reported) were cured by very high doses of vitamin D (50,000 IU/day) or its 1-alpha hydroxylated metabolites.

Needless to say, the aim of treatment in patients with hereditary hypocalcemic rickets, as in all patients with hypocalcemic rickets, is to keep extracellular calcium and phosphorous concentrations in a range that enables normal mineralization of newly formed organic bone and matrix. Thus, there is a need to provide calcium supplementation in doses adapted individually depending on age, rate of mineralization, existing osteoid, etc.

Treatment with high doses of vitamin D or its 1-alpha hydroxylated active metabolites in some patients, as well as calcium supplementation, needs close monitoring of serum calcium, phosphorous, PTH, and bone biochemical markers as well as measurements of 24-hour urinary calcium and creatinine excretion. This is aimed to follow the response to treatment and possible side effects related to high serum calcium concentration or hypercalciuria. The frequency of clinical and biochemical monitoring after the patient stabilizes, and the achievement of bone cure could be reduced accordingly.

A similar syndrome has been described and studied in a mutant strain of pigs, where the mode of inheritance and clinical and biochemical features are similar to those of the human disease (Fox et al., 1985; Harmeyer et al., 1982). Piglets affected by the disease have rickets, elevated 25(OH)D with low or undetectable $1,25(OH)_2D$ serum concentrations, normal specific tissue-binding sites for tritiated $1,25(OH)_2D$, and no detectable activity of 25(OH)D-1α-hydroxylase in renal cortical homogenates. Thus, there is strong evidence that the disease state in the pig is caused solely by an inherited defect in the renal enzyme.

Hereditary defects in the vitamin D receptor–effector system, or hereditary calcitriol-resistant rickets

Introduction

This is a rare disorder, and less than 100 patients have been reported (Balsan et al., 1983; Bear et al., 1981; Brooks et al., 1978; Castells et al., 1986; Chen et al., 1984, 2003; Clemens et al., 1983; Cockerill et al., 1997; Eil et al., 1981; Feldman et al., 1982; Fraher et al., 1986; Fujita et al., 1980; Griffin and Zerwekh, 1983; Hawa et al., 1996; Hewison et al., 1993; Hirst et al., 1985; Hochberg et al., 1984; Liberman et al., 1980, 1983b; Lin and Uttley, 1993; Lin et al., 1996; Malloy et al., 1997, 1999, 2001, 2002, 2002a, 2004, 2010, 2012; Marx et al., 1978, 1984; Mechica et al., 1997; Nguyen et al., 2002, 2006; Rosen et al., 1979; Saijo et al., 1991; Simonin et al., 1992; Sockalosky et al., 1980; Takeda et al., 1986, 1987, 1989; Tauchiya et al., 1980; Yagi et al., 1993; Whitfield et al., 1996; Zhu et al., 1998; and personal communications).

Brooks et al. (1978) described an adult patient with hypocalcemic osteomalacia and elevated serum concentration of $1,25(OH)_2D$. Treatment with vitamin D, causing a further increase in serum calcitriol levels, cured the patient. The term vitamin D–dependent rickets type II was suggested to describe this disorder. However, reports on additional patients,

slightly more than half of whom did not respond to any vitamin D therapy, as well as in vivo and in vitro studies to be discussed later, seem to prove that vitamin D dependency is a misnomer. The term hereditary defects in the vitamin D receptor–effector system, or hereditary calcitriol-resistant rickets (the abbreviation HCRR is suggested), is therefore more appropriate to describe the etiology and pathogenesis of this syndrome.

Clinical and biochemical features

General features

The clinical, radiological, histological, and biochemical features (except serum levels of vitamin D metabolites) are typical of hypocalcemic rickets and/or osteomalacia as previously discussed. Notable exceptions are two unrelated patients with hyperphosphatemia despite elevated serum levels of iPTH (Liberman et al., 1980; Yagi et al., 1993), which can be the end result of long-standing and severe hypocalcemia that paradoxically inhibits the phosphaturic response to PTH or represents an additional hereditary renal tubular defect.

In HCRR, there is no history of vitamin D deficiency and no clinical or biochemical response to physiological doses of vitamin D or its 1α-hydroxylated active metabolites. Serum levels of 25(OH)D are normal or elevated (depending on previous vitamin D therapy); $1,25(OH)_2D$ concentrations are markedly elevated before or during therapy with vitamin D preparations; and 24,25-dihydroxyvitamin D ($24,25(OH)_2D$) circulating levels, when measured, are inappropriately low (see Table 62.1).

The disease manifests itself as an active metabolic bone disease in early childhood. However, late onset at adolescence and adulthood was documented in several sporadic cases including the first reports by Brooks et al. (1978) and Fujita et al. (1980). These patients represented the mildest form of the disease and had complete remission when treated with vitamin D or its active metabolites. It is unclear whether the adult-onset patients belonged to the same hereditary entity because no further studies on their VDR status have been published.

Ectodermal anomalies

A peculiar clinical feature of HCRR patients, appearing in approximately half of the subjects, is total alopecia or sparse hair (Fig. 62.2). Alopecia usually appears during the first year of life, and in one patient at least, has been associated with additional ectodermal anomalies (Liberman et al., 1980). It seems that alopecia is a marker of a more severe form of the disease as judged by the earlier onset, severity of clinical features, proportion of patients who do not respond to treatment with high doses of vitamin D or its active metabolites, and extremely elevated levels of serum $1,25(OH)_2D$ recorded during therapy (Marx et al., 1984, 1986). Though some patients with alopecia could achieve clinical and biochemical remission of their bone disease, none have shown hair growth. The notion that total alopecia is probably a consequence of a defective vitamin D receptor–effector system is supported by the following: alopecia has only been associated with hereditary defects in the VDR system—i.e., with end-organ resistance to the action of the hormone—and has not been recorded with hereditary deficiency in $1,25(OH)_2D$ synthesis (i.e., low circulating levels of the hormone); alopecia is present in kindreds with different defects in VDRs; high-affinity uptake of tritiated $1,25(OH)_2D_3$ in the nucleus of the outer root sheath of the hair follicle of rodents has been demonstrated by autoradiography (Strumpf et al., 1979); and the epidermis and hair follicle contain a calcium-binding protein that is partially vitamin D–dependent (Marx et al., 1984). Finally, alopecia develops in homozygote VDR knockout mice (Li et al., 1997; Yoshizawa et al., 1997). Taken together, it could be hypothesized that an intact VDR–effector system is important for differentiation of the hair follicle in the fetus unrelated to mineral homeostasis.

Vitamin D metabolism

Serum concentrations of $1,25(OH)_2D$ range from upper normal to markedly elevated values before therapy, but on vitamin D treatment may reach the highest levels found in any living system (100 times and more than the upper normal range) (Marx et al., 1986). These values may represent the end results of four different mechanisms acting synergistically to strongly stimulate renal 25(OH)D-1α-hydroxylase. Three of the mechanisms are hypocalcemia, secondary hyperparathyroidism, and hypophosphatemia. The fourth mechanism may be a failure of the negative feedback loop by which the hormone inhibits the renal enzyme activity caused by the basic defect in the VDR–effector system. This was demonstrated in two patients with HCRR in remission (normal serum levels of calcium, phosphorus, and PTH) in whom a load of $25(OH)D_3$ caused a marked increase in serum $1,25(OH)_2D_3$ concentration (Balsan et al., 1983; Marx et al., 1984; Nguyen et al., 2006). It was reported that 1α-hydroxylase gene expression was not suppressed by $1,25(OH)_2D_3$ in renal tubular cells

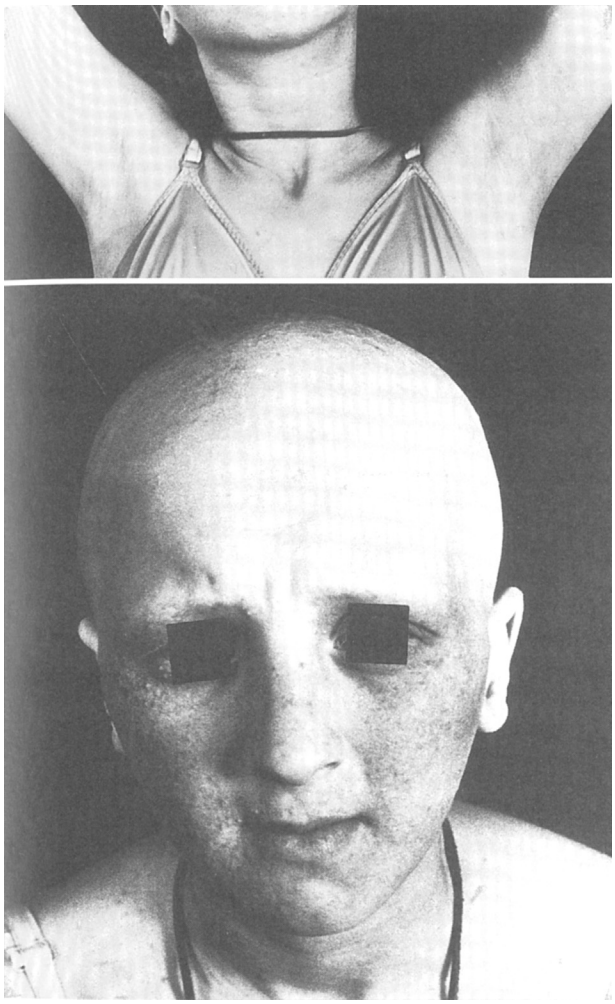

FIGURE 62.2 A patient with hereditary calcitriol-resistant rickets with total alopecia. Note: no scalp and axilla hair as well as no eyebrows and eyelashes.

from VDR knockout mice, whereas it was suppressed in cells with normal VDR or heterozygote for the null mutation (Murayama et al., 1999; Takeyama et al., 1997).

$1,25(OH)_2D$ is a potent inducer of the enzyme 25(OH)D-24-hydroxylase in vivo and in vitro. Serum levels of $24,25(OH)_2D$ have been very low or inappropriately low in the face of the elevated concentrations of the hormone in patients with HCRR (Castells et al., 1986; Fraher et al., 1986; Liberman et al., 1980; Marx et al., 1984). This probably reflects defective stimulation of $24,25(OH)_2D$ production owing to the basic deficiency in VDR activity. This assumption is supported by the observation that in mutant mice lacking VDR, expression of 24(OH)-hydroxylase was reduced to undetectable levels, and normal induction of the enzyme by $1,25(OH)_2D_3$ was not obtained (Takeyama et al., 1997).

Mode of inheritance

In approximately half of reported kindreds, parental consanguinity and multiple siblings with the same defect suggest an autosomal recessive mode of inheritance (Marx et al., 1984). Parents of patients who are expected to be obligate heterozygotes have been reported to be normal—i.e., no bone disease or alopecia, and normal blood biochemistry. However, studies on cells (cultured dermal fibroblasts, Epstein–Barr transformed lymphoblasts, and mitogen-stimulated lymphocytes) obtained from the parents of affected children revealed decreased bioresponse, decreased normal VDR protein and its mRNA, and a heterozygote genotype exhibiting both normal and mutant DNA alleles (Malloy et al., 1989, 1990; 1999, 2002; Nguyen et al., 2006; Ritchie et al., 1989; Takeda et al., 1990). There is a striking clustering of patients around the Mediterranean, including patients reported from Europe and America who originated from the same area.

A notable exception is a cluster of some kindreds from Japan (Fujita et al., 1980; Tauchiya et al., 1980, 1986, 1987, 1989; Yagi et al., 1993).

Cellular and molecular defects

Methods

The near ubiquity of a similar if not identical VDR–effector system among various cell types, including cells originating from tissues easily accessible for sampling, made it feasible to study the nature of intracellular and molecular defects in patients with HCRR. The cells used were mainly fibroblasts derived from skin biopsies (Balsan et al., 1983; Castells et al., 1986; Chen et al., 1984; Clemens et al., 1983; Eil et al., 1981; Feldman et al., 1982; Fraher et al., 1986; Griffin and Zerwekh, 1983; Hirst et al., 1985; Hughes et al., 1988; Liberman et al., 1983b; Malloy et al., 1989, 1990, 1997; 1999, 2002, 2004, 2010; Marx et al., 1984; Nguyen et al., 2002, 2006; Ritchie et al., 1989; Takeda et al., 1989) and peripheral blood mononuclear (PBM) cells (Koren et al., 1985; Ritchie et al., 1989; Takeda et al., 1986, 1990; Yagi et al., 1993). PBM cells contain high-affinity receptors for $1,25(OH)_2D_3$ that are expressed constitutively in monocytes and induced in mitogen-stimulated T lymphocytes and Epstein–Barr (EB)-transformed lymphoblasts. All cells have been used to assess most steps in $1,25(OH)_2D_3$ action, from cellular and subcellular uptake of the hormone to bioresponse, as well as to elucidate molecular aberrations in VDR protein, RNA, and DNA levels.

The hormone–receptor interaction has been analyzed by several methods including the binding characteristics of [3H] $1,25(OH)_2D_3$ to intact cells, nuclei or high-salt cellular soluble extracts, so-called cytosol (Balsan et al., 1983; Castells et al., 1986; Chen et al., 1984; Clemens et al., 1983; Eil et al., 1981; Feldman et al., 1982; Fraher et al., 1986; Hirst et al., 1985; Hochberg et al., 1984; Hughes et al., 1988; Koren et al., 1985; Liberman et al., 1983a,b; Malloy et al., 1989, 1990; Marx et al., 1984; Ritchie et al., 1989; Sone et al., 1990; Takeda et al., 1986; Yagi et al., 1993), measurements of VDR protein content by monoclonal antibodies with radiological immunoassay or Western blot analysis (Malloy et al., 1990; Ritchie et al., 1989), immunocytochemical methods in whole cells (Barsony et al., 1990), and characterization of the hormone–receptor complex on continuous sucrose gradient and nonspecific DNA-cellulose columns (Balsan et al., 1983; Chen et al., 1984; Clemens et al., 1983; Eil et al., 1981; Feldman et al., 1982; Hirst et al., 1985; Hochberg et al., 1984; Hughes et al., 1988; Liberman et al., 1983a,b; Malloy et al., 1989; Marx et al., 1984; Sone et al., 1990).

The cloning and nucleotide sequencing of the human VDR gene made it feasible to study molecular defects in patients with HCRR. The methods used included, among others, the isolation of genomic DNA that encodes the structural portion of the human VDR, PCR amplification, screening, and sequencing of the amplified DNA fragments (Hughes et al., 1988; Kristjansson et al., 1993; Malloy et al., 1990; Ritchie et al., 1989; Sone et al., 1990; Yagi et al., 1993); cloning and sequencing of VDR cDNA produced from isolated fibroblast total RNA by reverse transcription and PCR amplification (Rut et al., 1994; Saijo et al., 1991; Weise et al., 1993); and recreation of the mutant receptor in vitro by introducing the appropriate base change in normal VDR cDNA by site-directed mutagenesis that was transfected into cells that do not express endogenous VDR. Posttranscriptional action of $1,25(OH)_2D$ was tested in cells originating from patients or in cells cotransfected with VDR (either mutant or wild-type fused to a promotor containing VDRE) (Hewison et al., 1993; Hughes et al., 1988; Malloy et al., 1990, 1999; 2002, 2004; Nguyen et al., 2002, 2006; Ritchie et al., 1989; Sone et al., 1990; Yagi et al., 1993).

Types of defects

Studies with the above-mentioned methods in cells originating from a variety of patients with HCRR revealed heterogeneity of the cellular and molecular defects in the VDR–effector system. Based on the known functional properties of VDR, different classes of defects could be identified.

Defects in the hormone-binding region (including heterodimerization)

Deficient hormone binding

There are three subgroups in this class:

(i) No hormone binding. This is the most common abnormality observed and is characterized by the unmeasurable specific binding of [3H]$1,25(OH)_2D_3$ to intact cells, nuclei, or cell extracts (Balsan et al., 1983; Chen et al., 1984; Cockeril et al., 1997; Feldman et al., 1982; Fraher et al., 1986; Hawa et al., 1996; Koren et al., 1985; Kristjansson et al., 1993; Liberman et al., 1983a,b; Malloy et al., 1990, 2001; Marx et al., 1984; Mechica et al.,

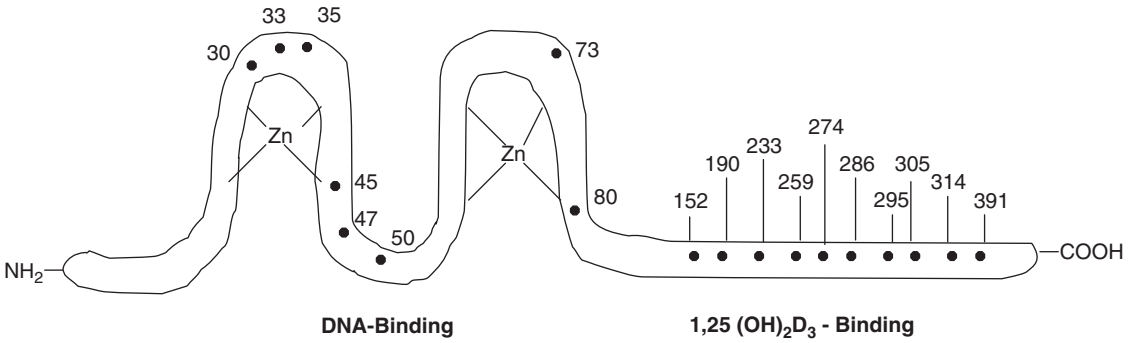

Normal	Mutant	Normal	Mutant
30 Arg (CGA)	Stop (TGA)	152 Gln (CAG)	Stop (TAG)
33 Gly (GGC)	Asp (GAC)	190 Cys (TGT)	Trp (TGG)
35 His (CAC)	Gln (CAG)	233 Leu (GTC)	fs (GTG)
45 Lys (AAA)	Glu (GAA)	259 Gln (CAG)	Pro (CCG)
47 Phe (TTC)	Lle (ATC)	274 Arg (CGC)	Leu (CTC)
50 Arg (CGA)	Gln (CAA)	286 Trp (TGG)	Arg (CGG)
73 Arg (CGC)	Stop (TGA)	295 Tyr (TAC)	Stop (TAA)
73 Arg (CGG)	Gln (CAA)	305 His (CAC)	Gln (CAG)
80 Arg (CGG)	Gln (CAG)	314 Lle (ATC)	Ser (AGC)
		391 Arg (CGC)	Cys (TGC)

FIGURE 62.3 Schematic presentation of the homozygous mutation in the VDR protein in some patients with hereditary calcitriol-resistant rickets. The asterisks depict sites of amino acid substitutions owing to point mutations and codon changes using the numbering system of Baker et al. (1988).

1997; Nguyen et al., 2002; Ritchie et al., 1989; Sone et al., 1989). Studies in several kindreds with this defect (including an extended kindred with eight patients studied) revealed undetectable levels of VDR by immunoblots on an immunoradiometric assay in most kindreds (Kristjansson et al., 1993; Malloy et al., 1990; Nguyen et al., 2002; Ritchie et al., 1989; Weise et al., 1993). DNA from these affected subjects exhibited a single base mutation in each kindred resulting in (1) conversion of a normal amino acid codon into a premature termination codon in the coding sequence of the VDR protein and (2) a frameshift in translation resulting in a premature stop codon. The truncated VDRs that were produced lacked hormone binding or both hormone-binding and DNA-binding domains (Fig. 62.3) (Cockeril et al., 1997; Hawa et al., 1996; Mechica et al., 1997; Weise et al., 1993). The recreated mutant VDR cDNA was expressed in mammalian cells, and the resulting mutant VDR was demonstrated to be the truncated protein that exhibited no specific hormone binding. Steady-state VDR mRNA levels were decreased or undetectable in patient cells from one kindred (Malloy et al., 1990; Ritchie et al., 1989). An immunoradiometric assay for VDR did not detect the 148- and 291 amino acid—long mutant VDR, though this portion of the receptor included both epitopes required for recognition (Weise et al., 1993). These observations may indicate an unstable transcript and/or increased turnover. In cells cultured from parents of some patients expected to be obligate heterozygotes, the binding of [3H]1,25$(OH)_2D_3$, VDR protein, and mRNA content of cells ranged from the lower limit of normal to about half the normal level.

In one patient representing a kindred with no hormone binding, a missense mutation resulted in the substitution of the hydrophobic basic arginine-274 by the hydrophilic nonpolar leucine in the hormone-binding region (Kristjansson et al., 1993) (see Fig. 62.3). In this patient, normal transcription in a transfection assay could be elicited by 1000-fold higher concentrations of calcitriol than needed for the wild-type receptor. However, no in vivo or in vitro stimulation of 25(OH)D-24-hydroxylase could be obtained by high concentrations of 1,25$(OH)_2D_3$.

Two siblings without alopecia and with no response to any dose of 1,25$(OH)_2D$ in vivo and in vitro had a missense mutation that caused a substitution of tryptophan by arginine at amino acid 286 of VDR (see Fig. 62.3) (Nguyen et al., 2002). This substitution in a normal-size VDR completely abolished the binding of 1,25$(OH)_2D$ to its receptor. The tryptophan in this position is critical for the positioning of calcitriol in VDR as was unveiled by the three-dimensional arrangement of VDR and its ligand based on its crystal structure (Rochel et al., 2000).

(ii) Defective hormone binding capacity. In a patient representing one kindred, the number of binding sites in nuclei and high-salt soluble cell extracts was 10% of control with an apparent normal affinity (Balsan et al., 1983; Liberman et al., 1983a,b; Sone et al., 1989).

Recently, a boy with total alopecia, severe rickets, and growth retardation was found to have two heterozygote-different molecular defects in the ligand-binding domain (Nguyen et al., 2006). The patient's VDR had a low hormone-binding capacity, 10%−30% of controls, with normal affinity and markedly deficient stimulation of 25(OH)D_3-24-hydroxylase. The recreated mutations, each one tested separately in vitro, also showed deficient heterodimerization and different transactivation of two gene promotors. This patient, similar to another one described more than 20 years ago, could be completely cured by very high doses of 25(OH) vitamin D, 250 μg/day initially followed by 100 μg/day and then 75 μg/day as a maintenance dose continuing for years, plus modest calcium supplementation. In both patients, it could be shown that during remission (normocalcemia, normophosphatemia, normal iPTH), 1,25$(OH)_2$D production is driven by the substrate—i.e., 25(OH) vitamin D concentrations.

(iii) Defective hormone binding affinity. Binding affinity of tritiated calcitriol was reduced 20- to 30-fold, with normal capacity, in high-salt soluble dermal fibroblast extracts from one kindred (Castells et al., 1986). An additional patient, representing a different kindred, had a modest decrease of VDR affinity when measured at 0°C (Malloy et al., 1997). No studies on the molecular defect were performed in patients with the last two defects.

Deficient nuclear uptake

Hormone−receptor−nuclear interaction in this defect is characterized by normal or near-normal binding capacity and affinity of [^{3}H]1,25$(OH)_2D_3$ to high-salt soluble cell extracts with low to unmeasurable hormone uptake into the nuclei of intact cells (Eil et al., 1981; Hewison et al., 1993; Liberman et al., 1983b; Takeda et al., 1989; Whitfield et al., 1996). These features were demonstrated in skin-derived fibroblasts in all kindreds, in cells cultured from a bone biopsy of one patient (Liberman et al., 1983b), and in EB-transformed lymphoblasts of one patient (Hewison et al., 1993). Occupied VDR obtained from high-salt fibroblast extracts of two kindreds demonstrated normal binding to nonspecific DNA cellulose (Liberman et al., 1986). Immunocytological studies in fibroblasts of a patient with this defect showed that immediately after 1,25$(OH)_2D_3$ treatment, VDR accumulated along the nuclear membrane with no nuclear translocation (Barsony et al., 1990). Patients with this defect included a kindred with normal hair and several kindreds with total alopecia. Finally, almost all patients responded with complete clinical remission to high doses of vitamin D and its active 1α-hydroxylated metabolites.

Attempts to characterize the molecular defect were carried out in six kindreds. In three of them, no mutation in the coding region of the VDR gene was observed (Hewison et al., 1993; personal communication). Studies in two kindreds revealed a normal molecular mass and quantitative expression of VDR as judged by immunoblotting (Whitfield et al., 1996). Complete sequencing of the VDR-coding region revealed a different single-nucleotide mutation in each kindred: ATC to AGC (isoleucine-314 to serine) in one kindred, CGC to TCG (altering arginine-391 to cysteine) in the second kindred, and CAG to CCG (altering glutamine-259 to proline) in the third kindred (see Fig. 62.3) (Cockeril et al., 1997; Whitfield et al., 1996), This region is considered to play a role in heterodimerization of VDR with RXR, and thus it has been suggested that these patients' receptors have defects that compromise RXR heterodimerization, which is essential for nuclear localization and probably for recognition of the vitamin D−responsive element as well. The fact that no mutation in the VDR-coding region was observed in three additional kindreds with the same phenotypical defect may suggest that the genetic defect affects another component of the receptor−effector system that is essential for VDR's function as a nuclear transcription factor. It has been shown that coactivation complexes are essential for the ligand-induced transactivation of VDR (Freedman, 1999). It is worthwhile to note that in one kindred originally described with this defect (Takeda et al., 1989) a missense mutation at position 140 in exon 3, encoding the DNA-binding domain, was observed (Saijo et al., 1991).

Concerning deficient coactivators of the calcitriol−VDR complex, a patient with HCRR without alopecia was described (Malloy et al., 1999). Sequencing of VDR-DNA revealed a missense mutation in the ligand-binding domain that caused a substitution of glutamic acid to lysine at amino acid 120 (see Fig. 62.3). This receptor exhibits many normal properties including calcitriol binding, dimerization, and binding to vitamin D−response elements in DNA but a marked impairment in the binding of coactivators essential for transactivation of the hormone−receptor complex and the initiation of physiological response.

Defects in the DNA-binding region

Deficient binding to DNA—cell preparations derived from patients with this defect demonstrate normal or near-normal binding capacity and affinity for [3H]1,25$(OH)_2D_3$ to the nuclei of intact cells and high-salt soluble cell extracts, as well as normal-molecular-size VDR of 48−50 kDa, as analyzed by immunoblot. Hormone−receptor complexes, however,

have decreased affinity to nonspecific DNA (peak elution from DNA-cellulose columns at 0.1 M KCl compared with 0.2 M in normals) (Hirst et al., 1985; Hughes et al., 1988; Liberman et al., 1986; Saijo et al., 1991; Yagi et al., 1993). A single-nucleotide missense mutation within exon 2 or 3, encoding the DNA-binding domain of VDR, was demonstrated in genomic DNA isolated from dermal fibroblasts and/or EB-transformed lymphoblasts from 10 unrelated kindreds (Hughes et al., 1988; Lin et al., 1996; Malloy et al., 1989, 1994; Mechica et al., 1997; Rut et al., 1994; Sone et al., 1990; Saijo et al., 1991; Yagi et al., 1993). Eight different single-nucleotide mutations were found in the 10 kindreds (see Fig. 62.3). Two apparently unrelated kindreds share the same mutation (Saijo et al., 1991; Sone et al., 1990).

All point mutations caused a single substitution of an amino acid that resides in the region of the two zinc fingers of the VDR protein that are essential for the functional interaction of the hormone−receptor complex with DNA. Interestingly, all these altered amino acids are highly conserved in the steroid receptor superfamily and seem to concentrate in three regions: the tip of the first zinc fingers (three mutations), the "knuckle" region—the C-terminal of the first zinc fingers (three mutations), and the C-terminal side of the second zinc fingers (two mutations). All of these single−amino acid residue substitutions are associated with charge changes and thus affect hydrogen bonding. These aberrations, as well as changes in hydrophobicity, will have a deleterious effect on the interaction of the hormone−receptor complex with DNA.

Each mutant was recreated by introducing the appropriate base change into the normal VDR cDNA and then transfecting the mutated cDNA into mammalian cells. The functional properties of the resultant VDR-expression product were indistinguishable from mutant DNA—i.e., normal hormone binding and deficient binding to nuclear extracts and nonspecific DNA (Hughes et al., 1988; Saijo et al., 1991; Sone et al., 1990). Studies on cells obtained from the parents of some of these patients revealed, as expected, a heterozygous state—i.e., expression of both normal and defective forms of VDR as well as normal and mutant gene sequences (Hughes et al., 1988; Malloy et al., 1989) but without any clinical or biochemical abnormalities.

In vitro posttranscriptional and transcriptional effects of *1,25(OH)$_2$D$_3$*

The in vitro bioeffects of the hormone on various cells in patients with HCRR have been assayed mainly by two procedures, induction of 25(OH)D-24-hydroxylase and inhibition of mitogen-stimulated PBM cells.

1,25(OH)$_2$D$_3$ induces 25(OH)D-24-hydroxylase activity in skin-derived fibroblasts (Balsan et al., 1983; Castells et al., 1986; Chen et al., 1984; Clemens et al., 1983; Feldman et al., 1982; Fraher et al., 1986; Gamblin et al., 1985; Griffin et al., 1983; Hewison et al., 1993; Hirst et al., 1985; Hughes et al., 1988; Liberman et al., 1983b; Malloy et al., 1990; Ritchie et al., 1989; Rut et al., 1994; Sone et al., 1990; Yagi et al., 1993), mitogen-stimulated lymphocytes (Takeda et al., 1990), and cells originating from bone (Balsan et al., 1986) in a dose-dependent manner. In cells from normal subjects, maximal and half-maximal induction of the enzyme was achieved by 10-8 and 10-9 M concentrations of 1,25(OH)$_2$D$_3$, respectively. Dermal fibroblast and PBM cells from HCRR patients with no calcemic response to maximal doses of vitamin D or its metabolites in vivo did not show any 25(OH)D-24-hydroxylase response to very high concentrations of 1,25(OH)$_2$D$_3$ in vitro, whereas dermal fibroblasts from patients with a calcemic response to high doses of vitamin D or its metabolites in vivo showed inducible 24-hydroxylase with supraphysiological concentrations of 1,25(OH)$_2$D$_3$—i.e., a shift to the right in vitro. Physiological concentrations of 1,25(OH)$_2$D$_3$ partially inhibit mitogen-induced DNA synthesis in peripheral lymphocytes, with half-maximal inhibition achieved at 10-10 M hormone (Koren et al., 1985; Takeda et al., 1986). Mitogen-stimulated lymphocytes from several kindreds with defects characterized as no hormone binding or deficient binding to DNA, with no calcemic response to high doses of vitamin D and its metabolites in vivo, showed no inhibition of lymphocyte proliferation in vitro with concentrations of up to 10-6 M 1,25(OH)$_2$D$_3$ (Fig. 62.4). Additional methods for measuring the bioeffects of 1,25(OH)$_2$D$_3$ on various cells in vitro were carried out in only a few patients and included the inhibition of dermal fibroblast proliferation (Clemens et al., 1983), induction of osteocalcin synthesis in cells derived from bone (Balsan et al., 1986), a mitogenic effect on dermal fibroblasts (Barsony et al., 1989), and stimulation of cGMP production in cultured skin fibroblasts (Barsony and Marx, 1988). It is noteworthy that in all assays mentioned, without exception, each patient's cells showed severely deficient responses.

With elucidation of the molecular defects in HCRR, the transactivation abilities of naturally occurring mutant or recreated mutant VDRs were evaluated in a transcriptional activation assay. The human osteocalcin gene promoter fused to chloramphenicol acetyltransferase (CAT) gene reporter plasmid was transfected into patients or normal fibroblasts (Hewison et al., 1993; Hughes et al., 1988; Malloy et al., 1990; Ritchie et al., 1989; Saijo et al., 1991; Sone et al., 1989; Yagi et al., 1993). Treating normal transfected cells with 1,25(OH)$_2$D$_3$ caused a concentration-dependent induction of transcription as measured by increased CAT activity. No induction of transcription was observed in cells originating from patients with defects characterized as no hormone binding (Kristjansson et al., 1993; Malloy et al., 1990; Ritchie et al., 1989) or deficient binding to DNA (Hughes et al., 1988; Saijo et al., 1991; Sone et al., 1990; Yagi et al., 1993). Moreover,

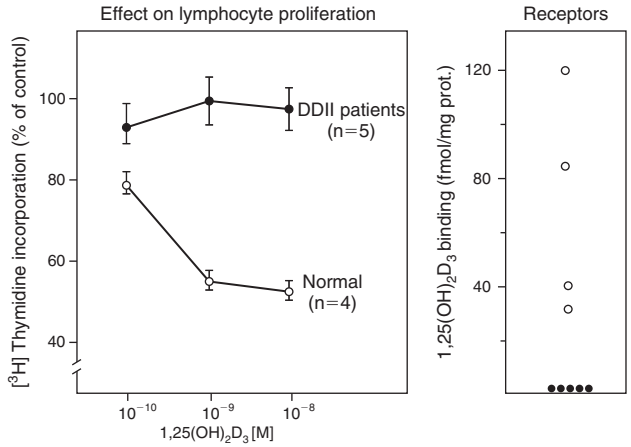

FIGURE 62.4 Effect of increasing concentrations of $1,25(OH)_2D_3$ on mitogen-induced lymphocyte proliferation from patients with hereditary calcitriol-resistant rickets (HCRR) and normal controls. The numbers of specific $[^3H]1,25(OH)_2D_3$-binding sites are depicted (right) in the same cell populations. HCRR patients tested here are with the defect characterized as no hormone binding.

in a cotransfection assay, the addition of a normal human VDR cDNA expression vector to the transfected plasmid that directed synthesis of a normal VDR restored the hormone responsiveness of resistant cells.

Finally, a 2 year-old girl with alopecia, hypocalcemic rickets, high circulating levels of $1,25(OH)_2$ vitamin D, and no response to recommended doses of vitamin D was characterized as having a deficient nuclear uptake defect; no mutation was identified within the coding region of the VDR gene, and no induction of 25(OH)D-24-hydroxylase activity by up to 10-6 M $1,25(OH)_2D_3$ was observed in cultured skin fibroblasts (Hewison et al., 1993). Cotransfection studies performed subsequently (Chen et al., 2003) showed that patient cells suppressed basal and hormone-induced transactivation by wild-type VDR. Electrophoretic mobility shift assays and western/southwestern blot analysis indicated that the suppressive effect was due to the overexpression of a nuclear protein that interacts specifically with a DNA response element known to bind RXR−VDR heterodimers. This dominant, negative-acting element belongs to the heterogenous nuclear ribonucleoproteins (hnRVP) family of nucleic acid binding proteins. Several members of this family, most notably hnRVPA1, were able to suppress calciferol-induced luciferase activity. The ability of hnRVPs to attenuate steroid hormones receptor genes transactivation also has been demonstrated in studies in New World primates known to have partial resistance to vitamin D and steroid hormones. These observations raise a few interesting questions. Are these proteins that interact with the DNA of the calciferol response element a part of the physiological control system of vitamin D and mineral homeostasis? The patient discussed has HCRR but with normal $1,25(OH)_2$ D receptors. The underlying cause for calcitriol resistance in this patient is overexpression of a response element binding protein that interacts with the DNA of the vitamin D−response element to block its biological activity. Most patients with HCRR have different defects within the coding region of VDR. As discussed, this patient, although being similar in clinical, radiological, and biochemical changes as well as dermal signs, has a different etiology and pathogenesis and therefore may deserve a different title such as HCRR type B. This patient had a complete cure of her rickets and normalization of all biochemical aberrations on treatment with high doses of $1,25(OH)_2$ vitamin D_3 (12 μg/day) plus 1 g/day of elemental calcium.

Cellular defects and clinical features

Normal hair was described with most phenotypes of the cellular defects, the exception being patients with deficient hormone-binding capacity and affinity, but this could be because only very few kindreds were described per subgroup. Normal hair is usually associated with a milder form of the disease as judged by the age of onset, severity of clinical features, and usually complete clinical and biochemical remission on high doses of vitamin D or its metabolites. Notable exceptions are two patients, from two separate kindreds, with normal hair that displayed resistance both in vivo (no clinical remission on a circulating calcitriol level of up to 100 times mean normal adult values) and in vitro—i.e., no induction of 25(OH)D-24-hydroxylase activity in dermal fibroblasts by up to 10-8 M $1,25(OH)_2D_3$ (Fraher et al., 1986; Malloy et al., 2002). Only about half of patients with alopecia have shown satisfactory clinical and biochemical remission in response to high doses of vitamin D or its active 1α-hydroxylated metabolites, but the dose requirement is 10-fold higher than in patients with normal hair (Marx et al., 1986).

It seems that patient defects characterized as deficient hormone-binding affinity and deficient nuclear uptake achieve complete clinical and biochemical remission on high doses of vitamin D or its active 1α-hydroxylated metabolites. Most patients with other types of defects could not be cured with high doses of vitamin D or its metabolites. However, it should be emphasized that not all patients received treatment for sufficiently long periods and at sufficiently high doses (see "Treatment").

Diagnosis

Clinical features of early-onset rickets with no history of vitamin D deficiency, total alopecia, parental consanguinity, additional siblings with the same disease, serum biochemistry of hypocalcemic rickets, elevated circulating levels of $1,25(OH)_2D$, and normal to high levels of 25(OH)D (see Table 62.1) support the diagnosis of HCRR. The issue becomes more complicated when clinical features are atypical—i.e., late onset of the disease, sporadic cases, and normal hair. Failure of a therapeutic trial with physiological replacement doses of vitamin D or its active metabolites plus calcium supplementation may support the diagnosis, but final direct proof requires the demonstration of a cellular, molecular, and functional defect in the VDR−effector system.

Based on clinical and biochemical features, the following additional disease states should be considered: (1) extreme calcium deficiency—a seemingly rare situation described in a group of children from a rural community in South Africa who consumed an exceptionally low-calcium diet of 125 mg/day (Pettifor et al., 1981). All had severe bone disease with histologically proven osteomalacia, biochemical features of hypocalcemic rickets with elevated serum levels of $1,25(OH)_2D$, and sufficient vitamin D. Calcium repletion caused complete clinical and biochemical remission. Nutritional history and the response to calcium supplementation support this diagnosis; (2) severe vitamin D deficiency—during initial stages of vitamin D therapy in children with severe vitamin D−deficiency rickets, the biochemical picture may resemble HCRR (i.e., hypocalcemic rickets with elevated serum calcitriol levels). This may represent a "hungry bone syndrome"—i.e., high calcium demands of the abundant osteoid tissue becoming mineralized. This is a transient condition that may be differentiated from HCRR by a history of vitamin D deficiency and the final therapeutic response to replacement doses of vitamin D.

Treatment

In about half of the kindreds with HCRR, the bioeffects of $1,25(OH)_2D_3$ were measured in vitro (see earlier). An invariable correlation (with one exception) was documented between the in vitro effect and the therapeutic response in vivo—i.e., patients with no calcemic response to high levels of serum calcitriol showed no effects of $1,25(OH)_2D_3$ on their cells in vitro (neither induction of 25(OH)D-24-hydroxylase nor inhibition of lymphocyte proliferation) and vice versa. If the predictive therapeutic value of the in vitro cellular response to $1,25(OH)_2D_3$ could be substantiated convincingly, it might eliminate the need for time-consuming and expensive therapeutic trials with massive doses of vitamin D or its active metabolites. In the meantime, it is mandatory to treat every patient with HCRR irrespective of the type of receptor defect.

An adequate therapeutic trial must include vitamin D at a dose sufficient to maintain high serum concentrations of $1,25(OH)_2D_3$, as patients can produce high hormone levels if supplied with enough substrate (Brooks et al., 1978; Marx et al., 1978). If high serum calcitriol levels are not achieved, it is advisable to treat with 1α-hydroxylated vitamin D metabolites in daily doses of up to 6 μg/kg, or a total of 30−60 μg, and calcium supplementation of up to 3 g of elemental calcium daily; therapy must be maintained for a period sufficient to mineralize the abundant osteoid (usually 3−5 months). Therapy may be considered a failure if no change in the clinical, radiological, or biochemical parameters occurs during continuous and frequent follow-up while serum $1,25(OH)_2D$ concentrations are maintained at 100 times the mean normal range.

In some patients with no response to adequate therapeutic trials with vitamin D or its active 1-alpha hydroxylated metabolites, a remarkable clinical and biochemical remission of their bone disease, including catch-up growth, was obtained by treatment with large amounts of calcium. This was achieved by long-term (months) intracaval infusions of up to 1000 mg of calcium daily (Balsan et al., 1986; Bliziotes et al., 1988; Weisman et al., 1987). Another way to increase calcium input into the extracellular compartment is to increase net gut absorption, independent of vitamin D, by increasing calcium intake (Sakati et al., 1986). This approach is limited by dose and patient tolerability and was used successfully in only a very few patients.

Several patients have shown unexplained fluctuations in response to therapy or in presentation of the disease. One patient, after a prolonged remission, became completely unresponsive to much higher doses of active 1α-hydroxylated vitamin D

metabolites (Balsan et al., 1983), and another patient seemed to show amelioration of resistance to $1,25(OH)_2D_3$ after a brief therapeutic trial with $24,25(OH)_2D_3$ (Liberman et al., 1980). In several patients, spontaneous healing occurred in their teens (Hochberg et al., 1984) or rickets did not recur for 14 years after the cessation of therapy (Takeda et al., 1989).

Animal models

Some New World primates (marmosets and tamarins) that develop osteomalacia in captivity are known to have high nutritional requirements for vitamin D and maintain high serum levels of $1,25(OH)_2D$, thus exhibiting a form of end-organ resistance to $1,25(OH)_2D$ (Adams and Gacad, 1988; Liberman et al., 1985; Shinki et al., 1983; Takahashi et al., 1985). Cultured dermal fibroblasts and EB-virus-transformed lymphoblasts have shown deficient hormone-binding capacity and affinity (Adams and Gacad, 1988; Liberman et al., 1985). It has been observed that marmoset lymphoblasts contain a soluble protein of 50–60 kDa that binds $1,25(OH)_2D_3$ with a low affinity but high capacity and thus may serve as a sink that interferes with hormone binding and its cognate receptor (Gacad and Adams, 1993). The same group described another protein present in the nuclear extract of these cells capable of inhibiting normal VDR-RXR binding to the vitamin D–response element (Arbelle et al., 1996).

It is of interest that these New World primates also exhibit a compensated hereditary end-organ resistance to true steroid hormones including glucocorticoids, estrogens, and progestins (Lipsett et al., 1985). This of course raises the interesting possibility that the defect in the hormone–receptor–effector system involves an element shared by all members of this superfamily of ligand-modulated transcription factors.

VDR knockout mice have been created by targeted ablation of the first or second zinc finger (Li et al., 1997; Yoshizawa et al., 1997). Only homozygotic mice were affected. Though phenotypically normal at birth, after weaning they become hypocalcemic and develop secondary hyperparathyroidism, rickets, osteomalacia, and progressive alopecia. Female mice with ablation of the first zinc finger are infertile and show uterine hypoplasia and impaired folliculogenesis. Otherwise, both VDR cell-mutant mice show clinical, radiological, histological, and biochemical features identical to those of the human disease HCRR. Supplementation with a calcium-enriched diet can prevent or treat most disturbances in mineral and bone metabolism in these animal models except alopecia (Delling and Demay, 1998). It is of interest that targeting the expression of human VDR to the keratinocytes of VDR-null mice prevented alopecia (Chen et al., 2001).

Concluding remarks

Hereditary deficiencies in vitamin D action are rare disorders. The importance of studying these diseases stems from the fact that they represent a naturally occurring experimental model that helps to elucidate the function and importance of vitamin D and the VDR–effector system in humans in vivo.

VDRs are abundant and widely distributed among most tissues studied, and multiple effects of calcitriol are observed on various cell functions in vitro. Yet the clinical and biochemical features in patients with HVDDR and HCRR seem to demonstrate that the only disturbances of clinical relevance are perturbations in mineral and bone metabolism. This demonstrates the pivotal role of $1,25(OH)_2D$ in transepithelial net calcium fluxes. Moreover, the fact that calcium infusions correct the disturbances in mineral homeostasis and cure the bone disease in patients with extreme end-organ resistance to calcitriol may support the notion that defective bone matrix mineralization in HVDDR and HCRR is secondary to disturbances in mineral homeostasis. Characterization of the molecular, cellular, and functional defects of the different natural mutants of human VDR in HCRR demonstrates the essentiality of VDR as the mediator of calcitriol action and the importance and function of its different domains. Furthermore, to function biologically, VDR must associate with additional partners—i.e., $1,25(OH)_2D$, an RXR isoform, a specifically defined DNA region, and coactivators and corepressor complexes. This notion has been based primarily on in vitro-created point mutations and in vitro functional assays. However, the acid test for the relevance of the structure–function relationship is the demonstration of in vivo effects in general and deficient function under pathological conditions in particular. Thus, studies in patients with hereditary deficiencies in vitamin D action are the essential link between molecular defects and physiologically relevant effects.

References

Adams, J.S., Gacad, M.A., 1988. Phenotypic diversity of the cellular 1,25-dihydroxyvitamin D_3-receptor interaction among different generations of new world primates. J. Clin. Endocrinol. Metab. 666, 224–229.

Akeno, N., Saikatsu, S., Kawane, T., Horiuchi, N., 1997. Mouse vitamin D-24 hydroxylase molecular cloning, tissue distribution, a transcriptional regulation by 1α,25-hydroxyvitamin D_3. Endocrinology 138, 2233–2240.

Al Mutair, A.N., Nasrat, G.H., Russell, D.W., 2012. Mutation of the CYP2R1 vitamin D 25-hydroxylase in a Saudi Arabian family with severe vitamin D deficiency. J. Clin. Endocrinol. Metab. 97, E2022–E2025.

Arbelle, J.E., Chen, H., Gacad, M.A., Allegretto, E.A., Pike, J.W., Adams, J.S., 1996. Inhibition of vitamin D receptor-retinoid X receptor-vitamin D response element complex formation by nuclear extracts of vitamin D-resistant New World primate cells. Endocrinology 137, 786–789.

Baker, A.R., McDonnel, D.P., Huges, M., Crisp, T.M., Mangelsdorf, D.J., Haussler, M.R., Pike, J.W., Shine, J., O'Malley, B.W., 1988. Cloning and expression of full-length cDNA encoding human vitamin receptor. Proc. Natl. Acad. Sci. U.S.A. 85, 3294–3298.

Balsan, A., Garabedian, M., Liberman, U.A., Eil, C., Bourdeau, A., Guillozo, H., Grimberg, R., DeDeunff, M.J., Lieberherr, M., Guimbaud, P., Broyer, M., Marx, S.J., 1983. Rickets and alopecia with resistance to 1,25-dihydroxyvitamin D: two different clinical courses with two different cellular defects. J. Clin. Endocrinol. Metab. 57, 824–830.

Balsan, S., Garabedian, M., Larchet, M., Gorski, A.M., Cournot, G., Tau, C., Bourdeau, A., Silve, C., Ricour, C., 1986. Long term nocturnal calcium infusions can cure rickets and promote normal mineralization in hereditary resistance to 1,25-dihydroxyvitamin D. J. Clin. Investig. 77, 1161–1167.

Barsony, J., Marx, S.J., 1988. A receptor-mediated rapid action of 1α, 25-dihydroxycholecalciferol: increase of intracellular cyclic GMP in human skin fibroblasts. Proc. Natl. Acad. Sci. U.S.A. 85, 1223–1226.

Barsony, J., McKoy, W., DeGrange, D.A., Liberman, U.A., Marx, S.J., 1989. Selective expression of a normal action of 1,25-dihydroxyvitamin D_3 receptor in human skin fibroblasts with hereditary severe defects in multiple action of this receptor. J. Clin. Investig. 83, 2093–2101.

Barsony, J., Pike, J.W., DeLuca, H.F., Marx, S.J., 1990. Immunocytology with microwave-fixed fibroblasts shows 1 alpha, 24-dihydroxyvitamin D_3-dependent rapid and estrogen-dependent slow reorganization of vitamin D receptors. J. Cell Biol. 111, 2385–2395.

Bear, S., Tieder, M., Kohelet, D., Liberman, U.A., Vine, E., Bar-Joseph, G., Gabizon, D., Borochowitz, Z.U., Varon, M., Modai, D., 1981. Vitamin D resistant rickets with alopecia: a form of end-organ resistance to 1,25-dihydroxyvitamin D. Clin. Endocrinol. 14, 395–402.

Bliziotes, M., Yergey, A.L., Nanes, M.S., Muenzer, J., Begley, M.G., Vieira, N.E., Kher, K.K., Brandi, M.L., Marx, S.J., 1988. Absent intestinal response to calciferols in hereditary resistance to 1,25-dihydroxyvitamin D: documentation and effective therapy with high dose intravenous calcium infusions. J. Clin. Endocrinol. Metab. 66, 294–300.

Brooks, M.H., Bell, N.H., Love, L., Stern, P.H., Ordei, E., Queener, S.J., 1978. Vitamin D dependent rickets type II resistance of target organs to 1,25-dihydroxyvitamin D. N. Engl. J. Med. 293, 996–999.

Burmester, J.K., Maeda, N., DeLuca, H.F., 1988. Isolation and expression of rat 1,25-dihydroxyvitamin D_3 receptor DNA. Proc. Natl. Acad. Sci. U.S.A. 85, 1005–1009.

Casella, S.J., Reiner, B.J., Chen, T.C., Holick, M.F., Harrison, H.E., 1994. A possible genetic defect in 25-hydroxylation as a cause of rickets. J. Pediatr. 124, 929–932.

Castells, S., Greig, F., Fusi, M.A., Finberg, L., Yasumura, S., Liberman, U.A., Eil, C., Marx, S.J., 1986. Severely deficient binding of 1,25-dihydroxyvitamin D to its receptor in a patient responsive to high doses of this hormone. J. Clin. Endocrinol. Metab. 63, 252–256.

Chen, C.H., Sakai, Y., Demay, M.B., 2001. Targeting expression of the human vitamin D receptor to the keratinocytes of vitamin D receptor null mice prevents alopecia. Endocrinology 142, 5386.

Chen, H., Hewison, M., Hu, B., Adams, J.S., 2003. Heterogenous nuclear ribonucleoprotein (hnRNP) binding to hormone response elements: a cause of vitamin D resistance. Proc. Natl. Acad. Sci. U.S.A. 100 (10), 6109–6114.

Chen, T.L., Hirst, M.A., Cone, C.M., Hochberg, Z., Tietze, H.U., Feldman, D., 1984. 1,25-Dihydroxyvitamin D resistance, rickets and alopecia: analysis of receptors and bioresponse in cultured skin fibroblasts from patients and parents. J. Clin. Endocrinol. Metab. 59, 383–388.

Clemens, T.L., Adams, J.C., Horiuchi, N., Gilchrist, B.A., Cho, H., Ysuchiya, Y., Matsuo, N., Suda, T., Holick, M.J., 1983. Interaction of 1,25-dihydroxyvitamin D_3 with keratinocytes and fibroblasts from skin of a subject with vitamin D-dependent rickets type II: a model for the study of action of 1,25-dihydroxyvitamin D_3. J. Clin. Endocrinol. Metab. 56, 824–830.

Cockerill, F.J., Hawa, N.S., Yousaf, N., Hewison, M., O'Riordan, J.F.L., Farrow, S.M., 1997. Mutations in the vitamin D receptor gene in three kindreds associated with hereditary vitamin D resistant rickets. J. Clin. Endocrinol. Metab. 82, 3156–3160.

Cole, D.E.C., Carpenter, T.O., Gundberg, C.M., 1985. Serum osteocalcin concentrations in children with metabolic bone disease. J. Pediatr. 106, 770–776.

De Braekeleer, M., Larochell, J., 1991. Population genetics of vitamin D-dependent rickets in Northeastern Quebec. Ann. Hum. Genet. 55, 283–290.

Delling, G., Demay, M.B., 1998. Normalization of mineral ion homeostasis by dietary means prevents hyperparathyroidism, rickets, and osteomalacia, but not alopecia in vitamin D receptor-ablated mice. Endocrinology 139, 4391–4396.

DeLuca, H.F., 1984. The metabolism, physiology and function of vitamin D. In: Kumar, R. (Ed.), Vitamin D: Basic and Clinical Aspects. Martinus Nijhoff, Boston, pp. 1–68.

Delvin, E.E., Arabian, A., 1987. Kinetics and regulation of 25-hydroxycholecalciferol 1α-hydroxylase from cells isolated from human term decidua. Eur. J. Biochem. 163, 659–662.

Delvin, E.E., Glorieux, F.H., Marie, P.J., Pettifor, J.M., 1981. Vitamin D dependency: replacement therapy with calcitriol. J. Pediatr. 99, 26–34.

Diaz, L., Sanchez, I., Avila, E., Halhali, A., Vilchis, F., Larrea, F., 2000. Identification of a 25-hydroxyvitamin D_3 1α-hydroxylase gene transcription product in cultures of human syncytiotrophoblast cells. J. Clin. Endocrinol. Metab. 85, 2543–2549.

Eil, C., Liberman, U.A., Rosen, J.F., Marx, S.J., 1981. A cellular defect in hereditary vitamin D-dependent rickets type II: defective nuclear uptake of 1,25-dihydroxyvitamin D in cultured skin fibroblasts. N. Engl. J. Med. 304, 1588–1591.

Evans, R.M., 1988. The steroid and thyroid hormone receptor super-family. Science 240, 889–895.

Feldman, D., Chen, T., Cone, C., Hirst, M., Shari, S., Benderli, A., Hochberg, Z., 1982. Vitamin D resistant rickets with alopecia: cultured skin fibroblasts exhibit defective cytoplasmic receptors and unresponsiveness to $1,25(OH)_2D_3$. J. Clin. Endocrinol. Metab. 55, 1020–1025.

Fox, J., Maunder, E.M.W., Ranall, V.A., Care, A.D., 1985. Vitamin D dependent rickets type I in pigs. Clin. Sci. 69, 541–548.

Fraher, L.J., Karmali, R., Hinde, F.R.J., Hendy, G.N., Jani, H., Nicholson, L., Grant, D., O'Riordan, J.L.H., 1986. Vitamin D-dependent rickets type II: extreme end organ resistance to 1,25-dihydroxyvitamin D_3 in a patient without alopecia. Eur. J. Pediatr. 145, 389–395.

Fraser, D., Kooh, S.W., Kind, P., Tanaka, Y., DeLuca, H.F., 1973. Pathogenesis of hereditary vitamin D-dependent rickets: an inborn error of metabolism involving defective conversion of 25-hydroxy-vitamin D to 1α, 25-dihydroxy-vitamin D. N. Engl. J. Med. 289, 817–822.

Freeman, L.P., 1999. Increasing the complexity of coactivation in nuclear receptor signaling. Cell 97, 5–8.

Fu, G.K., Portale, A.A., Miller, W.L., 1997a. Complete structure of the human gene for the vitamin D 1a-hydroxylase. Cell Biol. 16, 1499–1507.

Fu, G.K., Lin, D., Zhang, M.Y., Bikle, D.D., Shackleton, C.H., Miller, W.L., Portale, A.A., 1997b. Cloning of human 25-hydroxyvitamin D1a-hydroxylase and mutations causing vitamin D-dependent rickets type 1. Endocrinology 11, 1961–1970.

Fujita, T., Nomura, M., Okajima, S., Suzuya, H., 1980. Adult-onset vitamin D-resistant osteomalacia with unresponsiveness to parathyroid hormone. J. Clin. Endocrinol. Metab. 50, 927–931.

Gacad, M.A., Adams, J.S., 1993. Identification of competitive binding component in vitamin D resistant new world primate cells with a low affinity but high capacity for 1,25-dihydroxyvitamin D_3. J. Bone Miner. Res. 8, 27–35.

Gamblin, G.T., Liberman, U.A., Eil, C., Downs Jr., R.W., DeGrange, D.A., Marx, S.J., 1985. Vitamin D-dependent rickets type II, defective induction of 25-hydroxyvitamin D_3-24-hydroxylase by 1,25-dihydroxyvitamin D_3 in cultured skin fibroblasts. J. Clin. Investig. 75, 954–960.

Glorieux, F.H., Arabian, A., Delvin, E.E., 1995. Pseudo-vitamin D deficiency: absence of 25-hydroxyvitamin D 1α-hydroxylase activity in human placenta decidua cells. J. Clin. Endocrinol. Metab. 80, 2255–2258.

Griffin, J.E., Zerwekh, J.E., 1983. Impaired stimulation of 25-hydroxyvitamin D-24-hydroxylase in fibroblasts from a patient with vitamin D-dependent rickets, type II. J. Clin. Investig. 72, 1190–1199.

Harmeyer, J.V., Grabe, C., Winkley, I., 1982. Pseudovitamin D deficiency rickets in pigs. An animal model for the study of familial vitamin D dependency. Exp. Biol. Med. 7, 117–125.

Hawa, N.S., Cockerill, F.J., Vadher, S., Hewison, M., Rut, A.R., Pike, J.W., O'Riordan, J.L.H., Farrow, S.M., 1996. Identification of a novel mutation in hereditary vitamin D resistant rickets causing exon skipping. Clin. Endocrinol. 45, 85–92.

Hewison, M., Rut, A.R., Kristjansson, K., Walker, R.E., Dillon, M.J., Hughes, M.R., O'Riordan, J.L.H., 1993. Tissue resistance to 1,25-dihydroxyvitamin D without a mutation of the vitamin D receptor gene. Clin. Endocrinol. 39, 663–670.

Hirst, M.A., Hochman, H.I., Feldman, D., 1985. Vitamin D resistance and alopecia: a kindred with normal 1,25-dihydroxy-vitamin D_3 binding but decreased receptor affinity for deoxyribonucleic acid. J. Clin. Endocrinol. Metab. 60, 490–495.

Hochberg, Z., Benderli, Z., Levy, J., Weisman, Y., Chen, T., Feldman, D., 1984. 1,25-Dihydroxyvitamin D resistance, rickets and alopecia. Am. J. Med. 77, 805–811.

Hughes, M.R., Malloy, P.J., Kieback, D.G., Kesterson, R.A., Pike, J.W., Feldman, D., O'Malley, B.W., 1988. Point mutations in the human vitamin D receptor gene associated with hypocalcemic rickets. Science 242, 1702–1705.

Jehan, F., Ismail, R., Hanson, K., DeLuca, H.F., 1998. Cloning and expression of the chicken 25-hydroxyvitamin D_3 24-hydroxylase cDNA. Biochim. Biophys. Acta 1395, 259–265.

Jones, G., Ramshaw, H., Zhang, A., Cook, R., Byford, V., White, J., Petkovich, M., 1999. Expression and activity of vitamin D-metabolizing cytochrome P450s (CYP1a and CYP 24) in human nonsmall cell lung carcinomas. Endocrinology 140, 3303–3310.

Kitanaka, S., Takeyama, K., Murayama, A., Sato, T., Okumura, K., Nogami, M., Hasegawa, Y., Niimi, H., Yanagisawa, J., Tanaka, T., Kato, S., 1998. Inactivating mutations in the 25-hydroxyvitamin D_3 1α-hydroxylase gene in patients with pseudovitamin D-deficiency rickets. N. Engl. J. Med. 338, 653–661 [Comments].

Kitanaka, S., Murayama, A., Sakaki, T., Inoue, K., Seino, Y., Fukumoto, S., Shima, M., Yukizane, S., Takayanagi, M., Niimi, H., Takeyama, K., Kato, S., 1999. No enzyme activity of 25-hydroxyvitamin D_3 1α-hydroxylase geneproduct in pseudovitamin D-deficiency rickets with mild clinical manifestation. J. Clin. Endocrinol. Metab. 84, 4111–4117.

Koren, R., Ravid, A., Liberman, U.A., Hochberg, Z., Weisman, J., Novogrodsky, A., 1985. Defective binding and functions of 1,25-dihydroxyvitamin D_3 receptors in peripheral mononuclear cells of patients with end-organ resistance to 1,25-dihydroxyvitamin D. J. Clin. Investig. 76, 2012–2015.

Kristjansson, K., Rut, A.R., Hewison, M., O'Riordan, J.L.H., Hughes, M.R., 1993. Two mutations in the hormone binding domain of the vitamin D receptor causes tissue resistance to 1,25-dihydroxyvitamin D_3. J. Clin. Investig. 92, 12–16.

Labuda, M., Morgan, K., Glorieux, F.H., 1990. Mapping autosomal recessive vitamin D-dependency Type I to chromosome 12q14 by linkage analysis. Am. J. Hum. Genet. 46, 28–36.

Li, Y.C., Piroo, A.E., Amling, M., Delling, G., Baron, R., Bronson, R., Demay, M.B., 1997. Targeted ablation of the vitamin D receptor: an animal model of vitamin D-dependent rickets type II with alopecia. Proc. Natl. Acad. Sci. U.S.A. 94, 9831–9835.

Liberman, U.A., DeGrange, D., Marx, S.J., 1985. Low affinity of the receptor for 1 alpha, 25-dihydroxyvitamin D_3 in the marmoset, a New World monkey. FEBS Lett. 182, 385–389.

Liberman, U.A., Eil, C., Holst, P., Rosen, J.F., Marx, J.S., 1983a. Hereditary resistance to 1,25-dihydroxyvitamin D: defective function of receptors for 1,25-dihydroxyvitamin D in cells cultured from bone. J. Clin. Endocrinol. Metab. 57, 958–962.

Liberman, U.A., Eil, C., Marx, S.J., 1983b. Resistance 1,25-dihydroxyvitamin D: association with heterogeneous defects in cultured skin fibroblasts. J. Clin. Investig. 71, 192–200.

Liberman, U.A., Eil, C., Marx, S.J., 1986. Receptor positive hereditary resistance to 1,25-dihydroxyvitamin D. Chromatography of hormone-receptor complexes on DNA-cellulose shows two classes of mutations. J. Clin. Endocrinol. Metab. 62, 122–126.

Liberman, U.A., Samuel, R., Halabe, A., Kauli, R., Edelstein, S., Weisman, Y., Papapoulos, S.E., Clemens, T.L., Fraher, L.J., O'Riordan, J.L.H., 1980. End-organ resistance to 1,25-dihydroxy cholecalciferol. Lancet 1, 504–506.

Lin, J.P., Uttley, W.E., 1993. Intraatrial calcium infusions, growth and development in end-organ resistance to vitamin D. Arch. Dis. Child. 69, 689–692.

Lin, N.-T., Malloy, P.J., Sakati, N., Al-Ashwal, A., Feldman, D., 1996. A novel mutation in the deoxyribonucleic acid-binding domain of the vitamin D receptor causes hereditary 1,25-dihydroxyvitamin D resistant rickets. J. Clin. Endocrinol. Metab. 81, 2564–2569.

Lipsett, M.B., Chrousos, G.P., Tomita, M., Brandon, D.D., Loriaux, D.L., 1985. The defective glucocorticoid receptor in man and non-human primates. Recent Prog. Horm. Res. 41, 199–241.

Malloy, P.J., Eccleshall, T.R., Gross, C., van Maldergem, L., Bouillion, R., Feldman, D., 1997. Hereditary vitamin D resistant rickets caused by a novel mutation in the vitamin D receptor that results in decreased affinity for hormone and cellular hyporesponsiveness. J. Clin. Investig. 99, 297–304.

Malloy, P.J., Feldman, D., 2010. Genetic disorders and defects in vitamin D action. Endocrinol Metab. Clin. N. Am. 39, 333–346.

Malloy, P.J., Hochberg, Z., Pike, J.W., Feldman, D., 1989. Abnormal binding of vitamin D receptors to deoxyribonucleic acid in a kindred with vitamin D dependent rickets type II. J. Clin. Endocrinol. Metab. 68, 263–269.

Malloy, P.J., Hochberg, Z., Tiosano, D., Pike, J.W., Hughes, M.R., Feldman, D., 1990. The molecular basis of hereditary 1,25-dihydroxyvitamin D_3 resistant rickets in seven related families. J. Clin. Investig. 86, 2017–2079.

Malloy, P.J., Pike, J.W., Feldman, D., 1999. The vitamin D receptor and the syndrome of hereditary 1,25-dihydroxyvitamin D-resistant rickets. Endocr. Rev. 20, 156–188.

Malloy, P.J., Xu, R., Clark, P.A., Feldman, D., 2012. A novel mutation in helix 12 of the vitamin D receptor impairs coactivator interaction and causes hereditary 1,25-dihydroxyvitamin D-resistant rickets without alopecia. Mol. Endocrinol. 16, 2538–2546.

Malloy, P.J., Xu, R., Peng, L., Clark, P.A., Feldman, D., 2002a. A novel mutation in helix 12 of the vitamin D receptor impairs coactivator interaction and causes hereditary 1,25-dihydroxyvitamin D-resistant rickets without alopecia. Mol. Endocrinol. 16, 2538–2546.

Malloy, P.J., Xu, R., Peng, I., Peleg, S., Al-Ashwal, A., Feldman, D., 2004. Hereditary 1,25-dihydroxyvitamin D-resistant rickets due to a mutation causing multiple defects in vitamin D receptor function. Endocrinology 145, 5106–5114.

Malloy, P.J., Zhu, W., Bouillon, R., Feldman, D., 2002b. A novel non-sense mutation in the ligand binding domain of the vitamin D receptor causes hereditary 1,25-dihydroxyvitamin D-resistant rickets. Mol. Genet. Metabol. 77, 314–318.

Malloy, P.J., Zhu, W., Zhao, X.Y., Pehling, G.B., Feldman, D., 2001. A novel inborn error in the ligand-binding domain of the vitamin D receptor causes hereditary vitamin D-resistant rickets. Mol. Genet. Metabol. 73, 138–148.

Marx, S.J., Blizlotes, M.M., Nanes, M., 1986. Analysis of the relation between alopecia and resistance to 1,25-dihydroxyvitamin D. Clin. Endocrinol. 25, 373–381.

Marx, S.J., Liberman, U.A., Eil, C., Gamblin, G.T., DeGrange, D.A., Balsan, S., 1984. Hereditary resistance to 1,25-dihydroxyvitamin D. Recent Prog. Horm. Res. 40, 589–620.

Marx, S.J., Spiegel, A.M., Brown, E.M., Gardner, D.G., Downs Jr., R.W., Attie, M., Hamstra, A.J., DeLuca, H.F., 1978. A familial syndrome of decrease in sensitivity of 1,25-dihydroxyvitamin D. J. Clin. Endocrinol. Metab. 47, 1303–1310.

Mayer, E., Kadowabi, S., Williams, G., Norman, A.W., 1984. Mode of action of 1,25-dihydroxyvitamin D. In: Kumar, R. (Ed.), Vitamin D: Basic and Clinical Aspects. Martinus Nijhoff, Boston, p. 259.

Mechica, J.B., Leite, M.O.R., Mendoca, B.B., Frazzatto, E.S.T., Borelli, A., Latronico, A.C., 1997. A novel nonsense mutation in the first zinc finger of the vitamin D receptor causing hereditary 1,25-dihydroxyvitamin D resistant rickets. J. Clin. Endocrinol. Metab. 82, 3892–3894.

Miller, W.L., 2017. Genetic disorders of vitamin D biosynthesis and degradation. J. Steroid Biochem. Mol. Biol. 165, 101–108.

Monkawa, T., Yoshida, T., Wakino, S., Shinki, T., Anazawa, H., DeLuca, H.F., Suda, T., Hayashi, M., Saruta, T., 1997. Molecular cloning of cDNA and genomic DNA for human 25-hydroxyvitamin D_3 1α-hydroxylase. Biochem. Biophys. Res. Commun. 239, 527–533.

Murayama, A., Takeyama, K., Kitanaka, S., Kodera, Y., Kawaguchi, Y., Hosoya, T., Kato, S., 1999. Positive and negative regulations of the renal 25-hydroxyvitamin D_3 1α-hydroxylase gene by the parathyroid hormone, calcitonin and 1α, $25(OH)_2D_3$ in intact animals. Endocrinology 140, 2224–2231.

Nguyen, T.M., Adiceam, P., Kottler, M.L., Guillozo, M., Rizk-Rabin, F., Brouillard, F., Lagier, P., Palix, C., Garnier, J.M., Garabedian, M., 2002. Tryptophan missense mutation in the ligand-binding domain of the vitamin D receptor causes severe resistance to 1,25-dihyroxyvitamin D. J. Bone Miner. Res. 17, 1728–1737.

Nguyen, M., d'Alesio, A., Pascussi, J.M., Kumar, R., Griffin, M.D., Dong, X., Guillozo, H., Rizk-Rabin, M., Sinding, C., Bounéres, P., Jehan, F., Garabédian, M., 2006. Vitamin D resistant rickets and type 1 diabetes in a child with compound heterozygous mutations of the vitamin D receptor (L263R and R3915): dissociated responses of the CYP-24 and rel-B promotors to 1,25-dihydroxyvitamin D_3. J. Bone Miner. Res. 21, 886–894.

Ohyama, Y., Noshiro, M., Eggersten, G., Gotoh, O., Kato, Y., Bjorkhem, I., Okuda, K., 1993. Structural characterization of the gene encoding rate 25-hydroxyvitamin D_3 24-hydroxylase. Biochemistry 32, 76–82.

Owen, T.A., Aronow, M.S., Barone, L.M., Bettencourt, B., Stein, G.S., Lian, J.B., 1991. Pleiotropic effects of vitamin D on osteoblast gene expression are related to the proliferative and differentiated state of bone cell phenotype: dependency upon basal levels of gene expression, duration of exposure and bone matrix competency in normal rat osteoblast culture. Endocrinology 129, 3139–3146.

Ozur, K., Sone, T., Pike, J.W., 1991. The genomic mechanism of action of 1,25-dihydroxyvitamin D_3. J. Bone Miner. Res. 6, 1021–1027.

Parfitt, A.M., 1983. The physiologic and clinical significance of bone histomorphometric data. In: Recker, R. (Ed.), Bone Histomorphometric Data. CRC Press, Boca Raton, FL, p. 143.

Pettifor, J.M., Ross, F.P., Travers, R., Glorieux, F.H., DeLuca, H.F., 1981. Dietary calcium deficiency: a syndrome associated with bone deformities and elevated serum 1,25-dihydroxyvitamin D concentrations. Metab. Bone Dis. Relat. Res. 2, 301–305.

Prader, A., Illig, R., Heierli, E., 1961. Eline besondere from der primaren/vitamin D-resistenten Rachitis mit Hypocalcemie un autosomal-dominanten Erbgang: die hereditare Pseudo-Mangelrachi tis. Helv. Paediatr. Acta 16, 452–468.

Reichel, H., Koeffler, P., Norman, A.W., 1989. The role of the vitamin D endocrine system in health and disease. N. Engl. J. Med. 320, 980–991.

Ritchie, H.H., Hughes, M.R., Thompson, E.T., Hochberg, Z., Feldman, D., Pike, J.W., O'Mally, B.W., 1989. An ochre mutation in the vitamin D receptor gene causes hereditary 1,25-dihydroxyvitamin D_3 resistant rickets in three families. Proc. Natl. Acad. Sci. U.S.A. 86, 9783–9787.

Rochel, N., Wurtz, J.M., Mitschler, A., Klaholz, B., Moras, D., 2000. The crystal structure of the nuclear receptor for vitamin D bound to its natural ligand. Mol. Cell. 5, 173–179.

Roizen, J.D., Li, D., O'Lear, L., Javaid, M.K., Shaw, N.J., Ebeling, P.R., Nguyen, H.H., Radda, C.P., Thummel, K.E., Thacher, T.D., Hakonarson, H., Levine, M.A., 2018. CYP3A4 mutation causes vitamin D-dependent rickets type 3. J. Clin. Investig. 128 (5), 1913–1918.

Rosen, J.F., Fleischman, A.R., Fineberg, L., Hamstra, A., DeLuca, H.F., 1979. Rickets with alopecia: an inborn error of vitamin D metabolism. J. Pediatr. 94, 729–735.

Rut, A.R., Hewison, K., Kristjansson, K., Luisi, B., Hughes, M., O'Riordan, J.L.H., 1994. Two mutations causing vitamin D resistant rickets: modelling on the basis of steroid hormone receptor DNA-binding domain crystal structures. Clin. Endocrinol. 41, 581–590.

Saijo, T., Ito, M., Takeda, E., Mahbubul Huq, A.H.M., Naito, E., Yokota, I., Sine, T., Pike, J.W., Kuroda, Y., 1991. A unique mutation in the vitamin D receptor gene in three Japanese patients with vitamin D-dependent rickets type II: utility of single-strand conformation polymorphism analysis for heterozygous carrier detection. Am. J. Hum. Genet. 49, 668–673.

Sakati, N., Woodhouse, N.T.Y., Niles, N., Harji, H., DeGrange, D.A., Marx, S.J., 1986. Hereditary resistance to 1,25-dihydroxyvitamin D: clinical and radiological improvement during high-dose oral calcium therapy. Horm. Res. (Basel) 24, 280–287.

Shinki, T., Shiina, Y., Takanshi, N., Tamoika, Y., Koizumi, H., Suda, T., 1983. Extremely high circulating levels of 1,25-dihydroxyvitamin D_3 in the marmoset, a New World monkey. Biochem. Biophys. Res. Commun. 114, 452–457.

Shinki, T., Shimada, H., Wakino, S., Anazawa, H., Hayashi, M., Saruta, T., DeLuca, H.F., Suda, T., 1997. Cloning and expression of rat 25-hydroxyvitamin 1α-hydroxylase cDNA. Proc. Natl. Acad. Sci. U.S.A. 94, 12920–12925.

Simonin, G., Chabrol, B., Moulene, E., Bollini, G., Strouc, S., Mattei, J.F., Giraud, F., 1992. Vitamin D resistant rickets type II: apropos of 2 cases. Pediatrics 47, 817–820.

Smith, S.J., Rucka, A.K., Berry, J.L., Davies, M., Mylchreest, S., Paterson, C.R., Heath, D.A., Tassabehji, M., Read, A.P., Mee, A.P., Mawer, E.B., 1999. Novel mutations in the 1α-hydroxylase (p450cl) gene in three families with pseudovitamin D-deficiency rickets resulting in loss of functional enzyme activity in blood derived macrophages. J. Bone Miner. Res. 14, 730–739.

Sockalsosky, J.J., Westrom, R.A., DeLuca, H.F., Brown, D.M., 1980. Vitamin D-resistant rickets: end-organ unresponsiveness to 1,25 $(OH)_2D_3$. J. Pediatr. 96, 701–703.

Sone, T., Marx, S.J., Liberman, U.A., Pike, J.W., 1990. A unique point mutation in the human vitamin D receptor chromosomal gene confers hereditary resistance to 1,25-dihydroxyvitamin D_3. Mol. Endocrinol. 4, 623–631.

Sone, T., Scott, R.A., Hughes, M.R., Malloy, P.J., Feldman, D., O'Malley, B.W., Pike, J.W., 1989. Mutant vitamin D receptors which confer hereditary resistance to 1,25-dihydroxyvitamin D_3 in human are transcriptionally inactive in vitro. J. Biol. Chem. 264, 20230–20234.

St Arnaud, R., Messerlian, S., Moir, J.M., Omdahl, J.L., Glorieux, F.H., 1997. The 25-hydroxyvitamin 1 α-hydroxylase gene maps to the pseudovitamin D deficiency rickets (PDDR) disease locus. J. Bone Miner. Res. 12, 1552–1559.

Strumpf, W.E., Sar, M., Reid, F.A., 1979. Target cells for 1,25-dihydroxyvitamin D in intestinal tract, stomach, kidney, skin, pituitary and parathyroid. Science 206, 188–190.

Takahashi, N., Suda, S., Shinki, T., Horiuchi, N., Shina, Y., Tanioka, Y., Koizumi, H., Suda, T., 1985. The mechanisms of end-organ resistance to 1α,25-dihydroxycholecalciferol in the common marmoset. Biochem. J. 227, 555–563.

Takeda, E., Kuroda, Y., Saijo, T., Naito, E., Kobashi, H., Yokota, I., Miyao, M., 1987. 1 alpha-hydroxyvitamin D_3 treatment of three patients with 1,25-dihydroxyvitamin D-receptor-defect rickets and alopecia. Pediatrics 80, 97–101.

Takeda, E., Kuzoda, T., Saijo, T., Toshima, K., Naito, E., Kobashi, H., Iwakuni, Y., Miyao, M., 1986. Rapid diagnosis of vitamin D-dependent rickets type II by use of phyto-hemagglutinin-stimulated lymphocytes. Clin. Chim. Acta 155, 245–250.

Takeda, E., Yokota, I., Kawakami, I., Hashimoto, T.T., Kuroda, Y., Arase, S., 1989. Two siblings with vitamin D-dependent rickets type II: No recurrence of rickets for 14 years after cessation of therapy. Eur. J. Pediatr. 149, 54–57.

Takeda, E., Yokota, I., Ito, M., Kobashi, I., Saijo, T., Kuroda, Y., 1990. 25-Hydroxyvitamin D-24-hydroxylase in phyto-hemagglutinin-stimulated lymphocytes: intermediate bioresponse to 1,25-dihydroxyvitamin D_3 of cells from parents of patients with vitamin D dependent rickets type II. J. Clin. Endocrinol. Metab. 70, 1068–1074.

Takeyama, K., Kitanaka, S., Sato, T., Kobori, M., Yanagisawa, J., Kato, S., 1997. 25-hydroxyvitamin D_3 1α-hydroxylase and vitamin D synthesis. Science 277, 1827–1830.

Tauchiya, Y., Matsuo, N., Cho, H., Kumagai, M., Yasaka, A., Suda, T., Orimo, H., Shiraki, M., 1980. An unusual form of vitamin-D-dependent rickets in a child: alopecia and marked end-organ hyposensitivity to biological active vitamin D. J. Clin. Endocrinol. Metab. 51, 685–690.

Teitelbaum, S.L., Bollough, P.G., 1979. The pathophysiology of bone and disease. Am. J. Pathol. 96, 283.

Thacher, T.D., Fischer, P.R., Singh, R.J., Roizen, J.D., Levine, M.A., 2015. CYP2R1 mutations impair generation of 25-hydroxyvitamin D and cause an atypical form of vitamin D deficiency. J. Clin. Endocrinol. Metab. 100 (7), E1005–E1013.

Thacher, T.D., Levine, M.A., 2017. CYP2R1 mutations causing vitamin D-deficiency rickets. J. Steroid Biochem. Mol. Biol. 173, 333–336.

Wang, J.T., Lin, C.J., Burridge, S.M., Fu, G.K., Labuda, M., Portale, A.A., Miller, W.L., 1998. Genetics of vitamin D 1α-hydroxylase deficiency in 17 families. Am. J. Hum. Genet. 63, 1694–1702.

Weise, R.J., Goto, H., Prahl, J.M., Marx, S.J., Thomas, M., Al-Aqeel, A., DeLuca, H.F., 1993. Vitamin D-dependency rickets type II: truncated vitamin D receptor in three kindreds. Mol. Cell. Endocrinol. 90, 197–201.

Weisman, Y., Bab, I., Gazit, D., Spirer, Z., Jaffe, M., Hochberg, Z., 1987. Long-term intracaval calcium infusion therapy in end-organ resistance to 1,25-dihydroxyvitamin D. Am. J. Med. 83, 984–990.

Weisman, Y., Harell, A., Edelstein, S., David, M., Spirer, Z., Golander, A., 1979. 1α, 25-dihydroxyvitamin D_3 and 24, 25-dihydroxyvitamin D_3 in vitro synthesis by human decidua and placenta. Nature 281, 317–319.

Whitfield, G.K., Selznick, S.H., Haussler, C.A., Hsieh, J.C., Galligan, M.A., Jurutka, P.W., Thompson, P.D., Lee, S.M., Zerwekh, J.E., Haussler, M.R., 1996. Vitamin D receptors from patients with resistance to 1,25-dihydroxyvitamin D_3 point mutations confer reduced transactivation in response to ligand and impaired interaction with the retinoid x receptor heterodimeric partner. Mol. Endocrinol. 10, 1617–1631.

Yagi, H., Ozono, K., Miyake, H., Nagashima, K., Kuroume, T., Pike, J.W., 1993. A new point mutation in the deoxyribonucleic acid-binding domain of the vitamin D receptor in a kindred with hereditary 1,25-dihydroxyvitamin D resistant rickets. J. Clin. Endocrinol. Metab. 76, 509–512.

Yoshida, T., Monkawa, T., Tenehouse, H.S., Goodyear, P., Shinki, T., Suda, T., Wakino, S., Hayashi, M., Saruta, T., 1998. Two novel 1α-hydroxylase in French-Canadians with vitamin D dependency rickets type II. Kidney Int. 54, 1437–1443 [Comments].

Yoshizawa, T., Handa, Y., Uematsu, Y., Takeda, S., Sekine, K., Yoshihara, Y., Kawakami, T., Arioka, K., Sato, H., Uchiyama, Y., Masushige, S., Fukamizu, A., Matsumoto, T., Kato, S., 1997. Mice lacking the vitamin D receptor exhibit impaired bone formation, uterine hypoplasia and growth retardation after weaning. Nat. Genet. 16, 391–396.

Zhu, W.J., Malloy, P.J., Delvin, E., Chabot, G., Feldman, D., 1998. Hereditary 1,25-dihydroxyvitamin D-resistant rickets due to an opal mutation causing premature termination of the vitamin D receptor. J. Bone Miner. Res. 13, 259–264.

Further reading

Chen, K.S., DeLuca, H.F., 1995. Cloning of the human 1α, 25-hydroxyvitamin D_3 24-hydroxylase gene promoter and identification of two vitamin D-responsive elements. Biochim. Biophys. Acta 1263, 1–9.

Gill, R.K., Ramadan, D., Chesnut, C.H.,I.V., Lee, M.H., Patel, S.B., Bell, N.H., 2000. Vitamin D-25-hydroxylase deficiency does not map to the CYP27 or CYP2D6 gene loci. J. Bone Miner. Res. 15, S1–S329.

Malloy, P.J., Feldman, D., 2011. The role of vitamin D receptor mutations in the development of alopecia. Mol. Cell. Endocrinol. 347, 90–96.

Ozono, K., Yamagata, M., Ohyama, Y., Nakajima, S., 1998. Direct repeat 3-type element lacking the ability to bind to the vitamin D receptor enhances the function of a vitamin D-response element. J. Steroid Biochem. Mol. Biol. 66, 263–269.

Thacher, T.D., Hakonarson, H., Levine, M.A., 2018. CYP3A4 mutation causes vitamin D-dependent rickets type 3. J. Clin. Investig. 128 (5), 1913–1918.

Chapter 63

Fibroblast growth factor 23

Seiji Fukumoto

Fujii Memorial Institute of Medical Sciences, Institute of Advanced Medical Sciences, Tokushima University, Tokushima, Japan

Chapter outline

Identification of fibroblast growth factor 23

Serum phosphate level is maintained within a narrow range by intestinal phosphate absorption, proximal tubular phosphate reabsorption, and equilibrium between extracellular phosphate and that in bone or the intracellular space. Parathyroid hormone (PTH) reduces serum phosphate by suppressing proximal tubular phosphate reabsorption. In addition, 1,25-dihydroxyvitamin D ($1,25(OH)_2D$) works to increase serum phosphate by enhancing intestinal phosphate absorption. In addition to these hormones, the presence of some other humoral factor regulating serum phosphate level was postulated by analysis of hypophosphatemic diseases. Tumor-induced osteomalacia (TIO) is one of the paraneoplastic syndromes. Patients with TIO show hypophosphatemia with impaired proximal tubular phosphate reabsorption (Minisola et al., 2017). Hypophosphatemia usually enhances $1,25(OH)_2D$ production and increases serum $1,25(OH)_2D$ (Fukumoto, 2014). However, $1,25(OH)_2D$ is low to low normal in patients with TIO. In addition, serum calcium and PTH are usually normal in patients with TIO. TIO can be cured and biochemical abnormalities corrected by complete removal of the responsible tumors, indicating that some humoral factor produced by the tumors is causing hypophosphatemia and rather low $1,25(OH)_2D$. X-linked hypophosphatemic rickets (XLH) is the most prevalent cause of inherited hypophosphatemic rickets. Patients with XLH show biochemical features similar to those in subjects with TIO. The responsible gene for XLH was identified by positional cloning and named phosphate-regulating gene with homologies to endopeptidases on the X chromosome (*PHEX*) (The HYP Consortium, 1995). There is a murine model of XLH called the *Hyp* mouse. This mouse was shown to have a deletion in the *Phex* gene (Beck et al., 1997). Parabiosis experiments suggested that biochemical abnormalities in the *Hyp* mouse are caused by some humoral factor (Meyer et al., 1989). However, it was not clear whether biochemical abnormalities in TIO and *Hyp* are caused by the same humoral factor.

FGF23 was identified as a responsible gene for autosomal dominant hypophosphatemic rickets (ADHR) by positional cloning (ADHR Consortium, 2000). Patients with ADHR show clinical features similar to those in subjects with XLH. In addition, *Fgf23* was cloned by homology to *Fgf15* in mice (Yamashita et al., 2000). Furthermore, fibroblast growth factor

Principles of Bone Biology. https://doi.org/10.1016/B978-0-12-814841-9.00063-4

23 (FGF23) was identified as a responsible humoral factor for TIO (Shimada et al., 2001). FGF23 was later shown to be produced by bone, especially by osteocytes/osteoblasts (Liu et al., 2003), and to be the responsible humoral factor in XLH and *Hyp*.

Actions of fibroblast growth factor 23

The human *FGF23* gene encodes a protein of 251 amino acids. There is a signal peptide of 24 amino acids and a secreted FGF23 protein consists of 227 amino acids. A part of the FGF23 protein is proteolytically cleaved into inactive fragments between ^{179}Arg and ^{180}Ser before secretion by an enzyme that recognizes the ^{176}Arg−X−X−^{179}Arg motif (Shimada et al., 2001). While PHEX protein was originally postulated to mediate this processing of FGF23 protein, this hypothesis was later denied (Linglart et al., 2014).

FGF23 was shown to reduce the expression of type IIa and IIc sodium−phosphate cotransporters expressed in the brush border membrane of renal proximal tubules (Larsson et al., 2004; Shimada et al., 2004a). These cotransporters are physiological mediators of phosphate reabsorption. In addition, FGF23 suppresses the expression of *CYP27B1*, which encodes cytochrome P450 family 27, subfamily B member 1 (Shimada et al., 2004a). This enzyme converts 25-hydroxyvitamin D (25(OH)D) to 1,25$(OH)_2$D and is responsible for the production of 1,25$(OH)_2$D. FGF23 also enhances the expression of *CYP24A1* coding cytochrome P450 family 24, subfamily A member 1 (Shimada et al., 2004a). This enzyme converts 1,25$(OH)_2$D to 1,24,25- trihydroxyvitamin D and also 25(OH)D to 24,25-dihydroxyvitamin D. From these effects on vitamin D-metabolizing enzymes, FGF23 works to reduce the serum level of 1,25$(OH)_2$D. Because 1,25$(OH)_2$D is a hormone enhancing intestinal phosphate absorption, FGF23 reduces serum phosphate by suppressing intestinal phosphate absorption via reduction of serum 1,25$(OH)_2$D and also by inhibiting proximal tubular phosphate reabsorption (Fig. 63.1). In contrast, *Fgf23*-knockout mouse shows hyperphosphatemia with enhanced proximal tubular phosphate reabsorption and high 1,25$(OH)_2$D level (Shimada et al., 2004b; Sitara et al., 2004). These results indicate that FGF23 is a physiological humoral factor regulating phosphate and vitamin D metabolism and inspired the concept that bone works as an endocrine organ (Fukumoto and Martin, 2009).

Regulation of fibroblast growth factor 23 level

The regulatory mechanisms of FGF23 level are not fully elucidated. FGF23 levels can be regulated by changes in both *FGF23* expression and posttranslational processing of FGF23 protein as discussed later. A high-phosphate diet increases FGF23 levels in both rodents and humans (Ferrari et al., 2005; Perwad et al., 2005). However, it is not entirely clear how a high-phosphate diet causes high FGF23 levels. 1,25$(OH)_2$D and PTH were shown to enhance FGF23 production

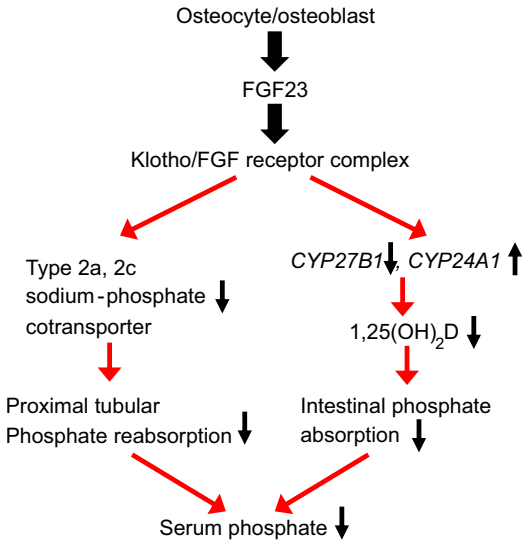

FIGURE 63.1 Actions of fibroblast growth factor 23 in kidney. Fibroblast growth factor 23 (FGF23) reduces serum phosphate by suppressing intestinal phosphate absorption via reduction of serum 1,25-dihydroxyvitamin D (1,25$(OH)_2$D and also by inhibiting proximal tubular phosphate reabsorption. *CYP24A1*, cytochrome P450 family 24, subfamily A member 1; *CYP27B1*, cytochrome P450 family 27, subfamily B member 1.

(Fan et al., 2016; Saito et al., 2005). Conversely, FGF23 reduces $1,25(OH)_2D$ level as previously mentioned. Furthermore, FGF23 was shown to inhibit PTH production and secretion (Ben-Dov et al., 2007). There seem to be negative feedback systems among PTH, $1,25(OH)_2D$, and FGF23.

PTH regulates serum calcium, and an increase in calcium activates the calcium-sensing receptor (CaSR) in parathyroid cells and suppresses PTH secretion (Brown et al., 1993). Therefore, there is a negative feedback between serum calcium and PTH via the CaSR. By an analogy to the relationship between calcium and PTH, it is suggested that serum phosphate affects FGF23 level. However, it is not known how serum phosphate is sensed in our body and whether serum phosphate can directly modulate FGF23 level.

A receptor for fibroblast growth factor 23

FGF23 belongs to the FGF family. FGF family members have an FGF homology region with a β-trefoil structure. FGF23 has an FGF homology region in the N-terminal portion of the processing site between ^{179}Arg and ^{180}Ser. FGF23 family members are divided into several subfamilies (Itoh and Ornitz, 2004). FGF23 belongs to the FGF19 subfamily together with FGF19 and FGF21. The prototypical FGF family members, such as FGF1 (acidic FGF) and FGF2 (basic FGF), work as autocrine/paracrine factors. These FGF family members have high affinity for heparin or heparan sulfate proteoglycan. Heparin or heparan sulfate proteoglycan enhances the affinity of FGF ligands to FGF receptors. In addition, because of this high affinity for heparin or heparan sulfate proteoglycan, these FGF family members are trapped in the extracellular matrix around cells producing these growth factors. This explains why some FGF family members work as local factors. In contrast, FGF23 is produced by bone and works in kidney and parathyroid glands. This means that FGF23 is a systemic factor. Actually, FGF19 subfamily members were shown to have a low affinity for heparin, explaining how these members work as systemic factors (Goetz et al., 2007). There are four FGF receptor genes, and alternative splicing from these genes produces several FGF receptor subtypes. The expression of most of these FGF receptors is not tissue specific. In vitro experiments showed that dissociation constants between FGF23 and these FGF receptors are much higher than the circulatory FGF23 level (Yu et al., 2005). These results indicate that FGF receptors alone cannot explain tissue-specific effects of FGF23.

Klotho was identified as a binding protein for FGF23 in kidney (Urakawa et al., 2006). *Klotho* was originally cloned as a gene whose expression is severely reduced in the genetically engineered *Klotho* mouse (Kuro-o et al., 1997). This mouse shows several phenotypes resembling aging, such as skin atrophy, infertility, emphysema, and reduced bone mass (Kuro-o et al., 1997). This mouse also shows high phosphate and $1,25(OH)_2D$ levels, like the *Fgf23*-knockout mouse, suggesting the involvement of Klotho in FGF23 signaling (Yoshida et al., 2002).

In vitro experiments showed that the Klotho−FGF receptor complex works as a specific receptor for FGF23 (Urakawa et al., 2006; Kurosu et al., 2006). Klotho is expressed in few tissues, such as kidneys and parathyroid glands. This tissue-specific expression of Klotho is considered to explain the target organs of FGF23. Klotho was shown to be expressed mainly in the renal distal convoluted tubules (Kuro-o et al., 1997). However, a 2012 study indicated that Klotho is also expressed in the proximal tubules (Andrukhova et al., 2012). It is postulated that a protein similar to Klotho, called β-Klotho, is necessary for the actions of FGF19 and FGF21 (Moore, 2007).

In contrast, there are several reports of Klotho-independent, FGF receptor−dependent actions of FGF23, such as suppression of PTH secretion and cardiac hypertrophy (Faul et al., 2011; Olauson et al., 2013). However, it has not been shown how FGF23 activates FGF receptors in a Klotho-independent way.

Hypophosphatemic diseases caused by excessive actions of fibroblast growth factor 23

After the cloning of *FGF23*, several kinds of hypophosphatemic diseases have been shown to be caused by excessive actions of FGF23 (Table 63.1). Establishment of assays for FGF23 helped to identify these hypophosphatemic diseases (Jonsson et al., 2003; Yamazaki et al., 2002). Circulatory FGF23 was shown to be high in hypophosphatemic patients caused by excessive actions of FGF23. In contrast, FGF23 is rather low in hypophosphatemic from other causes such as vitamin D deficiency and Fanconi syndrome (Endo et al., 2008). These results indicate that FGF23 level is regulated by serum phosphate or other associated metabolic changes, while it is not known how phosphate modulates FGF23 level as mentioned earlier. Chronic hypophosphatemia causes rickets and osteomalacia characterized by impaired mineralization of bone matrix. Rickets develops before the closure of growth plates. Growth retardation and bone deformities are major clinical problems in patients with rickets. In contrast, muscle weakness and bone pain are important symptoms of adult patients with hypophosphatemic osteomalacia.

TABLE 63.1 Diseases caused by aberrant actions of FGF23

Hypophosphatemic disease caused by excessive actions of FGF23	Responsible gene
Autosomal dominant hypophosphatemic rickets: ADHR	*FGF23*
X-linked hypophosphatemic rickets: XLH	*PHEX*
Autosomal recessive hypophosphatemic rickets 1: ARHR1	*DMP1*
Autosomal recessive hypophosphatemic rickets 2: ARHR2	*ENPP1*
Hypophosphatemia, dental anomalies and ectopic calcification	*FAM20C*
Jansen-type metaphyseal chondrodysplasia	*PTH1R*
McCune-Albright syndrome/Fibrous dysplasia of bone	*GNAS1*
Hypophosphatemia, skin and bone lesions	*HRAS, KRAS, NRAS*
Hypophosphatemic rickets and hyperparathyroidism	Translocation with a breakpoint adjacent to *Klotho*
Tumor-induced osteomalacia: TIO Hypophosphatemia by iron polymaltose, saccharated ferric oxide or ferric carboxymaltose Biliary atresia	
Hyperphosphatemic disease caused by impaired actions of FGF23	
Hyperphosphatemic familial tumoral calcinosis	*GALNT3, FGF23, Klotho*

DMP, dentin matrix protein 1; *ENPP1,* ectonucleotide pyrophosphatase/phosphodiesterase 1; *FAM20C,* family with sequence similarity 20, member C; *FGF23,* fibroblast growth factor 23; *GALNT3,* polypeptide N-acetylgalactosaminyltransferase 3; *GNAS1,* guanine nucleotide-binding protein, α stimulating;,*PHEX,* phosphate-regulating gene with homologies to endopeptidases on the X chromosome; *PTH1R,* parathyroid hormone 1 receptor.

Autosomal dominant hypophosphatemic rickets

Heterozygous mutations in *FGF23* cause ADHR. Mutations in patients with ADHR replace ^{176}Arg or ^{179}Arg with other amino acids, destroying the recognition site of ^{176}Arg−X−X−^{179}Arg by the processing enzyme (ADHR Consortium, 2000). This makes the mutant FGF23 proteins resistant to the processing. However, this resistance to the processing alone cannot explain the excessive actions of FGF23 in patients with ADHR. It is known that clinical presentation, including biochemical abnormalities, can wax and wane with time in patients with ADHR (Imel et al., 2007). This indicates that some patients can maintain serum phosphate level with mutations in *FGF23*. Even if the mutant FGF23 protein is resistant to the processing, these patients may be able to maintain FGF23 and phosphate levels by regulating the expression of *FGF23*.

Iron deficiency was shown to affect FGF23 level in patients with ADHR (Imel et al., 2011). Iron deficiency enhances *FGF23* expression and also processing of FGF23 protein, resulting in normal FGF23 and phosphate levels in healthy controls. In contrast, it is postulated that enhanced *FGF23* expression results in high FGF23 and hypophosphatemia in subjects with ADHR because the mutant FGF23 protein is resistant to the processing. However, it is not completely clear how iron deficiency affects FGF23 expression and processing. It is also possible that factors other than iron deficiency can modulate FGF23 level in patients with ADHR.

X-linked hypophosphatemic rickets

FGF23 is high in patients with XLH, suggesting that FGF23 is the humoral factor inducing hypophosphatemia in patients with XLH (Jonsson et al., 2003; Yamazaki et al., 2002). *Fgf23* was also shown to be overexpressed in bones of the *Hyp* mouse (Liu et al., 2003). *Phex* deletion in bone indicated that deficient Phex function in osteocytes/osteoblasts alone can explain *Hyp* phenotypes (Yuan et al., 2008). There are more than 300 kinds of *PHEX* mutations reported and assembled in a database (http://grch37.ensembl.org/Homo_sapiens/Gene/Variation_Gene/Table?db=core;g=ENSG00000102174;r=X:22050559-22269427). These mutations are considered to be inactivating ones. *PHEX* mutations were reported to change the expression of several proteins, including 7B2, resulting in high FGF23 (Yuan et al., 2013). However, it was not shown how deficient actions of PHEX cause decreased expression of 7B2. Furthermore, it is possible that there are other mechanisms for how inactivating mutations of *PHEX* cause elevated FGF23 levels.

Autosomal recessive hypophosphatemic rickets

Autosomal recessive hypophosphatemic rickets (ARHR) 1 and ARHR2 are caused by inactivating mutations in dentin matrix protein 1 (*DMP1*) and ectonucleotide pyrophosphatase/phosphodiesterase 1 (*ENPP1*), respectively (Feng et al., 2006; Levy-Litan et al., 2010; Lorenz-Depiereux et al., 2006, 2010). Enhanced expression of FGF23 in bone is considered to cause these diseases, while, again, the mechanisms of this overexpression of FGF23 are not completely understood. In vitro experiments showed that externally added DMP1 inhibits the production of FGF23 (Samadfam et al., 2009). However, the detailed mechanism of this inhibition of FGF23 production by DMP1 protein is not known. ENPP1 is an enzyme that hydrolyzes pyrophosphate. Pyrophosphate is a potent inhibitor of calcification, and inactivating mutations in *ENPP1* were shown to cause generalized arterial calcification of infancy (GACI) (Lorenz-Depiereux et al., 2010). GACI is usually fatal soon after birth. However, some surviving patients with mutations in *ENPP1* were shown to have hypophosphatemic rickets/osteomalacia with high FGF23.

Other hypophosphatemic diseases with known genetic causes

Mutations in family with sequence similarity 20, member C (*FAM20C*), cause hypophosphatemic disease with high FGF23, dental anomalies, and ectopic calcification (Rafaelsen et al., 2013). FAM20C is a Golgi serine/threonine protein kinase that phosphorylates secretory pathway proteins. Inactivating mutations in *FAM20C* have been shown to cause Raine syndrome, a neonatal osteosclerotic dysplasia (Simpson et al., 2007). This disease is usually fatal early in life. However, again, some surviving patients were shown to have hypophosphatemic rickets/osteomalacia with high FGF23. FAM20C can phosphorylate small integrin-binding ligand N-linked glycoproteins (SIBLINGs), including osteopontin and DMP1. It is likely that phosphorylation of these SIBLINGs affects mineralization of bone in patients with Raine syndrome. In addition, it is possible that deficient phosphorylation of DMP1 causes high FGF23, because inactivating mutations in *DMP1* result in ARHR1 (Kinoshita et al., 2014).

Activating mutations in PTH1 receptor (*PTH1R*) and guanine nucleotide-binding protein, α stimulating (*GNAS1*), cause hypophosphatemic disease with high FGF23, suggesting that FGF23 production is stimulated by the cyclic AMP pathway (Brown et al., 2009; Riminucci et al., 2003). In addition, there are several reports indicating that signals from FGF receptor regulate FGF23 production (Wohrle et al., 2011). Some activating mutations in FGF receptor 1 (*FGFR1*) were shown to cause hypophosphatemia with high FGF23 in patients with osteoglophonic dysplasia (White et al., 2005). FGF23 is high in hypophosphatemic patients with somatic mutations in *HRAS, KRAS* or *NRAS* (Lim et al., 2014), and there is a report of a hypophosphatemic patient with a de novo translocation with a breakpoint adjacent to the *Klotho* gene (Brownstein et al., 2008).

Acquired fibroblast growth factor 23-related hypophosphatemic disease

In addition to TIO, FGF23 is high in hypophosphatemic patients with iron-deficiency anemia treated with intravenous iron preparations (Schouten et al., 2009; Shimizu et al., 2009). Some patients treated with intravenous iron for a long time can present with severe hypophosphatemic osteomalacia. As discussed earlier, iron deficiency enhances both *FGF23* expression and processing of FGF23 protein. Therefore, it is possible that administration of intravenous iron preparations prevents the processing of FGF23 protein. However, it is not known how intravenous iron preparations affect the processing of FGF23 protein. High FGF23 level and hypophosphatemia are not reported with oral iron administration.

Hypophosphatemic rickets with high FGF23 was reported in some patients with biliary atresia (Wasserman et al., 2016). FGF23 was expressed in the liver of a patient. It is not known what triggers the expression of FGF23 in liver in this disease.

Treatment of fibroblast growth factor 23-related hypophosphatemic diseases

TIO can be cured by complete removal of the responsible tumors. Hypophosphatemia caused by intravenous iron preparations improves by stopping the drug. Other hypophosphatemic patients, including those with TIO, whose responsible tumors cannot be removed or found are usually treated with neutral phosphate and active vitamin D. However, these medications have limitations in both their effects and adverse events (Carpenter et al., 2011). Several methods to inhibit excessive FGF23 actions have been reported (Fukumoto, 2016). Of these, humanized anti-FGF23 blocking antibody has been tested in several clinical trials for patients with XLH and TIO. This antibody increases serum phosphate and

$1,25(OH)_2D$, and improves radiographic findings of rickets (Carpenter et al., 2014; Imel et al., 2015; Carpenter et al., 2018). The antibody was approved for patients with XLH in several countries in 2018.

Hyperphosphatemic diseases caused by impaired actions of fibroblast growth factor 23 (Table 63.1)

In contrast to hypophosphatemic diseases caused by excessive actions of FGF23, deficient actions of FGF23 result in hyperphosphatemic familial tumoral calcinosis. This disease is characterized by hyperphosphatemia with enhanced proximal tubular phosphate reabsorption and high $1,25(OH)_2D$ level (Lyles et al., 1988). These biochemical changes are also observed in *Fgf23*-knockout and *Klotho* mice. Patients with this disease have ectopic calcification and calcified mass, especially around large joints. These tumors can cause pain and white discharge from the skin.

There are three genes known to be responsible for hyperphosphatemic familial tumoral calcinosis. These are *GALNT3*, *FGF23*, and *Klotho* (Benet-Pages et al., 2005; Ichikawa et al., 2007; Topaz et al., 2004). *GALNT3* encodes a protein called UDP-*N*-acetyl-α-D-galactosamine:polypeptide *N*-acetylgalactosaminyltransferase 3 (GalNAc-T3). This enzyme attaches *N*-acetylgalactosamine to a Ser or Thr residue as an initial sugar of mucin-type O-linked glycosylation. There are 20 members of the GalNAc-Ts (Hurtado-Guerrero, 2016). While these 20 enzymes seem to have redundant substrate specificity, homozygous inactivating mutations in *GALNT3* cause hyperphosphatemic familial tumoral calcinosis, indicating that other GalNAc-Ts cannot compensate for the impaired actions of GalNAc-T3 in phosphate metabolism. FGF23 protein has three O-linked glycans at ^{171}Thr, ^{178}Thr, and ^{200}Thr. GalNAc-T3 was shown to initiate the O-linked glycosylation at ^{178}Thr, just before the processing site between ^{179}Arg and ^{180}Ser (Frishberg et al., 2007; Kato et al., 2006). This O-linked glycosylation at ^{178}Thr prevents the processing of FGF23 protein.

There are two kinds of assays for FGF23. The intact assay uses two kinds of antibodies that recognize the N-terminal and C-terminal portions of the processing site of FGF23. This assay measures only full-length biologically active FGF23 (Yamazaki et al., 2002). On the other hand, the C-terminal assay adopts two kinds of antibodies recognizing the C-terminal portion of FGF23. This C-terminal assay detects both full-length FGF23 and the processed C-terminal fragment of FGF23 (Jonsson et al., 2003). FGF23 levels in patients with mutations in *GALNT3* are very high by the C-terminal assay, but low to low normal by the intact assay (Frishberg et al., 2007). These results indicate that quite a lot of processed C-terminal fragment of FGF23 is present in the circulation of these patients, while there is only a little full-length FGF23. These clinical data also support the notion that deficient O-linked glycosylation at ^{178}Thr makes the FGF23 protein susceptible to the processing.

Patients with hyperphosphatemic familial tumoral calcinosis caused by mutations in *FGF23* also show similar FGF23 levels, high by C-terminal assay and rather low by full-length assay (Araya et al., 2005). The mutant FGF23 protein was shown to be trapped in the Golgi apparatus in in vitro experiments, while the detailed mechanism of the secretion of the processed C-terminal fragment is not known (Benet-Pages et al., 2005). On the other hand, it was also reported that the mutant protein can bypass the endoplasmic reticulum/Golgi quality control system and be secreted (Shawar et al., 2016). Further studies are necessary to clarify the mechanism of the impaired actions of FGF23 in patients with mutations in the *FGF23* gene.

There is a report of a patient with hyperphosphatemic tumoral calcinosis caused by a mutation in the *Klotho* gene (Ichikawa et al., 2007). FGF23 levels were high by both full-length and C-terminal assays in this patient. Because Klotho works as a coreceptor for FGF23, this hyperphosphatemic disease caused by a mutation in the *Klotho* gene is considered to be caused by resistance to FGF23. There is also a report of a patient with acquired hyperphosphatemic tumoral calcinosis caused by FGF23 autoantibodies (Roberts et al., 2018).

Treatment of hyperphosphatemic familial tumoral calcinosis

Surgery may be necessary for painful calcified masses. Dietary phosphate restriction and phosphate binders are used for hyperphosphatemia. There are a couple of reports suggesting the utility of acetazolamide for this condition (Lammoglia and Mericq, 2009; Yamaguchi et al., 1995). Theoretically, recombinant FGF23 can ameliorate hyperphosphatemia in patients with mutations in either *GALNT3* or *FGF23*.

Fibroblast growth factor 23 and chronic kidney disease–mineral and bone disorder

FGF23 is high in patients with chronic kidney disease (CKD) and can be extremely high in subjects with end-stage renal disease (Weber et al., 2003). FGF23 is also involved in the development of CKD–mineral and bone disorder. FGF23 starts

to increase in patients with CKD stage 2 during the progression of CKD before the increase in PTH or phosphate (Isakova et al., 2011). There is no clear abnormality in mineral metabolism when FGF23 begins to increase. It is not known what triggers this increase in FGF23 in patients with early CKD. However, this increase in FGF23 is considered to enhance urinary phosphate excretion and work to prevent the development of hyperphosphatemia. In vivo experiments showed that the inhibition of FGF23 activity by anti-FGF23 antibodies reduces urinary phosphate excretion and increases serum phosphate level in a rat model of early CKD (Hasegawa et al., 2010). On the other hand, FGF23 decreases $1,25(OH)_2D$ level and this reduced $1,25(OH)_2D$ may increase PTH synthesis. While FGF23 was shown to inhibit the synthesis and secretion of PTH (Ben-Dov et al., 2007), it is also reported that FGF23 is an inducer of parathyroid cell proliferation and PTH secretion (Kawakami et al., 2017). With the progression of CKD, the expression of Klotho in kidney and parathyroid glands decreases and FGF23 cannot work on these tissues in patients with end-stage renal disease (Koh et al., 2001; Komaba et al., 2010).

High FGF23 levels have been shown to be associated with various adverse events, especially in subjects with CKD. High FGF23 levels were reported to be associated with higher mortality, cardiovascular events, left-ventricular hypertrophy, arterial calcification, impaired vasodilation, decreased bone mineral density, fractures, progression of CKD, and so on (Fukumoto and Shimizu, 2011). Some of these associations were also reported in community-dwelling subjects. However, the reasons for these associations are not entirely clear. It was reported that FGF23 can induce left-ventricular hypertrophy by acting on cardiomyocytes (Faul et al., 2011). FGF23 was also shown to impair neutrophil recruitment and chemotaxis (Rossaint et al., 2016; Yang et al., 2017), and promote inflammation by acting on hepatocytes (Singh et al., 2016). Because Klotho is not shown to be expressed in these tissues, it is unknown at this writing how FGF23 induces these effects. In addition, it is not clear whether these direct actions of FGF23 in various tissues underlie the association between high FGF23 levels and all the reported adverse events. Further studies will clarify whether FGF23 has roles other than just working as a phosphotropic hormone and how FGF23 works in tissues without Klotho expression.

References

ADHR Consortium, 2000. Autosomal dominant hypophosphataemic rickets is associated with mutations in FGF23. Nat. Genet. 26, 345–348.

Andrukhova, O., Zeitz, U., Goetz, R., Mohammadi, M., Lanske, B., Erben, R.G., 2012. FGF23 acts directly on renal proximal tubules to induce phosphaturia through activation of the ERK1/2- SGK1 signaling pathway. Bone 51, 621–628.

Araya, K., Fukumoto, S., Backenroth, R., Takeuchi, Y., Nakayama, K., Ito, N., et al., 2005. A novel mutation in fibroblast growth factor 23 gene as a cause of tumoral calcinosis. J. Clin. Endocrinol. Metab. 90, 5523–5527.

Beck, L., Soumounou, Y., Martel, J., Krishnamurthy, G., Gauthier, C., Goodyer, C.G., et al., 1997. Pex/PEX tissue distribution and evidence for a deletion in the 3' region of the Pex gene in X-linked hypophosphatemic mice. J. Clin. Invest. 99, 1200–1209.

Ben-Dov, I.Z., Galitzer, H., Lavi-Moshayoff, V., Goetz, R., Kuro-o, M., Mohammadi, M., et al., 2007. The parathyroid is a target organ for FGF23 in rats. J. Clin. Investig. 117, 4003–4008.

Benet-Pagès, A., Orlik, P., Strom, T.M., Lorenz-Depiereux, B., 2005. An FGF23 missense mutation causes familial tumoral calcinosis with hyperphosphatemia. Hum. Mol. Genet. 14, 385–390.

Brown, E.M., Gamba, G., Riccardi, D., Lombardi, M., Butters, R., Kifor, O., et al., 1993. Cloning and characterization of an extracellular $Ca^{(2+)}$-sensing receptor from bovine parathyroid. Nature 366, 575–580.

Brown, W.W., Jüppner, H., Langman, C.B., Price, H., Farrow, E.G., White, K.E., et al., 2009. Hypophosphatemia with elevations in serum fibroblast growth factor 23 in a child with Jansen's metaphyseal chondrodysplasia. J. Clin. Endocrinol. Metab. 94, 17–20.

Brownstein, C.A., Adler, F., Nelson-Williams, C., Iijima, J., Li, P., Imura, A., et al., 2008. A translocation causing increased alpha-klotho level results in hypophosphatemic rickets and hyperparathyroidism. Proc. Natl. Acad. Sci. U. S. A. 105, 3455–3460.

Carpenter, T.O., Imel, E.A., Holm, I.A., Jan de Beur, S.M., Insogna, K.L., 2011. A clinician's guide to X-linked hypophosphatemia. J. Bone Miner. Res. 26, 1381–1388.

Carpenter, T.O., Imel, E.A., Ruppe, M.D., Weber, T.J., Klausner, M.A., Wooddell, M.M., et al., 2014. Randomized trial of the anti-FGF23 antibody KRN23 in X-linked hypophosphatemia. J. Clin. Investig. 124, 1587–1597.

Carpenter, T.O., Whyte, M.P., Imel, E.A., Boot, A.M., Högler, W., Linglart, A., et al., 2018. Burosumab therapy in children with X-linked hypophosphatemia. N. Engl. J. Med. 378, 1987–1998.

Endo, I., Fukumoto, S., Ozono, K., Namba, N., Tanaka, H., Inoue, D., et al., 2008. Clinical usefulness of measurement of fibroblast growth factor 23 (FGF23) in hypophosphatemic patients: proposal of diagnostic criteria using FGF23 measurement. Bone 42, 1235–1239.

Fan, Y., Bi, R., Densmore, M.J., Sato, T., Kobayashi, T., Yuan, Q., et al., 2016. Parathyroid hormone 1 receptor is essential to induce FGF23 production and maintain systemic mineral ion homeostasis. FASEB J. 30, 428–440.

Faul, C., Amaral, A.P., Oskouei, B., Hu, M.C., Sloan, A., Isakova, T., et al., 2011. FGF23 induces left ventricular hypertrophy. J. Clin. Investig. 121, 4393–4408.

Feng, J.Q., Ward, L.M., Liu, S., Lu, Y., Xie, Y., Yuan, B., et al., 2006. Loss of DMP1 causes rickets and osteomalacia and identifies a role for osteocytes in mineral metabolism. Nat. Genet. 38, 1310–1315.

Ferrari, S.L., Bonjour, J.P., Rizzoli, R., 2005. Fibroblast growth factor-23 relationship to dietary phosphate and renal phosphate handling in healthy young men. J. Clin. Endocrinol. Metab. 90, 1519–1524.

Frishberg, Y., Ito, N., Rinat, C., Yamazaki, Y., Feinstein, S., Urakawa, I., et al., 2007. Hyperostosis-hyperphosphatemia syndrome: a congenital disorder of O-glycosylation associated with augmented processing of fibroblast growth factor 23. J. Bone Miner. Res. 22, 235–242.

Fukumoto, S., 2014. Phosphate metabolism and vitamin D. Bone Rep. 3, 497.

Fukumoto, S., 2016. FGF23-FGF receptor/klotho pathway as a new drug target for disorders of bone and mineral metabolism. Calcif. Tissue Int. 98, 334–340.

Fukumoto, S., Martin, T.J., 2009. Bone as an endocrine organ. Trends Endocrinol. Metab. 20, 230–236.

Fukumoto, S., Shimizu, Y., 2011. Fibroblast growth factor 23 as a phosphotropic hormone and beyond. J. Bone Miner. Metab. 29, 507–514.

Goetz, R., Beenken, A., Ibrahimi, O.A., Kalinina, J., Olsen, S.K., Eliseenkova, A.V., et al., 2007. Molecular insights into the klotho-dependent, endocrine mode of action of fibroblast growth factor 19 subfamily members. Mol. Cell Biol. 27, 3417–3428.

Hasegawa, H., Nagano, N., Urakawa, I., Yamazaki, Y., Iijima, K., Fujita, T., et al., 2010. Direct evidence for a causative role of FGF23 in the abnormal renal phosphate handling and vitamin D metabolism in rats with early-stage chronic kidney disease. Kidney Int. 78, 975–980.

Hurtado-Guerrero, R., 2016. Recent structural and mechanistic insights into protein O-GalNAc glycosylation. Biochem. Soc. Trans. 44, 61–67.

Ichikawa, S., Imel, E.A., Kreiter, M.L., Yu, X., Mackenzie, D.S., Sorenson, A.H., et al., 2007. A homozygous missense mutation in human KLOTHO causes severe tumoral calcinosis. J. Clin. Investig. 117, 2684–2691.

Imel, E.A., Hui, S.L., Econs, M.J., 2007. FGF23 concentrations vary with disease status in autosomal dominant hypophosphatemic rickets. J. Bone Miner. Res. 22, 520–526.

Imel, E.A., Peacock, M., Gray, A.K., Padgett, L.R., Hui, S.L., Econs, M.J., 2011. Iron modifies plasma FGF23 differently in autosomal dominant hypophosphatemic rickets and healthy humans. J. Clin. Endocrinol. Metab. 96, 3541–3549.

Imel, E.A., Zhang, X., Ruppe, M.D., Weber, T.J., Klausner, M.A., Ito, T., et al., 2015. Prolonged correction of serum phosphorus in adults with X-linked hypophosphatemia using monthly doses of KRN23. J. Clin. Endocrinol. Metab. 100, 2565–2573.

Isakova, T., Wahl, P., Vargas, G.S., Gutiérrez, O.M., Scialla, J., Xie, H., et al., 2011. Fibroblast growth factor 23 is elevated before parathyroid hormone and phosphate in chronic kidney disease. Kidney Int. 79, 1370–1378.

Itoh, N., Ornitz, D.M., 2004. Evolution of the Fgf and Fgfr gene families. Trends Genet. 20, 563–569.

Jonsson, K.B., Zahradnik, R., Larsson, T., White, K.E., Sugimoto, T., Imanishi, Y., et al., 2003. Fibroblast growth factor 23 in oncogenic osteomalacia and X-linked hypophosphatemia. N. Engl. J. Med. 348, 1656–1663.

Kato, K., Jeanneau, C., Tarp, M.A., Benet-Pagès, A., Lorenz-Depiereux, B., Bennett, E.P., et al., 2006. Polypeptide GalNAc-transferase T3 and familial tumoral calcinosis. Secretion of fibroblast growth factor 23 requires O-glycosylation. J. Biol. Chem. 281, 18370–18377.

Kawakami, K., Takeshita, A., Furushima, K., Miyajima, M., Hatamura, I., Kuro, O.M., et al., 2017. Persistent fibroblast growth factor 23 signalling in the parathyroid glands for secondary hyperparathyroidism in mice with chronic kidney disease. Sci. Rep. 7, 40534.

Kinoshita, Y., Hori, M., Taguchi, M., Fukumoto, S., 2014. Functional analysis of mutant FAM20C in Raine syndrome with FGF23-related hypophosphatemia. Bone 67, 145–151.

Koh, N., Fujimori, T., Nishiguchi, S., Tamori, A., Shiomi, S., Nakatani, T., et al., 2001. Severely reduced production of klotho in human chronic renal failure kidney. Biochem. Biophys. Res. Commun. 280, 1015–1020.

Komaba, H., Goto, S., Fujii, H., Hamada, Y., Kobayashi, A., Shibuya, K., et al., 2010. Depressed expression of Klotho and FGF receptor 1 in hyperplastic parathyroid glands from uremic patients. Kidney Int. 77, 232–238.

Kuro-o, M., Matsumura, Y., Aizawa, H., Kawaguchi, H., Suga, T., Utsugi, T., et al., 1997. Mutation of the mouse klotho gene leads to a syndrome resembling ageing. Nature 390, 45–51.

Kurosu, H., Ogawa, Y., Miyoshi, M., Yamamoto, M., Nandi, A., Rosenblatt, K.P., et al., 2006. Regulation of fibroblast growth factor-23 signaling by klotho. J. Biol. Chem. 281, 6120–6123.

Lammoglia, J.J., Mericq, V., 2009. Familial tumoral calcinosis caused by a novel FGF23 mutation: response to induction of tubular renal acidosis with acetazolamide and the non-calcium phosphate binder sevelamer. Horm. Res. 71, 178–184.

Larsson, T., Marsell, R., Schipani, E., Ohlsson, C., Ljunggren, O., Tenenhouse, H.S., et al., 2004. Transgenic mice expressing fibroblast growth factor 23 under the control of the alpha1(I) collagen promoter exhibit growth retardation, osteomalacia, and disturbed phosphate homeostasis. Endocrinology 145, 3087–3094.

Levy-Litan, V., Hershkovitz, E., Avizov, L., Leventhal, N., Bercovich, D., Chalifa-Caspi, V., et al., 2010. Autosomal-recessive hypophosphatemic rickets is associated with an inactivation mutation in the ENPP1 gene. Am. J. Hum. Genet. 86, 273–278.

Lim, Y.H., Ovejero, D., Sugarman, J.S., Deklotz, C.M., Maruri, A., Eichenfield, L.F., et al., 2014. Multilineage somatic activating mutations in HRAS and NRAS cause mosaic cutaneous and skeletal lesions, elevated FGF23 and hypophosphatemia. Hum. Mol. Genet. 23, 397–407.

Linglart, A., Biosse-Duplan, M., Briot, K., Chaussain, C., Esterle, L., Guillaume-Czitrom, S., et al., 2014. Therapeutic management of hypophosphatemic rickets from infancy to adulthood. Endocr. Connect 3, R13–R30.

Liu, S., Guo, R., Simpson, L.G., Xiao, Z.S., Burnham, C.E., Quarles, L.D., 2003. Regulation of fibroblastic growth factor 23 expression but not degradation by PHEX. J. Biol. Chem. 278, 37419–37426.

Lorenz-Depiereux, B., Bastepe, M., Benet-Pagès, A., Amyere, M., Wagenstaller, J., Müller-Barth, U., et al., 2006. DMP1 mutations in autosomal recessive hypophosphatemia implicate a bone matrix protein in the regulation of phosphate homeostasis. Nat. Genet. 38, 1248–1250.

Lorenz-Depiereux, B., Schnabel, D., Tiosano, D., Häusler, G., Strom, T.M., 2010. Loss-of-function ENPP1 mutations cause both generalized arterial calcification of infancy and autosomal-recessive hypophosphatemic rickets. Am. J. Hum. Genet. 86, 267–272.

Lyles, K.W., Halsey, D.L., Friedman, N.E., Lobaugh, B., 1988. Correlations of serum concentrations of 1,25-dihydroxyvitamin D, phosphorus, and parathyroid hormone in tumoral calcinosis. J. Clin. Endocrinol. Metab. 67, 88–92.

Meyer Jr., R.A., Meyer, M.H., Gray, R.W., 1989. Parabiosis suggests a humoral factor is involved in X-linked hypophosphatemia in mice. J. Bone Miner. Res. 4, 493–500.

Minisola, S., Peacock, M., Fukumoto, S., Cipriani, C., Pepe, J., Tella, S.H., et al., 2017. Tumour-induced osteomalacia. Nat Rev Dis Primers 3, 17044.

Moore, D.D., 2007. Physiology. Sister act. Science 316, 1436–1438.

Olauson, H., Lindberg, K., Amin, R., Sato, T., Jia, T., Goetz, R., et al., 2013. Parathyroid-specific deletion of Klotho unravels a novel calcineurin-dependent FGF23 signaling pathway that regulates PTH secretion. PLoS Genet. 9, e1003975.

Perwad, F., Azam, N., Zhang, M.Y., Yamashita, T., Tenenhouse, H.S., Portale, A.A., 2005. Dietary and serum phosphorus regulate fibroblast growth factor 23 expression and 1,25- dihydroxyvitamin D metabolism in mice. Endocrinology 146, 5358–5364.

Rafaelsen, S.H., Raeder, H., Fagerheim, A.K., Knappskog, P., Carpenter, T.O., Johansson, S., et al., 2013. Exome sequencing reveals FAM20c mutations associated with fibroblast growth factor 23-related hypophosphatemia, dental anomalies, and ectopic calcification. J. Bone Miner. Res. 28, 1378–1385.

Riminucci, M., Collins, M.T., Fedarko, N.S., Cherman, N., Corsi, A., White, K.E., et al., 2003. FGF-23 in fibrous dysplasia of bone and its relationship to renal phosphate wasting. J. Clin. Investig. 112, 683–692.

Roberts, M.S., Burbelo, P.D., Egli-Spichtig, D., Perwad, F., Romero, C.J., Ichikawa, S., et al., 2018. Autoimmune hyperphosphatemic tumoral calcinosis in a patient with FGF23 autoantibodies. J. Clin. Invest. 128, 5368–5373.

Rossaint, J., Oehmichen, J., Van Aken, H., Reuter, S., Pavenstadt, H.J., Meersch, M., et al., 2016. FGF23 signaling impairs neutrophil recruitment and host defense during CKD. J. Clin. Investig. 126, 962–974.

Saito, H., Maeda, A., Ohtomo, S., Hirata, M., Kusano, K., Kato, S., et al., 2005. Circulating FGF-23 is regulated by 1alpha,25-dihydroxyvitamin D3 and phosphorus in vivo. J. Biol. Chem. 280, 2543–2549.

Samadfam, R., Richard, C., Nguyen-Yamamoto, L., Bolivar, I., Goltzman, D., 2009. Bone formation regulates circulating concentrations of fibroblast growth factor 23. Endocrinology 150, 4835–4845.

Schouten, B.J., Doogue, M.P., Soule, S.G., Hunt, P.J., 2009. Iron polymaltose-induced FGF23 elevation complicated by hypophosphataemic osteomalacia. Ann. Clin. Biochem. 46, 167–169.

Shawar, S.M., Ramadan, A.R., Ali, B.R., Alghamdi, M.A., John, A., Hudaib, F.M., 2016. FGF23-S129F mutant bypasses ER/Golgi to the circulation of hyperphosphatemic familial tumoral calcinosis patients. Bone 93, 187–195.

Shimada, T., Mizutani, S., Muto, T., Yoneya, T., Hino, R., Takeda, S., et al., 2001. Cloning and characterization of FGF23 as a causative factor of tumor-induced osteomalacia. Proc. Natl. Acad. Sci. U. S. A. 98, 6500–6505.

Shimada, T., Hasegawa, H., Yamazaki, Y., Muto, T., Hino, R., Takeuchi, Y., et al., 2004. FGF-23 is a potent regulator of vitamin D metabolism and phosphate homeostasis. J. Bone Miner. Res. 19, 429–435.

Shimada, T., Kakitani, M., Yamazaki, Y., Hasegawa, H., Takeuchi, Y., Fujita, T., et al., 2004. Targeted ablation of *Fgf23* demonstrates an essential physiological role of FGF-23 in phosphate and vitamin D metabolism. J. Clin. Investig. 113, 561–568.

Shimizu, Y., Tada, Y., Yamauchi, M., Okamoto, T., Suzuki, H., Ito, N., et al., 2009. Hypophosphatemia induced by intravenous administration of saccharated ferric oxide: another form of FGF23- related hypophosphatemia. Bone 45, 814–816.

Simpson, M.A., Hsu, R., Keir, L.S., Hao, J., Sivapalan, G., Ernst, L.M., et al., 2007. Mutations in FAM20C are associated with lethal osteosclerotic bone dysplasia (Raine syndrome), highlighting a crucial molecule in bone development. Am. J. Hum. Genet. 81, 906–912.

Singh, S., Grabner, A., Yanucil, C., Schramm, K., Czaya, B., Krick, S., et al., 2016. Fibroblast growth factor 23 directly targets hepatocytes to promote inflammation in chronic kidney disease. Kidney Int. 90, 985–996.

Sitara, D., Razzaque, M.S., Hesse, M., Yoganathan, S., Taguchi, T., Erben, R.G., et al., 2004. Homozygous ablation of fibroblast growth factor-23 results in hyperphosphatemia and impaired skeletogenesis, and reverses hypophosphatemia in Phex-deficient mice. Matrix Biol. 23, 421–432.

The HYP Consortium, 1995. A gene (PEX) with homologies to endopeptidases is mutated in patients with X-linked hypophosphatemic rickets. Nat. Genet. 11, 130–136.

Topaz, O., Shurman, D.L., Bergman, R., Indelman, M., Ratajczak, P., Mizrachi, M., et al., 2004. Mutations in GALNT3, encoding a protein involved in O-linked glycosylation, cause familial tumoral calcinosis. Nat. Genet. 36, 579–581.

Urakawa, I., Yamazaki, Y., Shimada, T., Iijima, K., Hasegawa, H., Okawa, K., et al., 2006. Klotho converts canonical FGF receptor into a specific receptor for FGF23. Nature 444, 770–774.

Wasserman, H., Ikomi, C., Hafberg, E.T., Miethke, A.G., Bove, K.E., Backeljauw, P.F., 2016. Two case reports of FGF23-induced hypophosphatemia in childhood biliary atresia. Pediatrics 138, e20154453.

Weber, T.J., Liu, S., Indridason, O.S., Quarles, L.D., 2003. Serum FGF23 levels in normal and disordered phosphorus homeostasis. J. Bone Miner. Res. 18, 1227–1234.

White, K.E., Cabral, J.M., Davis, S.I., Fishburn, T., Evans, W.E., Ichikawa, S., et al., 2005. Mutations that cause osteoglophonic dysplasia define novel roles for FGFR1 in bone elongation. Am. J. Hum. Genet. 76, 361–367.

Wöhrle, S., Bonny, O., Beluch, N., Gaulis, S., Stamm, C., Scheibler, M., et al., 2011. FGF receptors control vitamin D and phosphate homeostasis by mediating renal FGF-23 signaling and regulating FGF-23 expression in bone. J. Bone Miner. Res. 26, 2486–2497.

Yamaguchi, T., Sugimoto, T., Imai, Y., Fukase, M., Fujita, T., Chihara, K., 1995. Successful treatment of hyperphosphatemic tumoral calcinosis with long-term acetazolamide. Bone 16, 247S–250S.

Yamashita, T., Yoshioka, M., Itoh, N., 2000. Identification of a novel fibroblast growth factor, FGF-23, preferentially expressed in the ventrolateral thalamic nucleus of the brain. Biochem. Biophys. Res. Commun. 277, 494–498.

Yamazaki, Y., Okazaki, R., Shibata, M., Hasegawa, Y., Satoh, K., Tajima, T., et al., 2002. Increased circulatory level of biologically active full-length FGF-23 in patients with hypophosphatemic rickets/osteomalacia. J. Clin. Endocrinol. Metab. 87, 4957–4960.

Yang, K., Peretz-Soroka, H., Wu, J., Zhu, L., Cui, X., Zhang, M., et al., 2017. Fibroblast growth factor 23 weakens chemotaxis of human blood neutrophils in microfluidic devices. Sci. Rep. 7, 3100.

Yoshida, T., Fujimori, T., Nabeshima, Y., 2002. Mediation of unusually high concentrations of 1,25- dihydroxyvitamin D in homozygous klotho mutant mice by increased expression of renal 1alpha-hydroxylase gene. Endocrinology 143, 683–689.

Yu, X., Ibrahimi, O.A., Goetz, R., Zhang, F., Davis, S.I., Garringer, H.J., et al., 2005. Analysis of the biochemical mechanisms for the endocrine actions of fibroblast growth factor-23. Endocrinology 146, 4647–4656.

Yuan, B., Takaiwa, M., Clemens, T.L., Feng, J.Q., Kumar, R., Rowe, P.S., et al., 2008. Aberrant Phex function in osteoblasts and osteocytes alone underlies murine X-linked hypophosphatemia. J. Clin. Investig. 118, 722–734.

Yuan, B., Feng, J.Q., Bowman, S., Liu, Y., Blank, R.D., Lindberg, I., et al., 2013. Hexa-D-arginine treatment increases 7B2·PC2 activity in hyp-mouse osteoblasts and rescues the HYP phenotype. J. Bone Miner. Res. 28, 56–72.

Chapter 64

Tumor-induced osteomalacia

Michael T. Collins[1], Iris R. Hartley[2] and Pablo Florenzano[3]

[1]Skeletal Disorders and Mineral Homeostasis Section, National Institute of Dental and Craniofacial Research, National Institutes of Health, Bethesda, MD, United States; [2]Interinstitute Endocrine Training Program, Eunice Kennedy Shriver National Institute of Child Health and Human Development, National Institutes of Health, Bethesda, MD, United States; [3]Endocrine Department, School of Medicine, Pontificia Universidad Católica de Chile, Santiago, Chile

Chapter outline

Background

Tumor-induced osteomalacia (TIO), also known as oncogenic osteomalacia, is a rare paraneoplastic syndrome of abnormal phosphate and vitamin D metabolism caused by small tumors (phosphaturic mesenchymal tumors, PMTs) that secrete the phosphate- and vitamin D-regulating hormone fibroblast growth factor 23 (FGF23) (Jan de Beur, 2005; Drezner, 2001; Folpe et al., 2004; Jiang et al., 2012; Chong et al., 2011a; Minisola et al., 2017a; Florenzano et al., 2017). Biochemical hallmarks of the disorder are elevated or inappropriately normal blood FGF23 levels that cause renal phosphate wasting and hypophosphatemia, and impaired generation of 1,25-dihydroxyvitamin D. Low or inappropriately normal levels of 1,25-dihydroxyvitamin D can lead to secondary hyperparathyroidism, worsening renal phosphate wasting. Clinically, patients complain of bone pain and muscle weakness, and often present with pathologic fractures due to hypophosphatemic osteomalacia. When the disease occurs in children prior to growth plate fusion, it causes rickets. Rarely, TIO can be caused by multiple, synchronous PMTs (Peterson et al., 2010; Higley et al., 2015; Arai et al., 2017).

While "phosphatonins" other than FGF23 have been proposed to cause TIO (Schiavi and Moe, 2002; Bresler et al., 2004; Carpenter et al., 2005), the direct evidence to support their pathogenesis in TIO is weak, and there are no well-documented cases of TIO in which, when examined, FGF23 blood levels were not abnormally elevated. The time from onset of symptoms to diagnosis is often long, in large part due to lack of familiarity with the disease, combined with the fact that blood phosphorus levels are not routinely measured. As a result of delayed diagnosis, patients frequently present with significant morbidity, including multiple fractures, height loss, and a generalized debilitated status. If the condition develops before growth plate closure, linear growth is impaired, children fall below their previously established growth curve, and rickets is present.

There are patients with a TIO-like syndrome in whom a tumor is never found. Whether this is due to the inability to find the tumor or represents a separate syndrome is not known. Generally, patients with an acquired form of FGF23-mediated hypophosphatemia in which all causes of nontumorous FGF23-mediated hypophosphatemia have been excluded (see later) are considered to have TIO due to a tumor that has not been identified. It may take years to identify the tumor, and patients such as this should continue to undergo periodic testing to locate a tumor.

A TIO-like syndrome can also be seen in association with other diseases such as prostate cancer, oat cell cancer, hematologic malignancies, neurofibromatosis, cutaneous skeletal hypophosphatemia syndrome (CSHS), and polyostotic

Principles of Bone Biology. https://doi.org/10.1016/B978-0-12-814841-9.00064-6

fibrous dysplasia of bone (FD) (Nakahama et al., 1995; Konishi et al., 1991; Taylor et al., 1984; Carey et al., 1986; Reese and Rosen, 1997; Rao et al., 1987; Dent and Gertner, 1976; Saville et al., 1955; Ivker et al., 1997; Collins et al., 2001; Riminucci et al., 2003). In these cases, the primary disease is usually obvious, and the goal is treatment of the underlying disease. However, when the underlying disease is not amenable to cure or adequate treatment, as is the case in CSHS and FD, for example, medical treatment of the hypophosphatemic syndrome is the same as in cases of TIO caused by PMTs (see later).

Robert McCance is often credited with reporting the first case of TIO. In 1947, he reported a patient with manifestations of what was clearly TIO (McCance, 1947). The patient had pain, weakness, gait abnormalities, and low phosphorus levels. She was treated with high doses of vitamin D, but her symptoms did not completely resolve until a tumor in her femur was resected. McCance attributed her cure to the high-dose vitamin D therapy, not the tumor resection, and believed her disease was due to vitamin D resistance. At the time, vitamin D resistance was believed to be the mechanism of the disease that would eventually come to be understood as the FGF23-mediated phosphate wasting disorder X-linked hypophosphatemia (XLH) (Albright et al., 1937; Winters et al., 1957).

The first person to clearly recognize that the disease was the result of a "rachitogenic substance" was Andrea Prader. In 1959 he described an 11½-year-old girl who developed severe hypophosphatemic rickets over the course of a year (Prader et al., 1959). Her evaluation showed decreased tubular phosphate reabsorption but otherwise normal studies of kidney function. A tumor, classified as a giant cell granuloma, was identified in a rib and resected with resultant healing of her rickets. Prader made the association between resection of the tumor and cure of her rickets and posited that the granuloma was secreting a rachitogenic substance.

FGF23 was eventually identified as the rachitogenic substance causing TIO in 2003 (Jonsson et al., 2003). Approximately 500 cases of TIO have been reported in the English literature since Prader's original case (reviewed in Folpe et al., 2004; Chong et al., 2011a; Minisola et al., 2017a). The fact that over 300 of these cases have been reported since 2009 indicates a growing recognition of this disease. This recognition has paralleled the identification of FGF23 as the phosphaturic agent (White et al., 2001; ADHR, 2000). The discovery of FGF23 has not only paved the way toward a better understanding of the pathophysiology and treatment of TIO, but also provided a window into areas of mineral metabolism physiology that for years had been unexplained.

Phosphaturic mesenchymal tumors

There has been steady progress in elucidating the histopathology, cell biology, and molecular genetics of PMTs since Andreas Prader's first recognition in 1957 that a syndrome of TIO was caused by a "giant cell tumor." Weidner was the first to systematically characterize tumors that cause a TIO syndrome as distinct histopathological entities (Weidner and Santa Cruz, 1987). In 1991, Weidner et al. reviewed the literature of approximately 60 cases of TIO that had been described at that time (Weidner, 1991). They were the first to propose a classification system based on the histological findings and designated the tumors as "phosphaturic mesenchymal tumors." They subdivided PMTs into four categories: mixed connective tissue variant (PMTMCT), osteoblastoma-like variant, nonossifying fibroma-like variant, and ossifying fibroma-like variant. The first group, PMTMCT, comprised neoplasias containing primitive stromal cells, prominent vessels, and osteoclast-like giant cells. Osseous metaplasia and poorly formed cartilage-like areas with dystrophic calcification were also present. They noted that these tumors typically occurred in soft tissue and were almost invariably benign. The remaining three groups, also usually benign, tended to occur in bone.

In 2004, Folpe et al. reviewed the clinicopathological features of 32 new cases of TIO, re-reviewed all of the previously published cases, and made the assertion that virtually all of the cases fell into the category of PMTMCT (Folpe et al., 2004). The prototypical PMTMCT contains neoplastic cells that are spindled to stellate in shape, normochromatic, with small nuclei and indistinct nucleoli. The nuclear grade is low, and mitotic activity is usually absent or very low. The cells are typically embedded within a myxoid or myxochondroid "grungy matrix" that can resemble chondroid or osteoid. Osteoclast-like giant cells are often present and numerous; mature fat and even lamellar bone may also be seen. A prominent feature is an elaborate microvasculature with a mixture of vessel size and vascular pattern (Folpe et al., 2004). The most common diagnosis for these tumors prior to the moniker of PMTs was hemangiopericytoma, but it has also included hemangiomas, sarcomas, ossifying fibromas, granulomas, giant cell tumors, and osteoblastomas (Drezner, 2001; Folpe et al., 2004; Weidner, 1991). Typical features of PMTs are shown in Fig. 64.1.

Antigen expression was first evaluated in two immunohistochemical studies by Weidner et al. In their first study, tumors were negative for factor VIII (FVIII)-related antigen (endothelial marker), S-100 (epidermal marker), and cytokeratin (epithelial marker) (Weidner et al., 1985). The second study revealed only vimentin immunoreactivity (mesenchymal marker), in some cases within the tumor cells. All other antibodies, including desmin (mesenchymal

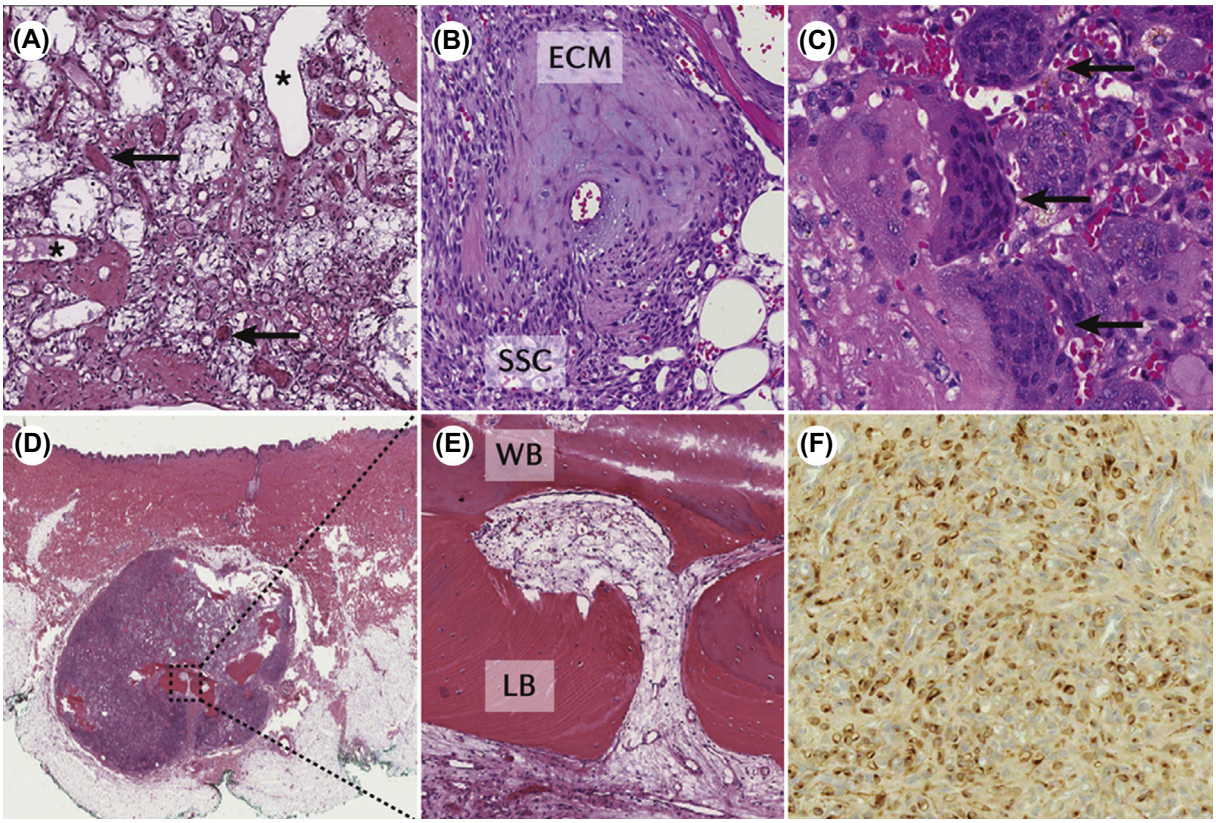

FIGURE 64.1 Histological features of phosphaturic mesenchymal tumors. (A) Low-power view demonstrates the marked vascularity of phosphaturic mesenchymal tumors (PMTs) (*arrows*, collections of fibroblast growth factor 23 (FGF23)-secreting tumor cells; *asterisks*, blood vessels). (B) The small spindle-shaped cells that predominate in PMTs often produce an abundant, "grungy" chondroid matrix. *ECM*, extracellular matrix; *SSCs*, spindle-shaped cells. (C) Multinucleated giant cells (*arrows*) are commonly seen in PMTs, and are often associated with the collagen-rich matrix, as in this case. (D and E) Low- (D) and high-power (E) views, respectively, of a small subcutaneous PMT (*dotted line* in D) that contained, as is sometimes the case in PMTs, both woven (*WB* in E) and lamellar bone (*LB* in E). (F) Immunohistochemical staining with a fibroblast growth factor 23 (FGF23)-specific polyclonal antibody demonstrates that it is the small spindle cells that predominate in the tumor that are the source of the FGF23. *Adapted from Minisola, S., Peacock, M., Fukumoto, S., Cipriani, C., Pepe, J., Tella, SH., et al., 2017. Tumour-induced osteomalacia. Nat. Rev. Dis. Primers. 3, 17044. Epub 2017/07/14.*

marker), leu-M1 and leukocyte common antigen (hematologic markers), and chromogranin and neuron-specific enolase (neuroendocrine tumor markers), were negative (Weidner et al., 1985). In their most recent series, Folpe et al. (Folpe et al., 2004) performed a series of immunohistochemical staining including pan-cytokeratin, desmin, S-100, smooth muscle actin, CD34, and FGF23, and with the exception of smooth muscle actin, which they found reactive in three cases, and FGF23, which was positive in about 70% of all the cases, all markers were negative. In terms of FGF23 staining, it was seen in the proliferating cells within the tumor. An example can be seen in Fig. 64.1.

In terms of ultrastructural features, Stone et al. described features consistent with a neuroendocrine tumor in a PMTMCT from a 33-year-old woman (Stone et al., 1992). Neurosecretory granules were also found in the case described by Wilkins et al. (Wilkins et al., 1995). However, immunostaining for S-100, neuron-specific enolase, chromogranin, and synaptophysin, typical markers of neurosecretory tumors, was negative, as was staining for actin, cytokeratin, and epithelial membrane antigen and FVIII. The only positive finding was vimentin, confirming what had already been described by Weidner at al. An additional case communicated by Shelekhova et al. also showed similar neurosecretory granules (Shelekhova et al., 2006). Somatostatin receptor expression is also a common feature of PMTs and accounts for the utility of imaging studies that utilize somatostatin receptor analogs, e.g., OctreoScan and DOTA-based scans (see later) (Seufert et al., 2001; Houang et al., 2013). However, the somatostatin receptors do not appear functional as far as regulating FGF23 expression, given that somatostatin analogs are not effective in treating TIO (Ovejero et al., 2017).

A potentially important recent finding is the identification of epithelial components in PMTs that arise from the maxilla and mandible (Wu et al., 2019). These tumors appear to have a much more aggressive clinical course and are perhaps more prone to metastasizing. Tumors that arise from the maxilla or mandible should be approached with greater care, assessing

for the presence of epithelial components and, if present, giving consideration to a more aggressive surgical approach, making sure to create wide margins. While the vast majority of tumors are benign, malignant transformation and metastases can occur (Harvey et al., 1992; Ogose et al., 2001; Rico et al., 1986; Uramoto et al., 2009; Wyman et al., 1977), a feature hard to predict from the benign histological appearance of even metastatic tumors (Bergwitz et al., 2011). While metastases are rare, benign tumors are not encapsulated, and infiltration into surrounding connective tissue is often present. This has significant implications for surgical management and emphasizes the importance of wide surgical margins to avoid persistence or recurrence. This is an important point that needs to be emphasized to surgeons caring for patients with TIO.

The most important recent finding in understanding the genetic and molecular pathophysiology of PMTs is the identification of fibronectin−FGF receptor 1 (FN1−FGFR1) translocations, that could be present in up to 60% of PMTs (Lee et al., 2015; Lee et al., 2016). Subsequent investigations of a larger group of tumors suggested that the percentage of tumors harboring FN1-FGFR1 translocations may be lower, and that other genetic abnormalities, such as fibronectin-FGF1 translocations, may be present (Lee et al., 2016). It is likely that additional genetic/molecular changes will be identified. There may be direct clinical implications for some of these genetic/molecular changes, as can be seen for FN1−FGFR1 translocations (see later).

To summarize, PMTMCTs are a group of tumors with a spectrum of histopathological findings that includes a background of spindle/stellate cells with low nuclear and mitotic activity. This is true even in cases of metastatic disease. Prominent vascularity is common and includes vessels of different sizes and patterns, consistent with the fact that they were historically most commonly classified as hemangiopericytomas. Osteoclast-like giant cells are frequently seen, and woven and/or lamellar bone can be present as well. Cytoplasmic FGF23 staining is a consistent feature. It is important to note that histopathological diagnosis of malignant disease is difficult to make, as even in clinically proven metastatic disease cellular features appear benign.

Clinical presentation and diagnosis

TIO typically presents with symptoms of chronic hypophosphatemia that include bone pain, muscle weakness, and fractures (Jan de Beur, 2005; Chong et al., 2011a). However, given the lack of specificity of the symptoms, diagnosis is often delayed, and patients are frequently misdiagnosed with several other more common rheumatologic, neurological, or psychiatric conditions, including osteoporosis, somatic syndrome, intervertebral disc herniation, and spondyloarthritis (Feng et al., 2017). Delay in diagnosis is not only due to nonspecific symptoms, but also the fact that blood phosphate levels are typically not checked as part of an initial panel of blood tests (El-Maouche et al., 2016). If left untreated, significant disability and deformity often develop, especially height loss due to vertebral compression fractures, which are common (Chong et al., 2011a). Patients can present at any age, including uncommonly in childhood (Chong et al., 2011a; Crossen et al., 2017; Jung et al., 2010), but are most often diagnosed between 40 and 45 years of age (Florenzano et al., 2017). What distinguishes the diagnosis of TIO in childhood from XLH, which is the most common form of genetic hypophosphatemia, is that in XLH the clinical presentation is early, usually appearing with weight-bearing ambulation. In TIO, the diagnosis is usually later, following a period of normal growth and development. And unlike autosomal dominant (ADHR) and autosomal recessive hypophosphatemic rickets (ARHR), rarer causes of familial hypophosphatemia that often present later in childhood, the signs and symptoms of hypophosphatemia in TIO are usually more profound and the FGF23 levels significantly higher than in ARHR or ADHR (Jan de Beur, 2005; Minisola et al., 2017a).

The characteristic biochemical findings of TIO include hypophosphatemia, renal phosphate wasting, low or inappropriately normal 1,25-dihydroxyvitamin D, and elevated or inappropriately normal FGF23 levels (Chong et al., 2011a; Florenzano et al., 2017; Gonzalez et al., 2017). The presence of renal phosphate wasting is confirmed by calculating either the tubular reabsorption of phosphate (TRP) or the ratio of the renal tubular maximum phosphate reabsorption rate to glomerular filtration rate (TmP/GFR). TmP/GFR is the most accurate reflection of renal phosphate reabsorption; however, TRP is simpler and more convenient (Minisola et al., 2017a). Both calculations require simultaneous urine and serum phosphate and creatinine measurements, but TmP/GFR requires fasting values at peak phosphate absorption, usually taken from a second morning void, while TRP can be calculated from random collections (Chong et al., 2011a). For accurate results, patients must have stopped phosphate supplementation and care should be taken to use consistent units when using either formula (Chong et al., 2011a). Online calculators and downloadable applications are available for the calculation of either of these values. Both TmP/GFR and blood phosphate levels vary with age, and care should be taken to use the appropriate age-specific normal ranges. Age-specific normal reference ranges for TmP/GFR are noted in Table 64.1. Under normal physiologic conditions, 85%−95% of filtered phosphate is reabsorbed by the proximal tubule. A TRP less than

TABLE 64.1 Normal ranges for ratio of renal tubular maximum phosphate reabsorption rate to glomerular filtration rate.

Age	Male, mg/dL (mmol/L)	Female, mg/dL (mmol/L)
Newborn	5.7–8.1 (1.27–2.59)	5.7–8.1 (1.27–2.59)
1 month–2 years	3.6–5.4 (1.15–1.73)	3.6–5.4 (1.15–1.73)
2–12 years	3.8–5.0 (1.22–1.60)	3.8–5.0 (1.22–1.60)
12–16 years	3.4–4.6 (1.09–1.47)	3.4–4.6 (1.09–1.47)
16–25 years	3.33–5.9 (1.07–1.89)	3.18–6.41 (1.02–2.05)
25–45 years	3.09–4.18 (0.99–1.34)	2.97–4.45 (0.95–1.42)
45–65 years	2.78–4.18 (0.89–1.34)	2.72–4.39 (0.87–1.40)
65–75 years	2.47–4.18 (0.79–1.34)	2.47–4.18 (0.79–1.34)

From Chong, W.H., Molinolo, A.A., Chen, C.C., Collins, M.T. 2011. Tumor-induced osteomalacia. Endocr. Relat. Cancer. 18(3), R53–R77.

85%–95% in the setting of hypophosphatemia or a TmP/GFR lower than the reference range is indicative of renal phosphate wasting.

Subsequent laboratory testing in patients with confirmed renal phosphate wasting should include serum calcium, 25-vitamin D, 1,25-dihydroxyvitamin D, parathyroid hormone (PTH), FGF23, and alkaline phosphate (see Fig. 64.2) (Minisola et al., 2017a). Vitamin D deficiency (25-vitamin D) must be corrected before making the diagnosis of TIO, as the frank or subtle secondary hyperparathyroidism associated with vitamin D deficiency can confound the determination of TRP or TmP/GFR. Patients with FGF23-mediated hypophosphatemia present with elevated (or inappropriately normal) FGF23 levels. It should be noted that an FGF23 value in the upper part of the normal range in the setting of hypophosphatemia is abnormal and consistent with TIO. 1,25-Dihydroxyvitamin D levels are low or inappropriately in the lower end of the normal range in TIO. Hypophosphatemia is considered to raise 1,25-dihydroxyvitamin D levels, so low levels of 1,25-dihydroxyvitamin D in the setting of hypophosphatemia are consistent with TIO. Alkaline phosphatase levels are generally elevated in TIO, and the degree of elevation reflects the degree of osteomalacia. In contrast, hypophosphatemia in the setting of low FGF23 and elevated 1,25-dihydroxyvitamin D levels would suggest an alternative etiology, such as an acquired or inherited Fanconi syndrome or, depending on the presentation, hereditary hypophosphatemic rickets with hypercalciuria. Calcium levels are typically normal in TIO. PTH levels can be normal or elevated. Patients with TIO commonly develop secondary hyperparathyroidism due to chronically low 1,25-vitamin D and the physiologic drive to maintain eucalcemia. Tertiary hyperparathyroidism can develop in longstanding disease, especially with prolonged phosphate supplementation (Jan de Beur, 2005; Chong et al., 2011a). C-terminal FGF-23 assays are commercially available, although at the time of this writing the more accurate intact FGF23 assay is available only for research purposes.

Familial causes of rickets, such as XLH, ADHR, and ARHR, can present with biochemical findings identical to TIO, and need to be considered in the differential diagnosis of hypophosphatemia (Chong et al., 2011a). As stated before, XLH usually presents in early childhood, especially when children begin to walk, at which time the legs begin to bow with weight bearing. However, XLH can have a broad phenotypic spectrum and diagnosis can be missed in childhood in patients with a subtler phenotype. Therefore, XLH should be considered even in adults. Clues to the diagnosis of XLH in adulthood that set it apart from TIO are short stature relative to predicted parental height, and a history of significant dental abnormalities, especially as a child, including enamel hypoplasia and dental abscesses. Certainly, a family history of hypophosphatemia and/or consanguinity suggests an inherited form of phosphate wasting and should suggest performing genetic testing. McCune–Albright syndrome, which consists of fibrous dysplasia, café-au-lait macules, and hyperfunctioning endocrinopathies, can also be associated with FGF23 hypersecretion from boney lesions, but the phosphate wasting in McCune–Albright syndrome occurs only in patients with extensive bone disease and the diagnosis is seldom confused with TIO (Boyce et al., 1993).

Tumor localization

After establishing the diagnosis of TIO, the next step in management is to determine the source of FGF23 (Fig. 64.3) (Minisola et al., 2017a). PMTs are typically small, slow-growing tumors that are notoriously difficult to locate

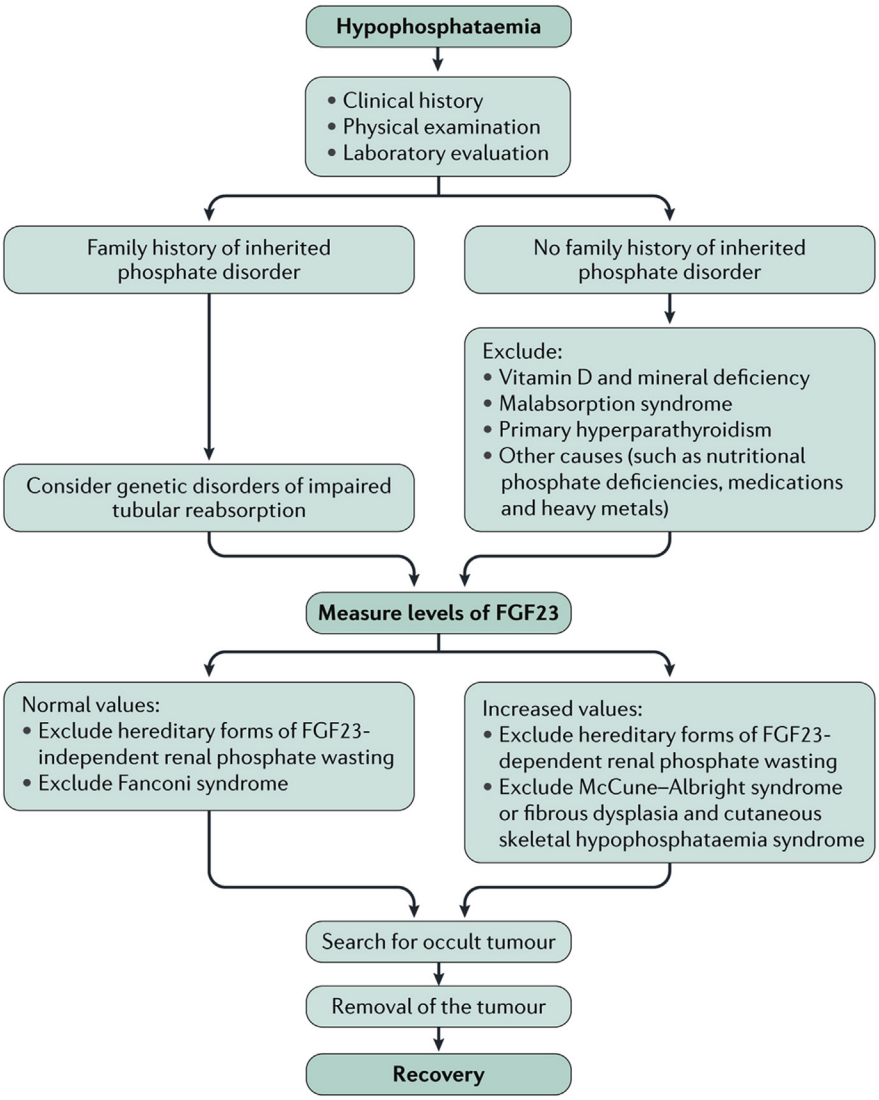

FIGURE 64.2 Diagnostic algorithm for tumor-induced osteomalacia. The clinical history should emphasize possible growth abnormalities and dental diseases (i.e., delayed dentition, previous dental abscesses). Physical examination is important for detecting limb abnormalities, which, in cases of inherited phosphate disorders, are more evident in the lower limbs. In adults, physical examination should attempt to detect small growths, including in the oral cavity, and assess any new lumps and bumps. Radiological investigations may be important, for example, for disclosing osteophytes or calcified entheses in patients with X-linked hypophosphatemic rickets or osteomalacia. *FGF23*, fibroblast growth factor 23. *Adapted from Minisola, S., Peacock, M., Fukumoto, S., Cipriani, C., Pepe, J., Tella, SH., et al., 2017. Tumour-induced osteomalacia. Nat. Rev. Dis. Primers. 3, 17044. Epub 2017/07/14.*

(El-Maouche et al., 2016). Surgical excision can result in cure, which is the gold standard treatment for TIO. A stepwise approach to localization is recommended and starts with a thorough medical history and physical examination. Occasionally tumors can be identified on physical examination. Asking the patient if there is a lump or bump that has arisen in the past several years, including in the oral cavity, and thoroughly examining the patient from head to toe can sometimes identify innocuous-appearing lesions that may be the offending tumor (Fig. 64.4) (Chong et al., 2011a) (Minisola et al., 2017a; Chong et al., 2013).

The three most effective functional imaging modalities at localizing PMTs, in order of accuracy, are DOTA-based positron emission tomography−computed tomography (PET/CT) studies, OctreoScan with single-photon emission CT (OctreoScan SPECT/CT), and [^{18}F]fluorodeoxyglucose PET/CT (FDG−PET) (El-Maouche et al., 2016). DOTA-based studies and OctreoScan both utilize analogs of somatostatin and target somatostatin receptors, which are highly expressed on PMTs. FDG−PET takes advantage of the increased metabolic activity of PMTs. DOTA is a chelator that is combined with positron emitter ^{68}Ga-labeled somatostatin analogs similar to octreotide. These can be ^{68}Ga PET/CT scans

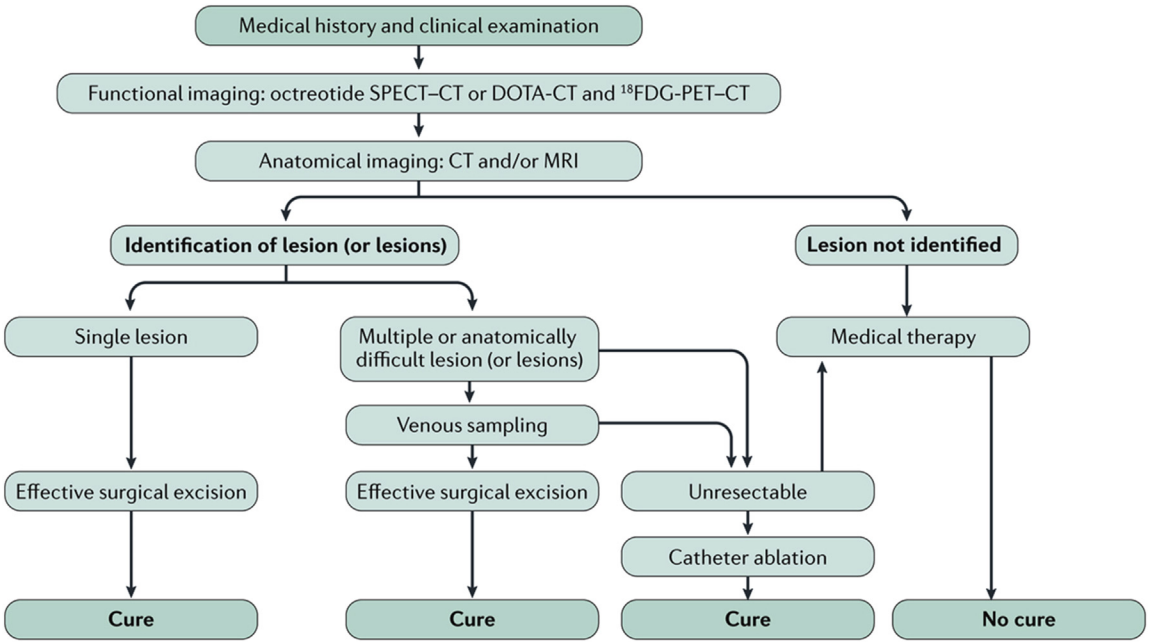

FIGURE 64.3 Localization algorithm. A suggested algorithm for the approach to tumor localization in a patient with a phosphaturic mesenchymal tumor. *DOTA−CT*, DOTA-chelated, ^{68}Ga-labeled somatostatin analog TATE, NOC, or TOC computed tomography (*CT*); *^{18}F-FDG−PET−CT*, ^{18}F-labeled fluorodeoxyglucose positron emission tomography/CT; *octreotide SPECT−CT*, octreotide scan with single-photon emission CT; *MRI*, magnetic resonance imaging. *Adapted from Minisola, S., Peacock, M., Fukumoto, S., Cipriani, C., Pepe, J., Tella, SH., et al., 2017. Tumour-induced osteomalacia. Nat. Rev. Dis. Primers. 3, 17044. Epub 2017/07/14.*

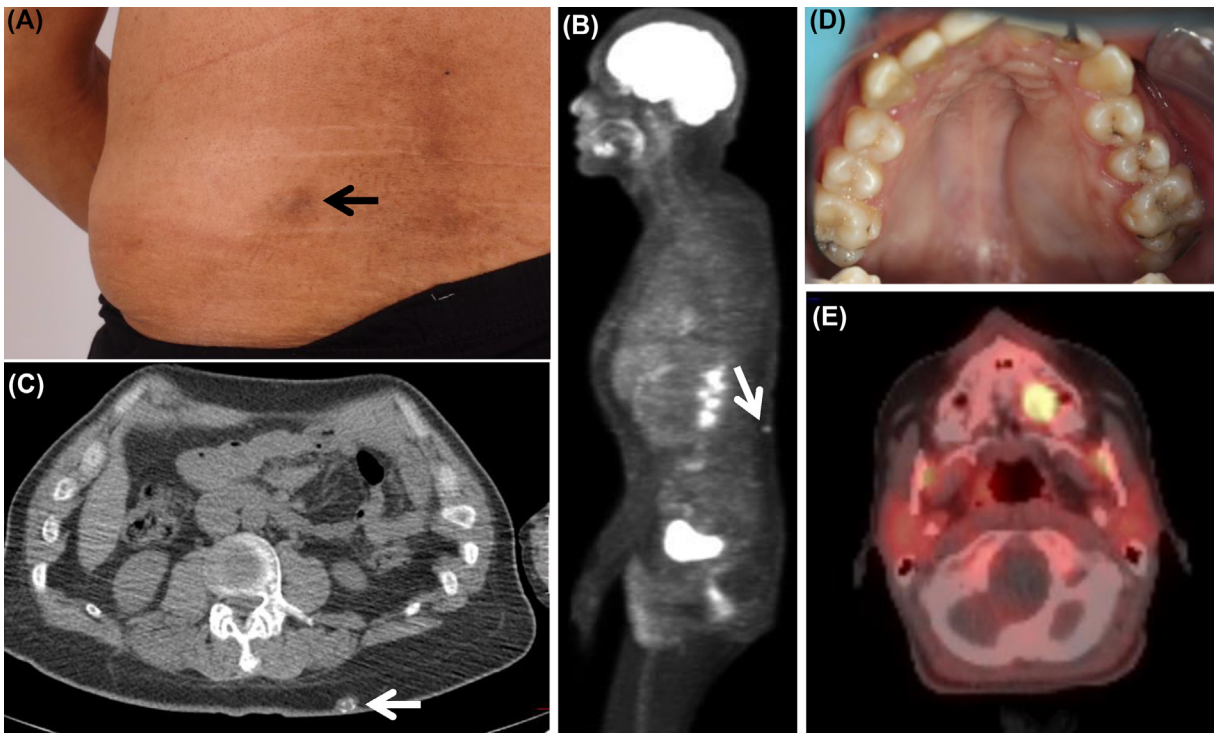

FIGURE 64.4 Tumors identified on physical examination. (A−C) The patient had a small, mobile, subcutaneous lesion on his back that he had noticed within the past several years (A, *arrow*). It showed marked metabolic activity on positron emission tomography/computed tomography (PET/CT) scan (B, *arrow*), and on CT windowing (C, *arrow*) it showed areas of calcification, which are often seen in phosphaturic mesenchymal tumors. (D and E) A 17-year-old girl was noted to have a mass in the roof of her mouth that she had noticed within the past several years (D). On merged ^{68}Ga-DOTA PET/CT scan (E) it was noted to have a high uptake of ^{68}Ga-DOTA, consistent with tumor-induced osteomalacia. In both cases, resection of the tumors led to complete remission.

with DOTA−TATE, DOTA−NOC, or DOTA−TOC. TATE, NOC, and TOC have been shown to have varying degrees of specificity for different somatostatin receptor subtypes, but as to whether these in vitro differences translate to varying degrees of clinical sensitivity or specificity remains to be seen. OctreoScans utilize pentetreotide conjugated with indium-111 and can be combined with SPECT/CT to produce 3D images. Full-body OctreoScan SPECT/CT can be time consuming, requiring 5−6 h of scanning over several days to optimize the diagnostic ability of this study, which may not be feasible in many centers (El-Maouche et al., 2016). It is important to note that cases have been identified wherein tumors were identified on FDG−PET, but were negative on somatostatin-based imaging studies. Therefore, if somatostatin receptor−based studies are negative, FDG−PET is the next imagining modality to perform (El-Maouche et al., 2016). Given that these tumors are often small, and all functional imaging studies have areas of false positive tracer uptake, there can be complementarity between somatostatin-based and FDG-based imaging that often make performing both of utility. Since tumors can be anywhere from head to toe, all scans must encompass the entire body, including the arms and hands (Chong et al., 2011b).

If a lesion is identified with functional imaging, the next step is to perform anatomical imaging of the area with contrast CT and/or magnetic resonance to assist with surgical planning. In cases with multiple suspicious lesions or a single lesion in a surgically challenging area, selective venous sampling is recommended to identify or confirm the location of the culprit lesion prior to surgery (Fig. 64.5) (Andreopoulou et al., 2011). Based on a cohort of nine subjects, a minimum ratio of FGF23 concentration gradient of 1.6 was identified as the cutoff between levels in venous drainage of the tumor bed and the general circulation (Andreopoulou et al., 2011). Venous sampling in the absence of pretest suspicious lesions has not been shown to be effective and is not recommended (Andreopoulou et al., 2011). Biopsy is generally discouraged due to the potential for tumor seeding; however, it may be required for tumor confirmation in rare cases prior to what might be a highly morbid surgery (Florenzano et al., 2017). Patients whose tumor cannot be localized even after extensive investigation can be treated medically (see later) with repeat attempts at localization periodically (Chong et al., 2011a; Florenzano et al., 2017).

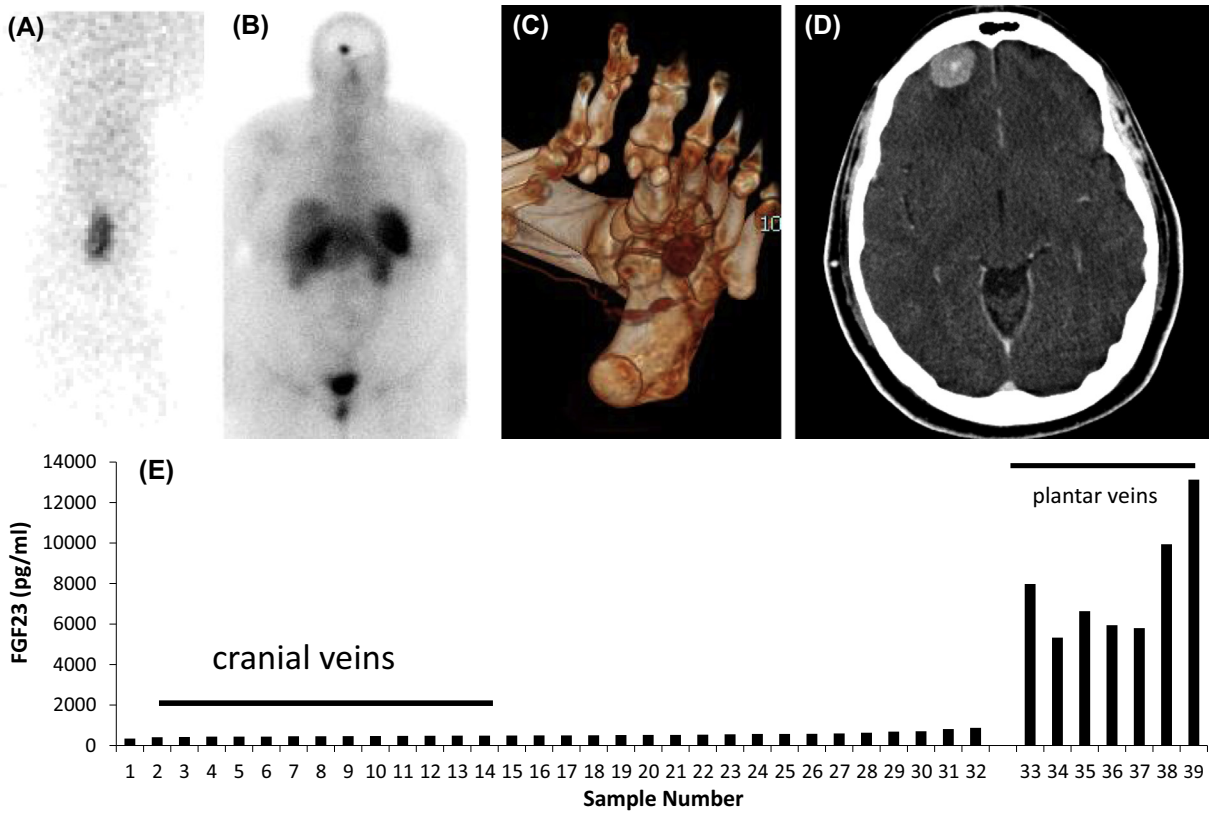

FIGURE 64.5 Utility of venous sampling in distinguishing between multiple foci. (A and B) A 43-year-old woman was noted to have tracer uptake in the foot and in the skull on OctreoScan. (C and D) On anatomic imaging (computed tomography) calcified masses were detected in both, either of which could represent a phosphaturic mesenchymal tumor. (E) Venous sampling revealed a clear step up in the plantar veins draining the foot, and not the skull, which suggested the lesion on the foot was the tumor. The lesion on the plantar surface of the foot was resected, and complete remission followed. *FGF23*, fibroblast growth factor 23.

Treatment

Surgical treatment

Surgery is considered the only definitive and curative treatment of TIO (Chong et al., 2011a; Minisola et al., 2017a), and therefore is the current standard of care. It is of utmost importance to aim for complete resection of the tumor with a wide margin of excision, as local recurrences have been reported (Chong et al., 2011a; Clunie et al., 2000), including cases that later developed malignant characteristics (Uramoto et al., 2009). When the tumor is located in soft tissue, as they are in about 50% of the cases, wide excision is less difficult, but not trivial, as the tumors are often not encapsulated and margins not immediately evident. Excision of tumors located in bone is more challenging. Distinction between tumor-bearing and normal bone is nearly impossible intraoperatively. While these tumors are often small and not locally aggressive, they are not encapsulated and tend to be locally infiltrative, especially along the trabeculae of bone. The preferred approach to ensure surgical cure of tumors located in bone is to completely resect the region of the bone in which the tumor is located (Florenzano et al., 2017). A more conservative surgical approach that entails curettage of the region in which the tumor resides is prone to persistence or recurrence. Despite an aggressive surgical approach, some patients require multiple interventions to remove the entire tumor (Sun et al., 2015). Postoperative radiotherapy for margin-positive tumors has been reported, but data on its utility are limited (Minisola et al., 2017a; Minisola et al., 2017b; Tarasova et al., 2013).

After complete resection, there is a rapid clinical recovery, with serum phosphorus and intact FGF23 returning to normal range within the first 5 days in most patients (Chong et al., 2013). In contrast, normalization of alkaline phosphatase, which reflects healing of osteomalacia, may take several weeks to months. Interestingly, serum 1,25-dihydroxyvitamin D levels begin to rise rapidly in the postoperative period, with levels elevated even above the normal range and a progressive decline toward normal during the second postoperative week (Chong et al., 2013).

Minimally invasive treatment

For many patients, surgery is not an option. Tumors may be located in areas difficult to access surgically, in which excision would likely cause significant morbidity. Operative morbidity may also be high in patients with poor performance status due to comorbid conditions (Florenzano et al., 2017; Tutton et al., 2012; Hesse et al., 2007). Ablative procedures include external beam radiation, radiofrequency ablation, and cryoablation, with or without prior embolization (Hesse et al., 2007; Jadhav et al., 2014; Tella et al., 2017). Multimodality, image-guided ablation with radiofrequency or cryoablation is a promising alternative for this group of patients. It has shown to be a technique with little morbidity and short hospital stays. Although surgery remains the treatment of choice, image-guided ablation may be an effective, less invasive, and safe treatment for patients with a difficult-to-remove tumor or who are poor surgical candidates (Tella et al., 2017). However, long-term efficacy of these modalities has not been demonstrated.

Conventional medical treatment

During the process of identifying the location of the culprit tumor, and in cases in which it is not possible to detect and/or completely resect the tumor, medical treatment is indicated. Phosphate plus active vitamin D (calcitriol or alfacalcidol) supplementation is the mainstay of treatment, with the goal of improving symptoms and healing osteomalacia. Biochemically, the goal is to maintain euphosphatemia, with blood phosphate in the lower end of the normal range, and PTH and urine calcium in the normal range (Tables 64.2 and 64.3) (Minisola et al., 2017a). The treatment regimen includes 15−60 mg/kg per day of elemental phosphorus (typically 1−3 g/day) divided into three to six doses and calcitriol or alfacalcidol 15−60 ng/kg per day (Chong et al., 2011a). Complications of medical therapy can include nephrocalcinosis and/or nephrolithiasis with an increased risk of reduced kidney function and/or secondary or tertiary hyperparathyroidism. Secondary hyperparathyroidism can also be seen at presentation as a consequence of decreased 1,25-dihydroxyvitamin D levels and reflects an appropriate physiological response to maintain eucalcemia (Florenzano et al., 2017). Secondary hyperparathyroidism can also develop as a consequence of treatment, especially if the dose of active vitamin D is not adequate and/or if there is insufficient dietary calcium to keep up with the rapid remineralization of the skeleton that occurs at the outset of treatment (Huang et al., 2000). Phosphorus supplementation is also thought to induce secondary hyperparathyroidism and parathyroid gland hyperplasia by an unclear mechanism (Huang et al., 2000; Reid et al., 1987). Prolonged secondary hyperparathyroidism can lead to the development of tertiary hyperparathyroidism with frank hypercalcemia (Huang et al., 2000). Active vitamin D (calcitriol or alfacalcidol) is used to prevent or treat secondary hyperparathyroidism. Addition of calcium supplements or increases in active vitamin D are indicated for difficult-to-normalize PTH, very low urinary calcium, or hypocalcemia. Secondary hyperparathyroidism can occur at the outset of

TABLE 64.2 Phosphorus supplements.

Phosphorus source	Amount of elemental phosphorus
Neutra-Phos	8 mmol (248 mg) per capsule/packet
Neutra-Phos-K	8 mmol (248 mg) per capsule/packet
K-Phos Neutral	8 mmol (248 mg) per tablet
K-Phos Original	3.68 mmol (114 mg) per tablet
Fleet Phospho-Soda	4.15 mmol (128.65 mg)/mL
Joulie's Solution	1.35 mmol (41.85 mg)/mL

Adapted from http://www.globalrph.com/phosphate_supplements.htm, http://www.newbornnetworks.org.uk/staffs/Nutrition.pdf.

TABLE 64.3 Medical treatment of tumor-induced osteomalacia.

Goal of therapy:	Low end of normal for age-appropriate normal range of phosphorus
Medication	**Dosing**
Phosphorus	15–60 mg/kg/day (approximately 1–3 g/day for adults) Dose should be divided four or five times/day to improve tolerance
Calcitriol or alfacalcidiol	15–60 ng/kg/day (approximately 0.75–3 μg/day for adults) Start 1.5 μg/day and titrate; dose can be divided two or three times/day
Monitoring	
Renal ultrasound to rule out nephrolithiasis and nephrocalcinosis at baseline. Repeat if concerning symptoms arise or persistent increase in urinary calcium.	
Serum calcium, phosphorus, and parathyroid hormone (PTH) every 3 months - If phosphorus below target, increase phosphorus supplements - If calcium below target, add/increase calcium supplements - If PTH elevated, increase calcitriol	
Urinary calcium (UCa) and creatinine (UCr) every 3 months (second morning void) - If UCa/UCr $\geq$ 0.2, check for urinary hemoglobin. Also check 24-h urinary calcium and creatinine with goal of normal-range urinary calcium. Decrease calcitriol dose if positive urinary hemoglobin or elevated 24-h urinary calcium. - If UCa/UCr $\leq$0.2, and serum phosphorus and PTH are okay, continue current regimen	

From Chong, W.H., Molinolo, A.A., Chen, C.C., Collins, M.T. 2011. Tumor-induced osteomalacia. Endocr. Relat. Cancer. 18(3), R53–R77.

treatment of severe cases of osteomalacia as the skeleton begins to mineralize at a high rate (Florenzano et al., 2017). Treatment with active vitamin D can induce the development of hypercalciuria and increase the risk for nephrocalcinosis/nephrolithiasis (Chong et al., 2011a). Given the described risk of significant side effects of medical therapy, monitoring with serum phosphorus, calcium, PTH, urinary calcium, and renal ultrasound should be routinely performed and treatment adjusted to meet therapeutic goals while avoiding complications (Chong et al., 2011a) (Table 64.3). In patients with more severe disease, doses of phosphate and vitamin D can be quite high at the outset of treatment. After the skeleton has healed significantly, the phosphate and vitamin D requirements decrease, and the doses of phosphate, and especially vitamin D, need to be lowered. Failure to do so can lead to renal calcification and impaired renal function. As is the case with XLH, some patients with mild disease may be treated with active vitamin D alone (Costa et al., 1981).

An adjuvant to conventional therapy with phosphate salts and active vitamin D is the calcimimetic cinacalcet (Geller et al., 2007). Its mechanism of action is based on the fact that FGF23 action is dependent on the presence of PTH for its full phosphaturic effect (Gupta et al., 2004). For this reason, lowering PTH with cinacalcet has been shown to decrease phosphaturia, reduce the need for phosphate and calcitriol supplements, and bring about bone healing (Geller et al., 2007). The main side effect of the use of cinacalcet is the development of hypercalciuria, thus requiring monitoring of 24-h urine calcium periodically and possibly requiring the use of a thiazide to prevent hypercalciuria. An even more dramatic approach along this line of thinking is total parathyroidectomy as a treatment for TIO (Bhadada et al., 2013). While this

approach may control blood phosphate, it will have other deleterious mineral homeostasis complications (e.g., hypercalciuria) and not address the underlying etiology of the disease, the PMT, which will still be in place with the potential to grow and/or metastasize.

Considering the presence of somatostatin receptors on PMTs, the somatostatin analog octreotide has been proposed as a potential treatment for TIO (Seufert et al., 2001). However, the preponderance of data to this point, albeit based on small, uncontrolled studies, is that octreotide is ineffective in treating TIO (Ovejero et al., 2017; Paglia et al., 2002). Likewise, the use of potentially tumoricidal treatment with lutetium-177 DOTATATE has failed to show a significant beneficial effect on tumor burden (Nair et al., 2017).

Future directions

Progress has been made and will continue to be made in the delineation of the underlying molecular/genetic pathophysiology, diagnosis, and treatment of TIO. Improvement in tumor molecular diagnostics in cancer biology can be directly applied to PMTs and will reveal novel molecular and genetic changes that underlie the development of PMTs beyond the FGFR changes that account for, at most, only about 40% of the cases of PMT. Data suggest a connection between the hypoxia-inducible factor/erythropoietin signaling pathway and the physiologic regulation of FGF23 production (Farrow et al., 2011; Toro et al., 2018; Hanudel et al., 2018). This points to another area of the physiological regulation of FGF23 that may be susceptible to pathophysiologic derangement and account for some cases of TIO, especially those in which a PMT cannot be identified.

DOTA-based imaging, which derives its utility from the fact that PMTs express somatostatin receptors, has significantly improved the localization of PMTs, allowing for the identification of tumors <2 cm in diameter. It is unlikely there will be significant progress in somatostatin receptor-based imaging, but it is possible that there are other epitopes expressed on PMTs that may lead to another avenue of tumor localization technologies.

The application of an array of ablative techniques, less invasive than surgery, in part enabled by the improvement in tumor localization, has opened the door for potentially lower morbidity treatment. It will be important going forward to be assured that the durability of remission brought about by these techniques is long lasting and that later recurrence, with or without metastatic spread, is not an issue.

The development of the anti-FGF23 humanized monoclonal antibody, burosumab (Kyowa Hakko Kirin, Tokyo, Japan, and Ultragenyx Pharmaceutical, Novato, CA, USA), which was recently approved for treatment of XLH (Carpenter et al., 2018; Insogna et al., 2018), opens a promising option for the treatment that will probably be applicable to patients with TIO. Burosumab is a blocking antibody that inhibits the formation of the FGF23−klotho receptor complex (Aono et al., 2011). Preliminary evidence shows that it significantly increases serum phosphate and 1,25-dihydroxyvitamin D in subjects with TIO (Carpenter et al., 2016). Here too, though, it should be noted that the PMT, the underlying cause of the disease with some potential for malignant transformation, is still in place and that medical treatment does not reflect cure, the primary goal.

The identification of aberrant FGFR expression/signaling in TIO has led to the study of drugs that target the FGF pathway (BGJ398) (Wohrle et al., 2011, 2013) and is currently an area of active investigation that may hold promise for patients with TIO.

Taken together, the future of the study and treatment of TIO is full of promise for both learning more about the biology of FGF23 and, most importantly, treating the patients who suffer from this debilitating disease.

References

ADHR, C., November 2000. Autosomal dominant hypophosphataemic rickets is associated with mutations in FGF23. The ADHR Consortium. Nat. Genet. 26 (3), 345−348.

Albright, F., Butler, A.M., Bloomber, E., 1937. Rickets resistant to vitamin D therapy. Am. J. Dis. Child. 529−547.

Andreopoulou, P., Dumitrescu, C.E., Kelly, M.H., Brillante, B.A., Cutler Peck, C.M., Wodajo, F.M., et al., June 2011. Selective venous catheterization for the localization of phosphaturic mesenchymal tumors. J. Bone. Miner. Res. 26 (6), 1295−1302. Epub 2011/05/26.

Aono, Y., Hasegawa, H., Yamazaki, Y., Shimada, T., Fujita, T., Yamashita, T., et al., April 2011. Anti-FGF-23 neutralizing antibodies ameliorate muscle weakness and decreased spontaneous movement of Hyp mice. J. Bone Miner. Res. 26 (4), 803−810.

Arai, R., Onodera, T., Terkawi, M.A., Mitsuhashi, T., Kondo, E., Iwasaki, N., February 13, 2017. A rare case of multiple phosphaturic mesenchymal tumors along a tendon sheath inducing osteomalacia. BMC Muscoskelet. Disord. 18 (1), 79.

Bergwitz, C., Collins, M.T., Kamath, R.S., Rosenberg, A.E., October 27, 2011. Case records of the Massachusetts General Hospital. Case 33-2011. A 56-year-old man with hypophosphatemia. N Engl J Med. 365 (17), 1625−1635. Epub 2011/10/28.

Bhadada, S.K., Palnitkar, S., Qiu, S., Parikh, N., Talpos, G.B., Rao, S.D., November 2013. Deliberate total parathyroidectomy: a potentially novel therapy for tumor-induced hypophosphatemic osteomalacia. J. Clin. Endocrinol. Metab. 98 (11), 4273–4278. Epub 2013/08/21.

Boyce, A.M., Florenzano, P., de Castro, L.F., Collins, M.T., 1993. Fibrous dysplasia/McCune-albright syndrome. In: Adam, M.P., Ardinger, H.H., Pagon, R.A., Wallace, S.E., Bean, L.J.H., Stephens, K., et al. (Eds.), GeneReviews((R)). Seattle (WA).

Bresler, D., Bruder, J., Mohnike, K., Fraser, W.D., Rowe, P.S., December 2004. Serum MEPE-ASARM-peptides are elevated in X-linked rickets (HYP): implications for phosphaturia and rickets. J. Endocrinol. 183 (3), R1–R9. Epub 2004/12/14.

Carey, D.E., Drezner, M.K., Hamdan, J.A., Mange, M., Ahmad, M.S., Mubarak, S., et al., December 1986. Hypophosphatemic rickets/osteomalacia in linear sebaceous nevus syndrome: a variant of tumor-induced osteomalacia. J. Pediatr. 109 (6), 994–1000.

Carpenter, T.O., Ellis, B.K., Insogna, K.L., Philbrick, W.M., Sterpka, J., Shimkets, R., February 2005. Fibroblast growth factor 7: an inhibitor of phosphate transport derived from oncogenic osteomalacia-causing tumors. J. Clin. Endocrinol. Metab. 90 (2), 1012–1020.

Carpenter, T.O., Miller, P., Weber, T., Peacock, M., Ruppe, M., Insogna, K., Osei, S., Luca, D., Skrinar, A., San Martin, J., Jan De Beur, S., 2016. Effects of KRN23, and anti-FGF23 antibody, in patients with tumor induced osteomalacia and epidermal nevus syndrome: results from an ongoing phase 2 study. In: Annual Meeting of the American Society for Bone and Mineral Research, p. 1098.

Carpenter, T.O., Whyte, M.P., Imel, E.A., Boot, A.M., Hogler, W., Linglart, A., et al., May 24, 2018. Burosumab therapy in children with X-linked hypophosphatemia. N. Engl. J. Med. 378 (21), 1987–1998.

Chong, W.H., Molinolo, A.A., Chen, C.C., Collins, M.T., June 2011. Tumor-induced osteomalacia. Endocr. Relat. Cancer 18 (3), R53–R77.

Chong, W.H., Yavuz, S., Patel, S.M., Chen, C.C., Collins, M.T., December 2011. The importance of whole body imaging in tumor-induced osteomalacia. J. Clin. Endocrinol. Metab. 96 (12), 3599–3600. Epub 2011/12/07.

Chong, W.H., Andreopoulou, P., Chen, C.C., Reynolds, J., Guthrie, L., Kelly, M., et al., June 2013. Tumor localization and biochemical response to cure in tumor-induced osteomalacia. J. Bone Miner. Res. 28 (6), 1386–1398.

Clunie, G.P., Fox, P.E., Stamp, T.C., December 2000. Four cases of acquired hypophosphataemic ('oncogenic') osteomalacia. Problems of diagnosis, treatment and long-term management. Rheumatology 39 (12), 1415–1421. Epub 2001/01/04.

Collins, M.T., Chebli, C., Jones, J., Kushner, H., Consugar, M., Rinaldo, P., et al., May 2001. Renal phosphate wasting in fibrous dysplasia of bone is part of a generalized renal tubular dysfunction similar to that seen in tumor-induced osteomalacia. J. Bone Miner. Res. 16 (5), 806–813.

Costa, T., Marie, P.J., Scriver, C.R., Cole, D.E., Reade, T.M., Nogrady, B., et al., March 1981. X-linked hypophosphatemia: effect of calcitriol on renal handling of phosphate, serum phosphate, and bone mineralization. J. Clin. Endocrinol. Metab. 52 (3), 463–472.

Crossen, S.S., Zambrano, E., Newman, B., Bernstein, J.A., Messner, A.H., Bachrach, L.K., et al., January 2017. Tumor-induced osteomalacia in a 3-year-old with unresectable central giant cell lesions. J. Pediatr. Hematol. Oncol. 39 (1), e21–e24. Epub 2016/11/08.

Dent, C.E., Gertner, J.M., July 1976. Hypophosphataemic osteomalacia in fibrous dysplasia. Q. J. Med. 45 (179), 411–420. Epub 1976/07/01.

Drezner, M.K., April 2001. Tumor-induced osteomalacia. Rev. Endocr. Metab. Disord. 2 (2), 175–186.

El-Maouche, D., Sadowski, S.M., Papadakis, G.Z., Guthrie, L., Cottle-Delisle, C., Merkel, R., et al., October 2016. (68)Ga-DOTATATE for tumor localization in tumor-induced osteomalacia. J. Clin. Endocrinol. Metab. 101 (10), 3575–3581. Epub 2016/08/18.

Farrow, E.G., Yu, X., Summers, L.J., Davis, S.I., Fleet, J.C., Allen, M.R., et al., November 15, 2011. Iron deficiency drives an autosomal dominant hypophosphatemic rickets (ADHR) phenotype in fibroblast growth factor-23 (Fgf23) knock-in mice. Proc. Natl. Acad. Sci. U. S. A. October 17, 108 (46). E1146–55.

Feng, J., Jiang, Y., Wang, O., Li, M., Xing, X., Huo, L., et al., July 28, 2017. The diagnostic dilemma of tumor induced osteomalacia: a retrospective analysis of 144 cases. Endocr. J. 64 (7), 675–683. Epub 2017/04/30.

Florenzano, P., Gafni, R.I., Collins, M.T., December 2017. Tumor-induced osteomalacia. BoneKEy Rep. 7, 90–97.

Folpe, A.L., Fanburg-Smith, J.C., Billings, S.D., Bisceglia, M., Bertoni, F., Cho, J.Y., et al., January 2004. Most osteomalacia-associated mesenchymal tumors are a single histopathologic entity: an analysis of 32 cases and a comprehensive review of the literature. Am. J. Surg. Pathol. 28 (1), 1–30.

Geller, J.L., Khosravi, A., Kelly, M.H., Riminucci, M., Adams, J.S., Collins, M.T., June 2007. Cinacalcet in the management of tumor-induced osteomalacia. J. Bone Miner. Res. 22 (6), 931–937.

Gonzalez, G., Baudrand, R., Sepulveda, M.F., Vucetich, N., Guarda, F.J., Villanueva, P., et al., July 2017. Tumor-induced osteomalacia: experience from a South American academic center. Osteoporos. Int. 28 (7), 2187–2193. Epub 2017/03/28.

Gupta, A., Winer, K., Econs, M.J., Marx, S.J., Collins, M.T., October 2004. FGF-23 is elevated by chronic hyperphosphatemia. J. Clin. Endocrinol. Metab. 89 (9), 4489–4492.

Hanudel, M.R., Eisenga, M.F., Rappaport, M., Chua, K., Qiao, B., Jung, G., et al., July 10, 2018. Effects of erythropoietin on fibroblast growth factor 23 in mice and humans. Nephrol. Dial. Transplant. 1–9.

Harvey, J.N., Gray, C., Belchetz, P.E., October 1992. Oncogenous osteomalacia and malignancy. Clin. Endocrinol. 37 (4), 379–382.

Hesse, E., Rosenthal, H., Bastian, L., July 26, 2007. Radiofrequency ablation of a tumor causing oncogenic osteomalacia. N. Engl. J. Med. 357 (4), 422–424.

Higley, M., Beckett, B., Schmahmann, S., Dacey, E., Foss, E., December 2015. Locally aggressive and multifocal phosphaturic mesenchymal tumors: two unusual cases of tumor-induced osteomalacia. Skeletal Radiol. 44 (12), 1825–1831.

Houang, M., Clarkson, A., Sioson, L., Elston, M.S., Clifton-Bligh, R.J., Dray, M., et al., December 2013. Phosphaturic mesenchymal tumors show positive staining for somatostatin receptor 2A (SSTR2A). Hum. Pathol. 44 (12), 2711–2718.

Huang, Q.L., Feig, D.S., Blackstein, M.E., April 2000. Development of tertiary hyperparathyroidism after phosphate supplementation in oncogenic osteomalacia. J. Endocrinol. Investig. 23 (4), 263–267. Epub 2000/06/15.

Insogna, K.L., Briot, K., Imel, E.A., Kamenicky, P., Ruppe, M.D., Portale, A.A., et al., August 2018. A randomized, double-blind, placebo-controlled, phase 3 trial evaluating the efficacy of burosumab, an anti-FGF23 antibody, in adults with X-linked hypophosphatemia: week 24 primary analysis. J. Bone Miner. Res. 33 (8), 1383−1393. Epub 2018/06/28.

Ivker, R., Resnick, S.D., Skidmore, R.A., December 1997. Hypophosphatemic vitamin D-resistant rickets, precocious puberty, and the epidermal nevus syndrome. Arch. Dermatol. 133 (12), 1557−1561. Epub 1998/01/08.

Jadhav, S., Kasaliwal, R., Shetty, N.S., Kulkarni, S., Rathod, K., Popat, B., et al., September 2014. Radiofrequency ablation, an effective modality of treatment in tumor-induced osteomalacia: a case series of three patients. J. Clin. Endocrinol. Metab. 99 (9), 3049−3054. Epub 2014/06/25.

Jan de Beur, S.M., September 14, 2005. Tumor-induced osteomalacia. Jama 294 (10), 1260−1267.

Jiang, Y., Xia, W.B., Xing, X.P., Silva, B.C., Li, M., Wang, O., et al., September 2012. Tumor-induced osteomalacia: an important cause of adult-onset hypophosphatemic osteomalacia in China: report of 39 cases and review of the literature. J. Bone Miner. Res. 27 (9), 1967−1975. Epub 2012/04/26.

Jonsson, K.B., Zahradnik, R., Larsson, T., White, K.E., Sugimoto, T., Imanishi, Y., et al., April 24, 2003. Fibroblast growth factor 23 in oncogenic osteomalacia and X-linked hypophosphatemia. N. Engl. J. Med. 348 (17), 1656−1663.

Jung, G.H., Kim, J.D., Cho, Y., Chung, S.H., Lee, J.H., Sohn, K.R., January 2010. A 9-month-old phosphaturic mesenchymal tumor mimicking the intractable rickets. J. Pediatr. Orthop. B 19 (1), 127−132. Epub 2009/10/06.

Konishi, K., Nakamura, M., Yamakawa, H., Suzuki, H., Saruta, T., Hanaoka, H., et al., May 1991. Hypophosphatemic osteomalacia in von Recklinghausen neurofibromatosis. Am. J. Med. Sci. 301 (5), 322−328. Epub 1991/05/01.

Lee, J.C., Jeng, Y.M., Su, S.Y., Wu, C.T., Tsai, K.S., Lee, C.H., et al., March 2015. Identification of a novel FN1-FGFR1 genetic fusion as a frequent event in phosphaturic mesenchymal tumour. J. Pathol. 235 (4), 539−545.

Lee, J.C., Su, S.Y., Changou, C.A., Yang, R.S., Tsai, K.S., Collins, M.T., et al., November 2016. Characterization of FN1-FGFR1 and novel FN1-FGF1 fusion genes in a large series of phosphaturic mesenchymal tumors. Mod. Pathol. 29 (11), 1335−1346.

McCance, R., January 1, 1947. Osteomalacia with looser's nodes (Milkman's Syndrome) Due To A Raised Resistance To Vitamin D Acquired About The Age Of 15 Years. QJM 16 (1), 33−46.

Minisola, S., Peacock, M., Fukumoto, S., Cipriani, C., Pepe, J., Tella, S.H., et al., July 13, 2017. Tumour-induced osteomalacia. Nat Rev Dis Primers 3, 17044. Epub 2017/07/14.

Minisola, S.P.M., Fukumoto, S., Cipriani, C., Pepe, J., Tella, S., Collins, M.T., 2017. Tumour-Induced Osteomalacia. Endocr Relat Cancer. Accepted for publication Nature Reviews Disease Primers.

Nair, A., Chakraborty, S., Dharmshaktu, P., Tandon, N., Gupta, Y., Khadgawat, R., et al., June 1, 2017. Peptide Receptor Radionuclide and Octreotide: A Novel Approach for Metastatic Tumor-Induced Osteomalacia. J. Endocr. Soc. 1 (6), 726−730. Epub 2017/12/22.

Nakahama, H., Nakanishi, T., Uno, H., Takaoka, T., Taji, N., Uyama, O., et al., 1995. Prostate cancer-induced oncogenic hypophosphatemic osteomalacia. Urol. Int. 55 (1), 38−40. Epub 1995/01/01.

Ogose, A., Hotta, T., Emura, I., Hatano, H., Inoue, Y., Umezu, H., et al., February 2001. Recurrent malignant variant of phosphaturic mesenchymal tumor with oncogenic osteomalacia. Skeletal Radiol. 30 (2), 99−103. Epub 2001/04/20.

Ovejero, D., El-Maouche, D., Brillante, B.A., Khosravi, A., Gafni, R.I., Collins, M.T., August 2017. Octreotide Is Ineffective in Treating Tumor-Induced Osteomalacia: Results of a Short-Term Therapy. J. Bone Miner. Res. 32 (8), 1667−1671.

Paglia, F., Dionisi, S., Minisola, S., May 30, 2002. Octreotide for tumor-induced osteomalacia. N. Engl. J. Med. 346 (22), 1748−1749 author reply -9. Epub 2002/05/31.

Peterson, N.R., Summerlin, D.J., Cordes, S.R., June 2010. Multiple phosphaturic mesenchymal tumors associated with oncogenic osteomalacia: case report and review of the literature. Ear Nose Throat J. 89 (6), E11−E15.

Prader, A., Illig, R., Uehlinger, E., Stalder, G., 1959. Rickets following bone tumor. Helv. Paediatr. Acta 14, 554−565.

Rao, D.S., Parfitt, A.M., Villanueva, A.R., Dorman, P.J., Kleerekoper, M., February 1987. Hypophosphatemic osteomalacia and adult Fanconi syndrome due to light-chain nephropathy. Another form of oncogenous osteomalacia. Am. J. Med. 82 (2), 333−338. Epub 1987/02/01.

Reese, D.M., Rosen, P.J., September 1997. Oncogenic osteomalacia associated with prostate cancer. J. Urol. 158 (3 Pt 1), 887. Epub 1997/09/01.

Reid, I.R., Teitelbaum, S.L., Dusso, A., Whyte, M.P., August 1987. Hypercalcemic hyperparathyroidism complicating oncogenic osteomalacia. Effect of successful tumor resection on mineral homeostasis. Am. J. Med. 83 (2), 350−354. Epub 1987/08/01.

Rico, H., Fernandez-Miranda, E., Sanz, J., Gomez-Castresana, F., Escriba, A., Hernandez, E.R., et al., 1986. Oncogenous osteomalacia: a new case secondary to a malignant tumor. Bone 7 (5), 325−329. Epub 1986/01/01.

Riminucci, M., Collins, M.T., Fedarko, N.S., Cherman, N., Corsi, A., White, K.E., et al., September 2003. FGF-23 in fibrous dysplasia of bone and its relationship to renal phosphate wasting. J. Clin. Investig. 112 (5), 683−692.

Saville, P.D., Nassim, J.R., Stevenson, F.H., Mulligan, L., Carey, M., May 28, 1955. Osteomalacia in Von Recklinghausen's neurofibromatosis; metabolic study of a case. Br. Med. J. 1 (4925), 1311−1313. Epub 1955/05/28.

Schiavi, S.C., Moe, O.W., July 2002. Phosphatonins: a new class of phosphate-regulating proteins. Curr. Opin. Nephrol. Hypertens. 11 (4), 423−430.

Seufert, J., Ebert, K., Muller, J., Eulert, J., Hendrich, C., Werner, E., et al., December 27, 2001. Octreotide therapy for tumor-induced osteomalacia. N. Engl. J. Med. 345 (26), 1883−1888.

Shelekhova, K.V., Kazakov, D.V., Hes, O., Treska, V., Michal, M., February 2006. Phosphaturic mesenchymal tumor (mixed connective tissue variant): a case report with spectral analysis. Virchows Arch. 448 (2), 232−235. Epub 2006/02/01.

Stone, M.D., Quincey, C., Hosking, D.J., June 1992. A neuroendocrine cause of oncogenic osteomalacia. J. Pathol. 167 (2), 181−185. Epub 1992/06/01.

Sun, Z.J., Jin, J., Qiu, G.X., Gao, P., Liu, Y., February 26, 2015. Surgical treatment of tumor-induced osteomalacia: a retrospective review of 40 cases with extremity tumors. BMC Muscoskelet. Disord. 16, 43. Epub 2015/04/17.

Tarasova, V.D., Trepp-Carrasco, A.G., Thompson, R., Recker, R.R., Chong, W.H., Collins, M.T., et al., November 2013. Successful Treatment of Tumor-Induced Osteomalacia due to an Intracranial Tumor by Fractionated Stereotactic Radiotherapy. J. Clin. Endocrinol. Metab. 98 (11), 4267–4272.

Taylor, H.C., Fallon, M.D., Velasco, M.E., December 1984. Oncogenic osteomalacia and inappropriate antidiuretic hormone secretion due to oat-cell carcinoma. Ann. Intern. Med. 101 (6), 786–788. Epub 1984/12/01.

Tella, S.H., Amalou, H., Wood, B.J., Chang, R., Chen, C.C., Robinson, C., et al., November 2017. Multimodality Image-Guided Cryoablation for Inoperable Tumor-Induced Osteomalacia. J. Bone Miner. Res. 32 (11), 2248–2256.

Toro, L., Barrientos, V., Leon, P., Rojas, M., Gonzalez, M., Gonzalez-Ibanez, A., et al., May 2018. Erythropoietin induces bone marrow and plasma fibroblast growth factor 23 during acute kidney injury. Kidney Int. 93 (5), 1131–1141. Epub 2018/02/06.

Tutton, S., Olson, E., King, D., Shaker, J.L., October 2012. Successful treatment of tumor-induced osteomalacia with CT-guided percutaneous ethanol and cryoablation. J. Clin. Endocrinol. Metab. 97 (10), 3421–3425.

Uramoto, N., Furukawa, M., Yoshizaki, T., February 2009. Malignant phosphaturic mesenchymal tumor, mixed connective tissue variant of the tongue. Auris Nasus Larynx 36 (1), 104–105.

Weidner, N., Santa Cruz, D., April 15, 1987. Phosphaturic mesenchymal tumors. A polymorphous group causing osteomalacia or rickets. Cancer 59 (8), 1442–1454. Epub 1987/04/15.

Weidner, N., Bar, R.S., Weiss, D., Strottmann, M.P., April 15, 1985. Neoplastic pathology of oncogenic osteomalacia/rickets. Cancer. Case Reports Research Support, U.S. Gov't, P.H.S. 55 (8), 1691–1705. Epub 1985/04/15.

Weidner, N., Jul-Oct. Review and update: oncogenic osteomalacia-rickets. Ultrastruct Pathol. 15 (4–5), 317–333. Epub 1991/07/01.

White, K.E., Jonsson, K.B., Carn, G., Hampson, G., Spector, T.D., Mannstadt, M., et al., February 2001. The autosomal dominant hypophosphatemic rickets (ADHR) gene is a secreted polypeptide overexpressed by tumors that cause phosphate wasting. J. Clin. Endocrinol. Metab. 86 (2), 497–500.

Wilkins, G.E., Granleese, S., Hegele, R.G., Holden, J., Anderson, D.W., Bondy, G.P., May 1995. Oncogenic osteomalacia: evidence for a humoral phosphaturic factor. J. Clin. Endocrinol. Metab. 80 (5), 1628–1634. Epub 1995/05/01.

Winters, R.W., Graham, J.B., Williams, T.F., Mc, F.V., Burnett, C.H., 1957. A genetic study of familial hypophosphatemia and vitamin D resistant rickets. Trans. Assoc. Am. Phys. 70, 234–242. Epub 1957/01/01.

Wohrle, S., Bonny, O., Beluch, N., Gaulis, S., Stamm, C., Scheibler, M., et al., October 2011. FGF receptors control vitamin D and phosphate homeostasis by mediating renal FGF-23 signaling and regulating FGF-23 expression in bone. J. Bone Miner. Res. 26 (10), 2486–2497.

Wohrle, S., Henninger, C., Bonny, O., Thuery, A., Beluch, N., Hynes, N.E., et al., April 2013. Pharmacological inhibition of fibroblast growth factor (FGF) receptor signaling ameliorates FGF23-mediated hypophosphatemic rickets. J. Bone Miner. Res. 28 (4), 899–911.

Wu, H., Bui, M.M., Zhou, L., Li, D., Zhang, H., Zhong, D., February 2019. Phosphaturic mesenchymal tumor with an admixture of epithelial and mesenchymal elements in the jaws: clinicopathological and immunohistochemical analysis of 22 cases with literature review. Mod. Pathol. 32 (2), 189–204.

Wyman, A.L., Paradinas, F.J., Daly, J.R., April 1977. Hypophosphataemic osteomalacia associated with a malignant tumour of the tibia: report of a case. J. Clin. Pathol. 30 (4), 328–335. Epub 1977/04/01.

Chapter 65

Osteopetrosis

Antonio Maurizi and Anna Teti
Department of Biotechnological and Applied Clinical Sciences, University of L'Aquila, L'Aquila, Italy

Chapter outline

Introduction

In 1904, Albers-Schönberg described a patient with extremely dense but fragile bones (Albers-Schönberg, 1904). This phenotype matches what is now called autosomal dominant osteopetrosis (ADO) and was named Albers-Schönberg or marble bone disease (Hill and Charlton, 1965). The term "osteopetrosis" (osteo + *petra*, stone, + *osis*, condition) was coined to better highlight the density of the bones, as opposed to osteoporosis, in which there is a reduction of bone mass, also leading to bone fragility. The disease is caused by abnormalities of osteoclasts, the cells deputed to the resorption of the bone matrix, described in detail in Chapter 17. Bone resorption is fundamental for harmonic bone accrual, the excavation of the bone cavities, and balanced bone remodeling, in concert with the bone formation implemented by osteoblasts (Teti, 2011; Cappariello et al., 2014).

In osteopetrosis, bone fragility is determined by the lack of bone renewal, with preservation of primary non-remodeled bone featuring persistent mineralized cartilage within the bone trabeculae (Rucci and Teti, 2016) (Fig. 65.1). This altered mineralized tissue does not retain the mechanical properties, losing resistance and fracturing with low energy. In this chapter we will describe the clinical, genetic, phenotypic, and molecular aspects of osteopetrosis and will provide information on existing and experimental therapies that we hope will cure in the future all forms of the disease.

Clinical features

Clinically, osteopetrosis is classified as lethal, intermediate, and mild forms. Lethal osteopetrosis has an autosomal recessive inheritance and is also called infantile or malignant osteopetrosis, or *autosomal recessive osteopetrosis* (ARO). A few cases have been demonstrated to have an X-linked inheritance and this group is called *X-linked osteopetrosis* (XLO). ARO and XLO are fatal within the first years of life. ARO has a prevalence of 1:250,000 live births (Whyte, 2013; Sobacchi et al., 2013, Teti and Econs, 2017), while the exact prevalence of XLO is unknown. Rarely, patients survive for the first decade, whereas most of them die within 2 years of birth (Whyte, 2013; Sobacchi et al., 2013; Teti and Econs, 2017). Symptoms include severe bone marrow failure signified by grave anemia, pancytopenia, impaired blood clotting, and susceptibility to infections, including osteomyelitis, and hepatosplenomegaly due to ectopic hematopoiesis. Patients also show hypocalcemia, hyperparathyroidism, stunted growth, pain, multiple atraumatic fractures affecting mostly the appendicular skeleton, cranial nerve compression syndromes leading to impaired vision and hearing, obstructive hydrocephalus due to overgrowth of the foramen magnum, nystagmus, frontal bossing, nasal sinus abnormalities, and impairment of tooth eruption (Schinke et al., 2009; Whyte, 2013; Sobacchi et al., 2013; Teti and Econs, 2017) (Table 65.1).

Principles of Bone Biology. https://doi.org/10.1016/B978-0-12-814841-9.00065-8

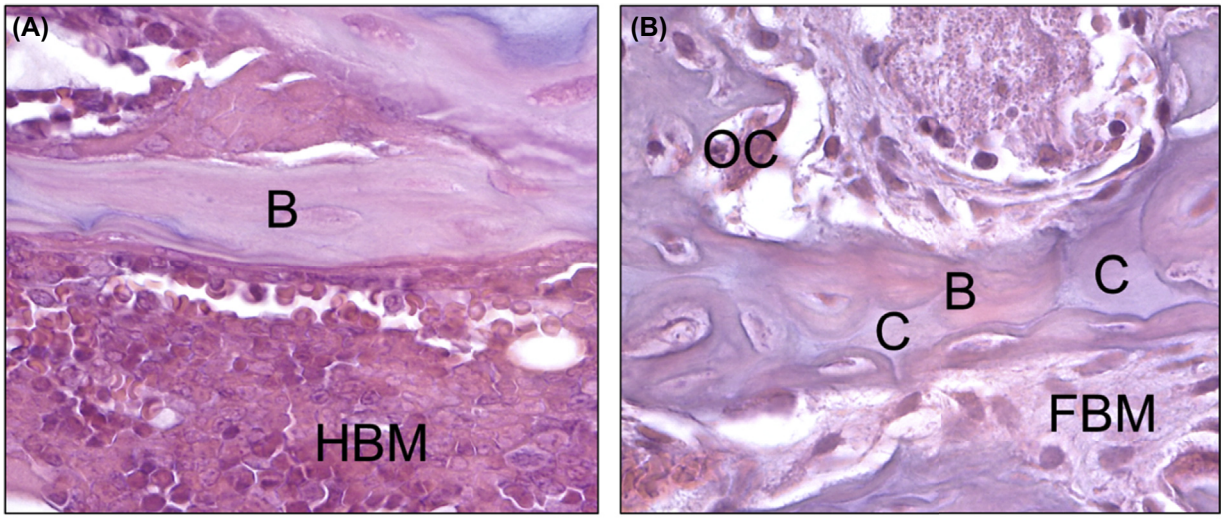

FIGURE 65.1 Histopathology of mouse osteopetrosis. Histological sections of C57BL/6 mouse proximal tibia trabecular bone stained with hematoxylin/eosin. (A) One-month-old wild-type mouse. (B) One-month-old osteopetrotic (autosomal recessive osteopetrosis) mouse. *B*, bone; *C*, cartilage; *FBM*, fibrotic bone marrow; *HBM*, hematopoietic bone marrow; *OC*, osteoclast. Bar: 15 μm.

Mental retardation is generally not seen in this form, although cerebral hemorrhage can occur due to thrombocytopenia. However, some osteopetrotic subtypes show primary neurodegeneration severely impairing neural functions (Kornak et al., 2001; Chalhoub et al., 2003).

Intermediate osteopetrosis has an autosomal recessive inheritance as well and presents with symptoms similar to those of the lethal forms, but less severe. It is also called *intermediate recessive osteopetrosis* (IRO) and its symptoms include renal tubular acidosis, cerebral calcification, and mental retardation, not seen in other types of osteopetrosis. Its prevalence is very low and not quantified, with about 50 cases described in the literature (Ohlsson et al., 1986; Bolt et al., 2005).

Mild osteopetrosis has an autosomal dominant inheritance and is generally called benign osteopetrosis. This definition is misleading as there are cases showing high morbidity and, rarely, early death, although generally patients achieve adulthood and have a normal life span. Mild osteopetrosis is also known as Albers-Schönberg disease to honor the very first publication on osteopetrosis by Albers-Schönberg (1904). Currently, the most accepted name of this form is ADO, which was previously classified as type 1 and type 2 (Bollerslev and Andersen, 1988). In the section describing the genetics of osteopetrosis we will highlight that ADO type 1 (ADO1) is not an osteoclast disease (Van Wesenbeeck et al., 2003) and that this syndrome should be reclassified as high bone mass (HBM) as it affects the function of osteoblasts rather than that of osteoclasts. ADO type 2 (ADO2) is instead a genuine osteoclast disease, so its current classification is correct, although there is some debate as to whether this should be called ADO or ADO2. In this chapter we will call it ADO2 as this is the most acknowledged name for this form.

ADO2 has a prevalence of 1:20,000 live births and an incomplete penetrance (66%), therefore more than 30% are healthy carriers who do not develop the syndrome (Waguespack et al., 2007; Bollerslev et al., 2013). The affected individuals have mild to rarely lethal outcome, frequently with high morbidity, especially due to multiple low-energy fractures that in some patients occur tens of times during their life. High bone density is observed especially at the skull base, in the vertebral bodies, and in the pelvis, and these observations are pathognomonic of ADO2 (Bénichou et al., 2000; Waguespack et al., 2007; Del Fattore et al., 2006; Bollerslev et al., 2013). Patients may also frequently suffer from anemia, mandibular osteomyelitis, dental problems, pain, hypovision, and hypoacusis (Bénichou et al., 2000; Del Fattore et al., 2006; Waguespack et al., 2007). Severe forms are seriously debilitating, with a very poor quality of life. These patients are often wheelchair bound and need life-long assistance. Very few cases are reported to exhibit cognitive failures (Del Fattore et al., 2006).

Radiographic features

Even though we are in the third millennium and many new sophisticated imaging diagnostic tools are available, the best method to diagnose osteopetrosis is still by radiography. Bones appear dense and medullary cavities are reduced or obliterated. Diffuse sclerosis is observed in the entire skeleton in ARO, XLO, and IRO, while ADO2 is characterized by a

TABLE 65.1 Radiographic and clinical features of osteopetrosis.

Type of osteopetrosis	Acronym	Radiographic features	Clinical features

Autosomal recessive	ARO	• Dense bone with reduced or obliterated medullary cavity
		• Diffuse sclerosis
		• Bone-in-bone appearance
		  ■ Spine
		  ■ Pelvis
		  ■ Long bones
		• Misshapen metaphysis
		• Incomplete dentition
		• Hypertelorism with "hair-on-end" appearance of the calvaria bone
			• Bone marrow failure
			• Anemia
			• Pancytopenia
			• Thrombocytopenia
			• Impaired blood clotting
			• Susceptibility to infections
			• Osteomyelitis
			• Hepatosplenomegaly
			• Hypocalcemia
			• Hyperparathyroidism
			• Stunted growth
			• Pain
			• Multiple low-energy fractures
			• Impaired vision and hearing
			• Obstructive hydrocephalus
			• Nasal sinus abnormalities
			• Impairment of tooth eruption

Intermediate	IRO	• Similar to ARO but less severe	• All ARO symptoms but less severe • Renal tubular acidosis • Cerebral calcification • Mental retardation

Autosomal dominant	ADO2	• Focal sclerosis
		  ■ Skull basis
		  ■ Vertebral bodies
		  ■ Pelvis
		• Sandwich vertebrae
		• Rugger-jersey spine
			• Multiple low-energy fractures
			• Anemia
			• Mandibular osteomyelitis
			• Dental problems
			• Pain
			• Hypovision
			• Hypoacusis
			• Cognitive failures (rare cases)

focal sclerosis of the skull basis, vertebral bodies, and pelvis (Bénichou et al., 2000; Waguespack et al., 2007; Del Fattore et al., 2006; Bollerslev et al., 2013). Specifically, the vertebral bodies present with dense bone tissue at their sub−end plates and for this feature they are called "sandwich vertebrae," while the entire spine is called "rugger-jersey spine" due to the prominent sub−end plate sclerosis of multiple contiguous vertebrae that produce alternating sclerotic−lucent−sclerotic areas (Bénichou et al., 2000; Waguespack et al., 2007; Del Fattore et al., 2006; Bollerslev et al., 2013). This aspect makes the diagnosis of ADO2 rather easy.

Osteopetrotic bones, especially in the most severe cases, show the so-called "bone-in-bone" appearance (Williams et al., 2004), which indicates a bone that has another bone inside, like a miniature version, seen in spine, pelvis, and long bones. Furthermore, long bones may present with alternating radiolucent and radiodense metaphyseal lines, which represent growth-arrest bands (Yao and Seeger, 1997; Bénichou et al., 2000; Waguespack et al., 2007; Del Fattore et al., 2006; Bollerslev et al., 2013). The metaphysis also appears misshapen, with an expanded funnel-like appearance. The length of bones is reduced for age, demonstrating stunted growth, confirmed by the short stature of patients. Mandibles present a triangular opacity due to calcification of the secondary condylar ossification center. Dentition is incomplete, with defective enamel formation and predisposition to caries. Patients may show hypertelorism, malformed calvariae with an expanded diploic space, which shows the so-called "hair-on-end" appearance. This consists of thin vertical striations resembling hairs due to the diploe trabecular pattern perpendicular to the curvature of the cranial vault (Azam and Bhatti, 2006).

Genetic features

The very first gene found in 1983 to affect osteopetrotic patients is called *CAII* and encodes carbonic anhydrase type II (Sly et al., 1983). This is a member of the large family of carbonic anhydrases that accelerate the spontaneous hydration of carbon dioxide. The resulting carbonic acid represents an efficient source of protons especially in cells that largely acidify the extracellular environment, including gastric parietal cells, renal tubular cells, and osteoclasts (Fig. 65.2). *CAII* was found to be mutated in the form of IRO now classified as OPTB3 osteopetrosis (Table 65.2), clinically recognizable for its intermediate severity, renal acidosis, and mental retardation (Sly et al., 1983, 1985). Given the significant spontaneous carbonic acid formation occurring in osteoclasts, some bone resorption is still possible in these patients, which explains the intermediate course.

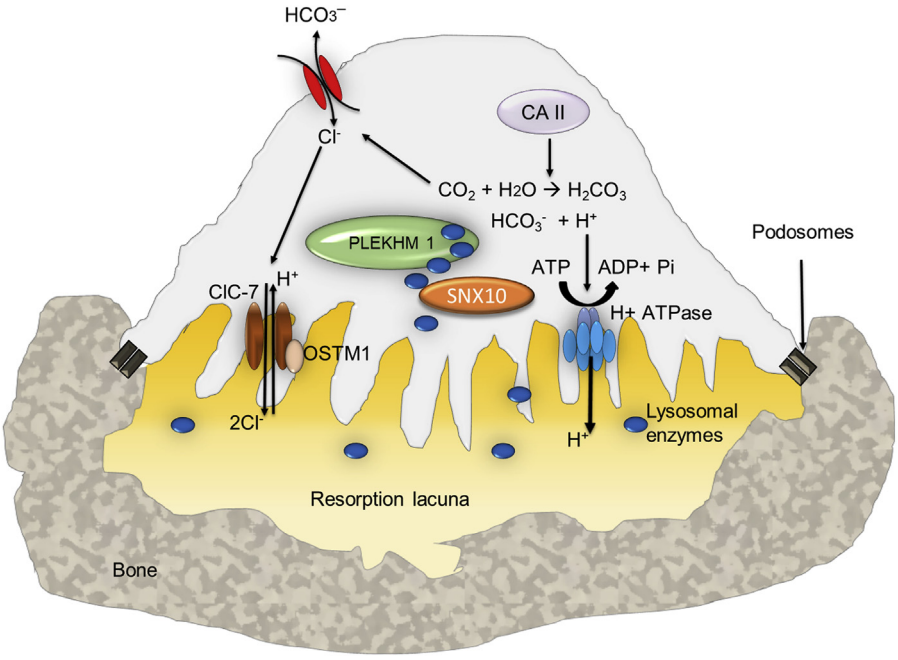

FIGURE 65.2 Osteoclast molecular mechanisms altered in osteopetrosis. Cartoon illustrating a polarized osteoclast in the process of bone resorption. The indicated proteins are mutated in the forms of osteopetrosis described in the text and in Table 65.2. *CAII*, carbonic anhydrase type II; *ClC-7*, chloride channel 7; *OSTM1*, osteopetrosis-transmembrane protein 1; *PLEKHM1*, pleckstrin homology domain-containing, family M (with RUN domain) member 1; *SNX10*, sorting nexin 10.

TABLE 65.2 Genetics of osteopetrosis.

Classification	OMIM number	Mutated gene	Encoded protein	Protein function	Osteopetrosis acronym	Frequency
OPTA1	607634	*LRP5*	LRP5	Induces bone formation	ADO1	Unknown
OPTA2	166600	*CLCN7*	ClC-7	Charge balances lysosomes and resorption lacunae	ADO2	70% of ADO
OPBT1	259700	*TCIRG1*	a3 subunit of the vacuolar H^+-ATPase	Acidifies lysosomes and resorption lacunae	ARO	50% of ARO
OPBT2	259710	*TNFS11*	RANKL	Induces osteoclastogenesis	ARO	5% of ARO
OPBT3	259730	*CAII*	Carbonic anhydrase II	Accelerates hydration of CO_2 in H_2CO_3	ARO	Unknown
OPBT4	611490	*CLCN7*	ClC-7	Charge balances lysosomes and resorption lacunae	ARO	10% of ARO
OPBT5	259720	*OSTM1*	OSTM1	Allows subcellular localization of ClC-7	ARO	5% of ARO
OPBT6	611497	*PLEKHM1*	PLEKHM1	Regulates vesicular trafficking	ARO	Unknown
OPBT7	612301	*TNFRS11A*	RANK	Induces osteoclastogenesis	ARO	5% of ARO
OPBT8	615085	*SNX10*	SNX10	Regulates endosome homeostasis	ARO	4% of ARO
-	300301	*NEMO*	NEMO	Regulates NF-κB activity	XLO	Unknown

The second gene found to affect osteopetrotic patients was identified 17 years later (Frattini et al., 2000). Building on the spontaneous osteopetrotic mouse model oc/oc, largely investigated to understand the molecular basis of bone resorption and identify the mechanisms inducing its impairment in osteopetrosis, Frattini et al. (2000) recognized the human homolog of the *atp6i* gene to be altered in about 50% of patients affected by ARO. This is now classified as OPTB1 (Table 65.2) osteopetrosis and the gene involved is called *TCIRG1*. This gene encodes the a3 subunit of the vacuolar H^+-ATPase (V-ATPase), a multimeric complex made up of a transmembrane V_0 domain transporting protons and a cytosolic V_1 domain representing the catalytic ATPase activity (Finbow and Harrison, 1997; Frattini et al., 2000) (Fig. 65.3). V_1 includes eight subunits, A−H, of which B, C, E, and G are tissue specific. For instance, mutations of the B1 isoform induce distal tubular acidosis and impair hearing (Karet et al., 1999). V_0 includes six subunits, a, d, c, c′, c″, and e. Subunits a and d are tissue specific, and biallelic loss-of-function mutations of the a3 isoform induce OPTB1 osteopetrosis. The a3 subunit is largely expressed in osteoclasts and in gastric parietal cells, where V-ATPase acidifies the extracellular environment: the resorption lacunae and the gastric lumen, respectively. In osteoclasts, V-ATPase is expressed in the lysosomal membrane and in the ruffled border membrane (Fig. 65.2). The latter derives from the fusion of lysosomes with the plasma membrane (Stenbeck, 2002); therefore, lysosomes contribute to inserting V-ATPase into this site and to modifying the resorption lacuna environment by releasing their acidic hydrolases (Baron et al., 1985; Stenbeck, 2002). Therefore, one can imagine the resorption lacuna as a giant modified lysosome. In fact, like lysosomes, this lacuna has a pH below 5 and contains lytic enzymes (Fig. 65.2). The low pH is essential to solubilize the hydroxyapatite crystals (Blair et al., 1986) and liberate the organic matrix underneath. This acidic environment is permissive for acidic enzymes that attack the organic matrix, especially type I collagen, which represents 95% of the matrix proteins and has been found to be sensitive to the proteolytic activity of cathepsin K (Zaidi et al., 2001). Mutations of cathepsin K do not disrupt the release of hydroxyapatite but prevent the hydrolysis of collagen, giving rise to a syndrome called pycnodysostosis or "Toulouse-Lautrec" disease (Motyckova and Fisher, 2002). The impairment of the acidification of the resorption lacunae disturbs bone resorption as is seen in OPTB1 osteopetrosis. OPTB1 affects at least 50% of ARO patients (Frattini et al., 2000) who are reported to harbor a severe disease. Given the expression of the a3 V-ATPase subunit in the gastric parietal cells as well, patients also present with high gastric pH that disturbs the absorption of calcium (Schinke et al., 2009; Barvencik et al., 2014). As a result, the

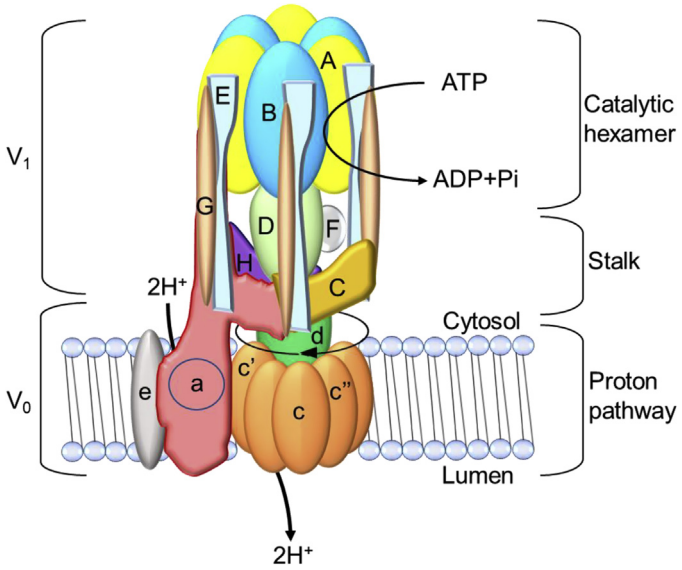

FIGURE 65.3 Molecular structure of the vacuolar H^+-ATPase. Osteoclasts express isoform 3 of the a subunit (a3) of the V_0 domain (*circle*).

bone matrix cannot mineralize properly. In fact, histopathologically, OPTB1 presents with unmineralized osteoid, reminiscent of rickets or osteomalacia. Therefore, this form of osteopetrosis has been proposed to be called osteopetrorickets or osteopetromalacia (Barvencik et al., 2014).

The second most frequent form of ARO is called OPTB4 and is caused by biallelic loss-of-function mutations of the *CLCN7* gene (Table 65.2). It affects about 10% of ARO patients. A peculiar phenotype of OPTB4 is a primary neurodegeneration, especially of the retina, hippocampus, and cerebral and cerebellar cortices (Kasper et al., 2005; Steward, 2003) (Fig. 65.4). For reasons yet to be elucidated, the penetrance of this symptom is incomplete, and some patients do not suffer from severe neurodegeneration. The *CLCN7* gene encodes a 2 chloride/1 proton antiporter (chloride channel 7; ClC-7) necessary to charge balance the electrogenic proton transport by V-ATPase (Cappariello et al., 2014). Like V-ATPase, it is inserted into the lysosomal membrane and transferred to the ruffled border membrane by an exocytosis process (Fig. 65.2). The source of chloride is through a chloride/bicarbonate exchanger located in the osteoclast basolateral membrane (Cappariello et al., 2014) (Fig. 65.2). This anion countertransporter effluxes the bicarbonate generated by the dissociation of the carbonic acid, whose formation is catalyzed by carbonic anhydrase type II, while influxing the chloride

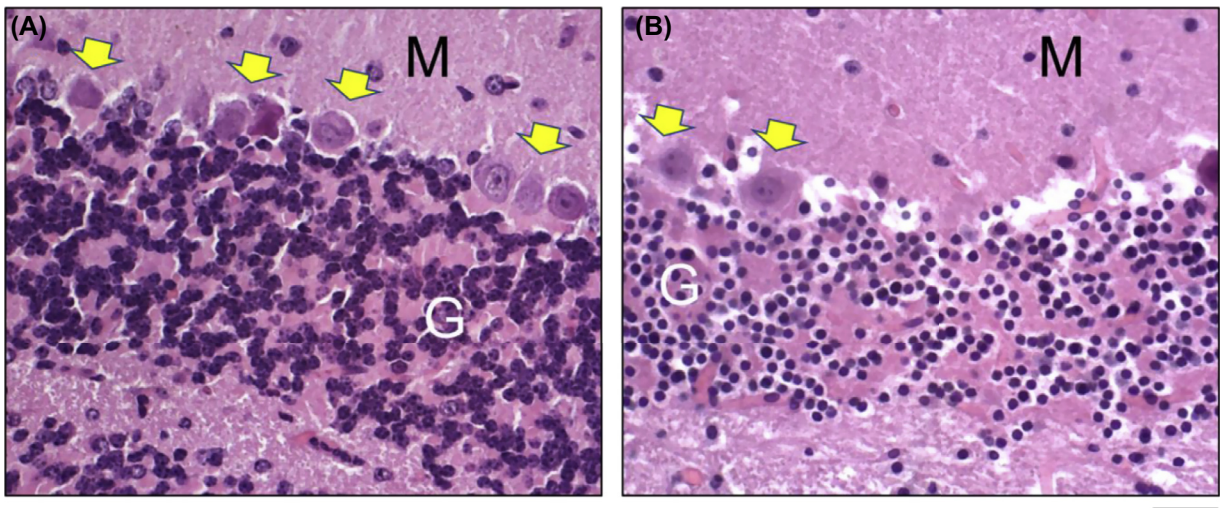

FIGURE 65.4 Histopathology of mouse cerebellar cortex. Histological sections of C57BL/6 mouse cerebellar cortex stained with hematoxylin and eosin. (A) One-month-old wild-type mouse. (B) One-month-old *Clcn7*^{G213R} ADO2 mouse. Note the hypocellularity in the Purkinje and in the granular layers compared with (A). *M*, molecular layer; *G*, granular layer. *Arrows*, Purkinje cells. Bar: 25 μm.

from the extracellular environment (Cappariello et al., 2014). Chloride is then released into the lysosomes or into the resorption lacuna by the ClC-7 protein (Fig. 65.2).

Associated with ClC-7 there is OSTM1, which is currently classified as the ClC-7 β subunit (Fig. 65.2). The role of OSTM1, encoded by the homonym gene, is to correctly subcellularly localize the ClC-7, contributing to the proper trafficking of the protein. Loss-of-function mutations of *OSTM1* induce OPBT5 osteopetrosis (Table 65.2), whose phenotype is very similar to that of OPTB4 osteopetrosis, albeit with a constant severe neurodegeneration (Pangrazio et al., 2006; Chalhoub et al., 2003). OPBT5 is even rarer than OPBT4, accounting for about 5% of patients (Pangrazio et al., 2006).

OPBT8 osteopetrosis (Table 65.2) is caused by mutations of the *SNX10* gene (Aker et al., 2012). The gene encodes a member of the sorting nexin protein family, involved in intracellular trafficking (Aker et al., 2012) (Fig. 65.3). The protein regulates endosome homeostasis and its mutations affect about 4% of ARO patients (Pangrazio et al., 2013). In this form of osteopetrosis, few and small osteoclasts are observed (Aker et al., 2012). In agreement with the role of the SNX10 protein, these osteoclasts show impairment of vesicular trafficking and endocytosis. They also show impaired extracellular acidification and altered ruffled border (Aker et al., 2012). In mice, SNX10 is not unique to osteoclasts. It is expressed in the stomach, where the phenotype is very similar to that induced by alteration of the *TCIRG1* gene: high pH and reduced calcium solubilization (Ye et al., 2015). In fact, the *SNX10*-coded protein contributes to the correct V-ATPase subcellular localization and is probably involved in the sorting of this complex to the ruffled border (Ye et al., 2015). In line with these alterations, the *SNX10* global knockout mouse skeleton is affected by osteopetrorickets or osteopetromalacia. In contrast, osteoclast-specific knockout mice show osteopetrosis but not rickets or osteomalacia (Ye et al., 2015).

The *PLEKHM1* gene, encoding the pleckstrin homology domain-containing, family M (with RUN domain) member 1 protein, is implicated in OPBT6 osteopetrosis (Table 65.2). This is another form of ARO in which the vesicular trafficking is altered (Fig. 65.2). It is milder than the other ARO forms, although the skeletal phenotype is still largely compromised (Van Wesenbeeck et al., 2007). PLEKHM1 functions as a multivalent adapter for the small GTP-binding protein Rab-7. It regulates Rab-7-dependent vesicular trafficking as well as lysosome−autophagosome fusion through interaction with the homotypic fusion and protein sorting complex (McEwan and Dikic, 2015), which associates the autophagic pathway with endocytic trafficking (McEwan and Dikic, 2015). Given the relevance of vesicular trafficking in the activity and cellular distribution of lysosomes and in their involvement in the formation of the osteoclast ruffled border, it is not difficult to imagine that the cellular impairment induced by PLEKHM1 loss-of-function mutations impairs bone resorption (Van Wesenbeeck et al., 2007). Through its interaction with Rab-7, PLEKHM1 also impairs the endocytic transport from early to late endosomes (McEwan and Dikic, 2015), also relevant for lysosome homeostasis (McEwan and Dikic, 2015). The literature on this form of ARO is scanty and the frequency of the mutation of this gene is not known. Interestingly, an R714C variant of PLEKHM1 has been found to induce a skeletal phenotype not related to osteopetrosis, characterized by osteopenia associated with focal osteosclerosis (Del Fattore et al., 2008), in which osteoclasts retained low tartrate-resistant acid phosphatase (TRAcP) intracellular activity, probably caused by exacerbated extracellular release of this lysosomal enzyme. Released TRAcP was observed to stimulate osteoblast activity, suggesting an increased osteoclast−osteoblast coupling potentially explaining the focal osteosclerosis seen in this patient (Del Fattore et al., 2008).

All the aforementioned ARO forms of osteopetrosis are defined as "osteoclast-rich" for their normal or high content of osteoclasts (Villa et al., 2009). The cellular nature of these AROs is related to the inability of osteoclasts to resorb bone, while the pattern of osteoclast differentiation remains unaltered (Villa et al., 2009). In several osteoclast-rich ARO patients (Villa et al., 2009), osteoclastogenesis is even increased, with no enhancement of osteoclast activity because of the alterations of genes involved in matrix reabsorption. This increase is thought to be due to the hypocalcemic phenotype caused by the lack of bone resorption, which stimulates the release of parathyroid hormone (PTH) from the parathyroid glands (Jacome-Galarzaet al., 2011; Hendy and Canaff, 2016). PTH is known to stimulate osteoclastogenesis by inducing the osteoblast expression of osteoclastogenic cytokines, including receptor activator of NF-κB ligand (RANKL) (Pierroz et al., 2009). In fact, in line with this hypothesis, osteoclast-rich ARO patients show high serum PTH concentration (Villa et al., 2009).

Two other forms of ARO do not show mature osteoclasts in their bone biopsies and are grouped as "osteoclast-poor" osteopetrosis. This histological feature is observed in two forms known as OPBT2 and OPBT7. OPBT2 is induced by loss-of-function mutations of the *TNFS11* gene encoding the osteoclastogenic protein RANKL (Table 65.2), while OPBT7 is caused by loss of function of the *TNFRS11A* gene encoding the RANKL receptor, RANK (Table 65.2; Fig. 65.5). OPBT2 and OPBT7 mutations affect 5% of ARO patients each. OPBT2 mutations are not osteoclast autonomous because the *TNFS11* gene is expressed by a variety of cell types, including lymphocytes and osteoblasts, but not by osteoclasts or their precursors (Pangrazio et al., 2012). However, osteoclasts are primarily affected by *TNFS11* gene mutations. In fact, RANKL is a member of the tumor necrosis factor family (Takahashi et al., 1999) and a proosteoclastogenic cytokine that

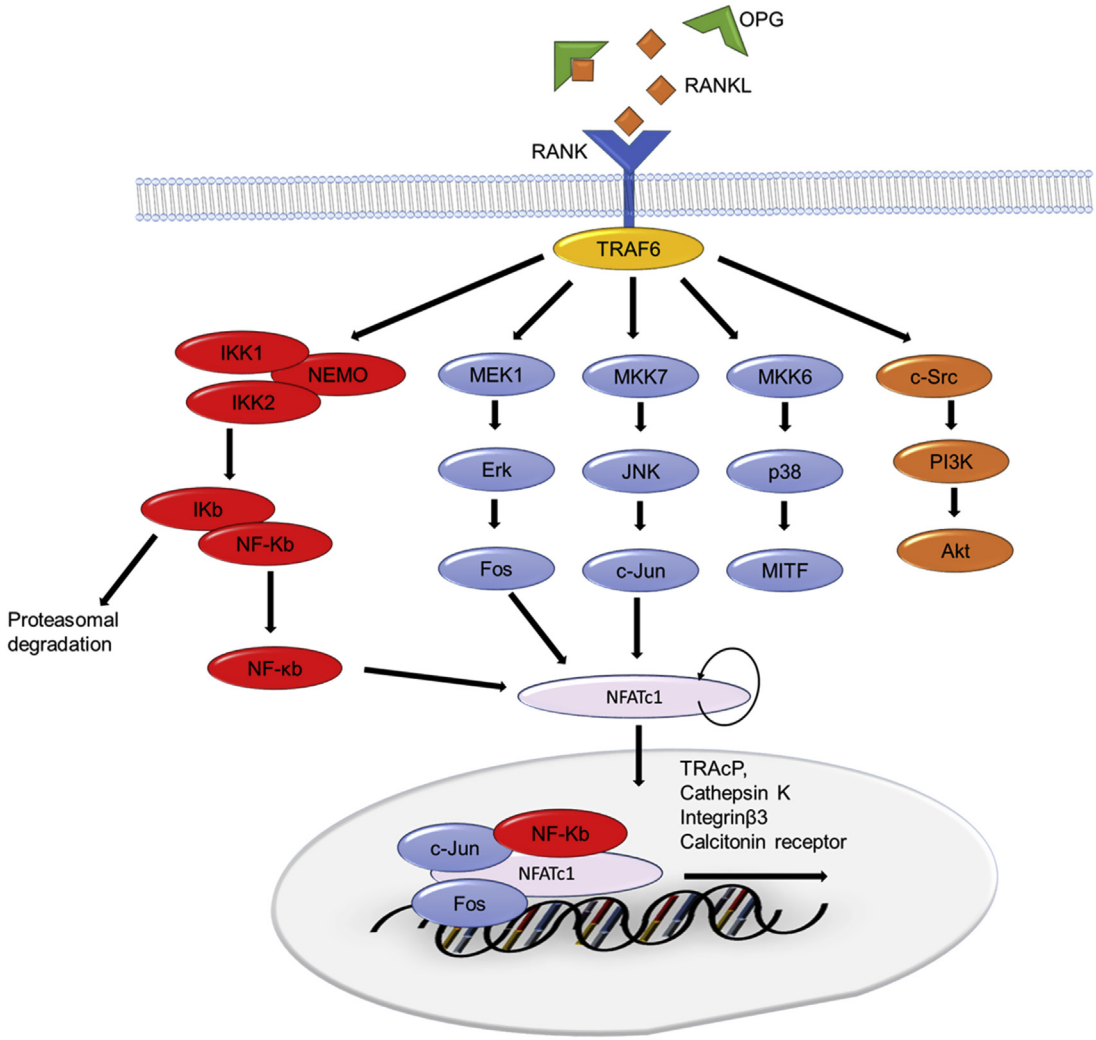

FIGURE 65.5 Osteoclastogenic receptor activator of NF-κB ligand (*RANKL*)/*RANK* intracellular signaling pathway. Cartoon illustrating the intracellular signaling pathway triggered by the RANKL/RANK axis, and the induced osteoclastogenic gene transcription. The pathway is physiologically antagonized by osteoprotegerin (*OPG*), which functions as a soluble RANKL decoy receptor.

binds its receptor RANK, expressed by osteoclast precursors, promoting their late differentiation. This event culminates in mononuclear precursor fusion into giant cells, which then polarize, maturate, and resorb bone (Takahashi et al., 1999). RANKL is also a prosurvival factor regulating osteoclast life span. The cytokine has many other roles in other cell types, especially in immune cells, such as dendritic cells and lymphocytes. In fact, an overall feature of *TNFS11* mutants is defective B and T differentiation and impaired immune response (Dougall et al., 1999). RANKL is also implicated in the development of the lobuloalveolar structure of the mammary gland (Asselin-Labat et al., 2010). Although severe, at variance with the osteoclast-rich osteopetrosis, this osteoclast-poor ARO form presents with a longer survival and a nonfibrotic bone marrow tissue (Sobacchi et al., 2007; Teti, 2012).

Phenotypically very similar to OPBT2, OPBT7 is caused by mutations in the RANKL counterpart (Table 65.2). In fact, the gene implicated, *TNFRS11A*, encodes the RANKL receptor RANK, expressed by osteoclast precursors (Guerrini et al., 2008). Therefore, dysfunctions are osteoclast autonomous although, as for the *TNFS11* gene mutations, also in this form of ARO there are lymphocyte deficiencies and impaired immune response. OPBT7 shares pathological features with OPBT2, but with an important therapeutic implication that will be described in the section on therapy.

So far, no other AROs are described in the literature. However, another lethal condition is the only XLO known, as of this writing, which is part of the complex syndrome called osteopetrosis, lymphedema, hypohidrotic ectodermal dysplasia and immunodeficiency (OL-HED-ID). OL-HED-ID is caused by mutations in the NF-κB essential modulator (*NEMO*)

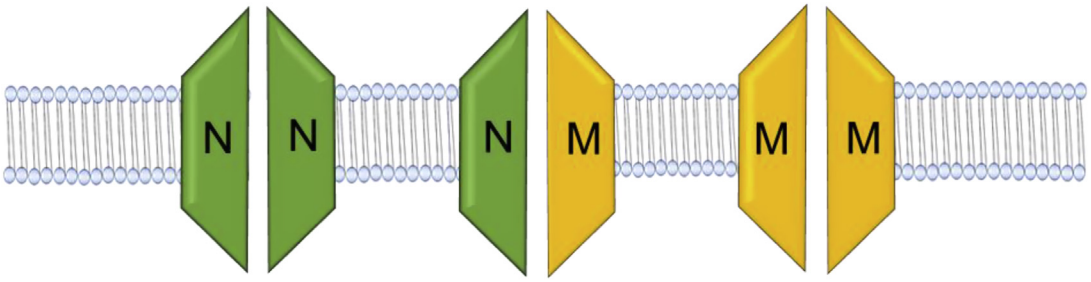

FIGURE 65.6 Assortment of chloride channel 7 (ClC-7) dimers in OPTA2 ADO2 osteopetrosis. Cartoon illustrating the potential ClC-7 subunit dimerization in OPTA2 osteopetrosis. Normal homodimers (*N/N*) are expressed together with mutated homodimers (*M/M*) and *N/M* heterodimers that are believed to be nonfunctional or malfunctional in their $Cl^-/2H^+$ exchange process.

gene (Table 65.2). This gene is also known as *IKKγ* or *IKBKG*, and its protein product exhibits a regulatory role in the IκB kinase (IKK) complex (Darwech et al., 2009). NEMO is an activator of the IKK complex, which is upstream of NF-κB and induces NF-κB translocation to the nucleus, where it functions as a proosteoclastogenic and pro-immune response transcription factor (Darwech et al., 2009) (Fig. 65.5). Given that NF-κB is also implicated in ectodermal tissue formation, including skin, hair, teeth, and sweat glands (Döffinger et al., 2001), its mutations cause alterations in these tissues as well, explaining the complexity of the disease. The bone histological phenotype of these patients is unknown, but the disease is assumed to be osteoclast poor given that the NF-κB pathway is involved in osteoclast differentiation. OL-HED-ID has the OMIM number 300301 (Table 65.2), but it is not classified with an OPBT number and the involved gene mutations have unknown frequency.

In addition to ARO and XLO, ADO patients have also received genetic diagnosis. As mentioned before, ADO1 is not an osteopetrosis but should be better classified as an HBM syndrome due to the involvement of exacerbated bone formation rather than impaired bone resorption (Van Wesenbeeck et al., 2003). This is not a trivial detail, as it has important clinical implications, because the HBM syndrome is characterized by strong bones that are not prone to fracture (Boyden et al., 2002; Van Wesenbeeck et al., 2003), while one relevant hallmark of osteopetrosis is bone fragility despite the increased bone mass (Teti and Econs, 2017). Nevertheless, OMIM lists ADO1 within the osteopetrotic disease family, where it is denominated OPTA1 (Table 65.2). Consistent with the HBM syndrome, the gene implicated in OPTA1 is *LRP5*, encoding a membrane receptor, low-density lipoprotein receptor–related protein 5 (LRP5), which, with its coreceptor Frizzled4, responds to members of the Wnt family of factors, affecting cell growth, adhesion, migration, and many other activities (Komiya and Habas, 2008). The pathway is highly conserved (Komiya and Habas, 2008) and was first identified in *Drosophila*, in which mutations impair segmentation (Wodarz and Nusse, 1998). LRP5 plays roles in the development of retina, inner ear, and bone. The Wnt/LRP5/Frizzled4 complex promotes bone formation, contributing to the regulation of bone mineral density and bone quality (Johnson, 2012), and is antagonized by specific inhibitors, including Dickkopf-1 (Niehrs, 2006) and sclerostin (Li et al., 2005). Some inactivating mutations of LRP5 induce juvenile primary osteoporosis, whereas many others cause osteoporosis–pseudoglioma syndrome. This is a very severe disease with extremely low bone mineral density, severe bone fragility, and eye abnormalities (Gong et al., 2001). Autosomal dominant *LRP5* mutations enhance bone mass, intensifying Wnt signaling or reducing the antagonistic effect of their inhibitors (Boyden et al., 2002). These mutations affect the first "B-propeller" module of LRP5 and may induce clinically recognizable HBM syndrome (Pangrazio et al., 2011). In line with this, a group of single-allele LRP5 mutations was identified in clinically diagnosed ADO1 patients, which should now be referred as a very mild form of HBM.

The only ADO form that is a genuine osteopetrosis disease is classified as OPTA2 (Table 65.2) and is caused by dominant negative mutations of the *CLCN7* gene (Cleiren et al., 2001), encoding the ClC-7 protein (Fig. 65.2) already described for OPBT4 ARO osteopetrosis. OPTA2 corresponds to the ADO2 phenotype and is caused mostly by single amino acid substitutions that alter the ClC-7 conformation. The frequency of these gene mutations accounts for about 70% of ADO2 cases, the remaining 30% still lacking a genetic diagnosis. Given that the ClC-7 protein is a homodimer, it is thought that OPTA2 patients express an assortment of mutated homodimers, normal homodimers, and heterodimers with one normal and one mutated subunit (Perdu et al., 2012) (Fig. 65.6). This condition reduces, but does not abolish, the chloride transport. The clinical result is a milder form of osteopetrosis, generally not lethal, but very heterogeneous in terms of penetrance, symptoms, and sufferance (Bénichou et al., 2000; Waguespack et al., 2007; Del Fattore et al., 2006; Bollerslev et al., 2013).

Current therapies

The turning point of the therapy of osteopetrosis was when the hematogenous and circulating origin of osteoclast precursors was discovered (Marks Jr and Walker, 1981) and when osteopetrosis was cured in mice by parabiosis (Walker, 1973) and by bone marrow transplantation (Walker, 1975). This was followed by the first osteopetrotic infant treated by bone marrow transplantation in 1980 (Coccia et al., 1980). Since then, hundreds of kids have been subjected to hematopoietic stem cell transplantation (HSCT) (Teti and Schulz, 2013), with outcomes that improved over the years (Driessen et al., 2003; Teti and Schulz, 2013). This therapy is not without limitations: (1) it is suitable only for ARO; (2) although most ARO patients can be treated, OPBT5 (*OSTM1* gene mutations) has severe neurodegeneration that HSCT cannot cure; (3) OPBT4 (*CLCN7* gene mutations) must be carefully evaluated neurologically before HSCT is performed due to the high likelihood of severe neurodegeneration in these patients as well; (4) OPBT2 (*TNFS11* gene mutations) is not osteoclast autonomous and cannot benefit from replacement of the osteoclast lineage by HSCT; (5) dwarfism and impaired vision and hearing do not improve if symptoms are already present at the time of HSCT; (6) lethal complications intrinsic to the procedure do not make HSCT suitable for intermediate osteopetrosis and ADO, such as OPTB3 (*CAII* mutations) and OPTA2 (*CLNC7* dominant negative mutations), respectively. Despite these limitations, HSCT is the only effective therapy that may provide patients an acceptable quality of life, especially in cases with no mental retardation (Teti and Schulz, 2013; Schulz et al., 2015).

Unfortunately, so far, other therapies have failed to substantially alleviate the osteopetrotic symptoms. Analgesics and antibiotics can treat pain and infections (Saigal et al., 2015). Calcium and vitamin D_3 supplementation and treatment with PTH, attempted in the far past, were not successful (Glorieux et al., 1981; Blazar et al., 1984; Key Jr et al., 1993; Askmyr et al., 2009). Interferon-γ has contradictory effects on osteoclast generation (Takayanagi et al., 2000; Gao et al., 2007) and induces several important adverse effects, although it delays the disease progression and improves hematopoiesis to some extent (Key et al., 1992, 1995). Erythropoietin and glucocorticoids are also used to improve hematopoiesis (Meletis et al., 1995). Furthermore, some patients are subjected to blood transfusions (Teti and Econs, 2017). However, these treatments are palliative and in general they are used while waiting for HSCT to be available or in cases that are not suitable for HSCT or in which HSCT failed. ARO patients with no options for HSCT will not be healed by any of these therapies, but they can be subjected to surgery to reduce fractures, decompress nerves, or treat hydrocephalus (Hwang et al., 2000).

No cure is available for ADO2 patients. The most harmful symptoms are pain and multiple fractures prone to developing osteomyelitis, which are treated with analgesics, surgery, and antibiotics, respectively (Landa et al., 2007; Saigal et al., 2015). HSCT is not performed given the intrinsic risky complications, unless symptoms are so severe as to become life threatening (Teti and Econs, 2017), which is a rare condition in ADO2. A phase II safety clinical trial has recently been completed, using an interferon-γ formulation, but results showed no efficacy (Imel et al., 2019). It is clear, though, that advanced research must be performed to overcome these bottlenecks and provide patients with effective therapeutic options.

Future therapeutic scenarios

Research does not arrest, and we are now in a phase of flourishing investigations on new therapies, also taking advantage of recent discoveries in other fields. Certainly, there is a substantial general progress in the HSCT technology under the pressure of medical needs for more frequent diseases, such as hematological cancers (Norkin and Wingard, 2017). These improvements are proving beneficial for the ARO forms suitable for HSCT as well, now infused also with hematopoietic stem cells (HSCs) donated by mismatched donors. Furthermore, the better understanding of the disease, the ease in finding useful information through certified websites, and the availability of genetic tests make early diagnosis of osteopetrosis more readily available also in nonspecialized centers. This is a *conditio sine qua non* for HSCT to be successful and to prevent irreversible symptoms, such hypovision and hypoacusis (Driessen e al., 2003). So, the HSCT field is already projected into the future also for osteopetrosis.

However, there is still very much that must be done for those conditions that have no cure at all. Gene therapy is under investigation for several diseases and could be a substantial advantage versus HSCT as it would allow the use of genetically modified patient HSCs instead of donor HSCs (Sessa et al., 2016). Gene therapy is being successfully employed for some congenital immunodeficiencies using lentivirus-transduced cells (Sessa et al., 2016). These studies have allowed important adverse effects noted in previous pioneer studies to be overwhelmed, making the therapy safe and effective (Sessa et al., 2016). Furthermore, there is great interest nowadays in the CRISPR/Cas9 genome editing technology, which is opening new doors to innovative genetic manipulations to cure diseases (Niu et al., 2016). One of these diseases could certainly be osteopetrosis, facilitated by its hematological etiology.

Gene therapy can also be associated with cell therapy and the paradigm for this innovation is the induced pluripotent stem cell (iPSC) technology (Neri et al., 2015; Fields et al., 2016). Autologous iPSCs could theoretically be genetically manipulated to replace the mutant gene and reinoculated into the patient, with the ultimate goal to engraft the bone marrow and provide corrected osteoclast lineage. Unfortunately, this procedure is still in its infancy and presents with a series of important drawbacks difficult to tackle: (1) reprogramming somatic cells requires transduction of several genes of pluripotency; (2) reprogramming technology is a long procedure during which osteopetrosis symptoms are likely to progress and become irreversible; (3) injected into experimental animals, iPSCs develop teratomas that are incompatible with safety; (4) hypothetically, corrected iPSCs could be predifferentiated and selected in vitro prior to their use in vivo: the inoculation of preosteoclasts into osteopetrotic mice has provided a proof of principle that the osteopetrotic phenotype could be improved, but the data has not yet demonstrated its efficacy as a therapy (Wakkach et al., 2008; Cappariello et al., 2010). However, given the great interest in the use of corrected iPSCs in medicine and the successful outcomes in local applications, such as in retinal disease (Fields et al., 2016), this therapy holds promise for future development.

As mentioned earlier, RANKL deficiency is not an osteoclast-autonomous disease, which prevents the employment of HSCT in OPBT2 (*TNFS11* gene mutations). These patients can receive only palliative interventions and are expected to die within their first decade of life. Two approaches could be anticipated for OPBT2: (1) pharmacological treatment with recombinant RANKL and (2) skeletal mesenchymal stem cell transplantation (SK-MSCT). Neither approach is available as of this writing, and research in these fields is experiencing important limitations. RANKL administration has been attempted in a mouse model of RANKL deficiency (Lo Iacono et al., 2012), with successful rescue of hematopoiesis, lymphopoiesis, and bone phenotype in mice treated for 1 month with soluble RANKL (Lo Iacono et al., 2012). Unfortunately, the study unveiled overdose complications causing expansion of lymphoid aggregates present in the lungs leading to respiratory impairment and death (Lo Iacono et al., 2012). The means to prevent accumulation of overdose over time can be investigated, for instance, by dose titration followed by dose scaling down at the time when the bone phenotype is normalized. An important limitation of this approach is the need for corporate interest to develop a pharmacological therapy for an extremely rare condition, estimated to affect only 5:25,000,000 live births.

SK-MSCT is very promising as a cure not only for osteopetrosis but also for other connective diseases. RANKL-producing cells, such as osteoblasts and osteocytes (Nakashima and Takayanagi, 2011), originate from SK-MSCs; therefore heterologous or corrected autologous SK-MSCs could be employed to provide patients with a source of RANKL, which could replenish the defective cytokine. Research on SK-MSCT has been ongoing for many years, but there are no substantial results yet supporting its therapeutic employment (Zhao and Liu, 2016). Therefore, a challenge for the future would be to optimize SK-MSCT and make it suitable for therapy. However, alternative approaches could be the subcutaneous implantation of devices incorporating RANKL-producing cells, which could exert a systemic effect, releasing soluble RANKL into the circulation. Calvarial osteoblasts have been used with this aim, implanted in diffusion chambers used long ago to investigate in vivo bone metabolism under controlled conditions (Gundle et al., 1995). Osteoblasts were cultured on hydroxyapatite supports functionalized to adsorb the catalytic domain of metalloproteinase-14, known to cleave the soluble domain of RANKL, which was then released into the circulation (Cappariello et al., 2015). Osteoclastogenesis was observed in RANKL-null mice receiving such devices, providing a proof of principle for future developments. Compared with pharmacological treatment with soluble RANKL, this method could prevent overdose, given that osteoblasts are physiologically regulated to produce RANKL, for instance, by PTH (Cappariello et al., 2014). Furthermore, caged into diffusion chambers, donor cells remain segregated from the host immune system, which should prevent or at least attenuate the immune response. Finally, donor cells could be engineered to express soluble RANKL in a controlled manner, theoretically improving efficacy while preventing overdose effects.

Most relevant is the lack of significant therapies for ADO2. The disease is generally nonlethal, but a large portion of patients live with debilitating symptoms, one being multiple and difficult to repair fractures. A 2015 approach resuscitated the interferon-γ therapy with a new indication for ADO2 (Alam et al., 2015). The approach was promising in ADO2 mice, in which interferon-γ improved the bone phenotype over an 8-week treatment. The reduction in bone volume induced by the treatment was approximately halfway between wild-type mice and ADO2 mutant mice. Therefore, although significant, the phenotypic rescue was unfortunately incomplete. However, based on these results and given that interferon-γ is approved for other diseases, such as chronic granulomatosis and ARO, a phase II safety clinical trial has recently been completed, unfortunately with negative results (Imel et al., 2019).

In an innovative perspective, because of its dominant negative nature, ADO2 is thought to be a target for RNA interference therapy. Our laboratory has been engaged for many years in this field and has patented a mutation-driven approach that proved effective in ADO2 mice in a variety of treatment regimens (Capulli et al., 2015; Maurizi et al., 2018). *Clcn7*^{G213R}

represents the mouse homolog of the most frequent human ADO2 mutation, and *Clcn7*^{G213R} heterozygous mice (Alam et al., 2014) have been challenged with *Clcn7*^{G213R}-specific small interfering (si) RNA proven to be effective in silencing the mutant, but not the normal, *Clcn7* mRNA (Capulli et al., 2015; Maurizi et al., 2018). The *Clcn7* gene is haplosufficient, as demonstrated by the normal phenotype of heterozygous carriers of *Clcn7* loss-of-function mutations. Therefore, we have created a condition of pseudohaplosufficiency that systemically rescued the bone phenotype upon 4 weeks of administration in young mice and 12 weeks in adult mice. Given that this siRNA complements the human *CLCN7*^{G215R} as well, and that the therapy is patented, corporate interest is expected to be in line with that for therapeutic siRNA developments in the search to cure other diseases (Chakraborty et al., 2017).

Conclusions

Over time, osteopetrosis moved from being an experiment of Nature to a family of, at least in part, treatable diseases. Instrumental to understanding the mechanisms of osteoclastogenesis and bone resorption, basic research has set the platform for genetic diagnosis and therapeutic approaches to osteopetrosis, which has given hope to patients and their families. The way to go is still demanding, but the results so far are encouraging and a tight interaction between basic and clinical scientists is anticipated to provide innovative solutions for the well-being of patients.

Acknowledgments

The original work performed by A.T. has been supported by the Telethon Grants GGP06019, GGP09018, and GGP14014, by the European Union−funded projects SYBIL−FP7-HEALTH-2013-INNOVATION−602300 and RUBICON−H2020-MSCA-RISE-2015−690850 and by the *Progetti di Rilevante Interesse Nazionale* (PRIN) grant 2015F3JHMB.

References

Aker, M., Rouvinski, A., Hashavia, S., Ta-Shma, A., Shaag, A., Zenvirt, S., Israel, S., Weintraub, M., Taraboulos, A., Bar-Shavit, Z., Elpeleg, O., 2012. An SNX10 mutation causes malignant osteopetrosis of infancy. J. Med. Genet. 49, 221−226.

Alam, I., Gray, A.K., Chu, K., Ichikawa, S., Mohammad, K.S., Capannolo, M., Capulli, M., Maurizi, A., Muraca, M., Teti, A., Econs, M.J., Del Fattore, A., 2014. Generation of the first autosomal dominant osteopetrosis type II (ADO2) disease models. Bone 59, 66−75.

Alam, I., Gray, A.K., Acton, D., Gerard-O'Riley, R.L., Reilly, A.M., Econs, M.J., 2015. Interferon gamma, but not calcitriol improves the osteopetrotic phenotypes in ADO2 mice. J. Bone Miner. Res. 30, 2005−2013.

Albers-Schönberg, H.E., 1904. Röntgenbilder einer seltenen Knock-enerkrankung. Munch Med Wochenscher 5, 365−368.

Askmyr, M., Flores, C., Fasth, A., Richter, J., 2009. Prospects for gene therapy of osteopetrosis. Curr. Gene Ther. 9, 150−159.

Asselin-Labat, M.-L., Vaillant, F., Sheridan, J.M., Pal, B., Wu, D., Simpson, E.R., Yasuda, H., Smyth, G.K., Martin, T.J., Lindeman, G.J., Visvader, J.E., 2010. Control of mammary stem cell function by steroid hormone signalling. Nature 465, 798−802.

Azam, M., Bhatti, N., 2006. Hair-on-end appearance. Arch. Dis. Child. 91, 735.

Baron, R., Neff, L., Louvard, D., Courtoy, P.J., 1985. Cell-mediated extracellular acidification and bone resorption: evidence for a low pH in resorbing lacunae and localization of a 100-kD lysosomal membrane protein at the osteoclast ruffled border. J. Cell Biol. 101, 2210−2222.

Barvencik, F., Kurth, I., Koehne, T., Stauber, T., Zustin, J., Tsiakas, K., Ludwig, C.F., Beil, F.T., Pestka, J.M., Hahn, M., Santer, R., Supanchart, C., Kornak, U., Fattore, A. Del, Jentsch, T.J., Teti, A., Schulz, A., Schinke, T., Amling, M., 2014. CLCN7 and TCIRG1 mutations differentially affect bone matrix mineralization in osteopetrotic individuals. J. Bone Miner. Res. 29, 982−991.

Bénichou, O.D., Laredo, J.D., De Vernejoul, M.C., 2000. Type II autosomal dominant osteopetrosis (Albers-Schonberg disease): clinical and radiological manifestations in 42 patients. Bone 26, 87−93.

Blair, H.C., Kahn, A.J., Crouch, E.C., Jeffrey, J.J., Teitelbaum, S.L., 1986. Isolated osteoclasts resorb the organic and inorganic components of bone. J. Cell Biol. 102, 1164−1172.

Blazar, B.R., Fallon, M.D., Teitelbaum, S.L., Ramsay, N.K., Brown, D.M., 1984. Calcitriol for congenital osteopetrosis. N. Engl. J. Med. 311 (1), 55.

Bollerslev, J., Andersen, P.E., 1988. Radiological, biochemical and hereditary evidence of two types of autosomal dominant osteopetrosis. Bone 9, 7−13.

Bollerslev, J., Henriksen, K., Nielsen, M.F., Brixen, K., Van Hul, W., 2013. Autosomal dominant osteopetrosis revisited: lessons from recent studies. Eur. J. Endocrinol. 169 (2), R39−R57.

Bolt, R.J., Wennink, J.M.B., Verbeke, J.I.M.L., Shah, G.N., Sly, W.S., Bokenkamp, A., 2005. Carbonic anhydrase type II deficiency. Am. J. Kidney Dis. 46 (A50), e71−e73.

Boyden, L.M., Mao, J., Belsky, J., Mitzner, L., Farhi, A., Mitnick, M.A., Wu, D., Insogna, K., Lifton, R.P., 2002. High bone density due to a mutation in LDL-receptor−related protein 5. N. Engl. J. Med. 346, 1513−1521.

Cappariello, A., Berardi, A.C., Peruzzi, B., Del Fattore, A., Ugazio, A., Bottazzo, G.F., Teti, A., 2010. Committed osteoclast precursors colonize the bone and improve the phenotype of a mouse model of autosomal recessive osteopetrosis. J. Bone Miner. Res. 25, 106−113.

Cappariello, A., Maurizi, A., Veeriah, V., Teti, A., 2014. The great beauty of the osteoclast. Arch. Biochem. Biophys. 561, 13−21.

Cappariello, A., Paone, R., Maurizi, A., Capulli, M., Rucci, N., Muraca, M., Teti, A., 2015. Biotechnological approach for systemic delivery of membrane Receptor Activator of NF-κB Ligand (RANKL) active domain into the circulation. Biomaterials 46, 58–69.

Capulli, M., Maurizi, A., Ventura, L., Rucci, N., Teti, A., 2015. Effective small interfering RNA therapy to treat CLCN7-dependent autosomal dominant osteopetrosis type 2. Mol. Ther. Nucleic Acids 4.

Chakraborty, C., Sharma, A.R., Sharma, G., Doss, C.G.P., Lee, S.S., 2017. Therapeutic miRNA and siRNA: moving from bench to clinic as next generation medicine. Mol. Ther. Nucleic Acids 8, 132–143.

Chalhoub, N., Benachenhou, N., Rajapurohitam, V., Pata, M., Ferron, M., Frattini, A., Villa, A., Vacher, J., 2003. Grey-lethal mutation induces severe malignant autosomal recessive osteopetrosis in mouse and human. Nat. Med. 9, 399–406.

Cleiren, E., Benichou, O., Van Hul, E., Gram, J., Bollerslev, J., Singer, F.R., Beaverson, K., Aledo, A., Whyte, M., Yoneyama, T., DeVernejoul, M., Van Hul, W., 2001. Albers-Schonberg disease (autosomal dominant osteopetrosis, type II) results from mutations in the ClCN7 chloride channel gene. Hum. Mol. Genet. 10, 2861–2867.

Coccia, P.F., Krivit, W., Cervenka, J., Clawson, C., Kersey, J.H., Kim, T.H., Nesbit, M.E., Ramsay, N.K., Warkentin, P.I., Teitelbaum, S.L., Kahn, A.J., Brown, D.M., 1980. Successful bone-marrow transplantation for infantile malignant osteopetrosis. N. Engl. J. Med. 302, 701–708.

Darwech, I., Otero, J., Alhawagri, M., Dai, S., Abu-Amer, Y., 2009. Impediment of NEMO oligomerization inhibits osteoclastogenesis and osteolysis. J. Cell. Biochem. 108, 1337–1345.

Del Fattore, A., Peruzzi, B., Rucci, N., Recchia, I., Cappariello, A., Longo, M., Fortunati, D., Ballanti, P., Iacobini, M., Luciani, M., Devito, R., Pinto, R., Caniglia, M., Lanino, E., Messina, C., Cesaro, S., Letizia, C., Bianchini, G., Fryssira, H., Grabowski, P., Shaw, N., Bishop, N., Hughes, D., Kapur, R.P., Datta, H.K., Taranta, A., Fornari, R., Migliaccio, S., Teti, A., 2006. Clinical, genetic, and cellular analysis of 49 osteopetrotic patients: implications for diagnosis and treatment. J. Med. Genet. 43, 315–325.

Del Fattore, A., Fornari, R., Van Wesenbeeck, L., De Freitas, F., Timmermans, J.P., Peruzzi, B., Cappariello, A., Rucci, N., Spera, G., Helfrich, M.H., Van Hul, W., Migliaccio, S., Teti, A., 2008. A new heterozygous mutation (R714C) of the osteopetrosis gene, Pleckstrin homolog domain containing family M (with run domain) member 1 (PLEKHM1), impairs vesicular acidification and increases TRACP secretion in osteoclasts. J. Bone Miner. Res. 23, 380–391.

Döffinger, R., Smahi, A., Bessia, C., Geissmann, F., Feinberg, J., Durandy, A., Bodemer, C., Kenwrick, S., Dupuis-Girod, S., Blanche, S., Wood, P., Rabia, S.H., Headon, D.J., Overbeek, P.A., Le Deist, F., Holland, S.M., Belani, K., Kumararatne, D.S., Fischer, A., Shapiro, R., Conley, M.E., Reimund, E., Kalhoff, H., Abinun, M., Munnich, A., Israël, A., Courtois, G., Casanova, J.L., 2001. X-linked anhidrotic ectodermal dysplasia with immunodeficiency is caused by impaired NF-κB signaling. Nat. Genet. 27, 277–285.

Dougall, W.C., Glaccum, M., Charrier, K., Rohrbach, K., Brasel, K., De Smedt, T., Daro, E., Smith, J., Tometsko, M.E., Maliszewski, C.R., Armstrong, A., Shen, V., Bain, S., Cosman, D., Anderson, D., Morrissey, P.J., Peschon, J.J., Schuh, J.A., 1999. RANK is essential for osteoclast and lymph node development. Genes Dev. 13, 2412–2424.

Driessen, G.J.A., Gerritsen, E.J.A., Fischer, A., Fasth, A., Hop, W.C.J., Veys, P., Porta, F., Cant, A., Steward, C.G., Vossen, J.M., Uckan, D., Friedrich, W., 2003. Long-term outcome of haematopoietic stem cell transplantation in autosomal recessive osteopetrosis: an EBMT report. Bone Marrow Transplant. 32, 657–663.

Fields, M., Cai, H., Gong, J., Del Priore, L., 2016. Potential of induced pluripotent stem cells (iPSCs) for treating age-related macular degeneration (AMD). Cells 5 (4).

Finbow, M.E., Harrison, M.A., 1997. The vacuolar H+-ATPase: a universal proton pump of eukaryotes. Biochem. J. 697–712.

Frattini, A., Orchard, P.J., Sobacchi, C., Giliani, S., Abinun, M., Mattsson, J.P., Keeling, D.J., Andersson, A.K., Wallbrandt, P., Zecca, L., Notarangelo, L.D., Vezzoni, P., Villa, A., 2000. Defects in TCIRG1 subunit of the vacuolar proton pump are responsible for a subset of human autosomal recessive osteopetrosis. Nat. Genet. 25, 343–346.

Gao, Y., Grassi, F., Ryan, M.R., Terauchi, M., Page, K., Yang, X., Weitzmann, M.N., Pacifici, R., 2007. IFN-gamma stimulates osteoclast formation and bone loss in vivo via antigen-driven T cell activation. J. Clin. Investig. 117, 122–132.

Glorieux, F.H., Pettifor, J.M., Marie, P.J., Delvin, E.E., Travers, R., Shepard, N., 1981. Induction of bone resorption by parathyroid hormone in congenital malignant osteopetrosis. Metab. Bone Dis. Relat. Res. 3, 143–150.

Gong, Y., Slee, R.B., Fukai, N., Rawadi, G., Roman-Roman, S., Reginato, A.M., Wang, H., Cundy, T., Glorieux, F.H., Lev, D., Zacharin, M., Oexle, K., Marcelino, J., Suwairi, W., Heeger, S., Sabatakos, G., Apte, S., Adkins, W.N., Allgrove, J., Arslan-Kirchner, M., Batch, J.A., Beighton, P., Black, G.C.M., Boles, R.G., Boon, L.M., Borrone, C., Brunner, H.G., Carle, G.F., Dallapiccola, B., De Paepe, A., Floege, B., Halfhide, M.L., Hall, B., Hennekam, R.C., Hirose, T., Jans, A., Jüppner, H., Kim, C.A., Keppler-Noreuil, K., Kohlschuetter, A., LaCombe, D., Lambert, M., Lemyre, E., Letteboer, T., Peltonen, L., Ramesar, R.S., Romanengo, M., Somer, H., Steichen-Gersdorf, E., Steinmann, B., Sullivan, B., Superti-Furga, A., Swoboda, W., Van den Boogaard, M.J., Van Hul, W., Vikkula, M., Votruba, M., Zabel, B., Garcia, T., Baron, R., Olsen, B.R., Warman, M.L., 2001. LDL receptor-related protein 5 (LRP5) affects bone accrual and eye development. Cell 107, 513–523.

Guerrini, M.M., Sobacchi, C., Cassani, B., Abinun, M., Kilic, S.S., Pangrazio, A., Moratto, D., Mazzolari, E., Clayton-Smith, J., Orchard, P., Coxon, F.P., Helfrich, M.H., Crockett, J.C., Mellis, D., Vellodi, A., Tezcan, I., Notarangelo, L.D., Rogers, M.J., Vezzoni, P., Villa, A., Frattini, A., 2008. Human osteoclast-poor osteopetrosis with hypogammaglobulinemia due to TNFRSF11A (RANK) mutations. Am. J. Hum. Genet. 83, 64–76.

Gundle, R., Joyner, C.J., Triffitt, J.T., 1995. Human bone tissue formation in-diffusion chamber culture in-vivo by bone-derived cells and marrow stromal fibroblastic cells. Bone 16, 597–601.

Hendy, G.N., Canaff, L., 2016. Calcium-sensing receptor, proinflammatory cytokines and calcium homeostasis. Semin. Cell Dev. Biol. 49, 37–43.

Hill, B.G., Charlton, W.S., 1965. Albers-Schonberg disease. Med. J. Aust. 2, 365–367.

Hwang, J.M., Kim, I.O., Wang, K.C., 2000. Complete visual recovery in osteopetrosis by early optic nerve decompression. Pediatr. Neurosurg. 33, 328–332.

Imel, E.A., Liu, Z., Acton, D., Coffman, M., Gebregziabher, N., Tong, Y., Econs, M.J., March 19, 2019. Interferon Gamma-1b Does Not Increase Markers of Bone Resorption in Autosomal Dominant Osteopetrosis. J. Bone Miner. Res. https://doi.org/10.1002/jbmr.3715 [Epub ahead of print].

Jacome-Galarza, C.E., Lee, S.K., Lorenzo, J.A., Aguila, H.L., 2011. Parathyroid hormone regulates the distribution and osteoclastogenic potential of hematopoietic progenitors in the bone marrow. J. Bone Miner. Res. 26, 1207–1216.

Johnson, M.L., 2012. LRP5 and bone mass regulation: where are we now? Bone Rep. 1.

Karet, F.E., Finberg, K.E., Nelson, R.D., Nayir, A., Mocan, H., Sanjad, S.A., Rodriguez-Soriano, J., Santos, F., Cremers, C.W.R.J., Di Pietro, A., Hoffbrand, B.I., Winiarski, J., Bakkaloglu, A., Ozen, S., Dusunsel, R., Goodyer, P., Hulton, S.A., Wu, D.K., Skvorak, A.B., Morton, C.C., Cunningham, M.J., Jha, V., Lifton, R.P., 1999. Mutations in the gene encoding B1 subunit of H+-ATPase cause renal tubular acidosis with sensorineural deafness. Nat. Genet. 21, 84–90.

Kasper, D., Planells-Cases, R., Fuhrmann, J.C., Scheel, O., Zeitz, O., Ruether, K., Schmitt, A., Poët, M., Steinfeld, R., Schweizer, M., Kornak, U., Jentsch, T.J., 2005. Loss of the chloride channel ClC-7 leads to lysosomal storage disease and neurodegeneration. EMBO J. 24, 1079–1091.

Key, L.L.,J., Ries, W.L., 1993. Osteopetrosis. The pharmaco-physiologic basis of therapy. Clin. Orthop. Relat. Res. 85–89.

Key, L.L.J., Ries, W.L., Rodriguiz, R.M., Hatcher, H.C., 1992. Recombinant human interferon gamma therapy for osteopetrosis. J. Pediatr. 121, 119–124.

Key Jr., L.L., Rodriguiz, R.M., Willi, S.M., Wright, N.M., Hatcher, H.C., Eyre, D.R., Cure, J.K., Griffin, P.P., Ries, W.L., 1995. Long-term treatment of osteopetrosis with recombinant human interferon gamma. N. Engl. J. Med. 332, 1594–1599.

Komiya, Y., Habas, R., 2008. Wnt signal transduction pathways. Organogenesis 4 (2), 68–75.

Kornak, U., Kasper, D., Bösl, M.R., Kaiser, E., Schweizer, M., Schulz, A., Friedrich, W., Delling, G., Jentsch, T.J., 2001. Loss of the CIC-7 chloride channel leads to osteopetrosis in mice and man. Cell 104, 205–215.

Landa, J., Margolis, N., Cesare, P. Di, 2007. Orthopaedic management of the patient with osteopetrosis. J. Am. Acad. Orthop. Surg. 15 (11), 654–662.

Li, X., Zhang, Y., Kang, H., Liu, W., Liu, P., Zhang, J., Harris, S.E., Wu, D., 2005. Sclerostin binds to LRP5/6 and antagonizes canonical Wnt signaling. J. Biol. Chem. 280, 19883–19887.

Lo Iacono, N., Blair, H.C., Poliani, P.L., Marrella, V., Ficara, F., Cassani, B., Facchetti, F., Fontana, E., Guerrini, M.M., Traggiai, E., Schena, F., Paulis, M., Mantero, S., Inforzato, A., Valaperta, S., Pangrazio, A., Crisafulli, L., Maina, V., Kostenuik, P., Vezzoni, P., Villa, A., Sobacchi, C., 2012. Osteopetrosis rescue upon RANKL administration to Rankl-/- mice: a new therapy for human RANKL-dependent ARO. J. Bone Miner. Res. 27, 2501–2510.

Marks, S.C., Walker, D.G., 1981. The hematogenous origin of osteoclasts: experimental evidence from osteopetrotic (microphthalmic) mice treated with spleen cells from beige mouse donors. Am. J. Anat. 161, 1–10.

Maurizi, A., Capulli, M., Patel, R., Curle, A., Rucci, N., Teti, A., 2018. RNA interference therapy for autosomal dominant osteopetrosis type 2. Towards the preclinical development. Bone 110, 343–354.

McEwan, D.G., Dikic, I., 2015. PLEKHM1: adapting to life at the lysosome. Autophagy 11 (4), 720–722.

Meletis, J., Samarkos, M., Michali, E., Vavourakis, S., Meletis, C., Poziopoulos, C., Stavrogianni, N., Konstantopoulos, K., Vaiopoulos, G., Yataganas, X., 1995. Correction of anaemia and thrombocytopenia in a case of adult type I osteopetrosis with recombinant human erythropoietin (rHuEPO). Br. J. Haematol. 89, 911–913.

Motyckova, G., Fisher, D.E., 2002. Pycnodysostosis: role and regulation of cathepsin K in osteoclast function and human disease. Curr. Mol. Med. 2, 407–421.

Nakashima, T., Takayanagi, H., 2011. New regulation mechanisms of osteoclast differentiation. Ann. N. Y. Acad. Sci. 1240.

Neri, T., Muggeo, S., Paulis, M., Caldana, M.E., Crisafulli, L., Strina, D., Focarelli, M.L., Faggioli, F., Recordati, C., Scaramuzza, S., Scanziani, E., Mantero, S., Buracchi, C., Sobacchi, C., Lombardo, A., Naldini, L., Vezzoni, P., Villa, A., Ficara, F., 2015. Targeted gene correction in osteopetrotic-induced pluripotent stem cells for the generation of functional osteoclasts. Stem Cell Reports 5, 558–568.

Niehrs, C., 2006. Function and biological roles of the Dickkopf family of Wnt modulators. Oncogene 25, 7469–7481.

Niu, X., He, W., Song, B., Ou, Z., Fan, D., Chen, Y., Fan, Y., Sun, X., 2016. Combining single strand oligodeoxynucleotides and CRISPR/Cas9 to correct gene mutations in beta-thalassemia-induced pluripotent stem Cells. J. Biol. Chem. 291, 16576–16585.

Norkin, M., Wingard, J.R., 2017. Recent advances in hematopoietic stem cell transplantation. F1000Research 6, 870.

Ohlsson, A., Cumming, W.A., Paul, A., Sly, W.S., 1986. Carbonic anhydrase II deficiency syndrome: recessive osteopetrosis with renal tubular acidosis and cerebral calcification. Pediatrics 77, 371–381.

Pangrazio, A., Poliani, P.L., Megarbane, A., Lefranc, G., Lanino, E., Di Rocco, M., Rucci, F., Lucchini, F., Ravanini, M., Facchetti, F., Abinun, M., Vezzoni, P., Villa, A., Frattini, A., 2006. Mutations in OSTM1 (grey lethal) define a particularly severe form of autosomal recessive osteopetrosis with neural involvement. J. Bone Miner. Res. 21, 1098–1105.

Pangrazio, A., Boudin, E., Piters, E., Damante, G., Iacono, N.L., D'Elia, A.V., Vezzoni, P., Van Hul, W., Villa, A., Sobacchi, C., 2011. Identification of the first deletion in the LRP5 gene in a patient with Autosomal Dominant Osteopetrosis type I. Bone 49, 568–571.

Pangrazio, A., Cassani, B., Guerrini, M.M., Crockett, J.C., Marrella, V., Zammataro, L., Strina, D., Schulz, A., Schlack, C., Kornak, U., Mellis, D.J., Duthie, A., Helfrich, M.H., Durandy, A., Moshous, D., Vellodi, A., Chiesa, R., Veys, P., Lo Iacono, N., Vezzoni, P., Fischer, A., Villa, A., Sobacchi, C., 2012. RANK-dependent autosomal recessive osteopetrosis: characterization of five new cases with novel mutations. J. Bone Miner. Res. 27, 342–351.

Pangrazio, A., Fasth, A., Sbardellati, A., Orchard, P.J., Kasow, K.A., Raza, J., Albayrak, C., Albayrak, D., Vanakker, O.M., De Moerloose, B., Vellodi, A., Notarangelo, L.D., Schlack, C., Strauss, G., Kuhl, J.-S., Caldana, E., Lo Iacono, N., Susani, L., Kornak, U., Schulz, A., Vezzoni, P., Villa, A., Sobacchi, C., 2013. SNX10 mutations define a subgroup of human autosomal recessive osteopetrosis with variable clinical severity. J. Bone Miner. Res. 28, 1041−1049.

Perdu, B., Mortier, G., Vanhoenacker, F., Van Hul, W., 2012. Sclerosing bone dysplasias. In: Pediatric Bone, pp. 541−556.

Pierroz, D.D., Rufo, A., Bianchi, E.N., Glatt, V., Capulli, M., Rucci, N., Cavat, F., Rizzoli, R., Teti, A., Bouxsein, M.L., Ferrari, S.L., 2009 May. Beta-Arrestin2 regulates RANKL and ephrins gene expression in response to bone remodeling in mice. J. Bone Miner. Res. 24 (5), 775−784. https://doi.org/10.1359/jbmr.081237.

Rucci, N., Teti, A., 2016. The "love−hate" relationship between osteoclasts and bone matrix. Matrix Biol. 52 (54), 176−190.

Saigal, A., Gopal, M., Mohanty, N., Misra, S.R., 2015. Recurrent osteomyelitis of the mandible in osteopetrosis: a common complication of an uncommon disease. BMJ Case Rep. 8.

Schinke, T., Schilling, A.F., Baranowsky, A., Seitz, S., Marshall, R.P., Linn, T., Blaeker, M., Huebner, A.K., Schulz, A., Simon, R., Gebauer, M., Priemel, M., Kornak, U., Perkovic, S., Barvencik, F., Beil, F.T., Del Fattore, A., Frattini, A., Streichert, T., Pueschel, K., Villa, A., Debatin, K.M., Rueger, J.M., Teti, A., Zustin, J., Sauter, G., Amling, M., 2009. Impaired gastric acidification negatively affects calcium homeostasis and bone mass. Nat. Med. 15, 674−681.

Schulz, A, Moshous D., Steward, C.G., Villa, A., Sobacchi, C., Osteopetrosis. Consensus Guidelines for Diagnosis, Therapy and Follow-Up. Version 3.

Sessa, M., Lorioli, L., Fumagalli, F., Acquati, S., Redaelli, D., Baldoli, C., Canale, S., Lopez, I.D., Morena, F., Calabria, A., Fiori, R., Silvani, P., Rancoita, P.M.V., Gabaldo, M., Benedicenti, F., Antonioli, G., Assanelli, A., Cicalese, M.P., del Carro, U., Sora, M.G.N., Martino, S., Quattrini, A., Montini, E., Di Serio, C., Ciceri, F., Roncarolo, M.G., Aiuti, A., Naldini, L., Biffi, A., 2016. Lentiviral haemopoietic stem-cell gene therapy in early-onset metachromatic leukodystrophy: an ad-hoc analysis of a non-randomised, open-label, phase 1/2 trial. Lancet 388, 476−487.

Sly, W.S., Hewett-Emmett, D., Whyte, M.P., Yu, Y.S., Tashian, R.E., 1983. Carbonic anhydrase II deficiency identified as the primary defect in the autosomal recessive syndrome of osteopetrosis with renal tubular acidosis and cerebral calcification. Proc. Natl. Acad. Sci. U. S. A 80, 2752−2756.

Sly, W.S., Whyte, M.P., Sundaram, V., Tashian, R.E., Hewett-Emmett, D., Guibaud, P., Vainsel, M., Baluarte, H.J., Gruskin, A., Al-Mosawi, M., Sakati, N., Ohlsson, A., 1985. Carbonic anhydrase II deficiency in 12 families with the autosomal recessive syndrome of osteopetrosis with renal tubular acidosis and cerebral calcification. N. Engl. J. Med. 313, 139−145.

Sobacchi, C., Frattini, A., Guerrini, M.M., Abinun, M., Pangrazio, A., Susani, L., Bredius, R., Mancini, G., Cant, A., Bishop, N., Grabowski, P., Del Fattore, A., Messina, C., Errigo, G., Coxon, F.P., Scott, D.I., Teti, A., Rogers, M.J., Vezzoni, P., Villa, A., Helfrich, M.H., 2007. Osteoclast-poor human osteopetrosis due to mutations in the gene encoding RANKL. Nat. Genet. 39, 960−962.

Sobacchi, C., Schulz, A., Coxon, F.P., Villa, A., Helfrich, M.H., 2013. Osteopetrosis: genetics, treatment and new insights into osteoclast function. Nat. Rev. Endocrinol. 9 (9), 522−536.

Stenbeck, G., 2002. Formation and function of the ruffled border in osteoclasts. Semin. Cell Dev. Biol. 13, 285−292.

Steward, C.G., 2003. Neurological aspects of osteopetrosis. Neuropathol. Appl. Neurobiol. 29 (2), 87−97.

Takahashi, N., Udagawa, N., Suda, T., 1999. A new member of tumor necrosis factor ligand family, ODF/OPGL/TRANCE/RANKL, regulates osteoclast differentiation and function. Biochem. Biophys. Res. Commun. 256, 449−455.

Takayanagi, H., Ogasawara, K., Hida, S., Chiba, T., Murata, S., Sato, K., Takaoka, A., Yokochi, T., Oda, H., Tanaka, K., Nakamura, K., Taniguchi, T., 2000. T-cell-mediated regulation of osteoclastogenesis by signalling cross-talk between RANKL and IFN-γ. Nature 408, 600−605.

Teti, A., 2011. Bone development: overview of bone cells and signaling. Curr. Osteoporos. Rep. 9 (4), 264−273.

Teti, A., 2012. Osteoclasts and hematopoiesis. BoneKEy Rep. 1 (3).

Teti, A., Econs, M.J., 2017. Osteopetroses, emphasizing potential approaches to treatment. Bone 102, 50−59.

Teti, A., Schulz, A., 2013. Haematopoietic Stem Cell Transplantation in Autosomal Recessive Osteopetrosis. Stem Cells and Bone Diseases (Chapter 15), pp. 267−288.

Van Wesenbeeck, L., Cleiren, E., Gram, J., Beals, R.K., Bénichou, O., Scopelliti, D., Key, L., Renton, T., Bartels, C., Gong, Y., Warman, M.L., De Vernejoul, M.-C., Bollerslev, J., Van Hul, W., 2003. Six novel missense mutations in the LDL receptor-related protein 5 (LRP5) gene in different conditions with an increased bone density. Am. J. Hum. Genet. 72, 763−771.

Van Wesenbeeck, L., Odgren, P.R., Coxon, F.P., Frattini, A., Moens, P., Perdu, B., MacKay, C.A., Van Hul, E., Timmermans, J.P., Vanhoenacker, F., Jacobs, R., Peruzzi, B., Teti, A., Helfrich, M.H., Rogers, M.J., Villa, A., Van Hul, W., 2007. Involvement of PLEKHM1 in osteoclastic vesicular transport and osteopetrosis in incisors absent rats and humans. J. Clin. Investig. 117, 919−930.

Villa, A., Guerrini, M.M., Cassani, B., Pangrazio, A., Sobacchi, C., 2009. Infantile malignant, autosomal recessive osteopetrosis: the rich and the poor. Calcif. Tissue Int. 84 (1), 1−12.

Waguespack, S.G., Hui, S.L., DiMeglio, L.A., Econs, M.J., 2007. Autosomal dominant osteopetrosis: clinical severity and natural history of 94 subjects with a chloride channel 7 gene mutation. J. Clin. Endocrinol. Metab. 92, 771−778.

Wakkach, A., Mansour, A., Dacquin, R., Coste, E., Jurdic, P., Carle, G.F., Blin-Wakkach, C., 2008. Bone marrow microenvironment controls the in vivo differentiation of murine dendritic cells into osteoclasts. Blood 112, 5074−5083.

Walker, D.G., 1973. Osteopetrosis cured by temporary parabiosis. Science 180, 875, 875.

Walker, D.G., 1975. Bone resorption restored in osteopetrotic mice by transplants of normal bone marrow and spleen cells. Science 190, 784−785.

Whyte, M.P., 2013. Sclerosing bone disorders. In: Clifford, J.,R., Keen, R.W. (Eds.), Primer on the Metabolic Bone Diseases and Disorders of Mineral Metabolism. John Wiley & Sons, pp. 769−785.

Williams, H.J., Davies, A.M., Chapman, S., 2004. Bone within a bone. Clin. Radiol. 59 (2), 132−144.

Wodarz, A., Nusse, R., 1998. Mechanisms of Wnt signaling in development. Annu. Rev. Cell Dev. Biol. 14, 59–88.

Yao, L., Seeger, L.L., 1997. Epiphyseal growth arrest lines MR findings. Clin. Imaging 21, 237–240.

Ye, L., Morse, L.R., Zhang, L., Sasaki, H., Mills, J.C., Odgren, P.R., Sibbel, G., Stanley, J.R.L., Wong, G., Zamarioli, A., Battaglino, R.A., 2015. Osteopetrorickets due to Snx10 deficiency in mice results from both failed osteoclast activity and loss of gastric acid-dependent calcium absorption. PLoS Genet. 11.

Zaidi, M., Troen, B., Moonga, B.S., Abe, E., 2001. Cathepsin K, osteoclastic resorption, and osteoporosis therapy. J. Bone Miner. Res. 16, 1747–1749.

Zhao, K., Liu, Q., 2016. The clinical application of mesenchymal stromal cells in hematopoietic stem cell transplantation. J. Hematol. Oncol. 9, 46.

Chapter 66

Hypophosphatasia: nature's window on alkaline phosphatase function in humans

Michael P. Whyte[1,2]

[1]*Center for Metabolic Bone Disease and Molecular Research, Shriners Hospitals for Children - St. Louis, St. Louis, MO, United States;* [2]*Division of Bone and Mineral Diseases, Department of Internal Medicine, Washington University School of Medicine at Barnes-Jewish Hospital, St. Louis, MO, United States*

Chapter outline

Introduction

Alkaline phosphatase (ALP) was discovered by Robert Robison, PhD, in 1923 (Robison, 1923). During the next decade, he and his coworkers would advance his hypothesis that this phosphomonoester phosphohydrolase functioned importantly in skeletal calcification, emphasizing the liberation of inorganic phosphate (Pi), perhaps from hexosephosphoric ester substrate. Liberation of Pi to bind with calcium (Ca^{++}) would allow for hydroxyapatite (HA) crystal formation and growth. However, by 1932 Robison had concluded that some additional unknown factor conditioned this process (Robison, 1932). As I will review, this proved to be the ALP natural substrate and inhibitor of biomineralization, inorganic pyrophosphate (PPi).

Principles of Bone Biology. https://doi.org/10.1016/B978-0-12-814841-9.00066-X

In the 1930s, physicians began to appreciate the important clinical insight that derives from quantitation of ALP activity in serum. Elevated levels (*hyper*phosphatasemia) usually denoted skeletal or hepatobiliary disease. In contrast, *hypo*-phosphatasemia usually went ignored (Wolf, 1978). Quantitation of serum ALP activity soon became the most frequently performed enzyme assay (McComb et al., 1979; Siller and Whyte, 2018).

In 1948, implication of the ubiquitously expressed "tissue nonspecific" (bone/liver/kidney) isoenzyme of ALP (TNSALP) as essential for skeletal mineralization began with the discovery by John C. Rathbun, MD, of hypophosphatasia (HPP) (Rathbun, 1948). In 1988, HPP was confirmed to be an inborn error of metabolism, as it was caused by loss-of-function mutation of the *ALPL* gene that encodes TNSALP (OMIM, 171760). The defective skeletal mineralization of HPP had been shown in the 1960s to involve deficient hydrolysis of PPi by TNSALP (Weiss et al., 1988a; Whyte, 1994). We now understand that ALPs are ubiquitous in nature (McComb et al., 1979; Harris, 1990; Moss, 1992; Whyte, 1994), yet there is uncertainty about the purpose of the three additional ALP isoenzymes in humans (Millán, 2006; Millán and Whyte, 2016).

In this chapter, I provide a brief history of the discovery of ALP, discuss the proposed function(s) of ALP in humans, and review the molecular and biological chemistry of the ALPs. Subsequently, HPP is described in some detail, and I summarize the most significant revelations about ALP from this "experiment-of-nature." Advances and refinements concerning the role of TNSALP revealed by mouse models of HPP are discussed (Millán, 2006; Millán and Whyte, 2016). Finally, the multinational approval in 2015 of asfotase alfa, a TNSALP-replacement therapy that restores "hard tissue" mineralization in HPP, returns us "full circle" concerning ALP.

History and proposed physiological roles of alkaline phosphatase

A 1923 publication by Robert Robison, PhD (Fig. 66.1**),** reported abundant phosphatase activity in bone and cartilage extracts from rats and rabbits, especially those with rickets. Thus, he hypothesized that the new enzyme acted in skeletal mineralization, perhaps by hydrolyzing a hexosephosphoric ester to increase the concentration of Pi available locally to bind with calcium (Ca^{++}) for HA crystal formation and growth (Robison, 1923). In 1924, he and Katherine Soames, PhD, reported that this phosphatase precipitated mineral into rachitic rat bone when monophosphate esters were the only source of Pi. In their laboratory, the enzyme became detectable using a distinctly alkaline pH optimum (Robison and Soames, 1924). However, Robison knew this pH was not physiological and called the enzyme "bone phosphatase" (Robison, 1932). The term "alkaline phosphatase" was introduced in the 1930s by others to distinguish it from a recently identified "acid phosphatase" that was becoming implicated in certain metastatic bone diseases (Siller and Whyte, 2018). However, concerns were emerging that challenged Robison's hypothesis (McComb et al., 1979). ALP activity was abundant not only in the skeleton but also in tissues that normally did not calcify (e.g., liver, intestine, and placenta). Furthermore, Robison had not identified its physiological substrate(s) (Neuman and Neuman, 1957).

FIGURE 66.1 Robert Robison, PhD, DSc, FRS (1883−1941), the discoverer of alkaline phosphatase in 1923. *Reproduced with permission from the Godfrey Argent Studio, as published in Obituary Notices of Fellows of The Royal Society, Vol. 3, 1941, p. 929.*

Then in the 1960s, electron microscopy rejuvenated Robison's hypothesis when the earliest site of HA crystal deposition in the skeleton was discovered by H. Clark Anderson, MD, to be within unique extracellular structures called "matrix vesicles" (MVs) (Anderson, 1969). MVs seem to be buds of the plasma membrane of chondrocytes and osteoblasts. They contain many enzymes including pyrophosphatase (PPi-ase) and ATPase (Anderson, 1992) and are especially rich in ALP (Ali, 1986). During the initial ("primary") phase of skeletal mineralization, HA crystals appear and then grow within MVs. When they rupture the MV, "secondary" mineralization features HA crystal growth for their deposition into the organic matrix of the skeleton (Ornoy et al., 1985). In 1975, nucleoside phosphate released from dying cells was proposed as the ALP substrate for Pi necessary to fulfill Robison's hypothesis (Majeska and Wuthier, 1975).

Further evidence that ALP functions in skeletal mineralization came from reports that used stereospecific inhibitors of ALP activity, such as L-tetramisole, which blocked calcification in vitro (Fallon et al., 1980). However, it was later shown that stereoisomers that did not block ALP activity would also impair mineralization (Whyte, 1994). In the clinic, it had been known for decades that circulating ALP activity correlated with the severity of disorders that involve accelerated bone formation (McComb et al., 1979), such as Paget bone disease (Kanis, 2002).

By the 1990s, many biological roles had been proposed for ALP (McComb et al., 1979; Harris, 1990; Moss, 1992; Whyte, 1989, 1994) and included provision of the nonphosphate moiety, transferase action in the synthesis of phosphate esters, regulation of Pi metabolism, maintenance of phosphoryl metabolite levels, and action as a phosphoprotein phosphatase (McComb et al., 1979; Alpers et al., 1990; Harris, 1990; Muller et al., 1991; Simko, 1991; Moss, 1992; Whyte, 1994; Millán and Whyte, 2016). Cell membrane ALP was hypothesized to condition not only the active transport of Pi but also Ca^{++}, fat, protein, carbohydrate, and Na^{+}/K^{+} (Muller et al., 1991; Simko, 1991). As the four isoenzymes of ALP in humans became recognized (see later), sequence analyses suggested they coupled to other proteins including collagen (Wu et al., 1992). In the placenta, ALP bound the Fc receptor of IgG and perhaps transcytosed this immunoglobulin (Makiya et al., 1992). During embryogenesis, ALP seemed to act intracellularly (Narisawa et al., 1992), although we now know that ALP functions importantly when bound to cell surfaces (see later).

Additional proposals also emerged for TNSALP action specifically in skeletal mineralization (Table 66.1) (Whyte, 1989, 1994). Perhaps TNSALP was a plasma membrane transporter for Pi (Wuthier and Register, 1985), an extracellular Ca^{++}-binding protein that stimulates Ca^{++}-Pi precipitation and orients mineral deposition into osteoid (DeBarnard et al., 1986), a Ca^{++}/Mg^{++}-ATPase (Birge and Gilbert, 1974), or a phosphoprotein phosphatase that conditions skeletal matrix for ossification (Lau et al., 1985; Tsonis et al., 1988). Certain structural domains of ALP suggested it could bind to types I, II, and X collagen in cartilage and bone (Tsonis et al., 1988; Wu et al., 1992). Nevertheless, a theory that captured Robison's missing "factor" (Robison, 1932) emerged and gained preeminence in the 1960s; i.e., TNSALP hydrolyzes an inhibitor of calcification (Neuman and Neuman, 1957; Caswell et al., 1991; Moss, 1992; Whyte, 1994; Heinonen, 2001; Millán, 2006; Millán and Whyte, 2016), with the principal candidate being PPi. High concentrations of extracellular PPi bind to HA and thereby impair HA crystal growth. TNSALP was shown to hydrolyze PPi (Moss et al., 1967). In fact (see later), plasma and urine levels of PPi became recognized as increased in HPP (Russell, 1965; Russell et al., 1971) consistent with PPi being a natural substrate of TNSALP.

Ironically, however, approaching a century after its discovery, methods for assaying ALP activity still do not deal with Robison's quandary of the alkaline pH optimum (McComb et al., 1979; Harris, 1990; Moss, 1992; Whyte, 1994; Coburn et al., 1998). In both clinical and research laboratories, ALP continues to be measured using nonphysiological alkalinity (e.g., pH 9.2 to 10.5). Furthermore, the assays involve high concentrations (millimolar) of artificial substrates whose

TABLE 66.1 Suggested roles for alkaline phosphatase in skeletal mineralization.

Locally increase Pi levels
Destruction of inhibitors of HA crystal growth
Transport of Pi
Ca^{++}-binding protein (Ca^{++} uptake by cells)
Ca^{++}/Mg^{++}-ATPase
Tyrosine-specific phosphoprotein phosphatase

Reproduced with permission from Whyte, M.P., 1989. Alkaline phosphatase: physiologic role explored in hypophosphatasemia. In: Peck, W.A. (Ed.), Bone and Mineral Research. Elsevier Science Publishers BV (Biomedical Division), Amsterdam.

hydrolysis products can be followed colorimetrically (e.g., p-nitrophenylphosphate) (McComb et al., 1979). Also, biological specimens for ALP assay are diluted into buffers without Pi, although Pi competitively inhibits TNSALP (Coburn et al., 1998). Such assays were devised especially for their clinical utility (Wolf, 1978), yet it had been known for decades that the pH optimum for ALP is considerably less alkaline for lower concentrations of physiological substrates, although hydrolytic rates are reduced (McComb et al., 1979; Moss, 1992). Until the discovery of the natural substrates for TNSALP in studies of HPP, the significance of this was unknown (McComb et al., 1979; Harris, 1990; Moss, 1992; Whyte, 1994).

To understand what HPP teaches us about ALP, it is helpful to review the genomic structure, protein chemistry, and enzymology of ALP.

Genomic structure, protein chemistry, and enzymology of alkaline phosphatase

ALP (orthophosphoric-monoester phosphohydrolase, alkaline optimum, EC 3.1.3.1) is found throughout nature in plants and animals (McComb et al., 1979). In humans, four ALP isoenzymes are encoded by four separate genes (Millán, 1988, 2006; Harris, 1990; Moss, 1992). Three of the isoenzymes have essentially tissue-specific expression and are designated intestinal, placental, and germ-cell (placental-like) ALP. The fourth ALP isoenzyme is expressed ubiquitously and therefore is designated TNSALP (Stigbrand and Fishman, 1984; Harris, 1990; Moss, 1992). Skeletal, hepatic, and renal tissue are especially rich in TNSALP. The distinctive physicochemical properties (heat stability, electrophoretic mobility, etc.) among ALPs purified from human bone, liver, and kidney are lost upon exposure to glycosidases (Moss and Whitaker, 1985), and TNSALP is therefore a family of "secondary" isoenzymes (I will call them "isoforms"). They are encoded by the same gene, have the identical polypeptide sequence, and differ only by posttranslational modifications involving carbohydrates (Harris, 1980).

The gene mapping symbol for TNSALP is *ALPL* ("ALP-liver"), although the function of the liver isoform of TNSALP is not known (see later). *ALPL* is located near the tip of the short arm of chromosome 1 (1p36.1−p34), whereas the genes for the intestinal, placental, and germ-cell ALPs are at the tip of the long arm of chromosome 2 (2q34−q37) (Harris, 1990; Millán, 2006). *ALPL* seems to represent the ancestral gene, whereas the tissue-specific ALPs were likely formed by gene duplication (Harris, 1990). *ALPL* is somewhat larger than 50 kb and contains 12 exons, 11 of which are translated to form the mature enzyme consisting of 507 amino acid residues (Weiss et al., 1988b). TATA and Sp1 sequences may be regulatory elements, but basal expression seems to reflect "housekeeping" promoter effects, whereas differential expression in various tissues may be mediated by a posttranscriptional mechanism (Kiledjian and Kadesch, 1990). *ALPL* has two promoters and two corresponding 5′-noncoding exons, 1a and 1b. Their expression results in two different mRNAs with differing 5′-untranslated regions (Nosjean et al., 1997). Transcription occurs preferentially from the upstream promoter (1a) in osteoblasts and from the downstream promoter (1b) in the liver and kidney (Millán, 2006).

The tissue-specific ALP genes are smaller than *ALPL*, primarily owing to shorter introns. Amino acid sequences deduced from their cDNAs suggest 87% positional identity between placental and intestinal ALP but only 50%−60% identity between the tissue-specific ALPs and TNSALP (Harris, 1990).

The amino acid residue sequence of TNSALP indicates five potential N-linked glycosylation sites (Weiss et al., 1988). N-glycosylation is necessary for catalytic activity. O-glycosylation characterizes the bone, but not the liver, isoform (Nosjean et al., 1997).

In 2000, the crystal structure for human placental ALP was delineated at 1.8-Å resolution (Le Due et al., 2000). The active site of TNSALP would derive from a nucleotide sequence conserved in ALPs throughout nature (Henthorn and Whyte, 1992), reflect six exons, and comprise 15 amino acid residues (Zurutuza et al., 1999).

ALPs are Zn^{++}-metalloenzymes (McComb et al., 1979). Catalytic activity requires a multimeric configuration of identical subunits with each monomer having one active site and two Zn^{++} atoms that stabilize the tertiary structure (Kim and Wycoff, 1991).

ALPs are generally considered homodimeric in the circulation (McComb et al., 1979). TNSALP, in its symmetrical dimeric form, has αβ topology for each subunit including a ten-stranded β-sheet at its center (Hoylaerts and Millán, 1991). However, in tissues, ALPs are tethered (see later) to cell surfaces, perhaps as homotetramers (Fedde et al., 1988).

In vitro, ALPs have broad substrate specificities and pH optima that depend on the type and concentration of phosphocompound undergoing catalysis (McComb et al., 1979). Catalytic activity requires Mg^{++} as a cofactor (McComb et al., 1979). PPi as well as phosphoesters can be hydrolyzed (Xu et al., 1991). The reaction involves phosphorylation−dephosphorylation of a serine residue. Dissociation of the covalently linked Pi seems to be the rate-limiting step. In fact, Pi is a potent competitive inhibitor of ALP (McComb et al., 1979; Kim and Wyckoff, 1991; Coburn et al., 1998). However, it may also be that Pi stabilizes the enzyme (Farley, 1991).

Uncertainties persist about the biosynthesis of ALP in higher organisms. The gene sequences of the human ALP isoenzymes indicate that the nascent polypeptides have a short signal sequence of 17−21 amino acid residues (Harris, 1990) and a hydrophobic domain at their carboxyl terminus (Weiss et al., 1988b). Intracellular degradation of ALPs can involve proteasomes (Cai et al., 1998). Nevertheless, these ALPs link to the external surface of plasma membranes tethered to the polar head group of a phosphatidylinositol−glycan moiety (Whyte et al., 1988; Whyte, 1994) and can be released by phosphatidylinositol-specific phospholipase (Fedde et al., 1988). However, their precise interaction with phosphatidylinositol may differ among ALP isoenzymes (Seetharam et al., 1987).

Lipid-free ALP is the moiety normally found in the circulation. Yet, the mechanisms for ALP release from cell surfaces are not known. The process could involve a phosphatidase of the C or D type, detergent action, proteolysis, membrane fractionation, or lipolysis (Alpers et al., 1990).

In healthy men and women, nearly all ALP activity in serum or plasma derives from approximately equal amounts of the bone and liver isoforms of TNSALP (Millán et al., 1980). Infants and children, particularly newborns and adolescents, have higher bloodstream levels of the bone isoform (McComb et al., 1979). Some individuals with B and O blood types who are "secretors" increase the small amount of intestinal ALP in their circulation after ingesting a fatty meal (Langman et al., 1966; McComb et al., 1979). Typically, however, intestinal ALP contributes just a few percent to serum total ALP activity (maximum 20%) (McComb et al., 1979; Mulivor et al., 1985). Placental ALP is usually expressed and circulates only during the last trimester of pregnancy (Birkett et al., 1966). Various cancers, however, release placental or germ-cell ("placental-like") ALP (Millán, 1988) into the bloodstream. Clearance of circulating ALP, as for many other glycoproteins, probably involves uptake and degradation by the liver (Young et al., 1984).

Hypophosphatasia

Subnormal extracellular levels of Ca^{++} and Pi, or Pi alone, cause nearly all types of rickets and osteomalacia (Whyte, 2002; Drezner and Whyte, 2018). In fact, some believe that hypophosphatemia is common to all such patients (Tiosano and Hochberg, 2009). HPP is, however, a distinctive and remarkably instructive exception. This heritable form of rickets and osteomalacia has hypophosphatasemia as its biochemical hallmark. In HPP, circulating levels of Ca^{++} and Pi are typically normal but often elevated, and the skeleton does not mineralize properly (Whyte, 1994, 2001). Thus, HPP has been "nature's window" for understanding the important physiological role of TNSALP in humans. With the discovery beginning in 1988 (Weiss et al., 1988a) of loss-of-function mutations in TNSALP in HPP, Robison's hypothesis that ALP acts in biomineralization became confirmed. TNSALP was necessary not only for skeletal mineralization but also for mineralization of the teeth (Whyte, 1994). However, undisturbed function of other organs/tissues in HPP, notably the liver and kidney, questioned the biological significance for TNSALP elsewhere (Whyte, 1994, 2001).

History

John C. Rathbun, MD (Fig. 66.2), a Canadian pediatrician, coined the term "hypophosphatasia" in 1948 when he reported an infant boy who died of seemingly acquired rickets and epilepsy whose ALP activity in serum, bone, and other tissues

FIGURE 66.2 John C. Rathbun, MD (1915−1972), who identified and characterized hypophosphatasia in 1948.

obtained at autopsy was paradoxically subnormal (Rathbun, 1948). Hundreds of case reports of HPP are now in the medical literature (Whyte, 1994, 2001), and we now know the disorder's etiology and its key clinical, radiographic, biochemical, and skeletal histopathological features, and in addition understand well (but not completely) its pathogenesis (Whyte, 2018). A PubMed (http://www.ncbi.nlm.nih.gov/sites/entrez/) search from 1948 onward shows 687 articles with "hypophosphatasia" in the title, and 1072 where it appears in the text. Reviewed following, our understanding of both the metabolic basis for HPP and the physiological function of TNSALP was advanced importantly by the discoveries of elevated endogenous levels of three phosphocompounds (i.e., TNSALP natural substrates) in affected individuals. In 1955, in the era of paper chromatography to diagnose inborn errors of metabolism, identification of increased amounts of phosphoethanolamine (PEA) in urine provided a second biochemical marker for HPP other than hypophosphatasemia (Fraser et al., 1955; McCance et al., 1955). In 1965 and 1971, the discovery of elevated levels of PPi in the urine (Russell, 1965) and plasma (Russell et al., 1971), respectively, of HPP patients would explain the disorder's defective skeletal mineralization, because PPi was now recognized as inhibiting this process (Heinonen, 2001). In 1985, the discovery of often markedly elevated plasma concentrations of pyridoxal 5′-phosphate (PLP), the major circulating form of vitamin B_6 in HPP, coupled with an understanding of vitamin B_6 metabolism, revealed that TNSALP functions as a cell-surface enzyme. This explained the extracellular accumulation of these three phosphocompounds in this "inborn-error-of-metabolism" (Whyte et al., 1985).

Clinical features

Hypophosphatasia (OMIM #146300, #241500, and #241510) seems to occur in all ethnicities (Whyte et al., 2006). However, it is especially prevalent in Mennonites in Manitoba, Canada, where about 1 in 25 individuals carries a "founder" *ALPL* missense mutation (Greenberg et al., 1993), and 1:2500 newborns manifests the severe autosomal recessive disease (Leung et al.). Canadian Hutterites too have a relatively high prevalence of HPP. In Toronto, Canada, the incidence for what would be the severest forms of HPP was estimated in 1957 to be 1 per 100,000 live births (Fraser, 1957). Inexplicably, HPP seems to be particularly rare in people of black ancestry (Whyte et al., 2006).

Despite the high expression of TNSALP in bone, cartilage, liver, kidney, and adrenal tissues (and at least some ubiquitous TNSALP) in healthy individuals (McComb et al., 1979), HPP seems to disrupt only the skeleton and dentition directly (Whyte, 2001). Discussed later, vitamin B_6–dependent seizures are a metabolic consequence of HPP when it is most severe (Baumgartner-Sigl et al., 2007). Muscle weakness is often an important finding, but its pathogenesis is not understood.

Nevertheless, a remarkable feature of HPP is its extraordinarily wide-ranging expressivity, spanning from death in utero with an essentially unmineralized skeleton to early shedding of deciduous "baby" teeth without skeletal disease (Fraser, 1957; Whyte, 2001). In fact, many individuals with relatively mild biochemical characteristics of HPP and harboring one defective *ALPL* allele seem, at least early in adult life, to have escaped the disorder's complications and can be considered "carriers" (Whyte et al., 1982a). I consider HPP to manifest the most broad-ranging severity of all skeletal diseases. This partly reflects the polymeric nature of the active enzyme, the many ($>$ 360) different deactivating predominantly missense mutations found throughout *ALPL*, and the two patterns of autosomal inheritance (Weiss et al., 1988; Henthorn et al., 1992; Mornet et al., 1998; Whyte, 2000; Mumm et al., 2002). Some *ALPL* mutations have dominant/negative effects and cause autosomal dominant disease. However, it is increasingly apparent that other unknown genetic or nongenetic factors can significantly condition HPP expressivity. This is obvious from the discordant HPP severity that sometimes occurs among siblings sharing identical *ALPL* defects (Henthorn et al., 1992; Whyte et al., 2006; Mumm et al., 2006) **(**Fig. 66.3**)**. Accordingly, the prevailing nosology for patients with HPP (Whyte, 2001) remains a clinical one based primarily on consideration of age-of-onset as suggested by Fraser beginning in 1957 (Fraser, 1957). Understandably, an alternative *ALPL* mutation-based nosology might add too little for prognostication (Whyte, 2001).

Six principal forms of HPP are now discussed. The age at which the disorder presents and is diagnosed distinguished early on the perinatal, infantile, childhood, and adult forms (Fraser, 1957; Whyte, 2001). Those affected individuals who do not have skeletal disease but instead manifest dental features only are said to have "odontohypophosphatasia" (odonto-HPP) (Whyte, 2001). With the approval in 2015 of asfotase alfa as a TNSALP-replacement therapy for HPP, it became important to recognize "mild" versus "severe" forms of childhood HPP (see later). Nevertheless, this nosology of six forms of HPP does not unambiguously classify all patients, and it is important to appreciate that the disorder features a continuum of expressivity. An extremely rare form of HPP called "pseudohypophosphatasia" recapitulates infantile HPP, except that serum ALP activity is not subnormal but instead within or above the age-appropriate reference range in the clinical laboratory, where the assay reflects highly nonphysiological conditions (see later) (Scriver and Cameron, 1969; Whyte, 2001). Importantly, a not uncommon "benign perinatal" form of HPP, characterized from fetal sonography, revealed that

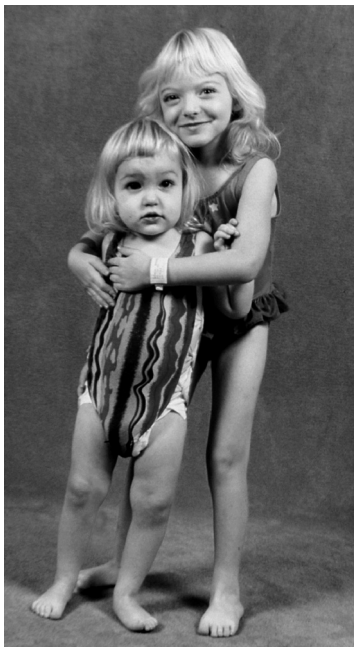

FIGURE 66.3 Variable clinical expressivity of hypophosphatasia is exemplified by these sisters who are compound heterozygotes sharing the same two *ALPL* missense mutations. The proposita (right) at age 5−3/12 years survived infantile HPP featuring poor weight gain, hypercalcemia with nephrocalcinosis, and severe rickets (Barcia et al., 1997) that was followed by short stature, premature loss of teeth, and craniosynostosis. Her younger sister (left) at age 2−2/12 years appears well and has mild rickets despite very similar hypophosphatasemia and endogenous elevations of the TNSALP substrates.

skeletal deformity in utero owing to HPP does not predict a lethal outcome (Moore et al., 1999; Pauli et al., 1999). This form of HPP manifests skeletal disease at birth but with spontaneous postnatal ex utero improvement, although with a broad-ranging clinical outcome (Wenkert et al., 2011).

The prognoses for the six major forms of HPP are determined by the severity of the skeletal disease. Typically, the earlier in life that skeletal signs and symptoms present, the worse the outcome (Fraser, 1957; Whyte, 2001). The benign prenatal form of HPP is, however, an important exception.

Perinatal hypophosphatasia

This most severe form of HPP (OMIM #241500), featuring profound generalized skeletal disease obvious in a neonate, reflects nearly a complete lack of mineralization of endochondral and membranous bone and typically causes death before or soon after birth. Remarkable skeletal softening can result in caput membranaceum and limbs that are short and deformed. Some affected newborns survive a few days or weeks but succumb to respiratory compromise owing to rachitic disease of the chest. In some, the lungs appear hypoplastic (Silver et al., 1988). There may be vitamin B_6−dependent seizures (Baumgartner-Sigl et al., 2007). Myelophthisic anemia can occur, perhaps from encroachment of excessive osteoid on the marrow space (Terheggen and Wischermann, 1984). Long-term survival is very rare (Whyte et al 2016a, 2019a).

Skeletal radiographs (Fig. 66.4) taken at birth readily distinguish perinatal HPP from even the most severe types of osteogenesis imperfecta or congenital dwarfism; the findings are diagnostic. Nevertheless, there is patient-to-patient variability (Shohat et al., 1991). In some stillborns, the bones appear nearly devoid of mineral (see Fig. 66.4A). In others, severe rachitic changes are apparent (see Fig. 66.4B). Occasionally, individual or sequential vertebrae appear completely or partly missing (Shohat et al., 1991). In the skull, the membranous bones may calcify only at their centers, giving the illusion that cranial sutures are widely separated ("open"), although they may be functionally closed (see Fig. 66.4C). Other unusual radiographic features (Whyte, 1988) include bony protrusions (Bowdler spurs) extending from the midshafts of the ulnas and fibulas (see Fig. 66.4D).

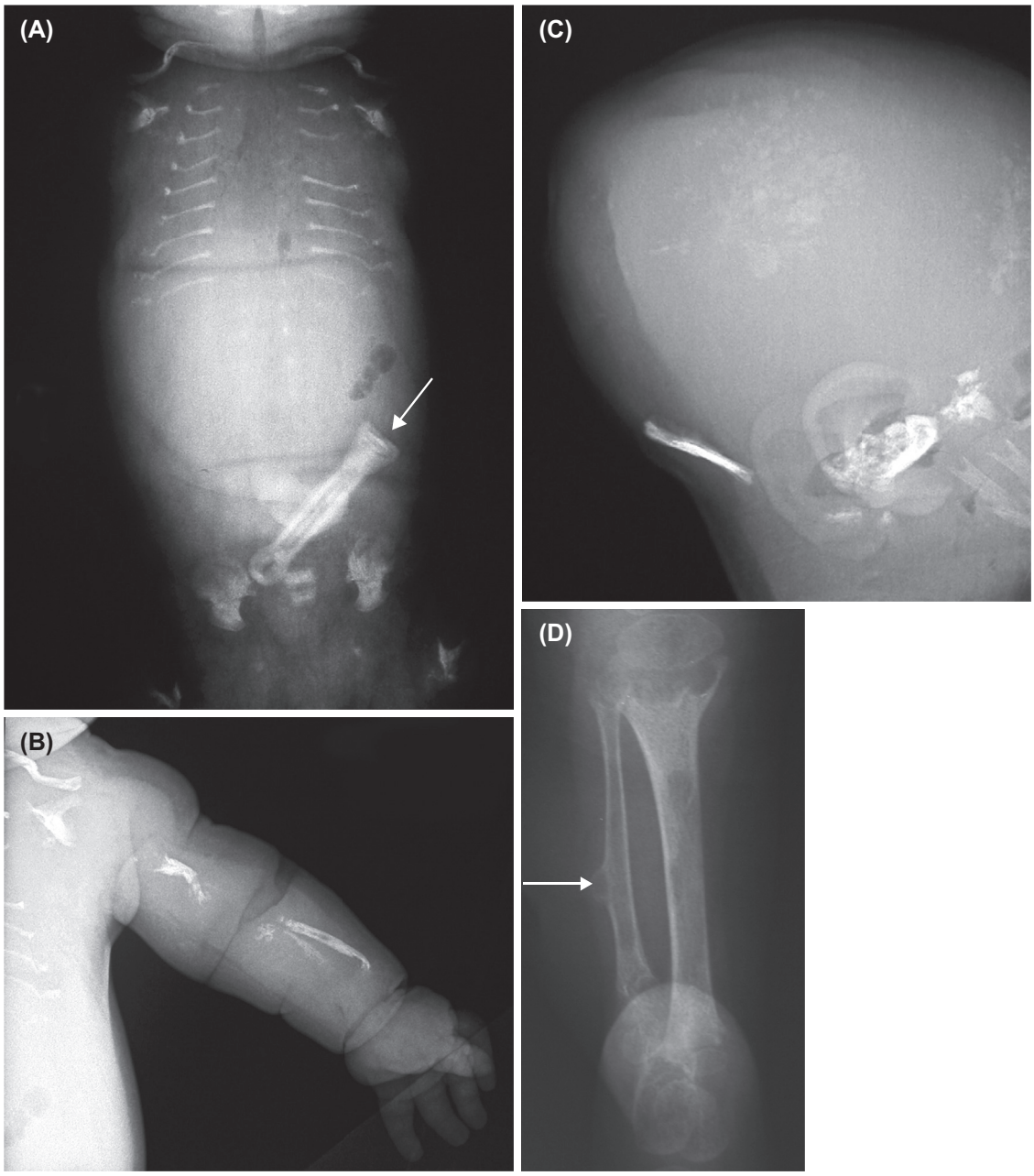

FIGURE 66.4 Perinatal hypophosphatasia. (A) Profound skeletal hypomineralization is obvious at birth (arrow points to umbilical cord clip). (B) The ends of the upper extremity long bones at 1 day of age show characteristic, extreme, rachitic changes. (C) Severe hypomineralization of the calvarium is present at 1 day of age. (D) A Bowdler spur (arrow) is found in some patients.

Infantile hypophosphatasia

This is the form of HPP (OMIM #241500) that was encountered by Rathbun (Rathbun, 1948). Signs and symptoms manifest after birth but before 6 months of age (Fraser, 1957; Whyte, 2001). Development may seem normal until there is hypotonia, poor feeding, and inadequate weight gain. At this time, the clinical and radiographic manifestations of rickets appear. Rarely, vitamin B_6–dependent epilepsy precedes the skeletal changes, and this complication predicts a lethal outcome (Baumgartner-Sigl et al., 2007). A flail chest from rib fractures, rachitic deformity, etc. often leads to pneumonia. Hypercalcemia and hypercalciuria are common and may explain episodes of recurrent vomiting as well as acquired nephrocalcinosis and renal compromise (Fraser, 1957; Whyte et al., 1982b, 2012).

Although the striking radiographic features of the skeletal disease of infantile HPP are diagnostic (see Fig. 66.5A), they are less severe than in perinatal HPP. Radiographs may suggest that the cranial sutures are wide open, but this can be an illusion from hypomineralization of the calvarium, and instead "functional" craniosynostosis can be present. Later, bony fusion of the sutures can occur if the patient survives infancy, causing the symptoms and complications of craniosynostosis (see Fig. 66.5B). In some babies, an abrupt transition from relatively normal-appearing diaphyses to poorly mineralized metaphyses (see Fig. 66.5C) suggests that metabolic deterioration occurred suddenly (Fraser, 1957). This observation is supported by the hypercalciuria and hypercalcemia that can develop in this form of HPP. Serial radiographs may reveal not only impaired skeletal mineralization (i.e., rickets) but also gradual, generalized demineralization of all osseous tissue (Whyte et al., 1982b) indicating a lethal outcome (Whyte et al., 2003; Cahill et al., 2007) (see Fig. 66.5D). However, spontaneous but unexplained improvement sometimes occurs (Ish-Shalom et al., 1986).

Childhood hypophosphatasia

This form of HPP (OMIM #241510) has especially wide-ranging expressivity (Fallon et al., 1984; Whyte, 2001). When asfotase alfa TNSALP-replacement therapy became available multinationally in 2015, characterization of mild versus

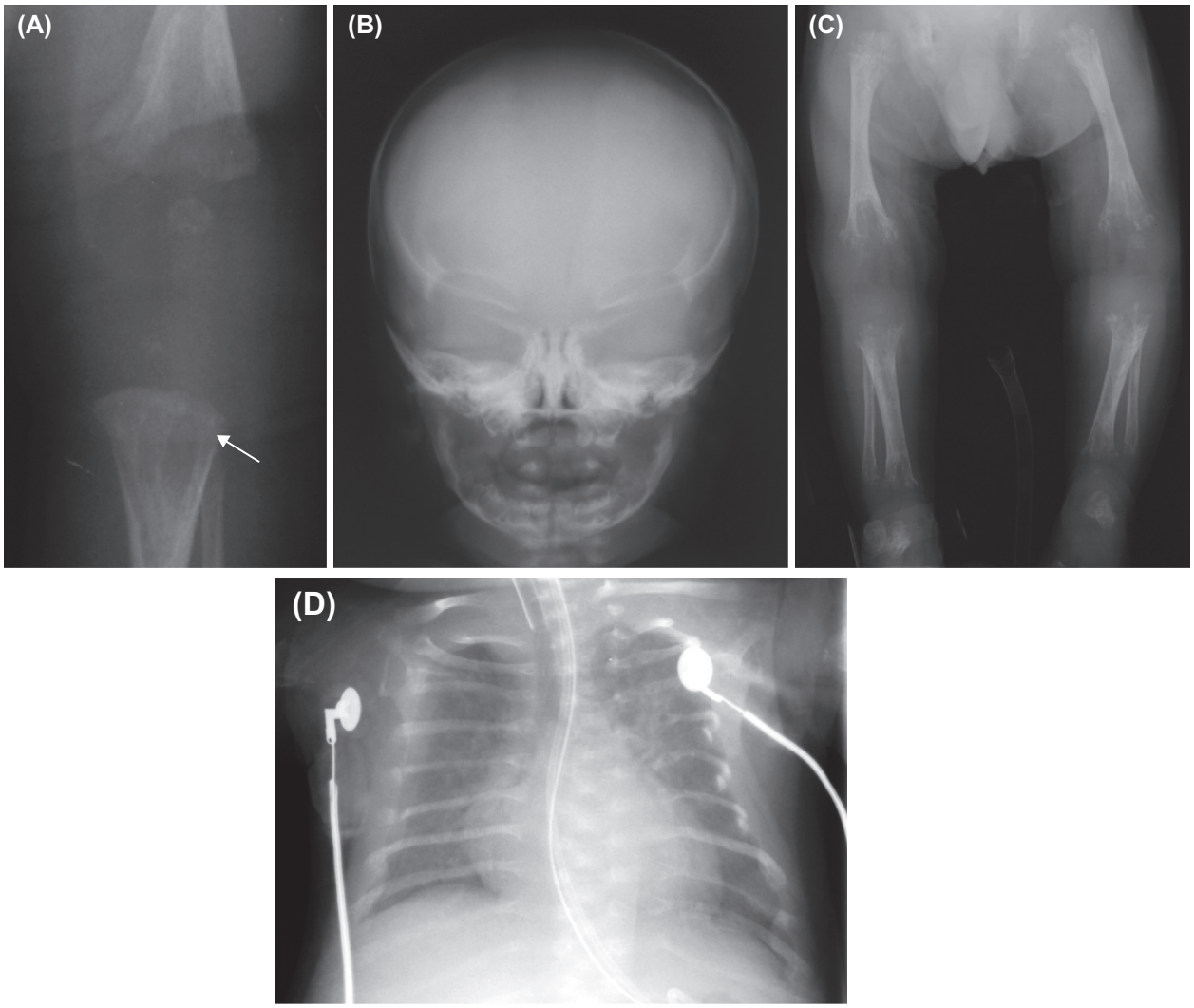

FIGURE 66.5 Infantile hypophosphatasia. (A) Characteristic tongues of radiolucency (arrow) extend from the growth plate into the metaphysis. (B) Cranial sutures appear widened in this hypomineralized skull at 1 month of age. (C) An abrupt transition seems to have occurred from well-mineralized diaphyses to poorly mineralized metaphyses by the age of 3 months. (D) The "bell-shaped" configuration of the chest from a soft thorax together with rib fractures will predispose to respiratory complications at 23 months of age.

severe childhood HPP helped in appreciating the clinical trial assessments of treatment (Whyte et al, 2015, 2016b). Childhood HPP is diagnosed when the presentation is after 6 months of age but before skeletal maturity. In 1953, premature loss of deciduous teeth was found to be a major clinical feature (Sobel et al., 1953). Early shedding of "baby" teeth (i.e., at less than 5 years of age) results from hypomineralization of aplastic or hypoplastic dental cementum (Van den Bos et al., 2005). Consequently, tooth roots are not bound sufficiently to the periodontal ligament (Lundgren et al., 1991), and teeth are shed painlessly, bloodlessly, and without trauma (see Fig. 66.6A). The mandibular incisors are typically lost first, and occasionally nearly all the primary dentition exfoliates prematurely. We have encountered premature loss of at least one deciduous tooth in 98% of our pediatric patients with HPP (Whyte et al., 2015). Delayed walking with a characteristic

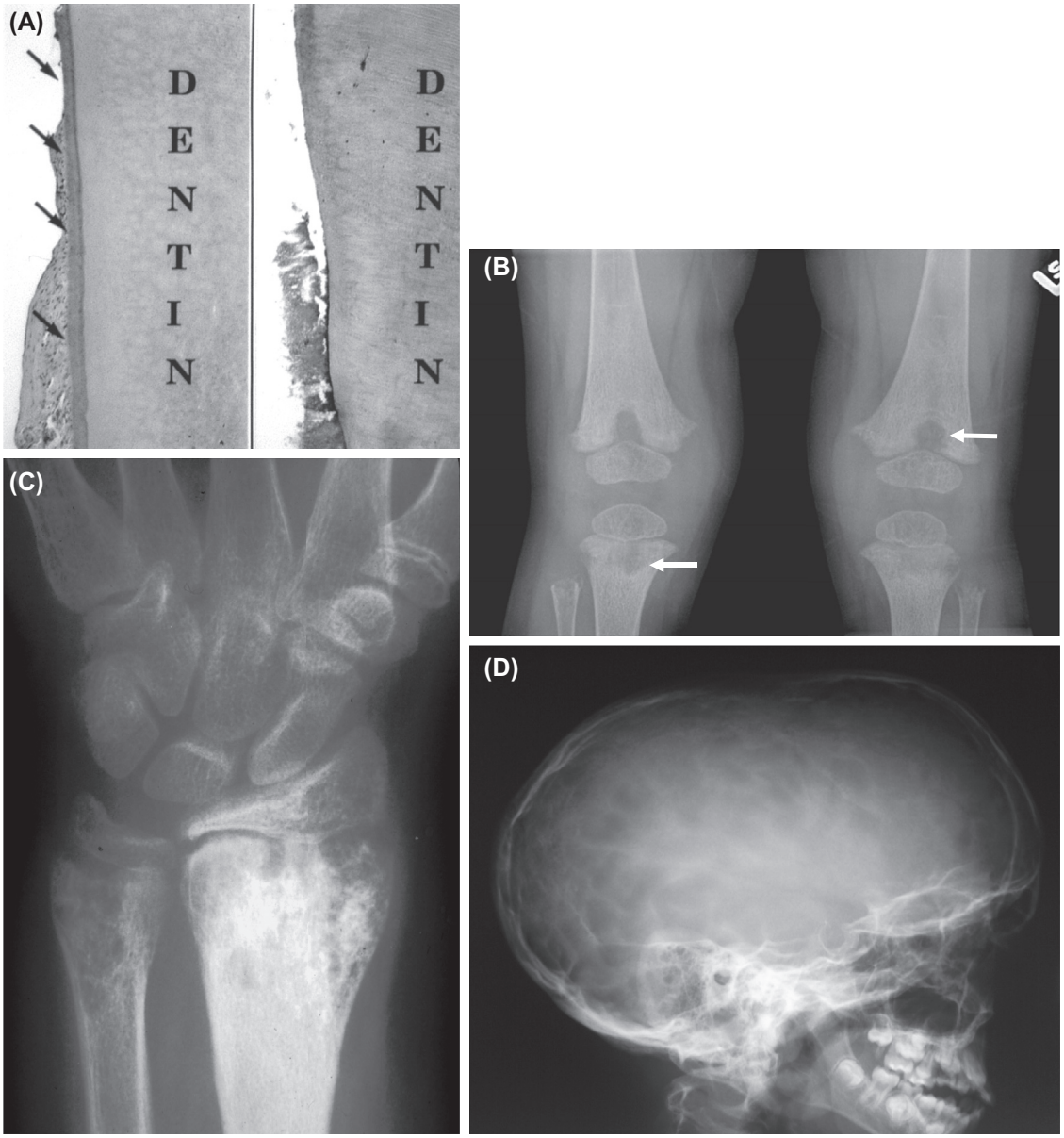

FIGURE 66.6 Childhood hypophosphatasia. (A) Dental findings. (Left) Decalcified section of part of the root of a maxillary incisor from a child with X-linked hypophosphatemia is essentially normal and shows primary cementum (delineated by arrows) at its surface (original magnification, ×150). (Right) In hypophosphatasia, cementum is absent (original magnification, ×150). (B) Characteristic tongues of radiolucency (arrows) project from growth plates into metaphyses at 16 months of age. (C) Idiopathic, patchy, metaphyseal osteosclerosis is a common finding. (D) A "beaten copper" appearance in the calvarium, here at 11 years of age, signifies premature closure of cranial sutures (craniosynostosis) that can lead to raised intracranial pressure. *(A) Reproduced with permission from Whyte, M.P., 2001. Hypophosphatasia. In: Scriver, C.R., Beaudet, A.L., Sly, W.S., Valle, D., (Eds.) The Metabolic and Molecular Bases of Inherited Disease, eighth ed., pp. 5313–5329. McGraw-Hill, New York.*

waddling gait is typical of severe childhood HPP. Patients may have appendicular muscle weakness (especially in the thighs) consistent with a nonprogressive myopathy (Seshia et al., 1990) and complain of stiffness and pain. There may also be delayed speech and language acquisition (unpublished observations).

Radiographs usually show characteristic focal "tongues" of radiolucency that project from rachitic growth plates into adjacent metaphyses (see Fig. 66.6B). Patchy metaphyseal osteosclerosis can occur (see Fig. 66.6C). True premature bony fusion of cranial sutures may raise intracranial pressure (see Fig. 66.6D). Dental radiographs sometimes show enlarged pulp chambers and root canals that characterize the "shell teeth" of various types of rickets.

Adult hypophosphatasia

This form of HPP (OMIM #146300) typically presents in middle age or later (Whyte, 2001; Whyte et al., 1982a). Not infrequently, however, such patients recall being told of early loss of their deciduous teeth followed by rickets or weakness in childhood. Subsequently, there is good health during young adult life (Weinstein and Whyte, 1981). Others among these patients may have been considered "carriers" of HPP until they manifested the characteristic complications of the disease (Sutton et al., 2012).

In adult HPP, osteomalacia often presents as recurrent metatarsal stress fractures (see Fig. 66.7A) (Whyte et al., 2007; Camacho et al., 2016). With more advanced disease, persistent aching or tenderness in the thighs or hips may be explained by femoral pseudofractures (see Fig. 66.7B) that will not heal spontaneously unless they progress to complete fractures (Coe et al., 1986; Khandwala et al., 2006; Whyte, 2009). Early loss or extraction of the secondary dentition is not uncommon, although the pathogenesis is not well understood (Whyte et al., 1982a). Calcium pyrophosphate dihydrate (CPPD) deposition disease troubles some patients, and occasionally overt attacks of pseudogout also reflect the increased endogenous levels of PPi (see later) (O'Duffy, 1970; Whyte et al., 1982a; McKiernan et al., 2014). Affected adults may suffer degeneration of articular cartilage from "pyrophosphate arthropathy" (Whyte et al., 1982a). Radiographs often reveal chondrocalcinosis and osteopenia (Lassere and Jones, 1990; Whyte et al., 1982a). In certain families manifesting hypophosphatasemia, Ca^{++}-Pi deposition manifests as "calcific periarthritis" (Guañabens et al., 2014) or ossification of ligaments (syndesmophytes) resembling spinal hyperostosis (Forestier's disease) (Lassere and Jones, 1990).

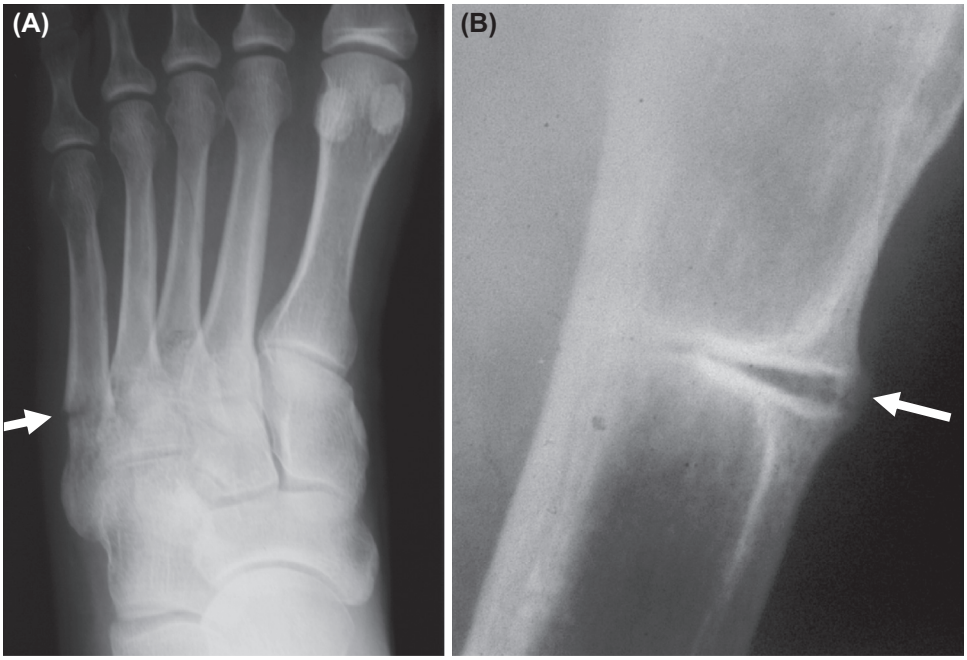

FIGURE 66.7 Adult hypophosphatasia. (A) Recurrent, poorly healing metatarsal stress fractures (arrow) may be the most common skeletal manifestation of the adult form of hypophosphatasia. (B) Femoral pseudofractures (arrow) are often painful and characteristically occur on the lateral aspect proximally in adult hypophosphatasia. They do not heal spontaneously unless a through-and-through break occurs.

Odontohypophosphatasia

This form of HPP is diagnosed when there are characteristic dental manifestations but no radiographic or histological evidence of rickets or osteomalacia.

Pseudohypophosphatasia

This extremely rare variant of HPP has been documented convincingly in two infants (Scriver and Cameron, 1969; Whyte, 2001). The clinical, radiographic, and biochemical findings are those of infantile HPP with one key exception—serum total ALP activity is not low but instead normal or increased (Whyte, 1994, 2001). The enzymatic explanation for pseudo-HPP involves defective TNSALP with diminished hydrolysis for PPi, PLP, and PEA endogenously, but normal or increased catalysis for artificial substrates in the nonphysiological conditions of the ALP assays used in clinical laboratories (see later) (Fedde et al., 1990).

Benign prenatal hypophosphatasia

Sonography may reveal a fetus with HPP showing bowing of major long bones that does not represent a lethal form of the disease. Spontaneous improvement of the skeletal deformities may occur later in the pregnancy as well as ex utero and then the severity range from infantile HPP to odonto-HPP (Moore et al., 1999; Pauli et al., 1999; Wenkert et al., 2005).

Laboratory diagnosis

Biochemical findings

HPP can be diagnosed with confidence from a consistent medical history and physical findings together with typical skeletal radiographic changes and serum ALP activity that is subnormal for the patient's age (Whyte, 2001, 2017b, Whyte et al., 2018). Even individuals with odonto-HPP are expected to have low serum ALP activity for their age, although their values can approach the lower end of carefully established reference ranges (see Fig. 66.8). Although HPP severity correlates inversely with age-appropriate serum ALP activity (Whyte et al., 2018), this correlation is not sufficiently strong to offer help with prognostication. In perinatal and infantile HPP, hypophosphatasemia is detectable at birth in umbilical cord blood (Whyte, 2001), while circulating ALP levels in carrier or affected mothers normalize or become elevated from placental ALP (Whyte et al., 1995).

Hypophosphatasemia can occur from other conditions (starvation, hypothyroidism, scurvy, severe anemia, Wilson's disease, celiac disease, multiple myeloma, hypomagnesemia, Zn^{++} deficiency, etc.), certain drugs (glucocorticoids, clofibrate, chemotherapy, vitamin D intoxication, milk-alkali syndrome, etc.), and exposure to radioactive heavy metals or a massive transfusion of blood or plasma (Macfarlane et al., 1992; McKiernan et al., 2014). These clinical situations should, however, be readily recognized and diagnosed. Especially rare cases of extremely severe osteogenesis imperfecta (Royce et al., 1988) and cleidocranial dysplasia in some infants (Unger et al., 2002; Wycoff et al., 2005) can also manifest hypophosphatasemia (apparently from the paucity of skeletal mass together with impaired cellular processing of bone ALP, or from osteoblast hypofunction, respectively). The skeletal changes of cleidocranial dysplasia might pose the greater confusion (Unger et al., 2002; Wycoff et al., 2005).

Transient increments in circulating bone ALP activity have been postulated for individuals with HPP after orthopedic surgery or significant fracturing (Whyte et al., 2013). In theory, circumstances that increase serum levels of any type of ALP (e.g., pregnancy, liver disease) could obscure the enzymatic and biochemical diagnosis of HPP. Thus, documenting hypophosphatasemia on more than one occasion during clinical stability, particularly from the earliest medical record, seems advisable for the exceptional, confusing patient. Quantitation of circulating ALP isoenzymes (Mulivor et al., 1985), isoforms of TNSALP (Whyte et al., 1996), or leukocyte ALP (Iqbal et al., 2000) in clinical laboratories may also be helpful.

Mineral homeostasis

Neither circulating Ca^{++} nor Pi levels are subnormal in HPP. Serum levels of 25(OH)D, $1,25(OH)_2D$, and parathyroid hormone (PTH) are typically normal (Whyte and Seino, 1982) unless altered physiologically by hypercalcemia or renal failure (Fallon et al., 1984). In fact, in infantile HPP there may be hypercalcemia, secondary hypoparathyroidism, and hyperphosphatemia together with hypercalciuria (Fraser, 1957; Shohat et al., 1991; Whyte et al., 1982b, 2012). The

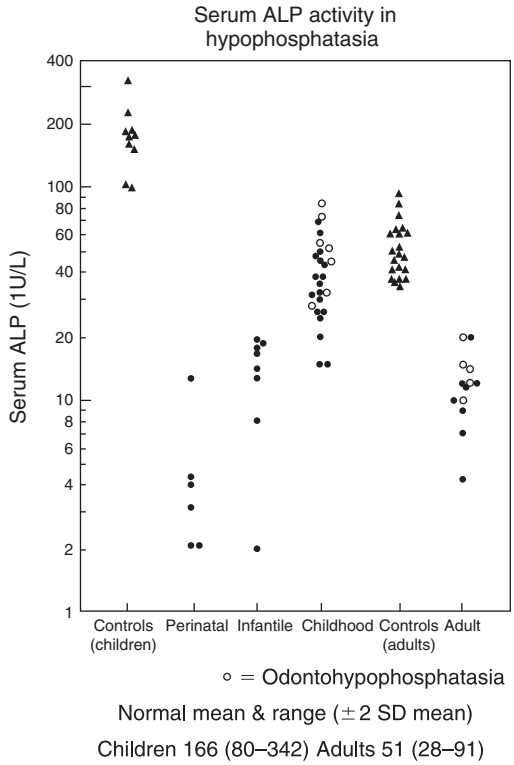

FIGURE 66.8 Serum alkaline phosphatase activity in hypophosphatasia. Serum total ALP activity in healthy children and adults and in 52 patients from 47 families with the various clinical forms of hypophosphatasia (note the logarithmic scale). All assays were performed at the Center for Metabolic Bone Disease and Molecular Research, Shriners Hospitals for Children-St. Louis, St. Louis, MO, USA. *Reproduced with permission from Whyte, M.P., 2001. Hypophosphatasia. In: Scriver, C.R., Beaudet, A.L., Sly, W.S., Valle, D., (Eds.) The Metabolic and Molecular Bases of Inherited Disease, eighth ed., pp. 5313–5329. McGraw-Hill, New York.*

disturbed mineral homeostasis seems largely due to impaired Ca^{++} and Pi uptake by a poorly mineralizing and growing skeleton, sometimes with progressive skeletal demineralization perhaps reflecting patient immobility. Low circulating levels of PTH, reflecting increased ionized Ca^{++} levels, are common in severely affected pediatric patients. In childhood HPP, affected individuals may manifest hypercalciuria but usually not with hypercalcemia. In the past, several HPP patients were reported to have elevated serum PTH levels, but impaired kidney function may have been the explanation in some (Whyte, 1994). Rarely, affected adults with HPP do have primary hyperparathyroidism (Faas et al., 1974; Whyte, 2001).

Of interest, individuals with the childhood or adult forms of HPP have serum Pi levels above average values for age-matched controls (Whyte, 2001). Indeed, >50% of these patients are distinctly hyperphosphatemic. Enhanced renal reclamation of Pi (increased TmP/GFR) underlies this finding (Whyte and Rettinger, 1987). However, in only some instances is suppressed circulating PTH contributory. The pathogenesis seems complex, perhaps involving low levels of TNSALP activity in the kidney tubules, subnormal or inappropriately normal circulating levels of phosphatonins, and/or elevated levels of urinary PPi (Whyte et al., 2019). In contrast, hypophosphatasemia with hypophosphatemia from renal Pi wasting was reported in 1981 (Juan and Lambert, 1981).

Phosphoethanolamine

Elevated urine levels of PEA support a diagnosis of HPP (Rasmussen, 1968) but are not pathognomonic. Licata et al. (1978) demonstrated that phosphoethanolaminuria occurs in other conditions including several metabolic bone diseases. Reference ranges for urine PEA vary according to patient age and somewhat by diet and follow a circadian rhythm. PEA values can be unremarkable in mildly affected HPP patients. Age-adjusted normal ranges (expressed as micromoles of PEA per gram of creatinine) are for less than age 15 years, 83 to 222; for 15–30 years, 42 to 146; for 31–41 years, 38 to 155; and for more than 45 years, 48 to 93 (Licata et al., 1978).

Pyridoxal 5′-phosphate

Increased plasma PLP ("vitamin B_6") is a sensitive and reliable marker for HPP (Coburn and Whyte, 1988; Whyte et al., 2018) including pseudo-HPP (Cole et al., 1986). Even patients with odonto-HPP manifest this biochemical finding (Whyte et al., 1985, 2018). However, the earliest studies showed that PLP values overlap between the different clinical forms of HPP (see Fig. 66.9). Now testing is available from commercial laboratories. In order to avoid false-positive results, vitamin supplements containing pyridoxine should not be taken, if possible, for 1 week before blood is obtained for the assay. HPP disease severity correlates positively but not precisely with the elevation in plasma PLP concentration (Whyte, 2001; Whyte et al., 2018). Quantitation of plasma PLP after challenge with pyridoxine given orally once each day for 6 days seems to distinguish HPP patients especially well (Whyte, 1994). The procedure has been used to identify Canadian Mennonite carriers of severe HPP (Chodirker et al., 1990).

Inorganic pyrophosphate

Assay of PPi in plasma or urine is not commercially available. Urine PPi levels are increased in most HPP patients but can be unremarkable in mildly affected individuals (Caswell et al., 1991). Nevertheless, this test may help with carrier detection (Whyte, 2001). Assays of both circulating PPi and PLP were used as efficacy and safety parameters during the clinical trials of asfotase alfa treatment for HPP (Whyte et al., 2016b, 2019b; Kishnani et al., 2019).

Radiographic findings

Radiographic features are illustrated elsewhere for the principal clinical forms of HPP (see Figs. 66.4 to 66.7).

Histopathological findings

Histopathological disturbances in HPP that are a direct consequence of TNSALP deficiency seem to be hard tissue hypomineralization and perhaps the seemingly paradoxical ectopic mineralization of calcific periarthritis and enthesopathy.

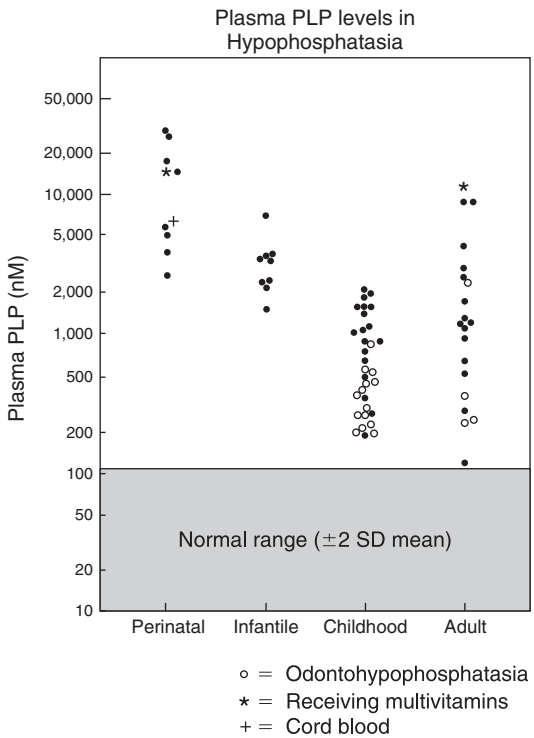

FIGURE 66.9 Plasma pyridoxal 5′-phosphate (PLP) levels in hypophosphatasia. PLP concentrations in plasma in various clinical forms of hypophosphatasia (hatched area is the normal range for children and adults). Note the logarithmic scale with some overlap between clinical forms (assays performed courtesy of Dr. Stephen P. Coburn, Fort Wayne State Developmental Center, Fort Wayne, IN). *Reproduced with permission from Whyte, M.P., 2001. Hypophosphatasia. In: Scriver, C.R., Beaudet, A.L., Sly, W.S., Valle, D., (Eds.) The Metabolic and Molecular Bases of Inherited Disease, eighth ed., pp. 5313–5329. McGraw-Hill, New York.*

Pulmonary hypoplasia (Silver et al., 1988) seems secondary to a small thorax. Myopathic changes are not observed despite muscle weakness.

Skeleton

In all but the mildest cases of HPP (i.e., odonto-HPP), nondecalcified sections of the skeleton reveal defective mineralization (Fallon et al., 1984; Ornoy et al., 1985). The degree of rickets or osteomalacia generally reflects the clinical severity overall (Fallon et al., 1984). Features of secondary hyperparathyroidism (present in rickets or osteomalacia associated with hypocalcemia) are typically absent (Fallon et al., 1984; Anderson et al., 1997). In severe cases, extramedullary hematopoiesis (Fallon et al., 1984; Ornoy et al., 1985) may reflect marrow space crowding owing to the osteomalacia.

In growth plates and osseous tissue, cellular sources of the bone isoform of TNSALP (chondrocytes and osteoblasts) are present (Anderson et al., 1997) but their TNSALP activity is deficient (Fallon et al., 1984; Ornoy et al., 1985). Other forms of rickets or osteomalacia cannot be excluded by their histopathological features unless ALP activity is assessed. In HPP, ALP activity in bone inversely reflects the degree of osteoid accumulation and therefore the severity of the skeletal disease (Fallon et al., 1984).

Electron microscopy of skeletal tissue obtained at autopsy from perinatal HPP has shown normal distribution of MVs, proteoglycan granules, and collagen fibers in the extracellular space of cartilage (Fallon et al., 1984; Ali, 1986), although the MVs lacked ALP activity. Early reports described only isolated or tiny groups of HA crystals (calcospherites) that frequently were not associated with vesicular structures (Ali, 1986; Shohat et al., 1991). Actually, HPP MVs do contain HA, but the crystals fail to enlarge due to the superabundance of extracellular PPi after these structures rupture (Anderson et al., 1997). Thus, "secondary," but not "primary," mineralization is compromised in HPP.

Dentition

Premature exfoliation of primary teeth occurs in a few diseases other than HPP, such as cyclical neutropenia and Papillon–Lefèvre syndrome (Van den Bos et al., 2005). In HPP, a paucity of mineralized cementum (despite the presence of cells that look like cementoblasts) seems to explain this complication (see Fig. 66.6A) (el-Labban et al., 1991; Lundgren et al., 1991). Desiccated teeth remain useful for histopathological examination. What cementum is present appears afibrillar (el-Labban et al., 1991). The severity of this defect varies from tooth to tooth but typically reflects the degree of skeletal disease (Whyte et al., 2015). Incisors are usually affected most and are the first to be shed.

In addition to defects in cementum, dentinogenesis seems to be impaired as shown by big pulp chambers. Dentin tubules may be enlarged although reduced in number. The excessive width of predentin, increased amounts of interglobular dentin, and impaired calcification of cementum are analogous to the osteoidosis found in bone. Reportedly, the enamel is not impacted directly (Lundgren et al., 1991). The histopathological changes of the permanent teeth are similar to those in deciduous teeth (el-Labban et al., 1991), but their prognosis early on is better (Lepe et al., 1997).

Biochemical and genetic defects

HPP is caused by mono- or biallelic loss-of-function mutation(s) in *ALPL*.

Tissue-nonspecific alkaline phosphatase deficiency

Early on, postmortem studies of perinatal and infantile HPP revealed selective deficiency of TNSALP isoenzyme activity and thereby identified HPP as an inborn error of metabolism while suggesting its genetic basis. Profound deficiency of ALP activity was discovered in bone, liver, and kidney tissue but not in intestine or placenta (fetal trophoblast) (Vanneuville and Leroy, 1981). This observation matched emerging amino acid sequence analyses from proteolytic peptide digests of ALPs purified from healthy human tissues (Stigbrand and Fishman, 1984) and indicated selective deficiency of the various isoforms within the TNSALP isoenzyme family. Leukocyte ALP activity can be subnormal in any form of HPP except perhaps pseudo-HPP, and therefore likely represents a type of TNSALP (Fallon et al., 1984).

Postmortem studies of children or adults with HPP have not been reported, but globally diminished TNSALP activity is indicated by deficiency in serum, bone, circulating granulocytes (Fallon et al., 1984), and skin fibroblasts (Vanneuville and Leroy, 1981; Whyte and Vrabel, 1985).

Hypophosphatasemia in HPP does not seem to involve accelerated clearance of TNSALP from the circulation (Gorodischer et al., 1976). Purified placental ALP (Whyte et al., 1992) as well as the bone isoform of TNSALP contained in the

plasma of patients with Paget bone disease (Whyte et al., 1982b) showed normal circulating half-lives of several days when infused intravenously into infants with life-threatening HPP during attempted ALP replacement therapy (see later).

Furthermore, coincubation experiments with mixtures of serum and coculture studies with fibroblasts provided evidence against the presence of an inhibitor or the absence of an activator of TNSALP in HPP (Fraser, 1957; O'Duffy, 1970; Whyte and Vrabel, 1985). Then, in 1985, skin fibroblast heterokaryon studies indicated a defect at a single gene locus causing severe HPP (Whyte and Vrabel, 1985).

ALP immunoreactivity has been studied in tissues obtained at autopsy as well as in skin fibroblasts from patients with severe HPP (Fallon et al., 1989; Fedde et al., 1996). In a preliminary report, a polyclonal antibody to the liver isoform of TNSALP indicated normal amounts of immunoreactive TNSALP in bone, liver, and kidney tissues from five patients (Fallon et al., 1989). Others, using isoelectric focusing and enzyme inhibition studies, suggested that the low ALP activity in one HPP patient reflected intestinal ALP (Mueller et al., 1983). In a fibroblast study, ALP had somewhat different physicochemical and immunological properties compared with ALP from healthy controls but seemed to be a type of TNSALP (Fedde et al., 1996). In studies of ALP in the circulation, monoclonal antibody-based immunoradiometric assays for polymeric TNSALP demonstrated low levels of the bone and liver isoforms in sera from patients with all clinical types of HPP except pseudo-HPP (Whyte et al., 1996). Upon release from cell surfaces into blood, TNSALP in HPP seemed altered in such a way that immunoreactivity was diminished and/or clearance was accelerated (Whyte et al., 1996). Fedde et al. (1996) concluded that the precise impact of the underlying *ALPL* mutation(s) (see later) must be understood to fully appreciate its effect(s). Now, these early findings are explained by the identification of >360 typically missense loss-of-function mutations of *ALPL* in HPP, including their effects on cellular processing of the enzyme as well as its structure (see later).

Inheritance

Mutational analysis of *ALPL* established both autosomal dominant and autosomal recessive patterns of inheritance for HPP. Perinatal and infantile HPP represent autosomal recessive disease (Weiss et al., 1988; Henthorn et al., 1992; Mumm et al., 2001; Whyte et al., 2003, 2006, 2012, 2015), whereas all milder forms of HPP can reflect either autosomal recessive (Henthorn et al., 1992) or autosomal dominant transmission of *ALPL* defects (Mumm et al., 2006; Whyte et al., 2007). Certain *ALPL* mutations have dominant-negative effects and account for multigenerational HPP (Mumm et al., 2006) (see later). Pseudo-HPP too involves *ALPL* defects (Madson et al., 2015). The utility of quantitating the biochemical parameters of HPP to identify carriers has been discussed (Sorensen et al., 1978; Chodiker et al., 1990; Whyte et al., 2017b).

ALPL gene defects

In 1988, proof that HPP can be caused by loss-of-function alteration of *ALPL* came with the discovery by Weiss and coworkers of a homozygous missense defect within *ALPL* in a consanguineous boy who died from perinatal HPP (Weiss et al., 1988). Transfection studies showed that his single-base transition in *ALPL* compromised the enzyme's activity, perhaps by impairing the binding of a metal ligand to an important arginine residue at the catalytic pocket (Weiss et al., 1988). In 1992, Henthorn et al. reported eight further missense mutations in four additional unrelated patients with perinatal or infantile HPP (Henthorn et al., 1992) and found two siblings with childhood HPP and one unrelated woman with adult HPP who were compound heterozygotes for the identical *ALPL* defects. In 1993, Greenberg and coworkers demonstrated that homozygosity for a "founder" tenth *ALPL* missense mutation accounts for the high prevalence of HPP in Mennonites living in Manitoba, Canada (Greenberg et al., 1993). Now, all clinical forms of HPP have been shown to involve loss-of-function mutation(s) in *ALPL* (Whyte, 2000, 2016, 2019), and all patients are expected, depending on sufficient rigor of the search, to carry one or two defective *ALPL* alleles (Whyte, 2017a; 2017b, 2018). There has not been genetic heterogeneity for HPP. A web site organized by Etienne Mornet, PhD, summarizes the *ALPL* mutations identified in HPP patients worldwide (http://www.sesep.uvsq.fr/Database.html). Currently, >360 different *TNSALP* mutations are recorded, of which the considerable majority are missense. Some seem to have increased regional or national prevalence (Mumm et al., 2006).

ALPL structural defects

Many *ALPL* mutations causing HPP (Taillander et al., 2001; Mumm et al., 2002) alter the amino acid residue in all mammals (Henthorn and Whyte, 1992; Mornet et al., 1998) and sometimes conserved in the ALPs of bacteria (Henthorn et al., 1992). Characterization of the three-dimensional structure of *Escherichia coli* ALP (Kim and Wyckoff, 1991) and human placental ALP (Le Due et al., 2000) by X-ray crystallography accelerated our understanding of the enzymatic basis for HPP (Henthorn et al., 1992; Kim and Wyckoff, 1991; Millán, 2006). Missense mutations in *ALPL* could now be

examined for their impact on the catalytically active dimeric TNSALP molecule (Chemscape Chime version 1.02 by MDL Information Systems, Inc., San Leandro, CA, at http://www.mdli.com and RasWin Molecular Graphics, Windows version 2.6 by Roger Sayle, Glaxo Wellcome Research and Development, Stevenage, Hertfordshire, UK, at http://www.umass.edu/microbio/rasmol/index.html). Some *ALPL* mutations would disturb the enzyme's catalytic pocket or structurally important metal ligand-binding sites; others possibly compromised the formation of TNSALP dimers (Mornet et al., 1998; Millán, 2006). Nevertheless, why all *ALPL* loss-of-function (Brunt-Heath et al., 2005) mutations associated with HPP are deleterious is not understood (Whyte, 2000; Millan and Whyte, 2016). For example, site-directed mutagenesis with the Ala161-Thr substitution first discovered to cause HPP (Weiss et al., 1988) did not compromise the catalytic activity of *E. coli* ALP (Chaidaroglou and Kantrowitz, 1993). In fact, some *ALPL* mutations alter the intracellular processing of TNSALP (Mornet et al., 1998; Shibata et al., 1998; Fukushi et al., 1998). Clinical, radiological, and perhaps histopathological studies of elderly individuals harboring the wide range of *ALPL* defects may prove especially helpful for understanding whether they ever cause HPP complications (Whyte, 2000, 2017a, b).

Prognosis

Untreated perinatal HPP is almost always rapidly fatal (Whyte et al., 2019). With intensive life support, these neonates may live for a short time, but long-term survival is rare. Now, however, asfotase alfa treatment can rescue these patients and lead to enjoyable health (Whyte et al., 2012; 2019b) (see later).

Infantile HPP, when first diagnosed, has a less certain outcome. Often there is clinical and radiographic deterioration, with historically ~50% of affected babies said to die from pneumonia and respiratory compromise owing to worsening skeletal disease particularly affecting the chest (Fraser, 1957; Whyte et al., 2003; Cahill et al., 2007). Sometimes instead, considerable spontaneous improvement occurs. The prognosis seems better if there is survival past infancy. In fact, a preliminary report in 1986 from Canada (Ish-Shalom et al., 1986) suggested that the adult stature of survivors of infantile HPP may be normal. Nevertheless, I am aware of less favorable outcomes (Whyte, 2001). Childhood HPP may also spontaneously improve, typically after growth plate fusion in young adult life. During childhood, however, the various pediatric forms of HPP usually do not alter their expressivity (Whyte et al., 2016c). Unfortunately, recurrence of skeletal symptoms and complications later in adulthood can occur (Fraser, 1957; Weinstein and Whyte, 1981; Khandwala et al., 2006; Whyte et al., 2007), but not predictably. Adult HPP often presents with recurrent metatarsal stress fractures and then further orthopedic difficulties become chronic (Whyte et al., 1982a). Worsening osteomalacia associated with osteopenia and fractures was not prevented in two affected women by estrogen replacement given at their menopause (personal observation).

Treatment

When the previous 2008 version of this chapter was published, clinical trials of HA-targeted asfotase alfa (Strensiq) for HPP had just begun. The results were transformative, especially for affected neonates, infants, and children, and this biologic was approved multinationally in 2015, typically for pediatric-onset HPP (Whyte, 2017b). The evolution of treatment trials for HPP is instructive concerning the physiological role of TNSALP.

Supportive

Symptoms from CPPD crystal deposition or periarticular HA precipitation (calcific periarthritis) may respond to nonsteroidal antiinflammatory agents.

Intramedullary rodding of femoral fractures or pseudofractures has been the mainstay of orthopedic management (Coe et al., 1986; Sutton et al., 2012). Recurrent metatarsal stress fractures have benefitted from wearing a boot.

Medical

Before asfotase alfa, there was no established medical treatment for HPP. Several informative approaches had been attempted (Fraser et al., 1955) including trials of nontargeted ALP replacement therapy (Whyte et al., 1982b, 1984, 1992), marrow cell transplantation (Whyte et al., 2003; Cahill et al., 2007), and teriparatide administration (Whyte et al., 2007). Cortisone given to a few pediatric patients with severe HPP reportedly coincided with periods of normalization of serum ALP activity and radiographic improvement (Fraser and Laidlaw, 1956) but was an inconsistent finding. Brief supplementation with Mg^{++} or Zn^{++} had been unsuccessful (Fraser, 1957). Because patients with HPP are often hyperphosphatemic (Whyte, 2001; Whyte et al., 2019), restriction and/or pharmacological binding of dietary Pi seemed

potentially useful for HPP (Wenkert et al., 2002). The superabundance of extracellular Pi might be competitively inhibiting TNSALP (McComb et al., 1979; Coburn et al., 1998) or suppressing *ALPL* gene expression (Goseki-Sone et al., 1999). Nevertheless, full clinical studies did not follow.

Hypercalcemia in infantile HPP can be treated by restriction of dietary Ca^{++} that hopefully does not exacerbate any progressive skeletal demineralization reflecting patient immobility (Whyte et al., 1982b, 1986). If necessary, glucocorticoids may be helpful for elevated blood Ca^{++} levels (Whyte et al., 1982b) but could pose an additional risk. Hypothetically, an antiresorptive treatment like subcutaneous injections of salmon calcitonin might address some of the hypercalcemia while blocking skeletal demineralization in HPP (Barcia et al., 1997), but experience has not been positive, likely because the skeletal disease involves osteoidosis covering bone surfaces. In fact, antiresorptive bisphosphonates have not had success and are derivatives of PPi that theoretically could exacerbate the rickets or osteomalacia (Whyte, 2001; Sutton et al., 2012). Some drugs that stimulate TNSALP biosynthesis in the skeleton, such as teriparatide, may benefit HPP, especially if there is only one defective *ALPL* allele (Whyte et al., 2007; Camacho et al., 2016).

Assessing therapy for infantile HPP can seem uncertain because some patients demonstrate spontaneous, and sometimes quite significant, improvement (Ish-Shalom et al., 1986; Whyte et al., 1986), whereas others show progressive skeletal demineralization leading to a fatal outcome (Whyte et al., 1982b). Now, we understand that the latter is more common (Lueng et al., 2013; Whyte et al., 2016a, 2019a).

Enzyme replacement therapy for HPP has been attempted by intravenous infusion of several types of ALP, but generally the results have been disappointing. In 1972, serum from a patient with Paget bone disease given to an affected infant was said to precede radiographic improvement (Macpherson et al., 1972). In 1982, weekly infusion of fresh plasma from healthy subjects was followed by clinical and radiographic advances in a child (Albeggiani and Cataldo, 1982). However, subsequent infusions of Paget plasma were without significant clinical or radiographic benefit for four patients with infantile HPP (Whyte et al., 1982b, 1984). One boy with infantile HPP showed remarkable but transient correction of hypophosphatasemia and substantial clinical, radiographic, and histological improvement after a brief trial of prednisone, bovine PTH 1−34, and then pooled plasma infusions from healthy individuals, but succumbed soon after to pneumonia (Whyte et al., 1986). He was later confirmed to have a homozygous *ALPL* missense mutation (Whyte et al., 2006). In follow-up to a brief report in 1989 that suggested infusions of ALP purified from liver improved the histological appearance of bone and decreased urinary PEA levels (Weninger et al., 1989), purified placental ALP was given to a severely affected infant, but despite repeated doses that led to transient hyperphosphatasemia there were only modest decrements of plasma PLP and urinary PEA concentrations, no change in urinary PPi levels, and no clinical or radiographic improvement (Whyte et al., 1992). Placental ALP was given because elevated concentrations of PLP in plasma and increased levels of PEA and PPi in urine diminished as endogenous natural production of this ALP isoenzyme corrected the hypophosphatasemia of pregnant women who were carriers of HPP (Whyte et al., 1995). Perhaps pregnancy with large amounts of placental ALP present physiologically in situ represents an "endogenous" form of enzyme replacement in HPP. However, the symptoms, radiology, skeletal histology, etc. of women who are carriers or affected by HPP have not been assessed across a pregnancy. Extreme skeletal disease in perinatal HPP despite placental ALP circulating in the mother shows that the in utero environment may not be protective for the fetus (Whyte, 2001).

These cumulative discouraging observations, showing that circulating ALP activity could be corrected in infantile HPP yet have no clinical benefit, suggested that ALP must be within the skeleton itself for physiological activity and therapeutic efficacy (Whyte et al., 1995). In fact, two subsequent reports of patient rescue and clinical and radiographic improvement in infantile HPP following mesenchymal cell transplantation suggested sufficient numbers of TNSALP-replete osteoblasts had formed (Whyte et al., 2003; Cahill et al., 2007). These improvements occurred without significant biochemical alterations of mineral metabolism, consistent with a beneficial effect limited to the skeleton.

In 2007, injections of teriparatide (recombinant PTH 1−34) were associated with clinical, biochemical, and radiographic improvement in a woman with adult HPP (Whyte et al., 2007), possibly from increased expression of her normal *ALPL* allele in her osteoblasts and/or PTH-induced phosphaturia documented by increased serum ALP and decreased Pi, respectively.

Later, I discuss the multinational availability of asfotase alfa to treat HPP.

Prenatal diagnosis

A number of reports have concluded that lethal perinatal HPP has been diagnosed in utero during the second trimester using ultrasonography with particular attention to the shape and mineralization of the skull and major long bones (van Dongen et al., 1990). However, relatively mild HPP, inherited either as an autosomal dominant or autosomal recessive trait, can bow major bones in utero and suggest the presence of this lethal form of HPP, yet the deformities correct postnatally,

reflecting instead the benign prenatal form of HPP (Moore et al., 1999; Pauli et al., 1999; Wenkert et al., 2005, 2011; Stevenson et al., 2008). The >360 specific defects possible in *ALPL* show that for mutation analysis it is necessary to examine *ALPL* exons 2−12 and their splice sites for new patients with HPP (Mumm et al., 2002). Microarray study for *ALPL* deletion/duplication is occasionally necessary. *ALPL* mutation analysis is possible to detect HPP prenatally (Henthorn and Whyte, 1995), but prognostication from the results and early fetal sonography can be problematic (Wenkert et al., 2011).

Physiological role of alkaline phosphatase explored in hypophosphatasia

As reviewed previously, several roles for TNSALP in skeletal formation have been proposed (Table 66.1). Hence, investigation of HPP has been a "window of opportunity" to explore a number of them directly in humans.

The discovery by Weiss and coworkers more than 3 decades ago that homozygosity for a loss-of-function missense mutation within *ALPL* caused severe HPP (Weiss et al., 1988) confirmed Robison's hypothesis; i.e., the enzyme that came to be called ALP functions crucially in skeletal mineralization (Robison, 1923). Subsequent characterization of the dental manifestations of HPP revealed that ALP is important also for the formation of teeth; i.e., "hard tissues." Now, it appears that all bona fide cases of HPP are explained by mono- or biallelic loss-of-function mutation(s) in *ALPL* (Whyte, 2016; 2017b, 2018, 2019).

Electron microscopy of bone and cartilage obtained at autopsy from patients representing the most severe forms of HPP demonstrated that deficient activity of TNSALP is associated with a fundamental disturbance in the process of "secondary" skeletal mineralization. Extravesicular mineralization is impeded in HPP (Anderson et al., 1997). HA crystal growth appears to fail after MVs rupture.

Mineralization defects in the cementum and dentin of HPP teeth have been considered as analogous to those in the skeleton (Lundgren et al., 1991). A prominent role for TNSALP during two critical phases of dental mineralization, initiation and completion, was proposed (Hotton et al., 1999). In 2005, Van den Bos and coworkers reported that both cellular and acellular cementum formation was impaired, but not mineralization of the dentin (Van den Bos et al., 2005).

Although healthy liver, kidneys, and adrenal glands are rich in TNSALP activity (McComb et al., 1979), they seem to function normally in HPP (see later) with the exception that reclamation of filtered Pi by the kidney is enhanced and hyperphosphatemia is common. This can be explained by suppression of circulating PTH levels in the often hypercalcemic perinatal and infantile forms of HPP (Whyte and Rettinger, 1987; Whyte et al., 2012), but otherwise seems to have a complex pathogenesis also involving a role for TNSALP in kidney tubules; phosphatonin deficiency or inappropriately normal levels despite hyperphosphatemia; and/or effects on TmP/GFR by the elevated levels of urinary PPi (Whyte et al., 2019).

It has been suggested that the TNSALP deficiency of severe HPP might impair the biosynthesis of phospholipids and thereby explain occurrences of pulmonary atelectasis (Silver et al., 1988). However, the respiratory problems of severely affected patients are attributable to rib cage fractures, thoracic deformity, and chest muscle weakness, perhaps also accounting for hypoplastic lungs.

In the 1980s, it became clear from investigation of HPP patients that TNSALP is important not only for hard tissue mineralization but also for dephosphorylation of extracellular PLP and therefore vitamin B_6 metabolism (Whyte, 1994). In severe pediatric HPP, insufficient hydrolysis of PLP to pyridoxal (PL) for entry into neurons impairs the biosynthesis of the neurotransmitter γ-aminobutyric acid (Baumgartner-Sigl et al., 2007). In fact, epilepsy is an important characteristic of the murine model of infantile HPP and is associated with low levels of γ-aminobutyric acid in the central nervous system (Waymire et al., 1995). Pyridoxine supplementation briefly extends the lives of these patients (Baumgartner-Sigl et al., 2007) and mice (Fedde et al., 1999) with HPP.

Tissue-nonspecific alkaline phosphatase substrates

The discoveries that PEA, PPi, and PLP accumulate endogenously in HPP were essential for elucidating the physiological role of TNSALP in humans. Each was thereby correctly inferred to be a natural substrate for TNSALP. However, a preliminary study using 31P-magnetic resonance spectroscopy of urine from patients with HPP suggested several additional phosphorylated TNSALP substrates (Whyte et al., 2000).

Phosphoethanolamine

The reports in 1955 by McCance and colleagues (1955) and Fraser and coworkers (1955) that PEA levels are elevated in the urine and plasma of HPP patients provided a second biochemical marker for the disorder and identified the first natural

substrate for TNSALP. In 1968, Rasmussen showed that this phosphocompound appears in the urine when plasma levels are scarcely detectable; i.e., there is essentially no renal threshold for PEA excretion (Rasmussen, 1968).

Although the metabolic origin of PEA is uncertain, the principal source of circulating PEA in HPP is considered to be the liver, which normally metabolizes PEA to ammonia, acetaldehyde, and Pi in a reaction catalyzed by O-phosphorylethanolamine phospholyase (Gron, 1978). In one family with adult HPP, urine levels of PEA correlated inversely with circulating activity of the liver but not the bone isoform of TNSALP (Millán et al., 1980). PEA is a component of the phosphatidylinositol-glycan linkage apparatus for cell surface proteins (Low and Zilversmit, 1980). Hence, PEA could be a degradation product of this link, but is not considered a degradation product of phosphatidylethanolamine; i.e., not from plasma membrane phospholipid breakdown.

Pyridoxal 5′-phosphate

The discovery in 1985 that circulating levels of PLP are elevated in HPP was key to understanding the physiological role of TNSALP (Whyte et al., 1985).

Reviewed later (Fig. 66.10), the forms of dietary vitamin B_6 (pyridoxine, pyridoxal, pyridoxamine, and their phosphorylated derivatives) are converted to PLP in the liver (Dolphin et al., 1986). Organ ablation studies of mammals identified hepatic tissue as the principal source of circulating PLP. PLP is released from hepatocytes into the bloodstream where more than 95% couples to albumin (Dolphin et al., 1986). Some PLP also binds in the circulation to various enzymes, but a small amount circulates freely.

Like many phosphorylated compounds, PLP cannot cross plasma membranes but must first be dephosphorylated to PL before it can enter tissues. Inside cells, PL is rephosphorylated to PLP or converted to pyridoxamine 5′-phosphate that then act as cofactors for many and varied enzymatic reactions. Ultimately, vitamin B_6 is degraded to 4-pyridoxic acid (4-PA), primarily in the liver, and then excreted into the urine (Dolphin et al., 1986; Coburn and Whyte, 1988).

In disorders that elevate circulating bone and liver TNSALP, plasma PLP concentrations are decreased (Anderson et al., 1980). Thus, discovery of elevated plasma PLP levels in HPP extended this reciprocal relationship. However, the wide-ranging elevated levels in circulating PLP are probably not of pathophysiological consequence in HPP because cell surface TNSALP controls extracellular but not intracellular dephosphorylation of PLP. Elevated plasma PLP levels in HPP do not reflect enhanced PLP synthesis but instead extracellular accumulation from diminished hydrolysis of PLP (Whyte

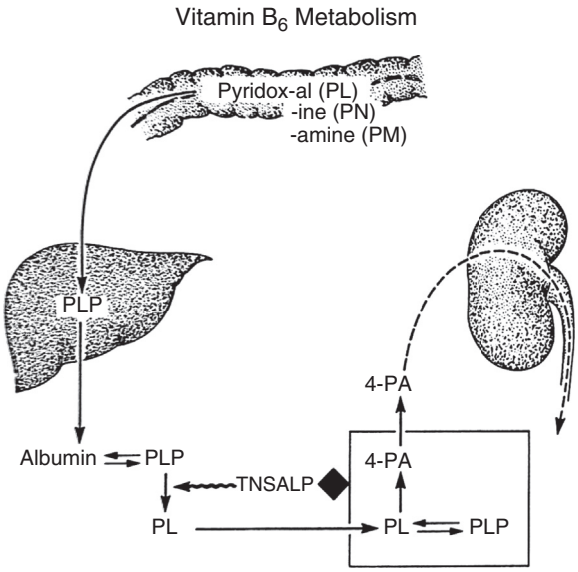

FIGURE 66.10 Role of tissue-nonspecific alkaline phosphatase (TNSALP) in vitamin B_6 metabolism. The various forms of vitamin B_6 are plentiful in the diet and absorbed into the hepatic portal circulation (phosphorylated forms are first dephosphorylated in the gut). In the liver, each is converted to PLP, which is then secreted bound to albumin into the plasma. In order to enter tissues, plasma PLP must be dephosphorylated to PL that can traverse membranes. 4-Pyridoxic acid (4-PA), the major degradation product of vitamin B_6, is excreted in the urine. High plasma levels of PLP in hypophosphatasia, yet normal plasma concentrations of PL, are consistent with a cell surface role for TNSALP in the extracellular dephosphorylation of PLP to PL. *Reproduced with permission from Whyte, M.P., 2001. Hypophosphatasia. In: Scriver, C.R., Beaudet, A.L., Sly, W.S., Valle, D., (Eds.) The Metabolic and Molecular Bases of Inherited Disease, eighth ed., pp. 5313–5329. McGraw-Hill, New York.*

et al., 1985). Clinical investigation of HPP led to this overview of vitamin B_6 metabolism because patients with HPP do not have symptoms of vitamin B_6 toxicity such as peripheral neuropathy (Dolphin et al., 1986) (see later). Similarly, in all types of HPP except the most severe perinatal and infantile forms where vitamin B_6–dependent epilepsy can occur, there are no signs or symptoms of chronic vitamin B_6 deficiency such as stomatitis, dermatitis, peripheral neuritis, anemia, or depression (Dolphin et al., 1986). Furthermore, a variety of biochemical findings indicated that intracellular levels of vitamin B_6 are unremarkable in HPP. First, urine levels of 4-pyridoxic acid are normal in patients with childhood HPP (Whyte et al., 1988). Second, these children respond normally to L-tryptophan loading—a test for vitamin B_6 deficiency (Whyte and Coburn, unpublished observation). Third, in homogenates of severely TNSALP-deficient HPP fibroblasts in culture, levels of PLP and the various other forms of vitamin B_6 are normal (Whyte et al., 1988). Finally, tissues obtained at autopsy from patients with perinatal HPP (plasma PLP concentrations elevated 50 to 900 times normal) contain essentially normal levels of PLP, PL, and total vitamin B_6 (Whyte et al., 1988). Accordingly, TNSALP seemed to function as a cell surface enzyme (Whyte et al., 1985; Fedde et al., 1988), and soon after how ALP and other proteins anchor to the plasma membrane was identified (Low and Saltiel, 1988).

Because TNSALP seemed responsible for the extracellular dephosphorylation of PLP to PL, plasma levels of PL could be low in HPP. However, only patients with the severest forms of HPP have low plasma PL concentrations, helping to explain the vitamin B_6–dependent seizures; the others show normal or sometimes elevated circulating PL levels (Whyte et al., 1985).

Vitamin B_6 deficiency is associated with renal stone disease and epilepsy. However, nephrocalcinosis in infants with HPP likely reflects hypercalciuria, although oxalate excess (a consequence of vitamin B_6 deficiency) has not been searched for in HPP (Dolphin et al., 1986). Epilepsy in severe HPP has the aforementioned metabolic explanation but also occurs in patients who may have cranial deformity, intracranial hemorrhage, periodic apnea, etc. Of interest, PEA reportedly caused seizures when given intravenously to an infant severely affected by HPP during a study of PEA metabolism (Takahashi et al., 1984). In two patients with perinatal HPP and epilepsy, both of whom had plasma PL levels below assay sensitivity, administration of vitamin B_6 as pyridoxine did not correct the seizure disorder (personal observation), perhaps because the pyridoxine was converted to more PLP rather than PL. Vitamin B_6–dependent seizures can be the first manifestation of infantile HPP. All reported cases of HPP with such seizures proved fatal (Baumgartner-Sigl et al., 2007). *Alpl* knockout mice manifest this type of epilepsy (see later), and require pyridoxine administration to extend their lives (Waymire et al., 1995; Fedde et al., 1999). Treatment of these mice, an excellent model for infantile HPP (Fedde et al., 1999), with asfotase alfa prevented their skeletal and dental disease and vitamin B_6-dependent epilepsy (Millán et al., 2008).

The clinical and biochemical observations concerning vitamin B_6 metabolism in HPP have indicated an extracellular role for TNSALP (Whyte et al., 1985). In 1988, Fedde and coworkers exposed cultivated human osteosarcoma cells (Fedde et al., 1988), and then dermal fibroblasts from patients with infantile HPP (Fedde et al., 1990), to PLP and PEA in the medium and confirmed that TNSALP is a plasma membrane-associated enzyme (see later). In 1980, characterization of porcine kidney ALP as membrane-bound by phosphatidylinositol (Low and Zilversmit, 1980) indicated this attachment apparatus for TNSALP (Low and Saltiel, 1988).

Inorganic pyrophosphate

Discovery in 1965 and 1971, respectively, that PPi levels are increased in HPP patient urine (Russell, 1965) and plasma (Russell et al., 1971) provided a plausible explanation for defective skeletal mineralization in HPP (Caswell et al., 1991) (Fig. 66.11). At that time, PPi was becoming recognized as a potent inhibitor of mineralization (Heinonen, 2001). Although low concentrations of PPi could enhance Ca^{++} and Pi precipitation from solution to form amorphous calcium phosphate, at higher concentrations PPi prevented the growth and dissolution of HA crystals (Caswell et al., 1991). Caswell and co-workers demonstrated that nucleoside triphosphate pyrophosphatase (NTP-PPi-ase, PC-1) activity is unremarkable in TNSALP-deficient fibroblasts from perinatal and infantile HPP patients. Extracellular generation of PPi from ATP by these cells was not hindered (Caswell et al., 1986). Therefore, NTP-PPi-ase seemed distinct from TNSALP. In 2000, this conclusion was supported by studies of osteoblasts from *Alpl* knockout mice (see later) (Johnson et al., 2000). From understanding PLP metabolism in HPP, it became clear how the clearance of 32PPi administered in the 1960s into the circulation of two adults with HPP was markedly delayed (R. G. G. Russell, personal communication). Endogenous accumulation of PPi in HPP reflects diminished extracellular hydrolysis (Caswell et al., 1991).

Consonant with the in vitro effects of PPi, several other abnormalities of mineralization in HPP may reflect the local concentration of PPi. Perhaps relatively minor excesses of extracellular PPi explain the precipitation of amorphous calcium phosphate and the calcific periarthritis observed in some adults with HPP (Lassere and Jones, 1990). Furthermore, ALP can dissolve CPPD crystals in vitro (Xu et al., 1991), and this PPi-ase activity seems additional to its capacity to hydrolyze

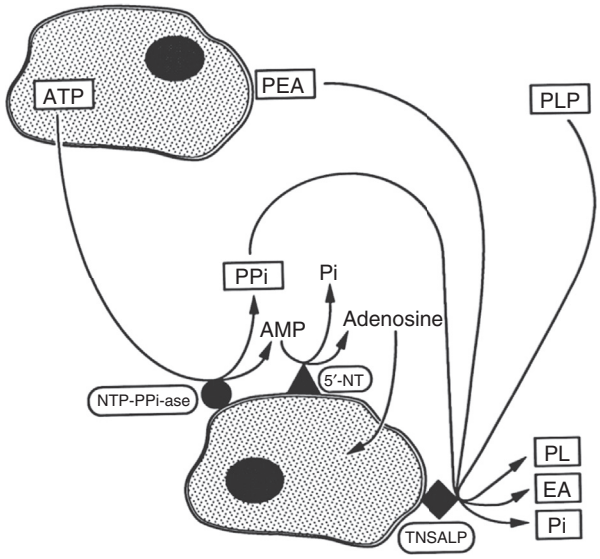

FIGURE 66.11 Metabolic basis for hypophosphatasia. Extracellular generation of PPi, presumably by the action of nucleoside triphosphate pyrophosphatase (NTP-PPi-ase), is normal. PPi is also pumped extracellularly from within cells via an ANK channel (not shown) (Millán, 2006). Extracellular degradation of PEA, PPi, and PLP is diminished because of deficient cell-surface TNSALP activity. Accumulation of PPi extracellularly accounts for CPPD precipitation and sometimes associated calcium phosphate crystal deposition. The inhibitory effect of PPi on extravesicular HA crystal growth accounts for the rickets/osteomalacia. *Reproduced with permission from Whyte, M.P., 2001. Hypophosphatasia. In: Scriver, C.R., Beaudet, A.L., Sly, W.S., Valle, D., (Eds.) The Metabolic and Molecular Bases of Inherited Disease, eighth ed., pp. 5313–5329. McGraw-Hill, New York.*

phosphoesters. Thus, CPPD crystal deposition leading to chondrocalcinosis, pseudogout, and pyrophosphate arthropathy could be explained by the failure of TNSALP to hydrolyze not only PPi but also CPPD crystals. The especially high extracellular concentrations of PPi in HPP would inhibit HA crystal formation and growth; hence, rickets or osteomalacia becomes readily explained. As discussed, electron microscopy of skeletal tissue from lethal HPP and in Tnsalp knockout mice (see later), showed that the precise pathogenesis involves secondary mineralization surrounding MVs (Anderson et al., 1997).

Circulating tissue-nonspecific alkaline phosphatase

Several observations suggest that circulating ALPs are physiologically inactive. Infants with severe HPP who received intravenous infusions of plasma from patients with Paget bone disease or purified placental ALP demonstrated no significant clinical or radiographic improvement despite transient correction in circulating ALP activity, sometimes to elevated levels. Such therapy failed to normalize urinary PEA or PPi levels or plasma PLP concentrations (Whyte et al., 1982b). The deficiency of TNSALP activity within the skeleton itself seemed to account for the rickets and osteomalacia of HPP. In fact, in studies reminiscent of Robison's work (Robison, 1932), Fraser and Yendt reported in 1955 that rachitic rat cartilage would calcify in serum obtained from an infant with HPP, yet slices of HPP costochondral junction would not mineralize in synthetic calcifying medium or in pooled serum from healthy children (Fraser and Yendt, 1955). Subsequently, transfection studies using ALP cDNA showed both catalysis against Pi esters and mineralization in a calcification system (Yoon et al., 1989; Farley et al., 1991). Nevertheless, there has been skepticism that such experiments reflect true biomineralization, because increased Pi in metastable solutions is expected to simply precipitate as calcium phosphate (Khouja et al., 1990). As discussed, it seemed necessary to augment ALP activity in the skeleton tissue itself to treat HPP. In fact, the aforementioned experience with marrow cell transplantation for infantile HPP suggested that even small increases in ALP activity within the skeleton can improve its mineralization in HPP (Whyte et al., 2003). Transient transfection studies of various *ALPL* mutations causing HPP also indicated that small differences in the magnitude of the deficiency of ALP activity within the skeleton can account for lethal versus nonlethal outcomes (Mornet et al., 1998).

Hypophosphatasia fibroblast studies

Healthy dermal fibroblasts in culture (Fedde et al., 1990; Whyte and Vrabel, 1985; Whyte et al., 1986) show some TNSALP-like activity that peaks at confluency (Whyte and Vrabel, 1987). Fibroblasts from severely affected HPP patients

are profoundly deficient in this ALP activity (less than 5% control) (Whyte et al., 1983), but the residual activity seems to be a type of TNSALP (Whyte et al., 1987). Using this model, preliminary studies indicated that the phospholipid composition and rates of 32Pi accumulation by these TNSALP-deficient cells were normal (Tsutsumi et al., 1986; Whyte and Vrabel, 1983). In 1990, Fedde et al. demonstrated that TNSALP is present primarily on the surface of these cells (Fedde et al., 1990) and hydrolyzed extracellular PEA and PLP under physiological conditions. Although some reports suggested that ALP conditions cell growth and differentiation by influencing the phosphorylation of nucleotide pools, HPP fibroblasts proliferated at normal rates in culture (Whyte et al., 1983), and TNSALP did not seem to be a phosphoprotein phosphatase acting at the plasma membrane (Fedde et al., 1993).

Alpl knockout animals

Since 1995, studies of *Alpl* knockout mice and then the creation of other murine models of ALP function have complimented and expanded the insights gained from investigation of HPP patients (Millan and Whyte, 2016). In 1995, Waymire and coworkers developed an *Alpl*-null mouse that manifested the deranged vitamin B_6 metabolism of HPP, including lethal seizures from deficient γ-aminobutyric acid in the brain (Waymire et al., 1995). With pyridoxine treatment, the epilepsy was controlled temporarily, and the animals survived long enough to develop dental disease. In 1997, Narisawa and colleagues created a different *Alpl*-null mouse with vitamin B_6–dependent epilepsy and dental defects that also manifested skeletal disease (Narisawa et al., 1997; Millán, 2006). In 1999, Fedde and coworkers demonstrated that both models recapitulated the infantile form of HPP remarkably well, including the acquired skeletal and dental disease and epilepsy together with endogenous accumulation of PPi, PLP, and PEA (Fedde et al., 1999). In 2000, the skeletal mineralization defect of HPP was reproduced in vitro using osteoblasts in culture from these mice (Wennberg et al., 2000). This disturbance did not seem to be related to the aberrations in vitamin B_6 metabolism (Narisawa et al., 2001). Defective secondary (extravesicular) skeletal mineralization was then confirmed by electron microscopy (Anderson et al., 2004). Subsequently, double-knockout mouse studies showed, as might be expected, that skeletal formation is essentially normal in mice that lack both Tnsalp and the PPi-generating enzyme PC-1 (NTP-PPi-ase) (Hessle et al., 2002). Furthermore, Tnsalp expressed under control of the APO-E promoter in the liver of *Alpl* knockout mice prevented the skeletal disease of HPP. It is uncertain, however, whether Tnsalp in the liver itself or in high amounts in the circulation of these mice explained the beneficial skeletal effects. In 2007, Hough and coworkers characterized a much milder, acquired, semi-dominant form of HPP in mice generated from N-ethyl-N-nitrosourea exposure. The adult mice manifested late-onset skeletal disease and arthropathy (Hough et al., 2007). Later, *Alpl*-null mice became the key preclinical model to test asfotase alfa therapy for HPP (Millán et al., 2008). Now, further mouse models of relatively mild HPP are undergoing investigation (Millán and Whyte, 2016; Foster et al., 2015). Recently, a large animal model (sheep) for HPP that includes dental findings has begun characterization (Williams et al., 2018). In 2019, infantile HPP was documented in a breed of dogs (Kyöstila et al., 2019).

Asfotase alfa treatment for hypophosphatasia

HPP was the last type of rickets or osteomalacia to have a medical treatment (Whyte, 2017a). In 2015, asfotase alfa was approved multinationally for HPP, typically if there was pediatric-onset disease. It is an expensive, HA-targeted, recombinant, human TNSALP-replacement therapy administered by subcutaneous injection with dosing based on the patient's weight (Whyte et al., 2012, 2016a; 2019b). The clinical trials encompassed patient ages ranging from newborn to adult life (Whyte et al., 2012, 2016a; Kishnani et al., 2019). Radiographic assessments using validated scales revealed relatively rapid and then sustained improvement in rickets—7 years for 1- to 3-year-old patients with perinatal or infantile HPP (Whyte et al., 2019b), and 5 years for 6- to 12-year-old survivors of infantile HPP or with severe childhood HPP (Whyte et al., 2016b). Osteomalacia seemed improved in both affected children and adults (Whyte et al., 2016b; Kishnani et al., 2019). Circulating ALP activity becomes markedly elevated with this treatment, but the clinical trials were reassuring against ectopic mineralization from excessive lowering of endogenous PPi levels. With treatment, circulating PPi and PLP levels were generally lower and often in the normal range. Rapid and marked improvements were demonstrated, especially by the most severely affected pediatric patients, but bony craniosynostosis was not prevented. Muscle weakness seemed to improve first. Thus, this experience has brought us "full circle," showing that today Rathbun's original patient (Rathbun, 1948) could overcome the pathogenesis of his TNSALP deficiency and enjoy good health. In the future, we must now aim to cure this highly informative inborn error of metabolism.

Summary and conclusions

HPP is the rare but remarkably instructive inborn error of metabolism that demonstrates a critical role for the tissue-nonspecific isoenzyme of ALP in hard tissue mineralization. Subnormal serum ALP activity (hypophosphatasemia), the biochemical hallmark of HPP, reflects a generalized deficiency of TNSALP activity. The three tissue-specific ALP isoenzymes (intestinal, placental, and germ-cell ALP) are not compromised in HPP, but the physiological function of these ALP isoenzymes is not certain.

HPP features impaired skeletal mineralization that manifests as rickets in newborns, infants, children, and adolescents and as osteomalacia in adults. Involvement of the dentition as well shows that all hard tissues are compromised. Clinical expressivity of HPP is, however, extremely broad-ranging and largely but not completely explained by autosomal dominant and autosomal recessive patterns of inheritance with a multitude of underlying loss-of-function mutations, primarily missense defects, in *ALPL*-encoding TNSALP. Perinatal HPP, apparent in utero, causes neonatal death from skeletal hypomineralization that is so severe that no calcification may be seen radiographically. Infantile HPP presents postnatally by the age of 6 months. Sometimes, there is nephrocalcinosis from hypercalcemia and hypercalciuria and functional craniosynostosis as well. Untreated, about 50% of these babies succumb to worsening rachitic disease that compromises pulmonary function. Vitamin B_6–dependent epilepsy indicates particularly severe TNSALP deficiency and a lethal outcome. Childhood HPP features premature loss of deciduous teeth, often preceding rickets and muscle weakness. Adult HPP causes recurrent metatarsal stress fractures, especially femoral pseudofractures, and often arthritis from CPPD crystal deposition, rarely calcific periarthritis from precipitation of amorphous calcium phosphate, and PPi arthropathy or pseudogout. Odonto-HPP refers to premature tooth loss from defective mineralization of dental cementum but no skeletal manifestations.

Perinatal and infantile HPP are transmitted as autosomal recessive traits involving >360 different loss-of-function, often missense, mutations scattered throughout *ALPL*. They compromise the catalytic site and/or structure of this cell surface homodimeric or homotetrameric phosphomonoester phosphohydrolase and sometimes its intracellular processing. All of the more mild forms of HPP can be inherited as an autosomal dominant trait owing to dominant-negative *ALPL* mutations. However, individuals with even the mildest forms of HPP can reflect autosomal recessive inheritance.

Prenatal diagnosis of HPP now involves *ALPL* mutation analysis. During the second trimester, fetal ultrasonography may identify skeletal disease; however, the considerable number and variety of *ALPL* mutations as well as the influence of other factors on the HPP phenotype preclude precise prognostication.

Discovery in HPP of increased endogenous levels of PEA, PPi, and then PLP demonstrated that TNSALP is a cell-surface phosphomonoester phosphohydrolase catalytically active toward a variety of natural substrates, acting also as a PPi-ase. However, additional substrates for TNSALP seem likely. Because these substrates are typically at nanomolar or micromolar concentrations, TNSALP acts physiologically at much lower pH and concentrations than those of the artificial substrates used in clinical and research assays of ALP activity. Clearly, "alkaline phosphatase" is a misnomer.

Clinical investigation of vitamin B_6 metabolism in HPP, supported by HPP fibroblast studies, confirmed that TNSALP acts as a cell-surface enzyme. Typically normal levels of PL in plasma, despite the superabundance of plasma membrane-impermeable PLP, explain the absence of signs or symptoms of vitamin B_6 deficiency (or toxicity) in all but the most severely affected HPP patients.

Attempts to treat HPP by intravenous infusions of ALPs purified from various human tissues was disappointing and suggested that circulating ALP is physiologically inactive. Marrow cell transplantation could be associated with clinical and radiographic improvement but without significant biochemical changes in blood or urine. Teriparatide stimulated bone ALP levels and appeared to heal fractures in several adults with HPP. Following successful treatment of *Alpl*-null mice with recombinant HA-targeted human TNSALP (asfotase alfa), clinical trials proved similarly beneficial, especially for the most severely affected pediatric patients.

Circulating PPi may be formed from extracellular ATP by cell surface NTP-PPi-ase and pumped there from cells by a channel protein called ANK. PLP appears to be from the liver. PEA seems to come from degradation of the phosphatidylinositol-glycan moiety that anchors many proteins to cells surfaces. Hyperphosphatemia owing to increased renal reclamation of Pi in HPP suggests that TNSALP plays a direct role in renal Pi excretion, although additional factors seem likely.

In HPP, PPi excess frequently results in chondrocalcinosis and sometimes in pseudogout or PPi arthropathy. Rickets and osteomalacia in HPP reflect the effect of high extracellular concentrations of PPi to inhibit HA crystal growth at sites of skeletal mineralization. Success using HA-targeted TNSALP-replacement therapy (asfotase alfa) for HPP was consistent with TNSALP acting physiologically within the skeleton but not in the circulation.

Acknowledgments

The staff at the Center for Metabolic Bone Disease and Molecular Research, Shriners Hospitals for Children-St. Louis, St. Louis, Missouri, USA made this chapter possible. My colleague, Steven Mumm, PhD, continues to importantly advance our understanding of the molecular basis for hypophosphatasia, radiologist William H. McAlister, MD, continues to facilitate the diagnosis, assessment, and treatment of our HPP patients, and Jose Luis Millan, PhD, continues to advance our understanding of the alkaline phosphatases. Gary S. Gottesman, MD, and Deborah Wenkert, MD, are providing their expertise as pediatric medical geneticist and rheumatologist, respectively, to manage HPP. Karen Mack, LPN, has now cared for more than 220 children with hypophosphatasia during the past 35 years at our Research Center. Sharon McKenzie provided expert secretarial help.

This work was supported by Shriners Hospitals for Children as well as by The Clark and Mildred Cox Inherited Metabolic Bone Disease Research Fund and The Hypophosphatasia Research Fund at the Barnes-Jewish Hospital Foundation, St. Louis, Missouri, USA.

References

Albeggiani, A., Cataldo, F., 1982. Infantile hypophosphatasia diagnosed at 4 months and surviving 2 years. Helv. Paediatr. Acta 37, 49–58.

Ali, S.Y., 1986. Cell Mediated Calcification and Matrix Vesicles. Elsevier Science, Amsterdam.

Alpers, D.H., Eliakim, R., DeSchruyver-Kecskemeti, K., 1990. Secretion of hepatic and intestinal alkaline phosphatases: similarities and differences. Clin. Chim. Acta 186, 211–223.

Anderson, B.B., O'Brien, H., Griffin, G.E., Mollin, D.L., 1980. Hydrolysis of pyridoxal 59-phosphate in plasma in conditions with raised alkaline phosphate. Gut. 21, 192–194.

Anderson, H.C., 1969. Vesicles associated with calcification in the matrix of epiphyseal cartilage. J. Cell Biol. 41, 59–72.

Anderson, H.C., 1992. Conference introduction and summary (fifth international conference on cell-mediated calcification and matrix vesicles). Bone Miner. 17, 107.

Anderson, H.C., Hsu, H.H.T., Morris, D.C., Fedde, K.N., Whyte, M.P., 1997. Matrix vesicles in osteomalacic hypophosphatasia bone contain apatite-like mineral crystals. Am. J. Pathol. 151, 1555–1561.

Anderson, H.C., Sipe, J.B., Hessle, L., Dhanyamraju, R., Atti, E., Camacho, N.P., Millán, J.L., 2004. Impaired calcification around matrix vesicles of growth plate and bone in alkaline phosphatase-deficient mice. Am. J. Pathol. 164, 841–847.

Barcia, J.P., Strife, C.F., Langman, C.B., 1997. Infantile hypophosphatasia: treatment options to control hypercalcemia, hypercalciuria, and chronic bone demineralization. J. Pediatr. 130, 825.

Baumgartner-Sigl, S.B., Haberlandt, E., Mumm, S., Sergi, C., Ryan, L., Ericson, K.L., Whyte, M.P., Högler, W., 2007. Pyridoxine-responsive seizures as the first symptom of infantile hypophosphatasia caused by two novel missense mutations (c.677T . C, p.M226T; c.1112C . T, p.T371I) of the tissue-nonspecific alkaline phosphatase gene. Bone 40, 1655–1661.

Birge, S.J., Gilbert, H.R., 1974. Identification of an intestinal sodium and calcium-dependent phosphate stimulated by parathyroid hormone. J. Clin. Investig. 54, 710–717.

Birkett, D.J., Dowe, J., Neale, F.C., Posen, S., 1966. Serum alkaline phosphatase in pregnancy: an immunological study. Br. Med. J. 5497, 1210–1212.

Brun-Heath, I., Taillandier, A., Serre, J.L., Nirbet, E., 2005. Characterization of 11 novel mutations in the tissue non-specific alkaline phosphatase gene responsible for hypophosphatasia and genotype-phenotype correlations. Mol. Genet. Metabol. 84, 273–277.

Cahill, R.A., Wenkert, D., Perlman, S.A., Steele, A., Coburn, S.P., McAlister, W.H., Mumm, S., Whyte, M.P., 2007. Infantile hypophosphatasia: trial of transplantation therapy using bone fragments and cultured osteoblasts. J. Clin. Endocrinol. Metab. 92, 2923–2930.

Cai, G., Michigami, T., Yamamoto, T., Yasui, N., Satomura, K., Yamagata, M., Shima, M., Nakajima, S., Mushiake, S., Okada, S., Ozono, K., 1998. Analysis of localization of mutated tissue-nonspecific alkaline phosphatase proteins associated with neonatal hypophosphatasia using green fluorescent protein chimeras. J. Clin. Endocrinol. Metab. 83, 3936–3942.

Camacho, P.M., Mazhari1, A.M., Wilczynski1, C., Kadanoff, R., Mumm, S., Whyte, M.P., 2016. Adult hypophosphatasia treated with teriparatide: report of 2 patients and review of the literature. Endocr. Pract. 22, 941–950.

Caswell, A.M., Whyte, M.P., Russell, R.G., 1991. Hypophosphatasia and the extracellular metabolism of inorganic pyrophosphate: clinical and laboratory aspects. CRC Crit. Rev. Clin. Lab. Sci. 28, 175–232.

Caswell, A.M., Whyte, M.P., Russell, R.G., 1986. Normal activity of nucleoside triphosphate pyrophosphatase in alkaline phosphatase-deficient fibroblasts from patients with infantile hypophosphatasia. J. Clin. Endocrinol. Metab. 63, 1237–1241.

Chaidaroglou, A., Kantrowitz, E.R., 1993. The Ala-161 β Thr substitution in *Escherichia coli* alkaline phosphatase does not result in loss of enzymatic activity although the homologous mutation in humans causes hypophosphatasia. Biochem. Biophys. Res. Commun. 193, 1104–1109.

Chodirker, B.N., Coburn, S.P., Seargeant, L.E., Whyte, M.P., Greenberg, C.R., 1990. Increased plasma pyridoxal-59-phosphate levels before and after pyridoxine loading in carriers of perinatal/infantile hypophosphatasia. J. Inherit. Metab. Dis. 13, 891–896.

Coburn, S.P., Whyte, M.P., 1988. Role of phosphatases in the regulation of vitamin B_6 metabolism in hypophosphatasia and other disorders. In: Leklem, J.E., Reynolds, R.D. (Eds.), Clinical and Physiological Applications of Vitamin B6. A. R. Liss, New York, pp. 65–93.

Coburn, S.P., Mahuren, J.D., Jain, M., Zubovic, Y., Wortsman, J., 1998. Alkaline phosphatase (EC 3.1.3.1) in serum is inhibited by physiological concentrations of inorganic phosphate. J. Clin. Endocrinol. Metab. 83, 3951–3957.

Coe, J.D., Murphy, W.A., Whyte, M.P., 1986. Management of femoral fractures and pseudofractures in adult hypophosphatasia. J. Bone Jt. Surg. 68-A, 981–990.

Cole, D.E.C., Stinson, R.A., Coburn, S.P., Ryan, L.M., Whyte, M.P., 1986. Increased serum pyridoxa1−5′−phosphate in pseudohypophosphatasia. N. Engl. J. Med. 314, 992−993.

DeBernard, B., Bianco, P., Bonucci, E., Costantini, M., Lunazzi, G.C., Martinuzzi, P., Modricky, C., Moro, L., Panfili, E., Pollesello, P., Stagni, N., Vittor, F., 1986. Biochemical and immunohistochemical evidence that in cartilage an alkaline phosphatase is a Ca21-binding glycoprotein. J. Cell Biol. 103, 1615−1623.

Dolphin, D., Poulson, R., Avramovic, O., 1986. Vitamin B_6 Pyridoxal Phosphate: Clinical, Biochemical and Medical Aspects: Part B. Wiley, New York.

Drezner, M.K., Whyte, M.P., 2018. Heritable renal phosphate wasting disorders, chapter #40. In: Thakker, R.V., Whyte, M.P., Eisman, J., Igarashi, T. (Eds.), Genetics of Bone Biology and Skeletal Disease. Elsevier (Academic Press), San Diego, CA, pp. 759−780.

El-Labban, N.G., Lee, K.W., Rule, D., 1991. Permanent teeth in hypophosphatasia: light and electron microscopic study. J. Oral Pathol. Med. 20, 352−360.

Faas, F.H., Wadkins, C.L., Daniels, J.S., Davis, G.R., Carter, W.J., Wynn, J.O., 1974. Hyperparathyroidism in an elderly adult with hypophosphatasia. Clin. Orthop. Relat. Res. 101, 216−219.

Fallon, M.D., Whyte, M.P., Teitelbaum, S.L., 1980. Stereospecific inhibition of alkaline phosphatase by L-tetramisole prevents in vitro cartilage calcification. Lab. Invest. 43, 489−494.

Fallon, M.D., Teitelbaum, S.L., Weinstein, R.S., Goldfischer, S., Brown, D.M., Whyte, M.P., 1984. Hypophosphatasia: clinicopathologic comparison of the infantile, childhood, and adult forms. Medicine 63, 12−24.

Fallon, M.D., Whyte, M.P., Weiss, M., Harris, H., 1989. Molecular biology of hypophosphatasia: a point mutation or small deletion in the bone/liver/kidney alkaline phosphatase gene results in an intact but functionally inactive enzyme. J. Bone Miner. Res. 4, S-304 [Abstract].

Farley, J.R., 1991. Phosphate regulates the stability of skeletal alkaline phosphatase activity in human osteosarcoma (SaOS-2) cells without equivalent effects on the level of skeletal alkaline phosphatase immuno-reactive protein. Calcif. Tissue Int. 57, 371−378.

Fedde, K.N., Lane, C.C., Whyte, M.P., 1988. Alkaline phosphatase in an ectoenzyme that acts on micromolar concentrations of natural substrates at physiologic pH in human osteosarcoma (SAOS-2) cells. Arch. Biochem. Biophys. 264, 400−409.

Fedde, K.N., Lane, C.C., Whyte, M.P., 1990. Alkaline phosphatase: (tissue nonspecific isoenzyme) is a phosphoethanolamine and pyridoxal 59-phosphate ectophosphatase: normal and hypophosphatasia fibroblast study. Am. J. Hum. Genet. 47, 767−775.

Fedde, K.N., Michel, M.P., Whyte, M.P., 1993. Evidence against a role for alkaline phosphatase in the dephosphorylation of plasma membrane proteins: hypophosphatasia fibroblast study. J. Cell. Biochem. 53, 43−50.

Fedde, K.N., Michell, M., Henthorn, P.S., Whyte, M.P., 1996. Aberrant properties of alkaline phosphatase in patient fibroblasts correlate with clinical expressivity in severe forms of hypophosphatasia. J. Clin. Endocrinol. Metab. 81, 2587−2594.

Fedde, K.N., Blair, L., Silverstein, J., Coburn, S.P., Ryan, L.M., Weinstein, R.S., Waymire, K., Narisawa, S., Millan, J.L., MacGregor, G.R., Whyte, M.P., 1999. Alkaline phosphatase knock-out mice recapitulate the metabolic and skeletal defects of infantile hypophosphatasia. J. Bone Miner. Res. 14, 2015−2026.

Foster, B.L., Sheen, C.R., Hatch, N.E., Liu, J., Cory, E., Narisawa, S., Kiffer-Moreira, T., Sah, R.L., Whyte, M.P., Somerman, M.J., Millan, J.L., 2015. Periodontal defects in the A116T knock-in mouse model of odontohypophosphatasia. J. Dent. Res. 94, 706−714.

Fraser, D., 1957. Hypophosphatasia. Am. J. Med. 22, 730−746.

Fraser, D., Laidlaw, J.C., 1956. Treatment of hypophosphatasia with cortisone, preliminary communication. Lancet 1, 553.

Fraser, D., Yendt, E.R., 1955. Metabolic abnormalities in hypophosphatasia. Am. J. Dis. Child. 90, 552−554.

Fraser, D., Yendt, E.R., Christie, F.H.E., 1955. Metabolic abnormalities in hypophosphatasia. Lancet 1, 286.

Fukushi, M., Amizuka, N., Hoshi, K., Ozawa, H., Kumagai, H., Omura, S., Misumi, Y., Ikehara, Y., Oda, K., 1998. Intracellular retention and degradation of tissue-nonspecific alkaline phosphatase with a Gly317-Asp substitution associated with lethal hypophosphatasia. Biochem. Biophys. Res. Commun. 246, 613−618.

Gorodischer, R., Davidson, R.G., Mosovich, L.L., Yaffe, S.J., 1976. Hypophosphatasia: a developmental anomaly of alkaline phosphatase? Pediatr. Res. 10, 650−656.

Goseki-Sone, M., Yamada, A., Asahi, K., Hirota, A., Ezawa, I., Iimura, T., 1999. Phosphate depletion enhances tissue-nonspecific alkaline phosphatase gene expression in a cultured mouse marrow stromal cell line ST2. Biochem. Biophys. Res. Commun. 265, 24−28.

Greenberg, C.R., Taylor, C.L.D., Haworth, J.C., Seargeant, L.E., Phillips, S., Triggs-Raine, B., Chodirker, B.N., 1993. A homoallelic Gly317 β Asp mutation in ALPL causes the perinatal (lethal) form of hypophosphatasia in Canadian Mennonites. Genomics 17, 215−217.

Gron, I.H., 1978. Mammalian O-phosphorylethanolamine phospholyase activity and its inhibition. Scand. J. Clin. Lab. Invest. 38, 107−112.

Guañabens, N., Mumm, S., Möller, I., González-Roca, E., Peris, P., Demertzis, J.L., Whyte, M.P., 2014. Calcific periarthritis as the only clinical manifestation of hypophosphatasia in middle-aged sisters. J. Bone Miner. Res. 29, 929−934.

Harris, H., 1980. The Principles of Human Biochemical Genetics, third ed. Elsevier, North Holland, Amsterdam.

Harris, H., 1990. The human alkaline phosphatases: what we know and what we don't know. Clin. Chim. Acta 186, 133−150.

Heinonen, J.K., 2001. Biological Role of Inorganic Pyrophosphate. Kluwer Academic Publishers, Norwell, MA.

Henthorn, P.S., Whyte, M.P., 1992. Missense mutations of the tissue nonspecific alkaline phosphatase gene in hypophosphatasia. Clin. Chem. 38, 2501−2505.

Henthorn, P.S., Whyte, M.P., 1995. Infantile hypophosphatasia: successful prenatal assessment by testing for tissue-nonspecific alkaline phosphatase gene mutations. Prenat. Diagn. 15, 1001−1006.

Henthorn, P.S., Raducha, M., Fedde, K.N., Lafferty, M.A., Whyte, M.P., 1992. Different missense mutations at the tissue-non-specific alkaline phosphatase gene locus in autosomal recessively inherited forms of mild and severe hypophosphatasia. Proc. Natl. Acad. Sci. U.S.A. 89, 9924−9928.

Hessle, L., Johnson, K.A., Anderson, H.C., Narisawa, S., Sali, A., Goding, J.W., Terkeltaub, R., Millan, J.L., 2002. Tissue-nonspecific alkaline phosphatase and plasma cell membrane glycoprotein-1 are central antagonistic regulators of bone mineralization. Proc. Natl. Acad. Sci. U.S.A. 99, 9445–9449.

Hotton, D., Mauro, N., Lézot, F., Forest, N., Berdal, A., 1999. Differential expression and activity of tissue-nonspecific alkaline phosphatase (TNAP) in rat odontogenic cells in vivo. J. Histochem. Cytochem. 47, 1541–1552.

Hough, T.A., Polewski, M., Johnson, K., Cheeseman, M., Nolan, P.M., Vizor, L., Rastan, S., Boyde, A., Pritzker, K., Hunter, A.J., Fisher, E.M., Terkeltaub, R., Brown, S.D., 2007. Novel mouse model of autosomal semidominant adult hypophosphatasia has a splice site mutation in the tissue nonspecific alkaline phosphatase gene Akp2. J. Bone Miner. Res. 22, 1397–1407.

Hoylaerts, M.F., Millan, J.L., 1991. Site-directed mutagenesis and epitope mapped monoclonal antibodies define a catalytically important conformational difference between human placental and germ cell alkaline phosphatase. Eur. J. Biochem. 202, 605–616.

Iqbal, S.J., Davies, T., Holland, S., Manning, T., Whittaker, P., 2000. Alkaline phosphatase isoenzymes and clinical features in hypophosphatasia. Ann. Clin. Biochem. 37, 775–780.

Ish-Shalom, S., Budden, F., Fraser, D., Harrison, J., Josse, R.G., Kirsh, J., Kooh, S.W., Patt, N., Reilly, B.J., Strauss, A., Tam, C., 1986. A follow-up of hypophosphatasia from infancy to adulthood. In: Presented at the Annual Meeting of the Pediatric Working Group, American Society for Bone and Mineral Research, 8th Annual Scientific Meeting, Anaheim, CA, June 21–24, 1986 [Abstract].

Johnson, K.A., Hessle, L., Vaingankar, S., Wennberg, C., Mauro, S., Narisawa, S., Goding, J.W., Sano, K., Millan, J.L., Terkeltaub, R., 2000. Osteoblast tissue-nonspecific alkaline phosphatase antagonizes and regulates PC-1. Am. J. Physiol. 279, R1365–R1377.

Juan, D., Lambert, P.W., 1981. Vitamin D. Metabolism and phosphorus absorption studies in a case of coexistent vitamin D resistant rickets and hypophosphatasia. In: Cohn, D.V., Talmage, R.V., Matthews, J.L. (Eds.), Hormonal Control of Calcium Metabolism. Excerpta Medica, Amsterdam. International Congress Series 511.

Kanis, J., 2002. Pathophysiology and Treatment of Paget's Disease of Bone, second ed. Lippincott Williams & Wilkins, Philadelphia, pp. 985–1020.

Khandwala, H.M., Mumm, S., Whyte, M.P., 2006. Low serum alkaline phosphatase activity with pathologic fracture: case report and brief review of adult hypophosphatasia. Endocr. Pract. 12, 676–680.

Khouja, H.I., Bevington, A., Kemp, G.J., Russell, R.G., 1990. Calcium and orthophosphate deposits in vitro do not imply osteoblast-medicated mineralization: mineralization by beta-glycerophosphate in the absence of osteoblasts. Bone 11, 385–391.

Kiledjian, M., Kadesch, T., 1990. Analysis of the human liver/bone/kidney alkaline phosphatase promoter in vivo and in vitro. Nucleic Acids Res. 18, 957–961.

Kim, E.E., Wyckoff, H.W., 1991. Reaction mechanism of alkaline phosphatase based on crystal structures. Two metal ion catalysis. J. Mol. Biol. 218, 449–464.

Kishnani, P.S., Rockman-Greenberg, C., Rauch, F., Bhatti, M.T., Moseley, S., Denker, A.E., Watsky, E., Whyte, M.P., 2019. Five-year efficacy and safety of asfotase alfa for adults and adolescents with hypophosphatasia. Bone 121, 149–162.

Kyöstilä, K., Syrjä, P., Lappalainen, A.K., Arumilli, M., Hundi, S., Karkamo, V., Viitmaa, R., Hytönen, M.K., Lohi, H., 2019. A homozygous missense variant in the alkaline phosphatase gene ALPL is associated with a severe form of canine hypophosphatasia. Sci. Rep. 9, 973.

Langman, M.J., Leuthold, E., Robson, E.B., Harris, J., Luffman, J.E., Harris, H., 1966. Influence of diet on the "intestinal" component of serum alkaline phosphatase in people of different ABO blood groups and secretor status. Nature 212, 41–43.

Lassere, M.N., Jones, J.G., 1990. Recurrent calcific periarthritis, erosive osteoarthritis and hypophosphatasia: a family study. J. Rheumatol. 17, 1244–1248.

Lau, K.H., Farley, J.R., Baylink, D.J., 1985. Phosphotyrosyl-specific protein phosphatase activity of a bovine skeletal acid phosphatase isoenzyme: comparison with the phosphotyrosyl protein phosphatase activity of skeletal alkaline phosphatase. J. Biol. Chem. 260, 4653–4660.

Le Due, H.M., Stigbrand, T., Taussig, M.J., Ménez, A., Stura, E.A., 2000. Crystal structure of alkaline phosphatase from human placenta at 1.8 Å resolution. J. Biol. Chem. 275 (2), 9158–9165.

Lepe, X., Rothwell, B.R., Banich, S., Page, R.C., 1997. Absence of adult dental anomalies in familial hypophosphatasia. J. Periodontal. Res. 32, 375–380.

Leung, E.C.W., Mhanni, A.A., Reed, M., Whyte, M.P., Landy, H., Greenberg, C.R., 2013. Outcome of perinatal hypophosphatasia in Manitoba Mennonites: a retrospective cohort analysis. JIMD Rep. 11, 73–78.

Licata, A.A., Radfor, N., Bartter, F.C., Bou, E., 1978. The urinary excretion of phosphoethanolamine in diseases other than hypophosphatasia. Am. J. Med. 64, 133–138.

Low, M.G., Saltiel, A.R., 1988. Structural and functional roles of glycosyl-phosphatidylinositol in membranes. Science 239, 268–275.

Low, M.G., Zilversmit, D.B., 1980. Role of phosphatidylinositol in attachment of alkaline phosphatase to membranes. Biochemistry 19, 3913–3918.

Lundgren, T., Westphal, O., Bolme, P., Modeer, T., Noren, J.G., 1991. Retrospective study of children with hypophosphatasia with reference to dental changes. Scand. J. Dent. Res. 99, 357–364.

Macfarlane, J.D., Souverijn, J.H., Breedveld, F.C., 1992. Clinical significance of a low serum alkaline phosphatase. Neth. J. Med. 40, 9–14.

Macpherson, R.I., Kroeker, M., Houston, C.S., 1972. Hypophosphatasia. Can. Assoc. Radiol. J. 23, 16–26.

Madson, K.L., Gill, S.S., Mumm, S., Whyte, M.P., 2015. Pseudohypophosphatasia: mutation identification and 46-year follow-up of the original patient. Submitted for presentation at the ASBMR 2015 Annual Meeting on October 9-12, 2015 in Seattle, Washington, USA J. Bone Miner. Res. 30 (Suppl. 1), S190.

Majeska, R.J., Wuthier, R.E., 1975. Studies on matrix vesicles isolated from chick epiphyseal cartilage. Association of pyrophosphatase and ATPase activities with alkaline phosphatase. Biochim. Biophys. Acta 391, 51–60.

Makiya, R., Thornell, L.E., Stigbrand, T., 1992. Placental alkaline phosphatase, a GPI-anchored protein, is clustered in clathrin-coated vesicles. Biochem. Biophys. Res. Commun. 183, 803–808.

McCance, R.A., Morrison, A.B., Dent, C.E., 1955. The excretion of phosphoethanolamine and hypophosphatasia. Lancet 1, 131.

McComb, R.B., Bowers Jr., G.N., Posen, S., 1979. Alkaline Phosphatase. Plenum, New York.

McKiernan, F.E., Berg, R.L., Fuehrer, J., 2014. Clinical and radiographic findings in adults with persistent hypophosphatasemia. J. Bone Miner. Res. 29, 1651–1660.

Millan, J.L., 1988. Oncodevelopmental expression and structure of alkaline phosphatase genes. Anticancer Res. 8, 995–1004.

Millan, J.L., 2006. Mammalian Alkaline Phosphatases: From Biology to Applications in Medicine and Biotechnology. Wiley-VCH, Weinheim, Germany.

Millan, J.L., Whyte, M.P., 2016. Alkaline phosphatase and hypophosphatasia. Calcif. Tissue Int. 98, 398–416.

Millan, J.L., Whyte, M.P., Avioli, L.V., Fishman, W.H., 1980. Hypophosphatasia (adult form): quantitation of serum alkaline phosphatase isoenzyme activity in a large kindred. Clin. Chem. 26, 840–845.

Millan, J.L., Narisawa, S., Lemire, I., Loisel, T.P., Boileau, G., Leonard, P., Gramatikova, S., Terkeltaub, R., Camacho, N.P., McKee, M., Crine, P., Whyte, M.P., 2008. Enzyme replacement therapy for murine hypophosphatasia. J. Bone Miner. Res. 23, 777–787.

Moore, C.A., Curry, C.J.R., Henthorn, P.S., Smith, J.A., Smith, J.C., O'Lague, P., Coburn, S.P., Weaver, D.D., Whyte, M.P., 1999. Mild autosomal dominant hypophosphatasia: in utero presentation in two families. Am. J. Med. Genet. 86, 410–415.

Mornet, E., Taillandier, A., Peyramaure, S., Kaper, F., Mulle, F., Brenner, R., Bussiere, P., Freisinger, P., Godard, J., Le Merrer, M., Oury, J.F., Plauchu, H., Puddy, R., Rival, J.M., Superti-Furga, A., Touraine, R.L., Serre, J.L., Simon-Bouy, B., 1998. Identification of fifteen novel mutations in the tissue-nonspecific alkaline phosphatase (TNSALP) gene in European patients with severe hypophosphatasia. Eur. J. Hum. Genet. 6, 308–845.

Moss, D.W., 1992. Perspectives in alkaline phosphatase research. Clin. Chem. 28, 2486–2492.

Moss, D.W., Whitaker, K.B., 1985. Modification of alkaline phosphatases by treatment with glycosidases. Enzyme 34, 212–216.

Moss, D.W., Eaton, R.H., Smith, J.K., Whitby, L.G., 1967. Association of inorganic pyrophosphatase activity with human alkaline phosphatase preparations. Biochem. J. 102, 53–57.

Mueller, H.D., Stinson, R.A., Mohyuddin, F., Milne, J.K., 1983. Isoenzymes of alkaline phosphatase in infantile hypophosphatasia. J. Lab. Clin. Med. 102, 24–30.

Mulivor, R.A., Boccelli, D., Harris, H., 1985. Quantitative analysis of alkaline phosphatases in serum and amniotic fluid: comparison of biochemical and immunologic assays. J. Lab. Clin. Med. 105, 342–348.

Muller, K., Schellenberger, V., Borneleit, P., Treide, A., 1991. The alkaline phosphatase from bone: transphosphorylating activity and kinetic mechanism. Biochim. Biophys. Acta 1076, 308–313.

Mumm, S.R., Jones, J., Finnegan, P., Whyte, M.P., 2001. Hypophosphatasia: molecular diagnosis of Rathbun's original case. J. Bone Miner. Res. 16, 1724–1727.

Mumm, S.R., Jones, J., Finnegan, P., Henthorn, P.S., Podgornik, M.N., Whyte, M.P., 2002. Denaturing gradient gel electrophoresis analysis of the tissue nonspecific alkaline phosphatase isoenzyme gene in hypophosphatasia. Mol. Genet. Metabol. 75, 143–153.

Mumm, S., Wenkert, D., Zhang, X., Geimer, M., Zerega, J., Whyte, M.P., 2006. Hypophosphatasia: the c.1133A . t, p.D378V transversion is the most common American TNSALP mutation. J. Bone Miner. Res. 21, S115 [Abstract].

Narisawa, S., Hofmann, M.C., Ziomek, C.A., Millan, J.L., 1992. Embryonic alkaline phosphatase is expressed at M-phase in the spermatogenic lineage of the mouse. Development 116, 159–165.

Narisawa, S., Fröhlander, N., Millán, J.L., 1997. Inactivation of two mouse alkaline phosphatase genes and establishment of a model of infantile hypophosphatasia. Dev. Dynam. 208, 432–465.

Narisawa, S., Wennberg, C., Millán, J.L., 2001. Abnormal vitamin B_6 metabolism in alkaline phosphatase knock-out mice causes multiple abnormalities, but not the impaired bone mineralization. J. Pathol. 193, 125–133.

Neuman, W.F., Neuman, M.W., 1957. Emerging concepts of the structure and metabolic functions of bone. Am. J. Med. 22, 123–131.

Nosjean, O., Koyama, I., Goseki, M., Roux, B., Komoda, T., 1997. Human tissue-nonspecific alkaline phosphatase: sugar-moiety-induced enzymic and antigenic modulations and genetic aspects. Biochem. J. 321, 297–303.

O'Duffy, J.D., 1970. Hypophosphatasia associated with calcium pyrophosphate dihydrate deposits in cartilage. Arthritis Rheum. 13, 381–388.

OMIM. Online Mendelian Inheritance in Man, OMIM (TM). Available at: http://www.ncbi.nlm.nih.gov/sites/entrez.

Ornoy, A., Adomian, G.E., Rimoin, D.L., 1985. Histologic and ultrastructural studies on the mineralization process in hypophosphatasia. Am. J. Med. Genet. 22, 743–758.

Pauli, R.M., Modaff, P., Sipes, S.L., Whyte, M.P., 1999. Mild hypophosphatasia mimicking severe osteogenesis imperfecta in utero: bent but not broken. Am. J. Med. Genet. 86, 434–438.

Rasmussen, K., 1968. Phosphorylethanolamine and hypophosphatasia. Dan. Med. Bull. 15 (Suppl. II), 1–112.

Rathbun, J.C., 1948. Hypophosphatasia, a new developmental anomaly. Am. J. Dis. Child. 75, 822–831.

Robison, R., 1923. The possible significance of hexosephosphoric esters in ossification. Biochem. J. 17, 286–293.

Robison, R., 1932. The Significance of Phosphoric Esters in Metabolism. New York University Press, New York.

Robison, R., Soames, K.M., 1924. The possible significance of hexosephosphoric esters in ossification. II. The phosphoric esterase of ossifying cartilage. Biochem. J. 18, 740–754.

Royce, P.M., Blumberg, A., Zurbrugg, R.P., Zimmermann, A., Colombo, J.P., Steinmann, B., 1988. Lethal osteogenesis imperfecta: abnormal collagen metabolism and biochemical characteristics of hypophosphatasia. Eur. J. Pediatr. 147, 626–631.

Russell, R.G.G., 1965. Excretion of inorganic pyrophosphate in hypophosphatasia. Lancet 2, 461–464.

Russell, R.G., Bisaz, S., Donath, A., Morgan, D.B., Fleisch, H., 1971. Inorganic pyrophosphate in plasma in normal persons and in patients with hypophosphatasia, osteogenesis imperfecta, and other disorders of bone. J. Clin. Investig. 50, 961–969.

Scriver, C.R., Cameron, D., 1969. Pseudohypophosphatasia. N. Engl. J. Med. 281, 604.

Seetharam, B., Tiruppathi, C., Alpers, D.H., 1987. Hydrophobic interactions of brush border alkaline phosphatases. The role of phosphatidyl inositol. Arch. Biochem. Biophys. 253, 189–198.

Seshia, S.S., Derbyshire, G., Haworth, J.C., Hoogstraten, J., 1990. Myopathy with hypophosphatasia. Arch. Dis. Child. 65, 130–131.

Shibata, H., Fukushi, M., Igarashi, A., Misumi, Y., Ikehara, Y., Ohashi, Y., Oda, K., 1998. Defective intracellular transport of tissue-nonspecific alkaline phosphatase with an Ala162-Thr mutation associated with lethal hypophosphatasia. J. Biochem. 123, 967–977.

Shohat, M., Rimoin, D.L., Gruber, H.E., Lachman, R.S., 1991. Perinatal lethal hypophosphatasia: clinical, radiologic and morphologic findings. Pediatr. Radiol. 21, 421–427.

Siller, A.F., Whyte, M.P., 2018. Alkaline phosphatase: discovery and naming of our favorite enzyme. J. Bone Miner. Res. 33, 362–364.

Silver, M.M., Vilos, G.A., Milne, K.J., 1988. Pulmonary hypoplasia in neonatal hypophosphatasia. Pediatr. Pathol. 8, 483–493.

Simko, V., 1991. Alkaline phosphatases in biology and medicine. Dig. Dis. 9, 189–209.

Sobel, E.H., Clark, L.C., Fox, R.P., Robinow, M., 1953. Rickets, deficiency of "alkaline" phosphatase activity and premature loss of teeth in childhood. Pediatrics 11, 309–321.

Sorensen, S.A., Flodgaard, H., Sorensen, E., 1978. Serum alkaline phosphatase, serum pyrophosphatase, phosphorylethanolamine and inorganic pyrophosphate in plasma and urine. A genetic and clinical study of hypophosphatasia. Monogr. Hum. Genet. 10, 66–69.

Stevenson, D. A., Carey, J. C., Coburn, S. P., Ericson, K. L., Byrne, J. L. B.,Mumm, S., and Whyte, M. P. Autosomal recessive hypophosphatasia manifesting *in utero* with long bone deformity but showing spontaneous postnatal improvement. J. Clin. Endocrinol. Metab. (in press).

Stigbrand, T., Fishman, W.H., 1984. Human Alkaline Phosphatases. A. R. Liss, New York.

Sutton, R.A.L., Mumm, S., Coburn, S.P., Ericson, K.L., Whyte, M.P., 2012. "Atypical femoral fractures" during bisphosphonate exposure in adult hypophosphatasia. J. Bone Miner. Res. 27, 987–994.

Taillander, A., Lia-Bladini, A.S., Mouchard, M., Robin, B., Muller, F., Simon-Bouy, B., Serre, J.L., Bera-Louville, M., Bondulle, M., Eckhrdt, J., Gaillard, D., Myhre, A.G., Kortge-Jung, S., Larget-Piet, L., Malou, E., Sillence, D., Temple, I.K., Viot, G., Mornet, E., 2001. Twelve novel mutations in the tissue-nonspecific alkaline phosphatase gene (ALPL) in patients with various forms of hypophosphatasia. Hum. Mutat. 18, 83–84.

Takahashi, T., Iwantanti, A., Mizuno, S., Morishita, Y., Nishio, H., Kodama, S., Matsuo, T., 1984. The relationship between phosphoethanolamine level in serum and intractable seizure on hypophosphatasia infantile form. In: Cohn, D.V., Fugita, T., Potts Sr., J.T., Talmage, R.V. (Eds.), Endocrine Control of Bone and Calcium Metabolism, vols. 8-B. Excerpta Medica, Amsterdam, pp. 93–94.

Terheggen, H.G., Wischermann, A., 1984. Congenital hypophosphatasia. Monatsschr. Kinderheilkd. 132, 512–522.

Tiosano, D., Hochberg, A., 2009. Hypophosphatemia: the common denominator of all rickets. J. Bus. Manag. Res. 27, 392, 40.

Tsonis, P.A., Argraves, W.S., Millan, J.L., 1988. A putative functional domain of human placental alkaline phosphatase predicted from sequence comparisons. Biochem. J. 254, 623–624.

Tsutsumi, M., Alvarez, U.M., Scott, M.J., Avioli, L.V., Whyte, M.P., 1986. Phospholipid metabolism in cultured skin fibroblasts from patients with infantile hypophosphatasia. J. Bone Miner. Res. 1, 72 [Abstract].

Unger, S., Mornet, E., Mondlos, S., Blaser, S., Cole, D.E.C., 2002. Severe cleidocranial dysplasia can mimic hypophosphatasia. Eur. J. Pediatr. 161, 623–626.

Van den Bos, T., Handoko, G., Niehof, A., Ryan, L.M., Coburn, S.P., Whyte, M.P., Beertsen, W., 2005. Cementum and dentin in hypophosphatasia. J. Dent. Res. 84, 1021–1025.

Van Dongen, P.W., Hamel, B.C., Nijhuis, J.G., de Boer, C.N., 1990. Prenatal follow-up of hypophosphatasia by ultrasound: case report. Eur. J. Obstet. Gynecol. Reprod. Biol. 34, 283–288.

Vanneuville, F.J., Leroy, L.G., 1981. Enzymatic diagnosis of congenital lethal hypophosphatasia in tissues, plasma, and diploid skin fibroblasts. J. Inherit. Metab. Dis. 4, 129–130.

Waymire, K.G., Mahuren, J.D., Jaje, J.M., Guilarte, T.R., Coburn, S.P., MacGregor, G.R., 1995. Mice lacking tissue non-specific alkaline phosphatase die from seizures due to defective metabolism of vitamin B-6. Nat. Genet. 11, 45–51.

Weinstein, R.S., Whyte, M.P., 1981. Fifty year follow-up of hypophosphatasia. Arch. Intern. Med. 141, 1720–1721 [Letter].

Weiss, M.J., Cole, D.E., Ray, K., Whyte, M.P., Lafferty, M.A., Mulivor, R.A., Harris, H., 1988a. A missense mutation in the human liver/bone/kidney alkaline phosphatase gene causing a lethal form of hypophosphatasia. Proc. Natl. Acad. Sci. U.S.A. 85, 7666–7669.

Weiss, M.J., Ray, K., Henthorn, P.S., Lamb, B., Kadesch, T., Harris, H., 1988b. Structure of the human liver/bone/kidney alkaline phosphatase gene. J. Biol. Chem. 263, 12002–12010.

Weninger, M., Stinson, R.A., Plenk Jr., H., Bock, P., Pollack, A., 1989. Biochemical and morphological effects of human hepatic alkaline phosphatase in a neonate with hypophosphatasia. Acta Paediatr. Scand. 360 (Suppl. l.), 154–160.

Wenkert, D., McAlister, W.H., Hersh, J.H., Mumm, S., Whyte, M.P., 2005. Hypophosphatasia: misleading in utero presentation for the childhood and odonto forms. J. Bone Miner. Res. 20 (Suppl. 1), S418 [Abstract].

Wenkert, D., Podgornik, M.N., Coburn, S.P., Ryan, L.M., Mumm, S., Whyte, M.P., 2002. Dietary phosphate restriction therapy for hypophosphatasia: preliminary observations. J. Bone Miner. Res. 17 (Suppl. 1), S384 [Abstract].

Wenkert, D., McAlister, W.H., Coburn, S.P., Zerega, J.A., Ryan, L.M., Ericson, K.L., Hersh, J.H., Mumm, S., Whyte, M.P., 2011. Hypophosphatasia: non-lethal disease despite skeletal presentation in utero (17 New Cases and Literature Review). J. Bone Miner. Res. 26, 2389–2398.

Wennberg, C., Hessle, L., Lundberg, P., Mauro, S., Narisawa, S., Lerner, U.H., Millán, J.L., 2000. Functional characterization of osteoblasts and osteoclasts from alkaline phosphatase knockout mice. J. Bone Miner. Res. 15, 1879–1888.

Whyte, M.P., 1988. Spur-limbed dwarfism in hypophosphatasia. Dysmorphol. Clin. Genet. 2, 126–127 [Letter].

Whyte, M.P., 1989. Alkaline phosphatase: physiologic role explored in hypophosphatasia. In: Peck, W.A. (Ed.), Bone and Mineral Research. Elsevier Science Publishers BV (Biomedical Division), Amsterdam.

Whyte, M.P., 1994. Hypophosphatasia and the role of alkaline phosphatase in skeletal mineralization. Endocr. Rev. 15, 439–461.

Whyte, M.P., 2000. Hypophosphatasia. In: Econs, M.J. (Ed.), The Genetics of Osteoporosis and Metabolic Bone Disease. Humana Press, Totowa, NJ, pp. 335–356.

Whyte, M.P., 2001. Hypophosphatasia. In: Scriver, C.R., Beaudet, A.L., Sly, W.S., Valle, D. (Eds.), The Metabolic and Molecular Bases of Inherited Disease, eighth ed. McGraw-Hill, New York, pp. 5313–5329.

Whyte, M.P., 2002. Rickets and osteomalacia (acquired and heritable forms). In: Wass, J.A.H., Shalet, S.M. (Eds.), The Oxford Textbook of Endocrinology and Diabetes. Oxford University Press, New York.

Whyte, M.P., 2009. Atypical femoral fractures, bisphosphonates, and adult hypophosphatasia. J. Bone Miner. Res. 24, 1132–1134.

Whyte, M.P., 2016. Hypophosphatasia: aetiology, nosology, pathogenesis, diagnosis and treatment. Nat. Rev. Endocrinol. 12, 233–246.

Whyte, M.P., 2017a. Hypophosphatasia: an overview for 2017. Bone 102, 15–25.

Whyte, M.P., 2017b. Hypophosphatasia: enzyme replacement therapy brings new opportunities and new challenges. J. Bone Miner. Res. 32, 667–675.

Whyte, M.P., 2018. Hypophosphatasia and how alkaline phosphatase promotes mineralization. Chapter #28. In: Thakker, R.V., Whyte, M.P., Eisman, J., Igarashi, T. (Eds.), Genetics of Bone Biology and Skeletal Disease. second ed. Elsevier (Academic Press), San Diego, CA, pp. 481–504.

Whyte, M.P., 2019. Hypophosphatasia and other enzyme deficiencies affecting the skeleton Chapter #115. In: Primer on Metabolic Bone Diseases and Disorders of Mineral Metabolism, ninth ed. American Society for Bone and Mineral Research, Wiley-Blackwell, pp. 886–890.

Whyte, M.P., Rettinger, S.D., 1987. Hyperphosphatemia due to enhanced renal reclamation of phosphate in hypophosphatasia. J. Bone Miner. Res. 2 (Suppl. 1) [Abstract 399].

Whyte, M.P., Seino, Y., 1982. Circulating vitamin D metabolite levels in hypophosphatasia. J. Clin. Endocrinol. Metab. 55, 178–181.

Whyte, M.P., Vrabel, L.A., 1983. Alkaline phosphatase-deficient hypophosphatasia fibroblasts: normal accumulation of inorganic phosphate in culture. Clin. Res. 31, 856A [Abstract].

Whyte, M.P., Vrabel, L.A., 1985. Infantile hypophosphatasia: genetic complimentation analyses with skin fibroblast heterokaryons suggest a defect(s) at a single gene locus. Clin. Res. 33, 332-A [Abstract].

Whyte, M.P., Vrabel, L.A., 1987. Infantile hypophosphatasia fibroblasts proliferate normally in culture: evidence against a role for alkaline phosphatase (tissue nonspecific isoenzyme) in the regulation of cell growth and differentiation. Calcif. Tissue Int. 40, 1–7.

Whyte, M.P., Murphy, W.A., Fallon, M.D., 1982a. Adult hypophosphatasia with chondrocalcinosis and arthropathy, variable penetrance of hypophosphatasemia in a large Oklahoma kindred. Am. J. Med. 72, 631–641.

Whyte, M.P., Valdes Jr., R., Ryan, L.M., McAlister, W.H., 1982b. Infantile hypophosphatasia: enzyme replacement therapy by intravenous infusion of alkaline phosphatase-rich plasma from patients with Paget's bone disease. J. Pediatr. 101, 379–386.

Whyte, M.P., Vrabel, L.A., Schwartz, T.D., 1983. Alkaline phosphatase deficiency in cultured skin fibroblasts from patients with hypophosphatasia: comparison of the infantile, childhood, and adult forms. J. Clin. Endocrinol. Metab. 57, 831–837.

Whyte, M.P., McAlister, W.H., Patton, L.S., Magill, H.L., Fallon, M.D., Lorentz, W.B., Herrod, H.G., 1984. Enzyme replacement therapy for infantile hypophosphatasia attempted by intravenous infusions of alkaline phosphatase-rich Paget plasma: results in three additional patients. J. Pediatr. 105, 926–933.

Whyte, M.P., Mahuren, J.D., Vrabel, L.A., Coburn, S.P., 1985. Markedly increased circulating pyridoxal-5′-phosphate levels in hypophosphatasia: alkaline phosphatase acts in vitamin B_6 metabolism. J. Clin. Investig. 76, 752–756.

Whyte, M.P., Magill, H.L., Fallon, M.D., Herrod, H.G., 1986. Infantile hypophosphatasia: normalization of circulating bone alkaline phosphatase activity followed by skeletal remineralization. Evidence for an intact structural gene for tissue nonspecific alkaline phosphatase. J. Pediatr. 108, 82–88.

Whyte, M.P., Rettinger, S.D., Vrabel, L.A., 1987. Infantile hypophosphatasia: enzymatic defect explored with alkaline phosphatase-deficient patient dermal fibroblasts in culture. Calcif. Tissue Int. 40, 244–252.

Whyte, M.P., Mahuren, J.D., Fedde, K.N., Cole, F.S., McCabe, E.R., Coburn, S.P., 1988. Perinatal hypophosphatasia: tissue levels of vitamin B_6 are unremarkable despite markedly increased circulating concentrations of pyridoxal-5′-phosphate. Evidence for an ectoenzyme role for tissue-nonspecific alkaline phosphatase. J. Clin. Investig. 81, 1234–1239.

Whyte, M.P., Habib, D., Coburn, S.P., Tecklenburg, F., Ryan, L., Fedde, K.N., Stinson, R.A., 1992. Failure of hyperphosphatasemia by intravenous infusion of purified placental alkaline phosphatase to correct severe hypophosphatasia: evidence against a role for circulating ALP in skeletal mineralization. J. Bone Miner. Res. 7 (Suppl. 1), S155 [Abstract].

Whyte, M.P., Landt, M., Ryan, L.M., Mulivor, R.A., Henthorn, P.S., Fedde, K.N., Coburn, S.P., 1995. Alkaline phosphatase: placental and tissue-nonspecific isoenzymes hydrolyze phosphoethanolamine, inorganic pyrophosphate, and pyridoxal 5′-phosphate (substrate accumulation in carriers of hypophosphatasia corrects during pregnancy). J. Clin. Investig. 95, 1440–1445.

Whyte, M.P., Walkenhorst, D.A., Fedde, K.N., Henthorn, P.S., Hill, C.S., 1996. Hypophosphatasia: levels of bone alkaline phosphatase isoenzyme immunoreactivity in serum reflect disease severity. J. Clin. Endocrinol. Metab. 81, 2142–2148.

Whyte, M.P., Eddy, M.C., D'Avignon, A., 2000. 31P-Nuclear magnetic resonance spectroscopy (NMRS) in hypophosphatasia: diagnostic urine profile indicating multiple new natural substrates for bone alkaline phosphatase. J. Bone Miner. Res. 15 (Suppl. 1), S483 [Abstract].

Whyte, M.P., Kurtzberg, J., McAlister, W.H., Mumm, S., Podgornik, M.N., Coburn, S.P., Ryan, L.M., Miller, C.R., Gottesman, G.S., Smith, A.K., Douville, J., Waters-Pick, B., Armstrong, R.D., Martin, P.L., 2003. Marrow cell transplantation for infantile hypophosphatasia. J. Bone Miner. Res. 18, 624–636.

Whyte, M.P., Essmyer, K., Geimer, M., Mumm, S., 2006. Homozygosity for TNSALP mutation 1348C.T (Arg433Cys) causes infantile hypophosphatasia manifesting transient disease correction and variably lethal outcome in a kindred of black ancestry. J. Pediatr. 148, 753–758.

Whyte, M.P., Mumm, S., Deal, C., 2007. Adult hypophosphatasia treated with teriparatide. J. Clin. Endocrinol. Metab. 92, 1203–1208.

Whyte, M.P., Wenkert, D., McAlister, W.H., Mughal, Z., Freemont, A.J., Whitehouse, R., Baildam, E., Mumm, S., 2009. Chronicrecurrent multifocal osteomyelitis mimicked in childhood hypophosphatasia. J. Bone Miner. Res. 24, 1493–1505.

Whyte, M.P., Greenberg, C.R., Salman, N.J., Bober, M.B., McAlister, W.H., Van Sickle, B., Wenkert, D., Edgar, T.S., Bauer, M.L., Hamdan, M., Simmons, J.H., Bishop, N., Lutz, R.E., McGinn, M., Craig, S., Moore, J.N., Taylor, J.W., Cleveland, R.H., Cranley, W.R., Lim, R., Thacher, T.D., Mayhew, J.E., Downs, M., Millan, J.L., Skrinar, A., Crine, P., Landy, H., 2012. Enzyme replacement therapy in life-threatening hypophosphatasia. N. Engl. J. Med. 366, 904–913.

Whyte, M.P., Leelawattana, R., Reinus, W.R., Yang, C., Mumm, S., Novack, D.V., 2013. Acute severe hypercalcemia after traumatic fractures and immobilization in hypophosphatasia complicated by chronic renal failure. J. Clin. Endocrinol. Metab. 98, 4606–4612.

Whyte, M.P., Zhang, F., Wenkert, D., McAlister, W.H., Mack, K.E., Benigno, M.C., Coburn, S.P., Wagy, S., Griffin, D.M., Ericson, K.L., Mumm, S., 2015. Hypophosphatasia: validation and expansion of the clinical nosology for children from 25 years experience with 173 pediatric patients. Bone 75, 229–239.

Whyte, M.P., Greenberg, C.R., Ozono, K., Riese, R., Moseley, S., Melian, A., Thompson, D., Hofmann, C., 2016a. Asfotase alfa treatment improves survival for perinatal and infantile hypophosphatasia. J. Clin. Endocrinol. Metab. 101, 334–342.

Whyte, M.P., Madson, K.L., Phillips, D., Reeves, A., McAlister, W.H., Yakimoski, A., Mack, K., Hamilton, K., Kagan, K., Melian, A., Thompson, D., Moseley, S., Odrljin, T., Greenberg, C.R., 2016b. Asfotase alfa therapy for children with hypophosphatasia. JCI Insight 1, e85971, 1-10.

Whyte, M.P., Mumm, S., McAlister, W.H., Mack, K., Benigno, M., Kempa, L.G., Franken, A., Lim, V.T., Ericson, K.L., Coburn, S.P., Ryan, L.M., Wenkert, D., Zhang, F., 2016c. Hypophosphatasia: natural history study of 101 affected children investigated at one research center. Bone 93, 125–138.

Whyte, M.P., Coburn, S.P., Ryan, L.M., Ericson, K.L., Zhang, F., 2018. Hypophosphatasia: biochemical hallmarks validate the expanded pediatric clinical nosology. Bone 110, 96–106.

Whyte, M.P., Leung, E., Wilcox, W.R., Liese, J., Argente, J., Martos-Moreno, G.A., Reeves, A., Fujita, K.P., Moseley, S., Hofmann, C., and on behalf of the Study 011-10 Investigators, 2019a. Natural history of perinatal and infantile hypophosphatasia: a retrospective study. J. Pediatr. 209, 116–124.

Whyte, M.P., Simmons, J.H., Moseley, S., Fujita, K.P., Bishop, N., Salman, N.J., Taylor, J., Phillips, D., McGinn, M., McAlister, W.H., 2019b. Asfotase alfa for infants and young children with hypophosphatasia: 7 year outcomes of a single-arm, open-label, phase 2 extension trial. Lancet Diab. & Endocrinol. 7, 93–105.

Williams, D., Huggins, S., Mitchell, A., Falck, A., Pryor, J., Skenandore, C., Read, G., Boyd, H., Long, S., Foster, B., Westhusin, M., Long, C., Suva, L., Gaddy, D., 2018. Development and characterization of a hypophosphatasia (HPP) tooth and muscle phenotype in sheep to model disease in an index HPP patient. (Abstract). J. Bone Miner. Res. 33 (Suppl. 1), 426.

Wolf, P.L., 1978. Clinical significance of an increased or decreased serum alkaline phosphatase level. Arch. Pathol. Lab Med. 102, 497–501.

Wu, L.N., Genge, B.R., Wuthier, R.E., 1992. Evidence for specific interaction between matrix vesicle proteins and the connective tissue matrix. Bone Miner. 17, 247–252.

Wuthier, R.E., Register, T.C., 1985. Role of alkaline phosphatase, a polyfunctional enzyme in mineralizing tissues. In: Butler, W.T. (Ed.), The Chemistry and Biology of Mineralized Tissues. EBSCO Media, Birmingham, pp. 113–124.

Wyckoff, M.H., El-Turk, C., Laptook, A., Timmons, C., Gannon, F.H., Zhang, X., Mumm, S., Whyte, M.P., 2005. Neonatal lethal osteochondrodysplasia with low serum levels of alkaline phosphatase and osteocalcin. J. Clin. Endocrinol. Metab. 90, 1233–1240.

Xu, Y., Cruz, T.F., Pritzker, K.P., 1991. Alkaline phosphatase dissolves calcium pyrophosphatase dihydrate crystals. J. Rheumatol. 18, 1606–1610.

Yoon, K., Golub, E., Rodan, G.A., 1989. Alkaline phosphatase cDNA transfected cells promote calcium and phosphate deposition. Connect. Tissue Res. 22, 53–61.

Young, G.P., Rose, I.S., Cropper, S., Seetharam, S., Alpers, D.H., 1984. Hepatic clearance of rat plasma intestinal alkaline phosphatase. Am. J. Physiol. 247, G419–G426.

Zurutuza, L., Muller, F., Gibrat, J.F., Tillandier, A., Simon-Bouy, B., Serre, J.L., Mornet, E., 1999. Correlations of genotype and phenotype in hypophosphatasia. Hum. Mol. Genet. 8, 1039–1046.

Chapter 67

Paget's disease of bone

Frederick R. Singer[1] and G. David Roodman[2]

[1]John Wayne Cancer Institute, Saint John's Health Center, Santa Monica, CA, United States; [2]Department of Medicine, Division of Hematology and Oncology, Indiana University School of Medicine, and Roudebush VA Medical Center, Indianapolis, IN, United States

Chapter outline

The patient

Paget's disease is a common disorder of the skeleton that is local in nature and extremely variable in its clinical manifestation (Singer and Krane, 1998). The majority of patients are without symptoms. When symptoms are present, skeletal deformity and pain are most common. Deformities are usually most apparent in the skull, face, and lower extremities. Pain is of several origins. Localized bone pain is surprisingly uncommon, but joint pain (hips and knees) is seen not infrequently, owing to degenerative arthritis. Pain of neural or spinal origin is unusual but the most severe.

A variety of complications may first bring the patient to medical attention. The complications depend on both the affected skeletal sites and the overall extent of the disease (six bones are commonly involved). Patients with Paget's disease in the skull often develop a hearing deficit if the temporal bone is affected. Massive enlargement of the cranium is associated with basilar impression and neurological impairment. Vertebral involvement may produce compression fractures, spinal stenosis, neurological impairment, and degenerative arthritis. Paget's disease in the pelvis and femurs commonly is associated with degenerative arthritis of the hips. Involvement of the femur and tibia may lead to pathological fractures of these long bones. Nonunion of a femoral fracture is relatively common. Degenerative arthritis in the knees is also a common feature when lower extremity long bones are extensively involved by Paget's disease. The most serious complication is the development of a sarcoma that, fortunately, occurs in less than 1% of patients. It always arises in a pagetic lesion and not in unaffected bone. Systemic complications of Paget's disease generally occur with more extensive disease.

Hypercalcemia, preceded by hypercalciuria, usually is noted with total bed rest and is related to the accelerated bone resorption induced by immobilization. Increased cardiac output, and less commonly, congestive heart failure, is a consequence of the great vascularity of bones affected by Paget's disease. Hyperuricemia has been observed in males with extensive disease and may reflect increased purine turnover.

Radiology and nuclear medicine

The diagnosis of Paget's disease is primarily accomplished by roentgenographic evaluation of the skeleton. Over the years it has become clear that the disease evolves through several stages, as observed by serial roentgenograms.

Principles of Bone Biology. https://doi.org/10.1016/B978-0-12-814841-9.00067-1

The initial stage of the disease is represented by a localized area of reduced bone density often referred to as an osteolytic lesion. This is most readily detected in the skull, where it is found as a discrete round or oval lesion in the frontal or occipital bones. It is called osteoporosis circumscripta. Paget's disease in the long bones almost always begins in the subchondral region of either epiphysis (uncommonly, both may be affected simultaneously). The osteolytic process has then been seen to advance proximally or distally at about 1 cm/year in the untreated patient. The advancing front usually has a V-shaped or arrowhead appearance.

In the most advanced stage of Paget's disease, the areas of previous osteolytic dominance now are characterized by a chaotic sclerotic appearance, a phase that is called osteoblastic or osteosclerotic. In long bones the osteolytic phase is commonly seen preceding the osteosclerotic region when much of the bone has been affected by the disease. Another feature of this phase is considerable thickening of the sclerotic bone, which can reach monumental proportions in the skull. Osteolytic activity of a secondary nature often can be observed as clefts in the thickened bone. It is likely that the evolution of the disease into its most severe form occurs over much of the life span of the patient. Two other features of the disease have been noted through serial roentgenographic observations. Although the disease can slowly course through an entire bone, it does not cross a joint space to affect an adjacent bone. Also it is extremely rare for new lesions of Paget's disease to be detected at any site in the skeleton after the diagnosis and extent of the disease has been determined initially.

Bone scans are the most sensitive means of detecting pagetic lesions. Radiolabeled bisphosphonates accumulate in regions where blood flow and bone formation are increased and can outline early lesions that are not detectable on roentgenograms. Radioactive gallium can also define areas of Paget's disease activity because of the uptake of gallium by osteoclasts (OCLs).

Histopathology

Beginning with the observations of Schmorl in 1932, it has become appreciated that the OCL is the dominant cell in the pathogenesis of Paget's disease. OCLs are increased in number in the haversian canals of the cortex in the absence of other abnormalities and are present in great numbers at the leading edge of the osteolytic front. The OCLs in Paget's disease may be far greater in size than OCLs in normal bone and contain as many as 100 nuclei in a cross section, compared with two or three nuclei in a normal OCL. OCLs of Paget's disease have a characteristic ultrastructural abnormality (Gherardi et al., 1980; Howatson and Fornasier, 1982; Mills and Singer, 1976; Rebel et al., 1974). This consists of microfilaments, sometimes grouped in a paracrystalline array, located in the nucleus and sometimes in the cytoplasm of OCLs (Fig. 67.1). These microfilaments are not seen in nonpagetic bone or bone marrow cells. These inclusions closely resemble nucleocapsids of viruses of the Paramyxoviridae family, a group of RNA viruses responsible for some of the most common childhood diseases. Despite the finding of these inclusions in the vast majority of patients studied, the budding off of an infectious virus from the OCLs has rarely been observed (Abe et al., 1995).

Osteoblasts (OBs) are another prominent feature of the cellular pathology of Paget's disease. Large numbers of OBs are often found near areas of resorbed bone and may even be prominent in a lesion that appears purely osteolytic by X-ray. The OBs are usually prism-shaped or polyhedral and contain abundant rough endoplasmic reticulum, mitochondria, and a well-developed Golgi zone. These signs of cellular activity are consistent with the increased bone formation in active lesions established by the use of double labeling with tetracycline.

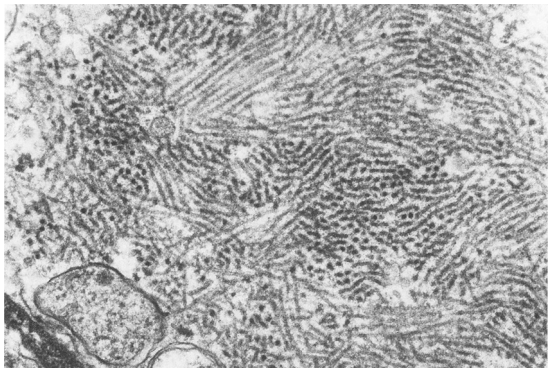

FIGURE 67.1 Electron micrograph of a nuclear inclusion in an osteoclast of a patient with Paget's disease. The microfilaments are seen both in longitudinal array and in paracrystalline array in cross section. *Provided by Dr. Barbara G. Mills.*

In addition to the increased numbers of OCLs and OBs, the marrow of pagetic lesions tends to be grossly abnormal. The normal hematopoietic elements are usually absent and replaced by mononuclear cells of indeterminate origin intermixed with highly vascular connective tissue.

The bone matrix in Paget's disease is highly abnormal in structure and arises as a consequence of disordered bone resorption and formation. The matrix consists of a "mosaic" of irregularly shaped pieces of lamellar bone with an erratic pattern of cement lines. The matrix is interspersed with numerous foci of woven bone, which, in adults, is ordinarily found associated with fracture healing. Analysis of bone biopsies indicates that there is a lower heterogeneous degree of bone mineralization and a younger tissue age than in control bone. This appears to result in less resistance to plastic deformation and a straighter crack path than in control bone (Singer, 2016).

Biochemistry

The biochemical findings in Paget's disease help to provide an integrated assessment of the cellular events occurring throughout the skeleton of affected patients.

Historically, the earliest index of bone matrix resorption was the measurement of urinary hydroxyproline excretion while ingesting a low-gelatin diet. This index is well correlated with the extent of the disease despite the fact that hydroxyproline is a prominent component of extraskeletal connective tissue as well as skeletal collagen. Measurement of collagen cross-link degradation products in serum and urine provides more specific measurements of skeletal matrix. Urinary N-telopeptide, C-telopeptide, pyridinoline, and deoxypyridinoline have all been reported to be more specific indices of skeletal matrix resorption and are not influenced by dietary gelatin (Alvarez et al., 1995; Reid et al., 2004; Shankar and Hosking, 2006). The telopeptide assays are most reliable.

Serum tartrate-resistant acid phosphatase, presumably released by OCLs, appears to be another index of bone resorption in Paget's disease but is not routinely available (Kraenzlin et al., 1990).

OB activity can be assessed by measurement of total alkaline phosphatase activity, bone-specific alkaline phosphatase activity, osteocalcin concentration, and procollagen type 1 N-terminal propeptide (P1NP) concentration in the serum. The most useful of these serum markers are the total alkaline phosphatase, bone-specific alkaline phosphatase, and P1NP (Alvarez et al., 1995; Reid et al., 2004; Shankar and Hosking, 2006). In the absence of liver disease, serum total alkaline phosphatase alone is least expensive and is adequate for following disease activity (Singer et al., 2014).

Treatment of Paget's disease

Salmon calcitonin by injection and etidronate disodium by the oral route were the first effective medications introduced in the 1980s. They generally suppress biochemical parameters of the disease by 50%. A variety of more potent bisphosphonates, including pamidronate, alendronate, risedronate, and ibandronate, have also proven to be effective in suppressing the activity of Paget's disease, but the most effective therapy has proven to be intravenous administration of zoledronic acid (Hosking et al., 2007). A 15-min infusion suppresses biochemical activity into the normal range for up to 6.5 years even in patients with markedly elevated parameters of bone resorption and formation (Reid et al., 2011). In patients with a mean age of 76 years a single infusion may produce a lasting remission for the remainder of their life (Cundy et al., 2017).

Surgery is sometimes necessary to treat patients with associated degenerative arthritis of the hip (total hip replacement) and of the knee (high tibial osteotomy). Orthopedic and/or neurosurgical procedures may occasionally be necessary after fractures and when skull or vertebral complications are present.

Evidence for the presence of paramyxoviruses in Paget's disease

Multiple environmental factors have been suggested as possible triggers for Paget's disease. These include dietary deficiencies (calcium, vitamin D), stress from repetitive use of affected bones, exposure to environmental toxins, a rural lifestyle or animal exposure, and chronic infection with a paramyxovirus such as measles virus (MV), canine distemper virus (CDV), and respiratory syncytial virus (RSV). A viral etiology of Paget's disease was first suggested by Rebel and coworkers (Rebel et al., 1974), who performed ultrastructural studies on OCLs from Paget's disease patients. These studies showed that nuclear and, less commonly, cytoplasmic inclusions resembling paramyxoviral nucleocapsids were present in pagetic OCLs, and immunologic and in situ hybridization studies suggested they were MV or a measles-like virus (Rebel et al., 1980a; Basle, 1986). Mills and colleagues (1984), using immunohistochemistry, found that RSV and MV nucleocapsid antigens were detectable in OCLs from Paget's disease patients, but not in OCLs from patients with other bone

diseases. More recently, however, other groups using a variety of techniques have been unable to detect MV or CDV in cells from Paget's disease patients (Ralston et al., 2007), making the role of a chronic paramyxoviral infection in Paget's disease controversial.

Additional evidence of paramyxovirus nucleocapsid transcripts in Paget's disease has come from the studies of Reddy and colleagues. They studied bone marrow mononuclear cells obtained from aspirations of the iliac crest of six patients with radiologically demonstrable Paget's disease and from the aspirations of 10 normal subjects (Reddy et al., 1995). Using reverse transcriptase−PCR techniques, they observed that five of the six patients had MV nucleocapsid transcripts, whereas none of the 10 normal subjects had detectable transcripts. Because granulocyte−macrophage colony-forming units (CFU-GM), the most likely OCL precursors, circulate in the peripheral blood, Reddy and colleagues (1996) examined peripheral blood samples for the presence of MV nucleocapsid transcripts by reverse transcriptase−PCR in Paget's disease and control subjects. In 9 of 13 patients, MV transcripts were detected. They were localized to peripheral blood monocytes (whose precursor is CFU-GM) by in situ hybridization. Results were negative in the 10 control subjects.

Three studies from the United Kingdom, one from the United States, and one from New Zealand have produced negative results with respect to detection of Paramyxoviridae mRNA in Paget's disease. In one study, RNA extracts of 10 bone specimens failed to exhibit MV, CDV, RSV, or parainfluenza 3 virus transcripts after reverse transcriptase−PCR evaluation (Ralston et al., 1991). In a second study, both bone cells cultured from pagetic explants and bone biopsies were studied similarly by reverse transcriptase−PCR techniques for the presence of MV and CDV transcripts (Birch et al., 1994). Completely negative results were obtained. A second UK study using the same primers also failed to find MV or CDV transcripts in long-term bone marrow cultures from lesions of Paget's disease (Ooi et al., 2000). In the US study, Nuovo and colleagues (1992) also could not detect MV-specific cDNA in pagetic specimens by using PCR and in situ hybridization in combination. The New Zealand study (Matthews et al., 2008) reported no evidence of MV ribonucleic acid in 13 OB and 13 bone marrow cell cultures. The explanation for the disparate results is unclear because these investigators demonstrated that they can detect very low levels of MV transcripts by PCR (Ralston et al., 2007).

Several studies have addressed the levels of circulating antibodies against various paramyxoviruses in patients with Paget's disease. Antibody titers have not been found to be greater in Paget's disease than in control subjects (Basle et al., 1983; Gordon et al., 1991; Pringle et al., 1985).

Cellular and molecular biology of Paget's disease

The development of in vitro techniques for the study of the ontogeny of human OCLs has made it possible to gain new insights into the pathogenesis of Paget's disease. Kukita and colleagues (1990) first established long-term cultures of marrow from involved bones of patients with Paget's disease and noted that the multinucleated cells that formed shared many of the characteristics of pagetic OCLs. Compared with OCL-like cells formed in normal marrow cultures, the pagetic OCL-like cells formed more rapidly and in much greater numbers (10- to 100-fold greater), had increased numbers of nuclei, and had higher levels of tartrate-resistant acid phosphatase. Examination of these cells by electron microscopy did reveal many features of OCLs found in pagetic bone biopsies, but the characteristic nuclear and cytoplasmic inclusions were not observed. As mentioned previously, the antigens of MV and RSV nucleocapsids were detectable in these cells (Mills et al., 1994); apparently the nucleocapsid structures do not form in this in vitro setting, perhaps because the formation of nucleocapsid structures requires more than the nucleocapsid gene alone.

Because the increased numbers of OCLs in pagetic lesions are of obvious importance in the pathogenesis of the disease, it seemed logical to examine OCL precursors in the marrow aspirates to determine whether they were abnormal or whether other cells in the marrow microenvironment were participants in the pathology. Demulder and colleagues (1993) examined CFU-GM in cultures of unfractionated marrow mononuclear cells and found that CFU-GM colony formation was significantly increased compared with that of normal cells. Using an antibody that recognizes the CD34 antigen present on most hematopoietic precursors, they also isolated enriched hematopoietic precursors and found similar numbers of OCL precursors in pagetic and normal marrow aspirations. Subsequent coculture experiments with highly purified hematopoietic precursors ($CD34^+$ cells) and nonhematopoietic marrow accessory cells ($CD34^-$ cells) demonstrated that the growth of pagetic precursors was significantly enhanced by both normal and pagetic $CD34^-$ cells. CFU-GM colony formation was also significantly increased when normal $CD34^+$ cells were cocultured with pagetic, but not with normal, $CD34^-$ cells. CFU-GM colony-derived cells from pagetic patients also formed OCL-like multinucleated cells with 1,25-dihydroxyvitamin D ($1,25(OH)_2D_3$) in concentrations 1/10 of that required for normal multinucleated cell formation. Thus, these experiments suggest that OCL precursors are abnormal in Paget's disease and that other cells in the pagetic marrow microenvironment may stimulate the growth and differentiation of these abnormal precursors. Menaa and coworkers (2000a) have extended the original studies of Demulder et al. (1993) to further understand the enhanced

sensitivity of OCL precursors from patients with Paget's disease to the marrow microenvironment and the enhanced osteoclastogenic potential of the marrow microenvironment from Paget's patients. Menaa and coworkers (2000a) showed that pagetic OCL precursors are hyperresponsive to receptor activator of NF-κB ligand (RANKL), a member of the tumor necrosis factor (TNF) gene family, which is absolutely required for OCL formation. The increased sensitivity to RANKL was caused by the additive effects of interleukin-6 (IL-6) produced by the pagetic marrow and RANKL on OCL formation. Furthermore, Menaa and coworkers (2000a) showed that marrow stromal cells from patients with Paget's disease expressed higher levels of RANKL than normal marrow stromal cells, although Naot and colleagues (2007) did not find increased RANKL expression by OBs from pagetic lesions by using gene expression profiling. Thus, in pagetic lesions the OCL precursors are hyperresponsive to RANKL, and increased amounts of RANKL may be expressed in the marrow microenvironment, further enhancing the osteoclastogenic potential of the pagetic lesion. In areas of bone not affected by Paget's disease, enhanced expression of RANKL was not detected.

As noted earlier, a strong candidate for a significant autocrine/paracrine factor involved in the increased OCL formation in Paget's disease is IL-6. Roodman and colleagues (1992) found that conditioned media from long-term pagetic marrow cultures increased multinucleated cell formation in normal marrow cultures, and antibodies to IL-6 blocked the stimulatory activity. Antibodies to IL-1, granulocyte−macrophage colony-stimulating factor, and TNFα had no effect on the stimulatory activity. In situ hybridization studies demonstrated that the multinucleated cells in the pagetic marrow cultures were actively transcribing IL-6 mRNA. In addition, bone marrow plasma samples obtained from sites of Paget's disease had increased levels of IL-6 in 9 of 10 patients compared with samples from normal subjects. Peripheral plasma also had elevated IL-6 levels in 17 of 27 patients. In another study, basal plasma IL-6 activity was increased in 19 of 22 patients (Schweitzer et al., 1995). The concept that IL-6 may be an important autocrine/paracrine factor in Paget's disease is also supported by the studies of Hoyland and colleagues (1994a), who used in situ hybridization to localize the expression of IL-6, IL-6 receptor, and IL-6 transcription factor in the bone of patients with Paget's disease in comparison with those with osteoarthritis. The OBs in both disorders expressed all three mRNAs, but in Paget's disease IL-6 and its receptor mRNA showed higher levels of expression. In the OCLs of both disorders, the receptor and transcription factor were expressed, but only in Paget's disease was IL-6 mRNA expressed in OCLs. Hoyland and Sharpe (1994b) also examined the expression of c-fos protooncogene in the bone of six patients with Paget's disease by in situ hybridization. c-fos has been found to be important in the regulation of OCLs and was markedly upregulated in pagetic OCLs and, to a lesser extent, in the OBs. It is possible that this is a consequence of IL-6 action (Korholz et al., 1992).

Ralston and colleagues (1994) also studied cytokine and growth factor expression in bone explants of Paget's disease and in control subjects (postmenopausal women with and without osteoporosis and young bone graft patients) and could not find differences between pagetic and nonpagetic bone. IL-6 mRNA was not detected in 40% of the pagetic specimens from severely affected individuals. There is no obvious explanation for their nonconfirmatory data.

Another abnormality of pagetic OCL precursors is that they are hyperresponsive to $1,25(OH)_2D_3$. OCL precursors form OCLs in vitro with concentrations of $1,25(OH)_2D_3$ that are 1−2 logs less than that required to induce OCL formation by normal OCL precursors (Kukita et al., 1990). Menaa and coworkers (2000b) have shown that this increased sensitivity to $1,25(OH)_2D_3$ is not caused by increased numbers of vitamin D receptors in pagetic OCL precursors or by mutations in the vitamin D receptor. Kurihara and colleagues (2000a) have used a GST−vitamin D receptor fusion protein to further examine the increased sensitivity of pagetic OCL precursors to $1,25(OH)_2D_3$. These workers found that TAFII-20, a component of the transcription factor IID transcription complex, was increased in OCL precursors from patients with Paget's disease compared with normal patients. This increase in expression of TAFII-20 did not require treatment of the cells with $1,25(OH)_2D_3$. These data suggest that pagetic OCL precursors express higher levels of TAFII-20 or have increased levels of a coactivator that can bind to TAFII-20 and the vitamin D receptor in the presence of lower concentrations of $1,25(OH)_2D_3$ to initiate transcription of vitamin D receptor-responsive genes.

Kurihara et al. (2000b) provided initial evidence for a pathophysiological role of MV in the abnormal OCL activity in Paget's disease. They found that OCL precursors from normal subjects transduced with retroviral vectors expressing the MV nucleocapsid protein (MVNP) gene formed OCLs that displayed many of the abnormal characteristics of pagetic OCL. Similarly, MV infection of bone marrow cells from mice that expressed the CD46 MV receptor formed OCLs that expressed the characteristics of pagetic OCL (Reddy, 2001). Further, transgenic mice with MVNP targeted to the OCL lineage formed OCL and bone lesions characteristic of Paget's disease (Fig. 67.2). These results demonstrated that MVNP expression in OCL was sufficient to induce OCL and bone lesions characteristic of Paget's disease.

Teramachi et al. (2014) then examined how MVNP expression in OCLs results in formation of OCLs that express a pagetic phenotype. They found that MVNP expression in OCLs induced them to secrete high levels of IL-6, and loss of IL-6 expression in MVNP mice abrogates the formation of pagetic OCLs and bone lesions in vivo. However, overexpression

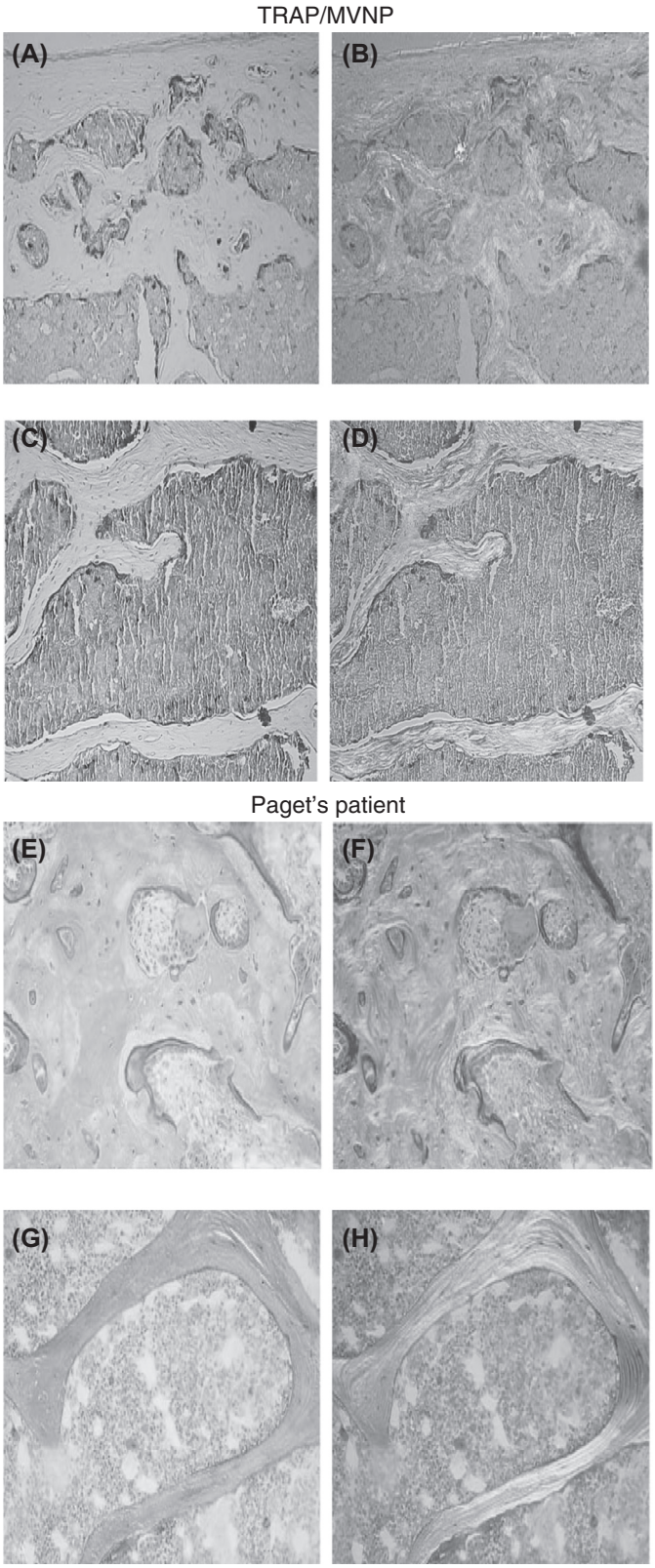

FIGURE 67.2 Histological features of a 12-month-old tartrate-resistant acid phosphatase/Edmonston strain measles virus nucleocapsid protein (*TRAP/MVNP*) transgenic mouse compared with wild-type (WT) control, a Paget's patient, and a normal subject. (A–D) Histological features in a TRAP/MVNP mouse (A and B) are compared with a WT control (C and D) at 12 months of age. Note thickened, irregular trabeculae, increased osteoclast number (A), tunneling resorption, and increased amounts of woven bone in the TRAP/MVNP mouse (B) compared with the WT control (C and D). (E–H) Provided for comparison are sections from a 58-year-old woman with Paget's disease (E and F) and a 58-year-old normal subject (G and H). (A and C) Viewed under polarized light. (E and G) Sections viewed under polarized light. Original magnification, ×3100. *From Kurihara, N., Zhou, H., Reddy, S.V., Garcia-Palacios, V., Subler, M.A., Dempster, D.W., Windle, J.J., and Roodman, G.D., 2006. Expression of the measles virus nucleocapsid protein in osteoclasts in vivo induces Paget's disease-like bone lesions in mice. J. Bone Miner. Res. 21, 446–455. (See plate section).*

of IL-6 in OCL precursors was not sufficient to induce pagetic OCL formation or pagetic bone lesions in mice (Teramachi et al., 2014).

Sun and coworkers (2014) reported that MVNP also regulates expression of TANK-binding kinase 1 (TBK1) and optineurin (OPTN) in OCL precursors, which also contribute to the generation of pagetic OCL. Prior to these studies, the roles of TBK1 and OPTN (members of the IκB kinase family) in bone metabolism were previously unknown. These authors found that MVNP interacts with TBK1−OPTN complexes in OCL precursors to increase the TBK1 kinase activity and protein stability, while decreasing OPTN levels. Overexpression of TBK1 alone in normal mouse OCL precursors increased endogenous IL-6 expression but did not induce formation of pagetic OCLs. However, overexpression of TBK1 in OCL precursors expressing MVNP synergized with MVNP to increase pagetic OCL formation. Similarly, TBK1 knockdown in OCL precursors expressing MVNP impaired the development of pagetic-like OCLs. These results demonstrate that TBK1 is an important contributor to MVNP's capacity to increase expression of IL-6 in OCL precursors and induce development of OCLs that express a pagetic phenotype.

Although much is known about the abnormal OCL activity in Paget's disease, very little is known about the mechanisms responsible for the abnormal OB activity in Paget's disease. Bone resorption and formation are tightly linked, with bone formation normally occurring only at sites of previous bone resorption. This "coupling" of bone remodeling is largely dependent on communication between OCLs and OBs with Eph receptors expressed on OBs, and ephrins on OCLs and OBs have been implicated as major regulators of coupling (Zhao et al., 2006). Ephs and ephrins are cell surface molecules that have bidirectional signaling and play major roles in tumor progression, angiogenesis, cell migration, and morphogenesis (Matsuo, 2012). Zhao and coworkers showed that OCLs express the nuclear factor of activated T cells 1 (NFATc1) target gene ephrinB2, while OBs express its receptor EphB4. Increased EphB4 signaling in OBs can increase bone mass in mice, while reverse signaling through ephrinB2 on OCLs suppresses OCL differentiation by inhibiting the c-fos/NFATc1 cascade. These data suggest that ephrinB2/EphB4 signaling can play a major role in coupling between bone resorption and new bone formation. Since Paget's disease represents the most exaggerated form of coupled bone formation, Teramachi et al. (2016) examined the expression of ephrins and their receptors in OCLs and OBs from MVNP, $p62^{P394L}$/MVNP, $p62^{P394L}$-knock-in, and wild-type mice. The presence of MVNP but not $p62^{P394L}$ in OCLs increased the expression of ephrinB2 in OCLs and EphB4 in OBs. Further, coculture of OCLs expressing MVNP with OBs from MVNP mice enhanced OB differentiation. These data suggested that increased ephrinB2/EphB4 expression induced by MVNP may drive the enhanced bone formation in MVNP mice. A preliminary gene expression profiling study of highly purified OCLs from MVNP, $p62^{P394L}$, and wild-type mice showed that OCLs from MVNP mice expressed elevated levels of insulin-like growth factor 1 (IGF-1) mRNA compared with wild-type mice, while OCLs from $p62^{P394L}$-knock-in mice did not (Teramachi et al., 2016). They further found that IL-6 regulated the increased IGF-1 protein expression in OCLs from MVNP mice, and IL-6 and IGF-1 in turn increased ephrinB2 expression by OCLs. IL-6 also increased EphB4 on OBs, while IGF-1 enhanced OB differentiation (Fig. 67.3). Importantly, OCLs from Paget's disease patients that express MVNP also express increased levels of IGF-1 and ephrinB2 compared with OCLs from normal donors. These results suggest that IL-6 and IGF-1 expression by pagetic OCLs contributes to the increased bone formation in Paget's disease.

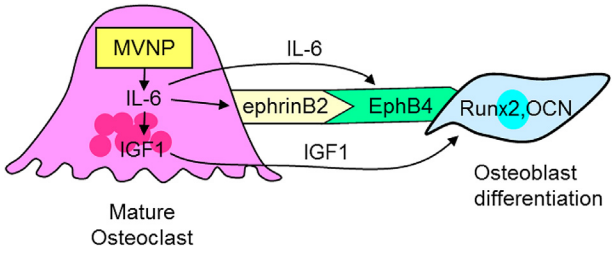

FIGURE 67.3 Model of osteoclast (OCL)/osteoblast (OB) coupling in Paget's disease. Measles virus nucleocapsid protein (*MVNP*) expression induces high levels of interleukin-6 (*IL-6*) in OCLs, which increases insulin-like growth factor 1 (*IGF1*) and ephrinB2 in OCLs and increases EphB4 in OBs to increase coupling. IGF1 further enhances ephrinB2 expression on OCLs and increases Runx2, a transcription factor required for osteoblast differentiation, and osteocalcin (*OCN*) levels in OBs to increase bone formation. *From Teramachi, J., Nagata, Y., Mohammad, K., Inagaki, Y., Ohata, Y., Guise, T., Michou, L., Brown, J.P., Windle, J.J., Kurihara, N., Roodman, G.D., 2016. Measles virus nucleocapsid protein increases osteoblast differentiation in Paget's disease. J. Clin. Investig.126, 1012−1022.*

Genetic mutations linked to Paget's disease

As noted earlier, genetic factors are an important contributor to the etiology of Paget's disease, with 15%–40% of affected patients having a first-degree relative with Paget's disease, and multiple families with Paget's disease have been reported with vertical transmission of Paget's disease in an autosomal dominant mode of inheritance (Morales-Piga et al., 1995). Not surprisingly, most of the mutations or single-nucleotide polymorphisms (SNPs) linked to or that predispose patients to Paget's disease affect OCL activity. Mutations in the coding regions of sequestosome 1 (SQSTM1) and valosin-containing protein (VCP/p97 or CDC48) have been linked to Paget's disease (Laurin et al., 2002, Mehta et al., 2013). SQSTM1 encodes the p62 protein, a multidomain scaffold protein that serves as a platform for the formation of cytokine signaling complexes, including RANKL and TNF, and acts as a cargo adaptor for polyubiquitinated proteins for proteasomal degradation and autophagy (Roodman, 2010). All 28 mutations in p62 identified in Paget's patients cause loss of function of the C-terminal ubiquitin association domain and result in increased cytokine activation of NF-κB. These p62 mutations increase RANKL responsivity of OCL precursors to enhance OCL formation. The most common p62 mutation linked to Paget's disease results in a proline (P) to leucine (L) substitution at codon 392 ($p62^{P392L}$). This mutation occurs in 10% of sporadic and 30% of familial Paget's patients (Hocking et al., 2000,Laurin et al., 2002,Morisette et al., 2006). Paget's disease patients with p62 mutations have an earlier onset and increased severity of disease compared with other Paget's disease patients, although the severity and age of onset of disease among affected members with the same p62 mutation vary (Bolland et al., 2007; Leach et al., 2006; Gennari et al., 2010). Further, mutations in p62 linked to Paget's disease demonstrate incomplete penetrance, because 15%–20% of patients with p62 mutations fail to develop Paget's disease (Bolland, 2013). In addition, Kurihara et al. (2011) found that mice with targeted expression of $p62^{P392L}$ in OCLs or mice with knock-in of the murine equivalent of human $p62^{P392L}$ ($p62^{P394L}$) develop increased numbers of OCLs, and do not develop bone lesions or OCLs characteristic of Paget's disease (Fig. 67.4). Importantly, Kurihara and colleagues (2011) showed that antisense knockdown of MVNP expression in MVNP-positive OCL precursors from Paget's patients harboring the $p62^{P392L}$ mutation resulted in loss of their ability to form OCLs that expressed a pagetic phenotype, although the OCL precursors still had increased responsivity to RANKL. These results indicated that $p62^{P392L}$ by itself was insufficient to induce a pagetic phenotype in OCLs from $p62^{P392L}$ patients, and that MVNP is a required cofactor for pagetic OCL formation in this subset of Paget's disease patients. However, when $p62^{P394L}$-knock-in mice were crossed

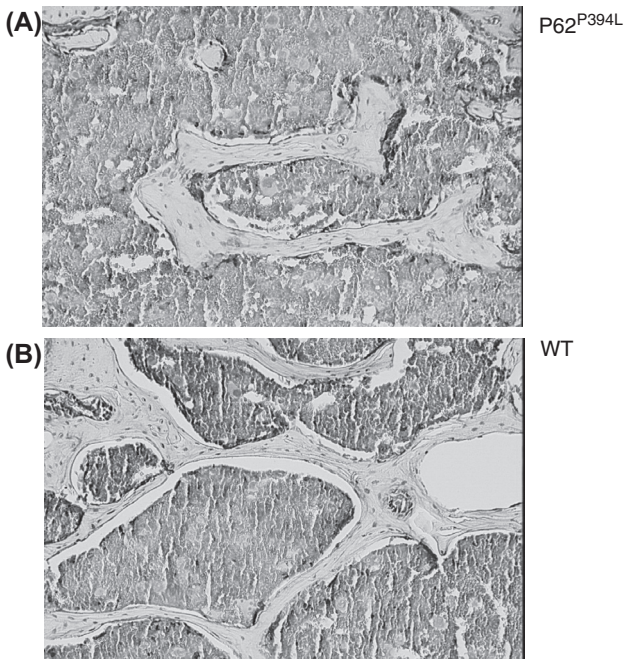

FIGURE 67.4 Histological studies of bone from TRAP-$p62^{P392L}$ mice. Vertebral cancellous bone from (A) TRAP-p62P392L mice or (B) wild-type (*WT*) littermates is shown. Note increased osteoclast perimeter, reduced cancellous bone volume, fewer and thinner trabeculae, and loss of trabecular connectivity in TRAP-p62P392L bone. *From Kurihara, N., Hiruma, Y., Zhou, H., Subler, M.A., Dempster, D.W., Singer, F.R., Reddy, S.V., Gruber, H.E., Windle, J.J., Roodman, G.D., 2007. Mutation of the sequestasome-1 (p62) gene increases osteoclastogenesis but does not induce Paget's disease. J. Clin. Investig. 117, 133–142. (See plate section).*

with mice expressing MVNP in cells of the OCL lineage, the $p62^{P394L}$/MVNP mice developed greater numbers of pagetic-like OCLs and more dramatic bone lesions that were strikingly similar to those seen in Paget's disease (Kurihara et al., 2011). These results suggest that p62 mutations linked to Paget's disease predispose patients to develop Paget's disease through their capacity to enhance RANKL responsivity of OCL precursors. However, since MVNP-negative Paget's patients carrying $p62^{P392L}$ also have pagetic lesions in vivo, these results suggest that a second genetic mutation or another environmental factor may have contributed to the development of their Paget's disease. In contrast, Daroszewska and coworkers (2011) generated similar $p62^{P394L}$-knock-in mice and reported that these mice developed small pagetic lesions in their long bones. It is unclear why the phenotypes of the two knock-in mouse lines differ, although differences in the genetic background and the phenotypic analyses performed may have contributed.

Like mutations in p62, mutations in VCP and a common variant of OPTN linked to Paget's disease also affect ubiquitin-dependent autophagy. Mutations in VCP are associated with a syndrome characterized by inclusion body myopathy, frontotemporal dementia, and early-onset Paget's disease. VCP mutations have also been linked to hereditary and spontaneous amyotrophic lateral sclerosis (ALS) (Mehta et al., 2013). OPTN is a negative regulator of NF-κB signaling and OCL formation that has been linked to glaucoma and ALS as well as Paget's disease (Obaid et al., 2015). Further, genome-wide association studies have identified at least seven loci with genetic polymorphisms (SNPs) linked to increased susceptibility to develop Paget's disease and that together account for 13% of the familial risk of Paget's disease (Albagha et al., 2010). Many but not all of these predisposition SNPs occur in genes that can affect OCL function, such as CSF1, OPTN, RANK, DC-STAMP, Ras, and RAB interactor 3. In contrast to mutations in p62 or VCP, these SNPs do not have an impact on the severity of Paget's disease (Bolland, 2013).

However, genetic causes alone cannot be responsible for the development of Paget's disease, since several epidemiologic studies showed that the prevalence and severity of Paget's disease has significantly decreased over the past 20–30 years (Doyle et al., 2002; van Staa et al., 2002; Cundy et al., 2004; Poor et al., 2006). These data suggest that additional factors are required for patients to develop Paget's disease, since this marked change in the epidemiology of Paget's disease is too rapid to be explained on a genetic basis. More likely, changes in environmental factors that contribute to Paget's disease have occurred.

Further, studies with families with Paget's disease linked to mutations in p62 also suggest that these mutations cannot completely account for the pathogenesis of Paget's disease, because the severity of the disease in family members carrying these mutations varies widely, and up to 83% of patients harboring the p62 mutation do not have Paget's disease (Laurin et al., 2002b; Bolland et al., 2007). These data suggest that additional factors may affect the pathogenesis of Paget's disease.

The etiology of Paget's disease

As reviewed earlier, Paget's disease is characterized by focal regions of highly exaggerated bone remodeling, with abnormalities in all phases of the bone remodeling process. In most affected individuals, it progresses slowly over many years without extending to new sites of involvement. The underlying pathophysiology appears to reflect a localized increase in the number of OCLs followed by a secondary increase in OB activity. These OCLs have striking characteristics by both light and electron microscopy. In Paget's disease, the OCLs may be far greater in size than OCLs in normal individuals and in patients with diseases in which OCLs are activated, such as primary hyperparathyroidism. Genetic and nongenetic factors have been implicated in the pathogenesis of Paget's disease, and genetic factors are clearly an important component of its etiology. However, microenvironmental factors appear to also play an important role. As indicated previously, the prevalence of Paget's disease has decreased over the past several decades, but not in all countries (Corral-Gudino et al., 2013). One possible explanation is that measles vaccination, beginning in 1963, was variably introduced over time into populations of different countries (Singer, 2015). Further, expression of the most common mutation linked to Paget's disease, the $p62^{P392L}$, when expressed in normal OCL precursors or targeted to the OCL lineage in transgenic mice, does not induce pagetic lesions or pagetic-like OCLs. In contrast, expression of the MVNP gene in vitro or in vivo results in formation of OCLs that express all the phenotypic characteristics of OCLs from patients with Paget's disease and form bone lesions that are very similar to those found in Paget's disease. The requirement for a nongenetic factor participating in the etiology of Paget's disease would explain why some individuals who have Paget's-associated mutations do not develop Paget's disease. One possibility is that such mutations predispose patients to Paget's disease by enhancing basal osteoclastogenesis, thereby creating a permissive environment for the development of Paget's disease. A second environmental factor, such as the expression of certain viral proteins, may further alter signaling pathways or the expression of specific transcription factors, which results in development of pagetic OCLs. These include changes in vitamin D receptor transcription as well as changes in the NF-κB signaling pathways and other signaling pathways

involved in OCL formation. Further, the increased numbers of OCLs would then secrete high levels of IL-6, which would then further expand OCL formation. Because OCL and OB activities remain coupled in Paget's disease, the increased OCL activity would result in increased OB numbers and rapid formation of new bone. In addition, Hiruma and colleagues (2008) found that marrow stromal cells expressing the $p62^{P392L}$ mutation express higher levels of RANKL than normal stromal cells when treated with low concentrations of $1,25(OH)_2D_3$. These results suggest that genetic mutations linked to Paget's disease may increase OCL formation both by enhancing OCL activity per se and by creating a more osteoclastogenic environment in the pagetic lesions. However, these mutations by themselves are not sufficient to induce Paget's disease in animal models or pagetic-like OCLs in human marrow cultures.

Thus, there has been a tremendous output of new information on the etiology and pathophysiology of Paget's disease. Identification of genes involved in osteoclastogenesis that are mutated in Paget's disease and the characterization of nongenetic factors such as MV that may be involved have provided important insights in the control of bone remodeling in Paget's disease as well as normal bone. Studies of abnormal bone remodeling in Paget's disease could result in identification of coupling factors produced by OCLs, which enhance new bone formation. Understanding the pathophysiology of Paget's disease should provide important insights into the mechanisms that control normal OCL differentiation and bone formation and may lead to both new therapies for patients with Paget's disease and the identification of new anabolic factors for treating patients with severe bone loss.

References

Abe, S., Ohno, T., Park, P., Higaki, S., Unno, K., Tateishi, A., 1995. Viral behavior of paracrystalline inclusions in osteoclasts of Paget's disease of bone. Ultrastruct. Pathol. 19 (6), 455–461.

Albagha, O.M., Visconti, M.R., Alonso, N., Langston, A.L., Cundy, T., Dargie, R., Dunlop, M.G., Fraser, W.D., Hooper, M.J., Isaia, G., Nicholson, G.C., del Pino Montes, J., Gonzalez-Sarmiento, R., di Stefano, M., Tenesa, A., Walsh, J.P., Ralston, S.H., 2010. Genome-wide association study identifies variants at CSF1, OPTN and TNFRSF11A as genetic risk factors for Paget's disease of bone. Nat. Genet. 42 (6), 520–524.

Alvarez, L., Guanabens, N., Peris, P., Monegal, A., Bedini, J.L., Deulofeu, R., Martinez De Osaba, M.J., Munoz-Gomez, J., Rivera-Fillat, F., Ballesta, A.M., 1995. Discriminative value of biochemical markers of bone turnover in assessing the activity of Paget's disease. J. Bone Miner. Res. 10 (3), 458–465.

Baslé, M.F., Fournier, J.G., Rozenblatt, S., Rebel, A., Bouteille, M., 1986. Measles virus RNA detected in Paget's disease bone tissue by *in situ* hybridization. J. Gen. Virol. **67** (5), 907–913.

Baslé, M.F., Rebel, A., Filmon, R., Pilet, P., 1983. Maladie osseuse de Paget. Anticorps seriques anti-rougeole. Presse Med. 12, 769–770.

Birch, M.A., Taylor, W., Fraser, W.D., Ralston, S.H., Hart, C.A., Gallagher, J.A., 1994. Absence of paramyxovirus RNA in cultures of pagetic bone cells in pagetic bone. J. Bone Miner. Res. 9 (1), 11–16.

Bolland, M.J., Tong, P.C., Naot, D., Callon, K.E., Wattie, D.J., Gamble, G.D., Cundy, T., 2007. Delayed development of Paget's disease in offspring inheriting SQSTM 1 mutations. J. Bone Miner. Res. 22 (3), 411–415.

Bolland, M.J., Cundy, T., 2013. Paget's disease of bone: clinical review and update. J. Clin. Pathol. 66 (11), 924–927.

Corral-Gudino, L., Borao-Cengotita-Bengoa, M., Del Pino-Montes, J., Ralston, S., 2013. Epidemiology of Paget's disease of bone: a systematic review and meta-analysis of secular changes. Bone 55 (2), 347–352. https://doi.org/10.1016/j.bone.2013.04.024. Epub 2013 May 1. Review. PMID:23643679.

Cundy, H.R., Gamble, G., Wattie, D., Rutland, M., Cundy, T., 2004. Paget's disease of bone in New Zealand: continued decline in disease severity. Calcif. Tissue Int. 75 (5), 358–364.

Cundy, T., Maslowski, K., Grey, A., Reid, I.R., 2017. Durability of response to zoledronate treatment and competing mortality in Paget's disease of bone. J. Bone Miner. Res. 32 (4), 753–756.

Daroszewska, A.L., van 't Hof, R.J., Rojas, J.A., Layfield, R., Landao-Basonga, E., Rose, L., Rose, K., Ralston, S.H., 2011. A point mutation in the ubiquitin-associated domain of SQSMT1 is sufficient to cause a Paget's disease-like disorder in mice. Hum. Mol. Genet. 20 (14), 2734–2744.

Demulder, A., Takahashi, S., Singer, F.R., Hosking, D.J., Roodman, G.D., 1993. Abnormalities in osteoclast precursors and marrow accessory cells in Paget's disease. Endocrinology 133, 1978–1982.

Doyle, T., Gunn, J., Anderson, G., Gill, M., Cundy, T., 2002. Paget's disease in New Zealand: evidence for declining prevalence. Bone 31, 616–619.

Gennari, L., Gianfrancesco, F., Di Stefano, M., Rendina, D., Merlotti, D., Esposito, T., Gallone, S., Fusco, P., Rainero, I., Fenoglio, P., Mancini, M., Martini, G., Bergui, S., De Filippo, G., Isaia, G., Strazzullo, P., Nuti, R., Mossetti, G., 2010. SQSTM1 gene analysis and gene-environment interaction in Paget's disease of bone. J. Bone Miner. Res. 25, 1375–1384.

Gherardi, G., Lo Cascio, V., Bonucci, E., 1980. Fine structure of nuclei and cytoplasm of osteoclasts in Paget's disease of bone. Histopathology 4, 63–74.

Gordon, M.T., Anderson, D.C., Sharpe, P.T., 1991. Canine distemper virus localised in bone cells of patients with Paget's disease. Bone 12, 195–201.

Hiruma, Y., Kurihara, N., Subler, M.A., Zhou, H., Boykin, C.S., Zhang, H., Ishizuka, S., Dempster, D.W., Roodman, G.D., Windle, J.J., 2008. A SQSTM1/p62 mutation linked to Paget's disease increases the osteoclastogenic potential of the bone microenvironment. Hum. Mol. Genet. 17 (23), 3708–3719.

Hocking, L., Slee, F., Haslam, S.I., Cundy, T., Nicholson, G., van Hul, W., Ralston, S.H., 2000. Familial Paget's disease of bone: patterns of inheritance and frequency of linkage to chromosome 18*q*. Bone 26, 577–580.

Hosking, D., Lyles, K., Brown, J.P., Fraser, W.D., Miller, P., Curiel, M.D., Devogelaer, J.P., Hooper, M., Su, G., Zelenakas, K., Pak, J., Fashola, T., Saidi, Y., Eriksen, E.F., Reid, I.R., 2007. Long-term control of bone turnover in Paget's disease with zoledronic acid and risedronate. J. Bone Miner. Res. 22 (1), 142−148.

Howatson, A.F., Fornasier, V.L., 1982. Microfilaments associated with Paget's disease of bone: comparison with nucleocapsids of measles virus and respiratory syncytial virus. Intervirology 18, 150−159.

Hoyland, J.A., Freemont, A.J., Sharpe, P.T., 1994. Interleukin-6, IL-6 receptor, and IL-6 nuclear factor gene expression in Paget's disease. J. Bone Miner. Res. 9, 75−80.

Hoyland, J., Sharpe, P.T., 1994. Upregulation of c-fos protooncogene expression in pagetic osteoclasts. J. Bone Miner. Res. 9, 1191−1194.

Korholz, D., Gerdon, S., Enczmann, J., Zessack, N., Burdach, S., 1992. Interleukin-6 induced differentiation of a human B cell line into IgM secreting plasma cells is mediated by c-fos. Eur. J. Immunol. 22, 607−610.

Kraenzlin, M.E., Lau, K.H., Liang, L., Freeman, T.K., Singer, F.R., Stepan, J., Baylink, D.J., 1990. Development of an immunoassay for human serum osteoclastic tartrate-resistant acid phosphatase. J. Clin. Endocrinol. Metab. 71, 442−451.

Kukita, A., Chenu, C., McManus, L.M., Mundy, G.R., Roodman, G.D., 1990. Atypical multinucleated cells form in long-term marrow cultures from patients with Paget's disease. J. Clin. Investig. 85, 1280−1286.

Kurihara, N., Reddy, S.V., Maeda, H., Kato, S., Araki, N., Ishizuka, S., Singer, F.R., Bruder, J.M., Roodman, G.D., 2000a. Identification of novel 60 and 15−17 kDa vitamin D receptor (VDR) binding peptides in osteoclast precursors infected with measles virus (MV) that are also present in patients with Paget's disease. J. Bone Miner. Res. 15 (Suppl. 1), S164.

Kurihara, N., Reddy, S.V., Menaa, C., Anderson, D., Roodman, G.D., 2000b. Osteoclasts expressing the measles virus nucleocapsid gene display a pagetic phenotype. J. Clin. Investig. 105, 607−614.

Kurihara, N., Zhou, H., Reddy, S.V., Garcia-Palacios, V., Subler, M.A., Dempster, D.W., Windle, J.J., Roodman, G.D., 2006. Expression of the measles virus nucleocapsid protein in osteoclasts in vivo induces Paget's disease-like bone lesions in mice. J. Bone Miner. Res. 21, 446−455.

Kurihara, N., Hiruma, Y., Zhou, H., Subler, M.A., Dempster, D.W., Singer, F.R., Reddy, S.V., Gruber, H.E., Windle, J.J., Roodman, G.D., 2007. Mutation of the sequestasome-1 (*p*62) gene increases osteoclastogenesis but does not induce Paget's disease. J. Clin. Investig. 117, 133−142.

Kurihara, N., Hiruma, Y., Yamana, K., Michou, L., Rousseau, C., Morissette, J., Galson, D.L., Teramachi, J., Zhou, H., Dempster, D.W., Windle, J.J., Brown, J.P., Roodman, G.D., 2011. Contributions of the measles virus nucleocapsid gene and the SQSTM1/p62$^{(P392L)}$ mutation to Paget's disease. Cell Metabol. 13, 23−34.

Laurin, N., Brown, J.P., Morissette, J., Raymond, V., 2002. Recurrent mutation of the gene encoding sequestosome 1 (SQSTM1/p62) in Paget disease of bone. Am. J. Hum. Genet. 70, 1582−1588.

Leach, R.J., Singer, F.R., Ench, Y., Wisdom, J.H., Pina, D.S., Johnson-Pais, T.L., 2006. Clinical and cellular phenotypes associated with sequestosome 1 (SQSTM1) mutations. J. Bone Miner. Res. 21 (Suppl. 2), P45−P50.

Matthews, B.G., Afzal, M.A., Minor, P.D., Bava, U., Callon, K.E., Pitto, R.P., Cundy, T., Cornish, J., Reid, I.R., Naot, D., 2008. Failure to detect measles virus ribonucleic acid in bone cells from patients with Paget's disease. J. Clin. Endocrinol. Metab. 93, 1398−1401.

Matsuo, K.L., Otaki, N., 2012. Bone cell interactions through Eph/ephrin: bone modeling, remodeling and associated diseases. Cell Adhes. Migrat. 6, 148−156.

Mehta, S.G., Khare, M., Ramani, R., Watts, G.D., Simon, M., Osann, K.E., Donkervoort, S., Dec, E., Nalbandian, A., Platt, J., Pasquali, M., Wang, A., Mozaffar, T., Smith, C.D., Kimonis, V.E., 2013. Genotype-phenotype studies of VCP-associated inclusion body myopathy with Paget disease of bone and/or frontotemporal dementia. Clin. Genet. 83, 422−431.

Menaa, C., Reddy, S.V., Kurihara, N., Anderson, D., Cundy, T., Cornish, J., Bruder, J.M., Roodman, G.D., 2000a. Enhanced RANK ligand expression and responsivity in Paget's disease of bone. J. Clin. Investig. 105, 1833−1838.

Menaa, C., Reddy, S.V., Barsony, J., Cornish, J., Cundy, T., Roodman, G.D., 2000b. 1,25-dihydroxyvitamin D3 hypersensitivity of osteoclast precursors from patients with Paget's disease. J. Bone Miner. Res. 15 (2), 1−9.

Mills, B.G., Frausto, A., Singer, F.R., Ohsaki, Y., Demulder, A., Roodman, G.D., 1994. Multinucleated cells formed *in vitro* from Paget's bone marrow express viral antigens. Bone 15, 443−448.

Mills, B.G., Singer, F.R., 1976. Nuclear inclusions in Paget's disease of bone. Science 194, 201−202.

Mills, B.G., Singer, F.R., Weiner, L.P., Suffin, S.C., Stabile, E., Holst, P., 1984. Evidence for both respiratory syncytial virus and measles virus antigens in the osteoclasts of patients with Paget's disease of bone. Clin. Orthop. Relat. Res. 183, 303−311.

Morales-Piga, A.A., Rey-Rey, J.S., Corres-Gonzalez, J., Garcia-Sagredo, J.M., Lopez-Abente, G., 1995. Frequency and characteristics of familial aggregation of Paget's disease of bone. J. Bone Miner. Res. 10, 663−670.

Morissette, J., Laurin, N., Brown, J.P., 2006. Sequestosome 1: mutation frequencies, haplotypes, and phenotypes in familial Paget's disease of bone. J. Bone Miner. Res. 21 (Suppl. 2), P38−P44.

Naot, D., Bava, U., Matthews, B., Callon, K.E., Gamble, G.D., Black, M., Song, S., Pitto, R.P., Cundy, T., Cornish, J., Reid, I.R., 2007. Differential gene expression in cultured osteoblasts and bone marrow stromal cells from patients with Paget's disease of bone. J. Bone Miner. Res. 22, 298−309.

Nuovo, M.A., Nuovo, G.J., MacConnell, P., Forde, A., Steiner, G.C., 1992. In situ analysis of Paget's disease of bone for measles-specific PCR-amplified cDNA. Diagn. Mol. Pathol. 1, 256−265.

Obaid, R., Wani, S.E., Azfer, A., Hurd, T., Jones, R., Cohen, P., Ralston, S.H., Albagha, O.M.E., 2015. Optineurin negatively regulates osteoclast differentiation by modulating NF-κB and interferon signaling: implications for Paget's disease. Cell Rep. 13 (6), 1096−1102.

Ooi, C.G., Walsh, C.A., Gallagher, J.A., Fraser, W.D., 2000. Absence of measles virus and canine distemper virus transcripts in long-term bone marrow cultures from patients with Paget's disease of bone. Bone 27 (3), 417−421.

Poór, G., Donath, J., Fornet, B., Cooper, C., 2006. Epidemiology of Paget's disease in Europe: the prevalence is decreasing. J. Bone Miner. Res. 21, 1545–1549.

Pringle, C.R., Wilkie, M.L., Elliot, R.M., 1985. A survey of respiratory syncytial virus and parainfluenza virus type 3 neutralising and immunoprecipitating antibodies in relation to Paget disease. J. Med. Virol. 17, 377–386.

Ralston, S.H., Digiovine, F.S., Gallacher, S.J., Boyle, I.T., Duff, G.W., 1991. Failure to detect paramyxovirus sequences in Paget's disease of bone using the polymerase chain reaction. J. Bone Miner. Res. 6, 1243–1248.

Ralston, S.H., Hoey, S.A., Gallacher, S.J., Adamson, B.B., Boyle, I.T., 1994. Cytokine and growth factor expression in Paget's disease: analysis by reverse-transcription/polymerase chain reaction. Br. J. Rheumatol. 33, 620–625.

Ralston, S.H., Afzal, M.A., Helfrich, M.H., Fraser, W.D., Gallagher, J.A., Mee, A., Rima, B., 2007. Multicentre blinded analysis of RT-PCR detection methods for paramyxoviruses in relation to Paget's disease. J. Bone Miner. Res. 22, 569–577.

Rebel, A., Malkani, K., Basle, M., 1974. Anomalies nucleaires des osteoclasts de la maladie osseuse de Paget. Nouv. Presse Med. 3, 1299–1301.

Rebel, A., Basle, M., Pouplard, A., Kouyoumdjian, S., Filmon, R., Lepatezour, A., 1980a. Viral antigens in osteoclasts from Paget's disease of bone. Lancet 2, 344–346.

Reddy, S.V., Singer, F.R., Roodman, G.D., 1995. Bone marrow mononuclear cells from patients with Paget's disease contain measles virus nucleocapsid messenger ribonucleic acid that has mutations in a specific region of the sequence. J. Clin. Endocrinol. Metab. 80, 2108–2111.

Reddy, S.V., Singer, F.R., Mallette, L., Roodman, G.D., 1996. Detection of measles virus nucleocapsid transcripts in circulating blood cells from patients with Paget's disease. J. Bone Miner. Res. 11, 1602–1607.

Reddy, S.V., Kurihara, N., Menaa, C., Landucci, G., Forthal, D., Koop, B.A., Windle, J.J., Roodman, G.D., 2001. Osteoclasts formed by measles virus-infected osteoclast precursors from hCD46 transgenic mice express characteristics of pagetic osteoclasts. Endocrinology 142, 2898–2905.

Reid, I.R., Davidson, J.S., Wattie, D., Wu, F., Lucas, J., Gamble, G.D., Rutland, M.D., Cundy, T., 2004. Comparative responses of bone turnover markers to bisphosphonate therapy in Paget's disease of bone. Bone 35, 224–230.

Reid, I.R., Lyles, K., Su, G., Brown, J.P., Walsh, J.P., del Pino-Montes, J., Miller, P.D., Fraser, W.D., Cafoncelli, S., Bucci-Rechtweg, C., Hosking, D.J., 2011. A single infusion of zoledronic acid produces sustained remissions in Paget disease: data to 6.5 years. J. Bone Miner. Res. 26, 2261–2270.

Roodman, G.D., Kurihara, N., Ohsaki, Y., Kukita, A., Hosking, D., Demulder, A., Smith, J.F., Singer, F.R., 1992. Interleukin-6, a potential autocrine/paracrine factor in Paget's disease of bone. J. Clin. Investig. 89, 46–52.

Roodman, G.D., 2010. Insights into the pathogenesis of Paget's disease. Ann. N. Y. Acad. Sci. 1192, 176–180.

Schmorl, G., 1932. Uber ostitis deformans Paget. Virchows Arch. Pathol. Anat. Physiol. 283, 694–751.

Schweitzer, D.H., Oostendorp-Van de Ruit, M., Van der Pluijm, G., Lowik, C.W.G., Papapoulos, S.E., 1995. Interleukin-6 and the acute phase response during treatment of patients with Paget's disease with the nitrogen-containing bisphosphonate dimethylaminohydroxypropylidene bisphosphonate. J. Bone Miner. Res. 10, 956–962.

Shankar, S., Hosking, D.J., 2006. Biochemical assessment of Paget's disease of bone. J. Bone Miner. Res. 21 (Suppl. 2), 22–27.

Singer, F.R., Krane, S.M., 1998. Paget's disease of bone. Metabolic Bone Disease 546–615.

Singer, F.R., Bone 3rd, H.G., Hosking, D.J., Lyles, K.W., Murad, M.H., Reid, I.R., Siris, E.S., Endocrine Society, 2014. Paget's disease of bone: an endocrine society clinical practice guideline. J. Clin. Endocrinol. Metab. 99, 4408–4422.

Singer, F.R., 2015. Paget's disease of bone-genetic and environmental factors. Nat. Rev. Endocrinol. 11, 662–671.

Singer, F.R., 2016. Bone quality in Paget's disease of bone. Curr. Osteoporos. Rep. 14, 39–42.

Sun, Q.L., Sammut, B., Wang, F.M., Kurihara, N., Windle, J.J., Roodman, G.D., Galson, D.L., 2014. TBK1 mediates critical effects of measles virus nucleocapsid protein (MVNP) on pagetic osteoclast formation. J. Bone Miner. Res. 29, 90–102.

Teramachik, J.L., Zhou, H., Subler, M.A., Kitagawa, Y., Galson, D.L., Dempster, D.W., Windle, J.J., Kurihara, N., Roodman, G.D., 2014. Increased IL-6 expression in osteoclasts is necessary but not sufficient for the development of Paget's disease of bone. J. Bone Miner. Res. 29, 1456–1465.

Teramachi, J., Nagata, Y., Mohammad, K., Inagaki, Y., Ohata, Y., Guise, T., Michou, L., Brown, J.P., Windle, J.J., Kurihara, N., Roodman, G.D., 2016. Measles virus nucleocapsid protein increases osteoblast differentiation in Paget's disease. J. Clin. Investig. 126, 1012–1022.

van Staa, T.P., Selby, P., Leufkens, H.G., Lyles, K., Sprafka, J.M., Cooper, C., 2002. Incidence and natural history of Paget's disease of bone in England and Wales. J. Bone Miner. Res. 17, 465–471.

Zhao, C.L., Irie, N., Takada, Y., Shimoda, K., Miyamoto, T., Nishiwaki, T., Suda, T., Matsuo, K., 2006. Bidirectional ephrinB2-EphB4 signaling controls bone homeostasis. Cell Metabol. 4, 111–121.

Further reading

Laurin, N., Brown, J.P., Lemainque, A., Duchesne, A., Huot, D., Lacourciere, Y., Drapeau, G., Verreault, J., Raymond, V., Morissette, J., 2001. Paget disease of bone: mapping of two loci at 5q35-qter and 5q31. Am. J. Hum. Genet. 69, 528–543.

Lucas, G.J., Riches, P.L., Hocking, L.J., Cundy, T., Nicholson, G.C., Walsh, J.P., Ralston, S.H., 2008. Identification of a major locus for Paget's disease on chromosome 10p13 in families of British desent. J. Bone Miner. Res. 23, 58–63.

Mee, A.P., Gordon, M.T., May, C., Bennett, D., Anderson, D.C., Sharpe, P.T., 1993. Canine distemper virus transcripts detected in the bone cells of dogs with metaphyseal osteopathy. Bone 14, 59–67.

Mee, A.P., Hoyland, J.A., Baird, P., Bennett, D., Sharpe, P.T., 1995. Canine bone marrow cell cultures infected with canine distemper virus: an *in vitro* model of Paget's disease. Bone 17, 461S–466S.

Mee, A.P., Webber, D.M., May, C., Bennett, D., Sharpe, P.T., Anderson, D.C., 1992. Detection of canine distemper virus in bone cells in the metaphyses of distemper-infected dogs. J. Bone Miner. Res. 7, 829–834.

Mills, B.G., Singer, F.R., Weiner, L.P., Holst, P.A., 1980. Cell cultures from bone affected by Paget's disease. Arthritis Rheum. 23, 1115–1120.

Mills, B.G., Singer, F.R., Weiner, L.P., Holst, P.A., 1981. Immunohistological demonstration of respiratory syncytial virus antigens in Paget's disease of bone. Proc. Natl. Acad. Sci. U.S.A. 78, 1209–1213.

O'Driscoll, J.B., Anderson, D.C., 1985. Past pets and Paget's disease. Lancet 2, 919–921.

Rebel, A., Basle, M., Pouplard, A., Malkani, K., Filmon, R., Lepatezour, A., 1980b. Bone tissue in Paget's disease of bone. Ultrastructure and immunocytology. Arthritis Rheum. 23, 1104–1114.

Chapter 68

Genetic determinants of bone mass and osteoporotic fracture

Yi-Hsiang Hsu[1], Charles R. Farber[2] and Douglas P. Kiel[1]

[1]Department of Medicine, Beth Israel Deaconess Medical Center and Harvard Medical School, Harvard School of Public Health, Hinda and Arthur Marcus Institute for Aging Research, Hebrew SeniorLife, Boston, MA, United States; [2]Center for Public Health Genomics, Departments of Public Health Sciences and Biochemistry and Molecular Genetics, University of Virginia School of Medicine, Charlottesville, VA, United States

Chapter outline

Introduction

Osteoporosis is a disease characterized by low bone mineral density (BMD), deteriorated bone microstructure, and increased risk of fracture that affects over 12 million individuals in the United States (Black and Rosen, 2016) https://paperpile.com/c/K3pMVk/i02VE). Family history is the strongest risk factor for development of osteoporosis, indicating a strong genetic basis (Christian et al., 1989; Ralston and de Crombrugghe, 2006; Ralston and Uitterlinden, 2010). Indeed, fracture-related traits, such as BMD, are among the most highly heritable disease-associated quantitative traits ($h^2 > 0.50$) (Christian et al., 1989; Ralston and de Crombrugghe, 2006; Ralston and Uitterlinden, 2010). As a result, developing a comprehensive biological understanding of bone requires a detailed understanding of the identity and function of the genes contributing to variation in bone traits.

Genome-wide association studies

Genome-wide association study (GWAS) using high-throughput microarrays to genotype hundreds of thousands and even millions of the most common genetic variants and relating them to phenotypic variation has transformed the field of genetics over the past decade. Table 68.1 lists resources of GWAS findings, disease-risk genetic variants, and their functional impact and druggable targets.

Conceptually, performing a GWAS is straightforward and consists of two main steps: (1) "data generation"—acquisition of genotypes and phenotypes and (2) "analysis"—associating genotype with phenotype (Bush and

Principles of Bone Biology. https://doi.org/10.1016/B978-0-12-814841-9.00068-3

TABLE 68.1 Resources for genome-wide association studies in humans.

Name	Description	Website
GWAS Catalog	A summary of genome-wide significant loci and genome-wide suggestive significant loci	https://www.ebi.ac.uk/gwas/
Genetic Factors for Osteoporosis Consortium	Summary statistics of published GWAS meta-analyses relevant to bone and muscle phenotypes	http://www.gefos.org/
GWAS Central	Summary statistics of published GWASs and GWAS meta-analyses	https://www.gwascentral.org/
Online Mendelian Inheritance in Man	Monogenic bone-relevant disorders	https://www.omim.org/
ClinVar	Variants associated with phenotypes and with strong clinical evidence to support their impact on diseases/phenotypes	https://www.ncbi.nlm.nih.gov/clinvar/
Global Variome	The Human Variome Project: curate all human genetic variation affecting human health	http://www.humanvariomeproject.org/ https://databases.lovd.nl/shared
Mitochondrial Disease Sequence Data Resource Consortium	Mitochondrial disease sequence data resource with bone-relevant disorders	https://mseqdr.org/
PharmGKB	Effect of human genetic variation on drug responses	https://www.pharmgkb.org/
Genotype-Tissue Expression project	Expression quantitative trait loci and expression single-nucleotide polymorphisms in multiple human tissues	https://gtexportal.org/

Moore, 2012). The first step of GWAS requires the generation of genome-wide single-nucleotide polymorphism (SNP) genotypes in a cohort of individuals who have been phenotyped for a trait of interest. In the osteoporosis field, the trait of interest most often has been DXA-derived BMD (Estrada et al., 2012; Rivadeneira et al., 2009), though other bone traits have been interrogated, such as bone size (Deng et al., 2013; Lei et al., 2012; Liu et al., 2008; Ran et al., 2013), trabecular density (Nielson et al., 2016), and estimated BMD of the heel measured by ultrasound (Kemp et al., 2016). Genotypes are generated using massively parallel genotyping arrays that simultaneously generate genotypes for 500,000 to 55,000,000 SNPs per individual. The most popular genotyping arrays are those produced by Illumina and Affymetrix (Chee et al., 1996; Gunderson et al., 2004). Array SNPs are spaced throughout the genome and typically designed to "capture" as much common genetic variation as possible in the human genome.

A key concept in the GWAS, and for that matter any genetic analysis, is linkage disequilibrium (LD). LD is often confusing to nongeneticists but provides the basis upon which GWAS is possible. LD is a phenomenon in which the alleles at two positions on a chromosome (SNPs or other variants) are not randomly distributed in a population. LD arises from the fact that alleles are inherited together on the same chromosome. Recombination during meiosis acts to separate alleles, but this takes many generations and is extremely rare for genetic variants in close proximity. If LD did not exist, all alleles would segregate independently. In this context, all variants would have to be tested in a GWAS to capture the majority of genetic variation potentially contributing to a disease. However, LD causes considerable redundancy among variants. For the vast majority of common genetic variants (those where the rarest allele is present in at least 5% of individuals), a number of other variants in the human genome will be in high LD. In practical terms this means that if the genotype is known for one variant, the genotype of any other variant in high LD is also known. Because of LD, it is possible to conduct a GWAS without genotyping all variants and still capture most variation from common variants across the genome. While this is a significant advantage of LD, it does have negative consequences when it comes to identifying variants that are truly causal for GWAS associations.

This approach interrogates the whole genome to search for associations without any prior assumptions about the underlying cause of a disease or the genetic architecture of a trait. GWASs have provided valuable information about the contribution of genetic variants to phenotypes including the following observations: (1) Most variants having a statistically significant association with phenotypes have small effect sizes and only explain a small percent of variance in a trait

(Manolio, 2009); (2) Many more variants with effect sizes that do not reach statistical significance account for some of the so-called "missing heritability" of complex diseases that have been studied (Yang et al., 2010); (3) Many rare variants with larger effect sizes also contribute to phenotypic variance (Marouli et al., 2017); (4) Most significant genetic associations from GWAS are located in noncoding regions of the genome such that their associations with phenotypic variation are mediated through regulatory effects (Maurano et al., 2012); (5) Current models of genetic associations with disease postulate that genetic variants collectively contribute multiple weak effects on key genes and regulatory pathways that confer the risk of various diseases.

The polygenic nature of complex disease has been well studied in the field of musculoskeletal genetics in a similar evolution as has been observed for other diseases. Thus, collaborative efforts across the world have enabled the scientific community interested in complex diseases of the skeleton to pool data to achieve the large sample sizes needed to characterize the genetic architecture of common diseases of the skeleton such as osteoporosis (Karasik et al., 2002, 2007, 2017a, 2017b), which has a high heritability regardless of how one measures the skeletal features and fracture (Michaelsson et al., 2005). Over time these collaborations have produced sample sizes that have now achieved upwards of half-a-million individuals.

Several large-scale GWAS meta-analyses of osteoporosis-related traits have been published (Estrada et al., 2012; Rivadeneira et al., 2009; Nielson et al., 2016; Hsu et al., 2010; Kung et al., 2010; Liu et al., 2012; Oei et al., 2012; Zheng et al., 2015). A summary of those loci can be found in a review article (Hsu and Kiel, 2012) as well as more recent publications (Nielson et al., 2016; Zheng et al., 2015; Hsu et al., 2016a). To date, the two largest GWAS meta-analyses for BMD have involved ~36,000 Caucasian men and women with 2.5 million HapMap-imputed common SNPs as well as one involving up to 31,016 fracture cases and 102,444 controls without fracture as part of the Genetic Factors for Osteoporosis consortium (Estrada et al., 2012). To date, ~70 genome-wide significant loci have been found to be associated with DXA-measured BMD of the lumbar spine (LS) and/or femoral neck (FN). Eighteen of these 70 BMD-associated loci were also associated with fracture risk in a case–control study (Estrada et al., 2012; Hsu and Kiel, 2012; Oei et al., 2011). As is true for many GWAS efforts, the identified common SNPs with the most significant *P*-values may not be the causal variants and are more likely to be in LD with underlying untyped causal variants or variants with less significant *P*-values. To illustrate the growing number of significant genetic associations observed with increasing sample sizes, one only has to consider that the first GWAS for DXA-derived BMD and hip geometry traits, the Framingham Study using a genotyping platform with only 100,000 SNPs in a sample of only 1,141 men and women, yielded no significant genome-wide findings. The most recent GWAS based on quantitative calcaneal ultrasound (estimated BMD—eBMD) in 445,326 individuals from the UK Biobank cohort identified 1,103 conditionally independent signals mapping to 515 loci and explained 18% of the variance in eBMD (Morris et al., 2019). At these 515 loci, 301 of which were novel when compared with the next largest GWAS in the same cohort when genotyping 140,623 individuals of European descent, 307 conditionally independent SNPs attained genome-wide significance at 203 loci (of which 153 were novel), altogether explaining 11.8% of the variance. These included the majority of SNPs previously associated with DXA-derived BMD as well as 308 novel loci, including many containing genes that had not been previously implicated in bone physiology. The growing number of loci for bone density highlights the value of expanding the sample size of GWASs and the great potential for identifying new biology as a next step toward driving these discoveries in the direction of clinical applications (e.g., drug targets). In fact, when all the GWAS signals are considered in pathway analyses, gene clusters are characterized by factors from major pathways critical to bone biology such as the RANK–RANKL–OPG pathway, mesenchymal–stem cell differentiation, endochondral ossification, and Wnt signaling. New targets may also be identified from GWAS. In a recent study, a low-frequency noncoding variant near a novel locus, engrailed homeobox-1 (*EN1*), with an effect size fourfold larger than the mean of previously reported common variants for BMD of the LS (rs11692564 (T), minor allele frequency (MAF) = 1.6%, replication effect size = +0.20 standard deviations, *P*-value for the meta-analysis = 2×10^{-14}), was confirmed. This variant's positive effect on BMD was accompanied by a decreased risk of fracture when comparing 598,742 fracture cases with 409,511 controls (odds ratio = 0.85; $P = 2 \times 10^{-11}$).

As more GWASs are performed, phenotypes other than BMD are being targeted. A GWAS of quantitative computed tomography of the spine identified a novel genetic variant associated with increased vertebral volumetric BMD (vBMD) not previously found to be significant for traditional spine DXA-derived BMD (Nielson et al., 2016). Also in this study, rs2468531 (5p13, near SLC1A3), the allele associated with higher vBMD, was found to be associated with a lower odds ratio of radiographic vertebral fracture after correction for multiple testing (odds ratio = 0.75 per minor allele; false discovery rate (FDR) $P = .01$). Finally, this GWAS identified SNP rs12742784 in the 1p36.12 locus as being associated with increased expression of *EPHB2*, which lies about 355 kb downstream ($\beta = 0.12$, FDR $P = 1.72 \times 10^{-3}$), but was only marginally associated ($P = .08$) with *ZBTB40*, the nearest gene in this GWAS locus (about 96 kb downstream).

With the advent of high-resolution peripheral quantitative computed tomography (HR-pQCT) scanning, further refinement of skeletal phenotypes may be realized. Bone microarchitecture assessed by HR-pQCT has been reported to be heritable even after adjusting for DXA-based areal BMD (aBMD) (Karasik et al., 2017, 2017a) and has been associated with fracture risks. Genetic studies of these phenotypes may reveal unique, novel genes that contribute to skeletal integrity not identifiable in previous GWASs of aBMD. Recently, results were reported from a study using data from 5,692 adult Caucasians obtained from seven cohort studies (Framingham Study, Mayo Clinic, Geneva Retirees Cohort, Os des Femmes de Lyon, Structure of the Aging Men's Bones, Osteoporotic Fractures in Men Sweden, and Gothenburg Osteoporosis and Obesity Determinants study) (Hsu et al., 2016b) with replication in 2,100 independent samples (Canadian Multicentre Osteoporosis Study and QUAlité Osseuse LYon Orléans, or QUALYOR, study). Multiple HR-pQCT phenotypes were assessed, all of the studies were genotyped by SNP chips, and whole-genome imputation to ~40 million SNPs was performed based on the Haplotype Reference Consortium. Meta-analysis was performed to combine association results.

Of the 17 genome-significant loci (386 SNPs with $p < 5 \times 10^{-8}$), 12 were not reported by previous aBMD GWAS meta-analyses: *SIX2, PNPT1, chr4q35.2, KCNIP1, chr5q11.2, chr7q31.31, CSMD1, NRG1, PTHLH-CCFC91, FAM155A, C3*, and *FMN2* loci. The majority of these loci were specifically associated with the phenotype of failure load calculated using finite element analysis (FEA-FL), total area, cortical thickness, trabecular spacing (TbSp), trabecular number, or cortical BMD. The most significantly associated SNP, rs10254825, was associated using FEA-FL ($P = 2.6 \times 10^{-22}$) and associated with a risk for fracture. The remaining 5 loci (*ZBTB40, SPTBN1, MEF2C-AS1, WNT16-FAM3C,* and *AKAP11-TNFSF11*) were previously reported by aBMD GWAS and are associated with multiple HR-pQCT phenotypes at both the radius and the tibia (e.g., Trabecular BMD, Total BMD, TbSp). These findings suggest that the genetic control of bone microarchitecture may provide additional insights into the pathogenesis of skeletal integrity not available from aBMD.

In the largest GWAS meta-analysis to date evaluating the influence of genetic variation on fracture risk, comprising 37,857 cases and 227,116 controls with replication in up to 147,200 fracture cases and 150,085 controls, the signals mapped to genes clustering in pathways known to be critical to bone biology (e.g., *SOST*, *WNT16*, and *ESR1*) and others identifying novel pathways (*FAM210A, GRB10*, and *ETS2*). Using the genetic variants as instrumental variables in a "Mendelian randomization" analyses demonstrated a causal effect of BMD on fracture risk, where each standard deviation decrease in genetically determined FN BMD was associated with a 55% increase in fracture risk (odds ratio = 1.55; 95% CI: 1.48−1.63; $P = 1 \times 10^{-68}$) (Trajanoska et al., 2018).

Focusing on the hallmark fracture of osteoporosis, the vertebral fracture, a recent GWAS was conducted in 1,553 postmenopausal women with clinical vertebral fractures and 4340 controls, with a two-stage replication involving 1,028 cases and 3,762 controls (Alonso et al., 2018). Potentially causal variants were identified using expression quantitative trait locus (eQTL) data from transiliac bone biopsies and bioinformatic studies. In contrast to much larger case−control studies, this modestly sized study identified a locus tagged by rs10190845 on chromosome 2q13 that was significantly associated with clinical vertebral fracture (odds ratio = 1.74; 95% CI: 1.06−2.6; $P = 1.04 \times 10^{-9}$). Bioinformatic analysis of this locus identified several potentially functional SNPs that are associated with expression of the positional candidate genes *TTL* and *SLC20A1*. Three other suggestive loci were identified on chromosomes 1p31, 11q12, and 15q11. The fact that this study identified loci that were novel and had not previously been associated with BMD or clinical fractures highlights the importance of studying various skeletal phenotypes. Available resources that may be used in conducting GWASs in human populations are shown in Table 68.1.

Follow-up of genome-wide association studies

Functional annotations

Given that the majority of significant GWAS associations are located in noncoding regions of the genome, one of the challenges of GWAS approaches is to be able to identify the most likely causal variant in a GWAS locus. Due to the LD structure, it is most likely that a cluster of SNPs all show strong associations with a phenotypes in each GWAS locus. Based on statistical association information alone, it is almost impossible to identify which variant(s) are potential causal variants and which gene(s) these causal variants map to. A growing number of tools have been developed to identify the likely causal noncoding variant such as fitness consequence scores (fitCons) (Gulko et al., 2015); prediction tools with machine learning algorithms such as DeepSEA (Zhou and Troyanskaya, 2015), deltaSVM (Lee et al., 2015), and Basset (Kelley et al., 2016); and epigenetic resources from ENCODE (Dunham et al., 2012), and the NIH Epigenetics RoadMap

Project (Roadmap Epigenomics et al., 2015). In addition, colocalization of eQTL (Heyn, 2016) and allelic specific expression in bone tissue (Jemtland et al., 2011), osteoclast cells (Mullin et al., 2018), multiple tissues of the Genotype-Tissue Expression (NIH GTEx) project (GTE, 2012), and miRBase databases for miRNA-coded regions and targets (Griffiths-Jones et al., 2006) can be used to narrow down the variants that may affect gene expression levels (see Fig. 68.1).

Expression quantitative trait loci in human bone tissue and cells

The limitation of currently available bone eQTL studies is their relatively small sample size, which makes it challenging to find associations with less common and rare variants. Two human eQTL studies have been reported. One is for osteoblasts and the other is for PBMC-derived osteoclast-like cells. Primary osteoblasts were derived from trabecular bone of proximal femora obtained from 95 Caucasians undergoing total hip replacement (Grundberg et al., 2009). A gene expression profile with 18,144 known genes via Illumina Human Ref8v2 BeadChips was measured. Genome-wide genotyping of 561,303 SNPs was done using Illumina 550k Duo chips. No imputation was done for this study. All gene expression levels were adjusted for sex and year of birth. Using a P-value $< 3.5 \times 10^{-8}$ (Bonferroni adjusted $P = .05/1{,}404{,}011$ tests), a total of 590 cis-eQTLs were identified. The osteoblast cis-eQTL findings are available through an interactive web-based browser (http://www.regulatorygenomics.org). Cultures of osteoclast-like cells from peripheral blood mononuclear cells were obtained from 158 female patients aged 30−70 years (Mullin et al., 2018). Genotyping was done by the Illumina Infinium

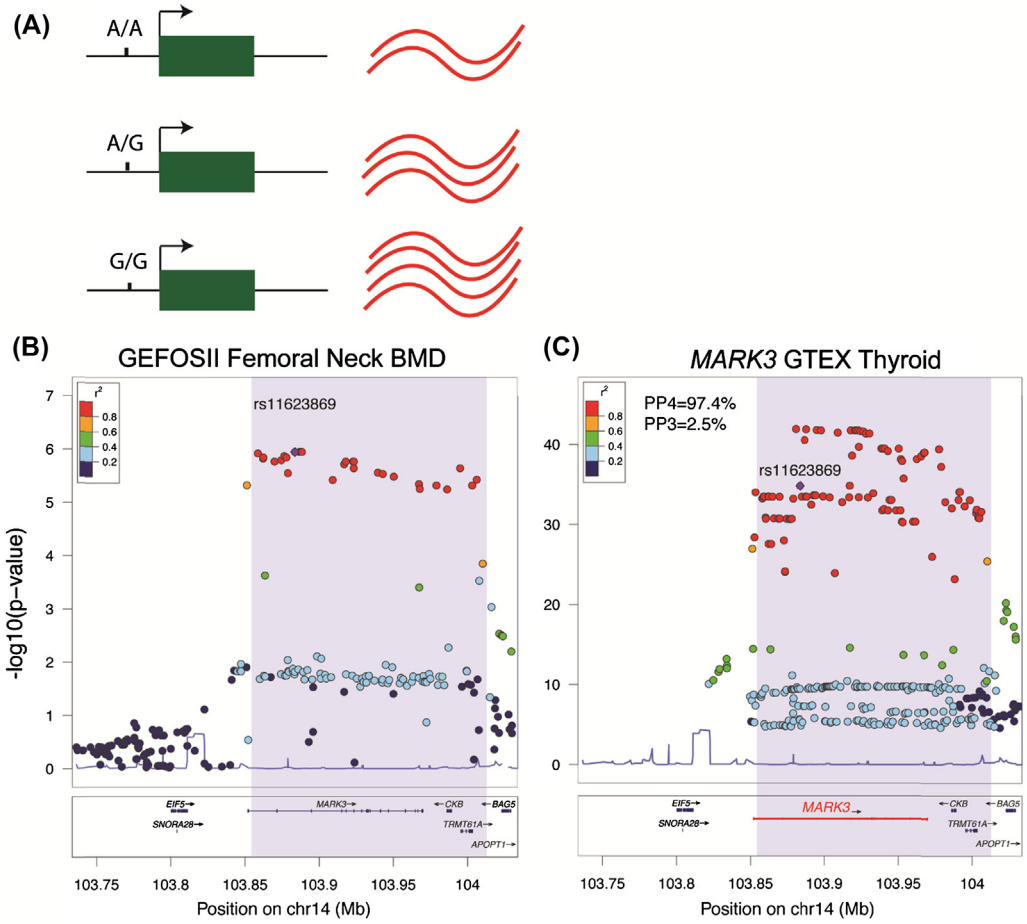

FIGURE 68.1 Using expression quantitative trait locus (eQTL) analysis to inform GWAS. (A) An eQTL is a genetic variant—single-nucleotide polymorphism (SNP), insertion/deletion, etc.—that alters the transcript levels of a gene. In this example, the "G" allele of an SNP increases transcription. eQTL can influence transcription, promoter usage, and posttranscriptional processes such as mRNA stability and splicing. (B and C) A locus influencing BMD and a colocalizing eQTL for *MARK3* in thyroid tissue. A colocalization approach was used to determine that the probability that a single shared variant is responsible for the two associations is 97.4% (PP4). Based on these data, one can hypothesize that variants in this region of chromosome 14 influence *MARK3* expression, which in turn influences BMD. *Data from GTEx.*

OmniExpress-24 BeadChip array and imputed by the Sanger Imputation Service using the Haplotype Reference Consortium release 1.1 reference panel. RNA samples extracted from the osteoclast-like cells and RNA-seq was done by 50 bp single-end reads on an Illumina (San Diego, CA, USA) HiSeq 2500 NGS machine. Several of the eQTL associations identified are relevant to genes that present strongly as having a role in bone, particularly IQGAP1, CYP19A1, CTNNB1, and COL6A3. In addition to specific bone cells, eQTLs on human whole bone have been performed. Iliac bone biopsies from 84 postmenopausal women from Oslo, Norway, were collected, and whole-bone gene expression was done by Affymetrix microarrays (Hsu et al., 2010; Grundberg et al., 2008). Genome-wide genotyping was performed using Affymetrix Genome-Wide Human SNP Array 6.0/Affymetrix Axiom Biobank array (1,000,000 and 700,000 SNPs assessed, respectively) (Reppe et al., 2017). Cis-eQTL analysis within a 2 Mb flanking region (1 Mb upstream and 1 Mb downstream) was performed to evaluate whether they influence transcript levels of genes in human whole bone (Hsu et al., 2010; Grundberg et al., 2008). A hypergeometric test was used to analyze clustered human bone eQTL and GWAS findings from 15 phenotypes from the NHGRI GWAS catalog. The top six phenotypes with their GWAS findings significantly enriched in the whole-bone cis-eQTLs include height, rheumatoid arthritis (RA), serum HbA1c level, ulcerative colitis, schizophrenia, and LS BMD. The enrichment analysis reflected the complexity and mixture of different cell types (including osteocytes, osteoblasts, osteoclasts, and bone marrow composed of hematopoietic and stromal stem cells and their lineages such as endothelial and fibroblast cells) in the whole-bone biopsies (Reppe et al., 2017). Given the mixture of cell types, there was still significant enrichment for the LS BMD GWAS. It is notable that the GWAS of human height, which was the most significantly enriched in human bone eQTLs, has been reported in several studies to be highly correlated with BMD (El-Bikai et al., 2015). The GWAS of RA also demonstrated a high correlation with human bone cis-eQTLs. In previous studies (Lodder et al., 2004), patients with low to moderately active RA have been found to have lower BMD at the hip and high radiological RA damage, which suggests a correlation between the severity of RA and the risk of bone loss. Hence, this correlation could corroborate the significant association between RA and human bone cis-eQTLs. To increase sample size, as part of the EU-supported Osteogene Consortium (PI: Drs. Kaare M. Gautvik (Jemtland et al., 2011; Reppe et al., 2006; Reppe et al., 2010), Sjur Reppe (Reppe et al., 2006, 2010, 2013), and Harish Datta (Reppe et al., 2013; Kalogeropoulos et al., 2010)), 120 low-trauma osteoporotic fracture patients (80 adult Caucasian women and 40 men, aged >50 years) undergoing hip replacement and 60 nonfracture controls were recruited from Diakonhjemmet Hospital, the Lovisenberg Hospital in Oslo, and the Oslo University Hospital. Bone biopsies are done for each patient during hip replacement surgery. Three bone samples are collected at the (1) FN, (2) FN near the fracture zone, and (3) intertrochanteric region. Whole-genome sequencing (WGS) and RNA-seq are planned.

Cell/tissue types targeted by genome-wide association study loci for bone mineral density and osteoporotic fractures

Previous work has shown that noncoding variants are enriched in tissue and cell type-specific enhancer regions, therefore suggesting disease-relevant cell types (Maurano et al., 2012; Ernst et al., 2011; Lo et al., 2014; Parker et al., 2013; Trynka and Raychaudhuri, 2013). Studying a diverse set of 66 GWAS traits in 127 human reference epigenomic maps from the NIH Roadmap Epigenomics Project has demonstrated that GWAS loci are enriched in gene regulatory elements in known disease-relevant tissue/cell types (for example, pancreatic islets for T2D and liver and intestine for cholesterol levels). In addition, in some instances new discoveries were found in those tissues/cell types that were not suspected as being relevant (for example, immune cell types for Alzheimer's disease), suggesting that GWAS loci may alter the differentiation of precursor cells of expected tissues of involvement (Roadmap Epigenomics et al., 2015; Farh et al., 2015). Several enrichment analytical approaches have been developed (Roadmap Epigenomics et al., 2015) to identify tissue/cell types whose regulatory elements (such as enhancer, promoter, bivalent, and repressed regulatory regions estimated by histone marks using the HMM algorithm; Ernst and Kellis, 2012) are significantly enriched in GWAS loci, which increases the chance of identifying potential underlying causal variants and their affected tissue and cell types. While osteoblasts and osteoclasts are clear candidate target cell types for BMD and osteoporotic fracture-associated GWAS loci, other cell/tissue types may also affected. For example, an unbiased search using cell type enrichment tests for the comprehensive set of all 127 cell/tissue types available in the NIH RoadMap Project that might be related to the previously identified 56 BMD GWAS loci (Estrada et al., 2012) identified a total of 6 cell types, including primary osteoblast, skeletal muscle, skeletal muscle myoblasts, muscle satellite cultured cells, and mesenchymal stem cells derived from chondrocyte cells and derived from adipocytes whose enhancers significantly overlap the BMD loci. Among the 56 loci, associated SNPs in 24 loci were enriched in candidate regulatory modules specific to human primary osteoblasts. The remaining loci were not enriched in regulatory modules in osteoblasts but in other cell/tissue types, suggesting potential additional pathophysiological pathways of osteoporosis that are not relevant to bone cells. The

identified tissue/cell types will also inform the design of in vitro experiments that will select relevant cells for functional validation of associated BMD variants.

Informing genome-wide association studies using biological knowledge and networks

GWAS is not expected to implicate genes that are random with respect to function. In fact, genes located within BMD GWAS associations are enriched for gene ontology terms such as "skeletal system development" and "Wnt signaling," among many others related to bone development (Estrada et al., 2012). These data suggest that truly causal genes participate in specific bone-relevant processes, such as osteoblast-mediated bone formation and osteoclast-mediated bone resorption. Although this observation is not unexpected, it has important implications. The most important is that by examining all genes within a locus it is possible to predict causality based on a gene's "connection" to or membership in a bone-relevant process or pathway.

There are a number of ways to group genes into functional groups. A common approach is to group genes based on prior knowledge or known function. Two examples of approaches developed to do this specifically in the context of GWAS are Gene Relationships Among Implicated Loci ("GRAIL") (Raychaudhuri et al., 2009) and Meta-Analysis Gene-set Enrichment of variaNT Associations ("MAGENTA") (Segre et al., 2010). GRAIL queries a set of genomic regions identified by GWAS and assesses relationships between genes across regions through a comprehensive cocitation analysis of PubMed. GRAIL was used in the largest GWAS meta-analysis for DXA-derived BMD and highlighted the RANK−RANKL−OPG, mesenchymal stem cell differentiation, and Wnt signaling pathways as functional groups whose members contribute to the genetic architecture of BMD (Estrada et al., 2012). MAGENTA identified very similar sets of pathways when applied to a recent GWAS for heel ultrasound-derived BMD (Kemp et al., 2016).

A second approach is to group genes based on empirical data. Data-driven Expression Prioritized Integration for Complex Traits (DEPICT) predicts gene function using coexpression relationships mined from a large compendium of ~78k expression profiles (Pers et al., 2015). It then uses predictions for all genes in the genome to identify functional groups containing more genes than would be expected by chance from a list of genes across a set of GWAS loci. Using this information, DEPICT prioritizes genes within a locus based on the likelihood they are causal. DEPICT also predicts the tissues and cell types responsible for a significant portion of the "genetic load" for a particular disease. When applied to the heel eBMD GWAS, 273 genes were identified as likely driving eBMD association signals (Kemp et al., 2016). For 189 of these genes, the mouse homologue had been characterized in a knockout line, and 62 (33%) were found to have skeletal abnormalities.

Another strategy for informing GWAS is the use of networks (Farber, 2013; Leiserson et al., 2013). The idea is very similar to DEPICT; however, genes are prioritized based on their network topology with known disease genes. Furthermore, such approaches can address more fundamental questions, such as "Are hub genes in protein−protein interactions more or less likely to be genetically associated with complex traits?" In the context of bone, a coexpression network generated from mouse cortical bone expression profiles was recently used to predict potential causal genes for 56 BMD GWAS loci (Estrada et al., 2012; Calabrese et al., 2017). A list of mouse homologues located within the loci were mapped onto the bone coexpression network. Two network modules were found to be enriched for genes implicated by GWAS. These modules were themselves enriched for genes important for osteoblast activity. The authors used this information to predict 33 potentially causal genes at 30 loci. Two loci were studied in depth, and experimental evidence supported *SPTBN1* and *MARK3* as causal for the two associations.

Knockout animal models for functional analysis

A more direct approach to provide functional evidence is the validation of GWAS genes and variants via animal models. However, due to challenges such as time and resource requirements as well as the difficulty of pinning down the variants and affected genes in each GWAS locus, such experiments are not always easy to conduct. Databases such as the International Mouse Phenotyping Consortium (IMPC, http://www.mousephenotype.org/) offer the opportunity to identify GWAS candidate genes in silico using reported bone phenotypes from characterized knockout mice. The IMPC has created knockout mice on 20,000 protein-coding genes. Another example is the Origins of Bone and Cartilage Disease (OBCD, http://www.boneandcartilage.com) project, which is an international collaboration identifying genetic causes of bone and cartilage disease through the systematic characterization of knockout strains. As part of this project, 733 knockout mice strains have gone through a comprehensive bone phenotyping protocol, including digital X-ray microradiography to measure femur length and bone mineral content; micro-CT to measure trabecular bone (BV/TV, Tb. N, Tb. Th) and cortical bone (Ct.Th, BMD); and biomechanical testing with three-point bending tests of the femur (yield, maximum and fracture

loads, stiffness, toughness) and vertebral compression testing (yield and maximum loads, stiffness) in adult and embryonic mice via the OBCD. Such resources can be used to prioritize GWAS candidate genes based on bone phenotyping from knockout mice as well as to obtain knockout mice strains for functional validation of GWAS findings. Previously, an SNP, rs11692564, was found to be associated with LS BMD (*P*-value for the meta-analysis $= 2 \times 10^{-14}$) (Zheng et al., 2015). The SNP is located 53 kb downstream from the *EN1* gene on chromosome 2. A cluster of SNPs in LD with rs11692654 and located in 5′ promoter and 3′ regulatory regions of the *EN1* gene was also found to be significantly associated with higher BMD and lower risk of osteoporotic fractures in Caucasians. The *En1* gene was conditioned knockout in mice. *En1* expression was detected during osteoblastogenesis in developing and mature cultured murine calvarial osteoblasts but not in marrow-derived osteoclasts. Conditional loss of *En1* resulted in low bone mass. Measured by μCT, mutants had lower trabecular bone volume fraction, number, and thickness in both lumbar L5 vertebrae. By histomorphometry, mutants had a statistically higher proportion of osteogenic and osteoclastic cells compared with littermate controls, suggesting low bone mass likely as a consequence of high bone turnover.

Genome-wide association studies for bone traits in mice

As discussed above, GWAS in humans has significantly informed our understanding of the genetics of BMD. It has provided the approximate location of hundreds of sites in the human genome that harbor genetic variants influencing BMD. This serves as the foundation to identify key genes responsible for the heritable component of BMD and begin to comprehensively unravel the complex genetic architecture of bone mass (Timpson et al., 2018). These findings have important implications for our understanding of bone biology, precision medicine, drug development, and ultimately the prevention and treatment of osteoporosis (Richards et al., 2012). However, a primary limitation of GWAS for osteoporosis is that large-scale (N ~ hundreds of thousands) studies have only been performed for BMD. In the context of fracture, this is problematic because BMD explains only part of the risk of fracture (Cummings et al., 2002; Dufresne et al., 2003; Lochmuller et al., 1998). Other aspects of bone, such as geometry and trabecular and cortical microarchitecture, have not been interrogated by large-scale GWAS, and such studies will likely take years to perform. Other characteristics such as bone cell activities, biomechanical bone strength, and bone quality will likely be impossible to study using human GWAS. Given the clinical importance of these independent predictors of fracture, how do we dissect their genetic architecture? One promising approach is to gain insight through GWAS in mice.

Mice have played a key and central role in our understanding of bone biology. In particular, mouse models have been used to generate the majority of our understanding of basic bone biology. Besides the obvious fact that mice possess a skeleton, there are a number of other reasons why mouse genetic mapping is a promising complementary approach to human GWAS. First, mouse genomes are highly similar to those of humans. Sequencing of the mouse reference genome revealed that ~40% of the mouse genome can be aligned at the sequence level (Mouse Genome Sequencing et al., 2002) to the human genome. This level of similarity rises to ~80% for coding genes (ranging from ~60% to 99%), and less than 1% of mouse genes do not have a clear human orthologue (Mouse Genome Sequencing et al., 2002). Second, it has been demonstrated that while only 5% of regulatory sites across a number of mouse tissues have been conserved in humans at the sequence level, 95% of the networks between transcription factors and the genes they regulate are the same between mice and humans (Stergachis et al., 2014). Third, while important differences exist, a large body of literature indicates a high level of similarity in gene function in the context of bone and overall bone physiology between rodents and humans. Fourth, there is evidence of correspondence between genes identified by mouse genetic means also playing a role in the genetic regulation of skeletal traits in humans (Ackert-Bicknell et al., 2008; Ghazalpour et al., 2012; Mesner et al., 2014; Tang et al., 2009).

Resources and the application of genome-wide association studies for skeletal traits in mice

In recent years there have been significant efforts placed toward developing state-of-the-art genetic mapping tools in mice (Flint and Eskin, 2012).

Similar to human approaches, early mouse genetic mapping strategies relied on linkage analysis in "families." The most popular approach was the generation of F2 populations of mice derived through the interbreeding of two classical inbred strains (Abiola et al., 2003; Darvasi, 1998). Such studies were extremely successful at localizing genomic regions harboring trait-associated variants (termed quantitative trait loci, or QTLs) (Shmookler Reis, 2003). In fact, hundreds of QTLs for BMD, trabecular and cortical architecture, bone geometry, bone strength, and other skeletal traits have been mapped using this approach (Ackert-Bicknell et al., 2010). The problem with F2 crosses, however, is that QTL confidence intervals are quite large (many centimorgans or megabase pairs [Mbp]), making it very difficult to identify the responsible causative genes. In fact, they are only a small number of cases in which this approach was successful for the purpose of

gene identification for bone traits (Mesner et al., 2014; Edderkaoui et al., 2007; Klein et al., 2004). As the mouse genome was sequenced (Mouse Genome Sequencing et al., 2002) (Mouse Genome Sequencing Consortium et al., 2002) and genotyping capabilities expanded, the ability to transition from linkage to GWAS emerged.

While this section is focused on the mouse, we should note that several other model organisms have made and will continue to make important contributions to our understanding of complex skeletal traits. For example, GWAS in outbred rats has been used to map a number of loci influencing BMD, bone architecture, and biomechanical bone strength (Alam et al., 2014; Levy et al., 2015; Rat Genome et al., 2013).

Inbred strains

The first application of GWAS in mice used panels of inbred strains (Cervino et al., 2007; Grupe et al., 2001; Pletcher et al., 2004). The strategy consists of performing an association analysis with existing genome-wide genotype profiles and phenotypes collected in a set of strains by treating the strain set like a group of unrelated individuals. In many cases, GWASs were performed "in silico" with archival sets of phenotypes that may have been collected years or decades prior (Grupe et al., 2001; Bogue et al., 2018). While this approach was superior in terms of the resolution of association (confidence intervals for associations were typically <1 Mbp), it had limitations (Payseur and Place, 2007). Because inbred strains share a common and complex breeding history, strains are not entirely unrelated. In fact, some sets of strains are highly related (the sets of B6 and 129 related strains are examples). Uneven relatedness (called population structure or population stratification) can lead to false positive associations if the phenotype under investigation also differs dependent on the complex patterns of relatedness (which is often the case). The other limitation was statistical power due to the small number of strains readily available for phenotyping—this resulted in the identification of only the largest genetic effects on complex traits. The limitations of using inbred strain panels were partly resolved through the development of analytical approaches that adjusted for population structure (EMMA, etc.; Kang et al., 2008) and leveraging QTL information from linkage study to mitigate false positive associations (Su et al., 2010).

Hybrid mouse diversity panel

The Hybrid Mouse Diversity Panel (HMDP) is a high-resolution resource for GWAS that was developed in part to solve the problem of low statistical power for GWAS in inbred strain panels (Ghazalpour et al., 2012; Bennett et al., 2010; Lusis et al., 2016). Instead of relying strictly on classical inbred strains, the HMDP combined these strains with recombinant inbred (RI) strains. RIs are F2 mice that have been inbred, and RI panels themselves have been used to map genes for complex bone phenotypes. By combining classical lab and RI strains, initial versions of the HMDP comprised approximately 100 strains. By boosting the number of strains surveyed, the HMDP had 80% probability of detecting an association explaining 5% of the variance in a complex trait (Bennett et al., 2010). Also, because of the inclusion of the classical lab strains, the resolution of associations in the HMDP was <1 Mbp. One of the first studies to use the HMDP identified *Asxl2* as a regulator of BMD (Farber et al., 2011). *Asxl2* was later shown to be a master regulator of skeletal, lipid, and glucose homeostasis (Izawa et al., 2015).

Collaborative cross and diversity outbred

Nearly 15 years ago the mouse genetics community set out to develop an "ideal" population for genetic mapping (Churchill et al., 2012). This population, termed the "Collaborative Cross" (CC) is a multiparental population created by "combining" eight genetically diverse inbred founders: A/J, C57BL/6J, 129S1/SvImJ, NZO/H1LtJ, NOD/LtJ, WSB/EiJ, PWK/PhJ, and CAST/EiJ (Collaborative Cross, 2012; Aylor et al., 2011; Churchill et al., 2004). The CC was created using funnel mating designs, each of which resulted in a unique recombinant inbred strain whose genome is a mosaic of the eight founders. Importantly, the genomes of the founders have been sequenced, leading to the discovery of at least 31.5 million SNPs and 6.1 million insertion/deletions (Srivastava et al., 2017). Importantly, the number of variants in the CC is roughly three times higher than existing mouse reference populations, increasing the likelihood that genes involved in the regulation of skeletal phenotypes are functionally polymorphic and can be identified through mapping.

Early in the generation of the CC, mice from 144 of the CC mating funnels were used to create the Diversity Outbred (DO) population (Churchill et al., 2012; Srivastava et al., 2017). The DO has all the characteristics of the CC except that mice are outbred and genetically unique. This offers the advantage of being highly heterozygous with the ability to characterize large populations for well-powered GWAS scans. It also means that the recombination number and the mapping resolution increase with each generation of the DO (Logan et al., 2013; Svenson et al., 2012). The disadvantage of the DO is that each mouse is unique, which excludes the ability to generate multiple phenotypes over time and in different

environments that the reproducible genetic background of the CC affords. Both the CC and DO have been shown to be powerful resources for the dissection of complex traits (Svenson et al., 2012; Chick et al., 2016; Recla et al., 2014; Shorter et al., 2018; Yuan et al., 2018) including bone (Levy et al., 2015). Large-scale efforts are underway to use CC/DO for high-resolution GWAS scans for a comprehensive suite of complex bone traits.

Advantages of genome-wide association studies in mice

We have already discussed one of the most important advantages of GWAS in mice, which is to study clinically relevant bone traits other than BMD. But there are a number of other advantages of GWAS in mice. Some advantages include the ability to investigate gene × environment interactions, genetic effects over time, and pleiotropy across large numbers of disparate disease-related traits. These advantages are particularly evident when using inbred strain collections (i.e., HMDP or CC). Since these strains are inbred and reproducible, one can sample the same genotype across environments or interventions that require multiple animals. These resources also represent a resource in which data can accumulate over time.

Identifying less common and rare variants associated with bone-relevant phenotypes via next generation sequencing

Although common-variant SNP chip–based GWASs have made strides in identifying loci that point to underlying disease pathophysiology, such approaches have inherent limitations. The narrow-sense heritability (h_g^2) of BMD has been estimated to be ∼85% of its variation, yet GWAS-identified common variants associated with DXA-BMD explained only ∼6% of the genetic variance of this trait. Thus, GWAS detects a small fraction of variance in BMD. Although genome-wide deep imputation using large reference panels is adequate to detect significant associations between common variants and quantitative traits like BMD (Walter et al., 2015), imputation for less common, rare, private mutations or even structural variations that might reveal unique pathways influencing bone metabolism is likely unavailable or will be associated with low imputation quality (McCarthy et al., 2016). Undiscovered, less common, rare, and private coding and noncoding variants as well as structural variations that have larger effect sizes are likely important for identifying novel genes and pathways influencing BMD and fractures. Recent studies (Zheng et al., 2015; Fuchsberger et al., 2016; Danjou et al., 2015; Morrison et al., 2013; Styrkarsdottir et al., 2003) have established the potential for next generation sequencing (NGS) to provide comprehensive enumeration of the sequence variation necessary for the detection of functional alleles that provide important clues to disease pathophysiology. The identification of causal variants underlying osteoporosis via NGS to provide complete coverage of genome variation now represents a compelling research opportunity.

To fine-map previous GWAS loci to identify potential causal variants responsible for GWAS signals, Hsu and colleagues performed targeted sequencing of four loci (chr1p31.3: *WLS,* 5q14.3: *MEF2C,* 11p11.2: *LRP4,* and 20p12.2: *JAG1*) using NGS in 1291 Caucasians from the Framingham Heart Study (n = 925) and Cardiovascular Health Study (n = 366) (Hsu et al., 2016a). Among them, 206 women and men had extremely low FN BMD. A total of 4,964 sequence variants (SNVs) were observed. Of them, 77% were novel variants and not imputed (or not well-imputed) using the 1000G Phase III reference panel. In addition, 80% are rare, with MAF <1%. The associations between previously identified SNPs in these loci and BMD, while nominally significant in sequenced participants, were no longer significant after multiple testing corrections. Conditional analyses did not find protein-coding variants that may be responsible for GWAS signals. On the other hand, in the sequenced subjects, novel associations were found in *WLS*, *ARHGAP1*, and *5′ of MEF2C* (*P*-values $< 8 \times 10^{-5}$; FDR q-value < 0.01) that were much more strongly associated with BMD than were GWAS SNPs. These associated SNVs were less common; independent from previous GWAS signals in the same loci; and located in gene regulatory elements. Our findings suggest that protein-coding variants in selected GWAS loci did not contribute to GWAS signals. By performing fine-mapping using the NGS approach in GWAS loci, less common and rare noncoding SNVs were found to be associated with BMD independently from GWAS common SNPs, suggesting both common and less common variants may associate with disease risks and phenotypes in the same loci, and that sequencing is required to discover these variants.

Whole-exome sequencing (WES) and WGS among Icelandic people with low versus high BMD revealed *LGR4* (Styrkarsdottir et al., 2013), *COL1A2* (Styrkarsdottir et al., 2016a), and *PTCH1* (Styrkarsdottir et al., 2016b) mutations that result in functional disruption of the protein. LGR4 plays a role in Wnt signaling, and embryonic mice lacking functional LGR4 were shown to have delayed osteoblast differentiation and mineralization (Styrkarsdottir et al., 2013). WES has identified functional coding variants for complex phenotypes, but only 5% of trait-associated SNPs from GWASs lie in coding regions (Maurano et al., 2012). If this proportion is representative of the distribution of truly causal

TABLE 68.2 Resources for genome-wide association studies in mice.

Population	Description	Advantages	Disadvantages
Hybrid Mouse Diversity Panel	~100 mouse strains treated as a population of unrelated individuals	• commercially available inbred strains • reproducible inbred strains • high mapping resolution	• low statistical power • population stratification • limited genetic variation
Collaborative Cross	~50 recombinant inbred strains derived from eight highly diverse inbred strains	• reproducible • genetically diverse • highly accurate genome reconstruction	• low statistical power • limited mapping resolution
Diversity Outbred	Outbred population derived from eight highly diverse inbred strains—at 30th generation of outbreeding as of August 2018	• high mapping resolution • genetically diverse • unlimited sample size; increasing power to detect subtle genetic effects • highly accurate genome reconstruction	• nonreproducible • each individual is unique and must be genotyped

variants, WGS will be required to discover variants underlying the majority of GWAS associations located in intronic, intergenic, and promoter regions. Indeed, Zheng and colleagues recently demonstrated that less common variants in noncoding regions of the *EN1* gene (Zheng et al., 2015) have an effect size two to four times larger than those of the common variants previously described in prominent genes (e.g., *LRP5*). In other fields, numerous examples now demonstrate the biological importance of rare variants in human disorders as well as the usefulness of this information in developing novel therapeutics.

The Trans-Omics for Precision Medicine (TOPMed), sponsored by the National Institutes of Health's National Heart, Lung, and Blood Institute, is the largest population-based WGS project for common/complex disorders/phenotypes. This resource may be utilized to identify less common and rare variants associated with bone density and fracture phenotypes. The TOPMed project is part of a broader Precision Medicine Initiative. In addition to WGS, the project is also measuring other omics, including metabolic profiles, protein and RNA expression pattern data with other phenomics, and environmental and clinical data. This resource will offer the opportunity to integrate different "omics" to understand pathophysiology of diseases as well as develop better therapeutic approaches. The current TOPMed project studies have a variety of study designs including population-based, family-based, case−control, pharmacogenomic, founder populations, and clinical studies. As of November 2018, over 120,000 deeply sequenced whole genomes have been done.

Future directions

Based on the richness of the growing number of GWASs and whole-genome association studies focusing on skeletal phenotypes and the increasing sample sizes available, understanding the genetic architecture underlying skeletal biology offers the promise of novel discovery of potential drug targets. In fact, there is a higher likelihood of successful drug development when a target is identified using genetic studies (Nelson et al., 2015) (Table 68.2).

As described in the commentary by the GTEx team, "Identifying any particular genetic variant's cascade of effects, from molecule to individual, requires assaying multiple layers of molecular complexity" (e GTEx Project, 2017), suggesting a complexity of gene function and gene expression regulations and the need to construct gene regulatory landscapes in multiple human primary cells and tissue types (see Fig. 68.2).

Future directions include the study of ethnic groups other than those of European ancestry and the follow-up of the novel genetic loci identified in these studies using cellular and animal models to identify the causal variants and their targeted genes.

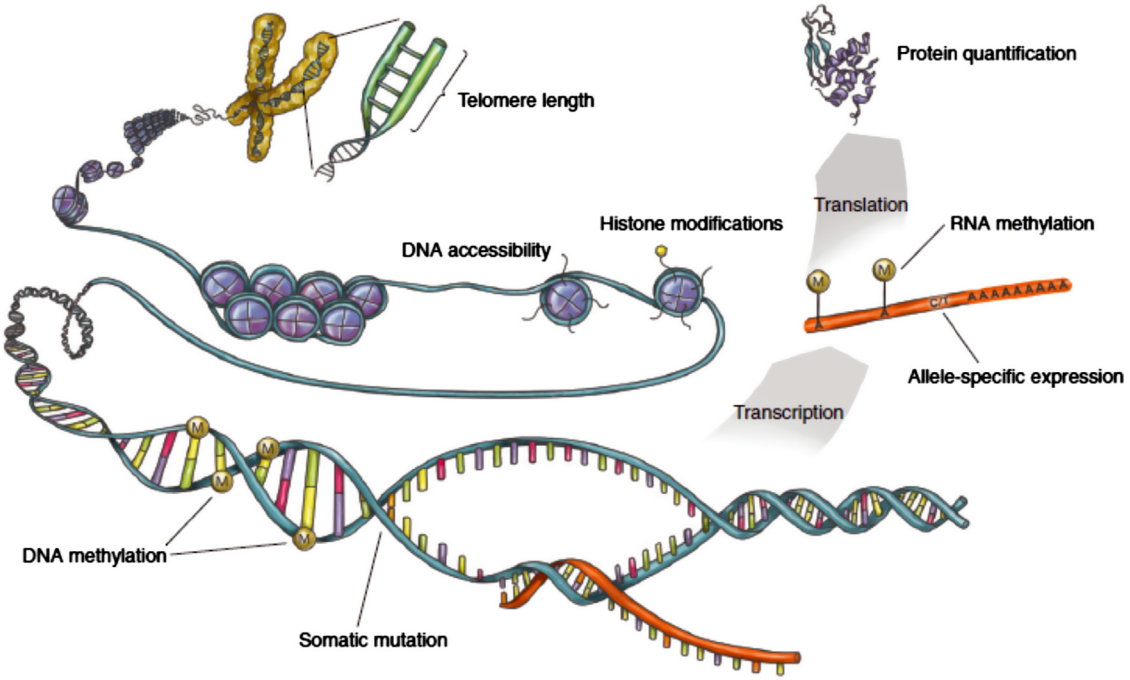

FIGURE 68.2 Quantifying layers of molecular and cellular phenotypes. The eGTEx project plans to study telomere length, DNA accessibility, histone modifications, DNA and RNA methylation, somatic mutation, allele-specific expression, and protein quantification across individuals and tissues.

References

Abiola, O., Angel, J.M., Avner, P., et al., 2003. The nature and identification of quantitative trait loci: a community's view. Nat. Rev. Genet. 4 (11), 911–916.

Ackert-Bicknell, C.L., Demissie, S., Marin de Evsikova, C., et al., 2008. PPARG by dietary fat interaction influences bone mass in mice and humans. J. Bone Miner. Res. 23 (9), 1398–1408.

Ackert-Bicknell, C.L., Karasik, D., Li, Q., et al., 2010. Mouse BMD quantitative trait loci show improved concordance with human genome wide association loci when recalculated on a new, common mouse genetic map. J. Bone Miner. Res. 25 (8), 1808–1820.

Alam, I., Koller, D.L., Canete, T., et al., 2014. High-resolution genome screen for bone mineral density in heterogeneous stock rat. J. Bone Miner. Res. 29 (7), 1619–1626.

Alonso, N., Estrada, K., Albagha, O.M.E., et al., 2018 Mar. Identification of a novel locus on chromosome 2q13, which predisposes to clinical vertebral fractures independently of bone density. Ann. Rheum. Dis. 77 (3), 378–385.

Aylor, D.L., Valdar, W., Foulds-Mathes, W., et al., 2011. Genetic analysis of complex traits in the emerging collaborative cross. Genome Res. 21 (8), 1213–1222.

Bennett, B.J., Farber, C.R., Orozco, L., et al., 2010. A high-resolution association mapping panel for the dissection of complex traits in mice. Genome Res. 20 (2), 281–290.

Black, D.M., Rosen, C.J., 2016. Postmenopausal osteoporosis. N. Engl. J. Med. 374 (21), 2096–2097.

Bogue, M.A., Grubb, S.C., Walton, D.O., et al., 2018. Mouse phenome database: an integrative database and analysis suite for curated empirical phenotype data from laboratory mice. Nucleic Acids Res. 46 (D1), D843–D850.

Bush, W.S., Moore, J.H., 2012. Chapter 11: Genome-wide association studies. PLoS Comput. Biol. 8 (12), e1002822.

Calabrese, G.M., Mesner, L.D., Stains, J.P., et al., 2017. Integrating GWAS and co-expression network data identifies bone mineral density genes SPTBN1 and MARK3 and an osteoblast functional module. Cell Syst. 4 (1), 46–59 e44.

Cervino, A.C., Darvasi, A., Fallahi, M., Mader, C.C., Tsinoremas, N.F., 2007. An integrated in silico gene mapping strategy in inbred mice. Genetics 175 (1), 321–333.

Chee, M., Yang, R., Hubbell, E., et al., 1996. Accessing genetic information with high-density DNA arrays. Science 274 (5287), 610–614.

Chick, J.M., Munger, S.C., Simecek, P., et al., 2016. Defining the consequences of genetic variation on a proteome-wide scale. Nature 534 (7608), 500–505.

Christian, J.C., Yu, P.L., Slemenda, C.W., Johnston Jr., C.C., 1989. Heritability of bone mass: a longitudinal study in aging male twins. Am. J. Hum. Genet. 44 (3), 429–433.

Churchill, G.A., Airey, D.C., Allayee, H., et al., 2004. The Collaborative cross, a community resource for the genetic analysis of complex traits. Nat. Genet. 36 (11), 1133–1137.

Churchill, G.A., Gatti, D.M., Munger, S.C., Svenson, K.L., 2012. The diversity outbred mouse population. Mamm. Genome 23 (9–10), 713–718.
Collaborative Cross, C., 2012. The genome architecture of the Collaborative cross mouse genetic reference population. Genetics 190 (2), 389–401.
Cummings, S.R., Karpf, D.B., Harris, F., et al., 2002. Improvement in spine bone density and reduction in risk of vertebral fractures during treatment with antiresorptive drugs. Am. J. Med. 112 (4), 281–289.
Danjou, F., Zoledziewska, M., Sidore, C., et al., 2015. Genome-wide association analyses based on whole-genome sequencing in Sardinia provide insights into regulation of hemoglobin levels. Nat. Genet. 47 (11), 1264–1271.
Darvasi, A., 1998. Experimental strategies for the genetic dissection of complex traits in animal models. Nat. Genet. 18 (1), 19–24.
Deng, F.Y., Dong, S.S., Xu, X.H., et al., 2013. Genome-wide association study identified UQCC locus for spine bone size in humans. Bone 53 (1), 129–133.
Dufresne, T.E., Chmielewski, P.A., Manhart, M.D., Johnson, T.D., Borah, B., 2003. Risedronate preserves bone architecture in early postmenopausal women in 1 year as measured by three-dimensional microcomputed tomography. Calcif. Tissue Int. 73 (5), 423–432.
Dunham, I., Kundaje, A., Aldred, S.F., et al., 2012. An integrated encyclopedia of DNA elements in the human genome. Nature 489 (7414), 57–74.
eGTEx Project, 2017. Enhancing GTEx by bridging the gaps between genotype, gene expression, and disease. Nat. Genet. 49 (12), 1664–1670.
Edderkaoui, B., Baylink, D.J., Beamer, W.G., Shultz, K.L., Wergedal, J.E., Mohan, S., 2007. Genetic regulation of femoral bone mineral density: complexity of sex effect in chromosome 1 revealed by congenic sublines of mice. Bone 41 (3), 340–345.
El-Bikai, R., Tahir, M.R., Tremblay, J., et al., 2015. Association of age-dependent height and bone mineral density decline with increased arterial stiffness and rate of fractures in hypertensive individuals. J. Hypertens. 33 (4), 727–735 discussion 735.
Ernst, J., Kellis, M., 2012. ChromHMM: automating chromatin-state discovery and characterization. Nat. Methods 9 (3), 215–216.
Ernst, J., Kheradpour, P., Mikkelsen, T.S., et al., 2011. Mapping and analysis of chromatin state dynamics in nine human cell types. Nature 473 (7345), 43–49.
Estrada, K., Styrkarsdottir, U., Evangelou, E., et al., 2012. Genome-wide meta-analysis identifies 56 bone mineral density loci and reveals 14 loci associated with risk of fracture. Nat. Genet. 44 (5), 491–501.
Farber, C.R., 2013. Systems-level analysis of genome-wide association data. G3 3 (1), 119–129.
Farber, C.R., Bennett, B.J., Orozco, L., et al., 2011. Mouse genome-wide association and systems genetics identify Asxl2 as a regulator of bone mineral density and osteoclastogenesis. PLoS Genet. 7 (4), e1002038.
Farh, K.K., Marson, A., Zhu, J., et al., 2015. Genetic and epigenetic fine mapping of causal autoimmune disease variants. Nature 518 (7539), 337–343.
Flint, J., Eskin, E., 2012. Genome-wide association studies in mice. Nat. Rev. Genet. 13 (11), 807–817.
Fuchsberger, C., Flannick, J., Teslovich, T.M., et al., 2016. The genetic architecture of type 2 diabetes. Nature 536 (7614), 41–47.
Ghazalpour, A., Rau, C.D., Farber, C.R., et al., 2012. Hybrid mouse diversity panel: a panel of inbred mouse strains suitable for analysis of complex genetic traits. Mamm. Genome 23 (9–10), 680–692.
Griffiths-Jones, S., Grocock, R.J., van Dongen, S., Bateman, A., Enright, A.J., 2006. miRBase: microRNA sequences, targets and gene nomenclature. Nucleic Acids Res. 34 (Database issue), D140–D144.
Grundberg, E., Brandstrom, H., Lam, K.C., et al., 2008. Systematic assessment of the human osteoblast transcriptome in resting and induced primary cells. Physiol. Genom. 33 (3), 301–311.
Grundberg, E., Kwan, T., Ge, B., et al., 2009. Population genomics in a disease targeted primary cell model. Genome Res. 19 (11), 1942–1952.
Grupe, A., Germer, S., Usuka, J., et al., 2001. In silico mapping of complex disease-related traits in mice. Science 292 (5523), 1915–1918.
GTE, 2012. Genotype-Tissue Expression (GTEx). https://commonfund.nih.gov/GTEx/.
Gulko, B., Hubisz, M.J., Gronau, I., Siepel, A., 2015. A method for calculating probabilities of fitness consequences for point mutations across the human genome. Nat. Genet. 47 (3), 276–283.
Gunderson, K.L., Kruglyak, S., Graige, M.S., et al., 2004. Decoding randomly ordered DNA arrays. Genome Res. 14 (5), 870–877.
Heyn, H., 2016. Quantitative trait loci identify functional noncoding variation in cancer. PLoS Genet. 12 (3), e1005826.
Hsu, Y.H., Kiel, D.P., 2012. Clinical review: genome-wide association studies of skeletal phenotypes: what we have learned and where we are headed. J. Clin. Endocrinol. Metab. 97 (10), E1958–E1977.
Hsu, Y.H., Zillikens, M.C., Wilson, S.G., et al., 2010. An integration of genome-wide association study and gene expression profiling to prioritize the discovery of novel susceptibility loci for osteoporosis-related traits. PLoS Genet. 6 (6), e1000977.
Hsu, Y.H., Li, G., Liu, C.T., et al., 2016. Targeted sequencing of genome wide significant loci associated with bone mineral density (BMD) reveals significant novel and rare variants: the cohorts for heart and aging research in genomic epidemiology (CHARGE) targeted sequencing study. Hum. Mol. Genet. 25 (23), 5234–5243.
Hsu, Y.H., Atkinson, E.J., Kinyua, F.K., et al., 2016. A genome-wide association study in adult Caucasians identifies novel loci and functional coding variants associated with bone microarchitecture assessed by HR-pQCT. J. Bone Miner. Res. 31 (Suppl. 1).
Izawa, T., Rohatgi, N., Fukunaga, T., et al., 2015. ASXL2 regulates glucose, lipid, and skeletal homeostasis. Cell Rep. 11 (10), 1625–1637.
Jemtland, R., Holden, M., Reppe, S., et al., 2011. Molecular disease map of bone characterizing the postmenopausal osteoporosis phenotype. J. Bone Miner. Res. 26 (8), 1793–1801.
Kalogeropoulos, M., Varanasi, S.S., Olstad, O.K., et al., 2010. Zic1 transcription factor in bone: neural developmental protein regulates mechano-transduction in osteocytes. FASEB J. 24 (8), 2893–2903.
Kang, H.M., Zaitlen, N.A., Wade, C.M., et al., 2008. Efficient control of population structure in model organism association mapping. Genetics 178 (3), 1709–1723.

Karasik, D., Myers, R.H., Hannan, M.T., et al., 2002. Mapping of quantitative ultrasound of the calcaneus bone to chromosome 1 by genome-wide linkage analysis. Osteoporos. Int. 13 (10), 796–802.

Karasik, D., Dupuis, J., Cupples, L.A., et al., 2007. Bivariate linkage study of proximal hip geometry and body size indices: the Framingham study. Calcif. Tissue Int. 81 (3), 162–173.

Karasik, D., Demissie, S., Lu, D., et al., 2017 Nov. Bone strength estimated by micro-finite element analysis (microFEA) is heritable and shares genetic predisposition with areal BMD: the Framingham study. J. Bone Miner. Res. 32 (11), 2151–2156.

Karasik, D., Demissie, S., Zhou, Y., et al., 2017a. Heritability and genetic correlations for bone microarchitecture: the Framingham study families. J. Bone Miner. Res. 32 (1), 106–114.

Kelley, D.R., Snoek, J., Rinn, J.L., 2016. Basset: learning the regulatory code of the accessible genome with deep convolutional neural networks. Genome Res. 26 (7), 990–999.

Kemp, J.P., Morris, J.A., Medina-Gómez, M., et al., October 20, 2016. Genome-wide association study of bone mineral density in the UK Biobank Study identifies over 376 loci associated with osteoporosis. Am. Soc. Hum. Genet. 2016. Vancouver, CA.

Klein, R.F., Allard, J., Avnur, Z., et al., 2004. Regulation of bone mass in mice by the lipoxygenase gene Alox15. Science 303 (5655), 229–232.

Kung, A.W., Xiao, S.M., Cherny, S., et al., 2010. Association of JAG1 with bone mineral density and osteoporotic fractures: a genome-wide association study and follow-up replication studies. Am. J. Hum. Genet. 86 (2), 229–239.

Lee, D., Gorkin, D.U., Baker, M., et al., 2015. A method to predict the impact of regulatory variants from DNA sequence. Nat. Genet. 47 (8), 955–961.

Lei, S.F., Shen, H., Yang, T.L., et al., 2012. Genome-wide association study identifies HMGN3 locus for spine bone size variation in Chinese. Hum. Genet. 131 (3), 463–469.

Leiserson, M.D., Eldridge, J.V., Ramachandran, S., Raphael, B.J., 2013. Network analysis of GWAS data. Curr. Opin. Genet. Dev. 23 (6), 602–610.

Levy, R., Mott, R.F., Iraqi, F.A., Gabet, Y., 2015. Collaborative cross mice in a genetic association study reveal new candidate genes for bone microarchitecture. BMC Genom. 16, 1013.

Liu, Y.Z., Wilson, S.G., Wang, L., et al., 2008. Identification of PLCL1 gene for hip bone size variation in females in a genome-wide association study. PLoS One 3 (9), e3160.

Liu, C.T., Estrada, K., Yerges-Armstrong, L.M., et al., 2012. Assessment of gene-by-sex interaction effect on bone mineral density. J. Bone Miner. Res. 27 (10), 2051–2064.

Lo, K.S., Vadlamudi, S., Fogarty, M.P., Mohlke, K.L., Lettre, G., 2014. Strategies to fine-map genetic associations with lipid levels by combining epigenomic annotations and liver-specific transcription profiles. Genomics 104 (2), 105–112.

Lochmuller, E.M., Zeller, J.B., Kaiser, D., et al., 1998. Correlation of femoral and lumbar DXA and calcaneal ultrasound, measured in situ with intact soft tissues, with the in vitro failure loads of the proximal femur. Osteoporos. Int. 8 (6), 591–598.

Lodder, M.C., de Jong, Z., Kostense, P.J., et al., 2004. Bone mineral density in patients with rheumatoid arthritis: relation between disease severity and low bone mineral density. Ann. Rheum. Dis. 63 (12), 1576–1580.

Logan, R.W., Robledo, R.F., Recla, J.M., et al., 2013. High-precision genetic mapping of behavioral traits in the diversity outbred mouse population. Genes Brain Behav. 12 (4), 424–437.

Lusis, A.J., Seldin, M.M., Allayee, H., et al., 2016. The hybrid mouse diversity panel: a resource for systems genetics analyses of metabolic and cardiovascular traits. J. Lipid Res. 57 (6), 925–942.

Manolio, T.A., 2009. Cohort studies and the genetics of complex disease. Nat. Genet. 41 (1), 5–6.

Marouli, E., Graff, M., Medina-Gomez, C., et al., 2017. Rare and low-frequency coding variants alter human adult height. Nature 542 (7640), 186–190.

Maurano, M.T., Humbert, R., Rynes, E., et al., 2012. Systematic localization of common disease-associated variation in regulatory DNA. Science 337 (6099), 1190–1195.

McCarthy, S., Das, S., Kretzschmar, W., et al., 2016. A reference panel of 64,976 haplotypes for genotype imputation. Nat. Genet. 48 (10), 1279–1283.

Mesner, L.D., Ray, B., Hsu, Y.H., et al., 2014. Bicc1 is a genetic determinant of osteoblastogenesis and bone mineral density. J. Clin. Investig. 124 (6), 2736–2749.

Michaelsson, K., Melhus, H., Ferm, H., Ahlbom, A., Pedersen, N.L., 2005. Genetic liability to fractures in the elderly. Arch. Intern. Med. 165 (16), 1825–1830.

Morris, J.A., Kemp, J.P., Youlten, S.E., 2019. An Atlas of Human and Murine Genetic Influences on Osteoporosis. Nat Gene 51 (2), 258–266. https://doi.org/10.1038/s41588-018-0302-x. Epub 2018 Dec 31. Erratum in: Nat Genet. 2019 May, 51 (5), 920.

Morrison, A.C., Voorman, A., Johnson, A.D., et al., 2013. Whole-genome sequence-based analysis of high-density lipoprotein cholesterol. Nat. Genet. 45 (8), 899–901.

Mouse Genome Sequencing, C., Waterston, R.H., Lindblad-Toh, K., et al., 2002. Initial sequencing and comparative analysis of the mouse genome. Nature 420 (6915), 520–562.

Mullin, B.H., Zhu, K., Xu, J., et al., 2018. Expression quantitative trait locus study of bone mineral density GWAS variants in human osteoclasts. J. Bone Miner. Res. 33 (6), 1044–1051.

Nelson, M.R., Tipney, H., Painter, J.L., et al., 2015. The support of human genetic evidence for approved drug indications. Nat. Genet. 47 (8), 856–860.

Nielson, C.M., Liu, C.T., Smith, A.V., et al., 2016. Novel genetic variants associated with increased vertebral volumetric BMD, reduced vertebral fracture risk, and increased expression of SLC1A3 and EPHB2. J. Bone Miner. Res. 31 (12), 2085–2097.

Oei, L., Zheng, H.F., Ntzani, E., et al., 2011. Large-scale meta-analysis of genome-wide association studies for fracture risk: the GEFOS consortium. J. Bone Miner. Res. 26 (Suppl. 1).

Oei, L., Zheng, H.F., Ntzani, E., et al., 2012. Fracture GWAS in the GEFOS consortium discovers new loci related to hormonal and neurological pathways. J. Bone Miner. Res. 27 (Suppl. 1).

Parker, S.C., Stitzel, M.L., Taylor, D.L., et al., 2013. Chromatin stretch enhancer states drive cell-specific gene regulation and harbor human disease risk variants. Proc. Natl. Acad. Sci. U. S. A 110 (44), 17921−17926.

Payseur, B.A., Place, M., 2007. Prospects for association mapping in classical inbred mouse strains. Genetics 175 (4), 1999−2008.

Pers, T.H., Karjalainen, J.M., Chan, Y., et al., 2015. Biological interpretation of genome-wide association studies using predicted gene functions. Nat. Commun. 6, 5890.

Pletcher, M.T., McClurg, P., Batalov, S., et al., 2004. Use of a dense single nucleotide polymorphism map for in silico mapping in the mouse. PLoS Biol. 2 (12), e393.

Ralston, S.H., de Crombrugghe, B., 2006. Genetic regulation of bone mass and susceptibility to osteoporosis. Genes Dev. 20 (18), 2492−2506.

Ralston, S.H., Uitterlinden, A.G., 2010. Genetics of osteoporosis. Endocr. Rev. 31 (5), 629−662.

Ran, S., Pei, Y.F., Liu, Y.J., et al., 2013. Bivariate genome-wide association analyses identified genes with pleiotropic effects for femoral neck bone geometry and age at menarche. PLoS One 8 (4), e60362.

Rat Genome, S., Mapping, C., Baud, A., et al., 2013. Combined sequence-based and genetic mapping analysis of complex traits in outbred rats. Nat. Genet. 45 (7), 767−775.

Raychaudhuri, S., Plenge, R.M., Rossin, E.J., et al., 2009. Identifying relationships among genomic disease regions: predicting genes at pathogenic SNP associations and rare deletions. PLoS Genet. 5 (6), e1000534.

Recla, J.M., Robledo, R.F., Gatti, D.M., Bult, C.J., Churchill, G.A., Chesler, E.J., 2014. Precise genetic mapping and integrative bioinformatics in diversity outbred mice reveals hydin as a novel pain gene. Mamm. Genome 25 (5−6), 211−222.

Reppe, S., Stilgren, L., Olstad, O.K., et al., 2006. Gene expression profiles give insight into the molecular pathology of bone in primary hyperparathyroidism. Bone 39 (1), 189−198.

Reppe, S., Refvem, H., Gautvik, V.T., et al., 2010. Eight genes are highly associated with BMD variation in postmenopausal Caucasian women. Bone 46 (3), 604−612.

Reppe, S., Sachse, D., Olstad, O.K., et al., 2013. Identification of transcriptional macromolecular associations in human bone using browser based in silico analysis in a giant correlation matrix. Bone 53 (1), 69−78.

Reppe, S., Datta, H.K., Gautvik, K.M., 2017. Omics analysis of human bone to identify genes and molecular networks regulating skeletal remodeling in health and disease. Bone 101 (Suppl. C), 88−95.

Richards, J.B., Zheng, H.F., Spector, T.D., 2012. Genetics of osteoporosis from genome-wide association studies: advances and challenges. Nat. Rev. Genet. 13 (8), 576−588.

Rivadeneira, F., Styrkarsdottir, U., Estrada, K., et al., 2009. Twenty bone-mineral-density loci identified by large-scale meta-analysis of genome-wide association studies. Nat. Genet. 41 (11), 1199−1206. https://doi.org/10.1038/ng.446. Published online 4 October 2009 (in press).

Roadmap Epigenomics, C., Kundaje, A., Meuleman, W., et al., 2015. Integrative analysis of 111 reference human epigenomes. Nature 518 (7539), 317−330.

Segre, A.V., Consortium, D., investigators, M., et al., 2010. Common inherited variation in mitochondrial genes is not enriched for associations with type 2 diabetes or related glycemic traits. PLoS Genet. 6 (8).

Shmookler Reis, R.J., 2003. From QTL mapping to genes: the long and winding road. J. Bone Miner. Res. 18 (2), 186−189.

Shorter, J.R., Huang, W., Beak, J.Y., et al., 2018. Quantitative trait mapping in diversity outbred mice identifies two genomic regions associated with heart size. Mamm. Genome 29 (1−2), 80−89.

Srivastava, A., Morgan, A.P., Najarian, M.L., et al., 2017. Genomes of the mouse collaborative cross. Genetics 206 (2), 537−556.

Stergachis, A.B., Neph, S., Sandstrom, R., et al., 2014. Conservation of trans-acting circuitry during mammalian regulatory evolution. Nature 515 (7527), 365−370.

Styrkarsdottir, U., Cazier, J.B., Kong, A., et al., 2003. Linkage of osteoporosis to chromosome 20p12 and association to BMP2. PLoS Biol. 1 (3), E69.

Styrkarsdottir, U., Thorleifsson, G., Sulem, P., et al., 2013. Nonsense mutation in the LGR4 gene is associated with several human diseases and other traits. Nature 497 (7450), 517−520.

Styrkarsdottir, U., Thorleifsson, G., Eiriksdottir, B., et al., 2016. Two rare mutations in the COL1A2 gene associate with low bone mineral density and fractures in Iceland. J. Bone Miner. Res. 31 (1), 173−179.

Styrkarsdottir, U., Thorleifsson, G., Gudjonsson, S.A., et al., 2016. Sequence variants in the PTCH1 gene associate with spine bone mineral density and osteoporotic fractures. Nat. Commun. 7, 10129.

Su, W.L., Sieberts, S.K., Kleinhanz, R.R., et al., 2010. Assessing the prospects of genome-wide association studies performed in inbred mice. Mamm. Genome 21 (3−4), 143−152.

Svenson, K.L., Gatti, D.M., Valdar, W., et al., 2012. High-resolution genetic mapping using the mouse diversity outbred population. Genetics 190 (2), 437−447.

Tang, P.L., Cheung, C.L., Sham, P.C., et al., 2009. Genome-wide haplotype association mapping in mice identifies a genetic variant in CER1 associated with BMD and fracture in southern Chinese women. J. Bone Miner. Res. 24 (6), 1013−1021.

Timpson, N.J., Greenwood, C.M.T., Soranzo, N., Lawson, D.J., Richards, J.B., 2018. Genetic architecture: the shape of the genetic contribution to human traits and disease. Nat. Rev. Genet. 19 (2), 110−124.

Trajanoska, K., Morris, J.A., Oei, L., et al., 2018. Assessment of the genetic and clinical determinants of fracture risk: genome wide association and mendelian randomisation study. BMJ 362, k3225.

Trynka, G., Raychaudhuri, S., 2013. Using chromatin marks to interpret and localize genetic associations to complex human traits and diseases. Curr. Opin. Genet. Dev. 23 (6), 635–641.

Walter, K., Min, J.L., Huang, J., et al., 2015. The UK10K project identifies rare variants in health and disease. Nature 526 (7571), 82–90.

Yang, J., Benyamin, B., McEvoy, B.P., et al., 2010. Common SNPs explain a large proportion of the heritability for human height. Nat. Genet. 42 (7), 565–569.

Yuan, J.T., Gatti, D.M., Philip, V.M., et al., 2018. Genome-wide association for testis weight in the diversity outbred mouse population. Mamm. Genome 29 (5-6), 310–324.

Zheng, H.F., Forgetta, V., Hsu, Y.H., et al., 2015. Whole-genome sequencing identifies EN1 as a determinant of bone density and fracture. Nature 526 (7571), 112–117.

Zhou, J., Troyanskaya, O.G., 2015. Predicting effects of noncoding variants with deep learning-based sequence model. Nat. Methods 12 (10), 931–934.

Chapter 69

Pharmacologic mechanisms of therapeutics: parathyroid hormone

Donovan Tay[1,2], Gaia Tabacco[1,3], Serge Cremers[4] and John P. Bilezikian[1]

[1]Division of Endocrinology, Department of Medicine, College of Physicians and Surgeons, Columbia University, New York, NY, United States; [2]Department of Medicine, Sengkang General Hospital, Singhealth, Singapore; [3]Endocrinology and Diabetes Unit, Department of Medicine, Campus Bio-Medico University of Rome, Rome, Italy; [4]Department of Pathology & Cell Biology and Department of Medicine, Vagelos College of Physicians and Surgeons, Columbia University Irving Medical Center, United States

Chapter outline

Introduction

Physiology of parathyroid hormone

Parathyroid hormone (PTH) is a full-length polypeptide hormone made up of 84 amino acids. The precursor hormone harbors a presequence of 25 amino acids and a prosequence of 6 amino acids, both of which are cleaved before the full-length mature PTH is released from the parathyroid glands. The classical biological properties of full-length PTH are resident in the first N-terminal 34-amino-acid sequence (Potts et al., 1971). The actions of PTH are physiologic and homeostatic. They are integral to maintaining normal calcium homeostasis. PTH tightly regulates and maintains the ambient extracellular ionized calcium concentration within a narrow range through its direct effects on the kidneys and bone and indirect effects on the gastrointestinal tract. In direct response to a reduction in the ionized calcium level, PTH secretion increases; in direct response to an increase in the ionized calcium level, PTH secretion falls. This physiological behavior is described by the well-known inverse sigmoid curve−shaped relationship between calcium and PTH (Brown, 1983). The proximal mediator of this relationship is the calcium-sensing receptor on the surface of parathyroid cells to which Ca^{2+} has affinity. The Ca^{2+}−calcium-sensing receptor interaction dictates to what extent PTH will be upregulated or downregulated. The renal actions of PTH include the stimulation of renal tubular reabsorption of calcium (at the thick ascending limb of the loop of Henle and distal convoluted tubule); thus, the renal actions of PTH are to conserve calcium. The skeletal actions of PTH include stimulation of osteoclast-mediated bone resorption to mobilize calcium stores. The third classical target organ of PTH is the gastrointestinal tract, but it is an indirect one. Through PTH's actions to stimulate the renal 1α-hydroxylase, 1,25-dihydroxyvitamin D ($1,25(OH)_2D$) is formed to increase gastrointestinal absorption of calcium in the duodenum and jejunum. In response to a hypocalcemic stimulus, these three servomechanisms, to varying extents and with different time courses, help to restore calcium levels. In response to a hypercalcemic signal, a reversal of these actions, also to varying extents and with different time courses, helps to restore calcium levels. In the case of high

Principles of Bone Biology. https://doi.org/10.1016/B978-0-12-814841-9.00069-5

extracellular calcium, under normal physiological conditions, PTH levels fall, leading to decreased renal tubular reabsorption, osteoclastic bone resorption, and intestinal absorption of calcium.

The secretion of PTH is best characterized by three components. A tonic component describes the continual secretion of PTH throughout the day at a constant rate. Superimposed upon this background constant secretory component, there is a circadian rhythm with an early morning peak and late morning trough and a smaller peak in the afternoon (el-Hajj Fuleihan et al., 1997). A third component, the pulsatile secretion of PTH exists that overlaps with the background secretroy rate and circadian rhythm that appears to be stochastic, occurring 10 or more times a day. These random bursts of PTH secretory activity account for about 30% of the total secretion (Chiavistelli et al., 2015). Circulating levels of PTH are determined mainly by the production rate of the hormone because PTH is rapidly metabolized by renal and hepatic tissue endopeptidases and its metabolites are excreted into the urine by glomerular filtration (Bringhurst et al., 1988). The biological half-life of endogenous PTH is thus very short. This very short half-life is illustrated well by patients undergoing parathyroidectomy for primary hyperparathyroidism (PHPT), who demonstrate a rapid decrease in circulating PTH levels very soon after removal of the parathyroid adenoma (Maier et al., 1998; Allgrove and O'Riordan, 1985; Leiker et al., 2013). Within 10 min after removal of the parathyroid adenoma, circulating levels of PTH are well below 50% of the preoperative values. From these studies, the biological half-life has been estimated to be about 3 min.

Apart from these physiologic homeostatic functions, PTH has been associated with anabolic or catabolic actions on the skeleton. This dual catabolic−anabolic aspect of PTH can be understood in pharmacokinetic, molecular, and cellular terms.

Pharmacokinetic mechanism: effects of ligand exposure

The duration of interaction between PTH and its receptor, PTH/PTH−related protein (PTHrP) type 1 receptor (PTH1R), is short. Depending on the duration of ligand exposure to its receptor, PTH can be predominantly anabolic or catabolic. Excessive and continuous PTH exposure favors bone resorption over bone formation, while intermittent PTH exposure favors bone formation over bone resorption. Intermittent PTH dosing more closely mimics a pulse of endogenous PTH secretion. This underlying principle has been exploited pharmacologically by utilizing once-daily injections of PTH to stimulate bone formation. The experimental basis for these functional distinctions was supported by Tam et al., who observed that continuous infusion of bovine PTH in rats leads to an increase in both formation and resorption surfaces and reduced trabecular bone, while intermittent daily injections of the hormone lead to an increase in formation surfaces without an increase in resorption surfaces along with an increase in trabecular volume (Tam et al., 1982). These findings were further clarified by Dobnig et al., who compared in rats the skeletal effects of daily subcutaneous injection, infusion (1, 2, or 6 h/day) and continuous 24-h exposure (Dobnig and Turner, 1997). Daily intermittent subcutaneous injections or 1 h/day infusion was associated with rapid anabolic effects in cancellous bone. Double-label perimeter, mineral apposition rate, and bone formation rate were higher in the setting of daily intermittent subcutaneous injections or 1 h/day infusions versus longer infusion times. In marked contrast, continuous infusion of PTH was associated with catabolic skeletal changes resembling PHPT. This body of knowledge led to the impression that low-dose intermittent use of PTH was likely to be anabolic, while chronic, continuous exposure of PTH was likely to be catabolic for bone.

Clinically, the best illustration of the catabolic actions of PTH is PHPT, a disorder in which tissues are exposed to continuous, excessive secretion of PTH. In PHPT, the excessive, continuous secretion of PTH leads to hypercalcemia. Basal secretion of PTH is higher and the amplitude of the pulses is higher, accounting for 50% of the total PTH secretion, virtually all emanating from the hyperactive parathyroid gland(s) (Harms et al., 1989). Renal tubular reabsorption of calcium is enhanced but the filtered load of calcium often exceeds the ability of the kidney to conserve the filtered load of calcium. If hypercalciuria follows, stone risk is higher, particularly if accompanied by other stone risk factors. The archives of yesteryear describe best the devastating potential of PTH to destroy the skeleton. The PHPT of Captain Charles Martell (Bauer and Federman, 1962) led to many fractures and dramatic height loss. He shrank in height until he was a shadow of his former athletic self. The eventual parathyroidectomy led to a severe hypocalcemic state and death, not long after removal of an ectopic mediastinal parathyroid adenoma, his seventh operation. Fortunately, such devastating manifestations of symptomatic PHPT are no longer common. What is more commonly seen in the current era is a form of PHPT that is discovered incidentally by the widespread use of the autoanalyzer that contains a serum calcium analysis channel. Even though this form of PHPT is much milder than the form seen more commonly 75 years ago, it nevertheless is associated with increased fracture risk and microarchitectural abnormalities seen best with high-resolution peripheral quantitative computed tomography. These abnormalities are seen in both the cortical and the trabecular compartments, though by bone mineral densitometry, there seems to be a predilection to affect cortical bone. Nevertheless, even by the trabecular bone score, involvement of trabecular bone is readily demonstrated. Both anabolic and catabolic markers of bone metabolism are typically elevated as a consequence of continuous exposure of PTH in PHPT (Costa and Bilezikian, 2013). The extent to

which these biochemical markers will be elevated is a function of the severity of the disease, but even in mild, asymptomatic PHPT, bone formation and resorption markers can be elevated or at the upper limits of normal (Guo et al., 1996; Silverberg et al., 1995). High bone turnover has been associated with increased fracture risk in many conditions, such as in PHPT and in postmenopausal osteoporosis (Vasikaran et al., 2011). Bone histomorphometric studies from the iliac crest bone biopsy in patients with PHPT confirm the detrimental effects of continuous exposure of PTH on cortical bone. Cortical porosity and cortical thinning are evident. Trabecular bone mass and structure were conserved, as assessed by structural indices such as trabecular bone volume, trabecular number, connectivity, and separation (Silverberg et al., 1989; Parisien et al., 1990, 1992; Dempster et al., 1999, 2007; Uchiyama et al., 1999; van Doorn et al., 1993). Dynamic parameters also demonstrate an increase in new bone formation as evidenced by an increased adjusted mineral apposition rate and active formation period in PHPT compared with normal postmenopausal women (Dempster et al., 1999; Parisien et al., 1995). These observations, along with relatively well-preserved lumbar spine bone density, helped to demonstrate, even under predominantly catabolic conditions, namely PHPT, that PTH has a potential to be anabolic.

Molecular mechanisms: ligand selectivity for receptor conformational state

The anabolic action of PTH depends upon its interaction with the PTH/PTHrP receptor. The PTH/PTHrP receptor type 1 (PTH1R) is a member of the B subfamily of G-protein-coupled receptors. In the skeleton, these receptors are found in osteoblasts and osteocytes (Fermor and Skerry, 1995). Binding to this receptor by the amino-terminal portion of PTH is an activation step. The receptor is coupled to both the adenylate cyclase-activating G protein (Gs) and the phospholipase C-activating G protein (Gq). Initiation of the Gs-mediated signaling cascade leads to an increase in cyclic AMP (cAMP) production, which results in protein kinase A (PKA) activation. Initiation of the Gq-mediated signaling cascade leads to activation of protein kinase C (PKC). The cAMP/PKA signaling is the dominant pathway that mediates PTH's anabolic response, since PTH ligands that lack the ability to initiate the Gq-mediated signaling cascade are still able to effect an anabolic response. For example, the truncated ligand [Gly^1,Arg^{19}] PTH (1−28), with substitution of glycine for alanine at position 1 and glutamic acid for arginine at position 19, lacks the ability to activate PKC, but it can stimulate cAMP production. This truncated ligand−receptor interaction led to an increase in bone formation, thus demonstrating that the PKC signaling cascade is not necessary for the anabolic effect of PTH (Yang et al., 2007). It was also shown that the Gq signaling cascade may inhibit the osteoanabolic effect of PTH. Daily PTH treatment in mice with loss of function of the Gq signal resulted in a higher increase in bone mass than in wild-type counterparts receiving the same therapy (Ogata et al., 2011). This implies that the Gq signaling cascade could mediate an inhibitory signal for the osteoanabolic response of PTH, since the loss of an inhibitory signal resulted in a greater osteoanabolic effect. Thus, cAMP signaling and downstream effects are considered to be the primary anabolic signaling system for PTH.

The PTH/PTHrP receptor (PTH1R) assumes at least two distinct conformation states. The two conformational states are R^G, when the receptor is coupled to heterotrimeric G proteins, and R^0, when it is free. Ligands that bind selectively to the R^G state induce a shorter signaling response, whereas ligands that bind selectively to the R^0 state induce a more prolonged signaling response (Dean et al., 2008; Okazaki et al., 2008). Also pertinent is the ratio of affinities of either of these two conformational states of the PTH/PTHrP receptor (PTH1R) for the ligand. Therefore, the state of the receptor and its affinity for a PTH ligand can determine biological activity (Dean et al., 2008). Since most PTHs have some affinity for either state of the PTH/PTHrP receptor (PTH1R), the behavior of a given PTH vis-à-vis duration of effect is determined by the ratio of binding affinities to each of these receptor states (Fig. 69.1).

Cellular mechanisms: Indirect effect on osteoclasts, and direct effects on osteoblast and osteocytes

The ultimate effect of PTH on the skeleton depends on the balance of the osteoblastic or osteoclastic activities stimulated by the ligand (Silva et al., 2015). Under physiological conditions, PTH stimulates bone remodeling, with a resultant increase in both bone formation and bone resorption through its direct effect on the osteoblasts and osteocytes and through its indirect effects on the osteoclasts. PTH increases bone formation by increasing osteoblast proliferation, decreasing osteoblast apoptosis, and converting quiescent lining cells into osteoblasts. PTH also increases osteoclast activity by enhancing receptor activator of nuclear factor-κB ligand (RANKL) production from osteoblasts and osteocytes (Bonewald, 2011). The stimulation of RANKL, a highly potent cytokine, is due, in part, to a decrease in osteoprotegerin, a decoy receptor to which RANKL binds (Huang et al., 2004). Therefore, PTH is anabolic by virtue of its ability to stimulate bone formation through remodeling-based formation (Ma et al., 2006), in which the bone formation phase of bone turnover is stimulated to

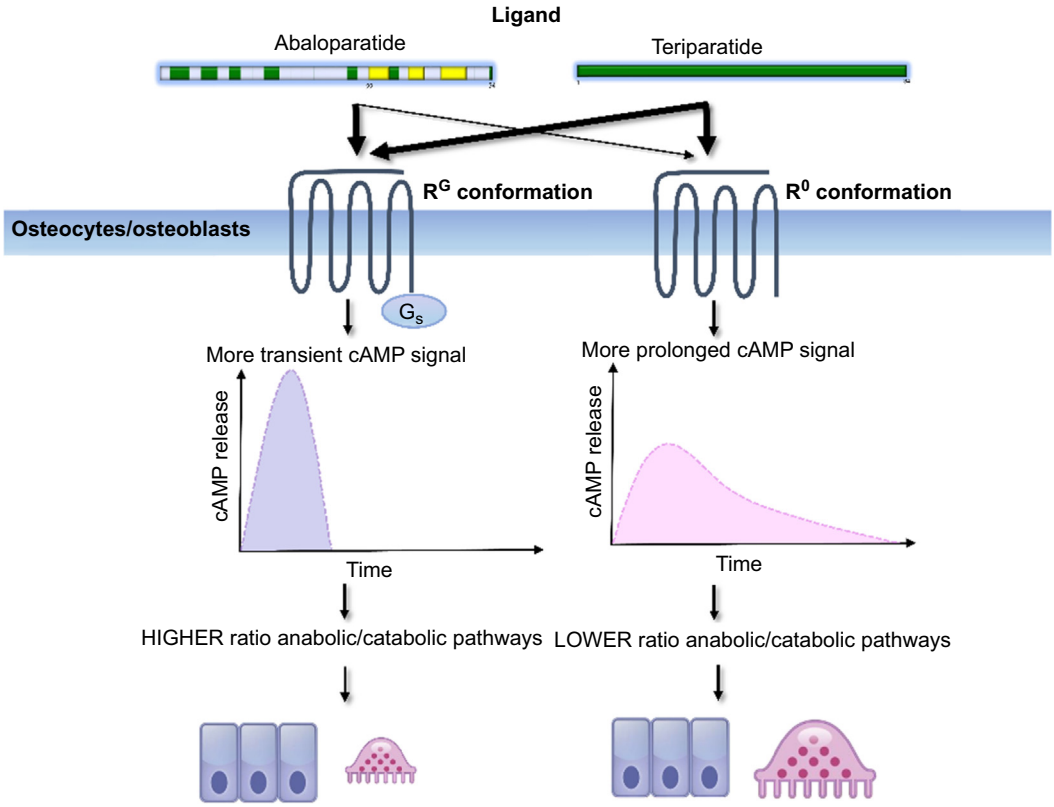

FIGURE 69.1 Different ligands have different binding selectivities for the different conformational states of the PTH/PTHrP receptor. Abaloparatide binds preferentially to the R^G state and elicit a more transient cyclic AMP signaling response favoring a less pronounced catabolic effect and a lower degree of hypercalcemia. Teriparatide has a preferential binding for the R^0 state and elicit a more prolonged cyclic AMP signaling response and a more pronounced catabolic effect and a relatively higher risk for hypercalcemia than abaloparatide.

a greater extent than the bone resorption phase. Remodeling-based accrual of bone is the primary mechanism by which PTH increases bone mass. The anabolic actions of PTH can also be affected by directly stimulating bone formation. This is known as modeling-based bone formation and is not preceded by bone resorption. Modeling-based bone formation occurs on quiescent surfaces of bone. It is typically evident during skeletal growth and development, but modeling, under very special circumstances, is now appreciated to occur throughout life, even in adults. With intermittent teriparatide administration, much of bone formation is remodeling based, but as much as 30% of bone accrual can be attributed to bone modeling. Bone modeling could not be demonstrated in control subjects not treated with teriparatide in that study (Lindsay et al., 2006). Modeling-based bone formation can be differentiated from remodeling-based bone formation on histomorphometry by the absence of scalloping beneath the surface of the newly formed bone. It can be inferred that smooth surfaces represent bone formation on quiescent surfaces (modeling), whereas scalloped surfaces indicate a site of bone resorption (remodeling). A third mechanism of bone accrual induced by PTH has been called "overflow remodeling" (Tabacco and Bilezikian, 2018). This occurs when osteoblasts refill the resorption cavity of the bone remodeling unit and "overflow" onto adjacent unresorbed quiescent surfaces (Lindsay et al., 2006).

The catabolic actions of PTH are thought to be based upon continuous exposure. Catabolic effects have been shown to depend on the presence or absence of SAA_3, serum amyloid A, an apolipoprotein. Released from preosteoclasts, SAA_3 inhibits osteoblastic differentiation during continuous PTH administration. This mechanism would account for the catabolic actions of PTH to be enhanced. In SAA_3-knockout mice (SAA_3 absent), Choudhary et al. showed that continuous PTH had anabolic effects on trabecular bone. PTH can directly or indirectly (via RANKL) stimulate the COX2 enzyme and in turn prostaglandin E_2 production, which subsequently results in secretion of SAA_3 from preosteoclasts. In that study, continuous PTH also increased osteoblast differentiation in osteoprogenitor cells when COX2 or RANKL activity was inhibited (Choudhary et al., 2018).

Not only does PTH directly influence osteoblastic activities, PTH can also indirectly influence osteoblastic activities via insulin-like growth factors, IGFs (McCarthy et al., 1989; Watson et al., 1995). Intermittent administration of PTH stimulates IGF-1 expression, which in turn leads to increased osteoblast differentiation (Xian et al., 2012). Both PTH and IGF-1 work in concert to regulate bone remodeling and thus couple bone resorption to bone formation (Elis et al., 2010). IGF-1 is deposited in the bone matrix bound by IGF-binding proteins. During PTH-induced bone remodeling, osteoclastic resorption leads to cleavage of the binding proteins and release of IGF-1 (Crane and Cao, 2014). Paracrine IGF-1 in turn stimulates the differentiation of mesenchymal stem cells to osteoblasts, therefore synergistically mediating the anabolic effects of PTH.

Complementary mechanisms can also enable PTH to exert its anabolic effects. One pathway is related directly to the osteocyte. Intermittent PTH reduces sclerostin, an osteocyte product (Keller and Kneissel, 2005). Sclerostin normally binds to low-density lipoprotein receptor−related protein (LRP) 5/6 and inhibits the canonical WNT signaling pathway, which leads to an inhibition of osteoblast-mediated bone formation. Activation of this WNT signaling pathway occurs when WNT binds to a receptor complex made up of LRP5 or LRP6 and the Frizzled receptor. This leads to an increase of intracellular β-catenin due to a reduction in its degradation. The degradation is prevented because activation of WNT signaling leads to the dissociation of the degradation complex formed by Dishevelled, Axin, adenomatous polyposis coli protein, protein phosphatase 2A, glycogen synthase kinase-3β (GSK-3β), and β-catenin. This occurs because activation of WNT leads to activation of Dishevelled, which in turn inhibits GSK-3β, which normally phosphorylates β-catenin, marking it for ubiquitination and proteolysis. β-Catenin, protected from cytoplasmic degradation in this manner, translocates to the nucleus where it modifies gene expression ultimately in an anabolic manner (Johnson and Kamel, 2007). Subsequent effects are associated with cellular changes that increase bone formation, such as differentiation of mesenchymal stem cells toward osteoblastogenesis, osteoblast proliferation, and inhibition of osteoblast apoptosis (Krishnan et al., 2006). This is an important complementary system that could account in a number of settings for the anabolic actions of PTH.

Both osteoblasts and marrow adipocytes originate from their skeletal precursors, mesenchymal stem cells. When these skeletal precursors are exposed to intermittent PTH, they are directed toward osteoblastogenesis and away from adipogenesis. Marrow adipocytes are a source of RANKL and are able to stimulate osteoclastogenesis. Fan et al. showed that deletion of the PTH/PTHrP receptor in mice resulted in increased marrow adiposity and that the marrow adipose tissue was capable of secreting RANKL, resulting in increased bone resorption and a resultant low bone mass phenotype (Fan et al., 2017). On the other hand, PTH (1−34) therapy in seven osteoporotic men showed a decrease in marrow adiposity in paired bone biopsies at baseline and 18 months (Dempster et al., 2001). These findings support the hypothesis that PTH is able to determine marrow mesenchymal cell fate. PTH may also in part regulate the provision of energy needed to fuel osteoblastic functions. Intermittent PTH can increase glycolysis via IGF signaling with increased anabolic effect (Esen et al., 2015). Intermittent PTH has also been shown to induce lipolysis in marrow adipocytes and release fatty acids to the osteoblasts to use as fuel for bone formation (Larsson et al., 2016).

Use of osteoanabolic agents in osteoporosis

Teriparatide

PTH is available pharmaceutically as teriparatide, human recombinant PTH (1−34). With teriparatide, we can appreciate how the pharmacokinetic properties of PTH can be manipulated to enhance its pharmacologic effect. The basic points are that the amino-terminal fragments demonstrate a much shorter half-life (of minutes), when injected subcutaneously, than the carboxy-terminal fragments and that the first 34 amino-terminal residues of PTH can produce a biological response as potent as that of the full-length peptide. Thus, PTH (1−34) administered as daily subcutaneous injections would allow it to function as an osteoanabolic agent since it is this form of administration that re-creates the desired brief intermittent ligand exposure to the PTH/PTHrP receptor (PTH1R). Intravenously administered PTH (1−34) has a very short half-life, measured in minutes (Fraher et al., 1995). When administered subcutaneously, the half-life approximates 1 h. The difference is accounted for by absorption kinetics from the subcutaneous reservoir, which delays uptake, rather than the metabolism of teriparatide (Satterwhite et al., 2010). In the pivotal trial that led to the approval of teriparatide [PTH (1−34)] by the US Food and Drug Administration (FDA), Neer et al. tested 20- and 40-μg doses against placebo in a double-blinded, randomized study. Once-daily injections of 20 μg PTH (1−34) reduced vertebral and non-vertebral fracture incidence by 65% and 53%, respectively. Bone mineral density (BMD) at the lumbar spine and femoral neck regions was increased by 9% and 3%, respectively, but not at the radius. There were, however, small declines at the radial site with the higher 40-μg dose (Neer et al., 2001). The 20-μg dose was developed further as the therapeutic dosage

because it was associated with fewer adverse events (less hypercalcemia and no reduction in radial BMD), while providing the same fracture protection as the 40-μg dose.

Abaloparatide

PTHrP is homologous to PTH in that the first eight amino-terminus residues are identical. It maintains three-dimensional functional homology through residue 34 (Martin, 2016). PTHrP is a longer peptide than PTH, with a linear sequence that is 141 amino acids long in humans. Nonetheless, PTHrP binds to the same receptor as PTH, and hence the designation of the receptor as PTH/PTHrP type 1 (PTH1R). Naturally occurring PTHrP has important physiological roles that include but are not limited to mammary gland development, lactation, tooth eruption, regulation of keratinocyte differentiation, vascular and uterine smooth muscle regulation, and placental calcium transport to the fetus. The pleiotropic effects of PTHrP expand concepts of PTH and PTHrP to evolutionary biology and nonskeletal actions of these peptides. In the skeleton, both PTHrP and PTH exert their distinct effects through binding and activation of a common PTH/PTHrP type 1 receptor (PTH1R) in osteoblasts. While both peptides share similar abilities to stimulate bone formation, PTH principally functions as a circulating endocrine response system, while PTHrP is believed to be primarily a paracrine regulator.

Abaloparatide was approved in April, 2017 by the US FDA for therapy of postmenopausal women with osteoporosis at high risk for fracture (Peterson and Riggs, 2010). Abaloparatide is identical to PTHrP through the first 22 residues, but thereafter, several substituent amino acids render this molecule very different in terms of its interactions at the receptor level. By virtue of these different primary sequences, empirically deduced, abaloparatide's interaction with the PTH/PTHrP type 1 receptor (PTH1R) appears to be more transient than that of PTHrP or teriparatide. Abaloparatide binds with lower affinity to the R^0 conformation state of the PTH/PTHrP type 1 receptor (PTH1R) but demonstrates an affinity to the R^G conformation state that is similar to that of teriparatide or PTHrP. Preferential binding of abaloparatide to the R^G state (ratio of binding affinities for the two receptor conformations favors R^G) elicits a transient cAMP signaling response, stimulating the mechanisms associated with greater anabolic potential (Hattersley et al., 2016).

The pharmacokinetic profiles of abaloparatide and teriparatide are similar. A single dose of subcutaneously administered abaloparatide (80 μg) has a half-life of 2.3 h, peaks at about 45 min, and remains in the circulation for about 7 h (Obaidi et al., 2010). In addition to greater selectivity, another distinguishing property that has clinical relevance is that abaloparatide does not require refrigeration.

In the dose-finding phase II trial, daily subcutaneous injections with 20, 40, or 80 μg of abaloparatide were compared with 20 μg of teriparatide for up to 24 weeks (Leder et al., 2015). There was a linear dose response to gains in BMD at the lumbar spine with increasing dose of abaloparatide. Both the 40- and the 80-μg doses were effective at increasing lumbar spine BMD compared with placebo (5.2% and 6.7% vs. 1.6%), with only the 80-μg dose showing similar efficacy compared with 20 μg of teriparatide. At the hip, only the 80-μg dose was effective at increasing the femoral neck or total hip BMD compared with placebo. At this dose, the change in femoral neck BMD was not different between abaloparatide and teriparatide, but the increase in total hip BMD was higher with abaloparatide compared with teriparatide. Of note, teriparatide did not significantly increase hip BMD at 24 weeks in this short study. The effects on bone-turnover markers were also different between the two anabolic agents. There was a linear dose response with bone formation markers with abaloparatide. The increase in formation markers was similar between 40- and 80-μg doses and 20 μg teriparatide. In contrast, and as expected, abaloparatide's effect on bone resorption markers was smaller than that of teriparatide.

The 80-μg abaloparatide dose was thus chosen for the definitive phase III double-blinded, randomized controlled clinical trial (ACTIVE) (Miller et al., 2016). Eighty micrograms of abaloparatide was compared with placebo and in an open-label comparison with teriparatide over 18 months. The primary end point was new vertebral fractures. The study was underpowered to appreciate the differences in the primary end point between abaloparatide and teriparatide, although both appeared similarly effective in reducing new vertebral fractures by 86% and 84%, respectively, compared with placebo. Abaloparatide reduced nonvertebral fractures by 43% compared with the 28% reduction in the teriparatide group, the latter of which did not reach statistical significance. If one takes into account the non-vertebral fracture efficacy from the original teriparatide phase III study, the reduction in non-vertebral fracture with teriparatide was appreciable only after 9–12 months of use (Neer et al., 2001; Miller et al., 2016). In contrast, fracture efficacy with abaloparatide was evident earlier compared with the time course from the report of Neer et al. for teriparatide.

Abaloparatide increased femoral neck BMD by 3.6%, total hip BMD by 4.2%, and lumbar spine BMD by 11.2% by 18 months. Abaloparatide demonstrated significantly greater BMD gains at the hip compared with teriparatide, but the gains at the lumbar spine were similar. The effects on bone-turnover markers were different between the two ligands. Increases in bone formation markers with abaloparatide were smaller from 3 months to the end of the study, and a transient and smaller increase in bone resorption markers from 3 to 12 months was observed compared with teriparatide.

Abaloparatide demonstrated less hypercalcemia than teriparatide (3.42% vs. 6.1%, respectively). The less prominent change in bone-turnover markers was mirrored by findings of lower eroded surface in the substudy evaluating the effect of abaloparatide on bone histomorphometry (Moreira et al., 2017). This is consistent with a smaller effect on parameters of bone resorption.

Use of parathyroid hormone in hypoparathyroidism

Recombinant human PTH (1−84)

Hypoparathyroidism is characterized by hypocalcemia with absent or deficient PTH associated with abnormal bone remodeling. The lack of PTH results in an inability to regulate calcium and phosphate homeostasis resulting in the characteristic biochemical profile of hypocalcemia and hyperphosphatemia. Typical symptoms of neuromuscular irritability, cognitive dysfunction, and renal and cardiac manifestations are prevalent in this disorder. They are not fully relieved with conventional therapy, namely calcium and active vitamin D (calcitriol) supplementation. Renal complications such as nephrolithiasis, nephrocalcinosis, and renal impairment, as well as systemic calcification, are typically seen as long-term complications of hypoparathyroidism. It is thought that both the natural history of the disease and the conventional therapy with large doses of supplemental calcium and calcitriol contribute to renal and other soft tissue calcifications in hypoparathyroidism. In the United States and many European countries, human recombinant (rh) PTH(1−84) is approved for the management of hypoparathyroidism not well controlled by conventional approaches (Clarke et al., 2014). PTH replacement therapy has been shown to reduce the burden of large supplemental doses of calcium and calcitriol while maintaining biochemical indices stably within the therapeutic range. By the psychometric SF-36 scale, it has also been shown to improve quality of life (Vokes et al., 2018; Cusano et al., 2014).

The ultimate therapeutic goal in hypoparathyroidism is total replacement of all three phases of normal PTH secretory dynamics. As a first step, a PTH ligand with a more prolonged state of binding to the PTH/PTHrP receptor (PTH1R) would be expected to approximate the homeostatic function PTH. This goal is opposite that of using PTH ligands in osteoporosis, in which the intention is to selectively stimulate the anabolic pathway of PTH action. Thus, teriparatide and abaloparatide function well in this regard but would not be as helpful in hypoparathyroidism. In hypoparathyroidism, it is the longer-lived configuration of the PTH−PTH1R interaction, not the shorter one, that is attractive therapeutically.

The difference in pharmacokinetics between intact PTH(1−84) and PTH (1−34) is further illustrated by the clinical experience with both molecules in the treatment of hypoparathyroidism. As anticipated by the foregoing discussion, PTH (1−34) requires at least twice-daily injections and sometimes three injections per day to achieve adequate control, whereas PTH (1−84) can be used successfully with a once-daily dosing regimen (Winer et al., 1998). Therapy with PTH replacement reduces the need for calcium and calcitriol. Mannstadt et al. showed that 53% of patients who received PTH (1−84) replacement were able to reduce their oral calcium and active vitamin D intake by 50% while maintaining stable and normal calcium levels at 24 weeks of therapy (Mannstadt et al., 2013). An even more physiological delivery of PTH may reduce urinary calcium excretion to a greater extent. Winer at al., for example, showed that continuous delivery of PTH (1−34) via continuous pump administration was able to reduce urinary calcium by 59% compared with twice-daily injections of PTH (1−34) which seems to suggest that a more physiological approach is beneficial (Winer et al., 2012).

Fox et al. compared four routes and sites of administration of PTH (1−84) (Fox and Garceau, 2011). Intravenously administered PTH(1−84) was cleared rapidly and provided the shortest calcium response, clearly not an attractive course for a disease like hypoparathyroidism. Subcutaneous routes were compared between the thigh and the abdomen. The thigh sites provide for slower absorption than the abdomen and therefore a more prolonged calcemic response. Subcutaneous thigh injection results in a biphasic profile with an initial peak 15 min post-injection, representing rather direct delivery of the drug into the circulation, and a second peak after 2 h (Sikjaer et al., 2013), indicating a slower uptake mechanism via the lymphatic system. PTH levels return to baseline after 12 h and calcium levels return to baseline after 24 h. For this reason, thigh injections are recommended for the treatment of hypoparathyroidism with PTH (1−84) (Clarke et al., 2014).

PTH replacement in hypoparathyroidism reverses the low bone turnover state characteristic of this disease. Intermittent replacement with PTH (1−34) increases bone-turnover markers above the normal range. Winer et al. showed that bone-turnover markers remained persistently elevated, with a twice a day regimen, for up to 3 years (Winer et al., 2003). A smaller increase in bone-turnover markers was observed in the twice a day regimen compared with the once a day regimen with PTH (1−34), although both bone formation and resorption markers were above the normal range (Winer et al., 1998). However, continuous administration of PTH (1−34) via pump delivery was able to keep both bone formation and resorption markers within normal range compared with the twice-daily regimen (Winer et al., 2012). In studies of PTH (1−84), once-daily injections of PTH (1−84) for up to 6 years also resulted in an increase in bone-turnover markers. Bone-

turnover markers peaked at 1 year of therapy and then fell, but remained elevated above baseline values by 6 years of therapy (Rubin et al., 2016). It remains to be studied, but we expect that more frequent regimens of PTH (1−84), either twice-daily injections or continuous administration via pump, will reverse the low bone turnover state, possibly keeping bone-turnover markers within the normal range without inducing bone remodeling excessively. Longitudinal observational studies with PTH (1−84) show an increase in BMD by dual-energy X-ray absorptiometry, which reflects the known site-specific effects of PTH seen from the use of these anabolic agents in osteoporotic patients, namely increases in lumbar spine and declines in distal one-third radius site. Although BMD at the lumbar spine and total hip was higher than that of age- and sex-matched reference standards prior to PTH replacement, lumbar spine BMD increased in the early years and seem to plateau after 4 years, while the increase in total hip BMD was seen in the later years of PTH therapy. Femoral neck BMD remained unchanged throughout the study. These changes seem to reflect the differential effects of PTH on cortical bone (distal one-third radius) and trabecular bone (lumbar spine). Histomorphometric analysis of bone biopsies from 13 subjects with hypoparathyroidism who were treated with rhPTH (1−84) for 8 years showed the presence of intratrabecular tunneling and increases in cancellous bone volume and trabecular number. PTH is known to increase cortical porosity and endosteal resorption (Rubin et al., 2011). Increased cortical porosity with PTH use is limited to the inner aspect of the cortex and is unlikely to contribute to a loss in bone strength. It must also be noted that PTH use is associated with an increase in bone size, and since the strength of a tube is related to the fourth power of its radius, this biomechanical advantage from the increase in bone size may offset the endosteal resorption and cortical porosity seen with PTH use in this disorder. Nonetheless, fracture data are ultimately needed to determine the clinical consequences of these observed structural changes. Long-term treatment of hypoparathyroidism with rhPTH (1−84) presents a unique opportunity to observe skeletal changes with long-term PTH exposure.

References

Allgrove, J., O'Riordan, J.L.H., 1985. Biological half-life of parathyroid hormone in the circulation. Bone 6 (1), 59.

Bauer, W., Federman, D.D., 1962. Hyperparathyroidism epitomized: the case of Captain Charles E. Martell. Metab.: Clin. Exp. 11, 21−29.

Bonewald, L.F., 2011. The amazing osteocyte. J. Bone Miner. Res. 26 (2), 229−238.

Bringhurst, F.R., Stern, A.M., Yotts, M., Mizrahi, N., Segre, G.V., Potts Jr., J.T., 1988. Peripheral metabolism of PTH: fate of biologically active amino terminus in vivo. Am. J. Physiol. 255 (6 Pt 1), E886−E893.

Brown, E.M., 1983. Four-parameter model of the sigmoidal relationship between parathyroid hormone release and extracellular calcium concentration in normal and abnormal parathyroid tissue. J. Clin. Endocrinol. Metab. 56 (3), 572−581.

Chiavistelli, S., Giustina, A., Mazziotti, G., 2015. Parathyroid hormone pulsatility: physiological and clinical aspects. Bone Res. 3, 14049.

Choudhary, S., Santone, E., Yee, S.-P., Lorenzo, J., Adams, D.J., Goetjen, A., et al., 2018. Continuous PTH in male mice causes bone loss because it induces serum amyloid A. Endocrinology 159 (7), 2759−2776.

Clarke, B.L., Kay Berg, J., Fox, J., Cyran, J.A., Lagast, H., 2014. Pharmacokinetics and pharmacodynamics of subcutaneous recombinant parathyroid hormone (1-84) in patients with hypoparathyroidism: an open-label, single-dose, phase I study. Clin. Ther. 36 (5), 722−736.

Costa, A.G., Bilezikian, J.P., 2013. Bone turnover markers in primary hyperparathyroidism. J. Clin. Densitom. 16 (1), 22−27.

Crane, J.L., Cao, X., 2014. Function of matrix IGF-1 in coupling bone resorption and formation. J. Mol. Med. (Berl.) 92 (2), 107−115.

Cusano, N.E., Rubin, M.R., McMahon, D.J., Irani, D., Anderson, L., Levy, E., et al., 2014. PTH(1-84) is associated with improved quality of life in hypoparathyroidism through 5 years of therapy. J. Clin. Endocrinol. Metab. 99 (10), 3694−3699.

Dean, T., Vilardaga, J.-P., Potts, J.J.T., Gardella, T.J., 2008. Altered selectivity of parathyroid hormone (PTH) and PTH-related protein (PTHrP) for distinct conformations of the PTH/PTHrP receptor. Mol. Endocrinol. 22 (1), 156−166.

Dempster, D.W., Parisien, M., Silverberg, S.J., Liang, X.G., Schnitzer, M., Shen, V., et al., 1999. On the mechanism of cancellous bone preservation in postmenopausal women with mild primary hyperparathyroidism. J. Clin. Endocrinol. Metab. 84 (5), 1562−1566.

Dempster, D.W., Cosman, F., Kurland, E.S., Zhou, H., Nieves, J., Woelfert, L., et al., 2001. Effects of daily treatment with parathyroid hormone on bone microarchitecture and turnover in patients with osteoporosis: a paired biopsy study. J. Bone Miner. Res. 16 (10), 1846−1853.

Dempster, D.W., Muller, R., Zhou, H., Kohler, T., Shane, E., Parisien, M., et al., 2007. Preserved three-dimensional cancellous bone structure in mild primary hyperparathyroidism. Bone 41 (1), 19−24.

Dobnig, H., Turner, R.T., 1997. The effects of programmed administration of human parathyroid hormone fragment (1-34) on bone histomorphometry and serum chemistry in rats. Endocrinology 138 (11), 4607−4612.

el-Hajj Fuleihan, G., Klerman, E.B., Brown, E.N., Choe, Y., Brown, E.M., Czeisler, C.A., 1997. The parathyroid hormone circadian rhythm is truly endogenous—a general clinical research center study. J. Clin. Endocrinol. Metab. 82 (1), 281−286.

Elis, S., Courtland, H.W., Wu, Y., Fritton, J.C., Sun, H., Rosen, C.J., et al., 2010. Elevated serum IGF-1 levels synergize PTH action on the skeleton only when the tissue IGF-1 axis is intact. J. Bone Miner. Res. 25 (9), 2051−2058.

Esen, E., Lee, S.Y., Wice, B.M., Long, F., 2015. PTH promotes bone anabolism by stimulating aerobic glycolysis via IGF signaling. J. Bone Miner. Res. 30 (11), 1959−1968.

Fan, Y., Hanai, J.I., Le, P.T., Bi, R., Maridas, D., DeMambro, V., et al., 2017. Parathyroid hormone directs bone marrow mesenchymal cell fate. Cell Metabol. 25 (3), 661−672.

Fermor, B., Skerry, T.M., 1995. PTH/PTHrP receptor expression on osteoblasts and osteocytes but not resorbing bone surfaces in growing rats. J. Bone Miner. Res. 10 (12), 1935−1943.

Fox, J.W.D., Garceau, R.J., 2011. Relationships between pharmacokinetic profile of human PTH(1-84) and serum calcium response in postmenopausal women following four different methods of administration (Abstract MO0173). In: 33rd Annual Meeting of the American Society of Bone and Mineral Research.

Fraher, L.J., Klein, K., Marier, R., Freeman, D., Hendy, G.N., Goltzman, D., et al., 1995. Comparison of the pharmacokinetics of parenteral parathyroid hormone-(1-34) [PTH-(1-34)] and PTH-related peptide-(1-34) in healthy young humans. J. Clin. Endocrinol. Metab. 80 (1), 60−64.

Guo, C.Y., Thomas, W.E., al-Dehaimi, A.W., Assiri, A.M., Eastell, R., 1996. Longitudinal changes in bone mineral density and bone turnover in postmenopausal women with primary hyperparathyroidism. J. Clin. Endocrinol. Metab. 81 (10), 3487−3491.

Harms, H.M., Kaptaina, U., KÜLpmann, W.R., Brabant, G., Hesch, R.D., 1989. Pulse amplitude and frequency modulation of parathyroid hormone in plasma. J. Clin. Endocrinol. Metab. 69 (4), 843−851.

Hattersley, G., Dean, T., Corbin, B.A., Bahar, H., Gardella, T.J., 2016. Binding selectivity of abaloparatide for PTH-type-1-receptor conformations and effects on downstream signaling. Endocrinology 157 (1), 141−149.

Huang, J.C., Sakata, T., Pfleger, L.L., Bencsik, M., Halloran, B.P., Bikle, D.D., et al., 2004. PTH differentially regulates expression of RANKL and OPG. J. Bone Miner. Res. 19 (2), 235−244.

Johnson, M.L., Kamel, M.A., 2007. The Wnt signaling pathway and bone metabolism. Curr. Opin. Rheumatol. 19 (4), 376−382.

Keller, H., Kneissel, M., 2005. SOST is a target gene for PTH in bone. Bone 37 (2), 148−158.

Krishnan, V., Bryant, H.U., Macdougald, O.A., 2006. Regulation of bone mass by Wnt signaling. J. Clin. Investig. 116 (5), 1202−1209.

Larsson, S., Jones, H.A., Goransson, O., Degerman, E., Holm, C., 2016. Parathyroid hormone induces adipocyte lipolysis via PKA-mediated phosphorylation of hormone-sensitive lipase. Cell. Signal. 28 (3), 204−213.

Leder, B.Z., O'Dea, L.S., Zanchetta, J.R., Kumar, P., Banks, K., McKay, K., et al., 2015. Effects of abaloparatide, a human parathyroid hormone-related peptide analog, on bone mineral density in postmenopausal women with osteoporosis. J. Clin. Endocrinol. Metab. 100 (2), 697−706.

Leiker, A.J., Yen, T.F., Eastwood, D.C., et al., 2013. Factors that influence parathyroid hormone half-life: determining if new intraoperative criteria are needed. JAMA Surg. 148 (7), 602−606.

Lindsay, R., Cosman, F., Zhou, H., Bostrom, M.P., Shen, V.W., Cruz, J.D., et al., 2006. A novel tetracycline labeling schedule for longitudinal evaluation of the short-term effects of anabolic therapy with a single iliac crest bone biopsy: early actions of teriparatide. J. Bone Miner. Res. 21 (3), 366−373.

Ma, Y.L., Zeng, Q., Donley, D.W., Ste-Marie, L.G., Gallagher, J.C., Dalsky, G.P., et al., 2006. Teriparatide increases bone formation in modeling and remodeling osteons and enhances IGF-II immunoreactivity in postmenopausal women with osteoporosis. J. Bone Miner. Res. 21 (6), 855−864.

Maier, G.W., Kreis, M.E., Renn, W., Pereira, P.L., Haring, H.U., Becker, H.D., 1998. Parathyroid hormone after adenectomy for primary hyperparathyroidism. A study of peptide hormone elimination kinetics in humans. J. Clin. Endocrinol. Metab. 83 (11), 3852−3856.

Mannstadt, M., Clarke, B.L., Vokes, T., Brandi, M.L., Ranganath, L., Fraser, W.D., et al., 2013. Efficacy and safety of recombinant human parathyroid hormone (1-84) in hypoparathyroidism (REPLACE): a double-blind, placebo-controlled, randomised, phase 3 study. Lancet Diabetes Endocrinol. 1 (4), 275−283.

Martin, T.J., 2016. Parathyroid hormone-related protein, its regulation of cartilage and bone development, and role in treating bone diseases. Physiol. Rev. 96 (3), 831−871.

McCarthy, T.L., Centrella, M., Canalis, E., 1989. Parathyroid hormone enhances the transcript and polypeptide levels of insulin-like growth factor I in osteoblast-enriched cultures from fetal rat bone. Endocrinology 124 (3), 1247−1253.

Miller, P.D., Hattersley, G., Riis, B., et al., 2016. Effect of abaloparatide vs placebo on new vertebral fractures in postmenopausal women with osteoporosis: a randomized clinical trial. J. Am. Med. Assoc. 316 (7), 722−733.

Moreira, C.A., Fitzpatrick, L.A., Wang, Y., Recker, R.R., 2017. Effects of abaloparatide-SC (BA058) on bone histology and histomorphometry: the ACTIVE phase 3 trial. Bone 97, 314−319.

Neer, R.M., Arnaud, C.D., Zanchetta, J.R., Prince, R., Gaich, G.A., Reginster, J.Y., et al., 2001. Effect of parathyroid hormone (1-34) on fractures and bone mineral density in postmenopausal women with osteoporosis. N. Engl. J. Med. 344 (19), 1434−1441.

Obaidi, M.C.R., Reinbolt, L., Offman, E., McKay, K., O'Dea, L.S., 2010. Pharmacokinetics and pharmacodynamics of subcutaneously (SC) administered doses of BA058, a bone mass density restoring agent, in healthy postmenopausal women [Abstract W5385].

Ogata, N., Shinoda, Y., Wettschureck, N., Offermanns, S., Takeda, S., Nakamura, K., et al., 2011. G alpha(q) signal in osteoblasts is inhibitory to the osteoanabolic action of parathyroid hormone. J. Biol. Chem. 286 (15), 13733−13740.

Okazaki, M., Ferrandon, S., Vilardaga, J.-P., Bouxsein, M.L., Potts, J.T., Gardella, T.J., 2008. Prolonged signaling at the parathyroid hormone receptor by peptide ligands targeted to a specific receptor conformation. Proc. Natl. Acad. Sci. U. S. A. 105 (43), 16525−16530.

Parisien, M., Silverberg, S.J., Shane, E., de la Cruz, L., Lindsay, R., Bilezikian, J.P., et al., 1990. The histomorphometry of bone in primary hyperparathyroidism: preservation of cancellous bone structure. J. Clin. Endocrinol. Metab. 70 (4), 930−938.

Parisien, M., Mellish, R.W., Silverberg, S.J., Shane, E., Lindsay, R., Bilezikian, J.P., et al., 1992. Maintenance of cancellous bone connectivity in primary hyperparathyroidism: trabecular strut analysis. J. Bone Miner. Res. 7 (8), 913−919.

Parisien, M., Cosman, F., Mellish, R.W., Schnitzer, M., Nieves, J., Silverberg, S.J., et al., 1995. Bone structure in postmenopausal hyperparathyroid, osteoporotic, and normal women. J. Bone Miner. Res. 10 (9), 1393−1399.

Peterson, M.C., Riggs, M.M., 2010. A physiologically based mathematical model of integrated calcium homeostasis and bone remodeling. Bone 46 (1), 49–63.

Potts Jr., J.T., Tregear, G.W., Keutmann, H.T., Niall, H.D., Sauer, R., Deftos, L.J., et al., 1971. Synthesis of a biologically active N-terminal tetratriacontapeptide of parathyroid hormone. Proc. Natl. Acad. Sci. U. S. A. 68 (1), 63–67.

Rubin, M.R., Dempster, D.W., Sliney Jr., J., Zhou, H., Nickolas, T.L., Stein, E.M., et al., 2011. PTH(1-84) administration reverses abnormal bone-remodeling dynamics and structure in hypoparathyroidism. J. Bone Miner. Res. 26 (11), 2727–2736.

Rubin, M.R., Cusano, N.E., Fan, W.-W., Delgado, Y., Zhang, C., Costa, A.G., et al., 2016. Therapy of hypoparathyroidism with PTH(1–84): a prospective six year investigation of efficacy and safety. J. Clin. Endocrinol. Metab. 101 (7), 2742–2750.

Satterwhite, J., Heathman, M., Miller, P.D., Marin, F., Glass, E.V., Dobnig, H., 2010. Pharmacokinetics of teriparatide (rhPTH[1-34]) and calcium pharmacodynamics in postmenopausal women with osteoporosis. Calcif. Tissue Int. 87 (6), 485–492.

Sikjaer, T., Amstrup, A.K., Rolighed, L., Kjaer, S.G., Mosekilde, L., Rejnmark, L., 2013. PTH(1-84) replacement therapy in hypoparathyroidism: a randomized controlled trial on pharmacokinetic and dynamic effects after 6 months of treatment. J. Bone Miner. Res. 28 (10), 2232–2243.

Silva, B.C., Kousteni, S., 2015. Chapter 8—cellular actions of PTH: osteoblasts, osteoclasts, and osteocytes A2. In: Bilezikian, J.P. (Ed.), The Parathyroids, third ed. Academic Press, San Diego, pp. 127–137.

Silverberg, S.J., Shane, E., de la Cruz, L., Dempster, D.W., Feldman, F., Seldin, D., et al., 1989. Skeletal disease in primary hyperparathyroidism. J. Bone Miner. Res. 4 (3), 283–291.

Silverberg, S.J., Gartenberg, F., Jacobs, T.P., Shane, E., Siris, E., Staron, R.B., et al., 1995. Longitudinal measurements of bone density and biochemical indices in untreated primary hyperparathyroidism. J. Clin. Endocrinol. Metab. 80 (3), 723–728.

Tabacco, G., Bilezikian, J.P., 2018. Osteoanabolic and dual action drugs. Br. J. Clin. Pharmacol. https://doi.org/10.1111/bcp.13766.

Tam, C.S., Heersche, J.N., Murray, T.M., Parsons, J.A., 1982. Parathyroid hormone stimulates the bone apposition rate independently of its resorptive action: differential effects of intermittent and continuous administration. Endocrinology 110 (2), 506–512.

Uchiyama, T., Tanizawa, T., Ito, A., Endo, N., Takahashi, H.E., 1999. Microstructure of the trabecula and cortex of iliac bone in primary hyperparathyroidism patients determined using histomorphometry and node-strut analysis. J. Bone Miner. Metab. 17 (4), 283–288.

van Doorn, L., Lips, P., Netelenbos, J.C., Hackeng, W.H., 1993. Bone histomorphometry and serum concentrations of intact parathyroid hormone (PTH(1-84)) in patients with primary hyperparathyroidism. Bone Miner. 23 (3), 233–242.

Vasikaran, S., Eastell, R., Bruyere, O., Foldes, A.J., Garnero, P., Griesmacher, A., et al., 2011. Markers of bone turnover for the prediction of fracture risk and monitoring of osteoporosis treatment: a need for international reference standards. Osteoporos. Int. 22 (2), 391–420.

Vokes, T.J., Mannstadt, M., Levine, M.A., Clarke, B.L., Lakatos, P., Chen, K., et al., 2018. Recombinant human parathyroid hormone effect on health-related quality of life in adults with chronic hypoparathyroidism. J. Clin. Endocrinol. Metab. 103 (2), 722–731.

Watson, P., Lazowski, D., Han, V., Fraher, L., Steer, B., Hodsman, A., 1995. Parathyroid hormone restores bone mass and enhances osteoblast insulin-like growth factor I gene expression in ovariectomized rats. Bone 16 (3), 357–365.

Winer, K.K., Yanovski, J.A., Sarani, B., Cutler Jr., G.B., 1998. A randomized, cross-over trial of once-daily versus twice-daily parathyroid hormone 1-34 in treatment of hypoparathyroidism. J. Clin. Endocrinol. Metab. 83 (10), 3480–3486.

Winer, K.K., Ko, C.W., Reynolds, J.C., Dowdy, K., Keil, M., Peterson, D., et al., 2003. Long-term treatment of hypoparathyroidism: a randomized controlled study comparing parathyroid hormone-(1-34) versus calcitriol and calcium. J. Clin. Endocrinol. Metab. 88 (9), 4214–4220.

Winer, K.K., Zhang, B., Shrader, J.A., Peterson, D., Smith, M., Albert, P.S., et al., 2012. Synthetic human parathyroid hormone 1-34 replacement therapy: a randomized crossover trial comparing pump versus injections in the treatment of chronic hypoparathyroidism. J. Clin. Endocrinol. Metab. 97 (2), 391–399.

Xian, L., Wu, X., Pang, L., Lou, M., Rosen, C.J., Qiu, T., et al., 2012. Matrix IGF-1 maintains bone mass by activation of mTOR in mesenchymal stem cells. Nat. Med. 18 (7), 1095–1101.

Yang, D., Singh, R., Divieti, P., Guo, J., Bouxsein, M.L., Bringhurst, F.R., 2007. Contributions of parathyroid hormone (PTH)/PTH-related peptide receptor signaling pathways to the anabolic effect of PTH on bone. Bone 40 (6), 1453–1461.

Chapter 70

Calcium

Connie M. Weaver[1] and Robert P. Heaney[2,†]
[1]Purdue University, West Lafayette, IN, United States; [2]Creighton University, Omaha, NE, United States

Chapter outline

Introduction

Calcium is the fifth most abundant element in the biosphere, after iron, silicon, oxygen, and aluminum. Unlike silicon and aluminum, whose compounds are quite insoluble, calcium salts exhibit an intermediate solubility that permits them both to be present in solution in the waters in which life evolved and to support development of various hard, solid organs for use by evolving life forms.

The radius of the Ca^{2+} ion is just right to fit naturally into the folds of many proteins, coordinating with up to eight oxygen atoms in the peptide chain and its side groups. Calcium thus stabilizes critical tertiary structures of both catalytic and structural proteins (Carafoli and Penniston, 1985). Calcium has an intermediate binding capacity, making it the perfect on−off switch. Zinc binds so tightly to proteins, it can stabilize them but cannot come off after a physiological action is complete. Magnesium, calcium's closest relative in the cell and, like calcium, a divalent alkaline earth element, has a smaller ionic radius and does not bind as strongly as does calcium. Calcium's functionality is so broad, in fact, that essentially all cells have found it necessary to restrict calcium concentration in the cell sap to something like 4−5 orders of magnitude below that in the extracellular fluid (ECF) surrounding the cell, about 1.25 mM. These low cytosolic concentrations are the context that permits cells to use calcium as a nearly universal second messenger. They do so by admitting controlled quantities into critical cellular compartments when specific functions are to be activated, and promptly pumping it out, either into the extracellular space or into intracellular vesicles, when the cell action is to be shut off. Intracellular storage of calcium is the rule, rather than the exception. Examples include the sarcoplasmic reticulum of muscle and calcium phosphate crystals in mitochondria. Calcium is so critical to intracellular function that most cells have developed a means to maintain their own supply. In general, their dependence on extracellular calcium is limited to initiating the cascade by opening calcium channels in the cell membrane. Movement of ECF calcium into the cytosol through these channels then activates a much larger release of calcium from intracellular stores, as in muscle contraction, neuronal synaptic transmission, and blood clotting.

† Deceased.

Principles of Bone Biology. https://doi.org/10.1016/B978-0-12-814841-9.00070-1

Bone as the body's calcium sink and reserve

Bone is the reservoir of calcium stored following a meal and tapped during fasting. Calcium is stored in bone mainly in the process of mineralizing newly deposited bone matrix, that is, by adding new volumes of bone tissue; and it is withdrawn from bone mainly by resorption of old bone tissue. Thus, the reservoir functions of bone are mediated by modulating, on a moment-to-moment basis, the balance between new bone formation and old bone resorption.

A good example of this modulation is afforded by what happens during calcium absorption from milk in infant mammals. The quantity of calcium ingested in a short period of time, coupled with the efficiency of absorption in infants and the small volume of the extracellular water into which that calcium is dumped, is such that near-fatal hypercalcemia would ensue if there were not some way to damp the absorptive rise in ECF [Ca^{2+}]. This is accomplished by calcitonin-mediated suppression of osteoclastic bone resorption. Because bone formation is continuing, the mineralization of recently deposited bone matrix effectively soaks up the absorbed calcium. Then, as absorptive input decreases, bony resorption resumes. The result is a nearly steady input of calcium into the ECF, with the relative contributions of bone and gut varying inversely.

Once suitable crystal nuclei are formed, mineralization is mainly passive. Most of the skeletal control of extracellular calcium levels throughout life is exerted on the resorptive side of the remodeling apparatus, for the simple reason that osteoclastic activity is susceptible to very rapid response to humoral mediators, whereas mineralization is not.

An example of the reservoir function of bone is seen during pregnancy, a period of more positive calcium balance than can be accounted for by fetal mineralization, and then, with substantial loss of bone, during the hypoestrin state of lactation (Heaney, 1996). For example, the nursing rat, across lactation of a full litter of pups, loses on the order of one-third of the skeletal mass she had at delivery (Brommage and DeLuca, 1985).

Bidirectional remodeling imbalances (decreasing and then augmenting local bone mass) are capable of both removing and replacing calcium from bone by tiny minute-to-minute alterations of bone mass. Except for the accumulation of remodeling errors, this in-and-out process would not be expected to exert a deleterious effect on bone; in fact, it probably has a net beneficial effect on bone quality, inasmuch as evoked remodeling seems to focus preferentially on old, fatigue-damaged tissue, replacing it with fresh, new bone. However, when withdrawals are protracted or payback is incomplete or absent, structural elements may be lost (Fig. 70.1). When this occurs, the loss becomes irreversible, inasmuch as the scaffolding for osteoblastic replacement vanishes. Nutrient repletion can be expected only to fatten up existing structures, not replace lost ones. In this sense, calcium differs from a nutrient such as iron for which full repletion of functional iron mass is possible even after loss of a major fraction of total body iron stores.

There is an important asymmetry about this bidirectional flux of calcium in and out of bone through the remodeling cycle. Although bone can be resorbed essentially without limit, there is a practical ceiling that governs how much calcium can be stored. Given an environmental abundance of calcium, bone mass is normally regulated not by nutrient availability but by a mechanical feedback loop that works to maintain bony strain under load at a constant level in all skeletal parts and

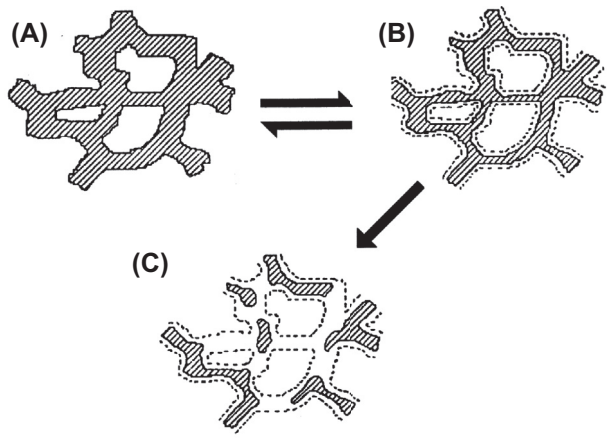

FIGURE 70.1 Schematic representation of the bidirectional flux of calcium in and out of the skeleton in a small volume of cancellous bone (A and B). Calcium is mobilized by resorbing bone tissue. So long as the basic structure is preserved (B), lost bone can be fully replaced. But when whole structures are resorbed (i.e., trabecular plates penetrated and trabecular beams severed; C), replacement of lost bone becomes difficult or impossible. *Reproduced from Heaney, R.P. 1994. The bone remodeling transient: implications for the interpretation of clinical studies of bone mass change. J. Bone Miner. Res. 9, 1515–1523, with permission. Copyright Robert P. Heaney 1995.*

regions. The bone set point (or "mechanostat") is poorly understood (as is true for most biological set points), but appears to involve the low-density lipoprotein receptor–related protein 5 (LRP5) that, in turn, controls osteoblast formation through the canonical Wnt signaling pathway (Robinson et al., 2006). Animals with functional mutation of the LRP5 gene produce more bone in response to mechanical loading than do animals with the wild-type gene (Robinson et al., 2006).

The regulation of this set point is complex and poorly understood, but in addition to mechanical loading, it is influenced, at least in part, by estrogen (which explains why bone tissue is added to the skeleton at puberty [Gilsanz et al., 1988] and during pregnancy [Heaney and Skillman, 1971], when estrogen levels rise, and withdrawn from it at menopause and during lactation [Brommage and DeLuca, 1985], when estrogen levels fall). But under a hormonal steady state, bone balance will become zero when the optimal level of strain is reached. Additional dietary calcium cannot be stored. The upshot is that, although the organism can withdraw calcium virtually without limit, storage is limited by the extent to which the skeleton continues to be subject to normal loading stresses, contingent upon preservation of structural elements and consistent with the set point of the bone mechanostat.

Calcium in bone

The adult human body contains, on average, slightly more than 1 kg of calcium, better than 99% of which is in the form of bone and teeth. Calcium is the principal cation of bone, comprising slightly less than 40% of the mass of the bone mineral and slightly less than 20% of the dry weight of bone. Calcium exists in bone in a mineral form that is usually characterized as hydroxyapatite, i.e., $Ca_{10}(PO_4)_6(OH)_2$. This is only approximately correct, and it is more accurate to say, after Posner (1987), that bone mineral is a "structurally imperfect analogue of hydroxyapatite." Bone mineral contains, for example, carbonate, citrate, potassium, magnesium, and fluoride among other ionic species. Carbonate content is especially high. It varies fairly substantially from species to species, in humans comprising in the neighborhood of 6%–9% of the mass of the mineral. Because the carbonate ion does not fit well into the hydroxyapatite crystal lattice, it is generally presumed to be located in superficial positions on the mineral crystals. The lability of bone carbonate, as reflected in changes in carbonate content with metabolic acidosis, suggests also that its location may be mostly on anatomic surfaces.

The crystals of bone exist in intimate association with the collagen fibers of the bone matrix. They are long and needle shaped, are ~70 Å in diameter and from 200 to 3000 Å long, and are constrained in size and orientation by the dense, orderly packing of the matrix collagen fibrils, which are laid down before mineralization begins. Matrix, as deposited, consists of about half protein and half water. As mineralization proceeds, mineral crystals displace the water, aligning themselves with the collagen fibrils. Ultimately, at full mineralization, the extracellular bony material contains virtually no free water. One consequence is the fact that mineral ions deep to anatomical surfaces are frozen in place, neither exchanging with nor supporting the level of the corresponding ionic species in solution in the ECF.

The calcification of matrix presents an interesting illustration of the importance of specificity of crystal habitus and takes advantage of the marginal solubility characteristics of calcium phosphate. Both calcium and phosphate, the latter in the form of H_2PO_4 and HPO_4^{2-}, circulate in the body fluids in solution and do not precipitate, neither in the bloodstream nor in healthy body tissues. However, the same minerals, in exactly the same concentrations, support mineralization when the blood flows past a bone-forming site. The reason, very simply, is that the concentrations of calcium and phosphate in ECF are such that body fluids are approximately half-saturated with respect to $CaHPO_4$ (the most likely crystal form at physiological pH and pCO_2). However, bone mineralization is not simple precipitation. Rather, it involves the creation of a template for formation of a crystal more like hydroxyapatite or tricalcium phosphate ($Ca_9(PO_4)_6$). Such minerals would not form spontaneously below pH 8; they are much less soluble, and body fluid concentrations of calcium and phosphate are approximately twice their K_{sp}. Local creation of such crystal nuclei is the means by which vertebrates have been able to control deposition of mineral, placing it only in loci specifically prepared to receive it, e.g., where it is needed to provide the necessary rigidity for the structural role of bone.

Noncollagenous matrix proteins are believed to play the critical role in configuring Ca^{2+} and PO_4^{3-} ions in space so as to create the hydroxyapatite template. Alkaline phosphatase, produced by the osteoblast late in the matrix deposition process, is believed to function by hydrolyzing pyrophosphate and organic phosphate esters present in the medium, which both makes extra phosphate available and removes components that otherwise function as crystal poisons, inhibiting crystal growth (Whyte, 2010). The chemistry of formation of the apatite mineral can be summarized as:

$$10Ca^{2+} + 3.5H_2PO_4^- + 2.5HPO_4^{2-} + 2H_2O$$

$$\rightleftarrows Ca_{10}(PO_4)_6(OH)_2 + 13.5H^+$$

The proportion of $H_2PO_4^-$ and HPO_4^{2-} in ECF at body pH is such that this reaction produces 13 protons for each unit cell[1] of hydroxyapatite formed. These must, of course, be removed from the mineralizing environment, or the reaction would cease or tend to run in reverse. By the same token, ~13 protons must be produced by osteoclasts to solubilize one unit cell of hydroxyapatite during bone resorption.

The calcium requirement

What the requirement ensures

The strength of bone, as with all material structures, resides in four features: the intrinsic strength of the mineral−matrix composite, the massiveness of the structure, the geometric arrangement of the bony elements in space, and the loading history of a structural element, expressed in accumulated fatigue damage. A major mechanism by which calcium is recognized to influence bone strength is through its effect on bone mass. Because bone functions as the calcium nutrient reserve, it follows inexorably that any depletion of that reserve (or failure to produce the genetically programmed skeletal mass during growth) will carry with it a corresponding decrease in bone strength.

In addition, at prevailing calcium intakes, bone remodeling occurs at a rate considerably in excess of the need to repair fatigue damage (Heaney, 2003; Parfitt, 2004), and this excess remodeling is a more important fracture risk factor than had been previously recognized. It is likely that contemporary calcium intakes, which are low by Paleolithic standards, are a part of the cause. In any event, supplementation reduces bone remodeling and reduces fracture risk as well (Heaney and Weaver, 2005).

As already noted, the calcium needed for critical cell metabolic functions is, in most cells, derived from intracellular stores of the mineral. Bone constitutes such a large reserve of calcium that cellular functions could virtually never deplete it, no matter how low the oral intake of the nutrient. The same is true for the maintenance of ECF Ca^{2+} concentration. A mere 5 g of bone contains as much calcium as the entire ECF space of an adult human. The requirement for calcium relates, thus, not to the metabolic role of the nutrient, but to building and maintaining the size of the calcium reserve, i.e., to its secondary function, bone strength.

The physiological adaptations to a low calcium intake

When the agricultural revolution positioned five cereal grains, i.e., wheat, corn, barley, oats, and rye, as the major source of energy largely replacing the roots, tubers, and other plants in the diet of early humans, intake of calcium as well as potassium and magnesium decreased markedly (Eaton and Nelson, 1991). Milk became the major source of calcium in the diet, and it is not usually consumed in sufficient quantities to meet the needs of hominids, who evolved in an environment of an abundance of calcium. Mammals typically have low intestinal calcium absorption efficacy, unregulated cutaneous losses, and poor renal conversion. Thus, humans are more often in a state of calcium deficiency, with homeostatic regulatory mechanisms trying, but largely failing, to adequately compensate.

When serum calcium levels fall, calcium-sensing receptors detect reduced Ca^{2+} concentrations in the ECF, and inhibition of parathyroid hormone (PTH) release from the parathyroids is removed and calcitonin release is suppressed. PTH activates conversion of vitamin D to its active form, $1,25(OH)_2D_3$, by cytochrome P450, subfamily 27A, polypeptide 1 (CYP27A1) in the liver and CYP27B1 in the kidney to activate three tissues, the gut, the kidney, and bone, to sustain blood calcium levels within the normal range (Fig. 70.2). Active calcium absorption is enhanced through upregulation of calcium transporters in the gut. PTH and $1,25(OH)_2D_3$ increase renal tubular calcium reabsorption to reduce urinary losses. Bone resorption ensues to mobilize calcium from this large reservoir. Sustained mobilization of bone to meet ECF Ca^{2+} concentrations comes at great cost to the skeleton over time.

Defining the calcium requirement

The calcium requirement can be defined as the intake needed to support genetically programmed acquisition of bone during growth and to sustain acquired bone during maturity and the declining years of life. Because of differing absorption and retention efficiencies, individuals will inevitably have differing requirements for a skeletal end point. Table 70.1 gives the adequate intake (AI), estimated average requirement (EAR), and recommended dietary allowance (RDA) for calcium, most recently revised in 2011 (IOM, 2011). The EAR is the value at which half the population is meeting their needs and the

1. A unit cell, in this case containing 10 calcium ions, is the smallest symmetrical repeating unit of the crystal lattice.

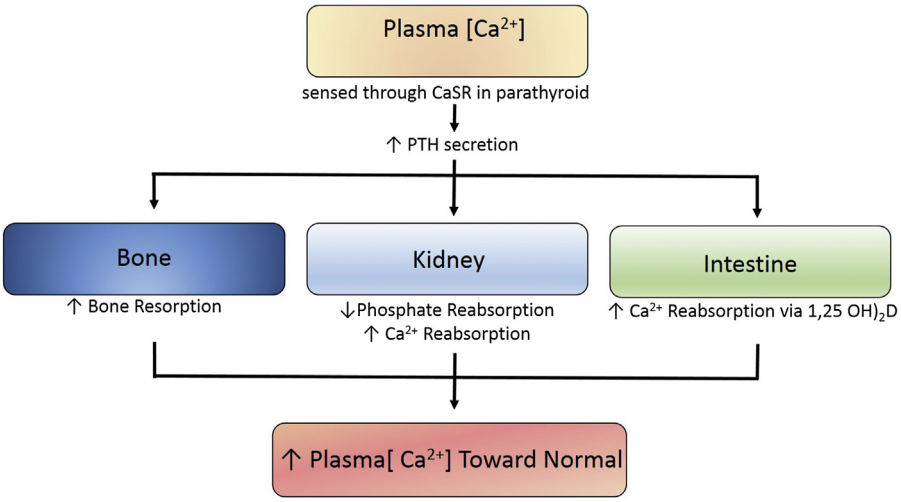

FIGURE 70.2 Homeostatic regulation of Ca^{2+} when plasma calcium falls to less than 2.5 mM. *CaSR*, calcium-sensing receptor; *PTH*, parathyroid hormone.

TABLE 70.1 Recommendations for calcium intake.

		Males (mg/day)		Females (mg/day)		
Life stage	**Age**	**EAR**	**RDA**	**EAR**	**RDA**	**UL**
Infants	0–6 months		200 (AI)		200 (AI)	1000
Infants	0–12 months		260 (AI)		260 (AI)	1500
Children	1–3 years	500	700	500	700	2500
Children	4–8 years	800	1000	800	1000	2500
Children	9–13 years	1100	1300	1100	1300	3000
Adolescents	14–18 years	1100	1300	1100	1300	3000
Adults	19–50 years	800	1000	800	1000	2500
Adults	51–70 years	800	1000	1000	1200	2000
Adults	71 years and older	1000	1200	1000	1200	2000
Pregnancy	14–18 years		–	1000	1300	3000
Pregnancy	19–50 years		–	800	1000	2500
Breastfeeding	14–18 years		–	1100	1300	3000
Breastfeeding	19–50 years		–	800	1000	2500

AI, adequate intake; *EAR*, estimated average requirement; *RDA*, recommended dietary allowance; *UL*, tolerable upper level.
From the Institute of Medicine, Dietary Reference Intakes for calcium and vitamin D. Washington, DC, 2011.

RDA provides a safety margin of 2 SDs so that 97% of the population are expected to meet their needs. AIs are used for infants to reflect intake from mother's milk for breastfed infants.

Calcium is a threshold nutrient. This means that, at subthreshold intakes, calcium retention is less than optimal. Bone gain during growth is then a direct function of intake (i.e., it is less than is genetically programmed), whereas in the mature organism, subthreshold intakes lead to actual bone loss. On the other hand, the threshold character of the relationship means that intakes above the threshold produce no additional bone effect. These relationships are depicted schematically in Fig. 70.4. Recommendations for calcium intake do not increase for pregnancy and lactation. Adaptations in calcium homeostasis during these life stages result in increased calcium absorption efficiency starting as early as 12 weeks in pregnancy to meet the needs of the fetus (Ritchie et al., 1998) and upon weaning of the infant following

cessation of lactation to recover bone loss experienced during lactation (Kalkwarf et al., 1997). In the elderly, optimizing calcium intake may not prevent a negative bone balance. In a randomized controlled trial (RCT) (McKane et al., 1996) in elderly women supplemented with calcium for 3 years, unsupplemented individuals, with intakes averaging close to 20 mmol (800 mg)/day, exhibited the high 24-h mean PTH levels, the enhanced PTH secretory reserve, and the elevated bone resorption that have all been taken to characterize the calcium and skeletal economies of the aged (Epstein et al., 1986). By contrast, women supplemented to 60 mmol (2400 mg)/day decreased both their bone remodeling and their parathyroid functional indices, restoring them to young adult normal values. The inference is that the increases in parathyroid cell mass and function represent not so much characteristics of old age as adaptive responses to long-standing calcium deprivation.

Contributing causes for this increased parathyroid activity in the elderly, aggravating the effect of low calcium intake, include a decline in vitamin D status with age (reflecting both decreased solar exposure and decreased efficiency of skin conversion of 7-dehydrocholesterol to previtamin D) and declining absorption and conservation efficiency for dietary calcium. Holding calcium intake constant at about 20 mmol (800 mg)/day, gross absorption efficiency declines from a mean at age 40 of 0.24, at a rate of 0.002/year through at least age 65, with a one-time additional drop of 0.02 at menopause (Heaney et al., 1989). Over that period, the decline thus amounts to 0.07, or a fall of 30% in absorptive efficiency. Nordin and others have shown also that renal conservation of calcium deteriorates across menopause (e.g., Nordin et al., 1991). The net result is that extraction of ingested calcium from food falls with age and conservation of that which is absorbed falls as well.

It must be noted that the absorption values cited earlier are *gross* absorption, such as would be measured by calcium tracer flux from the intestinal lumen into the bloodstream. They do not account for the contrary movement of calcium into the lumen in the digestive secretions and sloughed off mucosa (which turns over at a rate of 20%/day). In adult women, this calcium from endogenous sources entering the intestinal stream amounts to 3.5−3.75 mmol (140−150 mg)/day (Heaney and Recker, 1994). Most of this calcium is subject to the same absorptive probability as is ingested calcium, but given the low efficiency of calcium absorption in general, inevitably most endogenous calcium will be lost into the feces. Thus net absorption from intakes in the range of 20 mmol (800 mg)/day is on the order of only 10%−15% of ingested calcium. Not all of even this small amount of net calcium gain from the intestine can be retained, because the tiny elevation of blood calcium produced when calcium is absorbed elevates the filtered load at the kidney and leads to an increase in urinary calcium loss. The net result of the low net absorption and poor renal conservation is that, even during times of calcium need, only a small fraction of an ingested load is retained. Further, at the higher intakes achieved by calcium supplements, fractional retention is smaller still, because absorption fraction declines with the logarithm of the intake load size (Heaney et al., 1990, 2000).

Achieving the calcium requirement: dietary sources

Calcium must be consumed in sufficient quantities to replace obligatory losses through excretion and dermal sloughing and to supply needs for skeletal growth, or calcium balance will be more negative than optimal to build and maintain bone. The main sources of calcium are dairy products, fortified foods and beverages, and dietary supplements containing calcium.

Calcium is a shortfall nutrient around the globe, but even more so in Asian and African countries, where dairy product consumption is especially low. In US adults, surveyed in the 2009−12 National Health and Nutrition Examination Survey, 35.9 ± 1.0% of whites, 56.3 ± 1.4% of blacks, 36.4 ± 2.1% of Hispanics, and 61.4 ± 2.5% of Asians failed to meet the EAR from diet alone, which decreased to 24.2 ± 0.7% of whites, 48.2 ± 1.4% of blacks, 30.1 ± 2.0% of Hispanics, and 47.0 ± 2.6% of Asians when considering both diet and multivitamin and mineral supplement consumption (Blumberg et al., 2017). Calcium absorption from most of these sources, i.e., dairy, fortified foods and beverages, and supplements, is similar (Weaver and Heaney, 2006). However, other factors should be considered when planning how to achieve calcium recommendations.

Dairy foods not only provide calcium in high concentration, but also provide the whole package of nutrients needed for bone, including protein, phosphorus, magnesium, potassium, and B vitamins. Other natural sources of calcium in the diet typically have much less calcium in a serving than milk. Thus, even foods with very high calcium absorption efficiency due to absence of inhibitors such as oxalate and phytate cannot practically substitute for dairy recommendations. The number of servings to replace the absorbable calcium in one glass of milk is 3.5 for kale and 4.5 for broccoli. Fortified foods and beverages may contain good-quality protein and highly bioavailable calcium (Zhao et al., 2005). None of the other plant-based beverages becoming popular have been tested for calcium bioavailability. They have variable quantities of protein, potassium, and other nutrients important to bone and they all cost more than cow's milk. Supplements typically provide only calcium and maybe vitamin D; but not usually protein, potassium, magnesium, and other nutrient important to bone.

Nutritional factors influencing the calcium requirement

It is a truism of nutritional science that nutrients interact with one another and thereby alter their mutual requirements. Thus, requirements of certain of the B vitamins and of ascorbic acid vary with total energy intake (and expenditure). The lack of evolutionary development of efficient conservation of calcium has rendered this nutrient unusually sensitive to such nutrient−nutrient interactions. Most of this interaction is expressed in urinary calcium excretion, which, for example, is strongly influenced by the ingested load of sodium and by the acid/alkaline residue of the diet (Wigertz et al., 2005; Heaney, 1993b; Sebastian et al., 1994). The sodium effect is attributable to the fact that sodium and calcium share a common transport mechanism in the proximal tubule, and thus an increased filtered load of either ion will lead to increased excretion of the other. The magnitude of the sodium effect on the calcium economy is an increase of 0.5−1.5 mM urine calcium for every 100 mM sodium ingested (Devine et al., 1995; Nordin et al., 1993; Itoh and Suyama, 1996)).

These effects are linear across the full range of prevailing intakes from low to high, and are not thus consequences only of excessive intake. With diets characteristic of typical North American and European women, nutrients such as sodium account for 100 mg/day of obligatory calcium loss through the kidneys. Given the extremely poor net absorption efficiency for calcium, these nutrients can thus easily account for up to 1000 mg/day of the calcium requirement. It has been noted, for example, that individuals with low, but nutritionally adequate, intakes of sodium may have calcium requirements as low as 500 mg/day, whereas those with intakes more typical of contemporary patterns may have intake requirements closer to 2000 mg/day. This quite extraordinary sensitivity of calcium to the intake of other nutrients is but one more reflection of the lack of evolutionary acquisition of efficient mechanisms for calcium absorption and conservation.

The well-documented effect of the acid/alkaline residue of the diet (Berkelhammer et al., 1988; Sebastian et al., 1994) is probably a function of the "hard" anions (sulfate, chloride), either ingested with food or produced in metabolism. In any event, substitution of acetate or bicarbonate for chloride produces substantial reductions in urinary calcium loss and therefore in the ability to maintain calcium equilibrium on low calcium intakes.

It is important to stress this last point, that these nutrient interactions negatively affect calcium balance mainly at low calcium intakes. This is because they limit an individual's ability to adapt to a low intake. At the higher intakes near the RDA, adaptation is easily possible. High protein intakes do not have a negative effect on the skeleton, as once thought based on increased urinary calcium excretion (Ince et al., 2004). This increased loss through the kidney can be offset by increased calcium absorption (Kerstetter et al., 2005). A systematic review and meta-analysis of RCTs and observational studies showed no overall detrimental effect of dietary protein on bone (Shams-White et al., 2017). Protein supplementation in institutionalized elderly with recent hip fractures reduced bone loss (Schürch et al., 1998). There is evidence of an interaction of protein and calcium intakes on bone (Dawson-Hughes and Harris, 2002; Sahni et al., 2010). In the Framingham Study, those in the highest tertile of animal protein consumption taking <800 mg Ca/day had 2.8 times the risk of hip fracture of those in the lowest tertile of protein intake ($P = .02$), whereas protein decreased fracture incidence when calcium intakes were >800 mg/day (Sahni et al., 2010).

Another example of a dietary constituent influencing calcium metabolism is caffeine. Similar to the effect of protein, caffeine was considered detrimental to bone because of its impact on increasing urinary calcium excretion. However, at practical intakes, caffeine has little effect on calcium homeostasis or bone outcomes, including risk of fractures and falls, bone mineral density (BMD), and osteoporosis. In a systematic review of 14 studies, evidence of the effects of caffeine intake below 400 mg/day on these outcomes was of low magnitude and observed only under conditions of low calcium intake (Wikoff et al., 2017). A typical cup of coffee contains 50 mg, suggesting little effect up to eight cups of coffee or caffeine equivalent. The greater risk is displacement of milk consumption by caffeinated beverages.

Toxicity

It is possible to consume too much of any nutrient, and calcium is no exception. However, in healthy individuals, available evidence indicates that the toxic threshold is quite high. Many young adult males in the United States regularly consume more than 75 mmol (3000 mg)/day (Blumberg et al., 2017), and in pastoralist societies, such as the Maasai of East Africa, calcium intakes regularly average more than 150 mmol (6000 mg)/day. In both instances, there are no known ill effects associated with such intakes.

However, there are special circumstances in which high calcium intake can definitely be harmful. Even at the low-absorption fractions typical of high intakes, substantial quantities of calcium will enter the body and will need to be excreted in the urine (unless active bone building is occurring). Under conditions of dehydration or hypovolemia, perfusion of both bone and kidney can be sufficiently compromised so that absorbed calcium produces significant hypercalcemia. Likewise, under conditions of systemic alkalosis, large calcium intake can produce renal calcinosis and severe impairment

of kidney function. Furthermore, under these somewhat unusual and extreme circumstances, elements of positive feedback can cause the situation to deteriorate rapidly. Hypercalcemia impairs the ability of the kidney to retain water and thus aggravates a preexisting dehydration, with consequently worsening hypercalcemia. A fatal downward spiral can easily ensue. Published reports of such toxicity have generally involved intakes of more than 150 mmol (6000 mg)/day in individuals with preexisting impairments of water and electrolyte metabolism. Whatever the underlying cause, such problems can be easily handled by rehydration and by correction of the underlying abnormality, so long as these situations are recognized in time.

Kidney stones are the complication of most concern in setting tolerable upper levels (ULs) (see Table 70.1). Kidney stones are most often composed of calcium, oxalate, or calcium phosphate. Those with hypercalciuria are more at risk for kidney stones, which led to earlier recommendations to reduce calcium intake if risk of kidney stones was high (Curhan et al., 1993, 1997; Taylor et al., 2004; Taylor and Curhan, 2013). In these large prospective studies of men and women, there was an inverse correlation between calcium intake from either dairy or nondairy sources and stone formation; those with the highest calcium intakes had the lowest risk of kidney stones, although in elderly men, who experience lower incidence of stones, there was no relationship. This seeming paradox is explained by the fact that oxalate excretion in the urine is a more significant risk factor for calculi than is urine calcium. High calcium intake binds oxalate, both of dietary origin (when coingested) and produced by bacterial fermentation in the gut before it can be absorbed; dietary calcium thereby lowers the renal oxalate burden. In fact, very large calcium supplements have long been standard therapy for the kidney stones occurring with intestinal hyperoxalosis, sometimes found in patients with short-bowel syndrome. A protective effect of high calcium intake on both oxalate loads and stone recurrence was seen in an RCT in which those on a reduced calcium intake had twice the rate of stone occurrence as those on a high intake (Borghi et al., 2002).

In summary, the levels of calcium intake discussed in the foregoing sections of this chapter, as well as those needed to support osteoporosis pharmacotherapy (see next section on "Calcium and osteoporosis treatment"), are well within the safety limits for the ingestion of this nutrient. Mild adverse gastrointestinal events, including constipation, cramping, and bloating, have been associated with calcium supplementation (Lewis et al., 2012).

Calcium and osteoporosis treatment

Osteoporosis is a skeletal disorder characterized by increased risk of fracture and reduced BMD and bone strength. Effective osteoporosis treatments involve a combination of pharmacotherapy designed to reverse the negative remodeling balance prevailing in the skeleton and diet and physical therapy designed both to increase function and to increase mechanical loading on the skeleton. Currently recommended calcium intakes are presumably adequate to sustain bone mass, but they may not be sufficient to support bone gain in most individuals (i.e., net absorption from such intakes is just sufficient to offset obligatory losses). Furthermore, there is essentially no evidence that calcium alone, in any quantity, will lead to substantial gain in bone in individuals who already have osteoporosis. The small increase in BMD with supplementation in the classic study by Chapuy et al. (1992) illustrated in Fig. 70.3 probably reflects a remodeling transient (Heaney, 1994) and not a new steady-state rate of change. However, elevating calcium intake from 13 mmol (520 mg)/day to 42.5 mmol (1700 mg)/day in 1800 French women, average age 84, reduced fracture rates at the hip by an impressive 20% and at other sites by 40% within 18 months of supplementation (Chapuy et al., 1992). This occurred not due to the small increase in BMD in the supplemented group, but due to the prevention of erosion of bone mass observed in the control group. Participants in the intervention group were also given 800 IU vitamin D, which also would have resulted in fracture risk reduction.

Effective pharmacotherapy, including fluoride (Pak et al., 1995; Riggs et al., 1990), bisphosphonates (Liberman et al., 1995; Black et al., 1996; Cummings et al., 1998; Harris et al., 1999), selective estrogen receptor modulators (SERMs) (Ettinger et al., 1999), and PTH (Kurland et al., 2000; Neer et al., 2001), does increase bone mass, and for some of these agents at a rate of up to 8% per year. To realize this potential gain, and particularly to optimize it, calcium intake probably needs to be above the maintenance level. Most medications for osteoporosis treatment are prescribed with calcium and vitamin D supplementation as adjuvant therapy based on trials showing efficacy in that context (Harvey et al., 2017). Also, it is worth noting that the antiresorptive agents (principally bisphosphonates and SERMs, as well the receptor activator of NF-κB ligand and cathepsin K inhibitors), by blocking osteoclastic resorption, force higher levels of PTH secretion and hence better utilization of ingested calcium. Hence, the calcium intake requirement for optimal BMD response to these agents is unclear.

There is, however, some evidence. With respect to fluoride, Dure-Smith et al. (1996) showed, during effective fluoride therapy, an extraordinary degree of bone hunger, suggesting the need for calcium intake during fluoride therapy of perhaps

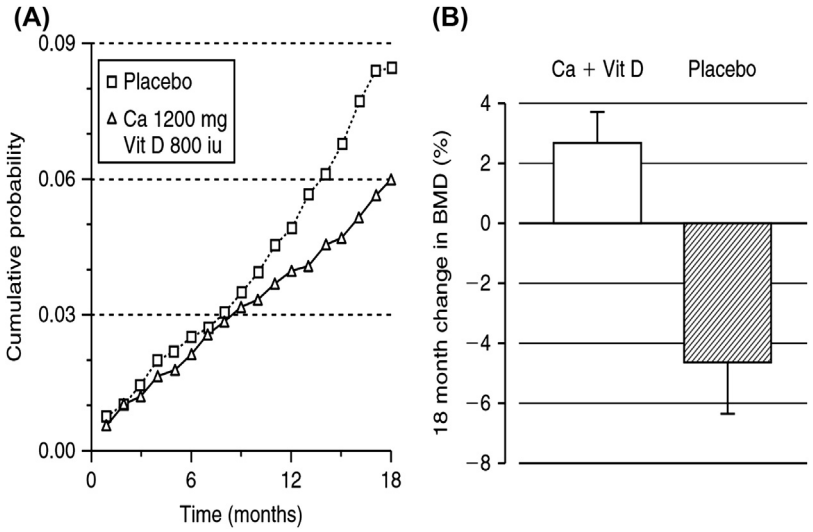

FIGURE 70.3 Effects of supplementation with calcium phosphate and vitamin D on hip fracture rate and hip bone mineral density (*BMD*). (A) The cumulative probability of fracture for the supplemented and unsupplemented groups is shown, as is (B) the change from baseline in hip BMD for the two groups. *Redrawn from the data of Chapuy, M.C., Arlot, M.E., Duboeuf, F., et al. 1992. Vitamin D3 and calcium to prevent hip fractures in elderly women. N. Engl. J. Med. 327, 1637–1642.*

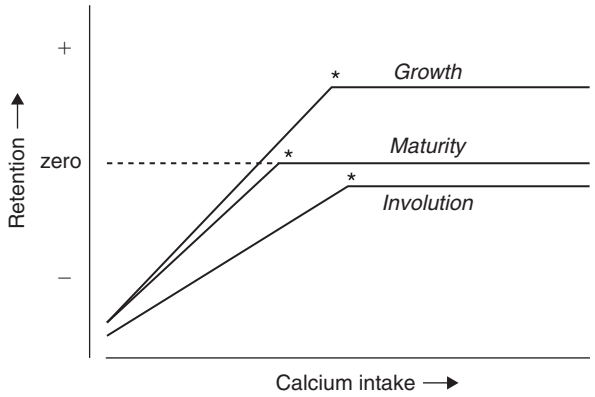

FIGURE 70.4 Schematic depiction of the relationship between calcium intake and skeletal retention at three life stages. Given sufficient intake, retention is positive during growth, zero at maturity, and variably negative during involution. Intakes above the threshold do not affect retention, but subthreshold intakes limit bone acquisition or lead to bone loss. The location of the minimum requirement is indicated by the *asterisk* above each line. *From Heaney, R.P. 1997. Nutrient effects: discrepancy between data from controlled trials and observational studies. Bone 21, 469–471, with permission. Copyright Robert P. Heaney 1998.*

as much as 62.5 mmol (2500 mg)/day. Other clear examples of the importance of ensuring adequate calcium intake when using other bone active agents are provided by a series of papers. First is a meta-analysis of 31 controlled trials of estrogen replacement therapy (Nieves et al., 1998), which showed that estrogen in trials using supplemental calcium (at an average intake of 1187 mg/day) produced bone responses more than twice as great as those that did not (at an average intake of 583 mg/day). In addition, Recker et al. (1999) showed that a reduced dose of estrogen (0.3 mg of conjugated equine estrogens) produced a 5% increase in bone mass in women given supplemental calcium and vitamin D. By contrast, in at least three earlier trials without supplemental calcium, this estrogen dose was essentially ineffective.

Calcium supplementation and bone health

The importance of a high calcium intake for bone health has often been questioned (e.g., Kanis and Passmore, 1989) and, even more often, has been termed "controversial." This is because some studies showed strong effects of calcium intake on bone status, but others showed no benefit at all. "Confusing" is the more accurate term. There are several reasons for this confusion.

First, osteoporotic fracture is a distinctly multifactorial disorder. Nutrition, and specifically calcium nutrition, is only one of many contributing factors. Although calcium intake is of critical importance in many individuals, it plays little or no role in others, just as iron intake is limiting in only certain forms of anemia. One example of this distinction is seen in menopausal bone loss, which is dominantly caused by estrogen deficiency and cannot be substantially influenced by calcium intake (although estrogen-related loss may be exaggerated if calcium intakes are very low) (Heaney, 1990). This is seen, for example, in the fact that even intakes of more than 75 mmol (3000 mg)/day, in the study by Elders et al. (1991), were able only to slow menopausal loss, not to prevent it. However, menopausal loss is self-limited and is mostly confined to the 5-year period surrounding cessation of ovarian function.

Observational studies do not always show a benefit of calcium supplementation or milk intake to bone, or they may show a benefit to one sex, but not the other, though which sex is not consistent (Bischoff-Ferrari et al., 2011; Michaelsson et al., 2014). There are many reasons for these discrepancies, including one sex being older with more comorbidities compared with the other sex (Sahni et al., 2017). Perhaps the more common and important reason for inconsistent results is the weak ability to estimate calcium intake from food records, or food frequency questionnaires, no matter how carefully these methods are applied, resulting in substantial classification bias (Heaney, 1991, 1997).

Results from RCTs are also inconsistent. Frequently, calcium and vitamin D supplementation are given together, making it difficult to distinguish the effects of calcium alone. Some systematic reviews or meta-analyses of RCTs fail to show a benefit of dietary calcium or supplements to lowering fracture risk (Zhao et al., 2017) and others show rather small benefits to BMD (<2%) (Tai et al., 2015).

Frequently, confounding issues also plague RCTs. Failure to consider baseline status is important, as calcium is a threshold nutrient and benefits will be realized only if status can be improved. Lack of compliance within either the intervention or the control group must be considered, as there is a tendency for convergence of intakes between the two arms (Atkinson et al., 2008). The largest of the RCTs is the Women's Health Initiative (WHI). A meta-analysis of eight RCTs with 30,970 subjects showed the powerful effect of supplementation on lowering hip fracture risk by 30% (Weaver et al., 2016). In this analysis, participants in the WHI study not consuming their own calcium and vitamin D supplements and who were not compliant were excluded. This contrasts with no significant association when this trial is not adjusted for compliance and baseline status. Additional confounding occurs when life stages are combined, such as perimenopausal women with women postmenopausal for greater than 5 years.

A final consideration relates to the uncritical use of transnational comparisons (e.g., Hegsted, 1986). Differences in fracture rate between ethnic and national populations have many bases, only some of them nutritional. An example is the lower hip fracture rates of contemporary Chinese and blacks, despite lower BMD values for Chinese (Walker et al., 2006) and despite mean calcium intakes for both groups that are lower than those of North American or European Caucasians. Behind this difference there is, first, the large effect of the other nutrients in the diet, previously described. Thus, the predominantly vegetable-based and low protein intakes of many Third World populations would be expected to lower their calcium requirements. Similarly, there are major racial differences in ability to conserve calcium. American blacks, for example, both absorb at higher efficiency for any given ingested intake and conserve better at the kidney than do Caucasians (Bryant et al., 2003; Abrams et al., 1995; Bell et al., 1985; Aloia et al., 1998; Cosman et al., 1997). Chinese American adolescents have a higher calcium absorption efficiency than other races (Wu et al., 2010). Thus they have lower calcium requirements. Finally, there are important racial differences in bone geometry that have their own effect on fracture rate. Hip axis length, for example, explains most or all of the difference between the hip fracture rates of Caucasians, on one hand, and Chinese and Japanese, on the other, after adjusting for bone mass (Faulkner et al., 1993; Nakamura et al., 1994).

Instead of making cross-cultural comparisons, the correct approach is to assess the effect of nutrient intakes within a cultural and ethnic group. When this has been done, bone mass and hip fracture rate are found to be inversely correlated with calcium intake (Anderson et al., 1995; Hu et al., 1993; Lau et al., 1988).

Calcium supplementation and cardiovascular risk

Calcium supplementation became associated with a risk of cardiovascular disease when a retrospective analysis of an RCT to determine the effect of calcium supplementation on BMD revealed an increased risk of myocardial infarction (Bolland et al., 2008). This finding spawned many additional retrospective analyses, prospective studies, and meta-analyses with mixed results with a variety of cardiovascular outcomes (Li et al., 2012; Xiao et al., 2013; Avenell et al., 2012; Samelson et al., 2012; Lewis et al., 2012, 2015; Khan et al., 2015). In an evaluation of the state of evidence base using Bradford Hill criteria, the association between calcium supplementation and cardiovascular risk was judged to fail because of a weak strength of relationship (relative risk <2.0), lack of consistent results, no dose−response relationship, and no biological

plausibility or proven mechanism (Heaney et al., 2012). A systematic review and meta-analysis examined four RCTs and 27 prospective cohort and nested case−control studies for the effects of calcium intake on cardiovascular disease among healthy adults (Chung et al., 2016). No statistically significant differences in risk for cardiovascular disease events or mortality between supplementation and placebo groups in the RCTs were observed. Nor were any consistent dose−response relationships between calcium intake from any source and cardiovascular mortality, risk for stroke, or stroke mortality observed in cohort studies.

In all of these studies, cardiovascular outcomes were secondary end points. Lacking are trials with cardiovascular end points as a primary outcome. The updated analysis by Chung et al. (2016) informed a joint position statement from the National Osteoporosis Foundation and American Society for Preventive Cardiology that concluded there is a B level, or moderate level, of evidence that calcium with or without vitamin D intake from food or supplements has no beneficial or harmful relationship to risk of cardiovascular or cerebrovascular disease, mortality, or all-cause mortality (Kopecky et al., 2016). Calcium intake up to the UL was considered safe from a cardiovascular standpoint.

Summary

Calcium is the principal cation of bone, making up 20% of its dry weight. Bone constitutes a very large nutrient reserve for calcium in terrestrial vertebrates, a reserve that has acquired a major mechanical function. The requirement for calcium is related to the protection of this mechanical function, not to the metabolic actions of calcium, which could be adequately protected by a reserve several orders of magnitude smaller. Calcium was abundant in the environment in which hominids evolved and in the foods they ate. Probably as a consequence, efficient calcium conservation mechanisms did not develop. Contemporary diets are low in calcium by comparison, and our Paleolithic physiologies are poorly adapted to them. Yet other features of the modern diet (e.g., high salt and low potassium) increase obligatory calcium loss and thereby reduce the ability to adapt to lowered intakes. The evidence is compelling that inadequate calcium intake weakens bone and contributes to the growing osteoporosis problem.

References

Abrams, S.A., O'Brien, K.O., Liang, L.K., Stuff, J.E., 1995. Differences in calcium absorption and kinetics between black and white girls aged 5−16 years. J. Bone Miner. Res. 10, 829−833.

Aloia, J.F., Mikhail, M., Pagan, C.D., et al., 1998. Biochemical and hormonal variables in black and white women matched for age and weight. J. Lab. Clin. Med. 132, 383−389.

Anderson, J.J.B., Tylavsky, F.A., Lacey, J.M., Adeleke, V.M., 1995. Ethnicity, nutrition, and bone mass. In: Burckhardt, P., Heaney, R.P. (Eds.), Challenges of Modern Medicine: Nutritional Aspects of Osteoporosis '94, vol. 7. Christengraf, Rome, pp. 27−44.

Atkinson, S.A., McCabe, G.P., Weaver, C.M., et al., 2008. Are Current calcium recommendations for adolescents higher than needed to achieve optimal peak bone mass? The Controversy. J. Nutr. 138, 1182−1186.

Avanell, A., MacLennan, G.S., Jenkinson, D.J., et al., 2012. Long−term follow-up for mortality and cancer in a randomized placebo-controlled trial of vitamin D(3) and/or calcium (RECORD trial). J. Clin. Endocrinol. Metab. 97 (Suppl. 2), 614−622.

Bell, N.H., Greene, A., Epstein, S., et al., 1985. Evidence for alteration of the vitamin D-endocrine system in blacks. J. Clin. Investig. 76, 470−473.

Berkelhammer, C.H., Wood, R.J., Sitrin, M.D., 1988. Acetate and hypercalciuria during total parenteral nutrition. Am. J. Clin. Nutr. 48, 1482−1489.

Bischoff-Ferrari, H.A., Dawson-Hughes, B., Baron, J.A., et al., 2011. Milk intake and risk of hip fracture in men and women: a meta-analysis of prospective cohort studies. J. Bone Miner. Res. 26, 833−839.

Black, D.M., Cummings, S.R., Karpf, D.B., et al., 1996. Randomised trial of effect of alendronate on risk of fracture in women with existing vertebral fractures. Lancet 348, 1535−1541.

Blumberg, J.B., Frei, B.B., Fulgoni, V.L., et al., 2017. Contribution of dietary supplements to nutritional adequacy in race/ethnic population subgroups in the United States. Nutrients 9, 1295−1304.

Bolland, M.J., Barber, P.A., Doughty, R.N., et al., 2008. Vascular events in healthy older women receiving calcium supplementation: randomized controlled trial. Br. Med. J. 336, 262−266.

Borghi, L., Schianchi, T., Meschi, T., et al., 2002. Comparison of two diets for the prevention of recurrent stones in idiopathic hypercalciuria. N. Engl. J. Med. 346, 77−84.

Brommage, R., DeLuca, H.F., 1985. Regulation of bone mineral loss during lactation. Am. J. Physiol. Endocrinol. Metab. 11, E182−E187.

Bryant, R.J., Wastney, M.E., Martin, B.R., et al., 2003. Racial differences in bone turnover and calcium metabolism in adolescent females. J. Clin. Endocrinol. Metab. 88 (Suppl. 3), 1043−1047.

Carafoli, E., Penniston, J.T., 1985. The calcium signal. Sci. Am. 253, 70−78.

Chapuy, M.C., Arlot, M.E., Duboeuf, F., et al., 1992. Vitamin D3 and calcium to prevent hip fractures in elderly women. N. Engl. J. Med. 327, 1637−1642.

Chung, M., Tang, A.M., Fu, Z., Wang, D.D., Newberry, S.J., 2016. Calcium intake and cardiovascular disease risk: an updated systematic review and meta-analysis. Ann. Intern. Med. 165 (Suppl. 12), 856–866.

Cosman, F., Morgan, D.C., Nieves, J.W., et al., 1997. Resistance to bone resorbing effects of PTH in black women. J. Bone Miner. Res. 12, 958–966.

Cummings, S.R., Black, D.M., Thompson, D.E., et al., 1998. Effect of alendronate on risk of fracture in women with low bone density but without vertebral fractures. J. Am. Med. Assoc. 280 (Suppl. 24), 2077–2082.

Curhan, G.C., Willett, W.C., Rimm, E.B., et al., 1993. A prospective study of dietary calcium and other nutrients and the risk of symptomatic kidney stones. N. Engl. J. Med. 328, 833–838.

Curhan, G.C., Willett, W.C., Speizer, F.E., et al., 1997. Comparison of dietary calcium with supplemental calcium and other nutrients as factors affecting the risk for kidney stones in women. Ann. Intern. Med. 126, 497–504.

Dawson-Hughes, B., Harris, S.S., 2002. Calcium intake influences the association of protein intake with rates of bone loss in elderly men and women. Am. J. Clin. Nutr. 75, 773–779.

Devine, A., Criddle, R.A., Dick, I.M., et al., 1995. A longitudinal study of the effect of sodium and calcium intakes on regional bone density in post-menopausal women. Am. J. Clin. Nutr. 62, 740–745.

Dure-Smith, B.A., Farley, S.M., Linkhart, S.G., et al., 1996. Calcium deficiency in fluoride-treated osteoporotic patients despite calcium supplementation. J. Clin. Endocrinol. Metab. 81, 269–275.

Eaton, S.B., Nelson, D.A., 1991. Calcium in evolutionary perspective. Am. J. Clin. Nutr. 54, 281S–287S.

Elders, P.J.M., Netelenbos, J.C., Lips, P., et al., 1991. Calcium supplementation reduces vertebral bone loss in perimenopausal women: a controlled trial in 248 women between 46 and 55 years of age. J. Clin. Endocrinol. Metab. 73, 533–540.

Epstein, S., Bryce, G., Hinman, J.W., et al., 1986. The influence of age on bone mineral regulating hormones. Bone 7, 421–425.

Ettinger, B., Black, D.M., Mitlak, B.H., et al., 1999. Reduction of vertebral fracture risk in postmenopausal women with osteoporosis treated with raloxifene. J. Am. Med. Assoc. 282, 637–645.

Faulkner, K.G., Cummings, S.R., Black, D.L., et al., 1993. Simple measurement of femoral geometry predicts hip fracture: the study of osteoporotic fractures. J. Bone Miner. Res. 8, 1211–1217.

Gilsanz, V., Gibbens, D.T., Roe, T.F., et al., 1988. Vertebral bone density in children: effect of puberty. Radiology 166, 847–850.

Harris, S.T., Watts, N.B., Genant, H.K., et al., 1999. Effects of risedronate treatment on vertebral and nonvertebral fractures in women with post-menopausal osteoporosis: a randomized controlled trial. J. Am. Med. Assoc. 282, 1344–1352.

Harvey, N.C., Biver, E., Kauffman, J.M., et al., 2017. The role of calcium supplementation in healthy musculoskeletal ageing : an expert consensus meeting of the European society for clinical and economic aspects of osteoporosis, osteoarthritis and musculoskeletal diseases (ESCEO) and the international foundation for osteoporosis (IOF). Osteoporos. Int. 28, 447–462.

Heaney, R.P., 1990. Estrogen-calcium interactions in the postmenopause: a quantitative description. Bone Miner. 11, 67–84.

Heaney, R.P., 1991. Assessment and consistency of calcium intake. In: Burckhardt, P., Heaney, R.P. (Eds.), Nutritional Aspects of Osteoporosis, vol. 85. Raven Press, New York, pp. 99–104.

Heaney, R.P., 1993b. Nutritional factors in osteoporosis. Annu. Rev. Nutr. 13, 287–316.

Heaney, R.P., 1994. The bone remodeling transient: implications for the interpretation of clinical studies of bone mass change. J. Bone Miner. Res. 9, 1515–1523.

Heaney, R.P., 1996. Nutrition and risk for osteoporosis. In: Marcus, R., Feldman, D., Kelsey, J. (Eds.), Osteoporosis. Academic Press, San Diego, CA, pp. 483–505.

Heaney, R.P., 1997. Nutrient effects: discrepancy between data from controlled trials and observational studies. Bone 21, 469–471.

Heaney, R.P., 2003. Is the paradigm shifting? Bone 33, 457–465.

Heaney, R.P., Recker, R.R., 1994. Determinants of endogenous fecal calcium in healthy women. J. Bone Miner. Res. 9, 1621–1627.

Heaney, R.P., Berner, B., Louie-Helm, J., 2000. Dosing regimen for calcium supplementation. J. Bone Miner. Res. 15, 2291.

Heaney, R.P., Recker, R.R., Stegman, M.R., et al., 1989. Calcium absorption in women: relationships to calcium intake, estrogen status, and age. J. Bone Miner. Res. 4, 469–475.

Heaney, R.P., Skillman, T.G., 1971. Calcium metabolism in normal human pregnancy. J. Clin. Endocrinol. Metab. 33, 661–670.

Heaney, R.P., Weaver, C.M., 2005. Newer perspectives on calcium nutrition and bone quality. J. Am. Coll. Nutr. 24, 574S–581S.

Heaney, R.P., Weaver, C.M., Fitzsimmons, M.L., 1990. The influence of calcium load on absorption fraction. J. Bone Miner. Res. 11, 1135–1138.

Heaney, R.P., Kopecky, S., Maki, K.C., et al., 2012. A review of calcium supplements and cardiovascular disease risk. Adv. Nutr 3, 763–771.

Hegsted, D.M., 1986. Calcium and osteoporosis. J. Nutr. 116, 2316–2319.

Hu, J.-F., Zhao, X.-H., Jia, J.-B., et al., 1993. Dietary calcium and bone density among middle-aged and elderly women in China. Am. J. Clin. Nutr. 58, 217–219.

Ince, B.A., Anderson, E., Neer, R.M., 2004. Lowering dietary protein to U.S. recommended dietary allowance levels reduces urinary calcium excretion and bone resorption in young women. J. Clin. Endocrinol. Metab. 89, 3801–3807.

Institute of Medicine, 2011. Dietary Reference Intakes for Calcium and Vitamin D. Washington, DC.

Itoh, R., Suyama, Y., 1996. Sodium excretion in relation to calcium and hydroxyproline excretion in a healthy Japanese population. Am. J. Clin. Nutr. 63, 735–740.

Kanis, J.A., Passmore, R., 1989. Calcium supplementation of the diet–I and II. Br. Med. J. 298, 137–140; 205–208.

Kalkwarf, H.J., Specker, B.L., Bianchi, C., et al., 1997. The effect of calcium supplementation on bone density during lactation and after weaning. N. Engl. J. Med. 337, 523–528.

Kerstetter, J.E., O'Brien, K.O., Caseria, D.M., et al., 2005. The impact of dietary protein on calcium absorption and kinetic measures of bone turnover in women. J. Clin. Endocrinol. Metab. 90, 26–31.

Khan, B., Nowson, C.A., Daly, R.M., et al., 2015. Higher dietary calcium intakes are associated with reduced risk of fractures, cardiovascular events, and mortality: a prospective cohort study of older men and women. J. Bone Miner. Res. 30, 1758–1766.

Kopecky, S.L., Bauer, D.C., Gulati, M., et al., 2016. Lack of evidence linking calcium with or without vitamin D supplementation to cardiovascular disease in generally healthy adults: a position statement from the National Osteoporosis Foundation and American Society for Preventive Cardiology. Ann. Intern. Med. 165, 867–868.

Kurland, E.S., Cosman, F., McMahon, D.J., et al., 2000. Parathyroid hormone as a therapy for idiopathic osteoporosis in men: effects on bone mineral density and bone markers. J. Clin. Endocrinol. Metab. 85, 3069–3076.

Lau, E., Donnan, S., Barker, D.J.P., Cooper, C., 1988. Physical activity and calcium intake in fracture of the proximal femur in Hong Kong. Br. Med. J. 297, 1441–1443.

Lewis, J.R., Radavelli-Bagatini, S., Rejnmark, L., 2015. The effects of calcium supplementation on verified coronary heart disease hospitalization and death in postmenopausal women: a collaborative meta-analysis of randomized controlled trials. J. Bone Miner. Res. 30, 165–175.

Lewis, J.R., Zhu, K., Prince, R.L., 2012. Adverse events from calcium supplementation relationship to errors in myocardial infarction self-reporting in randomized controlled trials of calcium supplementation. J. Bone Miner. Res. 27, 719–722.

Li, K., Kaaks, R., Linseisen, J., Rohrmann, S., 2012. Associations of dietary calcium intakes and calcium supplementation with myocardial infarction and stroke risk and overall cardiovascular morality in the Heidelberg cohort of the European prospective investigation into cancer and nutrition study (EPIC-Heidelberg). Heart 98, 920–925.

Liberman, U.A., Weiss, S.R., Broll, J., et al., 1995. Effect of oral alendronate on bone mineral density and the incidence of fractures in postmenopausal osteoporosis. N. Engl. J. Med. 333, 1437–1443.

McKane, W.R., Khosla, S., Egan, K.S., et al., 1996. Role of calcium intake in modulating age-related increases in parathyroid function and bone resorption. J. Clin. Endocrinol. Metab. 81, 1699–1703.

Michaëlsson, K., Wolk, A., Langenskiöld, S., et al., 2014. Milk intake and risk of mortality and fractures in women and men: cohort studies. Br. Med. J. 349, g6015.

Nakamura, T., Turner, C.H., Yoshikawa, T., et al., 1994. Do variations in hip geometry explain differences in hip fracture risk between Japanese and white Americans? J. Bone Miner. Res. 9, 1071–1076.

Neer, R.M., Arnaud, C.D., Zanchetta, J.R., et al., 2001. Effect of parathyroid hormone (1–34) on fractures and bone mineral density in postmenopausal women with osteoporosis. N. Engl. J. Med. 344, 1434–1441.

Nieves, J.W., Komar, L., Cosman, F., Lindsay, R., 1998. Calcium potentiates the effect of estrogen and calcitonin on bone mass: review and analysis. Am. J. Clin. Nutr. 67, 18–24.

Nordin, B.E.C., Need, A.G., Morris, H.A., Horowitz, M., 1993. The nature and significance of the relationship between urinary sodium and urinary calcium in women. J. Nutr. 123, 1615–1622.

Nordin, B.E.C., Need, A.G., Morris, H.A., Horowitz, M., Robertson, W.G., 1991. Evidence for a renal calcium leak in postmenopausal women. J. Clin. Endocrinol. Metab. 72, 401–407.

Pak, C.Y.C., Sakhaee, K., Adams-Huet, B., et al., 1995. Treatment of postmenopausal osteoporosis with slow-release sodium fluoride. Ann. Intern. Med. 123, 401–408.

Parfitt, A.M., 2004. What is the normal rate of bone remodeling? Bone 35, 1–3.

Posner, A.S., 1987. Bone mineral and the mineralization process. In: Peck, W.A. (Ed.), Bone and Mineral Research/5. Elsevier Science Publishers B.V., Amsterdam, Netherlands, pp. 65–116.

Recker, R.R., Davies, K.M., Dowd, R.M., Heaney, R.P., 1999. The effect of low dose continuous estrogen and progesterone therapy with calcium and vitamin D on bone in elderly women: a randomized controlled trial. Ann. Intern. Med. 130, 897–904.

Riggs, B.L., Hodgson, S.F., O'Fallon, W.M., et al., 1990. Effect of fluoride treatment on the fracture rate in postmenopausal women with osteoporosis. N. Engl. J. Med. 322, 802–809.

Ritchie, L.D., Fung, E.B., Halloran, B.D., et al., 1998. A longitudinal study of calcium homeostasis during human pregnancy and lactation and after resumption of menses. Am. J. Clin. Nutr. 67, 693–701.

Robinson, J.A., Chatterjee-Kishore, M., Yaworsky, P.J., et al., 2006. Wnt/ß-catenin signaling is a normal physiological response to mechanical loading in bone. J. Biol. Chem. 281, 31720–31728.

Sahni, S., Cuppels, A., McLean, R.R., et al., 2010. Protective effect of high protein and calcium intake on the risk of hip fracture in the Framingham offspring cohort. J. Bone Miner. Res. 25, 2494–2500.

Sahni, S., Soedamah-Muthu, S.S., Weaver, C.M., 2017. Higher milk intake increases fracture risk? Confounding or true association. Osteoporos. Int. https://doi.org/10.1007/s00198-017-4088-y.

Samelson, E.J., Booth, S.L., Fox, C.S., et al., 2012. Calcium intake is not associated with increased coronary artery calcification: the Framingham Study. Am. J. Clin. Nutr. 96, 1274–1280.

Schürch, M.-A., Rizzoli, R., Slosman, D., et al., 1998. Protein supplements increase serum insulin-like growth factor-I levels and attenuate proximal femur bone loss in patients with recent hip fracture. Ann. Intern. Med. 128, 801–809.

Sebastian, A., Harris, S.T., Ottaway, J.H., et al., 1994. Improved mineral balance and skeletal metabolism in postmenopausal women treated with potassium bicarbonate. N. Engl. J. Med. 330, 1776–1781.

Shams-White, M.M., Chung, M., Du, M., et al., 2017. Dietary protein and bone health: a systematic review and meta-analysis from the National Osteoporosis Foundation. Am. J. Clin. Nutr. 105, 1528−1543.

Tai, V., Lung, W., Grey, A., et al., 2015. Calcium intake and bone mineral density: systematic review and meta-analysis. Br. Med. J. 351, h1483.

Taylor, E.N., Stampfer, M.J., Curhan, G.C., 2004. Dietary factors and the risk of incident kidney stones in men: new insights after 14 years of follow-up. J. Am. Soc. Nephrol. 15, 3225−3232.

Taylor, E.N., Curhan, G.C., 2013. Dietary calcium from dairy and nondairy sources and risk of symptomatic kidney stones. J. Urol. 190, 1255−1259.

Walker, M.D., Babbar, R., Optowsky, A.R., et al., 2006. A referent bone mineral density database for Chinese American women. Osteoporos. Int. 17, 878−887.

Weaver, C.M., Heaney, R.P., 2006. Food sources, supplements and bioavailability. In: Weaver, C.M., Heaney, R.P. (Eds.), Calcium in Human Health. Humana Press, Totowa, NJ, pp. 129−142.

Weaver, C.M., Alexander, D.D., Boushey, C.J., et al., 2016. Calcium plus vitamin D supplementation and risk of fractures: an updated meta-analysis from the National Osteoporosis Foundation. Osteoporos. Int. 27, 367−376.

Whyte, M.P., 2010. Alkaline phosphatase: physiological role explored in hypophosphatasia. Ann NY Acad Sci 1192, 190−200.

Wigertz, K., Palacios, C., Jackman, L.A., Martin, B.R., McCabe, L.D., McCabe, G.P., Peacock, M., Pratt, J.H., Weaver, C.M., 2005. Racial differences in calcium retention in response to dietary salt in adolescent girls. Am. J. Clin. Nutr. 81, 845−850.

Wikoff, D., Welsh, B.T., Henderson, R., et al., 2017. Systematic review of the potential adverse effects of caffeine consumption in healthy adults, pregnant women, adolescents and children. Food Chem. Toxicol. 109, 585−648.

Wu, L., Martin, B.R., Braun, M.M., et al., 2010. Calcium requirements and metabolism in Chinese American boys and girls. J. Bone Miner. Res. 25 (Suppl. 8), 1842−1849.

Xiao, Q., Murphy, R.A., Houston, D.K., et al., 2013. Dietary and supplemental calcium intake and cardiovascular disease mortality: the National Institutes of Health-AARP diet and health study. JAMA Int. Med. 173, 639−646.

Zhao, J.-G., Zeng, X.-T., Wang, J., Liu, L., 2017. Association between calcium and vitamin D supplementation and fracture incidence in community-dwelling older adults a systematic review and meta-analysis. J. Am. Med. Assoc. 318, 2466−2482.

Zhao, Y., Martin, B.R., Weaver, C.M., 2005. Calcium bioavailability of calcium carbonate fortified soymilk is equivalent to cow's milk in young women. J. Nutr. 135, 2379−2392.

Further Reading

Heaney, R.P., 1993a. Is there a role for bone quality in fragility fractures? Calcif. Tissue Int. 53, S3−S5.

Weaver, C.M., Proulx, W.R., Heaney, R.P., 1990. Choices for achieving dietary calcium within a vegetarian diet. Am. J. Clin. Nutr. 70, 543S−438S.

Weaver, C.M., Gordon, C.M., Janz, K.F., Kalkwarf, H.J., Lappe, J.M., Lewis, R., O'Karma, M., Wallace, T.C., Zemel, B.S., 2016. The National Osteoporosis Foundation's position statement on peak bone mass development and lifestyle factors: a systematic review and implementation recommendations. Osteoporos Int 27 (4), 1281−1386.

Chapter 71

Drugs acting on the calcium receptor: calcimimetics and calcilytics

Cristiana Cipriani[1], Edward F. Nemeth[2] and John P. Bilezikian[3]

[1]*Department of Internal Medicine and Medical Disciplines, Sapienza University of Rome, Italy;* [2]*MetisMedica, Toronto, ON, Canada;* [3]*Division of Endocrinology, Department of Medicine, College of Physicians and Surgeons, Columbia University, New York, NY, United States*

Chapter outline

Introduction

The extracellular calcium sensing receptor (CaSR) is a G-protein-coupled receptor that monitors and maintains the level of ionized calcium (Ca^{2+}) in the blood and extracellular fluids (Brown, 2013). It is expressed at its highest levels in the parathyroid glands and the kidney, where it regulates, respectively, the secretion of parathyroid hormone (PTH) and the tubular reabsorption of Ca^{2+}. The essential molecule regulating systemic Ca^{2+} homeostasis, it has been rightly called the body's "calciostat." Because of this pivotal role, it was suggested, in the first edition of *Principles of Bone Biology*, that the CaSR might be a viable drug target to treat a number of bone and mineral-related disorders such as hyperparathyroidism (HPT) and osteoporosis (EF et al., 1996). Some of those predictions have proven to be correct, others have not.

A number of significant advances have been made since the last edition of this chapter, including understanding the genetic basis of some disorders associated with hyper- or hypocalcemia, the development of two new calcimimetic drugs, and insights into the molecular mechanisms of action of calcimimetic and calcilytic compounds (Nemeth et al., 2018). In addition, it has become clear that calcilytics are not suitable treatments for osteoporosis, as they fail to stimulate new bone formation (Nemeth and Goodman, 2016). There are, however, other indications that calcilytics might be therapeutically useful, but more work will be needed if this potential is to be realized.

Primary hyperparathyroidism

Primary HPT (PHPT) is a common endocrine disorder characterized by hyperfunction of one or more of the four parathyroid glands. The diagnosis is made readily by an elevated serum calcium in association with elevated or inappropriately normal PTH levels. Surgical removal of the hyperfunctioning gland(s) is the only definitive cure for this disease. It is indicated in symptomatic patients or in those who meet established guidelines (Bilezikian et al., 2014). In those who do not meet any of the surgical guidelines, parathyroidectomy is also an option if there are no medical contraindications. Those

Principles of Bone Biology. https://doi.org/10.1016/B978-0-12-814841-9.00071-3

who do not have parathyroid surgery typically do not meet any surgical criteria, have had previous unsuccessful surgery, or refuse surgery. If the patient's serum calcium is in the range where one would ordinarily recommend surgery but surgery is not going to occur, then pharmacological approaches to reducing the serum calcium may be indicated (Bilezikian et al., 2014). Cinacalcet is approved to reduce the serum calcium in these patients.

The indications in the United States are to control hypercalcemia in patients with either PHPT or parathyroid carcinoma for whom parathyroidectomy is not an option. In Europe, cinacalcet is registered for the reduction of hypercalcemia in patients with PHPT for whom parathyroidectomy is contraindicated.

In a randomized, double-blind, placebo-controlled, short-term, multicenter study Shoback et al. assessed the efficacy and safety of cinacalcet in PHPT. The drug was administered twice daily orally at different dosages, and the authors demonstrated that cinacalcet significantly reduced serum calcium, with maintenance of reduced levels during the 12-h interval between doses (Shoback et al., 2003). Decreased serum calcium levels were observed during the entire 15-day study period, with return of calcium levels to baseline values a week after discontinuation (Shoback et al., 2003). Cinacalcet also reduced PTH levels by 47%−51% 4 h after administration (Shoback et al., 2003). Although PTH levels increased after reaching their nadir, they remained below baseline levels in the 12-h interval between the two daily doses (Shoback et al., 2003). No safety signals emerged from this study, but paresthesias were noted commonly (Shoback et al., 2003).

A longer, randomized, double-blind, placebo-controlled study followed that clarified the long-term efficacy and safety of cinacalcet in PHPT (Peacock et al., 2005). Women and men (mean age, 62 years) with mild to moderate PHPT were randomized to receive cinacalcet (30 mg twice daily) or placebo and followed for up to 52 weeks (Peacock et al., 2005). Seventy-three percent of patients receiving cinacalcet experienced a $\geq$0.5 mg/dL decrease in serum calcium levels from baseline, reaching levels $\leq$10.3 mg/dL, a figure that was significantly lower than the placebo group. At week 52, mean serum calcium levels were normal in the cinacalcet group. A more modest 7.6% decrease in PTH remained significantly below the baseline up to week 12, with a return to baseline values thereafter (Peacock et al., 2005). Serum phosphorus, bone-specific alkaline phosphatase (BSAP), and N-telopeptide levels, although within the normal range, were significantly higher in the cinacalcet group at week 52 compared with placebo (Peacock et al., 2005). No significant differences between groups were observed in bone mineral density (BMD) or in safety parameters. Nausea and headache were reported as the most common adverse events.

Data from this clinical trial confirming the effectiveness and tolerability of cinacalcet as a nonsurgical approach to PHPT were further supported by results from an even longer 5-year study (Peacock et al., 2009). This experience was an open-label extension of the 52-week study of Peacock et al. The placebo group was crossed over to receive cinacalcet. The mean follow-up time was 4.5 years. Throughout the study period, those who received cinacalcet from the outset maintained reduced, normal serum calcium levels. The crossover group, receiving cinacalcet after 1 year of placebo, demonstrated a rapid reduction in serum calcium, similar to the observations in the 1-year study among those who originally received cinacalcet. Again, serum PTH levels fell by up to 21% but did not normalize during the extension period. Serum phosphorus and alkaline phosphatase rose in the first 12 weeks but remained within normal limits during the entire study with no further increases. No changes in BMD were observed. The only noteworthy adverse event was nausea, occurring more commonly compared with the placebo group in year 1 of the parent study.

The initial studies demonstrating the safety and efficacy of cinacalcet in PHPT were followed by several further clinical trials in which cinacalcet was tested in the context of patients with more severe PHPT and with parathyroid cancer. For example, Marcocci et al. reported the results from an open-label, single-arm, dose-titration study assessing the efficacy of cinacalcet in reducing serum calcium in patients with PHPT whose serum calcium was much higher (>12.5 mg/dL) (Marcocci et al., 2009). These individuals either had had unsuccessful parathyroid surgery or had contraindications to surgery. Notwithstanding the small number of patients, the study provided interesting data on the biochemical efficacy of cinacalcet in this setting. Eighty-eight percent of patients experienced a reduction in serum calcium concentration of at least 1 mg/dL; a majority showed normal serum calcium levels at the end of the titration phase. Quality of life measures were improved.

A pooled analysis of data from this study and those of Peacock et al. (2005, 2009) assessed the comparative efficacy of cinacalcet among patients with varying severity of PHPT (Peacock et al., 2011). Eighty-one patients were categorized into three groups: failed parathyroidectomy, indication for parathyroidectomy but not performed, and mild asymptomatic disease. More than 70% of patients from the entire cohort demonstrated normal serum calcium levels by 6 months with maintenance of control for up to 4 years. The serum PTH decreased within the first year of treatment. The serum phosphorus increased. There were no relevant changes in BMD, bone-turnover markers, or calcium excretion in any group. All groups responded similarly. This composite analysis demonstrated that cinacalcet effectively reduces the serum calcium

and maintains normal levels across a wide range of disease severity, with good tolerability. No group showed changes in BMD at any sites.

The further development of cinacalcet addressed patients with "nonoperable" PHPT (Khan et al., 2015). This phase III double-blind, placebo-controlled trial enrolled 67 patients who were randomized to cinacalcet at the initial dose of 30 mg twice daily that was titrated in the 12-week titration phase or to placebo. Serum calcium fell by at least 1 mg/dL in 84.8% and became normal (≤10.3 mg/dL) in 75.8% of study subjects, results that were significantly different from those of the placebo group. PTH levels fell, on average, by 23.8%. Although serum phosphorus rose, it remained within the normal range. No significant changes in the health-related quality of life as assessed by the parathyroid assessment of symptoms, medical outcomes scores - cognitive functioning scale, and short form-36 questionnaire were noted. Nausea and muscle spasm were the most common adverse events, but were not significantly different from the placebo group.

The benign, solitary parathyroid adenoma is the most common cause of PHPT (85%–90% of cases), while the involvement of more than 1 or all four glands as adenomatous or hyperplastic glands is observed in 10%–15% of cases (Silverberg et al., 2019). Most cases of parathyroid hyperplasia are in the setting of familial disease, whereby PHPT may occur as the only disorder or in association with other endocrinopathies (multiple endocrine neoplasia, MEN). In these cases, the surgical approach is the removal of all but one-half of a gland or total parathyroidectomy and autotransplantation. These procedures are associated with complications such as hypoparathyroidism and recurrence or persistence of disease. In these situations, nonsurgical approaches are worthy of consideration. A 2016 multicenter, phase IV, prospective, open-label, noncomparative trial evaluated the efficacy of cinacalcet in 33 patients with PHPT associated with MEN1 (Giusti et al., 2016). These patients either refused surgery or had contraindications that precluded further surgery. The initial dose of 30 mg once daily was maintained in 55% but was increased to 60 mg twice daily in the others during the 12-month follow-up period. The vast majority of patients showed normal serum calcium values by 6 (78.5%) or 12 (89.3%) months. No significant changes in serum PTH, bone-turnover markers, or BMD were observed (Giusti et al., 2016).

Parathyroid carcinoma is a rare form of PHPT occurring in less than 1% of hyperparathyroid patients. It is associated with a poor ultimate prognosis and high rate of local recurrence and metastatic disease (Silverberg et al., 2007, 2019). Typically, the serum calcium concentration is much higher than the degree of hypercalcemia in the benign form of the disease. In patients with recurrent and inoperable disease, therefore, management of hypercalcemia is a major challenge. Several clinical studies have clearly demonstrated that cinacalcet is an effective and safe treatment option in these patients. Silverberg et al. (2007) reported results from a multicenter, open-label, single-arm, dose-titration study of 29 patients with recurrent parathyroid carcinoma. The design of the trial permitted dose escalation from 30 mg twice daily during the 2–16 week "run-in" phase. The mean treatment duration was about 300 days. Under these circumstances, cinacalcet reduced and maintained serum calcium levels (Silverberg et al., 2007). In 62% of study subjects, the serum calcium fell by at least 1 mg/dL after the initial dosing and in 94% of them by the end of the titration period. The average reduction was 3.8 mg/dL. Given the wide range of initial serum calcium concentrations in these subjects, it was possible to relate the effect of the drug to starting calcium values. The strongest effect was observed in patients with the highest baseline serum calcium concentration. Serum PTH levels slightly declined in the first 4 h after dosing, with no significant changes during the entire observation period. The increase in serum phosphorus was significant but it remained within normal limits. No changes in the health-related quality of life scores were observed. The most common adverse events were nausea, vomiting, dehydration, and headache. It is interesting to note that these adverse events are also classic features of symptomatic hypercalcemia. It is possible that this calcimimetic is mimicking this calcemic symptomatology even though the serum calcium is actually lowered by the drug.

Since approval and registration of cinacalcet for management of the hypercalcemia of PHPT, additional studies have become available. The PRIMARA study in Europe described the clinical profile and main outcomes of patients with PHPT treated with cinacalcet (Schwarz et al., 2014). This prospective multicenter observational study was conducted in 303 patients with PHPT of various etiologies (adenoma, hyperplasia, carcinoma) and varying disease severity. The mean daily dose during the 1-year study period was 49.6 mg. At the end of the observation period, more than 70% of patients achieved the study target levels of serum calcium (≤10.3 mg/dL), with approximately 60% demonstrating a reduction of at least 1 mg/dL. An 8%–13% decrease in serum PTH and a 20% increase in serum phosphorus were observed. As was seen in most of the clinical trials, nausea and vomiting were the most common adverse events, in 13.5% and 3.7% of patients, respectively.

Other hypercalcemic disorders

The use of cinacalcet has been proposed in familial forms of PHPT associated with specific gene mutations (Arnold and Thakker, 2019). Among them, familial hypocalciuric hypercalcemia (FHH) has been an attractive model because the

disease is characterized by abnormalities in the calcium-sensing receptor (CaSR) gene. This autosomal dominant syndrome can be subtyped by three different mutations (Lee and Shoback, 2018). The most prevalent (about 65% of FHH cases) is FHH1, caused by a loss-of-function mutation of CaSR. The FHH2 and FHH3 subtypes are associated with inactivating mutations of the GNA11 gene encoding the G-protein subunit α11 and of the AP2S1 gene encoding the adaptor protein-2 σ subunit. These genes are intimately involved in the CaR signal and transduction systems, respectively (Lee and Shoback, 2018; Nesbit et al., 2013).

Based upon the pathogenesis of FHH, the rationale for expecting cinacalcet to be effective is clear. The calcimimetic could enhance the Ca−CaSR interaction and thus could amplify the weakened or dysfunctional signals arising from the mutations described in FHH. Further, the calcimimetic could amplify normal CaSR encoded by the normal gene (Brown, 2010). The case reports on the use of cinacalcet in all three subtypes of FHH describe high rates of success in terms of reducing serum calcium and improving hypercalcemia-related symptoms (Mayr et al., 2016; Gorvin et al., 2018). In 2016, Mayr et al. reviewed 16 cases of FHH1 and FHH3 treated with cinacalcet and reported a reduction in serum calcium and improvement of symptoms in 14 (Mayr et al., 2016). Adverse effects, reported in only three subjects, consisted of eye palpitations, hypotension, nausea, and paresthesia (Mayr et al., 2016). Notwithstanding substantial variability in the individual case reports, such as age, reason for starting cinacalcet treatment, and duration of therapy (from 8 days to 3 years) among these cases, the authors concluded that calcimimetics should be considered as a first-line option in patients with FHH who are symptomatic of hypercalcemia. Starting with a low dose of cinacalcet and titrating upward according to serum calcium levels was recommended. In 2018, a case report of FHH2 treated with cinacalcet was published (Gorvin et al., 2018). In this 33-year-old man who was symptomatic of hypercalcemia, cinacalcet at a daily dose of 60 mg was successful in reducing ionized calcium and PTH to normal levels (Gorvin et al., 2018). In vitro studies demonstrated that cinacalcet modulates and rectifies the loss-of-function mutation of the Gα11 (Gorvin et al., 2018).

The overall data need confirmation by randomized controlled trials, but an interesting perspective on the use of cinacalcet in these familial forms, particularly on the long-term effects of the drug, has become a topic of discussion. In this context, a prolonged cumulative effect on serum calcium in FHH has led to the suggestion of a drug holiday as an option (Mayr et al., 2016; Marx, 2017).

Neonatal severe PHPT (NSHPT) is a very rare disorder caused by inactivating homozygous or double heterozygous mutations of CaSR. It is characterized by severe, life-threatening hypercalcemia and very high PTH levels with consequent severe skeletal disease (Brown, 2010). A traditional primary therapeutic approach is urgent and life-saving parathyroidectomy and medical therapy with fluids and bisphosphonates. These approaches, however, have noteworthy drawbacks with only short-term or little beneficial outcomes (Brown, 2010). Cinacalcet has been proposed in children with NSHPT, with the idea that it would "rescue" CaSR function and stabilize calcium levels, with surgery an option thereafter (Arnold and Thakker, 2019; Brown, 2010). Cinacalcet use has been reported in nine infants with NSHPT, with successful results in five cases (Sun et al., 2018). Sun et al. hypothesized that different outcomes could be a function of mutation type (homozygous vs. double heterozygous), location of the mutation in the Ca^{2+}-binding domain, or residual function of CaSR (Sun et al., 2018).

Secondary hyperparathyroidism

Cinacalcet

The several disorders of mineral metabolism associated with chronic kidney disease (CKD) are included under the term "chronic kidney disease−mineral and bone disorder" (CKD−MB) (KDIGO, 2017). Among them is secondary HPT (SHPT), in which the multifactorial pathogenesis includes reduced $1,25(OH)_2D$ levels, hypocalcemia, hyperphosphatemia, and high fibroblast growth factor 23 (FGF23) levels (KDIGO, 2017). This is the only manifestation of CKD−MB that will be covered in this chapter. The severity of the SHPT is directly related to the level of renal dysfunction and is associated with negative cardiovascular and skeletal outcomes (Ganesh et al., 2001; Investigators et al., 2012). In addition, such patients, particularly those on hemodialysis, have increased morbidity and mortality (KDIGO, 2017). The therapeutic goal for this form of CKD−MB is to control PTH levels by several therapeutic modalities. In this regard, active vitamin D and related analogs are widely used. According to Kidney Disease Improving Global Outcomes guidelines, formulations of active vitamin D as well as precursor moieties such as parent vitamin D and calcifediol are recommended in patients with stage G3a−G5 and not on dialysis. In patients with stage G5 on dialysis (G5D), calcimimetic therapy is recommended (KDIGO, 2017). Calcimimetics may be used alone or in combination with calcitriol or vitamin D analogs in these patients (KDIGO, 2017). At this writing, cinacalcet is recommended as first-line therapy in stage G5D to lower PTH levels

(KDIGO, 2017). In the aggregate, these clinical trials, which have involved, in some cases, more than 1000 patients, have had as their end point reductions <250 pg/mL or 30% of baseline levels (Eidman and Wetmore, 2018).

Calciotropic end points

The clinical trials of cinacalcet in hemodialysis patients were first published in the early 2000s, showing collectively that cinacalcet had the potential to lower PTH with a good safety profile (Goodman et al., 2002; Quarles et al., 2003; Lindberg et al., 2003). Goodman et al. reported results from a single-dose and a multiple-dose randomized clinical trial (RCT) in which PTH levels declined by 40%−60% after 2 h of administration of cinacalcet at doses of 25−100 mg and by 30%−40% within a few days when administered for 8 days at doses of 25−50 mg (Goodman et al., 2002). Data from a subsequent double-blind, placebo-controlled, multicenter RCT showed, with doses up to 50 mg/day, a significant 26% decrease in mean PTH levels after a 12-week titration phase and a 6-week maintenance phase, compared with placebo (Lindberg et al., 2003). In addition, the calcium × phosphorus product fell by 11.9%, significantly different from placebo. Adverse events consisted mostly of nausea, dyspnea, and transient hypocalcemia (Lindberg et al., 2003). Similar results were reported by Quarles et al. in a placebo-controlled, double-blind RCT (Quarles et al., 2003). These investigators observed a progressive decline in PTH during the initial 12-week dose-titration phase (during which the 25-, 50-, 75-, and 100-mg doses were sequentially administered, as needed) and a 33% reduction in the 6-week maintenance phase (Quarles et al., 2003). The calcium × phosphorus product fell by 7.9% in the cinacalcet group.

Block et al. published, in 2004, results from two randomized, double-blind, placebo-controlled clinical trials conducted in North America, Europe, and Australia (Block et al., 2004).The two studies involving 741 study subjects were identical in design, consisting of a 12-week dose-titration phase and a 14-week efficacy-assessment phase (Block et al., 2004). The titration protocol started at 30 mg/day and could be increased sequentially every 3 weeks up to 180 mg/day if PTH levels remained >200 pg/mL (Block et al., 2004). Vitamin D and/or phosphate binders could be used as needed (Block et al., 2004). The primary end point, a mean reduction of PTH levels to ≤250 pg/mL, was met by 43% of patients in the cinacalcet group versus only 5% in the placebo group (Block et al., 2004).The magnitude of the reduction was independent of the vitamin D dose. The secondary end point, ≥30% decline in serum PTH, was met by 64% of the cinacalcet group versus 11% of the placebo group (Block et al., 2004). Other noteworthy findings were a 35% decrease (significantly lower than the placebo group) in bone alkaline phosphatase activity and reduction in serum calcium and phosphorus by 6.8% and 8.4%, respectively (Block et al., 2004). Mild to moderate upper gastrointestinal (GI) adverse events, mainly nausea and vomiting, along with hypocalcemia, were noted in the cinacalcet arm of the study (Block et al., 2004). The hypocalcemia was seen in 5% of patients on cinacalcet but was asymptomatic and not influenced by vitamin D (Block et al., 2004). Similar results have been observed in patients on peritoneal dialysis (Lindberg et al., 2005). Three multicenter trials involving over 1136 patients from 182 centers in North America, Europe, and Australia have confirmed these impressive results (Moe et al., 2005a).

Pharmacokinetics studies demonstrate a linear increase in plasma concentration of the drug for doses ranging from 25 to 200 mg, while no further increases in exposure are seen for doses >200 mg (Harris et al., 2004). The increase in plasma concentration of cinacalcet is inversely associated with changes in PTH levels (Harris et al., 2004). The greatest decline in PTH levels occurs 1 and 6 h after administration of drug, with return to baseline levels at 24 h and an increase at 48 h (Arenas et al., 2013). Long-term data from an open-label extension study in hemodialysis patients showed that the chronic administration of cinacalcet, up to 180 mg/day, is associated with reduced PTH levels for up to 3 years (Moe et al., 2005b).

Other clinical settings in which cinacalcet has been studied include tertiary HPT in patients after renal transplantation and SHPT in patients who are not dialysis dependent (Serra et al., 2005, 2007; Charytan et al., 2005). Small open-label studies in patients following renal transplantation collectively have shown good efficacy, tolerability, and safety when cinacalcet is administered for up to 6 months (Serra et al., 2005, 2007; Kruse et al., 2005). In patients who are not dialysis dependent, a multicenter, randomized, double-blind, placebo-controlled study conducted in 404 patients with CKD stage 3 or 4 reported a 43% decrease in PTH levels (Chonchol et al., 2009). Hypocalcemia, <8.4 mg/dL, was observed at least twice in 62% of patients along with a 21% increase in serum phosphorus levels (Chonchol et al., 2009).

Different combined regimens of cinacalcet and vitamin D in hemodialysis patients have been investigated (Block et al., 2008; Fishbane et al., 2008; Zawierucha et al., 2019; Chertow et al., 2006). In particular, combination therapy with cinacalcet and low-dose paricalcitol or doxercalciferol was compared with therapy with vitamin D sterols and cinacalcet alone in two multicenter, open-label studies (Block et al., 2008; Fishbane et al., 2008). Target levels of PTH, calcium × phosphorus product, or both were reached with the combination of cinacalcet + paricalcitol, but the cinacalcet arm performed as well (Block et al., 2008). In contrast, Fishbane et al. reported a greater reduction of PTH levels when combined therapy with cinacalcet + paricalcitol or doxercalciferol was compared with vitamin D alone (paricalcitol or

doxercalciferol), but there was no difference in the proportion of patients reaching target PTH and calcium × phosphorus product end points (Fishbane et al., 2008). In 2018, the combination of cinacalcet, calcitriol, and cholecalciferol was shown to reduce PTH levels even further (Zheng et al., 2018).

Some studies have tracked changes in FGF23 levels in the context of combination therapy with cinacalcet and vitamin D analogs. To this end, Wetmore et al. conducted a phase IV, open-label, placebo-controlled, multicenter RCT. FGF23 levels significantly declined with combination therapy of cinacalcet + paricalcitol or doxercalciferol compared with vitamin D (paricalcitol or doxercalciferol) (Wetmore et al., 2010).

Skeletal end points

Skeletal effects related to cinacalcet therapy in SHPT have been inconsistent when BMD has been measured. Tsuruta et al. observed a 7.3% increase in femoral BMD in a small group of hemodialysis patients treated with cinacalcet for 1 year. The increase in BMD was associated with a reduction in bone-turnover markers (Tsuruta et al., 2013). Changes in femur BMD were also evaluated as a secondary end point in an RCT. No differences between the cinacalcet and the placebo groups of renal transplantation recipients were noted (Evenepoel et al., 2014).

Histomorphometry data in hemodialysis patients showed that treatment with cinacalcet for 6−12 months is associated with a decline in measures of bone formation and resorption concomitant with the reduction in PTH levels (Behets et al., 2015).

The EVOLVE trial found no effect of cinacalcet on rate of fractures (Moe et al., 2015a). However, only clinical fractures were evaluated as a secondary end point of the study and no radiological assessment was routinely performed (Moe et al., 2015a).

Cardiovascular end points

Several studies have not been able to demonstrate beneficial effects of cinacalcet on cardiovascular outcomes such as cardiovascular disease, all-cause mortality, and vascular calcification (Investigators et al., 2012; Raggi et al., 2011; Floege et al., 2015; Moe et al., 2015b). EVOLVE, a multicenter, prospective, randomized, placebo-controlled trial (Investigators et al., 2012), enrolled 3883 dialysis patients with moderate-to-severe SHPT. Cinacalcet was used initially at 30 mg/day followed by a monthly dose titration protocol for 20 weeks and then an every-8-weeks follow-up period (Investigators et al., 2012). The primary end point, namely time to death or the first cardiovascular event, was not different between the cinacalcet and the placebo groups (Investigators et al., 2012). The incidence of parathyroidectomy was lower in the cinacalcet group (Investigators et al., 2012). Subsequent analyses showed that arterial calcifications were reduced by 69% −75% with cinacalcet treatment (Floege et al., 2015). Hypocalcemia was seen in as many as 58% of patients who received cinacalcet (Floege et al., 2018). Severe hypocalcemia was observed in 18% of patients, particularly in younger patients, those with prior parathyroidectomy and kidney transplantation, and those on phosphate binders (Floege et al., 2018). Finally, Moe et al. described the results of a secondary analysis of the EVOLVE trial showing that the reductions in FGF23 levels with cinacalcet were associated with declines in cardiovascular mortality and major cardiovascular events (Moe et al., 2015b).

The information we have at this writing argues for a key role of cinacalcet in the management of the SHPT associated with renal failure, particularly in those who are undergoing hemodialysis. The use of cinacalcet appears to ameliorate the secondary hyperparathyroid state, which in and of itself is a desirable goal. More work is needed to understand more completely the extent to which this calcimimetic might have beneficial effects on target organs such as the skeleton and the cardiovascular system.

Evocalcet

Evocalcet (Fig. 71.1) is a structural analog of cinacalcet that acts as a positive allosteric modulator of the CaSR. It increases $[Ca^{2+}]_i$ in HEK-293 cells expressing the human CaSR and shifts the concentration-response curve for extracellular Ca^{2+} to the left; it is without effect in the absence of extracellular Ca^{2+} (Kawata et al., 2018). The in vitro potencies of evocalcet and cinacalcet for increasing intracellular Ca^{2+} $[Ca^{2+}]_i$ in CaSR-expressing HEK-293 cells are similar (93 and 51 nM, respectively). The oral administration of evocalcet rapidly lowers circulating levels of PTH and Ca^{2+} in normal rats and in those with SHPT induced by a 5/6 nephrectomy. Again, these effects are very similar to those of cinacalcet but the oral bioavailability of evocalcet in the rat is much greater than that of cinacalcet (80% vs. 2%), so comparable efficacy in vivo occurs at much lower doses of evocalcet. Unlike cinacalcet, evocalcet does not affect the activity of a number of

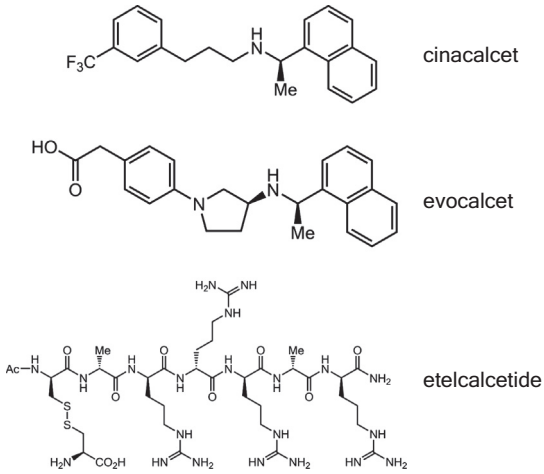

FIGURE 71.1 The structure of calcimimetics.

cytochrome P450 enzymes in vitro, including CYP2D6 (Miyazaki et al., 2018), nor does it affect the pharmacokinetic profiles of various drugs that are metabolized through P450 enzymes (Narushima et al., 2019). These findings indicate that evocalcet could be expected to be associated with fewer drug−drug interactions than cinacalcet.

The major adverse effects of cinacalcet are GI symptoms such as nausea and vomiting, which seriously limit compliance. A head-to-head comparator study of evocalcet and cinacalcet was performed to assess emetic responses in normal marmosets and gastric emptying time in the rat 5/6 nephrectomy model of SHPT. In marmosets, the incidence of emesis was lower for evocalcet compared with cinacalcet. In the rat, evocalcet did not affect gastric emptying time (compared with vehicle) at doses that maximally lowered plasma levels of PTH, whereas cinacalcet inhibited gastric emptying time by 46%. Evocalcet also had lower binding affinity to receptors associated with emesis (dopamine, cannabinoid, opioid, and serotonin) than did cinacalcet (Kawata et al., 2018).

A phase III head-to-head comparator trial of evocalcet and cinacalcet in Japanese patients with SHPT has been reported (Fukagawa et al., 2018). Both compounds were orally administered once a day for 30 weeks to patients on hemodialysis, and the primary end point was a plasma PTH level between 60 and 240 pg/mL. The proportions of patients achieving the primary end point were 72.7% in the evocalcet group and 76.7% in the cinacalcet group, a nonsignificant difference showing that evocalcet was noninferior to cinacalcet as regards efficacy. Secondary end points of efficacy (percentage of patients achieving $\geq$30% decrease in PTH from baseline and mean percentage change in PTH levels) were also similar for evocalcet- and cinacalcet-treated patients. Serum levels of calcium, phosphorus, and FGF23 were decreased by evocalcet and cinacalcet to similar extents. Evocalcet was superior to cinacalcet as regards safety. Specifically, the incidence of upper GI symptoms (nausea, vomiting, abdominal discomfort, abdominal distension, or decreased appetite) were significantly less in subjects treated with evocalcet (18.6% of patients) compared with those receiving cinacalcet (32.8%). Evocalcet was approved for the treatment of SHPT in patients on dialysis by the Ministry of Health, Labor, and Welfare in Japan in 2018.

The initial preclinical and clinical results obtained in comparator studies suggest that evocalcet might produce a lower incidence of upper GI symptoms than cinacalcet. However, the doses of cinacalcet used in preclinical gastric emptying time studies were 60- to 200-fold higher than the effective dose 50 for lowering plasma levels of PTH in the rat. Moreover, the incidence of upper GI symptoms in the clinical comparator trial was unusually high in patients treated with cinacalcet (it is typically 20%−25%). More real-world clinical experience with evocalcet will be required to determine if it has an improved GI side effect profile compared with cinacalcet.

Etelcalcetide

Etelcalcetide (Fig. 71.1) is a structurally novel calcimimetic for the treatment of SHPT in adult patients on dialysis (Hamano et al., 2017). Etelcalcetide is an octapeptide consisting of a linear chain of seven D-amino acids. Surprisingly, given the finding that polybasic peptides like protamine and poly-L-arginine are agonists at the CaSR (Nemeth et al., 2018), etelcalcetide behaves as an allosteric modulator with a unique mechanism of action. Etelcalcetide forms a covalent disulfide bond with Cys482 in the extracellular domain of the CaSR (Alexander et al., 2015). This binding to the extracellular domain of the CaSR is a reversible covalent linkage that undergoes thiol substitution with other sulfhydryl-donating

proteins and small endogenous molecules. The CaSR also undergoes continual recycling, and new receptors are constantly being added to the cell surface, so this covalent modification temporarily, but not permanently, activates the CaSR.

The D-amino acid backbone of etelcalcetide creates a molecule that is essentially metabolically inert and does not undergo proteolytic cleavage. Unlike cinacalcet, etelcalcetide does not affect the activity of cytochrome P450 enzymes (Subramanian et al., 2016, 2017). Nonclinical toxicology studies revealed no adverse effects other than those expected by the pharmacodynamic response of hypocalcemia (tremors, convulsions, and a prolongation of the QT interval; Fielden et al., 2016).

Etelcalcetide is not orally bioavailable and is administered by intravenous (iv) injection. Once injected, it is rapidly cleared from the circulation primarily by glomerular filtration; its pharmacokinetic profile is thus largely dependent on renal function. In healthy volunteers with normal kidney function, the terminal half-life for etelcalcetide is around 18 h, whereas in patients with CKD and on dialysis, the half-life can exceed 7 days (Shen et al., 2014). Etelcalcetide is mostly removed during a dialysis session and is therefore administered through the iv line at the end of a dialysis session.

In rat models of SHPT, the subcutaneous administration of etelcalcetide thrice weekly for 6 weeks lowered plasma levels of PTH and decreased vascular calcification. It also diminished parathyroid gland hyperplasia and increased expression of the CaSR, the vitamin D receptor, and the receptor for FGF23 (FGFR1) in parathyroid glands (Walter et al., 2013). Nephrocalcinosis and increased aortic calcium content in another rat model of SHPT were also reduced by etelcalcetide (Yu et al., 2017). These studies demonstrate the effectiveness of etelcalcetide in slowing the progression of SHPT. Etelcalcetide is also effective in a rodent model of established SHPT, in which it reduces plasma levels of PTH and FGF23 and halts parathyroid gland hyperplasia (Walter et al., 2014). The results obtained with etelcalcetide in rodent models of SHPT are similar to those obtained with other calcimimetics.

All the phase III registration trials for etelcalcetide involved adult hemodialysis patients with moderate to severe SHPT. Etelcalcetide was administered iv thrice weekly at the end of each dialysis session, and blood samples for determining PTH and other blood analytes were drawn just prior to a dialysis session. All the trial designs used a dose-titration period and in each study, patients assigned to etelcalcetide or placebo groups continued to receive standard of care (vitamin D sterols and phosphate binders) but had to be free of cinacalcet use for at least 4 weeks prior to screening for eligibility.

The primary end point of the study in Japanese hemodialysis patients was the proportion of patients achieving a serum PTH level between 60 and 240 pg/mL (Fukagawa et al., 2017). At the end of 12 weeks, 59.0% of patients treated with etelcalcetide achieved this target end point compared with only 1.3% of patients receiving placebo. Significant reductions from baseline in serum Ca and phosphorus persisted throughout the study, whereas there was no reduction in serum levels of either mineral in placebo-treated patients. There were no remarkable differences in serum levels of BSAP and tartrate-resistant acid phosphatase 5b (TRACP-5b) in patients treated with etelcalcetide compared with those treated with placebo. Serum FGF23 levels trended downward throughout the study in etelcalcetide-treated patients and by 12 weeks were 72.0% lower than baseline values, whereas FGF23 levels did not change in patients treated with placebo. The administration of etelcalcetide was generally safe and well tolerated. Adverse effects occurring in the etelcalcetide group but not in the placebo group were blood calcium decrease (6.4%), vomiting (3.8%), nausea (1.3%), and symptomatic hypocalcemia (1.3%). There were no clinically relevant cardiovascular complications in either treatment group (Fukagawa et al., 2017).

This phase III trial in Japan was followed by an open-label study with the ability to adjust the dose of etelcalcetide and concomitant medications to optimize serum levels of PTH and Ca (Shigematsu et al., 2018). Etelcalcetide was administered iv thrice weekly at the end of a dialysis session for 52 weeks. The percentage of patients achieving the primary end point (serum PTH levels between 60 and 240 pg/mL) increased from 6.3% on day 1 to 87.5% after 52 weeks of treatment with etelcalcetide. Although serum calcium levels were lower than baseline during the first 2 months of the study, they recovered toward baseline after adjustments to concomitant medications. The types and prevalence of adverse effects in the etelcalcetide-treated patients were similar to those in the earlier study.

The primary end point in two other phase III trials run in parallel was the percentage of patients achieving a $>30\%$ reduction in serum levels of PTH (Block et al., 2017a). The results for the two trials were similar and the averages of both are presented here. The primary end point was met in 74.6% of patients treated with etelcalcetide, but in only 8.9% of those treated with placebo. Decreases in serum PTH levels to ≤ 300 pg/mL (a secondary end point) were achieved by 51.4% of patients receiving etelcalcetide but by only 4.8% of patients in the placebo group. Treatment with etelcalcetide caused progressive decreases in serum calcium and phosphorus levels that reached a nadir between 10 and 12 weeks, whereas serum mineral levels in the placebo group remained at baseline values throughout the study. The percentage of patients taking calcium supplements, calcium-containing phosphate binders, and/or vitamin D sterols increased in the etelcalcetide group, as did the concentration of calcium in the dialysate compared with patients in the placebo group. Decreases in serum levels of FGF23, BSAP, and type I cross-linked C-telopeptide occurred in patients treated with etelcalcetide compared with those in patients receiving placebo.

Etelcalcetide was generally safe and well tolerated and the most frequent adverse event was blood calcium decrease (Ca <8.3 mg/dL), which occurred in 63.8% and 10.1% of patients treated with etelcalcetide and placebo, respectively. Overt symptomatic hypocalcemia occurred in 7% of patients in the etelcalcetide group and in 0.2% of patients in the placebo group. Hypocalcemic symptoms included muscle spasms (11.5% in the etelcalcetide group vs. 6.6% in the placebo group) and paresthesia (4.6% vs. 0.6%). Symptomatic hypocalcemia could also explain QT prolongation, which was 2.5-fold higher in etelcalcetide-treated patients compared with those receiving placebo. The incidences of nausea, vomiting, and diarrhea were also greater in the etelcalcetide group compared with the placebo group (see later). There were no major cardiovascular complications in either treatment group (Block et al., 2017a).

The fourth phase III trial was a head-to-head comparison of etelcalcetide and cinacalcet in patients randomized to receive iv etelcalcetide and oral placebo or oral cinacalcet and iv placebo (Block et al., 2017b). Etelcalcetide was administered three times a week and cinacalcet daily for 26 weeks. The primary end point was noninferiority of etelcalcetide to cinacalcet, specifically a >30% reduction from baseline in serum levels of PTH as measured during weeks 20−27. At the end of the study, 57.7% of patients treated with cinacalcet met the primary end point compared with 68.2% of patients treated with etelcalcetide ($P < 0.001$ for noninferiority; $P < 0.004$ for superiority). Significantly more patients treated with etelcalcetide achieved a >50% reduction from baseline in serum levels of PTH (52.4%) compared with those treated with cinacalcet (40.2%). Both calcimimetics decreased serum levels of calcium and phosphorus but the levels caused by etelcalcetide were greater in magnitude. Similarly, both calcimimetics decreased serum levels of FGF23, BSAP, and collagen type I cross-linked C but the magnitude was greater with etelcalcetide compared with cinacalcet. Taken together, the results of this study suggest that etelcalcetide is superior to cinacalcet as regards efficacy.

However, it is problematic to claim superiority or inferiority based on this trial because different routes of administration and different dosing regimens were used (Hai et al., 2017). And any superior efficacy came at the cost of safety. The most common adverse event in the head-to-head comparator trial was (as anticipated) decreased blood calcium, which occurred in 68.9% and 59.8% of patients treated with etelcalcetide and cinacalcet, respectively. Symptomatic hypocalcemia occurred twice as often in etelcalcetide-treated patients compared with those treated with cinacalcet, and heart failure events were fivefold higher in etelcalcetide-treated patients. High doses of cinacalcet would have efficacy comparable to that of etelcalcetide, but this would have caused greater decreases in serum calcium levels and compromised safety. Based on their mechanisms of action and the clinical results, there is no reason to suppose that the efficacy of these two calcimimetics differs.

What is perhaps most significant is the *similarity* of these two calcimimetics, especially in the incidence of upper GI symptoms like nausea and vomiting. Upper GI symptoms are the leading cause of stopping cinacalcet treatment in patients (note the EVOLVE study). It was anticipated that the iv route of administration, because it would eliminate exposure to a calcimimetic in the gut lumen, would diminish the incidence of GI symptoms. Because they were similar, GI symptoms might be an inherent pharmacodynamic property of calcimimetics resulting from actions on CaRs expressed throughout the GI tract.

Some features of etelcalcetide might prove superior to those of cinacalcet but at this writing it does not appear to be either efficacy or safety. One is the iv route of administration, which should improve adherence and will certainly reduce the pill burden in this patient population. Because etelcalcetide causes a sustained decrease in serum PTH levels, rather than the fluctuating one characteristic of cinacalcet, it will be easier to monitor these levels. Whether sustained decreases in serum PTH levels will translate into improved clinical outcomes is uncertain but this will obviously be the end point of future trials with etelcalcetide. Another is fewer concerns about drug−drug interactions because etelcalcetide does not affect the activity of P450 enzymes.

Calcilytics

Osteoporosis

The development of calcilytics as potential treatments for osteoporosis is based on their ability to stimulate secretion of PTH. Exogenously administered PTH or teriparatide stimulates new bone formation and the former peptide is an approved anabolic therapy for osteoporosis (Silva and Bilezikian, 2015). Despite encouraging preclinical results in rodent models of osteoporosis, three different calcilytic compounds lacked efficacy in clinical trials. It has been proposed that inhibitory effects of calcilytics on CaSR in bone block the stimulatory effects of PTH and explain, in whole or in part, the lack of efficacy (Nemeth et al., 2018; Nemeth and Goodman, 2016). Calcilytic compounds were, however, generally safe and well tolerated in clinical studies and because of this are being evaluated as therapies for alternative indications.

Repurposing calcilytics for new indications

Hypoparathyroidism

In all the clinical trials with calcilytics the magnitude and duration of increased circulating levels of PTH were sufficient to increase blood Ca^{2+} levels. Because of this, calcilytics are potentially useful for treating certain hypocalcemic disorders like hypoparathyroidism. While most cases of hypoparathyroidism arise from surgical removal of the thyroid gland, there are a number of rare genetic cases, of which the most prevalent is autosomal dominant hypoparathyroidism (ADH) (Abate and Clarke, 2016).

The conventional treatment for most hypoparathyroid disorders is supplementation with dietary calcium and active forms of vitamin D. Recombinant human PTH is also approved as an adjunct to calcium and vitamin D to control hypocalcemia in hypoparathyroidism. Calcilytics might be useful in postsurgical forms of hypoparathyroidism when there is some residual parathyroid tissue. They might also be useful even when no functional parathyroid tissue remains. Studies in rats show that the calcilytic NPS2143 (Fig. 71.2) can normalize serum Ca^{2+} levels in hypocalcemic rats whose parathyroid glands have been surgically removed (Loupy et al., 2012).

ADH is a rare genetic disorder resulting from germ-line activating mutations in either the CaSR gene (ADH type 1) or the gene encoding the G-protein subunit $G\alpha_{11}$ (ADH type 2; Hannan et al., 2016). These activating mutations increase the sensitivity of parathyroid cells to activation by extracellular Ca^{2+} and patients with ADH are therefore hypocalcemic with inappropriately low levels of PTH. Renal CaSRs are also affected and about a third of all patients are frankly hypercalciuric, while the remaining patients have unexpectedly normal urinary Ca^{2+} excretion given the prevailing hypocalcemia.

ADH is essentially a disorder of the set point of systemic Ca^{2+} homeostasis, and when the absolute level of blood Ca^{2+} is normalized (by calcium and vitamin D supplements), it will be sensed by the parathyroid glands and kidney as hypercalcemia, thereby further suppressing PTH secretion and increasing Ca^{2+} excretion. The resulting relative hypercalciuria often progresses to frank hypercalciuria leading to nephrocalcinosis, nephrolithiasis, and renal failure (Hannan et al., 2016; Hannan and Thakker, 2013). Therapy of ADH patients should strive to reset the set point by decreasing the sensitivity of parathyroid and renal CaSRs to extracellular Ca^{2+}. As negative allosteric modulators, this is precisely how calcilytics act, and they might provide an ideal therapy for ADH.

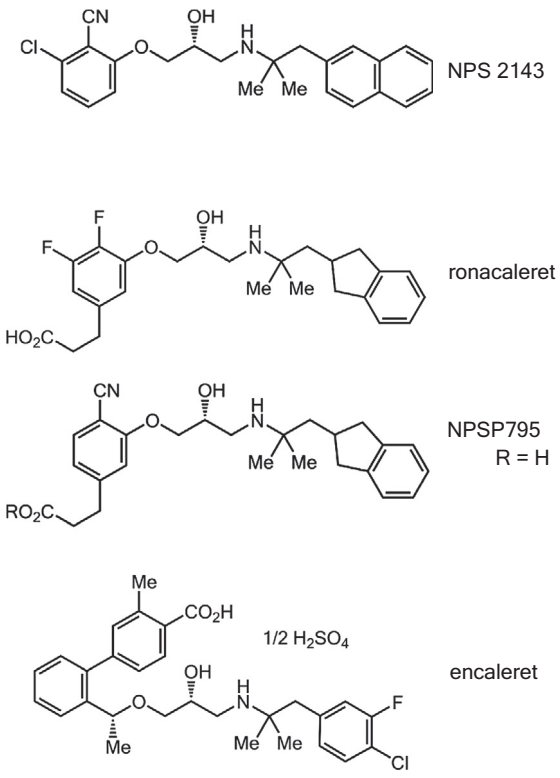

FIGURE 71.2 The structure of calcilytics.

In mouse models of ADH1, two different calcilytics (NPS2143 and JTT-305) have been shown to normalize serum Ca^{2+} (Dong et al., 2015; Hannan et al., 2015). Somewhat unexpectedly, NPS2143 also normalized serum Ca^{2+} levels in animal models of ADH2 (Gorvin et al., 2017). A small clinical trial in patients with ADH1 showed that NPSP795 caused small increases in plasma levels of PTH and tended to decrease renal Ca^{2+} excretion but, at the doses tested, did not increase blood Ca^{2+} levels (Ramnitz et al., 2015).

Pulmonary indications

There are other indications that are not associated with hypocalcemia and for which calcilytics might have some therapeutic benefit. The first is inflammatory lung disorders. In asthma, the expression of the CaSR is increased in airway smooth muscle cells. Airflow resistance in sensitized mice was depressed and airway hyperresponsiveness was reduced in a mouse model of allergic asthma (Yarova et al., 2015). In these in vivo studies, calcilytics were delivered directly into the lung and there were no changes in blood levels of Ca^{2+}.

Another indication is idiopathic pulmonary arterial hypertension (IPAH), a rare disease characterized by sustained pulmonary vasoconstriction that results in elevated vascular resistance and arterial pressure; it is progressive and fatal (Firth et al., 2010). As in certain inflammatory lung disorders, CaSR expression is increased in pulmonary arterial smooth muscle from humans with IPAH and in two different rodent models of this disease. Systemic administration of NPS2143 prevented the development of pulmonary hypertension and right-ventricular hypertrophy in both rodent models (Yamamura, 2014). Both IPAH and inflammatory lung disorders are attractive indications because the calcilytic can be delivered into the lung, thereby minimizing systemic exposure and avoiding changes in blood levels of PTH and Ca^{2+}.

Conclusion

- All allosteric modulators are really allosteric agonists, but as therapeutics they all behave as allosteric modulators.
- Newer calcimimetics might offer advantages over cinacalcet
  - evocalcet: fewer GI complications
    - caveat: only Japanese, only one study, not real world
  - etelcalcetide: better compliance
    - efficacy at cost of safety
    - GI side effects: inherent property of calcimimetics?
- Calcimimetics are generally applicable to a variety of hypercalcemic disorders, including FHH1−3
- Calcimimetics might be useful in treating some hypophosphatemic disorders.
- Calcilytics are not treatments for osteoporosis.
- Calcilytics might be useful in treating hypocalcemic disorders like ADH1 and 2 and certain forms of hypoparathyroidism.
- Calcilytics might be useful in treating certain pulmonary disorders.
- The ability of calcimimetics and calcilytics to normalize CaR signaling in FHH2 and 3 and ADH2 is surprising.

References

Abate, E.G., Clarke, B.L., 2016. Review of hypoparathyroidism. Front. Endocrinol. 7, 172.

Alexander, S.T., Hunter, T., Walter, S., Dong, J., Maclean, D., Baruch, A., et al., 2015. Critical cysteine residues in both the calcium-sensing receptor and the allosteric activator AMG 416 underlie the mechanism of action. Mol. Pharmacol. 88 (5), 853−865.

Arenas, M.D., de la Fuente, V., Delgado, P., Gil, M.T., Gutierrez, P., Ribero, J., et al., 2013. Pharmacodynamics of cinacalcet over 48 hours in patients with controlled secondary hyperparathyroidism: useful data in clinical practice. J. Clin. Endocrinol. Metab. 98 (4), 1718−1725.

Arnold, A.A.S., Thakker, R.V., 2019. Familial states of primary hyperparathyroidism. In: Primer on the Metabolic Bone Diseases and Disorders of Mineral Metabolism. John Wiley & Sons I, pp. 629−638.

Behets, G.J., Spasovski, G., Sterling, L.R., Goodman, W.G., Spiegel, D.M., De Broe, M.E., et al., 2015. Bone histomorphometry before and after long-term treatment with cinacalcet in dialysis patients with secondary hyperparathyroidism. Kidney Int. 87 (4), 846−856.

Bilezikian, J.P., Brandi, M.L., Eastell, R., Silverberg, S.J., Udelsman, R., Marcocci, C., et al., 2014. Guidelines for the management of asymptomatic primary hyperparathyroidism: summary statement from the Fourth International Workshop. J. Clin. Endocrinol. Metab. 99 (10), 3561−3569.

Block, G.A., Martin, K.J., de Francisco, A.L., Turner, S.A., Avram, M.M., Suranyi, M.G., et al., 2004. Cinacalcet for secondary hyperparathyroidism in patients receiving hemodialysis. N. Engl. J. Med. 350 (15), 1516−1525.

Block, G.A., Zeig, S., Sugihara, J., Chertow, G.M., Chi, E.M., Turner, S.A., et al., 2008. Combined therapy with cinacalcet and low doses of vitamin D sterols in patients with moderate to severe secondary hyperparathyroidism. Nephrol. Dial. Transplant. 23 (7), 2311−2318.

Block, G.A., Bushinsky, D.A., Cunningham, J., Drueke, T.B., Ketteler, M., Kewalramani, R., et al., 2017. Effect of etelcalcetide vs placebo on serum parathyroid hormone in patients receiving hemodialysis with secondary hyperparathyroidism: two randomized clinical trials. Jama 317 (2), 146–155.

Block, G.A., Bushinsky, D.A., Cheng, S., Cunningham, J., Dehmel, B., Drueke, T.B., et al., 2017. Effect of etelcalcetide vs cinacalcet on serum parathyroid hormone in patients receiving hemodialysis with secondary hyperparathyroidism: a randomized clinical trial. Jama 317 (2), 156–164.

Brown, E.M., 2010. Clinical utility of calcimimetics targeting the extracellular calcium-sensing receptor (CaSR). Biochem. Pharmacol. 80 (3), 297–307.

Brown, E.M., 2013. Role of the calcium-sensing receptor in extracellular calcium homeostasis. Best Pract. Res. Clin. Endocrinol. Metab. 27 (3), 333–343.

Charytan, C., Coburn, J.W., Chonchol, M., Herman, J., Lien, Y.H., Liu, W., et al., 2005. Cinacalcet hydrochloride is an effective treatment for secondary hyperparathyroidism in patients with CKD not receiving dialysis. Am. J. Kidney Dis. 46 (1), 58–67.

Chertow, G.M., Blumenthal, S., Turner, S., Roppolo, M., Stern, L., Chi, E.M., et al., 2006. Cinacalcet hydrochloride (Sensipar) in hemodialysis patients on active vitamin D derivatives with controlled PTH and elevated calcium x phosphate. Clin. J. Am. Soc. Nephrol. 1 (2), 305–312.

Chonchol, M., Locatelli, F., Abboud, H.E., Charytan, C., de Francisco, A.L., Jolly, S., et al., 2009. A randomized, double-blind, placebo-controlled study to assess the efficacy and safety of cinacalcet HCl in participants with CKD not receiving dialysis. Am. J. Kidney Dis. 53 (2), 197–207.

Dong, B., Endo, I., Ohnishi, Y., Kondo, T., Hasegawa, T., Amizuka, N., et al., 2015. Calcilytic ameliorates abnormalities of mutant calcium-sensing receptor (CaSR) knock-in mice mimicking autosomal dominant hypocalcemia (ADH). J. Bone Miner. Res. 30 (11), 1980–1993.

EF, N., 1996. Calcium receptors as novel drug targets. In: Bilezikian, J.P.R.L., Rodan, G.A. (Eds.), Principles of Bone Biology. Academic Press, New York, pp. 1019–1035.

Eidman, K.E., Wetmore, J.B., 2018. Treatment of secondary hyperparathyroidism: how do cinacalcet and etelcalcetide differ? Semin. Dial. 31 (5), 440–444.

Evenepoel, P., Cooper, K., Holdaas, H., Messa, P., Mourad, G., Olgaard, K., et al., 2014. A randomized study evaluating cinacalcet to treat hypercalcemia in renal transplant recipients with persistent hyperparathyroidism. Am. J. Transplant. 14 (11), 2545–2555.

Fielden, M.R., Dean Jr., C., Black, K., Sawant, S.G., Subramanian, R., Tomlinson, J.E., et al., 2016. Nonclinical safety profile of etelcalcetide, a novel peptide calcimimetic for the treatment of secondary hyperparathyroidism. Int. J. Toxicol. 35 (3), 294–308.

Firth, A.L., Mandel, J., Yuan, J.X., 2010. Idiopathic pulmonary arterial hypertension. Dis. Model. Mech. 3 (5–6), 268–273.

Fishbane, S., Shapiro, W.B., Corry, D.B., Vicks, S.L., Roppolo, M., Rappaport, K., et al., 2008. Cinacalcet HCl and concurrent low-dose vitamin D improves treatment of secondary hyperparathyroidism in dialysis patients compared with vitamin D alone: the ACHIEVE study results. Clin. J. Am. Soc. Nephrol. 3 (6), 1718–1725.

Floege, J., Kubo, Y., Floege, A., Chertow, G.M., Parfrey, P.S., 2015. The effect of cinacalcet on calcific uremic arteriolopathy events in patients receiving hemodialysis: the EVOLVE trial. Clin. J. Am. Soc. Nephrol. 10 (5), 800–807.

Floege, J., Tsirtsonis, K., Iles, J., Drueke, T.B., Chertow, G.M., Parfrey, P., 2018. Incidence, predictors and therapeutic consequences of hypocalcemia in patients treated with cinacalcet in the EVOLVE trial. Kidney Int. 93 (6), 1475–1482.

Fukagawa, M., Yokoyama, K., Shigematsu, T., Akiba, T., Fujii, A., Kuramoto, T., et al., 2017. A phase 3, multicentre, randomized, double-blind, placebo-controlled, parallel-group study to evaluate the efficacy and safety of etelcalcetide (ONO-5163/AMG 416), a novel intravenous calcimimetic, for secondary hyperparathyroidism in Japanese haemodialysis patients. Nephrol. Dial. Transplant. 32 (10), 1723–1730.

Fukagawa, M., Shimazaki, R., Akizawa, T., 2018. Evocalcet study g. Head-to-head comparison of the new calcimimetic agent evocalcet with cinacalcet in Japanese hemodialysis patients with secondary hyperparathyroidism. Kidney Int. 94 (4), 818–825.

Ganesh, S.K., Stack, A.G., Levin, N.W., Hulbert-Shearon, T., Port, F.K., 2001. Association of elevated serum PO(4), Ca x PO(4) product, and parathyroid hormone with cardiac mortality risk in chronic hemodialysis patients. J. Am. Soc. Nephrol. 12 (10), 2131–2138.

Giusti, F., Cianferotti, L., Gronchi, G., Cioppi, F., Masi, L., Faggiano, A., et al., 2016. Cinacalcet therapy in patients affected by primary hyperparathyroidism associated to Multiple Endocrine Neoplasia Syndrome type 1 (MEN1). Endocrine 52 (3), 495–506.

Goodman, W.G., Hladik, G.A., Turner, S.A., Blaisdell, P.W., Goodkin, D.A., Liu, W., et al., 2002. The Calcimimetic agent AMG 073 lowers plasma parathyroid hormone levels in hemodialysis patients with secondary hyperparathyroidism. J. Am. Soc. Nephrol. 13 (4), 1017–1024.

Gorvin, C.M., Hannan, F.M., Howles, S.A., Babinsky, V.N., Piret, S.E., Rogers, A., et al., 2017. Galpha11 mutation in mice causes hypocalcemia rectifiable by calcilytic therapy. JCI insight 2 (3), e91103.

Gorvin, C.M., Hannan, F.M., Cranston, T., Valta, H., Makitie, O., Schalin-Jantti, C., et al., 2018. Cinacalcet rectifies hypercalcemia in a patient with familial hypocalciuric hypercalcemia type 2 (FHH2) caused by a germline loss-of-function Galpha11 mutation. J. Bone Miner. Res. 33 (1), 32–41.

Hai, M.T.T., Guettier, J.M., Rosebraugh, C.J., 2017. Dosing of etelcalcetide and cinacalcet for secondary hyperparathyroidism. Jama 317 (20), 2132.

Hamano, N., Komaba, H., Fukagawa, M., 2017. Etelcalcetide for the treatment of secondary hyperparathyroidism. Expert Opin. Pharmacother 18 (5), 529–534.

Hannan, F.M., Thakker, R.V., 2013. Calcium-sensing receptor (CaSR) mutations and disorders of calcium, electrolyte and water metabolism. Best Pract. Res. Clin. Endocrinol. Metab. 27 (3), 359–371.

Hannan, F.M., Walls, G.V., Babinsky, V.N., Nesbit, M.A., Kallay, E., Hough, T.A., et al., 2015. The calcilytic agent NPS 2143 rectifies hypocalcemia in a mouse model with an activating calcium-sensing receptor (CaSR) mutation: relevance to autosomal dominant hypocalcemia type 1 (ADH1). Endocrinology 156 (9), 3114–3121.

Hannan, F.M., Babinsky, V.N., Thakker, R.V., 2016. Disorders of the calcium-sensing receptor and partner proteins: insights into the molecular basis of calcium homeostasis. J. Mol. Endocrinol. 57 (3), R127–R142.

Harris, R.Z., Padhi, D., Marbury, T.C., Noveck, R.J., Salfi, M., Sullivan, J.T., 2004. Pharmacokinetics, pharmacodynamics, and safety of cinacalcet hydrochloride in hemodialysis patients at doses up to 200 mg once daily. Am. J. Kidney Dis. 44 (6), 1070–1076.

Investigators, E.T., Chertow, G.M., Block, G.A., Correa-Rotter, R., Drueke, T.B., Floege, J., et al., 2012. Effect of cinacalcet on cardiovascular disease in patients undergoing dialysis. N. Engl. J. Med. 367 (26), 2482–2494.

Kawata, T., Tokunaga, S., Murai, M., Masuda, N., Haruyama, W., Shoukei, Y., et al., 2018. A novel calcimimetic agent, evocalcet (MT-4580/KHK7580), suppresses the parathyroid cell function with little effect on the gastrointestinal tract or CYP isozymes in vivo and in vitro. PLoS One 13 (4), e0195316.

KDIGO, 2017. KDIGO 2017 clinical practice guideline update for the diagnosis, evaluation, prevention, and treatment of chronic kidney disease–mineral and bone disorder (CKD-MBD). Kidney Int. Suppl. 7, 1–59.

Khan, A., Bilezikian, J., Bone, H., Gurevich, A., Lakatos, P., Misiorowski, W., et al., 2015. Cinacalcet normalizes serum calcium in a double-blind randomized, placebo-controlled study in patients with primary hyperparathyroidism with contraindications to surgery. Eur. J. Endocrinol. 172 (5), 527–535.

Kruse, A.E., Eisenberger, U., Frey, F.J., Mohaupt, M.G., 2005. The calcimimetic cinacalcet normalizes serum calcium in renal transplant patients with persistent hyperparathyroidism. Nephrol. Dial. Transplant. 20 (7), 1311–1314.

Lee, J.Y., Shoback, D.M., 2018. Familial hypocalciuric hypercalcemia and related disorders. Best Pract. Res. Clin. Endocrinol. Metab. 32 (5), 609–619.

Lindberg, J.S., Moe, S.M., Goodman, W.G., Coburn, J.W., Sprague, S.M., Liu, W., et al., 2003. The calcimimetic AMG 073 reduces parathyroid hormone and calcium x phosphorus in secondary hyperparathyroidism. Kidney Int. 63 (1), 248–254.

Lindberg, J.S., Culleton, B., Wong, G., Borah, M.F., Clark, R.V., Shapiro, W.B., et al., 2005. Cinacalcet HCl, an oral calcimimetic agent for the treatment of secondary hyperparathyroidism in hemodialysis and peritoneal dialysis: a randomized, double-blind, multicenter study. J. Am. Soc. Nephrol. 16 (3), 800–807.

Loupy, A., Ramakrishnan, S.K., Wootla, B., Chambrey, R., de la Faille, R., Bourgeois, S., et al., 2012. PTH-independent regulation of blood calcium concentration by the calcium-sensing receptor. J. Clin. Investig. 122 (9), 3355–3367.

Marcocci, C., Chanson, P., Shoback, D., Bilezikian, J., Fernandez-Cruz, L., Orgiazzi, J., et al., 2009. Cinacalcet reduces serum calcium concentrations in patients with intractable primary hyperparathyroidism. J. Clin. Endocrinol. Metab. 94 (8), 2766–2772.

Marx, S.J., 2017. Calcimimetic use in familial hypocalciuric hypercalcemia-A perspective in endocrinology. J. Clin. Endocrinol. Metab. 102 (11), 3933–3936.

Mayr, B., Schnabel, D., Dorr, H.G., Schofl, C., 2016. GENETICS IN ENDOCRINOLOGY: gain and loss of function mutations of the calcium-sensing receptor and associated proteins: current treatment concepts. Eur. J. Endocrinol. 174 (5), R189–R208.

Miyazaki, H., Ikeda, Y., Sakurai, O., Miyake, T., Tsubota, R., Okabe, J., et al., 2018. Discovery of evocalcet, a next-generation calcium-sensing receptor agonist for the treatment of hyperparathyroidism. Bioorg. Med. Chem. Lett 28 (11), 2055–2060.

Moe, S.M., Chertow, G.M., Coburn, J.W., Quarles, L.D., Goodman, W.G., Block, G.A., et al., 2005. Achieving NKF-K/DOQI bone metabolism and disease treatment goals with cinacalcet HCl. Kidney Int. 67 (2), 760–771.

Moe, S.M., Cunningham, J., Bommer, J., Adler, S., Rosansky, S.J., Urena-Torres, P., et al., 2005. Long-term treatment of secondary hyperparathyroidism with the calcimimetic cinacalcet HCl. Nephrol. Dial. Transplant. 20 (10), 2186–2193.

Moe, S.M., Abdalla, S., Chertow, G.M., Parfrey, P.S., Block, G.A., Correa-Rotter, R., et al., 2015. Effects of cinacalcet on fracture events in patients receiving hemodialysis: the EVOLVE trial. J. Am. Soc. Nephrol. 26 (6), 1466–1475.

Moe, S.M., Chertow, G.M., Parfrey, P.S., Kubo, Y., Block, G.A., Correa-Rotter, R., et al., 2015. Cinacalcet, fibroblast growth factor-23, and cardiovascular disease in hemodialysis: the evaluation of cinacalcet HCl therapy to lower cardiovascular events (EVOLVE) trial. Circulation 132 (1), 27–39.

Narushima, K., Maeda, H., Shiramoto, M., Endo, Y., Ohtsuka, S., Nakamura, H., et al., 2019. Assessment of CYP-mediated drug interactions for evocalcet, a new calcimimetic agent, based on in vitro investigations and a cocktail study in humans. Clin Transl Sci. 12 (1), 20–27.

Nemeth, E.F., Goodman, W.G., 2016. Calcimimetic and calcilytic drugs: feats, flops, and futures. Calcif. Tissue Int. 98 (4), 341–358.

Nemeth, E.F., Van Wagenen, B.C., Balandrin, M.F., 2018. Discovery and development of calcimimetic and calcilytic compounds. Prog. Med. Chem. 57 (1), 1–86.

Nesbit, M.A., Hannan, F.M., Howles, S.A., Reed, A.A., Cranston, T., Thakker, C.E., et al., 2013. Mutations in AP2S1 cause familial hypocalciuric hypercalcemia type 3. Nat. Genet. 45 (1), 93–97.

Peacock, M., Bilezikian, J.P., Klassen, P.S., Guo, M.D., Turner, S.A., Shoback, D., 2005. Cinacalcet hydrochloride maintains long-term normocalcemia in patients with primary hyperparathyroidism. J. Clin. Endocrinol. Metab. 90 (1), 135–141.

Peacock, M., Bolognese, M.A., Borofsky, M., Scumpia, S., Sterling, L.R., Cheng, S., et al., 2009. Cinacalcet treatment of primary hyperparathyroidism: biochemical and bone densitometric outcomes in a five-year study. J. Clin. Endocrinol. Metab. 94 (12), 4860–4867.

Peacock, M., Bilezikian, J.P., Bolognese, M.A., Borofsky, M., Scumpia, S., Sterling, L.R., et al., 2011. Cinacalcet HCl reduces hypercalcemia in primary hyperparathyroidism across a wide spectrum of disease severity. J. Clin. Endocrinol. Metab. 96 (1), E9–E18.

Quarles, L.D., Sherrard, D.J., Adler, S., Rosansky, S.J., McCary, L.C., Liu, W., et al., 2003. The calcimimetic AMG 073 as a potential treatment for secondary hyperparathyroidism of end-stage renal disease. J. Am. Soc. Nephrol. 14 (3), 575–583.

Raggi, P., Chertow, G.M., Torres, P.U., Csiky, B., Naso, A., Nossuli, K., et al., 2011. The ADVANCE study: a randomized study to evaluate the effects of cinacalcet plus low-dose vitamin D on vascular calcification in patients on hemodialysis. Nephrol. Dial. Transplant. 26 (4), 1327–1339.

Ramnitz, M.G.R., Brillante, B., et al., 2015. Treatment of autosomal dominant hypocalcemia with the calcilytic NPSP795. J. Bone Miner. Res. 30 (Suppl. 1).

Schwarz, P., Body, J.J., Cap, J., Hofbauer, L.C., Farouk, M., Gessl, A., et al., 2014. The PRIMARA study: a prospective, descriptive, observational study to review cinacalcet use in patients with primary hyperparathyroidism in clinical practice. Eur. J. Endocrinol. 171 (6), 727–735.

Serra, A.L., Schwarz, A.A., Wick, F.H., Marti, H.P., Wuthrich, R.P., 2005. Successful treatment of hypercalcemia with cinacalcet in renal transplant recipients with persistent hyperparathyroidism. Nephrol. Dial. Transplant. 20 (7), 1315–1319.

Serra, A.L., Savoca, R., Huber, A.R., Hepp, U., Delsignore, A., Hersberger, M., et al., 2007. Effective control of persistent hyperparathyroidism with cinacalcet in renal allograft recipients. Nephrol. Dial. Transplant. 22 (2), 577–583.

Shen, J., Xiao, J., Pickthorn, K., Huang, S., Bell, G., Vick, A., et al., 2014. A pharmacokinetic/pharmacodynamic model for AMG 416, a novel calcimimetic peptide, following a single intravenous dose in healthy subjects. J. Clin. Pharmacol. 54 (10), 1125–1133.

Shigematsu, T., Fukagawa, M., Yokoyama, K., Akiba, T., Fujii, A., Odani, M., et al., 2018. Long-term effects of etelcalcetide as intravenous calcimimetic therapy in hemodialysis patients with secondary hyperparathyroidism. Clin. Exp. Nephrol. 22 (2), 426–436.

Shoback, D.M., Bilezikian, J.P., Turner, S.A., McCary, L.C., Guo, M.D., Peacock, M., 2003. The calcimimetic cinacalcet normalizes serum calcium in subjects with primary hyperparathyroidism. J. Clin. Endocrinol. Metab. 88 (12), 5644–5649.

Silva, B.C., Bilezikian, J.P., 2015. Parathyroid hormone: anabolic and catabolic actions on the skeleton. Curr. Opin. Pharmacol. 22, 41–50.

Silverberg, S.J., Rubin, M.R., Faiman, C., Peacock, M., Shoback, D.M., Smallridge, R.C., et al., 2007. Cinacalcet hydrochloride reduces the serum calcium concentration in inoperable parathyroid carcinoma. J. Clin. Endocrinol. Metab. 92 (10), 3803–3808.

Silverberg, S.J.B.F., Liu, J., Marcocci, C., Walker, M.D., 2019. Primary Hyperparathyroidism. Primer on the Metabolic Bone Diseases and Disorders of Mineral Metabolism, ninth ed. ed. John Wiley & Sons, Inc, pp. 619–628.

Subramanian, R., Zhu, X., Kerr, S.J., Esmay, J.D., Louie, S.W., Edson, K.Z., et al., 2016. Nonclinical pharmacokinetics, disposition, and drug-drug interaction potential of a novel d-amino acid peptide agonist of the calcium-sensing receptor AMG 416 (etelcalcetide). Drug Metab. Dispos. 44 (8), 1319–1331.

Subramanian, R., Zhu, X., Hock, M.B., Sloey, B.J., Wu, B., Wilson, S.F., et al., 2017. Pharmacokinetics, biotransformation, and excretion of [(14)C] etelcalcetide (AMG 416) following a single microtracer intravenous dose in patients with chronic kidney disease on hemodialysis. Clin. Pharmacokinet. 56 (2), 179–192.

Sun, X., Huang, L., Wu, J., Tao, Y., Yang, F., 2018. Novel homozygous inactivating mutation of the calcium-sensing receptor gene in neonatal severe hyperparathyroidism responding to cinacalcet therapy: a case report and literature review. Medicine 97 (45), e13128.

Tsuruta, Y., Okano, K., Kikuchi, K., Tsuruta, Y., Akiba, T., Nitta, K., 2013. Effects of cinacalcet on bone mineral density and bone markers in hemodialysis patients with secondary hyperparathyroidism. Clin. Exp. Nephrol. 17 (1), 120–126.

Walter, S., Baruch, A., Dong, J., Tomlinson, J.E., Alexander, S.T., Janes, J., et al., 2013. Pharmacology of AMG 416 (Velcalcetide), a novel peptide agonist of the calcium-sensing receptor, for the treatment of secondary hyperparathyroidism in hemodialysis patients. J. Pharmacol. Exp. Ther. 346 (2), 229–240.

Walter, S., Baruch, A., Alexander, S.T., Janes, J., Sho, E., Dong, J., et al., 2014. Comparison of AMG 416 and cinacalcet in rodent models of uremia. BMC Nephrol. 15, 81.

Wetmore, J.B., Liu, S., Krebill, R., Menard, R., Quarles, L.D., 2010. Effects of cinacalcet and concurrent low-dose vitamin D on FGF23 levels in ESRD. Clin. J. Am. Soc. Nephrol. 5 (1), 110–116.

Yamamura, A., 2014. Pathological function of Ca^{2+}-sensing receptor in pulmonary arterial hypertension. J. Smooth Muscle Res. 50, 8–17.

Yarova, P.L., Stewart, A.L., Sathish, V., Britt Jr., R.D., Thompson, M.A., AP, P.L., et al., 2015. Calcium-sensing receptor antagonists abrogate airway hyperresponsiveness and inflammation in allergic asthma. Sci. Transl. Med. 7 (284), 284ra60.

Yu, L., Tomlinson, J.E., Alexander, S.T., Hensley, K., Han, C.Y., Dwyer, D., et al., 2017. Etelcalcetide, a novel calcimimetic, prevents vascular calcification in A rat model of renal insufficiency with secondary hyperparathyroidism. Calcif. Tissue Int. 101 (6), 641–653.

Zawierucha, J., Malyszko, J., Malyszko, J.S., Prystacki, T., Marcinkowski, W.P., Dryl-Rydzynska, T., 2019. Three therapeutic strategies: cinacalcet, paricalcitol or both in secondary hyperparathyroidism treatment in hemodialysed patients during 1-year observational study-A comparison. Front. Endocrinol. 10, 40.

Zheng, C.M., Wu, C.C., Hung, C.F., Liao, M.T., Shyu, J.F., Hsu, Y.H., et al., 2018. Cholecalciferol additively reduces serum parathyroid hormone levels in severe secondary hyperparathyroidism treated with calcitriol and cinacalcet among hemodialysis patients. Nutrients 10 (2).

Chapter 72

Clinical and translational pharmacology of bisphosphonates

Serge Cremers[1], Matthew T. Drake[2], Frank H. Ebetino[3,4], Michael J. Rogers[5], John P. Bilezikian[6] and R. Graham G Russell[4,7]

[1]Department of Pathology & Cell Biology and Department of Medicine, Vagelos College of Physicians and Surgeons, Columbia University Irving Medical Center, United States; [2]Department of Endocrinology and Kogod Center of Aging, Mayo Clinic College of Medicine, Rochester, MN, United States; [3]Department of Chemistry, University of Rochester, Rochester, NY, United States; [4]Mellanby Centre for Bone Research, Medical School, University of Sheffield, United Kingdom; [5]Garvan Institute of Medical Research and St Vincent's Clinical School; University of New South Wales, Sydney, Australia; [6]Division of Endocrinology, Department of Medicine, College of Physicians and Surgeons, Columbia University, New York, NY, United States; [7]Nuffield Department of Orthopaedics, Rheumatology and Musculoskeletal Sciences, The Oxford University Institute of Musculoskeletal Sciences, The Botnar Research Centre, Nuffield Orthopaedic Centre, Oxford, United Kingdom

Chapter outline

Introduction

The year 2019 marks 50 years since the first publications on the biological effects of bisphosphonates (BPs) (Fleisch et al., 1969a, 1969b; Francis et al., 1969).These agents have served for the past several decades as the pharmacological cornerstone for the treatment of skeletal disorders such as Paget's disease of bone, osteoporosis and cancers metastatic to bone. The early discovery and clinical development of BPs has been reviewed elsewhere (Fleisch, 2000; Russell, 2011). Abundant preclinical, translational and clinical research with BPs has led to a wealth of data that now enable us to rationally prescribe these drugs to the right patients using tailored dosing regimens to provide an optimal balance between efficacy and side effects. Better insight into the precise effects of BPs on various bone cell populations has resulted in continued efforts to develop new BPs for the treatment of metabolic bone diseases, while non-skeletal-related indications for these drugs have been more recently explored. In addition, BPs are currently under investigation as agents for the targeting of other drugs, such as antibiotics, to bone tissue. This chapter provides an overview of our current knowledge on the (pre-) clinical and translational pharmacology of BPs, and illustrates how this knowledge has been used both for the development of new compounds and for the treatment of patients.

Principles of Bone Biology. https://doi.org/10.1016/B978-0-12-814841-9.00072-5

- **Early BPs: non-nitrogen containing**

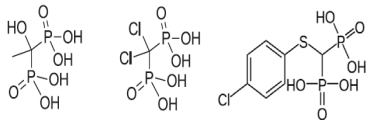

Etidronate Clodronate Tiludronate

- **"Second" generation: nitrogen-containing with short alkyl chains**

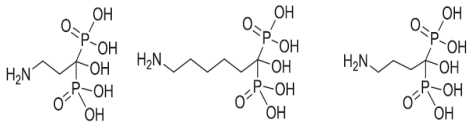

Pamidronate Neridronate Alendronate

- **"Third" generation: (from medicinal chemistry optimisation):**

N-containing with branched or ring structure, more potent

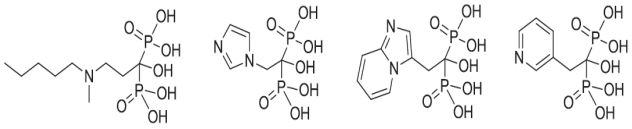

Ibandronate Zoledronate Minodronate Risedronate

Ten BPs which have been approved for clinical use in various countries.

Mechanisms of action

Therapeutic

BPs have several mechanisms of action which underlie their therapeutic use. Initially, they were studied for their ability to block calcification as reported by Francis et al. (Francis et al., 1969). Their antiresorptive mechanism is based on their mineral binding and biochemical effects on cells. Their ability to inhibit the dissolution of bone mineral was the action that was first described by Fleisch, Francis and Russell (Fleisch et al., 1969a, 1969b; Francis et al., 1969). Subsequently, it became clear that BPs also inhibit osteoclast-mediated bone resorption through effects on the osteoclast itself. It took until the late 1990s to determine the mechanism by which BPs inhibit osteoclast-mediated resorption. Following endocytic uptake into osteoclasts (Luckman et al., 1998; van Beek et al., 1999a, 1999b; Rogers, 2003), nitrogen (N)-containing BPs inhibit the intracellular enzyme farnesyl pyrophosphate pyrophosphate (FPP) synthase, a key-enzyme of the mevalonate pathway (Fig. 72.1). Inhibition of FPP synthase leads to decreases in FPP levels, as well as to levels of geranylgeraniol pyrophosphate (GGPP). Collectively, this results in the decreased prenylation of signal transduction proteins such as Ras, Rac and Rho, ultimately resulting in a loss of function of the osteoclasts. The subsequent elegant studies using X-ray crystallography have fully characterized the binding of N-containing BPs with the FPP synthase enzyme (Kavanagh et al., 2006), and have led to the rational design of even more potent and selective BPs such as OX14 (Lawson et al., 2017).

In contrast to the N-containing BPs, non-N-containing BPs undergo intracellular metabolism to non-hydrolyzable analogues of ATP, as catalyzed by aminoacyl-tRNA synthetase enzymes (Frith et al., 2001) (Fig. 72.1). Consequently, ATP analogue accumulation within the cytosol triggers osteoclast apoptosis via inhibition of the mitochondrial ADP/ATP translocase (Lehenkari et al., 2002). Interestingly, N-containing BPs have also been shown to have additional effects on osteoclasts by inducing formation of the intracellular apoptotic ATP analogue 1-adenosin-5′-yl ester 3-(-3-methylbut-3-enyl) ester triphosphoric acid (ApppI), a consequence of their inhibition of FPP synthase in the mevalonate pathway and the subsequent accumulation of intracellular isopentenyl pyrophosphate (IPP) (Raikkonen et al., 2009). In contrast to the intracellular ATP analogue metabolites of non-N-containing BPs, ApppI does not contain a BP in its structure (Raikkonen et al., 2009).

Bisphosphonates, both N-containing and non-N-containing, also appear to have effects on osteoblasts and osteocytes. The lifespan of both cell types is prolonged by the anti-apoptotic effects of BPs, an effect which is established through Connexin 43 (Cx43) and the downstream activation of extracellular signal-regulated kinases (ERKs) (Bellido and Plotkin,

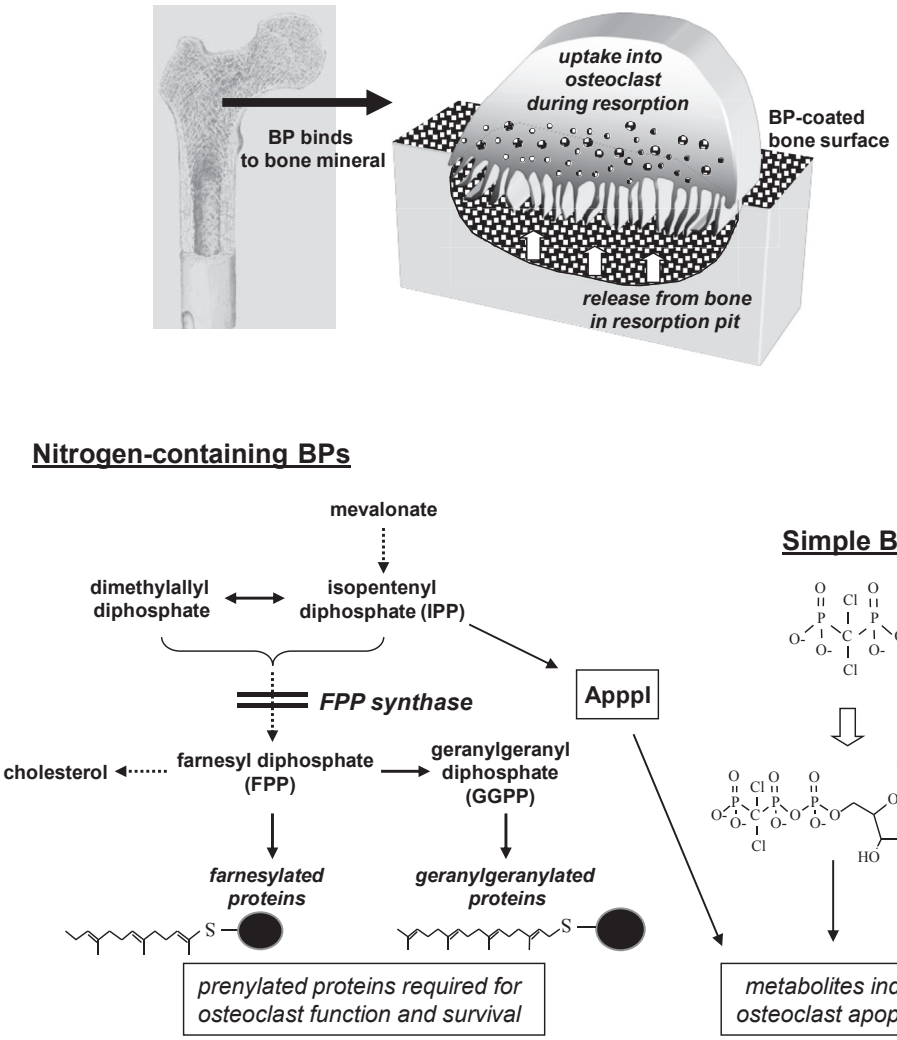

FIGURE 72.1 Mechanisms of action of bisphosphonates on osteoclasts. After binding to bone mineral, the drugs are internalized into bone-resorbing osteoclasts by endocytosis. Simple BPs (e.g., clodronate, etidronate) are metabolized in the osteoclast cytosol to ATP analogues that induce osteoclast apoptosis. Nitrogen-containing BPs inhibit FPP synthase, thereby preventing the prenylation of small GTPase proteins essential for the function and survival of osteoclasts. Inhibition of FPP synthase also causes the accumulation of IPP, which is incorporated into ApppI (an analogue of ATP capable of inducing osteoclast apoptosis).

2011). Interestingly these anti-apoptotic effects of BPs take place at very low concentrations, while the antiresorptive effects are evident at much higher concentrations of these drugs. These intriguing observations have led to the study of BPs such as IG9402 (Lidadronate) and NE11809 which show anti-apoptotic effects on osteoblasts and osteocytes, but without possessing the antiresorptive effect on osteoclasts (Bellido and Plotkin, 2011). Given these potentially positive effects of BPs on osteoblasts and especially osteocytes, the differential penetration of BPs into the canalicular network of bone, as discussed below in the PK section, might explain some of the clinically observed differences in effects of the various BPs, such as the differences between alendronate and risedronate (Roelofs et al., 2012; Russell et al., 2008; Ebetino et al., 2011). The different mechanisms of action of BPs on bone cells are illustrated in Fig. 72.2.

The effects of BPs on metastatic bone disease are thought to come mainly from their ability to decrease osteoclast-mediated bone resorption and to thereby effectively interrupt the vicious cycle that develops between metastatic tumor cells and bone cells (Croucher et al., 2016). However, direct anti-tumor cell activity has also been described for some BPs such as zoledronate which has been shown to inhibit cell viability, migration, invasion and metastasis (Mathew and Brufsky, 2015; Boissier et al., 2000; Jagdev et al., 2001). The anti-tumor effects of zoledronate might be exerted through the miRNA/PTEN/Akt signaling and activin signaling pathways (Fragni et al., 2016; Wilson et al., 2015). This pre-clinical data is consistent with the results of several clinical studies which have demonstrated a beneficial effect of the adjuvant use

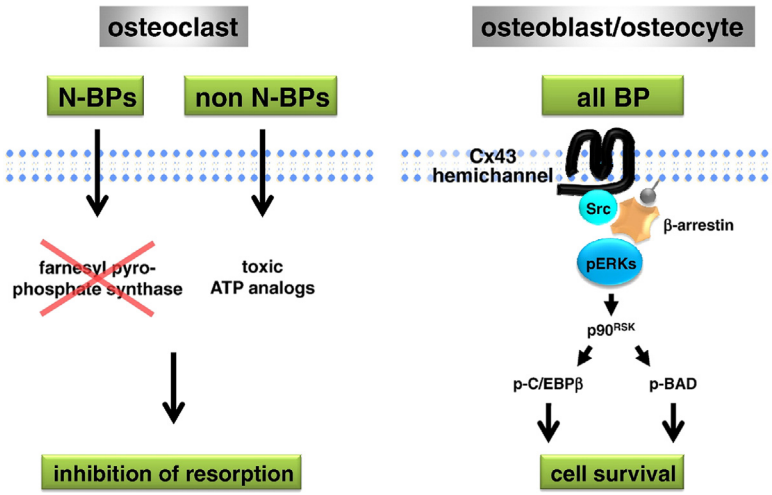

FIGURE 72.2 Bisphosphonates inhibit osteoclast activity and prevent osteoblast and osteocyte apoptosis via different mechanisms. For simplicity, only one of the six molecules of Cx43 that form the hemichannel is shown. See text for details (Bellido and Plotkin, 2011).

of zoledronate in elderly postmenopausal women with cancer, in addition to a role in preventing bone metastases (Mathew and Brufsky, 2015; Coleman et al., 2014; Chukir et al., 2018; Dionisio et al., 2019).

BPs are also currently under investigation as potential agents for the prevention and treatment of several neurodegenerative diseases including Alzheimer's Disease (AD), Parkinson's Disease and Huntington's Disease (Zameer et al., 2018). Some clinical studies suggest positive effects of BPs such as alendronate and etidronate on limiting brain calcifications, which may translate into alleviation of some of the symptoms that characterize these neurodegenerative diseases (Oliveira and Oliveira, 2016; Loeb et al., 2006). Several pre-clinical studies also suggest that the mechanism of action of BPs in neurodegenerative diseases is via inhibition of calcium crystal growth. However, the extent to which BPs might cross the blood brain barrier remains unclear. In contrast, other pre-clinical studies point toward the ability of BPs to inhibit FPP synthase and subsequently to decrease both protein prenylation and also cholesterol synthesis as a possible mechanism for their effects in neurodegenerative disease.

BPs have also been shown to prolong lifespan in pre-clinical models of progeria, an effect which may reflect their ability to inhibit FPP synthase (Varela et al., 2008; Gordon et al., 2014). Several human progerias, including Hutchinson–Gilford progeria syndrome (HGPS), are caused by the accumulation at the nuclear envelope of farnesylated forms of truncated prelamin A, a protein that is also altered during normal chronologic aging (Varela et al., 2008). Treatment with a combination of statins and zoledronate was shown to efficiently inhibit both farnesylation and geranylgeranylation of the proteins progerin and prelamin A and to markedly improve aging-like phenotypes of mice deficient in the metalloproteinase Zmpste24, including growth retardation, loss of weight, lipodystrophy, hair loss and bone defects (Varela et al., 2008). Likewise, the longevity of these mice was substantially extended. N-containing BPs might therefore be an interesting therapeutic approach for human progeroid syndromes associated with nuclear-envelope abnormalities (Varela et al., 2008). This pre-clinical data has been evaluated by clinical studies which suggest that farnesylation inhibition either by the farnsyltransferase inhibitor lonafarnib alone (Clinicaltrials.gov: NCT00425607) or by the combination of lonafarnib, pravastatin and zoledronate (NCT00879034 and NCT00916747), may improve the survival of patients with Hutchinson–Gilford progeria syndrome (Gordon et al., 2014).

Another potential application for N-containing BPs is to prevent the accumulation of DNA damage from radiation (Misra et al., 2016). Interestingly, this effect, which was demonstrated in vitro in mesenchymal stem cells, has been explained by the ability of BPs to inhibit FPP synthase and therefore to decrease the prenylation of signal transduction proteins such as Ras and Rheb, which in turns reduces activation of mTOR, a molecule implicated in lifespan extension (Misra et al., 2016). In addition, downstream effectors of mTOR, such as Forkhead Box O3 (FOXO3A), have been recognized as important effectors for the recruitment of DNA damage response proteins, such as the protein kinase ataxia telangiectasia mutated (ATM) (Misra et al., 2016).

Some BPs may also be useful in the treatment of certain ectopic calcification disorders. Etidronate has been used for more than 40 years to reduce flares in fibrodysplasia ossificans progressiva (FOP) and was registered for clinical use against heterotopic ossification (Wentworth et al., 2018). Interestingly, FOP results from activating mutations in the ACVR1 gene, which encodes the activin A Type 1 receptor. Aberrant signaling through this receptor leads to abnormal

activation of the pSMAD 1/5/8 pathway and triggers the formation of bone outside the skeleton. In FOP, BPs may have an effect on the abnormal extra-skeletal calcification as well as the locally increased bone (re)modeling, although definitive clinical data for BP use in this setting are sparse (Wentworth et al., 2018). Another rare ectopic calcification disorder for which BPs, especially etidronate, might be useful is pseudoxanthoma elasticum (PXE), in which an ABCC6 mutation has been shown to lead to reduced levels of circulating pyrophosphate, resulting in soft tissue mineralization (Li et al., 2018). Etidronate has been shown to prevent, but not to reverse, ectopic mineralization in a mouse model of PXE, which would be consistent with the proposed mechanism of action of BPs such as etidronate, which inhibits mineralization at clinically used doses (Li et al., 2018). It is currently unknown, however, if BP treatment might be beneficial to patients with PXE.

For some indications for which the potential effect of BPs is thought to depend on inhibition of osteoclast-mediated bone resorption, data is a more ambiguous and requires further investigation. Thus, for example, whereas preclinical data have suggested a beneficial effect of BPs on fracture healing, studies in humans have shown little to no effect, a potential benefit such that BPs can be started shortly after osteoporotic fracture (Kates and Ackert-Bicknell, 2016; Molvik and Khan, 2015). However, other approaches, such as treatment with intermittent parathyroid hormone (PTH) derivatives, might be more useful to improve fracture healing (Hegde et al., 2016). Another indication for which inhibition of bone resorption is thought to be effective is for the treatment of avascular necrosis of the femoral head (AVN) which can result from multiple causes such as Perthes Disease (an idiopathic childhood osteonecrosis of the femur head), sickle cell disease, or the use of high dose glucocorticoids (Guerado and Caso, 2016; Jamil et al., 2017). By inhibiting osteoclast-mediated bone resorption, BPs might be able to preserve femoral head strength and reduce the risk for femoral head collapse. Evidence that research for this indication is currently active both pre-clinically and clinically comes from a proposed multicenter, prospective, randomized controlled trial to evaluate the efficacy of zoledronate in Perthes Disease (Jamil et al., 2017). Changes in subchondral bone and crosstalk between subchondral bone and cartilage have been demonstrated to play an important role in the development of osteoarthritis (OA) (Bultink and Lems, 2013; Lems, 2018). In the early phase of OA, increased osteoclast activity, elevated bone remodeling and hypomineralization can be found (Bultink and Lems, 2013; Roman-Blas et al., 2014) It is therefore likely that BPs, via their effects as osteoclast resorption inhibitors, might be effective for the treatment of OA, especially in the early phase of the disease (Lems, 2018). Clinical trials (e.g., with risedronate) have shown equivocal results (Spector et al., 2005; Bingham et al., 2006). More recently, two large separate case-control studies suggest that BPs are effective for reducing the incidence of knee replacement in patients with OA (Lems, 2018; Fu et al., 2017; Neogi et al., 2018). While it is likely wise to treat patients with both osteoporosis and OA with antiresorptive drugs such as BPs, there is currently insufficient data to start antiresorptive therapy in patients with OA but without osteoporosis (Lems, 2018). Zoledronate has been shown to be able to reduce pain associated with bone marrow lesions in patients with osteoarthritis (Shabestari et al., 2016, 2017; Eriksen, 2015).

Another research direction for BPs is for the improvement of dental implants via local surface coating and/or direct application of BPs to the surgical site (Mendes et al., 2018). In animal models, local delivery of the BPs improves peri-implant bone formation (Ramalho-Ferreira et al., 2015; Meraw and Reeve, 1999; Back et al., 2012; Guimaraes et al., 2015) and in humans local BP delivery has been shown to improve the fixation of osteointegrated implants (Abtahi et al., 2012). While it has been suggested that systemic BP use may worsen dental implant outcomes, the available scientific evidence demonstrates that patients with a history of BP use do not have a higher risk of dental implant failure or marginal bone loss when compared to patients who have not used BPs (Mendes et al., 2018). In contrast, the existing literature does suggest that patients who undergo surgical trauma during dental implant installation may be more susceptible to BP-related osteonecrosis of the jaw (BRONJ, or ONJ, osteonecrosis of the jaw) (Mendes et al., 2018). Intriguingly, this potential side effect of BPs may be prevented by the use of pharmacologically non-active BPs, i.e., BPs with little to no effect on bone cells. The mechanism of this new approach appears to be via competitive equilibrium-based displacement of the pharmacologically active BPs (Hokugo et al, 2016, 2017, 2019; Sun et al., 2018; Ebetino et al., 2018).

Another side effect of N-containing BPs is an acute phase reaction (APR). This flu-like reaction is typically observed in a subset of patients, is more likely to occur with initial rather than subsequent intravenous (IV) administration (Anastasilakis et al., 2012), and is mediated by gamma-delta-T-cells (Kunzmann et al., 2000). The mechanism underlying this T-cell stimulation is N-containing BP inhibition of FPP synthase resulting in an increase in phospho-antigens for these cells such as isopentenyl pyrophosphate (IPP) and ApppI. This ability to stimulate gamma-delta T-cells has now been used for the development of cancer immunotherapies given that gamma-delta-T-cells have the ability to target cancer cells. The main challenge to this approach is the need to enhance uptake of the N-containing BPs into the cancer cells, an area for which nano-technology-based carriers such as ligand-targeted liposomes are actively being developed and investigated (Hodgins et al., 2017). Notably, this approach exemplifies how a side effect of the BPs is slowly but steadily being turned into a new indication.

Finally, N-containing BPs might also be applied to treat certain parasitic protozoan infections such as infections with Trypanosoma cruzi, the cause of Chagas' disease or American trypanosomiasis, infections with Schistosoma mansoni, also known as bilharzia, as well as Plasmodium falciparum, one of the causes of malaria (Montalvetti et al., 2001; Ziniel et al., 2013). In each of these species, a mevalonate pathway leads to the formation of sterols and polyisoprenoid compounds essential to survival, but which is susceptible to N-containing BPs which have shown to inhibit the growth of these parasites (Martin et al., 2001; Ghosh et al., 2004). Interestingly, the protozoan FPP synthase differs slightly from human FPP synthase; therefore, BP potency differs between species, as has been demonstrated for *Trypanosoma cruzi* (Montalvetti et al., 2001). These findings have been supported by both genetic and crystallographic studies and have led to the identification of more specific N-containing-BPs that may be useful for these infections (Rodriguez et al., 2016). Both current clinically used BPs as well as several more recently designed BPs are currently in various phases of pre-clinical development for these indications.

Side effects

Oral BPs are in some patients associated with gastrointestinal toxicity, where they can damage epithelial layers during absorption as demonstrated in vitro, in vivo and in humans (Cremers et al., 2019; Twiss et al., 1999, 2001, 2006). Some of the toxic effects on the GI tract have been linked to direct damaging effects of the BPs as acidic molecules, but the N-containing BPs' cellular mechanism of action including FPP synthase inhibition, as well as their effects on mitochondrial superoxide production and lipid peroxidation, may also play a role in the pathogenesis of GI toxicity (Cremers et al., 2019; Suri et al., 2001; Nagano et al., 2012). GI toxicity has been reduced by coating of the tablets, instructions to take the tablets with sufficient water and to not lie down immediately after intake, as well as the reduction of intake frequency from daily to weekly or monthly.

Renal toxicity is another potential side effect from BPs (Perazella and Markowitz, 2008) that has primarily been observed when high dose IV BP is provided as an injection or short infusion. It has also mainly been observed in patients already predisposed to renal impairment, such as those with multiple myeloma. The formation of precipitating aggregate complexes with bivalent cations such as calcium is one potential mechanism for nephrotoxicity, especially in subjects receiving high IV BP doses. However, FPP synthase inhibition has also been suggested to play a role in the nephrotoxicity of N-containing BPs (Luhe et al., 2008). Potential other mechanisms include dysregulation of fatty acid metabolism (Cheng et al., 2018), genotoxic effects, and/or cytotoxic effects (Singireesu et al., 2018). It is currently not clear how each mechanism may contribute to differences in the types of nephrotoxicity known to occur with the various BPs such as predominant glomerulotoxicity with pamidronate as compared to predominant tubular necrosis with zoledronate (Perazella and Markowitz, 2008). Here there is also controversy with respect to differences in nephrotoxicity between the clinically available BPs. As example, some investigators have reported differences, especially between IV ibandronate and zoledronate. Such differences might reflect differences in solubility between the two BPs, but alternative mechanisms have also been explored (Perazella and Markowitz, 2008). In comparison, others have reported no differences (Luedders et al., 2015).

An N-containing BP-specific side effect is the acute phase reaction that occurs in some patients after IV administration (Skjodt et al., 2018; Tsurukami, 2017). As discussed above, these flu-like symptoms of pyrexia and musculoskeletal pain are explained by an induction of gamma delta T cells through the formation of phospho-antigens formed as a result of FPP synthase inhibition. This side effect is manageable with acetaminophen, is most commonly seen after the first administration of the drug, and typically becomes less severe with subsequent administrations (Skjodt et al., 2018; Tsurukami, 2017).

One of the side effects first noted with use of BPs was the inhibition of mineralization seen with high doses of etidronate. This was attributed to direct physicochemical effects on inhibiting mineral deposition, which is not seen with other BPs used clinically where the window between inhibition of mineralization and bone resorption is much greater.

The mechanism of another severe side effect, BRONJ, remains unclear, despite much speculation about the role of suppressed bone turnover. FPP synthase inhibition in gingival fibroblasts leading to impaired wound healing might also play a role (Skjodt et al., 2018; Marolt et al., 2012; Cozin et al., 2011; Landesberg et al., 2011). ONJ occurs predominately in cancer patients, often associated with osteomyelitis after tooth extractions.

Finally, long-term BP use has been associated with the development of atypical femoral fractures. The precise mechanisms underlying this rare but serious side effect is not known, but again may reflect local reduction of bone resorption, perhaps combined with a pre-existing anatomic anomaly in the sub-trochanteric femur (Skjodt et al., 2018).

Other side effects of BPs may include cardiovascular harms or benefits, but these effects are controversial and potential mechanisms underlying these potential side effects are not fully understood (Skjodt et al., 2018).

Mathematical pharmacodynamic (PD) models of BPs

The effects of BPs on bone have been evaluated using a variety of preclinical in vitro and in vivo models in many animal species over the many decades since the first descriptions of their biological effects. In addition, the effects of BPs have been evaluated in healthy volunteers as well as patients. From this data, various quantitative parameters have been calculated that together describe BP potency in different models. A typical parameter is the LED_{50}, the lowest dose at which an antiresorptive effect is observed. A typical relationship between BP concentration and an antiresorptive effect might be described mathematically by a so-called inhibitory E_{max} − model: $E = E_0*(1 - E_{max} * C^{\gamma}/(EC_{50}^{\gamma} + C^{\gamma}))$. Parameters include the effect observed in the absence of BP (E_0), the maximum effect E_{max}, the BP concentration (C) at which 50% of the effect is seen (EC_{50}) and the Hill coefficient. These parameters differ from BP to BP for antiresorptive activity and also differ between experimental models. Other mathematical models include a so-called indirect inhibitory effect model, which is often used to describe the effect of BPs on bone resorption markers in patients. These models include a production rate and an elimination rate of bone resorption markers and have an effect of the BP concentration on the production rate, most often through an inhibitory E_{max} model. Other mathematical models have included the effect of BPs on bone multicellular units and subsequently on BMD (Hernandez et al., 2002), while others have developed more extensive and very complicated systems pharmacology approaches using differential equations (Riggs and Cremers, 2019). To our knowledge, there are few, if any, mathematical PD models for the many non-bone-related effects of BPs.

Pharmacokinetics (PK)

The general bio-distribution of BPs is illustrated in Fig. 72.3. Oral BPs are taken up in the stomach, duodenum and ileum via paracellular and active transport. All BPs have a low and variable bioavailability (Twiss et al., 2001; Lin, 1996), with the bioavailability of most BPs estimated at approximately 1% (Cremers et al., 2019). This declines to near zero if the drug is ingested with calcium- or magnesium-containing foods, drinks or drugs (Gertz et al., 1995). Various attempts to increase the bioavailability of BPs have included the use of pro-drugs as well as absorption enhancers such as caproic acid (Cremers et al., 2019). The influence of food can be decreased by slow release formulations that include chelators (McClung et al., 2012). The low bioavailability of oral BPs also increases when ingested with gastric pH raising drugs such as ranitidine and omeprazole (Gertz et al., 1995). The effects of most of these attempts to improve the oral bioavailability of BPs, however, are marginal.

BPs are bound to plasma and serum proteins, but the role of this protein binding for the PK and PD of BPs is not clear. Protein binding differs between BPs and depends on multiple factors including the BP concentration, local pH, presence of divalent cations such as calcium, as well as endogenous displacers (Lin, 1996). Protein binding also differs between species and has been reported to range between 5% and 90% (Cremers et al., 2019).

Once reaching the systemic circulation, BPs do distribute to various soft tissue organs including the liver but are not typically metabolized, with the exception of the metabolism of some non-N-containing BPs to ATP analogues within

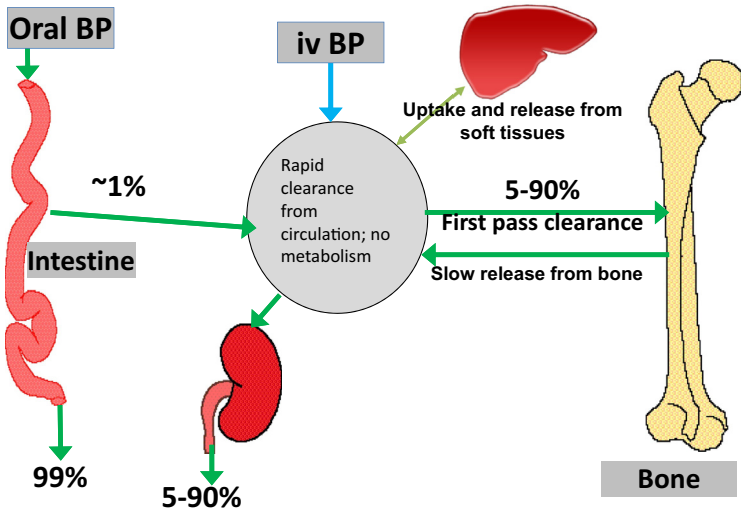

FIGURE 72.3 Schematic representation of the bio-distribution of BPs.

macrophages and osteoclasts as noted previously. Instead systemic BPs are either distributed to bone, or they are eliminated via the kidneys through glomerular filtration. Renal clearance of BPs correlates closely with creatinine clearance as has been demonstrated in various patient populations (Berenson et al., 1997; Bergner et al., 2007; Skerjanec et al., 2003). The United States FDA has used this correlation between renal function and the renal clearance of zoledronate to determine dose recommendations for zoledronate in patients with renal impairment (Booth et al., 2003). BPs remain contraindicated in patients with a creatinine clearance of less than 35 mL/min, although retrospective analyses of clinical trials suggest antifracture efficacy even in patients with low GFRs (Miller et al., 2005; Jamal et al., 2007). BPs are cleared from the systemic circulation by renal replacement therapy (Bergner et al., 2002; Buttazzoni et al., 2006; Beigel et al., 1995; Miller, 2007). However, most data on renal replacement therapy is relatively old and may not be applicable to the currently used dialyzers and membranes for patients on hemodialysis. Optimal BP dosing regimens for patients on dialysis are challenging to assess as there are effects of dialysis both on drug clearance and on the clearance of most biochemical markers of bone turnover, especially the resorption markers C-terminal and N-terminal peptides (CTX and NTX, respectively) (Miller, 2007). General recommendations for patients on hemodialysis are to decrease the BP dose by 50%, increase the infusion time, and to limit the overall number of doses provided (Miller, 2007). If the BP dose is given prior to a dialysis session, it is likely to result in elimination of at least part of the drug (Miller, 2007).

BPs are optimal drugs in terms of targeting the sites at which they are needed. They specifically bind to hydroxyapatite crystals and other calcium salts in bone, and thus are particularly available for binding at sites of active and increased bone turnover such as Pagetic lesions and bone metastases (Fleisch et al., 1969a; Fogelman et al., 1978). In bone, BPs bind strongly to sites of new mineral deposition at the 'calcification front' in osteoid as well as to resorption sites, most likely because of the exposure of calcium phosphate crystals during resorption. BPs bind specifically but not solely to high turnover sites. Binding to quiescent bone is less extensive, although numerically binding to quiescent bone can be substantial as for nearly all persons there is much more quiescent bone than bone that is actively turning over at any given time (Masarachia et al., 1996; Azuma et al., 1995). In the skeleton, comparatively more BP is taken up by trabecular as compared to cortical bone, which likely reflects the higher rate of bone turnover and the greater surface area available in the trabecular bone (Weiss et al., 2008). The distribution of BPs within the skeleton is therefore not homogeneous. BP deposition is even higher when bone turnover is increased locally, which is one reason why 99 mTc-labeled BPs are so successful for the diagnosis of diseases such as Paget's disease of bone and metastatic bone disease (Fogelman et al., 1978).

BPs differ from each other in terms of their binding affinity for hydroxyapatite (Dunford et al., 2008). This binding affinity might determine to some extent a BP's relative biodistribution between quiescent and actively remodeling bone, a function which differs between BPs (Masarachia et al., 1996; Azuma et al., 1995). It is, however, also likely that a BP's hydroxyapatite binding affinity determines not only the percentage of which a single IV dose will bind to the skeleton (Nancollas et al., 2006), but also how well a BP will penetrate the canalicular network within bone. As example, when compared to alendronate, risedronate has a weaker binding affinity for hydroxyapatite and lower skeletal retention, but exhibits higher penetration into the canalicular network and thus more pronounced access to osteocytes embedded within the bone matrix (Roelofs et al., 2012).

Most of an intravenously administered BP dose is either rapidly bound to bone or excreted into the urine, with only relatively small amounts accumulating in other tissues (Fig. 72.3). The amount of BP deposited in the skeleton can therefore be estimated from the IV dose and the amount of BP excreted into urine within a certain amount of time, e.g., 24 h, a technique developed and validated using 99 mTc-labeled BPs but also used to determine whole body retention (WBR) for multiple pharmacologically active BPs (Skerjanec et al., 2003; Fogelman et al., 1978; Khan et al., 1997; Cremers et al, 2003, 2005a; Pillai et al., 2004). These WBR_{24h} data correlate well with the hydroxyapatite affinity constants, illustrating that the amount of BP retained by the skeleton is determined by the binding properties of the BP (Nancollas et al., 2006). Skeletal retention, however, is also determined by additional patient related factors such as renal function, as well as the pretreatment rate of bone turnover, determined in cancer patients by the number of skeletal metastases and in patients with Paget's disease of bone by bone turnover levels (Cremers et al, 2003, 2005a; Chen et al., 2002). Interestingly, retention rates do not seem to change over time despite decreasing rates of bone turnover, which may illustrate that the biodistribution of BPs into bone may be more complex than suggested by currently available modeling efforts (Cremers et al, 2005a, 2019).

Once bound to bone, BPs may be either released by dissolution, or may become covered by new bone formed at resorption sites, with later release into the circulation during osteoclast-mediated bone resorption (Masarachia et al., 1996; Azuma et al., 1995). BPs are endocytosed into osteoclasts during resorption of bone (Coxon et al., 2008) (Fig. 72.4). While some BP is released into the circulation during this resorptive process, some BP may be released in association with osteoclast apoptosis and death. To our knowledge, however, there is no data on the actual contributions of either process to

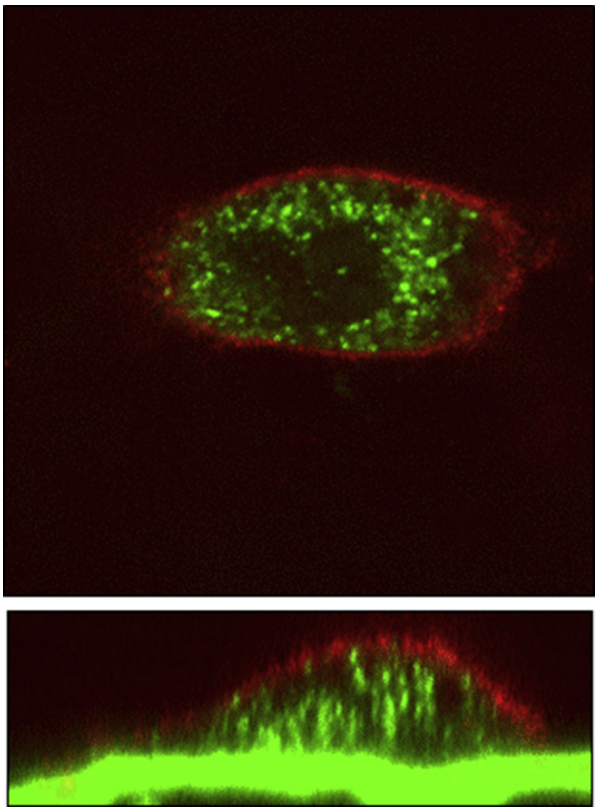

FIGURE 72.4 BP uptake into osteoclast. Rabbit osteoclasts were seeded onto dentine discs that had been pre-coated with 100 mM fluorescently labeled alendronate (green) and incubated for 18 h. Cells were then fixed, and actin stained with TRITC-phalloidin (red). Cells were examined by Light Scatter Confocal Microscopy (LSCM) (Luckman et al., 1998; Coxon et al., 2005, 2008).

long-term BP elimination in the urine. BPs released from bone may undergo re-uptake onto bone surfaces, a process that may depend on their relative affinity for hydroxyapatite. Importantly, BPs are detectable in urine for years after stopping treatment (Khan et al., 1997; Papapoulos and Cremers, 2007). Short-term and long-term urinary BP data are therefore highly informative about the overall amount of BP residing in bone, the latter especially when serum concentrations are too low to determine (Cremers et al., 2005b). Long-term (years) PK of BPs are characterized by half-lives determined by slow release from bone and subsequent excretion into urine. The few clinical studies which have collected blood and urine samples of sufficient duration to permit estimates of long-term half-lives suggest that the long-term half-lives of BPs in humans range between 1 and 10 years (Khan et al., 1997; Papapoulos and Cremers, 2007). Most studies, however, have been shorter such as one which directly compared alendronate and risedronate and followed urinary excretion of both BPs for a period of 4 weeks (Phipps et al., 2004). This study, which was originally planned as a 1 year study but for which only the 4 weeks results have been published, suggests that both short-term skeleton retention, as well as after 4 weeks, might be lower for risedronate than for alendronate. A fairly recent study comparing long-term excretion between BPs in $n = 43$ women previously treated for more than 4 years with either alendronate or risedronate showed that alendronate could be detected in the urine of some of the patients for more than a year after stopping treatment, whereas risedronate could not be detected even after 5 months after discontinuation of therapy (Peris et al., 2011). In more detail however, with a median time of discontinuation of 14 months for both groups alendronate was detected in $n = 15$ patients out of the $n = 36$ patients the alendronate group consisted of. Risedronate could not be detected in any of the $n = 7$ patients that the risedronate group consisted of (Peris et al., 2011). This data suggests differences in the elimination of alendronate and risedronate. However, it might also be the result of significantly differences in patient numbers between alendronate and risedronate users, a higher dose of alendronate versus risedronate for a period of more than 4 years prior to stop of treatment, as well as a more sensitive assay used in this study to quantify alendronate. The study might therefore also illustrate the potential influence of study design and methodologies on pharmacokinetic data reported in the literature (Cremers et al., 2005b).

Mathematical pharmacokinetic (PK) and pharmacokinetic-pharmacodynamic (PK-PD) models of BPs

PK of BPs can be described using compartmental mathematical models, the complexity of which is determined both by the drug modeled but also by available data (Riggs and Cremers, 2019; Cremers et al., 2005b). More extensive PK results for some BPs enable both short- and long-term PK models to be developed (Skerjanec et al., 2003; Chen et al., 2002; Cremers et al., 2002; Sedghizadeh et al., 2013). For other BPs, where such data were not available, simpler (e.g., kinetic) models have been developed and validated, although these latter models only describe the amount of BP delivered to the skeleton (Pillai et al., 2004). The common denominator in most of these models is typically the ability to describe the amount or concentration of BPs in the skeleton, which places these models in a good position to link them to mathematical pharmacodynamic (PD) models in a manner that is mechanism-based and results in so-called PK-PD and K-PD models.

A full integration of the PK and the PD of BPs comes from efforts to synthesize all available in vitro and in vivo experimental data, as well as all clinical studies. Various BP dosing regimens and their effects have been explored in several species as well as in humans across different disease states. Most of the effects observed in patients can be at least partially explained by accounting for a number of factors including the underlying disease, extent of the disease, disease progression, co-medication(s), mode of BP administration, dosing regimen, BP binding affinity and potency, pretreatment rate of bone turnover, bone turnover markers (BTMs), bone mineral density (BMD), fracture risk and renal function (Cremers et al., 2019). Many of these observations have been captured using mechanism-based mathematical models that simultaneously describe PK and PD of the BPs, with PD either restricted to bone resorption markers or expanded to include BTMs, BMD and fracture risk. Some models have also included the effects of co-medications such as calcium and vitamin D supplementation on BTMs, BMD and fracture risk, while other models have incorporated renal function (affecting both PK and PD) and disease progression (Pillai et al., 2004; Cremers et al., 2005b; Post et al., 2010; Berkhout et al., 2016; Schmidt et al., 2011; Peterson and Riggs, 2010, 2012; Riggs et al., 2012; Eudy-Byrne et al., 2017). To our knowledge, there exist no PK or PK-PD models focused on indications extrinsic to the skeleton.

Applications of the clinical and translational pharmacology of BPs

A major application of the clinical and translational pharmacology of BPs has been, and continues to be, the identification of optimal dosing regimens. Pharmacologic approaches have been used to identify optimal dosing regimens for first in human (FIH) studies, for phase 2 and 3 studies, and for modifications to dosing regimens after regulatory approval. To date, the PD markers of choice which have been used to address these challenges have been BTMs and BMD, which can provide helpful information during virtually all phases of drug development, and which subsequently often also are incorporated into the aforementioned mathematical PK/PD models used to simulate what happens to these markers across various dosing regimens (Cremers and Garnero, 2006; Leeming et al., 2006). For example, mathematical PK/PD models have been used to determine the oral monthly dosing regimen for ibandronate via simulations which found that changing from a dosing regimen of 2.5 mg daily to 150 mg monthly would result in a similar suppression of bone resorption (Fig. 72.5) (Zaidi et al., 2006). Likewise, a mathematical PK/PD model was earlier used to estimate the potential effects of

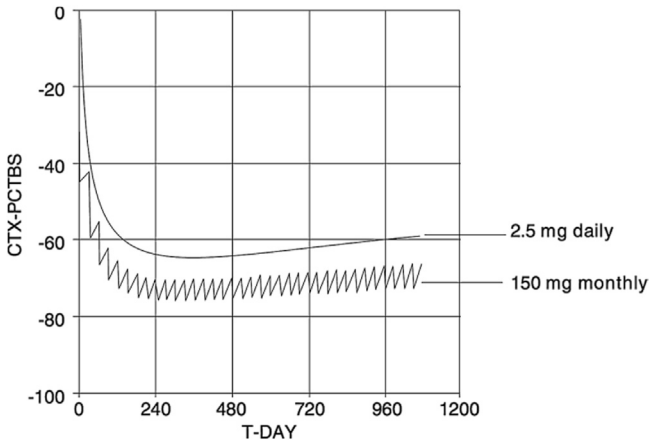

FIGURE 72.5 Kinetic-Pharmacodynamic (K-PD) model-based simulations of the median change in CTX from baseline with oral ibandronate 2.5 mg daily versus 150 mg monthly (Zaidi et al., 2006).

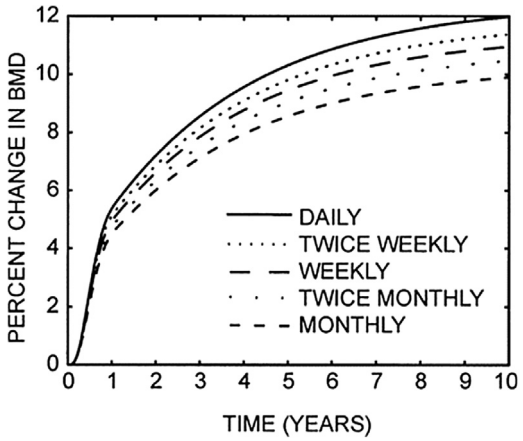

FIGURE 72.6 Model-based predicted changes in BMD in response to alendronate. Each line represents a different frequency of alendronate administration (Zaidi et al., 2006).

weekly alendronate 70 mg versus daily alendronate 10 mg on BMD changes, and contributed to the assumption that weekly administration would result in similar BMD effects as compared to daily treatment (Fig. 72.6) (Hernandez et al., 2002). Finally, a general knowledge of BP pharmacology combined with PK/PD studies and carefully derived mathematical models led to an initial dosing regimen of zoledronate 4 mg once monthly for the treatment of patients with metastatic bone disease, the subsequent exploration of a less intense dosing regimen of 4 mg every 3 months in these same patients, and an annual dose of zoledronate 5 mg in patients with osteoporosis (Berenson et al, 2001a, 2001b; Berenson, 2001; Reid et al., 2002).

Both mathematical PK/PD models and a deep understanding of the translational and clinical pharmacology of BPs have been instrumental in introducing so-called BP 'holidays' for patients provided with several years of continuous treatment with these drugs. Temporarily BP stoppage is mainly considered due to concerns for an increased risk of serious side effects such as atypical femur fractures and osteonecrosis of the jaw which might reflect over-suppression of bone turnover due to skeletal accumulation in the setting of prolonged BP treatment. A combination of bone resorption markers and BMD, two of the clinical PD markers for BPs, are typically used to monitor for the continued effects of BPs during these holidays. Collectively, these surrogate markers signal when the skeletal BP effects are waning and treatment may be reinstated. Interestingly, our knowledge of BP pharmacology explains why the effects of BPs are so protracted (especially when compared with other antiresorptive agents such as denosumab or cathepsin K inhibitors), and it may in part also explain differences in loss of the antiresorptive effect after treatment discontinuation for alendronate, risedronate, and ibandronate. In a head-to-head study which compared the effect of stopping alendronate, risedronate or ibandronate, BTM levels increased for all three BPs after treatment withdrawal, but remained below the pre-treatment baseline values with less BTM suppression in the risedronate group as compared to the alendronate and ibandronate groups up to 48 weeks after treatment cessation (Naylor et al., 2018). The only head-to-head study comparing the PK of BPs in humans used accelerator mass spectrometry to demonstrate that after IV administration, WBR of risedronate was less than that of alendronate [51.0% versus 55.5%, respectively after 24 h; 33.8% versus 44.9%, respectively after 4 weeks] (Phipps et al., 2004). This difference in retention might explain the difference in loss of the antiresorptive effect between alendronate and risedronate, despite the relatively small differences in both WBR and BTM levels. Interestingly, BMD changes evaluated 96 weeks after alendronate, risedronate or ibandronate discontinuation were the same (Naylor et al., 2018), which may reflect some of the other effects of BPs on bone such as their effects on osteocytes. Collectively, differences between BPs related to their effects on osteocytes, penetration into the canalicular network, FPP synthase inhibition potency, inhibition of osteoclast-mediated bone resorption, and skeletal retention, might also all contribute to the intriguing observation that risedronate 5 mg daily (or 35 mg weekly) and alendronate 10 mg daily (or 70 mg weekly) exhibit similar anti-fracture activity despite alendronate reducing biochemical BTMs to a greater extent than risedronate (Rosen et al., 2005).

The combination of BTMs and BMD has also been informative for so-called bridging trials, phase 2 studies designed to gain regulatory approval for comparable indications, i.e., seeking approval for glucocorticoid-induced osteoporosis based on BTM and BMD data if the BP has received previous approval for the treatment of postmenopausal osteoporosis. Drugs may be approved when similar effects on these PD parameters are observed in such studies (Kehoe et al., 2018). To our knowledge, there have been no full PK/PD studies of BPs conducted to support such bridging trial-based approvals. It is

therefore assumed that PK of the BPs, and PK/PD relationships are similar across these comparable but different patient populations.

BTMs, combined with BMD have also been very informative in studies which have examined treatment with BPs in combination with PTH derivatives. Thus, studies have examined BPs provided either continuously, prior to, or subsequent to intermittent PTH, either with or without intervening drug holidays (Cosman et al., 2017). While PK and PK/PD models exist for both BPs and for intermittent PTH (Tay et al., 2018), to our knowledge these models have not been used to predict the effects when these two classes of drugs are combined.

More recently, a renewed interest has emerged for the use of BPs to target other drugs, such as antibiotics and chemotherapeutics, to the skeleton via conjugation to BPs (Farrell et al., 2018; Sedghizadeh et al., 2017; Wang et al., 2018). The development of new chemical linkers now ensures that the active drugs are only released from the conjugates after reaching the bone. A challenge for the most efficacious use of these compounds lies in identifying optimal dosing regimens in both preclinical models and in patients. Knowledge of the PK and PD of BPs and the other compounds will be essential for approaches to resolve these issues.

Finally, in terms of the aforementioned new potential indications for BPs, PD models have been used to study BP effects in vitro. As noted previously, however, because traditional mathematical PK models for BPs have focused on assessing skeletal concentrations of BPs, they may be less useful for many of these new indications, the pathogeneses of which frequently lie outside the skeleton. Efforts to develop BPs for most of these new indications are currently preclinical, but will ultimately require the ability to quantify and simulate BP concentrations in brain, the GI tract, tumors, and other tissues, as well as their effects. We therefore anticipate that the translational and clinical pharmacology of BPs will need to look beyond the skeleton in the very near future.

Conclusions

Studies in the 1960s on the role of inorganic pyrophosphate (PPi) in controlling biological mineralization led to the search for stable PPi analogues. Studies with BPs showed that they also had effects on biological mineralization but had the added advantages that they were more stable and could be administered to animals orally without degradation. One of the early and somewhat unexpected observations was that BPs could also inhibit mineral dissolution and block bone resorption both in vitro and in living animals. This led rapidly to their clinical use. This began with the use of BPs as bone scanning agents and mineralization inhibitors, and then as resorption inhibitors in a variety of clinical disorders. Over the ensuing 50 years, the BPs have become established as leading drugs for the treatment of skeletal disorders characterized by increased bone resorption. BPs were first used in Paget's disease of bone and hypercalcemia of malignancy, and later to control skeletal-related-events associated with bone metastases and myeloma. When bone densitometry was developed and trials of sufficient size were conducted to demonstrate their remarkable efficacy in reducing fractures in patients with osteoporosis, several BPs were approved for osteoporosis on a world-wide basis.

There has been a vast amount of work done on BPs, with nearly 28,000 publications in PubMed alone. Much is now known about their biochemical actions within cells. A key intriguing discovery was that N-containing BPs appear to be specific inhibitors of enzymes in the mevalonate pathway of cholesterol biosynthesis, inhibition of which leads to interference with protein prenylation and intracellular signaling. Innovation continues to occur with new compounds and new applications. The safety and efficacy of this class of drugs ensure their continued use in clinical medicine, and potential extension to other applications for skeletal and non-skeletal conditions.

References

Abtahi, J., Tengvall, P., Aspenberg, P., 2012. A bisphosphonate-coating improves the fixation of metal implants in human bone. A randomized trial of dental implants. Bone 50, 1148−1151. https://doi.org/10.1016/j.bone.2012.02.001.

Anastasilakis, A.D., et al., 2012. Acute phase response following intravenous zoledronate in postmenopausal women with low bone mass. Bone 50, 1130−1134. https://doi.org/10.1016/j.bone.2012.02.006.

Azuma, Y., et al., 1995. Alendronate distributed on bone surfaces inhibits osteoclastic bone resorption in vitro and in experimental hypercalcemia models. Bone 16, 235−245.

Back, D.A., et al., 2012. Effect of local zoledronate on implant osseointegration in a rat model. BMC Musculoskelet Disord. 13, 42. https://doi.org/10.1186/1471-2474-13-42.

Beigel, A.E., Rienhoff, E., Olbricht, C.J., 1995. Removal of clodronate by haemodialysis in end-stage renal disease patients. Nephrol. Dial. Transplant. 10, 2266−2268.

Bellido, T., Plotkin, L.I., 2011. Novel actions of bisphosphonates in bone: preservation of osteoblast and osteocyte viability. Bone 49, 50−55. https://doi.org/10.1016/j.bone.2010.08.008.

Berenson, J.R., 2001. Zoledronic acid in cancer patients with bone metastases: results of Phase I and II trials. Semin. Oncol. 28, 25–34.
Berenson, J.R., et al., 1997. Pharmacokinetics of pamidronate disodium in patients with cancer with normal or impaired renal function. J. Clin. Pharmacol. 37, 285–290.
Berenson, J.R., et al., 2001. A Phase I, open label, dose ranging trial of intravenous bolus zoledronic acid, a novel bisphosphonate, in cancer patients with metastatic bone disease. Cancer 91, 144–154.
Berenson, J.R., et al., 2001. A phase I dose-ranging trial of monthly infusions of zoledronic acid for the treatment of osteolytic bone metastases. Clin. Cancer Res. 7, 478–485.
Bergner, R., Dill, K., Boerner, D., Uppenkamp, M., 2002. Elimination of intravenously administered ibandronate in patients on haemodialysis: a monocentre open study. Nephrol. Dial. Transplant. 17, 1281–1285.
Bergner, R., et al., 2007. Renal safety and pharmacokinetics of ibandronate in multiple myeloma patients with or without impaired renal function. J. Clin. Pharmacol. 47, 942–950. https://doi.org/10.1177/0091270007301801.
Berkhout, J., Stone, J.A., Verhamme, K.M., Danhof, M., Post, T.M., 2016. Disease systems analysis of bone mineral density and bone turnover markers in response to alendronate, placebo, and washout in postmenopausal women. CPT Pharmacometrics Syst. Pharmacol. 5, 656–664. https://doi.org/10.1002/psp4.12135.
Bingham 3rd, C.O., et al., 2006. Risedronate decreases biochemical markers of cartilage degradation but does not decrease symptoms or slow radiographic progression in patients with medial compartment osteoarthritis of the knee: results of the two-year multinational knee osteoarthritis structural arthritis study. Arthritis Rheum. 54, 3494–3507. https://doi.org/10.1002/art.22160.
Boissier, S., et al., 2000. Bisphosphonates inhibit breast and prostate carcinoma cell invasion, an early event in the formation of bone metastases. Cancer Research 60, 2949–2954.
Booth, B.P.R., Ibrahim, A., Scher, N., Williams, G., Schran, H., Ma, P., Hsu, C., Gobburu, J.V., 2003. In: Annual Meeting of the American Society for Clinical Pharmacology and Therapeutics, vol. 73. Clinical Pharmacology and Therapeutics, Washington D.C., p. 67
Bultink, I.E., Lems, W.F., 2013. Osteoarthritis and osteoporosis: what is the overlap? Curr. Rheumatol. Rep. 15, 328. https://doi.org/10.1007/s11926-013-0328-0.
Buttazzoni, M., et al., 2006. Elimination and clearance of pamidronate by haemodialysis. Nephrology 11, 197–200. https://doi.org/10.1111/j.1440-1797.2006.00569.x.
Chen, T., et al., 2002. Pharmacokinetics and pharmacodynamics of zoledronic acid in cancer patients with bone metastases. J. Clin. Pharmacol. 42, 1228–1236.
Cheng, L., et al., 2018. Zoledronate dysregulates fatty acid metabolism in renal tubular epithelial cells to induce nephrotoxicity. Arch. Toxicol. 92, 469–485. https://doi.org/10.1007/s00204-017-2048-0.
Chukir, T., Liu, Y., Farooki, A., 2018. Antiresorptive agents' bone-protective and adjuvant effects in postmenopausal women with early breast cancer. Br. J. Clin. Pharmacol. https://doi.org/10.1111/bcp.13834.
Coleman, R., et al., 2014. Adjuvant zoledronic acid in patients with early breast cancer: final efficacy analysis of the AZURE (BIG 01/04) randomised open-label phase 3 trial. Lancet Oncol. 15, 997–1006. https://doi.org/10.1016/S1470-2045(14)70302-X.
Cosman, F., Nieves, J.W., Dempster, D.W., 2017. Treatment sequence matters: anabolic and antiresorptive therapy for osteoporosis. J. Bone Miner. Res. 32, 198–202. https://doi.org/10.1002/jbmr.3051.
Coxon, F.P.T., Hughes, A., Ebetino, F.H., Rogers, M.J., 2005. In: Resorbing Osteoclasts Increase the Availability of Mineral-Bound Bisphosphonates to Non-resorbing Cells ASBMR Meeting, vol. 2005. Poster.
Coxon, F.P., Thompson, K., Roelofs, A.J., Ebetino, F.H., Rogers, M.J., 2008. Visualizing mineral binding and uptake of bisphosphonate by osteoclasts and non-resorbing cells. Bone 42, 848–860. https://doi.org/10.1016/j.bone.2007.12.225.
Cozin, M., et al., 2011. Novel therapy to reverse the cellular effects of bisphosphonates on primary human oral fibroblasts. J. Oral Maxillofac. Surg. 69, 2564–2578. https://doi.org/10.1016/j.joms.2011.03.005.
Cremers, S., Garnero, P., 2006. Biochemical markers of bone turnover in the clinical development of drugs for osteoporosis and metastatic bone disease: potential uses and pitfalls. Drugs 66, 2031–2058. https://doi.org/10.2165/00003495-200666160-00001.
Cremers, S., et al., 2002. A pharmacokinetic and pharmacodynamic model for intravenous bisphosphonate (pamidronate) in osteoporosis. Eur. J. Clin. Pharmacol. 57, 883–890.
Cremers, S.C., et al., 2003. Relationships between pharmacokinetics and rate of bone turnover after intravenous bisphosphonate (olpadronate) in patients with Paget's disease of bone. J. Bone Miner. Res. 18, 868–875. https://doi.org/10.1359/jbmr.2003.18.5.868.
Cremers, S.C., et al., 2005a. Skeletal retention of bisphosphonate (pamidronate) and its relation to the rate of bone resorption in patients with breast cancer and bone metastases. J. Bone Miner. Res. 20, 1543–1547. https://doi.org/10.1359/JBMR.050522.
Cremers, S.C., Pillai, G., Papapoulos, S.E., 2005b. Pharmacokinetics/pharmacodynamics of bisphosphonates: use for optimisation of intermittent therapy for osteoporosis. Clin. Pharmacokinet. 44, 551–570. https://doi.org/10.2165/00003088-200544060-00001.
Cremers, S., Drake, M.T., Ebetino, F.H., Bilezikian, J.P., Russell, R.G.G., 2019. Pharmacology of bisphosphonates. Br. J. Clin. Pharmacol. https://doi.org/10.1111/bcp.13867.
Croucher, P.I., McDonald, M.M., Martin, T.J., 2016. Bone metastasis: the importance of the neighbourhood. Nat. Rev. Canc. 16, 373–386. https://doi.org/10.1038/nrc.2016.44.
Dionisio, M.R., et al., 2019. Clinical and translational pharmacology of drugs for the prevention and treatment of bone metastases and cancer-induced bone loss. Br. J. Clin. Pharmacol. https://doi.org/10.1111/bcp.13852.

Dunford, J.E., et al., 2008. Structure-activity relationships among the nitrogen containing bisphosphonates in clinical use and other analogues: time-dependent inhibition of human farnesyl pyrophosphate synthase. J. Med. Chem. 51, 2187–2195. https://doi.org/10.1021/jm7015733.

Ebetino, F.H., et al., 2011. The relationship between the chemistry and biological activity of the bisphosphonates. Bone 49, 20–33. https://doi.org/10.1016/j.bone.2011.03.774.

Ebetino, F.H., et al., 2018. Prevention of zoledronate-induced MRONJ with Indocyanine Green labeled bisphosphonates in a mouse model. J. Bone Miner. Res. 32, S116.

Eriksen, E.F., 2015. Treatment of bone marrow lesions (bone marrow edema). Bone Rep. 4, 755. https://doi.org/10.1038/bonekey.2015.124.

Eudy-Byrne, R.J., Gillespie, W., Riggs, M.M., Gastonguay, M.R., 2017. A model of fracture risk used to examine the link between bone mineral density and the impact of different therapeutic mechanisms on fracture outcomes in patients with osteoporosis. J. Pharmacokinet. Pharmacodyn. 44, 599–609. https://doi.org/10.1007/s10928-017-9551-z.

Farrell, K.B., Karpeisky, A., Thamm, D.H., Zinnen, S., 2018. Bisphosphonate conjugation for bone specific drug targeting. Bone Rep. 9, 47–60. https://doi.org/10.1016/j.bonr.2018.06.007.

Fleisch, H., 2000. Bisphosphonates in Bone Disease : From the Laboratory to the Patient, fourth ed. Academic.

Fleisch, H., Russell, R.G., Francis, M.D., 1969. Diphosphonates inhibit hydroxyapatite dissolution in vitro and bone resorption in tissue culture and in vivo. Science 165, 1262–1264.

Fleisch, H., Russell, R.G., Simpson, B., Muhlbauer, R.C., 1969. Prevention by a diphosphonate of immobilization "osteoporosis" in rats. Nature 223, 211–212.

Fogelman, I., et al., 1978. The use of whole-body retention of Tc-99m diphosphonate in the diagnosis of metabolic bone disease. J. Nucl. Med. 19, 270–275.

Fragni, M., et al., 2016. The miR-21/PTEN/Akt signaling pathway is involved in the anti-tumoral effects of zoledronic acid in human breast cancer cell lines. N. Schmied. Arch. Pharmacol. 389, 529–538. https://doi.org/10.1007/s00210-016-1224-8.

Francis, M.D., Russell, R.G., Fleisch, H., 1969. Diphosphonates inhibit formation of calcium phosphate crystals in vitro and pathological calcification in vivo. Science 165, 1264–1266.

Frith, J.C., Monkkonen, J., Auriola, S., Monkkonen, H., Rogers, M.J., 2001. The molecular mechanism of action of the antiresorptive and antiinflammatory drug clodronate: evidence for the formation in vivo of a metabolite that inhibits bone resorption and causes osteoclast and macrophage apoptosis. Arthritis Rheum. 44, 2201–2210.

Fu, S.H., Wang, C.Y., Yang, R.S., Wu, F.L., Hsiao, F.Y., 2017. Bisphosphonate use and the risk of undergoing total knee arthroplasty in osteoporotic patients with osteoarthritis: a nationwide cohort study in taiwan. J. Bone Jt. Surg. 99, 938–946. https://doi.org/10.2106/JBJS.16.00385. American volume.

Gertz, B.J., et al., 1995. Studies of the oral bioavailability of alendronate. Clin. Pharmacol. Ther. 58, 288–298. https://doi.org/10.1016/0009-9236(95)90245-7.

Ghosh, S., et al., 2004. Effects of bisphosphonates on the growth of Entamoeba histolytica and Plasmodium species in vitro and in vivo. J. Med. Chem. 47, 175–187. https://doi.org/10.1021/jm030084x.

Gordon, L.B., et al., 2014. Impact of farnesylation inhibitors on survival in Hutchinson-Gilford progeria syndrome. Circulation 130, 27–34. https://doi.org/10.1161/CIRCULATIONAHA.113.008285.

Guerado, E., Caso, E., 2016. The physiopathology of avascular necrosis of the femoral head: an update. Injury 47 (Suppl. 6), S16–S26. https://doi.org/10.1016/S0020-1383(16)30835-X.

Guimaraes, M.B., Bueno, R.S., Blaya, M.B., Shinkai, R.S., Marques, L.M., 2015. Influence of the local application of sodium alendronate gel on osseointegration of titanium implants. Int. J. Oral Maxillofac. Surg. 44, 1423–1429. https://doi.org/10.1016/j.ijom.2015.05.013.

Hegde, V., Jo, J.E., Andreopoulou, P., Lane, J.M., 2016. Effect of osteoporosis medications on fracture healing. Osteoporos. Int. 27, 861–871. https://doi.org/10.1007/s00198-015-3331-7.

Hernandez, C.J., Beaupre, G.S., Marcus, R., Carter, D.R., 2002. Long-term predictions of the therapeutic equivalence of daily and less than daily alendronate dosing. J. Bone Miner. Res. 17, 1662–1666. https://doi.org/10.1359/jbmr.2002.17.9.1662.

Hodgins, N.O., Wang, J.T., Al-Jamal, K.T., 2017. Nano-technology based carriers for nitrogen-containing bisphosphonates delivery as sensitisers of gammadelta T cells for anticancer immunotherapy. Adv. Drug Deliv. Rev. 114, 143–160. https://doi.org/10.1016/j.addr.2017.07.003.

Hokugo, A., et al., 2016. Competitive equilibrium-based displacement of bisphosphonates for the prevention of BRONJ. J. Bone Miner. Res. 31, S105.

Hokugo, A., et al., 2017. Prevention of zoledronate-induced MRONJ in a mouse model of Bisphosphonate Displacement (BPD) prophylaxis therapy. J. Bone Miner. Res. 32, S116.

Hokugo, A., et al., 2019. Preventing bisphosphonate-related osteonecrosis of the jaw (ONJ) by competitive equilibrium-based bisphosphonate displacement. Bone (in press).

Jagdev, S.P., Coleman, R.E., Shipman, C.M., Rostami, H.A., Croucher, P.I., 2001. The bisphosphonate, zoledronic acid, induces apoptosis of breast cancer cells: evidence for synergy with paclitaxel. Br. J. Canc. 84, 1126–1134. https://doi.org/10.1054/bjoc.2001.1727.

Jamal, S.A., et al., 2007. Alendronate treatment in women with normal to severely impaired renal function: an analysis of the fracture intervention trial. J. Bone Miner. Res. 22, 503–508. https://doi.org/10.1359/jbmr.070112.

Jamil, K., et al., 2017. Protocol for a randomised control trial of bisphosphonate (zoledronic acid) treatment in childhood femoral head avascular necrosis due to Perthes disease. BMJ Paediatr. Open 1, e000084. https://doi.org/10.1136/bmjpo-2017-000084.

Kates, S.L., Ackert-Bicknell, C.L., 2016. How do bisphosphonates affect fracture healing? Injury 47 (Suppl. 1), S65–S68. https://doi.org/10.1016/S0020-1383(16)30015-8.

Kavanagh, K.L., et al., 2006. The molecular mechanism of nitrogen-containing bisphosphonates as antiosteoporosis drugs. Proc. Natl. Acad. Sci. U.S.A. 103, 7829–7834. https://doi.org/10.1073/pnas.0601643103.

Kehoe, T., Blind, E., Janssen, H., 2018. Regulatory aspects of the development of drugs for metabolic bone diseases - FDA and EMA perspective. Br. J. Clin. Pharmacol. https://doi.org/10.1111/bcp.13791.

Khan, S.A., et al., 1997. Elimination and biochemical responses to intravenous alendronate in postmenopausal osteoporosis. J. Bone Miner. Res. 12, 1700–1707. https://doi.org/10.1359/jbmr.1997.12.10.1700.

Kunzmann, V., et al., 2000. Stimulation of gammadelta T cells by aminobisphosphonates and induction of antiplasma cell activity in multiple myeloma. Blood 96, 384–392.

Landesberg, R., et al., 2011. Potential pathophysiological mechanisms in osteonecrosis of the jaw. Ann. N. Y. Acad. Sci. 1218, 62–79. https://doi.org/10.1111/j.1749-6632.2010.05835.x.

Lawson, M.A., et al., 2017. The pharmacological profile of a novel highly potent bisphosphonate, OX14 (1-Fluoro-2-(Imidazo-[1,2-alpha]Pyridin-3-yl)-Ethyl-Bisphosphonate). J. Bone Miner. Res. 32, 1860–1869. https://doi.org/10.1002/jbmr.3138.

Leeming, D.J., et al., 2006. An update on biomarkers of bone turnover and their utility in biomedical research and clinical practice. Eur. J. Clin. Pharmacol. 62, 781–792. https://doi.org/10.1007/s00228-006-0174-3.

Lehenkari, P.P., et al., 2002. Further insight into mechanism of action of clodronate: inhibition of mitochondrial ADP/ATP translocase by a non-hydrolyzable, adenine-containing metabolite. Mol. Pharmacol. 61, 1255–1262.

Lems, W.F., 2018. Bisphosphonates: a therapeutic option for knee osteoarthritis? Ann. Rheum. Dis. 77, 1247–1248. https://doi.org/10.1136/annrheumdis-2017-212364.

Li, Q., Kingman, J., Sundberg, J.P., Levine, M.A., Uitto, J., 2018. Etidronate prevents, but does not reverse, ectopic mineralization in a mouse model of pseudoxanthoma elasticum (Abcc6(-/-)). Oncotarget 9, 30721–30730. https://doi.org/10.18632/oncotarget.10738.

Lin, J.H., 1996. Bisphosphonates: a review of their pharmacokinetic properties. Bone 18, 75–85.

Loeb, J.A., Sohrab, S.A., Huq, M., Fuerst, D.R., 2006. Brain calcifications induce neurological dysfunction that can be reversed by a bone drug. J. Neurol. Sci. 243, 77–81. https://doi.org/10.1016/j.jns.2005.11.033.

Luckman, S.P., et al., 1998. Nitrogen-containing bisphosphonates inhibit the mevalonate pathway and prevent post-translational prenylation of GTP-binding proteins, including Ras. J. Bone Miner. Res. 13, 581–589. https://doi.org/10.1359/jbmr.1998.13.4.581.

Luedders, D.W., Steinhoff, J., Thill, M., Rody, A., Bohlmann, M.K., 2015. Lack of difference in acute nephrotoxicity of intravenous bisphosphonates zoledronic acid and ibandronate in women with breast cancer and bone metastases. Anticancer Res. 35, 1797–1802.

Luhe, A., et al., 2008. Preclinical evidence for nitrogen-containing bisphosphonate inhibition of farnesyl diphosphate (FPP) synthase in the kidney: implications for renal safety. Toxicol. Vitro 22, 899–909. https://doi.org/10.1016/j.tiv.2008.01.006.

Marolt, D., Cozin, M., Vunjak-Novakovic, G., Cremers, S., Landesberg, R., 2012. Effects of pamidronate on human alveolar osteoblasts in vitro. J. Oral Maxillofac. Surg. 70, 1081–1092. https://doi.org/10.1016/j.joms.2011.05.002.

Martin, M.B., et al., 2001. Bisphosphonates inhibit the growth of Trypanosoma brucei, Trypanosoma cruzi, Leishmania donovani, Toxoplasma gondii, and Plasmodium falciparum: a potential route to chemotherapy. J. Med. Chem. 44, 909–916.

Masarachia, P., Weinreb, M., Balena, R., Rodan, G.A., 1996. Comparison of the distribution of 3H-alendronate and 3H-etidronate in rat and mouse bones. Bone 19, 281–290.

Mathew, A., Brufsky, A., 2015. Bisphosphonates in breast cancer. Int. J. Cancer 137, 753–764. https://doi.org/10.1002/ijc.28965.

McClung, M.R., et al., 2012. Efficacy and safety of a novel delayed-release risedronate 35 mg once-a-week tablet. Osteoporos. Int. 23, 267–276. https://doi.org/10.1007/s00198-011-1791-y.

Mendes, V., Dos Santos, G.O., Calasans-Maia, M.D., Granjeiro, J.M., Moraschini, V., 2018. Impact of bisphosphonate therapy on dental implant outcomes: an overview of systematic review evidence. Int. J. Oral Maxillofac. Surg. https://doi.org/10.1016/j.ijom.2018.09.006.

Meraw, S.J., Reeve, C.M., 1999. Qualitative analysis of peripheral peri-implant bone and influence of alendronate sodium on early bone regeneration. J. Periodontol. 70, 1228–1233. https://doi.org/10.1902/jop.1999.70.10.1228.

Miller, P.D., 2007. Is there a role for bisphosphonates in chronic kidney disease? Semin. Dial. 20, 186–190. https://doi.org/10.1111/j.1525-139X.2007.00271.x.

Miller, P.D., et al., 2005. Safety and efficacy of risedronate in patients with age-related reduced renal function as estimated by the Cockcroft and Gault method: a pooled analysis of nine clinical trials. J. Bone Miner. Res. 20, 2105–2115. https://doi.org/10.1359/JBMR.050817.

Misra, J., et al., 2016. Zoledronate attenuates accumulation of DNA damage in mesenchymal stem cells and protects their function. Stem Cell. 34, 756–767. https://doi.org/10.1002/stem.2255.

Molvik, H., Khan, W., 2015. Bisphosphonates and their influence on fracture healing: a systematic review. Osteoporos. Int. 26, 1251–1260. https://doi.org/10.1007/s00198-014-3007-8.

Montalvetti, A., et al., 2001. Bisphosphonates are potent inhibitors of Trypanosoma cruzi farnesyl pyrophosphate synthase. J. Biol. Chem. 276, 33930–33937. https://doi.org/10.1074/jbc.M103950200.

Nagano, Y., et al., 2012. Bisphosphonate-induced gastrointestinal mucosal injury is mediated by mitochondrial superoxide production and lipid peroxidation. J. Clin. Biochem. Nutr. 51, 196–203. https://doi.org/10.3164/jcbn.12-41.

Nancollas, G.H., et al., 2006. Novel insights into actions of bisphosphonates on bone: differences in interactions with hydroxyapatite. Bone 38, 617–627. https://doi.org/10.1016/j.bone.2005.05.003.

Naylor, K.E., et al., 2018. Effects of discontinuing oral bisphosphonate treatments for postmenopausal osteoporosis on bone turnover markers and bone density. Osteoporos. Int. 29, 1407–1417. https://doi.org/10.1007/s00198-018-4460-6.

Neogi, T., Li, S., Peloquin, C., Misra, D., Zhang, Y., 2018. Effect of bisphosphonates on knee replacement surgery. Ann. Rheum. Dis. 77, 92−97. https://doi.org/10.1136/annrheumdis-2017-211811.

Oliveira, J.R., Oliveira, M.F., 2016. Primary brain calcification in patients undergoing treatment with the biphosphanate alendronate. Sci. Rep. 6, 22961. https://doi.org/10.1038/srep22961.

Papapoulos, S.E., Cremers, S.C., 2007. Prolonged bisphosphonate release after treatment in children. N. Engl. J. Med. 356, 1075−1076. https://doi.org/10.1056/NEJMc062792.

Perazella, M.A., Markowitz, G.S., 2008. Bisphosphonate nephrotoxicity. Kidney International 74, 1385−1393. https://doi.org/10.1038/ki.2008.356.

Peris, P., et al., 2011. Prolonged bisphosphonate release after treatment in women with osteoporosis. Relationship with bone turnover. Bone 49, 706−709. https://doi.org/10.1016/j.bone.2011.06.027.

Peterson, M.C., Riggs, M.M., 2010. A physiologically based mathematical model of integrated calcium homeostasis and bone remodeling. Bone 46, 49−63. https://doi.org/10.1016/j.bone.2009.08.053.

Peterson, M.C., Riggs, M.M., 2012. Predicting nonlinear changes in bone mineral density over time using a multiscale systems pharmacology model. CPT Pharmacometrics Syst. Pharmacol. 1, e14. https://doi.org/10.1038/psp.2012.15.

Phipps, R.J., et al., 2004. Head-to-Head comparison of risedronate and alendronate pharmacokinetics in clinical doses. Bone 34, S81−S82.

Pillai, G., et al., 2004. A semimechanistic and mechanistic population PK-PD model for biomarker response to ibandronate, a new bisphosphonate for the treatment of osteoporosis. Br. J. Clin. Pharmacol. 58, 618−631. https://doi.org/10.1111/j.1365-2125.2004.02224.x.

Post, T.M., Cremers, S.C., Kerbusch, T., Danhof, M., 2010. Bone physiology, disease and treatment: towards disease system analysis in osteoporosis. Clin. Pharmacokinet. 49, 89−118. https://doi.org/10.2165/11318150-000000000-00000.

Raikkonen, J., et al., 2009. Zoledronic acid induces formation of a pro-apoptotic ATP analogue and isopentenyl pyrophosphate in osteoclasts in vivo and in MCF-7 cells in vitro. Br. J. Pharmacol. 157, 427−435. https://doi.org/10.1111/j.1476-5381.2009.00160.x.

Ramalho-Ferreira, G., Faverani, L.P., Prado, F.B., Garcia Jr., I.R., Okamoto, R., 2015. Raloxifene enhances peri-implant bone healing in osteoporotic rats. Int. J. Oral Maxillofac. Surg. 44, 798−805. https://doi.org/10.1016/j.ijom.2015.02.018.

Reid, I.R., et al., 2002. Intravenous zoledronic acid in postmenopausal women with low bone mineral density. N. Engl. J. Med. 346, 653−661. https://doi.org/10.1056/NEJMoa011807.

Riggs, M.M., Cremers, S., 2019. Pharmacometrics and systems pharmacology for metabolic bone diseases. Br. J. Clin. Pharmacol. (in press).

Riggs, M.M., Peterson, M.C., Gastonguay, M.R., 2012. Multiscale physiology-based modeling of mineral bone disorder in patients with impaired kidney function. J. Clin. Pharmacol. 52, 45S−53S. https://doi.org/10.1177/0091270011412967.

Rodriguez, J.B., Falcone, B.N., Szajnman, S.H., 2016. Approaches for designing new potent inhibitors of farnesyl pyrophosphate synthase. Expert Opin. Drug Discov. 11, 307−320. https://doi.org/10.1517/17460441.2016.1143814.

Roelofs, A.J., et al., 2012. Influence of bone affinity on the skeletal distribution of fluorescently labeled bisphosphonates in vivo. J. Bone Miner. Res. 27, 835−847. https://doi.org/10.1002/jbmr.1543.

Rogers, M.J., 2003. New insights into the molecular mechanisms of action of bisphosphonates. Curr. Pharmaceut. Des. 9, 2643−2658.

Roman-Blas, J.A., Castaneda, S., Largo, R., Lems, W.F., Herrero-Beaumont, G., 2014. An OA phenotype may obtain major benefit from bone-acting agents. Semin. Arthritis Rheum. 43, 421−428. https://doi.org/10.1016/j.semarthrit.2013.07.012.

Rosen, C.J., et al., 2005. Treatment with once-weekly alendronate 70 mg compared with once-weekly risedronate 35 mg in women with postmenopausal osteoporosis: a randomized double-blind study. J. Bone Miner. Res. 20, 141−151. https://doi.org/10.1359/JBMR.040920.

Russell, R.G., 2011. Bisphosphonates: the first 40 years. Bone 49, 2−19. https://doi.org/10.1016/j.bone.2011.04.022.

Russell, R.G., Watts, N.B., Ebetino, F.H., Rogers, M.J., 2008. Mechanisms of action of bisphosphonates: similarities and differences and their potential influence on clinical efficacy. Osteoporos. Int. 19, 733−759. https://doi.org/10.1007/s00198-007-0540-8.

Schmidt, S., Post, T.M., Peletier, L.A., Boroujerdi, M.A., Danhof, M., 2011. Coping with time scales in disease systems analysis: application to bone remodeling. J. Pharmacokinet. Pharmacodyn. 38, 873−900. https://doi.org/10.1007/s10928-011-9224-2.

Sedghizadeh, P.P., et al., 2013. Population pharmacokinetic and pharmacodynamic modeling for assessing risk of bisphosphonate-related osteonecrosis of the jaw. Oral Surg. Oral Med. Oral Pathol. Oral. Radiol. Endod. 115, 224−232. https://doi.org/10.1016/j.oooo.2012.08.455.

Sedghizadeh, P.P., et al., 2017. Design, synthesis, and antimicrobial evaluation of a novel bone-targeting bisphosphonate-ciprofloxacin conjugate for the treatment of osteomyelitis biofilms. J. Med. Chem. 60, 2326−2343. https://doi.org/10.1021/acs.jmedchem.6b01615.

Shabestari, M., Vik, J., Reseland, J.E., Eriksen, E.F., 2016. Bone marrow lesions in hip osteoarthritis are characterized by increased bone turnover and enhanced angiogenesis. Osteoarthritis Cartil. 24, 1745−1752. https://doi.org/10.1016/j.joca.2016.05.009.

Shabestari, M., Vik, J., Reseland, J.E., Eriksen, E.F., 2017. Erratum to "Bone marrow lesions in hip osteoarthritis are characterized by increased bone turnover and enhanced angiogenesis" [Osteoarthritis Cartilage 24 (2016) 1745-1752]. Osteoarthritis Cartilage 25, 611. https://doi.org/10.1016/j.joca.2016.12.004.

Singireesu, S., Mondal, S.K., Yerramsetty, S., Misra, S., 2018. Zoledronic acid induces micronuclei formation, mitochondrial-mediated apoptosis and cytostasis in kidney cells. Life Sci. 203, 305−314. https://doi.org/10.1016/j.lfs.2018.04.059.

Skerjanec, A., et al., 2003. The pharmacokinetics and pharmacodynamics of zoledronic acid in cancer patients with varying degrees of renal function. J. Clin. Pharmacol. 43, 154−162.

Skjodt, M.K., Frost, M., Abrahamsen, B., 2018. Side effects of drugs for osteoporosis and metastatic bone disease. Br. J. Clin. Pharmacol. https://doi.org/10.1111/bcp.13759.

Spector, T.D., et al., 2005. Effect of risedronate on joint structure and symptoms of knee osteoarthritis: results of the BRISK randomized, controlled trial [ISRCTN01928173]. Arthritis Res Ther 7, R625−R633. https://doi.org/10.1186/ar1716.

Sun, S.T., et al., 2018. Prevention of zoledronate-induced MRONJ with indocyanine green (ICG) labeled bisphosphonates. J. Bone Miner. Res. 33, 22–23.

Suri, S., et al., 2001. Nitrogen-containing bisphosphonates induce apoptosis of Caco-2 cells in vitro by inhibiting the mevalonate pathway: a model of bisphosphonate-induced gastrointestinal toxicity. Bone 29, 336–343.

Tay, D., Cremers, S., Bilezikian, J.P., 2018. Optimal dosing and delivery of parathyroid hormone and its analogues for osteoporosis and hypoparathyroidism - translating the pharmacology. Br. J. Clin. Pharmacol. 84, 252–267. https://doi.org/10.1111/bcp.13455.

Tsurukami, H., 2017. Acute phase reaction following bisphosphonates. Clin. Calcium 27, 213–223. CliCa1702213223.

Twiss, I.M., Pas, O., Ramp-Koopmanschap, W., Den Hartigh, J., Vermeij, P., 1999. The effects of nitrogen-containing bisphosphonates on human epithelial (Caco-2) cells, an in vitro model for intestinal epithelium. J. Bone Miner. Res. 14, 784–791. https://doi.org/10.1359/jbmr.1999.14.5.784.

Twiss, I.M., et al., 2001. The sugar absorption test in the evaluation of the gastrointestinal intolerance to bisphosphonates: studies with oral pamidronate. Clin. Pharmacol. Ther. 69, 431–437.

Twiss, I.M., et al., 2006. A comparison of the gastrointestinal effects of the nitrogen-containing bisphosphonates pamidronate, alendronate, and olpadronate in humans. J. Clin. Pharmacol. 46, 483–487. https://doi.org/10.1177/0091270006286781.

van Beek, E., Pieterman, E., Cohen, L., Lowik, C., Papapoulos, S., 1999. Farnesyl pyrophosphate synthase is the molecular target of nitrogen-containing bisphosphonates. Biochem. Biophys. Res. Commun. 264, 108–111. https://doi.org/10.1006/bbrc.1999.1499.

van Beek, E., Pieterman, E., Cohen, L., Lowik, C., Papapoulos, S., 1999. Nitrogen-containing bisphosphonates inhibit isopentenyl pyrophosphate isomerase/farnesyl pyrophosphate synthase activity with relative potencies corresponding to their antiresorptive potencies in vitro and in vivo. Biochem. Biophys. Res. Commun. 255, 491–494. https://doi.org/10.1006/bbrc.1999.0224.

Varela, I., et al., 2008. Combined treatment with statins and aminobisphosphonates extends longevity in a mouse model of human premature aging. Nat. Med. 14, 767–772. https://doi.org/10.1038/nm1786.

Wang, H., et al., 2018. Synthesis of a bone-targeted bortezomib with in vivo anti-myeloma effects in mice. Pharmaceutics 10. https://doi.org/10.3390/pharmaceutics10030154.

Weiss, H.M., et al., 2008. Biodistribution and plasma protein binding of zoledronic acid. Drug Metab. Dispos. 36, 2043–2049. https://doi.org/10.1124/dmd.108.021071.

Wentworth, K.L., Masharani, U., Hsiao, E.C., 2018. Therapeutic advances for blocking heterotopic ossification in fibrodysplasia ossificans progressiva. Br. J. Clin. Pharmacol. https://doi.org/10.1111/bcp.13823.

Wilson, C., Ottewell, P., Coleman, R.E., Holen, I., 2015. The differential anti-tumour effects of zoledronic acid in breast cancer - evidence for a role of the activin signaling pathway. BMC Cancer 15, 55. https://doi.org/10.1186/s12885-015-1066-7.

Zaidi, M., Epstein, S., Friend, K., 2006. Modeling of serum C-telopeptide levels with daily and monthly oral ibandronate in humans. Ann. N. Y. Acad. Sci. 1068, 560–563. https://doi.org/10.1196/annals.1346.058.

Zameer, S., Najmi, A.K., Vohora, D., Akhtar, M., 2018. Bisphosphonates: future perspective for neurological disorders. Pharmacol. Rep. 70, 900–907. https://doi.org/10.1016/j.pharep.2018.03.011.

Ziniel, P.D., et al., 2013. Characterization of potential drug targets farnesyl diphosphate synthase and geranylgeranyl diphosphate synthase in Schistosoma mansoni. Antimicrob. Agents Chemother. 57, 5969–5976. https://doi.org/10.1128/AAC.00699-13.

Chapter 73

Pharmacological mechanisms of therapeutics: receptor activator of nuclear factor–kappa B ligand inhibition

Elena Tsourdi[1,2], Michael S. Ominsky[3], Tilman D. Rachner[1,2,4], Lorenz C. Hofbauer[1,2,5] and Paul J. Kostenuik[6,7]

[1]*Department of Medicine III, Technische Universität Dresden, Dresden, Germany;* [2]*Center for Healthy Aging, Technische Universität Dresden, Dresden, Germany;* [3]*Radius Health Inc., Waltham, MA, United States;* [4]*German Cancer Consortium (DKTK), Partner site Dresden and German Cancer Research Center (DKFZ), Heidelberg, Germany;* [5]*Center for Regenerative Therapies Dresden, Dresden, Germany;* [6]*Phylon Pharma Services, Newbury Park, CA, United States;* [7]*School of Dentistry, University of Michigan, Ann Arbor, MI, United States*

Chapter outline

History of osteoprotegerin/receptor activator of nuclear factor–kappa B ligand-based drug development

Before the mid-1990s, the molecular mechanisms underlying osteoclastogenesis were not well understood, and in vitro culturing of osteoclasts was technically challenging. As genetic mapping approaches progressed, parallel efforts from several commercial and academic groups began to unravel components of a key pathway that drives osteoclast formation, function, and survival. At Amgen, phenotypic screening of transgenic mice engineered to overexpress previously unknown secreted factors via the liver resulted in the discovery of osteoprotegerin (OPG) (Simonet et al., 1997). OPG, a secreted member of the TNF receptor superfamily, was identified based on increased radiographic density in OPG-overexpressing transgenic mice (Simonet et al., 1997). Histology demonstrated that OPG transgenic mice had few osteoclasts and

Principles of Bone Biology. https://doi.org/10.1016/B978-0-12-814841-9.00073-7

exhibited features reminiscent of human osteopetrosis. Subsequent experiments demonstrated that recombinant OPG inhibited osteoclast formation in vitro (Simonet et al., 1997), while genetic ablation of OPG resulted in severe osteopenia including fragility fractures (Bucay et al., 1998). Soon thereafter, independent investigators at the Snow Brand Milk Products Company reported an identical secreted protein with similar pharmacologic properties that they called osteoclast inhibitory factor (Yasuda et al., 1998).

The Amgen investigators then used OPG to find its binding partner, which OPG was presumably blocking to inhibit osteoclastogenesis. A longer-circulating recombinant form of OPG called OPG-Fc, which comprises the cysteine-rich TNF receptor-like domains of native OPG fused to the Fc portion of human IgG1, was found to bind to a molecule expressed on the surface of a myelomonocytic cell line (Lacey et al., 1998). The Amgen investigators named this molecule OPG ligand (OPGL), which they showed to be a potent promoter of osteoclast differentiation and activation (Lacey et al., 1998). Independent research by the investigators at Snow Brand Milk showed that an identical molecule, which they named osteoclast differentiation factor (ODF), stimulated osteoclastogenesis in vitro and caused hypercalcemia in vivo (Yasuda et al., 1998). Meanwhile, investigators at Immunex Corporation had identified the same "OPGL/ODF" molecule by direct sequencing of a myeloid dendritic cell cDNA library (Dougall et al., 1999; Hsu et al., 1999). They had initially identified a new member of the TNF receptor family they called "receptor activator of nuclear factor kappa B" (RANK) based on the key role of the transcription factor NF−κB in mediating its biological effects. Using an extracellular fragment of this receptor fused to Fc (RANK-Fc), they identified its binding partner via expression cloning and named this molecule RANK ligand (RANKL) (Anderson et al., 1997). The sequence of RANKL was identical to OPGL, and a nomenclature committee comprising representatives from the American Society for Bone and Mineral Research, along with esteemed advisors from the immunology field, proposed to adopt RANKL as the formal name with RANK as its receptor and OPG as the decoy receptor that binds RANKL and prevents it from activating RANK (American Society for Bone and Mineral Research President's Committee on Nomenclature, 2000; Fig. 73.1). Shortly after the Immunex group characterized roles for RANK and RANKL in T cells and dendritic cells (Anderson et al., 1997), investigators from Amgen, the Amgen Institute, and the University of Toronto demonstrated that RANKL was a critical mediator of osteoclastogenesis and that the genetic ablation of RANKL caused osteopetrosis in mice (Kong et al., 1999b). RANKL has since been demonstrated to exist in both membrane-bound and soluble forms (Ikeda et al., 2001), and soluble RANKL levels in peripheral blood and bone marrow appear to be regulatable (Abrahamsen et al., 2005; Li et al., 2009), which may allow RANKL to act in an endocrine, juxtacrine, or paracrine manner (Lacey et al., 2012).

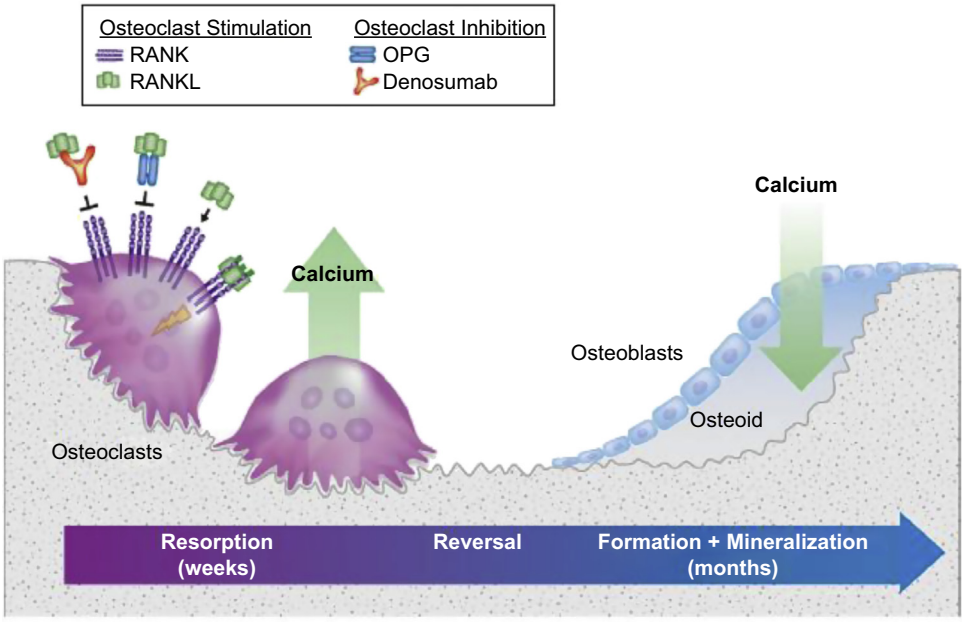

FIGURE 73.1 Role of the RANKL pathway and its inhibition on bone remodeling. Bone remodeling occurs as a coupled process of initiation of osteoclastic bone resorption followed by osteoblastic bone formation in the basic multicellular unit as shown here. Osteoclast formation, function, and survival are dependent on the binding of receptor activator of nuclear factor−kappa B ligand (RANKL) to its surface receptor (RANK). Prevention of this binding by the naturally occurring protein osteoprotegerin (OPG) and/or the engineered RANKL antibody denosumab results in the disruption of osteoclasts and their formation. This inhibition greatly reduces the rate of bone remodeling, resulting in increased bone mass. *Reproduced with Elsevier permission from Dempster et al., 2012. Clin. Ther. 34, 521−536.*

Recognizing the key and essential role of RANKL for bone resorption and bone loss, efforts were initiated to develop inhibitors of the RANK–RANKL pathway using a variety of therapeutic strategies. Investigators at Immunex developed RANK-Fc, which was an effective inhibitor of bone resorption, but preclinical studies indicated that immune responses arising against RANK-Fc had the potential to cause hypercalcemia via the activation of endogenous RANK, leading to the discontinuation of its development (Lacey et al., 2012). At Amgen, Fc-OPG was tested in Phase 1 clinical trials in postmenopausal women. Fc-OPG proved to be an effective inhibitor of bone resorption, with reductions in biochemical markers of bone resorption lasting for several weeks depending on dose (Bekker et al., 2001). In the pursuit of longer-acting versions that could be dosed less frequently for patient convenience, Amgen pivoted toward the development of OPG-Fc (AMGN-0007). OPG-Fc had a longer circulating half-life than that of Fc-OPG and also achieved more sustained reductions in bone resorption markers in subjects with breast cancer or multiple myeloma, with inhibitory effects lasting beyond the trial's 2-month endpoint (Body et al., 2003). However, concerns regarding potential anti-OPG-Fc immune responses that could also adversely affect the bioavailability of endogenous OPG led to the discontinuation of OPG-Fc development in favor of other approaches (Lacey et al., 2012). OPG-Fc remains a commonly used RANKL inhibitor in animal studies due to its ability to recognize and inhibit RANKL from various species including mice (Bonnet et al., 2016), rats (Ominsky et al., 2008), rabbits (Rodeo et al., 2007), cynomolgus monkeys (cynos) (Ominsky et al., 2007), and pigs (Sipos et al., 2011). Pharmacologic strategies were then initiated at Amgen to develop antibodies to inhibit RANKL (Lacey et al., 2012). The XenoMouse (Green, 1999) allowed the rapid generation of high-affinity, fully human monoclonal anti-RANKL antibodies including denosumab (Lacey et al., 2012). As outlined below, this RANKL-Ab strategy became the preferred therapeutic approach due to improved pharmacokinetics requiring less frequent administration compared with Fc-OPG or OPG-Fc, and the lack of potential for adverse immune-mediated perturbations of endogenous OPG or RANK activity. To date, there have been few if any cases of patients developing neutralizing immune responses against the fully human denosumab molecule, and the hypothetical impact of such a response might only involve loss of denosumab efficacy. In addition, unlike OPG, which can bind to TNF family member TRAIL, denosumab does not bind TRAIL or other TNF family members (Kostenuik et al., 2009). Beyond RANK, OPG, and antibody-based approaches to antagonize RANKL, there have been efforts to develop small-molecule (Idris et al., 2010) and peptide-based (Ta et al., 2010) approaches to inhibit RANKL. Although these modalities inhibit bone resorption in vitro and in animals, they have yet to demonstrate clinical efficacy. The section below summarizes some of the preclinical and clinical data generated during the development of the RANKL antibody denosumab.

Physiologic mechanisms and effects of receptor activator of nuclear factor–kappa B ligand inhibitors in bone

Numerous studies have examined the pharmacologic effects of RANKL inhibitors in healthy animals and in animal models of bone disease. The first such publications demonstrated that Fc-OPG and OPG-Fc inhibited RANKL-induced osteoclast formation in vitro and in vivo (Simonet et al., 1997; Lacey et al., 1998). Subsequent studies in bone disease models including rodent and nonhuman primate models of postmenopausal osteoporosis further demonstrated the impact of RANKL inhibitors on bone turnover, bone mass, bone microarchitecture, bone strength, and bone quality. Rodent studies have generally relied on recombinant RANK-Fc or OPG-based RANKL inhibitors because denosumab does not recognize mouse or rat RANKL (Kostenuik et al., 2009), though a number of pharmacology studies with denosumab were performed in nonhuman primates (Ominsky et al., 2011; Kostenuik et al., 2011, 2015) and in mice genetically engineered to express human or partially humanized RANKL (huRANKL) mice (Kostenuik et al., 2009; Rinotas et al., 2014).

The osteoclast-inhibiting effects of RANKL inhibitors are reflected in rapid decreases in biochemical markers of bone resorption followed by a delayed reduction in bone formation markers that reflects the coupled process of bone remodeling. In postmenopausal women with low bone mass, denosumab decreased bone resorption markers compared with placebo within 24 h after a single dose, and bone formation markers showed significant decreases several weeks later (Bekker et al., 2004). In growing male rats, a single injection of recombinant human OPG-Fc resulted in a significant decrease in the resorption marker serum TRACP within 48 h and a decline in the formation marker serum osteocalcin by day 10 (Capparelli et al., 2003). These inhibitory effects on bone turnover were associated with decreases in histological indices of osteoclasts and osteoblasts, effects that reversed over time as OPG-Fc concentrations diminished. Similar rapid declines in bone resorption markers were observed with OPG-Fc in OVX rats (Ominsky et al., 2008) and with denosumab in huRANKL mice (Li et al., 2009). Histomorphometry demonstrated that these changes corresponded to >95% reductions in the extent of trabecular osteoclast surfaces. Similar robust reductions in bone resorption and formation markers were reported in cynos treated with OPG-Fc (Ominsky et al., 2007) and denosumab (Ominsky et al., 2011) in association with marked

reductions in histomorphometric indices of resorption and formation at trabecular and cortical sites (Kostenuik et al., 2011).

Bone resorption and formation in adult animals occur predominantly in a coupled process known as remodeling, with resorption preceding formation as bone matrix is continually removed and replaced. Thus, the delayed reduction in bone formation indices after denosumab-mediated inhibition of bone resorption was expected, reflecting more remodeling spaces having completed their refilling with new bone matrix. In contrast, bone *modeling* represents temporally and spatially distinct mechanisms by which bone is formed or removed via uncoupled processes. Although bone modeling occurs predominantly during growth, there is evidence for continued bone modeling in adulthood. As denosumab was not thought to affect osteoblasts directly, its effects on bone modeling were investigated in OVX cynos (Ominsky et al., 2015). These results indicated that in the near absence of bone resorption and remodeling-based bone formation, modeling-based bone formation was present in the femur neck and ribs of denosumab-treated monkeys to a similar extent as that found in vehicle-treated controls. The extent of this modeling-based bone formation was small and location-dependent, but its presence and persistence over the 16-month treatment duration supported the hypothesis that bone modeling contributes to the uniquely progressive hip and femoral neck bone mineral density (BMD) gains observed in postmenopausal women receiving denosumab over a 10-year treatment period (Bone et al., 2017; Ominsky et al., 2015). In contrast, bisphosphonates do not induce incremental BMD gains at the hip or femoral neck beyond the first 3−4.5 years of therapy (Reid, 2015).

The reductions in bone turnover observed with RANKL inhibitors result in significant gains in bone mass and bone strength in various animal models. In OVX rats, 6 weeks of OPG-Fc resulted in increased in vivo DXA BMD and ex vivo bone volume by micro-CT at the lumbar vertebra and femur neck relative to OVX controls (Ominsky et al., 2008). Trabecular microarchitecture was also improved as reflected in increases in trabecular number and thickness. These improvements resulted in significant elevations in strength endpoint peak load in lumbar vertebrae and the femoral neck. Similar observations were made after 16 months of denosumab administration to OVX cynos, with denosumab-mediated gains in trabecular and cortical bone mass resulting in significantly greater peak load at the femoral neck (up to 34%), L3−L4 vertebral bodies (up to 55%), and L5−L6 cancellous cores (up to 82%) compared with OVX-Veh (Ominsky et al., 2011). In this study, microarchitectural improvements included increased cortical thickness and reduced cortical porosity as well as increased trabecular number.

Bone remodeling has long been considered by many to be essential for maintaining bone health via the removal and replacement of older bone matrix; as such, the longer-term effect of antiresorptives on bone quality has been a long-standing concern. Therefore, the demonstration that the near absence of bone turnover with up to 16 months of high-dose denosumab therapy led to gains in whole bone strength was reassuring. Linear regressions were performed to assess relationships between bone mass and bone strength variables, as such analyses were previously shown capable of identifying drug-related impairments in bone quality (Lafage et al., 1995). Regression analyses demonstrated that bone quality was maintained at the lumbar vertebra, femur neck, and femur diaphysis after 16 months of denosumab (Ominsky et al., 2011). In addition, calculated material properties from these tests, and destructive testing results for size-matched cortical samples machined from the humeral cortex, confirmed the maintenance of bone quality. A subsequent OVX cyno study verified these findings after 12 months of denosumab while also showing a lack of impaired bone quality measures with the bisphosphonate alendronate (Kostenuik et al., 2015). In addition, finite element strength estimates generated from vertebral CT images from the 16-month study strongly predicted measured bone strength, further supporting the interpretation that bone quality is maintained with denosumab (Lee et al., 2016).

Reduced bone remodeling, including that which results from RANKL inhibition, is expected to alter matrix mineralization properties primarily by affording remodeling sites more time to achieve a fuller degree of matrix mineralization. This effect often leads to a reduction in the heterogeneity of matrix mineralization distribution within the bone that some observational studies have associated with bone fragility (Lloyd et al., 2017). Aged OVX rats treated with OPG exhibited a higher average degree of matrix mineralization in femoral cancellous bone along with reduced heterogeneity of mineralization (Valenta et al., 2005), and the same femurs used for those analyses showed improved bone biomechanical properties with OPG treatment (Kostenuik et al., 2001). Vertebrae and femurs from huRANKL mice treated with denosumab or alendronate for 6 months also showed reduced heterogeneity of matrix mineralization, which was associated with improved biomechanical properties compared with vehicle-treated controls (Misof et al., 2011; Ominsky et al., 2008b). The degree of matrix mineralization in the vertebrae of OPG-treated OVX rats bore no relationship with vertebral bone strength, which was significantly increased in close association with increments in bone volume (Ominsky et al., 2008a). Increased matrix mineralization and reduced heterogeneity of mineralization is also observed in postmenopausal women treated with denosumab for up to 10 years (Dempster et al., 2018) in association with persistently reduced fracture rates (Bone et al., 2017). Together, these preclinical and clinical findings lend little support for the theory that potent inhibition

of bone turnover can impair bone biomechanics via changes in matrix mineralization parameters. Ultimately, even 5 years of denosumab therapy in postmenopausal women caused relatively modest absolute changes in matrix mineralization parameters, with no further changes between 5 and 10 years of therapy, despite extremely and persistently low remodeling rates (Dempster et al., 2018). Such findings may suggest the existence of self-regulatory mechanisms within bone that resist large excursions from biomechanically optimal matrix mineralization characteristics.

Clinical studies demonstrating the effects of denosumab (Table 73.1)

Osteoporosis indications

Postmenopausal osteoporosis

The efficacy and safety of denosumab administered as a 60 mg subcutaneous injection every 6 months was evaluated in several large clinical trials. Based on these data, described below, this regimen was approved by the FDA and EMA (trade name Prolia) for the treatment of postmenopausal women with osteoporosis at high risk for fracture.

The pivotal randomized, double-blind, placebo-controlled "FREEDOM" trial underscored the efficacy of denosumab treatment over 3 years to reduce the risk of new vertebral fractures by 68%, nonvertebral fractures by 20%, and hip fractures by 40% compared with placebo in postmenopausal women with osteoporosis (Cummings et al., 2009). Interestingly, the fracture reduction effect was independent of patient characteristics for vertebral fractures but was influenced by baseline body mass index and femoral neck T-score for nonvertebral fractures as depicted by a subgroup analysis (McClung et al., 2012). A post hoc analysis evaluating fracture incidence in women with known risk factors for fractures revealed that denosumab significantly reduced the risk of new vertebral and hip fractures in women at high fracture risk, whereas only new vertebral fractures were significantly reduced in women at low fracture risk (Boonen et al., 2011). Another post hoc analysis showed that the antifracture efficacy of denosumab was not dependent on renal function (Jamal et al., 2011). Long-term data support the antifracture efficacy of denosumab for up to 10 years according to data from the open-label extension of FREEDOM (Bone et al., 2017). Women originally randomized to denosumab (years 1−3) who remained on the drug during the extension (years 4−10) continued to exhibit low yearly rates of new vertebral, nonvertebral, and hip fracture, which were similar to the rates observed in denosumab-treated subjects during the first 3 years of the FREEDOM trial.

The effects of denosumab in FREEDOM were largely reproduced in the DIRECT study, which was a randomized, double-blind, placebo- and active comparator-controlled phase 3 trial in Japanese patients with osteoporosis (95% of whom were postmenopausal women) (Nakamura et al., 2014). Over 2 years, a 74% reduction in the risk of new vertebral fracture with denosumab versus placebo was noted, but the study was underpowered to assess differences in nonvertebral fracture risk. The antifracture benefit of denosumab was sustained in Japanese female and male patients with osteoporosis who continued to receive the drug in a 1-year open-label extension of DIRECT, while patients who switched from placebo to denosumab at the start of the extension had fracture rates similar to those of denosumab recipients in the original DIRECT trial (Sugimoto et al., 2015).

BMD, as evaluated by DXA, was significantly improved at various skeletal sites (total hip, lumbar spine, femoral neck) with denosumab treatment compared with placebo in the original FREEDOM trial (Bolognese et al., 2013). A substudy of FREEDOM analyzing changes in volumetric BMD as measured by quantitative CT yielded similar results (McClung et al., 2013). Furthermore, in the FREEDOM extension, BMD at the spine, hip, and femoral neck continued to progressively increase over a period of 10 years without reaching a plateau (Bone et al., 2017). Data from the 2-year DIRECT trial (Nakamura et al., 2014) conducted in Japan, and its 1-year extension (Sugimoto et al., 2015), were generally concordant with results of the FREEDOM trial while providing new evidence of a greater reduction in vertebral fracture risk with denosumab compared with open-label alendronate therapy. Several studies have investigated the effect of denosumab compared with bisphosphonates in improving BMD in postmenopausal women with osteopenia or osteoporosis. Denosumab significantly increased BMD at all sites when compared with once-weekly oral alendronate (Brown et al., 2009), once-monthly oral risedronate (Roux et al., 2014), and once-monthly oral ibandronate (Recknor et al., 2013). In a head-to-head study with once-yearly intravenous zoledronic acid in postmenopausal women with osteoporosis who were previously treated with oral bisphosphonates, denosumab significantly increased BMD at all skeletal sites compared with zoledronic acid (Miller et al., 2016).

Consistent with improved BMD, various subgroup analyses of the FREEDOM trial documented increased bone strength with denosumab treatment. In a subgroup of 99 patients in whom estimated bone strength was evaluated via QCT-based finite element analysis, denosumab treatment significantly increased bone strength in both trabecular and cortical

TABLE 73.1 Seminal denosumab clinical studies.

			Results			
Name	Phase	*n*	BTM	BMD	Fx/SRE	References
Postmenopausal osteoporosis						
Treatment of postmenopausal osteoporosis (FREEDOM)	3	7868	↓	↑	↓	Cummings et al. (2009)
Treatment of postmenopausal osteoporosis—extension study (FREEDOM extension)	4	2626	↓	↑	↓	Bone et al. (2017)
Comparison with alendronate in postmenopausal women with low BMD (DECIDE)	3	1189	↓	↑	NA	Brown et al. (2009)
Comparison with zoledronic acid in postmenopausal women with osteoporosis	3	643	↓	↑	NA	Miller et al. (2016)
Transition to denosumab after teriparatide treatment in women with postmenopausal osteoporosis (DATA)	4	94	↓	↑	NA	Leder et al. (2014, 2015)
Malignant bone disease						
Treatment of bone loss in men on androgen-deprivation treatment for nonmetastatic prostate cancer (HALT)	3	1468	NA	↑	↓	Smith et al. (2009)
Treatment of bone loss in women on aromatase inhibitors for nonmetastatic breast cancer	3	252	NA	↑	NA	Ellis et al. (2008)
Treatment of bone loss in women on aromatase inhibitors for early hormone receptor–positive breast cancer (ABCSG-18)	3	3425	NA	↑	↓	Gnant et al. (2015)
Denosumab versus zoledronic acid for the treatment of bone metastases in advanced breast cancer	3	2046	↓	NA	↓	Stopeck et al. (2010)
Denosumab versus zoledronic acid for the treatment of bone metastases in castration-resistant prostate cancer	3	1904	↓	NA	↓	Fizazi et al. (2011)
Denosumab versus zoledronic acid for the treatment of bone disease in patients with multiple myeloma	3	1718	NA	NA	↓	Raje et al. (2018)
Male osteoporosis						
Treatment of men with low BMD	3	242	↓	↑	NA	Orwoll et al. (2012)
Glucocorticoid-induced osteoporosis						
Comparison with risedronate in patients with glucocorticoid-induced osteoporosis	3	795	↓	↑	NA	Saag et al. (2018)

BMD, bone mineral density; *BTM,* bone turnover marker; *Fx,* fracture; *NA,* not available; *SRE,* skeletal-related event. *Arrows* indicate a significant effect of denosumab versus the comparator group.

departments compared with the effects of placebo (Keaveny et al., 2014). Similar results were noted for estimated strength of the radius (Simon et al., 2013). Furthermore, denosumab treatment over 3 years led to a significant increase in cortical thickness and mass and reduced cortical porosity at the proximal femur, which also correlated with increased bone strength (Zebaze et al., 2016). Nevertheless, these QCT-based findings were not reproduced in histological and micro-CT-based analyses of 112 iliac crest biopsies from FREEDOM, where significant differences between denosumab and placebo with regard to cortical thickness and porosity were not consistently observed (Chapurlat, 2017; Reid et al., 2010).

Consistent with the mechanism of action of denosumab in inhibiting osteoclast formation, function, and survival, clinical studies revealed a rapid decrease in serum markers of bone resorption after denosumab administration that was followed by later reductions in serum markers of bone formation (Bekker et al., 2004). In the pivotal FREEDOM trial, denosumab was associated with median reductions of 86%, 72%, and 72% in concentrations of the bone resorption marker C-telopeptide of type 1 collagen at months 1, 6, and 36, respectively. Concentrations of the bone formation marker

procollagen type 1 N-terminal propeptide decreased by 18%, 50%, and 76% at months 1, 6, and 36, respectively (Cummings et al., 2009). Bone turnover marker reductions were sustained for up to 10 years in patients who continued to receive denosumab treatment in the FREEDOM extension trial (Bone et al., 2017). In 1-year active comparator-controlled trials conducted in postmenopausal women with low bone mass or osteoporosis, denosumab was generally more effective than oral or intravenous bisphosphonates at reducing bone turnover markers (Brown et al., 2009; Roux et al., 2014; Recknor et al., 2013; Miller et al., 2016).

These bone turnover findings were mirrored in data obtained from iliac crest biopsies from 92 participants of the pivotal FREEDOM trial, where denosumab reduced histomorphometric measures of bone resorption (e.g., eroded surface, erosion depth, and osteoclast number) and measures of bone formation (osteoid surface, width, and volume) without impairing bone mineralization or microarchitecture (Chapurlat, 2017; Reid et al., 2010). Normal bone microarchitecture and sustained reduced bone turnover were also documented in 22 biopsies of patients who continued denosumab treatment over 10 years in the FREEDOM extension (Bone et al., 2017; Dempster, 2018, p. 39).

Male osteoporosis

Although women are more commonly affected by osteoporosis than men, up to 30%−40% of all osteoporotic fractures worldwide occur in men (Johnell and Kanis, 2006), underlining the necessity of screening and treating male patients with osteoporosis. Despite the fact that BMD measurements are less well standardized in men than in women, men with low BMD are at risk for fragility fractures, as shown in the large prospective analysis of the MrOS cohort (Cummings et al., 2006). Most pharmacological treatments for male osteoporosis have been initially approved for postmenopausal osteoporosis and then replicated in smaller randomized controlled trials in men, with change in BMD as a primary endpoint (Gennari and Bilezikian, 2018).

The study that led to the approval of denosumab (Prolia) by the FDA and EMA for the treatment of male osteoporosis was a phase 3 randomized-controlled trial in men with low BMD that showed significant increases in BMD at the lumbar spine and total hip region (5.7% and 2.4% increases, respectively, at 12 months) versus placebo (Orwoll et al., 2012). Although antiresorptive drugs are generally currently recommended as first line pharmacotherapy in male osteoporosis (Watts et al., 2012), considering that primary male osteoporosis is predominantly characterized by impaired bone formation, a case for the early application of osteoanabolic substances can be made (Gennari and Bilezikian, 2013).

Use of denosumab in combination/sequence with other osteoporosis agents

The sequence in which osteoporosis therapies are utilized in patients can be critical to their impact on BMD (Cosman et al., 2017) and transitions to and from denosumab have been tested in numerous studies. The transition from alendronate to denosumab has been examined in both OVX cynos and humans. In OVX cynos that initially received 6 months of ALN, transition to denosumab further decreased bone resorption and cortical porosity, and increased BMD and bone strength, without deleterious effects on serum calcium or bone quality (Kostenuik et al., 2015). In postmenopausal women receiving alendronate for at least 6 months, transition to denosumab also resulted in further decreases in bone turnover by serum biomarkers and histomorphometry, while BMD increased (as measured by DXA) and cortical porosity decreased (as measured by HRpQCT) (Reid et al., 2010; Kendler et al., 2010; Zebaze et al., 2014). A separate clinical study demonstrated that transitioning from alendronate to denosumab yielded larger BMD changes than transitioning from alendronate to zoledronic acid (Miller et al., 2016). Some of these differences have been attributed to greater inhibition of intracortical remodeling with denosumab; this greater inhibition may reflect denosumab's effects on osteoclastogenesis and may also relate to the limited uptake of bisphosphonates in dense cortical bone, which could contribute to the more pronounced effects of denosumab in the cortex (Zebaze et al., 2014).

Transition from the anabolic agent teriparatide to denosumab was also examined, as antiresorptive therapy is generally thought to be necessary to maintain bone mass gains after teriparatide therapy is discontinued. In the DATA study, the transition to 24 months of denosumab after 24 months of teriparatide resulted in positive gains in BMD at all sites examined (Leder et al., 2015) in association with improvements in finite element−estimated bone strength at the distal tibia and radius as evidenced by HRpQCT (Tsai et al., 2017). In the same study, the transition *from* denosumab to teriparatide was detrimental to estimated bone strength at these sites, further demonstrating the importance of sequence in the use of osteoporosis therapies.

The addition of denosumab to teriparatide as a combination therapy was also examined in the DATA study. Previous studies suggested that the addition of antiresorptive agents (oral bisphosphonates) did not consistently improve BMD when combined with parathyroid hormone—PTH(1−84) and/or teriparatide, PTH(1−34)—in postmenopausal women

(Black et al., 2003) or men (Finkelstein et al., 2003). In contrast, the DATA study demonstrated that the combination of denosumab and teriparatide for 24 months increased BMD to a significantly greater extent than either monotherapy alone (Leder et al., 2014). Similar findings were observed in rodent models when RANKL inhibitors were combined with PTH (Samadfam et al., 2007; Kostenuik et al., 2001; Pierroz et al., 2010). Transition from denosumab to other antiresorptives has also been examined because most BMD gains are lost within the first 12 months after denosumab discontinuation if no follow-on osteoporosis therapy is taken (Bone et al., 2011; Miller et al., 2008; Popp et al., 2018), as discussed below. In general, follow-on bisphosphonate therapy after denosumab discontinuation appears to prevent or partially mitigate bone loss (Freemantle et al., 2012; Lehmann and Aeberli, 2017; Reid et al., 2017), though the effects of these and other follow-on therapies on fracture risk remain unknown.

Cancer indications

Denosumab for cancer treatment–induced bone loss

Maintenance of bone health and strength is a continuous challenge in the adjuvant setting of cancer patients. In particular, patients with prostate or breast cancer receiving sex hormone ablation therapies are prone to excessive bone loss and osteoporotic fractures (Hadji et al., 2017; Adler, 2011), and several studies have addressed the ability of denosumab at 60 mg every 6 months to preserve or increase bone mass and reduce fracture risk in such patients. Based on the data below, Prolia was approved by the FDA and EMA as a treatment to increase bone mass in men at high risk for fracture who are receiving androgen deprivation therapy for nonmetastatic prostate cancer and in women at high risk for fracture who are receiving adjuvant aromatase inhibitor therapy for breast cancer.

Androgen deprivation in men with prostate cancer

In men with prostate cancer undergoing adjuvant hormone ablation therapy via gonadotropin-releasing hormone analogues, denosumab increased lumbar spine BMD by 5.6% compared with a loss of 1% in the placebo group after 24 months. In addition, vertebral fractures were significantly reduced in the denosumab group (1.5%) compared with placebo (3.9%) after 36 months (Smith et al., 2009).

Aromatase inhibitors in women with breast cancer

Aromatase inhibitors are commonly used as adjuvant hormone ablation therapies for the treatment of hormone receptor–positive breast cancer in postmenopausal women. While aromatase inhibitors significantly improve the prognosis of affected patients (Burstein et al., 2014), they exert distinct negative effects on bone mass and increase the risk of fractures (Hadji, 2015). Denosumab was the first osteoporosis drug to undergo clinical trials to specifically assess its efficacy in fracture risk reduction in breast cancer patients treated with aromatase inhibitors, which is a growing population. In an initial smaller trial with 252 patients, denosumab was shown to have positive effects on BMD compared with placebo—BMD at the lumbar spine increased by 5.5% and 7.6% in the denosumab group compared with placebo after 12 and 24 months, respectively, and denosumab also increased BMD at all other measured sites (Ellis et al., 2008). The larger ABCSG-18 phase 3 trial ($n = 3425$ subjects) was designed to assess the effects of adjuvant denosumab versus placebo on fracture risk reduction in postmenopausal women with early hormone-responsive breast cancer receiving aromatase inhibitor treatment. Denosumab reduced the number of fractures compared with placebo (92 vs. 172) and significantly delayed the time to first clinical fracture. Notably, fracture risk reduction was observed independent of baseline T-score, with significant reductions in the patient subgroup with a T-score of -1 or higher as well as in the subgroup with a T-score lower than -1 (Gnant et al., 2015).

Treatment of hypercalcemia of malignancy refractory to bisphosphonate therapy

Hypercalcemia of malignancy is a complication of patients with advanced cancer that denotes a poor prognosis. It is caused by enhanced osteoclast activity through either a humoral mechanism or local cancer-induced osteolysis. Optimal therapy requires treatment of the underlying malignancy, but in case of extensive disease a palliative approach to alleviate patients' symptoms is warranted. In addition to the initial correction of volume depletion through intravenous saline infusions and loop diuretics to promote renal calcium excretion, intravenous bisphosphonates have been the treatment of choice (Stewart, 2005). Alternatively, in cases of severe renal insufficiency or refractory hypercalcemia despite bisphosphonate use, denosumab was shown to be effective in lowering serum calcium in a single-arm international study (Hu et al., 2014). That study involved the subcutaneous administration of 120 mg denosumab on days 1, 8, 15, and 29 and then every 4 weeks to

subjects with BP-refractory hypercalcemia of malignancy. Denosumab reduced serum calcium in 64% of patients within 10 days, with an estimated median response duration of 104 days. Based on those findings, denosumab (XGEVA) received regulatory approval from the FDA under an orphan drug designation for the treatment of BP-refractory hypercalcemia of malignancy.

Breast cancer

Bone metastases are a frequent and dire complication in breast cancer patients with advanced disease, leading to a variety of SREs that include pathological fractures, radiation and/or surgery to bone, and spinal cord compression (Irelli et al., 2016). A phase 3 noninferiority study in patients with breast cancer and bone metastases assessed the effects of monthly denosumab (120 mg, $n = 1026$) or zoledronic acid (4 mg, $n = 1020$), with the primary endpoint being the time to first on-study SRE (Stopeck et al., 2010). Denosumab was shown to be noninferior and also superior to zoledronic acid in delaying the time to first on-study SRE. Denosumab was associated with fewer renal adverse events and fewer acute-phase reactions compared with zoledronic acid, whereas there were no significant differences in overall survival, breast cancer disease progression, or the occurrence of ONJ between the two treatment groups (Stopeck et al., 2010).

Prostate cancer

Bone metastases in men with prostate cancer are also associated with substantial morbidity and significant adverse impacts on health-related quality of life (Saad et al., 2017). A phase 3 trial was conducted in men with castration-resistant prostate cancer and bone metastases who were randomized to receive denosumab ($n = 950$) or zoledronic acid ($n = 951$), with the primary endpoint being the time to first on-study SRE (Fizazi et al., 2011). Denosumab significantly improved the time to first on-study SRE by 3.6 months compared with zoledronic acid. Hypocalcemia was more common in the denosumab group, while osteonecrosis of the jaw (ONJ) occurred at similarly infrequent rates in the denosumab (2%) and zoledronic acid (1%) arms (Fizazi et al., 2011). Preclinical data suggest that at least some human cancer cells express functional RANK and that RANKL can promote the migration and invasion of various cancer cell types including prostate cancer cells (Jones et al., 2006; Mori et al., 2007), suggesting a potential role for RANKL in the promotion of metastasis, and bone metastasis in particular. A phase 3 trial was conducted to assess the ability of denosumab to prevent bone metastases in men with nonmetastatic castration-resistant prostate cancer at high risk of developing bone metastases (Smith et al., 2012). Denosumab improved bone metastases–free survival by 4.2 months compared with placebo (median 29.5 vs. 25.2 months). Overall survival remained unaffected by the treatment. ONJ developed in 5% of patients on denosumab compared with none on placebo (Smith et al., 2012). While these results suggest efficacy of denosumab in preventing bone metastases, there is currently no FDA- or EMA-approved indication for the adjuvant treatment of prostate cancer patients with denosumab.

Other solid tumors

A third phase 3 trial compared denosumab and zoledronic acid in patients with bone metastases secondary to solid tumors (excluding breast and prostate) and myeloma (Henry et al., 2011). The primary endpoint was time to first on-study SRE, and denosumab proved noninferior to zoledronic acid in delaying time to first SRE. There were no differences in overall survival between the groups. A subanalysis of the lung cancer cohort within this trial revealed a significant survival benefit for patients with any form of lung cancer receiving denosumab, with an overall survival of 8.9 months compared with 7.7 months for those receiving zoledronic acid. Survival benefits were more pronounced in the non-small-cell lung cancer group (9.5 vs. 8.0 months), with the most pronounced effect on overall survival seen in patients with squamous cell carcinoma (8.6 vs. 6.4 months) (Scagliotti et al., 2012).

Multiple myeloma

Osteolytic lesions are a hallmark of multiple myeloma, which can also lead to SREs. In contrast to solid tumors, multiple myeloma is a hematological disease, and as such the classic metastatic pathway is not required for bone manifestations to occur. For the assessment of denosumab, patients with multiple myeloma were first included in the above-mentioned trial in combination with patients who had bone metastases secondary to solid tumor malignancies other than prostate or breast (Henry et al., 2011). While the primary endpoint of this trial, reduction in first on-trial SRE, was successfully reached by showing noninferiority over zoledronic acid, an ad hoc analysis of the myeloma subgroup ($n = 180$) revealed a lower overall survival in the patients who received denosumab compared with those who received zoledronic acid. Based on these findings, denosumab was approved by the FDA and EMA for the treatment of bone metastases from solid tumors but not multiple myeloma.

Further assessment of the myeloma subgroup revealed imbalances between the groups with regard to baseline risk characteristics such as ECOG score, renal function, and form of treatment, such as stem cell transplantation. A higher rate of early withdrawals was also noted in the zoledronic acid group (Raje et al., 2016). These results prompted the initiation of a larger ($n = 1718$) trial specific to patients with multiple myeloma. Patients were randomized to receive denosumab ($n = 859$) or zoledronic acid ($n = 859$), and the primary endpoint of noninferiority of denosumab compared with zoledronic acid was met. Adverse events were comparable between groups, although fewer renal treatment-emergent adverse events were observed in the denosumab group. ONJ occurrence was 4% and 3% in the denosumab and zoledronic acid groups, respectively. Based on these results, denosumab was approved by the FDA and EMA in early 2018 for the treatment of skeletal complications arising from multiple myeloma.

Giant cell tumors

GCTBs are benign tumors associated with an osteolytic phenotype and substantial skeletal morbidity (Sobti et al., 2016). In a phase 2 trial, 120 mg of denosumab was given to 37 patients with unresectable or recurrent GCTBs at days 1, 8, 15, and 28 followed by additional doses every 4 weeks. A tumor response was observed in 30 of 35 patients (Thomas et al., 2010). In a larger subsequent trial, 163/169 (96%) of surgically unsalvageable GCBT patients had no disease progression after a median follow-up 13 months after denosumab administration. In a separate cohort of this study, 74% (74/100) of patients with salvageable GCTBs whose surgery was associated with severe morbidity did not require surgery a median of 9.2 months after denosumab initiation; 62% (16/26) of those that did require surgery underwent a less extensive procedure than initially planned prior to therapy. Osteonecrosis occurred in 1% of all patients (Chawla et al., 2013).

Denosumab for the treatment of metastatic bone disease, multiple myeloma, and giant cell tumors

The efficacy and safety of denosumab has been extensively studied in patients with malignancy-associated bone lesions administered denosumab subcutaneously at a dose of 120 mg every 4 weeks. Based on the data described below, the FDA and EMA approved this regimen of denosumab (trade name XGEVA) for the prevention of skeletal-related events (SREs) in patients with multiple myeloma and those with bone metastases from solid tumors as well as for the treatment of adults and skeletally mature adolescents with giant cell tumor of bone (GCTB) that is unresectable or where surgical resection is likely to result in severe morbidity. For the latter indication, additional 120 mg doses are administered subcutaneously on Days 8 and 15 of the first month of therapy.

Additional denosumab data

Glucocorticoid-induced osteoporosis

Glucocorticoids exert manifold adverse effects on bone tissue, and while physiological concentrations of glucocorticoids are indispensable for bone accrual and growth, supraphysiological concentrations, either endogenously or more commonly iatrogenically, have detrimental effects on bone (Hofbauer and Rauner, 2009). Glucocorticoids dose-dependently inhibit the differentiation and proliferation of cultured osteoblasts, promote apoptosis of cultured osteoblasts and osteocytes, and slow the rate of bone matrix mineralization. In addition, glucocorticoids transiently enhance the activity of osteoclasts through upregulation of RANKL (Hofbauer and Rauner, 2009). In vitro data show that the treatment of osteoblast-like cells with glucocorticoids upregulates their expression of RANKL and downregulates OPG expression (Hofbauer et al., 1999). Denosumab was shown to prevent reductions in bone mass and bone strength in a mouse model of glucocorticoid-induced osteoporosis (GIOP) (Hofbauer et al., 2009). Antiresorptive and osteoanabolic drugs constitute the current therapeutic options for patients with GIOP. Clinical studies show that bisphosphonates are effective in reducing the occurrence of fractures in patients with GIOP to a degree comparable to that observed in trials of patients with postmenopausal osteoporosis (Kanis et al., 2007). A recently published double-blind, active-controlled study investigated the efficacy of denosumab compared with risedronate in patients with osteoporosis either initiating or continuing glucocorticoid treatment (Saag et al., 2018). At 12 months, treatment with denosumab (60 mg every 6 months) led to a significant BMD increase at the lumbar spine (4.4% vs. 2.3%) and total hip (2.1% vs. 0.6%) compared with risedronate. Based on these results, denosumab was approved by the FDA and EMA in 2018 for the treatment of bone loss associated with long-term systemic glucocorticoid therapy.

Rheumatoid arthritis

Inflammation in arthritic joints leads to joint destruction, in part through increased RANKL expression by activated T cells (Kong et al., 1999a). Therefore, the effects of RANKL inhibitors have been examined in multiple models of rheumatoid arthritis (RA) and in clinical trials of patients with RA. In adjuvant- and collagen-induced arthritis models in rats, RANKL inhibition via OPG treatment inhibited bone loss in arthritic joints without affecting local or systemic inflammation parameters (Kong et al., 1999a; Romas et al., 2002; Stolina et al., 2009). In clinical studies, denosumab was effective at inhibiting the progression of bone erosions (via Sharp erosion score) in RA patients receiving methotrexate, though denosumab did not affect joint space narrowing or RA disease activity (Cohen et al., 2008; Takeuchi et al., 2016, 2017). The combined use of RA biologics and denosumab did not lead to greater rates of serious infection in this patient population (Lau et al., 2018), which had been a potential concern based on results from the FREEDOM trial in postmenopausal women with osteoporosis, as described below. Based on these studies, in 2017 Daiichi Sankyo received regulatory approval from Japan's PMDA for the use of denosumab to inhibit the progression of bone erosions associated with RA. Although the pathogenesis of osteoarthritis (OA) differs somewhat from that of RA, the OPG/RANKL axis has also been implicated in OA. Early changes in subchondral bone have also been hypothesized to contribute to OA joint pathology, and therefore the prevention of these changes via RANKL inhibition may affect OA progression. OPG was shown to ameliorate pain in the monosodium iodoacetate OA rat model but did not improve pathology in joints with established damage (Sagar et al., 2014). Clinical data of the effects of denosumab on OA are limited, though at least one clinical trial is ongoing to examine denosumab's effects on erosive OA (NCT02771860).

Other potential applications

The effects of RANKL inhibitors have been examined in other conditions affecting bone including immobilization-induced bone loss (disuse osteopenia), periprosthetic osteolysis, fracture repair, and osteogenesis imperfecta (OI). Mechanical loading affects RANKL expression in bone; increased loading-induced strain reduced RANKL expression in marrow-derived stromal cell cultures (Rubin et al., 2000), while in vivo studies indicate that immobilization resulted in increased RANKL expression in murine bone (Aliprantis et al., 2012). Inhibition of RANKL by genetic modification (Xiong et al., 2011) or administration of OPG (Bateman et al., 2000) protected against disuse osteopenia in mice. Similarly, OPG ameliorated bone loss due to sciatic nerve damage (Bateman et al., 2001), transient muscle paralysis (Aliprantis et al., 2012), and space flight (Lloyd et al., 2015). Limited clinical data are available regarding the effects of denosumab on bone mass in immobilized patients, though clinical studies are ongoing (NCT01983475 and NCT03029442). One year of denosumab reduced bone turnover markers and increased BMD in a cohort of 14 patients with recent spinal cord injury (mean: 15 months postinjury) compared with their baseline values (Gifre et al., 2016).

Aseptic loosening due to wear debris–induced osteoclastic bone resorption is the most common cause of implant failure, and increased production of RANKL likely plays a critical role in this process (Haynes et al., 2001). Administration of RANKL inhibitors was able to prevent wear debris osteolysis in a mouse calvarial model (Childs et al., 2002; Tsutsumi et al., 2008) and improve screw fixation strength in a nonosteolysis model in rats (Bernhardsson et al., 2015). Initial results from a clinical trial of denosumab in postmenopausal women undergoing cementless total hip replacement indicated that although treatment ameliorated the loss of periprosthetic BMD, it did not prevent stem migration or improve functional recovery indices (Aro, 2017). These data remain preliminary and did not specifically examine the effect of denosumab in patients with aseptic loosening, which remains undetermined. A small clinical study in patients with established aseptic loosening is ongoing (NCT02299817).

Bone resorption plays a key role in the fracture repair process, primarily through callus remodeling that restores the fractured bone's original mass and shape. Because denosumab is primarily used in patients at increased risk of fracture, it is important to understand the effect of RANKL inhibitors on fracture healing. Studies in rodent models indicated that RANKL inhibitors do not impair fracture union or reduce callus structural strength (Gerstenfeld et al., 2009; Delos et al., 2008; Ulrich-Vinther and Andreassen, 2005). High-dose denosumab administration to human RANKL knock-in mice with a closed femoral fracture led to near-total ablation of callus osteoclasts that was predictably associated with delayed callus remodeling, a finding also seen in fractured rodents receiving other RANKL inhibitors (Gerstenfeld et al., 2009; Delos et al., 2008; Ulrich-Vinther and Andreassen, 2005). Delayed callus remodeling in denosumab-treated mice was associated with greater callus structural strength (Gerstenfeld et al., 2009). A subset of patients that experienced nonvertebral fractures during the FREEDOM study showed no indication of increased incidence of delayed healing or nonunion in the denosumab group (Adami et al., 2012).

OI is a genetic disorder that results in increased bone fragility. The effects of RANKL inhibitors have been examined in animals and humans with OI. In young oim/oim mice treated from 2 to 14 weeks of age, RANK-Fc improved bone microarchitecture and decreased fracture incidence compared with controls (Bargman et al., 2012). To date, clinical reports of denosumab use in OI patients have been limited, though current data indicate that lumbar spine BMD is increased (Li et al., 2018). In children with OI type IV treated with 1 mg per kg body mass denosumab every 3 months, hypercalcemia and hypercalciuria ensued, indicating that the dosing strategy may need adjustment in rapidly growing children with this unique form of OI (Trejo et al., 2018). A larger Amgen-sponsored clinical study of denosumab in OI patients is ongoing (NCT02352753).

Bone marrow edema syndrome is a painful and often difficult-to-treat condition characterized by an increase of interstitial fluid within bone. Since this "bone bruise" condition is accompanied by local bone resorption (Thiryayi et al., 2008), the use of an antiresorptive agent seems reasonable. Intravenous bisphosphonates were shown to be effective in reducing bone marrow edema in professional athletes (Simon et al., 2014). More recently, denosumab was used in a case-series of 14 patients with bone marrow edema, with an overall treatment success rate of 93% based on MRI findings (Rolvien et al., 2017).

Denosumab also has been recently used to treat alveolar bone destruction, which characterizes periodontitis. In a rodent model of periodontitis, systemic delivery of OPG-Fc preserved alveolar bone volume and decreased bone resorption markers (Jin et al., 2007). Similarly, rats treated with OPG-Fc displayed enhanced postorthodontic tooth stability (Hudson et al., 2012).

Denosumab safety

As with any drug, the clinical benefits of RANKL inhibitors should be weighed against their potential risk. The warnings and precautions section of the US label for Prolia and XGEVA indicate potential risks including hypocalcemia, ONJ, atypical subtrochanteric femoral fractures (AFFs), multiple vertebral fractures following discontinuation, hypersensitivity, serious infections, dermatologic adverse reactions, and musculoskeletal pain (Prolia/XGEVA PI).

Hypocalcemia

Decreases in serum calcium with denosumab secondary to decreased bone resorption may lead to or exacerbate hypocalcemia (Prolia/XGEVA PI). Higher baseline bone formation may contribute to hypocalcemia after denosumab therapy is initiated (Kinoshita et al., 2016; Kostenuik et al., 2015). Clinical monitoring of serum calcium is recommended within 14 days of denosumab administration for patients predisposed to hypocalcemia or altered mineral metabolism, including patients with renal impairment. Denosumab is contraindicated in patients with preexisting hypocalcemia. In contrast, discontinuation of denosumab in XGEVA-treated patients with growing skeletons should involve monitoring for hypercalcemia, which has been reported.

Osteonecrosis of the jaw

ONJ has been reported in patients taking Prolia and XGEVA, with a higher incidence reported for XGEVA. ONJ, which can occur spontaneously, is generally associated with tooth extraction and/or local infection with delayed healing. Therefore, a dental examination is recommended prior to treatment in patients who may require such procedures or have other risk factors that may predispose them to ONJ (Prolia/XGEVA PI). During the long-term extension of the FREEDOM trial in postmenopausal women with osteoporosis, in which all subjects received open-label denosumab, 12 cases of ONJ occurred, all but 1 of which followed invasive oral dental procedures or events comprising scaling or root planning, tooth extraction, dental implant, natural tooth loss, or jaw surgery. A total of 11 subjects developed ONJ among the 1621 subjects who underwent or experienced such procedures or events, for a rate of 0.7%, compared with 1 ONJ case among the 1970 subjects who did not undergo or experience such procedures or events (0.05%) (Watts et al., 2017). The pathophysiology of the increased incidence of ONJ is not clear, though increased ONJ risk is also associated with other antiresorptive agents (i.e., bisphosphonates) (Khan et al., 2017). The recent development of nonclinical models demonstrating induction of ONJ in the presence of periapical disease may provide additional insights (Aghaloo et al., 2014).

Atypical femoral fractures

AFFs have also been reported with denosumab (Prolia/XGEVA PI). First reported in patients receiving bisphosphonates, these transverse fractures occur in the femoral diaphysis below the lesser trochanter and are associated with minimal

trauma or comminution. Prodromal pain and bilaterality are frequent or occasional features of AFFs, and therefore patients on denosumab who experience new thigh or groin pain should seek medical attention, and the contralateral limb should be assessed should an AFF occur. The pathophysiology of these fractures is not clear, though the evidence suggests they may occur as stress or insufficiency fractures (Shane et al., 2014). Large-scale studies have reported that most radiographically confirmed AFFs occur in patients who were never dispensed any potent antiresorptive therapies (Feldstein et al., 2012), and that long-term bisphosphonate use is not associated with an overall increased risk of fractures in the specific femoral region where AFFs occur (Abrahamsen et al., 2016). These observations have led to suggestions that potent antiresorptives may lead to an atypical radiographic fracture pattern without necessarily causing the fracture itself (Feldstein et al., 2012). In support of that possibility, tibiae from OPG-treated mice subjected to destructive biomechanical testing exhibited more transverse and distal failure patterns than vehicle-treated mice, and these shifts were associated with greater, not lesser, bone strength (Bonnet et al., 2016).

Denosumab discontinuation: effects on bone turnover, bone mass, and fracture risk

Cessation of therapy with denosumab is associated with rapid reversal of BMD gains and an increase in bone turnover markers to above pretreatment baseline levels from around month 8 to around month 24 after the last denosumab dose, followed by a return of turnover markers to baseline levels (Bone et al., 2011; Miller et al., 2008). BMD levels also tend to return to pretreatment baseline levels after discontinuing denosumab but generally remain above the levels of patients who never received denosumab (Bone et al., 2011; Miller et al., 2008). Recent post hoc analyses of patients from FREEDOM and its open-label extension indicate that for subjects who discontinue denosumab without any follow-on osteoporosis therapy, overall fracture risk resumes at levels similar to those of subjects who never received denosumab. One analysis showed that for subjects in FREEDOM who discontinued placebo or denosumab after having received at least two doses of study drug and continued to participate in the study for at least 7 months after the last dose received, the exposure-adjusted rates of new vertebral fractures were 9.3 vs. 5.6 per 100 subject-years, respectively (Brown et al., 2013). A subsequent analysis wherein subjects from the FREEDOM extension study were also included reported similar exposure-adjusted rates of new or worsening vertebral fractures after discontinuing denosumab or placebo (Cummings et al., 2018). However, the latter study also reported that the rate of multiple new or worsening vertebral fractures was somewhat higher for subjects discontinuing denosumab than for those who discontinued placebo (4.2 vs. 3.2 per 100 subject-years, respectively). And among subjects from FREEDOM and its extension who experience at least one new off-treatment vertebral fracture, 60.7% of those who discontinued denosumab experienced multiple vertebral fractures, compared with 34.5% of such subjects who discontinued placebo (Cummings et al., 2018). Several published case series have also described multiple vertebral fractures in patients discontinuing denosumab (Popp et al., 2016; Aubry-Rozier et al., 2016; Anastasilakis et al., 2017). Accordingly, professional committees and national guidelines have issued statements advising against cessation of denosumab without an alternative treatment, especially in patients at high fracture risk (Tsourdi et al., 2017; Meier et al., 2017).

Mechanisms underlying the risk of multiple vertebral fractures after denosumab discontinuation are unclear, but a cogent pathophysiological hypothesis should reconcile with observations that overall vertebral and nonvertebral fracture risks were similar after discontinuing denosumab or placebo. One potential hypothesis relates to the potential for perturbed spinal alignment after an index off-treatment (or prevalent) vertebral fracture. Altered spinal alignment in subjects with vertebral fractures has been associated with increased mechanical loading on the other vertebrae (Briggs et al., 2006), and for subjects experiencing high turnover after discontinuing denosumab therapy, those increased mechanical loads may act on vertebrae that bear microstructural hallmarks of high bone turnover, such as more extensive resorption cavities and trabecular disconnections. Microstructural features of high turnover can be particularly deleterious to bone strength when placed in regions of higher strain or lower bone volume (Hernandez et al., 2006; Slyfield et al., 2012). This hypothesis suggests that the risk of multiple vertebral fractures after denosumab discontinuation may abate to some degree as transiently higher turnover subsides and biomechanically detrimental resorption cavities are refilled. On the other hand, index or prevalent vertebral fractures may continue to adversely influence spine alignment and vertebral biomechanics independent of bone turnover rates, which could represent an ongoing risk for additional vertebral fractures.

Hypersensitivity, serious infections, and musculoskeletal pain

Hypersensitivity has been reported with denosumab use, and treatment should be discontinued if clinically significant allergic reactions occur. Increased risk of serious infection that required hospitalization including endocarditis and infections of the skin, abdomen, urinary tract, and ear were reported more frequently in the Prolia group in the FREEDOM

trial (Prolia PI). Higher rates of skin reactions such as dermatitis, eczema, and rashes also occurred with Prolia in FREEDOM. Severe bone, joint, and/or muscle pain has also been reported in patients taking Prolia.

Use in women of reproductive age

Denosumab is contraindicated in patients who are pregnant based on data from animal studies suggesting that denosumab may cause fetal harm (Prolia PI/XGEVA). Administration of high-dose denosumab to cynos throughout pregnancy resulted in increased fetal loss, stillbirths, and postnatal mortality with absent peripheral lymph nodes, abnormal bone growth, and decreased neonatal growth. Some of these abnormalities improved following a recovery period from birth through 6 months of age (Boyce et al., 2014). Nonetheless, for women of reproductive age receiving denosumab, contraception is recommended for at least 5 months after the last dose.

Theoretical impact of receptor activator of nuclear factor−kappa B ligand inhibition on insulin resistance and vascular calcification

Additional animal studies have suggested the potential for RANKL inhibitors to affect other pathological processes including insulin resistance and vascular calcification. In a series of experiments in mouse models of type 2 diabetes, genetic inhibition of RANKL signaling or OPG administration improved insulin sensitivity and glucose metabolism (Kiechl et al., 2013). These data were supported by the authors' observation that high serum RANKL concentration was as an independent risk predictor of T2DM in humans. A separate set of studies demonstrated that RANKL inhibitors could induce β-cell proliferation in vitro and in vivo (Kondegowda et al., 2015). A post hoc analysis of the FREEDOM study did not demonstrate a clear effect of denosumab on fasting serum glucose in postmenopausal osteoporotic women with prediabetes or diabetes; however, some improvement was observed in a subset of diabetic patients not receiving antidiabetic medication (Napoli et al., 2018).

Early genetic studies suggested a link between RANKL signaling and vascular calcification based on the presence of calcified arteries in osteoporotic OPG-deficient mice (Bucay et al., 1998). A subsequent study demonstrated that denosumab reduced aortic calcium deposition in mice receiving prednisolone (Helas et al., 2009). A post hoc analysis of the FREEDOM study did not show an effect of treatment on the progression of aortic calcification (by lateral spine X-ray) or the incidence of cardiovascular adverse events, compared with placebo (Samelson et al., 2014).

Summary

Denosumab is an effective therapeutic agent for increasing BMD and reducing vertebral and nonvertebral fracture risk in patients with postmenopausal osteoporosis, glucocorticoid osteoporosis, and male osteoporosis. Denosumab also delays SREs, reduces the onset of bone metastases, and prevents fractures in patients with bone metastases from breast and prostate cancer. Denosumab's subcutaneous mode of administration renders it a practical and well-tolerated drug because it circumvents the gastrointestinal tract, and no infusion equipment or facility is required for denosumab administration. A further advantage lies in the possible utilization of denosumab in patients with renal insufficiency, a common condition in the elderly and/or patients with cancer. Denosumab displays a favorable safety profile, and the risks of hypocalcemia and ONJ can be reduced by preventive measures. Since denosumab is not deposited in the skeleton, there is no sustained effect on bone metabolism after its discontinuation. Therefore, regular denosumab administration during therapy is warranted, and a long-term therapeutic strategy is recommended if denosumab is discontinued, particularly in patients at increased risk for fracture.

References

Abrahamsen, B., Eiken, P., Prieto-Alhambra, D., Eastell, R., 2016. Risk of hip, subtrochanteric, and femoral shaft fractures among mid and long term users of alendronate: nationwide cohort and nested case-control study. BMJ 353, i3365.

Abrahamsen, B., Hjelmborg, J.V., Kostenuik, P., Stilgren, L.S., Kyvik, K., Adamu, S., Brixen, K., Langdahl, B.L., 2005. Circulating amounts of osteoprotegerin and RANK ligand: genetic influence and relationship with BMD assessed in female twins. Bone 36, 727−735.

Adami, S., Libanati, C., Boonen, S., Cummings, S.R., Ho, P.R., Wang, A., Siris, E., Lane, J., Group, F.F.-H.W., Adachi, J.D., Bhandari, M., De Gregorio, L., Gilchrist, N., Lyritis, G., Moller, G., Palacios, S., Pavelka, K., Heinrich, R., Roux, C., Uebelhart, D., 2012. Denosumab treatment in postmenopausal women with osteoporosis does not interfere with fracture-healing: results from the FREEDOM trial. J. Bone Jt. Surg. Am. 94, 2113−2119.

Adler, R.A., 2011. Management of osteoporosis in men on androgen deprivation therapy. Maturitas 68, 143−147.

Aghaloo, T.L., Cheong, S., Bezouglaia, O., Kostenuik, P., Atti, E., Dry, S.M., Pirih, F.Q., Tetradis, S., 2014. RANKL inhibitors induce osteonecrosis of the jaw in mice with periapical disease. J. Bone Miner. Res. 29, 843–854.

Aliprantis, A.O., Stolina, M., Kostenuik, P.J., Poliachik, S.L., Warner, S.E., Bain, S.D., Gross, T.S., 2012. Transient muscle paralysis degrades bone via rapid osteoclastogenesis. FASEB J. 26, 1110–1118.

American Society For Bone and Mineral Research President's Committee on Nomenclature, 2000. Proposed standard nomenclature for new tumor necrosis factor family members involved in the regulation of bone resorption. The American Society for Bone and Mineral Research President's Committee on Nomenclature. J. Bone Miner. Res. 15, 2293–2296.

Anastasilakis, A.D., Polyzos, S.A., Makras, P., Aubry-Rozier, B., Kaouri, S., Lamy, O., 2017. Clinical features of 24 patients with rebound-associated vertebral fractures after denosumab discontinuation: systematic review and additional cases. J. Bone Miner. Res. 32, 1291–1296.

Anderson, D.M., Maraskovsky, E., Billingsley, W.L., Dougall, W.C., Tometsko, M.E., Roux, E.R., Teepe, M.C., Dubose, R.F., Cosman, D., Galibert, L., 1997. A homologue of the TNF receptor and its ligand enhance T-cell growth and dendritic-cell function. Nature 390, 175–179.

Aro, H., Nazari-Farsani, S., Vuopio, M., Mattila, K., 2017. A Randomized, Double-Blind, Placebo-Controlled Trial of Denosumab in Postmenopausal Women Undergoing Cementless Total Hip Replacement. ASBMR.

Aubry-Rozier, B., Gonzalez-Rodriguez, E., Stoll, D., Lamy, O., 2016. Severe spontaneous vertebral fractures after denosumab discontinuation: three case reports. Osteoporos. Int. 27, 1923–1925.

Bargman, R., Posham, R., Boskey, A.L., Dicarlo, E., Raggio, C., Pleshko, N., 2012. Comparable outcomes in fracture reduction and bone properties with RANKL inhibition and alendronate treatment in a mouse model of osteogenesis imperfecta. Osteoporos. Int. 23, 1141–1150.

Bateman, T.A., Dunstan, C.R., Ferguson, V.L., Lacey, D.L., Ayers, R.A., Simske, S.J., 2000. Osteoprotegerin mitigates tail suspension-induced osteopenia. Bone 26, 443–449.

Bateman, T.A., Dunstan, C.R., Lacey, D.L., Ferguson, V.L., Ayers, R.A., Simske, S.J., 2001. Osteoprotegerin ameliorates sciatic nerve crush induced bone loss. J. Orthop. Res. 19, 518–523.

Bekker, P.J., Holloway, D., Nakanishi, A., Arrighi, M., Leese, P.T., Dunstan, C.R., 2001. The effect of a single dose of osteoprotegerin in postmenopausal women. J. Bone Miner. Res. 16, 348–360.

Bekker, P.J., Holloway, D.L., Rasmussen, A.S., Murphy, R., Martin, S.W., Leese, P.T., Holmes, G.B., Dunstan, C.R., Depaoli, A.M., 2004. A single-dose placebo-controlled study of AMG 162, a fully human monoclonal antibody to RANKL, in postmenopausal women. J. Bone Miner. Res. 19, 1059–1066.

Bernhardsson, M., Sandberg, O., Aspenberg, P., 2015. Anti-RANKL treatment improves screw fixation in cancellous bone in rats. Injury 46, 990–995.

Black, D.M., Greenspan, S.L., Ensrud, K.E., Palermo, L., Mcgowan, J.A., Lang, T.F., Garnero, P., Bouxsein, M.L., Bilezikian, J.P., Rosen, C.J., PaTH Study Investigators, 2003. The effects of parathyroid hormone and alendronate alone or in combination in postmenopausal osteoporosis. N. Engl. J. Med. 349, 1207–1215.

Body, J.J., Greipp, P., Coleman, R.E., Facon, T., Geurs, F., Fermand, J.P., Harousseau, J.L., Lipton, A., Mariette, X., Williams, C.D., Nakanishi, A., Holloway, D., Martin, S.W., Dunstan, C.R., Bekker, P.J., 2003. A phase I study of AMGN-0007, a recombinant osteoprotegerin construct, in patients with multiple myeloma or breast carcinoma related bone metastases. Cancer 97, 887–892.

Bolognese, M.A., Teglbjaerg, C.S., Zanchetta, J.R., Lippuner, K., Mcclung, M.R., Brandi, M.L., Hoiseth, A., Lakatos, P., Moffett, A.H., Lorenc, R.S., Wang, A., Libanati, C., 2013. Denosumab significantly increases DXA BMD at both trabecular and cortical sites: results from the FREEDOM study. J. Clin. Densitom. 16, 147–153.

Bone, H.G., Bolognese, M.A., Yuen, C.K., Kendler, D.L., Miller, P.D., Yang, Y.C., Grazette, L., San Martin, J., Gallagher, J.C., 2011. Effects of denosumab treatment and discontinuation on bone mineral density and bone turnover markers in postmenopausal women with low bone mass. J. Clin. Endocrinol. Metab. 96, 972–980.

Bone, H.G., Wagman, R.B., Brandi, M.L., Brown, J.P., Chapurlat, R., Cummings, S.R., Czerwinski, E., Fahrleitner-Pammer, A., Kendler, D.L., Lippuner, K., Reginster, J.Y., Roux, C., Malouf, J., Bradley, M.N., Daizadeh, N.S., Wang, A., Dakin, P., Pannacciulli, N., Dempster, D.W., Papapoulos, S., 2017. 10 years of denosumab treatment in postmenopausal women with osteoporosis: results from the phase 3 randomised FREEDOM trial and open-label extension. Lancet Diabetes Endocrinol. 5, 513–523.

Bonnet, N., Gerbaix, M., Ominsky, M., Ammann, P., Kostenuik, P.J., Ferrari, S.L., 2016. Influence of fatigue loading and bone turnover on bone strength and pattern of experimental fractures of the tibia in mice. Calcif. Tissue Int. 99, 99–109.

Boonen, S., Adachi, J.D., Man, Z., Cummings, S.R., Lippuner, K., Torring, O., Gallagher, J.C., Farrerons, J., Wang, A., Franchimont, N., San Martin, J., Grauer, A., Mcclung, M., 2011. Treatment with denosumab reduces the incidence of new vertebral and hip fractures in postmenopausal women at high risk. J. Clin. Endocrinol. Metab. 96, 1727–1736.

Boyce, R.W., Varela, A., Chouinard, L., Bussiere, J.L., Chellman, G.J., Ominsky, M.S., Pyrah, I.T., 2014. Infant cynomolgus monkeys exposed to denosumab in utero exhibit an osteoclast-poor osteopetrotic-like skeletal phenotype at birth and in the early postnatal period. Bone 64, 314–325.

Briggs, A.M., Wrigley, T.V., van Dieen, J.H., Phillips, B., Lo, S.K., Greig, A.M., Bennell, K.L., 2006. The effect of osteoporotic vertebral fracture on predicted spinal loads in vivo. Eur. Spine J. 15, 1785–1795.

Brown, J.P., Prince, R.L., Deal, C., Recker, R.R., Kiel, D.P., DE Gregorio, L.H., Hadji, P., Hofbauer, L.C., Alvaro-Gracia, J.M., Wang, H., Austin, M., Wagman, R.B., Newmark, R., Libanati, C., San Martin, J., Bone, H.G., 2009. Comparison of the effect of denosumab and alendronate on BMD and biochemical markers of bone turnover in postmenopausal women with low bone mass: a randomized, blinded, phase 3 trial. J. Bone Miner. Res. 24, 153–161.

Brown, J.P., Roux, C., Torring, O., Ho, P.R., Beck Jensen, J.E., Gilchrist, N., Recknor, C., Austin, M., Wang, A., Grauer, A., Wagman, R.B., 2013. Discontinuation of denosumab and associated fracture incidence: analysis from the fracture reduction evaluation of denosumab in osteoporosis every 6 Months (FREEDOM) trial. J. Bone Miner. Res. 28, 746–752.

Bucay, N., Sarosi, I., Dunstan, C.R., Morony, S., Tarpley, J., Capparelli, C., Scully, S., Tan, H.L., Xu, W., Lacey, D.L., Boyle, W.J., Simonet, W.S., 1998. osteoprotegerin-deficient mice develop early onset osteoporosis and arterial calcification. Genes Dev. 12, 1260–1268.

Burstein, H.J., Temin, S., Anderson, H., Buchholz, T.A., Davidson, N.E., Gelmon, K.E., Giordano, S.H., Hudis, C.A., Rowden, D., Solky, A.J., Stearns, V., Winer, E.P., Griggs, J.J., 2014. Adjuvant endocrine therapy for women with hormone receptor-positive breast cancer: American society of clinical oncology clinical practice guideline focused update. J. Clin. Oncol. 32, 2255–2269.

Capparelli, C., Morony, S., Warmington, K., Adamu, S., Lacey, D., Dunstan, C.R., Stouch, B., Martin, S., Kostenuik, P.J., 2003. Sustained antiresorptive effects after a single treatment with human recombinant osteoprotegerin (OPG): a pharmacodynamic and pharmacokinetic analysis in rats. J. Bone Miner. Res. 18, 852–858.

Chapurlat, R., P-M, N., Roux, J.P., Horlait, S., Dempster, D., Wang, A., Wagman, R., Chavassieux, P., 2017. Denosumab reduced bone remodeling, eroded surface, and erosion depth in cortical bone of iliac crest biopsies from postmenopausal women in the FREEDOM trial. J. Bone Miner. Res. 32. Abstract 1111.

Chawla, S., Henshaw, R., Seeger, L., Choy, E., Blay, J.Y., Ferrari, S., Kroep, J., Grimer, R., Reichardt, P., Rutkowski, P., Schuetze, S., Skubitz, K., Staddon, A., Thomas, D., Qian, Y., Jacobs, I., 2013. Safety and efficacy of denosumab for adults and skeletally mature adolescents with giant cell tumour of bone: interim analysis of an open-label, parallel-group, phase 2 study. Lancet Oncol. 14, 901–908.

Childs, L.M., Paschalis, E.P., Xing, L., Dougall, W.C., Anderson, D., Boskey, A.L., Puzas, J.E., Rosier, R.N., O'keefe, R.J., Boyce, B.F., Schwarz, E.M., 2002. In vivo RANK signaling blockade using the receptor activator of NF-kappaB:Fc effectively prevents and ameliorates wear debris-induced osteolysis via osteoclast depletion without inhibiting osteogenesis. J. Bone Miner. Res. 17, 192–199.

Cohen, S.B., Dore, R.K., Lane, N.E., Ory, P.A., Peterfy, C.G., Sharp, J.T., van der Heijde, D., Zhou, L., Tsuji, W., Newmark, R., Denosumab Rheumatoid Arthritis Study Group, 2008. Denosumab treatment effects on structural damage, bone mineral density, and bone turnover in rheumatoid arthritis: a twelve-month, multicenter, randomized, double-blind, placebo-controlled, phase II clinical trial. Arthritis Rheum. 58, 1299–1309.

Cosman, F., Nieves, J.W., Dempster, D.W., 2017. Treatment sequence matters: anabolic and antiresorptive therapy for osteoporosis. J. Bone Miner. Res. 32, 198–202.

Cummings, S.R., Cawthon, P.M., Ensrud, K.E., Cauley, J.A., Fink, H.A., Orwoll, E.S., Osteoporotic Fractures in Men Research Group & Study of Osteoporotic Fractures Research Group, 2006. BMD and risk of hip and nonvertebral fractures in older men: a prospective study and comparison with older women. J. Bone Miner. Res. 21, 1550–1556.

Cummings, S.R., Ferrari, S., Eastell, R., Gilchrist, N., Jensen, J.B., Mcclung, M., Roux, C., Torring, O., Valter, I., Wang, A.T., Brown, J.P., 2018. Vertebral fractures after discontinuation of denosumab: a post hoc analysis of the randomized placebo-controlled FREEDOM trial and its extension. J. Bone Miner. Res. 33, 190–198.

Cummings, S.R., San Martin, J., Mcclung, M.R., Siris, E.S., Eastell, R., Reid, I.R., Delmas, P., Zoog, H.B., Austin, M., Wang, A., Kutilek, S., Adami, S., Zanchetta, J., Libanati, C., Siddhanti, S., Christiansen, C., Trial, F., 2009. Denosumab for prevention of fractures in postmenopausal women with osteoporosis. N. Engl. J. Med. 361, 756–765.

Delos, D., Yang, X., Ricciardi, B.F., Myers, E.R., Bostrom, M.P., Camacho, N.P., 2008. The effects of RANKL inhibition on fracture healing and bone strength in a mouse model of osteogenesis imperfecta. J. Orthop. Res. 26, 153–164.

Dempster, D.W., Brown, J.P., Fahrleitner-Pammer, A., Kendler, D., Rizzo, S., Valter, I., Wagman, R.B., Yin, X., Yue, S.V., Boivin, G., 2018. Effects of long-term denosumab on bone histomorphometry and mineralization in women with postmenopausal osteoporosis. J. Clin. Endocrinol. Metab. 103 (7), 2498–2509.

Dougall, W.C., Glaccum, M., Charrier, K., Rohrbach, K., Brasel, K., DE Smedt, T., Daro, E., Smith, J., Tometsko, M.E., Maliszewski, C.R., Armstrong, A., Shen, V., Bain, S., Cosman, D., Anderson, D., Morrissey, P.J., Peschon, J.J., Schuh, J., 1999. RANK is essential for osteoclast and lymph node development. Genes Dev. 13, 2412–2424.

Ellis, G.K., Bone, H.G., Chlebowski, R., Paul, D., Spadafora, S., Smith, J., Fan, M., Jun, S., 2008. Randomized trial of denosumab in patients receiving adjuvant aromatase inhibitors for nonmetastatic breast cancer. J. Clin. Oncol. 26, 4875–4882.

Feldstein, A.C., Black, D., Perrin, N., Rosales, A.G., Friess, D., Boardman, D., Dell, R., Santora, A., Chandler, J.M., Rix, M.M., Orwoll, E., 2012. Incidence and demography of femur fractures with and without atypical features. J. Bone Miner. Res. 27, 977–986.

Finkelstein, J.S., Hayes, A., Hunzelman, J.L., Wyland, J.J., Lee, H., Neer, R.M., 2003. The effects of parathyroid hormone, alendronate, or both in men with osteoporosis. N. Engl. J. Med. 349, 1216–1226.

Fizazi, K., Carducci, M., Smith, M., Damiao, R., Brown, J., Karsh, L., Milecki, P., Shore, N., Rader, M., Wang, H., Jiang, Q., Tadros, S., Dansey, R., Goessl, C., 2011. Denosumab versus zoledronic acid for treatment of bone metastases in men with castration-resistant prostate cancer: a randomised, double-blind study. Lancet 377, 813–822.

Freemantle, N., Satram-Hoang, S., Tang, E.-T., Kaur, P., Macarios, D., Siddhanti, S., Borenstein, J., Kendler, D.L., 2012. Final results of the DAPS (Denosumab Adherence Preference Satisfaction) study: a 24-month, randomized, crossover comparison with alendronate in postmenopausal women. Osteoporos. Int. 23, 317–326.

Gennari, L., Bilezikian, J.P., 2013. Idiopathic osteoporosis in men. Curr. Osteoporos. Rep. 11, 286–298.

Gennari, L., Bilezikian, J.P., 2018. New and developing pharmacotherapy for osteoporosis in men. Expert Opin. Pharmacother. 19, 253–264.

Gerstenfeld, L.C., Sacks, D.J., Pelis, M., Mason, Z.D., Graves, D.T., Barrero, M., Ominsky, M.S., Kostenuik, P.J., Morgan, E.F., Einhorn, T.A., 2009. Comparison of effects of the bisphosphonate alendronate versus the RANKL inhibitor denosumab on murine fracture healing. J. Bone Miner. Res. 24, 196–208.

Gifre, L., Vidal, J., Carrasco, J.L., Muxi, A., Portell, E., Monegal, A., Guanabens, N., Peris, P., 2016. Denosumab increases sublesional bone mass in osteoporotic individuals with recent spinal cord injury. Osteoporos. Int. 27, 405–410.

Gnant, M., Pfeiler, G., Dubsky, P.C., Hubalek, M., Greil, R., Jakesz, R., Wette, V., Balic, M., Haslbauer, F., Melbinger, E., Bjelic-Radisic, V., Artner-Matuschek, S., Fitzal, F., Marth, C., Sevelda, P., Mlineritsch, B., Steger, G.G., Manfreda, D., Exner, R., Egle, D., Bergh, J., Kainberger, F., Talbot, S., Warner, D., Fesl, C., Singer, C.F., Austrian, B., Colorectal Cancer Study Group, 2015. Adjuvant denosumab in breast cancer (ABCSG-18): a multicentre, randomised, double-blind, placebo-controlled trial. Lancet 386, 433–443.

Green, L.L., 1999. Antibody engineering via genetic engineering of the mouse: XenoMouse strains are a vehicle for the facile generation of therapeutic human monoclonal antibodies. J. Immunol. Methods 231, 11–23.

Hadji, P., 2015. Cancer treatment-induced bone loss in women with breast cancer. Bonekey Rep. 4, 692.

Hadji, P., Aapro, M.S., Body, J.J., Gnant, M., Brandi, M.L., Reginster, J.Y., Zillikens, M.C., Gluer, C.C., de Villiers, T., Baber, R., Roodman, G.D., Cooper, C., Langdahl, B., Palacios, S., Kanis, J., Al-Daghri, N., Nogues, X., Eriksen, E.F., Kurth, A., Rizzoli, R., Coleman, R.E., 2017. Management of aromatase inhibitor-associated bone loss (AIBL) in postmenopausal women with hormone sensitive breast cancer: joint position statement of the IOF, CABS, ECTS, IEG, ESCEO IMS, and SIOG. J. Bone Oncol. 7, 1–12.

Haynes, D.R., Crotti, T.N., Potter, A.E., Loric, M., Atkins, G.J., Howie, D.W., Findlay, D.M., 2001. The osteoclastogenic molecules RANKL and RANK are associated with periprosthetic osteolysis. J. Bone Joint Surg. Br. 83, 902–911.

Helas, S., Goettsch, C., Schoppet, M., Zeitz, U., Hempel, U., Morawietz, H., Kostenuik, P.J., Erben, R.G., Hofbauer, L.C., 2009. Inhibition of receptor activator of NF-kappaB ligand by denosumab attenuates vascular calcium deposition in mice. Am. J. Pathol. 175, 473–478.

Henry, D.H., Costa, L., Goldwasser, F., Hirsh, V., Hungria, V., Prausova, J., Scagliotti, G.V., Sleeboom, H., Spencer, A., Vadhan-Raj, S., von Moos, R., Willenbacher, W., Woll, P.J., Wang, J., Jiang, Q., Jun, S., Dansey, R., Yeh, H., 2011. Randomized, double-blind study of denosumab versus zoledronic acid in the treatment of bone metastases in patients with advanced cancer (excluding breast and prostate cancer) or multiple myeloma. J. Clin. Oncol. 29, 1125–1132.

Hernandez, C.J., Gupta, A., Keaveny, T.M., 2006. A biomechanical analysis of the effects of resorption cavities on cancellous bone strength. J. Bone Miner. Res. 21, 1248–1255.

Hofbauer, L.C., Gori, F., Riggs, B.L., Lacey, D.L., Dunstan, C.R., Spelsberg, T.C., Khosla, S., 1999. Stimulation of osteoprotegerin ligand and inhibition of osteoprotegerin production by glucocorticoids in human osteoblastic lineage cells: potential paracrine mechanisms of glucocorticoid-induced osteoporosis. Endocrinology 140, 4382–4389.

Hofbauer, L.C., Rauner, M., 2009. Minireview: live and let die: molecular effects of glucocorticoids on bone cells. Mol. Endocrinol. 23, 1525–1531.

Hofbauer, L.C., Zeitz, U., Schoppet, M., Skalicky, M., Schuler, C., Stolina, M., Kostenuik, P.J., Erben, R.G., 2009. Prevention of glucocorticoid-induced bone loss in mice by inhibition of RANKL. Arthritis Rheum. 60, 1427–1437.

Hsu, H., Lacey, D.L., Dunstan, C.R., Solovyev, I., Colombero, A., Timms, E., Tan, H.L., Elliott, G., Kelley, M.J., Sarosi, I., Wang, L., Xia, X.Z., Elliott, R., Chiu, L., Black, T., Scully, S., Capparelli, C., Morony, S., Shimamoto, G., Bass, M.B., Boyle, W.J., 1999. Tumor necrosis factor receptor family member RANK mediates osteoclast differentiation and activation induced by osteoprotegerin ligand. Proc. Natl. Acad. Sci. USA. 96, 3540–3545.

Hudson, J.B., Hatch, N., Hayami, T., Shin, J.M., Stolina, M., Kostenuik, P.J., Kapila, S., 2012. Local delivery of recombinant osteoprotegerin enhances postorthodontic tooth stability. Calcif. Tissue Int. 90, 330–342.

Hu, MI., Glezerman, IG., Leboulleux, S., Insogna, K., Gucalp, R., Misiorowski, W., Yu, B., Zorsky, P., Tosi, D., Bessudo, A., Jaccard, A., Tonini, G., Ying, W., Braun, A., Jain, RK., 2014. Denosumab for treatment of hypercalcemia of malignancy. J. Clin. Endocrinol. Metab. 99, 3144–3152.

Idris, A.I., Coste, E., Greig, I.R., Ralston, S.H., van't Hof, R.J., 2010. The biphenyl-carboxylate derivative ABD328 is a novel orally active antiresorptive agent. Calcif. Tissue Int. 87, 525–532.

Ikeda, T., Kasai, M., Utsuyama, M., Hirokawa, K., 2001. Determination of three isoforms of the receptor activator of nuclear factor-κB ligand and their differential expression in bone and thymus. Endocrinology 142, 1419–1426.

Irelli, A., Cocciolone, V., Cannita, K., Zugaro, L., Di Staso, M., Lanfiuti Baldi, P., Paradisi, S., Sidoni, T., Ricevuto, E., Ficorella, C., 2016. Bone targeted therapy for preventing skeletal-related events in metastatic breast cancer. Bone 87, 169–175.

Jamal, S.A., Ljunggren, O., Stehman-Breen, C., Cummings, S.R., Mcclung, M.R., Goemaere, S., Ebeling, P.R., Franek, E., Yang, Y.C., Egbuna, O.I., Boonen, S., Miller, P.D., 2011. Effects of denosumab on fracture and bone mineral density by level of kidney function. J. Bone Miner. Res. 26, 1829–1835.

Jin, Q., Cirelli, J.A., Park, C.H., Sugai, J.V., Taba Jr., M., Kostenuik, P.J., Giannobile, W.V., 2007. RANKL inhibition through osteoprotegerin blocks bone loss in experimental periodontitis. J. Periodontol. 78, 1300–1308.

Johnell, O., Kanis, J.A., 2006. An estimate of the worldwide prevalence and disability associated with osteoporotic fractures. Osteoporos. Int. 17, 1726–1733.

Jones, D.H., Nakashima, T., Sanchez, O.H., Kozieradzki, I., Komarova, S.V., Sarosi, I., Morony, S., Rubin, E., Sarao, R., Hojilla, C.V., Komnenovic, V., Kong, Y.Y., Schreiber, M., Dixon, S.J., Sims, S.M., Khokha, R., Wada, T., Penninger, J.M., 2006. Regulation of cancer cell migration and bone metastasis by RANKL. Nature 440, 692–696.

Kanis, J.A., Stevenson, M., Mccloskey, E.V., Davis, S., Lloyd-Jones, M., 2007. Glucocorticoid-induced osteoporosis: a systematic review and cost-utility analysis. Health Technol. Assess. 11, 1–231. iii-iv, ix-xi.

Keaveny, T.M., Mcclung, M.R., Genant, H.K., Zanchetta, J.R., Kendler, D., Brown, J.P., Goemaere, S., Recknor, C., Brandi, M.L., Eastell, R., Kopperdahl, D.L., Engelke, K., Fuerst, T., Radcliffe, H.S., Libanati, C., 2014. Femoral and vertebral strength improvements in postmenopausal women with osteoporosis treated with denosumab. J. Bone Miner. Res. 29, 158–165.

Kendler, D.L., Roux, C., Benhamou, C.L., Brown, J.P., Lillestol, M., Siddhanti, S., Man, H.S., San Martin, J., Bone, H.G., 2010. Effects of denosumab on bone mineral density and bone turnover in postmenopausal women transitioning from alendronate therapy. J. Bone Miner. Res. 25, 72–81.

Khan, A.A., Morrison, A., Kendler, D.L., Rizzoli, R., Hanley, D.A., Felsenberg, D., Mccauley, L.K., O'ryan, F., Reid, I.R., Ruggiero, S.L., Taguchi, A., Tetradis, S., Watts, N.B., Brandi, M.L., Peters, E., Guise, T., Eastell, R., Cheung, A.M., Morin, S.N., Masri, B., Cooper, C., Morgan, S.L., Obermayer-Pietsch, B., Langdahl, B.L., Dabagh, R.A., Davison, K.S., Sandor, G.K., Josse, R.G., Bhandari, M., EL Rabbany, M., Pierroz, D.D., Sulimani, R., Saunders, D.P., Brown, J.P., Compston, J., International Task Force on Osteonecrosis of the Jaw, 2017. Case-based review of osteonecrosis of the jaw (ONJ) and application of the international recommendations for management from the international task force on ONJ. J. Clin. Densitom. 20, 8–24.

Kiechl, S., Wittmann, J., Giaccari, A., Knoflach, M., Willeit, P., Bozec, A., Moschen, A.R., Muscogiuri, G., Sorice, G.P., Kireva, T., Summerer, M., Wirtz, S., Luther, J., Mielenz, D., Billmeier, U., Egger, G., Mayr, A., Oberhollenzer, F., Kronenberg, F., Orthofer, M., Penninger, J.M., Meigs, J.B., Bonora, E., Tilg, H., Willeit, J., Schett, G., 2013. Blockade of receptor activator of nuclear factor-kappaB (RANKL) signaling improves hepatic insulin resistance and prevents development of diabetes mellitus. Nat. Med. 19, 358–363.

Kinoshita, Y., Arai, M., Ito, N., Takashi, Y., Makita, N., Nangaku, M., Shinoda, Y., Fukumoto, S., 2016. High serum ALP level is associated with increased risk of denosumab-related hypocalcemia in patients with bone metastases from solid tumors. Endocr. J. 63, 479–484.

Kondegowda, N.G., Fenutria, R., Pollack, I.R., Orthofer, M., Garcia-Ocana, A., Penninger, J.M., Vasavada, R.C., 2015. Osteoprotegerin and denosumab stimulate human beta cell proliferation through inhibition of the receptor activator of NF-kappaB ligand pathway. Cell Metabol. 22, 77–85.

Kong, Y.Y., Feige, U., Sarosi, I., Bolon, B., Tafuri, A., Morony, S., Capparelli, C., Li, J., Elliott, R., Mccabe, S., Wong, T., Campagnuolo, G., Moran, E., Bogoch, E.R., Van, G., Nguyen, L.T., Ohashi, P.S., Lacey, D.L., Fish, E., Boyle, W.J., Penninger, J.M., 1999a. Activated T cells regulate bone loss and joint destruction in adjuvant arthritis through osteoprotegerin ligand. Nature 402, 304–309.

Kong, Y.Y., Yoshida, H., Sarosi, I., Tan, H.L., Timms, E., Capparelli, C., Morony, S., Oliveira-Dos-Santos, A.J., Van, G., Itie, A., Khoo, W., Wakeham, A., Dunstan, C.R., Lacey, D.L., Mak, T.W., Boyle, W.J., Penninger, J.M., 1999b. OPGL is a key regulator of osteoclastogenesis, lymphocyte development and lymph-node organogenesis. Nature 397, 315–323.

Kostenuik, P.J., Capparelli, C., Morony, S., Adamu, S., Shimamoto, G., Shen, V., Lacey, D.L., Dunstan, C.R., 2001. OPG and PTH-(1-34) have additive effects on bone density and mechanical strength in osteopenic ovariectomized rats. Endocrinology 142, 4295–4304.

Kostenuik, P.J., Nguyen, H.Q., Mccabe, J., Warmington, K.S., Kurahara, C., Sun, N., Chen, C., Li, L., Cattley, R.C., Van, G., Scully, S., Elliott, R., Grisanti, M., Morony, S., Tan, H.L., Asuncion, F., Li, X., Ominsky, M.S., Stolina, M., Dwyer, D., Dougall, W.C., Hawkins, N., Boyle, W.J., Simonet, W.S., Sullivan, J.K., 2009. Denosumab, a fully human monoclonal antibody to RANKL, inhibits bone resorption and increases BMD in knock-in mice that express chimeric (murine/human) RANKL. J. Bone Miner. Res. 24, 182–195.

Kostenuik, P.J., Smith, S.Y., Jolette, J., Schroeder, J., Pyrah, I., Ominsky, M.S., 2011. Decreased bone remodeling and porosity are associated with improved bone strength in ovariectomized cynomolgus monkeys treated with denosumab, a fully human RANKL antibody. Bone 49, 151–161.

Kostenuik, P.J., Smith, S.Y., Samadfam, R., Jolette, J., Zhou, L., Ominsky, M.S., 2015. Effects of denosumab, alendronate, or denosumab following alendronate on bone turnover, calcium homeostasis, bone mass and bone strength in ovariectomized cynomolgus monkeys. J. Bone Miner. Res. 30, 657–669.

Lacey, D.L., Boyle, W.J., Simonet, W.S., Kostenuik, P.J., Dougall, W.C., Sullivan, J.K., San Martin, J., Dansey, R., 2012. Bench to bedside: elucidation of the OPG-RANK-RANKL pathway and the development of denosumab. Nat. Rev. Drug Discov. 11, 401–419.

Lacey, D.L., Timms, E., Tan, H.L., Kelley, M.J., Dunstan, C.R., Burgess, T., Elliott, R., Colombero, A., Elliott, G., Scully, S., Hsu, H., Sullivan, J., Hawkins, N., Davy, E., Capparelli, C., Eli, A., Qian, Y.X., Kaufman, S., Sarosi, I., Shalhoub, V., Senaldi, G., Guo, J., Delaney, J., Boyle, W.J., 1998. Osteoprotegerin ligand is a cytokine that regulates osteoclast differentiation and activation. Cell 93, 165–176.

Lafage, M.H., Balena, R., Battle, M.A., Shea, M., Seedor, J.G., Klein, H., Hayes, W.C., Rodan, G.A., 1995. Comparison of alendronate and sodium fluoride effects on cancellous and cortical bone in minipigs. A one-year study. J. Clin. Investig. 95, 2127–2133.

Lau, A.N., Wong-Pack, M., Rodjanapiches, R., Ioannidis, G., Wade, S., Spangler, L., Balasubramanian, A., Pannacciulli, N., Lin, C.J.F., Roy-Gayos, P., Bensen, W.G., Bensen, R., Adachi, J.D., 2018. Occurrence of serious infection in patients with rheumatoid arthritis treated with biologics and denosumab observed in a clinical setting. J. Rheumatol. 45, 170–176.

Leder, B.Z., Tsai, J.N., Uihlein, A.V., Burnett-Bowie, S.A., Zhu, Y., Foley, K., Lee, H., Neer, R.M., 2014. Two years of Denosumab and teriparatide administration in postmenopausal women with osteoporosis (The DATA Extension Study): a randomized controlled trial. J. Clin. Endocrinol. Metab. 99, 1694–1700.

Leder, B.Z., Tsai, J.N., Uihlein, A.V., Wallace, P.M., Lee, H., Neer, R.M., Burnett-Bowie, S.A., 2015. Denosumab and teriparatide transitions in postmenopausal osteoporosis (the DATA-Switch study): extension of a randomised controlled trial. Lancet 386, 1147–1155.

Lee, D.C., Varela, A., Kostenuik, P.J., Ominsky, M.S., Keaveny, T.M., 2016. Finite element analysis of denosumab treatment effects on vertebral strength in ovariectomized cynomolgus monkeys. J. Bone Miner. Res. 31, 1586–1595.

Lehmann, T., Aeberli, D., 2017. Possible protective effect of switching from denosumab to zoledronic acid on vertebral fractures. Osteoporos. Int. 28, 3067–3068.

Li, G., Jin, Y., Levine, M.A.H., Hoyer-Kuhn, H., Ward, L., Adachi, J.D., 2018. Systematic review of the effect of denosumab on children with osteogenesis imperfecta showed inconsistent findings. Acta Paediatr. 107, 534–537.

Li, X., Ominsky, M.S., Stolina, M., Warmington, K.S., Geng, Z., Niu, Q.T., Asuncion, F.J., Tan, H.L., Grisanti, M., Dwyer, D., Adamu, S., Ke, H.Z., Simonet, W.S., Kostenuik, P.J., 2009. Increased RANK ligand in bone marrow of orchiectomized rats and prevention of their bone loss by the RANK ligand inhibitor osteoprotegerin. Bone 45, 669–676.

Lloyd, A.A., Gludovatz, B., Riedel, C., Luengo, E.A., Saiyed, R., Marty, E., Lorich, D.G., Lane, J.M., Ritchie, R.O., Busse, B., Donnelly, E., 2017. Atypical fracture with long-term bisphosphonate therapy is associated with altered cortical composition and reduced fracture resistance. Proc. Natl. Acad. Sci. USA. 114, 8722–8727.

Lloyd, S.A., Morony, S.E., Ferguson, V.L., Simske, S.J., Stodieck, L.S., Warmington, K.S., Livingston, E.W., Lacey, D.L., Kostenuik, P.J., Bateman, T.A., 2015. Osteoprotegerin is an effective countermeasure for spaceflight-induced bone loss in mice. Bone 81, 562–572.

Mcclung, M.R., Boonen, S., Torring, O., Roux, C., Rizzoli, R., Bone, H.G., Benhamou, C.L., Lems, W.F., Minisola, S., Halse, J., Hoeck, H.C., Eastell, R., Wang, A., Siddhanti, S., Cummings, S.R., 2012. Effect of denosumab treatment on the risk of fractures in subgroups of women with postmenopausal osteoporosis. J. Bone Miner. Res. 27, 211–218.

Mcclung, M.R., Zanchetta, J.R., Hoiseth, A., Kendler, D.L., Yuen, C.K., Brown, J.P., Stonkus, S., Goemaere, S., Recknor, C., Woodson, G.C., Bolognese, M.A., Franek, E., Brandi, M.L., Wang, A., Libanati, C., 2013. Denosumab densitometric changes assessed by quantitative computed tomography at the spine and hip in postmenopausal women with osteoporosis. J. Clin. Densitom. 16, 250–256.

Meier, C., Uebelhart, B., Aubry-Rozier, B., Birkhauser, M., Bischoof-Ferrari, H.A., Frey, D., Kressig, R.W., Lamy, O., Lippuner, K., Stute, P., Suhm, N., Ferrari, S., 2017. Osteoporosis drug treatment: duration and management after discontinuation. A position statement from the SVGO/ASCO. Swiss Med. Wkly. 147, w14484.

Miller, P.D., Bolognese, M.A., Lewiecki, E.M., Mcclung, M.R., Ding, B., Austin, M., Liu, Y., San Martin, J., 2008. Effect of denosumab on bone density and turnover in postmenopausal women with low bone mass after long-term continued, discontinued, and restarting of therapy: a randomized blinded phase 2 clinical trial. Bone 43, 222–229.

Miller, P.D., Pannacciulli, N., Brown, J.P., Czerwinski, E., Nedergaard, B.S., Bolognese, M.A., Malouf, J., Bone, H.G., Reginster, J.Y., Singer, A., Wang, C., Wagman, R.B., Cummings, S.R., 2016. Denosumab or zoledronic acid in postmenopausal women with osteoporosis previously treated with oral bisphosphonates. J. Clin. Endocrinol. Metab. 101, 3163–3170.

Misof, B.R., Ominsky, M., Messmer, P., Kostenuik, P., Klaushofer, K., 2011. The effect of denosumab on the bone matrix mineralization in mice. J. Bone Miner. Res. 26, S94.

Mori, K., Le Goff, B., Charrier, C., Battaglia, S., Heymann, D., Redini, F., 2007. DU145 human prostate cancer cells express functional receptor activator of NFkappaB: new insights in the prostate cancer bone metastasis process. Bone 40, 981–990.

Nakamura, T., Matsumoto, T., Sugimoto, T., Hosoi, T., Miki, T., Gorai, I., Yoshikawa, H., Tanaka, Y., Tanaka, S., Sone, T., Nakano, T., Ito, M., Matsui, S., Yoneda, T., Takami, H., Watanabe, K., Osakabe, T., Shiraki, M., Fukunaga, M., 2014. Clinical Trials Express: fracture risk reduction with denosumab in Japanese postmenopausal women and men with osteoporosis: denosumab fracture intervention randomized placebo controlled trial (DIRECT). J. Clin. Endocrinol. Metab. 99, 2599–2607.

Napoli, N., Pannacciulli, N., Vittinghoff, E., Crittenden, D., Yun, J., Wang, A., Wagman, R., Schwartz, A.V., 2018. Effect of denosumab on fasting glucose in women with diabetes or prediabetes from the FREEDOM trial. Diabetes Metab. Res. Rev. 34 (4), e2991.

Ominsky, M.S., Kostenuik, P.J., Cranmer, P., Smith, S.Y., Atkinson, J.E., 2007. The RANKL inhibitor OPG-Fc increases cortical and trabecular bone mass in young gonad-intact cynomolgus monkeys. Osteoporos. Int. 18, 1073–1082.

Ominsky, M.S., Li, X., Asuncion, F.J., Barrero, M., Warmington, K.S., Dwyer, D., Stolina, M., Geng, Z., Grisanti, M., Tan, H.L., Corbin, T., Mccabe, J., Simonet, W.S., Ke, H.Z., Kostenuik, P.J., 2008a. RANKL inhibition with osteoprotegerin increases bone strength by improving cortical and trabecular bone architecture in ovariectomized rats. J. Bone Miner. Res. 23, 672–682.

Ominsky, M.S., Li, X., Tan, H., Asuncion, F.J., Barrero, M., Tian, X.Y., Warmington, K.S., Dwyer, D., Grisanti, M., Stolina, M., Jee, W.S., Simonet, W.S., Ke, H.Z., Kostenuik, P.J., 2008b. The effects of alendronate or denosumab on cortical and trabecular bone mass, bone strength, and bone mass-strength relationships in mice. J. Bone Miner. Res. 23, S40.

Ominsky, M.S., Libanati, C., Niu, Q.T., Boyce, R.W., Kostenuik, P.J., Wagman, R.B., Baron, R., Dempster, D.W., 2015. Sustained modeling-based bone formation during adulthood in cynomolgus monkeys may contribute to continuous BMD gains with denosumab. J. Bone Miner. Res. 30, 1280–1289.

Ominsky, M.S., Stouch, B., Schroeder, J., Pyrah, I., Stolina, M., Smith, S.Y., Kostenuik, P.J., 2011. Denosumab, a fully human RANKL antibody, reduced bone turnover markers and increased trabecular and cortical bone mass, density, and strength in ovariectomized cynomolgus monkeys. Bone 49, 162–173.

Orwoll, E., Teglbjaerg, C.S., Langdahl, B.L., Chapurlat, R., Czerwinski, E., Kendler, D.L., Reginster, J.Y., Kivitz, A., Lewiecki, E.M., Miller, P.D., Bolognese, M.A., Mcclung, M.R., Bone, H.G., Ljunggren, O., Abrahamsen, B., Gruntmanis, U., Yang, Y.C., Wagman, R.B., Siddhanti, S., Grauer, A., Hall, J.W., Boonen, S., 2012. A randomized, placebo-controlled study of the effects of denosumab for the treatment of men with low bone mineral density. J. Clin. Endocrinol. Metab. 97, 3161–3169.

Pierroz, D.D., Bonnet, N., Baldock, P.A., Ominsky, M.S., Stolina, M., Kostenuik, P.J., Ferrari, S.L., 2010. Are osteoclasts needed for the bone anabolic response to parathyroid hormone? A study of intermittent parathyroid hormone with denosumab or alendronate in knock-in mice expressing humanized RANKL. J. Biol. Chem. 285, 28164–28173.

Popp, A.W., Varathan, N., Buffat, H., Senn, C., Perrelet, R., Lippuner, K., 2018. Bone mineral density changes after 1 Year of denosumab discontinuation in postmenopausal women with long-term denosumab treatment for osteoporosis. Calcif. Tissue Int. 103 (1), 50–54.

Popp, A.W., Zysset, P.K., Lippuner, K., 2016. Rebound-associated vertebral fractures after discontinuation of denosumab-from clinic and biomechanics. Osteoporos. Int. 27, 1917–1921.

Raje, N., Terpos, E., Willenbacher, W., Shimizu, K., Garcia-Sanz, R., Durie, B., Legiec, W., Krejci, M., Laribi, K., Zhu, L., Cheng, P., Warner, D., Roodman, G.D., 2018. Denosumab versus zoledronic acid in bone disease treatment of newly diagnosed multiple myeloma: an international, double-blind, double-dummy, randomised, controlled, phase 3 study. Lancet Oncol. 19, 370−381.

Raje, N., Vadhan-Raj, S., Willenbacher, W., Terpos, E., Hungria, V., Spencer, A., Alexeeva, Y., Facon, T., Stewart, A.K., Feng, A., Braun, A., Balakumaran, A., Roodman, G.D., 2016. Evaluating results from the multiple myeloma patient subset treated with denosumab or zoledronic acid in a randomized phase 3 trial. Blood Canc. J. 6, e378.

Recknor, C., Czerwinski, E., Bone, H.G., Bonnick, S.L., Binkley, N., Palacios, S., Moffett, A., Siddhanti, S., Ferreira, I., Ghelani, P., Wagman, R.B., Hall, J.W., Bolognese, M.A., Benhamou, C.L., 2013. Denosumab compared with ibandronate in postmenopausal women previously treated with bisphosphonate therapy: a randomized open-label trial. Obstet. Gynecol. 121, 1291−1299.

Reid, I.R., 2015. Short-term and long-term effects of osteoporosis therapies. Nat. Rev. Endocrinol. 11, 418−428.

Reid, I.R., Horne, A.M., Mihov, B., Gamble, G.D., 2017. Bone loss after denosumab: only partial protection with zoledronate. Calcif. Tissue Int. 101 (4), 371−374.

Reid, I.R., Miller, P.D., Brown, J.P., Kendler, D.L., Fahrleitner-Pammer, A., Valter, I., Maasalu, K., Bolognese, M.A., Woodson, G., Bone, H., Ding, B., Wagman, R.B., San Martin, J., Ominsky, M.S., Dempster, D.W., Denosumab Phase 3 Bone Histology Study Group, 2010. Effects of denosumab on bone histomorphometry: the FREEDOM and STAND studies. J. Bone Miner. Res. 25, 2256−2265.

Rinotas, V., Niti, A., Dacquin, R., Bonnet, N., Stolina, M., Han, C.Y., Kostenuik, P., Jurdic, P., Ferrari, S., Douni, E., 2014. Novel genetic models of osteoporosis by overexpression of human RANKL in transgenic mice. J. Bone Miner. Res. 29, 1158−1169.

Rodeo, S.A., Kawamura, S., Ma, C.B., Deng, X.H., Sussman, P.S., Hays, P., Ying, L., 2007. The effect of osteoclastic activity on tendon-to-bone healing: an experimental study in rabbits. J. Bone Joint Surg. Am. 89, 2250−2259.

Rolvien, T., Schmidt, T., Butscheidt, S., Amling, M., Barvencik, F., 2017. Denosumab is effective in the treatment of bone marrow oedema syndrome. Injury 48, 874−879.

Romas, E., Sims, N.A., Hards, D.K., Lindsay, M., Quinn, J.W., Ryan, P.F., Dunstan, C.R., Martin, T.J., Gillespie, M.T., 2002. Osteoprotegerin reduces osteoclast numbers and prevents bone erosion in collagen-induced arthritis. Am. J. Pathol. 161, 1419−1427.

Roux, C., Hofbauer, L.C., Ho, P.R., Wark, J.D., Zillikens, M.C., Fahrleitner-Pammer, A., Hawkins, F., Micaelo, M., Minisola, S., Papaioannou, N., Stone, M., Ferreira, I., Siddhanti, S., Wagman, R.B., Brown, J.P., 2014. Denosumab compared with risedronate in postmenopausal women sub-optimally adherent to alendronate therapy: efficacy and safety results from a randomized open-label study. Bone 58, 48−54.

Rubin, J., Murphy, T., Nanes, M.S., Fan, X., 2000. Mechanical strain inhibits expression of osteoclast differentiation factor by murine stromal cells. Am. J. Physiol. Cell Physiol. 278, C1126−C1132.

Saad, F., Ivanescu, C., Phung, D., Loriot, Y., Abhyankar, S., Beer, T.M., Tombal, B., Holmstrom, S., 2017. Skeletal-related events significantly impact health-related quality of life in metastatic castration-resistant prostate cancer: data from PREVAIL and AFFIRM trials. Prostate Cancer Prostatic Dis. 20, 110−116.

Saag, K.G., Wagman, R.B., Geusens, P., Adachi, J.D., Messina, O.D., Emkey, R., Chapurlat, R., Wang, A., Pannacciulli, N., Lems, W.F., 2018. Denosumab versus risedronate in glucocorticoid-induced osteoporosis: a multicentre, randomised, double-blind, active-controlled, double-dummy, non-inferiority study. Lancet Diabetes Endocrinol. 6, 445−454.

Sagar, D.R., Ashraf, S., Xu, L., Burston, J.J., Menhinick, M.R., Poulter, C.L., Bennett, A.J., Walsh, D.A., Chapman, V., 2014. Osteoprotegerin reduces the development of pain behaviour and joint pathology in a model of osteoarthritis. Ann. Rheum. Dis. 73, 1558−1565.

Samadfam, R., Xia, Q., Goltzman, D., 2007. Co-treatment of PTH with osteoprotegerin or alendronate increases its anabolic effect on the skeleton of oophorectomized mice. J. Bone Miner. Res. 22, 55−63.

Samelson, E.J., Miller, P.D., Christiansen, C., Daizadeh, N.S., Grazette, L., Anthony, M.S., Egbuna, O., Wang, A., Siddhanti, S.R., Cheung, A.M., Franchimont, N., Kiel, D.P., 2014. RANKL inhibition with denosumab does not influence 3-year progression of aortic calcification or incidence of adverse cardiovascular events in postmenopausal women with osteoporosis and high cardiovascular risk. J. Bone Miner. Res. 29, 450−457.

Scagliotti, G.V., Hirsh, V., Siena, S., Henry, D.H., Woll, P.J., Manegold, C., Solal-Celigny, P., Rodriguez, G., Krzakowski, M., Mehta, N.D., Lipton, L., Gar-Saenz, J.A., Pereira, J.R., Prabhash, K., Ciuleanu, T.E., Kanarev, V., Wang, H., Balakumaran, A., Jacobs, I., 2012. Overall survival improvement in patients with lung cancer and bone metastases treated with denosumab versus zoledronic acid: subgroup analysis from a randomized phase 3 study. J. Thorac. Oncol. 7, 1823−1829.

Shane, E., Burr, D., Abrahamsen, B., Adler, R.A., Brown, T.D., Cheung, A.M., Cosman, F., Curtis, J.R., Dell, R., Dempster, D.W., Ebeling, P.R., Einhorn, T.A., Genant, H.K., Geusens, P., Klaushofer, K., Lane, J.M., Mckiernan, F., Mckinney, R., Ng, A., Nieves, J., O'keefe, R., Papapoulos, S., Howe, T.S., van der Meulen, M.C., Weinstein, R.S., Whyte, M.P., 2014. Atypical subtrochanteric and diaphyseal femoral fractures: second report of a task force of the American Society for Bone and Mineral Research. J. Bone Miner. Res. 29, 1−23.

Simon, J.A., Recknor, C., Moffett Jr., A.H., Adachi, J.D., Franek, E., Lewiecki, E.M., Mcclung, M.R., Mautalen, C.A., Ragi-Eis, S., Nicholson, G.C., Muschitz, C., Nuti, R., Torring, O., Wang, A., Libanati, C., 2013. Impact of denosumab on the peripheral skeleton of postmenopausal women with osteoporosis: bone density, mass, and strength of the radius, and wrist fracture. Menopause 20, 130−137.

Simon, M.J., Barvencik, F., Luttke, M., Amling, M., Mueller-Wohlfahrt, H.W., Ueblacker, P., 2014. Intravenous bisphosphonates and vitamin D in the treatment of bone marrow oedema in professional athletes. Injury 45, 981−987.

Simonet, W.S., Lacey, D.L., Dunstan, C.R., Kelley, M., Chang, M.S., Luthy, R., Nguyen, H.Q., Wooden, S., Bennett, L., Boone, T., Shimamoto, G., Derose, M., Elliott, R., Colombero, A., Tan, H.L., Trail, G., Sullivan, J., Davy, E., Bucay, N., Renshaw-Gegg, L., Hughes, T.M., Hill, D., Pattison, W., Campbell, P., Sander, S., Van, G., Tarpley, J., Derby, P., Lee, R., Boyle, W.J., 1997. Osteoprotegerin: a novel secreted protein involved in the regulation of bone density. Cell 89, 309−319.

Sipos, W., Zysset, P., Kostenuik, P., Mayrhofer, E., Bogdan, C., Rauner, M., Stolina, M., Dwyer, D., Sommerfeld-Stur, I., Pendl, G., Resch, H., Dall'Ara, E., Varga, P., Pietschmann, P., 2011. OPG-Fc treatment in growing pigs leads to rapid reductions in bone resorption markers, serum calcium, and bone formation markers. Horm. Metab. Res. 43, 944–949.

Slyfield, C.R., Tkachenko, E.V., Fischer, S.E., Ehlert, K.M., Yi, I.H., Jekir, M.G., O'brien, R.G., Keaveny, T.M., Hernandez, C.J., 2012. Mechanical failure begins preferentially near resorption cavities in human vertebral cancellous bone under compression. Bone 50, 1281–1287.

Smith, M.R., Egerdie, B., Toriz, N.H., Feldman, R., Tammela, T.L.J., Saad, F., Heracek, J., Szwedowski, M., Ke, C., Kupic, A., Leder, B.Z., Goessl, C., 2009. Denosumab in men receiving androgen-deprivation therapy for prostate cancer. N. Engl. J. Med. 361, 745–755.

Smith, M.R., Saad, F., Coleman, R., Shore, N., Fizazi, K., Tombal, B., Miller, K., Sieber, P., Karsh, L., Damiao, R., Tammela, T.L., Egerdie, B., Van Poppel, H., Chin, J., Morote, J., Gomez-Veiga, F., Borkowski, T., Ye, Z., Kupic, A., Dansey, R., Goessl, C., 2012. Denosumab and bone-metastasis-free survival in men with castration-resistant prostate cancer: results of a phase 3, randomised, placebo-controlled trial. Lancet 379, 39–46.

Sobti, A., Agrawal, P., Agarwala, S., Agarwal, M., 2016. Giant cell tumor of bone–an overview. Arch Bone Joint Surg. 4, 2–9.

Stewart, AF., 2005. Clinical practice. Hypercalcemia associated with cancer. N. Engl. J. Med. 352, 373–379.

Stolina, M., Schett, G., Dwyer, D., Vonderfecht, S., Middleton, S., Duryea, D., Pacheco, E., Van, G., Bolon, B., Feige, U., Zack, D., Kostenuik, P., 2009. RANKL inhibition by osteoprotegerin prevents bone loss without affecting local or systemic inflammation parameters in two rat arthritis models: comparison with anti-TNFalpha or anti-IL-1 therapies. Arthritis Res. Ther. 11, R187.

Stopeck, A.T., Lipton, A., Body, J.J., Steger, G.G., Tonkin, K., De Boer, R.H., Lichinitser, M., Fujiwara, Y., Yardley, D.A., Viniegra, M., Fan, M., Jiang, Q., Dansey, R., Jun, S., Braun, A., 2010. Denosumab compared with zoledronic acid for the treatment of bone metastases in patients with advanced breast cancer: a randomized, double-blind study. J. Clin. Oncol. 28, 5132–5139.

Sugimoto, T., Matsumoto, T., Hosoi, T., Miki, T., Gorai, I., Yoshikawa, H., Tanaka, Y., Tanaka, S., Fukunaga, M., Sone, T., Nakano, T., Ito, M., Matsui, S., Yoneda, T., Takami, H., Watanabe, K., Osakabe, T., Okubo, N., Shiraki, M., Nakamura, T., 2015. Three-year denosumab treatment in postmenopausal Japanese women and men with osteoporosis: results from a 1-year open-label extension of the Denosumab Fracture Intervention Randomized Placebo Controlled Trial (DIRECT). Osteoporos. Int. 26, 765–774.

Ta, H.M., Nguyen, G.T., Jin, H.M., Choi, J., Park, H., Kim, N., Hwang, H.Y., Kim, K.K., 2010. Structure-based development of a receptor activator of nuclear factor-kappaB ligand (RANKL) inhibitor peptide and molecular basis for osteopetrosis. Proc. Natl. Acad. Sci. USA. 107, 20281–20286.

Takeuchi, T., Tanaka, Y., Ishiguro, N., Yamanaka, H., Yoneda, T., Ohira, T., Okubo, N., Genant, H.K., van der Heijde, D., 2016. Effect of denosumab on Japanese patients with rheumatoid arthritis: a dose-response study of AMG 162 (Denosumab) in patients with RheumatoId arthritis on methotrexate to Validate inhibitory effect on bone Erosion (DRIVE)-a 12-month, multicentre, randomised, double-blind, placebo-controlled, phase II clinical trial. Ann. Rheum. Dis. 75, 983–990.

Takeuchi, T., Tanaka, Y., Soen, S., Yamanaka, H., Yoneda, T., Tanaka, S., Nitta, T., Okubo, N., Genant, H., van der Heijde, D., 2017. SAT0186 Effects of denosumab, a subcutaneous rankl inhibitor, on the progression of structural damage in Japanese patients with rheumatoid arthritis treated with csdmards: results from the 12-month double blind phase 3, desirable study. Ann. Rheum. Dis. 76, 841–842.

Thiryayi, W.A., Thiryayi, S.A., Freemont, A.J., 2008. Histopathological perspective on bone marrow oedema, reactive bone change and haemorrhage. Eur. J. Radiol. 67, 62–67.

Thomas, D., Henshaw, R., Skubitz, K., Chawla, S., Staddon, A., Blay, J.Y., Roudier, M., Smith, J., Ye, Z., Sohn, W., Dansey, R., Jun, S., 2010. Denosumab in patients with giant-cell tumour of bone: an open-label, phase 2 study. Lancet Oncol. 11, 275–280.

Trejo, P., Rauch, F., Ward, L., 2018. Hypercalcemia and hypercalciuria during denosumab treatment in children with osteogenesis imperfecta type VI. J. Musculoskelet. Neuronal Interact. 18, 76–80.

Tsai, J.N., Nishiyama, K.K., Lin, D., Yuan, A., Lee, H., Bouxsein, M.L., Leder, B.Z., 2017. Effects of denosumab and teriparatide transitions on bone microarchitecture and estimated strength: the DATA-switch HR-pQCT study. J. Bone Miner. Res. 32, 2001–2009.

Tsourdi, E., Langdahl, B., Cohen-Solal, M., Aubry-Rozier, B., Eriksen, E.F., Guanabens, N., Obermayer-Pietsch, B., Ralston, S.H., Eastell, R., Zillikens, M.C., 2017. Discontinuation of Denosumab therapy for osteoporosis: a systematic review and position statement by ECTS. Bone 105, 11–17.

Tsutsumi, R., Hock, C., Bechtold, C.D., Proulx, S.T., Bukata, S.V., Ito, H., Awad, H.A., Nakamura, T., O'keefe, R.J., Schwarz, E.M., 2008. Differential effects of biologic versus bisphosphonate inhibition of wear debris-induced osteolysis assessed by longitudinal micro-CT. J. Orthop. Res. 26, 1340–1346.

Ulrich-Vinther, M., Andreassen, T.T., 2005. Osteoprotegerin treatment impairs remodeling and apparent material properties of callus tissue without influencing structural fracture strength. Calcif. Tissue Int. 76, 280–286.

Valenta, A., Roschger, P., Fratzl-Zelman, N., Kostenuik, P.J., Dunstan, C.R., Fratzl, P., Klaushofer, K., 2005. Combined treatment with PTH (1-34) and OPG increases bone volume and uniformity of mineralization in aged ovariectomized rats. Bone 37, 87–95.

Watts, N.B., Adler, R.A., Bilezikian, J.P., Drake, M.T., Eastell, R., Orwoll, E.S., Finkelstein, J.S., Endocrine, S., 2012. Osteoporosis in men: an endocrine society clinical practice guideline. J. Clin. Endocrinol. Metab. 97, 1802–1822.

Watts, N.B., Butler, P.W., Binkley, N., Grbic, J.T., Mcclung, M., Tierney, A., Wagman, R.B., Yin, X., 2017. Evaluation of invasive oral procedures and events in women with postmenopausal osteoporosis treated for up to 10 years with denosumab: results from the phase 3 FREEDOM open-label extension. J. Bone Miner. Res. 32, S5.

Xiong, J., Onal, M., Jilka, R.L., Weinstein, R.S., Manolagas, S.C., O'brien, C.A., 2011. Matrix-embedded cells control osteoclast formation. Nat. Med. 17, 1235–1241.

Yasuda, H., Shima, N., Nakagawa, N., Yamaguchi, K., Kinosaki, M., Mochizuki, S., Tomoyasu, A., Yano, K., Goto, M., Murakami, A., Tsuda, E., Morinaga, T., Higashio, K., Udagawa, N., Takahashi, N., Suda, T., 1998. Osteoclast differentiation factor is a ligand for osteoprotegerin/osteoclastogenesis-inhibitory factor and is identical to TRANCE/RANKL. Proc. Natl. Acad. Sci. USA. 95, 3597−3602.

Zebaze, R., Libanati, C., Mcclung, M.R., Zanchetta, J.R., Kendler, D.L., Hoiseth, A., Wang, A., Ghasem-Zadeh, A., Seeman, E., 2016. Denosumab reduces cortical porosity of the proximal femoral shaft in postmenopausal women with osteoporosis. J. Bone Miner. Res. 31, 1827−1834.

Zebaze, R.M., Libanati, C., Austin, M., Ghasem-Zadeh, A., Hanley, D.A., Zanchetta, J.R., Thomas, T., Boutroy, S., Bogado, C.E., Bilezikian, J.P., Seeman, E., 2014. Differing effects of denosumab and alendronate on cortical and trabecular bone. Bone 59, 173−179.

Chapter 74

Pharmacologic basis of sclerostin inhibition

Hua Zhu Ke[1], Scott J. Roberts[2] and Gill Holdsworth[2]
[1]Angitia Biopharmaceuticals Limited, Guangzhou, China; [2]Bone Therapeutic Area, UCB Pharma, Slough, United Kingdom

Chapter outline

Introduction

Insights gained from rare genetic conditions can be used to identify potential new targets and pathways for therapeutic intervention. The function of the *SOST* gene product, sclerostin, as an inhibitor of bone formation in humans was discovered by genetic mapping studies that pinpointed loss-of-function mutations in the *SOST* gene as causative in the high bone mass (HBM) disorder sclerosteosis (Balemans et al., 2001; Brunkow et al., 2001). In mice, deletion of the *SOST* gene causes an increase in bone mass and strength due to increased bone formation, while overexpression of a human sclerostin transgene results in low bone mass and decreased bone strength (Ke et al., 2012). Significant efforts have been directed toward the development of neutralizing antibodies to sclerostin as novel bone-forming therapies for osteoporosis and other conditions of low bone mass.

In this chapter, we focus on the biology of sclerostin and its pharmacologic inhibition by monoclonal antibodies (Scl-Ab). We describe the biochemistry of sclerostin and its interactions with low-density lipoprotein receptor-related proteins (LRP) 4/5/6, which facilitate sclerostin's function as an antagonist of the canonical wingless-related integration site (Wnt) signaling pathway. The mechanism of action of sclerostin inhibition and its consequences for skeletal tissue in a number of animal models, including models of osteoporosis, are discussed. Finally, we briefly summarize the findings from clinical trials of Scl-Ab in postmenopausal osteoporosis, male osteoporosis, osteogenesis imperfecta (OI), and adult hypophosphatasia.

Principles of Bone Biology. https://doi.org/10.1016/B978-0-12-814841-9.00074-9

Sclerostin biology and biochemistry

Human monogenic high bone mass conditions related to sclerostin: sclerosteosis and van Buchem disease

Two very rare, severe sclerosing bone dysplasias, each caused by a genetic deficiency in sclerostin expression—sclerosteosis and van Buchem disease—have yielded important insights into the importance of sclerostin as a regulator of bone metabolism in the human skeleton.

Sclerosteosis (OMIM: 269500) is a rare, autosomal recessive, HBM disorder found principally within the Afrikaner population of South Africa and in a few individuals in other parts of the world (Van Lierop et al., 2017). Sclerosteosis is caused by inactivating mutations in the *SOST* gene (Balemans et al., 2001; Brunkow et al., 2001). *SOST* is located on chromosome 17q12−q21 and encodes the protein sclerostin. The most frequent mutation (c.69G>T) introduces a premature stop codon immediately following the signal peptide, resulting in the loss of sclerostin protein expression. Table 74.1 summarizes the known *SOST* mutations and clinical characteristics that have been reported in patients with sclerosteosis. The earliest observed postnatal feature of sclerosteosis is syndactyly, which is present in approximately two-thirds of patients. From an early age, affected individuals are typically of tall stature, and high skeletal density and cortical thickening are readily apparent on X-ray examination (Hamersma et al., 2003). In the skull, progressive bone overgrowth occurs, leading to facial feature deformities due to excessive mandibular growth and forehead bossing. Bone overgrowth also causes cranial nerve entrapment, facial palsy, hearing loss, and raised intracranial pressure, the most severe and life-threatening complication of the condition. Measurement of bone mineral density (BMD) by dual-energy X-ray absorptiometry (DXA) in patients with sclerosteosis reveals extremely high BMD Z scores, ranging from +7.7 to +14.4 at the lumbar spine and +7.8 to +11.5 at the hip (Van Lierop et al., 2017).

The HBM observed in individuals with sclerosteosis is driven by excessive osteoblast-mediated bone formation, rather than by any defect in osteoclastic bone resorption. In adults with sclerosteosis, serum levels of the bone-formation marker procollagen type 1 N-terminal propeptide (P1NP) have been shown to be approximately four times higher than in healthy controls; in contrast, serum levels of the bone-resorption marker C-terminal telopeptide of type I collagen (CTX) were normal, or lower, compared with healthy controls (Van Lierop et al., 2017). Importantly, the high BMD present in patients with sclerosteosis translates into enhanced bone strength, indicating that the bone formed is intrinsically of good quality. The hyperostotic skeleton appears resistant to trauma and there are no reports in the literature of patients experiencing a fracture. Changes in mineralization kinetics, resulting in a reduction in matrix mineralization and an increase in proteoglycan content, are seen in patients with sclerosteosis, indicating that the high BMD does not reflect increased bone matrix mineralization, as has been observed in other HBM disorders such as pycnodysostosis (Hassler et al., 2014).

Within the Afrikaner population, the carrier rate for sclerosteosis has been estimated at 1/140 (Beighton et al., 1976). Serum sclerostin levels in sclerosteosis carriers are reported to be approximately 60% lower than in healthy control subjects, while serum P1NP and BMD at the lumbar spine and hip were higher in sclerosteosis carriers than in age- and sex-matched healthy controls (Van Lierop et al., 2017). These heterozygous individuals do not show signs or symptoms of sclerosteosis, which is indicative of a gene-dose effect of the *SOST* mutation. This supports the idea that pharmacologic inhibition of sclerostin may have potential for the development of bone-forming therapeutics for osteoporosis and other bone-related disorders.

Patients with van Buchem disease (OMIM: 239100) display skeletal changes similar to those of patients with sclerosteosis. However, the skeletal phenotype in van Buchem disease is milder and individuals tend to be of normal height and do not display syndactyly. The condition is mostly restricted to inhabitants of a single isolated fishing village in the Netherlands, which was an island until its reconnection to the mainland following land reclamation in 1940. In contrast with the *SOST* gene-coding region mutations found in sclerosteosis patients, van Buchem disease is caused by deletion of a 52-kb, noncoding, *SOST*-specific regulatory element located 35 kb downstream of the *SOST* gene. This region contains at least one enhancer element that is required for postnatal expression of sclerostin in bone (Balemans et al., 2002; Loots et al., 2005).

More recently, an additional sclerostin−bone axis was reported following the discovery of novel missense mutations in the gene for LRP4 (also known as multiple epidermal growth factor-like domain 7) in patients with the HBM condition termed sclerosteosis 2 (OMIM: 614305), a condition that bears striking similarities to sclerosteosis (Leupin et al., 2011). Individuals carrying homozygous or heterozygous mutations in LRP4 exhibit the typical characteristics of sclerosteosis,

TABLE 74.1 Summary of *SOST* mutations reported to be associated with sclerosteosis, and selected clinical characteristics.

cDNA mutation	Protein change	Type	Number of cases	Geographical origin	Tall stature	Syndactyly	Facial involvement (distortion or palsy)	Hearing loss	Raised intracranial pressure or headaches	Increased BMD
c.69C>T	p.Glu24*	Nonsense	66	South Africa (Brunkow et al., 2001)	Y	Y	Y	Y	Y	Y
c.79C>T	p.Gln27*	Nonsense	1	Morocco (Belkhribchia et al., 2014)	N	Y	Y	Y	Y	Y
c.371G>A	p.Trp124*	Nonsense	1	Turkey (Yagi et al., 2015)	Y	Y	Y	Y	NR	Y
c.373G>A	p.Trp124*	Nonsense	7	Brazil (Balemans et al., 2001; Kim et al., 2008)	N	N	Y	Y	NR	Y
c.376C>T	p.Arg126*	Nonsense	9	USA (Balemans et al., 2001; Stein et al., 1983)	Y	Y	Y	Y	Y	Y
c.444_445TC>AA	p.Cys148*	Nonsense	2	China (He et al., 2016)	N	Y	Y	N	Y	Y
c.499T>C	p.Cys167Arg	Missense	2	Turkey (Piters et al., 2010)	Y	N	Y	Y	Y	Y
c.78_88insC	p.Lys30Glnfs*2	Frameshift	2	Egypt (Fayez et al., 2015)	Y	Y	Y	Y	Y	Y
c.296_297insC	p.Val100fs*128	Frameshift	1	India (Bhadada et al., 2013)	N	Y	Y	Y	Y	Y
IVS1+1G>C	–	Splice site	2	Germany (Balemans et al., 2005)	N	N	Y	Y	N	Y
IVS1+3A>T	–	Splice site	1	Senegal (Balemans et al., 2001)	Y	Y	Y	N	Y	Y

Original references are shown in the Geographical origin column. The * symbol in the protein change column indicates a stop codon. *Y* indicates that this clinical characteristic has been reported in association with the mutation shown; *N* indicates that this characteristic was not present in the cases described; *NR* indicates that there was no detail reported in relation to this clinical characteristic in the cases described.
BMD, bone mineral density.
Adapted from van Lierop, A.H., Appelman-Dijkstra, N.M., Papapoulos, S.E., 2017. Sclerostin deficiency in humans, Bone 96, 51–62, Copyright (2017), with permission from Elsevier.

including syndactyly and cortical thickening of the skull and long bones. The causative mutations, R1170Q/W and W1186S, are located within the central pocket of the third β propeller of LRP4 (Leupin et al., 2011; Fijalkowski et al., 2016). These mutations impair sclerostin binding to LRP4, leading to increased BMD, and suggest that LRP4 may act as a chaperone to facilitate the action of sclerostin.

Expression of sclerostin protein

During embryogenesis, sclerostin is expressed in the skeletal anlage and limb bud (Loots et al., 2005). Expression of sclerostin is maintained throughout aging and is largely limited to the skeleton, where it is expressed by mature osteocytes but not by early osteocytes, osteoblasts, or bone-lining cells (Poole et al., 2005). Low levels of sclerostin expression are also detected in mineralized matrix-associated cells, including cementocytes (Lehnen et al., 2012), hypertrophic chondrocytes in the growth plate and articular chondrocytes (Chan et al., 2011; Van Bezooijen et al., 2009; Winkler et al., 2003), synovial tissue cells from patients with rheumatoid arthritis (Wehmeyer et al., 2016), and mineralized lesions within the vascular system and aortic valves (Brandenburg et al., 2013; Koos et al., 2013; Zhu et al., 2011). Low levels of sclerostin are also found in nonmineralizing tissues, including aorta, kidney, and some regions of the developing embryonic and neonatal heart (although not adult cardiac tissue) (Balemans et al., 2001; Fijalkowski et al., 2016; Poole et al., 2005; Lehnen et al., 2012; Chan et al., 2011; Van Bezooijen et al., 2009; Winkler et al., 2003; Wehmeyer et al., 2016; Brandenburg et al., 2013; Koos et al., 2013; Zhu et al., 2011; Didangelos et al., 2010; Krishna et al., 2017; van Bezooijen et al., 2007).

Osteocytes are thought to fulfill a mechanosensing role in the skeleton, and sclerostin is a candidate mediator of mechanotransduction. Sclerostin is detected in the canalicular network of bone (Poole et al., 2005); its expression by osteocytes is reduced following mechanical loading and it is at increased levels in unloaded bone (Robling et al., 2008). In common with most cells, osteocytes release extracellular vesicles (EVs) in vivo (McCormick et al., 2016; Brown et al., 2016) and EVs released from osteocyte cell lines cultured in vitro have been shown to contain sclerostin (Brown et al., 2016; Wang et al., 2017). Sclerostin is also detected in the circulation (Van Lierop et al., 2017), although the relevance of serum sclerostin in the context of skeletal homeostasis is currently unclear.

The *SOST* gene is subject to epigenetic regulation, and methylation of the *SOST* proximal promoter has been proposed as the mechanism by which *SOST* expression is regulated during osteoblast-to-osteocyte transition (Delgado-Calle et al., 2012). The histone deacetylases SIRT1 and HDAC4/5 are reported to repress *SOST* expression, and HDAC4/5 have been associated with transcriptional downregulation of *SOST* in response to parathyroid hormone (PTH) (Cohen-Kfir et al., 2011; Wein et al., 2016).

Structure and functional domains of sclerostin

The secreted glycoprotein sclerostin was first identified as a member of the DAN/Cerberus family and thus was predicted to contain a cysteine knot motif (Balemans et al., 2001; Brunkow et al., 2001). While most cysteine-knot proteins exist as dimers, sclerostin lacks the classical free cysteine that typically mediates dimerization in this class of protein. Hence, sclerostin exists as a monomer of approximately 21 kDa. In 2009, two research groups determined the structure of sclerostin in solution using nuclear magnetic resonance (NMR) spectroscopy (Veverka et al., 2009; Weidauer et al., 2009). In addition to highly flexible N and C termini, sclerostin contains a variety of structural features arranged around the cysteine knot, including a structured core, which can bind heparin, and the disordered "loop 2" region that is important for binding to the LRP5/6 Wnt coreceptors. Efforts to generate a crystal structure of sclerostin, either as the apo-protein or in complex with antibody fragments or the extracellular domain(s) of any of its cognate receptors, have so far been unsuccessful. This probably reflects the highly dynamic and flexible nature of sclerostin.

Sclerostin mechanism of action in the skeleton

Sclerostin interaction with LRP4/5/6

At around the same time that mutations in the *SOST* gene were discovered as the cause of sclerosteosis, the discovery of low and high bone mass mutations in the first β propeller of the LRP5 Wnt coreceptor revealed the importance of the Wnt signaling pathway as a central regulator of bone formation (Gong et al., 2001; Van Wesenbeeck et al., 2003). Subsequently, sclerostin was demonstrated to function as an antagonist of Wnt signaling through high-affinity binding to the extracellular domains of LRP5/6 (Li et al., 2005; Semenov et al., 2005); crucially, the link was made demonstrating that the

presence of HBM mutations in LRP5 impaired sclerostin binding and function (Semenov and He, 2006). The highly flexible loop 2 region of sclerostin contains an NxI motif (where N represents asparagine; x, any amino acid; and I, isoleucine), which interacts with the central region of the first β propeller of the LRP5/6 Wnt coreceptors (Bourhis et al., 2011; Holdsworth et al., 2012). This interaction echoes the classical "shutter-binding" mechanism that typically occurs between β-propeller-containing lipoprotein receptors and their ligands (Andersen et al., 2013).

Despite its structural similarity to LRP5/6, LRP4 is not believed to participate directly in canonical Wnt signaling, which is initiated following the formation of a ternary complex with Wnt and Frizzled (Fzd). The presence of HBM LRP4 mutations and the blockade of sclerostin binding using an LRP4 antibody are both associated with an increase in serum sclerostin, as well as an increase in bone mass (Fijalkowski et al., 2016; Chang et al., 2014). This suggests that the role of LRP4 in bone is to anchor sclerostin within osseous tissue. Similarly, mice with the LRP4 HBM R1170Q knock-in mutation show elevated serum sclerostin and a decrease in the proportion of osteocytes staining positive for sclerostin in the tibia (Boudin et al., 2017). Sclerostin binds LRP4 with high affinity in vitro and LRP4 overexpression in a Wnt reporter cell line has been shown to enhance the efficacy of sclerostin as a Wnt signaling antagonist (Leupin et al., 2011), while silencing of LRP4 impairs sclerostin function. Although the LRP4 HBM mutations have identified the central region of the third β propeller as the site of interaction with sclerostin, the reciprocal region of sclerostin that binds LRP4 and the molecular basis of this interaction remain to be fully defined.

Sclerostin inhibition of the canonical Wnt signaling pathway

Due to its sequence homology with other secreted bone morphogenetic protein (BMP) antagonists, sclerostin was originally thought to function as a modulator of the BMP pathway. High-affinity interactions between sclerostin and several BMP family members resulting in decreased BMP binding to type 1 and 2 BMP receptors have been reported (Winkler et al., 2003). Sclerostin has also been found to promote the intracellular degradation of BMP7 in vitro (Nusse and Clevers, 2017). However, compared with the well-established role of sclerostin as an antagonist of Wnt signaling, its effects on the BMP pathway are poorly understood and the physiological relevance of the described observations is unclear.

Following the discovery of the first mammalian Wnt family member in 1982, the Wnt signaling pathway is now recognized as an evolutionarily conserved cascade that is a central regulator of developmental processes, normal physiology, and disease (reviewed by Nusse and Clevers, 2017). Three major Wnt signaling pathways are recognized: the Wnt/β-catenin pathway (also called the canonical Wnt pathway), the noncanonical Wnt/planar cell polarity pathway, and the Wnt/calcium pathway. While both the canonical and the noncanonical Wnt signaling cascades play a role in bone homeostasis, the canonical pathway has emerged as the predominant regulator of bone metabolism (reviewed by Baron and Kneissel, 2013) and is the pathway upon which sclerostin acts. Increased canonical Wnt signaling favors osteogenic commitment and the differentiation of mesenchymal stem cells (MSCs), with concomitant repression of differentiation along the chondrogenic and adipogenic lineages (Baron and Kneissel, 2013).

The Wnt signaling pathway is highly complex, with multiple Wnt ligands and receptor subtypes and intricate intracellular regulatory mechanisms. It is beyond the scope of this chapter to address this pathway in detail; rather, a simplified overview of the pathway is provided to describe the role and mechanism of action of sclerostin. Activation of the canonical Wnt pathway is triggered by the binding of soluble Wnt ligands to the extracellular domains of the Fzd and LRP5/6 cell surface receptors. Formation of this ternary complex results in the stabilization and accumulation of β-catenin, which translocates to the nucleus and associates with transcription factors to regulate target gene transcription. Binding of osteocyte-secreted sclerostin to LRP5/6 prevents LRP5/6 from interacting with Wnt, thereby inactivating the canonical Wnt pathway and targeting β-catenin for proteasomal degradation. This leads to the inhibition of Wnt target gene transcription and decreased bone formation. Antibodies that bind sclerostin and prevent its interaction with LRP4/5/6 restore canonical Wnt signaling, leading to an increase in bone formation. Fig. 74.1 shows a simplified representation of the action of sclerostin as a secreted antagonist of canonical Wnt signaling, and the restoration of Wnt/β-catenin pathway activation in the presence of Scl-Ab.

Sclerostin effects on mesenchymal stem cells

Sclerostin directly modulates osteoblast function. In vitro, recombinant sclerostin inhibits the proliferation, alkaline phosphatase activity, and mineralization of human MSCs, while apoptosis is increased by sclerostin (Winkler et al., 2003; Sutherland et al., 2004). Similarly, ex vivo osteogenic cultures of MSCs, and primary calvarial osteoblasts from transgenic mice overexpressing sclerostin (hereafter, referred to as *SOST* transgenic mice), show a decrease in alkaline phosphatase expression and a decrease in mineralization compared with control cultures or wild-type littermate controls (Winkler et al., 2003; Yorgan et al., 2015). Of the different stages of osteogenic differentiation of MSCs, it is the late osteoblast/

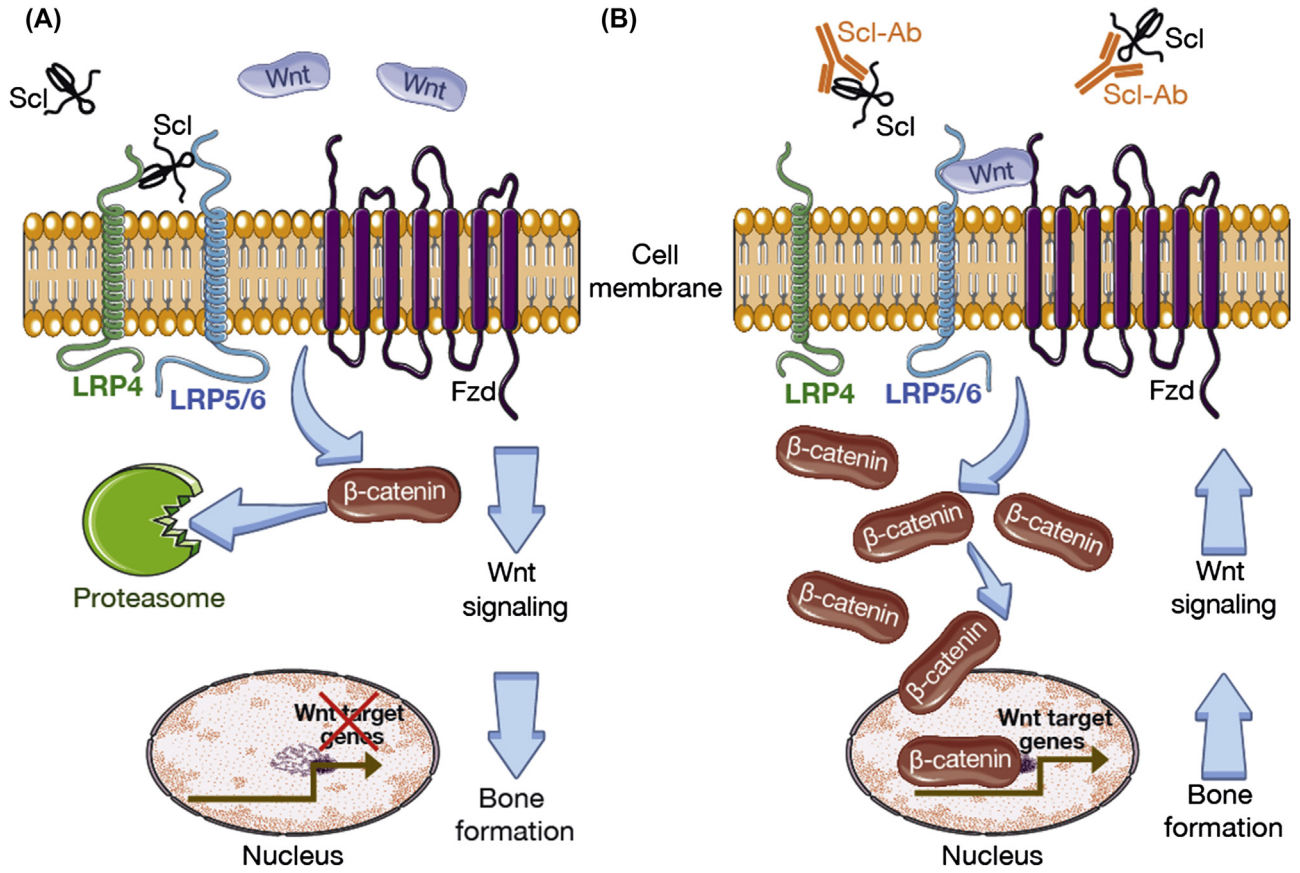

FIGURE 74.1 Mechanism of action of sclerostin as an antagonist of the canonical wingless-related integration site (*Wnt*) signaling pathway in bone tissue. (A) Sclerostin (*Scl*) binds the low-density lipoprotein receptor–related protein 4 (*LRP4*) and LRP5/6 cell surface receptors to block the interaction of Wnt with LRP5/6, thus preventing formation of the LRP5/6–Wnt–Frizzled (*Fzd*) ternary complex and inhibiting canonical Wnt signaling. Cytosolic β-catenin is targeted for proteasomal degradation and bone formation is inhibited. (B) Neutralizing antibodies to sclerostin (*Scl-Ab*) bind Scl to prevent the interaction between Scl and LRP4/5/6, thereby allowing Wnt to bind LRP5/6 and permitting formation of the LRP5/6–Wnt–Fzd ternary complex to stimulate canonical Wnt signaling. Cytosolic β-catenin accumulates and translocates to the nucleus, where it activates the transcription of Wnt target genes, leading to increased bone formation. This figure was produced using Servier Medical Art.

preosteocyte population that appears to be the most sensitive to sclerostin. Terminal differentiation of late osteoblasts into osteocytes is inhibited by sclerostin and in part reflects sclerostin-mediated regulation of the matrix extracellular phosphoglycoprotein (MEPE)–acidic serine aspartate-rich MEPE–associated motif axis, which is involved in mineralization of the newly formed bone matrix (Atkins et al., 2011). The action of sclerostin as an antagonist of Wnt signaling has also been shown in mouse preosteoblast MC-3T3 cells bearing a luciferase reporter of canonical Wnt pathway activation (Veverka et al., 2009).

Regulation of canonical Wnt signaling to control MSC differentiation has been demonstrated in vitro. In contrast to the widely studied effects of sclerostin on the osteoblast lineage, the action of sclerostin on chondrocytes and adipocytes is less well characterized. Addition of sclerostin to primary articular chondrocytes cultured in vitro reduces apoptosis and promotes chondrocyte homeostasis by inhibiting canonical Wnt signaling, decreasing expression of proteases implicated in cartilage degradation, and increasing expression of anabolic genes (Chan et al., 2011; Bouaziz et al., 2015). Inhibition of Wnt signaling by sclerostin was shown to induce adipogenesis in 3T3-L1 cells and bone marrow–derived MSCs (Fairfield et al., 2017), and promoted expression of UCP1, which is a marker of beige adipocytes (Fulzele et al., 2017).

Genetic manipulation of sclerostin expression in mice: *SOST* knockout and overexpression

Sclerostin is highly conserved across vertebrates and the amino acid sequences in rats and mice show at least 88% identity with the human sequence (Brunkow et al., 2001). Canonical Wnt signaling is an ancient and evolutionarily conserved pathway in metazoans. Animal models have proved to be highly informative translational models in which to study sclerostin function and have confirmed the significant role of sclerostin as an inhibitor of bone formation.

The sclerosteosis phenotype has been reproduced in mice through targeted deletion of the *SOST* gene. *SOST*-knockout (KO) mice exhibit increased BMD throughout the skeleton, which is apparent as early as 1 month of age (Kramer et al., 2010; Li et al., 2008; Lin et al., 2009). Progressive increases in leg and spine BMD have been observed from 1 to 4 months of age in male *SOST* KO mice, after which time leg BMD continues to increase, but at a slower rate, during months 4 to 12, with maintenance of peak BMD up to 18 months of age. Lumbar spine BMD in these mice peaks at 4 months of age and is sustained at this level up to 18 months (Ke et al., 2012). A similar profile of continuous increases in total and femoral BMD has also been observed in female *SOST*-KO mice compared with their wild-type littermates, with a rapid and progressive increase in BMD from 4 to 12 weeks of age, and a slower rate of BMD gain during weeks 12−40 (Lin et al., 2009).

Significant increases in trabecular thickness and bone volume fraction, as well as cortical thickness, have also been reported in *SOST*-KO mice (Ke et al., 2012; Kramer et al., 2010; Li et al., 2008; Lin et al., 2009). Dynamic histomorphometric analyses of bones from these mice demonstrated vastly greater mineralizing surface as a ratio to bone surface and markedly higher ratio of bone formation rate (BFR) to bone surface on trabecular bone surfaces. Elevated serum osteocalcin levels were also observed compared with wild-type littermates. The bones of *SOST*-KO mice display a normal lamellar bone structure, and the increased cortical thickness reflects accrual of bone on both endocortical and periosteal surfaces. Consistent with the increased bone formation and bone mass, bones from sclerostin-deficient male or female mice exhibited robust increases in mechanical strength upon testing of lumbar vertebral bodies and long bones (Li et al., 2008).

In agreement with the role of sclerostin as an antagonist of Wnt/β-catenin signaling, genetic deletion of *SOST* is associated with enhanced activation of this pathway in bone. A greater proportion of osteocytes show staining for β-catenin expression compared with osteocytes from wild-type mice. Furthermore, immunohistochemical staining revealed a significant reduction in apoptotic osteocytes in *SOST*-KO bone (Krause et al., 2010; Lin et al., 2009), suggesting a potential role for sclerostin in regulating osteocyte longevity. Bone composition analysis revealed that deletion of the *SOST* gene was associated with slower mineralization kinetics and a higher proteoglycan content of the endocortical bone matrix (Belkhribchia et al., 2014), which may contribute to the increased bone strength observed in the bones of *SOST*-deficient mice. Ovariectomy of female *SOST*-KO mice resulted in increased bone resorption, indicating that the impact of estrogen deficiency on bone resorption is maintained in mice lacking sclerostin (Ke et al., 2012).

As a counterpoint to the HBM phenotype in *SOST*-KO mice, *SOST* transgenic mice exhibit low bone mass and a reduction in bone strength due to decreased bone formation (Leupin et al., 2011; Winkler et al., 2003; Yorgan et al., 2015; Kramer et al., 2010). Three different approaches have been used to develop these models: one method expressed human sclerostin using a bacterial artificial chromosome (BAC) (Loots et al., 2005; Kramer et al., 2010), while other methods employed the mouse osteocalcin promoter, *OG2* (Winkler et al., 2003), or the mouse osteoblast-specific 2.3-kb *Col1a1* promoter (Yorgan et al., 2015) to overexpress human sclerostin in bone. Compared with their respective wild-type littermates, all three transgenic models exhibited reduced trabecular bone volume and cortical thickness within the axial and appendicular skeleton (lumbar spine, calvaria, and femur). The reduction in femoral cortical thickness was apparent in young mice and persisted through 8 months in the BAC−*SOST* model (Kramer et al., 2010), while vertebral trabecular bone volume was reduced at 6 weeks and persisted through 12 months in mice bearing the *Col1a1*−*SOST* transgene (Yorgan et al., 2015). Dynamic histomorphometry revealed a decreased BFR but no significant effect on bone resorption parameters in each transgenic model. Consistent with the reduction in bone formation and bone mass, the bones of *SOST* transgenic mice exhibit impaired mechanical strength and greater fragility compared with their wild-type littermate controls (Winkler et al., 2003).

Antibodies to neutralize sclerostin (Scl-Ab)

The concept of sclerostin inhibition has emerged as a potential approach for the treatment of osteoporosis and other skeletal disorders associated with low bone mass. Several Scl-Ab that block the function of sclerostin, including romosozumab (AMG785), blosozumab, and setrusumab (BPS804), have been tested in the clinical setting (Padhi et al., 2011; McColm et al., 2014; Seefried et al., 2017) and are briefly discussed later in this chapter. Various approaches have been used to generate Scl-Ab, including immunization-led antibody discovery campaigns and screening of synthetic human fragment antigen binding display libraries (Veverka et al., 2009; Back et al., 2012; Rothe et al., 2008). Neutralization of sclerostin function can be achieved by inhibiting its interaction with LRP4/5/6. NMR mapping experiments have revealed the binding sites of two research antibodies that interact with the sclerostin loop 2 region, the region that harbors the conserved NxI motif through which sclerostin binds LRP5/6 (Veverka et al., 2009; Boschert et al., 2016). While certain Scl-Ab, including romosozumab, block the interaction of sclerostin with LRP5/6 but not LRP4, other antibodies display the

converse effect and block binding to LRP4 but not LRP5/6 (Holdsworth et al., 2012; Gong et al., 2016). This may reflect differences in the epitopes recognized by individual Scl-Ab.

Pharmacologic inhibition of sclerostin by Scl-Ab: cell-level effects

Osteoblast lineage

Recombinant sclerostin inhibits mineralization of the mouse MC-3T3 osteoprogenitor cell line in vitro and addition of Scl-Ab to the culture medium reverses this effect (Li et al., 2009). In MC-3T3 cells modified to express a reporter of Wnt pathway activation, addition of Scl-Ab blocked the inhibitory effect of sclerostin on canonical Wnt signaling (Veverka et al., 2009). In vitro cultures of bone marrow stromal cells from mice treated with Scl-Ab form a greater number of alkaline phosphatase-positive colonies and mineralized nodules compared with cells from control mice (Shahnazari et al., 2012). Further evidence for the role of sclerostin on osteoblast lineage cells comes from in vivo experiments using Scl-Ab. For example, lineage tracing experiments show that Scl-Ab promotes the conversion of quiescent bone-lining cells into active osteoblasts on periosteal and endocortical surfaces in mice. This contributes to a rapid increase in osteoblast numbers and may involve activation of Wnt signaling in this cell population (Kim et al., 2017). Sclerostin may therefore contribute to the maintenance of bone-lining cells in a quiescent state on inactive bone surfaces.

In addition to the reactivation of bone-lining cells, administration of Scl-Ab in rodents increases osteoblast numbers concurrent with increased bone formation (Ominsky et al., 2015; Taylor et al., 2016), which is consistent with enhanced recruitment of osteoprogenitor cells to the bone surface (Greenbaum et al., 2017). The effects of Scl-Ab on individual osteoblasts were deduced through careful analysis of the time-dependent action of Scl-Ab on osteoblast lineage cells, characterized by the expression of runt-related transcription factor 2 (RUNX2) and neuroectodermal stem cell marker (Nestin) in osteoblasts and osteoprogenitors, respectively (Ominsky et al., 2015). In this study, at 4 and 26 weeks, the bone formation per osteoblast was higher in rats dosed with Scl-Ab compared with either the vehicle control or PTH(1−34). Both Scl-Ab and PTH(1−34) increased both osteoblast and osteoprogenitor number at the early (4-week) time point. While this effect was maintained in the PTH(1−34) group at the later (26-week) time point, it was attenuated in the Scl-Ab-treated group at this time point. This finding is indicative of the self-regulation of the bone-forming response, which occurs with prolonged Scl-Ab treatment in vivo. The mechanism for self-regulation of bone formation with longer-term treatment with Scl-Ab is a continuing area of investigation. As discussed later, the upregulation of other Wnt antagonists may contribute to this self-regulation.

Antibody-mediated inhibition of sclerostin promotes proliferation of osteogenic cells in the cambium layer of the periosteum in both young and geriatric (20-month-old) mice (Thompson et al., 2016). Lineage tracing approaches show that Scl-Ab promotes preferential differentiation of multipotent MSC-derived skeletal precursors toward early osteoblast precursors, increasing the number of osteoprogenitors through enhanced proliferation and decreased apoptosis (Trinh et al., 2017). Reduced apoptosis of osteoblasts and osteocytes was observed in mice treated with Scl-Ab following exposure to ionizing radiation, a finding that was associated with enhanced expression of DNA repair proteins by these cells in response to sclerostin inhibition (Chandra et al., 2017). Enhanced activity of individual osteoblasts ("osteoblast vigor") in response to Scl-Ab is reflected in studies performed in rats, where mineral apposition rate and bone formation per osteoblast were increased compared with controls (Ominsky et al., 2015).

Administration of Scl-Ab would be expected to cause enhanced Wnt signaling in target cells and, accordingly, treatment of male rats with Scl-Abs was found to increase β-catenin expression in endocortical osteoblasts (Suen et al., 2015). The temporal effects of Scl-Ab on the transcriptional profile of mature osteoblast lineage cells in bone samples enriched for bone-lining cells, osteoblasts, or osteocytes has been explored in vertebrae collected from ovariectomized (OVX) rats. In these studies, Scl-Ab rapidly increased expression of extracellular matrix genes and a subset of Wnt target genes. During the first week of treatment, bone-lining cells, osteoblasts, and osteocytes all displayed similar transcriptional patterns (Nioi et al., 2015). Longer-term treatment was associated with normalization of some Wnt target genes while the expression of secreted Wnt antagonists, including *SOST* and Dickkopf-related protein 1 (*DKK1*), was increased (Taylor et al., 2016; Holdsworth et al., 2017). Similar observations were made in femoral shafts collected from mice dosed with Scl-Ab. Interestingly, a synergistic bone-formation response has been observed when simultaneously inhibiting sclerostin and *DKK1*, further strengthening the role of additional Wnt regulators in the pharmacologic response to Scl-Ab (Florio et al., 2016). In addition to upregulation of *SOST* and *DKK1*, increased expression of mRNA transcripts encoding other secreted antagonists of Wnt signaling, including several secreted Fzd-related proteins and Wnt inhibitory factor 1, has been demonstrated (Holdsworth et al., 2017). Alterations in osteocyte expression of genes and pathways involved in the inhibition of cell cycle progression and mitogenesis, including activation of *p53* and inhibition of *c-Myc* signaling, occur

following chronic Scl-Ab treatment (Taylor et al., 2016). These changes are believed to contribute to self-regulation of the bone-forming response that occurs with longer-term Scl-Ab administration.

Further evidence for the effect of Scl-Ab on the osteocyte comes from observations that treatment with Scl-Ab restores osteocyte morphology and connectivity following spinal cord injury (Qin et al., 2015) or in the absence of periostin (Ren et al., 2015), and prevents the decrease in lacunar occupancy and osteocyte apoptosis following chronic exposure to glucocorticoids (Achiou et al., 2015).

Osteoclast lineage

Although sclerostin is not expressed by osteoclasts, there is evidence that it indirectly increases bone resorption by promoting osteoclast formation and activity. However, the mechanisms are not fully understood as of this writing. Experiments undertaken using in vitro cultures of mouse osteocyte-like MLO-Y4 cells suggest that sclerostin may regulate osteoclastogenesis by altering the ratio of receptor activator of nuclear factor-κB ligand (RANKL) to osteoprotegerin (OPG) expressed by these cells. In coculture of these cells with mouse splenocytes or human peripheral blood mononuclear cells, exogenous sclerostin enhanced osteoclastogenesis through RANKL-dependent formation of tartrate-resistant acid phosphatase form 5b (TRAP5b)-positive multinucleated cells that showed greater resorptive activity compared with control cocultures (Wijenayaka et al., 2011). Transcriptional analysis of osteoblast lineage cells in rats provides further evidence for Scl-Ab regulation of the RANKL/OPG ratio, as demonstrated by increased OPG expression and minimal effects on RANKL (Taylor et al., 2016). Ex vivo cultures of bone marrow osteoclast progenitors from OVX rats treated with Scl-Ab showed a reduction in the number of TRAP5b-positive osteoclast-like cells compared with controls, although serum concentrations of OPG and RANKL were unaffected in this study (Stolina et al., 2014). However, the expression of RANKL was reduced upon administration of Scl-Ab to in vitro organ cultures of mouse bones, with enhanced osteocyte Wnt signaling (Tu et al., 2015). Interestingly, mice with gain-of-function mutations in β-catenin resulting in elevated canonical Wnt signaling display increased bone resorption with enhanced expression of both *OPG* and *RANKL* (Tu et al., 2015). These data suggest that regulation of the OPG/RANKL balance is likely to play a pivotal role in the antiresorptive effect of Scl-Ab. In addition, increased expression of Wnt1-induced secreted protein 1 and decreased abundance of colony-stimulating factor 1 in osteoblast lineage cells (Taylor et al., 2016) may further contribute to the indirect inhibition of osteoclastogenesis by Scl-Ab. Fig. 74.2 illustrates the effects of Scl-Ab on osteoblast and osteoclast lineages within the bone microenvironment.

Pharmacologic inhibition of sclerostin by Scl-Ab in vivo

Effects of Scl-Ab in animal models of postmenopausal osteoporosis

Action of Scl-Ab on modeling- and remodeling-based bone formation

Scl-Ab promotes bone mass accrual with a unique mechanism of action resulting in increased osteoblast activity and decreased osteoclast activity. In OVX rats, a decrease in eroded and osteoclast surfaces is evident following 5 weeks of treatment with Scl-Ab (Li et al., 2009; Ominsky et al., 2014) and is maintained through 6 months of treatment (Li et al., 2014).

Increased bone formation, as indicated by transcriptional changes reflecting increased matrix production in osteoblast lineage cells, is observed soon (6 hours) after exposure to Scl-Ab in OVX rats (Nioi et al., 2015). These changes are later accompanied by further evidence of enhanced bone formation, including enlarged osteoblast surface, osteoid surface, and mineralization surface after 8 days. The process of osteoblast activation on quiescent surfaces results in an increase in modeling-based bone formation (MBF), defined as bone formation on bone surfaces where preexisting bone resorption is absent. An increase in MBF on the trabecular surfaces of vertebrae is observed in rats and cynomolgus monkeys following exposure to Scl-Ab for 5 and 10 weeks, respectively (Ominsky et al., 2014). Importantly, increases in MBF are not limited to the vertebrae, but are also detected within the long bones of the skeleton. For example, MBF is increased from 7% to 77% of the endocortical bone surface in the femur of cynomolgus monkeys (Ominsky et al., 2014). Furthermore, an increase in MBF in response to Scl-Ab is apparent on the periosteal surface, and the effect on each of these sites is dose-dependent (Ominsky et al., 2010). Similar bone formation events have been reported in the periosteal and endocortical regions of OVX rats (Li et al., 2014). Notably, promotion of MBF in the OVX rat has been documented with different sclerostin antibodies (Amgen, Inc./UCB Pharma, detailed above, and Eli Lilly and Company; Ma et al., 2017), further supporting the role of Scl-Ab in promoting bone formation.

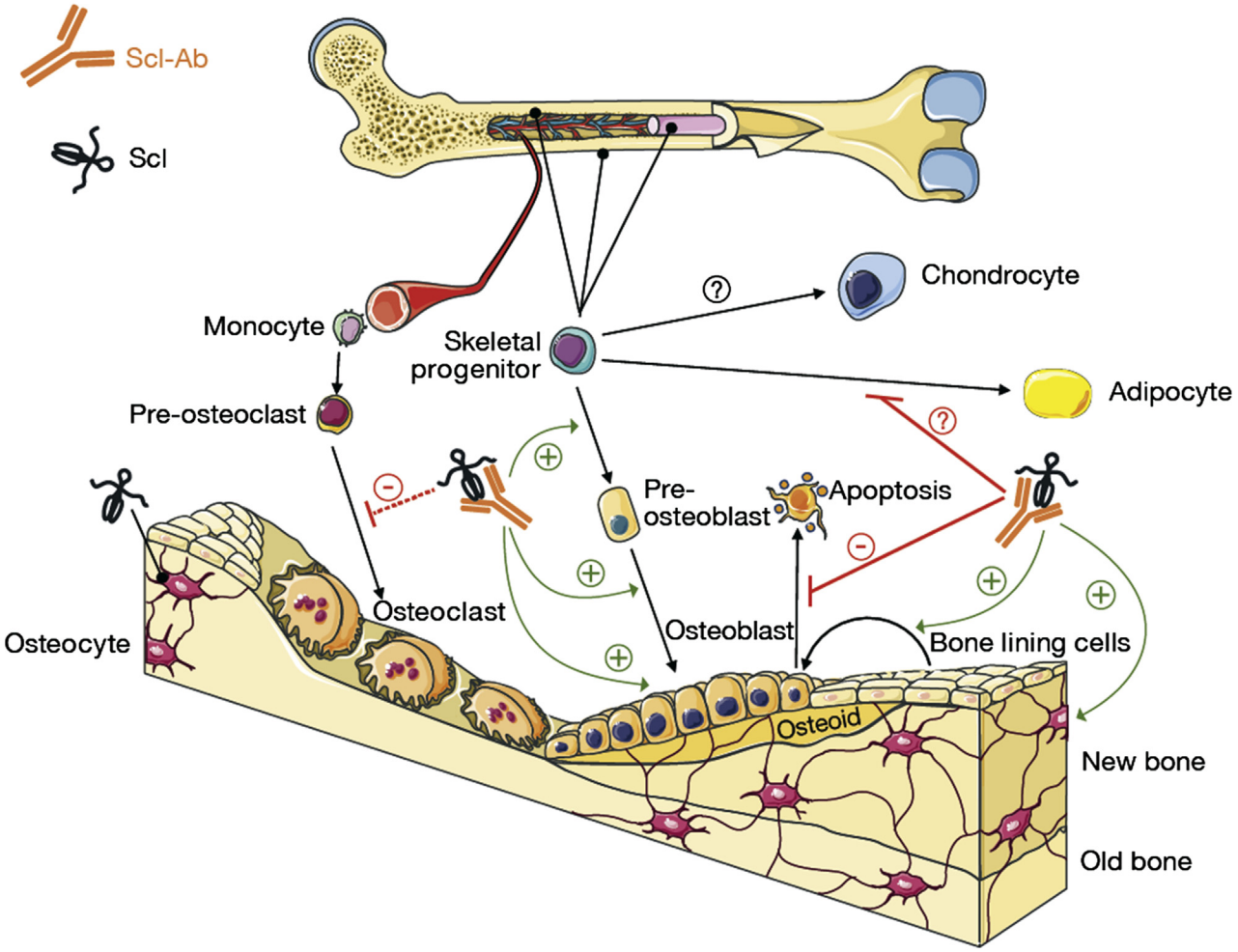

FIGURE 74.2 Effects of neutralizing antibodies to sclerostin (*Scl-Ab*) on bone formation and resorption. Inhibition of canonical Wnt signaling by sclerostin (*Scl*) in osteoblast lineage cells inhibits osteoblast-mediated bone formation and increases bone resorption by osteoclasts. Scl-Ab promotes bone formation via enhanced recruitment of osteoprogenitor cells, increased matrix production by osteoblasts, and reactivation of quiescent bone-lining cells. In addition, inhibition of osteoblast apoptosis by Scl-Ab contributes to the increased bone formation. Scl-Ab treatment also indirectly decreases bone resorption by modulating the expression of osteoclast regulators (produced by osteoblast lineage cells), including receptor activator for nuclear factor κB ligand/osteoprotegerin, colony-stimulating factor 1, and Wnt1-induced secreted protein 1. This figure was produced using Servier Medical Art.

The effects of Scl-Ab on remodeling-based bone formation (RBF) have been investigated in rat and cynomolgus monkey models. Scl-Ab increases the life span of the formative site (where walls of newly mineralized bone form following bone resorption) during RBF. This results in a positive net effect on bone volume at this site. However, this may be apparent only during the early stages of treatment, as shown in cynomolgus monkeys during weeks 2−10 of dosing, but not at week 28. Nevertheless, the remodeling sites in the vertebrae at the later time point did show a positive bone balance (increased wall thickness relative to resorption depth) (Boyce et al., 2017).

The positive effects on both modeling and remodeling bone formation lead to a large bone mass accrual; Fig. 74.3 summarizes the effects of sclerostin antibody on modeling- and remodeling-based bone formation. A transient bone formation response is observed following Scl-Ab treatment. Indeed, serum bone-formation markers, such as P1NP, bone-specific alkaline phosphatase (BSAP), and osteocalcin, are increased relative to vehicle control groups during the first 3 months of Scl-Ab treatment. Subsequently, these markers decrease toward baseline levels during months 6−12 of treatment (Ke et al., 2012; Li et al., 2014; Recker et al., 2015; Ominsky et al., 2012). The reduction in serum bone-formation markers correlates with a reduction in bone tissue formation, which is most evident within the lumbar vertebrae of OVX rats (Li et al., 2014) and intact cynomolgus monkeys (Ominsky et al., 2012). Interestingly, this attenuated response appears to be site specific; endocortical regions of the femoral diaphysis continue to display increases in bone

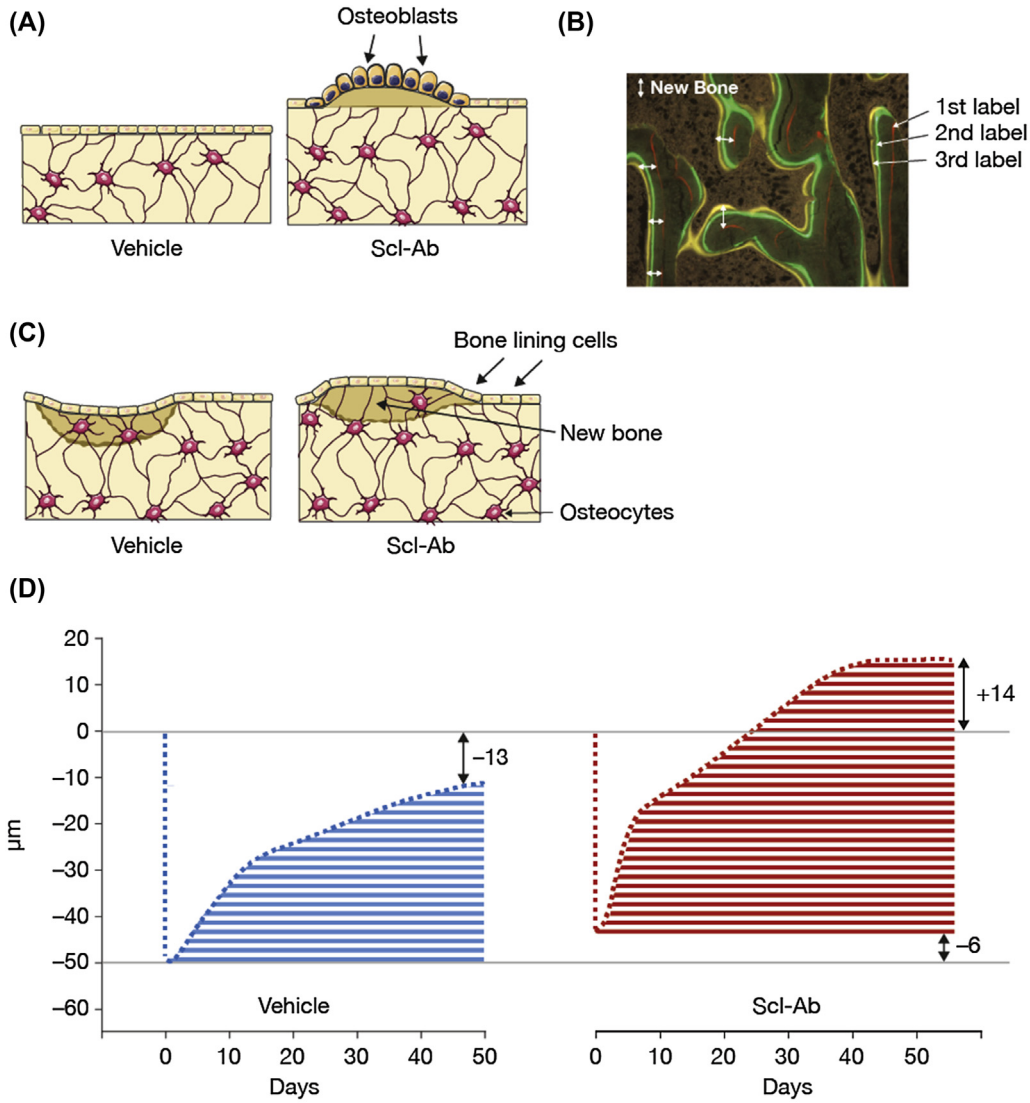

FIGURE 74.3 Tissue-level mechanisms of pharmacologic inhibition of sclerostin by sclerostin neutralizing antibody (*Scl-Ab*) on modeling-based bone formation and remodeling-based bone formation. (A) Modeling-based bone formation: illustration of bone formation by osteoblasts on a quiescent bone surface (i.e., without preexisting bone resorption) induced by Scl-Ab treatment. (B) An example of bone formation on a quiescent bone surface without preexisting bone resorption using dynamic histomorphometry. The fluorescence image shows an undecalcified 8-µm section of trabecular bone from the fifth lumbar vertebral body of an ovariectomized rat treated with Scl-Ab at 25 mg/kg, twice weekly by subcutaneous injection, for 5 weeks. The first fluorescent label was given on day 1 of Scl-Ab treatment, and the second and third fluorescent labels were given 12 and 2 days prior to autopsy. The first fluorescent label on the trabecular bone surface indirectly indicates bone formation on the quiescent surface without preexisting bone resorption. (C). Remodeling-based bone formation: illustration of bone formation following bone resorption. Scl-Ab treatment reduces the resorption pit depth and induces a greater extent of new bone formation than vehicle treatment. The amount of bone formed with Scl-Ab treatment exceeds that lost during the resorption phase of bone remodeling. Scl-Ab also extends new bone formation to include formation on the quiescent surface near the resorbed surface. (D) Illustration of the kinetic reconstruction of bone gain on the remodeling surface induced by Scl-Abs in a nonhuman primate model. The gray line at 0 µm represents the intact bone surface and the depth of the resorption site is shown by the vertical dashed lines. The filled area represents the formation of mineralized wall thickness at the formative site. Scl-Ab reduces the depth of the resorptive site (−6 µm compared with vehicle) and promotes greater wall thickness, resulting in a positive bone balance at the end of the resorption cycle (+14 µm compared with −13 µm in vehicle-treated animals). *(A and C) Modified from Ke, H.Z., Richards,W.G., Li, X., Ominsky, M.S., 2012. Sclerostin and Dickkopf-1 as therapeutic targets in bone diseases, Endocr. Rev. 33, 747−783. (D) Modified from Boyce, R.W., Niu, Q.T., Ominsky, M.S., 2017. Kinetic reconstruction reveals time-dependent effects of romosozumab on bone formation and osteoblast function in vertebral cancellous and cortical bone in cynomolgus monkeys, Bone 101, 77−87.*

formation beyond 6 months of treatment (Li et al., 2014). This extended response to Scl-Ab at cortical regions has also been documented in other studies with OVX rats (Ma et al., 2017).

Effects of Scl-Ab on bone mass and structure

The mechanism of action of Scl-Ab—increased bone formation and reduced bone resorption—leads to elevated bone mass and improved bone architecture in both cortical and trabecular compartments. In the OVX rat model, axial and peripheral BMD was restored following 5 weeks of Scl-Ab treatment versus sham treatment (Li et al., 2009). Furthermore, an increase in BMD was observed over 26 weeks at the lumbar vertebrae, which correlated with altered architecture, including increased trabecular thickness and thickness of the cortical shell (Li et al., 2014). These changes are not limited to the vertebral bones, as an increase in BMD and bone mineral content (BMC) at the femoral diaphysis was also noted. This is a direct result of increased periosteal and endosteal bone formation, with the net effect of increasing the cortical thickness. An increase in periosteal bone formation has also been reported at the femoral neck in response to Scl-Ab administration. Continued improvements in bone mass and geometry at the proximal tibial metaphysis and diaphysis were observed for up to 12 months of Scl-Ab treatment in OVX rats (Ominsky et al., 2017a). As in other animal models, bone-formation markers reached a plateau in the axial skeleton between months 6 and 12 despite continued administration of Scl-Ab.

Similar to the OVX rat model of osteoporosis, increases in bone formation have been reported in adolescent female (whole-body and distal radius metaphyseal BMC) and male cynomolgus monkeys (lumbar spine, femoral neck, and distal radius BMD) in response to treatment with Scl-Ab (romosozumab) (Ominsky et al., 2010, 2011). Interestingly, trabecular rods are converted to platelike structures because of increases in trabecular thickness (Matheny et al., 2017). This finding has great importance, as a low plate-to-rod ratio is known to be associated with increased fracture risk in osteoporosis (Wang et al., 2013; Liu et al., 2012).

Effects of Scl-Ab on bone strength and quality

The gains in bone mass and geometric bone changes in response to Scl-Ab improve bone strength at the lumbar vertebrae, femoral shaft, and femoral neck in OVX rats (Ominsky et al., 2017a). Increases in bone strength are also observed at the lumbar vertebrae, in male and female cynomolgus monkeys, in response to Scl-Ab treatment for up to 10 weeks (Ominsky et al., 2010, 2011). Consistent with this finding, adolescent cynomolgus monkeys display increased peak load strength at the lumbar vertebrae, femur midshaft, and neck following 6 months of treatment with Scl-Ab. Vertebral bone quality was maintained and a positive correlation between bone mass and bone strength (measured by peak load/force to failure) was observed with Scl-Ab at doses up to 100 mg/kg per week. Similarly, skeletally mature OVX cynomolgus monkeys dosed for 12 months with Scl-Ab displayed increased vertebral strength with maintenance of bone mass and strength relationship (Ominsky et al., 2017b).

Bone quality, as defined by the material properties and composition of the tissue, was maintained in cynomolgus monkeys dosed for 10 weeks with Scl-Ab (Ross et al., 2014). An important characteristic of bone matrix that reflects its ability to withstand mechanical strain is the level of mineralization within the tissue. Scl-Ab does not alter global mineralization of either cortical or trabecular bone tissue as assessed in male cynomolgus monkeys dosed for 10 weeks. The only change in the material properties of the matrix was an increase in lower mineralized areas due to enhanced new bone formation. No changes in tissue age-specific measurements of mineral-to-matrix ratio and no differences in hydroxyapatite crystallinity or collagen cross-linking in the endocortical, intracortical, or trabecular sites were detected. A significant increase in the trabecular compartment, of approximately 10% carbonate substitution for tissue older than 2 weeks, was observed. Interestingly, decreases in carbonate-to-phosphate ratios in bone are predictive of bone fragility fracture (Boskey et al., 2016). It is therefore unlikely that Scl-Ab treatment will negatively affect bone matrix quality or mineralization. The results from the 12-month bone quality studies using OVX rat and OVX cynomolgus monkey models (Ominsky et al., 2017a, 2017b) further demonstrated that Scl-Ab increased bone mass and strength, while maintaining bone quality in both trabecular and cortical bone compartments.

Probing Scl-Ab treatment regimens in preclinical models of osteoporosis

Clinical scenarios relating to Scl-Ab treatment have been investigated using preclinical models. The consequences of cotreatment with, or transition from and to, antiresorptive therapies have been tested in the OVX rat model. Transition from the bisphosphonate alendronate to Scl-Ab treatment did not alter the bone-forming capacity of Scl-Ab. Similar gains in mass and strength were observed in animals receiving Scl-Ab compared with those receiving vehicle alone (Li et al., 2011).

Furthermore, Scl-Ab maintained its bone-forming ability in the presence of alendronate when the agents were administered simultaneously. Similarly, when combined with zoledronate, Scl-Ab increased bone mass to a greater extent than either of the two agents alone when administered to OVX mice (Halleux et al., 2009).

It has been hypothesized that due to the attenuated response observed following 12 months of treatment with Scl-Ab, an initial Scl-Ab treatment period followed by an antiresorptive therapy may provide the optimal treatment strategy for patients with osteoporosis. Indeed, this strategy formed the treatment schedule for certain phase III clinical trials of romosozumab, a Scl-Ab in development by Amgen, Inc., and UCB Pharma. The consequences of follow-on treatment and discontinuation were deduced first in the OVX rat model. Following an initial 6-week treatment with Scl-Ab, the animals were transitioned to either vehicle or the antiresorptive RANKL inhibitor OPG-Fc for a further 20 weeks (Ominsky et al., 2017a). In this model, if transitioned to vehicle, bone mass was reduced to the level of the sham-operated controls in the Scl-Ab-treated group, but was still higher than that of OVX controls. However, transition to OPG-Fc treatment maintained the bone mass gains elicited by Scl-Ab treatment. Interestingly, the femoral diaphysis appeared to be more resistant to bone mass loss than the femoral neck or vertebrae following transition to vehicle, further underpinning the site specificity of the Scl-Ab response. The loss of bone due to transition from Scl-Ab to vehicle was also observed in OVX cynomolgus monkeys, where a gradual loss of bone mass was evident during the 6-month withdrawal period following 6 months of romosozumab treatment (Ominsky et al., 2017b). In addition to transition to OPG-Fc, transition to raloxifene and alendronate in the OVX rat (Ma et al., 2013), and zoledronate in the OVX mouse (Halleux et al., 2009), maintained Scl-Ab-mediated bone mass gains.

Re-treatment of OVX rats with Scl-Ab following withdrawal for 12 weeks restores bone mass to prewithdrawal levels, indicating restoration of pharmacologic response (Li et al., 2013). This has also been confirmed in mice, in which the bone-forming response to Scl-Ab is restored following treatment-free or "holiday" periods (Holdsworth et al., 2017) and in the clinical setting (Kendler et al., 2017). One caveat when interpreting these data is that bone loss occurs during the holiday period when all treatment is withdrawn. While it has not yet been shown that the bone-forming effects of Scl-Ab would be restored following the use of an antiresorptive agent during the Scl-Ab holiday, it has been shown that Scl-Ab treatment after alendronate effectively increases bone mass in preclinical and clinical settings (Li et al., 2011; Langdahl et al., 2017).

Effects of Scl-Ab in other animal models of low bone mass

In addition to the wealth of data generated in the OVX rat and cynomolgus monkey models of postmenopausal osteoporosis, inhibition of sclerostin by Scl-Ab has been shown to protect and restore bone mass and strength in several other animal models of low bone mass (Ke et al., 2012; Ominsky et al., 2017a). These include animal models of male osteoporosis, OI, immobilization-induced bone loss, glucocorticoid-induced osteoporosis, diabetic bone loss, radiation-induced bone loss, multiple myeloma bone diseases, and bone repair.

In an aged (16-month-old) male rat model with low bone mass, Scl-Ab treatment for 5 weeks significantly increased trabecular and cortical bone formation and restored trabecular and cortical bone mass and strength to the levels observed in young rats (Li et al., 2010). Similarly, Scl-Ab treatment for 6 weeks increased bone formation and decreased bone resorption, and completely restored bone mass and strength, in a male rat model of androgen deficiency induced by orchidectomy (Li et al., 2018). These data are consistent with the clinical observation that a dual effect of increasing bone formation and decreasing bone resorption results in significant gains in BMD at the spine and hip in men with osteoporosis following treatment with Scl-Ab (romosozumab) for 12 months (Lewiecki et al., 2016).

The efficacy of Scl-Ab in improving bone mass and bone strength has been tested in several animal models of OI, including Brtl/+ mice (a G349C point mutation on *Col1al*), Crtap$^{-/-}$ mice (a model of recessive OI), *Col1a2* G610C mice (mice with the Amish OI mutation), and *Col1a1*(Jrt)/+ mice (a model of severe dominant OI). Scl-Ab treatment showed improvements in bone formation, bone mass, and bone strength in these OI models (Little et al., 2017; Grafe et al., 2016; Sinder et al., 2013, 2014, 2016), although it may be less effective in a more severely affected model such as the *Col1a1(*Jrt)/+ mouse (Roschger et al., 2014). The efficacy of Scl-Ab in these models may be improved by use in combination with antiresorptive agents, such as bisphosphonates (Little et al., 2017), where bisphosphonates could preserve the bone gain upon cessation of Scl-Ab treatment (Perosky et al., 2016). It is worth noting that the improvements in bone mass and strength after treatment with Scl-Ab in these OI models are due to improvements in bone quantity, not bone quality. Importantly, the impaired bone quality in OI is unaffected by Scl-Ab (Sinder et al., 2016). Clinical trials to determine the benefits of Scl-Ab in patients with OI were ongoing at the time of writing.

Bone loss due to underloading—induced in animal models by hindlimb immobilization, tail suspension, neurotoxic protein (botulinum toxin)-induced muscle paralysis, and spinal cord injury—has been the subject of therapeutic agent testing. Sclerostin plays an important role in bone response to mechanical loading, as evidenced by increased sclerostin

expression with underloading and decreased expression with overloading (Robling et al., 2008; Moustafa et al., 2012). In addition, immobilization and underloading induce an increase in bone resorption and a decrease in bone formation, leading to rapid bone loss and structural damage. Scl-Ab may be a good choice of therapeutic agent for underloading-induced bone loss due to its dual action, increasing bone formation and decreasing bone resorption. Preclinical experiments of immobilization-induced bone loss models, including space shuttle-induced microgravity, demonstrate that Scl-Ab increases bone formation and decreases bone resorption, leading to increased bone mass, improved bone structure, and improved bone strength (Qin et al., 2015; Tian et al., 2011; Spatz et al., 2013; Beggs et al., 2015; Zhang et al., 2016; Bouxsein et al., 2012).

As with immobilization-induced bone loss, glucocorticoid treatment has also been shown to decrease bone formation and increase bone resorption. Scl-Ab impedes glucocorticoid-induced bone loss by preventing the decrease in osteoblast viability and bone formation, and the increase in bone resorption observed after glucocorticoid treatment (Achiou et al., 2015; Yao et al., 2016). Improvements in bone formation, bone mass, and bone strength after Scl-Ab treatment have been reported for several other forms of bone loss in animal models, including diabetic bone loss (Hamann et al., 2013), radiation-induced bone loss (Chandra et al., 2017), multiple myeloma bone diseases (Delgado-Calle et al., 2017; McDonald et al., 2017), and bone repair (see review by Ke et al., 2012).

Pharmacologic inhibition of sclerostin by Scl-Ab in humans

In humans, several Scl-Ab, namely romosozumab (AMG785), blosozumab (LY2541546), and setrusumab (BPS804), have been investigated in conditions associated with low bone mass and high risk of fragility fractures. These include postmenopausal osteoporosis (blosozumab and romosozumab), osteoporosis in men (romosozumab), adult hypophosphatasia (setrusumab), and adult moderate OI (setrusumab).

The most extensive clinical data sets have been generated in osteoporosis. These findings have been summarized in several reviews (Canalis, 2018; McClung, 2017; Lovato and Lewiecki, 2017) and will not be covered in depth in this chapter. Single- and multiple-dose phase I studies have been reported for both blosozumab and romosozumab in healthy volunteers with normal or low bone mass (Padhi et al., 2011, 2014; McColm et al., 2014). In these studies, each agent demonstrated dose-dependent increases in the serum bone-formation markers P1NP, osteocalcin, and BSAP; a dose-dependent decrease in the serum bone-resorption marker CTX; and an increase in BMD. In the follow-up phase II, dose-ranging studies in women with postmenopausal osteoporosis, administration of blosozumab or romosozumab dose-dependently increased BMD at the spine, total hip, and femoral neck, and recapitulated the rapid, dual effects on biochemical markers of bone formation and resorption reported in the phase I studies (Recker et al., 2015; McClung et al., 2014). Notably, the early response of serum markers of both bone formation and resorption to Scl-Ab is distinct from that seen following daily teriparatide (rhPTH(1−34)) or weekly alendronate treatment (McClung et al., 2014) (Fig. 74.4).

Results from phase III clinical studies evaluating the effect of romosozumab on reducing risk of fragility fractures in postmenopausal osteoporosis (Cosman et al., 2016; Saag et al., 2017) and the efficacy of the same molecule on markers of bone formation and resorption and BMD in men with osteoporosis have also been reported (Lewiecki et al., 2016). These results indicated that Scl-Ab increased bone formation and decreased bone resorption, which led to rapid and large increases in BMD in postmenopausal women and men with osteoporosis. Further, these studies also demonstrated that Scl-Ab decreased fragility fracture risk in postmenopausal women with osteoporosis compared with placebo and compared with alendronate. Increases in spine and hip BMD and estimated strength were also demonstrated versus teriparatide in postmenopausal women with osteoporosis who had transitioned from alendronate to romosozumab or teriparatide for 12 months (Langdahl et al., 2017).

In addition to the extensive clinical data generated for osteoporosis, preliminary clinical data for setrusumab have been reported following separate trials in patients with hypophosphatasia or adult moderate OI (Seefried et al., 2017; Glorieux et al., 2017). Consistent with the effects of other sclerostin antibodies in osteoporosis, administration of setrusumab to these patients resulted in increases in serum bone-formation markers and decreases in serum bone-resorption markers, leading to a mean increase in lumbar spine BMD.

Summary

Understanding the role of sclerostin in bone metabolism has led to the discovery and development of Scl-Ab as bone-forming agents for conditions associated with low bone mass, such as osteoporosis. In numerous animal models of bone loss, pharmacologic inhibition of sclerostin by Scl-Ab leads to a rapid increase in BMD and bone strength, while maintaining bone quality. The rapid bone gain induced by Scl-Ab arises from both an increase in bone formation and a

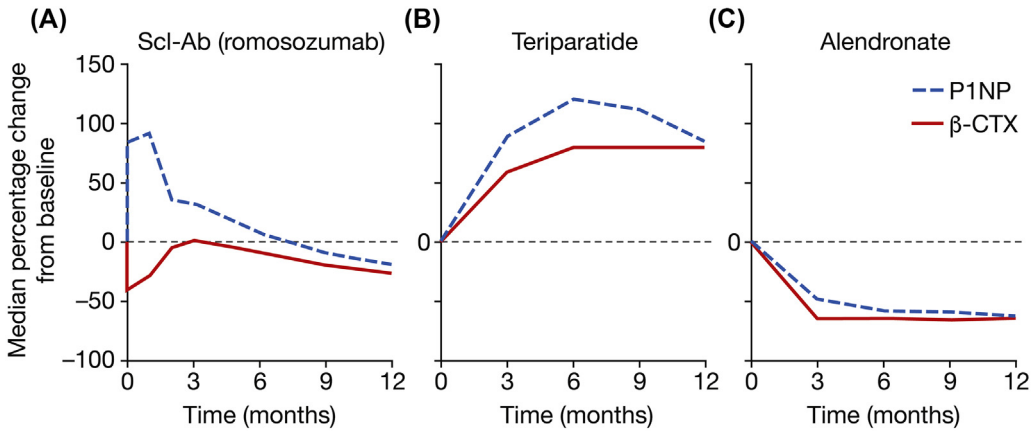

FIGURE 74.4 Effects of the sclerostin neutralizing antibody (*Scl-Ab*) romosozumab, teriparatide, and alendronate on serum markers of bone formation and bone resorption in postmenopausal women. Romosozumab increased bone formation and decreased bone resorption; teriparatide increased both bone formation and resorption, while alendronate decreased both bone formation and bone resorption. These data indicate differences in the mechanisms of action of the Scl-Ab romosozumab compared with teriparatide and alendronate. *β-CTX*, β-cross-linked C-terminal telopeptide of type I collagen; *P1NP*, procollagen type 1 N-terminal propeptide. *Modified and Reprinted from McClung, M.R., Grauer, A., Boonen, S., Bolognese, M.A., Brown, J.P., Diez-Perez, A., et al., 2014. Romosozumab in postmenopausal women with low bone mineral density, N. Engl. J. Med. 370, 412–420, Copyright (2014), with permission from Elsevier.*

decrease in bone resorption during the initial phase of treatment. Importantly, later gains in bone mass induced by Scl-Ab result primarily from a decrease in bone resorption, as the bone formation response is attenuated with continued treatment. The efficacy of Scl-Ab has been demonstrated in clinical trials of patients with osteoporosis, where treatment with Scl-Ab increases BMD and reduces vertebral, nonvertebral, and clinical fractures. The outcomes of trials investigating the efficacy of Scl-Ab in other indications such as OI, are ongoing at the time of writing and are eagerly awaited.

Abbreviations

ASARM acidic serine aspartate-rich MEPE-associated motif
BAC bacterial artificial chromosome
BFR bone formation rate
BFR/BS bone formation rate/bone surface referent
BMC bone mineral content
BMD bone mineral density
BMP bone morphogenetic protein
BSAP bone-specific alkaline phosphatase
CSF1 colony-stimulating factor 1
CTX cross-linked C-terminal telopeptide of type I collagen
DKK1 Dickkopf-related protein 1
DXA dual-energy X-ray absorptiometry
EV extracellular vesicle
Fab fragment antigen binding
Fzd Frizzled
HBM high bone mass
KO knockout
LRP4/5/6 low-density lipoprotein receptor-related protein 4/5/6
MBF modeling-based bone formation
MEGF7 multiple epidermal growth factor-like domain 7
MEPE matrix extracellular phosphoglycoprotein
MS/BS mineralizing surface/bone surface
MSC mesenchymal stem cell
Nestin neuroectodermal stem cell marker
NMR nuclear magnetic resonance
OI osteogenesis imperfecta

OPG osteoprotegerin
OVX ovariectomized
P1NP procollagen type 1 N-terminal propeptide
PBMC peripheral blood mononuclear cell
pQCT peripheral quantitative computed tomography
PTH parathyroid hormone
PTH(1−34) parathyroid hormone 1−34
RANKL receptor activator of nuclear factor-κB ligand
RBF remodeling-based bone formation
RUNX2 runt-related transcription factor 2
sc subcutaneous
Scl-Ab sclerostin neutralizing antibody
SFRP secreted Frizzled-related protein
TRAP5b tartrate-resistant acid phosphatase form 5b
WIF1 Wnt inhibitory factor 1
WISP1 Wnt1-induced secreted protein 1
Wnt wingless-related integration site

Acknowledgments

The authors thank the romosozumab teams at UCB Pharma and Amgen, Inc., for their support. Editorial support for this chapter in the form of styling, editing, and figure redrawing was provided by Angela Rogers, Ph.D., CMPP, Gardiner−Caldwell Communications, Macclesfield, United Kingdom, and was funded by UCB Pharma. The number of references cited is restricted due to space constraints.

References

Achiou, Z., Toumi, H., Touvier, J., Boudenot, A., Uzbekov, R., Ominsky, M.S., et al., 2015. Scl-Ab and interval treadmill training effects in a rodent model of glucocorticoid-induced osteopenia. Bone 81, 691−701.

Andersen, O.M., Dagil, R., Kragelund, B.B., 2013. New horizons for lipoprotein receptors: communication by beta-propellers. J. Lipid Res. 54, 2763−2774.

Atkins, G.J., Rowe, P.S., Lim, H.P., Welldon, K.J., Ormsby, R., Wijenayaka, A.R., et al., 2011. Sclerostin is a locally acting regulator of late-osteoblast/preosteocyte differentiation and regulates mineralization through a MEPE-ASARM-dependent mechanism. J. Bone Miner. Res. 26, 1425−1436.

Back, J.W., Frisch, C., Van Pee, K., Boschert, V., van Vught, R., Puijk, W., et al., 2012. Selecting highly structure-specific antibodies using structured synthetic mimics of the cystine knot protein sclerostin. Protein Eng. Des. Sel. 25, 251−259.

Balemans, W., Ebeling, M., Patel, N., Van Hul, E., Olson, P., Dioszegi, M., et al., 2001. Increased bone density in sclerosteosis is due to the deficiency of a novel secreted protein (SOST). Hum. Mol. Genet. 10, 537−543.

Balemans, W., Patel, N., Ebeling, M., Van Hul, E., Wuyts, W., Lacza, C., et al., 2002. Identification of a 52 kb deletion downstream of the SOST gene in patients with van Buchem disease. J. Med. Genet. 39, 91−97.

Balemans, W., Cleiren, E., Siebers, U., Horst, J., Van Hul, W., 2005. A generalized skeletal hyperostosis in two siblings caused by a novel mutation in the SOST gene. Bone 36, 943−947.

Baron, R., Kneissel, M., 2013. WNT signaling in bone homeostasis and disease: from human mutations to treatments. Nat. Med. 19, 179−192.

Beggs, L.A., Ye, F., Ghosh, P., Beck, D.T., Conover, C.F., Balaez, A., et al., 2015. Sclerostin inhibition prevents spinal cord injury-induced cancellous bone loss. J. Bone Miner. Res. 30 (4), 681−689.

Beighton, P., Cremin, B.J., Hamersma, H., 1976. The radiology of sclerosteosis. Br. J. Radiol. 49, 934−939.

Belkhribchia, M.R., Collet, C., Laplanche, J.L., Hassani, R., 2014. Novel SOST gene mutation in a sclerosteosis patient from Morocco: a case report. Eur. J. Med. Genet. 57, 133−137.

Bhadada, S.K., Rastogi, A., Steenackers, E., Boudin, E., Arya, A., Dhiman, V., et al., 2013. Novel SOST gene mutation in a sclerosteosis patient and her parents. Bone 52, 707−710.

Boschert, V., Frisch, C., Back, J.W., van Pee, K., Weidauer, S.E., Muth, E.M., et al., 2016. The sclerostin-neutralizing antibody AbD09097 recognizes an epitope adjacent to sclerostin's binding site for the Wnt co-receptor LRP6. Open Biol. 6, 160120.

Boskey, A.L., Donnelly, E., Boskey, E., Spevak, L., Ma, Y., Zhang, W., et al., 2016. Examining the relationships between bone tissue composition, compositional heterogeneity, and fragility fracture: a matched case-controlled FTIRI study. J. Bone Miner. Res. 31, 1070−1081.

Bouaziz, W., Funck-Brentano, T., Lin, H., Marty, C., Ea, H.K., Hay, E., et al., 2015. Loss of sclerostin promotes osteoarthritis in mice via beta-catenin-dependent and -independent Wnt pathways. Arthritis Res. Ther. 17, 24.

Boudin, E., Yorgan, T., Fijalkowski, I., Sonntag, S., Steenackers, E., Hendrickx, G., et al., 2017. The Lrp4R1170Q homozygous knock-in mouse recapitulates the bone phenotype of sclerosteosis in humans. J. Bone Miner. Res. 32, 1739−1749.

Bourhis, E., Wang, W., Tam, C., Hwang, J., Zhang, Y., Spittler, D., et al., 2011. Wnt antagonists bind through a short peptide to the first beta-propeller domain of LRP5/6. Structure 19, 1433−1442.

Bouxsein, M., Bateman, T.A., Hanson, A.H., et al., 2012. Sclerostin antibody treatment improves bone mass, microarchitecture and mechanical properties in mice exposed to microgravity: results from the STS-135 Shuttle Mission. J. Bone Miner. Res. 27 (Suppl. 1). ABSTRACT in Presentation 1063.

Boyce, R.W., Niu, Q.T., Ominsky, M.S., 2017. Kinetic reconstruction reveals time-dependent effects of romosozumab on bone formation and osteoblast function in vertebral cancellous and cortical bone in cynomolgus monkeys. Bone 101, 77–87.

Brandenburg, V.M., Kramann, R., Koos, R., Kruger, T., Schurgers, L., Muhlenbruch, G., et al., 2013. Relationship between sclerostin and cardiovascular calcification in hemodialysis patients: a cross-sectional study. BMC Nephrol. 14, 219.

Brown, G., Morrell, A., Robinson, S., Sattler, R., Guo, X., 2016. Mechanically-induced calcium oscillations in osteocytes facilitate release of RANKL, OPG, and sclerostin through extracellular vesicles and mediate skeletal adaptation. J. Bone Miner. Res. 31. ABSTRACT 1038.

Brunkow, M.E., Gardner, J.C., Van Ness, J., Paeper, B.W., Kovacevich, B.R., Proll, S., et al., 2001. Bone dysplasia sclerosteosis results from loss of the SOST gene product, a novel cystine knot-containing protein. Am. J. Hum. Genet. 68, 577–589.

Canalis, E., 2018. Management of endocrine disease: novel anabolic treatments for osteoporosis. Eur. J. Endocrinol. 178, R33.

Chan, B.Y., Fuller, E.S., Russell, A.K., Smith, S.M., Smith, M.M., Jackson, M.T., et al., 2011. Increased chondrocyte sclerostin may protect against cartilage degradation in osteoarthritis. Osteoarthritis Cartilage 19, 874–885.

Chandra, A., Lin, T., Young, T., Tong, W., Ma, X., Tseng, W.J., et al., 2017. Suppression of sclerostin alleviates radiation-induced bone loss by protecting bone-forming cells and their progenitors through distinct mechanisms. J. Bone Miner. Res. 32, 360–372.

Chang, M.K., Kramer, I., Huber, T., Kinzel, B., Guth-Gundel, S., Leupin, O., et al., 2014. Disruption of Lrp4 function by genetic deletion or pharmacological blockade increases bone mass and serum sclerostin levels. Proc. Natl. Acad. Sci. U. S. A. 111, E5187–E5195.

Cohen-Kfir, E., Artsi, H., Levin, A., Abramowitz, E., Bajayo, A., Gurt, I., et al., 2011. Sirt1 is a regulator of bone mass and a repressor of Sost encoding for sclerostin, a bone formation inhibitor. Endocrinology 152, 4514–4524.

Cosman, F., Crittenden, D.B., Adachi, J.D., Binkley, N., Czerwinski, E., Ferrari, S., et al., 2016. Romosozumab treatment in postmenopausal women with osteoporosis. N. Engl. J. Med. 375, 1532–1543.

Delgado-Calle, J., Sanudo, C., Bolado, A., Fernandez, A.F., Arozamena, J., Pascual-Carra, M.A., et al., 2012. DNA methylation contributes to the regulation of sclerostin expression in human osteocytes. J. Bone Miner. Res. 27, 926–937.

Delgado-Calle, J., Anderson, J., Cregor, M.D., Condon, K.W., Kuhstoss, S.A., Plotkin, L.I., et al., 2017. Genetic deletion of Sost or pharmacological inhibition of sclerostin prevent multiple myeloma-induced bone disease without affecting tumor growth. Leukemia. https://doi.org/10.1038/leu.2017.152.

Didangelos, A., Yin, X., Mandal, K., Baumert, M., Jahangiri, M., Mayr, M., 2010. Proteomics characterization of extracellular space components in the human aorta. Mol. Cell. Proteomics 9, 2048–2062.

Fairfield, H., Falank, C., Harris, E., Demambro, V., McDonald, M., Pettitt, J.A., et al., 2017. The skeletal cell-derived molecule sclerostin drives bone marrow adipogenesis. J. Cell. Physiol. 233, 1156–1167.

Fayez, A., Aglan, M., Esmaiel, N., El Zanaty, T., Abdel Kader, M., El Ruby, M., 2015. A novel loss-of-sclerostin function mutation in a first Egyptian family with sclerosteosis. BioMed Res. Int. 517815.

Fijalkowski, I., Geets, E., Steenackers, E., Van Hoof, V., Ramos, F.J., Mortier, G., et al., 2016. A novel domain-specific mutation in a sclerosteosis patient suggests a role of LRP4 as an anchor for sclerostin in human bone. J. Bone Miner. Res. 31, 874–881.

Florio, M., Gunasekaran, K., Stolina, M., Xiaodong, L., Ling, L., Tipton, B., et al., 2016. A bispecific antibody targeting sclerostin and DKK-1 promotes bone mass accrual and fracture repair. Nat. Commun. 7. Article number: 11505.

Fulzele, K., Lai, F., Dedic, C., Saini, V., Uda, Y., Shi, C., et al., 2017. Osteocyte-secreted Wnt signaling inhibitor sclerostin contributes to beige adipogenesis in peripheral fat depots. J. Bone Miner. Res. 32, 373–384.

Glorieux, F.H., Devogelaer, J.P., Durigova, M., Goemaere, S., Hemsley, S., Jakob, F., et al., 2017. BPS804 anti-sclerostin antibody in adults with moderate osteogenesis imperfecta: results of a randomized phase 2a trial. J. Bone Miner. Res. 32, 1496–1504.

Gong, Y., Slee, R.B., Fukai, N., Rawadi, G., Roman-Roman, S., Reginato, A.M., et al., 2001. Osteoporosis-Pseudoglioma Syndrome Collaborative G, LDL receptor-related protein 5 (LRP5) affects bone accrual and eye development. Cell 107, 513–523.

Gong, J., Cao, J., Ho, J., Chen, C., Paszty, C., 2016. Romosozumab blocks the binding of sclerostin to the two key Wnt signaling co-receptors, LRP5 and LRP6, but not to LRP4. J. Bone Miner. Res. 31. ABSTRACT MO0300.

Grafe, I., Alexander, S., Yang, T., Lietman, C., Homan, E.P., Munivez, E., et al., 2016. Scl-Ab treatment improves the bone phenotype of Crtap(-/-) mice, a model of recessive osteogenesis imperfecta. J. Bone Miner. Res. 31, 1030–1040.

Greenbaum, A., Chan, K.Y., Dobreva, T., Brown, D., Balani, D.H., Boyce, R., et al., 2017. Bone CLARITY: clearing, imaging, and computational analysis of osteoprogenitors within intact bone marrow. Sci. Transl. Med. 9 https://doi.org/10.1126/scitranslmed.aah6518.

Halleux, C., Hu, S., Diefenbach, B., Prassler, J., Merdes, M., Studer, A., et al., 2009. Infrequent co-treatment and sequential treatment of anti-sclerostin antibody with zoledronic acid restores and maintains bone mass in murine osteoporosis models. J. Bone Miner. Res. 24 (Suppl. 1). ABSTRACT in presentation 1063.

Hamann, C., Rauner, M., Hohna, Y., Bernhardt, R., Mettelsiefen, J., Goettsch, C., et al., 2013. Scl-Ab treatment improves bone mass, bone strength, and bone defect regeneration in rats with type 2 diabetes mellitus. J. Bone Miner. Res. 28, 627–638.

Hamersma, H., Gardner, J., Beighton, P., 2003. The natural history of sclerosteosis. Clin. Genet. 63, 192–197.

Hassler, N., Roschger, A., Gamsjaeger, S., Kramer, I., Lueger, S., van Lierop, A., et al., 2014. Sclerostin deficiency is linked to altered bone composition. J. Bone Miner. Res. 29, 2144–2151.

He, W.T., Chen, C., Pan, C., Zhang, M.X., Yu, X.F., Wang, D.W., et al., 2016. Sclerosteosis caused by a novel nonsense mutation of SOST in a consanguineous family. Clin. Genet. 89, 205–209.

Holdsworth, G., Slocombe, P., Doyle, C., Sweeney, B., Veverka, V., Le Riche, K., et al., 2012. Characterization of the interaction of sclerostin with the low density lipoprotein receptor-related protein (LRP) family of Wnt co-receptors. J. Biol. Chem. 287, 26464–26477.

Holdsworth, G., Greenslade, K., Stencel, Z., Jose, J., Kirby, H., Moore, A., et al., 2017. Dampening of the bone formation response following repeat dosing with sclerostin antibody in mice is associated with up-regulation of Wnt antagonists. Bone 107, 93–103.

Ke, H.Z., Richards, W.G., Li, X., Ominsky, M.S., 2012. Sclerostin and Dickkopf-1 as therapeutic targets in bone diseases. Endocr. Rev. 33, 747–783.

Kendler, D.L., Bone, H.G., Massari, F., Gielen, E., Palacios, S., Maddox, J., et al., 2017. Retreatment with romosozumab after 12 months of placebo demonstrates similar BMD efficacy compared with initial romosozumab treatment. Endocr. Rev. 38. OR08-1.

Kim, C.A., Honjo, R., Bertola, D., Albano, L., Oliveira, L., Jales, S., et al., 2008. A known SOST gene mutation causes sclerosteosis in a familial and an isolated case from Brazilian origin. Genet. Test. 12, 475–479.

Kim, S.W., Lu, Y., Williams, E.A., Lai, F., Lee, J.Y., Enishi, T., et al., 2017. Sclerostin antibody administration converts bone lining cells into active osteoblasts. J. Bone Miner. Res. 32, 892–901.

Koos, R., Brandenburg, V., Mahnken, A.H., Schneider, R., Dohmen, G., Autschbach, R., et al., 2013. Sclerostin as a potential novel biomarker for aortic valve calcification: an in-vivo and ex-vivo study. J. Heart Valve Dis. 22, 317–325.

Kramer, I., Loots, G.G., Studer, A., Keller, H., Kneissel, M., 2010. Parathyroid hormone (PTH)-induced bone gain is blunted in SOST overexpressing and deficient mice. J. Bone Miner. Res. 25, 178–189.

Krause, C., Korchynskyi, O., de Rooij, K., Weidauer, S.E., de Gorter, D.J., van Bezooijen, R.L., et al., 2010. Distinct modes of inhibition by sclerostin on bone morphogenetic protein and Wnt signaling pathways. J. Biol. Chem. 285, 41614–41626.

Krishna, S.M., Seto, S.W., Jose, R.J., Li, J., Morton, S.K., Biros, E., et al., 2017. Wnt signaling pathway inhibitor sclerostin inhibits angiotensin II-induced aortic aneurysm and atherosclerosis. Arterioscler. Thromb. Vasc. Biol. 37, 553–566.

Langdahl, B.L., Libanati, C., Crittenden, D.B., Bolognese, M.A., Brown, J.P., Daizadeh, N.S., et al., 2017. Romosozumab (sclerostin monoclonal antibody) versus teriparatide in postmenopausal women with osteoporosis transitioning from oral bisphosphonate therapy: a randomized, open-label, phase 3 trial. Lancet 390, 1585–1594.

Lehnen, S.D., Gotz, W., Baxmann, M., Jager, A., 2012. Immunohistochemical evidence for sclerostin during cementogenesis in mice. Ann. Anat. 194, 415–421.

Leupin, O., Piters, E., Halleux, C., Hu, S., Kramer, I., Morvan, F., et al., 2011. Bone overgrowth-associated mutations in the LRP4 gene impair sclerostin facilitator function. J. Biol. Chem. 286, 19489–19500.

Lewiecki, E., Horlait, S., Blicharski, T., Goemaere, S., Lippuner, K., Meisner, P., et al., 2016. Results of a phase 3 clinical trial to evaluate the efficacy and safety of romosozumab in men with osteoporosis. Arthritis Rheum. 68 (Suppl. 10). ABSTRACT 321.

Li, X., Zhang, Y., Kang, H., Liu, W., Liu, P., Zhang, J., et al., 2005. Sclerostin binds to LRP5/6 and antagonizes canonical Wnt signaling. J. Biol. Chem. 280, 19883–19887.

Li, X., Ominsky, M.S., Niu, Q.T., Sun, N., Daugherty, B., D'Agostin, D., et al., 2008. Targeted deletion of the sclerostin gene in mice results in increased bone formation and bone strength. J. Bone Miner. Res. 23, 860–869.

Li, X., Ominsky, M.S., Warmington, K.S., Morony, S., Gong, J., Cao, J., et al., 2009. Sclerostin antibody treatment increases bone formation, bone mass, and bone strength in a rat model of postmenopausal osteoporosis. J. Bone Miner. Res. 24, 578–588.

Li, X., Warmington, K.S., Niu, Q.T., Asuncion, F.J., Barrero, M., Grisanti, M., et al., 2010. Inhibition of sclerostin by monoclonal antibody increases bone formation, bone mass, and bone strength in aged male rats. J. Bone Miner. Res. 25, 2647–2656.

Li, X., Ominsky, M.S., Warmington, K.S., Niu, Q.-T., Asuncion, F.J., Barrero, M., et al., 2011. Increased bone formation and bone mass induced by sclerostin antibody is not affected by pretreatment or cotreatment with alendronate in osteopenic, ovariectomized rats. Endocrinology 152, 3312–3322.

Li, X., Warmington, K.S., Niu, Q.T., et al., 2013. Retreatment with sclerostin antibody increased bone formation and bone mass in ovariectomized rats. J. Bone Miner. Res. 28 (Suppl. 1). ABSTRACT 1072.

Li, X., Niu, Q.T., Warmington, K.S., Asuncion, F.J., Dwyer, D., Grisanti, M., et al., 2014. Progressive increases in bone mass and bone strength in an ovariectomized rat model of osteoporosis after 26 weeks of treatment with a sclerostin antibody. Endocrinology 155, 4785–4797.

Li, X., Ominsky, M.S., Villasenor, K.S., Niu, Q.-T., Asuncion, F.J., Xia, X., et al., 2018. Scl-Ab reverses bone loss by increasing bone formation and decreasing bone resorption in a rat model of male osteoporosis. Endocrinology 159, 260–271.

Lin, C., Jiang, X., Dai, Z., Guo, X., Weng, T., Wang, J., et al., 2009. Sclerostin mediates bone response to mechanical unloading through antagonizing Wnt/beta-catenin signaling. J. Bone Miner. Res. 24, 1651–1661.

Little, D.G., Peacock, L., Mikulec, K., Kneissel, M., Kramer, I., Cheng, T.L., et al., 2017. Combination sclerostin antibody and zoledronic acid treatment outperforms either treatment alone in a mouse model of osteogenesis imperfecta. Bone 101, 96–103.

Liu, X.S., Stein, E.M., Zhou, B., Zhang, C.A., Nickolas, T.L., Cohen, A., et al., 2012. Individual trabecula segmentation (ITS)-based morphological analyses and microfinite element analysis of HR-pQCT images discriminate postmenopausal fragility fractures independent of DXA measurements. J. Bone Miner. Res. 27, 263–272.

Loots, G.G., Kneissel, M., Keller, H., Baptist, M., Chang, J., Collette, N.M., et al., 2005. Genomic deletion of a long-range bone enhancer misregulates sclerostin in Van Buchem disease. Genome Res. 15, 928–935.

Lovato, C., Lewiecki, E.M., 2017. Emerging anabolic agents in the treatment of osteoporosis. Expert Opin. Emerg. Drugs 22, 247–257.

Ma, Y., Zeng, Q., Cain, R., et al., 2013. Bone anabolic effect of sclerostin antibody is maintained with antiresorptive agents in osteopenic, ovariectomized rats. J. Bone Miner. Res. 28 (Suppl. 1). ABSTRACT SA0405.

Ma, Y.L., Hamang, M., Lucchesi, J., Bivi, N., Zeng, Q., Adrian, M.D., et al., 2017. Time course of disassociation of bone formation signals with bone mass and bone strength in sclerostin antibody treated ovariectomized rats. Bone 97, 20–28.

Matheny, J.B., Torres, A.M., Ominskey, M.S., Hernandez, C.J., 2017. Romosozumab treatment converts trabecular rods into trabecular plates in male cynomolgus monkeys. Calcif. Tissue Int. 101, 82–91.

McClung, M.R., 2017. Sclerostin antibodies in osteoporosis: latest evidence and therapeutic potential. Ther. Adv. Musculoskel. Dis. 9, 263–270.

McClung, M.R., Grauer, A., Boonen, S., Bolognese, M.A., Brown, J.P., Diez-Perez, A., et al., 2014. Romosozumab in postmenopausal women with low bone mineral density. N. Engl. J. Med. 370, 412–420.

McColm, J., Hu, L., Womack, T., Tang, C.C., Chiang, A.Y., 2014. Single- and multiple-dose randomized studies of blosozumab, a monoclonal antibody against sclerostin, in healthy postmenopausal women. J. Bone Miner. Res. 29, 935–943.

McCormick, L., Grillo, M., Tiede-Lewis, L., Wang, K., Zhao, H., Dallas, S., 2016. Intravital imaging of osteoblast, osteocyte and GFP-collagen dynamics. J. Bone Miner. Res. 31. ABSTRACT 1079.

McDonald, M.M., Reagan, M.R., Youlten, S.E., Mohanty, S.T., Seckinger, A., Terry, R.L., et al., 2017. Inhibiting the osteocyte-specific protein sclerostin increases bone mass and fracture resistance in multiple myeloma. Blood 129, 3452–3464.

Moustafa, T., Sugiyama, J., Prasad, G., Zaman, G., Gross, T.S., Lanyon, L.E., et al., 2012. Mechanical loading-related changes in osteocyte sclerostin expression in mice are more closely associated with the subsequent osteogenic response than the peak strains engendered. Osteoporos. Int. 23, 1225–1234.

Nioi, P., Taylor, S., Hu, R., Pacheco, E., He, Y.D., Hamadeh, H., et al., 2015. Transcriptional profiling of laser capture microdissected subpopulations of the osteoblast lineage provides insight into the early response to sclerostin antibody in rats. J. Bone Miner. Res. 30, 1457–1467.

Nusse, R., Clevers, H., 2017. Wnt/beta-catenin signaling, disease, and emerging therapeutic modalities. Cell 169, 985–999.

Ominsky, M.S., Vlasseros, F., Jolette, J., Smith, S.Y., Stouch, B., Doellgast, G., et al., 2010. Two doses of sclerostin antibody in cynomolgus monkeys increases bone formation, bone mineral density, and bone strength. J. Bone Miner. Res. 25, 948–959.

Ominsky, M.S., Li, C., Li, X., Tan, H.L., Lee, E., Barrero, M., et al., 2011. Inhibition of sclerostin by monoclonal antibody enhances bone healing and improves bone density and strength of nonfractured bones. J. Bone Miner. Res. 26, 1012–1021.

Ominsky, M.S., Samadfam, R., Jolette, J., et al., 2012. Long-term sclerostin antibody treatment in cynomolgus monkeys: sustained in vertebral microarchitecture and bone strength following a temporal increase in cancellous bone formation. J. Bone Miner. Res. 27 (Suppl. 1), SA0406. ABSTRACT FR0406.

Ominsky, M.S., Niu, Q.T., Li, C., Li, X., Ke, H.Z., 2014. Tissue-level mechanisms responsible for the increase in bone formation and bone volume by sclerostin antibody. J. Bone Miner. Res. 29, 1424–1430.

Ominsky, M.S., Brown, D.L., Van, G., Cordover, D., Pacheco, E., Frazier, E., et al., 2015. Differential temporal effects of sclerostin antibody and parathyroid hormone on cancellous and cortical bone and quantitative differences in effects on the osteoblast lineage in young intact rats. Bone 81, 380–391.

Ominsky, M.S., Boyce, R.W., Li, X., Ke, H.Z., 2017. Effects of sclerostin antibodies in animal models of osteoporosis. Bone 96, 63–75.

Ominsky, M.S., Boyd, S.K., Varela, A., Jolette, J., Felx, M., Doyle, N., et al., 2017. Romosozumab improves bone mass and strength while maintaining bone quality in ovariectomized cynomolgus monkeys. J. Bone Miner. Res. 32 (4), 788–801.

Padhi, D., Jang, G., Stouch, B., Fang, L., Posvar, E., 2011. Single-dose, placebo-controlled, randomized study of AMG 785, a sclerostin monoclonal antibody. J. Bone Miner. Res. 26, 19–26.

Padhi, D., Alison, M., Kivits, A.J., Gutierrez, M.J., Stouch, B., Wang, C., et al., 2014. Multiple doses of sclerostin antibody romosozumab in healthy men and postmenopausal women with low bone mass: a randomized, double-blind, placebo-controlled study. J. Clin. Pharmacol. 54, 168–178.

Perosky, J.E., Khoury, B.M., Jenks, T.N., Ward, F.S., Cortright, K., Meyer, B., et al., 2016. Single dose of bisphosphonate preserves gains in bone mass following cessation of Scl-Ab in Brtl/+ osteogenesis imperfecta model. Bone 93, 79–85.

Piters, E., Culha, C., Moester, M., Van Bezooijen, R., Adriaensen, D., Mueller, T., et al., 2010. First missense mutation in the SOST gene causing sclerosteosis by loss of sclerostin function. Hum. Mutat. 31, E1526–E1543.

Poole, K.E., van Bezooijen, R.L., Loveridge, N., Hamersma, H., Papapoulos, S.E., Lowik, C.W., et al., 2005. Sclerostin is a delayed secreted product of osteocytes that inhibits bone formation. FASEB J. 19, 1842–1844.

Qin, W., Li, X., Peng, Y., Harlow, L.M., Ren, Y., Wu, Y., et al., 2015. Scl-Ab preserves the morphology and structure of osteocytes and blocks the severe skeletal deterioration after motor-complete spinal cord injury in rats. J. Bone Miner. Res. 30, 1994–2004.

Recker, R.R., Benson, C.T., Matsumoto, T., Bolognese, M.A., Robins, D.A., Alam, J., et al., 2015. A randomized, double-blind phase 2 clinical trial of blosozumab, a sclerostin antibody, in postmenopausal women with low bone mineral density. J. Bone Miner. Res. 30, 216–224.

Ren, Y., Han, X., Ho, S.P., Harris, S.E., Cao, Z., et al., 2015. Removal of SOST or blocking its product sclerostin rescues defects in the periodontitis mouse model. FASEB J. 29, 2702–2711.

Robling, A.G., Niziolek, P.J., Baldridge, L.A., Condon, K.W., Allen, M.R., Alam, I., et al., 2008. Mechanical stimulation of bone in vivo reduces osteocyte expression of Sost/sclerostin. J. Biol. Chem. 283, 5866–5875.

Roschger, A., Roschger, P., Keplingter, P., Klaushofer, K., Abdullah, S., Kneissel, M., et al., 2014. Effect of Scl-Ab treatment in a mouse model of severe osteogenesis imperfecta. Bone 66, 182–188.

Ross, R.D., Edwards, L.H., Acerbo, A.S., Ominsky, M.S., Virdi, A.S., Sena, K., et al., 2014. Bone matrix quality after sclerostin antibody treatment. J. Bone Miner. Res. 29, 1597–1607.

Rothe, C., Urlinger, S., Lohning, C., Prassler, J., Stark, Y., Jager, U., et al., 2008. The human combinatorial antibody library HuCAL GOLD combines diversification of all six CDRs according to the natural immune system with a novel display method for efficient selection of high-affinity antibodies. J. Mol. Biol. 376, 1182–1200.

Saag, K.G., Petersen, J., Brandi, M.L., Karaplis, A.C., Lorentzon, M., Thomas, T., et al., 2017. Romosozumab or alendronate for fracture prevention in women with osteoporosis. N. Engl. J. Med. 377, 1417–1427.

Seefried, L., Baumann, J., Hemsley, S., Hofmann, C., Kunstmann, E., Kiese, B., et al., 2017. Efficacy of anti-sclerostin monoclonal antibody BPS804 in adult patients with hypophosphatasia. J. Clin. Investig. 127, 2148–2158.

Semenov, M.V., He, X., 2006. LRP5 mutations linked to high bone mass diseases cause reduced LRP5 binding and inhibition by SOST. J. Biol. Chem. 281, 38276–38284.

Semenov, M., Tamai, K., He, X., 2005. SOST is a ligand for LRP5/LRP6 and a Wnt signaling inhibitor. J. Biol. Chem. 280, 26770–26775.

Shahnazari, M., Wronski, T., Chu, V., Williams, A., Leeper, A., Stolina, M., et al., 2012. Early response of bone marrow osteoprogenitors to skeletal unloading and sclerostin antibody. Calcif. Tissue Int. 91, 50–58.

Sinder, B.P., Eddy, M.M., Ominsky, M.S., Caird, M.S., Marini, J.C., Kozloff, K.M., 2013. Scl-Ab improves skeletal parameters in a Brtl/+ mouse model of osteogenesis imperfecta. J. Bone Miner. Res. 28, 73–80.

Sinder, B.P., White, L.E., Salemi, J.D., Ominsky, M.S., Caird, M.S., Marini, J.C., et al., 2014. Adult Brtl/+ mouse model of osteogenesis imperfecta demonstrates anabolic response to Scl-Ab treatment with increased bone mass and strength. Osteoporos. Int. 25, 2097–2107.

Sinder, B.P., Lloyd, W.R., Salemi, J.D., Marini, J.C., Caird, M.S., Morris, M.D., et al., 2016. Effect of anti-sclerostin therapy and osteogenesis imperfecta on tissue-level properties in growing and adult mice while controlling for tissue age. Bone 84, 222–229.

Spatz, J.M., Ellman, R., Cloutier, A.M., Louis, L., van Vliet, M., Suva, L.J., et al., 2013. Sclerostin antibody inhibits skeletal deterioration due to reduced mechanical loading. J. Bone Miner. Res. 28, 865–874.

Stein, S.A., Witkop, C., Hill, S., Fallon, M.D., Viernstein, L., Gucer, G., et al., 1983. Sclerosteosis: neurogenetic and pathophysiologic analysis of an American kinship. Neurology 33, 267–277.

Stolina, M., Dwyer, D., Niu, Q.T., Villasenor, K.S., Kurimoto, P., Grisanti, M., et al., 2014. Temporal changes in systemic and local expression of bone turnover markers during six months of sclerostin antibody administration to ovariectomized rats. Bone 67, 305–313.

Suen, P.K., Zhu, T.Y., Chow, D.H., Huang, L., Zheng, L.Z., Qin, L., 2015. Sclerostin antibody treatment increases bone formation, bone mass, and bone strength of intact bones in adult male rats. Sci. Rep. 5, 15632.

Sutherland, M.K., Geoghegan, J.C., Yu, C., Turcott, E., Skonier, J.E., Winkler, D.G., et al., 2004. Sclerostin promotes the apoptosis of human osteoblastic cells: a novel regulation of bone formation. Bone 35, 828–835.

Taylor, S., Ominsky, M.S., Hu, R., Pacheco, E., He, Y.D., Brown, D.L., et al., 2016. Time-dependent cellular and transcriptional changes in the osteoblast lineage associated with sclerostin antibody treatment in ovariectomized rats. Bone 84, 148–159.

Thompson, M.L., Chartier, S.R., Mitchell, S.A., Mantyh, P.W., 2016. Preventing painful age-related bone fractures: anti-sclerostin therapy builds cortical bone and increases the proliferation of osteogenic cells in the periosteum of the geriatric mouse femur. Mol. Pain 12 pii: 1744806916677147.

Tian, X., Jee, W.S., Li, X., Paszty, C., Ke, H.Z., 2011. Scl-Ab increases bone mass by stimulating bone formation and inhibiting bone resorption in a hindlimb-immobilization rat model. Bone 48, 197–201.

Trinh, S., Balani, D.H., Boyce, R., Kronenberg, H.M., 2017. Sclerostin antibody administration increases the numbers and differentiation of osteoblast precursors in vivo. J. Bone Miner. Res. ABSTRACT 1142.

Tu, X., Delgado-Calle, J., Condon, K.W., Maycas, M., Zhang, H., Carlesso, N., et al., 2015. Osteocytes mediate the anabolic actions of canonical Wnt/β-catenin signaling in bone. Proc. Natl. Acad. Sci. U. S. A. 112, E478–E486.

van Bezooijen, R.L., DeRuiter, M.C., Vilain, N., Monteiro, R.M., Visser, A., van der Wee-Pals, L., et al., 2007. SOST expression is restricted to the great arteries during embryonic and neonatal cardiovascular development. Dev. Dynam. 236, 606–612.

Van Bezooijen, R.L., Bronckers, A.L., Gortzak, R.A., Hogendoorn, P.C., van der Wee-Pals, L., Balemans, W., et al., 2009. Sclerostin in mineralized matrices and van Buchem disease. J. Dent. Res. 88, 569–574.

Van Lierop, A.H., Appelman-Dijkstra, N.M., Papapoulos, S.E., 2017. Sclerostin deficiency in humans. Bone 96, 51–62.

Van Wesenbeeck, L., Cleiren, E., Gram, J., Beals, R.K., Benichou, O., Scopelliti, D., et al., 2003. Six novel missense mutations in the LDL receptor-related protein 5 (LRP5) gene in different conditions with an increased bone density. Am. J. Hum. Genet. 72, 763–771.

Veverka, V., Henry, A.J., Slocombe, P.M., Ventom, A., Mulloy, B., Muskett, F.W., et al., 2009. Characterization of the structural features and interactions of sclerostin: molecular insight into a key regulator of Wnt-mediated bone formation. J. Biol. Chem. 284, 10890–10900.

Wang, J., Zhou, B., Parkinson, I., Thomas, C.D., Clement, J.G., Guo, X.E., et al., 2013. Trabecular plate loss and deteriorating elastic modulus of femoral trabecular bone in intertrochanteric hip fractures. Bone Res. 1, 346–354.

Wang, K., Tiede-Lewis, L., McCormick, L., Lara, N., Keightley, A., Farina, N., et al., 2017. Extracellular vesicle-mediated cell-cell communication in bone and potential role in muscle–bone crosstalk. J. Bone Miner. Res. 32. ABSTRACT 1149.

Wehmeyer, C., Frank, S., Beckmann, D., Bottcher, M., Cromme, C., Konig, U., et al., 2016. Sclerostin inhibition promotes TNF-dependent inflammatory joint destruction. Sci. Transl. Med. 8, 330ra35.

Weidauer, S.E., Schmieder, P., Beerbaum, M., Schmitz, W., Oschkinat, H., Mueller, T.D., 2009. NMR structure of the Wnt modulator protein sclerostin. Biochem. Biophys. Res. Commun. 380, 160–165.

Wein, M.N., Liang, Y., Goransson, O., Sundberg, T.B., Wang, J., Williams, E.A., et al., 2016. SIKs control osteocyte responses to parathyroid hormone. Nat. Commun. 7, 13176.

Wijenayaka, A.R., Kogawa, M., Lim, H.P., Bonewald, L.F., Findlay, D.M., Atkins, G.J., 2011. Sclerostin stimulates osteocyte support of osteoclast activity by a RANKL-dependent pathway. PLoS One 6, e25900.

Winkler, D.G., Sutherland, M.K., Geoghegan, J.C., Yu, C., Hayes, T., Skonier, J.E., et al., 2003. Osteocyte control of bone formation via sclerostin, a novel BMP antagonist. EMBO J. 22, 6267−6276.

Yagi, H., Takagi, M., Hasegawa, Y., Kayserili, H., Nishimura, G., 2015. Sclerosteosis (craniotubular hyperostosis-syndactyly) with complex hyperphalangy of the index finger. Pediatr. Radiol. 45, 1239−1243.

Yao, W., Dai, W., Jiang, L., Lay, E.Y., Zhong, Z., Ritchie, R.O., et al., 2016. Sclerostin-antibody treatment of glucocorticoid-induced osteoporosis maintained bone mass and strength. Osteoporos. Int. 27, 283−294.

Yorgan, T.A., Peters, S., Jeschke, A., Benisch, P., Jakob, F., Amling, M., et al., 2015. The anti-osteoanabolic function of sclerostin is blunted in mice carrying a high bone mass mutation of Lrp5. J. Bone Miner. Res. 30, 1175−1183.

Zhang, D., Hu, M., Chu, T., Lin, L., Wang, J., Li, X., et al., 2016. Scl-Ab prevented progressive bone loss in combined ovariectomized and concurrent functional disuse. Bone 87, 161−168.

Zhu, D., Mackenzie, N.C., Millan, J.L., Farquharson, C., MacRae, V.E., 2011. The appearance and modulation of osteocyte marker expression during calcification of vascular smooth muscle cells. PLoS One 6, e19595.

Chapter 75

Vitamin D and its analogs

Glenville Jones[1] **and J. Wesley Pike**[2]

[1]Department of Biomedical and Molecular Science, Queen's University, Kingston, ON, Canada; [2]Department of Biochemistry, University of Wisconsin—Madison, Madison, WI, United States

Chapter outline

Introduction

The association of vitamin D deficiency with a broad spectrum of common diseases, including breast, colorectal, and prostate cancers; cardiovascular disease; autoimmune conditions; and infections (Holick, 2007; Jones, 2007), has led to a renewed interest in using vitamin D metabolites and analogs to treat a host of clinical conditions. Since vitamin D regulates gene expression in functions as varied as calcium and phosphate homeostasis, cell growth regulation, and cell differentiation of a variety of cell types such as enterocytes, keratinocytes, and epithelial cells of the vasculature and gastrointestinal tract, it constitutes a valuable agent to modulate disease states. The discovery of the metabolites 25-hydroxyvitamin D_3 ($25(OH)D_3$; calcidiol) and 1α,25-dihydroxyvitamin D_3 ($1\alpha,25(OH)_2D_3$; calcitriol) in the early 1970s led to their chemical synthesis and, since the 1980s, the development of several generations of calcitriol analogs (Jones et al., 1998). The pharmaceutical industry has attempted to separate the *calcemic properties* of $1\alpha,25(OH)_2D_3$ from its *cell-differentiating properties* (Miyaura et al., 1981) so as to develop vitamin D analogs with specialized "calcemic" or "noncalcemic" (cell-differentiating) uses (Bouillon et al., 1995; Jones, 2008b). Several agents in the form of calcipotriol, 22-oxacalcitriol (OCT), 19-nor-$1\alpha,25\text{-}(OH)_2D_2$, and $1\alpha(OH)D_2$, with "reduced calcemic activity" have resulted, finding widespread use in the treatment of psoriasis and secondary hyperparathyroidism. Other vitamin D analogs, e.g., ED-71 and 2-MD, primarily targeted to bone, have been touted as drugs for treatment of osteoporosis. Research has also focused on the synthesis of vitamin D compounds with multiple transcriptional targets in addition to the vitamin D receptor (VDR), VDR antagonists, and cytochrome P450 family 24 (CYP24) inhibitors, which block VDR-mediated action or the catabolism of 25(OH)D and $1\alpha,25(OH)_2D$, to provide agents with possible utility in metabolic bone diseases, osteoporosis, and cancer (Jones et al., 1998; Masuda and Jones, 2006). Our perception of the importance of vitamin D/25(OH)D repletion has been modified by the concept that some $1\alpha,25(OH)_2D_3$ is produced locally by target cells, making this molecule an endocrine *and* a paracrine factor (Holick, 2007; Jones, 2007). This review will discuss the full spectrum of vitamin D compounds currently available and some of their possible uses and potential mechanisms of action.

Principles of Bone Biology. https://doi.org/10.1016/B978-0-12-814841-9.00075-0

Pharmacologically important vitamin D compounds

Vitamin D compounds can be subdivided into four major groups, listed in Tables 75.1—75.4 and described in the following sections.

Vitamin D and its natural metabolites

Table 75.1 shows the structures of vitamin D_3 and some of its important metabolites. Somewhat paradoxically, vitamin D_3, the natural form of vitamin D, is not approved for use as a drug in the United States, whereas it is found increasingly as an over-the-counter natural food supplement in the United States and is used in both roles in virtually every other country in the world.

TABLE 75.1 Vitamin D and its natural metabolites.

Vitamin D metabolite (ring structure)[a]	Side chain structure	Site of synthesis	Relative vitamin D receptor—binding affinity[b]	Relative vitamin D-binding protein—binding affinity[c]	References
Vitamin D_3 [1]	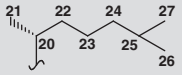	Skin	~0.001	3180	(Mellanby and Cantag, 1919; McCollum et al., 1922)
25(OH)D_3 [1]	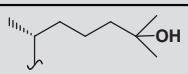	Liver	0.1	66,800	(Blunt et al., 1968)
1α,25(OH)$_2D_3$ [3]	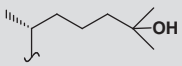	Kidney	100	100	(Fraser and Kodicek, 1970; Holick et al., 1971)
24(*R*),25(OH)$_2D_3$ [1]	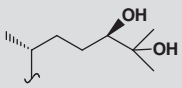	Kidney	0.02	33,900	(Holick et al., 1972)
1α,24(*R*),25(OH)$_3D_3$ [3]	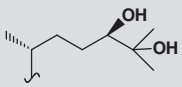	Target tissues[d]	10	21	(Holick et al., 1973)
25(*S*),26(OH)$_2D_3$ [1]	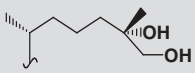	Liver?	0.02	26,800	(Suda et al., 1970)
25(OH)D_3-26,23-lactone [1]	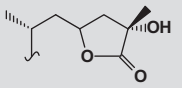	Kidney	0.01	250,000	(Horst, 1979)

[a]*Structure of the vitamin D nucleus (secosterol ring structure).*
[b]*Values reproduced from previously published data (Stern, 1981).*
[c]*Values reproduced from previously published data (Bishop et al., 1994).*
[d]*Known target tissues include intestine, bone, kidney, skin, and the parathyroid gland.*

Vitamin D nucleus

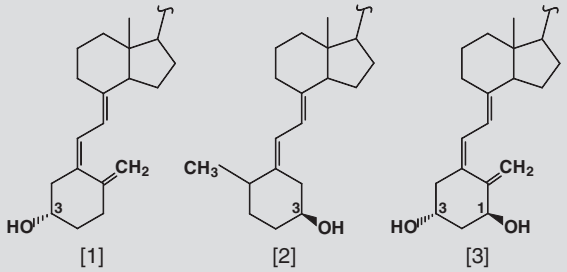

[1] [2] [3]

TABLE 75.2 Vitamin D prodrugs.

Vitamin D prodrug (ring structure)[a]	Side chain structure	Company	Status	Possible target diseases	Mode of delivery	References
25(OH)D_3)[1]	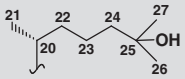	Generic	In use, Europe	Vitamin D deficiency	Rapid release, oral	US patent no. 3565924
		OPKO —Renal	In use, USA	CKD stage 3/4 Hyperparathyroidism	Controlled release, oral	
1α(OH)D_3 [3]	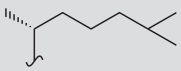	Leo	In use, Europe	Osteoporosis	Systemic	(Barton et al., 1973)
1α(OH)D_2 [3]	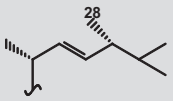	Genzyme	In use, USA	Secondary hyperparathyroidism	Systemic	(Paaren et al., 1978)
Dihydrotachysterol [2]	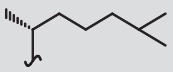	Duphar	Withdrawn	Renal failure	Systemic	(Jones et al., 1988)
Vitamin D_2 [1]	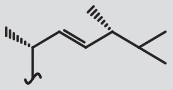	Various	In use, USA	Rickets Osteomalacia	Systemic Systemic	(Park, 1940)
1α(OH)D_5 [3]	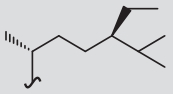	Various	In use, USA	Cancer	Systemic	(Mehta et al., 2000)

CKD, chronic kidney disease.
[a]*Structure of the vitamin D nucleus (secosterol ring structure).*

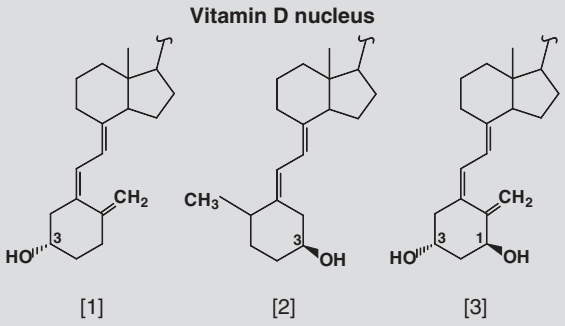

During the late 1960s and early 1970s, most of the principal vitamin D metabolites were first isolated and identified by gas chromatography—mass spectrometry and then their exact stereochemical structure was determined (Jones et al., 1998). This led to the chemical synthesis of the naturally occurring isomer and its testing in various biological assays in vitro and in vivo. Indeed all the major metabolites, namely, 25(OH)D_3 (Calderol, Rayaldee), 1α,25$(OH)_2D_3$ (Rocaltrol), and 24,25-dihydroxyvitamin D_3 (24*R*,25$(OH)_2D_3$; Secalciferol), are currently or have been available for use as drugs globally.

Vitamin D prodrugs

Table 75.2 lists some of the important prodrugs of vitamin D. All of these compounds require a step (or more) of activation in vivo before they are biologically active. Included here is vitamin D_2 (ergocalciferol), which is derived from the fungal sterol, ergosterol, by irradiation. When the nutritional basis of rickets and osteomalacia became apparent in the first half of the 20th century, vitamin D (particularly vitamin D_2 because it was less expensive and could be made by simply irradiating yeast) became the treatment of choice for these diseases. In North America, low-dose prophylactic vitamin D (400 IU) in the form of dietary supplements or fortification of milk, margarine, bread, or other food products replaced much of the need for therapeutic vitamin D to abolish overt rickets and osteomalacia. Florid vitamin D deficiency rickets has become

TABLE 75.3 Analogs of $1\alpha,25(OH)_2D_3$.

Vitamin D analog (ring structure)[a]	Side chain structure	Company	Status	Possible target diseases	Mode of delivery	References
Calcitriol, $1\alpha,25(OH)_2D_3$ [3]	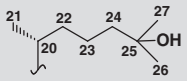	Roche Duphar	In use worldwide	Hypocalcemia Psoriasis	Systemic Topical	(Baggiolini et al., 1982)
26,27-F6-$1\alpha,25(OH)_2D_3$ [3]	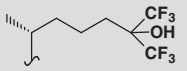	Sumitomo Taisho	In use, Japan	Osteoporosis Hypoparathyroidism	Systemic Systemic	(Kobayashi et al., 1982)
19-Nor-$1\alpha,25(OH)_2D_2$ [5]	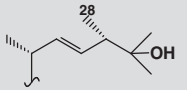	Abbott	In use, USA	Secondary hyperparathyroidism	Systemic	(Perlman et al., 1990)
22-Oxacalcitriol (OCT) [3]	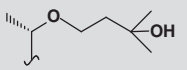	Chugai	In use, Japan	Secondary hyperparathy-roidism Psoriasis	Systemic Topical	(Murayama et al., 1986)
Calcipotriol (MC903) [3]	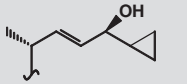	Leo	In use worldwide	Psoriasis Cancer	Topical Topical	(Calverley, 1987)
$1\alpha,25(OH)_2$-16-ene-23-yne-D_3 (Ro 23-7553) [6]	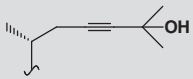	Roche	Preclinical	Leukemia	Systemic	(Baggiolini et al., 1989)
EB1089 [3]	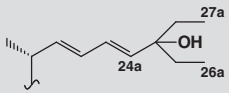	Leo	Clinical trials	Cancer	Systemic	(Binderup et al., 1991)
20-Epi-$1\alpha,25(OH)_2D_3$ [3]	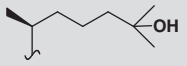	Leo	Preclinical	Immune diseases	Systemic	(Calverley et al., 1991)
2-Methylene-19-nor-20-epi-$1\alpha,25(OH)_2D_3$ (2MD) [7]	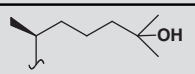	Deltanoid	Preclinical	Osteoporosis	Systemic	(Shevde et al., 2002)

2-Methylene-22-dehydro-19-nor-1,24*R*,25(OH)3D_3 (WT-51) [7]	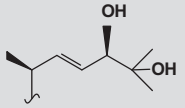	Deltanoid	Preclinical	Osteoporosis	Systemic	US patent application no. 2014/0206655
19-Nor-14-epi-23-yne-1,25$(OH)_2D_3$ (inecalcitol, TX-527) [8]	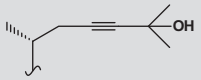	Hybrigenics	Clinical trials	Prostate cancer Leukemia	Systemic	(Medioni et al., 2014)
Eldecalcitol (ED-71) [4]	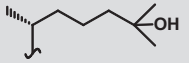	Chugai	In use, Japan	Osteoporosis	Systemic	(Nishii et al., 1993)
1α,24(*S*)-$(OH)_2D_2$ [3]	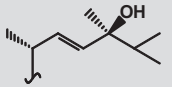	Sanofi	Preclinical	Psoriasis	Topical	(Strugnell et al., 1995)
1α,24(*R*)-$(OH)_2D_3$ (TV-02) [3]	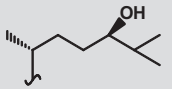	Teijin	In use, Japan	Psoriasis	Topical	(Morisaki et al., 1975)

[a]*Structure of the vitamin D nucleus (secosterol ring structure).*

Vitamin D nucleus

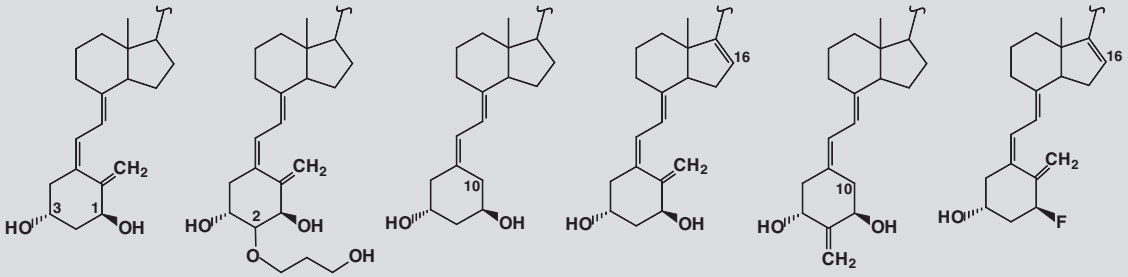

[3] [4] [5] [6] [7] [8]

TABLE 75.4 Miscellaneous vitamin D compounds.

Name	Structure	Name	Structure
LG190090 **Ligand Pharmaceuticals** Nonsteroidal VDR agonist (Boehm et al., 1999)	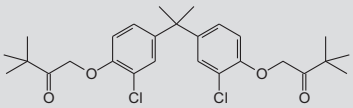	**LY2108491** **Eli Lilly** Nonsteroidal VDR agonist (Ma et al., 2006)	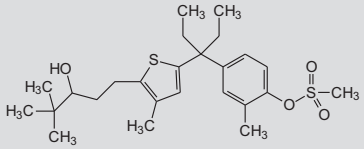
TEI-9647 **Teijin** VDR antagonist; dehydration product of 1α,25(*R*)-$(OH)_2D_3$-26,23(*S*)-lactone (Saito and Kittaka, 2006; Ochiai et al., 2005; Toell et al., 2001)	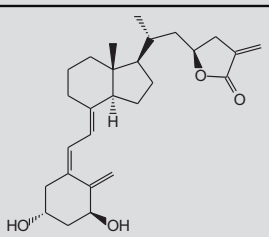	**ZK159222 Schering** VDR antagonist (Toell et al., 2001)	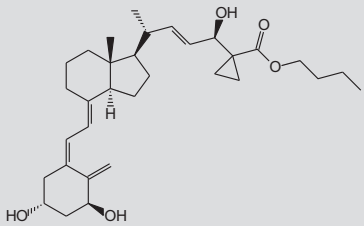
SDZ 89-443 Sandoz/ Novartis P450 inhibitor (Schuster et al., 2001)	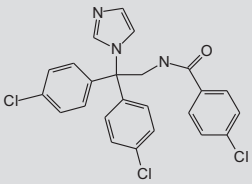	**VID-400 Sandoz/ Novartis** P450 inhibitor (Schuster et al., 2001)	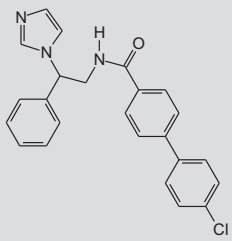
CTA016 **Cytochroma** CYP24A1 inhibitor (Posner et al., 2004)	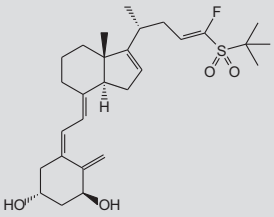	**ZG 1368** D-ring modified VDR agonist (Verstuyf et al., 2000)	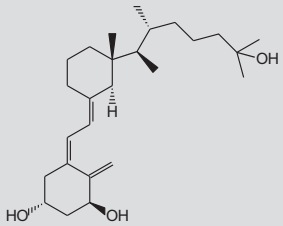
KS 176 C-ring-modified VDR agonist (Verstuyf et al., 2000)	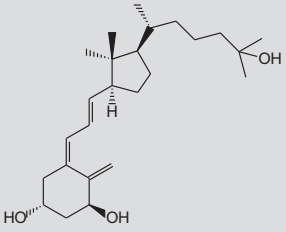	**SL 117** E-ring-modified VDR agonist (Verstuyf et al., 2000)	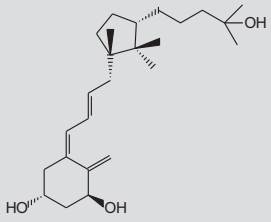
DK 406 VDR—histone deacetylase inhibitor hybrid (Bijian et al., 2018)	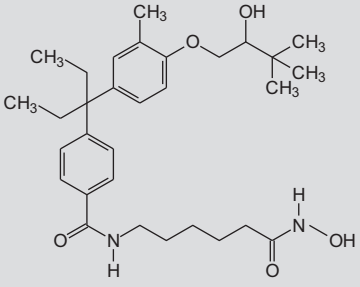		

VDR, vitamin D receptor.

uncommon in North America because of adherence to public health guidelines and the fact that vitamin D food fortification is required by law, in contrast to prior to fortification and it is still more prevalent in the world where food fortification is not practiced. In the United States, vitamin D_2 is the form of vitamin D used exclusively in pharmaceutical preparations, whereas vitamin D_3 is being increasingly incorporated into over-the-counter supplements. Vitamin D_2 differs only in that it possesses two specific modifications of the side chain (see Table 75.2) but these differences do not preclude the same series of activation steps as vitamin D_3, these giving rise to 25(OH)D_2, 1α,25(OH)$_2D_2$, and 24,25(OH)$_2D_2$, respectively. There has been controversy regarding the relative utility of dietary vitamin D_2 and vitamin D_3 to raise the circulating 25(OH)D level (Vieth et al., 2005). Evidence suggests that monthly oral pharmacological doses of vitamin D_3 are significantly more effective than equivalent doses of vitamin D_2 for increasing the 25(OH)D level into the sufficient range (20−50 ng/mL) (Armas et al., 2004), while there is ample evidence vitamin D_2 compounds are less toxic than their vitamin D_3 counterparts (Roborgh and de Man, 1960; Sjöden et al., 1985). On the other hand, other studies using smaller, daily oral dosing of vitamins D_2 and D_3 suggest a rough bioequivalence (Rapuri et al., 2004; Holick et al., 2008; Thacher et al., 2009).

25(OH)D_3 was developed and approved as the pharmaceutical preparation Calderol in the 1970s but was withdrawn in the United States in 2000 and at this writing is available only in Europe. A novel modified-release version of 25(OH)D_3 has been developed in the United States by OPKO−Renal (Miami, FL) and approved by the US FDA under the name Rayaldee and is approved for the treatment of stage 3/4 chronic kidney disease. Two other prodrugs, 1α(OH)D_3 and 1α(OH)D_2, were synthesized in the 1970s (Barton et al., 1973; Paaren et al., 1978) as alternative sources of 1α,25(OH)$_2D_3$ and 1α,25(OH)$_2D_2$, respectively, which in the process circumvent the renal 1α-hydroxylase enzyme, which was shown to be tightly regulated and prone to damage in renal disease. The prodrug 1α(OH)D_5 has been in clinical trials for the treatment of breast cancer (Mehta et al., 2000). The 1α-hydroxylated prodrugs have also been used in the treatment of osteoporosis. While the etiology of osteoporosis is complex and likely to be multifactorial (Seeman et al., 1995), there have been consistent claims that serum levels of 1α,25(OH)$_2D_3$ are low in osteoporosis (Riggs and Melton, 1992). In addition, evidence that certain VDR genotypes correlate with bone mineral density (Morrison et al., 1994; Uitterlinden et al., 2005) suggests that some genetically inherited basis involving vitamin D exists, leading to increased susceptibility to osteoporosis. As a consequence, it is not surprising that clinical trials of 1α(OH)D_3 (Orimo et al., 1987), 1α(OH)D_2 (Gallagher et al., 1994), and 1α,25(OH)$_2D_3$ (Gallagher et al., 1989; Ott and Chesnut, 1989; Tilyard et al., 1992) have led to reports of modest gains in bone mineral density and reductions in fracture rates in osteoporotic patients, a topic reviewed by Seeman et al. (1995).

The final compound in Table 75.2, dihydrotachysterol (DHT), lived a complex history as a prodrug. Originally it was believed to be "active" when converted to 25(OH)-DHT by virtue of an A ring rotated 180 degrees such that the 3β-hydroxyl function assumes a pseudo-1α-hydroxyl position (Jones et al., 1988). The mechanism of action of DHT has become less clear with the description of the extrarenal metabolism of 25(OH)-DHT to 1α,25(OH)$_2$-DHT and 1β,25(OH)$_2$-DHT, two further metabolites that have greater biological activity than either 25(OH)-DHT or DHT itself (Qaw et al., 1993).

Calcitriol analogs

Table 75.3 lists some of the most promising vitamin D analogs of 1α,25(OH)$_2D_3$ approved by governmental agencies, under development by various industrial/or university research groups as of this writing, or abandoned at various stages of the development process. Since the number of vitamin D analogs synthesized now lists in the thousands, the table is provided mainly to give a flavor of the structures experimented with thus far, the worldwide scope of the companies involved, and the broad spectrum of target diseases and uses.

The first generation of calcitriol analogs included molecules with fluorine atoms placed at metabolically vulnerable positions in the side chain and resulted in highly stable and potent calcemic agents such as 26,27-F_6-1α,25(OH)$_2D_3$. A second generation of analogs focused on features that make the molecule more susceptible to clearance, such as in calcipotriol (MC903), where a C22−C23 double bond, a 24-hydroxyl function, and a cyclopropane ring have been introduced into the side chain, or in OCT, where the 22-carbon has been replaced with an oxygen atom. Both modifications have given rise to highly successful analogs, calcipotriol and maxacalcitol, marketed in Europe and Japan, respectively (Kragballe et al., 1991; Nishii et al., 1993).

The C-24 position is a favorite site for modification, and numerous analogs contain 24-hydroxyl groups, e.g., 1α,24(*S*)-(OH)$_2D_2$ and 1α,24(*R*)-(OH)$_2D_3$ (Strugnell et al., 1995). Other analogs contain multiple changes in the side chain in combination, including unsaturation; 20-epimerization, 22-oxa replacement; homologation in the side chain; or terminal methyl groups. The resultant molecules such as EB1089 and KH1060 attracted the strong attention of researchers because of their increased potency in vitro and were pursued as possible anticancer and immunomodulatory compounds, respectively, but their development seems to have been stalled.

Attempts have been made to modify the nucleus of calcitriol. The Roche compound 1α,25(OH)$_2$-16-ene-23-yne-D$_3$, touted as an antitumor compound in vivo, possesses a D-ring double bond (Baggiolini et al., 1989). Declercq and Bouillon have made a novel 14-epi,19-nor-23-yne derivative with the same 23-yne feature (inecalcitol; TX-527), which also holds promise in the treatment of prostate cancer and various adult leukemias (Table 75.3; Medioni et al., 2014), and the same researchers have introduced a series of biologically active analogs without one of the other of the C/D rings but with a rigid backbone to maintain the spatial arrangement of the A-ring hydroxyl groups and the side chain (Table 75.4; Verstuyf et al., 2000). The A-ring-substituted 2-hydroxypropoxy-derivative ED-71 (Eldecalcitol), which by virtue of an A-ring substituent at C-2 and tighter binding affinity to vitamin D-binding protein (DBP) has a longer $t_{1/2}$ in the plasma (Nishii et al., 1993), is in use in Japan as an anti-osteoporosis drug. ED-71 performed well at restoring bone mass without causing hypercalcemia in long-term studies involving ovariectomized (OVX) rats and in phase I and II clinical trials (Matsumoto and Kubodera, 2007). Other bulky modifications at the C-2 position of the A ring are accommodated well by the VDR, as indicated by modeling and biological activity studies (Suhara et al., 2001; Shevde et al., 2002). Another C-2-substituted bone-specific analog is 2-MD (Shevde et al., 2002), at an early stage of pharmaceutical development, as of this writing, for the treatment of osteoporosis. It has a related 24-hydroxylated successor known as WT-51, which is (22E)-2-methylene-22-dehydro-1,24,25-trihydroxy-19-nor-vitamin D$_3$ and which markedly increases bone mass in OVX rats without causing hypercalcemia.

19-Nor-1α,25(OH)$_2$D$_2$ lacks a 19-methylene group and is similar to the in vivo active metabolite 1α,25(OH)$_2$-DHT$_2$, formed from DHT, because it lacks a functional group at the pseudo C-19 position. Many other compounds have been developed with rigid or altered *cis*-triene structures or modifications of the 1α-, 3β-, or 25-hydroxyl functions for use as drugs, but to allow us to establish minimal requirements for biological activity in structure/activity studies (Bouillon et al., 1995). BXL-628 combines 1-fluorination, 16-ene and 23-ene unsaturations, 26,27-homologation, and 20-epimerization, all found in earlier generations of analogs to make an antiproliferative agent used in clinical trials for the treatment of prostate cancer and prostatitis (Crescioli et al., 2004; Adorini et al., 2007).

Miscellaneous vitamin D analogs and associated drugs

One series of compounds depicted in Table 75.4 are the substituted biphenyls originally developed by Ligand, representing nonsteroidal scaffolds selected by high-throughput screening, which show weak VDR binding but good transactivation through vitamin D response element (VDRE)-driven, vitamin D-dependent genes and produce hypercalcemia in vivo (Boehm et al., 1999). This family has been extended by the synthesis of some highly potent, tissue-selective non-secosteroidal VDR modulators with nanomolar affinity (e.g., LY2109866) (Ma et al., 2006). This is the first class of vitamin D mimics that lack the conventional *cis*-triene secosteroid structure while maintaining the spatial separation of the A-ring and side-chain hydroxyl functions needed to bind to certain key residues of the ligand-binding pocket of the VDR. Although these nonsecosteroidal compounds are purported to exhibit an improvement of the therapeutic index over calcitriol in animal models, they are still to be tested clinically. In addition, Table 75.4 also shows the structures of two different classes of VDR/calcitriol antagonists. The former compounds, including TEI-9647, are dehydration products of the metabolite 1α,25(OH)$_2$D$_3$-26,23-lactone (Table 75.1) and have been used in the treatment of Paget's disease (Ishizuka et al., 2005; Saito and Kittaka, 2006; Toell et al., 2001).

Another group of compounds important to the vitamin D field that are under development are the CYP24A1 inhibitors. By blocking CYP24A1, the main catabolic pathway within the vitamin D-target cell, these agents extend the life of the natural agonist, calcitriol, giving rise to a longer lasting biological effect (Prosser and Jones, 2004). Sandoz/Novartis developed a group of molecules that exhibit greater specificity toward CYP24A1 and CYP27B1 compared with the general CYP inhibitor, ketoconazole, that showed utility in blocking cell proliferation in vitro, but these compounds were discontinued after early clinical trials (Schuster et al., 2001). Cytochroma (now OPKO—Renal) has developed a library of CYP24A1 inhibitors synthesized by Gary Posner based upon vitamin D templates, some of these being pure CYP24A1 inhibitors, while others are mixed VDR agonist/CYP24A1 inhibitors (Table 75.4). Some of these drugs have reached phase IIB human clinical trials for the treatment of psoriasis (Posner et al., 2004) and are now being tested systemically in the treatment of secondary hyperparathyroidism (Posner et al., 2009). Their promise stems from their ability to block the attenuating action of CYP24A1 on calcitriol-mediated prepro-parathyroid hormone (PTH) gene suppression.

There are several other compounds under development that have attracted interest because they have dual targets. James Gleason and John White have synthesized compounds with combined VDR-agonist and transcriptional histone deacetylase inhibitor activity for use as possible growth regulators in cancer therapy (Bijian et al., 2018), while Andrzej Kutner has developed vitamin D—retinoid combinations (retiferols), which target both VDR and their related retinoic acid/retinoid X nuclear receptors, where both agents are known to modulate cell differentiation and reduce cell division.

Clinical applications of vitamin D compounds

The clinical potential of vitamin D analogs has been covered comprehensively by others (Bikle, 1992; Bischoff-Ferrari et al., 2006) in published reviews. This section of the review focuses only on diseases currently treated with vitamin D analogs.

Secondary hyperparathyroidism

Chronic renal disease (CKD) is accompanied by a gradual fall in serum 1α,25$(OH)_2$D levels over the five-stage natural history of the disease, stages being defined by the decline in glomerular filtration rate (GFR). CKD culminates in the need for dialysis (stage 5). For 3 decades this reduction in serum 1α,25$(OH)_2$D has been assumed to be the result of a decline in 1α-hydroxylase (CYP27B1) activity, due in turn to loss of the protein itself, but the elucidation of the fibroblast growth factor 23 (FGF23)-regulated phosphate homeostatic pathway has opened up an alternative explanation. Since FGF23 triggers downregulation of CYP27B1 and upregulation of the catabolic 24-hydroxylase (CYP24A1), this hormone may also contribute to the progressive reduction in circulating 1α,25$(OH)_2$D levels (Quarles, 2008). Furthermore, FGF23 rises as early as CKD stage 1, preceding the decline in the 1α-hydroxylase activity, which occurs in CKD stage 2, and well before the hypocalcemia and secondary hyperparathyroidism that characterize the later stages of this disease. Unchecked, these biochemical events, together with the other sequelae of renal failure such as phosphate retention, can result in renal osteodystrophy. Active vitamin D analogs, such as 1α$(OH)D_3$ and 1α,25$(OH)_2D_3$, raise plasma Ca^{2+} concentrations and, in addition, lower PTH levels by direct suppression of PTH gene transcription at the level of the PTH gene promoter. Slatopolsky and colleagues (Delmez et al., 1989) showed that intravenous infusion of "active" vitamin D preparations results in a more effective suppression of plasma PTH levels without such a profound increase in plasma [Ca^{2+}] in end-stage renal disease (ESRD). Subsequent work has employed "low-calcemic" vitamin D analogs such as 1α$(OH)D_2$ (doxercalciferol), OCT, or 19-nor-1α,25$(OH)_2D_2$ (paricalcitol) as substitutes for the more calcemic natural hormone. The US FDA has approved both oral and intravenous versions of these drugs for the treatment of secondary hyperparathyroidism at stages 3 and 4 of the disease, as well as hemodialysis and peritoneal dialysis patients.

In 2003, a body of nephrologists released guidelines (National Kidney Foundation, 2003) recommending more aggressive use of vitamin D preparations and "active" vitamin D analogs in the treatment of secondary hyperparathyroidism in CKD. KDOQI guidelines suggested that treatment as early as stage 3 (GFR <60) might benefit the patient by limiting the extreme rises in plasma PTH levels and preventing the parathyroid gland resistance to vitamin D treatment often observed in ESRD. KDOQI guidelines also recognized the high frequency of vitamin D deficiency (25(OH)D <10 ng/mL) and vitamin D insufficiency (25(OH)D 10−30 ng/mL) in the CKD and ESRD population (Gonzalez et al., 2004) and made the opinion-based recommendation to make an initial attempt at vitamin D repletion with escalating doses of vitamin D_2 prior to administration of "active" vitamin D analog replacement therapy. This initial intervention to boost 25(OH)D levels has proven to be successful in stage 3 CKD patients in that it increases 1α,25$(OH)_2$D and mildly suppresses PTH levels but the strategy fails to produce the desired effects in stage 4 CKD patients due to reduced renal 1α-hydroxylase activity (Al-Aly et al., 2007; Zisman et al., 2007). As of this writing, both oral and intravenous formulations of various active vitamin D analogs are available for use in stage 3−5 patients to take over when vitamin D repletion fails to regulate PTH levels.

The emergence of the potential importance of the extrarenal 1α-hydroxylase in normal human physiology has led to a reevaluation of the vitamin D repletion and "active" hormone replacement arms of the CKD therapy (Jones, 2007). The value of vitamin D repletion is now seen as providing the substrate 25(OH)D for both the renal 1α-hydroxylase, which is the main determinant of circulating 1α,25$(OH)_2D_3$, and the extrarenal 1α-hydroxylase, which is postulated to augment 1α,25$(OH)_2D_3$ synthesis for local or intracrine actions around the body. While the decline of the renal enzyme during CKD is well established, the fate of the extrarenal 1α-hydroxylase in the face of uremia is largely a matter of conjecture. Evidence from anephric patients treated with large doses of 25$(OH)D_3$ (Dusso et al., 1988) suggests that the extrarenal enzyme survives in CKD patients, arguing that provision of a source of 25(OH)D to vitamin D-deficient and -insufficient patients throughout all stages of CKD is warranted. It also argues for the more judicious use of "active" vitamin D analogs as hormone replacement therapy layered on top of conventional vitamin D repletion therapy. Early attempts at this type of combined vitamin D/"active" vitamin D analog approach in a pediatric population have resulted in a more efficient PTH control without many of the usual problems of soft-tissue calcification observed in patients treated only with "active" vitamin D analogs (Fournier et al., 2007). The threefold higher susceptibility of CKD patients to cardiovascular disease (Teng et al., 2005; Tentori et al., 2006) may also point to the deleterious effects of untreated vitamin D deficiency on the vasculature and highlight the beneficial effects of both renally and locally produced 1α,25$(OH)_2$D for maintaining normal

blood pressure, for antiproliferative effects on myocardial cell hypertrophy, and for direct suppressive effects on vascular epithelial cell "osteoblastic" gene expression, e.g., Runx2 and Osterix (Mathew et al., 2008; Judd and Tangpricha, 2009).

On the other hand, a decade of availability of "active" vitamin D analogs has led some to question whether the overuse of such potent vitamin D compounds has contributed to accelerated calcification of the vascular tree and the increased incidence of cardiovascular disease in CKD patients (Razzaque, 2011). A new "milder" analog, in the form of Rayaldee (controlled-release $25(OH)D_3$) (Table 75.2), has been approved for use in stage 3/4 CKD patients for the treatment of secondary hyperparathyroidism. Clinical trial data show that Rayaldee suppresses serum PTH levels by over 30% (Sprague et al., 2016; Galassi et al., 2017) in such patients. Whether the same drug can be as successful in dialysis patients is still unknown.

Hyperproliferative conditions: psoriasis and cancer

The demonstration that $1\alpha,25(OH)_2D_3$ is an antiproliferative, prodifferentiating agent for certain cell types in vivo and many cell lines in vitro suggested that vitamin D analogs might offer some relief in hyperproliferative disorders such as psoriasis and cancer. Early psoriasis trials with systemic $1\alpha,25(OH)_2D_3$ were moderately successful but plagued with hypercalcemic side effects. Modifications to the protocol included:

(a) administration of calcitriol overnight when intestinal concentrations of $[Ca^{2+}]$ were low;
(b) substitution of low-calcemic analogs for the calcitriol.

Although oral calcitriol can be an effective treatment for psoriasis when administered using an overnight protocol, by far the most popular treatment for psoriasis is the topical administration of the low-calcemic analog calcipotriol, formulated as an ointment, which results in an improvement in over 75% of patients (Kragballe et al., 1991). Both $1\alpha,25(OH)_2D_3$ and calcipotriol are effective in psoriasis because they block hyperproliferation of keratinocytes, increase differentiation of keratinocytes, and help suppress local inflammatory factors through their immunomodulatory properties. Calcipotriol has now been marketed worldwide for use in psoriasis for over 25 years.

Several thousands of vitamin D analogs have been tested in vitro and in vivo with some degree of success in controlling the growth of tumor cells and thus offering potential for use as anticancer drug therapies (Masuda and Jones, 2006). Many vitamin D compounds are extremely effective antiproliferative or prodifferentiation agents in vitro, acting through a variety of mechanisms involving alterations in cell cycle genes and proapoptotic genes to produce their effects. Preclinical studies in laboratory animals have also resulted in promising data (Masuda and Jones, 2006). With the analog EB1089, the promising antiproliferative effects observed in vitro and in the NMU-induced mammary tumor and in LNCaP prostate cancer xenograft models (Colston et al., 2003) were also extended into the clinic. Early trials in limited numbers of breast cancer patients have been followed up with more extensive ongoing phase II and III clinical trials in a number of different cancers (Gulliford et al., 1998; Evans et al., 2002; Dalhoff et al., 2003). Several other analogs have entered clinical trials for the treatment of a variety of hyperproliferative diseases, usually involving VDR-positive tumors (see Masuda and Jones, 2006).

Despite the enormous promise of vitamin D analogs as anticancer agents, this has yet to result in an approved vitamin D analog for use in any type of cancer (Masuda and Jones, 2006). The principal problem in anticancer studies involving orally administered vitamin D compounds is hypercalcemia. Although the newer analogs appear to be less calcemic than calcitriol itself, they still retain some ability to raise serum calcium; they are not noncalcemic, as is sometimes claimed. Another problem emerging from experience with clinical trials is that effective doses needed to retard cell growth ($\sim$1 nM or higher) cannot be attained in vivo due to low bioavailability (Beer et al., 2004; Trump et al., 2004; Deeb et al., 2007). One of the determinants of tumor cell vitamin D analog levels is the catabolic enzyme CYP24A1, which is upregulated in vitamin D-target cells and limits the effective drug concentration reached. Thus, another approach to effective vitamin D therapy in cancer patients is the potential use of a CYP24-inhibitor (Table 75.4) with or without calcitriol or a calcitriol analog (Masuda and Jones, 2006). Nevertheless, it remains uncertain if a vitamin D compound can be developed that is sufficiently devoid of calcemic activity while retaining significant antiproliferative activity to be effective against tumors and also survive the catabolic processes that operate in vivo.

Criteria that influence pharmacological effects of vitamin D compounds

Three decades of work on vitamin D analogs have shown us that several factors play a role in dictating the success of synthetic compounds made to mimic some or all of the actions of calcitriol. These factors are discussed briefly next.

Activating enzymes

In vitro models show that some vitamin D compounds lacking 1α-hydroxylation (25(OH)D_3, 24(*R*),25(OH)$_2D_3$) are capable of interacting with VDR and transactivating reporter genes, but this occurs only at high (μM) concentrations of ligand (Uchida et al., 1994). It seems unlikely that these concentrations will be reached in vivo except in hypervitaminosis D (Jones, 2008a). Consequently, most of the compounds described in Tables 75.1 and 75.2 lack vitamin D biological activity *unless* they are activated in vivo. This is particularly the case for the parent vitamin D_3 itself, for its main circulating form 25(OH)D_3, or for any of the prodrugs listed in Table 75.2. Vitamins D_2 and D_3 depend upon both the liver 25-hydroxylase and the kidney 1α-hydroxylase enzyme systems to be activated, whereas most prodrugs require only a single step of activation. In particular, the 1α(OH)D drugs were designed to overcome the tightly regulated 1α-hydroxylase step, which is defective in chronic renal failure. In essence, prodrugs depend on the weakly regulated 25-hydroxylase step in the liver for activation. CYP27A1, the cytochrome P450 originally thought to be responsible for 25-hydroxylation of vitamin D_3, has been shown to be a bifunctional enzyme that can execute both activation of vitamin D_3 and the 27-hydroxylation of cholesterol during bile acid biosynthesis (Okuda et al., 1995). However, CYP27A1 has a relatively low affinity for vitamin D, does not 25-hydroxylate vitamin D_2, and when mutated results in cerebrotendinous xanthomatosis, not rickets. Consequently, the more "physiologically relevant" 25-hydroxylase within the group of candidate orphan P450s (Prosser and Jones, 2004) is likely to be CYP2R1 (Cheng et al., 2004), since this is a high-affinity microsomal enzyme with a known human mutation causing rickets and has been shown to 25-hydroxylate a D_2 prodrug, 1α(OH)D_2 (Jones et al., 2006). CYP2R1 has been crystallized with several vitamin D substrates in the active site, making it likely that it is the physiologically-relevant isoform (Strushkevich et al., 2008). Mutations of CYP2R1 result in vitamin D-dependency rickets type 1B (Thacher et al., 2015; Molin et al., 2017).

The role of extrarenal tissues in 1α-hydroxylating various 25-hydroxylated metabolites and analogs in normal physiology has always been a controversial story. However, it was widely accepted that extrarenal 1α-hydroxylase activity is pathologically relevant in granulomatous conditions (e.g., sarcoidosis) (Adams and Gacad, 1985). In sarcoid patients, 25(OH)D can be converted to 1α,25(OH)$_2$D in monocytes/macrophages, a step that, unlike the renal case, is not subject to tight regulation and thus potentially is more likely to result in hypercalcemia. Exposure of such patients to sunlight or administration of 25(OH)D can result in excessive plasma levels of 1α,25(OH)$_2$D. Following the cloning of the cytochrome P450 representing the 1α-hydroxylase (officially known as CYP27B1) (St. Arnaud et al., 1997; Takeyama et al., 1997), it was quickly shown that CYP27B1 can also be expressed extrarenally in skin, colon, and lung cancer cells (Fu et al., 1997; Jones et al., 1999). Our knowledge has been extended since 2005 with studies of CYP27B1 mRNA levels using real-time PCR and specific anti-CYP27B1 antibodies (Hewison et al., 2005) to show a widespread distribution of this enzyme in many normal tissues as well as pathological situations. Work using mouse models lacking positive and negative regulatory elements for the renal CYP27B1 suggest that in the absence of renal CYP27B1, serum levels of 1,25(OH)$_2D_3$ are reduced but do not disappear totally. This result is probably due to a failure to sufficiently suppress CYP27B1 activity in the kidney and to a corresponding complete suppression of renal CYP24A1, although it is possible that residual blood 1,25(OH)$_2D_3$ levels in these mice could be derived from extrarenal sources of CYP27B1 as well (Meyer et al., 2017). As alluded to earlier, the concept of the extrarenal 1α-hydroxylase suggests that this enzyme plays an important physiological as well as pathological role (Jones, 2007) and this has raised the level of importance given to ensuring maintenance of adequate 25(OH)D levels by vitamin D or direct 25(OH)D_3 supplementation in CKD patients.

Most of the calcitriol analogs listed in Table 75.3 are thought to be active as such, not requiring any step of activation prior to their action on the transcriptional machinery.

Vitamin D-binding protein

The DBP provides transport for all lipid-soluble vitamin D compounds, from vitamin D to 1α,25(OH)$_2D_3$, so it is not surprising that DBP also carries vitamin D analogs. Most of the analogs of calcitriol designed as of this writing contain modifications to the side chain, and this is usually detrimental to binding to DBP. Several analogs (e.g., calcipotriol, OCT, and 19-nor-1,25(OH)$_2D_2$) have very weak affinities for DBP, reduced by as much as 2−3 orders of magnitude relative to 1α,25(OH)$_2D_3$. This property has important implications for metabolic clearance rates, delivery to target cells, and tissue distribution (Bouillon et al., 1991; Kissmeyer et al., 1995). Detailed studies with one analog, OCT, have shown it to bind primarily to β-lipoprotein and exhibit an abnormal tissue distribution in vivo, with disproportionally high concentrations (ng/g tissue) in the parathyroid gland (Tsugawa et al., 1991). It was thus proposed that this unusual distribution may make OCT a useful systemically administered drug with a selective advantage in the treatment of hyperparathyroidism. Another vitamin D analog with a modified side chain is 20-epi-1α,25(OH)$_2D_3$, in which the 20-*S* configuration of the side chain is

opposite to the normal 20-*R* configuration. The DBP binding affinity of this analog is virtually unmeasurable as it does not displace [^{3}H]25(OH)D_3 from the plasma binding protein (Dilworth et al., 1994). Reporter gene transactivation assays show that 20-epi-1α,25$(OH)_2D_3$ transactivates equally well in COS cells incubated in the presence and absence of fetal calf serum (as a source of DBP), whereas 1α,25$(OH)_2D_3$-induced reporter gene expression is sensitive to DBP in the external growth medium, requiring two log units less hormone in the absence of DBP as in its presence (Dilworth et al., 1994). It therefore appears that analogs that bind DBP less well than 1α,25$(OH)_2D_3$ derive a target cell advantage over the natural hormone, *if they are able to find alternative plasma carrier proteins to transport them to their target cells.* However, these same alternative plasma carriers presumably result in changes in the tissue distribution and hepatic clearance of analogs over the natural metabolites of vitamin D. The development of a DBP-knockout mouse (Safadi et al., 1999) suggests that 25(OH)D_3 clearance is more rapid in the absence of DBP.

Vitamin D receptor/retinoid X receptor/vitamin D response element interactions

Three decades of work have established that 1α,25$(OH)_2D_3$ is able to work through a VDR-mediated genomic mechanism to stimulate transcriptional activity at vitamin D-dependent genes (Whitfield et al., 2005). Cloning of the VDR and elucidation of the 3D structure of its ligand-binding domain have provided a huge boost to delineating the precise conformational changes that take place when the natural ligand binds to the VDR (Rochel et al., 2001) and the nature of the post-ligand-binding transcriptional events that occur thereafter, particularly the nature of the coactivator proteins involved (Rachez and Freedman, 2000). Basic knowledge of the mechanism of action of vitamin D has also been aided by the opportunity to observe the lack of effects of calcitriol and its analogs in the VDR-knockout mouse (Yoshizawa et al., 1997; Li et al., 1997). These studies have largely refuted claims of alternative non-VDR-mediated mechanisms to produce physiologically relevant effects that might complicate our understanding of the pharmacological effects of vitamin D analogs.

Much evidence exists to support the viewpoint that vitamin D analogs mimic 1α,25$(OH)_2D_3$ and use primarily a genomic mechanism. In early work, Stern (1981) showed that there exists a strong correlation between chick intestinal VDR binding of an analog and its potency in a ^{45}Ca rat bone resorption assay, suggesting that a vitamin D analog is only as good as its affinity for the VDR. More recent work has suggested that this a highly simplified viewpoint and that VDR binding affinity may not even be the major factor; other factors may be transactivation activity stemming from a series of parameters such as conformation of the ligand/VDR complex, binding of the RXR partner, stability of the VDR/RXR/ligand complex, or even the nature of the coactivator proteins recruited to the complex. Data from the "superagonist" analogs (Yang and Freedman, 1999; Dilworth et al., 1997; Zella et al., 2009) suggest that 20-epi compounds including KH1060 are consistently only 1−2 orders of magnitude more potent than 1α,25$(OH)_2D_3$ in gene transactivation assays and/or differentiation assays. Thus it appears that the quantitative advantages claimed for some of the calcitriol analogs are modest. But it should also be pointed out that part of this advantage can also be explained by other factors such as differences in DBP binding or analog clearance.

Perhaps more important is whether analogs can be qualitatively different from 1α,25$(OH)_2D_3$ in their actions and work selectively in either calcium and phosphate homeostasis or cell differentiation. Freedman's group reported that the ability of various analogs to transactivate vitamin D-dependent genes or to stimulate differentiation of cells is best correlated with their ability to recruit the coactivator DRIP-205, one of the many components of the DRIP complex isolated by Freedman's group (Cheskis et al., 1995; Rachez et al., 1999). Among the other coactivators/transcription factors implicated in vitamin D analog action is GRIP-1 (TIF-2), which has been purported to have a particular propensity to interact with the analog OCT (Takeyama et al., 1999). In another study by Issa et al. (Issa et al., 2000), a broad panel of vitamin D analogs showed that GRIP-1 was more consistently recruited at levels closer to those of 1α,25$(OH)_2D_3$ than was another coactivator, AIB-1. Work by Peleg et al. (2003) offers an insight into the purported bone tissue selectivity of the Roche analog Ro 26-9228 (Table 75.3; renamed BXL-628) by showing recruitment of GRIP-1 in osteoblasts but not in CaCo-2 colon cancer cells; although paradoxically BXL-628 is now being pursued clinically for prostatic disease rather than osteoporosis treatment (Marchiani et al., 2006). Nevertheless, it appears that there is a fairly strong basis for the hypothesis that differences in the biopotency advantage of certain vitamin D analogs over 1α,25$(OH)_2D_3$ are due in part to changes in the recruitment of the RXR dimerization partner and/or coactivators (e.g., Eelen et al., 2008), but there is no consensus on which of these coactivator proteins is the important one or if these different coactivators can explain tissue/cell selectivity. Work using chromatin immunoprecipitation assays (Pike et al., 2007), which show temporal changes in coactivator recruitment at vitamin D-dependent gene promoters, may aid in our understanding of this complex transcriptional story.

The proposition that the interaction of analogs with the VDR might alter the receptor's conformation and therefore underlie its ability to interact with VDRE DNA sequences, to form RXR heterodimers, and/or to recruit coregulators such as DRIP, SRC, or any one of the other 300 or more coregulators that are now known, as has been described earlier, has been an attractive hypothesis since the 1990s (McKenna et al., 1999; O'Malley et al., 2008). This idea is supported by the discovery, through early proteolytic digestion studies and more recently through crystallography studies of the VDR, that receptor conformations may be different from that seen with $1,25(OH)_2D_3$ when complexed with certain analogs (Peleg et al., 1995; Orlov et al., 2012; Rochel et al., 2000, 2011; Tocchini-Valentini et al., 2001). These differences are extremely modest, however, and their actual effects on the transcription of specific genes as has been suggested is largely speculative. Consistent with these uncertainties is the observation that almost all of these effects of VDR mechanistic activity have been determined through either biochemical assays or highly modified cell-based assays that did not use endogenous gene output as an activity measure, and were rarely conducted in vivo. Indeed, even our most basic determination of the differential affinity of an analog for the VDR when bound to complex sites of DNA action in the cell has never been assessed. These and many additional uncertainties have prevented any definitive conclusions as to the underlying mechanisms that may be responsible for the differential actions of most analogs, which may include gene selectivity, tissue selectivity, or disease selectivity, which are the most sought-after features that have driven therapeutic analog development. Perhaps more importantly, these proposed mechanisms frequently neglect the possibility that the primary determinants of analog selectivity are due to other features described in this section, including aspects of metabolism and differential transport, as well as the unique pharmacokinetic and pharmacodynamics features of virtually every analog when tested in vivo. Returning to the VDR, it is also important to note that the VDR, like many transcription factors, binds to sites of action on cellular genomes that are highly chromatinized, dynamically active, and uniquely individualized for each of the genes with which they linked (Meyer et al., 2010, 2012). Thus, the uniqueness of each vitamin D target gene has also been neglected in assessing analog action in most if not all earlier studies. In a following section, we consider many of these newly emerging concepts, made possible through the use of new technical approaches that have enabled the investigation of VDR action in cells and tissues both in vitro and in vivo on a genome-wide scale. While none of these principles has been examined yet for their impact on vitamin D analog action, it seems very likely that they will play a central role as major determinants of the unique actions of these synthetic vitamin D ligands.

Target cell catabolic enzymes

Much evidence has accumulated to show that $1\alpha,25(OH)_2D_3$ is subject to target cell catabolism and side chain cleavage to calcitroic acid via a 24-oxidation pathway catalyzed by CYP24A1 (Makin et al., 1989). CYP24A1 is vitamin D inducible, since its gene promoter contains a double VDRE; carries out multiple steps in the side chain modification process; and is present in most (if not all) vitamin D-target cells (Prosser and Jones, 2004; Akiyoshi-Shibata et al., 1994); and its role appears to desensitize the target cell to continuing hormonal stimulation by $1\alpha,25(OH)_2D_3$ (Lohnes and Jones, 1992). The CYP24A1-knockout mouse shows 50% lethality at weaning and death resulting from hypercalcemia and nephrocalcinosis, and surviving mice show an inability to rapidly clear a bolus dose of $1\alpha,25(OH)_2D_3$ from the bloodstream and tissues (St-Arnaud et al., 2008; Masuda et al., 2005). CYP24A1-knockout mice also exhibit a metabolic bone disease reminiscent of the excessive osteoid bone pathology observed in rodents given excessive amounts of $1\alpha,25(OH)_2D_3$ (Hock et al., 1986). Moreover, work crossing the CYP24A1-knockout mouse with the VDR-knockout mouse rescues this bone defect (St Arnaud et al., 2000), suggesting that excessive VDR-mediated signaling is the cause, although the bone lesion can also be relieved by administration of $24,25(OH)_2D_3$ (Arnaud, 2009). The conclusion from the knockout mouse experiments that CYP24A1 primarily exists to catabolize $1,25(OH)_2D_3$ and its precursor $25(OH)D_3$ has now been reinforced by the finding that mutations of the human CYP24A1 gene result in hypercalcemia, hypercalciuria, nephrolithiasis, and nephrocalcinosis, in a syndrome known as idiopathic infantile hypercalcemia (IIH) (Schlingmann et al., 2011).

Given the demonstrated importance of CYP24A1 to $1\alpha,25(OH)_2D_3$ clearance, one must ask the question of whether vitamin D analogs might be subject to the same catabolic processes that determine their pharmacokinetics. Certainly there are vitamin D analogs such as calcipotriol, OCT, EB1089, and KH1060 that are metabolized by vitamin D-target cells to clearly defined and unique metabolites (Dilworth et al., 1997; Masuda et al., 1994, 1996; Shankar et al., 1997), which resemble products of the 24-oxidation pathway for $1\alpha,25(OH)_2D_3$. Furthermore, some of these metabolites are products only of vitamin D target cells and are calcitriol inducible, implying that CYP24A1 is involved in their formation, this having been confirmed with some analogs such as calcipotriol (Jones et al., 2006). Even in the cases of several analogs blocked at C-24 and subject to metabolism elsewhere on the side chain, the involvement of CYP24A1 is strongly implicated or proven, including 23-hydroxylation of 26,27-hexafluoro-$1\alpha,25(OH)_2D_3$, 26-hydroxylation of 24-difluoro-$1\alpha,25(OH)_2D_3$, 26-hydroxylation of $1\alpha,25(OH)_2$-16ene-23yne-D_3, and 26- and 28-hydroxylation of $1\alpha,25(OH)_2D_2$. Since

many of these same products are observed in vitro and in vivo and since pharmacokinetic parameters often parallel target cell metabolic parameters (Kissmeyer et al., 1995), one concludes that target cell metabolism of vitamin D analogs must contribute to the pharmacokinetics and biological activity observed in vitro and in vivo. Even studies such as that of Eelen et al. (2008), which claimed differences in VDR-mediated gene expression at the coactivator level, also show that a CYP24A1 inhibitor, VID-400 (Table 75.4), narrowed potency differences between 23yne analogs and 1α,25$(OH)_2D_3$ by blocking catabolism of the latter and revealed that analogs derive advantages at metabolic and transcriptional levels. Unfortunately, this metabolic blockade approach has not always been used in analog screening and there is little doubt that poor performance during in vivo testing is the result of poor metabolic stability of the studied analog.

Some of the calcitriol analogs with modifications in the vicinity of C-23, namely, 20-epi-1α,25$(OH)_2D_3$ (Dilworth et al., 1994), 1α,25$(OH)_2$-16ene-D_3 (Siu-Caldera et al., 1999), and 20-methyl-1α,25$(OH)_2D_3$ (Shankar et al., 2001), undergo 24-oxidation pathway metabolism that stalls at the level of the 24-oxo metabolite, seemingly because the enzyme CYP24A1 cannot efficiently carry out the usual 23-hydroxylation step and complete the catabolic sequence to the inactive cleaved product. The consequence, at least in vitro, is that the 24-oxo metabolite accumulates, and there have been claims that this metabolite retains significant biological activity (Siu-Caldera et al., 1999). This hypothesis has received a boost by the work of Zella et al. (2009), who have found that the superagonist 20-epi-1α,25$(OH)_2D_3$ exhibits a prolonged duration of action on intestinal calcium-regulating genes selectively, and these researchers have proposed that this advantage over 1α,25$(OH)_2D_3$ stems from a reduction in its catabolic rate.

Hepatic clearance or nonspecific metabolism

The poor DBP-binding properties of many side chain modified calcitriol analogs open up the possibility of alternative plasma carriers and accelerated degradation. The liver plays a major role in such metabolic clearance and a small number of detailed studies performed have included in vitro incubation with liver preparations. Calcipotriol (Sorensen et al., 1990), OCT (Masuda et al., 1996), EB1089 (Kissmeyer et al., 1997), and KH1060 (Rastrup-Anderson et al., 1992) are all subject to metabolism by liver enzymes. One such liver enzyme capable of nuclear and 23- and 24-hydroxylation of 1α,25$(OH)_2D_3$, and possibly some of its analogs, is the abundant general cytochrome P450, CYP3A4 (Xu et al., 2005). Indeed, this enzyme is upregulated by 1α,25$(OH)_2D_3$ in the duodenum, suggesting that a physiologically relevant loop exists (Thummel et al., 2001). Since over the years there have been frequent reports of drug-induced osteomalacia associated with coincidental use of anticonvulsants (e.g., diphenylhydantoin) or barbiturates with vitamin D preparations (Onodera et al., 2001), the direct association between CYP3A4 and 1α,25$(OH)_2D_3$ is potentially important to explain the putative accelerated clearance of some vitamin D metabolites (Gascon-Barre et al., 1984). One such phenomenon that might be explained by intestinal CYP3A4 action is the purported lower toxicity of vitamin D_2 compounds compared with their D_3 counterparts referred to earlier. Microsomes from an intestinal cell line and supersomes enriched in recombinant human CYP3A4 catabolize 1α,25$(OH)_2D_2$ at a significantly faster rate than 1α,25$(OH)_2D_3$ (Helvig et al., 2008). The implication of this finding is that 1α,25$(OH)_2D_2$ and possibly other synthetic analogs, such as the mixed VDR agonist/CYP24A1 inhibitor CTA-018 (Posner et al., 2009), are selectively broken down in intestine, potentially reducing their gene expression effects on intestinal calcium and PO_4 absorption but not on other tissues.

A 2017 demonstration that CYP3A4 might play a backup role to CYP24A1 in vitamin D catabolism was the use of rifampin in the treatment of IIH patients (Hawkes et al., 2017). Recall that IIH patients with mutations of CYP24A1 cannot catabolize 25$(OH)D_3$ or 1,25$(OH)_2D_3$ to 24-hydroxylated products efficiently, and the metabolites accumulate, causing hypercalcemia. Rifampin is a potent CYP3A4 inducer (Wang et al., 2013) and results in the appearance of biologically inactive 4α,25$(OH)_2D_3$ and 4β,25$(OH)_2D_3$ catabolites in the serum from 25$(OH)D_3$ metabolism. The IIH patients treated with rifampin have an alternative catabolic mechanism and show fewer hypercalcemic episodes (Hawkes et al., 2017).

The potential role of gene targets and the unique features of their regulation as major determinants of analog action

The previous section described studies suggesting that the differential actions of many vitamin D analogs in cells in vitro and in vivo may be due to metabolism, transport, tissue uptake, and/or the differential impact of certain analogs on VDR conformation, particularly as it relates to the receptor's ability to interact with RXR and/or to recruit and interact with the coregulator class of transcription factors. In the last case, however, almost all of the data used to support this idea that analogs promote unique VDR conformations with altered functional outcomes were derived using highly biased cellular techniques that were in vogue at the time but were simply incapable of delivering this type of mechanistic information. Since 2010, however, new approaches have emerged, which include chromatin immunoprecipitation linked to parallel

TABLE 75.5 Overarching principles of vitamin D action in target cells.

Vitamin D receptor (VDR) binding sites (the cistrome): 2000−8000 $1,25(OH)_2D_3$-sensitive binding sites/genome whose number and location are chromatin dependent and a function of cell-type
Active transcription unit for induction: the VDR/retinoid X receptor (RXR) heterodimer
Distal binding site locations: dispersed in *cis*-regulatory modules (CRMs or enhancers) across the genome; located in a cell-type-specific manner near promoters, but predominantly within introns and distal intergenic regions; frequently located in clusters of elements
VDR/RXR binding site sequence: induction mediated by classic hexameric half-sites (AGGTCA) separated by 3 bp; repression mediated by divergent sites
Mode of DNA binding: predominantly, but not exclusively, $1,25(OH)_2D_3$ dependent
Modular features of CRMs: contain binding sites for multiple transcription factors that facilitate either independent or synergistic interaction
Epigenetic CRM signatures: defined by the dynamically regulated posttranslational histone H3 and H4 modifications
VDR cistromes: dynamic alterations in the cellular epigenome during differentiation, maturation, and disease provoke changes to the VDR cistrome that qualitatively and quantitatively affect the vitamin D-regulated transcriptome

DNA sequencing (ChIP-seq) and derivative techniques, that have not only facilitated the study of gene transcription on a genome-wide scale, but have also begun to uncover novel roles for the epigenomic landscape that surrounds genes and defines their regulatory regions at levels of detail that are currently unparalleled (Hoffman et al., 2013; Ernst and Kellis, 2010; Ernst et al., 2011; Thurman et al., 2012; Bernstein et al., 2010; Kellis et al., 2014; Stamatoyannopoulos, 2012). This approach, as well as the striking ability to modify these regulatory regions easily both in cells in culture and in mice in vivo using gene editing techniques such as CRISPR/Cas9, now facilitates the study of gene regulation in an unprecedented fashion, providing new mechanistic insights that are of high significance (Cong et al., 2013; Hille and Charpentier, 2016; Singh et al., 2016). Perhaps most importantly, they have revealed that each gene, and often gene networks as well, represents a unique entity, and must therefore be studied in intact cells and tissues entirely in that context. This new approach has been applied to the vitamin D system, revealing a number of fundamental findings, as summarized in Table 75.5 and discussed briefly next. Unfortunately, none of these new concepts have been evaluated for their possible mechanistic contribution to analog-based gene-, cell-, or disease-based selectivity. Thus, while they represent only conceptual possibilities at present, they will have to be assessed in the future.

As summarized in Table 75.5, genome-wide studies have revealed that VDR binding to the genome is largely $1,25(OH)_2D_3$ dependent, is primarily colocalized to sites of RXR binding, and comprises from 2000 to 8000 sites per cell type (termed a VDR cistrome) (Pike et al., 2007; Meyer et al., 2014a, 2016; Heikkinen et al., 2011). While these sites often partially overlap, a subset is always highly cell-type specific, and all are highly enriched for the classic VDRE described in an earlier section of this review (Kerner et al., 1989; Ozono et al., 1990). Surprisingly, there is frequently more than one VDRE located within a given binding region, and thus more than one VDR/RXR complex exists within many of these regulatory segments, much like that first observed at the *Cyp24a1* gene (Zierold et al., 1995). Evidence that more than one VDRE leads to a facilitated response to $1,25(OH)_2D_3$ is prevalent (Kim et al., 2006; Stamatoyannopoulos et al., 2012). Given the fact that most genomes contain well over 100,000 typical VDRE-like sequences, ChIP-seq data clearly indicate that legitimate binding sites for the VDR/RXR heterodimer are highly chromatin restricted. We now know that these "functional" sites are determined by the presence of additional regulatory complexes that are essential for establishing sites of vitamin D regulation. This feature is well supported by parallel determinations of sites of DNase I hypersensitivity (Meyer et al., 2014b). Perhaps one of the most important discoveries is the observation that, while VDR binding sites can be located near gene promoters, most are located at intergenic and intronic sites frequently 10's if not 100's of kilobases from the genes they regulate (Meyer et al., 2014a, 2017). Even more profound is the fact that genes are modulated by multiple regulatory regions (termed enhancers), and that these enhancers are modular, and therefore typically capable of direct interaction with not only DNA-binding proteins like the VDR but also multiple additional transcription factors as well. A subset of these are likely to be determinants of enhancer structure, but others mediate regulation via additional signaling pathways, providing a mechanism at target genes that facilitates the integration of external signals at specific genes. These and many additional observations of the features of endogenous gene targets provide compelling support for much important detail that was never accounted for in the earlier studies of vitamin D analogs.

A second observation described in Table 75.5 is the finding that genomes and the individual genes within are maintained and regulated by an epigenetic chromatin environment that is both active and dynamic (Ernst and Kellis, 2010; Ernst et al., 2011). This environment is location specific and comprises, in part, distinct modifications to histone tails within nucleosomes that are preferentially enriched at gene transcription units, at the regulatory regions of genes, and at gene promoters. Virtually all binding sites for the VDR across individual genomes are located within epigenetic regions that are highlighted by the presence of epigenetic histone modifications that represent signatures of enhancer structure (Meyer et al., 2014b, 2016, 2017). These signatures are important, because they also reflect the presence of additional protein complexes that contribute to the type of response elicited by $1,25(OH)_2D_3$. The classes of proteins prebound to these sites are numerous; some are pioneering factors, others are lineage-determining factors and/or master regulators, and all are participants either in facilitating VDR binding or in enabling the assembly of a functional complex of which the VDR is a part (Meyer et al., 2014a, 2015; Lupien et al., 2008; Bi et al., 2012; Gosselin et al., 2014; Heinz et al., 2015). Thus, the overall activities of $1,25\text{-}(OH)_2D_3$ at these sites are fully framed within these enhancer environments, leading to activation, suppression, or qualified response. Previous analog studies would have been incapable of addressing these issues. Finally, given the frequency of multiple regulatory regions, and the often central roles of master regulators in gene output, enhancers frequently exhibit hierarchical activity in their ability to drive transcription. This occurs as a result of ubiquitous enhancer−enhancer interactions that enable one enhancer to dominate the activity of the others at a promoter. In some cases, this hierarchical activity prevails despite the fact that the dominant enhancer may be located many kilobases distal to the gene. This is illustrated by the *Mmp13* gene (Meyer et al., 2014c). These and other recently described features within genes are almost certain to influence the potential gene- and cell-specific biological actions of vitamin D analogs.

A final observation listed in Table 75.5 is that epigenomes are highly dynamic at numerous sites across the genome. Thus, this regulatory layer at many genes undergoes striking changes as a consequence of development, cellular differentiation, and maturation and, perhaps most importantly, as a function of disease. VDR cistromes are likewise highly dynamic and prone to substantial changes (Meyer et al., 2016; Ding et al., 2013a, 2013b). These changes in the epigenome lead to significant alterations in the availability of binding sites for transcription factors, thereby altering the regulatory potential of many genes within the entire genome (Meyer et al., 2014a). The consequences of this dynamism are significant alterations in cellular transcriptomes and, more importantly, in function. In the case of vitamin D, response to the VDR can be increased, decreased, prevented, or qualitatively modified, thereby altering the functional response to $1,25(OH)_2D_3$ in a temporal or spatial manner. Interestingly, while these changes occur typically in many disease states that are the focus of vitamin D analog therapy, they are particularly prevalent in cancer cells, a significant target of the antiproliferative activities identified for the vitamin D hormone. While the overall dynamism of the epigenome increases complexity, it also highlights the impact of disease in the selection of gene targets relevant to vitamin D as a therapeutic. Virtually none of these issues were addressable in earlier vitamin D analog studies. Future exploration of the mechanisms of action of novel vitamin D analogs will require the use of the aforementioned techniques and approaches if we are to fully understand exactly how vitamin D analogs operate in vivo.

Many of the basic principles of vitamin D-regulated gene expression as outlined in the foregoing section and in Table 75.5 are illustrated in a series of in vivo studies of the regulation of genes such as *Tnfsf11* (RANKL), the *VDR* itself, *LRP5*, *Mmp13*, *Cyp27b1*, and *Cyp24a1* (Meyer et al., 2017; Kim et al., 2006; Onal et al., 2015, 2016; Pike et al., 2016, 2017; Fretz et al., 2007). Details of the regulation of the *Tnfsf11* gene are illustrated in Fig. 75.1.

Proposed molecular mechanisms of action of vitamin D compounds

Fig. 75.2 contains a general model to predict how vitamin D analogs work. It allows for consideration of both prodrugs (those requiring 25-hydroxylation by CYP27A1 or CYP2R1 and those requiring 1α-hydroxylation by the kidney or extrarenal 1α-hydroxylase) and $1\alpha,25(OH)_2D_3$ analogs. This model therefore makes a distinction between those target cells that express an extrarenal 1α-hydroxylase (CYP27B1), and therefore have the ability to make and respond to their own "local" $1\alpha,25(OH)_2D_3$, and those that simply respond through their VDR with altered transcription. This model features a conventional VDR/RXR heterodimer working through a VDRE in most genes. Crucial parameters for each new analog include:

(1) affinity for DBP,
(2) affinity for VDR,
(3) ability to recruit RXR and coactivators followed by transactivation of genes,
(4) rate of target cell metabolism (reflected partly in pharmacokinetic parameters),
(5) rate of hepatic or nonspecific clearance (reflected partly in pharmacokinetic parameters).

Our view is that all listed parameters contribute significantly to the overall biological activity of any given analog.

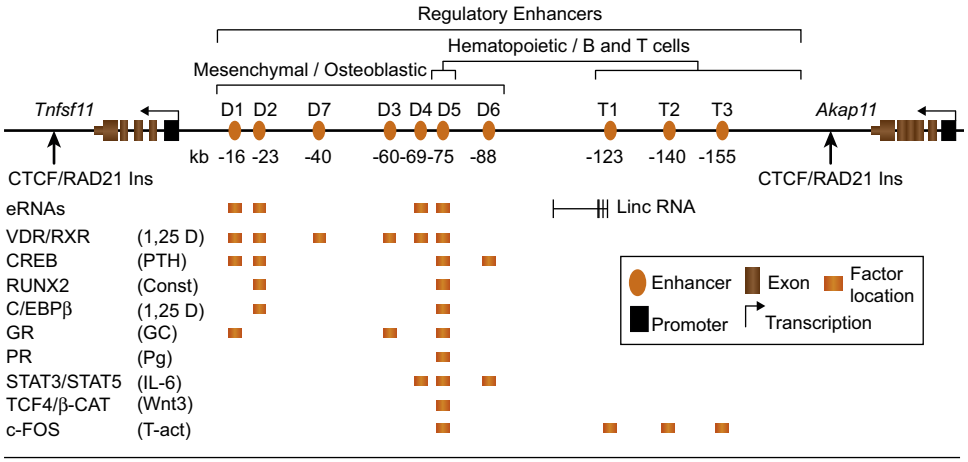

FIGURE 75.1 Regulatory enhancers involved in the regulation of the *Tnfsf11* gene. The *Tnfsf11* gene locus and its osteoblastic and hematopoietic regulatory regions are shown. *Arrows* indicate the CCCTC-binding factor (*CTCF*)/*RAD21*-defined boundaries of the locus that includes the transcription unit and its upstream noncoding regulatory control regions. Enhancers that mediate osteoblast lineage regulation (*D* regions) and hematopoietic regulation (*T* regions) are numbered and indicated by *orange ovals* (light gray in print version). Their distance from the *Tnfsf11* TS Snscription start site in kilobases is indicated below the oval. The *D5* enhancer is active in both cell lineage types. Factors that have been shown to bind to each enhancer by chromatin precipitation (ChIP)—chip and/or ChIP sequencing analysis are indicated below the gene locus by *orange blocks* (light gray in print version).

Future prospects

The elucidation of new details of the genomic mechanism of action of $1\alpha,25(OH)_2D_3$ will probably reveal novel post-VDR coactivator-based approaches by which the vitamin D signaling cascade can be exploited. Certainly, the significant progress made in characterizing the coactivator proteins and the rest of the transcriptional apparatus will continue and will benefit from parallel work on other transcriptional modulators (e.g., other steroids). The attempts to combine deacetylase inhibitors with VDR agonists (Bijian et al., 2018) will be followed with interest.

Studies of the vitamin D-binding pockets of VDR, DBP, and the three (or more) vitamin D-related CYPs will continue to be a major goal now that all these specific proteins have been cloned, overexpressed, and crystallized. Work on the ligand-binding domain of the VDR (Rochel et al., 2001; Rachez and Freedman, 2000; Tocchini-Valentini et al., 2001) will be extended to new analogs and coactivator complexes and the other major proteins in the vitamin D signal transduction pathway.

The wide availability of recombinant proteins for hundreds of CYPs from species across the phylogenetic tree, including 58 CYPs in the human genome, has allowed for the elucidation of some crystal structures and also modeling studies of the enzymes involved in vitamin D metabolism (Prosser et al., 2006; Hamamoto et al., 2006). Current models are starting to reveal key substrate side-chain contact residues (e.g., Ala326 within CYP24A1) associated with 24- and 23-hydroxylation that lead to bifurcation of the catabolic pathway into either calcitroic acid or 26,23-lactone production (Prosser et al., 2007). The crystallization and structural determination of the microsomal CYP2R1, the putative vitamin D 25-hydroxylase, is a harbinger of what is to come in this field (Strushkevich et al., 2008).

Access to full-length CYP24A1 and CYP27B1 has also permitted a more efficient search for potential inhibitors. Specific inhibitors of CYP24A1 (Schuster et al., 2001, 2003; Posner et al., 2004, 2009) may be of value in blocking $1\alpha,25(OH)_2D_3$ catabolism in certain clinical conditions where excessive breakdown is suspected (e.g., cancer therapy). CYP27B1 inhibitors (Schuster et al., 2001, 2003; Posner et al., 2004, 2009) might be useful in situations where $1,25(OH)_2D_3$ synthesis is excessive and serum levels are elevated. Alternatively, the development of specific or even nonspecific inducers of CYP24A1, or surrogates such as CYP3A4 (Hawkes et al., 2017), might aid in the treatment of $1,25(OH)_2D_3$ excess. In general, modeling of VDR and CYPs is expected to lead to more rational vitamin D analog design to take advantage of structural idiosyncrasies of all of these key proteins. Meanwhile, the not-so-rational synthesis of new analogs is likely to continue. The list of applications for these new vitamin D analogs continues to increase (Holick, 2007; Jones, 2007), making synthesis a worthwhile exercise.

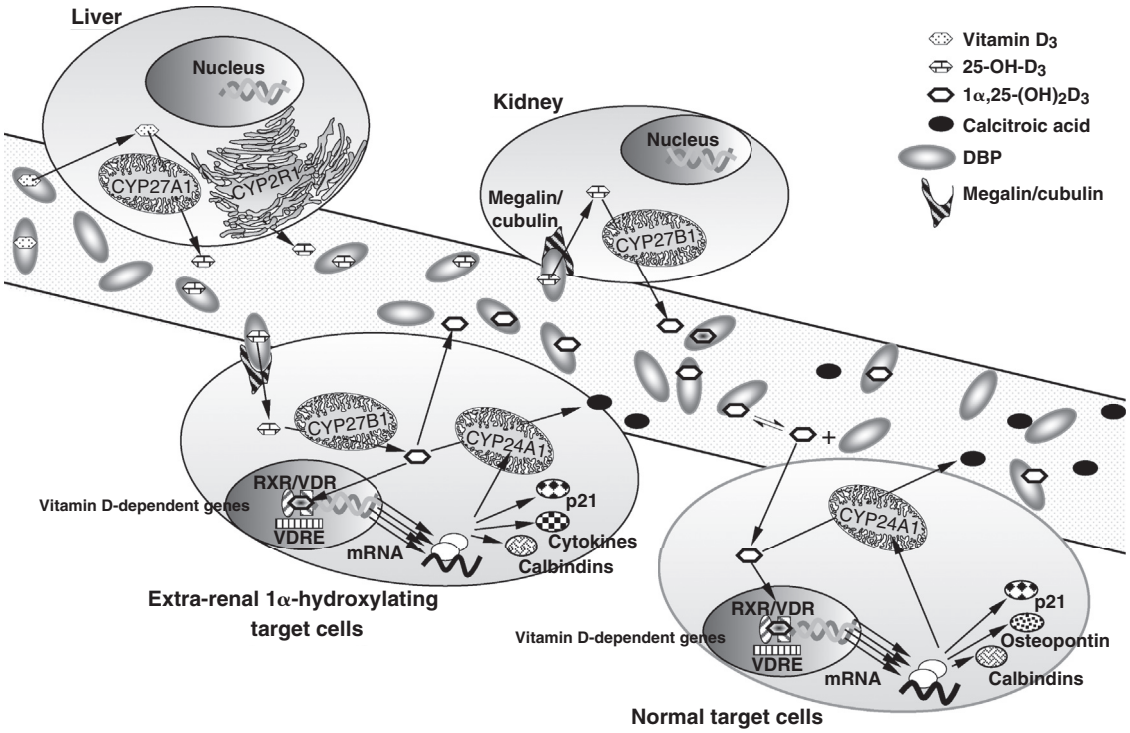

FIGURE 75.2 Current concepts of the activation, mechanism of action, and catabolism of vitamin D. The model incorporates a plasma-binding protein (vitamin D-binding protein, *DBP*), which acts as a carrier of vitamin D metabolites and analogs; activating enzymes (cytochrome P450s, CYPs) involved in activation of vitamin D or prodrug; target cell transcriptional machinery (vitamin D receptor, *VDR*; retinoid X receptor, *RXR*; coactivators) involved in the biological actions of $1\alpha,25(OH)_2D_3$ or its analogs; and a target cell catabolic enzyme system (CYP24A1) involved in the degradation of $1\alpha,25(OH)_2D_3$ or its analog. The metabolism of vitamin D in the context of the cells involved is shown. Going clockwise, top left: hepatocyte showing some of the candidate CYPs shown to 25-hydroxylate vitamin D and its prodrugs; note that VDR is believed to be absent from liver cells. Top middle: proximal tubular cell showing the key elements in the uptake of $25(OH)D_3$ and its conversion to $1\alpha,25(OH)_2D_3$. Megalin/cubulin are cell surface receptors that execute endocytosis of the DBP/$25(OH)D_3$ complex, while CYP27B1 is the main component of the 1α-hydroxylase, responsible for synthesis of circulating $1\alpha,25(OH)_2D_3$. Lower right: conventional target cell, which lacks megalin/cubulin and takes up only the free ligand, $1\alpha,25(OH)_2D_3$, and not the DBP originally involved in transporting the ligand to the target cell. The key elements of the transcriptional machinery are shown, including VDR/RXR as well as representative gene products such as cell division protein p21, the bone matrix protein osteopontin, the calcium transport protein calbindin, and the autoregulatory protein CYP24A1. The role of the highly inducible CYP24A1 is to convert the hormone (or analog) into inactive degradation products, such as calcitroic acid, which enter plasma and are excreted in bile. Lower left: target cell, which expresses extrarenal 1α-hydroxylase (CYP27B1) and the megalin/cubulin machinery to take up $25(OH)D_3$, and thus capable of making $1\alpha,25(OH)_2D_3$ locally. The cell can also respond in a likewise manner to the conventional target cell because it also possesses the VDR and other transcriptional machinery. The expectation is that cells involved in cell differentiation or controlling cell division require higher concentrations of $1\alpha,25(OH)_2D_3$ to modulate a different set of genes, and CYP27B1 boosts local production to augment that *circulating* $1\alpha,25(OH)_2D_3$ arriving from the kidney in the bloodstream. Under normal physiological processes, locally produced $1\alpha,25(OH)_2D_3$ would not enter the general circulation, although in pathological conditions (e.g., sarcoidosis) this could occur. At this time, it is not clear how many cell types can be considered simple target cells and how many possess the CYP27B1 and megalin/cubulin to allow for local production of hormone. *VDRE*, vitamin D response element. *Reproduced from* Jones, G., 2007. Expanding role for vitamin D in chronic kidney disease: importance of blood 25-OH-D levels & extrarenal 1α-hydroxylase in theclassical and non-classical actions of 1α,25-dihydroxyvitamin D3. Semin. Dial. 20, 316–324.

Acknowledgments

The authors acknowledge the contributions of Drs. David Prosser and Martin Kaufmann to the compilation of tables and Fig. 75.2 generated for this review. We thank Dr. Mark B. Meyer for his contribution to some of the work presented.

References

Adams, J.S., Gacad, M.A., 1985. Characterization of 1α-hydroxylation of vitamin D_3 sterols by cultured alveolar macrophages from patients with sarcoidosis. J. Exp. Med. 161, 755–765.

Adorini, L., Penna, G., Amuchastegui, S., et al., 2007. Inhibition of prostate growth and inflammation by the vitamin D receptor agonist BXL-628 (elocalcitol). J. Steroid Biochem. Mol. Biol. 103, 689–693.

Akiyoshi-Shibata, M., Sakaki, T., Ohyama, Y., et al., 1994. Further oxidation of hydroxycalcidiol by calcidiol 24- hydroxylase—a study with the mature enzyme expressed in *Escherichia coli*. Eur. J. Biochem. 224, 335−343.

Al-Aly, Z., Qazi, R.A., González, E.A., Zeringue, A., Martin, K.J., 2007. Changes in serum 25-hydroxyvitamin D and plasma intact PTH levels following treatment with ergocalciferol in patients with CKD. Am. J. Kidney Dis. 50, 59−68.

Armas, L.A., Hollis, B.W., Heaney, R.P., 2004. Vitamin D_2 is much less effective than vitamin D_3 in humans. J. Clin. Endocrinol. Metab. 89, 5387−5391.

St Arnaud. 24(R),25-$(OH)_2D_3$ administration corrects bone defect in cyp24-null mouse. 14th Workshop on Vitamin D. Brugge, Belgium. October 4−8, 2009.

Baggiolini, E.G., Wovkulich, P.M., Iacobelli, et al., 1982. Preparation of 1α-hydroxylated vitamin D metabolites by total synthesis. In: Norman, A.W., Schaefer, K., Herrath, D von, Grigoleit, H.-G. (Eds.), Vitamin D: Chemical, Biochemical and Clinical Endocrinology of Calcium Metabolism. De Gruyter, Berlin, pp. 1089−1100.

Baggiolini, E.G., Partridge, J.J., Shiuey, S.-J., et al., 1989. Cholecalciferol 23-yne derivatives, their pharmaceutical compositions, their use in the treatment of calcium related diseases, and their antitumor activity, US 4,804,502. Chem. Abstr. 111, 58160d. [Abstract].

Barton, D.H., Hesse, R.H., Pechet, M.M., et al., 1973. A convenient synthesis of 1α-hydroxy-vitamin D_3. J. Am. Chem. Soc. 95, 2748−2749.

Beer, T.M., Myrthue, A., Garzotto, M., 2004. Randomized study of high-dose pulse calcitriol or placebo prior to radical prostatectomy. Cancer Epidemiol. Biomark. Prev. 13, 2225−2232.

Bernstein, B.E., Stamatoyannopoulos, J.A., Costello, J.F., Ren, B., Milosavljevic, A., Meissner, A., Kellis, M., Marra, M.A., Beaudet, A.L., Ecker, J.R., Farnham, P.J., Hirst, M., Lander, E.S., Mikkelsen, T.S., Thomson, J.A., 2010. The NIH roadmap epigenomics mapping consortium. Nat. Biotechnol. 28 (10), 1045−1048.

Bi, L., Jung, S., Day, D., Neidig, K., Dusevich, V., Eick, D., Bonewald, L., 2012. Evaluation of bone regeneration, angiogenesis, and hydroxyapatite conversion in critical-sized rat calvarial defects implanted with bioactive glass scaffolds. J. Biomed. Mater. Res. A 100 (12), 3267−3275.

Bijian, K., Kaldre, D., Wang, T.-T., Su, J., Bouttier, M., Boucher, A., Alaoui-Jamali, M., White, J.H., Gleason, J.L., 2018. Efficacy of hybrid vitamin D receptor agonist/histone deacetylase inhibitors in vitamin D-resistant triple negative 4T1 breast cancer. J. Steroid Biochem. Mol. Biol. 177, 135−139.

Bikle, D.D., 1992. Clinical counterpoint: vitamin D: new actions, new analogs, new therapeutic potential. Endocr. Rev. 13, 765−784.

Binderup, E., Calverley, M.J., Binderup, L., 1991. Synthesis and biological activity of 1α-hydroxylated vitamin D analogues with poly-unsaturated side chains. In: Norman, A.W., Bouillon, R., Thomasset, M. (Eds.), Vitamin D: Proceedings of the 8th Workshop on Vitamin D, Paris, France. De Gruyter, Berlin, pp. 192−193.

Bischoff-Ferrari, H.A., Giovannucci, E., Willett, W.C., et al., 2006. Estimation of optimal serum concentrations of 25- hydroxyvitamin D for multiple health outcomes. Am. J. Clin. Nutr. 84, 18−28.

Bishop, J.E., Collins, E.D., Okamura, W.H., Norman, A.W., 1994. Profile of ligand specificity of the vitamin D binding protein for 1α,25-dihydroxyvitamin D_3 and its analogs. J. Bone Miner. Res. 9, 1277−1288.

Blunt, J.W., DeLuca, H.F., Schnoes, H.K., 1968. 25-Hydroxycholecalciferol. A biologically active metabolite of vitamin D_3. Biochemistry 7, 3317−3322.

Boehm, M.F., Fitzgerald, P., Zou, A., et al., 1999. Novel nonsecosteroidal vitamin D mimics exert VDR-modulating activities with less calcium mobilization than 1,25-dihydroxyvitamin D_3. Chem. Biol. 6, 265−275.

Bouillon, R., Allewaert, K., Xiang, D.Z., et al., 1991. Vitamin D analogs with low affinity for the vitamin D binding protein: enhanced in vitro and decreased in vivo activity. J. Bone Miner. Res. 6, 1051−1057.

Bouillon, R., Okamura, W.H., Norman, A.W., 1995. Structure-function relationships in the vitamin D endocrine system. Endocr. Rev. 16, 200−257.

Calverley, M.J., 1987. Synthesis of MC-903, a biologically active vitamin D metabolite analog. Tetrahedron 43, 4609−4619.

Calverley, M.J., Binderup, E., Binderup, L., 1991. The 20-epi modification in the vitamin D series: selective enhancement of "non-classical" receptor-mediated effects. In: Norman, A.W., Bouillon, R., Thomasset, M. (Eds.), Vitamin D: Proceedings of the 8th Workshop on Vitamin D, Paris, France. De Gruyter, Berlin, pp. 163−164.

Cheng, J.B., Levine, M.A., Bell, N.H., et al., 2004. Genetic evidence that the human CYP2R1 enzyme is a key vitamin D 25- hydroxylase. Proc. Natl. Acad. Sci. U. S. A. 101, 7711−7715.

Cheskis, B., Lemon, B.D., Uskokovic, M., Lomedico, P.T., Freedman, L.P., 1995. Vitamin D_3-retinoid X receptor dimerization, DNA binding, and transactivation are differentially affected by analogs of 1,25- dihydroxyvitamin D_3. Mol. Endocrinol. 9, 1814−1824.

Colston, K.W., Pirianov, G., Bramm, E., et al., 2003. Effects of Seocalcitol (EB1089) on nitrosomethyl urea-induced rat8mammary tumors. Breast Canc. Res. Treat. 80, 303−311.

Cong, L., Ran, F.A., Cox, D., Lin, S., Barretto, R., Habib, N., Hsu, P.D., Wu, X., Jiang, W., Marraffini, L.A., Zhang, F., 2013. Multiplex genome engineering using CRISPR/Cas systems. Science 339 (6121), 819−823.

Crescioli, C., Ferruzzi, P., Caporali, A., et al., 2004. Inhibition of prostate cell growth by BXL-628, a calcitriol analogue selected for a phase II clinical trial in patients with benign prostate hyperplasia. Eur. J. Endocrinol. 150, 591−603.

Dalhoff, K., Dancey, J., Astrup, L., et al., 2003. A phase II study of the vitamin D analogue, Seocalcitol in patients with inoperable hepatocellular carcinoma. Br. J. Canc. 89, 252−257.

Deeb, K.K., Trump, D.L., Johnson, C.S., 2007. Vitamin D signalling pathways in cancer: potential for anticancer therapeutics. Nat. Rev. Canc. 7, 684−700.

Delmez, J.A., Tindira, C., Grooms, P., et al., 1989. Parathyroid hormone suppression by intravenous 1,25-dihydroxyvitamin D. A role for increased sensitivity to calcium. J. Clin. Investig. 83, 1349−1355.

Dilworth, F.J., Calverley, M.J., Makin, H.L.J., Jones, G., 1994. Increased biological activity of 20-epi-1,25-dihydroxyvitamin D_3 is due to reduced catabolism and altered protein binding. Biochem. Pharmacol. 47, 987−993.

Dilworth, F.J., Williams, G.R., Kissmeyer, A.-M., et al., 1997. The vitamin D analog, KH1060 is rapidly degraded both in vivo and in vitro via several pathways: principal metabolites generated retain significant biological activity. Endocrinology 138, 5485–5496.

Ding, N., Yu, R.T., Subramaniam, N., Sherman, M.H., Wilson, C., Rao, R., Leblanc, M., Coulter, S., He, M., Scott, C., Lau, S.L., Atkins, A.R., Barish, G.D., Gunton, J.E., Liddle, C., Downes, M., Evans, R.M., 2013. A vitamin D receptor/SMAD genomic circuit gates hepatic fibrotic response. Cell 153 (3), 601–613.

Ding, N., Liddle, C., Evans, R.M., Downes, M., 2013. Hepatic actions of vitamin D receptor ligands: a sunshine option for chronic liver disease? Expert Rev. Clin. Pharmacol. 6 (6), 597–599.

Dusso, A., Lopez-Hilker, S., Rapp, N., Slatopolsky, E., 1988. Extra-renal production of calcitriol in chronic renal failure. Kidney Int. 34, 368–375.

Eelen, G., Valle, N., Sato, Y., et al., 2008. Superagonistic fluorinated vitamin D_3 analogs stabilize helix 12 of the vitamin D receptor. Chem. Biol. 15, 1029–1034.

Ernst, J., Kellis, M., 2010. Discovery and characterization of chromatin states for systematic annotation of the human genome. Nat. Biotechnol. 28 (8), 817–825.

Ernst, J., Kheradpour, P., Mikkelsen, T.S., Shoresh, N., Ward, L.D., Epstein, C.B., Zhang, X., Wang, L., Issner, R., Coyne, M., Ku, M., Durham, T., Kellis, M., Bernstein, B.E., 2011. Mapping and analysis of chromatin state dynamics in nine human cell types. Nature 473 (7345), 43–49.

Evans, T.R., Colston, K.W., Lofts, F.J., et al., 2002. A phase II trial of the vitamin D analogue Seocalcitol (EB1089) in patients with inoperable pancreatic cancer. Br. J. Canc. 86, 680–685.

Fournier, A., Harbouche, L., Mansour, J., Shahapuni, I., 2007. Impact of calcium and vitamin D therapy on arterial and cardiac disease in young adults with childhood-onset end stage renal disease. Nephrol. Dial. Transplant. 22, 956–957.

Fraser, D.R., Kodicek, E., 1970. Unique biosynthesis by kidney of a biologically active vitamin D metabolite. Nature 228, 764–766.

Fretz, J., Zella, L., Kim, S., Shevde, N., Pike, J., 2007. 1,25-Dihydroxyvitamin D3 induces expression of the Wnt signaling co-regulator LRP5 via regulatory elements located significantly downstream of the gene's transcriptional start site. J. Steroid Biochem. Mol. Biol. 103 (3–5), 440–445.

Fu, G.K., Lin, D., Zhang, M.Y., et al., 1997. Cloning of human 25-hydroxyvitamin D-1α-hydroxylase and mutations causing vitamin D-dependent rickets type 1. Mol. Endocrinol. 11, 1961–1970.

Galassi, A., Bellasi, A., Ciceri, P., Pivari, F., Conte, F., Cozzolino, M., 2017. Calcifediol to treat secondary hyperparathyroidism in patients with chronic kidney disease. Expert Rev. Clin. Pharmacol. 10, 1073–1084.

Gallagher, J.C., Riggs, B.L., Recker, R.R., Goldgar, D., 1989. The effect of calcitriol on patients with postmenopausal osteoporosis with special reference to fracture frequency. Proc. Soc. Exp. Biol. Med. 191, 287–292.

Gallagher, J.C., Bishop, C.W., Knutson, J.C., et al., 1994. Effects of increasing doses of 1α-hydroxyvitamin D_2 on calcium homeostasis in post-menopausal osteopenic women. J. Bone Miner. Res. 9, 607–614.

Gascon-Barre, M., Villeneuve, J.P., Lebrun, L.H., 1984. Effect of increasing doses of phenytoin on the plasma 25- hydroxyvitamin D and 1,25-dihydroxyvitamin D concentrations. J. Am. Coll. Nutr. 3, 45–50.

Gonzalez, E.A., Sachdeva, A., Oliver, D.A., Martin, K.J., 2004. Vitamin D insufficiency and deficiency in chronic kidney disease. A single center observational study. Am. J. Nephrol. 24, 503–510.

Gosselin, D., Link, V.M., Romanoski, C.E., Fonseca, G.J., Eichenfield, D.Z., Spann, N.J., Stender, J.D., Chun, H.B., Garner, H., Geissmann, F., Glass, C.K., 2014. Environment drives selection and function of enhancers controlling tissue-specific macrophage identities. Cell 159 (6), 1327–1340.

Gulliford, T., English, J., Colston, K.W., et al., 1998. A phase I study of the vitamin D analogue EB 1089 in patients with advanced breast and colorectal cancer. Br. J. Canc. 78, 6–13.

Hamamoto, H., Kusudo, T., Urushino, N., et al., 2006. Structure-function analysis of vitamin D 24-hydroxylase (CYP24A1) by site-directed mutagenesis: amino acid residues responsible for species-based difference of CYP24A1 between humans and rats. Mol. Pharmacol. 70, 120–128.

Hawkes, C.P., Li, D., Hakonarson, H., Meyers, K.E., Thummel, K.E., Levine, M.A., 2017. CYP3A4 induction by rifampin: an alternative pathway for vitamin D inactivation in patients with CYP24A1 mutations. J. Clin. Endocrinol. Metab. 102, 1440–1446.

Heikkinen, S., Väisänen, S., Pehkonen, P., Seuter, S., Benes, V., Carlberg, C., 2011. Nuclear hormone 1{alpha},25- dihydroxyvitamin D3 elicits a genome-wide shift in the locations of VDR chromatin occupancy. Nucleic Acids Res. 39 (21), 9181–9193.

Heinz, S., Romanoski, C.E., Benner, C., Glass, C.K., 2015. The selection and function of cell type-specific enhancers. Nat. Rev. Mol. Cell Biol. 16 (3), 144–154.

Helvig, C., Cuerrier, D., Kharebov, A., et al., 2008. Comparison of 1,25-dihydroxyvitamin D_2 and calcitriol effects in an adenine-induced uremic model of CKD reveals differential control over calcium and phosphate. Am. Soc. Bone Miner. Soc. 23, s1–s620. SU448, (abstract).

Hewison, M., Adams, J., 2005. Chapter 79: Extra-renal 1α-Hydroxylase activity and human disease. In: Feldman, D., Pike, W., Glorieux, F. (Eds.), Vitamin D, second ed. Academic Press, San Diego, CA, pp. 1379–1402.

Hille, F., Charpentier, E., 2016. CRISPR-Cas: biology, mechanisms and relevance. Philos. Trans. R. Soc. Lond. B Biol. Sci. 371 (1707).

Hock, J.M., Gunness-Hey, M., Poser, J., et al., 1986. Stimulation of undermineralized matrix formation by 1,25- dihydroxyvitamin D_3 in long bones of rats. Calcif. Tissue Int. 38, 79–86.

Hoffman, M.M., Ernst, J., Wilder, S.P., Kundaje, A., Harris, R.S., Libbrecht, M., Giardine, B., Ellenbogen, P.M., Bilmes, J.A., Birney, E., Hardison, R.C., Dunham, I., Kellis, M., Noble, W.S., 2013. Integrative annotation of chromatin elements from ENCODE data. Nucleic Acids Res. 41 (2), 827–841.

Holick, M.F., 2007. Vitamin D deficiency. N. Engl. J. Med. 357, 266–281.

Holick, M.F., Schnoes, H.K., DeLuca, H.F., et al., 1971. Isolation and identification of 1,25-dihydroxycholecalciferol: a metabolite of vitamin D active in intestine. Biochemistry 10, 2799–2804.

Holick, M.F., Schnoes, H.K., DeLuca, H.F., et al., 1972. Isolation and identification of 24,25-dihydroxycholecalciferol: a metabolite of vitamin D_3 made in the kidney. Biochemistry 11, 4251−4255.

Holick, M.F., Kleiner-Bossaller, A., Schnoes, H.K., et al., 1973. 1,24,25-Trihydroxyvitamin D_3. A metabolite of vitamin D_3 effective on intestine. J. Biol. Chem. 248, 6691−6696.

Holick, M.F., Biancuzzo, R.M., Chen, T.C., et al., 2008. Vitamin D_2 is as effective as vitamin D_3 in maintaining circulating concentrations of 25-hydroxyvitamin D. J. Clin. Endocrinol. Metab. 93, 677−681.

Horst, R.L., 1979. 25-OHD3-26,23-lactone: a metabolite of vitamin D3 that is 5 times more potent than 25-OHD3 in the rat plasma competitive protein binding radioassay. Biochem. Biophys. Res. Commun. 89, 286−293.

Ishizuka, S., Kurihara, N., Reddy, S.V., et al., 2005. (23S)-25-dehydro-1α-hydroxyvitamin D_3-26,23-lactone, a vitamin D receptor antagonist that inhibits osteoclast formation and bone resorption in bone marrow cultures from patients with Paget's disease. Endocrinology 146, 2023−2030.

Issa, L.L., Leong, G.M., Sutherland, R.L., Eisman, J.A., 2000. Vitamin D analogue-specific recruitment of vitamin D receptor coactivators. J. Bone Miner. Res. 17, 879−890.

Jones, G., 2007. Expanding role for vitamin D in chronic kidney disease: importance of blood 25-OH-D levels & extrarenal 1α-hydroxylase in the classical and non-classical actions of 1α,25-dihydroxyvitamin D_3. Semin. Dial. 20, 316−324.

Jones, G., 2008a. Pharmacokinetics of vitamin D toxicity. Am. J. Clin. Nutr. 88 (Suppl. l), 582S−586S.

Jones, G., 2008b. Chapter 83: Vitamin D and analogues. In: Bilezikian, J., Raisz, L., Rodan, G. (Eds.), Section: Pharmacological Mechanisms of Therapeutics, third ed., Principles of Bone Biology. Academic Press Inc, San Diego, pp. 1777−1799.

Jones, G., Edwards, N., Vriezen, D., et al., 1988. Isolation and identification of seven metabolites of 25- hydroxydihydrotachysterol$_3$ formed in the isolated perfused rat kidney: a model for the study of side-chain metabolism of vitamin D. Biochemistry 27, 7070−7079.

Jones, G., Strugnell, S., DeLuca, H.F., 1998. Current understanding of the molecular actions of vitamin D. Physiol. Rev. 78, 1193−1231.

Jones, G., Ramshaw, H., Zhang, A., et al., 1999. Expression and activity of vitamin D-metabolizing cytochrome P450s (CYP1α and CYP24) in human non-small cell lung carcinomas. Endocrinology 140, 3303−3310.

Jones, G., Byford, V., West, S., et al., 2006. Hepatic activation & inactivation of clinically-relevant vitamin D analogs and prodrugs. Anticancer Res. 26, 2589−2596.

Judd, S.E., Tangpricha, V., 2009. Vitamin D deficiency & risk for cardiovascular disease. Am. J. Med. Sci. 338, 40−44.

Kellis, M., Wold, B., Snyder, M.P., Bernstein, B.E., Kundaje, A., Marinov, G.K., Ward, L.D., Birney, E., Crawford, G.E., Dekker, J., Dunham, I., Elnitski, L.L., Farnham, P.J., Feingold, E.A., Gerstein, M., Giddings, M.C., Gilbert, D.M., Gingeras, T.R., Green, E.D., Guigo, R., Hubbard, T., Kent, J., Lieb, J.D., Myers, R.M., Pazin, M.J., Ren, B., Stamatoyannopoulos, J.A., Weng, Z., White, K.P., Hardison, R.C., 2014. Defining functional DNA elements in the human genome. Proc. Natl. Acad. Sci. U. S. A. 111 (17), 6131−6138.

Kerner, S.A., Scott, R.A., Pike, J.W., 1989. Sequence elements in the human osteocalcin gene confer basal activation and inducible response to hormonal vitamin D3. Proc. Natl. Acad. Sci. U. S. A. 86 (12), 4455−4459.

Kim, S., Yamazaki, M., Zella, L., Shevde, N., Pike, J., 2006. Activation of receptor activator of NF-kappaB ligand gene expression by 1,25-dihydroxyvitamin D3 is mediated through multiple long-range enhancers. Mol. Cell Biol. 26 (17), 6469−6486.

Kissmeyer, A.-M., Mathiasen, I.S., Latini, S., et al., 1995. Pharmacokinetic studies of vitamin D analogues: relationship to vitamin D binding protein (DBP). Endocrine 3, 263−266.

Kissmeyer, A.-M., Binderup, E., Binderup, L., et al., 1997. The metabolism of the vitamin D analog EB 1089: identification of in vivo and in vitro metabolites and their biological activities. Biochem. Pharmacol. 53, 1087−1097.

Kobayashi, Y., Taguchi, T., Mitsuhashi, S., et al., 1982. Studies on organic fluorine compounds. XXXIX. Studies on steroids. LXXIX. Synthesis of 1α,25-dihydroxy-26,26,26,27,27,27-hexaflurovitamin D_3. Chem. Pharm. Bull. (Tokyo) 30, 4297−4303.

Kragballe, K., Gjertsen, B.T., De Hoop, D., et al., 1991. Double-blind, right/left comparison of calcipotriol and betamethasone valerate in treatment of psoriasis vulgaris. Lancet 337, 193−196.

Li, Y.C., Pirro, A.E., Amling, M., et al., 1997. Targeted ablation of the vitamin D receptor: an animal model of vitamin D-dependent rickets type II with alopecia. Proc. Natl. Acad. Sci. U. S. A. 94, 9831−9835.

Lohnes, D., Jones, G., 1992. Further metabolism of 1α,25-dihydroxyvitamin D_3 in target cells. J. Nutr. Sci. Vitaminol. 75−78. Special Issue.

Lupien, M., Eeckhoute, J., Meyer, C.A., Wang, Q., Zhang, Y., Li, W., Carroll, J.S., Liu, X.S., Brown, M., 2008. FoxA1 translates epigenetic signatures into enhancer-driven lineage-specific transcription. Cell 132 (6), 958−970.

Ma, Y., Khalifa, B., Yee, Y.K., et al., 2006. Identification and characterization of noncalcemic, tissue-selective, nonsecosteroidal vitamin D receptor modulators. J. Clin. Investig. 116, 892−904.

Makin, G., Lohnes, D., Byford, V., Ray, R., Jones, G., 1989. Target cell metabolism of 1,25-dihydroxyvitamin D_3 to calcitroic acid. Evidence for a pathway in kidney and bone involving 24-oxidation. Biochem. J. 262, 173−180.

Marchiani, S., Bonaccorsi, L., Ferruzzi, P., et al., 2006. The vitamin D analogue BXL-628 inhibits growth factor-stimulated proliferation and invasion of DU145 prostate cancer cells, J. Cancer Res. Clin. Oncol. 132, 408−416.

Masuda, S., Jones, G., 2006. The promise of vitamin D analogs in the treatment of hyperproliferative conditions. Mol. Canc. Therapeut. 5, 797−808.

Masuda, S., Strugnell, S., Calverley, M.J., et al., 1994. In vitro metabolism of the anti-psoriatic vitamin D analog, calcipotriol, in two cultured human keratinocyte models. J. Biol. Chem. 269, 4794−4803.

Masuda, S., Byford, V., Kremer, R., et al., 1996. In vitro metabolism of the vitamin D analog, 22-oxacalcitriol, using cultured osteosarcoma, hepatoma and keratinocyte cell lines. J. Biol. Chem. 271, 8700−8708.

Masuda, S., Byford, V., Arabian, A., et al., 2005. Altered Pharmacokinetics of 1α,25-dihydroxyvitamin D_3 and 25- hydroxyvitamin D_3 in the blood and tissues of the 25-hydroxyvitamin D-24-hydroxylase (CYP24A1) null mouse. Endocrinology 146, 825–834.

Mathew, S., Lund, R.J., Chaudhary, L.R., et al., 2008. Vitamin D receptor activators can protect against vascular calcification. J. Am. Soc. Nephrol. 19, 1509–1519.

Matsumoto, T., Kubodera, N., 2007. ED-71, a new active vitamin D_3, increases bone mineral density regardless of serum 25(OH)D levels in osteoporotic subjects. J. Steroid Biochem. Mol. Biol. 103, 584–586.

McCollum, E.V., Simmonds, N., Becker, J.E., et al., 1922. Studies on experimental rickets. XXI. A demonstration of the existence of a vitamin which promotes calcium deposition. J. Biol. Chem. 53, 293–312.

McKenna, N.J., Lanz, R.B., O'Malley, B.W., 1999. Nuclear receptor coregulators: cellular and molecular biology. Endocr. Rev. 20 (3), 321–344.

Medioni, J., Deplanque, G., Ferrero, J.M., Maurina, T., Rodier, J.M., Raymond, E., Allyon, J., Maruani, G., Houillier, P., Mackenzie, S., Renaux, S., Dufour-Lamartinie, J.F., Elaidi, R., Lerest, C., Oudard, S., 2014. Phase I safety and pharmacodynamic of inecalcitol, a novel VDR agonist with docetaxel in metastatic castration-resistant prostate cancer patients. Clin. Cancer Res. 20, 4471–4477.

Mehta, R., Hawthorne, M., Uselding, L., et al., 2000. Prevention of N-methyl-N-nitrosourea-induced mammary carcinogenesis in rats by 1alpha-hydroxyvitamin D_5. J. Natl. Cancer Inst. 92, 1836–1840.

Mellanby, E., Cantag, M.D., 1919. Experimental investigation on rickets. Lancet 196, 407–412.

Meyer, M.B., Goetsch, P.D., Pike, J.W., 2010. Genome-wide analysis of the VDR/RXR cistrome in osteoblast cells provides new mechanistic insight into the actions of the vitamin D hormone. J. Steroid Biochem. Mol. Biol. 121 (1–2), 136–141.

Meyer, M.B., Goetsch, P.D., Pike, J.W., 2012. VDR/RXR and TCF4/β-catenin cistromes in colonic cells of colorectal tumor origin: impact on c-FOS and c-MYC gene expression. Mol. Endocrinol. 26 (1), 37–51.

Meyer, M.B., Benkusky, N.A., Lee, C.H., Pike, J.W., 2014. Genomic determinants of gene regulation by 1,25- dihydroxyvitamin D3 during osteoblast-lineage cell differentiation. J. Biol. Chem. 289 (28), 19539–19554.

Meyer, M.B., Benkusky, N.A., Pike, J.W., 2014. The RUNX2 cistrome in osteoblasts: characterization, down-regulation following differentiation, and relationship to gene expression. J. Biol. Chem. 289 (23), 16016–16031.

Meyer, M.B., Benkusky, N.A., Pike, J.W., 2014. 1,25-Dihydroxyvitamin D3 induced histone profiles guide discovery of VDR action sites. J. Steroid Biochem. Mol. Biol. 144 (Pt A), 19–21.

Meyer, M.B., Benkusky, N.A., Pike, J.W., 2015. Selective distal enhancer control of the Mmp13 gene identified through clustered regularly interspaced short palindromic repeat (CRISPR) genomic deletions. J. Biol. Chem. 290 (17), 11093–11107.

Meyer, M.B., Benkusky, N.A., Sen, B., Rubin, J., Pike, J.W., 2016. Epigenetic plasticity drives adipogenic and osteogenic differentiation of marrow-derived mesenchymal stem cells. J. Biol. Chem. 291 (34), 17829–17847.

Meyer, M.B., Benkusky, N.A., Kaufmann, M., Lee, S.M., Onal, M., Jones, G., Pike, J.W., 2017. A kidney-specific genetic control module in mice governs endocrine regulation of the cytochrome P450 gene, Cyp27b1, essential for vitamin D_3 activation. J. Biol. Chem. 292, 17541–17558.

Miyaura, C., Abe, E., Kuribayashi, T., et al., 1981. 1α,25-dihydroxyvitamin D_3 induces differentiation of human myeloid leukemia cells. Biochem. Biophys. Res. Commun. 102, 937–943.

Molin, A., Wiedemann, A., Demers, N., Kaufmann, M., Do Cao, J., Mainard, L., Dousset, B., Journeau, P., Abeguile, G., Coudray, N., Mittre, H., Richard, N., Weryha, G., Sorlin, A., Jones, G., Kottler, M.L., Feillet, F., 2017. Vitamin D-dependent rickets type 1B (25-hydroxylase deficiency): a rare condition or a misdiagnosed condition? J. Bone Miner. Res. 32, 1893–1899.

Morisaki, M., Koizumi, N., Ikekawa, N., et al., 1975. Synthesis of active forms of vitamin D. Part IX. Synthesis of 1α,24- dihydroxycholecalciferol. J. Chem. Soc. Perkin Trans. 1 (1), 1421–1424.

Morrison, N.A., Qi, J.C., Tokita, A., et al., 1994. Prediction of bone density from vitamin D receptor alleles. Nature 367, 284–287.

Murayama, E., Miyamoto, K., Kubodera, N., et al., 1986. Synthetic studies of vitamin D analogues. VIII. Synthesis of 22- oxavitamin D_3 analogues. Chem. Pharm. Bull. (Tokyo) 34, 4410–4413.

National Kidney Foundation, 2003. KDOQI clinical practise guidelines for bone metabolism and disease in chronic kidney disease. Am. J. Kidney Dis. 42 (Suppl. 3), S1–S202.

Nishii, Y., Sato, K., Kobayashi, T., 1993. The development of vitamin D analogues for the treatment of osteoporosis. Osteoporos. Int. 1 (Suppl. l), S190–S193.

O'Malley, B., Qin, J., Lanz, R., 2008. Cracking the coregulator codes. Curr. Opin. Cell Biol. 20 (3), 310–315.

Ochiai, E., Miura, D., Eguchi, H., et al., 2005. Molecular mechanism of the vitamin D antagonistic actions of (23S)-25- dehydro-1alpha-hydroxyvitamin D_3-26,23-lactone depends on the primary structure of the carboxylterminal region of the vitamin D receptor. Mol. Endocrinol. 19, 1147–1157.

Okuda, K.I., Usui, E., Ohyama, Y., 1995. Recent progress in enzymology and molecular biology of enzymes involved in vitamin D metabolism. J. Lipid Res. 36, 1641–1652.

Onal, M., Bishop, K.A., St John, H.C., Danielson, A.L., Riley, E.M., Piemontese, M., Xiong, J., Goellner, J.J., O'Brien, C.A., Pike, J.W., 2015. A DNA segment spanning the mouse Tnfsf11 transcription unit and its upstream regulatory domain rescues the pleiotropic biologic phenotype of the RANKL null mouse. J. Bone Miner. Res. 30 (5), 855–868.

Onal, M., St John, H.C., Danielson, A.L., Markert, J.W., Riley, E.M., Pike, J.W., 2016. Unique distal enhancers linked to the mouse Tnfsf11 gene direct tissue-specific and inflammation-induced expression of RANKL. Endocrinology 157 (2), 482–496.

Onodera, K., Takahashi, A., Mayanagi, H., et al., 2001. Phenytoin-induced bone loss and its prevention with alfacalcidol or calcitriol in growing rats. Calcif. Tissue Int. 69, 109–116.

Orimo, H., Shiraki, M., Hayashi, T., et al., 1987. Reduced occurrence of vertebral crush fractures in senile osteoporosis treated with 1α(OH)-vitamin D_3. Bone Miner. 3, 47–52.

Orlov, I., Rochel, N., Moras, D., Klaholz, B.P., 2012. Structure of the full human RXR/VDR nuclear receptor heterodimer complex with its DR3 target DNA. EMBO J. 31 (2), 291–300.

Ott, S., Chesnut, C.H., 1989. Calcitriol treatment is not effective in post-menopausal osteoporosis. Ann. Intern. Med. 110, 267–274.

Ozono, K., Liao, J., Kerner, S.A., Scott, R.A., Pike, J.W., 1990. The vitamin D-responsive element in the human osteocalcin gene. Association with a nuclear proto-oncogene enhancer. J. Biol. Chem. 265 (35), 21881–21888.

Paaren, H.E., Hamer, D.E., Schnoes, H.K., et al., 1978. Direct C-1 hydroxylation of vitamin D compounds: convenient preparation of 1α-hydroxyvitamin D_3, 1α, 25-dihydroxyvitamin D_3, and 1α-hydroxyvitamin D_2. Proc. Natl. Acad. Sci. U. S. A. 75, 2080–2081.

Park, E.A., 1940. The therapy of rickets. J. Am. Med. Assoc. 94, 370–379.

Peleg, S., Sastry, M., Collins, E.D., Bishop, J.E., Norman, A.W., 1995. Distinct conformational changes induced by 20-epi analogues of 1 alpha,25-dihydroxyvitamin D3 are associated with enhanced activation of the vitamin D receptor. J. Biol. Chem. 270 (18), 10551–10558.

Peleg, S., Ismail, A., Uskokovic, M.R., Avnur, Z., 2003. Evidence for tissue- and cell-type selective activation of the vitamin D receptor by Ro-26-9228, a noncalcemic analog of vitamin D_3. J. Cell. Biochem. 88, 267–273.

Perlman, K.L., Sicinski, R.R., Schnoes, H.K., DeLuca, H.F., 1990. 1α,25-Dihydroxy-19-nor-vitamin D_3, a novel vitamin D-related compound with potential therapeutic activity. Tetrahedron Lett. 31, 1823–1824.

Pike, J.W., Zella, L.A., Meyer, M.B., et al., 2007. Molecular actions of 1,25-dihydroxyvitamin D3 on genes involved in calcium homeostasis. J. Bone Miner. Res. 22 (Suppl. 2), V16–V19.

Pike, J.W., Meyer, M.B., Benkusky, N.A., Lee, S.M., St John, H., Carlson, A., Onal, M., Shamsuzzaman, S., 2016. Genomic determinants of vitamin D-regulated gene expression. Vitam. Horm. 100, 21–44.

Pike, J.W., Meyer, M.B., Lee, S.M., Onal, M., Benkusky, N.A., 2017. The vitamin D receptor: contemporary genomic approaches reveal new basic and translational insights. J. Clin. Investig. 127 (4), 1146–1154.

Posner, G.H., Crawford, K.R., Yang, H.W., et al., 2004. Potent low-calcemic selective inhibitors of CYP24 hydroxylase: 24- sulphone analogs of the hormone 1α,25-dihydroxyvitamin D_3. J. Steroid Biochem. Mol. Biol. 89–90, 5–12.

Posner G, Helvig C, Cuerrier D et al. Vitamin D analogues targeting CYP24 in chronic kidney disease. Proceedings of the 14th Workshop on Vitamin D-Brugge, Belgium, October 4–8, 2009. J. Steroid. Biochem. & Mol. Biol. (in press).

Prosser, D.E., Jones, G., 2004. Enzymes involved in the activation and inactivation of vitamin D. Trends Biochem. Sci. 29, 664–673.

Prosser, D.E., Guo, Y.-D., Geh, K.R., et al., 2006. Molecular modelling of CYP27A1 and site-directed mutational analyses affecting vitamin D hydroxylation. Biophys. J. 90, 1–21.

Prosser, D., Kaufmann, M., O'Leary, B., et al., 2007. Single A326G mutation converts hCYP24A1 from a 25-OH-D_3-24- hydroxylase into -23-hydroxylase generating 1α,25-$(OH)_2D_3$-26,23-lactone. Proc. Natl. Acad. Sci. U. S. A 104, 12673–12678.

Qaw, F., Calverley, M.J., Schroeder, N.J., et al., 1993. *In vivo* metabolism of the vitamin D analog, dihydrotachysterol. Evidence for formation of 1α,25- and 1β,25-dihydroxy-dihydrotachysterol metabolites and studies of their biological activity. J. Biol. Chem. 268, 282–292.

Quarles, L.D., 2008. Endocrine functions of bone in mineral metabolism regulation. J. Clin. Investig. 118, 3820–3828.

Rachez, C., Freedman, L.P., 2000. Mechanisms of gene regulation by vitamin D_3 receptor: a network of coactivator interactions. Gene 246, 9–21.

Rachez, C., Lemon, B.D., Suldan, Z., et al., 1999. Ligand-dependent transcription activation by nuclear receptors requires the DRIP complex. Nature 398, 824–828.

Rapuri, P.B., Gallagher, J.C., Haynatzki, G., 2004. Effect of vitamins D_2 and D_3 supplement use on serum 25OHD concentration in elderly women in summer and winter. Calcif. Tissue Int. 74, 150–156.

Rastrup-Anderson, N., Buchwald, F.A., Grue-Sorensen, G., 1992. Identification and synthesis of a metabolite of KH1060, a new potent 1α,25-dihydroxyvitamin D_3 analogue. Bioorg. Med. Chem. Lett 2, 1713–1716.

Razzaque, M.S., 2011. The dualistic role of vitamin D in vascular calcifications. Kidney Int. 79, 708–714.

Riggs, B.L., Melton III, L.J., 1992. The prevention and treatment of osteoporosis. N. Engl. J. Med. 327, 620–627.

Roborgh, J.R., de Man, T., 1960. The hypercalcemic activity of dihydrotachysterol-$_2$ and dihydrotachysterol-$_3$ and of the vitamins D_2 and D_3: comparative experiments in rats. Biochem. Pharmacol. 2, 1–6.

Rochel, N., Wurtz, J.M., Mitschler, A., Klaholz, B., Moras, D., 2000. The crystal structure of the nuclear receptor for vitamin D bound to its natural ligand. Mol. Cell 5 (1), 173–179.

Rochel, N., Tocchini-Valentini, G., Egea, P.F., et al., 2001. Functional and structural characterization of the insertion region in the ligand binding domain of the vitamin D nuclear receptor. Eur. J. Biochem. 268, 971–979.

Rochel, N., Ciesielski, F., Godet, J., Moman, E., Roessle, M., Peluso-Iltis, C., Moulin, M., Haertlein, M., Callow, P., Mély, Y., Svergun, D.I., Moras, D., 2011. Common architecture of nuclear receptor heterodimers on DNA direct repeat elements with different spacings. Nat. Struct. Mol. Biol. 18 (5), 564–570.

Safadi, F.F., Thornton, P., Magiera, H., et al., 1999. Osteopathy and resistance to vitamin D toxicity in mice null for vitamin D binding protein. J. Clin. Investig. 103, 239–251.

Saito, N., Kittaka, A., 2006. Highly potent vitamin D receptor antagonists: design, synthesis, and biological evaluation. Chembiochem 7, 1479–1490.

Schlingmann, K.P., Kaufmann, M., Weber, S., Irwin, A., Goos, C., John, U., Misselwitz, J., Klaus, G., Kuwertz-Bröking, E., Fehrenbach, H., Wingen, A.M., Güran, T., Hoenderop, J.G., Bindels, R.J., Prosser, D.E., Jones, G., Konrad, M., 2011. Mutations in CYP24A1 and idiopathic infantile hypercalcemia. N. Engl. J. Med. 365, 410–421.

Schuster, I., Egger, H., Astecker, N., et al., 2001. Selective inhibitors of CYP24: mechanistic tools to explore vitamin D metabolism in human keratinocytes. Steroids 66, 451–462.

Schuster, I., Egger, H., Nussbaumer, P., Kroemer, R.T., 2003. Inhibitors of vitamin D hydroxylases: structure-activity relationships. J. Cell. Biochem. 88, 372–380.

Seeman, E., Tsalamandris, C., Bass, S., et al., 1995. Present and future of osteoporosis therapy. Bone 17, 23S–29S.

Shankar, V.N., Dilworth, F.J., Makin, H.L.J., et al., 1997. Metabolism of the vitamin D analog EB1089 by cultured human cells: redirection of hydroxylation site to distal carbons of the side chain. Biochem. Pharmacol. 53, 783–793.

Shankar, V.N., Byford, V., Prosser, D.E., et al., 2001. Metabolism of a 20-methyl substituted series of vitamin D analogs by cultured human cells : apparent reduction of 23-hydroxylation of the side chain by 20-methyl group. Biochem. Pharmacol. 61, 893–902.

Shevde, N.K., Plum, L.A., Clagett-Dame, M., et al., 2002. A potent analog of 1α,25-dihydroxyvitamin D_3 selectively induces bone formation. Proc. Natl. Acad. Sci. U. S. A. 99, 13487–13491.

Singh, A., Chakraborty, D., Maiti, S., 2016. CRISPR/Cas9: a historical and chemical biology perspective of targeted genome engineering. Chem. Soc. Rev. 45 (24), 6666–6684.

Siu-Caldera, M.L., Sekimoto, H., Peleg, S., et al., 1999. Enhanced biological activity of 1α,25-dihydroxy-20-epi-vitamin D_3, the C-20 epimer of 1α,25-dihydroxyvitamin D_3, is in part due to its metabolism into stable intermediary metabolites with significant biological activity. J. Steroid Biochem. Mol. Biol. 71, 111–121.

Sjöden, G., Smith, C., Lindgren, U., et al., 1985. 1α-Hydroxyvitamin D_2 is less toxic than 1α-hydroxyvitamin D_3 in the rat. Proc. Soc. Exp. Biol. Med. 178, 432–436.

Sorensen, H., Binderup, L., Calverley, M.J., et al., 1990. In vitro metabolism of calcipotriol (MC 903), a vitamin D analogue. Biochem. Pharmacol. 39, 391–393.

Sprague, S.M., Crawford, P.W., Melnick, J.Z., Strugnell, S.A., Ali, S., Mangoo-Karim, R., Lee, S., Petkovich, P.M., Bishop, C.W., 2016. Use of extended-release calcifediol to treat secondary hyperparathyroidism in stages 3 and 4 chronic kidney disease. Am. J. Nephrol. 44, 316–325.

St Arnaud, R., Messerlian, S., Moir, J.M., et al., 1997. The 25-hydroxyvitamin D 1-α-hydroxylase gene maps to the pseudovitamin D-deficiency rickets (PDDR) disease locus. J. Bone Miner. Res. 12, 1552–1559.

St Arnaud, R., Arabian, A., Travers, R., et al., 2000. Deficient mineralization of intramembranous bone in vitamin D-24- hydroxylase-ablated mice is due to elevated 1,25-dihydroxyvitamin D and not to the absence of 24,25- dihydroxyvitamin D. Endocrinology 141, 2658–2666.

St-Arnaud, R., Arabian, A., Yu, V.W., et al., 2008. 1α,24(S)$(OH)_2D_2$ normalizes bone morphology and serum parathyroid hormone without hypercalcemia in 25-hydroxyvitamin D-1-hydroxylase (CYP27B1)-deficient mice, an animal model of vitamin D deficiency with secondary hyperparathyroidism. J. Endocrinol. Investig. 31, 711–717.

Stamatoyannopoulos, J.A., 2012. What does our genome encode? Genome Res. 22 (9), 1602–1611.

Stamatoyannopoulos, J.A., Snyder, M., Hardison, R., Ren, B., Gingeras, T., Gilbert, D.M., Groudine, M., Bender, M., Kaul, R., Canfield, T., Giste, E., Johnson, A., Zhang, M., Balasundaram, G., Byron, R., Roach, V., Sabo, P.J., Sandstrom, R., Stehling, A.S., Thurman, R.E., Weissman, S.M., Cayting, P., Hariharan, M., Lian, J., Cheng, Y., Landt, S.G., Ma, Z., Wold, B.J., Dekker, J., Crawford, G.E., Keller, C.A., Wu, W., Morrissey, C., Kumar, S.A., Mishra, T., Jain, D., Byrska-Bishop, M., Blankenberg, D., Lajoie1, B.R., Jain, G., Sanyal, A., Chen, K.B., Denas, O., Taylor, J., Blobel, G.A., Weiss, M.J., Pimkin, M., Deng, W., Marinov, G.K., Williams, B.A., Fisher-Aylor, K.I., Desalvo, G., Kiralusha, A., Trout, D., Amrhein, H., Mortazavi, A., Edsall, L., McCleary, D., Kuan, S., Shen, Y., Yue, F., Ye, Z., Davis, C.A., Zaleski, C., Jha, S., Xue, C., Dobin, A., Lin, W., Fastuca, M., Wang, H., Guigo, R., Djebali, S., Lagarde, J., Ryba, T., Sasaki, T., Malladi, V.S., Cline, M.S., Kirkup, V.M., Learned, K., Rosenbloom, K.R., Kent, W.J., Feingold, E.A., Good, P.J., Pazin, M., Lowdon, R.F., Adams, L.B., Consortium, M.E., 2012. An encyclopedia of mouse DNA elements (Mouse ENCODE). Genome Biol. 13 (8), 418.

Stern, P., 1981. A monolog on analogs. In vitro effects of vitamin D metabolites and consideration of the mineralisation question. Calcif. Tissue Int. 33, 1–4.

Strugnell, S., Byford, V., Makin, H.L.J., et al., 1995. 1α,24(*S*)-dihydroxyvitamin D_2: a biologically active product of 1α- hydroxyvitamin D_2 made in the human hepatoma, Hep3B. Biochem. J. 310, 233–241.

Strushkevich, N., Usanov, S.A., Plotnikov, A.N., Jones, G., Park, H.-W., 2008. Structural Analysis of CYP2R1 in complex with vitamin D_3. J. Mol. Biol. 380, 95–106.

Suda, T., DeLuca, H.F., Schnoes, H.K., et al., 1970. 25,26-dihydroxyvitamin D_3, a metabolite of vitamin D_3 with intestinal transport activity. Biochemistry 9, 4776–4780.

Suhara, Y., Nihei, K.I., Kurihara, M., et al., 2001. Efficient and versatile synthesis of novel 2α-substituted 1α,25- dihydroxyvitamin D_3 analogues and their docking to vitamin D receptors. J. Org. Chem. 66, 8760–8771.

Takeyama, K., Kitanaka, S., Sato, T., et al., 1997. 25-Hydroxyvitamin D_3 1α-hydroxylase and vitamin D synthesis. Science 277, 1827–1830.

Takeyama, K., Masuhiro, Y., Fuse, H., et al., 1999. Selective interaction of vitamin D receptor with transcriptional coactivators by a vitamin D analog. Mol. Cell Biol. 19, 1049–1055.

Teng, M., Wolf, M., Ofsthun, M.N., et al., 2005. Activated injectable vitamin D and hemodialysis survival: a historical cohort study. J. Am. Soc. Nephrol. 16, 1115–1125.

Tentori, F., Hunt, W.C., Stidley, C.A., et al., 2006. Mortality risk among hemodialysis patients receiving different vitamin D analogs. Kidney Int. 70, 1858–1865.

Thacher, T.D., Obadofin, M.O., O'Brien, K.O., et al., 2009. The effect of vitamin D_2 and vitamin D_3 on intestinal calcium absorption in Nigerian children with rickets. J. Clin. Endocrinol. Metab. 94.

Thacher, T.D., Fischer, P.R., Singh, R.J., Roizen, J., Levine, M.A., 2015. CYP2R1 mutations impair generation of 25- hydroxyvitamin D and cause an atypical form of vitamin D deficiency. J. Clin. Endocrinol. Metab. 100, E1005−E1013.

Thummel, K.E., Brimer, C., Yasuda, K., et al., 2001. Transcriptional control of intestinal cytochrome P-450 3A by 1α,25- dihydroxy vitamin D_3. Mol. Pharmacol. 60, 1399−1406.

Thurman, R.E., Rynes, E., Humbert, R., Vierstra, J., Maurano, M.T., Haugen, E., Sheffield, N.C., Stergachis, A.B., Wang, H., Vernot, B., Garg, K., John, S., Sandstrom, R., Bates, D., Boatman, L., Canfield, T.K., Diegel, M., Dunn, D., Ebersol, A.K., Frum, T., Giste, E., Johnson, A.K., Johnson, E.M., Kutyavin, T., Lajoie, B., Lee, B.K., Lee, K., London, D., Lotakis, D., Neph, S., Neri, F., Nguyen, E.D., Qu, H., Reynolds, A.P., Roach, V., Safi, A., Sanchez, M.E., Sanyal, A., Shafer, A., Simon, J.M., Song, L., Vong, S., Weaver, M., Yan, Y., Zhang, Z., Lenhard, B., Tewari, M., Dorschner, M.O., Hansen, R.S., Navas, P.A., Stamatoyannopoulos, G., Iyer, V.R., Lieb, J.D., Sunyaev, S.R., Akey, J.M., Sabo, P.J., Kaul, R., Furey, T.S., Dekker, J., Crawford, G.E., Stamatoyannopoulos, J.A., 2012. The accessible chromatin landscape of the human genome. Nature 489 (7414), 75−82.

Tilyard, M.W., Spears, G.F.S., Thomson, J., Dovey, S., 1992. Treatment of post-menopausal osteoporosis with calcium. N. Engl. J. Med. 326, 357−362.

Tocchini-Valentini, G., Rochel, N., Wurtz, J.M., Mitschler, A., Moras, D., 2001. Crystal structures of the vitamin D receptor complexed to superagonist 20-epi ligands. Proc. Natl. Acad. Sci. U. S. A. 98 (10), 5491−5496.

Toell, A., Gonzalez, M.M., Ruf, D., et al., 2001. Different molecular mechanisms of vitamin D_3 receptor antagonists. Mol. Pharmacol. 59, 1478−1485.

Trump, D.L., Hershberger, P.A., Bernardi, R.J., et al., 2004. Anti-tumor activity of calcitriol: pre-clinical and clinical studies. J. Steroid Biochem. Mol. Biol. 89−90, 519−526.

Tsugawa, N., Okano, T., Masuda, S., et al., 1991. A novel vitamin D_3 analogue, 22-oxacalcitriol (OCT): its different behaviour from calcitriol in plasma transport system. In: Norman, A.W., Bouillon, R., Thomasset, M. (Eds.), Vitamin D: Gene Regulation Structure-Function Analysis and Clinical Application. De Gruyter, Berlin, pp. 312−313.

Uchida, M., Ozono, K., Pike, J.W., 1994. Activation of the human osteocalcin gene by 24R,25-dihydroxyvitamin D_3 occurs through the vitamin D receptor & the vitamin D-responsive element. J. Bone Miner. Res. 9, 1980−1987.

Uitterlinden, A.G., Fang, Y., van Meurs JBJ, et al., 2005. Chapter 68: Analog metabolism. In: Feldman, D., Pike, W., Glorieux, F. (Eds.), Vitamin D, second ed. Academic Press, San Diego, pp. 1121−1158.

Verstuyf, A., Verlinden, L., van Etten, E., et al., 2000. Biological activity of CD-ring modified 1α,25-dihydroxyvitamin D analogues: C-ring and five-membered D-ring analogues. J. Bone Miner. Res. 15, 237−252.

Vieth, R., 2005. Chapter 61: The Pharmacology of Vitamin D, including fortification strategies. In: Feldman, D., Pike, J.W., Glorieux, F.H. (Eds.), Vitamin D, second ed. Elsevier Academic Press, New York, pp. 995−1015.

Wang, Z., Lin, Y.S., Dickmann, L.J., Poulton, E.J., Eaton, D.L., Lampe, J.W., Shen, D.D., Davis, C.L., Shuhart, M.C., Thummel, K.E., 2013. Enhancement of hepatic 4-hydroxylation of 25-hydroxyvitamin D_3 through CYP3A4 induction in vitro and in vivo: implications for drug-induced osteomalacia. J. Bone Miner. Res. 28, 1101−1116.

Whitfield, G.K., Jurutka, P.W., Haussler, C., et al., 2005. Chapter 13: Nuclear receptor: structure-function, molecular control of gene transcription and novel bioactions. In: Feldman, D., Pike, J.W., Glorieux, F.H. (Eds.), Vitamin D, second ed. Elsevier Academic Press, New York, pp. 219−262.

Xu, Y., Hashizume, T., Shuhart, M.C., et al., 2005. Intestinal and hepatic CYP3A4 catalyze hydroxylation of 1α,25- dihydroxyvitamin D_3: implications for drug-induced osteomalacia. Mol. Pharmacol. 69, 56−65.

Yang, W., Freedman, L.P., 1999. 20-Epi analogues of 1,25-dihydroxyvitamin D_3 are highly potent inducers of DRIP coactivator complex binding to the vitamin D_3 receptor. J. Biol. Chem. 274, 16838−16845.

Yoshizawa, T., Handa, Y., Uematsu, Y., et al., 1997. Mice lacking the vitamin D receptor exhibit impaired bone formation, uterine hypoplasia and growth retardation after weaning. Nat. Genet. 16, 391−396.

Zella, L.A., Meyer, M.B., Nerenz, R.D., Pike, J.W., 2009. The enhanced hypercalcemic response to 20-epi-1,25- dihydroxyvitamin D_3 results from a selective and prolonged induction of intestinal calcium-regulating genes. Endocrinology 150, 3448−3456.

Zierold, C., Darwish, H., DeLuca, H., 1995. Two vitamin D response elements function in the rat 1,25-dihydroxyvitamin D 24-hydroxylase promoter. J. Biol. Chem. 270 (4), 1675−1678.

Zisman, A.L., Hristova, M., Ho, L.T., Sprague, S.M., 2007. Impact of ergocalciferol treatment of vitamin D deficiency on serum parathyroid hormone concentrations in chronic kidney disease. Am. J. Nephrol. 27, 36−43.

Chapter 76

Mechanisms of exercise effects on bone quantity and quality

Vihitaben S. Patel[1], Stefan Judex[1], Janet Rubin[2] and Clinton T. Rubin[1]

[1]*Department of Biomedical Engineering, Bioengineering Building, State University of New York at Stony Brook, Stony Brook, NY, United States;*

[2]*Endocrine Division, Department of Medicine, University of North Carolina, Chapel Hill, NC, United States*

Chapter outline

Introduction

Weight-bearing exercise is an essential part of a comprehensive strategy to treat and prevent osteoporosis (Sinaki et al., 2010). The National Osteoporosis Foundation recommends both high- and low-impact weight-bearing exercises for 30 min per day 5−7 days a week to load the skeleton. Muscle-strengthening exercises, as complementary to weight-bearing exercises, improve posture and promote musculoskeletal anabolism (Kelly and Gilman, 2017), and help to coordinate

Principles of Bone Biology. https://doi.org/10.1016/B978-0-12-814841-9.00076-2

movement and prevent falls. A principal component of these exercises—mechanical signals—is anabolic to both bone and muscle, yet inhibitory to fat formation. This suggests that cells resident on and in the bone tissue are critical to the adaptive response, as well as cells in the bone marrow, including mesenchymal stem cells (MSCs), the shared progenitor for bone and fat cells, interpreting mechanical signals as stimulatory and inhibitory, respectively (Krishnan et al., 2006; Menuki et al., 2008; David et al., 2007; Luu et al., 2009a).

With exercise, dynamic ground-reaction forces transduce a range of signals across the skeleton (Martin et al., 2015; Nilsson and Thorstensson, 1989) and musculature, subjecting cells, tissues, and organs to mechanical strain (deformation) and acceleration. Key salutary outcomes of exercise include increased lean muscle, increased bone mineralization and turnover rate, decreased inflammation (Sakurai et al., 2009), and inhibition of marrow adipose tissue volume (Styner et al., 2014), improving health outcomes that combat the progression of osteoporosis and delay the onset of obesity.

Exercise represents a nondrug strategy to increase bone mass as well as decelerating bone loss, salutary outcomes achieved through bone tissue's sensitivity to its mechanical loading environment. A host of human-based studies have worked toward quantifying the impact of general and specific exercise regimens on bone mass and morphology, taking into account interdependent variables such as gender, age, and nutritional status of the individuals. Although some studies have provided encouraging results, the large majority of data have been equivocal, perhaps a reflection of our limited understanding of which specific components of the mechanical signal are perceived as influential by the resident bone cell populations (e.g., osteocytes, osteoblasts, lining cells, osteoclasts, bone marrow stem cells) and which are irrelevant by-products of loading. The design of an "optimal" exercise intervention (e.g., least amount of physical exertion for the greatest gain in skeletal strength) requires many critical questions to be addressed: should the exercise protocol incorporate large loads or could they be small if they are applied rapidly? How long does an individual have to exercise to maximize benefits? Are the attributes of mechanical loading accumulated, or is there a threshold past which additional challenges no longer are perceived as regulatory influences to the skeleton? Does an exercise program that works in one cohort (e.g., adolescents) translate to another (e.g., the elderly)?

Here, we first define the functional loading environment of bone to demonstrate that the ability of physical signals to influence bone morphology strongly depends on the character of the signal, and we provide an overview of the molecular and cellular events that play a role in transducing the mechanical signal into a biochemical message. Establishing a first-order approximation of the physical and molecular factors of the mechanically derived signal is critical toward developing exercise prophylaxes that are clinically feasible, enjoy high compliance, and can prevent the bone loss leading to osteoporosis.

Bone's sensitivity to mechanical signals

The skeleton's ability to adapt to altered levels and patterns of mechanical loading is well established but the difficulty lies in defining the specific regulatory component(s) that is embedded within the bone's complex loading environment. Numerous clinical exercise studies have been unable to correlate adaptive changes in bone to specific aspects of a particular exercise regimen, including exercise mode (e.g., running, swimming, weight lifting), intensity (e.g., percentage of maximal heart rate), duration, and repetition (number of times per month, week, day), emphasizing the need to characterize bone's mechanical environment generated by the prescribed exercise regimen.

At the organ level, the site specificity of exercise-induced bone adaptation is clear in tennis players, who display significant bone hypertrophy in the playing extremity but not in the contralateral arm that simply throws the ball into the air (Jones et al., 1977). During physical activity, changes in the loading environment are not uniform across the skeleton or bone. Reflecting this nonuniform environment, adaptation within a bone is also site specific, as some bone surfaces will change their osteoblastic or osteoclastic activity but others will not (Judex et al., 1997).

Since the early 1980s, specific components of the mechanical milieu have been proposed as the dominant stimulus for bone adaptation, including strain magnitude (Rubin and Lanyon, 1985), strain rate (O'Connor et al., 1982), electrokinetic streaming currents (Pollack et al., 1984), piezoelectric currents (Bassett, 1968), fluid shear flow (Weinbaum et al., 1994), and strain energy density (Fyhrie and Carter, 1986). Although several of these parameters correlate with specific skeletal morphologies, few have validated their regulatory role with an accurate, prospective prediction of adaptation as stimulated by changes in loading conditions (Gross et al., 1997). The difficulty in identifying a unifying principle that can anticipate the mechanical control of bone adaptation may be aggravated by an underlying "structural" presumption that tissue efficiency (minimal skeletal strain/minimal skeletal mass) is itself the driving stimulus that regulates the remodeling process.

Alternatively, bone cells may be responding to "biologically relevant" parameters of the functional milieu that are not necessarily linked to minimizing deformation of the structure under load. In support of "other than peak" signals regulating bone adaptation, examples of biological systems that perceive and respond to exogenous stimuli, such as vision, hearing,

and touch, are regulated in this fashion. It is also well accepted that too much loading will damage the bone matrix and predispose the skeleton to failure, just as too much light, noise, or pressure will overwhelm sight, hearing, and touch. To identify the criteria by which bone tissue responds to loading, it is important to look beyond the material consequences of a structure subject to dangerous levels of load and consider the biological benefit of a viable tissue/cell system subject to exercise.

Bone's mechanical milieu elicited by physical activity

Strains in bone

To gain insight into the structural demands that are placed onto the skeleton during daily activities, the mechanical environment that bone is subjected to can be characterized. In stark contrast to the notion that bone is purely loaded under compression, these experiments have definitively demonstrated that the long bones of the appendicular skeleton are also subject to a complex array of forces and moments produced by torsion and bending even during very simple activities such as steady-state locomotion (Rubin et al., 2013).

The mechanical state in the bone matrix is commonly quantified by spatial and temporal measures that are based on mechanical strain (ε), the dimensionless expression of deformation (ε = change in length, ΔL, normalized to the original length, L, of any given specimen). Because of the very small deformations that bone experiences during physiological loading, strain is typically expressed as microstrain (1% deformation = 0.01 strain = 10,000 $\times$ 10^{-6} strain = 10,000 $\mu\varepsilon$ = 10,000 microstrain).

Strain of a material is an inescapable product of load, regardless of its specific design or function. Pull a rubber band and it stretches, sit on a seat cushion and it compresses. Bend a pencil, and the concave surface is undergoing compression while the convex is stretching, undergoing tension; bend it too much, past the yield strain, and it snaps. In the case of bone, mechanical strain and its derivatives are considered an efficient means of translating mechanical load, including intensity, duration, and manner (e.g., twisting, bending), into a site-specific regulatory signal that can be recognized by the cell system that controls bone adaptation. One obvious goal of this strain-mediated form/function adaptation is to avoid catastrophic failure, or bone fracture. This requires that bone architecture is designed to control loading to avoid the tissue's yield strain of 0.7% (7000 $\mu\varepsilon$). Through strain gauges surgically implanted onto bone's surface, strain magnitudes have been determined during functional activities in a variety of species, including humans, dogs, primates, roosters, horses, sheep, and rats (Burr et al., 1996; Gross et al., 1992; Lanyon, 1971; Rubin and Lanyon, 1982). Although these gauges record deformation only from the specific sites they are attached to, engineering models can be used to extrapolate measured deformations to other sites within the bone.

Peak strain magnitudes measured in diverse vertebrates range from 2000 to 3000 microstrain (Rubin and Lanyon, 1984b). Whether measured in the third metacarpal of a galloping horse, the tibia of a running human, the humerus of a flying goose, the femur of a trotting sheep, or the mandible of a chewing macaque, this "dynamic strain similarity" suggests that skeletal morphology is adjusted such that functional activity elicits a very specific (and perhaps beneficial) level of strain to the bone tissue (Rubin et al., 1990). That strains of this magnitude are at least a factor of 2 below the yield point of bone material emphasizes that bone has a "safety factor to failure" of about 2−3 to defend against aberrant loading events. However, the realization of a mechanism by which the skeleton anticipates being loaded to about half its yield strength seems overly complex and unlikely. Instead, in vivo and in vitro data suggest that the functional criteria that regulate adaptation, and the means by which bone cells perceive and respond to their functional milieu, are more sophisticated than a mechanism that simply focuses on the magnitude of the deformation generated in the tissue.

Locomotion induces a nonuniform strain environment

During locomotion, bending is the dominant form of loading in the middiaphysis of limb bones; more than 85% of the strain measured in diaphyseal long bones is accounted for by bending moments (Rubin and Lanyon, 1982). These mid-diaphyseal bending moments are promoted, not negated, by bone curvature, and like the pencil, applied bending moments generate compressive strains on one side of the cortex and tensile strains on the opposite side (Fig. 76.1). The dominance of bending in the functional loading environment is somewhat counterintuitive because far less bone mass would be required to support the same loads if the bone were loaded axially. Bending fosters consistent, predictable loading conditions under which specific regions within the cortex are loaded in a similar fashion independent of the functional activity.

To demonstrate the stability of the functional strain environment, roosters were subjected to three distinct loading environments engendered by treadmill walking, treadmill running, or drop jumps for which roosters were released from a

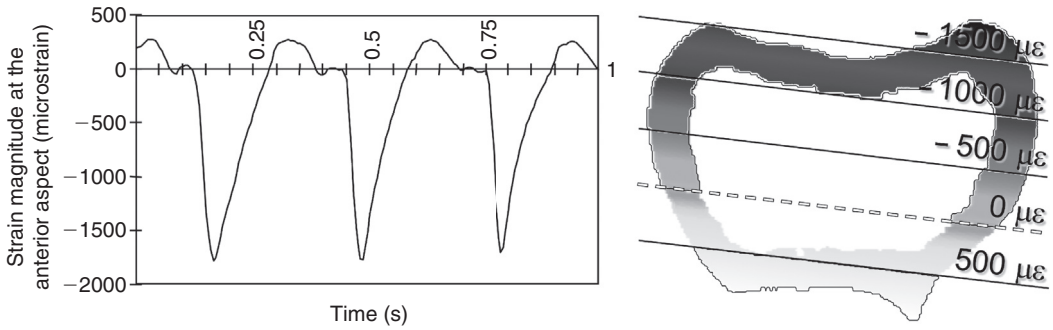

FIGURE 76.1 (Left) Recording from a strain gauge attached to the anterior aspect of the middiaphyseal tarsometatarsus while the animal is running on a treadmill at a high speed. (Right) The distribution of longitudinal normal strain magnitude about the middiaphysis of the rooster tarsometatarsus. The distribution was recorded at that point in the stride in which peak strain is achieved. While the distribution of peak strain is spatially very nonuniform, the manner in which the bone is loaded remains constant (i.e., the site of peak strain varies very little during the stance phase of a gait cycle). *Adapted from Judex, S., Gross, T.S., Zernicke, R.F., 1997. Strain gradients correlate with sites of exercise-induced bone-forming surfaces in the adult skeleton. J. Bone Miner. Res. 12(10), 1737–1745.*

50- to 60-cm height. Tarsometatarsal middiaphyseal strain magnitudes and distributions were determined via strain gauges and linear beam theory (Judex and Zernicke, 2000b). We found that peak compressive strains produced by these three activities increased from −1570 με for walking to −1870 με for running and −2070 με for jumping (nb, a negative strain denotes compression). Despite this increase in peak strains, the relative distribution of strain across the middiaphysis was essentially identical across the three activities.

With bending causing tension on one surface and compression on another, the transition between these two areas creates a region of the cortex that experiences very low peak strain magnitudes. Even though this neutral axis of zero strain is far removed from the area of the cortex subject to the peak strains, somehow tissue is retained in this low-magnitude strain state. It might be suggested that bone cells in different regions of the cortex are differentially sensitive to strain (e.g., some cells strive to 3000 με in compression, some to 1500 με in tension; others—near the neutral axis—are content with strains of 50 με). Although appealing in its simplicity, the apparent limitations of a spatially specific strain sensitivity are apparent with respect to the required genetic logistics.

Alternatively, it is possible that strain information is spatially integrated in three dimensions via a cell network facilitated by the osteocyte's canalicular network (Weinbaum et al., 2001) and gap junction intercellular communication (Donahue et al., 1995), such that the area of the cortex subject to 50 με resists resorption owing to sufficient homeostatic signals received from neighboring areas subject to higher strains. This "information integration" perspective is supported by the observation that the bone loss that parallels disuse occurs uniformly about the cortex and through the diaphysis, even though the net change in bone strain caused by the absence of function varies widely (Gross and Rubin, 1995). Since the early 2000s, many studies have confirmed the role of gap junction communication in signal transduction across osteocyte networks when bone cells are subjected to external mechanical cues (Jorgensen et al., 2000; Ishihara et al., 2013; Cherian et al., 2003, 2005).

The influence of muscle on bone's strain environment

The symbiotic relationship between muscle and bone is inherently obvious, and the musculoskeletal system might be considered in the context of one defining the other. In the absence of ground-reaction forces, the spectral components of muscle contraction typically impose smaller strains on the skeleton than those caused by functional impact loading. Even though muscle-induced strains may be small, they are sustained for extended periods of time (e.g., in postural muscle activity) and thus, over time, may dominate a bone's characteristic "strain history." Examining this hypothesis, strain data from a variety of animals reveal the existence of a broad frequency range of strains in the appendicular skeleton, even during activity such as quiet standing (Fritton et al., 2000; Fig. 76.2).

From a stimulus standpoint, these persistent, low-amplitude, high-frequency signals may, when summed, be at least as important as the seldom occurring, and somewhat unpredictable, peak strain events. If there is an age- or pathologically induced change in the dynamics of these muscle oscillations, it could be argued that bone mass may deteriorate, because these muscle-based signals also attenuate. To determine the role of muscle dynamics in the etiology of osteopenia, the spectral characteristics of muscle activity as a function of age were obtained through measurements of muscle surface vibration (Huang et al., 1999).

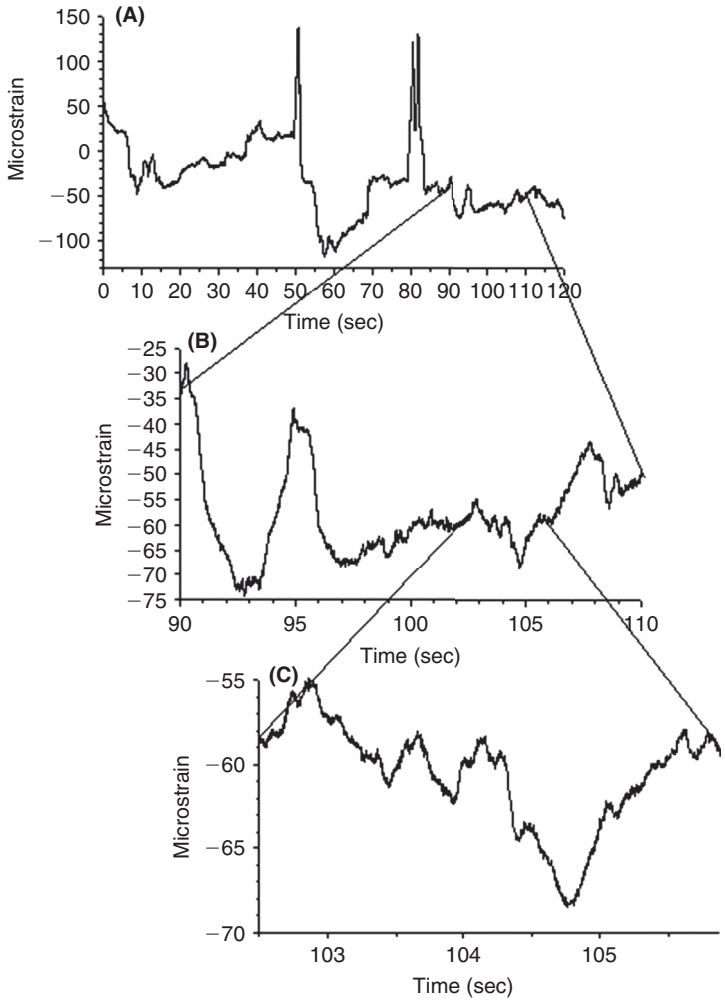

FIGURE 76.2 (A) A 2-min strain recording from the caudal longitudinal gauge of the sheep tibia while the animal took a few steps with peak strains on the order of 200 με. (B) A 20-s portion of that strain record shows peak strain events as large as 40 με. (C) Further scaling down to a 3-s stretch of the strain recording illustrates events on the order of 5 με. *Adapted from Fritton, S.P., McLeod, K.J., Rubin, C.T. 2000. Quantifying the strain history of bone: spatial uniformity and self-similarity of low-magnitude strains. J. Biomech. 33(3), 317–325.*

During the contraction of a muscle, radial expansion of the individual fibers results in fiber collisions and the production of muscle sound or acoustic vibrations of the muscle body. The frequency of these vibrations reflects the firing rate of the motor units and, correspondingly, the force output of the motor unit. When recorded in 40 volunteers (20–83 years of age) using a low-mass accelerometer, the spectra of the acoustic vibrations normal to the surface of the soleus muscle showed that muscle activity in the frequency range above 20 Hz decreased by a factor of 3 in the elderly compared with that seen in young adults, a sarcopenia consistent with loss of fast oxidative-type fibers. Simultaneous with the decay of high-frequency signals, there is a marked decrease in the amount of type IIa and IIb fibers (Lee et al., 2006), compounding the suppression of the source of the signal.

As the high-frequency components seen in bone during load bearing almost certainly arise through muscle activity, the deterioration of the muscle contraction spectra with age would consequently decrease the spectral content of bone strain above 20 Hz. From this perspective, it can be argued that the sarcopenia of aging may be a principal etiological factor in osteoporosis, as this portion of the strain spectrum is demonstrably osteogenic (see later). If aging leads to the loss of specific muscle fibers critical to the maintenance of bone mass, osteoporosis could presumably be inhibited by providing a "surrogate" for the lost spectral strain history.

Regulation of bone morphology by mechanical stimuli

Toward identifying the osteogenic parameters of the strain milieu

It is clear that the skeleton is subject to a wide range of mechanical signals, including low- to high-frequency strains, normal and shear strains, and compressive and tensile strains. It is also clear that the cells on and within the mineralized matrix are subject not only to mechanical parameters such as strain, but also to derivatives of tissue deformation such as fluid flow and electrokinetic currents, parameters that may represent an important physiological pathway in mediating an adaptive response. But which physical parameters are most important to regulating the adaptive response?

Models that have been used to investigate bone's adaptive response to its mechanical environment include overloads by osteotomies (Lanyon et al., 1982), vigorous exercise (Judex and Zernicke, 2000a), or exogenous loading models in which external forces are applied to the bone. Exercise represents a physiological means of enhanced mechanical loading, but the limited exercise repertoire of most laboratory animals makes it difficult to generate and control distinct mechanical milieus. Exogenous loading models such as the functionally isolated avian ulna (Rubin and Lanyon, 1984a), the axially loaded rat ulna (Torrance et al., 1994), or the rat tibia placed in a four-point bending apparatus (Turner et al., 1991) allow the generation of relatively controlled mechanical environments.

Strain magnitude

When holding strain frequency and number of loading events constant, longitudinal normal strain magnitude (strain in the direction of bone's longitudinal axis) is highly related to the osteogenic response. In other words, the larger the maximal deformation that is generated in the bone, the larger the overall response of the bone. Strains, when applied at 1 Hz (cycles per second) and that fail to reach a certain magnitude are permissive to bone loss. This relationship was first demonstrated in the functionally isolated turkey ulna preparation to which strains in the range of 400−500 με were applied at 1 Hz for 100 cycles per day. In this model, strains smaller than 1000 με caused bone loss, with strains larger than 1000 με leading to new bone formation in a dose-dependent relationship (Qin et al., 1998).

The question as to how much strain in bone has to be generated to obtain an osteogenic effect depends on the interrelationship between strain magnitude, strain rate, and strain frequency. While 100 loading cycles per day at 1 Hz inducing 1000 με prevented bone loss from occurring, this threshold can be reduced to 700 με when 600 loading cycles are applied at 1 Hz, to 270 με when 36,000 loading cycles are applied at 60 Hz, or to 100 με when 108,000 loading cycles are applied at 30 Hz. This demonstrates that the search for a particular strain (loading) threshold has to take other mechanical parameters into account as well and that this relationship can be exploited to design safer exercise regimens using smaller loads. Nevertheless, when considered in the clinic, a fascinating study has showed that higher intensity training has been shown to be more effectual than low intensity in peri- and postmenopausal women (Watson et al., 2018).

Differential bone remodeling to distinct components of the strain tensor

The goal of investigating the osteogenic effects of different aspects of the strain tensor has been approached using the turkey ulna model of disuse osteopenia, in which the modeling and remodeling response was quantified following 4 weeks of either axial or torsional loading or disuse (Rubin et al., 1996). Each of the two load groups was subjected to peak principal strains of 1000 με (predominately normal strain in the axial case, and shear strain when subjected to torsion). Of the three distinct groups, only disuse caused a significant change in gross areal properties compared with controls (13% loss of bone). This suggests that both axial and torsional loading conditions are substitutes for the functional signals normally responsible for retention of bone mass, leaving the periosteal and endosteal envelopes unfazed by disparate components of the strain tensor.

The intracortical response, however, was found to depend strongly on the manner in which the bone was loaded. Disuse failed to increase the *number* of sites within the cortex actively involved in bone turnover (intracortical events), yet significant area was lost within the cortex owing to a threefold *increase in the mean size* of each porotic site. Axial loading increased the degree of intracortical turnover compared with intact controls, yet the average size of each porotic event remained identical to that of controls. Conversely, torsion elevated neither the number of porotic events, the area of bone lost from within the cortex, nor the size of the porotic event. It appears that bone tissue can readily differentiate between distinct components of the strain tensor, with strain per se necessary to retain coupled formation and resorption, shear strain achieving this goal by maintaining the status quo, whereas normal strain elevates intracortical turnover, but retains coupling.

Strain rate

Although strain magnitude appears to be an important determinant of bone mass, it is critical to realize that dynamic but not static strains have osteogenic potential. At the extreme, static loading (strain rate = 0) at strain magnitudes capable of stimulating formation when applied dynamically produces a remodeling response similar to that to disuse, resulting in bone resorption (Lanyon and Rubin, 1984). Several studies support the notion that bone is sensitive to the applied strain rate, with higher strain rates being more osteogenic (LaMothe et al., 2005; O'Connor et al., 1982).

Extrapolated for the design of exercise interventions, these results imply that loads should be applied rapidly. Although exercise studies have been unable to identify a specific exercise intervention that is most effective in producing beneficial skeletal effects, a trend has emerged with high-impact exercise being more efficient than low-impact exercises in terms of stimulating new bone formation (Gabel et al., 2017). This trend may support the notion that high strain rates have a critical impact on bone morphology, as high-impact exercises ostensibly induce higher strain rates (MacKelvie et al., 2003).

Cycle number

A threshold behavior exists for the number of loading cycles, with the full response being triggered after only a limited number of loading cycles (Umemura et al., 1997; Rubin and Lanyon, 1984a). Focusing on the turkey ulna preparation, a loading regimen inducing peak strains of approximately 2000 με maintained bone mass with only 4 cycles a day. When the cycle number was increased, this loading regimen stimulated new bone formation. Thirty-six load cycles saturated the osteogenic response, with as many as 1800 cycles failing to be more effective than 36 cycles. Once the system is "on," additional information appears to be ignored.

Studies have indicated that the manner in which loading cycles are distributed plays an important role in defining the magnitude of the anabolic response. Partitioning a given bout of loading cycles into several loading sessions can increase bone's response to the mechanical intervention (Robling et al., 2002). Going one step further, studies have shown that this concept can be exploited to produce a mechanical intervention that is more efficacious despite providing fewer loading cycles (Gross et al., 2004), achieved by inserting a 10- to 15-s rest period between loading cycles to increase the osteogenic response in both young and aged mice (Srinivasan et al., 2002, 2003). This loading strategy can transform an otherwise ineffective loading regimen into a highly osteogenic stimulus. Specifically, varying the peak strain magnitudes (at a fixed cycle number) and varying cycle numbers (at a fixed strain magnitude) both result in increased bone formation rate (BFR) when a 10-s rest is inserted between loading cycles, compared with cyclic loading (Srinivasan et al., 2007). The mechanism by which the sensitivity of cells to mechanical signals is increased by rest-inserted loading may be associated with high cell refractory periods that, upon the application of a single loading event, impose a "time out" to the cell during which it cannot respond to another cycle (Sen et al., 2011). Translated to the human, perhaps incorporating rest periods into training regimens could increase the salutary response to exercise.

Strain distribution

Although a relation between bone's peak strain magnitude and the adaptive response has been proposed, bone also appears to be sensitive to how the strains are distributed across a bone section. Simply imposing a strain distribution that produces peak strain magnitudes similar to those of habitual loading conditions—but at different locations within the section (i.e., rotating the strain distribution)—may initiate new bone formation (Rubin and Lanyon, 1987). Thus, unusual strain events (strain errors) have been suggested to drive bone adaptation. Running, for instance, may not be the optimal exercise for bone formation, partly because it may generate strain distributions that are very similar to strain distributions induced by walking. Interestingly, sports that involve a great variety of changes in loading directions, such as squash, aerobic dancing, and speed skating, lead to site-specific benefits in bone mineral density in the areas that are subjected to loads during a given activity (Heinonen et al., 1995). Specifically, squash players had increased bone mineral density at lumbar spine (13.8%), femoral neck (16.8%), distal femur (11.2%), patella (6.7%), proximal tibia (12.6%), calcaneus (18.5%), and distal radius (11.3%), compared with sedentary controls. The speed skaters had a higher bone mineral density only at the distal femur (7.2%).

Sport-induced enhancement in bone has also been shown to be dependent on the intensity of the sport, such that high-impact sports (i.e., football) are more effective in increasing bone mass compared with low-impact sports (i.e., swimming and cycling) (Vlachopoulos et al., 2017). In addition, exposing the skeleton to the mechanical forces from childhood may also aid in maximizing the potential gains, as evident by the correlation between physical activity and bone strength from childhood to early adulthood (Gabel et al., 2017). Hence, physical activity that varies in loading directions has been shown

to result in enhanced osteogenic responses, although it has not been confirmed that these changes in loading directions actually cause altered bone strain distributions.

Strain gradient

Rather than exclusively considering the peak magnitude of the stimulus and averaging the morphological response through a given cross section, one could investigate whether new bone is actually deposited in those regions where the applied stimulus is the largest (i.e., does bone adaptation correlate with strain distribution?). If such a site-specific relationship exists, then the knowledge of this specific osteogenic component may provide information about a mechanism by which bone cells perceive their mechanical environment.

To a degree, this issue was addressed in an exercise study in which young adult roosters were run on a treadmill for 9 min per day (~1500 gait cycles) for 3 weeks. The brief daily running regimen activated periosteal surfaces, but the amount of periosteal mineralizing surfaces per sector was only weakly associated with strain magnitude ($R^2 = 0.24$, negative correlation). In contrast, circumferential strain gradients (changes in strain magnitude across a volume of tissue) correlated strongly ($R^2 = 0.63$) with the sites of periosteal activation, consistent with earlier results from an external loading model (Judex et al., 1997). In general, circumferential strain gradients are largest where strains (deformations) are the smallest.

Although counterintuitive from a structural perspective, activating bone formation at sites subjected to low strains rather than large strains, strain gradients drive fluid flow in bone in the matrix, a process that has been suggested to play an important role in mechanotransduction in bone. These data further emphasize that bone adaptation is not necessarily guided by form–function relations, rather that bone cells respond to a biological signal resulting from the application of mechanical loads.

Fluid flow

Cells on and within the mineralized matrix are subject to mechanical parameters such as strain, as well as derivatives of tissue deformation such as fluid flow and electrokinetic currents, parameters that may represent an important physiological pathway in mediating an adaptive response. Bone cells, in particular osteocytes, are surrounded by extracellular fluid (Weinbaum et al., 1994). The driving force for fluid to flow is a differential pressure between two ends of a lacunar–canalicular system that experience different amounts of mechanical strain, both temporally and spatially. Fluid flow is thus a direct by-product of mechanical strain, and a large body of in vitro studies has shown the sensitivity of bone cells to flow (Rubin et al., 2006; Bancroft et al., 2002). Because of the tight coupling between mechanical strain and fluid flow under physiological conditions in vivo, only few studies have successfully increased fluid flow in controlled animal models (Qin et al., 2003). Similar to in vitro data, raising intramedullary pressure, and thus enhancing interstitial bone fluid flow, can increase bone formation (Stevens et al., 2006). The in vivo mechanism(s) by which bone cells sense and respond to fluid flow may be related to one of the following processes: (1) fluid pressurization that directly stimulates cells, (2) interstitial fluid flow that excites osteocytes through fluid shear stresses, (3) drag forces that perturb the osteocytic processes in the pericellular matrix, (4) fluid flow that aids in the transport of nutrients to bone cells, or (5) electrokinetic effects such as streaming potentials (Bonewald and Johnson, 2008).

Evidence of this is provided by a novel fluorescence recovery after photobleaching technique, combined with synchronized mechanical loading and imaging, used to show a 31% increase in real-time solute transport within the lacunar–canalicular system following cyclic end compression of mouse tibia (400 με of surface strain at 0.5 Hz, 4 s rest between adjacent loading cycles) (Price et al., 2011). This model provides a foundation through which the effect of mechanical stimulation of osteocytic cellular responses could be quantified in vivo. Together, in vitro and in vivo studies clearly demonstrate that bone fluid flow is capable of transducing mechanical signals from the matrix to the cell.

Low-magnitude, high-frequency mechanical signals

A common theme of the exercise-induced adaptation in bone is that only peak events are considered (e.g., exercise intensity, peak strain magnitude, peak strain rate). From this, one could conclude that mechanical modulation of bone physiology depends on large signals to have any morphological impact. However, the weak correlation of new bone formation with exercise intensity or with the specific sites of peak strain magnitudes suggests that other factors may also help define bone mass and morphology.

As discussed earlier, in vivo data suggest a nonlinear interdependence between cycle number, strain frequency, and strain magnitude. When the turkey ulna was loaded at 1 Hz, peak strains larger than 700 με were necessary to maintain bone mass. This loading threshold can be reduced to 400 με at 30 Hz and to 270 με at 60 Hz. Although the reduction in strain threshold could be associated with an increase in cycle number, it is also possible that the increase in frequency at which loading occurred played a large role, just as the eye sees color based on frequency and the ear hears pitch based on frequency. Indeed, since the early 2000s, we and others have demonstrated that bone can sense and respond to even extremely small mechanical signals if they are applied at frequencies considered "high" based on typical locomotion (walk at 1 Hz, run at 3 Hz).

Low-level mechanical signals increase bone quantity and strength

To examine the long-term influence of applying short bouts of extremely low magnitude, high-frequency signals, adult sheep stood in a chute where only the hindlimbs were subjected to a vertical ground-based vibration, oscillating at 30 Hz, to create peak−peak accelerations of 0.3*g* (Rubin et al., 2001a). When the animals were not being treated, they pastured with controls. After 1 year of stimulation, peripheral quantitative computed tomography of the femur demonstrated a 34.2% increase in trabecular density in mechanically stimulated sheep ($P < .01$). Micro-computed tomography indicated that not only the quantity of trabecular bone had benefited but also its microarchitecture (Rubin et al., 2002b). The trabecular bone pattern factor, an index of connectivity, decreased 24.2% in animals subjected to the noninvasive stimulus ($P < .03$), reflecting an increase in connectivity of the trabecular struts. Histomorphometry emphasized that the increase in volume fraction was achieved through an anabolic stimulus (Rubin et al., 2002a). The elastic modulus and stiffness of the bone subject to the low-level mechanical stimulus also increased significantly (Fig. 76.3) and analyses of the tissue-level stresses and strains indicated that, micromechanically, the bone had to adapt to become a mechanically more efficient structure (Judex et al., 2003).

Translating this to the human, a pilot study in children with low bone density showed a similar trend wherein a 30-min vibration intervention (30 Hz, 0.3*g*) for 8 weeks led to 6.2% increase in cancellous bone density, 2.1% increase in cortical bone density, and 16.6% increase in bone-specific alkaline phosphatase, an indicator for increase in bone formation (Pitukcheewanont and Safani, 2006). Low-level leisure time physical activity such as walking or bicycling for less than 20 min per day has also been shown to reduce the risk of hip fracture (hazard ratio = 0.77) and any fracture (hazard ratio = 0.87) in both men and women (Stattin et al., 2017). These studies suggest that bone may be "tuned" to higher frequency loading, and it may represent a sort of "surrogate" for strenuous exercise (Ozcivici et al., 2010).

Low-level mechanical signals normalize bone formation

Disuse osteopenia models have been used to determine whether resorptive remodeling, as stimulated by disuse, could be suppressed with brief exposure to these low-level vibrations. A single-element strain gauge, attached to the tibia of

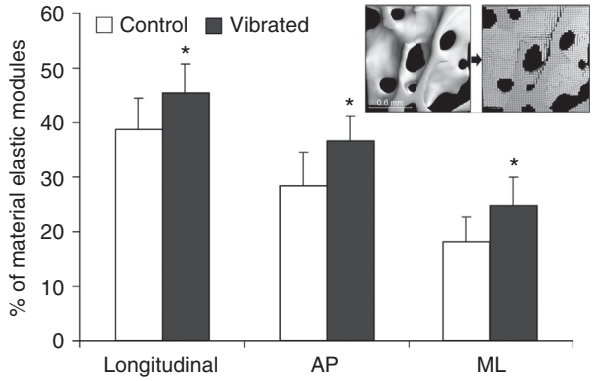

FIGURE 76.3 Finite element modeling was used to convert the trabecular structure into a mechanical model. Simulated mechanical testing in all three orthogonal loading directions indicated that the application of short bouts of high-frequency mechanical signals increased trabecular stiffness. Shown is the apparent tissue elastic modulus expressed as percentage of the tissue elastic modulus for control and experimental sheep in the three directions (mean + SD). *AP*, anterior−posterior direction; *ML*, medial−lateral direction. *$P < .05$. *Adapted from Judex, S., Boyd, S., Qin, Y.X., Turner, S., Ye, K., Muller, R., Rubin, C. 2003. Adaptations of trabecular bone to low magnitude vibrations result in more uniform stress and strain under load. Ann. Biomed. Eng. 31(1), 12−20.*

calibration rats, showed that the oscillation, at 0.3*g*, generated strains less than 5 με at 45 Hz, more than 2 orders of magnitude below the strains that can protect bone when induced at 1 Hz. Compared with long-term controls, 28 days of tail suspension caused mineralizing surface (MS/bone surface (BS)) of the tibiae to drop 52% ($P < .004$) and BFR per bone volume (BFR/BV) to drop 72% ($P < .0002$) (Rubin et al., 2001b). The suppression of formation was not significantly different from that in the animals subjected to disuse for most of the day (23 h, 50 min) and then allowed to freely bear weight for 10 min per day. However, 10 min/day of weight bearing on an active vibration platform normalized mineralizing surfaces and BFRs to normal weight-bearing levels.

Translating this to humans, a 6-month vibration intervention (90 Hz, 0.3*g*, 10 min/day, 5 days/week) in children with immobility-induced disability resulted in 6.3% increase in trabecular bone mineral density of the proximal tibia, compared with children who did not receive a vibration treatment, who had a 12% decrease in bone mineral density relative to baseline (Ward et al., 2004). Taking this to an extreme, negative implications of a prolonged 56-day bed rest, in terms of reduced bone mass and increased bone resorption, were mitigated with a twice-daily resistive vibration exercise for 4−6 min per bout, ranging in frequency from 18 to 26 Hz (Armbrecht et al., 2010), although the *g* forces were much higher.

Vibrations can decrease resorptive activity

To test the effects of these higher frequency mechanical signals in the growing skeleton in which resorptive activity is relatively high, 8-week-old mice were subjected to daily 15-min bouts of whole-body vibrations at 45 Hz and 0.3*g*. After 3 weeks, osteoclastic activity in the trabecular metaphysis and epiphysis of the tibia was ~30% lower ($P < .05$) in vibrated mice than in age-matched controls. BFR/BS on the endocortical surface of the metaphysis was 30% greater ($P < .05$) in whole-body vibration than in age-matched control mice, but trabecular and middiaphyseal BFRs were not significantly altered (Xie et al., 2006).

Translated to humans, 8 weeks of whole-body vibration intervention (15 min/day, 30 Hz, 0.3*g*) in postmenopausal women reduced the hip fracture risk by mitigating the bone loss at the trochanter and lumbar spine (Beck and Norling, 2010). In addition, whole-body vibration (frequency ranging from 25 to 35 Hz) combined with exercise also resulted in increased bone mineral density at the lumbar spine and decreased fall risk in postmenopausal women (von Stengel et al., 2011).

Genetic variations modulate bone's response to mechanical signals

It is well accepted that the genetic makeup of any given individual is a strong predictor of risk of osteoporosis (Deng et al., 2001). What is not as clear is if the genetic template can account for variability in the response to bone's ability to adapt to mechanical signals. To address this question, inbred mouse strains with distinct bone phenotypes (Judex et al., 2004) were used to examine whether they were differentially sensitive to changes in their habitual mechanical environment (Judex et al., 2002). Adult female mice, with relatively thin (C57BL/6J), medium (BALB/cByJ), and robust (C3H/HeJ) skeletons were subjected to 10 min/day of low-level, high-frequency mechanical signals (0.25*g* at 45 Hz). After 3 weeks, BFR, with tissue volume as referent of C57BL/6J mice subjected to the low-level mechanical signal, was 69% greater ($P < .04$) than in intrastrain control mice. Increased trabecular BFRs coincided with an 85% ($P < .01$) larger BV (BV/TV) and 50% larger trabecular thickness ($P < .009$) in the vibrated mice. In BALB/cByJ mice, the low-level mechanical signals increased BFR/BV by 34% ($P < .02$), but bone structural indices, including BV/TV, remained unaffected. In contrast to the responsiveness of the C57BL/6J and BALB/cByJ strains, no significant effects of mechanical stimulation were measured in tibial trabecular bone of C3H mice. Extrapolating these results to the human skeleton may provide insight into the preferential efficacy of mechanical interventions, such as exercise or low-level vibrations. The results of this study also suggest that some people who benefit from a genetically predetermined higher bone mass may ultimately be less sensitive to any form of physical intervention (Torvinen et al., 2003).

Inhibition of postmenopausal bone loss by low-level vibrations

With the demonstration that mechanical factors can be anabolic and anticatabolic to the skeleton, a challenge becomes whether these "regulatory factors" can be safely and effectively administered in the clinic to inhibit or reverse osteopenia. Many animal studies have shown the efficacy of low-level whole-body vibration intervention in mitigating ovariectomy-induced bone loss (Flieger et al., 1998; Rubinacci et al., 2008; Butezloff et al., 2015; Krishnamoorthy et al., 2016). However, the effect of whole-body vibration in postmenopausal women in the clinic remains ambiguous. The ability of a

low-magnitude (0.2g), high-frequency (30 Hz) mechanical stimulation to inhibit postmenopausal osteopenia was evaluated in a prospective, randomized, double-blind, placebo-controlled clinical trial (Rubin et al., 2004). Sixty-two postmenopausal women were enrolled in the study. Thirty-one women underwent mechanical loading of the lower appendicular and axial skeleton for two 10-min periods per day, induced via floor-mounted devices that produced the mechanical stimulus, whereas 31 women received placebo devices and underwent daily treatment for the same period of time.

An intention-to-treat analysis of dual-energy X-ray absorptiometry data of the spine (L1−4), proximal femur, and nondominant radius showed little effect of the intervention. In a post hoc analysis of those subjects who used the device at least 60% of the prescribed time, a linear regression of the means was used to show that lumbar spine bone mineral density declined by 3.3% (±0.83) in the placebo group compared with only 0.8% (±0.82) in the treated group ($P < .03$), reflecting a 2.5% benefit of the biomechanical intervention. A 3.3% treatment benefit was observed in the trochanter region of the hip, with a 2.9% (±1.2) loss observed in the placebo group, yet with a 0.4% (±1.2) gain in the treated group ($P < .03$). At the distal radius, no significant differences were observed as a function of time or between groups, emphasizing the mechanical influence to be locally delivered.

On the other hand, another randomized controlled trial on 202 osteopenic postmenopausal women showed no significant improvement in overall trabecular, femoral neck, total hip, or lumbar spine bone mineral density after 1 year of whole-body vibration intervention (20 min/day, 37 or 90 Hz, 0.3g) (Slatkovska et al., 2011). This clinical trial, however, had some limitations including low patient compliance and a lack of subjects with low bone density, and the placebo group did not lose significant bone density over the course of 1 year. Hence, more studies are needed to determine the efficacy of low-intensity whole-body vibration intervention in tackling postmenopausal bone loss. In any case, physical activity has been independently shown to be associated with thicker cortex and higher bone strength at the distal tibia in elderly women, suggesting that physical activity in old age may aid in mitigating bone loss (Nilsson et al., 2017). However, low-magnitude, high-frequency mechanical signals failed to reverse osteoporosis in the frail elderly (Kiel et al., 2015).

Low-level mechanical signals mitigate bone loss due to cancer

Cancer progression, along with the treatment strategies such as chemotherapy, irradiation, and immunosuppressive therapies, can put a tremendous stress on the musculoskeletal system, leading to rapid bone loss and increased fracture risk. Multiple studies have shown the efficacy of low-magnitude whole-body vibration in tackling the bone loss and osteopenia resulting from cancer and radiation therapies. In an ovarian cancer murine model, a 1-year intervention with whole-body vibration (15 min/day, 5 days/week, 90 Hz, 0.3g) increased BV by 25% in proximal tibia and by 16% in L5 vertebrae, compared with age-matched control mice (Pagnotti et al., 2012).

Similarly, in a murine model of multiple myeloma, 8 weeks of whole-body vibration intervention (15 min/day, 5 days/week, 90 Hz, 0.3g) resulted in a 76% increase in trabecular BV fraction, 30% increase in cortical BV, and 45% reduction in tartrate-resistant acid phosphatase 5b activity, compared with mice with multiple myeloma (Pagnotti et al., 2016).

Extending this to the clinic, pediatric cancer survivors who had a bone mineral density Z score of ≤ -1 improved their Z score by 0.25 ± 0.78 after 1-year of whole-body vibration intervention (2 × 10 min/day, 7 days/week, 32−37 Hz, 0.3g), while the placebo group's Z scores reduced by −0.19 ± 0.79 ($P = .05$) (Mogil et al., 2016). Improvement in bone mineral density was correlated with circulating osteocalcin ($P = .02$), suggesting increased bone formation as a result of whole-body vibration.

Low-level mechanical signals are anabolic to the musculoskeletal system

Susceptibility to osteopenia is present early in life, the amount of bone gained during adolescence is a main contributor to peak bone mass in the young adult, and peak bone mass in the young adult is a determinant of osteoporosis in the elderly (Loro et al., 2000). A study was designed to establish if brief, daily exposure to extremely low level mechanical stimuli (10 min/day, 30 Hz, 0.3g) was anabolic to musculoskeletal development in young females, 15−20 years of age, each in the lowest quartile of bone density in this age cohort and who had already sustained a fracture (Gilsanz et al., 2006). Using an intention-to-treat analysis, cancellous bone in the lumbar vertebrae and cortical bone in the femoral midshaft of the experimental group were 2.0% ($P = .06$) and 2.3% ($P = .04$) greater, respectively, compared with controls. Cross-sectional area of paraspinous musculature was 4.9% greater ($P = .002$) in the experimental group versus controls. When a per-protocol analysis was performed, gains in both muscle and bone were strongly correlated to a threshold in compliance, where the benefit of the mechanical intervention compared with controls was realized once the device was used for at least 2 min per day ($n = 18$), as reflected by a 3.9% increase in cancellous bone of the spine ($P = .007$), 2.9% increase in

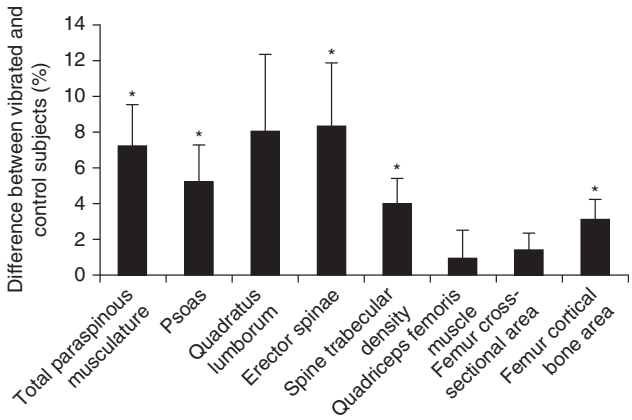

FIGURE 76.4 The difference in the change (mean + SE) in musculoskeletal parameters measured over 1 year for young women who used the device for more than 2 min per day, compared with controls and women who stood on the vibrating plate for less than 2 min per day. With the exception of musculature around the femur and femoral cross-sectional area, the musculoskeleton of the experimental group benefited significantly (*$P < .05$) from the brief low-level mechanical intervention. *Adapted from Gilsanz, V., Wren, T.A., Sanchez, M., Dorey, F., Judex, S., Rubin, C. 2006. Low-level, high-frequency mechanical signals enhance musculoskeletal development of young women with low BMD. J. Bone Miner. Res. 21(9), 1464–1474.*

cortical bone of the femur ($P = .009$), and 7.2% increase in musculature of the spine ($P = .001$), compared with controls plus the low compliers (Fig. 76.4).

Short bouts of extremely low level mechanical signals, several orders of magnitude below that associated with vigorous exercise, increased both trabecular and cortical bone in weight-bearing regions of the skeleton. Further, muscle mass of the paraspinous region increased, suggesting that risk factors for fracture beyond bone quantity and quality could be mitigated. Low-level, high-frequency mechanical signals, even lower than those used in this study, have also been shown to preserve postural stability in an aging population (Gravelle et al., 2002), providing evidence that physical signals can serve to reduce risk factors of osteopenia, falling, and sarcopenia.

Low-level mechanical stimulation has also been shown to aid in muscle strength loss during extended bed rest (Muir et al., 2011). During a 90-day bed rest, healthy adults were subjected to either low-magnitude whole-body vibration (10 min/day, 30 Hz, 0.3g or 0.5g) or no treatment. Subjects that underwent whole-body vibration intervention retained their postural stability as quantified by 73% reduction in displacement and 97% reduction in velocity after 60 days of bed rest, compared with controls. In addition, although vibration did not mitigate loss in muscle extension strength, it resulted in 46.2% improved retention in flexion strength, compared with controls ($P = .01$). Preserving postural control and improving muscle strength, whole-body vibration can aid in reducing the risk of debilitating falls and represent a system-level approach to controlling fractures due to low bone density.

The reason for improvement in muscle strength and postural stability due to whole-body vibration is not yet clearly understood. Satellite cells are quiescent myogenic cells that are capable of differentiating into skeletal muscle cells in response to injury or an external stimulus (Morgan and Partridge, 2003). A study utilizing a murine model of ovariectomy demonstrated depletion in the satellite cell population (−21%, $P < .05$) in the muscle compared with control. The depletion of muscle satellite cells was mitigated when the mice were subjected to whole-body vibration (−11% compared with control, $P > .05$) (Frechette et al., 2015), suggesting a possible mechanism through which low-level vibration can preserve muscle mass and muscle strength, and possibly mitigate fall risk. Should these musculoskeletal enhancements be preserved through adulthood, this intervention may prove a deterrent to osteoporosis in the elderly.

How can bone sense a signal so small?

The aforementioned studies, contrasting with a more-is-better principle, suggest that bone strains 2 orders of magnitude below a previously suggested threshold (Frost, 1987) can be anabolic to bone. The means by which such low-level mechanical signals can be anabolic to a tissue such as bone is not clear. If cortical matrix deformations of less than 0.001% strain, measured at the periosteum, were transduced directly to the resident osteoblast or osteocyte population, the deformation of the cell itself would be less than 1 Å. Given that such deformations may be too small to be recognized by cells (Han et al., 2004), by-products of matrix deformation, such as fluid flow–induced shear stresses, streaming potentials, fluid drag on pericellular processes, or enhanced nutrient transport, may contribute to a cell's responsiveness to mechanical

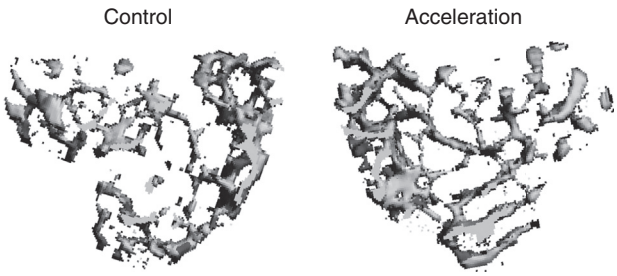

FIGURE 76.5 By applying very low level oscillatory accelerations to one leg of the anesthetized mouse while the other leg serves as a contralateral control, the efficacy of very small and unconstrained motions that do not directly apply deformation to the matrix can be tested. *Adapted from Garman, R., Gaudette, G., Donahue, L.R., Rubin, C., Judex, S. 2007a. Low-level accelerations applied in the absence of weight bearing can enhance trabecular bone formation. J. Orthop. Res. 25(6), 732–740.*

signals (Malone et al., 2007a). Yet even these alternative pathways are dependent on matrix deformation and therefore will be very small in magnitude during low-level mechanical stimulation.

In contrast to a matrix deformation–dependent pathway for mechanotransduction, the frequency sensitivity of the adaptive system points toward a more fundamental, perhaps unrecognized, pathway by which physical signals interact with the tissues and cells (Luu et al., 2009b). Indeed, a mechanism that would allow a cell to sense mechanical signals directly without reliance on matrix strain would obviate the need for compensatory tissue-level amplification mechanisms and reduce complexity in the system, and may provide cells with mechanical information without the potential for damaging the surrounding tissue. Physical acceleration of a cell may present such a signal that can transmit physical challenges to a receptive cell population in an efficient and safe manner (Garman et al., 2007a). This hypothesis was tested by removing bone's habitual loading environment and imposing very small amplitude oscillatory accelerations that induce motion but no direct deformation (Garman et al., 2007b).

To this end, a device was developed that can deliver high-frequency accelerations to skeletal segments in the absence of weight bearing (Fig. 76.5). In an anesthetized murine model, the left tibia of each mouse was subjected to oscillatory 0.6*g* accelerations at 45 Hz for 20 min/day and the right tibia served as control. Oscillatory accelerations, applied in the absence of weight bearing, resulted in 70% greater BFRs in the trabeculae of the metaphysis but similar levels of bone resorption, compared with contralateral controls. Quantity and quality of trabecular bone also improved as a result of the acceleration stimulus. As expected, the matrix deformations induced by these motions are extremely small, indicating that mechanosensory elements of resident bone cell populations can perceive and respond to acceleratory signals, and point to an efficient means of introducing subtle physical signals into a biological system without putting the matrix at risk of overloading.

Biochemical modulation of mechanical signals

Which cells sense the stimulus?

It is clear that bone cells are able to sense their mechanical environment via a number of proposed mechanisms, including direct matrix deformations, pressure and transient pressure waves, accelerations, fluid shear stresses, fluid drag forces, or even dynamic electric fields as interstitial fluid flows past charged bone crystals (Fig. 76.6). It is much less clear, however, which of the cells within a bone are the key sensory elements in mechanotransduction. Mechanical responses of

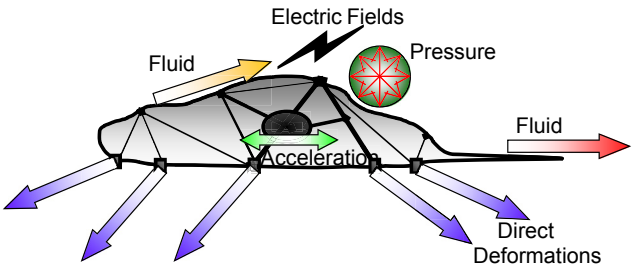

FIGURE 76.6 Proposed mechanisms by which bone cells may sense the application of mechanical forces to the skeleton.

osteoprogenitor cells, including stromal cells, osteoblasts, and osteocytes, have all been documented without identifying the critical responding cell: for example, exposure to microgravity results in a decreased number of osteoblasts—but what cell senses and responds to the loss of gravity, the undifferentiated mesenchymal precursor, the differentiated osteoblast, or the distant, entombed osteocyte?

Bone marrow mesenchymal stem cells

Bone marrow stromal cells change their proliferation rate and gene expression patterns in response to mechanical stimulation (Li et al., 2004; Baskan et al., 2017) and alter lineage selection as well, moving toward osteoblastogenesis and away from adipogenesis (David et al., 2007; Luu et al., 2009a). Low-level mechanical stimulation has also been shown to suppress adiposity and adipogenesis in vivo as evident by 27.4% reduction in fat volume in the torso and 19% lower ratio of adipocytes to marrow-based MSCs in the epididymal fat pad in mice that underwent whole-body vibration treatment (15 min/day, 5 days/week, 90 Hz, 0.2*g*), compared with controls (Rubin et al., 2007a).

Returning to the importance of "timing" of the signal, when low-magnitude vibration was separated into multiple bouts throughout the day, separated by a refractory period between bouts of stimulation, the suppression of adipogenesis was enhanced in MSCs in vitro. Following 7 days of low-magnitude whole-body vibration treatment (90 Hz, 0.7*g*), the cells that were vibrated 40 min/day failed to suppress adipogenesis. On the other hand, the cells that were vibrated for two bouts of 20 min per day suppressed adipogenesis by 30 ± 8% ($P < .05$) and 70 ± 5% ($P < .01$) when the bouts were separated by 1 and 3 h, respectively (Sen et al., 2011). When the length of the refractory period was increased from 3 to 6 h, there was no further improvement in adipogenesis suppression in MSCs.

These studies suggest that not only are the stromal cells in the body responsive to low-level mechanical stimulation, but their response is also dependent on how the signals are delivered, in terms of the bout duration, number of bouts delivered per day, and length of the refractory period between bouts of stimulation. Indeed, similar response is demonstrated in vivo such that when adult C57BL/6 mice are subjected to 6 week of low-magnitude whole-body vibration (90 Hz, 0.2*g*), the visceral adiposity is suppressed when the vibration was delivered in two bouts of 15 min per day, separated by a 5-h refractory period, but not when the vibration was delivered in one bout of 30 min per day (Patel et al., 2017). Again, timing may be as important as the signal itself.

Osteoblasts

Low-magnitude high-frequency mechanical stimulation at 35 Hz and 0.3*g* for 10 min/day has been shown to restore mineralization and osteogenic gene expression (alkaline phosphatase, RUNX2, osteomodulin, osteoglycin, parathyroid hormone receptor 1) in preosteoblast cells (2T3) that were exposed to a random positioning machine, which can mimic disuse and microgravity conditions in vitro (Patel et al., 2009). In another preosteoblast cell line, MC3T3-E1, subjecting the cells to low-magnitude mechanical stimulation (35 Hz, 0.25*g*) for either 30 min per day or two bouts of 15 min per day (separated by 0.5, 1, 2, 3, or 6-h refractory periods) has been shown to increase the expression of osteogenic proteins (alkaline phosphatase, osteocalcin, and collagen type I) (Zhao et al., 2018). The osteogenic protein expression was the highest when the mechanical loading was delivered in two bouts of 15 min per day, separated by a 0.5-h refractory period.

Osteoclasts

With respect to osteoclasts and bone resorption, stromal cell expression of the osteoclast differentiation factor is sensitive to mechanical force (Rubin et al., 2000), suggesting that the number of osteoclasts present is controlled through mechanical regulation sensed by stromal cells. Osteocytes are another mechanosensitive cell embedded in the bone that can affect osteoclast activity. Low-level mechanical stimulation (1 h/day, 60 Hz, 0.3*g*) of MLO-Y4 osteocyte-like cells led to 55% reduction ($P < .01$) in receptor activator of nuclear factor κB ligand (RANKL), 36% attenuation ($P < .05$) of formation of large osteoclasts (≥10 nuclei), and 20% reduction ($P = .07$) in osteoclastic resorption, compared with control (Lau et al., 2010). In addition, low-magnitude high-frequency vibration has also been shown to inhibit RANKL-induced differentiation of monocyte-like cells (RAW264.7) into mature osteoclasts (Wu et al., 2012), adding another layer of control by which mechanical force might limit bone resorption and influence the system level of bone turnover.

Osteocytes

Finally, the majority of cells in cortical bone are osteocytes, and owing to their pervasive, three-dimensional distribution throughout both trabecular and cortical bone, these cells are potentially well placed to sense the magnitude and direction of

mechanical strain within the tissue (Bonewald, 2011). Osteocytes, although enclosed in calcified tissue, are interconnected through a network of canaliculi through which these cells cast long cell processes. Osteocytes respond to strain in vivo as shown by increased glucose-6-phosphate dehydrogenase activity (Skerry et al., 1989) or earlier response of c-*fos* mRNA (Inaoka et al., 1995) after loading. As well, unloading causes osteopontin expression in osteocytes (Gross et al., 2005). Dentin matrix protein 1, which is a secreted matrix protein expressed in late osteoblasts and osteocytes, has been shown to increase in osteocytes after tooth movement in the jaw (Gluhak-Heinrich et al., 2003).

If we consider that strain signals of even very low magnitude can stimulate an anabolic response in bone tissue, the osteocyte may be best placed to sense such a signal (Santos et al., 2009). This might occur through fluid flow through canaliculi, as well as through deformation, both of which have been shown to cause changes in osteocyte function (Plotkin et al., 2005). It has also been suggested that, owing to the modulus mismatch of the bone material and the lacunae, the osteocytes within the cavity would be subject to strains as high as 30,000 με, even though the bulk material was strained only to 3000 με (Nicolella et al., 2006). In other words, the microarchitecture of the bone tissue could serve to indirectly (fluid pressure through canaliculi) or directly (strain amplification via the lacunae and then again via membrane to nucleus via linker of nucleoskeleton and cytoskeleton [LINC]) amplify the strain signal.

Bone marrow vasculature

Other cells present in bone, such as endothelial and smooth muscle cells in the penetrating vasculature, might also contribute to the skeleton's adaptive response to loading. After all, endothelial cells respond to shear stress and tensile strain generated by increased heart rate during exercise, by producing nitric oxide (Boo and Jo, 2003). Nitric oxide is an important humoral factor to transduction of mechanical input in vascular cells (Lane and Gross, 1999). Increased vascular release of nitric oxide is likely to regulate bone cell response: nitric oxide has pleiotropic effects in bone cells and potently decreases resorption by decreasing osteoclast formation and activity (Fan et al., 2004). But bone stromal cells also release nitric oxide as a result of mechanical input (Rubin et al., 2003), providing a secondary cell target for mechanical induction of this freely diffusible antiresorptive agent. Thus, targets of skeletal loading may include extraskeletal cells and systems. In any case, cells contributing to bone remodeling directly (osteoblasts and osteoclasts), indirectly (osteoprogenitor cells and osteocytes), and distantly (muscle and vascular systems) are all known to be mechanosensitive.

Mechanoreceptors in bone cells

The ability of cells to read their biomechanical environment requires either that their mechanoreceptors be in contact with the outside, through the cell membrane and its attachment to substrate, or that the mechanoreceptor be able to sense changes in a loading-induced physical intermediary such as fluid shear on the apical membrane. Although there are examples of channels that are regulated by movement of mechanosensory bristles (Sukharev and Corey, 2004), or by tension waves (Morris, 1990), a unified model of the most proximal events that lead to intracellular signal transduction in nonsensory tissues does not yet exist.

Theoretical considerations may be moving toward an architectural/spatial concept that integrates positional changes between signaling proteins, scaffolds, membrane domains, and structural components of the cell. All can be perturbed by mechanical force. Whether each aspect is a mechanoreceptor in itself or works in a holistic context combining many aspects of cell architecture and response is yet to be determined. With the multiplicity of mechanical signals presented to the cell, it is at least likely that no single mechanosensor or receptor mechanism is responsible for all of the integrated cell response to the mechanical environment.

Integrins and integrin-associated proteins

Membrane deformation and shear across the membrane, as well as pressure transients, can be transmitted to the cytoskeleton and ultimately to the cell-matrix adhesion proteins that anchor the cell in place (Katsumi et al., 2004). Thus, the cell represents a load transmission network whereby surface forces will affect proteins that span or are associated with the plasma membrane, including the cytoskeleton, linker proteins at sites of cell attachment, and membrane-spanning integrin adhesion proteins. In this way, mechanotransduction might be expected to depend on the mechanical integrity of this network with constituents of this network serving as molecular mechanotransducers.

Indeed, in particular the β1-integrin subunit has been implicated in mechanotransduction on osteocytes and osteoblasts (Bennett et al., 2001). In osteoblasts, steady fluid flow can upregulate β1 expression (Kapur et al., 2003), even though blocking β3 with RGD-containing peptides did not affect extracellular signal-regulated kinase (ERK) activation (Weyts et al., 2002). Other focal adhesion proteins such as focal adhesion kinase (FAK) may be critical to integrin clustering as

well as molecular signaling in bone cells (Rezzonico et al., 2003). Mechanical stimulation stimulates tyrosine phosphorylation, predominantly in FAK, in osteoblasts (Boutahar et al., 2004). Upon phosphorylation, FAK contributes to mitogen-activated protein kinase (MAPK) activation via interaction with c-src, Grb2, and the small GTPase Ras (Schlaepfer et al., 1999). This is significant because MAPK activation is also one of the effectors of oscillatory flow in bone cells and this pathway has been observed in response to fluid flow in endothelial cells (Berk et al., 1995). More molecular definition has lately been assigned to this pathway: involvement of a β1-integrin-linked kinase is stimulated through mechanical input via, leading to AKT activation (Nho et al., 2005), a pathway that links to downstream processes regulated by canonical Wnt/catenin.

Connexins

Connexins are membrane-spanning proteins that form regulated channels that allow the direct exchange of small molecules with adjacent cells resulting in intercellular communication between cells. Intercellular communication via gap junctions has been suggested to be central to the transmission of information about the mechanical environment of a given cell and ultimately allowing a sensing cell to elicit a change in behavior at an actor cell some distance removed from the mechanosensing event (Yellowley et al., 2000). Interconnected cells have also been proposed to form a cellular network that can exhibit an enhanced sensitivity to biophysical stimuli than occur in individual cells. This application might occur owing to the larger area occupied by a cell network, and therefore larger net effect of the biophysical signal than by individual cells. Indeed, when the communication of an ensemble of cells is interrupted, a reduced sensitivity has been observed in response to biophysical signals such as electric fields (Vander Molen et al., 2000) or fluid flow (Saunders et al., 2001). In addition, mechanical signals may increase the expression of connexins in vitro and in vivo, increasing the gap junction intracellular communication and becoming better connected with their neighbors, perhaps acting as a sort of positive feedback loop (Alford et al., 2003; Uzer et al., 2014). Fluid shear stress has been shown to result in opening and phosphorylation of connexin 43 in osteocytic cells, following increased level of active AKT (Batra et al., 2014).

Channels

Alterations in ion channel activity in osteoblasts have been associated with bone cell activation, whether through alteration in conductance stimulated by parathyroid hormone (Ferrier et al., 1986) or by stretch/strain (Duncan et al., 1992). There are at least three classes of mechanosensitive ion channels in human osteoblasts (Davidson et al., 1990). Through this set of channels, a mechanical stimulus could induce membrane hyper- and depolarization or a complex multiphasic response. Cyclical strain has been shown to modulate the activity of certain channels: chronically strained osteoblasts had significantly larger increases in whole-cell conductance when subjected to additional mechanical strain than unstrained controls (Duncan and Hruska, 1994). More recently, radial membrane strains of 800% were shown to be necessary to open half of the mechanosensitive channels in bone cells (Charras et al., 2004). Mechanosensitive channels have also been implicated in the response of bone cells to fluid shear stress (Ryder and Duncan, 2001). In addition to direct activation of intracellular signaling cascades, influx of a charged species such as calcium can also alter membrane potential and activate voltage-sensitive channels that are not directly mechanosensitive (Li et al., 2002). Studies have identified activation of piezo-type mechanosensitive ion channel component 1 as a driving factor for enhanced osteoblastogenesis and suppressed osteoclastogenesis in human periodontal ligament cells and suppressed adipogenesis in MSCs when the cells are subjected to compressive loading or hydrostatic pressure, respectively (Sugimoto et al., 2017; Jin et al., 2015). Further studies are needed to identify the exact channel(s) in different types of cells that responds to external mechanical cues.

Membrane structure

Cells possess a complex organizational structure that supports compartmentalization of signals within an equally complex plasma membrane. Certain proteins are integral to membrane structure while creating docking positions for signaling complexes. Caveolins 1 and 2 have been described in human fetal osteoblasts and in murine MC3T3-E1 cells along with multiple caveolar flasks in the membrane (Solomon et al., 2000) and in osteoblasts in adult bone (Lofthouse et al., 2001). Bone cell caveolae are associated with important signaling molecules, including G proteins, Ras, nitric oxide synthase (NOS), and tyrosine kinases. These membrane domains, whether caveolae or noncaveolar lipid rafts, provide a microenvironment that modulates efficiency and fidelity of mechanical signal transduction.

The organized membrane may have greater significance for mechanical response than for parsing signals arising from liganded receptors. Noncaveolar and caveolar organized membranes have been shown to be critical for mechanically induced signals in a variety of cells. In the vascular endothelium, for instance, increased flow causes the translocation of

signaling molecules to caveolae; if caveolae are disassembled, both proximal and downstream signaling events, including activation of the MAPK pathway, are abrogated (Rizzo et al., 1998). Stretch activation of small GTPases in cardiac myocytes has, as well, been associated with caveolae: the stretch activation of the guanine nucleotide exchange factors (GEFs) RhoA and Rac1 fails to occur when caveolae are disrupted by treatment with methyl-β-cyclodextrin (Kawamura et al., 2003).

The role of caveolae in processing signals in bone is being studied: caveolin-1-null mice have bigger bones, perhaps resulting from accelerated development (Rubin et al., 2007b). The accumulation of β-catenin, following mechanical stimulation, has been shown to be dependent on the cross talk between caveolin-1 and ERK, emphasizing the interaction between caveolin-1/ERK and Wnt/β-catenin signaling pathways in transducing mechanical cues for osteocytic survival and bone formation (Bilic et al., 2007; Case et al., 2008; Gortazar et al., 2013).

Primary cilium

Another potential avenue for mechanical signal transduction has arisen with the reevaluation of the role of the primary cilium, a microtubule-based structure extending from almost every mammalian cell studied. The primary cilium has been known to function as a sensory organelle, but is now recognized as receiving both mechanical and chemical signals from the environment (Michaud and Yoder, 2006). Epithelial cells in the kidney have been shown to recognize fluid shear stress in the lumen of the nephron through their primary cilium, and mutations leading to abnormal cilia, such as are found in polycystic kidney disease, lead to gross abnormalities in function (Nauli and Zhou, 2004). Indeed, when ciliary polycystin-1 is knocked out, in addition to developing polycystic kidney disease, mice have delayed endochondral and intramembranous bone formation (Xiao et al., 2006). Further, interesting data have shown that bone cell primary cilia translate fluid flow into calcium signals (Malone et al., 2007b).

Nuclear connectivity

Considering a means of translating mechanical information to the nucleus, studies suggest that the MSC response to low-level mechanical stimulation is dependent on cytoskeletal remodeling, rather than fluid-induced shear stress, as evident by enhanced cell proliferation and mineralization following actin remodeling (Uzer et al., 2012, 2013). Specifically, cell mechanosensitivity is enabled by mechanical coupling between the nucleus and the cytoskeleton through LINC complexes. When LINC complexes were disrupted, cells' response to low-level mechanical stimulation diminished. Interestingly, cells' response to high-magnitude mechanical stimulation did not alter when LINC complexes were disrupted, suggesting LINC as a novel and specific mechanism for cells' response to low-level mechanical stimulation (Uzer et al., 2015). The role of LINC complexes in controlling the sensitivity of cells to mechanical cues is further demonstrated in enucleated cells that showed lower contractile energy and lower traction tress values when the LINC complexes were disrupted in the cells (Graham et al., 2018).

Mechanically activated intracellular signaling

Application of mechanical force to bone cells causes modulation of cell function, including changes in proliferation and function. Indeed, most aspects of cell behavior can be elucidated by a number of mechanical forces. Thus, straining osteoprogenitor cells can cause them to proliferate (Zhuang et al., 1996) and to secrete extracellular matrix (Harter et al., 1995). Similarly, shear stress, in addition to strain-induced effects, can induce β-catenin signaling (Norvell et al., 2004) and secretion of osteopontin (You et al., 2001). To achieve these ends, it is quite clear that multiple classical signaling pathways are activated after force application.

Because the distal responses to mechanical factors are similar to those elicited by ligand−receptor pairing, and result in changes in gene expression, mechanotransduction must eventually end up utilizing similar intracellular signaling cascades. In essence, mechanical forces have been shown to activate every type of signal transduction cascade, from increases in intracellular cAMP (Lavandero et al., 1993) to inositol trisphosphate and intracellular calcium, guanine regulatory proteins (Gudi et al., 2003), and MAPK (Waterman et al., 2002). Next, rather than reviewing each mechanosignaling cascade, we provide four examples.

MAPK signaling

Mechanical force can activate MAPK in every cell type studied to date. In bone cells many groups have shown activation of ERK1/2, in particular. Mechanical activation of ERK1/2 is required for certain measurable responses to strain in bone

stromal and osteoblast-like cells. The strained bone cell downregulates its expression of RANKL, and upregulates expression of endothelial NOS. Although strain also activates c-jun kinase (JNK), JNK inhibition does not prevent strain effects on either RANKL or endothelial NOS. Reduced display of RANKL by cells present in bone diminishes the local osteoclastogenic potential. As a result of increased endothelial NOS expression, nitric oxide synthesis is enhanced.

ERK1/2 activation by mechanical stress has been linked to other specific genes, such as strain induction of collagenase-3 (Yang et al., 2004), as well as to proliferation. Both FosB and its spliced variant, ΔFosB, which has been shown to stimulate increases in bone density in vivo, are induced by mechanical loading of the mouse hindlimb and by fluid shear stress in mouse calvarial osteoblasts (Inoue et al., 2004). The ERK1/2-dependent increase in the fos gene targets a CRE/AP-1 type element in the promoter that binds CREB. The proximal events leading to ERK1/2 activation are the subject of much continued research. This may certainly involve integrins (Whedon, 1984) as well as multiple other effectors, including small GEFs (Jin et al., 2005) or changes in membrane structure (Boyd et al., 2003).

MAPK has been also shown to play a role in adipogenic differentiation of multipotent stromal cells during low-magnitude high-frequency vibration (15 min/day, 40 Hz, 0.3*g*). Under the influence of adipogenic medium and vibration, phosphorylation of p38 MAPK was enhanced, leading to increased secretion of PPARγ, C/EBPα, and adiponectin, and increased number of oil droplets. The adipogenic differentiation of stromal cells was inhibited when p38 inhibitor was added to the cells (Zhao et al., 2017). Interestingly, in the absence of adipogenic medium, vibration has been shown to promote osteogenic differentiation in MSCs in vitro as evident by increased alkaline phosphatase activity, matrix mineralization, and osteogenic gene expression (Runx2, collagen type I, alkaline phosphatase, osteocalcin, and osteopontin). Vibration-mediated increase in osteogenic differentiation is driven by phosphorylation of p38 MAPK, and inhibition of p38 MAPK leads to reduction in alkaline phosphatase activity and osteogenic gene expression (Lu et al., 2018).

Activation of Wnt/catenin signals

Increased expression of Wnt/β-catenin target genes is another response of osteoblasts to mechanical loading (Robinson et al., 2006). Multiple known genes with catenin response elements are quickly transcribed when strain is applied to osteoblast cells in culture, or when bone cells are studied after whole-animal loading; these are probably related to the anabolic response of bone tissue to exercise. Increased canonical β-catenin signaling through a gain-of-function mutation in low-density lipoprotein−related protein 5 (G171V) has further been shown to increase the response of osteoblasts to mechanical loading (Sawakami et al., 2006). The Wnt/β-catenin signaling pathway also plays a role in bone marrow MSC adhesion and osteogenic differentiation on a hydroxyapatite-coated surface, as evident by increased alkaline phosphatase activity and osteogenic gene expression, following low-level vibration (Chen et al., 2016).

β-Catenin regulation in the cytoplasm has been well studied, but its nuclear trafficking and function are not yet well studied. A 2018 study suggests that inactivation of glycogen synthase kinase-3β leads to β-catenin association with the nucleoskeleton following low-level vibration or substrate strain. However, concurrently depleting LINC complex elements (SUN1 and SUN2) leads to reduced nucleoskeleton association and nuclear entry of β-catenin, suggesting that nucleus access of β-catenin is one of the mechanisms through which mechanical signals are transmitted by the cytoskeleton to the nuclear surface (Uzer et al., 2018). Mechanical activation of catenin signaling, of crucial importance to osteoprogenitor proliferation and lineage selection, will continue to be of great interest to this field.

Nitric oxide signaling

Nitric oxide has pleiotropic effects on bone cells (Ralston, 1997), and may have a role in mechanical signaling in bone. Nitric oxide is released shortly after shear stress from osteoblasts and osteocytes (Smalt et al., 1997) probably owing to activation of endothelial NOS (Klein et al., 2004), similar to known effects of shear in vascular cells. The rapid activation of nitric oxide in endothelial cells requires, in part, an intact plasma membrane, including lipid rafts (Park et al., 1998) and cytoskeleton (Knudsen and Frangos, 1997), and this is likely to be true for the mechanical release of nitric oxide in bone cells.

Endothelial NOS is the predominant NOS isoform in adult bone (Helfrich et al., 1997), and expression of this gene with subsequent increase in nitric oxide production is upregulated by strain in marrow stromal cells. Nitric oxide has also been independently shown to induce osteogenic differentiation in osteoprogenitor cells in the absence of osteogenic growth factors (Mostafa et al., 2015). Downstream nitric oxide signaling can depend on activation of guanylate cyclase or on direct actions of the molecule to nitrosylate proteins as has been shown for nitric oxide action to decrease the RANKL/osteoprotegerin ratio in stromal cells (Fan et al., 2004). Nitric oxide has also been shown to be necessary for the response to

in vivo loading in rodents, although whether the nitric oxide derives from bone or the vasculature in bone is not yet clear (Kunnel et al., 2004).

Prostaglandins

In bone's anabolic response to loading, prostaglandins may be important as indicated by their increased levels during loading (Rawlinson et al., 1991). Indeed, a variety of mechanical signals, including direct stretch (Zaman et al., 1997), pressure (Burger et al., 1992), and fluid flow (Klein-Nulend et al., 1997), can markedly upregulate prostaglandin production, whereas the disruption of the osteocyte cytoskeleton, and thus the transmission of the signal to the nucleus, completely disrupts the responsiveness of the cell (Ajubi et al., 1996). Although greater detail of the mechanism of action of prostaglandins is provided elsewhere in this book, it is important to note that administration of prostaglandin E_2 to rodents will increase the stiffness of trabecular bone (Akhter et al., 2001), and that perhaps the EP2 receptor is most important in coordinating the prostaglandin response to mechanical signals into improved bone strength. Indeed, strain-induced upregulation of osteocalcin has been shown to be mediated by the EP2 receptor, whereas strain-induced downregulation of sclerostin, which is a potent inhibitor of bone formation, has been shown to be mediated by the EP4 receptor (Galea et al., 2011). Considering the role of prostaglandins as potent regulators of bone remodeling (Raisz, 1995), and their responsiveness to both mechanical and humoral signals, it will ultimately be important to more definitively understand the physiological responses of the skeleton to exercise and mechanical signals and the role of biochemical messengers such as prostaglandins that can modulate bone quantity and quality.

Summary

The critical contribution of exercise in general, and mechanical stimuli in particular, to the achievement and maintenance of bone quantity and quality is clear. In contrast to systemic, pharmaceutical interventions, the attributes of such mechanical strategies are that they are native to the bone tissue, are safe at low intensities, incorporate all aspects of the remodeling cycle, and will ultimately suppress osteopenia. Further, these signals appear to influence tissues beyond "simply" bone, with evidence that they can help retain musculature and postural stability, thus providing a more "systems-based" intervention for osteoporosis. However, the design and widespread use of effective and clinically acceptable exercise prophylaxes and treatments that are based on bone's sensitivity to mechanical stimuli will be delayed until we achieve a better understanding of the operative mechanisms at the levels of the tissue, cell, and gene. Until that time, it is safe to conclude that you should get up and run around your office a few times, to stimulate your brain and your skeleton.

Acknowledgments

This work has been supported by grants from the National Institutes of Health, National Aeronautics and Space Administration, US Army, and National Science Foundation. We are grateful for the many contributions made by our colleagues.

References

Ajubi, N.E., Klein-Nulend, J., Nijweide, P.J., Vrijheid-Lammers, T., Alblas, M.J., Burger, E.H., 1996. 'Pulsating fluid flow increases prostaglandin production by cultured chicken osteocytes—a cytoskeleton-dependent process. Biochem. Biophys. Res. Commun. 225 (1), 62–68.

Akhter, M.P., Cullen, D.M., Gong, G., Recker, R.R., 2001. Bone biomechanical properties in prostaglandin EP1 and EP2 knockout mice. Bone 29 (2), 121–125.

Alford, A.I., Jacobs, C.R., Donahue, H.J., 2003. 'Oscillating fluid flow regulates gap junction communication in osteocytic MLO-Y4 cells by an ERK1/2 MAP kinase-dependent mechanism. Bone 33 (1), 64–70.

Armbrecht, G., Belavy, D.L., Gast, U., Bongrazio, M., Touby, F., Beller, G., Roth, H.J., Perschel, F.H., Rittweger, J., Felsenberg, D., 2010. 'Resistive vibration exercise attenuates bone and muscle atrophy in 56 days of bed rest: biochemical markers of bone metabolism. Osteoporos. Int. 21 (4), 597–607.

Bancroft, G.N., Sikavitsas, V.I., van den Dolder, J., Sheffield, T.L., Ambrose, C.G., Jansen, J.A., Mikos, A.G., 2002. 'Fluid flow increases mineralized matrix deposition in 3D perfusion culture of marrow stromal osteoblasts in a dose-dependent manner. Proc. Natl. Acad. Sci. U. S. A. 99 (20), 12600–12605.

Baskan, O., Mese, G., Ozcivici, E., 2017. 'Low-intensity vibrations normalize adipogenesis-induced morphological and molecular changes of adult mesenchymal stem cells. Proc. Inst. Mech. Eng. H 231 (2), 160–168.

Bassett, C.A., 1968. Biologic significance of piezoelectricity. Calcif. Tissue Res. 1 (4), 252–272.

Batra, N., Riquelme, M.A., Burra, S., Kar, R., Gu, S., Jiang, J.X., 2014. Direct regulation of osteocytic connexin 43 hemichannels through AKT kinase activated by mechanical stimulation. J. Biol. Chem. 289 (15), 10582–10591.

Beck, B.R., Norling, T.L., 2010. The effect of 8 mos of twice-weekly low- or higher intensity whole body vibration on risk factors for postmenopausal hip fracture. Am. J. Phys. Med. Rehabil. 89 (12), 997–1009.

Bennett, J.H., Carter, D.H., Alavi, A.L., Beresford, J.N., Walsh, S., 2001. Patterns of integrin expression in a human mandibular explant model of osteoblast differentiation. Arch. Oral Biol. 46 (3), 229–238.

Berk, B.C., Corson, M.A., Peterson, T.E., Tseng, H., 1995. Protein kinases as mediators of fluid shear stress stimulated signal transduction in endothelial cells: a hypothesis for calcium-dependent and calcium-independent events activated by flow. J. Biomech. 28 (12), 1439–1450.

Bilic, J., Huang, Y.L., Davidson, G., Zimmermann, T., Cruciat, C.M., Bienz, M., Niehrs, C., 2007. Wnt induces LRP6 signalosomes and promotes dishevelled-dependent LRP6 phosphorylation. Science 316 (5831), 1619–1622.

Bonewald, L.F., 2011. The amazing osteocyte. J. Bone Miner. Res. 26 (2), 229–238.

Bonewald, L.F., Johnson, M.L., 2008. Osteocytes, mechanosensing and Wnt signaling. Bone 42 (4), 606–615.

Boo, Y.C., Jo, H., 2003. Flow-dependent regulation of endothelial nitric oxide synthase: role of protein kinases. Am. J. Physiol. Cell Physiol. 285 (3), C499–C508.

Boutahar, N., Guignandon, A., Vico, L., Lafage-Proust, M.H., 2004. Mechanical strain on osteoblasts activates autophosphorylation of focal adhesion kinase and proline-rich tyrosine kinase 2 tyrosine sites involved in ERK activation. J. Biol. Chem. 279 (29), 30588–30599.

Boyd, N.L., Park, H., Yi, H., Boo, Y.C., Sorescu, G.P., Sykes, M., Jo, H., 2003. Chronic shear induces caveolae formation and alters ERK and Akt responses in endothelial cells. Am. J. Physiol. Heart Circ. Physiol. 285 (3), H1113–H1122.

Burger, E.H., Klein-Nulend, J., Veldhuijzen, J.P., 1992. Mechanical stress and osteogenesis in vitro. J. Bone Miner. Res. 7 (Suppl. 2), S397–S401.

Burr, D.B., Milgrom, C., Fyhrie, D., Forwood, M., Nyska, M., Finestone, A., Hoshaw, S., Saiag, E., Simkin, A., 1996. In vivo measurement of human tibial strains during vigorous activity. Bone 18 (5), 405–410.

Butezloff, M.M., Zamarioli, A., Leoni, G.B., Sousa-Neto, M.D., Volpon, J.B., 2015. Whole-body vibration improves fracture healing and bone quality in rats with ovariectomy-induced osteoporosis. Acta Cir. Bras. 30 (11), 727–735.

Case, N., Ma, M., Sen, B., Xie, Z., Gross, T.S., Rubin, J., 2008. Beta-catenin levels influence rapid mechanical responses in osteoblasts. J. Biol. Chem. 283 (43), 29196–29205.

Charras, G.T., Williams, B.A., Sims, S.M., Horton, M.A., 2004. Estimating the sensitivity of mechanosensitive ion channels to membrane strain and tension. Biophys. J. 87 (4), 2870–2884.

Chen, B., Lin, T., Yang, X., Li, Y., Xie, D., Zheng, W., Cui, H., Deng, W., Tan, X., 2016. Low-magnitude, high-frequency vibration promotes the adhesion and the osteogenic differentiation of bone marrow-derived mesenchymal stem cells cultured on a hydroxyapatite-coated surface: the direct role of Wnt/beta-catenin signaling pathway activation. Int. J. Mol. Med. 38 (5), 1531–1540.

Cherian, P.P., Cheng, B., Gu, S., Sprague, E., Bonewald, L.F., Jiang, J.X., 2003. Effects of mechanical strain on the function of Gap junctions in osteocytes are mediated through the prostaglandin EP2 receptor. J. Biol. Chem. 278 (44), 43146–43156.

Cherian, P.P., Siller-Jackson, A.J., Gu, S., Wang, X., Bonewald, L.F., Sprague, E., Jiang, J.X., 2005. Mechanical strain opens connexin 43 hemichannels in osteocytes: a novel mechanism for the release of prostaglandin. Mol. Biol. Cell 16 (7), 3100–3106.

David, V., Martin, A., Lafage-Proust, M.H., Malaval, L., Peyroche, S., Jones, D.B., Vico, L., Guignandon, A., 2007. Mechanical loading down-regulates peroxisome proliferator-activated receptor gamma in bone marrow stromal cells and favors osteoblastogenesis at the expense of adipogenesis. Endocrinology 148 (5), 2553–2562.

Davidson, R.M., Tatakis, D.W., Auerbach, A.L., 1990. Multiple forms of mechanosensitive ion channels in osteoblast-like cells. Pflugers Arch 416 (6), 646–651.

Deng, H.W., Lai, D.B., Conway, T., Li, J., Xu, F.H., Davies, K.M., Recker, R.R., 2001. Characterization of genetic and lifestyle factors for determining variation in body mass index, fat mass, percentage of fat mass, and lean mass. J. Clin. Densitom. 4 (4), 353–361.

Donahue, H.J., McLeod, K.J., Rubin, C.T., Andersen, J., Grine, E.A., Hertzberg, E.L., Brink, P.R., 1995. Cell-to-cell communication in osteoblastic networks: cell line-dependent hormonal regulation of gap junction function. J. Bone Miner. Res. 10 (6), 881–889.

Duncan, R.L., Hruska, K.A., 1994. Chronic, intermittent loading alters mechanosensitive channel characteristics in osteoblast-like cells. Am. J. Physiol. 267 (6 Pt 2), F909–F916.

Duncan, R.L., Hruska, K.A., Misler, S., 1992. Parathyroid hormone activation of stretch-activated cation channels in osteosarcoma cells (UMR-106.01). FEBS Lett. 307 (2), 219–223.

Fan, X., Roy, E., Zhu, L., Murphy, T.C., Ackert-Bicknell, C., Hart, C.M., Rosen, C., Nanes, M.S., Rubin, J., 2004. Nitric oxide regulates receptor activator of nuclear factor-kappaB ligand and osteoprotegerin expression in bone marrow stromal cells. Endocrinology 145 (2), 751–759.

Ferrier, J., Ward, A., Kanehisa, J., Heersche, J.N., 1986. Electrophysiological responses of osteoclasts to hormones. J. Cell. Physiol. 128 (1), 23–26.

Flieger, J., Karachalios, T., Khaldi, L., Raptou, P., Lyritis, G., 1998. Mechanical stimulation in the form of vibration prevents postmenopausal bone loss in ovariectomized rats. Calcif. Tissue Int. 63 (6), 510–514.

Frechette, D.M., Krishnamoorthy, D., Adler, B.J., Chan, M.E., Rubin, C.T., 2015. Diminished satellite cells and elevated adipogenic gene expression in muscle as caused by ovariectomy are averted by low-magnitude mechanical signals. J. Appl. Physiol. (1985) 119 (1), 27–36.

Fritton, S.P., McLeod, K.J., Rubin, C.T., 2000. Quantifying the strain history of bone: spatial uniformity and self-similarity of low-magnitude strains. J. Biomech. 33 (3), 317–325.

Frost, H.M., 1987. The mechanostat: a proposed pathogenic mechanism of osteoporoses and the bone mass effects of mechanical and nonmechanical agents. Bone Miner. 2 (2), 73–85.

Fyhrie, D.P., Carter, D.R., 1986. A unifying principle relating stress to trabecular bone morphology. J. Orthop. Res. 4 (3), 304–317.

Gabel, L., Macdonald, H.M., Nettlefold, L., McKay, H.A., 2017. Physical activity, sedentary time, and bone strength from childhood to early adulthood: a mixed longitudinal HR-pQCT study. J. Bone Miner. Res. 32 (7), 1525–1536.

Galea, G.L., Sunters, A., Meakin, L.B., Zaman, G., Sugiyama, T., Lanyon, L.E., Price, J.S., 2011. Sost down-regulation by mechanical strain in human osteoblastic cells involves PGE2 signaling via EP4. FEBS Lett. 585 (15), 2450–2454.

Garman, R., Gaudette, G., Donahue, L.R., Rubin, C., Judex, S., 2007a. Low-level accelerations applied in the absence of weight bearing can enhance trabecular bone formation. J. Orthop. Res. 25 (6), 732–740.

Garman, R., Rubin, C., Judex, S., 2007b. Small oscillatory accelerations, independent of matrix deformations, increase osteoblast activity and enhance bone morphology. PLoS One 2 (7), e653.

Gilsanz, V., Wren, T.A., Sanchez, M., Dorey, F., Judex, S., Rubin, C., 2006. Low-level, high-frequency mechanical signals enhance musculoskeletal development of young women with low BMD. J. Bone Miner. Res. 21 (9), 1464–1474.

Gluhak-Heinrich, J., Ye, L., Bonewald, L.F., Feng, J.Q., MacDougall, M., Harris, S.E., Pavlin, D., 2003. Mechanical loading stimulates dentin matrix protein 1 (DMP1) expression in osteocytes in vivo. J. Bone Miner. Res. 18 (5), 807–817.

Gortazar, A.R., Martin-Millan, M., Bravo, B., Plotkin, L.I., Bellido, T., 2013. Crosstalk between caveolin-1/extracellular signal-regulated kinase (ERK) and beta-catenin survival pathways in osteocyte mechanotransduction. J. Biol. Chem. 288 (12), 8168–8175.

Graham, D.M., Andersen, T., Sharek, L., Uzer, G., Rothenberg, K., Hoffman, B.D., Rubin, J., Balland, M., Bear, J.E., Burridge, K., 2018. Enucleated cells reveal differential roles of the nucleus in cell migration, polarity, and mechanotransduction. J. Cell Biol. 217 (3), 895–914.

Gravelle, D.C., Laughton, C.A., Dhruv, N.T., Katdare, K.D., Niemi, J.B., Lipsitz, L.A., Collins, J.J., 2002. Noise-enhanced balance control in older adults. Neuroreport 13 (15), 1853–1856.

Gross, T.S., Edwards, J.L., McLeod, K.J., Rubin, C.T., 1997. Strain gradients correlate with sites of periosteal bone formation. J. Bone Miner. Res. 12 (6), 982–988.

Gross, T.S., King, K.A., Rabaia, N.A., Pathare, P., Srinivasan, S., 2005. Upregulation of osteopontin by osteocytes deprived of mechanical loading or oxygen. J. Bone Miner. Res. 20 (2), 250–256.

Gross, T.S., McLeod, K.J., Rubin, C.T., 1992. Characterizing bone strain distributions in vivo using three triple rosette strain gages. J. Biomech. 25 (9), 1081–1087.

Gross, T.S., Poliachik, S.L., Ausk, B.J., Sanford, D.A., Becker, B.A., Srinivasan, S., 2004. Why rest stimulates bone formation: a hypothesis based on complex adaptive phenomenon. Exerc. Sport Sci. Rev. 32 (1), 9–13.

Gross, T.S., Rubin, C.T., 1995. Uniformity of resorptive bone loss induced by disuse. J. Orthop. Res. 13 (5), 708–714.

Gudi, S., Huvar, I., White, C.R., McKnight, N.L., Dusserre, N., Boss, G.R., Frangos, J.A., 2003. Rapid activation of Ras by fluid flow is mediated by Galpha(q) and Gbetagamma subunits of heterotrimeric G proteins in human endothelial cells. Arterioscler. Thromb. Vasc. Biol. 23 (6), 994–1000.

Han, Y., Cowin, S.C., Schaffler, M.B., Weinbaum, S., 2004. Mechanotransduction and strain amplification in osteocyte cell processes. Proc. Natl. Acad. Sci. U. S. A. 101 (47), 16689–16694.

Harter, L.V., Hruska, K.A., Duncan, R.L., 1995. Human osteoblast-like cells respond to mechanical strain with increased bone matrix protein production independent of hormonal regulation. Endocrinology 136 (2), 528–535.

Heinonen, A., Oja, P., Kannus, P., Sievanen, H., Haapasalo, H., Manttari, A., Vuori, I., 1995. Bone mineral density in female athletes representing sports with different loading characteristics of the skeleton. Bone 17 (3), 197–203.

Helfrich, M.H., Evans, D.E., Grabowski, P.S., Pollock, J.S., Ohshima, H., Ralston, S.H., 1997. Expression of nitric oxide synthase isoforms in bone and bone cell cultures. J. Bone Miner. Res. 12 (7), 1108–1115.

Huang, R.P., Rubin, C.T., McLeod, K.J., 1999. Changes in postural muscle dynamics as a function of age. J. Gerontol., Ser. A 54 (8), B352–B357.

Inaoka, T., Lean, J.M., Bessho, T., Chow, J.W., Mackay, A., Kokubo, T., Chambers, T.J., 1995. Sequential analysis of gene expression after an osteogenic stimulus: c-fos expression is induced in osteocytes. Biochem. Biophys. Res. Commun. 217 (1), 264–270.

Inoue, D., Kido, S., Matsumoto, T., 2004. Transcriptional induction of FosB/DeltaFosB gene by mechanical stress in osteoblasts. J. Biol. Chem. 279 (48), 49795–49803.

Ishihara, Y., Sugawara, Y., Kamioka, H., Kawanabe, N., Hayano, S., Balam, T.A., Naruse, K., Yamashiro, T., 2013. Ex vivo real-time observation of Ca(2+) signaling in living bone in response to shear stress applied on the bone surface. Bone 53 (1), 204–215.

Jin, Y., Li, J., Wang, Y., Ye, R., Feng, X., Jing, Z., Zhao, Z., 2015. Functional role of mechanosensitive ion channel Piezo1 in human periodontal ligament cells. Angle Orthod. 85 (1), 87–94.

Jin, Z.G., Wong, C., Wu, J., Berk, B.C., 2005. Flow shear stress stimulates Gab1 tyrosine phosphorylation to mediate protein kinase B and endothelial nitric-oxide synthase activation in endothelial cells. J. Biol. Chem. 280 (13), 12305–12309.

Jones, H.H., Priest, J.D., Hayes, W.C., Tichenor, C.C., Nagel, D.A., 1977. Humeral hypertrophy in response to exercise. J. Bone Joint Surg. Am. 59 (2), 204–208.

Jorgensen, N.R., Henriksen, Z., Brot, C., Eriksen, E.F., Sorensen, O.H., Civitelli, R., Steinberg, T.H., 2000. Human osteoblastic cells propagate intercellular calcium signals by two different mechanisms. J. Bone Miner. Res. 15 (6), 1024–1032.

Judex, S., Boyd, S., Qin, Y.X., Turner, S., Ye, K., Muller, R., Rubin, C., 2003. Adaptations of trabecular bone to low magnitude vibrations result in more uniform stress and strain under load. Ann. Biomed. Eng. 31 (1), 12–20.

Judex, S., Donahue, L.R., Rubin, C., 2002. Genetic predisposition to low bone mass is paralleled by an enhanced sensitivity to signals anabolic to the skeleton. FASEB J. 16 (10), 1280–1282.

Judex, S., Garman, R., Squire, M., Busa, B., Donahue, L.R., Rubin, C., 2004. Genetically linked site-specificity of disuse osteoporosis. J. Bone Miner. Res. 19 (4), 607–613.

Judex, S., Gross, T.S., Zernicke, R.F., 1997. Strain gradients correlate with sites of exercise-induced bone-forming surfaces in the adult skeleton. J. Bone Miner. Res. 12 (10), 1737–1745.

Judex, S., Zernicke, R.F., 2000a. Does the mechanical milieu associated with high-speed running lead to adaptive changes in diaphyseal growing bone? Bone 26 (2), 153–159.

Judex, S., Zernicke, R.F., 2000b. High-impact exercise and growing bone: relation between high strain rates and enhanced bone formation. J. Appl. Physiol. (1985) 88 (6), 2183–2191.

Kapur, S., Baylink, D.J., Lau, K.H., 2003. Fluid flow shear stress stimulates human osteoblast proliferation and differentiation through multiple interacting and competing signal transduction pathways. Bone 32 (3), 241–251.

Katsumi, A., Orr, A.W., Tzima, E., Schwartz, M.A., 2004. Integrins in mechanotransduction. J. Biol. Chem. 279 (13), 12001–12004.

Kawamura, S., Miyamoto, S., Brown, J.H., 2003. Initiation and transduction of stretch-induced RhoA and Rac1 activation through caveolae: cytoskeletal regulation of ERK translocation. J. Biol. Chem. 278 (33), 31111–31117.

Kelly, O.J., Gilman, J.C., 2017. Can unconventional exercise be helpful in the treatment, management and prevention of osteosarcopenic obesity? Curr. Aging Sci. 10 (2), 106–121.

Kiel, D.P., Hannan, M.T., Barton, B.A., Bouxsein, M.L., Sisson, E., Lang, T., Allaire, B., Dewkett, D., Carroll, D., Magaziner, J., Shane, E., Leary, E.T., Zimmerman, S., Rubin, C.T., 2015. Low-magnitude mechanical stimulation to improve bone density in persons of advanced age: a randomized, placebo-controlled trial. J. Bone Miner. Res. 30 (7), 1319–1328.

Klein-Nulend, J., Burger, E.H., Semeins, C.M., Raisz, L.G., Pilbeam, C.C., 1997. Pulsating fluid flow stimulates prostaglandin release and inducible prostaglandin G/H synthase mRNA expression in primary mouse bone cells. J. Bone Miner. Res. 12 (1), 45–51.

Klein, R.F., Allard, J., Avnur, Z., Nikolcheva, T., Rotstein, D., Carlos, A.S., Shea, M., Waters, R.V., Belknap, J.K., Peltz, G., Orwoll, E.S., 2004. Regulation of bone mass in mice by the lipoxygenase gene Alox15. Science 303 (5655), 229–232.

Knudsen, H.L., Frangos, J.A., 1997. Role of cytoskeleton in shear stress-induced endothelial nitric oxide production. Am. J. Physiol. 273 (1 Pt 2), H347–H355.

Krishnamoorthy, D., Frechette, D.M., Adler, B.J., Green, D.E., Chan, M.E., Rubin, C.T., 2016. Marrow adipogenesis and bone loss that parallels estrogen deficiency is slowed by low-intensity mechanical signals. Osteoporos. Int. 27 (2), 747–756.

Krishnan, V., Bryant, H.U., MacDougald, O.A., 2006. Regulation of bone mass by Wnt signaling. J. Clin. Invest 116 (5), 1202–1209.

Kunnel, J.G., Igarashi, K., Gilbert, J.L., Stern, P.H., 2004. Bone anabolic responses to mechanical load in vitro involve COX-2 and constitutive NOS. Connect. Tissue Res. 45 (1), 40–49.

LaMothe, J.M., Hamilton, N.H., Zernicke, R.F., 2005. Strain rate influences periosteal adaptation in mature bone. Med. Eng. Phys. 27 (4), 277–284.

Lane, P., Gross, S.S., 1999. Cell signaling by nitric oxide. Semin. Nephrol. 19 (3), 215–229.

Lanyon, L.E., 1971. Strain in sheep lumbar vertebrae recorded during life. Acta Orthop. Scand. 42 (1), 102–112.

Lanyon, L.E., Goodship, A.E., Pye, C.J., MacFie, J.H., 1982. Mechanically adaptive bone remodelling. J. Biomech. 15 (3), 141–154.

Lanyon, L.E., Rubin, C.T., 1984. Static vs dynamic loads as an influence on bone remodelling. J. Biomech. 17 (12), 897–905.

Lau, E., Al-Dujaili, S., Guenther, A., Liu, D., Wang, L., You, L., 2010. Effect of low-magnitude, high-frequency vibration on osteocytes in the regulation of osteoclasts. Bone 46 (6), 1508–1515.

Lavandero, S., Cartagena, G., Guarda, E., Corbalan, R., Godoy, I., Sapag-Hagar, M., Jalil, J.E., 1993. Changes in cyclic AMP dependent protein kinase and active stiffness in the rat volume overload model of heart hypertrophy. Cardiovasc. Res. 27 (9), 1634–1638.

Lee, W.S., Cheung, W.H., Qin, L., Tang, N., Leung, K.S., 2006. Age-associated decrease of type IIA/B human skeletal muscle fibers. Clin. Orthop. Relat. Res. 450, 231–237.

Li, J., Duncan, R.L., Burr, D.B., Turner, C.H., 2002. L-type calcium channels mediate mechanically induced bone formation in vivo. J. Bone Miner. Res. 17 (10), 1795–1800.

Li, Y.J., Batra, N.N., You, L., Meier, S.C., Coe, I.A., Yellowley, C.E., Jacobs, C.R., 2004. Oscillatory fluid flow affects human marrow stromal cell proliferation and differentiation. J. Orthop. Res. 22 (6), 1283–1289.

Lofthouse, R.A., Davis, J.R., Frondoza, C.G., Jinnah, R.H., Hungerford, D.S., Hare, J.M., 2001. Identification of caveolae and detection of caveolin in normal human osteoblasts. J Bone Joint Surg. Br. 83 (1), 124–129.

Loro, M.L., Sayre, J., Roe, T.F., Goran, M.I., Kaufman, F.R., Gilsanz, V., 2000. Early identification of children predisposed to low peak bone mass and osteoporosis later in life. J. Clin. Endocrinol. Metab. 85 (10), 3908–3918.

Lu, Y., Zhao, Q., Liu, Y., Zhang, L., Li, D., Zhu, Z., Gan, X., Yu, H., 2018. Vibration loading promotes osteogenic differentiation of bone marrow-derived mesenchymal stem cells via p38 MAPK signaling pathway. J. Biomech. 71, 67–75.

Luu, Y.K., Capilla, E., Rosen, C.J., Gilsanz, V., Pessin, J.E., Judex, S., Rubin, C.T., 2009a. Mechanical stimulation of mesenchymal stem cell proliferation and differentiation promotes osteogenesis while preventing dietary-induced obesity. J. Bone Miner. Res. 24 (1), 50–61.

Luu, Y.K., Pessin, J.E., Judex, S., Rubin, J., Rubin, C.T., 2009b. Mechanical signals as a non-invasive means to influence mesenchymal stem cell fate, promoting bone and suppressing the fat phenotype. Bonekey Osteovision 6 (4), 132–149.

MacKelvie, K.J., Khan, K.M., Petit, M.A., Janssen, P.A., McKay, H.A., 2003. A school-based exercise intervention elicits substantial bone health benefits: a 2-year randomized controlled trial in girls. Pediatrics 112 (6 Pt 1), e447.

Malone, A.M., Anderson, C.T., Tummala, P., Kwon, R.Y., Johnston, T.R., Stearns, T., Jacobs, C.R., 2007b. Primary cilia mediate mechanosensing in bone cells by a calcium-independent mechanism. Proc. Natl. Acad. Sci. U. S. A. 104 (33), 13325–13330.

Malone, A.M., Batra, N.N., Shivaram, G., Kwon, R.Y., You, L., Kim, C.H., Rodriguez, J., Jair, K., Jacobs, C.R., 2007a. The role of actin cytoskeleton in oscillatory fluid flow-induced signaling in MC3T3-E1 osteoblasts. Am. J. Physiol. Cell Physiol. 292 (5), C1830–C1836.

Martin, R.B., Burr, D.B., Sharkey, N.A., Fyhrie, D.P., 2015. Skeletal Tissue Mechanics. Springer, New York.

Menuki, K., Mori, T., Sakai, A., Sakuma, M., Okimoto, N., Shimizu, Y., Kunugita, N., Nakamura, T., 2008. Climbing exercise enhances osteoblast differentiation and inhibits adipogenic differentiation with high expression of PTH/PTHrP receptor in bone marrow cells. Bone 43 (3), 613–620.

Michaud, E.J., Yoder, B.K., 2006. The primary cilium in cell signaling and cancer. Cancer Res. 66 (13), 6463–6467.

Mogil, R.J., Kaste, S.C., Ferry Jr., R.J., Hudson, M.M., Mulrooney, D.A., Howell, C.R., Partin, R.E., Srivastava, D.K., Robison, L.L., Ness, K.K., 2016. Effect of low-magnitude, high-frequency mechanical stimulation on BMD among young childhood cancer survivors: a randomized clinical trial. JAMA Oncol. 2 (7), 908–914.

Morgan, J.E., Partridge, T.A., 2003. Muscle satellite cells. Int. J. Biochem. Cell Biol. 35 (8), 1151–1156.

Morris, C.E., 1990. Mechanosensitive ion channels. J. Membr. Biol. 113 (2), 93–107.

Mostafa, E., Gayathri, S., Halim, A., Eda, Y.-A., 2015. Exogenous nitric oxide (NO) generated by NO-plasma treatment modulates osteoprogenitor cells early differentiation. J. Phys. D Appl. Phys. 48 (34), 345401.

Muir, J., Judex, S., Qin, Y.X., Rubin, C., 2011. Postural instability caused by extended bed rest is alleviated by brief daily exposure to low magnitude mechanical signals. Gait Posture 33 (3), 429–435.

Nauli, S.M., Zhou, J., 2004. Polycystins and mechanosensation in renal and nodal cilia. Bioessays 26 (8), 844–856.

Nho, R.S., Xia, H., Kahm, J., Kleidon, J., Diebold, D., Henke, C.A., 2005. Role of integrin-linked kinase in regulating phosphorylation of Akt and fibroblast survival in type I collagen matrices through a beta1 integrin viability signaling pathway. J. Biol. Chem. 280 (28), 26630–26639.

Nicolella, D.P., Moravits, D.E., Gale, A.M., Bonewald, L.F., Lankford, J., 2006. Osteocyte lacunae tissue strain in cortical bone. J. Biomech. 39 (9), 1735–1743.

Nilsson, J., Thorstensson, A., 1989. Ground reaction forces at different speeds of human walking and running. Acta Physiol. Scand. 136 (2), 217–227.

Nilsson, M., Sundh, D., Mellstrom, D., Lorentzon, M., 2017. Current physical activity is independently associated with cortical bone size and bone strength in elderly Swedish women. J. Bone Miner. Res. 32 (3), 473–485.

Norvell, S.M., Alvarez, M., Bidwell, J.P., Pavalko, F.M., 2004. Fluid shear stress induces beta-catenin signaling in osteoblasts. Calcif. Tissue Int. 75 (5), 396–404.

O'Connor, J.A., Lanyon, L.E., MacFie, H., 1982. The influence of strain rate on adaptive bone remodelling. J. Biomech. 15 (10), 767–781.

Ozcivici, E., Luu, Y.K., Adler, B., Qin, Y.X., Rubin, J., Judex, S., Rubin, C.T., 2010. Mechanical signals as anabolic agents in bone. Nat. Rev. Rheumatol. 6 (1), 50–59.

Pagnotti, G.M., Adler, B.J., Green, D.E., Chan, M.E., Frechette, D.M., Shroyer, K.R., Beamer, W.G., Rubin, J., Rubin, C.T., 2012. Low magnitude mechanical signals mitigate osteopenia without compromising longevity in an aged murine model of spontaneous granulosa cell ovarian cancer. Bone 51 (3), 570–577.

Pagnotti, G.M., Chan, M.E., Adler, B.J., Shroyer, K.R., Rubin, J., Bain, S.D., Rubin, C.T., 2016. Low intensity vibration mitigates tumor progression and protects bone quantity and quality in a murine model of myeloma. Bone 90, 69–79.

Park, H., Go, Y.M., St John, P.L., Maland, M.C., Lisanti, M.P., Abrahamson, D.R., Jo, H., 1998. Plasma membrane cholesterol is a key molecule in shear stress-dependent activation of extracellular signal-regulated kinase. J. Biol. Chem. 273 (48), 32304–32311.

Patel, M.J., Chang, K.H., Sykes, M.C., Talish, R., Rubin, C., Jo, H., 2009. Low magnitude and high frequency mechanical loading prevents decreased bone formation responses of 2T3 preosteoblasts. J. Cell. Biochem. 106 (2), 306–316.

Patel, V.S., Chan, M.E., Pagnotti, G.M., Frechette, D.M., Rubin, J., Rubin, C.T., 2017. Incorporating refractory period in mechanical stimulation mitigates obesity-induced adipose tissue dysfunction in adult mice. Obesity 25 (10), 1745–1753.

Pitukcheewanont, P., Safani, D., 2006. Extremely low-level, short-term mechanical stimulation increases cancellous and cortical bone density and muscle mass of children with low bone density: a pilot study. Endocrinololgist 16 (3), 128–132.

Plotkin, L.I., Mathov, I., Aguirre, J.I., Parfitt, A.M., Manolagas, S.C., Bellido, T., 2005. Mechanical stimulation prevents osteocyte apoptosis: requirement of integrins, Src kinases, and ERKs. Am. J. Physiol. Cell Physiol. 289 (3), C633–C643.

Pollack, S.R., Salzstein, R., Pienkowski, D., 1984. Streaming potentials in fluid-filled bone. Ferroelectrics 60 (1), 297–309.

Price, C., Zhou, X., Li, W., Wang, L., 2011. Real-time measurement of solute transport within the lacunar-canalicular system of mechanically loaded bone: direct evidence for load-induced fluid flow. J. Bone Miner. Res. 26 (2), 277–285.

Qin, Y.X., Kaplan, T., Saldanha, A., Rubin, C., 2003. Fluid pressure gradients, arising from oscillations in intramedullary pressure, is correlated with the formation of bone and inhibition of intracortical porosity. J. Biomech. 36 (10), 1427–1437.

Qin, Y.X., Rubin, C.T., McLeod, K.J., 1998. Nonlinear dependence of loading intensity and cycle number in the maintenance of bone mass and morphology. J. Orthop. Res. 16 (4), 482–489.

Raisz, L.G., 1995. Physiologic and pathologic roles of prostaglandins and other eicosanoids in bone metabolism. J. Nutr. 125 (7 Suppl. l), 2024s-27s.

Ralston, S.H., 1997. The michael mason prize essay 1997. Nitric oxide and bone: what a gas! Br. J. Rheumatol. 36 (8), 831–838.

Rawlinson, S.C., el-Haj, A.J., Minter, S.L., Tavares, I.A., Bennett, A., Lanyon, L.E., 1991. Loading-related increases in prostaglandin production in cores of adult canine cancellous bone in vitro: a role for prostacyclin in adaptive bone remodeling? J. Bone Miner. Res. 6 (12), 1345–1351.

Rezzonico, R., Cayatte, C., Bourget-Ponzio, I., Romey, G., Belhacene, N., Loubat, A., Rocchi, S., Van Obberghen, E., Girault, J.A., Rossi, B., Schmid-Antomarchi, H., 2003. 'Focal adhesion kinase pp125FAK interacts with the large conductance calcium-activated hSlo potassium channel in human osteoblasts: potential role in mechanotransduction. J. Bone Miner. Res. 18 (10), 1863–1871.

Rizzo, V., Sung, A., Oh, P., Schnitzer, J.E., 1998. Rapid mechanotransduction in situ at the luminal cell surface of vascular endothelium and its caveolae. J. Biol. Chem. 273 (41), 26323–26329.

Robinson, J.A., Chatterjee-Kishore, M., Yaworsky, P.J., Cullen, D.M., Zhao, W., Li, C., Kharode, Y., Sauter, L., Babij, P., Brown, E.L., Hill, A.A., Akhter, M.P., Johnson, M.L., Recker, R.R., Komm, B.S., Bex, F.J., 2006. Wnt/beta-catenin signaling is a normal physiological response to mechanical loading in bone. J. Biol. Chem. 281 (42), 31720−31728.

Robling, A.G., Hinant, F.M., Burr, D.B., Turner, C.H., 2002. Improved bone structure and strength after long-term mechanical loading is greatest if loading is separated into short bouts. J. Bone Miner. Res. 17 (8), 1545−1554.

Rubin, C., Gross, T., Qin, Y.X., Fritton, S., Guilak, F., McLeod, K., 1996. Differentiation of the bone-tissue remodeling response to axial and torsional loading in the Turkey ulna. J Bone Joint Surg. Am. 78 (10), 1523−1533.

Rubin, C., Recker, R., Cullen, D., Ryaby, J., McCabe, J., McLeod, K., 2004. Prevention of postmenopausal bone loss by a low-magnitude, high-frequency mechanical stimuli: a clinical trial assessing compliance, efficacy, and safety. J. Bone Miner. Res. 19 (3), 343−351.

Rubin, C., Turner, A.S., Bain, S., Mallinckrodt, C., McLeod, K., 2001a. Anabolism. Low mechanical signals strengthen long bones. Nature 412 (6847), 603−604.

Rubin, C., Turner, A.S., Mallinckrodt, C., Jerome, C., McLeod, K., Bain, S., 2002a. Mechanical strain, induced noninvasively in the high-frequency domain, is anabolic to cancellous bone, but not cortical bone. Bone 30 (3), 445−452.

Rubin, C., Turner, A.S., Muller, R., Mittra, E., McLeod, K., Lin, W., Qin, Y.X., 2002b. Quantity and quality of trabecular bone in the femur are enhanced by a strongly anabolic, noninvasive mechanical intervention. J. Bone Miner. Res. 17 (2), 349−357.

Rubin, C., Xu, G., Judex, S., 2001b. The anabolic activity of bone tissue, suppressed by disuse, is normalized by brief exposure to extremely low-magnitude mechanical stimuli. FASEB J. 15 (12), 2225−2229.

Rubin, C.T., Capilla, E., Luu, Y.K., Busa, B., Crawford, H., Nolan, D.J., Mittal, V., Rosen, C.J., Pessin, J.E., Judex, S., 2007a. Adipogenesis is inhibited by brief, daily exposure to high-frequency, extremely low-magnitude mechanical signals. Proc. Natl. Acad. Sci. U. S. A. 104 (45), 17879−17884.

Rubin, C.T., Lanyon, L.E., 1982. Limb mechanics as a function of speed and gait: a study of functional strains in the radius and tibia of horse and dog. J. Exp. Biol. 101, 187−211.

Rubin, C.T., Lanyon, L.E., 1984a. Regulation of bone formation by applied dynamic loads. J.Bone Joint Surg. Am. 66 (3), 397−402.

Rubin, C.T., Lanyon, L.E., 1984b. Dynamic strain similarity in vertebrates; an alternative to allometric limb bone scaling. J. Theor. Biol. 107 (2), 321−327.

Rubin, C.T., Lanyon, L.E., 1985. Regulation of bone mass by mechanical strain magnitude. Calcif. Tissue Int. 37 (4), 411−417.

Rubin, C.T., Lanyon, L.E., 1987. Kappa Delta Award paper. Osteoregulatory nature of mechanical stimuli: function as a determinant for adaptive remodeling in bone. J. Orthop. Res. 5 (2), 300−310.

Rubin, C.T., McLeod, K.J., Bain, S.D., 1990. Functional strains and cortical bone adaptation: epigenetic assurance of skeletal integrity. J. Biomech. 23 (Suppl. 1), 43−54.

Rubin, C.T., Seeherman, H., Qin, Y.X., Gross, T.S., 2013. The mechanical consequences of load bearing in the equine third metacarpal across speed and gait: the nonuniform distributions of normal strain, shear strain, and strain energy density. FASEB J. 27 (5), 1887−1894.

Rubin, J., Murphy, T., Nanes, M.S., Fan, X., 2000. Mechanical strain inhibits expression of osteoclast differentiation factor by murine stromal cells. Am. J. Physiol. Cell Physiol. 278 (6), C1126−C1132.

Rubin, J., Murphy, T.C., Zhu, L., Roy, E., Nanes, M.S., Fan, X., 2003. Mechanical strain differentially regulates endothelial nitric-oxide synthase and receptor activator of nuclear kappa B ligand expression via ERK1/2 MAPK. J. Biol. Chem. 278 (36), 34018−34025.

Rubin, J., Rubin, C., Jacobs, C.R., 2006. Molecular pathways mediating mechanical signaling in bone. Gene 367, 1−16.

Rubin, J., Schwartz, Z., Boyan, B.D., Fan, X., Case, N., Sen, B., Drab, M., Smith, D., Aleman, M., Wong, K.L., Yao, H., Jo, H., Gross, T.S., 2007b. Caveolin-1 knockout mice have increased bone size and stiffness. J. Bone Miner. Res. 22 (9), 1408−1418.

Rubinacci, A., Marenzana, M., Cavani, F., Colasante, F., Villa, I., Willnecker, J., Moro, G.L., Spreafico, L.P., Ferretti, M., Guidobono, F., Marotti, G., 2008. Ovariectomy sensitizes rat cortical bone to whole-body vibration. Calcif. Tissue Int. 82 (4), 316−326.

Ryder, K.D., Duncan, R.L., 2001. Parathyroid hormone enhances fluid shear-induced [Ca2+]i signaling in osteoblastic cells through activation of mechanosensitive and voltage-sensitive Ca2+ channels. J. Bone Miner. Res. 16 (2), 240−248.

Sakurai, T., Izawa, T., Kizaki, T., Ogasawara, J.E., Shirato, K., Imaizumi, K., Takahashi, K., Ishida, H., Ohno, H., 2009. Exercise training decreases expression of inflammation-related adipokines through reduction of oxidative stress in rat white adipose tissue. Biochem. Biophys. Res. Commun. 379 (2), 605−609.

Santos, A., Bakker, A.D., Zandieh-Doulabi, B., Semeins, C.M., Klein-Nulend, J., 2009. Pulsating fluid flow modulates gene expression of proteins involved in Wnt signaling pathways in osteocytes. J. Orthop. Res. 27 (10), 1280−1287.

Saunders, M.M., You, J., Trosko, J.E., Yamasaki, H., Li, Z., Donahue, H.J., Jacobs, C.R., 2001. Gap junctions and fluid flow response in MC3T3-E1 cells. Am. J. Physiol. Cell Physiol. 281 (6), C1917−C1925.

Sawakami, K., Robling, A.G., Ai, M., Pitner, N.D., Liu, D., Warden, S.J., Li, J., Maye, P., Rowe, D.W., Duncan, R.L., Warman, M.L., Turner, C.H., 2006. The Wnt co-receptor LRP5 is essential for skeletal mechanotransduction but not for the anabolic bone response to parathyroid hormone treatment. J. Biol. Chem. 281 (33), 23698−23711.

Schlaepfer, D.D., Hauck, C.R., Sieg, D.J., 1999. Signaling through focal adhesion kinase. Prog. Biophys. Mol. Biol. 71 (3−4), 435−478.

Sen, B., Xie, Z., Case, N., Styner, M., Rubin, C.T., Rubin, J., 2011. Mechanical signal influence on mesenchymal stem cell fate is enhanced by incorporation of refractory periods into the loading regimen. J. Biomech. 44 (4), 593−599.

Sinaki, M., Pfeifer, M., Preisinger, E., Itoi, E., Rizzoli, R., Boonen, S., Geusens, P., Minne, H.W., 2010. The role of exercise in the treatment of osteoporosis. Curr. Osteoporos. Rep. 8 (3), 138−144.

Skerry, T.M., Bitensky, L., Chayen, J., Lanyon, L.E., 1989. Early strain-related changes in enzyme activity in osteocytes following bone loading in vivo. J. Bone Miner. Res. 4 (5), 783–788.

Slatkovska, L., Alibhai, S.M., Beyene, J., Hu, H., Demaras, A., Cheung, A.M., 2011. Effect of 12 months of whole-body vibration therapy on bone density and structure in postmenopausal women: a randomized trial. Ann. Intern. Med. 155 (10), 668–679. W205.

Smalt, R., Mitchell, F.T., Howard, R.L., Chambers, T.J., 1997. Mechanotransduction in bone cells: induction of nitric oxide and prostaglandin synthesis by fluid shear stress, but not by mechanical strain. Adv. Exp. Med. Biol. 433, 311–314.

Solomon, K.R., Danciu, T.E., Adolphson, L.D., Hecht, L.E., Hauschka, P.V., 2000. Caveolin-enriched membrane signaling complexes in human and murine osteoblasts. J. Bone Miner. Res. 15 (12), 2380–2390.

Srinivasan, S., Agans, S.C., King, K.A., Moy, N.Y., Poliachik, S.L., Gross, T.S., 2003. Enabling bone formation in the aged skeleton via rest-inserted mechanical loading. Bone 33 (6), 946–955.

Srinivasan, S., Ausk, B.J., Poliachik, S.L., Warner, S.E., Richardson, T.S., Gross, T.S., 2007. Rest-inserted loading rapidly amplifies the response of bone to small increases in strain and load cycles. J. Appl. Physiol. (1985) 102 (5), 1945–1952.

Srinivasan, S., Weimer, D.A., Agans, S.C., Bain, S.D., Gross, T.S., 2002. Low-magnitude mechanical loading becomes osteogenic when rest is inserted between each load cycle. J. Bone Miner. Res. 17 (9), 1613–1620.

Stattin, K., Michaelsson, K., Larsson, S.C., Wolk, A., Byberg, L., 2017. Leisure-time physical activity and risk of fracture: a cohort study of 66,940 men and women. J. Bone Miner. Res. 32 (8), 1599–1606.

Stevens, H.Y., Meays, D.R., Frangos, J.A., 2006. Pressure gradients and transport in the murine femur upon hindlimb suspension. Bone 39 (3), 565–572.

Styner, M., Thompson, W.R., Galior, K., Uzer, G., Wu, X., Kadari, S., Case, N., Xie, Z., Sen, B., Romaine, A., Pagnotti, G.M., Rubin, C.T., Styner, M.A., Horowitz, M.C., Rubin, J., 2014. Bone marrow fat accumulation accelerated by high fat diet is suppressed by exercise. Bone 64C, 39–46.

Sugimoto, A., Miyazaki, A., Kawarabayashi, K., Shono, M., Akazawa, Y., Hasegawa, T., Ueda-Yamaguchi, K., Kitamura, T., Yoshizaki, K., Fukumoto, S., Iwamoto, T., 2017. Piezo type mechanosensitive ion channel component 1 functions as a regulator of the cell fate determination of mesenchymal stem cells. Sci. Rep. 7 (1), 17696.

Sukharev, S., Corey, D.P., 2004. Mechanosensitive channels: multiplicity of families and gating paradigms. Sci. STKE 2004 (219), re4.

Torrance, A.G., Mosley, J.R., Suswillo, R.F., Lanyon, L.E., 1994. Noninvasive loading of the rat ulna in vivo induces a strain-related modeling response uncomplicated by trauma or periostal pressure. Calcif. Tissue Int. 54 (3), 241–247.

Torvinen, S., Kannus, P., Sievanen, H., Jarvinen, T.A., Pasanen, M., Kontulainen, S., Nenonen, A., Jarvinen, T.L., Paakkala, T., Jarvinen, M., Vuori, I., 2003. Effect of 8-month vertical whole body vibration on bone, muscle performance, and body balance: a randomized controlled study. J. Bone Miner. Res. 18 (5), 876–884.

Turner, C.H., Akhter, M.P., Raab, D.M., Kimmel, D.B., Recker, R.R., 1991. A noninvasive, in vivo model for studying strain adaptive bone modeling. Bone 12 (2), 73–79.

Umemura, Y., Ishiko, T., Yamauchi, T., Kurono, M., Mashiko, S., 1997. Five jumps per day increase bone mass and breaking force in rats. J. Bone Miner. Res. 12 (9), 1480–1485.

Uzer, G., Bas, G., Sen, B., Xie, Z., Birks, S., Olcum, M., McGrath, C., Styner, M., Rubin, J., 2018. Sun-mediated mechanical LINC between nucleus and cytoskeleton regulates betacatenin nuclear access. J. Biomech. 74, 32–40.

Uzer, G., Manske, S.L., Chan, M.E., Chiang, F.P., Rubin, C.T., Frame, M.D., Judex, S., 2012. 'Separating fluid shear stress from acceleration during vibrations in vitro: identification of mechanical signals modulating the cellular response. Cell. Mol. Bioeng. 5 (3), 266–276.

Uzer, G., Pongkitwitoon, S., Ete Chan, M., Judex, S., 2013. Vibration induced osteogenic commitment of mesenchymal stem cells is enhanced by cytoskeletal remodeling but not fluid shear. J. Biomech. 46 (13), 2296–2302.

Uzer, G., Pongkitwitoon, S., Ian, C., Thompson, W.R., Rubin, J., Chan, M.E., Judex, S., 2014. Gap junctional communication in osteocytes is amplified by low intensity vibrations in vitro. PLoS One 9 (3), e90840.

Uzer, G., Thompson, W.R., Sen, B., Xie, Z., Yen, S.S., Miller, S., Bas, G., Styner, M., Rubin, C.T., Judex, S., Burridge, K., Rubin, J., 2015. Cell mechanosensitivity to extremely low-magnitude signals is enabled by a LINCed nucleus. Stem Cell. 33 (6), 2063–2076.

Vander Molen, M.A., Donahue, H.J., Rubin, C.T., McLeod, K.J., 2000. Osteoblastic networks with deficient coupling: differential effects of magnetic and electric field exposure. Bone 27 (2), 227–231.

Vlachopoulos, D., Barker, A.R., Ubago-Guisado, E., Fatouros, I.G., Knapp, K.M., Williams, C.A., Gracia-Marco, L., 2017. Longitudinal adaptations of bone mass, geometry, and metabolism in adolescent male athletes: the PRO-BONE study. J. Bone Miner. Res. 32 (11), 2269–2277.

von Stengel, S., Kemmler, W., Engelke, K., Kalender, W.A., 2011. Effects of whole body vibration on bone mineral density and falls: results of the randomized controlled ELVIS study with postmenopausal women. Osteoporos. Int. 22 (1), 317–325.

Ward, K., Alsop, C., Caulton, J., Rubin, C., Adams, J., Mughal, Z., 2004. Low magnitude mechanical loading is osteogenic in children with disabling conditions. J. Bone Miner. Res. 19 (3), 360–369.

Waterman, H., Katz, M., Rubin, C., Shtiegman, K., Lavi, S., Elson, A., Jovin, T., Yarden, Y., 2002. A mutant EGF-receptor defective in ubiquitylation and endocytosis unveils a role for Grb2 in negative signaling. EMBO J. 21 (3), 303–313.

Watson, S.L., Weeks, B.K., Weis, L.J., Harding, A.T., Horan, S.A., Beck, B.R., 2018. High-intensity resistance and impact training improves bone mineral density and physical function in postmenopausal women with osteopenia and osteoporosis: the LIFTMOR randomized controlled trial. J. Bone Miner. Res. 33 (2), 211–220.

Weinbaum, S., Cowin, S.C., Zeng, Y., 1994. A model for the excitation of osteocytes by mechanical loading-induced bone fluid shear stresses. J. Biomech. 27 (3), 339–360.

Weinbaum, S., Guo, P., You, L., 2001. A new view of mechanotransduction and strain amplification in cells with microvilli and cell processes. Biorheology 38 (2–3), 119–142.

Weyts, F.A., Li, Y.S., van Leeuwen, J., Weinans, H., Chien, S., 2002. ERK activation and alpha v beta 3 integrin signaling through Shc recruitment in response to mechanical stimulation in human osteoblasts. J. Cell. Biochem. 87 (1), 85–92.

Whedon, G.D., 1984. Disuse osteoporosis: physiological aspects. Calcif. Tissue Int. 36 (Suppl. 1), S146–S150.

Wu, S.H., Zhong, Z.M., Chen, J.T., 2012. Low-magnitude high-frequency vibration inhibits RANKL-induced osteoclast differentiation of RAW264.7 cells. Int. J. Med. Sci. 9 (9), 801–807.

Xiao, Z., Zhang, S., Mahlios, J., Zhou, G., Magenheimer, B.S., Guo, D., Dallas, S.L., Maser, R., Calvet, J.P., Bonewald, L., Quarles, L.D., 2006. Cilia-like structures and polycystin-1 in osteoblasts/osteocytes and associated abnormalities in skeletogenesis and Runx2 expression. J. Biol. Chem. 281 (41), 30884–30895.

Xie, L., Jacobson, J.M., Choi, E.S., Busa, B., Donahue, L.R., Miller, L.M., Rubin, C.T., Judex, S., 2006. Low-level mechanical vibrations can influence bone resorption and bone formation in the growing skeleton. Bone 39 (5), 1059–1066.

Yang, C.M., Chien, C.S., Yao, C.C., Hsiao, L.D., Huang, Y.C., Wu, C.B., 2004. Mechanical strain induces collagenase-3 (MMP-13) expression in MC3T3-E1 osteoblastic cells. J. Biol. Chem. 279 (21), 22158–22165.

Yellowley, C.E., Li, Z., Zhou, Z., Jacobs, C.R., Donahue, H.J., 2000. Functional gap junctions between osteocytic and osteoblastic cells. J. Bone Miner. Res. 15 (2), 209–217.

You, J., Reilly, G.C., Zhen, X., Yellowley, C.E., Chen, Q., Donahue, H.J., Jacobs, C.R., 2001. Osteopontin gene regulation by oscillatory fluid flow via intracellular calcium mobilization and activation of mitogen-activated protein kinase in MC3T3-E1 osteoblasts. J. Biol. Chem. 276 (16), 13365–13371.

Zaman, G., Suswillo, R.F., Cheng, M.Z., Tavares, I.A., Lanyon, L.E., 1997. Early responses to dynamic strain change and prostaglandins in bone-derived cells in culture. J. Bone Miner. Res. 12 (5), 769–777.

Zhao, B., Li, R., Cheng, S., Dong, X., Tan, L., Chen, Y., Hao, B., Zhu, D., 2018. Intermittent low-magnitude high-frequency vibration promotes osteogenic protein expression and inhibits osteoclastogenic cytokine secretion in osteoblasts. Biomed. Res. 29 (5), 988–994.

Zhao, Q., Lu, Y., Gan, X., Yu, H., 2017. Low magnitude high frequency vibration promotes adipogenic differentiation of bone marrow stem cells via P38 MAPK signal. PLoS One 12 (3), e0172954.

Zhuang, H., Wang, W., Tahernia, A.D., Levitz, C.L., Luchetti, W.T., Brighton, C.T., 1996. Mechanical strain-induced proliferation of osteoblastic cells parallels increased TGF-beta 1 mRNA. Biochem. Biophys. Res. Commun. 229 (2), 449–453.

Chapter 77

Application of genetically modified animals in bone research

Matthew J. Hilton[1] and Karen M. Lyons[2,3]

[1]Department of Orthopaedic Surgery, Department of Cell Biology, Duke University School of Medicine, Durham, NC, United States; [2]Department of Orthopaedic Surgery/Orthopaedic Hospital, University of California, Los Angeles, CA, United States; [3]Department of Molecular, Cell, & Developmental Biology, University of California, Los Angeles, CA, United States

Chapter outline

Introduction

Studies involving genetically manipulated animals have contributed enormously to our understanding of cellular and molecular mechanisms controlling skeletal development, homeostasis, and disease progression. The mouse and zebrafish have been the most widely utilized organisms for genetic studies. The zebrafish has been used to great advantage in forward genetic screens to identify novel genes that affect skeletal patterning and development, and it is possible to generate defined mutations in zebrafish that enable the development of human skeletal disease models (reviewed in Luderman et al., 2017). However, the mouse is the most widely used organism for genetic studies of bone biology and thus will be the focus of this review. Public repositories of genetically modified embryonic stem (ES) cells and mice have greatly facilitated the genetic analysis of bone biology. The adaptation of CRISPR/Cas9 technology has made the production of genetically modified animals more feasible and enabled the generation of mouse models carrying disease-causing mutations found in humans. Large-scale publicly supported phenotyping efforts include assessments of bone morphology and bone density, enabling investigators to screen through public databases for novel genes that may have an impact on bone formation and/or maintenance.

Large-scale phenotyping resources and repositories

Several large-scale government-sponsored research programs including the Knockout Mouse Project (USA), European Conditional Mouse Mutagenesis Program, North American Conditional Mouse Mutagenesis project (Canada), and Texas

Principles of Bone Biology. https://doi.org/10.1016/B978-0-12-814841-9.00077-4

A&M Institute for Genomic Medicine (USA) are coordinated into the International Mouse Phenotyping Consortium (IMPC) (www.mousephenotype.org). The goal of the IMPC is to produce loss-of-function alleles for 20,000 known and predicted genes in the mouse genome and provide high-throughput initial phenotypic assessments. The IMPC has provided access to targeting vectors, ES cells, and mice harboring a large number of mutated alleles. Some of the alleles have been created by gene targeting, while others have been generated through gene-trapping technologies or large-scale chemical mutagenesis screens. The IMPC publishes a searchable list of all available vectors, ES cell clones, and mice (http://www.knockoutmouse.org).

The phenotyping pipeline includes an assessment of body weight, bone mineral density (DEXA), and bone morphology (X-ray). The database can be searched by gene name or phenotype. For example, at the time of this writing, the IMPC database contains over 200 mutant alleles that lead to abnormal appendicular skeleton morphology. There are nearly 200 entries for abnormal bone mineral density and nearly 100 for abnormal autopod morphology. Many of the genes have not been implicated previously in skeletal biology. Modified ES cells and mice can be obtained from the IMPC, greatly accelerating the process of generating and characterizing mutant mouse strains. The IMPC bone phenotype screen is designed for high throughput and therefore cannot identify subtle morphological alterations or abnormalities in bone mechanical properties, material properties, or structure. The Origins of Bone and Cartilage Disease (OBCD) project (www.boneandcartilage.com), affiliated with IMPC, performs micro-CT, biomechanical testing, and digital X-ray microradiography on a subset of mice generated through the IMPC (Freudenthal et al., 2016; Kemp et al., 2017). As of March 2018, some micro-CT data were available on the OBCD website for 620 conventional knockout strains.

Overexpression approaches to assess gene function in skeletal tissues

The production of transgenic mice that overexpress target genes in specific skeletal tissues is a widely employed strategy. Different transgenic lines that display variable levels of transgene expression can be generated from a single DNA construct, which can enable the discovery of dose-dependent effects on target cells. However, a major caveat of this approach is that these transgenic models often yield nonphysiological levels of gene expression, confounding interpretations of the role(s) of the gene under normal conditions. Moreover, the site of transgene integration and variability in transgene copy number insertion can have significant consequences on tissue specificity and levels of expression. Although this can be exploited to examine dose-dependent effects, the levels and sites of expression must be documented carefully.

A common limitation of standard transgenic approaches is that the overexpression of genes can lead to embryonic lethality, prohibiting the establishment of stable transgenic lines. Furthermore, this can lead to selection for lines expressing only low levels of the transgene, which can confound interpretations of the function of the gene under investigation. This limitation can be addressed by the generation of inducible transgenic strains. The most widely used method is to generate a construct that contains a strong transcriptional stop sequence flanked by LoxP sites located upstream of the gene of interest. By crossing such strains to mice expressing Cre recombinase (discussed later), transgene expression can be activated in a tissue-specific or inducible manner in skeletal cells (Liu et al., 2015).

In addition to overexpressing genes of interest, the transgenic approach can be used for loss-of-function studies. For some genes, it is possible to design and express a dominant-negative variant in order to block its activity (see, e.g., Hiramatsu et al., 2011). The use of transgenics to drive overexpression of dominant-negative variants or natural antagonists leads to loss of function and thus targets pathways in their normal physiological contexts.

The overexpression of siRNA targeting a gene of interest is another transgenic loss-of-function approach that has been used to interrogate gene function in skeletal tissues (e.g., Guo et al., 2016). Although not widely utilized, this strategy can reveal aspects of gene function that are not evident using Cre-loxP technology (discussed later) to delete specific genes. For example, Mutsaers et al. compared osteosarcoma features using osteoblast-restricted Cre-loxP-mediated loss of the tumor suppressor Trp53 (p53) with osteoblast-restricted expression of shRNA against Trp53 (Mutsaers et al., 2013). The two approaches yielded distinct subtypes of osteosarcoma, likely due to differences in the acute versus gradual loss of p53 in knockout and shRNA models, respectively.

Transgenic-overexpression approaches to ablate specific skeletal cell populations can be achieved by driving overexpression of the diphtheria toxin receptor (DTR); this strategy has been used to indicate that osteocytes are transducers of mechanical signals in bone (Tatsumi et al., 2007). However, another study reported effects in multiple organs using the same transgenic construct (Al-Jazzar et al., 2017), highlighting the importance of analyzing tissue specificity in different background strains and experimental contexts when using these transgenic approaches.

Over the past decade, transgenic strains in which marker genes such as *LacZ, GFP,* and/or *ALP* are expressed under the control of tissue-specific promoters (discussed below) have been extensively characterized and are now widely employed

to track gene expression and specific cell lineages in skeletal tissues. These transgenic lineage tracers allow visualization of specific cell types and their descendants in vivo and permit the isolation of these cells for more detailed analyses of gene expression and functional characteristics (Roeder et al., 2016). Most lineage-tracing approaches utilize promoters that drive the expression of Cre recombinase (discussed below).

Several promoter constructs, discussed following, have been well characterized and widely used to drive gene expression in skeletal tissues.

Tendon and ligament

Tendon patterning and differentiation have been difficult to study using transgenic overexpression approaches due to a lack of tendon-specific promoters. This is because there are no genes expressed at high levels, such as those encoding matrix components, whose expressions are restricted specifically to tendon. Tendon-specific enhancers of more widely expressed genes have not been described. *Scleraxis* (*Scx*) encodes a transcription factor expressed in developing tendons and ligaments, although expression has also been reported in cartilage and nonskeletal tissue (Sugimoto et al., 2013). An *Scx* promoter capable of driving high levels of tendon-specific gene expression has not yet been reported. *Scx-Cre* strains (discussed later) provide a potential strategy for inducing the expression of Cre-inducible transgenes with reasonable specificity in tendon.

Chondrocytes

The most commonly used cartilage-specific promoter is derived from the mouse *pro a1(II) collagen* gene *(Col2a1).* This promoter drives expression in the sclerotomic compartment prior to the migration of these cells to become vertebral bodies and in nascent chondrocytes beginning during the condensation stage in appendicular elements (Ovchinnikov et al., 2000). The *Col11a2* promoter has also been used, but some *Col11a2*-based promoters drive expression in perichondrium and osteoblasts in addition to doing so in chondrocytes (Horiki et al., 2004).

Osteoblasts/osteocytes

Proximal promoter fragments (2.3 kb) derived from rat or mouse *Col1a1* genes have been used extensively to drive overexpression in osteoblasts. Strong activity is seen in fetal and adult mature osteoblasts and osteocytes (Dacquin et al., 2002). The 3.6 kb proximal *Col1a1* promoter drives robust expression earlier (in preosteoblasts) but is also active in tendon, skin, muscle, and brain (Liu et al., 2004; Scheller et al., 2011). Promoters based on osteocalcin have been used extensively because they exhibit excellent specificity for osteolineage cells. The 3.5−3.9 kb human osteocalcin promoter fragments drive expression in the majority of mature osteoblasts and osteocytes (Zhang et al., 2002).

The identification of a promoter whose activity is restricted to mature osteocytes has been a challenge. A 10 kb *dentin matrix protein 1 (Dmp1)* promoter has been described, but reportedly drives gene expression in osteoblasts and myoblasts in addition to osteocytes; an 8 kb *Dmp1* promoter appears to have higher specificity for osteocytes (reviewed in Kalajzic et al., 2013).

Osteoclasts

A variety of promoters drive high levels of gene expression in osteoclasts and their progenitors. These include *Cd11b,* expressed in monocytes, macrophages, and along the osteoclast differentiation pathway from mononucleated progenitor cells and into mature osteoclasts (Ferron and Vacher, 2005), and *Tracp,* expressed in mature osteoclasts and their precursors (Kim et al., 2016).

Transgenic mouse reporters of signaling pathways

Transgenic reporter lines can also be used to monitor signaling pathway activity. For example, WNT pathway activity has been monitored in vivo using TOPGAL mice to track β-catenin activity during endochondral bone formation (Day et al., 2005). Specifically, this transgene harbors the *LacZ* gene cassette under the control of a promoter consisting of three TCF/LEF consensus binding sites that serve β-catenin-dependent enhancers positioned upstream of a minimal *Fos* promoter. Tools have also been developed to monitor canonical BMP pathway activity in vivo (Monteiro et al., 2004; Javier et al., 2012). These mice carry a SMAD1/5-specific response element derived from the *Id1* promoter coupled to *lacZ* or luciferase reporters. Similar approaches have been employed to monitor canonical or RBPJ-dependent Notch signaling

activity. For example, one such reporter consists of an open reading frame for the histone H2B-Venus fusion protein under the control of four tandem copies of the RBPJ-binding consensus sequence from the Epstein−Barr virus major latency C promoter upstream of a basal Sv40 promoter (Nowotschin et al., 2013).

Other approaches, such as gene targeting (described later), have also been utilized to monitor signaling pathway activity. For example, a *LacZ* cassette has been targeted to both *Ptch1* and *Gli1* loci, which are direct transcriptional targets of Hedgehog signaling, and β-galactosidase staining can then be used to monitor Hedgehog-responsive cells. While these "knockin" approaches ablate one allele of the targeted gene, heterozygotes have been used to monitor Hedgehog signaling in several skeletal cells (Mak et al., 2008; Zhao et al., 2015). These represent just a few genetic reporter tools being utilized to study cell signaling during normal skeletal development, disease, and repair.

Gene targeting

Gene targeting in mouse ES cells is the most widely used technique for genetic manipulation. Basic methodologies can be found in review articles (Bouabe and Okkenhaug, 2013). The International Mouse Knockout Consortium (IMKC) maintains a searchable list of all available vectors, ES cells, and mice (http://www.knockoutmouse.org). The goal of the consortium is to generate conditional loss-of-function alleles for 20,000 genes, with new mouse strains being added weekly. The Jackson Laboratories Mouse Genome Informatics website (www.informatics.jax.org) provides information on all published genetic modifications, results of ongoing phenotypic analysis, and links to publicly available ES and mouse resources. Since all genetic modifications are included on this website, one can request strains that have not been deposited into a public repository by contacting the investigator directly.

Advantages and disadvantages of conventional gene deletion

Phenotypes caused by conventional gene deletion and loss of function can be used to generate animal models of human disease. As discussed previously, skeletal analysis performed on conventional loss-of-function mutants by the IMKC has revealed previously unknown skeletal phenotypes. However, deletion of genes essential for early embryonic development may lead to lethality, thus precluding analysis of skeletal tissues. Moreover, it is often challenging to discriminate direct effects in skeletal tissues from indirect ones related to the roles of targeted genes in metabolic, cardiovascular, neuroendocrine, or other systems and/or processes. On the other hand, conventional gene knockouts play an essential role in detecting the indirect effects of genes on skeletal tissue formation and maintenance.

Conditional loss-of-function approaches

The ability to ablate or overexpress genes in a tissue-specific manner has revolutionized our understanding of gene function in distinct cell types and lineages, at specific stages of development, and in adults in response to disease or injury. Most methods used to realize tissue-specific gene knockout or activation rely on site-specific recombinases from yeast (Flp) or bacteriophage (Cre) (Birling et al., 2009). These recombinases recognize specific short palindromic sequences in DNA; the target gene is modified to add these sequences (Birling et al., 2009). For the most widely used Cre-loxP system, two mouse strains are required: the "floxed" strain, in which a region of the gene under investigation is flanked by loxP sites, and a second transgenic or "knockin" strain in which Cre recombinase is expressed under the control of an inducible and/or tissue-selective promoter/enhancer sequence. In mice carrying both the floxed alleles and Cre transgene, the Cre recombinase deletes the sequence located between the loxP sites. LoxP sites are placed in noncoding regions, often within introns flanking important exons (i.e., the exon is "floxed"); often the exon containing the translational start site of the encoded protein is chosen. The floxed target gene usually functions normally in the absence of Cre. Fig. 77.1 shows a typical IMKC vector design and various targeting strategies used by the IMKC to generate mice and ES cells carrying conditional alleles that can be obtained from this repository.

Most studies have employed constitutively active forms of Cre. However, ligand-regulated forms that enable inducible control of Cre activity are rapidly gaining precedence. This approach enables simultaneous tissue and temporal control of gene deletion or activation. The most popular strategy for regulating Cre activity involves fusion of the Cre recombinase to a ligand binding domain derived from a mutated estrogen receptor (ER) (Metzger and Chambon, 2001). The mutated ER domain recognizes the synthetic estrogen antagonist 4-OH tamoxifen (T) but is insensitive to endogenous β-estradiol. In the absence of T, the Cre-ER(T) fusion protein is retained in the cytoplasm. Binding of T to the ER domain permits the fusion protein to enter the nucleus and catalyze recombination. Sensitivity to T is greatly improved in mice expressing a Cre-ER(T2) fusion protein in which additional point mutations were introduced into the ligand binding domain of ER

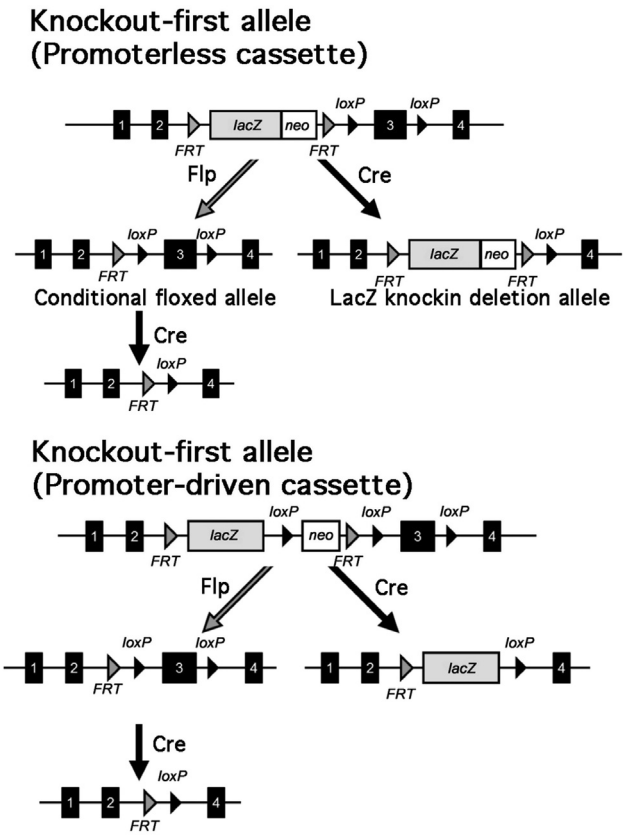

FIGURE 77.1 Schematic of a Knockout-first allele generated by the International Mouse Knockout Consortium (IMKC). The targeting strategies used by IMKC rely on the identification of a "critical" exon. The generation of the knockout-first allele is flexible and can produce reporter knockouts, conditional knockouts, and null alleles following exposure to site-specific recombinases Cre and Flp (Osterwalder et al., 2010).

(Indra et al., 1999). A complete list of Cre lines can be obtained by downloading the Jackson Laboratories Mouse Genome Informatics *MGI Recombinase Alleles Report* (www.informatics.jax.org/home/recombinase). The Jackson Laboratories website also includes a link with expression data for some of these lines (www.creportal.org).

The Cre-loxP system permits exploration of gene function in distinct tissues at multiple time points. However, there are some important considerations. Depending on the Cre line used, excision of the target gene may not be complete; this is highly dependent on the floxed allele. Floxed alleles also vary with respect to the kinetics of Cre-mediated recombination. This must be born in mind when attempting to compare phenotypes caused by excision of different genes using the same Cre transgenic line, especially at prenatal stages.

As discussed following, the promoters most widely used for analysis of skeletal phenotypes often exhibit expression in multiple skeletal cell types, at multiple stages of differentiation within a lineage, and for some genes, in nonskeletal cell types as well. For this reason, every study should verify the extent and location of Cre-mediated recombination of the floxed line of interest. Lineage controls and activity reporters are discussed briefly in the following section.

T can have effects on cartilage, bone, and osteoclasts independently of target gene deletion. Even low doses of T used to catalyze Cre-ER(T)-mediated excision can affect osteoblast function (Starnes et al., 2007). Hence, a control group of Cre-negative mice treated with T may be needed to examine the impact of this variable on the mutant phenotype.

Some of the constitutive and inducible Cre lines most widely used to study skeletal biology are discussed in the following and outlined in Table 77.1.

Uncondensed mesenchyme and precartilage condensations

Prrx1-Cre utilizes a 2.4 kb region of the *Prrx1* promoter to drive Cre expression in early uncondensed mesenchyme largely restricted to the limbs and head (Logan et al., 2002). This mesenchyme eventually gives rise to differentiated chondrocytes, osteoblasts, adipocytes, and vessel-associated pericytes within these anatomical regions. Two *Prrx1-CreERT2* mouse

TABLE 77.1 Commonly used Cre lines for skeletal analysis.

Precondensed mesenchyme	Description	Primary sites of expression
Dermo1-Cre (Twist2-Cre) Twist2$^{tm1.1(cre)Dor}$	Cre knockin that abolishes function of *Twist2* allele	Craniofacial and splanchnic mesenchyme; skeletal condensations
Prrx1-Cre Tg(Prrx1-Cre)1Cjt	Transgene insertion	Limb bud mesenchyme, skull vault
Prrx1-CreER-GFP Tg(Prrx1-cre/ERT2,-GFP)1Smkm	Transgene insertion Inducible, GFP activity tracer	Limb bud mesenchyme, skull vault
Prrx1-CreERT2 Tg(Prrx1-cre/ERT2)1Mlgn	Transgene insertion Inducible Cre activity	Limb bud and skull mesenchyme
Cartilage		
Sox9-Cre Sox9$^{tm3(cre)Crm}$	IRES-Cre cassette inserted into 3′UTR of Sox9	Skeletal condensations; other sites: intestine, testes, etc.
Sox9-CreERT2	IRES-CreERT2 cassette inserted into 3′UTR of *Sox9*	Skeletal condensations; other sites: intestine, testes, etc.
Col2a1-Cre Tg(Col2a1-cre)1Bhr	Transgene insertion	Differentiating chondrocytes in appendicular elements, sclerotome Other sites: heart valves, notochord
Col2a1-CreERT Tg(Col2a1-cre/ERT)KA3Smac	Transgene insertion Inducible; not responsive in adults	Tamoxifen-inducible in differentiating chondrocytes
Col2a1-CreERT2 Tg(Col2a1-cre/ERT2)1Dic	Transgene insertion Inducible in embryos and adults	Tamoxifen-inducible in differentiating chondrocytes
Aggrecan-CreERT2 Acan$^{tm1(cre/ERT2)Crm}$	CreERT2 knockin into 3′ UTR of *Acan* locus Inducible in embryos and adults	Growth plate and articular cartilage, ligament, fibrocartilage of meniscus, trachea, intervertebral disc
Col10a1-Cre Tg(Col10a1-cre)1421/1427/1465Vdm	Transgene insertion of a bacterial artificial chromosome (BAC) encoding *Col10a1* modified by insertion of a Cre cassette	Hypertrophic chondrocytes and descendants in bone marrow regions; detected in skin
Col10a1-Cre Col10a1$^{tm2.1(cre)Ksec}$	Transgene insertion containing a 10.5 kb *Col10a1* promoter/enhancer region upstream of Cre recombinase	Hypertrophic chondrocytes and descendants in bone marrow regions
Col10a1-CreERT2 Col10a1$^{tm3.1(cre/ERT)Ksec}$	Transgene insertion containing a 10.5 kb *Col10a1* promoter/enhancer region upstream of CreERT2 inducible recombinase	Tamoxifen inducible in hypertrophic chondrocytes; lineage traces to descendants in bone marrow regions
GDF5-Cre Tg(Gdf5-cre-ALPP)1Kng	Transgene insertion of a BAC encoding *Gdf5* modified by insertion of a Cre-IRES-ALPP cassette into the translational start site	Joint interzone in embryos; derivatives contribute to synovium and articular cartilage
Prg4-CreERT2 Prg4$^{tm1(GFP/cre/ERT2)Abl}$	GFP/CreERT2 cassette inserted into translation initiation codon of the Prg4 gene; abolishes function of the modified Prg4 locus Inducible in embryos and adults	Superficial zone cartilage; descendant cells contribute extensively to full thickness articular cartilage
FSP1-Cre Tg(S100a4-cre)1Egn	Transgene insertion	Broadly in a subset of fibroblasts; fibrous periosteum/perichondrium

Bone		
Prrx1-CreER-GFP Tg(Prrx1-cre/ERT2,-GFP)1Smkm	Transgene insertion Inducible, GFP activity tracer	Osteochondroprogenitors
Prrx1-CreERT2 Tg(Prrx1-cre/ERT2)1Mlgn	Transgene insertion Inducible Cre activity	Osteochondral progenitors; periosteal cells; bone marrow mesenchymal progenitors
Grem1-CreERT Tg(Grem1-cre/ERT)3Tcw	Transgenic insertion of a BAC encoding Gremlin-1 modified by insertion of CreERT	Osteochondroreticular progenitors
Sp7-Cre (Osx-Cre) g(Sp7-tTA,tetO-EGFP/cre)1Amc	Transgene insertion. A tetracycline-regulated transactivator (tTA) upstream of a tetracycline-responsive element (tetO)-controlled EGFP/Cre fusion protein placed in exon 1 of a BAC construct encoding Sp7 (Osterix) Inducible in embryos and adults	Neonatal mesenchymal stromal cells that give rise to osteochondroprogenitors and bone marrow adipocytes; the transgene itself impacts bone mass and causes a craniofacial defect
LepR-Cre $LepR^{tm2(cre)Rck}$	A cre inserted into the endogenous LepR gene, generating a loss-of-function allele of Lepr	Adult mesenchymal stromal cells that give rise to osteochondroprogenitors and bone marrow adipocytes
Col1a1(2.3 kb)-Cre Tg(Col1a1-cre)1Kry	Transgene insertion of 2.3 kb promoter	Mature osteoblasts throughout differentiation
Col1a1(3.6 kb)-Cre Tg(Col1a1-creBek	Transgene insertion of 3.6 kb promoter	Immature osteoblasts throughout differentiation
Col1a1(2.3 kb)-CreERT2 Tg(Col1a1-cre/ERT2)1Crm	Transgene insertion of 2.3 kb promoter Inducible	Mature osteoblasts throughout differentiation
Col1a1(3.2 kb)-CreERT2 TG(Col1a1-cre/ERT)#Hmk	Transgene insertion 3.2 kb promoter	Immature osteoblasts throughout differentiation
Bglap-Cre (Oc-Cre) Tg(BGLAP-cre)1Clem	Transgene insertion	Mature osteoblasts
Dmp1-Cre Tg(Dmp1-cre)1Jqfe	Transgene insertion; 14 kb promoter	Odontoblasts, osteoblasts, osteocytes
Dmp1-Cre Tg(Dmp1-cre)1Btm	Transgene insertion; 8 kb promoter	Odontoblasts, osteoblasts, osteocytes
Dmp1-CreERT2 Tg(Dmp1-cre/ERT2)D77Pdp	Transgene insertion; 10 kb promoter Inducible in embryos and adults	Mature osteoblasts and osteocytes
Osteoclasts		
LysM-Cre $Lyz2^{tm1(cre)Ifo}$	A Cre inserted into the ATG start site of the endogenous *Lyz2* gene	Myeloid lineage cells
CD11b-Cre Tg(ITGAM-cre)2781Gkl	Transgene insertion	Myeloid lineage cells
TRAP-Cre Tg(Acp5-cre)4Rda	Transgene insertion containing promoters 1B and 1C of *Acp5* gene	Myeloid lineage cells

Continued

TABLE 77.1 Commonly used Cre lines for skeletal analysis.—cont'd

Precondensed mesenchyme	Description	Primary sites of expression
Ctsk-Cre Ctsktm1(cre)Ska	Targeted insertion of the Cre cassette into the endogenous *Ctsk* locus replacing first 4 exons	Myeloid lineage cells
Ctsk-Cre Tg(Ctsk-cre)1Rda	Transgene insertion of a 5 kb *Ctsk* promoter driving Cre expression	Myeloid lineage cells
Cre reporters and ROSA locus tools		
R26R Gt(ROSA)26Sor^{tm1Sor}	Targeted insertion of a loxP-flanked stop cassette upstream of a lacZ coding sequence within the Rosa26 locus between exons 1 and 2	LacZ expressed in all cells where Cre is active and in their descendants
R26R-Confetti Gt(ROSA)26Sor$^{tm1(CAG-Brainbow2.1)Cle}$	Targeted insertion of a strong CAGG promoter, a loxP site, a PGK-Neo-pA cassette (serving as a transcriptional roadblock), and the Brainbow 2.1 construct inserted between exons 1 and 2 of the Gt(ROSA)26Sor locus	Individual cells and their descendants can be tracked upon Cre activation
R26-tdTomato (Ai9) Gt(ROSA)26Sor$^{tm9(CAG-tdTomato)Hze}$	Targeted insertion of a CAGG promoter upstream of a loxP-flanked stop cassette and the coding sequence for a DsRed protein (tdTomato)	Cellular tdTomato-derived red fluorescence in all cells where Cre is active and in their descendants
R26-ntdTomato (Ai75D) Gt(ROSA)26Sor$^{tm75.1(CAG-tdTomato*)Hze}$	Targeted insertion of a CAGG promoter upstream of a loxP-flanked stop cassette and coding sequences for a DsRed protein (tdTomato) containing a nuclear localization signal	Nuclear tdTomato-derived red fluorescence in all cells where Cre is active and in their descendants
mTmG Gt(ROSA)26Sor$^{tm4(ACTB-tdTomato,-EGFP)Luo}$	Targeted insertion of a CAGG promoter upstream of a loxP-flanked coding sequence for a DsRed protein (tdTomato) and poly adenylation sequence, which is followed by a membrane-tagged EGFP protein	Red fluorescence in all tissues; EGFP in Cre-expressing cells and in their descendants
nTnG Gt(ROSA)26Sor$^{tm1(CAG-tdTomato*,\ -EGFP)Ees}$	Targeted insertion of a CAGG promoter upstream of a loxP-flanked coding sequence for a nuclear localized DsRed protein (ntdTomato), which is followed by a nuclear localized EGFP protein	Red fluorescence in nuclei of all tissues; EGFP in the nuclei of Cre-expressing cells and in their descendants
R26-rtTA Gt(ROSA)26Sor$^{tm1(rtTA,\ -EGFP)Nagy}$	Targeted insertion of a loxP-flanked stop cassette upstream of a reverse tetracycline trans-activator coding sequence, internal ribosomal entry site (IRES), and EGFP coding sequence	A doxycycline inducible transactivator protein is expressed in all Cre-expressing cells and in their descendants; rtTA interacts with transgenic promoters containing tet-responsive elements to drive expression of exogenous transgenes only in the presence of doxycycline
R26-iDTR Gt(ROSA)26Sor$^{tm1(HBEGF)Awai}$	Targeted insertion of a loxP-flanked stop cassette upstream of the simian diphtheria toxin receptor coding sequence	Diphtheria toxin receptor (DTR)-inducible expression in all Cre-expressing cells; DTR-expressing cells are susceptible to ablation following administration of diphtheria toxin
R26-DTA Gt(ROSA)26Sor$^{tm1(DTA)Lky}$	Targeted insertion of a loxP-flanked stop cassette upstream of the diphtheria toxin alpha chain (DTA) coding sequence	Inducible expression of diphtheria toxin and cell death/toxicity in all Cre-expressing cells

strains utilizing the same promoter region have been developed, and these mice also demonstrate expression within the previously mentioned mesenchymal progenitor populations (Hasson et al., 2007; Kawanami et al., 2009). One of the two *Prrx1-CreERT2* strains (Kawanami et al., 2009) contains a CreERT2-GFP fusion protein, allowing for both Cre activity and the detection of cells with an active *Prrx1* transgene promoter. The *Dermo1-Cre* (*Twist2*-Cre) is a "knockin" mouse line used in heterozygosity that exhibits Cre expression within mesenchymal condensations (Yu et al., 2003); however, it is not restricted to the skeletal mesenchyme and can be observed more broadly in the mesenchyme of other organs. A *Sox9-Cre* "knockin" that targeted an internal ribosomal entry site (IRES)-Cre to the *Sox9* 3′UTR successfully drives Cre-mediated excision within precursors of osteoblasts and chondrocytes in skeletogenic condensations (Akiyama et al., 2005; Chan et al., 2011); however, it is also active in other sites of endogenous *Sox9* expression.

Chondrocytes

The most widely used Cre strain for chondrocyte-mediated gene deletion/activation is *Col2a1-Cre* (Ovchinnikov et al., 2000). Transgene expression of the *Col2a1-Cre* line is robustly driven in chondrocytes; however, most lines exhibit Cre activity in joint mesenchymal and perichondrial cells that give rise to many if not most osteoblasts (Long et al., 2001; Ono et al., 2014). Three *Col10a1-Cre* lines permit gene deletion specifically within hypertrophic chondrocytes of the developing growth plate (Yang et al., 2005, 2014bbib_Yang_et_al_2005; Golovchenko et al., 2013bib_Yang_et_al_2014b). These *Col10a1-Cre* lines were derived using transgenic approaches: one using a transgenic approach including a 10.5 kb *Col10a1* promoter region (Yang et al., 2005), the second using a bacterial artificial chromosome (BAC) transgene containing much of the *Col10a1* gene (Gebhard et al., 2008; Golovchenko et al., 2013), and the third by knockin of Cre into the endogenous gene (Tsang et al., 2007; Yang et al., 2014b). Several of these mouse lines have been used to demonstrate that hypertrophic chondrocytes give rise to a great number of osteoblasts and osteocytes during endochondral bone development, thereby illustrating that "chondrocyte-specific" gene deletion/activation is transient at best, while the growth plate actively contributes cells to the osteoblast lineage within the bone marrow.

T-inducible recombination in chondrocytes is enabled via the use of transgenic lines expressing a CreERT or CreERT2 cassette under the control of *Col2a1* promoter/enhancer fragments. These mice permit efficient ablation or activation of genes in prenatal cartilage up to 2 weeks after birth; however, for most lines, efficiency is significantly lower in adults. One more widely used *Col2a1-CreERT2* line is more efficient in adult mice (e.g., Grover and Roughley, 2006; Chen et al., 2007). To overcome these issues, *aggrecan-CreERT2* mice were developed in which an IRES-CreERT2 cassette has been "knocked in" to the *aggrecan* gene 3′UTR. These mice exhibit robust inducible Cre expression in both prenatal and adult growth plate and articular chondrocytes as well as chondrocytes within fibrocartilage (Henry et al., 2009). Finally, a *Col10a1-CreERT2* mouse line was generated using a transgenic approach similar to that of the *Col10a1-Cre* mouse line that utilizes a 10.5 kb Col10a1 promoter/enhancer sequence. This line has been important in lineage-tracing hypertrophic chondrocytes into cells within the bone marrow (Zhou et al., 2014b). However, since *Col10a1*-expressing hypertrophic chondrocytes are a transient population, continuous delivery of T would be required to examine the long-term skeletal effects of hypertrophic chondrocyte and descendant gene deletion/activation.

No Cre lines drive Cre-mediated recombination specifically within articular chondrocytes alone. However, transgenic mice in which a Cre-IRES-ALPP (alkaline phosphatase used as a reporter of Cre expression) cassette was inserted into a *Gdf5* BAC clone (*Gdf5-Cre*) drive Cre expression within joint interzone cells, synovial cells, and articular chondrocytes (Koyama et al., 2008). More recently, a *Prg4GFPCreERT2* strain, in which GFP and CreERT2 have been introduced into the *Prg4* locus, has been shown to drive Cre expression in superficial zone cartilage in young mice. This work also demonstrated that superficial zone cells give rise to descendants that end up spanning the depth of articular cartilage in adults (Kozhemyakina et al., 2015).

Osteoprogenitors/osteoblasts/osteocytes

In addition to the lateral plate mesoderm and skull mesenchyme of embryos, *Prrx1-CreERT2* activity can be induced in osteochondroprogenitors of postnatal mice within the cranial suture mesenchyme, the periosteum, and bone marrow (Ouyang et al., 2014). Similarly, the *Grem1-CreERT2* mouse, which was generated by BAC recombineering techniques utilizing the *Grem1* gene, marks a skeletal stem cell population with chondrogenic, osteogenic, and reticular potential (Worthley et al., 2015). BAC recombineering approaches utilizing a clone containing the *Sp7 (Osterix)* locus and a doxycycline regulatable Cre-GFP fusion cassette was generated to create an inducible "Tet-OFF" *Sp7-Cre* mouse line (Rodda and McMahon, 2006). Originally characterized as a marker of osteoprogenitors, *Sp7* and Cre-GFP are now known to be expressed in cells that give rise to chondrocytes, osteoblasts, stromal cells, adipocytes, and perivascular cells in bone

marrow (Chen et al., 2014). Similar to *Sox9-Cre* mice, *leptin receptor* Cre *(LepR-Cre)* utilized a "knockin" approach positioning an IRES-Cre cassette in the *LepR* 3′UTR. *LepR-Cre* drives Cre-mediated excision within most mesenchymal progenitor cells of late embryonic and adult bone marrow (Zhou et al., 2014a). Over the course of weeks to months, these *LepR-Cre* expressing progenitors give rise to most osteoblasts and many osteocytes in adult mouse bone.

Unlike previous Cre-expressing mice that initiated gene recombination in mesenchymal or osteochondral progenitors, the *Col1a1(3.6 kb)-Cre* utilizes a 3.6 kb *Col1a1* promoter transgene to drive Cre expression in more committed osteoblasts; however, it also targets tendon and fibrous cells in cranial sutures, skin, and other organs (Liu et al., 2004). A smaller 2.3 kb *Col1a1* promoter transgene permits *Col1a1 (2.3 kb)-Cre* to have a restricted pattern of expression in mature osteoblasts; however, ectopic expression has been noted in the brain (Dacquin et al., 2002; Scheller et al., 2011). A fragment of the human *bone gamma carboxyglutamate* protein or *osteocalcin* promoter/enhancer has been used to direct expression of Cre to mature osteoblasts in the *Bglap-Cre* (or *Oc-Cre*) transgenic mouse line, which is activated in mature osteoblasts just prior to birth (Zhang et al., 2002). Several transgenic Cre lines have been developed utilizing the *Dmp1* promoter to drive Cre expression in osteocytes; however, they are not specific to these cells (reviewed in Kalajzic et al., 2013). Lines containing 10 kb or longer *Dmp1* proximal promoter regions exhibit expression in osteoblasts in addition to osteocytes. An 8 kb *Dmp1-Cre* strain is reported to have more osteocyte-selective expression (Bivi et al., 2012). Several inducible Cre transgenic strains have been developed for committed osteoblast-derived gene deletions or activations in postnatal mice. These include the *Col1a1* (2.3 kb)-*CreERT*, *Col1a1* (3.2 kb)-*CreERT*, and 8 kb *Dmp1-CreERT2* strains (Maes et al., 2010, p. 1471; Kim et al., 2012).

Osteoclasts

Several Cre strains permit ablation in myeloid cells of the hematopoietic lineage. LysM-Cre mice, in which a Cre was targeted to the endogenous *Lys2* gene locus, demonstrate constitutive Cre expression in the myeloid cell lineage including monocytes, granulocytes, mature macrophages, and osteoclasts (Clausen et al., 1999). The *Cd11b-Cre* transgenic mouse line utilizes a 1.7 kb promoter fragment of the human *ITGAM* (*CD11b*) gene to drive Cre expression in murine macrophages and osteoclasts (Nakamura et al., 2007). Additional transgenic lines expressing Cre under the control of *Acp5* (*TRAP-Cre*) and *Ctsk* (*Ctsk-Cre*) promoters have been generated and characterized (Nakamura et al., 2007); however, each line exhibits promiscuous Cre expression in nonmyeloid cells. An excellent review compares the most commonly used myeloid-specific promoters (Hume, 2011).

Lineage tracing and overexpression tools of the *Rosa26* locus

Lineage tracing

Genetically modified mice have enabled the elucidation of cell lineage relationships in bone with unprecedented resolution, as illustrated in Fig. 77.2. These studies employ strains carrying a floxed reporter gene, such as *LacZ, GFP,* or *RFP* (*tdTomato*), whose expression is activated in specific cells and maintained in their descendants. The reporter allele *R26R* carries a LacZ cassette under the control of a floxed strong transcriptional stop sequence that has been introduced into the ubiquitously expressed *Rosa26* locus. When bred to a Cre-expressing strain, β-galactosidase is expressed in all cells in which the Cre is expressed. The use of R26R in bone is limited by the fact that osteoblasts express endogenous LacZ, but major insights have been made using R26R and other lineage tracers to study osteoprogenitors. These are discussed in several comprehensive reviews (Roeder et al., 2016; Scott and Underhill, 2016). Examples are the previously discussed demonstrations that immature osteoblasts move into developing bone along with invading blood vessels (Maes et al., 2010) and that hypertrophic chondrocytes give rise to osteoblasts (Ono et al., 2014; Yang et al., 2014b). More recently, multiple lines have been generated that permit live imaging of the expression of fluorescent proteins in specific organelles (cell membrane, nucleus, etc.) in a tissue-specific and inducible manner (Abe and Fujimori, 2013).

Overexpression using the *Rosa26* locus

The *Rosa26* locus has also been exploited to conditionally express a variety of genes that serve as useful tools to study skeletal biology. Conditional overexpression of diphtheria toxin alpha chain (DTA) or diphtheria toxin receptor (DTR) is often used to study the function of specific cell populations when R26-DTA or R26-DTR mice are crossed with Cre-expressing or inducible Cre−expressing mice. R26-DTA mice were developed by inserting a loxP-flanked stop cassette upstream of the DTA coding sequence (Voehringer et al., 2008) that when Cre-activated induces cell toxicity and cell

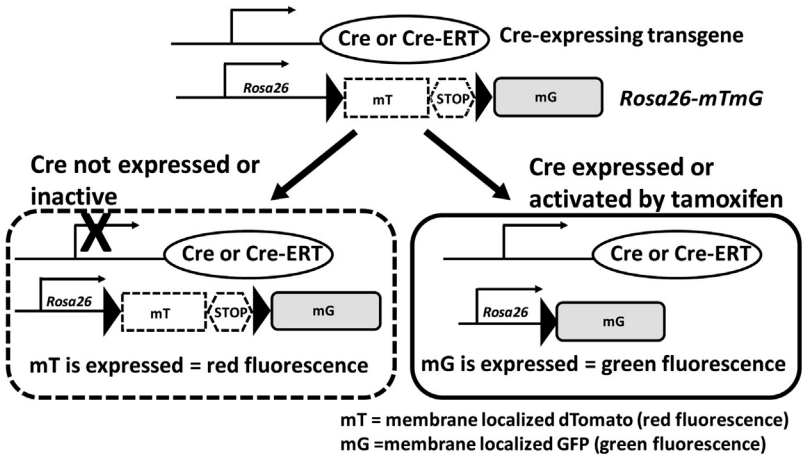

FIGURE 77.2 Lineage tracing with Cre strains and the *Rosa26-mTmG* reporter line. Schematic depicting the general principle behind Cre/lox-mediated lineage tracing. *Rosa26-mTmG* mice (*top*) are crossed with a Cre-expressing or CreERT—expressing strain. Double-heterozygous offspring will produce Cre recombinase in cells in which the promoter driving Cre (or CreERT) expression is active. If the Cre is unmodified, it will be active in these cells. If a CreERT is used, Cre will be expressed but will be inactive unless tamoxifen is supplied. In cells in which Cre is not present or is inactive, cells will be red due to the expression of membrane-bound dTomato (mT), which is expressed from the *Rosa26* reporter allele *(bottom left).* Expression of Cre or administration of tamoxifen to CreERT-expressing mice will lead to Cre-mediated excision of the mT-STOP cassette (*bottom right*). This removes the strong transcriptional STOP sequence and enables expression of membrane-bound GFP (mG). Because the Cre-mediated switch is genetic, it is permanent and will remain for the life span of the recombined cell. It will be passed on to the cell's offspring, allowing its lineage (i.e., the cell types to which the recombined cell gives rise to) to be traced.

death. R26-iDTR mice contain a loxP-flanked stop cassette upstream of the DTR coding sequence that when Cre-activated induces DTR expression (Buch et al., 2005); however, cell death induction requires the delivery of diphtheria toxin, affording temporal control of cell death induction. A recent study investigated the importance of surface chondrocyte death in articular cartilage by overexpressing diphtheria toxin within surface chondrocytes using *Prg4-GFPCreERT2* (Zhang et al., 2016). Although cell death has been proposed as a contributor to the onset or progression of osteoarthritis, this study revealed that the death of surface chondrocytes did not initiate joint cartilage degeneration.

Finally, inducible and tunable overexpression of genes can be achieved utilizing a reverse tetracycline transactivator (rtTA) and tetracycline-inducible transgene overexpression system. In this approach, a Rosa26 mouse line containing a loxP-flanked stop cassette upstream of an rtTA, IRES, and GFP cassette allows for doxycycline-inducible rtTA and GFP protein expression when crossed with a Cre-expressing mouse line. Upon Cre-mediated activation and delivery of doxycycline, the rtTA interacts with additional transgenic promoters containing tet-responsive elements to drive the expression of exogenous transgenes only in the presence of doxycycline. This model has been used recently to study transient versus sustained Notch signaling in chondrocytes and their descendants (Liu et al., 2015).

Genomic engineering using CRISPR/Cas9

The development of CRISPR/Cas9 technology has revolutionized genomic engineering. CRISPR/Cas9 is a genome editing technique in which the generation of 20-nt guide RNA sequences (gRNAs) determines the site of genomic editing. Error-prone DNA repair mechanisms are exploited to introduce insertions or deletions. The technology can also be used to generate specific point mutations or conditional alleles. In addition to the efficiency of the technique, CRISPR/Cas9 gRNAs can be injected directly into fertilized eggs to generate mutant offspring, bypassing the need to inject ES cells into blastocysts. Thus, genetically modified mice can be produced in as few as 4 weeks compared with homologous recombination using ES cells, which typically requires 6—12 months. Detailed methodologies for generating mutant animals using CRISPR/Cas9 are rapidly evolving but can be found in work by Yang et al. (2014a). Many core facilities and commercial groups cost-effectively generate mouse models using CRISPR/Cas9 technology.

Conclusions

With all of the successes in genetic manipulation and the rapidly growing number of modified mouse strains available in public repositories, the real bottleneck is phenotyping. Many knockout and mutant strains exhibit no obvious skeletal

phenotypes due to functional redundancy. Therefore, the creation of double or even triple knockouts may be necessary to discover gene function. Furthermore, inbred strains vary considerably in their peak BMD. ES cells from the 129 strain have been frequently used. However, 129 mice exhibit abnormal immunological characteristics that could impact bone density (McVicar et al., 2002). Genetically modified mice frequently have 129, C56Bl/6, and C3H backgrounds, but unmodified mice of these strains have different BMD profiles (Rosen et al., 2001) and different responses to mechanical loading (Li et al., 2005) that need to be considered when interpreting skeletal phenotypes. Moreover, environmental factors such as housing, diet, and intestinal microbiota can have a significant impact on metabolic parameters and BMD (Nagy et al., 2002; Li et al., 2016).

Finally, it is well recognized that caution must be taken when extrapolating findings in mouse models to functions in humans. Biomechanical loading and hormonal effects on bones are clearly different in mice and humans. Nonetheless, similarities outweigh the differences by far, and genetic models are likely to play an increasingly prominent role in every aspect of research within the field of skeletal biology.

Acknowledgments

This work was supported by funding from the NIH to KML (AR052686 and AR044528) and MJH (AR063071).

References

Abe, T., Fujimori, T., 2013. Reporter mouse lines for fluorescence imaging. Dev. Growth Differ. 55, 390–405.

Akiyama, H., Kim, J.E., Nakashima, K., Balmes, G., Iwai, N., Deng, J.M., Zhang, Z., Martin, J.F., Behringer, R.R., Nakamura, T., de Crombrugghe, B., 2005. Osteo-chondroprogenitor cells are derived from Sox9 expressing precursors. Proc. Natl. Acad. Sci. U. S. A. 102, 14665–14670.

Al-Jazzar, A., Javaheri, B., Prideaux, M., Boyde, A., Scudamore, C.L., Cherifi, C., Hay, E., Hopkinson, M., Boyd, M., Cohen-Solal, M., Farquharson, C., Pitsillides, A.A., 2017. Dmp1 promoter-driven diphtheria toxin receptor transgene expression directs unforeseen effects in multiple tissues. Int. J. Mol. Sci. 18.

Birling, M.C., Gofflot, F., Warot, X., 2009. Site-specific recombinases for manipulation of the mouse genome. Methods Mol. Biol. 561, 245–263.

Bivi, N., Condon, K.W., Allen, M.R., Farlow, N., Passeri, G., Brun, L.R., Rhee, Y., Bellido, T., Plotkin, L.I., 2012. Cell autonomous requirement of connexin 43 for osteocyte survival: consequences for endocortical resorption and periosteal bone formation. J. Bone Miner. Res. 27, 374–389.

Bouabe, H., Okkenhaug, K., 2013. Gene targeting in mice: a review. Methods Mol. Biol. 1064, 315–336.

Buch, T., Heppner, F.L., Tertilt, C., Heinen, T.J., Kremer, M., Wunderlich, F.T., Jung, S., Waisman, A., 2005. A Cre-inducible diphtheria toxin receptor mediates cell lineage ablation after toxin administration. Nat. Methods 2, 419–426.

Chan, H.Y., V, S., Xing, X., Kraus, P., Yap, S.P., Ng, P., Lim, S.L., Lufkin, T., 2011. Comparison of IRES and F2A-based locus-specific multicistronic expression in stable mouse lines. PLoS One 6, e28885.

Chen, J.Q., Shi, Y., Regan, J., Karuppaiah, K., Ornitz, D.M., Long, F.X., 2014. Osx-Cre targets multiple cell types besides osteoblast lineage in postnatal mice. PLoS One 9.

Chen, M., Lichtler, A.C., Sheu, T.J., Xie, C., Zhang, X., O'Keefe, R.J., Chen, D., 2007. Generation of a transgenic mouse model with chondrocyte-specific and tamoxifen-inducible expression of Cre recombinase. Genesis 45, 44–50.

Clausen, B.E., Burkhardt, C., Reith, W., Renkawitz, R., Forster, I., 1999. Conditional gene targeting in macrophages and granulocytes using LysMcre mice. Transgenic Res. 8, 265–277.

Dacquin, R., Starbuck, M., Schinke, T., Karsenty, G., 2002. Mouse alpha1(I)-collagen promoter is the best known promoter to drive efficient Cre recombinase expression in osteoblast. Dev. Dynam. 224, 245–251.

Day, T.F., Guo, X., Garrett-Beal, L., Yang, Y., 2005. Wnt/beta-catenin signaling in mesenchymal progenitors controls osteoblast and chondrocyte differentiation during vertebrate skeletogenesis. Dev. Cell 8, 739–750.

Ferron, M., Vacher, J., 2005. Targeted expression of Cre recombinase in macrophages and osteoclasts in transgenic mice. Genesis 41, 138–145.

Freudenthal, B., Logan, J., Pipelines, S.I.M., Croucher, P.I., Williams, G.R., Bassett, J.H.D., 2016. Rapid phenotyping of knockout mice to identify genetic determinants of bone strength. J. Endocrinol. 231, R31–R46.

Gebhard, S., Hattori, T., Bauer, E., Schlund, B., Bosl, M.R., de Crombrugghe, B., von der Mark, K., 2008. Specific expression of Cre recombinase in hypertrophic cartilage under the control of a BAC-Col10a1 promoter. Matrix Biol. 27, 693–699.

Golovchenko, S., Hattori, T., Hartmann, C., Gebhardt, M., Gebhard, S., Hess, A., Pausch, F., Schlund, B., von der Mark, K., 2013. Deletion of beta catenin in hypertrophic growth plate chondrocytes impairs trabecular bone formation. Bone 55, 102–112.

Grover, J., Roughley, P.J., 2006. Generation of a transgenic mouse in which Cre recombinase is expressed under control of the type II collagen promoter and doxycycline administration. Matrix Biol. 25, 158–165.

Guo, Y., Tang, C.Y., Man, X.F., Tang, H.N., Tang, J., Wang, F., Zhou, C.L., Tan, S.W., Feng, Y.Z., Zhou, H.D., 2016. Insulin receptor substrate-1 time-dependently regulates bone formation by controlling collagen Ialpha2 expression via miR-342. FASEB J. 30, 4214–4226.

Hasson, P., Del Buono, J., Logan, M.P., 2007. Tbx5 is dispensable for forelimb outgrowth. Development. 134, 85–92.

Henry, S.P., Jang, C.W., Deng, J.M., Zhang, Z., Behringer, R.R., de Crombrugghe, B., 2009. Generation of aggrecan-CreERT2 knockin mice for inducible Cre activity in adult cartilage. Genesis 47, 805–814.

Hiramatsu, K., Iwai, T., Yoshikawa, H., Tsumaki, N., 2011. Expression of dominant negative TGF-beta receptors inhibits cartilage formation in conditional transgenic mice. J. Bone Miner. Metab. 29, 493−500.

Horiki, M., Imamura, T., Okamoto, M., Hayashi, M., Murai, J., Myoui, A., Ochi, T., Miyazono, K., Yoshikawa, H., Tsumaki, N., 2004. Smad6/Smurf1 overexpression in cartilage delays chondrocyte hypertrophy and causes dwarfism with osteopenia. J. Cell Biol. 165, 433−445.

Hume, D.A., 2011. Applications of myeloid-specific promoters in transgenic mice support in vivo imaging and functional genomics but do not support the concept of distinct macrophage and dendritic cell lineages or roles in immunity. J. Leukoc. Biol. 89, 525−538.

Indra, A.K., Warot, X., Brocard, J., Bornert, J.M., Xiao, J.H., Chambon, P., Metzger, D., 1999. Temporally-controlled site-specific mutagenesis in the basal layer of the epidermis: comparison of the recombinase activity of the tamoxifen-inducible Cre-ERT and Cre-ERT2 recombinases. Nucleic Acids Res. 27, 4324−4327.

Javier, A.L., Doan, L.T., Luong, M., Reyes de Mochel, N.S., Sun, A., Monuki, E.S., Cho, K.W., 2012. Bmp indicator mice reveal dynamic regulation of transcriptional response. PLoS One 7, e42566.

Kalajzic, I., Matthews, B.G., Torreggiani, E., Harris, M.A., Divieti Pajevic, P., Harris, S.E., 2013. In vitro and in vivo approaches to study osteocyte biology. Bone 54, 296−306.

Kawanami, A., Matsushita, T., Chan, Y.Y., Murakami, S., 2009. Mice expressing GFP and CreER in osteochondro progenitor cells in the periosteum. Biochem. Biophys. Res. Commun. 386, 477−482.

Kemp, J.P., Morris, J.A., Medina-Gomez, C., Forgetta, V., Warrington, N.M., Youlten, S.E., Zheng, J., Gregson, C.L., Grundberg, E., Trajanoska, K., Logan, J.G., Pollard, A.S., Sparkes, P.C., Ghirardello, E.J., Allen, R., Leitch, V.D., Butterfield, N.C., Komla-Ebri, D., Adoum, A.T., Curry, K.F., White, J.K., Kussy, F., Greenlaw, K.M., Xu, C.J., Harvey, N.C., Cooper, C., Adams, D.J., Greenwood, C.M.T., Maurano, M.T., Kaptoge, S., Rivadeneira, F., Tobias, J.H., Croucher, P.I., Ackert-Bicknell, C.L., Bassett, J.H.D., Williams, G.R., Richards, J.B., Evans, D.M., 2017. Identification of 153 new loci associated with heel bone mineral density and functional involvement of GPC6 in osteoporosis. Nat. Genet. 49, 1468−1475.

Kim, J.H., Kim, K., Kim, I., Seong, S., Nam, K.I., Lee, S.H., Kim, K.K., Kim, N., 2016. Role of CrkII signaling in RANKL-induced osteoclast differentiation and function. J. Immunol. 196, 1123−1131.

Kim, S.W., Pajevic, P.D., Selig, M., Barry, K.J., Yang, J.Y., Shin, C.S., Baek, W.Y., Kim, J.E., Kronenberg, H.M., 2012. Intermittent parathyroid hormone administration converts quiescent lining cells to active osteoblasts. J. Bone Miner. Res. 27, 2075−2084.

Koyama, E., Shibukawa, Y., Nagayama, M., Sugito, H., Young, B., Yuasa, T., Okabe, T., Ochiai, T., Kamiya, N., Rountree, R.B., Kingsley, D.M., Iwamoto, M., Enomoto-Iwamoto, M., Pacifici, M., 2008. A distinct cohort of progenitor cells participates in synovial joint and articular cartilage formation during mouse limb skeletogenesis. Dev. Biol. 316, 62−73.

Kozhemyakina, E., Zhang, M., Ionescu, A., Ayturk, U.M., Ono, N., Kobayashi, A., Kronenberg, H., Warman, M.L., Lassar, A.B., 2015. Identification of a Prg4-expressing articular cartilage progenitor cell population in mice. Arthritis Rheum. 67, 1261−1273.

Li, J., Liu, D., Ke, H.Z., Duncan, R.L., Turner, C.H., 2005. The P2X7 nucleotide receptor mediates skeletal mechanotransduction. J. Biol. Chem. 280, 42952−42959.

Li, J.Y., Chassaing, B., Tyagi, A.M., Vaccaro, C., Luo, T., Adams, J., Darby, T.M., Weitzmann, M.N., Mulle, J.G., Gewirtz, A.T., Jones, R.M., Pacifici, R., 2016. Sex steroid deficiency-associated bone loss is microbiota dependent and prevented by probiotics. J. Clin. Investig. 126, 2049−2063.

Liu, F., Woitge, H.W., Braut, A., Kronenberg, M.S., Lichtler, A.C., Mina, M., Kream, B.E., 2004. Expression and activity of osteoblast-targeted Cre recombinase transgenes in murine skeletal tissues. Int. J. Dev. Biol. 48, 645−653.

Liu, Z., Chen, J., Mirando, A.J., Wang, C., Zuscik, M.J., O'Keefe, R.J., Hilton, M.J., 2015. A dual role for NOTCH signaling in joint cartilage maintenance and osteoarthritis. Sci. Signal. 8, ra71.

Logan, M., Martin, J.F., Nagy, A., Lobe, C., Olson, E.N., Tabin, C.J., 2002. Expression of Cre recombinase in the developing mouse limb bud driven by a Prxl enhancer. Genesis 33, 77−80.

Long, F., XZhang, X., Karp, S., Yang, Y., McMahon, A., 2001. Genetic manipulation of hedgehog signaling in the endorchondral skeleton reveals a direct role in the regulation of chondrocyte proliferation. Development. 128, 5099−5108.

Luderman, L.N., Unlu, G., Knapik, E.W., 2017. Zebrafish developmental models of skeletal diseases. Curr. Top. Dev. Biol. 124, 81−124.

Maes, C., Kobayashi, T., Selig, M.K., Torrekens, S., Roth, S.I., Mackem, S., Carmeliet, G., Kronenberg, H.M., 2010. Osteoblast precursors, but not mature osteoblasts, move into developing and fractured bones along with invading blood vessels. Dev. Cell 19, 329−344.

Mak, K.K., Bi, Y., Wan, C., Chuang, P.T., Clemens, T., Young, M., Yang, Y., 2008. Hedgehog signaling in mature osteoblasts regulates bone formation and resorption by controlling PTHrP and RANKL expression. Dev. Cell 14, 674−688.

McVicar, D.W., Winkler-Pickett, R., Taylor, L.S., Makrigiannis, A., Bennett, M., Anderson, S.K., Ortaldo, J.R., 2002. Aberrant DAP12 signaling in the 129 strain of mice: implications for the analysis of gene-targeted mice. J. Immunol. 169, 1721−1728.

Metzger, D., Chambon, P., 2001. Site- and time-specific gene targeting in the mouse. Methods 24, 71−80.

Monteiro, R.M., de Sousa Lopes, S.M., Korchynskyi, O., ten Dijke, P., Mummery, C.L., 2004. Spatio-temporal activation of Smad1 and Smad5 in vivo: monitoring transcriptional activity of Smad proteins. J. Cell Sci. 117, 4653−4663.

Mutsaers, A.J., Ng, A.J., Baker, E.K., Russell, M.R., Chalk, A.M., Wall, M., Liddicoat, B.J., Ho, P.W., Slavin, J.L., Goradia, A., Martin, T.J., Purton, L.E., Dickins, R.A., Walkley, C.R., 2013. Modeling distinct osteosarcoma subtypes in vivo using Cre:lox and lineage-restricted transgenic shRNA. Bone 55, 166−178.

Nagy, T.R., Krzywanski, D., Li, J., Meleth, S., Desmond, R., 2002. Effect of group vs. single housing on phenotypic variance in C57BL/6J mice. Obes. Res. 10, 412−415.

Nakamura, T., Imai, Y., Matsumoto, T., Sato, S., Takeuchi, K., Igarashi, K., Harada, Y., Azuma, Y., Krust, A., Yamamoto, Y., Nishina, H., Takeda, S., Takayanagi, H., Metzger, D., Kanno, J., Takaoka, K., Martin, T., Chambon, P., Kato, S., 2007. Estrogen prevents bone loss via estrogen receptor alpha and induction of Fas ligand in osteoclasts. Cell 130, 811−823.

Nowotschin, S., Xenopoulos, P., Schrode, N., Hadjantonakis, A.K., 2013. A bright single-cell resolution live imaging reporter of Notch signaling in the mouse. BMC Dev. Biol. 13, 15.

Ono, N., Ono, W., Nagasawa, T., Kronenberg, H.M., 2014. A subset of chondrogenic cells provides early mesenchymal progenitors in growing bones. Nat. Cell Biol. 16, 1157−1167.

Osterwalder, M., Galli, A., Rosen, B., Skarnes, W.C., Zeller, R., Lopez-Rios, J., 2010. Dual RMCE for efficient re-engineering of mouse mutant alleles. Nat. Methods 7, 893−895.

Ouyang, Z.F., Chen, Z.J., Ishikawa, M., Yue, X.Z., Greenfield, E., Murakami, S., 2014. Prx1 and3.2 kb Col1a1 promoters target distinct bone cell populations in transgenic mice. Bone 58, 136−145.

Ovchinnikov, D.A., Deng, J.M., Ogunrinu, G., Behringer, R.R., 2000. Col2a1-directed expression of Cre recombinase in differentiating chondrocytes in transgenic mice. Genesis 26, 145−146.

Rodda, S.J., McMahon, A.P., 2006. Distinct roles for Hedgehog and canonical Wnt signaling in specification, differentiation and maintenance of osteoblast progenitors. Development. 133, 3231−3244.

Roeder, E., Matthews, B.G., Kalajzic, I., 2016. Visual reporters for study of the osteoblast lineage. Bone 92, 189−195.

Rosen, C.J., Beamer, W.G., Donahue, L.R., 2001. Defining the genetics of osteoporosis: using the mouse to understand man. Osteoporos. Int. 12, 803−810.

Scheller, E.L., Leinninger, G.M., Hankenson, K.D., Myers Jr., M.G., Krebsbach, P.H., 2011. Ectopic expression of Col2.3 and Col3.6 promoters in the brain and association with leptin signaling. Cells Tissues Organs 194, 268−273.

Scott, R.W., Underhill, T.M., 2016. Methods and strategies for lineage tracing of mesenchymal progenitor cells. Methods Mol. Biol. 1416, 171−203.

Starnes, L.M., Downey, C.M., Boyd, S.K., Jirik, F.R., 2007. Increased bone mass in male and female mice following tamoxifen administration. Genesis 45, 229−235.

Sugimoto, Y., Takimoto, A., Hiraki, Y., Shukunami, C., 2013. Generation and characterization of ScxCre transgenic mice. Genesis 51, 275−283.

Tatsumi, S., Ishii, K., Amizuka, N., Li, M., Kobayashi, T., Kohno, K., Ito, M., Takeshita, S., Ikeda, K., 2007. Targeted ablation of osteocytes induces osteoporosis with defective mechanotransduction. Cell Metabol. 5, 464−475.

Tsang, K.Y., Chan, D., Cheslett, D., Chan, W.C., So, C.L., Melhado, I.G., Chan, T.W., Kwan, K.M., Hunziker, E.B., Yamada, Y., Bateman, J.F., Cheung, K.M., Cheah, K.S., 2007. Surviving endoplasmic reticulum stress is coupled to altered chondrocyte differentiation and function. PLoS Biol. 5, e44.

Voehringer, D., Liang, H.E., Locksley, R.M., 2008. Homeostasis and effector function of lymphopenia-induced "memory-like" T cells in constitutively T cell-depleted mice. J. Immunol. 180, 4742−4753.

Worthley, D.L., Churchill, M., Compton, J.T., Tailor, Y., Rao, M., Si, Y.L., Levin, D., Schwartz, M.G., Uygur, A., Hayakawa, Y., Gross, S., Renz, B.W., Setlik, W., Martinez, A.N., Chen, X.W., Nizami, S., Lee, H.G., Kang, H.P., Caldwell, J.M., Asfaha, S., Westphalen, C.B., Graham, T., Jin, G.C., Nagar, K., Wang, H.S., Kheirbek, M.A., Kolhe, A., Carpenter, J., Glaire, M., Nair, A., Renders, S., Manieri, N., Muthupalani, S., Fox, J.G., Reichert, M., Giraud, A.S., Schwabe, R.F., Pradere, J.P., Walton, K., Prakash, A., Gumucio, D., Rustgi, A.K., Stappenbeck, T.S., Friedman, R.A., Gershon, M.D., Sims, P., Grikscheit, T., Lee, F.Y., Karsenty, G., Mukherjee, S., Wang, T.C., 2015. Gremlin 1 identifies a skeletal stem cell with bone, cartilage, and reticular stromal potential. Cell 160, 269−284.

Yang, G., Cui, F., Hou, N., Cheng, X., Zhang, J., Wang, Y., Jiang, N., Gao, X., Yang, X., 2005. Transgenic mice that express Cre recombinase in hypertrophic chondrocytes. Genesis 42, 33−36.

Yang, H., Wang, H., Jaenisch, R., 2014a. Generating genetically modified mice using CRISPR/Cas-mediated genome engineering. Nat. Protoc. 9, 1956−1968.

Yang, L., Tsang, K.Y., Tang, H.C., Chan, D., Cheah, K.S., 2014b. Hypertrophic chondrocytes can become osteoblasts and osteocytes in endochondral bone formation. Proc. Natl. Acad. Sci. U. S. A. 111, 12097−12102.

Yu, K., Xu, J., Liu, Z., Sosic, D., Shao, J., Olson, E.N., Towler, D.A., Ornitz, D.M., 2003. Conditional inactivation of FGF receptor 2 reveals an essential role for FGF signaling in the regulation of osteoblast function and bone growth. Development. 130, 3063−3074.

Zhang, M., Mani, S.B., He, Y., Hall, A.M., Xu, L., Li, Y., Zurakowski, D., Jay, G.D., Warman, M.L., 2016. Induced superficial chondrocyte death reduces catabolic cartilage damage in murine posttraumatic osteoarthritis. J. Clin. Investig. 126, 2893−2902.

Zhang, M., Xuan, S., Bouxsein, M.L., von Stechow, D., Akeno, N., Faugere, M.C., Malluche, H., Zhao, G., Rosen, C.J., Efstratiadis, A., Clemens, T.L., 2002. Osteoblast-specific knockout of the insulin-like growth factor (IGF) receptor gene reveals an essential role of IGF signaling in bone matrix mineralization. J. Biol. Chem. 277, 44005−44012.

Zhao, H., Feng, J., Ho, T.V., Grimes, W., Urata, M., Chai, Y., 2015. The suture provides a niche for mesenchymal stem cells of craniofacial bones. Nat. Cell Biol. 17, 386−396.

Zhou, B.O., Yue, R., Murphy, M.M., Peyer, J.G., Morrison, S.J., 2014a. Leptin-receptor-expressing mesenchymal stromal cells represent the main source of bone formed by adult bone marrow. Cell Stem Cell 15, 154−168.

Zhou, X., von der Mark, K., Henry, S., Norton, W., Adams, H., de Crombrugghe, B., 2014b. Chondrocytes transdifferentiate into osteoblasts in endochondral bone during development, postnatal growth and fracture healing in mice. PLoS Genet. 10, e1004820.

Chapter 78

Bone turnover markers

Patrick Garnero[1] **and Serge Cremers**[2]

[1]INSERM Research Unit 1033-Lyos, Lyon, France; [2]Department of Pathology & Cell Biology and Department of Medicine, Vagelos College of Physicians and Surgeons, Columbia University Irving Medical Center, United States

Chapter outline

Introduction

Bone metabolism is characterized by an intimate cooperation of bone cells including osteoblasts, osteoclasts, and osteocytes in order to maintain bone tissue quantity and the integrity of bone structure. In metabolic bone diseases such as osteoporosis, bone metabolism is altered, leading to bone loss that is often accompanied by changes in the microarchitecture that result in bone fragility and ultimately fracture. The development of serum and urinary assays for biochemical markers, reflecting either enzymatic activities of osteoblasts and osteoclasts or breakdown products of bone tissue, has been very useful for investigating the complex pathways of bone metabolism and their alterations in bone diseases. Novel biological markers have been developed, and studies suggest that they may be valuable research tools for investigating the mechanisms of bone metabolism and assessing the activity of osteocytes, and some of them may be of value for the management of patients with osteoporosis and other bone diseases. In this chapter we will present briefly the established biochemical markers, review the new data on emerging biomarkers, and then discuss their clinical utility in osteoporosis and other metabolic bone diseases.

Principles of Bone Biology. https://doi.org/10.1016/B978-0-12-814841-9.00078-6

Established biochemical markers of bone metabolism

The structure, biology, and clinical utility of classical biochemical markers in different diseases including osteoporosis has been reviewed in several recent review papers (Naylor and Eastell, 2012; Eastell and Szulc, 2017). At present, the most specific and sensitive markers of bone formation (Table 78.1) are serum total osteocalcin; the bone isoenzyme of alkaline phosphatase (bone ALP); and the procollagen type I N-terminal propeptide (PINP), this last marker reflecting the rate of synthesis of the main constituent of bone tissue. For the evaluation of bone resorption, most currently available assays are based on serum or urine detection of breakdown products of type I collagen, the most abundant protein of bone matrix. These include the intermolecular cross-links pyridinoline (PYD) and deoxypyridinoline (DPD); cathepsin K−generated C-terminal telopeptide of collagen type I (CTX) and cross-linked N-terminal telopeptide of type I collagen (NTX); and matrix metalloproteinase (MMP)-generated cross-linked carboxyterminal telopeptide of type I collagen (CTX-MMP or ICTP); all of which are type I collagen fragments. Serum 5b isoenzyme of tartrate-resistant acid phosphatase (TRACP5b) is also a valuable biochemical marker reflecting mainly the number and activity of osteoclasts. An expert group from the International Osteoporosis Foundation (IOF) and the International Federation of Clinical Chemistry and Laboratory Medicine (IFCC) has performed a comprehensive review of the available data, and based on this assessment has recommended the systematic use of serum PINP and serum betaCTX as biochemical reference markers of bone formation and bone resorption, respectively, but only in clinical research studies in osteoporosis (Vasikaran et al., 2011; Johansson et al., 2014).

A study performed in 371 untreated postmenopausal women with osteoporosis aged between 50 and 84 years analyzed the correlation of bone markers including PINP and serum CTX with static and dynamic histomorphometric parameters measured on iliac crest biopsies (Chavassieux et al., 2015). PINP was found to be significantly associated with both static and dynamic parameters of formation ($0.21 \leq r \leq 0.36$, $.01 \geq P \geq .0001$), whereas serum CTX correlated with all resorption parameters ($0.18 \leq r \leq 0.24$, $.02 \geq P \geq .0001$). These associations are rather modest, but this is not surprising, as systemic bone markers reflect the turnover of the entire skeleton including the periosteal, cortical, endocortical, and cancellous compartments, whereas histomorphometric parameters assess a small part of the iliac crest. A combined calcium balance and tracer study in women with osteoporosis (Eastell et al., 1997) also showed positive correlation between the estimated resorption and concentration of bone resorption markers, with DPD having the highest correlation coefficient. The available studies of bone turnover marker (BTM) validation have shortfalls including limitations of the reference methods such as availability, cost, and small sample size.

BTM selection depends on the clinical context. In metabolic bone diseases such as Paget's disease of bone and patients with bone metastases (BMs), some type I collagen degradation markers are more sensitive than serum beta CTX. These include urinary NTX and the nonisomerized form of CTX (αCTX) (Garnero et al., 1997; Leeming et al., 2006). Bone ALP, intact PINP (bone formation), and TRAP5b (bone resorption) would be appropriate for assessing bone disorders in chronic kidney disease (because these markers are excreted not by the kidney but by the liver), and osteocalcin (bone formation) or CTX (bone resorption) would be appropriate for assessing glucocorticoid-induced osteoporosis.

However, the established biochemical markers, including serum CTX and PINP, have some limitations. These include (1) a lack of tissue specificity for bone, as type I collagen is widely distributed in different organs, (2) an inability to distinguish the metabolic activity of the different skeletal compartments even though they can be differently affected by

TABLE 78.1 Established markers of bone turnover.

Bone formation (serum marker)	Bone resorption (serum or urine marker)
Osteocalcin: intact, total, or undercarboxylated	*Serum* and urine ***cross-linked C-telopeptide of type I collagen (S-βCTX,*** CTX)
Bone alkaline phosphatase	Serum and urine cross-linked N-telopeptide of type I collagenS
Procollagen type I N-terminal propeptide	Serum cross-linked C-telopeptide of type I collagen generated by matrix metalloproteinases (CTX-MMP or ICTP[a])
Procollagen type I C-terminal propeptide	Urinary free and total deoxypyridinoline
	Serum tartrate-resistant acid phosphatase isoenzyme 5b
	Urinary free and total deoxypyridinoline

The markers recommended by the IOF−IFCC as reference markers for use in clinical studies are indicated in bold italic.
[a]CTX-MMP *is the official abbreviation;* ICTP *is the most commonly used abbreviation.*

TABLE 78.2 New biological markers of bone metabolism.

Noncollagenous protein	Osteoclastic enzyme	Regulatory molecule	Hormone	"Omics"
Total periostin CatK-periostin	Cathepsin K	Osteoprotegerin RANKL Dkk1 Sclerostin Sphingosine-1 phosphate	FGF-23 Klotho	Proteomic Metabolomic miRNAs

diseases and treatments, (3) reflecting mainly the function of osteoblasts or osteoclasts and not the activity of osteocytes even though these cells are the most abundant of bone tissue and play a pivotal role in the maintenance of skeletal integrity, and (4) all of them being single protein-based markers, although circulating proteomic, metabolomic, or microRNA (miRNA generally; miR for specific numbers) signature could provide an earlier and/or a more integrated view of bone remodeling alterations. The new biochemical markers described in the following section may overcome some of these limitations (Table 78.2).

Novel biological markers of bone metabolism

The novel markers can be classified in different groups as shown in Table 78.2. These include the measurements of some noncollagenous proteins, osteoclastic enzymes other than TRACP5b, osteocyte-secreted factor, molecules involved in coupling between osteoclast−osteoblasts, hormones, and "omics" markers such as proteomic and metabolomic patterns and circulating miRNAs. The most promising candidates in each category and their clinical relevance for the investigation of patients with osteoporosis and other metabolic bone diseases are discussed next.

Periostin

The periosteum covers long bones, and although in adults its metabolism is considered low, it plays an important role for controlling the diameter of bones and thus bone strength (Seeman, 2007). Currently, however, there are no available noninvasive biological tools allowing the assessment of periosteal metabolism, as current bone markers reflect mainly endosteal bone remodeling (Szulc et al., 2005). Periostin (POSTN) may be a candidate marker of periosteal metabolism. Detailed reviews of the structure, regulation, and involvement of this protein in bone metabolism have been recently published (Merle and Garnero, 2012; Bonnet et al., 2016).

POSTN is mainly expressed by periosteal osteoblasts and osteocytes—although osteoclasts may also express low levels (Merle et al., 2014). At the protein level, it is composed of a signal sequence followed by an Emilin domain rich in cysteine, four repeated and conserved Fasciclin-1 (FAS-1) domains, and a C-terminal hydrophilic and variable domain. Alternative splicing of the C-terminal domain gives rise to at least five different human isoforms. Each FAS-1 domain is rich in glutamate residues and contains an N-terminal recognition site for the vitamin K-dependent enzyme γ-glutamyl carboxylase (γ-carboxylase recognition sites) responsible for posttranslational modification of glutamic residues to γ-carboxyglutamate. This protein belongs to the matricellular protein family because it contains binding sites for extracellular matrix proteins, such as type I and type V collagens, and the cell surface receptor integrins. In adults, POSTN has been shown to be overexpressed at the periosteal surface as well as in other collagen-rich tissues subjected to mechanical strain such as periodontal ligaments, heart valves, and tendons (Merle and Garnero, 2012; Bonnet et al., 2016).

The most informative data on the function of POSTN in bone metabolism have been obtained from studies using POSTN-deficient mice. These mice develop periodontitis and osteoporosis with lower bone mineral density (BMD), altered microarchitecture, and decreased bone strength (Bonnet et al., 2009). These studies have also shown POSTN to be an important mediator of the effects of mechanical factors and parathyroid hormone (PTH) on cortical BMD and bone strength by modulating the canonical Wnt signaling pathway via downregulation of sclerostin (SOST) expression (Bonnet et al., 2009, 2012).

POSTN not only is involved in regulating bone formation and BMD but also could have an effect on bone strength by regulating collagen cross-linking (Kii et al., 2010). POSTN interacts in bone tissue with bone morphogenic protein 1, which catalyzes the lysyl oxidase activation that promotes collagen cross-linking (Maruhashi et al., 2010).

Circulating periostin as a potential clinical biomarker

Because POSTN is a secreted protein, it can be measured in peripheral biological fluids including serum. Several clinical studies have been performed using various research enzyme-linked immunosorbent assays (ELISAs) based on polyclonal or monoclonal antibodies with different specificities. There are several commercially available immunoassays but the most widely used are the following three. The USCN (China) assay uses a polyclonal antibody raised against the FAS-1 domain of POSTN and is expected to detect all POSTN isoforms (Rousseau et al., 2014, 2015). This assay has been used in most published clinical studies. Two other ELISAs, from Adipogen (Switzerland) and Biomedica (Austria), were more recently developed. These two site assays use a combination of a monoclonal and polyclonal antibodies raised against human recombinant POSTN. However, the exact specificity of the antibodies is unknown, and it remains unclear which molecular forms they are detecting in the serum. Because research and commercial assays are not standardized, it is difficult to compare the results between studies, and this could influence the interpretation of the data. In young adults, serum POSTN measured by the Biomedica assay was shown to correlate with serum insulin-like growth factor 1 (IGF-1) and high-resolution peripheral quantitative computed tomography (HR-pQCT) measures of cortical bone. This suggests that POSTN could have a role in IGF-1-driven cortical modeling and consolidation (Walsh et al., 2017). In postmenopausal women, serum POSTN had zero or weak correlation (Rousseau et al., 2014, 2015; Walsh et al., 2017; Anastasilakis et al., 2014) with spine and hip areal BMD. Similarly, serum POSTN was not or only slightly associated with conventional markers of bone formation and bone resorption (Rousseau et al., 2015; Walsh et al., 2017; Anastasilakis et al., 2014). These data indicate that when assayed in serum, POSTN levels reflect biological processes different from those captured by static (BMD) or dynamic (bone marker) indices of bone metabolism. In a cohort of healthy elderly men and women, a positive correlation between serum POSTN and HR-pQCT-assessed cortical bone thickness was observed; it correlated negatively with cortical porosity, although these associations were no longer significant after adjusting for gender and age. In the same individuals, serum POSTN was not correlated with trabecular bone volume fraction (BV/TV) after adjustment by PINP, serum CTX, BMD, gender, or age (Bonnet et al., 2015). There was also an association of POSTN levels between parents and adult offspring, with an estimated heritability of 50%, and a genetic covariance was found between serum POSTN and bone microarchitecture. In a cohort of postmenopausal women, the highest quartile of serum total POSTN measured by the USCN assay was associated with an increased risk of all incident fractures independently of BMD and conventional bone markers (Rousseau et al., 2014). These data were more recently confirmed in another case−control study of postmenopausal women from Korea (Kim et al., 2015). A positive association was found between serum POSTN and all incident fractures independently of BMD (Kim et al., 2015). When vertebral and nonvertebral fractures were analyzed separately, POSTN levels were associated only with the latter type of fracture, which is in agreement with the predominant role of POSTN on cortical bone metabolism (Kim et al., 2015). Altogether, available clinical data suggest that serum total POSTN could be a new biological marker of fracture risk, and more specifically nonvertebral fracture in postmenopausal women. The fact that it is independent of both BMD and bone markers suggests that the measurement of serum POSTN could be useful in combination with these two key risk factors to improve risk assessment. These data, however, need to be confirmed in larger independent studies.

Because POSTN has been shown to be an important mediator of the anabolic activity of PTH in animal studies, circulating POSTN may be useful in assessing the effects of PTH and its derivatives in humans. A recent open-label single-arm study showed that serum POSTN was moderately but significantly increased after 52 weeks of treatment with teriparatide in postmenopausal women with osteoporosis (Gossiel et al., 2018). In addition, the change in serum POSTN was significantly and positively associated with changes in lumbar spine and hip BMD after 1 and 2 years, respectively.

Total serum POSTN as measured by commercially available immunoassays is not specific, however, as serum levels represent the additional contribution of the metabolism of other tissues. It is possible that bone-specific isoforms or POSTN fragments could be a more sensitive index of fracture risk. In that respect, it is interesting to note that specific POSTN isoforms have been described in other tissues such in fibrotic lung, heart and skin (Kuhn et al., 2007; Uchida et al., 2012; Masuoka et al., 2012). Thus, it may be possible to identify bone-specific POSTN isoforms or POSTN bone-specific fragments. It has recently been shown that mouse and human POSTN are efficiently degraded by the osteoclast-specific enzyme cathepsin K (Garnero et al., 2017). Cathepsin K−generated POSTN fragment(s) may thus be a candidate of such a bone-specific biochemical marker. Based on these assumptions, we recently developed a competitive ELISA that specifically detects a fragment of POSTN generated by the catalytic action of cathepsin K (Garnero et al., 2017). We found that serum levels of this new marker (so-called K-POST) was not associated with areal hip BMD, serum PINP, and CTX, but was negatively correlated with cortical bone parameters of the tibia assessed by HR-pQCT in a cohort of elderly women. Interestingly, increased levels of this marker were also significantly associated with the risk of low-trauma clinical fracture even after multiple adjustments including serum CTX, PINP, areal BMD, and the Fracture Risk Assessment Tool index, whereas total POSTN measured by the USCN commercial assay was not predictive (Bonnet et al., 2017).

Receptor activator of NF-kB ligand and osteoprotegerin

Measurements of regulators of osteoclastic and osteoblastic differentiation and activity have been suggested as useful in assessing bone metabolism in osteoporosis, arthritis, and metastatic bone diseases. The receptor activator of *NF-kB ligand (RANKL)/RANK/osteoprotegerin (OPG)* system is one of the main regulators of osteoclast formation and function as demonstrated by a series of preclinical and clinical studies (for a review, see Kearns et al., 2008). It has been shown that serum RANKL levels were increased in patients with systemic autoimmune diseases before glucocorticoid therapy compared with healthy controls (Kaneko et al., 2012). Patients with high baseline RANKL levels demonstrated an increase in BMD after therapy, whereas BMD decreased in those with lower RANKL values. This suggests that serum pretreatment RANKL may be useful for predicting the response to glucocorticoid in patients with systemic autoimmune diseases. In order to increase the sensitivity of systemic measurements, OPG and RANKL expression have been measured in peripheral blood mononuclear cells (PBMCs). No changes in OPG or RANKL expression could be demonstrated in PBMCs of postmenopausal women after treatment with either ibandronate or strontium ranelate (Stuss et al., 2013). Measuring circulating RANKL and OPG remains challenging, especially RANKL, because their levels are very low. It is also unlikely that circulating levels of OPG and RANKL adequately reflect local bone marrow production. These limitations explain the conflicting data on the association of circulating OPG and RANKL with BMD and biochemical BTMs in postmenopausal women and elderly men (Findlay and Atkins, 2011). The OPG/RANKL system is also likely to play a role in the bone−vascular axis. Indeed, in postmenopausal women with osteoporosis and hypercholesterolemia, statin treatment leads to a significant increase of serum OPG and RANKL expression in T cells (Rattazzi et al., 2016).

Dickkopf-related protein 1

The Wingless (Wnt) signaling pathway plays a pivotal role in the differentiation and activity of osteoblastic cells (Day et al., 2005). The primary receptors of Wnt molecules are the seven-transmembrane Frizzled-related proteins (FRPs), each of which interacts with a single transmembrane low-density lipoprotein receptor-related protein 5/6 (LRP5/6). Different secreted proteins including soluble FRPs (sFRPs), Wnt inhibitory factor 1, and Dickkopf (Dkk) 1 to Dkk4 prevent ligand−receptor interactions and consequently inhibit the Wnt signaling pathway. Alterations of the Wnt signaling pathway and its regulatory molecules including Dkk1 and sFRPs play an important role in bone turnover abnormalities associated with osteoporosis, arthritis, multiple myeloma (MM), and BMs from prostate and breast cancer. Immunoassays for circulating Dkk1 have been developed. Serum Dkk1 levels have been reported to be increased in clinical situations characterized by depressed bone formation such as MM (Tian et al., 2003) but also in diseases characterized by focal osteolysis such as MM (Tian et al., 2003), BMs from breast or lung cancer (Voorzanger-Rousselot et al., 2007), and rheumatoid arthritis (Diarra et al., 2007). Conversely, in patients with osteoarthritis of the hip, a clinical situation characterized by focal sclerosis of subchondral bone, lower serum Dkk1 levels have been associated with a decreased risk of joint destruction (Lane et al., 2007; Voorzanger-Rousselot et al., 2009a). In postmenopausal osteoporosis, a negative association of Dkk1 with BMD has been reported (Butler et al., 2011; Anastasilakis et al., 2010). Dkk1 was decreased after 12 months of glucocorticoids (Gifre et al., 2013). Interestingly, serum Dkk1 has been reported to increase after 12 and 18 months of teriparatide treatment in women with postmenopausal osteoporosis, which may explain the waning of the anabolic effect of this drug (Gatti et al., 2011). After treatment with yearly zoledronic acid, serum Dkk1 transiently increases within 1 month and declines thereafter (Gatti et al., 2014; Anastasilakis et al., 2013), whereas with an intramuscular monthly injection of a non-nitrogen-containing bisphosphonate such as clodronate, the level of Dkk1 is not affected (Gatti et al., 2012a). Dkk1 serum levels are unaffected 3 months after treatment with denosumab (Anastasilakis et al., 2013). In another longer-term study, serum Dkk1 decreased within the first 6 months of denosumab treatment and reached statistical significance compared with placebo at 18 months. The changes in Dkk1 were significantly and positively related to serum CTX and bone ALP (Gatti et al., 2012a). In patients with active RA, it was shown that 6-month anti-TNF therapy induces a small but significant decrease of serum Dkk1 (Adami et al., 2016). As for the assessment of OPG and RANKL, circulating Dkk1 might not adequately reflect local bone contribution. One way to increase the sensitivity of circulating Dkk1 measurements may be to use an assay based on the binding of Dkk1 on LRP6, or so-called functional Dkk1. Circulating functional Dkk1 was associated with radiological progression in patients with ankylosing spondylitis (AS), whereas total Dkk1 was not predictive (Heiland et al., 2012). In AS, it was also shown that increased serum Dkk1 is associated with low BMD and a higher prevalence of vertebral fracture (Rossini et al., 2016).

From a practical point of view, measurements of Dkk1 in plasma are recommended, as platelets activated during the clotting process to obtain serum are major contributors to circulating Dkk1 (Voorzanger-Rousselot et al., 2009b).

Sphingosine-1-phosphate

Sphingosine-1-phosphate (S1P) is a lipid mediator that acts on different functions of cells through S1P receptors (SP1R, SP1R1, and SP1R2) of the G-protein-coupled receptor family (During et al., 2015; Meshcheryakova et al., 2017). Although S1P may affect the proliferation, survival, and migration of osteoblasts (Grey et al., 2002, 2004; Roelofsen et al., 2008), the dominant effect of this protein on bone metabolism seems to be on osteoclastogenesis. Indeed, in vitro and in vivo experiments have shown that S1P significantly potentiates osteoclast differentiation by increasing RANKL in osteoblasts (Ryu et al., 2006). When substantial gradients exist between S1P concentrations in blood and bone, the migration of osteoclast precursors from blood (high S1P state) to bone (low S1P state) is facilitated (Ishii et al., 2009, 2010). The deletion of SP1R1 in monocyte cells leads to an accumulation of osteoclast precursors and a resultant increase in bone resorption (Lee et al., 2012). Conversely, SP1R2-deficient mice exhibit moderate osteopetrosis as a result decreased osteoclastic bone resorption (Ishii et al., 2010). Thus, SP1R1 exerts positive chemotaxis to an S1P gradient, whereas SP1R2 induces migration in the inverse direction—so-called chemorepulsion. Increased serum S1P levels were found to be associated with high levels of bone resorption—but not bone formation—markers, low BMD, and a higher risk of prevalent vertebral fractures in postmenopausal women (Lee et al., 2012; Kim et al., 2012). The predictive value of plasma S1P was investigated in 248 postmenopausal women who were either untreated or receiving HRT or bisphosphonate and followed prospectively over 3.5 years. It was reported that women with baseline levels of S1P in the highest tertile had a 5.5-fold increased risk of incident vertebral fracture compared with women with levels in the two lower tertiles, independently of BMD and prevalent fracture (Bae et al., 2016). A case–control study also reported that in patients with hip fracture, the plasma/bone marrow ratio of S1P was elevated compared with controls, whereas neither plasma nor bone marrow level alone could discriminate the two groups (Kim et al., 2016). Thus, the effect of S1P on bone fragility may depend on the ratio between levels in the peripheral circulation and bone marrow compartment. Altogether, these data suggest that the measurement of circulating S1P levels and/or its plasma/bone marrow ratio could be a new biological marker of fracture risk, although these data obtained in small number of Asian subjects require confirmation in larger prospective studies and other ethnicities.

Sclerostin

SOST is a 22 kD secreted protein that binds LRP5 and LRP6 and thereby inhibits the Wnt signaling pathway and consequently bone formation (Li et al., 2005; Semenov et al., 2005). SOST can also stimulate the secretion of osteocyte-derived RANKL, thereby activating directly osteoclast activity (Wijenayaka et al., 2011; Xiong and O'Brien, 2012). Placebo-controlled studies in postmenopausal women demonstrated that injection of monoclonal blocking antibodies against SOST, romosozumab, and blosozumab transiently increased bone-formation markers and BMD and was associated with decreased bone resorption markers (McClung et al., 2014; McColm et al., 2014; Recker et al., 2015; Appelman-Dijkstra and Papapoulos, 2016).

Different immunoassays including three commercially available tests have been developed to detect SOST changes in blood. The two ELISAs from Biomedica and TECOmedical, and the Meso Scale Discovery (MSD) electrochemiluminescence assay, use antibodies recognizing different epitopes on the SOST molecule. They are likely detecting different circulating immunoreactive forms (Durosier et al., 2013). The MSD test recognizes only the intact molecule, whereas the two ELISAs also measure fragments from SOST and possible other structurally similar but unrelated molecules. It has been shown that although all three assays were highly correlated, especially the two ELISAs (Costa et al., 2014), absolute levels can differ markedly, and their association with bone turnover and PTH may also vary (Durosier et al., 2013). Because circulating SOST highly correlates with bone marrow plasma values, serum level is likely to reflect local bone production (Costa et al., 2014).

SOST levels are slightly higher in girls prior to puberty, tend to decrease in both sexes during puberty, but remain significantly higher in boys than in girls after puberty (Kirmani et al., 2012). SOST was found to be significantly higher in postmenopausal women than in premenopausal controls (Mirza et al., 2010). In healthy women and men, SOST levels increased over lifetime by respective averages of 2.4-fold and 4.6-fold (Modder et al., 2011a; Ardawi et al., 2011). In postmenopausal women, SOST correlated negatively with total and free estradiol and with intact PTH (Modder et al., 2011b).

The association of SOST with fracture risk has been investigated in elderly women and men, with discordant data (Arasu et al., 2012; Ardawi et al., 2012; Garnero et al., 2013; Szulc et al., 2013) between studies. This suggests that the clinical utility of this marker to predict fracture risk in osteoporosis is probably limited. SOST levels are higher in patients with type 2 diabetes (T2D) (Gennari et al., 2012; Garcia-Martin et al., 2012; Ardawi et al., 2013; Yamamoto et al., 2013).

In these subjects, serum SOST was negatively associated with BTMs and positively with BMD. Postmenopausal women with T2D and increased serum SOST had a higher risk of prevalent fractures independently of BMD and bone turnover. These findings suggest that SOST could be a determinant of skeletal fragility in patients with T2D (Starup-Linde et al., 2016), although they require confirmation by longitudinal studies. SOST expression has been reported in the wall of calcifying arteries (Caira et al., 2006; Roman-Garcia et al., 2010), and serum SOST is associated with vascular calcification in postmenopausal women (Hampson et al., 2013), patients with T2D (Morales-Santana et al., 2013), patients with rheumatoid arthritis (Paccou et al., 2014), and chronic kidney disease subjects (Thambiah et al., 2012; Evenepoel et al., 2015; Lv et al., 2016a). Thus, serum SOST could be a new biological marker of vascular calcification.

Fibroblast growth factor 23 and klotho

Fibroblast growth factor 23 (FGF-23) is a circulating factor expressed predominantly in osteocytes that negatively regulates serum levels of inorganic phosphorous and 1,25-dihydroxyvitamin D_3 (Riminucci et al., 2003; Liu et al., 2003; Shimada et al., 2004). The release of FGF-23 by both young and old osteocytes may be a mechanism whereby osteocytes can control mineralization (Wang et al., 2008) and phosphate homeostasis. A cofactor, α-klotho, is needed for FGF-23 to bind to FGF receptors (Kuro-o, 2013). α-Klotho heterodimerizes with the FGFR1 receptor in the parathyroid tissue and distal convoluted tubule of the kidney, yielding a high-affinity receptor for FGF-23 (Urakawa et al., 2006). Several clinical skeletal disorders that result in mineralization abnormalities and elevated FGF-23 serum levels have been reported and include autosomal-dominant hypophosphatemic rickets, tumor-induced osteomalacia, and X-linked hypophosphatemic rickets (Wang et al., 2008; Bonewald and Wacker, 2013). Moreover, mice overexpressing FGF-23 have low cortical and trabecular BMD (Larsson et al., 2004). Given the importance of FGF-23 as a regulator of phosphate homeostasis, it is possible that this osteocyte factor could be associated with bone strength and fracture risk.

FGF-23 is synthesized as a molecule of 251 amino acids including a leader sequence coding for a signal peptide of 24 amino acids. During secretion, FGF-23 can be proteolytically cleaved between Arg179 and Ser180 to generate N-terminal and C-terminal fragments. Thus, in circulation, FGF-23 can be present as the intact form and C- and N-terminal fragments (Komaba and Fukagawa, 2012). Circulating FGF-23 can be measured by immunoassays that detect only the intact molecule, or with a C-terminal assay that detects both intact FGF-23 and C-terminal fragments. Currently it remains unclear whether the C-terminal assay will give results comparable to the intact one in different clinical situations.

Two prospective studies have analyzed the relationships between serum intact FGF-23 and fracture risk in elderly men. Mirza et al. (2011) measured baseline intact FGF-23 in 2868 elderly Swedish men (mean age 75 years) followed prospectively for more than 3 years. They found that increased baseline intact FGF-23 was associated with increased risk of all fractures and vertebral fractures. For nonvertebral and hip fracture, the relationship was not linear—only patients with serum levels of FGF-23 in the highest quartile have increased risk of fracture. Interestingly, the association remained significant after adjustment for several potentially confounding factors such as BMD, PTH, and glomerular filtration rate (GFR). Lane et al. (2013) performed a case–control investigation in 387 men with incident nonvertebral fractures including 75 hip fractures and a random sample of 1385 elderly men (>65 years, mean 74 years) participating in the US MrOS study. In contrast to the findings in Swedish men, they overall found no significant association of serum FGF-23 analyzed in quartiles and the risk of nonvertebral or hip fracture. When subjects were stratified according to renal function, however, there was a twofold higher risk of nonvertebral fracture for patients with levels of serum FGF-23 in the highest quartile—only among those with a GFR <60 mL/min/1.73 m^2. The reasons for the discrepancy between these two studies remain unclear, and additional data in prospective studies in men and postmenopausal women with various degrees of renal function would be helpful. Recently, the association of serum klotho with BMD loss and incidence of fracture was investigated in the Health, Aging and Body Composition Study (commonly known as the Health ABC Study) comprising 2776 older individuals followed prospectively for 5 years. There was no association of baseline serum klotho with spinal and hip bone loss nor with the risk of vertebral, nonvertebral, and hip fracture (Chalhoub et al., 2016).

Proteomic signature

As reviewed previously, conventional biochemical marker studies focus on a limited number of molecules and are usually based on previously established biological relevance. Proteomic studies, on the other hand, allow for an unconstrained approach to the analysis of a broad array of proteins or their fragment peptides without the need for a priori knowledge of their involvement in a particular disease state. Such an approach has been utilized particularly in the cancer field (Petricoin et al., 2002; Liotta and Petricoin, 2006). More recently, serum proteomic analyses have expanded to other diseases such as metabolic syndrome (Lamers et al., 2011) and type 1 diabetes (Moulder et al., 2015). Proteomic analysis is usually

performed on serum samples that are first depleted of abundant proteins such as albumin. Samples are subsequently digested by trypsin, and the tryptic peptide samples are analyzed using an LC−MS−MS platform (Baker et al., 2014). Detection and quantification of LC−MS−MS features with characteristics (mass, charge, LC elution time, MS drift time, and abundance) are performed using specific software. The detected features are then identified by mapping their mass, elution time, and drift time using other software tools (Crowell et al., 2013; Zimmer et al., 2006).

This proteomic approach has been used recently to predict hip bone loss and the incidence of hip fracture in MrOS study (Nielson et al., 2017). Twenty proteins were found to be significantly associated with accelerated BMD loss, and among them, five were also predictive of hip fracture risk. Some of these proteins have been previously associated with fracture risk (e.g., CD14 and SHBG), whereas others have roles in cellular senescence and aging (B2MG and TIMP1) and complement activation and innate immunity (CO7, CO9, CFAD). Selective reaction monitoring allows detection of multiple proteins in a single sample and can thus be used to easily assess a proteomic signature provided that it can be replicated in other studies, reliably yielding more robust predictions of outcomes than do the measurements of single molecules.

Metabolomic signature

Metabolomic is an emerging "omics" science that involves comprehensive and systematic profiling of low-molecular-weight end product metabolites from tissues, cells, or biological fluids (Wilson et al., 2005). This is a potentially powerful technology, as small changes in gene and protein expression could be amplified at the metabolic level. Alterations in the composition and concentration of metabolites may also enable the screening of potential biomarkers closely related to diseases. Up to now, metabolomics has found applications in many chronic metabolic disorders, such as diabetes, lung disease, neurodegenerative diseases, cancer, hypertension, and cardiovascular diseases (Tan et al., 2016; Wang et al., 2012a; Blekherman et al., 2011). The application of metabolomics in osteoporosis has just begun.

From a technical point of view, metabolomics is a method of systematic, qualitative, and quantitative analysis of metabolites in organism. Proton nuclear magnetic resonance (1H NMR) and mass spectrum (MS)-based techniques used in metabolomics exhibit properties of relatively high sensitivity, high resolution, and high throughout. However, metabolomic data are influenced by several preanalytical factors—including how samples are collected and processed—that need to be carefully controlled.

Metabolomics has been used in several preclinical osteoporosis studies as reviewed recently (Lv et al., 2016b). A few studies investigated serum metabolic profiles in osteoporosis clinical studies. The study from Qi et al. (2016) involved 364 female subjects from China divided into four groups (premenopausal women with normal BMD, postmenopausal women with normal BMD, postmenopausal women with osteopenia, and postmenopausal women with osteoporosis) (Qi et al., 2016). It was reported that women with low BMD had increased linoleic acid, oleic acid, arachidonic acid, 11,14-eicosadienoic acid, eicosapentaenoic acid, and tryptophan as well as lower 3-hydroxy-L-proline, which suggests alterations in lipid, amino acid, and energy metabolism. You et al. (2014) performed a cross-sectional metabolomic study in 601 Taiwanese women separated into two groups of postmenopausal women with high or low BMD (You et al., 2014). This study demonstrated that women with low BMD are characterized by increased acetate and glutamine and decreased glucose, VLDLs, lactate, acetone, and lipids, suggesting alteration in the metabolism of pyruvate, fatty acid, carbohydrate, D-glutamine, and D-glutamate. Sheedy et al. (Sheedy et al., 2014) used a 1H NMR-based metabolomics approach to analyze urine samples from participants recruited for an 18-month randomized controlled trial of a multicomponent progressive resistance training exercise program and calcium−vitamin D3-fortified milk consumption in healthy middle-aged and older men (Sheedy et al., 2014). There was no change in urinary metabolome in response to calcium−vitamin D3 intervention, while significant metabolite alterations following exercise intervention were observed, notably a reduction in creatinine and an increase in choline, guanidinoacetate, and hypoxanthine. Finally, Miyamoto et al. (2017) compared serum metabolome analyzed using capillary electrophoresis/MS in postmenopausal women with low and normal BMD. They could detect 57 different serum metabolites. Compared with women with normal BMD ($n = 42$), women with low BMD ($n = 5$) had significantly lower levels of Gly-Gly dipeptide and cystine, whereas hydroxyproline was increased. However, because the number of subjects was very limited, these data should be interpreted cautiously and need to be replicated in larger studies.

To date, metabolomic-based osteoporosis studies have been performed using the untargeted metabolomic approach. While the untargeted metabolomics method can provide comprehensive information on molecular weight and sample composition, it has limitations including poor specificity, large fluctuations from the instrument, and poor reproducibility of results. To improve selectivity and accuracy, it would be important in the future to combine targeted metabolomic studies with untargeted metabolomics.

MicroRNAs

The miRNAs are a class of small (~22 nucleotides), single-stranded noncoding RNAs (Hobert, 2008). They induce either translational repression or cleavage of target messenger RNAs (mRNAs) by imperfect or perfect base-pairing with specific sequences in the 3′ untranslated regions (UTRs) of target mRNAs. Interactions between mRNAs and miRNAs demonstrate two important characteristics: (1) a single miRNA is capable of binding to 100 or more distinct mRNA species, and (2) UTRs of most mRNAs contain binding sites for several miRNAs. The resulting pleiotropy of interactions and cooperative activities of miRNAs enables the regulation of complex gene expression networks in a fashion similar to that of transcription factors. Several in vitro and a few in vivo animal studies have shown that miRNAs play important roles in osteoblast (Lian et al., 2012) and osteoclast (Sugatani and Hruska, 2009) differentiation and function. As recently reviewed, miRNAs are not only involved in normal osteoblast and osteoclast function but also can be deregulated in bone disease states including osteoporosis (van Wijnen et al., 2013; Hackl et al., 2016; Wang et al., 2013).

A study showed that miR-214 levels are elevated in bone tissue specimens from older individuals with fracture, and that levels correlated with several biological and histological indices of bone formation (Wang et al., 2013). The target gene of miR-214 was identified; it is *ATF4*, which codes for an important transcription factor required for osteoblast function (Wang et al., 2013). miRNAs are released from cellular cytoplasm into biological fluids within extracellular vesicles (Valadi et al., 2007) or vesicles formed by high-density lipoproteins (Vickers et al., 2011) as well as in association with RNA-binding proteins such as nucleoplasmin or proteins of the argonaut family (Wang et al., 2010; Arroyo et al., 2011).

From a diagnostic point of view, measuring circulating miRNAs would be very attractive, as they may provide valuable information about alterations of bone metabolism and possibly earlier than protein-based biomarkers. The vesicular or protein association of circulating miRNAs accounts for their remarkable stability in biological fluids. They are resistant to RNase activity in the peripheral blood and thus may serve as excellent biomarkers (Gilad et al., 2008; Mitchell et al., 2008). However, as protein-based biomarkers, measurement of circulating miRNAs has some limitations. Blood levels may vary significantly with lifestyle and comorbidities, circadian rhythm (Shende et al., 2011), liver and kidney functions, smoking habits, and diet (Witwer, 2012). Thus, measurements of circulating miRNAs require a strict definition of inclusion and exclusion criteria in order to minimize the impact of these sources of variability and maximize the signal/noise ratio. For example, miRNA assessment can be improved by limiting measurements to patients with normal renal function (>30 mL/min/1.73 m^2) and the use of samples taken early in the morning after overnight fasting. Analytical factors can also substantially affect miRNA measurement variability. The different qPCR platforms are not standardized and can introduce variability. Similarly, levels can vary according to PCR protocols even on the same platform. In addition, most miRNA data are relative expression values rather than absolute levels, and there is currently no consensus on which selected reference gene, global mean normalization, or other approach performs best.

Although many studies have analyzed circulating miRNAs in different diseases including cancer, data on osteoporosis are limited. The first attempt to identify circulating miRNAs as biomarkers of osteoporosis focused on measuring them in monocytes, which are a circulatory reservoir of osteoclast precursors. Wang et al. (Wang et al., 2012b) showed that miR-133a was upregulated in peripheral monocytes from 10 patients with low BMD compared with 10 healthy controls, although such a difference could not be found when miRNA was isolated from B cells. CXCL11, CXCR3, and SLC39A1, which are involved in osteoclast differentiation, were identified as putative target genes. Li et al. (2014) replicated the upregulation of miR-133a in cell-free plasma samples of osteoporotic compared with osteopenic women from a cohort of 120 Chinese postmenopausal women. Besides miR-133a, Li et al. (2014) also reported a downregulation of circulating miR-21-5p. Both miRNA levels correlated with spinal and hip BMD (Li et al., 2014). Conversely, levels of miR-503 were reported to be decreased in CD14+ monocytic PBMCs of 10 untreated postmenopausal women with osteoporosis compared with those of 10 women with normal BMD (Chen et al., 2014). In ovariectomized mice, the authors showed that silencing of miR-503 using a specific antagomir increased RANK protein expression, promoted bone resorption, and decreased bone mass. Conversely, the overexpression of miR-503 with agomir inhibited bone resorption and prevented bone loss. Cell-free miRNAs were analyzed in the serum of 60 patients with hip fracture who were categorized as osteoporotic and nonosteoporotic based on dual-energy X-ray absorptiometry (DXA) BMD assessments (Seeliger et al., 2014). Nine miRNAs were found to be upregulated in patients with osteoporosis, and among those, six [miRs 21, 23a, 24, 25, 100, and 125b] were also significantly increased in the corresponding hip bone tissue. Weilner et al. (2015) compared the serum miRNA of patients who had recent fractures with that of healthy controls and identified 10 miRNAs differentially expressed including miRs let-7g, 10b, 133b, 22, and 328. Two other studies analyzed circulating miRNA in patients with osteoporosis compared with controls. Panach et al. (2015) reported 12 differently expressed miRNAs among the 179 analyzed in patients with fractures compared with subjects with osteoarthritis used as controls. They confirmed that among those, miRs 122, 125, and 21 were upregulated in an independent validation sample. Interestingly, these miRNAs

were also identified by Seeliger (Seeliger et al., 2014), and miR-21 levels were significantly correlated with the bone-resorption marker CTX. The regulation of 331 miRNAs in whole blood samples was investigated in 48 postmenopausal women stratified according to BMD levels (Meng et al., 2015). The investigators initially identified six miRNAs differently expressed between 25 osteoporotic women and 23 women with osteopenia. In a replicative study, five (miRs 130b, 151a, 151b, 194, and 590) of six miRNAs were confirmed to be increased in patients with osteoporosis. miR-194 expression levels were found to be significantly different between 24 postmenopausal women with normal BMD values, 32 osteopenic subjects, and 32 individuals with osteoporosis, with values correlating with BMD T-scores. Finally, Yavropoulou et al. (2017) analyzed the serum level of 14 targeted miRNAs in 35 women with fracture, 35 women with low BMD and no fracture, and 30 healthy controls. Among them, 2 were found to be increased in cases versus controls (miRs 124 and 2861), whereas 3 others were downregulated (miRs 21-5p, 23a, and 23a-3p).

A recent study investigated circulating miRNA expression according to the presence and absence of fracture in 80 postmenopausal women with T2D (Heilmeier et al., 2016). The identification of new risk factors for fragility fracture in T2D is critically needed, as BMD and conventional protein-based biochemical markers are poorly predictive. Using miRNA−qPCR arrays, the investigators showed that 48 miRNAs can differentiate fracture status in T2D women, and that several combinations of four miRNAs were able to discriminate diabetes-related fractures with high specificity and sensitivity (AUCs: 0.92−0.96; 95% CI: 0.88−0.98). Among the most discriminative miRNAs, in vitro studies showed that miR-382 significantly enhanced osteogenic differentiation, while miR-550a inhibited this process. These two miRNAs impaired adipogenic differentiation.

Other situations where new predictive biomarkers are awaited are in men with idiopathic osteoporosis, premenopausal women, and postmenopausal women with osteopenia (Kocijan et al., 2016). A recent study investigated serum miRNA profiling in 10 premenopausal women, 10 postmenopausal women, 16 men with idiopathic osteoporosis, and 39 age-matched controls. It was found that among the 187 circulating miRNAs investigated, expression was altered in 19 of them in patients compared with controls. Interestingly, a combination of eight of them was highly predictive with an area under the ROC greater than 0.9. Some of these miRNAs—including miR-29b-3, which has been found to be involved in the regulation of extracellular matrix formation via collagen type I expression—correlated with PINP, a marker of type I collagen synthesis.

As shown from Table 78.3, the available studies that investigated blood levels of miRNAs are all cross-sectional and included a limited number of subjects. Data between studies are difficult to compare, as the criteria to classify cases and controls were different and the technical platforms were not standardized. Before these candidate miRNAs can be used clinically to investigate alterations of bone metabolism in osteoporosis, data need to be confirmed in substantially larger studies, ideally prospective in design with fracture incidence as an outcome. It can be foreseen that in the future this field will markedly expand and may lead to the discovery of a signature of circulating miRNAs, thus demonstrating clinical utility for the investigation of patients with osteoporosis.

Variability of biochemical markers of bone turnover

The measurement of established protein bone markers is subject to variability that is important to consider when interpreting data. Different sources of variability have been identified including preanalytical conditions, assay technical precision, and biological variability. Among the sources of preanalytical variability that have been reviewed in detail elsewhere (Naylor and Eastell, 2012; Garnero, 2008; Hlaing and Compston, 2014), the most important are (1) the circadian variation, which is of greater magnitude for markers of bone resorption—except serum TRACP and CTX-MMP—than for markers of bone formation, (2) diet and food intake, especially for markers such as serum CTX (Qvist et al., 2002; Clowes et al., 2002), and (3) recent fracture. Indeed, bone marker levels are markedly increased during fracture healing starting from month 1 and remain elevated for about 6 months, with a return to levels before the fracture by the end of 1 year (Ivaska et al., 2007). The extent of increase differs between markers (highest for serum PINP) and according to the size of the fractured bone (Ivaska et al., 2007). For example, BTMs increase more after trochanteric fracture than femoral neck fracture (Ikegami et al., 2009). Recently, the National Bone Health Alliance published recommendations to standardize sample handling and patient preparation to reduce preanalytical variability of the two reference markers CTX and PINP (Szulc et al., 2017).

Commercial CTX assays include manual ELISA (Immunodiagnostic Systems [IDS], Boldon, UK), automated electrochemiluminescence immunoassays (ECLIA; Roche Diagnostics, Mannheim, Germany), and automated chemiluminescence immunoassay (CLIA; IDS). PINP measurements include intact PINP by radioimmunoassay (Orion Diagnostica, Espoo, Finland), which measures only native trimeric peptide; total PINP with ECLIA by automated Roche Diagnostics platforms, which measures both trimeric PINP peptide and the low-molecular-weight peptides of α1 and α2

TABLE 78.3 Circulating/bone miRNA in osteoporosis studies.

Study (reference)	Population sample	Deregulated miRNA	Target gene when known
Wang et al. (2013)	Bone tissue specimens	miR-214	AFT4
Wang et al. (2012b)	PBMCs from women with low ($n = 10$) versus normal ($n = 10$) BMD	miR-133a	CXCL11, CXCR3, SLC39A1
Li et al. (2014)	Plasma: non-OP ($n = 40$), OP ($n = 40$), osteopenic ($n = 40$)	miR-133a miR-21-5p	SPRY1, DKK2, BMP3
Chen et al. (2014)	CD14 + PBMCs: low ($n = 10$) versus normal BMD ($n = 10$)	miR-503	RANK
Seeliger et al. (2014)	Serum and bone samples: Serum: OP ($n = 30$) versus non-OP ($n = 30$) Bone; OP ($n = 20$) versus non-OP ($n = 20$)	miR-21 miR-23a miR-24 miR-25 miR-100 miR-125b	SPRY1, SMAD7 RUNX2, SATB2
Weilner et al. (2015)	Serum: Discovery: postmenopausal women with hip Fx ($n = 7$) versus controls ($n = 7$) Validation: Fx ($n = 12$) versus controls ($n = 11$)	miR-let-7g miR-10b miR-133b miR-22 miR-328	
Panach et al. (2015)	Serum: Fx ($n = 15$) versus OA ($n = 12$)	miR-122 miR-125 miR-21	FASC, PDCD4
Meng et al. (2015)	Serum: OP ($n = 32$) versus low BMD ($n = 32$) versus controls ($n = 32$)	miR-130b miR-151a miR-151b miR-194-5p miR-590	
Yavropoulou et al. (2017)	Serum: Fx ($n = 35$) versus low BMD ($n = 35$) versus controls ($n = 30$)	miR-124 miR-2861 miR-21-5p miR-23a miR-29a-3p	NFATC1, NFATC2, HDAC5 HDAC5 See above; COL3A, COL5A3, PTHLH, DUSP2
Heilmeier et al. (2016)	Serum T2D study: Fx ($n = 19$) versus controls ($n = 19$) OP study: Fx ($n = 17$) versus controls ($n = 19$)	T2D[a]: most discriminative miRNA—miR-550a-5p miR-382-3p OP[b]: most discriminative miRNA—miR-382-2p miR-188-3p	

OA, osteoarthritis; *OP*, osteoporosis; *PBMCs*, peripheral blood mononuclear cells (monocytic); *T2D*, type 2 diabetes.
[a]*Among 48.*
[b]*Mmong 23 identified to be deregulated in T2D and osteoporotic patients, respectively.*

chains; and intact PINP with CLIA by automated IDS platform, which measures native trimeric peptides only. To obtain the most precise measurements of these two reference markers, the recommendation is to collect blood fasting between 7:30 and 10:00 a.m., although random sampling is acceptable for PINP because it is only slightly affected by diet and circadian variability. Other factors that should be considered when interpreting the results of bone markers include age, gender, ethnicity, underlying diseases such as kidney insufficiency (which may alter renal excretion of the markers and thus serum levels), concomitant medications, such as glucocorticoids, that induce a rapid decrease of markers of bone formation, and geographical location (Naylor and Eastell, 2012; Hlaing and Compston, 2014; Szulc et al., 2017). Although such influences cannot be modified, having their effects on biomarker data in mind is important. When biochemical BTMs are measured on adequately collected samples and with a well-performing assay, the within patient variability is in the range of 8%−12% for serum bone formation markers and 15% (serum based) to 40% for markers (urinary assays) of bone resorption. Such figures are used to determine the least significant change (LSC) when evaluating the efficacy of bone active therapy (see below).

Reference ranges

Each laboratory should establish reference intervals (RIs) for cutoff levels that identify subjects at risk for fracture or for assessing response to treatment (see later). However, when this is not feasible, laboratories can refer to published RIs that have been determined specifically for a given bone marker measured by a given assay platform—because the different assays are not standardized—in the same type of specimen. Interestingly, in the last decade several studies have been performed to establish these reference ranges for most assays (Glover et al., 2008, 2009; Adami et al., 2008; de Papp et al., 2007), which were recently reviewed (Morris et al., 2017). Because bone marker levels vary with age with a marked increase at the time of the menopause, healthy untreated premenopausal women from 30 or 35 to 40 years of age should be selected. The subjects must have optimum vitamin D status, the number of subjects must be large enough, and geographical variation should be considered when reference ranges are established.

Clinical uses of bone markers in osteoporosis

The IOF and IFCC recommend the use of a marker of bone formation (serum PINP) and bone resorption (serum CTX) as reference analytes in clinical studies (Vasikaran et al., 2011). In osteoporosis, the main potential uses for BTMs are for monitoring the treatment and assessment of fracture risk, although some studies have reported an association with the level of BMD and rate of bone loss.

Diagnosis of osteoporosis and prognosis of bone loss

Bone marker levels have been shown to correlate negatively with BMD assessed by DXA at different skeletal sites (Biver et al., 2012), with a higher association with advancing age in postmenopausal women (Garnero et al., 1996a). The association is too weak, however, to accurately identify women at low BMD, and thus bone markers are not recommended for diagnosing osteoporosis. However, if levels are substantially raised (more than 1.5 times higher than the upper limit of the RI), causes of high bone turnover other than osteoporosis should be investigated including myeloma, BMs, kidney disease, primary hyperparathyroidism, thyrotoxicosis, or recent fracture.

Several studies have also shown that increased BTMs, and especially markers of bone resorption, are associated with a higher magnitude of bone loss in the 2−5 years that follow (Garnero et al., 1999; Chopin et al., 2012). Although this association is significant at a cohort level, it is not strong enough to predict the rate of bone loss at the individual level with a single assessment of bone markers. One approach to improve the predictive value of BTMs is to combine indices of bone formation and bone resorption into a single integrated measure reflecting the bone balance index at the level of the whole body. Such an index has been recently proposed and based on the relationship between resorption (urinary NTX) and formation (osteocalcin) seen in a patient cohort with stable BMD (premenopausal women more than 5 years before final menstrual period) (Shieh et al., 2016). Then patients are assessed relative to this regression standard to investigate whether their level of NTX relative to osteocalcin is above or below the amount expected to correspond to stable BMD. Initial validation in early postmenopausal women suggests that this bone balance index may be more useful than urinary NTX alone in predicting BMD loss at the lumbar spine over the subsequent 3−4 years. However, further large studies are required to see whether this approach is useful in predicting bone loss in individual subjects. Such a bone balance index should also be developed using the IOF−IFCC recommended serum markers, CTX and PINP.

Prediction of fracture risk

Several prospective studies have shown that some bone markers predict the risk of osteoporotic fractures over the next 2–5 years, including spinal, hip, and nonvertebral fractures in postmenopausal women (reviewed in Garnero, 2000). The association is somewhat inconsistent for bone formation markers—except bone ALP—whereas stronger and more consistent relationships were observed for bone resorption markers including serum CTX. The association between resorption markers and fracture is largely independent of BMD, and when combined, these two risk factors allow for the prediction of fracture risk more accurately than one parameter alone (Garnero et al., 1996b; Johnell et al., 2002). In 2011, Vasikaran et al. (2011) reviewed all prospective studies of bone markers for fracture prediction in untreated men and women. They confirmed that several studies found that bone markers can identify early and late postmenopausal women at increased risk for fracture. The value of markers to predict fracture appears to decrease with longer follow-up (Ivaska et al., 2010). In healthy elderly men, the association seems to be weaker than it is in postmenopausal women. For example, in a case–control study of the large US MrOS study, it was reported that serum PINP—but not serum CTX or TRAP—predicted the risk of nonvertebral and hip fracture, but this association was was no longer significant after adjustment for BMD (Bauer et al., 2009). However, the association of bone formation markers including PINP in men and women may be not linear. A study in elderly men and women followed prospectively for 7.3 years found no significant association overall between baseline PINP and the risk of hip fracture (Finnes et al., 2014). However, spline analysis suggested a U-shaped curve association, with increased risk of hip fracture for very high or very low PINP levels. A recent meta-analysis including six prospective studies in elderly men and postmenopausal women confirmed a modest but significant association of both reference markers—serum CTX and PINP—with the risk of fracture (Chavassieux et al., 2015). This study reported that each SD increase in serum PINP and CTX was associated with a hazard ratio of fracture of 1.2. Since the publication of this meta-analysis, three additional prospective studies have been reported. In the Australian Health in Men study, which included 100 men with incident hip fracture and 3896 subjects with no fracture, it was found that each SD increase in serum total osteocalcin was associated with a 1.2-fold increased risk of fracture independent of multiple variables including age and glucocorticoid use (Chubb et al., 2015). In contrast, neither serum CTX, nor PINP were independent predictors of fracture in this study. Yoshimura et al. (2011) analyzed 400 men and women participating to the Taiji cohort followed prospectively for 10 years. They reported no significant association between a panel of different bone markers including osteocalcin, bone ALP, procollagen type I C-terminal propeptide (PICP), PINP, serum CTX, serum NTX, serum ICTP, urinary PYD and DPD, and fracture risk. However, this study was performed in relatively young subjects, resulting in only 32 incident fractures, and thus was insufficiently powered to use fracture as an endpoint. Finally, the predictive value of bone markers was analyzed in a nested case–control analysis of the Singapore Chinese Health Study, a 5-year prospective study in healthy women and men (45–74 years) (Dai et al., 2016). It was found that both serum PINP and serum CTX were significantly associated with the risk of hip fracture, with ORs (95% CI) of 6.63 (2.02–21.18) and 4.92 (1.67–14.51), respectively, for the highest versus lowest quartile. Interestingly, when subjects at risk were identified as those with both high serum PINP and high serum CTX, the odds ratio of fracture increased to 7.5 (2.53–21.41).

Predicting and monitoring treatment efficacy

It has been hypothesized that the response to antiresorptive therapy and anabolic treatment could be related to pretreatment levels of bone markers. For example, in the Fracture Intervention Study, it was shown that patients with high pretreatment levels of bone ALP or PINP had a greater response to alendronate in terms of reduction of nonspine fracture than that shown by subjects with lower levels (Bauer et al., 2006). In postmenopausal osteoporosis, lower PINP was associated with slower bone loss before treatment and lower response to treatment with zoledronate (Eastell et al., 2015). With anabolic therapies such as PTH and PTH analogs, one could argue that these drugs will particularly benefit patients with low turnover. However, randomized studies indicate that teriparatide increases BMD and reduces fracture risk whether pretreatment levels of bone markers are suppressed or not (Delmas et al., 2006). In fact, in that study it was shown that the reduction in absolute risk of spinal fracture was larger in those women with high pretreatment bone turnover (Delmas et al., 2006). However, because the association in these studies was modest, nonconsistent (Seibel et al., 2004), and may vary according to the drugs even within the same class, it is still unclear whether the baseline levels of bone markers predict which individual patients will benefit more from one treatment or another. The role of bone markers to identify patients who are candidates for new therapies with novel and unique mechanisms of action such as cathepsin K or SOST inhibitors remains to be investigated.

Treatment for osteoporosis primarily aims to prevent bone loss and reduce fracture risk. The magnitude of change in BMD in response to antiresorptive therapy is small, and taking the precision of the measurement into account, it is

necessary to wait 2 years to determine efficacy. The level of BTMs changes rapidly with therapy and can help to identify nonresponse and/or poor adherence to therapeutic regimens. It has been shown that larger changes in bone marker levels are associated with better adherence to bisphosphonate treatment and subsequent reduction in fracture risk (Eastell et al., 2011a). However, other studies did not show any difference in the persistence of oral bisphosphonate between women receiving the feedback of bone markers and subjects with no feedback (Clowes et al., 2004; Silverman et al., 2012). The IOF and the European Calcified Tissue Society have proposed that the BTMs CTX and PINP be used to identify non-adherence to oral bisphosphonate therapy (Diez-Perez et al., 2017). The recommendation was based on the results of the TRIO study, which compared the effects of oral alendronate, ibandronate, and risedronate on BMD and bone markers in postmenopausal women with osteoporosis. The working group recommends measuring PINP and CTX at baseline and 3 months after starting therapy to check for a decrease greater than the LSC (a decrease of more than 38% for PINP and 56% for CTX). If a significant decrease is observed, treatment can continue. If no significant decrease is observed, the clinician should reassess to identify problems with the treatment, mainly low adherence. However, it remains to be seen whether this screening strategy has a direct effect on adherence in real-life settings.

Several randomized placebo controlled studies have shown that antiresorptive therapies including estrogens, selective estrogen-receptor modulators, bisphosphonates, the anti-RankL antibody, denosumab, and cathepsin K inhibitors induce a dose-dependent decrease of resorption markers within 1−3 months. The decrease in bone formation markers is delayed and reaches a plateau after 3−6 months, reflecting the physiological coupling of bone resorption and formation (for a review, see Cremers and Garnero, 2006; Fig. 78.1A and B). The onset and magnitude of decrease in BTMs with antiresorptive therapy depends on the mechanism of action of the drug, the category of bisphosphonate, the route of administration (faster for intravenous than for oral bisphosphonate), and the marker used. For example, although serum TRACP5b levels decrease significantly with bisphosphonate and the anti-RANKL denosumab, they remain stable or even increase with cathepsin K inhibitors (Eisman et al., 2011). Indeed, both bisphosphonates and denosumab markedly suppress the differentiation and number of osteoclasts reflected by serum TRACP5b, whereas cathepsin K inhibitors do not interfere with osteoclast formation. With cathepsin K inhibitors, ICTP concentrations increase, which could be due to a compensatory increase in MMP activity and/or the decrease of cathepsin K−mediated degradation of the ICTP peptide. In contrast, the other collagen markers of bone resorption, such as NTX and CTX, are suppressed by these agents (Eisman et al., 2011).

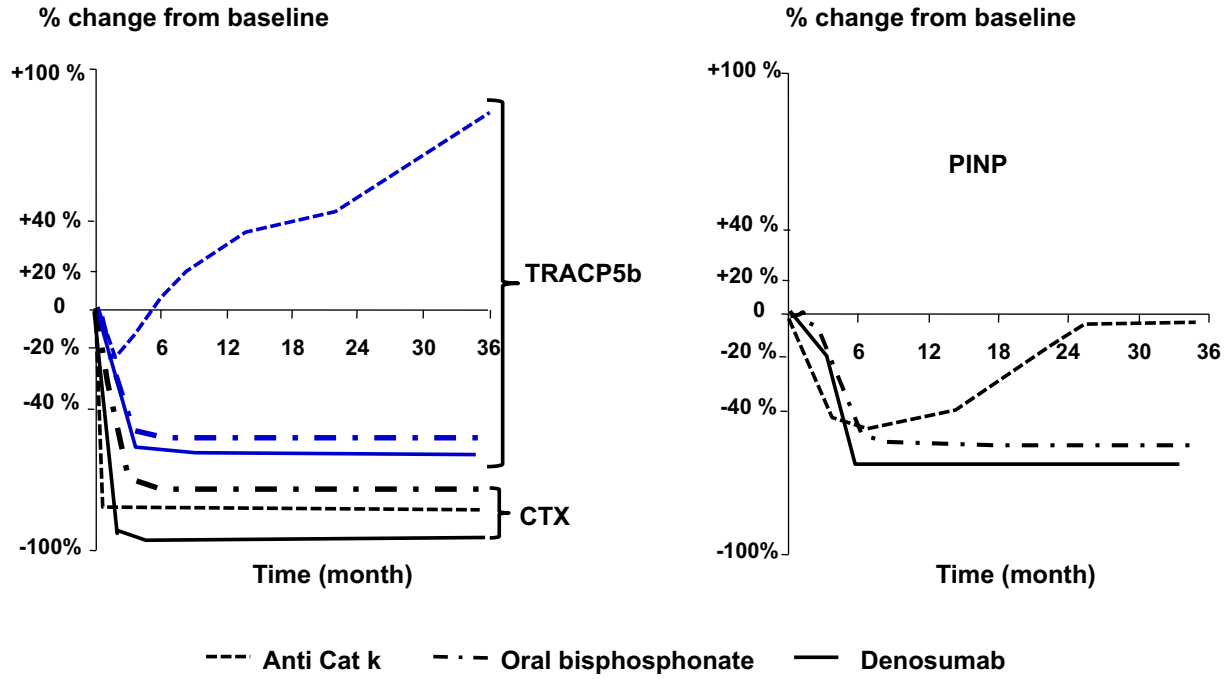

FIGURE 78.1 Schematic changes of bone turnover with antiresorptive treatments. Left panel: Bone resorption markers; Right panel: PINP as a representative bone formation marker. *Anti-Cat K*, anti−cathepsin K; *CTX*, C-terminal telopeptide of collagen type I; *PINP*, procollagen type I N-terminal propeptide; *TRACP5b*, tartrate-resistant acid phosphatase isoenzyme 5b.

The relationships between changes of BTMs and fracture risk have been investigated in several placebo-controlled studies. These include investigations of bisphosphonates and raloxifene and were reviewed by Vasikaran et al. (2011). In this review, there was a significant relationship between the magnitude of change of bone markers over 3−12 months and the reduction in spinal fracture risk at 3 years. The changes in bone markers explained from 27% to 77% of the antifracture efficacy. Since then, two additional randomized trials of antiresorptive drugs have been reported. Jacques et al. (2012) looked at the relationships between change in bone marker and BMD and the risk reduction of new vertebral fracture risk at 3 years in postmenopausal women receiving 5 mg intravenous injection of zoledronic acid once a year (the Horizon trial). Among the 7736 women randomized to zoledronic acid or placebo injection, PINP data were available at baseline and at 1 year for 1132 of them. The changes in absolute levels of PINP explained up to 58% of the antifracture efficacy, which was largely independent of changes in BMD. Thus, with this drug, changes in both BMD and bone markers could be useful in predicting its clinical efficacy. Bruyere et al. (2012) analyzed the relationships between BMD or BTM changes and vertebral fracture incidence in women treated with the selective estrogen receptor modulator bazedoxifene in a post hoc analysis of a 3-year randomized, placebo-controlled study. Data for serum CTX and osteocalcin were available in all 5244 randomized subjects at baseline. It was found that the 1-year change in CTX and osteocalcin explained 16% and 6%, respectively, of the reduction in the 3-year risk of new vertebral fracture (both significant). Thus, all these studies with antiresorptive treatments are consistent and show that bone marker monitoring effectively predicts clinical efficacy, at least as well as prediction based on changes in BMD.

From a clinical point of view, it would be very helpful to determine whether there is a threshold level of bone markers under treatment that will translate into optimal antifracture efficacy. In the risedronate study, it was shown that the relationship between vertebral fracture risk and the levels of CTX reached after 3−6 months was not linear and that there may be a level of bone resorption reduction below which there are no further fracture benefits (Eastell et al., 2003). Two methods of assessing bone marker response have been proposed, and both have limitations. The LSC approach signifies the minimum change in the bone marker that can be attributed to treatment effect rather than random variation of the marker (usually with 95% certainty). This is most commonly expressed as a percentage change or alternatively as absolute units. The approach, which has only a statistical and not a clinical basis, requires that a sample be taken before starting therapy. This could be overlooked, or the patient may have low turnover due to previous treatment. In these cases, the RI approach, established in young healthy women who do not lose bone, is particularly useful. However, this also has its limitations. Some untreated women may already be in the lower half of the reference for some bone markers (e.g., serum CTX) at baseline. In that case, another bone marker (e.g., PINP) could be measured for comparison. Interestingly, a recent head-to-head study (TRIO study) of three oral bisphosphonates (ibandronate, alendronate, and risedronate) in postmenopausal women with osteoporosis compared the response at 12 weeks of serum CTX and PINP using both LSC and the pre-menopausal women's RI (Naylor et al., 2016). It showed that the proportion of bone marker responders was high (70% −100%) with these bisphosphonates and similar in the two approaches (LSC and RI). Ultimately, however, optimal cutoffs will need to be validated in prospective studies using incidence of fracture as an endpoint.

Biochemical BTMs are also useful for monitoring the efficacy of anabolic treatment including teriparatide (Fig. 78.2), a synthetic form of PTH, and possibly new drugs such as abaloparatide, a synthetic peptide analog of PTH-related protein

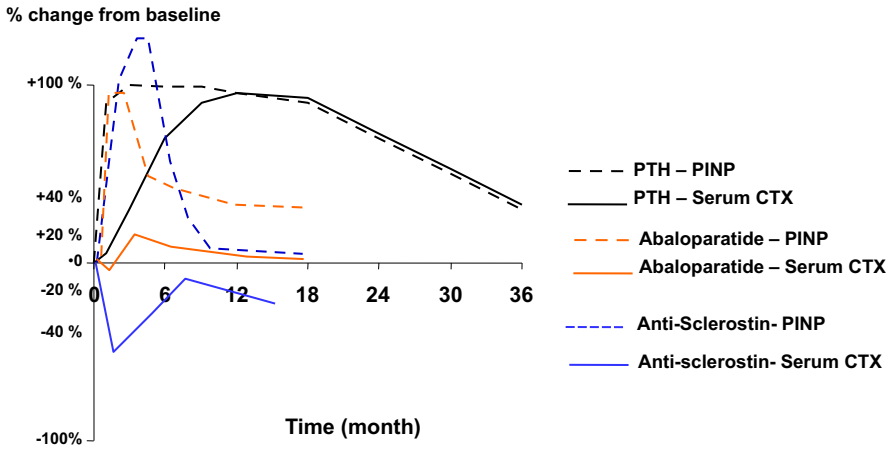

FIGURE 78.2 Schematic changes of bone turnover with anabolic treatments. *PINP*, procollagen type I N-terminal propeptide; *PTH*, parathyroid hormone*; serum CTX*, serum C-terminal telopeptide of collagen type I.

and the anti-SOST romosozumab (McClung et al., 2014). As reviewed recently (Krege et al., 2014), serum PINP appears to be the most useful bone marker for monitoring and predicting the efficacy of teriparatide for the following reasons: (1) it increases markedly within 1 month of therapy and has the highest signal-to-noise ratio compared with other bone formation (PICP, bone ALP) and bone resorption (urinary NTX, DPD) markers (Chen et al., 2005), (2) at the individual level it has a great specificity and sensitivity to differentiate patients treated with teriparatide versus placebo when a positive response is defined as an increase of 10 ng/mL in PTH (Tsujimoto et al., 2011) (3) levels during teriparatide therapy highly correlate with bone formation, defined by the mineralizing surface of transiliac bone biopsies ($r = 0.85$) (Dempster et al., 2012) or by the increase in skeletal uptake of technetium-99m methylene diphosphonate on a bone scan (Moore et al., 2010), confirming that PINP concentration is related to bone formation at the skeletal level, (4) changes at 1 and 3 months are strongly predictive of spinal BMD increase at 12 and 18 months as shown in several clinical studies reviewed by Krege et al. (2014), and (5) changes at 1−3 months correlated with changes of bone strength at 18 months as estimated from quantitative computed tomography scans with finite element modeling of the spine (Keaveny et al., 2007; Farahmand et al., 2013). Data validating the use of PINP for predicting fracture risk reduction during teriparatide treatment are not yet available. Abaloparatide stimulates bone formation and bone resorption rapidly and dose-dependently in women with postmenopausal osteoporosis, but less and more transiently than does teriparatide (Fig. 78.2), leading to a greater increase in BMD compared with the effect of teriparatide (Miller et al., 2016). Differences in the effects of teriparatide and abaloparatide may be related to differences in biologic effects. The differential binding of abaloparatide compared with teriparatide leads to parathyroid type 1 receptor conformation binding selectivity that favors anabolic activity. As a result, abaloparatide may provide more transient stimulation of osteoblast cyclic adenosine monophosphate production and result in lower expression of osteoblast-derived RANKL. This could result in less stimulation of bone resorption. A recent study comparing the effects of teriparatide and abaloparatide on BMD and bone markers in postmenopausal women with osteoporosis showed that an early change in PINP correlates with a change in lumbar spine BMD more strongly with abaloparatide than it does with teriparatide (Eastell, 2017).

Monitoring side effects of osteoporosis therapies

Severe bone resorption suppression—e.g., at the beginning of the treatment with denosumab—might induce hypocalcemia. In postmenopausal women, hypocalcemia was more frequent in patients with increased BTM concentrations before treatment (Ishikawa et al., 2016). Long-term suppression of bone turnover during treatment with bisphosphonates or denosumab is associated with increased risk of osteonecrosis of the jaw. However, no study has shown a difference in BTMs between patients with osteonecrosis of the jaw and controls or a predictive value for low BTMs (Khan et al., 2015). Long-term suppression of bone turnover might also be associated with increased risk of subtrochanteric and femoral shaft fractures—so-called atypical femur fractures. In patients with atypical femur fractures, BTMs were within the RI for healthy young premenopausal women (Franceschetti et al., 2013). Because BTMs increase substantially after fracture, however, measurements after atypical femur fractures are difficult to interpret (Black et al., 2012; Adler et al., 2016).

Treatment holiday monitoring

The possibility of drug holidays has been suggested because of concern over long-term harm with antiresorptive therapy (Bone et al., 2011). Denosumab withdrawal results in a rebound in BTMs, accelerated bone loss, and increased vertebral fracture risk (Aubry-Rozier et al., 2016; Tsourdi et al., 2017). Consequently, a discontinuation is not appropriate with denosumab without considering an alternative treatment to prevent bone loss (Tsourdi et al., 2017).

With bisphosphonates, however, suppressed bone turnover is observed for several years after treatment is stopped (Black et al., 2012). However, a recent assessment of the extension studies of the pivotal FLEX (with alendronate) and Horizon (with zoledronate) trials reported that after stopping alendronate or zoledronate for 3 years, 53% and 34% of patients, respectively, had either total hip BMD loss exceeding the LSC cutoff or PINP levels above the target premenopausal range (Kim, 2017). This supports the ASBMR task force's recommendation to reassess risk 3 years after drug discontinuation.

In postmenopausal osteoporosis, BTM concentrations after 5 years of treatment with alendronate or 3 years of treatment with zoledronate did not predict the rate of bone loss after stopping treatment (McNabb et al., 2013; Cosman et al., 2014), but bone loss was small, decreasing the power of the study. Furthermore, 1-year changes in bone ALP and urine NTX after treatment discontinuation did not predict fracture rates, although the power of this study was limited due to the low rate of clinical vertebral fractures (Bauer et al., 2014). Based on these findings, measuring bone markers after treatment is not recommended at the present time, although this issue remains of great interest and deserves additional prospective studies.

Diagnosis and monitoring of treatment in Paget's disease of bone

BTMs are used for diagnosis, monitoring of treatment, and monitoring for relapse in patients with Paget's disease of bone (Singer et al., 2014; Muschitz et al., 2017; Paul Tuck et al., 2017). BTMs are sensitive but not specific enough to diagnose Paget's, which is usually diagnosed by imaging (Al Nofal et al., 2015). Levels are significantly elevated in the majority of pretreatment patients but can be in the upper range of normal in patients with monostotic disease. A recent systemic review and meta-analysis demonstrated moderate to strong correlations between most BTMs in untreated patients (Al Nofal et al., 2015). In addition, moderate to strong correlations were found with scintigraphic assessment of disease activity. There were no statistically significant differences between the various BTMs in terms of their correlation with scintigraphic activity. The Endocrine Society recommends that basically all BTMs can be used in patients with Paget's disease of bone with the exception of osteocalcin, which seems less useful in these patients (Singer et al., 2014). Because of its low costs and adequate performance, total ALP is mostly recommended (Singer et al., 2014). Abnormalities in the RANKL/OPG dipole have been implicated in the pathogenesis of Paget's disease (Ralston et al., 2008; Vega et al., 2007; Idolazzi et al., 2017). However, two of the circulating Wnt antagonists, SOST and Dkk1, did not differ between untreated patients with Paget's disease of bone and gender- and age-matched controls (Idolazzi et al., 2017). To our knowledge, other newer BTMs such as POSTN have not yet been explored in Paget's disease of bone.

Dkk1 and SOST have been described to increase in response to BP treatment (Gatti et al., 2012b), but to our knowledge these have not been explored as markers for response to BP treatment in patients with Paget's disease of bone. Other BTMs have been explored and have been found very useful in the monitoring of oral and IV BP therapy as well as monitoring of denosumab therapy (Singer et al., 2014; Muschitz et al., 2017; Paul Tuck et al., 2017), with rapid decreases in bone resorption markers followed by decreases in bone formation markers. The time scale of the decrease depends on the drug, the dose, and the mode of administration. The earlier mentioned systemic review also demonstrated good correlations between BTMs and between BTMs and disease activity in Paget patients assessed using scintigraphic imaging a few months after treatment (Al Nofal et al., 2015). The biochemical target of pharmacotherapy in patients with Paget's disease of bone is usually normalization of the BTMs (Singer et al., 2014; Muschitz et al., 2017; Paul Tuck et al., 2017), and BP therapy combined with BTM monitoring is indeed generally seen as a best practice. However, it must be mentioned that studies such as the PRISM study (with all its caveats) failed to demonstrate differences in bone pain between BP-treated patients and symptomatically treated patients with Paget's disease of bone (Langston et al., 2010). Retreatment of patients with Paget's disease of bone is either based on symptoms or an increase in BTM levels. Most BTMs seem useful for this purpose (Singer et al., 2014; Muschitz et al., 2017; Paul Tuck et al., 2017).

Bone turnover markers for rare bone diseases

The last couple of years have been characterized by exciting developments in the diagnosis and treatment options for rare metabolic bone diseases. While the investigation of some rare bone diseases such as van Buchem disease, sclerosteosis, and pycnodysostosis has led to the development of potential compounds for osteoporosis such as the SOST antibody romosozumab and the cathepsin K inhibitors (Costa and Bilezikian, 2012; Bandeira et al., 2017; Stoch and Wagner, 2008), investigation of other rare bone diseases has led to the development of compounds that will probably be applicable only to those diseases, such as an activin A antibody for *fibrodysplasia ossificans progressiva (FOP)* (Upadhyay et al., 2017). Much credit goes to the regulatory authorities that have enabled these life-changing developments for the few patients seriously affected by these diseases. BTMs can be helpful in diagnosis and treatment monitoring in some of these diseases and may also be useful during various stages of drug development. The following gives a brief overview of the value of BTMs in some of the more than 400 rare metabolic bone diseases (Masi et al., 2015).

Fibrous dysplasia

In a relatively large group of patients with fibrous dysplasia and McCune–Albright syndrome (MAS) studied retrospectively, BTMs (total ALP, PINP, and CTX) were elevated prior to treatment, and levels correlated with skeletal involvement (as determined by imaging using 99mTc-skeletal scintigraphy and skeletal burden scores as described by Collins et al., 2005 of the disease) as well as pain scores (Majoor et al., 2017). BTMs were successfully used to monitor BP therapy in these patients with normalization of BTM levels as the target (Majoor et al., 2017). Correlating with higher skeletal involvement, BTM levels in MAS were higher than in polyostotic fibrous dysplasia (PFD). This study and others clearly suggest that BTMs seem useful in determining the skeletal involvement and monitoring of BP treatment in MAS and PFD.

Hypophosphatasia

BTMs seem to have a limited role, if any, in the diagnosis or monitoring of the treatment of hypophosphatasia (HPP). A consensus document reports that in adult patients, bone biopsies might be considered for patients with additional skeletal risk factors beyond HPP such as chronic kidney disease, history of fractures, or very low BMD (Kishnani et al., 2017). BTMs may provide support in deciding whether bone biopsies are indicated; albeit that is left to the discretion of the clinician (Kishnani et al., 2017). A case−control study investigating the predictive value of the ALP:PINP ratio for a loss-of-function mutation in the gene that encodes for the "tissue-non-specific" isoenzyme of ALP (TNSALP) is currently ongoing in adult untreated patients (NCT02796885). In various forms of HPP (infantile, severe childhood, mild childhood, and "odonto"), total ALP and bone ALP were found to be invariably below control ranges (Whyte, 2017a). Recently, a recombinant bone-targeted ALP, called asfotase alpha, has become available to correct the inborn error caused by a loss-of-function mutation of the TNSALP (*ALPL* gene) (Whyte, 2017b). To our knowledge, the effects of asfotase alpha on BTMs, and the potential role of BTMs in the development of the drug as well as monitoring of treatment, have not yet been published.

Fibrodysplasia ossificans progressiva (FOP)

Little is known for the role of BTMs in FOP, although it has been reported that, for example, total ALP might increase during flare-ups. Three drugs are currently in clinical development for this disease: palovarotene, ACE-011, and REGN2477. BTMs are part of the various clinical studies for the development of these drugs (Kaplan, 2017). Given the limited data on the BTMs in these patients, interpretation of the markers collected during these trials will be challenging. At the same time, these studies will provide us with a wealth of BTM data in these patients, even pretreatment and during placebo treatment.

Osteogenesis imperfecta

Compared with controls, BTMs do not seem to be altered in untreated osteogenesis imperfecta (OI) patients (Brunetti et al., 2016). OI patients treated with BPs have expected decreases in BTMs such as serum CTX and bone ALP. BTMs may therefore be useful for monitoring BP treatment that increases BMD but may have little effect on fractures or clinical status (pain, growth, functional mobility) in these patients. Interestingly, circulating SOST and OPG levels are similar between controls and OI patients, and BP treatment does not appear to change their levels. In contrast, Dkk1 and RANKL circulating levels are increased in OI patients. Dkk1 seems unaffected by BPs, but RANKL seems to increase (Brunetti et al., 2016). In 2014, excessive TGF-beta was identified as a common mechanism in OI (Grafe et al., 2014). A phase 1 trial with a TGF-antibody (fresolimumab) is currently ongoing (NCT03064074). The effects of fresolimumab on BTMs in patients with OI are currently still unknown.

X-linked hypophosphatemia

In children with X-linked hypophosphatemia (XLH), FGF-23-mediated hypophosphatemia impairs skeletal mineralization and causes rickets. Treatment consists of oral phosphate and active vitamin D. New treatment consists of burosumab, an FGF-23 monoclonal antibody. Little is known about BTMs in XLH, nor about the effects of burosumab on BTMs in these patients. Recent data from burosumab in patients with tumor-induced osteolysis demonstrated statistically significant increases from baseline levels of PINP (51%) and CTX (38%) (De Beur, 2017).

Bone turnover markers in metastatic bone disease

Multiple myeloma

In MM, skeletal complications are caused by an increased activation of osteoclasts that is not followed by reactive formation by osteoblasts (Terpos et al., 2010, 2017). Bone resorption is therefore increased in MM while bone formation seems inhibited. Of the BTMs, bone resorption markers have proven useful in the management of the disease. BTMs such as uNTX/Cr, serum CTX, and serum ICTP are increased in patients with MM, and their levels correlate with skeletal involvement of the disease, disease stage, and biomarkers of disease activity such as Beta2-microglobulin and IL6 (Terpos et al., 2003, 2010; Fonseca et al., 2000; Corso et al., 2001; Abildgaard et al., 2000). In addition, BTM levels correlate with the risk for skeletal-related events (SREs) and with overall survival (Terpos et al., 2010). In MM patients undergoing

conventional chemotherapy, bone resorption markers such as ICTP and uNTX/Cr have demonstrated prognostic significance for disease progression and survival (Terpos et al., 2010). Bone resorption markers such as uNTX/Cr seem useful to monitor the effect of antiresorptive treatment, especially bisphosphonates. Patients with persistently elevated BTM levels are at higher risk for SREs and disease progression compared with patients who respond well to BPs and have normalized bone resorption (Terpos et al., 2010). Other potentially interesting markers for diagnosis, prognosis, and/or monitoring of treatment include RANKL/OPG, Bone sialoprotein (BSP), and Dkk1.

In addition to antiresorptive therapy such as BPs and denosumab, BTMs may also be affected by immunomodulatory drugs such as thalidomide and lenalidomide in combination with steroids. From the available data, it seems that immunomodulatory drugs reduce osteoclastic function but have little to no effect on osteoblastic activity. The proteasome inhibitor bortezomib has been reported to have beneficial effects on bone formation (Mohty et al., 2014). Monotherapy in MM patients reduces Dkk1 and soluble RANKL associated with a reduction in bone resorption (TRAP5b and serum CTX) and an increase in bone formation markers (BALP and OC). However, when combined with other antimyeloma agents Bortezomib might lose its beneficial effects on bone formation.

Related to the pathophysiology of uncoupled bone turnover, with increased bone resorption and decreased bone formation, the levels of RANKL and the RANKL/OPG ratio are increased, while circulating levels of Dkk1 and SOST are increased in these patients (Terpos et al., 2017). Encouraging results from trials with RANKL, Dkk1, and SOST antibodies are slowly appearing in the literature.

Metastatic bone disease from solid tumors

Most BTMs are increased in patients with BMs from solid tumors and seem to correlate with the extent of skeletal involvement (D'Oronzo et al., 2017). However, at present BTMs are not used for routine diagnosis of BMs from solid tumors such as breast, prostate, and lung cancers predominantly because of suboptimal specificity, sensitivity, and diagnostic efficiency (D'Oronzo et al., 2017). Other biomarkers related to metastatic bone disease include tumor-derived genes, proteins, and miRNAs, some of which may indicate osteotropism of cancer cells and have prognostic possibilities. Again, at the moment none of these are routinely used in patient care (D'Oronzo et al., 2017).

BTMs have been demonstrated to be useful for the prognosis of BMs both with and without antiresorptive treatment, with increased BTMs correlating with increased risk for SREs seemingly irrespective of what antiresorptive drug is used (D'Oronzo et al., 2017). For example, elevated baseline BTMs such as high uNTX levels have demonstrated the potential to predict treatment efficacy, especially from BPs (Coleman et al., 2013). Elevated uNTX and/or BALP levels collected after 3 months of ZOL or denosumab treatment correlated with significantly reduced overall survival, increased disease progression, and worsening of BMs (Lipton et al., 2016).

Bone turnover markers for the development of bone drugs

Roughly three classes of drugs with effects on bone currently can be used for osteoporosis and/or metastatic bone disease: antiresorptive, anabolic, and dual-action. The response of BTMs as well as the relationship with disease activity and endpoints such as fracture risk or risk for SREs depends on the class of drugs, and within each class of drug it is determined by the mechanism of action of the specific drug as well as the specific pharmacokinetics and pharmacokinetic/pharmacodynamic relationships of that particular drug (Cremers and Garnero, 2006; Cremers et al., 2005; Russell et al., 2008). Another key point relevant to drug development is the translation or transfer of the relationship between BTM levels during treatment between related diseases, which might be useful when seeking regulatory approval for similar indications (Cremers and Garnero, 2006). The best example of this is the use of BTM levels during BP treatment for postmenopausal osteoporosis in seeking approval for that BP for another type of osteoporosis such as glucocorticoid-induced osteoporosis (Saag et al., 1998; Wallach et al., 2000; Lukert and Raisz, 1990). BTM levels combined with BMD response during treatment can sometimes serve as a surrogate for a true fracture-intervention study (Cremers and Garnero, 2006).

Bisphosphonates

Osteoporosis

BTMs have been very successful in dose-finding studies, with maximum suppression of BTMs being a successful target during phases 1 and 2 of drug development (Cremers and Garnero, 2006; Ravn et al., 1996; Chesnut et al., 1995; Reid et al., 2002). Phase 3 trials have subsequently revealed the relationship between BTM levels and clinical outcome (Eastell

et al., 2015; Cremers and Garnero, 2006). Simplified, antiresorptive drugs such as bisphosphonates decrease the levels of BTMs, and continued suppression of both resorption and formation markers beyond a certain degree is generally associated with antifracture efficacy (Eastell et al., 2011a; Cremers and Garnero, 2006). Too little suppression and too much fluctuation in the levels seem associated with suboptimal efficacy of BP treatment (Cremers and Garnero, 2006). It is this relationship that has been used to support the development of new dose regimens for bisphosphonates such as alendronate (from daily to weekly) and ibandronate (from daily to monthly) (Miller et al., 2005a; Schnitzer et al., 2000). This relationship between a certain level of suppression of bone turnover and antifracture efficacy is recognized by most regulatory authorities and has been used in combination with effects on BMD for approval of bisphosphonates for glucocorticoid-induced osteoporosis and osteoporosis in men (Cremers and Garnero, 2006; Saag et al., 1998; Wallach et al., 2000; Lukert and Raisz, 1990).

While generally perceived as rational, and noting that BTM targets have been defined for clinical use of BPs and drug development in general, the differences between the various BPs and the consequences for the relationships between BTMs and antifracture efficacy should be acknowledged, too. Risedronate, for example, leads, despite its higher potency, to a smaller decrease in BTMs than alendronate while having similar antifracture efficacy (Bonnick et al., 2006). It is highly likely that part of the effects of BPs are not captured by BTMs yet result in antifracture efficacy (Russell et al., 2008; Roelofs et al., 2012). Such effects may include effects on osteocytes, which may also be related to differences in the binding properties of the various BPs (Russell et al., 2008; Roelofs et al., 2012).

Last but not least, it is important to set any target for BTMs during BP therapy for the specific BTM and sometimes even the specific assay used to measure it (Vasikaran et al., 2011; Cremers et al., 2005; Greenblatt et al., 2017). There are substantial differences in the sensitivity and kinetics of the various BTMs, and therefore care should be given to extrapolating results generated with one BTM to another BTM, including during drug development (Vasikaran et al., 2011; Cremers et al., 2005; Greenblatt et al., 2017).

Metastatic bone disease

BTMs have played an essential role in defining the dose regimens of BPs used to treat metastatic bone disease (Berenson et al., 2001a, 2001b; Rosen et al., 2001; Body et al., 1995). Continued suppression of BTMs in most patients has been the basis for monthly 4 mg zoledronic acid infusions in these patients (Berenson et al., 2001a, 2001b), which made sense at a time when long-term high-dose IV BPs were generally regarded as safe provided the infusion rate was not too fast, as that is known to cause nephrotoxicity (Perazella and Markowitz, 2008). BTMs also played a role when rare complications such osteonecrosis of the jaw and subtrochanteric fractures prompted the search for alternative regimens with either smaller doses or longer dose intervals (Coleman et al., 2011). Again, continued suppression of BTMs, often measured using uNTX/Cr, has been the aim during the various decreased dosing efforts, such as q3mo treatment dosing after an initial period of monthly infusions (Hortobagyi et al., 2017).

Denosumab

BTMs have been used to determine dose and dose interval during the clinical development of denosumab for the treatment of postmenopausal osteoporosis (Bekker et al., 2004; McClung et al., 2006) as well as the treatment of metastatic bone disease (Body et al., 2006). For postmenopausal osteoporosis, short- and long-term changes in BTMs correlate with changes in BMD (Eastell et al., 2011b). BTMs also revealed rebound-increased bone turnover after stopping denosumab treatment in patients with postmenopausal osteoporosis accompanied by rapid bone loss (Tsourdi et al., 2017). Because of this rebound effect, patients at particular risk for fracture are advised to continue treatment after 5 years of denosumab treatment. Treatment is either continued with denosumab or with a BP. BTMs can be useful for monitoring the effect of such a switch in treatment. Long-term BMD outcomes during denosumab treatment can be predicted from changes in BTMs after a single dose using a semimechanistic mathematical bone cycle model that includes descriptions of denosumab pharmacokinetics and its relations with BTMs and lumbar spine BMD (Zheng et al., 2015). Treatment data for 5 and 8 years demonstrate sustained suppression of BTMs, continued increases in BMD, and persistent low-fracture incidence in patients treated with denosumab 60 mg q6mo (Papapoulos et al., 2015). BTMs in combination with BMD have been used to explore the effect of denosumab in osteoporosis other than postmenopausal such as glucocorticoid-induced osteoporosis (Dore et al., 2010; Mok et al., 2015; Sawamura et al., 2017). BTMs in combination with BMD have also demonstrated the efficacy of denosumab for the treatment and prevention of androgen-deprived and estrogen-deprived bone loss in prostate and breast cancer, respectively (Smith et al., 2009; Ellis et al., 2008). Recently, Lipton et al. reanalyzed data from phase 3 trials with antiresorptive drugs in patients with advanced cancer and BMs and concluded that relatively high levels of

BTMs (uNTX/Cr and PINP) after 3 months of antiresorptive treatment were associated with reduced overall survival and increased risk of disease progression and disease progression in bone. BTMs might therefore be useful for identifying those patients at risk for worsened clinical outcomes while on either BP or denosumab treatment (Lipton et al., 2016).

Cathepsin K inhibitors

BTMs have been extremely useful for the clinical development of cathepsin K inhibitors, despite the termination of development for most of them including odanacatib (Eastell et al., 2011c; Nagase et al., 2012; Stoch et al., 2009, 2013). Dose-finding studies were conducted based largely on BTMs, with continued suppression of BTMs in the majority of patients as a target, similar to that of other antiresorptive drugs. Interestingly, bone formation markers during cathepsin K inhibitor treatment are decreased less than they are during treatment with BPs or denosumab, suggesting continued signaling of osteoclasts to osteoblasts during treatment that results in additional bone mass increases (Costa et al., 2011). Also interesting, very low doses of odanacatib were associated with relatively small decreases in bone resorption markers but increases in bone formation markers, which in itself could perhaps also lead to renewed clinical development of low-dose cathepsin K inhibitor therapy for osteoporosis. Further phase 2 and 3 studies with strong antiresorptive doses of this compound in postmenopausal women with low bone mass revealed continued suppression of BTMs and increases in BMD. Similar to denosumab (and for that matter estrogen therapy), cessation of cathepsin K inhibitors is also characterized by a rebound effect in BTMs that is accompanied by bone loss (Eisman et al., 2011).

Odanacatib seemed to have strong antifracture efficacy in postmenopausal women with low bone mass, and its efficacy on bone loss was also investigated in other populations (Drake et al., 2017). Unfortunately, the development program was terminated before relationships between BTMs and BMD, as well as antifracture efficacy, could be established. In addition, a potential transfer of such a relationship in postmenopausal women to other osteoporosis populations such as patients with glucocorticoid-induced osteoporosis was not applied to seek approval of odanacatib for this indication based on antifracture efficacy in postmenopausal osteoporosis and its effects on BTMs and BMD in both postmenopausal women and patients with glucocorticoid-induced osteoporosis.

In a short 4-week study, odanacatib suppressed bone resorption in patients with breast cancer and BMs (Jensen et al., 2010) and might be a potentially interesting agent for the treatment of metastatic bone disease.

Overall antiresorptive treatment

Several reviews summarize the relationship between changes in BMD and antifracture efficacy during the use of various antiresorptive drugs (Eastell et al., 2003; Bjarnason et al., 2001; Greenspan et al., 1998, 2000, 2005; Iwamoto et al., 2005; Bjarnason and Christiansen, 2000; Delmas et al., 2000). Also, several reviews summarize the relationship between changes in BTMs, BMD, and antifracture efficacy during the use of various antiresorptive drugs (Vasikaran et al., 2011; Cremers and Garnero, 2006; Miller et al., 2005b). It is from these papers that a general consensus may be derived with respect to the targets of BTMs during the development of new drugs. BTMs seem useful in determining the most effective dose of antiresorptive therapy with more extensive suppression of bone resorption during a dose-ranging study, most likely resulting in more extensive gain in bone mass and perhaps more antifracture efficacy, schematically represented in Fig. 78.3 (Bonjour et al., 2014). Between various antiresorptive drugs and even between compounds of the same class, drugs decrease BTMs to different extents even when they have similar antifracture efficacy (Table 78.4; Bonjour et al., 2014). It is therefore very difficult to assess exact target levels for BTMs for the development of new antiresorptive agents. Previously assessed levels for a drug might be useful, however, for the development of alternative dose regimens as well as for studies of the same drug with the same dose regimen for a different but similar indication (such as steroid-induced osteoporosis), all in conjunction with BMD measurements.

Anabolic agents

Anabolic drugs such as intermittent PTH increase BTMs, increase BMD, and decrease fracture risk. It seems as if higher increases in bone formation markers lead to higher bone mass and thereby perhaps more antifracture efficacy (Fig. 78.3; Bonjour et al., 2014). Interestingly, various forms of PTH seem to increase BTMs to a different extent while having similar antifracture efficacy (Table 78.4; Bonjour et al., 2014). The relationship between BTMs, BMD, and antifracture efficacy is very complex for PTH, but it is used to develop new modes of administration of PTH as well as new forms of PTH such as abaloparatide (Tay et al., 2018). Given that various forms of PTH have different effects on osteoblasts, osteocytes, and osteoclasts and that these effects clearly depend on the dose regimen, one should be very careful not to overinterpret BTM

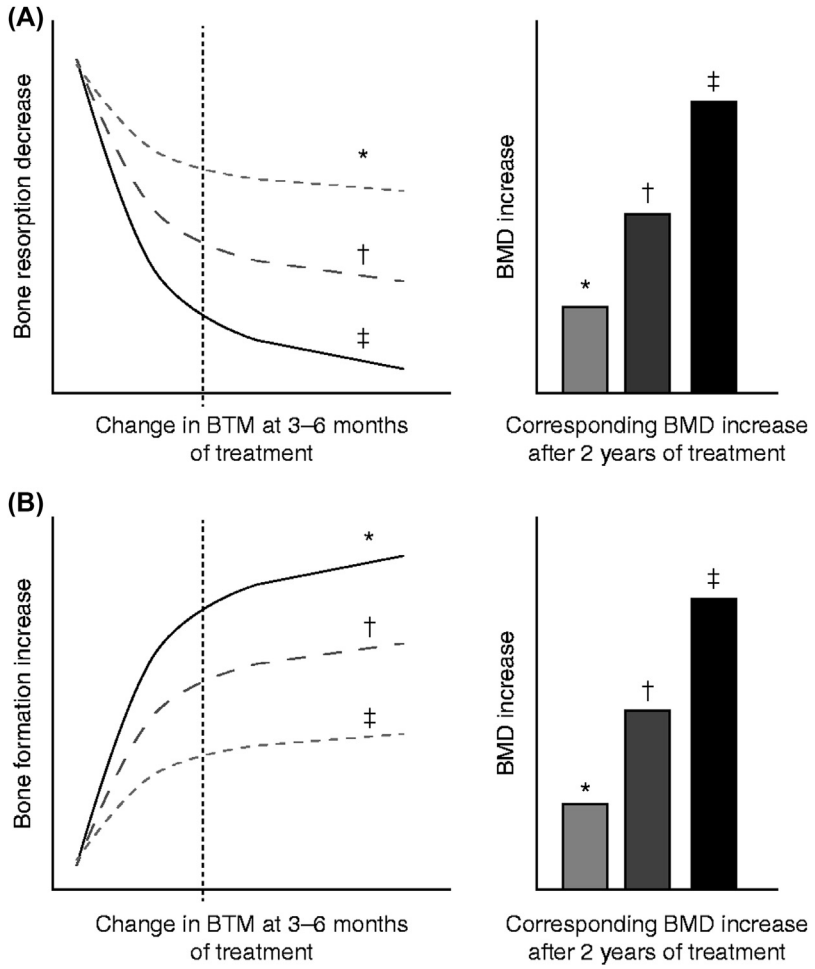

FIGURE 78.3 Schematic representation of changes in bone turnover markers (BTMs) at 3−6 months and corresponding increase in bone mineral density (BMD) during the treatment of osteoporosis. (A) Bone antiresorptive treatment (i.e., bisphosphonate); a more pronounced decrease in bone resorption marker at 3−6 months is associated with larger increases in BMD. (B) Bone formation-stimulating treatment (i.e., recombinant parathyroid hormone); a greater increase in bone formation marker is associated with a larger increase in BMD. * Mild response in changes in BTM and BMD. † Moderate response in changes in BTM and BMD. ‡ Pronounced response in changes in BTM and BMD. The diagrams show the relationship between early changes (3−6 months) in BTM and changes in BMD after 2 years of either bone resorption inhibition (A) or bone formation stimulation (B). Fig. 78.3(A) is based on quantitative data obtained by antiresorptive treatment with alendronate, documenting tertile changes at 6 months in the bone resorption marker urinary N-terminal telopeptide, and changes in BMD as assessed by dual-energy X-ray absorptiometry (DXA) in total hip, trochanter, and spine at 3 years in postmenopausal women. Fig. 78.3(B) is based on quantitative data obtained by anabolic treatment with parathyroid hormone, documenting tertile changes at 3 months in the bone formation marker N-terminal procollagen I propeptide, and the change in areal and volumetric BMD at 12 months, as assessed in the spine by DXA and quantitative computed tomography in postmenopausal women (Bonjour et al., 2014).

levels of new forms of PTH, even in conjunction with BMD measurements. BTM levels remain to be validated by bone biopsies for all novel bone agents, including bone anabolic drugs in development. Generally, intermittent PTH treatment rapidly increases bone formation followed by an increase in bone resorption marker levels, which has been repetitively confirmed by bone biopsies (Dempster et al., 2001, 2012; Rubin et al., 2011). This differential increase gives rise to a rapid gain in bone mass and has been coined the anabolic window (Rubin and Bilezikian, 2005). Besides confirming that BTMs indeed reflect increases in bone remodeling, the biopsies also demonstrate increased bone modeling, which may explain to some extent the rapid increases in bone formation markers (Dempster et al., 2018). Increases in BTMs during intermittent PTH are transient, however, with normalization of BTM levels after 12−18 months of treatment, which is also confirmed by bone biopsies (Dempster et al., 2001, 2012, 2018; Rubin et al., 2011). It is not entirely clear at the moment why normalization of levels is associated with a continued increase in BMD. Bone biopsies as well as HR-pQCT scans seem to reveal the differential effects of intermittent PTH on various bone envelopes not entirely reflected by BTMs (Nishiyama et al., 2014), which nicely illustrates that BTMs only reflect part of what is happening at the bone level.

TABLE 78.4 Changes from baseline in serum tartrate-resistant acid phosphatase (s-TRAP), serum carboxyterminal telopeptide of collagen type I (s-CTX), and serum procollagen type I N-terminal propeptide (s-PINP) in response to antiresorptive and bone-formation-stimulating treatments (Bonjour et al., 2014).

	Change from baseline (%)			
Compound	Dose and route of administration	s-TRAP	s-CTX	s-PINP
Ca + vitamin D	500–1000 mg + 10–20 μg/d (p.o.)	−20 to −25	−20 to −30	−10 to −20
Alendronate	70 mg/week (p.o.)	−30 to −40	−70 to −80	−60 to −70
Risedronate	35 mg/week (p.o.)		−50 to −60	−40 to −50
Ibandronate	150 mg/month (p.o.)			
	3 mg/3 months (i.v.)		−60 to −80	−60 to −70
Zoledronate	5 mg/year (i.v.)		−50 to −60	−50 to −60
Raloxifene	60 mg/d (p.o.)	−10 to −15	−20 to −50	−30 to −40
Denosumab	60 mg/6 months (s.c.)		−70 to −90	−60 to −70
PTH 1–34 (teriparatide)	20 μg/d (s.c.)		Up to 80	Up to 200
PTH 1–84	100 μg/d (s.c.)		10–100	90–150

Dual-action drugs such as romosozumab

Changes in BTMs during antiresorptive or anabolic therapy are fairly complex, but these changes and their apparent relationship with changes in BMD and fracture risk still seem rather straightforward compared with the transient changes during SOST-antibody treatment. During romosozumab treatment, bone formation levels increase initially and bone resorption markers decrease, with very transient dose-dependent changes and levels decreasing again after a few months of treatment (Fig. 78.2; McClung et al., 2014). In contrast, BMD perhaps surprisingly continues to increase despite the normalization of BTM levels (McClung et al., 2014). BTM levels were used to identify the seemingly most appropriate dose. However, it is presently not clear how much short-term and/or long-term changes in the BTM levels correlate with gains in bone mass or antifracture efficacy of the drug in postmenopausal women with low bone mass. The use of BTMs in conjunction with BMD might therefore also be challenging for romosozumab studies seeking approval for other indications without performing a proper phase 3 trial that includes fracture risk as an outcome. From the transient BTM levels during both romosozumab and PTH treatment, it can be appreciated that BTMs do not simply reflect bone turnover as always being a function of bone remodeling. In both cases, they probably reflect a mixture of bone modeling and remodeling, with both contributing differently during the time course of treatment. It is therefore important that BTM levels during drug development are correlated with histomorphometric data from bone biopsies in animals as well as humans.

The challenge for new drugs with new mechanisms of action

As detailed above there are numerous examples of differential use of BTMs during drug development. Results can sometimes be extrapolated to similar new drugs and similar indications, albeit that one needs to remain careful when doing so. More challenging is the use of BTMs for the development of drugs with completely new mechanisms of action. Basically, BTMs need to be revalidated completely in terms of their relationships with actual bone turnover, gain in BMD, other surrogate parameters including biomechanical properties, as well as clinical outcomes such as fracture risk.

Bone turnover markers to assess skeletal safety of new drugs

Many drugs have an unwanted effect on bone. These include NSAIDs, DMARDs, psychotropic drugs, antiepileptic drugs, vitamin K, statins, antacids, estrogens, androgens, progestins, corticosteroids, anabolic steroids, hormonal contraceptives, chemotherapeutics, targeted cancer agents, therapies that cause hypogonadism and depletion of peripheral production of sex hormones, antihypertensives, antiretrovirals, and immunosuppressants, to name a few (Goodman et al., 2007; Compston and Rosen, 2013). Effects on bone are established through various mechanisms of action and can be related to

changes in hormone levels, changes in mineral transporters in various organs, and also through direct effects on bone cells. In many cases such effects are observed after being in clinical use for a few years, and BTMs might be useful to identify the mechanism behind observed changes in bone mass or fracture risk. CTX and PINP, for example, were used to demonstrate decreased bone turnover caused by older (carbamazepine, valproic acid) as well as newer (levetiracetam) antiepileptic drugs (Hakami et al., 2016). CTX and PINP were also used to demonstrate increased bone turnover during TNF-alpha inhibitor therapy, which helps explain the loss of bone in the femoral neck that was also observed in patients on this treatment (Orsolini et al., 2016). In other cases, BTMs provide early information on potential effects of drugs on bone initially identified from routine chemistry parameters such as calcium and phosphate. NTX and osteocalcin, for example, were used to further explore the effects of the tyrosine kinase inhibitor imatinib on bone after low phosphate levels were found in a subgroup of patients treated with the drug (Berman et al., 2006).

In combination with other chemistries, BTMs could therefore be useful to assess the skeletal safety of not only established drugs but also new compounds in development. To our knowledge, this is not a routine assessment during drug development and could be a new and exciting application for these very informative biomarkers.

References

Abildgaard, N., et al., 2000. Biochemical markers of bone metabolism reflect osteoclastic and osteoblastic activity in multiple myeloma. Eur. J. Haematol. 64 (2), 121–129.

Adami, S., et al., 2008. Determinants of bone turnover markers in healthy premenopausal women. Calcif. Tissue Int. 82 (5), 341–347.

Adami, G., et al., 2016. Effects of TNF inhibitors on parathyroid hormone and wnt signaling antagonists in rheumatoid arthritis. Calcif. Tissue Int. 99 (4), 360–364.

Adler, R.A., et al., 2016. Managing osteoporosis in patients on long-term bisphosphonate treatment: report of a task force of the American society for bone and mineral research. J. Bone Miner. Res. 31 (10), 1910.

Al Nofal, A.A., et al., 2015. Bone turnover markers in Paget's disease of the bone: a systematic review and meta-analysis. Osteoporos. Int. 26 (7), 1875–1891.

Anastasilakis, A.D., et al., 2010. The effect of teriparatide on serum Dickkopf-1 levels in postmenopausal women with established osteoporosis. Clin. Endocrinol. 72 (6), 752–757.

Anastasilakis, A.D., et al., 2013. Comparative effect of zoledronic acid versus denosumab on serum sclerostin and dickkopf-1 levels of naive postmenopausal women with low bone mass: a randomized, head-to-head clinical trial. J. Clin. Endocrinol. Metab. 98 (8), 3206–3212.

Anastasilakis, A.D., et al., 2014. Circulating periostin levels do not differ between postmenopausal women with normal and low bone mass and are not affected by zoledronic acid treatment. Horm. Metab. Res. 46 (2), 145–149.

Appelman-Dijkstra, N.M., Papapoulos, S.E., 2016. Sclerostin inhibition in the management of osteoporosis. Calcif. Tissue Int. 98 (4), 370–380.

Arasu, A., et al., 2012. Serum sclerostin and risk of hip fracture in older Caucasian women. J. Clin. Endocrinol. Metab. 97 (6), 2027–2032.

Ardawi, M.S., et al., 2011. Determinants of serum sclerostin in healthy pre- and postmenopausal women. J. Bone Miner. Res. 26 (12), 2812–2822.

Ardawi, M.S., et al., 2012. High serum sclerostin predicts the occurrence of osteoporotic fractures in postmenopausal women: the center of excellence for osteoporosis research study. J. Bone Miner. Res. 27 (12), 2592–2602.

Ardawi, M.S., et al., 2013. Increased serum sclerostin and decreased serum IGF-1 are associated with vertebral fractures among postmenopausal women with type-2 diabetes. Bone 56 (2), 355–362.

Arroyo, J.D., et al., 2011. Argonaute2 complexes carry a population of circulating microRNAs independent of vesicles in human plasma. Proc. Natl. Acad. Sci. U. S. A. 108 (12), 5003–5008.

Aubry-Rozier, B., et al., 2016. Severe spontaneous vertebral fractures after denosumab discontinuation: three case reports. Osteoporos. Int. 27 (5), 1923–1925.

Bae, S.J., et al., 2016. The circulating sphingosine-1-phosphate level predicts incident fracture in postmenopausal women: a 3.5-year follow-up observation study. Osteoporos. Int. 27 (8), 2533–2541.

Baker, E.S., et al., 2014. Advancing the high throughput identification of liver fibrosis protein signatures using multiplexed ion mobility spectrometry. Mol. Cell. Proteomics 13 (4), 1119–1127.

Bandeira, L., Lewiecki, E.M., Bilezikian, J.P., 2017. Romosozumab for the treatment of osteoporosis. Expert Opin. Biol. Ther. 17 (2), 255–263.

Bauer, D.C., et al., 2006. Pretreatment levels of bone turnover and the antifracture efficacy of alendronate: the fracture intervention trial. J. Bone Miner. Res. 21 (2), 292–299.

Bauer, D.C., et al., 2009. Biochemical markers of bone turnover, hip bone loss, and fracture in older men: the MrOS study. J. Bone Miner. Res. 24 (12), 2032–2038.

Bauer, D.C., et al., 2014. Fracture prediction after discontinuation of 4 to 5 years of alendronate therapy: the FLEX study. JAMA Intern. Med. 174 (7), 1126–1134.

Bekker, P.J., et al., 2004. A single-dose placebo-controlled study of AMG 162, a fully human monoclonal antibody to RANKL, in postmenopausal women. J. Bone Miner. Res. 19 (7), 1059–1066.

Berenson, J.R., et al., 2001. A phase I, open label, dose ranging trial of intravenous bolus zoledronic acid, a novel bisphosphonate, in cancer patients with metastatic bone disease. Cancer 91 (1), 144–154.

Berenson, J.R., et al., 2001. A phase I dose-ranging trial of monthly infusions of zoledronic acid for the treatment of osteolytic bone metastases. Clin. Cancer Res. 7 (3), 478–485.

Berman, E., et al., 2006. Altered bone and mineral metabolism in patients receiving imatinib mesylate. N. Engl. J. Med. 354 (19), 2006–2013.

Biver, E., et al., 2012. Bone turnover markers for osteoporotic status assessment? A systematic review of their diagnosis value at baseline in osteoporosis. Jt. Bone Spine 79 (1), 20–25.

Bjarnason, N.H., Christiansen, C., 2000. Early response in biochemical markers predicts long-term response in bone mass during hormone replacement therapy in early postmenopausal women. Bone 26 (6), 561–569.

Bjarnason, N.H., et al., 2001. Six and twelve month changes in bone turnover are related to reduction in vertebral fracture risk during 3 years of raloxifene treatment in postmenopausal osteoporosis. Osteoporos. Int. 12 (11), 922–930.

Black, D.M., et al., 2012. The effect of 3 versus 6 years of zoledronic acid treatment of osteoporosis: a randomized extension to the HORIZON-pivotal fracture trial (PFT). J. Bone Miner. Res. 27 (2), 243–254.

Blekherman, G., et al., 2011. Bioinformatics tools for cancer metabolomics. Metabolomics 7 (3), 329–343.

Body, J.J., et al., 1995. Intravenous pamidronate in patients with tumor-induced osteolysis: a biochemical dose-response study. J. Bone Miner. Res. 10 (8), 1191–1196.

Body, J.J., et al., 2006. A study of the biological receptor activator of nuclear factor-kappaB ligand inhibitor, denosumab, in patients with multiple myeloma or bone metastases from breast cancer. Clin. Cancer Res. 12 (4), 1221–1228.

Bone, H.G., et al., 2011. Effects of denosumab treatment and discontinuation on bone mineral density and bone turnover markers in postmenopausal women with low bone mass. J. Clin. Endocrinol. Metab. 96 (4), 972–980.

Bonewald, L.F., Wacker, M.J., 2013. FGF23 production by osteocytes. Pediatr. Nephrol. 28 (4), 563–568.

Bonjour, J.P., et al., 2014. Biochemical markers for assessment of calcium economy and bone metabolism: application in clinical trials from pharmaceutical agents to nutritional products. Nutr. Res. Rev. 27 (2), 252–267.

Bonnet, N., et al., 2009. The matricellular protein periostin is required for sost inhibition and the anabolic response to mechanical loading and physical activity. J. Biol. Chem. 284 (51), 35939–35950.

Bonnet, N., Conway, S.J., Ferrari, S.L., 2012. Regulation of beta catenin signaling and parathyroid hormone anabolic effects in bone by the matricellular protein periostin. Proc. Natl. Acad. Sci. U. S. A. 109 (37), 15048–15053.

Bonnet, N., et al., 2015. Additive genetic effects on circulating periostin contribute to the heritability of bone microstructure. J. Clin. Endocrinol. Metab. 100 (7), E1014–E1021.

Bonnet, N., Garnero, P., Ferrari, S., 2016. Periostin action in bone. Mol. Cell. Endocrinol. 432, 75–82.

Bonnet, N., et al., 2017. Serum levels of a cathepsin-K generated periostin fragment predict incident low-trauma fractures in postmenopausal women independently of BMD and FRAX. J. Bone Miner. Res. 32 (11), 2232–2238.

Bonnick, S., et al., 2006. Comparison of weekly treatment of postmenopausal osteoporosis with alendronate versus risedronate over two years. J. Clin. Endocrinol. Metab. 91 (7), 2631–2637.

Brunetti, G., et al., 2016. Impaired bone remodeling in children with osteogenesis imperfecta treated and untreated with bisphosphonates: the role of DKK1, RANKL, and TNF-alpha. Osteoporos. Int. 27 (7), 2355–2365.

Bruyere, O., et al., 2012. Relationships between changes in bone mineral density or bone turnover markers and vertebral fracture incidence in patients treated with bazedoxifene. Calcif. Tissue Int. 91 (4), 244–249.

Butler, J.S., et al., 2011. The role of Dkk1 in bone mass regulation: correlating serum Dkk1 expression with bone mineral density. J. Orthop. Res. 29 (3), 414–418.

Caira, F.C., et al., 2006. Human degenerative valve disease is associated with up-regulation of low-density lipoprotein receptor-related protein 5 receptor-mediated bone formation. J. Am. Coll. Cardiol. 47 (8), 1707–1712.

Chalhoub, D., et al., 2016. Association of serum klotho with loss of bone mineral density and fracture risk in older adults. J. Am. Geriatr. Soc. 64 (12), e304–e308.

Chavassieux, P., et al., 2015. Are biochemical markers of bone turnover representative of bone histomorphometry in 370 postmenopausal women? J. Clin. Endocrinol. Metab. 100 (12), 4662–4668.

Chen, P., et al., 2005. Early changes in biochemical markers of bone formation predict BMD response to teriparatide in postmenopausal women with osteoporosis. J. Bone Miner. Res. 20 (6), 962–970.

Chen, C., et al., 2014. MiR-503 regulates osteoclastogenesis via targeting RANK. J. Bone Miner. Res. 29 (2), 338–347.

Chesnut III, C.H., et al., 1995. Alendronate treatment of the postmenopausal osteoporotic woman: effect of multiple dosages on bone mass and bone remodeling. Am. J. Med. 99 (2), 144–152.

Chopin, F., et al., 2012. Prognostic interest of bone turnover markers in the management of postmenopausal osteoporosis. Joint Bone Spine 79 (1), 26–31.

Chubb, S.A., et al., 2015. Reference intervals for bone turnover markers and their association with incident hip fractures in older men: the health in men study. J. Clin. Endocrinol. Metab. 100 (1), 90–99.

Clowes, J.A., et al., 2002. Effect of feeding on bone turnover markers and its impact on biological variability of measurements. Bone 30 (6), 886–890.

Clowes, J.A., Peel, N.F., Eastell, R., 2004. The impact of monitoring on adherence and persistence with antiresorptive treatment for postmenopausal osteoporosis: a randomized controlled trial. J. Clin. Endocrinol. Metab. 89 (3), 1117–1123.

Coleman, R., et al., 2011. Consensus on the utility of bone markers in the malignant bone disease setting. Crit. Rev. Oncol. Hematol. 80 (3), 411–432.

Coleman, R.E., et al., 2013. Possible survival benefits from zoledronic acid treatment in patients with bone metastases from solid tumours and poor prognostic features-An exploratory analysis of placebo-controlled trials. J. Bone Oncol. 2 (2), 70–76.

Collins, M.T., et al., 2005. An instrument to measure skeletal burden and predict functional outcome in fibrous dysplasia of bone. J. Bone Miner. Res. 20 (2), 219–226.

Compston, J., 2013. Skeletal effects of drugs. In: Rosen, C. (Ed.), Primer on Metabolic Bone Diseases and Disorders of Mineral Metabolism. Wiley and Sons, New York, NY, pp. 520–526.

Corso, A., et al., 2001. Biochemical markers of bone disease in asymptomatic early stage multiple myeloma. A study on their role in identifying high risk patients. Haematologica 86 (4), 394–398.

Cosman, F., et al., 2014. Reassessment of fracture risk in women after 3 years of treatment with zoledronic acid: when is it reasonable to discontinue treatment? J. Clin. Endocrinol. Metab. 99 (12), 4546–4554.

Costa, A.G., Bilezikian, J.P., 2012. Sclerostin: therapeutic horizons based upon its actions. Curr. Osteoporos. Rep. 10 (1), 64–72.

Costa, A.G., et al., 2011. Cathepsin K: its skeletal actions and role as a therapeutic target in osteoporosis. Nat. Rev. Rheumatol. 7 (8), 447–456.

Costa, A.G., et al., 2014. Comparison of two commercially available ELISAs for circulating sclerostin. Osteoporos. Int. 25 (5), 1547–1554.

Cremers, S., Garnero, P., 2006. Biochemical markers of bone turnover in the clinical development of drugs for osteoporosis and metastatic bone disease: potential uses and pitfalls. Drugs 66 (16), 2031–2058.

Cremers, S.C., Pillai, G., Papapoulos, S.E., 2005. Pharmacokinetics/pharmacodynamics of bisphosphonates: use for optimisation of intermittent therapy for osteoporosis. Clin. Pharmacokinet. 44 (6), 551–570.

Crowell, K.L., et al., 2013. Increasing confidence of LC-MS identifications by utilizing ion mobility spectrometry. Int. J. Mass Spectrom. 354–355, 312–317.

D'Oronzo, S., Brown, J., Coleman, R., 2017. The value of biomarkers in bone metastasis. Eur. J. Cancer Care 26 (6).

Dai, Z., et al., 2016. Bone turnover biomarkers and risk of osteoporotic hip fracture in an Asian population. Bone 83, 171–177.

Day, T.F., et al., 2005. Wnt/beta-catenin signaling in mesenchymal progenitors controls osteoblast and chondrocyte differentiation during vertebrate skeletogenesis. Dev. Cell 8 (5), 739–750.

De Beur, S.J., 2017. Effects of Burosumab (KRN23), a Human Monoclonal Antibody to FGF23, in Patients with Tumor-Induced Osteomalacia (TIO) or Epidermal Nevus Syndrome (ENS). ASBMR, p. SU0305.

de Papp, A.E., et al., 2007. A cross-sectional study of bone turnover markers in healthy premenopausal women. Bone 40 (5), 1222–1230.

Delmas, P.D., et al., 2000. Monitoring individual response to hormone replacement therapy with bone markers. Bone 26 (6), 553–560.

Delmas, P.D., et al., 2006. Fracture risk reduction during treatment with teriparatide is independent of pretreatment bone turnover. Bone 39 (2), 237–243.

Dempster, D.W., et al., 2001. Effects of daily treatment with parathyroid hormone on bone microarchitecture and turnover in patients with osteoporosis: a paired biopsy study. J. Bone Miner. Res. 16 (10), 1846–1853.

Dempster, D.W., et al., 2012. Skeletal histomorphometry in subjects on teriparatide or zoledronic acid therapy (SHOTZ) study: a randomized controlled trial. J. Clin. Endocrinol. Metab. 97 (8), 2799–2808.

Dempster, D.W., et al., 2018. Longitudinal effects of teriparatide or zoledronic acid on bone modeling- and remodeling-based formation in the SHOTZ study. J. Bone Miner. Res. 33, 627–633.

Diarra, D., et al., 2007. Dickkopf-1 is a master regulator of joint remodeling. Nat. Med. 13 (2), 156–163.

Diez-Perez, A., et al., 2017. International osteoporosis foundation and european calcified tissue society working group. Recommendations for the screening of adherence to oral bisphosphonates. Osteoporos. Int. 28 (3), 767–774.

Dore, R.K., et al., 2010. Effects of denosumab on bone mineral density and bone turnover in patients with rheumatoid arthritis receiving concurrent glucocorticoids or bisphosphonates. Ann. Rheum. Dis. 69 (5), 872–875.

Drake, M.T., et al., 2017. Cathepsin K inhibitors for osteoporosis: biology, potential clinical utility, and lessons learned. Endocr. Rev. 38 (4), 325–350.

During, A., Penel, G., Hardouin, P., 2015. Understanding the local actions of lipids in bone physiology. Prog. Lipid Res. 59, 126–146.

Durosier, C., et al., 2013. Association of circulating sclerostin with bone mineral mass, microstructure, and turnover biochemical markers in healthy elderly men and women. J. Clin. Endocrinol. Metab. 98 (9), 3873–3883.

Eastell, R., 2017. Early Change in PINP Correlates with Lumbar Spine BMD More Strongly Wit Abaloparatide than with Teriparatide: Results of the ACTIVE Trial. ASBMR.

Eastell, R., Szulc, P., 2017. Use of bone turnover markers in postmenopausal osteoporosis. Lancet Diabetes Endocrinol. 5 (11), 908–923.

Eastell, R., et al., 1997. Biochemical markers of bone resorption compared with estimates of bone resorption from radiotracer kinetic studies in osteoporosis. J. Bone Miner. Res. 12 (1), 59–65.

Eastell, R., et al., 2003. Relationship of early changes in bone resorption to the reduction in fracture risk with risedronate. J. Bone Miner. Res. 18 (6), 1051–1056.

Eastell, R., et al., 2011. Bone turnover markers and bone mineral density response with risedronate therapy: relationship with fracture risk and patient adherence. J. Bone Miner. Res. 26 (7), 1662–1669.

Eastell, R., et al., 2011. Effects of denosumab on bone turnover markers in postmenopausal osteoporosis. J. Bone Miner. Res. 26 (3), 530–537.

Eastell, R., et al., 2011. Safety and efficacy of the cathepsin K inhibitor ONO-5334 in postmenopausal osteoporosis: the OCEAN study. J. Bone Miner. Res. 26 (6), 1303–1312.

Eastell, R., et al., 2015. Relationship between pretreatment rate of bone loss and bone density response to once-yearly ZOL: HORIZON-PFT extension study. J. Bone Miner. Res. 30 (3), 570–574.

Eisman, J.A., et al., 2011. Odanacatib in the treatment of postmenopausal women with low bone mineral density: three-year continued therapy and resolution of effect. J. Bone Miner. Res. 26 (2), 242–251.

Ellis, G.K., et al., 2008. Randomized trial of denosumab in patients receiving adjuvant aromatase inhibitors for nonmetastatic breast cancer. J. Clin. Oncol. 26 (30), 4875–4882.

Evenepoel, P., et al., 2015. Sclerostin serum levels and vascular calcification progression in prevalent renal transplant recipients. J. Clin. Endocrinol. Metab. 100 (12), 4669–4676.

Farahmand, P., et al., 2013. Early changes in biochemical markers of bone formation during teriparatide therapy correlate with improvements in vertebral strength in men with glucocorticoid-induced osteoporosis. Osteoporos. Int. 24 (12), 2971–2981.

Findlay, D.M., Atkins, G.J., 2011. Relationship between serum RANKL and RANKL in bone. Osteoporos. Int. 22 (10), 2597–2602.

Finnes, T.E., et al., 2014. Procollagen type 1 amino-terminal propeptide (P1NP) and risk of hip fractures in elderly Norwegian men and women. A NOREPOS study. Bone 64, 1–7.

Fonseca, R., et al., 2000. Prognostic value of serum markers of bone metabolism in untreated multiple myeloma patients. Br. J. Haematol. 109 (1), 24–29.

Franceschetti, P., et al., 2013. Risk factors for development of atypical femoral fractures in patients on long-term oral bisphosphonate therapy. Bone 56 (2), 426–431.

Garcia-Martin, A., et al., 2012. Circulating levels of sclerostin are increased in patients with type 2 diabetes mellitus. J. Clin. Endocrinol. Metab. 97 (1), 234–241.

Garnero, P., 2000. Markers of bone turnover for the prediction of fracture risk. Osteoporos. Int. 11 (Suppl. 6), S55–S65.

Garnero, P., 2008. Biomarkers for osteoporosis management: utility in diagnosis, fracture risk prediction and therapy monitoring. Mol. Diagn. Ther. 12 (3), 157–170.

Garnero, P., et al., 1996. Increased bone turnover in late postmenopausal women is a major determinant of osteoporosis. J. Bone Miner. Res. 11 (3), 337–349.

Garnero, P., et al., 1996. Markers of bone resorption predict hip fracture in elderly women: the EPIDOS prospective study. J. Bone Miner. Res. 11 (10), 1531–1538.

Garnero, P., et al., 1997. Decreased beta-isomerization of the C-terminal telopeptide of type I collagen alpha 1 chain in Paget's disease of bone. J. Bone Miner. Res. 12 (9), 1407–1415.

Garnero, P., et al., 1999. Markers of bone turnover predict postmenopausal forearm bone loss over 4 years: the OFELY study. J. Bone Miner. Res. 14 (9), 1614–1621.

Garnero, P., et al., 2013. Association of serum sclerostin with bone mineral density, bone turnover, steroid and parathyroid hormones, and fracture risk in postmenopausal women: the OFELY study. Osteoporos. Int. 24 (2), 489–494.

Garnero, P., Bonnet, N., Ferrari, S.L., 2017. Development of a new immunoassay for human cathepsin K-generated periostin fragments as a serum biomarker for cortical bone. Calcif. Tissue Int. 101 (5), 501–509.

Gatti, D., et al., 2011. The waning of teriparatide effect on bone formation markers in postmenopausal osteoporosis is associated with increasing serum levels of DKK1. J. Clin. Endocrinol. Metab. 96 (5), 1555–1559.

Gatti, D., et al., 2012. Sclerostin and DKK1 in postmenopausal osteoporosis treated with denosumab. J. Bone Miner. Res. 27 (11), 2259–2263.

Gatti, D., et al., 2012. Bisphosphonate treatment of postmenopausal osteoporosis is associated with a dose dependent increase in serum sclerostin. Bone 50 (3), 739–742.

Gatti, D., et al., 2014. Distinct effect of zoledronate and clodronate on circulating levels of DKK1 and sclerostin in women with postmenopausal osteoporosis. Bone 67, 189–192.

Gennari, L., et al., 2012. Circulating sclerostin levels and bone turnover in type 1 and type 2 diabetes. J. Clin. Endocrinol. Metab. 97 (5), 1737–1744.

Gifre, L., et al., 2013. Effect of glucocorticoid treatment on Wnt signalling antagonists (sclerostin and Dkk-1) and their relationship with bone turnover. Bone 57 (1), 272–276.

Gilad, S., et al., 2008. Serum microRNAs are promising novel biomarkers. PLoS One 3 (9), e3148.

Glover, S.J., et al., 2008. Establishing a reference range for bone turnover markers in young, healthy women. Bone 42 (4), 623–630.

Glover, S.J., et al., 2009. Establishing a reference interval for bone turnover markers in 637 healthy, young, premenopausal women from the United Kingdom, France, Belgium, and the United States. J. Bone Miner. Res. 24 (3), 389–397.

Goodman, S.B., et al., 2007. The effects of medications on bone. J. Am. Acad. Orthop. Surg. 15 (8), 450–460.

Gossiel, F., et al., 2018. The effect of teriparatide treatment on circulating periostin and its relationship to regulators of bone formation and BMD in postmenopausal women with osteoporosis. J. Clin. Endocrinol. Metab. 103, 1302–1309.

Grafe, I., et al., 2014. Excessive transforming growth factor-beta signaling is a common mechanism in osteogenesis imperfecta. Nat. Med. 20 (6), 670–675.

Greenblatt, M.B., Tsai, J.N., Wein, M.N., 2017. Bone turnover markers in the diagnosis and monitoring of metabolic bone disease. Clin. Chem. 63 (2), 464–474.

Greenspan, S.L., et al., 1998. Early changes in biochemical markers of bone turnover predict the long-term response to alendronate therapy in representative elderly women: a randomized clinical trial. J. Bone Miner. Res. 13 (9), 1431–1438.

Greenspan, S.L., Rosen, H.N., Parker, R.A., 2000. Early changes in serum N-telopeptide and C-telopeptide cross-linked collagen type 1 predict long-term response to alendronate therapy in elderly women. J. Clin. Endocrinol. Metab. 85 (10), 3537–3540.

Greenspan, S.L., Resnick, N.M., Parker, R.A., 2005. Early changes in biochemical markers of bone turnover are associated with long-term changes in bone mineral density in elderly women on alendronate, hormone replacement therapy, or combination therapy: a three-year, double-blind, placebo-controlled, randomized clinical trial. J. Clin. Endocrinol. Metab. 90 (5), 2762–2767.

Grey, A., et al., 2002. The phospholipids sphingosine-1-phosphate and lysophosphatidic acid prevent apoptosis in osteoblastic cells via a signaling pathway involving G(i) proteins and phosphatidylinositol-3 kinase. Endocrinology 143 (12), 4755–4763.

Grey, A., et al., 2004. Osteoblastic cells express phospholipid receptors and phosphatases and proliferate in response to sphingosine-1-phosphate. Calcif. Tissue Int. 74 (6), 542–550.

Hackl, M., et al., 2016. Circulating microRNAs as novel biomarkers for bone diseases - complex signatures for multifactorial diseases? Mol. Cell. Endocrinol. 432, 83–95.

Hakami, T., et al., 2016. Monotherapy with levetiracetam versus older AEDs: a randomized comparative trial of effects on bone health. Calcif. Tissue Int. 98 (6), 556–565.

Hampson, G., et al., 2013. The relationship between inhibitors of the Wnt signalling pathway (Dickkopf-1(DKK1) and sclerostin), bone mineral density, vascular calcification and arterial stiffness in post-menopausal women. Bone 56 (1), 42–47.

Heiland, G.R., et al., 2012. High level of functional dickkopf-1 predicts protection from syndesmophyte formation in patients with ankylosing spondylitis. Ann. Rheum. Dis. 71 (4), 572–574.

Heilmeier, U., et al., 2016. Serum miRNA signatures are indicative of skeletal fractures in postmenopausal women with and without type 2 diabetes and influence osteogenic and adipogenic differentiation of adipose tissue-derived mesenchymal stem cells in vitro. J. Bone Miner. Res. 31 (12), 2173–2192.

Hlaing, T.T., Compston, J.E., 2014. Biochemical markers of bone turnover - uses and limitations. Ann. Clin. Biochem. 51 (Pt 2), 189–202.

Hobert, O., 2008. Gene regulation by transcription factors and microRNAs. Science 319 (5871), 1785–1786.

Hortobagyi, G.N., et al., 2017. Continued treatment effect of zoledronic acid dosing every 12 vs 4 weeks in women with breast cancer metastatic to bone: the OPTIMIZE-2 randomized clinical trial. JAMA Oncol. 3 (7), 906–912.

Idolazzi, L., et al., 2017. Circulating Dickkopf-1 and sclerostin in patients with Paget's disease of bone. Clin. Rheumatol. 36 (4), 925–928.

Ikegami, S., et al., 2009. Comparison in bone turnover markers during early healing of femoral neck fracture and trochanteric fracture in elderly patients. Orthop. Rev. 1 (2), e21.

Ishii, M., et al., 2009. Sphingosine-1-phosphate mobilizes osteoclast precursors and regulates bone homeostasis. Nature 458 (7237), 524–528.

Ishii, M., et al., 2010. Chemorepulsion by blood S1P regulates osteoclast precursor mobilization and bone remodeling in vivo. J. Exp. Med. 207 (13), 2793–2798.

Ishikawa, K., et al., 2016. High bone turnover elevates the risk of denosumab-induced hypocalcemia in women with postmenopausal osteoporosis. Ther. Clin. Risk Manag. 12, 1831–1840.

Ivaska, K.K., et al., 2007. Effect of fracture on bone turnover markers: a longitudinal study comparing marker levels before and after injury in 113 elderly women. J. Bone Miner. Res. 22 (8), 1155–1164.

Ivaska, K.K., et al., 2010. Bone turnover markers and prediction of fracture: a prospective follow-up study of 1040 elderly women for a mean of 9 years. J. Bone Miner. Res. 25 (2), 393–403.

Iwamoto, J., et al., 2005. Early changes in urinary cross-linked N-terminal telopeptides of type I collagen level correlate with 1-year response of lumbar bone mineral density to alendronate in postmenopausal Japanese women with osteoporosis. J. Bone Miner. Metab. 23 (3), 238–242.

Jacques, R.M., et al., 2012. Relationship of changes in total hip bone mineral density to vertebral and nonvertebral fracture risk in women with post-menopausal osteoporosis treated with once-yearly zoledronic acid 5 mg: the HORIZON-pivotal fracture trial (PFT). J. Bone Miner. Res. 27 (8), 1627–1634.

Jensen, A.B., et al., 2010. The cathepsin K inhibitor odanacatib suppresses bone resorption in women with breast cancer and established bone metastases: results of a 4-week, double-blind, randomized, controlled trial. Clin. Breast Canc. 10 (6), 452–458.

Johansson, H., et al., 2014. A meta-analysis of reference markers of bone turnover for prediction of fracture. Calcif. Tissue Int. 94 (5), 560–567.

Johnell, O., et al., 2002. Biochemical indices of bone turnover and the assessment of fracture probability. Osteoporos. Int. 13 (7), 523–526.

Kaneko, K., et al., 2012. Changes of serum soluble receptor activator for nuclear factor-kappaB ligand after glucocorticoid therapy reflect regulation of its expression by osteoblasts. J. Clin. Endocrinol. Metab. 97 (10), E1909–E1917.

Kaplan, F.S., 2017. Efficacy and Safety of Palovarotene in Fibrodysplasia Ossificans Progressiva (FOP): A Randomized, Placebo-Controlled, Double-Blind Study. ASBMR, p. FR0334.

Kearns, A.E., Khosla, S., Kostenuik, P.J., 2008. Receptor activator of nuclear factor kappaB ligand and osteoprotegerin regulation of bone remodeling in health and disease. Endocr. Rev. 29 (2), 155–192.

Keaveny, T.M., et al., 2007. Effects of teriparatide and alendronate on vertebral strength as assessed by finite element modeling of QCT scans in women with osteoporosis. J. Bone Miner. Res. 22 (1), 149–157.

Khan, A.A., et al., 2015. Diagnosis and management of osteonecrosis of the jaw: a systematic review and international consensus. J. Bone Miner. Res. 30 (1), 3–23.

Kii, I., et al., 2010. Incorporation of tenascin-C into the extracellular matrix by periostin underlies an extracellular meshwork architecture. J. Biol. Chem. 285 (3), 2028–2039.

Kim, T.H., 2017. Comparison of BMD Changes Ad Bone Turnover Levels 3 Years after Bisphosphonate Discontinuation: FLEX and HORIZON Studies. ASBMR.

Kim, B.J., et al., 2012. Plasma sphingosine 1-phosphate levels and the risk of vertebral fracture in postmenopausal women. J. Clin. Endocrinol. Metab. 97 (10), 3807–3814.

Kim, B.J., et al., 2015. Plasma periostin associates significantly with non-vertebral but not vertebral fractures in postmenopausal women: clinical evidence for the different effects of periostin depending on the skeletal site. Bone 81, 435–441.

Kim, B.J., et al., 2016. The effect of sphingosine-1-phosphate on bone metabolism in humans depends on its plasma/bone marrow gradient. J. Endocrinol. Investig. 39 (3), 297–303.

Kirmani, S., et al., 2012. Sclerostin levels during growth in children. Osteoporos. Int. 23 (3), 1123–1130.
Kishnani, P.S., et al., 2017. Monitoring guidance for patients with hypophosphatasia treated with asfotase alfa. Mol. Genet. Metabol. 122 (1–2), 4–17.
Kocijan, R., et al., 2016. Circulating microRNA signatures in patients with idiopathic and postmenopausal osteoporosis and fragility fractures. J. Clin. Endocrinol. Metab. 101 (11), 4125–4134.
Komaba, H., Fukagawa, M., 2012. The role of FGF23 in CKD—with or without Klotho. Nat. Rev. Nephrol. 8 (8), 484–490.
Krege, J.H., et al., 2014. PINP as a biological response marker during teriparatide treatment for osteoporosis. Osteoporos. Int. 25 (9), 2159–2171.
Kuhn, B., et al., 2007. Periostin induces proliferation of differentiated cardiomyocytes and promotes cardiac repair. Nat. Med. 13 (8), 962–969.
Kuro-o, M., 2013. Klotho, phosphate and FGF-23 in ageing and disturbed mineral metabolism. Nat. Rev. Nephrol. 9 (11), 650–660.
Lamers, D., et al., 2011. Dipeptidyl peptidase 4 is a novel adipokine potentially linking obesity to the metabolic syndrome. Diabetes 60 (7), 1917–1925.
Lane, N.E., et al., 2007. Wnt signaling antagonists are potential prognostic biomarkers for the progression of radiographic hip osteoarthritis in elderly caucasian women. Arthritis Rheum. 56 (10), 3319–3325.
Lane, N.E., et al., 2013. Association of serum fibroblast growth factor 23 (FGF23) and incident fractures in older men: the osteoporotic fractures in men (MrOS) study. J. Bone Miner. Res. 28 (11), 2325–2332.
Langston, A.L., et al., 2010. Randomized trial of intensive bisphosphonate treatment versus symptomatic management in Paget's disease of bone. J. Bone Miner. Res. 25 (1), 20–31.
Larsson, T., et al., 2004. Transgenic mice expressing fibroblast growth factor 23 under the control of the alpha1(I) collagen promoter exhibit growth retardation, osteomalacia, and disturbed phosphate homeostasis. Endocrinology 145 (7), 3087–3094.
Lee, S.H., et al., 2012. Higher circulating sphingosine 1-phosphate levels are associated with lower bone mineral density and higher bone resorption marker in humans. J. Clin. Endocrinol. Metab. 97 (8), E1421–E1428.
Leeming, D.J., et al., 2006. Alpha CTX as a biomarker of skeletal invasion of breast cancer: immunolocalization and the load dependency of urinary excretion. Cancer Epidemiol. Biomark. Prev. 15 (7), 1392–1395.
Li, X., et al., 2005. Sclerostin binds to LRP5/6 and antagonizes canonical Wnt signaling. J. Biol. Chem. 280 (20), 19883–19887.
Li, H., et al., 2014. Plasma miRNA levels correlate with sensitivity to bone mineral density in postmenopausal osteoporosis patients. Biomarkers 19 (7), 553–556.
Lian, J.B., et al., 2012. MicroRNA control of bone formation and homeostasis. Nat. Rev. Endocrinol. 8 (4), 212–227.
Liotta, L.A., Petricoin, E.F., 2006. Serum peptidome for cancer detection: spinning biologic trash into diagnostic gold. J. Clin. Investig. 116 (1), 26–30.
Lipton, A., et al., 2016. Changes in bone turnover marker levels and clinical outcomes in patients with advanced cancer and bone metastases treated with bone antiresorptive agents. Clin. Cancer Res. 22 (23), 5713–5721.
Liu, S., et al., 2003. Regulation of fibroblastic growth factor 23 expression but not degradation by PHEX. J. Biol. Chem. 278 (39), 37419–37426.
Lukert, B.P., Raisz, L.G., 1990. Glucocorticoid-induced osteoporosis: pathogenesis and management. Ann. Intern. Med. 112 (5), 352–364.
Lv, W., et al., 2016. Sclerostin as a new key factor in vascular calcification in chronic kidney disease stages 3 and 4. Int. Urol. Nephrol. 48 (12), 2043–2050.
Lv, H., et al., 2016. Metabolomics and its application in the development of discovering biomarkers for osteoporosis research. Int. J. Mol. Sci. 17 (12).
Majoor, B.C., et al., 2017. Outcome of long-term bisphosphonate therapy in McCune-albright syndrome and polyostotic fibrous dysplasia. J. Bone Miner. Res. 32 (2), 264–276.
Maruhashi, T., et al., 2010. Interaction between periostin and BMP-1 promotes proteolytic activation of lysyl oxidase. J. Biol. Chem. 285 (17), 13294–13303.
Masi, L., et al., 2015. Taxonomy of rare genetic metabolic bone disorders. Osteoporos. Int. 26 (10), 2529–2558.
Masuoka, M., et al., 2012. Periostin promotes chronic allergic inflammation in response to Th2 cytokines. J. Clin. Investig. 122 (7), 2590–2600.
McClung, M.R., et al., 2006. Denosumab in postmenopausal women with low bone mineral density. N. Engl. J. Med. 354 (8), 821–831.
McClung, M.R., et al., 2014. Romosozumab in postmenopausal women with low bone mineral density. N. Engl. J. Med. 370 (5), 412–420.
McColm, J., et al., 2014. Single- and multiple-dose randomized studies of blosozumab, a monoclonal antibody against sclerostin, in healthy postmenopausal women. J. Bone Miner. Res. 29 (4), 935–943.
McNabb, B.L., et al., 2013. BMD changes and predictors of increased bone loss in postmenopausal women after a 5-year course of alendronate. J. Bone Miner. Res. 28 (6), 1319–1327.
Meng, J., et al., 2015. Identification of miR-194-5p as a potential biomarker for postmenopausal osteoporosis. PeerJ 3, e971.
Merle, B., Garnero, P., 2012. The multiple facets of periostin in bone metabolism. Osteoporos. Int. 23 (4), 1199–1212.
Merle, B., et al., 2014. Periostin and transforming growth factor beta-induced protein (TGFbetaIp) are both expressed by osteoblasts and osteoclasts. Cell Biol. Int. 38 (3), 398–404.
Meshcheryakova, A., Mechtcheriakova, D., Pietschmann, P., 2017. Sphingosine 1-phosphate signaling in bone remodeling: multifaceted roles and therapeutic potential. Expert Opin. Ther. Targets 21 (7), 725–737.
Miller, P.D., et al., 2005. Monthly oral ibandronate therapy in postmenopausal osteoporosis: 1-year results from the MOBILE study. J. Bone Miner. Res. 20 (8), 1315–1322.
Miller, P.D., et al., 2005. How useful are measures of BMD and bone turnover? Curr. Med. Res. Opin. 21 (4), 545–554.
Miller, P.D., et al., 2016. Effect of abaloparatide vs placebo on new vertebral fractures in postmenopausal women with osteoporosis: a randomized clinical trial. J. Am. Med. Assoc. 316 (7), 722–733.
Mirza, F.S., et al., 2010. Serum sclerostin levels negatively correlate with parathyroid hormone levels and free estrogen index in postmenopausal women. J. Clin. Endocrinol. Metab. 95 (4), 1991–1997.

Mirza, M.A., et al., 2011. Serum fibroblast growth factor-23 (FGF-23) and fracture risk in elderly men. J. Bone Miner. Res. 26 (4), 857–864.
Mitchell, P.S., et al., 2008. Circulating microRNAs as stable blood-based markers for cancer detection. Proc. Natl. Acad. Sci. U. S. A. 105 (30), 10513–10518.
Miyamoto, T., et al., 2017. A serum metabolomics-based profile in low bone mineral density postmenopausal women. Bone 95, 1–4.
Modder, U.I., et al., 2011. Relation of age, gender, and bone mass to circulating sclerostin levels in women and men. J. Bone Miner. Res. 26 (2), 373–379.
Modder, U.I., et al., 2011. Regulation of circulating sclerostin levels by sex steroids in women and in men. J. Bone Miner. Res. 26 (1), 27–34.
Mohty, M., et al., 2014. The effects of bortezomib on bone disease in patients with multiple myeloma. Cancer 120 (5), 618–623.
Mok, C.C., Ho, L.Y., Ma, K.M., 2015. Switching of oral bisphosphonates to denosumab in chronic glucocorticoid users: a 12-month randomized controlled trial. Bone 75, 222–228.
Moore, A.E., et al., 2010. Assessment of regional changes in skeletal metabolism following 3 and 18 months of teriparatide treatment. J. Bone Miner. Res. 25 (5), 960–967.
Morales-Santana, S., et al., 2013. Atherosclerotic disease in type 2 diabetes is associated with an increase in sclerostin levels. Diabetes Care 36 (6), 1667–1674.
Morris, H.A., et al., 2017. Clinical usefulness of bone turnover marker concentrations in osteoporosis. Clin. Chim. Acta 467, 34–41.
Moulder, R., et al., 2015. Serum proteomes distinguish children developing type 1 diabetes in a cohort with HLA-conferred susceptibility. Diabetes 64 (6), 2265–2278.
Muschitz, C., et al., 2017. Diagnosis and treatment of Paget's disease of bone: a clinical practice guideline. Wien Med. Wochenschr. 167 (1–2), 18–24.
Nagase, S., et al., 2012. Serum and urine bone resorption markers and pharmacokinetics of the cathepsin K inhibitor ONO-5334 after ascending single doses in post menopausal women. Br. J. Clin. Pharmacol. 74 (6), 959–970.
Naylor, K., Eastell, R., 2012. Bone turnover markers: use in osteoporosis. Nat. Rev. Rheumatol. 8 (7), 379–389.
Naylor, K.E., et al., 2016. Response of bone turnover markers to three oral bisphosphonate therapies in postmenopausal osteoporosis: the TRIO study. Osteoporos. Int. 27 (1), 21–31.
Nielson, C.M., et al., 2017. Identification of hip BMD loss and fracture risk markers through population-based serum proteomics. J. Bone Miner. Res. 32 (7), 1559–1567.
Nishiyama, K.K., et al., 2014. Teriparatide increases strength of the peripheral skeleton in premenopausal women with idiopathic osteoporosis: a pilot HR-pQCT study. J. Clin. Endocrinol. Metab. 99 (7), 2418–2425.
Orsolini, G., et al., 2016. Short-term effects of TNF inhibitors on bone turnover markers and bone mineral density in rheumatoid arthritis. Calcif. Tissue Int. 98 (6), 580–585.
Paccou, J., et al., 2014. The relationships between serum sclerostin, bone mineral density, and vascular calcification in rheumatoid arthritis. J. Clin. Endocrinol. Metab. 99 (12), 4740–4748.
Panach, L., et al., 2015. Serum circulating MicroRNAs as biomarkers of osteoporotic fracture. Calcif. Tissue Int. 97 (5), 495–505.
Papapoulos, S., et al., 2015. The effect of 8 or 5 years of denosumab treatment in postmenopausal women with osteoporosis: results from the FREEDOM extension study. Osteoporos. Int. 26 (12), 2773–2783.
Paul Tuck, S., et al., 2017. Adult Paget's disease of bone: a review. Rheumatol. (Oxford) 56 (12), 2050–2059.
Perazella, M.A., Markowitz, G.S., 2008. Bisphosphonate nephrotoxicity. Kidney Int. 74 (11), 1385–1393.
Petricoin, E.F., et al., 2002. Use of proteomic patterns in serum to identify ovarian cancer. Lancet 359 (9306), 572–577.
Qi, H., et al., 2016. Association between the metabolome and bone mineral density in pre- and post-menopausal Chinese women using GC-MS. Mol. Biosyst. 12 (7), 2265–2275.
Qvist, P., et al., 2002. Circadian variation in the serum concentration of C-terminal telopeptide of type I collagen (serum CTx): effects of gender, age, menopausal status, posture, daylight, serum cortisol, and fasting. Bone 31 (1), 57–61.
Ralston, S.H., Langston, A.L., Reid, I.R., 2008. Pathogenesis and management of Paget's disease of bone. Lancet 372 (9633), 155–163.
Rattazzi, M., et al., 2016. Atorvastatin reduces circulating osteoprogenitor cells and T-cell RANKL expression in osteoporotic women: implications for the bone-vascular Axis. Cardiovasc. Ther. 34 (1), 13–20.
Ravn, P., et al., 1996. The effect on bone mass and bone markers of different doses of ibandronate: a new bisphosphonate for prevention and treatment of postmenopausal osteoporosis: a 1-year, randomized, double-blind, placebo-controlled dose-finding study. Bone 19 (5), 527–533.
Recker, R.R., et al., 2015. A randomized, double-blind phase 2 clinical trial of blosozumab, a sclerostin antibody, in postmenopausal women with low bone mineral density. J. Bone Miner. Res. 30 (2), 216–224.
Reid, I.R., et al., 2002. Intravenous zoledronic acid in postmenopausal women with low bone mineral density. N. Engl. J. Med. 346 (9), 653–661.
Riminucci, M., et al., 2003. FGF-23 in fibrous dysplasia of bone and its relationship to renal phosphate wasting. J. Clin. Investig. 112 (5), 683–692.
Roelofs, A.J., et al., 2012. Influence of bone affinity on the skeletal distribution of fluorescently labeled bisphosphonates in vivo. J. Bone Miner. Res. 27 (4), 835–847.
Roelofsen, T., et al., 2008. Sphingosine-1-phosphate acts as a developmental stage specific inhibitor of platelet-derived growth factor-induced chemotaxis of osteoblasts. J. Cell. Biochem. 105 (4), 1128–1138.
Roman-Garcia, P., et al., 2010. High phosphorus diet induces vascular calcification, a related decrease in bone mass and changes in the aortic gene expression. Bone 46 (1), 121–128.
Rosen, L.S., et al., 2001. Zoledronic acid versus pamidronate in the treatment of skeletal metastases in patients with breast cancer or osteolytic lesions of multiple myeloma: a phase III, double-blind, comparative trial. Cancer J. 7 (5), 377–387.

Rossini, M., et al., 2016. Higher level of dickkopf-1 is associated with low bone mineral density and higher prevalence of vertebral fractures in patients with ankylosing spondylitis. Calcif. Tissue Int. 98 (5), 438–445.

Rousseau, J., et al., 2014. Serum periostin is associated with fracture risk in postmenopausal women: a 7 years prospective analysis of the OFELY study. J. Clin. Endocrinol. Metab. 3893, 1–7.

Rousseau, J.C., et al., 2015. Serum periostin is associated with prevalent knee osteoarthritis and disease incidence/progression in women: the OFELY study. Osteoarthritis Cartilage 23 (10), 1736–1742.

Rubin, M.R., Bilezikian, J.P., 2005. Parathyroid hormone as an anabolic skeletal therapy. Drugs 65 (17), 2481–2498.

Rubin, M.R., et al., 2011. Parathyroid hormone stimulates circulating osteogenic cells in hypoparathyroidism. J. Clin. Endocrinol. Metab. 96 (1), 176–186.

Russell, R.G., et al., 2008. Mechanisms of action of bisphosphonates: similarities and differences and their potential influence on clinical efficacy. Osteoporos. Int. 19 (6), 733–759.

Ryu, J., et al., 2006. Sphingosine 1-phosphate as a regulator of osteoclast differentiation and osteoclast-osteoblast coupling. EMBO J. 25 (24), 5840–5851.

Saag, K.G., et al., 1998. Alendronate for the prevention and treatment of glucocorticoid-induced osteoporosis. Glucocorticoid-nduced Osteoporosis Intervention Study Group. N. Engl. J. Med. 339 (5), 292–299.

Sawamura, M., et al., 2017. Effects of denosumab on bone metabolic markers and bone mineral density in patients treated with glucocorticoids. Intern. Med. 56 (6), 631–636.

Schnitzer, T., et al., 2000. Therapeutic equivalence of alendronate 70 mg once-weekly and alendronate 10 mg daily in the treatment of osteoporosis. Alendronate Once-Weekly Study Group. Aging (Milano) 12 (1), 1–12.

Seeliger, C., et al., 2014. Five freely circulating miRNAs and bone tissue miRNAs are associated with osteoporotic fractures. J. Bone Miner. Res. 29 (8), 1718–1728.

Seeman, E., 2007. The periosteum—a surface for all seasons. Osteoporos. Int. 18 (2), 123–128.

Seibel, M.J., et al., 2004. Relationship between pretreatment bone resorption and vertebral fracture incidence in postmenopausal osteoporotic women treated with risedronate. J. Bone Miner. Res. 19 (2), 323–329.

Semenov, M., Tamai, K., He, X., 2005. SOST is a ligand for LRP5/LRP6 and a Wnt signaling inhibitor. J. Biol. Chem. 280 (29), 26770–26775.

Sheedy, J.R., et al., 2014. (1)H-NMR analysis of the human urinary metabolome in response to an 18-month multi-component exercise program and calcium-vitamin-D3 supplementation in older men. Appl. Physiol. Nutr. Metabol. 39 (11), 1294–1304.

Shende, V.R., et al., 2011. Expression and rhythmic modulation of circulating microRNAs targeting the clock gene Bmal1 in mice. PLoS One 6 (7), e22586.

Shieh, A., et al., 2016. Quantifying the balance between total bone formation and total bone resorption: an index of net bone formation. J. Clin. Endocrinol. Metab. 101 (7), 2802–2809.

Shimada, T., et al., 2004. FGF-23 is a potent regulator of vitamin D metabolism and phosphate homeostasis. J. Bone Miner. Res. 19 (3), 429–435.

Silverman, S.L., et al., 2012. Impact of bone turnover markers and/or educational information on persistence to oral bisphosphonate therapy: a community setting-based trial. Osteoporos. Int. 23 (3), 1069–1074.

Singer, F.R., et al., 2014. Paget's disease of bone: an endocrine society clinical practice guideline. J. Clin. Endocrinol. Metab. 99 (12), 4408–4422.

Smith, M.R., et al., 2009. Denosumab in men receiving androgen-deprivation therapy for prostate cancer. N. Engl. J. Med. 361 (8), 745–755.

Starup-Linde, J., et al., 2016. Bone structure and predictors of fracture in type 1 and type 2 diabetes. J. Clin. Endocrinol. Metab. 101 (3), 928–936.

Stoch, S.A., Wagner, J.A., 2008. Cathepsin K inhibitors: a novel target for osteoporosis therapy. Clin. Pharmacol. Ther. 83 (1), 172–176.

Stoch, S.A., et al., 2009. Effect of the cathepsin K inhibitor odanacatib on bone resorption biomarkers in healthy postmenopausal women: two double-blind, randomized, placebo-controlled phase I studies. Clin. Pharmacol. Ther. 86 (2), 175–182.

Stoch, S.A., et al., 2013. Odanacatib, a selective cathepsin K inhibitor to treat osteoporosis: safety, tolerability, pharmacokinetics and pharmacodynamics—results from single oral dose studies in healthy volunteers. Br. J. Clin. Pharmacol. 75 (5), 1240–1254.

Stuss, M., et al., 2013. Assessment of OPG/RANK/RANKL gene expression levels in peripheral blood mononuclear cells (PBMC) after treatment with strontium ranelate and ibandronate in patients with postmenopausal osteoporosis. J. Clin. Endocrinol. Metab. 98 (5), E1007–E1011.

Sugatani, T., Hruska, K.A., 2009. Impaired micro-RNA pathways diminish osteoclast differentiation and function. J. Biol. Chem. 284 (7), 4667–4678.

Szulc, P., et al., 2005. Biochemical markers of bone formation reflect endosteal bone loss in elderly men—MINOS study. Bone 36 (1), 13–21.

Szulc, P., et al., 2013. Lower fracture risk in older men with higher sclerostin concentration: a prospective analysis from the MINOS study. J. Bone Miner. Res. 28 (4), 855–864.

Szulc, P., et al., 2017. Use of CTX-I and PINP as bone turnover markers: national bone health alliance recommendations to standardize sample handling and patient preparation to reduce pre-analytical variability. Osteoporos. Int. 28 (9), 2541–2556.

Tan, Y., et al., 2016. Potential metabolic biomarkers to identify interstitial lung abnormalities. Int. J. Mol. Sci. 17 (7).

Tay, D., Cremers, S., Bilezikian, J.P., 2018. Optimal dosing and delivery of parathyroid hormone and its analogues for osteoporosis and hypoparathyroidism—translating the pharmacology. Br. J. Clin. Pharmacol. 84 (2), 252–267.

Terpos, E., et al., 2003. Soluble receptor activator of nuclear factor kappaB ligand-osteoprotegerin ratio predicts survival in multiple myeloma: proposal for a novel prognostic index. Blood 102 (3), 1064–1069.

Terpos, E., et al., 2010. The use of biochemical markers of bone remodeling in multiple myeloma: a report of the international myeloma working group. Leukemia 24 (10), 1700–1712.

Terpos, E., et al., 2017. Mechanisms of bone destruction in multiple myeloma. Eur. J. Cancer Care 26 (6).

Thambiah, S., et al., 2012. Circulating sclerostin and Dickkopf-1 (DKK1) in predialysis chronic kidney disease (CKD): relationship with bone density and arterial stiffness. Calcif. Tissue Int. 90 (6), 473–480.

Tian, E., et al., 2003. The role of the Wnt-signaling antagonist DKK1 in the development of osteolytic lesions in multiple myeloma. N. Engl. J. Med. 349 (26), 2483–2494.

Tsourdi, E., et al., 2017. Discontinuation of Denosumab therapy for osteoporosis: a systematic review and position statement by ECTS. Bone 105, 11–17.

Tsujimoto, M., et al., 2011. PINP as an aid for monitoring patients treated with teriparatide. Bone 48 (4), 798–803.

Uchida, M., et al., 2012. Periostin, a matricellular protein, plays a role in the induction of chemokines in pulmonary fibrosis. Am. J. Respir. Cell Mol. Biol. 46 (5), 677–686.

Upadhyay, J., et al., 2017. The expansion of heterotopic bone in fibrodysplasia ossificans progressiva is activin A-dependent. J. Bone Miner. Res. 32 (12), 2489–2499.

Urakawa, I., et al., 2006. Klotho converts canonical FGF receptor into a specific receptor for FGF23. Nature 444 (7120), 770–774.

Valadi, H., et al., 2007. Exosome-mediated transfer of mRNAs and microRNAs is a novel mechanism of genetic exchange between cells. Nat. Cell Biol. 9 (6), 654–659.

van Wijnen, A.J., et al., 2013. MicroRNA functions in osteogenesis and dysfunctions in osteoporosis. Curr. Osteoporos. Rep. 11 (2), 72–82.

Vasikaran, S., et al., 2011. Markers of bone turnover for the prediction of fracture risk and monitoring of osteoporosis treatment: a need for international reference standards. Osteoporos. Int. 22 (2), 391–420.

Vega, D., Maalouf, N.M., Sakhaee, K., 2007. Clinical Review #: the role of receptor activator of nuclear factor-kappaB (RANK)/RANK ligand/osteoprotegerin: clinical implications. J. Clin. Endocrinol. Metab. 92 (12), 4514–4521.

Vickers, K.C., et al., 2011. MicroRNAs are transported in plasma and delivered to recipient cells by high-density lipoproteins. Nat. Cell Biol. 13 (4), 423–433.

Voorzanger-Rousselot, N., et al., 2007. Increased Dickkopf-1 expression in breast cancer bone metastases. Br. J. Canc. 97 (7), 964–970.

Voorzanger-Rousselot, N., Ben-Tabassi, N.C., Garnero, P., 2009. Opposite relationships between circulating Dkk-1 and cartilage breakdown in patients with rheumatoid arthritis and knee osteoarthritis. Ann. Rheum. Dis. 68 (9), 1513–1514.

Voorzanger-Rousselot, N., et al., 2009. Platelet is a major contributor to circulating levels of Dickkopf-1: clinical implications in patients with multiple myeloma. Br. J. Haematol. 145 (2), 264–266.

Wallach, S., et al., 2000. Effects of risedronate treatment on bone density and vertebral fracture in patients on corticosteroid therapy. Calcif. Tissue Int. 67 (4), 277–285.

Walsh, J.S., et al., 2017. Effect of age and gender on serum periostin: relationship to cortical measures, bone turnover and hormones. Bone 99, 8–13.

Wang, H., et al., 2008. Overexpression of fibroblast growth factor 23 suppresses osteoblast differentiation and matrix mineralization in vitro. J. Bone Miner. Res. 23 (6), 939–948.

Wang, K., et al., 2010. Export of microRNAs and microRNA-protective protein by mammalian cells. Nucleic Acids Res. 38 (20), 7248–7259.

Wang, D.C., et al., 2012. Serum fatty acid profiles using GC-MS and multivariate statistical analysis: potential biomarkers of Alzheimer's disease. Neurobiol. Aging 33 (6), 1057–1066.

Wang, Y., et al., 2012. MiR-133a in human circulating monocytes: a potential biomarker associated with postmenopausal osteoporosis. PLoS One 7 (4), e34641.

Wang, X., et al., 2013. miR-214 targets ATF4 to inhibit bone formation. Nat. Med. 19 (1), 93–100.

Weilner, S., et al., 2015. Differentially circulating miRNAs after recent osteoporotic fractures can influence osteogenic differentiation. Bone 79, 43–51.

Whyte, M., 2017. Hypophosphatasia: Principal Biochemical Features Validate the Clinical Nosology for Affected Children. ASBMR, p. MO0705.

Whyte, M.P., 2017. Hypophosphatasia: enzyme replacement therapy brings new opportunities and new challenges. J. Bone Miner. Res. 32 (4), 667–675.

Wijenayaka, A.R., et al., 2011. Sclerostin stimulates osteocyte support of osteoclast activity by a RANKL-dependent pathway. PLoS One 6 (10), e25900.

Wilson, I.D., et al., 2005. HPLC-MS-based methods for the study of metabonomics. J. Chromatogr. B: Anal. Technol. Biomed. Life Sci. 817 (1), 67–76.

Witwer, K.W., 2012. XenomiRs and miRNA homeostasis in health and disease: evidence that diet and dietary miRNAs directly and indirectly influence circulating miRNA profiles. RNA Biol. 9 (9), 1147–1154.

Xiong, J., O'Brien, C.A., 2012. Osteocyte RANKL: new insights into the control of bone remodeling. J. Bone Miner. Res. 27 (3), 499–505.

Yamamoto, M., Yamauchi, M., Sugimoto, T., 2013. Elevated sclerostin levels are associated with vertebral fractures in patients with type 2 diabetes mellitus. J. Clin. Endocrinol. Metab. 98 (10), 4030–4037.

Yavropoulou, M.P., et al., 2017. Expression of microRNAs that regulate bone turnover in the serum of postmenopausal women with low bone mass and vertebral fractures. Eur. J. Endocrinol. 176 (2), 169–176.

Yoshimura, N., et al., 2011. Biochemical markers of bone turnover as predictors of osteoporosis and osteoporotic fractures in men and women: 10-year follow-up of the Taiji cohort. Mod. Rheumatol. 21 (6), 608–620.

You, Y.S., et al., 2014. Association between the metabolome and low bone mineral density in Taiwanese women determined by (1)H NMR spectroscopy. J. Bone Miner. Res. 29 (1), 212–222.

Zheng, J., et al., 2015. Using early biomarker data to predict long-term bone mineral density: application of semi-mechanistic bone cycle model on denosumab data. J. Pharmacokinet. Pharmacodyn. 42 (4), 333–347.

Zimmer, J.S., et al., 2006. Advances in proteomics data analysis and display using an accurate mass and time tag approach. Mass Spectrom. Rev. 25 (3), 450–482.

Chapter 79

Microimaging

Steven Boyd[1] **and Ralph Müller**[2]

[1]*McCaig Institute for Bone and Joint Health, The University of Calgary, Calgary, AB, Canada;* [2]*Institute for Biomechanics, ETH Zurich, Zurich, Switzerland*

Chapter outline

Introduction

Bone plays an important role in the skeleton by providing both mechanical and physiological functions. At the macroscopic level, bone is described in terms of its overall size, shape, and geometry, whereas the microscopic scale captures important structural features that underpin its mechanical and physiological functions. Structurally, we differentiate the cortical compartment containing compact bone from the trabecular compartment containing cancellous bone. The cortical bone is relatively dense, with porosity ranging from 5% to 30%, and makes up approximately 80% of the total bone mass in the body (Langton and Njeh, 2004). The trabecular bone is less dense, with a porosity up to 90%, and is mostly found in the epiphysis of long bones and in vertebrae.

Bone is one of the most investigated biological materials due to its primary function of providing skeletal stability. Bone is susceptible to different local stimuli including mechanical forces and has great capabilities in adapting its mechanical properties to the changes in its environment. Nevertheless, aging or hormonal changes can make bone lose its ability to remodel appropriately, with loss of strength and increased fracture risk as a result. Due to the emergence of accurate and precise bone densitometry over the last 2 decades, bone mass has become a primary endpoint in osteoporosis diagnosis and monitoring. Strong correlations between bone mass and mechanical properties of trabecular bone have been demonstrated for large populations using power-law regressions (Carter and Hayes, 1977; Keaveny et al., 1994; Keller, 1994; McElhaney et al., 1970; Odgaard and Linde, 1991; Rice et al., 1988; Williams and Lewis, 1982). However, changes in mass can only partially explain the variation of trabecular bone strength of individuals, leaving sometimes up to 90% of the strength variation unexplained (Ciarelli et al., 1991). Thus, accurate diagnosis of bone fracture risk in a clinical environment solely based on bone densitometry is difficult. With up to 90% unexplained variation, other factors such as bone macro- and microarchitecture, bone cell distribution, bone remodeling, the distribution of microcracks or microdamage and bone matrix material properties must play important roles too. All these factors together, including bone mineral density (BMD), are often referred to as bone quality (Bouxsein, 2003; Felsenberg and Boonen, 2005; Seeman and

Principles of Bone Biology. https://doi.org/10.1016/B978-0-12-814841-9.00079-8

Delmas, 2006). However, the relative contribution of the different factors to define overall bone competence is still relatively poorly understood.

Macroarchitecture is often measured in terms of bone size/shape and BMD, either of the bone as a whole or in specific cortical or trabecular compartments, and can be readily assessed in vivo using a variety of imaging modalities in both animals and humans. Typical radiographic techniques used include radiography (X-ray), dual-energy X-ray absorptiometry (DXA), and quantitative computed tomography (QCT). There is also work in this area using magnetic resonance imaging (MRI) (Jara et al., 1993; Majumdar, 2002; Majumdar et al., 1998; Wehrli et al., 2001b); however, MRI is less frequently applied than radiographic techniques.

Microarchitecture is typically defined as structures measured at resolutions of 100 μm or less, and these can be found in both cortical and trabecular compartments of the bone. Measurements may include the thickness of the trabeculae, their interconnectivity, or the porosity of the cortical bone, for example. As imaging resolution increases, it is possible to move down the hierarchical scale of bone—for example, to osteocyte lacunae and lamellae. Traditionally, microarchitectural features of bone were captured using histological techniques based on stereological measurement techniques applied to physical slices in order to characterize the bone microarchitecture, and those approaches are still critical for understanding the dynamic modeling processes in bone. However, those approaches require invasive techniques and are destructive to the tested tissue. With the advent of advanced imaging, it is now possible to measure features on the submicron scale nondestructively in three dimensions (3D), albeit limited to in vitro measurements at ultrahigh resolutions due to the practical limitations of the high radiation dose and scanning times required. Synchrotron microcomputed tomography (micro-CT) provides the opportunity to have incredible insight into bone structures at the level of cells and lamellae, and while these systems are relatively rare, there are current advances toward so-called X-ray tomographic microscopes that are now approaching similar resolutions, albeit with the disadvantage of using a polychromatic X-ray source.

Using in vivo techniques while accounting for the potential harming effects of radiation and the minimization of scan time, it is possible to resolve microarchitecture down to approximately 10 μm in animals such as rats and mice, and with that, measure bone remodeling parameters using dynamic morphometry. In humans, in vivo measurements at extremities can assess structures on the order of 60 μm while keeping acquisition parameters to safe and reasonable measures. The peripheral skeleton can be examined using single-slice methods, such as peripheral QCT (pQCT), or multislice methods, such as high-resolution pQCT (HR-pQCT). On the other hand, the axial skeleton is more difficult to assess at high resolution, so QCT is often used for measures at the spine and hip and is typically limited to resolutions on the order of 200 μm, which are not enough to resolve individual trabeculae.

Overall, the options for nondestructive imaging have never been greater, and we are fortunate to have tools available that provide imaging resolutions down to the submicron level for in vitro work and well within the resolution of individual trabeculae for in vivo measures. These advances are accompanied by quantitative approaches for evaluating these rich data sets including techniques for measuring 3D structural features, numerical approaches based on the finite element (FE) method to noninvasively assess strength, and supporting tools such as 3D image registration to track bone changes over time in longitudinal studies.

From a clinical point of view, the determination of bone microarchitecture is a new opportunity to understand how bone develops and changes in disease and ultimately can provide important insight into preventing the development of fragile bones and predicting the fracture risk of patients within the context of age, disease, and treatments. While BMD remains an important feature to measure in bones, the opportunity to explore what underpins BMD is enormous, and using the vast array of imaging technologies today, we are on the cusp of making important advancements in our ability to understand the pathophysiology and progression of bone-related diseases such as osteoporosis.

In vitro microimaging

Imaging endpoints have become an important factor for success in basic research and the development of novel therapeutic strategies in biology and medicine. Biomedical imaging of biological structures has therefore received increased attention, for it is often the basis on which both qualitative (i.e., visualization) and quantitative (i.e., morphometry) image processing is performed. Especially for the assessment of microstructural tissue properties, a number of new imaging modalities have been introduced in recent years. These techniques can typically be used to image a variety of different biological materials ranging from soft to hard tissues. Whereas soft tissue imaging is actually a much larger market and is nowadays regularly used as a standard procedure to image and visualize biological structures (Badea et al., 2005; Bullitt et al., 2007; Heinzer et al., 2006; Paulus et al., 2001; Ritman, 2004), hard tissue imaging (i.e., bone) has made great progress not only with respect to qualitative imaging but also with respect to structural and functional assessment of microstructural images in

both animal and human bone (Bouxsein, 2008; Genant et al., 1999; Goldstein et al., 1993; Ito et al., 1998; Link and Majumdar, 2004; McCreadie et al., 2001; Müller, 2002; Müller and Rüegsegger, 1997; Porter et al., 2005; Wehrli, 2007).

Hierarchical imaging of bone microarchitecture

Hierarchical imaging denotes the ability to resolve anatomical features at a variety of resolutions and size scales using basically the same imaging modality and ideally covering a few orders of magnitude in resolution. This ability will allow measurements starting at the organ level (500 μm resolution) and going down to the structural level (50 μm), tissue level (5 μm), and even cell level (0.5 μm) using the same technology.

As already introduced, computed tomography (CT) is such an approach to imaging and quantifying trabecular bone in 3D, providing multiscale biological imaging capabilities with isotropic resolutions ranging from a few millimeters (clinical CT) to a few tens of micrometers (micro-CT) and further down to 100 nanometers (nano-CT) (Fig. 79.1). Early implementations of 3D micro-CT focused on the methodological aspects of the systems and required equipment that was not widely available (Feldkamp et al., 1989); recent developments have emphasized the practical aspects of microtomographic imaging (Rüegsegger et al., 1996). This and other similar types of in vitro systems, now also commercially available, can be used routinely in basic research and clinical laboratories. Also referred to as desktop or laboratory micro-CT, they provide spatial resolutions ranging from roughly 0.5−100 μm. Specimens with diameters ranging from a few millimeters to 100 mm can be measured. Micro-CT is a precise and validated technique (Balto et al., 2000; Graichen et al., 1998; Kapadia et al., 1998; Kuhn et al., 1990; Müller et al., 1998b; Uchiyama et al., 1997; Yamashita et al., 2000) and has been used extensively in the assessment of microarchitectural bone (Fig. 79.2) in the context of investigating different diseases

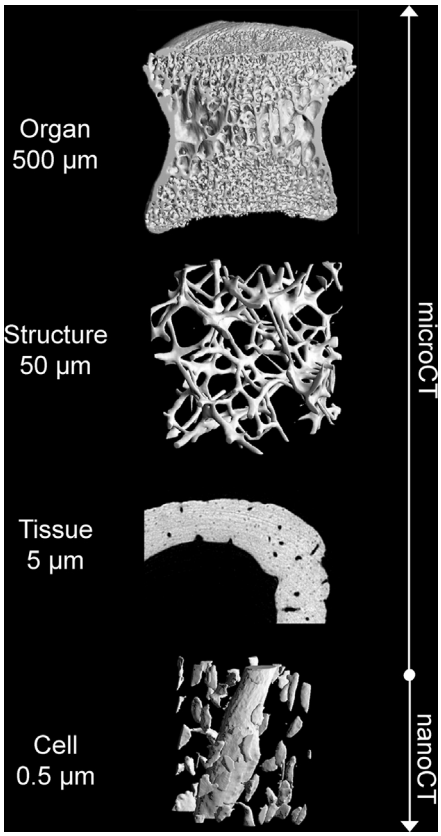

FIGURE 79.1 Schematic overview of hierarchical imaging with micro-CT and nano-CT. At the organ level, an image of a cut-through vertebral body, obtained using desktop micro-CT, demonstrates the extensive heterogeneity in the vertebra of a macaque. At the structural level, desktop micro-CT illustrates the three-dimensional trabecular microarchitecture in a human vertebral sample. At the tissue level, synchrotron radiation micro-CT of a cortical bone sample from a mouse femur illustrates vascular channels (*large holes*) and cell lacunae (*small holes*). Synchrotron radiation micro-CT at the cellular level shows osteocytic lacunae arranged around a microvessel in mouse cortical bone.

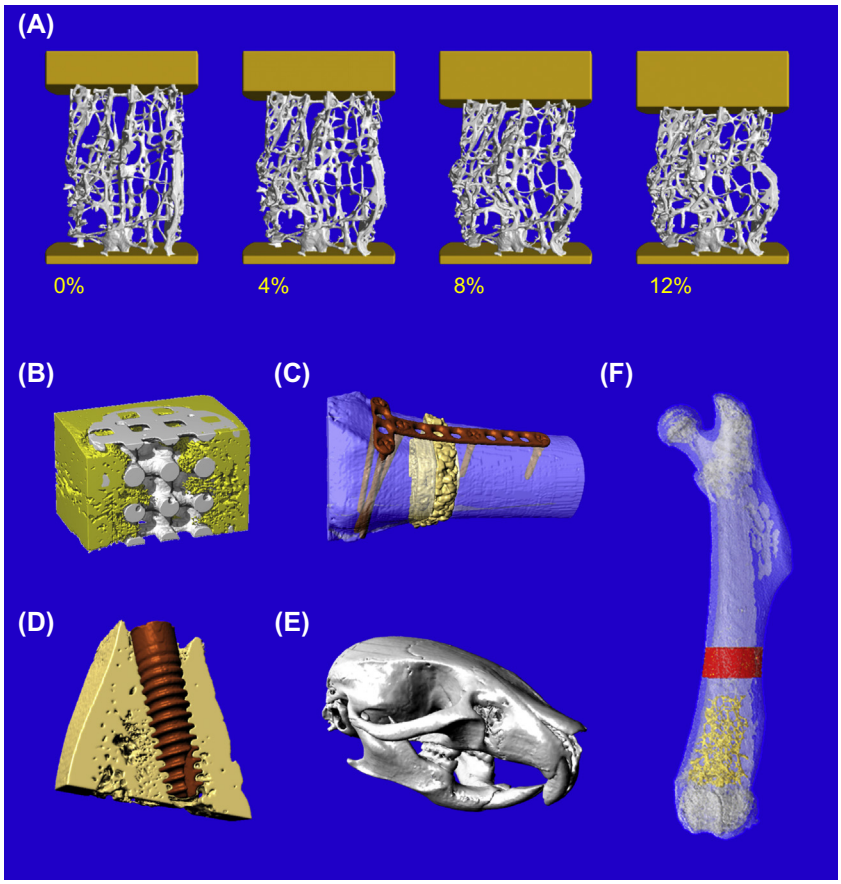

FIGURE 79.2 Typical applications of micro-CT in the imaging of bone. (A) Human spine trabecular bone structure in a two-plate compression testing experiment. (B) Three-dimensional reconstruction of scaffold and bone ingrowth in a minipig model of bone regeneration. Only part of the cylindrical scaffold is displayed to enable a view of the inside of the scaffold. (C) Performance analysis of a bone replacement material in a sheep fracture repair model. A gap was cut in the long bone and filled with bone replacement material; the fracture was fixed using a conventional T-plate. (D) Mouse femur. Typically in bone research, different compartments (full bone; cortical ring; trabecular region) are selected to compute morphometric indices. (E) Titanium screw in rat bone. (F) Mouse cranium.

and their treatment, such as osteoporosis (Alexander et al., 2001; Babij et al., 2003; Borah et al., 2002, 2004; Dempster et al., 2001; Ding and Hvid, 2000; Goulet et al., 1994; Ulrich et al., 1999; Yoshitake et al., 1999) or osteoarthritis (Badger et al., 2000; Day et al., 2001; Dedrick et al., 1993; Pettit et al., 2001); genetics and gene therapy (Bouxsein et al., 2004; Huang et al., 2005; Moutsatsos et al., 2001; Turner et al., 2000), dental research and implants (Duyck et al., 2001; Giesen and van Eijden, 2000; Peters et al., 2000; Sasaki et al., 2000), tissue engineering and biomaterials (Jones et al., 2004; Lin et al., 2003; Lutolf et al., 2003; Porter et al., 2005; Williams et al., 2005; Zeltinger et al., 2001), and the validation of other techniques aimed at investigating bone microstructure in a more clinical setting (Gluer et al., 1994; Laib and Rüegsegger, 1999; Nicholson et al., 1998).

Since the introduction of these systems, there has been an increasing demand for microtomographic technology throughout the world. With the advent of third-generation synchrotron radiation (SR) facilities, micro-CT with resolutions of 1 μm and even better became feasible (Bonse et al., 1994; Engelke et al., 1993; Salome et al., 1999). SR has several advantages over conventional X-rays, including its high brilliance, which allows higher resolutions in nanotomographic applications (Stampanoni et al., 2003) and the use of a monochromatic beam for accurate density representations (Borah et al., 2005; Nuzzo et al., 2002). The high resolution of SR micro-CT and SR nano-CT systems (systems with resolutions < 1 μm) opened a new level of magnification, which in bone research was necessary to investigate 3D properties of ultrastructural features, such as the canal network (Bousson et al., 2004; Matsumoto et al., 2007), osteocyte lacunae (Schneider et al., 2007; Fig. 79.3) and even single cells (Weiss et al., 2000) as well as direct functional outcomes such as microcracks and microfractures (Koester et al., 2008; Larrue et al., 2007; Thurner et al., 2006).

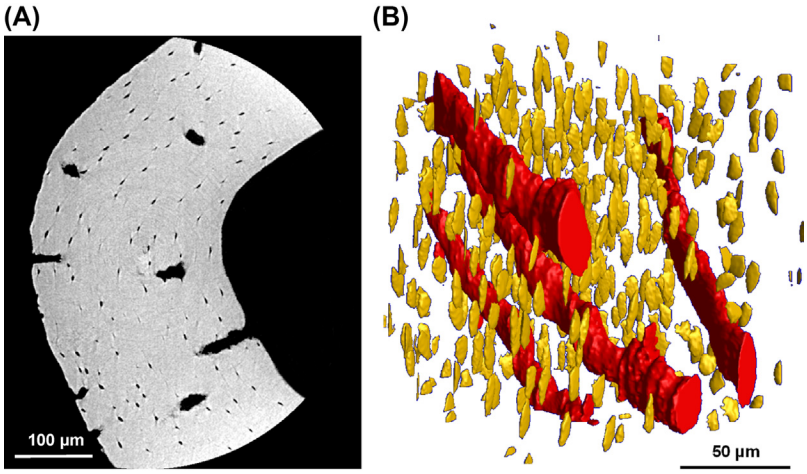

FIGURE 79.3 Ultrastructural representation of void spaces within cortical bone of a mouse femur. (A) Two-dimensional nano-CT slice of the cortical middiaphysis in transverse view showing sections through canals and osteocyte lacunae. Data were assessed at the Swiss Light Source at 700 nm nominal resolution. (B) Three-dimensional representation of the cortical subvolume visualizing the extent of the canal network (*red*) (dark gray in print version) and osteocyte lacunae (*yellow*) (light gray in print version). Volumetric information was extracted from the same data using negative imaging.

Biomechanical imaging of bone competence

Although the assessment of bone microarchitecture is important in the determination of bone quantity and quality, bone competence eventually is responsible for the mechanical and fracture behavior of bone. The gold standard to determine bone competence is mechanical testing of bone. Classical mechanical testing (Turner and Burr, 1993) provides detailed information on whole bone mechanical and bone matrix material properties but fails in revealing local failure properties. Bone failure is a time-dependent, nonlinear event including high local deformations and local fractures that build up to macroscopic failure in the final stage (Bay et al., 1999). Although some work on bone failure characteristics has been done, basic knowledge of how failure originates within both trabecular and cortical bone is still lacking. However, for estimating the risk of fractures for individual patients, an extended understanding of the failure behavior of bone is essential. For this reason, imaging techniques that allow the study of bone tissue in a nondestructive and time-lapsed fashion in situ are very important. Incorporation of such biomechanical or functional imaging methods in mechanical setups will allow better insight into bone deformation and failure characteristics on various levels of structural organization.

For this reason, a biomechanical imaging techniques have been developed and validated, allowing direct time-lapse 3D visualization and quantification of fracture initiation and progression on the microscopic level (Müller et al., 1998a; Nazarian and Müller, 2004). Additionally, novel image analysis approaches have been implemented to identify and classify individual rods and plates, to then track those elements over the time course of failure, and eventually to compute local displacements and strains from consecutive compression steps (Müller et al., 2002). In an initial study, trabecular bone specimens were compressed in steps of 0%, 1%, 2%, 4%, 8%, and 12%, and local strains were determined experimentally. The results showed that average strains were much smaller than the externally applied strain, but maximum local strain values were 5−8 times greater than the externally applied strain, providing further evidence for a bandlike, local failure behavior of trabecular bone (Fig. 79.2A). These high strains were mostly found in rodlike elements aligned with the main strain axis or platelike elements that were fenestrated. Some of these elements bend, others buckle, and some are compressed. Although internodal strains can indicate active structural elements, they cannot distinguish the different behaviors of these elements and how much energy is absorbed. They also do not correlate well with the amount of deformation in an element. Therefore, internodal strains alone cannot fully explain the failure mechanisms of trabecular bone.

Previously, histological damage labeling, micro-CT imaging, and image-based FE analysis were combined to detect regions of trabecular bone microdamage (Nagaraja et al., 2005). For the purpose of that study, bovine tibial trabecular bone cores underwent a stepwise uniaxial compression routine in which specimens were micro-CT imaged following each compression step. Regions of trabecular bone microdamage were then coregistered to estimated microstructural stresses and strains. The results indicate that the mode of trabecular failure observed by micro-CT imaging agreed well with the polarity and distribution of stresses within an individual trabecula as assessed from FE analysis. Analysis of on-axis subsections within specimens provided significant positive relationships between microdamage and estimated tissue

stress and strain. In a more localized analysis, individual microdamaged and undamaged trabeculae were extracted from specimens loaded within the elastic region and to the apparent yield point. As expected, damaged trabeculae in both groups possessed significantly higher local stresses and strains than undamaged trabeculae (Nagaraja et al., 2005).

Where micro-CT studies thus far had focused mostly on the microstructural level of analysis, SR micro-CT and nano-CT allowed for the next level of hierarchy. With this, the exploration of bone failure at the micrometer and even submicrometer level facilitates direct observation of microcracks and microfractures in a fully nondestructive and even time-lapsed fashion. To better investigate the different failure mechanisms on the micro level, a novel in situ mechanical compression device was recently developed at a synchrotron site capable of exerting both static and dynamic displacements on experimental samples (Thurner et al., 2006). To study different failure mechanisms in trabecular bone, a fatigued and a nonfatigued bovine bone sample were compared with respect to failure initiation and propagation. Where the nonfatigued sample exhibited an as-expected distinct localized failure band, the fatigued sample failed in a burstlike fashion. Moreover, microscopic cracks—microcracks and microfractures—were uncovered directly in 3D, illustrating the failure process in great detail and with true representation. Almost all of these cracks were connected to a clearly recognizable bone surface. The data also showed that the classification of microcracks and microfractures from a single two-dimensional (2D) section can sometimes be ambiguous, which is also true for the identification of diffuse and distinct microdamage. Detailed investigation of the failure mechanism in these samples illustrated that trabecular bone often fails in delamination, providing a mechanism for energy dissipation while conserving trabecular bone architecture.

The concept of hierarchical functional imaging was recently also introduced for investigating failure behavior in cortical bone (Voide et al., 2008). In that study, femoral testing in a single-legged stance configuration was performed concurrently with SR tomography to observe fracture initiation and propagation in an intact proximal mouse femur and in 3D. During femoral head compression, image-guided failure assessment showed that fracture occurred were the ratio of the bending moment relative to the cross-sectional moment of inertia was highest. In other words, bone failed at the location where the tensile stresses were the highest in the cortical bone—i.e., the superior femoral neck (Fig. 79.4A and B). Subsequently a cortical notch model was used to better investigate local postyield behavior of bone where microcracks and uncracked ligament bridging play an important role in providing additional material toughness. Uncracked ligament bridging in bone was first reported as a toughening mechanism involving 2D uncracked regions along the crack path that can bridge the crack on opening (Nalla et al., 2005). The reason for the toughening effect is that microcracking causes dilation and increases the compliance of the region surrounding the crack. In other words, uncracked ligament bridges increase resistance to fracture by sustaining part of the applied load that would otherwise contribute to crack continuation. In this study, uncracked ligament bridges were imaged for the first time in 3D at a nominal resolution of 700 nm, displaying not only the relationship of the microcrack to the canal network but also to the much smaller osteocyte lacunae (Fig. 79.4C and D). The results showed that the osteocyte lacunae did not contribute to the initiation of cracks but were important in their propagation. Many cracks actually initiated at the open surfaces of the canal network, something that was recently shown to also play an important role in human cortical bone (Koester et al., 2008). Three-dimensional visualization revealed that the uncracked ligament bridges were not 2D uncracked regions along the crack path, as reported previously (Nalla et al., 2005), but had proper 3D shapes. Their thickness varied between 1 and 3 μm. SR micro-CT also uncovered uncracked ligament bridging at two different phases. Initially, shortly after microcrack initiation, the long axes of the uncracked ligament bridges are mostly aligned parallel to the direction of crack propagation or the long axis of the crack. This can be explained by the fact that at the nanoscale, bone fails through the delamination of mineralized collagen fibrils (Thurner et al., 2007), which are the basic building blocks of bone matrix at the supramolecular level (Weiner et al., 1999). When failure progresses and the crack openings become larger, the uncracked ligament bridges rotate and eventually their long axes become oriented perpendicular to the long axis of the crack (Fig. 79.4E). New developments at synchrotron sites, which allow high-speed imaging that takes full tomographic images at microscopic resolution in only a few seconds (Di Michiel et al., 2005), will facilitate higher throughput in biomechanical imaging and therefore also allow imaging of dynamic failure behavior (Christen et al., 2012; Levchuk et al., 2018; Meier et al., 2008).

Quantitative image processing

Image processing is a large field, and to cover all aspects would be beyond the scope of this chapter. This section describes the most commonly applied procedures to extract and quantify microstructural features as they are used in the bone field. A number of guideline papers will give the reader more in-depth information on image processing, quantitative image analysis, and bone morphometry (Bouxsein et al., 2010; Dempster et al., 2013; Parfitt et al., 1987).

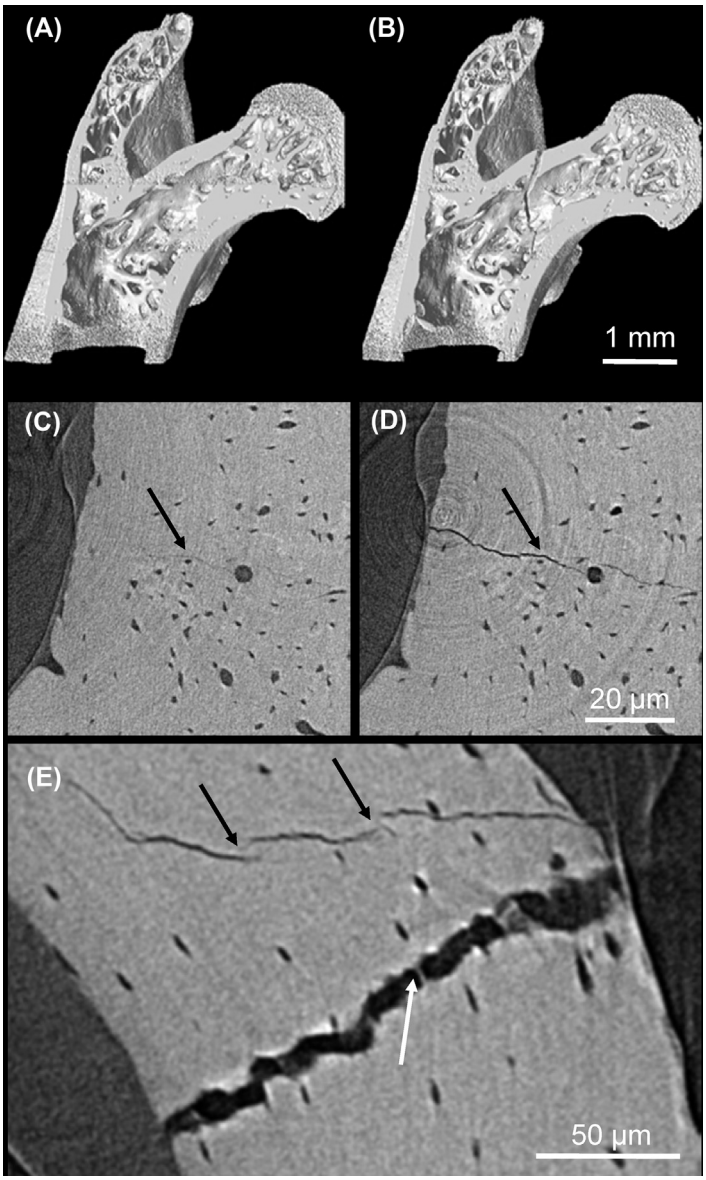

FIGURE 79.4 Hierarchical imaging of bone function with synchrotron radiation CT. Image-guided failure assessment illustrates compression and fracture at a proximal mouse femur (A) in the uncompressed femoral neck, and (B) after displacement of the femoral neck. Nominal resolution 3.5 µm for both images. (C) Reconstructed slices of mouse femoral bone from the cortical middiaphysis. Nominal resolution 700 nm; 1% apparent strain. A microcrack is faintly visible (*black arrow*). (D) At 2% apparent strain, the microcrack has propagated and is now clearly visible (*black arrow*). Nominal resolution 700 nm. (E) Cortical bone at 1% strain with a microcrack and a microfracture. Uncracked ligament bridges intersect the microcrack (*black arrows*) and span the microfracture (*white arrow*). Nominal resolution 700 nm.

Filtration and segmentation

Reconstructed image data inherently include noise that should be reduced by filtering while maintaining sharp contrast between bone and marrow (Stauber and Müller, 2008). Photon statistics, fluctuations of the CCD, and thermal fluctuations are all factors that may increase noise in final images. To reduce this noise and be better able to extract the desired features, a large set of different filtering methods have been introduced. Examples are Gauss, Hamming, Hann, Blackman, Bartlett, Welch, and Wiener filters (Gonzalez and Woods, 2002). Most filters are applied in the Fourier space, where the filters are classified as either low- or high-pass filters according their function to remove either high or low frequencies from images. High-pass filters are commonly used for feature extraction and edge enhancement, whereas low-pass filters are commonly used for noise reduction. Where high-pass filters may increase some noise, low-pass filters blur images. This trade-off can

be solved optimally using Gaussian filtration. Furthermore, the Fourier transform of the Gaussian function yields the Gaussian function again, whereby this filter can be applied in direct space, which makes this filter easily implementable and fast in computation. For these reasons, Gaussian filtration is one of the most commonly used filters for noise reduction. However, since the Gaussian filter also blurs the edges, more advanced smoothing techniques have been developed to normalize the image while preserving the edges. An example of such an edge-preserving smoothing filter is the anisotropic diffusion filter. Other filters frequently used are median, minimum, and maximum filters, which can also be applied in direct space.

The segmentation process is a critical step in bone analysis and generally involves separating an object or multiple objects from the background for subsequent quantitative analysis. An example of a typical three-phase object application is a bone with an implant, where the third phase is the background. Segmenting images is a difficult topic and has led to many publications trying to establish new methods for special purposes. The main problem is that because of beam hardening, aliasing artifact, partial volume effect, or ring artifact, the values of different materials in a single image may not be clearly distinguishable anymore. Therefore, it becomes relatively difficult to select all voxels of a certain value range and to assign it to an object. Nevertheless, the most common segmentation technique is still so-called thresholding, where all voxels above a certain value are set to white (1) and all remaining voxels are set to black (0). This procedure can also be applied to two, three, or more levels if image quality is good enough and image contrast is sufficient for the different materials to be resolved.

For structural analysis, it might in certain cases be reasonable to remove small, unconnected objects from the main object that may arise from image noise or from improper sample preparation. This is accomplished by the so-called component labeling algorithm, which first labels all components in the structure. Depending on the software, it can then be decided whether the largest, the smallest, or all components of a certain size should be kept for further evaluation.

Quantitative morphometry

A method of quantitatively describing bone architecture and changes associated with the age or stage of a disease is the calculation of morphometric indices, also referred to as quantitative bone morphometry. In the past, structural properties of trabecular bone have been investigated by the examination of 2D sections of bone biopsies. Three-dimensional morphometric parameters were then derived from 2D images using stereological methods (Parfitt et al., 1983). Highly significant correlations between 2D histology and 3D micro-CT have been found for bone volume density (BV/TV) and bone surface density (BS/TV) (Müller et al., 1998b). While measurements like BV/TV and BS/TV can be directly obtained from 2D images, a range of important parameters such as trabecular thickness (Tb.Th), trabecular separation (Tb.Sp), and trabecular number (Tb.N) are derived indirectly assuming a fixed-structure model. Typically, an ideal plate or ideal rod model is used; however, such assumptions are critical because the type of trabecular bone architecture differs for different anatomical sites, which will lead to an unpredictable error of the indirectly derived parameters.

For these reasons, and in order to take full advantage of volumetric measurements, several new 3D image processing methods have been presented that allow for direct quantification of bone microarchitecture (Hildebrand et al., 1999; Odgaard et al., 1997). These techniques calculate actual distances in 3D space and therefore do not rely on an assumed model type and are not biased by possible deviations. In addition to the computation of direct metric parameters, nonmetric parameters can be calculated to describe the 3D nature of a bone structure. An estimation of how platelike or rodlike a bone structure is can be achieved using the structure model index (SMI) (Hildebrand and Rüegsegger, 1997b). Several studies show that the degree of anisotropy (i.e., a description of how the structural elements are oriented) together with bone volume fraction may explain a significant part of the mechanical properties of a 3D structure. Therefore, several methods, such as mean intercept length (Whitehouse, 1974), volume orientation (Odgaard et al., 1990), star volume distribution (Cruz-Orive et al., 1992), and star length distribution, have been proposed to estimate the degree of anisotropy of trabecular bone. These and other measures of architectural anisotropy are reviewed in detail elsewhere (Odgaard, 1997). An index called connectivity density (Conn.D) has been introduced to characterize the number of possible paths that connect the analyzed bone structure from one end to the other. Conn.D expresses the number of connections per cubic mm and is derived from the Euler number (Odgaard and Gundersen, 1993) as follows: $\text{Conn.D} = (1 - \text{Euler number})/\text{TV}$.

Quantitative assessment of 3D bone morphometry typically applies to porous structures as a whole and not to their individual elements. Although studies demonstrate the importance of architectural bone properties in a statistical sense, they do not explain the real physical contribution of the microarchitecture to the mechanical failure behavior of bone. A recent project aimed to calculate the structural properties of individual trabecular elements using a method called volumetric spatial decomposition (Stauber and Müller, 2006). The ability to break down the bone microarchitecture and extract individual structural elements, such as trabecular rods and plates, allows performing of local bone morphometry; i.e., it

allows determining of the shape and form of each single bone element individually. With this method it is hence possible to perform more detailed analyses of 3D structures, and it has now become possible to analyze the individual contribution of rods and plates to the competence of trabecular bone (Liu et al., 2008; Stauber et al., 2006).

Finite element analysis

Although the inclusion of architectural parameters has strongly improved the prediction of the competence of bone (Müller et al., 2004; Yang et al., 1998), they only do so in a statistical sense. They do not explain the real physical contribution of the microarchitecture to the mechanical failure behavior of bone. To understand how differences in bone microarchitecture influence bone competence, insight into load transfer through the bone architecture is needed. With the advent of fast and powerful computers, simulation techniques are becoming popular for investigating the mechanical properties of bone.

Using microstructural FE models generated directly from computer reconstructions of trabecular bone, it is now possible to perform a "virtual experiment"—i.e., to simulate a mechanical test in great detail and with high precision. Detailed FE models of trabecular bone can be created using 3D microstructural images as described before. They are often denoted as "high-resolution," "large-scale," or "microstructural" FE (micro-FE) models. After assigning appropriate material properties to the elements defining the structure, these computer models provide realistic response characteristics to simulated loading. For linear deformation conditions, comparison between biomechanical compression tests and micro-FE shows very good agreement when a homogeneous, isotropic tissue modulus is applied (Kabel et al., 1999; Ladd et al., 1998). This holds true for normal as well as osteoporotic bone (Homminga et al., 2003). These computer models allow calculation of loads at the microstructural or even tissue level (Ladd et al., 1998; van Rietbergen et al., 1995) and have been used extensively to accurately determine the mechanical properties of bone.

Later, it was shown that these micro-FE models can also accurately predict trabecular bone failure for bovine (Niebur et al., 2000) as well as human trabecular bone (Bayraktar et al., 2004); micro-FE-predicted apparent stresses and strains at failure were equal to experimentally measured values for the same bone specimens, demonstrating that the quality of micro-FE analyses has reached such accuracy that the use of such simulation techniques can be an effective way to reduce experimental errors (Van Rietbergen et al., 1998) and can be used as an alternative to destructive mechanical tests (Niebur et al., 2000). A great advantage of micro-FE analysis is that models can be analyzed multiple times under different conditions to simulate various types of loading. Furthermore, bone micro-FE models provide better insight into the relationship of structure and strength by allowing one to look inside the bone to see where strains and stresses are localizing and therefore where they may cause fracture (Borah et al., 2001).

In vivo microimaging

In parallel with the advancement of in vitro imaging modalities, the past 2 decades have seen major developments in the area of in vivo imaging. For bone, X-ray methods are particularly well suited to measure microarchitecture, and the availability of 3D methods based on CT provides opportunities to simultaneously explore changes in the composition of the bone tissue, its microarchitecture, and its macroarchitecture. While the resolution of in vivo techniques is limited by the importance of ensuring that safe X-ray dose levels are delivered (not a limitation for in vitro imaging), this drawback is offset by the exciting ability to nondestructively monitor bone at multiple time points in a living being (Waarsing et al., 2004).

The shift from study designs focused on cross-sectional analysis to longitudinal analysis has important implications for providing insight into bone adaptation. It is through time-lapse imaging that we can truly explore the dynamic nature of bone adaptation. In animal studies, the design of a longitudinal study means relatively fewer animals are needed to answer a scientific question due to the increased statistical power of the repeated measures. In contrast, cross-sectional study designs typically need larger numbers so that normal population variation does not mask the effect being studied. A longitudinal design is a powerful approach to studying an animal model of human disease, and in fact one of the challenges a scientist often faces is reining in the enthusiasm to perform longitudinal measurements too frequently and/or maximize imaging resolution, as both decisions have implications on the X-ray dose delivered to the animal and can even influence the adaptive behavior of bone if too high (Klinck et al., 2008).

In human studies, the development of high-resolution in vivo measurement techniques offers new insight into bone microarchitecture that was previously only possible using ex vivo imaging or biopsies. Both cross-sectional and longitudinal study designs can be employed, although there is a much higher proportion of cross-sectional studies (Cheung et al., 2013) despite the value of longitudinal research. Of course, a major reason for that disproportionate number of cross-sectional studies is that the time course of human research can be long, thus making those studies expensive and

time-consuming. Nevertheless, since the introduction of pQCT and HR-pQCT technologies in past decades, an increasing number of longitudinal studies have been published. This is evident in the area of fracture prediction based on microarchitecture, where there is a shift from the establishment of large cohort studies that are cross-sectional in design and focused on prevalent fractures, toward longitudinal cohort studies where incident fractures can be investigated.

In human and animal studies using in vivo techniques, common challenges must be overcome. First, if using an X-ray-based technique, it is important to minimize the X-ray dose while balancing that with maximized resolution, field of view, and frequency of follow-up exams. Second, in a living being, movement during scan acquisition is inevitable. While this can be minimized in an animal by anesthetizing it, or minimized in a human by using supporting braces, movements will inevitably occur during scanning acquisition, and depending on the magnitude of the artifact, can have a significantly negative impact on the measurement of microarchitecture (Pauchard et al., 2012). Third, it is important to measure the same region of interest in the bone at each exam. While most imaging devices have built-in software and hardware designed to maximize the repositioning of follow-up scans, it is not possible to be perfectly realigned. The problem of misalignment becomes more acute when the region of interest is small. For example, in HR-pQCT only a 1 cm length of bone is typically scanned at the wrist and ankle, and therefore small perturbations of the positioning can unduly influence the ability to track changes in bone. This problem can be mitigated using postprocessing techniques, in particular region-matching approaches based on 3D image registration to maximize reproducibility (Boyd et al., 2006; Ellouz et al., 2014), and in some cases, they are critical (and nontrivial) to employ.

In the following sections, we outline strategies and techniques for both animal and human in vivo imaging of bone microarchitecture.

In vivo animal microimaging

The primary tools for assessing microarchitecture by in vivo imaging of animals are X-ray-based due to excellent contrast for bone tissue and high resolution. Although other methods have been developed using techniques, such as micro-MRI, that avoid ionizing radiation to the animal (Majumdar, 2002; Majumdar et al., 1998; Wehrli et al., 2001a), they are challenged by lower resolution, longer imaging times, and the fundamental inability to collect an imaging signal from bone (rather than marrow and soft tissues). While micro-MRI is a promising noninvasive tool for microimaging, our focus here is on X-ray-based techniques.

The most frequently applied tool for measuring microarchitecture is micro-CT, and its extension from desktop in vitro micro-CT to in vivo systems has provided the exciting ability to study processes of bone remodeling and adaptation in research related to fracture healing (Taiani et al., 2014), mechanical loading (Schulte et al., 2013) and aging (Razi et al., 2015), hind limb unloading (Manske et al., 2015a), osteoporosis (Campbell et al., 2008), osteoarthritis (Panahifar et al., 2012), orthopedics (Li et al., 2017), bone metastases (Bondareva et al., 2009; Buie et al., 2013), bone development (Buie and Boyd, 2010), and many more.

Many of the challenges for in vivo animal assessment are the same as for in vivo human assessment. That includes issues of subject movement during image acquisition, radiation exposure, maximizing reproducibility, and quantification of microarchitecture parameters.

A fixture to support the animal is required to ensure that minimal movement occurs during the scanning protocol while at the same time providing a method to deliver anesthetic to the animal. Although manufacturers of in vivo systems provide commercially available devices, it is frequently the case that customized versions need to be developed for the specific needs of the research. Taking the scanning of a mouse vertebra as an example, it is challenging to prevent excessive movement caused by expansion of the mouse's lungs during respiration. A custom jig developed for in vivo studies of mouse vertebra (Buie et al., 2008) was designed to allow the mouse to be anesthetized with a mask, reducing exposure to the operator and minimizing the risk of a mouse awakening during setup. The mouse could be positioned on its stomach or back, the latter of which reduces motion of the vertebra. The lower limbs were held in place on opposite sides of a partition using a single orthodontic elastic band around both ankles. A latex glove finger is used to cover the body to catch feces and keep the tail contained. The small size of the fixture enabled a scan resolution of 12.5 μm, and the resolution of the whole-body device was limited to 19 μm because of the large diameter of the tube (Fig. 79.5).

Radiation considerations

A major consideration for in vivo micro-CT imaging is whether the ionizing radiation delivered during an exam is sufficient to cause damage to the bone. It has been shown that with high-resolution imaging ($\sim$10 μm) and weekly scans, a significant effect on bone microarchitecture in a mouse can be detected (Klinck et al., 2008). It is prudent to establish an

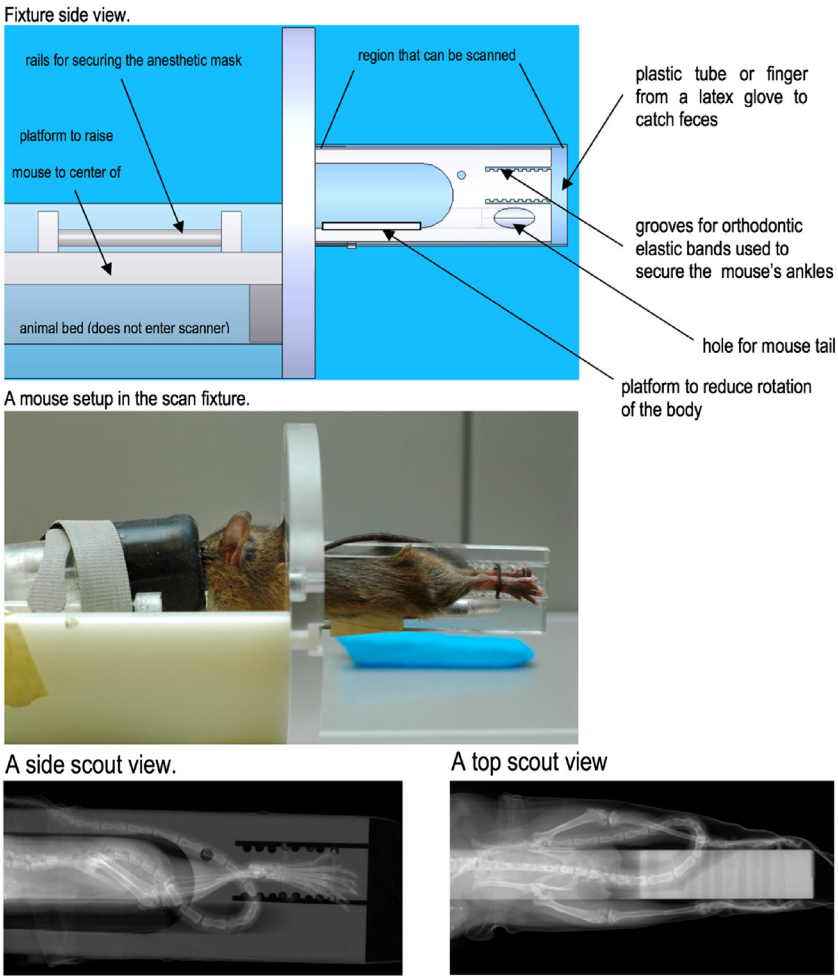

FIGURE 79.5 A custom fixture designed for in vivo mouse scans of the lumbar spine and lower extremities is shown. The left and right limbs can be aligned and scanned simultaneously.

appropriate protocol for an in vivo micro-CT study that ensures that radiation effects are avoided or minimized (Brouwers et al., 2007; Laperre et al., 2011), and this is typically considered in study design. For example, in a study with many time points, having a control group that is measured only at the start and end of the protocol would provide evidence of the effect (or lack thereof) of repeated in vivo micro-CT measurements on bone adaptation. Interestingly, although most studies seek to avoid radiation effects on bone, there are some exceptions where those effects are specifically of interest and might be applied intentionally to study effects on bone microarchitecture (Michel et al., 2015). Nevertheless, the majority of in vivo animal research is focused on understanding the processes of bone adaptation in disease models while minimizing any effects the micro-CT measurements themselves may have on bone.

Reproducibility

The challenges of measuring the same region of bone at each time point in an in vivo study is significant, and in anatomic regions where the bone varies strongly as a function of the distance along its length such as at the ends of long bones (Boyd, 2008), the effects of misalignment are exacerbated. The use of a 2D X-ray, often referred to as a scout view (Fig. 79.6), prior to image acquisition significantly improves follow-up accuracy; however, the application of other postprocessing tools can further improve reproducibility. The most common approach is to use 3D image registration to align scans so that a common region of analysis can be identified for an entire time series of data (Boyd et al., 2006). Using the standard repeated-measures approach to measure imaging reproducibility (Gluer et al., 1995), it has been shown that the use of image registration maximizes the sensitivity of in vivo micro-CT to detect bone microarchitecture changes (Nishiyama et al., 2010; Schulte et al., 2014).

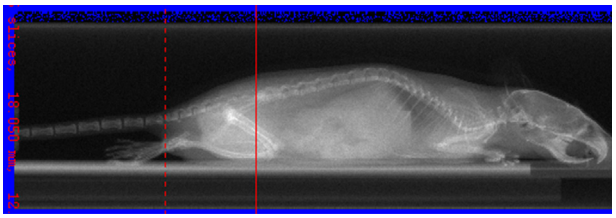

FIGURE 79.6 A two-dimensional X-ray acquired prior to the full three-dimensional scanning protocol helps assure that the same region of the skeleton is scanned at each follow-up measurement. Shown here is a scout view of a mouse body.

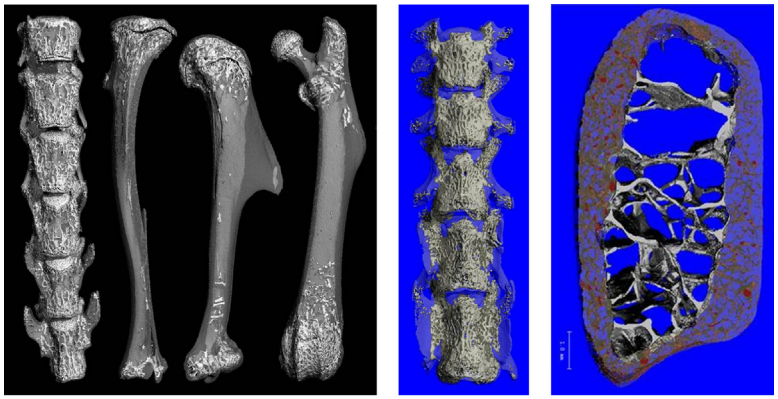

FIGURE 79.7 Automated segmentation of the cortical and trabecular compartments is shown for whole mouse bones, rat vertebra, and a human rib. The versatility of the method is important to accelerate in vivo microarchitecture studies due to the ability to efficiently segment compartments for subsequent morphological analysis.

Another important component of generating reproducible results is how bony compartments, such as the trabecular and cortical compartment, are consistently identified. The endocortical margin defining the border between the trabecular and cortical compartments is a region of particular interest in terms of adaptive remodeling and is also important for defining microarchitecture parameters related to the cortex, such as cortical porosity. Two major approaches have been developed to define the compartments (Buie et al., 2007; Zebaze et al., 2013), both based on an image analysis approach, and are designed to generate highly reproducible results (Burghardt et al., 2010). One method focuses on the gradient change between the cortical and trabecular compartments to define the border (Zebaze et al., 2013), and the other uses a series of thresholding procedures to distinguish the compartments (Buie et al., 2007). While both are used in the context of human in vivo imaging, typically only the threshold-based approach has been applied with in vivo animal studies to date (Fig. 79.7).

Altogether, image processing techniques for 3D registration as well as defining bony compartments play an important role in maximizing the reproducibility of in vivo imaging outcomes for microarchitecture and improving the sensitivity of longitudinal studies to detect subtle changes related to bone adaptation in growth, aging, disease processes, and treatment effects.

Dynamic morphometry

In time-lapse or longitudinal in vivo imaging, several images of the same object are taken over time fully noninvasively. This allows for the following of changes that occur in that object over time. To determine such changes, follow-up images need to be aligned to each other, and the differences need to be defined (Christen and Müller, 2017). Images of bone are usually aligned using rigid image registration. In that approach, an optimization algorithm is used to find the transformation that translates and rotates images onto each other until they overlap well enough such that a certain objective function is met. Once the transformation is found, it is applied to the image, and interpolation is used on the follow-up image to assign each voxel its new coordinates. In a final step, registered images are superimposed, revealing the differences between follow-up images, to visualize and quantify bone resorption and bone formation.

In cases where image resolution is high and the changes occurring over time are small, rigid image registration has been successfully used in animal experiments to align and subsequently superimpose baseline with follow-up images (Boyd et al., 2006). This approach also allows for determination of sites of bone resorption and bone formation. A total of six parameters for both bone resorption and bone formation were determined and described: bone formation rate, bone resorption rate, mineral apposition rate, mineral resorption rate, mineralizing surface, and eroded surface (Lambers et al., 2013; Razi et al., 2015; Schulte et al., 2011). It is important to note that with this approach, not only bone formation but also bone resorption, can be quantified, which is not possible with dynamic histomorphometry because there are no labels for bone resorption as these are removed when bone is resorbed.

The approach has been applied to the mouse caudal vertebra as assessed by in vivo micro-CT at a voxel size of 10.5 μm (Lambers et al., 2013; Schulte et al., 2011). Time-lapse imaging was performed at baseline and 4 weeks and then every 2 weeks for 14 weeks. Grayscale images were aligned using 3D rigid image registration based on an intensity-based least-squares objective function and B-spline interpolation. Sites of bone resorption and bone formation were quantified and visualized by overlaying segmented follow-up images. This revealed good agreement with histomorphometry and erroneously resorbed bone volume of 4.9% ± 1.8% (mean ± standard deviation) and formed bone volume of 5.3% ± 2.1% (mean ± standard deviation). In another example, the approach has been applied to mouse tibia also imaged with micro-CT at a voxel size of 10.5 μm (Razi et al., 2015). Time-lapse in vivo imaging was performed at baseline and on days 5, 10, and 15. Also in this case, grayscale images were aligned using 3D rigid image registration but based on a normalized mutual information objective function and Lanczos interpolation. Sites of bone resorption and bone formation were again determined by overlaying segmented follow-up images. This study revealed good agreement with histomorphometry and reported an error of 3.49% ± 3.42% classifying voxels into bone resorption and bone formation. Newest developments extended this approach to track bone resorption and bone formation events over time and thus study sequences of bone resorption and bone formation in the mouse tibia (Birkhold et al., 2015).

In vivo human microimaging

Advancements in the area of in vivo CT imaging of animals have largely been paralleled by advancements in human imaging. As noted for animal studies, technologies such as micro-MRI can be used to assess bone microarchitecture; however, the best contrast and resolution can be obtained using X-ray-based methods. The most common clinical tool is DXA, which is primarily used to assess areal BMD of key skeletal sites for major osteoporotic fracture (hip, spine, forearm). Although the 2D approach of DXA is not well suited to distinguish trabecular and cortical compartments, and hence bone microarchitecture, the recent introduction of the trabecular bone score appears to generate an index related to microarchitecture. There is currently significant interest in its use as an independent predictor of osteoporotic fracture, although the field is still evaluating its effectiveness in that area (Bousson et al., 2015).

The most common modalities used to measure 3D bone microarchitecture in humans in vivo include CT, pQCT, micro-CT, and HR-pQCT. Of course, MRI can also be used (Wehrli et al., 1998, 2001b), and it holds the advantage that it does not use ionizing radiation; however, resolution of the images provided is at the limit for detecting human bone microarchitecture. Furthermore, an MRI image provides geometric information but no information about the tissue material itself. This is in contrast, for example, to X-ray methods such as CT that simultaneously acquire geometric information and density information about the tissue. In general, the highest in vivo imaging resolutions by CT are achieved when measuring at peripheral skeletal sites. The smaller gantry size necessary for an extremity is better suited for allowing high-resolution images to be acquired while keeping within safe doses of ionizing radiation exposure for the patient.

Clinical computed tomography

CT is the basis of most 3D methods to acquire bone microarchitecture, although the implementation of the technology can vary widely for specific purposes, with varying gantry size, resolution, number of slices, etc. The clinical use of CT is widespread, and although the technology is constantly evolving, it generates a series of 2D axial slices ranging between 0.3 and 5 mm in thickness with an in-plane resolution on the order of 0.2−0.5 mm. The advancing of the body inside the gantry allows the acquisition of a large number of 2D slices that are the basis of the 3D volumetric analysis. The scalar data represented in the CT data set are typically expressed as Hounsfield units, which can then be calibrated to a measure of the density of the object (Kalender et al., 1987; Lang et al., 1999). Although clinical CT is highly versatile and provides a rich data set representing bone that can be used as input for FE models to assess bone strength, those models typically include a continuum-level distribution of bone mass (Cody et al., 1999, 2000) because the resolution is insufficient to capture detailed bone microarchitecture.

Peripheral quantitative computed tomography

Peripheral CT systems began with single-slice methods such as pQCT (Dambacher and Ruegsegger, 1994; Rittweger et al., 2000, 2005). The advantage of a pQCT system is that it can capture BMD of the cortical and trabecular compartments at peripheral sites and requires very low radiation doses (Hangartner et al., 1985; Fig. 79.8). Also, it is well suited to measure muscle cross-sectional areas in the lower limbs, which can provide important functional information to help understand the relationship between bone and muscle adaptation. The pQCT systems function on the same principles as whole-body QCT but are smaller, easier to site, and cheaper to operate and purchase. The resolution of these systems is on the order of 200 μm, and due to the ability to separate cortical from trabecular bone compartments, small changes in volume and mineral content can be identified (Ferretti et al., 1995). It is not well suited to measure structural features of trabecular bone microarchitecture but is able to measure moments of inertia, volume, cortical thickness, and other gross measurements. It has applications in both animal and human work and in the detection of osteoporosis (Butz et al., 1994; Takagi et al., 1995), monitoring treatment effects (Ruegsegger et al., 1995; Schneider et al., 1999), and studying growth and development in relation to physical exercise (Burt et al., 2012, 2013; Gabel et al., 2015).

High-resolution peripheral quantitative computed tomography

In contrast to pQCT, an HR-pQCT system is capable of collecting multiple slices in the same acquisition, thus providing a 3D volumetric measure of the bone microarchitecture (Müller et al., 1994). The systems are self-enclosed with lead shielding to avoid stray radiation and are relatively simple to operate for image acquisition (Cheung et al., 2013). Numerous studies have demonstrated an association of microarchitecture with major osteoporotic fracture (Boutroy et al., 2008; Burt et al., 2018; Christen et al., 2013; Nishiyama et al., 2013; Sornay-Rendu et al., 2009; Stein et al., 2010; Vico et al., 2008; Vilayphiou et al., 2010, 2011).

The first-generation system allowed the acquisition of a 9 mm thick region of interest at the tibia or radius at an isotropic resolution of 82 μm in under 3 min with an effective radiation dose of less than 3 μSv. The second-generation system captures a 10 mm thick region at 61 μm voxel size in about 2 min with an effective dose of less than 5 μSv. For all HR-pQCT systems, the extremity is supported in a cast to minimize movement during image acquisition, and similar to micro-CT, a scout view is acquired so that the scanning region is precisely located (Fig. 79.9).

Following acquisition, analysis of the data is not very different from analysis of in vivo micro-CT systems because essentially it is the same type of data, albeit collected on a human instead of an animal. However, in the first-generation systems (Boutroy et al., 2005), which could achieve in vivo nominal isotropic resolutions of 82 μm, some standard morphometric parameters such as Tb.Th, Tb.Sp, and Tb.N were determined by derivations rather than by the direct analysis approaches typically applied for micro-CT. For example, BV/TV was derived by determining the BMD of the trabecular compartment and then dividing that by a density of 1200 mg HA/ccm (the assumed density of fully mineralized trabecular tissue). Although Tb.N was measured using the standard direct approach (Hildebrand and Rüegsegger, 1997a), Tb.Th and Tb.Sp were derived from the Tb.N and BV/TV measures in the trabecular compartment (Laib et al., 1998).

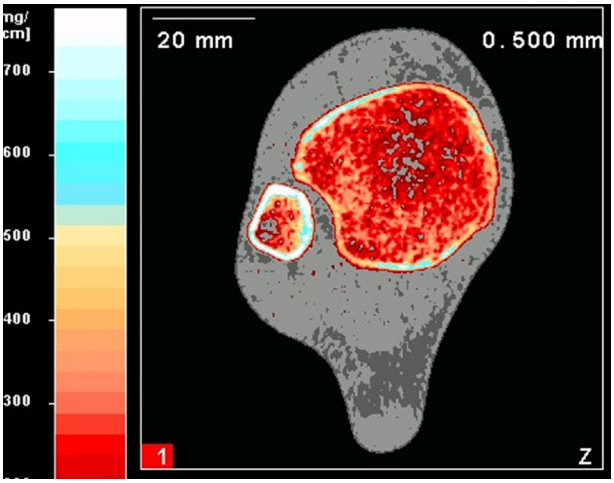

FIGURE 79.8 Sample image of the distal tibia showing variations of density of the tibia and fibula as well as the muscle and interstitial fat.

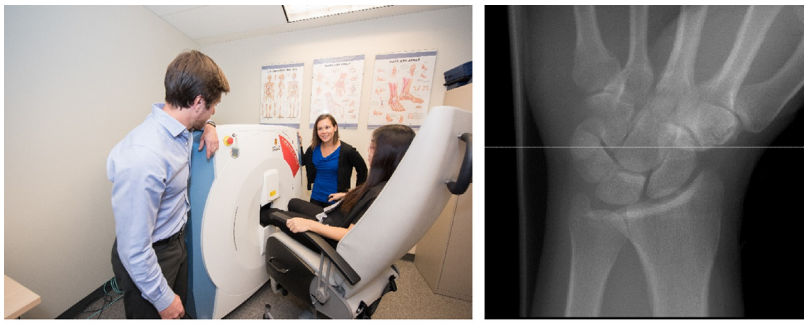

FIGURE 79.9 An HR-pQCT of the distal tibia is acquired with the leg supported in a cast to prevent movement. A scout view (right) is shown for a distal radius scan and is typically used to identify the scanning site.

Additionally, the cortical compartment was originally segmented using a relatively simple thresholding approach to determine its mask and measures of thickness and porosity, but that was later replaced by a more robust approach to identifying the cortical compartment based on a series of thresholding steps (Buie et al., 2007). Other morphological parameters such as Conn.D, SMI, and the different anisotropy measures are limited by the 82 μm voxel size. Even some standard measures, such as Tb.Th, do not appear to be accurately measured by the first-generation HR-pQCT (MacNeil and Boyd, 2007). On the other hand, advanced morphological decomposition has been validated for HR-pQCT systems (Liu et al., 2010a).

The development of the second-generation HR-pQCT system provides a higher resolution and slightly larger field of view, as previously noted. The accuracy of morphological measures by second-generation HR-pQCT is improved (Manske et al., 2015b), albeit with absolute values that are slightly altered due to the higher resolution. Therefore, significant work has attempted to establish the conversion between parameters measured on both generations so that the data generated on each system can be compared (Agarwal et al., 2016; Manske et al., 2017) and so that the field continues to move forward with improved ability to measure microarchitecture in vivo in humans.

Subject movement during scans is important to minimize, as it has a direct effect on the accuracy of microarchitecture measurements. Based on reproducibility studies, it has been shown that density measures such as total density, cortical density, and trabecular density can be measured with a precision of about 1%, whereas morphological measures such as Tb.N and cortical thickness are measured with a precision closer to 5% (MacNeil and Boyd, 2008b). Density measures are more precisely measured than morphological measures because they are less sensitive to movement artifact. Clearly, a human trabecula having a thickness of about 100 μm cannot be accurately measured if there is any small patient movement, especially given the relatively similar structure size to the imaging resolution. There are automated approaches to assessing patient movement during HR-pQCT scans (Pauchard et al., 2012) and even proposals for how the sinogram can be manipulated to "correct" for that motion (Pauchard and Boyd, 2008). However, the most frequently (and practically) used approach is to provide a subjective measure of the motion grade on a scale from 1 to 5 (lowest to highest motion artifact) and to perform a repeat scan if the subject is available for a second measurement attempt (Pialat et al., 2012).

Although the primary utilization of HR-pQCT is for the assessment of bone microarchitecture in the distal tibia and radius, there is increasing interest in learning about bone microarchitecture at other skeletal sites. For example, there is increasing interest in using HR-pQCT to understand the development and treatment of bony erosions that occur in rheumatoid arthritis (Barnabe et al., 2013), and with the larger gantry of the HR-pQCT system, the possibility to study microarchitecture in acutely injured knees (Kroker et al., 2017b).

Radiation dose

An important safety consideration for in vivo imaging is the X-ray dose delivered to the person, which is measured as effective radiation dose and reported as sieverts (Sv). This measure is a function of the amount of radiation emitted by the system, that absorbed by the body, and the sensitivity of the organs that receive radiation. The effective dose in DXA is low, with an estimated 5 μSv being reported for a total body exam (Scafoglieri et al., 2011) and less than 10 μSv for a spine or hip bone exam. An HR-pQCT system measurement at the wrist or ankle is typically less than 5 μSv, although it can be higher if a larger-than-normal region of interest is measured or for a different measurement site. For example, a scan of the knee covering about 6 cm in length results in about 50 μSv (Kroker et al., 2017b).

The X-ray dose of a pQCT system is very small, typically under 1 μSv. On the other hand, clinical exams using standard radiography and QCT can vary widely in effective X-ray dose depending on the site measured and imaging protocol used. For example, a spine X-ray with two views may result in over 400 μSv, and a QCT exam of the spine of a large patient can be as much as 10,000 μSv. These are all approximations, and the risk to the patient depends on many factors including how frequently they are scanned using X-ray methods. For reference, the average background radiation that a person in North America receives is approximately 3000 μSv, and the dose received on a transatlantic flight is roughly 60 μSv. Translating the effective dose into the risk of cancer mortality is approximated by International Commission on Radiological Protection guidelines (ICRP, 2007), which suggest 5% increased risk per Sv, which translates to approximately a 2.5×10^{-5}% increased risk of cancer per HR-pQCT.

Normative data

The 3D microarchitecture measured by HR-pQCT provides novel insight into the structure of bones, but without a reference cohort to compare those data against, it is difficult to interpret them. It is important to know the normal range of values for the morphological parameters measured by HR-pQCT as a function of sex, age, and ethnic background. In Canada, the Canadian Multicentre Osteoporosis Study (CaMos) (Tenenhouse et al., 2000) has been the basis to establish normative values of predominantly Caucasian men and women (Burt et al., 2016). Using these published data, it is possible for studies involving HR-pQCT to make conclusions about special populations, and this avoids the unnecessary and challenging task of establishing a control cohort for each study. This has been done, for example, in a recent study looking at bone microarchitecture in persons with hemophilia (Lee et al., 2015). Furthermore, while published data can be a rigorous way to share information about population variations, it can be much more practical to make those data available in a public domain, and this has been the basis of developing a web page (normative.ca) that provides an opportunity for scientists around the world to compare their patients' results with a normative population and even provide individual reports that can be shared with those patients. While the CaMos cohort provides important normative information, it is specific to the Canadian population. For this reason, other parts of the world have established normative data representing their own populations such as Hong Kong (Hung et al., 2015), the USA (Khosla et al., 2006), and Europe (Hansen et al., 2014). Furthermore, all these reference data are focused on adults, and there is a need to incorporate reference data for pediatrics as well (Gabel et al., 2017), although the challenge has been how to determine a standardized measurement site in growing children. Overall, reference data is an active and necessary area of research if HR-pQCT is ever to be used in a more clinical setting.

Fracture prediction

Microarchitectural information can provide insight into the progression of diseases or the effects of treatments; however, it is challenging to translate that knowledge into a predictor of fracture. Early attempts at linking microarchitecture to fracture prediction have focused on *prevalent* fractures. These studies are cross-sectional designs where the subjects recruited have suffered a fracture prior to study entry. While significant knowledge can be gained from these studies, their limitation is that by the time HR-pQCT scanning is performed, other factors (bedrest, changes in activity levels, etc.) may have influenced their microarchitecture. Subsequently, using *incident* fractures as a basis for study requires longitudinally following a cohort of people who have not yet suffered a fracture. Eventually, fractures will occur within the population, and from that information the linkage between fracture risk and microarchitectural features can be established and are not confounded by the same problems found in studies of prevalent fractures. The major challenge of studies with incident fractures is that larger populations must be included in the study, and it requires longitudinally monitoring the cohort—both of which result in increased costs and time.

Cross-sectional studies have identified key microarchitectural features in the radius and tibia that are most highly associated with fractures; typically these parameters include trabecular BMD, Tb.N, and total BMD (Boutroy et al., 2005; Melton et al., 2007; Sornay-Rendu et al., 2007; Vico et al., 2008). In addition to microarchitectural features, estimated bone strength from FE modeling has consistently been shown to be a good predictor of fracture (Boutroy et al., 2008; Kirmani et al., 2009; MacNeil and Boyd, 2008a; Nishiyama et al., 2013; Stein et al., 2010; Vilayphiou et al., 2010). The advantage of an FE approach to predicting fracture is that it intrinsically includes all microarchitectural features in a single outcome measure of bone strength, and based on this fact it would appear logical that bone strength would be related to fracture risk. Furthermore, it seems that despite the fact that measurements are taken at the radius and tibia, these sites are relevant to overall skeletal health (Kroker et al., 2017a; Liu et al., 2010b). Increasingly, studies with incident fractures are becoming available now that the technology has been accessible for over a decade and there has been time to follow longitudinal

cohorts. The microarchitectural features that seem most highly related to fractures are surprisingly consistent with earlier cross-sectional studies (Boutroy et al., 2016; Burt et al., 2017, 2018; Sornay-Rendu et al., 2017). Currently, the most ambitious project to date is close to completion, where groups from around the world have combined their prospective data to establish the parameters most highly associated with fracture risk (Samelson et al., 2019), and consistent with previous work, bone strength has been identified as an important outcome measure. These data, combined with the establishment of large normative databases, are paving the way for HR-pQCT to become a new and important contributor to the assessment of skeletal health and prediction of fracture in the future.

Summary

During the last 2 decades, bone microimaging based on high-resolution CT has become the method of choice for quantifying 3D bone microstructure and architecture in vitro. It is a nondestructive, noninvasive, and precise procedure allowing the measurement of trabecular and cortical bone as well as the computation of microstructural and micromechanical properties, both static and dynamic. It has demonstrated its effectiveness in evaluating many applications such as the characterization of genetic effects in different mouse models and in quantifying microarchitectural changes resulting from diseases such as osteoporosis, the effects of hormones and medications such as estrogen and bisphosphonates, and effects of bone adaptation, such as those due to mechanical loading. Recent studies have shown the great potential of time-lapse in vivo micro-CT for a better understanding of structural changes in bone geometry and bone microstructure as well as mechanical properties. These structural changes can be quantified using morphometric measures derived from the 3D data sets, and effects on bone competence can be estimated from micro-FE analyses. The ability to noninvasively track changes over time is likely to establish in vivo micro-CT as a standard methodology in the coming decade. The procedure might help improve predictions of fracture risk, clarify the pathophysiology of skeletal diseases, and define the response to therapy in both preclinical and clinical settings. We expect these findings to improve our understanding of the influence of densitometric, morphological, and also loading factors in the etiology of traumatic and spontaneous fractures of the forearm, hip, and spine as well as detection of longitudinal changes related to bone remodeling and adaptation in growth, aging, disease processes, and treatment effects.

References

Agarwal, S., Rosete, F., Zhang, C., McMahon, D.J., Guo, X.E., Shane, E., Nishiyama, K.K., 2016. In vivo assessment of bone structure and estimated bone strength by first- and second-generation HR-pQCT. Osteoporos. Int. 27, 2955−2966.

Alexander, J.M., Bab, I., Fish, S., Müller, R., Uchiyama, T., Gronowicz, G., Nahounou, M., Zhao, Q., White, D.W., Chorev, M., Gazit, D., Rosenblatt, M., 2001. Human parathyroid hormone 1-34 reverses bone loss in ovariectomized mice. J. Bone Miner. Res. 16, 1665−1673.

Babij, P., Zhao, W., Small, C., Kharode, Y., Yaworsky, P.J., Bouxsein, M.L., Reddy, P.S., Bodine, P.V., Robinson, J.A., Bhat, B., Marzolf, J., Moran, R.A., Bex, F., 2003. High bone mass in mice expressing a mutant LRP5 gene. J. Bone Miner. Res. 18, 960−974.

Badea, C.T., Fubara, B., Hedlund, L.W., Johnson, G.A., 2005. 4-D micro-CT of the mouse heart. Mol. Imag. 4, 110−116.

Badger, A.M., Griswold, D.E., Kapadia, R., Blake, S., Swift, B.A., Hoffman, S.J., Stroup, G.B., Webb, E., Rieman, D.J., Gowen, M., Boehm, J.C., Adams, J.L., Lee, J.C., 2000. Disease-modifying activity of SB 242235, a selective inhibitor of p38 mitogen-activated protein kinase, in rat adjuvant-induced arthritis. Arthritis Rheum. 43, 175−183.

Balto, K., Müller, R., Carrington, D.C., Dobeck, J., Stashenko, P., 2000. Quantification of periapical bone destruction in mice by micro-computed tomography. J. Dent. Res. 79, 35−40.

Barnabe, C., Buie, H., Kan, M., Szabo, E., Barr, S.G., Martin, L., Boyd, S.K., 2013. Reproducible metacarpal joint space width measurements using 3D analysis of images acquired with high-resolution peripheral quantitative computed tomography. Med. Eng. Phys. 35, 1540−1544.

Bay, B.K., Yerby, S.A., McLain, R.F., Toh, E., 1999. Measurement of strain distributions within vertebral body sections by texture correlation. Spine 24, 10−17.

Bayraktar, H.H., Morgan, E.F., Niebur, G.L., Morris, G.E., Wong, E.K., Keaveny, T.M., 2004. Comparison of the elastic and yield properties of human femoral trabecular and cortical bone tissue. J. Biomech. 37, 27−35.

Birkhold, A.I., Razi, H., Weinkamer, R., Duda, G.N., Checa, S., Willie, B.M., 2015. Monitoring in vivo (re)modeling: a computational approach using 4D microCT data to quantify bone surface movements. Bone 75, 210−221.

Bondareva, A., Downey, C.M., Ayres, F., Liu, W., Boyd, S.K., Hallgrìmsson, B., Jirik, F.R., 2009. The lysyl oxidase inhibitor, beta-aminopropionitrile, diminishes the metastatic colonization potential of circulating breast cancer cells. PLoS One 4, e5620.

Bonse, U., Busch, F., Gunnewig, O., Beckmann, F., Pahl, R., Delling, G., Hahn, M., Graeff, W., 1994. 3D computed X-ray tomography of human cancellous bone at 8 microns spatial and 10(-4) energy resolution. Bone Miner. 25, 25−38.

Borah, B., Dufresne, T.E., Chmielewski, P.A., Gross, G.J., Prenger, M.C., Phipps, R.J., 2002. Risedronate preserves trabecular architecture and increases bone strength in vertebra of ovariectomized minipigs as measured by three-dimensional microcomputed tomography. J. Bone Miner. Res. 17, 1139−1147.

Borah, B., Dufresne, T.E., Chmielewski, P.A., Johnson, T.D., Chines, A., Manhart, M.D., 2004. Risedronate preserves bone architecture in post-menopausal women with osteoporosis as measured by three-dimensional microcomputed tomography. Bone 34, 736–746.

Borah, B., Gross, G.J., Dufresne, T.E., Smith, T.S., Cockman, M.D., Chmielewski, P.A., Lundy, M.W., Hartke, J.R., Sod, E.W., 2001. Three-dimensional microimaging (MRμI and μCT), finite element modeling, and rapid prototyping provide unique insights into bone architecture in osteoporosis. Anat. Rec. 265, 101–110.

Borah, B., Ritman, E.L., Dufresne, T.E., Jorgensen, S.M., Liu, S., Sacha, J., Phipps, R.J., Turner, R.T., 2005. The effect of risedronate on bone mineralization as measured by micro-computed tomography with synchrotron radiation: correlation to histomorphometric indices of turnover. Bone 37, 1–9.

Bousson, V., Bergot, C., Sutter, B., Thomas, T., Bendavid, S., Benhamou, C.L., Blain, H., Brazier, M., Breuil, V., Briot, K., Chapurlat, R., Chapuis, L., Cohen Solal, M., Fardellone, P., Feron, J.M., Gauvain, J.B., Laroche, M., Legrand, E., Lespessailles, E., Linglart, A., Marcelli, C., Roux, C., Souberbielle, J.C., Tremollieres, F., Weryha, G., Cortet, B., Groupe de Recherche et d'Information sur les, O., 2015. Trabecular Bone Score: where are we now? Joint Bone Spine 82, 320–325.

Bousson, V., Peyrin, F., Bergot, C., Hausard, M., Sautet, A., Laredo, J.D., 2004. Cortical bone in the human femoral neck: three-dimensional appearance and porosity using synchrotron radiation. J. Bone Miner. Res. 19, 794–801.

Boutroy, S., Bouxsein, M.L., Munoz, F., Delmas, P.D., 2005. In vivo assessment of trabecular bone microarchitecture by high-resolution peripheral quantitative computed tomography. J. Clin. Endocrinol. Metab. 90, 6508–6515.

Boutroy, S., Khosla, S., Sornay-Rendu, E., Zanchetta, M.B., McMahon, D.J., Zhang, C.A., Chapurlat, R.D., Zanchetta, J., Stein, E.M., Bogado, C., Majumdar, S., Burghardt, A.J., Shane, E., 2016. Microarchitecture and peripheral BMD are impaired in postmenopausal white women with fracture independently of total hip T-score: an international multicenter study. J. Bone Miner. Res. 31, 1158–1166.

Boutroy, S., Van Rietbergen, B., Sornay-Rendu, E., Munoz, F., Bouxsein, M.L., Delmas, P.D., 2008. Finite element analysis based on in vivo HR-pQCT images of the distal radius is associated with wrist fracture in postmenopausal women. J. Bone Miner. Res. 23, 392–399.

Bouxsein, M.L., 2003. Bone quality: where do we go from here? Osteoporos. Int. 14 (Suppl. 5), 118–127.

Bouxsein, M.L., 2008. Technology insight: noninvasive assessment of bone strength in osteoporosis. Nat. Clin. Pract. Rheumatol. 4, 310–318.

Bouxsein, M.L., Boyd, S.K., Christiansen, B.A., Guldberg, R.E., Jepsen, K.J., Müller, R., 2010. Guidelines for assessment of bone microstructure in rodents using micro-computed tomography. J. Bone Miner. Res. 25, 1468–1486.

Bouxsein, M.L., Uchiyama, T., Rosen, C.J., Shultz, K.L., Donahue, L.R., Turner, C.H., Sen, S., Churchill, G.A., Müller, R., Beamer, W.G., 2004. Mapping quantitative trait loci for vertebral trabecular bone volume fraction and microarchitecture in mice. J. Bone Miner. Res. 19, 587–599.

Boyd, S.K., 2008. Site-specific variation of bone micro-architecture in the distal radius and tibia. J. Clin. Densitom. 11, 424–430.

Boyd, S.K., Davison, P., Müller, R., Gasser, J.A., 2006. Monitoring individual morphological changes over time in ovariectomized rats by in vivo micro-computed tomography. Bone 39, 854–862.

Brouwers, J.E., van Rietbergen, B., Huiskes, R., 2007. No effects of in vivo micro-CT radiation on structural parameters and bone marrow cells in proximal tibia of wistar rats detected after eight weekly scans. J. Orthop. Res. 25, 1325–1332.

Buie, H.R., Bosma, N.A., Downey, C.M., Jirik, F.R., Boyd, S.K., 2013. Micro-CT evaluation of bone defects: applications to osteolytic bone metastases, bone cysts, and fracture. Med. Eng. Phys. 35, 1645–1650.

Buie, H.R., Boyd, S.K., 2010. Reduced bone mass accrual in swim-trained prepubertal mice. Med. Sci. Sports Exerc. 42, 1834–1842.

Buie, H.R., Campbell, G.M., Klinck, R.J., MacNeil, J.A., Boyd, S.K., 2007. Automatic segmentation based on a dual threshold technique for in vivo micro-CT bone analysis. Bone 41, 505–515.

Buie, H.R., Moore, C.P., Boyd, S.K., 2008. Postpubertal architectural developmental patterns differ between the L3 vertebra and proximal tibia in three inbred strains of mice. J. Bone Miner. Res. 23, 2048–2059.

Bullitt, E., Reardon, D.A., Smith, J.K., 2007. A review of micro- and macrovascular analyses in the assessment of tumor-associated vasculature as visualized by MR. Neuroimage 37 (Suppl. 1), S116–S119.

Burghardt, A.J., Buie, H.R., Laib, A., Majumdar, S., Boyd, S.K., 2010. Reproducibility of direct quantitative measures of cortical bone microarchitecture of the distal radius and tibia by HR-pQCT. Bone 47, 519–528.

Burt, L.A., Greene, D.A., Ducher, G., Naughton, G.A., 2013. Skeletal adaptations associated with pre-pubertal gymnastics participation as determined by DXA and pQCT: a systematic review and meta-analysis. J. Sci. Med. Sport 16, 231–239.

Burt, L.A., Hanley, D.A., Boyd, S.K., 2017. Cross-sectional versus longitudinal change in a prospective HR-pQCT study. J. Bone Miner. Res. 32, 1505–1513.

Burt, L.A., Liang, Z., Sajobi, T.T., Hanley, D.A., Boyd, S.K., 2016. Sex- and site-specific normative data curves for HR-pQCT. J. Bone Miner. Res. 31, 2041–2047.

Burt, L.A., Manske, S.L., Hanley, D.A., Boyd, S.K., 2018. Lower bone density, impaired microarchitecture, and strength predict future fragility fracture in postmenopausal women: 5-year follow-up of the calgary CaMos cohort. J. Bone Miner. Res. 33, 589–597.

Burt, L.A., Naughton, G.A., Greene, D.A., Courteix, D., Ducher, G., 2012. Non-elite gymnastics participation is associated with greater bone strength, muscle size, and function in pre- and early pubertal girls. Osteoporos. Int. 23, 1277–1286.

Butz, S., Wüster, C., Scheidt-Nave, C., Götz, M., Ziegler, R., 1994. Forearm BMD as measured by peripheral quantitative computed tomography (pQCT) in a German reference population. Osteoporos. Int. 4, 179–184.

Campbell, G.M., Buie, H.R., Boyd, S.K., 2008. Signs of irreversible architectural changes occur early in the development of experimental osteoporosis as assessed by in vivo micro-CT. Osteoporos. Int. 19, 1409–1419.

Carter, D.R., Hayes, W.C., 1977. The compressive behavior of bone as a two-phase porous structure. J. Bone Joint Surg. Am. 59, 954–962.

Cheung, A.M., Adachi, J.D., Hanley, D.A., Kendler, D.L., Davison, K.S., Josse, R., Brown, J.P., Ste-Marie, L.G., Kremer, R., Erlandson, M.C., Dian, L., Burghardt, A.J., Boyd, S.K., 2013. High-resolution peripheral quantitative computed tomography for the assessment of bone strength and structure: a review by the Canadian bone strength working group. Curr. Osteoporos. Rep. 11, 136–146.

Christen, D., Levchuk, A., Schori, S., Schneider, P., Boyd, S.K., Müller, R., 2012. Deformable image registration and 3D strain mapping for the quantitative assessment of cortical bone microdamage. J. Mech. Behav. Biomed. Mater. 8, 184–193.

Christen, D., Melton, L.J., Zwahlen, A., Amin, S., Khosla, S., Müller, R., 2013. Improved fracture risk assessment based on nonlinear micro-finite element simulations from HRpQCT images at the distal radius. J. Bone Miner. Res. 28, 2601–2608.

Christen, P., Müller, R., 2017. In vivo visualisation and quantification of bone resorption and bone formation from time-lapse imaging. Curr. Osteoporos. Rep. 15, 311–317.

Ciarelli, M.J., Goldstein, S.A., Kuhn, J.L., Cody, D.D., Brown, M.B., 1991. Evaluation of orthogonal mechanical properties and density of human trabecular bone from the major metaphyseal regions with materials testing and computed tomography. J. Orthop. Res. 9, 674–682.

Cody, D.D., Divine, G.W., Nahigian, K., Kleerekoper, M., 2000. Bone density distribution and gender dominate femoral neck fracture risk predictors. Skeletal Radiol. 29, 151–161.

Cody, D.D., Gross, G.J., Hou, F.J., Spencer, H.J., Goldstein, S.A., Fyhrie, D.P., 1999. Femoral strength is better predicted by finite element models than QCT and DXA. J. Biomech. 32, 1013–1020.

Cruz-Orive, L., Karlsson, L., Larsen, S., Wainschtein, F., 1992. Characterizing anisotropy: a new concept. Micron Microsc. Acta 23, 75–76.

Dambacher, M.A., Ruegsegger, P., 1994. [Bone density measurements and their indications]. Orthopä 23, 38–44.

Day, J.S., Ding, M., van der Linden, J.C., Hvid, I., Sumner, D.R., Weinans, H., 2001. A decreased subchondral trabecular bone tissue elastic modulus is associated with pre-arthritic cartilage damage. J. Orthop. Res. 19, 914–918.

Dedrick, D.K., Goldstein, S.A., Brandt, K.D., O'Connor, B.L., Goulet, R.W., Albrecht, M., 1993. A longitudinal study of subchondral plate and trabecular bone in cruciate-deficient dogs with osteoarthritis followed up for 54 months. Arthritis Rheum. 36, 1460–1467.

Dempster, D.W., Compston, J.E., Drezner, M.K., Glorieux, F.H., Kanis, J.A., Malluche, H., Meunier, P.J., Ott, S.M., Recker, R.R., Parfitt, A.M., 2013. Standardized nomenclature, symbols, and units for bone histomorphometry: a 2012 update of the report of the ASBMR histomorphometry nomenclature committee. J. Bone Miner. Res. 28, 2–17.

Dempster, D.W., Cosman, F., Kurland, E.S., Zhou, H., Nieves, J., Woelfert, L., Shane, E., Plavetic, K., Müller, R., Bilezikian, J., Lindsay, R., 2001. Effects of daily treatment with parathyroid hormone on bone microarchitecture and turnover in patients with osteoporosis: a paired biopsy study. J. Bone Miner. Res. 16, 1846–1853.

Di Michiel, M., Merino, J.M., Fernandez-Carreiras, D., Buslaps, T., Honkimäki, V., Falus, P., Martins, T., Svensson, O., 2005. Fast microtomography using high energy synchrotron radiation. Rev. Sci. Instrum. 76.

Ding, M., Hvid, I., 2000. Quantification of age-related changes in the structure model type and trabecular thickness of human tibial cancellous bone. Bone 26, 291–295.

Duyck, J., Ronold, H.J., Van Oosterwyck, H., Naert, I., Vander Sloten, J., Ellingsen, J.E., 2001. The influence of static and dynamic loading on marginal bone reactions around osseointegrated implants: an animal experimental study. Clin. Oral Implant. Res. 12, 207–218.

Ellouz, R., Chapurlat, R., van Rietbergen, B., Christen, P., Pialat, J.B., Boutroy, S., 2014. Challenges in longitudinal measurements with HR-pQCT: evaluation of a 3D registration method to improve bone microarchitecture and strength measurement reproducibility. Bone 63, 147–157.

Engelke, K., Graeff, W., Meiss, L., Hahn, M., Delling, G., 1993. High spatial resolution imaging of bone mineral using computed microtomography. Comparison with microradiography and undecalcified histologic sections. Investig. Radiol. 28, 341–349.

Feldkamp, L.A., Goldstein, S.A., Parfitt, A.M., Jesion, G., Kleerekoper, M., 1989. The direct examination of three-dimensional bone architecture in vitro by computed tomography. J. Bone Miner. Res. 4, 3–11.

Felsenberg, D., Boonen, S., 2005. The bone quality framework: determinants of bone strength and their interrelationships, and implications for osteoporosis management. Clin. Ther. 27, 1–11.

Ferretti, J.L., Gaffuri, O., Capozza, R., Cointry, G., Bozzini, C., Olivera, M., Zanchetta, J.R., Bozzini, C.E., 1995. Dexamethasone effects on mechanical, geometric and densitometric properties of rat femur diaphyses as described by peripheral quantitative computerized tomography and bending tests. Bone 16, 119–124.

Gabel, L., Macdonald, H.M., McKay, H.A., 2017. Sex differences and growth-related adaptations in bone microarchitecture, geometry, density, and strength from childhood to early adulthood: a mixed longitudinal HR-pQCT study. J. Bone Miner. Res. 32, 250–263.

Gabel, L., Nettlefold, L., Brasher, P.M., Moore, S.A., Ahamed, Y., Macdonald, H.M., McKay, H.A., 2015. Reexamining the surfaces of bone in boys and girls during adolescent growth: a 12-year mixed longitudinal pQCT study. J. Bone Miner. Res. 30, 2158–2167.

Genant, H.K., Gordon, C., Jiang, Y., Lang, T.F., Link, T.M., Majumdar, S., 1999. Advanced imaging of bone macro and micro structure. Bone 25, 149–152.

Giesen, E.B., van Eijden, T.M., 2000. The three-dimensional cancellous bone architecture of the human mandibular condyle. J. Dent. Res. 79, 957–963.

Gluer, C.C., Blake, G., Lu, Y., Blunt, B.A., Jergas, M., Genant, H.K., 1995. Accurate assessment of precision errors: how to measure the reproducibility of bone densitometry techniques. Osteoporos. Int. 5, 262–270.

Gluer, C.C., Wu, C.Y., Jergas, M., Goldstein, S.A., Genant, H.K., 1994. Three quantitative ultrasound parameters reflect bone structure. Calcif. Tissue Int. 55, 46–52.

Goldstein, S.A., Goulet, R.W., McCubbrey, D., 1993. Measurement and significance of three-dimensional architecture to the mechanical integrity of trabecular bone. Calcif. Tissue Int. 53, 127–132.

Gonzalez, R., Woods, R., 2002. Digital Image Processing. Prentice Hall.

Goulet, R.W., Goldstein, S.A., Ciarelli, M.J., Kuhn, J.L., Brown, M.B., Feldkamp, L.A., 1994. The relationship between the structural and orthogonal compressive properties of trabecular bone. J. Biomech. 27, 375–389.

Graichen, H., Lochmüller, E.M., Wolf, E., Langkabel, B., Stammberger, T., Haubner, M., Renner-Müller, I., Englmeier, K.H., Eckstein, F., 1998. A non-destructive technique for 3-D microstructural phenotypic characterisation of bones in genetically altered mice: preliminary data in growth hormone transgenic animals and normal controls. Anat. Embryol. 199, 239–248.

Hangartner, T.N., Overton, T.R., Harley, C.H., van den Berg, L., Crockford, P.M., 1985. Skeletal challenge: an experimental study of pharmacologically induced changes in bone density in the distal radius, using gamma-ray computed tomography. Calcif. Tissue Int. 37, 19–24.

Hansen, S., Shanbhogue, V., Folkestad, L., Nielsen, M.M., Brixen, K., 2014. Bone microarchitecture and estimated strength in 499 adult Danish women and men: a cross-sectional, population-based high-resolution peripheral quantitative computed tomographic study on peak bone structure. Calcif. Tissue Int. 94, 269–281.

Heinzer, S., Krucker, T., Stampanoni, M., Abela, R., Meyer, E.P., Schuler, A., Schneider, P., Müller, R., 2006. Hierarchical microimaging for multiscale analysis of large vascular networks. Neuroimage 32, 626–636.

Hildebrand, T., Laib, A., Müller, R., Dequeker, J., Rüegsegger, P., 1999. Direct three-dimensional morphometric analysis of human cancellous bone: microstructural data from spine, femur, iliac crest, and calcaneus. J. Bone Miner. Res. 14, 1167–1174.

Hildebrand, T., Rüegsegger, P., 1997a. A new method for the model-independent assessment of thickness in three-dimensional images. J. Microsc. 185, 67–75.

Hildebrand, T., Rüegsegger, P., 1997b. Quantification of bone microarchitecture with the structure model index. Comput. Methods Biomech. Biomed. Eng. 1, 15–23.

Homminga, J., McCreadie, B.R., Weinans, H., Huiskes, R., 2003. The dependence of the elastic properties of osteoporotic cancellous bone on volume fraction and fabric. J. Biomech. 36, 1461–1467.

Huang, Y.C., Simmons, C., Kaigler, D., Rice, K.G., Mooney, D.J., 2005. Bone regeneration in a rat cranial defect with delivery of PEI-condensed plasmid DNA encoding for bone morphogenetic protein-4 (BMP-4). Gene Ther. 12, 418–426.

Hung, V.W., Zhu, T.Y., Cheung, W.H., Fong, T.N., Yu, F.W., Hung, L.K., Leung, K.S., Cheng, J.C., Lam, T.P., Qin, L., 2015. Age-related differences in volumetric bone mineral density, microarchitecture, and bone strength of distal radius and tibia in Chinese women: a high-resolution pQCT reference database study. Osteoporos. Int. 26, 1691–1703.

ICRP, 2007. The 2007 recommendations of the international commission on radiological protection. ICRP publication. Ann. ICRP 37, 2–4.

Ito, M., Nakamura, T., Matsumoto, T., Tsurusaki, K., Hayashi, K., 1998. Analysis of trabecular microarchitecture of human iliac bone using micro-computed tomography in patients with hip arthrosis with or without vertebral fracture. Bone 23, 163–169.

Jara, H., Wehrli, F.W., Chung, H., Ford, J.C., 1993. High-resolution variable flip angle 3D MR imaging of trabecular microstructure in vivo. Magn. Reson. Med. 29, 528–539.

Jones, A.C., Milthorpe, B., Averdunk, H., Limaye, A., Senden, T.J., Sakellariou, A., Sheppard, A.P., Sok, R.M., Knackstedt, M.A., Brandwood, A., Rohner, D., Hutmacher, D.W., 2004. Analysis of 3D bone ingrowth into polymer scaffolds via micro-computed tomography imaging. Biomaterials 25, 4947–4954.

Kabel, J., Van Rietbergen, B., Dalstra, M., Odgaard, A., Huiskes, R., 1999. The role of an effective isotropic tissue modulus in the elastic properties of cancellous bone. J. Biomech. 32, 673–680.

Kalender, W.A., Klotz, E., Suess, C., 1987. Vertebral bone mineral analysis: an integrated approach with CT. Radiology 164, 419–423.

Kapadia, R.D., Stroup, G.B., Badger, A.M., Koller, B., Levin, J.M., Coatney, R.W., Dodds, R.A., Liang, X., Lark, M.W., Gowen, M., 1998. Applications of micro-CT and MR microscopy to study pre-clinical models of osteoporosis and osteoarthritis. Technol. Health Care 6, 361–372.

Keaveny, T.M., Guo, X.E., Wachtel, E.F., McMahon, T.A., Hayes, W.C., 1994. Trabecular bone exhibits fully linear elastic behavior and yields at low strains. J. Biomech. 27, 1127–1136.

Keller, T.S., 1994. Predicting the compressive mechanical behavior of bone. J. Biomech. 27, 1159–1168.

Khosla, S., Riggs, B.L., Atkinson, E.J., Oberg, A.L., McDaniel, L.J., Holets, M., Peterson, J.M., Melton III, L.J., 2006. Effects of sex and age on bone microstructure at the ultradistal radius: a population-based noninvasive in vivo assessment. J. Bone Miner. Res. 21, 124–131.

Kirmani, S., Christen, D., van Lenthe, G.H., Fischer, P.R., Bouxsein, M.L., McCready, L.K., Melton, L.J., Riggs, B.L., Amin, S., Müller, R., Khosla, S., 2009. Bone structure at the distal radius during adolescent growth. J. Bone Miner. Res. 24, 1033–1042.

Klinck, R.J., Campbell, G.M., Boyd, S.K., 2008. Radiation effects on bone architecture in mice and rats resulting from in vivo micro-computed tomography scanning. Med. Eng. Phys. 30, 888–895.

Koester, K.J., Ager III, J.W., Ritchie, R.O., 2008. The true toughness of human cortical bone measured with realistically short cracks. Nat. Mater. 7, 672–677.

Kroker, A., Plett, R., Nishiyama, K.K., McErlain, D.D., Sandino, C., Boyd, S.K., 2017a. Distal skeletal tibia assessed by HR-pQCT is highly correlated with femoral and lumbar vertebra failure loads. J. Biomech. 59, 43–49.

Kroker, A., Zhu, Y., Manske, S.L., Barber, R., Mohtadi, N., Boyd, S.K., 2017b. Quantitative in vivo assessment of bone microarchitecture in the human knee using HR-pQCT. Bone 97, 43–48.

Kuhn, J.L., Goldstein, S.A., Feldkamp, L.A., Goulet, R.W., Jesion, G., 1990. Evaluation of a microcomputed tomography system to study trabecular bone structure. J. Orthop. Res. 8, 833–842.

Ladd, A.J., Kinney, J.H., Haupt, D.L., Goldstein, S.A., 1998. Finite-element modeling of trabecular bone: comparison with mechanical testing and determination of tissue modulus. J. Orthop. Res. 16, 622–628.

Laib, A., Hauselmann, H.J., Rüegsegger, P., 1998. In vivo high resolution 3D-QCT of the human forearm. Technol. Health Care 6, 329–337.

Laib, A., Rüegsegger, P., 1999. Calibration of trabecular bone structure measurements of in vivo three-dimensional peripheral quantitative computed tomography with 28-microm-resolution microcomputed tomography. Bone 24, 35–39.

Lambers, F.M., Koch, K., Kuhn, G., Ruffoni, D., Weigt, C., Schulte, F.A., Müller, R., 2013. Trabecular bone adapts to long-term cyclic loading by increasing stiffness and normalization of dynamic morphometric rates. Bone 55, 325–334.

Lang, T.F., Li, J., Harris, S.T., Genant, H.K., 1999. Assessment of vertebral bone mineral density using volumetric quantitative CT. J. Comput. Assist. Tomogr. 23, 130–137.

Langton, C.M., Njeh, C.F., 2004. In: Orton, C.G., Spaan, J.A., Webster, J.G. (Eds.), The Physical Measurement of Bone. Institute of Physics Publishing, London.

Laperre, K., Depypere, M., van Gastel, N., Torrekens, S., Moermans, K., Bogaerts, R., Maes, F., Carmeliet, G., 2011. Development of micro-CT protocols for in vivo follow-up of mouse bone architecture without major radiation side effects. Bone 49, 613–622.

Larrue, A., Rattner, A., Laroche, N., Vico, L., Peyrin, F., 2007. Feasibility of micro-crack detection in human trabecular bone images from 3D synchrotron microtomography. Conf. Proc. IEEE Eng. Med. Biol. Soc. 2007, 3918–3921.

Lee, A., Boyd, S.K., Kline, G., Poon, M.C., 2015. Premature changes in trabecular and cortical microarchitecture result in decreased bone strength in hemophilia. Blood 125, 2160–2163.

Levchuk, A., Schneider, P., Meier, M., Vogel, P., Donaldson, F., Müller, R., 2018. An automated step-wise micro-compression device for 3D dynamic image-guided failure assessment of bone tissue on a microstructural level using time-lapsed tomography. Front. Mater. 5.

Li, Z., Kuhn, G., Schirmer, M., Müller, R., Ruffoni, D., 2017. Impaired bone formation in ovariectomized mice reduces implant integration as indicated by longitudinal in vivo micro-computed tomography. PLoS One 12, e0184835.

Lin, A.S., Barrows, T.H., Cartmell, S.H., Guldberg, R.E., 2003. Microarchitectural and mechanical characterization of oriented porous polymer scaffolds. Biomaterials 24, 481–489.

Link, T.M., Majumdar, S., 2004. Current diagnostic techniques in the evaluation of bone architecture. Curr. Osteoporos. Rep. 2, 47–52.

Liu, X.S., Cohen, A., Shane, E., Stein, E., Rogers, H., Kokolus, S.L., Yin, P.T., McMahon, D.J., Lappe, J.M., Recker, R.R., Guo, X.E., 2010a. Individual trabeculae segmentation (ITS)-based morphological analysis of high-resolution peripheral quantitative computed tomography images detects abnormal trabecular plate and rod microarchitecture in premenopausal women with idiopathic osteoporosis. J. Bone Miner. Res. 25, 1496–1505.

Liu, X.S., Cohen, A., Shane, E., Yin, P.T., Stein, E.M., Rogers, H., Kokolus, S.L., McMahon, D.J., Lappe, J.M., Recker, R.R., Lang, T., Guo, X.E., 2010b. Bone density, geometry, microstructure, and stiffness: relationships between peripheral and central skeletal sites assessed by DXA, HR-pQCT, and cQCT in premenopausal women. J. Bone Miner. Res. 25, 2229–2238.

Liu, X.S., Sajda, P., Saha, P.K., Wehrli, F.W., Bevill, G., Keaveny, T.M., Guo, X.E., 2008. Complete volumetric decomposition of individual trabecular plates and rods and its morphological correlations with anisotropic elastic moduli in human trabecular bone. J. Bone Miner. Res. 23, 223–235.

Lutolf, M.P., Weber, F.E., Schmoekel, H.G., Schense, J.C., Kohler, T., Müller, R., Hubbell, J.A., 2003. Repair of bone defects using synthetic mimetics of collagenous extracellular matrices. Nat. Biotechnol. 21, 513–518.

MacNeil, J.A., Boyd, S.K., 2007. Accuracy of high-resolution peripheral quantitative computed tomography for measurement of bone quality. Med. Eng. Phys. 29, 1096–1105.

MacNeil, J.A., Boyd, S.K., 2008a. Bone strength at the distal radius can be estimated from high-resolution peripheral quantitative computed tomography and the finite element method. Bone 42, 1203–1213.

MacNeil, J.A., Boyd, S.K., 2008b. Improved reproducibility of high-resolution peripheral quantitative computed tomography for measurement of bone quality. Med. Eng. Phys. 30, 792–799.

Majumdar, S., 2002. Magnetic resonance imaging of trabecular bone structure. Top. Magn. Reson. Imag. 13, 323–334.

Majumdar, S., Kothari, M., Augat, P., Newitt, D.C., Link, T.M., Lin, J.C., Lang, T., Lu, Y., Genant, H.K., 1998. High-resolution magnetic resonance imaging: three-dimensional trabecular bone architecture and biomechanical properties. Bone 22, 445–454.

Manske, S.L., Davison, E.M., Burt, L.A., Raymond, D.A., Boyd, S.K., 2017. The estimation of second-generation HR-pQCT from first-generation HR-pQCT using in vivo cross-calibration. J. Bone Miner. Res. 32, 1514–1524.

Manske, S.L., Vijayaraghavan, S., Tuthill, A., Brutus, O., Yang, J., Gupta, S., Judex, S., 2015a. Extending rest between unloading cycles does not enhance bone's long-term recovery. Med. Sci. Sports Exerc. 47, 2191–2200.

Manske, S.L., Zhu, Y., Sandino, C., Boyd, S.K., 2015b. Human trabecular bone microarchitecture can be assessed independently of density with second generation HR-pQCT. Bone 79, 213–221.

Matsumoto, T., Yoshino, M., Uesugi, K., Tanaka, M., 2007. Biphasic change and disuse-mediated regression of canal network structure in cortical bone of growing rats. Bone 41, 239–246.

McCreadie, B.R., Goulet, R.W., Feldkamp, L.A., Goldstein, S.A., 2001. Hierarchical structure of bone and micro-computed tomography. Adv. Exp. Med. Biol. 496, 67–83.

McElhaney, J.H., Fogle, J.L., Melvin, J.W., Haynes, R.R., Roberts, V.L., Alem, N.M., 1970. Mechanical properties of cranial bone. J. Biomech. 3, 495–511.

Meier, M., Vogel, P., Schneider, P., Müller, R., 2008. Investigation of microdamage in murine bone under dynamic load. J. Biomech. 41, S76.

Melton III, L.J., Riggs, B.L., van Lenthe, G.H., Achenbach, S.J., Müller, R., Bouxsein, M.L., Amin, S., Atkinson, E.J., Khosla, S., 2007. Contribution of in vivo structural measurements and load/strength ratios to the determination of forearm fracture risk in postmenopausal women. J. Bone Miner. Res. 22, 1442–1448.

Michel, G., Blery, P., Pilet, P., Guicheux, J., Weiss, P., Malard, O., Espitalier, F., 2015. Micro-ct analysis of radiation-induced osteopenia and bone hypovascularization in rat. Calcif. Tissue Int. 97, 62–68.

Moutsatsos, I.K., Turgeman, G., Zhou, S., Kurkalli, B.G., Pelled, G., Tzur, L., Kelley, P., Stumm, N., Mi, S., Müller, R., Zilberman, Y., Gazit, D., 2001. Exogenously regulated stem cell-mediated gene therapy for bone regeneration. Mol. Ther. 3, 449–461.

Müller, R., 2002. The Zurich experience: one decade of three-dimensional high-resolution computed tomography. Top. Magn. Reson. Imag. 13, 307–322.

Müller, R., Boesch, T., Jarak, D., Stauber, M., Nazarian, A., Tantillo, M., Boyd, S.K., 2002. Micro-mechanical evaluation of bone microstructures under load. In: Bonse, U. (Ed.), Developments in X-Ray Tomography III. SPIE, San Diego, CA, pp. 189–200.

Müller, R., Gerber, S.C., Hayes, W.C., 1998a. Micro-compression: a novel technique for the nondestructive assessment of local bone failure. Technol. Health Care 6, 433–444.

Müller, R., Hannan, M., Smith, S.Y., Bauss, F., 2004. Intermittent ibandronate preserves bone quality and bone strength in the lumbar spine after 16 months of treatment in the ovariectomized cynomolgus monkey. J. Bone Miner. Res. 19, 1787–1796.

Müller, R., Hildebrand, T., Rüegsegger, P., 1994. Noninvasive bone-biopsy—a new method to analyze and display the 3-dimensional structure of trabecular bone. Phys. Med. Biol. 39, 145–164.

Müller, R., Rüegsegger, P., 1997. Micro-tomographic imaging for the nondestructive evaluation of trabecular bone architecture. Stud. Health Technol. Inf. 40, 61–79.

Müller, R., Van Campenhout, H., Van Damme, B., Van Der Perre, G., Dequeker, J., Hildebrand, T., Rüegsegger, P., 1998b. Morphometric analysis of human bone biopsies: a quantitative structural comparison of histological sections and micro-computed tomography. Bone 23, 59–66.

Nagaraja, S., Couse, T.L., Guldberg, R.E., 2005. Trabecular bone microdamage and microstructural stresses under uniaxial compression. J. Biomech. 38, 707–716.

Nalla, R.K., Stolken, J.S., Kinney, J.H., Ritchie, R.O., 2005. Fracture in human cortical bone: local fracture criteria and toughening mechanisms. J. Biomech. 38, 1517–1525.

Nazarian, A., Müller, R., 2004. Time-lapsed microstructural imaging of bone failure behavior. J. Biomech. 37, 55–65.

Nicholson, P.H., Müller, R., Lowet, G., Cheng, X.G., Hildebrand, T., Rüegsegger, P., van der Perre, G., Dequeker, J., Boonen, S., 1998. Do quantitative ultrasound measurements reflect structure independently of density in human vertebral cancellous bone? Bone 23, 425–431.

Niebur, G.L., Feldstein, M.J., Yuen, J.C., Chen, T.J., Keaveny, T.M., 2000. High-resolution finite element models with tissue strength asymmetry accurately predict failure of trabecular bone. J. Biomech. 33, 1575–1583.

Nishiyama, K.K., Campbell, G.M., Klinck, R.J., Boyd, S.K., 2010. Reproducibility of bone micro-architecture measurements in rodents by in vivo micro-computed tomography is maximized with three-dimensional image registration. Bone 46, 155–161.

Nishiyama, K.K., Macdonald, H.M., Hanley, D.A., Boyd, S.K., 2013. Women with previous fragility fractures can be classified based on bone micro-architecture and finite element analysis measured with HR-pQCT. Osteoporos. Int. 24, 1733–1740.

Nuzzo, S., Lafage-Proust, M.H., Martín-Badosa, E., Boivin, G., Thomas, T., Alexandre, C., Peyrin, F., 2002. Synchrotron radiation microtomography allows the analysis of three- dimensional microarchitecture and degree of mineralization of human iliac crest biopsy specimens: effects of etidronate treatment. J. Bone Miner. Res. 17, 1372–1382.

Odgaard, A., 1997. Three-dimensional methods for quantification of cancellous bone architecture. Bone 20, 315–328.

Odgaard, A., Gundersen, H.J., 1993. Quantification of connectivity in cancellous bone, with special emphasis on 3-D reconstructions. Bone 14, 173–182.

Odgaard, A., Jensen, E.B., Gundersen, H.J., 1990. Estimation of structural anisotropy based on volume orientation. A new concept. J. Microsc. 157, 149–162.

Odgaard, A., Kabel, J., Van Rietbergen, B., Dalstra, M., Huiskes, R., 1997. Fabric and elastic principal directions of cancellous bone are closely related. J. Biomech. 30, 487–495.

Odgaard, A., Linde, F., 1991. The underestimation of Young's modulus in compressive testing of cancellous bone specimens. J. Biomech. 24, 691–698.

Panahifar, A., Maksymowych, W.P., Doschak, M.R., 2012. Potential mechanism of alendronate inhibition of osteophyte formation in the rat model of post-traumatic osteoarthritis: evaluation of elemental strontium as a molecular tracer of bone formation. Osteoarthritis Cartilage 20, 694–702.

Parfitt, A.M., Drezner, M.K., Glorieux, F.H., Kanis, J.A., Malluche, H., Meunier, P.J., Ott, S.M., Recker, R.R., 1987. Bone histomorphometry: standardization of nomenclature, symbols, and units. Report of the ASBMR histomorphometry nomenclature committee. J. Bone Miner. Res. 2, 595–610.

Parfitt, A.M., Mathews, C.H., Villanueva, A.R., Kleerekoper, M., Frame, B., Rao, D.S., 1983. Relationships between surface, volume, and thickness of iliac trabecular bone in aging and in osteoporosis. Implications for the microanatomic and cellular mechanisms of bone loss. J. Clin. Investig. 72, 1396–1409.

Pauchard, Y., Boyd, S.K., 2008. Landmark based compensation of patient motion artifacts in computed tomography. Proc. SPIE: Med. Imaging 6913, 69133C-69131–69133C-69110.

Pauchard, Y., Liphardt, A.M., Macdonald, H.M., Hanley, D.A., Boyd, S.K., 2012. Quality control for bone quality parameters affected by subject motion in high-resolution peripheral quantitative computed tomography. Bone 50, 1304–1310.

Paulus, M.J., Gleason, S.S., Easterly, M.E., Foltz, C.J., 2001. A review of high-resolution X-ray computed tomography and other imaging modalities for small animal research. Lab. Anim. (NY) 30, 36–45.

Peters, O.A., Laib, A., Ruegsegger, P., Barbakow, F., 2000. Three-dimensional analysis of root canal geometry by high-resolution computed tomography. J. Dent. Res. 79, 1405–1409.

Pettit, A.R., Ji, H., von Stechow, D., Müller, R., Goldring, S.R., Choi, Y., Benoist, C., Gravallese, E.M., 2001. TRANCE/RANKL knockout mice are protected from bone erosion in a serum transfer model of arthritis. Am. J. Pathol. 159, 1689–1699.

Pialat, J.B., Burghardt, A.J., Sode, M., Link, T.M., Majumdar, S., 2012. Visual grading of motion induced image degradation in high resolution peripheral computed tomography: impact of image quality on measures of bone density and micro-architecture. Bone 50, 111–118.

Porter, B., Zauel, R., Stockman, H., Guldberg, R., Fyhrie, D., 2005. 3-D computational modeling of media flow through scaffolds in a perfusion bioreactor. J. Biomech. 38, 543–549.

Razi, H., Birkhold, A.I., Weinkamer, R., Duda, G.N., Willie, B.M., Checa, S., 2015. Aging leads to a dysregulation in mechanically driven bone formation and resorption. J. Bone Miner. Res. 30, 1864–1873.

Rice, J.C., Cowin, S.C., Bowman, J.A., 1988. On the dependence of the elasticity and strength of cancellous bone on apparent density. J. Biomech. 21, 155–168.

Ritman, E.L., 2004. Micro-computed tomography—current status and developments. Annu. Rev. Biomed. Eng. 6, 185–208.

Rittweger, J., Beller, G., Ehrig, J., Jung, C., Koch, U., Ramolla, J., Schmidt, F., Newitt, D., Majumdar, S., Schiessl, H., Felsenberg, D., 2000. Bone-muscle strength indices for the human lower leg. Bone 27, 319–326.

Rittweger, J., Frost, H.M., Schiessl, H., Ohshima, H., Alkner, B., Tesch, P., Felsenberg, D., 2005. Muscle atrophy and bone loss after 90 days' bed rest and the effects of flywheel resistive exercise and pamidronate: results from the LTBR study. Bone 36, 1019–1029.

Ruegsegger, P., Keller, A., Dambacher, M.A., 1995. Comparison of the treatment effects of ossein-hydroxyapatite compound and calcium-carbonate in osteoporotic females. Osteoporos. Int. 5, 30–34.

Rüegsegger, P., Koller, B., Müller, R., 1996. A microtomographic system for the nondestructive evaluation of bone architecture. Calcif. Tissue Int. 58, 24–29.

Salome, M., Peyrin, F., Cloetens, P., Odet, C., Laval-Jeantet, A.M., Baruchel, J., Spanne, P., 1999. A synchrotron radiation microtomography system for the analysis of trabecular bone samples. Med. Phys. 26, 2194–2204.

Samelson E.J., Broe K.E., Xu H., Yang L., Boyd S., Biver E., Szulc P., Adachi J., Amin S., Atkinson E., Berger C., Burt L., Chapurlat R., Chevalley T., Ferrari S., Goltzman D., Hanley D.A., Hannan M.T., Khosla S., Liu C.T., Lorentzon M., Mellstrom D., Merle B., Nethander M., Rizzoli R., Sornay-Rendu E., Van Rietbergen B., Sundh D., Wong A.K.O., Ohlsson C., Demissie S., Kiel D.P., Bouxsein M.L. 2019. Cortical and trabecular bone microarchitecture as an independent predictor of incident fracture risk in older women and men in the Bone Microarchitecture International Consortium (BoMIC): a prospective study. Lancet Diabetes Endocrinol. 7, 34–43

Sasaki, H., Hou, L., Belani, A., Wang, C.Y., Uchiyama, T., Müller, R., Stashenko, P., 2000. IL-10, but not IL-4, suppresses infection-stimulated bone resorption in vivo. J. Immunol. 165, 3626–3630.

Scafoglieri, A., Provyn, S., Wallace, J., Louis, O., Tresignie, J., Bautmans, I., 2011. Whole body composition by hologic QDR 4500/A DXA system: system reliability versus user accuracy and precision. In: Ivanov, O. (Ed.), Applications and Experiences of Quality Control. InTech, pp. 45–62.

Schneider, P., Stauber, M., Voide, R., Stampanoni, M., Donahue, L.R., Müller, R., 2007. Ultrastructural properties in cortical bone vary greatly in two inbred strains of mice as assessed by synchrotron light based micro- and nano-CT. J. Bone Miner. Res. 22, 1557–1570.

Schneider, P.F., Fischer, M., Allolio, B., Felsenberg, D., Schroder, U., Semler, J., Ittner, J.R., 1999. Alendronate increases bone density and bone strength at the distal radius in postmenopausal women. J. Bone Miner. Res. 14, 1387–1393.

Schulte, F.A., Lambers, F.M., Kuhn, G., Müller, R., 2011. In vivo micro-computed tomography allows direct three-dimensional quantification of both bone formation and bone resorption parameters using time-lapsed imaging. Bone 48, 433–442.

Schulte, F.A., Lambers, F.M., Mueller, T.L., Stauber, M., Müller, R., 2014. Image interpolation allows accurate quantitative bone morphometry in registered micro-computed tomography scans. Comput. Methods Biomech. Biomed. Eng. 17, 539–548.

Schulte, F.A., Ruffoni, D., Lambers, F.M., Christen, D., Webster, D.J., Kuhn, G., Müller, R., 2013. Local mechanical stimuli regulate bone formation and resorption in mice at the tissue level. PLoS One 8, e62172.

Seeman, E., Delmas, P.D., 2006. Bone quality—the material and structural basis of bone strength and fragility. N. Engl. J. Med. 354, 2250–2261.

Sornay-Rendu, E., Boutroy, S., Duboeuf, F., Chapurlat, R.D., 2017. Bone microarchitecture assessed by HR-pQCT as predictor of fracture risk in postmenopausal women: the OFELY study. J. Bone Miner. Res. 32, 1243–1251.

Sornay-Rendu, E., Boutroy, S., Munoz, F., Delmas, P.D., 2007. Alterations of cortical and trabecular architecture are associated with fractures in postmenopausal women, partially independent of decreased BMD measured by DXA: the OFELY study. J. Bone Miner. Res. 22, 425–433.

Sornay-Rendu, E., Cabrera-Bravo, J.L., Boutroy, S., Munoz, F., Delmas, P.D., 2009. Severity of vertebral fractures is associated with alterations of cortical architecture in postmenopausal women. J. Bone Miner. Res. 24, 737–743.

Stampanoni, M., Borchert, G., Abela, R., Rüegsegger, P., 2003. Nanotomography based on double asymmetrical Bragg diffraction. Appl. Phys. Lett. 82, 2922–2924.

Stauber, M., Müller, R., 2006. Volumetric spatial decomposition of trabecular bone into rods and plates—a new method for local bone morphometry. Bone 38, 475–484.

Stauber, M., Müller, R., 2008. Micro-computed tomography: a method for the non-destructive evaluation of the three-dimensional structure of biological specimens. Methods Mol. Biol. 455.

Stauber, M., Rapillard, L., van Lenthe, G.H., Zysset, P., Müller, R., 2006. Importance of individual rods and plates in the assessment of bone quality and their contribution to bone stiffness. J. Bone Miner. Res. 21, 586–595.

Stein, E.M., Liu, X.S., Nickolas, T.L., Cohen, A., Thomas, V., McMahon, D.J., Zhang, C., Yin, P.T., Cosman, F., Nieves, J., Guo, X.E., Shane, E., 2010. Abnormal microarchitecture and reduced stiffness at the radius and tibia in postmenopausal women with fractures. J. Bone Miner. Res. 25, 2572–2581.

Taiani, J.T., Buie, H.R., Campbell, G.M., Manske, S.L., Krawetz, R.J., Rancourt, D.E., Boyd, S.K., Matyas, J.R., 2014. Embryonic stem cell therapy improves bone quality in a model of impaired fracture healing in the mouse; tracked temporally using in vivo micro-CT. Bone 64, 263–272.

Takagi, Y., Fujii, Y., Miyauchi, A., Goto, B., Takahashi, K., Fujita, T., 1995. Transmenopausal change of trabecular bone density and structural pattern assessed by peripheral quantitative computed tomography in Japanese women. J. Bone Miner. Res. 10, 1830–1834.

Tenenhouse, A., Joseph, L., Kreiger, N., Poliquin, S., Murray, T.M., Blondeau, L., Berger, C., Hanley, D.A., Prior, J.C., 2000. Estimation of the prevalence of low bone density in Canadian women and men using a population-specific DXA reference standard: the Canadian multicentre osteoporosis study (CaMos). Osteoporos. Int. 11, 897–904.

Thurner, P.J., Erickson, B., Jungmann, R., Schriock, Z., Weaver, J.C., Fantner, G.E., Schitter, G., Morse, D.E., Hansma, P.K., 2007. High-speed photography of compressed human trabecular bone correlates whitening to microscopic damage. Eng. Fract. Mech. 74, 1928–1941.

Thurner, P.J., Wyss, P., Voide, R., Stauber, M., Stampanoni, M., Sennhauser, U., Müller, R., 2006. Time-lapsed investigation of three-dimensional failure and damage accumulation in trabecular bone using synchrotron light. Bone 39, 289–299.

Turner, C.H., Burr, D.B., 1993. Basic biomechanical measurements of bone: a tutorial. Bone 14, 595–608.

Turner, C.H., Hsieh, Y.F., Müller, R., Bouxsein, M.L., Baylink, D.J., Rosen, C.J., Grynpas, M.D., Donahue, L.R., Beamer, W.G., 2000. Genetic regulation of cortical and trabecular bone strength and microstructure in inbred strains of mice. J. Bone Miner. Res. 15, 1126–1131.

Uchiyama, T., Tanizawa, T., Muramatsu, H., Endo, N., Takahashi, H.E., Hara, T., 1997. A morphometric comparison of trabecular structure of human ilium between microcomputed tomography and conventional histomorphometry. Calcif. Tissue Int. 61, 493–498.

Ulrich, D., van Rietbergen, B., Laib, A., Ruegsegger, P., 1999. The ability of three-dimensional structural indices to reflect mechanical aspects of trabecular bone. Bone 25, 55–60.

Van Rietbergen, B., Odgaard, A., Kabel, J., Huiskes, R., 1998. Relationships between bone morphology and bone elastic properties can be accurately quantified using high-resolution computer reconstructions. J. Orthop. Res. 16, 23–28.

van Rietbergen, B., Weinans, H., Huiskes, R., Odgaard, A., 1995. A new method to determine trabecular bone elastic properties and loading using micromechanical finite-element models. J. Biomech. 28, 69–81.

Vico, L., Zouch, M., Amirouche, A., Frere, D., Laroche, N., Koller, B., Laib, A., Thomas, T., Alexandre, C., 2008. High-resolution pQCT analysis at the distal radius and tibia discriminates patients with recent wrist and femoral neck fractures. J. Bone Miner. Res. 23, 1741–1750.

Vilayphiou, N., Boutroy, S., Sornay-Rendu, E., Van Rietbergen, B., Munoz, F., Delmas, P.D., Chapurlat, R., 2010. Finite element analysis performed on radius and tibia HR-pQCT images and fragility fractures at all sites in postmenopausal women. Bone 46, 1030–1037.

Vilayphiou, N., Boutroy, S., Szulc, P., van Rietbergen, B., Munoz, F., Delmas, P.D., Chapurlat, R., 2011. Finite element analysis performed on radius and tibia HR-pQCT images and fragility fractures at all sites in men. J. Bone Miner. Res. 26, 965–973.

Voide, R., Van Lenthe, G.H., Stauber, M., Schneider, P., Thurner, P., Wyss, P., Stampanoni, M., Mueller, R., 2008. Functional microimaging: a hierarchical investigation of bone failure behavior. J. Jpn. Soc. Bone Morphom. 9–21.

Waarsing, J.H., Day, J.S., van der Linden, J.C., Ederveen, A.G., Spanjers, C., De Clerck, N., Sasov, A., Verhaar, J.A., Weinans, H., 2004. Detecting and tracking local changes in the tibiae of individual rats: a novel method to analyse longitudinal in vivo micro-CT data. Bone 34, 163–169.

Wehrli, F.W., 2007. Structural and functional assessment of trabecular and cortical bone by micro magnetic resonance imaging. J. Magn. Reson. Imaging 25, 390–409.

Wehrli, F.W., Gomberg, B.R., Saha, P.K., Song, H.K., Hwang, S.N., Snyder, P.J., 2001a. Digital topological analysis of in vivo magnetic resonance microimages of trabecular bone reveals structural implications of osteoporosis. J. Bone Miner. Res. 16, 1520–1531.

Wehrli, F.W., Hwang, S.N., Ma, J., Song, H.K., Ford, J.C., Haddad, J.G., 1998. Cancellous bone volume and structure in the forearm: noninvasive assessment with MR microimaging and image processing. Radiology 206, 347–357.

Wehrli, F.W., Hwang, S.N., Song, H.K., Gomberg, B.R., 2001b. Visualization and analysis of trabecular bone architecture in the limited spatial resolution regime of in vivo micro-MRI. Adv. Exp. Med. Biol. 496, 153–164.

Weiner, S., Traub, W., Wagner, H.D., 1999. Lamellar bone: structure-function relations. J. Struct. Biol. 126, 241–255.

Weiss, D., Schneider, G., Niemann, B., Guttmann, P., Rudolph, D., Schmahl, G., 2000. Computed tomography of cryogenic biological specimens based on X-ray microscopic images. Ultramicroscopy 84, 185–197.

Whitehouse, W.J., 1974. The quantitative morphology of anisotropic trabecular bone. J. Microsc. 101, 153–168.

Williams, J.L., Lewis, J.L., 1982. Properties and an anisotropic model of cancellous bone from the proximal tibial epiphysis. J. Biomech. Eng. 104, 50–56.

Williams, J.M., Adewunmi, A., Schek, R.M., Flanagan, C.L., Krebsbach, P.H., Feinberg, S.E., Hollister, S.J., Das, S., 2005. Bone tissue engineering using polycaprolactone scaffolds fabricated via selective laser sintering. Biomaterials 26, 4817–4827.

Yamashita, T., Nabeshima, Y., Noda, M., 2000. High-resolution micro-computed tomography analyses of the abnormal trabecular bone structures in klotho gene mutant mice. J. Endocrinol. 164, 239–245.

Yang, G., Kabel, J., van Rietbergen, B., Odgaard, A., Huiskes, R., Cowin, S.C., 1998. The anisotropic Hooke's law for cancellous bone and wood. J. Elast. 53, 125–146.

Yoshitake, H., Rittling, S.R., Denhardt, D.T., Noda, M., 1999. Osteopontin-deficient mice are resistant to ovariectomy-induced bone resorption. Proc. Natl. Acad. Sci. U. S. A. 96, 8156–8160.

Zebaze, R., Ghasem-Zadeh, A., Mbala, A., Seeman, E., 2013. A new method of segmentation of compact-appearing, transitional and trabecular compartments and quantification of cortical porosity from high resolution peripheral quantitative computed tomographic images. Bone 54, 8–20.

Zeltinger, J., Sherwood, J.K., Graham, D.A., Müller, R., Griffith, L.G., 2001. Effect of pore size and void fraction on cellular adhesion, proliferation, and matrix deposition. Tissue Eng. 7, 557–572.

Chapter 80

Macroimaging

Klaus Engelke[1,2], **Harry K. Genant**[3] and **James Griffith**[4]

[1]Department of Medicine, FAU University Erlangen-Nürnberg and Universitätsklinikum Erlangen, Erlangen, Germany; [2]Bioclinica, Hamburg, Germany; [3]Departments of Radiology and Medicine, University of California, San Francisco, CA, United States; [4]Department of Imaging and Interventional Radiology, The Chinese University of Hong Kong, Hong Kong, China

Chapter outline

Introduction

In vivo imaging of bone in the context of osteoporosis primarily refers to radiographs for fracture assessment and dual-energy X-ray absorptiometry (DXA) and quantitative computed tomography (QCT) to quantify bone mineral density (BMD). For the clinician, radiographs and DXA are the main imaging techniques to support the diagnosis of osteoporosis, to assess the risk of osteoporotic fracture, and to monitor the effectiveness of intervention. Today about 50−100 patients with osteoporosis must be treated to prevent one fracture (Albert and Reddy, 2017), while about 50% of subjects who do fracture do not have osteoporosis as judged by DXA analysis using World Health Organization (WHO) criteria (Schuit et al., 2004; Siris et al., 2004).

Many different avenues have been pursued to improve fracture risk prediction and to better identify high-risk patients. One approach is the 3D quantification of trabecular architecture, initially imaged in samples of trabecular bone using micro-computed tomography (micro-CT). Nowadays trabecular architecture can be directly measured in vivo in the peripheral skeleton. In the spine and hip, in vivo CT- and DXA-based techniques are being explored to determine bone texture as a surrogate for bone microarchitecture because the spatial resolution achievable in the central skeleton is not adequate to separate individual trabeculae.

An exciting development is so-called opportunistic screening, which utilizes existing CT examinations obtained for various diagnostic purposes, such as routine abdominal or thorax examinations performed in every radiological department. These examinations may be used for detection of vertebral fractures and to quantify BMD either of the hip or of the spine. However, since these scans are not obtained using routine QCT protocols appropriate BMD calibration routines must be used.

Principles of Bone Biology. https://doi.org/10.1016/B978-0-12-814841-9.00080-4

A different approach is the determination of bone strength by CT-based finite element analysis (FEA), a method originally developed to solve complex elasticity and structural analysis problems in civil and aeronautical engineering. With respect to bone strength FEA combines the distribution of BMD with the geometry of a given bone. Individual components contributing to bone strength, such as cortical thickness, moments of inertia, and other geometrical measures, can also directly be measured by CT or estimated from DXA scans. Of course, with CT cancellous (also referred to as trabecular) and cortical bone can be assessed separately.

More recently, advanced statistical methods in combination with progress in computational power have facilitated analytic approaches such as voxel-based and tensor-based morphometry methods, cortical thickness mapping, and statistical shape analysis. These approaches were originally developed to distinguish pathologic brain anatomy from the wide range of normal variations (Li et al., 2009; Toga and Thompson, 2002). Recent efforts have extended this approach to spinal radiography and CT examinations of the hip and spine, spatially heterogeneous skeletal sites with large subject-specific density and geometric variations.

Magnetic resonance imaging (MRI) has been used for imaging of trabecular architecture in the wrist and calcaneus in the past, but due to rather complicated scan protocols not routinely available on most magnetic resonance (MR) systems and long scan times, it has largely been replaced by high-resolution peripheral QCT (HR-pQCT). More recently, MRI has been used to quantify cortical water and to differentiate it into components of bound water, characterizing collagen content, and free water, characterizing cortical porosity. Another application is imaging of marrow fat content and composition, marrow perfusion, and marrow molecular diffusion (Griffith, 2017).

Another interesting development is imaging of muscle as a reflection of systemic disorders. The main application is in frailty, cachexia, and sarcopenia, but the paradigm of the bone−muscle unit has triggered expanding research into the relation of muscle properties and fractures. Of course it is of high interest whether parameters describing muscle and the distribution of muscle and adipose tissue in general can improve fracture risk prediction of BMD.

Radiography

Radiography is the most widely available, noninvasive technique of visualizing bone structure. The term osteopenia, "paucity of bone," is used to describe visually decreased bone density—or radiolucency—on radiographs. Thus, it also provides qualitative information on bone density. However, radiographs are rather insensitive to changes in BMD. In the spine, for example, it has been estimated that as much as 20%−40% of bone mass must be lost before a decrease in bone visual density can be seen in lateral spine radiographs. The decrease in density is primarily a result of a decrease in mineralized bone volume since in osteoporosis and osteopenia the amount of calcium per unit of mineralized bone volume remains constant at about 35%. Alone or in conjunction with other advanced imaging techniques, radiography is still widely used to diagnose osteoporotic fractures and to differentiate various disorders associated with osteoporosis and osteomalacia.

Changes in the axial skeleton and the ends of the long tubular bones are most prominent, since these sites have a relatively greater proportion of trabecular bone. Trabecular bone has more surface and responds more quickly than cortical bone. As bone mineral is lost, non-weight-bearing connecting trabeculae are resorbed first, leaving the remaining weight-bearing trabeculae more widely separated. Some may undergo compensatory thickening in the direction of mechanical stress. Trabecular anisotropy increases, resulting in distinct patterns on radiographs, such as the organized sequential trabecular changes along the compressive and tensile stress in the proximal femur and an appearance of vertical striation in the lumbar spine in the early stages of osteopenia caused by rarefaction of the horizontal trabeculae and a relative reinforcement of the vertical trabeculae (Fig. 80.1). At a later stage, vertebrae may appear on radiographs as a "picture frame" or as an "empty box" because of accentuation of the cortical margins surrounding the lucent trabecular center. Osteopenic vertebrae may also demonstrate increased bioconcavity of the vertebral end plates owing to protrusion of the intervertebral disk into the weakened vertebral body.

Vertebral fracture, the hallmark of osteoporosis, has a wide range of morphologic appearances, from increased concavity of the end plates, anterior wedging, to a complete destruction of the vertebral morphology in vertebral crush fractures (Fig. 80.2). Fractures can be graded by radiologists or experienced clinicians and quantified with morphometric methods to reduce the subjectivity inherent in grading (Genant et al., 1996; Wu et al., 2000). The Genant semiquantitative scoring method (Genant et al., 1993; Lentle et al., 2007) shown in Fig. 80.3 grades 0 for normal, 1 for mildly deformed (20%−25% reduction in anterior, middle, and/or posterior height, and 10%−20% reduction in the projected area of the vertebral body), 2 for moderately deformed (25%−40% reduction in height, and 20%−40% in area), and 3 for severely deformed (40% or greater reduction in height and in area). This method offers high reproducibility (Wu et al., 2000). It has been widely used to evaluate fracture end points in most epidemiological and clinical studies investigating the efficacy of osteoporotic drugs (Black et al., 2007; Boonen et al., 2011; Ettinger et al., 1999; Genant et al., 2005; Grados et al., 2004).

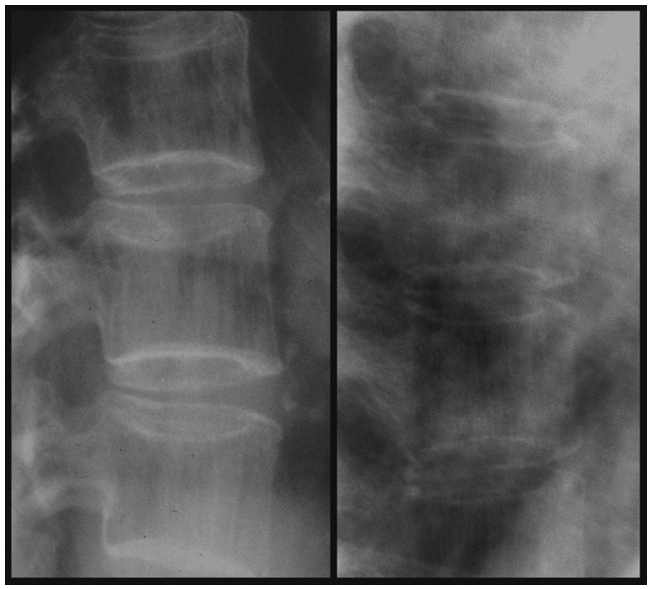

FIGURE 80.1 (Left) Increased vertical striation due to the proportionally greater loss of horizontal trabeculae and compensatory hypertrophy of the vertical trabeculae. (Right) Severe osteoporosis: the vertebrae can hardly be distinguished on the lateral lumbar spine radiograph. There are multiple end-plate and compression fractures.

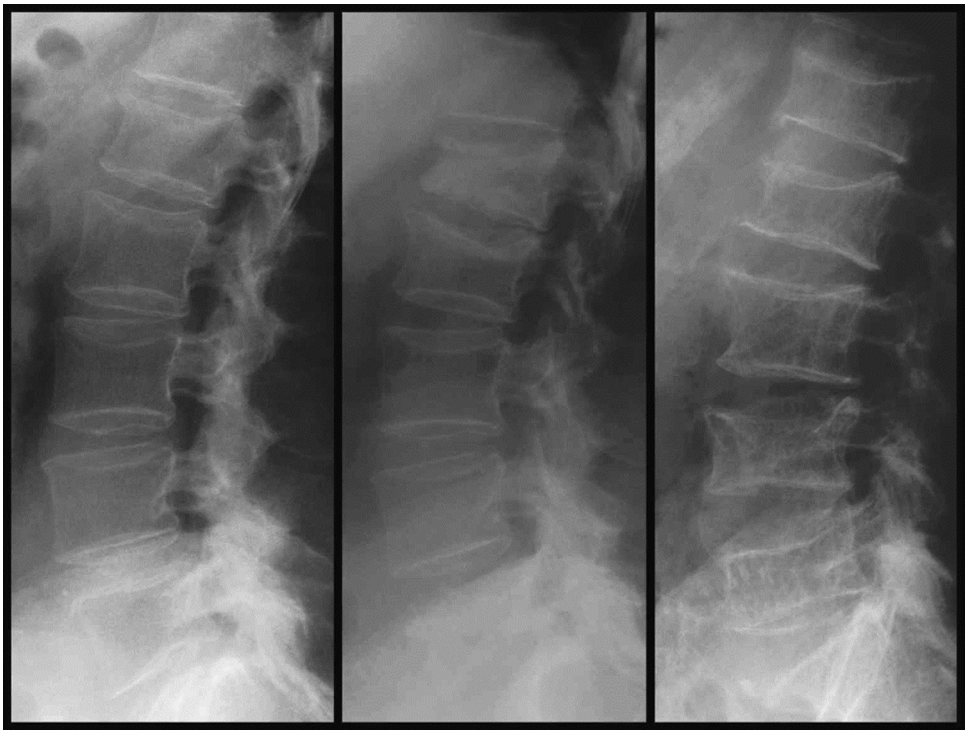

FIGURE 80.2 Multiple fractures in the thoracic spine in advanced involutional osteoporosis, including (left) end-plate, (middle) wedge, and (right) compression fractures.

Of most concern in osteoporosis are fractures of the hips, spine, and wrists. Changes in the bone cortex or spongiosa may make such injuries more likely to occur. Fractures of the vertebral bodies are a result of predominantly axial compressive loads. One reason for the decreased load-bearing capacity is the increased absorption and removal of the horizontal trabeculae or lateral support cross-ties (Mosekilde et al., 1985). The vertical trabecular bone, therefore, behaves as a column and is prone to critical buckling loads (Townsend et al., 1975). A 50% decrease in cross-sectional area (CSA)

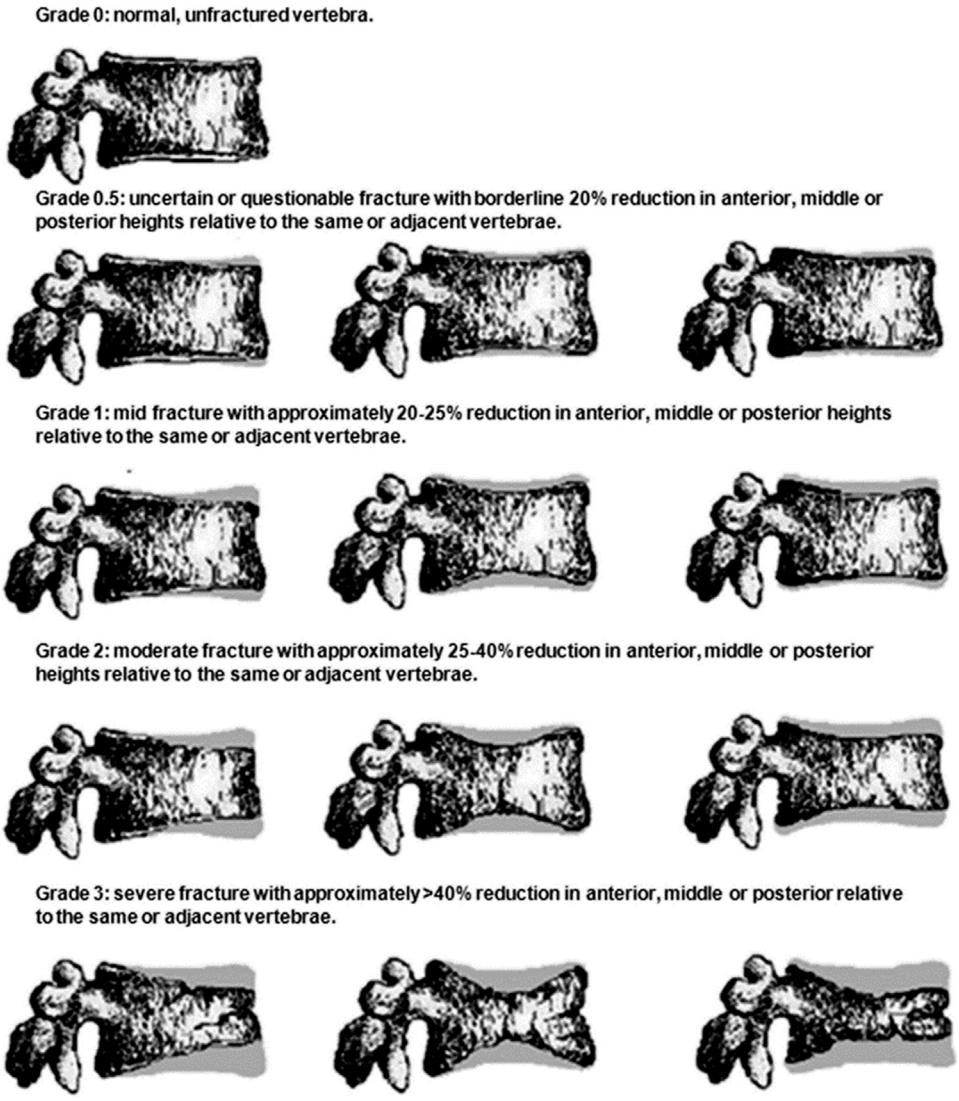

FIGURE 80.3 The Genant grading method for a semiquantitative evaluation of osteoporotic vertebral fracture grades: fracture severity from normal (grade 0) to severe deformity (grade 3). The scoring scheme illustrates reductions in the anterior height that correspond to the grade of deformity. Reductions in the middle or posterior heights or combinations thereof can be evaluated accordingly.

as a result of absorption of the horizontal trabeculae is associated with a 75% decrease in the load-bearing capacity of the vertebral body (Einhorn, 1992).

In the hip and forearm, radiographs are typically used to diagnose a fracture. Quantitative grading has not gained much attention, although in the hip the Singh index has been developed to grade differences in the trabecular pattern (Singh et al., 1973). The trabecular compartment is of interest because osteoporotic fractures of the hip and the forearm typically occur in trabecular-rich locations: at the neck and trochanter region of the hip and at the ultradistal site of the radius, whereas osteoporotic fractures are much less frequent in the shaft, where bone strength depends only on compact bone (Smith and Smith, 1976).

Standard DXA

DXA technique

DXA is the most widely used technique to determine areal BMD (aBMD) of the central (spine and hip, Fig. 80.4) and peripheral (forearm) skeleton. Further routine applications include whole-body measurements to assess aBMD and soft-

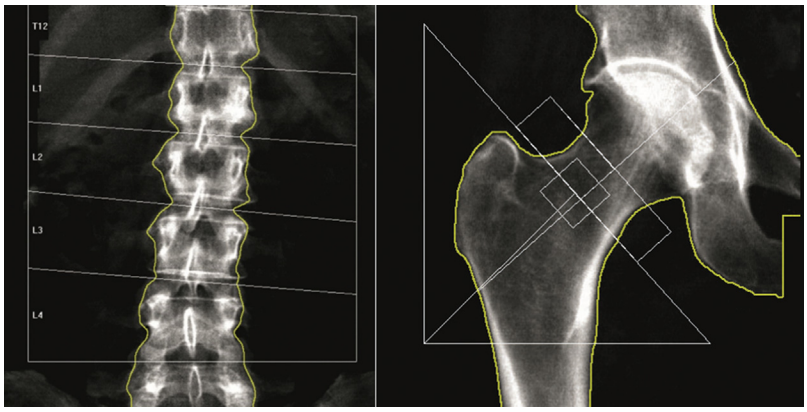

FIGURE 80.4 Dual-energy X-ray absorptiometry. (Left) Spine scan. (Right) Hip scan.

tissue composition of various body segments as well as vertebral fracture assessment (VFA) of the spine. DXA has emerged as the gold standard for the diagnosis of osteoporosis, fracture risk assessment, and monitoring of age-, disease-, and treatment-related changes in aBMD. DXA has been used in all major epidemiological studies on fracture risk and in almost all clinical trials to monitor the longitudinal effectiveness of pharmacological treatment of osteoporosis. Other reasons that made DXA a success were low precision errors; early commercialization, which provided wide accessibility to DXA equipment; ease of use; standardization across DXA manufacturers; and the availability of reference data from a large variety of different populations. The basic DXA technology has not changed significantly since 2009, and most technical reviews were published some years ago (Blake and Fogelman, 1997; Kalender et al., 2009). Recommendations on the clinical use of DXA are periodically updated by the International Society for Clinical Densitometry (ISCD) and other national and international organizations (Verdijk et al., 2009; Crabtree et al., 2014; Camacho et al., 2016).

DXA is a projection technique to determine aBMD in grams per square centimeter. aBMD is measured in a segmented area termed the region of interest (ROI). Bone mineral content (BMC) is then derived as aBMD × area. The projection approach is associated with a number of technical limitations. The bone dimension perpendicular to the projected area, i.e., the true bone volume, is not considered. This complicates, for example, longitudinal BMD monitoring in children because of bone growth (Adams et al., 2014). A larger problem in elderly subjects is degenerative and hypertrophic changes in the spine, which typically result in an overestimation of vertebral aBMD (Rand et al., 1997). In the hip, differences in the rotation of the leg relative to the scanner table have an impact on aBMD and dedicated positioning devices ensuring constant leg rotation should be used (Rosenthall, 2004; Goh et al., 1995). Frequently the acetabulum overlaps with the proximal neck; thus in DXA only a small neck box positioned either in the center of the neck or adjacent to the greater trochanter is analyzed as the neck ROI.

Experienced DXA operators achieve short-term in vivo precision errors of about 1%−1.5% in the spine and 1.5%−2% in the hip. Long-term errors are 30%−50% higher (Fan et al., 2008; Tothill and Hannan, 2007). In individual patients longitudinal changes are significant if they are larger than the least significant change defined as 2.7 × precision error. Based on in situ measurements and on simulations, accuracy errors of up to 30% have been reported (Hagiwara et al., 1994; Sabin et al., 1995; Bolotin, 2001). Accuracy errors arise from the heterogeneous distribution of adipose tissue external to bone and variations in marrow, obesity, beam hardening, scatter (Kalender et al., 2009), and potentially intake of strontium ranelate (Blake and Fogelman, 2007). Accuracy errors primarily affect the diagnosis of osteoporosis. In longitudinal measurements they are of concern if long-term precision is affected by changes in inaccuracy between measurements of a given patient. One example of such an effect is severe weight change in obese patients after bariatric surgery (Ko et al., 2016; Yu et al., 2014; Rajamanohara et al., 2011).

aBMD figures obtained from DXA scanners of different manufacturers are highly correlated, but differences in BMD calibration materials cause a bias of up to 10% in aBMD. Standardization efforts have suggested using a standardized aBMD (sBMD) to correct this bias (Genant et al., 1994; Shepherd et al., 2002), but in clinical practice the use of T scores and standardized reference data has replaced sBMD. T scores express an aBMD result in terms of standard deviations (STD) relative to aBMD of a young normal (YN) reference population:

$$\text{T score} = \frac{\text{aBMD} - \text{aBMD}_{\text{YN}}}{\text{STD}_{\text{YN}}}$$

For the hip, the use of the NHANES III reference data (Looker et al., 1997) is suggested. DXA T scores are also the basis for the operational WHO definition of osteoporosis (WHO, 1994). T scores of the hip are used in the FRAX algorithm (http://www.shef.ac.uk/FRAX) for calculation of fracture risk (Kanis et al., 2009; Lewiecki et al., 2011). There are no universal reference data for spine or forearm DXA, typically manufacturer-specific reference values are used. The use of T scores and reference data decreases the clinical impact of aBMD accuracy errors because any constant bias is eliminated. The remaining accuracy errors will increase the standard deviation of the normal population, thus lowering the T score (Blake and Fogelman, 2008). Accuracy errors of a given aBMD measurement that largely differ from those inherent in the reference population will affect the diagnosis of an individual patient. There is a vast body of literature on discordance between spine and hip T scores and on the use of gender-, ethnic-, and country-specific reference data, but a more detailed discussion is beyond the scope of this chapter.

Fracture prediction using areal bone mineral density

One of the important clinical advantages of DXA compared with other types of bone density measurements is that its ability to identify patients at risk of fracture has been assessed and proven in a large number of epidemiological studies (Johnell et al., 2005; Stone et al., 2003; Marshall et al., 1996). The Marshall meta-analysis (Marshall et al., 1996), which included women only, was based on more than 2000 osteoporotic fractures from 90,000 person-years of follow-up. Different BMD measurement sites showed similar abilities to predict fractures (relative risk [RR] 1.5; 95% confidence interval [CI] 1.4−1.6), with the exception of hip BMD predicting hip fractures (RR 2.6; CI 2.0−3.5) and spine BMD predicting vertebral fractures (RR 2.3; CI 1.9−2.8). The authors concluded that hip and spine BMD values were the best measurements for predicting hip and spine fractures, respectively. The Johnell meta-analysis (Johnell et al., 2005) included both men and women and was based on 971 hip fractures from 168,000 person-years of follow-up from 12 different fracture studies from Australia, Canada, Europe, and Japan. There was no significant difference in hip fracture risk between men and women (women: RR 2.2; CI 2.0−2.4; men: RR 2.3; CI 1.8−2.9). The RR decreased progressively with increasing age, varying from an RR of 3.7 (CI 2.6−5.2) at age 50 to an RR of 1.9 (CI 1.8−2.1) at age 85. A 2017 study showed that hip aBMD was a persistent long-term predictor of hip (relative hazard per standard deviation (RH/SD) 2.6; CI 2.2−3.0 for 0−5 years, to RH/SD 1.8; CI 1.4−2.4 for 20−25 years) and nonvertebral fracture (Black et al., 2017). Of course in clinical practice, BMD is combined with other factors for a comprehensive fracture risk assessment (Johansson et al., 2009; Krege et al., 2013; Siris et al., 2007; Robbins et al., 2005).

Monitoring osteoporosis treatment with DXA

Measurement of aBMD was part of almost all clinical trials investigating the efficacy of osteoporosis treatments. Interestingly, the relationship between gains in aBMD and reduction in fracture risk is still a topic of investigation (Cummings et al., 2002; Delmas et al., 2004; Hochberg et al., 2002). In particular for antiresorptive drugs, small aBMD increases of below 10% are associated with a 50% or even higher reduction of vertebral fractures. At the study level, the relationship appears to be robust. However, for the individual patient, aBMD seems not to be a strong predictor of effects of osteoporosis treatment on fracture risk, questioning the utility of serial BMD measurements to assess treatment efficacy (Compston, 2009). In contrast, a more recent study reported that on a patient level, the change in total hip BMD explained 35% (CI 20%−61%) of the treatment effect with denosumab in reducing new or worsening vertebral fracture risk and 87% (CI 35%−100%) in reducing nonvertebral fracture risk (Austin et al., 2012).

Vertebral fracture assessment

VFA is a special DXA analysis to detect spinal fractures from a lateral image of the spine. The main advantage of VFA compared with radiography is the much lower radiation exposure and the possibility of adding a quick VFA scan after a standard aBMD assessment. The main disadvantage is the lower spatial resolution of VFA. In the absence of scoliosis, VFA compared favorably with standard spine radiography for diagnosis of moderate and severe vertebral fractures. In women over the age of 65 years, a sensitivity of 87%−93% and a specificity of 93%−95% was reported (Schousboe and Debold, 2006), but sensitivity dropped significantly for mild vertebral fractures. Also visualization of vertebral levels T4−T7 is often poor (Rea et al., 2000). Thus VFA does not replace radiography but its integration into the workflow for diagnosis of osteoporosis would help to detect many fractures that remain unnoticed otherwise (Zeytinoglu et al., 2017). This is important as in particular moderate or severe vertebral fractures present a high risk factor for the risk of future fractures (Black et al., 1999).

Computed tomography

CT is an X-ray-based technique that generates a cross-sectional image of so-called CT values, measured in Hounsfield units (HU), i.e., a map of the X-ray absorption coefficient calibrated to water. QCT denotes the specific method to quantify BMD on CT images, which requires a second calibration from CT to BMD values (Kalender et al., 2009; Genant et al., 1982). Since the early development of QCT to measure trabecular BMD in single transverse CT slices at the lumbar midvertebral levels and the distal forearm, proponents of QCT have always claimed its superiority over DXA. A true measurement of physical density in grams per square centimeter must be better than the measurement of aBMD in grams per square centimeter. Also, trabecular and cortical bone compartments can be separately assessed by QCT.

Standard quantitative computed tomography to assess bone mineral density

aBMD of the spine and hip are strong predictors of future fracture risk but still not strong enough to predict whether an individual patient will eventually fracture. aBMD is a surrogate parameter and its assessment does not differentiate pathophysiological causes for low BMD. In addition, aBMD has limitations to characterizing bone status under treatment. Since the late 1990s, one important focus of the technical development of QCT and of advanced techniques based on QCT such as FEA was the compensation for DXA deficiencies.

Volumetric QCT of the spine and hip (Fig. 80.5) is now an established technique widely used in research studies and clinical trials and also increasingly in clinical routine with precision errors comparable to DXA (Engelke et al., 2009; Lang et al., 1997; Museyko et al., 2016). Early single-slice peripheral QCT (pQCT) of the forearm or tibia is now mostly restricted to use in children (Adams et al., 2014). Table 80.1 summarizes recommendations of the ISCD on the clinical use

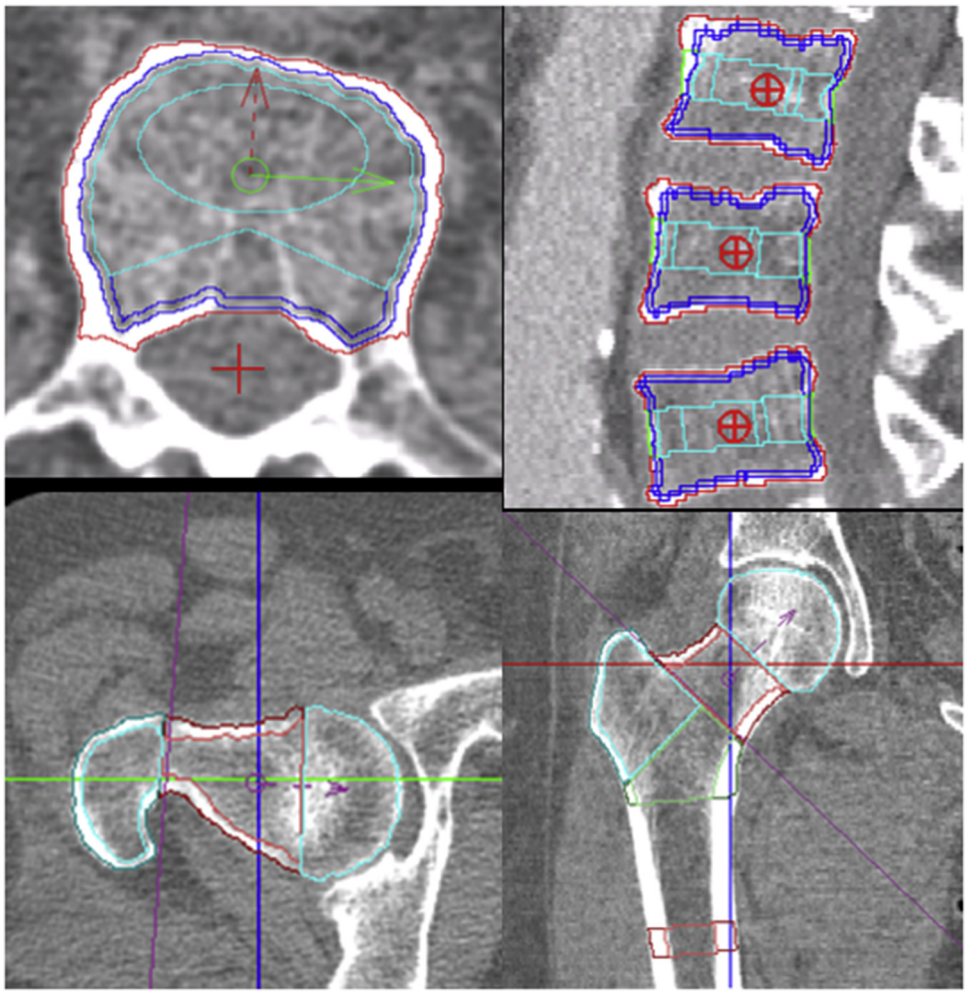

FIGURE 80.5 Advanced 3D quantitative computed tomography at spine and hip (slice thickness 1 mm, in-plane resolution 300 μm) to analyze regional bone mineral density and geometry such as cortical thickness. Left axial, right coronal multi-planar reformations of 3D data sets.

TABLE 80.1 Official positions for women of the International Society of Clinical Densitometry on clinical utility of dual-energy X-ray absorptiometry and quantitative computed tomography.

	Location	Diagnosis of osteoporosis	Site-matched fracture prediction	Monitoring age-related changes	Monitoring treatment effects	Initialization of treatment
Integral BMD	Spine	No		0[b]	0[b]	Yes
	Hip	No		Yes	Yes	
Trabecular BMD	Spine	No	Yes	Yes	Yes	Yes
	Hip	No	Yes	Yes	Yes	
CTXA	Hip	Yes				
Integral BMD	pQCT UD radius	No	Yes[a]	Yes		Yes
Trabecular BMD		No	Yes[a]	Yes		Yes
FEA strength	Spine	No	Yes	Yes	Yes	Yes
	Hip	No	Yes	Yes	Yes	Yes

For a complete list of positions, see www.ISCD.org. *BMD*, bone mineral density; *CTXA*, computed tomography X-ray absorptiometry; *FEA*, finite element analysis; *No*, technique should not be used; *Yes*, technique can be used.

[a]*Predicts hip fracture, no position for radius fracture.*

[b]*There was insufficient evidence at the time (2007) when International Society of Clinical Densitometry positions for quantitative computed tomography of the spine were issued; however, there is now plenty of evidence that integral BMD of the spine can be used for monitoring. Note: in men, there are fewer studies and several of the positions that are supported for women are not supported for men because of missing evidence.*

of QCT of the spine and hip (Engelke et al., 2008, 2015a; Zysset et al., 2015). As can be seen from the table, QCT BMD assessments of the hip and spine cannot be used for a diagnosis of osteoporosis because the exclusive applicability of the WHO diagnostic classification to DXA is inherent to the definition. T scores define an age-independent threshold that depends on the mean BMD and standard deviation of the young normals of the DXA reference population. It is an intrinsic deficiency of the WHO definition that it cannot be adapted to other densitometric techniques, as standard deviation and age-related decline are different from those of DXA.

The only exception is CTXA (CT X-ray absorptiometry) of the hip, a technique to simulate DXA using projectional data from 3D CT images to estimate aBMD. US FDA−approved implementations of CTXA are available for QCT Pro from Mindways Software, Inc. (Austin, TX) (Cann et al., 2014), and for VirtuOst from O.N. Diagnostics (Berkeley, CA) (Weber et al., 2014). A projectional option is also available in the UCSF QCT hip software developed by Lang (Lang et al., 2012). CTXA DXA equivalent T scores (Khoo et al., 2009) and aBMD for the femoral neck have been integrated into FRAX, which calculates 10-year fracture probability (World Health Organization Collaborating Center for Metabolic Bone Diseases, 2015).

According to Table 80.1 QCT BMD assessments of the spine and hip can be used for fracture prediction. Overall evidence on fracture prediction is still limited; in many studies the number of fractures is often low, resulting in large CIs and hiding potential significance. Existing data suggest that QCT BMD measured in vivo at the hip does not predict hip fracture risk better than hip aDXA (Engelke et al., 2015a). In the spine an analysis of the prospective AGES−Reykjavik study indicated a significantly better fracture prediction using QCT BMD of the spine compared with spinal aBMD but after adjustment for aBMD, QCT BMD did not remain significant in a multivariate analysis although relative hazards were only slightly decreased by the adjustment (Wang et al., 2012). The area under the curve (AUC) value for integral BMD of 0.83 was significantly higher than for aBMD (0.67).

Compared with DXA the interpretation of longitudinal changes of trabecular and cortical BMD measured by QCT needs special attention because absolute values of trabecular BMD are much lower than those of cortical and integral BMD. As a consequence, percentage changes typically used to report age-, disease-, or treatment-related BMD changes may be rather high for trabecular BMD. For example, in the hip with mostly fatty marrow, trabecular BMD values below 20 mg/cm^3 are frequently encountered. At this level, even a small change of, for example, 5 mg/cm^3 results in a 25% change. However, the same absolute change amounts to just 5% if trabecular volumetric BMD (vBMD) is 100 mg/cm^3, a typical value for osteopenic subjects in the lumbar spine. Thus, a percentage change of trabecular vBMD has to be interpreted also in the context of the absolute value. The use of absolute vBMD or even BMC also provides additional insights into the differential actions of pharmaceutical treatment on cortical and trabecular bone. For example, in studies with denosumab (Genant et al., 2013) and cathepsin-K inhibitors (Engelke et al., 2014, 2015b) in which this analysis was used, absolute cortical vBMD increases were higher than absolute trabecular vBMD increases and more than 60% of the newly formed bone was deposited in cortical and subcortical compartments.

Components of bone quality

Apart from the straightforward assessment of BMD, QCT opens many avenues to assess components of bone quality, defined broadly as all geometric, microarchitectural, and material factors (e.g., trabecular architecture, collagen cross-linking, mineralization, microcracks, …) (Donnelly, 2011). Not all of them can be measured in vivo but specific HR-pQCT using dedicated scanners has been developed to quantify trabecular architecture. High-resolution CT (HR-CT) has also been applied to the spine to characterize trabecular architecture of the vertebrae. Three-dimensional geometry can be quantified from standard QCT images of the spine, hip, and forearm.

FEA is a computer-based simulation of the strains and stresses induced by mechanical loading of an object and is widely used in engineering. The object is described as a connected set of simply shaped elements, which are ascribed elastic properties. FEA is based on QCT acquisitions. Currently, the elastic properties of each voxel are derived from the corresponding BMD values. FEA potentially integrates density and geometry and accounts for regional variations better than the separation of a bone into subvolumes. It is primarily promoted to calculate an integral parameter of bone strength, which is easy to explain in clinical practice: if bone strength is too low for a given external load the bone will fracture. Mechanical experiments in which bones are loaded until they fracture have indeed shown that bone strength of the hip or vertebrae as determined by FEA is a better predictor of failure load than corresponding DXA or QCT measurements of BMD or content (Cody et al., 1999; Dall'Ara et al., 2012; Danielson et al., 2012; Pottecher et al., 2016). However, similar to QCT, in vivo FEA showed significantly better fracture prediction than DXA only at the spine and not at the hip (Wang et al., 2012; Imai et al., 2009).

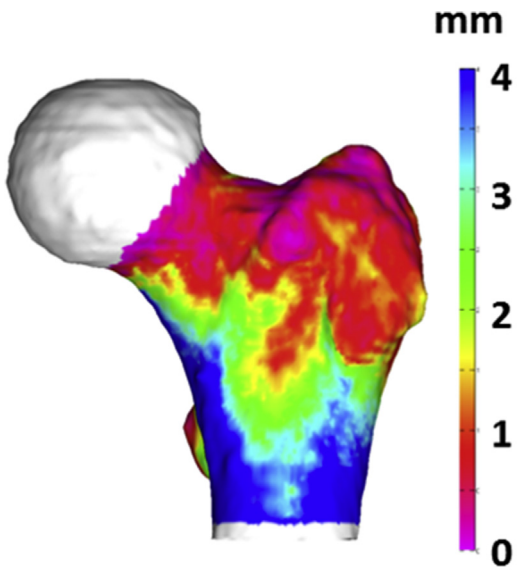

FIGURE 80.6 Cortical thickness map: proximal femur right. *Courtesy: Julio Carballido-Gamio, UCSF.*

Interestingly, at the hip, several QCT studies found a BMD-independent contribution of cortical geometry to fracture risk (Museyko et al., 2016; Bousson et al., 2011; Chappard et al., 2010; Cheng et al., 2007; Yang et al., 2014a, 2017; Borggrefe et al., 2016). These findings have triggered further research into a more comprehensive characterization of cortical and subcortical bone compartments as discussed in the next section. Although a multivariate analysis of BMD, cortical thickness, and strength has not been published as of this writing, the added effort of FEA may not be required after combining BMD and cortical geometry. At the spine, vertebral compressive strength has been estimated as a linear combination of integral BMD and CSA, two parameters that also can easily be determined from QCT alone (Bouxsein et al., 2006; Bruno et al., 2014). Of course, in clinical practice it is intriguing to use only bone strength as a single parameter, as the combination of BMD and geometry is more difficult to understand.

With FEA, the distribution under load can be calculated, which may give important insights into the fracture process and fracture load patterns (Faisal and Luo, 2017; Haider et al., 2018; Bessho et al., 2004). Methods of statistical parameter mapping can be used to compare an individual stress pattern with that of an average subject represented mathematically by a so-called atlas. This procedure eliminates residual anatomic variability so that a given spatial coordinate in one scan is mapped to the anatomically homologous coordinate in the scans comprising the atlas. Statistical tests are then usually performed on a voxel-by-voxel basis generating statistical maps to identify regions where the feature of interest is significantly related with the effect or outcome of interest. Typical features have been cortical thickness (Poole et al., 2012, 2015) and BMD (Li et al., 2009; Carballido-Gamio et al., 2013a, 2013b; Bredbenner et al., 2014).

Results are often displayed as a feature map, for example, as a colored surface of an average femur indicating the local cortical thickness variation in a group of subjects under treatment (Fig. 80.6). The interpretation is challenging and the clinical utility of these methods still has to be established (Engelke et al., 2015c), but in combination with machine learning techniques, these methods could be able to delineate feature variations in relation to specific clinical end points such as fracture (Poole et al., 2017), and to interventions such as medication or exercise regimes. These methods also allow for an integration of the various parameters that can be obtained from QCT data (Carballido-Gamio et al., 2015). One critical issue is the generation of a representative atlas, which usually requires a large number of data sets to capture the population variance.

Cortical bone

The separate assessment of cortical bone, a key feature of QCT, is important not only because of the independent contribution to strength and fracture risk (Reeve, 2017; Tang et al., 2018; Johannesdottir et al., 2011), but also to better understand age-related changes of bone geometry and density (Nicks et al., 2013; Carpenter et al., 2011) and to explore differential effects of pharmaceutical drugs used to treat osteoporotic patients (Fitzpatrick et al., 2012; Langdahl et al., 2017).

State of the art spiral CT offers almost isotropic spatial resolution of about 0.5 mm when using high-resolution acquisition and reconstruction protocols, but for standard QCT a slice thickness of 1 or 1.25 mm and medium sharp reconstruction kernels are used to limit noise or to allow for lower dose protocols. Thus, in particular in the femoral neck and the vertebral body where cortical thicknesses of 200−500 μm are frequently encountered in elderly people, the measurement of cortical parameters is impaired by partial volume artifacts, causing an overestimation of cortical thickness and an underestimation of cortical BMD (Dougherty and Newman, 1999; Newman et al., 1998). An additional difficulty is the definition of the endosteal border because of a more or less continuous transition from the cortical to the trabecular compartment characterized by increasing porosity transitioning to trabecular architecture (Zebaze et al., 2010).

Measurements of cortical thickness and BMD differ among QCT analysis programs because fundamentally different segmentation approaches are used. This is confusing for the user unfamiliar with image processing details. The software program VirtuOst simply defines a 3 (2)-mm outer shell in the hip (spine) in separating finite elelment based strength measurements in cortical and trabecular compartments, but does not report cortical BMD or thickness. The MIAF software from the University of Erlangen uses locally adaptive 50% thresholds, which theoretically is the best approach as long as the cortex is thick enough (1−3 mm for current CT equipment and scan protocols) (Prevrhal et al., 1999). The Stradwin software from the University of Cambridge implements a deconvolution algorithm reversing the blurring effects. Cortical thickness is more accurate compared with the other methods but this technique requires input of BMD of the unblurred cortex, a so-called reference BMD. This can be determined in locations with a thick cortex, largely unaffected by blurring (Treece et al., 2010). Further refinements have been reported to determine the reference BMD closer to the location of the cortical measurement (Treece and Gee, 2015; Treece et al., 2012). A hybrid approach combining deconvolution for thin cortices with 50% local thresholds for thicker cortices has been developed for MIAF (Museyko et al., 2017). Fig. 80.7 compares the standard 50% local threshold used in MIAF with the new hybrid segmentation using a deconvolution for thin cortices.

A comparison of the MIAF (Genant et al., 2013) and Stradwin softwares (Poole et al., 2015) to assess changes in cortical parameters after 3-year treatment with denosumb versus placebo suggests the use of cortical BMC for longitudinal measurements. Stradwin's deconvolution-based method resulted in higher changes in cortical thickness but lower changes in cortical BMD than MIAF's standard local 50% thresholds. However, increases in cortical BMC, which balance the overestimation of cortical thickness and the underestimation of cortical BMD, were similar and may prove more useful in longitudinal studies. Obviously, the use of BMC in cross-sectional studies is more problematic as people with larger bones by definition have higher BMC.

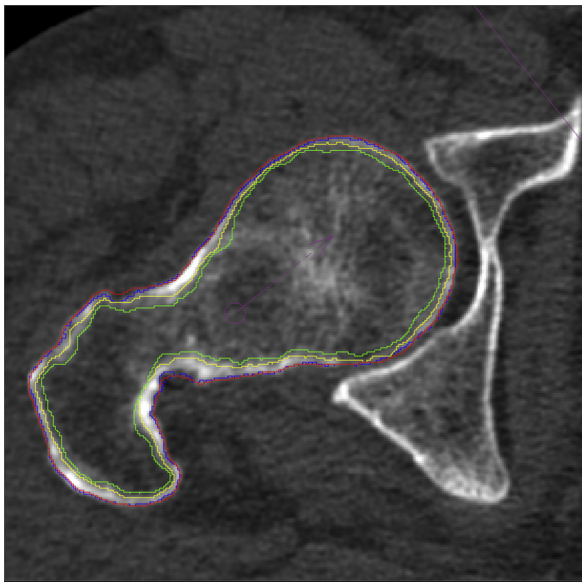

FIGURE 80.7 Effects of different cortical segmentations in the hip: periosteal (*red*, 50% local thresholds - outermost contour; *blue*, deconvolution technique - contour almost identical to 50% local threshold contour) and endosteal (*green*, 50% local thresholds - innermost contour; *yellow - between blue and green contour*, deconvolution technique) surfaces of the cortex (Engelke, 2017).

High-resolution computed tomography

The primary aim of high-resolution tomography is the assessment of trabecular structure and increasingly of cortical porosity. The accuracy of cortical thickness measurements also increases with higher spatial resolution. In the past many attempts have been reported to determine trabecular architecture with clinical whole-body CT scanners also used for standard QCT measurements. With appropriate acquisition and tomographic reconstruction protocols, an almost isotropic spatial resolution of approximately 0.5 mm can be obtained in the axial skeleton. Dedicated single-slice pQCT scanners have improved in-plane resolution by about a factor of 2−3 but use slice thicknesses of 1−2 mm. However, given typical dimensions of trabeculae (100−400 μm) and trabecular spaces (200−2000 μm) this resolution is still insufficient for an accurate determination of standard stereological parameters.

This is illustrated in Fig. 80.8, where HR-CT images were simulated from a stack of 21 sagittal grindings (thickness 5 μm) of a trabecular network from a human calcaneus. The thickness of each grinding was 5 μm and the distance between two adjacent grindings was 51 μm. A stack of binary images with isotropic voxels $(12\ \mu m)^3$ was obtained from the digitized grindings. The images of the stack were averaged along the direction indicated in Fig. 80.8. The first row of simulated images shows two radiographic-type images. The one on the left resulted from averaging half the stack and the one on the right from averaging all images of the stack. Thus a total slice thickness of 0.51 mm and of 1.02 mm was simulated, respectively. The in-plane pixel area in these radiographic type images is unchanged at $12 \times 12\ \mu m^2$. There are still artificial discontinuities in the gray value variations. They would be avoided by averaging more images. The second and third rows show simulated hrCT images with pixel sizes of 100 and 200 μm. The images were blurred with a Gaussian filter to give a more realistic impression of what can be expected in vivo.

The simulations demonstrate that in HR-CT images only the dominant structures are preserved, details of the trabecular network cannot be extracted. The textures in the CT-like and in the radiographic-like images are similar and a major deterioration of the network will be noticeable in the HR-CT images. However, a determination of parameters typically used in histomorphometry is problematic. It is evident that parameters like Tb.Th, Tb.Sp, or Tb.N change drastically and artifactually. To indicate that structural parameters measured in HR-CT and HR-MR images differ significantly from those

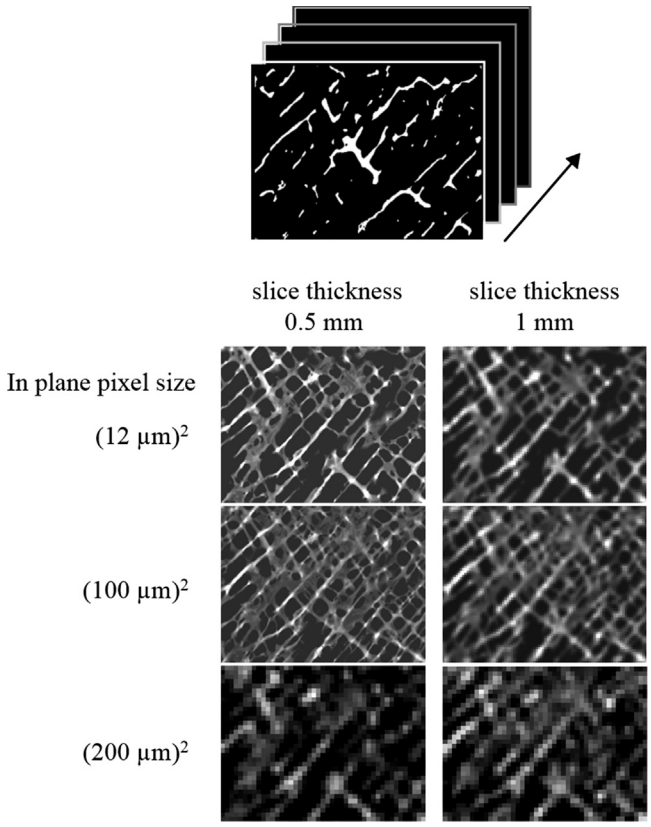

FIGURE 80.8 Effects of slice thickness and in-plane pixel size on trabecular structure. Simulation of radiographic and high-resolution computed tomography (HR-CT) images based on a stack of stained grindings. Stack of grindings (top). Simulated radiographic and hrCT images (bottom).

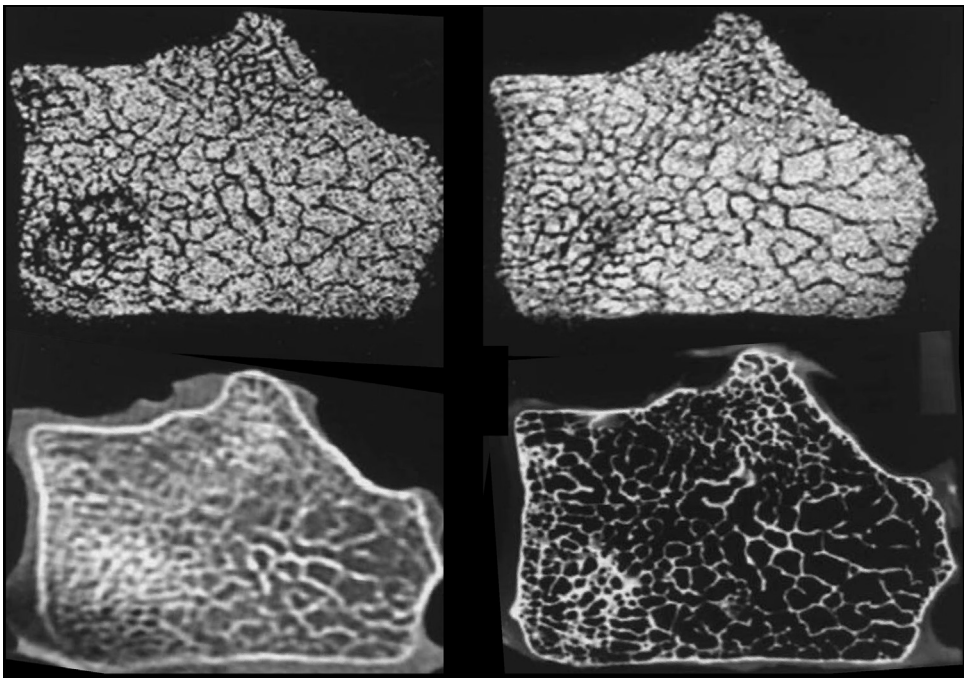

FIGURE 80.9 Comparison of trabecular structure a calcaneus specimen imaged with high-resolution magnetic resonance imaging (HR-MRI), high-resolution computed tomography (HR-CT), and microradiography. (Top) 3D HR-MRI spin echo sequence, in-plane pixel size 150 μm, slice thickness 300 μm (left) and 900 μm (right). (Bottom) Left, HR-CT plane pixel size 250 μm, slice thickness 1000; right, contact radiograph of a 1-mm-thick section cut from the calcaneus, slice of plane pixel size 5 μm (Link et al., 2003).

measured by microscopic histomorphometry of thin section it is recommended to call them apparent trabecular thickness, etc., and to use the prefix "app," such as appTb.Th, appTb.Sp, or appTb.N.

A number of cadaver and specimen studies have explored potentials and limitations of using whole-body spiral CT scanners for high-resolution imaging of trabecular structure of the calcaneus and the lumber vertebral bodies (Fig. 80.9). However, only a few in vivo studies have been published more recently (Grados et al., 2004; Graeff et al., 2013; Ito, 2005; Link and Bauer, 2002). Similar to techniques of high-resolution radiography, HR-CT of the spine and calcaneus has not been widely used in clinical practice. Potentially advanced analysis techniques using texture parameters (Milovanovic et al., 2014; Wolfram et al., 2009; Checefsky et al., 2016; Baum et al., 2010) that do not require the segmentation of individual trabeculae may stimulate further progress in this field.

HR-pQCT

For high-resolution in vivo scanning at the forearm and tibia the XtremeCT (Scanco Medical, Brüttisellen, Switzerland) has been introduced (Boutroy et al., 2005). The first version of this device provides an isotropic voxel size of 82 μm^3 resulting in a spatial resolution of about 120 μm (Burghardt et al., 2013; Fig. 80.10). The trabecular dimensions of the forearm and tibia are similar to those of the spine, but due to the much smaller cross section compared with the central body, the spatial resolution can be increased without a radiation dose penalty. In contrast, as the forearm tissue is less radiation sensitive than that of the spine, the effective dose per scan is below 10 μSv.

As suggested by Laib (Laib and Ruegsegger, 1999), histomorphometric parameters are determined from a measurement of bone volume fraction (BV/TV) and apparent trabecular number (Tb.N). BV/TV is obtained from the BMD of the trabecular compartment by assuming a density of 1200 mg/cm^3 for fully mineralized bone. Tb.N is directly measured using ridge extraction methods. A critical step in the analysis of follow-up scans is the registration of baseline and follow-up scans with an accuracy error that should be lower than 100 μm. Thus during the scans even slight motion of the forearm must be avoided, which is not an easy task given a scan time of 3 min. Motion causes artifacts in the reconstructed images.

Most information on HR-pQCT scanner technology (Burghardt et al., 2011; Nishiyama and Shane, 2013) is available for the first-generation device. The second-generation XtremeCT II provides higher spatial resolution using a voxel size of 61 μm^3 and a reduced scan time of 2 min. The higher spatial resolution allows for a direct quantification of trabecular

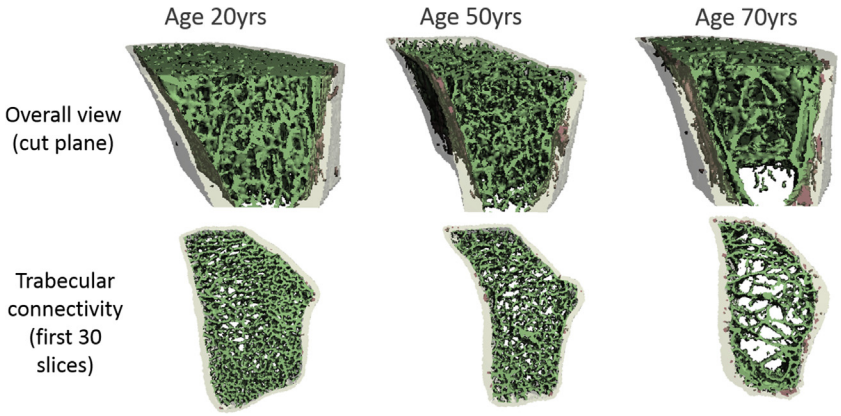

FIGURE 80.10 Characteristic age-related changes in trabecular bone of the distal radius imaged by HR-pQCT (82 × 82 × 82 μm).

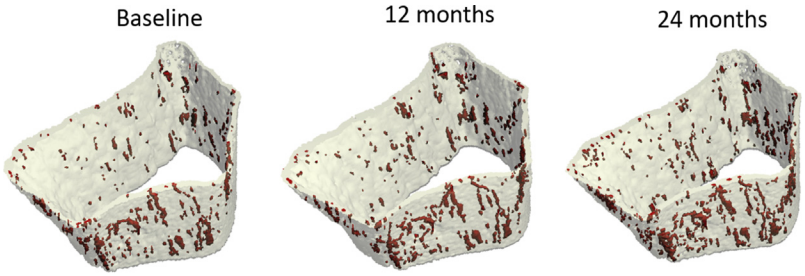

FIGURE 80.11 Cortical porosity of the distal radius imaged by high-resolution peripheral quantitative computed tomography (82 × 82 × 82 μm). A 2-year follow-up of a 58-year-old menopausal woman is shown. Notice the increase cortical porosity at the palmar side.

structure independent of trabecular BMD (Manske et al., 2015). Both XtremeCT versions apply 2D slice by slice−based area matching between baseline and follow-up scans. A full 3D registration reduces motion artifacts and improves precision but expands the time required for image processing (Ellouz et al., 2014).

The resolution of HR-pQCT is high enough to directly detect larger cortical pores (Fig. 80.11). The quantification of cortical porosity has received considerable attention as an increase in number and size of pores is largely responsible for the decrease in cortical BMD as long as mineralization is stable. Porosity (p) increases with age (Bousson et al., 2001) and is increased in diabetes type 2 (Paccou et al., 2016; Patsch et al., 2013a). However, so far it is not known whether porosity-related parameters such as the pore size distribution themselves carry clinical information not obtainable from easier to measure parameters such as cortical BMD. It has been argued that differences in bone tissue mineralization do not account for elastic properties (Zebaze et al., 2011), which are an essential input to FEA, but the combination of porosity and mineralization is reflected by cortical BMD.

Two different approaches exist to quantify cortical porosity in HR-pQCT data. With the software implemented by the manufacturer, pores are segmented directly using a threshold of 450 mg/cm^3 (Jorgenson et al., 2015). Smaller pores are missed and porosity is underestimated. The second technique is based on cortical BMD. It assumes that the density of fully mineralized bone is 1200 mg/cm^3; that within 20% of this upper limit, i.e., for voxels with cortical BMD larger than 960 mg/cm^3, cortical bone may be slightly less mineralized but that no pores exist, i.e., $p = 0$; and that for voxels with cortical BMD below 960 mg/cm^3 $p = (1 - \text{BMD}/1200) \times 100$ (Jorgenson et al., 2015). Compared with synchrotron radiation (SR)−based micro-CT measurements, the density approach overestimates porosity. However, results from the direct segmentation and the density-based technique were highly correlated with SR results ($r^2 > 0.94$) (Jorgenson et al., 2015).

HR-pQCT is predominantly used as a research tool because the number of deployed scanners is still below 100 worldwide, since the equipment is far more expensive than DXA systems. A review of clinical imaging of bone microarchitecture with HR-pQCT was published in 2014 (Nishiyama and Shane, 2013). More recent clinical in vivo studies examined differences between fractured and nonfractured subjects (Zhu et al., 2016; Sornay-Rendu et al., 2017; Macdonald et al., 2018; Sundh et al., 2017; Boutroy et al., 2016), collected normative data (Gabel et al., 2018; Alvarenga et al., 2017; Burt et al., 2014), or reported on monitoring age-related changes (Vilayphiou et al., 2016; Burt et al., 2017) or the

effects of osteoporosis drugs on cortical and trabecular bone microstructure (Lespessailles et al., 2016; Lima et al., 2018; Tsai et al., 2017). Quite a number of further studies focused on technical details or explored changes in trabecular architecture and porosity in specific diseases or differences between populations.

Opportunistic screening

In the field of osteoporosis the term "opportunistic screening" refers to the use of existing clinical CT images for the diagnosis of osteoporosis and prediction of fracture risk. If widely implemented, opportunistic screening could significantly improve the identification of patients at high risk for fracture. First ideas were published as early as 2000 (Hopper et al., 2000) and reviewed more recently (Engelke et al., 2015c; Gausden et al., 2017). The major challenges of opportunistic screening are missing a calibration phantom, lack of standardization of CT scanners with respect to BMD measurements, large variation of CT acquisition parameters affecting BMD measurements such as tube voltage and table height, and the use of contrast agents in many routine CT examinations. The simultaneous calibration typically used in QCT can be replaced by an asynchronous calibration, as modern CT scanners are rather stable over time (Pickhardt et al., 2015). DXA scanners from Lunar also use an asynchronous BMD calibration. A step further facilitating the clinical workflow is an internal calibration based on the absorption of air, of internal organs, and of the aorta. Good agreement between simultaneous and a scanner-specific internal calibration has been reported but exact details of the method were not published (Lee et al., 2017).

Many authors advocate the direct use of HU values (Gausden et al., 2017), arguing that clinical CT scanners are regularly calibrated to air and water. However, this calibration ensures only that CT values of water equivalent materials, i.e., to a first approximation of soft tissues, are comparable across scanners and are also independent of the specific tube voltage. Because X-ray mass absorption coefficients of bone and water are very different, this is not the case for bone (Kalender et al., 2009). As a consequence, HU values for trabecular and cortical bone may vary widely between different CT scanners. Any HU thresholds reported in the literature for opportunistic screening may be valid only for the specific scanner and tube voltage used for the study. They should not be generalized automatically. The same is true for correction factors that have been applied to account for elevated BMD caused by X-ray contrast (Baum et al., 2011). Here additional difficulties apply, such as the amount of contrast and the timing of the CT scan after contrast injection (Emohare et al., 2014; Pickhardt et al., 2016).

Prior to the widespread introduction of opportunistic screening into clinical routine, a thorough standardization is required. If the accuracy error of a BMD measurement is high, a secondary analysis of CT data obtained for tumor and other routine clinical diagnoses could be used to categorize fracture risk as low, medium, or high. It has been suggested that subjects with high fracture risk could be followed up with DXA or could be directly referred to counseling on appropriate intervention even without an additional DXA scan. Both scenarios are convenient and cost effective because DXA scans and associated logistics are not required. An additional benefit of the dual use of CT scans is the possibility of using a lateral scout view or a sagittal reconstruction of the spinal column to assess fractures.

DXA beyond bone mineral density

Several advanced analyses such as trabecular bone score (TBS), hip structure analysis, FEA, and 3D DXA have been introduced to obtain information from DXA scans beyond BMD. Most of these techniques are implemented in a fashion so that large data sets can be analyzed automatically. As so much DXA data are available, the techniques can be rapidly validated.

Trabecular bone score

Some of the underlying ideas for the TBS analysis were originally developed for the texture analysis of high-resolution X-ray films (Pothuaud et al., 2000, 2001). TBS is a specific texture analysis applied to DXA images. It is based on the gray level variogram. When applied to trabecular samples, TBS reflects bone microarchitecture (Hans et al., 2011; Pothuaud et al., 2008). In vivo the relation may be less obvious because of soft tissue, spinal, and transverse processes, and degenerative changes alter the texture of the pure trabecular bone. Nevertheless, a recent meta-analysis (Harvey et al., 2015) impressively demonstrated the potential of TBS. Low TBS is associated with an increase in prevalent and incident fractures partly independent of clinical risk factors and of aBMD at the lumbar spine and proximal femur. According to the ISCD positions "TBS can be used in association with FRAX and aBMD to adjust FRAX-probability of fracture in

postmenopausal women and older men" but "is not useful for monitoring bisphosphonate treatment in postmenopausal women with osteoporosis" (Silva et al., 2015).

Hip geometry, hip structure analysis, and finite element analysis

Several investigations have found that projectional measurements of parameters describing femur geometry can predict hip fractures independent of BMD. One prominent example is the hip axis length (HAL) determined from conventional radiographs or DXA. It predicts hip fracture, as a longer HAL is associated with an increase in femoral neck and trochanteric fracture risk (Faulkner et al., 1994; Glüer et al., 1994). Instead of varying with age after midadolescence, the HAL seems to be mainly influenced by genetic factors (Flicker et al., 1996), which supports other reports that differences in the HAL may partially explain racial differences in hip fractures (Cummings et al., 1994).

A more comprehensive approach to estimate geometrical and mechanical properties from DXA of the hip is hip structural or hip strength analysis (HSA), which was first applied to cross-sectional bone mineral absorption curves generated by single-photon absorptiometry at the forearm (Martin and Burr, 1984). This early work was extended to DXA data at the proximal femur to automatically estimate cross-sectional moments of inertia (CSMI) and CSAs of the neck, the trochanter, and the shaft, as well as the femoral neck shaft angle, bending moments, and HAL (Beck et al., 1990).

For HSA 1D profiles are extracted from narrow regions across the neck, the intertrochanter, and the shaft by averaging pixel values perpendicular to the profile directions (Fig. 80.12). For each pixel along the profile, aBMD is obtained from the DXA measurement, and BMC is determined using the known pixel dimensions. The BMC distribution along the profile is used to calculate p_c, the position of its center of mass. Under the assumption that the specific axis through p_c, which is perpendicular to the plane of the DXA image, is also the main bending axis, the CSMI of the cross section defined by the profile can (apart from a multiplicative constant) be accurately calculated from the DXA images by:

$$\mathrm{CSMI} = \frac{1}{\mathrm{BMD}_{\mathrm{cort}}} \sum_i \mathrm{BMC}_i [\Delta(p_c - i)]^2$$

$\mathrm{BMD}_{\mathrm{cort}}$ is the areal density of cortical bone, and a value of 1.051 g/cm^2 is assumed. Δ denotes the length of a profile pixel.

A comprehensive review of the clinical utility of HSA and of parameters describing hip geometry was published in the 2015 official positions of the ISCD (Broy et al., 2015). According to these recommendations none of the parameters should be used for fracture prediction, with the exception of HAL, which predicted hip fractures independent of BMD in multiple studies of postmenopausal women. There was also good evidence that HSA structural parameters predicted hip fracture in postmenopausal women, but not independent of BMD, questioning their clinical relevance. None of the parameters should

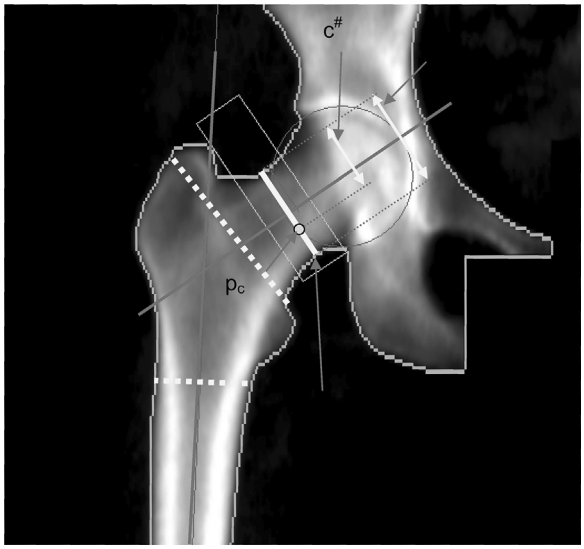

FIGURE 80.12 Hip strength analysis: p_c, center of mass of cross section; $C^{\#}$, defined by hip strength analysis (see text). In hip structure analysis, cross-sectional moment of inertia (CSMI) is estimated along the three yellow profiles; in hip strength analysis CSMI is estimated only along the solid profile (arrow).

be used for monitoring intervention, because either the expected changes were less than the least significant change of the measurement or there were no expected changes as for HAL and neck shaft angle. Thus, the main value of these parameters is their use in dedicated research studies.

A further extension of the structural analysis of DXA is its direct use for FEA. Early results showed surprisingly good agreement to strain-gauge measurements and to a 3D finite element model (Testi et al., 1999). More recent publications showed significant hip fracture discrimination of femoral strength and load-to-strength ratio determined from DXA even after adjustment for standard DXA aBMD of the neck (Naylor et al., 2013). A post hoc analysis of the Study of Osteoporotic Fractures in postmenopausal females showed a prediction of incident hip fracture by femoral strength after adjustment for age, body mass index (BMI), and DXA neck aBMD with a hazard ratio of 1.71 (Yang et al., 2014b). However, in males from the Osteoporotic Fractures in Men (MrOS) study the results were less convincing (Yang et al., 2017). In the large Manitoba registry study increased hip fracture risk was significantly associated (OR = 1.36) with lower femoral strength after adjusting for FRAX hip fracture (Yang et al., 2018). So far, fracture prediction or discrimination with FEA has not been compared between QCT and DXA data in the same study.

Three-dimensional DXA

Three-dimensional DXA is a technique to simulate a 3D data set from a projectional 2D DXA scan. Initially it was termed VXA (Ahmad et al., 2010) and based on five projections of the hip obtained with a C-arm scanner under different angles. These projections were fitted to a statistical 3D atlas of the femur generated from volumetric CT data of 100 subjects. It was shown that 95% of the individual anatomical variations from the atlas could be described by 10–20 different parameters (Whitmarsh et al., 2011), the so-called eigenvectors, suggesting that a limited number of 2D projections suffice to obtain accurate 3D geometrical and densitometric information of the femur. The result is a simulated QCT image.

Newer implementations now known as 3D DXA are based on a single projection, the standard DXA images, and can therefore also be implemented on DXA scanners without a C-arm. Nowadays, one direction of the development of 3D DXA seems to be the differentiation of cortical and trabecular compartments. A recent cross-sectional study in 157 subjects demonstrated the potential of the method: correlations between QCT and 3D DXA were 0.95 for total hip cortical density and 0.91 for total hip cortical thickness with mean absolute differences of 72 mg/cm^3 or 7.6% and 0.33 mm or 18.3% for density and thickness, respectively (Whitmarsh et al., 2011). The 3D DXA images still looked somewhat blurred (Fig. 80.13). CT scans were obtained on two different scanners, one of them using a soft tissue reconstruction kernel that would also generate a blurred cortex in the QCT images.

Magnetic resonance imaging

Hydrogen is the most abundant atom in the body. MRI imparts a very short burst of energy via the MR radio-frequency (RF) coil, which is placed near to the body part being examined. The freely mobile hydrogen atoms, mainly in the form of water or fat, take up this energy momentarily but hydrogen atoms in fat release the energy faster than hydrogen atoms in water. This differential energy release forms the basis of MRI, which essentially differentiates all tissues in the body into those composed of fat or water. MRI looks at the concentration of free hydrogen atoms and determines whether these are contained in fat or water. Trabecular and cortical bone contain very little fat or water and appear dark with no emitted signal (hypointense) on MR images. MR depicts trabecular bone as a negative image by virtue of its signal void contrasting against the strong signal generated by the marrow fat and water in the adjacent marrow tissue. Marrow fat increases with increasing age and particularly in osteoporotic bone, allowing better contrast differentiation between fatty marrow and trabecular bone than between red marrow and trabecular bone.

Trabecular structure

Bone trabecular macrostructure has been studied mainly in the distal radius and the calcaneus, as these are bone areas close to the skin surface. This close proximity to the RF coil allows a high signal-to-noise ratio (SNR) to be generated. For good contrast of bone structure imaging by MRI a minimal SNR of 10 is recommended (Chang et al., 2017). The SNR can be increased by scanning at higher field strength, using multichannel coils with individual smaller coil dimensions and using SNR-efficient pulse sequences (Chang et al., 2017). Both spin-echo (Magland et al., 2006) and gradient-echo sequences (Majumdar et al., 1995) have been used to image trabecular structure but HR-pQCT has largely replaced MRI for this purpose.

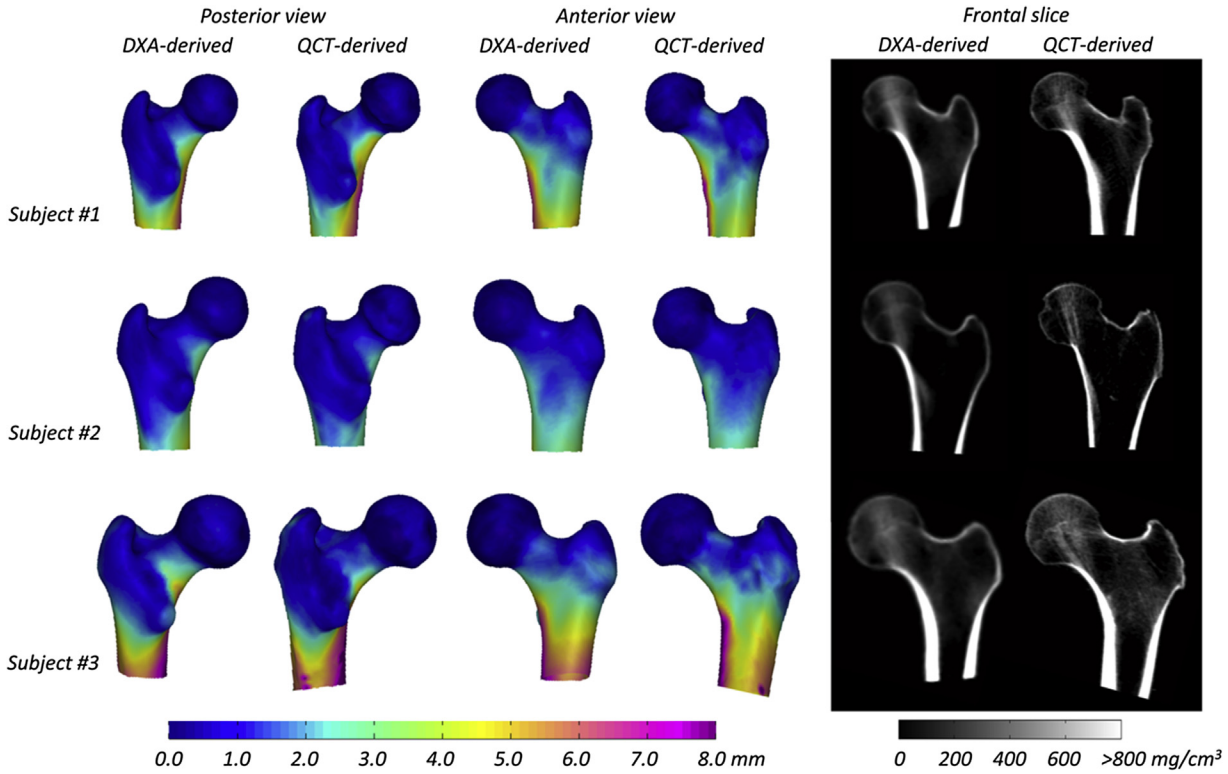

FIGURE 80.13 Comparison between dual-energy X-ray absorptiometry (*DXA*)- and quantitative computed tomography (*QCT*)-derived femoral shapes: cortical thickness distributions (left) and frontal slices showing bone density values (right). *Courtesy: Ludovic Humbert, Galgo Medical, Barcelona, Spain; Reproduced from Humbert, L., Martelli, Y., Fonolla, R., Steghofer, M., Di Gregorio, S., Malouf, J., et al. 2017. 3D-DXA: assessing the femoral shape, the trabecular macrostructure and the cortex in 3D from DXA images. IEEE Trans. Med. Imaging 36(1), 27–39; IEEE copyright line © 2017 IEEE.*

Fast 3D spin-echo approaches are less sensitive to local T2* differences between bone and bone marrow. Overestimation of trabecular size is more pronounced on gradient echo images (Boutry et al., 2004), especially when the echo time (TE) is increased, as this leads to local magnetic field inhomogeneities at the trabecular to marrow interface. These inhomogeneities lead to a signal void and hence artifactual broadening of the trabeculae. This "ballooning effect" can be used to advantage to enhance the visibility of trabecular bone structure. Gradient echo sequences provide higher signal-to-noise characteristics allowing for shorter scan times, important for in vivo imaging (Majumdar et al., 1995). Scanning at higher field strength such as at 3T and 7T allows one to reduce the voxel size and scan time and investigate more proximal sites such as the biologically relevant femoral neck.

Cortical water

An advantage of MRI over traditional imaging techniques such as DXA and CT is its specific ability to investigate cortical water content. The collagen matrix and water contribute significantly to bone strength and account for about half of the cortical bone volume. Cortical bone contains free water within cortical pores (cortical pore water; CPW), which also includes the water residing within haversian canals and the lacunar–canalicular system lacunae and collagen-bound water (CBW), which is water bound to collagen within the bone matrix. CPW has a T2 relaxation time of >1 ms, while that of CBW is 0.3–0.4 ms; thus collagen-bound water essentially emits no signal using standard MR pulse sequences. This limitation can be overcome by using ultrashort TE (UTE) sequences, with nominal TEs of less than 100 μs. Studies have mainly used the anterior tibial cortex and, to a lesser extent, the distal radius and proximal femur, as these areas possess relatively thick cortical bone. Using a water phantom, one of the earliest UTE cortical bone studies performed on a clinical 3T MRI scanner, and looking at new water content of cortical bone, showed that renal osteodystrophy patients had a 43% higher cortical bone water content than postmenopausal subjects and a 135% higher bone water content than premenopausal subjects (Techawiboonwong et al., 2008).

It is advantageous to distinguish between CPW and CBW signals as cortical bone strength increases with higher concentrations of bound water but decreases with higher concentrations of free water. With recently developed variations of the UTE technique such as antibiotic inversion recovery (Manhard et al., 2015), radial cones trajectory (Chen et al., 2016), or a suppression ratio technique (Li et al., 2016), CPW and CBW components of cortical water can be distinguished. Bound water is an indirect marker of collagen matrix content, while pore water is an indirect measure of porosity. Cortical bone specimens with more bound water tend to have higher peak and yield stress values and elastic toughness, while cortical bone specimens with a greater concentration of pore water generally tend to have higher porosity and lower peak stress, yield stress, and toughness (Manhard et al., 2015). In 40 healthy women, the mean free water concentration and bound water concentration were 5.9% and 19.6%, respectively, with cortical bone free water concentration showing a strong positive correlation ($r^2 = 0.62$) with age (Abbasi-Rad and Saligheh Rad, 2017).

Bone marrow

MRI also provides information on marrow fat content and composition, marrow perfusion, and marrow molecular diffusion (Griffith, 2017). Marrow fat content can be measured using either MR spectroscopy or fat–water separation techniques such as IDEAL imaging. MR spectroscopy provides information on marrow fat composition as well as content but can examine only a limited area of about 1 cm^3 at any one time (Fig. 80.14). Fat–water separation techniques can examine much larger areas but do not provide information on fat composition.

Lifelong studies addressing physiological changes in marrow fat content show a gradual physiological increase in percentage marrow fat content with advancing years (Duda et al., 1995; Kugel et al., 2001). As a rule of thumb vertebral body marrow fat content increases from 25% at 25 years of age to 65% at 65 years (Montazel et al., 2003; Patsch et al., 2013b; Yeung et al., 2005; Fig. 80.15). In addition, there is a distinct sex difference in marrow fat content (Kugel et al., 2001; Griffith et al., 2012). From the time of skeletal maturation to extreme old age, males show a gradual increase in lumbar vertebral marrow fat content of 7% per life decade (Kugel et al., 2001; Griffith et al., 2012). In contrast, females show a less steep increase in marrow fat of about 5% per decade up to 55 years and a dramatic increase in marrow fat content between the ages of 55 and 65 years (Kugel et al., 2001; Griffith et al., 2012), corresponding to the known reduction in bone mass that occurs at that time (Fig. 80.16).

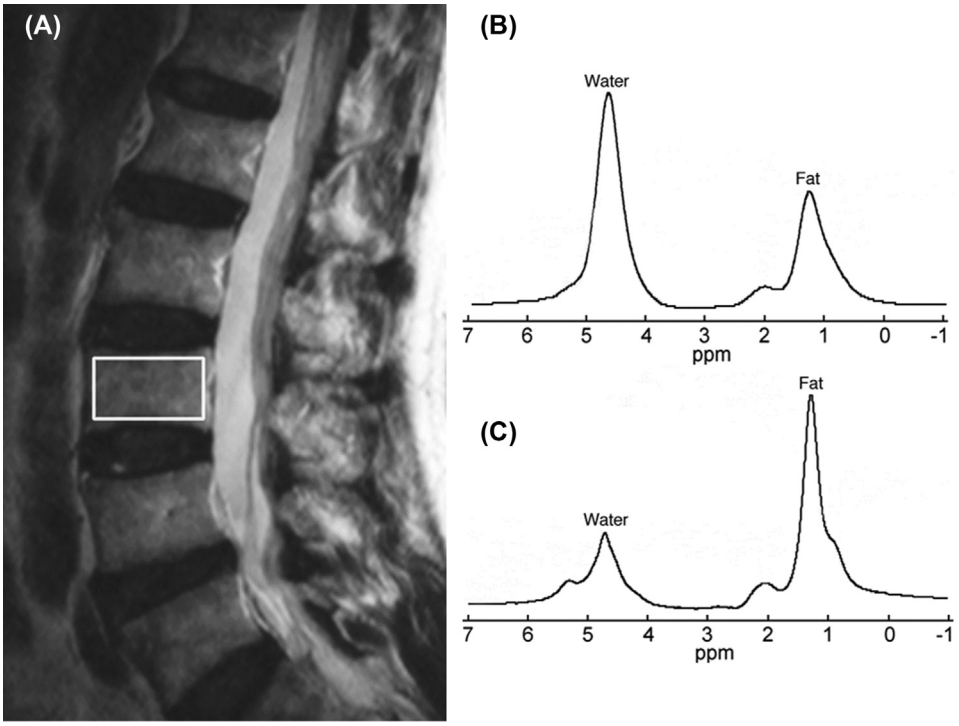

FIGURE 80.14 ^{1}H MR spectroscopy examination. (A) Sagittal T2-weighted MR image showing positioning of volume of interest (white rectangle) for proton spectroscopy of L3 vertebral body. (B) Typical ^{1}H MR spectra in a normal subject with little marrow fat and (C) an osteoporotic subject with a large amount of marrow fat.

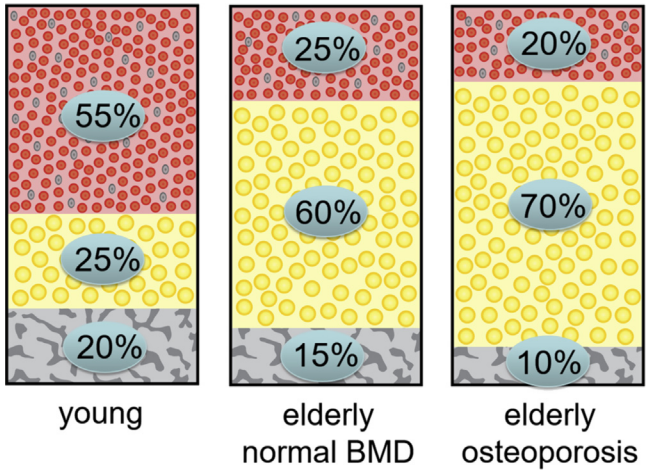

FIGURE 80.15 Distribution of trabecular bone, fatty marrow, and red marrow. For young subjects in the confined space of the bone marrow, there is about 20% trabecular bone, 25% fatty marrow, and 55% red marrow (dark gray in print version). With aging, the amount of trabecular bone and red marrow decreases, while the amount of fatty marrow increases. *BMD*, bone mineral density.

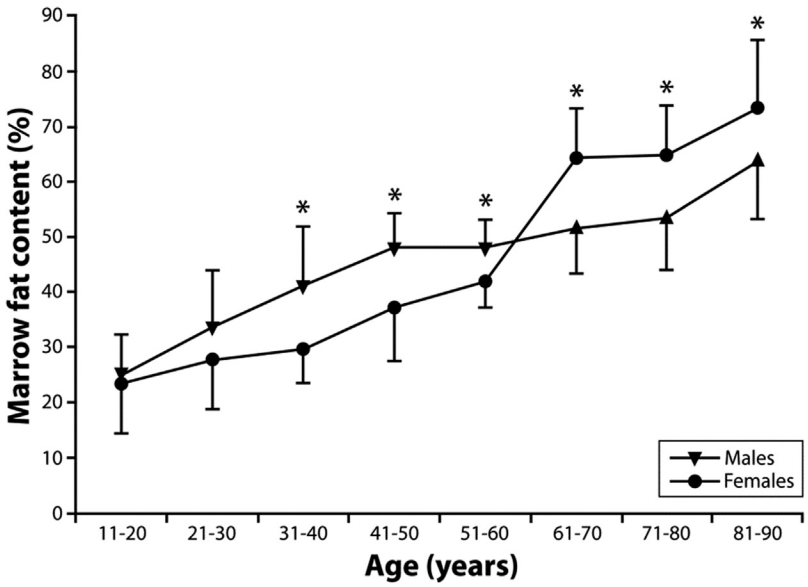

FIGURE 80.16 Marrow fat content (%) of lumbar vertebral body stratified for age and sex. Marrow fat increases slowly and steadily for males, while for females there is a dramatic increase around the time of menopause. * significant ($p < 0.05$) differences between males and females.

An increase in marrow fat is associated with a reduction in BMD. There is also an increase in marrow fat in conditions associated with reduced BMD such as anorexia nervosa, alcohol abuse, spinal cord injury, and prolonged bed rest (Schwartz, 2015). Higher prevalent marrow fat predicts future increased bone loss. Postmenopausal women with a marrow fat content above the median experienced average bone loss of 4.7% over 4 years, while those with a marrow fat content below the median experienced a bone loss of only 1.6% (Griffith et al., 2011). Increased marrow fat may also increase fracture risk. Mean vertebral marrow fat was 55% in those with a prevalent vertebral fracture compared with 45% ($p < .001$) in those without a prevalent vertebral fracture, even after adjusting for the effect of marrow fat on DXA measurements (Wehrli et al., 2000). A knowledge of the marrow fat content would also help to correct accuracy errors in DXA and in particular in single-energy QCT BMD measurements (Blake et al., 2009; Glüer and Genant, 1989), but so far is not routinely done.

MR spectroscopy also has the ability to evaluate the type as well as the quantity of fat. Young normal controls have a higher (0.127) portion of unsaturated fat in the bone marrow than postmenopausal females with osteoporosis (0.091) (Yeung et al., 2005). Vertebral insufficiency fracture patients were shown to have 1.7% lower unsaturation levels and 2.9%

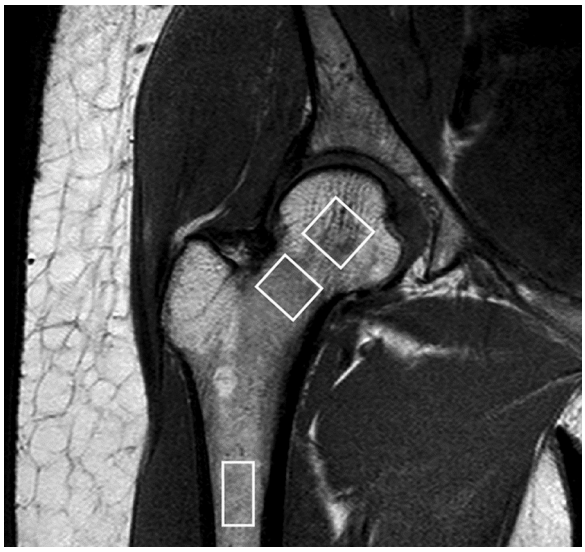

FIGURE 80.17 Dynamic contrast-enhanced MRI. Coronal oblique T1-weighted image of proximal femur showing regions of interest used to measure marrow perfusion in the femoral head, neck, and shaft.

higher vertebral marrow fat saturation levels (Patsch et al., 2013b). In the same study, diabetics had 1.3% lower unsaturation and 3.3% higher vertebral marrow fat saturation levels. Diabetics with fractures had the lowest marrow unsaturation and highest saturation. Although changing marrow fat composition was associated with diabetes and insufficiency fracture, the marrow fat content (%) per se did not change with either diabetes or fracture (Patsch et al., 2013b).

Further techniques are dynamic contrast-enhanced MRI to measure marrow perfusion (Fig. 80.17), and diffusion-weighted MRI is able to measure the apparent diffusion coefficient (ADC) of water. Bone perfusion is a critical element in bone fracture healing, including microfracture healing, which is highly relevant in osteoporosis (Griffith and Guglielmi, 2013; Griffith et al., 2013). The ADC is associated with marrow compaction (Griffith and Guglielmi, 2013; Griffith et al., 2013). It decreases with the accumulation of fat cells within the bony trabeculae, which restricts extracellular diffusion. ADC values in females age less than 50 years were significantly higher than in males (presumably reflecting reduced fat packing), while ADC values of postmenopausal females were lower than in premenopausal females (Jie et al., 2016).

Quantitative muscle imaging

The paradigm of the bone−muscle unit has steered interest in quantitative muscle assessments such as muscle volume, CT muscle density and content, and distribution of adipose tissue. Fields of application are falls, fractures, and sarcopenia, where muscle function and perhaps muscle mass are important parameters to measure. The typical anatomical location is the lower appendicular skeleton. Lean and fat mass can also be differentiated by DXA or bioelectrical impedance but these techniques do not provide a spatially resolved distribution of muscle and adipose tissue. This is the domain of CT and MRI.

At the thigh and calf, standard MR T1 sequences show excellent contrast between muscle and fat and display the inter- and intramuscular adipose tissue. Larger agglomerations of adipose tissue can be identified but the true fat content of muscle cannot be measured from T1-weighted images because the gray values do not scale in a known way with fat content (Hollingsworth et al., 2012). More quantitative MR techniques to determine fat fraction are spectroscopy and Dixon sequences (Grimm et al., 2018a, 2018b). In spectroscopy typically only a very small volume of interest ($\approx 1\ cm^3$) is analyzed, which is often not representative of the muscle−fat distribution, in particular in elderly and diseased subjects with a high muscle fat infiltration. MR Dixon sequences provide a scalable map of the fat fraction from 1% to 100%, in which a gray value of 1 corresponds to a fat fraction of 0.1% and a gray value of 1000 to a fat fraction of 100%. Intra- and extracellular lipids can be distinguished with MR spectroscopy (Velan et al., 2007) but not with Dixon sequences.

In contrast to MR, CT is faster, more widely available, and accessible and cheaper. Another advantage of CT is the possibility of quantifying muscle density, which linearly depends on the fat content of muscle. MRI and CT can both be used to measure muscle volume, but the spatial resolution of CT images is higher. Typical MR parameters are a slice

thickness of 3−5 mm and an in-plane pixel size of 0.4−0.8 mm, whereas in CT a slice thickness of 1 mm and an in-plane pixel size of 300 μm are state of the art parameters.

MR techniques have mostly been applied in sarcopenia and muscle diseases, whereas the association of muscle parameters with hip fracture risk has been investigated in some studies (Wong et al., 2014a, 2014b; Lang et al., 2008, 2010; Hahn and Won, 2016) using QCT or pQCT. In a CT study of the pelvis from Lang (Lang et al., 2008), CSA of total fat and extensor and adductor muscles, and CT attenuation of adductor muscles, remained significantly lower in fractured subjects after adjustment for age and BMI. Compared with DXA aBMD alone, fracture discrimination was improved by the inclusion of the soft tissue descriptors in a multivariate model. In the Health, Aging, and Body Composition (Health ABC) Study (Lang et al., 2010), CT attenuation of the thigh muscle predicted hip fracture with a RR of 1.4 after adjustment for aBMD. In the MrOS study, composite descriptors combining the stress strain index or bending strength of bone with muscle cross-sectional area were determined by pQCT of the lower limb. These descriptors predicted hip fracture with a hazard ratio of 1.2 after adjustment for aBMD of the spine and total hip (Wong et al., 2014a). In the EFFECT study the amount of adipose tissue of the upper thigh and the distribution of the adipose tissue in the muscles discriminated hip fracture (AUC 0.85) as well as trochanteric trabecular BMD combined with neck cortical thickness (AUC 0.84) (Mühlberg et al., 2019; Muhlberg et al., 2017).

Summary

Musculoskeletal quantitative and semiquantitative in vivo imaging has matured considerably since 2009. While radiography is the mainstay of fracture diagnosis, most attempts to improve hip fracture prediction using QCT, FEA, or trabecular bone architecture beyond the use of aBMD determined by DXA were not unduly successful. In osteoporosis, bone is lost and fracture risk increased but the remaining bone is optimally distributed so that the integral density remains the essential parameter to be determined. In the spine the projectional DXA technique often overestimates aBMD, particularly in older subjects due to degenerative change and aortic calcification, so for vertebral fracture prediction the use of QCT is better. This is important because prevalent vertebral fractures are an important risk factor for new fractures. The technique of opportunistic screening and the use of existing clinical CT scans may open new strategies for identifying patients with high fracture risk. Imaging of muscle and adipose tissue in the upper thigh and pelvis region may improve hip fracture risk prediction because they are associated with muscle function and therefore probably with falls, the component so far not considered in hip fracture prediction.

The introduction of HR-pQCT has enabled in vivo quantification of trabecular architecture and cortical parameters at the distal radius and tibia. Together with the differentiation of cortical and trabecular compartments at the spine and hip by QCT and the analysis of strength by FEA, a wealth of new quantitative parameters characterizing bone quality has been introduced that already have greatly improved the understanding of pathophysiology and the mechanisms of anti-osteoporotic medication. However, the multitude of parameters is confusing for the non-expert and these should be consolidated into those that are really independent of one another and thus provide unique information.

There are several new developments in MRI that should gain more attention in the bone field. Quantitative imaging of cortical water may be an important component to better understand bone strength. Current FEA techniques use only the BMD distribution as measured by QCT as input. The second important achievement is the possibility of marrow fat imaging, including the differentiation of red and yellow marrow. While in elderly subjects most of the bone marrow is composed of fat, at age 50, in the spine about 50% is red marrow. However, this portion decreases with advancing age. Thus in particular in QCT, changes in BMD observed beyond 5 years or associated with diabetes may be overestimated and MRI marrow measurements may offer a correction strategy. MRI remains the most important technique for muscle imaging, but in the periphery where radiation exposure is low, CT may be an alternative. Also in opportunistic screening muscle analysis of existing CT images may be an alternative.

References

Abbasi-Rad, S., Saligheh Rad, H., 2017. Quantification of human cortical bone bound and free water in vivo with ultrashort echo time MR imaging: a model-based approach. Radiology 283 (3), 862−872.

Adams, J.E., Engelke, K., Zemel, B.S., Ward, K.A., International Society of Clinical D, 2014. Quantitative computer tomography in children and adolescents: the 2013 ISCD pediatric official positions. J. Clin. Densitom. 17 (2), 258−274.

Ahmad, O., Ramamurthi, K., Wilson, K.E., Engelke, K., Prince, R.L., Taylor, R.H., 2010. Volumetric DXA (VXA): a new method to extract 3D information from multiple in vivo DXA images. J. Bone Miner. Res. 25 (12), 2744−2751.

Albert, S.G., Reddy, S., 2017. Clinical evaluation of cost efficacy of drugs for treatment of osteoporosis: a meta-analysis. Endocr. Pract. 23 (7), 841−856.

Alvarenga, J.C., Fuller, H., Pasoto, S.G., Pereira, R.M., 2017. Age-related reference curves of volumetric bone density, structure, and biomechanical parameters adjusted for weight and height in a population of healthy women: an HR-pQCT study. Osteoporos. Int. 28 (4), 1335−1346.

Austin, M., Yang, Y.C., Vittinghoff, E., Adami, S., Boonen, S., Bauer, D.C., et al., 2012. Relationship between bone mineral density changes with denosumab treatment and risk reduction for vertebral and nonvertebral fractures. J. Bone Miner. Res. 27 (3), 687−693.

Baum, T., Carballido-Gamio, J., Huber, M.B., Muller, D., Monetti, R., Rath, C., et al., 2010. Automated 3D trabecular bone structure analysis of the proximal femur—prediction of biomechanical strength by CT and DXA. Osteoporos. Int. 21 (9), 1553−1564.

Baum, T., Muller, D., Dobritz, M., Rummeny, E.J., Link, T.M., Bauer, J.S., 2011. BMD measurements of the spine derived from sagittal reformations of contrast-enhanced MDCT without dedicated software. Eur. J. Radiol. 80 (2), e140−e145.

Beck, T.J., Christopher, B.R., Warden, K.E., Scott, W.W., Rao, G.U., 1990. Predicting femoral neck strength from bone mineral data: a structural approach. Investig. Radiol. 25, 6−18.

Bessho, M., Ohnishi, I., Okazaki, H., Sato, W., Kominami, H., Matsunaga, S., et al., 2004. Prediction of the strength and fracture location of the femoral neck by CT-based finite-element method: a preliminary study on patients with hip fracture. J. Orthop. Sci. 9 (6), 545−550.

Black, D.M., Arden, N.K., Palermo, L., Pearson, J., Cummings, S.R., 1999. Prevalent vertebral deformities predict hip fractures and new vertebral deformities but not wrist fractures. Study of Osteoporotic Fractures Research Group. J. Bone Miner. Res. 14 (5), 821−828.

Black, D.M., Delmas, P.D., Eastell, R., Reid, I.R., Boonen, S., Cauley, J.A., et al., 2007. Once-yearly zoledronic acid for treatment of postmenopausal osteoporosis. N. Engl. J. Med. 356 (18), 1809−1822.

Black, D.M., Cauley, J.A., Wagman, R., Ensrud, K., Fink, H.A., Hillier, T.A., et al., 2018. The ability of a single BMD and fracture history assessment to predict fracture over 25 years in postmenopausal women: the study of osteoporotic fractures. J. Bone Miner. Res. 33 (3), 389−395.

Blake, G.M., Fogelman, I., 1997. Technical principles of dual energy x-ray absorptiometry. Semin. Nucl. Med. 27 (3), 210−228.

Blake, G.M., Fogelman, I., 2007. Effect of bone strontium on BMD measurements. J. Clin. Densitom. 10 (1), 34−38.

Blake, G.M., Fogelman, I., 2008. How important are BMD accuracy errors for the clinical interpretation of DXA scans? J. Bone Miner. Res. 23 (4), 457−462.

Blake, G.M., Griffith, J.F., Yeung, D.K., Leung, P.C., Fogelman, I., 2009. Effect of increasing vertebral marrow fat content on BMD measurement, T-score status and fracture risk prediction by DXA. Bone 44 (3), 495−501.

Bolotin, H.H., 2001. Inaccuracies inherent in dual-energy X-ray absorptiometry in vivo bone mineral densitometry may flaw osteopenic/osteoporotic interpretations and mislead assessment of antiresorptive therapy effectiveness. Bone 28 (5), 548−555.

Boonen, S., Adachi, J.D., Man, Z., Cummings, S.R., Lippuner, K., Torring, O., et al., 2011. Treatment with denosumab reduces the incidence of new vertebral and hip fractures in postmenopausal women at high risk. J. Clin. Endocrinol. Metab. 96 (6), 1727−1736.

Borggrefe, J., de Buhr, T., Shrestha, S., Marshall, L.M., Orwoll, E., Peters, K., et al., 2016. Association of 3D geometric measures derived from quantitative computed tomography with hip fracture risk in older men. J. Bone Miner. Res. 31 (8), 1550−1558.

Bousson, V., Meunier, A., Bergot, C., Vicaut, E., Rocha, M.A., Morais, M.H., et al., 2001. Distribution of intracortical porosity in human midfemoral cortex by age and gender. J. Bone Miner. Res. 16 (7), 1308−1317.

Bousson, V.D., Adams, J., Engelke, K., Aout, M., Cohen-Solal, M., Bergot, C., et al., 2011. In vivo discrimination of hip fracture with quantitative computed tomography: results from the prospective European femur fracture study (EFFECT). J. Bus. Manag. Res. 26 (4), 881−893.

Boutroy, S., Bouxsein, M.L., Munoz, F., Delmas, P.D., 2005. In vivo assessment of trabecular bone microarchitecture by high-resolution peripheral quantitative computed tomography. J. Clin. Endocrinol. Metab. 90 (12), 6508−6515.

Boutroy, S., Khosla, S., Sornay-Rendu, E., Zanchetta, M.B., McMahon, D.J., Zhang, C.A., et al., 2016. Microarchitecture and peripheral BMD are impaired in postmenopausal white women with fracture independently of total hip T-score: an international multicenter study. J. Bone Miner. Res. 31 (6), 1158−1166.

Boutry, N., Cortet, B., Chappard, D., Dubois, P., Demondion, X., Marchandise, X., et al., 2004. Bone structure of the calcaneus: analysis with magnetic resonance imaging and correlation with histomorphometric study. Osteoporos. Int. 15 (10), 827−833.

Bouxsein, M.L., Melton III, L.J., Riggs, B.L., Muller, J., Atkinson, E.J., Oberg, A.L., et al., 2006. Age- and sex-specific differences in the factor of risk for vertebral fracture: a population-based study using QCT. J. Bone Miner. Res. 21 (9), 1475−1482.

Bredbenner, T.L., Mason, R.L., Havill, L.M., Orwoll, E.S., Nicolella, D.P., Osteoporotic Fractures in Men Study, 2014. Fracture risk predictions based on statistical shape and density modeling of the proximal femur. J. Bone Miner. Res. 29 (9), 2090−2100.

Broy, S.B., Cauley, J.A., Lewiecki, M.E., Schousboe, J.T., Shepherd, J.A., Leslie, W.D., 2015. Fracture risk prediction by non-BMD DXA measures: the 2015 ISCD official positions part 1: hip geometry. J. Clin. Densitom. 18 (3), 287−308.

Bruno, A.G., Broe, K.E., Zhang, X., Samelson, E.J., Meng, C.A., Manoharan, R., et al., 2014. Vertebral size, bone density, and strength in men and women matched for age and areal spine BMD. J. Bone Miner. Res. 29 (3), 562−569.

Burghardt, A.J., Link, T.M., Majumdar, S., 2011. High-resolution computed tomography for clinical imaging of bone microarchitecture. Clin. Orthop. Relat. Res. 469 (8), 2179−2193.

Burghardt, A.J., Pialat, J.B., Kazakia, G.J., Boutroy, S., Engelke, K., Patsch, J.M., et al., 2013. Multicenter precision of cortical and trabecular bone quality measures assessed by high-resolution peripheral quantitative computed tomography. J. Bone Miner. Res. 28 (3), 524−536.

Burt, L.A., Macdonald, H.M., Hanley, D.A., Boyd, S.K., 2014. Bone microarchitecture and strength of the radius and tibia in a reference population of young adults: an HR-pQCT study. Arch. Osteoporos. 9, 183.

Burt, L.A., Bhatla, J.L., Hanley, D.A., Boyd, S.K., 2017. Cortical porosity exhibits accelerated rate of change in peri- compared with post-menopausal women. Osteoporos. Int. 28 (4), 1423−1431.

Camacho, P.M., Petak, S.M., Binkley, N., Clarke, B.L., Harris, S.T., Hurley, D.L., et al., 2016. American Association of Clinical Endocrinologists and American College of Endocrinology Clinical Practice Guidelines for the diagnosis and treatment of postmenopausal osteoporosis—2016—executive summary. Endocr. Pract. 22 (9), 1111−1118.

Cann, C.E., Adams, J.E., Brown, J.K., Brett, A.D., 2014. CTXA hip—an extension of classical DXA measurements using quantitative CT. PLoS One 9 (3), e91904.

Carballido-Gamio, J., Harnish, R., Saeed, I., Streeper, T., Sigurdsson, S., Amin, S., et al., 2013. Proximal femoral density distribution and structure in relation to age and hip fracture risk in women. J. Bone Miner. Res. 28 (3), 537−546.

Carballido-Gamio, J., Harnish, R., Saeed, I., Streeper, T., Sigurdsson, S., Amin, S., et al., 2013. Structural patterns of the proximal femur in relation to age and hip fracture risk in women. Bone 57 (1), 290−299.

Carballido-Gamio, J., Bonaretti, S., Saeed, I., Harnish, R., Recker, R., Burghardt, A.J., et al., 2015. Automatic multi-parametric quantification of the proximal femur with quantitative computed tomography. Quant. Imag. Med. Surg. 5 (4), 552−568.

Carpenter, R.D., Sigurdsson, S., Zhao, S., Lu, Y., Eiriksdottir, G., Sigurdsson, G., et al., 2011. Effects of age and sex on the strength and cortical thickness of the femoral neck. Bone 48 (4), 741−747.

Chang, G., Boone, S., Martel, D., Rajapakse, C.S., Hallyburton, R.S., Valko, M., et al., 2017. MRI assessment of bone structure and microarchitecture. J. Magn. Reson. Imaging 46 (2), 323−337.

Chappard, C., Bousson, V., Bergot, C., Mitton, D., Marchadier, A., Moser, T., et al., 2010. Prediction of femoral fracture load: cross-sectional study of texture analysis and geometric measurements on plain radiographs versus bone mineral density. Radiology 255 (2), 536−543.

Checefsky, W.A., Abidin, A.Z., Nagarajan, M.B., Bauer, J.S., Baum, T., Wismuller, A., 2016. Assessing vertebral fracture risk on volumetric quantitative computed tomography by geometric characterization of trabecular bone structure. Proc. SPIE-Int. Soc. Opt. Eng. 9785.

Chen, J., Carl, M., Ma, Y., Shao, H., Lu, X., Chen, B., et al., 2016. Fast volumetric imaging of bound and pore water in cortical bone using three-dimensional ultrashort-TE (UTE) and inversion recovery UTE sequences. NMR Biomed. 29 (10), 1373−1380.

Cheng, X., Li, J., Lu, Y., Keyak, J., Lang, T., 2007. Proximal femoral density and geometry measurements by quantitative computed tomography: association with hip fracture. Bone 40 (1), 169−174.

Cody, D.D., Gross, G.J., Hou, F.J., Spencer, H.J., Goldstein, S.A., Fyhrie, D.P., 1999. Femoral strength is better predicted by finite element models than QCT and DXA. J. Biomech. 32 (10), 1013−1020.

Compston, J., 2009. Monitoring osteoporosis treatment. Best Pract. Res. Clin. Rheumatol. 23 (6), 781−788.

Crabtree, N.J., Arabi, A., Bachrach, L.K., Fewtrell, M., El-Hajj Fuleihan, G., Kecskemethy, H.H., et al., 2014. Dual-energy X-ray absorptiometry interpretation and reporting in children and adolescents: the revised 2013 ISCD pediatric official positions. J. Clin. Densitom. 17 (2), 225−242.

Cummings, S.R., Cauley, J.A., Palermo, L., Ross, P.D., Wasnich, R.D., Black, D., et al., 1994. Racial differences in hip axis lengths might explain racial differences in rates of hip fractures. Osteoporos. Int. 4, 226−229.

Cummings, S.R., Karpf, D.B., Harris, F., Genant, H.K., Ensrud, K., LaCroix, A.Z., et al., 2002. Improvement in spine bone density and reduction in risk of vertebral fractures during treatment with antiresorptive drugs. Am. J. Med. 112 (4), 281−289.

Dall'Ara, E., Pahr, D., Varga, P., Kainberger, F., Zysset, P., 2012. QCT-based finite element models predict human vertebral strength in vitro significantly better than simulated DEXA. Osteoporos. Int. 23 (2), 563−572.

Danielson, M.E., Beck, T.J., Karlamangla, A.S., Greendale, G.A., Atkinson, E.J., Lian, Y., et al., 2012. A comparison of DXA and CT based methods for estimating the strength of the femoral neck in post-menopausal women. Osteoporos. Int.

Delmas, P.D., Li, Z., Cooper, C., 2004. Relationship between changes in bone mineral density and fracture risk reduction with antiresorptive drugs: some issues with meta-analyses. J. Bone Miner. Res. 19 (2), 330−337.

Donnelly, E., 2011. Methods for assessing bone quality: a review. Clin. Orthop. Relat. Res. 469 (8), 2128−2138.

Dougherty, G., Newman, D., 1999. Measurement of thickness and density of thin structures by computed tomography: a simulation study. Med. Phys. 26 (7), 1341−1348.

Duda, S.H., Laniado, M., Schick, F., Strayle, M., Claussen, C.D., 1995. Normal bone marrow in the sacrum of young adults: differences between the sexes seen on chemical-shift MR imaging. AJR Am. J. Roentgenol. 164 (4), 935−940.

Einhorn, T.A., 1992. Bone strength: the bottom line. Calcif. Tissue Int. 51 (5), 333−339.

Ellouz, R., Chapurlat, R., van Rietbergen, B., Christen, P., Pialat, J.B., Boutroy, S., 2014. Challenges in longitudinal measurements with HR-pQCT: evaluation of a 3D registration method to improve bone microarchitecture and strength measurement reproducibility. Bone 63, 147−157.

Emohare, O., Cagan, A., Polly Jr., D.W., Gertner, E., 2014. Opportunistic computed tomography screening shows a high incidence of osteoporosis in ankylosing spondylitis patients with acute vertebral fractures. J. Clin. Densitom.

Engelke, K., 2017. Quantitative computed tomography-current status and new developments. J. Clin. Densitom. 20 (3), 309−321.

Engelke, K., Adams, J.E., Armbrecht, G., Augat, P., Bogado, C.E., Bouxsein, M.L., et al., 2008. Clinical use of quantitative computed tomography and peripheral quantitative computed tomography in the management of osteoporosis in adults: the 2007 ISCD official positions. J. Clin. Densitom. 11 (1), 123−162.

Engelke, K., Mastmeyer, A., Bousson, V., Fuerst, T., Laredo, J.D., Kalender, W.A., 2009. Reanalysis precision of 3D quantitative computed tomography (QCT) of the spine. Bone 44 (4), 566−572.

Engelke, K., Nagase, S., Fuerst, T., Small, M., Kuwayama, T., Deacon, S., et al., 2014. The effect of the cathepsin K inhibitor ONO-5334 on trabecular and cortical bone in postmenopausal osteoporosis: the OCEAN study. J. Bone Miner. Res. 29 (3), 629−638.

Engelke, K., Lang, T., Khosla, S., Qin, L., Zysset, P., Leslie, W.D., et al., 2015. Clinical use of quantitative computed tomography (QCT) of the hip in the management of osteoporosis in adults: the 2015 ISCD official positions-part I. J. Clin. Densitom. 18 (3), 338−358.

Engelke, K., Fuerst, T., Dardzinski, B., Kornak, J., Ather, S., Genant, H.K., et al., 2015. Odanacatib treatment affects trabecular and cortical bone in the femur of postmenopausal women: results of a two-year placebo-controlled trial. J. Bone Miner. Res. 30 (1), 30–38.

Engelke, K., Lang, T., Khosla, S., Qin, L., Zysset, P., Leslie, W.D., et al., 2015. Clinical use of quantitative computed tomography-based advanced techniques in the management of osteoporosis in adults: the 2015 ISCD official positions-part III. J. Clin. Densitom. 18 (3), 393–407.

Ettinger, B., Black, D.M., Mitlak, B.H., Knickerbocker, R.K., Nickelsen, T., Genant, H.K., et al., 1999. Reduction of vertebral fracture risk in postmenopausal women with osteoporosis treated with raloxifene: results from a 3-year randomized clinical trial. Multiple Outcomes of Raloxifene Evaluation (MORE) Investigators. JAMA 282 (7), 637–645.

Faisal, T.R., Luo, Y., 2017. Study of the variations of fall induced hip fracture risk between right and left femurs using CT-based FEA. Biomed. Eng. Online 16 (1), 116.

Fan, B., Lewiecki, E.M., Sherman, M., Lu, Y., Miller, P.D., Genant, H.K., et al., 2008. Improved precision with hologic apex software. Osteoporos. Int. 19 (11), 1597–1602.

Faulkner, K.G., McClung, M., Cummings, S.R., 1994. Automated evaluation of hip axis length for predicting hip fracture. J. Bone Miner. Res. 9 (7), 1065–1070.

Fitzpatrick, L.A., Dabrowski, C.E., Cicconetti, G., Gordon, D.N., Fuerst, T., Engelke, K., et al., 2012. Ronacaleret, a calcium-sensing receptor antagonist, increases trabecular but not cortical bone in postmenopausal women. J. Bone Miner. Res. 27 (2), 255–262.

Flicker, L., Faulkner, K.G., Hopper, J.L., Green, R.M., Kaymacki, B., Nowson, C.A., et al., 1996. Determinants of hip axis length in women aged 10-89: a twin study. Bone 18, 41–45.

Gabel, L., Macdonald, H.M., Nettlefold, L.A., McKay, H.A., 2018. Sex-, ethnic-, and age-specific centile curves for pQCT- and HR-pQCT-derived measures of bone structure and strength in adolescents and young adults. J. Bone Miner. Res.

Gausden, E.B., Nwachukwu, B.U., Schreiber, J.J., Lorich, D.G., Lane, J.M., 2017. Opportunistic use of CT imaging for osteoporosis screening and bone density assessment: a qualitative systematic review. J. Bone Joint Surg. Am. 99 (18), 1580–1590.

Genant, H., Cann, C., Ettinger, B., Gordon, G., 1982. Determination of bone mineral loss in the axial skeleton of oophorectomized women using quantitative computed tomography. J. Comput. Assist. Tomogr. 6, 217–218.

Genant, H.K., Wu, C.Y., van Kuijk, C., Nevitt, M., 1993. Vertebral fracture assessment using a semi-quantitative technique. J. Bone Miner. Res. 8, 1137–1148.

Genant, H.K., Grampp, S., Glüer, C.C., Faulkner, K.G., Jergas, M., Engelke, K., et al., 1994. Universal standardization for dual x-ray absorptiometry: patient and phantom cross-calibration results. J. Bone Miner. Res. 9 (10), 1503–1514.

Genant, H.K., Jergas, M., Palermo, L., Nevitt, M., Valentin, R.S., Black, D., et al., 1996. Comparison of semiquantitative visual and quantitative morphometric assessment of prevalent and incident vertebral fractures in osteoporosis the study of osteoporotic fractures research group. J. Bone Miner. Res. 11 (7), 984–996.

Genant, H.K., Siris, E., Crans, G.G., Desaiah, D., Krege, J.H., 2005. Reduction in vertebral fracture risk in teriparatide-treated postmenopausal women as assessed by spinal deformity index. Bone 37 (2), 170–174.

Genant, H.K., Libanati, C., Engelke, K., Zanchetta, J.R., Hoiseth, A., Yuen, C.K., et al., 2013. Improvements in hip trabecular, subcortical, and cortical density and mass in postmenopausal women with osteoporosis treated with denosumab. Bone 56 (2), 482–488.

Glüer, C.C., Genant, H.K., 1989. Impact of marrow fat on accuracy of quantitative CT. J. Comput. Assist. Tomogr. 13 (6), 1023–1035.

Glüer, C.C., Cummings, S.R., Pressman, A., Li, J., Glüer, K., Faulkner, K.G., et al., 1994. Prediction of hip fractures from pelvic radiographs: the study of osteoporotic fractures. J. Bone Miner. Res. 9, 671–677.

Goh, J.C., Low, S.L., Bose, K., 1995. Effect of femoral rotation on bone mineral density measurements with dual energy X-ray absorptiometry. Calcif. Tissue Int. 57 (5), 340–343.

Grados, F., Marcelli, C., Dargent-Molina, P., Roux, C., Vergnol, J.F., Meunier, P.J., et al., 2004. Prevalence of vertebral fractures in French women older than 75 years from the EPIDOS study. Bone 34 (2), 362–367.

Graeff, C., Marin, F., Petto, H., Kayser, O., Reisinger, A., Pena, J., et al., 2013. High resolution quantitative computed tomography-based assessment of trabecular microstructure and strength estimates by finite-element analysis of the spine, but not DXA, reflects vertebral fracture status in men with glucocorticoid-induced osteoporosis. Bone 52 (2), 568–577.

Griffith, J., 2017. Age-related changes in the bone marrow. Curr. Radiol. Rep. 5, 24.

Griffith, J., 2013. Bone marrow changes in osteoporosis. In: Guglielmi, G. (Ed.), Medical Radiology, Osteoporosis and Bone Densitometry Measurements. Springer, pp. 69–85.

Griffith, J.F., Yeung, D.K., Leung, J.C., Kwok, T.C., Leung, P.C., 2011. Prediction of bone loss in elderly female subjects by MR perfusion imaging and spectroscopy. Eur. Radiol. 21 (6), 1160–1169.

Griffith, J.F., Yeung, D.K., Ma, H.T., Leung, J.C., Kwok, T.C., Leung, P.C., 2012. Bone marrow fat content in the elderly: a reversal of sex difference seen in younger subjects. J. Magn. Reson. Imaging 36 (1), 225–230.

Griffith, J., 2013. Age-related physiological changes of the bone marrow and immune system. In: Guglielmi, G., Peh, W., Guermazi, A. (Eds.), Geriatric Imaging. Springer.

Grimm, A., Meyer, H., Nickel, M.D., Nittka, M., Raithel, E., Chaudry, O., et al., 2018. A comparison between 6-point Dixon MRI and MR spectroscopy to quantify muscle fat in the thigh of subjects with sarcopenia. JFA (online).

Grimm, A., Meyer, H., Nickel, M.D., Raithel, E., Chaudry, O., Friedberger, A., et al., 2018. Evaluation of 2-point, 3-point, and 6-point dixon magnetic resonance imaging with flexible echo timing for muscle fat quantification. Eur. J. Radiol. 103, 57–64.

Hagiwara, S., Engelke, K., Yang, S.-O., Dhillon, M.S., Guglielmi, G., Nelson, D.S., et al., 1994. Dual x-ray absorptiometry forearm software: accuracy and intermachine relationship. J. Bone Miner. Res. 9, 1425−1427.

Hahn, M.H., Won, Y.Y., 2016. Bone mineral density and fatty degeneration of thigh muscles measured by computed tomography in hip fracture patients. J. Bone Metab. 23 (4), 215−221.

Haider, I.T., Goldak, J., Frei, H., 2018. Femoral fracture load and fracture pattern is accurately predicted using a gradient-enhanced quasi-brittle finite element model. Med. Eng. Phys.

Hans, D., Barthe, N., Boutroy, S., Pothuaud, L., Winzenrieth, R., Krieg, M.A., 2011. Correlations between trabecular bone score, measured using anteroposterior dual-energy X-ray absorptiometry acquisition, and 3-dimensional parameters of bone microarchitecture: an experimental study on human cadaver vertebrae. J. Clin. Densitom. 14 (3), 302−312.

Harvey, N.C., Gluer, C.C., Binkley, N., McCloskey, E.V., Brandi, M.L., Cooper, C., et al., 2015. Trabecular bone score (TBS) as a new complementary approach for osteoporosis evaluation in clinical practice. Bone 78, 216−224.

Hochberg, M.C., Greenspan, S., Wasnich, R.D., Miller, P., Thompson, D.E., Ross, P.D., 2002. Changes in bone density and turnover explain the reductions in incidence of nonvertebral fractures that occur during treatment with antiresorptive agents. J. Clin. Endocrinol. Metab. 87 (4), 1586−1592.

Hollingsworth, K.G., de Sousa, P.L., Straub, V., Carlier, P.G., 2012. Towards harmonization of protocols for MRI outcome measures in skeletal muscle studies: consensus recommendations from two TREAT-NMD NMR workshops, 2 May 2010, Stockholm, Sweden, 1−2 October 2009, Paris, France. Neuromuscul. Disord. 22 (Suppl. 2), S54−S67.

Hopper, K.D., Wang, M.P., Kunselman, A.R., 2000. The use of clinical CT for baseline bone density assessment. J. Comput. Assist. Tomogr. 24 (6), 896−899.

Humbert, L., Martelli, Y., Fonolla, R., Steghofer, M., Di Gregorio, S., Malouf, J., et al., 2017. 3D-DXA: assessing the femoral shape, the trabecular macrostructure and the cortex in 3D from DXA images. IEEE Trans. Med. Imaging 36 (1), 27−39.

Imai, K., Ohnishi, I., Matsumoto, T., Yamamoto, S., Nakamura, K., 2009. Assessment of vertebral fracture risk and therapeutic effects of alendronate in postmenopausal women using a quantitative computed tomography-based nonlinear finite element method. Osteoporos. Int. 20 (5), 801−810.

Ito, M., 2005. Assessment of bone quality using micro-computed tomography (micro-CT) and synchrotron micro-CT. J. Bone Miner. Metab. 23 (Suppl. l), 115−121.

Jie, H., Hao, F., Na, L.X., 2016. Vertebral bone marrow diffusivity in healthy adults at 3T diffusion-weighted imaging. Acta Radiol. 57 (10), 1238−1243.

Johannesdottir, F., Poole, K.E., Reeve, J., Siggeirsdottir, K., Aspelund, T., Mogensen, B., et al., 2011. Distribution of cortical bone in the femoral neck and hip fracture: a prospective case-control analysis of 143 incident hip fractures; the AGES-REYKJAVIK study. Bone 48 (6), 1268−1276.

Johansson, H., Kanis, J.A., Oden, A., Johnell, O., McCloskey, E., 2009. BMD, clinical risk factors and their combination for hip fracture prevention. Osteoporos. Int. 20 (10), 1675−1682.

Johnell, O., Kanis, J.A., Oden, A., Johansson, H., De Laet, C., Delmas, P., et al., 2005. Predictive value of BMD for hip and other fractures. J. Bone Miner. Res. 20 (7), 1185−1194.

Jorgenson, B.L., Buie, H.R., McErlain, D.D., Sandino, C., Boyd, S.K., 2015. A comparison of methods for in vivo assessment of cortical porosity in the human appendicular skeleton. Bone 73, 167−175.

Kalender, W., Engelke, K., Fuerst, T., Glüer, C.-C., Laugier, P., Shepherd, J., 2009. ICRU report 81: quantitative aspects of bone densitometry. J. ICRU 9 (1).

Kanis, J.A., Oden, A., Johansson, H., Borgstrom, F., Strom, O., McCloskey, E., 2009. FRAX and its applications to clinical practice. Bone 44 (5), 734−743.

Khoo, B.C., Brown, K., Cann, C., Zhu, K., Henzell, S., Low, V., et al., 2009. Comparison of QCT-derived and DXA-derived areal bone mineral density and T scores. Osteoporos. Int. 20 (9), 1539−1545.

Ko, B.J., Myung, S.K., Cho, K.H., Park, Y.G., Kim, S.G., Kim do, H., et al., 2016. Relationship between bariatric surgery and bone mineral density: a meta-analysis. Obes. Surg. 26 (7), 1414−1421.

Krege, J.H., Wan, X., Lentle, B.C., Berger, C., Langsetmo, L., Adachi, J.D., et al., 2013. Fracture risk prediction: importance of age, BMD and spine fracture status. Bonekey Rep. 2, 404.

Kugel, H., Jung, C., Schulte, O., Heindel, W., 2001. Age- and sex-specific differences in the 1H-spectrum of vertebral bone marrow. J. Magn. Reson. Imaging 13 (2), 263−268.

Laib, A., Ruegsegger, P., 1999. Calibration of trabecular bone structure measurements of in vivo three-dimensional peripheral quantitative computed tomography with 28-microm-resolution microcomputed tomography. Bone 24 (1), 35−39.

Lang, T.F., Keyak, J.H., Heitz, M.W., Augat, P., Lu, Y., Mathur, A., et al., 1997. Volumetric quantitative computed tomography of the proximal femur: precision and relation to bone strength. Bone 21 (1), 101−108.

Lang, T., Koyama, A., Li, C., Li, J., Lu, Y., Saeed, I., et al., 2008. Pelvic body composition measurements by quantitative computed tomography: association with recent hip fracture. Bone 42 (4), 798−805.

Lang, T., Cauley, J.A., Tylavsky, F., Bauer, D., Cummings, S., Harris, T.B., et al., 2010. Computed tomographic measurements of thigh muscle cross-sectional area and attenuation coefficient predict hip fracture: the health, aging, and body composition study. J. Bone Miner. Res. 25 (3), 513−519.

Lang, T.F., Sigurdsson, S., Karlsdottir, G., Oskarsdottir, D., Sigmarsdottir, A., Chengshi, J., et al., 2012. Age-related loss of proximal femoral strength in elderly men and women: the age gene/environment susceptibility study—Reykjavik. Bone 50 (3), 743−748.

Langdahl, B.L., Libanati, C., Crittenden, D.B., Bolognese, M.A., Brown, J.P., Daizadeh, N.S., et al., 2017. Romosozumab (sclerostin monoclonal antibody) versus teriparatide in postmenopausal women with osteoporosis transitioning from oral bisphosphonate therapy: a randomised, open-label, phase 3 trial. Lancet 390 (10102), 1585−1594.

Lee, D.C., Hoffmann, P.F., Kopperdahl, D.L., Keaveny, T.M., 2017. Phantomless calibration of CT scans for measurement of BMD and bone strength-inter-operator reanalysis precision. Bone 103, 325−333.

Lentle, B.C., Brown, J.P., Khan, A., Leslie, W.D., Levesque, J., Lyons, D.J., et al., 2007. Recognizing and reporting vertebral fractures: reducing the risk of future osteoporotic fractures. Can. Assoc. Radiol. J. 58 (1), 27−36.

Lespessailles, E., Hambli, R., Ferrari, S., 2016. Osteoporosis drug effects on cortical and trabecular bone microstructure: a review of HR-pQCT analyses. Bonekey Rep. 5, 836.

Lewiecki, E.M., Compston, J.E., Miller, P.D., Adachi, J.D., Adams, J.E., Leslie, W.D., et al., 2011. FRAX((R)) bone mineral density task force of the 2010 joint international society for clinical densitometry & international osteoporosis foundation position development conference. J. Clin. Densitom. 14 (3), 223−225.

Li, W., Kornak, J., Harris, T., Keyak, J., Li, C., Lu, Y., et al., 2009. Identify fracture-critical regions inside the proximal femur using statistical parametric mapping. Bone 44 (4), 596−602.

Li, C., Seifert, A.C., Rad, H.S., Bhagat, Y.A., Rajapakse, C.S., Sun, W., et al., 2016. Cortical bone water concentration: dependence of MR imaging measures on age and pore volume fraction. Radiology 280 (2), 653.

Lima, G.L., Paupitz, J.A., Aikawa, N.E., Alvarenga, J.C., Pereira, R.M.R., 2018. A randomized double-blind placebo-controlled trial of vitamin D supplementation in juvenile-onset systemic lupus erythematosus: positive effect on trabecular microarchitecture using HR-pQCT. Osteoporos. Int. 29 (3), 587−594.

Link, T.M., Bauer, J.S., 2002. Imaging of trabecular bone structure. Semin. Muscoskel. Radiol. 6 (3), 253−261.

Link, T.M., Vieth, V., Langenberg, R., Meier, N., Lotter, A., Newitt, D., et al., 2003. Structure analysis of high resolution magnetic resonance imaging of the proximal femur: in vitro correlation with biomechanical strength and BMD. Calcif. Tissue Int. 72 (2), 156−165.

Looker, A.C., Orwoll, E.S., Johnston Jr., C.C., Lindsay, R.L., Wahner, H.W., Dunn, W.L., et al., 1997. Prevalence of low femoral bone density in older U.S. adults from NHANES III. J. Bone Miner. Res. 12 (11), 1761−1768.

Macdonald, H.M., Maatta, M., Gabel, L., Mulpuri, K., McKay, H.A., 2018. Bone strength in girls and boys after a distal radius fracture: a 2-year HR-pQCT double cohort study. J. Bone Miner. Res. 33 (2), 229−240.

Magland, J., Vasilic, B., Wehrli, F.W., 2006. Fast low-angle dual spin-echo (FLADE): a new robust pulse sequence for structural imaging of trabecular bone. Magn. Reson. Med. 55 (3), 465−471.

Majumdar, S., Newitt, D., Jergas, M., Gies, A., Chiu, D., Osman, D., et al., 1995. Evaluation of technical factors affecting the quantification of trabecular bone structure using magnetic resonance imaging. Bone 17, 417−430.

Manhard, M.K., Horch, R.A., Gochberg, D.F., Nyman, J.S., Does, M.D., 2015. In vivo quantitative MR imaging of bound and pore water in cortical bone. Radiology 277 (1), 221−229.

Manske, S.L., Zhu, Y., Sandino, C., Boyd, S.K., 2015. Human trabecular bone microarchitecture can be assessed independently of density with second generation HR-pQCT. Bone 79, 213−221.

Marshall, D., Johnell, O., Wedel, H., 1996. Meta-analysis of how well measures of bone mineral density predict occurrence of osteoporotic fractures. BMJ 312 (7041), 1254−1259.

Martin, R.B., Burr, D.B., 1984. Non-invasive measurements of long bone cross-sectional moment of intertia by photon absorptiometry. J. Biomech. 17, 195−201.

Milovanovic, P., Rakocevic, Z., Djonic, D., Zivkovic, V., Hahn, M., Nikolic, S., et al., 2014. Nano-structural, compositional and micro-architectural signs of cortical bone fragility at the superolateral femoral neck in elderly hip fracture patients vs. healthy aged controls. Exp. Gerontol. 55, 19−28.

Montazel, J.L., Divine, M., Lepage, E., Kobeiter, H., Breil, S., Rahmouni, A., 2003. Normal spinal bone marrow in adults: dynamic gadolinium-enhanced MR imaging. Radiology 229 (3), 703−709.

Mosekilde, L., Viidik, A., Mosekilde, L., 1985. Correlation between the compressive strength of iliac and vertebral trabecular bone in normal individuals. Bone 8, 79−85.

Mühlberg, A., Museyko, O., Bousson, V., Pottecher, P., Laredo, J.D., Engelke, K., 2019. Three-dimensional distribution of muscle and adipose tissue of the thigh at CT: association with acute hip fracture, Radiology 290 (2), 426−434.

Muhlberg, A., Museyko, O., Laredo, J.D., Engelke, K., 2017. A reproducible semi-automatic method to quantify the muscle-lipid distribution in clinical 3D CT images of the thigh. PLoS One 12 (4), e0175174.

Museyko, O., Bousson, V., Adams, J., Laredo, J.D., Engelke, K., 2016. QCT of the proximal femur-which parameters should be measured to discriminate hip fracture? Osteoporos. Int. 27 (3), 1137−1147.

Museyko, O., Gerner, B., Engelke, K., 2017. A new method to determine cortical bone thickness in CT images using a hybrid approach of parametric profile representation and local adaptive thresholds: accuracy results. PLoS One 12 (11), e0187097.

Naylor, K.E., McCloskey, E.V., Eastell, R., Yang, L., 2013. Use of DXA-based finite element analysis of the proximal femur in a longitudinal study of hip fracture. J. Bone Miner. Res. 28 (5), 1014−1021.

Newman, D.L., Dougherty, G., al Obaid, A., al Hajrasy, H., 1998. Limitations of clinical CT in assessing cortical thickness and density. Phys. Med. Biol. 43 (3), 619−626.

Nicks, K.M., Amin, S., Melton III, L.J., Atkinson, E.J., McCready, L.K., Riggs, B.L., et al., 2013. Three-dimensional structural analysis of the proximal femur in an age-stratified sample of women. Bone 55 (1), 179−188.

Nishiyama, K.K., Shane, E., 2013. Clinical imaging of bone microarchitecture with HR-pQCT. Curr. Osteoporos. Rep. 11 (2), 147−155.

Paccou, J., Ward, K.A., Jameson, K.A., Dennison, E.M., Cooper, C., Edwards, M.H., 2016. Bone microarchitecture in men and women with diabetes: the importance of cortical porosity. Calcif. Tissue Int. 98 (5), 465−473.

Patsch, J.M., Burghardt, A.J., Yap, S.P., Baum, T., Schwartz, A.V., Joseph, G.B., et al., 2013. Increased cortical porosity in type 2 diabetic postmenopausal women with fragility fractures. J. Bone Miner. Res. 28 (2), 313–324.

Patsch, J.M., Li, X., Baum, T., Yap, S.P., Karampinos, D.C., Schwartz, A.V., et al., 2013. Bone marrow fat composition as a novel imaging biomarker in postmenopausal women with prevalent fragility fractures. J. Bone Miner. Res. 28 (8), 1721–1728.

Pickhardt, P.J., Bodeen, G., Brett, A., Brown, J.K., Binkley, N., 2015. Comparison of femoral neck BMD evaluation obtained using lunar DXA and QCT with asynchronous calibration from CT colonography. J. Clin. Densitom. 18 (1), 5–12.

Pickhardt, P.J., Lauder, T., Pooler, B.D., Munoz Del Rio, A., Rosas, H., Bruce, R.J., et al., 2016. Effect of IV contrast on lumbar trabecular attenuation at routine abdominal CT: correlation with DXA and implications for opportunistic osteoporosis screening. Osteoporos. Int. 27 (1), 147–152.

Poole, K.E., Treece, G.M., Mayhew, P.M., Vaculik, J., Dungl, P., Horak, M., et al., 2012. Cortical thickness mapping to identify focal osteoporosis in patients with hip fracture. PLoS One 7 (6), e38466.

Poole, K.E., Treece, G.M., Gee, A.H., Brown, J.P., McClung, M.R., Wang, A., et al., 2015. Denosumab rapidly increases cortical bone in key locations of the femur: a 3D bone mapping study in women with osteoporosis. J. Bone Miner. Res. 30 (1), 46–54.

Poole, K.E.S., Skingle, L., Gee, A.H., Turmezei, T.D., Johannesdottir, F., Blesic, K., et al., 2017. Focal osteoporosis defects play a key role in hip fracture. Bone 94, 124–134.

Pothuaud, L., Porion, P., Lespessailles, E., Benhamou, C.L., Levitz, P., 2000. A new method for three-dimensional skeleton graph analysis of porous media: application to trabecular bone microarchitecture. J. Microsc. 199 (Pt 2), 149–161.

Pothuaud, L., Levitz, P., Benhamou, C.L., 2001. Simulation of osteoporosis bone changes: effects on the degree of anisotropy. Adv. Exp. Med. Biol. 496, 111–121.

Pothuaud, L., Carceller, P., Hans, D., 2008. Correlations between grey-level variations in 2D projection images (TBS) and 3D microarchitecture: applications in the study of human trabecular bone microarchitecture. Bone 42 (4), 775–787.

Pottecher, P., Engelke, K., Duchemin, L., Museyko, O., Moser, T., Mitton, D., et al., 2016. Prediction of hip failure load: in vitro study of 80 femurs using three imaging methods and finite element models-the european fracture study (EFFECT). Radiology 280 (3), 837–847.

Prevrhal, S., Engelke, K., Kalender, W.A., 1999. Accuracy limits for the determination of cortical width and density: the influence of object size and CT imaging parameters. Phys. Med. Biol. 44, 751–764.

Rajamanohara, R., Robinson, J., Rymer, J., Patel, R., Fogelman, I., Blake, G.M., 2011. The effect of weight and weight change on the long-term precision of spine and hip DXA measurements. Osteoporos. Int. 22 (5), 1503–1512.

Rand, T., Seidl, G., Kainberger, F., Resch, A., Hittmair, K., Schneider, B., et al., 1997. Impact of spinal degenerative changes on the evaluation of bone mineral density with dual energy X-ray absorptiometry (DXA). Calcif. Tissue Int. 60 (5), 430–433.

Rea, J.A., Li, J., Blake, G.M., Steiger, P., Genant, H.K., Fogelman, I., 2000. Visual assessment of vertebral deformity by X-ray absorptiometry: a highly predictive method to exclude vertebral deformity. Osteoporos. Int. 11 (8), 660–668.

Reeve, J., 2017. Role of cortical bone in hip fracture. Bonekey Rep. 6, 867.

Robbins, J.A., Schott, A.M., Garnero, P., Delmas, P.D., Hans, D., Meunier, P.J., 2005. Risk factors for hip fracture in women with high BMD: EPIDOS study. Osteoporos. Int. 16 (2), 149–154.

Rosenthall, L., 2004. Range of change of measured BMD in the femoral neck and total hip with rotation in women. J. Bone Miner. Metab. 22 (5), 496–499.

Sabin, M.A., Blake, G.M., MacLaughlin-Black, S.M., Fogelman, I., 1995. The accuracy of volumetric bone density measurements in dual x-ray absorptiometry. Calcif. Tissue Int. 56 (3), 210–214.

Schousboe, J.T., Debold, C.R., 2006. Reliability and accuracy of vertebral fracture assessment with densitometry compared to radiography in clinical practice. Osteoporos. Int. 17 (2), 281–289.

Schuit, S.C., van der Klift, M., Weel, A.E., de Laet, C.E., Burger, H., Seeman, E., et al., 2004. Fracture incidence and association with bone mineral density in elderly men and women: the Rotterdam study. Bone 34 (1), 195–202.

Schwartz, A.V., 2015. Marrow fat and bone: review of clinical findings. Front. Endocrinol. 6, 40.

Shepherd, J.A., Cheng, X.G., Lu, Y., Njeh, C., Toschke, J., Engelke, K., et al., 2002. Universal standardization of forearm bone densitometry. J. Bone Miner. Res. 17 (4), 734–745.

Silva, B.C., Broy, S.B., Boutroy, S., Schousboe, J.T., Shepherd, J.A., Leslie, W.D., 2015. Fracture risk prediction by non-BMD DXA measures: the 2015 ISCD official positions part 2: trabecular bone score. J. Clin. Densitom. 18 (3), 309–330.

Singh, M., Riggs, B.L., Beabout, J.W., Jowsey, J., 1973. Femoral trabecular pattern index for evaluation of spinal osteoporosis. A detailed methodologic description. Mayo Clin. Proc. 48 (3), 184–189.

Siris, E.S., Chen, Y.T., Abbott, T.A., Barrett-Connor, E., Miller, P.D., Wehren, L.E., et al., 2004. Bone mineral density thresholds for pharmacological intervention to prevent fractures. Arch. Intern. Med. 164 (10), 1108–1112.

Siris, E.S., Genant, H.K., Laster, A.J., Chen, P., Misurski, D.A., Krege, J.H., 2007. Enhanced prediction of fracture risk combining vertebral fracture status and BMD. Osteoporos. Int. 18 (6), 761–770.

Smith, C.B., Smith, D.A., 1976. Relations between age, mineral density and mechanical properties of human femoral compacta. Acta Orthop. Scand. 47 (5), 496–502.

Sornay-Rendu, E., Boutroy, S., Duboeuf, F., Chapurlat, R.D., 2017. Bone microarchitecture assessed by HR-pqct as predictor of fracture risk in postmenopausal women: the OFELY study. J. Bone Miner. Res. 32 (6), 1243–1251.

Stone, K.L., Seeley, D.G., Lui, L.Y., Cauley, J.A., Ensrud, K., Browner, W.S., et al., 2003. BMD at multiple sites and risk of fracture of multiple types: long-term results from the study of osteoporotic fractures. J. Bone Miner. Res. 18 (11), 1947–1954.

Sundh, D., Nilsson, A.G., Nilsson, M., Johansson, L., Mellstrom, D., Lorentzon, M., 2017. Increased cortical porosity in women with hip fracture. J. Intern. Med. 281 (5), 496–506.

Tang, T., Cripton, P.A., Guy, P., McKay, H.A., Wang, R., 2018. Clinical hip fracture is accompanied by compression induced failure in the superior cortex of the femoral neck. Bone 108, 121–131.

Techawiboonwong, A., Song, H.K., Leonard, M.B., Wehrli, F.W., 2008. Cortical bone water: in vivo quantification with ultrashort echo-time MR imaging. Radiology 248 (3), 824–833.

Testi, D., Viceconti, M., Baruffaldi, F., Cappello, A., 1999. Risk of fracture in elderly patients: a new predictive index based on bone mineral density and finite element analysis. Comput. Methods Progr. Biomed. 60 (1), 23–33.

Toga, A.W., Thompson, P.M., 2002. New approaches in brain morphometry. Am. J. Geriatr. Psychiatry 10 (1), 13–23.

Tothill, P., Hannan, W.J., 2007. Precision and accuracy of measuring changes in bone mineral density by dual-energy X-ray absorptiometry. Osteoporos. Int. 18 (11), 1515–1523.

Townsend, P.R., Rose, R.M., Radin, E.L., 1975. Buckling studies of single human trabeculae. J. Biomech. 8 (3–4), 199–201.

Treece, G.M., Gee, A.H., 2015. Independent measurement of femoral cortical thickness and cortical bone density using clinical CT. Med. Image Anal. 20 (1), 249–264.

Treece, G.M., Gee, A.H., Mayhew, P.M., Poole, K.E., 2010. High resolution cortical bone thickness measurement from clinical CT data. Med. Image Anal. 14 (3), 276–290.

Treece, G.M., Poole, K.E., Gee, A.H., 2012. Imaging the femoral cortex: thickness, density and mass from clinical CT. Med. Image Anal. 16 (5), 952–965.

Tsai, J.N., Nishiyama, K.K., Lin, D., Yuan, A., Lee, H., Bouxsein, M.L., et al., 2017. Effects of denosumab and teriparatide transitions on bone microarchitecture and estimated strength: the DATA-switch HR-pQCT study. J. Bone Miner. Res. 32 (10), 2001–2009.

Velan, S.S., Durst, C., Lemieux, S.K., Raylman, R.R., Sridhar, R., Spencer, R.G., et al., 2007. Investigation of muscle lipid metabolism by localized one- and two-dimensional MRS techniques using a clinical 3T MRI/MRS scanner. J. Magn. Reson. Imaging 25 (1), 192–199.

Verdijk, N.A., Romeijnders, A.C., Ruskus, J.J., van der Sluijs, C., Pop, V.J., 2009. Validation of the Dutch guidelines for dual X-ray absorptiometry measurement. Br. J. Gen. Pract. 59 (561), 256–260.

Vilayphiou, N., Boutroy, S., Sornay-Rendu, E., Van Rietbergen, B., Chapurlat, R., 2016. Age-related changes in bone strength from HR-pQCT derived microarchitectural parameters with an emphasis on the role of cortical porosity. Bone 83, 233–240.

Wang, X., Sanyal, A., Cawthon, P.M., Palermo, L., Jekir, M., Christensen, J., et al., 2012. Prediction of new clinical vertebral fractures in elderly men using finite element analysis of CT scans. J. Bone Miner. Res. 27 (4), 808–816.

Weber, N.K., Fidler, J.L., Keaveny, T.M., Clarke, B.L., Khosla, S., Fletcher, J.G., et al., 2014. Validation of a CT-derived method for osteoporosis screening in IBD patients undergoing contrast-enhanced CT enterography. Am. J. Gastroenterol. 109 (3), 401–408.

Wehrli, F.W., Hopkins, J.A., Hwang, S.N., Song, H.K., Snyder, P.J., Haddad, J.G., 2000. Cross-sectional study of osteopenia with quantitative MR imaging and bone densitometry. Radiology 217 (2), 527–538.

Whitmarsh, T., Fritscher, K.D., Humbert, L., Del Rio Barquero, L.M., Roth, T., Kammerlander, C., et al., 2011. A statistical model of shape and bone mineral density distribution of the proximal femur for fracture risk assessment. Med. Image Comput. Comput. Assist. Interv. 14 (Pt 2), 393–400.

WHO, 1994. Assessment of Osteoporotic Fracture Risk and its Application to Screening for Postmenopausal Osteoporosis. World Health Organization, Geneva. Report No.: Technical Report Series no. 843.

Wolfram, U., Schmitz, B., Heuer, F., Reinehr, M., Wilke, H.J., 2009. Vertebral trabecular main direction can be determined from clinical CT datasets using the gradient structure tensor and not the inertia tensor—a case study. J. Biomech. 42 (10), 1390–1396.

Wong, A.K., Cawthon, P.M., Peters, K.W., Cummings, S.R., Gordon, C.L., Sheu, Y., et al., 2014. Bone-muscle indices as risk factors for fractures in men: the osteoporotic fractures in men (MrOS) study. J. Musculoskelet. Neuronal Interact. 14 (3), 246–254.

Wong, A.K., Beattie, K.A., Min, K.K., Gordon, C., Pickard, L., Papaioannou, A., et al., 2014. Peripheral quantitative computed tomography-derived muscle density and peripheral magnetic resonance imaging-derived muscle adiposity: precision and associations with fragility fractures in women. J. Musculoskelet. Neuronal Interact. 14 (4), 401–410.

World Health Organization Collaborating Centre for Metabolic Bone Diseases, 2015. U.o.S., UK FRAX ® WHO Fracture Risk Assessment Tool. Available from: http://www.shef.ac.uk/FRAX/.

Wu, C., van Kuijk, C., Li, J., Jiang, Y., Chan, M., Countryman, P., et al., 2000. Comparison of digitized images with original radiography for semi-quantitative assessment of osteoporotic fractures. Osteoporos. Int. 11 (1), 25–30.

Yang, L., Udall, W.J., McCloskey, E.V., Eastell, R., 2014. Distribution of bone density and cortical thickness in the proximal femur and their association with hip fracture in postmenopausal women: a quantitative computed tomography study. Osteoporos. Int. 25 (1), 251–263.

Yang, L., Palermo, L., Black, D.M., Eastell, R., 2014. Prediction of incident hip fracture with the estimated femoral strength by finite element analysis of DXA Scans in the study of osteoporotic fractures. J. Bone Miner. Res. 29 (12), 2594–2600.

Yang, L., Parimi, N., Orwoll, E.S., Black, D.M., Schousboe, J.T., Eastell, R., et al., 2018. Association of incident hip fracture with the estimated femoral strength by finite element analysis of DXA scans in the osteoporotic fractures in men (MrOS) study. Osteoporos. Int. 29 (3), 643–651.

Yang, S., Luo, Y., Yang, L., Dall'Ara, E., Eastell, R., Goertzen, A.L., et al., 2018. Comparison of femoral strength and fracture risk index derived from DXA-based finite element analysis for stratifying hip fracture risk: a cross-sectional study. Bone 110, 386–391.

Yeung, D.K., Griffith, J.F., Antonio, G.E., Lee, F.K., Woo, J., Leung, P.C., 2005. Osteoporosis is associated with increased marrow fat content and decreased marrow fat unsaturation: a proton MR spectroscopy study. J. Magn. Reson. Imaging 22 (2), 279–285.

Yu, E.W., Bouxsein, M.L., Roy, A.E., Baldwin, C., Cange, A., Neer, R.M., et al., 2014. Bone loss after bariatric surgery: discordant results between DXA and QCT bone density. J. Bone Miner. Res. 29 (3), 542–550.

Zebaze, R.M., Ghasem-Zadeh, A., Bohte, A., Iuliano-Burns, S., Mirams, M., Price, R.I., et al., 2010. Intracortical remodelling and porosity in the distal radius and post-mortem femurs of women: a cross-sectional study. Lancet 375 (9727), 1729–1736.

Zebaze, R.M., Jones, A.C., Pandy, M.G., Knackstedt, M.A., Seeman, E., 2011. Differences in the degree of bone tissue mineralization account for little of the differences in tissue elastic properties. Bone 48 (6), 1246–1251.

Zeytinoglu, M., Jain, R.K., Vokes, T.J., 2017. Vertebral fracture assessment: enhancing the diagnosis, prevention, and treatment of osteoporosis. Bone 104, 54–65.

Zhu, T.Y., Hung, V.W., Cheung, W.H., Cheng, J.C., Qin, L., Leung, K.S., 2016. Value of measuring bone microarchitecture in fracture discrimination in older women with recent hip fracture: a case-control study with HR-pqct. Sci. Rep. 6, 34185.

Zysset, P., Qin, L., Lang, T., Khosla, S., Leslie, W.D., Shepherd, J.A., et al., 2015. Clinical use of quantitative computed tomography-based finite element analysis of the hip and spine in the management of osteoporosis in adults: the 2015 ISCD official positions-part II. J. Clin. Densitom. 18 (3), 359–392.

Chapter 81

Methods in lineage tracing

Brya G. Matthews[1], Noriaki Ono[2] and Ivo Kalajzic[3]

[1]Department of Molecular Medicine and Pathology, University of Auckland, Auckland, New Zealand; [2]Department of Orthodontics and Pediatric Dentistry, University of Michigan School of Dentistry, Ann Arbor, MI, United States; [3]Department of Reconstructive Sciences, UConn Health, Farmington, CT, United States

Chapter outline

Introduction

Lineage tracing is an approach that has been widely used in developmental biology to identify the origin and fate of cells. Lineage tracing studies have been performed in numerous organisms for over a century using various methods to identify and track cells (reviewed in Stern and Fraser, 2001). Cells, or more commonly cell populations, have been identified using various vital dyes, radioactivity, genetic markers, or physical characteristics. Their fate can then be traced to later stages of development or to the adult organism. Many of these studies utilized organisms with transparent embryos to facilitate labeling and analysis. Ideal systems for tracking cells require the ability to deliberately label a specific cell or population of interest in an appropriate model system. The optimal label should be permanent, without loss of signal following cell division or change of phenotype or the ability to transfer to unlabeled neighboring cells. Finally, the labeling procedure ideally should not affect other aspects of the cell's biology.

In recent years, the ability to perform lineage tracing in animals at various stages of life has been greatly facilitated by genetic mouse models. This has enabled extensive study of various stem and progenitor populations in vivo. In addition to studying embryonic development, these models have been utilized to identify adult stem and progenitor cells. In this chapter, we provide an overview of models and reporters that can be used for lineage tracing in the skeleton and outline their use in different settings including development, postnatal growth, adulthood, and after injury. To date, lineage tracing studies in the field have primarily focused on characterizing cell fate within the osteoblast and chondrocyte lineages, so this chapter will focus primarily on these cell types.

Cre recombinase

Genetic manipulation has been utilized to direct the specific overexpression or deletion of genes. As described in previous chapters, targeted deletion of genes has often been achieved using a Cre/lox system, a genome site-specific recombination model allowing for spatial and in some cases temporal gene activation or deletion (Feil et al., 2009; Carlone, 2016). Briefly, Cre recombinase is an enzyme derived from P1 bacteriophage that catalyzes recombination between two 34−base pair loxP sequences. Depending on the orientation of the loxP sequence, Cre will catalyze excision, inversion, or translocation

Principles of Bone Biology. https://doi.org/10.1016/B978-0-12-814841-9.00081-6

of the sequence between the loxP sites. Spatial control of recombination is achieved by using tissue-specific promoters or other regulatory sequences to drive Cre. Temporal regulation of recombination is achieved by using a ligand-dependent Cre enzyme. CreER is a fusion protein composed of Cre and a mutated hormone binding domain of the estrogen receptor (Metzger et al., 1995). Cre activation is achieved by the binding of 4-hydroxytamoxifen (4-OHT, a metabolite of tamoxifen), which enables translocation of Cre to the nucleus. A number of modifications were made to improve ligand-independent activity and tamoxifen sensitivity, with CreERT^2 representing the optimized and most frequently used tamoxifen-inducible Cre (Feil et al., 1997). In order to activate CreER activity, mice are administered either 4-OHT or tamoxifen. Tamoxifen is most frequently used, primarily because it is cheaper, and is administered in oil either IP or orally. In order to perform lineage tracing, a Cre model must be combined with a suitable reporter gene.

Reporters

Reporters are genetic constructs that express a marker gene following activation, in this case by Cre recombination. Many lineage tracing studies have utilized a well-known reporter gene, β-galactosidase (detected as lacZ staining), ubiquitously expressed under the ROSA26 locus and controlled by a flox-Stop cassette (Fig. 81.1A; Soriano, 1999). Although useful in developmental biology, detection of lacZ activity requires a staining procedure usually performed on whole mount tissue. In tissues such as bone, penetration of the stain can give variable results. It is also possible to overstain, making it difficult to distinguish labeled cells from background signal. Use of fluorescent protein (FP) reporters has a number of benefits over staining-based approaches, including eliminating staining steps that can introduce experimental variability and enabling the isolation of live cells for further characterization. An early version utilized expression of enhanced green FP (GFP) following Cre-mediated lacZ deletion (Z/EG) (Novak et al., 2000; Lobe et al., 1999; Fig. 81.1B). There are a number of drawbacks associated with Z/EG mice including lack of ubiquitous expression of the transgene and the possibility of silencing that inhibits Cre-mediated recombination in adult cells (Long and Rossi, 2009). These phenomena were observed in postnatal life in tissues including hematopoietic cells, adult kidney, liver, testis, and other organs.

The next improvements were the generation of R26R-EYFP and R26R-CFP strains that were cloned in the ROSA26 locus to achieve ubiquitous expression (Fig. 81.1C). In this case, Cre recombination would remove a sequence between floxed sites containing a PGK promoter and neo cassette to activate the downstream FP. Indeed, these constructs were useful during developmental stages, but in adult bone samples they exhibit very weak fluorescence, particularly the cyan

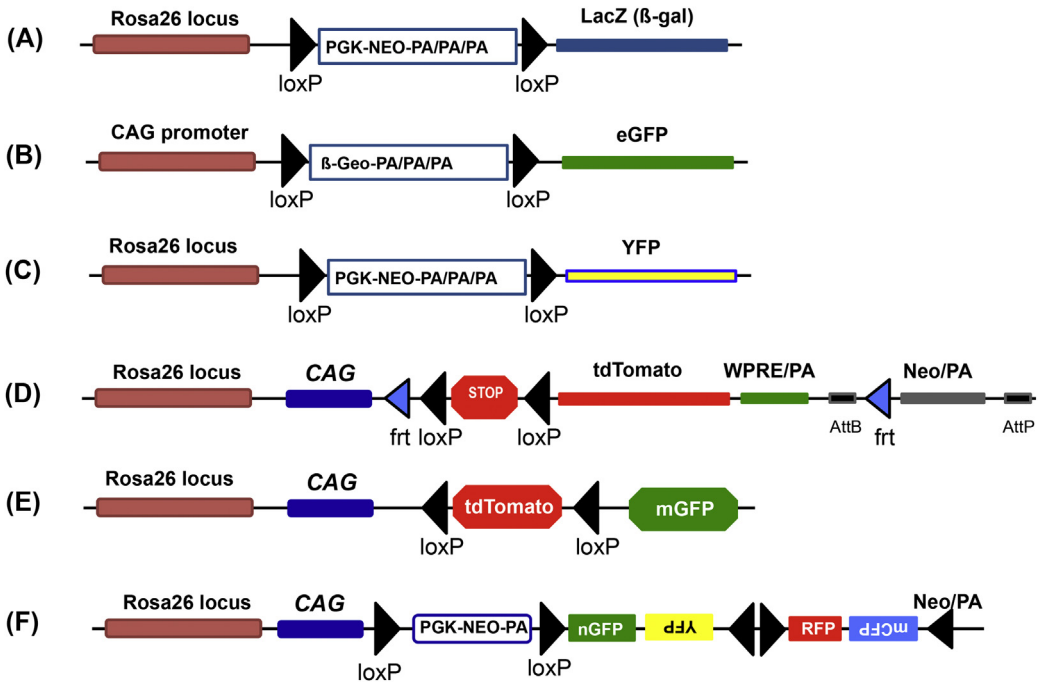

FIGURE 81.1 Reporter genes for Cre activation. (A) R26R reporter, Jackson Labs stock # 003474. (B) Z/EG reporter, stock # 004178. (C) R26R-EYFP, stock # 006148. (D) Ai9 reporter, stock # 007909. (E) mT/mG reporter, stock # 007676. (F) R26R-Confetti, stock # 017492.

FP (CFP) variant (Srinivas et al., 2001). One reporter construct allows for better temporal and spatial localization of recombination, as it contains double fluorescence markers, a membrane-targeted tdTomato and membrane-targeted GFP (Fig. 81.1D). Transgenes are expressed ubiquitously under the control of a CAG promoter cloned into the ROSA26 locus. Following Cre excision, ubiquitously expressed tdTomato is deleted and cells cease to be red and express GFP (Muzumdar et al., 2007). The minor disadvantage is that membrane-bound forms of tdTomato and GFP are harder to detect on histological sections. Madisen et al. (2010) developed a series of constructs that exhibit robust expression of various GFP forms under the control of a CAG promoter and ROSA26 locus with the addition of a woodchuck hepatitis virus post-transcriptional regulatory element that provides stability to the mRNA transcript. These constructs were termed Ai2, Ai3, Ai6, Ai9, and Ai14 (Fig. 81.1E). Strong and reliable fluorescence has been reported using numerous Cre lines. Recently, a multiplex reporter approach has been developed to assist with identification of clones (Snippert et al., 2010; Livet et al., 2007). This strategy utilized the R26R locus and CAG promoter with a neomycin resistance that is excised following recombination, and a Brainbow 2.1 construct randomly activates to generate four different outcomes (Fig. 81.1F). A GFP reporter is localized in nucleus and CFP is membrane-bound while RFP and yellow FP (YFP) are cytoplasmic. Unfortunately, the fluorescent signal generated by this reporter is weak, which makes imaging technically challenging, particularly in tissues with high autofluorescence such as bone marrow. At least one other four-color ubiquitous reporter has been published; however, it does not appear to be available from Jackson Labs (Rinkevich et al., 2011). Numerous other reporters are available for specific purposes, but for basic lineage tracing analysis, Ai3 (YFP), Ai6 (ZsGreen), and Ai9/Ai14 (tdTomato) provide a bright signal easily detected for microscopy including intravital or whole mount imaging as well as flow cytometry.

Experimental design for lineage tracing

Both temporal and spatial factors need to be considered when designing lineage tracing studies. For spatial regulation, it is necessary to identify a "marker" gene and a promoter/enhancer element that can specifically mark a homogeneous group of cells at a specific stage of cell lineage development. If we can identify a marker gene and a promoter/enhancer element specifically expressed by "stem cells" but not by their downstream progeny cells, an inducible genetic tool utilizing this particular gene would unambiguously demonstrate cell fates of these stem cells in unperturbed conditions. Conversely, if we can identify a marker gene and a promoter/enhancer element specifically expressed by "terminally differentiated cells" but not by their upstream precursor cells, an inducible genetic tool utilizing this gene would unravel the plasticity and/or transdifferentiation of such cells. In reality, no gene or promoter/enhancer element is specifically active in "stem cells" or "terminally differentiated cells"—rather, they always mark a heterogeneous group of cells at different stages, and therefore a deliberate characterization of the cell population initially labeled is essential for interpreting the result of lineage tracing experiments.

Lineage tracing with inducible Cre typically involves a pulse−chase experimental design. The "pulse" component allows for identification of cells in which recombination occurs, and it is usually completed by sacrificing animals within 12 h to 2 days after tamoxifen treatment and evaluating labeling histologically. Careful analysis of the cell population initially labeled is critical for accurate interpretation of results. Further characterization by immunostaining, flow cytometry, or cell sorting followed by gene expression or other ex vivo analyses can be performed. The "chase" component is completed days, weeks, or months following initial labeling and indicates the progeny of the initially labeled cells. CreER can exhibit "leakiness" or recombination in the absence of tamoxifen, so it is important to examine reporter expression in mice that have not received tamoxifen, at least at later time points or following injury manipulations. Control mice should be housed separately from animals receiving tamoxifen to avoid inadvertent exposure. The half-life of tamoxifen in vivo is reported to be around 16 h, although how long the Cre remains active depends on the initial dose of tamoxifen as well as various other factors including the level of CreER expression (Wilson et al., 2014). Generally, tamoxifen can remain active for 24−48 h after administration. Alternatively, 4-OH tamoxifen, which activates recombination more rapidly, can be injected to reduce the window of action, typically to 6−9 h after injection. Dosage should be determined experimentally for each system. In some cases, less efficient labeling is desirable—for example, if trying to identify clones, in which case tamoxifen dosage can be reduced. Timing of labeling will depend on the experimental question, but for studies attempting to identify tissue-resident cells contributing to injury, a washout period of at least 24 h after the last tamoxifen dose is helpful to avoid the labeling of cells that activate the promoter after injury.

Lineage tracing can also be used to determine the number and type of cells derived from a single clone in vivo. Generally this involves the use of a Brainbow-type reporter that produces multiple colors and requires labeling a relatively small number of cells initially. Statistical analysis should be performed to determine the probability of adjacent cells receiving the same label to ensure that sufficient samples are analyzed. Clonal analysis is simpler in tissues with clear

organization such as growth plate and more complicated in regions like bone marrow. Ideally, the ability for clones to expand over three dimensions should be considered, although this makes analysis more challenging technically.

Effects of tamoxifen on bone

CreER is the most common inducible system; however, it should be noted that tamoxifen or 4-OHT required to induce Cre activity has actions in the bone that should be taken into account. Tamoxifen is a selective estrogen receptor modulator, and in bone its effects mimic those of estrogen and thus promote bone formation while inhibiting resorption (Zhong et al., 2015). Trabecular bone volume is increased in male and female mice in response to a range of doses of tamoxifen, with effects reported for a cumulative dose as low as 1 mg/kg (Zhong et al., 2015; Perry et al., 2005; Sugiyama et al., 2010). The effect of tamoxifen can be dramatic, with threefold increased trabecular bone volume reported with high-dose tamoxifen (100 mg/kg daily for 4 days) 1 month after treatment of 1-, 2-, or 3-month-old animals (Zhong et al., 2015). Trabecular effects are evident in both actively growing mice around 1 month of age and more mature animals and have been noted in both inbred strains (C57Bl/6 and CBA-1) and mixed-background animals. Similar anabolic effects have been reported with administration of 4-OHT (Starnes et al., 2007). We performed a pilot experiment that clearly demonstrates the dramatic effects of tamoxifen treatment on bone during adolescent growth (Fig. 81.2). Four-week-old female αSMA-CreER mice (C57Bl/6) were given three doses of 75 mg/kg tamoxifen over 9 days, and μCT analysis was performed on femora 3 weeks after the initial dose. As expected, αSMA-CreER mice do not show any differences in bone parameters compared with wild-type littermates. In contrast, tamoxifen treatment dramatically increases trabecular bone while also altering the overall size and shape of bones. Tamoxifen-treated bones were longer, with a smaller periosteal and endosteal perimeter and increased cortical thickness. Others have reported increased cortical thickness and increased biomechanical strength when growing mice are exposed to similar doses of tamoxifen (Zhong et al., 2015; Starnes et al., 2007), and even 10-week-old animals showed growth plate changes in response to much lower doses of tamoxifen (28 days of 0.1, 1, or 10 mg/kg) (Perry et al., 2005). Notably, the effects on the growth plate are the opposite of those from 17β-estradiol, which reduces longitudinal growth (Perry et al., 2005). Interestingly, low-dose tamoxifen (1 mg/kg total given over 10 days) also increased the anabolic response to mechanical loading (Sugiyama et al., 2010). 4-OHT (1 μM) also reduced CFU-F formation when added to cultures of cells derived from a ubiquitous CreER mouse, but not with wild-type cells (McHaffie et al., 2016).

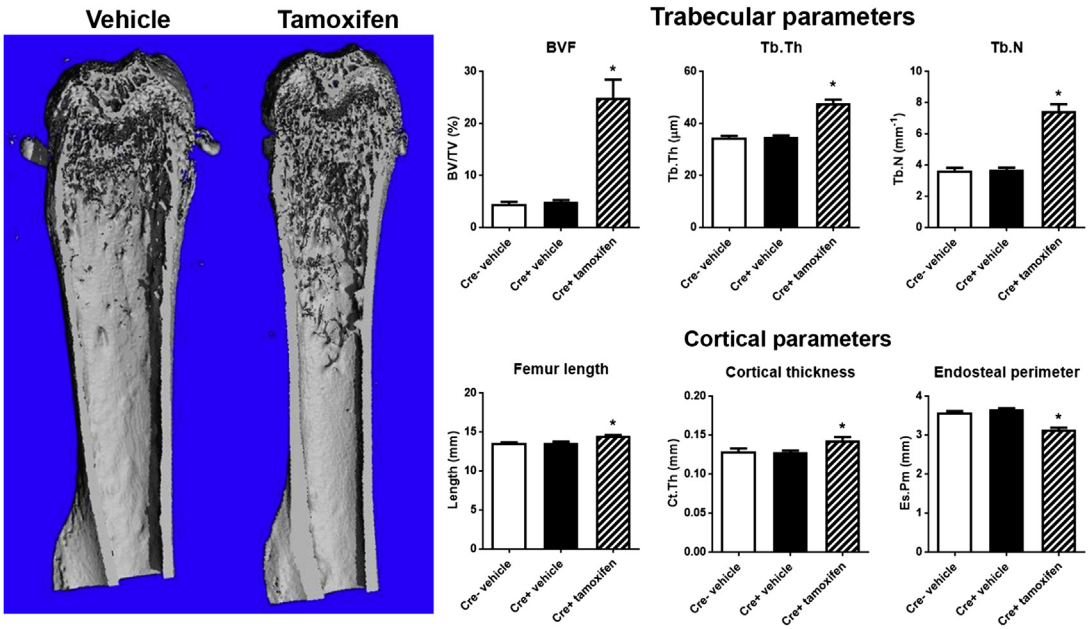

FIGURE 81.2 Tamoxifen effects on bone parameters of growing mice. Female C57Bl/6 mice, either with or without the αSMA-CreERT2 transgene, were treated with 75 mg/kg body weight of tamoxifen or vehicle on P28, P32, and P37. At 7 weeks of age, bones were collected and μCT analysis was performed on the femurs ($n = 5–7$). Reconstructions of representative bones from Cre+ mice are shown. Selected parameters representing changes in trabecular and cortical bone are depicted graphically. *$P < .05$ 1-way ANOVA with Dunnett's posttest compared with Cre+ vehicle.

While doses of tamoxifen or 4-OHT used for lineage tracing studies vary, the majority of studies using tamoxifen-inducible Cre in the bone field use one or more doses of 50−100 mg/kg, although in some studies high total cumulative doses of around 1000 mg/kg have been used (Shi et al., 2017; Worthley et al., 2015). Clearly this is not ideal and should be carefully considered in studies where inducible Cre is used to target genes in order to evaluate the bone phenotype. It may also mean that the contribution of various cell populations to osteoblasts and osteocytes, particularly in the short term, is overestimated in many studies.

Tet expression systems

The Tet-On and Tet-Off systems are widely used genetic systems that enable inducible control using the antibiotic tetracycline or more commonly its derivative doxycycline (Dox). In order to be useful for lineage tracing, Tet systems need to be coupled with Cre under the control of a tetracycline-responsive promoter element (TRE) (for example, the tetO-Cre mouse, Jackson Labs stock #006234). This therefore comprises a three-part system. In a Tet-Off system, the tetracycline-controlled transactivator protein (tTA) is expressed under control of a tissue-specific promoter, and is active under normal conditions but inactive when bound to Dox. In the Tet-On system, reverse tTA (rtTA) is expressed under control of the tissue-specific promoter, and is only able to activate the TRE (and thus Cre) when doxycycline is present. The Tet-On system is therefore more suitable for lineage tracing studies, as it allows transient activation of Cre activity without chronic antibiotic treatment. This system has not been used in many studies in the bone field but has been used to identify stem cells in calvarial sutures and mammary gland (Maruyama et al., 2016; Van Keymeulen et al., 2011; Rios et al., 2014). Dox can be administered via food, water, or intraperitoneal injection, providing flexibility in terms of dosage and timing of administration. Tet systems frequently suffer from leakiness, so untreated controls as described for CreER should always be included.

The Osx-GFP::Cre mouse that has been widely used for targeting osteoblast lineage utilizes the Tet-Off system, although both components are contained within a single construct (Rodda and McMahon, 2006). This mouse shows delayed craniofacial mineralization and small body size early in life, so its use has declined in recent years (Wang et al., 2015; Davey et al., 2012). Interestingly, these phenotypes can be avoided by Dox administration to the mothers during development. Given that other osteoprogenitor-directed Cre models do not have this phenotype, this may be due to tTA binding to DNA during development. Like tamoxifen, Dox has widespread actions that may affect bone. Dosage in different studies varies widely, although most are within the range of antibiotic activity, meaning there is potential to alter the microbiome, especially when administered orally over a long period. It is also notable that tetracyclines are contra-indicated in humans during pregnancy and childhood due to tooth discoloration and some indications of skeletal deformities (Mylonas, 2011). In mouse studies, Dox was shown to inhibit osteoclastogenesis but not alter osteoblast growth or differentiation in vitro or in vivo (Kinugawa et al., 2012). The in vivo effects of Dox on osteoclastogenesis have been demonstrated in situations of enhanced resorption but are likely negligible under normal conditions (Kinugawa et al., 2012; Fowlkes et al., 2015). Finally, members of the tetracycline family bind to bone mineral and can be used as mineralization labels for dynamic histomorphometry (Pautke et al., 2010). It is therefore plausible that the half-life of Dox activity is extended in bone tissue.

Intersectional strategies to identify cells

The aforementioned methods rely on the use of one promoter or promoter fragment to identify a specific cell type or population. In reality, most promoters are expressed in multiple cell types or at least a heterogeneous cell population. A number of strategies have been developed to address this issue by requiring that two different promoters are expressed in the same cell prior to labeling. Split Cre systems allow two parts of the Cre molecule that are not active individually to be expressed from different promoters, enabling activity only in cells where both are expressed simultaneously (Casanova et al., 2003; Wang et al., 2012). These can be combined with standard Cre reporters or any other construct containing lox sites. In the more recently developed version of this system, the split Cre-induced reporter identified more cells than in situ hybridization for both components, suggesting high efficiency (Wang et al., 2012). Alternatively, a number of reporter mouse lines are now available that require the activity of two different recombinases in order to activate the reporter (Madisen et al., 2015). Most commonly this involves a combination of Cre and Flp activity, although reporters are also available for Cre and tTA or Cre and Dre. This system would not necessarily require simultaneous expression of both recombinases, although CreER and/or FlpER could be used to enable the labeling to remain inducible. Presumably, a loss in efficiency will result from combining multiple recombinases and should be considered.

Lineage tracing during embryonic development

Embryonic development is a highly dynamic and organized process in which a simple primordial structure increases its complexity over time and differentiates into functional tissues. The reproducibility of this process makes it particularly attractive for studying cell lineage within the native environment. The basic principle here is to mark a particular group of "early" cells within undifferentiated, relatively simple primordial structures and observe how these cells produce their progeny and contribute to more differentiated cells in later stages as the tissue architecture becomes more complex. The lineage tracing technique is particularly advantageous for unraveling this important aspect and has been successfully applied to a number of major organ systems. Timing of initial labeling is particularly important in analyzing cell lineages during embryonic development, as tissue formation occurs very rapidly.

In the bone research field, a number of marker genes have been utilized to identify various stages of cells in the chondrocyte and osteoblast lineage. These genes include *SRY-Box 9* (*Sox9*), *type II collagen alpha-1* (*Col2a1*), *aggrecan* (*Acan*), and *type X collagen* for the chondrocyte lineage; and *osterix* (*Osx*), *alpha-smooth muscle actin* (αSMA), *type I collagen alpha*-1, *osteocalcin* (*Oc*), and *dentin matrix protein-1* (*Dmp1*) for the osteoblast lineage. It is important to note that essentially all "early marker" genes are also expressed in late cells of the lineage with the exception of αSMA-CreER, which is not expressed in mature osteoblasts or chondrocytes (Grcevic et al., 2012). For example, *Sox9* and *Col2a1* are expressed by more differentiated chondrocytes including proliferating and articular chondrocytes, and *Osx* is also expressed by matrix-producing osteoblasts and osteocytes. Conversely, seemingly "late marker" genes can be expressed by some cells earlier within the lineage. For example, *Dmp1* is expressed not only by osteocytes but also by matrix-producing osteoblasts and possibly some other cells within bone marrow (Matic et al., 2016). Therefore, no single set of available makers can define cells at a specific stage in bone cell lineages. One way to circumvent this limitation is to mark these early cells in the primordial stage before more differentiated cells appear in the structure. This becomes possible when recombination is induced at a specific stage of development before these marked cells move down the lineage. Several studies over the last decade have undertaken this approach using tamoxifen-inducible $CreER^{T2}$ genetic tools and successfully revealed the nature of early cells of the chondrocyte and osteoblast lineages during development. For example, Osx-CreER can mark osteoblast precursor cells in the perichondrium that have the capability to move into the nascent marrow cavity (Maes et al., 2010), whereas Sox9-CreER and Col2a1-CreER can mark osteo-chondro-progenitor cells in mesenchymal condensations that can robustly continue to produce both chondrocytes and osteoblasts (Ono et al., 2014). To better understand how available genetic tools can be utilized to unravel the dynamics of putative progenitor and precursor populations, it is important to know the sequence of embryonic bone development. Endochondral bone development of major long bones (e.g., femurs and tibias) in mice is described next as an example.

Endochondral bone development is a highly organized process in which the lineage development of chondrocytes, osteoblasts, and their precursors occurs sequentially, following highly reproducible trails. In mice, the limb bud, a primordial structure for future limb skeletal elements, is formed at embryonic day (E) 10.5. At E11.5, mesenchymal cells start to condense, establish bone anlage free of vasculature, and first express *Sox9*, a master transcription factor of chondrogenesis, and then *Col2a1*, the major collagenous extracellular matrix of the cartilage. Tamoxifen injection at these stages (e.g., E10.5−E11.5 for Sox9-CreER, and E11.5 for Col2a1-CreER) can effectively mark osteo-chondro-perichondro-progenitor cells in mesenchymal condensations, which demonstrate diverse differentiation potential by contributing to chondrocytes, perichondrial cells, and osteoblasts at later stages (Ono et al., 2014). At E12.5, condensed mesenchymal cells start to differentiate into chondrocytes and become hierarchically organized. Tamoxifen injection at this stage (E12.5) for Col2a1-CreER can mark these nascent chondrocytes and their precursors that contribute to a majority of chondrocytes and osteoblasts at later stages. By contrast, these cells contribute to perichondrial cells to a much lesser extent, indicating that perichondrial cells diverge from these nascent chondrocytes at an earlier stage. At E13.5, chondrocytes in the center of cartilage templates undergo hypertrophy, and subsequently the first osteoblast precursor cells appear in the adjacent perichondrium. These perichondrial osteoblast precursors can be effectively marked by Osx-CreER at these stages (E12.5−E13.5) (Maes et al., 2010). These cells further move into the nascent marrow space and contribute to osteoblasts and stromal cells at later stages. However, perichondrial cells marked by Osx-CreER appear to be transient precursor cells, as they do not stay in the perichondrium at later stages and eventually disappear from most marrow cavity (Maes et al., 2010; Mizoguchi et al., 2014). Earlier precursor cells for *Osx*-expressing cells should exist in the fetal perichondrium, although their identity has not been revealed. The formation of the primary ossification center and marrow cavity starts at E14.5, and hematopoiesis in bone marrow starts at E15.5. By this time, the complexity of the skeletal structure is well developed, and the diversity of the bone cell lineage has been fully established. Tamoxifen injection any time after this point (E14.5−E15.5) in the CreER lines mentioned above marks a wide spectrum of cells over the lineage, therefore making it more challenging to determine the definitive precursor−progeny relationships. For example, tamoxifen injection

of Osx-CreER after E15.5 results in marking a variety of bone cells, including perichondrial cells, osteoblasts and their precursors, and stromal cells in the marrow cavity. At later stages, these cells proliferate within the marrow space well into postnatal development but then gradually disappear in the metaphysis, while a small population remains in the metaphyseal marrow space (Ono et al., 2014; Mizoguchi et al., 2014; Liu et al., 2013). It cannot be ascertained which initially Osx-expressing cells contribute to persisting marrow stromal cells because of the heterogeneity of the cell population initially labeled by Osx-CreER. Similarly, tamoxifen injection for Sox9-CreER or Col2a1-CreER after E15.5 results in marking cells beyond chondrocytes and their precursor cells, including osteoblast precursor cells (Ono et al., 2014; Balani et al., 2017). At later stages, these cells continue to feed into osteoblasts and stromal cells for a long period well into adult and aged stages.

Below is the summary of discoveries from lineage tracing during embryonic endochondral bone development in mice so far:

1. Osteo-chondro-perichondro-progenitor cells in mesenchymal condensations
   a. *Sox9-CreER*: tamoxifen at E10.5−E11.5
   b. *Col2a1-CreER*: tamoxifen at E11.5
2. Osteo-chondro-progenitor cells in cartilage templates
   a. *Sox9-CreER* and *Col2-CreER*: tamoxifen at E12.5−E14.5
3. Osteoblast precursor cells in perichondrium
   a. *Osx-CreER*: tamoxifen at E12.5−E14.5

For the purpose of studying cell fates of the chondrocyte and osteoblast lineage using available CreER genetic tools, a tamoxifen pulse at a late stage of development between E15.5 and E18.5 is particularly challenging. Delivering a relatively high dose of tamoxifen into late pregnant dams is technically difficult because of antiestrogenic activities of tamoxifen that often induce abortion. An equal amount of progesterone can be added into the mixture to mitigate the risk for abortion (Danielian et al., 1998), but still the success rate is quite low if chased more than 3 days (∼15% in our experience, if outbred CD-1 mice are used as breeders). More acute pulse experiments require administration of 4-OH tamoxifen, but this reagent is more difficult to handle and costlier than standard tamoxifen. In addition, part of administered tamoxifen is accumulated in a pregnant dam's fat pads due to its high hydrophobicity. Therefore, if high doses of tamoxifen are given to pregnant dams, there is a chance that pups are reexposed to a new wave of tamoxifen as soon as the delivered mother starts to lactate. For these reasons, injecting an extremely low dose of tamoxifen shortly after birth to newly born pups would be a better option for studying the cell fates of bone cells after the marrow space is fully established.

Postnatal lineage tracing

There is great interest in the identity of postnatal stem cells, particularly in the context of their utility in regenerative medicine. Mice grow rapidly up to about 6 weeks of age when they reach sexual maturity, then continue to grow more slowly until about 4 months of age when they reach peak bone mass. Their growth plates narrow over this time period, but unlike those of humans, they never fully close. A number of markers used in lineage tracing identify progenitor cells in the primary spongiosa or trabecular region that are abundant during rapid growth around 1 month of age but are rare or absent in adulthood. These include *Gli1*, which identifies "metaphyseal mesenchymal progenitors" that contribute primarily to trabecular osteoblasts over a long period, *Gremlin1*, which labels a very rare population of "osteo-chondro-reticular progenitor cells," and αSMA, which labels a transient osteoprogenitor population (Shi et al., 2017; Worthley et al., 2015; Grcevic et al., 2012). Notably, *Gli1*and *Gremlin1* also label a subset of chondrocytes. In contrast, leptin receptor (LepR)-labeled cells do not appear until around 2 months of age (Zhou et al., 2014a). Unfortunately, all the lineage tracing studies of LepR+ cells utilized a noninducible Cre, making it difficult to determine whether the increasing contribution to osteoblasts as the mice age is because LepR identifies a self-renewing population or LepR is activated at a later stage in the lineage.

Mature osteoblast markers have been used to trace the fate of osteoblasts as well as estimate their life spans. Live cell imaging using Osx-CreER in calvaria showed peak labeling after 30 days followed by a gradual drop in cell number. Oc-CreER, which identifies more mature osteoblasts, shows peak labeling by 14 days followed by a drop and returning close to baseline by 60 days, suggesting that osteoblasts have a maximal life span around 60 days in young mice (Park et al., 2012). Both Oc-CreER and Dmp1-CreER, which efficiently labels the majority of osteoblasts despite being considered primarily an osteocyte marker, have been used to label and characterize bone lining cells that were previously very difficult to identify given their similarity to osteoblasts (Matic et al., 2016; Kim et al., 2012, 2017; Jang et al., 2016). This was achieved either by labeling osteoblasts, then waiting for the majority to disappear from the bone surface and leave bone

lining cells (and osteocytes within the matrix), or by genetically ablating osteoblasts. This technique has allowed unique characterization of these cells that had not been possible using other methods.

Osteoblast-to-chondrocyte transition

Lineage tracing has been used to address the hypothesis that chondrocyte-to-osteoblast or chondrocyte-to-osteoblast precursor transformation continues to occur during postnatal growth. It is technically challenging to formally prove this process because of the heterogeneity of the cell population initially labeled by so-called chondrocyte-specific transgenes such as Sox9-CreER, *Col2a1-CreER*, *Acan-CreER*, and *ColX-CreER*. In recent years, a series of studies have suggested that the chondrocyte-to-osteoblast transition is the major route providing new osteoblasts in the epiphyseal growth plates of long bones (Yang et al., 2014a, 2014b; Zhou et al., 2014b) and mandibular condylar cartilage of lower jaws (Jing et al., 2015) as well as during fracture healing (Zhou et al., 2014b; Hu et al., 2017). However, as discussed previously, these "chondrocyte-specific" constructs can simultaneously mark other closely associated cell types, especially osteoblast precursors, upon tamoxifen injection in postnatal mice. For example, one recent study shows that Sox9-CreER can mark osteoblast precursors in adult mice that can robustly respond to intermittent administration of PTH (Balani et al., 2017). Therefore, the significance of this chondrocyte-to-osteoblast transition route in providing new osteoblasts needs to be further validated using more sophisticated genetic tools. We have developed a resting chondrocyte-specific genetic tool (PTHrP-CreER) and demonstrated that PTHrP^{+} resting chondrocytes can differentiate not only proliferating and hypertrophic chondrocytes as expected, but also osteoblasts and reticular stromal cells in bone marrow (N.O., unpublished data). Although our data unambiguously show that the chondrocyte-to-osteoblast transition does occur, the extent of osteoblastogenesis to which this process contributes appears to be rather modest, at least based on our genetic model in normal bone growth.

Lineage tracing following injury

Lineage tracing has proved a valuable technique to identify cell types involved in healing processes as well as the pathological processes of inappropriate bone formation. Genetic lineage tracing has the benefit of not requiring the additional manipulations involved in transplantation studies, to either the transplanted cells or the recipient animal, that may affect growth and differentiation potential. Since these processes involve de novo tissue formation, many studies have utilized constitutive Cre models to evaluate contribution. While lineage tracing with constitutive Cre simplifies experimental design and is useful for proving lack of contribution or very limited contribution to a system, results showing contribution are more difficult to interpret, particularly if the promoter in question may be injury responsive and therefore activated in cells that were not labeled prior to injury.

Rinkevich et al. (2011) used lineage tracing to investigate the contribution of different cell types to digit tip regeneration in mice. This process involves generation of a blastema at the wound site, which was hypothesized to contain pluripotent cells prior to regeneration of multiple tissue types. Their data confirm lineage-restricted contribution to new tissues, with ectoderm-specific Cre-labeled cells contributing to the regenerated epidermis and related structures, while Prx1-Cre-labeled mesenchymal cells contributed to bone, tendon, and dermis, and endothelial cells were derived from Tie2-Cre and VE-cadherin-CreER endothelial lineages. This indicated that lineage-restricted tissue stem/progenitor cells, as opposed to pluripotent blastema cells, were responsible for regeneration.

Lineage tracing has also been utilized in fracture healing. Colnot (2009) performed an elegant series of studies using transplantation of bone grafts from a LacZ reporter mouse. The results demonstrate that matrix-forming cells were primarily derived locally, and the periosteum but not the endosteum was the source of chondrocytes, while both were capable of contributing to osteoblasts. A number of subsequent studies have identified markers of osteo-chondro-progenitors in the periosteum. Prx1-CreER identifies some osteoblasts and chondrocytes in fracture calluses, although many cells are not labeled and tamoxifen was administered after the fracture, so the role of resident Prx1+ cells in fracture remains unclear (Kawanami et al., 2009). αSMA-CreER identifies cells in the periosteum that contribute to a large proportion of osteoblasts, chondrocytes, and fibrous tissue in a fracture callus (Grcevic et al., 2012; Matthews et al., 2014). When tamoxifen is given at the time of fracture, some animals show contribution to over 90% of osteoblasts, suggesting that the vast majority of osteoprogenitors express αSMA at some point in their lineage (B.G.M. unpublished data). LepR-driven Cre (non-inducible) identifies cells that contribute to around 50% of osteoblasts and chondrocytes in a fracture callus (Zhou et al., 2014a), as does Gli1-CreER when tamoxifen is administered at 1 month of age with fractures performed at 2 months of age (Shi et al., 2017). Gremlin1-labeled cells also contribute to fracture callus, albeit for a smaller fraction of cells (28% of osteoblasts and 14% of chondrocytes) (Worthley et al., 2015). Mx1-Cre, an interferon-inducible promoter that is activated

in a number of different types of stem cells, also identifies osteoprogenitors that contribute to fracture healing, although not chondroprogenitors (Park et al., 2012). In contrast to other studies, which used long bone fractures to assess contribution to both cell types, this study used different microfracture models to assess contribution to the lineages separately, so the presence of lineage-restricted progenitors in the context of periosteal fracture healing has yet to be proven. Finally, lineage tracing has been used to evaluate the contribution of muscle to fracture healing. MyoD-Cre-labeled myogenic cells make little or no contribution to closed fractures with intact periosteum but can contribute to both osteoblasts and chondrocytes in an open fracture model (Liu et al., 2011). Another study showed contribution of muscle-derived cells to chondrocytes in an open fracture, although given the ubiquitous nature of the reporter used in the muscle graft, it is unclear whether this contribution was myogenic or a different muscle-resident cell type (Abou-Khalil et al., 2015). Many of the markers utilized in fracture studies also identify stem or progenitor populations in the bone marrow compartment involved in growth or adult turnover, but in most cases the periosteal resident populations involved in fracture healing were not characterized separately despite clear indications that these cells have different functions and differentiation capacity in vivo (Colnot, 2009). To date, we do not have any selective markers of periosteal progenitors, and it is unclear how the populations identified by different markers overlap. Further studies combining lineage tracing with other characterization are required to better understand the heterogeneity and source of progenitors contributing to fracture callus formation.

A number of recent studies have identified progenitor populations in calvarial sutures. By combining lineage tracing studies with diphtheria toxin—mediated cell ablation studies, Zhao et al. (2015) demonstrated that Gli1-CreER identifies cells in the suture that contribute to osteoblasts in the calvaria during postnatal growth and into adulthood. Ablation of these cells causes premature suture fusion and prevents bone defect healing. Axin2-rtTA also identifies cells in the suture that show some stem cell characteristics, particularly upon isolation and transplantation, although they appear to make a much smaller contribution to bone growth and adult turnover than the Gli1 lineage (Maruyama et al., 2016). They also appear to contribute to injury healing. Finally, Prx1-CreER also identifies progenitors in the suture that contribute to defect healing (Wilk et al., 2017). These cells are likely a subset of the Gli1 population but separate from Axin2-labeled cells. Ablation studies indicate that this population is not necessary for postnatal growth but is critical for the healing of a cranial defect. Together these studies indicate that at least in the cranium, the cells that respond to injury may be separate from the populations involved in normal growth and turnover. To date, there is no evidence of a similar phenomenon in long bones.

Lineage tracing in heterotopic ossification

One setting where lineage tracing has been used extensively to identify the source of progenitors is heterotopic ossification (HO), covered in a recent review (Lees-Shepard and Goldhamer, 2018). HO involves pathological formation of bony tissue in muscle or other soft connective tissues. Acquired HO can occur as a complication of severe injury or orthopedic surgery. There are also rare genetic forms of HO, most notably fibrodysplasia ossificans progressive (FOP). FOP is caused by mutations in the BMP receptor *Acvr1* that sensitize the receptor to activin A, resulting in inappropriate BMP signaling (Hatsell et al., 2015). Excessive BMP signaling is likely a common mechanism for all types of HO, and identifying the cell type that transforms into bonelike tissue has been a major focus of the field. The majority of studies evaluating cellular contribution to HO have utilized ectopic administration of BMP or the Nse-Bmp4 mouse. Recently, mice that selectively express Acvr1 mutations found in FOP or other constitutively active forms only following Cre activity have been developed and used to identify cell populations involved in pathological bone formation (Lees-Shepard et al., 2018; Dey et al., 2016). If these mutants are expressed in permissive cell populations, HO forms either spontaneously or following a muscle injury. Studies using various Cre lines have clearly ruled out the possibility that hematopoietic lineages could directly contribute to the lesions in both BMP-mediated and FOP HO (Dey et al., 2016; Kan et al., 2009). The muscle lineage was another potential candidate, based on the ability of satellite cells and myoblasts to differentiate into osteoblasts with in vitro BMP treatment. Again, lineage tracing results using both satellite cell-specific (*Pax7*) Cre and other models that target later in the muscle lineage (*MyoD, Myf5, Myf6*) showed negligible contribution of the muscle lineage to the lesions and total absence of HO when Acvr1 mutants were targeted to the muscle lineage, indicating that the in vitro differentiation capacity of these cells was not indicative of their capability in vivo, even under pathological conditions (Lees-Shepard et al., 2018; Dey et al., 2016; Kan et al., 2009; Matthews et al., 2016; Lounev et al., 2009). Endothelial cells were another candidate based on lineage tracing data using Tie2-Cre, in addition to histological studies from human FOP lesions and in vitro results suggesting that endothelial-to-mesenchymal transition was occurring during HO (Lounev et al., 2009; Medici et al., 2010). However, other markers of endothelial cells, including a different Tie2-Cre line that shows more restricted expression, failed to show contribution to HO (Lees-Shepard et al., 2018; Dey et al., 2016; Kolind et al., 2015; Wosczyna et al., 2012), and follow-up studies indicated that the population labeled by Tie2-Cre that could contribute to HO was actually a nonhematopoietic, nonendothelial interstitial population that expressed Sca1 and PDGFRα (Wosczyna

et al., 2012). Therefore, confirming what cells are targeted by Cre in the tissue of interest is vital for correctly interpreting the results. Cells identified by a number of different mesenchymal markers have been shown to contribute to HO in muscle, including perivascular markers—αSMA and *Glast*, and *Mx1* and PDGFRα—that identify interstitial cells (Lees-Shepard et al., 2018; Dey et al., 2016; Matthews et al., 2016; Kan et al., 2013). Whether these markers identify one overlapping population or different types of cells that can contribute to HO is still unclear.

Conclusions

To summarize, despite some weaknesses associated with lineage tracing approaches, a tremendous amount of knowledge has been obtained using this technique. Besides identifying different population of cells during development and postnatal differentiation and injury, lineage tracing has been critical in indicating what stage or cell population we can target for gene deletions or overexpression. It is increasingly indicating that in vitro assays are not a clear indicator of plasticity and the differentiation potential of cells in vivo. Future improvements should be directed toward developing inducible models that would avoid the use of the compounds that affect bone metabolism, and strategies that target more defined cell populations.

References

Abou-Khalil, R., Yang, F., Lieu, S., Julien, A., Perry, J., Pereira, C., et al., 2015. Role of muscle stem cells during skeletal regeneration. Stem Cell. 33 (5), 1501−1511.

Balani, D.H., Ono, N., Kronenberg, H.M., 2017. Parathyroid hormone regulates fates of murine osteoblast precursors in vivo. J. Clin. Investig. 127 (9), 3327−3338.

Carlone, D.L., 2016. Identifying adult stem cells using Cre-mediated lineage tracing. Curr. Protoc. Stem Cell Biol. 36, 5A.2.1−5A.2.18.

Casanova, E., Lemberger, T., Fehsenfeld, S., Mantamadiotis, T., Schutz, G., 2003. Alpha complementation in the Cre recombinase enzyme. Genesis 37 (1), 25−29.

Colnot, C., 2009. Skeletal cell fate decisions within periosteum and bone marrow during bone regeneration. J. Bone Miner. Res. 24 (2), 274−282.

Danielian, P.S., Muccino, D., Rowitch, D.H., Michael, S.K., McMahon, A.P., 1998. Modification of gene activity in mouse embryos in utero by a tamoxifen-inducible form of Cre recombinase. Curr. Biol. 8 (24), 1323−1326.

Davey, R.A., Clarke, M.V., Sastra, S., Skinner, J.P., Chiang, C., Anderson, P.H., et al., 2012. Decreased body weight in young Osterix-Cre transgenic mice results in delayed cortical bone expansion and accrual. Transgenic Res. 21 (4), 885−893.

Dey, D., Bagarova, J., Hatsell, S.J., Armstrong, K.A., Huang, L., Ermann, J., et al., 2016. Two tissue-resident progenitor lineages drive distinct phenotypes of heterotopic ossification. Sci. Transl. Med. 8 (366).

Feil, R., Wagner, J., Metzger, D., Chambon, P., 1997. Regulation of Cre recombinase activity by mutated estrogen receptor ligand-binding domains. Biochem. Biophys. Res. Commun. 237 (3), 752−757.

Feil, S., Valtcheva, N., Feil, R., 2009. Inducible Cre mice. Methods Mol. Biol. 530, 343−363.

Fowlkes, J.L., Nyman, J.S., Bunn, R.C., Cockrell, G.E., Wahl, E.C., Rettiganti, M.R., et al., 2015. Effects of long-term doxycycline on bone quality and strength in diabetic male DBA/2J mice. Bone Rep. 1 (Suppl. C), 16−19.

Grcevic, D., Pejda, S., Matthews, B.G., Repic, D., Wang, L.P., Li, H.T., et al., 2012. In vivo fate mapping identifies mesenchymal progenitor cells. Stem Cell. 30 (2), 187−196.

Hatsell, S.J., Idone, V., Wolken, D.M., Huang, L., Kim, H.J., Wang, L., et al., 2015. ACVR1R206H receptor mutation causes fibrodysplasia ossificans progressiva by imparting responsiveness to activin A. Sci. Transl. Med. 7 (303), 303ra137.

Hu, D.P., Ferro, F., Yang, F., Taylor, A.J., Chang, W., Miclau, T., et al., 2017. Cartilage to bone transformation during fracture healing is coordinated by the invading vasculature and induction of the core pluripotency genes. Development (Camb.) 144 (2), 221−234.

Jang, M.G., Lee, J.Y., Yang, J.Y., Park, H., Kim, J.H., Kim, J.E., et al., 2016 Sep. Intermittent PTH treatment can delay the transformation of mature osteoblasts into lining cells on the periosteal surfaces. J. Bone Miner. Metab. 34 (5), 532−539.

Jing, Y., Zhou, X., Han, X., Jing, J., von der Mark, K., Wang, J., et al., 2015. Chondrocytes directly transform into bone cells in mandibular condyle growth. J. Dent. Res. 94 (12), 1668−1675.

Kan, L., Liu, Y., McGuire, T.L., Berger, D.M., Awatramani, R.B., Dymecki, S.M., et al., 2009. Dysregulation of local stem/progenitor cells as a common cellular mechanism for heterotopic ossification. Stem Cell. 27 (1), 150−156.

Kan, L.X., Peng, C.Y., McGuire, T.L., Kessler, J.A., 2013. Glast-expressing progenitor cells contribute to heterotopic ossification. Bone 53 (1), 194−203.

Kawanami, A., Matsushita, T., Chan, Y.Y., Murakami, S., 2009. Mice expressing GFP and CreER in osteochondro progenitor cells in the periosteum. Biochem. Biophys. Res. Commun. 386 (3), 477−482.

Kim, S.W., Pajevic, P.D., Selig, M., Barry, K.J., Yang, J.Y., Shin, C.S., et al., 2012. Intermittent parathyroid hormone administration converts quiescent lining cells to active osteoblasts. J. Bone Miner. Res. 27 (10), 2075−2084.

Kim, S.W., Lu, Y., Williams, E.A., Lai, F., Lee, J.Y., Enishi, T., et al., 2017. Sclerostin antibody administration converts bone lining cells into active osteoblasts. J. Bone Miner. Res. 32 (5), 892−901.

Kinugawa, S., Koide, M., Kobayashi, Y., Mizoguchi, T., Ninomiya, T., Muto, A., et al., 2012. Tetracyclines convert the osteoclastic-differentiation pathway of progenitor cells to produce dendritic cell-like cells. J. Immunol. 188 (4), 1772−1781.

Kolind, M., Bobyn, J.D., Matthews, B.G., Mikulec, K., Aiken, A., Little, D.G., et al., 2015. Lineage tracking of mesenchymal and endothelial progenitors in BMP-induced bone formation. Bone 81, 53−59.

Lees-Shepard, J.B., Goldhamer, D.J., 2018. Stem cells and heterotopic ossification: lessons from animal models. Bone 109, 178−186.

Lees-Shepard, J.B., Yamamoto, M., Biswas, A.A., Stoessel, S.J., Nicholas, S.E., Cogswell, C.A., et al., 2018. Activin-dependent signaling in fibro/adipogenic progenitors causes fibrodysplasia ossificans progressiva. Nat. Commun. 9 (1), 471.

Liu, R., Birke, O., Morse, A., Peacock, L., Mikulec, K., Little, D.G., et al., 2011. Myogenic progenitors contribute to open but not closed fracture repair. BMC Muscoskelet. Disord. 12, 288.

Liu, Y.L., Strecker, S., Wang, L.P., Kronenberg, M.S., Wang, W., Rowe, D.W., et al., 2013. Osterix-Cre labeled progenitor cells contribute to the formation and maintenance of the bone marrow stroma. PLoS One 8 (8).

Livet, J., Weissman, T.A., Kang, H., Draft, R.W., Lu, J., Bennis, R.A., et al., 2007. Transgenic strategies for combinatorial expression of fluorescent proteins in the nervous system. Nature 450 (7166), 56−62.

Lobe, C.G., Koop, K.E., Kreppner, W., Lomeli, H., Gertsenstein, M., Nagy, A., 1999. Z/AP, a double reporter for cre-mediated recombination. Dev. Biol. 208 (2), 281−292.

Long, M.A., Rossi, F.M., 2009. Silencing inhibits Cre-mediated recombination of the Z/AP and Z/EG reporters in adult cells. PLoS One 4 (5), e5435.

Lounev, V.Y., Ramachandran, R., Wosczyna, M.N., Yamamoto, M., Maidment, A.D.A., Shore, E.M., et al., 2009. Identification of progenitor cells that contribute to heterotopic skeletogenesis. J. Bone Joint Surg. Am. 91A (3), 652−663.

Madisen, L., Zwingman, T.A., Sunkin, S.M., Oh, S.W., Zariwala, H.A., Gu, H., et al., 2010. A robust and high-throughput Cre reporting and characterization system for the whole mouse brain. Nat. Neurosci. 13 (1), 133−140.

Madisen, L., Garner Aleena, R., Shimaoka, D., Chuong Amy, S., Klapoetke Nathan, C., Li, L., et al., 2015. Transgenic mice for intersectional targeting of neural sensors and effectors with high specificity and performance. Neuron 85 (5), 942−958.

Maes, C., Kobayashi, T., Selig, M.K., Torrekens, S., Roth, S.I., Mackem, S., et al., 2010. Osteoblast precursors, but not mature osteoblasts, move into developing and fractured bones along with invading blood vessels. Dev. Cell 19 (2), 329−344.

Maruyama, T., Jeong, J., Sheu, T.J., Hsu, W., 2016. Stem cells of the suture mesenchyme in craniofacial bone development, repair and regeneration. Nat. Commun. 7.

Matic, I., Matthews, B.G., Wang, X., Dyment, N.A., Worthley, D.L., Rowe, D.W., et al., 2016. Quiescent bone lining cells are a major source of osteoblasts during adulthood. Stem Cell. 34 (12), 2930−2942.

Matthews, B.G., Grcevic, D., Wang, L., Hagiwara, Y., Roguljic, H., Joshi, P., et al., 2014. Analysis of alphaSMA-labeled progenitor cell commitment identifies Notch signaling as an important pathway in fracture healing. J. Bone Miner. Res. 29 (5), 1283−1294.

Matthews, B.G., Torreggiani, E., Roeder, E., Matic, I., Grcevic, D., Kalajzic, I., 2016. Osteogenic potential of alpha smooth muscle actin expressing muscle resident progenitor cells. Bone 84, 69−77.

McHaffie, S.L., Hastie, N.D., Chau, Y.Y., 2016. Effects of CreERT2, 4-OH tamoxifen, and gender on CFU-F assays. PLoS One 11 (2), e0148105.

Medici, D., Shore, E.M., Lounev, V.Y., Kaplan, F.S., Kalluri, R., Olsen, B.R., 2010. Conversion of vascular endothelial cells into multipotent stem-like cells. Nat. Med. 16 (12), 1400−1406.

Metzger, D., Clifford, J., Chiba, H., Chambon, P., 1995. Conditional site-specific recombination in mammalian cells using a ligand-dependent chimeric Cre recombinase. Proc. Natl. Acad. Sci. U. S. A. 92 (15), 6991−6995.

Mizoguchi, T., Pinho, S., Ahmed, J., Kunisaki, Y., Hanoun, M., Mendelson, A., et al., 2014. Osterix marks distinct waves of primitive and definitive stromal progenitors during bone marrow development. Dev. Cell 29 (3), 340−349.

Muzumdar, M.D., Tasic, B., Miyamichi, K., Li, L., Luo, L., 2007. A global double-fluorescent Cre reporter mouse. Genesis 45 (9), 593−605.

Mylonas, I., 2011. Antibiotic chemotherapy during pregnancy and lactation period: aspects for consideration. Arch. Gynecol. Obstet. 283 (1), 7−18.

Novak, A., Guo, C., Yang, W., Nagy, A., Lobe, C.G., 2000. Z/EG, a double reporter mouse line that expresses enhanced green fluorescent protein upon Cre-mediated excision. Genesis 28 (3−4), 147−155.

Ono, N., Ono, W., Nagasawa, T., Kronenberg, H.M., 2014. A subset of chondrogenic cells provides early mesenchymal progenitors in growing bones. Nat. Cell Biol. 16 (12), 1157−1167.

Park, D., Spencer, J.A., Koh, B.I., Kobayashi, T., Fujisaki, J., Clemens, T.L., et al., 2012. Endogenous bone marrow MSCs are dynamic, fate-restricted participants in bone maintenance and regeneration. Cell Stem Cell 10 (3), 259−272.

Pautke, C., Vogt, S., Kreutzer, K., Haczek, C., Wexel, G., Kolk, A., et al., 2010. Characterization of eight different tetracyclines: advances in fluorescence bone labeling. J. Anat. 217 (1), 76−82.

Perry, M.J., Gujra, S., Whitworth, T., Tobias, J.H., 2005. Tamoxifen stimulates cancellous bone formation in long bones of female mice. Endocrinology 146 (3), 1060−1065.

Rinkevich, Y., Lindau, P., Ueno, H., Longaker, M.T., Weissman, I.L., 2011. Germ-layer and lineage-restricted stem/progenitors regenerate the mouse digit tip. Nature 476 (7361), 409−413.

Rios, A.C., Fu, N.Y., Lindeman, G.J., Visvader, J.E., 2014. In situ identification of bipotent stem cells in the mammary gland. Nature 506 (7488), 322−327.

Rodda, S.J., McMahon, A.P., 2006. Distinct roles for Hedgehog and canonical Wnt signaling in specification, differentiation and maintenance of osteoblast progenitors. Development 133 (16), 3231−3244.

Shi, Y., He, G., Lee, W.C., McKenzie, J.A., Silva, M.J., Long, F., 2017. Gli1 identifies osteogenic progenitors for bone formation and fracture repair. Nat. Commun. 8 (1), 2043.

Snippert, H.J., van der Flier, L.G., Sato, T., van Es, J.H., van den Born, M., Kroon-Veenboer, C., et al., 2010. Intestinal crypt homeostasis results from neutral competition between symmetrically dividing Lgr5 stem cells. Cell 143 (1), 134–144.

Soriano, P., 1999. Generalized lacZ expression with the ROSA26 Cre reporter strain. Nat. Genet. 21 (1), 70–71.

Srinivas, S., Watanabe, T., Lin, C.S., William, C.M., Tanabe, Y., Jessell, T.M., et al., 2001. Cre reporter strains produced by targeted insertion of EYFP and ECFP into the ROSA26 locus. BMC Dev. Biol. 1, 4.

Starnes, L.M., Downey, C.M., Boyd, S.K., Jirik, F.R., 2007. Increased bone mass in male and female mice following tamoxifen administration. Genesis 45 (4), 229–235.

Stern, C.D., Fraser, S.E., 2001. Tracing the lineage of tracing cell lineages. Nat. Cell Biol. 3, E216.

Sugiyama, T., Galea, G.L., Lanyon, L.E., Price, J.S., 2010. Mechanical loading-related bone gain is enhanced by tamoxifen but unaffected by fulvestrant in female mice. Endocrinology 151 (12), 5582–5590.

Van Keymeulen, A., Rocha, A.S., Ousset, M., Beck, B., Bouvencourt, G., Rock, J., et al., 2011. Distinct stem cells contribute to mammary gland development and maintenance. Nature 479 (7372), 189–193.

Wang, P., Chen, T., Sakurai, K., Han, B.X., He, Z., Feng, G., et al., 2012. Intersectional Cre driver lines generated using split-intein mediated split-Cre reconstitution. Sci. Rep. 2, 497.

Wang, L., Mishina, Y., Liu, F., 2015. Osterix-Cre transgene causes craniofacial bone development defect. Calcif. Tissue Int. 96 (2), 129–137.

Wilk, K., Yeh, S.C.A., Mortensen, L.J., Ghaffarigarakani, S., Lombardo, C.M., Bassir, S.H., et al., 2017. Postnatal calvarial skeletal stem cells expressing PRX1 reside exclusively in the calvarial sutures and are required for bone regeneration. Stem Cell Rep. 8 (4), 933–946.

Wilson, C.H., Gamper, I., Perfetto, A., Auw, J., Littlewood, T.D., Evan, G.I., 2014. The kinetics of ER fusion protein activation in vivo. Oncogene 33 (40), 4877–4880.

Worthley, D.L., Churchill, M., Compton, J.T., Tailor, Y., Rao, M., Si, Y., et al., 2015. Gremlin 1 identifies a skeletal stem cell with bone, cartilage, and reticular stromal potential. Cell 160 (1–2), 269–284.

Wosczyna, M.N., Biswas, A.A., Cogswell, C.A., Goldhamer, D.J., 2012. Multipotent progenitors resident in the skeletal muscle interstitium exhibit robust BMP-dependent osteogenic activity and mediate heterotopic ossification. J. Bone Miner. Res. 27 (5), 1004–1017.

Yang, L., Tsang, K.Y., Tang, H.C., Chan, D., Cheah, K.S., 2014. Hypertrophic chondrocytes can become osteoblasts and osteocytes in endochondral bone formation. Proc. Natl. Acad. Sci. U. S. A. 111 (33), 12097–12102.

Yang, G., Zhu, L., Hou, N., Lan, Y., Wu, X.M., Zhou, B., et al., 2014. Osteogenic fate of hypertrophic chondrocytes. Cell Res. 24 (10), 1266–1269.

Zhao, H., Feng, J.F., Ho, T.V., Grimes, W., Urata, M., Chai, Y., 2015. The suture provides a niche for mesenchymal stem cells of craniofacial bones. Nat. Cell Biol. 17 (4), 386.

Zhong, Z.A., Sun, W., Chen, H., Zhang, H., Lay, Y.A., Lane, N.E., et al., 2015. Optimizing tamoxifen-inducible Cre/loxp system to reduce tamoxifen effect on bone turnover in long bones of young mice. Bone 81, 614–619.

Zhou, B.O., Yue, R., Murphy, M.M., Peyer, J.G., Morrison, S.J., 2014. Leptin-receptor-expressing mesenchymal stromal cells represent the main source of bone formed by adult bone marrow. Cell Stem Cell 15 (2), 154–168.

Zhou, X., von der Mark, K., Henry, S., Norton, W., Adams, H., de Crombrugghe, B., 2014. Chondrocytes transdifferentiate into osteoblasts in endochondral bone during development, postnatal growth and fracture healing in mice. PLoS Genet. 10 (12), e1004820.

Chapter 82

Bone histomorphometry in rodents

Y. Linda Ma[1], David B. Burr[2] and Reinhold G. Erben[3]

[1]Biotechnology and Autoimmunity Research, Eli Lilly and Company, Indianapolis, IN, United States; [2]Department of Anatomy and Cell Biology, Indiana Center for Musculoskeletal Health, Indiana University School of Medicine, Indianapolis, IN, United States; [3]Department of Biomedical Research, University of Veterinary Medicine Vienna, Vienna, Austria

Chapter outline

Introduction

Rodents have proven to be useful models to study metabolic and genetic bone diseases. Bone histomorphometry is a unique technique that histologically and quantitatively assesses bone cells, growth, tissue remodeling, bone architecture, and repair. It provides critical information for understanding tissue-level mechanisms of action and plays an important role in documenting the biological effects and possible side-effects of new drug treatments. In this chapter, we introduce histomorphometric techniques that can be applied to rodent bone including in vivo labeling, sample preparation, parameter readouts, and their biological significances. We also include histomorphometric evaluation of microdamage and bone healing. Histomorphometric changes found in common rodent models of bone loss and skeletal drug effects also are reviewed.

Methodologies

In vivo labeling

One of the most important endpoints in rodent histomorphometry is the assessment of the rates of osteoblastic bone formation and bone mineralization. These measurements are made on bones harvested from animals given fluorochrome

Principles of Bone Biology. https://doi.org/10.1016/B978-0-12-814841-9.00082-8

labels in vivo. Fluorochromes are fluorescent, calcium-seeking substances incorporated into the mineralization front of mineralizing surfaces (MSs). Once incorporated into a specific bone site, fluorochromes persist and are not released until resorption of the fluorochrome-containing bone matrix by osteoclasts. In histological bone sections, fluorochrome labels can be visualized by excitation with UV or blue light or with light in the red−green range. Typical fluorochromes used for dynamic histomorphometry in rodents are calcein green, alizarin complexone, tetracyclines, and xylenol orange (Erben, 2003). For the calculation of the mineral apposition rate (MAR) and bone formation rate (BFR), two labels given at different time points are necessary. Due to its low toxicity and bright fluorescence, the authors generally recommend using double labeling with calcein green at a dosage of 10−20 mg/kg in young and 10 mg/kg in aged rats and mice. In most cases, two different labels do not offer any advantage unless the information contained within the individual labels is used—for example, in multiple labeling regimens (Erben et al., 1997).

In most cases, fluorochromes are given subcutaneously or intraperitoneally in mice and rats. An exception to this rule may be tetracyclines, mainly due to animal welfare considerations because the injection solutions must be slightly acidic to keep the tetracyclines in solution. Therefore, subcutaneous or intraperitoneal injection may cause transient pain that can be avoided by intravenous administration. However, intravenous injection of fluorochromes needs to be done slowly, especially with alizarin, due to their calcium-complexing nature. For details of preparation of fluorochrome injection solutions, the reader is referred to more specialized textbook chapters (Erben, 2003).

An important aspect of experimental planning is to use an appropriate time interval between individual fluorochrome labels and between the last fluorochrome label and necropsy. The reason the time interval between the last label and necropsy should be at least 1 day in mice and 2 days in rats is that the last label needs to be covered with new bone matrix to prevent elution during subsequent sample processing. The time difference between the two labels is called the interlabel time (Ir.L.t) or marker interval. To appreciate the major consequences of the Ir.L.t on dynamic histomorphometric parameters in cancellous bone of rodents, it is essential to understand the nature of label escape error and skewed sampling error. The label escape error describes the influence of the Ir.L.t on the proportion of double-labeled remodeling sites. The magnitude of the label escape error depends on the ratio between the Ir.L.t and the formation period (FP), or Ir.L.t/FP ratio. The shorter the Ir.L.t, the higher is the proportion of double-labeled remodeling sites. When the Ir.L.t is greater than the FP, remodeling units may not be double labeled, making it impossible to measure MARs and BFRs. Therefore, keeping the Ir.L.t as short as possible is important for reliable data generation. It is obvious that a limiting factor in this context is the distance between the fluorochrome labels because for accurate assessment of MAR, the double labels need to be clearly separated. Hence, in practical terms, the trade-off between label escape error and accurate measurement of MAR determines the appropriate marker intervals. There is general agreement that an Ir.L.t/FP ratio below 0.2 results in an acceptable label escape error (Frost, 1983a). Even with appropriate Ir.L.ts, label escape will occur because some sites will either begin bone formation or cease formation between the time the initial label is given and the time the second is administered. Therefore, a correction for label escape should always be made (Martin, 1989).

The skewed sampling error describes the error in the measurement of MAR introduced by an inappropriately long Ir.L.t. Osteoblastic matrix formation and MAR are more rapid during the early phase of the FP. Moreover, osteoblasts may temporarily stop their bone-forming activity, especially during the late phases of the FP (so-called OFF periods). Therefore, the longer the marker interval, the lower the measured values of MAR will be (Frost, 1983b) and the less accurate relative to actual MAR.

In conclusion, use of appropriate marker intervals is necessary to avoid large label escape and skewed sampling errors. The authors recommend the use of a marker interval of 1 day in 3−4 week-old mice, of 2−3 days in 6−12 week-old mice, of 3−5 days in mice older than 4 months, and of 5−7 days in rats older than 3 months (Erben, 2003). If the study also analyzes cortical bone, longer label intervals are needed for older mice and rats. For a more detailed description and explanation of label escape and skewed sampling errors, the reader is referred to other textbooks (Erben, 2003; Frost, 1983b).

When periosteal bone formation is measured in studies involving aged rats or mice, an Ir.L.t suitable for cancellous bone histomorphometry may result in inseparable double labels at periosteal surfaces. Periosteal MAR shows an age-dependent decline in all species including mice and rats. Therefore, periosteal MAR may be much lower than cancellous and endocortical MAR in aged rodents. This problem can be solved by introducing a second pair of fluorochrome labels with a different color and a longer Ir.L.t. For example, a calcein double label with a marker interval of 3−5 days is given for the measurement of cancellous BFRs in an aged mouse study, and an alizarin complexone double label with a marker interval of 10 days is given for the measurement of periosteal BFR. In some experimental situations, introducing a single baseline fluorochrome label for the assessment of periosteal bone formation over the whole experimental period can add useful information.

Sample preparation

An important consideration with major implications for later analytic possibilities is how to embed the bone samples. This decision depends on the planned endpoints of a study. If the endpoint is standard bone histomorphometry, the bones are usually embedded undecalcified in methylmethacrylate (MMA), because MMA embedding yields the highest quality undecalcified bone sections. Decalcification with subsequent paraffin embedding is often used for bone and bone marrow histopathology but plays only a minor role in rodent bone histomorphometry, mainly because decalcification results in complete loss of fluorochromes. As described above, fluorochromes are bound to calcium in mineralized bone matrix. Therefore, dynamic bone histomorphometry is not possible in decalcified, paraffin-embedded bone samples. If done properly, MMA embedding and histological processing result in high-quality sections of undecalcified bone, a prerequisite for any sound histomorphometric evaluation. However, the downside of standard MMA embedding is that radicals formed during the exothermic chain reaction occur during MMA polymerization. This will covalently alter all macromolecules present in the sample, resulting in almost complete loss of antigenic determinants and enzyme activities. Therefore, any reliable histochemical or immunohistochemical analysis is not possible on bone specimens embedded in standard MMA. There are two options to circumvent this. One is to use low-temperature MMA embedding methods that reduce covalent modification of biomolecules by slowing down the polymerization process and the number of radicals formed through the lowering of the polymerization temperature to about −20°C (Erben, 1997). These low-temperature MMA embedding methods are suitable for histochemistry and immunohistochemistry, and the histological section quality is not inferior to conventional MMA embedding (Erben, 1997). Because TRAPc histochemistry is necessary for the quantification of osteoclast numbers (Oc.Ns) in mice, we embed all our mouse bones using low-temperature MMA embedding. The other option is to use cryoembedding and cryosectioning of bones. Although previously considered fraught with unsurmountable technical difficulties, the latter technology has made significant progress during recent years, and it is now possible to routinely prepare high-quality frozen sections of undecalcified bone.

Fixation

To avoid autolysis of tissue and preserve optimal cellular detail, it is important that the bones are fixed immediately after necropsy. Careful cleaning of the bones from adherent muscles and tendons helps with later orientation of the blocks in the microtome. To achieve optimal fixation results, the marrow cavity should be opened in larger bones such as femora, tibiae, or larger rat vertebrae before fixation. In long bones, this is best done by transversally cutting the bone with a low-speed or small oscillating saw to isolate the different parts of the bone (distal femur, proximal tibia, and shaft) for separate analysis. There are many different fixation protocols. The most commonly used in bone histomorphometry are ethanol preservation and fixation in formalin/paraformaldehyde (PFA). We recommend fixation in 40% ethanol at 4°C for 48 h in rat bones, and 4% PFA in 0.1 M phosphate buffer at pH 7.4 and 4°C for 24 h in mice. After fixation in 40% ethanol, the specimens are transferred to 70% ethanol. After PFA fixation, the samples are washed overnight in 0.1 M phosphate buffer, pH 7.4, containing 10% (w/v) sucrose. Thereafter, they are also transferred to 70% ethanol for long-term storage.

Standard methylmethacrylate embedding

The dehydration and infiltration steps shown in Table 82.1 should be carried out at 4°C using a magnetic stirrer. Incubation times for the individual steps depend on the sample size and ages of the animals. Larger samples and samples from older animals or those treated with antiresorptives require longer durations.

For polymerization, the infiltrated bones are placed in 25 mL glass vials containing a plastic base. The bases are prepared by pouring 5 mL of freshly prepared MMA solution III (see next section) in the empty vials, capping them with an airtight plastic cap, and polymerizing the plastic at 40°C for 24 h. For optimal positioning of the blocks in the microtome, a plastic base is helpful because the sample is surrounded by plastic on all sides after polymerization. A label is added to identify the sample. The glass vials are then filled to the top with freshly prepared MMA solution III and capped airtight with a plastic cap. The vials are kept in a water bath overnight at 26°C. The next morning, the temperature is increased to 28°C. Subsequently, the temperature is increased by 0.5°C every 12 h until the final temperature of 31°C is reached. Using this protocol, polymerization usually occurs at about 29−30°C (Schenk et al., 1984).

TABLE 82.1 Dehydration and methylmethacrylate (MMA) infiltration procedure.

Step	Time (days)
70% ethanol	1–4
96% ethanol	1–4
100% propan-2-ol, repeat twice	1–4
Xylene, repeat twice	1–4
MMA solution I	2–4
MMA solution II	2–4
MMA solution III	2–4

MMA solution I: methylmethacrylate with 20% (v/v) dibutyl phthalate; MMA solution II: MMA solution I with 1% (w/v) dry benzoyl peroxide; MMA solution III: MMA solution I with 3% (w/v) dry benzoyl peroxide.

Low temperature methylmethacrylate embedding

The infiltration is done according to the regimen given in Table 82.1. However, the chemistry of MMA infiltration solutions is different to allow for low-temperature polymerization and the preservation of enzyme activities and antigenic determinants:

MMA solution I—methylmethacrylate with 35% (v/v) butyl methacrylate, 5% (v/v) methyl benzoate, and 1.2% polyethylene glycol 400
MMA solution II—MMA solution I with 0.4% (w/v) dry benzoyl peroxide
MMA solution III—MMA solution I with 0.8% (w/v) dry benzoyl peroxide

Similar to the process for the routine MMA embedding procedure, glass vials with plastic bases are used. To prepare the bases, add 600 μL of *N*,*N*-dimethyl-*p*-toluidine to 100 mL of freshly prepared MMA solution III at 4°C and stir for a few minutes. Five mL of the polymerization mixture is poured into each glass vial. Before capping each vial with an airtight plastic cap, it needs to be gassed with N_2 or CO_2 for 20–30 s to remove O_2 from the vial. Polymerization of the bases is achieved by incubating vials for at least 24 h at 4°C.

To prepare the polymerization mixture, 400 μL of *N*,*N*-dimethyl-*p*-toluidine is added to 100 mL of MMA III solution at 4°C and stirred for a few minutes. The infiltrated bones are placed on the plastic bases in the prechilled glass vials (around 0°C on ice), filled with the polymerization mixture to the top, and the vials are capped with airtight plastic caps. The vials are then transferred to a cooling unit at −23°C for 16 h. It is critical for the quality of the embedding protocol that the temperature, and thus the velocity of the polymerization, is well controlled. It is recommended that a programmable climate chamber is used for this purpose. The polymerization is initiated by gradually increasing the temperature from −23°C to −22°C over 1 h and thereafter from −22°C to −20°C over 46 h. Subsequently, the temperature is increased from −20°C to −18°C over 24 h and from −18°C to +2°C over 12 h. The polymerized blocks should be stored frozen at −20°C.

Sectioning of plastic-embedded bone specimens

Microtome sectioning

Sectioning of undecalcified plastic-embedded bone specimens can be performed on rotary or sledge microtomes. In our hands, the best section quality can be achieved on sledge microtomes with a knife angle of 40 degrees. Typical section thickness is between 3 and 7 μm. To achieve optimal section quality, the drying process should be performed in a slide press. To improve reproducibility and reduce interindividual variance, it is important to standardize the sectioning planes. Standard bone sites for cancellous bone histomorphometry are the proximal tibia and lumbar vertebrae (L1 or L2) in rats and the distal femur and L1 or L2 in mice. We use midsagittal sectioning planes for rat tibiae and vertebrae as well as for mouse distal femora. Alternatively, rat tibiae may be sectioned using a coronal sectioning plane through the cruciate

ligaments. Mouse vertebrae should be sectioned in a frontal plane to make sure that enough cancellous bone is available for histomorphometric analysis. It is also possible to use the proximal tibia in mice for cancellous bone histomorphometry. However, due to the strong curvature of the murine tibia, sectioning is more difficult than it is with the distal femur. In addition, the amount of cancellous bone is lower in the proximal tibial metaphysis than in the distal femoral metaphysis, making the distal femur the preferred long bone site in mice.

Micromilled cross sections of cortical bone

For cortical bone histomorphometry, the tibial shaft at 2−3 mm proximal to the insertion of the fibula is the standard sampling site in rats, whereas in mice the midshaft of the femur is usually used. To reduce the interindividual variance, the sampling site should be exactly defined and standardized within an experiment. The bones are embedded in standard MMA, cut perpendicular to the long axis of the bones with a water-cooled precision diamond band saw, microtome saw, or diamond-embedded wire saw into 80−200 μm-thick slices, glued to 3-aminopropyltriethoxysilane (APES)-pretreated glass slides using adhesive (e.g., Loctite 420, Henkel) and a splicer, and finally microground with a microgrinder or by hand to provide ∼20-μm-thick transverse sections. To prepare the APES-pretreated slides, immerse acetone-cleaned glass slides in APES for 5 min, rinse in distilled water, and allow them to dry.

Cryoembedding and cryosectioning

As mentioned above, it was previously thought impossible to prepare high-quality cryosections of undecalcified bone. However, with the advent of tape technology, the situation has considerably changed (Hong et al., 2012). Using this technology, it is now possible to prepare high-quality cryosections of undecalcified bones employing a standard cryotome. The advantages are immediately evident: (1) enzyme activities and antigenic determinants are optimally preserved, (2) the technology saves 4−5 weeks of time because the time-consuming plastic embedding of the specimens is not necessary, and (3) it opens up new methodological horizons beyond bone histomorphometry such as laser capture microdissection. We recently employed this technology to elucidate the cellular mechanisms by which estrogen deficiency causes bone loss (Streicher et al., 2017). Cryosections of bone also can be used for standard dynamic cancellous bone histomorphometry (Hong et al., 2012).

Immediately after harvesting, the bones are snap-frozen in liquid nitrogen using an appropriate cryoembedding medium such as TissueTek (SAKURA, Finetek, USA). Thereafter, the blocks can be stored at −80°C. Before sectioning, the blocks should be brought to −25°C for at least 2 h to make them less brittle. Sectioning at 4−8 μm-thickness can be done with a standard cryotome (e.g., Leica) equipped with a tungsten carbide knife. Before the section is taken, the block is covered with an adhesive tape (Section Lab Co. Ltd., Hiroshima, Japan). Air bubbles between the block and the tape need to be avoided. The section is collected together with the tape and mounted on a glass slide with the tape facing the slide and the bone section facing upward. It is not necessary to use any glue between the tape and glass slide. Further processing of the cryosections depends on the intended purpose. For histochemistry or immunohistochemistry, the cryosections are briefly (2 min) fixed in methanol or acetone at −20°C before incubation with primary antibodies or enzyme substrates.

Staining

Von Kossa/MacNeal's stain

The von Kossa stain with MacNeal's tetrachrome counterstain combines good cellular detail with a clear distinction between mineralized and unmineralized bone (Schenk et al., 1984). It is the standard stain for static cancellous bone histomorphometry in mice and rats. A disadvantage is that mineralized bone and calcified cartilage are uniformly stained black. Therefore, information about structural details within the mineralized bone matrix such as remodeling units or calcified cartilage remnants is lost. Before staining, the MMA is removed from the sections.

Toluidine blue stain

The toluidine blue stain at acid pH is a nuclear stain and gives very good cellular detail. It also provides a good distinction between mineralized and unmineralized bone (Baron et al., 1983). It is often used for histomorphometric measurement of cellular parameters in rats and can be used for measuring osteoid. It also is frequently used for evaluation of non-mineralized skeletal tissues, such as cartilage.

Masson–Goldner stain

Masson-Goldner, or Masson's trichrome, staining is a multicolor staining commonly used for bone to distinguish cells from surrounding connective tissue. The staining can be used on formalin-fixed material and for paraffin, frozen, or MMA embedding sections. Though there can be a slightly difference in the solution ratio, most recipes produce red keratin and muscle fibers, blue or green collagen and bone, light red or pink cytoplasm, and dark brown to black cell nuclei (Gruber, 1992).

Cement line stain

The cement line stain is a surface-staining technique for demonstration of cement lines in undecalcified sections (Erben, 1996). For this stain, the MMA is *not* removed, but the surface of the bone should be acid-etched prior to staining. Alternatively, the toluidine blue can be mixed with tetraborate and formic acid: 1% (w/v) toluidine blue O, 1% (w/v) sodium tetraborate, and 0.1% (v/v) formic acid in distilled water (filter before use, can be used several times).

Histochemical tartrate resistant acid phosphatase staining

This protocol is used for histochemical identification of osteoclasts in undecalcified sections of mouse and rat bones that have been embedded using the low-temperature MMA protocol described above. Osteoclasts will stain red and provide an easier and more accurate count for the measurement of osteoclast Oc.N and perimeter (Oc.Pm).

Staining of micromilled cross sections

Micromilled cross sections of cortical bone can be stained with toluidine blue after etching the surface with H_2O_2 (Reim et al., 2008). The plastic is not removed before staining. This stain provides a nice representation for the measurement of cortical porosity, osteoid, cellular detail, and cement lines.

Cancellous bone histomorphometry

Cancellous bone histomorphometry is an indispensable tool for the assessment of bone turnover, bone mineralization, and bone remodeling dynamics. Although structural bone parameters also are measured during routine histomorphometry procedures, high-resolution μCT technology is far superior to histomorphometry with regard to the assessment of bone structure, because the latter technology is able to assess bone architecture in three dimensions (3D) in a much larger volume and an assumption-free manner. However, it is important to consider that this is only true under the condition that bone mineralization is normal. By definition, the term "bone" comprises both mineralized and unmineralized matrix (osteoid). μCT scanners pick up only mineralized bone. Therefore, μCT-based structural parameters are associated with a large error when bone mineralization is impaired.

The primary spongiosa beneath the growth plate is normally excluded from measurement by keeping a certain distance from the growth plate. This distance depends on the longitudinal elongation rate at a specific site. In the tibial metaphysis of young rats, bone within 1 mm of the growth plate should be excluded from measurements. In rats beyond 5 months of age, this distance can be reduced to 0.5 mm. In lumbar vertebrae of rats at all ages, it is safe to exclude bone within 0.5 mm from the cranial and caudal growth plates. In mice, these values can be halved—i.e., 0.5 mm in the distal femoral metaphysis in rapidly growing mice and 0.25 mm in the vertebrae as well as distal femoral metaphysis of older mice. In addition, cancellous bone within 0.25 mm of endocortical bone surfaces should generally be excluded from measurements to avoid inclusion of endocortical bone turnover activities.

Structural parameters

All two-dimensional and 3D structural parameters are derived from the primary measurements, namely total (measuring or tissue) area, bone area, and bone surface (Table 82.2). Of note, calculation of the 3D parameters bone surface, trabecular thickness, trabecular number, and trabecular separation is based on the model assumption that the structure is isotropic (Parfitt et al., 1987). It is clear that structural bone elements are not oriented in a spatially random fashion in mouse and rat cancellous bone. Therefore, 3D histomorphometric parameters calculated on the basis of this model are always associated with some systematic error and may deviate from assumption-free assessment of the same parameters by μCT.

TABLE 82.2 Structural trabecular histomorphometric parameters.[a]

Primary parameters (abbreviation)	(Unit)
Total area (Tt.Ar; bone + bone marrow)	(mm^2)
Bone area (B.Ar)	(mm^2)
Bone surface (B.Pm)	(mm)
Two-dimensional derived parameters	
Bone area (B.Ar/T.Ar) = B.Ar/T.Ar × 100	(%)
Bone surface ratio (B.Pm/B.Ar) = B.Pm/B.Ar	(mm/mm^2)
Trabecular width (Tb.Wi) = B.Ar/B.Pm × 2000	(μm)
Trabecular number (Tb.N) = 0.5 × B.Pm/T.Ar	(no./mm)
Trabecular separation (Tb.Sp) = 1/Tb.N × 1000 − Tb.Wi	(μm)
Three-dimensional derived parameters	
Bone volume (BV/TV) = B.Ar/T.Ar × 100	(%)
Bone surface ratio (BS/BV) = B.Pm/B.Ar × 4/π	(mm^2/mm^3)[b]
Trabecular thickness (Tb.Th) = B.Ar/B.Pm × 2000 × π/4	(μm)
Tb.N = 4/π × 0.5 × B.Pm/T.Ar	(no./mm)
Tb.Sp = 1/Tb.N × 1000 − Tb.Th	(μm)

[a]*For formula explanation, interpretation, and complete histomorphometric indices lists, refer to (Dempster et al., 2013).*
[b]*The obliquity correction often is not used for measurements in rodents but is used in larger animal species. If a correction is used, the values 1.199/2.00 for trabecular number or 2000/1.199 for trabecular width and separation are recommended.*

Bone formation

Bone formation is best assessed by dynamic, fluorochrome-based bone histomorphometry (Table 82.3). These measurements represent a functional determination of matrix synthesis by an osteoblast team and its subsequent mineralization and are clearly superior to a purely morphology-based assessment of osteoblastic activity such as osteoblast perimeter/surface or osteoblast number as long as there is no mineralization deficit. Fluorochrome-based measurements are made on unstained sections, mounted in nonfluorescent media such as Fluoromount (Serva) or Eukitt's without removal of the plastic. The Ir.L.t is the time interval between the administration of the labels. The MAR is given in μm/day and is the mean distance between the labels divided by the Ir.L.t. In cases where broader diffuse labels are present, the interlabel distance should be measured from midpoint to midpoint of the labels (Frost, 1983c). Fluorochrome labels appear in the form of bands in sections, whereby the width of a band depends on the angle at which a 3D label plane has been sectioned, speed of

TABLE 82.3 Dynamic histomorphometric indices of bone formation.

Primary parameters (abbreviation)	(Unit)
Bone surface (B.Pm)	(mm)
Double-labeled surface (dLS.Pm)	(mm)
Single-labeled surface (sLS.Pm)	(mm)
Interlabel distance (Ir.L.D)	(μm)
Derived parameters	
Mineral apposition rate (MAR) = Ir.L.D/Ir.L.t	(μm/day)
Mineralizing surface (MS/BS) = (dL.Pm + 0.5 × sL.Pm)/B.Pm × 100	(%)
Bone formation rate/BS (BFR/BS) = MS/BS/100 × MAR	($μm^2$/μm/day or $μm^3/μm^2$/day)

matrix mineralization, and time the fluorochrome was present in the extracellular fluid. The mineralizing bone perimeter (M.Pm) is either defined as the double-labeled perimeter (dL.Pm) or the sum of dL.Pm and one-half the single-labeled perimeter. The latter definition is widely used in nonrodent species. Which calculation of M.Pm is most suitable for rodents is a controversial issue. The definition M.Pm = dL.Pm underestimates the "true" M.Pm, but on the other hand reduces the likelihood of errors introduced by nonspecific labeling of resting or resorptive bone surfaces, which is often a problem in mice and rats. Therefore, to be "on the safe side," many labs use the latter definition of M.Pm. BFR is the amount of mineralized bone matrix produced per unit of bone surface, tissue volume, or time. The authors recommend using surface-based BFR because it best reflects the intensity of bone formation per unit of bone perimeter/surface and is not directly influenced by differences in cancellous bone mass. This is particularly relevant in osteopenia models such as gonadectomized mice and rats in which there is substantial loss of bone volume.

The essential information about the intensity of cancellous bone formation is contained in the three parameters MAR, MS/bone surface (BS), and BFR/BS. Therefore, static histomorphometric indices of bone formation such as osteoblast perimeter/surface (Table 82.4) are dispensable when only a minimum data set is required.

Bone mineralization

Histomorphometry is indispensable for reliably assessing alterations in bone formation and mineralization. One of the key parameters that needs to be measured for the assessment of bone mineralization is osteoid width (O.Wi). Osteoid measurements are usually performed on sections stained with von Kossa/MacNeal's, toluidine blue, Goldner's trichrome, or Villanueva staining (Villanueva et al., 1994). O.Wi either can be calculated from osteoid area (O.Ar) and perimeter as shown in Table 82.4, or measured directly by a two-point distance measurement, sampling osteoid seams every 50 μm. However, compared with those of humans and higher mammals, osteoid seams are very thin in rodents with normal bone mineralization, which makes it difficult to measure reliably unless one uses very high magnification. Increases in bone formation can lead to moderate increases in osteoid perimeter (O.Pm) and O.Ar in the absence of impaired bone mineralization. The most sensitive parameter indicative of impaired bone mineralization is osteoid maturation time (Omt). Impaired bone mineralization is typically reflected in increased Omt. The calculation of mineralization lag time (osteoid thickness/Aj.Ar; with adjusted apposition rate Aj.Ar = MAR × M.Pm/O.Pm) is not useful in rodents in most cases, because the M.Pm/O.Pm ratio often is greater than 1 in mice and rats. However, there are specific cases, such as in chronic kidney disease, in which Aj.Ar is much more sensitive than Omt in detecting a defect in mineralization. Severe impairments in bone mineralization often result in complete lack of fluorochrome double labeling, making the calculation of Omt impossible. In these cases, the impaired bone mineralization is reflected in profound increases in O.Wi and O.Ar.

TABLE 82.4 Histomorphometric indices of bone formation and of bone mineralization.

Primary parameters (abbreviation)	(Unit)
Bone surface (B.Pm)	
Bone area (B.Ar)	
Osteoid surface (O.Pm)	
Osteoid area (O.Ar)	
Osteoblast surface (Ob.Pm)	
Osteoid width (O.Wi)	
Derived parameters	
O.Pm = O.Pm/B.Pm × 100	(%)
Ob.Pm = Ob.Pm/B.Pm × 100	(%)
O.Ar/B.Ar = osteoid volume (OV)/BV = O.Ar/B.Ar × 100 (%)	
O.Wi = O.Ar/O.Pm × 1000	(μm)
Osteoid maturation time (Omt) = O.Wi/MAR	(d)
Osteoid thickness (O.Th)[a] = O.Wi × π/4	(μm)

[a]*Many labs do not normalize for obliquity of section in rats, so this may only apply to large nonrodent animal models.*

Bone resorption

In contrast to the assessment of bone formation by dynamic histomorphometry, histomorphometric measurements aimed at assessing bone resorption are purely based on morphology. Histomorphometry cannot provide a functional determination of osteoclast activity. In part this is because erosion surfaces are shallow and can be difficult to detect in rodents. In other cases, such as some conditions of osteopetrosis or low bone remodeling due to pharmaceutical treatment, osteoclasts are prevalent but inactive and unable to resorb bone. To assess osteoclast activity, measurements of collagen cross-link excretion in urine or collagen cross-link serum levels are necessary.

In rats, osteoclasts can be reliably detected in toluidine blue, Goldner's trichrome, and von Kossa/MacNeal's-stained sections on the basis of their typical morphology (Fig. 82.1). In mice, a large proportion of osteoclasts are mononuclear, and Howship lacunae are often shallow, making it much more difficult to recognize osteoclasts. Therefore, histochemical tartrate-resistant acid phosphatase (TRAcP) staining is routinely used to quantify osteoclasts in mice. Another possibility is using cathepsin-K immunohistochemistry to sensitively detect osteoclasts in mice. Since TRAcP staining makes all osteoclast profiles readily visible, it is important to count only TRAcP-positive nucleated cells in contact with bone as osteoclasts. TRAcP-positive cells within bone marrow or osteoclast profiles lacking a nucleus are not included in the measurements. The most commonly used primary and derived measurements of Oc.N and bone resorption are shown in Table 82.5. Oc.Pm is defined as the contact perimeter between the osteoclast and the bone surface.

An important point to consider is that Oc.Ns expressed per tissue area (N.Oc./T.Ar) can lead to erroneous conclusions when the amount of cancellous bone differs between groups of animals. Therefore, Oc.Ns should always be expressed per mm of bone perimeter (N.Oc/B.Pm) to avoid this pitfall. Osteoclasts can normally be found only on mineralized bone surfaces. Therefore, it can be useful to express Oc.Ns per mineralized perimeter to correct for osteoid surfaces, especially when O.Pm differs between different groups of animals. The measurement of eroded perimeter (E.Pm) includes prior and currently active sites of bone resorption. This parameter is sometimes assessed in rats, although the measurement is not always reliable because the erosion cavities are shallow. The authors recommend using a certain cutoff (e.g., at least 3 μm resorption depth) to exclude very shallow lacunae and increase reproducibility of the measurement.

Bone remodeling dynamics

Although aged mice also show clear evidence of remodeling units, remodeling-based parameters are usually assessed only in rats. The most commonly used variables reflecting bone remodeling indices in rat studies are wall width (W.Wi), active FP, and activation frequency. Because the relative proportion of cancellous bone remodeling versus modeling increases with age, especially in the long bones of the appendicular skeleton (Erben, 1996), rats older than 6 months of age are used for the measurement of remodeling-based parameters in most cases. As shown in Table 82.6, measurement of W.Wi forms the basis of all remodeling-based parameters. W.Wi is the mean width of completed remodeling packages. Wall thickness (W.Th) is the corresponding 3D parameter. In rodents, W.Wi is most reliably measured using cement line-stained sections viewed under polarized light (Fig. 82.1). Similar to O.Wi, W.Wi can either be measured directly by two-point distance measurements, using evenly distributed perpendicular distance measurements between the reversal line and the bone surface per remodeling unit, or indirectly by tracing the bone surface and the reversal line of the remodeling package. It is important to exclude remodeling units with a scalloped bone surface indicative of earlier resorptive activities and units with active bone formation at the bone surface, because both would reduce the measured values for W.Wi. We recommend measuring the width of at least 15 remodeling units per sample to arrive at reliable values. However, if bone subjected to a potent antiresorptive agent is being measured, it may be difficult to find 15 units. In these cases, W.Wi changes can underestimate the impact of the pharmaceutical agent. Therefore, W.Wi is more useful when evaluating bone anabolic agents or the effects of skeletal aging.

Cortical bone histomorphometry

For the measurement of structural parameters, we use ~20-μm-thick microground sections stained with toluidine blue. Primary measurements are cross-sectional tissue area (Tt.Ar), cortical area (Ct.Ar), marrow area (Ma.Ar), cortical thickness, and number and area of intracortical pores (N.Po and Po.Ar). To be consistent and to reduce measurement variation, we recommend that only porosities >30 μm in diameter are measured. From these data, the relative values for cortical and marrow areas (Ct.Ar/Tt.Ar and Ma.Ar/Tt.Ar, %) and intracortical pore area (Po.Ar/Ct.Ar, %) can be calculated. Relative

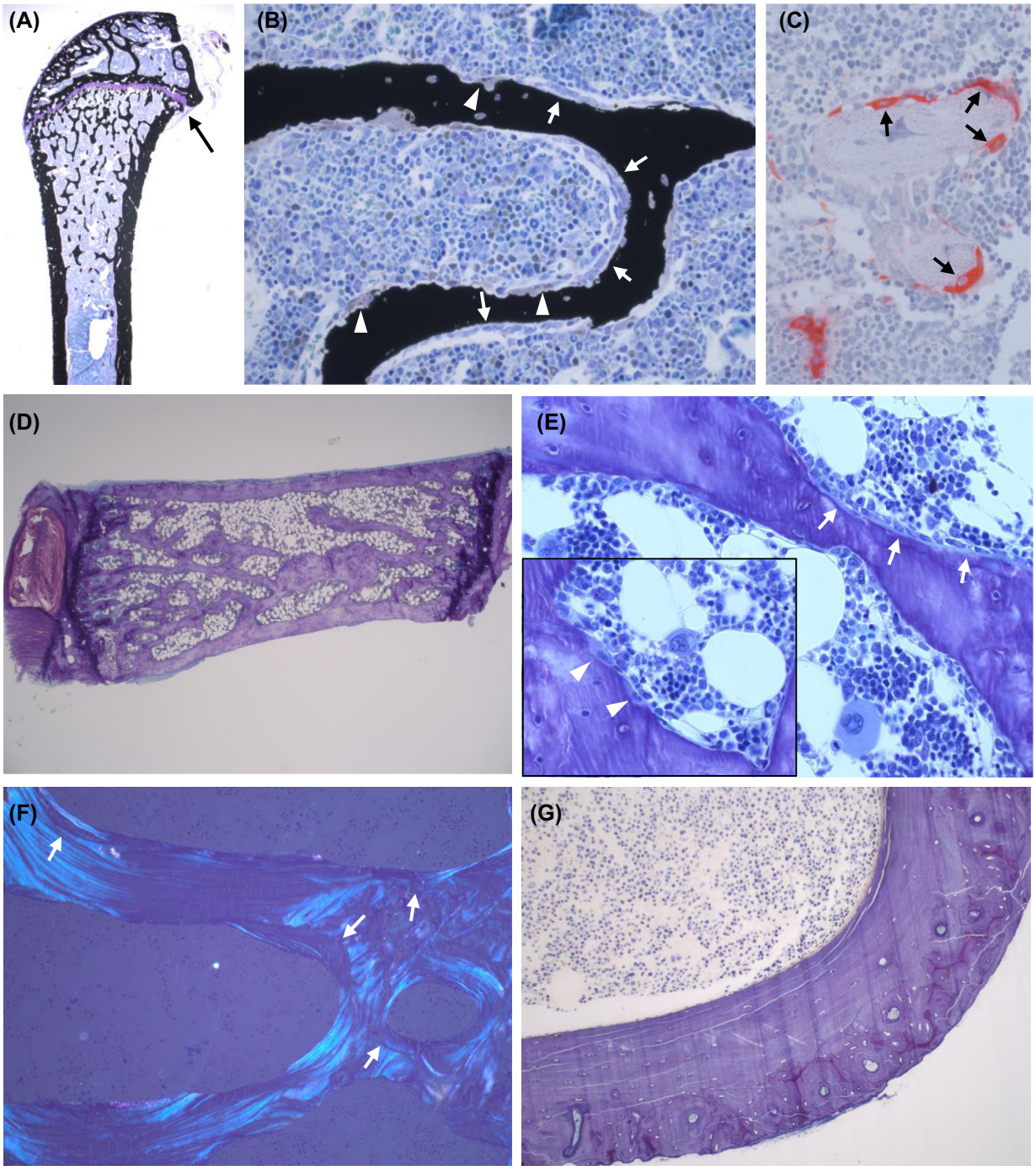

FIGURE 82.1 Staining of undecalcified bone sections. (A–B) Von Kossa/MacNeal's stain of 3-µm-thick undecalcified MMA sections of a murine distal femur. (A) low-power image of the distal femur; *arrow marks* growth plate. Original magnification ×25. (B) High-power view of cancellous bone in the distal metaphysis. Osteoblasts are marked by arrows, multinucleated osteoclasts by arrowheads. Original magnification ×400. (C) Three-µm-thick MMA section of murine distal femur stained histochemically for TRAP activity and counterstained with Mayer's hematoxylin. TRAP-positive osteoclasts at bone surfaces are marked by *arrows*. Original magnification ×400. (D) Toluidine blue-stained, 5-µm-thick undecalcified MMA sections of a rat lumbar vertebra. low-power view. Original magnification ×20. (E) High-power view of rat lumbar vertebral cancellous bone shown under low power in (D). Osteoblasts located on an osteoid seam are marked by arrows. Inset shows osteoclasts in Howship lacunae (*arrowheads*). Original magnification ×400. (F) Cement line-stained section of rat vertebral cancellous bone viewed under polarized light. *Arrows* mark scalloped cement lines of remodeling units. Original magnification ×200. (G) Twenty-µm-thick micromilled cross section of the femoral midshaft of a 9-month-old mouse stained with toluidine blue showing porosities in outer cortex region. Original magnification ×200. *Photomicrographs courtesy of Christiane Schüler, Department of Biomedical Research, University of Veterinary Medicine, Vienna, Austria.*

TABLE 82.5 Histomorphometric indices of bone resorption.

Primary parameters (abbreviation)	(Unit)
Bone surface (B.Pm)	
Number of osteoclasts (N.Oc)	
Osteoclast surface (Oc.Pm)	
Eroded surface (E.Pm)	
Derived parameters	
N.Oc—surface referent (N.Oc/B.Pm) = N.Oc/B.Pm	(no./mm)
N.Oc - tissue referent (N.Oc/T.Ar) = N.Oc/T.Ar	(N./mm^2)
Oc.Pm = Oc.Pm/B.Pm × 100	(%)
E.Pm = E.Pm/B.Pm × 100	(%)

TABLE 82.6 Remodeling-based parameters.

Derived parameters (abbreviation)	(Unit)
Active formation period (FP) = W.Wi/MAR	(d)
[a]FP = W.Wi/Aj.AR	(d)
Resorption period (Rs.P) = FP × E.Pm/O.Pm	(d)
Active resorption period (Rs.P act.) = FP × Oc.Pm/O.Pm	(d)
Reversal period (Rv.P) = FP × (E.Pm − Oc.Pm)/O.Pm	(d)
Remodeling period = FP × (E.Pm + O.Pm)/O.Pm	(d)
Total period (Tt.P) = FP × B.Pm/O.Pm	(d)
Activation frequency (Ac.F) = 1/Tt.P	(N/y)

[a]*Not often used in rodent studies.*

values often show less variability than the absolute values for Ct.Ar, Ma.Ar, and Po.Ar and can partially compensate for small variations in sampling site. Analogous to cancellous bone, μCT analysis of cortical bone is the gold standard for assessing cortical bone structure because μCT analysis is based on a whole stack of sections, not only on one or two sections as in histomorphometry.

Rats and mice do not show genuine Haversian intracortical remodeling. Therefore, changes in N.Po and Po.Ar are not indicative of changes in intracortical remodeling. Rather, increased intracortical porosity, which can occur in sex steroid-deficient aged rats, low-calcium diets, or with underloading in the vicinity of the marrow cavity, reflects increases in a primitive remodeling activity originating from endocortical bone surfaces (Reim et al., 2008) (true intracortical remodeling can occur in rats with a significant challenge, such as occurs with a low-calcium diet or fatigue loading (Bentolila et al., 1998).

The fluorochrome-based measurement of endocortical and periosteal BFR follows identical principles as in cancellous bone. These measurements are made on unstained ~20-μm-thick microground sections. Primary measurements are the endocortical and periosteal MAR and M.Pm, from which endocortical and periosteal BFR/BS can be calculated. Because of the lack of intracortical remodeling in rats and mice, intracortical BFR is usually not measured.

Osteoclasts are not found on periosteal bone surfaces at the tibial or femoral midshaft in rodents and are only rarely observed on endocortical bone surfaces in microground sections. Therefore, the only useful histomorphometric index of endocortical bone resorption is the endocortical eroded perimeter (Ec.E.Pm/B.Pm, %). Analogous to cancellous bone, a cutoff value of at least 3 μm resorption depth should be used to exclude very shallow erosions.

Histomorphometric measurement of longitudinal bone growth

In studies involving growing rats or mice, it is sometimes necessary to assess longitudinal bone elongation rate, which is measured directly, using fluorochrome labeling. Although the routine double label administered for the measurement of cancellous BFRs can also be employed to measure longitudinal bone elongation, use of a separate single label with a different color results in more reliable measurements in most cases. When using a single label, longitudinal growth rate is assessed by measuring the mean distance between the most proximal traces of the fluorochrome label and the first calcified cartilage spicules found in the growth plate, divided by the time interval between administration of the label and necropsy. This time interval must not be too long, because metaphyseal cancellous bone is resorbed toward the diaphyseal marrow cavity in a growing animal, leading to disappearance of the label.

Microdamage measurement technique

The importance of bone microcrack accumulation in vivo was first identified by Frost nearly 50 years ago (Frost, 1960). But it was not until after validation of the *en bloc* basic fuchsin staining technique (Burr and Stafford, 1990; Burr and Hooser, 1995), originally proposed by Frost, that the role and consequences of damage accumulation in bone began to be studied in earnest. It is now clear that, at least under experimental conditions, microdamage accumulation can reduce the residual strength and stiffness of bone (Burr et al., 1997, 1998a) and is also associated in animal models with reduced bone toughness (Mashiba et al., 2000, 2001; Komatsubara et al., 2003; Allen et al., 2006). It is widely considered to be one of the five "bone quality indicators" together with architecture, turnover rate, matrix/collagen properties, and mineralization.

There are now several techniques for staining tissues *en bloc* to label microdamage. The "standard" technique is still staining with basic fuchsin (Burr and Hooser, 1995), but newer fluorescent techniques have also been developed and validated (Lee et al., 1998, 2000, 2003). Recently, a contrast-enhanced micro-CT technique using $BaSO_4$ was proposed as a 3D technique for identifying regions of microdamage (Turnbull et al., 2014), although this approach does not separate microcracks from other tissue voids such as pores.

Basic fuchsin acts by simple diffusion and will appear wherever there are spaces that it can occupy—including Haversian canals, lacunae, and canaliculi as well as microcracks. Staining under load does not improve the diffusion of dye into cracks nor does it prevent the stain from entering cracks that may have closed (Burr et al., 1998b). Fluorescent techniques rely on the presence of exposed calcium along the walls of cracks. Basic fuchsin has fluorescent properties as well, and viewing basic fuchsin staining of cracks under fluorescent microscopy improves the resolution of the microcracks in bone slightly (Huja et al., 1999). Times of en bloc staining vary depending on the size of the bone, its porosity, and the patency of its canaliculi. These are not always known, but reasonable estimates can be made using values shown in Table 82.7.

Several groups have now explored the possibility of using positron emission tomography for detecting areas of damage in vivo without the need for histological techniques (Li et al., 2005; Silva et al., 2006). These techniques do not have the resolution to detect individual microcracks, but they hold promise and with future development may provide a means to identify damaged regions in living individuals.

Microcracks are best viewed in sections that are 80−150 μm thick. Microcracks stained with basic fuchsin are difficult to see in thinner sections (3−5 μm thick) because there is not sufficient depth of staining to be easily and consistently detected in such thin sections. Because sections this thin must be used for cancellous bone histomorphometry to minimize the imprecise definition of bone surfaces caused by section thickness, it may not be possible to accurately measure microcrack numerical densities on the same section as one would measure static and dynamic histomorphometric parameters (Fig. 82.2).

In addition to brightfield microscopy, confocal microscopy can be used in conjunction with staining agents (Zioupos et al., 1994; Boyce et al., 1998) and is particularly sensitive for identifying smaller cracks within diffusely stained areas (Fazzalari et al., 1998). Confocal microscopy can discriminate between patchy areas of stain that represent poorly mineralized regions of bone and areas that are stained diffusely because they are damaged (Vashishth et al., 2000).

Microdamage comes in many varieties (Boyce et al., 1998) and is a general term that describes both various microcrack morphologies as well as "diffuse damage" that consists of very tiny (<10 um; Fazzalari et al., 1998; Seref-Ferlengez et al., 2014) cracks that may never develop into a linear microcrack (Vashishth et al., 2000). Microcracks are defined by their shape (more jagged than canaliculi or vascular canals), some depth of field, and permeation of stain into the bone matrix through the crack walls. They are typically 40−80 μm "long" in cross section (or in trabecular bone) but can run 2−3 mm or more longitudinally in cortical bone (Burr and Martin, 1993). In 3D they are elliptical with an aspect ratio of 4:1 or 5:1 (Larrue et al., 2011). Diffuse damage is more difficult to quantify and is usually assessed by the stained area representative

TABLE 82.7 Times for *en bloc* staining of different samples.

Type of bone		Time per step[a]
Mouse	Femur/tibia	1 h
Rat		
	Ulna	2 h
	Proximal tibia	2 h
Dog		
	Rib (periosteum removed)	4 h
	L3 vertebra	4 h
	Femoral neck	4 h
Human		
	9th rib	2 h
	Femoral neck	4 h
	Femoral neck cores	2 h
	Femoral cortical beams (5 mm diameter)	2 h
	Iliac crest biopsy	2.5 h
	L3 vertebra	4 h
	Trabecular cores (5 × 5 × 5 mm)	2 h
	Isolated trabecula	1 h
Necrotic bone		24 h

[a]*Specimens should be soaked under vacuum in 1% basic fuchsin in 70%, 80%, 90%, and 100% EtOH, two washes each.*

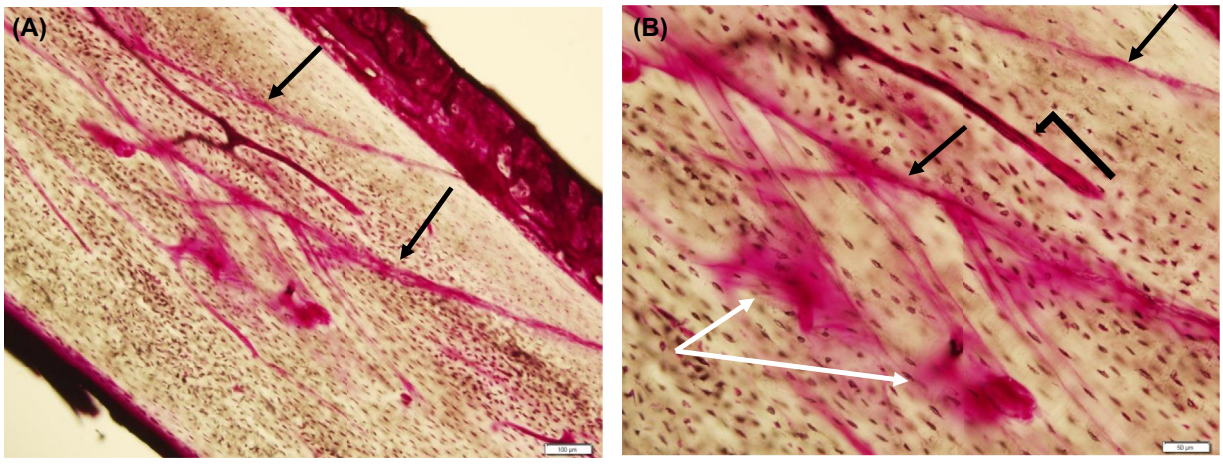

FIGURE 82.2 Bone microdamage in longitudinal section in a rat that was mechanically loaded. *Arrows* identify two linear microcracks that appear to be emanating from the periosteal surface of the bone; 100× magnification. *Black arrows* identify the linear cracks from (A). Note that the basic fuchsin stain diffuses in an irregular way into the bone matrix outside the cracks. (B) *White arrows* show areas of diffuse microdamage. In these areas, individual cracks are much smaller (10 μm) and more numerous, and require a higher magnification or confocal microscopy to identify. However, because there is a collection of damage here, the basic fuchsin stain is able to diffuse into the crack spaces and create an area of intense staining. The perpendicular arrow points to a vascular space. Note that there is no diffusion into the bone matrix as there is for the linear microcracks. This is one way to distinguish microcracks from vascular spaces, which will also be stained. 200× magnification. *Photomicrographs courtesy of Dr. Jiliang Li, Department of Biology, Indiana University—Purdue University, Indianapolis.*

TABLE 82.8 Intraclass correlation coefficients for microdamage measurement.

Variable	Intraclass correlation coefficient (brightfield)	Intraclass correlation coefficient (fluorescence)
Crack density	0.70	0.83
Crack surface density	0.82	0.90
Damage area	0.82	0.89

Crack density (Cr.Dn) = crack number/area. Crack surface density = Cr.Dn × Cr.Le, where Cr.Le = average crack length. Damage area = area of diffuse damage.
From Li, J., Miller, M.A., Hutchins, G.D., Burr, D.B. 2005. Imaging bone microdamage in vivo with positron emission tomography. Bone 37(6), 819–824.

of damage, normalized to bone area (Burr et al., 1998a). Typically, three measurement parameters are used to describe the burden of microdamage in bone: crack density (crack number (Cr.N) / bone area (B.Ar)), crack length (Cr.Le), and crack surface density (= Cr.N/B.Ar x Cr.Le). It is crack surface density that best describes the overall amount of damage in a specimen. Diffuse damage cannot be evaluated in this way because the cracks are too small and numerous to be characterized by number and length. Diffuse damage can be quantified by the area of intense stain that is different from surrounding undamaged matrix, termed the damage area, with B.Ar as the referent.

Variability in microdamage measurements occurs between laboratories and between individuals, but the intraobserver reliability of measurements is relatively good (Huja et al., 1999). Table 82.8 shows the intraclass correlation coefficients for crack density, crack surface density and damage area—all of which range between 0.70 and 0.90. Most variability occurs because of individual variation in how cracks are counted. Because of the *en bloc* staining protocol, artifactual cracks do not contribute significantly to measurement reliability. Nevertheless, particularly for bone biopsies that are taken in vivo, substantial artifacts can occur and render the biopsy unusable for damage analysis.

Intraobserver reliability is slightly better for measurements made under fluorescent light than in brightfield. Even so, averaging two to three sections per bone can reduce the number of crackless specimens and improve measurement reliability and accuracy (Martin et al., 2007).

Histomorphometry of rodent models of bone healing

Typical healing of long bones proceeds through three distinct, consecutive, but overlapping stages: inflammation, repair/callus formation, and remodeling (Einhorn and Gerstenfeld, 2015; Brighton and Hunt, 1991; Marsell and Einhorn, 2011; Ghiasi et al., 2017). The early stage is characterized by trauma-induced soft tissue damage resulting in a hematoma followed by cell infiltration and vascular invasion that result in granulation tissue formation. Bone repair proceeds through both intramembranous and endochondral ossification, which starts by depositing collagen matrix and fibrocartilage that converts granulation tissue into the soft callus. The soft callus or cartilage callus is mineralized to form a hard callus that bridges the fracture gap. Subsequently, osteoclasts remove the calcified cartilage, and osteoblasts form a woven bone bridge that eventually, through revascularization and extensive remodeling, becomes mineralized lamellar bone matrix. During the remodeling stage, the bone is restored to its original shape, structure, and mechanical strength via both modeling and remodeling processes (Einhorn, 1998; Schindeler et al., 2008a; Gerstenfeld et al., 2005), with a few exceptions (such as vertebra or with nonunion fractures).

Histomorphometry of the fracture callus is challenging but can provide unique perspectives into cellular activity and differentiation during the complex bone healing process. Histological and immunohistochemical analyses are essential in preclinical bone healing studies to clarify the biological course of healing, clarify regulating factors, and quantify the effects of pharmacological intervention. Specimens with the periosteum and callus carefully preserved are critical to allow the investigator to see the entire extent of the bridging callus. Therefore, longitudinal sections are recommended. Depending upon the study design, decalcified sections are usually prepared for histological and immunohistochemical quantitation. Undecalcified sections are prepared when mineralization status or BFR analyses are needed. For longitudinal sections, the section with the largest medial-lateral marrow cavity diameter should be obtained. If transverse sections are used, multiple serial sections at fixed increments along the long axis of the entire length of the fracture callus for each animal should be prepared. While hematoxylin and eosin staining is the basic stain for histological evaluation, Safranin-O/fast green (Hacker et al., 1997; O'Driscoll et al., 1999) or Alcian blue with hematoxylin and eosin (Kon et al., 2001; Tiyapatanaputi et al., 2004; Kratzel et al., 2008; Zhang et al., 2002) are commonly used for bone repair evaluations because

they can differentiate cartilage and soft tissues in the callus. To evaluate mineralization of the callus, von Kossa or MacNeal's tetrachrome stains can be useful on undecalcified sections. To visualize cellular details, stains such as TRAP for osteoclasts (Gruber, 1992; Schindeler et al., 2008b) and toluidine blue (Sridharan and Shankar, 2012) for osteoid, osteoblasts, and cartilage chondrocytes also are commonly used on undecalcified sections for the evaluation of bone healing. Because morphological changes during bone repair are driven by a dynamic interplay of molecular, cellular, and biomechanical processes, sampling at multiple time points is highly recommended.

Histomorphometric analyses of bone healing usually require multiple endpoints including determination of hematopoietic tissues, fibrous tissue, cartilage, hard callus area, callus composition at the healing repair site, grading of fracture union (by bridging), fracture-gap tissue type, new bone formation, cell kinetics, microstructure, and tissue vascularity. Due to the high degree of tissue heterogeneity and dynamic matrix turnover, quantitative analyses of bone repair primarily focuses on assessing the time course for cellular response, callus composition (i.e., the volume fraction of mineralized tissue), osteoblast and osteoclast activity in callus remodeling, and the structural features of mineralized bone at different healing stages. All endpoints should be normalized to per-unit T.Ar or presented as a percentage of total callus area. Time courses for the phases of the fracture healing process in rats and mice for three common models are summarized in Table 82.9.

A review of histomorphometric methods applied to the study of long bone fracture repair was published by Gerstenfeld et al. (Gerstenfeld et al., 2005). When interpreted together with other radiographic and biomechanical data, histomorphometry can provide insights into the role of cells, tissues, biological pathways, and the effects of pharmacological or mechanical intervention upon the different stages of bone repair.

Histomorphometry of bone loss rodent models

Rats and mice have been widely used to model human skeletal physiology and disease states including processes leading to bone loss and the efficacy of possible therapeutic interventions. The ovariectomized (OVX) rat model is the most common animal model in osteoporosis research (Wronski et al., 1989a; Kalu, 1991; Lelovas et al., 2008; Kimmel, 1996; Jee and Yao, 2001). OVX-induced bone loss in rats mimics several key features to those observed in postmenopausal women. These similarities include increased rate of bone turnover with resorption exceeding formation, an initial rapid bone loss followed by a steady slower phase of bone loss, and greater loss of cancellous than cortical bone. The rat 4–5 day estrus or menstrual

TABLE 82.9 Time course of repair in common rodent bone healing models.

Models (reference)	Granulation formation phase	Early bone repair phase	Late bone repair phase	Peak 2nd bone remodeling phase[a]
Closed fracture[b] (Brighton and Hunt, 1991; Hacker et al., 1997; Tiyapatanaputi et al., 2004; Turner et al., 2001; Alkhiary et al., 2005)	~3–5 days of hematoma, inflammation cells, granulation tissue	5–16 days of fibrous, angiogenic cells, osteoblasts, osteoid, chondroclasts, fibrocartilage, or soft callus	10–28 days of cartilage tissue, osteoblast, osteoclast, hard callus, and mineralized or woven bone formation	21–35 days of actively remodeling hard tissue and woven bone by osteoclast to lamellar and anatomically shape bone
Stabilized osteotomy[c] (Zhang et al., 2002; Minkwitz et al., 2015; Cao et al., 2002; Komatsubara et al., 2005; Li et al., 1999)	3–5 days of hematoma, inflammation cells, granulation tissue	3–16 days of fibrous, angiogenic cells, osteoblasts, osteoid, chondroclasts, fibrocartilages, or soft callus	7–28 days of cartilage tissue, osteoblast, osteoclast, hard callus, and mineralized or woven bone formation	14–42 of actively remodeling hard tissue and woven bone by osteoclast to lamellar and anatomically shape bone
Femoral cortical defect (Komatsu et al., 2009; Tanaka et al., 2005; Monfoulet et al., 2010)	1–3 days of hematoma, inflammation cells, granulation tissue	3–11 days of intramembranous ossification healing with osteoid, intramarrow woven bone	7–18 days of bone marrow trabecular woven bone converting to cortical bone, resolving granulation tissue	14–21 days of marrow trabecular converting to lamellar and compact cortex

[a] *The chronic callus remodeling phase lasts months until original bone shape, structure, and mechanical strength recover.*
[b] *Data are for both rat and mouse models.*
[c] *Healing time also depends on osteotomy gap size.*

cycle makes this skeleton sensitive to the loss of estrogen (Butcher et al., 1974; Miller et al., 1986). Following OVX in the rat, cancellous osteoclast surface increases quickly within a week from baseline. Osteoclast surface continues to increase and peaks at threefold to fourfold the levels of age-matched sham controls after 4−5 weeks. It then declines but maintains a slight increase over sham-operated animals for a long time (Dempster et al., 1995; Sims et al., 1996). Bone formation indices such as osteoblast surface, MS/BS, MAR, BFR/BS, and BFR/TV are increased about onefold to twofold following OVX but with a time delay relative to bone resorption, representing the coupling of bone resorption and formation and the reversal phase (Wronski et al., 1989a, 1989b; Turner et al., 1993). Significantly increased osteoblast surface can be detected by 7−10 days post-OVX, while increases in MS/BS, MAR, BFR/BS, and BFR/TV usually do not reach statistical significance until 2−3 weeks post-OVX, typically peaking by 5−6 weeks. Bone formation gradually declines to become only slightly higher than age-matched sham controls by 3 months post-OVX (Wronski et al., 1988a, 1989b). Although it is a technical challenge to accurately quantify the bone remodeling cycle in rats, mainly because the eroded surface is shallow and difficult to clearly identify morphometrically, a few studies have indicated that similar to humans, the cancellous bone remodeling period is shorter after OVX than in age-matched intact females (Mori et al., 1990; Ma et al., 1994, 1995a, 1995b, 2003; Chen et al., 1995; Erben et al., 2002). A detectable trabecular bone loss by histomorphometry of the proximal tibia can be seen by 2 weeks, reaches ∼50% bone loss by 30−60 days, and slows to a steady state by ∼90 days after OVX (Wronski et al., 1988a, 1989a). For example, bone volume fraction (bone volume/total volume) in the proximal tibia of a 6-month-old rat is about 17% and declines to 4% in 2 months and 3% in 5 months following ovariectomy (OVX) (Ma et al., 2008). Bone loss in lumbar vertebral cancellous bone is ∼1−3 weeks slower than in the proximal tibial metaphysis, probably due to a relatively slower bone remodeling rate (Wronski et al., 1989b). Morphometric analyses show that OVX-induced bone loss in rats is related to decreased trabecular number and connectivity parameters, and greater trabecular separation, but not related to decreased trabecular width (Ma et al., 2002, 2011; Shen et al., 1993).

Studies also show that not all cancellous bone sites lose bone after OVX in rats. For example, estrogen depletion does not induce cancellous bone loss in the calvaria, epiphysis, distal tibia, or caudal vertebrae in rats, even though bone turnover is increased after OVX in all these sites (Jee and Yao, 2001; Ma et al., 1994; Li et al., 1996a). One common feature for these sites is the presence of yellow marrow, while red marrow tends to dominate at skeletal sites with pronounced cancellous bone loss in the OVX rat, such as the proximal tibia, distal femur, and lumbar vertebra.

The low level of intracortical remodeling in rat long bones makes them unsuitable for modeling estrogen-deficiency effects on human cortical bone. However, studies show that increased endocortical bone turnover and eroded surface are seen in the tibial and femoral shafts of OVX rats (Jee et al., 1990). Periosteal bone formation is increased, which may be partly a mechanical compensation for the loss of endocortical bone and partly due to the mechanical stimulation of body weight gain after OVX (Ma et al., 2002; Wronski et al., 1987). Body weight has been observed to increase by 10%−14% within 4−6 weeks of OVX. The combination of endocortical bone loss and periosteal growth increases total T.Ar, enlarges the bone marrow cavity, thins the cortex, and modestly decreases the cortical area 8−10 weeks after OVX (Ma et al., 1995a, 1997, 2017). Ovariectomy combined with a low-calcium diet or disuse accelerates cortical bone loss (Bagi et al., 1993; Zhang et al., 2016; Keune et al., 2015; Shen et al., 1995, 1997). Although it may not be informative to study cortical remodeling in rats for agents that suppress bone remodeling, rat cortical bone does respond well to bone anabolic agents such as parathyroid hormone analogues (PTH) or parathyroid hormone receptor protein (PTHrp), as described later in this chapter.

Because of its clinical significance, a few histomorphometric studies have attempted to study age-related or OVX-associated femoral neck changes in the rat (Bagi et al., 1995, 1996; Li et al., 1997; Yamamoto et al., 1995). Compared with humans, the rat femoral neck has a much higher cortical-to-trabecular bone ratio (Bagi et al., 1997). OVX induces cellular responses in the femoral neck similar to those observed at other bone sites. Bone resorption and formation changes can be detected as early as 4 weeks post-OVX, while microstructural changes such as enlarged marrow cavity, thinner cortex, and loss of marrow trabecular bone can be detected 6−8 weeks post-OVX. One advantage of the rat femoral neck is the ability to analyze both cortical and cancellous bone parameters from the same histological section.

Mice are another useful small animal model for skeletal research, commonly used for genetic profiling, heritability studies, or evaluating the efficacy of antibodies. Genetically modified mice have powerful advantages in being able to provide insights into how genes regulate the skeletal phenotype, understanding the interaction between important biological pathways, and allowing evaluation of potential therapeutic targets and pharmacologic agents. The magnitudes and rates of cancellous bone loss, cellular activation, and dynamic bone remodeling in response to OVX or mechanical stimulation vary between mouse strains and skeletal sites, and in general are less pronounced and less consistent than in rats (Iwaniec et al., 2006; Bouxsein et al., 2005). As pointed out earlier in the chapter, when evaluating cancellous bone changes, lumbar vertebrae and the distal femur are the preferred sites for histomorphometry in mice rather than the proximal tibia, which has very little cancellous bone. The percentage of cancellous bone area in C57/B6J female mice is

reported to be only 4% in the proximal tibial metaphysis versus 7%−12% in the distal femur and 14%−24% in lumbar vertebrae (Iwaniec et al., 2006; Bouxsein et al., 2005; Amblard et al., 2003).

Orchidectomy (ORX) of aged male rats models closely models conditions in adult men suffering from androgen withdrawal. Because both androgen and estrogen levels are decreased (Erben et al., 2000), some differences in skeletal histomorphometry are observed between ORX and OVX rats. Similar to OVX in female rats, ORX rats show increased bone turnover with bone resorption exceeding bone formation leading to bone loss on both cancellous and endocortical surfaces (Erben et al., 2000; Erben, 2001; Ke et al., 2001; Turner et al., 1990; Vanderschueren et al., 1992). However, different from OVX, periosteal apposition in ORX rats is rapidly suppressed with no periosteal bone growth. This may result from the combination of androgen receptor deactivation, muscle weakening, and loss of body weight following ORX (Ke et al., 2001; Turner et al., 1990). Because both androgen and estrogen levels are closely related to peak bone mass, studies of young growing and aged male ORX rats differ with regard to time and rate of cortical bone changes. The loss of androgen in young rats mainly reduces age-dependent bone growth (i.e., failure to gain bone), whereas later loss of androgen during adulthood leads to a net loss in bone balance causing osteoclast-induced bone loss.

Many rodent models have been developed to study disuse-induced bone loss. Rodent models of reduced weight-bearing include reversible and nonreversible underloading. Hind limb suspension (HS) is the most commonly used reversible underloading model (Morey-Holton and Globus, 1998). Skeletal effects in this model are compartment specific and mimic many of the physiological changes associated with prolonged bed rest or space flight. Histomorphometry of the unloaded proximal tibia, midtibia, or femoral shaft show a 60%−70% decline in cancellous osteoblast surface and BFR and a 70%−90% decline in cortical periosteal BFR within 1−2 weeks of HS in both growing and adult rats (Shen et al., 1997; Bloomfield et al., 2002; Matsumoto et al., 1998; Barou et al., 1999). Trabecular Oc.N in this model may be increased (Kodama et al., 1997) or may not change (Barou et al., 1999). Trabecular area and width are decreased, whereas trabecular number may be increased transiently from early rapid perforation of trabeculae. However, trabecular number later is decreased. Most studies show no cortical bone loss or at least reduced age-related cortical gain in growing rats, likely due to depression of periosteal bone formation caused by reduced loading. Another hind limb immobilization model is the rat unilateral bandage immobilization bone loss model (Ma et al., 1995b; Li et al., 1990; Ijiri et al., 1995). A comprehensive review of this model was published by Jee and Ma (Jee and Ma, 1999). Mice also are commonly used for HS studies because of cost advantages and possibly greater tolerance by mice than rats for the procedures (Milstead et al., 2004; Lloyd et al., 2014).

Glucocorticoid-induced osteoporosis is the most common secondary osteoporosis in patients (Canalis and Delany, 2002; Dempster, 1989). Although rats do not consistently lose bone with excess glucocorticoid treatment (Li et al., 1996b), mice have demonstrated a loss of cancellous bone with treatment. An early prolongation of osteoclast life span and later promotion of osteoblast and osteocyte apoptosis in mice treated with prednisolone have been reported by Weinstein et al. (Jia et al., 2006; Weinstein et al., 1998). Histomorphometric analyses show remarkably reduced osteoblast surface, BFR, and bone turnover rates with 30%−40% cancellous bone loss. A significant decrease in Oc.Ns after a 2−4 week period is thought to be due to a later suppression of osteoclastogenesis with glucocorticoids in mice (Weinstein et al., 1998; Yao et al., 2008).

Histomorphometry of pharmacological efficacy in rodents

Bone histomorphometry has played a critical role in helping understand pharmacological effects on the coupling of bone resorption−formation at the multicellular unit (BMU) level. In OVX rats, studies showed that raloxifene, a selective estrogen receptor modulator, prevents cancellous bone loss by maintaining the osteoclast surface and activation frequency at sham control levels. Bone formation indices of MS/BS, MAR, and BFR/BS are either preserved at sham control levels or reduced to levels between those of OVX and sham controls. The bone histomorphometric profiles of raloxifene in OVX rats are similar to what has been seen with estrogen treatment (Turner et al., 1993; Ma et al., 2003, 2005; Evans et al., 1994; Wronski et al., 1988b). Vitamin D analogs, which are frequently the first-line supplement for preventing bone loss in postmenopausal women, have shown a biphasic effect in animal studies. At low or nonhypercalcemic doses, bone effects of vitamin D and analogs reduce bone resorption and prevent bone loss with subtle suppression or no change in bone formation indices (Erben et al., 1998; Takeda et al., 2013). At high doses, vitamin D analogs do stimulate new trabecular bone formation, but the doses are usually not clinically relevant due to hypercalcemia (Erben et al., 1997; Li et al., 2003).

The mechanism of action of bisphosphonates is to suppress osteoclast function and bone remodeling (Fleisch, 1998). In contrast to the remarkable ability of bisphosphonates to decrease circulation of bone resorption biomarkers, most OVX rat bone histomorphometry studies show that bisphosphonates slightly decrease, do not change, or even increase osteoclast surface (Erben et al., 2002; Balena et al., 1993); however eroded surface is significantly reduced (Ma et al., 2003). These

findings indicate that the primary effect of bisphosphonates is to decrease osteoclast activity rather than numbers. As powerful bone-resorption inhibitors, bisphosphonates markedly reduce bone-formation indices and activation frequency due to the bone resorption−formation coupling mechanism in rats and humans (Balena et al., 1993). In rodents, there is a reduction in bone formation on modeling (periosteal and endocortical) surfaces that is independent of coupling (Iwata et al., 2006). Although to a lesser degree than seen in human studies, bone formation activity in bisphosphonate-treated animals can also be severely suppressed to the degree that no double label is detected. For specimens without double labels, three methods have been used to calculate MAR: assign a zero, impute a value of 0.1−0.3 μm/day, or treat as a missing value. Bone formation rate is calculated accordingly (Recker et al., 2011). As a single label indicates that MAR is not zero (i.e., there is formation, at some rate, albeit too slow to measure), the recommended approach is to impute an MAR of 0.1 um/day in rodents (0.3 um/day in larger animal models and humans), which allows for maintenance of an adequate sample size to allow robust statistical analysis. Although there is debate about whether the artificial imputation of MAR is scientifically correct, for rodent studies, double labels should be detected in all control rats to confirm that the in vivo fluorochrome label schedules are appropriate.

Despite a significant increase in BMD in humans treated with antiresorptive agents, bone histomorphometry analyses show that antiresorptives including bisphosphonates reduce bone turnover to prevent further bone loss in animal models without substantially restoring architecture or volumetric bone mass. However, bisphosphonates are able to improve bone strength in rodent models by preventing bone deterioration and preserving the trabecular microstructure.

The bone anabolic efficacy of human PTH, either the amino terminal fragment teriparatide (PTH 1−34) or the full length hormone PTH1-84, has been well studied in rats. PTH was shown to restore lost bone in OVX (Ma et al., 2005, 2011; Shen et al., 1993), ORX (Martin-Fernandez et al., 2014), and disuse (Ma et al., 1995b) rat models. Histomorphometric analyses illustrate a fundamentally different mechanism of action of PTH from that of antiresorptive agents. In contrast to the antiresorptive agents' decrease in bone turnover, PTH stimulates osteoblastic activity and increases bone remodeling with a net positive bone balance to volumetrically gain new bone. Daily treatment with PTH increases osteoblast surface, single- and double-labeled surfaces, MAR, BFR, and activation frequency (Ma et al., 2003, 2011). Osteoclast surface is usually increased with time but to a lesser extent than osteoblast surface. As a result, more bone is formed than is resorbed in each BMU, as evidenced by increased mean wall thickness. Trabecular area can be increased beyond that of baseline, intact, or sham control levels depending on duration of treatment and dose (Sato et al., 1998). PTH improves trabecular microstructure mainly by thickening trabeculae with a smaller effect on trabecular number (Ma et al., 2011; Shen et al., 1993). Although the rat is not a good model for cortical bone remodeling, studies do show that PTH increases cortical bone area, thickens the cortex, and stimulates periosteal bone formation (Ma et al., 1995b, 2011; Fig. 82.3).

Abaloparatide is a newly approved human PTHrP (1−34) analog that also works through the PTH1 receptor. Abaloparatide increased bone mass and bone formation without significantly increasing osteoclast surface after 12 months of treatment in OVX rats (Varela et al., 2017). A head-to-head study comparing dose-adjusted exposures of abaloparatide with PTH at earlier time points would be informative to assess whether there are different bone histomorphometry profiles between these anabolic agents in the OVX rat skeleton.

The sclerostin−antibody (Scl-ab) is emerging as a new therapy for osteoporosis. Time course studies in OVX rats show that Scl-ab increases bone mass by a combination of early stimulation of bone formation while gradually reducing bone

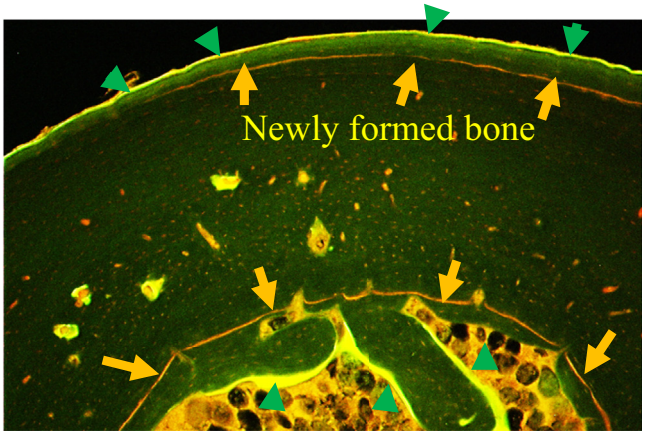

FIGURE 82.3 hPTH stimulates new periosteal and endocortical bone formation in the OVX rat. Bone formed between the xylenol orange label (*arrows*, given at day 1 of treatment) and calcein label (*arrowheads*, given at day 47 posttreatment) was formed during the experimental period.

resorption. Scl-ab rapidly stimulates bone formation activity as reflected in increased serum bone formation biomarkers and histomorphometric parameters of osteoblast surface and BFR. Different from PTH, which stimulates bone formation through both increased remodeling and modeling with daily treatment, Scl-ab−stimulated bone formation is modeling dominated; bone formation initially increases but then quickly declines. Osteoclast surface is gradually and slightly but significantly decreased (Ma et al., 2017; Stolina et al., 2014; Ominsky et al., 2014). Scl-ab histomorphometry in OVX rats parallels what has been observed in humans (McClung et al., 2014; Roux et al., 2017).

Conclusion

With proper study design, a carefully considered in vivo bone double-labeling schedule, and meticulous specimen preparation and staining, histomorphometry can provide unique information on tissue-level qualitative and quantitative changes in bone cellular activity as well as on bone structure, growth, remodeling, and repair. Together with other methods such as measurement of circulating biomarkers, bone imaging, and biomechanical testing, bone histomorphometry is an essential research tool for the comprehensive evaluation of skeletal adaptation and response to hormonal deficiency, pharmaceutical treatments, and other experimental challenges.

References

Alkhiary, Y.M., Gerstenfeld, L.C., Krall, E., Westmore, M., Sato, M., Mitlak, B.H., Einhorn, T.A., 2005. Enhancement of experimental fracture-healing by systemic administration of recombinant human parathyroid hormone (PTH 1-34). J. Bone. Joint Surg. Am. 87 (4), 731−741.

Allen, M.R., Iwata, K., Phipps, R., Burr, D.B., 2006. Alterations in canine vertebral bone turnover, microdamage accumulation, and biomechanical properties following 1-year treatment with clinical treatment doses of risedronate or alendronate. Bone 39 (4), 872−879.

Amblard, D., Lafage-Proust, M.H., Laib, A., Thomas, T., Ruegsegger, P., Alexandre, C., Vico, L., 2003. Tail suspension induces bone loss in skeletally mature mice in the C57BL/6J strain but not in the C3H/HeJ strain. J. Bone Miner. Res. 18 (3), 561−569.

Bagi, C.M., Mecham, M., Weiss, J., Miller, S.C., 1993. Comparative morphometric changes in rat cortical bone following ovariectomy and/or immobilization. Bone 14 (6), 877−883.

Bagi, C.M., DeLeon, E., Brommage, R., Rosen, D., Sommer, A., 1995. Treatment of ovariectomized rats with the complex of rhIGF-I/IGFBP-3 increases cortical and cancellous bone mass and improves structure in the femoral neck. Calcif. Tissue Int. 57 (1), 40−46.

Bagi, C.M., DeLeon, E., Ammann, P., Rizzoli, R., Miller, S.C., 1996. Histo-anatomy of the proximal femur in rats: impact of ovariectomy on bone mass, structure, and stiffness. Anat. Rec. 245 (4), 633−644.

Bagi, C.M., Wilkie, D., Georgelos, K., Williams, D., Bertolini, D., 1997. Morphological and structural characteristics of the proximal femur in human and rat. Bone 21 (3), 261−267.

Balena, R., Toolan, B.C., Shea, M., Markatos, A., Myers, E.R., Lee, S.C., Opas, E.E., Seedor, J.G., Klein, H., Frankenfield, D., et al., 1993. The effects of 2-year treatment with the aminobisphosphonate alendronate on bone metabolism, bone histomorphometry, and bone strength in ovariectomized nonhuman primates. J. Clin. Invest. 92 (6), 2577−2586.

Baron, R., Vignery, A., Neff, L., Silverglate, A., Santa Maria, A., 1983. Processing of undecalcified bone specimens for bone histomorphometry. In: Recker, R.R. (Ed.), Bone Histomorphometry: Techniques and Interpretation. CRC Press, Boca Raton, FL, pp. 13−35.

Barou, O., Lafage-Proust, M.H., Martel, C., Thomas, T., Tirode, F., Laroche, N., Barbier, A., Alexandre, C., Vico, L., 1999. Bisphosphonate effects in rat unloaded hindlimb bone loss model: three-dimensional microcomputed tomographic, histomorphometric, and densitometric analyses. J. Pharmacol. Exp. Ther. 291 (1), 321−328.

Bentolila, V., Boyce, T.M., Fyhrie, D.P., Drumb, R., Skerry, T.M., Schaffler, M.B., 1998. Intracortical remodeling in adult rat long bones after fatigue loading. Bone 23 (3), 275−281.

Bloomfield, S.A., Allen, M.R., Hogan, H.A., Delp, M.D., 2002. Site- and compartment-specific changes in bone with hindlimb unloading in mature adult rats. Bone 31 (1), 149−157.

Bouxsein, M.L., Myers, K.S., Shultz, K.L., Donahue, L.R., Rosen, C.J., Beamer, W.G., 2005. Ovariectomy-induced bone loss varies among inbred strains of mice. J. Bone Miner. Res. 20 (7), 1085−1092.

Boyce, T.M., Fyhrie, D.P., Glotkowski, M.C., Radin, E.L., Schaffler, M.B., 1998. Damage type and strain mode associations in human compact bone bending fatigue. J. Orthop. Res. 16 (3), 322−329.

Brighton, C.T., Hunt, R.M., 1991. Early histological and ultrastructural changes in medullary fracture callus. J Bone Joint Surg. Am. 73 (6), 832−847.

Burr, D.B., Hooser, M., 1995. Alterations to the en bloc basic fuchsin staining protocol for the demonstration of microdamage produced in vivo. Bone 17 (4), 431−433.

Burr, D.B., Martin, R.B., 1993. Calculating the probability that microcracks initiate resorption spaces. J. Biomech. 26 (4−5), 613−616.

Burr, D.B., Stafford, T., 1990. Validity of the bulk-staining technique to separate artifactual from in vivo bone microdamage. Clin. Orthop. Relat. Res. 260, 305−308.

Burr, D.B., Forwood, M.R., Fyhrie, D.P., Martin, R.B., Schaffler, M.B., Turner, C.H., 1997. Bone microdamage and skeletal fragility in osteoporotic and stress fractures. J. Bone Miner. Res. 12 (1), 6−15.

Burr, D.B., Turner, C.H., Naick, P., Forwood, M.R., Ambrosius, W., Hasan, M.S., Pidaparti, R., 1998. Does microdamage accumulation affect the mechanical properties of bone? J. Biomech. 31 (4), 337–345.

Burr, D.B., Turner, C.H., Naick, P., Forwood, M.R., Pidaparti, R., 1998. En bloc staining of bone under load does not improve dye diffusion into microcracks. J. Biomech. 31 (3), 285–288.

Butcher, R.L., Collins, W.E., Fugo, N.W., 1974. Plasma concentration of LH, FSH, prolactin, progesterone and estradiol-17beta throughout the 4-day estrous cycle of the rat. Endocrinology 94 (6), 1704–1708.

Canalis, E., Delany, A.M., 2002. Mechanisms of glucocorticoid action in bone. Ann. N. Y. Acad. Sci. 966, 73–81.

Cao, Y., Mori, S., Mashiba, T., Westmore, M.S., Ma, L., Sato, M., Akiyama, T., Shi, L., Komatsubara, S., Miyamoto, K., Norimatsu, H., 2002. Raloxifene, estrogen, and alendronate affect the processes of fracture repair differently in ovariectomized rats. J. Bone. Miner. Res. 17 (12), 2237–2246.

Chen, H.K., Ke, H.Z., Jee, W.S., Ma, Y.F., Pirie, C.M., Simmons, H.A., Thompson, D.D., 1995. Droloxifene prevents ovariectomy-induced bone loss in tibiae and femora of aged female rats: a dual-energy X-ray absorptiometric and histomorphometric study. J. Bone Miner. Res. 10 (8), 1256–1262.

Dempster, D.W., 1989. Bone histomorphometry in glucocorticoid-induced osteoporosis. J. Bone Miner. Res. 4 (2), 137–141.

Dempster, D.W., Birchman, R., Xu, R., Lindsay, R., Shen, V., 1995. Temporal changes in cancellous bone structure of rats immediately after ovariectomy. Bone 16 (1), 157–161.

Dempster, D.W., Compston, J.E., Drezner, M.K., Glorieux, F.H., Kanis, J.A., Malluche, H., Meunier, P.J., Ott, S.M., Recker, R.R., Parfitt, A.M., 2013. Standardized nomenclature, symbols, and units for bone histomorphometry: A 2012 update of the report of the ASBMR Histomorphometry Nomenclature Committee. J. Bone. Miner Res. 28 (1), 2–17.

Einhorn, T.A., 1998. The cell and molecular biology of fracture healing. Clin. Orthop. Relat. Res. (355 Suppl. l), S7–S21.

Einhorn, T.A., Gerstenfeld, L.C., 2015. Fracture healing: mechanisms and interventions. Nat. Rev. Rheumatol. 11 (1), 45–54.

Erben, R.G., 1996. Trabecular and endocortical bone surfaces in the rat: modeling or remodeling? Anat. Rec. 246 (1), 39–46.

Erben, R.G., 1997. Embedding of bone samples in methylmethacrylate: an improved method suitable for bone histomorphometry, histochemistry, and immunohistochemistry. J. Histochem. Cytochem. 45 (2), 307–313.

Erben, R.G., 2001. Skeletal effects of androgen withdrawal. J. Musculoskelet. Neuronal Interact. 1 (3), 225–233.

Erben, R.G., 2003. Bone labeling techniques. In: An, Y.H., Martin, K.L. (Eds.), Handbook of Histology Methods for Bone and Cartilage. Humana Press Inc, Totowa, NJ, pp. 99–117.

Erben, R.G., Scutt, A.M., Miao, D., Kollenkirchen, U., Haberey, M., 1997. Short-term treatment of rats with high dose 1,25-dihydroxyvitamin D3 stimulates bone formation and increases the number of osteoblast precursor cells in bone marrow. Endocrinology 138 (11), 4629–4635.

Erben, R.G., Bromm, S., Stangassinger, M., 1998. Therapeutic efficacy of 1alpha,25-dihydroxyvitamin D3 and calcium in osteopenic ovariectomized rats: evidence for a direct anabolic effect of 1alpha,25-dihydroxyvitamin D3 on bone. Endocrinology 139 (10), 4319–4328.

Erben, R.G., Eberle, J., Stahr, K., Goldberg, M., 2000. Androgen deficiency induces high turnover osteopenia in aged male rats: a sequential histomorphometric study. J. Bone Miner. Res. 15 (6), 1085–1098.

Erben, R.G., Mosekilde, L., Thomsen, J.S., Weber, K., Stahr, K., Leyshon, A., Smith, S.Y., Phipps, R., 2002. Prevention of bone loss in ovariectomized rats by combined treatment with risedronate and 1alpha,25-dihydroxyvitamin D3. J. Bone Miner. Res. 17 (8), 1498–1511.

Evans, G., Bryant, H.U., Magee, D., Sato, M., Turner, R.T., 1994. The effects of raloxifene on tibia histomorphometry in ovariectomized rats. Endocrinology 134 (5), 2283–2288.

Fazzalari, N.L., Forwood, M.R., Manthey, B.A., Smith, K., Kolesik, P., 1998. Three-dimensional confocal images of microdamage in cancellous bone. Bone 23 (4), 373–378.

Fleisch, H., 1998. Bisphosphonates: mechanisms of action. Endocr. Rev. 19 (1), 80–100.

Frost, H.M., 1960. Presence of microscopic cracks in vivo in bone. Henry Ford Hosp. Med. Bull. 25–35.

Frost, H.M., 1983a. Bone histomorphometry: correction of labeling 'escape error'. In: Recker, R.R. (Ed.), Bone Histomorphometry: Techniques and Interpretation. CRC Press, Boca Raton, FL, pp. 133–142.

Frost, H.M., 1983b. Bone histomorphometry: choice of marking agent and labeling schedule. In: Recker, R.R. (Ed.), Bone Histomorphometry: Techniques and Interpretation. CRC Press, Boca Raton, FL, pp. 37–52.

Frost, H.M., 1983c. Bone histomorphometry: analysis of trabecular bone dynamics. In: Recker, R.R. (Ed.), Bone Histomorphometry: Techniques and Interpretation. CRC Press, Boca Raton, FL, pp. 109–131.

Gerstenfeld, L.C., Wronski, T.J., Hollinger, J.O., Einhorn, T.A., 2005. Application of histomorphometric methods to the study of bone repair. J. Bone Miner. Res. 20 (10), 1715–1722.

Ghiasi, M.S., Chen, J., Vaziri, A., Rodriguez, E.K., Nazarian, A., 2017. Bone fracture healing in mechanobiological modeling: a review of principles and methods. Bone Rep. 6, 87–100.

Gruber, H.E., 1992. Adaptations of Goldner's Masson trichrome stain for the study of undecalcified plastic embedded bone. Biotech. Histochem. 67 (1), 30–34.

Hacker, S.A., Healey, R.M., Yoshioka, M., Coutts, R.D., 1997. A methodology for the quantitative assessment of articular cartilage histomorphometry. Osteoarthritis Cartilage 5 (5), 343–355.

Hong, S.H., Jiang, X., Chen, L., Josh, P., Shin, D.G., Rowe, D., 2012. Computer-automated static, dynamic and cellular bone histomorphometry. J. Tissue Sci. Eng. Suppl. 1, 004.

Huja, S.S., Hasan, M.S., Pidaparti, R., Turner, C.H., Garetto, L.P., Burr, D.B., 1999. Development of a fluorescent light technique for evaluating microdamage in bone subjected to fatigue loading. J. Biomech. 32 (11), 1243–1249.

Ijiri, K., Ma, Y.F., Jee, W.S., Akamine, T., Liang, X., 1995. Adaptation of non-growing former epiphysis and metaphyseal trabecular bones to aging and immobilization in rat. Bone 17 (4 Suppl. l), 207S–212S.

Iwaniec, U.T., Yuan, D., Power, R.A., Wronski, T.J., 2006. Strain-dependent variations in the response of cancellous bone to ovariectomy in mice. J. Bone Miner. Res. 21 (7), 1068–1074.

Iwata, K., Li, J., Follet, H., Phipps, R.J., Burr, D.B., 2006. Bisphosphonates suppress periosteal osteoblast activity independently of resorption in rat femur and tibia. Bone 39 (5), 1053–1058.

Jee, W.S., Ma, Y., 1999. Animal models of immobilization osteopenia. Morphologie 83 (261), 25–34.

Jee, W.S., Yao, W., 2001. Overview: animal models of osteopenia and osteoporosis. J. Musculoskelet. Neuronal Interact. 1 (3), 193–207.

Jee, W.S., Mori, S., Li, X.J., Chan, S., 1990. Prostaglandin E2 enhances cortical bone mass and activates intracortical bone remodeling in intact and ovariectomized female rats. Bone 11 (4), 253–266.

Jia, D., O'Brien, C.A., Stewart, S.A., Manolagas, S.C., Weinstein, R.S., 2006. Glucocorticoids act directly on osteoclasts to increase their life span and reduce bone density. Endocrinology 147 (12), 5592–5599.

Kalu, D.N., 1991. The ovariectomized rat model of postmenopausal bone loss. Bone Miner. 15 (3), 175–191.

Ke, H.Z., Crawford, D.T., Qi, H., Chidsey-Frink, K.L., Simmons, H.A., Li, M., Jee, W.S., Thompson, D.D., 2001. Long-term effects of aging and orchidectomy on bone and body composition in rapidly growing male rats. J. Musculoskelet. Neuronal Interact. 1 (3), 215–224.

Keune, J.A., Branscum, A.J., Iwaniec, U.T., Turner, R.T., 2015. Effects of spaceflight on bone microarchitecture in the axial and appendicular skeleton in growing ovariectomized rats. Sci. Rep. 5, 18671.

Kimmel, D.B., 1996. Animal models for in vivo experimentation in osteoporosis research. In: Marcus, R., Feldman, D., Kelsey, J. (Eds.), Osteoporosis. Academic Press, San Diego, pp. 671–690.

Kodama, Y., Nakayama, K., Fuse, H., Fukumoto, S., Kawahara, H., Takahashi, H., Kurokawa, T., Sekiguchi, C., Nakamura, T., Matsumoto, T., 1997. Inhibition of bone resorption by pamidronate cannot restore normal gain in cortical bone mass and strength in tail-suspended rapidly growing rats. J. Bone Miner. Res. 12 (7), 1058–1067.

Komatsu, D.E., Brune, K.A., Liu, H., Schmidt, A.L., Han, B., Zeng, Q.Q., Yang, X., Nunes, J.S., Lu, Y., Geiser, A.G., Ma, Y.L., Wolos, J.A., Westmore, M.S., Sato, M., 2009. Longitudinal in vivo analysis of the region-specific efficacy of parathyroid hormone in a rat cortical defect model. Endocrinology 150 (4), 1570–1579.

Komatsubara, S., Mori, S., Mashiba, T., Ito, M., Li, J., Kaji, Y., Akiyama, T., Miyamoto, K., Cao, Y., Kawanishi, J., Norimatsu, H., 2003. Long-term treatment of incadronate disodium accumulates microdamage but improves the trabecular bone microarchitecture in dog vertebra. J. Bone Miner. Res. 18 (3), 512–520.

Komatsubara, S., Mori, S., Mashiba, T., Nonaka, K., Seki, A., Akiyama, T., Miyamoto, K., Cao, Y., Manabe, T., Norimatsu, H., 2005. Human parathyroid hormone (1-34) accelerates the fracture healing process of woven to lamellar bone replacement and new cortical shell formation in rat femora. Bone 36 (4), 678–687.

Kon, T., Cho, T.J., Aizawa, T., Yamazaki, M., Nooh, N., Graves, D., Gerstenfeld, L.C., Einhorn, T.A., 2001. Expression of osteoprotegerin, receptor activator of NF-kappaB ligand (osteoprotegerin ligand) and related proinflammatory cytokines during fracture healing. J. Bone Miner. Res. 16 (6), 1004–1014.

Kratzel, C., Bergmann, C., Duda, G., Greiner, S., Schmidmaier, G., Wildemann, B., 2008. Characterization of a rat osteotomy model with impaired healing. BMC Musculoskelet. Disord. 9, 135.

Larrue, A., Rattner, A., Peter, Z.A., Olivier, C., Laroche, N., Vico, L., Peyrin, F., 2011. Synchrotron radiation micro-CT at the micrometer scale for the analysis of the three-dimensional morphology of microcracks in human trabecular bone. PLoS One 6 (7), e21297.

Lee, T.C., Myers, E.R., Hayes, W.C., 1998. Fluorescence-aided detection of microdamage in compact bone. J. Anat. 193 (Pt 2), 179–184.

Lee, T.C., Arthur, T.L., Gibson, L.J., Hayes, W.C., 2000. Sequential labelling of microdamage in bone using chelating agents. J. Orthop. Res. 18 (2), 322–325.

Lee, T.C., Mohsin, S., Taylor, D., Parkesh, R., Gunnlaugsson, T., O'Brien, F.J., Giehl, M., Gowin, W., 2003. Detecting microdamage in bone. J. Anat. 203 (2), 161–172.

Lelovas, P.P., Xanthos, T.T., Thoma, S.E., Lyritis, G.P., Dontas, I.A., 2008. The laboratory rat as an animal model for osteoporosis research. Comp. Med. 58 (5), 424–430.

Li, J., Mori, S., Kaji, Y., Mashiba, T., Kawanishi, J., Norimatsu, H., 1999. Effect of bisphosphonate (incadronate) on fracture healing of long bones in rats. J. Bone. Miner. Res. 14 (6), 969–979.

Li, X.J., Jee, W.S., Chow, S.Y., Woodbury, D.M., 1990. Adaptation of cancellous bone to aging and immobilization in the rat: a single photon absorptiometry and histomorphometry study. Anat. Rec. 227 (1), 12–24.

Li, M., Shen, Y., Qi, H., Wronski, T.J., 1996. Comparative study of skeletal response to estrogen depletion at red and yellow marrow sites in rats. Anat. Rec. 245 (3), 472–480.

Li, M., Shen, Y., Halloran, B.P., Baumann, B.D., Miller, K., Wronski, T.J., 1996. Skeletal response to corticosteroid deficiency and excess in growing male rats. Bone 19 (2), 81–88.

Li, M., Shen, Y., Wronski, T.J., 1997. Time course of femoral neck osteopenia in ovariectomized rats. Bone 20 (1), 55–61.

Li, M., Healy, D.R., Simmons, H.A., Ke, H.Z., Thompson, D.D., 2003. Alfacalcidol restores cancellous bone in ovariectomized rats. J. Musculoskelet. Neuronal Interact. 3 (1), 39–46.

Li, J., Miller, M.A., Hutchins, G.D., Burr, D.B., 2005. Imaging bone microdamage in vivo with positron emission tomography. Bone 37 (6), 819–824.

Lloyd, S.A., Lang, C.H., Zhang, Y., Paul, E.M., Laufenberg, L.J., Lewis, G.S., Donahue, H.J., 2014. Interdependence of muscle atrophy and bone loss induced by mechanical unloading. J. Bone Miner. Res. 29 (5), 1118–1130.

Ma, Y.F., Ke, H.Z., Jee, W.S., 1994. Prostaglandin E2 adds bone to a cancellous bone site with a closed growth plate and low bone turnover in ovariectomized rats. Bone 15 (2), 137–146.

Ma, Y.F., Li, X.J., Jee, W.S., McOsker, J., Liang, X.G., Setterberg, R., Chow, S.Y., 1995. Effects of prostaglandin E2 and F2 alpha on the skeleton of osteopenic ovariectomized rats. Bone 17 (6), 549–554.

Ma, Y.F., Jee, W.S., Ke, H.Z., Lin, B.Y., Liang, X.G., Li, M., Yamamoto, N., 1995. Human parathyroid hormone-(1-38) restores cancellous bone to the immobilized, osteopenic proximal tibial metaphysis in rats. J. Bone Miner. Res. 10 (3), 496–505.

Ma, Y.F., Pan, Z., Jee, W.S., Lin, C.H., Liang, H.H., Chen, H., Pun, S., Li, X.J., 1997. Intermittent on/off prostaglandin E2 and risedronate are equally anabolic as daily PGE2 alone treatment in cortical bone of ovariectomized rats. J. Bone Miner. Res. 12 (12), 2108–2112.

Ma, Y.L., Bryant, H.U., Zeng, Q., Palkowitz, A., Jee, W.S., Turner, C.H., Sato, M., 2002. Long-term dosing of arzoxifene lowers cholesterol, reduces bone turnover, and preserves bone quality in ovariectomized rats. J. Bone Miner. Res. 17 (12), 2256–2264.

Ma, Y.L., Bryant, H.U., Zeng, Q., Schmidt, A., Hoover, J., Cole, H.W., Yao, W., Jee, W.S., Sato, M., 2003. New bone formation with teriparatide [human parathyroid hormone-(1-34)] is not retarded by long-term pretreatment with alendronate, estrogen, or raloxifene in ovariectomized rats. Endocrinology 144 (5), 2008–2015.

Ma, Y.L., Bryant, H.U., Zeng, Q., Schmidt, A., Jee, W.S., Sato, M., 2005. Raloxifene and teriparatide (hPTH 1-34) have complementary effects on the osteopenic skeleton of ovariectomized rats. J. Bone Miner. Metab. 23 (Suppl. l), 62–68.

Ma, Y.L., Zeng, Q.Q., Porras, L.L., Harvey, A., Moore, T.L., Shelbourn, T.L., Dalsky, G.P., Wronski, T.J., Aguirre, J.I., Bryant, H.U., Sato, M., 2011. Teriparatide [rhPTH (1-34)], but not strontium ranelate, demonstrated bone anabolic efficacy in mature, osteopenic, ovariectomized rats. Endocrinology 152 (5), 1767–1778.

Ma, Y.L., Hamang, M., Lucchesi, J., Bivi, N., Zeng, Q., Adrian, M.D., Raines, S.E., Li, J., Kuhstoss, S.A., Obungu, V., Bryant, H.U., Krishnan, V., 2017. Time course of disassociation of bone formation signals with bone mass and bone strength in sclerostin antibody treated ovariectomized rats. Bone 97, 20–28.

Marsell, R., Einhorn, T.A., 2011. The biology of fracture healing. Injury 42 (6), 551–555.

Martin, R.B., 1989. Label escape theory revisited: the effects of resting periods and section thickness. Bone 10 (4), 255–264.

Martin, R.B., Yeh, O.C., Fyhrie, D.P., 2007. On sampling bones for microcracks. Bone 40 (4), 1159–1165.

Martin-Fernandez, M., Martinez, E., Diaz-Curiel, M., Guede, D., Caeiro, J.R., De la Piedra, C., 2014. Effects of PTH (1-84) on bone quality in a validated model of osteoporosis due to androgenic deprivation. Aging Male 17 (1), 42–50.

Mashiba, T., Hirano, T., Turner, C.H., Forwood, M.R., Johnston, C.C., Burr, D.B., 2000. Suppressed bone turnover by bisphosphonates increases microdamage accumulation and reduces some biomechanical properties in dog rib. J. Bone Miner. Res. 15 (4), 613–620.

Mashiba, T., Turner, C.H., Hirano, T., Forwood, M.R., Johnston, C.C., Burr, D.B., 2001. Effects of suppressed bone turnover by bisphosphonates on microdamage accumulation and biomechanical properties in clinically relevant skeletal sites in beagles. Bone 28 (5), 524–531.

Matsumoto, T., Nakayama, K., Kodama, Y., Fuse, H., Nakamura, T., Fukumoto, S., 1998. Effect of mechanical unloading and reloading on periosteal bone formation and gene expression in tail-suspended rapidly growing rats. Bone 22 (5 Suppl. l), 89S–93S.

McClung, M.R., Grauer, A., Boonen, S., Bolognese, M.A., Brown, J.P., Diez-Perez, A., Langdahl, B.L., Reginster, J.Y., Zanchetta, J.R., Wasserman, S.M., Katz, L., Maddox, J., Yang, Y.C., Libanati, C., Bone, H.G., 2014. Romosozumab in postmenopausal women with low bone mineral density. N. Engl. J. Med. 370 (5), 412–420.

Miller, S.C., Shupe, J.G., Redd, E.H., Miller, M.A., Omura, T.H., 1986. Changes in bone mineral and bone formation rates during pregnancy and lactation in rats. Bone 7 (4), 283–287.

Milstead, J.R., Simske, S.J., Bateman, T.A., 2004. Spaceflight and hindlimb suspension disuse models in mice. Biomed. Sci. Instrum. 40, 105–110.

Minkwitz, S., Fassbender, M., Kronbach, Z., Wildemann, B., 2015. Longitudinal analysis of osteogenic and angiogenic signaling factors in healing models mimicking atrophic and hypertrophic non-unions in rats. PLoS One 10 (4), e0124217.

Morey-Holton, E.R., Globus, R.K., 1998. Hindlimb unloading of growing rats: a model for predicting skeletal changes during space flight. Bone 22 (5 Suppl. l), 83S–88S.

Monfoulet, L., Rabier, B., Chassande, O., Fricain, J.C., 2010. Drilled hole defects in mouse femur as models of intramembranous cortical and cancellous bone regeneration. Calcif. Tissue Int. 86 (1), 72–81.

Mori, S., Jee, W.S., Li, X.J., Chan, S., Kimmel, D.B., 1990. Effects of prostaglandin E2 on production of new cancellous bone in the axial skeleton of ovariectomized rats. Bone 11 (2), 103–113.

O'Driscoll, S.W., Marx, R.G., Fitzsimmons, J.S., Beaton, D.E., 1999. Method for automated cartilage histomorphometry. Tissue Eng. 5 (1), 13–23.

Ominsky, M.S., Niu, Q.T., Li, C., Li, X., Ke, H.Z., 2014. Tissue-level mechanisms responsible for the increase in bone formation and bone volume by sclerostin antibody. J. Bone Miner. Res. 29 (6), 1424–1430.

Parfitt, A.M., Drezner, M.K., Glorieux, F.H., Kanis, J.A., Malluche, H., Meunier, P.J., Ott, S.M., Recker, R.R., 1987. Bone histomorphometry: standardization of nomenclature, symbols, and units. Report of the ASBMR Histomorphometry Nomenclature Committee. J. Bone Miner. Res. 2 (6), 595–610.

Recker, R.R., Kimmel, D.B., Dempster, D., Weinstein, R.S., Wronski, T.J., Burr, D.B., 2011. Issues in modern bone histomorphometry. Bone 49 (5), 955–964.

Reim, N.S., Breig, B., Stahr, K., Eberle, J., Hoeflich, A., Wolf, E., Erben, R.G., 2008. Cortical bone loss in androgen-deficient aged male rats is mainly caused by increased endocortical bone remodeling. J. Bone Miner. Res. 23 (5), 694–704.

Roux, J., Chavassieux, P., Chapurlat, R., Portero-Muzy, N., Garcia, P., Brown, J.P., Libanati, C., Boyce, R., Wang, A., Grauer, A., 2017. Effects of Romosozumab in postmenopausal women with osteoporosis after 2 and 12 months: bone histomorphometry substudy. In: Annual Meeting of American Society of Bone and Mineral Research. Denver Colorado, September 8–11. Abstract# 1072.

Sato, M., Zeng, G.Q., Rowley, E., Turner, C.H., 1998. LY353381 x HCl: an improved benzothiophene analog with bone efficacy complementary to parathyroid hormone-(1-34). Endocrinology 139 (11), 4642–4651.

Schenk, R.K., Olah, A.J., Herrmann, W., 1984. Preparation of calcified tissues for light microscopy. In: Dickson, G.R. (Ed.), Methods of Calcified Tissue Preparation. Elsevier, Amsterdam, pp. 1–56.

Schindeler, A., McDonald, M.M., Bokko, P., Little, D.G., 2008. Bone remodeling during fracture repair: the cellular picture. Semin. Cell Dev. Biol. 19 (5), 459–466.

Schindeler, A., Morse, A., Harry, L., Godfrey, C., Mikulec, K., McDonald, M., Gasser, J.A., Little, D.G., 2008. Models of tibial fracture healing in normal and Nf1-deficient mice. J. Orthop. Res. 26 (8), 1053–1060.

Seref-Ferlengez, Z., Basta-Pljakic, J., Kennedy, O.D., Philemon, C.J., Schaffler, M.B., 2014. Structural and mechanical repair of diffuse damage in cortical bone in vivo. J. Bone Miner. Res. 29 (12), 2537–2544.

Shen, V., Dempster, D.W., Birchman, R., Xu, R., Lindsay, R., 1993. Loss of cancellous bone mass and connectivity in ovariectomized rats can be restored by combined treatment with parathyroid hormone and estradiol. J. Clin. Invest. 91 (6), 2479–2487.

Shen, V., Birchman, R., Xu, R., Lindsay, R., Dempster, D.W., 1995. Short-term changes in histomorphometric and biochemical turnover markers and bone mineral density in estrogen-and/or dietary calcium-deficient rats. Bone 16 (1), 149–156.

Shen, V., Liang, X.G., Birchman, R., Wu, D.D., Healy, D., Lindsay, R., Dempster, D.W., 1997. Short-term immobilization-induced cancellous bone loss is limited to regions undergoing high turnover and/or modeling in mature rats. Bone 21 (1), 71–78.

Silva, M.J., Uthgenannt, B.A., Rutlin, J.R., Wohl, G.R., Lewis, J.S., Welch, M.J., 2006. In vivo skeletal imaging of 18F-fluoride with positron emission tomography reveals damage- and time-dependent responses to fatigue loading in the rat ulna. Bone 39 (2), 229–236.

Sims, N.A., Morris, H.A., Moore, R.J., Durbridge, T.C., 1996. Increased bone resorption precedes increased bone formation in the ovariectomized rat. Calcif. Tissue Int. 59 (2), 121–127.

Sridharan, G., Shankar, A.A., 2012. Toluidine blue: a review of its chemistry and clinical utility. J. Oral Maxillofac. Pathol. 16 (2), 251–255.

Stolina, M., Dwyer, D., Niu, Q.T., Villasenor, K.S., Kurimoto, P., Grisanti, M., Han, C.Y., Liu, M., Li, X., Ominsky, M.S., Ke, H.Z., Kostenuik, P.J., 2014. Temporal changes in systemic and local expression of bone turnover markers during six months of sclerostin antibody administration to ovariectomized rats. Bone 67, 305–313.

Streicher, C., Heyny, A., Andrukhova, O., Haigl, B., Slavic, S., Schuler, C., Kollmann, K., Kantner, I., Sexl, V., Kleiter, M., Hofbauer, L.C., Kostenuik, P.J., Erben, R.G., 2017. Estrogen regulates bone turnover by targeting RANKL expression in bone lining cells. Sci. Rep. 7 (1), 6460.

Takeda, S., Sakai, S., Shiraishi, A., Koike, N., Mihara, M., Endo, K., 2013. Combination treatment with eldecalcitol (ED-71) and raloxifene improves bone mechanical strength by suppressing bone turnover and increasing bone mineral density in ovariectomized rats. Bone 53 (1), 167–173.

Tanaka, M., Sakai, A., Uchida, S., Tanaka, S., Nagashima, M., Katayama, T., Yamaguchi, K., Nakamura, T., 2004. Prostaglandin E2 receptor (EP4) selective agonist (ONO-4819.CD) accelerates bone repair of femoral cortex after drill-hole injury associated with local upregulation of bone turnover in mature rats. Bone 34 (6), 940–948.

Tiyapatanaputi, P., Rubery, P.T., Carmouche, J., Schwarz, E.M., O'Keefe, J.R., Zhang, X., 2004. A novel murine segmental femoral graft model. J. Orthop. Res. 22 (6), 1254–1260.

Turnbull, T.L., Baumann, A.P., Roeder, R.K., 2014. Fatigue microcracks that initiate fracture are located near elevated intracortical porosity but not elevated mineralization. J. Biomech. 47 (12), 3135–3142.

Turner, R.T., Wakley, G.K., Hannon, K.S., 1990. Differential effects of androgens on cortical bone histomorphometry in gonadectomized male and female rats. J. Orthop. Res. 8 (4), 612–617.

Turner, R.T., Evans, G.L., Wakley, G.K., 1993. Mechanism of action of estrogen on cancellous bone balance in tibiae of ovariectomized growing rats: inhibition of indices of formation and resorption. J. Bone Miner. Res. 8 (3), 359–366.

Turner, R.T., Maran, A., Lotinun, S., Hefferan, T., Evans, G.L., Zhang, M., Sibonga, J.D., 2001. Animal models for osteoporosis. Rev. Endocr. Metab. Disord. 2 (1), 117–127.

Vanderschueren, D., Van Herck, E., Suiker, A.M., Visser, W.J., Schot, L.P., Bouillon, R., 1992. Bone and mineral metabolism in aged male rats: short and long term effects of androgen deficiency. Endocrinology 130 (5), 2906–2916.

Varela, A., Chouinard, L., Lesage, E., Smith, S.Y., Hattersley, G., 2017. One year of Abaloparatide, a selective activator of the PTH1 receptor, increased bone formation and bone mass in osteopenic ovariectomized rats without increasing bone resorption. J. Bone Miner. Res. 32 (1), 24–33.

Vashishth, D., Koontz, J., Qiu, S.J., Lundin-Cannon, D., Yeni, Y.N., Schaffler, M.B., Fyhrie, D.P., 2000. In vivo diffuse damage in human vertebral trabecular bone. Bone 26 (2), 147–152.

Villanueva, A.R., Longo III, J.A., Weiner, G., 1994. Staining and histomorphometry of microcracks in the human femoral head. Biotech. Histochem. 69 (2), 81–88.

Weinstein, R.S., Jilka, R.L., Parfitt, A.M., Manolagas, S.C., 1998. Inhibition of osteoblastogenesis and promotion of apoptosis of osteoblasts and osteocytes by glucocorticoids. Potential mechanisms of their deleterious effects on bone. J. Clin. Invest. 102 (2), 274–282.

Wronski, T.J., Schenck, P.A., Cintron, M., Walsh, C.C., 1987. Effect of body weight on osteopenia in ovariectomized rats. Calcif. Tissue Int. 40 (3), 155–159.

Wronski, T.J., Cintron, M., Dann, L.M., 1988. Temporal relationship between bone loss and increased bone turnover in ovariectomized rats. Calcif. Tissue Int. 43 (3), 179–183.

Wronski, T.J., Cintron, M., Doherty, A.L., Dann, L.M., 1988. Estrogen treatment prevents osteopenia and depresses bone turnover in ovariectomized rats. Endocrinology 123 (2), 681–686.

Wronski, T.J., Dann, L.M., Scott, K.S., Cintron, M., 1989. Long-term effects of ovariectomy and aging on the rat skeleton. Calcif. Tissue Int. 45 (6), 360–366.

Wronski, T.J., Dann, L.M., Horner, S.L., 1989. Time course of vertebral osteopenia in ovariectomized rats. Bone 10 (4), 295–301.

Yamamoto, N., Jee, W.S., Ma, Y.F., 1995. Bone histomorphometric changes in the femoral neck of aging and ovariectomized rats. Anat. Rec. 243 (2), 175–185.

Yao, W., Cheng, Z., Pham, A., Busse, C., Zimmermann, E.A., Ritchie, R.O., Lane, N.E., 2008. Glucocorticoid-induced bone loss in mice can be reversed by the actions of parathyroid hormone and risedronate on different pathways for bone formation and mineralization. Arthritis Rheum. 58 (11), 3485–3497.

Zhang, X., Schwarz, E.M., Young, D.A., Puzas, J.E., Rosier, R.N., O'Keefe, R.J., 2002. Cyclooxygenase-2 regulates mesenchymal cell differentiation into the osteoblast lineage and is critically involved in bone repair. J. Clin. Invest. 109 (11), 1405–1415.

Zhang, D., Hu, M., Chu, T., Lin, L., Wang, J., Li, X., Ke, H.Z., Qin, Y.X., 2016. Sclerostin antibody prevented progressive bone loss in combined ovariectomized and concurrent functional disuse. Bone 87, 161–168.

Zioupos, P., Currey, J.D., Sedman, A.J., 1994. An examination of the micromechanics of failure of bone and antler by acoustic emission tests and laser scanning confocal microscopy. Med. Eng. Phys. 16 (3), 203–212.

Chapter 83

Bone strength testing in rodents

Mary L. Bouxsein[1,2,3] and Frank C. Ko[1]

[1]Center for Advanced Orthopaedic Studies, Beth Israel Deaconess Medical Center, Boston, MA, United States; [2]Department of Orthopaedic Surgery, Harvard Medical School, Boston, MA, United States; [3]Endocrine Unit, Department of Medicine, Massachusetts General Hospital, Boston, MA, United States

Chapter outline

Introduction

Despite advances in biomedical science and healthcare, skeletal fragility and its associated fractures remain as leading causes of disability and increased burden of care among the elderly population. Rodent models of skeletal fragility provide useful insights into bone biology and biomechanics that may assist in the development of interventions to prevent fractures. In particular, the application of various mechanical testing methods has allowed assessment of the functional outcomes (e.g., strengths, failure modes, and/or material properties) resulting from genetic, pharmacologic, and/or environmental interventions in rodents, thereby allowing for inferences about their potential effects on skeletal fracture incidents in humans. Accordingly, as the field continues to utilize rodent models to develop novel therapeutic interventions for skeletal fragility, functional assessment of skeleton by mechanical testing will continue to be among the key preclinical pharmacological assessments.

Mechanical testing methods for rodent skeleton have been adapted from the American Society for Testing and Materials standards that have tested the mechanical properties of steel, concrete, glass, and other common materials used for structures that need to pass rigorous safety criteria. However, unlike these materials, which are generally homogeneous, elastic, and isotropic, bone is an orthotropic and heterogeneous material that is a mixture of minerals and organic and inorganic matrix. Rodent bones in particular present additional challenges due to their diminutive sizes compared with larger mammalian bones. Despite these challenges, several studies have successfully assessed the functional alterations in rodent bones with wide-ranging mechanical testing techniques, such as whole-bone three-point bending to failure, fracture toughness, and microindention/nanoindentation. For a scientist who has a limited background in the mechanics of materials, these various testing methods can be overwhelming and perplexing. In this chapter, we will review the mechanical testing methods that have been implemented on rodent skeleton to better equip scientists with the knowledge to select appropriate testing methods and properly interpret their results. We will broadly categorize these testing methods from a whole-bone to a nanoscale assessment of mechanical properties (Fig. 83.1).

Principles of Bone Biology. https://doi.org/10.1016/B978-0-12-814841-9.00083-X

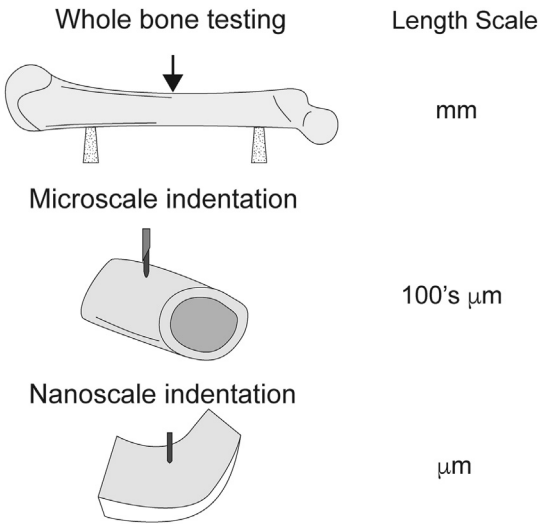

FIGURE 83.1 Common biomechanical assessment techniques of bone at different length scales in rodent models.

Whole-bone mechanical testing

Assessing the strength of a rodent bone using whole-bone mechanical testing has become a standard measure of functional outcomes in response to pharmacological therapies or genetic alterations. These testing methods are used to assess long bone or vertebral body stiffness, strength, and energy-absorbing capability, and can be combined with theoretical approaches to estimate the material (or tissue-level) properties of bone. Depending on scientific questions and observed phenotypes, investigators should select appropriate testing methods to assess functional outcomes in rodent bones.

Specimen preparation

Prior to biomechanical testing, investigators need to ensure that specimens are harvested and stored in appropriate conditions to minimize introducing environmental variables that can influence rodent bone biomechanical properties. For example, dry bone is more brittle than wet bone, which translates to increased Young's modulus and decreased toughness (Evans and Lebow, 1951). Also, use of fixatives such as ethanol, formalin, or glutaraldehyde for specimen preservation can alter mechanical properties such as modulus or strength compared with those of fresh bones (Linde and Sorensen, 1993; Unger et al., 2010). While a single or repeated freeze−thaw cycles do not alter the biomechanical properties of bone (Panjabi et al., 1985; Borchers et al., 1995; Kang et al., 1997), one study suggests potential alterations in cortical bone compositional properties following multiple freeze−thaw cycles that may influence tissue-level mechanical properties (McElderry et al., 2011). Finally, the temperature at which the tests are conducted can influence the mechanical properties of bone, where testing at a room temperature (23−25°C) slightly increases modulus (2%−4%) of bone compared with testing at a physiologically relevant temperature (37°C) (Bonfield and Li, 1968; Smith and Walmsley, 1959). However, maintaining 37°C using water baths during mechanical testing is a technical challenge to many investigators. Thus, the generally accepted specimen harvest and storage procedure is to clear soft tissues from rodent bones, wrap in saline soaked gauze, and store in a −20°C freezer until mechanical testing at a room temperature.

Standard three-point and four-point bending to failure

Bending tests are used to assess diaphyseal cortical bone biomechanical properties. The tests are performed with the bones placed on two supports at the ends and loaded at a constant rate at the center until failure. The difference between three- and four-point bending is the number of loading points applied at the center of bone; the three-point bending test applies load at a single point that generates maximum moment at the center of bone, whereas four-point applies load at two points that generate constant maximum moment between two loading points (Fig. 83.2). Since the moment is maximum at the center load point, a three-point bending test predisposes the bone to fracture at the loading point. In contrast, in four-point bending the constant moment between two loading points allows the bone to fracture at the weakest point testing the loading region. While both three- and four-point bending tests have been used previously to assess rodent bone strengths,

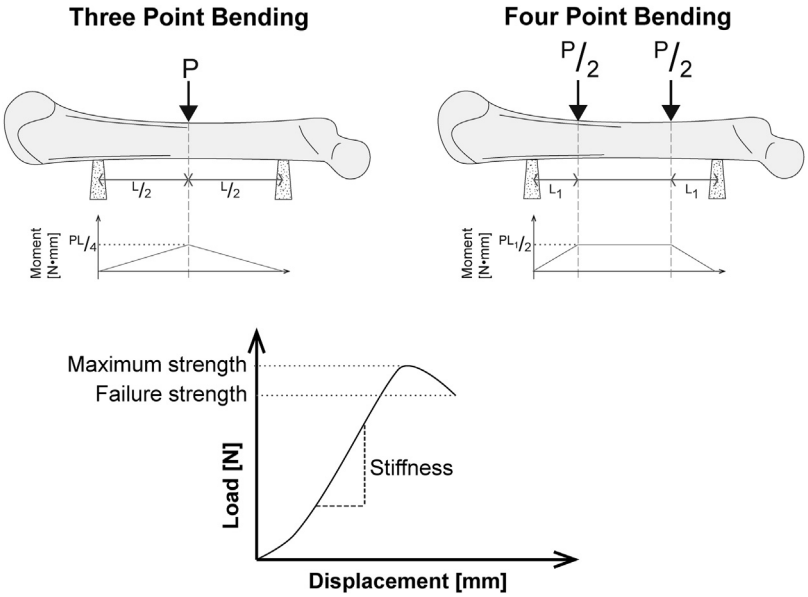

FIGURE 83.2 Experimental setup for three and four point bending, moment diagram along the bone, and typical load-displacement curve where maximum/failure strengths and stiffness can obtained. These strengths and stiffness outcomes can be converted to bending moments and bending stiffness. *P*, applied load; *L*, bottom support span length; L_1, distance between the loading point and support.

the choice between these two depends on the size of rodents and availability of fixtures, as finding four support and loading points on some small mouse bones is more challenging than it is on an older and bigger mouse or a rat bone.

The outcomes from a standard three- or four-point bending test are derived from the load−displacement curve and include stiffness (slope of linear portion), maximum strength, failure strength, and work to failure (area under the curve) (Table 83.1). These outcomes can be converted to bending stiffness and bending strengths by multiplying by the span length used. In addition, estimated cortical bone material properties (elastic modulus) can also be calculated according to beam theory, adjusting the cortical bone stiffness by the appropriate moment of inertia, which is often calculated from microcomputed tomography (micro-CT) scans (Jepsen et al., 2015). Depending on rodent models, span length can vary from 6 to 8 mm for a mouse femur to 13−20 mm for a rat femur. While these span lengths do not satisfy the assumption in beam theory that the aspect ratio of "span length:width" needs to be higher than 16:1 to calculate tissue-level properties (stress, modulus, etc.), estimated cortical bone material properties nonetheless provide some insights about whether the alterations in the whole-bone mechanical properties are due to structural or material changes. Commonly used loading rates are from 0.01 to 5 mm/s. The slower the loading rate (i.e., quasistatic), the better the test will be at capturing the postyield behavior of bone.

TABLE 83.1 Whole-bone outcomes and their respective tissue-level outcomes from mechanical tests.

	Whole-bone outcomes	Tissue-level outcomes
Three-point bending	M = max moment [N•mm] K = bending stiffness [N•mm^2] Work to failure [N•mm]	Ultimate stress [N/mm^2] = M•c/I Elastic modulus [N/mm^2] = FL^3/(48dI) Toughness = "not recommended"[a]
Torsion	T = max torque [N•mm] S = torsional stiffness [N•mm/rad] Work to failure [N•mm]	Ultimate sheer stress [N/mm^2] = T•R/J Elastic shear modulus [N/mm^2] = SL/J Toughness = "not recommended"[a]
Compression	F = max load [N] K = compressive stiffness [N/mm]	Ultimate stress [N/mm^2] = F/A Elastic modulus [N/mm^2] = stress/strain

A, cross-sectional area; *c*, maximum distance between the centroid and outermost cortical bone; *d*, displacement; *F*, applied load; *I*, area moment of inertia; *J*, polar moment of inertia; *L*, span/gage length; *R*, maximum cortical bone radius.
[a]*Because toughness involves both linear and nonlinear behavior, applying linear beam theory approximation is not recommended.*

Torsion to failure

While both bending and torsion tests predict strength and stiffness of cortical bone, the differences in functional implications as well as technical challenges occasionally lead to choosing torsional tests for rodent bone. For example, in mouse models of fracture healing, bulky and weak callus at the center of the bone presents a significant challenge for traditional three-point and even four-point bending tests, which need to apply loads at a region where the callus is formed. Thus, investigators opt for the torsional test, which applies constant torque throughout the whole bone to assess callus strength and stiffness (Gerstenfeld et al., 2009). Similar to the four-point bending test, the torsion test applies constant torque through the whole bone, allowing the bone to fail at the weakest point.

Prior to torsional testing, both ends of bone are embedded in polymethyl methacrylate at a fixed gage length. The bone is then tested under constant radial displacement (radian) until failure. Similar to bending tests, the torsion test generates a torque versus radian curve, which can then be used to calculate maximum torque, torsional stiffness (slope), and work to maximum/failure torque (Table 83.1).

Compression testing

Compression testing is used to assess whole vertebral mechanical properties in rodents. In general when testing rat vertebrae, the vertebral posterior elements are removed and endplates are cut to ensure parallel surfaces for compression testing (Glatt et al., 2004). Due to its smaller size, cutting endplates and posterior elements is generally not performed in a mouse vertebra (Tommasini et al., 2005). The main outcomes of the compression test include compressive stiffness and strength, which reflect both cortical and trabecular bone mechanical properties (Table 83.1). By performing both bending and compressive tests at these two different skeletal sites, investigators can assess mechanical properties in both the appendicular and the axial skeleton and determine whether the environmental, genetic, or pharmacological perturbations have site-specific responses.

Summaries of whole-bone outcomes and their respective tissue-level outcomes for the bending and compressive tests are in Table 83.1. As noted earlier, investigators should cautiously select appropriate whole-bone testing methods to assess functional outcomes in rodent bones based on their observed phenotypes, skeletal sites of interest, and scientific inquiries.

Whole-bone testing in preclinical drug development

While the testing methods described above are applicable to all investigations in musculoskeletal research, they are particularly important in the development of new therapeutic agents. In particular, it is critical to demonstrate that any new therapeutic agent maintains or increases bone strength in rodent models and maintains or increases "bone quality." While bone quality is ill defined, in this context one can interpret this to mean that the intervention maintains the normally observed relationship between bone mass and bone biomechanical outcomes. For example, there is generally a strong association between femoral bone mass and femoral failure load (or moment) from three-point bending tests. A new therapeutic agent should maintain this relationship, or perhaps improve bone failure load for a given bone mass as has been shown for all approved osteoporosis therapies in the past 2 decades (Kostenuik, 2013).

Fracture toughness testing

While not used as commonly as the aforementioned whole-bone mechanical tests, fracture toughness tests can be used to estimate tissue-level mechanical properties of rodent bone that reflect different mechanical behavior than whole-bone bending, torsion, and compression tests. Indeed, fracture toughness tests reflect the ability of the bone material to resist the initiation and growth of a crack. Similar to the three-point bending test, bones undergoing a fracture toughness test are loaded at the center (Fig. 83.3). However, by artificially creating a notch (usually by low-speed saw or razor blade) in the middle and loading at a significantly lower rate (0.001 mm/s), investigators can determine the bone's resistance to crack growth (fracture toughness).

Fracture toughness in rodent bones can be calculated using crack-initiation, maximum load, or instability methods, which are based on different crack angles from scanning electron microscopy (SEM) images or loads from a load–displacement curve. While the initial notched crack angle can be obtained from micro-CT images, it is best to use SEM to obtain both the notched and instability crack angles (for a detailed description, see review by Ritchie et al., 2008).

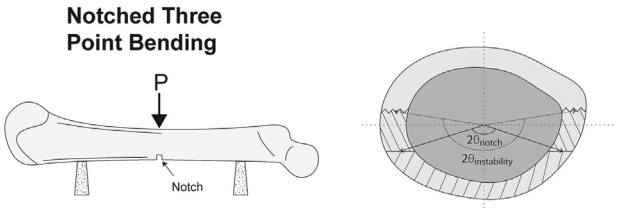

$$K_c = F_b \frac{P_c S R_o}{\pi (R_o^4 - R_i^4)} \sqrt{\pi R_m \theta_c}$$

FIGURE 83.3 Experimental setup for fracture toughness testing. P_c, maximum or failure loads; S, span length; R_o and R_i, mean outer and inner radii of the femoral cortex; R_m, average of R_o and R_i; q_c, notched or instability crack angles; F_b, geometry factor.

The majority of whole-bone bending and fracture toughness tests use rodent femurs due to their predominantly straight and hollow cylindrical cross-sectional properties. Several excellent tutorial and review articles have also been published describing these mechanical testing techniques in detail (Jepsen et al., 2015; Turner and Burr, 1993; Ritchie et al., 2008).

Finite element analysis

Unlike the previously mentioned destructive tests that "fracture" bones to assess biomechanical properties, finite element analysis (FEA) uses computational approaches to predict bone mechanical properties in a nondestructive manner (Spatz et al., 2013). In particular, high-resolution micro-CT images of rodent bone can be converted to an FEA model with appropriate software. After creating the FEA model, investigators conduct a virtual mechanical test to estimate bone biomechanical properties, thereby leaving the bone available for other evaluations, such as histology, immunohistochemistry, or dynamic histomorphometry. FEA may be particularly useful for assessing mechanical properties of trabecular bone in rodents, as the specimens are too small to experimentally test isolated trabecular bone. Another application is predicting strain distribution along the whole bone during in vivo mechanical loading of mouse tibia, allowing investigators to interrogate the relationships between high-strain regions and biological responses (Moustafa et al., 2012). Altogether, FEA provides avenues to uniquely integrate mechanical and biological events in rodent bones. However, despite these advantages, FEA is not free from challenges and limitations. For example, images generated from micro-CT can contain five million voxels or more, and performing voxel-based FEA can require large computational resources. Furthermore, the assumptions applied to FEA, such as boundary conditions and isotropic and linear elastic material properties, can misrepresent bone's physiological mechanical properties. These limitations are now being addressed by new computational algorithms to incorporate anisotropic and nonlinear material behaviors as well as experimental validations (Dos Santos et al., 2017; Imai, 2015). For example, in a mouse vertebra, predicted vertebral strength from FEA was well correlated with experimentally tested compressive strength and was able to assess the effects of pharmacological treatments or genetic background (Nyman et al., 2015).

Microscale and nanoscale bone material assessment

The advancement of material testing techniques has translated to allow for the assessment of bone mechanical properties at a smaller scale, such as on the order of microns, by applying a force using micrometer/nanometer sized tips. Complementing the assessment of mechanical properties at a whole-bone scale, these smaller-scale testing methods can potentially examine alterations in the material properties of an individual trabecular, perilacunar regions of osteocytes, or collagen/mineral components of bone. While multiple indentation tests have been applied to bones, we will focus on the techniques that have been applied to rodent bones.

Cyclic reference point indentation

The reference point indentation (RPI) technique was first introduced as a tool to evaluate tissue-level mechanical properties in ex vivo bone specimens (Hansma et al., 2009; Randall et al., 2009) and was subsequently applied to assess in vivo tissue mechanical properties in humans (Diez-Perez et al., 2010). Since then, two RPI devices have been introduced, OsteoProbe and BioDent. OsteoProbe administers a single impact force and records the distance that the probe subsequently descends into the bone to calculate a "bone material strength index." In comparison, BioDent performs cyclic indentations and then

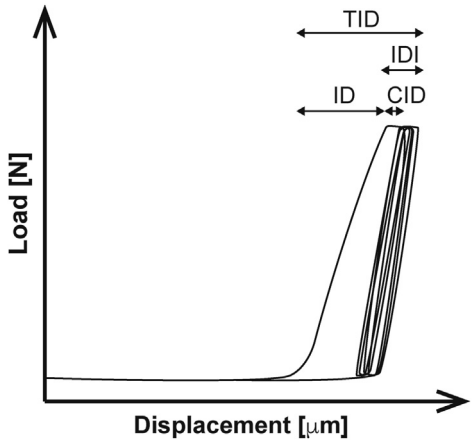

FIGURE 83.4 Load-displacement curve from cRPI test. *IDI,* indentation distance increase; *ID*, indentation distance; *TID*, total indentation distance; *CID*, creep indentation distance.

computes several outcome variables including total indentation distance, indentation distance increase, and creep indentation distance as well as loading and unloading slopes (Fig. 83.4; Allen et al., 2015; Karim et al., 2018). The indentation tip has a 2.5 um radius, and measurements can be taken at multiple locations a minimum of 500 um apart. RPI outcomes from rodent bone testing are weakly correlated or not correlated to traditional whole-bone mechanical properties and stress-intensity fracture toughness (Carriero et al., 2014; Gallant et al., 2013; Krege et al., 2016). These results indicate that cyclic RPI (cRPI) reflects mechanical properties distinct from those captured by whole-bone mechanical testing. Notably, indentation distances are increased in mouse models of diabetes (Rubin et al., 2016; Devlin et al., 2014). Also, the total indentation distance is decreased in the caudal site, but not in the cranial site, after mechanical loading of mouse tibia (Bergstrom et al., 2017). Investigations into the factors that influence cRPI and correlations with other mechanical testing variables are ongoing. However, RPI's ability to assess mechanical properties in vivo provides unique opportunities for longitudinal assessment of the material behavior of rodent bones. Investigators still need to be cognizant that in vivo cRPI measurements can be highly variable, which will affect the sample size. In a recent in vivo reproducibility study, within-animal coefficients of variation of cRPI outcomes varied from 13% to 33% in 16-week-old C57Bl/6 mice (Srisuwananukorn et al., 2015).

Nanoindentation

Nanoindentation has been used for decades to characterize the intrinsic mechanical properties of different types of materials including bone (Rho et al., 1997). Similar to other indentation methods, nanoindentation applies a static force on a rodent bone, using a diamond tip typically 100 nm in radius. The smaller tip size allows greater spatial resolution than that of the RPI method. Outcomes include measures of elastic modulus and hardness obtained from the force−displacement curve and indentation area. While this high spatial resolution technique can be used to determine local tissue-level alterations, such as the effects of tissue age on rat cortical bone (Donnelly et al., 2010), nanoindentation cannot be used in vivo due to the requirement of extensive sample preparation, including dehydration and surface polishing, prior to testing. The technique nonetheless can assess unique tissue-level mechanical properties, such as the effects of age or osteopontin deficiency, on mouse tibial cortical bone (Miller et al., 2007; Thurner et al., 2010).

Summary and discussion

Significant advancements in material science and engineering technologies now allow scientists to examine rodent bone mechanical properties from nanometer to whole-bone levels (Fig. 83.1). Which mechanical testing method(s) to choose will depend on the scientific questions asked. For example, one can design a study to determine variations in mechanical properties within a single cortex, which would require the use of nanoindentation, and integrate with whole-bone scale mechanical assessment in rodents (Kim et al., 2012). Also, an investigator may see a phenotype where mouse intact bone is unusually short, which can present significant technical challenges to performing three- or four-point bending tests. Whole-bone mechanical properties in these bones can alternatively be assessed by torsion test to failure (Liu et al., 2016). Finally,

specific cancellous and cortical bone mechanical properties from a single rodent bone can be predicted by FEA (Yang et al., 2014), where assessing such compartment-specific alterations is a significant challenge using conventional experimental approaches.

As musculoskeletal scientists continue to use rodent models to gain insight into skeletal fragility and fracture healing, appropriately assessing and interpreting the functional outcomes of genetic, pharmacologic, and environmental interventions is a crucial first step in the development of new therapies to reduce the burden of musculoskeletal diseases.

References

Allen, M.R., McNerny, E.M., Organ, J.M., Wallace, J.M., 2015. True gold or pyrite: a review of reference point indentation for assessing bone mechanical properties in vivo. J. Bone Miner. Res. 30, 1539−1550.

Bergstrom, I., Kerns, J.G., Tornqvist, A.E., Perdikouri, C., Mathavan, N., Koskela, A., Henriksson, H.B., Tuukkanen, J., Andersson, G., Isaksson, H., Goodship, A.E., Windahl, S.H., 2017. Compressive loading of the murine tibia reveals site-specific micro-scale differences in adaptation and maturation rates of bone. Osteoporos. Int. 28, 1121−1131.

Bonfield, W., Li, C.H., 1968. The temperature dependence of the deformation of bone. J. Biomech. 1, 323−329.

Borchers, R.E., Gibson, L.J., Burchardt, H., Hayes, W.C., 1995. Effects of selected thermal variables on the mechanical properties of trabecular bone. Biomaterials 16, 545−551.

Carriero, A., Bruse, J.L., Oldknow, K.J., Millan, J.L., Farquharson, C., Shefelbine, S.J., 2014. Reference point indentation is not indicative of whole mouse bone measures of stress intensity fracture toughness. Bone 69, 174−179.

Devlin, M.J., Van Vliet, M., Motyl, K., Karim, L., Brooks, D.J., Louis, L., Conlon, C., Rosen, C.J., Bouxsein, M.L., 2014. Early-onset type 2 diabetes impairs skeletal acquisition in the male TALLYHO/JngJ mouse. Endocrinology 155, 3806−3816.

Diez-Perez, A., Guerri, R., Nogues, X., Caceres, E., Pena, M.J., Mellibovsky, L., Randall, C., Bridges, D., Weaver, J.C., Proctor, A., Brimer, D., Koester, K.J., Ritchie, R.O., Hansma, P.K., 2010. Microindentation for in vivo measurement of bone tissue mechanical properties in humans'. J. Bone Miner. Res. 25, 1877−1885.

Donnelly, E., Boskey, A.L., Baker, S.P., van der Meulen, M.C., 2010. Effects of tissue age on bone tissue material composition and nanomechanical properties in the rat cortex. J. Biomed. Mater. Res. A 92, 1048−1056.

Dos Santos, M.B.F., Meloto, G.O., Bacchi, A., Correr-Sobrinho, L., 2017. Stress distribution in cylindrical and conical implants under rotational micromovement with different boundary conditions and bone properties: 3-D FEA. Comput. Methods Biomech. Biomed. Eng. 20, 893−900.

Evans, F.G., Lebow, M., 1951. 'Regional differences in some of the physical properties of the human femur. J. Appl. Physiol. 3, 563−572.

Gallant, M.A., Brown, D.M., Organ, J.M., Allen, M.R., Burr, D.B., 2013. Reference-point indentation correlates with bone toughness assessed using whole-bone traditional mechanical testing. Bone 53, 301−305.

Gerstenfeld, L.C., Sacks, D.J., Pelis, M., Mason, Z.D., Graves, D.T., Barrero, M., Ominsky, M.S., Kostenuik, P.J., Morgan, E.F., Einhorn, T.A., 2009. Comparison of effects of the bisphosphonate alendronate versus the RANKL inhibitor denosumab on murine fracture healing. J. Bone Miner. Res. 24, 196−208.

Glatt, M., Pataki, A., Evans, G.P., Hornby, S.B., Green, J.R., 2004. Loss of vertebral bone and mechanical strength in estrogen-deficient rats is prevented by long-term administration of zoledronic acid. Osteoporos. Int. 15, 707−715.

Hansma, P., Yu, H., Schultz, D., Rodriguez, A., Yurtsev, E.A., Orr, J., Tang, S., Miller, J., Wallace, J., Zok, F., Li, C., Souza, R., Proctor, A., Brimer, D., Nogues-Solan, X., Mellbovsky, L., Pena, M.J., Diez-Ferrer, O., Mathews, P., Randall, C., Kuo, A., Chen, C., Peters, M., Kohn, D., Buckley, J., Li, X., Pruitt, L., Diez-Perez, A., Alliston, T., Weaver, V., Lotz, J., 2009. 'The tissue diagnostic instrument. Rev. Sci. Instrum. 80, 054303.

Imai, K., 2015. Analysis of vertebral bone strength, fracture pattern, and fracture location: a validation study using a computed tomography-based nonlinear finite element analysis. Aging Dis. 6, 180−187.

Jepsen, K.J., Silva, M.J., Vashishth, D., Guo, X.E., van der Meulen, M.C., 2015. Establishing biomechanical mechanisms in mouse models: practical guidelines for systematically evaluating phenotypic changes in the diaphyses of long bones. J. Bone Miner. Res. 30, 951−966.

Kang, Q., An, Y.H., Friedman, R.J., 1997. Effects of multiple freezing-thawing cycles on ultimate indentation load and stiffness of bovine cancellous bone. Am. J. Vet. Res. 58, 1171−1173.

Karim, L., Van Vliet, M., Bouxsein, M.L., 2018. Comparison of cyclic and impact-based reference point indentation measurements in human cadaveric tibia. Bone 106, 90−95.

Kim, G., Boskey, A.L., Baker, S.P., van der Meulen, M.C., 2012. 'Improved prediction of rat cortical bone mechanical behavior using composite beam theory to integrate tissue level properties. J. Biomech. 45, 2784−2790.

Kostenuik, P., 2013. On the evolution and contemporary roles of bone remodeling. In: Feldman, D., Marcus, R., Dempster, D.W., Luckey, M., Cauley, J.A. (Eds.), Osteoporosis, fourth ed. Academic Press.

Krege, J.B., Aref, M.W., McNerny, E., Wallace, J.M., Organ, J.M., Allen, M.R., 2016. Reference point indentation is insufficient for detecting alterations in traditional mechanical properties of bone under common experimental conditions. Bone 87, 97−101.

Linde, F., Sorensen, H.C., 1993. The effect of different storage methods on the mechanical properties of trabecular bone. J. Biomech. 26, 1249−1252.

Liu, E.S., Martins, J.S., Raimann, A., Chae, B.T., Brooks, D.J., Jorgetti, V., Bouxsein, M.L., Demay, M.B., 2016. 1,25-Dihydroxyvitamin D alone improves skeletal growth, microarchitecture, and strength in a murine model of XLH, despite enhanced FGF23 expression. J. Bone Miner. Res. 31, 929−939.

McElderry, J.D., Kole, M.R., Morris, M.D., 2011. Repeated freeze-thawing of bone tissue affects Raman bone quality measurements. J. Biomed. Opt. 16, 071407.

Miller, L.M., Little, W., Schirmer, A., Sheik, F., Busa, B., Judex, S., 2007. Accretion of bone quantity and quality in the developing mouse skeleton. J. Bone Miner. Res. 22, 1037−1045.

Moustafa, A., Sugiyama, T., Prasad, J., Zaman, G., Gross, T.S., Lanyon, L.E., Price, J.S., 2012. Mechanical loading-related changes in osteocyte sclerostin expression in mice are more closely associated with the subsequent osteogenic response than the peak strains engendered. Osteoporos. Int. 23, 1225−1234.

Nyman, J.S., Uppuganti, S., Makowski, A.J., Rowland, B.J., Merkel, A.R., Sterling, J.A., Bredbenner, T.L., Perrien, D.S., 2015. Predicting mouse vertebra strength with micro-computed tomography-derived finite element analysis. Bonekey Rep. 4, 664.

Panjabi, M.M., Krag, M., Summers, D., Videman, T., 1985. Biomechanical time-tolerance of fresh cadaveric human spine specimens. J. Orthop. Res. 3, 292−300.

Randall, C., Mathews, P., Yurtsev, E., Sahar, N., Kohn, D., Hansma, P., 2009. The bone diagnostic instrument III: testing mouse femora. Rev. Sci. Instrum. 80, 065108.

Rho, J.Y., Tsui, T.Y., Pharr, G.M., 1997. Elastic properties of human cortical and trabecular lamellar bone measured by nanoindentation. Biomaterials 18, 1325−1330.

Ritchie, R.O., Koester, K.J., Ionova, S., Yao, W., Lane, N.E., Ager III, J.W., 2008. 'Measurement of the toughness of bone: a tutorial with special reference to small animal studies. Bone 43, 798−812.

Rubin, M.R., Paschalis, E.P., Poundarik, A., Sroga, G.E., McMahon, D.J., Gamsjaeger, S., Klaushofer, K., Vashishth, D., 2016. Advanced glycation endproducts and bone material properties in type 1 diabetic mice. PLoS One 11, e0154700.

Smith, J.W., Walmsley, R., 1959. Factors affecting the elasticity of bone. J. Anat. 93, 503−523.

Spatz, J.M., Ellman, R., Cloutier, A.M., Louis, L., van Vliet, M., Suva, L.J., Dwyer, D., Stolina, M., Ke, H.Z., Bouxsein, M.L., 2013. Sclerostin antibody inhibits skeletal deterioration due to reduced mechanical loading. J. Bone Miner. Res. 28, 865−874.

Srisuwananukorn, A., Allen, M.R., Brown, D.M., Wallace, J.M., Organ, J.M., 2015. In vivo reference point indentation measurement variability in skeletally mature inbred mice. Bonekey Rep. 4, 712.

Thurner, P.J., Chen, C.G., Ionova-Martin, S., Sun, L., Harman, A., Porter, A., Ager III, J.W., Ritchie, R.O., Alliston, T., 2010. Osteopontin deficiency increases bone fragility but preserves bone mass. Bone 46, 1564−1573.

Tommasini, S.M., Morgan, T.G., van der Meulen, M.C., Jepsen, K.J., 2005. Genetic variation in structure-function relationships for the inbred mouse lumbar vertebral body. J. Bone Miner. Res. 20, 817−827.

Turner, C.H., Burr, D.B., 1993. Basic biomechanical measurements of bone: a tutorial. Bone 14, 595−608.

Unger, S., Blauth, M., Schmoelz, W., 2010. Effects of three different preservation methods on the mechanical properties of human and bovine cortical bone. Bone 47, 1048−1053.

Yang, H., Butz, K.D., Duffy, D., Niebur, G.L., Nauman, E.A., Main, R.P., 2014. Characterization of cancellous and cortical bone strain in the in vivo mouse tibial loading model using microCT-based finite element analysis. Bone 66, 131−139.

Chapter 84

Regulation of energy metabolism by bone-derived hormones

Mathieu Ferron[1] and Gérard Karsenty[2]

[1]Institut de Recherches Cliniques de Montréal, Montréal, QC, Canada; [2]Department of Genetics and Development, Columbia University Medical Center, New York, NY, United States

Chapter outline

Introduction

As a tissue unique to vertebrates, bone fulfills a number of essential physiological functions viewed as classical functions of this tissue. It acts as a scaffold for muscle and the other organs and hence allows locomotion. Bone is also an important reservoir for several minerals including calcium, phosphate, and magnesium. Finally, bone cells are involved in the maintenance of the hematopoietic stem cell niche and therefore in the production of lymphocytes, erythrocytes, and platelets. These functions of bone are regulated by specific hormonal and neuronal input on bone cells. This topic has been extensively covered in other chapters.

Bone modeling and remodeling, the biological mechanisms by which bone grows, maintains its integrity, and repairs fractures, involve the coordinated bone-resorbing action of osteoclasts and the bone-forming action of osteoblasts. The nature of the cell biological processes involved strongly suggests that bone remodeling is an energy-consuming function. Furthermore, the energetic cost of this physiological process is necessarily proportional to the considerable area covered by bone in the body. The hypothesis that bone remodeling is tightly linked to energy metabolism is best illustrated by the observation that anorexia nervosa, a state of low energy intake, is associated with osteoporosis in humans (Legroux-Gerot et al., 2005; Misra and Klibanski, 2011). Accordingly, several hormones and neuropeptides implicated in the control of energy metabolism, such as insulin, adiponectin, leptin, NPY, orexins, and Agrp, do influence bone mass accrual (Fulzele et al., 2010; Ducy et al., 2000; Cornish et al., 2002; Kajimura et al., 2013; Horsnell and Baldock, 2016; Wei et al., 2014a; Kim et al., 2015). As a matter of fact, the regulation of bone mass by leptin and other hormones implicated in the control of energy metabolism was a reason to consider the hypothesis that, in a classical feedback loop, bone may be implicated in the control of energy metabolism. Moreover, that bone and other organs regulating energy metabolism are not adjacent to each other implied that if bone should have such a function, it must be through endocrinal means. This hypothesis was verified

Principles of Bone Biology. https://doi.org/10.1016/B978-0-12-814841-9.00084-1

by the demonstration that osteocalcin is a hormone influencing pancreatic β cell proliferation, insulin secretion, insulin sensitivity, and muscle function during exercise. More recently, lipocalin-2 (LCN2) was identified as a second bone-specific hormone involved in the control of appetite and glucose metabolism. Hence, bone is a bona fide endocrine organ that influences energy metabolism through the production of at least two hormones. This chapter will review in detail the mechanisms of action and regulation of osteocalcin and LCN2.

Osteocalcin: a bone-derived hormone regulating glucose metabolism

Osteocalcin is a short protein, 46 amino acids long in the mouse and 49 amino acids long in humans, that is produced and secreted specifically by osteoblasts. Inactivation of the two genes encoding osteocalcin (*Bglap1* and *Bglap2*) has profound metabolic consequences in mice fed a normal chow diet (Lee et al., 2007). Most strikingly, osteocalcin-deficient mice ($Ocn^{-/-}$) are characterized by increased adiposity, low circulating levels of insulin, reduced peripheral insulin sensitivity, and decreased glucose tolerance. They also display liver steatosis and signs of inflammation in the liver and white adipose tissue. In addition, the absence of osteocalcin causes a marked reduction in global energy expenditure, which likely contributes to the increased fat mass of these animals. Intermittent injections of recombinant osteocalcin in lean or obese mice or rats resulted in phenotypes opposite to the ones observed in $Ocn^{-/-}$ mice—i.e., they increased energy expenditure,

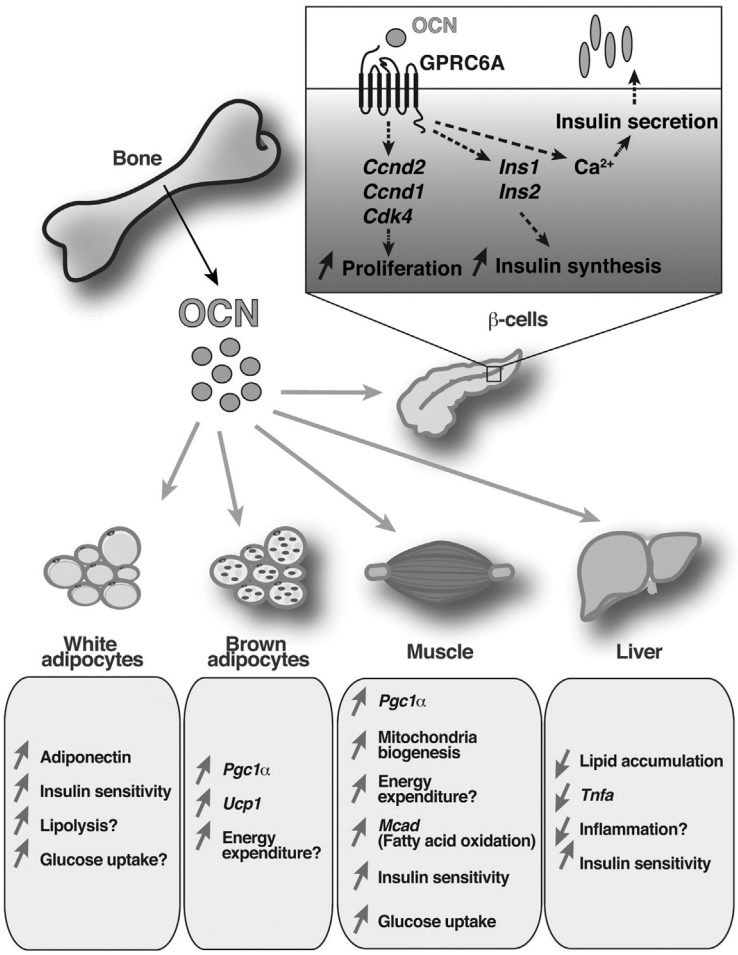

FIGURE 84.1 Endocrinal functions of osteocalcin. Once released in the circulation, undercarboxylated bioactive osteocalcin affects glucose metabolism mainly in two ways. First, osteocalcin directly affects β cell function by binding to the receptor GPRC6A and increasing its capacity to proliferate as well as to synthetize and secrete insulin. Second, osteocalcin improves insulin sensitivity and energy expenditure through multiple mechanisms. Osteocalcin stimulates energy expenditure by increasing mitochondrial biogenesis in the muscle and by regulating the expression of genes implicated in energy consumption in brown adipose tissue and skeletal muscle. Osteocalcin also affects insulin sensitivity, possibly by increasing adiponectin expression in white fat and decreasing lipid accumulation and inflammation in steatotic liver. The direct impact of osteocalcin as an insulin-sensitizing hormone is speculative and remains to be established.

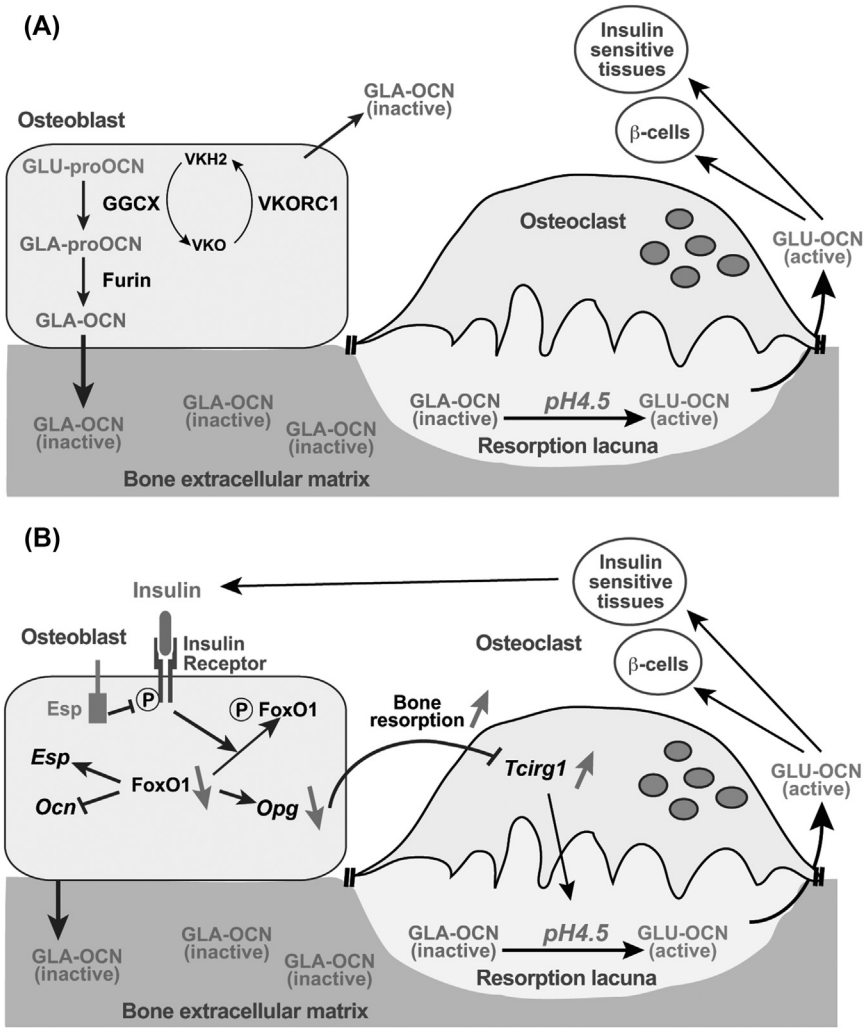

FIGURE 84.2 Regulation of osteocalcin activity. (A) Once γ-carboxylated, processed by the proprotein convertase furin, and secreted by osteoblasts, osteocalcin is stored in the bone extracellular matrix in an inactive form. To fulfill its beneficial effect on glucose metabolism, osteocalcin has to be activated—i.e., decarboxylated. This is accomplished through osteoclastic bone resorption that generates the acid pH necessary for osteocalcin decarboxylation. (B) Insulin signaling in osteoblasts affects osteocalcin activity by increasing bone resorption through osteoprotegerin (*Opg*) downregulation. Since osteocalcin stimulates insulin secretion, a feed-forward loop exists between osteocalcin and insulin activity. Esp, a tyrosine phosphatase, negatively regulates insulin receptor signaling and decreases osteocalcin activity.

reduced fat mass, improved insulin sensitivity, and prevented liver steatosis (Ferron et al., 2008, 2012; Huang et al., 2017; Gupte et al., 2014). Similarly, mouse models in which the circulating level of the active form of osteocalcin is increased—e.g., $Esp^{-/-}$ or osteoblast-specific knockout of *Ggcx* (see also sections "Regulation of the endocrine function of osteocalcin by gamma-carboxylation" and "Osteocalcin decarboxylation and activation during bone resorption" and Fig. 84.2)—are characterized by increased insulin secretion, increased β cell proliferation, improved insulin sensitivity, increased energy expenditure, and reduced fat mass (Lee et al., 2007; Ferron et al., 2015). These results indicated what has become a hallmark of osteocalcin biology—it is necessary and sufficient to favor the physiological processes it regulates (Oury et al., 2013a; Mera et al., 2016a; Khrimian et al., 2017).

The acute effect of osteocalcin on insulin secretion appears to be mediated by calcium (Ca^{2+}) signaling in β cells (Hinoi et al., 2008; Fig. 84.1). A receptor to which osteocalcin binds in pancreatic β cells, G-protein-coupled receptor family C group 6 member A (GPRC6A), which acts through G-protein α-subunit (Gsα) and cAMP response element-binding protein, mediates osteocalcin regulation of cell proliferation, insulin expression, and insulin secretion. This receptor is also expressed in myofibers and regulates the functions of osteocalcin myofibers during exercise (Mera et al., 2016a; see section "Osteocalcin regulation of skeletal muscle energy metabolism during exercise"). Remarkably, in white adipocytes,

osteocalcin stimulates the expression of adiponectin, a hormone that regulates bone mass accrual in animals fed a normal diet, but this action appears to be independent of GPRC6A not expressed in adipocytes (Kajimura et al., 2013). In addition, osteocalcin suppresses lipolysis, directly promotes glucose uptake, and can suppress the secretion of proinflammatory cytokines in white adipocytes (Lee et al., 2007; Hill et al., 2014; Fig. 84.1). Osteocalcin also promotes mitochondria biogenesis in the muscle when injected in obese mice (Ferron et al., 2012) and stimulates the expression of genes involved in thermogenesis (*Pgc1α* and *Ucp1*) in brown adipocytes in vivo and ex vivo (Ferron et al., 2008). Altogether, these observations suggest that the protective effect of this hormone on obesity and insulin resistance could be at least partially caused by its capacity to enhance energy expenditure in muscle and brown adipose tissue.

Several cell-based assays provided evidence that osteocalcin also stimulates insulin secretion in rat and human islets ex vivo (Sabek et al., 2015; Gao et al., 2016a, 2016b; Kover et al., 2015). Likewise, genetic studies further support an impact of osteocalcin polymorphisms in glucose and energy metabolism in humans (Korostishevsky et al., 2012; Das et al., 2010). Finally, two meta-analyses demonstrated respectively that circulating levels of total osteocalcin are higher in subjects with normal glucose tolerance than in patients with type 2 diabetes (Kunutsor et al., 2015), and that osteocalcin serum level is an independent risk factor for the development of type 2 diabetes (Liu et al., 2015).

GPRC6A osteocalcin receptor in β cells

As alluded to previously, and like most known peptide hormones, osteocalcin mediates its functions through the binding of at least one specific receptor, GPRC6A (Fig. 84.1). This G-protein-coupled receptor shares some sequence identity with calcium-sensing receptors involved in calcium homeostasis through the regulation of parathyroid hormone release. Based on ex vivo experiments, GPRC6A was proposed to be a cation-sensing receptor, and more recently a receptor for amino acids, steroids, and osteocalcin (Pi and Quarles, 2012; Wei et al., 2014b). *Gprc6a*$^{-/-}$ mice phenocopied osteocalcin-deficient animals with regard to their defects in insulin secretion and glucose tolerance (Pi et al., 2008). Moreover, inactivation of *Gprc6a*, specifically in the pancreas, resulted in reduced β cell proliferation and decreased insulin secretion in response to glucose (Wei et al., 2014b; Pi et al., 2016). Two pieces of genetic evidence demonstrate that in vivo, osteocalcin is the ligand of GPRC6A that accounts for the regulation of insulin secretion by this receptor. First, whereas single heterozygous *Gprc6a*$^{+/-}$ or *Ocn* $^{+/-}$ mice have normal pancreatic β cell proliferation and insulin secretion, compound heterozygous (*Gprc6a*$^{+/-}$;*Ocn*$^{+/-}$) mice have the same defect in insulin secretion and glucose homeostasis as that of *Ocn*$^{-/-}$ and *Gprc6a*$^{-/-}$ mice (Wei et al., 2014b). Second, osteocalcin capacity to induce insulin secretion is abrogated in *Gprc6a*$^{-/-}$ islets (Wei et al., 2014b; Pi et al., 2016). Additional genetic experiments in mice demonstrated that GPRC6A also acts as an osteocalcin receptor in Leydig cells, where osteocalcin-dependent signaling promotes testosterone synthesis (Oury et al., 2011; De Toni et al., 2014).

Many lines of evidence suggest that GPRC6A's function as an osteocalcin receptor is conserved in humans. First, human osteocalcin can bind and activate human GPRC6A receptor as was reported for the mouse proteins (De Toni et al., 2016a). Second and more directly, a mutation in the human *GPRC6A* gene that disrupts GPRC6A trafficking to the plasma membrane is associated with insulin resistance and testicular failure in humans, two phenotypes caused by osteocalcin deficiency in mice (Oury et al., 2013b). Third, polymorphisms in the human *GPRC6A* gene were also shown to be associated with insulin resistance and testicular failure (De Toni et al., 2016b; Di Nisio et al., 2017).

Regulation of the endocrine function of osteocalcin by gamma-carboxylation

Before it is secreted by the osteoblast, osteocalcin is γ-carboxylated on three glutamic acid residues (Glus) that are converted to γ-carboxyglutamic acid (Gla). This posttranslational modification that occurs in the endoplasmic reticulum of the osteoblast is accomplished by γ-glutamyl carboxylase (GGCX), an enzyme requiring reduced vitamin K as a cofactor (Fig. 84.2A). For each carboxylation reaction, one molecule of reduced vitamin K is oxidized to vitamin K epoxide by GGCX. A second enzyme, called vitamin K oxidoreductase, is responsible for reducing vitamin K epoxide, allowing the recycling of vitamin K and further γ-carboxylation reactions (Lacombe et al., 2018). The presence of Gla residues in osteocalcin allows its binding with high affinity to hydroxyapatite, the mineral component of bone, explaining why the majority of carboxylated osteocalcin (Gla-Ocn) accumulates in the bone extracellular matrix, where it is the most abundant noncollagenous protein (Fig. 84.2A). Yet in the circulation, osteocalcin exists in two forms, carboxylated and undercarboxylated. In vitro and in vivo studies in mice have established that γ-carboxylation of osteocalcin, particularly on its first Glu residue (Glu13 in mice and Glu17 in human), inhibits osteocalcin endocrine action on energy metabolism and that undercarboxylated osteocalcin is the bioactive form of this hormone for all known functions (Ferron et al., 2008; Zhou et al., 2013). For instance, inactivation of GGCX in osteoblasts results in increased circulating levels of undercarboxylated

osteocalcin and improved glucose tolerance in mice (Ferron et al., 2015). A cross-sectional study in postmenopausal obese women also demonstrated that the level of osteocalcin carboxylation on its Glu17 residue positively correlates with insulin resistance and low-grade inflammation (Bonneau et al., 2017), suggesting that γ-carboxylation of osteocalcin negatively regulates the function of this hormone in humans as it does in rodents.

Osteocalcin decarboxylation and activation during bone resorption

If osteocalcin is γ-carboxylated prior to its secretion by osteoblasts, how does it get converted to undercarboxylated and bioactive before reaching the general circulation? It turns out that decarboxylation of osteocalcin is a nonenzymatic process that occurs outside the osteoblast in the osteoclastic resorption lacunae (Fig. 84.2B). Indeed, it is the low pH (∼4.5) generated by the osteoclasts in the resorption lacunae that decarboxylates at least one of the Gla residues present in osteocalcin (Ferron et al., 2010), thus allowing the release of bioactive osteocalcin (Glu13-Ocn). This explains why mice with increased bone resorption also display increased circulating levels of bioactive osteocalcin and improved glucose tolerance and insulin sensitivity, while mice lacking osteoclasts have reduced levels of bioactive osteocalcin and decreased glucose tolerance (Lacombe et al., 2013). Interestingly, bone resorption couples insulin and osteocalcin in a feed-forward endocrine loop controlling glucose metabolism. Indeed, insulin signaling in osteoblasts, through a signaling pathway involving the inhibition of the transcription factor FOXO1, reduced the expression of *osteoprotegerin*, a negative regulator of bone resorption (Ferron et al., 2010; Rached et al., 2010); this has the consequence of increasing osteoclastic activity and thereby the release of bioactive osteocalcin (Fig. 84.2B).

Regulation of osteocalcin by the proprotein convertase furin

Like many other peptide hormones, osteocalcin is first synthesized as a prohormone, proosteocalcin (pro-Ocn). Yet until recently, the biological importance of pro-Ocn maturation in regulating osteocalcin and the identity of the endopeptidase responsible for pro-Ocn cleavage in osteoblasts were unknown. Based on biochemical and genetic arguments, the proprotein convertase furin was recently identified as the endopeptidase responsible for pro-Ocn processing in osteoblasts (Al Rifai et al., 2017). Proteolysis of pro-Ocn is critical for the activation of this hormone, since inactivation of furin in osteoblasts in mice results in decreased circulating levels of active osteocalcin, impaired glucose tolerance, and reduced energy expenditure. At the mechanistic level, it appears that retention of the propeptide in osteocalcin reduces its ability to be decarboxylated during the process of bone resorption. Of note, *furin* deletion in osteoblasts also reduces appetite, a function not regulated by osteocalcin. This observation suggests that osteoblasts must secrete other hormones that regulate different aspects of energy metabolism such as, for instance, appetite (see section "Are there additional osteocalcin- or lipocalin-2-independent endocrine functions of bone?").

A role for osteocalcin in adaptation to exercise

A question raised by the beneficial influence of osteocalcin on glucose homeostasis is whether there is any difference between osteocalcin and insulin endocrine actions. Considering the significant role of skeletal muscle in the maintenance of whole-body glucose homeostasis, it became important to determine whether osteocalcin influences any aspect of energy metabolism in skeletal muscle. One experimental approach to address this question was to determine whether osteocalcin exerts any function in muscle during exercise, a physiological situation characterized by an increase in glucose uptake in skeletal muscle and a simultaneous decrease in circulating insulin levels. That circulating levels of bioactive osteocalcin triple in mice and also increase in humans after a single bout of endurance exercise were additional reasons to test this hypothesis (Mera et al., 2016a).

Osteocalcin regulation of skeletal muscle energy metabolism during exercise

A common feature of all known osteocalcin functions is that they decline quite early during adult life (Lee et al., 2007; Oury et al., 2011, 2013a). The identification of a receptor for osteocalcin in testis and β cell, the G-protein coupled receptor GPRC6A (see section "GPRC6A osteocalcin receptor in β cells"), provided the necessary tool to study the role, if any, of osteocalcin signaling in skeletal muscle aside from its functions in other organs. Analysis of 3-month-old $Ocn^{-/-}$ mice and mice lacking GPRC6A only in skeletal muscle ($Gprc6a^{Mck-/-}$) revealed that when forced to run on a treadmill at a constant speed until exhausted, $Ocn^{-/-}$ and $Gprc6a^{Mck-/-}$ mice run 20%−30% less than control littermates (Mera et al., 2016a). Further investigation of this phenotype reveals that osteocalcin regulates the uptake and catabolism of glucose and

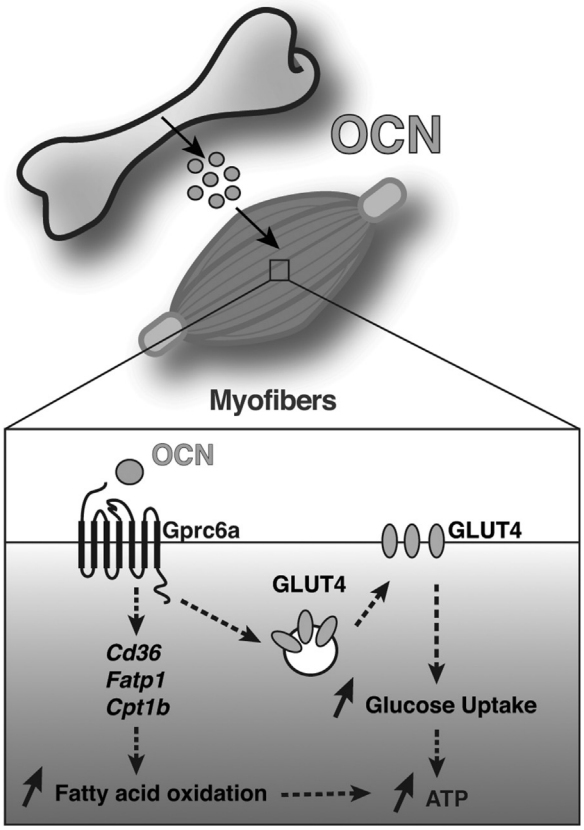

FIGURE 84.3 Mechanism of action of osteocalcin in skeletal muscle during exercise. During exercise, bioactive osteocalcin is released by osteoblasts and binds to the receptor GPRC6A in myofibers where it promotes the uptake and utilization of nutrients. First, osteocalcin favors the expression of fatty acid transporters and stimulates β-oxidation. Second, osteocalcin favors translocation of the glucose transporter GLUT4 to the plasma membrane. This in turn allows the increase in glucose uptake and catabolism.

fatty acids (FAs) in muscle during exercise (Fig. 84.3). The uptake and utilization of these nutrients by contracting myofibers is absolutely essential for adaptation to exercise. Consequently, the regulation of nutrient catabolism in skeletal muscle by osteocalcin certainly explains, at least in part, the decreased performance during exercise observed in $Ocn^{-/-}$ and $Gprc6a^{Mck-/-}$ mice. Hence, in that respect osteocalcin differs from insulin, an anabolic hormone.

Osteocalcin supports muscle function during exercise through an additional mechanism—it stimulates the production and release of interleukin-6 (IL-6), one of the first myokines ever identified (Pedersen and Febbraio, 2008; Steensberg et al., 2000). IL-6 circulating levels increase after exercise in humans and rodents in a manner proportional to the length of exercise and the degree of muscle involvement (Febbraio et al., 2004; Febbraio and Pedersen, 2002; Nielsen et al., 2007). Additionally, IL-6 is expressed in cultured myotubes and myofibers, and skeletal muscle is the major source of circulating IL-6 during exercise (Keller et al., 2001; Steenbergen et al., 2002). During exercise, IL-6 acts in an autocrine, paracrine and endocrine manner to promote skeletal muscle nutrient utilization, glucose production in the liver, and lipolysis in white adipose tissue (Pedersen and Febbraio, 2008). Considering experimental observations showing that IL-6 also signals in bone cells (Tamura et al., 1993), the regulation of IL-6 by osteocalcin during exercise raised another fundamental question: Could IL-6 signal back to bone to modulate the release of bioactive osteocalcin?

The next aspect in this work was to determine whether osteocalcin regulates skeletal muscle function and adaptation to exercise, a physiological process severely affected during early aging. Supporting this premise is the fact that circulating levels of bioactive osteocalcin decline early in adult life in mice, monkeys, and humans of both genders. This reduction in circulating bioactive osteocalcin occurs at the same time that the ability to perform exercise declines, at least in mice (Mera et al., 2016a). These observations were an incentive to test whether administration of exogenous osteocalcin to wild-type (WT) mice might increase their endurance during exercise. A single injection of exogenous osteocalcin immediately before exercise or a chronic delivery of this hormone for 1 month not only improved the exercise capacity of young mice but also restored aerobic endurance in older mice to a level similar to those seen in young adult mice (Mera et al., 2016a).

Moreover, chronic delivery of osteocalcin also favors a gain in muscle mass in older mice (Mera et al., 2016b). These experiments demonstrate that osteocalcin signaling in myofibers is necessary and sufficient to increase muscle function during exercise, highlighting the therapeutic potential of osteocalcin to reverse the age-induced decline in exercise capacity and muscle mass observed in humans.

Modulating adaptation to exercise through bone and skeletal muscle cross talk

Interestingly, after a single bout of exercise, blood markers of bone resorption and bioactive osteocalcin increase in WT mice but not IL-6-deficient mice ($Il6^{-/-}$) (Mera et al., 2016a). Recombinant IL-6 increases the expression of *Rankl*, a cytokine essential to osteoclast differentiation, and decreases *osteoprotegerin*, a decoy receptor for RANKL and an inhibitor of bone resorption (Teitelbaum and Ross, 2003) in cultured calvaria osteoblasts (Mera et al., 2016a). These results suggest that in vivo, IL-6 acts during exercise, when its circulating levels increase in the cells of osteoblast lineage to increase *Rankl* expression, bone resorption, and the production of bioactive osteocalcin (see also Fig. 84.2). Extensive genetic and molecular studies will be needed to fully understand the regulation of bioactive osteocalcin by IL-6 during exercise.

Altogether, analyses of $Ocn^{-/-}$, $Gprc6a^{Mck-/-}$, and $Il6^{-/-}$ mice revealed the existence of a feed-forward loop between bone (via osteocalcin) and muscle (via IL-6) promoting adaptation to exercise through at least three different synergistic mechanisms (Fig. 84.4): (1) osteocalcin promotes nutrient uptake and catabolism in myofibers; (2) osteocalcin signaling in myofibers increases the expression and secretion of IL-6, which in turn might allow the generation of extramuscular glucose and FAs (Febbraio et al., 2004; van Hall et al., 2003); and (3) IL-6 increases the production of bioactive osteocalcin. This model does not exclude the possibility that osteocalcin and IL-6 might have additional functions to modulate adaptation to exercise. Similarly, other molecules made by bone cells or skeletal muscle cells could contribute to this cross talk.

IL-6 and osteocalcin regulate similar aspects of skeletal muscle metabolism during exercise—e.g., the increase in glucose and FA catabolism. Experiments studying the effect of exogenous osteocalcin on glucose and FA utilization in WT and $Il6^{-/-}$-cultured myotubes showed that osteocalcin can induce these functions independently of IL-6 signaling in myofibers (Mera et al., 2016a). Whether osteocalcin and IL-6 might have synergistic functions in order to increase glucose and FA uptake and utilization in skeletal muscle during exercise remains to be established.

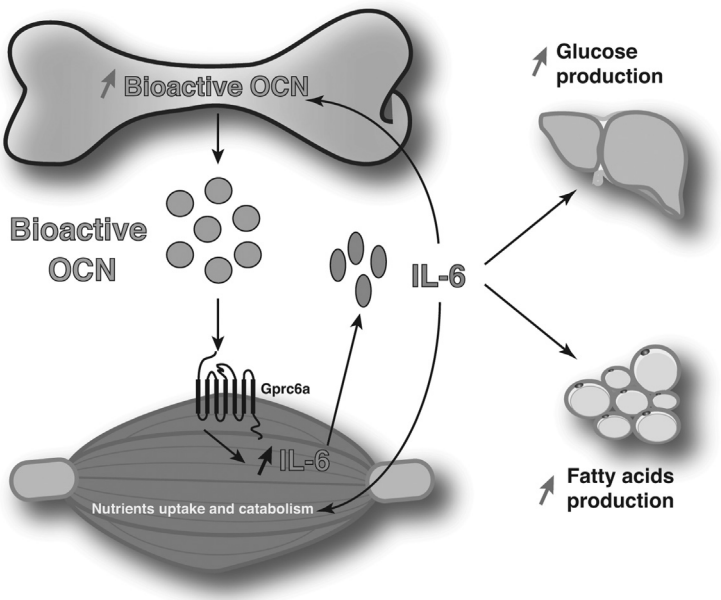

FIGURE 84.4 Cross talk between bone via osteocalcin, and skeletal muscle via IL-6, promotes adaptation to exercise. Circulating levels of bioactive osteocalcin increase during exercise. Osteocalcin signals in myofibers through GPRC6A, where it induces the expression of *Il6* and increased circulating levels of this myokine. IL-6 signals back to skeletal muscle, where it favors glucose and fatty acid (FA) utilization. IL-6 also stimulates FA production in white adipose tissue and glucose production in the liver. Furthermore, IL-6 signals to bone to increase the production of bioactive osteocalcin.

Bone as a regulator of appetite: the anorexigenic function of osteoblast-derived lipocalin-2

Taken at face value, the discovery of osteocalcin regulation of glucose metabolism established a new concept—i.e., that bone is an endocrine organ affecting energy metabolism. It also raised a fascinating question: Do additional bone-derived hormones exist and contribute to the regulation of energy metabolism? To address this question, osteoblasts were conditionally ablated in mice. As expected, a 50% decrease in osteoblast numbers decreased osteocalcin circulating levels and impacted glucose metabolism. However, and more intriguingly, another metabolic function was affected—appetite. Reduced osteoblast numbers increased food intake, a function not regulated by osteocalcin (Al Rifai et al., 2017; Yoshikawa et al., 2011). These findings implied that appetite is one more metabolic function regulated by osteoblasts, most probably mediated by at least one additional osteoblast-derived hormone.

The identification of this hormone was achieved by taking advantage of another mouse model of bone-related improved energy metabolism, the mice lacking *Foxo1* in osteoblasts (Rached et al., 2010). FOXO1 is a transcription factor regulating osteoblast function and energy metabolism at least through its ability to regulate osteocalcin activity (Ferron et al., 2010; Rached et al., 2010), raising the prospect that additional hormones involved in energy metabolism may be downstream targets of FOXO1. Comparative gene expression analysis pointed to an increase in the expression of the gene encoding LCN2 in $Foxo1^{-/-}$ osteoblasts, and therefore higher LCN2 serum levels were observed in the same mice. LCN2, also known as neutrophil gelatinase-associated lipocalin, is a secreted glycoprotein previously thought to be an adipocyte-derived hormone (Yan et al., 2007). However, expression profiling showed that *Lcn2* is expressed at least 10-fold higher in bone than in white adipose tissue or any other organ. Analysis of mice lacking *Lcn2* specifically in osteoblasts ($Lcn2^{osb-/-}$ mice) showed that inactivation of *Lcn2* in osteoblasts increases food intake (Mosialou et al., 2017). As a consequence, $Lcn2^{osb-/-}$ mice exhibit increased adiposity and body weight as well as decreased glucose tolerance and insulin sensitivity. Interestingly, the increase in food intake precedes changes in blood glucose levels and body weight and partly contributes to the development of impaired glucose metabolism. Normalization of food intake by pair-feeding $Lcn2^{osb-/-}$ to their WT littermates restores body weight, fat mass and insulin sensitivity. Finally, chronic administration of exogenous LCN2 in lean and obese mice suppresses food intake, fat mass, and body weight gain and improves glucose homeostasis (Mosialou et al., 2017), providing further evidence that LCN2 regulates energy metabolism.

Suggesting a physiological role of LCN2 in the regulation of food intake, osteoblastic expression and circulating levels of LCN2 increase threefold 3 h postprandially in mice. Interestingly, this increase in serum levels correlates with a suppression of food intake. Following its rise in the serum, LCN2 crosses the blood—brain barrier and accumulates mainly in the hypothalamus where it activates neurons in the paraventricular nucleus (PVN), as indicated by *c-Fos* induction and electrophysiological recordings. The PVN is involved in feeding regulation partly due to the actions of the well-established melanocortin 4 receptor (MC4R) anorexigenic pathway. Indeed, mice and humans with MC4R defects exhibit hyperphagia and early onset obesity, increased fat mass, decreased energy expenditure, and hyperinsulinemia (Tao, 2010). A series of molecular and biochemical studies showed that LCN2 activates the MC4R pathway, promotes cAMP production, and induces MC4R target genes through direct binding to MC4R, establishing a central role for MC4R in mediating the LCN2 anorexigenic response (Fig. 84.5). The LCN2/MC4R interaction may be extended to humans, since some obese subjects carrying mutations in MC4R had elevated LCN2 plasma levels compared with those of weight-matched people without mutations. This observation implies increased ligand levels in the case of desensitization or inactivation of the cognate G-protein-coupled receptor in an attempt to overcome resistance and reestablish homeostasis.

Altogether, these observations add the control of food intake to the endocrinal properties of bone. The regulation of appetite by osteoblasts also provides a feedback mechanism to the well-established central control of bone mass, consisting mainly of hypothalamic pathways regulating feeding, such as leptin, the Agrp neuronal circuit, orexins, NPY, Neuromedin U, and the MC4R pathway, further reinforcing the powerful cross talk between bone and the brain.

Are there additional osteocalcin- or lipocalin-2-independent endocrine functions of bone?

The identification of the anorexigenic function of LCN2 widens the range of bone metabolic functions and supports the hypothesis that more than one osteoblast-derived signal contributes to bone endocrinal function. Besides food intake, other osteocalcin-independent effects on fat mass and energy expenditure were observed in mice with partial osteoblast ablation. Gonadal fat was decreased and energy expenditure increased, which was the opposite of what would be expected with osteocalcin deficiency. This observation was confirmed by a subsequent study in mice harboring a β-catenin deletion in early

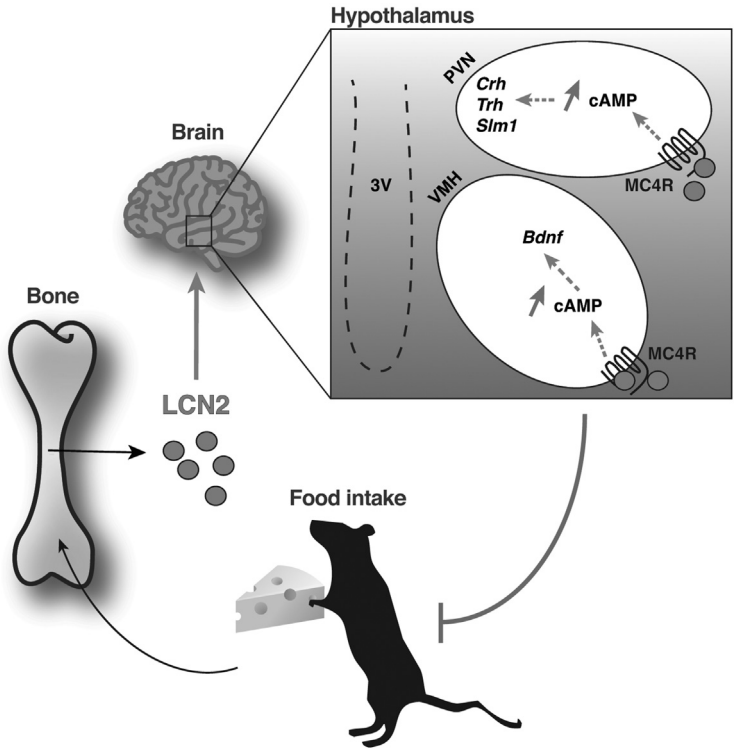

FIGURE 84.5 Regulation of food intake by lipocalin-2. Following feeding, lipocalin-2 is released by osteoblasts and accumulates in the hypothalamus where it binds the melanocortin 4 receptor (MC4R) in the paraventricular (PVN) and ventromedial (VMH) neurons of the hypothalamus. Activation of MC4R by lipocalin-2 induces cAMP and the expression of *Crh, Trh, Sim1*, and *Bdnf*, suppressing food intake.

lineage osteoblasts that led to an osteocalcin-independent increase in food intake and energy expenditure, and decreased fat mass (Yao et al., 2017). LCN2 cannot explain these effects, since one would expect to observe increase fat mass in its absence. This suggests an additional factor counteracting the effects of osteocalcin and LCN2 on adiposity. Intriguingly, the inactivation of the proprotein convertase furin in osteoblasts resulted in reduced food intake without affecting the circulating levels of LCN2. Moreover, LCN2 does not appear to be processed by furin in vitro and in vivo, suggesting that furin in osteoblasts influences appetite through an LCN2-independent mechanism (Al Rifai et al., 2017). In line with these finding, bone cells including osteocytes were proposed to act as a "gravitostat" to regulate appetite in response to body weight changes through a yet to be identified factor that is neither osteocalcin nor LCN2 (Jansson et al., 2018).

Regulation of body adiposity by the skeleton may also require osteocytes. Partial osteocyte deletion in mice led to significant fat and body weight loss through a yet to be identified cooperation with the hypothalamic nuclei regulating energy balance (Sato et al., 2013). Similarly, constitutive and inducible deletion of *Gsα* in osteocytes, which is associated with an increase in the circulating level of the osteocyte-secreted factor sclerostin, led to the expected decrease in bone mass, but also to a significant decrease in adiposity due to induction of beige adipogenesis by sclerostin (Fulzele et al., 2017). In contrast to these findings, another group reported that sclerostin-deficient mice ($Sost^{-/-}$) exhibit a reduction in adipose tissue accumulation associated with increased insulin sensitivity, while sclerostin overproduction results in the opposite metabolic phenotype due to adipocyte hypertrophy (Kim et al., 2017). Hence, the exact role of sclerostin in fat metabolism remains to be determined.

In general, glucose metabolism does not appear to be altered by genetic manipulations in osteocytes, suggesting that compared with those of osteoblasts, osteocyte functions may be limited to the regulation of fat metabolism. Additional bone-derived hormones and bone metabolic functions may yet be identified, and their exploration may shed new light on the endocrine-regulating properties of bone.

Concluding remarks

Bone has recently emerged as an endocrine organ. This was unexpected because of both the nature of bone and the increasingly broad spectrum of its functions. A more complete understanding of all the roles and the regulation of bone-

derived hormones needs to be achieved before osteocalcin- or LCN2-based therapies for metabolic disorders can be developed for humans. Nonetheless, wherever future research on bone endocrine function will take us, it is clear that these findings have significantly broadened the definition of what is bone physiology.

Acknowledgments

We thank P. Mera for her help with preparing the figures. This work was supported by funding from the Canada Research Chair program (M.F.), by the Canadian Institutes of Health Research (M.F., MOP-133652), by the Natural Sciences and Engineering Research Council of Canada (M.F.), NIA (G.K., 2P01AG032959-06A1), and NIDDK (G.K., RO1DK104727).

References

Al Rifai, O., Chow, J., Lacombe, J., Julien, C., Faubert, D., Susan-Resiga, D., Essalmani, R., Creemers, J.W., Seidah, N.G., Ferron, M., 2017. Proprotein convertase furin regulates osteocalcin and bone endocrine function. J. Clin. Investig. 127 (11), 4104–4117.

Bonneau, J., Ferland, G., Karelis, A.D., Doucet, E., Faraj, M., Rabasa-Lhoret, R., Ferron, M., 2017. Association between osteocalcin gamma-carboxylation and insulin resistance in overweight and obese postmenopausal women. J. Diabet. Complicat. 6.

Cornish, J., Callon, K.E., Bava, U., Lin, C., Naot, D., Hill, B.L., Grey, A.B., Broom, N., Myers, D.E., Nicholson, G.C., Reid, I.R., 2002. Leptin directly regulates bone cell function in vitro and reduces bone fragility in vivo. J. Endocrinol. 175 (2), 405–415.

Das, S.K., Sharma, N.K., Elbein, S.C., 2010. Analysis of osteocalcin as a candidate gene for type 2 diabetes (T2D) and intermediate traits in Caucasians and African Americans. Dis. Markers 28 (5), 281–286.

Ducy, P., Amling, M., Takeda, S., Priemel, M., Schilling, A.F., Beil, F.T., Shen, J., Vinson, C., Rueger, J.M., Karsenty, G., 2000. Leptin inhibits bone formation through a hypothalamic relay: a central control of bone mass. Cell 100 (2), 197–207.

Febbraio, M.A., Pedersen, B.K., 2002. Muscle-derived interleukin-6: mechanisms for activation and possible biological roles. FASEB J. 16 (11), 1335–1347.

Febbraio, M.A., Hiscock, N., Sacchetti, M., Fischer, C.P., Pedersen, B.K., 2004. Interleukin-6 is a novel factor mediating glucose homeostasis during skeletal muscle contraction. Diabetes 53 (7), 1643–1648.

Ferron, M., Hinoi, E., Karsenty, G., Ducy, P., 2008. Osteocalcin differentially regulates beta cell and adipocyte gene expression and affects the development of metabolic diseases in wild-type mice. Proc. Natl. Acad. Sci. U. S. A. 105 (13), 5266–5270.

Ferron, M., Wei, J., Yoshizawa, T., Del Fattore, A., DePinho, R.A., Teti, A., Ducy, P., Karsenty, G., 2010. Insulin signaling in osteoblasts integrates bone remodeling and energy metabolism. Cell 142 (2), 296–308.

Ferron, M., McKee, M.D., Levine, R.L., Ducy, P., Karsenty, G., 2012. Intermittent injections of osteocalcin improve glucose metabolism and prevent type 2 diabetes in mice. Bone 50 (2), 568–575.

Ferron, M., Lacombe, J., Germain, A., Oury, F., Karsenty, G., 2015. GGCX and VKORC1 inhibit osteocalcin endocrine functions. J. Cell Biol. 208 (6), 761–776.

Fulzele, K., Riddle, R.C., DiGirolamo, D.J., Cao, X., Wan, C., Chen, D., Faugere, M.C., Aja, S., Hussain, M.A., Bruning, J.C., Clemens, T.L., 2010. Insulin receptor signaling in osteoblasts regulates postnatal bone acquisition and body composition. Cell 142 (2), 309–319.

Fulzele, K., Lai, F., Dedic, C., Saini, V., Uda, Y., Shi, C., Tuck, P., Aronson, J.L., Liu, X., Spatz, J.M., Wein, M.N., Divieti Pajevic, P., 2017. Osteocyte-secreted Wnt signaling inhibitor sclerostin contributes to beige adipogenesis in peripheral fat depots. J. Bone Miner. Res. 32 (2), 373–384.

Gao, J., Zhong, X., Ding, Y., Bai, T., Wang, H., Wu, H., Liu, Y., Yang, J., Zhang, Y., 2016. Inhibition of voltage-gated potassium channels mediates uncarboxylated osteocalcin-regulated insulin secretion in rat pancreatic beta cells. Eur. J. Pharmacol. 777, 41–48.

Gao, J., Bai, T., Ren, L., Ding, Y., Zhong, X., Wang, H., Guo, Y., Li, J., Liu, Y., Zhang, Y., 2016. The PLC/PKC/Ras/MEK/Kv channel pathway is involved in uncarboxylated osteocalcin-regulated insulin secretion in rats. Peptides 86, 72–79.

Gupte, A.A., Sabek, O.M., Fraga, D., Minze, L.J., Nishimoto, S.K., Liu, J.Z., Afshar, S., Gaber, L., Lyon, C.J., Osama Gaber, A., Hsueh, W.A., 2014. Osteocalcin protects against non-alcoholic steatohepatitis in a mouse model of metabolic syndrome. Endocrinology 155. https://doi.org/10.1210/en.2014-1430.

van Hall, G., Steensberg, A., Sacchetti, M., Fischer, C., Keller, C., Schjerling, P., Hiscock, N., Moller, K., Saltin, B., Febbraio, M.A., Pedersen, B.K., 2003. Interleukin-6 stimulates lipolysis and fat oxidation in humans. J. Clin. Endocrinol. Metab. 88 (7), 3005–3010.

Hill, H.S., Grams, J., Walton, R.G., Liu, J., Moellering, D.R., Garvey, W.T., 2014. Carboxylated and uncarboxylated forms of osteocalcin directly modulate the glucose transport system and inflammation in adipocytes. Horm. Metab. Res. 46 (5), 341–347.

Hinoi, E., Gao, N., Jung, D.Y., Yadav, V., Yoshizawa, T., Myers Jr., M.G., Chua Jr., S.C., Kim, J.K., Kaestner, K.H., Karsenty, G., 2008. The sympathetic tone mediates leptin's inhibition of insulin secretion by modulating osteocalcin bioactivity. J. Cell Biol. 183 (7), 1235–1242.

Horsnell, H., Baldock, P.A., 2016. Osteoblastic actions of the neuropeptide Y system to regulate bone and energy homeostasis. Curr. Osteoporos. Rep. 14 (1), 26–31.

Huang, L., Yang, L., Luo, L., Wu, P., Yan, S., 2017. Osteocalcin improves metabolic profiles, body composition and arterial stiffening in an induced diabetic rat model. Exp. Clin. Endocrinol. Diabetes 125 (4), 234–240.

Jansson, J.O., Palsdottir, V., Hagg, D.A., Schele, E., Dickson, S.L., Anesten, F., Bake, T., Montelius, M., Bellman, J., Johansson, M.E., Cone, R.D., Drucker, D.J., Wu, J., Aleksic, B., Tornqvist, A.E., Sjogren, K., Gustafsson, J.A., Windahl, S.H., Ohlsson, C., 2018. Body weight homeostat that regulates fat mass independently of leptin in rats and mice. Proc. Natl. Acad. Sci. U. S. A. 115 (2), 427–432.

Kajimura, D., Lee, H.W., Riley, K.J., Arteaga-Solis, E., Ferron, M., Zhou, B., Clarke, C.J., Hannun, Y.A., DePinho, R.A., Guo, E.X., Mann, J.J., Karsenty, G., 2013. Adiponectin regulates bone mass via opposite central and peripheral mechanisms through FoxO1. Cell Metabol. 17 (6), 901–915.

Keller, C., Steensberg, A., Pilegaard, H., Osada, T., Saltin, B., Pedersen, B.K., Neufer, P.D., 2001. Transcriptional activation of the IL-6 gene in human contracting skeletal muscle: influence of muscle glycogen content. FASEB J. 15 (14), 2748–2750.

Khrimian, L., Obri, A., Ramos-Brossier, M., Rousseaud, A., Moriceau, S., Nicot, A.S., Mera, P., Kosmidis, S., Karnavas, T., Saudou, F., Gao, X.B., Oury, F., Kandel, E., Karsenty, G., 2017. Gpr158 mediates osteocalcin's regulation of cognition. J. Exp. Med. 214 (10), 2859–2873.

Kim, J.G., Sun, B.H., Dietrich, M.O., Koch, M., Yao, G.Q., Diano, S., Insogna, K., Horvath, T.L., 2015. AgRP neurons regulate bone mass. Cell Rep. 13 (1), 8–14.

Kim, S.P., Frey, J.L., Li, Z., Kushwaha, P., Zoch, M.L., Tomlinson, R.E., Da, H., Aja, S., Noh, H.L., Kim, J.K., Hussain, M.A., Thorek, D.L.J., Wolfgang, M.J., Riddle, R.C., 2017. Sclerostin influences body composition by regulating catabolic and anabolic metabolism in adipocytes. Proc. Natl. Acad. Sci. U. S. A. 114 (52), E11238–E11247.

Korostishevsky, M., Malkin, I., Trofimov, S., Pei, Y., Deng, H.W., Livshits, G., 2012. Significant association between body composition phenotypes and the osteocalcin genomic region in normative human population. Bone 51 (4), 688–694.

Kover, K., Yan, Y., Tong, P.Y., Watkins, D., Li, X., Tasch, J., Hager, M., Clements, M., Moore, W.V., 2015. Osteocalcin protects pancreatic beta cell function and survival under high glucose conditions. Biochem. Biophys. Res. Commun. 462 (1), 21–26.

Kunutsor, S.K., Apekey, T.A., Laukkanen, J.A., 2015. Association of serum total osteocalcin with type 2 diabetes and intermediate metabolic phenotypes: systematic review and meta-analysis of observational evidence. Eur. J. Epidemiol. 30 (8), 599–614.

Lacombe, J., Karsenty, G., Ferron, M., 2013. In vivo analysis of the contribution of bone resorption to the control of glucose metabolism in mice. Mol. Metab. 2 (4), 498–504.

Lacombe, J., Rishavy, M.A., Berkner, K.L., Ferron, M., 2018. VKOR paralog VKORC1L1 supports vitamin K-dependent protein carboxylation in vivo. JCI Insight 3 (1).

Lee, N.K., Sowa, H., Hinoi, E., Ferron, M., Ahn, J.D., Confavreux, C., Dacquin, R., Mee, P.J., McKee, M.D., Jung, D.Y., Zhang, Z., Kim, J.K., Mauvais-Jarvis, F., Ducy, P., Karsenty, G., 2007. Endocrine regulation of energy metabolism by the skeleton. Cell 130 (3), 456–469.

Legroux-Gerot, I., Vignau, J., Collier, F., Cortet, B., 2005. Bone loss associated with anorexia nervosa. Joint Bone Spine 72 (6), 489–495.

Liu, C., Wo, J., Zhao, Q., Wang, Y., Wang, B., Zhao, W., 2015. Association between serum total osteocalcin level and type 2 diabetes mellitus: a systematic review and meta-analysis. Horm. Metab. Res. 47 (11), 813–819.

Mera, P., Laue, K., Ferron, M., Confavreux, C., Wei, J., Galan-Diez, M., Lacampagne, A., Mitchell, S.J., Mattison, J.A., Chen, Y., Bacchetta, J., Szulc, P., Kitsis, R.N., de Cabo, R., Friedman, R.A., Torsitano, C., McGraw, T.E., Puchowicz, M., Kurland, I., Karsenty, G., 2016. Osteocalcin signaling in myofibers is necessary and sufficient for optimum adaptation to exercise. Cell Metabol. 23 (6), 1078–1092.

Mera, P., Laue, K., Wei, J., Berger, J.M., Karsenty, G., 2016. Osteocalcin is necessary and sufficient to maintain muscle mass in older mice. Mol. Metab. 5 (10), 1042–1047.

Misra, M., Klibanski, A., 2011. The neuroendocrine basis of anorexia nervosa and its impact on bone metabolism. Neuroendocrinology 93 (2), 65–73.

Mosialou, I., Shikhel, S., Liu, J.M., Maurizi, A., Luo, N., He, Z., Huang, Y., Zong, H., Friedman, R.A., Barasch, J., Lanzano, P., Deng, L., Leibel, R.L., Rubin, M., Nicholas, T., Chung, W., Zeltser, L.M., Williams, K.W., Pessin, J.E., Kousteni, S., 2017. MC4R-dependent suppression of appetite by bone-derived lipocalin 2. Nature 543 (7645), 385–390.

Nielsen, A.R., Mounier, R., Plomgaard, P., Mortensen, O.H., Penkowa, M., Speerschneider, T., Pilegaard, H., Pedersen, B.K., 2007. Expression of interleukin-15 in human skeletal muscle effect of exercise and muscle fibre type composition. J. Physiol. 584 (Pt 1), 305–312.

Di Nisio, A., Rocca, M.S., Fadini, G.P., De Toni, L., Marcuzzo, G., Marescotti, M.C., Sanna, M., Plebani, M., Vettor, R., Avogaro, A., Foresta, C., 2017. The rs2274911 polymorphism in GPRC6A gene is associated with insulin resistance in normal weight and obese subjects. Clin. Endocrinol. 86 (2), 185–191.

Oury, F., Sumara, G., Sumara, O., Ferron, M., Chang, H., Smith, C.E., Hermo, L., Suarez, S., Roth, B.L., Ducy, P., Karsenty, G., 2011. Endocrine regulation of male fertility by the skeleton. Cell 144 (5), 796–809.

Oury, F., Khrimian, L., Denny, C.A., Gardin, A., Chamouni, A., Goeden, N., Huang, Y.Y., Lee, H., Srinivas, P., Gao, X.B., Suyama, S., Langer, T., Mann, J.J., Horvath, T.L., Bonnin, A., Karsenty, G., 2013. Maternal and offspring pools of osteocalcin influence brain development and functions. Cell 155 (1), 228–241.

Oury, F., Ferron, M., Huizhen, W., Confavreux, C., Xu, L., Lacombe, J., Srinivas, P., Chamouni, A., Lugani, F., Lejeune, H., Kumar, T.R., Plotton, I., Karsenty, G., 2013. Osteocalcin regulates murine and human fertility through a pancreas-bone-testis axis. J. Clin. Investig. 123 (6), 2421–2433.

Pedersen, B.K., Febbraio, M.A., 2008. Muscle as an endocrine organ: focus on muscle-derived interleukin-6. Physiol. Rev. 88 (4), 1379–1406.

Pi, M., Quarles, L.D., 2012. Multiligand specificity and wide tissue expression of GPRC6A reveals new endocrine networks. Endocrinology 153 (5), 2062–2069.

Pi, M., Chen, L., Huang, M.Z., Zhu, W., Ringhofer, B., Luo, J., Christenson, L., Li, B., Zhang, J., Jackson, P.D., Faber, P., Brunden, K.R., Harrington, J.J., Quarles, L.D., 2008. GPRC6A null mice exhibit osteopenia, feminization and metabolic syndrome. PLoS One 3 (12), e3858.

Pi, M., Kapoor, K., Ye, R., Kenneth Nishimoto, S., Smith, J.C., Baudry, J., Darryl Quarles, L., 2016. Evidence for osteocalcin binding and activation of GPRC6A in beta-cells. Endocrinology 157. https://doi.org/10.1210/en.2015-2010.

Rached, M.T., Kode, A., Silva, B.C., Jung, D.Y., Gray, S., Ong, H., Paik, J.H., DePinho, R.A., Kim, J.K., Karsenty, G., Kousteni, S., 2010. FoxO1 expression in osteoblasts regulates glucose homeostasis through regulation of osteocalcin in mice. J. Clin. Investig. 120 (1), 357–368.

Sabek, O.M., Nishimoto, S.K., Fraga, D., Tejpal, N., Ricordi, C., Gaber, A.O., 2015. Osteocalcin effect on human beta-cells mass and function. Endocrinology 156 (9), 3137–3146.

Sato, M., Asada, N., Kawano, Y., Wakahashi, K., Minagawa, K., Kawano, H., Sada, A., Ikeda, K., Matsui, T., Katayama, Y., 2013. Osteocytes regulate primary lymphoid organs and fat metabolism. Cell Metabol. 18 (5), 749–758.

Steenbergen, R.D., OudeEngberink, V.E., Kramer, D., Schrijnemakers, H.F., Verheijen, R.H., Meijer, C.J., Snijders, P.J., 2002. Down-regulation of GATA-3 expression during human papillomavirus-mediated immortalization and cervical carcinogenesis. Am. J. Pathol. 160 (6), 1945–1951.

Steensberg, A., van Hall, G., Osada, T., Sacchetti, M., Saltin, B., Klarlund Pedersen, B., 2000. Production of interleukin-6 in contracting human skeletal muscles can account for the exercise-induced increase in plasma interleukin-6. J. Physiol. 529 (Pt 1), 237–242.

Tamura, T., Udagawa, N., Takahashi, N., Miyaura, C., Tanaka, S., Yamada, Y., Koishihara, Y., Ohsugi, Y., Kumaki, K., Taga, T., et al., 1993. Soluble interleukin-6 receptor triggers osteoclast formation by interleukin 6. Proc. Natl. Acad. Sci. U. S. A. 90 (24), 11924–11928.

Tao, Y.X., 2010. The melanocortin-4 receptor: physiology, pharmacology, and pathophysiology. Endocr. Rev. 31 (4), 506–543.

Teitelbaum, S.L., Ross, F.P., 2003. Genetic regulation of osteoclast development and function. Nat. Rev. Genet. 4 (8), 638–649.

De Toni, L., De Filippis, V., Tescari, S., Ferigo, M., Ferlin, A., Scattolini, V., Avogaro, A., Vettor, R., Foresta, C., 2014. Uncarboxylated osteocalcin stimulates 25-Hydroxy vitamin D production in Leydig cell line through a GPRC6a-dependent pathway. Endocrinology 155 (11), 4266–4274.

De Toni, L., Guidolin, D., De Filippis, V., Tescari, S., Strapazzon, G., Santa Rocca, M., Ferlin, A., Plebani, M., Foresta, C., 2016. Osteocalcin and sex hormone binding globulin compete on a specific binding site of GPRC6A. Endocrinology 157 (11), 4473–4486.

De Toni, L., Di Nisio, A., Speltra, E., Rocca, M.S., Ghezzi, M., Zuccarello, D., Turiaco, N., Ferlin, A., Foresta, C., 2016. Polymorphism rs2274911 of GPRC6A as a novel risk factor for testis failure. J. Clin. Endocrinol. Metab. 101 (3), 953–961.

Wei, W., Motoike, T., Krzeszinski, J.Y., Jin, Z., Xie, X.J., Dechow, P.C., Yanagisawa, M., Wan, Y., 2014. Orexin regulates bone remodeling via a dominant positive central action and a subordinate negative peripheral action. Cell Metabol. 19 (6), 927–940.

Wei, J., Hanna, T., Suda, N., Karsenty, G., Ducy, P., 2014. Osteocalcin promotes beta-cell proliferation during development and adulthood through Gprc6a. Diabetes 63 (3), 1021–1031.

Yan, Q.W., Yang, Q., Mody, N., Graham, T.E., Hsu, C.H., Xu, Z., Houstis, N.E., Kahn, B.B., Rosen, E.D., 2007. The adipokine lipocalin 2 is regulated by obesity and promotes insulin resistance. Diabetes 56 (10), 2533–2540.

Yao, Q., Yu, C., Zhang, X., Zhang, K., Guo, J., Song, L., 2017. Wnt/beta-catenin signaling in osteoblasts regulates global energy metabolism. Bone 97, 175–183.

Yoshikawa, Y., Kode, A., Xu, L., Mosialou, I., Silva, B.C., Ferron, M., Clemens, T.L., Economides, A.N., Kousteni, S., 2011. Genetic evidence points to an osteocalcin-independent influence of osteoblasts on energy metabolism. J. Bone Miner. Res. 26 (9), 2012–2025.

Zhou, B., Li, H., Liu, J., Xu, L., Zang, W., Wu, S., Sun, H., 2013. Intermittent injections of osteocalcin reverse autophagic dysfunction and endoplasmic reticulum stress resulting from diet-induced obesity in the vascular tissue via the NFkappaB-p65-dependent mechanism. Cell Cycle 12 (12), 1901–1913.

Index for Volumes 1 and 2

'*Note:* Page numbers followed by "f" indicate figures, "t" indicate tables and "b" indicate boxes.'

B

C

D

E

F

H

M

N

O

P

Q

R

T

U

V

W

X

Y

Z

Principles of Bone Biology

FOURTH EDITION

Volume 2

Edited by John P. Bilezikian, T. John Martin, Thomas L. Clemens and Clifford J. Rosen

Preface from the first edition (1996): "The world of modern science is undergoing a number of spectacular events that are redefining our understanding of ourselves. As with any revolution, we should take stock of where we have been, where we are, and where we are going. Our special world of bone biology is participating in and taking advantage of the larger global revolution in modern science… we assembled experts from all over the world and asked them to focus on the current state of knowledge and the prospects for new knowledge in their area of expertise. To this end, Principles of Bone Biology was conceived." - John P. Bilezikian, Lawrence G. Raisz, Gideon A. Rodan

Praise for the previous edition: "Students, teachers, and practitioners will benefit from reading it, and investigators will use it as a reference work; it will certainly be consulted frequently."—The New England Journal of Medicine

For over two decades, "Big Gray" has been the go-to repository of knowledge in the disciplines related to bone and mineral metabolism. The fourth edition is a must-have for students new to the field; young investigators at the graduate or postgraduate level beginning their research careers; established scientists who need to keep up with the changing nature of the field, looking to enrich their own research programs, or who are changing their career direction; clinicians who want ready access to up-to-date relevant basic science.

This new edition builds on the successful formula from previous editions, taking the reader from the basic elements of fundamental research to the most sophisticated concepts in therapeutics. ***Principles of Bone Biology, Fourth Edition*** provides the most comprehensive, authoritative reference on the study of bone biology and related diseases. Bone research continues to generate enormous attention, due to the broad public health implications of osteoporosis and related bone disorders. This classic, fully updated, two volume reference is designed for anyone involved in the study of bone biology.

Key Features:

- Provides a "one-stop" shopping paradise. Anything you want to find about bone biology is here and written by the world's experts
- ***THE*** essential resource for anyone involved in the study of the skeleton and metabolic bone diseases
- Covers everything from the basic scientific concepts to the underlying principles of therapeutics and management
- Allows readers to easily search and locate information quickly in the online format

Volumes include:

- Basic Principles
- Molecular Mechanisms of Metabolic Bone Disease
- Pharmacological Mechanisms of Therapeutics
- Methods in Bone Research

Science / Life Sciences / General

ISBN 978-0-12-814841-9

9 780128 148419

SET ISBN

ISBN 978-0-12-819933-6

9 780128 199336

VOLUME 2

ELSEVIER

ACADEMIC PRESS

An imprint of Elsevier

elsevier.com/books-and-journals